VOLUME 23
1985
ACC. NOS N85-10001 TO N85-36162

STAR
AN ABSTRACT JOURNAL

Scientific and Technical Aerospace Reports

Annual Index 1985

Part One
SUBJECT

PRODUCED BY THE
SCIENTIFIC AND TECHNICAL
INFORMATION
BRANCH

NASA



NATIONAL AERONAUTICS AND SPACE ADMINISTRATION

WHAT YOU CAN DO FOR *STAR*

All users of this abstract service are urged to forward reports to be considered for announcement in *STAR*. This will aid NASA in its efforts to provide the fullest possible coverage of all scientific and technical publications that might support aeronautics and space research and development. If you have prepared relevant reports (other than those that you will transmit to NASA, DoD, or DOE through the usual contract- or grant-reporting channels), please send them for consideration to the NASA Scientific and Technical Information Facility, P.O. Box 8757, B.W.I. Airport, Maryland 21240.

Reprints of journal articles, book chapters, and conference papers are also welcome. These will be considered for announcement in *STAR's* companion journal, *International Aerospace Abstracts*.

You may specify a particular source to be included in a report announcement if you wish; otherwise the report will be placed on public sale at the National Technical Information Service. Copyrighted publications will be announced but not distributed or sold.

PURCHASE OF *STAR*

The semimonthly issues are available postpaid on subscription and in single copy from the Superintendent of Documents, United States Government Printing Office, Washington, D.C. 20402, United States of America.

PUBLISHED BY:

UNITED STATES GOVERNMENT
NATIONAL AERONAUTICS AND SPACE ADMINISTRATION
SCIENTIFIC AND TECHNICAL INFORMATION BRANCH
Scientific and Technical Aerospace Reports, Volume 23, is prepared by the NASA Scientific and Technical Information Facility operated for the National Aeronautics and Space Administration by RMS Associates.

The Administrator of the National Aeronautics and Space Administration has determined that the publication of this periodical is necessary in the transaction of the public business required by law of this Agency. Use of funds for printing this periodical has been approved by the Director of the Office of Management and Budget through March 22, 1988.

US ISSN 0036-8741

SPECIAL NOTICE

The abstract sections of the semimonthly *STAR* journals can be bound separately. Individual abstracts can be located readily be means of the page numbers given at each entry, e.g., p 2207. To assist the user in binding *STAR* Volume 23, four (4) title pages are included in the back of Part I of the Annual Index.

For sale by the Superintendent of Documents, U.S. Government Printing Office Washington, D.C. 20402

AT

VOLUME 23 NUMBERS 1-24

Scientific and Technical Aerospace Reports

Annual Index (Part I) January – December 1985

TABLE OF CONTENTS

Page

PART I

Introduction iii
Subject Index A-1

PART II

Introduction iii
Personal Author Index B-1
Corporate Source Index C-1
Contract Number Index D-1
Report/Accession Number Index E-1

INTRODUCTION

WHAT STAR ANNUAL INDEXES ARE

This Annual Index is an edited consolidation of the indexes to the individual issues of *Scientific and Technical Aerospace Reports (STAR)* for the calendar year 1985 (Volume 23 Numbers 1 through 24). For the convenience of the user, it is divided into two parts, each bound separately. Part I contains the Subject Index. Part II contains the Personal Author Index, Corporate Source Index, Contract Number Index, and Report/Accession Number Index. The Annual Index supersedes the semimonthly indexes previously issued during 1985.

Each entry in this index includes a group of identifying numbers in the following form: 23 p 3906 N85-34200. The first two digits (23) identify the issue in which the document was announced. The "p" and the four digits that follow (3906) refer to the page number, in the designated issue, on which the abstract of the document appears. The next group of numbers (N85-34200) is the NASA Accession Number, a unique identification number assigned by NASA to each document that was acquired, indexed, and announced in *STAR* during the year.

In addition to these identifying numbers each entry in the Subject Index contains a title or title and title extension. Each entry in the Personal Author and Corporate Source Indexes contains the title of the document.

At the beginning of each index in this cumulation, a typical listing is illustrated with each of its elements identified to assist the reader in using the different types of index entries.

HOW TO USE THE SUBJECT INDEX

Subject terms in this cumulative index are arranged alphabetically, and are supplemented with cross-references which are intended to serve as directions that will enable the user to modify, enlarge, or narrow his search in accordance with his specific interests. The subject headings have been selected from the latest revision of the *NASA Thesaurus*. Two types of cross-references are used:

1. Use (U) references direct the user to alternate headings under which material on the subject may be found. For example:

   ANNULAR JETS
   U ANNULAR FLOW
   U JET FLOW
   COLUMBIAN
   U NIOBIUM

2. Narrower Term (NT) references refer the user to more specific headings in the same subject area, under which additional material on the subject may be found. For example:

   EMISSION
   NT ELECTRON EMISSION
   NT NEUTRON EMISSION
   NT THERMAL EMISSION

Finally, a searcher should use the titles and title extensions in the index to narrow further his quest for particular items. This is because subject terms can readily refer to more than one class of document. For example:

CATHODES
Cesium plasma cathodes as sources of high intensity electron beams
Cathode material testing in electrochemical half cells

This illustrates a case where two references on different topics are listed under the same subject term.

HOW TO USE THE PERSONAL AUTHOR INDEX

All personal authors identified in the abstract-section citations in the individual *STAR* issues appear in this index. Differences in transliteration schemes may require multiple searching of the index for variants of an author's name. For example:

EMELIANOV, M. D.
YEMELYANOV, M. D.

HOW TO USE THE CORPORATE SOURCE INDEX

The corporate source index entries are abridged versions of the corporate sources used in the abstract-section citations in the individual issue supplements. The corporate source supplementary (organizational component) does not appear in the index. For example:

PRINCETON UNIV., N.J. DEPT. OF CHEMICAL ENGINEERING.
(Corporate source at citation)
PRINCETON UNIV., N.J.
(Corporate source index entry)

HOW TO USE THE CONTRACT NUMBER INDEX

All contract numbers that are identified in the abstract-section citations in the individual *STAR* issues appear in this index. Changes by agencies in the style in which contract numbers are presented may require multiple searching for variants. For example:

AF 33(615)-67-C-1758
F33615-67-C-1758

HOW TO USE THE REPORT/ACCESSION NUMBER INDEX

All report numbers that have been assigned by the corporate source, monitoring activity, or cataloging activity appear in this index. Variations in initial input may result in different report number series. For example:

TP-924
ONERA-TP-924

A COMPREHENSIVE INFORMATION SERVICE

The National Aeronautics and Space Administration makes the results of worldwide research and development activities in aeronautics, space, and supporting disciplines promptly available to participants in its programs. NASA's scientific and technical information system now contains over two million documents, which are abstracted, indexed, and obtained through retrieval and dissemination services. These services which include the abstract journal, *Scientific and Technical Aerospace Reports (STAR),* are described fully in a bulletin, *The NASA Scientific and Technical Information System ... and How to Use It,* available at no charge from the NASA Scientific and Technical Information Facility, P.O. Box 8757, B.W.I. Airport, Maryland 21240.

AVAILABILITY OF DOCUMENTS

Information concerning the availability of documents announced in the *STAR* issues covered in this index is found in the Introduction to the most currently issued semimonthly issue.

PUBLIC COLLECTIONS OF NASA DOCUMENTS

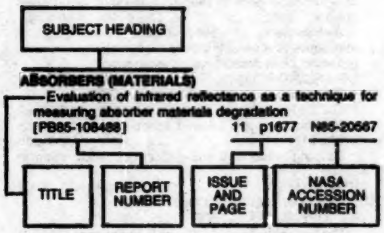
DOMESTIC: NASA and NASA-sponsored documents and a large number of aerospace publications are available to the public for reference purposes at the library maintained by the American Institute of Aeronautics and Astronautics, Technical Information Service, 555 West 57th Street, 12th Floor, New York, New York 10019.

EUROPEAN: An extensive collection of NASA and NASA-sponsored publications is maintained by the British Library Lending Division, Boston Spa, Wetherby, Yorkshire, England for public access. The British Library Lending Division also has available many of the non-NASA publications cited in *STAR*. European requesters may purchase facsimile copy or microfiche of NASA and NASA-sponsored documents, those identified by both the symbols # and * from ESA — Information Retrieval Service European Space Agency, 8-10 rue Mario-Nikis, 75738 CEDEX 15, France.

FEDERAL DEPOSITORY LIBRARY PROGRAM

In order to provide the general public with greater access to U.S. Government publications, Congress established the Federal Depository Library Program under the Government Printing Office (GPO), with 50 regional depositories responsible for permanent retention of material, inter-library loan, and reference services. Over 1,300 other depositories also exists. A list of the regional GPO libraries appears on the inside back cover.

Typical Subject Index Listing



The subject heading is the key to the subject content of the document. Titles, issues, page numbers, report numbers, and accession numbers of pertinent documents are provided under each subject heading. When the title is insufficiently descriptive of the document content, a title extension has been added, separated by three hyphens. The report number helps to indicate the type of document cited (e.g., NASA report, translation, NASA contractor report). The issue and page identify the *STAR* issue in which the document was announced and the page number on which the citation appears. The accession number denotes the number by which the citation is identified on that page. The titles are arranged under each subject heading in ascending accession number order. The subject headings have been selected from the latest revision of the *NASA Thesaurus* (NASA SP-7051).

A

A STARS
Hyades moving group 05 p0740 N85-14757
The velocity-age relation for B and A stars 05 p0740 N85-14762
Kinematics of B and A stars 05 p0741 N85-14766
A type stars as probes of the local interstellar medium 06 p0874 N85-15550

A-7 AIRCRAFT
The development of a performance and mission planning program for the A-7E aircraft
[AD-A151717] 15 p2471 N85-25258

A-10 AIRCRAFT
Peripheral vision horizon display on the single seat night attack A-10 01 p0009 N85-10053
Performance evaluation of A-10 aircraft maintenance units and aircraft using constrained facet analysis
[AD-A146955] 07 p0893 N85-15660

A-310 AIRCRAFT
Statistical study of the dynamic analysis of the workload in the A310 certification campaign 16 p2544 N85-27531

A-320 AIRCRAFT
Description of MBB computerized design techniques for A320 08 p1141 N85-17194
Design of the nacelle for the A-320 aircraft
[SNIAS-851-111-111] 20 p3363 N85-31046

ABEL FUNCTION
A continuous Helson surface in R3 11 p1698 N85-20674

ABERRATION
Effect of aberration in optical system on illuminance distribution over image of strip in semicoherent light 06 p0777 N85-14870
Light scattered from polished optical surfaces: Wings of the point spread function 08 p1252 N85-17911
Aberration characteristics of plane-parallel compensator plate 14 p2276 N85-24100
Stimulated Brillouin scattering reflectivity in the presence of various aberrators
[AD-A151750] 15 p2563 N85-25812
Method of measuring spherical aberration and apparatus therefor
[AD-D011706] 19 p3367 N85-30882
Theoretical modeling of laser induced optical degradation
[AD-A155302] 21 p3592 N85-32323
New method for correcting chromatism of mirror-lens objectives 21 p3696 N85-32965

ABILITIES
An investigation of the effect of correlated abilities on observed test characteristics
[AD-A144869] 01 p0113 N85-10765
Trends in skill and accuracy of National Weather Service pop forecasts
[PB84-229053] 06 p0840 N85-15335
Training high performance skills: Fallacies and guidelines
[AD-A148574] 08 p1196 N85-17545
A theorem on the optimal allocation of effort
[AD-A148028] 08 p1211 N85-17623

ABIOGENESIS
Estuaries of the Cape. Part 2: Synopses of available information on individual systems. Report 13: Silvermine (CSW 3)
[CSIR-RR-412-PT-2] 01 p0066 N85-10582
Estuaries of the Cape. Part 2: Synopses of available information on individual systems. Report no. 16: Eerste (CSW 6)
[CSIR-RR-415-PT-2] 01 p0067 N85-10585

ABLATION
A T-matrix theory of galactic heavy-ion fragmentation
[NASA-TP-2363] 08 p1221 N85-17690
Laser ablation studies using RIS
[DE85-001118] 09 p1326 N85-18336
Atmospheric profile imprint in firewall ablation coefficient 11 p1662 N85-20473
Charge-to-mass dispersion methods for abrasion-ablation fragmentation models
[NASA-TM-86340] 11 p1726 N85-20657
Alternate nozzle ablative materials program
[NASA-CR-175658] 14 p2246 N85-23924
Examination of a method for predicting the properties of railgun plasmas
[AR-004-322] 17 p3039 N85-28799
Numerical studies of ablation and ionization of railgun materials
[DE85-010741] 19 p3223 N85-29983
One method of solving the problem of unsteady heat exchange of a body and its ablation 22 p3733 N85-33146
Laser effects on opaque targets. Part 2C: Thermal effects of a time-variable beam intensity
[ISL-R-105/84-PT-2C] 22 p3791 N85-33486
Thermal transport measurements of UV laser irradiated spherical targets
[DE85-011038] 23 p3931 N85-34365
A study of the chemistry of alkali metals in the upper atmosphere
[AD-A156349] 24 p4117 N85-35524

ABLATIVE MATERIALS
Thermal design of the space shuttle solid rocket booster 08 p1103 N85-16878
Adequacy of metal ablation process with laser radiation and a shock-compressed plasma 13 p2028 N85-22708
Experimental study of enthalpy of quasimonocrystal of graphite and carbon glass in temperature range of 2890-3818 deg K 13 p2036 N85-22751
Seven-wavelength pyrometer for determining surface temperature of ablation materials
[NASA-TM-77832] 14 p2305 N85-24288
Thermal protection systems for reentry vehicles
[CNES-NT-113] 23 p3900 N85-34157

ABORT TRAJECTORIES
Study of several factors affecting crew escape trajectories from the Space Shuttle Orbiter at low-subsonic speeds
[NASA-TM-86303] 10 p1428 N85-19008

ABRASION
Structure and wear workshop colloquium 01 p0054 N85-10356
The influence of the carbide distribution on the abrasive wear of ledeburitic chromium steels 01 p0054 N85-10359
Structure and abrasive resistance of iron based alloys rich in hardening components 01 p0054 N85-10360
Microstructural effects in abrasive wear
[DE84-016155] 04 p0509 N85-13247
A T-matrix theory of galactic heavy-ion fragmentation
[NASA-TP-2363] 08 p1221 N85-17690
Effect of microstructure on solid particle erosion in multiphase materials
[DE85-000426] 11 p1608 N85-20109
Charge-to-mass dispersion methods for abrasion-ablation fragmentation models
[NASA-TM-86340] 11 p1726 N85-20657
A comparison of terrestrial saltation flux in the laboratory and the field 13 p2189 N85-23582
Abrasive cutting-off wheel 15 p2566 N85-25843
Microstructure-abrasive wear characteristics of low carbon dual phase steels
[DE85-010666] 19 p3239 N85-30083
Impact dynamics research on composite transport structures
[NASA-TM-86391] 19 p3284 N85-30967
Three body abrasive wear in various metal combinations 23 p3908 N85-34200

ABRASION RESISTANCE
Experimental AC (Asphalt Concrete) overlays of PCC pavement
[PB84-218171] 03 p0342 N85-12203
Effects of B, Ti and Ta implantation on the wear resistance of Fe and Ni-plated Fe
[AD-A149947] 12 p1806 N85-21330
Effect of zero-wear in friction pairs operating in abrasive media 13 p2045 N85-22801
Role of fluid lubricant-coolant in fine grinding of optical glass by diamond tool 14 p2280 N85-24125
Wear improvement in titanium alloys by ion implantation
[AD-D011694] 19 p3239 N85-30081

ABRASIVES
Abrasive products study
[PB84-223636] 01 p0033 N85-10205
Effect of microstructure on solid particle erosion in multiphase materials
[DE85-000426] 11 p1608 N85-20109
The effect of abrasive blasting on the fatigue and corrosion of an aluminium-copper alloy
[AD-A154954] 21 p3566 N85-32182

ABSORBENTS
Desorption efficiences of vapor phase polynuclear aromatic compounds on solid adsorbents
[DE85-001303] 10 p1436 N85-19052
The effects of water and hydrogen on materials used in integrated circuit packages
[AD-A151883] 15 p2518 N85-25529
Flight-service program for advanced composite rudders on transport aircraft
[NASA-CR-174637] 19 p3217 N85-29950
Improved catalysts for liquid hydrocarbon fuels from syngas
[DE85-011082] 20 p3421 N85-31234
Molecular and macromolecular sieving by asymmetric ultrafiltration membranes
[PB85-157766] 24 p4077 N85-35266

ABSORBERS (MATERIALS)
Evaluation of infrared reflectance as a technique for measuring absorber materials degradation
[PB85-108488] 11 p1677 N85-20667
Correctness of reflection characteristics of radio absorbent materials 13 p2061 N85-22966
Capture of liquid hydrogen boiloff with metal hydride absorbers
[NASA-CR-175677] 14 p2249 N85-23939
Measured acoustic properties of variable and low density bulk absorbers
[NASA-TM-87065] 19 p3351 N85-30770
Choice of optimum saturable absorber for YAG passive mode-locking laser 21 p3695 N85-32993

SELECT

ABSORPTANCE
Changes in spectral properties of detached leaves
[E85-10042] 07 p0983 N85-16243
Effect of integration time on precision of absorbances measured with a diode array UV-VIS spectrophotometer
[AD-A149952] 07 p1043 N85-16624
A calorimetric approach for measuring emittance and normal spectral absorptance at elevated temperatures
[AD-A151292] 15 p2651 N85-26351
Thermal consequences of localized SAR from RFR exposures 16 p2775 N85-27130

ABSORPTION
Water absorption and conductivity in poly(ethylene oxide)-lithium tetrafluoroborate films
[AD-A147969] 10 p1450 N85-19138
Nebulization reflux concentrator
[NASA-CASE-LAR-13254-1] 11 p1615 N85-20154
Collaborative shock tube studies of benzene pyrolysis
[DE85-006347] 14 p2253 N85-23962
Process for clarification of water
[DE85-007864] 17 p2923 N85-28023
Chromophores with auxochrome-like function
[NASA-TM-77849] 20 p3421 N85-31233
Quasi-steady-state melting mode during combined laser irradiation of semiconductor materials 21 p3682 N85-32674

ABSORPTION BANDS
U ABSORPTION SPECTRA

ABSORPTION COEFFICIENT
U ABSORPTIVITY

ABSORPTION COOLING
Mathematical models for the boiling diagram of the ideal two-component mixture
[DFVLR-FB-84-22] 04 p0471 N85-13000
Performance evaluation of an active solar cooling system utilizing low cost plastic collectors and an evaporatively-cooled absorption chiller
[DE84-010813] 12 p1860 N85-21798
Testing and further development of a solar absorption cooling plant
[BMFT-FB-T-84-264] 15 p2588 N85-25954
Ten degree Kelvin hydride refrigerator
[NASA-CASE-NPO-16393-1-CU] 18 p3085 N85-29084

ABSORPTION CROSS SECTIONS
Remote sensing of atmospheric gases with CO2 lasers. Continuation and conclusion of spectroscopic investigations
[BMFT-FB-W-84-030] 07 p0989 N85-16285
MSG-7: Molecular absorption processes related to the penetration of ultraviolet solar radiation into the middle atmosphere 11 p1658 N85-20449
Chemical kinetics and photochemical data for use in stratospheric modeling. Evaluation number 6
[NASA-CR-175564] 12 p1868 N85-21849
Workshop report on new directions in soft X-ray photoabsorption
[DE85-006150] 14 p2419 N85-24923
Tables of nuclear cross sections for galactic cosmic rays: Absorption cross sections
[NASA-RP-1134] 16 p2864 N85-27665
Hydrogen absorption in metals: A field ion microscopy study
[DE85-010299] 18 p3076 N85-29026
Opticals constant at X-ray wavelengths
[DE85-009743] 19 p3355 N85-30795
Absorption of 10.6 micrometer laser radiation in electron-hole condensate in germanium 21 p3681 N85-32870
An attempt to detect induced neutron capture in laser radiation field 21 p3690 N85-32928
Determination of band oscillator strengths of atmospheric molecules from high resolution vacuum ultraviolet cross section measurements
[NASA-CR-176150] 22 p3814 N85-33624
Monte Carlo learning-biasing experiment with intelligent random numbers
[DE85-010713] 22 p3834 N85-33742
Dissociative and double photoionization cross sections of NO from threshold to 120 A
[NASA-CR-176185] 24 p4147 N85-35713

ABSORPTION SPECTRA
NT FRAUNHOFER LINES
Middle infrared spectral studies of geologic materials in their natural state using photothermal beam deflection spectroscopy
[AD-A144894] 01 p0120 N85-10820
Nonlinear absorption of laser radiation in InP and in GaAs 02 p0266 N85-11740
Simultaneous measuring absorption spectrometer
[BMFT-FB-T-84-132] 03 p0365 N85-12339
Ice-soil mixtures: Visual and near-infrared remote sensing techniques
[NASA-CR-174087] 04 p0525 N85-13358
Saturation phenomena in LIF measurements, appendix B 05 p0676 N85-14339
Evidence for pairing of implanted nitrogen in silicon
[DE84-015622] 06 p0868 N85-15517
Absorption line studies and the distribution of neutral gas in the local interstellar medium 06 p0873 N85-15544
A type stars as probes of the local interstellar medium 06 p0874 N85-15550
Optical observations of nearby interstellar gas 06 p0875 N85-15557
Observations of absorption lines from highly ionized atoms 06 p0876 N85-15562
Detection of narrow C 4 and Si 4 absorption features in spectra of stars within 200 pc f the Sun 06 p0876 N85-15564
The smallest sizes of diffuse interstellar clouds 06 p0878 N85-15578
Stromgren trails of hot white dwarfs 06 p0879 N85-15589
Measurement of soft X-ray absorption spectra with a fluorescent ion chamber detector
[AD-A142213] 07 p0922 N85-15836
Narrow absorption components in Be star winds 06 p1232 N85-17760
Low excitation absorptions in the spectrum of the quasar PKS 1327-206 due to the galaxy MCG 03-34-085 08 p1237 N85-17801
The extragalactic nature of H0323+022 08 p1237 N85-17802
A study of the K-edge absorption spectra of selected vanadium compounds
[AD-A149334] 10 p1435 N85-19045
Quantum mechanical and semiclassical approaches to molecular dynamics
[DE85-003458] 10 p1555 N85-19803
IUE absorption line studies of highly ionized interstellar gas 11 p1743 N85-20962
Galactic absorption lines measured from the IUE low dispersion spectra of active galaxies 11 p1745 N85-20977
High-velocity interstellar gas in the line-of-sight to HD 50896 11 p1749 N85-20999
An episodic red-wing structure of SiIV, lambda 1394A, in gamma Cas 11 p1750 N85-21009
FP Cygni profiles in HL CMa 11 p1752 N85-21022
Ultraviolet spectroscopy of the interacting binary U Sagittae 11 p1755 N85-21042
Ultraviolet observations of circumstellar matter in Algol type binary systems 11 p1756 N85-21043
Ultraviolet, radio and X-ray observations of hybrid stars 11 p1759 N85-21063
The effects of atmospheric water vapor on infrared propagation
[AD-A150030] 12 p1934 N85-22150
Below-room-temperature water-vapor continuum absorption within the 8- to 10 micron atmospheric transmission window
[TR-0084(4945-09)-1] 13 p2132 N85-23266
Studies of galactic HI in 21-centimeter absorption 13 p2170 N85-23466
First direct detection of clay minerals on Mars 13 p2194 N85-23612
Reassignment of the iron (3) absorption bands in the spectra of Mars 13 p2195 N85-23614
Determination of mineral type, abundance, and grain size with remotely obtained reflectance spectra 13 p2196 N85-23623
An atlas of pure water vapor spectra from 500 to 5000/cm, volume 1
[AD-A151756] 15 p2505 N85-25454
X-ray spectroscopy of solids under pressure
[DE85-006939] 15 p2507 N85-25465
Possible uses of tunable diode lasers in infrared spectroscopy
[ESA-TT-869] 15 p2564 N85-25818
High-frequency microwave observations of convective precipitation 15 p2596 N85-26000
A measurement of the vibrational band strength for the upsilon sub 3 band of the HO2 radical
[NASA-CR-175858] 16 p2744 N85-26936
An atlas of pure water vapor spectra from 500 to 5000/cm, Volume 2
[AD-A151757] 16 p2745 N85-26940
Effects of temperature on remotely sensed mafic mineral absorption features 16 p2809 N85-27323
Hydrogen absorption in metals: A field ion microscopy study
[DE85-010299] 18 p3076 N85-29026
Thermal donor removal by rapid thermal annealing: Infrared absorption
[DE85-010092] 18 p3081 N85-29059
The development of new techniques in laser spectroscopy 19 p3233 N85-30041
Separation of Drude and band-to-band spectra in polyvalent metals
[DE85-010247] 19 p3240 N85-30093
A study of Co and Mn in ZnO varistors
[DE85-011193] 19 p3263 N85-30233
Combustion control with smart sensors
[DE85-009419] 19 p3274 N85-30303
Sensitive detection of tunable diode laser absorption by polarization rotation
[DE85-009821] 19 p3277 N85-30322
Structure and chemistry of sol-gel derived transparent silica aerogel
[DE85-009902] 20 p3434 N85-31303
Doppler spectrometer for measuring narrow photochemical gaps in inhomogeneously broadened spectra 21 p3689 N85-32921
Determination of band oscillator strengths of atmospheric molecules from high resolution vacuum ultraviolet cross section measurements
[NASA-CR-176150] 22 p3814 N85-33624
The universal spectrum of AGNs and QSOs
[OG-2.7-9] 22 p3872 N85-33982
Time-resolved and infrared spectroscopy of excitons
[DE85-011879] 23 p3912 N85-34235
Dangling bonds and sub-gap optical absorption in silicon
[DE85-011752] 24 p4082 N85-35302

ABSORPTION SPECTROSCOPY
NT OPTOGALVANIC SPECTROSCOPY
The X-ray Absorption Coefficient Fine Structure (EXAFS) study on precipitates in AlCu
[DESY-SR-84-15] 01 p0025 N85-10153
Experimental capabilities and prospects for measuring soft X-ray photoabsorption
[DE84-015468] 02 p0278 N85-11813
Mossbauer spectroscopic investigations of the diffusion and correlation of lattice defects (complementary to neutron spectroscopic investigations) 03 p0429 N85-12736
Direct measurements of nitrous acid, nitrogen dioxide and formaldehyde in auto exhaust by differential optical absorption spectroscopy
[PB84-229269] 06 p0767 N85-14905
Effect of ultraviolet radiation on transparent polymer films as determined using in situ FTIR-RA spectroscopy. Volume 2: Photophysics of poly(vinylidene fluoride) films
[DE84-013040] 09 p1299 N85-18159
Carbon monoxide adsorption on a platinum electrode studied by polarization modulated FT-IRRAS (Fourier Transform-IR Reflections Adsorption Spectroscopy). Part 1: CO adsorbed in the double layer potential region and its oxidation in acids
[AD-A149751] 12 p1800 N85-21288
Effect of ultraviolet radiation on transparent polymer films as determined using in situ FTIR-RA spectroscopy. Volume 1: Photodegradation of transparent polymer films
[DE84-013039] 12 p1814 N85-21377
Spectroscopic studies of lead oxide in a flow tube
[AD-A151849] 15 p2505 N85-25455
High resolution spectroscopy of C13O16 in gas mixtures
[AD-A152625] 17 p2919 N85-27991
Spectroscopy of surface adsorbed molecules
[DE85-009452] 17 p3034 N85-28766
Recent advances in optical measurement methods in physics and chemistry
[DE85-008695] 17 p3037 N85-28792
Digital control of diode laser for atmospheric spectroscopy
[NASA-CASE-NPO-16000-1] 18 p3112 N85-29264
Formation and fate of toxic chemicals in California's atmosphere
[PB85-172609] 18 p3134 N85-29414
Structural and physical studies on a new class of low-dimensional conducting material: FeOCl intercalated with TTF and related molecules
[DE85-009701] 18 p3196 N85-29824
Clay identification and amount measured by laboratory techniques compared to well log responses: Application to tight gas sands and shales
[DE85-010411] 19 p3362 N85-30843
Differential optical absorption techniques for diagnostics of coal gasification
[DE85-010177] 19 p3368 N85-30890
X-ray spectroscopy of solids under pressure
[DE85-011466] 22 p3745 N85-33213

ABSORPTIVE INDEX
U ABSORPTIVITY

ABSORPTIVITY
In vivo dermal absorption method and system for laboratory animals
[AD-D011231] 01 p0094 N85-10635
Change in Venusian atmosphere absorption coefficient with altitude 02 p0163 N85-11103
Laboratory investigation of coefficients of absorption of air at Lambda = 10.6 microns 02 p0263 N85-11723

Characteristics of absorption and frequency filtration of ULF electromagnetic waves in the ionosphere
03 p0376 N85-12402
Ice-soil mixtures: Visual and near-infrared remote sensing techniques
[NASA-CR-174087] 04 p0525 N85-13358
GaAs material properties and models
05 p0665 N85-14277
Anti-reflection coatings materials and models
05 p0665 N85-14278
Analysis of optical and electrical performance of a TCP-coated solar cell 06 p0832 N85-15293
Absorption and emission of EUV radiation by the local ISM 06 p0876 N85-15563
Optical properties of composite materials
[AD-A146768] 07 p0920 N85-15828
Continuum absorption by H2O in the 700-1200 cm(-1) and 2400-280 cm(-1) windows
[AD-A147391] 07 p0997 N85-16334
Estimate of sound absorption due to magnetoelastic interactions
[AD-A148216] 08 p1218 N85-17671
USSR report: Physics and mathematics
[JPRS-UPM-85-001] 11 p1715 N85-20786
Phonon-impurity relaxation and acoustic wave absorption in yttrium-aluminum garnet crystals with impurities 11 p1715 N85-20790
Effect of impurities on absorption in semiconductors and lasing of semiconductor lasers 11 p1716 N85-20797
A method for determining in situ the absorption coefficient of particulate media using pulsed laser technique
[AD-D011548] 12 p1799 N85-21281
Investigation of absorptive electrochemical systems for display applications
[BMFT-FB-T-84-301] 15 p2507 N85-25467
Kinetic studies following state selective laser excitations
[DE85-007173] 15 p2584 N85-25816
Submillimeter-band solid state distributed feedback laser 15 p2644 N85-26307
Comprehensive silicon solar cell computer modeling
[NASA-CR-175959] 17 p2987 N85-28461
Selective radiative cooling with MgO and/or LiF layers
[DE85-011595] 19 p3262 N85-30228
Optical stability, atmospheric transparency and aerosol absorption 19 p3297 N85-30442
Variability of rural aerosols under stable weather conditions 21 p3647 N85-32663
Absorption of laser radiation in substance with absorption coefficient depending linearly upon temperature 21 p3684 N85-32953
Coefficient of optical absorption and scattered light capture effect 21 p3695 N85-32959
Aluminum work function: Effect of oxidation, mechanical scraping and ion bombardment
[NASA-TM-87079] 23 p3915 N85-34265
Acoustical absorption coefficient in a diffuse field of a plane, rectangular material of finite dimensions placed on an infinite perfectly reflecting surface
[NRC/CNR-TT-2113] 23 p3968 N85-34599
X-ray spectra of bursting neutron stars
23 p3981 N85-34686
Underwater measurements of muon intensity
[HE-5.1-16] 24 p4202 N85-36078

ABSTRACTS

Center for Electronics and Electrical Engineering Technical Bulletin covering center programs with 1984 CEEE events calendar
[PB84-222785] 01 p0045 N85-10292
Center for Electronics and Electrical Engineering Technical Bulletin covering center programs with 1984 CEEE events calendar
[PB84-223684] 01 p0045 N85-10293
Center for Electronics and Electrical Engineering Technical Bulletin covering center programs
[PB84-219716] 01 p0045 N85-10295
Center for Electronics and Electrical Engineering Technical Bulletin covering center programs
[PB84-218056] 01 p0045 N85-10296
Geology and geomorphology of the southern central Blue Ridge: An indexed bibliography
[PB84-225119] 01 p0072 N85-10480
Publications of the National Bureau of Standards, 1983 catalog
[PB84-218031] 01 p0126 N85-10669
European Scientific Notes, Number 38-9
[AD-A145683] 02 p0306 N85-11975
National Photovoltaics Program Annual Review Meeting, abstracts
[DE84-013003] 04 p0530 N85-13390
Abstract and index collection
[PB85-119501] 10 p1569 N85-19892
Model of information-reference dialogue system for working with document abstracts
12 p1903 N85-21949
Aerospace Medicine and Biology: A continuing bibliography with indexes, supplement 267, January 1985
[NASA-SP-7011(267)] 12 p1904 N85-21959
Evaluation of the vocabulary switching systems
[PB85-127157] 12 p1951 N85-22260
Schema theory in the representation and analysis of text 14 p2433 N85-25004
Air Force Office of Scientific Research (AFOSR): Technical report summaries. Fourth quarter (CY)
[AD-A150860] 14 p2456 N85-25167
A summary of the Naval Postgraduate School research program
[AD-A151721] 16 p2875 N85-27738
Compilation of abstracts of theses submitted by candidates for degrees
[AD-A151722] 16 p2875 N85-27739
Summary of Research, Academic Departments, 1983 - 1984
[AD-A151724] 16 p2875 N85-27741
Bibliography of Lewis Research Center technical publications announced in 1984
[NASA-TM-87012] 17 p3049 N85-28876
Proceedings of the 10th Annual Conference of the Finnish Physical Society
[REPT-104] 20 p3532 N85-31974
Seventh Symposium on Biotechnology for Fuels and Chemicals: Program and abstracts
[DE85-011197] 22 p3742 N85-33192
1985 Amorphous Silicon Review Meeting
[DE85-008794] 22 p3807 N85-33582
A hierarchy of knowledge levels implemented in a rule-based production system to calculate bounds on the size of intersections and unions of simple sets
[AD-A155291] 22 p3848 N85-33836
NASA patent abstracts bibliography: A continuing bibliography. Section 1: Abstracts (supplement 27)
[NASA-SP-7039(27)-SECTION-1]
22 p3849 N85-33840
Monitoring building energy performance: An informal review and characterization of research in progress
[BNL-51765] 23 p3923 N85-34308
Center for Electronics and Electrical Engineering technical progress bulletin covering center programs, July-September with 1985 CEEE events calendar
[PB85-191393] 24 p4091 N85-35363

ABUNDANCE

Giacobini-Zinner comet: Polarimetric and physical observations
[NASA-TM-77771] 01 p0130 N85-10894
Contribution to the radiogeology of Sao Roque, SP, granites
[INPE-3079-PRE/492] 03 p0391 N85-12503
Ge abundances in the lunar mantle and implications for the origin of the Moon 04 p0582 N85-13721
Origin of the Moon 04 p0587 N85-13745
Pioneer 10 and Voyager observations of the interstellar medium in scattered emission of the He 584 A and H Lya 1216 A lines 06 p0873 N85-15541
Deuterium abundance in the local interstellar medium
06 p0874 N85-15552
Boron cosmochemistry 06 p0888 N85-15642
Differentiated meteorites and the components of chondrites
[NASA-CR-174201] 06 p0890 N85-15649
The abundance of deuterium in the outer solar system from ground-based measurements of monodeuterated methane 07 p1060 N85-16725
Measurements of H2O in Jupiter's atmosphere from 5 microns airborne observations 08 p1244 N85-17854
Elemental abundances of mercury-manganese stars and the population 2 type star HD 109995
[NASA-CR-174298] 08 p1255 N85-17913
Boundary conditions for the paleoenvironment: Chemical and physical processes in the pre-solar nebula — molecular clouds, interstellar matter, and abundance
[NASA-CR-174370] 10 p1570 N85-19001
IUE observations of planetary nebulae in the Magellanic Clouds 11 p1747 N85-20986
The Jovian Stratosphere in the ultraviolet
11 p1760 N85-21069
Cosmic ray composition and origin
12 p1955 N85-22287
A Jamin interferometer to determine the helium abundance in the atmosphere of Jupiter
[BONN-IR-83-17] 12 p1961 N85-22329
Relative abundances of sub-iron to iron nuclei in low energy (50-250 MeV/N) cosmic rays as observed in the Skylab experiment
[OG-4.1-4] 22 p3876 N85-34010
Cosmic ray charge and energy spectrum measurements using a new large area Cerenkov x dE/dx telescope
[OG-4.1-5] 22 p3876 N85-34011
The energy dependence of the neon-22 excess in the cosmic radiation
[OG-4.3-7] 22 p3879 N85-34032
Initial results from the Caltech/DRSI balloon-borne isotope experiment
[OG-4.3-8] 22 p3879 N85-34033
Ariel 6 measurements of ultra-heavy cosmic ray fluxes in the region 34 or = Z or = 48
[OG-4.4-3] 22 p3879 N85-34036
Ariel 6 measurements of ultra-heavy cosmic ray fluxes in the region Z or = 48
[OG-4.4-4] 22 p3880 N85-34037
Elemental abundances of cosmic rays with Z 33 as measured on HEAO-3
[OG-4.4-5] 22 p3880 N85-34038
Abundances of secondary elements among the ultra heavy cosmic rays: Results from HEAO-3
[OG-4.4-6] 22 p3880 N85-34039
Capabilities of the LDEF-2 heavy nuclei collection
[OG-4.4-8] 22 p3880 N85-34040
Ultraheavy cosmic ray tracks in meteorites: A reappraisal, based on calibrations with relativistic ions
[OG-4.4-10] 22 p3880 N85-34041
Solar Coronal and photospheric abundances from solar energetic particle measurements
[SH-2.1-5] 23 p3998 N85-34788
Variations in elemental composition of several MEV/nucleon ions observed in interplanetary space
[SH-2.1-7] 23 p3998 N85-34788
Anomalous abundances of solar energetic particles and coronal gas: Coulomb effects and First Ionization Potential (FIP) ordering
[SH-2.1-10] 23 p3999 N85-34791
Abundances from solar-flare gamma-ray line spectroscopy
[SH-2.1-13] 23 p3999 N85-34794
Solar flare gamma-ray line spectroscopy
[SH-2.1-14] 23 p3999 N85-34795
Elemental abundance differences between nuclei accelerated in CIR shocks and solar flares
[SH-2.2-6] 23 p4000 N85-34801
The heavy ion composition in 3HE-rich solar flares
[SH-2.2-7] 23 p4000 N85-34802
Germanium and lead: Significant differences between meteoritic and photospheric abundances?
[OG-7.1-2] 23 p4012 N85-34864
Lead and uranium group abundances in cosmic rays
[OG-7.1-3] 23 p4013 N85-34865
Implications of source abundances of ultraheavy cosmic rays
[OG-7.1-4] 23 p4013 N85-34866
Alfven wave scattering and the secondary to primary ratio
[OG-7.2-9] 23 p4015 N85-34878
Do supernovae of type 1 paly a role in cosmic-ray production?
[OG-8.2-5] 23 p4019 N85-34905
Bursting star formation and the oversabundance of Wolf-Rayet stars
[OG-8.2-8] 23 p4019 N85-34907
Measurement of low energy cosmic rays aboard Spacelab-1
[SH-10.1-6] 23 p4053 N85-35137

AC (CURRENT)

U ALTERNATING CURRENT

AC GENERATORS

The microprocessor control of a motor-alternator
[RAE-TM-NAV-ENG-1023(L)] 02 p0244 N85-11501
Vibroacoustic control diagnostics of selected machines based on research on the slide bearing of an automobile engine and the alternator
[ISSN-0208-5658] 05 p0641 N85-14112
Two-rotor alternators with superconductor field winding 06 p0795 N85-15082
The ferrite permanent magnet AC motor: A technical and economical assessment
[DE85-002480] 13 p2066 N85-22903
Batteryless magneto-driven portable radiac
[DE85-011622] 22 p3760 N85-33300

ACCELERATED LIFE TESTS

Cyclic endurance testing of the RB211-22B cast HP turbine blade — high pressure (HP)
[PNR-90210] 03 p0320 N85-12063
Accelerated viscoelastic characterization of T300/5208 graphite-epoxy laminates 03 p0325 N85-12091
Accelerated stress facility 1976-1983
[AD-A146101] 03 p0359 N85-12303
NBS (National Bureau of Standards) solar collector durability-reliability test program
[PB85-113603/GAR] 09 p1346 N85-18489
Forced corrosion tests of construction components of passenger aircraft fuselages 11 p1600 N85-20082
A note on some simple influence diagnostics in accelerated life testing
[AD-A149583] 12 p1862 N85-21677
Life testing of rubber seals — aircraft hydraulic systems
[AD-A143193] 13 p2066 N85-23086

Advanced life analysis methods. Volume 2: Crack growth analysis methods for attachment lugs
[AD-A150420] 13 p2103 N85-23109
Parallel test method for LSI (Large Scale Integration) microprocessors
[AD-A150237] 13 p2144 N85-23310
Advanced life analysis methods. Volume 3: Experimental evaluation of crack growth analysis methods for attachment lugs
[AD-A151058] 14 p2317 N85-24319
Module performance and failure analysis area: Flat-plate solar array project
[NASA-CR-175689] 15 p2585 N85-25936
Natural and accelerated aging of plastics
17 p2936 N85-28123
A test methodology for an automated and interactive software development environment
[AD-A152857] 17 p3011 N85-28618
Accelerated and real-time geosynchronous life cycling test performance of nickel-hydrogen batteries
20 p3448 N85-31405
Understanding and laboratory prediction of the atmospheric corrosion behavior of steels and of non-ferrous metals and alloys
[AD-A154642] 21 p3566 N85-32179
High temperature electronics technology: Life test report
[AD-A154681] 21 p3580 N85-32257
Accelerated stress factors and failure/degradation mechanisms in terrestrial solar cells
21 p3613 N85-32451
Degradation mechanisms and accelerated aging test design
[TI85-003251] 23 p3940 N85-34420

ACCELERATION
What is being done to control motion sickness?
15 p2687 N85-26599
Accelerator experiments on the contribution of secondary particles to the production of cosmogenic nuclides in meteorites
[SH-7.1-8] 23 p4048 N85-35100

ACCELERATION (PHYSICS)
NT ANGULAR ACCELERATION
NT DECELERATION
NT ELECTRON ACCELERATION
NT HIGH ACCELERATION
NT HIGH GRAVITY ENVIRONMENTS
NT IMPACT ACCELERATION
NT PARTICLE ACCELERATION
NT PLASMA ACCELERATION
NT SPIN REDUCTION
NT TRANSVERSE ACCELERATION
Design of a digital ride quality augmentation system for commuter aircraft
[NASA-CR-172419] 01 p0006 N85-10037
The Reports of Aeromedical Laboratory, volume 25, no. 1/2
[ISSN-0023-2858] 01 p0090 N85-10605
The effects of isotonic training on +Gz tolerance
01 p0090 N85-10607
Acceleration waves 02 p0207 N85-11367
Study of the solar corona using radio and space observations
[NASA-CR-174094] 02 p0304 N85-11963
Magnetospheric plasma studies using data from the dynamics high and low altitude plasma instruments
[AD-A145751] 03 p0392 N85-12505
Geomagnetic secular variation: A jerk in 1970
04 p0521 N85-13329
Acceleration of bluff bodies through fluids
05 p0593 N85-13786
Diffusion in metals under high mechanical strain and acceleration
[JUEL-1913] 07 p0928 N85-15887
Superconducting rotor dynamics
[AD-A147176] 07 p0947 N85-16000
Comparative visualization of accelerating flow around various bodies, starting from rest
[AD-P004159] 09 p1264 N85-17944
Primer for mass metrology
[PB85-121424/GAR] 09 p1305 N85-18199
Acceleration responses of typical LRU's subjected to bench handling and installation shock
09 p1334 N85-18385
Alternative shock characterizations for consistent shock test specifications 09 p1335 N85-18396
Numerical simulations of liquid propellant combustion instability: Onset and growth
[DE85-000743] 10 p1458 N85-19186
Tether fundamentals 11 p1643 N85-20345
Artificial gravity: Tethers and containers
11 p1645 N85-20367
Development of high field Nb-Ti accelerator dipoles
[DE85-000821] 11 p1714 N85-20782
Averaging of equations of cometary orbital motion with allowance for nongravitational effects
13 p1978 N85-22411
Physics of the inner heliosphere: Mechanisms, models and observational signatures
[NASA-CR-175632] 13 p2205 N85-23677
Problems of space biology. Volume 50: Nystagmometry for evaulation of the status of the vestibular function
[NASA-TM-77616] 14 p2385 N85-24694
Comets and nongravitational forces
14 p2437 N85-25038
Unsteady Navier-Stokes calculations in an accelerated reference frame
[AD-A151751] 15 p2557 N85-25774
Effects of magnetic shear on lower hybrid waves in the supraurcral region
[AD-A151980] 15 p2656 N85-26392
Empirical development of ground acceleration, velocity and displacement for accidental explosions at J5 or the proposed large altitude rocket cell at Arnold Engineering Development Center
[DE85-008324] 16 p2758 N85-27020
Acceleration resistant combination of opposite-handed piezoelectric crystals
[AD-D011626] 16 p2778 N85-27143
Acceleration-resistant crystal resonator
[AD-D011627] 16 p2778 N85-27144
Acceleration sensitivity reduction method
[AD-D011631] 16 p2778 N85-27146
Acceleration insensitive oscillator
[AD-D011621] 17 p2953 N85-28236
A counterpart of Faxen's formula in potential flow
[REPT-84-09] 17 p2960 N85-28279
Design of SC cut 10 MHZ H.Q. crystals with G. sensitivity better than 2.10(-10)/G 17 p2966 N85-28319
Wake fields and wake field acceleration
[DE85-008054] 17 p3031 N85-28750
Multiple time-scale methods in particle simulations of plasmas
[DE85-007519] 17 p3040 N85-28808
Spacecraft, straight-tube evaporator design
[AD-A154462] 19 p3226 N85-30003
Seakeeping and vibration tests of the Coast Guard 110 foot surface effect ship SEA BIRD class (WSES)
[AD-A154150] 19 p3252 N85-30166
Effect of periodic accelerations on physiochemical properties and Ca2+ reactivity of actomyosin in white rat myocardium and skeletal muscles
19 p3324 N85-30594
Physics with low temperature antiproton
[DE85-009627] 19 p3355 N85-30798
Recovery of pyroshock data from distorted acceleration records
[NASA-TP-2494] 20 p3407 N85-31141
Update on the evolution of the LAGEOS orbit
20 p3491 N85-31698
Pulsed hydrojet propulsion
[DE85-010771] 22 p3784 N85-33446
Acceleration of polarized H(-) in the BNL 200 MeV linac
[DE85-011836] 22 p3840 N85-33777
Long term variability of the cosmic ray intensity
[OG-3.1-11] 22 p3874 N85-33999
Injection of energetic particles following the gamma-ray flares on June 7, 1980, as observed on Helios 1
[SH-1.3-9] 23 p3993 N85-34756
The cosmic-ray shock structure problem for relativistic shocks
[OG-8.1-1] 23 p4017 N85-34891
Time-dependent nonlinear cosmic ray shocks confirming abstract
[OG-8.1-3] 23 p4017 N85-34893
Relativistic cosmic ray spectra in the full non-linear theory of shock acceleration
[OG-8.1-8] 23 p4018 N85-34896
Acceleration of cosmic rays in supernova-remnants
[OG-8.1-9] 23 p4018 N85-34899
Evaluation of parameters for particles acceleration by the zero-point field of quantum electrodynamics
[OG-8.2-16] 23 p4020 N85-34912
Matched filtering of visual evoked potentials to detect acceleration (+Gz) induced blackout
[AD-A155912] 24 p4131 N85-35609

ACCELERATION PROTECTION
Improving inflight negative Gz restraint for aircrewmen
[AD-A151909] 16 p2703 N85-26688

ACCELERATION STRESSES (PHYSIOLOGY)
NT CENTRIFUGING STRESS
Frequency and nature of electrocardiographic disturbances in dogs during single and repeated exposure to +G sub z accelerations 01 p0092 N85-10619
Analysis of the transient response of temporal artery blood flow data relative to various anti-G suit pressure schedules 10 p1533 N85-19660
Space adaptation syndrome: Incidence and operational implications for the space transportation system program
11 p1695 N85-20655
Homeostasis in primates in the hyperdynamic environment — circadian timekeeping and effects of lower body positive pressure on sleep
15 p2610 N85-26085
The European vestibular experiments of the Spacelab-1 mission 20 p3508 N85-31808
Some results of the European vestibular experiments in the Spacelab-1 mission 20 p3508 N85-31809
Oxygenation and regional circulation in gingival mucosa during exposure to lower body negative pressure
23 p3953 N85-34498
The effect of +Gx acceleration on platelet activation as determined by plasma platelet factor 4 levels
[AD-A155881] 24 p4131 N85-35608

ACCELERATION TOLERANCE
The Reports of Aeromedical Laboratory, volume 25, no. 1/2
[ISSN-0023-2858] 01 p0090 N85-10605
The effects of isotonic training on +Gz tolerance
01 p0090 N85-10607
Assessment of the inflating characteristics of the modified anti-G suit 01 p0090 N85-10609
Effect of fluid and salt supplements to food allowance on endurance of head-to-pelvis accelerations following 7-day dry immersion and under ordinary motor activity conditions 01 p0092 N85-10618
Frequency and nature of electrocardiographic disturbances in dogs during single and repeated exposure to +G sub z accelerations 01 p0092 N85-10619
Random pattern tracking acceleration tolerance tester
[AD-D011404] 07 p1017 N85-16459
Tolerance, fatigue, physiological and performance effects of sustained and oscillating lateral accelerations
10 p1533 N85-19659
Positive Gz accelerations tolerance of individuals 41 to 58 years of age 19 p3323 N85-30588
Analysis of the transient response of temporal artery blood flow data relative to various anti-G suit pressure schedules
[AD-A155242] 21 p3666 N85-32775
Tolerance to +Gz and +Gx accelerations of individuals in older age groups in good health and with early signs of arteriosclerosis 23 p3952 N85-34496
Effect of hypokinesia and +Gz accelerations on transport function of human blood
23 p3952 N85-34497
Matched filtering of visual evoked potentials to detect acceleration (+Gz) induced blackout
[AD-A155912] 24 p4131 N85-35609
Simulation of high +Gz onset in the dynamic environment simulator
[AD-A155963] 24 p4131 N85-35610

ACCELERATORS
Superconducting magnet technology for accelerators
[DE85-004192] 12 p1926 N85-22102

ACCELEROMETERS
NT STRAIN GAGE ACCELEROMETERS
Keeping up with operational loads in the French Air Force: Defining new equipment
07 p0896 N85-15681
Flight simulation for inertial navigation system
14 p2273 N85-24081
Preguidance and piloting with the aid of composite inertial sensors 16 p2696 N85-26846
Low cost two gimbal inertial platform and its system integration 16 p2698 N85-26861
Simulation of a low orbit restitution. Covariance analysis of the position-velocity by Doppler and accelerometer measurements
[CNES-CT/DTI/MS/AE/166] 16 p2728 N85-26836
Research and development of subsurface acoustic wave devices for sensor applications
[AD-A152197] 16 p2861 N85-27642
Principles of designing digital compensating accelerometers 17 p2944 N85-28172
Uniaxial angular accelerometers
17 p2944 N85-28173
Study on a flexure hinged pendulum accelerometer
[NAL-TR-844] 18 p3104 N85-29220
Passivation on high Q acoustic strain sensor for accelerometer
[AD-A153565] 18 p3177 N85-29695
Investigation of fast reaction SAW (Surface Acoustic Wave) accelerometer
[AD-A153876] 19 p3216 N85-29943
The DREO (Defence Research Establishment Ottawa) Inertial Navigation Laboratory: Development and test capabilities
[AD-A154425] 19 p3216 N85-29945
R and D activities of the Systems Engineering Division
20 p3540 N85-32027

Application of satellite accelerometer data to improve density models
[AD-A154904] 21 p0631 N85-32558
Multiple-stage integrating accelerometer
[DE85-006505] 23 p3935 N85-34388

ACCEPTABILITY
Development of acceptance criteria for batches of silane primer for external tank thermal protection system bonding applications
[NASA-CR-171436] 15 p2518 N85-25523
Development of acceptance criteria for batches of silane primer for external tank thermal protection system bonding applications
[NASA-CR-175850] 16 p2754 N85-26995
A critique of Deming's discussion of acceptance sampling procedures
[AD-A154305] 19 p3348 N85-30751
Atmospheric modeling of organics for risk assessment: A Chemist's view
[DE85-009770] 23 p3909 N85-34217

ACCEPTANCE
U ACCEPTABILITY

ACCEPTOR MATERIALS
Electrochemistry of polymer films. Applications to chemical analysis and energy conversion
[AD-A147737] 08 p1132 N85-17136

ACCESS CONTROL
Throughput characteristics of Carrier Sense Multiple Access (CSMA) networks
[FUB-25-1983] 01 p0106 N85-10713
Heterogeneous data base access
05 p0735 N85-14724
Some experiences of testing protocol implementations — open systems interconnection
[NPL-DITC-48/84] 08 p1204 N85-17574
Performance evaluation and control of distributed computer communication networks
[AD-A148103] 08 p1208 N85-17598
Analytical modeling of a polling protocol — airline information network
[ENST-84H001] 09 p1277 N85-18029
Design and analysis of an access control system for a multi-backend database system
[AD-A148750] 09 p1367 N85-18588
AID: Access to Informal Documentation
[DE85-000418] 11 p1740 N85-20939
Access path optimization for network database retrieval
16 p2877 N85-27749
Optimizing data access in the LAMPF control system
[DE85-012653] 24 p4140 N85-35663

ACCIDENT INVESTIGATION
NT AIRCRAFT ACCIDENT INVESTIGATION
Structural design guidelines for heliports
[FAA-PM-84-23] 02 p0149 N85-11010

ACCIDENT PREVENTION
Development and certification of a new stall warning and avoidance system 05 p0702 N85-14507
A manual control test for the detection and deterrence of impaired drivers 05 p0709 N85-14550
The use of falconry as mean to persuade the birds to stay out of the airport vicinity 11 p1580 N85-19856
Safety with industrial manufacturing lasers
14 p2308 N85-24281
MELCOR Accident Consequence Code System (MACCS)
[DE85-009712] 19 p3339 N85-30689
A review of the SIMMER-2 analyses of liquid-metal-cooled fast breeder reactor core-disruptive accident fuel escape
[DE85-010803] 19 p3366 N85-30876
General Aviation Airworthiness Alerts, no. 85
[FAA-AC-43-16] 22 p3729 N85-33117
Transient three-phase three-component systems. Part 1: Formulation of the system of differential equations
[DE85-013257] 24 p4095 N85-35364

ACCIDENT PRONENESS
Calculation of trajectories of detached wind turbine blades and prediction of site risk levels associated with failures of HAWT's 24 p4110 N85-35475

ACCIDENTS
NT BIRD-AIRCRAFT COLLISIONS
Volatility of vanadium from a candidate fusion tractor alloy
[DE84-015277] 05 p0618 N85-13955
HS and E environmental sciences
[DE84-016183] 05 p0672 N85-14314
Ballistic/detonic transition of propellants
08 p1117 N85-17041
Control of tractors on sloping ground
[AD-P004292] 09 p1406 N85-18869
The medical results of human exposures to radio frequency radiation
[AD-A149718] 12 p1905 N85-21982
Two phase discharge of liquefied gases through pipes. Field experiments with ammonia and theoretical model
[FOA-B-40139-C1] 18 p3103 N85-29209
Hazardous air pollutants
[GPO-43-064] 21 p3613 N85-32458
The 1983 international intercomparison of nuclear accident dosimetry systems at Oak Ridge National Laboratory
[DE85-011303] 23 p3934 N85-34382
Computer code calculations of the TMI-2 accident: Initial and boundary conditions
[DE85-012613] 24 p4140 N85-35666
Thermal hydraulic features of the TMI accident
[DE85-014569] 24 p4152 N85-35747

ACCLIMATIZATION
NT ALTITUDE ACCLIMATIZATION
NT COLD ACCLIMATIZATION
NT HEAT ACCLIMATIZATION
Introduction to human biometeorology
05 p0687 N85-14415
Aerobic and anaerobic exercise tolerance in the heat: Effect and acclimatization 14 p2368 N85-24707
Exercise-heat strain during hypohydration: Interaction with heat acclimation and aerobic fitness
[AD-A151023] 14 p2389 N85-24717

ACCOUNTING
The analysis of tank calibration data from several runs
[DE84-015529] 02 p0200 N85-11337
Management control systems and interdependencies: An empirical study
[AD-A152280] 16 p2876 N85-27746
Computer center policy
[AD-A154416] 19 p3338 N85-30681
Energy accounting software
[DE85-010612] 19 p3340 N85-30694
DOD Value Engineering Conference report. Value Engineering (VE): A tool that benefits line management held at Leesburg, Virginia on 1-2 November 1984. Part 1. Executive summary
[AD-A156067] 24 p4163 N85-35810

ACCRETION
U DEPOSITION

ACCRETION DISKS
Spherical accretion onto a protostellar core
03 p0442 N85-12817
The lunar angular momentum problem
04 p0588 N85-13752
Formation of the preluner accretion disk
04 p0588 N85-13755
X-ray spectra of accretion disks — active galactic nuclei 08 p1239 N85-17614
Shock acceleration in active galactic nuclei and quasars 08 p1241 N85-17628
Models of nonkeplerian accretion disks based on dynamo magnetic field: Application to Active Galactic Nuclei (AGN) 08 p1242 N85-17634
X-ray spectra of accretion disks — active galactic nuclei 08 p1242 N85-17638
Circumstellar dust disks around young stars
08 p1247 N85-17670
The vertical structure and stability of alpha model accretion disks 09 p1417 N85-18938
EXOSAT observations of the galactic bulge X-ray source GX17+2 — X ray binary star 11 p1742 N85-20951
Thermal convection and magnetic fields in accretion disks of black holes 12 p1955 N85-22285
Drift-accretion theory of the spiral structure of galaxies
12 p1957 N85-22296
Hydrodynamics of astrophysical jets — active galactic nuclei 12 p1958 N85-22307
Formation of optical-line emitting regions in the jets of SS433 12 p1959 N85-22318
Evolution of grains in a turbulent solar nebula
13 p2179 N85-23525
A numerical study of nonspherical black hole accretion 16 p2881 N85-27760
Ultra high energy gamma rays, cosmic rays and neutrinos from accreting degenerate stars
[OG-2.2-5] 22 p3864 N85-33931
500 TeV gamma rays from Hercules X-1
[OG-2.2-7] 22 p3865 N85-33933
A model for the UHE gamma-rays from Hercules X-1
[OG-2.2-8] 22 p3865 N85-33934

ACCUMULATORS
NT DUST COLLECTORS
NT SOLAR COLLECTORS
NT SOLAR REFLECTORS
Development and evaluation of cloud water collectors
[PB84-232529] 04 p0540 N85-13437
Power transfer from natural emitters to collection apertures at microwave wavelengths
[NASA-CR-174275] 07 p0945 N85-15989
Application of fiber optics and compound collectors
08 p1253 N85-17912
Antiproton source beam position system
[DE84-016716] 09 p1380 N85-18679
Development of a second-generation linear Fresnel Photovoltaic and Thermal (PVT) concentrator array, including fabrication and installation of a 200 square meter collector field
[DE85-008473] 17 p2968 N85-28485
Integrated current collector and catalyst support
[DE85-011616] 22 p3761 N85-33311
Multistage spent particle collector and a method for making same
[NASA-CASE-LEW-13914-1] 22 p3791 N85-33489
Vapor phase heat transport concepts
[DE85-009550] 23 p3931 N85-34366

ACCURACY
NT GEODETIC ACCURACY
NT GEOMETRIC ACCURACY
Research on large, highly accurate, inflatable reflectors
[AD-A145080] 01 p0016 N85-10099
Economic model of calibration improvements for automatic test equipment
[PB84-217827] 01 p0051 N85-10335
Evaluation of laser profile and deflection measuring system
[FAA-PM-84-24] 02 p0201 N85-11341
Observations of lightweight Doppler system accuracy
[AD-A145988] 03 p0317 N85-12049
Portable real-time clock
[AD-A146218] 03 p0364 N85-12336
Comparability and accuracy of industry codes in different data systems
[PB84-215807] 04 p0548 N85-13482
Magnetic constraints on early lunar evolution revisited: Limits on accuracy imposed by methods of paleointensity measurements 04 p0582 N85-13716
Improvement of the accuracy of reflection factor measurements by a computer 05 p0629 N85-14039
Treatment and expression of measurement uncertainties 05 p0630 N85-14042
The Georges Bank monitoring program 1983: Analysis of trace metals in bottom sediments
[CIRC-915] 05 p0668 N85-14423
Reducing numerical diffusion for incompressible flow calculations
[NASA-TM-83821] 06 p0756 N85-14840
Resolution and accuracy of radar measurements
06 p0789 N85-15044
Summary of photovoltaic performance models
06 p0832 N85-15298
Trends in skill and accuracy of National Weather Service pop forecasts
[PB84-229053] 06 p0840 N85-15335
Power of deterministic thinking in machine tool accuracy
[DE85-001751] 07 p0974 N85-16198
Development of a Helicopter integrated navigation system 08 p1073 N85-16802
High accuracy Doppler navigation employing optimum integrated position fix information
08 p1073 N85-16803
An application of discriminant analysis to the selection of software cost estimating models
[AD-A147632] 09 p1204 N85-17580
Study on steerability of articulated tracked vehicles
[AD-P004308] 09 p1410 N85-18885
Geometric accuracy of LANDSAT-4 MSS image data
11 p1667 N85-20503
Influence of individual reflections on the precision of parameter estimates in least squares refinement
[DE85-000830] 11 p1735 N85-20909
Modal control of structural systems
[AD-A149734] 12 p1790 N85-21235
Speed and accuracy in automated manufacture
[DE85-003913] 12 p1819 N85-21410
Accuracy of typhoon center determined by GMS imagery 12 p1864 N85-21867
AFOS (Automation of Field Operations and Services)-ERA forecast verification, September 1984
[PB85-137578] 12 p1897 N85-21912
Method for determining the number of correlative measurements required to validate the SBUV/2 ozone retrievals 13 p2105 N85-23114
Measurement requirements for the detection of ozone trends 13 p2105 N85-23115
Automated extraction of absorption bands from reflectance specta 13 p2197 N85-23624
Innovation in earthquake and natural hazards research: Determining soil liquefaction potential
[PB85-148573] 14 p2374 N85-24678
Arithmetic and elementary functions on mini and microcomputers 14 p2398 N85-24761
Accuracy of the calculated stress field around a craze
[DE85-005520] 16 p2901 N85-27272
Optimal relative data weights
16 p2905 N85-27296
Studies into location accuracy — ARGOS system
16 p2911 N85-27334

Evaluation of the PROFS (Program for Regional Observing and Forecasting Services) 1982, real-time forecast experiment
[PB85-158747] 16 p2837 N85-27495
Separating the variances of noise components in the Global Positioning System
[AD-P004578] 17 p2963 N85-28295
An empirical comparison of the accuracy of univariate and multivariate corrections for range restriction
[AD-A153071] 17 p3019 N85-28670
Study of the accuracy of astrometric observations of comets
[ESA-CR(P)-1964] 17 p3054 N85-28903
On the accuracy of Ca beam primary frequency standards 18 p3105 N85-29224
Time transfer techniques: Historical overview, current practices and future capabilities 18 p3108 N85-29245
New GOES satellite synchronized time code generation 18 p3109 N85-29247
Accepting error to make less error
[AD-A153949] 18 p3171 N85-29651
Accuracy in determining velocity of fluid movement by Doppler method 19 p3293 N85-30419
Study of the interferences of 2 GHz radio beams with a DORIS system — precise low orbit determination system (DORIS)
[CNES-CT/DRT/TIT/RL-84/140-T] 20 p3442 N85-31362
TOPEX error budget 20 p3493 N85-31717
Accuracy and operational use of medium and extended range numerical atmospheric forecasts: A review
[AD-A155027] 21 p3635 N85-32579
Medium range atmospheric forecast system: Evaluation report
[AD-A155240] 21 p3637 N85-32580
Resource allocation in cerebral specialization of function: Behavioral and electrophysiological studies
[AD-A155092] 21 p3664 N85-32750
A method of accurizing rail guns
[LA-10028-MS] 22 p3737 N85-33166
Art of programming programmable microcalculators, part 4: errors of calculations 22 p3778 N85-33411
Determining an azimuth with a north seeking gyro
[AD-A156880] 24 p4063 N85-35180
Accuracy and error analysis — airborne instruments 24 p4123 N85-35557

ACEE PROGRAM

Fuel efficiency through new airframe technology
[NASA-TM-84548] 02 p0133 N85-10809
Energy efficient engine combustor test hardware detailed design report
[NASA-CR-167945] 02 p0140 N85-10950
Energy efficient engine component development and integration program
[NASA-CR-170034] 02 p0146 N85-10990
Energy efficient engine. Volume 2. Appendix A: Component development and integration program
[NASA-CR-173085] 02 p0146 N85-10991
Energy efficient engine. Volume 1: Component development and integration program
[NASA-CR-173084] 02 p0146 N85-10992
Energy efficient engine. Low pressure turbine test hardware detailed design report
[NASA-CR-167956] 02 p0147 N85-10994
Energy efficient engine high pressure turbine test hardware detailed design report
[NASA-CR-167955] 02 p0147 N85-10995
Energy efficient engine high pressure turbine ceramic shroud support technology report
[NASA-CR-168036] 02 p0147 N85-10996
Energy efficient engine ICLS engine bearings, drives and configuration: Detail design report
[NASA-CR-167871] 02 p0147 N85-10997
Energy efficient engine. High pressure compressor detail design report
[NASA-CR-165556] 02 p0147 N85-10998
Investigation of toughened neat resins and their relations to advanced composite mechanical properties 04 p0464 N85-12949
Steady- and unsteady-pressure measurements on a supercritical-wing model with oscillating control surfaces at subsonic and transonic speeds
[NASA-TM-84543] 08 p1077 N85-16831
Transonic steady- and unsteady-pressure measurements on a high-aspect-ratio supercritical-wing model with oscillating control surfaces
[NASA-TM-81886] 09 p1273 N85-18003
Subsonic and transonic pressure measurements on a high-aspect-ratio supercritical-wing model with oscillating control surfaces
[NASA-TM-83201] 09 p1273 N85-18004
Energy efficient engine high-pressure turbine component rig performance test report
[NASA-CR-168189] 19 p3218 N85-29955
Energy efficient engine integrated core/low spool test hardware design report
[NASA-CR-168137] 19 p3218 N85-29956
Energy Efficient Engine (E3) controls and accessories detail design report
[NASA-CR-168017] 19 p3218 N85-29957
Energy efficient engine component development and integration program
[NASA-CR-172946] 19 p3219 N85-29958
Energy efficient engine. Fan and quarter-stage component performance report
[NASA-CR-168070] 23 p3897 N85-34141
Energy efficient engine, high pressure turbine thermal barrier coating. Support technology report
[NASA-CR-168037] 24 p4066 N85-35199

ACETALDEHYDE

(Vinyloxy)fluorocyclotriphosphazenes
[AD-A147448] 07 p0924 N85-15850

ACETATES

Fatal hemorrhagic shock and acetate solutions
[AD-A146754] 07 p1014 N85-16444
1-Fluoro-1,1,5-Trinitro-3-Oxa-5-Azahexane and method of preparation
[AD-D011421] 08 p1136 N85-17158
Pre-flight report on cultured human embryonic kidney cell handling and cell electrophoresis. Prepared prior to continuous-flow electrophoretic separation experiments aboard space shuttle flight STS-8 20 p3503 N85-31775
Microbiological and biochemical studies towards optimization of substrate utilization by methanogenic bacteria
[PB85-188332] 24 p4064 N85-35310

ACETONE

Biocatalyzed processes for production of commodity chemicals: Assessment of future research advances for N-butanol production
[NASA-CR-174264] 07 p0919 N85-15819
ECUT, Energy Conversion and Utilization Technologies program: Technical and economic assessment of processes for the production of butanol and acetone. Phase 2: Analysis of research advances
[NASA-CR-175471] 10 p1434 N85-19034
Brittle fracture resistance of electron beam-welded joints in titanium Alpha alloys 15 p2500 N85-25419
Microstructural characteristics during the controlled solidification of a binary system
[DE85-005200] 15 p2507 N85-25461

ACETYL COMPOUNDS

Method of obtaining polychalcones
[AD-A145051] 01 p0018 N85-10107
Use and disuse and the control of acetylcholinesterase activity in fast and slow twitch muscle of rat
[NASA-CR-175717] 15 p2614 N85-26109
Phenoxy resins containing pendent ethynyl groups and cured resins obtained therefrom
[NASA-CASE-LAR-13262-1] 18 p3068 N85-28973

ACETYLACETONE

Investigation of the Ostwald ripening of separated particles in liquid-liquid systems under microgravity conditions
[BMFT-FB-W-84-037] 05 p0615 N85-13927

ACETYLENE

Preparation of polymers of functionalized acetylenes
[AD-D011296] 06 p0771 N85-14935
Vibrational spectroscopy of chemisorption phenomena on model catalyst surfaces
[AD-A146753] 07 p0922 N85-15840
Conduction in polymerized polyfunctional diacetylenes
[AD-A149104] 10 p1451 N85-19145
Characterization of acetylene-terminated resin cure states
[AD-A149463] 10 p1452 N85-19148
Synthesis and thermomechanical properties of new AT-Phenylene R systems
[AD-A149961] 12 p1813 N85-21372
Collaborative shock tube studies of benzene pyrolysis
[DE85-006347] 14 p2253 N85-23962
The mechanisms of phenylacetylene polymerization by molybdenum and titanium initiators
[AD-A150993] 14 p2260 N85-24007
C2H(n) fragments on metal surfaces
[AD-A151474] 15 p2505 N85-25449
Crossed molecular beam studies of the reactions of oxygen and fluorine atoms
[AD-A153302] 17 p2921 N85-28008
Lifetime and quenching measurements of C2H emission produced by vacuum ultraviolet photolysis of C2H2
[DE85-010769] 19 p3278 N85-30330
Metal alkoxides: Models for metal oxides. Alkoxide ligands in early transition metal organometallic chemistry
[DE85-011366] 23 p3916 N85-34269
The photodissociation of acetylene at 193.3 NM
[AD-A155775] 24 p4075 N85-35255

ACHIEVEMENT

The impact of group processing on achievement in cooperative learning groups
[AD-A153168] 17 p3001 N85-28551
Oral discussion, group-to-individual transfer and achievement in cooperative learning groups
[AD-A153209] 17 p3001 N85-28552

ACID BASE EQUILIBRIUM

A potentiometric study of chloroaluminate equilibria in the aluminum chloride - 1-methyl-2-ethylimidazolium chloride ionic liquid
[AD-A144729] 01 p0023 N85-10144
Monitoring approaches for assessing quality of high altitude lakes: Colorado Flat Tops Wilderness Area
[PB85-117232] 11 p1679 N85-20679

ACID RAIN

Acid rain and transported air pollutants: Implications for public policy
[PB84-222967] 01 p0071 N85-10469
Analysis of potential combustion sorce impacts on acid deposition using an independently derived inventory, volume 1
[DE84-012005] 02 p0225 N85-11471
Estimation of the potential and probable source regions for acid precipitation
[DE84-015119] 02 p0225 N85-11472
Potential for acidification of six remote ponds in the White Mountains of New Hampshire
[PB84-207349] 02 p0225 N85-11475
Selection, procurement and description of Salem Limestone samples used to study the effects of acid rain
[PB84-231067] 04 p0484 N85-13066
Effects of acid rain on plant microbial associations in California
[PB84-242122] 04 p0532 N85-13404
Transformation processes and wet deposition on the urban scale
[DE84-015294] 04 p0539 N85-13432
Acid rain and tree physiology: Some hypotheses for observed changes in forest productivity
[DE84-016566] 05 p0672 N85-14318
Analysis of terrestrial conditions and dynamics
[E85-10063] 08 p1174 N85-17401
Mesoscale storm and dry period parameters from hourly precipitation data: Program documentation
[DE85-001366] 09 p1357 N85-18538
Sequential precipitation chemistry sampling program at Brookhaven National Laboratory with an analytical summary of 1978-1982 data
[DE85-002768] 10 p1513 N85-19545
Non-photochemical interactions of sulfur and nitrogen compounds in acid deposition
[DE84-016141] 10 p1513 N85-19548
National Acid Precipitation Assessment Program. Report to the President and Congress (1983)
[PB85-116713] 11 p1679 N85-20581
National Performance Audit Program ambient air audits of analytical proficiency
[PB85-138204] 11 p1680 N85-20586
Effects of air pollution and acid rain on forest decline
[GPO-37-459] 12 p1883 N85-21618
Report on the Second Annual Review Meeting of the National Acid Precipitation Assessment Program. Research to assist decisionmaking: Summary
[DE85-003003] 12 p1884 N85-21620
Combined effects of atmospheric deposition, internal acid production, and harvesting on nutrient gains and losses from forest ecosystems
[DE85-002325] 12 p1884 N85-21621
Gas-liquid chemistry of natural waters, volume 1
[DE85-002603] 12 p1884 N85-21622
Rationale and basic design for experimental acidification of a lake ecosystem in Northern Wisconsin
[PB85-116077] 12 p1885 N85-21629
Non-precipitating cumulus cloud study
[DE85-002352] 12 p1886 N85-21902
Studies of the mechanisms and rates with which nitrogen species are incorporated into cloud water and precipitation
[PB85-144350] 12 p1886 N85-21914
Areas with forest soils sensitive to acidic deposition under alternative damage hypotheses
[DE85-005257] 13 p2130 N85-23257
PLUVIUS: A generalized 1-dimensional model of reactive pollutant behavior, including dry deposition, precipitation formation, and wet removal, 2nd edition
[DE85-005542] 14 p2353 N85-24538
MAP3S precipitation chemistry network
[DE85-005324] 14 p2353 N85-24539
An analysis of issues concerning acid rain, report to the Congress of the United States
[TI85-901070] 15 p2589 N85-25859
A comparative evaluation of the effects of acid precipitation, natural acid production and harvesting of cation removal from forests
[DE85-005254] 15 p2589 N85-25861

Emission inventory applications to regional acid deposition modeling
[PB85-157386] 16 p2760 N85-27033
Interactive effects of acid rain and gaseous air pollutants on natural terrestrial vegetation
[DE85-006255] 16 p2821 N85-27401
Acid rain: Effects on fish and wildlife
[PB85-154672] 16 p2821 N85-27402
Acid precipitation in North America: 1980, 1981 and 1982 annual data summaries from acid deposition system data base
[PB85-162477] 16 p2822 N85-27410
Acid rain: Towards automated monitoring
16 p2829 N85-27444
Oxygen isotopic study of the oxidation of SO2 by H2O2 in the atmosphere
[DE85-004017] 17 p2968 N85-28468
Chemical transformations in acid rain. Volume 2: Investigation of kinetics and mechanism of aqueous-phase peroxide formation
[PB85-173433] 18 p3135 N85-29416
North American acid deposition data base system (ADS) and its use in spatial analysis
[PB85-173235] 18 p3201 N85-29856
Evaluation of methods used for the determination of acidity in acid rain samples
[PB85-178309] 19 p3237 N85-30070
Environmental Sciences Division report
[DE85-010452] 19 p3308 N85-30506
A comparative evaluation of the effects of acid precipitation, natural acid production and harvesting on cation removal from forests
[DE85-010621] 19 p3309 N85-30511
Chemical transformation in acid rain. Volume 1: New methodologies for sampling and analysis of gas-phase peroxide
[PB85-173425] 19 p3311 N85-30527
An interim user's manual for the advanced scavenging module version 1.2
[PB85-173904] 19 p3318 N85-30572
Design of the National Trends Network for monitoring the chemistry of atmospheric precipitation
[GS-CIRC-964] 20 p3486 N85-31664
Atmospheric Tracer Workshop
[DE85-010573] 20 p3486 N85-31666
Historic emissions of sulfur and nitrogen oxides in the U.S. from 1900 to 1980. Volume 1: Results
[PB85-191195] 20 p3487 N85-31674
Historic emissions of sulfur and nitrogen oxides in the U.S. from 1900 to 1980. Volume 2: Data
[PB85-191203] 20 p3487 N85-31675
EPA (Environmental Protection Agency) research program guide, FY-1985, October 1, 1984 - September 30, 1985
[PB85-181881] 20 p3487 N85-31676
Acid rain in Europe
[COMMITTEE-PRINT-99-F] 22 p3810 N85-33601
Practical consequences of the assessment of different energy health risks
[DE85-004538] 22 p3825 N85-33696
Effects of acid rain on forest nutrient status
[DE85-012486] 23 p3947 N85-34463
Throughfall rate and chemistry studies: Whiteface Mountain
[DE85-012407] 23 p3947 N85-34464

ACIDITY
Acid Deposition: Processes of Lake Acidification
[PB84-216175] 01 p0070 N85-10486
Potential for acidification of six remote ponds in the White Mountains of New Hampshire
[PB84-207349] 02 p0225 N85-11475
Monitoring approaches for assessing quality of high altitude lakes: Colorado Flat Tops Wilderness Area
[PB85-117232] 11 p1679 N85-20579
Evidence that resorption of bone by rat peritoneal macrophages occurs in an acidic environment
15 p2612 N85-26098
Evaluation of methods used for the determination of acidity in acid rain samples
[PB85-178309] 19 p3237 N85-30070
Granulometric study of the acidity and sulfate excess in marine aerosols 21 p3652 N85-32691

ACIDS
NT ALANINE
NT AMINO ACIDS
NT ASPARTIC ACID
NT BENZOIC ACID
NT BUTYRIC ACID
NT CARBOXYLIC ACIDS
NT CHROMIC ACID
NT CITRIC ACID
NT DEOXYRIBONUCLEIC ACID
NT DICARBOXYLIC ACIDS
NT FATTY ACIDS
NT GLUTAMINE
NT GLUTATHIONE
NT GLYCINE
NT HYDROBROMIC ACID
NT HYDROCHLORIC ACID
NT HYDROFLUORIC ACID
NT METHIONINE
NT NITRIC ACID
NT OXIDASE
NT PEPTIDES
NT PHOSPHORIC ACID
NT RIBONUCLEIC ACIDS
NT SULFURIC ACID
NT TRYPTOPHAN
Spectrophotometric studies of iodine complexes in an aluminum chloride - butylpyridinium chloride ionic liquid
[AD-A145074] 01 p0024 N85-10150
Computer-assisted Gran titration procedure for strong acid determination
[DE85-006801] 15 p2507 N85-25462
A comparative evaluation of the effects of acid precipitation, natural acid production and harvesting of cation removal from forests
[DE85-005254] 15 p2589 N85-25861
Correlation of zeolite ZSM-5 acid strength with catalytic activity and selectivity
[DE85-005415] 17 p2922 N85-28013
Improved acid electrolytes for fuel cells
[PB85-176053] 18 p3132 N85-29397
An interim user's manual for the advanced scavenging module version 1.2
[PB85-173904] 19 p3318 N85-30572
Method for extracting lanthanides and actinides from acid solutions by modification of Purex solvent
[DE85-005763] 23 p3909 N85-34220
Origin of sedimentary humic acids, potential carriers of ore-forming elements 24 p4104 N85-35443

ACOUSTIC ATTENUATION
NT SHOCK WAVE ATTENUATION
The role of dislocations in ultrasonic attenuation
[AERE-R-11384] 12 p1904 N85-21317
Surface forward scattering and reflection
[AD-A150115] 12 p1928 N85-22112
Long range downwind propagation of low-frequency sound
[NASA-TM-86409] 15 p2545 N85-26318
Interaction of finite-amplitude sound with air-filled porous materials
[NASA-CR-174865] 16 p2860 N85-27637
Study of sound attenuation in sediments
[AD-A153690] 18 p3177 N85-29697
Airborne sound transmission loss characteristics of wood-frame construction
[AD-A154174] 20 p3524 N85-31919
Overground Excess Sound Attenuation (ESA). Volume 3: Application of ESA data in NOISEFILE
[AD-A154820] 21 p3699 N85-32964
Lateral attenuation of aircraft flight noise
[AD-A154958] 21 p3700 N85-32966
Acoustical absorption coefficient in a diffuse field of a plane, rectangular material of finite dimensions placed on an infinite perfectly reflecting surface
[NRC/CNR-TT-2113] 23 p3968 N85-34599

ACOUSTIC COMBUSTION
U COMBUSTION STABILITY

ACOUSTIC DUCTS
Investigations of reactive and non reactive acoustic boundary layers in porous walled ducts
13 p2000 N85-22535
On the solution for the sound field in a semi-infinite uniform duct with sheared mean flow
20 p3523 N85-31912
Models for describing active noise control in ducts
[ISVR-TR-127] 20 p3525 N85-31922

ACOUSTIC EMISSION
Acoustic emission linear pulse holography
[DE84-014519] 01 p0050 N85-10330
Detection of hydrogen assisted crack growth by measurement of modulus changes and acoustic emission
[DE84-015752] 02 p0184 N85-11236
Contributions to the 7th International Acoustic Emission Symposium
[AD-A146366] 02 p0275 N85-11792
Acoustic emission monitoring of fatigue in 7010 aluminum alloys
[AERE-R-11167] 03 p0394 N85-12152
Technical activities 1983, Office of Nondestructive Evaluation
[PB84-217074] 03 p0370 N85-12360
Rotary-wing aircraft noise measurements: Analysis of variations and proposed measurement standard
[AD-A146207] 03 p0416 N85-12662
Acoustic emission waveforms in a half space
[AD-A146322] 03 p0417 N85-12664
Three-dimensional crack location by acoustic emission
[AERE-R-11277] 06 p0618 N85-15193
Identification of leaks: Internal acoustic method, phase 2
[PB85-101947/GAR] 07 p0936 N85-15927
Quantitative acoustic emission techniques
[AERE-R-11262] 07 p0977 N85-16203
In-situ stress determination in soil and rock using the acoustic emission method
[AD-A147459] 07 p0979 N85-16215
Journal of Research of the National Bureau of Standards, Volume 89, Number 1, January-February, 1984
[PB84-235530] 08 p1262 N85-17931
Contribution of the study of light aircraft propeller noise
[ESA-TT-865] 09 p1378 N85-18667
Leak monitoring in high pressure preheaters by a noninvasive ultrasonic method
[CISE-2373] 11 p1650 N85-20394
Leak detection by acoustic emission monitoring in power plant high pressure preheaters
[CISE-2392] 11 p1650 N85-20395
Defect characterization and monitoring by acoustic emission
[AERE-R-11409] 12 p1863 N85-21683
Characterization of fatigue crack extension by quantitative acoustic emission
[AERE-R-11289] 12 p1868 N85-21721
Method and apparatus for detecting acoustic emissions from metal matrix wire
[AD-D011553] 12 p1927 N85-22107
Use of acoustical emission method to study specifics of fracture of boron reinforced plastic structural elements 13 p2026 N85-22698
Optimal synthesis of surface acoustic wave filters
13 p2070 N85-22933
Sound emission by particle beam passing through hole in rigid shield 15 p2525 N85-25570
Acoustic emission of semiconductor devices
15 p2529 N85-25593
Contribution to the study of equivalent noise source identification in fast cold jets
[ISL-R-114/83] 16 p2961 N85-27645
Method of assessment of start of slow crack growth by acoustic emission technique
[BLL-BISI-TRANS-21762-(9022.09)]
17 p3027 N85-28722
Acoustic emission study of fatigue crack extension position in a stress cycle 19 p3283 N85-30355
Propagation of acoustic pulse in atmospheric waveguide 19 p3297 N85-30443
Production verification of the acoustic emission weld monitor
[AD-A154168] 20 p3464 N85-31519
Simulation model of acoustic emission due to microscopic fracture in metals
[BLL-BISI-TRANS-22367-(9022.09)]
20 p3523 N85-31909
Source characterization of point-like and distributed sources of acoustic emission 20 p3523 N85-31910
Acoustic emission during transformation of austenite in 36KhN3MF steel
[BLL-M-35825-(9828.4)] 23 p3914 N85-34256
Contribution to the properties of carbon fiber reinforced composites — structural mechanics
[ESA-TT-849] 24 p4074 N85-35246

ACOUSTIC EXCITATION
Behavior of charged particles in lower ionosphere with acoustical effects 02 p0161 N85-11089
Optoacoustic spectroscopy
[AD-A145995] 03 p0419 N85-12679
Response measurements for two building structures excited by noise from a large horizontal axis wind turbine generator
[NASA-CR-172482] 04 p0558 N85-13552
Spacecraft structural acoustic studies: Development of structural acoustic design guides
[ESA-CR(P)-1918] 05 p0804 N85-13849
Preliminary analysis of tone-excited two-stream jet velocity decay
[NASA-TM-86951] 12 p1770 N85-21114
Acoustic agglomeration methods and apparatus
[NASA-CASE-NPO-15498-1] 12 p1927 N85-22104
Vibroacoustic study of the NASA Goddard Space Flight Center OSS-1 payload
[NASA-CR-175320] 13 p1988 N85-22465
Acoustic noise associated with the MOD-1 wind turbine: Its source, impact, and control
[DE85-002947] 16 p3175 N85-29700
Acoustic radiation from concentric shells containing an inner fluid
[AD-A155476] 21 p3700 N85-32991

ACOUSTIC GENERATORS
U SOUND GENERATORS

ACOUSTIC IMPEDANCE
Determination of the pressure sensitivity of 1 inch condenser microphones
[PTB-AK-26] 05 p0833 N85-14058

The effect of grazing flow on the impedance of the Helmholtz resonator 05 p0635 N85-14076
Characteristic impedance of a porous center during transmission of quasi-static sinusoidal vibrations [ISSN-0208-5658] 05 p0647 N85-14155
On the long range propagation of sound over irregular terrain [NASA-CR-3662] 07 p1038 N85-16589
Interaction of finite-amplitude sound with air-filled porous materials [NASA-CR-174685] 16 p2650 N85-27637
Reactanceless synthesized impedance bandpass amplifier [NASA-CASE-GSC-12786-1] 18 p3093 N85-29145
Method for thermal monitoring subcutaneous tissue [NASA-CASE-LAR-13028-1] 19 p3328 N85-30618
Spectral methods for the estimation of acoustic intensity, energy density, and surface velocity using a multimicrophone probe 20 p3524 N85-31916

ACOUSTIC INSTABILITY
Theoretical study of collective ion acceleration in the Luce diode [AD-A150107] 12 p1929 N85-22116
Acoustic energy balance method 13 p2000 N85-22537
Investigation of the characteristics of the velocity-coupled response functions of solid propellants 13 p2001 N85-22540
Measurements of distributed combustion 13 p2001 N85-22542
Distributed combustion: A mechanism of acoustic suppression 13 p2001 N85-22543

ACOUSTIC LEVITATION
Development of the sonic pump levitator [NASA-CR-171362] 12 p1782 N85-21186
High temperature acoustic levitator [NASA-CASE-NPO-16022-1] 12 p1927 N85-22105
Gravity enhanced acoustic levitation method and apparatus [NASA-CASE-NPO-16147-1-CU] 18 p3177 N85-29693

ACOUSTIC MEASUREMENT
NT NOISE MEASUREMENT
YO-3A acoustics research aircraft systems manual [NASA-TM-85968] 01 p0012 N85-10074
Electromagnetic-acoustic-transducer e system for thick-weld inspection [PB84-219492] 01 p0051 N85-10336
Low-frequency sound absorption measurements in air [NASA-RP-1126] 02 p0275 N85-11789
Pulse-echo method for flaw detection in concrete [PB84-234509] 06 p0775 N85-14953
Analytical and physical modeling program for the NASA Lewis Research Center's Altitude Wind Tunnel (AWT) [NASA-TM-86919] 07 p0909 N85-15757
Acoustic transducers for fast reactor instrumentation [BLL-RISLEY-TR-4979-(9091.9F)] 07 p0961 N85-16091
External cavity diode laser sensor [AD-D011341] 07 p0969 N85-16152
Quantitative acoustic emission techniques [AERE-R-11252] 07 p0977 N85-16203
Acoustic tomographic reconstruction of anomalies in three-dimensional bodies [DE84-017035] 09 p1378 N85-18666
USSR report: Physics and mathematics [JPRS-UPM-85-001] 11 p1715 N85-20786
Nondestructive method for detecting machine damage in beryllium [DE85-001074] 12 p1862 N85-21681
Defect characterisation and monitoring by acoustic emission [AERE-R-11409] 12 p1863 N85-21683
The measurement of residual stresses using ultrasonics [AERE-R-11415] 12 p1868 N85-21722
Calibration method for acoustic scattering measurements using a spherical target [AD-D011521] 12 p1927 N85-22106
Numerical results of acoustic radiation, transmission and reflection of steel plate in water [AMTE(N)-TM-84037] 13 p2155 N85-23378
Properties of materials using acoustic waves [AD-A150465] 13 p2155 N85-23382
Surface pressure produced by Space Transportation System flight 41B [AD-A150793] 14 p2242 N85-23901
Investigation of errors of acoustic goniometer information-measurement systems on rocking base 14 p2283 N85-24139
Optical monitoring of photo-acoustic pulse propagation in silicon wafers [AD-A151333] 15 p2651 N85-26352
Development of a modified time delay spectrometry technique for underwater acoustic measurements in a multipath environment [AD-A152111] 16 p2660 N85-27639
Experimental investigation of the pulsed photoacoustic effect produced on a solid surface [AD-A152114] 16 p2660 N85-27640
Measurement of cochlear acoustic pressure in guinea pigs [ISL-CO-234/83] 16 p2661 N85-27644
The Shock and Vibration Digest, volume 17, no. 1 [AD-A151051] 17 p2977 N85-28397
Sound intensity measurement 17 p2977 N85-28398
Correlation of predicted and measured sonic boom characteristics from the reentry of STS-1 orbiter [NASA-TP-2475] 18 p3177 N85-29694
Study of sound attenuation in sediments [AD-A153690] 18 p3177 N85-29697
Crosswell acoustic surveying in gas sands: Travel-time pattern recognition, seismic Q and channel waves [DE85-010777] 19 p3352 N85-30776
On the solution for the sound field in a semi-infinite uniform duct with sheared mean flow 20 p3523 N85-31912
Gas sensing with surface acoustic wave devices [DE85-009125] 20 p3524 N85-31921
Ultrasonic position reference systems for an autonomous sentry robot and a robot manipulator arm [AD-A155481] 21 p3586 N85-32336
FAA/GAMA (Federal Aviation Administration/General Aviation Manufacturer's Association) propeller aircraft noise test program, Salina Municipal Airport, Salina, Kansas [AD-A154818] 21 p3699 N85-32563
Acoustic cross-correlation flowmeter for solid-gas flow [DE85-005988] 23 p3935 N85-34391
Acoustical absorption coefficient in a diffuse field of a plane, rectangular material of finite dimensions placed on an infinite perfectly reflecting surface [NRC/CNR-TT-2113] 23 p3968 N85-34599
Search for acoustic signals from high energy cascades [HE-7.1-1] 24 p4213 N85-36155
Experimental investigation of radiative-acoustic effects in the water by the thermodynamical conditions of Dumand [HE-7.1-2] 24 p4213 N85-36156
Exploring results of the possibility on detecting cosmic ray particles by acoustic way [HE-7.1-3] 24 p4213 N85-36157
Acoustic detection of air shower cores [HE-7.1-4] 24 p4213 N85-36158

ACOUSTIC MICROSCOPES
High resolution acoustic microstructural characterization of titanium with interstitial contamination [AD-P004128] 08 p1127 N85-17103
Research on nondestructive testing [AD-A148375] 08 p1171 N85-17380
Acoustic microscopy at cryogenic temperatures [AD-A148755] 09 p1384 N85-18704
Scanning photoacoustic microscopy of aluminum with aluminum oxide, roughness standards and rubber [AD-A149460] 10 p1441 N85-19081
Nondestructive method for detecting machine damage in beryllium [DE85-001074] 12 p1862 N85-21681
Reliability of void detection in structural ceramics using scanning laser acoustic microscopy [NASA-TM-87036] 21 p3597 N85-32337

ACOUSTIC PROPAGATION
A description and discussion of FREDDEX oceanographic measurements [AD-A145032] 01 p0088 N85-10596
Behavior of charged particles in lower ionosphere with acoustical effects 02 p0161 N85-11089
The numerical solution of the Helmholtz equation for wave propagation problems in underwater acoustics [NASA-CR-172454] 02 p0250 N85-11634
The acoustic pressure in a wedge-shaped water layer overlying a fast fluid bottom [AD-A145517] 02 p0276 N85-11795
The S-matrix and acoustic signal structure in simple and compound waveguides [PP-583] 03 p0415 N85-12652
Deep water mass circulation in the Western Alboran Basin: Measurements in July and September 1980 (Alboran I experiment) [AD-A148566] 08 p1191 N85-17504
SAI (Science Applications, Inc.) Interim Scattering Model/Ice (SISM/ICE) [AD-A148596] 08 p1213 N85-17638
A critical analysis of ocean thermal analysis models in operation at FNOC (Fleet Numerical Oceanography Centers) [AD-A148731] 09 p1359 N85-18547
Preliminary results of study of space-time variability of shallow sea on steady acoustical path 10 p1499 N85-19459
Arctic acoustic propagation model with ice scattering [AD-A149430] 10 p1553 N85-19795
A stochastic-mechanical approach to acoustic pulse propagation in the deep ocean sound channel [AD-A149598] 12 p1928 N85-22110
Acoustic energy exchange in sheared mean flows — solid rocket motors 13 p1999 N85-22534
Transmission of gear noise to aircraft interiors prediction methods 14 p2223 N85-23788
Abatement of noise and vibration in pipelines of hydro systems 14 p2276 N85-24102
Acoustic radiation from bilaminar plates 14 p2415 N85-24903
Propagation of sound in matter [AD-A151013] 14 p2416 N85-24907
Propagation of sound in matter [AD-A151052] 14 p2416 N85-24908
Recent progress in the development and application of the parabolic equation [AD-A151475] 15 p2637 N85-26265
Long range downwind propagation of low-frequency sound [NASA-TM-86409] 15 p2645 N85-26318
Acoustic propagation in a thermally stratified atmosphere [NASA-CR-175787] 16 p2660 N85-27636
Propagation of acoustic pulse in atmospheric waveguide 19 p3297 N85-30443
Microwave SAW (Surface Acoustic Wave) monochromator [AD-D011718] 21 p3590 N85-32311

ACOUSTIC PROPERTIES
NT ACOUSTIC IMPEDANCE
NT ACOUSTIC INSTABILITY
NT ACOUSTIC SCATTERING
NT ACOUSTIC VELOCITY
NT REVERBERATION
NT SOUND INTENSITY
Vibration, acoustic, and shock design and test criteria for components on the Solid Rocket Boosters (SRB), Lightweight External Tank (LWT), and Space Shuttle Main Engines (SSME) [NASA-RP-1127] 01 p0061 N85-10405
Nonlinear acoustics [AD-A145580] 02 p0276 N85-11796
Sources, paths, and concepts for reduction of noise in the test section of the NASA Langley 4x7m wind tunnel [NASA-CR-172446-VOL-1] 05 p0726 N85-14666
Comparison of options for reduction of noise in the test section of the NASA Langley 4x7m wind tunnel, including reduction of nozzle area [NASA-CR-172446-VOL-2] 05 p0726 N85-14667
Noise measurement flight test: Data-analyses, Sikorsky S-76A helicopter [AD-A148525] 08 p1218 N85-17673
Effect of sealants of the sound absorption coefficients of acoustical friable insulating materials [AD-A148541] 08 p1218 N85-17674
Methods of computer-aided analysis of non-Gaussian noise and application to robust adaptive detection, part 2 [AD-A148879] 10 p1539 N85-19704
Acoustic scaling: A re-evaluation of the acoustic model of Manchester Studio 7 [BBC-RD-1984/18] 12 p1822 N85-21432
Interaction of a turbulent vortex with a lifting surface 15 p2464 N85-25214
Phase-lock fiber optic interferometer [AD-D011603] 16 p2786 N85-27191
Geoacoustic models: Washington state continental margin [AD-A153761] 18 p3177 N85-29699
Chemical-acoustic interactions in combustion systems [AD-A153657] 19 p3233 N85-30046
Measured acoustic properties of variable and low density bulk absorbers [NASA-TM-87065] 19 p3351 N85-30770
Airborne sound transmission loss characteristics of wood-frame construction [AD-A154174] 20 p3524 N85-31919
Acoustic scaling: The development of improved instrumentation [BBC-RD-1985/7] 24 p4145 N85-35694
Analysis of two-parameter constant background born inversion for acoustic synthetic data [AD-A156364] 24 p4145 N85-35696
Acoustic resonances in cylinder bundles oscillating in a compressible fluid [DE85-004086] 24 p4145 N85-35699

ACOUSTIC RADIATION
U SOUND WAVES

ACOUSTIC RETROFITTING
Noise in small portable motocompressors. Experiments on limited-cost acoustic treatments to obtain progressive improvements
[CETIM-11-H-445] 04 p0558 N85-13557
Aircraft cabin noise prediction and optimization
[NASA-CR-175982] 19 p3350 N85-30766
Design of sidewall treatment of cabin noise control of a twin engine turboprop aircraft
[NASA-CR-172245] 19 p3351 N85-30771
ACOUSTIC SCATTERING
NT REVERBERATION
Analytical modeling of random thermal fluctuations in the NORDA high-frequency sound scattering facility
[AD-A145024] 01 p0116 N85-10790
High-frequency asymptotic behavior of reflected and transmitted waves during scattering of sound by hollow elastic sphere filled with fluid 02 p0266 N85-11738
Acoustic scattering cross sections for truly composite wind-wave surfaces. Scattering without bubbles
[AD-A145672] 03 p0415 N85-12655
Selective observation of elastic-body resonances via their ringing in transient acoustic scattering
[AD-A145868] 03 p0416 N85-12656
USSR report: Physics and mathematics
[JPRS-UPM-84-007] 05 p0723 N85-14651
Resonant scattering of acoustic waves by elastic spherical shell in fluid 06 p0778 N85-14972
Research on acoustical and optical scattering, optics of bubbles, diffraction catastrophes, laser generation of sound, and shock induced cavitation
[AD-A146703] 06 p0860 N85-15466
SAI (Science Applications, Inc.) interim Scattering Model/Ice (SISM/ICE)
[AD-A148596] 08 p1213 N85-17638
Arctic acoustic propagation model with ice scattering
[AD-A149430] 10 p1553 N85-19795
Calibration method for acoustic scattering measurements using a spherical target
[AD-D011521] 12 p1927 N85-22106
Surface forward scattering and reflection
[AD-A150115] 12 p1928 N85-22112
Surface scattering
[AD-A150252] 13 p2153 N85-23366
Elastic wave scattering from cavities and sound inclusions analyzed by the resonance method
[AD-A150315] 13 p2155 N85-23381
Properties of materials using acoustic waves
[AD-A150465] 13 p2155 N85-23382
Scattering of sounds by piezoceramic cylindrical shell near rigid surface 17 p2943 N85-28168
Toward the theory of acoustic scattering on uneven free surface 21 p3680 N85-32862
Understanding coherence losses incurred by bottom-retained signals
[AD-A155559] 21 p3701 N85-32992
Second Colloquim on the Scattering of Ultrasonic Waves
[AD-A156298] 24 p4145 N85-35697
ACOUSTIC SOUNDING
Characterization of stressed metals using acoustic shear waves 05 p0648 N85-14159
Influence of refraction effects on informativeness of bistatic acoustical atmospheric sounding systems 06 p0825 N85-15237
Specifics of backscattering of sound by bottom of bank in open sea 10 p1499 N85-19460
Average sound intensity decrease rule in irregular hydroecoustical waveguide 10 p1499 N85-19461
Ultrasonic large-diameter pipe weld testing installations 11 p1603 N85-20061
Quantitative non-destructive evaluation of damage in composite materials using transmitted and reflected ultrasound
[NASA-CR-175550] 12 p1796 N85-21269
Experimental results of temperature-wind soundings of the atmosphere by the radio acoustical method 14 p2340 N85-24471
ACOUSTIC STABILITY
U FREQUENCY STABILITY
ACOUSTIC VELOCITY
Active remote sensing of ocean parameters, an engineering study 02 p0213 N85-11403
CHORDS: A new temperature or sound speed profile thinning algorithm
[AD-A145464] 02 p0275 N85-11793
Project review on geophysical and ocean sound speed profile inversion
[AD-A145717] 02 p0276 N85-11797
Influence of pressure on speed of sound in single-phase region of stratifying mixtures 11 p1715 N85-20788
Sound velocity of carbon at high pressures
[DE85-002016] 12 p1928 N85-22113
Coupling between velocity oscillations and solid propellant combustion 13 p2000 N85-22536
Coupled acoustic and hydrodynamic wave instabilities 13 p2000 N85-22538
Investigation of the characteristics of the velocity-coupled response functions of solid propellants 13 p2001 N85-22540
Coupling between velocity oscillations and solid propellant combustion
[AD-A151061] 14 p2247 N85-23927
Field of point source of low-frequency sound in atmosphere with altitudinally nonuniform wind 15 p2524 N85-25566
Wave description of sound propagation through stratified moving atmosphere 15 p2525 N85-25567
Apparatus for measuring velocity of sound in fluids 17 p2944 N85-28175
Spectral methods for the estimation of acoustic intensity, energy density, and surface velocity using a multimicrophone probe 20 p3524 N85-31916
Trailing edge flow and aerodynamic sound. Part 1: Tonal pressure and velocity fluctuations. Part 2: Random pressure and velocity fluctuations
[AD-A154947] 21 p3552 N85-32097
Toward the propagation of waves in unsteady media 21 p3683 N85-32861
Sound speed measurements in liquid oxygen-liquid nitrogen mixtures
[NASA-TP-2464] 24 p4083 N85-35307
Experimental investigation of radiative-acoustic effects in the water by the thermodynamical conditions of Dumand
[HE-7.1-2] 24 p4213 N85-36156
ACOUSTIC VIBRATIONS
U SOUND WAVES
ACOUSTICAL HOLOGRAPHY
Heterodyne holographic interferometry for visualization of surface acoustic waves
[AD-A155405] 22 p3836 N85-33753
ACOUSTICS
NT AEROACOUSTICS
NT GEOMETRICAL ACOUSTICS
NT MAGNETOACOUSTICS
NT PSYCHOACOUSTICS
NT UNDERWATER ACOUSTICS
Scattering of plane wave on cylindrical shell in low-frequency region 02 p0256 N85-11677
Influence of radiation wavelength on elastic pulse shape during laser excitation 02 p0257 N85-11681
Laminar-to-turbulent flow transition under influence of acoustic oscillations 02 p0260 N85-11701
USSR report: Physics and mathematics
[JPRS-UPM-84-004] 02 p0266 N85-11737
Coupling of airborne sound into the Earth
[AD-A146231] 03 p0416 N85-12663
Research activities of the Illinois University Coordinated Science Laboratory
[AD-A145589] 03 p0449 N85-12856
USSR report: Electronics and electrical engineering
[JPRS-UEE-84-010] 04 p0485 N85-13095
Perceptibility of nonlinear distortions in power amplifier 06 p0789 N85-15041
A miniature urethane molded acoustic transducer
[AD-A146459] 06 p0804 N85-15114
An extension of the Born inversion method to a depth dependent reference profile
[AD-A146469] 06 p0859 N85-15461
Human engineer's guide to auditory displays. Volume 2: Elements of signal reception and resolution affecting auditory displays
[AD-A146513] 06 p0859 N85-15462
Basic research in electronic (JSEP): Joint Services Electronics Program
[AD-A147891] 07 p0948 N85-16007
Statistical filtering as method for detecting transcrustal acoustic anomalies 07 p0962 N85-16237
Analysis of the surface load and radiated sound of a vibrating airfoil with application to the experiment of Brooks
[NASA-CR-3864] 07 p1038 N85-16590
Estimate of sound absorption due to magnetoelastic interactions
[AD-A148216] 08 p1218 N85-17671
Digital sound: Programme-modulated noise levels in sound signals subjected to a number of digital companding processes
[BBC-RD-1984/11] 09 p1310 N85-18233
On the interaction of a sound pulse with the shear layer of an axisymmetric jet. Part 3: Nonlinear effects
[NASA-CR-172512] 09 p1378 N85-18663
Acoustic resonance in heat exchanger tube banks
[DE85-004396] 11 p1632 N85-20281
USSR report: Electronics and electrical engineering
[JPRS-UEE-85-004] 12 p1837 N85-21531
Methods of progressing waves in turbulent media with applications to acoustics
[AD-A149599] 12 p1920 N85-22055
Ice statistics and acoustic scattering in the Arctic basin
[AD-A150141] 13 p2140 N85-23269
Noise measurement flight test: Data/Analyses, hughes 500 D/E helicopter
[AD-A148110] 14 p2219 N85-23758
Propagation of sound in matter
[AD-A151013] 14 p2416 N85-24907
Propagation of sound in matter
[AD-A151052] 14 p2416 N85-24908
Psychological and physiological basis of stereophonic effect 15 p2526 N85-25574
An evaluation of proposed acoustic treatments for the NASA LaRC 4 x 7 meter wind tunnel
[NASA-CR-172577] 15 p2646 N85-26319
Analysis of combustion oscillations in heterogeneous systems
[AD-A151999] 16 p2745 N85-26942
Phase-lock fiber optic interferometer
[AD-D011603] 16 p2786 N85-27191
Acoustic oscillations of rods and plates 17 p2944 N85-28170
Theoretical investigations of the propagation and interactions of surface waves
[AD-A153548] 18 p3185 N85-29753
Activities of Istituto Elettrotecnico Nazionale Galileo Ferraris 18 p3199 N85-29845
Hot Dry Rock Geothermal Energy Developement Program
[DE85-010570] 19 p3268 N85-30264
Acoustic particle separation
[NASA-CASE-NPO-155559-1] 19 p3350 N85-30765
Acoustic imaging systems (for robotic object acquisition)
[AD-A154043] 19 p3351 N85-30772
USSR report: Physics and mathematics
[JPRS-UPM-85-004] 21 p3680 N85-32860
Lateral attenuation of aircraft flight noise
[AD-A154958] 21 p3700 N85-32966
Heterodyne holographic interferometry for visualization of surface acoustic waves
[AD-A155405] 22 p3836 N85-33753
Applications of the Kirchoff-Helmholtz integral to problems in body wave seismology 24 p4116 N85-35515
Acoustic scaling: The development of improved instrumentation
[BBC-RD-1985/7] 24 p4145 N85-35694
ACOUSTO-OPTICS
Guided-wave optic devices for integrated optic information processing
[AD-A145695] 02 p0260 N85-11827
Characteristics of light diffraction by two acoustic waves, one with complex frequency composition 03 p0348 N85-12243
USSR report: Physics and mathematics
[JPRS-UPM-84-007] 05 p0723 N85-14651
Laser excitation of coupled surface electromagnetic and acoustic waves and of static structures in solids 05 p0723 N85-14652
A single optical fiber telephone system
[AD-D011293] 06 p0799 N85-15107
USSR report: Electronics and electrical engineering
[JPRS-UEE-84-018] 07 p0949 N85-16014
Optimization piezoelectric transducer width of acousto-optical devices 07 p0950 N85-16024
Study of optical sound generation and amplification
[AD-A147359] 07 p1039 N85-16592
Tunable heterodyne receiver from 100 micron to 1,000 micron for airborne observations 08 p1249 N85-17888
Optical data processing for missile guidance
[AD-A149346] 10 p1422 N85-18972
Photoacoustic effect and its applications 12 p1820 N85-21421
Acousto-optically addressed Fourier transform matched filters
[AD-A150298] 13 p2063 N85-22889
USSR report: Electronics and electrical engineering
[JPRS-UEE-85-002] 13 p2066 N85-22907
Space-time response characteristics of acoustooptic filter for compression of linearly frequency-modulated signal 13 p2071 N85-22937
Integrated optical components utilizing acoustooptic and electrooptic diffraction in micro-waveguides 13 p2089 N85-23044
Acoustooptic demodulation of frequency-modulated signals 13 p2090 N85-23050
Acoustooptic cell as space-frequency filter 13 p2090 N85-23051
Accuracy of random signal spectral parameter estimation against interference background in acoustooptical spectrum analyzers 13 p2090 N85-23052
Optoacoustic receiver with semiconductor-type radiator and photodetector 14 p2274 N85-24086

Photoacoustic imaging
[AD-A150823] 14 p2416 N85-24905
Optical monitoring of photo-acoustic pulse propagation in silicon wafers
[AD-A151333] 15 p2651 N85-26352
The development and implementation of an optical communications laboratory
[AD-A151682] 16 p2772 N85-27111
Acousto-optical spectrometers at Itapetinga Radio Observatory
[INPE-3479-PRE/722] 16 p2881 N85-27776
An introductory view of Raman-Nath type equations
[PREPRINT-422] 18 p3172 N85-29664
High accuracy digital acousto-optic matrix computer
[AD-D011692] 19 p3343 N85-30716
Acoustic imaging systems (for robotic object acquisition)
[AD-A154043] 19 p3351 N85-30772
The sound field of a moving laser-induced acoustic array (theory)
[AD-A154553] 21 p3699 N85-32441
Fundamentals of radio optical theory of resonant and directional quasi-optical devices
22 p3780 N85-33420
Binary signal detection in acoustooptic receivers
22 p3782 N85-33430
Asymmetry of diffraction orders with light diffraction at surface acoustic wave 22 p3782 N85-33431

ACQUISITION
NT DATA ACQUISITION
NT TARGET ACQUISITION
Systems analysis for microcomputer acquisitions
[AD-A145447] 02 p0239 N85-11556
Survey relating to the implementation of cost/schedule control systems criteria within the Department of Defense and industry
[AD-A146664] 06 p0870 N85-15526
Acquisition planning at the Defense Communications Agency
[AD-A146877] 07 p1051 N85-16669
Food acquisition: Food ingredients, raw materials and supply 14 p2393 N85-24737
Capital investment motivational techniques used by prime contractors on subcontractors
[AD-A153660] 18 p3198 N85-29837
Producibility Engineering and Planning (PEP): Program management guidelines
[AD-A153730] 19 p3379 N85-30966
Second Colloquim on the Scattering of Ultrasonic Waves
[AD-A156298] 24 p4145 N85-35697

ACRYLATES
Properties of ultra-violet cured poly(dimethylsiloxane)-urea acrylates
[AD-A148570] 06 p1134 N85-17146
Chiral polymers
[AD-A150366] 13 p2037 N85-22760
New air-curing lacquer systems with high solids content
[BMFT-FB-T-85-005] 17 p2936 N85-28124

ACRYLIC RESINS
Fluorinated diacrylic esters
[AD-D011328] 07 p0929 N85-15889
Process for preparation of crosslinked poly(tri-n-butyltin) methacrylate with simultaneous particle size reduction
[AD-D011313] 07 p0932 N85-15905
Study for a large area acrylic scintillator detector — magnetic monopoles
[NOTA-INTERNA-827] 18 p3097 N85-29174
Measurement of the attenuation length of an acrylic scintillator — magnetic monopoles
[NOTA-INTERNA-828] 18 p3097 N85-29175
New corrosion protection concept for very high voltage line towers
[BLL-OA-TRANS-2691-(6196.300)] 20 p3429 N85-31270
Effect of polymer additives on characteristics of direct-current motor with liquid dielectric filler
22 p3772 N85-33376

ACRYLONITRILES
Morphology and dynamic mechanical properties of diglycidyl ether of bisphenol-A toughened with carboxyl-terminated butadiene-acrylonitrile
04 p0466 N85-12958
Properties of polycaproamide fibers modified by grafted polyacrylonitrile 06 p0761 N85-14867
The adsorption of acrylonitrile at a gold electrode: An EMIRS measurement of the electrochemical stark effect
[AD-A148664] 08 p1123 N85-17082

ACTH
U ADRENOCORTICOTROPIN (ACTH)

ACTINIDE SERIES
NT AMERICIUM
NT AMERICIUM ISOTOPES
NT AMERICIUM 241
NT CALIFORNIUM ISOTOPES
NT CURIUM
NT CURIUM 244
NT PLUTONIUM
NT PLUTONIUM ISOTOPES
NT PLUTONIUM 238
NT PLUTONIUM 239
NT RADIUM
NT THORIUM
NT THORIUM ISOTOPES
NT TRANSURANIUM ELEMENTS
NT URANIUM
NT URANIUM ISOTOPES
NT URANIUM 235
Influence of 5f electrons on structures and bonding in the actinide-hydrogen intermetallics
[DE84-013893] 01 p0118 N85-10607
Actinides, the narrowest bands
[DE84-016463] 05 p0733 N85-14710
Method for fluorination of actinide fluorides and oxyfluorides using O2F2
[DE85-011648] 22 p3743 N85-33202
Capabilities of the LDEF-2 heavy nuclei collection
[OG-4.4-8] 22 p3880 N85-34040

ACTINIDE SERIES COMPOUNDS
NT NEPTUNIUM COMPOUNDS
NT PLUTONIUM OXIDES
NT URANIUM CARBIDES
NT URANIUM COMPOUNDS
NT URANIUM FLUORIDES
Mossbauer effect and contactless conductivity studies of superconducting actinides intermetallics and hydrides. Mossbauer high pressure studies
03 p0430 N85-12743
Method for extracting lanthanides and actinides from acid solutions by modification of Purex solvent
[DE85-005763] 23 p3909 N85-34220

ACTINOGRAPHS
U ACTINOMETERS

ACTINOMETERS
NT INFRARED DETECTORS
NT INFRARED SCANNERS
NT INFRARED SPECTROMETERS
NT INFRARED SPECTROPHOTOMETERS
NT MICROWAVE RADIOMETERS
NT PASSIVE L-BAND RADIOMETERS
NT PYRANOMETERS
NT RADIOMETERS
NT SOLAR SPECTROMETERS
NT SPECTROHELIOGRAPHS
NT SPECTROPHOTOMETERS
NT SPECTRORADIOMETERS
NT ULTRAVIOLET SPECTROMETERS
NT ULTRAVIOLET SPECTROPHOTOMETERS
Impact of fluctuations in optical properties of atmosphere on the ratio of spectral brightness from remote sensing of agricultural land 22 p3734 N85-33149

ACTIVATED CARBON
A study of the chemical interaction of gases with activated carbon
[AD-A147342] 07 p0923 N85-15846
Versatility of peat emphasized
07 p0994 N85-16316
The reaction of oxygen-nitrogen mixtures with granular activated carbons below the spontaneous ignition temperature
[AD-A149041] 10 p1434 N85-19039
Low pressure storage of methane on interlayered clays for potential vehicular applications
[DE85-006949] 16 p2758 N85-27017
Radiocarbon content in the annual tree rings during last 150 years and time variation of cosmic rays
[SH-7.1-15] 23 p4048 N85-35106

ACTIVATION
Study of proton and neutron activation of metal samples in low Earth orbit
[NASA-CR-171183] 01 p0026 N85-10164
A comment on Rosen's comments on activation and inhibition
[CTH-MATH-1984-24] 05 p0719 N85-14617
Impact of activation optimization on the Vandenberg Ground Support System using Q-GERT analysis
[AD-A148448] 08 p1105 N85-16986
Activation of Si-N modes in silicon by pulsed laser annealing
[DE85-003988] 13 p2097 N85-23082
CO adsorption on (111) and (100) surfaces of the Pt sub 3 Ti alloy. Evidence for parallel binding and strong activation of CO
[NASA-CR-176077] 21 p3565 N85-32176
A simple model to investigate the activation process in waterclouds 21 p3649 N85-32675
Measurements of the critical supersaturation of 0.029 to 0.035 micron radius particles at Washington, District of Columbia 21 p3649 N85-32676
Fog activation and supersaturation
21 p3650 N85-32678
Luminescence and absorption of indium-activated potassium-borate glasses subjected to high-power excitation 21 p3681 N85-32868
The effect of +Gx acceleration on platelet activation as determined by plasma platelet factor 4 levels
[AD-A155881] 24 p4131 N85-35608

ACTIVATION ANALYSIS
NT NEUTRON ACTIVATION ANALYSIS
Non-invasive techniques for determining musculoskeleton body composition
[DE84-015718] 04 p0545 N85-13470
Measurement and evaluation of selected 14-MeV neutron cross sections for fusion
[DE85-010295] 19 p3365 N85-30667
NBS (National Bureau of Standards) reactor: Summary of activities Jul. 1983 through Jun. 1984
[PB85-184836] 20 p3522 N85-31907
Study of proton and neutron activation of metal samples in low Earth orbit
[NASA-CR-171596] 21 p3558 N85-32130

ACTIVATION ENERGY
Fire retardant cellulosehydrate fibers
06 p0761 N85-14870
Deer control using 7 strand vertical fence
11 p1581 N85-19958
Detonations of solid explosives
[AD-A152012] 15 p2521 N85-25540
Thermoelectric properties of beta-boron and some boron compounds
[DE85-011976] 21 p3582 N85-32270
Activation analysis of natural water using neutrons of various energies 21 p3690 N85-32924
Three-dimensional hydrodynamic hot-spot model
[DE85-009587] 23 p3922 N85-34301
Grain boundary and surface diffusion in oxide systems
[DE85-007291] 23 p3985 N85-34715

ACTIVE CONTROL
Active control technology experience with the Space Shuttle in the landing regime
[NASA-TM-85910] 01 p0012 N85-10071
Fuel efficiency through new airframe technology
[NASA-TM-84548] 02 p0133 N85-10909
Energy efficient engine. Low pressure turbine test hardware detailed design report
[NASA-CR-167956] 02 p0147 N85-10994
Integrated Application of Active Controls (IAAC) technology to an advanced subsonic transport project-longitudinal handling qualities study of a relaxed-stability airplane
[NASA-CR-3660] 02 p0148 N85-11005
Development and flight evaluation of an augmented stability active controls concept: Executive summary
[NASA-CR-166009] 02 p0149 N85-11006
The microprocessor control of a motor-alternator
[RAE-TM-NAV-ENG-1023(L)] 02 p0244 N85-11591
Flying qualities and control system characteristics for superaugmented aircraft
[NASA-CR-170419] 05 p0596 N85-13800
Active sticks: A new dimension in controller design
05 p0706 N85-14531
Integrated Application of Active Controls (IAAC) technology to an advanced subsonic transport project. ACT/Control/Guidance System study, volume 1
[NASA-CR-165963-VOL-1] 06 p0754 N85-14837
Integrated Application of Active Controls (IAAC) technology to an advanced subsonic transport project. ACT/Control/Guidance System study. Volume 2: Appendices
[NASA-CR-165963-VOL-2] 06 p0754 N85-14838
Efficiency in integral active antennas
06 p0792 N85-15060
Study to eliminate ground resonance using active controls
[NASA-CR-166609] 07 p0902 N85-15715
Helicopter active control with rotor blades relaxation
08 p1075 N85-16819
Challenges in the development of the orbiter active thermal control subsystem 08 p1098 N85-16923
Active control of forward swept wings with divergence and flutter aeroelastic instabilities
09 p1282 N85-18063
The experimental performance of an off-road vehicle utilizing a semi-active suspension — off-road motorcyles
09 p1339 N85-18421
Ground and flight testing for aircraft guidance and control
[AGARD-AG-262] 13 p1966 N85-22350
Dynamic wind tunnel testing for active control research 13 p1966 N85-22352
Dynamic wind-tunnel testing of active controls by the NASA Langley Research Center
13 p1966 N85-22353
Passive and Active Control of Space Structures (PACOSS) 14 p2234 N85-23648
ACOSS 11 (Active Control Of Space Structures)
[AD-A150639] 14 p2248 N85-23922

Active dispersion control for a Doppler broadened laser
[AD-D011570] 14 p2310 N85-24297
The design and operation of a simple low-speed flutter-suppression model
[AD-A151610] 15 p2474 N85-25269
Active control of forward swept wings with divergence and flutter aeroelastic instabilities
[AD-A151837] 15 p2474 N85-25270
The ONERA establishment at Cannes in the service of aeronautical research
[ESA-TT-875] 15 p2475 N85-25276
Numerical simulation of boundary layer excitation by surface heating/cooling
[NASA-CR-172575] 15 p2554 N85-25756
Technical evaluation report on the Flight Mechanics Symposium on Active Control Systems: Review, Evaluation and Projections
[AGARD-AR-220] 16 p2711 N85-26730
Active control technology: Past, present, future
16 p2711 N85-26731
The state-of-the-art and future of flight control systems 16 p2712 N85-26732
A perspective on superaugmented flight control advantages and problems 16 p2712 N85-26733
Aspects of application of ACT systems for pilot workload alleviation 16 p2712 N85-26734
Application of AFTI/F-16 task-tailored control modes in advanced multirole fighters 16 p2712 N85-26735
X-29A digital flight control system design
16 p2712 N85-26736
The evaluation of ACS for helicopters: Conceptual simulation studies to preliminary design
16 p2712 N85-26737
ACT applied to helicopter flight control
16 p2712 N85-26738
An update on experience on the fly by wire Jaguar equipped with a full-time digital flight control system
16 p2712 N85-26740
ACT flight research experience
16 p2713 N85-26741
Operational and developmental experience with the F/A-18A digital flight control system
16 p2713 N85-26742
OLGA: An open loop gust alleviation
16 p2713 N85-26744
Active control technology experience with the Space Shuttle in the landing regime 16 p2713 N85-26747
The aerodynamics of controls
16 p2713 N85-26748
Active control landing gear for ground loads alleviation
16 p2714 N85-26749
Wing buffeting active control testing on a transport aircraft configuration in a large sonic tunnel
16 p2714 N85-26750
How to handle failures in advanced flight control systems of future transport aircraft 16 p2714 N85-26752
The certification of airborne complex digital systems
16 p2714 N85-26754
Automatic flight control modes for the AFTI/F-111 mission adaptive wing aircraft 16 p2714 N85-26756
The evolution of active control technology systems for the 1990's helicopter 16 p2715 N85-26758
Active Control Systems: Review, Evaluation and Projections
[AGARD-CP-384] 17 p2901 N85-27883
Active Control Technology (ACT): Past, present and future 17 p2901 N85-27884
The state-of-the-art and future of flight control systems 17 p2901 N85-27885
A perspective on superaugmented flight control advantages and problems 17 p2901 N85-27886
Aspects of application of ACT systems for pilot workload alleviation 17 p2901 N85-27887
X-29 digital flight control system design
17 p2901 N85-27889
The evolution of ACS for helicopters: Conceptual simulation studies to preliminary design
17 p2902 N85-27890
Some flight test results with redundant digital flight control systems 17 p2902 N85-27892
ACT flight research experience
17 p2902 N85-27894
Flight testing and development of the F/A-18A digital flight control system 17 p2902 N85-27896
OLGA: An open loop gust alleviation system
17 p2903 N85-27897
Demonstration of relaxed static stability on a commercial transport 17 p2903 N85-27898
Active control technology experience with the Space Shuttle in the landing regime 17 p2903 N85-27900
Active control landing gear for ground load alleviation
17 p2903 N85-27902
Wing buffeting active control testing on a transport aircraft configuration in a large sonic windtunnel
17 p2904 N85-27903
A modular dissimilar redundant computer designed for high integrity control 17 p2904 N85-27904
How to handle failures in advanced flight control systems of future transport aircraft 17 p2904 N85-27905
The evolution of active control technology systems for the 1990's helicopter 17 p2905 N85-27911
Vibration control of rotor shaft
[NASA-TM-87053] 18 p3117 N85-29292
NASA Space controls research and technology program 20 p3408 N85-31149
Characteristic elastic systems of time-limited optimal manouvers 20 p3413 N85-31184
Models for describing active noise control in ducts
[ISVR-TR-127] 20 p3525 N85-31922
R and D activities of the Systems Engineering Division
20 p3540 N85-32027

ACTIVE GLACIERS
U GLACIERS

ACTIVE VOLCANOES
U VOLCANOES

ACTIVITY (BIOLOGY)
Primary light harvesting system: The relationship of phycobiliosomes to photosystem 1 and 2
[DE85-009075] 11 p1689 N85-20622
Sulfur Cycle 21 p3662 N85-32748

ACTIVITY CYCLES (BIOLOGY)
Biogeochemical cycles: Interactions in global metabolism 05 p0652 N85-14184
Spontaneous motility of goldfish in absence of terrestrial zeitgebers: Space flight simulation in a mine
05 p0689 N85-14432
Circadian dynamics of potassium excretion in urine as related to working on one and two shifts
19 p3325 N85-30596

ACTUATION
Systems study for an integrated Digital-Electric Aircraft (IDEA)
[NASA-CR-3840] 07 p0902 N85-15714
Space shuttle rudder/speedbrake actuation subsystem
08 p1102 N85-16965
Development of the space shuttle body flap actuation subsystem 08 p1102 N85-16966
Magentically actuated compressor
[NASA-CASE-GSC-12799-1] 12 p1818 N85-21404

ACTUATOR DISKS
Turbine blade damping study
[NASA-CR-171255] 04 p0456 N85-12880
Users manual for a computer program for dynamic response analysis of bladed systems
[UDR-TR-84-38] 04 p0456 N85-12883

ACTUATORS
Development and flight evaluation of an augmented stability active controls concept: Executive summary
[NASA-CR-168009] 02 p0149 N85-11006
Autonomous momentum management for space station, exhibit A
[NASA-CR-171256] 04 p0462 N85-12933
Overview of magnetic bearing control and linearization approaches for annular magnetically suspended devices
05 p0607 N85-13872
Precise control of flexible manipulators
[NASA-CR-174210] 07 p0973 N85-16178
Mirror actuator control system
[AD-D011383] 07 p1042 N85-16619
Space shuttle rudder/speedbrake actuation subsystem
08 p1102 N85-16965
Development of the space shuttle body flap actuation subsystem 08 p1102 N85-16966
Design and test of a four channel motor for electromechanical flight control actuation
[NASA-CR-171838] 08 p1156 N85-17294
Neural compensation, muscle load distribution and muscle function in control of biped models
09 p1314 N85-18257
The development of a microprocessor-controlled linearly-actuated valve assembly
[NASA-CR-174437] 10 p1491 N85-19415
Fine figuring actuator
[AD-D011476] 10 p1557 N85-19619
Solar optical telescope primary mirror controller
[NASA-CR-174416] 10 p1570 N85-19903
Laser Doppler Anemometry (LDA) signal triggering and effective particle size range
[KU-SFB-210/E/5] 11 p1634 N85-20290
Slow opening valve — valve design for shuttle portable oxygen system
[NASA-CASE-MSC-20112-1] 11 p1642 N85-20338
Solar powered actuator with continuously variable auxiliary power control
[NASA-CASE-MFS-25637-1] 12 p1876 N85-21769
A quantitative comparison of active and passive damping for large space structures
[UTIAS-TN-249] 13 p1998 N85-22524
Optimum design of electrical motors for multilink manipulators and automated manufacturing systems
13 p2062 N85-22880
Analysis and design of hydraulic servo systems within the scope of the improvement of a fatigue testing installation of the Royal Dutch Army
[LEOK-TR-1984-09] 14 p2265 N85-24033
Vibration isolator actuator
[AD-D011574] 14 p2321 N85-24343
Surveillance program for the dissection and analysis of explosive and pyrotechnic components
[DE85-006105] 16 p2757 N85-27016
Fully redundant mechanical release actuator
[NASA-CASE-LAR-13196-1] 18 p3116 N85-29287
The effect of sensor and actuator errors on static shape control for large space structures
[NASA-TM-86445] 19 p3225 N85-29898
Thermal expansion coefficients of a 30% glass fiber filled PEEK pyrotechnic charge holder
[DE85-010905] 19 p3251 N85-30155
Thermo-electric valve
[AD-D011682] 19 p3252 N85-30165
Spillover minimization: An approach for actuators and sensors placement in distributed parameter study
[INPE-3525-PRE/746] 19 p3272 N85-30289
Experiments in structural dynamics and control using a grid 20 p3410 N85-31166
The experimental computer control of a two-dimensional hyperbolic system 20 p3411 N85-31168
Stiffness control of large space structures
20 p3414 N85-31189
Wideband disturbance accomodation in precision flexible space structures 20 p3415 N85-31194
Self-tuning adaptive-controller using online frequency identification 20 p3417 N85-31205
Comparison of the response of shape memory alloy actuators using air-cooling and water-cooling
[AD-A155216] 21 p3557 N85-32185
Automatic rotary valve actuator
[DE85-012797] 22 p3794 N85-33505
Design and development of a linear thermal actuator
22 p3796 N85-33515
A dual, fault-tolerant aerospace actuator
22 p3796 N85-33530
Design of a dual fault tolerant space shuttle payload deployment actuator 22 p3796 N85-33531
Intelligent redundant actuation system requirements and preliminary system design
[NASA-CR-177366] 23 p3896 N85-34136
Actuator rigging test set electromagnetic interference test (CE03)
[AD-A156619] 24 p4066 N85-36327
Computer simulation of a cruise missile using brushless dc motor fin control
[AD-A155935] 24 p4069 N85-36349

ACUITY
NT VISUAL ACUITY
Quantitative measurement of human auditory acuity
10 p1524 N85-19614

ADA (PROGRAMMING LANGUAGE)
Ada (trademark) training curriculum. Using the Ada language reference manual l402 teacher's guide
[AD-A143582] 01 p0103 N85-10685
Ada (trademark) training curriculum. Basic Ada programming l202 teacher's guide. Laboratory manual and exercises
[AD-A143583] 01 p0103 N85-10687
Ada (trademark) training curriculum. Real-time concepts l303 teacher's guide
[AD-A145093] 01 p0104 N85-10694
Ada (trademark) training curriculum. Software engineering for managers m101 teacher's exercise guide
[AD-A145094] 01 p0104 N85-10695
Advanced Ada (trademark)
[AD-A146257] 03 p0407 N85-12802
Real-time Ada (trademark)
[AD-A146258] 03 p0407 N85-12803
Experimenting with the Rolm Ada language workshop for specifying and designing 03 p0408 N85-12807
A proposal for standard basic functions in Ada
[NPL-DITC-45/84] 05 p0715 N85-14584
Ada compiler validation summary report: New York University (NYU Ada/Ed) compiler, version 1.4 for VAX 11/780, using VMS 3.5
[AD-A146824] 07 p1022 N85-16483
Ada compiler validation summary report: TeleSoft (TeleSoft Ada) compiler, version 2.0a for Sun 120 Motorola M68010, using 4.2 BSD UNIX-Sun Version 1.1
[AD-A146825] 07 p1022 N85-16484
NYU Ada/Ed user's guide: Version 1.4 for VAX/VMS systems
[AD-A146758] 07 p1024 N85-16495
Ada training curriculum. Real-time systems in Ada l401 teacher's guide, volume 1
[AD-A146782] 07 p1024 N85-16496
Ada training curriculum. Real-time systems in Ada l401 teacher's guide, volume 2
[AD-A146783] 07 p1024 N85-16497

Software testing in an Ada programming environment
08 p1065 N85-16748
Concept paper for the development of a DOD Ada (trademark) software engineering education and training plan
[AD-A148774] 08 p1206 N85-17592
Ada (trademark) primer
[AD-A148855] 10 p1539 N85-19703
Ada compiler validation summary report, Dansk Datamatik Center, VAX 11 compiler version 1.1
[AD-A149340] 11 p1699 N85-20681
A Gypsy-to-Ada program compiler
[TR-39] 12 p1913 N85-22005
Selection and use of general-purpose programming-language: Program examples, volume 2
[PB85-122000] 12 p1917 N85-22039
Selection and use of general-purpose programming language: Overview, volume 1
[PB85-122018] 12 p1917 N85-22040
Software library: A reusable software issue
[AD-A150722] 14 p2403 N85-24816
Reusable software: A concept for cost reduction
16 p2697 N85-26655
Evaluation of Ada (trademark) as a communications programming language, volume 1
[AD-A152314] 16 p2848 N85-27559
Evaluation of Ada (trademark) as a communications programming language. Volume 2: Communications protocols application
[AD-A152315] 16 p2848 N85-27560
Evaluation of Ada (trademark) as a communications programming language. Volume 3: Trusted software application
[AD-A152316] 16 p2848 N85-27561
Automatic distribution of programs in MASCOT and Ada (trademark) environments: A feasibility study
[AD-A152665] 17 p3010 N85-28614
AFIT GKS: A GKS implementation in the Ada programming language
[AD-A152954] 17 p3012 N85-28620
Evaluation and Validation (E/V) team public report, volume 1
[AD-A153600] 18 p3161 N85-29584
Ada validation summary report. ALS AdaVAX version 1.1 VAX-11/780 using VAX/VMS release 3.6
[AD-A153684] 18 p3162 N85-29588
Ada (trademark) compiler validation summary report. Honeywell Information systems GCOS6 Ada version 1.1
[AD-A153746] 18 p3162 N85-29590
Ada compiler validation summary report, University of Karlsruhe-GMD/German MOD Siemens - BS 2000 version 7.30
[AD-A153747] 18 p3163 N85-29591
Ada (trademark) compiler validation summary report: ALSYS ALSYCOMP-0001
[AD-A153750] 18 p3163 N85-29592
Ada developments
[REPT-84-28] 18 p3164 N85-29604
Ada compiler validation summary report: University of Karlsruhe-GMD/German MOD VAX 11 compiler, version v1.0
[AD-A154370] 19 p3337 N85-30678
Survey of Ada (Trademark)-based PDLs (Program Design Language)
[AD-A154402] 19 p3338 N85-30680
Study of the applicability of higher order languages for on-board satellite software production
[ESA-CR(P)-2024] 20 p3516 N85-31864
Artificial intelligence in Ada (trademark): Pattern-directed processing
[AD-A156230] 24 p4141 N85-35671

ADAPTATION
NT ACCLIMATIZATION
NT ALTITUDE ACCLIMATIZATION
NT COLD ACCLIMATIZATION
NT DARK ADAPTATION
NT HEAT ACCLIMATIZATION
NT LIGHT ADAPTATION
NT RETINAL ADAPTATION
Functional capacities of elderly subjects exposed to simulated spaceflight factors 01 p0091 N85-10617
Assessment of lift- and blockage-induced wall interference in a three-dimensional adaptive-wall tunnel
03 p0312 N85-12016
A data base for three-dimensional all-interference code evaluation 03 p0312 N85-12017
Wall adaptation at Mach 1.2 — wind tunnel tests
[ONERA-RTS-26/3075-AY-402]
04 p0453 N85-12873
Loss of bone substance in consequence of amputation as a model for the adaptation to microgravity
05 p0694 N85-14484
Effects of external loads on human head movement control systems 05 p0707 N85-14534
Use of shanks transformation for speeding up adaptation process in antenna arrays 07 p0951 N85-16029
Vityaz specialists study human adaptability to ocean depths 07 p0980 N85-16225
Research on adaptive antenna techniques 6
[AD-A149341] 11 p1624 N85-20228
Prediction of the space adaptation syndrome
11 p1693 N85-20646
Space adaptation syndrome: Incidence and operational implications for the space transportation system program
11 p1695 N85-20655
Multiple regression method used to assess animal adaptation to hypoxic hypoxia 12 p1902 N85-21947
Plans for adaptation research during Antarctic expedition 14 p2333 N85-24426
Biological investigations of adaptive networks. Neuronal control of conditioned responding
[AD-A150959] 14 p2385 N85-24695
Principal patterns of functional changes of human respiratory system in adaptation to high pressure
14 p2387 N85-24704
Fluid-electrolyte responses during prolonged space flight: A review and interpretation of significant findings
[NASA-CR-171678] 15 p2617 N85-26124
Mathematical modeling of fluid-electrolyte alterations during weightlessness
[NASA-CR-171881] 15 p2617 N85-26125
The design of an adaptive predictive coder using a single-chip digital signal processor
[AD-A152461] 17 p2952 N85-28231
Predictors of transfer adjustment: A longitudinal study
[AD-A152462] 17 p3000 N85-28548
Adaptive aiding for symbiotic human-computer control: Conceptual model and experimental approach
[AD-A153870] 19 p3332 N85-30644
The European vestibular experiments of the Spacelab-1 mission 20 p3508 N85-31808
Some results of the European vestibular experiments in the Spacelab-1 mission 20 p3508 N85-31809
Learning and self adaptation applied to the simulation of a human pilot
[ONERA-RT-24/5122-SY] 20 p3511 N85-31828
Intracardiac hemodynamics and human heart function in simulated weightlessness 22 p3733 N85-33140
Mathematical analysis of heart rhythm assessment of distinctive features in adaptation to spaceflight conditions 22 p3733 N85-33142
Effect of hypokinesia and +Gz accelerations on transport function of human blood
23 p3952 N85-34497
Lipid hydrolysis in man during antiorthostatic hypokinesia 23 p3953 N85-34500

ADAPTERS
Low voltage two wire to four wire telephone circuit converter apparatus
[AD-D011449] 10 p1488 N85-19261
Structure of SYLDA double launch system for Ariane
17 p2946 N85-28185

ADAPTIVE CONTROL
NT ACTIVE CONTROL
NT LEARNING MACHINES
NT SELF ADAPTIVE CONTROL SYSTEMS
Robotization of electric welding processes
03 p0345 N85-12225
Architecture of adaptive space-frequency-time signal processing system 04 p0486 N85-13103
Evaluation of automated decisionmaking methodologies and development of an integrated robotic system simulation
[NASA-CR-172401] 04 p0552 N85-13516
Adaptive mutual interference suppression method
[AD-D011268] 05 p0628 N85-14024
Phase only adaptive nulling in a monopulse antenna
[AD-D011289] 05 p0628 N85-14026
An apparatus for and a method of controlling multiple time-varying processes
[AD-D011253] 05 p0631 N85-14045
Improvement of electromechanical systems by utilization of microelectronic technology 07 p0955 N85-16053
Logic elements for systems with variable structure
07 p0955 N85-16054
Precise control of flexible manipulators
[NASA-CR-174210] 07 p0973 N85-16178
Bibliography of adaptive control
[OUEL-1544/84] 08 p1209 N85-17802
Research on optimal control, stabilization and computational algorithms for aerospace applications
[NASA-CR-174318] 08 p1209 N85-17803
Simplified grasping and manipulation with dextrous robot hands
[AD-A148982] 10 p1492 N85-19419
Dual adaptive control based upon sensitivity functions
[NASA-CR-169331] 10 p1543 N85-19727
Research in adaptive and decentralized control
[AD-A148964] 10 p1543 N85-19728
Adaptive regulation of transmitter radiation power in radio lines during delays of control signals
12 p1841 N85-21551
System dynamics and network control
[AD-A149420] 13 p2054 N85-22863
Electronics Engineering Department EE Technical Review
[UCRL-50025-84-1] 13 p2063 N85-22887
Adaptive control of airborne radar antennas
13 p2080 N85-22989
Adaptive techniques for control of large space structures
[AD-A150957] 14 p2246 N85-23923
Construction of high speed guaranteed regulators
14 p2270 N85-24063
Synthesis of hyperstable control system with adaptive model 14 p2273 N85-24084
Noise cancellation using adaptive arrays
[AD-A150721] 14 p2292 N85-24206
Practical methods for the compensation and control of multivariable systems
[AD-A151047] 14 p2407 N85-24841
Feasibility analysis of moving bank multiple model adaptive estimation and control algorithms
[AD-A152015] 15 p2641 N85-26292
Algorithms for determining the relative complexity of dynamic signals
[BLL-M-36111-(5828.4)] 16 p2851 N85-27574
Automatic flight control modes for the AFTI/F-111 mission adaptive wing aircraft 17 p2905 N85-27909
Adaptive nulling at HF using a compact array of active parasitic antennas
[AD-A152582] 17 p2948 N85-28203
In orbit infrastructure
[DM-51/CC-FL-044-83] 18 p3066 N85-28966
A simulation study of jammer nulling trade-offs in a reactively steered adaptive array
[AD-A153461] 18 p3090 N85-29124
Standard Generic approach for Spacecraft Autonomy and Automation, phase 2 (SGASA-2). Volume 1: Executive summary
[ESA053-1-VOL-1] 18 p3167 N85-29623
Standard Generic Approach for Spacecraft Autonomy and Automation, phase 2 (SGASA-2). Volume 2: Technical report
[ESA053-1-VOL-2] 18 p3167 N85-29624
Standard Generic Approach for Spacecraft Autonomy and Automation, phase 2 (SGASA-2). Volume 3: Appendices
[ESA053-1-VOL-3] 18 p3167 N85-29625
Research on optimal control, stabilization and computational algorithms for aerospace applications
[NASA-CR-172528] 19 p3221 N85-29970
Adaptive aiding for symbiotic human-computer control: Conceptual model and experimental approach
[AD-A153870] 19 p3332 N85-30644
High gain adaptive control of decentralized systems
[DE85-001566] 19 p3343 N85-30717
Adaptive identification and control of structural dynamics systems using recursive lattice filters
[NASA-TP-2371] 20 p3407 N85-31142
NASA Space controls research and technology program 20 p3408 N85-31149
Space station dynamic modeling, disturbance accommodation, and adaptive control
20 p3409 N85-31154
New directions in asymptotically stable finite-dimensional adaptive control of linear distributed parameter systems 20 p3412 N85-31177
Proceedings of the Workshop on Identification and Control of Flexible Space Structures, volume 3
[NASA-CR-176053] 20 p3415 N85-31195
Adaptive control: Actual status and trends
20 p3416 N85-31202
A nonlinear dual-adaptive control strategy for identification and control of flexible structures
20 p3416 N85-31203
Stable direct adaptive control of linear infinite-dimensional systems using a command generator tracker approach 20 p3416 N85-31204
Self-tuning adaptive-controller using online frequency identification 20 p3417 N85-31205
Robust adaptive control 20 p3417 N85-31207
Fixed gain and adaptive techniques for rotorcraft vibration control
[NASA-CR-177344] 22 p3728 N85-33111
Gradiental adaptive corrector with optimum tuning step 22 p3776 N85-33403
Recursive partitioning estimation
24 p4141 N85-35670

ADAPTIVE CONTROL SYSTEMS
U ADAPTIVE CONTROL

ADAPTIVE FILTERS
Noise removal in multichannel images
[NASA-CR-174116] 04 p0554 N85-13526
Suppression of biodynamic interference by adaptive filtering 05 p0706 N85-14530
Studies in statistical signal processing
[AD-A147130] 07 p0940 N85-15959

Multiple channel adaptive filtering using a fast orthogonalization network: An application to efficient pulsed Doppler radar processing
[AD-A147929] 08 p1211 N85-17619
One-dimensional processing for adaptive image restoration
[AD-A149314] 10 p1557 N85-19815
Synthesis of optimum algorithms for secondary processing 13 p2080 N85-22992
Methods of digital correction for channels of multichannel radar receivers 13 p2082 N85-23005
Noise cancellation using adaptive arrays
[AD-A150721] 14 p2292 N85-24206
Basic research in electronics (JSEP)
[AD-A151002] 14 p2298 N85-24230
The performance of a new adaptive filter for digital communications
[AD-A151890] 15 p2543 N85-25702
Correlating and adaptive digital filters
[BMFT-FB-T-84-299] 15 p2551 N85-25744
Transform domain adaptive filtering using a recursive DFT
[DE85-008965] 18 p3172 N85-29656
Adaptive filtering for large space structures: A closed-form solution 20 p3417 N85-31206
Application of adaptive noise cancellation to Coast Guard voice communications
[AD-A154798] 21 p3574 N85-32230
Introduction to adaptive techniques for voice signal processing
[FUB-52-1983] 22 p3756 N85-33287
Synthesis of adaptive filters for tracking radio systems 22 p3763 N85-33325
High-speed adaptation algorithm for harmonic corrector 22 p3765 N85-33336
Adaptive corrector operating in frequency domain 22 p3765 N85-33337
Transformation of spectrum of phase-code keyed signal for scanning in time 22 p3765 N85-33338

ADAPTIVE OPTICS

Fast Hartmann method for problems in astronomical adaptive optics 02 p0161 N85-11094
Investigations relating to the simultaneous use of Combined Optical Adaptive Techniques (COAT) and angle-tracking
[ESA-TT-844] 09 p1385 N85-18712
Bibliography of Soviet Laser Developments, Number 67, September-October 1983
[AD-A151199] 15 p2582 N85-25805
Solar adaptive optics
[AD-A155434] 21 p3724 N85-33101

ADDERS (CIRCUITS)

U ADDING CIRCUITS

ADDING CIRCUITS

Hardware realization of digital filters without multipliers 22 p3766 N85-33340

ADDITION RESINS

NT ACRYLIC RESINS
NT VINYL COPOLYMERS

ADDITIVES

NT ADMIXTURES
NT ANTIFREEZES
NT ANTIKNOCK ADDITIVES
NT PLASTICIZERS
NT PROPELLANT ADDITIVES
NT PROPELLANT BINDERS
NT SOLID ROCKET BINDERS
An investigation of the solubility and diffusivity of chromium in gallium arsenide
[AD-A144949] 01 p0024 N85-10148
Eutectic explosives containing ammonium nitrate
[DE84-015705] 01 p0034 N85-10213
Effects of additives and KOH electrolyte concentration on dissolution of iron electrodes
[DE84-014840] 02 p0173 N85-11162
P-doping of (CH)x to the metallic regime with gaseous oxygen. Application to oxygen fuel cell type electrodes
[AD-A145477] 02 p0186 N85-11242
The concept of doping of conducting polymers. The role of reduction potentials
[AD-A145480] 02 p0186 N85-11243
A study of defects in neutron transmutation doped silicon: Gallium by hall effect analysis
[AD-A146047] 03 p0433 N85-12758
Effect of doping on the voltage holdoff performance of alumina insulators in vacuum
[DE84-017163] 04 p0480 N85-13060
Effect of lubricant extreme-pressure additives on surface fatigue life of AISI 9310 spur gears
[NASA-TP-2408] 04 p0507 N85-13234
Synthesis of transit practice: Diesel fuel quality and effects of fuel additives
[PB84-235688] 05 p0621 N85-13973
Fluorinated aliphatic polyalkylether lubricant with an additive composed of an aromatic phosphine substituted with perfluoroalkylether groups
[AD-D011286] 06 p0770 N85-14927
Development of technology of silicon single-crystal production semiconductor power devices: State of art outlook 06 p0795 N85-15078
Process research of non-Cz silicon material 06 p0830 N85-15275
Effect of five lubricants on life of AISI 9310 spur gears
[NASA-TP-2419] 07 p0962 N85-16099
An investigation of chemiluminescent reactions
[AD-A148460] 08 p1122 N85-17073
Tensile test of pressureless-sintered silicon nitride at elevated temperature
[NASA-TM-77777] 08 p1172 N85-17390
Densification of submicron YSZ (Yttria-Stabilized Zirconia) powders with alumina and borate additives
[AD-A149520] 10 p1452 N85-19150
Investigation of fuel additive effects on sooting flames
[AD-A149154] 10 p1457 N85-19179
Improved operation of transversely exited N2O lasers
[AD-D011488] 10 p1490 N85-19409
Development of AK18 alloy production technology based on electrothermic silumin 11 p1598 N85-20048
Effect of rhodamine-B on the electrodeposition of lead on copper, revision
[DE85-000674] 11 p1606 N85-20101
Characterization of lubricated bearing surfaces operated under high loads
[NASA-TM-86964] 12 p1811 N85-21357
Plasmachemical evaporation and doping of amorphous silicon 12 p1879 N85-21790
Investigation of the effects of NaOH dopant level on the physical and mechanical properties of carbon/phenolic composite material 12 p1945 N85-22213
Effects of HMX addition on the combustion of energetic binders 13 p2004 N85-22560
The effects of lithium counterdoping on radiation damage and annealing in n(+)p silicon solar cells 13 p2007 N85-22586
Microstructure and properties of ferrous alloy weldments
[DE85-005582] 14 p2257 N85-23987
Dopant incorporation in silicon during nonequilibrium solidification: Comparison of 2 processes
[DE85-005568] 14 p2430 N85-24968
Status of French research in plastic batteries 15 p2530 N85-25803
Effect of nickel addition on the thermal, magnetic and magnetomechanical properties of Fe(80)B(15)Si(5)
[AD-A152281] 16 p2749 N85-26967
Jet fuel instability mechanisms
[NASA-CR-175856] 17 p2936 N85-28127
Lubricant and additive effects on spur gear fatigue life
[NASA-TM-87044] 17 p2974 N85-28373
The microstructural state of Nb3Sn in a multifilamentary titanium doped bronze-process wire
[DE85-010979] 19 p3240 N85-30089
High-temperature oxidation of reaction-roasted silicon nitride with various additives 19 p3244 N85-30114
A method for predicting additive drag reduction from small-diameter pipe flows
[AD-A154411] 19 p3268 N85-30254
Improved catalysts for liquid hydrocarbon fuels from syngas
[DE85-011062] 20 p3421 N85-31234
Phenomena simulation for heavy doping and surface recombination velocity 20 p3482 N85-31636
Process and design considerations for high-efficiency solar cells 20 p3482 N85-31641
The effect of alloy additions on superplasticity in thermomechanically processed high magnesium aluminum-magnesium alloys
[AD-A155142] 21 p3567 N85-32184
Z-contrast imaging and electron channeling analysis of dopants in semiconductors
[DE85-011410] 21 p3582 N85-32269
Thermoelectric properties of beta-boron and some boron compounds
[DE85-011978] 21 p3582 N85-32270
Injection of drag reducing additives into turbulent water flows: Two-component velocity measurements and mixing length model predictions
[AD-A154604] 21 p3583 N85-32274
Experimental test for interpreting the increase in sensibility of doped CR-39
[OG-4.4-11] 22 p3860 N85-34042

ADDRESSING

Thin film transistors for addressing flat panel displays
[BMFT-FB-T-84-210] 08 p1227 N85-17726
Automatic multi-banking of memory for microprocessors
[NASA-CASE-NPO-15295-1] 12 p1911 N85-21992
A secure high-speed transaction protocol
[CWI-CS-R8417] 17 p3009 N85-28605

ADENINES

NT RIBONUCLEIC ACIDS

ADENOSINE DIPHOSPHATE

The DNA metabolism and poly-(ADP-ribose) synthesis in lymphocytes of persons exposed to low doses of ionizing radiation
[OEFZS-4307] 20 p3507 N85-31800

ADENOSINE TRIPHOSPHATE

Neutron small angle scattering of the free and membrane-bound ATPase — adenosine triphosphate (ATP) 03 p0431 N85-12746
Chemical, biological, and physical measurements from the subtropical western North Atlantic Ocean. Summer 1982, USNS Lynch, cruise 710-82
[AD-A153823] 18 p3201 N85-29857
Influence of underwater volcanic mountains of Atlantic on microplankton distribution 19 p3294 N85-30424
Radioprotective efficacy of ATP and adenosine with exposure to high energy protons 19 p3325 N85-30602

ADENOSINES

NT ADENOSINE DIPHOSPHATE
NT ADENOSINE TRIPHOSPHATE
Radioprotective efficacy of ATP and adenosine with exposure to high energy protons 19 p3325 N85-30602
Molecular toxicology of chromatin: The role of Poly(ADP-Ribose) in gene control
[AD-A154415] 19 p3327 N85-30611

ADHEROMETERS

U ADHESION TESTS

ADHESION

Zero adhesion system
[AD-D011237] 01 p0015 N85-10093
Optical contacting for gravity probe star tracker
[NASA-TM-86475] 01 p0120 N85-10819
The adhesion of hard and wear resistant coatings 02 p0179 N85-11203
The role of molecular diffusion in the adhesion of elastomers
[AD-A145576] 02 p0186 N85-11245
Universal binding energy relations in metallic adhesion
[NASA-TM-86889] 03 p0931 N85-12132
Polyimide-glass multilayer printed wiring boards
[DE84-015092] 05 p0631 N85-14048
Fundamental tribological properties of ceramics
[NASA-TM-86915] 07 p0930 N85-15893
Cryogenic glass-to-metal seal
[AD-D011370] 07 p0933 N85-15911
Application of electrochemical engineering methods and theory to solving corrosion and adhesion problems with organic coatings
[AD-A147799] 08 p1129 N85-17115
Mod silver metallization for photovoltaics
[NASA-CR-174444] 10 p1509 N85-19518
Humidity effects on adhesion of nickel-zinc ferrite in elastic contact with magnetic tape and itself
[NASA-TP-2449] 12 p1811 N85-21359
Monte Carlo lattice models for adsorbed polymer conformation
[NASA-TP-2453] 14 p2426 N85-24961
Aging of gold thick-film solder joints
[DE85-009647] 18 p3077 N85-29037
Adherence of ash particles from the combustion of micronized coal
[DE85-008600] 19 p3229 N85-30023

ADHESION TESTS

An improved torsional method for determining the fracture toughness of stiff materials and of adhesive joints
[AD-A152091] 16 p2800 N85-27267
A study of adherent oxide scales
[AD-A155554] 21 p3567 N85-32188
Study of an ultrasonic detection method to inspect bonding effects in light alloy bonded structures, test report no. 43-954/F — aircraft structures
[PV-43-954/F] 22 p3795 N85-33510

ADHESIVE BONDING

Ceramic microstructure and adhesion
[NASA-TM-83804] 01 p0031 N85-10188
Deformations and strains in adhesive joints by moire interferometry
[NASA-CR-172474] 02 p0185 N85-11236
Evaluation of the alkaline peroxide pre-bond surface treatment for titanium
[AD-A147352] 07 p0928 N85-15881
Laboratory investigation on adhesives for Naval facilities construction
[AD-A147453] 07 p0932 N85-15909
Mechanical properties of adhesively bonded aluminum structures protected with hydration inhibitors
[AD-A148123] 08 p1133 N85-17139

The development of a method for the shock-resistant securing of large batteries in submarines
09 p1335 N85-18391
Single crystal silicon as a low-temperature structural material
[DE84-017469] 09 p1400 N85-18810
Procedures for the bonding of the E.M.C. mirror onto its INVAR mirror flange --- United Kingdom Infrared Telescope
[UKIRT-19] 09 p1414 N85-18917
Characterization of a thermoplastic polyimidesulfone
[NASA-TM-86358] 10 p1450 N85-19135
Reliability of adhesive bonds under severe environments. Report of the Committee on Reliability of Adhesive Bonds in Severe Environments
[AD-A149010] 10 p1451 N85-19140
Adhesive joint formation under field conditions
[AD-D011478] 10 p1453 N85-19153
Characterization and adhesive bonding of poly(etheretherketone) resins and composites
[DE85-002526] 11 p1593 N85-20023
Hot melt adhesive attachment pad
[NASA-CASE-LAR-12894-1] 11 p1610 N85-20125
Characterization of mode 1 and mixed-mode failure of adhesive bonds between composite adherends
[NASA-TM-86355] 12 p1797 N85-21270
On the stress analysis of bonded inserts
[ARL/STRUC-R-407] 12 p1865 N85-21696
Study of character of adhesive interaction and breaking of polyimid-aluminum foil junction during process of hardening 13 p2014 N85-22637
The characterisation of oxide films on treated aluminium alloys
[MOAD-R-849] 13 p2022 N85-22667
Elasticity solution of an adhesively bonded joint
[NASA-CR-175591] 13 p2101 N85-23097
Development of acceptance criteria for batches of silane primer for external tank thermal protection system bonding applications
[NASA-CR-171428] 14 p2259 N85-23998
Fracture surface analysis in composite and titanium bonding: Part 1: Titanium bonding
[NASA-CR-175750] 15 p2502 N85-25434
Development of acceptance criteria for batches of silane primer for external tank thermal protection system bonding applications
[NASA-CR-171436] 15 p2518 N85-25523
A study of the time dependence in fracture processes relating to service prediction of adhesive joints and advanced composites
[AD-A152084] 15 p2579 N85-25910
Bond test data acquisition and analysis system
[DE85-007021] 16 p2780 N85-27158
Mechanical properties of adhesively bonded aluminum structures protected with hydration inhibitors
[AD-A153755] 18 p3079 N85-29047
Adhesive evaluation of LARC-TPI and a water-soluble version of LARC-TPI
[NASA-TM-86426] 19 p3248 N85-30136
Influence of interface ply orientation on fatigue damage of adhesively bonded composite joints
[NASA-TM-86443] 19 p3264 N85-30365
Fundamental studies related to failure of adhesively bonded structures
[AD-A154072] 19 p3285 N85-30374
Description of an holographic interferometry nondestructive test installation: Application to bond tests
[SNIAS-851-430-101] 20 p3464 N85-31521
Improved materials for composites and adhesive joints
[AD-A154918] 21 p3561 N85-32152
Improved materials for composite and adhesive joints
[AD-A155065] 21 p3562 N85-32153
Experimental and theoretical assessment of a new technique for the non-destructive evaluation of laminated panels
[AD-A155622] 21 p3562 N85-32155
Molecular orbital studies in oxidation: Sulfate formation and metal-metal oxide adhesion
[NASA-CR-176070] 21 p3565 N85-32174
A cracked orthotropic sheet stiffened by a semi-infinite orthotropic sheet
[NASA-TP-2455] 21 p3597 N85-32339
Method of bonding silver to glass and mirrors produced according to this method
[DE85-011642] 22 p3792 N85-33496
Study of an ultrasonic detection method to inspect bonding effects in light alloy bonded structures, test report no. 43-954/F --- aircraft structures
[PV-43-954/F] 22 p3795 N85-33510
Nonlinear adhesive behavior effects in a cracked orthotropic sheet stiffened by a semi-infinite orthotropic sheet
[NASA-TM-87584] 23 p3941 N85-34426

ADHESIVES
NT GLUES
NT PASTES
Volatile organic emissions from adhesives with indoor applications
[DE84-015965] 05 p0620 N85-13966
Encapsulation materials and processing
06 p0830 N85-15269
Laboratory investigation on adhesives for Naval facilities construction
[AD-A147453] 07 p0932 N85-15909
Corrosion properties of second-generation conductive materials 07 p1000 N85-16348
Evaluation and prediction of long-term environmental effects of nonmetallic materials
[NASA-CR-171353] 10 p1450 N85-19137
Elastomer toughened polyimide adhesives --- bonding metal and composite material structures for aircraft and spacecraft
[NASA-CASE-LAR-12775-2] 12 p1809 N85-21349
Rubber modified epoxy adhesive
[AD-D011527] 12 p1810 N85-21354
Study of character of adhesive interaction and breaking of polyimid-aluminum foil junction during process of hardening 13 p2014 N85-22637
Research on composite materials for structural design
[AD-A150802] 14 p2260 N85-24004
Prediction of the long term stability of polyester-based recording media
[PB85-160133] 14 p2262 N85-24019
Development of a polystyrene insulation system
[DE85-006950] 16 p2784 N85-27180
Adhesive evaluation of LARC-TPI and a water-soluble version of LARC-TPI
[NASA-TM-86428] 19 p3248 N85-30136
Working with flammable solvents, thinners, paints and adhesives
[HSE-TRANS-11066] 19 p3250 N85-30154
Optical effects of thin film adhesives in multijunction solar cells
[DE85-010120] 19 p3305 N85-30488
Synthesis and characterization of copolyimides with varying flexibilizing groups
[NASA-TM-86416] 20 p3433 N85-31296
STPI/LARC: A 200 deg C polyimide adhesive
[NASA-TM-86447] 20 p3433 N85-31297
Influence of the resin on interlaminar mixed-mode fracture
[NASA-TM-87571] 21 p3561 N85-32150

ADIABATIC CONDITIONS
Further developments of a nongradient theory of premixed turbulent flames
[NAL-TR-802T] 01 p0023 N85-10143
On the cause of X-line formation in the near-Earth plasma sheet: Results of adiabatic convection of Plasma-Sheet-Plasma
[AD-A145835] 03 p0396 N85-12525
Generation of available potential energy and other diagnostic studies during FGGE
05 p0683 N85-14388
Estimations of diabatic heating for an explosively-developing maritime cyclone
[AD-A147678] 06 p1188 N85-17483
Acceleration of an electron ring in a modified betatron with transverse pressure
[AD-A148626] 08 p1221 N85-17688
The Adiabatic invariant: A tool for the study of the dynamics of the solar system 15 p2676 N85-26519
Investigations of the material factors in the adiabatic shearing of steels
[AD-A153084] 17 p2979 N85-28418
A numerical study of the mean trajectory approximation in a non-adiabatic process
[AD-A152763] 17 p3030 N85-28737
Adiatatic approach in the theory of polyatomic photodissociation: Application to C2N2
[DE85-006515] 18 p3071 N85-28996
Some recent developments in numerical modelling at ECMWF 18 p3147 N85-29481
Study of intermediate velocity penetration of steel spheres into deep aluminum targets
[DE85-010419] 19 p3287 N85-30365
Diagnostics of severe convection and subsynoptic scale ageostrophic circulations
[NASA-CR-171581] 21 p3634 N85-32571
Spectral evolution of gamma-rays from adiabatically expanding sources in dense clouds
[OG-2.5-2] 22 p3869 N85-33959
A theoretical study of non-adiabatic surface effects for a model in the NTF cryogenic wind tunnel
[NASA-CR-3924] 23 p3929 N85-34352
Why do leaky-box models work so fine?
[OG-7.2-8] 23 p4014 N85-34877
Relativistic transport theory for cosmic-rays
[OG-8.3-8] 23 p4022 N85-34926

ADIABATIC EQUATIONS
An interactive computer code for calculation of gas-phase chemical equilibrium (EQLBRM)
[NASA-CR-166337] 02 p0140 N85-10948
Adiabatic thermal models for planetary bodies
22 p3857 N85-33881

ADJOINTS
Use of adjoint equations in problems of evaluating state of random hydrodynamic fields
19 p3289 N85-30398
Monte Carlo techniques for analyzing deep penetration problems
[DE85-011426] 23 p3968 N85-34598

ADJUSTING
A strategy for the adjustment and analysis of densification networks --- geodetic networks
[SER-C-295] 01 p0063 N85-10420
Impact tests of adjusters for the HBU-12 lap belt
[AD-A148021] 08 p1080 N85-16843
Adjustment structure
[AD-D011461] 10 p1459 N85-19193
The 1980 diagnostic adjustment of the German main triangulation network. 4: Network adjustment (part 3)
[SER-B-267-PT-3-MITT-168] 11 p1665 N85-20494
The 1980 diagnostic adjustment of the German main triangulation network. 4: Network adjustment (part 1)
[SER-B-267-PT-1-MITT-168] 11 p1670 N85-20525
The 1980 diagnostic adjustment of the German main triangulation network. 4: Network adjustment (part 2)
[SER-B-267-PT-2-MITT-168] 11 p1670 N85-20526
Adjustment of the national dispersion model for air pollution from elevated sources
[KNMI-TR-57] 14 p2353 N85-24540
Adjustment of the frequency-temperature characteristics of crystal oscillators
[AD-D011588] 15 p2548 N85-25726
Predictors of transfer adjustment: A longitudinal study
[AD-A152462] 17 p3000 N85-28548

ADJUSTMENT
U ADJUSTING

ADMINISTRATION
U MANAGEMENT

ADMITTANCE
U ELECTRICAL IMPEDANCE

ADMIXTURES
On the co-variant formulation of the law of motion of passive particles in a field of turbulence
[REPT-564] 03 p0377 N85-12407
Algebra of hydrodynamic flows of an ideal fluid and the prediction of the behaviour of a system of particles of a passive admixture on Riemann surfaces with a variable curvature
[REPT-565] 03 p0377 N85-12408
Influence of background electrically neutral argon admixture on mechanical strength of silicon crystals
21 p3683 N85-32878
High temperature polymer concrete
[DE85-005756] 23 p3920 N85-34290

ADOBE FLATS
U FLATS (LANDFORMS)

ADP
U ADENOSINE DIPHOSPHATE

ADRENAL GLAND
Skeletal muscle metabolism in hypokinetic rats
[NASA-CR-174059] 02 p0233 N85-11520
Biochemical status of adrenocortical dysfunction following spaceflight 12 p1901 N85-21935
Distinctive morphological manifestations of acute stress reaction in adrenal cortex of hypokinetic rats
12 p1902 N85-21944
Primate adrenal reactions to antiorthostatic hypokinesia 19 p3324 N85-30591

ADRENAL METABOLISM
Role of glucocorticoids in the response to unloading of muscle protein and amino acid metabolism
15 p2609 N85-26077
Primate adrenal reactions to antiorthostatic hypokinesia 19 p3324 N85-30591

ADRENALINE
U EPINEPHRINE

ADRENERGICS
The effect of beta adrenergic blockade on ratings of perceived exertion
[AD-A148053] 08 p1195 N85-17530

ADRENOCORTICOTROPIN (ACTH)
Biochemical status of adrenocortical dysfunction following spaceflight 12 p1901 N85-21935
Rat plasma hormone levels following flight aboard Cosmos-1129 biosatellite 22 p3823 N85-33681

ADSORBENTS
A study of gas solid reactions using coated piezoelectric detectors
[AD-A153047] 17 p2920 N85-28001

ADSORPTION
NT CHEMISORPTION

Inhibition of hydrogen absorption during plating of high strength steels
[AD-A144882] 01 p0028 N85-10174
The use of fixed-bed adsorber models to predict the fluxes of toxic substances in groundwaters and soil environments
[PB84-202553] 01 p0071 N85-10488
Reversible change in parameters of GaAs-based surface-barrier metal-semiconductor diodes induced by hydrogen absorption-desorption
02 p0258 N85-11690
Calculation of the scattering function of rotating molecules with emphasis on the tunnel spectra of absorbed molecules 03 p0427 N85-12725
Structure and kinetics of physisorption, properties of helium during reduction of the dimension
03 p0432 N85-12749
USSR report: Chemistry
[JPRS-UCH-84-012] 06 p0761 N85-14885
Polymer-carbon black interaction in electrically conducting fiber-forming composites
06 p0762 N85-14875
Structure determination of molecular adsorbates with dynamical LEED and HREELS
[DE85-002007] 06 p0861 N85-15473
The adsorption of CO and oxygen on Cu layers on a W(110) surface
[AD-A147345] 07 p0923 N85-15847
Modulated surface vibrational spectroscopies at electrode/electrolyte interfaces
[AD-A148885] 08 p1123 N85-17083
Effect of microstructure and trapping on the hydrogen embrittlement susceptibility of a ti-bearing HSLA steel
[AD-A148810] 08 p1130 N85-17122
Metal-support interactions: Their effects upon adsorption, electronics, and activity/selectivity properties of cobalt in hydrogenation
[DE85-003316] 09 p1292 N85-18113
Mechanisms of gas permeation through polymer membranes
[DE84-017423] 09 p1293 N85-18117
Prediction of retention indices of polynuclear aromatic hydrocarbons. Part 2: Capillary gas chromatography
[DE85-001301] 10 p1437 N85-19053
Separation of gas mixtures with coordination complexes
[DE85-000363] 10 p1438 N85-19062
Adsorption thermodynamics and surface transport of metal catalyst poisons
[DE85-002868] 10 p1441 N85-19084
Optical second harmonic generation for surface studies
[DE85-000670] 11 p1640 N85-20333
Adsorption thermodynamics and surface transport of metal catalyst poisons
[DE85-003750] 12 p1802 N85-21301
In situ monitoring of electrochemical reactions by surface enhanced Raman scattering
[PB85-149789] 12 p1803 N85-21312
Some unique aspects of fouling on copper as compared to titanium or nickel
[AD-A150072] 12 p1806 N85-21332
Critical events in inelastic deformation of glassy polymers in adsorptive medium
13 p2014 N85-22634
Adsorption behaviour of nitrogen compounds on to porous polymer beads and applications to atmospheric sampling
[BLL-DRIC-TRANS-7399-(3623.66)]
13 p2036 N85-22753
Determining adsorption of surface-active substances by sea bottom deposits 13 p2107 N85-23128
Adsorption site, adsorption energy and normal vibration frequency of H/Ni(100) via total energy calculations
[AD-A150555] 13 p2156 N85-23388
Hydrogen on impurity-covered iron surfaces
14 p2254 N85-23968
Interaction of low energy electrons with surface lattice vibrations
[DE85-005475] 14 p2428 N85-24975
Experimental testing of cooling by low pressure adsorption in a zeolite
[DE85-007509] 16 p2716 N85-26763
Correlation of zeolite ZSM-5 acid strength with catalytic activity and selectivity
[DE85-005415] 17 p2922 N85-28013
Methanol adsorption on Pt(111)
[DE85-006802] 17 p2923 N85-28017
Theory of laser-stimulated surface process. 2: A generalized-master-equation approach to energy transfer between an IR laser, an aspecties and phonons
[AD-A153083] 17 p2970 N85-28344
Multiple scattering effects in low energy alkali ion scattering: Application to the analysis of adsorbate ordering and bonding geometry
[DE85-007575] 17 p3032 N85-28757
Spectroscopy of surface adsorbed molecules
[DE85-009452] 17 p3034 N85-28768
Adsorption of Hg on lunar samples
[DE85-007948] 17 p3054 N85-28906
Coadsorption studies on transition metals
[PB85-183713] 18 p3072 N85-29003
Technique for measuring surface diffusion by laser-beam-localized surface photochemistry
[DE85-007885] 18 p3113 N85-29273
Electronic structure calculations for low coverage adlayers
[DE85-007733] 18 p3179 N85-29709
Cation promotion effects in zeolite-supported F-T catalysts
[DE85-009969] 19 p3233 N85-30044
Method for production of ceramic oxide and carbide bodies by polymer inclusion and decomposition
[DE85-011668] 19 p3250 N85-30152
Statistical mechanics of adsorption and wetting
[DE85-010093] 19 p3269 N85-30271
Adsorption of O2, SO2, and SO3 on nickel oxide. Mechanism for sulfate formation
[NASA-CR-176072] 21 p3565 N85-32175
CO adsorption on (111) and (100) surfaces of the Pt sub 3 Ti alloy. Evidence for parallel binding and strong activation of CO
[NASA-CR-176077] 21 p3565 N85-32176
Cloud condensation on insoluble particles
21 p3648 N85-32670
Characterization of catalysts with metal-support effects and of the species adsorbed on their surfaces
[DE85-012254] 24 p4096 N85-35394
Size and shape dependence of CO adsorption sites on sapphire supported Fe microcrystals
[NASA-CR-176171] 24 p4160 N85-35794

ADSORPTIVITY
Functional and structural changes in human erythrocyte surface after irradiation by UV waves of various wavelentghts. Report 2: Adsorption of alcyan blue by external premembranous components
09 p1361 N85-18565

ADVANCED X RAY ASTROPHYSICAL FACILITY
U X RAY ASTROPHYSICS FACILITY

ADVANCED X RAY ASTROPHYSICS FACILITY
U X RAY ASTROPHYSICS FACILITY

ADVANCING GLACIERS
U GLACIERS

ADVANCING SHORELINES
U BEACHES

ADVECTION
The development of objective forecast techniques based on advection of surface weather parameters
01 p0078 N85-10522
Pointwise iterations of finite element modeling of advection-diffusion equations
[DE84-015284] 02 p0253 N85-11656
Generalized formulation of TVD Lax-Wendroff schemes
[NASA-CR-172478] 04 p0554 N85-13526
Razrezy program research in the tropical Atlantic
07 p0981 N85-16229
An evaluation of an advection fog prediction model
[AD-A147436] 07 p1008 N85-16403
A scheme for short-term prediction of hydrometeors using advection and physical forcing
[AD-A148011] 08 p1188 N85-17487
Measurements of sediment temperatures, conductivity and heat flow in the North Atlantic and their relevance to radioactive waste disposal
[IOS-172] 09 p1359 N85-18551
Evaluation of two numerical integrator schemes
[PB85-138196] 11 p1683 N85-20603
Two-dimensional numerical model of sensible and latent heat transport in an irrigated field under advective conditions 13 p2131 N85-23261
Variation of Arctic cloud cover in summer
[DE85-004507] 13 p2139 N85-23285
Fog advection in the Namib 16 p2831 N85-27454
A multilevel-multigrid method for recirculating flows
21 p3583 N85-32271
Mesoscale features and atmospheric refraction conditions of the Arctic marginal ice zone
[AD-A155139] 21 p3636 N85-32584
New semi-implicit method for solving the time-dependent conservation equations for incompressible flow
[DE85-010926] 23 p3931 N85-34367

AE-C SATELLITE
U EXPLORER 51 SATELLITE

AEOLIAN TONES
Statistics of Aeolian surface of Mars
13 p2199 N85-23637

AERATION
In-lake water quality management for Lake Eureka: Highlights of third year (1983) operation
[PB85-104149/GAR] 07 pC990 N85-16289

AERIAL EXPLOSIONS
The HEMP (High-altitude Electromagnetic Pulse) response of a long transmission line buried in the earth
[AD-A146517] 06 p0800 N85-15108
Long-distance propagation of infrasound in atmosphere near Earth's surface 06 p0825 N85-15238
Environmental airblast around large shock tubes
[DE85-010654] 20 p3483 N85-31512
Explosion in flight 21 p3683 N85-32883
Study to assess the effects of magnetohydrodynamic electromagnetic pulse on electric power systems, phase 1, volume 3
[DE85-011301] 24 p4156 N85-35771

AERIAL IMAGERY
U AERIAL PHOTOGRAPHY

AERIAL PHOTOGRAPHY
Remote sensing for landforms and soils in the arid southwest United States 03 p0378 N85-12410
Some principles of plant resources evaluation using remotely sensed data 04 p0543 N85-13459
EARSeL/ESA Symposium on Integrative Approaches in Remote Sensing
[ESA-SP-214] 05 p0655 N85-14202
Integrative investigation on forest damage detection based on airborne Multispectral Scanner data
05 p0656 N85-14215
Landform evaluation through integrated remote sensing methods. A case study in parts of Haryana, India
05 p0657 N85-14221
The need for integrating ground thermal measurements with thermal aircraft imagery 05 p0660 N85-14243
Photo-reconnaissance system
[AD-D011287] 06 p0626 N85-15245
Evidence accumulation for spatial reasoning
07 p0985 N85-16261
Forest area estimates from LANDSAT MSS and forest inventory plot data
[PB85-105617/GAR] 07 p0990 N85-16290
Interactive digital image processing for terrain data extraction
[AD-A146580] 08 p1176 N85-17417
Exploring the solar system with stellar occultations
08 p1245 N85-17857
Geoindication method for interpreting aerial and space photographs: Status and prospects
13 p1984 N85-22445
Combined analysis of the dynamics of complex ecosystems based on repeated remote measurements
13 p1985 N85-22450
Comprehensive, integrated, remote sensing at DOE sites
[DE85-004867] 13 p2126 N85-23240
Accomplishments of Institute of Cartography summarized 13 p2166 N85-23435
Calculation of image shift in panoramic photography
15 p2488 N85-25357
Identification of structure of soil-vegetation cover using aerial and space photographs 16 p2726 N85-26826
Diffusion coefficients for coastal water determined from aerial photographs
[INPE-3413-PRE/679] 16 p2810 N85-27331
Comparative study of the digital analysis of areas of the Earth's surface prepared for planting using different classification algorithms
[INPE-3359-PRE/637] 16 p2846 N85-27545
Airphoto interpretation of vegetation and landforms for soil mapping 17 p2983 N85-28436
Air photo analysis, photo interpretation logic, and feature extraction
[AD-A153926] 18 p3124 N85-29347
Handbook for obtaining and using aerial photography to map aquatic plant distribution
[AD-A154584] 21 p3605 N85-32388
Coastal erosion along Monterey Bay
[AD-A155610] 21 p3655 N85-32707
Cataloging the spectral brightness coefficients of the forested region of the European territory of the USSR
22 p3735 N85-33155

AERIAL RECONNAISSANCE
Satellite, airborne remote sensing development outlined 03 p0342 N85-12189
Earth Resources, A Continuing Bibliography with Indexes
[NASA-SP-7041(43)] 03 p0378 N85-12411
Measurements of atmospheric carbon disulfide using aircraft platforms and a GC/MS isotopic dilution analysis technique 03 p0391 N85-12500
The need for a dedicated public service helicopter design 06 p0753 N85-14828
Geological effectiveness of automated processing of highly precise aeromagnetic surveys in Caspian region
06 p0821 N85-15218
Photo-reconnaissance system
[AD-D011287] 06 p0626 N85-15245

Hybrid state estimation approach to multiobject tracking for airborne surveillance radars
[AD-A148459] 08 p1153 N85-17279
Earth resources: A continuing bibliography with indexes
[NASA-SP-7041(44)] 10 p1503 N85-19484
1981 wC-130 airborne lightning characterization program data review
[AD-A150230] 13 p2138 N85-23275
A constant altitude flight survey method for mapping atmospheric ambient pressures and systematic radar errors
[NASA-TM-86733] 19 p3217 N85-29951
Electronic reconnaissance aircraft of the Soviet Union Navy
[AD-A154706] 21 p3551 N85-32091

AERIAL RUDDERS
Space shuttle rudder/speedbrake actuation subsystem 08 p1102 N85-16965
Translating rudder pedal system
[AD-D011510] 12 p1780 N85-21172

AEROACOUSTICS
Results of tests of advanced flexible insulation vortex and flow environments in the North American Aerodynamics Laboratory lowspeed wind tunnel using 0.0405-scale Space Shuttle Orbiter model 16-0 (test OA-309)
[NASA-CR-167692] 01 p0015 N85-10096
Turbofan noise generation. Volume 2: Computer programs
[NASA-CR-167952] 02 p0275 N85-11791
Aeroacoustic data for high Reynolds number supersonic axisymmetric jets
[NASA-TM-86296] 07 p1038 N85-16587
Aeroacoustics at the DFVLR Brunswick Research Center: A survey on recent and current activities
[DFVLR-MITT-84-14] 08 p1219 N85-17677
Analysis of selected problems involving vortical flows
[NASA-CR-177347] 15 p2463 N85-25212

AEROASSIST
OTV Propulsion Issues
[NASA-CP-2347] 08 p1106 N85-16989
NASA OAST perspective 08 p1106 N85-16990
Performance assessment of aero-assisted orbital transfer vehicles 08 p1106 N85-16993
Low lift-to-drag aero-assisted orbit transfer vehicles 08 p1107 N85-16994
Moderate lift-to-drag aeroassist 08 p1107 N85-16995
Benefits of high aerodynamic efficiency to orbital transfer vehicles 08 p1107 N85-16996
Space science and applications 11 p1644 N85-20362
Nonequilibrium air radiation (Nequair) program: User's manual
[NASA-TM-86707] 19 p3353 N85-30780

AEROBES
Aerobic sulfur-oxidizing bacteria: Environmental selection and diversification 21 p3656 N85-32712
Distribution and abundance of organic thiols 21 p3657 N85-32717

AEROBIOLOGY
Growth of soil bacteria in presence of Martian soil analog, carbon dioxide and hydrogen peroxide 09 p1361 N85-18580

AEROBRAKING
An optimization method for the preliminary design of interplanetary aerobraking missions 08 p1076 N85-16822
Design study of an integrated aerobraking orbital transfer vehicle
[NASA-TM-58264] 12 p1795 N85-21262

AERODYNAMIC AXIS
U AERODYNAMIC BALANCE

AERODYNAMIC BALANCE
Data input, processing and presentation — helicopter rotor balance measurement
[NASA-TM-77739] 01 p0125 N85-10656
Aerodynamic research efforts at SERI Wind Energy Research Center at Rocky Flats
[DE85-000529] 12 p1881 N85-21805
Dispersion sensitivity of the eight inch advanced ramjet munitions technology projectile due to wind and minor thrust errors
[AD-A152145] 16 p2727 N85-26835
Recent developments in rotary-balance testing of fighter aircraft configurations at NASA Ames Research Center
[NASA-TM-86714] 21 p3551 N85-32090

AERODYNAMIC BRAKES
NT DRAG CHUTES
NT LEADING EDGE SLATS
NT TRAILING EDGE FLAPS
NT WING FLAPS
An experimental study of airfoil-spoiler aerodynamics
[NASA-CR-177328] 06 p0748 N85-14796

AERODYNAMIC BUZZ
U FLUTTER

AERODYNAMIC CENTER
U AERODYNAMIC BALANCE

AERODYNAMIC CHARACTERISTICS
NT AERODYNAMIC BALANCE
NT AERODYNAMIC DRAG
NT AERODYNAMIC STABILITY
NT INTERFERENCE DRAG
NT INTERFERENCE LIFT
NT LIFT
NT STATIC AERODYNAMIC CHARACTERISTICS
NT ZERO LIFT
A study of aerodynamic characteristics of wing-body combinations. Part 2: Low-wing airplane
[NAL-TR-798] 01 p0002 N85-10010
Inlet and airframe compatibility for a V/STOL fighter/attack aircraft with top-mounted inlets
[NASA-TM-84252] 01 p0003 N85-10015
Prediction of aerodynamic characteristics of fighter wings at high angles of attack
[AD-A145107] 01 p0003 N85-10017
Experimental data base for computers program assessment. Report of the Fluid Dynamics Panel Working Group 04: Addendum
[AGARD-AR-138-ADD] 01 p0004 N85-10020
Pressure distribution on a swept wing aircraft in flight 01 p0004 N85-10025
Design and wind tunnel evaluation of a symmetric airfoil series for large wind turbine applications
[NASA-CR-174764] 02 p0135 N85-10919
VORCOR: A computer program for calculating characteristics of wings with edge vortex separation by using a vortex-filament and-core model
[NASA-CR-165902] 02 p0135 N85-10921
Results of winglet development studies for DC-10 derivatives
[NASA-CR-3677] 02 p0138 N85-10936
Energy efficient engine ICLS Nacelle detail design report
[NASA-CR-167870] 02 p0148 N85-10993
Definition of acceptable levels of mismatch for equivalent systems of augmented CTOL (Conventional Take-Off and Landing) aircraft
[AD-A145619] 02 p0149 N85-11007
The lateral-directional characteristics of a 74-degree Delta wing employing gothic planform vortex flaps
[NASA-CR-3848] 03 p0311 N85-12009
Flow visualization study of a vortex-wing interaction
[NASA-TM-86656] 03 p0316 N85-12040
Nonlinear system identification methodology development based on F-4S flight test data analysis
[AD-A146289] 03 p0318 N85-12053
Numerical simulation of the subsonic wing-rock phenomenon 03 p0320 N85-12064
A study of flow past an airfoil with a jet issuing from its lower surface
[NASA-CR-166610] 04 p0451 N85-12860
Application of the ONERA model of dynamic stall
[NASA-TP-2399] 04 p0451 N85-12862
Space Shuttle Orbiter trimmed center-of-gravity extension study. Volume 8: Effects of configuration modifications on the aerodynamic characteristics of the 140 A/B Orbiter at a Mach number of 5.97
[NASA-TM-72861-VOL-8] 04 p0452 N85-12867
Evaluation of the unsteady effects for a class of wind turbines 05 p0592 N85-13772
Influence of stationary components on unsteady flow in industrial centrifugal compressors 05 p0645 N85-14140
Aerodynamic characteristics of some lifting reentry concepts applicable to transatmospheric vehicle design studies
[NASA-TM-86331] 06 p0747 N85-14787
Details of export A-5 close-support aircraft given — Qiang-5 aircraft 06 p0748 N85-14793
PROGRAM VSAERO: A computer program for calculating the non-linear aerodynamic characteristics of arbitrary configurations: User's manual
[NASA-CR-166476] 06 p0749 N85-14802
Aerodynamic and thermal characteristics of stellate bodies in hypersonic flow of rarefied gas at angle of attack 06 p0778 N85-14974
Effects of body shape on the aerodynamics of a body of revolution at Mach numbers from 1.6 to 4.6
[NASA-TM-86345] 07 p0893 N85-15657
Analytical modeling of circuit aerodynamics in the new NASA Lewis wind tunnel
[NASA-TM-86912] 07 p0897 N85-15688
An investigation of vortex-induced aerodynamic characteristics of supersonic cruise configurations
[NASA-CR-174290] 07 p0898 N85-15690
Downwash in the plane of symmetry of an elliptically loaded wing
[NASA-TP-2414] 07 p0898 N85-15693
Aileron effectiveness for a subsonic transport model with a high-aspect-ratio supercritical wing
[NASA-TM-85674] 07 p0898 N85-15695
Effect of aerodynamic and angle-of-attack uncertainties on the May 1979 entry flight control system of the Space Shuttle from Mach 8 to 1.5
[NASA-TP-2365] 07 p0913 N85-15778
Designer on civil aircraft design trends in USSR 08 p1068 N85-16768
Improvement of Aerodynamic Performance Through Boundary Layer Control and High Lift Systems
[AGARD-CP-365] 08 p1068 N85-16771
Operational requirements versus technological capabilities 08 p1072 N85-16796
Study of winglets applied to biplanes
[NASA-TM-86350] 08 p1083 N85-16862
Airworthiness and flight characteristics test of the RC-12D Guardrail V
[AD-A148046] 08 p1084 N85-16864
Optimum performance parameters for ski-jump operations of USAF fighter aircraft
[AD-A148532] 08 p1084 N85-16867
The aerodynamic challenges of the design and development of the space shuttle orbiter 08 p1093 N85-16909
The development and application of aerodynamic uncertainties: And flight test verification for the space shuttle orbiter 08 p1093 N85-16910
Performance assessment of aero-assisted orbital transfer vehicles 08 p1106 N85-16993
Benefits of high aerodynamic efficiency to orbital transfer vehicles 08 p1107 N85-16996
Exploratory investigation of the aerodynamic characteristics of a biwing vehicle at Mach 20.3
[NASA-TM-86314] 08 p1113 N85-17021
Proceedings of the workshop on unsteady separated flow held at the United States Air Force Academy on August 10-11, 1983
[AD-A148249] 09 p1263 N85-17937
Calculations for aerodynamic characteristics on a 3-D lifting body in a subsonic flow using boundary element method
[NAL-TR-835] 09 p1272 N85-17998
Icing flight research: Aerodynamic effects of ice and ice shape documentation with stereo photography
[NASA-TM-86906] 09 p1279 N85-18049
Theory of wing rock 09 p1282 N85-18064
The Altitude Wind Tunnel (AWT): A unique facility for propulsion system and adverse weather testing
[NASA-TM-86921] 09 p1283 N85-18067
The S2MA wind tunnel at the Modane-Avrieux aerodynamic test center
[ESA-TT-862] 09 p1284 N85-18071
Influence of normalized frequency on time-dependent aerodynamic characteristics of vane blading profiles 09 p1306 N85-18204
Computation of noise radiation from a free jet perpendicular to its axis via laser anemometry measurements
[ESA-TT-870] 09 p1379 N85-18669
Some fighter aircraft trends
[NASA-TM-86352] 10 p1420 N85-18954
Space Shuttle Orbiter trimmed center-of-gravity extension study. Volume 9: Effects of configuration modifications on the aerodynamic characteristics of the 140 A/B Orbiter at Mach numbers of 1.5, 2.0, and 2.5 — wind tunnel tests
[NASA-TM-72861-VOL-9] 10 p1420 N85-18956
A method for estimating the rolling moment due to spin rate for arbitrary planform wings
[NASA-TM-86365] 10 p1425 N85-18990
Noise constraints effecting optimal propeller designs
[NASA-TM-86967] 11 p1575 N85-19923
Wind-tunnel investigation of a full-scale canard-configured general aviation airplane
[NASA-TP-2382] 11 p1575 N85-19925
STS-1 Pogo analysis
[NASA-TM-57433] 11 p1591 N85-20007
Measured unsteady transonic aerodynamic characteristics of an elastic supercritical wing with an oscillating control surface
[NASA-TM-86376] 12 p1771 N85-21116
A calculation of slender delta wing with leading-edge separation by quasi-vortex-lattice method 12 p1821 N85-21423
Supersonic Tactical Missile (STM) radome development
[AD-P004360] 12 p1825 N85-21454
Aerodynamic behavior of ventilated wind tunnel walls 13 p1968 N85-22363
The application of some lifting-body reentry concepts to missile design
[NASA-TM-86394] 13 p1969 N85-22366
Calculation of vortex-flap aerodynamic characteristics
[NASA-CR-175524] 13 p1969 N85-22367

Large-scale Advanced Propfan (LAP) performance, acoustic and weight estimation, January, 1984
[NASA-CR-174782] 13 p1969 N85-22388
Determination of aerodynamic and propulsion parameters of general aviation aircraft using steady state flight test data 13 p1971 N85-22377
Redesign of fuselage compartments by method of special contours 13 p2042 N85-22784
Oscillating airfoils and their wake
[NASA-TM-77831] 14 p2209 N85-23701
Missions and vehicle concepts for modern, propelled, lighter-than-air vehicles
[NASA-TM-87461] 15 p2457 N85-25170
Transonic Unsteady Aerodynamics and Its Aeroelastic Applications
[AGARD-CP-374] 15 p2457 N85-25171
Analysis of transonic aerodynamic characteristics for a supercritical airfoil oscillating in heave, pitch and with oscillating flap 15 p2458 N85-25175
A semi-empirical unsteady transonic method with supersonic free stream 15 p2458 N85-25179
Special course on V/STOL aerodynamics: An assessment of European jet lift aircraft
[AGARD-R-710-ADDENDUM] 15 p2460 N85-25188
Unsteady analysis of rotor blade tip flow
[NASA-CR-3868] 15 p2462 N85-25202
Transonic aerodynamic and aeroelastic characteristics of a variable sweep wing
[NASA-TM-86677] 15 p2462 N85-25203
Effects of side-stick controllers on rotorcraft handling qualities for terrain flight
[NASA-TM-86688] 15 p2473 N85-25267
Mach-10 high Reynolds number development in the NSWC (Naval Surface Weapons Center) hypervelocity facility
[AD-A151241] 15 p2474 N85-25274
Numerical analyses in aerodynamic design of aero-engine fan 16 p2692 N85-26618
Low Reynolds number vehicles
[AGARD-AG-286] 16 p2699 N85-26666
Rotor blade flap-lag stability and response in forward flight in turbulent flows 16 p2705 N85-26698
Low-speed aerodynamic test of an axisymmetric supersonic inlet with variable cowl slot
[NASA-TM-87039] 16 p2706 N85-26710
OLGA: An open loop gust alleviation 16 p2713 N85-26744
The aerodynamics of controls 16 p2713 N85-26748
Observations, theoretical ideas and modeling of turbulent flows: Past, present and future
[NASA-TM-86679] 16 p2782 N85-27167
Analyses of orderly structures in jets and the relationship with emitted noise
[ISL-R-117/83] 16 p2861 N85-27646
Some effects of sweep direction and strakes for wings with sharp leading edges
[CA-8421] 17 p2892 N85-27826
A method to calculate the parameters of wings of arbitrary planform
[AD-A152689] 17 p2892 N85-27831
Design of robust controllers for a multiple input-multiple output control system with uncertain parameters application to the lateral and longitudinal modes of the KC-135 transport aircraft
[AD-A153100] 17 p2900 N85-27877
The aerodynamics of control 17 p2903 N85-27901
Wind-tunnel evaluation of a 21-percent-scale powered model of a prototype advanced scout helicopter
[NASA-TP-2420] 18 p3058 N85-29023
Wake effects on the aerodynamic performance of horizontal axis wind turbines
[NASA-CR-174920] 18 p3127 N85-29364
Nonlinear potential analysis techniques for supersonic-hypersonic configuration design
[NASA-CR-166078] 19 p3212 N85-29917
High Reynolds number tests of a NASA SC(3)-0712(B) airfoil in the Langley 0.3-meter transonic cryogenic tunnel
[NASA-TM-86371] 19 p3213 N85-29926
Two approaches for the prediction of plume-induced separation
[AD-A154098] 19 p3215 N85-29935
Low-speed tests of a high-aspect-ratio, supercritical-wing transport model equipped with a high-lift flap system in the Langley 4- by 7-meter and Ames 12-foot pressure tunnels
[NASA-TP-2067] 20 p3368 N85-31010
Real scale test of the Petit Canard aircraft in the number 3 section, 47 sqm, of the SIMA wind tunnel, May 1984
[ONERA-PV-1/0772-GY] 20 p3369 N85-31018
Aerodynamic measurement of the wind flow in the number two section of the SIMA wind tunnel
[ONERA-PV-1/8138-GY] 20 p3369 N85-31019
Compendium of unsteady aerodynamic measurements, addendum 1
[AGARD-R-702-ADD-1] 20 p3390 N85-31028
Heat transfer in aeropropulsion systems
[NASA-TM-87066] 20 p3453 N85-31444
Quest for performance: The evolution of modern aircraft
[NASA-SP-468] 21 p3551 N85-32089
Trailing edge flow and aerodynamic sound. Part 1: Tonal pressure and velocity fluctuations. Part 2: Random pressure and velocity fluctuations
[AD-A154947] 21 p3552 N85-32097
Flight control system for a computer controlled aircraft with limited sensors
[AD-A155107] 21 p3555 N85-32115
Conceptual design and analysis of high-speed electronic imaging
[LA-10072-MS] 22 p3758 N85-33292
Aerodynamic analysis of a horizontal axis wind turbine by use of helical vortex theory, volume 2: Computer program users manual
[NASA-CR-174921] 22 p3804 N85-33563
The aerodynamic characteristics of a GU25-5(11)8 aerofoil for low Reynolds numbers
[GU-AERO-8410] 23 p3894 N85-34121

AERODYNAMIC CHORDS
U AIRFOIL PROFILES

AERODYNAMIC COEFFICIENTS
Fitting aerodynamic forces in the Laplace domain: An application of a nonlinear nongradient technique to multilevel constrained optimization
[NASA-TM-86317] 02 p0134 N85-10917
An investigation of vortex-induced aerodynamic characteristics of supersonic cruise configurations
[NASA-CR-174299] 07 p0698 N85-15690
Transport processes in the upper atmosphere 11 p1646 N85-20375
Unsteady aerodynamic characterization of a military aircraft in vertical gusts
[NASA-TM-77810] 12 p1770 N85-21110
Flight-measured laminar boundary-layer transition phenomena including stability theory analysis
[NASA-TP-2417] 12 p1771 N85-21118
Low-speed characteristics of a circulation control airfoil with AFT camber and a spiral trailing edge
[AD-A150851] 14 p2213 N85-23725
Design of apparatus for the determination of aerodynamic drag coefficients of automobiles
[AD-A151842] 15 p2464 N85-25219
A study of transonic flutter of a two-dimensional airfoil using the U-g and p-k methods
[AD-A151463] 15 p2473 N85-25268
Wind tunnel wall interference
[AD-A151212] 15 p2474 N85-25273
La Recherche Aerospatiale Bimonthly Bulletin Number 1984-3, 220/May-June
[ESA-TT-882] 16 p2695 N85-26638
Measurements of the symmetric aerodynamic coefficients for flat faced cylinders in the angle of attack regime 0 to 90 deg for transonic and supersonic speeds
[FFA-TN-1984-04] 16 p2700 N85-26675
Subsonic and transonic aerodynamics of a wraparound fin configuration
[AD-A153646] 18 p3059 N85-28927

AERODYNAMIC CONFIGURATIONS
NT WING NACELLE CONFIGURATIONS
Inlet and airframe compatibility for a V/STOL fighter/attack aircraft with top-mounted inlets
[NASA-TM-84252] 01 p0003 N85-10015
Experimental data base for computers program assessment. Report of the Fluid Dynamics Panel Working Group 04: Addendum
[AGARD-AR-138-ADD] 01 p0004 N85-10020
DFVLR rotorcraft: Construction and engineering
[NASA-TM-77740] 01 p0006 N85-10035
Stress-derivative control of keystoning deformation in finite element codes 01 p0058 N85-10385
PAN AIR: A computer program for predicting subsonic or supersonic linear potential flows about arbitrary configurations using a higher order panel method. Volume 3: Case manual (version 1.0)
[NASA-CR-3253] 02 p0135 N85-10922
Role of research aircraft in technology development
[NASA-TM-85913] 02 p0137 N85-10932
Energy efficient engine ICLS Nacelle detail design report
[NASA-CR-167870] 02 p0146 N85-10993
Simulator study of flight characteristics of several large, dissimilar, cargo transport airplanes during approach and landing
[NASA-TP-2357] 02 p0148 N85-11002
Comparative flow calculation on transonic cone/cylinder standard models in connection with the wall interference problem
[FW-FO-1689] 04 p0453 N85-12878
The preliminary checkout, evaluation and calibration of a 3-component force measurement system for calibrating propulsion simulators for wind tunnel models
[NASA-CR-174113] 04 p0458 N85-12903
An overview of some monoplanar missile programs
[NASA-TM-86330] 06 p0747 N85-14786
The aerodynamics of some guided projectiles
[NASA-TM-86334] 06 p0747 N85-14788
F-7 supersonic day fighter viewed — Jian-7 aircraft 06 p0747 N85-14791
A-5 supersonic attack aircraft described — Qiang-5 aircraft 06 p0747 N85-14792
Hypersonic flow of mixture around blunt body 06 p0779 N85-14979
A collection of flow visualization techniques used in the Aerodynamic Research Branch
[NASA-TM-85998] 06 p0808 N85-15135
Systems study for an Integrated Digital-Electric Aircraft (IDEA)
[NASA-CR-3840] 07 p0902 N85-15714
Aircraft drag reduction technology 08 p1070 N85-16782
Theoretical study of boundary-layer control 08 p1070 N85-16784
Aerodynamic-structural study of canard wing, dual wing, and conventional wing systems for general aviation applications
[NASA-CR-172529] 08 p1077 N85-16829
Study of winglets applied to biplanes
[NASA-TM-86350] 08 p1083 N85-16862
The space shuttle ascent vehicle aerodynamic challenges configuration design and data base development 08 p1093 N85-16906
The aerodynamic challenges of the design and development of the space shuttle orbiter 08 p1093 N85-16909
Exploratory investigation of the aerodynamic characteristics of a biwing vehicle at Mach 20.3
[NASA-TM-86314] 08 p1113 N85-17021
Generation of 3-dimensional body fitted coordinates using hyperbolic partial differential equations
[AD-A148059] 09 p1274 N85-18006
The S2MA wind tunnel at the Modane-Avrieux aerodynamic test center
[ESA-TT-862] 09 p1284 N85-18071
Effects of airfoil shape, thickness, camber, and angle of attack on calculated transonic unsteady airloads
[NASA-TM-86320] 10 p1420 N85-18957
Space Shuttle orbiter trimmed center-of-gravity extension study
[NASA-TP-2284] 10 p1428 N85-19003
Parametric study of a canard-configured transport using conceptual design optimization
[NASA-TP-2400] 11 p1584 N85-19979
Semianalytic modeling of aerodynamic shapes
[NASA-TP-2413] 12 p1771 N85-21120
Calculation of vortex-flap aerodynamic characteristics
[NASA-CR-175624] 13 p1969 N85-22367
The generation of three-dimensional body-fitted coordinate systems for viscous flow problems
[AD-A150861] 14 p2408 N85-24848
Experience with transonic unsteady aerodynamic calculations 15 p2458 N85-25178
Automatic Dynamic Aircraft Modeler (ADAM) for the computer program NASTRAN 15 p2574 N85-25875
Computational aerodynamics in designing aircraft 16 p2693 N85-26622
Numerical example of three-dimensional flying object in shockless transonic flow 16 p2693 N85-26623
Navier-Stokes solution of hypersonic blunt-nosed body flowfields 16 p2693 N85-26624
Recent progress in computational aerodynamics 16 p2693 N85-26626
Computational aerodynamics for aircraft wing design 16 p2693 N85-26627
Comparison of computational results of a few representative three-dimensional transonic potential flow analysis programs 16 p2693 N85-26628
A numerical design method for three-dimensional transonic wings 16 p2694 N85-26631
ESP (External-Stores Program): A pilot computer program for determining flutter-critical external-store configurations. Volume 1: User's manual
[AD-A152268] 16 p2710 N85-26725
ESP (External-Stores Program): A pilot computer program for determining flutter-critical external-store configurations. Volume 2: Final report on program enhancement and delivery
[AD-A152269] 16 p2711 N85-26726
ESP (External-Stores Program): A pilot computer program for determining flutter-critical external-store configurations. Volume 3, part 1: Program compilation
[AD-A152270] 16 p2711 N85-26727
The evaluation of ACS for helicopters: Conceptual simulation studies to preliminary design 16 p2712 N85-26737

Supersonic aerodynamic characteristics of canard, tailless, and aft-tail configurations for 2 wing planforms
[NASA-TP-2434] 17 p2891 N85-27822
Static and dynamic pressure measurements on a NACA 0012 airfoil in the Ames High Reynolds Number Facility
[NASA-TP-2485] 17 p2891 N85-27823
Methods for design aerodynamics of modern transport aircraft
[DFVLR-FB-85-05] 17 p2893 N85-27838
Addition of flexible body option to the TOLA computer program, part 1
[NASA-CR-132732-1] 17 p2896 N85-27855
The flight control system for the Experimental Aircraft Programme (EAP) demonstration aircraft
17 p2904 N85-27906
Propulsion efficiency of vibrating bodies in subsonic gas stream 17 p2942 N85-28159
Nonlinear potential analysis techniques for supersonic-hypersonic configuration design
[NASA-CR-166078] 19 p3212 N85-29917
Performance comparison between NACA 23024 and NACA 64(3)-618 airfoil configurated rotors for horizontal-axis wind turbines
[NASA-TM-83471] 19 p3303 N85-30477
Compendium of unsteady aerodynamic measurements, addendum 1
[AGARD-R-702-ADD-1] 20 p3390 N85-31028
Data set 8: ZKP wing, oscillating aileron
20 p3390 N85-31029
Data set 9: LANN wing. Pitching oscillation
20 p3390 N85-31030
Recent developments in rotary-balance testing of fighter aircraft configurations at NASA Ames Research Center
[NASA-TM-86714] 21 p3551 N85-32090
Wind tunnel drag evaluations of helicopter nose sections
[AD-A155489] 21 p3553 N85-32100
Study of an efficient long-range Mach 2.7 supersonic transport configuration concept
[NASA-TM-86414] 21 p3554 N85-32110
Aerodynamic characteristics of a distinct wing-body configuration at Mach 6: Experiment, theory, and the hypersonic isolation principle
[NASA-TP-2467] 22 p3727 N85-33107
Energy efficient transport technology: Program summary and bibliography
[NASA-RP-1135] 22 p3729 N85-33116
Proceedings of the 14th Army Science Conference. Volume 2: Principal authors I through O
[AD-A149201] 24 p4144 N85-35680

AERODYNAMIC DRAG

Optimum design of nonplanar wings: Minimum induced drag for a given lift and wing root bending moment
[NAL-TR-797] 01 p0002 N85-10011
Airworthiness and Flight Characteristics (A and FC) test of the EH - 1X/EH - 1H helicopter configurations
[AD-A144681] 01 p0007 N85-10039
A comparison of Wortmann airfoil computer-generated lift and drag polars with flight and wind tunnel results
[NASA-TM-86035] 04 p0452 N85-12868
Investigations into the effects of scale and compressibility on lift and drag in the RAE 5m pressurized low-speed wind tunnel 06 p1068 N85-16773
An optimization method for the preliminary design of interplanetary aerobraking missions
06 p1076 N85-16822
Profile design for wings and propellers
[NASA-TM-77785] 10 p1419 N85-18953
Hypothetical zero yaw drag trajectory of spinning projectiles between M = 5 and M = 10
[AD-A148699] 10 p1421 N85-18963
Techniques to analyze vehicle coastdown data
[DE85-005159] 12 p1772 N85-21127
Determination of the drag of free flying particles in supersonic flow with a pulsed laser
12 p1773 N85-21129
Technical evaluation report on the FDP Symposium on Flight Test Techniques
[AGARD-AR-208] 12 p1777 N85-21157
Investigations into the effects of scale and compressibility on lift and drag in the RAE 5m pressurised low-speed wind tunnel
[RAE-TM-AERO-2006] 13 p1969 N85-22372
Preliminary assessment of power-generating tethers in space and of propulsion for their orbit maintenance
13 p1997 N85-22520
Investigation of the Vortex Tab
[NASA-CR-172586] 15 p2463 N85-25209
Flow past a flat plat with a vortex/sink combination
[JIAA-TR-59] 15 p2464 N85-25215
Design of apparatus for the determination of aerodynamic drag coefficients of automobiles
[AD-A151842] 15 p2464 N85-25219
The development of a performance and mission planning program for the A-7E aircraft
[AD-A151717] 15 p2471 N85-25258
Mercedes-Benz auto 2000 achieves low drag coefficient 15 p2530 N85-25602
A computer program for the drag prediction of subsonic, turbine powered aircraft in the en-route configuration
[VTH-LR-412] 16 p2701 N85-26681
Atmospheric density model 16 p2805 N85-27297
Aerodynamic performance of a wing in ground effect using the PANAIR program
[AD-A153303] 17 p2892 N85-27832
Ice shapes and the resulting drag increase for a NACA 0012 airfoil
[NASA-TM-83556] 17 p2894 N85-27839
Urban vehicle research project
[DE85-005444] 17 p3052 N85-28889
Consummative expressions for satellite drag perturbations in a spherically symmetrical atmosphere
[AD-A154230] 19 p3222 N85-29981
SANDRAG: A computer code for predicting drag of bodies of revolution at zero angle of attack in incompressible flow
[DE85-011170] 19 p3338 N85-30684
Wind tunnel drag evaluations of helicopter nose sections
[AD-A155489] 21 p3553 N85-32100
The influence of helicopter tail shape on drag: An aerodynamic study using a low speed wind tunnel
[AD-A156304] 24 p4062 N85-35174

AERODYNAMIC FORCES

NT AERODYNAMIC DRAG
NT AERODYNAMIC INTERFERENCE
NT AERODYNAMIC LOADS
NT BLAST LOADS
NT GUST LOADS
NT INTERFERENCE LIFT
NT LIFT
NT WING LOADING
NT ZERO LIFT

Integral equation of lifting surfaces in Laplace domain and analytic continuation of its pressure kernel
[NAL-TR-795T] 01 p0002 N85-10009
Fitting aerodynamic forces in the Laplace domain: An application of a nonlinear nongradient technique to multilevel constrained optimization
[NASA-TM-86317] 02 p0134 N85-10917
Force and moment measurements on a 74 deg delta wing with an apex flap
[NASA-CR-166081] 02 p0134 N85-10918
Unsteady aerodynamic response of cascades and turborotors 03 p0319 N85-12058
Effect of a variable camber and twist wing at transonic Mach numbers
[NASA-TM-86281] 04 p0452 N85-12869
A preliminary study of using a strain-gauged balance and parameter estimation techniques for the determination of aerodynamic forces on a model in a very short duration wind tunnel
[AD-A146473] 06 p0810 N85-15145
An exploratory study of finite difference grids for transonic unsteady aerodynamics
[NASA-TM-84583] 07 p0899 N85-15696
Theoretical study of non-linear unsteady aerodynamics of a non-rigid lifting body
[AD-P004169] 09 p1266 N85-17954
Experimental study of aerodynamic shielding of turbojet engine air intake against exhaust gases
09 p1307 N85-18210
Flight dynamics of axisymmetrical rotating bodies in air medium 13 p2043 N85-22791
Estimating unsteady aerodynamic forces on a cascade in a three-dimensional turbulence field
[NASA-TM-86701] 14 p2209 N85-23704
Investigation of the aerodynamic forces on bluff bodies at high Reynolds numbers
[DFVLR-MITT-84-19] 14 p2213 N85-23727
Effect of drag behind nozzle array on its force and energy characteristics 14 p2277 N85-24107
Calculation of harmonic aerodynamic forces of aerofoils and wings from the Euler equations
15 p2458 N85-25177
Application of CFD techniques toward the validation of nonlinear aerodynamic models
[NASA-TM-86715] 16 p2700 N85-26671
Preliminary wind tunnel study of the influence of a jet on the unsteady aerodynamics of a turbojet engine
[ONERA-RT-12/5115-RY-230-R-231G]
16 p2701 N85-26679
Flow around rotating and nonmoving circular cylinder near flat screen. Report 1: Aerodynamic forces in cylinder 16 p2765 N85-27059
Aerodynamic forces developing in channels between vanes in turbine drive wheels 16 p2765 N85-27062
Turbine blade-tip clearance excitation forces
[NASA-CR-171534] 19 p3220 N85-29963
A review of shock waves around aeroassisted orbital transfer vehicles
[NASA-TM-86769] 22 p3739 N85-33177

AERODYNAMIC HEAT TRANSFER

NT HYPERSONIC HEAT TRANSFER

Results of a M = 5.3 heat transfer test of the integrated vehicle using phase-change paint techniques on the 0.0175-scale model 56-OTS in the NASA/Ames Research Center 3.5-foot hypersonic wind tunnel
[NASA-CR-167695] 13 p1988 N85-22468
Unsteady transonic heat transfer in a transient facility
[NASA-CR-176145] 23 p3930 N85-34354
Mach 14 flow restrictor thermal stress analysis
[AD-A156215] 24 p4067 N85-35208

AERODYNAMIC HEATING

NT SHOCK HEATING

Experimental and predicted heating distributions for biconics at incidence in air at Mach 10
[NASA-TP-2334] 03 p0361 N85-12313
Columbia: The first 5 flights entry heating data series. Volume 1: An overview
[NASA-CR-171820] 07 p0913 N85-15777
Challenges in the development of the orbiter radiator system 08 p1096 N85-16925
Shuttle system ascent aerodynamic and plume heating 08 p1103 N85-16975
Aerothermal tests of a 12.5 percent cone at Mach 6.7 for various Reynolds numbers, angles of attack and nose shapes — conducted in Langley 8-foot high temperature tunnel
[NASA-TP-2345] 08 p1161 N85-17322
Aerodynamic heating rate distributions induced by trailing edge controls on hypersonic aircraft configurations at Mach 8
[NASA-TM-87453] 13 p1969 N85-22370
Results of aeroheating DFI and ET design-data test on a 0.0175-scale model 60-OTS conducted in the Von Karman Gas Dynamics Facility (VKF) 40' supersonic and the 50' hypersonic wind tunnels A and C
[NASA-CR-167693] 13 p1988 N85-22466
Navier-Stokes solution of hypersonic blunt-nosed body flowfields 16 p2693 N85-26624
Unsteady heat transfer due to time-dependent free stream velocity 17 p2911 N85-27947
The role of thermal motions of air particles for fireballs
[PUBL-59] 17 p3053 N85-28900
SRB thermal protection systems materials test results in an arc-heated nitrogen environment
[NASA-CR-170881] 24 p4072 N85-35236
Results of tests of weathered K5NA closeout material in the MSFC Hot Gas Facility
[NASA-CR-170893] 24 p4073 N85-35239
Study of NSI and related cable performance during tests performed in the NASA Hot Gas Facility
[NASA-CR-170886] 24 p4101 N85-35423

AERODYNAMIC INTERFERENCE

Wind Tunnel Wall Interference Assessment and Correction, 1983
[NASA-CP-2319] 03 p0311 N85-12011
Wall interference measurements for three-dimensional models in transonic wind tunnels: Experimental difficulties 03 p0311 N85-12012
Survey of ONERA activities on adaptive-wall applications and computation of residual corrections
03 p0312 N85-12013
Wind tunnel wall interference in closed, ventilated and adaptive test sections 03 p0312 N85-12014
Two- and three-dimensional model and wall data from a flexible-walled transonic test section
03 p0312 N85-12015
Assessment of lift- and blockage-induced wall interference in a three-dimensional adaptive-wall tunnel
03 p0312 N85-12016
Interference from slotted walls
03 p0314 N85-12028
An interference assessment approach for a three-dimensional slotted tunnel with sparse wall pressure data 03 p0314 N85-12030
Determination of equivalent model geometry for tunnel wall interference assessment/correction
03 p0314 N85-12031
Adaptation of a four-wall interference assessment/correction procedure for airfoil tests in the 0.3-m TCT 03 p0315 N85-12035
Modeling of propulsive jet plumes--extension of modeling capabilities by utilizing wall curvature effects
[AD-A146262] 03 p0362 N85-12324
Detection, classification, and extraction of helicopter-radiated noise
[AD-A145993] 03 p0416 N85-12661
Flow separation induced by periodic aerodynamic interference
[AD-P004174] 09 p1266 N85-17959
Unsteady transonic flow calculations for two-dimensional canard-wing configurations with aeroelastic applications
[NASA-TM-86375] 10 p1420 N85-18960

Experimental study of main rotor tip geometry and tail rotor interactions in hover. Volume 1: Text and figures
[NASA-CR-177336-VOL-1] 13 p1965 N85-22344
Experimental study of main rotor tip geometry and tail rotor interactions in hover. Volume 2: Run log and tabulated data
[NASA-CR-177336-VOL-2] 13 p1965 N85-22345
Study for prediction of rotor/wake/fuselage interference, part 1
[NASA-CR-177340-VOL-1] 13 p1965 N85-22346
Study for prediction of rotor/wake/fuselage interference. Part 2: Program users guide
[NASA-CR-177340-VOL-2] 13 p1966 N85-22347
F-14A aircraft high-speed flow simulations
[NASA-CR-172559] 14 p2209 N85-23702
Approximate neutral point of a subsonic canard aircraft
[NASA-TM-86694] 15 p2462 N85-25205
Unsteady gas dynamics problems related to flight vehicles
[AD-A151187] 15 p2464 N85-25218
Wind tunnel wall interference
[AD-A151212] 15 p2474 N85-25273
An experimental and analytical study of the aerodynamic interference effects between two Sears-Haack bodies at Mach 2.7
[NASA-TM-85729] 16 p2700 N85-26673
Synthesis study: Validation of a gust generator in the presence of a model in a wind tunnel
[ONERA-RT-16/5108-RY-051] 16 p2701 N85-26678
Adaptive wall wind tunnels and wall interference correction methods
[DFVLR-IB-222-84-A-37] 17 p2905 N85-27912
Effect of ground and/or ceiling planes on thrust of rotors in hover
[NASA-TM-86754] 20 p3388 N85-31014

AERODYNAMIC LIFT
U LIFT

AERODYNAMIC LOADS
NT BLAST LOADS
NT GUST LOADS
An experimental study on the induced normal force on tail-fins due to wing-tail interference
[NAL-TR-814] 03 p0318 N85-12051
Low power laminar aircraft structures 04 p0451 N85-12857
Operational loads measurement: A philosophy and its implementation 07 p0894 N85-15665
Navy operational loads data sources and systems 07 p0895 N85-15668
Operational loads data evaluation for individual aircraft fatigue monitoring 07 p0895 N85-15669
Structural flight load measurement demonstration of structural integrity 07 p0895 N85-15670
Aeroelastic analysis and the identification of flight loads — Mirage 2000 aircraft 07 p0896 N85-15679
Keeping up with operational loads in the French Air Force: Defining new equipment 07 p0896 N85-15681
Loads and Aeroelasticity Division research and technology accomplishments for FY 1984 and plans for FY 1985
[NASA-TM-86356] 07 p0898 N85-15691
Comparison of analytical and experimental steadyand unsteady-pressure distributions at Mach number 0.78 for a high-aspect-ratio supercritical wing model with oscillating control surfaces
[NASA-TM-84589] 07 p0899 N85-15697
Speed benefits of tilt-rotor designs for LHX
[NASA-CR-166437] 07 p0902 N85-15717
Flutter control with unsteady aerodynamic models
[AD-A147858] 07 p0909 N85-15753
Unsteady aerodynamic loading of an airfoil due to vortices released intermittently from its upper surface
[AD-P004162] 09 p1265 N85-17947
Modeling stochastic wind loads on vertical axis wind turbines
[DE85-001148] 09 p1340 N85-18426
Airbus fatigue tests 11 p1618 N85-20186
A study for calculating rotor loads using free vortex concept 11 p1620 N85-20194
Parachute inflation dynamics 11 p1715 N85-20792
Calculation of the flow around thick wings with separation vortices 12 p1821 N85-21424
Determination of stresses and deformations in linearly elastic conical shell subjected to aerodynamic loading and heating 13 p2047 N85-22812
Preliminary study of inphase gusts and moment force wind loads over the first 150 meters at KSC, Florida
[NASA-TM-86501] 13 p2137 N85-23273
Advanced life analysis methods. Volume 3: Experimental evaluation of crack growth analysis methods for attachment lugs
[AD-A151058] 14 p2317 N85-24319
Prediction of vortex-induced loads on wind-tunnel turning vanes
[NASA-TM-86678] 15 p2462 N85-25204
Description of a computer program treating transonic steady state aeroelastic effects for a canard or tail airplane
[FFA-TN-1983-23] 16 p2700 N85-26674
The effect of load factor on aircraft handling qualities
[AD-A152118] 16 p2710 N85-26724
Application of AFTI/F-16 task-tailored control modes in advanced multirole fighters 16 p2712 N85-26735
Some flight test results with redundant digital flight control systems 16 p2712 N85-26739
Study of stresses on surface of flat barrier immersed in under expanded jet of rarefied gas 16 p2765 N85-27061
Overview of aerothermodynamic loads definition study 17 p2910 N85-27942
Research on structures and materials — aircraft structures
[B8580080] 17 p2981 N85-28432
Acroswind response of towers and stacks of circular cross-section 19 p3282 N85-30354
A new finite element approach: Progress in inviscid flow computations
[NASA-TM-86434] 20 p3454 N85-31450
Flight control system for a computer controlled aircraft with limited sensors
[AD-A155107] 21 p3555 N85-32115

AERODYNAMIC MOMENTS
U STABILITY DERIVATIVES

AERODYNAMIC NOISE
Analysis of noise measured from a propeller in a wake
[NASA-TP-2358] 02 p0274 N85-11788
Noise constraints effecting optimal propeller designs
[NASA-TM-86967] 11 p1575 N85-19923
Noise transmission loss of a rectangular plate in an infinite baffle
[NASA-TP-2398] 12 p1927 N85-22109
Large-scale Advanced Propfan (LAP) performance, acoustic and weight estimation, January, 1984
[NASA-CR-174782] 13 p1969 N85-22368
Laboratory studies of spacecraft response to transient discharge pulses 13 p1995 N85-22506
An experimental study of the noise generated by vaporous cavitation in turbulent shear flows produced by confined orifice plates 15 p2645 N85-26316
La Recherche Aerospatiale Bimonthly Bulletin Number 1984-3, 220/May-June
[ESA-TT-882] 16 p2695 N85-26636
Rotorcraft noise 18 p3057 N85-28916
Trailing edge flow and aerodynamic sound. Part 1: Tonal pressure and velocity fluctuations. Part 2: Random pressure and velocity fluctuations
[AD-A154947] 21 p3552 N85-32097
Nozzle wall roughness effects on free-stream noise and transition in the pilot low-disturbance tunnel
[NASA-TM-86389] 23 p3930 N85-34355
Optimally designed propellers constrained by noise 24 p4085 N85-35196

AERODYNAMIC STABILITY
Some considerations on Aeroelastic instabilities caused by coupling between propeller-type rotor and its supporting structure
[NAL-TR-804] 01 p0003 N85-10013
Aircrew-aircraft integration: A summary of US Army research programs and plans
[NASA-TM-85991] 02 p0148 N85-11004
Oil-flow study of a Space Shuttle orbiter tip-fin controller
[NASA-TM-86276] 04 p0460 N85-12920
Flutter parametric studies of cantilevered twin-engine transport type wing with and without winglet. Volume 2: Transonic and density effect investigations
[NASA-CR-172410-VOL-2] 04 p0513 N85-13270
Flutter control with unsteady aerodynamic models
[AD-A147858] 07 p0909 N85-15753
Active control of forward swept wings with divergence and flutter aeroelastic instabilities 09 p1282 N85-18063
Viscous effects on transonic airfoil stability and response
[NASA-TM-86374] 10 p1421 N85-18961
Acta Aeronautica et Astronautic Sinica (selected articles)
[AD-A148630] 11 p1575 N85-19922
An experimental study of aerodynamic damping characteristics of a compressor annular cascade in high speed flow and the visualization of annular cascade flow
[NAL-TR-838] 15 p2554 N85-25750
Aerodynamic detuning analysis of an unstalled supersonic turbofan cascade
[NASA-TM-87001] 16 p2700 N85-26670
Optimum parameters of aerogyroscopic satellite orientation system 16 p2718 N85-26782
Dynamic and aeroelastic action of guy cables
[VTT-18] 16 p2802 N85-27276
Static and dynamic pressure measurements on a NACA 0012 airfoil in the Ames High Reynolds Number Facility
[NASA-TP-2485] 17 p2891 N85-27823
Proceedings of the 9th US Air Force and the Federal Republic of Germany Data Exchange Agreement Meeting, Viscous and Interacting Flow Field Effects
[AD-A153020] 17 p2958 N85-28286
Research on optimal control, stabilization and computational algorithms for aerospace applications
[NASA-CR-172528] 19 p3221 N85-29970
Ground effect on helicopter aerodynamics and stability 20 p3395 N85-31083
Interactive aircraft flight control and aeroelastic stabilization
[NASA-CR-176035] 20 p3396 N85-31084
Aerodynamic characteristics of the standard dynamics model in coning motion at Mach 0.6
[NASA-TM-86717] 21 p3552 N85-32094
The physical and empirical basis for a specific clear-air turbulence risk index
[NASA-CR-178522] 24 p4120 N85-35540

AERODYNAMIC STALLING
Application of the ONERA model of dynamic stall
[NASA-TP-2399] 04 p0451 N85-12862
Development and certification of a new stall warning and avoidance system 05 p0702 N85-14507
Flight test results on stall characteristics of a large jet transport
[NAL-TR-817] 06 p0754 N85-14835
Prediction of dynamic stall characteristics using advanced non-linear panel methods
[AD-A148453] 08 p1078 N85-16838
Supermaneuverability
[AD-P004153] 09 p1263 N85-17938
Wing rock flow phenomena
[AD-P004154] 09 p1264 N85-17939
Unsteady stall penetration of an oscillating swept wing
[AD-P004156] 09 p1264 N85-17941
A Navier-Stokes calculation of the airfoil dynamic stall process
[AD-P004163] 09 p1265 N85-17948
Theoretical investigation of dynamic stall using a momentum integral method
[AD-P004170] 09 p1266 N85-17955
Syntheeized airfoil data method for prediction of dynamic stall and unsteady airloads
[NASA-CR-3672] 09 p1274 N85-18005
Rocky Flats Wind Energy Research Center FY 1983 report
[DE85-004500] 10 p1511 N85-19535
The unsteady boundary layer on an elliptic cylinder following the impulsive oneet of translational and rotational motion — dynamic stall 14 p2209 N85-23699
Nonlinear problems in flight dynamics involving aerodynamic bifurcations
[NASA-TM-86706] 15 p2462 N85-25206
Flight investigation of stall, spin and recovery characteristics of a low-wing, single-engine, T-tail light airplane
[NASA-TP-2427] 15 p2470 N85-25248
Simulator study of the stall departure characteristics of a light general aviation airplane with and without a wing-leading-edge modification
[NASA-TM-86309] 15 p2470 N85-25250
Investigation of potential and viscous flow effects contributing to dynamic stall
[AD-A151696] 15 p2557 N85-25773
Unsteady Navier-Stokes calculations in an accelerated reference frame
[AD-A151751] 15 p2557 N85-25774
Preliminary airworthiness evaluation of a National Aeronautics and Space Administration automated stall warning system for an OV-1 aircraft
[AD-A152010] 16 p2707 N85-26708
Wing tunnel investigation of dynamic stall of an NACA 0018 airfoil oscillating in pitch
[NAE-AN-27] 17 p2892 N85-27830
Turbulence structure in the boundary layers of an oscillating airfoil
[AD-A153631] 18 p3059 N85-28926
Calculation of steady and unsteady airfoil flow fields via the Navier-Stokes equations
[NASA-CR-3899] 22 p3727 N85-33105
Flutter clearance of the Schweizer 1-36 deep-stall sailplane
[NASA-TM-85917] 22 p3729 N85-33118
A design procedure to modify the trailing edge upper surface pressure gradient of a given aerofoil
[GU-AERO-8408] 23 p3894 N85-34120
An investigation into the three-dimensional stall development on a modified NACA 23012 aerofoil
[GU-AERO-8414] 23 p3894 N85-34124
Comments on the prediction of dynamic stall
[GU-AERO-8501] 23 p3894 N85-34125

AERODYNAMIC VEHICLES
U AIRCRAFT
AERODYNAMICS
NT AEROTHERMODYNAMICS
NT ROTOR AERODYNAMICS
NT SUPERSONICS
Aerodynamics of airfoils subject to 3-dimensional periodic gusts
[AD-A145149] 01 p0003 N85-10018
Rotor systems research aircraft airplane configuration flight-test results
[NASA-TM-85911] 01 p0006 N85-10034
Characteristic boundary conditions for three-dimensional transonic unsteady aerodynamics
[NASA-TM-86292] 02 p0134 N85-10915
Energy efficient engine combustor test hardware detailed design report
[NASA-CR-167945] 02 p0140 N85-10950
Aeronautical Engineering, A Continuing Bibliography With Indexes
[NASA-SP-7037(179)] 03 p0307 N85-11976
Inverse design technique for cascades
[NASA-CR-3836] 03 p0311 N85-12008
Estimation of helicopter performance using a program based on blade element analysis
[AD-A146341] 03 p0318 N85-12055
Aeronautical Engineering, a continuing bibliography with indexes
[NASA-SP-7037(180)] 04 p0451 N85-12858
Development of computational fluid dynamics at NASA Ames Research Center
[NASA-TM-86021] 04 p0452 N85-12868
Autonomous momentum management for space station
[NASA-CR-174065] 04 p0462 N85-12931
Subsynchronous vibrations in a high pressure centrifugal compressor: A case history 05 p0642 N85-14118
Performance measures for aircraft landings as a function of aircraft dynamics 05 p0712 N85-14565
Closing the design loop on HIMAT (highly maneuverable aircraft technology)
[NASA-TM-85923] 06 p0754 N85-14836
Circulation control: A bibliography of DTNSRDC research and selected outside references: Update
[AD-A146966] 07 p0893 N85-15661
Aero-optics experimental techniques
[AD-A146755] 07 p0957 N85-16067
Aeronautical Engineering: A continuing bibliography with indexes (supplement 182)
[NASA-SP-7037(182)] 08 p1057 N85-16758
International aviation (selected articles)
[AD-A148704] 08 p1067 N85-16762
Aerodynamic issues in the design of high-lift systems for transport aircraft 08 p1069 N85-16780
Joined wing transonic design and test validation
[AD-A148355] 08 p1078 N85-16834
Aeronautical engineering, a continuing bibliography with indexes
[NASA-SP-7037(181)] 09 p1263 N85-17932
Numerical approach for the aerodynamic analysis if airfoils with laminar separation
[NASA-CR-172496] 09 p1273 N85-18001
A first-order Green's function approach to supersonic oscillatory flow: A mixed analytic and numeric treatment
[NASA-CR-172207] 09 p1273 N85-18002
Generation of 3-dimensional body fitted coordinates using hyperbolic partial differential equations
[AD-A148059] 09 p1274 N85-18006
Aeronautical engineering: A continuing bibliography with indexes
[NASA-SP-7037(184)] 10 p1419 N85-18949
LOVEL-84: A LOw-VELocity aerodynamic heating code for flat plates, wedges, and cones
[DE85-002604] 11 p1576 N85-19933
New air supply-prime mover facility for engine tests detailed 11 p1621 N85-20204
A locally linearized panel method for tran-/subsonic flow past an oscillating wing 11 p1622 N85-20212
Air Force Academy Aeronautics Digest
[AD-A149614] 12 p1769 N85-21104
An investigation of aerowindows for solar receivers
[DE84-010931] 12 p1877 N85-21772
List of RAE (Royal Aircraft Establishment) translations issued during the period 1 March 1983 - 31 March 1984
[AD-A149787] 12 p1951 N85-22257
Aeronautical Engineering: A continuing bibliography with indexes, supplement 185
[NASA-SP-7037(185)] 13 p1965 N85-22342
Aeronautical Engineering: A cumulative index to the 1984 issues of the continuing bibliography
[NASA-SP-7037(183)] 13 p1965 N85-22343
Absolute stability of unsteady movement of axisymmetrical rotating flight vehicle
13 p2044 N85-22793
Aeronautical engineering, a continuing bibliography with indexes
[NASA-SP-7037(186)] 14 p2207 N85-23682
Problem of reduction to ideal tube in experimental aerodynamics 14 p2268 N85-24179
A fundamental study of liquid phase particle breakup. Revision
[AD-A150791] 14 p2301 N85-24249
Nonlinear problems in flight dynamics involving aerodynamic bifurcations
[NASA-TM-86708] 15 p2462 N85-25206
Three-Dimensional Boundary Layers
[AGARD-R-719] 15 p2558 N85-25784
A perspective on superaugmented flight control advantages and problems 16 p2712 N85-26733
Wind energy technology program summary
[DE85-007349] 16 p2820 N85-27392
Adaptive grid generation for numerical solution of Burger's equation
[AD-A152217] 16 p2855 N85-27606
Research and development. Technical and scientific reports 1984 16 p2873 N85-27724
New flow physical aspects in aerodynamics
[MBB-FE-122/S/PUB/133] 16 p2873 N85-27725
Upwind-difference methods for aerodynamic problems governed by the Euler equations
[REPT-84-23] 17 p2893 N85-27834
Test devices for aeronautical research and technology
[NASA-TM-77651] 17 p2905 N85-27914
Helicopter aeromechanics: Introduction and historical review 18 p3057 N85-28914
Subsonic and transonic aerodynamics of a wraparound fin configuration
[AD-A153646] 18 p3059 N85-28927
A computational method for wings of arbitrary planform
[AD-A153788] 18 p3059 N85-28929
Acoustic noise associated with the MOD-1 wind turbine: Its source, impact, and control
[DE85-002947] 18 p3178 N85-29700
Aeronautical Engineering: A continuing bibliography with indexes
[NASA-SP-7037(187)] 19 p3211 N85-29911
Aerodynamic analysis of a horizontal axis wind turbine by use of helical vortex theory. Volume 1: Theory
[NASA-CR-168054] 19 p3212 N85-29916
A first-order time-domain Green's function approach to supersonic unsteady flow
[NASA-CR-172208] 19 p3214 N85-29930
Compendium of unsteady aerodynamic measurements, addendum 1
[AGARD-R-702-ADD-1] 20 p3390 N85-31028
Data set 8: ZKP wing, oscillating aileron
20 p3390 N85-31029
Data set 9: LANN wing. Pitching oscillation
20 p3390 N85-31030
R and D programmes at the National Aeronautical Laboratory
[AR-22] 20 p3539 N85-32022
R and D activities of the Aerodynamics Division
20 p3539 N85-32023
Aeronautical engineering: A continuing bibliography with indexes (supplement 189)
[NASA-SP-7037(189)] 22 p3727 N85-33104
Nineteenth Aerospace Mechanisms Symposium
[NASA-CP-2371] 22 p3795 N85-33512
Aeronautical engineering: A continuing bibliography with indexes, supplement 190
[NASA-SP-7037(190)] 24 p4059 N85-35152
Analysis of incompressible cascade flows using state-of-the-art computer programs
[AD-A155850] 24 p4062 N85-35173
AEROELASTIC RESEARCH WINGS
Transonic calculations for a flexible supercritical wing and comparison with experiment
[NASA-TM-86439] 20 p3388 N85-31012
AEROELASTICITY
Some considerations on Aeroelastic instabilities caused by coupling between propeller-type rotor and its supporting structure
[NAL-TR-804] 01 p0003 N85-10013
Characteristics of controlled-oscillating annular cascade test facility with Freon gas
[NAL-TR-812] 01 p0003 N85-10014
Aeroelastic stability analysis with interacting structural nonlinearities 02 p0207 N85-11364
Extended aeroelastic analysis for helicopter rotors with prescribed hub motion and blade appended pendulum vibration absorbers
[NASA-CR-172455] 03 p0315 N85-12038
Unsteady aerodynamic response of cascades and turborotors 03 p0319 N85-12058
Propulsive efficiency of vibrating wing in supersonic flow 05 p0724 N85-14656
Verification of a computer program for vibration analysis of composite wing cores
[NAL-TR-825] 06 p0817 N85-15187
Aeroelastic analysis and the identification of flight loads — Mirage 2000 aircraft 07 p0896 N85-15679
Stereo Electro-optical Tracking System (SETS)
[NASA-CR-172471] 07 p0962 N85-16098
Active control of forward swept wings with divergence and flutter aeroelastic instabilities
09 p1282 N85-18063
Unsteady transonic flow calculations for two-dimensional canard-wing configurations with aeroelastic applications
[NASA-TM-86375] 10 p1420 N85-18960
Viscous effects on transonic airfoil stability and response
[NASA-TM-86374] 10 p1421 N85-18961
Three-dimensional unsteady lifting surface theory in the subsonic range
[NASA-TM-77812] 12 p1770 N85-21111
A study of transonic flutter of a two-dimensional airfoil using the U-g and p-k methods
[LR-615] 12 p1771 N85-21121
Study for the optimization of a transport aircraft wing for maximum fuel efficiency. Volume 1: Methodology, criteria, aeroelastic model definition and results
[NASA-CR-172551] 13 p1971 N85-22378
Simple theoretical models for composite rotor blades
[NASA-CR-175620] 13 p1971 N85-22382
Structural response of a rotating bladed disk to rotor whirl
[NASA-CR-175605] 13 p1973 N85-22391
Oscillating airfoils and their wake
[NASA-TM-77831] 14 p2209 N85-23701
A research program in active control/aeroelasticity
[NASA-CR-175674] 14 p2218 N85-23752
Flutter taming: A new tool for the aeroelastic designer
[AD-A150834] 14 p2226 N85-23802
Some optimization problems in static aeroelasticity for wings made of composite materials
14 p2277 N85-24104
Transonic Unsteady Aerodynamics and its Aeroelastic Applications
[AGARD-CP-374] 15 p2457 N85-25171
Experience with transonic unsteady aerodynamic calculations 15 p2458 N85-25176
Computation of unsteady transonic flows about two-dimensional and three-dimensional AGARD standard configurations 15 p2459 N85-25183
Calculation of unsteady transonic flow around a high swept wing 15 p2459 N85-25184
The development of unsteady transonic 3-D full potential code and its aeroelastic applications
15 p2460 N85-25187
Transonic aerodynamic and aeroelastic characteristics of a variable sweep wing
[NASA-TM-86677] 15 p2462 N85-25203
Unsteady gas dynamics problems related to flight vehicles
[AD-A151187] 15 p2464 N85-25218
Active control of forward swept wings with divergence and flutter aeroelastic instabilities
[AD-A151837] 15 p2474 N85-25270
Description of a computer program treating transonic steady state aeroelastic effects for a canard or tail airplane
[FFA-TN-1983-23] 16 p2700 N85-26674
Dynamic and aeroelastic action of guy cables
[VTT-18] 16 p2802 N85-27276
An assessment of the suitability of the BHGA structural test rig for aerodynamic testing of hang gliders
[CA-8505] 17 p2896 N85-27853
Flight trials of a modified gulfstream commander carrying external stores
[AD-A153376] 17 p2896 N85-27859
On the wind-induced vibrations of a mass-spring system
[REPT-84-04] 17 p2981 N85-28428
Helicopter Aeromechanics
[AGARD-LS-139] 18 p3057 N85-28913
Recent developments in the dynamics of advanced rotor systems 18 p3057 N85-28917
The static aeroelasticity of a composite wing
18 p3121 N85-29321
Selected topics in experimental aeroelasticity at the NASA Langley Research Center
[NASA-TM-86436] 19 p3284 N85-30364
Interactive aircraft flight control and aeroelastic stabilization
[NASA-CR-176035] 20 p3396 N85-31064
Aeroelastic constraints for a wing weight minimization procedure
[FFA-TN-1985-4] 23 p3895 N85-34126
The application of bispectral analyses to aeroelastic phenomena 24 p4060 N85-35157

Analysis of flexible aircraft longitudinal dynamics and handling qualities. Volume 1: Analysis methods
[NASA-CR-177943-VOL-1] 24 p4066 N85-35202
Analysis of flexible aircraft longitudinal dynamics and handling qualities. Volume 2: Data
[NASA-CR-177943-VOL-2] 24 p4067 N85-35203

AEROLOGY
Optimization of system for observing Northern Hemisphere atmospheric pressure field
15 p2485 N85-25338
Lightweight aerological radiosonde MARZ
16 p2807 N85-27309
Reports from the German Meteorological Service. No. 167: Results of aerological soundings in the model area upper Rhine: Heat release project upper Rhine area, part 3
[ISBN-3-88148-216-4] 23 p3950 N85-34479

AEROMAGNETISM
Long-wavelength magnetic and gravity anomaly correlations on Africa and Europe
20 p3476 N85-31597

AEROMAGNETO FLUTTER
U FLUTTER

AEROMANEUVERING
Report of the Transportation Panel
11 p1645 N85-20364

AERONAUTICAL ENGINEERING
Aeronautical systems technology needs: Escape, rescue and survival, test facilities and test equipment and training-simulation equipment
[AD-A145059] 01 p0001 N85-10002
ACEE program rationale and implementation
[NASA-TM-84549] 02 p0133 N85-10908
Characteristics of systems engineering in aviation science research
[AD-A145602] 02 p0292 N85-11899
Research and technology
[NASA-TM-86321] 02 p0305 N85-11973
Aeronautical Engineering, A Continuing Bibliography With Indexes
[NASA-SP-7037(179)] 03 p0307 N85-11976
Activities report of the Department of Engineering
03 p0342 N85-12202
Aeronautical Engineering, a continuing bibliography with indexes
[NASA-SP-7037(180)] 04 p0451 N85-12858
USSR report: Engineering and equipment
[JPRS-UEQ-84-007] 06 p0775 N85-14954
Aeronautical Engineering: A continuing bibliography with indexes (supplement 182)
[NASA-SP-7037(182)] 06 p1067 N85-16758
Aeronautical engineering, a continuing bibliography with indexes
[NASA-SP-7037(181)] 09 p1283 N85-17932
The Prandtl Hergesell project of a national research establishment for aeronautics
[ESA-TT-835] 09 p1272 N85-17993
Aeronautical engineering: A continuing bibliography with indexes
[NASA-SP-7037(184)] 10 p1419 N85-18949
Calendar of selected aeronautical and space meetings
[AGARD-CAL-84/2] 10 p1573 N85-19917
Air Force Academy Aeronautics Digest
[AD-A149614] 12 p1789 N85-21104
Bibliography of Lewis Research Center technical publications announced in 1983
[NASA-TM-83693] 12 p1951 N85-22255
List of RAE (Royal Aircraft Establishment) translations issued during the period 1 March 1983 - 31 March 1984
[AD-A149787] 12 p1951 N85-22257
Aeronautical Engineering: A continuing bibliography with indexes, supplement 185
[NASA-SP-7037(185)] 13 p1965 N85-22342
Aeronautical Engineering: A cumulative index to the 1984 issues of the continuing bibliography
[NASA-SP-7037(183)] 13 p1965 N85-22343
Aeronautical engineering, a continuing bibliography with indexes
[NASA-SP-7037(186)] 14 p2207 N85-23682
Model research: The National Advisory Committee for Aeronautics, 1915-1958, volume 1
[NASA-SP-4103-VOL-1] 14 p2207 N85-23683
Model research, the National Advisory Committee for Aeronautics, 1915-1958, volume 2
[NASA-SP-4103-VOL-2] 14 p2207 N85-23684
Future directions in aeropropulsion technology
[NASA-TM-87010] 14 p2207 N85-23685
USSR report: Engineering and equipment
[JPRS-UEQ-84-005] 14 p2285 N85-24157
Fiscal year 1986 technical objective document
[AD-A151039] 14 p2432 N85-25000
Research and technology
[NASA-TM-86662] 14 p2456 N85-25166
The 1985 long-range program plan
[NASA-TM-87464] 15 p2664 N85-26440
Activities of the Aeronautics and Space Engineering Board
[NASA-CR-175825] 16 p2691 N85-28610
Alternatives for jet engine control
[NASA-CR-175832] 16 p2709 N85-26714
Alternatives for jet engine control
[NASA-CR-175833] 16 p2709 N85-26715
Guide for the execution of reliability tests in the laboratory — aeronautical equipment
16 p2796 N85-27237
Simulation for human factors research. A central question: Fidelity 18 p3159 N85-29568
Aeronautical Engineering: A continuing bibliography with indexes (supplement 188)
[NASA-SP-7037(188)] 19 p3211 N85-29910
Aeronautical Engineering: A continuing bibliography with indexes
[NASA-SP-7037(187)] 19 p3211 N85-29911
The economics of private sector R and D decisionmaking in aeronautics
[NASA-CR-176007] 19 p3379 N85-30962
National aeronautical R and D goals: Technology for America's future 19 p3379 N85-30964
Some applications of aeronautical engineering in the construction of yachts
[NLR-MP-83042-U] 20 p3394 N85-31052
The Naval Postgraduate School Flight Mechanics Laboratory: A feasibility study
[AD-A154578] 21 p3557 N85-32127
DYNA3D, INGRID, and TAURUS: An integrated, interactive software system for crashworthiness engineering
[DE85-010928] 21 p3677 N85-32846
Aeronautical engineering: A continuing bibliography with indexes (supplement 189)
[NASA-SP-7037(189)] 22 p3727 N85-33104
Aeronautical engineering: A continuing bibliography with indexes, supplement 190
[NASA-SP-7037(190)] 24 p4059 N85-35152

AERONAUTICAL SATELLITES
Experimental satellite system for determining coordinates of maritime distress
09 p1306 N85-18216

AERONAUTICS
Large scale computing in aeronautical design
01 p0007 N85-10043
AGARD Highlights
[AGARD-HIGHLIGHTS-84/2] 02 p0305 N85-11972
Natural laminar flow airfoil design considerations for winglets on low-speed airplanes
[NASA-CR-3853] 04 p0452 N85-12863
Operation of aviation support bases
04 p0544 N85-13461
Research and technology highlights of the Lewis Research Center
[NASA-TM-86899] 06 p1261 N85-17928
On the frontier: Flight research at Dryden 1946-1981
[NASA-SP-4303] 09 p1263 N85-17934
The Prandtl Hergesell project of a national research establishment for aeronautics
[ESA-TT-835] 09 p1272 N85-17993
National airspace system: Operational requirements
[AD-A149349] 10 p1422 N85-18973
Flight investigation of stall, spin and recovery characteristics of a low-wing, single-engine, T-tail light airplane
[NASA-TP-2427] 15 p2470 N85-25248
West European report: Science and technology
[JPRS-WST-84-036] 18 p3066 N85-28960
AEV local verification for aviation, precipitation, and temperature programs: AV, REL, TEM
[PB85-179125] 19 p3318 N85-30568
Aeronautical engineering: A continuing bibliography with indexes (supplement 189)
[NASA-SP-7037(189)] 22 p3727 N85-33104
Aeronautical engineering: A continuing bibliography with indexes, supplement 190
[NASA-SP-7037(190)] 24 p4059 N85-35152

AERONOMY
Aeronomy
02 p0298 N85-11930
Summary presentation of the Science Applications Panel 11 p1644 N85-20355
Aeronomical aspects of mesospheric photodissociation: Processes resulting from the solar H Lyman alpha line
[AERONOMICA-ACTA-A-285-1984] 11 p1680 N85-20587
Sounding rocket program Aeronomia. The payload M-I in the project MAP-WINE
[BMFT-FB-W-84-048] 12 p1790 N85-21238
Atmospheric chemistry
[INPE-3190-PRE/554] 16 p2826 N85-27430
Equitorial scintillations: Advances since ISEA-6
[AD-A154962] 21 p3631 N85-32559
Activities report of the Aeronomy Department
[G-774-1984] 21 p3633 N85-32569

AEROPHYSICS
U ATMOSPHERIC PHYSICS

AEROS SATELLITE
Sources of information concerning the ionosphere
04 p0521 N85-13334

AEROSOLS
NT FOG
Gravitational effects on premixed particle cloud flames
02 p0171 N85-11144
Spectroradiometric calibration of the Thematic Mapper and Multispectral Scanner system
[E85-10026] 02 p0218 N85-11439
Aerosol sampling bias from differential electrostatic charge and particle size 02 p0224 N85-11467
A dispersion model for airborne particulates inside a building
[DE84-014961] 02 p0225 N85-11473
Development of a global model for atmospheric backscatter at CO2 wavelengths
[NASA-CR-174053] 02 p0228 N85-11489
Arctic haze: Meteorological aspects of long-range transport 02 p0230 N85-11499
Evaluation of an aerosol prediction model for coastal regions using marine aerosol generation and transport data
[AD-A145443] 02 p0231 N85-11510
Laboratory investigation of coefficients of absorption of air at Lambda = 10.6 microns 02 p0263 N85-11723
Ultraviolet observations of Uranus and Neptune below 3000 Angstrom 02 p0298 N85-11932
Organic aerosol formation: OH(hydroxyl radical) versus ozone oxidation pathways
[PB84-219880] 03 p0388 N85-12484
A system for monitoring radon and its decay products in the atmosphere
[INPE-3085-PRE/494] 03 p0391 N85-12502
Atmospheric extinction in critical environments
[AD-A146102] 03 p0396 N85-12527
Characteristics of aerosol volume distributions measured at Meppen, W. Germany
[AD-A146138] 03 p0396 N85-12528
Deposition in the human lung during respiration of small particles suspended in the air
[BLL-RISLEY-TR-5021-(9091.9F)] 03 p0400 N85-12549
Intermediate results of a 1-year study of a laser spectrometer in the DOE filter test facilities
[DE84-016478] 04 p0508 N85-13228
Urban aerosol modeling
[PB84-233469] 04 p0532 N85-13401
Parallel flow diffusion battery
[DE84-005984] 05 p0631 N85-14047
Certain optimal parameters of high-velocity Venturi ejection tubes
[BLL-M-35924-(5828.4)] 05 p0634 N85-14066
Utilization of SAGE aerosol profiles in the analysis of Mauna Loa stratospheric lidar data
[NASA-CR-174198] 05 p0675 N85-14332
Assessment of Techniques for Measuring Tropospheric H sub x O sub y: Summary 05 p0675 N85-14337
Aerosol reactor for silicon processing
06 p0832 N85-15292
Comparison measurements on optical particle counters
[BLL-DOUNREAY-TR-934-(9091.9F)] 07 p0961 N85-16092
Middle Atmosphere program. Handbook for MAP. Volume 13: Ground-based techniques
[NASA-CR-174345] 08 p1183 N85-17452
Lidar systems for aerosol studies: An outline
08 p1183 N85-17457
Satellite stratospheric aerosol measurement validation
[NASA-TM-86003] 08 p1187 N85-17479
Optical wave propagation and imaging in the atmosphere 08 p1222 N85-17694
Carbon dioxide laser radar for monitoring atmospheric transmittance and atmospheric aerosol
09 p1354 N85-18518
Condensational transformation of atmospheric aerosol particle distribution functions 10 p1500 N85-19486
Airborne lidar measurements of El Chichon stratospheric aerosols, October 1982 to November 1982
[NASA-RP-1136] 10 p1514 N85-19550
Upper atmosphere research at INPE
[INPE-3281-PRE/604] 10 p1515 N85-19557
Aerosol limb absorption — stratosphere
[NASA-TM-77733] 10 p1515 N85-19562
Imaging through a multiple scattering medium
[DE85-002051] 10 p1557 N85-19821
Effect of water vapor and water droplets on the RAM-1 (Real-Time Aerosol Monitor): Preliminary results
[PB85-109429] 11 p1637 N85-20313
MAP in Japan: Organization and projects
11 p1655 N85-20425

The Middle Atmosphere Program: A special project for the Antarctic Middle Atmosphere (AMA)
11 p1656 N85-20430
The concentration of sulfate in broken cloud layers
[DE85-000228] 11 p1678 N85-20574
Continued research in mesoscale air pollution simulation modeling. Volume 7: Mathematical modeling of urban aerosol dynamics
[PB85-137366] 11 p1679 N85-20584
Continued research in mesoscale air pollution simulation modeling. Volume 5: Refinements in numerical analysis, transport, chemistry, and pollutant removal
[PB85-137362] 11 p1680 N85-20585
Lidar observations of stratospheric aerosol over Mauna Loa Observatory, 1974 - 1981
[PB85-115061] 11 p1682 N85-20597
Novel photo-thermal technique for flow and spectroscopic measurements in a dense aerosol stream
[AD-A149745] 12 p1800 N85-21287
Photo-thermal detection of the onset of photo-chemical nucleation (laser-snow) in vapor
[AD-A150111] 12 p1801 N85-21295
Aerosol multiple-scanning code, ASCAT
[LA-10046-MS] 12 p1823 N85-21440
Study of electric field and ion effects on HVDC lines
[DE85-002975] 12 p1833 N85-21503
Transmission and reflection of laser beams propagating through aerosol clouds in space
[LA-9986-MS] 12 p1856 N85-21638
Spectroradiometric calibration of the Thematic Mapper and Multispectral Scanner system
[E85-10094] 12 p1874 N85-21758
Phase function, backscatter, extinction, and absorption for standard radiation atmosphere and El Chichon aerosol models at visible and near-infrared wavelengths
[NASA-TM-86379] 12 p1892 N85-21874
Impact of aerosols on visibility and climate: A report prepared for Panel 3, Environmental Impact, of the NATO/CCMS Air Pollution Pilot Study on Air Pollution Control Strategies and Impact Modelling
[PB85-106744] 12 p1897 N85-21906
Studies of the mechanisms and rates with which nitrogen species are incorporated into cloud water and precipitation
[PB85-144350] 12 p1898 N85-21914
Chemical characterization and toxicologic evaluation of airborne mixtures. Inhalation toxicology of diesel fuel obscurant aerosol in Sprague-Dawley rats. Phase 3. Subchronic exposures
[AD-A150100] 12 p1905 N85-21968
Microstructure of Venus cloud layer based on spectrophotometric data from Venera-11 spacecraft
13 p1982 N85-22436
Effects of temperature variation among droplets in an evaporating fuel spray 13 p2004 N85-22562
Multiple element neutron-activation analysis of atmospheric aerosols with X-ray and gamma-spectrometric recording of radionuclides formed
13 p2013 N85-22631
One mechanism of formation of organic fraction in atmospheric aerosol 13 p2014 N85-22632
Size and velocity distributions of particles and droplets in spray combustion systems
[AD-A150055] 13 p2017 N85-22648
The orientation distribution of nonspherical aerosol particles within a cloud
[AD-A150600] 13 p2092 N85-23061
Infrared aerosol absorption index
13 p2110 N85-23147
The relationship between marine aerosol particles and satellite-detected radiance 13 p2131 N85-23263
Cumulus cloud venting of mixed layer ozone
[NASA-TM-87429] 13 p2132 N85-23269
Analysis of biological particles by mass spectrometry
[AD-A149952] 13 p2141 N85-23291
Physical chemistry of exothermic gas-aerosol calorimetry
[AD-A150872] 14 p2251 N85-23950
The detonation of aerosols and vapors of combustible substances under controlled conditions. Part 1: Construction of a test installation
[ISL-R-109/83-PT-1] 14 p2254 N85-23966
The significance for laser anemometry of particles carried along in a gas flow
[ISL-CO-206/83] 14 p2301 N85-24251
Measurement of the expansion velocity of an aerosol cloud during pyrotechnical dispersion
[ISL-R-125/83] 14 p2303 N85-24262
Classification of atmospheric aerosol for evaluation of its effect on climate 14 p2333 N85-24428
Chemical composition of coastal haze aerosol
14 p2338 N85-24456
Study of integral and spectral direct solar radiation over Atlantic 14 p2341 N85-24475
Visibility of small objects in turbid atmosphere
14 p2342 N85-24482
Influence of aerosol on formation of outgoing thermal radiation 14 p2342 N85-24483
Characteristics and behavior of atmospheric aerosols; application to prediction of infrared extinction
[AD-A150691] 14 p2372 N85-24685
Sea surface temperatures from VAS MSI data
[NASA-CR-175706] 14 p2382 N85-24689
Computer-assisted Gran titration procedure for strong acid determination
[DE85-006801] 15 p2507 N85-25462
Skywave radar detectability of volcanic aerosols
[AD-A151448] 15 p2542 N85-25694
Particle curtain generator for optical property measurements of solid particles
[DE85-005784] 15 p2560 N85-25797
Results of recent large-scale NH3 and N2O4 dispersion experiments
[DE85-004988] 15 p2589 N85-25960
Size distributions of elemental carbon in atmospheric aerosols
[PB85-153534] 15 p2589 N85-25963
SAM 2 measurements of the polar stratospheric aerosol, volume 5
[NASA-RP-1140] 15 p2590 N85-25970
Development of global model for atmospheric backscatter at CO2 wavelengths
[NASA-CR-175879] 15 p2591 N85-25971
Development of algorithms for using satellite meteorological data sets to study global transport of stratospheric aerosols and ozone
[NASA-CR-172540] 15 p2591 N85-25974
Aerosol deposition along the respiratory tract at zero gravity: A theoretical study
[DE85-006703] 15 p2619 N85-26136
Studies of electro-optical attenuation in the vicinity of cloud base
[AD-A151745] 15 p2653 N85-26360
French and West German equipment for Vega Project
16 p2722 N85-26805
SAM II measurements of the polar stratospheric aerosol. Volume 6: April to October 1981
[NASA-RP-1141] 16 p2825 N85-27422
Atmospheric radon measurements in the Antarctic Peninsula: A preliminary report
[INPE-3308-PRE/667] 16 p2827 N85-27436
Evolution of stratospheric aerosol size distribution from ground-based radiometric measurements: A study of El Chichon aerosol
[DE85-007555] 16 p2827 N85-27439
Geophysical monitoring for climatic change, number 12
[PB85-172278] 16 p2837 N85-27496
Study of the formation of sulfuric acid aerosols
[DE85-008102] 17 p2922 N85-28011
Equipment development for rapid detection of microorganisms in air and water
[FOA-A-40046-B2] 18 p3134 N85-29410
Optical stability, atmospheric transparency and aerosol absorption 19 p3297 N85-30442
Clearing of polydisperse aqueous aerosol by laser radiation pulses 19 p3298 N85-30445
Haze over eastern North America. Part 1: Haze properties
[PB85-161657] 19 p3311 N85-30526
Effects of relative humidity gradients on the evaluation of submicron aerosol flux measurements in the atmospheric surface layer
[DE85-010510] 19 p3316 N85-30555
Satellite measurements of atmospheric aerosols
[AD-A153607] 19 p3316 N85-30556
Source Term Experiments Project (STEP): Aerosol characterization system
[DE85-010248] 19 p3361 N85-30839
Modeling of chemical transformations of SO(x) and NO(x) in the polluted atmosphere: An overview of approaches and current status
[PB85-173169] 20 p3487 N85-31677
Function of a device for detection of biological aerosols in field testing
[FOA-C-40194-B2] 20 p3504 N85-31782
Efficiency tests of samplers for microbiological aerosols, a review
[FOA-C-40199-B1] 20 p3504 N85-31783
Investigation of variation in the concentration of bacteria in outdoor testing, with the use of a detector for aerosols of bacteria
[FOA-C-40201-B2] 20 p3504 N85-31784
Aerosol analysis and emission spectrometry with free jets
[DE85-010576] 21 p3564 N85-32168
Silicon production in an aerosol reactor
21 p3609 N85-32416
Data analysis for lidar and quartz crystal microbalance systems
[NASA-CR-172601] 21 p3615 N85-32464
Nuclear thermal transmittance in the atmosphere using LOWTRAN-6 computer code
[AD-A154689] 21 p3630 N85-32553
Absorption and scattering properties of aerosols of aggregated particles in the infrared spectral region
[AD-A155475] 21 p3637 N85-32591
Eleventh International Conference on Atmospheric Aerosols, Condensation and Ice Nuclei, volume 2
[PB85-182418] 21 p3638 N85-32596
Mechanism of heterogeneous deposition ice nucleation near water-saturation 21 p3638 N85-32597
Inactivation of silver iodide by atmospheric nucleation inhibitors 21 p3638 N85-32599
Ice nucleation by silver iodine particles with nearly critical sizes 21 p3638 N85-32600
Photoinduced active sites on ice nucleating aerosol of silver iodide 21 p3639 N85-32601
Experimental investigation of properties of ice-forming reagents 21 p3639 N85-32602
The effect of supersaturation, temperature and particle size on ice-nucleating ability of atmospheric aerosol
21 p3639 N85-32604
Ice crystal nucleation on hygroscopic aerosols
21 p3639 N85-32605
On the efficiency of the mechanism of ice particles formation in the vapor supersaturation field around a freezing droplet 21 p3639 N85-32606
Generation of lead, lead iodide and iodide aerosols and their ice nucleation 21 p3639 N85-32607
Aircraft observations of condensation and ice nuclei at a tropical station 21 p3640 N85-32613
A statistical analysis of ice nuclei concentrations at urban and rural sites in Valladolid, Spain
21 p3640 N85-32614
Supersaturation spect A of Ice Nuclei at different locations in Europe and over the North-Atlantic
21 p3640 N85-32615
The capture of ice nucleating and non ice-nucleating aerosols by ice phase precipitation
21 p3641 N85-32620
The 100 years of Aitken Nuclei (AN) study-reminiscence, current and future problems 21 p3641 N85-32621
Properties of aerosol particles detected by satellites in coastal regions 21 p3641 N85-32622
Multi-channel electric aerosol spectrometer
21 p3642 N85-32623
Supersaturation obtained in a condensation nucleus counter 21 p3642 N85-32624
The investigation of natural and artificial ice nuclei by the improved membrane filter method
21 p3642 N85-32626
Stable generation of highly monodisperse aerosols
21 p3642 N85-32628
Eleventh International Conference on Atmospheric Aerosols, Condensation and Ice Nuclei, volume 1
[PB85-182400] 21 p3644 N85-32636
Photochemical aerosol formation in polluted atmosphere 21 p3644 N85-32642
The influence of Brownian coagulation on the size distributions of atmospheric aerosols
21 p3645 N85-32643
A study of time transformation of natural photochemical aerosols 21 p3645 N85-32644
A new hypothesis for the observed vertical distribution of atmospheric aerosols 21 p3645 N85-32646
On the mechanisms responsible for the formation of typical size spectra and vertical distribution of tropospheric aerosol particles 21 p3645 N85-32647
On the transformation regularities of time series of solid aerosol concentrations in the surface atmospheric layer
21 p3645 N85-32648
Our knowledge about the atmospheric aerosol
21 p3646 N85-32650
Characteristics of aerosol composition in a nonurban area, north China 21 p3646 N85-32651
Trace element concentrations in atmospheric aerosol over Hungary 21 p3646 N85-32652
Chemical composition of atmospheric aerosol at Delhi
21 p3646 N85-32653
Mineral aerosols and source identification
21 p3646 N85-32654
Physical and chemical aerosol characteristics in extremely clean air masses at Cape Grim, Tasmania
21 p3646 N85-32655
Aitken particle size distribution in Antarctica
21 p3646 N85-32656
Airborne measurements of the vertical distribution of Arctic haze 21 p3647 N85-32657
Condensation nuclei and aerosol size distribution measurements in Arctic haze 21 p3647 N85-32658
Aircraft investigations of the distribution of aerosols in the lower troposphere 21 p3647 N85-32659
The variability of aerosol microstructure in continental and oceanic surface layers of the atmosphere in anticyclones 21 p3647 N85-32660

Variation of the submicron aerosol structure
21 p3647 N85-32661
Some considerations about the natural atmospheric radioactive aerosol
21 p3647 N85-32662
Variability of rural aerosols under stable weather conditions
21 p3647 N85-32663
Marine aerosols at the Dutch North Sea coast: Size distributions and fractionation of trace elements
21 p3648 N85-32664
Application of Particle Induced X-ray Emission analysis (PIXE) to aerosol long range transport studies
21 p3648 N85-32665
Scavenging of submicron aerosol particles by snow crystals: Theory and experiments
21 p3648 N85-32667
A probabilistic method for particle size analysis of aerosols
21 p3648 N85-32669
Cloud condensation on insoluble particles
21 p3648 N85-32670
Observations of cloud droplets, aerosol particles and cloud condensation nuclei in continental air masses
21 p3649 N85-32671
Condensation properties of atmospheric aerosol
21 p3649 N85-32672
Investigation of the formation of cloud particle spectrum on natural condensation nuclei
21 p3649 N85-32674
A simple model to investigate the activation process in watercloude
21 p3649 N85-32675
Measurements of the critical supersaturation of 0.029 to 0.035 micron radius particles at Washington, District of Columbia
21 p3649 N85-32676
On the question to the effect of surfactants on the spectrum of cloud drops in the process of their condensation growth
21 p3650 N85-32679
Influence on an industrial site on the characteristics of CCN supersaturation with air masses of different origin
21 p3650 N85-32683
Theoretical studies of structure and stability of hydrates of atmospheric sulfur species
21 p3650 N85-32684
A review on the formation of aerosol particles in the atmosphere
21 p3651 N85-32687
Aerosol formation by wave action over Ross Sea, Antartica
21 p3651 N85-32688
An electron microscopic study of urban aerosol
21 p3651 N85-32689
Sulfates in marine aerosols over the tropical Western Pacific Ocean
21 p3651 N85-32690
Granulometric study of the acidity and sulfate excess in marine aerosols
21 p3652 N85-32691
Variations of particulate sulfur concentrations in a coastal atmospheric environment in connection with the change of air masses origin
21 p3652 N85-32692
Characterization of insoluble particles associated with cloud droplets
21 p3652 N85-32693
The measured rate of condensation nucleation to droplets using the techniques of chemical kinetics
21 p3652 N85-32694
Development of a microorifice uniform deposit cascade impactor
[DE85-006765]
22 p3812 N85-33614
Nordic Association for Aerosol Research (NOSA) Aerosol Symposium: Program and abstracts
[FOA-E-40019]
22 p3812 N85-33616
Evaluation of source strength and dispersion model predications with data from large nitrogen tetroxide field experiments
[DE85-011855]
23 p3947 N85-34465
MATADOR (Methods for the Analysis of Transport And Deposition Of Radionuclides) code description and user's manual
[TI85-901402]
23 p3966 N85-34592
Downstream behavior of volatile fission product species
[DE85-012124]
23 p3971 N85-34617
System for the continuous generation of phosphorous aerosols from red phosphorus-butyl rubber
[DE85-013527]
24 p4072 N85-35232
Experimental lithium system
[DE85-013252]
24 p4094 N85-35382
Linear absorption and scattering of laser beams
[AD-A156167]
24 p4096 N85-35401
Incorporating meteorological data into receptor analysis: RAPS (Regional Air Pollution Study) revisited
[PB85-186944]
24 p4114 N85-35503
Literature search for new physical methods for biological aerosol detection
[AD-A155883]
24 p4128 N85-35592
Calculation of the diffusion of light by aerosols: Description of the MIELOR software and results obtained
[REPT-80]
24 p4137 N85-35638

AEROSPACE ENGINEERING
NT AERONAUTICAL ENGINEERING

Aerospatiale's experimentations of vectorization on supercomputers for aircraft structural problems
01 p0007 N85-10041
Impact of new computing systems on computational mechanics and flight-vehicle structures technology
01 p0007 N85-10042
Large scale computing in aeronautical design
01 p0007 N85-10043
Development of space instrumentation of Intercosmos member countries
02 p0163 N85-11106
Report of the Department of Aerospace Engineering
03 p0307 N85-11977
NSSDC and WDC-A-R and S document availability and distribution services
[NASA-TM-87374]
03 p0438 N85-12787
Reduction method for thermal analysis of complex aerospace structures
[NASA-TP-2373]
07 p0957 N85-16066
SNAP (Space Nuclear Auxiliary Power) reactor overview
[AD-A146831]
07 p1041 N85-16612
Activities report of the aerospace industry in West Germany
[ISSN-0722-3838]
07 p1053 N85-16686
Activities report of the aerospace industry in West Germany
[ISSN-0722-3838]
07 p1054 N85-16687
Random equations in aerodynamics
[NASA-CR-174279]
08 p1077 N85-16825
S-3A ballast block final design and engineering tests
[AD-A147685]
08 p1080 N85-16842
Orbiter processing facility: Access platforms Kennedy Space Center, Florida, from challenge to achievement
08 p1102 N85-16968
Summary of activities of Aeronautics and Space Engineering Board
[NASA-CR-174294]
08 p1228 N85-17729
Scientific and technical information output of the Langley Research Center for calendar year 1984
[NASA-TM-86336]
08 p1229 N85-17740
Space Station engineering and technology development
[NASA-CR-174383]
09 p1287 N85-18079
Activities report in aerospace in West Germany
[ISSN-0070-3966]
09 p1418 N85-18947
West Europe report: Science and technology
[JPRS-WST-85-004]
10 p1460 N85-19204
Calendar of selected aeronautical and space meetings
[AGARD-CAL-84/2]
10 p1573 N85-19917
West Europe report: Science and technology
[JPRS-WST-85-008]
11 p1617 N85-20174
China report: Science and technology
[JPRS-CST-84-032]
11 p1621 N85-20202
Biomechanics finds practical applications in aerospace research
11 p1621 N85-20205
Where are we going in tethers
11 p1644 N85-20354
Space science and applications
11 p1644 N85-20362
Bibliography of Lewis Research Center technical publications announced in 1983
[NASA-TM-83693]
12 p1951 N85-22255
USSR report: Engineering and equipment
[JPRS-UEQ-85-003]
13 p2042 N85-22782
Authorizing appropriations to the National Aeronautics and Space Administration for fiscal year 1986
[H-REPT-99-32]
13 p2168 N85-23452
Spatial acquisition algorithms and systems for intersatellite optical communication links
[AD-A150794]
14 p2292 N85-24207
Technology for large space systems: A bibliography with indexes, supplement 11
[NASA-SP-7046(11)]
15 p2475 N85-25277
A decision support methodology for space technology advocacy
[AD-A151895]
15 p2476 N85-25283
USSR report: Space
[JPRS-USP-85-003]
15 p2476 N85-25284
West Europe report: Science and technology
[JPRS-WST-85-014]
15 p2489 N85-25362
In-plane shear properties of graphite Fibre/Epoxy composites for aerospace applications: Evaluation of test methods by the decision analysis technique
[AD-A151599]
15 p2503 N85-25440
West Europe report: Science and technology
[JPRS-WST-84-007]
15 p2530 N85-25600
West Europe report: Science and technology
[JPRS-WST-84-010]
15 p2535 N85-25644
Multikilowatt hydrogen-nickel oxide battery system
[DE85-003339]
15 p2550 N85-25737
IPAD: Integrated Programs for Aerospace-vehicle Design
[NASA-CR-3890]
15 p2632 N85-26221
The 1985 long-range program plan
[NASA-TM-87464]
15 p2664 N85-26440

Application of space methods in geodesy
16 p2724 N85-26817
A study of spacecraft technology and design concepts, volume 1
[NASA-CR-172579-VOL-1]
16 p2730 N85-26844
A study of spacecraft technology and design concepts. Volume 2: Appendices
[NASA-CR-172579-VOL-2]
16 p2730 N85-26845
Space Station Engineering and Technology Development
[NASA-CR-175806]
16 p2731 N85-26851
Space Station Spartan study
[NASA-TM-86215]
16 p2731 N85-26852
Activities in aerospace
17 p2991 N85-27821
Technical services at NLR
[B8561898]
17 p3049 N85-28871
West Europe report: Science and technology
[JPRS-WST-84-031]
18 p3086 N85-29089
West Europe report: Science and technology
[JPRS-WST-84-035]
18 p3087 N85-29102
Research on structural analysis at the DFVLR, Brunswick
18 p3120 N85-29314
Space research at NLR
20 p3397 N85-31075
Visualization of computation results. Definition of a graphics satellite computer
[ONERA-RT-2/3587-CY]
20 p3514 N85-31845
USSR report: Space
[JPRS-USP-84-006]
22 p3731 N85-33128
Special tools used by cosmonauts in EVA
22 p3731 N85-33129

AEROSPACE ENVIRONMENTS
NT DEEP SPACE
NT INTERPLANETARY SPACE
NT INTERSTELLAR SPACE
Metal oxide semiconductors power transistors
[CNES-84/QPE/FT/190]
04 p0496 N85-13166
Effects of the solar and extraterrestrial environments on space power systems
05 p0610 N85-13898
Environmental interactions working group report
05 p0611 N85-13908
Spacelab 1 experiment: Microorganisms in space hard environment
05 p0691 N85-14443
Activities report in Earth and planetary environments physics
[CRPE-NT-134]
05 p0734 N85-14720
Testing changes in visual function due to orbital environment
[AD-A147259]
07 p1016 N85-16453
Evaluation and prediction of long-term environmental effects of nonmetallic materials
[NASA-CR-171353]
10 p1450 N85-19137
Instrumentation for Application Number 1: Mass spectrometric analysis of the boundary layer associated with the tethered satellite
11 p1646 N85-20372
Study proposal for the possible use of ISS as an aerodynamic facility for aerospace applications
11 p1646 N85-20374
Earth observations and the polar platform
[NOAA-TR-NESDIS-18]
11 p1669 N85-20517
Aviation medicine's role in modern airforce discussed
11 p1696 N85-20682
Assessment of satellite collision hazards by simulated sampling in space
12 p1784 N85-21195
Transmission and orbital constraints in space-related programs: Briefing summary
12 p1787 N85-21216
Natural environment design criteria for the Space Station definition and preliminary design
[NASA-TM-86496]
12 p1789 N85-21232
On the P1 data from GMS-SEM
12 p1894 N85-21890
Interactions between large space power systems and low-Earth-orbit plasmas
13 p1992 N85-22480
The Giotto spacecraft impact-induced plasma environment
[ESA-SP-224]
14 p2243 N85-23905
Spacecraft environment during the Giotto-Halley encounter: A summary
14 p2246 N85-23921
A FORTRAN program for deep space sensor analysis
[AD-A151700]
15 p2489 N85-25366
Analysis of space station operations in the space debris environment
[AD-A151872]
15 p2493 N85-25380
West Europe report: Science and technology
[JPRS-WST-84-008]
15 p2531 N85-25609
Space brain research in China reported
15 p2537 N85-25657
Nondestructive equipment study
[NASA-CR-171865]
15 p2571 N85-25853
Structural development and gravity
15 p2608 N85-26071
Research on zero-gravity botany apparatus
16 p2723 N85-26811
Forecasts on long-range development of space programs
16 p2727 N85-26830

Solar activity monitoring satellite (SAMSAT): Impact on space environment services
[PB85-165066] 16 p2888 N85-27818
Spray applicator for spraying coatings and other fluids in space
[NASA-CASE-MSC-18852-1] 18 p3115 N85-29283
Current concepts and future directions of CELSS 18 p3155 N85-29532
Survey of CELSS concepts and preliminary research in Japan 18 p3155 N85-29533
Human productivity experience and undersea habitat design 18 p3159 N85-29563
Considerations for space station interior architecture 18 p3159 N85-29564
Human factors in space station architecture: The ECLSS module concept 18 p3159 N85-29565
Ion beam sputter-deposited thin film coatings for protection of spacecraft polymers in low Earth orbit
[NASA-TM-87051] 19 p3248 N85-30137
Measurement of material damping in a simulated space environment 20 p3397 N85-31070
On the measurement of material damping in a simulated space environment 20 p3411 N85-31169
Evaluation of Results of Space Experiments in Physiology and Medicine and Informal Briefings by the F-16 Medical Working Group 20 p3506 N85-31606
Three-dimensional ballistocardiography in microgravity 20 p3510 N85-31618
Special tools used by cosmonauts in EVA 22 p3731 N85-33129
Effects of environment on spacecraft materials 22 p3733 N85-33144
Microorganisms in space flight 23 p3951 N85-34490
Effect of seeds of heavy charged particles of galactic cosmic radiation 23 p3954 N85-34505
Problems of aviation and space medicine and psychology discussed at 14th Gagarin lectures 23 p3954 N85-34509
Determination of characteristic values for fiber reinforced materials 24 p4074 N85-35247

AEROSPACE INDUSTRY
NT AIRCRAFT INDUSTRY
Comments on the commercialization of expendable launch vehicles 02 p0153 N85-11034
Space know-how, twenty years' space experience 04 p0461 N85-12926
Electronic components for space applications
[CNES-NT-109] 04 p0496 N85-13169
Component reliability and assembling technologies
[CNES-NT-108] 04 p0511 N85-13258
An electronic documentation system
[SNIAS-842-111-101] 04 p0577 N85-13683
BDLI memorandum on the future of space flight in the Federal Republic of Germany
[NASA-TM-77624] 07 p0911 N85-15765
Activities report in aerospace in West Germany
[ISSN-0070-3966] 09 p1418 N85-18947
Activities in French aerospace 11 p1587 N85-19995
Aerospace Safety Advisory Panel
[NASA-TM-87426] 13 p1970 N85-22373
Welcome to the Saclay Propeller Testing Center
[NASA-TM-77648] 14 p2225 N85-23799
West Europe report: Science and technology
[JPRS-WST-84-008] 15 p2531 N85-25606
Characteristics and applications of superplastic materials for aeronautics
[MBB-BB-565/84-O] 16 p2873 N85-27727
Managerial benefits of Helios for the European industry 16 p2887 N85-27809
The technological gains of Helios for the European industry 16 p2887 N85-27810
Activities in aerospace 17 p2891 N85-27821
Note for a research feasibility project: High reliability design in the aeronautical field
[REPT-84-RR-350] 20 p3367 N85-31005
Description of an holographic interferometry nondestructive test installation: Application to bond tests
[SNIAS-851-430-101] 20 p3464 N85-31521
Philosophy of nondestructive control in aeronautics quality control. Knowledge of and improvements to nondestructive test safety
[SNIAS-851-551-101] 20 p3465 N85-31522
Management of Corrosion
[AGARD-LS-141] 22 p3749 N85-33238
Corrosion management strategies for aircraft and related systems 22 p3749 N85-33239
Theoretical aspects of corrosion and practical implications for aircraft and related systems 22 p3749 N85-33240
Environmental factors in corrosion and deterioration of materials 22 p3750 N85-33241
Investment justification of robotic technology in aerospace manufacturing. User's manual
[AD-A156193] 24 p4099 N85-35410

AEROSPACE MEDICINE
Personal experience with the PVHD and opinion of situations in which a wide Field Of View (FOV) PVHD might be helpful 01 p0008 N85-10045
USSR report: Space Biology and Aerospace Medicine, volume 18, no. 4, July - August 1984
[JPRS-USB-84-006] 01 p0091 N85-10611
Potential use of dialogue with computers in biomedical research 01 p0091 N85-10614
Space medicine and biology, continuing bibliography (supplement 263)
[NASA-SP-7011(263)] 01 p0094 N85-10636
USSR report: Space
[JPRS-USP-84-005] 02 p0156 N85-11060
Cosmonauts complete 4th month aboard Salyut-7 02 p0157 N85-11065
Applications of aerospace technology in biology and medicine
[NASA-CR-165872] 02 p0234 N85-11521
Aerospace Medicine and Biology, a continuing bibliography with indexes
[NASA-SP-7011(264)] 02 p0234 N85-11525
AGARD bulletin technical programme, 1985
[AGARD-BUL-84-2] 02 p0305 N85-11971
The effects of helicopter vibration on the spinal system
[AD-A146274] 03 p0402 N85-12562
USSR report: Life sciences. Biomedical and behavioral sciences
[JPRS-UBB-84-025] 04 p0543 N85-13453
USSR report: Life Sciences: Biomedical and behavioral sciences
[JPRS-UBB-84-028] 04 p0543 N85-13457
Impact of space medicine on Earth-based medicine: Academician Ye. I. Chazov comments on the work in orbit of physician O. Atkov 04 p0543 N85-13458
A survey of space biology and space medicine
[ESA-BR-17] 04 p0545 N85-13466
Aerospace Medicine and Biology, a continuing bibliography with indexes
[NASA-SP-7011(265)] 04 p0545 N85-13467
Space medicine research publications: 1983-1984
[NASA-CR-3860] 04 p0545 N85-13469
Overview of German microgravity activities in the field of life science 05 p0696 N85-14476
USSR report: Life sciences. Biomedical and behavioral sciences
[JPRS-UBB-84-015] 07 p1010 N85-16416
USSR report: Life sciences. Biomedical and behavioral sciences
[JPRS-UBB-84-027] 07 p1012 N85-16426
Aerospace medicine and biology: A continuing bibliography with indexes
[NASA-SP-7011(266)] 08 p1194 N85-17525
Aerospace medicine and biology: A continuing bibliography with indexes, supplement 268
[NASA-SP-7011(266)] 08 p1194 N85-17526
Efforts to improve aviation medical examiner performance through continuing medical education and annual performance reports
[AD-A148078] 08 p1195 N85-17531
Health examination findings among active civil airmen
[AD-A148325] 08 p1195 N85-17533
USSR report: Life sciences. Biomedical and behavioral sciences
[JPRS-UBB-85-002] 09 p1360 N85-18559
USSR report: Life sciences. Biomedical and behavioral sciences
[JPRS-UBB-85-011] 10 p1525 N85-19616
Be healthy, pilot 10 p1526 N85-19626
Aerospace medicine and biology: A continuing bibliography with indexes
[NASA-SP-7011(269)] 10 p1526 N85-19628
Report of the Artificial Gravity Panel 11 p1645 N85-20365
Motion Sickness: Mechanisms, Prediction, Prevention and Treatment
[AGARD-CP-372] 11 p1693 N85-20642
Susceptability to kineloses and the amplitude perceived from sensory illusions 11 p1694 N85-20651
China report: Science and technology
[JPRS-CST-84-036] 11 p1696 N85-20661
Aviation medicine's role in modern airforce discussed 11 p1696 N85-20662
Symposium on Military Aviation Medicine summarized 11 p1696 N85-20663
Research and technology activities at Ames Research Center's Biomedical Research Division
[NASA-TM-86692] 12 p1899 N85-21925
USSR report: Space Biology and Aerospace Medicine, volume 18, no. 6, November - December 1984
[JPRS-USB-85-002] 12 p1900 N85-21931
Review of US manual of clinical aviation medicine 12 p1904 N85-21957
Review of US guide on medication and flying 12 p1904 N85-21958
Aerospace Medicine and Biology: A continuing bibliography with indexes, supplement 267, January 1985
[NASA-SP-7011(267)] 12 p1904 N85-21959
Second generation USAFSAM (United States Air Force School of Aerospace Medicine) microprocessor audiometer
[AD-A149938] 12 p1905 N85-21963
The clinical and biomedical evaluation of trauma and fatalities associated with aircrew ejection and crash. A Working Group report
[AGARD-AR-194] 12 p1906 N85-21969
Lyakhov and Aleksandrov on 150-day flight 13 p1977 N85-22405
China report: Science and technology
[JPRS-CST-84-030] 13 p2041 N85-22777
Research opportunities in human behavior and performances
[NASA-CR-3886] 13 p2142 N85-23290
USSR report: Life sciences. Biomedical and behavioral sciences
[JPRS-UBB-85-012] 14 p2386 N85-24697
Second Soviet-French Symposium on Space Cytology 14 p2386 N85-24699
Results of a longitudinal study of airsickness during naval flight officer training: Executive summary
[AD-A150887] 14 p2388 N85-24712
Second Soviet-French Symposium on Space Technology 15 p2483 N85-25326
Aerospace Medicine and Biology: A continuing bibliography with indexes
[NASA-SP-7011(270)] 15 p2615 N85-26114
Computer simulation studies in fluid and calcium regulation and orthostatic intolerance
[NASA-CR-171869] 15 p2616 N85-26117
Psychometric evaluation of head injury among fliers referred to the AF School of Aerospace Medicine
[AD-A151479] 15 p2617 N85-26129
Cardiovascular effects of weightlessness 15 p2688 N85-26607
Aerospace medicine and biology: A continuing bibliography with indexes, supplement 271, May 1985
[NASA-SP-7011(271)] 16 p2840 N85-27514
USSR report: Space Biology and Aerospace Medicine, volume 18, no. 5, September - October 1984
[JPRS-USB-84-007] 19 p3322 N85-30583
Development of guidelines for setting physiological and hygienic standards for noise levels in aerospace medicine 19 p3323 N85-30584
Applications of aerospace technology in biology and medicine
[NASA-CR-166100] 19 p3328 N85-30619
Aerospace Medicine and Biology: A continuing bibliography with indexes (supplement 272)
[NASA-SP-7011(272)] 19 p3328 N85-30620
Space-flight simulations of calcium metabolism using a mathematical model of calcium regulation
[NASA-CR-171883] 19 p3328 N85-30621
Longitudinal study of cardiovascular disease in US Navy pilots
[AD-A154331] 19 p3328 N85-30623
Effects of coating rectangular microscopic electrophoresis chamber with methylcellulose 20 p3498 N85-31748
Results of Space Experiments in Physiology and Medicine and Informal Briefings by the F-16 Medical Working Group
[AGARD-CP-377] 20 p3507 N85-31605
Spatial orientation in weightlessness and readaptation to Earth's gravity 20 p3509 N85-31611
Cardiovascular research in space: Problems and results 20 p3510 N85-31617
Sleep and wake physiology in weightlessness 20 p3510 N85-31619
USSR Space Life Sciences Digest
[NASA-CR-3922] 21 p3656 N85-32709
USSR report: Life sciences. Biomedical and behavioral sciences
[JPRS-UBB-85-020] 21 p3663 N85-32752
Remote medical diagnosis 21 p3663 N85-32753
Aerospace medicine and biology: A continuing bibliography with indexes, supplement 273
[NASA-SP-7011(273)] 21 p3663 N85-32755
Air force technical objective document, Aerospace Medical Division, Fiscal Year 1986
[AD-A155195] 21 p3664 N85-32762
Results and prospects of physiological research during spaceflights 22 p3732 N85-33130
Mechanisms of osteodystrophy in weightlessness 22 p3733 N85-33143

USSR report: Space Biology and Aerospace Medicine, volume 19, no. 2, March - April 1985
[JPRS-USB-85-004] 22 p3820 N85-33867
Labyrinthine and extralabyrinthine mechanisms of development of motion sickness in weightlessness
22 p3821 N85-33868
Aerospace Medicine and Biology: A continuing bibliography with indexes (supplement 274)
[NASA-SP-7011(274)] 23 p3952 N85-34491
USSR report: Space Biology and Aerospace Medicine, vol. 19, no. 3, May - June 1985
[JPRS-USB-85-005] 23 p3952 N85-34494
Problems of aviation and space medicine and psychology discussed at 14th Gagarin lectures
23 p3954 N85-34509
Proceedings of a Scientic Meeting on the Occasion of the Inauguration of New Buildings for the DFVLR Institute for Aerospace Medicine
[ESA-TT-857] 24 p4129 N85-35595
The research programme of the Institute for Aerospace Medicine 24 p4129 N85-35596
Simulation of high +Gz onset in the dynamic environment simulator
[AD-A155963] 24 p4131 N85-35610

AEROSPACE SAFETY
Space Nuclear Safety Program
[DE84-016973] 05 p0728 N85-14679
FAA (Federal aviation administration) assessment of satellite concepts and aviation spectrum requirements
[AD-A152338] 17 p2948 N85-28199
Space station crew safety alternatives study. Volume 3: Safety impact of human factors
[NASA-CR-3856] 19 p3223 N85-29984
Space Station crew safety alternatives study. Volume 2: Threat development
[NASA-CR-3855] 21 p3558 N85-32133

AEROSPACE SCIENCES
Canada report to COSPAR 01 p0131 N85-10906
USSR report: Space
[JPRS-USP-84-005] 02 p0156 N85-11060

AEROSPACE SYSTEMS
Material problems for high-temperature, high-power space energy-conversion systems
[AD-A145940] 03 p0385 N85-12466
Conceptual design for scaled truss antenna flight experiment
[NASA-TM-85804] 04 p0462 N85-12932
Robotic technology: An assessment and forecast
[AD-A146872] 06 p0615 N85-15171
SNAP (Space Nuclear Auxiliary Power) reactor overview
[AD-A146831] 07 p1041 N85-16812
Space System Applications to Tactical Operations
[AGARD-CP-344] 11 p1709 N85-20751
Tactical operations and space applications
11 p1709 N85-20752
Fiscal year 1986 technical objective document
[AD-A151039] 14 p2432 N85-25000
Research and technology
[NASA-TM-86662] 14 p2456 N85-25166
Application of space methods in geodesy
16 p2724 N85-26817
The replacement of precious metal thick film inks using conductive polymer technology
[AD-A152002] 16 p2749 N85-26985
European Science Notes, Volume 39, Number 3
[AD-A152446] 17 p3027 N85-28717
Air Force technical objective document FY 86
[AD-A152730] 17 p3047 N85-28855
Overhead management guide for aerospace procurements
[AD-A153626] 18 p3198 N85-29835
Space research at NLR 20 p3397 N85-31075
Robust control of multivariable and large space systems
[AD-A155117] 21 p3559 N85-32140
Nineteenth Aerospace Mechanisms Symposium
[NASA-CP-2371] 22 p3795 N85-33512
A spacefaring people: Perspectives on early spaceflight
[NASA-SP-4405] 23 p4056 N85-35142
Space science and exploration: A historical perspective 23 p4056 N85-35143
The next assignment: The state of the literature on space 23 p4057 N85-35146
Evaluation of nuclear detonation location capability under high attack scenario
[AD-A155761] 24 p4149 N85-35729

AEROSPACE TECHNOLOGY TRANSFER
Aeronautics Technology Possibilities for 2000: Report of a workshop
[NASA-CR-174018] 01 p0001 N85-10001
Rotor systems research aircraft airplane configuration flight-test results
[NASA-TM-85911] 01 p0006 N85-10004
West Europe report: Science and technology
[JPRS-WST-84-004] 03 p0309 N85-11998
Fokker wants to start new Netherlands space program
03 p0310 N85-11999
Loads and Aeroelasticity Division research and technology accomplishments for FY 1984 and plans for FY 1985
[NASA-TM-86356] 07 p0898 N85-15691
West Europe report: Science and technology
[JPRS-WST-84-039] 07 p0936 N85-15929
West Europe report: Science and technology
[JPRS-WST-85-001] 08 p1141 N85-17190
Space research in the Federal Republic of Germany
09 p1285 N85-18074
Activities report in aerospace in West Germany
[ISSN-0070-3966] 09 p1418 N85-18947
European Scientific Notes. Volume 39, number 1
[AD-A149498] 10 p1568 N85-19866
Authorizing appropriations to the National Aeronautics and Space Administration for fiscal year 1986
[H-REPT-99-32] 13 p2166 N85-23452
Technology and Economics, Inc. Technology Application Team
[NASA-CR-175630] 13 p2168 N85-23454
AGARD bulletin: Meetings, publications, membership
[AGARD-BUL-85-1] 15 p2686 N85-26589
Symbiosis between postgraduate training and research projects: A successful experience
[INPE-3216-PRE/569] 16 p2810 N85-27330
The technological gains of Helios for the European industry 16 p2867 N85-27810
European Science Notes, Volume 39, Number 3
[AD-A152446] 17 p3027 N85-28717
West Europe report: Science and technology
[JPRS-WST-84-037] 18 p3088 N85-29108
FRG weighs ESA participation, budget issues
18 p3088 N85-29110
Some applications of aeronautical engineering in the construction of yachts
[NLR-MP-83042-U] 20 p3394 N85-31052
NASA Space controls research and technology program 20 p3408 N85-31149
Civilian Space Stations and the US future in Space
[OTA-STI-242] 20 p3418 N85-31215
USSR report: Life sciences. Biomedical and behavioral sciences
[JPRS-UBB-85-020] 21 p3663 N85-32752
USSR report: Space
[JPRS-USP-84-006] 22 p3731 N85-33128
Product definition: Technical specification of needs
[SNIAS-851-430-104] 23 p3910 N85-34228
New technologies at the forefront of industrial developments 24 p4061 N85-35168

AEROSPACE VEHICLES
NT FLEXIBLE SPACECRAFT
Aerodynamic characteristics of some lifting reentry concepts applicable to transatmospheric vehicle design studies
[NASA-TM-86331] 06 p0747 N85-14787
A theoretical method for selecting space craft and space suit atmospheres
[AD-A148219] 08 p1200 N85-17559
An overview of the MIL-HDBK-5 program
[AD-A147788] 14 p2254 N85-23970

AEROSTATS
U AIRSHIPS

AEROTHERMOCHEMISTRY
Sandia Cooperative Group on the Aerothermochemistry of Turbulent Combustion. Discussion record of fourth meeting
[DE85-004720] 20 p3423 N85-31246
Intermittency, conditional sampling and turbulent combustion 20 p3424 N85-31249
Conditional modeling in turbulent shear flows
20 p3424 N85-31250
Non-equilibrium effects in turbulent diffusion flames
20 p3425 N85-31258
Sandia Cooperative Group on the Aerothermochemistry of Turbulent Combustion
[DE85-004720] 20 p3455 N85-31453
Sandia Cooperative Group on the Aerothermochemistry of Turbulent Combustion
[DE85-007493] 20 p3455 N85-31454
Sandia Cooperative Group on the Aerothermochemistry of Turbulent Combustion. Discussion record of the second meeting
[DE85-007493] 22 p3743 N85-33203

AEROTHERMODYNAMICS
Aerothermal modeling program
02 p0145 N85-10983
Space Shuttle wind tunnel testing program
[NASA-RP-1125] 02 p0167 N85-11127
Experimental and predicted heating distributions for biconics at incidence in air at Mach 10
[NASA-TP-2334] 03 p0361 N85-12313
Optimum thermogasdynamic design of gas turbine engines by characteristics of element prototypes
06 p0777 N85-14985
Heat transfer results and operational characteristics of the NASA Lewis Research Center Hot Section Cascade Test Facility
[NASA-TM-86690] 06 p0808 N85-15133
Analytical and physical modeling program for the NASA Lewis Research Center's Altitude Wind Tunnel (AWT)
[NASA-TM-86919] 07 p0909 N85-15757
Columbia: The first 5 flights entry heating data series. Volume 1: An overview
[NASA-CR-171820] 07 p0913 N85-15777
Shuttle system ascent aerodynamic and plume heating 08 p1103 N85-16975
Orbiter entry aerothermodynamics
08 p1104 N85-16978
Orbiter thermal protection system
08 p1104 N85-16979
Combustion research for gas turbine engines
[NASA-TM-86963] 12 p1778 N85-21184
Results of aeroheating DFI and ET design-data test on a 0.0175-scale model 60-OTS conducted in the Von Karman Gas Dynamics Facility (VKF) 40" supersonic and the 50" hypersonic wind tunnels A and C
[NASA-CR-167693] 13 p1968 N85-22466
Results of a M = 5.3 heat transfer test of the integrated vehicle using phase-change paint techniques on the 0.0175-scale model 56-OTS in the NASA/Ames Research Center 3.5-foot hypersonic wind tunnel
[NASA-CR-167695] 13 p1968 N85-22468
Space Shuttle aerothermodynamic data report, phase C
[NASA-CR-171858] 14 p2241 N85-23867
NASA R and T aerospace plane vehicles: Progress and plans
[NASA-TM-86429] 15 p2491 N85-25368
Future fundamental combustion research for aeropropulsion systems
[NASA-TM-87049] 17 p2898 N85-27870
Structural Integrity and Durability of Reusable Space Propulsion Systems
[NASA-CP-2381] 17 p2910 N85-27941
Overview of aerothermodynamic loads definition study
17 p2910 N85-27942
Heating parameter estimation using coaxial thermocouple gages in wind tunnel test articles
[AD-A153039] 17 p2968 N85-28328
A new finite element approach: Progress in inviscid flow computations
[NASA-TM-86434] 20 p3454 N85-31450

AFC (CONTROL)
U AUTOMATIC FREQUENCY CONTROL

AFCS (CONTROL SYSTEM)
U AUTOMATIC FLIGHT CONTROL

AFFECTS
U EFFECTS

AFFINITY
Thermally modulated electron affinity detector for priority pollutant analysis
[PB85-158145] 15 p2508 N85-25469

AFRICA
Operating experiences of reverse osmosis plants treating Rand Water Board (RWB) water: Pitfalls and problems 01 p0023 N85-10142
Mineral nutrients in Mediterranean ecosystems
[REPT-71] 01 p0069 N85-10458
Short period forecasts in West Africa using Meteosat data 01 p0079 N85-10526
Estuaries of the Cape. Part 2: Synposes of available information on individual systems. Report no. 19: Groot (WES) (CMS 23) and Sout (CMS 22)
[CSIR-RR-418] 01 p0087 N85-10588
The identification of rain-bearing synoptic systems through principal component analysis
02 p0212 N85-11394
The application of principal component analysis in a study of rainfall 02 p0212 N85-11396
Archean sedimentation and tectonics in southern Africa
[NASA-CR-174156] 04 p0533 N85-13408
The mineralogy of global magnetic anomalies
[E85-10061] 07 p0987 N85-16272
Satellite definition of the bio-optical and thermal variation of coastal eddies associated with the African current
[AD-A147910] 07 p0989 N85-16282
Synthesis of proterozoic data as a prerequisite for tectonic and thermal modeling
[NASA-CR-174252] 07 p0995 N85-16323
Reduced to pole long-wavelength magnetic anomalies of Africa and Europe 20 p3475 N85-31585
Euro-African MAGSAT anomaly-tectonic observations
20 p3475 N85-31586
Long-wavelength magnetic and gravity anomaly correlations on Africa and Europe
20 p3476 N85-31587

Microwave hydrology: A trilogy
[NASA-CR-176042] 20 p3477 N85-31603
AFTERBODIES
Navier-Stokes solution of 3-dimensional hypersonic afterbody flowfields over capsule-type vehicles
[NAL-TR-819] 03 p0311 N85-12010
Empirical formulas for the prediction of the base pressure of missile bodies at subsonic velocities
[DFVLR-FB-84-23] 03 p0316 N85-12044
Effects of body shape on the aerodynamics of a body of revolution at Mach numbers from 1.6 to 4.6
[NASA-TM-86345] 07 p0893 N85-15657
On the evaluation of boundary layer measurements on boattailed bodies of revolution in axisymmetric compressible subsonic flow
[ESA-TT-883] 20 p3457 N85-31471
SRB TPS closeout materials characterization
[NASA-CR-170885] 24 p4070 N85-35222
Study of NSI and related cable performance during tests performed in the NASA Hot Gas Facility
[NASA-CR-170866] 24 p4101 N85-35423
AFTERBURNERS
U AFTERBURNING
AFTERBURNING
Flameholder with integrated air mixer
[AD-D011549] 12 p1778 N85-21161
Some unique features in operation of two-stage turbojet engine with afterburner 13 p2049 N85-22828
Effect of water injection into air for turbine cooling on economy of operation of gas turbine engine with afterburning 13 p2050 N85-22830
AFTERGLOWS
Ionic reactions of atmospheric importance
[AD-A147354] 07 p0997 N85-16333
Gas phase ion-molecule chemistry of carbon, nitrogen and oxygen compounds
[AD-A152876] 17 p2919 N85-27996
AGC (CONTROL)
U AUTOMATIC GAIN CONTROL
AGE DETERMINATION
U CHRONOLOGY
AGE FACTOR
Functional capacities of elderly subjects exposed to simulated spaceflight factors 01 p0091 N85-10617
The dynamical behavior of the age-size-distribution of a cell population
[CWI-AM-R8414] 17 p2998 N85-28538
Positive Gz accelerations tolerance of individuals 41 to 58 years of age 19 p3323 N85-30588
AGE HARDENING
U PRECIPITATION HARDENING
AGENTS
Optical 3-D signature device for detecting chemical agents
[AD-D011669] 19 p3272 N85-30293
AGGLOMERATION
Acoustic agglomeration methods and apparatus
[NASA-CASE-NPO-15466-1] 12 p1927 N85-22104
Gasification of boron oxide drops and boron slurry agglomerates in combustion gases 13 p1999 N85-22529
AGGLUTINATION
Functional and structural changes in human erythrocyte surface after irradiation by UV waves of various wavelengths. Report 1: Expression of ABO and Rhesus system antigen 09 p1361 N85-18564
Functional and structural changes in human erythrocyte surface after irradiation by UV waves of various wavelenghts. Report 2: Adsorption of alcyan blue by external premembranous components 09 p1361 N85-18565
AGGREGATES
Unexplained Fe, Ni and S anomalies in CV chondrite components 06 p0884 N85-15618
Electrochemical features of the ferric sulfate leaching of CuFeS2/C aggregates
[AD-A148661] 08 p1123 N85-17081
Field validation of statistically-based acceptance plan for bituminous airport pavements. Volume 1: Correlation analysis of Marshall properties of laboratory-compacted specimens
[FAA-PM-84-12-VOL-1] 12 p1781 N85-21180
Texture independent determination of residual stress in polycrystalline aggregates using Rayleigh waves
[AERE-R-11483] 12 p1943 N85-22203
Characterization of atomic defects and their aggregates using positron annihilation spectroscopy
[DE85-006206] 14 p2418 N85-24918
High temperature polymer concrete
[DE85-005756] 23 p3920 N85-34290
AGING (BIOLOGY)
Blood pressure levels of active pilots compared with those of air traffic controllers
[AD-A146845] 06 p0846 N85-15373
Changes in spectral properties of detached leaves
[E85-10042] 07 p0963 N85-16243
Toxicity, mutagenesis and aging due to endogenous oxygen radicals
[AD-A150121] 12 p1900 N85-21928
Sleep deprivation and performance: Older age performance and limited sleep period use
[AD-A153102] 17 p2999 N85-28540
Tolerance to +Gz and +Gx accelerations of individuals in older age groups in good health and with early signs of arteriosclerosis 23 p3952 N85-34496
AGING (MATERIALS)
NT AGING (METALLURGY)
Weldability of aged heat resistant nickel alloys 01 p0021 N85-10125
System engineering and integration contract for implementation of the National Airspace System plan, volume 1, sections 1.0-4.0, 6.0
[AD-A145763] 03 p0317 N85-12048
Long-term thermal aging of 2 graphite-polyimide composite materials
[NASA-TP-2369] 03 p0325 N85-12094
Free volume considerations in thermoplastic and thermosetting resins 04 p0485 N85-12952
Influence of relaxation on the mechanical characteristics of a carbon-epoxy composite. Report no. 45.427/1 04 p0488 N85-12980
Solidification and aging behavior of types 308 and 308CRE stainless steel welds
[DE84-016552] 04 p0476 N85-13029
Encapsulation materials and processing 06 p0830 N85-15269
Photothermal degradation of encapsulants 06 p0830 N85-15270
Determination of the decomposition behavior of double base propellants at low temperatures 08 p1117 N85-17045
Compressive strength-maturity relationships of mortar containing fly ash
[AD-A148705] 09 p1339 N85-18423
Accelerated aging of aluminized acrylic solar mirror materials
[DE85-002683] 11 p1612 N85-20138
Chemical and photographic evaluation of rigid explosive transfer lines
[AD-A149303] 11 p1613 N85-20145
Sol-gel-derived AR coatings for solar receivers
[DE85-000192] 11 p1673 N85-20541
Synthesis and thermomechanical properties of new AT-Phenylene R systems
[AD-A149961] 12 p1813 N85-21372
NBS solar collector durability/reliability test program
[DE85-003489] 12 p1881 N85-21801
TEM/FIM study of modulated microstructures in the Fe-Be system
[DE85-005379] 13 p2023 N85-22678
Effect of alternative aging and accident simulations on polymer properties
[DE85-002642] 13 p2037 N85-22762
Stability of highly nonlinear oxide-zinc resistors under continuous voltage of industrial frequency 13 p2087 N85-23030
Synthesis and properties of elevated temperature P/M aluminum alloys
[AD-A151031] 14 p2256 N85-23981
Influence of short-range order on deformation mechanisms in solid solutions
[DE85-006374] 14 p2258 N85-23989
Retroreflective armbands: Influences of wearing mode, aging and other factors on the visibility distance
[IZF-1984-28] 14 p2422 N85-24942
Characterization-curing-property studies of HBRF 55A resin formulations
[NASA-CR-175836] 16 p2753 N85-26989
Damage caused to polyurethane foams by aging, simulated sunlight exposure, heat and fire
[AD-A152040] 16 p2754 N85-26998
Natural and accelerated aging of plastics 17 p2936 N85-28123
Qualitative and quantitative determination of aging by mechanical tests — plastics 17 p2977 N85-28393
Recycling agent selection and tentative specification
[AD-A153529] 18 p3070 N85-28988
Aging study of copper alloy 172
[DE85-009848] 18 p3075 N85-29023
Aging of gold thick-film solder joints
[DE85-009847] 18 p3077 N85-29037
Investigation of fast reaction SAW (Surface Acoustic Wave) accelerometer
[AD-A153676] 19 p3216 N85-29943
Study of the kinetics of hydrogenation using aged catalysts
[DE85-010427] 19 p3230 N85-30025
Ten year environmental test of glass fiber/epoxy pressure vessels
[NASA-TM-87058] 19 p3231 N85-30034
Internal structure of GP zones in dilute Al-Cu alloys 19 p3238 N85-30073
CP DDT detonators. 4: Thermal aging
[DE85-011172] 19 p3251 N85-30160
Long-term thermal aging of Celion/V378A composite materials
[NASA-TM-86362] 20 p3421 N85-31236
Thermomechanical deformation in the presence of metallurgical changes 20 p3466 N85-31533
Hot isostatically pressed Sm(2)(TM)17 magnets
[AD-A155479] 21 p3582 N85-32267
Near-threshold fatigue: An overview of the role of microstructure and environment
[DE85-009903] 23 p3941 N85-34431
Conduction and aging of piezoelectric PZT ceramics 24 p4089 N85-35346
A kinetic model for predicting oxidative degradation rates in combined radiation-thermal environments
[TI85-002629] 24 p4100 N85-35414
AGING (METALLURGY)
Thermal ageing studies of 9%Cr 1%Mo steel
[AERE-R-11109] 03 p0333 N85-12149
Investigation of the isothermal precipitation behavior of nickel-base alloys using electrochemical phase extraction
[JUEL-1903] 05 p0619 N85-13958
Strength and aging behaviour of soft soldered joints
[BLL-T6385/BG/WH800/84] 07 p0925 N85-15662
On reversion phenomena in Cu-Zr-Cr alloys
[NASA-TM-77791] 08 p1125 N85-17092
Reversion phenomena of Cu-Cr alloys
[NASA-TM-77780] 08 p1125 N85-17094
Comparison of property regeneration techniques and life prediction procedures applied to laboratory tested and service exposed Ni-Cr alloys
[NPL-DMA(A)-91] 09 p1333 N85-18374
Initial aging phenomena in copper-chromium alloys
[NASA-TM-77790] 10 p1439 N85-19070
Study of influence of cold plastic deformation on aging of VT30 alloy 10 p1448 N85-19124
Evaluation of 7010 aluminium alloy extruded tube in the T76 condition
[BR92019] 11 p1596 N85-20039
Mechanism of titanium impact on brittle tendency in delayed deformation of martensite-aging steels 11 p1604 N85-20087
Effects of neutron irradiation at 450(0)C and 16 dpa on the properties of various commercial copper alloys
[DE85-005716] 13 p2024 N85-22684
Decomposition of VTAN alloy solid solution upon irradiation and thermal aging 13 p2029 N85-22712
Structure and aging of amorphous chromium-germanium alloys 15 p2497 N85-25401
Structural changes with one- and two-stage aging of alloys Ti-Al-Mo-Fe and Ti-Zr-V-Al-Sn 15 p2499 N85-25415
Effect of thermal ageing on the mechanical properties of PWR pressure vessel steels and weldments
[AERE-R-11460] 24 p4078 N85-35275
AGREEMENTS
The structures and the role of an international agency for the control of satellites
[NASA-TM-76765] 03 p0441 N85-12806
The effects of controversy and concurrence seeking on effective decision making
[AD-A153370] 17 p3002 N85-28555
AGRICULTURAL AIRCRAFT
Effectiveness of agricultural aviation 04 p0544 N85-13460
Director on institute's civil aviation projects 08 p1067 N85-16764
Improved sprayer for AN-2 cropdusting work 08 p1068 N85-16769
AGRICULTURE
Agribusiness and space: No limits to growth 02 p0152 N85-11029
USSR report: Life sciences. Biomedical and behavioral sciences
[JPRS-UBB-84-025] 04 p0543 N85-13453
USSR report: Life Sciences: Biomedical and behavioral sciences
[JPRS-UBB-84-026] 04 p0543 N85-13457
A field control methodology of remotely sensed data for statistical purposes: An example of SPOT simulated data in eastern Belgium — land use statistics 05 p0660 N85-14241
Renewable energy: Energy from agricultural products
[TI84-901769] 05 p0669 N85-14307
Detecting agricultural to urban land use change from multi-temporal MSS digital data — Salt Lake County, Utah
[E85-10049] 07 p0983 N85-16245
Exploring the use of structural models to improve remote sensing agricultural estimates 07 p0985 N85-16259
Image variance and spatial structure in remotely sensed scenes — South Dakota, California, Missouri, Kentucky, Louisiana, Tennessee, District of Columbia, and Oregon 07 p0986 N85-16265

USSR report: Life sciences. Biomedical and behavioral sciences
[JPRS-UBB-84-015] 07 p1010 N85-16416
An investigation of the driving wheel thrust of paddy field tractors
[AD-P004284] 09 p1407 N85-18861
Study of the motion of agricultural vehicles on steep grass-covered slopes
[AD-P004290] 09 p1408 N85-18867
Pressure tests in soil below tires of agricultural vehicles
[AD-P004294] 09 p1408 N85-18871
Turning behaviour of articulated frame steering tractor
[AD-P004304] 09 p1409 N85-18881
An integrated GIS/remote sensing data base in North Cache soil conservation district, Utah: A pilot project for the Utah Department of Agriculture's RIMS (Resource Inventory and Monitoring System)
[E85-10073] 10 p1504 N85-19487
Anayeis of the quality of image data required by the LANDSAT-4 Thematic Mapper and Multispectral Scanner — agricultural and forest cover types in California
[E85-10074] 10 p1504 N85-19488
Birds and airport agriculture in the conterminous United States: A review of literature
[AD-P004208] 11 p1583 N85-19975
Remote sensing technology now playing practical roles 11 p1619 N85-20190
Moisture variation in northern hemisphere temperate latitudes 13 p2105 N85-23119
Characterization of LANDSAT-4 TM and MSS image quality for the interpretation of California's agricultural resources — Central Valley 13 p2118 N85-23190
Atlas of archived vegetation, land-use and seasonal Albedo data sets
[NASA-TM-86199] 14 p2346 N85-24508
NASTRAN's application in agricultural engineering 15 p2575 N85-25880
Function of remote sensing in Brazil
[INPE-3314-PRE/621] 16 p2810 N85-27329
Symposium on Atmospheric Sciences in South Africa
[CSIR-S-331] 16 p2829 N85-27442
A weather service for agriculture 16 p2830 N85-27450
Genetic engineering of plants: Agricultural research opportunities and policy concerns
[DE85-006771] 16 p2840 N85-27513
Preliminary technology utilization assessment of the robotic fruit harvester
[NASA-CR-175834] 16 p2844 N85-27532
Meteorology and food production: The theme of the 16 meteorology day
[AD-A152372] 17 p2996 N85-28518
Earth Resources: A continuing bibliography with indexes, issue 45
[NASA-SP-7041(45)] 18 p3123 N85-29336
Screening Prosopis (mesquite) species for biofuel production on semi-arid lands
[DE85-010048] 19 p3302 N85-30471
Agricultural weather report for the Ijsselmeer polders in the 1984 summer season; a verification report
[KNMI-TR-61] 20 p3496 N85-31737
USSR report: Life sciences. Biomedical and behavioral sciences
[JPRS-UBB-85-017] 20 p3504 N85-31785
Deficit irrigation feasibility study and demonstration project
[DE85-011531] 22 p3802 N85-33555
Salinity driven oceanographic upwelling
[DE85-011664] 22 p3818 N85-33652
USSR report: Life sciences. Biomedical and behavioral sciences
[JPRS-UBB-85-018] 22 p3819 N85-33660
Snow cover in the Siberian forest-steppe
[NASA-TM-77914] 23 p3943 N85-34435

AGRISTARS PROJECT
Shortwave infrared detection of vegetation
[E85-10064] 08 p1174 N85-17402
Analysis of data acquired by synthetic aperture radar and LANDSAT Multispectral Scanner over Kershaw County, South Carolina, during the summer season
[E85-10071] 10 p1503 N85-19485
NOAA-AISC user's guide for implementing CERES maize model for large area yield estimation
[E85-10083] 12 p1873 N85-21748
NOAA-AISC user's guide for implementing CERES wheat model for large area yield estimation
[E85-10085] 12 p1873 N85-21750
Estimating solar radiation for plant simulation models
[E85-10089] 12 p1873 N85-21751
Thematic Mapper data quality and performance assessment in renewable resources/agriculture/remote sensing 13 p2120 N85-23201
Supplement to evaluation of satellite derived estimates of solar radiation
[E85-10086] 14 p2346 N85-24506
Evaluation of satellite derived estimates of solar radiation
[E85-10087] 14 p2346 N85-24507

AGROCLIMATOLOGY
An integrated remote sensing approach for identifying ecological range sites — parker mountain
[E85-10050] 07 p0983 N85-16246
The climate in food production in Latin America 07 p1001 N85-16359
Crop yield forecasting 07 p1001 N85-16360
The challenge of food production: The importance of climate 07 p1001 N85-16361
Socio-economic impact of climate — Mexico 07 p1003 N85-16372
Evaluation of the climatic resources of Cuba applied to agricultural work 07 p1004 N85-16380

AGROMETEOROLOGY
Short period forecasts in West Africa using Meteosat data 01 p0079 N85-10526
Frost nowcasting in the agricultural area of Valencia (Spain) — meteorological satellites 05 p0658 N85-14225
Climate Conference for Latin America and the Caribbean
[WMO-632] 07 p1000 N85-16352
Crop yield forecasting 07 p1001 N85-16360
The challenge of food production: The importance of climate 07 p1001 N85-16361
The management of atmospheric resources in food production 07 p1002 N85-16362
Water and climate, study of one case 07 p1002 N85-16369
Evaluation of the climatic resources of Cuba applied to agricultural work 07 p1004 N85-16380
The El Nino phenomenon and its agrometeorological implications 07 p1004 N85-16382
Agricultural weather report for the Ijsselmeer polders in the 1984 summer season; a verification report
[KNMI-TR-61] 20 p3496 N85-31737

AGT
U AUTOMATED GUIDEWAY TRANSIT VEHICLES

AILERONS
NT FLAPERONS
Aileron controls for wind turbine applications
[NASA-TM-86867] 02 p0222 N85-11458
Aileron effectiveness for a subsonic transport model with a high-aspect-ratio supercritical wing
[NASA-TM-85674] 07 p0898 N85-15695
Shutdown characteristics of the Mod-O wind turbine with aileron controls
[NASA-TM-86918] 07 p0992 N85-16299
Flight service evaluation of advanced composite ailerons on the L-1011 transport aircraft
[NASA-CR-172483] 08 p1118 N85-17049
Gust load alleviation of a cantilevered rectangular elastic wing. Wind tunnel experiment and analysis
[NAK-TR-86] 18 p3063 N85-28950
Compendum of unsteady aerodynamic measurements, addendum 1
[AGARD-R-702-ADD-1] 20 p3390 N85-31028
Data set 8: ZKP wing, oscillating aileron 20 p3390 N85-31029
Reflection plane tests of a wind turbine blade tip section with ailerons
[NASA-TM-87018] 23 p3945 N85-34444

AIR
NT COMPRESSED AIR
NT EXPIRED AIR
NT LIQUID AIR
Electron energy loss rates in N-2, O-2 and air
[AD-A145158] 01 p0072 N85-10476
Diagnostics of ionization in air produced by infrared radiation from A pulse CO2 laser
[AD-A145376] 02 p0201 N85-11342
Laboratory investigation of coefficients of absorption of air at Lambda = 10.6 microns 02 p0263 N85-11723
Low-frequency sound absorption measurements in air
[NASA-RP-1128] 02 p0275 N85-11789
Pathogenesis and treatment of cerebral air embolism and associated disorders
[AD-A146723] 07 p1014 N85-16443
Theoretical studies of the ignition and combustion of silane-hydrogen-air mixtures
[NASA-CR-3676] 10 p1433 N85-19032
Self-Optimized Sector (SOS) model of self-consistent energy loss and scattering for an electron beam propagating in air
[DE85-003161] 11 p1722 N85-20831
Hydrogen flame acceleration and transition to detonation
[DE85-000611] 12 p1802 N85-21299
Continuous measurement of zircaloy corrosion in air with an ultrasonic corrosion monitor
[DE85-003663] 12 p1807 N85-21337
Pseudo-stationary oblique-shock-wave reflections in a polyatomic gas, sulfur hexafluoride
[UTIAS-TN-253] 12 p1845 N85-21577
The effect of air holes on combustor liner wall temperature profile: Experiments
[NAL-TR-840] 15 p2504 N85-25443
Modeling the role of radicals in the ignition of and flame propagation in hydrogen-air and methane-air mixtures 16 p2744 N85-29035
Aluminum-air power cell research and development
[DE85-006117] 17 p2966 N85-28456
Air Weather Service (AWS) climatic briefs: Europe
[AD-A152528] 17 p2996 N85-28519
Research test facility for evaporation and combustion of alternative jet fuels at high air temperatures
[AD-A153830] 18 p3083 N85-29073
A model for the combustion of polymethyl methacrylate in air in a laminar diffusion flame
[VTH-LR-439] 18 p3165 N85-29606
Air bag restraint system
[AD-D011671] 19 p3215 N85-29936
Rayleigh scattering for density measurements in premixed flames: One point, time series data 20 p3424 N85-31253
Supersaturation obtained in a condensation nucleus counter 21 p3642 N85-32624
Recombination and ionization in a nitrogen plasma
[AD-A155426] 22 p3845 N85-33613
Influence of technology of atomization of naturally alloyed iron on grain-size characteristics of powder material
[BLL-M-35810-(5828.4)] 23 p3914 N85-34257
Cerenkov radiation from periodic electron bunches for finite emission length in air
[AD-A156158] 24 p4090 N85-35352
Proton-air and proton-proton cross sections from air shower data
[HE-1.1-1] 24 p4170 N85-35849
Proton-air inelastic cross section at S(1/2) = 30 TeV
[HE-1.1-2] 24 p4170 N85-35850

AIR BEARINGS
U GAS BEARINGS

AIR BLASTS
U AERIAL EXPLOSIONS

AIR BREATHING BOOSTERS
Integral boost, heat protection, port covers and transition 07 p0918 N85-15813

AIR BREATHING ENGINES
NT GAS TURBINE ENGINES
NT J-85 ENGINE
NT JET ENGINES
NT RAMJET ENGINES
NT SUPERSONIC COMBUSTION RAMJET ENGINES
NT TURBOFAN ENGINES
NT TURBOJET ENGINES
NT TURBOPROP ENGINES
An experimental investigation of two-dimensional thrust augmenting ejectors, part 1
[NASA-CR-174111] 04 p0456 N85-12894
An experimental investigation of two-dimensional thrust augmenting ejectors, part 2
[NASA-CR-174110] 04 p0456 N85-12895
Combustion in high speed air flows
[AD-A148371] 08 p1122 N85-17070
A study of air breathing rockets. Part 4: Direct fuel injection into a secondary combustor
[NAL-TR-832] 09 p1287 N85-18083
An air-breathing ballistic space transporter for Europe
[NASA-TM-77645] 12 p1792 N85-21244
Status of boron combustion research 13 p1998 N85-22526
Fiscal year 1986 technical objective document
[AD-A151039] 14 p2432 N85-25000
Status of boron combustion research
[AD-A154762] 21 p3563 N85-32160

AIR CONDITIONING
An assessment of ground-coil heat-pump technology
[DE85-002567] 10 p1486 N85-19362
Performance evaluation of an active solar cooling system utilizing low cost plastic collectors and an evaporatively-cooled absorption chiller
[DE84-010813] 12 p1860 N85-21796
Latent heat storage in cooling systems
[DE85-005355] 13 p2129 N85-23248
A review of development and application of heat pump technology
[CSIR-RR-585] 14 p2300 N85-24241
Evaporatively cooled chiller for solar air conditioning systems design and field test
[DE84-014154] 20 p3484 N85-31652

AIR CONDITIONING EQUIPMENT
Modeling of a second-generation solar-driven Rankine air conditioner
[DE84-015132] 01 p0036 N85-10223
Turbine test report, addendum
[DE84-015130] 02 p0205 N85-11353
New control design principles based on measured performance and energy analysis of HVAC (Heating, Ventilating, and Air-Conditioning) systems
[AD-A151708] 15 p2522 N85-25546
The influence of oil contamination on the nucleate pool-boiling behavior of R-114 from a structured surface
[AD-A155609] 21 p3585 N85-32284

AIR CONDUCTIVITY
Natural convection in square partitioned enclosures
[AD-A153707] 18 p3197 N85-29828

AIR COOLING
Cooling system investigation of the 3-kW MEP models 016A, 021A, and 026A (60Hz, 400-Hz and 28-V dc) gasoline-engine-driven generator sets
[AD-A147571] 07 p0974 N85-16185
Improvement of gas turbine engine performance by water injection into turbine cooling air
09 p1307 N85-18209
Method for refining microstructures of cast titanium articles
[AD-D011518] 12 p1804 N85-21318
Effect of water injection into air for turbine cooling on economy of operation of gas turbine engine with afterburning 13 p2050 N85-22830
effect of gas stream sweeping past the effluent of a perforated plate on heat transfer inside the perforations
13 p2051 N85-22836
Comparison of the response of shape memory alloy actuators using air-cooling and water-cooling
[AD-A155216] 21 p3567 N85-32185

AIR CURRENTS
NT JET STREAMS (METEOROLOGY)
NT MERIDIONAL FLOW
NT VERTICAL AIR CURRENTS
Numerical calculations of stratified Ekman layer flow over ridges with a finite element model
[DE84-014482] 04 p0499 N85-13179
High-frequency wind wave spectrum in storm basin
14 p2336 N85-24444
Radon concentration inversion in the troposphere: Still unexplained
[INPE-3360-PRE/638] 16 p2826 N85-27431
The physical and empirical basis for a specific clear-air turbulence risk index
[NASA-CR-178522] 24 p4120 N85-35540

AIR CUSHION VEHICLES
U GROUND EFFECT MACHINES

AIR DEFENSE
NT ANTIMISSILE DEFENSE
A methodology for the determination of rotary wing aircraft vulnerabilities in air-to-air combat simulation
[AD-A148984] 10 p1424 N85-18984
Close air support mission: Development of a unitary measure of pilot performance
[AD-A149285] 11 p1697 N85-20685
Visual simulation requirements for aircraft aspect recognition at real world distances
[AD-A151040] 14 p2228 N85-23810
Inertial navigation system - LAS II for SGT YORK testing
[AD-A154204] 19 p3216 N85-29944
Program Manager: The journal of the defense systems management college, volume 14, number 2, March-April 1985
[AD-A154219] 20 p3540 N85-32031
Assured information flow capping architecture
[AD-A155392] 22 p3756 N85-33283

AIR DROP OPERATIONS
60,000 pound capacity extraction system
[AD-A145841] 03 p0318 N85-12052

AIR DUCTS
A numerical procedure on three-dimensional parabolic flow in duct 16 p2692 N85-26820

AIR FILTERS
Fabric filter system study
[PB84-229749] 03 p0342 N85-12206
Electrostatic augmentation of fabric filtration: Reverse-air pilot unit experience
[PB84-230002] 03 p0343 N85-12207
Development of a mass transfer machine for gas/liquid operations in the absence of gravity
[BMFT-FB-W-84-027] 05 p0637 N85-14091
Gas contamination detection device
[AD-D011386] 07 p0921 N85-15833
Diffusion deposition in fibrous filters for parallel and transverse flow models
[DE85-006149] 13 p2093 N85-23066
The investigation of natural and artificial ice nuclei by the improved membrane filter method
21 p3642 N85-32626

AIR FLOW
NT AIR CURRENTS
NT JET STREAMS (METEOROLOGY)
NT MERIDIONAL FLOW
NT VERTICAL AIR CURRENTS
Stall elimination and restart enhancement device
[AD-D011217] 01 p0010 N85-10062
Turbine heat transfer 02 p0142 N85-10964
Energy efficient engine. High pressure compressor detail design report
[NASA-CR-165558] 02 p0147 N85-10998
A dispersion model for airborne particulates inside a building
[DE84-014961] 02 p0225 N85-11473
Microburst wind structure and evaluation of Doppler radar for wind shear detection
[DOT/FAA/PM-84/29] 02 p0230 N85-11501
Problem of reduction to ideal wind tunnel in experimental aerodynamics 02 p0260 N85-11702
Investigation of heat exchange on models in subsonic jets of induction plasmatron 02 p0269 N85-11756
Aircraft flow effects on cloud droplet images and concentrations
[AD-A146176] 03 p0396 N85-12529
Simple mesoscale models for operational use in regions of topographic and thermal forcing: Development and evaluation
[AD-A146667] 06 p0839 N85-15325
The 500 millibar sign frequency teleconnection charts: Winter
[PB85-106276/GAR] 07 p1009 N85-16410
Combustion in high speed air flows
[AD-A148371] 08 p1122 N85-17070
Studies on reactive mufflers. Part 2: Mufflers with air flow 09 p1303 N85-18184
Control technology for fiber reinforced plastics industry at AMF Hatteras Yachts, New Bern Division, New Bern, North Carolina
[PB85-109015] 10 p1460 N85-19198
New air supply-prime mover facility for engine tests detailed 11 p1621 N85-20204
A probe for direct measurement of flow direction
[ESA-TT-953] 11 p1637 N85-20310
Flameholder with integrated air mixer
[AD-D011549] 12 p1778 N85-21161
Liquid fuel spray processes in high-pressure gas flow
[NASA-TM-86944] 12 p1844 N85-21570
Surface-slip equations for multicomponent nonequilibrium air flow
[NASA-TM-85820] 12 p1845 N85-21573
Multi-year plan for Experimental Systems Research: Passive and hybrid solar energy program
[DE85-004698] 12 p1882 N85-21810
Study for prediction of rotor/wake/fuselage interference, part 1
[NASA-CR-177340-VOL-1] 13 p1965 N85-22346
Study for prediction of rotor/wake/fuselage interference. Part 2: Program users guide
[NASA-CR-177340-VOL-2] 13 p1966 N85-22347
Diffusion deposition in fibrous filters for parallel and transverse flow models
[DE85-006149] 13 p2093 N85-23066
The ASCOT Data Analysis Workshop
[DE85-004407] 13 p2139 N85-23283
Planning of air cushion transport vehicles
14 p2285 N85-24160
A computer program to calculate the supersonic flow over a solid cone in air or water
[AD-A151102] 15 p2464 N85-25217
Air flow of the western coastal boundary of South Africa and its influence on the ocean 16 p2631 N85-27459
Aerodynamic performance of a wing in ground effect using the PANAIR program
[AD-A153303] 17 p2892 N85-27832
On Long's solution to hydrostatic flow over mountains
[DFVLR-MITT-84-02] 17 p2994 N85-28503
Multiple equilibria of the barotropic vorticity equation on a sphere 18 p3146 N85-29475
Approximate factorization method for computation of nonhydrostatic mesoscale flows
[DE85-007259] 19 p3313 N85-30537
A study of the adequacy of quasi-geostrophic dynamics for modeling the effect of frontal cyclones on the larger scale flow
[NASA-CR-176065] 20 p3495 N85-31731
Mesoscale features and atmospheric refraction conditions of the Arctic marginal ice zone
[AD-A155139] 21 p3636 N85-32584
The influence of helicopter tail shape on drag: An aerodynamic study using a low speed wind tunnel
[AD-A156304] 24 p4062 N85-35174
Experimental study of free and mixed convective flow of air in a heated cavity
[DE85-012538] 24 p4094 N85-35380

AIR INLETS
U AIR INTAKES

AIR INTAKES
NT ENGINE INLETS
NT INLET AIRFRAME CONFIGURATIONS
NT SUPERSONIC INLETS
Variable inlet vane assembly for a gas turbine combustion
[AD-D011220] 01 p0010 N85-10063
Interest of internal bleed for a two-dimensional air intake operating in a wide Mach number range (1.8-3 plus)
08 p1071 N85-16793
Selection of air intake parameters for supersonic-flow operation 13 p2051 N85-22837
West Europe report: Science and technology
[JPRS-WST-84-012] 15 p2523 N85-25552
MBB uses new CFC form tool for titanium alloy air intake 15 p2523 N85-25553
Low-speed aerodynamic test of an axisymmetric supersonic inlet with variable cowl slot
[NASA-TM-87039] 16 p2708 N85-26710

AIR JETS
Jet array impingement flow distributions and heat transfer characteristics: Effects of initial crossflow and nonuniform array geometry 02 p0142 N85-10967
Rayleigh and Raman scattering for density in a swirling flow combustor 08 p1120 N85-17060
Flow visualization study of the effect of injection hole geometry on an inclined jet in crossflow
[NASA-TM-86936] 11 p1631 N85-20269
Improved silicon grinding method and apparatus
[NASA-CASE-NPO-16336-1-CU] 12 p1819 N85-21407
Comparison of measured and computed boundary layers at the tail-end of an axisymmetric body in an air-jet
[AMTE(N)-TM-83053] 14 p2209 N85-23700
Experimental investigation of annular air curtain domes
[UTIAS-288] 15 p2521 N85-25543
Study of stresses on surface of flat barrier immersed in under expanded jet of rarefied gas
16 p2765 N85-27061
Moist barotropic instability in the tropics
20 p3489 N85-31683
Mean and large-scale turbulence characteristics of the noise-producing region of an acoustically excited round jet 20 p3523 N85-31911
Jets in air-jet family
[HE-3.2-1] 24 p4179 N85-35912

AIR LAND INTERACTIONS
Boundary layer-cloud interactions as potential storm predictors 01 p0081 N85-10543
Biosphere/atmosphere interactions
05 p0679 N85-14364
Theory and modeling of the interaction between subgrid scale orography and large scale flow
[DM-43] 16 p2827 N85-27440
Quasi stationary states in the Southern Hemisphere
16 p3144 N85-29465
Global model of transport of pollutants in atmosphere
19 p3297 N85-30439
An atmospheric boundary layer model forced by the operational ECMWV-model
[WSR-3] 24 p4120 N85-35541

AIR LAUNCHING
An artificial intelligence based framework for planning air launched cruise missile missions
[AD-A154466] 19 p3344 N85-30722

AIR LAW
Civil air code international flights section explained
15 p2460 N85-25194
Rotterdam Airport and the Common Market
17 p2894 N85-27840
Thirty years' activities for aircraft safety
20 p3391 N85-31033
The 121.5 MHz ELT: Past, present and future — Emergency Locator Transmitter (ELT)
20 p3401 N85-31105

AIR LOCKS
Fokker wants to start new Netherlands space program
03 p0310 N85-11999

AIR MASSES
The atmospheric extinction problem
08 p1251 N85-17901
Variation of Arctic cloud cover in summer
[DE85-004507] 13 p2139 N85-23265
Atmospheric cross sections for the Arctic gas and aerosol sampling program, March - April 1983
[NASA-CR-176027] 19 p3314 N85-30541
A statistical analysis of ice nuclei concentrations at urban and rural sites in Valladolid, Spain
21 p3640 N85-32614
Observations of cloud droplets, aerosol particles and cloud condensation nuclei in continental air masses
21 p3649 N85-32671
Variations of particulate sulfur concentrations in a coastal atmospheric environment in connection with the change of air masses origin 21 p3652 N85-32692

AIR NAVIGATION
NT ALL-WEATHER AIR NAVIGATION
NT AREA NAVIGATION
NT NAP-OF-THE-EARTH NAVIGATION
National airspace review 02 p0136 N85-10926
National airspace system: Operational requirements [AD-A149349] 10 p1422 N85-18973
Terrain following without use of forward looking sensors 16 p2698 N85-26659
Low cost two gimbal inertial platform and its system integration 16 p2698 N85-26661
The AFTI/F16 terrain-aided navigation system [DE85-008411] 18 p3060 N85-28935
Simulations of strapdown-system errors and error compensation methods — transport aircraft navigation [DFVLR-MITT-84-22] 20 p3392 N85-31040
Flight testing the Litton LTN 90 laser gyro strapdown system for civil aviation [ESA-TT-904] 20 p3392 N85-31042

AIR PIRACY
Semiannual report to Congress on the effectiveness of the civil aviation security program [AD-A149522] 10 p1421 N85-18967

AIR POLLUTION
NT GLOBAL AIR POLLUTION
NT INDOOR AIR POLLUTION
Demonstrating air quality improvements: A review of alternatives [DE84-014274] 01 p0070 N85-10462
Acid rain and transported air pollutants: Implications for public policy [PB84-222967] 01 p0071 N85-10469
Size specific total particulate emission factors for mobile sources [PB84-226653] 01 p0071 N85-10471
Mobile source exposure estimation [PB84-224518] 01 p0095 N85-10643
Aerosol sampling bias from differential electrostatic charge and particle size 02 p0224 N85-11467
The changing pattern of fossil fuel CO2 emissions [DOE/OR-21400/2] 02 p0224 N85-11469
Green River air quality model development: Meteorological and tracer data, July/August 1982. Field study in Brush Valley, Colorado [DE84-014975] 02 p0225 N85-11474
Arctic haze: Meteorological aspects of long-range transport 02 p0230 N85-11499
Bibliography of climate textbooks and studies [WCP-84] 02 p0231 N85-11505
Review of the NAAQS (National Ambient Air Quality Standards) for carbon monoxide: Reassessment of scientific and technical information [PB84-231315] 03 p0388 N85-12485
Analysis of Santa Barbara oxidant study [PB84-229277] 03 p0388 N85-12486
Review of the attributes and performance of six urban diffusion models [PB84-236850] 04 p0484 N85-13087
Thermodynamic conditions of the Earth's atmosphere with pollution processes 04 p0523 N85-13345
Outline of a new emissions model for military and civilian aircraft facilities [DE84-016455] 04 p0531 N85-13394
Aircraft measurements of tracer gas during the 1983 cross Appalachian tracer experiment (CAPTEX) [DE84-015292] 04 p0531 N85-13395
Impact of alcohol fuels on urban air pollution: Methanol photochemistry study [DE84-012950] 04 p0531 N85-13397
Regional-scale (1000 KM) model of photochemical air pollution. Part 2: Input processor network design [PB84-232051] 04 p0532 N85-13400
Atmospheric tracer experiments in a deep narrow valley [PB84-234590] 04 p0532 N85-13402
VOC emissions from volatile organic liquid storage tanks: Background information for proposed standards [PB84-237320] 04 p0532 N85-13403
Climatological variability in modeling of long-term regional transport and deposition of air pollutants [DE84-014726] 04 p0539 N85-13430
Calms processor (CALMPRO) user's guide [PB84-229467] 04 p0540 N85-13439
Fundamental molecular physics and chemistry, part 1 [DE84-009127] 04 p0561 N85-13571
Carbon cycle: Terrestrial interactions 05 p0652 N85-14167
Global carbon - nitrogen - phosphorus cycle interactions: A key to solving the atmospheric CO2 balance problem? 05 p0652 N85-14188
Mean maximum mixing heights for northern Asia for the winter of 1978 [DE84-015980] 05 p0672 N85-14315
Portable instrument for the detection and identification of air pollutants [DE84-014767] 05 p0672 N85-14316
Carbon monoxide study, Anchorage, Alaska, November 22, 1982 to February 11, 1983 [PB84-236595] 05 p0673 N85-14321
Cross-Appalachian Tracer Experiment (CAPTEX '83) [PB84-238641] 06 p0834 N85-15307
NAAQS (National Ambient Air Quality Standards) Exposure Model (NEM) applied to carbon monoxide [PB84-242551] 06 p0834 N85-15310
Climate and water quality 07 p1002 N85-16368
Determination of the laws governing the changes in the standard deviations of the distribution of pollution based on observations of the atmospheric turbulence spectrum and the possibility of simulating it in the laboratory [BLL-TR-T6373/BG/MRS14883/84] 08 p1179 N85-17431
Air quality assessment model validation in complex terrain [AD-A147690] 08 p1180 N85-17434
Impact of aircraft emissions on air quality in the vicinity of airports. Volume 3: Air quality and emission modeling needs [AD-A147951] 08 p1180 N85-17435
Modeling of turbulent dispersion of neutral and buoyant contaminants released from two dimensional sources — air pollution [VKI-TN-150] 08 p1180 N85-17438
Atmospheric photochemical modeling of turbine engine fuels. Phase 1: Experimental studies. Volume 2: Environmental chamber data tabulations [AD-A147786] 08 p1185 N85-17470
The application of emissions trading to DoD installations [AD-P004136] 09 p1346 N85-18472
Quality assurance for environmental analytical chemistry, 1983 [DE84-016045] 09 p1349 N85-18489
Meteorological factors responsible for high CO (carbon monoxide) levels in Alaskan cities [PB85-115137/GAR] 09 p1350 N85-18493
Stratospheric concentration of nitric acid, ozone and carbonyl sulfide: Measurement of nitric acid absorption in the Q branch of the V4 band as a function of temperature [ESA-TT-864] 09 p1355 N85-18524
Laser air pollution monitoring system planned for Moscow 10 p1500 N85-19465
TRAN-STAT: Statistics for environmental studies [DE85-000829] 10 p1513 N85-19547
Application of SIMCA (Soft Independent Modeling of Class Analogy) pattern recognition to air pollutant analytical data [PB85-124683] 10 p1513 N85-19549
Evaluation of recent SO/sub x/ and NO/sub x/ emission inventories [DE85-002649] 11 p1677 N85-20570
The concentration of sulfate in broken cloud layers [DE85-000226] 11 p1678 N85-20574
Meteorological support for the 1983 Deep Creek, Maryland experiment [DE85-002616] 11 p1678 N85-20575
Air quality for ozone and other photochemical oxidants. External review draft, volume 1 [PB85-128035] 11 p1679 N85-20582
Continued research in mesoscale air pollution simulation modeling. Volume 7. Mathematical modeling of urban aerosol dynamics [PB85-137386] 11 p1679 N85-20584
Continued research in mesoscale air pollution simulation modeling. Volume 5: Refinements in numerical analysis, transport, chemistry, and pollutant removal [PB85-137362] 11 p1680 N85-20585
Lidar observations of stratospheric aerosol over Mauna Loa Observatory, 1974 - 1981 [PB85-115061] 11 p1682 N85-20597
Turbulence parameters impacting dispersion in an urban convection boundary layer [PB85-116036] 11 p1682 N85-20598
User's guide for the Photochemical Box Model (PBM) [PB85-137164] 11 p1682 N85-20602
Evaluation of two numerical integrator schemes [PB85-138196] 11 p1683 N85-20603
Effects of air pollution and acid rain on forest decline [GPO-37-459] 12 p1863 N85-21818
Atlantic Coast Unique Regional Atmospheric Tracer Experiment (ACURATE) [PB85-128460] 12 p1886 N85-21839
Hazardous air pollutants: Wet removal rates and mechanisms [PB85-138626] 12 p1887 N85-21842
Hazardous air pollutants: Dry-deposition phenomena [PB85-138279] 12 p1887 N85-21843
Continued research in mesoscale air pollution simulation modeling. Volume 6. Further studies in the modeling of microscale phenomena [PB85-137370] 12 p1887 N85-21844
Sector analysis of relevant meteorological parameters for long range transport of air pollutants [NR-27] 12 p1893 N85-21882
Impact of aerosols on visibility and climate: A report prepared for Panel 3, Environmental Impact, of the NATO/CCMS Air Pollution Pilot Study on Air Pollution Control Strategies and Impact Modelling [PB85-106744] 12 p1897 N85-21906
Adsorption behaviour of nitrogen compounds on to porous polymer beads and applications to atmospheric sampling [BLL-DRIC-TRANS-7399-(3623.66)] 13 p2036 N85-22753
Spectroscopic study of gas pollutants in atmosphere over large cities: A review 14 p2341 N85-24478
Adjustment of the national dispersion model for air pollution from elevated sources [KNMI-TR-57] 14 p2353 N85-24540
Field validation of 8-particle puff model [DE85-004073] 15 p2589 N85-25982
Analytical methods for determination of POHC (Principal Organic Hazardous Constituents) in combustion products [PB85-161578] 16 p2747 N85-28955
Emission inventory applications to regional acid deposition modeling [PB85-157386] 16 p2760 N85-27033
Interactive effects of acid rain and gaseous air pollutants on natural terrestrial vegetation [DE85-005255] 16 p2821 N85-27401
Acid rain: Effects on fish and wildlife [PB85-154672] 16 p2821 N85-27402
Review of national emission standards for mercury [PB85-153906] 16 p2822 N85-27406
Utilization of remote sensing data in the evaluation of air pollution characteristics in the south coast/Southeast Desert Air Basin [PB85-162063] 16 p2822 N85-27407
Symposium on Atmospheric Sciences in South Africa [CSIR-S-331] 16 p2829 N85-27442
Elemental analysis of aerosols in Transvaal urban and power-producing areas using time and size-resolved samples 16 p2829 N85-27443
A wind-bivane/microprocessor system for on-line prediction and display of pollutant distributions 16 p2830 N85-27449
Effect of traffic and meteorology on air pollution 16 p2830 N85-27452
Ground-based remote sensing of atmospheric pollution 16 p2832 N85-27462
Testing of materials and coatings for jet engine components under simulated operational conditions [86580073] 17 p2899 N85-27873
A study of gas solid reactions using coated piezoelectric detectors [AD-A153047] 17 p2920 N85-28001
Investigation of air pollution impact in Eastern Bavaria: Measurement results from August and September, 1984 [DFVLR-FB-85-03] 17 p2986 N85-29471
DFVLR measuring system for the determination of the spatial distribution of environmental parameters of the atmosphere by means of mobile instrumented platforms [DFVLR-FB-85-09] 17 p2989 N85-29472
Quality assurance for RESOLVE (Research on Operations-Limiting Visual Extinction). A viability study in the California desert [AD-A152383] 17 p2992 N85-28494
Impact of alcohol fuels on urban air pollution: Methanol photochemistry study [DE85-009539] 18 p3133 N85-29403
Environmental Research Division report: Atmospheric physics [DE85-009859] 18 p3133 N85-29404
Analysis and model/data comparisons of large-scale releases of nitrogen tetroxide [DE85-009989] 18 p3133 N85-29406
Elemental tracers of source regions of contaminants in precipitation [DE85-007366] 18 p3133 N85-29407
Equipment development for rapid detection of microorganisms in air and water [FOA-A-40046-B2] 18 p3134 N85-29410
Formation and fate of toxic chemicals in California's atmosphere [PB85-172609] 18 p3134 N85-29414
Hellmut Berg issue — meteorology [MITT-39] 18 p3147 N85-29483
Urban climate and air hygiene before, during, and after the lifework of Hellmut Berg. Overview of a branch of applied meteorology 18 p3147 N85-29487
Diffusion of trace gases in the ground level boundary layer 18 p3148 N85-29489
Application of climatological analysis to minimize air pollution impacts in California [PB85-172963] 18 p3149 N85-29502

Ambient air contamination: Characterization and detection techniques 18 p3157 N85-29546
Internal contamination in the space station 18 p3157 N85-29549
Control of acid deposition precursors through dry scrubbing
[DE85-010281] 19 p3235 N85-30056
Institute works on modeling thermonuclear plasma processes 19 p3296 N85-30435
Reduction of pollutant formation in combustion processes
[DE85-010161] 19 p3309 N85-30512
The Terrain-Responsive Atmospheric Code (TRAC) for plume growth and dispersion in complex terrain
[DE85-010541] 19 p3309 N85-30513
Technical guide for estimating fugitive dust impacts from coal handling operations, volume 2
[DE85-010939] 19 p3309 N85-30514
Technical guide for estimating fugitive dust impacts from coal handling operations. Volume 1: Project summary
[DE85-010948] 19 p3309 N85-30515
MELSAR: A mesoscale air quality model for complex terrain. Volume 2: Appendices
[DE85-010991] 19 p3310 N85-30519
Sources of copper air emissions
[PB85-191138] 19 p3310 N85-30523
Factor analysis of atmospheric pollution by polycyclic aromatic hydrocarbons
[HSE-TRANS-10968] 19 p3311 N85-30528
Analysis of aldehydes and ketones in the gas phase
[PB85-181865] 20 p3426 N85-31261
New corrosion protection concept for very high voltage line towers
[BLL-OA-TRANS-2601-(6196.300)] 20 p3429 N85-31270
Environmental concerns related to natural gas vehicles
[DE85-010246] 20 p3486 N85-31666
State of knowledge of environmental concerns related to natural-gas-fueled vehicles
[DE85-009746] 20 p3486 N85-31667
Atmospheric Tracer Workshop
[DE85-010573] 20 p3486 N85-31668
Organic air pollutants during manufacturing and handling of PVC floor tiles
[FOA-E-40018] 20 p3487 N85-31669
Historic emissions of sulfur and nitrogen oxides in the U.S. from 1900 to 1980. Volume 1: Results
[PB85-191195] 20 p3487 N85-31674
Historic emissions of sulfur and nitrogen oxides in the U.S. from 1900 to 1980. Volume 2: Data
[PB85-191203] 20 p3487 N85-31675
EPA (Environmental Protection Agency) research program guide, FY-1985, October 1, 1984 - September 30, 1985
[PB85-181881] 20 p3487 N85-31676
Modeling of chemical transformations of SO(x) and NO(x) in the polluted atmosphere: An overview of approaches and current status
[PB85-173169] 20 p3487 N85-31677
Manual for the computer program for the Gaussian plume model with percentile calculations
[KNMI-TR-80] 20 p3517 N85-31867
Hazardous air pollutants
[GPO-43-064] 21 p3613 N85-32458
VALMET: A valley air pollution model
[DE85-010820] 21 p3614 N85-32463
Eleventh International Conference on Atmospheric Aerosols, Condensation and Ice Nuclei, volume 2
[PB85-182418] 21 p3638 N85-32596
Observations of the atmospheric ice nucleus at northwest China 21 p3641 N85-32618
Photochemical aerosol formation in polluted atmosphere 21 p3644 N85-32642
Human activity and production rate of secondary nuclei 21 p3645 N85-32645
Characteristics of aerosol composition in a nonurban area, north China 21 p3646 N85-32651
Trace element concentrations in atmospheric aerosol over Hungary 21 p3646 N85-32652
Physical and chemical aerosol characteristics in extremely clean air masses at Cape Grim, Tasmania 21 p3646 N85-32655
Condensation nuclei and aerosol size distribution measurements in Arctic haze 21 p3647 N85-32658
Some considerations about the natural atmospheric radioactive aerosol 21 p3647 N85-32662
Influence on an industrial site on the characteristics of CCN supersaturation with air masses of different origin 21 p3650 N85-32683
Variations of particulate sulfur concentrations in a coastal atmospheric environment in connection with the change of air masses origin 21 p3652 N85-32692
on the transport of large condensation nuclei in the atmosphere at various altitudes over the territory of the USSR 21 p3653 N85-32698
Laser Elektronika-01 for air pollution control lidar 21 p3684 N85-32887
Acid rain in Europe
[COMMITTEE-PRINT-99-F] 22 p3810 N85-33601
The 1984 effluent and environmental monitoring report for the Bettis Atomic Power Laboratory
[DE85-011533] 22 p3810 N85-33602
ARAC status report, 1985
[DE85-012835] 22 p3810 N85-33603
Environmental summary for calendar year 1984
[DE85-012020] 22 p3810 N85-33604
Environmental monitoring at Lawrence Livermore National Laboratory: 1984 report
[DE85-011593] 22 p3811 N85-33606
The 1984 environmental monitoring report, Sandia National Laboratories, Albuquerque, New Mexico
[DE85-011175] 22 p3811 N85-33607
Control technology for radioactive emissions to the atmosphere at US Department of Energy facilities: The Los Alamos Meson Physics Facility
[DE85-011402] 22 p3811 N85-33609
Technology of off-gas treatment for liquid-fed ceramic melters
[DE85-012467] 22 p3812 N85-33610
The 1984 environmental monitoring program report for Idaho National Engineering Laboratory site
[DE85-011209] 22 p3812 N85-33611
Evaluation of the 2DFLOW and hybrid complex-terrain dispersion models with the 1980 ASCOT data base from the Geysers
[DE85-012960] 22 p3812 N85-33613
Atmospheric reaction products from hazardous air pollutant degradation
[PB85-185841] 22 p3813 N85-33620
Practical consequences of the assessment of different energy health risks
[DE85-004538] 22 p3825 N85-33696
Atmospheric modeling of organics for risk assessment: A Chemist's view
[DE85-009770] 23 p3909 N85-34217
Description of a test site for large-scale heavy gas dispersion and combustion experiments
[DE85-004967] 23 p3911 N85-34231
Forecasting future industrial SO2 and NC/sub x/ emissions, revised 23 p3947 N85-34461
User's guide to the MATHEW/ADPIC models
[DE85-012952] 23 p3966 N85-34587
Basic research on pulse-combustion phenomena
[PB85-200228] 24 p4077 N85-35265
Studies in photochemical smog chemistry. 1: Atmospheric chemistry of toulene. 2: Analysis of chemical reaction mechanisms for photochemical smog 24 p4113 N85-35497
Incorporating meteorological data into receptor analysis: RAPS (Regional Air Pollution Study) revisited
[PB85-188944] 24 p4114 N85-35503

AIR PURIFICATION
Ventilation flow: Submerged 18 p3156 N85-29545
Space shuttle revitalization system 18 p3157 N85-29548
Third US/USSR Symposium on Particulate Control
[PB85-190690] 19 p3310 N85-30522

AIR QUALITY
Space Shuttle Environmental Effects: The First 5 Flights
[NASA-CR-171812] 01 p0069 N85-10457
Demonstrating air quality improvements: A review of alternatives
[DE84-014274] 01 p0070 N85-10462
Review of the NAAQS (National Ambient Air Quality Standards) for carbon monoxide: Reassessment of scientific and technical information
[PB84-231315] 03 p0388 N85-12485
Analysis of Santa Barbara oxidant study
[P384-229277] 03 p0388 N85-12486
Airliner cabin air quality
[S-REPT-98-468] 03 p0402 N85-12560
Outline of a new emissions model for military and civilian aircraft facilities
[DE84-016455] 04 p0531 N85-13394
Proceedings of a Workshop on Atmospheric Research Needs for the Western United States
[DE84-015069] 04 p0534 N85-13412
Relationship between model complexity and data base quality for complex terrain tracer experiments
[DE84-015022] 04 p0539 N85-13429
Calms processor (CALMPRO) user's guide
[PB84-229467] 04 p0540 N85-13439
NAAQS (National Ambient Air Quality Standards) Exposure Model (NEM) applied to carbon monoxide
[PB84-242551] 06 p0834 N85-15310
Visibility monitoring in the southern California desert for the Department of Defense: Research on operations-limiting visual extinction, RESOLVE protocol
[AD-A146617] 06 p0835 N85-15315
Air quality assessment model validation in complex terrain
[AD-A147690] 08 p1180 N85-17434
Impact of aircraft emissions on air quality in the vicinity of airports. Volume 3: Air quality and emission modeling needs
[AD-A147951] 08 p1180 N85-17435
Impact of aircraft emissions on air quality in the vicinity of airports. Volume 4. Nitrogen dioxide and hydrocarbons
[AD-A148253] 08 p1180 N85-17436
Atmospheric photochemical modeling of turbine engine fuels. Phase 1: Experimental studies. Volume 2: Environmental chamber data tabulations
[AD-A147786] 08 p1185 N85-17470
The application of emissions trading to DoD installations
[AD-P004136] 09 p1346 N85-18472
Measurement and analysis of ambient carbon monoxide concentrations for project-level air quality impact studies
[PB85-104602/GAR] 09 p1350 N85-18492
Atmospheric science and power production
[DE84-005177] 09 p1354 N85-18521
Laser air pollution monitoring system planned for Moscow 10 p1500 N85-19485
Evaluation of recent SO/sub x/and NO/sub x/ emission inventories
[DE85-002649] 11 p1677 N85-20570
Air quality for ozone and other photochemical oxidants. External review draft, volume 1
[PB85-126035] 11 p1679 N85-20582
Air quality criteria for ozone and other photochemical oxidants. External review draft, volume 5
[PB85-126076-VOL-5] 11 p1679 N85-20583
Continued research in mesoscale air pollution simulation modeling. Volume 7. Mathematical modeling of urban aerosol dynamics
[PB85-137388] 11 p1679 N85-20584
Legislation to improve airline safety
[GPO-38-222] 12 p1773 N85-21132
Evaluation of complex terrain air quality simulation models
[PB85-119485] 12 p1886 N85-21635
Air quality criteria for ozone and other photochemical oxidants. External review draft, volume 2
[PB85-126043] 12 p1886 N85-21636
Air quality criteria for ozone and other photochemical oxidants, external review draft, volume 3
[PB85-126050] 12 p1886 N85-21637
Air quality criteria for ozone and other photochemical oxidants. External review draft, volume 4
[PB85-126068] 12 p1886 N85-21638
Papers from the Symposium on Emissions: The Value of Incentives and Guidelines for Control
[S-336] 15 p2590 N85-25967
Air quality benefit analysis for Los Angeles and San Francisco based on housing values and visibility
[PB85-166049] 16 p2822 N85-27409
Urban climate and air hygiene before, during, and after the lifework of Helmut Berg. Overview of a branch of applied meteorology 18 p3147 N85-29487
Environmental Research Laboratories (of the National Oceanic and Atmospheric Administration) programs and plans: FY 1984 programs and FY 1985 plans
[PB85-171494] 18 p3149 N85-29501
Qualitative and quantitative examination of the performance of regional air quality models representing different modeling approaches
[DE85-010508] 19 p3310 N85-30518
MELSAR: A mesoscale air quality model for complex terrain. Volume 2: Appendices
[DE85-010991] 19 p3310 N85-30519
Assessment of the role of nitrogen oxides in nonurban ozone formation
[PB85-173680] 19 p3311 N85-30524
Identification and quantification of nitropolynuclear aromatic hydrocarbons in ambient and indoor air particulate samples
[PB85-176790] 19 p3311 N85-30525
Annual environmental monitoring report, January-December 1984
[DE85-011689] 20 p3486 N85-31665
Environmental concerns related to natural gas vehicles
[DE85-010246] 20 p3486 N85-31666
State of knowledge of environmental concerns related to natural-gas-fueled vehicles
[DE85-009746] 20 p3486 N85-31667
Soil extraction kit
[AD-D011736] 22 p3742 N85-33190
Environmental surveillance at Los Alamos during 1984
[DE85-011886] 22 p3811 N85-33605
The 1984 environmental monitoring report, Sandia National Laboratories, Albuquerque, New Mexico
[DE85-011175] 22 p3811 N85-33607

MELSAR: A mesoscale air quality model for complex terrain. Volume 1: Overview, technical description and user's guide
[DE85-010943] 22 p3811 N85-33608
Evaluation of the 2DFLOW and hybrid complex-terrain dispersion models with the 1980 ASCOT data base from the Geysers
[DE85-012960] 22 p3812 N85-33613
Modeling of auto exhaust smog chamber data for EKMA development
[PB85-186492] 22 p3813 N85-33619
Review of US NOx abatement technology
[PB85-193522] 24 p4114 N85-35501

AIR SAMPLING
Aerosol sampling bias from differential electrostatic charge and particle size 02 p0224 N85-11467
Aircraft measurements of tracer gas during the 1983 cross Appalachian tracer experiment (CAPTEX)
[DE84-015282] 04 p0531 N85-13395
Integrated global background monitoring network
[DE84-016996] 04 p0532 N85-13398
Portable instrument for the detection and identification of air pollutants
[DE84-014767] 05 p0672 N85-14316
Carbon monoxide study, Anchorage, Alaska, November 22, 1982 to February 11, 1983
[PB84-236595] 05 p0673 N85-14321
Direct measurements of nitrous acid, nitrogen dioxide and formaldehyde in auto exhaust by differential optical absorption spectroscopy
[PB84-229269] 06 p0767 N85-14905
Attempted measurement of gaseous H-2O-2 in the ambient atmosphere
[DE85-001937] 06 p0834 N85-15306
The CSIRO (Australia) atmospheric carbon dioxide monitoring program: Surface data
[CSIRO-TP-6] 07 p0996 N85-16324
Methodology for the collection and analysis of trace metals in atmospheric precipitation
[CM-67] 09 p1350 N85-18491
Measurement and analysis of ambient carbon monoxide concentrations for project-level air quality impact studies
[PB85-104602/GAR] 09 p1350 N85-18492
Comparative evaluation of GC/MS (Gas Chromatography/Mass Spectrometry) data analysis processing
[PB85-125684] 11 p1596 N85-20037
Solid sorbent air sampler
[NASA-CASE-MSC-20653-1] 11 p1636 N85-20301
The concentration of sulfate in broken cloud layers
[DE85-000228] 11 p1678 N85-20574
Evaluation of complex terrain air quality simulation models
[PB85-119485] 12 p1886 N85-21835
Atlantic Coast Unique Regional Atmospheric Tracer Experiment (ACURATE)
[PB85-128460] 12 p1886 N85-21839
Acid rain: Towards automated monitoring
16 p2829 N85-27444
SCPP (Sierra Cooperative Pilot Project) data collection and analysis. Volume 1: Executive summary
[PB85-156065] 16 p2837 N85-27494
Theoretical basis for the determination of the concentration of radon decay products in air from the activity of a particulate air sample
[IRI-190-83-07] 17 p3035 N85-28774
Program RNTHR/2: An HP-41 C program for the calculation of RaA, RaB, and RaC concentrations in air based on three measurements of an air-dust sample
[IRI-190-83-10] 18 p3134 N85-29412
Density and confinement effects on mixing characteristics of an axisymmetrical CO(2) jet
[AD-A154468] 19 p3267 N85-30258
Optical waveguide sensor for methane gas
[AD-D011691] 19 p3273 N85-30284
Mathematical model of global processes in the biosphere 19 p3295 N85-30431
Quasi non-intrusive sampling and analysis of gases associated with the boundary layer on the tethered satellite and similar supersonic and hypersonic research vehicles
[NASA-CR-176075] 20 p3407 N85-31140
On the design of a global detection system for airborne radioactivity
[CM-68] 20 p3487 N85-31670
Particulate contamination control in clean rooms by particle fallout (PFO) measurements
[ESA-PSS-01-204-ISSUE-1] 20 p3487 N85-31673
Ames Laboratory measurements of alkali levels in the Curtiss-Wright PFBC gas stream
[DE85-011357] 22 p3745 N85-33214
Control technology for radioactive emissions to the atmosphere at US Department of Energy facilities: The Los Alamos Meson Physics Facility
[DE85-011402] 22 p3811 N85-33609
The 1984 environmental monitoring program report for Idaho National Engineering Laboratory site
[DE85-011209] 22 p3812 N85-33611
Development of a microorifice uniform deposit cascade impactor
[DE85-006765] 22 p3812 N85-33614

AIR SEA ICE INTERACTIONS
Ice dynamics
[AD-A147376] 07 p0988 N85-16278
Southern ocean sea-ice morphology and kinematics
08 p1144 N85-17217
MIZEX. A program for mesoscale Air-Ice-Ocean interaction experiments in arctic marginal ice zones. 4: Initial results and analysis from MIZEX 83
[AD-A148255] 08 p1173 N85-17399
Passive microwave remote sensing for sea ice research
[NASA-CR-175570] 12 p1874 N85-21758
Carbonate chemistry of the Weddell Sea
[DOE/EV-110611/4] 12 p1898 N85-21916
Large space antenna technology applied to radar-imaging, rain-rate measurements, and ocean wind sensing 14 p2230 N85-23320
Possible sea ice impacts on oceanic deep convection
15 p2603 N85-26041
Results of the MIZEX preliminary campaign: 29 June to 19 July 1983 — Marginal Ice Zone Experiment (MIZEX), satellite observation
[CNES-84/142/T/CT/DRT/TIT/RL]
20 p3478 N85-31609

AIR SEA INTERACTIONS
U AIR WATER INTERACTIONS

AIR SICKNESS
U MOTION SICKNESS

AIR TO AIR MISSILES
NT SIDEWINDER MISSILES

AIR TO AIR REFUELING
Technical evaluation report on the FDP Symposium on Flight Test Techniques
[AGARD-AR-208] 12 p1777 N85-21157

AIR TO SURFACE MISSILES
Cost-effective missile guidance through distributed architecture and standard processes
16 p2698 N85-26662
Next generation gunship
[AD-A156361] 24 p4085 N85-35193

AIR TRAFFIC
MERIT: A man/computer data management and enhancement system for upper air nowcasting/forecasting in the United States — Minimum Energy Routes using Interactive Techniques (MERIT)
01 p0083 N85-10558
Activities report in air traffic control
03 p0317 N85-12047
TCAS 2 logic performance during phase one operational evaluation
[DOT/FAA/PM-84/20] 05 p0595 N85-13793
Activities report of the aerospace industry in West Germany
[ISSN-0176-5086] 05 p0734 N85-14718
FAA (Federal Aviation Administration) statistical handbook of aviation, calendar year 1983
[AD-A148171] 08 p1067 N85-16760
Airport activity statistics of certificated route air carriers
[AD-A148472] 08 p1081 N85-16846
Air traffic management concepts for the UK in the 1990's: A review of recent RSRE work
[AD-A147850] 08 p1082 N85-16853
Ultralight aircraft technology and public safety
[GPO-38-948] 12 p1773 N85-21131
Disturbance to the population due to flight operations at landing fields. Questionnaire on community reaction to non-commercial and sporting aviation
[NASA-TM-76531] 14 p2353 N85-24537
National airspace review. Implementation plan. Revised
[AD-A151412] 15 p2468 N85-25238
Air traffic: Instruments, airports, companies, post, cargo and passengers 18 p3060 N85-28932
Traffic alert and collision avoidance system: Operational simulation
[FAA-PM-85-10] 19 p3216 N85-29941
FAA air traffic activity, fiscal year 1984
[AD-A154318] 19 p3216 N85-29942
Status of air traffic control system
[S-HRG-98-1197] 20 p3391 N85-31036
System safety study of minimum TCAS 2 for instrument weather conditions
[FAA-PM-85-12] 22 p3728 N85-33113
The contribution made by flight mechanics to civil aviation 24 p4061 N85-35169

AIR TRAFFIC CONTROL
NT AUTOMATED EN ROUTE ATC
NT RADAR APPROACH CONTROL
National airspace review 02 p0136 N85-10926
Enhanced TCAS 2/CDTI traffic Sensor digital simulation model and program description
[NASA-CR-172445] 02 p0136 N85-10927
System engineering and integration contract for implementation of the National Airspace System Plan. Volume 2: Section 5.0
[AD-A145710] 02 p0137 N85-10929
A proof-of-principle getaway special free-flying satellite demonstration 02 p0155 N85-11051
New airport ground traffic control system planned
03 p0310 N85-12008
Activities report in air traffic control
03 p0317 N85-12047
System engineering and integration contract for implementation of the National Airspace System plan, volume 1, sections 1.0-4.0, 6.0
[AD-A145763] 03 p0317 N85-12048
Aircraft navigation and landing technology: Status of implementation
[GPO-38-615] 04 p0454 N85-12883
Closely spaced independent parallel runway simulation
[DOT/FAA/CT-84/45] 04 p0457 N85-12902
The construction of auditive tests of attention and spatial orientation and their factorial structure
[DFVLR-FB-84-21] 05 p0699 N85-14485
Predictions of cockpit simulator experimental outcome using system models 05 p0702 N85-14504
National airspace review: Airport radar service area operational confirmation report
[DOT/FAA/AT-84/2] 07 p0901 N85-15707
A bird strike handbook for base-level managers
[AD-A147928] 07 p0948 N85-16008
Designer on Aeroflot automated COMMO system development 08 p1067 N85-16765
National airspace review enhancement plan, revision 3
[AD-A150743] 08 p1082 N85-16852
Air traffic management concepts for the UK in the 1990's: A review of recent RSRE work
[AD-A147850] 08 p1082 N85-16853
A cockpit-display concept for executing a multiple glide-slope approach for wake-vortex avoidance
[NASA-TP-2386] 08 p1085 N85-16869
Test of dispersal of turbojet aircraft departure tracks at washington National Airport (1983-84), volume 1 report
[AD-A148111] 08 p1218 N85-17689
Research at automated ATC Scientific-Experimental Center 09 p1278 N85-18037
Improvements in Kazan airport equipment, facilities
09 p1278 N85-18039
Improvements under way at Gorkiy airport
09 p1278 N85-18040
Design and realization of a multiradar tracking system for air traffic control
[ENST-84E010] 09 p1279 N85-18044
Denver ARTCC (Air Route Traffic Control Center) evaluation of PROFS (Program for Regional Observing and Forecasting Services) mesoscale weather products
[PB85-120301/GAR] 09 p1279 N85-18045
Prototype concept design for US Army type 3A Air Traffic Control Tower (ATCT)
[AD-A148840] 09 p1284 N85-18070
National airspace system: Operational requirements
[AD-A149349] 10 p1422 N85-18973
Collision avoidance for Naval training aircraft
[FAA-PM-84-4] 12 p1774 N85-21136
The evolution of methods of air traffic control
[AD-A149606] 12 p1774 N85-21137
Operations concept for the advanced automation system man-machine interface
[AD-A149797] 12 p1774 N85-21139
A radome for air traffic control SSR radar systems
[AD-P004373] 12 p1827 N85-21467
Civil avionics flight testing with the RAE(B) BAC1-11
13 p1967 N85-22354
A flight management algorithm and guidance for fuel-conservative descents in a time-based metered air traffic environment: Development and flight test results
13 p1967 N85-22356
Planned office and facility consolidations: To improve system effectiveness and efficiency, FY 1985-87
[AD-A150441] 13 p1970 N85-22376
Analysis of estimation algorithms for CDTI and CAS applications
[NASA-CR-172444] 13 p1973 N85-22387
FAA aviation forecasts: Fiscal years 1985-1996
[AD-A151050] 14 p2216 N85-23747
Safety recommendation(s), A-84-82 through -84
[REPT-3957] 14 p2217 N85-23748
An analysis of the impacts of the Airport Radar Service Area (ARSA)
[AD-A150954] 14 p2217 N85-23749
Development concerns for satellite-based air traffic control surveillance systems 14 p2230 N85-23816

Multiple resources and display formatting: The implications of task integration in a simulated air traffic control task
[AD-A150713] 14 p2292 N85-24205
Administration chief on air traffic control improvements
15 p2460 N85-25193
Calculation and display of stack departure times for aircraft inbound to Heathrow Airport
[AD-A151991] 15 p2469 N85-25241
Wind modelling for increased aircraft operational efficiency 16 p2697 N85-26652
National Airspace System Plan: Facilities, equipment and associated development 16 p2704 N85-26692
Probabilistic computer model of optimal runway turnoffs
[NASA-CR-172549] 16 p2715 N85-26760
National airspace review, change 1
[AD-A152369] 17 p2894 N85-27844
Developments in the area of air traffic control systems and the relation with meteorology
[NLR-MP-84029-U] 17 p2895 N85-27848
A general area air traffic controller simulation using colour graphics
[AD-A153634] 18 p3060 N85-28933
FAA air traffic activity, fiscal year 1984
[AD-A154318] 19 p3216 N85-29942
Definition and layout of a traffic generator for an air traffic control simulation
[ESA-TT-886] 20 p3391 N85-31034
Status of air traffic control system
[S-HRG-98-1197] 20 p3391 N85-31036
A feasibility study for the use of electronic flight strips in ATC controller workstations
[DFVLR-FB-85-08] 20 p3392 N85-31039
Simulation studies of time-control procedures for the advanced air traffic control system
[NASA-TP-2493] 21 p3553 N85-32101
Status of the air traffic control system
[GPO-40-343] 21 p3554 N85-32107
System safety study of minimum TCAS 2 for instrument weather conditions
[FAA-PM-85-12] 22 p3726 N85-33113
Performance of rolling ball and isometric joystick on a 2-D target alignment task
[RSRE-MEMO-3695] 22 p3826 N85-33699
Effect of interference on the performance of a minimum TCAS 2
[FAA-PM-84-33] 23 p3895 N85-34131
Introduction to European air traffic control
[AD-A156328] 24 p4062 N85-35176
FAA requirements for model to support capacity, delay, noise and energy programs
[AD-A155815] 24 p4063 N85-35179
Analogies of control mechanisms in flight guidance and medicine 24 p4129 N85-35597

AIR TRAFFIC CONTROLLERS (PERSONNEL)
The Reports of Aeromedical Laboratory, volume 25, no. 1/2
[ISSN-0023-2858] 01 p0090 N85-10605
A study of fatigue of shiftworkers in air traffic control and weather service groups in JASDF
01 p0090 N85-10610
Blood pressure levels of active pilots compared with those of air traffic controllers
[AD-A146545] 06 p0646 N85-15373
Training high performance skills: Fallacies and guidelines
[AD-A148574] 08 p1198 N85-17545
Operations concept for the advanced automation system man-machine interface
[AD-A149797] 12 p1774 N85-21139
Administration chief on air traffic control improvements
15 p2460 N85-25193
Calculation and display of stack departure times for aircraft inbound to Heathrow Airport
[AD-A151991] 15 p2469 N85-25241
Construction of a job-oriented test for the selection of air traffic controllers
[DFVLR-FB-84-51] 17 p3002 N85-28558
Investigation of biochemical and psychological parameters of air traffic controllers in prestart state before beginning to work 19 p3325 N85-30599
A feasibility study for the use of electronic flight strips in ATC controller workstations
[DFVLR-FB-85-08] 20 p3392 N85-31039
Status of the air traffic control system
[GPO-40-343] 21 p3554 N85-32107
Performance of rolling ball and isometric joystick on a 2-D target alignment task
[RSRE-MEMO-3695] 22 p3826 N85-33699
U.S. Civil airmen statistics for calendar year 1984
[AD-A156326] 24 p4059 N85-35153

AIR TRANSPORTATION
Activities report in air traffic control
03 p0317 N85-12047
German domestic scheduled air transport in the year 2000
[ESA-TT-828] 05 p0595 N85-13792
FAA (Federal Aviation Administration) statistical handbook of aviation, calendar year 1983
[AD-A148171] 08 p1067 N85-16780
Utilization of Increased Airlift Capability (UIAC) study
[AD-A148669] 08 p1081 N85-16847
Tolerance endpoint for evaluating the effects of heat stress in dogs
[AD-A148104] 08 p1192 N85-17511
Issues in air transport
[PB85-121374/GAR] 09 p1277 N85-18030
Semiannual report to Congress on the effectiveness of the civil aviation security program
[AD-A149522] 10 p1421 N85-18967
Airport system development
[PB85-127793] 11 p1587 N85-19993
Assessing the behavior and performance of teams in organizations: The case of air transport crews
[AD-A150359] 13 p2143 N85-23302
USSR report: Transportation
[JPRS-UTR-84-008] 14 p2208 N85-23694
Bugayev on civil aviation ministry's 1983 achievements 14 p2208 N85-23696
FAA aviation forecasts: Fiscal years 1985-1996
[AD-A151050] 14 p2216 N85-23747
USSR report: Transportation
[JPRS-UTR-85-008] 15 p2460 N85-25189
Civil air code international flights section explained
15 p2460 N85-25194
Aviation system delays
[S-HRG-98-1241] 21 p3553 N85-32102
The research programme of the Institute for Aerospace Medicine 24 p4129 N85-35596

AIR WATER INTERACTIONS
NT AIR SEA ICE INTERACTIONS
Large-scale ocean-atmosphere interactions in the mid-latitudes and equatorial regions: A literature review
[CSIR-T/SEA-8302] 01 p0073 N85-10482
Excitation of quasi-static magnetic fields with axial structure 02 p0259 N85-11696
Dynamics of coupled ice-ocean system in the marginal ice zone: Study of the mesoscale processes and of constitutive equations for sea ice
[NASA-CR-174171] 04 p0542 N85-13448
Biogeochemical cycles: Interactions in global metabolism 05 p0652 N85-14184
Global biogeochemical cycles: Studies of interaction and change, some views on the strategy of approach
05 p0652 N85-14185
Some aspects of understanding changes in the global carbon cycle 05 p0652 N85-14186
Interactions of the marine phosphorus and carbon cycles 05 p0653 N85-14190
Air-sea heat exchange, an element of the water cycle
05 p0653 N85-14195
An investigation of the marine boundary layer during cold air outbreak 05 p0680 N85-14368
Structure and growth of the marine boundary layer
05 p0680 N85-14369
Numerical modeling of the atmosphere
05 p0680 N85-14370
Air-sea interaction during cold air outbreaks
05 p0685 N85-14401
Cage regional energy budgets from the GLAS ATH order model 05 p0685 N85-14402
Diagnostics of rainfall anomalies in the nordeste during the global weather experiment 05 p0685 N85-14405
Energy active areas of ocean
06 p0820 N85-15204
Studies of the ocean surface and the coupling between the sea and the atmosphere
[AD-A146546] 06 p0841 N85-15339
Spectral model for subtidal variability in the Chesapeake Bay
[PB84-226679] 06 p0842 N85-15345
Razrezy program research in the tropical Atlantic
07 p0981 N85-16229
Frazil ice formation
[AD-A147425] 07 p0988 N85-16279
Meteorological aspects of the 1982-83 El Nino/southern oscillation episode 07 p1001 N85-16356
The ocean and the dynamics of the tropical atmosphere; its possible predicability 07 p1002 N85-16366
A one dimensional dynamical model of ocean/atmosphere interactions
09 p1358 N85-18545
Analysis of flow within the coastal boundary layer off Long Island, New York
[DE85-001384] 09 p1359 N85-18550
The effect of stochastic surface heat fluxes on the climatology of the seasonal thermocline
[AD-A149957] 12 p1889 N85-21857
Intensification of tropical instabilities
[AD-A149985] 12 p1896 N85-21899
Oceanic role in terrestrial climate
[DE85-004422] 12 p1896 N85-21904
Modeling of mechanism of positive feedback between mean Earth surface temperature and atmospheric carbon dioxide in geologic time scale 13 p2106 N85-23122
Numerical investigation of evolution of energy spectrum of slightly nonlinear Rossby waves
13 p2106 N85-23124
Contribution to theory of ocean-atmosphere gas exchange 13 p2106 N85-23134
Sea-ice motion in response to geostrophic winds
14 p2323 N85-24357
A large-scale air sea interaction project over the Pacific basin 14 p2326 N85-24373
Atmosphere ice-ocean interactions in the Antarctic (IAGO) 14 p2326 N85-24375
The French Ocean Climate in Equatorial Atlantic (FOCAL) Drifter Program, 1983-1984
14 p2329 N85-24399
The Tropical Ocean and Global Atmosphere program (TOGA) 14 p2330 N85-24411
Applications of ARGOS measurements in equatorial Pacific Ocean-atmosphere interaction studies
14 p2331 N85-24414
An overview of NDBC drifting buoy development programs — NOAA Data Buoy Center (DBC)
14 p2332 N85-24422
Influence of interaction between ocean and atmosphere on intensity of moving tropical cyclone
14 p2333 N85-24431
Influence of bubbles formed upon breaking of waves on gas exchange between ocean and atmosphere
14 p2335 N85-24439
Structure of cold film in water-air boundary layer
14 p2335 N85-24443
Parameterization of apparent and latent heat fluxes above water surface in calm weather under natural conditions 14 p2337 N85-24454
A study of the turbulent layer in the water at an air-water interface 14 p2378 N85-24679
Sensitivity analysis of a coupled atmospheric-oceanic boundary layer model
[AD-A150760] 14 p2382 N85-24690
Analysis of the inflow and air-sea interactions in hurricane Frederic 15 p2595 N85-25990
North Atlantic Deep Water Formation
[NASA-CP-2367] 15 p2601 N85-26028
Changes in the high-latitude ocean as possible causes of atmosphere CO2 variations 15 p2602 N85-26038
Climatic impact of a change in North Atlantic Deep Water formation 15 p2603 N85-26045
Deepwater wind wave growth with fetch and duration
[AD-A151604] 15 p2604 N85-26051
China's integrated circuit production
16 p2606 N85-27302
Tropical Oceans-Global Atmosphere (TOGA) experiment planning for the Brazilian participation in TOGA global climate program
[INPE-3499-PRE/735] 16 p2834 N85-27477
Simulation of a synchronously coupled atmosphere-ocean prediction model
[AD-A152020] 16 p2835 N85-27482
NASA Oceanic Processes Program annual review
[NASA-TM-87565] 16 p2838 N85-27503
Time-dependence of CO2-induced climate change
[DE85-007568] 17 p2997 N85-28525
On the global distribution of three-dimensional Eliassen-Palm fluxes by stationary waves
18 p3145 N85-29469
A GCM study of the atmospheric response to tropical SST anomalies 18 p3146 N85-29477
Global model of transport of pollutants in atmosphere
19 p3297 N85-30439
Northeast Brazil droughts and Atlantic SST anomalies
[INPE-3536-PRE/754] 19 p3316 N85-30553
Atmospheric chlorofluromethanes as tracers of ocean circulation and mixing: Measurement and calibration techniques and studies in the Greenland and Norwegian Seas 19 p3319 N85-30573
Experiments using atmospheric forcing from a FGGE analysis to drive an upper ocean model
[INPE-3503-PRE/738] 19 p3319 N85-30576
A study of the turbulent layer in the water at an air-water interface
[AD-A154117] 19 p3319 N85-30578
Some remarks on the constitutive equations of stratified gas-liquid flow
[EME-137] 20 p3456 N85-31466
Geodynamics Branch research program
[NASA-TM-86223] 20 p3489 N85-31668
Southern oscillation/El Nino excitation of the Earth's Chandler wobble 20 p3490 N85-31695
Tropical Ocean and Global Atmosphere (TOGA) heat exchange project: A summary report
[NASA-CR-176038] 20 p3498 N85-31738

Mesoscale features and atmospheric refraction conditions of the Arctic marginal ice zone
[AD-A155139] 21 p3636 N85-32584
Bacterial ice nuclei of marine origin: Some recent observations 21 p3640 N85-32611
Properties of aerosol particles detected by satellites in coastal regions 21 p3641 N85-32622
Numerical simulations of the response of intense ocean currents to atmospheric forcing
[AD-A155161] 21 p3655 N85-32704
Simulation of the coupled atmospheric and oceanic boundary layer model during MILDEX
[AD-A155166] 21 p3655 N85-32705
Study of molecular diffusivity influence on mass transfer rate at a water-atmosphere interface
22 p3747 N85-33222
Air-sea interaction with SSM/I and altimeter
[NASA-CR-176105] 22 p3818 N85-33650
Meteorological data from the OPTOMA (Ocean Prediction Through Observations, Modeling and Analysis) program OPTOMA 2, leg D2. 30 Jun. - 10 Jul. 1984
[AD-A156134] 24 p4123 N85-35560
Mean cloudiness over the global tropics from satellite observations
[AD-A156188] 24 p4123 N85-35561

AIRBORNE EQUIPMENT

NT AIRBORNE/SPACEBORNE COMPUTERS
Effectiveness of agricultural aviation
04 p0544 N85-13480
USAF approach to airborne structural data recording: Airborne Data Acquisition Multifunction System (ADAMS)
07 p0897 N85-15683
Realization and testing of an experimental color display system for general aviation helicopters and aircraft
[BMFT-FB-W-84-042] 09 p1086 N85-16672
Optical studies of nitrogen oxides in the stratosphere
08 p1183 N85-17455
A far infrared Echelle spectrometer for the Kuiper Airborne Observatory 08 p1249 N85-17886
A 150 micron heterodyne spectrometer for airborne astronomy 08 p1249 N85-17887
Tunable heterodyne receiver from 100 micron to 1,000 micron for airborne observations
08 p1249 N85-17888
Instrumentation for submillimeter polarimetry
08 p1250 N85-17889
Design and analysis of airborne scanning optical systems 11 p1623 N85-20218
Airborne remote sensing CCD imaging system
11 p1623 N85-20220
MAP-related activities in the United States
11 p1655 N85-20427
Atmospheric research aircraft — conductivity/charge measurements
[ONERA-RS-87/7154/PY] 11 p1682 N85-20596
A subaperture approach to the calculation of flashlobes introduced by airborne radomes
[AD-P004355] 12 p1825 N85-21449
Intra-eruption geologic map from an x-band radar image during the May 18, 1980 eruption of Mount St. Helens, Washington 13 p2199 N85-23639
Radar observations of fissure-fed basaltic lava flows, Craters of the Moon, Idaho 13 p2199 N85-23640
DFVLR measuring system for the determination of the spatial distribution of environmental parameters of the atmosphere by means of mobile instrumented platforms
[DFVLR-FB-85-09] 17 p2969 N85-28472
Convective storm downdraft outflows detected by NASA/MSFC's Airborne 10.6 micron pulsed Doppler Lidar System
[NASA-CR-3898] 17 p2995 N85-28511
Dynamic rectification of airborne scanner digital image recordings 18 p3124 N85-29344
Altitude variations of cosmic-ray soft and hard components observed by airborne detectors
[SH-6.1-5] 23 p4045 N85-35079
The principles of wind measurement with the help of aircraft 24 p4123 N85-35558

AIRBORNE RADAR APPROACH

Development and flight test of a helicopter, X-band, portable precision landing system concept
[NASA-TM-86710] 16 p2710 N85-26721
Investigation of imaging and flight guidance concepts for rotorcraft zero visibility approach and landing
[NASA-CR-166571] 17 p2994 N85-27843

AIRBORNE/SPACEBORNE COMPUTERS

Analytical redundancy management mechanization and flight data analysis for the F-8 digital fly-by-wire aircraft flight control sensors
[NASA-CR-170396] 06 p0757 N85-14844
NOAA (National Oceanic and Atmospheric Administration) Aircraft Satellite Data Link (ASDL)
[PB84-243773] 07 p0942 N85-15976
Investigation of semiautomatic aircraft control processes en..loying time redundancy in on-board digital trajectory control computers 07 p0954 N85-16048
Data and results of a laboratory investigation of microprocessor upset caused by simulated lightning-induced analog transients
07 p0999 N85-16345
Documentation and separate test program development is most important for test/maintenance
08 p1085 N85-16745
Experience in using on-aircraft software for testing integrated systems 08 p1085 N85-16747
Automatic error detection and recovery techniques in onboard intelligent units for space and avionic application 08 p1086 N85-16756
The design and development of an integrated core system for battlefield helicopters
08 p1074 N85-16811
Development and implementation of the verification process for the shuttle avionics system
08 p1091 N85-16896
Satellite description 09 p1412 N85-18900
Feasibility of self-structured current accessed bubble devices in spacecraft recording systems
[NASA-CR-172554] 13 p1998 N85-22525
Spaceborne automatic data processing
14 p2397 N85-24769
A cost-efficient control procedure for the benefit of all airspace users 16 p2697 N85-26851
The interactive generation of specifications for an onboard software series (GISELE)
17 p2904 N85-27906
Certifying complex digital systems on civil aviation aircraft 17 p2904 N85-27907
The Department of Defense statement on the Science and Technology Program by Colonel Donald I. Carter, USAF Acting Deputy Under Secretary of Defense for Research and Advanced Technology before the Subcommittee on Research and Development of the Committee on Armed Services of the United States House of Representatives, 99th Congress, first session
[AD-A152467] 17 p3046 N85-28850
Space station automation study-satellite servicing. Volume 1: Executive summary
[NASA-CR-171512] 19 p3226 N85-29999
Development and evaluation of a Fault-Tolerant Multiprocessor (FTMP) computer. Volume 2: FTMP software
[NASA-CR-166072] 19 p3341 N85-30706
Development and evaluation of a Fault-Tolerant Multiprocessor (FTMP) computer. Volume 3: FTMP test and evaluation
[NASA-CR-166073] 19 p3341 N85-30707
A micro/PDP-11 system for 406 MHz COSPAS/SARSAT processing 20 p3403 N85-31117
Informatics Division 20 p3449 N85-31416
Microprocessor AirborneData Acquisition and Replay (MADAR) system
[AD-A151728] 20 p3514 N85-31843
Comparative study on data system architecturec --- spacecraft data processing
[ESA-CR(P)-2015] 21 p3675 N85-32828
Effects of space radiation on advanced semiconductor devices. Part 3: Further cosmic ray simulation studies of single event upsets and latch-up in CMOS memories
[AERE-G-3366-PT-3] 22 p3848 N85-33833
Development and operation of a measuring data acquisition system for use in light airplanes
24 p4123 N85-35556

AIRBUS

U EUROPEAN AIRBUS

AIRCRAFT

Three degree of freedom steady state point performance program: Updated version 1
[CSIR-NIAST-83/48] 01 p0001 N85-10005
Auditory information systems in military aircraft: Current configurations versus the state of the art
[AD-A145469] 02 p0275 N85-11794
Logistics support costs for the B-1B aircraft can be reduced
[AD-A145846] 03 p0309 N85-11906
The beginnings of airborne astronomy, 1920 - 1930: An historical narrative 08 p1244 N85-17849
On the frontier: Flight research at Dryden 1946-1981
[NASA-SP-4303] 09 p1263 N85-17934
Advanced life analysis methods. Volume 1: Cracking data survey and NDI (nondestructive inspection) assessment for attachment lugs
[AD-A150419] 13 p2103 N85-23106
Low-profile fastener
[AD-D011667] 19 p3260 N85-30343
Removable cleanable antireflection shield
[AD-D011735] 22 p3844 N85-33810

AIRCRAFT ACCIDENT INVESTIGATION

Review of aircraft accident data: US General Aviation
[PB84-230960] 01 p0005 N85-10027
Aircraft accident report. Central Airlines flight 27, Hughes Charter Air, Gates Learjet model 25 (N51CA) Newark International Airport, Newark, New Jersey, March 30, 1983
[PB84-910411] 02 p0136 N85-10024
Aircraft accident report, Western Helicopters, Inc., Bell UH-1B, N67701, Valencia, California, July 23, 1982
[PB84-910414] 05 p0594 N85-13789
Aircraft accident report Air Canada, Lockheed L-1011, C-FTNJ, near Charleston, South Carolina, November 24, 1983
[PB84-910413] 05 p0594 N85-13790
Annual review of aircraft accident data: US general aviation, calendar year, 1981
[PB84-230960] 06 p0750 N85-14805
Proceedings of the 6th Human Factors Workshop on Aviation
[AD-A150043] 12 p1909 N85-21982
Safety recommendation(s), A-84-126 through -133
[REPT-3998C/41] 15 p2466 N85-25221
Safety recommendation(s), A-84-123 and -124
[REPT-3804B/83] 15 p2466 N85-25222
Safety recommendation(s), A-84-96
[REPT-3963A/217] 15 p2466 N85-25223
Safety recommendation(s), A-84-76 through -78
[REPT-3751E] 15 p2466 N85-25224
Aircraft accident report: United Airlines Flight 663, Boeing 727-222, N7647U, Denver, Colorado, May 31, 1984
[PB85-910405] 16 p2703 N85-26686
General Aviation Crashworthiness Project. Phase 2: Impact severity and potential injury prevention in general aviation accidents
[PB85-917002] 19 p3215 N85-29938

AIRCRAFT ACCIDENTS

NT BIRD-AIRCRAFT COLLISIONS
Review of aircraft accident data: US General Aviation
[PB84-230960] 01 p0005 N85-10027
Proceedings of the Aviation Accident Investigation Symposium
[PB84-917004] 01 p0005 N85-10029
Aircraft accident report. Central Airlines flight 27, Hughes Charter Air, Gates Learjet model 25 (N51CA) Newark International Airport, Newark, New Jersey, March 30, 1983
[PB84-910411] 02 p0136 N85-10024
Aircraft accident report: Flying Tigers, Inc., Flight 2468, McDonell Douglas DC8-63, N797FT, Chambers Field, Naval Air Station, Norfolk, Virginia, October 25, 1983
[PB84-910408] 02 p0136 N85-10025
Aircraft accident report, Scandinavian Airlines System, Flight 901, McDonnell Douglas DC-10-30, John F. Kennedy International Airport, Jamaica, New York, February 28, 1984
[PB84-910415] 05 p0594 N85-13788
Crew communication as a factor in aviation accidents
05 p0710 N85-14555
Communication on the flight deck
05 p0711 N85-14557
Annual review of aircraft accident data: US general aviation, calendar year, 1981
[PB84-230960] 06 p0750 N85-14805
Human factors in cockpit automation
06 p0752 N85-14819
Establishment of posture and working movements of pilot in air crash enquiries 07 p1010 N85-16417
FAA (Federal Aviation Administration) statistical handbook of aviation, calendar year 1983
[AD-A148171] 08 p1067 N85-16760
SPH-4 US Army flight helmet performance, 1972 - 1983
[AD-A148674] 08 p1201 N85-17562
Safety awareness, pilot education, and incident reporting programs 09 p1276 N85-18020
The aviation safety reporting system
09 p1276 N85-18021
Annual review of aircraft accident data: US air carrier operations calendar year 1981
[NTSB/ARC-85/01] 12 p1774 N85-21134
TCAS II: Design and validation of the high-traffic-density surveillance subsystem
[DOT/FAA/PM-84/5] 13 p1970 N85-22375
Safety recommendation(s), A-84-93 through -95
[REPT-3963/33] 14 p2216 N85-23746
Safety recommendation(s), A-84-96
[REPT-3963A/217] 15 p2466 N85-25223
Aircraft accident report: United Airlines Flight 663, Boeing 727-222, N7647U, Denver, Colorado, May 31, 1984
[PB85-910405] 16 p2703 N85-26686
Frangibility of obstacles at airports
[NLR-MP-84002-U] 17 p2981 N85-28431
DYNA3D, INGRID, and TAURUS: An integrated, interactive software system for crashworthiness engineering
[DE85-010928] 21 p3677 N85-32946

AIRCRAFT ANTENNAS
Measurements of polarization characteristics of radiation field of on-board aircraft antennas
03 p0346 N85-12230
On aircraft antennas and basic scattering studies
[AD-A146017] 03 p0355 N85-12262
Microstrip antenna for multichannel radiometer
06 p0791 N85-15058
Proceedings of the Symposium on Electromagnetic Windows (17th) held at Georgia Inst. of Technology, Engineering Experiment Station, Atlanta, Georgia on 25-27 July 1984. Part 2
[AD-A149125] 12 p1824 N85-21444
Comparison of spherical wave ray tracing and exact boundary value solutions for spherical radomes
[AD-P004353] 12 p1824 N85-21447
Coordinate determination errors in measuring characteristics of radiation field of airborne antennas
13 p2068 N85-22919
Simulation and analysis of airborne antenna radiation patterns
20 p3439 N85-31342
AIRCRAFT APPROACH SPACING
National airspace review enhancement plan, revision 3
[AD-A150743] 06 p1062 N85-16852
AIRCRAFT BASES
U MILITARY AIR FACILITIES
AIRCRAFT BRAKES
NT LEADING EDGE SLATS
NT TRAILING EDGE FLAPS
NT WING FLAPS
AIRCRAFT CABINS
U AIRCRAFT COMPARTMENTS
AIRCRAFT CARRIERS
An update of the functional requirements of the Naval Aviation Logistics Command Management Information System (NALCOMIS)
[AD-A146565] 06 p0871 N85-15532
An interactive environment for the development of an expert system in ZOG
[AD-A149054] 12 p1915 N85-22025
Visual and part-task manipulations for teaching simulated carrier landings
[AD-A153622] 18 p3154 N85-29529
AIRCRAFT COMMUNICATION
Ministry wants better commo facilities for agroaviation
03 p0310 N85-12003
Designer on Aeroflot automated COMMO system development
06 p1067 N85-16765
Tactical HF communication for military helicopters using the NVIS mode
08 p1074 N85-16807
National airspace system: Operational requirements
[AD-A149349] 10 p1422 N85-18973
EHF air-to-air communications
10 p1469 N85-19273
Spectrum resource assessment of the Aeronautical Mobile Service between 400 MHz and 17.7 GHz
[PB85-125995] 11 p1626 N85-20241
The effects of atmospheric turbulence on an air-to-air optical communication link
[AD-A151840] 15 p2543 N85-25700
Survey of narrow band vocoder technology
[AD-A151919] 16 p2773 N85-27114
AIRCRAFT COMPARTMENTS
Aircraft cabin pressurization control system tester
[AD-D011225] 01 p0013 N85-10061
The pyrolysis toxic gas analysis of aircraft interior materials
[AD-A146285] 03 p0328 N85-12115
Airliner cabin air quality
[S-REPT-98-468] 03 p0402 N85-12580
Modeling of aircraft cabin fires
[NBS-GCR-84-473] 04 p0454 N85-12880
An improved source model for aircraft interior noise studies
[NASA-CR-172517] 08 p1217 N85-17668
Modeling of aircraft cabin fires
[PB85-137685/GAR] 09 p1277 N85-18031
Pathophysiological study of poisoning due to thermal degradation of materials — aircraft cabins
[CERMA-84-15] 11 p1692 N85-20640
Legislation to improve airline safety
[GPO-38-222] 12 p1773 N85-21132
Suppression and control of Class C cargo compartment fires
[FAA-CT-84-21] 12 p1773 N85-21133
Simultaneous cabin and ambient ozone measurements on two Boeing 747 airplanes. Volume 3: October 1978 - July 1979
[NASA-TM-86683] 12 p1892 N85-21672
Thermal response of aircraft cabin ceiling materials during a post-crash, external fuel-spill, fire scenario
[PB85-145647] 14 p2220 N85-23764
Transmission of gear noise to aircraft interiors prediction methods
14 p2223 N85-23788
A study of interior noise levels, noise sources and transmission paths in light aircraft
[NASA-CR-172152] 19 p3350 N85-30766
Effects of propeller rotation direction on airplane interior noise levels
[NASA-TP-2444] 19 p3350 N85-30767
Design of sidewall treatment of cabin noise control of a twin engine turboprop aircraft
[NASA-CR-172245] 19 p3351 N85-30771
The role of aircraft panel materials in cabin fires and their properties
[FAA-CT-84-30] 21 p3553 N85-32104
Aviation safety (aircraft passenger survivability and cabin safety)
[GPO-39-847] 23 p3895 N85-34130
AIRCRAFT CONFIGURATIONS
Preliminary airworthiness evaluation of the Rutan Aircraft Factory (RAF), Inc. LONG-EZ airplane with external sight
[AD-A145381] 02 p0136 N85-10937
Second sailplane project: The RP-2
04 p0468 N85-12977
An in-flight investigation of a twin fuselage configuration in approach and landing
[NASA-CR-172366] 05 p0596 N85-13801
Design of an airfoil leading edge slat using an inverse aerodynamic calculation method
08 p1069 N85-16777
Integrated digital/electric aircraft concepts study
[NASA-CR-3841] 08 p1083 N85-16861
A first-order Green's function approach to supersonic oscillatory flow: A mixed analytic and numeric treatment
[NASA-CR-172207] 09 p1273 N85-18002
Over the wing propeller
[NASA-CASE-LAR-13134-1] 11 p1584 N85-19980
Study for prediction of rotor/wake/fuselage interference, part 1
[NASA-CR-177340-VOL-1] 13 p1965 N85-22346
Study for prediction of rotor/wake/fuselage interference. Part 2: Program users guide
[NASA-CR-177340-VOL-2] 13 p1966 N85-22347
Boundary layer transition control for takeoff and landing configurations
14 p2211 N85-23714
Experiences with transition fixation in the high-speed regime at NLR
14 p2211 N85-23715
Recent developments in the dynamics of advanced rotor systems
[NASA-TM-86669] 14 p2317 N85-24320
Computation of unsteady transonic flows about two-dimensional and three-dimensional AGARD standard configurations
15 p2459 N85-25183
The application of transonic unsteady methods for calculation of flutter airloads
15 p2460 N85-25186
Tensile and fracture toughness properties of Mirage III spars
[AR-003-019] 15 p2578 N85-25869
A first-order time-domain Green's function approach to supersonic unsteady flow
[NASA-CR-172208] 19 p3214 N85-29930
Calculation of transonic flows around an aircraft configuration with motorized nacelle
[SNIAS-851-111-106] 20 p3387 N85-31008
Quest for performance: The evolution of modern aircraft
[NASA-SP-468] 21 p3551 N85-32089
Flight testing the fixed-wing configuration of the Rotor Systems Research Aircraft (RSRA)
[NASA-TM-86762] 23 p3896 N85-34135
AIRCRAFT CONSTRUCTION
U AIRCRAFT STRUCTURES
AIRCRAFT CONSTRUCTION MATERIALS
NT AIRFRAME MATERIALS
Near-threshold fatigue crack growth and crack closure in 17-4 precipitation hardening steel and 2043-T3 aluminum alloy
[FFA-TN-1984-16] 02 p0210 N85-11385
The pyrolysis toxic gas analysis of aircraft interior materials
[AD-A146285] 03 p0328 N85-12115
Tensile and crack propagation tests on aluminum alloys of the 2000 and 7000 series in laminated plate and forged products
[M2-678300] 03 p0373 N85-12383
Low power laminar aircraft structures
04 p0451 N85-12857
Modern structural materials. Present situation and evolution prospects — aircraft materials
[SNIAS-842-551-101] 04 p0455 N85-12886
Characterizing delamination resistance of toughened resin composites
04 p0464 N85-12943
Electroforming of nickel
[SNIAS-841-501-101] 04 p0484 N85-13085
Preliminary evaluation of an improved flammability test method for aircraft materials
[FAA-CT-84-22] 06 p1060 N85-16840
Composite structure repair, addendum
[AGARD-R-716-ADD] 08 p1120 N85-17057
Repair of composites
08 p1120 N85-17058
FRG firms jump into market for auto, aircraft ceramics
09 p1309 N85-18225
Fatigue-creep interaction in + or - 45 deg carbon-resin composites — aircraft construction materials
[ONERA-RT/40/7086/M] 11 p1594 N85-20027
High-strength composite materials for aircraft, body armor
11 p1599 N85-20057
Forced corrosion tests of construction components of passenger aircraft fuselages
11 p1600 N85-20062
Composite structural materials
[NASA-CR-175515] 12 p1796 N85-21268
Corrosion of aircraft Al and Al-Zn ion plated steel fasteners
13 p2021 N85-22666
An overview of the MIL-HDBK-5 program
[AD-A147788] 14 p2254 N85-23970
Development of a field repair technique for mini-sandwich Kevlar/epoxy aircraft skin
[AD-A151369] 15 p2503 N85-25439
Mechanical properties of cast Martensitic high-strength multicomponent titanium alloys
15 p2514 N85-25514
Pechiney strategy includes development of new materials
15 p2531 N85-25607
Aluminum-lithium alloys: The answer of the aluminum industry to the threat of advanced fiber-reinforced materials
[VTH-LR-406] 17 p2932 N85-28102
Research on structures and materials — aircraft structures
[B8580080] 17 p2981 N85-28432
DFVLR research in aluminum-lithium alloys
18 p3067 N85-29105
Study of the influence of metallurgical factors on fatigue and fracture of aerospace structural materials
[AD-A153913] 18 p3122 N85-29328
Mechanical properties of aligned short carbon fiber reinforced PES and PI laminates
[ESA-TT-898] 20 p3422 N85-31240
Influence of recrystallization and solution on the tenacity of the 7010 and 7475 alloys. Oligocyclic fatigue of the 7010 alloy
[ONERA-RT-19/5069-M] 20 p3432 N85-31289
R and D activities of the Materials Science Division
20 p3539 N85-32024
R and D activities of the Structural Sciences Division
20 p3539 N85-32026
New materials needs in aeronautics
[SNIAS-851-502-101] 22 p3729 N85-33120
AIRCRAFT CONTROL
NT HELICOPTER CONTROL
Aircraft accident report: Flying Tigers, Inc., Flight 2468, McDonell Douglas DC8-63, N797FT, Chambers Field, Naval Air Station, Norfolk, Virginia, October 25, 1983
[PB84-910408] 02 p0136 N85-10925
High-temperature optically activated GaAs power switching for aircraft digital electronic control
[NASA-CR-174711] 04 p0457 N85-12901
Accounting for error stochasticity in terminal homing of aircraft
04 p0469 N85-13115
A unified method for evaluating real-time computer controllers: A case study — aircraft control
[NASA-CR-174166] 04 p0547 N85-13478
Integrated Application of Active Controls (IAAC) technology to an advanced subsonic transport project. ACT/Control/Guidance System study, volume 1
[NASA-CR-165963-VOL-1] 06 p0754 N85-14837
Integrated Application of Active Controls (IAAC) technology to an advanced subsonic transport project. ACT/Control/Guidance System study. Volume 2: Appendices
[NASA-CR-165963-VOL-2] 06 p0754 N85-14838
Aircraft thrust control scheme for terrain following system
[AD-D011367] 07 p0901 N85-15711
Investigation of semiautomatic aircraft control processes employing time redundancy in on-board digital trajectory control computers
07 p0954 N85-16048
Integrated digital/electric aircraft concepts study
[NASA-CR-3841] 08 p1083 N85-16861
Time series analysis of closed-loop pilot vehicle dynamics
08 p1087 N85-16876
Use of airplanes for loft training
09 p1276 N85-18019
Preliminary performance of a vertical-attitude takeoff and landing, supersonic cruise aircraft concept having thrust vectoring integrated into the flight control system
[NASA-CR-172530] 10 p1423 N85-18977
Pilot workload, performance and aircraft control automation
10 p1534 N85-19670
Acta Aeronautica et Astronautic Sinica (selected articles)
[AD-A148830] 11 p1575 N85-19922

Leading edge flap system for aircraft control augmentation
[NASA-CASE-LAR-12787-2] 11 p1585 N85-19985
Robustness of continuous multivariable flight controls
[ONERA-RT-12/7224-SY] 11 p1586 N85-19987
Robustness of continuous multivariable flight controls
[ONERA-RT-11/7224-SY] 11 p1586 N85-19988
In-flight investigation of the effects of time delay in control system on flying qualities in landing approach
[DFVLR-FB-84-35] 11 p1586 N85-19989
Optimal symmetric flight studies
[NASA-CR-172508] 12 p1780 N85-21176
Aeronautical Engineering: A continuing bibliography with indexes, supplement 185
[NASA-SP-7037(185)] 13 p1965 N85-22342
Reference systems for the evaluation of dead-reckoning navigation equipment 13 p1967 N85-22358
Relative control effectiveness technique with application to airplane control coordination
[NASA-TP-2416] 14 p2218 N85-23753
Multivariable control law design for the AFTI/F-16 with a failed control surface
[AD-A151908] 15 p2474 N85-25271
Cost Effective and Affordable Guidance and Control Systems
[AGARD-CP-360] 16 p2695 N85-26638
A method of estimating aircraft attitude from fly by wire flight control system data 16 p2697 N85-26653
Application of linear optimal control theory to the design of the elevator control system of the DHC-2 Beaver experimental aircraft
[VTH-LR-411] 16 p2711 N85-26729
Controller requirements for uncoupled aircraft motion, volume 1
[AD-A153173] 17 p2900 N85-27878
In-flight investigation of the influence of pitch damping and pitch control effectiveness on landing approach flying qualities of statically unstable transport aircraft
[DFVLR-FB-84-12] 17 p2900 N85-27880
Proposals for the determination of necessary elevator handling characteristics of sailplanes in high speed range
[DFVLR-FB-84-52] 17 p2900 N85-27882
Active Control Technology (ACT): Past, present and future 17 p2901 N85-27884
The state-of-the-art and future of flight control systems 17 p2901 N85-27885
Aspects of application of ACT systems for pilot workload alleviation 17 p2901 N85-27887
Some flight test results with redundant digital flight control systems 17 p2902 N85-27892
An update of experience on the fly by wire Jaguar equipped with a full-time digital flight control system 17 p2902 N85-27893
Demonstration of relaxed static stability on a commercial transport 17 p2903 N85-27896
The aerodynamics of control 17 p2903 N85-27901
The STOL and maneuver technology program integrated control system development 17 p2905 N85-27910
A survey of the turbulence in the marine surface layer for the operation of low-Reynolds number aircraft
[AD-A154133] 19 p3316 N85-30658
Learning and self adaptation applied to the simulation of a human pilot
[ONERA-RT-24/5122-SY] 20 p3511 N85-31828
R and D activities of the Systems Engineering Division 20 p3540 N85-32027
Seat experiments for the full-scale transport aircraft controlled impact demonstration
[AD-A155024] 21 p3553 N85-32106
Flight control system for a computer controlled aircraft with limited sensors
[AD-A155107] 21 p3555 N85-32115
Development of control laws for a flight test maneuver autopilot for an F-15 aircraft
[NASA-TM-86736] 22 p3730 N85-33122
Energy management of three-dimensional minimum-time intercept
[NASA-CR-176174] 24 p4084 N85-35186
Control variables in vertical wind determination using simple flight-mechanical equations 24 p4121 N85-35546

AIRCRAFT DESIGN

NT HELICOPTER DESIGN

Optimum design of nonplanar wings: Minimum induced drag for a given lift and wing root bending moment
[NAL-TR-797] 01 p0002 N85-10011
The Influence of Large Scale Computing on Aircraft Structural Design
[AGARD-R-706] 01 p0007 N85-10040
Observations from varying the lift and drag inputs to a noise prediction method for supersonic helical tip speed propellers
[NASA-TM-83757] 01 p0115 N85-10788
ACEE program rationale and implementation
[NASA-TM-84549] 02 p0133 N85-10908
Energy efficient engine component development and integration program
[NASA-CR-168496] 02 p0146 N85-10989
Energy efficient engine component development and integration program
[NASA-CR-170034] 02 p0146 N85-10990
Energy efficient engine. Volume 2. Appendix A: Component development and integration program
[NASA-CR-173085] 02 p0146 N85-10991
Effect of stress concentrations in composite structures
[NASA-CR-173976] 02 p0170 N85-11140
Low power laminar aircraft structures 04 p0451 N85-12857
Natural laminar flow airfoil design considerations for winglets on low-speed airplanes
[NASA-CR-3853] 04 p0452 N85-12863
Physics on aircraft wakes
[NASA-CR-174105] 04 p0453 N85-12871
Solvent resistant thermoplastic composite matrices 04 p0466 N85-12960
Increase in the economy of design and process planning by integrated and graphic data processing, phase 2 — aircraft design
[BMFT-FB-W-84-028] 05 p0716 N85-14589
Aerodynamic characteristics of some lifting reentry concepts applicable to transatmospheric vehicle design studies
[NASA-TM-86331] 06 p0747 N85-14787
New fighter aircraft reported — Jian-8 aircraft 06 p0747 N85-14790
F-7 supersonic day fighter viewed — Jian-7 aircraft 06 p0747 N85-14791
A-5 supersonic attack aircraft described — Qiang-5 aircraft 06 p0747 N85-14792
Details of export A-5 close-support aircraft given — Qiang-5 aircraft 06 p0748 N85-14793
Civil law enforcement missions 06 p0751 N85-14812
HH-65A Dolphin digital integrated avionics 06 p0751 N85-14815
Integrated cockpit design for the Army helicopter improvement program 06 p0751 N85-14816
United States Air force aircraft modification process: A system dynamics analysis
[AD-A146054] 07 p0893 N85-15659
Design study of technology requirements for high performance single-propeller-driven business airplanes
[NASA-CR-3863] 07 p0898 N85-15692
Missions and vehicle concepts for modern, propelled, lighter-than-air vehicles
[NASA-TM-86672] 08 p1066 N85-16757
Computer sizing of fighter aircraft
[NASA-TM-86351] 08 p1067 N85-16759
International aviation (selected articles)
[AD-A148704] 08 p1067 N85-16762
Designer on civil aircraft design trends in USSR 08 p1068 N85-16768
Recent progress of development and understanding of high lift systems 08 p1068 N85-16772
Design of an airfoil leading edge slat using an inverse aerodynamic calculation method 08 p1069 N85-16777
Aerodynamic issues in the design of high-lift systems for transport aircraft 08 p1069 N85-16780
Design studies of thick laminar flow airfoils for low speed flight employing turbulent boundary layer suction over the rear part 08 p1070 N85-16786
Technology developments for laminar boundary layer control on subsonic transport aircraft 08 p1071 N85-16787
Integrated digital/electric aircraft concepts study
[NASA-CR-3841] 08 p1083 N85-16861
Study of winglets applied to biplanes
[NASA-TM-86350] 08 p1083 N85-16862
A description of a logistically ideal aircraft
[AD-A148425] 08 p1084 N85-16866
The aircraft engine of the future
[PNR-90226] 08 p1087 N85-16875
Description of MBB computerized design techniques for A320 08 p1141 N85-17194
The development of a dynamic model of a generalised combat aircraft with forward wings for the identification of stability and control characteristics
[CAR-84-33] 09 p1280 N85-18050
Profile design for wings and propellers
[NASA-TM-77785] 10 p1419 N85-18953
Some fighter aircraft trends
[NASA-TM-86352] 10 p1420 N85-18954
Deployment sequence mode selection system for aircraft ejection seat
[AD-D011484] 10 p1422 N85-18968
The design of sport and touring aircraft
[NASA-TM-77783] 10 p1423 N85-18975
Preliminary performance of a vertical-attitude takeoff and landing, supersonic cruise aircraft concept having thrust vectoring integrated into the flight control system
[NASA-CR-172530] 10 p1423 N85-18977
Details of export A-5 close-support aircraft given 10 p1424 N85-18983
Study of advanced fuel system concepts for commercial aircraft and engines
[NASA-CR-174752] 10 p1456 N85-19176
Noise constraints effecting optimal propeller designs
[NASA-TM-86967] 11 p1575 N85-19923
Parametric study of a canard-configured transport using conceptual design optimization
[NASA-TP-2400] 11 p1584 N85-19979
Current development, applications of airships in USSR 12 p1769 N85-21109
Towards a renewal of the propeller in aeronautics
[NASA-TM-77803] 12 p1779 N85-21169
Translating rudder pedal system
[AD-D011510] 12 p1780 N85-21172
Some aspects of the design of a fly-by-wire flying control system for a supersonic V/STOL fighter aircraft
[COLL-AERON-8413] 12 p1780 N85-21175
Lubrication and performance of high-speed rolling-element bearings
[NASA-TM-86958] 12 p1859 N85-21658
Introduction: The clinical and biomedical evaluation for trauma and fatalities associated with aircrew ejection and crash 12 p1906 N85-21970
Aeronautical Engineering: A continuing bibliography with indexes, supplement 185
[NASA-SP-7037(185)] 13 p1965 N85-22342
Dynamic wind-tunnel testing of active controls by the NASA Langley Research Center 13 p1966 N85-22353
Study for the optimization of a transport aircraft wing for maximum fuel efficiency. Volume 1: Methodology, criteria, and realistic model definition and results
[NASA-CR-172551] 13 p1971 N85-22378
China report: Science and technology
[JPRS-CST-84-008] 13 p1972 N85-22384
Uses of composite materials 13 p2027 N85-22698
Redesign of fuselage compartments by method of special contours 13 p2042 N85-22784
Problems of the application of wind tunnel results to aerodynamic performance of large aircraft 14 p2211 N85-23713
The design of high-performance gliders
[NASA-TM-77772] 14 p2217 N85-23750
Design considerations for high-altitude, long-endurance, microwave-powered aircraft
[NASA-TM-86403] 14 p2218 N85-23751
Transmission error measurements in gearbox development 14 p2224 N85-23794
Do new aircraft need new technologies and certification rules? 14 p2224 N85-23795
Missions and vehicle concepts for modern, propelled, lighter-than-air vehicles
[NASA-TM-87461] 15 p2457 N85-25170
Special course on V/STOL aerodynamics: An assessment of European jet lift aircraft
[AGARD-R-710-ADDENDUM] 15 p2460 N85-25188
USSR report: Transportation
[JPRS-UTR-84-014] 15 p2467 N85-25229
Flying objects
[CH-634516-A5] 15 p2469 N85-25242
Aircraft
[CH-642598-A5] 15 p2470 N85-25246
Simulator study of the stall departure characteristics of a light general aviation airplane with and without a wing-leading-edge modification
[NASA-TM-86309] 15 p2470 N85-25250
The ONERA establishment at Cannes in the service of aeronautical research
[ESA-TT-875] 15 p2475 N85-25276
MBB cost-reduction plan for Airbus construction described 15 p2532 N85-25616
YAV-8B Harrier 15 p2688 N85-26605
Computer software for aerodynamic design of aircraft developed within the National Aerospace Laboratory 16 p2691 N85-26613
Numerical analyses in aerodynamic design of aero-engine fan 16 p2692 N85-26618
Computational aerodynamics in designing aircraft 16 p2693 N85-26622
Numerical example of three-dimensional flying object in shockless transonic flow 16 p2693 N85-26623
Computational aerodynamics for aircraft wing design 16 p2693 N85-26627
Comparison of computational results of a few representative three-dimensional transonic potential flow analysis programs 16 p2693 N85-26628
Three-dimensional wing boundary layer analysis program BLAY and its application 16 p2694 N85-26632

ACT flight research experience
16 p2713 N85-26741
The introduction of new cockpit technology: A human factors study
[NASA-TM-86659] 16 p2843 N85-27528
Research and development. Technical and scientific reports 1984 16 p2873 N85-27724
Utilization of an automated riveting system in aircraft construction
[MBB-UT-11/84-O] 16 p2875 N85-27736
Methods for design aerodynamics of modern transport aircraft
[DFVLR-FB-85-05] 17 p2893 N85-27836
Test flight of IL-76TD long-range transport variant
17 p2894 N85-27842
Technical services at NLR
[B8561888] 17 p3049 N85-28871
Future of V/STOL aircraft systems: A survey of opinions
[NASA-TM-86689] 18 p3061 N85-28937
MBB expands CADAM system for a 320 program
18 p3067 N85-29099
Aeronautical Engineering: A continuing bibliography with indexes (supplement 188)
[NASA-SP-7037(188)] 19 p3211 N85-29910
Impact dynamics research on composite transport structures
[NASA-TM-86391] 19 p3284 N85-30367
Avionics and civil aircraft systems: The present and the future
[SNIAS-851-111-104] 20 p3392 N85-31038
Design of the nacelle for the A-320 aircraft
[SNIAS-851-111-111] 20 p3393 N85-31046
Design of a basic airfoil for a slightly swept wing. Part 1: Theoretical transonic airfoil design
[ESA-TT-892] 20 p3394 N85-31054
Corrosion in civil aircraft structures
[SNIAS-851-111-105] 20 p3432 N85-31291
Preliminary sizing and performance of aircraft
[NASA-TM-86357] 21 p3554 N85-32111
Design of an expert-system flight status monitor
[NASA-TM-86739] 21 p3669 N85-32784
Energy efficient transport technology: Program summary and bibliography
[NASA-RP-1135] 22 p3729 N85-33116
Qualification needs for advanced integrated aircraft
[NASA-TM-86731] 22 p3729 N85-33119
New materials needs in aeronautics
[SNIAS-851-502-101] 22 p3729 N85-33120
Maintenance and the military environment
22 p3750 N85-33243
A guide to USAF helicopter instrument flight procedures
[AD-A156102] 24 p4063 N85-35182
Design and testing of an energy-absorbing crewseat for the F/FB-111 aircraft. Volume 2: Data from seat testing
[NASA-CR-3917] 24 p4064 N85-35184
Proceedings of the 14th Army Science Conference. Volume 2: Principal authors I through O
[AD-A149201] 24 p4144 N85-35690
A research program to reduce the interior noise in general aviation aircraft, index and summary
[NASA-CR-176176] 24 p4145 N85-35695

AIRCRAFT DETECTION
National airspace system: Operational requirements
[AD-A149349] 10 p1422 N85-18973

AIRCRAFT ENERGY EFFICIENCY PROGRAM
U ACEE PROGRAM

AIRCRAFT ENGINES
NT J-52 ENGINE
NT TF-34 ENGINE
NT VARIABLE CYCLE ENGINES
A study of bird ingestions into large high bypass ratio turbine aircraft engines
[DOE/FAA/CT-84/13] 01 p0005 N85-10028
Turbine Engine Hot Section Technology (HOST)
[NASA-TM-83022] 02 p0140 N85-10951
Equivalent damage: A critical assessment
02 p0140 N85-10952
Benchmark notch test for life prediction
02 p0140 N85-10953
Nonlinear structural and life analyses of a turbine blade 02 p0141 N85-10954
Nonlinear structural and life analyses of a combustor liner 02 p0141 N85-10955
Pre-HOST high temperature crack propagation
02 p0141 N85-10956
Structural analysis 02 p0143 N85-10969
Burner liner thermal/structural load modelling
02 p0143 N85-10970
Component-specific modeling
02 p0143 N85-10971
The 3-D inelastic analysis methods for hot section components: Brief description 02 p0143 N85-10972
Constitutive model development for isotropic materials
02 p0144 N85-10975
Airfoil deposition model 02 p0144 N85-10979
Effects of surface chemistry on hot corrosion life: Overview 02 p0145 N85-10980
Combustion hot section technology
02 p0145 N85-10981
Combustion system for radiation investigations
02 p0145 N85-10986
Energy efficient engine component development and integration program
[NASA-CR-170034] 02 p0146 N85-10990
Energy efficient engine. Low pressure turbine test hardware detailed design report
[NASA-CR-167956] 02 p0147 N85-10994
Energy efficient engine high pressure turbine test hardware detailed design report
[NASA-CR-167955] 02 p0147 N85-10995
Energy efficient engine. High pressure compressor detail design report
[NASA-CR-165558] 02 p0147 N85-10998
Air force engine repair - Oklahoma City Air Logistics Center, Propulsion Division
[AD-P003999] 03 p0307 N85-11980
Performance deterioration of cascades exposed to solid particles 03 p0319 N85-12057
Basic study of bladed disk structural response
[AD-A146226] 03 p0319 N85-12061
Propulsion — jet aircraft engines
[PNR-90208] 03 p0320 N85-12062
Cyclic endurance testing of the RB211-22B cast HP turbine blade — high pressure (HP)
[PNR-90210] 03 p0320 N85-12063
The applications of fibre optics in gas turbine engine instrumentation
[PNR-90209] 03 p0420 N85-12687
Static jet noise test results of four 0.35 scale-model QCGAT mixer nozzles
[NASA-TM-86871] 04 p0558 N85-13551
Random vibrations of aircraft engine blades
06 p0777 N85-14967
Predicted performance benefits of an adaptive digital engine control system of an F-15 airplane
[NASA-TM-85916] 07 p0905 N85-15729
Monitoring engine thermal stresses
07 p0906 N85-15735
Accelerated Mission Endurance Testing (AMET)
07 p0906 N85-15736
Design and test requirements for development of today's engines 07 p0906 N85-15737
Contamination and distortion of steady flow field induced by discrete frequency in aircraft gas turbines
[AD-A147092] 07 p0958 N85-16073
The aircraft engine of the future
[PNR-90226] 08 p1087 N85-16875
Rolls-Royce experience with thermal barrier coatings — in aircraft engines
[PNR-90222] 08 p1135 N85-17152
Flow measurement device
[AD-D011432] 08 p1168 N85-17369
An improved source model for aircraft interior noise studies
[NASA-CR-172517] 08 p1217 N85-17668
Design description of a microprocessor based Engine Monitoring and Control unit (EMAC) for small turboshaft
[NASA-TM-86860] 09 p1263 N85-17935
Research and development for semi-spherical inflow control device
[NAL-TR-833] 09 p1281 N85-18056
Improvement of gas turbine engine performance by water injection into turbine cooling air
09 p1307 N85-18209
On limits of applicability of linear models to dynamics of gas channels in aircraft engines
09 p1308 N85-18219
FRG firms jump into market for auto, aircraft ceramics
09 p1309 N85-18225
NASA Lewis Research Center/University Graduate Research Program on Engine Structures
[NASA-TM-86916] 09 p1333 N85-18375
Preliminary performance of a vertical-attitude takeoff and landing, supersonic cruise aircraft concept having thrust vectoring integrated into the flight control system
[NASA-CR-172530] 10 p1423 N85-18977
Analytical fuel property effects: Small combustors, phase 2
[NASA-CR-174848] 10 p1456 N85-19175
Study of advanced fuel system concepts for commercial aircraft and engines
[NASA-CR-174752] 10 p1456 N85-19176
Study of advanced fuel system concepts for commercial aircraft
[NASA-CR-174751] 11 p1584 N85-19978
Over the wing propeller
[NASA-CASE-LAR-13134-1] 11 p1584 N85-19980
Assuring structural integrity in Army systems
[NASA-CR-175492] 11 p1651 N85-20398
A theory of post-stall transients in multistage axial compression systems
[NASA-CR-3678] 12 p1771 N85-21117
Description of a technique to measure spray distribution in an air stream
[AD-A149780] 12 p1771 N85-21122
Stratified charge rotary aircraft engine technology enablement program
[NASA-CR-174812] 12 p1778 N85-21163
Tribological systems as applied to aircraft engines
[NASA-TM-86985] 12 p1858 N85-21657
Effects of inlet distortion on a static pressure probe mounted on the engine hub in an F-15 airplane
[NASA-TP-2411] 13 p1974 N85-22394
Hydrodynamic simulation of transient processes in injection system of aircraft engines during pump unswirling 13 p2050 N85-22829
Effect of water injection into air for turbine cooling on economy of operation of gas turbine engine with afterburning 13 p2050 N85-22830
T700 cutter life improvement program
[AD-A150450] 13 p2099 N85-23089
Welcome to the Saclay Propeller Testing Center
[NASA-TM-77648] 14 p2225 N85-23799
High frequency estimation of 2-dimensional cavity scattering
[AD-A151697] 15 p2542 N85-25696
Advanced smoke meter development survey and analysis
[NASA-CR-168287] 15 p2560 N85-25792
Nondestructive tests of ceramic components for aircraft turbines 16 p2709 N85-26718
Test devices for aeronautical research and technology
[NASA-TM-77651] 17 p2905 N85-27914
An investigation into the soot production processes in a gas turbine engine
[AD-A152710] 17 p2919 N85-27992
Compressor and turbine models - numerical stability and other aspects
[AD-A153811] 18 p3063 N85-28948
Hold-time effects in elevated temperature fatigue crack propagation
[AD-A154146] 19 p3286 N85-30376
Component-specific modeling
[NASA-CR-174925] 21 p3556 N85-32119
Elevated temperature crack growth
[NASA-CR-174857] 22 p3799 N85-33540
Performance improvements from surfacing in aero engine components
[PNR-90257] 23 p3897 N85-34142
Directionally solidified gas turbine alloys
[PNR-90264] 23 p3917 N85-34279
Towards the year 2000: Developments in inspection and product assurance to be anticipated during the next 15 years — aircraft engines
[PNR-90258] 23 p3940 N85-34421
Cost effective single crystals: The Rolls Royce approach — gas turbine components
[PNR-90262] 23 p3985 N85-34717

AIRCRAFT EQUIPMENT
NT AIRCRAFT HYDRAULIC SYSTEMS
NT AIRCRAFT LIGHTS
NT AIRCRAFT TIRES
NT BOMBING EQUIPMENT
NT EJECTION SEATS
Moving object detection system using infrared scanning
[AD-D011222] 01 p0120 N85-10822
Flares and photoflash items
[AD-A145442] 02 p0187 N85-11253
Electronics/avionics depots in the United States Air Force Warner Robins Air Logistics Center
[AD-P004000] 03 p0307 N85-11981
Wear and corrosion of components under stress and subjected to motion
[AD-A145781] 03 p0372 N85-12372
The effect of aircraft generated electromagnetic interference (EMI) on future avionics systems: A compendium
[AD-A146380] 06 p0799 N85-15101
Voice command weapons launching system
[AD-D011378] 07 p0937 N85-15940
cost and benefits optimization model for fault-tolerant aircraft electronic systems
[NASA-CR-166043] 07 p0946 N85-15993
Military vital sign monitor
[AD-A147257] 07 p1016 N85-16452
Managing recoverable aircraft components in the PPB and related processes: Executive summary
[AD-A146808] 07 p1050 N85-16667
Design for Tactical Avionics Maintainability
[AGARD-CP-361] 08 p1063 N85-16731
Objectives in studying the maintainability of aircraft systems 08 p1063 N85-16732

Joint service design for testability program
08 p1063 N85-16733
Study and realisation of a 3rd level maintenance center based on ATE systems utilization
08 p1063 N85-16735
A practical example of reducing life cycle costs and increased availability 08 p1063 N85-16736
Director on institute's civil aviation projects
08 p1067 N85-16764
Impact tests of automatic lap belt configurations
[AD-A148034] 08 p1081 N85-16844
NASA three-laser airborne differential absorption lidar system electronics
[NASA-CR-174293] 08 p1166 N85-17353
Improvements under way at Gorkiy airport
09 p1278 N85-18040
FRG firms jump into market for auto, aircraft ceramics
09 p1309 N85-18225
The susceptibility of aeronautical navigational aids to interference from adjacent-band broadcast transmissions
[BBC-RD-1984/12] 09 p1311 N85-18234
Laser clock
[AD-D011513] 12 p1855 N85-21634
Advanced life analysis methods. Volume 3: Experimental evaluation of crack growth analysis methods for attachment lugs
[AD-A151058] 14 p2317 N85-24319
US Army Aviation Engineering Flight Activity (USAAEFA) report bibliography update 1983 - 1984
[AD-A151381] 15 p2457 N85-25168
Managing recoverable aircraft components in the PPB (Planning, Programming and Budgeting) and related processes. Technical volume
[AD-A152014] 15 p2457 N85-25169
A description of the process of elaborating man-machine dialog in an aircraft equipped with cathode tubes: Rules and specifications of piloted simulation methods
16 p2698 N85-26658
Terrain following without use of forward looking sensors 16 p2698 N85-26659
Improving inflight negative Gz restraint for aircrewmen
[AD-A151909] 16 p2703 N85-26668
Earth Resources: A continuing bibliography with indexes, issue 45
[NASA-SP-7041(45)] 18 p3123 N85-29336
Aeronautical Engineering: A continuing bibliography with indexes (supplement 188)
[NASA-SP-7037(188)] 19 p3211 N85-29910
Air bag restraint system
[AD-D011671] 19 p3215 N85-29936
Simulation studies of time-control procedures for the advanced air traffic control system
[NASA-TP-2493] 21 p3553 N85-32101
General Aviation Airworthiness Alerts, no. 85
[FAA-AC-43-16] 22 p3729 N85-33117

AIRCRAFT FUEL SYSTEMS

Aircraft wing fuel tank environmental simulator tests for evaluation of antimisting fuels
[FAA-CT-84-15] 07 p0934 N85-15920
Flow measurement device
[AD-D011432] 08 p1168 N85-17369
Study of advanced fuel system concepts for commercial aircraft and engines
[NASA-CR-174752] 10 p1456 N85-19176
Study of advanced fuel system concepts for commercial aircraft
[NASA-CR-174751] 11 p1584 N85-19978
Interactions between F-111 fuselage fuel tank sealants. Part 2: Variation in performance properties of polysulfides after contact with polyester degradation products
[AD-A149777] 12 p1812 N85-21368
Hydrodynamic simulation of transient processes in injection system of aircraft engines during pump unswirling 13 p2050 N85-22829

AIRCRAFT FUELS

Variability of major organic components in aircraft fuels. Volume 1: Technical discussion
[AD-A145574] 02 p0188 N85-11256
Variability of major organic components in aircraft fuels. Volume 2: Illustrations
[AD-A145831] 04 p0481 N85-13067
Distribution and storage of aviation turbine fuel for military operations in northern Australia
[AD-A147180] 07 p0935 N85-15921
Study of advanced fuel system concepts for commercial aircraft
[NASA-CR-174751] 11 p1584 N85-19978
A study of intumescent reaction mechanisms
[AD-A149605] 12 p1812 N85-21365
A standard aircraft diffusion flame: Spectral characteristics and a feasibility study for developing an alternate calibration source for aircraft optical fire detection systems
[AD-A150231] 13 p2039 N85-22768
FAA aviation forecasts: Fiscal years 1985-1996
[AD-A151050] 14 p2216 N85-23747
Applications of high pressure differential scanning calorimetry to aviation fuel thermal stability research
[NASA-TM-87002] 14 p2249 N85-23941
Trends of petroleum fuels
[DE85-000116] 14 p2263 N85-24023
USSR report: Transportation
[JPRS-UTR-84-017] 15 p2461 N85-25196
Chronic fuel shortages in Volga civil aviation administration 15 p2461 N85-25198
Ilyushin bureau designer on fuel conservation research
15 p2467 N85-25231
Aviation turbine fuels from tar sands bitumen and heavy oils. Part 1: Process analysis
[AD-A151319] 15 p2521 N85-25539
Realisation of relaxed static stability on a commercial transport 16 p2713 N85-26748
Jet fuel property changes and their effect on producibility and cost in the U.S., Canada, and Europe
[NASA-CR-174840] 16 p2757 N85-27012
Fuel freeze point investigations
[AD-A152801] 17 p2937 N85-28129
Heat management system for aircraft
[AD-D011658] 18 p3081 N85-29936
Detailed studies of aviation fuel flowability
[NASA-CR-174938] 20 p3435 N85-31308
A comparison of two bench scale tests of fuel low temperature flow properties
[AD-A154477] 20 p3435 N85-31311
Observations of the use of the setapoint detector
[AD-A154533] 21 p3571 N85-32208
Comparative analysis of operational forecasts versus actual weather conditions in airline flight planning, volume 1
[NASA-CR-167862] 24 p4119 N85-35534
Comparative analysis of operational forecasts versus actual weather conditions in airline flight planning, volume 4
[NASA-CR-167865] 24 p4120 N85-35537
Comparative analysis of operational forecasts versus actual weather conditions in airline flight planning: Summary report
[NASA-CR-167866] 24 p4120 N85-35538

AIRCRAFT GUIDANCE

Guidance and navigation programs and plans
06 p0751 N85-14809
Helicopter Guidance and Control Systems for Battlefield Support
[AGARD-CP-359] 08 p1072 N85-16797
Implications of guidance and control technology on human factors considerations 10 p1532 N85-19656
Algorithms for automatic four-dimensional aircraft guidance, considering the momentary wind situation
[DFVLR-FB-84-40] 12 p1775 N85-21146
Optimal symmetric flight studies
[NASA-CR-172506] 12 p1780 N85-21176
A flight management algorithm and guidance for fuel-conservative descents in a time-based metered air traffic environment: Development and flight test results
13 p1967 N85-22356
Reference systems for the evaluation of dead-reckoning navigation equipment 13 p1967 N85-22358
Cost Effective and Affordable Guidance and Control Systems
[AGARD-CP-360] 16 p2695 N85-26638
Investigation of imaging and flight guidance concepts for rotorcraft zero visibility approach and landing
[NASA-CR-166571] 17 p2894 N85-27843
Simulation studies of time-control procedures for the advanced air traffic control system
[NASA-TP-2493] 21 p3553 N85-32101

AIRCRAFT HAZARDS

The microburst as a hazard to aviation: Structure, mechanisms, and nowcasting 01 p0074 N85-10491
Automated aircraft icing forecast technique
[AD-A144853] 01 p0085 N85-10571
A bird strike handbook for base-level managers
[AD-A147928] 07 p0948 N85-16008
A study of the effects of triggered lightning
[AD-A148296] 08 p1189 N85-17494
Don't fowl out
[AD-P004179] 11 p1578 N85-19941
Accidents and serious incidents to civil aircraft due to birstrikes
[AD-P004180] 11 p1578 N85-19942
Analysis of bird strikes reported by European airlines, 1976 - 1980
[AD-P004181] 11 p1578 N85-19943
1983 Air Force bird strikes
[AD-P004182] 11 p1579 N85-19944
Birds and aircraft engine strike rates
[AD-P004184] 11 p1579 N85-19946
Review of engine ingestions to wide body transport aircraft
[AD-P004185] 11 p1579 N85-19947
Reducing gull use of some attractions near airports
[AD-P004195] 11 p1581 N85-19962
Evaluation of effectiveness of bird scaring operations at a sanitary landfill site near CFB Trenton, Ontario, Canada
[AD-P004201] 11 p1582 N85-19968
Development of bird hazard reduction for airport operational safety
[AD-P004202] 11 p1582 N85-19969
The bird strike situation and its ecological background in the Copenhagen Airport, Kastrup
[AD-P004203] 11 p1582 N85-19970
Bird control program Orlando International Airport
[AD-P004204] 11 p1583 N85-19971
Staff assistance to bases for bird hazards
[AD-P004205] 11 p1583 N85-19972
Bird strike avoidance system for Dover AFB, Delaware
[AD-P004206] 11 p1583 N85-19973
The potential of the NEXRAD radar system for warning of bird hazards
[AD-P004210] 11 p1583 N85-19977
Annual review of aircraft accident data: US air carrier operations calendar year 1981
[NTSB/ARC-85/01] 12 p1774 N85-21134
Direct-strike lightning photographs, swept-flash attachment patterns, and flight conditions for storm hazards 1982
[NASA-TM-86347] 12 p1892 N85-21877
Wind shear detection technology
[GPO-38-920] 12 p1893 N85-21879
Aircraft skin penetrator and agent applicator. Volume 1: Working model development and construction
[AD-A150498] 13 p1970 N85-22374
Thermal response of aircraft cabin ceiling materials during a post-crash, external fuel-spill, fire scenario
[PB85-145647] 14 p2220 N85-23764
USSR report: Transportation
[JPRS-UTR-84-017] 15 p2461 N85-25196
Effects of lightning on aircraft studied at Sheremetyevo 15 p2461 N85-25199
Safety recommendation(s), A-84-96
[REPT-3983A/217] 15 p2466 N85-25223
Safety recommendation(s), A-84-76 through -78
[REPT-3751E] 15 p2466 N85-25224
The impact of weather on aviation safety
[GPO-35-520] 16 p2703 N85-26685
Lightning strikes on aircraft. The TRIP 82 experiment and 3-dimensional electromagnetic interferometry
[ONERA-RF-88/7154-PY] 16 p2703 N85-26690
Status of air traffic control system
[S-HRG-98-1197] 20 p3391 N85-31096
On the state of knowledge on meteorologically caused icing of aircraft in clouds
[ESA-TT-861] 20 p3496 N85-31736

AIRCRAFT HYDRAULIC SYSTEMS

Space shuttle rudder/speedbrake actuation subsystem
06 p1102 N85-16965
Life testing of rubber seals — aircraft hydraulic systems
[AD-A143193] 13 p2096 N85-23086

AIRCRAFT INDUSTRY

Development of a production order release methodology
[AD-A145213] 01 p0124 N85-10852
For the sacred air space of our motherland; an interview with our country's famous aircraft designer, Lu Hsiao-Peng
[AD-A146291] 03 p0309 N85-11997
The embedded test (BIT): Impact on the total cost of possession 08 p1063 N85-16734
Innovation in British industry (notably the aircraft industry) and its value: Collected papers
[BAE-KRS-N-GEN-286] 09 p1263 N85-17933
FAA aviation forecasts: Fiscal years 1985-1996
[AD-A151050] 14 p2216 N85-23747
Aviation workers plenum reviews fuel conservation progress 15 p2461 N85-25197
National airspace review. Implementation plan. Revised
[AD-A151412] 15 p2468 N85-25238
Characterization of solderless minivrapping connections
[CNES-NT-112] 16 p2706 N85-27236
The evolution of the U.S. helicopter industry
[AD-A154290] 19 p3211 N85-29913
Automated fabrication of composite structures for helicopters
[SNIAS-851-210-104] 20 p3393 N85-31049
DOD Value Engineering Conference report. Value Engineering (VE): A tool that benefits line management held at Leesburg, Virginia on 1-2 November 1984. Part 2. Plenary session
[AD-A156068] 24 p4163 N85-35811

AIRCRAFT INSTRUMENTS

NT ALTIMETERS
NT ANEMOMETERS
NT APPROACH INDICATORS
NT ATTITUDE INDICATORS

NT AUTOMATIC PILOTS
NT COMPASSES
NT GYRO HORIZONS
NT GYROCOMPASSES
NT HOT-WIRE ANEMOMETERS
NT MAGNETIC COMPASSES
NT PLAN POSITION INDICATORS
NT POSITION INDICATORS
NT RADIO ALTIMETERS
NT RADIO DIRECTION FINDERS
NT SPACECRAFT POSITION INDICATORS
NT SPEED INDICATORS
NT TACHOMETERS

Realistic localizer courses for aircraft instrument landing simulators
[NASA-CR-172333] 04 p0455 N85-12885

System status display information
[NASA-CR-172347] 04 p0455 N85-12889

Airspeed sensing pressure valve system
[AD-D011472] 10 p1425 N85-16987

Electronic displays: Their strengths and weaknesses for advanced high performance aircraft
10 p1533 N85-19664

Changing system and display concepts and their impact on aircrew performance 10 p1533 N85-19665

Combinatorial performance/cost analysis of an autonomous navigation system for aircraft
16 p2695 N85-28840

Navigation and flight director guidance for the NASA/FAA helicopter MLS curved approach flight test program
[NASA-CR-177350] 16 p2704 N85-26691

Geomagnetic velocimeter
[AD-D011672] 19 p3218 N85-29953

MIZEX, 1984, NASA CV-990 flight report
[NASA-TM-86216] 19 p3299 N85-30451

The development and evaluation of color display systems for airborne applications. Phase 1: Fundamental visual, perceptual, and display system considerations
[FAA/PM-85-19] 22 p3826 N85-33700

Determination of instrument errors by compatibility checking: Results from dynamic flight test data
[ARL/AERO-R-162] 23 p3896 N85-34137

AIRCRAFT LANDING
NT CRASH LANDING
NT DITCHING (LANDING)
NT SKID LANDINGS

Aircraft accident report: Flying Tigers, Inc., Flight 2468, McDonell Douglas DC8-63, N797FT, Chambers Field, Naval Air Station, Norfolk, Virginia, October 25, 1983
[PB84-910408] 02 p0136 N85-10925

Preliminary airworthiness evaluation of the Rutan Aircraft Factory (RAF), Inc. LONG-EZ airplane with external sight
[AD-A145381] 02 p0138 N85-10937

Aircraft accident report, Scandinavian Airlines System, Flight 901, McDonnell Douglas DC-10-30, John F. Kennedy International Airport, Jamaica, New York, February 28, 1984
[PB84-910415] 05 p0594 N85-13786

To take off and to land safely, Hoechst 1678 for ice and snow free runways 05 p0595 N85-13791

An in-flight investigation of a twin fuselage configuration in approach and landing
[NASA-CR-172366] 05 p0596 N85-13801

Alternatives for runway rubber removal from porous friction surfaces
[DOT/FAA/PM-84/28] 05 p0597 N85-13803

Performance measures for aircraft landings as a function of aircraft dynamics 05 p0712 N85-14565

Multi-crew model analytic assessment of landing performance and decision-making demands
05 p0712 N85-14567

Guidance and navigation programs and plans
06 p0751 N85-14809

Critical conditions for the automatic control of landing from decision height in variable winds
[UTIAS-284] 06 p0753 N85-14830

Simulation evaluation of two VTOL control/display systems in IMC approach and shipboard landing
[NASA-TM-85996] 06 p0756 N85-14841

The effect of changes in the angle of incidence in the event of a richochet at a float step
[RAE-TRANS-2120] 07 p0902 N85-15712

Development of a preliminary ALRS stabilized material pavement analysis system (SPAS)
[AD-A147116] 07 p0910 N85-15760

Aircraft barricade
[AD-D011316] 07 p0910 N85-15761

Testing solution for IL-76 braking system problem
06 p1067 N85-16766

Airport activity statistics of certificated route air carriers
[AD-A146472] 08 p1081 N85-16848

Evaluation of arctic test of improved tritium radioluminescent lighting
[AD-A148215] 08 p1089 N85-16864

Why vertical landing — aircraft
[BAE-KRS-N-GEN-301] 09 p1279 N85-18048

In-flight investigation of the effects of time delay in control system on flying qualities in landing approach
[DFVLR-FB-84-35] 11 p1586 N85-19989

New runway enables IL-76 flights to Tenkeli in far north 12 p1769 N85-21106

Runway rubber removal specification development field evaluation procedures development
[FAA-PM-84-27] 12 p1781 N85-21179

Boundary layer transition control for takeoff and landing configurations 14 p2211 N85-23714

Total energy-rate feedback for automatic glide-slope tracking during wind-shear penetration
[NASA-TP-2412] 14 p2226 N85-23801

Trajectory measurements for take-off and landing tests and other short-range applications, volume 16
[AGARD-AG-160-VOL-16] 15 p2561 N85-25801

The use of pressure sensing tape on the aircraft wing as sensor for flight control systems
16 p2696 N85-26660

Study of longitudinal landing flying qualities evaluation using pilot model theory
[AD-A152194] 16 p2706 N85-26702

A system for take-off and landing measurements (STALINS)
[B8580072] 17 p2895 N85-27849

Addition of flexible body option to the TOLA computer program, part 1
[NASA-CR-132732-1] 17 p2896 N85-27855

Addition of flexible body option to the TOLA computer program. Part 2: User and programmer documentation
[NASA-CR-132732-2] 17 p2896 N85-27856

In-flight investigation of the influence of pitch damping and pitch control effectiveness on landing approach flying qualities of statically unstable transport aircraft
[DFVLR-FB-84-12] 17 p2900 N85-27860

Visual and part-task manipulations for teaching simulated carrier landings
[AD-A153622] 18 p3154 N85-29529

Application of frequency domain handling qualities criteria to the longitudinal landing task
[NASA-TM-86728] 22 p3730 N85-33124

The integrated manual and automatic control of complex flight systems
[NASA-CR-176166] 24 p4066 N85-35201

AIRCRAFT LIGHTS
Flares and photoflash items
[AD-A145442] 02 p0187 N85-11253

AIRCRAFT MAINTENANCE
Aircraft cabin pressurization control system tester
[AD-D011225] 01 p0013 N85-10061

Expert systems in maintenance diagnostics for self-repair of digital flight control systems
[AD-P003933] 02 p0247 N85-11613

DoD Robotics Application Workshop Proceedings
[AD-A145867] 03 p0307 N85-11978

Air force engine repair - Oklahoma City Air Logistics Center, Propulsion Division
[AD-P003999] 03 p0307 N85-11980

Electronics/avionics depots in the United States Air Force Warner Robins Air Logistics Center
[AD-P004000] 03 p0307 N85-11981

Air force landing gear repair - Ogden Air Logistics Center Industrial Products and Landing Gear Division
[AD-P004001] 03 p0307 N85-11982

Jet engine blade repair at the Oklahoma Air Logistics Center, Propulsion Division
[AD-P004003] 03 p0307 N85-11983

Air Force honeycomb shaping at SM-ALC (Sacramento Air Logistics Center)
[AD-P004005] 03 p0308 N85-11985

Laser paint removal
[AD-P004009] 03 p0308 N85-11989

Future robotics program at San Antonio ALC (Air Logistics Center)
[AD-P004011] 03 p0309 N85-11991

Robotics in nondestructive inspection at Sacramento Air Logistics Center
[AD-P004012] 03 p0309 N85-11992

USSR report: Transportation
[JPRS-UTR-84-028] 03 p0310 N85-12002

Editorial urges improved aviation repair work quality
03 p0310 N85-12004

Maintenance Management Information and Control System (MMICS): Administrative boon or burden
[AD-A145762] 03 p0438 N85-12790

DYNA-SIM: A nonstationary queuing simulation with application to the automated test equipment problem
[AD-A146384] 06 p0957 N85-15450

An update of the functional requirements of the Naval Aviation Logistics Command Management Information System (NALCOMIS)
[AD-A146565] 06 p0871 N85-15532

Performance evaluation of A-10 aircraft maintenance units and aircraft using constrained facet analysis
[AD-A146955] 07 p0893 N85-15660

Parametric estimates of propulsion system maintenance manhours
[AD-A147120] 07 p0894 N85-15662

A Q-GERT network simulation model for examining pipeline time in the Navy's J-52 intermediate level jet engine repair cycle
[AD-A147269] 07 p0894 N85-15663

Operational Loads Data
[AGARD-CP-375] 07 p0894 N85-15664

F-16 force management, yesterday, today and tomorrow 07 p0895 N85-15674

Managing recoverable aircraft components in the PPB and related processes: Executive summary
[AD-A146806] 07 p1050 N85-16667

Design for Tactical Avionics Maintainability
[AGARD-CP-361] 08 p1063 N85-16731

Objectives in studying the maintainability of aircraft systems 08 p1063 N85-16732

Joint service design for testability program
08 p1063 N85-16733

Study and realisation of a 3rd level maintenance center based on ATE systems utilization
08 p1063 N85-16735

A practical example of reducing life cycle costs and increased availability 08 p1063 N85-16736

Avionics fault tree analysis and artifical intelligence for future aircraft maintenance 08 p1066 N85-16755

International projects, other work of Aeroproyekt Institute 08 p1068 N85-16767

Composite structure repair, addendum
[AGARD-R-716-ADD] 08 p1120 N85-17057

Composite repair of aircraft structures
08 p1120 N85-17059

Mobile accelerator neutron radiography system
[AD-A148806] 09 p1323 N85-18311

National airspace system: Operational requirements
[AD-A149349] 10 p1422 N85-18973

Transportation
[JPRS-UTR-85-004] 12 p1769 N85-21105

Aviation repair plant directors on quality control measures 12 p1769 N85-21108

Proceedings of the 6th Human Factors Workshop on Aviation
[AD-A150043] 12 p1909 N85-21982

Aviation maintenance computerized management information systems: Perspective for the future
[AD-A150637] 13 p1966 N85-22349

Ministry officials on improving aircraft technical servicing 14 p2208 N85-23697

Development of a field repair technique for mini-sandwich Kevlar/epoxy aircraft skin
[AD-A151369] 15 p2503 N85-25439

Graphic simulation of a machine-repairman model
[AD-A151761] 16 p2694 N85-26633

Deployable Core Automated Maintenance System (DCAMS)
[AD-A153695] 18 p3198 N85-29639

Air Force bid sample testing 20 p3437 N85-31323

Corrosion management strategies for aircraft and related systems 22 p3749 N85-33239

Relating corrosion maintenance to environmental factors 22 p3750 N85-33247

Implications of artificial intelligence on the design of future onboard systems
[SFENA-DPS/C/S3/84252A] 23 p3967 N85-34566

AIRCRAFT MANEUVERS
Directional solidification of flake and nodular cast iron during KC-135 low-g manouvers
02 p0154 N85-11040

Measuring workload differences between short-term memory and long-term memory scenarios in a simulated flight environment 05 p0703 N85-14513

Algorithm for tracking manuevering object with ambiguous measurements 06 p0791 N85-15057

Evaluation of operational loads to verify structural design 07 p0896 N85-15677

Modeling of aircraft performance from flight test results using quasi steady-state test techniques
09 p1279 N85-18047

Coordinate determination errors in measuring characteristics of radiation field of airborne antennas
13 p2068 N85-22919

Minimum time turns using vectored thrust
[AD-A151693] 15 p2471 N85-25256

High specific power aircraft turn maneuvers: Tradeoff of time-to-turn versus change in specific energy
[AD-A151701] 15 p2471 N85-25257

Application of CFD techniques toward the validation of nonlinear aerodynamic models
[NASA-TM-86715] 16 p2700 N85-26671
Autofocus motion compensation for synthetic aperture radar and its compatibility with strapdown inertial navigation sensors on highly maneuverable aircraft
[AD-A151940] 16 p2704 N85-26693
Piloted simulation of one-on-one helicopter air combat at NOE flight levels
[NASA-TM-86686] 16 p2710 N85-26720
Parameter identification results of tests in nonsteady symmetric flight with the Hawker Hunter Mk 7
[NLR-TR-83042-U] 17 p2897 N85-27860
The STOL and maneuver technology program integrated control system development 17 p2905 N85-27910
System safety study of minimum TCAS 2 for instrument weather conditions
[FAA-PM-85-12] 22 p3728 N85-33113
Development of control laws for a flight test maneuver autopilot for an F-15 aircraft
[NASA-TM-86736] 22 p3730 N85-33122
Control variables in vertical wind determination using simple flight-mechanical equations
24 p4121 N85-35546

AIRCRAFT MODELS
Wind tunnel wall interference correction for aircraft models 03 p0314 N85-12029
On aircraft antennas and basic scattering studies
[AD-A146017] 03 p0355 N85-12282
Differences in health risks by aircraft model among US Navy pilots
[AD-A146147] 03 p0401 N85-12556
Unsteady aerodynamic characterization of a military aircraft in vertical gusts
[NASA-TM-77810] 12 p1770 N85-21110
Structural design of the Sandia 34-M Vertical Axis Wind Turbine
[DE85-002631] 13 p2129 N85-23247
Hover test results of a small-scale twin-tilt nacelle model
[NASA-TM-86665] 14 p2210 N85-23706
Automatic Dynamic Aircraft Modeler (ADAM) for the computer program NASTRAN 15 p2574 N85-25875
Wing buffeting active control testing on a transport aircraft configuration in a large sonic tunnel
16 p2714 N85-26750
Parameter identification results of tests in nonsteady symmetric flight with the Hawker Hunter Mk 7
[NLR-TR-83042-U] 17 p2897 N85-27860
Pressure distribution data from tests of 2.29 M (7.5 feet) span EET high-lift transport aircraft model in the Ames 12-foot pressure tunnel
[NASA-TM-84517] 19 p3211 N85-29912
Flight-mechanics test with a restricted flying aircraft model in a wind tunnel
[ESA-TT-885] 20 p3394 N85-31053
Design and implementation of input signals for identification of pilot/aircraft models
[ESA-TT-880] 20 p3394 N85-31055
Development and validation of a general purpose linearization program for rigid aircraft models
[NASA-TM-86737] 21 p3556 N85-32122

AIRCRAFT NOISE
NT JET AIRCRAFT NOISE
NT SONIC BOOMS
Jet noise suppression by porous plug nozzles
[NASA-CR-3613] 02 p0275 N85-11790
Airport noise impact prediction and measurement
03 p0387 N85-12476
Prediction and modeling of helicopter noise
[AD-A145764] 03 p0415 N85-12656
Detection, classification, and extraction of helicopter-radiated noise
[AD-A145993] 03 p0416 N85-12661
Rotary-wing aircraft noise measurements: Analysis of variations and proposed measurement standard
[AD-A146207] 03 p0416 N85-12662
Static jet noise test results of four 0.35 scale-model COGAT mixer nozzles
[NASA-TM-86671] 04 p0558 N85-13551
Evaluation of the Langley 4- by 7-meter tunnel for propeller noise measurements
[NASA-TM-85721] 04 p0558 N85-13553
NOISEMAP 4.4 computer program update, operator's manual, addendum 1
[AD-A147091] 07 p1025 N85-16503
Helicopter noise survey performed at Las Vegas, Nevada, 19-21 January, 1984
[AD-A147392] 07 p1039 N85-16583
Noise measurement flight test: Data-analyses aerospatiale AS-355F TwinStar helicopter
[AD-A147497] 07 p1039 N85-16585
Helicopter model rotor-blade vortex interaction impulsive noise: Scalability and parametric variations
[NASA-TM-86007] 08 p1077 N85-16826
An improved source model for aircraft interior noise studies
[NASA-CR-172517] 08 p1217 N85-17668
Test of dispersal of turbojet aircraft departure tracks at washington National Airport (1983-84), volume 1 report
[AD-A148111] 08 p1218 N85-17669
Noise measurement flight test for Boeing Vertol 234/CH 47-d helicopter: Data/analyses
[AD-A148172] 08 p1218 N85-17670
Noise measurement flight test: Data-analyses Aerospatiale AS 350D AStar helicopter
[AD-A148495] 08 p1218 N85-17672
Noise measurement flight test: Data-analyses, Sikorsky S-76A helicopter
[AD-A148525] 08 p1218 N85-17673
Aeroacoustics at the DFVLR Brunswick Research Center: A survey on recent and current activities
[DFVLR-MITT-84-14] 08 p1219 N85-17677
Aircraft noise effects: An interdisciplinary study of the effects of aircraft noise on man. Part 1: Basic report
[NASA-TM-75819] 10 p1526 N85-19629
Aircraft noise effects: An interdisciplinary study of the effect of aircraft noise on man. Part 2: Appendix
[NASA-TM-75818] 10 p1527 N85-19630
Aircraft noise effects: An inter-disciplinary study of the effect of aircraft noise on man. Part 3: Supplementary analyses of the social-scientific portion of the study on aircraft noise conducted by the DFG
[NASA-TM-75802] 10 p1527 N85-19631
Fluctuating pressures on fan blades of a turbofan engine, flight test investigation
[NASA-TP-2381] 10 p1553 N85-19790
A community survey of helicopter noise annoyance conducted under controlled noise exposure conditions
[NASA-TM-86400] 13 p2154 N85-23374
Research on the effect of noise at different times of day: Models, methods and findings
[NASA-CR-3888] 13 p2154 N85-23375
An experimental investigation of the chopping of helicopter main rotor tip vortices by the tail rotor
[NASA-CR-177338] 13 p2154 N85-23376
Wind tunnel acoustic study of a propeller installed behind an airplane empennage: Data report
[NASA-CR-177335] 13 p2154 N85-23377
Noise measurement flight test: Data/Analyses, hughes 500 D/E helicopter
[AD-A148110] 14 p2219 N85-23758
Disturbance to the population due to flight operations at landing fields. Questionnaire on community reaction to non-commercial and sporting aviation
[NASA-TM-76531] 14 p2353 N85-24537
Interaction of a turbulent vortex with a lifting surface
15 p2464 N85-25214
Fundamental studies of structure borne noise for advanced turboprop applications
[NASA-CR-175737] 15 p2648 N85-26320
Prediction of free-field noise levels from aircraft flyover measurements
[VTH-LR-427] 16 p2661 N85-27647
Effects of propeller rotation direction on airplane interior noise levels
[NASA-TP-2444] 19 p3350 N85-30767
Aircraft cabin noise prediction and optimization
[NASA-CR-175982] 19 p3350 N85-30768
Data on noise environments at different times of day around airports
[NASA-CR-172612] 19 p3351 N85-30769
Design of sidewall treatment of cabin noise control of a twin engine turboprop aircraft
[NASA-CR-172245] 19 p3351 N85-30771
Aviation noise effects
[AD-A154319] 19 p3352 N85-30776
Impulsive noise due to transonic blade-vortex interactions 20 p3523 N85-31913
FAA/GAMA (Federal Aviation Administration/General Aviation Manufacturer's Association) propeller aircraft noise test program, Salina Municipal Airport, Salina, Kansas
[AD-A154818] 21 p3699 N85-32983
Overground Excess Sound Attenuation (ESA). Volume 3: Application of ESA data in NOISEFILE
[AD-A154820] 21 p3699 N85-32984
Helicopter noise survey for selected cities in the contiguous US
[AD-A154883] 21 p3699 N85-32985
Lateral attenuation of aircraft flight noise
[AD-A154958] 21 p3700 N85-32988
A theoretical appraisal of the use of ground-plane microphones for aircraft noise measurements
[NPL-AC-103] 22 p3836 N85-33752
Langley aeronautics and space test highlights, 1984
[NASA-TM-87585] 23 p4057 N85-35151

AIRCRAFT NOISE PREDICTION
U NOISE PREDICTION (AIRCRAFT)

AIRCRAFT PARTS
Determination of parameters of cupped aircraft landing ski 06 p0775 N85-14956
US Army helicopter operational flight loads
07 p0895 N85-15675
Helicopter data acquisition in WHL
07 p0896 N85-15676
All-composite Airbus empennage
07 p0936 N85-15931
Managing recoverable aircraft components in the PPB and related processes: Executive summary
[AD-A146806] 07 p1050 N85-16667
The Air Force can improve its forecasts of aircraft spare parts requirements
[AD-A147911] 07 p1053 N85-16682
Estimating wartime support resource requirements. Statistical and related policy issues
[AD-A147923] 07 p1053 N85-16685
Alternative shock characterizations for consistent shock test specifications 09 p1335 N85-18396
Flexible manufacturing system for the production of aircraft parts
[PNR-90237] 14 p2207 N85-23687
Fiber optics applications for MIL-STD-1760
[AD-A151113] 15 p2470 N85-25251

AIRCRAFT PERFORMANCE
NT HELICOPTER PERFORMANCE
Performance capabilities of the C-5 and C-17 cargo aircraft
[AD-A145518] 02 p0138 N85-10939
Airborne performance measurement system design: C-5 aircraft
[AD-A145436] 02 p0236 N85-11539
Speed benefits of tilt-rotor designs for LHX
[NASA-CR-166437] 07 p0902 N85-15717
Missions and vehicle concepts for modern, propelled, lighter-than-air vehicles
[NASA-TM-86672] 08 p1066 N85-16757
Modeling of aircraft performance from flight test results using quasi steady-state test techniques
09 p1279 N85-18047
The design of sport and touring aircraft
[NASA-TM-77783] 10 p1423 N85-18975
Preliminary performance of a vertical-attitude takeoff and landing, supersonic cruise aircraft concept having thrust vectoring integrated into the flight control system
[NASA-CR-172530] 10 p1423 N85-18977
Details of export A-5 close-support aircraft given
10 p1424 N85-18983
Acta Aeronautica et Astronautic Sinica (selected articles)
[AD-A148830] 11 p1575 N85-19922
AIRLAB: A laboratory for flight-crucial-electronics system research 13 p1968 N85-22362
Boundary layer control by transition fixing — conference
[DFVLR-MITT-84-17] 14 p2211 N85-23712
Problems of the application of wind tunnel results to aerodynamic performance of large aircraft
14 p2211 N85-23713
The design of high-performance gliders
[NASA-TM-77772] 14 p2217 N85-23750
Simulation of aircraft behaviour on and close to the ground
[NASA-TM-87460] 14 p2218 N85-23754
Glider Nimbus 3-24.5. Partial certification test results for importation in the U category
[REPT-CEV/IS/SE/AV/84] 14 p2220 N85-23763
Structures and Dynamics Division research and technology plans for FY 1985 and accomplishments for FY 1984
[NASA-TM-86417] 15 p2577 N85-25895
Parameter identification results of tests in nonsteady symmetric flight with the Hawker Hunter Mk 7
[NLR-TR-83042-U] 17 p2897 N85-27860
Demonstration of relaxed static stability on a commercial transport 17 p2903 N85-27898
Realisation of relaxed static stability on a commercial transport 17 p2903 N85-27899
Mission analysis of solar powered aircraft
[NASA-CR-172583] 20 p3397 N85-31072
Qualification needs for advanced integrated aircraft
[NASA-TM-86731] 22 p3729 N85-33119
Comparative analysis of operational forecasts versus actual weather conditions in airline flight planning, volume 1
[NASA-CR-167862] 24 p4119 N85-35534

AIRCRAFT PILOTS
Effects of foveal information processing
01 p0009 N85-10052
The Reports of Aeromedical Laboratory, volume 25, no. 1/2
[ISSN-0023-2858] 01 p0090 N85-10805

Psychological states (mood, affect or emotion) experienced by JASDF pilots through flying duties. 3: Flying conditions causing pilots psychological disturbance 01 p0090 N85-10806
The relationship between emotional tension scale and psychological uneasiness of JASDF pilots in flying situations 01 p0090 N85-10808
Assessment of the inflating characteristics of the modified anti-G suit 01 p0090 N85-10809
Air-to-air visual acquisition performance with TCAS 2 [FAA-PM-84-17] 02 p0236 N85-11537
What pilots like (and don't like) about the new cockpit technology 05 p0710 N85-14554
Management training for cockpit crews at Piedmont flight 09 p1276 N85-18013
Video concepts in CRM training 09 p1276 N85-18015
Be healthy, pilot 10 p1526 N85-19826
Grasp of information by the pilot in future combat aircraft 10 p1533 N85-19862
Traffic alert and collision avoidance system: Operational simulation [FAA-PM-85-10] 19 p3216 N85-29941
Psychophysiological nature of aircraft feel 19 p3323 N85-30587
A systematic determination of skill and simulator requirements for airline transport pilot certification [AD-A154135] 19 p3330 N85-30830
Learning and self adaptation applied to the simulation of a human pilot [ONERA-RT-24/5122-SY] 20 p3511 N85-31828

AIRCRAFT POWER SOURCES
U AIRCRAFT ENGINES

AIRCRAFT POWER SUPPLIES
Advanced secondary power system for transport aircraft [NASA-TP-2463] 18 p3062 N85-28944

AIRCRAFT PRODUCTION
Flexible manufacturing system for the production of aircraft parts [PNR-90237] 14 p2207 N85-23687

AIRCRAFT PRODUCTION COSTS
MBB automates aircraft production in many FRG facilities 14 p2289 N85-24186
FRG journal analyzes state, prospects of airbus programs: General analysis 15 p2535 N85-25638

AIRCRAFT RELIABILITY
Airworthiness and flight characteristics test of the JOH-6A light combat helicopter configured with a wire strike protection system [AD-A144880] 01 p0006 N85-10038
Airworthiness and Flight Characteristics (A and FC) test of the EH - 1X/EH - 1H helicoptur configurations [AD-A144881] 01 p0007 N85-10039
Preliminary airworthiness evaluation of the Rutan Aircraft Factory (RAF), Inc. LONG-EZ airplane with external sight [AD-A145381] 02 p0138 N85-10937
The DG400 propulsed glider [CEV/IS/SE/AV/84] 05 p0595 N85-13785
Nondestructive inspection: Improved capabilities of technicians [AD-A147388] 07 p0975 N85-16196
Airworthiness and flight characteristics test of the RC-12D Guardrail V [AD-A148046] 08 p1084 N85-16864
Preliminary airworthiness evaluation AH-1S (MC) helicopter with external fuel tanks installed [AD-A148091] 08 p1084 N85-16865
Standardization of helicopter certification requirements in the western world [SNIAS-951-210-103] 20 p3393 N85-31048

AIRCRAFT SAFETY
Study of effects of lightning on aircraft systems stressed 03 p0310 N85-12005
Flight phase status monitor study. Phase 1: Systems concepts [DOT/FAA/PM-84/18] 03 p0317 N85-12048
Crew communication as a factor in aviation accidents 05 p0710 N85-14555
A bird strike handbook for base-level managers [AD-A147926] 07 p0948 N85-16006
Safety awareness, pilot education, and incident reporting programs 09 p1276 N85-18020
Why vertical landing — aircraft [BAE-KRS-N-GEN-301] 09 p1279 N85-18048
Bird Strike Committee Europe [AD-P004207] 11 p1583 N85-19974
The FAA grant-in-aid assurances: FAR part 139, and airport hazards [AD-P004209] 11 p1583 N85-19976
Pathophysiological study of poisoning due to thermal degradation of materials — aircraft cabins [CERMA-84-15] 11 p1692 N85-20840
Legislation to improve airline safety [GPO-39-222] 12 p1773 N85-21132
Annual review of aircraft accident data: US air carrier operations calendar year 1981 [NTSB/ARC-85/01] 12 p1774 N85-21134
A safety evaluation of the relocation of the ACM (Air Combat Maneuver) panel in the F-14 ( )/AIP (Avionics Integration Program) [AD-A149596] 12 p1777 N85-21158
Wind shear detection technology [GPO-38-920] 12 p1893 N85-21879
FTASUM: Aviation forecast summaries [PB85-112977] 12 p1897 N85-21908
Safety recommendation(s), A-84-65 [REPT-3908] 14 p2216 N85-23743
Safety recommendation(s), A-84-103 [REPT-3909B/101B] 14 p2216 N85-23745
Safety recommendation(s), A-84-93 through -95 [REPT-3963/33] 14 p2216 N85-23746
Safety recommendation(s), A-84-82 through -84 [REPT-3957] 14 p2217 N85-23748
Preliminary design of a limb restraint evaluator [AD-A151749] 15 p2466 N85-25226
Aircraft safety improvement 15 p2688 N85-26802
Generalized escape system simulation: Its purpose, recent modifications and potential [DE85-005571] 16 p2703 N85-26689
Flying in spite of the weather [NLR-MP-84021-U] 17 p2895 N85-27847
Traffic alert and collision avoidance system: Operational simulation [FAA-PM-85-10] 19 p3216 N85-29941
Thirty years' activities for aircraft safety 20 p3391 N85-31033
The 121.5 MHz ELT: Past, present and future — Emergency Locator Transmitter (ELT) 20 p3401 N85-31105
The role of aircraft panel materials in cabin fires and their properties [FAA-CT-84-30] 21 p3553 N85-32104
General Aviation Airworthiness Alerts, no. 85 [FAA-AC-43-16] 22 p3729 N85-33117
Aviation safety (aircraft passenger survivability and cabin safety) [GPO-39-847] 23 p3895 N85-34130
Investigation of experimental lightweight firewall materials for A/C engine bay applications [AD-A155765] 24 p4062 N85-35175

AIRCRAFT SPECIFICATIONS
Details of export A-5 close-support aircraft given 10 p1424 N85-18983
An overview of the MIL-HDBK-5 program [AD-A147788] 14 p2254 N85-23970
US Army Aviation Engineering Flight Activity (USAAEFA) report bibliography update 1963 - 1984 [AD-A151361] 15 p2457 N85-25168
NASA/aircraft industry standard specification for graphite fiber toughened thermoset resin composite material [NASA-RP-1142] 16 p2742 N85-26923

AIRCRAFT SPIN
Determination of corrections to flow direction measurements obtained with a wing-tip mounted sensor [NASA-CR-174412] 10 p1421 N85-18962
Extended moment arm anti-spin device [NASA-CASE-LAR-12979-1] 12 p1776 N85-21147
Flight investigation of stall, spin and recovery characteristics of a low-wing, single-engine, T-tail light airplane [NASA-TP-2427] 15 p2470 N85-25248
Dual towline spin-recovery device [NASA-CASE-LAR-13076-1] 24 p4066 N85-35200

AIRCRAFT STABILITY
Preliminary airworthiness evaluation of the Rutan Aircraft Factory (RAF), Inc. LONG-EZ airplane with external sight [AD-A145381] 02 p0138 N85-10937
Preliminary performance of a vertical-attitude takeoff and landing, supersonic cruise aircraft concept having thrust vectoring integrated into the flight control system [NASA-CR-172530] 10 p1423 N85-18977
Acta Aeronautica et Astronautic Sinica (selected articles) [AD-A148830] 11 p1575 N85-19922
A Lagrange-D'Alembert formulation of the equations of motion of a helicopter carrying an externally suspended load [NASA-TM-85864] 12 p1776 N85-21149
Aeronautical Engineering: A continuing bibliography with indexes, supplement 185 [NASA-SP-7037(185)] 13 p1965 N85-22342
Relative control effectiveness technique with application to airplane control coordination [NASA-TP-2416] 14 p2218 N85-23753
A perspective on superaugmented flight control advantages and problems 17 p2901 N85-27866
Demonstration of relaxed static stability on a commercial transport 17 p2903 N85-27899
Realisation of relaxed static stability on a commercial transport 17 p2903 N85-27899
Experimental and theoretical determination of the wing-induced lateral wind on the tail surfaces in oscillating rolling motion. Part 1: Application of the Mobile Oscillating Derivatives (MOD) on an experimental part [IFD-1/84-PT-1] 18 p3061 N85-28939
Experimental and theoretical determination of the wing-induced lateral wind on the tail surfaces in oscillating rolling motion. Part 2: Theoretical investigations for calculation of the lateral wind [IFD-1/84-PT-2] 18 p3061 N85-28940
Contributions on the subject of longitudinal movements of aircraft in wind shears [NASA-TM-77837] 18 p3139 N85-29432

AIRCRAFT STRUCTURES
NT AFTERBODIES
NT AIRFRAMES
NT FOREBODIES
NT FUSELAGES
NT NOSES (FOREBODIES)
Method for measuring haze in transparencies [AD-D011233] 01 p0120 N85-10823
Quasi-steady analysis of aircraft panel flammability [AD-A145461] 02 p0138 N85-10938
Advanced manufacturing development of a composite empennage component for L-1011 aircraft [NASA-CR-165885] 02 p0170 N85-11141
Development of powder metallurgy 2XXX series Al alloys for high temperature aircraft structural applications [NASA-CR-172408] 02 p0182 N85-11220
Measurement of the inertial constants of a rigid or flexible structure of arbitrary share through a vibration test [NASA-TM-77557] 02 p0209 N85-11381
Air Force honeycomb shaping at SM-ALC (Sacramento Air Logistics Center) [AD-P004005] 03 p0308 N85-11985
Crack resistance of pressed and rolled semifinished goods of aluminum alloys used in load-bearing aircraft wing structures 03 p0348 N85-12245
Low power laminar aircraft structures 04 p0451 N85-12657
Graphics software for the display of body deformation motion [FW-FO-1640] 04 p0455 N85-12888
Composite fracture toughness and impact characterization 04 p0466 N85-12963
Composite structural materials [NASA-CR-174077] 04 p0467 N85-12966
Defect detection threshold in riveted joints, test report no.44-833/F — in aircraft 04 p0511 N85-13260
Increase in the economy of design and process planning by integrated and graphic data processing, phase 2 — aircraft design [BMFT-FB-W-84-028] 05 p0716 N85-14589
A study of crashworthiness of light aircraft fuselage structures: A numerical and experimental investigation [UTIAS-286] 06 p0750 N85-14803
Analytical construction of flight vehicle surfaces 06 p0775 N85-14957
Verification of a computer program for vibration analysis of composite wing cores [NAL-TR-825] 06 p0817 N85-15167
Operational Loads Data [AGARD-CP-375] 07 p0894 N85-15664
Operational loads data evaluation for individual aircraft fatigue monitoring 07 p0895 N85-15669
Structural flight load measurement demonstration of structural integrity 07 p0895 N85-15670
Advanced fatigue monitoring on service aircraft 07 p0895 N85-15671
F-16 force management, yesterday, today and tomorrow 07 p0895 N85-15674
US Army helicopter operational flight loads 07 p0895 N85-15675
Evaluation of operational loads to verify structural design 07 p0896 N85-15677
Tornado: Structural Usage Monitoring System (SUMS) 07 p0896 N85-15680
All-composite Airbus empennage 07 p0936 N85-15931
The influence of fastener flexibility on load transfer and fatigue life predictions for multirow bolted and riveted joints — aircraft structures [LBF-FB-172/84] 07 p0979 N85-16219
Composite structure repair, addendum [AGARD-R-716-ADD] 08 p1120 N85-17057
Composite repair of aircraft structures 08 p1120 N85-17059
Flexible manufacturing system for the production of aircraft parts [BLL-PNR-90237-(8019.3153)] 08 p1137 N85-17159
Icing flight research: Aerodynamic effects of ice and ice shape documentation with stereo photography [NASA-TM-86906] 09 p1279 N85-18049

USSR report: Engineering and equipment
[JPRS-UEQ-85-001] 09 p1305 N85-18200
On solving nonlinear problems of aircraft structural mechanical design 09 p1309 N85-18223
Some fighter aircraft trends
[NASA-TM-86352] 10 p1420 N85-18954
Integrated paratroop door
[AD-D011507] 12 p1776 N85-21148
Fatigue crack propagation in mirage 1110 wing main spar specimens and the effects of spectrum truncation on life
[ARL/STRUC-R-405] 12 p1776 N85-21152
A history of full-scale testing of aircraft structures at the National Aeronautical Establishment
[NAE-AN-24] 12 p1777 N85-21153
Elastomer toughened polyimide adhesives — bonding metal and composite material structures for aircraft and spacecraft
[NASA-CASE-LAR-12775-2] 12 p1809 N85-21349
Finite element analysis of problems associated with life enhancement techniques
[ARL/STRUC-R-404] 12 p1862 N85-21676
Normal mode calculations for fuselage type intricate structures by regarding them as systems with superposed constraints 13 p2048 N85-22817
Operational loads measurement: A philosophy and its implementation — aircraft structures
[AD-A149445] 13 p2144 N85-23308
Durability calculation of wing panel element 14 p2285 N85-24159
Two recent cases of marker load applications on cargo/fighter aircraft fatigue tests 14 p2318 N85-24325
Aircraft structure for application to training aircraft
[CH-635286-A5] 15 p2469 N85-25244
Automatic Dynamic Aircraft Modeler (ADAM) for the computer program NASTRAN 15 p2574 N85-25875
Protective coatings for aircraft structures: A review
[VTH-LR-413] 16 p2706 N85-26704
ESP (External-Stores Program): A pilot computer program for determining flutter-critical external-store configurations. Volume 3, part 1: Program compilation
[AD-A152270] 16 p2711 N85-26727
Investigation of the influence of some paint systems and water displacing corrosion inhibitors on anodic undermining corrosion of aluminum 2024 clad alloy — aircraft structures
[VTH-LR-443] 16 p2756 N85-27009
The application of computer aided structural optimization to the design of aircraft components
[MBB-UT-21/84-O] 16 p2873 N85-27728
New materials and techniques for aircraft structures
[B6580074] 17 p2897 N85-27861
Heat resistant Carbon Fiber Reinforced Plastics (CFRP) hardening equipment
[MBB/LFA33/CFK/PUB/007] 17 p2916 N85-27976
Proceedings of the 9th US Air Force and the Federal Republic of Germany Data Exchange Agreement Meeting, Viscous and Interacting Flow Field Effects
[AD-A153020] 17 p2958 N85-28266
Research on structures and materials — aircraft structures
[B6580080] 17 p2961 N85-28432
Further investigations to improve the fatigue life of the Mirage 1110 wing main span
[ARL/STRUC-TM-397] 18 p3061 N85-28938
MBB expands CADAM system for a 320 program 18 p3067 N85-29099
Structural Analysis
[DFVLR-MITT-84-21] 18 p3120 N85-29313
Research on structural analysis at the DFVLR, Brunswick 18 p3120 N85-29314
Activities of the Department of Aerospace Engineering 18 p3199 N85-29844
Aeronautical Engineering: A continuing bibliography with indexes (supplement 188)
[NASA-SP-7037(188)] 19 p3211 N85-29910
Fuel containment and damage tolerance in large composite primary aircraft structures
[NASA-CR-166063] 19 p3231 N85-30032
Automated fabrication of composite structures for helicopters
[SNIAS-851-210-104] 20 p3393 N85-31049
Elastomers used in aeronautics industry
[SNIAS-851-551-109] 20 p3434 N85-31304
Influence of the molding joint plane on the fatigue resistance of the alloys 7010 and 7050. Test Report No. M1-631600
[PV-M1-631600] 20 p3470 N85-31562
R and D programmes at the National Aeronautical Laboratory
[AR-22] 20 p3539 N85-32022
R and D activities of the Materials Science Division 20 p3539 N85-32024
R and D activities of the Structural Sciences Division 20 p3539 N85-32026
Quest for performance: The evolution of modern aircraft
[NASA-SP-468] 21 p3551 N85-32089
Preliminary sizing and performance of aircraft
[NASA-TM-86357] 21 p3554 N85-32111
Study of an ultrasonic detection method to inspect bonding effects in light alloy bonded structures, test report no. 43-954/F — aircraft structures
[PV-43-954/F] 22 p3795 N85-33510
Flight service evaluation of composite helicopter components
[NASA-CR-172582] 23 p3909 N85-34222
An automated technique for encasing specific payloads with low-drag fairings 24 p4063 N85-35183
Fatigue lives of specimens representing critical locations in Mirage 3 spars under Australian and Swiss test spectra
[ARL-STRUC-R-415] 24 p4064 N85-35187
Analysis of flexible aircraft longitudinal dynamics and handling qualities. Volume 1: Analysis methods
[NASA-CR-177943-VOL-1] 24 p4066 N85-35202
Analysis of flexible aircraft longitudinal dynamics and handling qualities. Volume 2: Data
[NASA-CR-177943-VOL-2] 24 p4067 N85-35203

AIRCRAFT SURVIVABILITY
F-16 force management, yesterday, today and tomorrow 07 p0895 N85-15674
An empirical self-protection chaff model
[AD-A151928] 16 p2773 N85-27115
General Aviation Crashworthiness Project. Phase 2: Impact severity and potential injury prevention in general aviation accidents
[PB85-917002] 19 p3215 N85-29938

AIRCRAFT TIRES
Aircraft chocks
[AD-A145135] 01 p0012 N85-10077
Alternatives for runway rubber removal from porous friction surfaces
[DOT/FAA/PM-84/28] 05 p0597 N85-13803
The space shuttle program from challenge to achievement: Space exploration rolling on tires 08 p1101 N85-16960
Selection of effective arrangement of heavy undercarriage systems for use with concrete runways 14 p2285 N85-24158
A feasibility study for using low boiling point fluids to change aircraft tire deflection
[AD-A152096] 16 p2706 N85-26701

AIRCRAFT WAKES
NT HELICOPTER WAKES
NT PROPELLER SLIPSTREAMS
NT SLIPSTREAMS
Preliminary results using a rapid photographic wake traverse system — in a wind tunnel
[RAE-TM-AERO-1967] 02 p0200 N85-11332
Analysis of noise measured from a propeller in a wake
[NASA-TP-2358] 02 p0274 N85-11788
Recent advances in computational methods to solve the high-lift multi-component airfoil problem 08 p1068 N85-16774

AIRCREWS
U FLIGHT CREWS

AIRFIELD SURFACE MOVEMENTS
New airport ground traffic control system planned 03 p0310 N85-12006
Simulation of aircraft behaviour on and close to the ground
[NASA-TM-87460] 14 p2218 N85-23754

AIRFIELDS
U AIRPORTS

AIRFOIL CHARACTERISTICS
U AIRFOILS

AIRFOIL FENCES
An exploratory study of apex fence flaps on a 74 deg delta wing
[NASA-CR-172463] 15 p2463 N85-25208

AIRFOIL PROFILES
NT WING PROFILES
NT WING SPAN
First cryogenic test of the CAST 7 profile in the T2 wind tunnel. Comparison with calculations — airfoils
[ONERA-RTS-56/1665-AY-035-D] 04 p0577 N85-13682
Effects of aircraft and flight parameters on energy-efficient profile descents in time-based metered traffic
[NASA-CR-172336-ADD] 07 p0901 N85-15706
Detailed study of the flow around a multi-element airfoil. Comparison with calculations 08 p1069 N85-16775
Laminar separation bubble with transition: Prediction test with local interaction — airfoils
[PNR-90231] 09 p1274 N85-18008
Profile design for wings and propellers
[NASA-TM-77785] 10 p1419 N85-18953
Skin friction measurements for 2 relatively thick airfoil sections at high Reynolds number
[AD-A150021] 12 p1772 N85-21125
Investigation of the aerodynamic forces on bluff bodies at high Reynolds numbers
[DFVLR-MITT-84-19] 14 p2213 N85-23727
Airfoil wing with flap
[CH-634787-A5] 15 p2469 N85-25243
Investigation of potential and viscous flow effects contributing to dynamic stall
[AD-A151696] 15 p2557 N85-25773
Design of a basic profile for a low sweep airfoil. Part 2: Experimental investigation on the DFVLR-W1 airfoil profile in the Brunswick transonic wind tunnel
[DFVLR-FB-85-01-PT-2] 17 p2892 N85-27833
Integral profile method for production of carbon fiber sheets
[MBB/LFA34/CFK/PUB/008] 17 p2916 N85-27975
Experimental investigations on airfoils with different geometries in the domain of high angles of attack-flow separation
[NASA-TM-77892] 22 p3728 N85-33110
An investigation into the three-dimensional stall development on a modified NACA 23012 aerofoil
[GU-AERO-8414] 23 p3894 N85-34124

AIRFOIL SECTIONS
U AIRFOIL PROFILES

AIRFOIL THICKNESS
U AIRFOIL PROFILES

AIRFOILS
NT AERIAL RUDDERS
NT AEROELASTIC RESEARCH WINGS
NT AILERONS
NT AIRFOIL FENCES
NT BEARINGLESS ROTORS
NT CAMBERED WINGS
NT CIRCULATION CONTROL AIRFOILS
NT DELTA WINGS
NT ELEVATORS (CONTROL SURFACES)
NT ELEVONS
NT FIXED WINGS
NT FLAPERONS
NT FLAPS (CONTROL SURFACES)
NT FLEXIBLE WINGS
NT HORIZONTAL TAIL SURFACES
NT JET FLAPS
NT LAMINAR FLOW AIRFOILS
NT LEADING EDGE SLATS
NT LIFTING ROTORS
NT LOW ASPECT RATIO WINGS
NT PROPELLER BLADES
NT RECTANGULAR WINGS
NT RIGID ROTORS
NT RIGID WINGS
NT ROTARY WINGS
NT SLENDER WINGS
NT SPOILERS
NT SUPERCRITICAL AIRFOILS
NT SUPERCRITICAL WINGS
NT SUPERSONIC AIRFOILS
NT SWEPT FORWARD WINGS
NT SWEPT WINGS
NT SWEPTBACK WINGS
NT TABS (CONTROL SURFACES)
NT THIN AIRFOILS
NT THIN WINGS
NT TILTING ROTORS
NT TIP DRIVEN ROTORS
NT TRAILING EDGE FLAPS
NT TWISTED WINGS
NT UNSWEPT WINGS
NT VARIABLE SWEEP WINGS
NT VORTEX FLAPS
NT WING FLAPS
NT WINGS
Development and applications of algorithms for calculating the transonic flow about harmonically oscillating wings
[NASA-CR-172376] 01 p0002 N85-10007
Computational methods for complex flowfields
[AD-A145219] 01 p0004 N85-10019
Embedded-grid generation with complete continuity across interfaces for multi-element airfoils 02 p0133 N85-10911
Design and wind tunnel evaluation of a symmetric airfoil series for large wind turbine applications
[NASA-CR-174784] 02 p0135 N85-10919
Turbine heat transfer 02 p0142 N85-10964
Gas side heat transfer: 2-D flow 02 p0142 N85-10965
Jet array impingement flow distributions and heat transfer characteristics: Effects of initial crossflow and nonuniform array geometry 02 p0142 N85-10967
Life prediction and constitutive models for anisotropic materials 02 p0144 N85-10976

Interactive aircraft flight control and aeroelastic stabilization
[NASA-CR-174025] 02 p0148 N85-11003
Performance of two transonic airfoil wind tunnels utilizing limited ventilation 03 p0313 N85-12020
Experiments suitable for wind tunnel wall interference assessment/correction 03 p0313 N85-12021
Asymptotic methods for wind tunnel wall corrections at transonic speed 03 p0313 N85-12022
Progress in wind tunnel wall interference assessment/correction procedures at the NAE 03 p0314 N85-12025
Review of the advanced technology airfoil test program in the 0.3-meter transonic cryogenic tunnel 03 p0315 N85-12033
Some experience with Barnwell-Sewall type correction to two-dimensional airfoil data 03 p0315 N85-12034
Interaction between an airfoil and a streamwise vortex
[AD-A145823] 03 p0316 N85-12041
Design of a basic airfoil for a slightly swept wing. Part 1: Theoretical transonic airfoil design
[DFVLR-FB-84-19-PT-1] 03 p0316 N85-12043
An experimental study on the induced normal force on tail-fins due to wing-tail interference
[NAL-TR-814] 03 p0318 N85-12051
Unsteady aerodynamic response of cascades and turborotors 03 p0319 N85-12058
Numerical studies of unsteady transonic flow over an oscillating airfoil
[NASA-TM-86011] 03 p0361 N85-12316
A study of flow past an airfoil with a jet issuing from its lower surface
[NASA-CR-166610] 04 p0451 N85-12860
Natural laminar flow airfoil design considerations for winglets on low-speed airplanes
[NASA-CR-3853] 04 p0452 N85-12863
A comparison of Wortmann airfoil computer-generated lift and drag polars with flight and wind tunnel results
[NASA-TM-86035] 04 p0452 N85-12868
Effect of a variable camber and twist wing at transonic Mach numbers
[NASA-TM-86281] 04 p0452 N85-12869
The role of freestream turbulence scale in subsonic flow separation
[NASA-CR-174172] 04 p0452 N85-12870
Tailored airfoils for vertical axis wind turbines
[DE84-013618] 04 p0529 N85-13380
Simulation of separated transonic airfoil flow by finite-difference viscous-inviscid interaction 05 p0591 N85-13768
Evaluation of the unsteady effects for a class of wind turbines 05 p0592 N85-13772
Experimental studies of transonic airfoil trailing edge and wake flowfield properties 05 p0592 N85-13773
An experimental study of airfoil-spoiler aerodynamics
[NASA-CR-177328] 06 p0748 N85-14796
Comparison of uniform perturbation solutions and numerical solutions for some potential flows past slender bodies
[NASA-CR-172485] 06 p0749 N85-14799
Development of the code NSFOIL for analyzing high Reynolds number transonic flow around an airfoil
[NAL-TR-816] 06 p0749 N85-14801
Laminar separation bubble with transition: Prediction test with local interaction
[BLL-PNR-90231-(8019.3153)] 06 p0808 N85-15132
Unsteady pressure measurements on a biconvex airfoil in a transonic oscillating cascade
[NASA-TM-86914] 07 p0898 N85-15689
Aircraft wing fuel tank environmental simulator tests for evaluation of antimisting fuels
[FAA-CT-84-15] 07 p0934 N85-15920
Some important problems in unsteady boundary layers including separation. 1: Nature of singularity on oscillating airfoils
[AD-A147897] 07 p0960 N85-16087
High temperature thermocouple and heat flux gauge using a unique thin film-hardware hot juncture
[NASA-TM-86696] 07 p0962 N85-16096
Analysis of the surface load and radiated sound of a vibrating airfoil with application to the experiment of Brooks
[NASA-CR-3864] 07 p1036 N85-16590
Recent advances in computational methods to solve the high-lift multi-component airfoil problem 08 p1066 N85-16774
Inviscid compressible flow past a multi-element aerofoil 08 p1069 N85-16776
Turbulent bubbles behind airfoils and wings at high angle of attack 08 p1069 N85-16779
Design studies of thick laminar flow airfoils for low speed flight employing turbulent boundary layer suction over the rear part 08 p1070 N85-16786
Pneumatic turbulators: A device for drag reduction at Reynolds numbers below 5 million 08 p1071 N85-16791
Results of S5 CH tests with an ARL (Aerospace Research Laboratory) cascade
[NASA-TM-77510] 08 p1089 N85-16882
Unsteady aerodynamic loading of an airfoil due to vortices released intermittently from its upper surface
[AD-P004162] 09 p1265 N85-17947
A Navier-Stokes calculation of the airfoil dynamic stall process
[AD-P004163] 09 p1265 N85-17948
Unsteady separated flow: Forced and common vorticity about oscillating airfoils
[AD-P004167] 09 p1265 N85-17952
Leading edge separation criterion for an oscillating airfoil
[AD-P004175] 09 p1267 N85-17960
Corrections for attached sidewall boundary-layer effects in 2-dimensional airfoil testing
[NASA-CR-3873] 09 p1272 N85-17997
Flow instabilities in transonic small disturbance theory
[NASA-TM-86251] 09 p1273 N85-18000
Numerical approach for the aerodynamic analysis if airfoils with laminar separation
[NASA-CR-172496] 09 p1273 N85-18001
Synthesized airfoil data method for prediction of dynamic stall and unsteady airloads
[NASA-CR-3672] 09 p1274 N85-18005
Study of controlled diffusion stator blading
[NASA-CR-167995] 09 p1281 N85-18058
The boundary layer on compressor cascade blades
[NASA-CR-174369] 09 p1319 N85-18292
On the flow processes in sharply inclined and stalled airfoils in parallel movement and rotation
[NASA-TM-77509] 10 p1419 N85-18952
Analysis of inviscid transonic flow around an airfoil by diagonal form of IAF scheme
[NAL-TR-831] 10 p1420 N85-18955
Effects of airfoil shape, thickness, camber, and angle of attack on calculated transonic unsteady airloads
[NASA-TM-86320] 10 p1420 N85-18957
Viscous effects on transonic airfoil stability and response
[NASA-TM-86374] 10 p1421 N85-18961
Wall interference estimation of the NAL's two-dimensional wind tunnel
[NAL-TR-829] 10 p1426 N85-18992
A multistage time-stepping scheme for the Navier-Stokes equations
[NASA-CR-172527] 10 p1483 N85-19365
Post stall airfoil data for wind turbines: Wind tunnel test results
[DE85-004052] 10 p1511 N85-19534
Rocky Flats Wind Energy Research Center FY 1983 report
[DE85-004500] 10 p1511 N85-19535
A fast algorithm of the finite difference method for computation of the transonic flow past an arbitrary airfoil with the conservative full-potential equation 11 p1619 N85-20191
On relaxation of transonic flows around zero-lift airfoils and convergence of self-correcting wing tunnels 11 p1622 N85-20214
Finite difference computation of the flow around airfoils in two-dimensional transonic slotted wall wind tunnel 11 p1623 N85-20216
The Satellite sail 11 p1647 N85-20376
Three-dimensional unsteady lifting surface theory in the subsonic range
[NASA-TM-77812] 12 p1770 N85-21111
A study of transonic flutter of a two-dimensional airfoil using the U-g and p-k methods
[LR-615] 12 p1771 N85-21121
Tailored airfoils for vertical axis wind turbines
[DE85-004626] 12 p1772 N85-21128
Numerical integration of the unsteady full-potential equation with applications to transonic flow about a two-dimensional airfoil
[NLR-MP-84022-U] 12 p1773 N85-21130
Hypersonic flow about triangular airfoil at large angles of attack 13 p2044 N85-22792
T700 cutter life improvement program
[AD-A150450] 13 p2099 N85-23089
Structural design of the Sandia 34-M Vertical Axis Wind Turbine
[DE85-002631] 13 p2129 N85-23247
Oscillating airfoils and their wake
[NASA-TM-77831] 14 p2209 N85-23701
The structure of separated flow regions occurring near the leading edge of airfoils, including transition
[NASA-CR-175670] 14 p2209 N85-23703
Computations of two-dimensional airfoil-vortex interactions --- helicopter rotor flowfields
[NASA-CR-3885] 14 p2210 N85-23709
Flutter taming: A new tool for the aeroelastic designer
[AD-A150834] 14 p2226 N85-23802
Transonic Unsteady Aerodynamics and its Aeroelastic Applications
[AGARD-CP-374] 15 p2457 N85-25171
Numerical studies of unsteady transonic flow over oscillating airfoil 15 p2458 N85-25174
Experience with transonic unsteady aerodynamic calculations 15 p2458 N85-25176
Calculation of harmonic aerodynamic forces of aerofoils and wings from the Euler equations 15 p2458 N85-25177
Unsteady transonic aerodynamic and aeroelastic calculations about airfoils and wings 15 p2459 N85-25185
A study of transonic flutter of a two-dimensional airfoil using the U-g and p-k methods
[AD-A151463] 15 p2473 N85-25268
Transient technique for measuring heat transfer coefficients on stator airfoils in a jet engine environment
[NASA-TM-87005] 15 p2560 N85-25794
Investigation to optimize the passive shock wave/boundary layer control for supercritical airfoil drag reduction
[NASA-CR-175788] 16 p2699 N85-26665
Low Reynolds number vehicles
[AGARD-AG-288] 16 p2699 N85-26666
Automatic flight control modes for the AFTI/F-111 mission adaptive wing aircraft 16 p2714 N85-26756
Static and dynamic pressure measurements on a NACA 0012 airfoil in the Ames High Reynolds Number Facility
[NASA-TP-2485] 17 p2891 N85-27823
Users manual for coordinate generation code CRDSRA
[NASA-CR-172584] 17 p2891 N85-27824
User's manual for airfoil flow field computer code SRAIR
[NASA-CR-172585] 17 p2891 N85-27825
Numerical study of porous airfoils in transonic flow
[NASA-TM-86713] 17 p2892 N85-27828
Wing tunnel investigation of dynamic stall of an NACA 0018 airfoil oscillating in pitch
[NAE-AN-27] 17 p2892 N85-27830
Ice shapes and the resulting drag increase for a NACA 0012 airfoil
[NASA-TM-83556] 17 p2894 N85-27839
Proposals for the determination of necessary elevator handling characteristics of sailplanes in high speed range
[DFVLR-FB-84-52] 17 p2900 N85-27882
New facility to study unsteady wake effects on turbine airfoil heat transfer 17 p2911 N85-27948
Constitutive cyclic deformation behavior in single-crystal and directionally solidified SSME high-pressure fuel turbopump airfoil materials 17 p2914 N85-27965
A 5-year research plan, 1985-1990. Wind energy technology: Generating power from the wind
[DE85-008427] 17 p2987 N85-28463
Turbulence structure in the boundary layers of an oscillating airfoil
[AD-A153831] 18 p3059 N85-28926
A study of aerodynamic control in stalled flight leading-edge vortex formation analysis
[AD-A153758] 18 p3059 N85-28928
A study of aerodynamic control in stalled flight long laminar separation bubble analysis
[AD-A153650] 18 p3059 N85-28930
Post-stall wind tunnel data for NACA 44XX series airfoil sections
[DE85-002948] 18 p3060 N85-28931
Inviscid analysis of two supercritical laminar-flow-control airfoils at design and off-design conditions
[NASA-TM-84657] 19 p3212 N85-29920
Application of two-dimensional unsteady aerodynamic to a free-tip rotor response analysis
[NASA-CR-177348] 19 p3215 N85-29933
Aircraft rotor blade with passive tuned tab
[NASA-CASE-ARC-11444-1] 19 p3217 N85-29947
Performance comparison between NACA 23024 and NACA 64(3)-618 airfoil configurated rotors for horizontal-axis wind turbines
[NASA-TM-83471] 19 p3303 N85-30477
Computer programs for smoothing and scaling airfoil coordinates
[NASA-TM-84866] 20 p3388 N85-31011
Interactive aircraft flight control and aeroelastic stabilization
[NASA-CR-176035] 20 p3396 N85-31064
Sidewall boundary-layer effects in two-dimensional airfoil testing
[NASA-CR-176034] 20 p3396 N85-31065
Heat transfer in aeropropulsion systems
[NASA-TM-87066] 20 p3453 N85-31444
An evaluation of four methods of numerical analysis for two-dimensional airfoil flows
[AD-A155202] 21 p3552 N85-32098

Calculation of steady and unsteady airfoil flow fields via the Navier-Stokes equations
[NASA-CR-3899] 22 p3727 N85-33105
Experimental investigations on airfoils with different geometries in the domain of high angles of attack-flow separation
[NASA-TM-77892] 22 p3728 N85-33110
Generation by conformal mappings of aerofoil sections and of certain other simple shapes suitable for both aerodynamic and stress-concentration problems
[AD-A154901] 22 p3728 N85-33112
Local heat-transfer measurements on a large, scale-model turbine blade airfoil using a composite of a heater element and liquid crystals
[NASA-TM-86900] 22 p3782 N85-33435
An evaluation of three helicopter rotor sections
[NASA-TM-86719] 23 p3893 N85-34115
A design procedure to modify the trailing edge upper surface pressure gradient of a given aerofoil
[GU-AERO-8408] 23 p3894 N85-34120
Modelling of unsteady, incompressible separation on an aerofoil using an inviscid flow algorithm
[GU-AERO-8412] 23 p3894 N85-34122
The collected data for ramp function tests on a NACA 23012 aerofoil. Volume 1: Description and pressure data
[GU-AERO-8413-VOL-1] 23 p3894 N85-34123
A comparison of laser Doppler anemometry and probe measurements within the boundary layer of an airfoil at subsonic flow
[ISL-CO-219/84] 23 p3895 N85-34127
A stream function approach to solving the conservative Euler equations for transonic flows
24 p4059 N85-35156
Heat transfer characteristics for two-dimensional arrays of impinging jets with initial crossflow
24 p4092 N85-35365

AIRFRAME MATERIALS
Fuel efficiency through new airframe technology
[NASA-TM-84548] 02 p0133 N85-10909
Full-scale crash-test evaluation of two load-limiting subfloors for general aviation airframes
[NASA-TP-2380] 04 p0512 N85-13267
A comparison of fatigue lives under a complex and a much simplified flight-by-flight testing sequence --- Mirage 3 aircraft
[ARL/STRUC-TM-386] 09 p1280 N85-18052
Fatigue Crack Topography
[AGARD-CP-376] 14 p2318 N85-24321
New materials and techniques for aircraft structures
[B6580074] 17 p2897 N85-27861

AIRFRAMES
The Influence of Large Scale Computing on Aircraft Structural Design
[AGARD-R-706] 01 p0007 N85-10040
Fuel efficiency through new airframe technology
[NASA-TM-84548] 02 p0133 N85-10909
Iterative method of calculating strength of airframe members using finite element method
06 p0775 N85-14955
Analysis of thin-walled airframe members in geometrically nonlinear statement
06 p0780 N85-14965
Some aspects of engine and airframe integration for Ramjet and Ramrocket powered missiles
07 p0918 N85-15812
High-strength composite materials for aircraft, body armor
11 p1599 N85-20057
Aircraft skin penetrator and agent applicator. Volume 2: Test and evaluation
[AD-A151609] 15 p2466 N85-25225
Design, fabrication and test of composite curved frames for helicopter fuselage structure
[NASA-CR-172438] 15 p2470 N85-25247
Tensile and fracture toughness properties of Mirage III spars
[AR-003-019] 15 p2578 N85-25899
Initial quality of advanced joining concepts
[AD-A152241] 16 p2759 N85-27027
USAF damage tolerant design handbook: Guidelines for the analysis and design of damage tolerant aircraft structures, revision B
[AD-A153161] 17 p2896 N85-27858

AIRGLOW
NT GEOCORONAL EMISSIONS
NT NIGHTGLOW
NT TWILIGHT GLOW
Nocturnal increases of ionization in the ionospheric F region in the low latitude of Brazil during magnetic storms
[INPE-3271-PRE/596] 05 p0675 N85-14334
Study of infrared atmospheric emission
[AD-A147517] 07 p0998 N85-18336
Application of Fabry-Perot spectrometers for measurement of upper atmosphere temperatures and winds
08 p1183 N85-17454
Upper atmosphere research at INPE
[INPE-3281-PRE/604] 10 p1515 N85-19557
Analysis and interpretation of observations of airglow at 297 nm in the Venus thermosphere
13 p2172 N85-23473
A measurement of the intensity of the cosmic background radiation at 3.9 cm
13 p2206 N85-23681
Determination of total moisture content in cloud-free atmosphere by relative radio emission measurements
14 p2340 N85-24472
Fabry-Perot interferometer and skymapping photometer determinations of midlatitude f-region neutral winds and temperatures and airglow enhancement/depletions
[AD-A150730] 14 p2373 N85-24666
Observations of airglow O2(1-Sigma) atmospheric band at 8645 A and the rotational temperature at 23 deg S
[INPE-3378-PRE/653] 16 p2826 N85-27435
Thermospheric winds observed by OI6300A Doppler shifts at 23 deg S in the Brazilian sector
[INPE-3384-RPE/470] 16 p2834 N85-27479
SCRIBE data of October 23, 1983 flight
[AD-A154864] 21 p3705 N85-33012
Atmospheric Emission Photometric Imaging (AEPI)
23 p3902 N85-34170

AIRLINE OPERATIONS
Activities report of the aerospace industry in West Germany
[ISSN-0176-5086] 05 p0734 N85-14718
Activities report of the aerospace industry in West Germany
[ISSN-0722-3838] 07 p1053 N85-16686
Activities report of the aerospace industry in West Germany
[ISSN-0722-3838] 07 p1054 N85-16687
Simulation 09 p1277 N85-18024
Analytical modeling of a polling protocol --- airline information network
[ENST-84H001] 09 p1277 N85-18029
First deputy minister on 1984 civil aviation performance 09 p1277 N85-18033
Finnair, LOT, SAS reps in USSR on present operations, plans 09 p1278 N85-18035
Sunset of the Civil Aeronautics Board
[S-HRG-98-940] 09 p1403 N85-18829
Digest of the Deutsche Lufthansa report, 1983
[ISSN-0415-603X] 09 p1418 N85-18848
Rotterdam Airport and the Common Market
17 p2894 N85-27840

AIRPORT LIGHTS
NT RUNWAY LIGHTS

AIRPORT PLANNING
Airport site selection and design
[AD-P004193] 11 p1581 N85-19959
Landscape management on airports for reduction of bird populations
[AD-P004194] 11 p1581 N85-19960
Airport system development
[PB85-127793] 11 p1587 N85-19993
Deputy minister on civil aviation construction projects
14 p2208 N85-23692
OWEMA report: A project study concerning the possibilities and the desirability of a east-west runway for Maastricht Airport (Netherlands) as a Euro-regional air freight center
[B8476490] 18 p3084 N85-28955
Aviation system delays
[S-HRG-98-1241] 21 p3553 N85-32102

AIRPORT TOWERS
Prototype concept design for US Army type 3A Air Traffic Control Tower (ATCT)
[AD-A148840] 09 p1284 N85-18070
Planned office and facility consolidations: To improve system effectiveness and efficiency, FY 1985-87
[AD-A150441] 13 p1970 N85-22376

AIRPORTS
NT HELIPORTS
Evaluation of laser profile and deflection measuring system
[FAA-PM-84-24] 02 p0201 N85-11341
New airport ground traffic control system planned
03 p0310 N85-12006
Start-2 ATC system installation progresses at Leningrad 03 p0311 N85-12007
Airport noise impact prediction and measurement
03 p0367 N85-12476
Operation of aviation support bases
04 p0544 N85-13461
TAF verification (airport weather forecasts)
[GEOPHYSBDBW-FM-205] 05 p0687 N85-14420
FAA (Federal Aviation Administration) statistical handbook of aviation, calendar year 1983
[AD-A148171] 08 p1067 N85-16780
International projects, other work of Aeroproyekt Institute 08 p1068 N85-16787
Activities report on West German civil airports. Part 1: Text
[ISBN-3-87977-055-7-PT-1] 08 p1090 N85-16887
Activities report for the West German Civil Airports. Part 2: Tables
[ISBN-3-87977-055-7-PT-2] 08 p1090 N85-16888
Impact of aircraft emissions on air quality in the vicinity of airports. Volume 3: Air quality and emission modeling needs
[AD-A147951] 08 p1180 N85-17435
Impact of aircraft emissions on air quality in the vicinity of airports. Volume 4. Nitrogen dioxide and hydrocarbons
[AD-A148253] 08 p1180 N85-17436
Test of dispersal of turbojet aircraft departure tracks at washington National Airport (1983-84), volume 1 report
[AD-A148111] 08 p1218 N85-17669
Improvements in Kazan airport equipment, facilities
09 p1278 N85-18039
Improvements under way at Gorkiy airport
09 p1278 N85-18040
Denver ARTCC (Air Route Traffic Control Center) evaluation of PROFS (Program for Regional Observing and Forecasting Services) mesoscale weather products
[PB85-120301/GAR] 09 p1279 N85-18045
Aircraft noise effects: An inter-disciplinary study of the effect of aircraft noise on man. Part 3: Supplementary analyses of the social-scientific portion of the study on aircraft noise conducted by the DFG
[NASA-TM-75802] 10 p1527 N85-19631
The use of small mobile radars to detect, monitor, and quantify bird movements
[AD-P004188] 11 p1580 N85-19951
Blackbirds and starlings: Population ecology and habits related to airport environments
[AD-P004190] 11 p1580 N85-19953
Birds on airports: The reason for their presence
11 p1580 N85-19955
The use of falconry as mean to persuade the birds to stay out of the airport vicinity 11 p1580 N85-19956
Control of mammals at airports
[AD-P004192] 11 p1580 N85-19957
Inexpensive multipurpose landscaping
11 p1581 N85-19961
Reducing gull use of some attractions near airports
[AD-P004195] 11 p1581 N85-19962
FAA policy regarding solid waste disposal facilities
[AD-P004196] 11 p1581 N85-19963
Airport bird hazards associated with solid waste disposal facilities
[AD-P004197] 11 p1581 N85-19964
Successful control of gulls and other birds at a sanitary landfill
[AD-P004198] 11 p1582 N85-19965
Development of bird hazard reduction for airport operational safety
[AD-P004202] 11 p1582 N85-19969
The bird strike situation and its ecological background in the Copenhagen Airport, Kastrup
[AD-P004203] 11 p1582 N85-19970
Bird control program Orlando International Airport
[AD-P004204] 11 p1583 N85-19971
Birds and airport agriculture in the conterminous United States: A review of literature
[AD-P004208] 11 p1583 N85-19975
The FAA grant-in-aid assurances: FAR part 139, and airport hazards
[AD-P004209] 11 p1583 N85-19976
Light your runways and taxiways without electricity
[DE85-000269] 11 p1586 N85-19991
International airport study: How to improve the effect of airports on trade and on export-related industries
[PB85-124923] 11 p1586 N85-19992
Airport system development
[PB85-127793] 11 p1587 N85-19993
Examination of the feasibility for demonstration and use of radioluminescent lights for Alaskan remote runway lighting
[DE85-002503] 12 p1782 N85-21185
FTASUM: Aviation forecast summaries
[PB85-112977] 12 p1807 N85-21906
An analysis of the impacts of the Airport Radar Service Area (ARSA)
[AD-A150954] 14 p2217 N85-23749
Disturbance to the population due to flight operations at landing fields. Questionnaire on community reaction to non-commercial and sporting aviation
[NASA-TM-76531] 14 p2353 N85-24537
A study of the methods for evaluating the noise impact of a proposed airport on a community
15 p2588 N85-25957
Probabilistic computer model of optimal runway turnoffs
[NASA-CR-172549] 16 p2715 N85-26760

Study of acceptance criteria for joint densities in bituminous airport pavements
[FAA-PM-85-5] 16 p2715 N85-26761
Radioluminescent lighting for rural Alaskan runway lighting and marking
[DE85-007022] 16 p2716 N85-26764
Acceptability testing of radioluminescent lights for VFR-night air taxi operations
[DE85-007303] 16 p2716 N85-26765
Rotterdam Airport and the Common Market
17 p2894 N85-27840
Airport and airway system cost allocation model. Volume 7: User's manual
[AD-A152877] 17 p2906 N85-27917
Frangibility of obstacles at airports
[NLR-MP-84002-U] 17 p2981 N85-28431
Air traffic: Instruments, airports, companies, post, cargo and passengers 18 p3060 N85-28932
Data on noise environments at different times of day around airports
[NASA-CR-172612] 19 p3351 N85-30769

AIRSHIPS
Missions and vehicle concepts for modern, propelled, lighter-than-air vehicles
[NASA-TM-86672] 08 p1066 N85-16757
Current development, applications of airships in USSR
12 p1769 N85-21109
Missions and vehicle concepts for modern, propelled, lighter-than-air vehicles
[NASA-TM-87461] 15 p2457 N85-25170

AIRSPACE
System engineering and integration contract for implementation of the National Airspace System Plan. Volume 2: Section 5.0
[AD-A145710] 02 p0137 N85-10929
System engineering and integration contract for implementation of the National Airspace System plan, volume 1, sections 1.0-4.0, 6.0
[AD-A145763] 03 p0317 N85-12048
National airspace review: Airport radar service area operational confirmation report
[DOT/FAA/AT-84/2] 07 p0901 N85-15707
National airspace review enhancement plan, revision 3
[AD-A150743] 08 p1082 N85-16852
National airspace review. Implementation plan. Revised
[AD-A151412] 15 p2468 N85-25238
Airport and airway system cost allocation model. Volume 7: User's manual
[AD-A152877] 17 p2906 N85-27917
Introduction to European air traffic control
[AD-A156326] 24 p4062 N85-35176

AIRSPEED
Critical conditions for the automatic control of landing from decision height in variable winds
[UTIAS-284] 06 p0753 N85-14830
Recent methods for calibrating the anemometry of helicopters at low speeds 08 p1074 N85-16809
Simulating speed and height cues in the C-130 weapon system trainer
[AD-P004313] 09 p1268 N85-17967
Determination of corrections to flow direction measurements obtained with a wing-tip mounted sensor
[NASA-CR-174412] 10 p1421 N85-18962
Airspeed sensing pressure valve system
[AD-D011472] 10 p1425 N85-18987
Miniature electrooptical air flow sensor
[NASA-CASE-LAR-13065-1] 11 p1635 N85-20295
Safety recommendation(s), A-84-123 and -124
[REPT-3894B/93] 15 p2466 N85-25222
High specific power aircraft turn maneuvers: Tradeoff of time-to-turn versus change in specific energy
[AD-A151701] 15 p2471 N85-25257
Formulation and implementation of nonstationary adaptive estimation algorithm with applications to air-data reconstruction
[NASA-TM-86727] 16 p2706 N85-26699
Using regression analysis for determining air data sensor errors by means of an inertial navigation system
[ESA-TT-866] 20 p3392 N85-31041

AIRWORTHINESS
U AIRCRAFT RELIABILITY

AIRWORTHINESS REQUIREMENTS
U AIRCRAFT RELIABILITY

AIRY FUNCTION
Brownian motion with a parabolic drift and Airy functions
[CWI-MS-R8413] 12 p1925 N85-22097

AITKEN NUCLEI
Eleventh International Conference on Atmospheric Aerosols, Condensation and Ice Nuclei, volume 2
[PB85-182418] 21 p3638 N85-32596
Inactivation of silver iodide by atmospheric nucleation inhibitors 21 p3638 N85-32599
Ice nucleus measurements 21 p3640 N85-32609
The 100 years of Aitken Nuclei (AN) study-reminiscence, current and future problems 21 p3641 N85-32621
Analysis of performance of dynamic thermal diffusion chamber 21 p3642 N85-32625
Eleventh International Conference on Atmospheric Aerosols, Condensation and Ice Nuclei, volume 1
[PB85-182400] 21 p3644 N85-32636
The first condensation nucleus conference
21 p3644 N85-32637
Study of the formation of particles from natural hydrocarbons released by vegetation
21 p3644 N85-32640
Experimental studies of the formation of Aitken nuclei in the atmosphere 21 p3644 N85-32641
Human activity and production rate of secondary nuclei 21 p3645 N85-32645
Aitken particle size distribution in Antarctica
21 p3645 N85-32656
Properties of forest derived cloud condensation nuclei
21 p3650 N85-32682
The nuclei of cloud formation
21 p3651 N85-32685
Transport and formation of summertime cloud condensation nuclei over the Arctic Ocean
21 p3651 N85-32686
A review on the formation of aerosol particles in the atmosphere 21 p3651 N85-32687
The interaction of polynuclear aromatic hydrocarbons PAH's with water vapor and their role as condensation nuclei in the formation of haze and fog
21 p3652 N85-32695
Applicability of surface CCN measurements
21 p3652 N85-32696
on the transport of large condensation nuclei in the atmosphere at various altitudes over the territory of the USSR 21 p3653 N85-32698

ALABAMA
Operational evaluation of 5 cm Doppler radar. Two contributions: Review of WSR-74C Doppler radar operations at WSO Montgomery, Alabama (April 1982 - August 1983). The Johnson-Effect resolving ambiguous Doppler velocities
[PB84-207521] 01 p0041 N85-10269
Alabama Tin Belt: Metallogenesis and mineral resource evaluation. Year-end report
[DE84-901335] 07 p0989 N85-16283
Water resources data for Alabama, water year 1983
[PB85-123842] 10 p1507 N85-19507
Geodetic accuracy of LANDSAT 4 Multispectral Scanner and Thematic Mapper data — Washington, DC, California, Alabama, South Dakota, and Illinois
11 p1667 N85-20504

ALADIN 2 AIRCRAFT
Presentation of the acoustic and aerodynamic results of the Aladin 2 concept qualification testing
[NASA-TM-77883] 24 p4060 N85-35161

ALANINE
Response of amino acids in hindlimb muscles to recovery from hypogravity and unloading by tail-cast suspension
[NASA-CR-176183] 24 p4128 N85-35589
Response of rat hindlimb muscles to 12 hours recovery from tail-cast suspension
[NASA-CR-176182] 24 p4128 N85-35590

ALARMS
U WARNING SYSTEMS

ALASKA
The Alaskan mineral resources assessment program: Guide to information contained in the folio of geologic and mineral-resource maps of the Medfra Quadrangle, Alaska
[GS-CIRC-928] 02 p0219 N85-11443
A paleomagnetic study of the Prince William terrane and Nixon Fork terrane, Alaska 02 p0226 N85-11478
Late quarterly glaciolacustrine and vegetational history of the Copper River Basin, south-central Alaska
03 p0391 N85-12489
The United States Geological Survey in Alaska: Accomplishments during 1981
[USGS-CIRC-868] 04 p0515 N85-13283
Summary of LANDSAT quadrangle studies in Alaska
04 p0515 N85-13284
Digital elevation models improve processing of Alaskan gravity data 04 p0515 N85-13285
Seismic studies in southern Alaska
04 p0515 N85-13286
Horizontal-strain observations in the Shumagin Island and Yakataga seismic gaps, Alaska
04 p0515 N85-13287
Computer-generated latitude and longitude templates for rapid determination of geographic positions in Alaska
04 p0516 N85-13288
The Kanayut Conglomerate in the westernmost Brooks Range, Alaska 04 p0516 N85-13289
Geothermal studies in Alaska: Conditions at Prudhoe Bay 04 p0516 N85-13290
Reconnaissance geology of the northern part of the Unalakleet quadrangle 04 p0516 N85-13291
Newly recognized sedimentary environments in the Shelikof Formation, Alaska 04 p0516 N85-13292
New ages of radiolarian chert from the Rampart district, east-central Alaska 04 p0516 N85-13293
Concordant bands of augen gneiss within metasedimentary rocks in the Big Delta C-2 quadrangle, east-central Alaska 04 p0516 N85-13294
Metamorphic petrology of the Table Mountain area, Circle quadrangle, Alaska 04 p0516 N85-13295
Paleozoic limestones of the Crazy Mountains and vicinity, Circle quadrangle, east-central Alaska
04 p0517 N85-13296
Late Paleozoic and early Mesozoic radiolarians in the Circle quadrangle, east-central Alaska
04 p0517 N85-13297
Structural observations in the Circle quadrangle, Yukon-Tanana Upland, Alaska 04 p0517 N85-13298
Lacustrine and eolian deposits of Wisconsin age at Riverside Bluff in the upper Tanana River valley, Alaska
04 p0517 N85-13299
The northern coast plutonic-metamorphic complex, southeastern Alaska and northwestern British Columbia
04 p0518 N85-13305
Cretaceous plutonic rocks, Mitkof and Kupreanof Islands, Petersburg quadrangle, southeastern Alaska
04 p0518 N85-13306
Late oligocene gabbro near Ketchikan, southeastern Alaska 04 p0518 N85-13307
Geology and geochemical evolution of the Lost River, Alaska, tin deposit 04 p0533 N85-13405
Carbon monoxide study, Anchorage, Alaska, November 22, 1982 to February 11, 1983
[PB84-236595] 05 p0673 N85-14321
Revised Uniform Summary of Surface Weather Observations (RUSSWO). Shemya AFB, Alaska, parts A-F
[AD-A146917] 07 p1005 N85-16388
Shore ice ride-up and pile-up features. Part 2. Alaska's Beaufort Sea coast, 1983 - 1984
[AD-A148428] 08 p1190 N85-17501
Meteorological factors responsible for high CO (carbon monoxide) levels in Alaskan cities
[PB85-115137/GAR] 09 p1350 N85-18493
Mountain barrier baroclinity effects on surface winds along the Alaskan Arctic coast 14 p2238 N85-23877
Characteristics of fast sea ice collected near Barrow, Alaska 15 p2582 N85-25925
The ecology of tundra ponds of the Arctic coastal plain: A community profile
[TI85-900650] 15 p2589 N85-25958
Glossary of landscape and vegetation ecology for Alaska
[PB85-153831] 16 p2816 N85-27372
Structural analysis of terrane accretions in the eastern Brooks Range and adjacent areas in central Alaska and Canada
[DE85-008279] 17 p2993 N85-28501
Deep source gas
[DE85-001984] 18 p3126 N85-29358
The U.S. Geological Survey in Alaska: Accomplishments during 1982
[US-GEOL-SURV-CIRC-939] 20 p3493 N85-31719
Pacific Northwest and Alaska bioenergy program glossary
[DE85-011740] 22 p3808 N85-33591
The United States Geological Survey in Alaska: Accomplishments during 1983
[USGS-CIRC-945] 23 p3948 N85-34468
Some geophysical guides to ore in southern and southwestern Alaska 24 p4103 N85-35438

ALBEDO
NT COSMIC RAY ALBEDO
NT EARTH ALBEDO
Ultraviolet observations of Uranus and Neptune below 3000 Angstrom 02 p0298 N85-11932
Satellite masses in the Uranus and Neptune systems
[PSI-CONTRIB-198] 02 p0301 N85-11947
Dust properties determined from backscattering in the interplanetary and interstellar medium
03 p0446 N85-12838
Influence of the atmosphere on remotely sensed reflection from vegetation surfaces
[DE85-000658] 11 p1670 N85-20521
Atlas of relectance patterns for uniform earth and cloud surfaces (NIMBUS-7ERB-81 days)
[PB85-116382] 12 p1891 N85-21870
GMS operational calibration procedure and status
12 p1895 N85-21893
Snow reflectance from Thematic Mapper
13 p2120 N85-23205
Seasonal and secular variation of the Solis Lacus albedo feature: Relation to the Martian dust-transport cycle
13 p2188 N85-23576

Accurate albedos of the brightest regions on Io
13 p2195 N85-23618
Determination of mineral type, abundance, and grain size with remotely obtained reflectance spectra
13 p2196 N85-23623
Mars planimetric mapping 13 p2203 N85-23666
Atlas of archived vegetation, land-use and seasonal Albedo data sets
[NASA-TM-86199] 14 p2346 N85-24508
Current ideas on the nature of comets
14 p2435 N85-25017
Evaluating radiation distortions of optical image of Earth's surface in horizontally inhomogeneous atmosphere 15 p2486 N85-25345
Selection of a model of Earth's albedo radiation, practical calculation of its effect on the trajectory of a satellite
[NASA-TM-77870] 15 p2591 N85-25972
Sea ice, climate and Fram Strait
15 p2603 N85-26042
Earth Albedo and the orbit of LAGEOS
[NASA-TM-86210] 21 p3558 N85-32131
The distribution of compositional classes in the asteroid belt: A cosmochemical fingerprint?
22 p3852 N85-33856
Interpretation of photometric measurements of airless bodies 22 p3855 N85-33871
Monte Carlo techniques for analyzing deep penetration problems
[DE85-011426] 23 p3968 N85-34598
Additional flux of particles and albedo-electrons in upper atmosphere
[SH-6.1-6] 23 p4045 N85-35080
Observation of energy spectrum of electron albedo in low latitude region at Hyderabad, India
[SH-6.1-7] 23 p4045 N85-35081
Proton albedo spectrum observation in low latitude region at Hyderabad, India
[SH-6.1-8] 23 p4045 N85-35082

ALCOHOLS
NT ETHYL ALCOHOL
NT GLYCOLS
NT METHYL ALCOHOLS
NT PHENOLS
NT POLYVINYL ALCOHOL
Workload demand and CNS depressant stressor effects on spatial orientation information processing
[AD-A145211] 01 p0098 N85-10651
Converting gasoline farm tractors to run efficiently on farm-produced alcohol
[DE84-015796] 02 p0205 N85-11350
Development of acceptance criteria for batches of silane primer for external tank thermal protection system bonding applications
[NASA-CR-171266] 04 p0478 N85-13043
DOE supported research in alcohol fuel technology development
[DE84-007686] 06 p0774 N85-14948
Research and development of alcohol fuel usage in spark ignited engines 09 p1301 N85-18175
ECUT, Energy Conversion and Utilization Technologies program: Technical and economic assessment of processes for the production of butanol and acetone. Phase 2: Analysis of research advances
[NASA-CR-175471] 10 p1434 N85-19034
Fluorinated polyurethanes
[AD-D011526] 12 p1810 N85-21353
Trifunctional catalysts for conversion of syngas to alcohols
[DE85-004577] 13 p2040 N85-22771
Urban vehicle research project
[DE85-005444] 17 p3052 N85-28689
Alcohol: An alternate energy resource for community use
[DE85-007731] 18 p3084 N85-29075
Alkaline battery containing a separator of a cross-linked copolymer of vinyl alcohol and unsaturated carboxylic acid
[NASA-CASE-LEW-13102-1] 18 p3093 N85-29144
Impact of alcohol fuels on urban air pollution: Methanol photochemistry study
[DE85-009539] 18 p3133 N85-29403
Galactose oxidase in stereospecific oxidation of primary alcohols
[AD-A154059] 19 p3234 N85-30048
Phase behavior and QLS (Quasielastic Light Scattering) in potassium linoleate/n-alkanol microemulsions
[AD-A155028] 21 p3563 N85-32163
Metal alkoxides: Models for metal oxides. Alkoxide ligands in early transition metal organometallic chemistry
[DE85-011366] 23 p3916 N85-34269
Air university commander's and supervisor's guide on substance abuse
[AD-A156336] 24 p4133 N85-35822

ALDEHYDES
NT ACETALDEHYDE
NT FORMALDEHYDE
Highly dispersed metal atoms in zeolites
[DE85-010515] 19 p3354 N85-30792
Analysis of aldehydes and ketones in the gas phase
[PB85-181865] 20 p3426 N85-31281

ALDOSTERONE
Biochemical status of adrenocortical dysfunction following spaceflight 12 p1901 N85-21935

ALERTNESS
Shape with and without redundant colour as coding mechanism for simulated radar displays in a time-extended simple vigilance task
[AD-A151683] 16 p2844 N85-27533
Effects of low level carbon monoxide (CO) on tracking and monitoring. An attempt to replicate the findings of Putz et al. (1976) protocol 2
[AD-A155722] 22 p3825 N85-33694

ALEUTIAN ISLANDS (US)
Geology and geochemistry of early Tertiary submarine volcanic rocks of the Aleutian Islands, and their bearing on the development of the Aleutian Island Arc
03 p0389 N85-12493
Kuril-Aleutian subduction 19 p3290 N85-30402

ALFALFA
Multi crop area estimation in Idaho using EDITOR
[E85-10054] 06 p0827 N85-15251
Two-dimensional numerical model of sensible and latent heat transport in an irrigated field under advective conditions 13 p2131 N85-23251

ALFVEN WAVES
U MAGNETOHYDRODYNAMIC WAVES

ALGAAS
U ALUMINUM GALLIUM ARSENIDES

ALGAE
NT BLUE GREEN ALGAE
Response of algal populations to changes in stream water quality
[PB84-202464] 01 p0070 N85-10465
Modeling effects of toxicants on aquatic systems
[DE84-016594] 04 p0531 N85-13396
Cultivation and conversion of marine macroalgae — biomass energy production
[DE84-004522] 04 p0544 N85-13464
Problems associated with the utilization of algae in bioregenerative life support systems
[NASA-CR-166615] 07 p1019 N85-16469
Algal culture studies related to a Closed Ecological Life Support System (CELSS)
[NASA-CR-177322] 07 p1019 N85-16470
Petrography, sedimentology, diagenesis, and reservoir characteristics of some Pennsylvanian phylloid algal limestones: Kansas and Utah, USA
09 p1352 N85-18507
Artificial photosynthesis with algal and reconstituted systems
[DE85-002557] 10 p1523 N85-19604
Research and development of shallow algal mass culture systems for the production of oils
[DE85-000518] 11 p1690 N85-20624
Microalgae culture collection, 1984-1985
[DE84-013035] 11 p1690 N85-20626
Photosynthetic water splitting
[DE85-002460] 11 p1690 N85-20627
Characteristic vector analysis of inflection ratio spectra: New technique for analysis of ocean color data
[NASA-TP-2426] 13 p2126 N85-23237
Studies of photosynthetic Energy Conversion
[DE85-005973] 15 p2586 N85-25844
Technical and economic analysis of liquid fuel production from microalgae
[DE85-002926] 16 p2758 N85-27018
The role of sulfur in osmoregulation and salinity tolerance in cyanobacteria, algae, and plants
21 p3660 N85-32736
Salinity driven oceanographic upwelling
[DE85-011664] 22 p3818 N85-33652
Production of liquid fuels and chemicals by microalgae
[DE85-008780] 22 p3819 N85-33658
Composition and dynamics of bacteriocenosis associated with algae in human life-support systems
22 p3823 N85-33684
Resource evaluation and site selection for microalgae production systems
[DE85-008607] 23 p3951 N85-34485
Screening and characterizing oleaginous microalgal species from the southeastern United States
[DE85-008787] 23 p3951 N85-34488

ALGAL BLOOM
U ALGAE

ALGEBRA
NT ADJOINTS
NT AUTOMORPHISMS
NT BANACH SPACE
NT BINOMIALS
NT CANONICAL FORMS
NT CURRENT ALGEBRA
NT DETERMINANTS
NT EIGENVALUES
NT EIGENVECTORS
NT GROUP THEORY
NT HERMITIAN POLYNOMIAL
NT HILBERT SPACE
NT HOMOMORPHISMS
NT JORDAN FORM
NT LIE GROUPS
NT LINEAR EQUATIONS
NT LINEAR EVOLUTION EQUATIONS
NT LINEAR TRANSFORMATIONS
NT MATRICES (MATHEMATICS)
NT MONGE-AMPERE EQUATION
NT NONLINEAR EQUATIONS
NT NONLINEAR EVOLUTION EQUATIONS
NT POLYNOMIALS
NT QUADRATIC EQUATIONS
NT SOBOLEV SPACE
NT SPINOR GROUPS
NT STATE VECTORS
NT STIFFNESS MATRIX
NT STOKES THEOREM (VECTOR CALCULUS)
NT STRESS TENSORS
NT TENSORS
NT VECTOR SPACES
NT VECTORS (MATHEMATICS)
NT VORTICITY
Mathmatics and Computer Science Division activities
[DE84-014842] 01 p0104 N85-10701
PASCAL-MP algebraic and numerical manipulator for polynomials
[INPE-3229-TDL/176] 02 p0240 N85-11562
Algebraic functions of H-functions with specific dependency structure
[AD-A145598] 02 p0252 N85-11647
United States Air Force on research on algebraic manipulation
[AD-A145737] 02 p0253 N85-11655
Process algebra for communication and mutual exclusion
[CWI-CS-R8409] 05 p0720 N85-14622
Algebraic techniques in systolic array design
[AD-A146417] 06 p0857 N85-15451
The algebraic structure of convolutional codes with application to code construction and decoding
[AD-A148770] 08 p1206 N85-17591
Computing the Kac determinant using dual mode techniques and more about the No-ghost theorem
[DE85-001329] 09 p1375 N85-18640
Towards the construction of periodic solutions of pseudodifferential equations with the aid of algebraic operators 10 p1535 N85-19674
MACSYMA usage at Langley
[NASA-CR-172518] 10 p1537 N85-19688
Checking microcode algebraically
[AD-A149441] 10 p1547 N85-19759
Process algebra with asynchronous communication mechanisms
[CWI-CS-R8410] 11 p1625 N85-20235
Generalization of Beurling algebras
11 p1698 N85-20675
Object-oriented algebraic specification: Proposal for a notation and 12 examples
[CWI-CS-R8411] 11 p1707 N85-20744
Accidental degeneracies, hidden supersymmetries, and spectrum-generating superalgebras
[DE85-003547] 11 p1738 N85-20930
Parallel linear algebra library for the Denelcor HEP
[DE85-004685] 12 p1917 N85-22034
An algebraic specification language and a syntax directed editor
[AD-A150664] 14 p2403 N85-24815
BLAS (Basic Linear Algebra Subroutines), linear algebra modules and supercomputers
[AD-A151504] 15 p2628 N85-26199
Alternatives for jet engine control
[NASA-CR-175831] 16 p2709 N85-26713
Proposal for an extended set of FORTRAN Basic Linear Algebra subprograms
[DE85-007241] 16 p2848 N85-27562
Schubert varieties are arithmetically Cohen-Macaulay
16 p2853 N85-27592
Quadratic spaces over discrete Hodge algebras
16 p2853 N85-27593
Algebra of communicating processes
[CWI-CS-R8421] 17 p2950 N85-28214
Boundary to constructive solid geometry mappings: A focus on 2-D issues 17 p3004 N85-28570
A complete inference system for regular processes with silent moves
[CWI-CS-R8420] 17 p3014 N85-28638
A high-accuracy optical linear algebra processor for finite element applications
[NASA-CR-175894] 17 p3017 N85-28658
Discrete mathematics for communications systems
[AD-A152814] 17 p3018 N85-28664

Tenth-order expansion formulae for the orbital eccentricity function K (sub lpq)(e) obtained using a symbolic algebraic manipulation system
[AD-A153754] 18 p3170 N85-29647
On MGR (Upsilon) multigrid methods
[AD-A153867] 19 p3345 N85-30733
Parametric stiffness control of flexible structures
20 p3414 N85-31187
Symposium on Computational Mathematics-State-of-the-Art: Informal Proceedings
[DE85-008122] 20 p3516 N85-31858
A cracked orthotropic sheet stiffened by a semi-infinite orthotropic sheet
[NASA-TP-2455] 21 p3597 N85-32339
Gradient scaling for nonuniform meshes
[DE85-009625] 22 p3784 N85-33443
A study of the second and third order closure models of turbulence for prediction of separated shear flows
[NASA-CR-176127] 23 p3920 N85-34353
Stress analysis of axisymmetric sandwich shells of variable thickness 24 p4101 N85-35419

ALGORITHMS
NT PARSING ALGORITHMS
NT SIMPLEX METHOD
Computational methods for complex flowfields
[AD-A145219] 01 p0004 N85-10019
Impact of new computing systems on computational mechanics and flight-vehicle structures technology
01 p0007 N85-10042
Comparison of numerical techniques for integration of stiff ordinary differential equations arising in combustion chemistry
[NASA-TP-2372] 01 p0011 N85-10065
CREKID: A computer code for transient, gas-phase combustion of kinetics
[NASA-TM-83806] 01 p0011 N85-10066
Planarity criteria in electromagnetic topology
[AD-A145279] 01 p0036 N85-10241
Augmented weak forms and element-by-element preconditioners: Efficient iterative strategies for structural finite elements. A preliminary study
01 p0058 N85-10384
A Monte Carlo comparison of the recovery of winds near upwind and downwind from the SASS-1 model function by means of the sum of squares algorithm and a maximum likelihood estimator
[NASA-CR-3839] 01 p0064 N85-10421
Function algorithms for MPP scientific subroutines, volume 1
[NASA-CR-175246] 01 p0102 N85-10678
Numerical algorithms and parallel tasking
[AD-A145090] 01 p0104 N85-10693
Markovian control problems: Functional equations and algorithms
[MCTH-97] 01 p0107 N85-10717
Recursive algorithms for adaptive arrays based on estimates
[REPT-5-84] 01 p0107 N85-10718
A comparative evaluation of algorithms for generalized network problems
[TWISK-289] 01 p0107 N85-10721
Vertical compression algorithms
[DE84-015040] 01 p0126 N85-10864
Shock capturing finite difference algorithms for supersonic flow past fighter and missile type configurations
[NASA-CR-174051] 02 p0134 N85-10913
Accelerated convergence for incompressible flow calculations
[NASA-TM-86663] 02 p0140 N85-10949
Routing the power and ground wires on a VLSI chip
[AD-A145356] 02 p0194 N85-11296
An automated immittance measuring system for electroacoustic transducers
[AD-A145701] 02 p0200 N85-11336
Efficient methods for mechanical and structural reliability analysis and design 02 p0205 N85-11355
Quasi-Newton algorithms for large scale nonlinear systems 02 p0208 N85-11370
Parallel searching and merging on ZMOB
[AD-A145424] 02 p0241 N85-11574
Research on distributed languages and algorithms
[AD-A145661] 02 p0242 N85-11580
Research topics: Multiprocessing algorithms for computational logic
[DE84-015500] 02 p0242 N85-11583
A fast, compact assignment algorithm
[NRIMS-TWISK-331] 02 p0250 N85-11632
Inverse problems, optimization and algorithms
[AD-A145397] 02 p0250 N85-11638
An algorithm for least squares projections onto the intersection of shifted, convex cones
[AD-A145428] 02 p0251 N85-11640
Rapidly convergent algorithms for nonsmooth optimization
[AD-A145556] 02 p0251 N85-11643
Control and identification of time varying systems
[AD-A145638] 02 p0252 N85-11649
Likelihood estimation for generalized mixed exponential distributions
[AD-A145675] 02 p0252 N85-11651
Design of edge detectors for reduced images
[AD-A145700] 02 p0252 N85-11653
CHORDS: A new temperature or sound speed profile thinning algorithm
[AD-A145484] 02 p0275 N85-11793
Active regions --- and the Solar Maximum Mission
[NASA-CR-170628] 02 p0304 N85-11965
A digital algorithm for composite laminate analysis: FORTRAN, Revised
[AD-A145833] 03 p0326 N85-12096
Multielement bend discontinuities in oversize rectangular waveguides
[PR-200] 03 p0354 N85-12275
Signal processing algorithms
[AD-A145748] 03 p0406 N85-12590
A sequential quadratic programming algorithm for solving large, sparse nonlinear programs
[AD-A145854] 03 p0407 N85-12597
Analysis and design methodology for VLSI computing networks
[AD-A146030] 03 p0409 N85-12611
A decomposable algorithm for contour surface display generation
[AD-A145783] 03 p0410 N85-12619
Statistical analysis of some traveling salesman algorithms
[AD-A145786] 03 p0410 N85-12620
The ML (Maximum Likelihood) method for frequency estimation of real sinusoids in noise
[AD-A146053] 03 p0411 N85-12628
A two-segment approximation algorithm for separable convex programming with linear constraints
[AD-A146215] 03 p0412 N85-12634
Designing optimal AOQL sampling plans a computerized approach
[AD-A146288] 03 p0413 N85-12639
Algorithm for astronomical, extended source, signal-to-noise radio calculations
[NASA-TP-2396] 03 p0445 N85-12833
Algorithm for astronomical, point source, signal to noise ratio calculations
[NASA-TP-2397] 03 p0445 N85-12834
Microprocessor implementation of algorithms of nonlinear filtration 04 p0486 N85-13104
Comparison analysis of algorithm for construction of functional tests for combined large-scale integrated circuits 04 p0490 N85-13121
Quasi-three dimensional modeling of functionally-integrated elements of large-scale integrated circuits 04 p0490 N85-13122
Long-range predictive control using weighting-sequence models
[OUEL-1542/84] 04 p0553 N85-13521
On the formal development of graph theoretical algorithms by transformation
[TUM-I8403] 04 p0553 N85-13522
Restoration of multichannel microwave radiometric images
[NASA-CR-174115] 04 p0554 N85-13527
Generalized formulation of TVD Lax-Wendroff schemes
[NASA-CR-172478] 04 p0554 N85-13528
Transformation of two and three-dimensional regions by elliptic systems
[NASA-CR-174176] 04 p0554 N85-13529
Parallel processing of numerical transport algorithms
[DE84-016825] 04 p0555 N85-13534
TCAS 2 logic performance during phase one operational evaluation
[DOT/FAA/PM-84/20] 05 p0595 N85-13793
A generalized LQG approach to self-tuning control. Part 1: Aspects of design. Part 2: Implementation and simulation
[OUEL-1536/84] 05 p0622 N85-13976
The adaptive spectrum analyser
05 p0622 N85-13978
On estimating the phase of periodic waveform in additive Gaussian noise, part 2 05 p0622 N85-13982
VLSI architectures for the multiplication of integers modulo a Fermat number 05 p0624 N85-13993
Documentation of earthquake algorithms
[PB84-235324] 05 p0677 N85-14351
Applications of sequential estimation to numerical weather prediction 05 p0681 N85-14374
Determining training device requirements in Army aviation systems 05 p0711 N85-14558
Research in computer science
[NASA-CR-174086] 05 p0713 N85-14572
Fast algorithms and specialized architectures
05 p0714 N85-14579
Integrated resource management algorithms for computer systems 05 p0715 N85-14582
Efficient sorting routines in FORTRAN 77
[OUEL-1529/84] 05 p0716 N85-14590
Automatic determination of motion in an image sequence. The interest for interpretation
[ENST-84E012] 05 p0716 N85-14592
On an algorithm for Pythagorean sums and its connection with continued fractions
[NPL-DITC-42/84] 05 p0718 N85-14603
Most wanted factorizations using the quadratic sieve
[DE84-016208] 05 p0718 N85-14609
Some implementations of multigrid linear system solvers
[CWI-NM-R8401] 05 p0720 N85-14626
Numerical method for computing supersonic flow over wings of flight vehicles 05 p0725 N85-14659
Molarity principle: Foundation for parallel digital signal processes 05 p0725 N85-14663
Multi-disciplinary techniques for understanding time-varying space-based imagery
[AD-A144357] 05 p0728 N85-14681
Analytical redundancy management mechanization and flight data analysis for the F-8 digital fly-by-wire aircraft flight control sensors
[NASA-CR-170396] 06 p0757 N85-14844
Primary data processing in very long baseline radiointerferometer 06 p0783 N85-15006
Asymptotically optimal ranking algorithms for quasi-determinate signal detection
06 p0792 N85-15064
A geometric approach to high resolution TVD schemes
[NASA-CR-172484] 06 p0857 N85-15449
Selecting a leader in a clique in O(N log N) messages
[AD-A146581] 06 p0857 N85-15453
Tristatic tracking filter used by the multistatic measurement system
[AD-A146885] 07 p0911 N85-15769
cost and benefits optimization model for fault-tolerant aircraft electronic systems
[NASA-CR-166043] 07 p0946 N85-15993
Influence of Faraday effect in ionosphere on nonmutuality of meteor radio channel
07 p0952 N85-16037
A second-order accurate parabolized Navier-Stokes algorithm for internal flows
[NASA-CR-174258] 07 p0956 N85-16059
An evaluation and comparison of vertical profile data from the VISSR Atmospheric Sounder (VAS)
[NASA-TP-2425] 07 p1000 N85-16351
Decentralized control of scheduling in distributed systems
[AD-A147446] 07 p1022 N85-16487
An algorithm for assembly of stiffness matrices into a compacted data structure
[AD-A146727] 07 p1023 N85-16492
Monotone operators in mathematical programming
[AD-A147309] 07 p1025 N85-16506
Continuity of the null space basis and constrained optimization
[AD-A147036] 07 p1030 N85-16538
Techniques for vector quantization
[AD-A147052] 07 p1030 N85-16539
A dual quadratic programming algorithm
[AD-A147237] 07 p1031 N85-16547
Extracting embedded generalized networks from linear programming problems
[AD-A147565] 07 p1033 N85-16558
Structural optimization and other large-scale processes
[AD-A147895] 07 p1034 N85-16564
Efficient computation of optimal time for transaction processing in a database system
[AD-A147568] 07 p1054 N85-16603
High accuracy Doppler navigation employing optimum integrated position fix information
08 p1073 N85-16803
Vectorizable multigrid algorithms for transonic flow calculations
[NASA-CR-174326] 08 p1077 N85-16827
Research into topics in transonic flow theory
[AD-A148526] 08 p1078 N85-16837
Information extraction and transmission techniques for spaceborne synthetic aperture radar images
[NASA-CR-174341] 08 p1150 N85-17256
Coding for reliable satellite communications
[NASA-CR-174315] 08 p1150 N85-17257
Hierarchical data structures and algorithms for digital stereoscopical mensuration 08 p1175 N85-17410
An efficient algorithm for the computation of the inverse in bundle adjustment systems --- photogrammetry
08 p1175 N85-17411
The algebraic structure of convolutional codes with application to code construction and decoding
[AD-A148770] 08 p1206 N85-17591

Asynchronous distributed flow control algorithms
[AD-A148452] 08 p1208 N85-17600
Research on optimal control, stabilization and computational algorithms for aerospace applications
[NASA-CR-174318] 08 p1209 N85-17603
Algorithm for space-time analysis of data on geomagnetic field
[NASA-TM-77804] 08 p1209 N85-17609
Signal reconstruction from Fourier transform sign information
[AD-A148039] 08 p1211 N85-17624
The EM algorithm for censored data
[AD-A148136] 08 p1212 N85-17626
Use of iterative linear and nonlinear algebraic methods for solving large stiff systems of ODEs
[AD-A148516] 08 p1213 N85-17636
Probabilistic analysis of algorithms for NP-Complete problems
[AD-A148207] 08 p1215 N85-17653
A variable span smoother
[AD-A148241] 08 p1215 N85-17655
Decentralized control of scheduling in distributed systems
[AD-A147668] 08 p1226 N85-17731
On one design principle of surge protector for gas turbine engine compressor 09 p1306 N85-18206
A public key cryptographic algorithm based on a generalization of the knapsack problem
[FUB-7-1984] 09 p1313 N85-18250
Development of multigrid algorithms for problems from fluid dynamics
[GMD-111] 09 p1321 N85-18305
The optimal control and design of a flexible manipulator arm 09 p1327 N85-18340
An optimal parallel processing method for inverting sparse matrices 09 p1367 N85-18588
Modeling relationships using groups and items 09 p1367 N85-18591
Parallel algorithms for robot dynamics
[DE84-016563] 09 p1369 N85-18605
Where are the parallel algorithms?
[NASA-CR-172516] 09 p1373 N85-18627
Initialization of Thompson-Plaarenko's algorithm — sinusoidal signal parameter estimation
[FUB-46-1983] 09 p1375 N85-18641
Methodology for evaluating related databases and a computerized algorithm for merging their output 09 p1401 N85-18821
A multistage time-stepping scheme for the Navier-Stokes equations
[NASA-CR-172527] 10 p1483 N85-19365
A generalized ordering constraint for stereo correspondence
[AD-A149182] 10 p1487 N85-19390
Planning of minimum-time trajectories for robot arms
[AD-A148956] 10 p1492 N85-19415
Cyclone diagnostics — rainfall estimation, backscatter, and lidar
[NASA-CR-171337] 10 p1518 N85-19567
Equations and algorithms for meteorological applications in air weather service
[AD-A148694] 10 p1519 N85-19575
Relative performance of micro and mainframe computers
[AD-A149281] 10 p1538 N85-19695
Algorithms for the Euler and Navier-Stokes equations for supercomputers
[NASA-CR-172543] 10 p1539 N85-19701
Efficient algorithm for fuzzy linear programming with multiple objectives
[AD-A149012] 10 p1544 N85-19736
Smoothing with split linear fits
[AD-A149032] 10 p1545 N85-19740
Vectorization and implementation of an efficient multigrid algorithm for the solution of elliptic partial differential equations
[AD-A149049] 10 p1545 N85-19743
Blunder detection using a sequential least squares adjustment
[AD-A149514] 10 p1546 N85-19765
Order picking in an aisle
[AD-A149553] 10 p1546 N85-19766
Robust Kalman filtering and its applications
[AD-A149044] 10 p1550 N85-19775
One-dimensional processing for adaptive image restoration
[AD-A149314] 10 p1557 N85-19815
Optical implementation of the synthetic discriminant function
[AD-A149562] 10 p1557 N85-19817
Finite-(beta) optimization of tandem mirors
[DE85-002658] 10 p1560 N85-19835
Distribution of hydrogen in multi-layer welded joints of alloyed steels 11 p1603 N85-20079
Simulation of the electrochemical machining process
[DE85-003797] 11 p1616 N85-20159
Guidepost routing algorithm for distributed computer networks 11 p1622 N85-20210
Numerical simulation of turbulent reacting flows
[DE84-016777] 11 p1632 N85-20278
Real time algorithms for robotic control of teleoperators
[DE85-001137] 11 p1647 N85-20380
Continued research in mesoscale air pollution simulation modeling. Volume 5: Refinements in numerical analysis, transport, chemistry, and pollutant removal
[PB85-137362] 11 p1680 N85-20585
Parallel processing experiences on the Denelcor HEP computer
[DE85-000653] 11 p1702 N85-20703
Three algorithms for parametric frequency domain system identification
[DE85-002801] 11 p1706 N85-20735
New approach for solving large residual nonlinear least squares problems
[DE85-002655] 11 p1707 N85-20742
Bayesian analysis of time series 1: Householder transformation analyses
[DE85-004449] 11 p1708 N85-20749
Precise measurements of radial velocities of emission lines in the far-ultraviolet spectra of late-type stars 11 p1758 N85-21062
Cometary atmospheres: Modeling the spatial distribution of observed neutral radicals
[NASA-CR-175485] 11 p1765 N85-21098
A study of transonic flutter of a two-dimensional airfoil using the U-g and p-k methods
[LR-615] 12 p1771 N85-21121
Algorithms for automatic four-dimensional aircraft guidance, considering the momentary wind situation
[DFVLR-FB-84-40] 12 p1775 N85-21146
A comparison of the efficiency of numerical methods for integrating chemical kinetic rate equations
[NASA-TM-83590] 12 p1776 N85-21162
Modal control of structural systems
[AD-A149734] 12 p1790 N85-21235
Estimating algorithmic error of digital recursive filters 12 p1839 N85-21543
Algorithm for statistical simulation of electromagnetic compatibility characteristics of high-frequency transmission channels in radioelectronic facilities 12 p1842 N85-21560
Synthesis of digital control for object with lag 12 p1843 N85-21562
Mathematical simulation of thermal processes involved in electron-beam treatment 12 p1843 N85-21565
Modeling of transient heat pipe operation
[NASA-CR-175496] 12 p1844 N85-21571
A three-dimensional spectral algorithm for simulations of transition and turbulence
[NASA-CR-172561] 12 p1845 N85-21575
Algorithm for the simulation of transient viscoelastic flows with free surfaces
[DE85-002713] 12 p1848 N85-21590
Robust calculation of three-dimensional transonic potential flow based on the nonlinear gas multigrid method and a mixed incomplete lower upper decomposition/strongly implicit procedure (ILU/SIP) algorithm
[NLR-MP-84003-U] 12 p1848 N85-21593
Velocity inversion using a stratified reference
[AD-A150082] 12 p1889 N85-21858
RAPIDbus: Design of an extensible multiprocessor structure
[AD-A150061] 12 p1912 N85-21998
A linear characteristic-nodal transport method for the two-dimensional (X,Y)-geometry multigroup discrete ordinates equations over an arbitrary triangle mesh
[LA-10092-T] 12 p1913 N85-22006
User's guide for NPSOL (Version 2.1): A FORTRAN package for quadratic programming
[AD-A150078] 12 p1916 N85-22026
Software for special functions
[DE85-004884] 12 p1917 N85-22033
Parallel linear algebra library for the Denelcor HEP
[DE85-004885] 12 p1917 N85-22034
Determining conductivity by boundary measurements. Part 2: Interior results
[AD-A149750] 12 p1921 N85-22063
Parallel processing of encoded bit strings
[AD-A149812] 12 p1921 N85-22064
Distributed asynchronous deterministic and stochastic gradient optimization algorithms: Revision
[AD-A149997] 12 p1921 N85-22068
Statistics for the maximum of several positive random variables with application to networking
[AD-A150005] 12 p1922 N85-22069
A review of some aspects of robust inference for time series
[AD-A149706] 12 p1923 N85-22082
Needs, opportunities, and options for large scale systems research
[DE85-004842] 12 p1925 N85-22091
Determining object orientation from a single image using multiple information sources
[AD-A149980] 12 p1933 N85-22146
Multiple resolution representation and probabilistic matching of 2-D gray-scale shape
[AD-A149981] 12 p1933 N85-22147
Evaluation of expert systems 12 p1947 N85-22229
Problems in decentralized decision making and computation
[AD-A150025] 12 p1950 N85-22251
A flight management algorithm and guidance for fuel-conservative descents in a time-based metered air traffic environment: Development and flight test results 13 p1967 N85-22358
On the solution of the three-dimensional flowfield about a flow-through nacelle
[NASA-TM-87448] 13 p1969 N85-22371
Analysis of estimation algorithms for CDTI and CAS applications
[NASA-CR-172444] 13 p1973 N85-22387
Computation of elliptical functions in problems of celestial mechanics 13 p1979 N85-22418
Algorithm for determining optimal three impulse point-to-orbit transfer with limited transfer time 13 p1979 N85-22419
Assembly robot control algorithms 13 p2046 N85-22808
Nonlinear behavior and stability of thin spherical shells subjected to non-axisymmetrical loading 13 p2048 N85-22821
Efficiency of algorithms for gas-air channel diagnostics in gas turbine engines based on gas thermodynamic parameters 13 p2048 N85-22823
Advanced mixed-mode simulation techniques 13 p2062 N85-22983
Factorized algorithms for combined spatial and temporal processing of radar signals 13 p2081 N85-22997
Algorithm in Walsh function basis for analysis of integrated microcircuits on MOS-structures 13 p2083 N85-23006
Use of Bigaussian approximation to describe fading in scattering communications channel 13 p2084 N85-23017
Computing convolution of multifrequency signal employing truncated fast Fourier transform algorithms 13 p2085 N85-23019
Synthesis of quasi-optimum algorithms for signal recognition against background of correlated noise employing discrete spectral transformations 13 p2085 N85-23020
New convolution and discrete Fourier transformation algorithms based on rectangular transformations over field of roots of unity 13 p2085 N85-23022
Discrimination of normal and anomalous magnetic and electric fields in geoelectromagnetic variations 13 p2114 N85-23166
Polynomial parameterization in inverse gravimetric problem 13 p2115 N85-23174
Primary processing of experimental magnetovariation sounding data using spline functions 13 p2115 N85-23175
Orphan detection in the Argus system
[AD-A150562] 13 p2148 N85-23331
Implementation of some concurrent algorithms
[DE85-004687] 13 p2148 N85-23334
Algorithms for reconstruction of partially known, band limited Fourier transform pairs from noisy data
[AD-A150194] 13 p2150 N85-23347
Image data compression using uneven knots selection
[AD-A150602] 13 p2152 N85-23359
Algorithm for singular decomposition
[DE85-016488] 13 p2152 N85-23361
Motion planning with six degrees of freedom
[AD-A150312] 13 p2165 N85-23432
Quantitative analyses of planetary reflectance spectra 13 p2197 N85-23625
Progress in planetary radarclinometry 13 p2198 N85-23630
Thermal response of aircraft cabin ceiling materials during a post-crash, external fuel-spill, fire scenario
[PB85-145847] 14 p2220 N85-23764
An eigensystem realization algorithm for application to modal testing 14 p2233 N85-23842
Linearization of digital derived rate algorithm for use in linear stability analysis
[NASA-TM-87000] 14 p2243 N85-23904
Quaternion algorithms of 3-dimensional inertial navigational systems 14 p2257 N85-24173
Spatial acquisition algorithms and systems for intersatellite optical communication links
[AD-A150794] 14 p2292 N85-24207

An improved battery state-of-charge indicator
[NASA-CR-175701] 14 p2296 N85-24227
Some methods of computing platform transmitter terminal location estimates — ARGOS system; whale tracking 14 p2332 N85-24420
Perceptual organization and visual recognition
[AD-A150626] 14 p2391 N85-24723
Finite element methods in space mathematics 14 p2396 N85-24757
Propagation of numerical errors in computers and numerical quality 14 p2396 N85-24760
Execution of cellular logic operations in spatially continuous, bit slice processor 14 p2401 N85-24796
Nonlinear 0-1 programming. 1: Linearization techniques, revision
[AD-A150860] 14 p2405 N85-24826
A simple and efficient algorithm to compute tail probabilities from transforms
[AD-A150928] 14 p2409 N85-24849
Probalistic analysis of combinatorial algorithms: An annotated bibliography
[CWI-OS-R8411] 14 p2411 N85-24864
Disproof of the Mertens conjecture
[CWI-NM-R8412] 14 p2414 N85-24896
Some historical and other notes about the Mertens conjecture and its recent disproof
[CWI-NM-R8415] 14 p2414 N85-24898
Parametric coherence estimation via convolved correlations
[DE85-003946] 14 p2416 N85-24909
A fast ray tracing routine for laterally inhomogeneous media
[AD-A150864] 14 p2421 N85-24936
On the orbit improvement results obtained by referring old cometary observations to the SAO Star Catalog 14 p2438 N85-25042
Implementation of an inertial navigation algorithm using a limited wordlength microprocessor for a strapdown navigation computer
[BAE-BT-12792] 15 p2468 N85-25234
Multistep orbital correction algorithms for an Earth satellite using low thrust engine 15 p2479 N85-25303
Calculation of image shift in panoramic photography 15 p2488 N85-25357
An analysis of grid-based line drawing quantization methods
[AD-A151647] 15 p2522 N85-25647
Margin leveling algorithm for fully saturated satellite transponder with CDMA (Code Division Multiple Access) signalling
[AD-A151710] 15 p2543 N85-25699
Development of robots and application to industrial processes
[NASA-CR-175754] 15 p2567 N85-25840
Control of a flexible beam
[DE85-007243] 15 p2580 N85-25914
Effective microinstruction pipeline organization in a high-capacity microprocessor 15 p2625 N85-26176
Care 3 model overview and user's guide, first revision
[NASA-TM-86404] 15 p2627 N85-26192
The design and analysis of a complete hierarchical interface for the multi-backend database system
[AD-A151550] 15 p2629 N85-26203
On the throughput of channel access algorithms with limited sensing
[AD-A151984] 15 p2630 N85-26208
Censored observations, repeated measures and mixed effects models: An approach using the EM algorithm and normal errors
[MATHEMATICS-RESEARCH-183] 15 p2636 N85-26256
Vortex dynamics
[AD-A151278] 15 p2637 N85-26260
Communication complexity of the Gaussian elimination algorithm on multiprocessors
[AD-A151891] 15 p2638 N85-26267
Solution of coupled system of PDE by the transistorized multigrid method
[DE85-006377] 15 p2639 N85-26276
Sliding interfaces with contact-impact in large scale Lagrangian computations
[DE85-006451] 15 p2639 N85-26277
Construction of efficient algorithms for the estimation of multivariate probability densities
[AD-A151509] 15 p2640 N85-26285
Feasibility analysis of moving bank multiple model adaptive estimation and control algorithms
[AD-A152015] 15 p2641 N85-26292
Design and implementation of the digital engineering laboratory distributed database management system
[AD-A151694] 15 p2985 N85-26450
Developing an automated technique for translating a relational database into an equivalent network one
[AD-A151844] 15 p2686 N85-26451
Generation of flight paths using heuristic search
[AD-A151949] 16 p2704 N85-26694
Formulation and implementation of nonstationary adaptive estimation algorithm with applications to air-data reconstruction
[NASA-TM-86727] 16 p2706 N85-26699
Method for evaluating perturbation in algorithms for solving navigational problems 16 p2718 N85-26783
The effect of inaccuracies in structural models on the control of large space structures
[AD-A151794] 16 p2732 N85-26858
Control of motion of manipulator robots on basis of first-order kinematic algorithms 16 p2762 N85-27047
Optimal control of electric drive with simultaneous control inputs for motor current and flux 16 p2763 N35-27049
Approximate solution of the problem of fluid oscillations in cavities of revolution 16 p2764 N85-27056
Automation of the process of speech signal segmentation in an analogic-numeric system
[REPT-5/1984] 16 p2768 N85-27082
Development and application of optimum sensitivity analysis of structures
[NASA-CR-175857] 16 p2799 N85-27257
Basic research for the geodynamics program
[NASA-CR-175751] 16 p2825 N85-27424
Parallel time 0(log N) acceptance of deterministic CFLs
[AD-A152255] 16 p2845 N85-27539
A general purpose scatter storage subsystem and a comparison of hashing methods
[NASA-CR-175814] 16 p2845 N85-27542
Comparative study of the digital analysis of areas of the Earth's surface prepared for planting using different classification algorithms
[INPE-3359-PRE/637] 16 p2846 N85-27545
Character recognition using correlation techniques
[AD-A152006] 16 p2847 N85-27549
A data based algorithm for choosing the window width when estimating the integral of f2(x)
[AD-A152093] 16 p2847 N85-27553
Numerical optimization algorithm for engineering problems using microcomputer
[AD-A152135] 16 p2847 N85-27554
Multigrid algorithms on the hypercube multiprocessor
[AD-A152200] 16 p2847 N85-27556
Squeezing the most out of Eigenvalue solvers on high-performance computers
[DE85-007569] 16 p2849 N85-27565
Local uniform mesh refinement on locally-coupled parallel processors
[AD-A152199] 16 p2850 N85-27571
Corrective-predictive systems
[BLL-M-36063-(5828.4)] 16 p2851 N85-27573
Algorithms for determining the relative complexity of dynamic signals
[BLL-M-36111-(5828.4)] 16 p2851 N85-27574
A fast hidden line algorithm with contour option
[NASA-CR-175803] 16 p2852 N85-27582
Finite elements and the method of conjugate gradients on a concurrent processor
[NASA-CR-175812] 16 p2853 N85-27586
Born inversion with a stratified reference velocity
[AD-A149222] 16 p2853 N85-27594
Scene analysis using recursive frequency domain correlation with energy normalization
[AD-A151777] 16 p2854 N85-27596
Complexity of dense linear system solution on a multiprocessor ring
[AD-A151970] 16 p2854 N85-27598
Evaluation of an algorithm for the solution of the time-dependent Euler equations
[AD-A151993] 16 p2854 N85-27600
A heuristic solution to the spacing problem: Maximizing the minimum Euclidean distance among N points in a convex region
[AD-A152116] 16 p2855 N85-27603
Efficient parallel pseudo-random number generation
[AD-A152235] 16 p2855 N85-27608
Probabilistic algorithms in group theory
[AD-A152253] 16 p2859 N85-27630
Computing the singular value decomposition of a product of two matrices
[DE85-006977] 16 p2859 N85-27631
On the choice of coordinates for semiconductor simulation
[AD-A152214] 16 p2870 N85-27708
Discrete foundation for physics and experience
[DE85-008172] 16 p2872 N85-27720
An adaptive technique and its application in database design 16 p2877 N85-27748
Access path optimization for network database retrieval 16 p2877 N85-27749
Incorporating control into the optimal structural design of large flexible space structures
[AD-A152858] 17 p2909 N85-27937
Enhacements to the TTS-502 time transfer system 17 p2963 N85-28296
The steering of GPS time 17 p2964 N85-28301
Automatic detection of gust fronts
[FAA-PM-85-11] 17 p2995 N85-28516
A comparison of three curve intersection algorithms 17 p3007 N85-28592
Tracking algorithm performance analysis program (TRAPP)
[DE85-007304] 17 p3009 N85-28601
The addition of advanced scene rendering techniques to a general purpose graphics package
[AD-A153323] 17 p3012 N85-28625
Evidential reasoning in expert systems for image analysis
[AD-A153379] 17 p3013 N85-28627
Ray tracing general sweep defined objects
[REPT-84-36] 17 p3014 N85-28636
Efficient parallel solution of linear systems with hyperbolic rotations
[AD-A152355] 17 p3018 N85-28661
Numerical methods for stiff ordinary and elliptic partial differential equations
[AD-A153247] 17 p3020 N85-28675
Parallel Cholesky factorization on a multiprocessor
[DE85-008762] 17 p3021 N85-28682
Montonicity preserving bicubic interpolation, revision 1
[DE85-007976] 17 p3021 N85-28683
A greedy algorithm for the transhipment along a single road problem
[AD-A152343] 17 p3025 N85-28709
Maximum flow in planar networks with exponentially distributed arc capacities
[AD-A153158] 17 p3026 N85-28710
Kirchhoff modeling via wave equation datuming
[AD-A152399] 17 p3028 N85-28727
The AFTI/F16 terrain-aided navigation system
[DE85-008411] 18 p3060 N85-28935
Piloted simulation of an algorithm for onboard control of time-optimal intercept
[NASA-TP-2445] 18 p3063 N85-28949
Application of model following control and estimation techniques to attitude control of maneuvering spacecraft. Part 1: Theory and simulation results
[NLR-TR-82116-U-PT-1] 18 p3065 N85-28957
Computer-aided thermohydraulic design of TEMA type E shell and tube heat exchangers for use in low pressure, liquid-to-liquid, single phase applications
[AD-A153779] 18 p3100 N85-29191
Automatic volume calibration system
[DE85-008955] 18 p3102 N85-29204
Recent developments in nonlinear normal mode initialization 18 p3142 N85-29451
Three-dimensional data display on the two-dimensional screen
[AD-A153699] 18 p3160 N85-29577
A global optimization algorithm using stochastic differential equations
[AD-A153526] 18 p3161 N85-29583
Parallel computation of multiple-scale problems, revision 1
[DE85-009447] 18 p3164 N85-29598
Solving elliptic partial differential equations on the hypercube multiprocessor
[AD-A153464] 18 p3168 N85-29629
A quadratic programming algorithm
[AD-A153476] 18 p3168 N85-29631
Finding the largest l(p)-ball in a polyhedral set
[AD-A153542] 18 p3170 N85-29643
High performance asynchronous limited sensing algorithms for CSMA and CSMA-CD channels
[AD-A153919] 18 p3171 N85-29650
Pipelined Givens method for computing the QR factorization of a sparse matrix
[DE85-009772] 18 p3171 N85-29653
Monotonicity preserving bicubic interpolation
[DE85-004206] 18 p3172 N85-29657
Constructing a bit string universe
[DE85-008317] 18 p3197 N85-29829
Distributed database design tool
[AD-A153760] 18 p3200 N85-29850
On the numerical computation of nonlinear force-free magnetic fields 18 p3203 N85-29871
Research on optimal control, stabilization and computational algorithms for aerospace applications
[NASA-CR-172528] 19 p3221 N85-29970
Study of second order upwind differencing in a recirculating flow
[NASA-CR-174939] 19 p3264 N85-30243
A probabilistic forecasting model of tropical cyclone-generated storm surge for a straight coastline 19 p3314 N85-30544

Performance envelopes and optimal appropriateness measurement
[AD-A154129] 19 p3330 N85-30629
On the step size in Karmarkar's algorithm
[AD-A154040] 19 p3335 N85-30661
An algorithm to test for confluence in a system of left to right rewrite rules
[AD-A154066] 19 p3335 N85-30662
An algorithm for the influence numbers in the expansion of the lumped gravitational potential coefficients in the presence of resonant inclination variation
[AD-A154229] 19 p3336 N85-30669
The origin of the binary-search paradigm
[AD-A154367] 19 p3337 N85-30677
A parallelized point successive over-relaxation method on a multiple instruction multiple data stream computer
[AD-A154377] 19 p3337 N85-30679
A dynamic programming approach to time-staged convex programs
[DE85-010616] 19 p3340 N85-30700
High gain adaptive control of decentralized systems
[DE85-001566] 19 p3343 N85-30717
An iterative method for indefinite systems of linear equations
[NASA-CR-172345] 19 p3345 N85-30728
On MGR (Upsilon) multigrid methods
[AD-A153887] 19 p3345 N85-30733
Numerical algorithms for solving linear algebra problems
[DE85-010310] 19 p3346 N85-30738
An extension to complex-valued functions of an algorithm for numerically inverting the Laplace transform
[DE85-010701] 19 p3347 N85-30743
Bayesian factor analysis
[AD-A154184] 19 p3347 N85-30747
A critique of Deming's discussion of acceptance sampling procedures
[AD-A154305] 19 p3348 N85-30751
Target discrimination using infrared techniques: Theoretical considerations
[AD-A154070] 19 p3350 N85-30762
Measurement problem in PROGRAM UNIVERSE
[DE85-008179] 19 p3378 N85-30959
Modified dynamic hashing
[DE85-011166] 19 p3381 N85-30974
Approximation techniques for parameter estimation and feedback control for distributed models of large flexible structures 20 p3413 N85-31179
An integrated control and minimum mass structural optimization algorithm for large space structures 20 p3413 N85-31183
Experimental verification of identification algorithms for control of flexible structures 20 p3418 N85-31211
An Eigensystem Realization Algorithm (ERA) for modal parameter identification and model reduction 20 p3418 N85-31212
Self-adaptive echo cancellation for telephony
[ENST-84E013] 20 p3441 N85-31353
Computer methods in manipulator kinematics, dynamics and control: A comparative study 20 p3462 N85-31506
Study of new computing algorithms for supercomputers. Application to parallel processing computation
[SNIAS-440-070/84] 20 p3516 N85-31860
Inference in hierarchic classification — data bases
[ENST-84E014] 20 p3518 N85-31873
Efficient solution methods for nonlinear finite element analysis 20 p3519 N85-31886
Time-implicit Monte-Carlo collision algorithm for particle-in-cell electron transport models
[DE85-010758] 20 p3521 N85-31900
New O(6) region near A = 130 and the interplay of triaxiality and gamma-softness in the IBA
[DE85-010957] 20 p3530 N85-31961
Globally-asynchronous locally-synchronous systems
[AD-A154624] 21 p3573 N85-32222
Routing algorithms and stochastic analysis for large communications networks
[AD-A154654] 21 p3573 N85-32225
A multilevel-multigrid method for recirculating flows 21 p3583 N85-32271
Non-model based estimation with applications to sensor calibration using multiple sensors
[AD-A154736] 21 p3589 N85-32308
Emergency modeling of hazardous air pollutants
[AD-A155441] 21 p3614 N85-32481
Practical use of a tropopause height determination algorithm on an MST radar data set, part 1.8B 21 p3618 N85-32479
Criteria and algorithms for spectrum parameterization of MST radar signals 21 p3626 N85-32527
Automated cell detection as a mesocyclone precursor tool
[AD-A154952] 21 p3635 N85-32577
Real-time automated detection of mesocyclones and tornado vortex signatures
[AD-A154968] 21 p3635 N85-32578
Consensus in the presence of partial synchrony (Preliminary version)
[AD-A154705] 21 p3670 N85-32799
SIGMA - A stochastic-integration global minimization algorithm
[AD-A154878] 21 p3671 N85-32806
A comparison and analysis of Vintr's global routing algorithm with the Lee routing algorithm in two-layer printed circuit boards
[AD-A155600] 21 p3673 N85-32816
A practical approach to Karmarkar's algorithm
[AD-A155714] 21 p3673 N85-32818
Evaluation and implementation of a functional microprogram generator
[AD-A155164] 21 p3674 N85-32823
Broadcasting topology and routing information in computer networks
[AD-A155668] 21 p3674 N85-32827
On the dependence of the convergence of Gummel's algorithm on the regularity of the solution
[AD-A154628] 21 p3675 N85-32832
A new fault-tolerant algorithm for clock synchronization
[AD-A154771] 21 p3676 N85-32836
A vectorized nearest-neighbors algorithm of order N using a monotonic logical grid
[AD-A155169] 21 p3679 N85-32853
Poisson formula for radon transformation and numerical image reconstruction algorithm 21 p3697 N85-32973
An image compression survey and algorithm switching based on scene activity
[NASA-TP-2458] 22 p3727 N85-33106
Implementation of the SITAN algorithm in the digital terrain management and display system
[DE85-010659] 22 p3729 N85-33115
Enhancing precision of remote temperature sensing data from satellites under cloudy atmospheric conditions 22 p3734 N85-33148
High-speed adaptation algorithm for harmonic corrector 22 p3765 N85-33336
State of art and development problems in computer-aided design of electronic circuits 22 p3768 N85-33342
Modeling of electronic circuits with high degree of component integration 22 p3768 N85-33343
Diakoptic calculation of characteristics for optimization of linear circuits with respect to parameters of individual branches 22 p3767 N85-33346
Algorithms for constructing models of circuit elements in input language of computer-aided design software 22 p3768 N85-33356
Algorithm for determination of isomorphic graphs 22 p3769 N85-33357
Method of estimating convergence of Haar coefficients in message compression problems 22 p3769 N85-33358
Determination of sensitivity functions for discrete dynamic systems from results of function modeling on digital computer 22 p3769 N85-33359
Analysis of crosstalk in nonhomogeneous multiconductor lines 22 p3769 N85-33360
Gradiental adaptive corrector with optimum tuning step 22 p3776 N85-33403
Multishaker modal testing
[NASA-CR-176139] 22 p3800 N85-33544
Solar energy meteorological research and training program: Region 4
[DE85-011783] 22 p3816 N85-33640
Optimal Bayesian estimators for image segmentation and surface reconstruction
[AD-A155732] 22 p3827 N85-33704
DECODE: A software manual for use with the Serial ASCII Instrumentation Loop (SAIL) system
[AD-A155358] 22 p3828 N85-33709
Parallel Cholesky factorization in message-passing multiprocessor environments
[DE85-012079] 22 p3830 N85-33717
An algorithm for the generation of primitive polynomials
[FUB-17-1984] 22 p3831 N85-33730
Research on distributed artificial intelligence
[AD-A155356] 22 p3833 N85-33733
Some ideas for decomposing the domain of elliptic partial differential equations in the Schwarz process
[DE85-011844] 22 p3834 N85-33739
Modelling of unsteady, incompressible separation on an aerofoil using an inviscid flow algorithm
[GU-AERO-8412] 23 p3904 N85-34122
A versatile computer package for mechanism analysis, part 2: Dynamics and balance 23 p3924 N85-34315
The improved display of 625-line television pictures: Adaptive interpolation
[BBC-RD-1985/5] 23 p3925 N85-34328
Sequential regularization solution of the inverse heat conduction problem
[DE85-010657] 23 p3931 N85-34362
Algorithm for calculation of strain state from measurements of node coordinates of arbitrary curvilinear grid
[BLL-M-36304-(5828.4)] 23 p3940 N85-34422
Short-time creep of ice
[NRC/CNR-TT-2111] 23 p3941 N85-34428
Reordering computations for parallel execution
[NASA-CR-177961] 23 p3957 N85-34522
A theoretical and empirical analysis of coherent ray-tracing 23 p3957 N85-34524
Computer analysis techniques for the temporal evaluation of cardiac wall motion 23 p3958 N85-34530
An analysis and algorithm for filling propagation 23 p3961 N85-34551
A curvilinear coordinate method for the solutions of initial value problems using the third-order upwind differencing scheme
[IPPJ-734] 23 p3975 N85-34642
Cubic interpolated pseudo-particle method (CIP) for solving hyperbolic-type equation 23 p3979 N85-34673
Numerical simulation in astrophysics: Smoothed particle methods 23 p3979 N85-34674
Vector calculation of particle code 23 p3981 N85-34688
Energy management of three-dimensional minimum-time intercept
[NASA-CR-176174] 24 p4064 N85-35186
Communication complexity of distributed shortest path algorithms
[AD-A156049] 24 p4067 N85-35332
An evaluation of a class of practical optimization techniques for structural dynamics applications
[PB85-195766] 24 p4103 N85-35434
Optimal estimation of a high degree gravity field from a global set of 1 deg x 1 deg anomalies to degree and order 250
[AD-A156008] 24 p4117 N85-35519
Comparative analysis of operational forecasts versus actual weather conditions in airline flight planning, volume 2
[NASA-CR-167863] 24 p4119 N85-35535
Reachable grasps on a polygon: The convex rope algorithm
[AD-A155913] 24 p4138 N85-35647
L-step sequential decoding
[AD-A156121] 24 p4138 N85-35649
Pruned error-trellis decoding of certain non-systematic convolutional codes
[AD-A156122] 24 p4138 N85-35650
Three-dimensional finite deformation viscoelastic model accounting for damage effects
[DE85-012951] 24 p4139 N85-35660
Recursive partitioning estimation 24 p4141 N85-35670
Algorithmic approaches in sets of good answers in inverse problems
[PM/84/18] 24 p4142 N85-35677
Smoothing surface data by spline functions
[AD-A155829] 24 p4142 N85-35678

ALIGNMENT
NT SELF ALIGNMENT
Linac quadrupole connections
[DE84-014894] 01 p0118 N85-10810
Gyrodynamic fixture for measuring thrust force components
[AD-D011258] 06 p0760 N85-14860
Measurement of parameters defining orientation of liquid crystals in electrooptic cells 06 p0777 N85-14971
Magnetic alignment theory and the interpretation of polarization 06 p0880 N85-15590
Upgrading flexible infrared waveguides
[AD-A146763] 07 p0970 N85-16160
An alignment fixture for a 2-Degree-of-Freedom (TDF) gyroscope
[AD-A148865] 10 p1422 N85-18969
An evaluation of the 64-meter antenna radial bearing for use on the 70-meter antenna 10 p1464 N85-19238
Mask aligner for solar cell fabrication
[AD-D011450] 10 p1510 N85-19529
Ingot slicing machine and method
[NASA-CASE-NPO-15483-1] 12 p1857 N85-21650
Error analysis of heliostat alignment methods 14 p2281 N85-24128
Modernization of running gear of crane 14 p2286 N85-24163

Non-linear methods for inertial navigation system alignment
[BAE-BT-12663] 15 p2468 N85-25232
Assessment of a nonlinear method of INS alignment — inertial navigation systems (INS)
[BAE-BT-12664] 15 p2468 N85-25233
Surveying and optical tooling technologies combined to align a skewed beamline at the LAMPF accelerator
[DE85-005902] 16 p2864 N85-27664
Alignment and assembly tool for very large diameter cylinders
[NASA-CASE-MFS-28003-1] 18 p3116 N85-29269
Accelerator vibration issues
[DE85-010766] 22 p3842 N85-33791

ALIPHATIC COMPOUNDS
NT ACETALDEHYDE
NT ACETONE
NT ACETYL COMPOUNDS
NT ACETYLACETONE
NT ACETYLENE
NT ACRYLATES
NT ACRYLONITRILES
NT ADENOSINE DIPHOSPHATE
NT ADENOSINE TRIPHOSPHATE
NT ADENOSINES
NT ALKANES
NT ALKENES
NT ALKYL COMPOUNDS
NT ALKYNES
NT ANTHRACENE
NT BUTADIENE
NT BUTANES
NT BUTENES
NT CARBON TETRACHLORIDE
NT CARBON TETRAFLUORIDE
NT CELLULOSE
NT CHLOROETHYLENE
NT CHLOROFORM
NT CHOLINE
NT CITRIC ACID
NT CYANOGEN
NT CYCLIC HYDROCARBONS
NT CYCLOPROPANE
NT DDT
NT DIISOCYANATES
NT ETHANE
NT ETHYL ALCOHOL
NT ETHYLENE
NT ETHYLENEDIAMINE
NT FATTY ACIDS
NT GALACTOSE
NT GLUCOSE
NT GLUTAMATES
NT GLUTAMINE
NT GLUTATHIONE
NT GLYCOGENS
NT GLYCOLS
NT HEXENES
NT HYDRAZINES
NT KETONES
NT MALEATES
NT METHANE
NT METHYL ALCOHOLS
NT METHYL COMPOUNDS
NT NITRATE ESTERS
NT NITROPROPANE
NT NUCLEOSIDES
NT PARAFFINS
NT PENTANES
NT PENTOSE
NT PROPANE
NT PROPYL COMPOUNDS
NT PROPYLENE
NT RIBOSE
NT STARCHES
NT SUCROSE
NT SUGARS
NT THIOLS
NT TRIAMINOGUANIDINIUM AZIDE
NT TRIMETHYL COMPOUNDS
NT URETHANES
NT VINYLIDENE
Converting gasoline farm tractors to run efficiently on farm-produced alcohol
[DE84-015796] 02 p0205 N85-11350
Fluorinated polyurethanes
[AD-D011525] 12 p1810 N85-21353

ALKALI HALIDES
NT CESIUM IODIDES
NT SODIUM CHLORIDES
NT SODIUM IODIDES
Thresholds of optical breakdown in alkali-halide crystals under pulses from CO2-laser 14 p2282 N85-24134
Polarimetric image recorder
[AD-D011605] 16 p2787 N85-27192
Perturbative treatment of quasi-resonant proton neutralization at alkali-halide surfaces
[AD-A154143] 19 p3356 N85-30806

ALKALI METALS
NT CESIUM
NT CESIUM ISOTOPES
NT CESIUM 134
NT CESIUM 137
NT LIQUID LITHIUM
NT LIQUID POTASSIUM
NT LIQUID SODIUM
NT LITHIUM
NT POTASSIUM
NT POTASSIUM 40
NT RUBIDIUM
NT RUBIDIUM ISOTOPES
NT SODIUM
NT SODIUM ISOTOPES
NT SODIUM VAPOR
Corrosion in alkali metal/molybdenum heat pipes
[DE84-014039] 02 p0164 N85-11233
Electrochemical investigations of novel electrode materials
[DE84-014352] 04 p0495 N85-13158
Origin of the Moon: Constraints from volatile elements 04 p0584 N85-13727
The effect of temperature and pressure on the composition density of alkaline metals
[BLL-M-35940-(5828.4)] 05 p0616 N85-13934
Homogeneous reaction involving components of different redox couples. 2: Polarographic studies of the interactions of alkali metal cations with anthracene and fluoroenthene dianions in N,N-dimethylformamide and acetonitrile
[AD-A148667] 08 p1124 N85-17085
S-11 and S-20 photocathode research activity, revision 1
[DE84-017164] 09 p1326 N85-18335
Calorimetric investigation into the possibility of a charge density wave ground state in alkali metals
[DE85-002006] 09 p1397 N85-18795
Classical rainbow scattering of alkali ions on metal surfaces. Application to the investigation of unknown surface structures
[MPIS-10/1984] 11 p1726 N85-20854
Heterocontact effects in point contact electron-phonon spectroscopy of the alkali metals
[AD-A149760] 12 p1800 N85-21290
Studies of metal/carbon surface chemistry
[DE85-005513] 15 p2507 N85-25463
Analysis of alkali liquid metal Rankine space power systems
[DE85-005089] 16 p2741 N85-26917
Ames Laboratory measurements of alkali levels in the Curtiss-Wright PFBC gas stream
[DE85-011357] 22 p3745 N85-33214
Infrared studies of the influence of alkali metals on the C-O bond in chemisorbed carbon monoxide
[DE85-005306] 23 p3911 N85-34232
Metal alkoxides: Models for metal oxides. Alkoxide ligands in early transition metal organometallic chemistry
[DE85-011368] 23 p3916 N85-34269
A study of the chemistry of alkali metals in the upper atmosphere
[AD-A156349] 24 p4117 N85-35524

ALKALIES
NT POTASSIUM HYDROXIDES
Optical detection of alkali compounds
[DE84-015505] 03 p0328 N85-12117
Laser spectroscopy of alkali atom-tetrahaloethylene reactions
[AD-A147431] 07 p0923 N85-15848
Lidar studies of the alkali metals 08 p1184 N85-17460
Resistance of optical coatings to alkali solutions and sea water 14 p2281 N85-24129
Bifunctional oxygen electrodes
[DE85-006871] 17 p2955 N85-28248
Multiple scattering effects in low energy alkali ion scattering: Application to the analysis of adsorbate ordering and bonding geometry
[DE85-007575] 17 p3032 N85-28757
Cation promotion effects in zeolite-supported F-T catalysts
[DE85-009969] 19 p3233 N85-30044
Alkali atom - SbCl(5) reactions: Blue-green chemiluminescence from an inverted population in SbCl
[AD-A154371] 19 p3276 N85-30315
Photofragment fluorescence as a sensitive probe for gas-phase alkali compounds and their photochemistry
[DE85-010707] 22 p3746 N85-33219
Photoionization of alkali and alkaline earth atoms: Na and Mg
[DE85-011812] 22 p3837 N85-33755

ALKALINE BATTERIES
Research on separators for alkaline zinc batteries
[DE85-003062] 12 p1836 N85-21523
Alkaline battery containing a separator of a cross-linked copolymer of vinyl alcohol and unsaturated carboxylic acid
[NASA-CASE-LEW-13102-1] 18 p3093 N85-29144
Low-rate discharge of various electrochemical batteries for use with oceanographic instruments
[AD-A153965] 18 p3095 N85-29159
Electrochemical and morphological study of the effect of temperature on the restructuring and loss of capacity of alkaline battery electrodes
[DE85-008869] 18 p3129 N85-29378

ALKALINE EARTH METALS
Inoculation of non-metallic inclusions in steel 17GS
[BLL-BISI-TRANS-22431-(9022.06)] 17 p2925 N85-28042

ALKALINE EARTH OXIDES
NT BARIUM OXIDES
NT BERYLLIUM OXIDES
NT CALCIUM OXIDES
NT MAGNESIUM OXIDES
Electronically excited alkaline earth oxides: Chemical production and collisional energy transfer processes
[AD-A153172] 17 p3044 N85-28833

ALKALINITY
Tectonic position and formation of young alkaline provinces of continents and oceans 10 p1502 N85-19480
Carbonate chemistry of the Weddell Sea
[DOE/EV-110611/4] 12 p1898 N85-21916
Ohmic potential drop and gas bubble radius distribution in alkaline water electrolysis 17 p2924 N85-28025

ALKALOIDS
NT ATROPINE
NT QUINOLINE

ALKALOSIS
Respiratory chain of alkalophilic bacteria
[DE84-012558] 09 p1360 N85-18558

ALKANES
NT BUTANES
NT ETHANE
NT HEXENES
NT METHANE
NT NITROPROPANE
NT PARAFFINS
NT PENTANES
NT PROPANE
Liquid phase products and solid deposit formation from thermally stressed model jet fuels
[NASA-TM-86874] 04 p0481 N85-13066
Review of the toxicokinetics of n-hexane
[AD-P004018] 06 p0843 N85-15352
Molecular mechanisms of n-hexane neurotoxicity
[AD-P004020] 06 p0843 N85-15354
Electrochemistry at very high potentials: The use of ultramicroelectrodes in the anodic oxidation of short chain alkanes
[AD-A148654] 08 p1123 N85-17078
Fuels combustion research
[AD-A149106] 10 p1457 N85-19178
Transitional metal activation and functionalization of C-H bonds
[DE85-006816] 16 p2746 N85-26949
The distribution of higher n-alkanes in partially frozen middle distillate fuels
[AD-A159940] 18 p3083 N85-29074
Phase behavior and QLS (Quasielastic Light Scattering) in potassium linoleate/n-alkanol microemulsions
[AD-A155028] 21 p3563 N85-32163
Soil extraction kit
[AD-D011736] 22 p3742 N85-33190

ALKENES
NT BUTADIENE
NT BUTENES
NT ETHYLENE
NT HEXENES
NT PROPYLENE
NT VINYLIDENE
A metal-catalyzed rearrangement of alkene-alkynes and the stereochemistry of metallacyclobutene ring opening
[AD-A149064] 10 p1435 N85-19042
Rep rated long life capacitor development: Phase 1 and 2
[DE85-000719] 11 p1629 N85-20256

ALKYD RESINS
New air-curing lacquer systems with high solids content
[BMFT-FB-T-85-005] 17 p2936 N85-28124

ALKYL COMPOUNDS
NT TRIMETHYL COMPOUNDS
Fluorinated aliphatic polyalkylether lubricant with an additive composed of an aromatic phosphine substituted with perfluoroalkylether groups
[AD-D011286] 06 p0770 N85-14927

Super hydrides
[AD-A153499] 18 p3070 N85-28986
Pyrophoric alkylaluminum compounds in decoy flares
[FOA-C-20562-E4] 18 p3078 N85-29039
Improved acid electrolytes for fuel cells
[PB85-176053] 18 p3132 N85-29397
Spray pyrolysis as a synthetic tool
[AD-A153891] 19 p3234 N85-30047
Self-developing polysilane deep-UV resists: Photochemistry, photophysics and submicron lithography
[DE85-007608] 19 p3237 N85-30067

ALKYLATION
Study of application of organic semiconductors to electronic components
[BMFT-FB-T-84-142] 02 p0289 N85-11890
Effects of introduction of alkyl groups into aluminium anodized coatings
[DRIC-T-7244] 03 p0331 N85-12133

ALKYNES
NT ACETYLENE
A metal-catalyzed rearrangement of alkene-alkynes and the stereochemistry of metallacyclobutene ring opening
[AD-A149084] 10 p1435 N85-19042

ALL SKY PHOTOGRAPHY
The ROSAT all-sky survey in X-rays
08 p1243 N85-17843
The ROSAT XUV wide field camera
08 p1243 N85-17844

ALL-WEATHER AIR NAVIGATION
Coverage and buildup of the Navstar constellation
11 p1711 N85-20764
Flying in spite of the weather
[NLR-MP-84021-U] 17 p2895 N85-27847

ALL-WEATHER LANDING SYSTEMS
Development and flight test of a helicopter compact, portable, precision landing system concept
08 p1076 N85-16821

ALLENDE METEORITE
Minor elements and cathodoluminescence of Mg-rich olivines from Murchison and Allende carbonaceous meteorites
06 p0684 N85-15619
X-radiography of slices of the Allende Meteorite
06 p0685 N85-15622
Dynamic thermal episodes in the protosolar nebula: Development of models from observations on CAI's
06 p0687 N85-15633
Mineralogical investigations of lunar samples and meteorites
[NASA-CR-174291] 08 p1258 N85-17918
Lunar sample analysis — Allende meteorite
[NASA-CR-171851] 10 p1572 N85-19911
Interstellar Al-26 and excess Mg-26
15 p2680 N85-26551

ALLOCATIONS
NT RESOURCE ALLOCATION
Spectrum resource assessment of the 1530-1660.5 MHz band
[NTIA/REPT-84/160] 10 p1469 N85-19268
Summary of activities of the Committee on Science and Technology
[H-REPT-98-1189] 12 p1964 N85-22341
An analysis of a dynamic project cost problem
[CSIR-TWISK-338] 13 p2149 N85-23341
Criteria for qualifying for FRG federal CAD/CAM subsidies
15 p2536 N85-25651
Airport and airway system cost allocation model. Volume 7: User's manual
[AD-A152877] 17 p2906 N85-27917
Geostationary orbit capacity study
[REPT-44-3558] 18 p3091 N85-29134
Department of Housing and Urban Development-Independent Agencies Appropriation Act, 1986
20 p3542 N85-32041
National Aeronautics and Space Administration research and development
20 p3542 N85-32042
Progress report on implementing the recommendations of the White House Science Council's Federal Laboratory Review Panel, volume 1
[PB85-185072] 24 p4184 N85-35819

ALLOYS
NT ALUMINUM ALLOYS
NT ANTIMONY ALLOYS
NT ARSENIC ALLOYS
NT AUSTENITIC STAINLESS STEELS
NT BARIUM ALLOYS
NT BEARING ALLOYS
NT BERYLLIUM ALLOYS
NT BINARY ALLOYS
NT BISMUTH ALLOYS
NT BORON ALLOYS
NT BRASSES
NT BRONZES
NT CARBON STEELS
NT CAST ALLOYS
NT CESIUM ALLOYS
NT CHROMIUM ALLOYS
NT CHROMIUM STEELS
NT COBALT ALLOYS
NT COPPER ALLOYS
NT EUTECTIC ALLOYS
NT FERRITIC STAINLESS STEELS
NT GERMANIUM ALLOYS
NT GOLD ALLOYS
NT HAFNIUM ALLOYS
NT HASTELLOY (TRADEMARK)
NT HEAT RESISTANT ALLOYS
NT HIGH STRENGTH ALLOYS
NT HIGH STRENGTH STEELS
NT INCONEL (TRADEMARK)
NT IRON ALLOYS
NT KOVAR (TRADEMARK)
NT LEAD ALLOYS
NT LIGHT ALLOYS
NT LIQUID ALLOYS
NT LITHIUM ALLOYS
NT LOW CARBON STEELS
NT MAGNESIUM ALLOYS
NT MANGANESE ALLOYS
NT MARAGING STEELS
NT MARTENSITIC STAINLESS STEELS
NT MOLYBDENUM ALLOYS
NT MONEL (TRADEMARK)
NT NEODYMIUM ALLOYS
NT NICKEL ALLOYS
NT NICKEL STEELS
NT NIOBIUM ALLOYS
NT NITINOL ALLOYS
NT PALLADIUM ALLOYS
NT PLATINUM ALLOYS
NT POTASSIUM ALLOYS
NT QUATERNARY ALLOYS
NT RARE EARTH ALLOYS
NT REFRACTORY METAL ALLOYS
NT RENE 95
NT RHENIUM ALLOYS
NT RUTHENIUM ALLOYS
NT SELENIUM ALLOYS
NT SHAPE MEMORY ALLOYS
NT SILICON ALLOYS
NT SILVER ALLOYS
NT SODIUM ALLOYS
NT SOLDERS
NT STAINLESS STEELS
NT STEELS
NT TANTALUM ALLOYS
NT TERNARY ALLOYS
NT TIN ALLOYS
NT TITANIUM ALLOYS
NT TUNGSTEN ALLOYS
NT UDIMET ALLOYS
NT URANIUM ALLOYS
NT VANADIUM ALLOYS
NT WASPALOY
NT WROUGHT ALLOYS
NT ZINC ALLOYS
NT ZIRCALOYS (TRADEMARK)
NT ZIRCONIUM ALLOYS
Effects of cobalt, boron, and zirconium on the microstructure of Udimet 738
[NASA-CR-174762] 01 p0027 N85-10166
Minor element effects on gas tungsten arc weld penetration
[PB84-222579] 01 p0056 N85-10370
Materials studies for magnetic fusion energy applications at low temperatures, 7
[DE84-013487] 01 p0122 N85-10837
Method for calculating linear shrinkage and expansion of metals and alloys
[BLL-M-35747-(5828.4)] 02 p0175 N85-11173
Alloying effects of reactive elements in ferritic stainless steels
02 p0178 N85-11196
Erosion of sintered WC-Co alloys
02 p0179 N85-11201
The influence of metallurgical aspects on the pitting corrosion behaviour of high alloy stainless steels
02 p0179 N85-11202
Recent developments on the role of molybdenum in irons and steels
02 p0180 N85-11206
Metastable phase formation in ion implanted metals
[DE84-014945] 02 p0183 N85-11229
Use of magnetic compression based on amorphous alloys as a drive for induction linacs
[DE84-014524] 02 p0277 N85-11805
The modification of metallic corrosion by ion implantation: Engineering applications and fundamentals studies
[AD-P003954] 02 p0286 N85-11870
Application of positron annihilation in materials science
[DE84-014733] 02 p0288 N85-11883
Structural uses for ductile ordered alloys. Report of the committee on application potential for ductile ordered alloys
[AD-A146313] 03 p0332 N85-12139
USSR report: Materials science and metallurgy
[JPRS-UMS-84-007] 03 p0348 N85-12244
Parameters of structural relaxation and mechanical properties of amorphous alloys
03 p0349 N85-12246
HgCdTe surface and defect study program
[AD-A146343] 03 p0434 N85-12764
Change in the nitrogen content when nitrided alloys are heated
[BLL-M-35946-(5828.4)] 05 p0615 N85-13929
Testing of production of silicon-titanium-magnesium alloying composition
[BLL-M-35904-(5828.4)] 05 p0616 N85-13937
Material selection consideration for solar ponds
05 p0666 N85-14284
Modelling of deformation and fracture in high-temperature structural materials
[DE84-016906] 06 p0818 N85-15191
The growth of metastable peritectic compounds
[NASA-CR-171290] 07 p0920 N85-15825
The influence of porosity on the deformation and fracture of alloys
[AD-A148766] 08 p1130 N85-17124
Structural studies of amorphous Mo-Ge alloys using synchrotron radiation
[DE85-002081] 08 p1131 N85-17125
Alloying effects and microstructure of iron aluminides
[DE85-000903] 09 p1295 N85-18137
Behavior of pressurized tubes of candidate alloys in a simulated low-Btu environment
[DE85-003403] 09 p1296 N85-18141
Ion beam studies of hydrogen in metals
[DE84-017422] 09 p1297 N85-18145
Advanced artificial dielectric materials for millimeter wavelength applications
[AD-A148960] 10 p1431 N85-19027
Characterization of erosion of metallic materials under cavitation attack in a mineral oil
[NASA-TM-86934] 10 p1440 N85-19075
Cobalt-free permanent magnet alloys
[AD-A149272] 10 p1441 N85-19079
Radiation-induced compositional redistribution and local phase transformation in irradiated alloys
[DE85-000080] 10 p1441 N85-19082
Kinetics of reaction of metals and non-metals during diffusion welding
11 p1602 N85-20076
Weldability of alloy ABM1 to alloy 1201
11 p1603 N85-20080
Structure of transient zone in diffusion welding of TaTS-19 piezoceramic with AMg6 alloy
11 p1603 N85-20082
Alloys based on NiAl for high temperature applications
[NASA-TM-86976] 12 p1805 N85-21322
Advanced thin film thermocouples
[NASA-CR-175541] 12 p1850 N85-21607
Viscoplastic constitutive relationships with dependence on thermomechanical history
[NASA-CR-174836] 12 p1864 N85-21691
Creep crack growth in ductile alloys
[DE85-003937] 13 p2023 N85-22676
New tooling for plasma cutting technology
13 p2051 N85-22842
Annealing effects in ferromagnetic amorphous alloys
[AD-A150648] 14 p2255 N85-23972
Exploratory corrosion tests on alloys in molten salts at 900(0)C
[DE85-000511] 14 p2257 N85-23983
Tracer diffusion in an ordered alloy: Application of the path probability and Monte Carlo methods
[DE85-002768] 14 p2257 N85-23986
Influence of short-range order on deformation mechanisms in solid solutions
[DE85-006374] 14 p2258 N85-23989
Exploratory corrosion tests on materials and fluids for advanced high-temperature molten-salt storage
[DE85-002911] 14 p2258 N85-23991
Measurements of radiation-induced segregation and diffusion in ion irradiated alloy using implanted manganese
[AERE-R-11529] 14 p2258 N85-23994
Characterization of atomic defects and their aggregates using positron annihilation spectroscopy
[DE85-006206] 14 p2418 N85-24918
USSR report: Materials science and metallurgy
[JPRS-UMS-85-001] 15 p2496 N85-25395
Structural changes with one- and two-stage aging of alloys Ti-Al-Mo-Fe and Ti-Zr-V-Al-Sn
15 p2496 N85-25415
Effects of surface chemistry on hot corrosion life
[NASA-CR-174915] 16 p2708 N85-26711

Properties and microstructures for dual alloy combinations of three superalloys with alloy 901
[NASA-TM-86987] 16 p2749 N85-26963
On the feasibility of Ab Initio calculations of ordering alloy phase diagrams
[DE85-007073] 16 p2751 N85-26979
The influence of melting practice and of microalloying, with rare earth metals and with boron, on the quality of low-carbon steel
[BLL-BISI-22467-(9022.06)] 17 p2925 N85-28036
Powder-metallurgy alloys and steels
[BLL-BISI-TRANS-22239-(9022.06)] 17 p2926 N85-28050
New process for production of bimetal with corrosion-resistant cladding layer
[BLL-BISI-TRANS-22371-(9022.06)] 17 p2927 N85-28056
Production and compaction of amorphous metal powders
[BLL-BISI-TRANS-22367-(9022.06)] 17 p2929 N85-28060
In situ HVEM studies of electron beam-driven composition changes in thin film alloys: Displacement-rate gradient effects
[DE85-007992] 17 p2931 N85-28092
Temperature and manganese content dependences of tensile deformation in iron-high manganese binary alloys
[DE85-007656] 17 p2932 N85-28098
Submerged arc welding of new Czechoslovak micro-alloy steels
[BLL-BISI-TRANS-22193-(9022.06)] 17 p2972 N85-28356
Unalloyed and alloyed line wires of improved properties
[BLL-BISI-TRANS-21930-(9022.06)] 18 p3073 N85-29008
Interfacial segregation and fracture
[DE85-009779] 18 p3075 N85-29019
Local density theory of heats of formation and short-range order parameters in substitutionally disordered alloys
[DE85-009811] 18 p3075 N85-29021
Cavitation erosion of plasma sprayed alloys
[DE85-009542] 18 p3077 N85-29036
Theory of positron annihilation in vacancies in concentrated disordered alloys
[DE85-010267] 18 p3183 N85-29734
Alloy development for irradiation performance
[DE85-010454] 19 p3240 N85-30091
Structure and properties of VT23 alloy welded joints after thermocyclic processing 19 p3246 N85-30125
Fatigue-crack propagation behavior of alloy A-286
[DE85-007460] 19 p3288 N85-30391
Durability of reinforced hard-alloy draw plates
[BLL-M-36278-(5828.4)] 20 p3465 N85-31526
Determination of deformation speed during high-speed deformation of cylindrical shells
[BLL-M-36280-(5828.4)] 20 p3465 N85-31527
Thermomechanical deformation in the presence of metallurgical changes 20 p3466 N85-31533
Results of an interlaboratory fatigue test program conducted on alloy 800H at room and elevated temperatures
[NASA-CR-174940] 21 p3597 N85-32340
Management of Corrosion
[AGARD-LS-141] 22 p3749 N85-33238
Corrosion management strategies for aircraft and related systems 22 p3749 N85-33239
Maintenance and the military environment 22 p3750 N85-33243
Protective systems and maintenance policies for marine environments 22 p3750 N85-33245
The study of the effect of residual microimpurities on the fatigue strength of 55S2 steel
[BLL-M-36317-(5828.4)] 23 p3913 N85-34246
Pitting corrosion of ferrous alloys
[AERE-R-11490] 24 p4078 N85-35273
Fatigue damage detection in steels by optical correlation
[AD-A155830] 24 p4079 N85-35277
X-ray fluorescence analysis of 304L stainless steel
[DE85-013254] 24 p4080 N85-35288

ALLUVIUM
Attenuation of seismic waves at regional distances
[AD-A150198] 13 p2132 N85-23267

ALMUCANTAR
U ELEVATION ANGLE

ALOUETTE SATELLITES
NT ALOUETTE 2 SATELLITE

ALOUETTE 2 SATELLITE
Actual altitudes of radioacoustic sounding in decimeter wavelength band 06 p0826 N85-15243

ALPHA DECAY
International program to improve decay data for transactinium nuclides
[DE85-011258] 20 p3529 N85-31954
Production of stable embryo particles in dense ion tracks of alpha particle emissions in the atmosphere 21 p3644 N85-32638

ALPHA PARTICLES
A system for monitoring radon and its decay products in the atmosphere
[INPE-3085-PRE/494] 03 p0391 N85-12502
Alpha-particle diagnostics with high energy neutral beams
[IPPJ-695] 06 p0863 N85-15485
Feasibility of alpha particle measurement by CO2 laser Thomson scattering
[DE85-001764] 09 p1326 N85-18334
Effect of alpha particles on the stability of Elmo Bumpy Torus (EBT) reactor
[DE84-017266] 09 p1392 N85-18759
Feasibility of alpha particle measurement by CO2 laser Thomson scattering
[DE85-004938] 13 p2097 N85-23081
Noninductive current drive in Tokamaks
[DE85-005427] 14 p2424 N85-24951
An alpha particle diagnostic beam line system to generate an intense Li(O) beam with an ORNL SITEX source
[DE85-010564] 18 p3182 N85-29730
New concept for a wall detector for alpha particles
[DE85-009037] 18 p3183 N85-29740
Effect of polarized radiative transfer on the Hanle magnetic field determination in prominences: Analysis of hydrogen H alpha line observations at Pic-du-Midi 18 p3207 N85-29894
The effects of alpha particle production on the stability of an Elmo Bumpy Torus (EBT) reactor 19 p3369 N85-30695
Production of stable embryo particles in dense ion tracks of alpha particle emissions in the atmosphere 21 p3644 N85-32638
Calculated neutron-induced cross sections for /sup 63,65/Cu/sup 58,60/Ni and (52) Cr from 1 to 20 MeV and comparisons with experiments
[DE85-011926] 22 p3844 N85-33808
Injection of energetic particles following the gamma-ray flares on June 7, 1980, as observed on Helios 1
[SH-1.3-9] 23 p3993 N85-34756
Observations of solar energetic particles at a synchronous orbit
[SH-3.1-1] 23 p4001 N85-34806
Calculation of heavy-ion tracks in liquid water
[DE85-012101] 24 p4149 N85-35725
Gamma-ray production cross sections for alpha-particle induced reactions on F-19 and Na-23
[DE85-012603] 24 p4150 N85-35732
Some nuclear data needs in astrophysics
[DE85-012916] 24 p4168 N85-35842
Determination of primary energy in nucleus-nucleus collisions and the high P(sub)T tail of alpha-particles 24 p4173 N85-35875

ALPHA RADIATION
U ALPHA PARTICLES

ALPHABETS
Character recognition using correlation techniques
[AD-A152006] 16 p2847 N85-27549

ALPHANUMERIC CHARACTERS
NT BINARY DIGITS
Plotting TDL coastal wind forecasts
[PB84-220789] 03 p0397 N85-12533
Axial representations of shape
[AD-A150387] 13 p2151 N85-23356
Comparative study of the digital analysis of areas of the Earth's surface prepared for planting using different classification algorithms
[INPE-3359-PRE/637] 16 p2846 N85-27545

ALPINE METEOROLOGY
Frontal motion in mountainous terrain: Analysis and implications for 0 to 12 hour forecasts 01 p0076 N85-10502
Simple methods in very short-range forecasting based on data from a mesoscale network of automatic stations (ANETZ) and from satellite (Meteosat) and radar — Swiss Alps 01 p0082 N85-10548
Some aspects of matching nowcasting and Very-Short-Range Forecasting (VSRF) products with the need of a multilingual community of a mountainous country — Swiss Alps 01 p0084 N85-10566
Alpine meteorology: Translations of classic contributions by Wagner, A., Ekhart, E. and Defant, F.
[DE84-014929] 01 p0085 N85-10574
Data catalog for the 1982 DFVLR observational Foehn experiment — alpine wind
[DFVLR-FB-84-33] 09 p1358 N85-18543
Measurement of water equivalent of mountain snow cover — ARGOS system 14 p2327 N85-24386
Observation of precipitating clouds by a vertically pointing radar at Morino in the Iburi District, Hokkaido, Japan 15 p2582 N85-25922
Statistical comparison of radar echoes of convective precipitation between the northern Alps and its foreland
[DFVLR-FB-85-07] 17 p2950 N85-28215

ALPS MOUNTAINS (EUROPE)
Alpine meteorology: Translations of classic contributions by Wagner, A., Ekhart, E. and Defant, F.
[DE84-014929] 01 p0085 N85-10574
Crustal stretching and subsidence in sedimentary eastern Switzerland and permo-carboniferous basins in the continental United States
[DE85-000622] 11 p1681 N85-20592

ALTERATION
U REVISIONS

ALTERNATING CURRENT
Induction voltmeter
[DE84-014321] 01 p0050 N85-10329
High-current measurement techniques
[PB85-100444] 11 p1637 N85-20311
Power control for ac motor
[NASA-CASE-MFS-25861-1] 13 p2062 N85-22877
Dynamic characteristics of ac arc in welding aluminum alloys 15 p2500 N85-25424
The performance of an alternating-current thyristor-controlled motor induction heating gun 15 p2548 N85-25716
[NASA-CASE-LAR-13161-1] 16 p3085 N85-29083
Alternating current OHMIC heating in a toroidal stellerator 20 p3534 N85-31988
Tailored vacuum chambers for ac magnets
[DE85-010767] 21 p3591 N85-32319
Optimization of design parameters for alternating current stabilizer based on magnetic suspension 22 p3772 N85-33374

ALTERNATING CURRENT GENERATORS
U AC GENERATORS

ALTERNATIVES
Diesel fuel alternatives for engines in civil works prime movers
[AD-A149736] 12 p1617 N85-21400

ALTERNATORS (GENERATORS)
U AC GENERATORS

ALTIMETERS
NT RADIO ALTIMETERS
TCAS 2 logic performance during phase one operational evaluation
[DOT/FAA/PM-84/20] 05 p0595 N85-13793
Theoretical and experimental analyses of laser altimeters for barometric measurements over the ocean 08 p1165 N85-17351
A method for determining mesoscale dynamic topography
[AD-D011412] 08 p1191 N85-17506
Along-track deflection of the vertical from SEASAT: GEBCO (General Bathymetric Chart of the Oceans) overlays
[PB85-129641] 12 p1876 N85-21767
Application of space methods in geodesy 16 p2724 N85-26817
Global mean sea surface based upon a combination of the GEOS-3 and SEASAT altimeter data 20 p3492 N85-31710
SEASAT altimetry for surface height of inland seas 20 p3493 N85-31714
TOPEX error budget 20 p3493 N85-31717
Global geoid and gravity anomaly predictions using the collocation and point mass techniques
[AD-A154517] 21 p3605 N85-32367

ALTITUDE
NT FLIGHT ALTITUDE
NT HIGH ALTITUDE
NT LOW ALTITUDE
NT SEA LEVEL
Change in Venusian atmosphere absorption coefficient with altitude 02 p0163 N85-11103
Critical conditions for the automatic control of landing from decision height in variable winds
[UTIAS-284] 06 p0753 N85-14830
Analytical and physical modeling program for the NASA Lewis Research Center's Altitude Wind Tunnel (AWT)
[NASA-TM-86919] 07 p0909 N85-15757
On the altitudinal distribution of birds and bird strikes in the Netherlands
[AD-P004189] 11 p1580 N85-19952
Atmospheric environment for Space Shuttle (STS-51A) launch
[NASA-TM-86497] 12 p1892 N85-21875
Altitude of auroral scattering observed along auroral electrojets 14 p2339 N85-24465
Statistical comparison of pooled nitrogen washout data of various altitude decompression response groups
[NASA-TM-58265] 15 p2639 N85-26278
A constant altitude flight survey method for mapping atmospheric ambient pressures and systematic radar errors
[NASA-TM-86733] 19 p3217 N85-29951

Comparison of tropopause altitude determination by the Platteville Radar, Sunset Radar and the NWS Rawinsonde 21 p3617 N85-32477
Observations of mesospheric turbulence by rocket probe and VHF radar, part 2.4A 21 p3619 N85-32484
Terrain illumination conditions when taking scanning photographs from space 22 p3736 N85-33159
Altitude variations of cosmic-ray soft and hard components observed by airborne detectors [SH-6.1-5] 23 p4045 N85-35079
Long-period cosmic ray variations and their altitude dependence [SH-6.1-19] 23 p4046 N85-35091
Particle distributions in approximately 10(13) - 10(16) eV air shower cores at mountain altitude and comparison with Monte Carlo simulations [HE-4.2-18] 24 p4190 N85-35994

ALTITUDE ACCLIMATIZATION
Results of study of hypoxia problems 04 p0544 N85-13462
Dynamics of external respiration and gas metabolism under combined effect of hypoxia and hypercapnia 06 p1193 N85-17519
Multiple regression method used to assess animal adaptation to hypoxic hypoxia 12 p1902 N85-21947
Structural changes in thyroid due to high-altitude adaptation in Kirghizia 22 p3820 N85-33666
Effect of dibazol on parameters of nonspecific resistance of subjects in pressurized cabins 23 p3954 N85-34504

ALTITUDE CONTROL
Altitude control using action-demanding interactive displays: Toward an active psychophysics [AD-P004311] 09 p1267 N85-17965

ALTITUDE SICKNESS
The effect of naproxen on acute mountain sickness and vascular responses to hypoxia [AD-A145144] 01 p0095 N85-10638
Simulator sickness: Sensorimotor disturbances induced in flight simulators [AD-P004334] 09 p1271 N85-17988
Airsickness control using biofeedback to self-regulate psychophysiological responses [AD-A151167] 15 p2617 N85-26128
Effect of spironolactone on acute mountain sickness [AD-A153780] 18 p3153 N85-29525

ALTITUDE SIMULATION
Analytical modeling of circuit aerodynamics in the new NASA Lewis wind tunnel [NASA-TM-86912] 07 p0897 N85-15688
The NASA Altitude Wind Tunnel (AWT): Its role in advanced icing research and development [NASA-TM-86920] 07 p0910 N85-15758
An environmentally-controlled extended-use small animal hypobaric chamber [AD-A153735] 19 p3221 N85-29974

ALTITUDE TESTS
NT HIGH ALTITUDE TESTS
The KZD-85 engine test. Engine type: 1 cylinder, 2 stroke motor 2100 Husquarna [FWE-FO-1717] 02 p0205 N85-11354
Oxygen uptake as an indicator of animal adaptation to altitude hypoxia 19 p3324 N85-30595

ALTITUDE TOLERANCE
Hemodynamics and neurodynamics of the human brain during exposure to moderate hypoxic hypoxia 01 p0094 N85-10630
Effect of acute hypoxia on coronary and systemic hemodynamics 23 p3953 N85-34503

ALU (COMPUTER COMPONENTS)
U ARITHMETIC AND LOGIC UNITS

ALUMINA
U ALUMINUM OXIDES

ALUMINATES
Glass corrosion in liquid lithium [DE85-002086] 09 p1299 N85-18162
Alloys based on NiAl for high temperature applications [NASA-TM-86976] 12 p1805 N85-21322
Ionic conduction and water diffusion in Li (BETA)-alumina [DE85-007548] 16 p2755 N85-27005

ALUMINIZING
U ALUMINUM COATINGS

ALUMINUM
NT ALUMINUM ISOTOPES
NT ALUMINUM 26
NT POWDERED ALUMINUM
NT SINTERED ALUMINUM POWDER
The influence of aluminum on the qualities of low and medium carbon steel [BLL-M-35754-(5828.4)] 03 p0330 N85-12123
Influence of aluminum oxide film on thermocompression bonding of gold wire to evaporated aluminum film [NASA-TM-77503] 03 p0330 N85-12127
Universal binding energy relations in metallic adhesion [NASA-TM-86889] 03 p0331 N85-12132
Effects of introduction of alkyl groups into aluminium anodized coatings [DRIC-T-7244] 03 p0331 N85-12133
Research approaches to quality aluminum for Ocean Thermal Energy Conversion (OTEC) systems [DE84-013007] 04 p0476 N85-13034
Thermite and Fe/KClO4: Some thermodynamic calculations [DE84-016945] 04 p0573 N85-13653
Abundancies of Ni, Cr, CO and major elements in the silicate portion of the Moon: Constraints from primary lunar magmas 04 p0582 N85-13720
Investigation of materials for inert electrodes in aluminum electrodeposition cells [DE84-015036] 05 p0617 N85-13947
Multiaxial yield behavior of 1100 aluminum following various magnitudes of prestrain [DE84-013904] 05 p0617 N85-13949
Development and testing of TiB2, used as cathode material in Al-electrolysis cells [BMFT-FB-T-84-176] 06 p0633 N85-14060
Thermal conductivity of aluminum, copper, iron and tungsten for temperature from 1 K to the melting point [PB84-235878] 06 p0770 N85-14924
Microstructure, texture and formability of thin aluminium sheets 06 p0796 N85-15088
Recommended aluminum pipe welding procedures for corps of engineers construction [AD-A146712] 06 p0815 N85-15172
Ultrasonic girth weld evaluation for aluminum substrate of spherical Kevlar-epoxy test specimens [DE85-001502] 06 p0816 N85-15181
Bulk compositions of Al-rich chondrules in ordinary and carbonaceous chondrites: Variations and similarities 06 p0881 N85-15601
The growth of metastable peritectic compounds [NASA-CR-171289] 07 p0920 N85-15824
Optimization of the NiCrAl-Y/ZrO-Y2O3 thermal barrier system [NASA-TM-86905] 07 p0927 N85-15878
Experimental compliance calibration of the NASA Lewis Research Center Mode 2 fatigue specimen [NASA-TM-86908] 07 p0977 N85-16205
A study of constitutive relations for polycrystalline aluminum during finite dynamic plastic deformation 08 p1172 N85-17388
Advanced NMR characterization of zeolite catalysts [DE85-000456] 09 p1291 N85-18104
Alloying effects and microstructure of iron aluminides [DE85-000903] 09 p1295 N85-18137
Beam-foil spectroscopy of highly ionized aluminum atoms 09 p1390 N85-18748
High temperature properties of equiatomic FeAl with ternary additions [NASA-TM-86938] 10 p1439 N85-19072
Chemistry Institute's advances in making extra-pure aluminum 10 p1443 N85-19093
Mechanical properties of Be-Al composite 10 p1443 N85-19094
Aluminum in biogenic cycle and forms of its occurence in ocean 10 p1499 N85-19463
USSR report: Materials science and metallurgy [JPRS-UMS-84-005] 11 p1597 N85-20044
Study of phase composition of Al-B plasma coatings 11 p1598 N85-20050
Structure and properties of copper-titanium-aluminum composites obtained by thermoreactive sintering 11 p1600 N85-20061
Patterns in the occurrence of the brittle topologically close-packed phases: Al [DE85-000592] 11 p1607 N85-20106
Chemically amplified laser direct-writing of aluminum [DE85-000308] 11 p1639 N85-20324
A computerized study of rigid cones penetrating aluminum targets [FOA-C-20561-D4] 11 p1648 N85-20384
Effects of chromium and aluminum on mechanical and oxidation properties of iron-nickel-base superalloys based on CG-27 [NASA-TP-2443] 12 p1805 N85-21323
Measurements of distributed combustion 13 p2001 N85-22542
Study of character of adhesive interaction and breaking of polyimid-aluminum foil junction during process of hardening 13 p2014 N85-22637
Directional dependent engineering properties of aluminum-aramid-epoxy laminates [CCMS-85-02] 13 p2015 N85-22638
An electrochemical study of the corrosion behavior of primer coated 2219-T87 aluminum [NASA-TP-2459] 13 p2021 N85-22662
Dependence of superplastic flow on state of grain boundaries 13 p2025 N85-22689
Method of calculating strength of joint produced by cold welding of aluminum under discrete loading 13 p2034 N85-22743
AL-124 light-emitting diode in 30 Mbit/s fiber-optic communication line 13 p2069 N85-22925
Microstructure and properties of ferrous alloy weldments [DE85-005582] 14 p2257 N85-23987
Use of optical techniques in studies of wear rates of anodized aluminum and polymer coatings on aluminum 14 p2259 N85-23997
Fatigue crack topography and crack growth analysis — wrought and cast aluminum 14 p2319 N85-24333
Development of coating for protection of backside of seam in welding of titanium alloys 15 p2500 N85-25421
Ultrasonic SH wave velocity in textured aluminum plates [AERE-R-11516] 15 p2509 N85-25475
Ion beam mixing of marker layers in Al and Si [DE85-006227] 15 p2511 N85-25490
Temperature, velocity, and species mapping in an induction plasma [DE85-004005] 15 p2512 N85-25499
Structure of condensed aluminum thin film metallizations 15 p2512 N85-25501
Reduced-chromium stainless steel substitutes containing silicon and aluminum [PB85-160786] 15 p2513 N85-25502
Measurement of material properties to Mbar pressures using time-resolved shock wave techniques [DE85-007319] 15 p2558 N85-25780
Ultrasonic characterization of porosity: Theory [DE85-005922] 15 p2646 N85-26325
Spectroscopic studies of a railgun muzzle flash [MRL-R-952] 16 p2728 N85-26837
Ignition of metals in high pressure oxygen 16 p2735 N85-26874
Effect of low-velocity or ballistic impact damage on the strength of thin composite and aluminum shear panels [NASA-TP-2441] 16 p2742 N85-26924
Microscopic study of the influence of impurities on interface bonding [AD-A151725] 16 p2743 N85-26928
The application of BRILES rivets for mechanical jointing of Aramid Reinforced Aluminum Laminate (ARALL) [VTH-LR-387] 16 p2802 N85-27279
Friction and wear behavior of aluminum and composite I-beam stiffened airplane skins [NASA-TM-86418] 17 p2895 N85-27852
Influence of manganese and heat treatment on structure and properties of Fe-0.1 percent-C-14 percent Cr-based steels [BLL-BISI-TRANS-22299-(9022.06)] 17 p2928 N85-28071
Preventing the formation of an anomalous structure in chemically sealed low carbon steel [BLL-BISI-TRANS-22373-(9022.06)] 17 p2930 N85-28085
Research on design of cryotransformers and its prospects for the future [AD-A152400] 17 p2952 N85-28230
Aluminum-air power cell research and development [DE85-008117] 17 p2966 N85-28456
Possible indication of an A-dependence of R in deep-inelastic electron scattering from nuclei [DE85-008174] 17 p3033 N85-28783
Strain fields for aluminum at different tooling temperatures and extrusion ratios [DE85-006257] 18 p3075 N85-29020
Mechanical properties of adhesively bonded aluminum structures protected with hydration inhibitors [AD-A153755] 18 p3079 N85-29047
Aluminum-air power cell: The M3-3 experiment [DE85-008878] 18 p3096 N85-29168
Establishment of a methodology for predicting lifetimes in active solar systems [DE85-008629] 18 p3130 N85-29383
Study of the equilibrium vacancy ensemble in aluminum using 1D- and 2D-angular correlation of annihilation radiation [DE85-008967] 18 p3194 N85-29813
Characteristics of charge transfer in the dispersed phase of electrorheological suspensions [RAE-TRANS-2125] 19 p3233 N85-30040
Separation of Drude and band-to-band spectra in polyvalent metals [DE85-010247] 19 p3240 N85-30093
Producing titanium-sapphire items by solid-phase bonding through aluminum gasket 19 p3246 N85-30127
Diffusion welding of aluminum with vacuum-tight corundum ceramic 19 p3247 N85-30130
Effect of confinement on failure in 95 TATB/5 KEL-F [DE85-010790] 19 p3251 N85-30158
Impact dynamics research on composite transport structures [NASA-TM-86391] 19 p3284 N85-30367

Study of intermediate velocity penetration of steel spheres into deep aluminum targets
[DE85-010419] 19 p3267 N85-30385
Environmental background measurement program
[AD-A153860] 19 p3319 N85-30577
Magnetoconductance in aluminum films, wires, and cylinders 19 p3374 N85-30928
An update of the JPL program to develop Li-SOCl2 cells 20 p3445 N85-31384
Excitation of some alkaline Earth-like ions
[DE85-010737] 20 p3529 N85-31951
Defect production and recovery in FCC metals irradiated at 4.2 K
[DE85-010477] 20 p3538 N85-32014
Thermoelectric properties of beta-boron and some boron compounds
[DE85-011978] 21 p3582 N85-32270
Plasma mass and effective inductance in a small railgun
[AD-A154644] 21 p3589 N85-32304
Laser beam interactions with vapor plumes during Nd:YAG laser welding on aluminum
[DE85-009793] 21 p3593 N85-32326
Properties of Ti-6Al-4V spun formed fuze supports
[DE85-011968] 22 p3792 N85-33498
A new analysis of cosmic ray isotopes at 3 GeV/n from HEAO3-C2 data
[OG-4.3-6] 22 p3879 N85-34031
Fracture behavior of aluminum composites reinforced with fiber 23 p3907 N85-34207
Enthalpies of formation of liquid Fe-Ce-Si and Fe-Ce-Al three-component alloys
[BLL-M-36296-(5828.4)] 23 p3913 N85-34247
The properties of VSt3ap inoculated steel
[BLL-M-35894-(5828.4)] 23 p3915 N85-34263
Aluminum work function: Effect of oxidation, mechanical scraping and ion bombardment
[NASA-TM-87079] 23 p3915 N85-34265
Electrically conductive containment vessel for molten aluminum
[DE85-006518] 23 p3939 N85-34415
Elliptical X-ray analyzer spectrograph application to a laser-produced plasma
[DE85-013790] 24 p4097 N85-35396
Few-particles generation channels in inelastic hadron-nuclear interactions at energy approximately equals 400 GeV
[HE-3.2-9] 24 p4179 N85-35917

ALUMINUM ALLOYS
USSR report: Materials science and metallurgy, no. 93
[JPRS-84810] 01 p0018 N85-10110
Effect of scandium on the structure and properties of Al-Zn-Mg alloys 01 p0018 N85-10111
Influence of parameters of aluminun alloy anodizing process on oxide coating thickness 01 p0018 N85-10113
Suppressing porosity in weld joints of 1420 aluminum alloy 01 p0020 N85-10123
Effect of welding method on corrosion resistance of welded compositions made of 1201 alloy 01 p0020 N85-10124
Implantation of ionized monomer into aluminum alloy 6061 for marine corrosion protection
[AD-A144874] 01 p0028 N85-10172
Bilouling and corrosion studies at the Seacoast Test Facility in Hawaii
[DE84-014843] 01 p0029 N85-10180
Effect of penetrant on fatigue of aluminum alloy lap joints
[NLR-TR-82104-U] 01 p0056 N85-10373
Flight simulation fatigue crack propagation in metal/carbon-epoxy laminates
[NLR-TR-83008-U] 01 p0063 N85-10416
Containerless drop tube solidification and grain refinement of NiAl3 02 p0154 N85-11042
A study of environmental characterization of conventional and advanced aluminum alloys for selection and design. Phase 1: Literature review
[NASA-CR-172387-PHASE-1] 02 p0181 N85-11218
A study of environmental characterization of conventional and advanced aluminum alloys for selection and design. Phase 2: The breaking load test method
[NASA-CR-172387-PHASE-2] 02 p0182 N85-11219
Development of powder metallurgy 2XXX series Al alloys for high temperature aircraft structural applications
[NASA-CR-172408] 02 p0182 N85-11220
The transient oxidation of single crystal NiAl+Zr
[NASA-CR-174756] 02 p0182 N85-11221
Near-threshold fatigue crack growth and crack closure in 17-4 precipitation hardening steel and 2043-T3 aluminum alloy
[FFA-TN-1984-16] 02 p0210 N85-11385
Short cracks and crack closure in AL 2024-T3
[FFA-TN-1984-40] 02 p0210 N85-11387
Plastic deformation and microstructural transformations of metals under shock waves 02 p0272 N85-11775
Feasibility of the electrochemical method of determining nitrogen content in metallic melts
[BLL-M-35730-(5828.4)] 03 p0330 N85-12124
Observation of oxide skin in powder metallurgy aluminum alloys
[AD-A145919] 03 p0331 N85-12135
Acoustic emission monitoring of fatigue in 7010 aluminum alloys
[AERE-R-11167] 03 p0334 N85-12152
Crack resistance of pressed and rolled semifinished goods of aluminum alloys used in load-bearing aircraft wing structures 03 p0348 N85-12245
One-dimensional model of thin films. Analysis of aluminum surface 03 p0350 N85-12254
Study of deformation and fracture of AMg6N weldable aluminum alloy by method of acoustic emission 03 p0352 N85-12266
Tensile and crack propagation tests on aluminum alloys of the 2000 and 7000 series in laminated plate and forged products
[M2-678300] 03 p0373 N85-12383
The Al-Be system: The effects of RSP on structure and phase relating
[DE84-015604] 04 p0474 N85-13019
Electrochemical pitting evaluation of aluminum alloy 7075 in machining coolant
[DE84-016844] 04 p0475 N85-13026
Nondestructive determination of mechanical properties — aluminum alloys 04 p0512 N85-13266
Characterization of aluminum alloy 7010 in moderate width plate and T651 and T7651 metallurgical states
[REPT-44-606/F] 05 p0619 N85-13961
The variable polarity plasma arc welding process: Its application to the Space Shuttle external tank
[NASA-TM-86482] 05 p0641 N85-14115
Evaluation of the crack initiation life behavior of fatigue loaded automotive components made from high strength aluminium alloys
[ESA-TT-733] 05 p0651 N85-14181
Carbon fibre reinforced aluminum matrix composites: A critical review
[AD-A146367] 06 p0764 N85-14883
Phase equilibria of stored chemical energy reactants
[AD-A146527] 06 p0765 N85-14896
Fractographic observation and estimation of crack growth curve of aluminum alloy under ramdom flight simulation loading
[NAL-TR-824] 06 p0768 N85-14913
Wear of anodic oxide films on aluminum alloys in cryogenic liquids
[NAL-TR-818] 06 p0768 N85-14914
The effect of potential on the corroion fatigue behavior of a precipitation hardened aluminum alloy
[AD-A146537] 06 p0768 N85-14916
Application of solidification theory to rapid solidification processing
[AD-A146619] 06 p0769 N85-14917
Improvement of the ladle deoxidizing of Al-killed steel
[BMFT-FB-T-84-172] 06 p0769 N85-14923
Three-dimensional crack location by acoustic emission
[AERE-R-11277] 06 p0818 N85-15193
Mechanical property data 7050-t736511 alloy
[AD-A147365] 07 p0926 N85-15882
Design of ordered intermetallic alloys for high-temperature structural use
[DE85-000897] 07 p0926 N85-15885
Influence of constant amplitude and variable amplitude loading on crack initiation and micro crack propagation in Al 2024-T3
[DFVLR-FB-84-29] 07 p0979 N85-16220
Electronic structure and properties of magnetic defects in Co(1+x)Al(1-x) and Fe(1+x)Al(1-x) alloys
[NASA-TM-77498] 07 p1047 N85-16648
Application of electrochemical engineering methods and theory to solving corrosion and adhesion problems with organic coatings
[AD-A147799] 08 p1129 N85-17115
Fluctuation phenomena studies in chemically sensitive field effect transistor. Part 1: Corrosion of aluminum
[AD-A148240] 08 p1129 N85-17118
Rapid solidification processing and powder metallurgy of Al alloys
[AD-A148427] 08 p1130 N85-17120
Engineering property comparisons of PM and IM aluminum alloy forgings
[AD-B086146L] 08 p1173 N85-17398
A study of spectrum fatigue crack propagation in two aluminum alloys. 1: Spectrum simplification
[NASA-TM-86929] 09 p1293 N85-18124
A study of spectrum fatigue crack propagation in two aluminum alloys. 2: Influence of microstructures
[NASA-TM-86930] 09 p1294 N85-18125
Ion implantation of surgical Ti-6Al-4V alloy
[DE85-000943] 09 p1296 N85-18142
Ti-6Al-4V alloy castings prepared in zircon sand molds and the effect of hot isostatic pressing
[PB85-109932/GAR] 09 p1298 N85-18150
Antifriction nickel-phosphorous coatings on aluminum alloy products 09 p1309 N85-18221
Laser-initiated combustion studies on metallic alloys in pressurized oxygen
[PB85-128114] 10 p1438 N85-19066
Radiation-induced compositional redistribution and local phase transformation in irradiated alloys
[DE85-000060] 10 p1441 N85-19082
Characterization of Nb-8 wt % Al wires by analytical electron microscopy
[DE85-002726] 10 p1442 N85-19086
Development of surface cracks in AMg6 alloy under low-cycle loading conditions 10 p1442 N85-19089
K sub 1° -n diagram of cyclical crack resistance of aluminum alloys 10 p1442 N85-19090
Influence of excess phases on fracture toughness of cast alumiun-magnesium-zinc alloy 10 p1442 N85-19091
Study of superplastic alloys based on Al-Zn-Ca 10 p1442 N85-19092
Excitation modes and parameters of stress waves in metal exposed to single laser pulses 10 p1446 N85-19109
Estimate of quality of aluminum alloy surface preparation for arc welding 10 p1449 N85-19128
Computation of thermal shock-free straightening conditions for aluminum-magnesium alloy welded structures 10 p1449 N85-19131
Evaluation of 7010 aluminium alloy extruded tube in the T76 condition
[BR92019] 11 p1596 N85-20039
Rapidly solidified NiAl and FeAl
[NASA-TM-86941] 11 p1597 N85-20042
USSR report: Materials science and metallurgy
[JPRS-UMS-84-005] 11 p1597 N85-20044
Effect of ingot structure of failure ductility of pressed semifinished products of high-durability aluminum alloys 11 p1597 N85-20045
Structure-phase state and properties of high-durability VAL8 alloy 11 p1597 N85-20046
Mechanism and pattern of fatigue crack growth in aluminum alloys 11 p1597 N85-20047
Development of AK18 alloy production technology based on electrothermic alumin 11 p1598 N85-20048
Estimating deformability upon pressing of aluminum alloys based on results of mechanical testing 11 p1598 N85-20049
Study of microstructure of aluminum and copper alloys after processing with continuous CO2 laser beam 11 p1601 N85-20066
Bending two-layer metal-polymer plates 11 p1604 N85-20085
Effect of form memory in alloys based on Cu-Al systems 11 p1604 N85-20088
Influence of work-hardening on the Portevin-LeChatelier effect
[DE85-002505] 11 p1605 N85-20093
Initial development of nickel and nickel-iron aluminides for structural uses
[DE84-016641] 11 p1606 N85-20106
Effect of mill run and temper variations on barrier anodic film format ion on 6061 aluminum alloy
[DE85-000447] 11 p1608 N85-20112
Micrographic and fractographic examination of alloys 2214 and 2024 for conditions which would cause burning of the metal on being put into solution, trial 17/175
[DGT-23.419] 11 p1609 N85-20117
Fatigue crack growth in Aramid Reinforced Aluminum Laminates (ARALL): Mechanisms and predictions
[DFVLR-FB-84-37] 11 p1609 N85-20118
Crack growth geometry in aluminum alloy sheet material under flight simulation loading: 1: A comparison between TWIST and miniTWIST FALSTAFF and short FALSTAFF. 2: Effect of truncating high loads
[VTH-LR-441] 11 p1609 N85-20119
Carbon filter plates for aluminum filtration at casting
[BMFT-FB-T-84-242] 12 p1808 N85-21343
Performance of Chromel versus Alumel and Nicrosil versus Nisil thermocouple assemblies in vacuum and argon between 1000 deg C and 1200 deg C
[DE85-000810] 12 p1853 N85-21624
Defect characterisation and monitoring by acoustic emission
[AERE-R-11409] 12 p1863 N85-21683
Characterisation of fatigue crack extension by quantitative acoustic emission
[AERE-R-11289] 12 p1868 N85-21721
The strength and characteristics of VPPA welded 2219-T87 aluminum alloy 12 p1946 N85-22224
Ignition phenomena of bulk aluminum alloy as a function of oxygen pressure 13 p1999 N85-22531

Structures of ordered linear dislocation multipoles in Cu-Al alloys
[ISSN-0379-6906] 13 p2021 N85-22664
The characterisation of oxide films on treated aluminium alloys
[MQAD-R-849] 13 p2022 N85-22667
Magnetic studies of Ni3Al(Fe) compounds
[DE85-005262] 13 p2025 N85-22686
USSR report: Materials science and metallurgy
[JPRS-UMS-85-002] 13 p2025 N85-22688
Dependence of superplastic flow on state of grain boundaries 13 p2025 N85-22689
Fatigue and corrosion fatigue resistance of aluminum casting alloy VAL10 and forging alloy AK8 13 p2025 N85-22690
Structural strenght of strip D16T aluminum alloy with low copper and magnesium content 13 p2025 N85-22691
Temperature effects of heterogenizated annealing on structure and properties of V95 aluminum alloy 13 p2025 N85-22692
Anomalies of aluminum structure and properties 13 p2026 N85-22693
New deformable secondary aluminum alloys 13 p2026 N85-22694
Study of processes of modification of Al-Si alloys 13 p2026 N85-22695
Aluminum alloy ATs5K5 (5% Zn + 5% Ca) for superplastic forming 13 p2026 N85-22697
Segregation of silicon in silumin-carbon fiber composites 13 p2026 N85-22706
Composition and thickness of oxide coatings on granule surfaces of aluminum alloys 13 p2030 N85-22719
Basis and pyramidal slipping in single crystals of alpha-alloy Ti-Al-Sn 13 p2032 N85-22730
Problem of pore formation mechanism in welded joints of aluminum alloys in the system aluminum-magnesium-lithium 13 p2032 N85-22732
Analysis of strength and ductility of welded joints in AMtsS and AMg5 aluminum alloys 13 p2033 N85-22737
Effect of moisture in inert gases on density of seam metal and on mechanical characteristics of welded joints of aluminum and aluminum alloys 13 p2034 N85-22744
Characteristics of surface crack development in ATtsS aluminum alloy during slow-cycle loading 13 p2034 N85-22745
China report: Science and technology
[JPRS-CST-84-030] 13 p2041 N85-22777
Experimental investigation of crippling strength of Chinese aluminum alloy (LY12CZ) sections 13 p2041 N85-22779
Use of ferrofluids in machining of metals 13 p2045 N85-22802
The effect of notch acuity on the fracture toughness of silicon carbide/aluminum metal matrix composites
[AD-A150970] 14 p2248 N85-23936
The role of hydrogen in the stress corrosion failure of high strength Al-Zn-Mg alloys
[AD-A150891] 14 p2256 N85-23976
Synthesis and properties of elevated temperature P/M aluminum alloys
[AD-A151031] 14 p2256 N85-23981
Fatigue crack propagation and fracture in 7050 and 7091 aluminum alloy forgings 14 p2318 N85-24324
Effect of deep cooling on crack resistance and low-temperature hardening of aluminum alloys 15 p2496 N85-25396
Fatigue of clad aluminum materials D16T and 2024-T3 with stepped loading 15 p2496 N85-25397
Dynamic characteristics of ac arc in welding aluminum alloys 15 p2500 N85-25424
Pressure welding of corrosion-resistant steel with AMg6 aluminum 15 p2501 N85-25426
Thermocompression welding of parts made from AMts and VT1 alloys 15 p2501 N85-25430
Mechanical properties of welded joints of 1201 aluminum alloy 15 p2502 N85-25431
Mechanisms of corrosion fatigue in high strength I/M (Ingot Metallurgy) and P/M (Powder Metallurgy) aluminum alloys
[AD-A151177] 15 p2509 N85-25478
Mossbauer spectrometry: Testing of a new computer based system and its application to a study of an aluminum-iron-cerium alloy
[AD-A151826] 15 p2510 N85-25483
Metallurgical characterization of aluminum powder consolidation
[AD-A151990] 15 p2510 N85-25484
Superplasticity in a thermo-mechanically processed Aluminum-10.2%Mg-0.52%Mn alloy
[AD-A152016] 15 p2510 N85-25485
Design of ductile polycrystaline Ni3Al alloys
[DE85-005572] 15 p2511 N85-25491
Weldability of Ni3Al-type aluminide alloys
[DE85-006932] 15 p2512 N85-25496
Oxidation of nickel-aluminum and iron-aluminum alloys
[DE85-006930] 15 p2512 N85-25497
USSR report: Materials science and metallurgy
[JPRS-UMS-85-004] 15 p2513 N85-25503
Effect of zirconium on forming ultrafine-grained structure in Al-Mg-Zr alloy 15 p2513 N85-25504
Corrosion behavior of Al4 aluminum alloy hardened by CO2 laser radiation 15 p2514 N85-25512
Pechiney strategy includes development of new materials 15 p2531 N85-25607
Fatigue life, fatigue crack propagation and fracture toughness study of 7075 aluminum alloy subjected to thermomechanical processing 15 p2573 N85-25662
Tensile and fracture toughness properties of Mirage III spars
[AR-003-019] 15 p2578 N85-25899
Transition region for corner cracks at holes
[AD-A151835] 15 p2579 N85-25908
Experimental studies of the electronic structure of 1-2 and 1-3 intermetallic compounds
[DE85-006978] 15 p2662 N85-26432
Durability of Aramid reinforced aluminum laminate (ARALL)
[VTH-LR-423] 16 p2744 N85-26933
Microstructures and properties of rapidly solidified alloys
[NASA-CR-172377] 16 p2748 N85-26961
Evaluation of the corrosion properties of aluminum alloy 5083 weldments
[DE85-007729] 16 p2751 N85-26977
The effect of low sheet thicknesses on the fracture toughness of an Al alloy (7075-T6) --- Aramid Reinforced Aluminum Laminate (ARALL)
[VTH-LR-425] 16 p2752 N85-26984
Influence of pretreatment, environment and strain rate on stress corrosion cracking of the aluminum alloy 7075-T6
[VTH-LR-433] 16 p2752 N85-26985
Investigation of the pitting potential of rapidly solidified aluminum-lithium alloys
[VTH-LR-434] 16 p2752 N85-26986
Investigation of the influence of some paint systems and water displacing corrosion inhibitors on anodic undermining corrosion of aluminum 2024 clad alloy --- aircraft structures
[VTH-LR-443] 16 p2756 N85-27009
Special features of the one-sided automatic welding of structures of Al-Mg alloys 16 p2792 N85-27222
Aluminum-lithium alloys: The answer of the aluminum industry to the threat of advanced fiber-reinforced materials
[VTH-LR-406] 17 p2932 N85-28102
Erosion of multiphase materials
[DE85-008895] 18 p3068 N85-28978
Evaluation of 7XXX-series aluminum alloys for the W87 aft support ring
[DE85-009087] 18 p3076 N85-29027
Age hardening and atomic structure of an aluminum-6 at. % silver alloy
[DE85-009977] 18 p3077 N85-29031
The precipitation mechanism in a metallic solid solution crystal: Case of the aluminum-copper and aluminum-silver systems
[DE85-009981] 18 p3077 N85-29032
West Europe report: Science and technology
[JPRS-WST-84-035] 18 p3087 N85-29102
Study of the influence of metallurgical factors on fatigue and fracture of aerospace structural materials
[AD-A153913] 18 p3122 N85-29328
Studies of strain rate effects in the deformation of solids by means of stress pulses and ultrasonic methods
[DE85-009463] 18 p3122 N85-29329
Aluminum pressure die casting process for the production of low porosity castings and new casting alloys
[BMFT-FB-T-84-286] 18 p3123 N85-29335
Anisotropic electron-impurity scattering in dilute AlLi: (Small) corrections to the local density approximation
[DE85-002948] 19 p3238 N85-30076
Corrosion fatigue cooperative testing program statistical analysis
[AD-A153886] 19 p3238 N85-30077
Effects of annealing treatments on superplasticity in a thermomechanically processed Aluminum-10.2%Mg-0.52%Mn
[AD-A154414] 19 p3239 N85-30080
USSR report: Materials Science and Metallurgy
[JPRS-UMS-85-005] 19 p3241 N85-30095
Effect of ScAl3 phase dispersion on hardening of alloy Al-6.3 percent Mg-0.21 percent Sc 19 p3241 N85-30096
Mechanical modification of friction surfaces of aluminum alloys by friction transfer 19 p3241 N85-30097
Study of phase equilibria and crystallization processes in Al-Zn-Mg alloy systems 19 p3241 N85-30098
Possible causes of modification and strengthening of aluminum by scandium 19 p3241 N85-30099
Action of plasma and explosion products on silumins 19 p3242 N85-30100
Crystallization of aluminum-based alloys in weightlessness 19 p3242 N85-30101
Specifics of fine structure of pressed aluminum alloys manufactured by plasma atomization 19 p3242 N85-30102
Physical-mechanical characteristics and wear resistance of coatings applied by microarc oxidation 19 p3242 N85-30104
Resistance to corrosion fatigue in aluminum alloy 1561 in sea water 19 p3243 N85-30108
Atomized magnetism-aluminum protective coatings 19 p3244 N85-30116
Welding of steel-aluminum cooling panels for the holds of refrigerator vessels 19 p3246 N85-30129
Chemical composition and kinetics of libration of gases upon welding of aluminum alloys 19 p3247 N85-30131
Means for reducing hydrogen concentration upon surfacing of antifriction aluminum alloys with powder electrode 19 p3247 N85-30132
Properties of heat resistant Ni-Al-Nb alloys with unidirectional eutectic structure 19 p3247 N85-30133
concentration variation of work function of alloys in the system nickel-titanium-aluminum 19 p3247 N85-30134
Optimisation of MCr Al coating compositions for marine gas turbines
[BR91159] 20 p3394 N85-31066
Crack growth data for two aluminum alloys 7050-T73651 and 2024-T3
[FFA-TN-1984-51] 20 p3432 N85-31290
Influence of the molding joint plane on the fatigue resistance of the alloys 7010 and 7050. Test Report No. M1-631600
[PV-M1-631600] 20 p3470 N85-31562
Modifications of flight-by-flight load sequences to provide for good fracture surface readability
[NLR-MP-84012-U] 20 p3472 N85-31577
Understanding and laboratory prediction of the atmospheric corrosion behavior of steels and of non-ferrous metals and alloys
[AD-A154642] 21 p3566 N85-32179
The effect of abrasive blasting on the fatigue and corrosion of an aluminium-copper alloy
[AD-A154954] 21 p3566 N85-32182
The effect of alloy additions on superplasticity in thermomechanically processed high magnesium aluminum-magnesium alloys
[AD-A155142] 21 p3567 N85-32184
Experimental studies of the geometric and electronic structure of chemisorption bonding
[PB85-192250] 22 p3747 N85-33228
Mechanical properties of plasma arc cut steel 23 p3905 N85-34188
The influence of temperature on static and dynamic SCC crack growth behavior in aluminum alloy 23 p3905 N85-34190
A fractographic study on mode 2 and mode 3 SCC crack growth in an Al-Zn-Mg alloy 23 p3905 N85-34191
Fatigue crack retardation phenomenon caused by single-multiple overloads in 2017-T3 aluminum allow 23 p3906 N85-34196
Method for preparing high purity vanadium
[DE85-006412] 23 p3913 N85-34242
Influence of particle erosion on the microstructural changes in metals and alloys
[TI85-901384] 23 p3917 N85-34276
Fatigue lives of specimens representing critical locations in Mirage 3 spars under Australian and Swiss test spectra
[ARL-STRUC-R-415] 24 p4064 N85-35167
Studies of the crystallization process of aluminum-silicon alloys using a high temperature microscope
[NASA-TM-77869] 24 p4078 N85-35272
Development of a mathematical model for predicting the percentage fatigue life increase resulting from shot peened components
[AD-A155774] 24 p4101 N85-35425
Prediction of plasticity characteristics for three-dimensional fracture specimens comparison with experiment
[AD-A156425] 24 p4102 N85-35430

ALUMINUM ARSENIDES

AlAs/GaAs superlattice barrier unipolar diode structure
[DE85-001904] 11 p1736 N85-20921
A study of Ga(.47)In(.53)As and Al(.48)In(.52)As for very high frequency device applications
[AD-A151995] 16 p2570 N85-27706

Summary of recent studies on AlGaAs/GaAs radiation hardened photodiodes
[DE85-009501] 18 p3194 N85-29812

ALUMINUM BORON COMPOSITES

Influence of 3% NaCl solution on rate of accumulation of damage and residual strength of aluminum-boron composite 13 p2027 N85-22690
Division boundary in Al-B composite material with boron in contact with solid and liquid aluminum 13 p2027 N85-22704
Estimating degree of development of physical-chemical interaction among components in Al-B fiber composite material 13 p2027 N85-22705
Effect of operating medium on cyclic durability of AD33-W composite 13 p2029 N85-22716
Effect of surface state on durability of aluminized boron fibers 19 p3244 N85-30115
Features of the interaction between fibers and matrix in production of aluminum-boron composite material 19 p3244 N85-30117

ALUMINUM CARBIDES

Segregation of silicon in silumin-carbon fiber composites 13 p2026 N85-22706

ALUMINUM CHLORIDES

A potentiometric study of chloroaluminate equilibria in the aluminum chloride - 1-methyl-2-ethylimidazolium chloride ionic liquid
[AD-A144729] 01 p0023 N85-10144
Spectrophotometric studies of iodine complexes in an aluminum chloride - butylpyridinium chloride ionic liquid
[AD-A145074] 01 p0024 N85-10150
Electrochemistry and electrochemical methodology in molten salts
[AD-A149813] 12 p1799 N85-21284

ALUMINUM COATINGS

Influence of aluminum metallization coatings on corrosion fatigue properties of steel 01 p0018 N85-10112
The experimental mod 3 firefighters' aluminized crash-rescue, fire-proximity hood
[AD-A144993] 01 p0096 N85-10855
Qualitative and quantitative compositional analysis of shale derived by gas chromatography and combined gas Chromatography/Mass spectrometry. Executive summary
[AD-A146369] 07 p0924 N85-15851
Accelerated aging of aluminized acrylic solar mirror materials
[DE85-002663] 11 p1612 N85-20138
Corrosion of aircraft Al and Al-Zn ion plated steel fasteners 13 p2021 N85-22666
Impact ionization from gold, aluminum and PCB-Z — Giotto spacecraft paint PCB-Z 14 p2244 N85-23910
Mechanisms of buildup and properties of aluminum coatings on heat-resistant nickel alloys 15 p2513 N85-25506
Technology development for thin-film-trace humidity sensors
[BMFT-FB-T-84-268] 17 p2969 N85-28338
Action of wear-inhibiting Al2O3-coatings when applied to hard metal cutting tools
[BLL-RISLEY-TR-5041-(9091.9F)] 24 p4081 N85-35292

ALUMINUM COMPOUNDS

NT ALUMINATES
NT ALUMINUM ARSENIDES
NT ALUMINUM CARBIDES
NT ALUMINUM CHLORIDES
NT ALUMINUM NITRIDES
NT ALUMINUM OXIDES
NT ALUMINUM SILICATES
NT BERYL
NT FELDSPARS
NT SAPPHIRE

The X-ray Absorption Coefficient Fine Structure (EXAFS) study on precipitates in AlCu
[DESY-SR-84-15] 01 p0025 N85-10153
The B2 aluminides as alternative materials
[NASA-TM-86937] 10 p1440 N85-19076

ALUMINUM GALLIUM ARSENIDES

Effect of liquid phase composition on thickness of epitaxial Ga sub (1-x) Al sub x As films 02 p0257 N85-11683
Thin film (Al, Ga)As heterojunction solar cells 02 p0258 N85-11691
Gallium arsenide/AlGaAs multilayer structures with special doping profiles for microwave and optoelectronic devices
[BMFT-FB-T-84-207] 08 p1227 N85-17725
Fabrication and I-V characterization of AlGaAs/GaAs MODFETs with P-type surface layers grown by molecular beam epitaxy
[AD-A151695] 15 p2660 N85-26415

ALUMINUM GRAPHITE COMPOSITES

Localized corrosion currents from graphite/aluminum and welded SiC/Al metal matrix composites
[AD-A150988] 14 p2256 N85-23980

ALUMINUM ISOTOPES

NT ALUMINUM 26
Cosmogenic Na-22 and Al-26 in Luna-24 lunar drill core soil samples 13 p1981 N85-22427
SMM detection of interstellar Al-26 gamma radiation
[OG-3.2-1] 22 p3874 N85-34001
Galactic distribution of interstellar Al-26
[OG-3.2-3] 22 p3874 N85-34002

ALUMINUM NITRIDES

Aluminum nitride insulator for 3-5 MIS (Metal-Insulator-Semiconductor) applications
[AD-A147842] 07 p1049 N85-16662
AlN insulator for 3-5 MIS applications
[AD-A150674] 14 p2426 N85-24962
Passivation on high Q acoustic strain sensor for accelerometer
[AD-A153565] 18 p3177 N85-29695

ALUMINUM OXIDES

NT SAPPHIRE
Fundamental studies of structure property relationship in transformation toughened ceramics
[DE84-015344] 01 p0033 N85-10204
Trivalent ion exchange in beta alumina
[AD-A145373] 02 p0172 N85-11151
The transient oxidation of single crystal NiAl+Zr
[NASA-CR-174756] 02 p0182 N85-11221
Influence of aluminum oxide film on thermocompression bonding of gold wire to evaporated aluminum film
[NASA-TM-77503] 03 p0330 N85-12127
Annealing of implanted Al-2O-3 in a reducing environment
[DE84-015370] 03 p0332 N85-12140
Reinforcement of molybdenum disilicide with nematic crystals of aluminum oxide 03 p0353 N85-12269
Phase transformations of AlPO4 with SiO2 structures 03 p0425 N85-12713
Structural changes during milling of aluminum oxide powders
[NASA-TM-77488] 04 p0472 N85-13008
Tests and modeling for sintering theory
[DE84-015110] 04 p0473 N85-13012
Erosion of multiphase materials
[DE84-015816] 04 p0474 N85-13018
Formation of subsurface Al2O3 layers in aluminum by oxygen ion implantation
[DE84-015599] 04 p0474 N85-13020
Surface diffusion of high temperature vapors in porous alumina
[DE84-015968] 04 p0479 N85-13053
Effect of doping on the voltage holdoff performance of alumina insulators in vacuum
[DE84-017163] 04 p0480 N85-13060
An optical and mass spectrometric study of the aluminum-oxygen flame
[AD-A147434] 07 p0923 N85-15849
Microbiological method for the desiliconization of high-silica bauxites
[BLL-MINTEK-TR-1168-(5810.5759)] 07 p0925 N85-15864
Fundamental tribological properties of ceramics
[NASA-TM-86915] 07 p0930 N85-15893
Dispersed metal-toughened ceramics and ceramic brazing
[NASA-CR-174284] 07 p0933 N85-15916
Transformation toughened ceramics for the heavy duty diesel engine technology program
[NASA-CR-174689] 07 p1055 N85-16698
Mechanical properties of adhesively bonded aluminum structures protected with hydration inhibitors
[AD-A148123] 08 p1133 N85-17139
Ionic and molecular transport in beta- and beta''-alumina
[DE85-000984] 09 p1380 N85-18680
High temperature laser interferometric studies of solid electrolytes 09 p1396 N85-18785
Formation of amorphous layers in Al2O3 by ion implantation
[DE85-001269] 09 p1397 N85-18794
Sub-eutectic densification and second phase formation in Al2O3 - CaO
[DE85-002065] 09 p1398 N85-18796
Scanning photoacoustic microscopy of aluminum with aluminum oxide, roughness standards and rubber
[AD-A149460] 10 p1441 N85-19081
Amorphization of ceramics by ion beams
[DE85-000936] 10 p1453 N85-19156
Modeling thermal plasma material processing experiments
[DE85-001551] 10 p1560 N85-19838
Material growth and characterization for solid state devices
[NASA-CR-174410] 10 p1561 N85-19847
Laser processing of ceramics
[DE85-001184] 11 p1612 N85-20135
Slit-ring test for evaluating fracture in tubular cross sections
[DE85-003550] 11 p1654 N85-20416
Electrochemical processes at the sodium (BETA)'' alumina interface
[DE85-004653] 12 p1802 N85-21305
The Valence- and conduction-band structure of the sapphire (1102) surface
[AD-A150001] 12 p1940 N85-22184
Distributed combustion: A mechanism of acoustic suppression 13 p2001 N85-22543
Formation of alumina layers on iron-base alloys
[BLL-T6418/BG/LRS/LRST737/84] 13 p2020 N85-22657
Composition and thickness of oxide coatings on granule surfaces of aluminum alloys 13 p2030 N85-22719
Dispersed-metal-toughened alumina
[NASA-CR-174687] 13 p2037 N85-22758
Research directed advanced high temperature coating system beyond current state-of-the art systems
[AD-A150698] 14 p2255 N85-23974
Density and thermal expansion measurements of several mixed oxide glasses in the solid and liquid regions
[DE85-006134] 14 p2261 N85-24014
Structure and properties of ion-implanted Al sub 2 O sub 3
[DE85-005374] 14 p2430 N85-24987
Temperature, velocity, and species mapping in an induction plasma
[DE85-004005] 15 p2512 N85-25499
France develops own aluminum-based composite ceramic 15 p2534 N85-25836
Degradation phenomena in solid electrolytes
[DE85-007066] 15 p2587 N85-25949
Particulate and whisker toughened alumina composites
[DE85-005239] 16 p2743 N85-26930
Thermal annealing of Fe implanted Al2O3 in oxidizing and reducing environment: Revised version
[DE85-007546] 16 p2752 N85-26983
Test and modeling for sintering theory
[DE85-007761] 16 p2755 N85-27004
Microstructure-mechanical property relationships in transformation-toughened ceramics
[DE85-009722] 17 p2935 N85-28117
Diffusion welding of aluminum with vacuum-tight corundum ceramic 19 p3247 N85-30130
Vibrational properties of disordered solids: Far infrared studies
[DE85-010400] 19 p3377 N85-30951
Improved materials for composite and adhesive joints
[AD-A155065] 21 p3562 N85-32153
The Faraday effect in ruby and corundum in strong magnetic fields 21 p3697 N85-32967
Method for preparing Pb-(beta)-aluminum ceramic
[DE85-011665] 22 p3752 N85-33256
Preparation and use of very pure o-D2
[DE85-009415] 22 p3843 N85-33800
Electrolytic synthesis of colored eta alumina film 23 p3906 N85-34201
Rotating bending fatigue strength of silicon carbide and alumina-fiber reinforced aluminum 23 p3907 N85-34206
Grain boundary and surface diffusion in oxide systems
[DE85-007291] 23 p3985 N85-34715
Action of wear-inhibiting Al2O3-coatings when applied to hard metal cutting tools
[BLL-RISLEY-TR-5041-(9091.9F)] 24 p4081 N85-35292
Noise in silver beta alumina ceramics
[AD-A156135] 24 p4082 N85-35297
Size and shape dependence of CO adsorption sites on sapphire supported Fe microcrystals
[NASA-CR-176171] 24 p4160 N85-35794
Noise in sodium beta alumina crystals
[AD-A156025] 24 p4161 N85-35798

ALUMINUM SILICATES

Modified aluminosilicide coating for heat-resistant nickel alloys 15 p2514 N85-25509
Conditions for formation of paragenesses containing kyanite-orthoclase in region of Mount Provender and Pratt Peak (Shackleton Range, Antarctica) 19 p3298 N85-30447

ALUMINUM 26

Interstellar Al-26 and excess Mg-26 15 p2680 N85-26551
Gamma-ray line emission from Al-26 produced by Wolf-Rayet stars
[OG-3.2-5] 22 p3875 N85-34003

ALVEOLI

Pulmonary blood flow and oxygenation of arterial blood in a healthy subject upon 7 days hypokinesia 07 p1014 N85-16439

AMAZON REGION (SOUTH AMERICA)
Systematic data interpretation of remote sensing in the reception of hydrocarbons, volume 1
[E85-10008] 02 p0215 N85-11421
Eddy correlation measurements of energy partition for Amazonian forest
[INPE-3195-PRE/559] 06 p0827 N85-15252
Water and climate, study of one case
07 p1002 N85-16369
The water balance and climate — Amazon region
07 p1003 N85-16370
Ecological impacts of hydroelectric projects in Amazonia 07 p1003 N85-16374
The Amazon and climate 07 p1003 N85-16376
Deforestation, floodplain dynamics, and carbon biogeochemistry in the Amazon Basin
08 p1144 N85-17216
Information for space radar designers: Required dynamic range vs resolution and antenna calibration using the Amazon rain forest 08 p1147 N85-17239
Meridional penetration of frontal systems in South America and its relation to organized convection in the Amazon
[INPE-3407-PRE/676] 10 p1518 N85-19572
System of interpretation of remote sensing data when hydrocarbons are present, volume 2
[INPE-3087-TDL/162-VOL-2] 16 p2810 N85-27326
The ARGOS system in Brazil — hydrology
16 p2813 N85-27349
The micrometeorology of an Amazonian rainforest
[INPE-3515-PRE/740] 19 p3315 N85-30551
On the dynamical climatology of the Amazon Basin and associated rain producing mechanisms
[INPE-3531-RPE/477] 19 p3315 N85-30552

AMBIENCE
Characterization of material surfaces exposed to atomic oxygen on space shuttle missions
12 p1946 N85-22220

AMBIENT TEMPERATURE
Advances in room-temperature solid-state gamma-ray spectrometry
[DE84-015944] 04 p0469 N85-12967
Attempted measurement of gaseous H-2O-2 in the ambient atmosphere
[DE85-001937] 06 p0834 N85-15306
NBS (National Bureau of Standards) daylight availability database
[PB84-245745] 07 p1054 N85-16688
Microwave surface resistivity of several materials at ambient temperature 10 p1463 N85-19226
Short duration winter-time performances of different passive solar systems
[DE85-000850] 11 p1675 N85-20557
The temperature of a glass-encapsulated solar cell estimated from ambient air temperature and global radiation
[GKSS-84-E-36] 11 p1676 N85-20563
Portable Automated Mesonet (PAM) data from the 1980 experiment in Anderson Creek Valley
[DE85-004361] 13 p2139 N85-23282
Soil temperature extrema recovery rates after precipitation cooling 20 p3401 N85-31697
Results of an interlaboratory fatigue test program conducted on alloy 800H at room and elevated temperatures
[NASA-CR-174940] 21 p3597 N85-32340
Improved Nominal Operating Cell Temperature (NOCT) test procedure 21 p3612 N85-32449
Lake ice occurence as a possible detector of atmospheric CO2 effects on climate
[DE85-012987] 23 p3950 N85-34480

AMBIGUITY
About ambiguity and Q-functions
[AD-A145293] 02 p0250 N85-11636
Ambiguity and uncertainty in probabilistic inference
[AD-A147378] 07 p1035 N85-16572
The ambiguity function of random binary-phase-coded waveforms
[AD-A148906] 10 p1466 N85-19249
The ambiguity function and the Wigner distribution
[AD-A150095] 12 p1829 N85-21482
Language design, computers and brains
[AD-A152819] 17 p3008 N85-28594

AMBIPOLAR DIFFUSION
Breakdown of intrinsic ambipolarity for the radial diffusion due to a rotating RF field 23 p3977 N85-34660
Effect of ECH and ICH on ambipolar potential in NBT-1M 23 p3978 N85-34661
Analytic and numerical calculations of the ambipolar electric field in a stellarator 23 p3978 N85-34665

AMBIT
U FIELD THEORY (PHYSICS)

AMERICIUM
NT AMERICIUM ISOTOPES
NT AMERICIUM 241
Americium thermodynamic data for the EQ3/6 database
[DE84-017085] 04 p0573 N85-13656
Americium metal preparation on the multigram scale
[DE85-003735] 13 p2024 N85-22683
Thermodynamic systematics of oxides of americium, curium and neighboring elements
[DE85-009704] 16 p3197 N85-29831

AMERICIUM ISOTOPES
NT AMERICIUM 241
Historical review of californium-252 discovery and development
[DE85-010223] 19 p3362 N85-30844

AMERICIUM 241
Role of natural dissolved organic compounds in determining the concentrations of americium in natural waters
[DE85-010266] 19 p3229 N85-30022
Determination of the average neutron activation cross section with an annular-shaped 241 Am/Be neutron source and a NaI(T1) detector for the 27 Al (n,p)27 Mg-reaction
[REPT-4/1984] 20 p3532 N85-31975
The 1984 environmental monitoring program report for Idaho National Engineering Laboratory site
[DE85-011209] 22 p3812 N85-33611

AMIDES
NT POLYIMIDES
NT UREAS
Properties of polycaproamide fibers modified by grafted polyacrylonitrile 06 p0761 N85-14867
Low temperature synthesis of polycaproamide copolymers grafted with polydimethylaminothylmethacrylate
06 p0761 N85-14868
Preparation of fire-resistant infusible polycaproamide fiber 06 p0763 N85-14877
Working medium for sorption heat pumps
[BLL-T8360/BG/WH785/84] 06 p0807 N85-15131

AMINES
NT ANILINE
NT CATECHOLAMINE
NT DIAMINES
NT ETHYLENEDIAMINE
NT TRIAMINOGUANIDINIUM AZIDE
The 7-Amino-4,6-Dinitrobenzofuroxan, an insensitive high explosive
[AD-A145665] 02 p0188 N85-11257
Study of reaction kinetics and development of elastic properties in network polymerization systems by the impulse technique
[AD-A148187] 08 p1133 N85-17141
Molecular dynamics in nitramines and modified nitramines
[AD-A148515] 08 p1220 N85-17686
Amine salts as bonding agents
[AD-D011543] 12 p1817 N85-21396
Chemical interpretation of the relaxed permittivity during epoxy resin cure
[AD-A150955] 14 p2260 N85-24005
Polyamines as possible modulators of gravity induced calcium transport in plants 15 p2606 N85-25060
Processable and stable conductive polymers
[AD-D011684] 19 p3249 N85-30143
Nuclear magnetic resonance study of the intramolecular rearrangement of 2-(5-cyanotetrazolato)pentaammine cobalt (III) perchlorate
[DE85-010810] 22 p3839 N85-33772
Metal (2) 4,4',4',4''' phthalocyanine tetrasmines as curing agents for epoxy resins
[NASA-CASE-ARC-11424-1] 23 p3919 N85-34281

AMINO ACIDS
NT ALANINE
NT ASPARTIC ACID
NT GLUTAMINE
NT GLUTATHIONE
NT GLYCINE
NT METHIONINE
NT PEPTIDES
NT POLYPEPTIDES
NT TRYPTOPHAN
Skeletal muscle metabolism in hypokinetic rats
[NASA-CR-174059] 02 p0233 N85-11520
Effects of hyperthermia on free amino acids in rat brain and in subcellular fractions 11 p1691 N85-20631
USSR report: Space Biology and Aerospace Medicine, volume 18, no. 6, November - December 1984
[JPRS-USB-85-002] 12 p1900 N85-21931
Cosmonauts' blood plasma free amino acid levels during preflight training 12 p1901 N85-21937
Remarks on preparation of indandione detection reagents
[NASA-TM-77905] 21 p3560 N85-32146
Cytochromes and iron sulfur proteins in sulfur metabolism of phototrophic bacteria
21 p3657 N85-32718
Investigation of some aspects of amino acid metabolism in man during brief exposure to anticorthostatic hypokinesia combined with ultraviolet radiation
22 p3822 N85-33678

AMMETERS
Pulsed-power system diagnostics: Electromagnetic data interpretation along pulse lines
[AD-A146607] 08 p0810 N85-15148
High-current measurement techniques
[PB85-100444] 11 p1637 N85-20311
Beam current sensor
[DE85-011600] 20 p3459 N85-31482

AMMONIA
NT LIQUID AMMONIA
Electrochemistry in near-critical and supercritical fluids. I. Ammonia
[AD-A146429] 06 p0785 N85-14894
Silazane precursors to silicon nitride
[AD-A146791] 07 p0931 N85-15899
Photosynthesis of ammonia
[DE85-001482] 11 p1585 N85-20029
Studies of the kinetics and mechanisms of ammonia synthesis and hydrodesulfurization on metal single crystal surfaces
[DE85-001650] 11 p1595 N85-20030
Meteorological support for the 1983 Deep Creek, Maryland experiment
[DE85-002616] 11 p1678 N85-20575
Effect of high ammonia content in closed environment on some parameters of human nitrogen and carbohydrate metabolism against background of a controlled diet
12 p1903 N85-21948
Ammonia formation caused by the presence of water in the wet grinding of silicon nitride powder
[NASA-TM-77746] 14 p2249 N85-23937
Results of recent large-scale NH3 and N2O4 dispersion experiments
[DE85-004988] 15 p2589 N85-25980
Cation promotion effects in zeolite-supported F-T catalysts
[DE85-009969] 19 p3233 N85-30044
Facility for large-scale hazardous gas testing
[DE85-011652] 21 p3564 N85-32169
Metal alkoxides: Models for metal oxides. Alkoxide ligands in early transition metal organometallic chemistry
[DE85-011368] 23 p3916 N85-34269
Determination of properties of zeolite/refrigerant combinations for solar refrigeration systems
[DE85-012009] 23 p3945 N85-34448

AMMONIUM COMPOUNDS
NT AMMONIUM NITRATES
NT AMMONIUM PERCHLORATES
Additives for heat engine coal slurry fuels
[DE84-016434] 05 p0621 N85-13971
Synthesis of antimicrobial chemical fibers and fibrous materials containing quaternary ammonium compounds and their utilization 06 p0762 N85-14872
Michelle-derived catalysts for extended Schulz-Flory
[DE85-005656] 17 p2922 N85-28012
Throughfall rate and chemistry studies: Whiteface Mountain
[DE85-012407] 23 p3947 N85-34464

AMMONIUM NITRATES
Eutectic explosives containing ammonium nitrate
[DE84-015705] 01 p0034 N85-10213
The IMX double direct process
[AD-A146250] 03 p0340 N85-12188
Application of Monte Carlo and molecular dynamics methods to the calculation of thermodynamic properties of molten salts
[AD-A148897] 10 p1565 N85-19669
Explosibility of ammonium nitrate
[HSE-TRANS-11111] 19 p3252 N85-30164

AMMONIUM PERCHLORATES
The heat sensitivity of solid propellants
06 p1117 N85-17043
Mechanism of burning rate enhancement by ferric oxide 13 p2002 N85-22548

AMMUNITION
Effects of perforation L/D ratio and slotting on slick propellant combustion
[AD-A148854] 10 p1456 N85-19177
Laboratory vibration schedules
[AD-A155656] 24 p4064 N85-35188

AMOR ASTEROID
The discovery circumstances of Earth-approaching asteroids
[NASA-CR-174327] 08 p1256 N85-17920

AMORPHOUS MATERIALS
Deuteron NMR (Nuclear Magnetic Resonance) in relation to the glass transition in polymers
[AD-P003910] 01 p0032 N85-10196
Studies of laser melting and rapid solidification using amorphous silicon
[DE84-014737] 02 p0202 N85-11345

Use of magnetic compression based on amorphous alloys as a drive for induction linacs
[DE84-014524] 02 p0277 N85-11805
Characterization of amorphous surface layers in Fe implanted with Ti and C
[DE84-014980] 02 p0289 N85-11885
USSR report: Materials science and metallurgy
[JPRS-UMS-84-007] 03 p0348 N85-12244
Parameters of structural relaxation and mechanical properties of amorphous alloys
03 p0349 N85-12246
Effect of annealing in transverse magnetic field on magnetic permeability of amorphous Fe5Co70Si15B10 alloy 03 p0349 N85-12247
Magnetic properties of and superline interactions in amorphous Fe-Cr-Co-Si-B alloys
03 p0349 N85-12248
Static and dynamic disordering in amorphous magnets and crystals 03 p0422 N85-12699
Radiation effects in amorphous metallic alloys
[DE84-014302] 04 p0475 N85-13025
Structural properties of amorphous metals by Raman scattering
[DE84-016947] 04 p0475 N85-13027
Development of rapidly quenched alloys with special physical properties and of processes for their continuous production
[BMFT-FB-T-84-179] 04 p0477 N85-13039
Advanced amorphous materials for photovoltaic conversion
[DE84-017198] 04 p0529 N85-13384
Amorphous metallic layers in Si metallization systems
06 p0830 N85-15277
Advances and opportunities in the amorphous silicon research field
[DE84-004526] 06 p0833 N85-15304
Recent developments in photovoltaics
[DE84-004528] 06 p0833 N85-15305
Application of the diffraction model to amorphous magnesium zinc alloys
[AD-A147369] 07 p0928 N85-15883
Structural relaxation and isoconfigurational flow of a metallic glass near equilibrium
[AD-A147888] 07 p0933 N85-15915
Electronic properties of intercalated graphite and amorphous metals
[AD-A147864] 08 p1225 N85-17716
Plasma deposition of amorphous metal alloys
[DE85-000768] 09 p1295 N85-18132
Amorphous materials and recrystallization
[DE85-001873] 09 p1398 N85-18801
Reactivity of ion implanted silicon carbide
[DE85-001543] 09 p1399 N85-18802
Amorphization of ceramics by ion beams
[DE85-000936] 10 p1453 N85-19156
Electron-diffraction structural examination of amorphous iron-tin alloys 11 p1604 N85-20084
Amorphous Ni-Ti alloys: A new method of synthesis
[DE85-002744] 11 p1605 N85-20094
Structural studies of sputtered Ni-As-O films
[DE85-003229] 11 p1605 N85-20095
Properties and thermal stabilities of amorphous transition metal hydrides
[DE85-002117] 11 p1607 N85-20104
Effects of hydrogen on magnetic properties of amorphous zirconium alloys
[DE85-003303] 11 p1607 N85-20107
Mossebauer study of amorphous Fe(67)Co(18)B(14)Si(1)
[AERE-R-11528] 11 p1737 N85-20928
Corrosion-resistant amorphous alloys
13 p2035 N85-22748
Structure of amorphous films of alloys based on Fe, condensed from laser erosion products
13 p2035 N85-22749
Energy spectrum of processes of structural relaxation of amorphous alloy FeCo70Si15B10
13 p2035 N85-22750
Electronic transport in hydrogenated amorphous silicon films
[DE85-002901] 13 p2164 N85-23426
Annealing effects in ferromagnetic amorphous alloys
[AD-A150648] 14 p2255 N85-23972
SEM (Scanning Electron Microscopy) studies of magnetic domains in amorphous metals
[AD-A150983] 14 p2256 N85-23979
Characterization of poly(ethylene oxide) drawn by solid state extrusion
[AD-A150967] 14 p2260 N85-24006
USSR report: Materials science and metallurgy
[JPRS-UMS-85-001] 15 p2496 N85-25395
Determination of symmetry of immediate surroundings in amorphous Co-P alloys 15 p2496 N85-25398
Temperature variation of resistivity of certain alloys based on transition and simple metals in amorphous and crystalline states 15 p2496 N85-25399
Conversions in amorphous zirconium-vanadium alloy
15 p2496 N85-25400
Structure and aging of amorphous chromium-germanium alloys 15 p2497 N85-25401
Study of amorphous strips and microconductors by ferromagnetic resonance method
15 p2497 N85-25402
Optical properties of hydrogenated amorphous carbon films grown from methane plasma
[NASA-TM-86995] 15 p2658 N85-26406
Structural inhomogeneities in amorphous nickel-phosphorus alloy
[BLL-M-36103-(5828.4)] 16 p2748 N85-26980
Solid state hydrogen pumping and storage material
[AD-D011610] 16 p2757 N85-27011
Electrical resistivity in amorphous metals: Consequences of phonon ineffectiveness in the diffraction model
[AD-A152130] 16 p2779 N85-27150
Glassy metals: New highly resistant material
[BLL-BISI-TRANS-21764-(9022.06)]
17 p2926 N85-28049
Obtaining amorphous coatings of FeW and Fe-Cr-P-B alloys using laser sputtering
[BLL-BISI-22493-(9022.06)] 17 p2927 N85-28057
Production and compaction of amorphous metal powders
[BLL-BISI-TRANS-22387-(9022.06)]
17 p2929 N85-28080
Thermal expansion effects in electrical transport in amorphous metals
[AD-A152477] 17 p2930 N85-28089
Corrosion resistant coating
[NASA-CASE-NPO-15928-1] 18 p3073 N85-29005
Application of the reference intensity method to coal analysis
[DE85-009528] 19 p3228 N85-30015
Investigation for low-cost permanent magnets
[AD-A154387] 19 p3260 N85-30212
Amorphous alloys of ion-implanted Fe-Ti-C
[DE85-010656] 19 p3360 N85-30834
Amorphous metallic films in silicon metallization systems 21 p3610 N85-32427
Mirror reflection of charged particles from +amorphous and polycrystalline surfaces 21 p3690 N85-32827
The development and evaluation of point defect models for the growth of passive films on single crystal, polycrystalline, and amorphous metal surfaces
[AD-A154685] 21 p3709 N85-33023
Long-term research in Japan: Amorphous metals, metal oxide varistors, high-power semiconductors and superconducting generators
[DE85-010827] 22 p3748 N85-33230
In-situ observations of the development of heavy-ion damage in semiconductors
[DE85-010289] 22 p3761 N85-33307
1985 Amorphous Silicon Review Meeting
[DE85-006794] 22 p3807 N85-33582
Process for improving the quality of epitaxial silicon films grown on insulating substrates
[AD-D011730] 22 p3847 N85-33828
The effect of liquid-liquid phase separation of glass on the properties and crystallization behavior
[NASA-TM-77690] 23 p3919 N85-34285
Size and shape dependence of CO adsorption sites on sapphire supported Fe microcrystals
[NASA-CR-176171] 24 p4160 N85-35794

AMORPHOUS SEMICONDUCTORS
Studies of hydrogenated amorphous silicon
[DE84-013038] 01 p0057 N85-10443
Solar generators made of amorphous silicon
05 p0662 N85-14257
Laser annealing of ion implanted semiconductors
[AD-A146979] 07 p1047 N85-16652
Density of states and recombination in amorphous silicon (a-Si:H)
[BMFT-FB-T-84-216] 08 p1135 N85-17151
Stability of amorphous metals on semiconductor substrates
[DE84-017256] 09 p1295 N85-18134
Infrared modulation of photoluminescence in glow discharge amorphous silicon
[DE85-016993] 11 p1737 N85-20922
International Congress Centrum Berlin report on photovoltaics 12 p1877 N85-21773
Pin solar cells made of amorphous silicon
12 p1879 N85-21787
Development of an amorphous silicon panel
12 p1879 N85-21788
Amorphous silicon solar cells with a view to cheap production processes 12 p1879 N85-21789
Plasmachemical evaporation and doping of amorphous silicon 12 p1879 N85-21790
Production and characterization of amorphous silicon (a-Si:H) as base material for solar cells
12 p1879 N85-21791
Thin-film solar cells from sputtered and vapor-deposited amorphous silicon 12 p1879 N85-21792
Chemical vapor deposition of amorphous semiconductor films
[DE85-002917] 15 p2661 N85-28421
Investigation of a Si and related semiconductors as materials for photovoltaic conversion
[DE85-002932] 18 p3096 N85-29163
Carrier loss in dispersive transport in amorphous semiconductors
[DE85-009122] 18 p3194 N85-29811
Drift mobilities by time-of-flight methods and time-dependent phototransport in the nanosecond regime in amorphous semiconductors
[DE85-008729] 18 p3194 N85-29815
Glow discharge deposition at high rates using disilane
[DE85-010236] 19 p3263 N85-30235
Microscopic structure of two-dimensional electron glass
[DE85-010265] 19 p3376 N85-30942
Chemistry and physics of silicon-based amorphous semiconductors
[DE85-001931] 19 p3377 N85-30949
Defects in tetrahedrally coordinated amorphous semiconductors
[AD-A155150] 21 p3581 N85-32263
Thin-film reliability and engineering overview
21 p3612 N85-32450
Raman scattering studies in solids
[AD-A155528] 21 p3710 N85-33032
1985 Amorphous Silicon Review Meeting
[DE85-008794] 22 p3807 N85-33582
Formation of amorphous silicon by light ion damage
[DE85-012605] 23 p3972 N85-34623

AMOUNT
Models for mixture experiments when the response depends on the total amount
[DE85-000370] 09 p1374 N85-18637

AMPERAGE
U ELECTRIC CURRENT

AMPHIBIA
NT FROGS
The development of the vestibular apparatus under conditions of weightlessness
[NASA-TM-77517] 07 p1011 N85-16422
Simulated microgravity as a probe for understanding the mechanisms of early pattern specification
15 p2611 N85-26092
Report of Amphibian Development Group
24 p4127 N85-35583

AMPLIFICATION
NT SOUND AMPLIFICATION
NT WAVE AMPLIFICATION
Transverse field interaction multibeam amplifier
[AD-D011241] 01 p0043 N85-10282
Narrowband tunable dye laser with amplifier pumped by powerful nitrogen laser 02 p0262 N85-11716
Calculation of energy characteristics of double-passage amplifier 03 p0347 N85-12238
Vorticity amplification in viscous flow around a body
03 p0360 N85-12309
Investigation of effect of photocurrent amplification in meta-dielectric-semiconductor structures based on silicon 04 p0488 N85-13110
Analysis of a coded, M-ary orthogonal input optical channel with random-gain photomultiplier detection
05 p0624 N85-13990
Coherent amplification of ultrasonic pulses in activated crystals 05 p0724 N85-14653
The dc SQUID as a tuned radiofrequency amplifier
[DE85-000701] 06 p0805 N85-15123
Array sidelobes, error tolerance, gain, and beamwidth
[AD-A147004] 07 p0940 N85-15956
New construction principles for oscillator power summing devices 07 p0949 N85-16016
Adaptive antenna arrays for weak interfering signals
[NASA-CR-174336] 08 p1150 N85-17258
Gain instabilities in photomultipliers: How accurate are photon counting measurements?
08 p1251 N85-17903
Resonance between betatron and synchrotron oscillations in a free electron laser: A 3-D numerical study
[AD-A150059] 12 p1857 N85-21645
Design and testing of gyroklystron amplifiers
[AD-A151026] 14 p2298 N85-24231
Earth station antenna sidelobe characteristics
[PB85-164966] 16 p2780 N85-27159
Conversion efficiencies of charged particle beam driven free electron lasers
[AD-A154404] 19 p3276 N85-30316
Fin-line horn antennas
[AD-A154597] 21 p3580 N85-32255
Fixed gain and adaptive techniques for rotorcraft vibration control
[NASA-CR-177344] 22 p3728 N85-33111

AMPLIFICATION FACTOR
U AMPLIFICATION
AMPLIFIER DESIGN
Feasibility study for a 34 GHz (Ka band) gyroamplifier
[NASA-CR-174439] 10 p1477 N85-19325
A circuit grammar for operational amplifier design
[AD-A149566] 10 p1481 N85-19348
Cascode and differential amplifier using field-effect transistors 15 p2529 N85-25591
Reactanceless synthesized impedance bandpass amplifier
[NASA-CASE-GSC-12788-1] 18 p3093 N85-29145
Design and fabrication of monolithic broadband microwave GaAs low noise FET amplifiers 20 p3443 N85-31370
Thirty GHz low noise GaAs FET amplifiers — satellite-ground communication
[CD.6500666] 20 p3449 N85-31413
AMPLIFIERS
NT BROADBAND AMPLIFIERS
NT CURRENT AMPLIFIERS
NT DIFFERENTIAL AMPLIFIERS
NT FEEDBACK AMPLIFIERS
NT FLUID AMPLIFIERS
NT LIGHT AMPLIFIERS
NT LIMITER AMPLIFIERS
NT MICROWAVE AMPLIFIERS
NT OPERATIONAL AMPLIFIERS
NT PARAMETRIC AMPLIFIERS
NT PHOTOMULTIPLIER TUBES
NT POWER AMPLIFIERS
NT PREAMPLIFIERS
NT TRANSISTOR AMPLIFIERS
Transverse field interaction multibeam amplifier
[AD-D011241] 01 p0043 N85-10282
An optically isolated amplifier
[CSIR-SR-ELEK-257] 01 p0049 N85-10321
Calculation of energy characteristics of double-passage amplifier 03 p0347 N85-12238
Forced oscillations theory for resonant extended interaction electron devices
[PR-206] 03 p0358 N85-12296
The 30 GHz solid state amplifier for low cost low data rate ground terminals
[NASA-CR-174795] 03 p0358 N85-12300
Design, construction, and operational results of an 800-A, 10-kV hot deck amplifier
[DE84-014044] 04 p0496 N85-13162
China report: Science and technology
[JPRS-CST-84-001] 04 p0557 N85-13545
Present status, future prospects of domestic acoustical instruments 04 p0557 N85-13548
The dc SQUID as a tuned radiofrequency amplifier
[DE85-000701] 06 p0805 N85-15123
Feasibility study for a 34 GHz (Ka band) gyroamplifier
[NASA-CR-174439] 10 p1477 N85-19325
Enhancing the performance of a high-gain free electron laser operating at millimeter wavelengths
[DE85-000662] 12 p1857 N85-21646
Transient processes in tuned amplifier during phase-shift keying with smooth phase variation 15 p2527 N85-25581
Temperature sensitive oscillator
[NASA-CASE-GSC-12958-1] 19 p3258 N85-30201
Development and application of a high power ND-glass laser instrument
[AD-A154366] 19 p3278 N85-30314
Comparative characteristics of optical multiposition pulse signals with intersymbol distortion 22 p3764 N85-33329
Synthesis of high-speed devices using integrated operational amplifiers 22 p3781 N85-33428
Wide-band phase locked loop amplifier apparatus
[AD-D011720] 23 p3927 N85-34337
Solid state high power amplifier for driving the SLC injector klystron
[DE85-013063] 24 p4090 N85-35356
AMPLITUDE DISTRIBUTION ANALYSIS
The estimation of persistence statistics from cumulative probabilities of wave height
[NMI-R183] 03 p0397 N85-12534
Piezoelectric filter with low-Q inductances 13 p2070 N85-22932
Cosmic ray variations with the period close to 27 days and their connection with solar activity longitudinal distribution
[SH-4.4-19] 23 p4035 N85-35015
AMPLITUDE MODULATION
The spectral distribution of field components for a sinusoidal power modulated monofrequency optical carrier source
[FI-44-TBR-84] 04 p0565 N85-13601
Parameters of amplitude-modulated signal upon reflections 13 p2076 N85-22966
Transient processes in tuned amplifier during phase-shift keying with smooth phase variation 15 p2527 N85-25581
The distortion of AM broadcast antenna patterns as caused by nearby towers and highrise buildings
[CRC-1379] 15 p2538 N85-25668
A sampling phasemeter design for pulsed continuous wave signals
[AD-A155237] 21 p3581 N85-32264
A new description of combined trellis coding with asymmetric modulation
[NASA-CR-176197] 24 p4086 N85-35323
AMPLITUDE PROBABILITY ANALYSIS
U AMPLITUDE DISTRIBUTION ANALYSIS
AMPLITUDES
NT PULSE AMPLITUDE
NT SCATTERING AMPLITUDE
Pattern reversal visual evoked potentials and reaction time
[CSIR-SR-PERS-354] 01 p0097 N85-10844
Nonlinear propagation in a depth-dependent ocean
[AD-A145079] 01 p0116 N85-10791
Local photometric standards for CaII emission stars 01 p0126 N85-10883
The investigation of short wave signal structure in the vicinity of the caustic by means of a high-directed antenna
[PR-194] 03 p0354 N85-12277
Standardization of amplitude characteristics of galvanometric seismographs in the KAPG network
[REPT-552] 03 p0375 N85-12395
Shear-layer correction after Amiet under consideration of additional temperature gradient. Working diagrams for correction of signals
[NASA-TM-77741] 03 p0415 N85-12654
Accurate measurement of heat capacity by differential scanning calorimetry 04 p0468 N85-12975
On derivation and significance of geomagnetic equivalent amplitude indices 04 p0520 N85-13321
Recent observations of tides and tidal currents from the northeastern Bering Sea shelf
[PB84-241785] 04 p0543 N85-13452
Helicopter pilot performance for discrete-maneuver flight tasks 05 p0702 N85-14502
Artificial defocusing lens in ionosphere 05 p0724 N85-14654
Measuring large amplitudes of mechanical vibrations with laser interferometers 06 p0787 N85-15028
The use of an optical data acquisition system for bladed disk vibration analysis
[NASA-TM-86891] 06 p0817 N85-15184
Spectral model for subtidal variability in the Chesapeake Bay
[PB84-226679] 06 p0842 N85-15345
Low noise multiple crystal-controlled oscillator
[AD-D011401] 07 p0948 N85-16010
An analytical model of periodic waves in shallow water
[AD-A147501] 07 p0960 N85-16085
An analytical model of periodic waves in shallow water
[AD-A147502] 07 p0960 N85-16086
Real-time estimation of amplitude and group delay distortion in a PSK line-of-sight communications channel
[AD-A147735] 08 p1151 N85-17266
The atmospheric extinction problem 08 p1251 N85-17901
The Midway Atoll coral cap: Meteoric diagenesis, amplitude of sea-level fluctuation and dolomitization 09 p1351 N85-18499
Coherent receiver phase and amplitude alignment circuit
[AD-D011487] 10 p1468 N85-19265
Autumn and winter anomalies in ionospheric absorption as measured by riometers 11 p1660 N85-20460
Resonance between betatron and synchrotron oscillations in a free electron laser: A 3-D numerical study
[AD-A150059] 12 p1857 N85-21645
Surface forward scattering and reflection
[AD-A150115] 12 p1928 N85-22112
Reduction of amplitude-phase distortions of movable microwave coupling circuit for antenna field measurements 13 p2068 N85-22920
Programmable filter with fanned interdigital surface acoustic wave transducer 13 p2083 N85-23008
Nature of seismic images with amplitude and time fluctuations of recorded oscillations 13 p2112 N85-23156
A theoretical study of the ozone quasi-biennial oscillation in the tropical stratosphere 13 p2132 N85-23264
Analytical studies and experimental measurements of amplitude and phase of near-field range antenna probes
[AD-A150922] 14 p2293 N85-24212
Determining geometrical divergence using seismic observation data 14 p2343 N85-24489
Observations of intermediate-degree solar oscillations 14 p2442 N85-25089
Fatigue damage and small crack growth during biaxial loading 16 p2797 N85-27247
Studies of collisional and nonlinear radiative process for development of coherent UV and XUV sources
[AD-A152001] 16 p2865 N85-27670
High voltage power supply
[NASA-CASE-GSC-12818-1] 18 p3093 N85-29147
Interaction of large amplitude stress waves in layered elastic-plastic materials
[AD-A153519] 18 p3121 N85-29323
Mechanistic experiments to determine the origin of Southern Hemisphere stationary waves 18 p3143 N85-29461
An objective analysis technique for extrapolating tidal fields 20 p3493 N85-31715
Huffman-coded pulse compression waveforms
[AD-A155322] 21 p3576 N85-32243
Amplitude stabilization of pulse signals 22 p3762 N85-33320
Synthesis of high-speed devices using integrated operational amplifiers 22 p3781 N85-33428
Generalized string amplitude and wave equation for hadrons
[DE85-011492] 22 p3842 N85-33796
Cosmic ray intensity variations at primary rigidities near 1900 GV
[OG-5.3-0] 22 p3885 N85-34075
Reducing grating lobes due to subarray amplitude tapering
[AD-D011723] 23 p3927 N85-34339
Applications of the Kirchoff-Helmholtz integral to problems in body wave seismology 24 p4116 N85-35515
Average features of the muon component of EAS or = 10(17) eV
[HE-4.3-10] 24 p4191 N85-36004
AMPOULES
Reusable thermal cycling clamp
[NASA-CASE-LAR-12868-1] 12 p1858 N85-21651
ANAEROBES
Anaerobic digestion of biomass: status summary and research development needs, 1983
[PB85-161925] 13 p2040 N85-22772
Comparative anaerobic power of males and females
[AD-A151960] 16 p2842 N85-27523
Anaerobic reduction of elemental sulfur by Chromatium vinosum and Beggiatoa alba 21 p3660 N85-32739
Anaerobic microbial transformations in subsurface environments
[DE85-012790] 22 p3819 N85-33659
ANALOG CIRCUITS
Analog voice processing for FM transmission in a telephone channel
[INPE-2798-PRE/359] 03 p0354 N85-12279
Ensuring required metrological reliability of analog instrument channels by parametric compensation 07 p0955 N85-16050
A general theory of circuit analogy in fracture diagnosis
[AD-A147177] 07 p0978 N85-16212
System for computer-aided design of analog electronic circuits 22 p3768 N85-33353
Microcomputer controlled image processor
[AD-D011734] 22 p3833 N85-33735
Analog, still without fear
[AD-A155920] 24 p4089 N85-35348
ANALOG COMPUTERS
NT UNIVAC 1100 SERIES COMPUTERS
Microcomputer: Controlled statistics analyzer
[BLL-CE-TRANS-7971-(9022.09)] 13 p2144 N85-23306
ANALOG DATA
Optical waveguide spatial filters
[AD-A145674] 02 p0280 N85-11825
Analog disc recorder system: Operator's reference manual
[DE84-016926] 04 p0503 N85-13209
A scanning alarm electronic processor
[AD-D011419] 08 p1158 N85-17309
Complexity, testability, and fault analysis of digital, analog and hybrid systems
[AD-A148485] 08 p1213 N85-17634
Solid state research
[AD-A147640] 08 p1225 N85-17714
A description of the NRL oblique-incidence-ionogram data base
[AD-A148625] 08 p1230 N85-17748
Study on steerability of articulated tracked vehicles
[AD-P004308] 09 p1410 N85-18885
Photonic methods of high speed analog data recording
[DE84-016723] 11 p1637 N85-20308
Electrical characterization of analog microprocessors
[AD-A149629] 12 p1911 N85-21995

User's guide to calibration of analog electronic controllers in HVAC systems
[AD-A150803] 14 p2296 N85-24229
Parallel programmable charge domain device
[AD-D011599] 15 p2549 N85-25733
Pipelined programmable charge domain device
[AD-D011598] 17 p2951 N85-26225
Investigation and construction of the Mini Remote Terminal Unit (mRTU-M) Analog Processor Module (AP-M), volume 1
[MR-DS-01-VOL-1] 18 p3166 N85-29619
Investigation and construction of the Mini Remote Terminal Unit (mRTU-M), Analog Processor Module (AP-M), volume 2
[MR-DS-01-VOL-2] 18 p3166 N85-29620
Analog frequency modulated laser using magnetostriction
[AD-D011701] 19 p3276 N85-30318
Defense Mapping Agency (DMA) raster-to-Vector analysis
[AD-A154153] 19 p3336 N85-30668
Self-adaptive echo cancellation for telephony
[ENST-84E013] 20 p3441 N85-31353
Development of a dedicated speech work station
[AD-A155465] 21 p3674 N85-32824
Solid state research
[AD-A154783] 21 p3709 N85-33025
Design of high-order analog and digital filters with identical sections 22 p3766 N85-33341

ANALOG SIMULATION
Estimating algorithmic error of digital recursive filters 12 p1839 N85-21543
Experimental simulation of the flows in front of and behind a projectile with and without gas slippage
[ISL-CO-232/83] 14 p2302 N85-24258
The utilization of a light-gas gun to simulate interior ballistic flow
[ISL-CO-233/83] 14 p2303 N85-24259
Feasibility study of an installation to simulate the flow of propellant gases in a gun barrel, part 2
[ISL-R-128/83-PT-2] 14 p2303 N85-24263
Stress in axially symmetrical heavy metal projectiles during discharge — numerical simulation
[ISL-CO-219/83] 14 p2321 N85-24345

ANALOG TO DIGITAL CONVERTERS
Digital radio receivers and problems of analog-to-digital conversion of narrow-band signals 04 p0486 N85-13101
Development of components for micro-C oriented sensor systems
[BMFT-FB-T-84-126] 04 p0504 N85-13215
User-oriented development and production of integrated circuits in small and medium quantities
[BMFT-FB-T-84-171] 05 p0633 N85-14059
Formation of reference signals in laser-type gas analyzers with mechanical switching of optical channels 06 p0787 N85-15027
Analog to digital converter
[AD-D011336] 07 p0945 N85-15983
Power spectrum analysis of astronomical photographs digitised with small apertures 07 p0965 N85-16127
Medium speed computer interface (digitizer) for general purpose data acquisition
[DE85-001595] 09 p1367 N85-18587
Low voltage two wire to four wire telephone circuit converter apparatus
[AD-D011449] 10 p1468 N85-19261
Some propagation experimental results on protection techniques for line-of-sight digital systems 10 p1472 N85-19286
RELTIM: A library of routines used in real time machine control applications
[PB85-116507] 10 p1542 N85-19725
Quantization study for ERS-1 wave mode
[DFVLR-FB-84-39] 11 p1625 N85-20234
The study of certain aspects of probability with applications in communications theory
[AD-A149820] 12 p1829 N85-21476
Multichannel digital processing of wideband signals 12 p1840 N85-21548
EZPIX: A tablet entry method for computer-generated slides, drawings, and graphs
[DE85-005234] 12 p1916 N85-22030
The use of a high-speed 12-bit A/D converter for digital sampling of communication signal carriers
[AD-A150578] 13 p2056 N85-22872
Synthesis of quasi-optimum two-level signal discriminator with level changing at unknown point 13 p2083 N85-23010
Microcomputer controlled image acquisition system 15 p2537 N85-25654
Microcomputer controlled automatic peak locking of laser circuit 15 p2537 N85-25655
A portable pulse analyzer for nuclear geophysics using a Sinclair-TK microcomputer
[INPE-3278-PRE/601] 16 p2864 N85-27666
The HURRA high resolution experimental radar system sampling unit
[FOA-C-30376-E1] 18 p3091 N85-29133
A stored data acquisition system: Update
[DE85-010534] 18 p3166 N85-29616
R, L, C, G measurement 21 p3668 N85-32784
Development of a dedicated speech work station
[AD-A155465] 21 p3674 N85-32824
Method of and apparatus for generating an interstitial point in a data stream having an even number of data points
[NASA-CASE-MFS-25319-1] 22 p3827 N85-33701
Microcomputer controlled image processor
[AD-D011734] 22 p3833 N85-33735
Using an LSI-11/23 and RT-11 to digitize analog tapes
[DE85-012736] 24 p4139 N85-35656
The structure of the shower disk observed at Mt. Norikura
[HE-4.7-1] 24 p4196 N85-36052
Thickness of the particle swarm in cosmic ray air showers
[HE-4.7-14] 24 p4200 N85-36064
Search for acoustic signals from high energy cascades
[HE-7.1-1] 24 p4213 N85-36155

ANALOGIES
NT HYDRAULIC ANALOGIES
A similarity analysis of phase change heat conduction in corners 05 p0634 N85-14069
A general theory of circuit analogy in fracture diagnosis
[AD-A147177] 07 p0978 N85-16212
Explorations into thermodynamics analogies and critical points in reference to gas-solid transport
[DE85-000616] 11 p1738 N85-20929
Terrestrial analogs for planetary wrinkle ridges 13 p2199 N85-23644
On the absence of strike-slip faults from the planets and satellites 13 p2200 N85-23645
Application of field similitude theory to calculation of stripline heating 22 p3780 N85-33419
Some plant location problems — computer networks
[FUB-14-1984] 22 p3835 N85-33746
Analogies of control mechanisms in flight guidance and medicine 24 p4129 N85-35597

ANALOGS
A total dose characterization of five commercial analog multiplexers
[AD-A146866] 07 p0946 N85-15997
Growth of soil bacteria in presence of Martian soil analog, carbon dioxide and hydrogen peroxide 09 p1361 N85-18560

ANALYSIS
U ANALYZING

ANALYSIS (MATHEMATICS)
NT ABEL FUNCTION
NT AIRY FUNCTION
NT ANALYTIC FUNCTIONS
NT APPROXIMATION
NT ASYMPTOTES
NT ASYMPTOTIC SERIES
NT BANACH SPACE
NT BESSEL FUNCTIONS
NT BETHE-SALPETER EQUATION
NT BIHARMONIC EQUATIONS
NT BLASIUS EQUATION
NT BOREL SETS
NT BORN APPROXIMATION
NT BURGER EQUATION
NT CALCULUS
NT CALCULUS OF VARIATIONS
NT CHANDRASEKHAR EQUATION
NT CHEBYSHEV APPROXIMATION
NT COLLINEARITY
NT COMBINATIONS (MATHEMATICS)
NT COMBINATORIAL ANALYSIS
NT COMPLEX VARIABLES
NT COMPOSITE FUNCTIONS
NT COMPUTATIONAL CHEMISTRY
NT COMPUTATIONAL FLUID DYNAMICS
NT CONFORMAL MAPPING
NT CONJUGATE GRADIENT METHOD
NT CONJUGATE POINTS
NT CONTINUITY (MATHEMATICS)
NT CONVOLUTION INTEGRALS
NT COPLANARITY
NT DELTA FUNCTION
NT DEPENDENT VARIABLES
NT DIFFERENCE EQUATIONS
NT DIFFERENTIAL CALCULUS
NT DIFFERENTIAL EQUATIONS
NT EDDINGTON APPROXIMATION
NT EINSTEIN EQUATIONS
NT ELLIPTIC DIFFERENTIAL EQUATIONS
NT ELLIPTIC FUNCTIONS
NT ENTIRE FUNCTIONS
NT ERROR ANALYSIS
NT EULER-CAUCHY EQUATIONS
NT EXISTENCE THEOREMS
NT EXPONENTIAL FUNCTIONS
NT EXTREMUM VALUES
NT FACTORIALS
NT FALKNER-SKAN EQUATION
NT FINITE DIFFERENCE THEORY
NT FINITE ELEMENT METHOD
NT FOKKER-PLANCK EQUATION
NT FOURIER ANALYSIS
NT FOURIER SERIES
NT FOURIER TRANSFORMATION
NT FREDHOLM EQUATIONS
NT FUNCTION SPACE
NT FUNCTIONAL ANALYSIS
NT GAMMA FUNCTION
NT GAUSS EQUATION
NT GREEN'S FUNCTIONS
NT HALF PLANES
NT HALF SPACES
NT HARMONIC ANALYSIS
NT HARMONIC FUNCTIONS
NT HARTREE APPROXIMATION
NT HELMHOLTZ VORTICITY EQUATION
NT HILBERT SPACE
NT HILBERT TRANSFORMATION
NT HYPERBOLIC DIFFERENTIAL EQUATIONS
NT HYPERBOLIC FUNCTIONS
NT HYPERGEOMETRIC FUNCTIONS
NT INTEGRAL CALCULUS
NT INTEGRAL EQUATIONS
NT INTEGRAL TRANSFORMATIONS
NT INTERPOLATION
NT ITERATION
NT J INTEGRAL
NT JACOBI MATRIX METHOD
NT KERNEL FUNCTIONS
NT LAGUERRE FUNCTIONS
NT LAME WAVE EQUATIONS
NT LAPLACE TRANSFORMATION
NT LEAST SQUARES METHOD
NT LEGENDRE FUNCTIONS
NT LIAPUNOV FUNCTIONS
NT LIMITS (MATHEMATICS)
NT LINEAR EQUATIONS
NT LINEAR EVOLUTION EQUATIONS
NT LIOUVILLE EQUATIONS
NT LIPSCHITZ CONDITION
NT LOGARITHMS
NT MAXIMA
NT MEAN SQUARE VALUES
NT MEASURE AND INTEGRATION
NT MEROMORPHIC FUNCTIONS
NT MONGE-AMPERE EQUATION
NT MONTE CARLO METHOD
NT NEUMANN PROBLEM
NT NEWTON-RAPHSON METHOD
NT NOMOGRAPHS
NT NONLINEAR EQUATIONS
NT NONLINEAR EVOLUTION EQUATIONS
NT NUMERICAL ANALYSIS
NT NUMERICAL DIFFERENTIATION
NT NUMERICAL INTEGRATION
NT ORTHOGONAL FUNCTIONS
NT PADE APPROXIMATION
NT PARABOLIC DIFFERENTIAL EQUATIONS
NT PARTIAL DIFFERENTIAL EQUATIONS
NT PARTICLE IN CELL TECHNIQUE
NT PARTITIONS (MATHEMATICS)
NT PERIODIC FUNCTIONS
NT PHASE-SPACE INTEGRAL
NT POISSON EQUATION
NT POWER SERIES
NT QUADRATIC EQUATIONS
NT REAL VARIABLES
NT RELAXATION METHOD (MATHEMATICS)
NT RITZ AVERAGING METHOD
NT RUNGE-KUTTA METHOD
NT SERIES (MATHEMATICS)
NT SINGULAR INTEGRAL EQUATIONS
NT SINGULARITY (MATHEMATICS)
NT SOBOLEV SPACE
NT SPHERICAL HARMONICS
NT STURM-LIOUVILLE THEORY
NT TANGENTS
NT TAYLOR SERIES
NT TESSERAL HARMONICS
NT VECTOR ANALYSIS
NT VLASOV EQUATIONS
NT VOLTERRA EQUATIONS
NT VORTICITY
NT WEIGHTING FUNCTIONS
NT WIENER HOPF EQUATIONS
NT ZONAL HARMONICS

Performance of the h, p and h-p versions
01 p0058 N85-10383
Numerical methods for solving systems of linear equations
[INPE-3240-RPE/463] 02 p0250 N85-11633
USSR report: Physics and mathematics
[JPRS-UPM-84-004] 02 p0266 N85-11737
Nonlinear semigroups and evolution governed by accretive operators
[AD-A147556] 07 p1033 N85-16557
Complexity, testability, and fault analysis of digital, analog and hybrid systems
[AD-A148465] 08 p1213 N85-17634
Optical flow and texture variables useful in detecting decelerating and accelerating self-motion
[AD-A148718] 09 p1384 N85-18703
Symmetry breaking for a class of semi-linear elliptic problems
[AD-A149093] 10 p1546 N85-19748
Effects of assuming independent component failure times, if they are actually dependent, in a series system
[AD-A150582] 13 p2101 N85-23092
Interaction of metals and metalloids with biomembranes
[DE85-004902] 13 p2141 N85-23293
Twenty questions on ordered spaces
14 p2413 N85-24880
A note on perfect normality in generalized ordered spaces 14 p2413 N85-24881
Metrization theorems for continuous images of compact ordered spaces 14 p2413 N85-24882
A pathological homogeneous subspace of the real line
14 p2413 N85-24883
A note on topological groups with dense orderable subspaces 14 p2413 N85-24884
The Kappa sub n property in small Omega sub 1 trees
14 p2413 N85-24885
On compactifications of generalized order GO-spaces
14 p2413 N85-24886
The orderability of compact scattered spaces
14 p2413 N85-24887
Submetrizable topologies on the ordinals
14 p2414 N85-24888
Local bases and product partial order II
14 p2414 N85-24890
Mappings of finite oscillations at local separating points 14 p2414 N85-24891
Orderable subspaces of compact F-spaces
14 p2414 N85-24892
The nonlinear analysis of thick composite plates using a cubic spline function
[AD-A152115] 16 p2801 N85-27268
Symbiosis between postgraduate training and research projects: A successful experience
[INPE-3216-PRE/569] 16 p2810 N85-27330
Impact of ozone on vegetation
[PB85-159937] 16 p2821 N85-27403
An interactive computer package for use with simulation models which performs multidimensional sensitivity analysis by employing the techniques of response surface methodology
[AD-A151956] 16 p2846 N85-27548
Performance evaluation of stochastic timed decision-free Petri Nets
[AD-A153987] 18 p3171 N85-29652
Symposium on Computational Mathematics-State-of-the-Art: Informal Proceedings
[DE85-008122] 20 p3516 N85-31858
USSR report: Physics and mathematics
[JPRS-UPM-85-004] 21 p3660 N85-32860
Stability of two-dimensional immiscible flow to viscous fingering
[DE85-011403] 23 p3931 N85-34364
Analytic and numerical calculations of the ambipolar electric field in a stellarator 23 p3978 N85-34665
Polylith: The early goals
[DE85-012534] 24 p4139 N85-35658

ANALYSIS OF VARIANCE

Individual geopotential coefficients of order 15 and 30, from resonant satellite orbits
[AD-A146667] 06 p0628 N85-15256
Estimation of variance of the regression estimator
[AD-A149407] 10 p1551 N85-19780
On the characterization of nonnegatively estimable linear combinations of variance components
[AD-A153786] 18 p3174 N85-29678
Overhead management guide for aerospace procurements
[AD-A153626] 18 p3198 N85-29835
Corrosion fatigue cooperative testing program statistical analysis
[AD-A153886] 19 p3238 N85-30077
The distribution and dynamics of planetary nebulae in M32 and the Andromeda Galaxy
20 p3546 N85-32068

ANALYTIC FUNCTIONS

NT ENTIRE FUNCTIONS

Some families of near-orthonormal analytic and harmonic functions
[AD-A144722] 01 p0110 N85-10748
On the rate of mean convergence of finite linear predictors of multivariate stationary stochastic processes
[AD-A145609] 02 p0254 N85-11664
Interpolating sequences for H to infinity in the ball
[CTH-MATH-1984-15] 04 p0556 N85-13542
Annuals of the Finnish Academy of Sciences, series A. 1: Mathematics, volume 8, part 2
[ISSN-0066-1953] 10 p1535 N85-19673
On the spherical derivative of a meromorphic function with a Nevanlinna deficient value
10 p1535 N85-19676
On harmonic functions with integrable maximum modulus 10 p1536 N85-19681
Close-to-convex functions and linear-invariant families
10 p1536 N85-19683
Annals of the Fourier Institute, volume 34, no. 4
11 p1698 N85-20668
An extension of the Gleason problem in pseudoconvex domains 11 p1698 N85-20671
Contribution of the cup-product of Milnor's fiber with /1/ sup 2 lambda poles 11 p1698 N85-20672
Classic Fourier microdistributions in the real analytic case 11 p1698 N85-20673
Annals of the Scientific Academy of Finland, series A. 1: Mathematics, volume 9
[ISSN-0066-1953] 15 p2633 N85-26229
Harmonic univalent functions
15 p2633 N85-26230
Fourier-Stieltjes coefficients and continuation of functions 15 p2633 N85-26231
On meromorphic functions continuous on the Stollow boundary 15 p2633 N85-26232
Remarks of the maximal dilation of the Beurling-Ahlfors extension 15 p2634 N85-26239
Entire functions with spiral limits
15 p2634 N85-26241
Conditions for the possibility of conformal sewing
[ST-AASF-IMD-58] 16 p2858 N85-27625
Analysis of two-parameter constant background born inversion for acoustic synthetic data
[AD-A156394] 24 p4145 N85-35698

ANALYTIC GEOMETRY

NT CATENARIES
NT CIRCUMFERENCES
NT CONICS
NT ELLIPSES
NT EPICYCLOIDS
NT HYPERBOLAS
NT LOCI
NT MERCATOR PROJECTION
NT OBLATE SPHEROIDS
NT PARABOLAS
NT SPHEROIDS
NT TANGENTS
NT TORUSES

COM-GEOM Interactive Display Debugger (CIDD)
[AD-A145001] 01 p0104 N85-10692
Numerical improvement of asymptotic solutions and nonlinear shell analysis 05 p0648 N85-14158

ANALYTICAL CHEMISTRY

USSR report: Chemistry
[JPRS-UCH-84-012] 06 p0761 N85-14865
Ion microscopy of metals and semiconductors
[AD-A147118] 07 p1043 N85-16626
Chemical information from ion scattering spectrometry
[AD-A148287] 08 p1121 N85-17069
Background detection and correction in multicomponent analysis
[AD-A148251] 08 p1212 N85-17628
Multicomponent calibration and quantitation methods
[AD-A148252] 08 p1212 N85-17629
Quality assurance for environmental analytical chemistry, 1983
[DE84-016045] 09 p1349 N85-18489
Two-dimensional measurements of OH concentration and temperature in reactive flows
[AD-A149849] 12 p1800 N85-21292
Compositional and structural analysis of Air Force materials
[AD-A150092] 14 p2252 N85-23957
Abstracts of the 36th Southeastern Regional Meeting of the American Chemical Society
[AD-A151506] 15 p2496 N85-25394
The development of laser analytical methods for the characterization of solid-liquid and solid-high pressure gas interfaces
[AD-A152362] 17 p2918 N85-27988
Analytical Chemistry Division
[DE85-010585] 18 p3068 N85-28974
Principles of quality assurance of chemical measurements
[PB85-177947] 18 p3072 N85-28997
The determination of dinitrotoluene in single base propellants
[AD-A154672] 21 p3571 N85-32209
Marine environmental quality assessment program, five-year plan (FY 1984 - 1988)
[AD-A154715] 21 p3613 N85-32459

ANALYZERS

NT ENGINE ANALYZERS
NT SIGNAL ANALYZERS

Program flow analyzer, volume 1
[AD-A145320] 02 p0241 N85-11572
Bragg cell spectrum analyzer specification
[AD-D011320] 07 p1044 N85-16629
Battery charger
[AD-D011420] 08 p1178 N85-17425
Calculation and computer simulation of the Paraboloidal Mirror Analyzer (PMA)
[DE85-001417] 09 p1364 N85-18705
Microcomputer: Controlled statistics analyzer
[BLL-CE-TRANS-7971-(0022.00)]
13 p2144 N85-23306
Possibility of developing charged-particle energy analyzer based on hyperboloidal axisymmetrical lens
21 p3691 N85-32933

ANALYZING

Analyzing two-level fractional factorial experiments for possible dispersion effects
[AD-A149456] 10 p1548 N85-19760
Using a logic analyser and trigger unit to de-bug a program
[BAE-881/ELO/1487] 15 p2626 N85-26180

ANATOMY

NT ADRENAL GLAND
NT ARM (ANATOMY)
NT ARTERIES
NT BLADDER
NT BLOOD VESSELS
NT BONES
NT BRAIN
NT BRAIN STEM
NT BRONCHI
NT CARDIAC VENTRICLES
NT CARDIOVASCULAR SYSTEM
NT CEREBELLUM
NT CEREBRAL CORTEX
NT CEREBRAL VENTRICLES
NT CEREBRUM
NT CHEMORECEPTORS
NT CIRCULATORY SYSTEM
NT COCHLEA
NT DIAPHRAGM (ANATOMY)
NT EAR
NT ELBOW (ANATOMY)
NT ERYTHROCYTES
NT EYE (ANATOMY)
NT FEET (ANATOMY)
NT FEMUR
NT FINGERS
NT GASTROINTESTINAL SYSTEM
NT GRAVIRECEPTORS
NT HAND (ANATOMY)
NT HEAD (ANATOMY)
NT HEART
NT HEMATOPOIESIS
NT HEMATOPOIETIC SYSTEM
NT HUMAN BODY
NT INTESTINES
NT JOINTS (ANATOMY)
NT KIDNEYS
NT KNEE (ANATOMY)
NT LABYRINTH
NT LEG (ANATOMY)
NT LIMBS (ANATOMY)
NT LIVER
NT LUNGS
NT LYMPHOCYTES
NT MARROW
NT MECHANORECEPTORS
NT MUSCULOSKELETAL SYSTEM
NT MYOCARDIUM
NT NECK (ANATOMY)
NT OCULOMOTOR NERVES
NT ORGANS
NT OTOLITH ORGANS
NT PANCREAS
NT PARATHYROID GLAND
NT PELVIS
NT PHOTORECEPTORS
NT PITUITARY GLAND
NT PROPRIOCEPTORS
NT RECTUM
NT RESPIRATORY SYSTEM
NT RETINA

NT SCIATIC REGION
NT SKULL
NT SPLEEN
NT TEETH
NT THYMUS GLAND
NT THYROID GLAND
NT TORSO
NT VASCULAR SYSTEM
NT VEINS
NT VERTEBRAE
NT VERTEBRAL COLUMN
NT VESTIBULES
NT WRIST

ANCHORS (FASTENERS)
Vehicle anchoring system
[AD-D011282] 06 p0615 N85-15173
Expedient runway surfacing with post tensioning system for expeditionary airfields
[AD-D011677] 19 p3222 N85-29976

ANDES MOUNTAINS (SOUTH AMERICA)
Mesoscale lee cyclogenesis 09 p1355 N85-18527

ANDROMEDA GALAXIES
The distribution and dynamics of planetary nebulae in M32 and the Andromeda Galaxy
20 p3546 N85-32068

ANECHOIC CHAMBERS
Near-field effects on radome boresight errors
[AD-P004356] 12 p1825 N85-21450
Acoustic detection of air shower cores
[HE-7.1-4] 24 p4213 N85-36158

ANEMIAS
Research opportunities in loss of red blood cell mass in space flight
[NASA-CR-175808] 16 p2841 N85-27517

ANEMOMETERS
NT HOT-FILM ANEMOMETERS
NT HOT-WIRE ANEMOMETERS
NT LASER ANEMOMETERS
Hot section laser anemometry
02 p0142 N85-10962
Laser anemometer optimization
02 p0142 N85-10963
Laser Doppler Anemometry (LDA) signal triggering and effective particle size range
[KU-SFB-210/E/5] 11 p1634 N85-20290
Wind: Measuring for energy
[DE85-900227] 11 p1687 N85-20607
Flow measurement by laser Doppler anemometry in a nuclear fuel assembly
[DE85-003260] 12 p1848 N85-21592

ANEMOMETRY
U VELOCITY MEASUREMENT

ANESTHESIA
NT ELECTROANESTHESIA
Smith predictor and self-tuning control of muscle relaxant drug administration
[RR-257] 02 p0235 N85-11534

ANESTHESIOLOGY
Smith predictor and self-tuning control of muscle relaxant drug administration
[RR-257] 02 p0235 N85-11534

ANESTHETICS
NT CHLOROFORM
NT CYCLOPROPANE
NT METHYL CHLORIDE
Changes in the impedance and bioelectrical activity of the cerebral cortex of rats under the action of anaesthetic drugs
[HSE-TRANS-10371] 19 p3327 N85-30617
Studies of circulatory and metabolic changes during ketamine narcosis
[AD-A154512] 21 p3663 N85-32756

ANGLE OF ATTACK
Wind tunnel calibration of a hemispherical head angle of attack and angle of sideslip indicator
[FFA-TN-1984-11] 02 p0135 N85-10923
Navier-Stokes solution of 3-dimensional hypersonic afterbody flowfields over capsule-type vehicles
[NAL-TR-819] 03 p0311 N85-12010
Heat transfer and pressure drop in blade cooling channels with turbulence promoters
[NASA-CR-3837] 03 p0361 N85-12315
Review of requirements and status of simulation and scaling of transonic, viscous flows
[AD-A146357] 06 p0608 N85-15137
Experiences with the use of a side-strut model support system for high angles of attack in the Trinsonik wind tunnel TMK
[DFVLR-MITT-84-09] 07 p0910 N85-15763
Effect of aerodynamic and angle-of-attack uncertainties on the May 1979 entry flight control system of the Space Shuttle from Mach 8 to 1.5
[NASA-TP-2365] 07 p0913 N85-15778
Unsteady stall penetration of an oscillating swept wing
[AD-P004156] 09 p1264 N85-17941
Theoretical investigation of dynamic stall using a momentum integral method
[AD-P004170] 09 p1266 N85-17955
Determination of corrections to flow direction measurements obtained with a wing-tip mounted sensor
[NASA-CR-174412] 10 p1421 N85-18962
Study of several factors affecting crew escape trajectories from the Space Shuttle Orbiter at low-subsonic speeds
[NASA-TM-86303] 10 p1428 N85-19008
Effect of inclination, transverse intertip spacing, and logitudinal pitch on crossflow heat transfer from an array of finned tubes 10 p1482 N85-19359
Implications of guidance and control technology on human factors considerations 10 p1532 N85-19656
Hypersonic flow about triangular airfoil at large angles of attack 13 p2044 N85-22792
The structure of separated flow regions occurring near the leading edge of airfoils, including transition
[NASA-CR-175670] 14 p2209 N85-23703
Low-speed stability and control wind-tunnel investigations of effects of spanwise blowing on fighter flight characteristics at high angles of attack — Langely 12-ft low-speed tunnel and 30- by 60-ft tunnel
[NASA-TP-2431] 14 p2210 N85-23708
Performance and surge limits of a TF30-P-3 turbofan engine/axisymmetric mixed-compression inlet propulsion system at Mach 2.5
[NASA-TP-2461] 15 p2472 N85-25261
Investigation of potential and viscous flow effects contributing to dynamic stall
[AD-A151696] 15 p2557 N85-25773
Measurements of the symmetric aerodynamic coefficients for flat faced cylinders in the angle of attack regime 0 to 90 deg for transonic and supersonic speeds
[FFA-TN-1984-04] 16 p2700 N85-26675
Experiences with the use of a side-strut model support system for high angles for attack in the TMK Trinsonik Wind Tunnel
[ESA-TT-895] 20 p3396 N85-31069
Recent developments in rotary-balance testing of fighter aircraft configurations at NASA Ames Research Center
[NASA-TM-86714] 21 p3551 N85-32090
Aerodynamic characteristics of the standard dynamics model in coning motion at Mach 0.6
[NASA-TM-86717] 21 p3552 N85-32094
Numerical solutions of turbulent models for flow over a flat plate with angle of attack
[DE85-010380] 21 p3585 N85-32286
Experimental investigations on airfoils with different geometries in the domain of high angles of attack-flow separation
[NASA-TM-77892] 22 p3728 N85-33110

ANGLES (GEOMETRY)
NT ANGLE OF ATTACK
NT BRAGG ANGLE
NT ELEVATION ANGLE
NT GRAZING INCIDENCE
Design sensitivity analysis of an antisymmetric angle-ply laminate
[CSIR-TWISK-318] 01 p0021 N85-10128
The effect of changes in the angle of incidence in the event of a richochet at a float step
[RAE-TRANS-2120] 07 p0902 N85-15712
Tolerance synthesis of multilayer radome walls
07 p0953 N85-16041
Quantitative use of multiincidence-angle SAR for geologic mapping 08 p1145 N85-17220
Investigation of SIR-B images for lithologic mapping
08 p1148 N85-17241
Australian Multiexperimental Assessment of SIR-B (AMAS) 08 p1148 N85-17243
German Radar Observation Shuttle Experiment (ROSE) 08 p1148 N85-17245
Influence of setting angle of jet cooling nozzles on temperature and stress state of a turbine wheel
09 p1306 N85-18208
Forces on undriven, angled wheels
[AD-P004303] 09 p1409 N85-18880
Polarization angles of linearly polarized antennas and radio waves in satellite communications
[PB85-131613] 11 p1626 N85-20240
Angular measurement system
[NASA-CASE-MFS-25825-1] 11 p1635 N85-20298
Detection of angular modulated electromagnetic signals
[AD-D011563] 12 p1823 N85-21437
Mathematical model of discriminator for signals with fluctuations and thermal noise 13 p2072 N85-22943
Examination of the contact wetting angle in the vicinity of critical temperature
[BLL-T6416/BG/CRS/LR-ST735/84]
13 p2091 N85-23054
Characterization of terrestrial solar cells for space applications: Electrical characteristics of thin Westinghouse dendritic web cells as a function of solar intensity, temperature, and incidence angle
[NASA-CR-175842] 14 p2349 N85-24516
Free-surface phenomena under low- and zero-gravity conditions
[NASA-CR-175835] 16 p2782 N85-27166
Measurement and interpretation of electron angle at MABE beam stop
[DE85-008583] 17 p3032 N85-28755
Two-degree-of-freedom linear and planar microwave array lenses
[AD-A153701] 18 p3095 N85-29156
Inherent angular tracking error in an amplitude comparison monopulse radar
[AD-A154212] 19 p3255 N85-30185
Integrated dual beam line scanning antenna and negative resistance diode oscillator
[AD-D011717] 19 p3261 N85-30223
On design of off-axis specimens
[AD-A154328] 19 p3266 N85-30379
Aerodynamic measurement of the wind flow in the number two section of the SIMA wind tunnel
[ONERA-PV-1/8138-GY] 20 p3389 N85-31019
Solid surface characterization by contact angle measurements
[FOA-C-40209-C,B2] 20 p3459 N85-31483
Intersatellite optical links: The point ahead angle
[CNES-83/DRT/TIT/TR/150] 20 p3533 N85-31984
Arrival directions of cosmic rays of E .4 EeV
[OG-5.3-4] 22 p3884 N85-34071
Comprehensive fracture diagnostics experiement. Part 2: Comparison of seven fracture azimuth measurements
[DE85-011707] 23 p3948 N85-34470
OMEGA: Optoelectronic measurement of the incidence angle of a projectile
[ISL-CO-223/84] 23 p3974 N85-34634
The response of ionization chambers to relativistic heavy nuclei
[OG-9.1-13] 23 p4024 N85-34939
Reachable grasps on a polygon: The convex rope algorithm
[AD-A155913] 24 p4138 N85-35647
Geophysical searches for three-neutrino oscillations
[HE-5.3-9] 24 p4205 N85-36103

ANGULAR ACCELERATION
Influence of gravitoinertial force level on apparent magnitude of coriolis cross-coupled angular accelerations and motion sickness 11 p1693 N85-20644
Results of a longitudinal study of airsickness incidence during Naval flight officer training
11 p1694 N85-20649
Uniaxial angular accelerometers
17 p2944 N85-28173
Effect of experimental motion sickness on postrotory nystagmus and counterrotation illusion
22 p3824 N85-33690

ANGULAR CORRELATION
Electronic structure and lattice dynamics of solid state substances from gamma nuclear resonance absorption and angular correlation measurements
03 p0427 N85-12728

ANGULAR DISTRIBUTION
Focusing beam of 1-GeV protons with volumetric capture to the mode of channeling by bent single crystal
02 p0268 N85-11750
Structural studies of sputtered MOS(2) films by angle-resolved photoelectron spectroscopy
[AD-A146052] 03 p0433 N85-12759
Fast neutron capture with a white neutron source
[DE84-016799] 04 p0562 N85-13580
Coincidence techniques to study electron emission in ion-atom collisions
[DE85-003635] 11 p1724 N85-20846
Angular dependence of the Rayleigh-surface wave velocity in polycrystalline metals with small anisotropy
[AERE-R-11595] 15 p2509 N85-25476
Theoretical studies of heavy ion scattering processes
[DE85-008823] 17 p3032 N85-28753
SPECTER: Neutron damage calculations for materials irradiations
[DE85-005791] 18 p3180 N85-29716
Electron multiple, plural and single scattering
[DE85-010325] 18 p3181 N85-29721
Fast-neutron-spectrum measurements for the thick-target (9)Be(d/ = 7 MeV
[DE85-010481] 18 p3183 N85-29735
Investigation of thick-target neutron emission from Be-9(d,n)B-10 at E(d) = 7 MeV for angles other than zero degrees
[DE85-010254] 20 p3528 N85-31947
Evaluated nuclear-data file for niobium
[DE85-012095] 21 p3704 N85-33009

Low-energy sputterings with the Monte Carlo Program ACAT
[IPPJ-AM-40] 23 p3982 N85-34690
On the angular and energy distribution of solar neutrons generated in P-P reactions
[SH-1.4-9] 23 p3995 N85-34789
Additional flux of particles and albedo-electrons in upper atmosphere
[SH-6.1-6] 23 p4045 N85-35080
Neutron production by Ne and Si ions on a thick Cu target at 670 MeV/A with application to radiation protection
[DE85-014526] 24 p4152 N85-35746
1Single particle momentum and angular distributions in hadron-hadron collisions at ultrahigh energies
[HE-1.2-1] 24 p4171 N85-35860
Angular distribution and multiplicity of backward hadrons in hFe interactions at 0.5-5.0 TeV energies (PION Experiment)
[HE-1.2-8] 24 p4172 N85-35866
Anugar distribution of shower particles produced in the collisions of 20-GeV/c and 300-GeV negative pions with emulsion nuclei 24 p4172 N85-35868
Inclusive angular distribution of alpha and Li fragments produced in the Fe-C and Fe-Pb collisions at 1.88 GeV/u
[HE-1.4-11] 24 p4177 N85-35898
Characteristics of anomalously high multiplicity cosmic ray interactions
[HE-3.3-1] 24 p4180 N85-35920
Peculiarities of gamma-quanta distribution at 20 TeV energy
[HE-3.7-10] 24 p4186 N85-35967
The thickness of the shower disc as observed in showers produced by primaries above 10 (19)eV
[HE-4.7-6] 24 p4199 N85-36057
Thickness of the particle swarm in cosmic ray air showers
[HE-4.7-14] 24 p4200 N85-36064
Measurement of neutrino oscillations in MACRO experiment
[HE-5.3-10] 24 p4206 N85-36104

ANGULAR MOMENTUM
A packed storage program for angular momentum coupling coefficients
[TWISK-316] 01 p0102 N85-10680
A reappraisal of Darwin's fission hypothesis and a possible limit to the primordial angular momentum of the Earth 04 p0585 N85-13736
Numerical simulations of fission 04 p0585 N85-13737
Models of angular momentum input to a circumterrestrial swarm from encounters with heliocentric planetesimals 04 p0587 N85-13750
The lunar angular momentum problem 04 p0588 N85-13752
Formation of the prelunar accretion disk 04 p0588 N85-13755
Description of a laborstory model Annular Momentum Control Device (AMCD) 05 p0806 N85-13863
Winds from rotating, magnetic, hot stars 08 p1234 N85-17775
Suspension torques on a gimballed electrostatically supported gyroscope and requirements on the gyroscope and spacecraft for the relativity gyroscope experiment 12 p1851 N85-21606
Models of angular momentum input to a circum-terrestrial swarm from encounters with heliocentric planetesimals 13 p2179 N85-23521
Flight investigation of stall, spin and recovery characteristics of a low-wing, single-engine, T-tail light airplane
[NASA-TP-2427] 15 p2470 N85-25248
Microscopic analysis of angular momentum projected HFB-states in terms of interacting bosons
[DE85-007629] 16 p2863 N85-27661
Multi-particle quantum mechanics obeying fractional statistics
[DE85-007830] 16 p2873 N85-27723
Spin distributions in heavy ion fusion at and below the Coulomb barrier
[DE85-007817] 17 p3031 N85-28751
Analysis and modeling of variations in length of day 19 p3349 N85-30761
Interacting Boson approximation
[DE85-003016] 22 p3837 N85-33756
Duality of two-point functions for confined non-relativistic quark-antiquark systems
[DE85-012334] 23 p3971 N85-34618

ANGULAR MOTION
U ANGULAR VELOCITY

ANGULAR RESOLUTION
Limitation of VLBI angular resolution 07 p1057 N85-16710
Opportunities for high angular and temporal resolutions of galactic objects at radio frequencies — QUASAT 07 p1059 N85-16723
Image processing instrumentation for speckle interferometry and imaging
[AD-A149306] 11 p1762 N85-21084
Determination of angular resolution of coded aperture gamma-ray telescope 13 p1961 N85-22432
Spectra and positions of galactic gamma-ray sources
[OG-2.5-7] 22 p3869 N85-33963
A search for sources of ultra high energy gamma rays at air shower energies with Ooty EAS array
[OG-2.6-8] 22 p3870 N85-33970
The gamma-ray telescope Gamma-1
[OG-9.2-10] 23 p4026 N85-34949
Lapsc: A Phoswich balloon experiment for hard X-ray astronomy
[OG-9.3-1] 23 p4027 N85-34956
A new ultra high energy gamma ray telescope at Ohya mine
[OG-9.4-3] 23 p4029 N85-34970
An EAS experiment at mountain altitude for the detection of gamma-ray sources
[OG-9.4-6] 23 p4029 N85-34972
A new array for the study of ultra high energy gamma-ray sources
[OG-9.4-7] 23 p4029 N85-34974
Shower disc sampling and the angular resolution of gamma-ray shower detectors
[OG-9.5-2] 23 p4030 N85-34980
A method to improve observations of gamma-ray sources near 10 (15) eV
[OG-9.5-5] 23 p4030 N85-34982
Angular resolution of air-shower array-telescopes
[OG-9.5-6] 23 p4030 N85-34983
Astrophysical applications of high angular resolution array-telescopes
[OG-9.5-7] 23 p4031 N85-34984
Angular resolution of an EAS array for gamma ray astronomy energies 5 x 10 (13) eV
[OG-9.5-8] 23 p4031 N85-34985
Note on the detection of high energy primary cosmic gamma rays by air shower observation
[OG-9.5-9] 23 p4031 N85-34986
The angular resolution of air shower gamma ray telescopes
[OG-9.5-14] 23 p4031 N85-34990
Measurement of low energy cosmic rays aboard Spacelab-1
[SH-10.1-6] 23 p4053 N85-35137
Preliminary results of the Cerenkov EAS flashes the Crimean Astrophysical Observatory
[HE-4.4-17] 24 p4194 N85-36023
Thickness of the particle swarm in cosmic ray air showers
[HE-4.7-14] 24 p4200 N85-36064

ANGULAR VELOCITY
Rotational motion of a satellite 13 p1981 N85-22428
Status of and outlook for producing means of transmitting units of plane angle, angular velocity and acceleration with ring lasers 13 p2074 N85-22955
Investigation of errors of acoustic goniometer information-measurement systems on rocking base 14 p2283 N85-24139
Models of solar differential rotation 14 p2446 N85-25097
Optimum rotation of solid body with 1 axis of symmetry 16 p2718 N85-26781
Fluidic angular velocity sensor
[NASA-CASE-NPO-16479-1-CU] 18 p3104 N85-29219

ANHYDRIDES
NT INORGANIC PEROXIDES
NT ORGANIC PEROXIDES
NT PEROXIDES
Condensation of anhydrides or dicarboxylic acids with compounds containing active methylene groups. Part 19: Condensation of phthalic and substituted phthalic anhydrides with benzoylacetic ester
[NASA-TM-77685] 19 p3227 N85-30009
Condensation of anhydrides or dicarboxylic acids with compounds containing active methylene groups. Part 1: Condensation of phthalic anhydride with acetoacetic and malonic ester
[NASA-TM-77686] 19 p3227 N85-30010
Remarks on preparation of indandione detection reagents
[NASA-TM-77905] 21 p3560 N85-32148

ANIK SATELLITES
SLIM TDMA ANIK B pilot project
[CRC-REPT-1366] 03 p0354 N85-12278

ANILINE
Homogeneous reaction involving components of different redox couples. 1: Theoretical considerations and digital simulation
[AD-A148666] 08 p1124 N85-17084
Supersonic molecular jet study of the liquid state
[AD-A147416] 09 p1379 N85-18671
Influence of pressure on speed of sound in single-phase region of stratifying mixtures 11 p1715 N85-20788
Resistance of polyaniline films as a function of electrochemical potential and the fabrication of polyaniline-based microelectronic devices
[AD-A154999] 21 p3569 N85-32201

ANIMALS
NT AMPHIBIA
NT BABOONS
NT BEARS
NT BIRDS
NT CATS
NT DEER
NT DOGS
NT DOLPHINS
NT FISHES
NT FROGS
NT GUINEA PIGS
NT HETEROTROPHS
NT HUMAN BEINGS
NT INSECTS
NT INVERTEBRATES
NT LARVAE
NT MAMMALS
NT MICE
NT MONKEYS
NT PRIMATES
NT PROTOZOA
NT RABBITS
NT RATS
NT SEALS (ANIMALS)
NT SHARKS
NT SHEEP
NT SPIDERS
NT TURTLES
NT WHALES
NT WILDLIFE
Estuaries of the Cape. Part 2: Synopses of available information on individual systems. Report 13: Silvermine (CSW 3)
[CSIR-RR-412-PT-2] 01 p0086 N85-10582
Estuaries of the Cape. Part 2: Synopses of available information on individual systems. Report no. 16: Eerste (CSW 6)
[CSIR-RR-415-PT-2] 01 p0087 N85-10585
Estuaries of the Cape. Part 2: Synopses of available information on individual systems. Report no. 17: Lourens (CSW 7)
[CSIR-RR-416-PT-2] 01 p0087 N85-10586
In vivo dermal absorption method and system for laboratory animals
[AD-D011231] 01 p0094 N85-10635
Small animal hypobaric chamber
[AD-A146196] 03 p0364 N85-12335
Oxygen delivery during exercise: Limitations to maximum flow 05 p0688 N85-14424
Effect of broad-band constant noise on some systems of animal body 14 p2387 N85-24705
NASA Space Biology Program: 9th Annual Symposium
[NASA-CP-2336] 15 p2605 N85-26054
Effects of weightlessness of Aurelia Ephyra differentiation and statolith synthesis 15 p2605 N85-26056
Gravity perception in a Cladoceran-Zooplankter: Anatomy of antennal socket setae of Daphnia magna 15 p2605 N85-26057
Review and annotated bibliography of benthic studies in coastal and estuarine areas of Florida with a selected compilation of worldwide benthic methodological references and southeastern United States benthic taxonomic references
[PB85-151041] 16 p2822 N85-27405
MARMAP survey of the continental shelf from Cape Hatteras, North Carolina to Cape Sable, Nova Scotia (1977 - 1983). Atlas 1: Summary of operations
[PB85-150985] 16 p2839 N85-27506
An environmentally-controlled extended-use small animal hypobaric chamber
[AD-A153735] 19 p3221 N85-29974
The 1984 environmental monitoring report, Sandia National Laboratories, Albuquerque, New Mexico
[DE85-011175] 22 p3811 N85-33607
Antihypertensive neutral lipid
[DE85-011625] 22 p3819 N85-33658
The 1984 biotic studies of Yucca Mountain, Nevada test site, Nye County, Nevada
[DE85-011715] 23 p3951 N85-34487

ANIMATION
U MOTION
ANIONS
Electronic and redox properties of stacked-ring silicon phthalocyanines from molecular orbital theory
[AD-A147161] 07 p0922 N85-15844
Homogeneous reaction involving components of different redox couples. 1: Theoretical considerations and digital simulation
[AD-A148686] 08 p1124 N85-17084
Microstructural analysis of ion containing polymers
[DE85-001594] 10 p1453 N85-19157
The synthesis, structural characterization and reactions of closo-Rhodacarborane Anions containing a formal d8 metal vertex 1,2
[AD-A149640] 12 p1799 N85-21265
Theoretical studies of kinetic mechanisms of negative ion formation in plasmas
[AD-A150820] 14 p2423 N85-24946
The electronic spectra of phthalocyanine radical anions and cations
[AD-A152326] 17 p2918 N85-27986
Gas phase ion-molecule chemistry of carbon, nitrogen and oxygen compounds
[AD-A152876] 17 p2919 N85-27996
An alpha particle diagnostic beam line system to generate an intense Li(O) beam with an ORNL SITEX source
[DE85-010564] 18 p3182 N85-29730
Method of reducing impurity and antisite defects in semiconductor crystal materials, and device and apparatus respectively produced from and utilizing same
[AD-D011698] 19 p3260 N85-30216
Electron photoejection in carbanions
[DE85-011747] 23 p3911 N85-34230
Electron photoejection in carbanions
[DE85-011748] 23 p3912 N85-34237
Throughfall rate and chemistry studies: Whiteface Mountain
[DE85-012407] 23 p3947 N85-34464
ANISOTROPIC MEDIA
Identification of pulse-echo rays in austenitic steels
[AERE-R-11265] 03 p0369 N85-12356
Microwave measurement of the complex dielectric tensor at anisotropic slab materials
[DE84-017050] 04 p0493 N85-13144
Reflection theorems for some anisotropic media
07 p0953 N85-16038
Angular dependence of the Rayleigh-surface wave velocity in polycrystalline metals with small anisotropy
[AERE-R-11595] 15 p2509 N85-25476
Multiple scattering of electromagnetic waves in discrete random media
[AD-A151766] 16 p2772 N85-27112
Examination of anisotropic films by resonance method
22 p3778 N85-33412
ANISOTROPIC PLATES
Quantification of Saint-Venant's principle for a general prismatic member 04 p0467 N85-12972
A refinement of the transverse shear deformation theory for multilayered anisotropic plates
[STN-5] 20 p3471 N85-31571
ANISOTROPIC SHELLS
Normal mode method of solving problem forced oscillations of rib-reinforced shell of revolution in liquid
02 p0273 N85-11781
Stability of anisotropic cylindrical sandwich shells
16 p2766 N85-27065
ANISOTROPY
Theory of nuclear magnetic relaxation
[AD-P003911] 01 p0032 N85-10197
Fracture, failure, and fragmentation
01 p0059 N85-10390
A finite element projection method for the solution of particle transport problems with anisotropic scattering
[AD-A145382] 02 p0250 N85-11637
Improved beam theory for anisotropic materials
04 p0468 N85-12973
Collective processes and formation of star clusters
05 p0736 N85-14743
Anisotropy and microstructure of rare earth permanent magnet materials
[AD-A146549] 06 p0859 N85-15460
Irradiation creep induced anisotropy in a/2110 dislocation populations
[DE84-016623] 06 p0868 N85-15520
Low cycle fatigue of MAR-M 200 single crystals at 760 and 870 deg C
[NASA-TM-86933] 10 p1440 N85-19074
On shrinkage and molecular extension
[AD-A149100] 10 p1451 N85-19144
Imaging through a multiple scattering medium
[DE85-002051] 10 p1557 N85-19821
Ferromagnetic resonance in a Ni-Mo superlattice
[DE85-003039] 11 p1735 N85-20911
Calculation of ionospheric profiles by inverting VLF/LF reflection data. 2. Anisotropic propagation
[AD-A150105] 12 p1880 N85-21859
Correlation of interplanetary medium parameters in transition region of high-velocity solar wind streams
13 p1978 N85-22412
Orientation and temperature dependence of some mechanical properties of the single-crystal nickel-base superalloy Rene N4. 3: Tension-compression anisotropy
[NASA-TM-86962] 13 p2021 N85-22660
Investigations of ultrasonic wave interactions at boundaries separating anisotropic materials
[DE85-003506] 13 p2155 N85-23384
Measurement of the large-scale anisotropy of the cosmic background radiation at 3 MM 13 p2206 N85-23680
Solid/melt interface studies of high-speed silicon sheet growth
[NASA-CR-175698] 14 p2350 N85-24525
Energetic electron anisotropy and ELF waves onboard GEOS. How does quasi-linear diffusion work
14 p2366 N85-24623
Models of solar differential rotation
14 p2446 N85-25097
Effect of nickel addition on the thermal, magnetic and magnetomechanical properties of Fe(80)B(15)Si(5)
[AD-A152281] 16 p2749 N85-26967
Polarimetric image recorder
[AD-D011605] 16 p2787 N85-27192
Active and passive remote sensing of ice
[AD-A151741] 16 p2815 N85-27369
The soft X-ray background as a supernova blast wave viewed from inside: Solar abundance models
[NASA-CR-175767] 16 p2887 N85-27813
Investigation for low-cost permanent magnets
[AD-A154387] 19 p3260 N85-30212
Investigation of thick-target neutron emission from Be-9(d,n)B-10 at E(d) = 7 MeV for angles other than zero degrees
[DE85-010254] 20 p3528 N85-31947
Drift anisotropy instability of a finite Beta magnetospheric plasma
[IFSI-84-12] 20 p3536 N85-32005
Anisotropy of the permittivity field inferred from aspect-sensitive radar echoes 21 p3620 N85-32492
Influence of mirror anisotropy and Brewster window orientation on radiation characteristics of ring lasers
21 p3684 N85-32889
Low frequency instabilities driven by an ion temperature anisotropy
[AD-A154902] 21 p3707 N85-33016
Shear wave transducer for boreholes
[DE85-011662] 22 p3787 N85-33461
The effect of anisotropic emission on the log N-log S curve of gamma-ray bursts
[OG-1.2-4] 22 p3862 N85-33914
Search for ultra high energy gamma-rays from various sources
[OG-2.6-7] 22 p3870 N85-33969
Long term variability of the cosmic ray intensity
[OG-3.1-11] 22 p3874 N85-33999
Arrival directions of large air showers, low-mu showers and old-age low-mu air showers observed at St. Chacaltaya
[OG-5.3-2] 22 p3884 N85-34069
Anisotropy of cosmic rays of energy 10 (15) eV to 10 (17) eV observed at Akeno
[OG-5.3-3] 22 p3884 N85-34070
Arrival directions of cosmic rays of E .4 EeV
[OG-5.3-4] 22 p3884 N85-34071
The sidereal anisotropy of cosmic rays around 3 x 10 (15) eV observed at a middle north latitude
[OG-5.3-6] 22 p3884 N85-34072
Arrival direction distribution of cosmic rays of energy 10 (18) eV
[OG-5.3-7] 22 p3885 N85-34073
Air shower arrival directions measured at Buckland Park
[OG-5.3-11] 22 p3885 N85-34077
A simulation of high energy cosmic ray propagation 2
[OG-5.4-2] 22 p3885 N85-34079
Implications of the experimental results on high energy cosmic rays with regard to their origin
[OG-5.4-5] 22 p3886 N85-34082
Virgo cluster as a high energy cosmic rays source
[OG-5.4-8] 22 p3886 N85-34085
Modeling cosmic ray anisotropies near 10(18) eV
[OG-5.4-9] 22 p3886 N85-34086
Anisotropy and the knee of the energy spectrum
[OG-5.4-10] 22 p3887 N85-34087
A model for the proton spectrum and cosmic ray anisotropy
[OG-5.4-12] 22 p3887 N85-34089
On galactic origin of cosmic rays with energy up to 10(19) eV
[OG-5.4-15] 22 p3887 N85-34091
Flux-line lattice anisotropy in V3Si: Observation and interpretation
[DE85-011935] 23 p3985 N85-34713
Helios 1 energetic particle observations of the solar gamma ray flare events of 7, 21 June 1980 and 3 June 1982
[SH-1.3-8] 23 p3993 N85-34755
Ultrarelativistic electrons and solar flare gamma-radiation
[SH-1.3-11] 23 p3993 N85-34757
Cosmic ray north-south anisotropy 1961 - 1983
[SH-4.2-6] 23 p4007 N85-34844
Effects of a wavy neutral sheet on cosmic ray anisotropies
[SH-4.2-11] 23 p4008 N85-34849
The expected cosmic ray density and stream distributions at the heliolatitudinal asymmetry of solar wind
[SH-4.2-14] 23 p4008 N85-34852
The effect of the neutral sheet structure of the interplanetary magnetic field on cosmic ray distribution in space
[SH-4.2-18] 23 p4008 N85-34855
On the cosmic ray diffusion in a violent interstellar medium
[OG-7.2-14] 23 p4015 N85-34881
Gradients and anisotropies of high energy cosmic rays in the outer heliosphere
[SH-4.3-7] 23 p4032 N85-34992
IMF-sense-dependent cosmic ray anisotropy produced from diffusion-convection in heliosphere
[SH-4.3-9] 23 p4032 N85-34994
Influence of the neutral sheet on the Swinson's type north-south anisotropy of cosmic rays
[SH-4.3-10] 23 p4032 N85-34995
Characteristics of cosmic ray pole-equator anisotropy derived from spherical harmonic analysis of neutron monitor data
[SH-4.3-12] 23 p4032 N85-34996
First zonal harmonic component of cosmic ray neutron intensity
[SH-4.3-13] 23 p4032 N85-34997
The corotating variation of the north-south anisotropy of cosmic rays
[SH-4.3-15] 23 p4033 N85-34999
Sidereal anisotropies in the median rigidity range 60-600GV in 1978-1983
[SH-4.4-3] 23 p4033 N85-35001
The effect of the interplanetary magnetic field on sidereal variations observed at medium depth underground detectors
[SH-4.4-5] 23 p4033 N85-35003
The sidereal semi-diurnal variation observed at high zenith angles at Mawson, 1968-1984, and the polarity of the solar main field
[SH-4.4-6] 23 p4033 N85-35004
Sidereal anisotropy of cosmic rays
[SH-4.4-8] 23 p4034 N85-35006
Formulation of cosmic-ray solar daily variation and its seasonal variation, produced from generalized stationary anisotropy of solar origin
[SH-4.5-2] 23 p4036 N85-35020
Solar tri-diurnal variation of cosmic rays in a wide range of rigidity
[SH-4.5-3] 23 p4036 N85-35021
Upper cut-off rigidity for corotation anisotropy during solar activity cycles 20 and 21
[SH-4.5-4] 23 p4036 N85-35022
Diurnal anisotropy during solar activity cycle twenty and diffusion-convection model
[SH-4.5-7] 23 p4036 N85-35025
Comparative study of the phase of diurnal anisotropy on quiet and disturbed days on a long term basis up to recent period
[SH-4.5-9] 23 p4037 N85-35027
Study of spectral exponent on quiet and disturbed days
[SH-4.5-10] 23 p4037 N85-35028
The modulation features of the long-period cosmic ray variations in connection with the sign change of the general magnetic field of the Sun
[SH-4.5-15] 23 p4037 N85-35032
Cosmic ray density gradient and its dependence on the north-south asymmetry in solar activity
[SH-4.5-17] 23 p4038 N85-35034
Anomalous increase of solar anisotropy above 150GV in 1981-1983
[SH-4.5-18] 23 p4038 N85-35035
Diagnostic of electromagnetic conditions in space using cosmic rays
[SH-4.5-19] 23 p4038 N85-35036
Change of cosmic ray anisotropy with solar activity
[SH-4.5-20] 23 p4038 N85-35037
Magnetic fluctuation and cosmic ray diurnal variations
[SH-4.5-21] 23 p4038 N85-35038

The theoretical and experimental investigation of cosmic ray Forbush-effects
[SH-5.1-20] 23 p4044 N85-35072
Peculiarities of Galactic Cosmic Ray (GCR) anisotropy variation in connection with the recurrent and sporadic Forbush effects
[SH-5.1-21] 23 p4044 N85-35073
A comparative analysis of gamma and hadron families at the superhigh energies recorded in experiment Pamir
[HE-3.7-1] 24 p4185 N85-35960
Character of energy flow in air shower core 24 p4189 N85-35985
An underground cosmic ray muon telescope for observation of cosmic ray anisotropy 24 p4196 N85-36037
Underground measurements on secondary cosmic rays
[HE-5.4-1] 24 p4207 N85-36116

ANNEALING
NT LASER ANNEALING
NT PULSE HEATING
Influence of annealing on properties of AT3 alloy welded joints 01 p0019 N85-10118
Kinetics of short-range ordering in metallic glasses: Analysis of the crossover effect
[DE84-015524] 02 p0187 N85-11251
Complex formation and temperature stability of electrophysical properties of GaAs seminsulating single crystals 02 p0258 N85-11689
The effect of heat treatment on wear resistance of gas-plasma eutectic coatings
[BLL-M-35756-(5828.4)] 03 p0329 N85-12122
Annealing of implanted Al-2O-3 in a reducing environment
[DE84-015370] 03 p0332 N85-12140
Parameters of structural relaxation and mechanical properties of amorphous alloys 03 p0349 N85-12246
Effect of annealing in transverse magnetic field on magnetic permeability of amorphous Fe5Co70Si15B10 alloy 03 p0349 N85-12247
Structural recrystallization in titanium 03 p0351 N85-12258
A study of defects in neutron transmutation doped silicon: Gallium by hall effect analysis
[AD-A146047] 03 p0433 N85-12758
On the origins of structural defects in BF2(+)-implanted and rapid thermally annealed silicon: Conditions for defect free regrowth
[DE84-016060] 04 p0572 N85-13650
Impact toughness of wire after cold deformation and annealing
[BLL-M-35941-(5828.4)] 05 p0615 N85-13930
Multiaxial yield behavior of 1100 aluminum following various magnitudes of prestrain
[DE84-013904] 05 p0617 N85-13949
Development of technology of silicon single-crystal production semiconductor power devices: State of art outlook 06 p0795 N85-15078
Oxide charge characteristics of low temperature MOS (Metal-Oxide-Silicon) oxide films
[AD-A146447] 06 p0803 N85-15113
Atmospheric heating of meteorites: Results from nuclear track studies 06 p0882 N85-15607
Defective nature of the crystalline lattice of nickel ferrite-based solid solutions
[BLL-WH-595-(9091.9F)] 07 p1046 N85-16645
X-ray and backscattering analysis of ion implantation phenomena in GaAs and related compounds
[AD-A147449] 07 p1048 N85-16659
Study of the mechanism for annealing embrittlement of an iron-based metallic glass
[DE84-016856] 09 p1300 N85-18164
Radiation effects in Strain-Layer Superlattice (SLS) structures
[DE85-001713] 09 p1398 N85-18799
Ion beam processes in Si
[DE85-001254] 09 p1399 N85-18808
Damage to boron fibers during thermal cycling and annealing 10 p1445 N85-19107
Study of the volumetric changes in VT23 alloy upon heating 10 p1448 N85-19123
Mod silver metallization for photovoltaics
[NASA-CR-174444] 10 p1509 N85-19518
Pulsed excimer laser processing for cost-effective solar cells
[NASA-CR-175465] 10 p1509 N85-19520
Dependence of mechanical properties of large VT3-1 alloy forgings on microstructure parameters 11 p1602 N85-20072
Low cost, sprayed CuInSe2 solar cell research
[DE85-003487] 12 p1881 N85-21799
Investigation of device and electronic interactions in Ga-.s device processing
[AD-A149747] 12 p1940 N85-22182
The effects of lithium counterdoping on radiation damage and annealing in n(+)p silicon solar cells 13 p2007 N85-22586
Temperature effects of heterogenizated annealing on structure and properties of V95 aluminum alloy 13 p2025 N85-22692
Influence of annealing on cyclic and short-term strength of thin sheets of VT1-0 titanium and OTR4 alloy 13 p2031 N85-22727
Thermal hardening of welded joints in titanium alloys with various structures 13 p2032 N85-22734
Investigation of the effect of annealing on the dislocation and sub-grain boundary content of solvent-evaporation-grown CdTe
[AD-A144087] 13 p2182 N85-23415
Influence of substrate heating and thermal annealing on the surface crystallinity in single Si crystals implanted with high doses of (16)O
[DE85-005264] 13 p2164 N85-23428
Annealing effects in ferromagnetic amorphous alloys
[AD-A150648] 14 p2255 N85-23972
Possible use of rapid heating for improving mechanical properties of titanium alloys 15 p2498 N85-25409
Effect of annealing procedures on structure and properties of VT6 alloy with initial large-grained structure 15 p2498 N85-25410
Effect of aluminum on nature of titanium alloy failure 15 p2498 N85-25411
Study of oxidized surface coating on titanium after annealing 15 p2498 N85-25412
Brittle fracture resistance of electron beam-welded joints in titanium Alpha alloys 15 p2500 N85-25419
Structure and properties of VT20L titanium alloy with 0.1-0.3 percent content 15 p2515 N85-25517
Characterization of thin films and layered structures using X-ray absorption and reflection at grazing incidence
[DE85-006560] 15 p2662 N85-26429
Relationships between microstructure and microfissuring in alloy 718 16 p2735 N85-26876
Solution softening in molybdenum-rhenium alloys
[DE85-006706] 16 p2750 N85-26972
Thermal annealing of Fe implanted Al2O3 in oxidizing and reducing environment: Revised version
[DE85-007546] 16 p2752 N85-26983
Thermomechanical softening treatment for bearing and tool steels
[BLL-BISI-TRANS-22432-(9022.06)] 17 p2925 N85-28035
Influence of preliminary cold deformation on fineness of pearlite
[BLL-BISI-TRANS-22409-(9022.06)] 17 p2927 N85-28054
The characteristic structure of weld metal of high temperature alloy X20CrMoV 121
[BLL-BISI-TRANS-21623-(9022.06)] 17 p2928 N85-28069
Kinetics of the formation of a complex alloyed boride coating on iron and its properties
[BLL-BISI-TRANS-22303-(9022.06)] 17 p2930 N85-28084
Activities of the Solid State Physics Research Institute
[NASA-CR-175899] 17 p3042 N85-28818
Thermal donor removal by rapid thermal annealing: Infrared absorption
[DE85-010092] 18 p3081 N85-29059
Post-deposition heat treatments of CdS/CuInSe2 solar cells
[DE85-002943] 18 p3128 N85-29373
Electronic states in silicon and on its interfaces
[AD-A153864] 18 p3193 N85-29807
Effects of annealing treatments on superplasticity in a thermomechanically processed Aluminum-10.2%Mg-0.52%Mn
[AD-A154414] 19 p3239 N85-30080
Fatigue resistance of homogeneous and heterogeneous welded joints of TS5 titanium alloy 19 p3246 N85-30126
Investigation for low-cost permanent magnets
[AD-A154387] 19 p3260 N85-30212
Method for producing high quality germanium-germanium nitride interfaces for germanium semiconductors and device produced thereby
[AD-D011702] 19 p3260 N85-30218
Electrical properties of bulk grown nitrogen doped silicon
[AD-A155471] 21 p3581 N85-32266
Metallic glass composition
[DE85-011594] 22 p3751 N85-33253
Ultra-trace analysis of sinter tantalum with SIMS
[BLL-RARDE-TR-1220-(7291.7965)] 23 p3913 N85-34245
Changes in lattice cell parameter of film intermetallic compounds RT2
[BLL-M-35874-(5828.4)] 23 p3915 N85-34261
An X-ray diffraction study of titanium oxidation
[NASA-CR-176263] 23 p3915 N85-34264
Rapid annealing of temperature-compensated, precision voltage references following fast-neutron irradiation
[DE85-009821] 23 p3970 N85-34609
Decomposition of martensite in R6M5 and R6AM5 steels after direct immersion in liquid nitrogen
[BLL-M-36305] 24 p4077 N85-35268
Advanced detectors and signal processing
[NASA-CR-176193] 24 p4088 N85-35343
Size and shape dependence of CO adsorption sites on sapphire supported Fe microcrystals
[NASA-CR-176171] 24 p4160 N85-35794
Laser and electron beam processing of semiconductors
[AD-A155914] 24 p4161 N85-35796

ANNIHILATION REACTIONS
NT POSITRON ANNIHILATION
Performance of a large area flash chamber prototype
[NOTA-INTERNA-807] 02 p0201 N85-11336
Experimental medium energy physics
[DE84-014825] 02 p0278 N85-11807
Fermilab research program workbook
[DE84-012568] 06 p0882 N85-15476
Experimental investigations in particle physics at intermediate energies
[DE85-001481] 11 p1722 N85-20832
Parton dynamics in hadronic processes
[DE85-006072] 14 p2418 N85-24922
Experimental methods of heavy quark detection
[DE85-006316] 17 p3036 N85-28781
Control technology for radioactive emissions to the atmosphere at US Department of Energy facilities: The Los Alamos Meson Physics Facility
[DE85-011402] 22 p3811 N85-33609
Annihilation radiation in cosmic gamma-ray bursts
[OG-1.1-3] 22 p3861 N85-33905
Unthermalized plasma in bursts sources
[OG-1.1-5] 22 p3861 N85-33907
Neutrino-antineutrino annihilation around collapsing star
[OG-1.1-10] 22 p3861 N85-33911
Diffuse galactic annihilation radiation from supernova nucleosynthesis
[OG-3.2-8] 22 p3875 N85-34004
Galactic cosmic ray antiprotons and supersymmetry
[OG-6.1-9] 22 p3888 N85-34100

ANNUAL VARIATIONS
Predictor model for seasonal variations in skid resistance, volume 1
[PB84-226612] 01 p0036 N85-10229
Predictor model for seasonal variations in skid resistance. Volume 2: Comprehensive report
[PB84-226620] 01 p0037 N85-10230
The climate of Denmark. Summaries of observations from light vessels. 3: Sea temperature
[ISBN-87-7478-215-0] 01 p0073 N85-10481
Return wave heights off South Uist estimated from seven years of data
[IOS-164] 01 p0089 N85-10601
Observations of the pulsating hydrogen: Deficient star BD+13 deg 3224, during 1980 - 1981 01 p0128 N85-10682
Remote sensing as a mineral prospecting technique
[E85-10010] 02 p0216 N85-11423
Northern Hemisphere atlas of 1-minute rainfall rates
[AD-A145411] 02 p0231 N85-11508
Seasonal variations in Triton's atmospheric mass and composition 02 p0301 N85-11948
Seasonal variations of reflexibility and transmissibility of ULF waves propagating through the ionosphere of geomagnetic mid-latitudes
[REPT-560] 03 p0376 N85-12403
On the annual and semiannual variation of S sub R at l'Aquila --- geomagnetism 04 p0520 N85-13326
On some new features of semiannual variation of the geomagnetic field 04 p0520 N85-13327
Image texture study for the operational meteorological satellites NOAA 6 and NOAA 7 and its variation with time. Application to the Beauce region
[ENST-84E009] 05 p0661 N85-14249
Solar pond research at Argonne National Laboratory 05 p0667 N85-14291
Interannual variability in the observed circulation 05 p0686 N85-14409
The influence of synoptic scales on low-frequency modes of variability 05 p0687 N85-14412
Annual energy spectrum for tracking arrays 06 p0832 N85-15297
Monthly and seasonal climatology over the global tropics and subtropics for the decade 1973 to 1983. Volume 1: 200 mb winds
[AD-A146521] 06 p0838 N85-15322

Diurnal and seasonal patterns of temperature and wind flow in the planetary boundary layer for ten locations in complex terrain
[PB85-106606/GAR] 08 p0840 N85-15333
Satellite definition of the bio-optical and thermal variation of coastal eddies associated with the African current
[AD-A147910] 07 p0969 N85-16282
The problem of climate and climate variation
07 p1001 N85-16353
Evaluation of the climatic resources of Cuba applied to agricultural work 07 p1004 N85-16360
The use of hydrometeorological data in explaining shrimp cycles in Guyana 07 p1004 N85-16361
Interrelationship of atmospheric parameters in Honduras
[AD-A147371] 07 p1007 N85-16401
North American vegetation patterns observed with the NOAA-7 advanced very high resolution radiometer — North America
[E85-10062] 08 p1174 N85-17400
Regional and seasonal variations in snow-cover density in the USSR
[AD-A148429] 08 p1189 N85-17496
The atmospheric extinction problem
08 p1251 N85-17901
An analysis of the seasonal variations in the water vapor transport fields over the Southern Hemisphere
09 p1356 N85-18531
Weather data for simplified energy calculation methods. Volume 3: Western United States: TRY data
[DE85-000495] 09 p1358 N85-18540
Calculation of optical characteristics of shelf ecological system based on its mathematical model
10 p1496 N85-19453
Growth and reflectance characteristics of winter wheat canopies
[E85-10080] 10 p1505 N85-19494
Study of low energy density photovoltaic applications under varying rate structures
[DE85-000185] 10 p1511 N85-19538
Sequential precipitation chemistry sampling program at Brookhaven National Laboratory with an analytical summary of 1976-1982 data
[DE85-002786] 10 p1513 N85-19545
Interannual variations of the winter circulation in the Northern Hemisphere and in the southern oscillation (meridian) and their possible connections with the climate of Northeast Brazil
[INPE-3333-TDL/182] 10 p1519 N85-19573
Cut-off lows and their influence on the weather in Switzerland
[REPT-45] 10 p1519 N85-19574
The Middle Atmosphere Program: Winter in Northern Europe (MAP/WINE) 11 p1655 N85-20429
Autumn and winter anomalies in ionospheric absorption as measured by riometers 11 p1660 N85-20460
A model of the influence of neutral air dynamics on the seasonal variation in the low ionosphere
11 p1660 N85-20462
Explanation of the normal winter anomaly from the seasonal variation of short wave absorption
11 p1660 N85-20463
Seasonal characteristics of mesospheric plasma and their transitions 11 p1660 N85-20464
Spring changeover of the middle atmosphere circulation compared with rocket wind data up to 80 km
11 p1661 N85-20466
Monthly and seasonal weather outlook for October 1984, volume 38, number 19, 29 September 1984
[PB85-113536] 11 p1687 N85-20610
OSCAR experiment high-density network data report
[DE85-004907] 12 p1884 N85-21626
The effect of stochastic surface heat fluxes on the climatology of the seasonal thermocline
[AD-A149957] 12 p1889 N85-21857
Solar-geophysical data number 479, July 1984. Part 1: (Prompt reports). Data for June 1984, May 1984 and later data
[NASA-CR-175542] 12 p1962 N85-22333
Empirical and modeled synoptic cloud climatology of the Arctic Ocean
[NASA-CR-175628] 13 p2137 N85-23272
Seasonal and secular variation of the Solis Lacus albedo feature: Relation to the Martian dust-transport cycle
13 p2188 N85-23576
Water-ice clouds on Mars: Location and seasonal variation 13 p2194 N85-23611
The Tropical Ocean and Global Atmosphere program (TOGA) 14 p2330 N85-24411
Small component spectral model of annual course of zonal atmospheric circulation 14 p2337 N85-24453
Ionspheric effects of seasonal and diurnal variations of electric fields in equatorial F-region
14 p2338 N85-24459
Diurnal variations in terrestrial magnetic field and structure of magnetosphere 14 p2344 N85-24493
MAP3S precipitation chemistry network
[DE85-005324] 14 p2353 N85-24539
Monthly and Seasonal Weather Outlook for mid-December 1984 mid-January 1985, volume 38, number 24, 14 December 1984
14 p2379 N85-24687
Analysis of hydrometeorological conditions in Antarctic coastal waters according to data from hydrological and satellite observations 15 p2487 N85-25354
Development of algorithms for using satellite meteorological data sets to study global transport of stratospheric aerosols and ozone
[NASA-CR-172540] 15 p2591 N85-25974
Annual cycle. Part 1: The annual variation of surface temperatures over the United States and Canada
[PB85-147676] 15 p2600 N85-26026
Annual cycle. Part 2: The annual variation of precipitation over the United States and Canada
[PB85-147684] 15 p2600 N85-26027
Oceanographic variations in recent decades and their impact on the fertility of the Iceland Sea
15 p2602 N85-26034
Mars: Seasonally variable radar reflectivity
15 p2683 N85-26570
Year-to-year variability of components of Earth's radiation budget according to satellite measurement data 16 p2725 N85-26821
The seasonal cycle of atmospheric CO in the Southern Hemisphere 16 p2830 N85-27447
Fog advection in the Namib 16 p2831 N85-27454
Air flow of the western coastal boundary of South Africa and its influence on the ocean 16 p2831 N85-27459
Forecast of Atlantic seasonal hurricane activity for 1985 16 p2833 N85-27470
AWS (Air Weather Service) climatic briefs: North America
[AD-A152161] 16 p2835 N85-27483
Solar-Geophysical Data Number 484, December 1984. Part 1 (prompt reports): Data for November 1984, October 1984 and late data
[NASA-CR-175629] 16 p2888 N85-27819
Precipitation and snow cover data, 1977
[ISBN-951-697-215-2] 17 p2995 N85-28514
Observations of surface water temperature in the Netherlands since 1860: Statistics
[KNMI-WR-84-3] 17 p2997 N85-28531
Observations of surface water temperature in the Netherlands since 1860: Tables for light vessels
[KNMI-WR-84-4] 17 p2998 N85-28532
Observations of surface water temperature in the Netherlands since 1860: Series from KNMI-RWS
[KNMI-WR-84-5] 17 p2998 N85-28533
Measurements of VHF/UHF radio propagation in a maritime temperate climate
[CRC-1380] 18 p3089 N85-29119
Permafrost, seasonally frozen ground, snow cover and vegetation in the USSR
[AD-A153628] 18 p3124 N85-29346
The seasonal cycle of storminess as measured by band-pass fluctuations 18 p3144 N85-29467
The contrasting Northern Hemisphere winters of 1980-81 and 1981-82 18 p3144 N85-29468
Monthly and seasonal weather outlook for mid-February to mid-March 1985, volume 39, number 4, February 14, 1985
[PB85-164580] 18 p3149 N85-29500
Application of climatological analysis to minimize air pollution impacts in California
[PB85-172963] 18 p3149 N85-29502
The influence of global dust storms on the mean seasonal daily insolations at the Martian surface
[AERONOMICA-ACTA-A-289-1984]
18 p3203 N85-29868
Categorization of nocturnal drainage flows within the Brush Creek valley in western Colorado and the variability of sigma theta in complex terrain
[DE85-011291] 19 p3300 N85-30461
Calibration of relevant measuring sensors
[DE85-009820] 19 p3306 N85-30492
Tropical ozone: Seasonal variations in the troposphere at 6 deg S
[INPE-3555-PRE/766] 19 p3313 N85-30535
Atmospheric cross sections for the Arctic gas and aerosol sampling program, March - April 1983
[NASA-CR-176027] 19 p3314 N85-30541
On the dynamical climatology of the Amazon Basin and associated rain producing mechanisms
[INPE-3531-RPE/477] 19 p3315 N85-30552
Northeast Brazil droughts and Atlantic SST anomalies
[INPE-3538-PRE/754] 19 p3316 N85-30553
On the interannual variability of the Indian monsoon and the Southern Oscillation 20 p3495 N85-31728
The worldwide distribution of the seasonal cycle of mean sea level
[IOS-190] 20 p3497 N85-31743
Insolation changes on Pluto caused by orbital element variations
[AERONOMICA-ACTA-A-290-1984]
20 p3546 N85-32070
Trace element concentrations in atmospheric aerosol over Hungary 21 p3646 N85-32652
Chemical composition of atmospheric aerosol at Delhi
21 p3646 N85-32653
The variability of aerosol microstructure in continental and oceanic surface layers of the atmosphere in anticyclones 21 p3647 N85-32660
Numerical modeling of sea ice dynamics and ice thickness characteristics
[AD-A154600] 21 p3654 N85-32700
Comparisons of the North Polar Cap of Mars and the Earth's Northern Hemisphere snow cover
[NASA-TM-86191] 23 p3989 N85-34728
Characteristics of cosmic ray pole-equator anisotropy derived from spherical harmonic analysis of neutron monitor data
[SH-4.3-12] 23 p4032 N85-34996
Cosmic ray intensity distribution perpendicular to solar equatorial plane at 1 A.U. during 1978-83
[SH-4.3-14] 23 p4032 N85-34998
The corotating variation of the north-south anisotropy of cosmic rays
[SH-4.3-15] 23 p4033 N85-34999
Cosmic ray intensity variations observed at Matsushiro (220 M.W.E. in depth)
[SH-4.4-9] 23 p4034 N85-35007
Cosmic ray biannual variation
[SH-4.4-15] 23 p4034 N85-35011
Cosmic ray modulation by high-speed solar wind fluxes
[SH-5.1-22] 23 p4044 N85-35074
The influence of quiet asymmetric magnetosphere on the cutoff rigidities of the main cone
[SH-6.1-10] 23 p4045 N85-35083
A possible mechanism to cause the quasi-biennial variability on the solar neutrino flux
[SH-8.1-5] 23 p4049 N85-35110
Subseasonal variability in a two-level atmospheric general circulation model 24 p4114 N85-35504

ANNULAR DUCTS

Stall elimination and restart enhancement device
[AD-D011217] 01 p0010 N85-10062
Unsteady free-convection heat transfer inside an annular cavity
[CFD/84/16] 08 p1163 N85-17339
High-pressure rocket engine turnaround duct computational fluid dynamics analysis
13 p2003 N85-22556

ANNULAR FLOW

Characteristics of controlled-oscillating annular cascade test facility with Freon gas
[NAL-TR-812] 01 p0003 N85-10014
Stability of fluid flow in a cylindrical annulus
[NASA-TM-77720] 01 p0046 N85-10300
Identification of dynamic coefficients of annular turbulent seals 05 p0644 N85-14133
Analysis and testing for rotordynamic coefficients of turbulent annular seals with different, directionally homogeneous surface-roughness treatment for rotor and stator elements 05 p0644 N85-14134
Analysis for leakage and rotordynamic coefficients of surface roughened tapered annular gas seals
05 p0644 N85-14135
An improved computer model for prediction of axial gas turbine performance losses
[NASA-CR-174246] 07 p0904 N85-15724
Unsteady free-convection heat transfer inside an annular cavity
[CFD/84/16] 08 p1163 N85-17339
Determination of total pressure losses in stepped annular diffusors with curvilinear outer walls and uniform velocity field at inlet 09 p1306 N85-18203
An experimental study of aerodynamic damping characteristics of a compressor annular cascade in high speed flow and the visualization of annular cascade flow
[NAL-TR-838] 15 p2554 N85-25759
Flow visualization study of inverted annular flow of post dryout heat transfer region
[DE85-010482] 19 p3269 N85-30275

ANNULAR NOZZLES

Experimental investigation of shock-cell noise reduction for single stream nozzles in simulated flight
[NASA-CR-3845] 04 p0557 N85-13550

ANNULI

Birkhoff orbits for non-monotone twist maps
[AD-A144718] 01 p0110 N85-10747

ANODES

NT CELL ANODES
NT SHELL ANODES
NT TUBE ANODES
Advanced fuel cell development
[DE84-014847] 01 p0044 N85-10289

The driving-force dependence of electrochemical rate parameters: Origins of anodic-cathodic asymmetries for metal aquo redox couples
[AD-A145605] 02 p0172 N85-11153
Oxygen diffusion from anodic surface oxide films on titanium subhydride studies by auger electron spectroscopy and electron energy loss spectroscopy
[DE84-016942] 04 p0572 N85-13648
Behaviour of lead-silver anodes in zinc electrodeposition from sulphuric acid baths
[BLL-MINTEK-TR-1180-(5810.5759)] 06 p0764 N85-14887
The anode mechanism of a thermal argon arc
[NASA-TM-77754] 07 p0921 N85-15835
The development and test of ultra-large-format multi-anode microchannel array detector systems
[NASA-CR-174247] 07 p1043 N85-16822
Electrochemistry at very high potentials: The use of ultramicroelectrodes in the anodic oxidation of short chain alkanes
[AD-A148654] 08 p1123 N85-17078
Photometry with Multi-Anode Microchannel Arrays (MAMAs) and Charge Injection Devices (CIDs) 08 p1252 N85-17909
Thermal investigation of an electrical high-current arc with porous gas-cooled anode
[NASA-TM-77789] 11 p1627 N85-20245
Development of a low cost electrochemical CO monitor based on anodic scanning voltammetry in nonaqueous electrolyte
[PB85-113488] 11 p1637 N85-20314
Alternative anodic reactions in water splitting
[DE85-004159] 12 p1802 N85-21300
Review of anode phenomena in vacuum arcs
[DE85-002736] 12 p1926 N85-22101
Application of modulated hydrodynamic voltammetry to the study of anodic electrocatalysis
[DE85-004182] 13 p2018 N85-22653
Molten carbonate fuel cell performance model update, draft
[DE85-005423] 13 p2129 N85-23252
Oxygen evolution on NiCo2O4 electrodes 17 p2924 N85-28026
Bifunctional oxygen electrodes
[DE85-006871] 17 p2955 N85-28248
Streak tube characterization
[DE85-009874] 17 p2956 N85-28255
Molten carbonate fuel cell performance model update
[DE85-003356] 17 p2986 N85-28454
Spectrographic investigation of low-voltage arc discharge in argon atmosphere
[BLL-M-36276-(5828.4)] 20 p3422 N85-31242
Method of production of metals by cathodic solution of their compounds in electrolytic cells
[BLL-OA-TRANS-3207-(6198.300)] 20 p3429 N85-31266
Deposition of nickel-cobalt alloys by controlled-potential electrolysis
[PB85-198562] 24 p4081 N85-35291

ANODIC COATINGS

Influence of parameters of aluminum alloy anodizing process on oxide coating thickness 01 p0018 N85-10113
Effects of introduction of alkyl groups into aluminium anodized coatings
[DRIC-T-7244] 03 p0331 N85-12133
Wear of anodic oxide films on aluminum alloys in cryogenic liquids
[NAL-TR-818] 06 p0768 N85-14914
Method for bonding insulator to insulator
[AD-D011340] 07 p0929 N85-15891
Improved ceramic anodes for corrosion protection
[AD-A149492] 10 p1452 N85-19149
Effect of mill run and temper variations on barrier anodic film format ion on 6061 aluminum alloy
[DE85-000447] 11 p1608 N85-20112
Resistance of polyaniline films as a function of electrochemical potential and the fabrication of polyaniline-based microelectronic devices
[AD-A154999] 21 p3569 N85-32201

ANODIC STRIPPING

Microprocessor-controlled anodic stripping voltammeter for trace metal analysis in tap water
[DE85-002781] 12 p1852 N85-21619

ANODIZING

Effect of mill run and temper variations on barrier anodic film format ion on 6061 aluminum alloy
[DE85-000447] 11 p1608 N85-20112
Corrosion characteristics of some steels produced through a self-cleaning rotating electrode
[BLL-BISI-TRANS-22046-(9022.06)] 17 p2925 N85-28034
Electrolytic synthesis of colored eta alumina film 23 p3906 N85-34201

ANOMALIES

NT GEOMAGNETIC HOLLOW
NT GEOTHERMAL ANOMALIES
NT GRAVITY ANOMALIES
NT MAGNETIC ANOMALIES

The de Tifini star pointer characterization and conclusions on the 1982 transmediterranean flight
[CESR-83-1070] 02 p0139 N85-10946
Systematic data interpretation of remote sensing in the reception of hydrocarbons, volume 1
[E85-10008] 02 p0215 N85-11421
Remote sensing as a mineral prospecting technique
[E85-10010] 02 p0216 N85-11423
Digital Terrain Elevation Data (DTED) anomaly removal through the use of an interactive Fourier frequency filtering process
[AD-A145433] 02 p0219 N85-11445
Anomalies in frequency characteristics of solid-state ring laser 02 p0271 N85-11765
Anomalon search — heavy cosmic ray interactions
[NOTA-INTERNA-825] 02 p0305 N85-11970
The winter anomaly in ionospheric absorption (with special reference to the results obtained in Spain) 04 p0522 N85-13338
Possible anomaly prediction system for the middle atmosphere — ionospheric absorption 04 p0522 N85-13339
Heat sources in the tropics and large scale flow anomalies associated with precipitation anomalies in northeast Brazil
[INPE-3211-TDL/175] 04 p0538 N85-13421
Kohn anomaly in metastable fcc lanthanum at low temperatures
[DE84-015459] 04 p0569 N85-13628
Implications of the chiral anomaly for quantum Hall effect devices
[NUB-2662] 05 p0629 N85-14029
Diagnostics of rainfall anomalies in the nordeste during the global weather experiment 05 p0685 N85-14405
Linear studies of stationary, extratropical anomalies in the troposphere 05 p0686 N85-14410
Unexplained Fe, Ni and S anomalies in CV chondrite components 06 p0884 N85-15618
Chemical evolution of the solar nebula: A new model 06 p0887 N85-15631
Statistical filtering as method for detecting transcrustal acoustic anomalies 07 p0982 N85-16237
Ocean and climate, an example. The interannual variability of the tropical Pacific Ocean 07 p1002 N85-16365
Climate and fisheries: A Peruvian case study 07 p1003 N85-16373
The 500 millibar sign frequency teleconnection charts: Winter
[PB85-106276/GAR] 07 p1009 N85-16410
Solid rocket motor certification to meet space shuttle requirements from challenge to achievement 08 p1098 N85-16941
An investigation of ionospheric irregularity effects on SIR-B image processing and information extraction 08 p1149 N85-17247
Droughts and floods in South America due to the 1982-83 El Nino-southern oscillation episode
[INPE-3408-PRE/677] 09 p1357 N85-18535
Acoustic tomographic reconstrution of anomalies in three-dimensional bodies
[DE84-017035] 09 p1378 N85-18666
Nonlinear seismology 10 p1503 N85-19482
Recent investigations at INPE in magnetospheric physics and geomagnetism
[INPE-3280-PRE/603] 10 p1514 N85-19555
Planetary scale circulation anomalies associated with droughts over northeast Brazil
[INPE-3351-PRE/630] 10 p1518 N85-19570
Large scale circulation anomalies and prediction of northeast Brazil droughts
[INPE-3405-PRE/674] 10 p1518 N85-19571
Winter anomaly of the lower ionosphere and its possible causes 11 p1660 N85-20459
Winter anomaly 1982/83 in comparison with earlier winters (1960-82) 11 p1660 N85-20461
Explanation of the normal winter anomaly from the seasonal variation of short wave absorption 11 p1660 N85-20463
Dependence of the high latitude middle atmosphere ionization on structures in interplanetary space 11 p1664 N85-20487
Interacting binary systems 11 p1744 N85-20967
Workshop on Remote Sensing/Lineament Applications for Energy Extraction
[DE84-009291] 12 p1875 N85-21763
Moisture variation in northern hemisphere temperate latitudes 13 p2105 N85-23119
El Nino, the capricious child 13 p2106 N85-23121
Diurnal variations in terrestrial magnetic field and structure of magnetosphere 14 p2344 N85-24493
Temperature anomalies above ore bodies 14 p2345 N85-24500
A study of terrain reductions, density anomalies and geophysical inversion methods in gravity field modelling
[AD-A150788] 14 p2373 N85-24868
Real-time enhancement of a climatology or forecast of ocean thermal structure using observed ocean temperatures
[AD-A151118] 15 p2804 N85-26049
On geoid heights and flexure of the lithosphere at seamounts
[AD-A151220] 15 p2804 N85-26050
A spectacular nitrogen isotope anomaly in Bencubbin 15 p2883 N85-26589
Effect of nickel addition on the thermal, magnetic and magnetomechanical properties of Fe(80)B(15)Si(5)
[AD-A152281] 16 p2749 N85-26967
Quasi stationary states in the Southern Hemisphere 16 p3144 N85-29466
Northeast Brazil droughts and Atlantic SST anomalies
[INPE-3538-PRE/754] 19 p3316 N85-30553
The nature of the anomalies on the polytherms of the properties of molten metallic alloys
[BLL-M-36265-(5828.4)] 20 p3430 N85-31277
Short meridional scale anomalies in the lower stratosphere and upper troposphere 20 p3489 N85-31684
Dynamic compensation of Venus's geoid: A comparison with Earth 22 p3858 N85-33688
Anomalous abundances of solar energetic particles and coronal gas: Coulomb effects and First Ionization Potential (FIP) ordering
[SH-2.1-10] 23 p3999 N85-34791
Search for anomalous C-jets in Chacaltaya emulsion chamber experiment
[HE-3.2-5] 24 p4179 N85-35913
Anomalous correlation between hadron and electromagnetic particles in hadron and gamma-ray families
[HE-3.3-6] 24 p4180 N85-35924
Anomalies in cosmic rays: New particles versus charm?
[HE-5.4-9] 24 p4208 N85-36120

ANOMALOUS TEMPERATURE ZONES

Thermal energy resources of thermal waters in Kazakhstan 06 p0820 N85-15208
Temperature anomalies above ore bodies 14 p2345 N85-24500
A GCM study of the atmospheric response to tropical SST anomalies 18 p3148 N85-29477

ANORTHOSITE

Particle velocity experiments in anorthosite and gabbro
[NASA-CR-174158] 04 p0533 N85-13407
Primordial magmaspheres and their lasting consequences 22 p3857 N85-33882

ANOXIA

Armed forces special Symposium on Medicine of Altitudes 13 p2166 N85-23441

ANTARCTIC ENVIRONMENT

U ICE ENVIRONMENTS

ANTARCTIC REGIONS

NT ROSS ICE SHELF

South African Antarctic research report to SCAR, no. 24, 1982. 1: Record of activities: April 1981 - September 1982. 2: Planned activities: October 1982 - September 1983. 3: Recent publications: 1981/1982
[CSIR-SR-SCAR-24] 01 p0063 N85-10417
Sea ice data buoys in the Weddell Sea
[AD-A144953] 01 p0068 N85-10594
Marine geological and geophysical investigations of the Antarctic Continental Margin, 1984
[GS-CIRC-935] 02 p0212 N85-11400
MIZEX. A program for mesoscale air-ice-ocean interaction experiments in arctic marginal ice zones. III: Modeling the marginal ice zone
[AD-A145351] 02 p0233 N85-11517
Feasibility of long duration ballooning in Antarctica
[PB84-240571] 04 p0541 N85-13443
Report on United States Antarctic research activities, February 1983 - October 1984 and United States Antarctic research activities planned for October 1984 - September 1985
[PB84-231265] 05 p0677 N85-14352
Environmental data inventory for the antarctic area
[PB85-107944] 06 p0819 N85-15195
USSR report: Earth sciences
[JPRS-UES-84-007] 06 p0819 N85-15196
Surging as a potential response of ice sheets to CO2-induced changes in the polar environment (SPICAE)
[DE84-016472] 06 p0841 N85-15341
Peculiar spherules from Antarctica and their origin 06 p0863 N85-15612
Meteorite concentrations in Antarctica: How complete is the picture? 06 p0889 N85-15844

Earth science investigations in the United States Antarctic Research Program (USARP)
[PB84-240506] 07 p0990 N85-16286
The viability climatology of McMurdo Sound-Williams Field, Antarctica
[AD-A148108] 08 p1189 N85-17492
Survey of VLF-OMEGA transmissions received during summer at Antarctic peninsula
[INPE-3369-PRE/666] 10 p1462 N85-19223
USSR report: Earth sciences
[JPRS-UES-85-003] 10 p1497 N85-19446
Brazil future plans in upper atmosphere research in Antarctica
[INPE-3400-PRE/669] 10 p1515 N85-19559
Some aspects of atmospheric circulation near South America and interactions with the Antarctic regions
[INPE-3308-PRE/618] 10 p1515 N85-19561
MAP in Japan: Organization and projects
11 p1655 N85-20425
The Middle Atmosphere Program: A special project for the Antarctic Middle Atmosphere (AMA)
11 p1656 N85-20430
Proceedings of a Workshop on Environment of West Antarctica: Potential CO2-induced changes
[PB85-110757] 11 p1671 N85-20527
Los Alamos MINI-Review: Tracking Antarctic winds
[DE85-004597] 12 p1896 N85-21903
USSR report: Earth sciences
[JPRS-UES-85-002] 13 p2105 N85-23116
Antarctic glaciation, or what are catastrophes in Earth's history
13 p2105 N85-23118
China report: Science and technology
[JPRS-CST-85-003] 13 p2166 N85-23433
Planetary analogs in Antarctica: Mars
13 p2193 N85-23604
Planetary analogs in Antarctica: Icy satellites
13 p2193 N85-23605
Chemical weathering of soils from the dry valleys of Antarctica: A terrestrial analog of Martian weathering processes
13 p2197 N85-23628
The use of the ARGOS system for the study of the drift of Antarctic icebergs
14 p2240 N85-23890
Automatic weather stations in Antarctica
14 p2324 N85-24360
Main features of Antarctic Ocean circulation as revealed by satellite tracking of icebergs
14 p2325 N85-24372
Atmosphere ice-ocean interactions in the Antarctic (IAGO)
14 p2326 N85-24375
Antarctic automatic weather stations
14 p2329 N85-24397
Plans for adaptation research during Antarctic expedition
14 p2333 N85-24426
Results of comparison of long-wave radiation fluxes measured by Soviet and Japanese actinometric radiosounds
14 p2333 N85-24427
Observations of the MF-HF plasma wave emissions in active auroras by the sounding rocket experiments at Syowa station
14 p2366 N85-24620
VLF wave-particle interaction experiments by EXOS-B/Siple station transmissions
14 p2366 N85-24622
Whistler mode waves near the plasmapause: Results from the IMS VLF experiment at Halley, Antarctica
14 p2367 N85-24626
Designer O. K. Antonov on new AN-74 arctic transport
15 p2467 N85-25230
Analysis of hydrometeorological conditions in Antarctic coastal waters according to data from hydrological and satellite observations
15 p2467 N85-25354
North Atlantic Deep Water formation: Information from ice cores
15 p2602 N85-26035
USSR report: Earth sciences
[JPRS-UES-85-005] 16 p2807 N85-27307
Atmospheric radon measurements in the Antarctic Peninsula: A preliminary report
[INPE-3398-PRE/667] 16 p2827 N85-27456
Information relative to cartography and geodesy. Series 2: Translations, Number 42, Volume 2 — maps
[ISSN-0489-4244] 18 p3123 N85-29337
Digital image mapping of Antarctica using NOAA-7 AVHRR imagery
18 p3124 N85-29340
German contributions to the cartography of Antarctica by means of photogrammetry and remote sensing
18 p3124 N85-29342
Microbial ecology of extreme environments: Antarctic yeasts and growth in substrate-limited habitats
[NASA-CR-176005] 19 p3326 N85-30609
Antarctica
[S-HRG-86-1181] 20 p3473 N85-31584
Petroleum and mineral resources of Antarctica
[US-GEOL-SURV-CIRC-909] 20 p3477 N85-31605
Use of the synoptic view: Examples from Earth and other planets
21 p3602 N85-32371
Aerosol formation by wave action over Ross Sea, Antarctica
21 p3651 N85-32688

ANTARCTICA
U ANTARCTIC REGIONS
ANTENNA ARRAYS
NT LINEAR ARRAYS
NT STEERABLE ANTENNAS
Nowcasting using lightning location techniques
01 p0084 N85-10568
Recursive algorithms for adaptive arrays based on estimates
[REPT-5-84] 01 p0107 N85-10718
The study of microstrip antenna arrays and related problems
[NASA-CR-174054] 02 p0189 N85-11265
Possibility of realization of highly-directional antenna arrays
03 p0344 N85-12220
A dynamical model for a towed linear sonar antenna
[REPT-6-84] 04 p0512 N85-13263
Modern radioastronomical aperture synthesis systems (review)
06 p0782 N85-14997
Phase problem in aperture synthesis systems
06 p0782 N85-15002
Synthesis of zeros in radiation pattern of linear antenna array
06 p0784 N85-15015
Remote sounding of fields in feed radiators of multi-element antenna system with allowance for interaction with sounding device
06 p0790 N85-15047
Characteristics of circular-polarized printed radiators in planar phased antenna array
06 p0790 N85-15049
Investigation of characteristics of phased antenna array considering interaction between radiators and properties of power divider
06 p0790 N85-15051
Scattering matrix of antenna array with Joule losses in radiators
06 p0791 N85-15053
Characteristics of two-frequency combined dipole antenna arrays
06 p0791 N85-15055
Peculiarities of microprocessor implementation of algorithms for processing radio signals and noise in large antenna arrays
06 p0792 N85-15059
Characterization of MMIC devices for active array antennas
[NASA-TM-86907] 07 p0913 N85-15779
Array sidelobes, error tolerance, gain, and beamwidth
[AD-A147004] 07 p0940 N85-15956
Parallel processor configuration for adaptive antenna arrays
[AD-D011347] 07 p0942 N85-15970
Basic research in electronic (JSEP): Joint Services Electronics Program
[AD-A147891] 07 p0948 N85-16007
Use of shanks transformation for speeding up adaptation process in antenna arrays
07 p0951 N85-16029
Analysis of effectiveness of partial optimization of spatial processing systems
07 p0952 N85-16031
Determination of row-and-column control principle of phase antenna array from amplitude-phase distribution of field in aperture
07 p0952 N85-16033
Infrared technology for satellite power conversion — antenna arrays and bolometers
[NASA-CR-174266] 07 p0991 N85-16293
Dual mode radio frequency-infrared frequency system
[AD-D011402] 08 p1081 N85-16850
Adaptive antenna arrays for weak interfering signals
[NASA-CR-174336] 08 p1150 N85-17258
Spaceborne distributed SAR antenna
[NASA-CR-171835] 08 p1150 N85-17259
Millimeter wave antenna technology
[AD-A146694] 08 p1155 N85-17291
Partial reflection spaced antenna wind measurements
08 p1185 N85-17467
Broad-band UHF dipole array
[NASA-TM-86373] 10 p1462 N85-19222
Condensed antenna structural models for dynamics analysis
10 p1463 N85-19230
Conformal phased array antenna pattern corrector
[AD-D011489] 10 p1468 N85-19266
Overview of RADC adaptive antenna developments for communications
10 p1474 N85-19299
Interleaved array antenna technology development
[NASA-CR-171845] 10 p1477 N85-19326
Research on adaptive antenna techniques 6
[AD-A149341] 11 p1624 N85-20228
Multiple loop sidelobe canceller
[AD-D011533] 12 p1823 N85-21434
Method and apparatus for self-calibration and phasing of array antenna
[NASA-CASE-NPO-15920-1] 12 p1832 N85-21493
Wide angle phased array dome lens antenna with a reflection/transmission switch
[AD-D011562] 12 p1833 N85-21502
Phased antenna array for wind profiling applications
[PB85-132884] 12 p1837 N85-21529
KAM-250 antenna switch
13 p2068 N85-22916
Studies of galactic HI in 21-centimeter absorption
13 p2170 N85-23466
Microstrip comb array design
[R-NIAS-24] 14 p2290 N85-24195
An examination of signal-to-noise enhancement at the Edzell CDAA (Circular Disposed Antenna Array)
[AD-A150708] 14 p2291 N85-24204
Noise cancellation using adaptive arrays
[AD-A150721] 14 p2292 N85-24206
Interference immunity of optical radar system with phased antenna array
15 p2526 N85-25575
Cophasal horizontal wideband array antennas for transmitting with asymmetric output
15 p2526 N85-25576
Design and swept-frequency measurement of printed circuit board log-periodic dipole arrays
[R-NIAS-23] 15 p2539 N85-25671
Mobile antenna and beam pointing studies for satellite mobile communications
[NASA-CR-175736] 15 p2540 N85-25679
Trade-off between land vehicle antenna cost and gain for satellite mobile communications
[NASA-CR-175732] 15 p2540 N85-25681
Land vehicle antennas for satellite mobile communications
[NASA-CR-175735] 15 p2540 N85-25682
A study of computational techniques for nonconanical microstrip antennas and arrays
[AD-A152216] 16 p2774 N85-27123
Performance analysis of the DSN baseband assembly (Bba) Real-Time Combiner (RTC)
[NASA-CR-175878] 17 p2946 N85-28190
Performance analysis of the DSN baseband assembly (Bba) Real-Time Combiner (RTC)
[NASA-CR-175877] 17 p2947 N85-28193
Adaptive nulling at HF using a compact array of active parasitic antennas
[AD-A152582] 17 p2948 N85-28203
Two-degree-of-freedom linear and planar microwave array lenses
[AD-A153701] 18 p3095 N85-29156
Computer simulation of the effects of a distributed array antenna on synthetic aperture radar images
[NASA-CR-171866] 19 p3254 N85-30176
Theoretical investigation of single-frequency 8-element localizer signal scattering for critical area determination
[FAA-PM-85-4] 20 p3391 N85-31037
Antenna pointing of large flexible telecommunications spacecraft
20 p3409 N85-31156
Phase synchronizing large antenna arrays using the spatial correlation properties of radar clutter
20 p3439 N85-31344
ECM multiple-target retrodirective antenna
[AD-D011528] 20 p3439 N85-31346
New concepts in free electron lasers
20 p3460 N85-31493
New VLBI technology developments
20 p3491 N85-31702
Null synthesis with phase and amplitude controls at the subarray outputs
[AD-A155187] 21 p3576 N85-32241
Evaluation of the effects of roll angle on the natural convection heat transfer from an array of cylindrical spines
[AD-A154594] 21 p3583 N85-32273
A simple model for testing the effects of gravity-wave-produced vertical oscillations of scattering irregularities on spaced-antenna, horizontal drift measurements
21 p3619 N85-32469
Criteria for optimum spacing of spaced antenna, part 3.2A
21 p3620 N85-32491
Increase of antenna area instead of transmitter power, part 6.3A
21 p3624 N85-32517
Summary of progress at the Poker Flat Observatory in Alaska
21 p3626 N85-32539
Radio telescope with 256 antennas built in Siberia
22 p3732 N85-33136
Digital holographic systhesis of pattern-forming transparencies for ring antenna arrays
22 p3783 N85-33326
Adaptive synthesis of antennas with separation of signals by direction of arrival
22 p3764 N85-33328
USSR report: Electronics and electrical engineering
[JPRS-UEE-84-003] 22 p3773 N85-33361
Frequency independent parabolic phased antenna array of log periodic antennas
22 p3774 N85-33367
Minimizing field scattered by slender dipoles
22 p3774 N85-33368
Adaptive antenna arrays for satellite communications: Design and testing
[NASA-CR-176162] 23 p3926 N85-34329
A planar version of a 4.0 gigahertz reactively steered adaptive array
[AD-A156029] 24 p4067 N85-35330
Signal space models for antenna arrays
[AD-A156063] 24 p4067 N85-35335

Theory of mutual impedances and multiple reflections in an N-element array environment
[PB85-191419] 24 p4092 N85-35364
ANTENNA COMPONENTS
NT ANTENNA COUPLERS
NT ANTENNA FEEDS
NT DIRECTIONAL COUPLERS
Invariance of mean-square effective area of synthesized apertures 06 p0784 N85-15009
Antenna matching device tuning for type ZhRU radiostations 06 p0785 N85-15017
Characterization of MMIC devices for active array antennas
[NASA-TM-86907] 07 p0913 N85-15779
Feasibility study for a 34 GHz (Ka band) gyroamplifier
[NASA-CR-174439] 10 p1477 N85-19325
The 60 GHz antenna system analyses for intersatellite links, phase A
[NASA-CR-175285] 12 p1823 N85-21439
Deployable folded antenna apparatus
[AD-D011503] 12 p1832 N85-21495
System of light protection of antenna-mast structures of radio-relay lines 15 p2527 N85-25583
Two-degree-of-freedom linear and planar microwave array lenses
[AD-A153701] 18 p3095 N85-29156
A simplified GPS C/A reciever front end with low noise performance 18 p3109 N85-29251
ANTENNA COUPLERS
NT COUPLING CIRCUITS
NT DIPLEXERS
NT DIRECTIONAL COUPLERS
Hardwire missile receiver coupler
[AD-D011350] 07 p0937 N85-15936
Mutual coupling analysis for conformal microstrip antennas 20 p3439 N85-31343
ANTENNA DESIGN
A generalized solution to a class of printed circuit antennas
[AD-A145626] 02 p0191 N85-11278
Some considerations on the capacitive calibration used for the 2.3 ton cryogenic antenna at CERN — gravitational antennas
[NOTA-INTERNA-809] 02 p0192 N85-11284
Possibility of realization of highly-directional antenna arrays 03 p0344 N85-12220
Conceptual design for scaled truss antenna flight experiment
[NASA-TM-85804] 04 p0462 N85-12932
Workshop on Mechanical Technology for Antennas — conferences; satellite antennas
[ESA-SP-225] 05 p0625 N85-13999
Antenna mechanical technologies within ESA 05 p0625 N85-14000
High performance deployable antenna structures 05 p0625 N85-14001
Offset unfurlable antenna concepts 05 p0625 N85-14002
The UK and Netherlands millimetre-wave telescope — Netherlands (NL) 05 p0625 N85-14003
Electrical consequences of mechanical antenna characteristics 05 p0625 N85-14006
Structural aspects of SAR antenna for Japanese Earth Resources Satellite 1 05 p0626 N85-14007
Technology for the ERS-1 SAR antenna 05 p0626 N85-14008
Mechanical/thermal design of a polarization sensitive reflector — communication satellites 05 p0626 N85-14009
CASA technological effort in the field of antennas — satellite radar antennas 05 p0626 N85-14010
BAe antenna hardware technology for current satellite projects 05 p0626 N85-14011
Technology and performances of structural thermal mechanical equipment used for antenna of TV.SAT-TDF 1 program 05 p0626 N85-14012
CASA activities in antenna technology — satellite antennas 05 p0627 N85-14015
ARABSAT spacecraft: Rx and Tx antenna mechanisms 05 p0628 N85-14022
Characteristics of circular-polarized printed radiators in planar phased antenna array 06 p0790 N85-15049
Green function in theory of microstrip antennas 06 p0790 N85-15050
Efficiency in integral active antennas 06 p0792 N85-15060
Broadband pillbox antennas
[AD-A146569] 06 p0799 N85-15104
The 20 GHz proof-of-concept test model results for a multiple scan beam dual reflector antenna
[NASA-CR-174268] 07 p0938 N85-15944
A low-sidelobe space feed lens
[AD-A147883] 07 p0942 N85-15972
Dual band, low sidelobe, high efficiency mirror antenna
[AD-D011329] 07 p0944 N85-15980
Compact wideband multiple conductor monopole antenna
[AD-D011331] 07 p0944 N85-15981
Configuration study for a 30 GHz monolithic receive array: Technical assessment
[NASA-CR-174697] 09 p1311 N85-18238
Configuration study for a 30 GHz monolithic receive array, volume 1
[NASA-CR-174697-VOL-1] 09 p1311 N85-18239
Configuration study for a 30 GHz monolithic receive array, volume 2
[NASA-CR-174697-VOL-2] 09 p1311 N85-18240
The effects of mode impurity of Ka-band system performance 10 p1463 N85-19227
Condensed antenna structural models for dynamics analysis 10 p1463 N85-19230
Design procedure for the new 70-meter antenna subreflector positioner 10 p1463 N85-19232
HF broadband whip antenna evaluation
[AD-A149527] 10 p1467 N85-19258
Shuttle S-band high gain switched beam breadboard antennas
[NASA-CR-171852] 10 p1478 N85-19327
Compensator development and examination of performance and robustness
[NASA-CR-175470] 11 p1627 N85-20244
Monte Carlo studies of tandem mirror plasmas interacting with waves in the Ion Cyclotron Range of Frequencies (ICRF)
[DE85-002988] 11 p1731 N85-20883
The 60 GHz antenna system analyses for intersatellite links, phase A
[NASA-CR-175285] 12 p1823 N85-21439
Image lobe analysis for large radomes
[AD-P004359] 12 p1825 N85-21453
3-D Dome/Rotman lens antenna breadboard demonstration
[AD-A149609] 12 p1828 N85-21475
Wide angle phased array dome lens antenna with a reflection/transmission switch
[AD-D011562] 12 p1833 N85-21502
Performance ranges of helical antenna made of conductor with extra bends 12 p1836 N85-21536
Computer aided antenna design and frequency selection for HF communications
[AD-A150485] 13 p2055 N85-22869
Variational and moment method solutions of the fields in a parallel-plate waveguide-aperture system
[DE85-006288] 13 p2057 N85-22876
A generalized solution to a class of printed circuit antennas 13 p2062 N85-22882
Experimental verification of beam deflection from hybrid reflector antenna within wide-angle sector 13 p2079 N85-22984
Large Space Antenna Systems Technology, 1984
[NASA-CP-2368-PT-1] 14 p2229 N85-23813
NASA mobile satellite program 14 p2229 N85-23814
Application of pushbroom altimetry from space using large space antennas 14 p2230 N85-23817
LDR system concepts and technology 14 p2231 N85-23823
Development of the 15-meter hoop-column antenna system 14 p2231 N85-23825
Box truss development and its application 14 p2231 N85-23826
Synchronously deployable tetrahedral truss reflector 14 p2231 N85-23827
Antenna Technology for QUASAT application — radio antenna for very long base interferometry missions 14 p2231 N85-23828
Cable-catenary large antenna concept 14 p2231 N85-23829
Extreme precision antenna reflector study results 14 p2232 N85-23830
Large Space Antenna Systems Technology, 1984
[NASA-CP-2368-PT-2] 14 p2233 N85-23840
Large antenna control methods: Current status and future trends 14 p2234 N85-23845
Design and measured performance of a broadband Archimedes spiral antenna
[R-NIAS-22] 14 p2290 N85-24194
A compact, aperture-matched, balanced transmission line antenna
[R-NIAS-28] 14 p2290 N85-24196
Prime-focus parabolic reflector antenna: Theory and measurement
[R-NIAS-20] 14 p2291 N85-24199
Spheroidal functions: Properties and tabulation. Application to antenna synthesis 14 p2296 N85-24758
Antenna with outboard exciter for 3.4-13.25 GHz frequency range 15 p2526 N85-25577
Design and swept-frequency measurement of printed circuit board log-periodic dipole arrays
[R-NIAS-23] 15 p2539 N85-25671
Compensator development and examination of performance and robustness
[NASA-CR-175703] 15 p2540 N85-25678
Concepts and cost trade-offs for land vehicle antennas in satellite mobile communications
[NASA-CR-175731] 15 p2540 N85-25680
A simplified GPS C/A reciever front end with low noise performance 18 p3109 N85-29251
A special antenna for SARSAT EPIRBs providing circular polarization and hemispheric coverage for reliable transmission to satellites — Emergency Position Indicating Radio Beacon (EPIRB) 20 p3404 N85-31122
Dynamic performance of several large antenna concepts 20 p3409 N85-31155
Design and evaluation of control systems for large communications satellites 20 p3409 N85-31157
Control of large antennas based on electromagnetic performance criteria 20 p3409 N85-31158
Large space structure flight experiment 20 p3410 N85-31163
Design of a shuttle-borne SAR for the DFVLR's planning study
[ERYS-019/84] 20 p3419 N85-31219
Fin-line horn antennas
[AD-A154597] 21 p3580 N85-32255
Most desirable terrain, e.g., flat vs valley location, part 5.1B 21 p3624 N85-32513
Summary of session on optimum transmitter and antenna configuration for MST radar, part 6 21 p3624 N85-32514
Frequency independent parabolic phased antenna array of log periodic antennas 22 p3774 N85-33367
Polarization diversity addition to the 10 centimeter Doppler weather radar
[AD-A156062] 24 p4087 N85-35334
ANTENNA FEEDS
Remote sounding of fields in feed radiators of multi-element antenna system with allowance for interaction with sounding device 06 p0790 N85-15047
Hardwire missile receiver coupler
[AD-D011350] 07 p0937 N85-15936
Dual offset reflector antenna systems with rotationally symmetric aperture distributions
[AD-A147346] 07 p0940 N85-15961
A low-sidelobe space feed lens
[AD-A147883] 07 p0942 N85-15972
The effects of mode impurity of Ka-band system performance 10 p1463 N85-19227
A reflectometer unit for a 500 kW HF balanced screened feeder
[BBC-RD-1984/13] 10 p1477 N85-19322
Printed circuit balun with a dipole antenna
[AD-D011534] 12 p1833 N85-21498
Wide angle phased array dome lens antenna with a reflection/transmission switch
[AD-D011562] 12 p1833 N85-21502
KAM-250 antenna switch 13 p2068 N85-22916
Measured performance of a broadband matching section for peripherally fed helical antennas
[R-NIAS-25] 15 p2539 N85-25670
Beam forming network
[NASA-CASE-NPO-15743-1] 18 p3089 N85-29118
MMIC devices for active phased array antennas
[NASA-CR-178015] 19 p3254 N85-30177
A hardware demonstration of distributed control for a flexible offset-feed antenna 20 p3410 N85-31160
Multitrunk high-frequency multiplexing of antenna-waveguide channels 22 p3774 N85-33365
Method of constructing folding umbrella-type antenna 22 p3774 N85-33366
Minimizing field scattered by slender dipoles 22 p3774 N85-33368
ANTENNA FIELDS
U ANTENNA RADIATION PATTERNS
ANTENNA RADIATION PATTERNS
NT SIDELOBES
An error analysis for the use of presently available lunar radio flux data in broadbeam antenna-system measurements
[PB84-218361] 01 p0016 N85-10097
Case study of sample spacing in planar near-field measurement of high gain antennas
[NASA-TM-86872] 01 p0037 N85-10234
A proof-of-principle getaway special free-flying satellite demonstration 02 p0155 N85-11051
Apparatus of short baseline centrimetric wave radiointerferometer with cable communication lines for astrophysical research 06 p0782 N85-15001
Invariance of mean-square effective area of synthesized apertures 06 p0784 N85-15009
Synthesis of zeros in radiation pattern of linear antenna array 06 p0784 N85-15015
Measurement of external antenna characteristics with allowance for distorting factors (review) 06 p0790 N85-15048

Remote sounding of fields in feed radiators of multi-element antenna system with allowance for interaction with sounding device
06 p0790 N85-15047
Fast method for calculating radiation patterns of nonequidistant radiator systems
06 p0791 N85-15052
System of equations for finding antenna radiation pattern from near-field samples 06 p0791 N85-15054
Efficiency in integral active antennas
06 p0792 N85-15060
The 20 GHz proof-of-concept test model results for a multiple scan beam dual reflector antenna
[NASA-CR-174268] 07 p0936 N85-15944
Dual offset reflector antenna systems with rotationally symmetric aperture distributions
[AD-A147346] 07 p0940 N85-15961
Efficient computation of reflector antenna aperture distributions and far field patterns
[AD-A147367] 07 p0940 N85-15962
Tactical HF communication for military helicopters using the NVIS mode 08 p1074 N85-16807
Information for space radar designers: Required dynamic range vs resolution and antenna calibration using the Amazon rain forest 08 p1147 N85-17239
The effects of soil moisture on bistatic clutter power
[AD-A147636] 08 p1150 N85-17261
Loop radiating elements
[AD-D011409] 08 p1156 N85-17306
Propagation measurements for land-mobile satellite services in the 800 MHz band
[CRC-TN-724] 09 p1310 N85-18231
Radiation patterns of a pyramidal horn antenna
09 p1311 N85-18236
Multivariable Autoregressive Moving Average (ARMA) models: A time approach to antenna processing
[ENST-84E015] 09 p1313 N85-18252
Measurement procedures for the radar spectrum engineering criteria
[PB85-119022/GAR] 09 p1313 N85-18254
The effects of mode impurity of Ka-band system performance 10 p1463 N85-19227
Subreflector focusing techniques applied to new DSS-15 and DSS-45 34-meter antennas
10 p1464 N85-19233
Conformal phased array antenna pattern corrector
[AD-D011469] 10 p1466 N85-19266
Comparison of measured and calculated mutual coupling in the near field between microwave antennas
[PB85-105963] 11 p1625 N85-20237
Landing control centrals
[AD-A149800] 12 p1775 N85-21140
Technical evaluation report on the FDP Symposium on Flight Test Techniques
[AGARD-AR-208] 12 p1777 N85-21157
The 60 GHz antenna system analyses for intersatellite links, phase A
[NASA-CR-175285] 12 p1823 N85-21439
A subaperture approach to the calculation of flashlobes introduced by airborne radomes
[AD-P004355] 12 p1825 N85-21449
Automated radome testing
[AD-P004362] 12 p1826 N85-21456
USSR report: Electronics and electrical engineering
[JPRS-UEE-85-002] 13 p2066 N85-22907
Coordinate determination errors in measuring characteristics of radiation field of airborne antennas
13 p2068 N85-22919
Reduction of amplitude-phase distortions of movable microwave coupling circuit for antenna field measurements 13 p2068 N85-22920
Experimental verification of beam deflection from hybrid reflector antenna within wide-angle sector
13 p2079 N85-22964
Synthesis of multistep directional couplers with nonminimum-phase characteristics
13 p2079 N85-22966
Scattering of waves by axisymmetrical edge
13 p2080 N85-22967
Electromagnetic analysis for surface tolerance effects on large space antennas 14 p2234 N85-23850
Microstrip comb array design
[R-NIAS-24] 14 p2290 N85-24195
Prime-focus parabolic reflector antenna: Theory and measurement
[R-NIAS-20] 14 p2291 N85-24199
Analytical studies and experimental measurements of amplitude and phase of near-field range antenna probes
[AD-A150922] 14 p2293 N85-24212
Spheroidal functions: Properties and tabulation. Application to antenna synthesis
14 p2396 N85-24758
COSPAS-SARSAT satellite orbit predictor, volume 5
[NASA-TM-85015-VOL-5] 14 p2439 N85-25052
Space processing of acoustic signals in plane-parallel waveguide — antenna arrays 15 p2525 N85-25572
Interference immunity of optical radar system with phased antenna array 15 p2526 N85-25575
Cophasal horizontal wideband array antennas for transmitting with asymmetric output
15 p2526 N85-25576
Antenna with outboard exciter for 3.4-13.25 GHz frequency range 15 p2526 N85-25577
The distortion of AM broadcast antenna patterns as caused by nearby towers and highrise buildings
[CRC-1379] 15 p2538 N85-25668
Mobile antenna and beam pointing studies for satellite mobile communications
[NASA-CR-175736] 15 p2540 N85-25679
Land vehicle antennas for satellite mobile communications
[NASA-CR-175735] 15 p2540 N85-25682
Null generation using discs on a reflector
[AD-A151697] 15 p2544 N85-25703
Radiation and scattering of spiral antennas
[AD-A151929] 16 p2773 N85-27116
Earth station antenna sidelobe characteristics
[PB85-184986] 16 p2780 N85-27159
Performance analysis of the DSN baseband assembly (Bba) Real-Time Combiner (RTC)
[NASA-CR-175877] 17 p2947 N85-28193
A simulation study of jammer nulling trade-offs in a reactively steered adaptive array
[AD-A153461] 18 p3090 N85-29124
Computer simulation of the effects of a distributed array antenna on synthetic aperture radar images
[NASA-CR-171888] 19 p3254 N85-30176
Inherent angular tracking error in an amplitude comparison monopulse radar
[AD-A154212] 19 p3255 N85-30185
Theoretical investigation of single-frequency 8-element localizer signal scattering for critical area determination
[FAA-PM-85-4] 20 p3391 N85-31037
Phase synchronizing large antenna arrays using the spatial correlation properties of radar clutter
20 p3439 N85-31344
Offset reflector with horn feed array, used as an experimental sensor for radiometric measurements
[ESA-TT-830] 20 p3443 N85-31369
Deterministic and random phase noise of oscillators — synthetic aperture radar
[ESA-TT-848] 20 p3449 N85-31415
Null synthesis with phase and amplitude controls at the subarray outputs
[AD-A155187] 21 p3576 N85-32241
Anisotropy of the permittivity field inferred from aspect-sensitive radar echoes 21 p3620 N85-32492
Effects of line-of-sight velocity on spaced-antenna measurements, part 3.5A 21 p3621 N85-32496
Problems and solutions in analyzing partial-reflection drift data by correlation techniques
21 p3626 N85-32529
Comprehensive radio direction finder with electronically stabilized radiation pattern 22 p3762 N85-33318
Method of constructing folding umbrella-type antenna
22 p3774 N85-33386
Minimizing field scattered by slender dipoles
22 p3774 N85-33388
Box truss analysis and technology development. Task 1: Mesh analysis and control
[NASA-CR-172570] 23 p3900 N85-34156
Adaptive antenna arrays for satellite communications: Design and testing
[NASA-CR-176162] 23 p3926 N85-34329
Characteristic modes for slots in a ground plane TE case
[AD-A155757] 24 p4086 N85-35326
A planar version of a 4.0 gigahertz reactively steered adaptive array
[AD-A156029] 24 p4087 N85-35330
Theory of mutual impedances and multiple reflections in an N-element array environment
[PB85-191419] 24 p4092 N85-35364

ANTENNAS

NT AIRCRAFT ANTENNAS
NT CASSEGRAIN ANTENNAS
NT CYLINDRICAL ANTENNAS
NT DIPOLE ANTENNAS
NT DIRECTIONAL ANTENNAS
NT FURLABLE ANTENNAS
NT GRAVITATIONAL WAVE ANTENNAS
NT HELICAL ANTENNAS
NT HOOP COLUMN ANTENNAS
NT HORN ANTENNAS
NT LENS ANTENNAS
NT LOG PERIODIC ANTENNAS
NT LOOP ANTENNAS
NT MICROWAVE ANTENNAS
NT MISSILE ANTENNAS
NT MONOPOLE ANTENNAS
NT MONOPULSE ANTENNAS
NT MULTIPLE BEAM INTERVAL SCANNERS
NT PARABOLIC ANTENNAS
NT RADAR ANTENNAS
NT RADIO ANTENNAS
NT RECTENNAS
NT RHOMBIC ANTENNAS
NT SATELLITE ANTENNAS
NT SLOT ANTENNAS
NT SPACECRAFT ANTENNAS
NT SPACETENNAS
NT SPIRAL ANTENNAS
NT STEERABLE ANTENNAS
NT TWO REFLECTOR ANTENNAS
NT WAVEGUIDE ANTENNAS
NT WHIP ANTENNAS

Case study of sample spacing in planar near-field measurement of high gain antennas
[NASA-TM-86872] 01 p0037 N85-10234
Center for Electronics and Electrical Engineering Technical Bulletin covering center programs
[PB84-218056] 01 p0045 N85-10296
RF characteristics of the hoop column antenna for the land mobile satellite system mission
[NASA-CR-3842] 02 p0189 N85-11264
A generalized solution to a class of printed circuit antennas
[AD-A145626] 02 p0191 N85-11278
USSR report: Electronics and electrical engineering
[JPRS-UEE-84-014] 03 p0344 N85-12215
Conceptual design for scaled truss antenna flight experiment
[NASA-TM-85804] 04 p0462 N85-12932
Fundamental limitations in antenna resolution by maximum entropy methods
[DE84-017052] 04 p0493 N85-13145
Active nutation control of spacecraft using a magnetic bearing momentum wheel with Vernier gimballing capability
[NAL-TR-8201] 06 p0759 N85-14857
USSR report: Electronics and electrical engineering
[JPRS-UEE-84-012] 06 p0781 N85-14991
Antenna matching device tuning for type ZhRU radiostations 06 p0785 N85-15017
USSR report: Electronics and electrical engineering
[JPRS-UEE-84-011] 06 p0789 N85-15042
Fast method for calculating radiation patterns of nonequidistant radiator systems
06 p0791 N85-15052
MMIC devices for active phased array antennas
[NASA-CR-174281] 07 p0938 N85-15943
Data appendix: F-number=1.0 EMR with a flexible back electrode
[NASA-CR-172477] 07 p0946 N85-15994
USSR report: Electronics and electrical engineering
[JPRS-UEE-84-017] 07 p0951 N85-16025
Reduction method for thermal analysis of complex aerospace structures
[NASA-TP-2373] 07 p0957 N85-16066
Integrated defense communications system antijamming antenna system
[AD-D011423] 08 p1154 N85-17285
Antenna axis drive torques for the 70-meter antenna
10 p1464 N85-19237
An evaluation of the 64-meter antenna radial bearing for use on the 70-meter antenna
10 p1464 N85-19238
Elevation bearing maximum load, 70-meter antenna
10 p1464 N85-19239
Characteristics of the elevation drive suspension of the 64-meter antennas 10 p1464 N85-19240
Hydrostatic bearing pad maximum load and overturning conditions for the 70-meter antenna
10 p1465 N85-19241
A technical solution to fadings in tactical satellite digital transmissions 10 p1473 N85-19297
Overview of RADC adaptive antenna developments for communications 10 p1474 N85-19299
Direction finder set, radio
[AD-A149958] 12 p1775 N85-21142
A computer analysis of the RF performance of a ground-mounted, air-supported radome
[AD-P004352] 12 p1824 N85-21446
Generalized radome BSE (radome boresight error) characterization using superposition techniques
[AD-P004354] 12 p1825 N85-21448
A radome for air traffic control SSR radar systems
[AD-P004373] 12 p1827 N85-21467
Gain enhancement methods for printed circuit antennas
[AD-A150090] 12 p1835 N85-21517
Preliminary investigation into using the sun as a source for G/T (Gain to System Noise Temperature) measurements
[PB85-128148] 12 p1952 N85-22265
USSR report: Electronics and electrical engineering
[JPRS-UEE-85-002] 13 p2066 N85-22907
KAM-250 antenna switch 13 p2068 N85-22916

Large space antenna technology applied to radar-imaging, rain-rate measurements, and ocean wind sensing 14 p2230 N85-23820
Advanced 2-frequency ocean sensing radar using high resolution antenna beams 14 p2230 N85-23821
WRAP-RIB antenna technology development 14 p2231 N85-23824
Development of the 15-meter hoop-column antenna system 14 p2231 N85-23825
Box truss development and its application 14 p2231 N85-23826
Precision space structures 14 p2232 N85-23833
An eigensystem realization algorithm for application to modal testing 14 p2233 N85-23842
Electromagnetic analysis for surface tolerance effects on large space antennas 14 p2234 N85-23850
Feed system design considerations for large space antenna systems. Part 2: Single aperture with overlapping feeds 14 p2235 N85-23853
Diffraction analysis of mesh deployable reflector antennas 14 p2235 N85-23854
Shuttle attached antenna Flight Experiment Definition Study (FEDS) 14 p2237 N85-23865
Electro-science requirements for shuttle-attached antenna flight experiments 14 p2237 N85-23866
Analytical studies and experimental measurements of amplitude and phase of near-field range antenna probes [AD-A150922] 14 p2293 N85-24212
Ways of optimization of light energy transformation in primary stages of photosyntheels. Necessity of optimization of photosynthetic unit structure and method for calculating efficiency 14 p2386 N85-24700
Ways of optimization of light energy transformation in primary stages of photosyntheels. Optimization of lattice structure of uniform photosynthetic unit 14 p2386 N85-24701
ANTENA user guide [DE85-004961] 14 p2424 N85-24953
Electromagnetic scattering by arbitrarily shaped reflectors: Subreflector efficiency [AD-A149224] 15 p2541 N85-25687
Calibration methods in millimeter-wave radioastronomy [INPE-3481-PRE/724] 16 p2881 N85-27778
Avionics data base [AD-A152415] 17 p2897 N85-27863
Mathematical modeling and control of a large space structure as applied to a shuttle-antenna configuration [AD-A153269] 17 p2910 N85-27939
LFMR definition study [AD-A153691] 18 p3090 N85-29126
Upgrade of the LLNL EM transient range monocone antenna [DE85-006639] 18 p3097 N85-29172
The effect of sensor and actuator errors on static shape control for large space structures [NASA-TM-86446] 19 p3225 N85-29998
High switching speed electrically tuned microwave magnetic resonance devices [AD-D011699] 19 p3269 N85-30217
ICRF antenna coupling and wave propagation in a tokamak plasma 19 p3369 N85-30893
Proceedings of the Workshop on Identification and Control of Flexible Space Structures, volume 3 [NASA-CR-176053] 20 p3415 N85-31195
Mutual coupling analysis for conformal microstrip antennas 20 p3439 N85-31343
The use of the glistening surface concept in rough surface scattering [AD-A154922] 21 p3575 N85-32234
Field antenna handbook [AD-A155204] 21 p3576 N85-32242
Numerical modeling of subsurface communication [DE85-012818] 21 p3577 N85-32249
Middle Atmosphere Program. Handbook for MAP. Volume 14: URSI/SCOSTEP Workshop on Technical Aspects of MST Radar [NASA-CR-176085] 21 p3615 N85-32466
USSR report: Electronics and electrical engineering [JPRS-UEE-84-015] 22 p3762 N85-33314
Multitrunk high-frequency multiplexing of antenna-waveguide channels 22 p3774 N85-33385
Method of constructing folding umbrella-type antenna 22 p3774 N85-33386
High-field launch electron cyclotron heating experiments in the ELMO Bumpy Torus [DE85-012098] 22 p3846 N85-33825
Reducing grating lobes due to subarray amplitude tapering [AD-D011723] 23 p3927 N85-34339
Moment-method formulation of the cavity-probe aperture antenna [DE85-013264] 24 p4088 N85-35336
Center for Electronics and Electrical Engineering technical progress bulletin covering center programs, July-September with 1985 CEEE events calendar [PB85-191393] 24 p4091 N85-35363

ANTHRACENE
Homogeneous reaction involving components of different redox couples. 2: Polarographic studies of the interactions of alkali metal cations with anthracene and fluoroanthene dianions in N,N-dimethylformamide and acetonitrile [AD-A148667] 08 p1124 N85-17085
Studies on organic semiconductors. 15: Effects of the substituents on the photoconductivities of substituted anthracenes [NASA-TM-77788] 08 p1225 N85-17712
Thermal reactions of aromatics with CaO [DE85-010888] 22 p3742 N85-33193

ANTHROPOMETRY
Anthropometric cockpit compatibility assessment of US Army aircraft for large and small personnel wearing a training, warm-weather clothing configuration [AD-A145208] 01 p0099 N85-10656
Anthropometric cockpit compatibility assessment of US Army aircraft for large and small personnel wearing A cold weather, armored vest, chemical defense protective clothing configuration [AD-A145472] 02 p0238 N85-11547
Challenges of developing an electro-optical system for measuring man's operational envelope 08 p1095 N85-16921
Technique for measuring body circumferences and skinfold thicknesses [AD-A148166] 08 p1195 N85-17532
An investigation of spinal injury potential from the use of the ACES 2 ejection seat by lower weight female pilots [AD-A148449] 08 p1196 N85-17537
Crewstation assessment of reach as applied to the OH-58A helicopter [AD-A149413] 10 p1531 N85-19650
The application of anthropometric survey data to aircrew clothing sizing [AD-A150545] 13 p2143 N85-23304
Preliminary design of a limb restraint evaluator [AD-A151749] 15 p2468 N85-25226
Comparative anaerobic power of males and females [AD-A151960] 16 p2842 N85-27523
Relationship between the Army two mile run test and maximal oxygen uptake [AD-A153914] 18 p3154 N85-29526

ANTIADRENERGICS
The effect of beta adrenergic blockade on ratings of perceived exertion [AD-A148053] 08 p1195 N85-17530

ANTIAIRCRAFT MISSILES
NT SIDEWINDER MISSILES

ANTIBODIES
Induction of immunity to toxins with anti-idiotypic antibody [AD-A146793] 07 p1014 N85-16445
Armed forces special Symposium on Medicine of Altitudes 13 p2166 N85-23441
Isolation of hybridomas for golgi-associated proteins and a plant calmodulin 15 p2613 N85-26103
Rapid rate-kinetic turbidometric assay for quantitation of antiviral complement-fixing antibodies [AD-A153644] 18 p3152 N85-29516

ANTICHOLINERGICS
Effects of pyridostigmine on psychomotor and visual performance [AD-A148553] 08 p1196 N85-17539

ANTICLINES
Structural development of the west-central Grant Range, Nye County, Nevada 24 p4115 N85-35506

ANTICLINORIA
U ANTICLINES

ANTICOAGULANTS
Management of microcirculatory disorders in vibration sickness 10 p1524 N85-19611

ANTICYCLONES
Mesoscale features and atmospheric refraction conditions of the Arctic marginal ice zone [AD-A155139] 21 p3636 N85-32584
The variability of aerosol microstructure in continental and oceanic surface layers of the atmosphere in anticyclones 21 p3647 N85-32660
Maintenance of blocking anticyclones in a general circulation model [PB85-190866] 24 p4124 N85-35567

ANTIEMETICS AND ANTIHAUSEANTS
Medication interference with space research: An example from a mass-discrimination experiment on Spacelab 1 05 p0695 N85-14472

ANTIFERROMAGNETISM
Fermi surface study of CeSb [DE85-002532] 10 p1564 N85-19662
Investigation of electric and magnetic properties of intercalated graphite [AD-A149601] 12 p1797 N85-21274
Coexistence of antiferromagnetism and spin-glass ordering in the Ising system FeO 55MgO 45Cl2 [DE85-004164] 12 p1942 N85-22197
Peltier heat of a small polaron in a magnetic semiconductor [DE85-000470] 14 p2430 N85-24963

ANTIFOULING
An electrochemical approach to the prevention of biofouling phenomena [PB84-202613] 01 p0025 N85-10155
Process for preparation of crosslinked poly(tri-n-butyltin) methacrylate with simultaneous particle size reduction [AD-D011313] 07 p0932 N85-15905

ANTIFREEZES
Development of a high-temperature coolant for advanced diesel engines [AD-A153660] 18 p3117 N85-29297

ANTIFRICTION BEARINGS
NT BALL BEARINGS
NT ROLLER BEARINGS
Testing the antifriction properties of alloys for heavily loaded bearings 06 p0780 N85-14990
Applications of vibration analysis to the condition monitoring of rolling element bearings [ARL/AERO-R-163] 12 p1859 N85-21663
Powder metallurgy bearings for advanced rocket engines 16 p2736 N85-26581

ANTIGENS
Functional and structural changes in human erythrocyte surface after irradiation by UV waves of various wavelengths. Report 1: Expression of ABO and Rhesus system antigen 09 p1361 N85-18584
Functional and structural changes in human erythrocyte surface after irradiation by UV waves of various wavelenghts. Report 2: Adsorption of alcyan blue by external premembranous components 09 p1361 N85-18585
Differences in susceptibility of inbred mice to bacillus anthracis [AD-A155646] 21 p3662 N85-32750
Genetic and physiological control of protective antigen synthesis by bacillus anthracis [AD-A156324] 24 p4133 N85-35617

ANTIGRAVITY
Analysis of the transient response of temporal artery blood flow data relative to various anti-G suit pressure schedules 10 p1533 N85-19980
Simulation of high +Gz onset in the dynamic environment simulator [AD-A155963] 24 p4131 N85-35610

ANTIKNOCK ADDITIVES
Knock syndrome: Its cures and its victims [NASA-CR-174395] 10 p1458 N85-19185

ANTIMATTER
NT ANTINEUTRINOS
NT ANTINUCLEONS
NT ANTIPARTICLES
NT ANTIPROTONS
NT POSITRONS
On the nature of the baryon asymmetry [NASA-TM-86156] 05 p0748 N85-14784
Gravitational properties of antimatter [DE85-009601] 18 p3197 N85-29832

ANTIMISSILE DEFENSE
Directed energy missile defense in space [PB84-210111] 01 p0015 N85-10095

ANTIMISSILE MISSILES
Arms control and The President's Strategic Defense Initiative [AD-A156334] 24 p4066 N85-35212

ANTIMISTING FUELS
Aircraft wing fuel tank environmental simulator tests for evaluation of antimisting fuels [FAA-CT-84-15] 07 p0934 N85-15920
A brief review of the technology of microemulsions and other micellar systems [AD-A149759] 12 p1800 N85-21289
Practical real-time quality control of antimisting kerosene [DE/FAA/CT-85/1] 18 p3083 N85-29072

ANTIMONIDES
NT GALLIUM ANTIMONIDES
NT INDIUM ANTIMONIDES

ANTIMONY
Dopant incorporation in silicon during nonequilibrium solidification: Comparison of 2 processes [DE85-005568] 14 p2430 N85-24968
Optically bistable devices using InSb 18 p3186 N85-29758
Control of acid deposition precursors through dry scrubbing [DE85-010281] 19 p3295 N85-30056

ANTIMONY ALLOYS
Comparative analysis of laboratory and fullscale experimental data for metal flow displacements and speeds
[BLL-M-36266-(5828.4)] 20 p3430 N85-31276

ANTIMONY COMPOUNDS
NT GALLIUM ANTIMONIDES
NT INDIUM ANTIMONIDES
Fermi surface study of CeSb
[DE85-002532] 10 p1584 N85-19862
Alkali atom - SbCl(5) reactions: Blue-green chemiluminescence from an inverted population in SbCl
[AD-A154371] 18 p3276 N85-30315

ANTINEUTRINOS
Neutrino-antineutrino annihilation around collapsing star
[OG-1.1-10] 22 p3861 N85-33911
QCD analysis of neutrino charged current structure function F2 in deep inelastic scattering
[HE-5.3-23] 24 p4207 N85-36114

ANTINUCLEONS
Discussion session: Nucleon- and antinucleon-nucleus inelastic scattering and charge exchange
[DE85-010723] 19 p3364 N85-30860

ANTIPARTICLES
NT ANTINEUTRINOS
NT ANTINUCLEONS
NT ANTIPROTONS
NT POSITRONS
Search for heavy antinuclei in the cosmic radiation
[OG-6.1-2] 22 p3887 N85-34093
The flux of secondary anti-deuterons and antihelium produced in the interstellar medium
[OG-6.1-5] 22 p3888 N85-34096

ANTIPROTONS
Antiproton source beam position system
[DE84-016716] 09 p1380 N85-16679
Bunch coalescing in the main ring to form intense proton and antiproton bunches without RF counterphasing
[DE85-001364] 09 p1382 N85-16682
High energy physics study
[DE84-015803] 09 p1383 N85-16700
Low energy antiproton interaction studies at Brookhaven
[DE85-001228] 11 p1720 N85-20620
Gravitational properties of antimatter
[DE85-009601] 18 p3197 N85-29632
Physics with low temperature antiproton
[DE85-009627] 19 p3355 N85-30796
Spectral evolution of gamma-rays from adiabatically expanding sources in dense clouds
[OG-2.5-2] 22 p3869 N85-33958
Nineteenth International Cosmic Ray Conference. OG sessions, volume 2
[NASA-CP-2376-VOL-2] 22 p3875 N85-34006
Abundance of low energy (50-150 MeV) antiprotons in cosmic rays
[OG-6.1-1] 22 p3887 N85-34092
Propagation and secondary production of low energy antiprotons in the atmosphere
[OG-6.1-3] 22 p3887 N85-34094
Secondary antiproton production in relativistic plasmas
[OG-6.1-4] 22 p3888 N85-34095
The flux of secondary anti-deuterons and antihelium produced in the interstellar medium
[OG-6.1-5] 22 p3888 N85-34096
Analysis of experimental data on interstellar antiprotons in the light of measurements of high-energy electrons and He-3 nuclei
[OG-6.1-6] 22 p3888 N85-34097
Observed antiprotons and energy dependent confinement of cosmic rays: A conflict?
[OG-6.1-7] 22 p3888 N85-34098
Antiparticles in the extragalactic cosmic radiation
[OG-6.1-8] 22 p3888 N85-34099
Galactic cosmic ray antiprotons and supersymmetry
[OG-6.1-9] 22 p3888 N85-34100
Galactic antiprotons of 0.2-2 GeV energy
[OG-6.1-11] 22 p3888 N85-34101
The design of an experiment to detect low energy antiprotons
[OG-9.1-1] 23 p4022 N85-34928
An experiment to measure the energy spectrum of cosmic ray antiprotons from 100 to 1000 MeV
[OG-9.1-3] 23 p4022 N85-34929
Studies of relativistic heavy ion collisions
[DE85-014666] 24 p4152 N85-35745
P(P bar)P elastic scattering and cosmic ray data
[HE-1.1-6] 24 p4170 N85-35854
Some remarks about simulation of cosmic ray phenomena with use of nuclear interaction models based on the current SPS proton-antiproton data
[HE-1.2-6] 24 p4172 N85-35864
A test of the Feynman scaling in the fragmentation region
[HE-1.2-9] 24 p4172 N85-35867

ANTIRADIATION DRUGS
Chemical protection against ionizing radiation
[AD-A147822] 07 p1016 N85-16457
Radioprotective efficacy of ATP and adenosine with exposure to high energy protons
19 p3325 N85-30802

ANTIREFLECTION COATINGS
Effect of an underlayer of cadmium telluride on the reflection-reducing properties of zinc sulfide on mercury cadmium telluride
[AD-A146195] 03 p0414 N85-12649
Material models and device structures for GaAs solar cells, introduction
05 p0665 N85-14276
Anti-reflection coatings materials and models
05 p0665 N85-14278
Effective antireflection coatings of transparent polymeric materials by gas-phase surface fluorination
[DE84-013027] 09 p1385 N85-18711
Sol-gel-derived AR coatings for solar receivers
[DE85-000192] 11 p1673 N85-20541
1.5 to 1.7 micrometers LEDs (Light-Emitting Diode)
[AD-A149685] 12 p1834 N85-21508
Resistance of optical coatings to alkali solutions and sea water
14 p2281 N85-24129
Nonuniform interference coatings with thickness-dependent refractive index
14 p2281 N85-24131
Gyrotron traveling-wave device including quarter wavelength anti-reflective dielectric layer to enhance microwave absorption
[AD-D011690] 19 p3271 N85-30285
Technical and historical overview of the study at Lawrence of porous antireflection coatings
[DE85-010925] 20 p3434 N85-31302
Process and design considerations for high-efficiency solar cells
20 p3482 N85-31641
Los Alamos optical materials reliability, maintainability, and exposure testing program
[DE85-011894] 21 p3613 N85-32456
Effects of laser radiation on surfaces and coatings
[DE85-010475] 22 p3790 N85-33484
Removable cleanable antireflection shield
[AD-D011735] 22 p3844 N85-33810

ANTISEPTICS
Synthesis of antimicrobial chemical fibers and fibrous materials containing quaternary ammonium compounds and their utilization
06 p0762 N85-14872

ANTISHIP WARFARE
Optimizing the specifications for an air-surface laser system
16 p2696 N85-26644

ANTISUBMARINE WARFARE
Development of a Helicopter integrated navigation system
08 p1073 N85-16802
Real-time enhancement of a climatology or forecast of ocean thermal structure using observed ocean temperatures
[AD-A151118] 15 p2604 N85-26049
The NAVTAG (Naval Tactical Game) system and its modification to include the SH-60B helicopter
[AD-A152004] 16 p2858 N85-27624

ANTISUBMARINE WARFARE AIRCRAFT
NT P-3 AIRCRAFT
The NAVTAG (Naval Tactical Game) system and its modification to include the SH-60B helicopter
[AD-A152004] 16 p2858 N85-27624

ANTISYMMETRY
Design sensitivity analysis of an antisymmetric angle-ply laminate
[CSIR-TWISK-318] 01 p0021 N85-10128

ANTONOV AIRCRAFT
Designer O. K. Antonov on new AN-74 arctic transport
15 p2467 N85-25230

ANVIL CLOUDS
Anvil structure of severe thunderstorms
15 p2595 N85-25993

ANVILS
Electrical resistance measurements of metals to 40 GPa in the diamond cell
[DE85-001009] 11 p1629 N85-20262

ANXIETY
Psychological states (mood, affect or emotion) experienced by JASDF pilots through flying duties. 3: Flying conditions causing pilots psychological disturbances
01 p0090 N85-10606

AO-1 AIRCRAFT
U OV-1 AIRCRAFT

AOIPS
U ATMOSPHERIC & OCEANOGRAPHIC INFORM SYS

APATITES
U CALCIUM PHOSPHATES
U MINERALS

APERTURES
NT SYNTHETIC APERTURES
RF characteristics of the hoop column antenna for the land mobile satellite system mission
[NASA-CR-3842] 02 p0189 N85-11264
Formation of radio images by scanning around circle
02 p0264 N85-11727
Comparison of wide aperture and short residence time ion lenses
[DE84-015274] 03 p0420 N85-12685
Characterization of MMIC devices for active array antennas
[NASA-TM-86907] 07 p0913 N85-15779
Dual offset reflector antenna systems with rotationally symmetric aperture distributions
[AD-A147346] 07 p0940 N85-15961
Efficient computation of reflector antenna aperture distributions and far field patterns
[AD-A147367] 07 p0940 N85-15962
Power transfer from natural emitters to collection apertures at microwave wavelengths
[NASA-CR-174275] 07 p0945 N85-15989
Aperture studies with PATRICIA and RACETRACK on simple attices containing SSC dipoles
[DE85-004163] 11 p1724 N85-20642
An investigation of aerowindows for solar receivers
[DE84-010931] 12 p1877 N85-21772
Beam loss due to the aperture limitation resulting from intrabeam scattering
[DE85-005138] 12 p1930 N85-22124
Determination of angular resolution of coded aperture gamma-ray telescope
13 p1961 N85-22432
Variational and moment method solutions of the fields in a parallel-plate waveguide-aperture system
[DE85-006288] 13 p2057 N85-22876
Application of modern Aperture Integration (AI) and Geometrical Theory of Diffraction (GTD) techniques for analysis of large reflector antennas
14 p2234 N85-23851
Feed system design considerations for large space antenna systems. Part 1: Multiple apertures with non-overlapping feeds
14 p2234 N85-23852
Feed system design considerations for large space antenna systems. Part 2: Single aperture with overlapping feeds
14 p2235 N85-23853
Small aperture analysis of the dual TEM (transverse electromagnetic) cell and an investigation of test object scattering in a single TEM cell
[PB85-159952] 14 p2306 N85-24277
Development of the microwave antenna range of the national antenna test facility at Paardefontein
[R-NIAS-21] 15 p2539 N85-25669
Modeling and analysis of pinhole occulter experiment: Initial study phase
[NASA-CR-175978] 19 p3272 N85-30287
Method of precisely modifying predetermined surface layers of a workpiece by cluster ion impact therewith
[DE85-006519] 23 p3984 N85-34710
Hexagonal uniformly redundant arrays for coded-aperture imaging
[OG-9.2-1] 23 p4024 N85-34940
SONTRAC: A solar neutron track chamber detector
[SH-9.1-12] 23 p4052 N85-35127
Moment-method formulation of the cavity-probe aperture antenna
[DE85-013264] 24 p4088 N85-35338

APEXES
An experimental study of the pressure in a fast bottom beneath the apex of an overlying fluid wedge
[AD-A153618] 18 p3177 N85-29696

APNEA
U RESPIRATION

APOLLO APPLICATIONS PROGRAM
The evolution of civilian in-space infrastructure, i.e., space station concepts in the United States
07 p0914 N85-15788

APOLLO ASTEROIDS
The discovery circumstances of Earth-approaching asteroids
[NASA-CR-174327] 08 p1258 N85-17920

APOLLO PROJECT
The evolution of civilian in-space infrastructure, i.e., space station concepts in the United States
07 p0914 N85-15788
Feoktistov says manned lunar, Mars flights lack justification
13 p1985 N85-22452

APOLLO SPACECRAFT
On the Apollo subsatellite evidance for a lunar core
04 p0581 N85-13714
Ground man-machine interfaces for orbiter checkout
08 p1091 N85-16897
Challenges in the development of the shuttle extravehicular mobility unit
08 p1095 N85-16922
Hypervelocity impacts on Skylab 4/Apollo windows
12 p1785 N85-21202
Hypervelocity impact investigations and meteoroid shielding experience related to Apollo and Skylab
12 p1785 N85-21206
Analysis of systematic errors in systems of selenodetic coordinates
13 p1982 N85-22435

APPALACHIAN MOUNTAINS (NORTH AMERICA)
Aircraft measurements of tracer gas during the 1983 cross Appalachian tracer experiment (CAPTEX)
[DE84-015292] 04 p0531 N85-13395
Late precambrian to ordovician metamorphism and orogenesis in the Blue Ridge and western Piedmont, Virginia Appalachians 09 p1352 N85-18503
Lithologic and environmental atlas of Berea Sandstone (Mississippian) in the Appalachian Basin
[PB85-129039] 11 p1682 N85-20600

APPARATUS
U EQUIPMENT

APPENDAGES
NT ARM (ANATOMY)
NT ELBOW (ANATOMY)
NT HAND (ANATOMY)
NT KNEE (ANATOMY)
NT LEG (ANATOMY)
The design and development of a spacecraft appendage tie down mechanism 22 p3797 N85-33522

APPLICATION
U UTILIZATION

APPLICATIONS OF MATHEMATICS
Complexity, testability, and fault analysis of digital, analog and hybrid systems
[AD-A148465] 08 p1213 N85-17634
Computing environments for data analysis. Part 1. Introduction
[AD-A146677] 09 p1373 N85-18632
Sensitivity of inferred subphotospheric velocity field to mode selection, analysis technique and noise 14 p2442 N85-25085
Compilation of abstracts of theses submitted by candidates for degrees
[AD-A151722] 16 p2875 N85-27739

APPLICATIONS PROGRAMS (COMPUTERS)
Toward an improved FIPS cost-benefit methodology. Phase 2: Descriptive models, general purpose application software development and maintenance
[PB84-226943] 06 p0870 N85-15527
METC VAX-IBM guide to ASPEN
[DE85-001974] 12 p1916 N85-22031
Executive control systems in the engineering design environment
[NASA-CR-172582] 14 p2406 N85-24835
Mapping principles for the standards interface for computer aided design
[PB85-177905] 16 p2849 N85-27566

APPLICATIONS TECHNOLOGY SATELLITES
U ATS

APPROACH
NT AIRBORNE RADAR APPROACH
NT INSTRUMENT APPROACH
Aircraft accident report. Central Airlines flight 27, Hughes Charter Air, Gates Learjet model 25 (N51CA) Newark International Airport, Newark, New Jersey, March 30, 1983
[PB84-910411] 02 p0136 N85-10924
An in-flight investigation of a twin fuselage configuration in approach and landing
[NASA-CR-172366] 05 p0566 N85-13801
A cockpit-display concept for executing a multiple glide-slope approach for wake-vortex avoidance
[NASA-TP-2386] 08 p1085 N85-16869
A frozen vorticity approach to the axisymmetric strong interaction problem
[AD-A149101] 10 p1484 N85-19369
Safety recommendation(s), A-84-62 through -84
[REPT-3957] 14 p2217 N85-23748
An IKBS approach to image understanding
[AD-A151992] 16 p2854 N85-27599
Ground-based and in-flight simulator studies of flight characteristics of a twin-fuselage passenger transport airplane during approach and landing
[NASA-TP-2451] 23 p3898 N85-34144

APPROACH AND LANDING TESTS (STS)
Aerodynamic challenges of ALT 08 p1094 N85-16911
The orbiter air data system 08 p1094 N85-16912

APPROACH CONTROL
NT RADAR APPROACH CONTROL
Aspects of application of ACT systems for pilot workload alleviation 16 p2712 N85-26734
Construction of a job-oriented test for the selection of air traffic controllers
[DFVLR-FB-84-51] 17 p3002 N85-28558
A preliminary investigation of handling qualities requirements for helicopter instrument flight during decelerating approach maneuvers and overshoot
[AD-A154650] 21 p3557 N85-32125
Guidelines for the evaluation of visual approach slope indicators
[ARL/SYS-R-32] 23 p3896 N85-34132
The integrated manual and automatic control of complex flight systems
[NASA-CR-176166] 24 p4066 N85-35201

APPROACH INDICATORS
Evaluation of arctic test of improved tritium radioluminescent lighting
[AD-A148215] 08 p1089 N85-16884
Safety recommendation(s), A-84-123 and -124
[REPT-3894B/93] 15 p2466 N85-25222

APPROPRIATIONS
Department of Housing and Urban Development, and certain independent agencies appropriations for fiscal year 1985, part 2
[S-REPT-98-889-PT-2] 01 p0127 N85-10870
An agenda for a study of government science policy
[GPO-40-860] 12 p1949 N85-22245
National Telecommunications and Information Administration authorization
[GPO-38-660] 16 p2879 N85-27768
National Aeronautics and Space Administration Authorization Act, 1986
[S-REPT-99-91] 17 p3051 N85-28885
National Aeronautics and Space Administration Authorization Act, 1986
[S-REPT-99-91] 19 p3381 N85-30978
Department of Housing and Urban Development-Independent Agencies Appropriation Bill, 1986
[H-REPT-99-212] 19 p3382 N85-30979
National Aeronautics and Space Administration 19 p3382 N85-30980
Department of Housing and Urban Development-Independent Agencies Appropriation Act, 1986 20 p3542 N85-32041
National Aeronautics and Space Administration research and development 20 p3542 N85-32042
Testimony of Robert A. Frosch before the Subcommittee on HUD and Independent Agencies of the Senate Committee on Appropriations
[NASA-TM-87496] 22 p3736 N85-33173
Department of Housing and Urban Development Independent Agencies Appropriation Bill, 1986
[S-REPT-99-129] 23 p3987 N85-34720
National Aeronautics and Space Administration research and development: Program description 23 p3987 N85-34721

APPROXIMATION
NT BORN APPROXIMATION
NT CHEBYSHEV APPROXIMATION
NT EDDINGTON APPROXIMATION
NT FINITE DIFFERENCE THEORY
NT FINITE ELEMENT METHOD
NT HARTREE APPROXIMATION
NT LEAST SQUARES METHOD
NT MEAN SQUARE VALUES
NT NEWTON-RAPHSON METHOD
NT NUMERICAL DIFFERENTIATION
NT PADE APPROXIMATION
NT PARTICLE IN CELL TECHNIQUE
NT RELAXATION METHOD (MATHEMATICS)
NT RITZ AVERAGING METHOD
Design proposals for torsional buckling of stiffeners
[AD-A144783] 01 p0062 N85-10409
On the treatment of material laws for approximate J-estimation methods
[GKSS-84-E-15] 01 p0062 N85-10414
Normal approximation for response time in a processor-shared computer system model
[AD-A144997] 01 p0103 N85-10690
Approximating hierarchical normal priors using a vague component
[CSIR-TWISK-284] 01 p0107 N85-10720
Some concepts in multi-criteria optimization
[CSIR-TWISK-299] 01 p0108 N85-10722
The approximation of nonsmooth solutions of hyperbolic partial differential equations
[CSIR-TWISK-297] 01 p0108 N85-10723
Simultaneous rational approximation of a function and its derivatives in the complex plane
[CSIR-TWISK-311] 01 p0109 N85-10733
Sensitivity analysis in generalized rational approximation with restricted denominator
[CSIR-TWISK-319] 01 p0109 N85-10734
The convergence of Galerkin approximation schemes for second-order hyperbolic equations with dissipation
[CSIR-TWISK-325] 01 p0109 N85-10736
Spline-Galerkin solution of integral equations for 3-body scattering above break-up
[TWISK-327] 01 p0109 N85-10738
Legendre-Tau approximation for functional differential equations. Part 3: Eigenvalue approximations and uniform stability
[NASA-CR-172447] 01 p0110 N85-10744
Partitions of unity and approximation
[AD-A144717] 01 p0110 N85-10746
Some families of near-orthonormal analytic and harmonic functions
[AD-A144722] 01 p0110 N85-10748
Methods for numerical differentiation
[AD-A145058] 01 p0112 N85-10758
Credibility approximations for Bayesian prediction of second moments
[AD-A144996] 01 p0113 N85-10766
Comment on the validity of an L2 treatment of the center of mass problem
[CSIR-TWISK-324] 01 p0114 N85-10779
Fast Fourier transform for unequally spaced data 01 p0128 N85-10876
Fitting aerodynamic forces in the Laplace domain: An application of a nonlinear nongradient technique to multilevel constrained optimization
[NASA-TM-86317] 02 p0134 N85-10917
Approximation methods for inverse problems involving the vibration of beams with tip bodies
[NASA-CR-172468] 02 p0209 N85-11379
Approximation of discontinuous solutions of hyperbolic partial differential equations
[NRIMS-TWISK-302] 02 p0250 N85-11631
Sinc method of solution of singular integral equations
[AD-A146155] 03 p0411 N85-12631
A two-segment approximation algorithm for separable convex programming with linear constraints
[AD-A146215] 03 p0412 N85-12634
Coherent amplification of ultrasonic pulses in activated crystals 05 p0724 N85-14653
A geometric approach to high resolution TVD schemes
[NASA-CR-172484] 06 p0857 N85-15449
Determination of moments of initial estimate during linear approximation of distribution of ejected impurity 07 p0954 N85-16045
Numerical methods and approximation and modelling problems in stochastic control theory
[AD-A146927] 07 p1029 N85-16533
A counterexample to a result of Strang and Fix concerning controlled approximation
[AD-A147360] 07 p1032 N85-16550
Spline methods for approximating quantile functions and generating random samples
[NASA-TP-2389] 07 p1035 N85-16585
Multivariable flight control with time-scale separation
[NASA-CR-174320] 08 p1087 N85-16873
Computer subroutines for estimation of human exposure to radiation in low Earth orbit
[NASA-TM-86324] 08 p1199 N85-17550
Improved stability and performance bounds using approximate models — control system design
[RR-280] 08 p1209 N85-17606
Asymptotic methods for the analysis, estimation, and control of stochastic dynamic systems
[AD-A147758] 08 p1211 N85-17618
The performance of variable sampling plans when the normal distribution is truncated
[AD-A147717] 08 p1215 N85-17649
Electronic structure of liquid metal alloys
[DE85-000904] 09 p1295 N85-18136
Resistivity of alloys
[DE85-000906] 09 p1296 N85-18138
Modeling of real UT transducer field/flaw interactions
[DE85-000341] 09 p1329 N85-18351
A 3-dimensional mass conserving element for compressible flows
[NASA-CR-172513] 09 p1373 N85-18626
On the connection between multigrid and cyclic reduction
[NASA-TM-86020] 09 p1373 N85-18629
Simple approximate variances for b-letter values. A sampling enquiry: Supplement
[DE85-001410] 09 p1376 N85-18647
Nonlocal and nonlinear effects on solar oscillations 09 p1416 N85-18934
Diffeomorphic approximation of quasiconformal and quasisymmetric homeomorphisms 10 p1536 N85-19678
A Galerkin method for the estimation of parameters in hybrid systems governing the vibration of flexible beams with tip bodies
[NASA-CR-172537] 10 p1544 N85-19734
Controlled approximation and a characterization of the local approximation order
[AD-A149095] 10 p1545 N85-19750
A new method of approximating normal and t-tail areas
[AD-A149457] 10 p1548 N85-19761
A remark on regularization in Hilbert spaces
[AD-A149046] 10 p1552 N85-19787
Imaging through a multiple scattering medium
[DE85-002051] 10 p1557 N85-19821
Theoretical and experimental study of crack resistance and macrocrack growth rate in organic fiber reinforced plastic under pure shear condition 11 p1598 N85-20053

The eigenvalues of the pseudospectral Fourier approximation to the operator sin (2x) d/dx
[NASA-CR-172536] 11 p1706 N85-20729
Alternative approximation concepts for space frame synthesis
[NASA-CR-172526] 12 p1776 N85-21150
Recovering pointwise values of discontinuous data within spectral accuracy
[NASA-CR-172535] 12 p1919 N85-22049
A two-dimensional smoothing spline and a regression problem
[AD-A149824] 12 p1921 N85-22067
Inference for censored matched pairs using signed ranks
[MATHEMATICS-RESEARCH-162] 12 p1923 N85-22078
Rates of convergence of semistochastic approximation procedures for solving stochastic optimization problems 12 p1924 N85-22088
Approximation order from certain spaces of smooth bivariate splines on a 3-direction mesh
[AD-A149833] 12 p1925 N85-22092
Preliminary development of an approximation procedure for supercritical wing design optimization applications
[AD-A150177] 13 p1972 N85-22363
Computing convolution of multifrequency signal employing truncated fast Fourier transform algorithms 13 p2085 N85-23019
Significance of the thin-layer Navier-Stokes approximation
[DE85-002630] 13 p2092 N85-23063
Confidence intervals using the regenerative method for simulation output analysis
[AD-A150147] 13 p2149 N85-23343
Approximation in optimal control and identification of large space structures
[AD-A150323] 13 p2151 N85-23351
Accumulation of the terrestrial planets 13 p2179 N85-23524
Some approximations of geophysical hydrodynamics 14 p2336 N85-24448
Properties of systems which lead to efficient computation of reliability
[AD-A151033] 14 p2409 N85-24853
Algorithms and approximations for queueing systems
[CWI-TRACT-8] 14 p2410 N85-24859
On the stability of predictor-corrector methods for parabolic equations with delay
[CWI-NM-R8410] 14 p2410 N85-24860
Estimation of optimum scores for partition detectors using stochastic approximation techniques 14 p2411 N85-24865
One method for constructing model of point masses of planetary gravity field 15 p2479 N85-25300
Natural convection in cylindrical containers 15 p2555 N85-25783
Approximating posterior distributions of system reliability derived from component test data
[AD-A152057] 15 p2572 N85-25857
Truncated nonlinear filters 15 p2635 N85-26249
Scattered data interpolation and approximation
[DE85-007495] 15 p2641 N85-26290
An approximation theory for nonlinear evolution equations and single conservation laws 16 p2691 N85-26614
A numerical procedure on three-dimensional parabolic flow in duct 16 p2692 N85-26620
Application of conformal mapping to grid generation 16 p2692 N85-26621
Approximate solution of the problem of fluid oscillations in cavities of revolution 16 p2764 N85-27058
An incremental multigrid strategy for the fluid dynamics equations
[AD-A151953] 16 p2783 N85-27172
An approximation to the problem of a pin-loaded hole in an orthotropic plate
[VTH-LR-366] 16 p2802 N85-27276
Solving the minimal least squares problem subject to bounds on the variables
[TRITA-NA-8215] 16 p2852 N85-27560
Uniformly high-order accurate non-oscillatory schemes, 1
[NASA-CR-175768] 16 p2853 N85-27569
Eigenvalue approximation methods for quantum lattice Hamiltonians 16 p2858 N85-27627
Characteristics of steady-state hypersonic flow about blunted bodies with discontinuities in generators 17 p2941 N85-28155
SC filters and design centering of integrated circuits. Part 2: Design centering of integrated circuits
[BMFT-FB-T-84-265-PT-2] 17 p2956 N85-28257
Curved finite elements and curve approximation 17 p3007 N85-28590
An inequality and its application to the truncated distributions 17 p3020 N85-28673
Spatial differencing for finite difference codes
[DE85-006902] 17 p3021 N85-28684
On the accuracy of the Poincare-Lindstedt method
[REPT-84-37] 17 p3022 N85-28690
On the condition number of modified moment matrices arising from least squares approximation in the complex plane
[AD-A152353] 17 p3026 N85-28714
A numerical study of the mean trajectory approximation in a non-adiabatic process
[AD-A152763] 17 p3030 N85-28737
The mean trajectory approximation for charge and energy transfer processes at surfaces
[AD-A152706] 17 p3043 N85-28830
Quantum model of dephasing-enhanced laser desorption: Master equation approach
[AD-A153769] 18 p3112 N85-29269
Sigma filter 18 p3142 N85-29450
The vertical structure of global rotational normal modes 18 p3144 N85-29464
Effect of some estimators on a large sample approximation to the non-null distribution of the pearson chi-square statistic
[AD-A153515] 18 p3173 N85-29673
Development of the relativistic impulse approximation
[DE85-006505] 18 p3179 N85-29711
Evaluation of the eigenvalue method in the solution of transient heat conduction problems
[AD-A154434] 19 p3266 N85-30256
Well-posedness of one-way wave equations and absorbing boundary conditions
[NASA-CR-172619] 19 p3345 N85-30727
Calculation of Franck-Condon factors for diatomic molecules
[AD-A154463] 19 p3353 N85-30784
Activities of Rutgers - The State University Department of Mathematics
[AD-A154158] 19 p3370 N85-30904
Plasma radiation sources. Quasi-adiabatic theory and numerical modeling in the electro-diffusive approximation
[AD-A154375] 19 p3370 N85-30906
Tables of generalized hydrogen diffusion profiles and permeating fluxes for fusion applications
[DE85-006876] 19 p3372 N85-30919
Approximation techniques for parameter estimation and feedback control for distributed models of large flexible structures 20 p3413 N85-31179
Approximation of optimal infinite dimensional compensators for flexible structures 20 p3413 N85-31181
Influence of error of determination of moire isotach orders on the stability of their approximation
[BLL-M-36277-(5828.4)] 20 p3450 N85-31423
Reduced order models and simulation data in control systems design
[RR-267] 20 p3463 N85-31516
Memory effects in dynamical many-body systems: The isomnesic (constant-memory) approximation
[AD-A154160] 20 p3520 N85-31889
Improved Nominal Operating Cell Temperature (NOCT) test procedure 21 p3612 N85-32449
Toward the propagation of waves in unsteady media 21 p3683 N85-32861
On the problem of linear programming with approximate data 21 p3698 N85-32978
Discrete-element acoustic analysis of submerged structures using doubly asymptotic approximations
[AD-A154959] 21 p3700 N85-32987
Maximally flat approximation of attenuation characteristics of coupled-line filters 22 p3775 N85-33393
Interacting Boson approximation
[DE85-003016] 22 p3837 N85-33756
Multiaxial stress analysis taking account of penetration depth of X-rays. A solution by means of polynomial approximation 23 p3907 N85-34204
Building an octree from a set of parallelepipeds 23 p3964 N85-34572
Guiding center distribution function and longitudinal invariant 23 p3978 N85-34663
The role of cosmic rays in magnetic hydrodynamics of interstellar medium
[OG-7.2-15] 23 p4015 N85-34882
Finite analytic solutions of supersonic flows in two-dimensional non-symmetrical channels 24 p4059 N85-35154
Prediction of turbulent internal recirculating flows with K-epsilon models 24 p4092 N85-35366
Vibrations of free hollow circular cylindrical bodies 24 p4100 N85-35416
An evaluation of a class of practical optimization techniques for structural dynamics applications
[PB85-195766] 24 p4103 N85-35434
A new theory for multistep discretizations of stiff ordinary differential equations: Stability with large step sizes
[NASA-CR-177941] 24 p4142 N85-35675
Model robust response surface designs: Scaling two-level factorials
[AD-A156218] 24 p4143 N85-35686
Applications and misapplications of the channel-capture formalism of direct neutron capture
[DE85-013992] 24 p4152 N85-35748
Optical receivers using rough reflectors
[NASA-CR-176200] 24 p4154 N85-35750
Study of the parameters affecting the collapse of a rotating protostellar cloud 24 p4168 N85-35837

APPROXIMATION METHODS
U APPROXIMATION

APSIDAL ANGLES
U APSIDES

APSIDES
NT PERIGEES
NT PERIHELIONS

The stellar wind in the BO V-type eclipsing binary Y Cygni 11 p1755 N85-21040

APTITUDE

The application of basic control laws to human medicine
[DFVLR-MITT-84-13] 05 p0697 N85-14482
Cognitive asymmetry and occupation. Computer programmers, students, and bank personnel, part 1 and part 2
[AD-A147125] 08 p1197 N85-17540
Technical evaluation of the Naval Automated Pilot Aptitude Measurement System (NAPAMS)
[AD-A152361] 17 p3000 N85-28547
Estimating ability with the wrong model
[AD-A154071] 19 p3335 N85-30663
Equipercentile test equating: The effects of presmoothing and postsmoothing on the magnitude of sample-dependent errors
[AD-A154110] 19 p3347 N85-30746

AQUATIC PLANTS

Aquatic plant control research program. Evaluation of Fusarium roseum Culmorum as a biological control agent for Hydrilla verticillata
[AD-A145228] 01 p0069 N85-10459
Estuaries of the Cape. Part 2: Synopses of available information on individual systems. Report 13: Silvermine (CSW 3)
[CSIR-RR-412-PT-2] 01 p0086 N85-10582
Estuaries of the Cape. Part 2: Synopses of available information on individual systems. Report no. 16: Eerste (CSW 6)
[CSIR-RR-415-PT-2] 01 p0087 N85-10585
Effects of low temperatures on the growth and unfrozen water content of an aquatic plant
[AD-A147107] 07 p1011 N85-16424
Review and annotated bibliography of benthic studies in coastal and estuarine areas of Florida with a selected compilation of worldwide benthic methodological references and southeastern United States benthic taxonomic references
[PB85-151041] 16 p2622 N85-27405
Handbook for obtaining and using aerial photography to map aquatic plant distribution
[AD-A154584] 21 p3605 N85-32388

AQUEOUS SOLUTIONS

Experiments on turbulent mixing and chemical reactions in a liquid mixing layer 02 p0134 N85-10912
Transport phenomena in the boundary layer during solution solidification under microgravity. Ice growth from a water-salt solution
[BMFT-FB-W-84-031] 03 p0329 N85-12121
Electrokinetic potential and stability of SiC suspensions in electrolyte solutions
[NASA-TM-77482] 04 p0469 N85-12984
Investigations regarding process analysis of liquids in the 1 to 2 micrometer spectral range
[BMFT-FB-T-84-169] 05 p0614 N85-13926
Current and potential transients during localized corrosion of stainless steel
[DE84-014100] 05 p0618 N85-13954
Measuring system with ion selective electrodes
[BMFT-FB-T-84-170] 05 p0639 N85-14100
Photoacoustic spectroscopy at electrode-solution interface
[DE85-001872] 09 p1292 N85-18111
Thermodynamic properties of aqueous NaCl from 273 to 823 K with estimates for higher temperatures
[DE85-000392] 09 p1292 N85-18116
Contributions of segregated phosphorus to the intergranular stress corrosion cracking of nickel
[DE85-003112] 11 p1606 N85-20099
Compiled and thermodynamic data sources for aqueous and biochemical systems: An annotated bibliography, 1930 - 1983
[PB85-137693] 12 p1944 N85-22208
Applications of photoinduced electron transfer and hydrogen abstraction reactions to chemical and electrochemical conversion processes
[DE85-006068] 15 p2508 N85-25459

Kinetics of hydrolysis and products of hydrolysis and photolysis of tetryl
[AD-A153144] 17 p2921 N85-26005
Properties of nitrogen containing stainless alloy designed for high resistance to pitting
[DE85-006282] 17 p2931 N85-26095
Corrosion Research Center of the University of Minnesota
[DE85-009418] 18 p3075 N85-29022
Chemical transformations in acid rain. Volume 2: Investigation of kinetics and mechanism of aqueous-phase peroxide formation
[PB85-173433] 18 p3135 N85-29416
Systematic view of transition intensities in the spectra of actinides and lanthanides in condensed phases
[DE85-010272] 19 p3354 N85-30789
Experimental evaluation of the thermodynamic properties of concentrated aqueous potassium hydroxide solutions
[DE85-010628] 23 p3912 N85-34236

AQUICULTURE
Cultivation and conversion of marine macroalgae — biomass energy production
[DE84-004522] 04 p0544 N85-13464
Research and development of shallow algal mass culture systems for the production of oils
[DE85-000518] 11 p1690 N85-20624
Aquatic Invertebrate Development Working Group
24 p4127 N85-35585

AQUIFERS
Definition of global dispersion coefficients — aquifers
[PSE-83/4-B] 01 p0064 N85-10426
Water resources by orbital remote sensing: Examples of applications
[E85-10015] 02 p0217 N85-11428
Geothermal resource assessment for North Dakota
[DE84-016128] 04 p0526 N85-13367
Steady flow model user's guide
[DE85-002001] 08 p1163 N85-17337
Field testing of aquifer thermal energy storage
[DE85-000399] 09 p1344 N85-18457
Protocol for aquifer cleanup decision making at military installations
[AD-P004151] 09 p1349 N85-18487
Evaluation of subsurface fracture geometry using fluid pressure response to solid earth tidal strain
[DE85-003294] 12 p1890 N85-21864
Determining deep heat flow and rate of horizontal percolation from temperature measurements in aquifer
13 p2116 N85-23180
Report on regional groundwater flow modeling for the Palo Duro Basin, Texas
[DE85-007490] 16 p2815 N85-27370
Central solar heating plants with seasonal storage. Evaluation of systems concepts based on heat storage in aquifers
[DE85-006788] 16 p2820 N85-27396
Groundwater model for an island aquifer: Bribie Island groundwater study
[CE-44] 16 p2821 N85-27398
Occurrence of uranium in ground water in the vicinity of the US Department of Energy Feed Materials Production Center, Fernald, Ohio
[DE85-010340] 19 p3364 N85-30662
State-of-the-art of aquifer restoration. Volume 1: Sections 1 through 8
[PB85-181071] 20 p3478 N85-31612
State-of-the-art of aquifer restoration. Volume 2: Appendices A through G
[PB85-181089] 20 p3478 N85-31613
Detailed validation of a liquid and heat flow code against field performance
[DE85-009901] 23 p3932 N85-34368
Depletion modeling of liquid dominated geothermal reservoirs
[DE85-009823] 23 p3943 N85-34437
The geostatistical approach to the inverse problem in two-dimensional steady state groundwater modeling
24 p4107 N85-35462
Hydrogeology of the lower Glen Rose Aquifer, south-central Texas 24 p4108 N85-35466

ARABIAN SEA
Arabian gulf circulation — pollution monitoring
14 p2331 N85-24412
Mineralogical-geochemical characteristics of ferromanganese formations in Arabian-Indian Ocean Ridge 19 p3293 N85-30416
On the interannual variability of the Indian monsoon and the Southern Oscillation 20 p3495 N85-31728

ARABSAT
ARABSAT spacecraft: Rx and Tx antenna mechanisms 05 p0626 N85-14022

ARC CHAMBERS
Study of a constricted electric arc cooled by transpiration
[NASA-TM-77846] 17 p3038 N85-28798

ARC CLOUDS
The arc cloud complex: A case study
[AD-A145384] 02 p0231 N85-11507

ARC DISCHARGES
Gas pressure and electron density at the level of the active zone of hollow cathode arc discharges
[NASA-TM-77477] 03 p0414 N85-12648
The discharge mechanism of the high-temperature arc
[NASA-TM-77794] 07 p0922 N85-15837
Gas pressure and electron density in the active zone level of hollow cathode arc discharges
[NASA-TM-77468] 07 p0945 N85-15968
An investigation of arc discharging on negatively biased dielectric conductor samples in a plasma
13 p1994 N85-22498
Phenomenology of discharges in space: Application to a solar generator — SPOT satellite
13 p2007 N85-22583
Electrostatic discharge testing on a carbon fiber solar panel structure 13 p2007 N85-22584
The loss of material from the cathode of metal arcs
[NASA-TM-77845] 17 p2918 N85-27985
Spectrographic investigation of low-voltage arc discharge in argon atmosphere
[BLL-M-36276-(5828.4)] 20 p3422 N85-31242
High pressure working mode of hollow cathode arc discharges
[NASA-TM-77880] 20 p3535 N85-31992
Hollow cathodes in high pressure arc discharges
[NASA-TM-87096] 23 p3903 N85-34179

ARC GENERATORS
Experimental research on electric propulsion. Note 7: Analysis of the performance of an arc-jet driven by means of hydrogen and nitrogen
[NASA-TM-77473] 06 p0760 N85-14861
Experimental research on electrical propulsion. Note 2: Experimental research on a plasma jet with vortex type stabilization for propulsion
[NASA-TM-77874] 18 p3067 N85-28966

ARC JET ENGINES
Experimental research on electric propulsion. Note 7: Analysis of the performance of an arc-jet driven by means of hydrogen and nitrogen
[NASA-TM-77473] 06 p0760 N85-14861
Axisymmetric electromagnetic field influence on the characteristic velocity of an arc-jet
[NASA-TM-77475] 07 p0938 N85-15942
Electrode erosion in arc discharges at atmospheric pressure
[NASA-TM-87087] 23 p3903 N85-34178
Hollow cathodes in high pressure arc discharges
[NASA-TM-87096] 23 p3903 N85-34179

ARC LAMPS
Investigation of light source and scattering medium related to vapor-screen flow visualization in a supersonic wind tunnel
[NASA-TM-86290] 06 p0810 N85-15144
Life study of RF excited Hg arc lamps and CO2 waveguide lasers
[AD-A149618] 12 p1856 N85-21640
Electrodeless HID lamp study
[DE85-010626] 18 p3096 N85-29167
Optical output stabilization method for direct current arc lamps
[AD-A154987] 21 p3705 N85-33013

ARC SPRAYING
Arc spray fabrication of metal matrix composite monotape
[NASA-CASE-LEW-13828-1] 19 p3230 N85-30027

ARC WELDING
NT GAS TUNGSTEN ARC WELDING
NT PLASMA ARC WELDING
Utility of the M.I.T. (Massachusetts Institute of Technology) underwater stud welding gun
[AD-A144793] 01 p0055 N85-10365
Optical seam tracking of robotic arc welding
[VTT-272] 01 p0055 N85-10368
Design, construction, demonstration and delivery of an automated narrow gap welding system
[AD-A145497] 02 p0204 N85-11348
New welding equipment for mechanized welding and trends in further development 03 p0352 N85-12284
Prediction of weld defects using welding condition data
[VTT-RR-264] 03 p0370 N85-12359
Optimization of toughness properties of HSCA shielded metal arc welding electrodes
[BMFT-FB-T-84-186] 05 p0646 N85-14148
ONR (Office of Naval Research) Far East Scientific Bulletin, volume 9, number 3, July to September 1984
[AD-A147282] 08 p1282 N85-17930
Effect of tempering on the strength and toughness of 2 1/4 Cr-1 Mo steel weldments
[DE85-003818] 09 p1296 N85-18140
Mechanical properties of Shielded Metal Arc (SMA) and Submerged Arc (SA) welded joints for quenched and tempered steel StE 470.
[VTT-319] 09 p1328 N85-18346
Estimate of quality of aluminum alloy surface preperation for arc welding 10 p1449 N85-19128
The effect of filler wire and flux compositions on the microstructure and properties of microalloyed steel weld metal
[AD-A149529] 10 p1492 N85-19423
Weldability of alloy ABM1 to alloy 1201
11 p1603 N85-20080
Properties of welded joints in argon arc welding of titanium alloy using a protective coating
13 p2032 N85-22733
Reliability of robotized welding apparatus
13 p2034 N85-22741
Structure and mechanical characteristics of heterogeneous joints produced by laser welding
13 p2034 N85-22742
Study of experimental robotized system for arc welding based on Universal-15 manipulator
15 p2500 N85-25423
Dynamic characteristics of ac arc in welding aluminum alloys 15 p2500 N85-25424
Effectiveness of use of heat-dissipating clamps to reduce deformation during argon arc welding of thin sheets of AMg6 alloy 15 p2501 N85-25427
Hardening of titanium alloy electric-arc welded joints
15 p2514 N85-25513
Welding technology and organisation in steel construction 15 p2568 N85-25828
Robotic arc welding 15 p2568 N85-25830
Automation and robotics in welding
15 p2568 N85-25831
Recent advances in arc welding equipment and their application 15 p2568 N85-25832
A critical review of selected recent advancements in arc welding equipment and processes
15 p2568 N85-25833
Underwater pipeline: Welding by high frequency induction
[BLL-WI-TRANS-682-(9312.57)]
16 p2792 N85-27221
Welder training/welder testing
[BLL-WI-TRANS-683-(9312.57)]
16 p2792 N85-27223
Submerged arc welding of new Czechoslovak micro-alloy steels
[BLL-BISI-TRANS-22193-(9022.06)]
17 p2972 N85-28356
Application of 4-wire submerged arc method to welding UOE pipe
[BLL-BISI-TRANS-22417-(9022.06)]
17 p2972 N85-28358
High-speed longitudinal welding of pipes by automatic submerged arc process
[BLL-BISI-TRANS-22340-(9902.06)]
17 p2973 N85-28366
Effect of protective method on cyclic durability and nature of failure of titanium alloy welded joints
19 p3245 N85-30122
Low pressure arc butt welding of dissimilar metals
19 p3246 N85-30128
Welding of steel-aluminum cooling panels for the holds of refrigerator vessels 19 p3246 N85-30129
Hot cracking of austenitic stainless steels: The debut of the Sigmajig
[DE85-010560] 20 p3431 N85-31287
Chromium-base powder alloys for welding cladding layer of bimetal
[BLL-M-35776-(5828.4)] 23 p3915 N85-34260
Electronic imaging system and technique
[DE85-005740] 23 p3935 N85-34393

ARCHAEOLOGY
Methodological research in connection with the handling of LANDSAT satellite data for archaeology
05 p0655 N85-14207
Multivariate analyses of sedimentological data at two early Bronze age sites, Bab edh-Dhra and Numeira, southeast Dead Sea Graben, Jordan
05 p0674 N85-14328
Paleoenvironmental investigations at seed cave (Windust cave H-45FR46), Franklin County, Washington
[AD-A154777] 21 p3635 N85-32576

ARCHES
Investigation of internal friction of free-flowing material during discharge
[BLL-M-36141-(5828.4)] 15 p2553 N85-25752

ARCHITECTURE
Patterns of behavior in lodgings exposed to traffic noise
[NASA-TM-77750] 03 p0387 N85-12479
The human role in space. Volume 3: Generalizations on human roles in space
[NASA-CR-171225] 04 p0546 N85-13475

Seismic performance of low-rise light-framed wood buildings 08 p1171 N85-17384
Prototype concept design for US Army type 3A Air Traffic Control Tower (ATCT)
[AD-A148840] 09 p1284 N85-18070
Report of the Artificial Gravity Panel 11 p1645 N85-20365
Photovoltaic roofing tile systems 12 p1878 N85-21783
Evaluating wind flow around buildings on heliport placement
[FAA-PM-84-25] 12 p1893 N85-21881
Progress through cooperation and exchange of ideas and experiences 15 p2626 N85-26186
Design of computer-related workstations in relation to job functions and productivity
[AD-A151938] 16 p2844 N85-27534
Overview: Human factors issues in space station architecture 18 p3158 N85-29558
Assured information flow capping architecture
[AD-A155392] 22 p3756 N85-33283
Generative design in architecture using an expert system 23 p3965 N85-34582

ARCHITECTURE (COMPUTERS)
Aerospatiale's experimentations of vectorization on supercomputers for aircraft structural problems 01 p0007 N85-10041
Impact of new computing systems on computational mechanics and flight-vehicle structures technology 01 p0007 N85-10042
Electronics Engineering Department: EE technical review
[DE84-016124] 01 p0044 N85-10286
The FLEX/32 multicomputing environment 01 p0057 N85-10378
Performance of the h, p and h-p versions 01 p0058 N85-10383
Activities of the MIT Laboratory for Computer Science
[AD-A145134] 01 p0100 N85-10661
Data flow computer architecture
[DE84-014362] 01 p0100 N85-10664
Analysis of three database system architectures using benchmarks
[PB84-217512] 01 p0105 N85-10706
A technique to model and design physical database systems
[DE84-015337] 01 p0126 N85-10863
The computer-communication link for the innovative use of Space Station 02 p0150 N85-11016
Supercomputers and VLSI: The effect of large scale integration on computer architecture
[AD-A145408] 02 p0239 N85-11555
Design and descriptive tools for systolic architectures
[DE84-015521] 02 p0239 N85-11557
Parallel searching and merging on ZMOB
[AD-A145424] 02 p0241 N85-11574
Parallel, iterative solution of sparse linear systems: Models and architectures
[NASA-CR-172457] 02 p0243 N85-11586
Fault tolerant computing research
[AD-A145640] 02 p0244 N85-11590
Application of the CSRL language to the design of expert diagnosis systems: The Auto-Mech experience
[AD-P003922] 02 p0245 N85-11602
Study on the conversion and test of protocols
[ENST-84E005] 03 p0356 N85-12293
Application of a silicon compiler to VLSI (Very Large Scale Integrated circuits) design of digital pipelined multipliers
[AD-A146328] 03 p0403 N85-12569
Analysis and design methodology for VLSI computing networks
[AD-A146030] 03 p0409 N85-12611
A decomposable algorithm for contour surface display generation
[AD-A145783] 03 p0410 N85-12619
USSR report: Electronics and electrical engineering
[JPRS-UEE-84-010] 04 p0485 N85-13095
Architecture of adaptive space-frequency-time signal processing system 04 p0486 N85-13103
A control scheme for microcomputers being used in multiprocessor arrays
[DE84-014590] 04 p0547 N85-13479
Physical database processor preliminary interface specifications
[PB84-217561] 04 p0548 N85-13483
New directions in software for advanced computer architectures
[DE84-017435] 04 p0550 N85-13502
A distributed expert system for Space Shuttle flight control 05 p0602 N85-13836
VLSI architectures for the multiplication of integers modulo a Fermat number 05 p0624 N85-13993
Massively parallel processor 05 p0680 N85-14366
Memory hierarchies for Directly Executed Language microprocessors 05 p0713 N85-14570
Requirements and overview of the LINCS distributed operating system architecture
[DE84-013721] 05 p0714 N85-14577
Fast algorithms and specialized architectures 05 p0714 N85-14579
S-MICRO: A system for simulating a microprogrammed control unit
[INPE-3224-PRE/575] 05 p0715 N85-14585
Avionics/crew station integration 06 p0752 N85-14818
Internal structure of microprocessor 06 p0785 N85-15020
Workshop on Computer Architecture
[AD-A146455] 06 p0847 N85-15378
Architecture, design, and system; performance assessment and development methodology for computer-based systems. Volume 1: Methodology description, discussion, and assessment
[AD-A146577] 06 p0847 N85-15379
Distributed database components in a DBMS (Database Management System) component architecture
[PB84-217546] 06 p0848 N85-15382
Specialized silicon compilers for language recognition
[AD-A146526] 06 p0853 N85-15425
A framework for the development of Navy computer-based systems: Combat system architecture and combat system engineering put into perspective
[AD-A146460] 06 p0856 N85-15445
Algebraic techniques in systolic array design
[AD-A146417] 06 p0857 N85-15451
Two-dimensional signal processing and storage and theory and applications of electromagnetic measurements. Supplemental appendix
[AD-A146848] 07 p0939 N85-15953
Upset susceptibility study employing circuit analysis and digital simulation --- digital systems and electromagnetic interference 07 p0999 N85-16344
Future database machine architectures
[AD-A146786] 07 p1022 N85-16481
Computer science research in Europe
[AD-A146905] 07 p1022 N85-16482
Local area network evaluation by MICROSS extensions
[AD-A146773] 07 p1027 N85-16521
Built-in test and self repair mechanisms in a digital correlator integrated circuit 08 p1064 N85-16741
Hardware/software codesign for maintainable systems 08 p1066 N85-16753
Evolution toward a multi-bus architecture for Army helicopter avionic systems 08 p1074 N85-16812
Restructurable VLSI program
[AD-A148145] 08 p1157 N85-17301
Kernel Ada Programming Support Environment (KAPSE) interface team public report, volume 4
[AD-A147648] 08 p1205 N85-17581
Matrix-matrix multiplication using an electrooptical systolic-engagement array processing architecture
[AD-D011410] 08 p1223 N85-17704
Raster graphics extensions to the core system
[NASA-CR-174348] 09 p1367 N85-18590
Integrating heterogeneous non-geometric information systems using RIM
[DE84-017600] 09 p1402 N85-18823
The feasibility of a multiprocessor architecture for real-time contour surface display generation
[AD-A149427] 10 p1538 N85-19697
Meta-level control through fault detection and diagnosis
[AD-A149064] 10 p1540 N85-19709
Siemens introduces fast computer with pipeline architecture 11 p1618 N85-20178
ESOP expert system model described 11 p1619 N85-20187
PASLIB programmer's guide for the finite element machine, revision 2.1-A
[NASA-CR-172281] 11 p1705 N85-20727
Needs, opportunities, and options for large scale systems research
[DE85-002664] 11 p1709 N85-20750
RAPIDbus: Design of an extensible multiprocessor structure
[AD-A150061] 12 p1912 N85-21998
Towards the generation of efficient code from verified programs
[TR-40] 12 p1914 N85-22017
Feasibility of self-structured current accessed bubble devices in spacecraft recording systems
[NASA-CR-172554] 13 p1998 N85-22525
Periodic binary sequence generators: VLSI circuits considerations
[NASA-CR-175649] 13 p2063 N85-22886
Synthesis of tree-structured computing systems through use of closures
[AD-A150502] 13 p2147 N85-23326
Performance evaluation of distributed systems with unbalanced flows: An analysis of the INFOPLEX data storage hierarchy
[AD-A150528] 13 p2147 N85-23328
General design considerations of an Air Force information system
[AD-A150611] 13 p2168 N85-23449
Multidimensional digital signal processing
[AD-A150833] 14 p2292 N85-24209
Comparative architectures for a multiple function speech processor
[AD-A150873] 14 p2292 N85-24211
USSR report: Cybernetics, computers, and automation technology
[JPRS-UCC-85-002] 14 p2400 N85-24794
Systems design and application of computers with flexible architecture 14 p2401 N85-24800
The Multimission Image Processing Laboratory's virtual frame buffer interface
[NASA-CR-175655] 14 p2402 N85-24805
Executive control systems in the engineering design environment
[NASA-CR-172582] 14 p2406 N85-24835
Design and analysis of ordering and join for a multi-backed database system
[AD-A150711] 14 p2433 N85-25006
Rotorcraft digital advanced avionics system (RODAAS) functional description
[NASA-CR-166611] 15 p2468 N85-25237
Conversion of algorithms to custom integrated circuit devices
[AD-A151288] 15 p2547 N85-25720
Posing of the problem, status, and future of parallel computer architecture for image processing 15 p2622 N85-26155
The EGPA multiprocessor system and its possible application for pattern recognition tasks --- computer architecture 15 p2622 N85-26156
Computer architecture for image processing and pattern recognition in the Federal Republic of Germany. Status 1983, a review 15 p2623 N85-26161
Supercomputers and symbolic computation
[AD-A151376] 15 p2623 N85-26166
Role of supercomputers in energy research programs
[DE85-006865] 15 p2624 N85-26172
Computer technology advances exhibited 15 p2625 N85-26175
High-capacity real-time computer system for processing hydrophysical data 15 p2625 N85-26178
Mini- and microcomputer local control network architecture and design principles 15 p2625 N85-26179
Communication complexity of the Gaussian elimination algorithm on multiprocessors
[AD-A151891] 15 p2638 N85-26267
Recent advances in supercomputers 16 p2693 N85-26625
Navigation: Accounting for copy 16 p2695 N85-26641
A modular dissimilar redundant computer designed for high integrity control 16 p2714 N85-26751
Design and specification of a local area network architecture for use in real-time flight simulation
[AD-A152242] 16 p2716 N85-26762
Reliability models for dataflow computer systems
[NASA-CR-175813] 16 p2846 N85-27543
Evaluation of Ada (trademark) as a communications programming language, volume 1
[AD-A152314] 16 p2848 N85-27559
Evaluation of Ada (trademark) as a communications programming language. Volume 3: Trusted software application
[AD-A152316] 16 p2848 N85-27561
Continued development and implementation of the Universal Network Interface Device (UNID) 2, Digital Engineering Laboratory Network (DELNET), volume 1
[AD-A151935] 16 p2850 N85-27569
Continued development and implementation of the Universal Network Interface Device (UNID) 2 in the Digital Engineering Laboratory Network (DELNET), volume 2
[AD-A151947] 16 p2850 N85-27570
Complexity of dense linear system solution on a multiprocessor ring
[AD-A151970] 16 p2854 N85-27598
Multiple array processors for ocean acoustic problems
[AD-A152174] 16 p2860 N85-27641
Computational plasma physics and supercomputers, revision 1
[DE85-007228] 16 p2867 N85-27667
A modular dissimilar redundant computer designed for high integrity control 17 p2904 N85-27904
VLSI workshop and project: February - November 1982
[WSRL-0374-TR] 17 p2951 N85-28223

System Analysis for the Huntsville Operation Support Center, Distributed Computer System
[NASA-CR-171506] 17 p3015 N85-28642
Synchronization and fault-masking in redundant real-time systems
[NASA-TM-87478] 17 p3015 N85-28644
Interfacing the VAX 11/780 using Berkeley Unix 4.2 BSD and Ethernet based Xerox network systems, volume 1
[AD-A152953] 17 p3015 N85-28645
Interfacing the VAX 11/780 using berkeley UNIX 4.2BSD and Ethernet based Xerox Network Systems
[AD-A153174] 17 p3016 N85-28647
A high-accuracy optical linear algebra processor for finite element applications
[NASA-CR-175894] 17 p3017 N85-28658
Efficient parallel solution of linear systems
[AD-A152663] 17 p3018 N85-28663
France's use of Cray 1, plans for national supercomputer 18 p3066 N85-29093
Distributed database design tool
[AD-A153760] 18 p3200 N85-29850
A single chip VLSI architecture for radar signal processing 19 p3257 N85-30195
The BLAZE language: A parallel language for scientific programming
[NASA-CR-172615] 19 p3334 N85-30656
A parallelized point successive over-relaxation method on a multiple instruction multiple data stream computer
[AD-A154377] 19 p3337 N85-30679
Fault-tolerant computing research
[AD-A154082] 19 p3342 N85-30710
MECA: A multiprocessor concept specialized to Monte Carlo
[DE85-010791] 19 p3346 N85-30737
Design and implementation of an intelligence database
[AD-A154095] 19 p3361 N85-30973
Distributed implementation of functional program evaluation
[DE85-009573] 20 p3514 N85-31844
PIPE-1000: An implementation of piping on an HP-1000 minicomputer
[PB85-191955] 20 p3514 N85-31847
Proceedings of the 1st Workshop for the Design of Expert System Partial Differential Equation Solvers
[AD-A154192] 20 p3515 N85-31853
Globally-asynchronous locally-synchronous systems
[AD-A154624] 21 p3573 N85-32222
Secure digital voice communications in the Defense Data Network (DDN)
[AD-A154677] 21 p3574 N85-32226
Characteristics of a numerical fluid dynamics simulator
[DE85-009602] 21 p3586 N85-32290
Resource management for the tagged token dataflow architecture
[AD-A154773] 21 p3667 N85-32779
Real-time contour surface display generation
[AD-A155232] 21 p3668 N85-32780
Software for interactive on-line conferences
[AD-A154742] 21 p3670 N85-32801
HLLM software support
[AD-A154826] 21 p3671 N85-32805
Comparative study on data system architectures — spacecraft data processing
[ESA-CR(P)-2015] 21 p3675 N85-32828
Simulation of complex three-dimensional flows
[NASA-TM-86773] 21 p3675 N85-32831
New developments on the core function for efficient implementation of the difficult residue number system operations
[AD-A154678] 21 p3676 N85-32834
Basic features of personal computers
22 p3766 N85-33344
Flat is not necessarily good
[DE85-012819] 22 p3830 N85-33723
Modular digital holographic fringe data processing system
[NASA-CR-177952] 23 p3933 N85-34376
The parser generator as a general purpose tool
[NASA-CR-177955] 23 p3957 N85-34521
Architecture of languages for large CAD systems development 23 p3962 N85-34557
A methodology for the design of testable custom large-scale integrated circuits
[AD-A156098] 24 p4090 N85-35351
Design for MISP: A multiple instruction stream shared pipeline processor
[AD-A156314] 24 p4136 N85-35635
Distribution of computer functionality for accelerator control at the Brookhaven AGS
[DE85-012520] 24 p4141 N85-35669
Report on the SLC control system
[DE85-013076] 24 p4148 N85-35722

ARCTIC ENVIRONMENTS
U ICE ENVIRONMENTS

ARCTIC OCEAN
Sea-level in the world ocean. Part 5: The North-East Pacific and Arctic Oceans, a catalogue of measurements
[CSIR-T/SEA-8303-5] 01 p0087 N85-10589
Active microwave measurements of sea ice under fall conditions: The RADARSAT/FIREX fall experiment — in the Canadian Arctic
[E85-10019] 02 p0217 N85-11432
One-year records of current and bottom pressure in the strait between Nordaustlandet and Kvitoeya and Svalbard, 1980 - 1981
[AD-A145594] 02 p0233 N85-11518
Eastern-Western Arctic Sea ice analysis 1983
[AD-A146133] 03 p0398 N85-12541
Arctic ice island and sea ice movements and mechanical properties
[DE84-016323] 04 p0542 N85-13450
Satellite photographs suggest arctic volcano
07 p0982 N85-16239
Arctic marine acoustics
[AD-A147492] 07 p1039 N85-16594
Data report on variations in the composition of sea ice during MIZEX/East'83 with the Nimbus-7 SMMR
[NASA-TM-86170] 09 p1342 N85-18443
Ice statistics and acoustic scattering in the Arctic basin
[AD-A150141] 13 p2140 N85-23289
Sea-ice motion in response to geostrophic winds
14 p2323 N85-24357
Sea ice, climate and Fram Strait
15 p2603 N85-26042
Arctic mixed layer dynamics
[AD-A153582] 18 p3150 N85-29505
Transport and formation of summertime cloud condensation nuclei over the Arctic Ocean
21 p3651 N85-32686

ARCTIC REGIONS
Response of arctic ecosystems to elevated carbon dioxide regimes, volume 2
[DE84-015236] 01 p0069 N85-10460
Forecasting of polar lows 01 p0075 N85-10495
Arctic haze: Meteorological aspects of long-range transport 02 p0230 N85-11499
MIZEX. A program for mesoscale air-ice-ocean interaction experiments in arctic marginal ice zones. III: Modeling the marginal ice zone
[AD-A145351] 02 p0233 N85-11517
Evaluation of arctic test of improved tritium radioluminescent lighting
[DE84-014887] 05 p0597 N85-13805
USSR report: Earth sciences
[JPRS-UES-84-007] 06 p0819 N85-15196
Development of radar to measure sea ice merits prize nomination 06 p0826 N85-15244
Satellite photographs suggest arctic volcano
07 p0982 N85-16239
Parachute expedition to Arctic
07 p0982 N85-16240
MIZEX. A program for mesoscale Air-Ice-Ocean interaction experiments in arctic marginal ice zones. 4: Initial results and analysis from MIZEX 83
[AD-A148255] 08 p1173 N85-17399
Regional and seasonal variations in snow-cover density in the USSR
[AD-A148420] 08 p1189 N85-17496
Technology development for unmanned untethered submersible vehicle systems
[AD-A148794] 09 p1304 N85-18190
USSR report: Earth sciences
[JPRS-UES-85-003] 10 p1497 N85-19446
Types of placer formation of eastern Arctic shelf
10 p1498 N85-19452
MIZEX (Marginal Ice Zone Program): A program for mesoscale air-ice-ocean interaction experiments in Arctic marginal ice zones. 5. MIZEX 84. Summer experiment PI (Principal Investigator) preliminary reports
[AD-A148966] 10 p1521 N85-19594
Arctic acoustic propagation model with ice scattering
[AD-A149430] 10 p1553 N85-19795
Cold Arctic Mesopause Project (CAMP): Scientific objectives 11 p1656 N85-20433
High time resolution thermospheric temperature and wind studies in the Arctic
[AD-A150114] 12 p1880 N85-21860
USSR report: Earth sciences
[JPRS-UES-85-002] 13 p2105 N85-23116
Arctic-North Atlantic rift megasystem
13 p2105 N85-23117
Application of field X-ray: Radiometric analysis in exploratory geology and means for its improvement
13 p2115 N85-23176
Empirical and modeled synoptic cloud climatology of the Arctic Ocean
[NASA-CR-175828] 13 p2137 N85-23272
Variation of Arctic cloud cover in summer
[DE85-004507] 13 p2139 N85-23285
Ice statistics and acoustic scattering in the Arctic basin
[AD-A150141] 13 p2140 N85-23289
High-frequency acoustic variability in the arctic
[AD-A150550] 13 p2155 N85-23383
Applications of ARGOS data collection systems in Arctic regions 14 p2238 N85-23675
Mountain barrier baroclinity effects on surface winds along the Alaskan Arctic coast 14 p2238 N85-23677
Applications of ARGOS data collection system for automatic meteorological observatories in Arctic regions
14 p2240 N85-23693
MI-8 helicopter cargo loading experiment for Arctic shipping 14 p2332 N85-24425
Substorm associated Pc 1 emission in the morning sub-cleft latitudes 14 p2368 N85-24637
Designer O. K. Antonov on new AN-74 arctic transport
15 p2467 N85-25230
The ecology of tundra ponds of the Arctic coastal plain: A community profile
[TI85-900650] 15 p2589 N85-25958
Mining cosmic dust from the blue ice lakes of Greenland 15 p2682 N85-26563
USSR report: Earth sciences
[JPRS-UES-85-005] 16 p2807 N85-27307
Operational experiences with the ARGOS system in Greenland 16 p2813 N85-27353
An assessment of atmospheric refractivity in the northern marginal ice zone
[AD-A152346] 17 p2992 N85-28493
Atmospheric cross sections for the Arctic gas and aerosol sampling program, March - April 1983
[NASA-CR-176027] 19 p3314 N85-30541
Arctic acoustic tomography MIZEX 84
[AD-A154426] 19 p3320 N85-30580
The COSPAS/SARSAT local user terminal in Tromso, Norway. Special considerations and experience with high latitude location (69 deg, 43 min N)
20 p3402 N85-31109
Mesoscale features and atmospheric refraction conditions of the Arctic marginal ice zone
[AD-A155139] 21 p3636 N85-32584
Condensation nuclei and aerosol size distribution measurements in Arctic haze 21 p3647 N85-32658
Arctic and offshore research
[DE85-001995] 22 p3818 N85-33653

AREA NAVIGATION
Evaluation of radio navigation systems and their configuration with respect to minimum cost
[ESA-TT-847] 20 p3392 N85-31043

ARGENTINA
Tectonic, volcanic, and climatic geomorphology study of the Sierras Pampeanas Andes, northwestern Argentina 08 p1144 N85-17215
Meteorological and oceanographic support during the Falklands conflict 11 p1712 N85-20769

ARGON
NT ARGON ISOTOPES
Experimental studies of atomic inner shell ionization phenomena
[DE84-013448] 01 p0118 N85-10805
Diffusion of gases in porous solids: Simulation and measurements
[DE84-016292] 04 p0500 N85-13191
The discharge mechanism of the high-temperature arc
[NASA-TM-77794] 07 p0922 N85-15837
Study of opacity effects on line radiation from pellet implosions
[DE85-000380] 10 p1491 N85-19413
The effect of inert gases on ion transport across the erythrocyte membrane
[AD-A148889] 10 p1527 N85-19635
Pseudo-stationary oblique-shock-wave reflections in a polyatomic gas, sulfur hexafluoride
[UTIAS-TN-253] 12 p1845 N85-21577
Performance of Chromel versus Alumel and Nicrosil versus Nisil thermocouple assemblies in vacuum and argon between 1000 deg C and 1200 deg C
[DE85-000810] 12 p1853 N85-21624
Argon ion pollution of the magnetosphere
13 p1986 N85-22523
Properties of welded joints in argon arc welding of titanium alloy using a protective coating
13 p2032 N85-22733
Threshold double photoionization of argon with synchrotron radiation
[AD-A150615] 13 p2157 N85-23380
Effectiveness of use of heat-dissipating clamps to reduce deformation during argon arc welding of thin sheets of AMg6 alloy 15 p2501 N85-25427
Spectroscopy of quasimolecular X-rays with H-like decelerated ions
[DE85-006565] 15 p2849 N85-28337
Welding of 11 458.1 steel in shielding atmospheres [BLL-BISI-TRANS-21763-(9022.06)]
17 p2972 N85-29353

Hall mobility in fluid argon
[DE85-007268] 17 p3045 N85-28840
Structure and properties of VT23 alloy welded joints after thermocyclic processing 19 p3246 N85-30125
Environmental monitoring at Argonne National Laboratory
[DE85-010613] 19 p3309 N85-30516
Vibrational energy transfer in benzene-argon collisions
[DE85-009603] 19 p3355 N85-30797
Energy transfer and excimer formation in rare gas solids 19 p3374 N85-30830
Spectrographic investigation of low-voltage arc discharge in argon atmosphere
[BLL-M-36276-(5828.4)] 20 p3422 N85-31242
New metal coating method developed 21 p3566 N85-32191
Supersaturation obtained in a condensation nucleus counter 21 p3642 N85-32624
Influence of background electrically neutral argon admixture on mechanical strength of silicon crystals 21 p3683 N85-32678
Measurements of Fe and Ar fragmentation cross sections
[PAPER-OG-7.2-20] 21 p3714 N85-33047
Liquid crystal light valve structures
[NASA-CASE-MSC-20036-1] 22 p3847 N85-33626
Apparatus and method for the horizontal, crucible-free growth of silicon sheet crystals
[DE85-011588] 22 p3847 N85-33629
Thermodynamics of the corrosion of chromium in molten carbonates
[DE85-011407] 24 p4079 N85-35282
Size and shape dependence of CO adsorption sites on sapphire supported Fe microcrystals
[NASA-CR-176171] 24 p4160 N85-35794

ARGON ISOTOPES
Investigation of the daytime lunar atmosphere
[NASA-CR-175636] 14 p2440 N85-25057
The degassing history of the Earth: Noble gas studies of Archaean cherts and zero age glassy submarine basalts 21 p3718 N85-33072
The 1984 environmental monitoring report, Sandia National Laboratories, Albuquerque, New Mexico
[DE85-011175] 22 p3811 N85-33607
Control technology for radioactive emissions to the atmosphere at US Department of Energy facilities: The Los Alamos Meson Physics Facility
[DE85-011402] 22 p3811 N85-33609
Measurements of the fragmentation of (40)Ar, (28)Si and (12)C in CH2C and H targets between 300 and 1500 MeV/nuc at the Bevalac
[OG-7.2-19] 23 p4016 N85-34886
Measurements of Fe and Ar fragmentation cross sections
[OG-7.2-20] 23 p4016 N85-34887
Correlation between solar neutrino flux and other solar phenomena 23 p4049 N85-35109
The conjecture concerning time variations in the solar neutrino flux
[SH-8.1-6] 23 p4049 N85-35111

ARGON LASERS
Excimer laser photofragmentation of organophosphonates. 1: Detection of the PO radical from dimethyl methyl phosphonate (DMMP)
[AD-A149471] 10 p1490 N85-19407
Linewidth and bandwidth measurements of the q-branch of h2 using CW coherent anti-Stokes Raman spectroscopy
[AD-A151868] 15 p2506 N85-25456
Fiber optic Raman thermometer for Space Shuttle main engine preburner profiling 16 p2739 N85-28904
A study of mode-locked argon ion-dye laser systems 16 p2789 N85-27205
Photochemical ignition studies. 1: Laser ignition of flowing premixed gases
[AD-A153048] 17 p2920 N85-28002
Investigation of several low-lying levels of X doublet pi state of NCO using argon laser excited fluorescence
[AD-A153693] 18 p3071 N85-28994

ARGON PLASMA
Spatial resolution of small particles in silane discharge
[AD-A150953] 14 p2423 N85-24948
Temperature, velocity, and species mapping in an induction plasma
[DE85-004005] 15 p2512 N85-25499
Experiments in plasma initiation and laser absorption in flowing gases
[AD-A154303] 19 p3276 N85-30313
Synthesis of ultrafine ceramic and metallic powders in a thermal argon rf plasma
[DE85-009634] 23 p3983 N85-34696

ARGUMENTS (MATHEMATICS)
U INDEPENDENT VARIABLES

ARIANE LAUNCH VEHICLE
View of Ariane countdown procedures, Kourou launch facilities 03 p0310 N85-12001
Launching systems
[CNES-NT-111] 04 p0460 N85-12917
Relationships between Ariane trajectories and satellite orbits 05 p0599 N85-13815
British aerospace studies HOTOL satellite launcher 10 p1460 N85-19206
The ARIANE family 11 p1712 N85-20774
Ignition, separation of boosters, stages in Ariane 3 14 p2289 N85-24185
Studies on rocket engines for future European launchers
[SEP-TPRL/K-19572/84] 15 p2495 N85-25393
Calendar of Ariane launches 1984 - 1987 15 p2523 N85-25554
Costs, payload of Ariane, US Space Shuttle compared 15 p2530 N85-25601
West Europe report: Science and technology
[JPRS-WST-84-027] 15 p2532 N85-25612
France officially proposes development of Ariane 5 to ESA 15 p2532 N85-25613
SEP of France to make Ariane HM-60 cryogenic engine 15 p2532 N85-25614
West Europe report: Science and technology
[JPRS-WST-84-026] 15 p2532 N85-25617
French CNES official describes Ariane V launcher 15 p2532 N85-25619
The Ariane launch vehicle is the key of the Europeans to the space market 17 p2908 N85-27931
Structure of SYLDA double launch system for Ariane 17 p2946 N85-28185
Documentation for the West German Federal Cabinet's space policy decision 17 p3051 N85-28886
Space insurance firms view shuttle, Ariane reliability 18 p3066 N85-29090
Ariane space general director on satellite launcher market 18 p3067 N85-29103
FRG weighs ESA participation, budget issues 18 p3068 N85-29110
DFVLR study recommends European independence in space systems 18 p3068 N85-29111
Ariane launcher system. Pyrotechnics subsystem: Definition of chains and pyrotechnic components
[CNES-84/CT/DRT/SST/SE/242(1)] 20 p3396 N85-31081

ARID LANDS
Australian Multiexperimental Assessment of SIR-B (AMAS) 06 p1148 N85-17243
Vegetation analysis for arid lands geobotany
[NASA-CR-175455] 10 p1506 N85-19500
Work physiology of operating personnel at power plants in arid regions 10 p1523 N85-19606
Evaluation of carrying capacity and landscape damage in northern Kenya by multistage remote sensing
[DFVLR-FB-84-47] 14 p2347 N85-24514
Screening Prosopis (mesquite) species for biofuel production on semi-arid lands
[DE85-010048] 19 p3302 N85-30471
Comprehensive mapping of arid territories of Arizona using space photography 22 p3737 N85-33164
Resource evaluation and site selection for microalgae production systems
[DE85-006807] 23 p3951 N85-34485
Remote sensing of hydrologic transport processes using spot simulation data
[DE85-012412] 24 p4108 N85-35467

ARIETID METEOROIDS
Observations of RR Lyrae and X Arietis with the IUE satellite 11 p1754 N85-21030

ARIP (IMPACT PREDICTION)
U COMPUTERIZED SIMULATION
U IMPACT PREDICTION

ARITHMETIC
NT FIXED POINT ARITHMETIC
NT FLOATING POINT ARITHMETIC
Electrooptical matrix multiplication using the twos complement arithmetic for improved accuracy
[AD-D011252] 05 p0726 N85-14682
Digital high speed programmable convolver
[AD-D011455] 10 p1481 N85-19348
Propagation of numerical errors in computers and numerical quality 14 p2396 N85-24760
Arithmetic and elementary functions on mini and microcomputers 14 p2396 N85-24761
Numerical optical computing at the Ohio State University 18 p3188 N85-29775

ARITHMETIC AND LOGIC UNITS
Hardware multiplier processor
[DE84-006174] 05 p0713 N85-14574

ARIZONA
Hydrogeochemical investigation of thermal springs in the Black Canyon-Hoover Dam area, Nevada and Arizona
[PB84-202472] 01 p0064 N85-10428
Control aspects of the Schuchuli Village stand-alone photovoltaic power system
[NASA-TM-83790] 04 p0495 N85-13157
CO-2-silica geothermometer for low temperature geothermal resource assessment, with application to resources in the Safford Basin, Arizona
[DE84-013958] 04 p0534 N85-13411
Intraband radiometric performance of the LANDSAT 4 Thematic Mapper — Washington, DC, Arkansas, Massachusetts, Virginia, and Arizona 12 p1871 N85-21736
The geology of Mt. Hope, a silicic volcanic center in West Central Arizona 13 p2187 N85-23571
Preliminary assessment of climatic change during late Wisconsin time, southwest Great Basin and vicinity, Arizona, California and Nevada
[DE85-008343] 16 p2836 N85-27468

ARKANSAS
Sedimentary petrology and provenance of the upper Jackforth Sandstone (Morrowan) Quachita Mountains, Arkansas, USA 08 p1182 N85-17447
Scan angle and detector effects in Thematic Mapper radiometry — Iowa and Arkansas 12 p1871 N85-21735
Intraband radiometric performance of the LANDSAT 4 Thematic Mapper — Washington, DC, Arkansas, Massachusetts, Virginia, and Arizona 12 p1871 N85-21736

ARM (ANATOMY)
NT ELBOW (ANATOMY)
Simple nonrestrictive arm restraint system
[AD-D011216] 01 p0005 N85-10026
Electromyographic patterns associated with discrete limb movements 05 p0710 N85-14551
Windblast arm protector assembly
[AD-D011512] 12 p1909 N85-21984
Postural adjustments associated with arm movements in weightlessness 20 p3509 N85-31813

ARMATURES
Metal armatures for railguns
[AD-A152129] 16 p2728 N85-26838

ARMED FORCES
NT ARMED FORCES (FOREIGN)
NT ARMED FORCES (UNITED STATES)
NT NAVY
Maintenance and the military environment 22 p3750 N85-33243

ARMED FORCES (FOREIGN)
Conceptual model of critical requirements for effective pilot performance in high performance aircraft 10 p1533 N85-19063
A review of fatality, impairment of consciousness and head and neck injury on Royal Air Force ejections 1968-1981 12 p1907 N85-21975
Correlations between selection ratings and success as army aviators
[FOA-C-53020-H2] 15 p2620 N85-26144
Investigation of the requirement for auxiliary heating of Canadian forces personnel
[AD-A151950] 16 p2841 N85-27522
Soviet weapons development and the scientific community
[AD-P004562] 17 p3047 N85-28857
The revolution in military affairs and the Soviet system
[AD-P004568] 17 p3048 N85-28863

ARMED FORCES (UNITED STATES)
Self-paced instruction. Factors critical to implementation in Air Force technical training: A preliminary inquiry
[AD-A145096] 01 p0097 N85-10647
Air Force Human Resources Laboratory report: Fiscal year, 1983
[AD-A145647] 02 p0238 N85-11548
AFHRL (Air Force Human Resources Laboratory) program for artificial intelligence applications to maintenance and training
[AD-P003931] 02 p0247 N85-11611
United States Air Force on research on algebraic manipulation
[AD-A145737] 02 p0253 N85-11655
NEO robotic application development at Letterkenny Army Depot: The application of robotics to agricultural blast cleaning
[AD-P004007] 03 p0308 N85-11987
Air Force Materials Laboratory plans/projects
[AD-P004010] 03 p0308 N85-11990
Potential application of robotics and state-of-the art end effectors at Letterkenny Army Depot
[AD-P004015] 03 p0309 N85-11994
Field applications for robotic materiel handling
[AD-P004016] 03 p0309 N85-11995
The role of physical and physiological capacities and their modification on the tolerance to various stress experienced by Air Force personnel
[AD-A145779] 03 p0400 N85-12550
Cardiovascular disease among U.S. Navy pilots
[AD-A145871] 03 p0400 N85-12552
An update on the capabilities of the Air Force Computerized Occupational Health Program (COHP)
[AD-P004037] 06 p0845 N85-15967

The Air Force stock fund and aircraft availability
[AD-A148653] 08 p1067 N85-16761
Utilization of Increased Airlift Capability (UIAC) study
[AD-A148669] 08 p1081 N85-16847
Design of an evaluation system to measure performance degradation due to continuous operations
[AD-A148188] 08 p1200 N85-17558
Reflections on trends in dynamics: The Navy's perspective 09 p1334 N85-18382
Compatible goals: Defense and environmental protection
[AD-P004137] 09 p1347 N85-18473
Closed-loop concepts for the Army: Water conservation, recycle, and reuse
[AD-A148839] 09 p1365 N85-18581
Catalog of completed studies, US Army health care studies and clinical investigation activity
[AD-A149450] 10 p1568 N85-19985
Air Force Office of Scientific Research (AFOSR) technical report summaries. Third quarter (CY)
[AD-A148965] 10 p1573 N85-19918
1983 Air Force bird strikes
[AD-P004182] 11 p1579 N85-19944
Tactical operations and space applications
11 p1709 N85-20752
US MILSATCOM: Present and future
11 p1709 N85-20753
Military applications of meteorological satellite (METSAT) data 11 p1711 N85-20767
Air Force Academy Aeronautics Digest
[AD-A149614] 12 p1769 N85-21104
A review of fatality, impairment of consciousness, and head/neck injury on USAF ejections 1971 - July 1983
12 p1906 N85-21974
Fiscal year 1986 technical objective document
[AD-A151039] 14 p2432 N85-25000
Air Force Office of Scientific Research (AFOSR): Technical report summaries. Fourth quarter (CY)
[AD-A150860] 14 p2456 N85-25167
Manufacturing methods and technology CAD/CAM (Computer-Aided Design/Computer-Aided Manufacturing) related efforts (FY 1980 - 1986)
[AD-A151817] 16 p2846 N85-27547
Continued development and implementation of the Universal Network Interface Device (UNID) 2 in the Digital Engineering Laboratory Network (DELNET), volume 2
[AD-A151947] 16 p2850 N85-27570
Computer assisted flight schedule optimization
[AD-A151689] 16 p2858 N85-27623
Summary of Research, Academic Departments, 1983 - 1984
[AD-A151724] 16 p2875 N85-27741
Rome Development Center Air Force technical objective document CSI FY-86
[AD-A152476] 17 p3047 N85-28851
Air Force technical objective document FY 86
[AD-A152730] 17 p3047 N85-28855
Air Force Federal Photovoltaic Utilization Program
[DE85-010812] 20 p3484 N85-31648
Air force technical objective document, Aerospace Medical Division, Fiscal Year 1986
[AD-A155195] 21 p3664 N85-32762
Feasibility of applications of Competition Decision Assist Package (CDAP) to spare parts
[AD-A154716] 21 p3712 N85-33036
Air Force Office of Scientific Research (AFOSR). Technical report summaries: First quarter (CY)
[AD-A154757] 21 p3713 N85-33041
U.S. Civil airmen statistics for calendar year 1984
[AD-A156328] 24 p4059 N85-35153
Laboratory vibration schedules
[AD-A155856] 24 p4064 N85-35186
United States Army welding research and development topical and coordination meeting
[AD-A155834] 24 p4099 N85-35409
Solar pond technology for Navy applications
[AD-A155877] 24 p4112 N85-35488
Air university commander's and supervisor's guide on substance abuse
[AD-A156336] 24 p4133 N85-35622

ARMOR

Penetrator/armour interactions: Background to Australian work
[MRL-R-936] 03 p0387 N85-12353
Thermal contact conductance measurements on Doublet 3 armor tile trophie
[DE84-013554] 05 p0613 N85-13916
Production verification of the acoustic emission weld monitor
[AD-A154166] 20 p3484 N85-31519

AROMATIC COMPOUNDS

Liquid phase products and solid deposit formation from thermally stressed model jet fuels
[NASA-TM-86674] 04 p0481 N85-13068
Prediction of retention indices of polynuclear aromatic hydrocarbons. Part 1: HPLC on nitrogen containing normal phase packing materials
[DE85-001302] 10 p1436 N85-19051
Desorption efficiences of vapor phase polynuclear aromatic compounds on solid adsorbents
[DE85-001303] 10 p1436 N85-19052
Fuels combustion research
[AD-A149106] 10 p1457 N85-19178
Quantitative determination of compound classes in jet turbine fuels by high performance liquid Chromatography/Differential refractive index detection: Part 2
[AD-A149298] 11 p1613 N85-20144
Electrostatic potentials: A new method for interpreting and predicting molecular reactivities and for designing synthetic pathways. Applications to nitroaromatics, nitramines and nitrated
[AD-A150120] 12 p1801 N85-21298
Spray pyrolysis as a synthetic tool
[AD-A153891] 19 p3234 N85-30047
Experimental studies of chemical reactivity during shock initiation of hexanitrostilbene
[DE85-011726] 22 p3754 N85-33270

ARRAYS

NT ANTENNA ARRAYS
NT LINEAR ARRAYS
NT MULTISPECTRAL LINEAR ARRAYS
NT PHASED ARRAYS
NT SOLAR ARRAYS
NT SOLAR BLANKETS
NT STEERABLE ANTENNAS

Data flow computer architecture
[DE84-014362] 01 p0100 N85-10684
Automated installation methods for photovoltaic arrays 2
[SAND-84-7035] 02 p0222 N85-11453
Modular photovoltaic array field
[SAND-83-7028] 02 p0222 N85-11454
Modular detonator device
[AD-D011232] 03 p0340 N85-12184
Chemical derivatization of an array of three gold microelectrodes with polypyrrole: Fabrication of a molecule-based transistor
[AD-A148221] 03 p0359 N85-12304
Heatsink requirements for coherent operation of high-power semiconductor laser arrays
[AD-A148184] 03 p0366 N85-12346
Use of monitors in FORTRAN: A tutorial on the barrier, self-scheduling DO-loop and Askfor monitors
[DE84-016506] 05 p0715 N85-14587
Fly's eye sensor nonlinear signal processing
[AD-D011290] 05 p0729 N85-14684
Algebraic techniques in systolic array design
[AD-A148417] 06 p0857 N85-15451
Transmission line biased coherent array of Josephson oscillators
[AD-D011323] 07 p0944 N85-15979
RF laser array driver apparatus
[AD-D011375] 07 p0969 N85-16155
Phased locked array laser systems
[AD-D011317] 07 p0971 N85-16184
The development and test of ultra-large-format multi-anode microchannel array detector systems
[NASA-CR-174247] 07 p1043 N85-16622
Switchable zero order diffraction gratings as light valves
[AD-A147575] 07 p1044 N85-16633
A variable length and sensor spacing thermistor array
[AD-D011416] 08 p1113 N85-17017
Coherent array of Josephson oscillators with external bias leads
[AD-D011367] 08 p1156 N85-17293
The use of self-scanned silicon photodiode arrays for astronomical spectrophotometry
08 p1252 N85-17907
Photometry with Multi-Anode Microchannel Arrays (MAMAs) and Charge Injection Devices (CIDs)
09 p1252 N85-17909
Signal Hill solar-powered repeater report and recommendations
[DE85-000487] 09 p1316 N85-18273
An electronically controlled array for simulation of passive target/background signatures at millimeter wavelengths
[AD-D011456] 10 p1468 N85-19263
An evaluation of wind measurements by four Doppler sodars
[PB85-115301] 10 p1520 N85-19586
Natural convection heat transfer between arrays of horizontal cylinders and their enclosure
[DE85-003773] 11 p1632 N85-20280
Double pinhole spatial phase correlator apparatus
[AD-D011495] 11 p1729 N85-20572
Experimental test of the three subaperture method for estimating target elevation angle
[AD-A149687] 12 p1851 N85-21614
Monolithic short wave infrared (SWIR) detector array
[NASA-CR-175284] 12 p1874 N85-21769
Stability of vortex structures during separation flow past array of wings 14 p2278 N85-24110
Bipolar nonswitching logic arrays: Universal components of function expanders for computation of elementary functions 14 p2400 N85-24797
A multi-element ultrasonic ranging array
[AD-A150898] 14 p2416 N85-24906
Performance of charge-injection-device infrared detector arrays at low and moderate backgrounds
[NASA-TM-86667] 15 p2580 N85-25793
Method and apparatus for generating a structured light beam array
[AD-D011590] 15 p2652 N85-26357
Maintenance of photovoltaic power systems
[AD-A152299] 16 p2819 N85-27390
Analysis and modeling for thermal focal plane arrays
[AD-A153156] 17 p2988 N85-28329
Chemometric analysis of multisensor arrays
[AD-A153805] 18 p3174 N85-29680
Physiochemically controlled scour jet array system
[AD-D011668] 19 p3308 N85-30505
Nested dissection on a mesh-connected processor array
[AD-A154068] 19 p3342 N85-30711
Hierarchical beamforming with application to a large aperture array system 20 p3439 N85-31345
A multiplying slot array
[AD-A155570] 21 p3576 N85-32245
The dynamics of slack marine cables
[AD-A155022] 21 p3599 N85-32349
The Norwegian seismic array (NORSAR)
[AD-A154751] 21 p3631 N85-32555
The moving thermoacoustic array: A theoretical feasibility study
[AD-A154510] 21 p3699 N85-32980
Estimating angular position of optical radiation source when received by array of photodetectors
22 p3778 N85-33413
Synthesis of metrico-topological model for layout of topology of large-scale-integration arrays
22 p3781 N85-33427
Mosaic Infrared Sensor for Space Astronomy (MIRSSA)
[NASA-CR-176154] 22 p3786 N85-33456
Electromagnetic inspection of wire ropes using sensor arrays
[AD-A155412] 22 p3795 N85-33509
MORSE-CGA: A Monte Carlo radiation transport code with array geometry capability
[DE85-012063] 22 p3830 N85-33718
Air shower arrival directions measured at Buckland Park
[OG-5.3-11] 22 p3885 N85-34077
Hexagonal uniformly redundant arrays for coded-aperture imaging
[OG-9.2-1] 23 p4024 N85-34840
Mini and super mini arrays for the study of highest energy cosmic rays
[OG-9.4-6] 23 p4029 N85-34976
Angular resolution of air-shower array-telescopes
[OG-9.5-6] 23 p4030 N85-34983
Astrophysical applications of high angular resolution array-telescopes
[OG-9.5-7] 23 p4031 N85-34984
Angular resolution of an EAS array for gamma ray astronomy energies 5 x 10 (13) eV
[OG-9.5-8] 23 p4031 N85-34985
The ISAVF opto-mechanical test bed
[NASA-TM-87505] 24 p4067 N85-35206
Heat transfer characteristics for two-dimensional arrays of impinging jets with initial crossflow
24 p4092 N85-35365
Measurement of shower electrons and muons using a small air shower array
[HE-4.3-11] 24 p4192 N85-36005

ARRESTING GEAR

Aircraft barricade
[AD-D011316] 07 p0910 N85-15761

ARRHYTHMIA

Mapping of mammalian arrhythmias with the cardiac laser scanner 03 p0399 N85-12545

ARSENIC

The influence of manganese on intercrystalline internal adsorption of arsenic in low carbon steel
[BLL-M-35905-(5828.4)] 05 p0615 N85-13931
Environmental surveillance at Los Alamos during 1984
[DE85-011886] 22 p3811 N85-33805

ARSENIC ALLOYS

Structural studies of sputtered Ni-As-O films
[DE85-003229] 11 p1605 N85-20095

ARSENIC COMPOUNDS
NT ALUMINUM GALLIUM ARSENIDES
NT GALLIUM ARSENIDES
NT INDIUM ARSENIDES
Effect of light pulses on film of chalcogenide vitreous semiconductors 02 p0258 N85-11687
Compositional, structural, and physical studies of some graphite hexafluoroarsenates and their relatives
[DE85-000855] 10 p1432 N85-19030

ARSENIDES
NT ALUMINUM ARSENIDES
NT ALUMINUM GALLIUM ARSENIDES
NT GALLIUM ARSENIDES
NT INDIUM ARSENIDES

ARTERIES
Pulmonary blood flow and oxygenation of arterial blood in a healthy subject upon 7 days hypokinesia 07 p1014 N85-16439
Analysis of the transient response of temporal artery blood flow data relative to various anti-G suit pressure schedules 10 p1533 N85-19660
Analysis of the transient response of temporal artery blood flow data relative to various anti-G suit pressure schedules
[AD-A155242] 21 p3866 N85-32775

ARTERIOSCLEROSIS
Tolerance to +Gz and +Gx accelerations of individuals in older age groups in good health and with early signs of arteriosclerosis 23 p3952 N85-34496

ARTHROPODS
NT INSECTS
NT LARVAE
NT SPIDERS

ARTIFICIAL CLOUDS
NT BARIUM ION CLOUDS

ARTIFICIAL GRAVITY
Proceedings of a Workshop on Applications of Tethers in Space, Volume 2
[NASA-CR-171197] 03 p0322 N85-12077
Tethers open new space options 11 p1642 N85-20340
Physiological considerations of artificial gravity 11 p1643 N85-20351
Summary presentation to the Artificial Gravity Panel 11 p1644 N85-20358
Physiological considerations of artificial gravity 11 p1645 N85-20366
Artificial gravity: Tethers and containers 11 p1645 N85-20367

ARTIFICIAL INTELLIGENCE
NT COGNITIVE PSYCHOLOGY
NT EXPERT SYSTEMS
Terrain navigation concepts for autonomous vehicles
[AD-A144994] 01 p0005 N85-10031
A review of selected studies of computerized speech recognition conducted at the Naval Postgraduate School
[AD-A144841] 01 p0037 N85-10235
Feature discovery by competitive learning
[AD-A145052] 01 p0097 N85-10648
Office of Technology Assessment 01 p0127 N85-10672
Toward a computational neuropsychology of high-level vision
[AD-A145711] 02 p0236 N85-11540
Artificial Intelligence in Maintenance: Proceedings of the Joint Services Workshop
[AD-A145349] 02 p0244 N85-11592
The need for improvements in weapon system maintenance: What can AI (Artificial Intelligence) contribute?
[AD-P003913] 02 p0244 N85-11593
Artificial intelligence applications to maintenance
[AD-P003914] 02 p0244 N85-11594
On applying AI (Artificial Intelligence) to maintenance and troubleshooting
[AD-P003915] 02 p0244 N85-11595
Overview of training and aiding
[AD-P003917] 02 p0245 N85-11597
AI (Artificial Intelligence) approaches to troubleshooting
[AD-P003918] 02 p0245 N85-11598
Failure detection processes by pattern recognition and expert systems
[AD-P003924] 02 p0246 N85-11604
GUIDON
[AD-P003925] 02 p0246 N85-11605
Designing an expert system for training automotive electrical troubleshooting
[AD-P003926] 02 p0246 N85-11606
Models of natural intelligence in fault diagnosis tasks: Implications for training and aiding of maintenance personnel
[AD-P003927] 02 p0246 N85-11607
The psychology of technical devices and technical discourse
[AD-P003928] 02 p0246 N85-11609
Artificial intelligence approaches to monitoring system integrity
[AD-P003930] 02 p0246 N85-11610
AFHRL (Air Force Human Resources Laboratory) program for artificial intelligence applications to maintenance and training
[AD-P003931] 02 p0247 N85-11611
Artificial intelligence contributions to training and maintenance
[AD-P003934] 02 p0247 N85-11614
NAVAIR's (Naval air systems command) AI (Artificial intelligence) program for ATE (Automated Test Equipment)
[AD-P003935] 02 p0247 N85-11615
Artificial intelligence applications to automatic test equipment
[AD-P003936] 02 p0247 N85-11616
Model-based probabilistic reasoning for electronics troubleshooting
[AD-P003937] 02 p0247 N85-11617
Implications of artificial intelligence for a user defined technical information system
[AD-P003938] 02 p0248 N85-11618
Application of artificial intelligence to equipment maintenance
[AD-P003939] 02 p0248 N85-11619
DELTA: An expert system for diesel electric locomotive repair
[AD-P003941] 02 p0248 N85-11621
An effective graphics user interface for rules and inference mechanisms
[AD-P003942] 02 p0248 N85-11622
The ACE (Automated Cable Expert) experiment: Initial evaluation of an expert system for preventive maintenance
[AD-P003943] 02 p0248 N85-11623
The application of artificial intelligence to a maintenance and diagnostic information system
[AD-P003945] 02 p0249 N85-11625
Intelligent information retrieval from on-line technical documentation
[AD-P003946] 02 p0249 N85-11626
On the requirements of expert systems for fault isolation
[AD-P003947] 02 p0249 N85-11627
Memory-based expert systems
[AD-A145812] 02 p0249 N85-11628
Constraint-based scheduling in an intelligent logistics support system: An artificial intelligence approach
[AD-A145613] 02 p0293 N85-11900
Air Force Materials Laboratory plans/projects
[AD-P004010] 03 p0306 N85-11990
Status and prospects of computational fluid dynamics for unsteady transonic viscous flows
[NASA-TM-86018] 03 p0315 N85-12037
West Europe report: Science and technology, no. 166
[JPRS-84845] 03 p0341 N85-12190
French firms develop artificial intelligence robot 03 p0341 N85-12192
East Europe report: Scientific affairs, no. 791
[JPRS-84624] 03 p0341 N85-12195
Technological institute director views artificial intelligence 03 p0341 N85-12197
The search for regularity: Four aspects of scientific discovery
[AD-A145939] 03 p0368 N85-12355
Research in knowledge representation for natural language understanding
[AD-A145807] 03 p0409 N85-12613
Test-bed for programmable automation research. Phase 1
[AD-A145872] 03 p0409 N85-12614
Knowledge representation and natural-language semantics
[AD-A146025] 03 p0409 N85-12615
Psychological issues in the design of expert systems
[AD-A146061] 03 p0438 N85-12792
Technologies for space station autonomy
[NASA-CR-174112] 04 p0458 N85-12906
Definition of technology development missions for early Space Station satellite servicing. Volume 1: Executive summary
[NASA-CR-171228] 04 p0460 N85-12922
Soviet robot exhibition reviewed 04 p0491 N85-13128
Development, new application of Soviet robots 04 p0491 N85-13129
Expert systems in design and manufacture
[DE84-005522] 04 p0550 N85-13496
Minimal cut-set methodology for artificial intelligence applications
[DE84-016674] 04 p0553 N85-13518
Real-time planning by an intelligent robot
[DE84-016669] 04 p0553 N85-13519
Induction of fuzzy decision rules
[INPE-3053-PRE/474] 04 p0554 N85-13525
Getting mental models and computer models to cooperate 05 p0709 N85-14548
Knowledge-based communication and management support in a system development environment 05 p0717 N85-14596
Use of artificial intelligence and simple mathematics to analyze a physiological model 05 p0717 N85-14597
Multi-disciplinary techniques for understanding time-varying space-based imagery
[AD-A144357] 05 p0728 N85-14681
Interpretation of natural language database queries using optimization methods 05 p0735 N85-14723
Crewstation design and validation 06 p0752 N85-14822
Recent advances in data compression
[DE85-001133] 06 p0854 N85-15432
Research on introspective systems
[AD-A146406] 06 p0870 N85-15530
Vision by man and machine: How the brain processes visual information may be suggested by studies in computer vision (and vice versa)
[AD-A147890] 07 p1017 N85-16458
Interaction of human cognitive models and computer based models in supervisory control
[AD-A142547] 07 p1020 N85-16474
Implementation of a constraint machine for prism - A parallel problem solver
[AD-A147844] 07 p1026 N85-16512
Avionics fault tree analysis and artifical intelligence for future aircraft maintenance 08 p1066 N85-16755
New applications for robot loaders, unloaders 08 p1139 N85-17175
East Europe report: Science and technology
[JPRS-ESA-84-046] 08 p1139 N85-17176
Researchers on third generation robotics development 08 p1140 N85-17184
Robotics research, integration overview presented. Application objectives cited 08 p1142 N85-17201
Probabilistic analysis of algorithms for NP-Complete problems
[AD-A148207] 08 p1215 N85-17653
The optimal control and design of a flexible manipulator arm 09 p1327 N85-18340
Strategy planning by an intelligent machine
[DE84-016609] 09 p1372 N85-18624
Researchers, projects at French intelligent machine center 10 p1460 N85-19207
French firm develops 2D, 3D computer vision system 10 p1461 N85-19208
Dean of Kiev State University on impact of robots 10 p1461 N85-19213
On motion planning with uncertainty: Revised
[AD-A149521] 10 p1492 N85-19421
Research on knowledge delivery
[AD-A149565] 10 p1538 N85-19698
Qualitative process theory
[AD-A148967] 10 p1543 N85-19729
French plans for fifth generation computer systems
[AD-A149435] 10 p1544 N85-19732
Proceedings of the 14th Army Science Conference. Volume 1: Principal Authors A through H
[AD-A149200] 10 p1573 N85-19920
A functional vehicle for autonomous mobile robot research
[AD-A150052] 12 p1860 N85-21666
Dynamic visual servo control of robots: An adaptive image-based approach
[AD-A150057] 12 p1860 N85-21667
The automated reasoning system ITP
[ANL-84-27] 12 p1914 N85-22016
Characterizing the parallelism in rule-based expert systems
[DE85-002432] 12 p1919 N85-22047
Aviation maintenance computerized management information systems: Perspective for the future
[AD-A150637] 13 p1966 N85-22349
Advancing automation and robotics technology for the Space Station and for the US economy. Volume 1: Executive overview
[NASA-TM-87566-VOL-1] 13 p1966 N85-22460
Advancing automation and robotics technology for the Space Station and for the US economy, volume 2
[NASA-TM-87566-VOL-2] 13 p1967 N85-22461
The potential for advanced computerized aids for comprehensible writing of technical documents
[AD-A150501] 13 p2055 N85-22870
Artificial Intelligence and Bionics Workshop held at Stowe, Vermont on 11-15 June 1984
[AD-A150463] 13 p2149 N85-23339
Research needs for artificial intelligence applications in support of C3 (Command, Control, and Communication)
[AD-A150867] 14 p2292 N85-24210
Some critical factors that limit the effectiveness of machine intelligence technology in military systems applications
[AD-A150684] 14 p2407 N85-24838

Artificial intelligence applications to testability
[AD-A150694] 14 p2407 N85-24839
Semantic networks and neural nets
[AD-A150750] 14 p2407 N85-24840
Our future in the cosmos: Computers
14 p2432 N85-24997
Documentation for the machine-readable version of the Stellar Spectrophotometric Atlas, 3130 A lambda 10800 A of Gunn and Stryker (1983)
[NASA-TM-87437] 14 p2438 N85-25045
Documentation for the machine-readable version of A Library of Stellar Spectra (Jacoby, Hunter and Christian 1984)
[NASA-TM-87438] 14 p2438 N85-25046
Documentation for the machine-readable version of A Finding List for the Multiplet Tables of NSRDS-NBS 3, Sections 1-10 (Adelman, Adelman, Fischel and Warren 1984)
[NASA-TM-87440] 14 p2438 N85-25048
Documentation for the machine-readable version of the Cordoba Durchmusterung (CD)
[NASA-TM-87441] 14 p2439 N85-25049
Documentation for the machine-readable version of the Cape Photographic Durchmusterung (CPD)
[NASA-TM-87442] 14 p2439 N85-25050
Documentation for the machine readable version of the Yale Catalogue of the Positions and Proper Motions of Stars between Declinations -60 deg and -70 deg (Fallon 1983)
[NASA-TM-87443] 14 p2439 N85-25051
Status and prospects of computational fluid dynamics for unsteady transonic flow 15 p2459 N85-25180
An approach to planning in the inflight emergency domain
[AD-A151869] 15 p2467 N85-25228
Artificial intelligence based control of a sensor-driven machine
[DE85-006972] 15 p2633 N85-26227
Generation of flight paths using heuristic search
[AD-A151949] 16 p2704 N85-26694
Symbiosis between postgraduate training and research projects: A successful experience
[INPE-3216-PRE/569] 16 p2810 N85-27330
Diagnosis: Using automatic test equipment and an artificial intelligence expert system
[AD-A151918] 16 p2851 N85-27576
Artificial intelligence in space platforms
[AD-A152078] 16 p2851 N85-27578
Research in knowledge representation for natural language understanding
[AD-A152260] 16 p2851 N85-27579
Application of artificial intelligence (AI) to radar image understanding
[AD-A152519] 17 p3017 N85-28654
A study of user-defined searching requirements for the on-line version of the directory of DOD-sponsored R and D data bases on the Defense Gateway computer system
[AD-A153000] 17 p3050 N85-28878
Applications of some artificial intelligence methods to satellite soundings 18 p3141 N85-29446
Hybrid uncertainty theory
[DE85-008357] 18 p3167 N85-29622
The application of artificial intelligence techniques to large distributed networks
[NASA-CR-177346] 19 p3344 N85-30721
An artificial intelligence based framework for planning air launched cruise missile missions
[AD-A154466] 19 p3344 N85-30722
Data communications-Oriented Production System Language (CPSL)
[DE85-011457] 20 p3440 N85-31352
Distributed implementation of functional program evaluation
[DE85-009573] 20 p3514 N85-31844
Proceedings of the 1st Workshop for the Design of Expert System Partial Differential Equation Solvers
[AD-A154192] 20 p3515 N85-31853
The documentation assistant: An intelligent system for documentation
[AD-A154709] 21 p3670 N85-32800
Space station automation and robotics study. Operator-systems interface
[NASA-CR-176095] 22 p3738 N85-33172
Space robot simulator vehicle
[NASA-CR-176133] 22 p3739 N85-33176
Future of robots in nuclear plants and processes
[DE85-011505] 22 p3793 N85-33500
Machine intelligence for robotics applications
[DE85-011430] 22 p3793 N85-33503
Flat is not necessarily good
[DE85-012619] 22 p3830 N85-33723
Knowledge engineering application in image processing 23 p3965 N85-34583
Heuristic rules for visualization
23 p3965 N85-34584
Robot environment expert system
[NASA-CR-3915] 23 p3967 N85-34593
Implications of artificial intelligence on the design of future onboard systems
[SFENA-DPS/C/S3/84252A] 23 p3967 N85-34596
Monte Carlo techniques for analyzing deep penetration problems
[DE85-011426] 23 p3968 N85-34598
Testbed for sensory control of intelligent machines
[DE85-012355] 24 p4099 N85-35412
Justified generalization: Acquiring procedures from examples
[AD-A156406] 24 p4135 N85-35626
Polylith: The early goals
[DE85-012534] 24 p4139 N85-35658
Artificial intelligence in Ada (trademark): Pattern-directed processing
[AD-A156230] 24 p4141 N85-35671

ARTIFICIAL RESPIRATION
U RESUSCITATION

ARTIFICIAL SATELLITES
NT AERONAUTICAL SATELLITES
NT AEROS SATELLITE
NT ALOUETTE 2 SATELLITE
NT ANIK SATELLITES
NT ARABSAT
NT ASTRONOMICAL SATELLITES
NT ATS
NT BIOSATELLITES
NT COMMUNICATION SATELLITES
NT COMMUNICATIONS TECHNOLOGY SATELLITE
NT COS-B SATELLITE
NT COSMOS SATELLITES
NT COSMOS 936 SATELLITE
NT COSMOS 1129 SATELLITE
NT COSPAS
NT DYNAMICS EXPLORER 1 SATELLITE
NT EOSS
NT ERS-1 (ESA SATELLITE)
NT EUROPEAN COMMUNICATIONS SATELLITE
NT EXOSAT SATELLITE
NT EXPLORER SATELLITES
NT EXPLORER 10 SATELLITE
NT EXPLORER 43 SATELLITE
NT EXPLORER 46 SATELLITE
NT EXPLORER 50 SATELLITE
NT EXPLORER 51 SATELLITE
NT EXTREME ULTRAVIOLET EXPLORER SATELLITE
NT FAR UV SPECTROSCOPIC EXPLORER
NT GEODETIC SATELLITE$_{Ge}$
NT GEOPHYSICAL SATELLITES
NT GEOS SATELLITES (ESA)
NT GEOS 1 SATELLITE
NT GEOS 2 SATELLITE
NT GEOS 3 SATELLITE
NT GOES SATELLITES
NT GOES 5
NT GRAVITY GRADIENT SATELLITES
NT HEAO 1
NT HEAO 2
NT HEAO 3
NT HELIOS SATELLITES
NT HELIOS 1
NT HELIOS 2
NT HEOS B SATELLITE
NT HUBBLE SPACE TELESCOPE
NT IMP
NT INFRARED ASTRONOMY SATELLITE
NT INTELSAT SATELLITES
NT INTERCOSMOS SATELLITES
NT INTERNATIONAL SUN EARTH EXPLORER 1
NT INTERNATIONAL SUN EARTH EXPLORER 2
NT INTERNATIONAL SUN EARTH EXPLORER 3
NT INTERNATIONAL SUN EARTH EXPLORERS
NT ISIS SATELLITES
NT IUE
NT L-SAT
NT LAGEOS (SATELLITE)
NT LANDSAT SATELLITES
NT LANDSAT 1
NT LANDSAT 4
NT LANDSAT 5
NT LONG DURATION EXPOSURE FACILITY
NT LUNAR SATELLITES
NT MAGSAT SATELLITES
NT MARISAT SATELLITES
NT MARITIME SATELLITES
NT METEOROLOGICAL SATELLITES
NT METEOSAT SATELLITE
NT MIRANDA SATELLITE
NT MULTISPECTRAL RESOURCE SAMPLER
NT NAVIGATION SATELLITES
NT NAVSTAR SATELLITES
NT NIMBUS SATELLITES
NT NIMBUS 5 SATELLITE
NT NIMBUS 7 SATELLITE
NT NOAA SATELLITES
NT NOAA 6 SATELLITE
NT NOAA 7 SATELLITE
NT NOAA 8 SATELLITE
NT OAO 3
NT OGO
NT ORBITAL SPACE STATIONS
NT OTS (ESA)
NT PASSIVE SATELLITES
NT PROGNOZ SATELLITES
NT QUASAT
NT ROSAT MISSION
NT SAGE SATELLITE
NT SARSAT
NT SCATHA SATELLITE
NT SCIENTIFIC SATELLITES
NT SEASAT SATELLITES
NT SEASAT 1
NT SIRIO SATELLITE
NT SIRS B SATELLITE
NT SKYNET SATELLITES
NT SOLAR MESOSPHERE EXPLORER
NT SOLAR POWER SATELLITES
NT SPACE INFRARED TELESCOPE FACILITY
NT SPARTAN SATELLITES
NT SPOT (FRENCH SATELLITE)
NT STORMSAT SATELLITE
NT SYMPHONIE SATELLITES
NT SYNCHRONOUS SATELLITES
NT TETHERED SATELLITES
NT TIROS N SERIES SATELLITES
NT TIROS SATELLITES
NT TRANSIT SATELLITES
NT UK SATELLITES
NT VELA SATELLITES
NT VENERA SATELLITES
NT VENERA 11 SATELLITE
Development of the Engineering Test Satellite-3 (ETS-3) ion engine system
[NASA-TM-77536] 01 p0017 N85-10101
Problem of determining highly accurate coordinates of artificial satellites by photographic methods
02 p0162 N85-11096
Space research benefits national economy
02 p0163 N85-11107
NESDIS international activities, appendix 2
02 p0295 N85-11917
Sweden's Kiruna may be future launch site for satellites 03 p0310 N85-12000
Study of instrument design options for the Columbus spectroscopy mission
[NASA-CR-174072] 04 p0502 N85-13205
Theory of the orbital motion of an artificial Earth satellite
[NAL-TR-807] 06 p0758 N85-14847
Aerodynamic and thermal characteristics of stellate bodies in hypersonic flow of rarefied gas at angle of attack 06 p0778 N85-14974
Upper Atmosphere Research Satellite (UARS) trade analysis
[NASA-CR-175269] 07 p0912 N85-15774
Theory of the orbital motion of an artificial Earth Satellite
[NAL-TR-807] 09 p1285 N85-18075
Study of factors affecting an HF/VHF direct broadcasting satellite service
[PB85-120889/GAR] 09 p1313 N85-18255
Transdigitizer for relaying signals from Global Positioning System (GPS) satellites
[AD-D011442] 10 p1422 N85-18970
A semianalytical, artificial satellite orbit propagation procedure based on optimal parameter estimation
[INPE-3301-PRE/613] 10 p1427 N85-18997
One rocket multiple satellite launch technology
[AD-A149228] 10 p1427 N85-19002
Telemetry systems of Interkosmos satellites
11 p1617 N85-20173
A system simulator for the solar generator of artificial satellites
[INPE-3320-TDL/180] 11 p1672 N85-20534
NORAD's PARCS small satellite tests (1976 and 1978) 12 p1783 N85-21191
NASA/JSC orbital debris study: Debris model
12 p1783 N85-21193
The long term behaviour of Earth orbits and the implications for debris control 12 p1786 N85-21213
Passive microwave remote sensing for sea ice research
[NASA-CR-175570] 12 p1874 N85-21758
Plans for Interbol satellite experiment
13 p1977 N85-22407
Nontraditional method for determining unperturbed orbits of unknown space objects using incomplete optical observational data 13 p1979 N85-22417
China report: Science and technology
[JPRS-CST-84-030] 13 p2041 N85-22777

Nation said to rank high with 15 satellites
13 p2041 N85-22778
Periodic movements of axisymmetrical satellite about center of mass due to gravitational moment
13 p2042 N85-22783
Development, prospect of satellite dynamics discussed
13 p2052 N85-22847
Multistep orbital correction algorithms for an Earth satellite using low thrust engine
15 p2479 N85-25303
Electric potential of satellite in electron emitting experiments in initial stage of electron beam injection in steady-state mode
15 p2480 N85-25309
Czech institute develops microcomputer for satellites
15 p2484 N85-25331
Selection of optimal control program for solar cell panels of Earth satellites
15 p2484 N85-25335
Application of perturbation theory to problem in orbital theory
15 p2537 N85-25656
Margin leveling algorithm for fully saturated satellite transponder with CDMA (Code Division Multiple Access) signalling
[AD-A151710] 15 p2543 N85-25699
Positions of relative equilibrium of satellite-gyrostat
16 p2718 N85-26777
Observability in problem of correction of inertial navigation systems using additional information from artificial Earth satellite
16 p2719 N85-26785
Satellite selection criteria
16 p2804 N85-27268
Atmospheric density model
16 p2805 N85-27297
Simultaneous Earth observations from 2 satellites
[NASA-TM-86204] 16 p2810 N85-27325
Altimetry data and the elastic stress tensor of subduction zones
[NASA-CR-175796] 16 p2825 N85-27425
West Europe report: Science and technology
[JPRS-WST-84-024] 17 p2945 N85-28183
Structure of SYLDA double launch system for Ariane
17 p2946 N85-28185
Swedish space program includes research satellites
18 p3088 N85-29113
Balanced system for ranging and synchronization between satellite pairs
[AD-D011697] 19 p3224 N85-29992
Global geoid and gravity anomaly predictions using the collocation and point mass techniques
[AD-A154517] 21 p3605 N85-32387
Far travelers: The exploring machines
[NASA-SP-480] 22 p3731 N85-33126
On the principle of uniformity of satellite communications systems
22 p3773 N85-33382
Magnetospheric multiprobes: MMP/CHEMSAT
23 p3902 N85-34171

ARTILLERY
The electronic typesetting program programmer's manual
[AD-A147500] 07 p1025 N85-16508

ARTS
NT ABILITIES
NT GRAPHIC ARTS

ARYABHATA
U INDIAN SPACECRAFT

ARYL COMPOUNDS
U AROMATIC COMPOUNDS

ASBESTOS
Early detection of environmental exposure
[AD-P004030] 06 p0845 N85-15389
Effect of sealants of the sound absorption coefficients of acoustical friable insulating materials
[AD-A148541] 08 p1216 N85-17674
Substitution of asbestos by aramid fibers and fiber blends in industrial textiles and composites with organic binders
[BMFT-FB-T-85-006] 23 p3920 N85-34294

ASCENT
NT CLIMBING FLIGHT

ASCENT PROPULSION SYSTEMS
The space shuttle ascent vehicle aerodynamic challenges configuration design and data base development
08 p1093 N85-16906

ASCENT TRAJECTORIES
The space shuttle launch vehicle aerodynamic verification challenges
08 p1093 N85-16907

ASHES
NT FLY ASH
Ash contents of Costa Rican peat deposits
[DE85-010734] 19 p3301 N85-30462
Ice nucleating characteristics of Capparis Aphylla, an Indian herb
2? p3841 N85-32619

ASIA
Mean maximum mixing heights for northern Asia for the winter of 1978
[DE84-015980] 05 p0672 N85-14315
Lateral inhomogeneity of mantle surface in western Eurasia
14 p2344 N85-24497
Location of continental Permian volcanites of central Asia and its tectonic interpretation
14 p2346 N85-24505
Frequency dependence of Q in the mantle underlying the shield areas of eurasia
[AD-A151367] 15 p2592 N85-25978
AWS (Air Weather Service) climatic briefs: Asia
[AD-A151944] 16 p2835 N85-27481
The 2nd World Meteorological Association Regional Association (Asia), 8th session
[WMO-642] 22 p3617 N85-33643

ASPARTATES
Response of rat hindlimb muscles to 12 hours recovery from tail-cast suspension
[NASA-CR-176182] 24 p4128 N85-35590

ASPARTIC ACID
Blood amino acids of cosmonauts before and after 211-day spaceflight
12 p1900 N85-21933

ASPECT RATIO
NT HIGH ASPECT RATIO
NT LOW ASPECT RATIO
Blind zones and aspect ratio bias in acquisition of discontinuity orientation data
[DE84-002718] 04 p0533 N85-13410
Detailed pressure distribution measurements obtained on several configurations of an aspect-ratio-7 variable twist wing
[NASA-TM-86306] 10 p1419 N85-18950
Basic studies of multiple free and confined jets
[AD-A149556] 10 p1485 N85-19374
Visual simulation requirements for aircraft aspect recognition at real world distances
[AD-A151040] 14 p2228 N85-23810
Some optimization problems in static aeroelasticity for wings made of composite materials
14 p2277 N85-24104
Wind tunnel wall interference
[AD-A151212] 15 p2474 N85-25273
Visual search strategy predictions: The use of aspect ratio as a cue
[BAE-BT-12565] 15 p2619 N85-26136
Hypersonic nonequilibrium gas flow past zero-aspect wing
16 p2765 N85-27063
Multiple scattering of electromagnetic waves in discrete random media
[AD-A151786] 16 p2772 N85-27112
Aerodynamic performance of a wing in ground effect using the PANAIR program
[AD-A153303] 17 p2892 N85-27832
Solution to eigenvalue problems of antisymmetric cross-ply and antisymmetric angle-ply laminated plates using affine transformations
[AD-A153040] 17 p2917 N85-27980
A numerical study of Taylor-Vortex flow
[AD-A154787] 21 p3584 N85-32277
Object identification and manipulation using silhouette moments
[AD-A154755] 21 p3705 N85-33011
Neoclassical diffusion including ellipticity in a heliotron-like configuration
23 p3978 N85-34667
Generalized reduced fluid model with finite ion-gyroradius effects
[DE85-013123] 24 p4157 N85-35777

ASPHALT
Design of alternate launch and recovery surfaces for environmental effects
[AD-A145800] 03 p0320 N85-12066
Related studies to cathodic protection of reinforced concrete structures
[PB84-216114] 03 p0333 N85-12145
Experimental AC (Asphalt Concrete) overlays of PCC pavement
[PB84-218171] 03 p0342 N85-12203
Development of a rapid test method for asphalt concrete content determination in hot-mix paving mixtures
[PB84-218692] 03 p0342 N85-12204
Evaluation of moduli and thicknesses of pavement systems by spectral-analysis-of-surface-waves method
[PB84-219112] 03 p0342 N85-12205
Alternatives for runway rubber removal from porous friction surfaces
[DOT/FAA/PM-84/28] 05 p0597 N85-13803
Field validation of statistically-based acceptance plan for bituminous airport pavements. Volume 1: Correlation analysis of Marshall properties of laboratory-compacted specimens
[FAA-PM-84-12-VOL-1] 12 p1781 N85-21180
Field validation of statistically-based acceptance plan for bituminous airport pavements. Volume 2: Statistical analysis of Marshall properties of plant-produced bituminous materials
[FAA-PM-84-12-VOL-2] 12 p1781 N85-21181
Field validation of statistically-based acceptance plan for bituminous airport pavements. Volume 3: Statistical analysis of 3 methods for determining maximum specific gravity of bituminous concrete mixtures
[FAA-PM-84-12-VOL-3] 12 p1781 N85-21182
Field validation of statistically-based acceptance plan for bituminous airport pavements. Volume 5: Summary of validation studies
[FAA-PM-84-12-VOL-5] 12 p1782 N85-21184
Overlays for plain jointed concrete pavements
[PB85-156297] 15 p2523 N85-25557
Anticorrosion protection of reinforcing steel in prestressed gypsum and anhydrite concrete
[BLL-BISI-TRANS-22079-(9022.06)] 17 p2926 N85-29044
Recycling agent selection and tentative specification
[AD-A153529] 18 p3070 N85-29968
Pycnometer shaker
[PB85-174985] 20 p3460 N85-31491

ASPHYXIA
Basic cryogenics and materials. Phase 1
[NASA-CR-177932] 21 p3572 N85-32215

ASPIRATION
U VACUUM

ASSAULTING
U ATTACKING (ASSAULTING)

ASSAYING
Development of a new class of chemical and biological ultrasensors: Ribonuclease contamination and control
[NASA-CR-175466] 11 p1635 N85-20296
Compact L-edge densitometer for uranium concentration assay
[DE85-010344] 18 p3110 N85-29261
Quantitative passive technique for assay of near-surface tritium in materials
[DE85-010661] 19 p3360 N85-30833
Carcinogenesis of nitrated toluenes and benzenes skin and lung tumor assays in mice
[AD-A155723] 22 p3818 N85-33655
Improved flow cytometer measurement of binding assays
[DE85-006407] 23 p3935 N85-34390

ASSEMBLER ROUTINES
MC68CRX cross-assembler users manual
[AD-A148031] 08 p1205 N85-17584

ASSEMBLIES
NT SUBASSEMBLIES
NT TAIL ASSEMBLIES
The development of an optoelectronic assembly applied to computer systems
[AD-A145028] 01 p0120 N85-10621
SMP: A solid modeling program
[NASA-CR-172473] 02 p0241 N85-11570
Emitted vibration measurement device and method
[NASA-CASE-MFS-25981-1] 11 p1635 N85-20299
Performance of Chromel versus Alumel and Nicrosil versus Nisil thermocouple assemblies in vacuum and argon between 1000 deg C and 1200 deg C
[DE85-000810] 12 p1853 N85-21624
Releasable cable connector assembly for use between a mobile and stationary object
[AD-D011538] 12 p1858 N85-21655
Development of a sintered shim
[DE85-006183] 13 p2025 N85-22665
Direct transient analysis of a fuze assembly by axisymmetric solid elements
15 p2576 N85-25890
A Gimbal sizing analysis for an IPACS rotating assembly
[NASA-CR-172524] 16 p2741 N85-26913
Fully redundant mechanical release actuator
[NASA-CASE-LAR-13198-1] 18 p3116 N85-29287
Self-locking mechanical center joint
[NASA-CASE-LAR-12864-1] 19 p3279 N85-30336
Voyager 0.2-lbf thruster valve assembly short pulse test report
[NASA-CR-176121] 22 p3741 N85-33185
Latch assembly
[DE85-011660] 22 p3792 N85-33492
Two-plane balance and slip-ring design
22 p3799 N85-33536

ASSEMBLING
NT ORBITAL ASSEMBLY
Automation of assembly of electrical products
03 p0346 N85-12228
Mathematical modeling of assembly processes involving use of sensitized robots
04 p0488 N85-13111
Component reliability and assembling technologies
[CNES-NT-108] 04 p0511 N85-13258
External tank processing from barge to pad
06 p1096 N85-16927
Automated assembly of Gallium Arsenide and 50-micron thick silicon solar cell modules
[NASA-CR-174331] 08 p1168 N85-17364
Ground test article for deployable space structure systems
[NASA-CR-171301] 10 p1429 N85-19011

Double pinch-push contact insertion end-effector
[AD-D011485] 10 p1459 N85-19196
Investigation of dynamics of manipulator with elastic sections 13 p2048 N85-22819
Advanced life analysis methods. Volume 2: Crack growth analysis methods for attachment lugs
[AD-A150420] 13 p2103 N85-23109
Extreme precision antenna reflector study results 14 p2232 N85-23830
Large Deployable Reflector (LDR) requirements for space station accommodations 14 p2236 N85-23858
Classification of holding jigs for objects of robotized assembly 14 p2266 N85-24039
Construction in space 15 p2484 N85-25328
Robot use in FRG increases but sensor technology lags 15 p2531 N85-25605
Robots, automatic devices inside VW's Wolfsburg plant 17 p2946 N85-28186
Alignment and assembly tool for very large diameter cylinders
[NASA-CASE-MFS-28001-1] 18 p3116 N85-29289
X-ray satellite
[NASA-TM-77898] 20 p3407 N85-31144
Automatic assembly of space stations 20 p3409 N85-31153
Field testing of a lightweight relocatable structure in a temperate environment
[AD-A155171] 21 p3599 N85-32350
Multi-robot assembly of IC's 23 p3964 N85-34577

ASSEMBLY LANGUAGE
MC68CRX cross-assembler users manual
[AD-A148031] 08 p1205 N85-17584
Topics in optical materials and device research, 3. Volume 2
[AD-A149727] 12 p1911 N85-21996
ZTL: A subroutine package for the IBM personal computer to support the Zlatech ZT1488 IEEE-488 controller
[LA-10141-MS] 12 p1913 N85-22010
HGRAPH: A subroutine package for the IBM personal computer to support the Hercules Graphic Card
[LA-10144-MS] 12 p1914 N85-22013
ZTLCK: A subroutine package for the IBM personal computer to support the Zlatech ZT1488 real time clock
[LA-10146-MS] 12 p1914 N85-22014
TRANIO: A subroutine package for the IBM personal computer to support the transfer 6002 CAMAC crate controller
[LA-10145-MS] 12 p1914 N85-22015
A quickly tested Pascal random number generator for microcomputers
[AD-A156059] 24 p4136 N85-35633

ASSESSMENTS
NT DAMAGE ASSESSMENT
NT TECHNOLOGY ASSESSMENT
DC-10 winglet flight evaluation
[NASA-CR-3704] 19 p3217 N85-29949
Description of a test site for large-scale heavy gas dispersion and combustion experiments
[DE85-004987] 23 p3911 N85-34231
The role of regional subsurface geochemistry in resource assessment in the central United States 24 p4104 N85-35440
Some recent deposit modeling efforts 24 p4106 N85-35453

ASSIGNMENT
U ALLOCATIONS

ASSIMILATION
A simulation experiment on the impact of geostationary temperature retrievals in numerical models 15 p2597 N85-26005
VAS/model impact study 15 p2597 N85-26006
Users guide for optimum interpolation method of global data assimilation
[AD-A155929] 24 p4138 N85-35648
Two methods of global data assimilation
[AD-A155981] 24 p4143 N85-35684

ASSOCIATIONS
U ORGANIZATIONS

ASSOCIATIVE PROCESSING (COMPUTERS)
Linear associative mapping
[ESA-TT-856] 05 p0719 N85-14611
Evaluation of the RSTN (Regional Seismic Test Network) network and further improvement to automatic association
[AD-A146395] 08 p0835 N85-15312
Toward a model of attention and the development of automatic processing
[AD-A149348] 10 p1567 N85-19682

ASSURANCE
Measurement assurance programs. Part 2: Development and implementation
[PB84-217876] 01 p0051 N85-10338
Measurement assurance programs. Part 1: General introduction
[PB84-217868] 01 p0051 N85-10339
The ESA product assurance specification system: Explanatory note 04 p0511 N85-13259
Toward a non-bureaucratic approach to quality assurance in data processing
[DE84-007484] 04 p0550 N85-13497
Quality assurance for environmental analytical chemistry, 1983
[DE84-016045] 09 p1349 N85-18489
Characteristics of quality data
[DE85-001203] 10 p1568 N85-19689
Examination of steels by chemical analysis for quality assurance
[BLL-BISI-TRANS-22068-(9022.06)] 17 p2929 N85-28074
Principal quality assurance measures in the manufacture of HF-welded high-pressure linepipe
[BLL-BISI-TRANS-21600-(9022.06)] 17 p2976 N85-28389
Principles of quality assurance of chemical measurements
[PB85-177947] 18 p3072 N85-28997
Towards the year 2000: Developments in inspection and product assurance to be anticipated during the next 15 years — aircraft engines
[PNR-90258] 23 p3940 N85-34421

ASTEROID BELTS
NT AMOR ASTEROID
NT APOLLO ASTEROIDS
NT ASTEROIDS
NT VESTA ASTEROID
The asteroid ring 15 p2678 N85-26536
Asteroid compositional rings: Clues to the compositions of primordial planetesimals in the middle solar system 15 p2678 N85-26537
Collisional outcomes in the asteroid belt 15 p2678 N85-26538
The distribution of compositional classes in the asteroid belt: A cosmochemical fingerprint? 22 p3852 N85-33856

ASTEROID MISSIONS
Asteroid amphitrite: Surface composition and prospects for the possible Galileo flyby 15 p2680 N85-26549
Space ventures and society long-term perspectives
[NASA-CR-176012] 19 p3379 N85-30963

ASTEROIDS
NT AMOR ASTEROID
NT APOLLO ASTEROIDS
NT VESTA ASTEROID
The asteroidal source region of ordinary chondrites 06 p0681 N85-15600
How many Earth-approaching asteroids are there?
[NASA-CR-174209] 06 p0690 N85-15650
The discovery circumstances of Earth-approaching asteroids
[NASA-CR-174327] 08 p1258 N85-17920
The geology of the terrestrial planets
[NASA-SP-469] 09 p1410 N85-18888
Asteroids, comets and planet formation 09 p1410 N85-18889
Asteroid taxonomy from cluster analysis of Photometry 09 p1411 N85-18897
Research in planetary studies and operation of Mauna Kea Observatory
[NASA-CR-175618] 13 p2169 N85-23460
Study and estimation of planet-crossing asteroid populations: Discoveries and analysis 13 p2175 N85-23498
The olivine asteroids: Discovery, mineralogy, and relationship to palasites 13 p2175 N85-23500
Convex-profile inversion of asteroid lightcurves 13 p2176 N85-23502
Surfaces of asteroids and cometary nuclei 13 p2176 N85-23503
The asteroid ring 15 p2678 N85-26536
Asteroid compositional rings: Clues to the compositions of primordial planetesimals in the middle solar system 15 p2678 N85-26537
Collisional outcomes in the asteroid belt 15 p2678 N85-26538
Asteroid amphitrite: Surface composition and prospects for the possible Galileo flyby 15 p2680 N85-26549
Mining cosmic dust from the blue ice lakes of Greenland 15 p2682 N85-26563
A search for evidence of large body Earth impacts associated with biological crisis zones in the fossil record 15 p2682 N85-26567
An analysis of alternate hydrogen sources for lunar manufacture
[DE85-007234] 16 p2884 N85-27792
Speckle interferometry applied to asteroids and other solar system objects
[NASA-CR-175976] 19 p3384 N85-30995
The 13 November 1984 occultation of BD +08 deg 0471 by (1) Ceres
[NASA-CR-176106] 23 p3987 N85-34725
The nature and origin of outer solar system asteroids from reflectance spectrophotometry 24 p4168 N85-35838

ASTHMA
Short-term human respiratory effects of nitrogen dioxide: Determination of quantitative dose-response profiles. Phase 2: Exposure of asthmatic volunteers to 4 PPM NO2
[PB85-104388/GAR] 07 p1017 N85-16462

ASTRO MISSIONS (STS)
The 1986 National Aeronautics and Space Administration authorization
[GPO-47-635] 24 p4166 N85-35829

ASTROBIOLOGY
U EXOBIOLOGY

ASTRODYNAMICS
Method for prompt modeling of quasiperiodic movement of solid near-axisymmetrical body in atmosphere 13 p2043 N85-22790
Application of quaternions to problems of solid body dynamics in the atmosphere 15 p2481 N85-25313
Solved und unsolved problems in planetary ring dynamics 15 p2674 N85-26502
Dynamics of neutral small particles — in the solar system 15 p2676 N85-26521
Accuracy in predicting orbital motion of artificial Earth satellite 16 p2720 N85-25793
Optimal relative data weights 16 p2805 N85-27296

ASTROGRAPHY
NGC 2024: Multi-wavelength infrared and radio observations 06 p1246 N85-17865
Far-infrared photometry of low-mass pre-main-sequence stars with broad CO wings 06 p1246 N85-17866
The astrometry programme at Mt. John Observatory 14 p2436 N85-25026
The astrometry network of observers in China 14 p2436 N85-25027
Obtaining accurate comet positions despite some inaccurate catalog stars 14 p2437 N85-25032
Reduction of astrographic catalogues 14 p2437 N85-25033

ASTROLABES
Timing-system design considerations for a mobile astrolabe 17 p2965 N85-28309

ASTROMASTS
U LONGERONS

ASTROMETRY
The present state of the International Star Cluster Photometry Programme 05 p0737 N85-14741
Plate measurements and reductions at Muenster — astronomical photography 07 p0966 N85-16129
First tests on the astrometric performance of the new PDS1010G at Hamburg Observatory — granite microdensitometer 07 p0966 N85-16135
Astrometric applications of the Mt. Stromlo PDS 1010A — microdensitometer 07 p0967 N85-16136
Automated star counts in nebulous areas 07 p0967 N85-16137
Cometary Astrometry
[NASA-CR-175660] 14 p2435 N85-25015
The astrometry network of the IHW and the P/Crommelin trial run results 14 p2435 N85-25016
Remarks on cometary astrometry 14 p2435 N85-25019
Cometary astrometry with Schmidt cameras 14 p2435 N85-25020
Astrometry of comets using hypersensitized type 2415 film 14 p2435 N85-25021
Astrometric plates obtained at the primary focus of large aperture reflectors 14 p2436 N85-25022
Kitt Peak measurements of P/Halley positions 14 p2436 N85-25023
Problems and procedures of cometary astrometry 14 p2436 N85-25024
Astrometry at La Silla 14 p2436 N85-25025
The astrometry programme at Mt. John Observatory 14 p2436 N85-25026
The astrometry network of observers in China 14 p2436 N85-25027
The astrometry network of observers in Japan 14 p2436 N85-25028
The astrometry network of observers in USSR 14 p2436 N85-25029
Desired characteristics of catalogs for cometary astrometry 14 p2436 N85-25030
The IHW reference star catalogs for Comets Halley and Giacobini-Zinner 14 p2436 N85-25031
Obtaining accurate comet positions despite some inaccurate catalog stars 14 p2437 N85-25032
Measuring: The quantifying art 14 p2437 N85-25035

Least squares reduction technique
14 p2437 N85-25036
Reduction of astrometric plates
14 p2437 N85-25037
The work on Comet Halley's orbit at ESOC
14 p2438 N85-25041
Study of the accuracy of astrometric observations of comets
[ESA-CR(P)-1984] 17 p3054 N85-28903

ASTRONAUT PERFORMANCE
Ultrasonic study of early cardiovascular adaptation to zero gravity 05 p0691 N85-14445
NASA: Model development for human factors interfacing
[NASA-CR-175584] 12 p1910 N85-21985
Psychological issues relevant to astronaut selection for long-duration space flight: A review of the literature
[AD-A154051] 19 p3330 N85-30627

ASTRONAUT TRAINING
25th anniversary of the Gagarin Cosmonaut Training Center
[NASA-TM-77644] 09 p1286 N85-18076

ASTRONAUTS
Approaches to radiation guidelines for space travel
[DE85-001248] 09 p1363 N85-18576
Astronaut hazard during free-flight polar EVA
13 p1997 N85-22522
Psychological issues relevant to astronaut selection for long-duration space flight: A review of the literature
[AD-A154051] 19 p3330 N85-30627
Experience of science astronaut on the Spacelab-1 mission 20 p3508 N85-31807
Results of microbiological studies conducted during operation of Salyut-6 orbital station
22 p3823 N85-33882
The effect of +Gx acceleration on platelet activation as determined by plasma platelet factor 4 levels
[AD-A155861] 24 p4131 N85-35608

ASTRONAVIGATION
Optimization of orientation in navigation by two heavenly bodies 07 p0951 N85-16027
Errors of analog of inertial coordinate systems modeled in astronavigation system 07 p0951 N85-16028

ASTRONOMICAL CATALOGS
The catalogue of the discrete sources in the declination range from -13 deg to -2 deg
[NASA-TM-77594] 01 p0129 N85-10687
Documentation for the machine-readable version of A Catalogue of Extragalactic Radio Source Identifications (Veron-Cetty and Veron 1983)
[NASA-TM-87373] 03 p0405 N85-12587
Documentation for the machine-readable version of The Revised AFGL Infrared Sky Survey Catalog (Price and Murdock 1983)
[NASA-TM-87377] 03 p0405 N85-12588
Documentation for the machine-readable version of the MK classification extension catalogue Morris-Kennedy (1983)
[NASA-TM-87372] 04 p0549 N85-13491
Documentation for the machine-readable version of the Perth 75: A Catalogue of Positions of 2589 FK4 and FK4S Stars (Nikoloff and Hog 1982)
[NASA-TM-87376] 04 p0549 N85-13492
Documentation for the machine-readable version of the AGK3 Star Catalogue of Positions and Proper Motions North of -2 deg .5 declination (Dieckvoss and Collaborators 1975)
[NASA-TM-87378] 04 p0549 N85-13493
The Lund catalogue of open cluster parameters
05 p0738 N85-14742
Catalogue of observations of total occultations of stars by the Moon for the years 1972 to 1980 and of grazing occultations for the years 1963 to 1980
[BULL-192] 05 p0741 N85-14768
Dark cloud and globule distribution for galactic longitudes 230 to 360 degrees 06 p0878 N85-15575
Data reduction 09 p1412 N85-18903
Flux reconstruction and calibration
09 p1412 N85-18904
Analysis of processing 09 p1412 N85-18905
Sky coverage, confusion, completeness and reliability
09 p1412 N85-18906
The formats of the IRAS catalogs and atlases
09 p1413 N85-18908
IUE low-dispersion reference atlas
11 p1760 N85-21073
Statistical classification of IUE low-dispersion stellar spectra: Progress report 11 p1760 N85-21075
Herstmonceux observations of the Sun, planets and Moon, 1957 - 1982
[BULL-193] 11 p1762 N85-21087
Materialization of a reference system via a star catalog 14 p2399 N85-24787
Desired characteristics of catalogs for cometary astrometry 14 p2436 N85-25030
The IHW reference star catalogs for Comets Halley and Giacobini-Zinner 14 p2436 N85-25031
Obtaining accurate comet positions despite some inaccurate catalog stars 14 p2437 N85-25032
Reduction of astrographic catalogues
14 p2437 N85-25033
On the orbit improvement results obtained by referring old cometary observations to the SAO Star Catalog
14 p2438 N85-25042
Documentation for the machine-readable version of the Stellar Spectrophotometric Atlas, 3130 A lambda 10800 A of Gunn and Stryker (1983)
[NASA-TM-87437] 14 p2438 N85-25045
Documentation for the machine-readable version of A Library of Stellar Spectra (Jacoby, Hunter and Christian 1984)
[NASA-TM-87438] 14 p2438 N85-25046
Documentation for the machine-readable version of the Revised S210 Catalog of Far-Ultraviolet Objects (Page, Carruthers and Heckathorn 1982)
[NASA-TM-87439] 14 p2438 N85-25047
Documentation for the machine-readable version of the Cordoba Durchmusterung (CD)
[NASA-TM-87441] 14 p2439 N85-25049
Documentation for the machine-readable version of the Cape Photographic Durchmusterung (CPD)
[NASA-TM-87442] 14 p2439 N85-25050
Documentation for the machine readable version of the Yale Catalogue of the Positions and Proper Motions of Stars between Declinations -60 deg and -70 deg (Fallon 1983)
[NASA-TM-87443] 14 p2439 N85-25051
A second catalog of gamma ray bursts: 1978 - 1980 localizations from the interplanetary network
[OG-1.2-1] 22 p3861 N85-33912
Limits to the burster repetition rate as deduced from the 2nd catalog of the interplanetary network
[OG-1.2-5] 22 p3862 N85-33915

ASTRONOMICAL COORDINATES
Optimization of orientation in navigation by two heavenly bodies 07 p0951 N85-16027
Data reduction 09 p1412 N85-18903
Analysis of processing 09 p1412 N85-18905
Reduction of astrographic catalogues
14 p2437 N85-25033
On the orbit improvement results obtained by referring old cometary observations to the SAO Star Catalog
14 p2438 N85-25042
Basic formulae for the computation of the deflection of the vertical from astronomical star observations
[AD-A154912] 21 p3605 N85-32390
Jets in air-jet family
[HE-3.2-1] 24 p4179 N85-35912

ASTRONOMICAL MAPS
Infrared mapping of galaxian centers: Star forming regions with kiloparsec scale sizes
03 p0444 N85-12827
Synthesis of radio image on RATAN-600 radiotelescope 06 p0783 N85-15004
Automated star counts in nebulous areas
07 p0967 N85-16137
The formats of the IRAS catalogs and atlases
09 p1413 N85-18908
Infrared observations of the Uranian rings
15 p2672 N85-26488
Far-infrared observations of young clusters embedded in the R Coronae Australinae and RHO Ophiuchi dark clouds
[NASA-TM-86681] 24 p4167 N85-35834

ASTRONOMICAL MODELS
NT DENSITY WAVE MODEL
NT STELLAR MODELS
Time-dependent chemistry of molecular clouds
03 p0443 N85-12822
The Martian climate: Energy balance models with CO2/H2O atmospheres
[NASA-CR-174073] 03 p0448 N85-12849
Far-infrared photometry of compact extragalactic sources: OJ 187 and BL Lac
[NASA-TM-86022] 04 p0580 N85-13701
Galaxy and cluster formation in a universe dominated by cold dark matter
[DE84-015879] 04 p0580 N85-13706
Bulk composition of the Moon in the context of models for condensation in the solar nebula
04 p0583 N85-13725
Tidal disruption and the origin of the Moon
04 p0586 N85-13739
A numerical investigation of planetesimal collision trajectories with a Moon accumulating in Earth orbit
04 p0586 N85-13740
Stochastic does not equal ad hoc — theories of lunar origin 04 p0586 N85-13741
A testable gravitational capture model for the origin of the Earth's Moon 04 p0586 N85-13742
Directional properties of circular Maria: Interpretation in the context of a testable gravitational capture model for lunar origin 04 p0586 N85-13743
The problem of iron partition between Earth and Moon during simultaneous formation as a double planet system 04 p0587 N85-13744
An integrated dynamical and geochemical approach to lunar origin modelling 04 p0587 N85-13748
Lunar origin from impact on the Earth
04 p0588 N85-13757
Stability of stellar disk and ratio of halo to disk masses in the galaxy 05 p0740 N85-14763
Structure and evolution of the large scale solar and heliospheric magnetic fields 05 p0746 N85-14782
Local Interstellar Medium. International Astronomical Union Colloquium No. 81
[NASA-CP-2345] 06 p0672 N85-15539
Supersymmetric inflationary cosmology
[DE85-001331] 06 p0681 N85-15598
BL Lacertae objects: Multifrequency observations and model applications 08 p1236 N85-17792
Shock acceleration in active galactic nuclei and quasars 08 p1241 N85-17826
On the hydrodynamical equations of astrophysical jets — active galactic nuclei 08 p1241 N85-17831
An alternative to relativistic beaming in AGN — Active Galactic Nuclei (AGN) 08 p1242 N85-17833
Models of nonkeplerian accretion disks based on dynamo magnetic field: Application to Active Galactic Nuclei (AGN) 08 p1242 N85-17834
Macroscopic currents and wind perturbations in the frame of the wind and shock model — galactic nuclei
08 p1242 N85-17836
Duelling winds: A model for broad-line regions — galactic nuclei 08 p1242 N85-17837
Theoretical studies of emission line variability in type 1 Seyfert galaxies 08 p1242 N85-17839
A model for the climatic behavior of water on Mars
09 p1415 N85-18931
Coordinated multifrequency observations of the BL LAC objects MRK 180, MRK 421, and MRK 501
11 p1746 N85-20983
A model for the variable continuum of the Seyfert 1 galaxy NGC 5548 11 p1747 N85-20985
The changing ultraviolet spectrum of Herbig-Haro object No. 1 11 p1747 N85-20989
Accretion in the zeta Aurigae and 32 Cygni shock cones 11 p1754 N85-21036
Consequences of hot gas in the broad line region of active galactic nuclei
[NASA-TM-86176] 11 p1763 N85-21090
The axisymmetric pulsar magnetosphere
12 p1955 N85-22279
Dynamics of elliptical galaxies and the r sup 1/4 luminosity law 12 p1955 N85-22282
Nonlinear evolution of astrophysical Alfven waves
12 p1956 N85-22294
About static and dynamic solutions of the aligned rotator model — pulsar magnetospheres
12 p1958 N85-22306
Hydrodynamics of astrophysical jets — active galactic nuclei 12 p1958 N85-22307
Equilibrium model of thin magnetic flux tubes — solar atmosphere 12 p1958 N85-22310
An analytic model for hydromagnetospheres — stellar winds; pulsars; cosmic jets 12 p1959 N85-22313
The influence of the local solar wind structures on the propagation of low energy particles
12 p1959 N85-22314
Small scale structure and the Spinar model for active galactic nuclei 12 p1959 N85-22316
Viking radio science data analysis and synthesis
[NASA-CR-175631] 13 p2171 N85-23471
An idealized short period comet model: Surface insolation, H2O flux, dust flux and mantle evolution
13 p2176 N85-23504
Planetary Rings. Colloquium 75 — conferences
[ISBN-2-85428-100-4] 15 p2670 N85-26473
A model containing blobs for the A ring of Saturn
15 p2671 N85-26479
The rings of Uranus 15 p2672 N85-26486
Evolution of collisional systems — planetary disks
15 p2674 N85-26505
A simple model of Saturn's rings revisited
15 p2674 N85-26506
Viscosity in Saturn's rings 15 p2674 N85-26507
Comments on collision mechanics in ring systems — planetary rings
[PSI-CONTRIB-186] 15 p2675 N85-26510
Diffusion instability in a bimodal disc — planetary rings
15 p2675 N85-26513
Stochastic modeling of planetary ring systems
15 p2675 N85-26516
The Adiabatic invariant: A tool for the study of the dynamics of the solar system 15 p2676 N85-26519

The formation of the terrestrial planets from lunar sized planetesimals 15 p2678 N85-26533
The evolution of meteor streams 15 p2678 N85-26539
Some features of the interplanetary medium during Forbush decreases
[NOTA-INTERNA-836] 18 p3202 N85-29866
First-order shock acceleration in solar flares
[SH-1.1-5] 23 p3989 N85-34732
Variations in the propagation of UH-nuclei
[OG-7.1-1] 23 p4012 N85-34863
An experiment to measure the energy spectrum of cosmic ray antiprotons from 100 to 1000 MeV
[OG-9.1-3] 23 p4022 N85-34929

ASTRONOMICAL OBSERVATORIES
NT ASTRONOMICAL SATELLITES
NT GAMMA RAY OBSERVATORY
NT HEAO
NT HEAO 1
NT HEAO 2
NT HEAO 3
NT HUBBLE SPACE TELESCOPE
NT INFRARED ASTRONOMY SATELLITE
NT IUE
NT OAO 3
NT QUASAT
NT ROSAT MISSION
NT SPACE INFRARED TELESCOPE FACILITY
NT SPARTAN SATELLITES
Study of instrument design options for the Columbus spectroscopy mission
[NASA-CR-174072] 04 p0502 N85-13205
The Ebro Observatory and international scientific organizations 04 p0518 N85-13309
Aperture synthesis for radioastronomy 06 p0781 N85-14992
Pointing and control system design study for the space infrared telescope facility (SIRTF)
[NASA-CR-166612] 07 p0915 N85-15795
Recalibration of the KPNO spot sensitometers — Kitt Peak National Observatory 07 p0963 N85-16103
Some nonatlas work at the European Southern Observatory (ESO) Sky Atlas Laboratory — astronomical photography 07 p0964 N85-16117
The work of the photolabs at the Royal Observatory, Edinburgh — astronomical photography 07 p0965 N85-16122
SIRTF: The next step
[NASA-TM-86663] 07 p1059 N85-16724
Airborne Astronomy Symposium. A symposium commemorating the tenth anniversary of operations of the Kuiper Airborne Observatory
[NASA-CP-2353] 08 p1244 N85-17848
The Lear Jet Observatory: Fifteen years of discovery and rebirth 08 p1244 N85-17850
Simultaneous determination of the xi and eta components of vertical deflection with a prism astrolabe
[SER-B-270-MITT-171] 09 p1343 N85-18450
Astronomy and sodium lighting
[RAND/N-2069-RC] 09 p1413 N85-18914
The astrometry network of observers in China 14 p2436 N85-25027
The astrometry network of observers in Japan 14 p2436 N85-25028
The astrometry network of observers in USSR 14 p2436 N85-25029
A program of ground-based astronomy to complement einstein observations
[AD-A151111] 15 p2668 N85-26466
A priority of space exploration: Observation of Saturn's rings from a Saturn orbiter 15 p2679 N85-26542
Program for observations of Halley's comet 22 p3732 N85-33136
Research of advanced techniques for X-ray detectors and telescopes with applications to rockets and the LAMAR facility
[NASA-CR-176161] 23 p4054 N85-35141

ASTRONOMICAL PHOTOGRAPHY
Problem of determining highly accurate coordinates of artificial satellites by photographic methods 02 p0162 N85-11096
Astronomical photography 1984 — conferences
[ROE-OR-14] 07 p0962 N85-16102
SENSIT.FOR: A program for sensitometric reduction 07 p0963 N85-16105
A spectrosensitometer with an absolute calibration 07 p0963 N85-16106
Comparison of the fine grain compensation hypersensitization (FAH) process with gas hypersensitizing techniques — astronomical photography plates 07 p0963 N85-16107
The results of hydrogen hypersensitization of photoemulsions — astronomical photography 07 p0963 N85-16108
Nitrogen flushing during exposure of large Schmidt telescope plates 07 p0963 N85-16109
The most effective astronomical photographic emulsions for recording of faint and low-contrast objects 07 p0963 N85-16110
Astronomical applications of new infrared films 07 p0964 N85-16111
The 3a-F emulsion and the quasar redshift cut-off 07 p0964 N85-16112
Microspots on spectroscopic plates — astronomical photography 07 p0964 N85-16113
Where to next in astronomical photography? — tabular grain emulsions 07 p0964 N85-16114
What do we want: Increased speed, resolution, contrast or DQE? — astronomical photography 07 p0964 N85-16115
Some aspects of photography with a small Schmidt camera — astronomical photography 07 p0964 N85-16116
Some nonatlas work at the European Southern Observatory (ESO) Sky Atlas Laboratory — astronomical photography 07 p0964 N85-16117
Using a Gossen light meter to produce enlarged interpositive film copies from glass plates — astronomical photography 07 p0964 N85-16118
Unsharp masking at the enlarger — astronomical photography 07 p0964 N85-16119
Processing of photographic observing material at the National Astronomical Observatory Rozhen 07 p0965 N85-16120
The UK Schmidt telescope and the facilities in Edinburgh 07 p0965 N85-16121
The work of the photolabs at the Royal Observatory, Edinburgh — astronomical photography 07 p0965 N85-16122
An investigation into the fidelity of reproduction of UKST original objective prism plates on to film — United Kingdom Schmidt Telescope (UKST) 07 p0965 N85-16123
Power spectrum analysis of astronomical photographs digitised with small apertures 07 p0965 N85-16127
Recent developments on the COSMOS plate-scanning machine — microdensitometer 07 p0966 N85-16128
Plate measurements and reductions at Muenster — astronomical photography 07 p0966 N85-16129
The Torun measuring system for astronomical spectra 07 p0966 N85-16130
The Malin effect in stellar photography 07 p0966 N85-16131
Some applications of signal-to-noise in photographic stellar photometry 07 p0966 N85-16132
Stellar photographic photometry using a double wedge technique with a focal reducer system 07 p0966 N85-16133
Design and fabrication of a CCD camera for use with relay optics in solar X-ray astronomy
[NASA-CR-174334] 08 p1164 N85-17344
An objective prism quasar survey with the Schmidt telescope on Calar Alto (Spain) 08 p1243 N85-17845
Development of a portable zenith chamber and its use on the 47th parallel
[SER-C-287] 11 p1741 N85-20946
Analysis of white dwarf Lyman alpha profiles 11 p1752 N85-21018
Evaluating accuracy in orientation of topographic photograph and satellite-centered direction from star photograph 13 p1983 N85-22442
Remarks on cometary astrometry 14 p2435 N85-25019
Cometary astrometry with Schmidt cameras 14 p2435 N85-25020
Astrometry of comets using hypersensitized type 2415 film 14 p2435 N85-25021
Astrometric plates obtained at the primary focus of large aperture reflectors 14 p2436 N85-25022
Problems and procedures of cometary astrometry 14 p2436 N85-25024
Astometry at La Silla 14 p2436 N85-25025
Least squares reduction technique 14 p2437 N85-25036
Variability of the structure of the granulation over the solar activity cycle 14 p2447 N85-25100
One aspect of determination of direction of space survey base from photographs of planetary surface and star sky 15 p2487 N85-25352
Summary of optical groundbased E ring observations at the University of Arizona 15 p2671 N85-26482
Analysis and modeling of variations in length of day 19 p3349 N85-30761
A star camera aspect system suitable for use in balloon experiments
[OG-9.3-10] 23 p4028 N85-34965

ASTRONOMICAL PHOTOMETRY
NT STELLAR SPECTROPHOTOMETRY
South African Astronomical Observatory Circulars, no. 7
[SAAOC-7] 01 p0127 N85-10675
Observations of the pulsating hydrogen: Deficient star BD+13 deg 3224, during 1980 - 1981 01 p0128 N85-10682
Spectral components at visual and infrared wavelengths in active galactic nuclei
[NASA-CR-174133] 03 p0445 N85-12832
Time series photometry with a CCD camera 06 p1252 N85-17906
The use of self-scanned silicon photodiode arrays for astronomical spectrophotometry 06 p1252 N85-17907
Photodiodes for astronomical stellar radiometry 06 p1252 N85-17908
Photometry with Multi-Anode Microchannel Arrays (MAMAs) and Charge Injection Devices (CIDs) 06 p1252 N85-17909
Filter and passband problems 06 p1252 N85-17910
Light scattered from polished optical surfaces: Wings of the point spread function 06 p1252 N85-17911
Application of fiber optics and compound collectors 06 p1253 N85-17912
Asteroid taxonomy from cluster analysis of Photometry 09 p1411 N85-18897
Study of the pulsations of the ZZ Ceti stars 09 p1414 N85-18923
Improved continuum definition in high-background IUE images 11 p1761 N85-21078
Convex-profile inversion of asteroid lightcurves 13 p2176 N85-23502
Offerings of the Astronomical Institute of Bonn 15 p2667 N85-26459
Photoelectric observations of contact binary stars
[REPT-96] 15 p2667 N85-26460
Photoelectric observations of the dwarf nova VW Hydri during the November 1977 supermaximum
[REPT-97] 15 p2667 N85-26461
Photoelectric observations of the eclipsing binary V 836 Cygni
[REPT-98] 15 p2668 N85-26462

ASTRONOMICAL SATELLITES
NT HEAO
NT HEAO 1
NT HEAO 2
NT HEAO 3
NT HUBBLE SPACE TELESCOPE
NT INFRARED ASTRONOMY SATELLITE
NT IUE
NT OAO 3
NT QUASAT
NT SPACE INFRARED TELESCOPE FACILITY
NT SPARTAN SATELLITES
QUASAT: An orbiting very long baseline interferometer program using large space antenna systems 14 p2230 N85-23822
China report: Science and technology
[JPRS-CST-85-007] 15 p2533 N85-25621
Professional Committee on Solid Propulsion hold conference 15 p2533 N85-25623
Mapping with QUASAT (quasar satellite) using short observation times
[AD-A155155] 21 p3559 N85-32141

ASTRONOMICAL SPECTROSCOPY
A spectroscopic survey of 113 nearby red dwarf stars 01 p0129 N85-10686
Forbidden lines of oxygen in comet spectra 02 p0163 N85-11105
Solar neutrino spectroscopy
[DE84-015518] 02 p0304 N85-11968
Fr. Angelo Secchi, a pioneer in the study of solar-terrestrial relationships 04 p0519 N85-13312
Oblique focus ICCD laboratory evaluation
[NASA-CR-174205] 06 p0662 N85-15480
Optical and UV emission of active galactic nuclei 08 p1236 N85-17791
The 1.5 - 3.5 micron spectroscopy of the Orion H2 source 08 p1246 N85-17864
High sensitivity, high angular resolution far-infrared photometry from the KAO 08 p1246 N85-17867
Carbon stars: There is no such thing as a dead leg 08 p1247 N85-17871
Mid-infrared spectroscopy of planetary nebulae 08 p1247 N85-17872
Interstellar grain mantles 08 p1247 N85-17874
Far-infrared spectroscopy of galaxies: The 158 micron C(+) line 08 p1249 N85-17882
High precision measurement of stellar radial velocity variations 08 p1250 N85-17896
International Ultraviolet Explorer observations of amorphous hot galaxies
[NASA-CR-174354] 10 p1571 N85-19904
A new generation of spectrometer designs for ultraviolet astronomy 11 p1761 N85-21079
The multi-anode microchannel array detector system: Current status and future prospects 11 p1761 N85-21080

Interactions of galaxies and their nuclear activity
20 p3545 N85-32060
Development of observational and instrumental techniques in hard X-ray and medium energy gamma-ray astronomy
[NASA-CR-176172] 24 p4168 N85-35841

ASTRONOMICAL TELESCOPES
NT HELIOMETERS
NT INFRARED TELESCOPES
NT PYROHELIOMETERS
NT SPACE INFRARED TELESCOPE FACILITY
NT SPECTROSCOPIC TELESCOPES
NT ULTRAVIOLET TELESCOPES
NT X RAY TELESCOPES
Study of a coded mask telescope for astronomical measurements in the hard X-ray domain
[MPE-182] 01 p0129 N85-10689
Construction of a superheterodyne receiver for 10 micron waves to be put on a Cassegrain optics telescope for spectroscopic research on the Mars and Venus atmospheres
[MPE-183] 06 p0872 N85-15538
Image quality on the KAO 08 p1249 N85-17885
A 150 micron heterodyne spectrometer for airborne astronomy 08 p1249 N85-17887
A new generation of sub mm telescopes, made of carbon fiber reinforced plastic 08 p1250 N85-17890
The ground based photometric limitations to the search for light variations due to 5-minute solar-type oscillations in other stars 08 p1251 N85-17896
Light scattered from polished optical surfaces: Wings of the point spread function 08 p1252 N85-17911
Dall-Null tester for spaceborne applications
[AD-A151772] 16 p2881 N85-27779
Optical observations of HEAO-B objects
17 p3052 N85-28895
Radio telescope with 256 antennas built in Siberia
22 p3732 N85-33136
High energy neutrino astronomy with MACRO
[HE-5.3-12] 24 p4206 N85-36106

ASTRONOMY
NT GAMMA RAY ASTRONOMY
NT INFRARED ASTRONOMY
NT RADAR ASTRONOMY
NT RADIO ASTRONOMY
NT SPACEBORNE ASTRONOMY
NT ULTRAVIOLET ASTRONOMY
NT X RAY ASTRONOMY
NT X RAY BINARIES
NT X RAY SOURCES
National Science Foundation grants and awards for fiscal year 1983, volume 2
[PB84-212323] 01 p0125 N85-10854
South African Astronomical Observatory Circulars, no. 7
[SAAOC-7] 01 p0127 N85-10875
Observations of four Beta Cephei stars in NGC6231
01 p0128 N85-10877
Research and technology, 1984: Marshall Space Flight Center
[NASA-TM-86476] 04 p0590 N85-13765
The beginnings of airborne astronomy, 1920 - 1930: An historical narrative 08 p1244 N85-17849
Global meteor observation system (GLOBMET)
11 p1656 N85-20438
Research and technology: Fiscal year 1984 report
[NASA-TM-85231] 12 p1964 N85-22340
Activities report of the Institute for Astronomy and Astrophysics
[MITT-5] 14 p2434 N85-25012
Cometary Astrometry
[NASA-CR-175660] 14 p2435 N85-25015
USSR report: Space
[JPRS-USP-85-003] 15 p2476 N85-25264
Astrometric method advances Astronomy, geodesy
16 p2806 N85-27306
Basic formulae for the computation of the deflection of the vertical from astronomical star observations
[AD-A154912] 21 p3605 N85-32390
Space research in the United Kingdom: An assessment
[AD-A155334] 21 p3712 N85-33038
The 13 November 1984 occultation of BD +08 deg 0471 by (1) Ceres
[NASA-CR-176106] 23 p3987 N85-34725
Neutrino astronomy and the atmospheric background
[HE-5.3-17] 24 p4207 N85-36111

ASTROPHYSICS
NT COMPUTATIONAL ASTROPHYSICS
NT SOLAR PHYSICS
South African Astronomical Observatory Circulars, no. 7
[SAAOC-7] 01 p0127 N85-10875
Observations of four Beta Cephei stars in NGC6231
01 p0128 N85-10877
USSR report: Space
[JPRS-USP-84-005] 02 p0156 N85-11060
Cosmonauts complete 4th month aboard Salyut-7
02 p0157 N85-11065
Salyut-7 crew in orbit 150 days
02 p0157 N85-11068
Tass reports astrophysical, atmospheric studies on Salyut-7 02 p0158 N85-11075
The solar wind at 20-30 AU 02 p0301 N85-11950
Study of the solar corona using radio and space observations
[NASA-CR-174034] 02 p0304 N85-11963
RS CV sub n binary systems
[NASA-CR-174164] 04 p0580 N85-13704
Evolution of globular clusters
05 p0738 N85-14745
Investigation of central parts of globular clusters, performed in Pulkovo 05 p0738 N85-14747
The distribution of dust in the region of the Rosette Nebula and MON OB2 association
05 p0739 N85-14753
Proper motions and kinematical properties of Orion trapezium type stellar systems 05 p0739 N85-14755
Research in nuclear astrophysics: Stellar collapse and supernovae
[DE84-015559] 05 p0743 N85-14776
Method of aperture synthesis: Fundamental relations and data processing in aperture synthesis systems (review) 06 p0781 N85-14994
Interferometry with decametric waves (review)
06 p0781 N85-14996
Metric-wave and decimetric-wave aperture synthesis systems (review) 06 p0782 N85-14998
Testing theories of superluminal motion — QUASAT
07 p1058 N85-16714
Comments on the physics of active galactic nuclei
08 p1240 N85-17823
Experimental determination of the 1 sigma(+) state electron-dipole-moment function of carbon monoxide up to a large internuclear separation
[NASA-TM-85979] 09 p1379 N85-18670
Molecular hydrogen and thermal phases in astrophysics 09 p1414 N85-18922
Cosmic axions
[DE85-001330] 09 p1418 N85-18944
Report of the Electrodynamic Interactions Panel
11 p1645 N85-20363
National solar-terrestrial research program, part 1. Solar-terrestrial research for the 1980's, part 2
[AD-A149542] 11 p1681 N85-20591
JPL highlights, 1983
[NASA-CR-175558] 12 p1951 N85-22256
Plasma Astrophysics — conference
[ESA-SP-207] 12 p1953 N85-22270
Research in particles and fields
[NASA-CR-175472] 12 p1963 N85-22337
Research and technology: Fiscal year 1984 report
[NASA-TM-85231] 12 p1964 N85-22340
Theoretical and observational studies of stellar activity
13 p2171 N85-23468
Giant planets and their satellites: Cosmochemistry, evolution and structure 13 p2175 N85-23494
The structure and composition of Uranus and Neptune
13 p2175 N85-23495
Introduction to the Space Physics Analysis Network (SPAN)
[NASA-TM-86499] 14 p2290 N85-24198
Activities report of the Institute for Astronomy and Astrophysics
[MITT-5] 14 p2434 N85-25012
Cometary Astrometry
[NASA-CR-175660] 14 p2435 N85-25015
The structure and angular momentum content of dark clouds 14 p2439 N85-25054
X-ray polarimetry: The measurement of the polarization of solar flare X-rays and the design of a Compton polarimeter 14 p2441 N85-25059
Rotational inversion from global solar oscillations
14 p2442 N85-25064
Satellite research on solar flares
16 p2717 N85-26776
The soft X-ray background as a supernova blast wave viewed from inside: Solar abundance models
[NASA-CR-175767] 16 p2887 N85-27813
Activities report of the Institute for Extraterrestrial Physics
[MPI-PAE/EXTRATERR-187] 17 p3053 N85-28898
Institute works on modeling thermonuclear plasma processes 19 p3296 N85-30435
Slow tearing modes: Transitions to instability
20 p3534 N85-31989
Activities report of the Department of Astrophysics
20 p3546 N85-32064
Solar-geophysical data no. 485, January 1985. Part 1 (prompt reports): Data for December 1984, November 1984 and late data
[PB85-181360] 20 p3548 N85-32079
Space research in the United Kingdom: An assessment
[AD-A155334] 21 p3712 N85-33038
Research in particles and fields
[NASA-CR-176069] 21 p3724 N85-33103
Yakutsk Institute's cosmic ray research facility
22 p3732 N85-33135
Program for observations of Halley's comet
22 p3732 N85-33138
Numerical simulation in astrophysics: Smoothed particle methods 23 p3979 N85-34674
Research of advanced techniques for X-ray detectors and telescopes with applications to rockets and the LAMAR facility
[NASA-CR-176161] 23 p4054 N85-35141
Pulsed-neutron-source models for the astrophysical s-process
[DE85-012927] 24 p4151 N85-35740
Development of observational and instrumental techniques in hard X-ray and medium energy gamma-ray astronomy
[NASA-CR-176172] 24 p4168 N85-35841
Some nuclear data needs in astrophysics
[DE85-012916] 24 p4168 N85-35842
The research program of the Liquid Scintillation Detector (LSD) in the Mont Blanc Laboratory
[HE-5.3-6] 24 p4205 N85-36100
A search for cosmic sources of high energy neutrinos with small underground detectors
[HE-5.3-16] 24 p4206 N85-36110
Monopole, astrophysics and cosmic ray observatory at Gran Sasso
[HE-6.1-4] 24 p4209 N85-36130

ASYMMETRY
Cognitive asymmetry and occupation. Computer programmers, students, and bank personnel, part 1 and part 2
[AD-A147125] 08 p1197 N85-17540
Multiple resources and brain laterality
[AD-A148912] 10 p1530 N85-19643
Skewed stable variables and processes
[AD-A150549] 13 p2153 N85-23372
Stability of permanent rotation modes of asymmetric heavy solid body 14 p2279 N85-24118
Attempts to localize and identify the gravity sensing device of plant seedlings 15 p2607 N85-26064
Plant growth biophysics: The basis for growth asymmetry induced by gravity 15 p2611 N85-26089
Asymmetric flux generation and its relaxation in reversed field pinch
[IPPJ-712] 15 p2656 N85-26387
Predicting fully plastic mode 2 crack growth from an asymmetric defect
[AD-A152227] 16 p2801 N85-27269
Theoretical prediction of stationary positions in the rectangular chamber during asymmetric electroosmotic flow 20 p3499 N85-31750
The longitudinal asymmetry of the interplanetary perturbation producing Forbush decreases
[IFSI-84-18] 20 p3546 N85-32065
Search for the north-south asymmetry in solar activity
[AD-A155525] 21 p3724 N85-33102
Multidiode integrated-circuit protective device
22 p3781 N85-33425
Assessment of magnetic field asymmetries in ELMO Bumpy square
[DE85-011905] 22 p3846 N85-33819
Model of azimuthal non-uniformities induced by RF heating in RFC-XXM 23 p3977 N85-34658
Assessment of magnetic field asymmetries in ELMO Bumpy square
[DE85-011559] 23 p3984 N85-34705
North-south asymmetry in activity on the Sun and cosmic ray density gradients
[SH-4.2-7] 23 p4007 N85-34845
The expected cosmic ray density and stream distributions at the heliolatitudinal asymmetry of solar wind
[SH-4.2-14] 23 p4008 N85-34852
The influence of quiet asymmetric magnetosphere on the cutoff rigidities of the main cone
[SH-6.1-10] 23 p4045 N85-35083
New Matsushiro underground cosmic ray station (220 M.W.E. in depth)
[SH-9.1-14] 23 p4052 N85-35129
A new description of combined trellis coding with asymmetric modulation
[NASA-CR-176197] 24 p4086 N85-35323

ASYMPTOTES
Numerical improvement of asymptotic solutions and nonlinear shell analysis 05 p0648 N85-14158

A limit theorem for the superposition of renewal processes
[CWI-MS-R8408] 05 p0722 N85-14636
On the global asymptotic stabilization of nonlinear systems
[PREPRINT-838] 08 p1209 N85-17604
Velocity inversion using a stratified reference
[AD-A150082] 12 p1889 N85-21858
Asymptotic behavior of matrix coefficients related to reductive symmetric spaces
[CWI-PM-R8410] 12 p1925 N85-22095
Extended semiclassical calculations
[DE85-007824] 19 p3346 N85-30736

ASYMPTOTIC METHODS
Singular asymptotic expansions in nonlinear rotordynamics
[NASA-CR-174012] 01 p0017 N85-10100
Estimates of Freud-Christoffel functions for some weights with the whole real line as support
[CSIR-TWISK-323] 01 p0114 N85-10775
An asymptotic theory for logistic regression when some predictors are measured with error
[AD-A145673] 02 p0254 N85-11666
Asymptotic methods for wind tunnel wall corrections at transonic speed 03 p0313 N85-12022
Least squares estimation of conditionally heteroscedastic autoregressions
[AD-A145994] 03 p0411 N85-12626
Analysis and testing for rotordynamic coefficients of turbulent annular seals with different, directionally homogeneous surface-roughness treatment for rotor and stator elements 05 p0644 N85-14134
Approximating the percentage points of Greenwood's statistic with Cornish-Fisher expansions
[CWI-MS-R8405] 05 p0721 N85-14634
An operator method for computing the asymptotics of a collision resolution interval
[AD-A146637] 07 p1028 N85-16528
Local likelihood estimation
[AD-A147317] 07 p1035 N85-16571
Asymptotic methods for the analysis, estimation, and control of stochastic dynamic systems
[AD-A147758] 08 p1211 N85-17618
Robust linear filtering for multivariable stationary time series, part 3
[AD-A148169] 08 p1212 N85-17627
Low-dimensional behavior of the pattern formation Cahn-Hilliard equation
[DE85-003727] 12 p1922 N85-22072
Singular asymptotic expansions in nonlinear rotordynamics 12 p1945 N85-22218
Investigation of dynamics of manipulator with elastic sections 13 p2048 N85-22819
Domain of applicability of asymptotic description of radio pulse fields near critical frequency 13 p2073 N85-22949
Scattering of waves by axisymmetrical edge 13 p2080 N85-22987
Asymptotically optimum multialternative sequential procedures for discernment of processes minimizing average length of observations 13 p2084 N85-23012
Confidence intervals using the regenerative method for simulation output analysis
[AD-A150147] 13 p2149 N85-23343
Asymptotic methods especially in combustion
[AD-A151505] 15 p2505 N85-25450
Point processes associated with extreme value theory
[AD-A151211] 15 p2640 N85-26280
Asymptotic solutions of MHD equations with finite conductivity
[REPT-12/1984] 16 p2852 N85-27581
Comments on the paper by F. Pegoraro, L. Sugiyama: Spatial diffusion of charged high-energy fusion products by shear Alfven perturbations
[INPE-3291-PRE/606] 16 p2866 N85-27675
On the accuracy of the Poincare-Lindstedt method
[REPT-84-37] 17 p3022 N85-28690
Extrapolation methods in the finite element method
[BONNER-MATHE-SCHR-158] 19 p3345 N85-30729
Asymptotic expansions for finite element eigenvalues and finite element solution 19 p3345 N85-30730
Asymptotic expansions for the finite element approximation of parabolic functions 19 p3345 N85-30731
Some asymptotic problems in the optimal control of distributed systems 20 p3412 N85-31175
Turbulent mixing and combustion 22 p3744 N85-33207

ASYMPTOTIC PROPERTIES
Estimates of Freud-Christoffel functions for some weights with the whole real line as support
[CSIR-TWISK-323] 01 p0114 N85-10775
On the coupling of an anchored flame with an acoustic field
[COLL-AERON-8434] 12 p1799 N85-21282
Accuracy of approximation of Bayes estimates in presence of noninformative parameters 13 p2084 N85-23015
On the length of asymptotic paths of meromorphic functions of order zero 15 p2633 N85-26234
On asymptotic joint distribution of the eigenvalues of the noncentral manova matrix for nonnormal populations
[AD-A151886] 15 p2642 N85-26294
Asymptotic expansion of Jacobi polynomials
[REPT-84-35] 17 p3021 N85-28689
Error-correcting codes for computer memories 24 p4136 N85-35636

ASYMPTOTIC SERIES
Scattering by a parabolic cylinder: A uniform asymptotic expansion
[AD-A145688] 02 p0252 N85-11652
Asymptotically optimal ranking algorithms for quasi-determinate signal detection 06 p0792 N85-15064
An asymptotic analysis of a transient p-n junction model
[AD-A147270] 07 p0947 N85-16004
Asymptotic representation of solutions of the basic semiconductor device equations
[AD-A149040] 10 p1545 N85-19741
The asymptotic behavior of the likelihood ratio statistic for testing a shift in mean in a sequence of independent normal variates
[AD-A149329] 10 p1550 N85-19779
Asymptotic distributions of the sample mean, autocovariances and autocorrelations of long-memory time series
[AD-A149409] 10 p1551 N85-19781
Tests of fit based on normalized spacings
[AD-A149749] 12 p1921 N85-22062
Asymptotics for configural estimators
[AD-A150106] 12 p1924 N85-22087
Theory of oriented nucleation with asymmetric single elements. 2: Effects of rotational diffusion
[IFTR-32/1984] 12 p1939 N85-22179
Asymptotic expansions of the distribution of test statistics associated with several two parameter exponential distributions
[AD-A151906] 15 p2641 N85-26289
Asymptotic expansion of Jacobi polynomials
[REPT-84-35] 17 p3021 N85-28689
A class of polynomials related to those of Laguerre
[CWI-AM-R8411] 17 p3022 N85-28693
Uniform asymptotic expansions of integrals
[CWI-AM-R8412] 17 p3022 N85-28694
Instability at the interface between two shearing fluids in a channel
[AD-A153532] 18 p3099 N85-29185
Towards a statistical analysis of genetic sequences data with particular reference to protein sequences
[AD-A153605] 18 p3152 N85-29515
Least-squares approximation to minimum chi-square estimators of location and scale parameters and their effect on the Pearson chi-square test
[AD-A153534] 18 p3169 N85-29638
Limit behaviour for stochastic monotonicity and applications
[AD-A153814] 18 p3170 N85-29648
Nonparametric renewal function estimation
[AD-A153474] 18 p3173 N85-29672
Extent to which least-squares cross-validation minimizes integrated square error in nonparametric density estimation
[AD-A153789] 18 p3174 N85-29679
Discrete-element acoustic analysis of submerged structures using doubly asymptotic approximations
[AD-A154959] 21 p3700 N85-32987

ASYNCHRONOUS MOTORS
Full load testing in the platform module prior to tow-out: A case history of subsynchronous instability 05 p0642 N85-14117

ATHEROSCLEROSIS
U ARTERIOSCLEROSIS

ATHLETES
Influence of geomagnetic disturbances on cardiovascular function of athletes 08 p1193 N85-17516

ATHODYDS
U RAMJET ENGINES

ATLANTIC OCEAN
Sea-level in the world ocean. Part 6: The South Atlantic and South Pacific Oceans, a catalogue of measurements
[CSIR-T/SEA-8303-6] 01 p0087 N85-10580
Late quaternary glacial cycles in the Bahamian deep basins and in the adjacent Atlantic Ocean 02 p0226 N85-11476
Submarine sand ridges: Geology and development, New Jersey, USA 02 p0227 N85-11482
Summary of 1984 Atlantic seasonal tropical cyclone activity and verification of author's forecast 03 p0395 N85-12520
The structure of the Iceland-Faeroe ridge, derived from geophysical measurements
[DRIC-T-7255] 03 p0397 N85-12535
The Long Term Upper Ocean Study (LOTUS). Cruise summary
[AD-A145767] 03 p0397 N85-12536
Variations with time of the carbon dioxide partial pressure in central and south Atlantic surface waters
[AD-A145825] 03 p0398 N85-12537
Heat sources in the tropics and large scale flow anomalies associated with precipitation anomalies in northeast Brazil
[INPE-3211-TDL/175] 04 p0538 N85-13421
Measurements of electric fields obtained by stratospheric balloons in the region of the South Atlantic anomaly
[INPE-3218-PRE/571] 05 p0675 N85-14335
Razrezy program research in the tropical Atlantic 07 p0981 N85-16229
Conditions governing the formation of stratocumulus clouds over the western Atlantic during cold air outbreaks
[AD-A146760] 07 p1004 N85-16383
A compilation of moored current meter and wind recorder data. Volume 35: Long-Term Upper Ocean Study (LOTUS) (Moorings 764, 765, 766, 767, 770), May 1982 - April 1983
[AD-A147103] 07 p1009 N85-16412
The long term upper ocean study (LOTUS). Cruise summary and hydrographic data report, OCEANUS 154, May 1984
[AD-A147808] 07 p1009 N85-16414
Oceanographic data for development of the US exclusive economic zone
[PB85-106458/GAR] 07 p1010 N85-16415
Detailed oceanic crustal modeling
[AD-A148589] 08 p1191 N85-17507
Preliminary post-emplacement safety analysis of the subseabed disposal of high-level nuclear waste
[DE84-011162] 08 p1221 N85-17692
Measurements of sediment temperatures, conductivity and heat flow in the North Atlantic and their relevance to radioactive waste disposal
[IOS-172] 09 p1359 N85-18551
Benthic boundary layer, IOS observational programme: Discovery Gap measurements, March 1984 — Institute of Oceanographic Sciences (IOS)
[ISO-180] 09 p1359 N85-18552
Hurricane experience levels of coastal county populations: Texas to Maine
[PB85-111383] 10 p1520 N85-19581
The imaging of internal waves by the SEASAT-A synthetic aperture radar
[AD-A149808] 12 p1875 N85-21761
Atlantic Coast Unique Regional Atmospheric Tracer Experiment (ACURATE)
[PB85-128460] 12 p1886 N85-21839
Report of the International Ice Patrol Services in the North Atlantic Ocean, season of 1982
[AD-A149595] 12 p1898 N85-21917
The imaging of internal waves by the SEASAT-A synthetic aperture radar
[ARE(PORTLAND)TN-720/84] 13 p2054 N85-22660
Automatic buoys to assist the tuna fishery off the Azores 14 p2238 N85-23879
Circulation pattern of the North Atlantic, part of the warmwater sphere research effort at Kiel University 14 p2239 N85-23888
Evaluation of wave energy resources on the French Atlantic seaboard 14 p2325 N85-24369
Transatlantic migration study of the leathery turtle using the ARGOS system. Transatlantic turtle race 14 p2326 N85-24379
The French Ocean Climate in Equatorial Atlantic (FOCAL) Drifter Program, 1983-1984 14 p2329 N85-24399
Most important geochemical barrier zones in ocean (with example of Atlantic Ocean basin) 14 p2343 N85-24491
North Atlantic Deep Water Formation
[NASA-CP-2367] 15 p2601 N85-26028
Review of North Atlantic source waters 15 p2601 N85-26029
Deep water formation 15 p2601 N85-26030
Temporal and spatial scales of Labrador Sea water formation 15 p2601 N85-26031
Chemical signatures associated with the freshening of Northern Atlantic waters between 1972 and 1981 15 p2601 N85-26032

North Atlantic Deep Water and the world ocean
15 p2602 N85-26033
Oceanographic variations in recent decades and their impact on the fertility of the Iceland Sea
15 p2602 N85-26034
Quaternary North Atlantic surface paleoceanography in regions of potential deep-water formation
15 p2602 N85-26036
Glacial-to-interglacial changes in NADW fluxes?
15 p2602 N85-26037
Ocean modeling of the North Atlantic
15 p2602 N85-26039
Numerical simulation of North Atlantic Sea ice variability, 1951 - 1980
15 p2603 N85-26040
Climatic impact of a change in North Atlantic Deep Water formation
15 p2603 N85-26045
Ocean circulation and meteorology off the Georgia coast. Part 1: Real-time telemetry system for data collection
[PB85-155935] 15 p2605 N85-26052
ARGOS-tracked drifters in the Rockall Trough
16 p2812 N85-27340
Contribution of the NOAA-7 and 8 and ARGOS partnership to white tuna fishing in the northeast Atlantic
16 p2813 N85-27355
X-ray intensification at balloon altitudes of the South Atlantic magnetic anomaly in association with geomagnetic activity
[INPE-3469-PRE/712] 16 p2827 N85-27437
The sea level response to weather along the coast of southern Africa
16 p2829 N85-27446
On the 1983 drought in northeast Brazil
[INPE-3412-PRE/678] 16 p2834 N85-27476
Tropical Oceans-Global Atmosphere (TOGA) experiment planning for the Brazilian participation in TOGA global climate program
[INPE-3499-PRE/735] 16 p2834 N85-27477
An evaluation of discretized conditional probability and linear regression threshold techniques in model output statistics forecasting of visibility over the north Atlantic Ocean
[AD-A151955] 16 p2857 N85-27619
Summary of archived Atlantic coast wave information study pressure, wind, wave, and water level data
[AD-A153782] 18 p3151 N85-29508
Chemical, biological, and physical measurements from the subtropical western North Atlantic Ocean. Summer 1982, USNS Lynch, cruise 710-82
[AD-A153823] 18 p3201 N85-29857
Density characteristics of asthenosphere in Atlantic Ocean
19 p3294 N85-30423
Influence of underwater volcanic mountains of Atlantic on microplankton distribution
19 p3294 N85-30424
Tectonic structure features of some deep faults in Atlantic and Pacific Oceans (according to deep seismic sounding-reflected waves method data)
19 p3295 N85-30428
Mariners weather log, volume 29, number 1, winter 1985
[PB85-177483] 19 p3318 N85-30570
Research, progress and the mark A box model for physical, biological and chemical transports
[DE85-010574] 19 p3320 N85-30581
Forecast of Atlantic seasonal hurricane activity for 1985
20 p3495 N85-31732
An evaluation of discretized conditional probability and linear regression threshold techniques in model output statistics forecasting of cloud amount and ceiling over the North Atlantic Ocean
[AD-A155100] 21 p3636 N85-32581
Research at the Institute of Oceanographic Sciences related to the possible disposal of radioactive waste on or beneath the seafloor
[IOS-204] 23 p3973 N85-34628
Marine phosphorite deposits model for exploration, with emphasis on deposits in the US Atlantic coastal plain
24 p4104 N85-35439
Atlantic coast hindcast. Phase 2: Wave information, additional extremal estimates
[AD-A156137] 24 p4125 N85-35575

ATLAS CENTAUR LAUNCH VEHICLE
Assessment of candidate-expendable launch vehicles for large payloads
[NASA-CR-175540] 14 p2237 N85-23867

ATLAS LAUNCH VEHICLES
NT ATLAS CENTAUR LAUNCH VEHICLE

ATMOSPHERE EXPLORER C
U EXPLORER 51 SATELLITE

ATMOSPHERES
On the angular and energy distribution of solar neutrons generated in P-P reactions
[SH-1.4-9] 23 p3995 N85-34769

ATMOSPHERIC & OCEANOGRAPHIC INFORM SYS
A wind-bivane/microprocessor system for on-line prediction and display of pollutant distributions
16 p2830 N85-27449

ATMOSPHERIC ABSORPTION
U ATMOSPHERIC ATTENUATION

ATMOSPHERIC ATTENUATION
Atmospheric channel performance measurements at 10 to 100 GHz
[PB84-211325] 01 p0042 N85-10271
Using measured variance of skywave radar sea-echo power spectra to estimate ionospheric Doppler broadening of mean spectra
[PB84-214071] 03 p0399 N85-12544
Multiple scattering effects on transmission through the atmosphere
[AD-A147527] 07 p0941 N85-15969
Propagation and scattering considerations for the 0.2-3.0 GHz frequency range for a space-based radar
[AD-A148504] 08 p1153 N85-17282
Atmospheric wind and diffusion from analysis of an SF6 release at 350 km altitude
[AD-A147965] 08 p1185 N85-17471
Carbon dioxide laser radar for monitoring atmospheric transmittance and atmospheric aerosol
09 p1354 N85-18516
Digital controller for the Wave Propagation Laboratory's VHF and UHF wind-profiling radars
[PB85-112142] 11 p1626 N85-20238
MSG-7: Atmospheric penetration of solar radiation in the range of Schumann-Runge bands
11 p1657 N85-20443
Synopsis of mid-latitude radio wave absorption in Europe
11 p1659 N85-20454
Evaluation of the radiometric integrity of LANDSAT 4 Thematic Mapper band 6 data
12 p1869 N85-21726
Spectroradiometric calibration of the Thematic Mapper and Multispectral Scanner system
[E85-10094] 12 p1874 N85-21756
Atmospheric handbook: Atmospheric data tables available on computer tape
[PB85-108512] 12 p1891 N85-21867
The effects of atmospheric water vapor on infrared propagation
[AD-A150030] 12 p1934 N85-22150
Infrared aerosol absorption index
13 p2110 N85-23147
Below-room-temperature water-vapor continuum absorption within the 8- to 10 micron atmospheric transmission window
[TR-0084(4945-09)-1] 13 p2132 N85-23266
Applicability of vertically homogeneous atmospheric models for remote soundings
14 p2341 N85-24477
Development of an auroral absorption subsform
14 p2360 N85-24586
Rain rate determinations from electronic weight measurements: Instrument description and data reduction techniques
[AD-A150785] 14 p2378 N85-24681
Sound propagation studies for a large horizontal axis wind turbine
[NASA-CR-172564] 14 p2415 N85-24904
Evaluating radiation distortions of optical image of Earth's surface in horizontally inhomogeneous atmosphere
15 p2486 N85-25345
Field of point source of low-frequency sound in atmosphere with altitudinally nonuniform wind
15 p2524 N85-25566
Wave description of sound propagation through stratified moving atmosphere
15 p2525 N85-25567
ILUM code: Solar and lunar flux calculations for multi-cloud layered atmospheres
[DE85-005578] 15 p2600 N85-26025
Studies of electro-optical attenuation in the vicinity of cloud base
[AD-A151745] 15 p2653 N85-26360
Meteorological factors in Earth-Satellite propagation
[NASA-CR-175764] 16 p2769 N85-27069
Synchronizing heavily encoded data in bad weather
16 p2770 N85-27099
EHF attenuation derived from emission temperatures in light rain
[AD-A151166] 16 p2772 N85-27110
Radar study of the melting layer
[ESA-CR(P)-1974] 17 p2997 N85-28527
Atmospheric limitations to clock synchronization at microwave frequencies
18 p3107 N85-29236
Comparison of 8 to 12 micrometer and 3 to 5 micrometer CVF transmissometer data with LOWTRAN calculations
[AD-A154218] 19 p3350 N85-30763
Radiometry: A useful prediction tool — atmospheric attenuation
[ESA-SP-1071] 20 p3399 N85-31064
Ship-to-ship propagation: Maritime data analyses
[AD-A155484] 21 p3592 N85-32325
Linear absorption and scattering of laser beams
[AD-A156167] 24 p4098 N85-35401
Sensitivity of depth of maximum and absorption depth of EAS to hadron production mechanism
24 p4186 N85-35982
EAS development curve at energy of 10(16) - 10(18) eV measured by optical Cerenkov light
[HE-4.4-7] 24 p4193 N85-36015

ATMOSPHERIC BOUNDARY LAYER
Evaluation of an integrated mixed-layer model for single station prediction in a marine regime
01 p0080 N85-10535
Boundary layer-cloud interactions as potential storm predictors
01 p0081 N85-10543
The lifting condensation level and its relation to convective cloud base
[AD-A145654] 02 p0232 N85-11513
Development of a microcomputer coupled atmospheric and oceanic boundary layer prediction model
[AD-A146334] 03 p0397 N85-12530
Energy diagnostics and impact studies of FGGE global data sets and GLAS GCM simulations
05 p0683 N85-14390
Air-sea interaction during cold air outbreaks
05 p0685 N85-14401
Mixed layers and satellite retrievals
05 p0686 N85-14411
Study of low-frequency sound with point source in stream with shear
06 p0825 N85-15239
Modeling influence of three layer cloud cover on outgoing thermal radiation
06 p0825 N85-15242
Indirect estimation of convective boundary layer structure for use in routine dispersion models
[PB84-238260] 06 p0834 N85-15308
Simulation of entrainment at the top of the atmospheric boundary layer for use in General Circulation Models (GCM)
[DM-42] 09 p1355 N85-18525
Radiosodar system for remote synchronous measurements of wind speed, temperature and its fluctuations
13 p2110 N85-23145
The BALSAMINE experiment
14 p2238 N85-23876
Statistical/Trend analysis of the marine atmospheric boundary layer model
[AD-A151053] 14 p2374 N85-24673
Deepwater wind wave growth with fetch and duration
[AD-A151604] 15 p2604 N85-26051
Study of the functions of similarity of the planetary boundary layer. Part 2: Results
[INPE-3130-PRE/521-VOL-2] 16 p2826 N85-27429
Three powered sailplanes as meteorological instrumentation for atmospheric boundary layer studies at DFVLR
[DFVLR-FB-84-50] 17 p2897 N85-27862
On the improvement of satellite temperature retrievals by means of boundary layer models
18 p3140 N85-29443
On Fofonoff's mode
18 p3145 N85-29471
Use of radar with frequency modulation for studying atmospheric boundary layer
19 p3296 N85-30437
Excitation of turbulence by density waves
[NASA-CR-3905] 19 p3314 N85-30546
Effects of relative humidity gradients on the evaluation of submicron aerosol flux measurements in the atmospheric surface layer
[DE85-010510] 19 p3316 N85-30555
A survey of wind and turbulence modeling methods
[AD-A154470] 20 p3496 N85-31733
Facility for large-scale hazardous gas testing
[DE85-011852] 21 p3564 N85-32189
Properties of aerosol particles detected by satellites in coastal regions
21 p3641 N85-32622
Simulation of the coupled atmospheric and oceanic boundary layer model during MILDEX
[AD-A155166] 21 p3655 N85-32705
Verification of Doppler sodar measurements — atmospheric boundary layer
[KNMI-WR-85-2] 22 p3817 N85-33645
An atmospheric boundary layer model forced by the operational ECMWV-model
[WSR-3] 24 p4120 N85-35541
Measurements for the determination of the vertical structure of the convective boundary layer — atmospheric boundary layer
24 p4122 N85-35550
Partitioning of the vertical turbulent energy transport into positive and negative contributions — meteorology
24 p4122 N85-35551
Aircraft measurements during the Bonn Experiment (BONEX 1) — meteorology
24 p4122 N85-35552

ATMOSPHERIC CHEMISTRY
Estimation of the potential and probable source regions for acid precipitation
[DE84-015119] 02 p0225 N85-11472
Organic aerosol formation: OH(hydroxyl radical) versus ozone oxidation pathways
[PB84-219880] 03 p0388 N85-12484
Thermodynamic conditions of the Earth's atmosphere with pollution processes
04 p0523 N85-13345

Impact of alcohol fuels on urban air pollution: Methanol photochemistry study
[DE84-012950] 04 p0531 N85-13397
Regional-scale (1000 KM) model of photochemical air pollution. Part 2: Input processor network design
[PB84-232851] 04 p0532 N85-13400
Proceedings of a Workshop on Atmospheric Research Needs for the Western United States
[DE84-015069] 04 p0534 N85-13412
Fundamental molecular physics and chemistry, part 1
[DE84-009127] 04 p0561 N85-13571
Research and technology, 1984: Marshall Space Flight Center
[NASA-TM-86476] 04 p0590 N85-13785
The use of tracers for the study of atmospheric chemical and physical transformation processes
[DE84-015287] 05 p0671 N85-14313
Determination of Toluene's degradation products under simulated atmospheric conditions
05 p0674 N85-14331
Assessment of Techniques for Measuring Tropospheric H sub x O sub y
[NASA-CP-2332] 05 p0675 N85-14336
Assessment of Techniques for Measuring Tropospheric H sub x O sub y: Summary 05 p0675 N85-14337
Chemical kinetics and Earth's atmosphere
06 p0822 N85-15218
Application of quantum chemistry of atmospheric chemistry
[AD-A147035] 07 p0922 N85-15843
Remote sensing of atmospheric gases with CO2 lasers. Continuation and conclusion of spectroscopic investigations
[BMFT-FB-W-84-030] 07 p0989 N85-16285
Ionic reactions of atmospheric importance
[AD-A147354] 07 p0997 N85-16333
Electronically excited atomic and molecular oxygen
[AD-A147732] 08 p1121 N85-17064
A new fast response probe for diffusion studies in atmospheric air — pollution modeling
[IC-AERO-84-01] 08 p1180 N85-17437
Atmospheric photochemical modeling of turbine engine fuels. Phase 1: Experimental studies. Volume 2: Environmental chamber data tabulations
[AD-A147786] 08 p1185 N85-17470
On the importance of light hydrocarbons in multiphase atmospheric systems
[JUEL-1942] 08 p1190 N85-17498
Atmospheric acidification chemistry: A review
[PB84-215490] 09 p1350 N85-18495
Atmospheric science and power production
[DE84-005177] 09 p1354 N85-18521
Sequential precipitation chemistry sampling program at Brookhaven National Laboratory with an analytical summary of 1976-1982 data
[DE85-002788] 10 p1513 N85-19545
Non-photochemical interactions of sulfur and nitrogen compounds in acid deposition
[DE84-016141] 10 p1513 N85-19546
Upper atmosphere research at INPE
[INPE-3281-PRE/804] 10 p1515 N85-19557
Infrared excitation of clusters and ions of atmospheric interest
[DE85-002098] 10 p1516 N85-19564
MAP in India 11 p1655 N85-20424
Cold Arctic Mesopause Project (CAMP): Scientific objectives 11 p1656 N85-20433
MAP activities in Hungary 11 p1657 N85-20440
Ozone measurements in the mesosphere during a solar proton event 11 p1665 N85-20490
The concentration of sulfate in broken cloud layers
[DE85-000228] 11 p1678 N85-20574
Meteorological support for the 1983 Deep Creek, Maryland experiment
[DE85-002616] 11 p1678 N85-20575
Middle atmosphere NO and NO2 observed by means of the Spacelab one grille spectrometer
[AERONOMICA-ACTA-A-293-1984]
11 p1680 N85-20588
Applicability of laboratory kinetics studies to the evaluation of aqueous phase atmospheric oxidation of sulfur-4
[DE85-000586] 12 p1883 N85-21819
Gas-liquid chemistry of natural waters, volume 1
[DE85-002603] 12 p1884 N85-21822
Gas-liquid chemistry of natural waters, volume 2
[DE85-002457] 12 p1884 N85-21823
OSCAR experiment high-density network data report
[DE85-004907] 12 p1884 N85-21826
Continued research in mesoscale air pollution simulation modeling. Volume 6. Further studies in the modeling of microscale phenomena
[PB85-137370] 12 p1887 N85-21844
Chemical kinetics and photochemical data for use in stratospheric modeling. Evaluation number 6
[NASA-CR-175564] 12 p1888 N85-21849
Global tropospheric chemistry: A plan for action
[NASA-CR-175545] 12 p1891 N85-21865
Non-precipitating cumulus cloud study
[DE85-002352] 12 p1896 N85-21902
Multiple element neutron-activation analysis of atmospheric aerosols with X-ray and gamma-spectrometric recording of radionuclides formed
13 p2013 N85-22631
One mechanism of formation of organic fraction in atmospheric aerosol 13 p2014 N85-22632
One-dimensional nonstationary model of photochemical transformations of gas impurities in stratosphere
14 p2342 N85-24484
PLUVIUS: A generalized 1-dimensional model of reactive pollutant behavior, including dry deposition, precipitation formation, and wet removal, 2nd edition
[DE85-005542] 14 p2353 N85-24538
Magnetospheric effects on the upper atmosphere
14 p2365 N85-24616
High altitude sampling program: Radioactivity in the stratosphere
[DE85-005924] 14 p2374 N85-24676
Emission inventory applications to regional acid deposition modeling
[PB85-157366] 16 p2760 N85-27033
Measurement of elements in the stratosphere
[NASA-CR-175891] 16 p2823 N85-27414
Free radicals in the stratosphere: A new observational technique 16 p2824 N85-27415
Atmospheric chemistry
[INPE-3190-PRE/554] 16 p2826 N85-27430
Oxygen isotopic study of the oxidation of SO2 by H2O2 in the atmosphere
[DE85-004017] 17 p2968 N85-28468
Homogeneous processes of atmospheric interest
[NASA-CR-175770] 17 p2989 N85-28475
Absolute calibrations of SO2 and NO analyzers by photographic methods
[DFVLR-MITT-85-02] 17 p2994 N85-28504
Reconstruction of past atmospheric CO/sub 2/ contents from the chemistry of the contemporary ocean: An evaluation
[DE85-008426] 18 p3133 N85-29401
Environmental Research Division report: Atmospheric physics
[DE85-009659] 18 p3133 N85-29404
Kinetics and intensity of photochemical processes in the atmosphere
[BPT-10/84] 18 p3134 N85-29411
Formation and fate of toxic chemicals in California's atmosphere
[PB85-172609] 18 p3134 N85-29414
Chemical transformations in acid rain. Volume 2: Investigation of kinetics and mechanism of aqueous-phase peroxide formation
[PB85-173433] 18 p3135 N85-29416
Conceptual Design for a Gulf Coast Oxidant Transport and Transformation Experiment: Workshop proceedings and recommendations
[PB85-173789] 18 p3135 N85-29417
Investigation of the reaction system NOX/ClOX/HOX under tropospheric and stratospheric conditions
[BPT-11/84] 18 p3137 N85-29427
Atmosphere monitoring requirements
18 p3158 N85-29553
Quantitative studies for photoabsorption and fluorescence of HCl
[NASA-CR-175965] 19 p3233 N85-30043
Evaluation of methods used for the determination of acidity in acid rain samples
[PB85-178309] 19 p3237 N85-30070
Applied Science Division's Environmental Research Program
[DE85-010637] 19 p3308 N85-30510
Analysis of aldehydes and ketones in the gas phase
[PB85-181885] 20 p3426 N85-31261
Modeling of chemical transformations of SO(x) and NO(x) in the polluted atmosphere: An overview of approaches and current status
[PB85-173169] 20 p3487 N85-31677
Activities report of the Aeronomy Department
[G-774-1984] 21 p3633 N85-32569
Eleventh International Conference on Atmospheric Aerosols, Condensation and Ice Nuclei, volume 2
[PB85-182418] 21 p3638 N85-32596
Ice nucleation by silver iodine particles with nearly critical sizes 21 p3638 N85-32600
Airborne measurements of atmospheric ice nuclei
21 p3640 N85-32612
A statistical analysis of ice nuclei concentrations at urban and rural sites in Valladolid, Spain
21 p3640 N85-32614
Experimental studies of the formation of Aitken nuclei in the atmosphere 21 p3644 N85-32641
Photochemical aerosol formation in polluted atmosphere 21 p3644 N85-32642
The influence of Brownian coagulation on the size distributions of atmospheric aerosols
21 p3645 N85-32643
The nuclei of cloud formation
21 p3651 N85-32665
Characterization of insoluble particles associated with cloud droplets 21 p3652 N85-32693
Sulfur Cycle 21 p3662 N85-32748
Evaluation of the 2DFLOW and hybrid complex-terrain dispersion models with the 1980 ASCOT data base from the Geysers
[DE85-012960] 22 p3812 N85-33613
Ozone during sudden stratospheric warming: A three-dimensional simulation
[AERONOMICA-ACTA-A-292-1984]
22 p3813 N85-33621
Acetonitrile in the Earth's atmosphere: An upper limit deduced from infrared solar spectra
[AERONOMICA-ACTA-A-295-1985]
22 p3813 N85-33623
Middle Atmosphere Program. Handbook for MAP, volume 11
[NASA-CR-176107] 22 p3814 N85-33625
Elemental tracers of source regions of contaminants in precipitation
[DE85-012858] 24 p4113 N85-35499
Atmospheric nitrogen oxides: Their detection and chemistry
[PB85-193910] 24 p4114 N85-35502
Air chemistry measurements 2
[AD-A156041] 24 p4117 N85-35520
A study of the chemistry of alkali metals in the upper atmosphere
[AD-A156349] 24 p4117 N85-35524
Time-dependent response of the climate to increasing atmospheric carbon dioxide 24 p4119 N85-35532

ATMOSPHERIC CIRCULATION

Large-scale ocean-atmosphere interactions in the mid-latitudes and equatorial regions: A literature review
[CSIR-T/SEA-8302] 01 p0073 N85-10482
About the influence of nonadiabatic processes on frontogenesis near the ground 01 p0075 N85-10498
Evaluation of surface sensible heat flux effects on the generation and modification of mesoscale circulations
01 p0079 N85-10527
Development of an operational system for Very-Short-Range Forecasting (VSRF) at Swedish Meteorological and Hydrological Institute (SMHI)
01 p0083 N85-10559
Some aspects of post-frontal convective areas along the west coast of the united states
[AD-A144895] 01 p0085 N85-10572
Quasi-stationary atmospheric responses to large-scale forcing 02 p0227 N85-11484
A comparison of 2- and 3-dimensional transport within a stratospheric circulation model
02 p0227 N85-11485
Arctic haze: Meteorological aspects of long-range transport 02 p0230 N85-11499
Atmospheric dynamics of Uranus and Neptune: Theoretical considerations 02 p0299 N85-11936
Conditional symmetric instability and mesoscale rainbands 05 p0678 N85-14358
Global Scale Atmospheric Processes Research Program Review
[NASA-CP-2344] 05 p0679 N85-14360
GLAS fourth order model 05 p0679 N85-14361
Orographic effects in atmospheric circulation
05 p0679 N85-14362
Spectral general circulation model development
05 p0679 N85-14363
Biosphere/atmosphere interactions
05 p0679 N85-14364
Fully implicit numerical methods for the baroclinic primitive equations 05 p0679 N85-14365
A vertically resolved planetary boundary layer
05 p0680 N85-14367
Generation of available potential energy and other diagnostic studies during FGGE
05 p0683 N85-14388
Comparison of forecast and observed energetics
05 p0683 N85-14389
Energy diagnostics and impact studies of FGGE global data sets and GLAS GCM simulations
05 p0683 N85-14390
Spectral energetics diagnoses and FGGE spectral observing periods and energetics analyses of forecast experiments with GLAS GCM 05 p0683 N85-14391
Jet stream errors and tropospheric-stratospheric interactions in the GLAS general circulation model
05 p0683 N85-14392
Analysis of diabatic heating during FGGE
05 p0683 N85-14393
Global scale diagnosis of FGGE data
05 p0683 N85-14394

Theoretical modeling for numerical weather prediction
05 p0684 N85-14395
Large scale rossby waves during FGGE
05 p0684 N85-14396
Planetary scale interactions 05 p0684 N85-14397
Structure and energetics of medium-scale atmospheric waves in the southern hemisphere summer
05 p0685 N85-14403
Investigation of cloud feedback in the GLAS model
05 p0685 N85-14404
Diagnostics of rainfall anomalies in the nordeste during the global weather experiment 05 p0685 N85-14405
Application of the bounded derivative initialization method 05 p0686 N85-14407
Implicit numerical methods in meteorology
05 p0686 N85-14408
Interannual variability in the observed circulation
05 p0686 N85-14409
Linear studies of stationary, extratropical anomalies in the troposphere 05 p0686 N85-14410
The influence of synoptic scales on low-frequency modes of variability 05 p0687 N85-14412
A new physical Lagrangian tracer
[DE84-016212] 05 p0687 N85-14419
Polar regions and climatic change
[PB84-237023] 05 p0688 N85-14421
Characteristic scale of inner mixing layers in stably stratified atmosphere 06 p0824 N85-15235
Simple mesoscale models for operational use in regions of topographic and thermal forcing: Development and evaluation
[AD-A148667] 06 p0839 N85-15325
Towing tank studies of stratified flow over ridges and valleys
[DE84-011418] 06 p0839 N85-15329
The 500 millibar sign frequency teleconnection charts: Winter
[PB85-106276/GAR] 07 p1009 N85-16410
A 2-dimensional second order closure model of the upper atmosphere 08 p1182 N85-17450
Spectral modeling of a potential vorticity equation for a barotropic flow on a beta-plane
[CWI-AM-R8408] 08 p1186 N85-17478
Dynamics of the low-latitude thermosphere and ionosphere 09 p1351 N85-18501
Simulation of entrainment at the top of the atmospheric boundary layer for use in General Circulation Models (GCM)
[DM-42] 09 p1355 N85-18525
Behavior and characteristics of storm cold outflows
09 p1356 N85-18529
Global scale diagnoses of FGGE data
[NASA-CR-174356] 09 p1356 N85-18533
Discovery about temperature fluctuations in turbulent air flows 10 p1500 N85-19466
Some aspects of atmospheric circulation near South America and interactions with the Antarctic regions
[INPE-3308-PRE/618] 10 p1515 N85-19561
Planetary scale circulation anomalies associated with droughts over northeast Brazil
[INPE-3351-PRE/630] 10 p1518 N85-19570
Large scale circulation anomalies and prediction of northeast Brazil droughts
[INPE-3405-PRE/674] 10 p1518 N85-19571
Interannual variations of the winter circulation in the Northern Hemisphere and in the southern oscillation (meridian) and their possible connections with the climate of Northeast Brazil
[INPE-3333-TDL/182] 10 p1519 N85-19573
PMP-2: Equatorial wave dynamics
11 p1655 N85-20422
French activities relevant to middle atmosphere research 11 p1655 N85-20423
UK participation in the Middle Atmosphere Programme
11 p1655 N85-20426
The global meteor observation system (GLOBMET)
11 p1656 N85-20432
MAP activities in Hungary 11 p1657 N85-20440
Middle Atmosphere Program. Handbook for MAP, volume 10
[NASA-CR-175477] 11 p1658 N85-20450
Middle atmosphere temperature and dynamics as revealed from D-region observations
11 p1659 N85-20453
Abnormal circulation changes in the winter stratosphere, detected through variations of D region ionospheric absorption 11 p1659 N85-20458
Seasonal characteristics of mesospheric plasma and their transitions 11 p1660 N85-20464
Spring changeover of the middle atmosphere circulation compared with rocket wind data up to 80 km
11 p1661 N85-20466
Large scale winter time disturbances in meteor winds over central and eastern Europe
11 p1661 N85-20467
Changes in the ozone content over central Europe during reversals of stratospheric circulation in late winter
11 p1661 N85-20469
Some aspects of general circulation and tides in the middle atmosphere 11 p1661 N85-20470
Meteor wind results from Atlanta, USA, and Ramey, Puerto Rico 11 p1662 N85-20474
Basic features of global circulation in the mesopause lower thermosphere region 11 p1662 N85-20475
Winds and waves (4 min - 11 yra) in the upper middle atmosphere (60-110 km) at Saskatoon, Canada (52 deg N, 107 deg W): MF radar (2.2 MHz) soundings 1973 - 1983 11 p1662 N85-20476
The dynamics of ionospheric D region over East Siberia 11 p1662 N85-20477
Stratwarm effects in the ionospheric D region wind field 11 p1663 N85-20479
Investigation of aeronomic processes on the basis of ionospheric sporadic E 11 p1663 N85-20482
Comparison of MESOI atmospheric dispersion estimates with data and estimates from other models
[DE85-002372] 11 p1678 N85-20572
A study of eddy-mean flow interactions using Eliassen-Palm diagnostics: FGGE SOP-1 data and the NASA GLAS general circulation model compared
[NASA-CR-175508] 11 p1686 N85-20604
The 500 millibar sign frequency teleconnection charts: Fall
[PB85-110930] 11 p1687 N85-20612
The 500 millibar sign frequency teleconnection charts: Summer
[PB85-111359] 11 p1688 N85-20613
The 500 millibar sign frequency teleconnection charts: Spring
[PB85-111367] 11 p1688 N85-20614
Structure and forcing of teleconnection patterns occurring in general circulation model simulations
[DE85-002434] 12 p1690 N85-21862
Analysis of the NASA/MSFC Airborne Doppler Lidar results from San Gorgonio Pass, California
[NASA-CR-171355] 12 p1892 N85-21873
Navy tactical applications guide. Volume 4. Part 1. Eastern North Pacific weather analysis and forecast applications
[AD-A150097] 12 p1896 N85-21900
Non-precipitating cumulus cloud study
[DE85-002352] 12 p1896 N85-21902
Empirical and modeled synoptic cloud climatology of the Arctic Ocean
[NASA-CR-175628] 13 p2137 N85-23272
Variation of Arctic cloud cover in summer
[DE85-004507] 13 p2139 N85-23285
Mountain barrier baroclinity effects on surface winds along the Alaskan Arctic coast 14 p2238 N85-23877
Atmosphere ice-ocean interactions in the Antarctic (IAGO) 14 p2326 N85-24375
Considering zonal wind in semidiurnal tide problem
14 p2335 N85-24440
Small component spectral model of annual course of zonal atmospheric circulation 14 p2337 N85-24453
Comparison of observations of orographic disturbances in the troposphere and upper atmosphere
14 p2341 N85-24479
PLUVIUS: A generalized 1-dimensional model of reactive pollutant behavior, including dry deposition, precipitation formation, and wet removal, 2nd edition
[DE85-005542] 14 p2353 N85-24538
A study of the turbulent layer in the water at an air-water interface 14 p2378 N85-24679
Circulation statistics based on FGGE (First GARP Global Experiment) level 3-B analyses produced by GFDL (Geophysics Fluid Dynamics Laboratory)
[PB85-149318] 14 p2379 N85-24688
Cyclic flows in the solar convection zone due to the dynamo reaction 14 p2451 N85-25137
Field validation of 6-particle puff model
[DE85-004073] 15 p2589 N85-25962
The South Pacific convergence zone and energy balance of the southern hemisphere
15 p2593 N85-25980
Monitoring tropical cyclone growth using GOES VISSR/VAS and Nimbus-7 TOMS data
15 p2595 N85-25989
Analysis of the inflow and air-sea interactions in hurricane Frederic 15 p2595 N85-25990
Role of jet streaks and boundary layer processes in organizing a pre-convective environment
15 p2597 N85-26008
Impact of soil moisture in organizing a severe storm outbreak 15 p2597 N85-26009
Role of frontal circulations and gravity waves in initiating convective storm systems 15 p2598 N85-26010
Meso-S scale numerical simulations of the jet streak adjustments which organized the Carolina tornado outbreak and the subsequent explosive coastal cyclogenesis 15 p2598 N85-26011
A study of the effect of gently varying terrain on atmospheric flow near the surface
16 p2823 N85-27411
Wave dynamics and transport in the stratosphere
[NASA-CR-175789] 16 p2823 N85-27413
Study of the functions of similarity of the planetary boundary layer. Part 1: Theory
[INPE-3129-PRE/520-PT-1] 16 p2826 N85-27428
Study of the functions of similarity of the planetary boundary layer. Part 2: Results
[INPE-3130-PRE/521-VOL-2] 16 p2826 N85-27429
Radon concentration inversion in the troposphere: Still unexplained
[INPE-3360-PRE/638] 16 p2826 N85-27431
Upper-air data collection during CAPTEX
[DE85-006300] 16 p2827 N85-27438
Evolution of stratospheric aerosol size distribution from ground-based radiometric measurements: A study of El Chichon aerosol
[DE85-007555] 16 p2827 N85-27439
Theory and modeling of the interaction between subgrid scale orography and large scale flow
[DM-43] 16 p2827 N85-27440
Geophysical monitoring for climatic change, number 12
[PB85-172278] 16 p2837 N85-27496
Circulation statistics from January and July: Simulation with the NCAR (National Center for Atmospheric Research) community climate model (CCMOB)
[PB85-165637] 16 p2837 N85-27497
Great Lakes winter weather and ice conditions for 1982-83
[PB85-165009] 16 p2837 N85-27498
NASA Oceanic Processes Program annual review
[NASA-TM-87565] 16 p2838 N85-27503
Potential climatic impacts of increasing atmospheric CO2 with emphasis on water availability and hydrology in the United States
[NASA-TM-87479] 17 p2995 N85-28517
Mathematical modeling and simulation of climate and climatic change
[DE85-008974] 17 p2997 N85-28526
Conceptual Design for a Gulf Coast Oxidant Transport and Transformation Experiment: Workshop proceedings and recommendations
[PB85-173789] 18 p3135 N85-29417
Propagation of gravity waves in the atmosphere and around critical levels
[KNMI-WR-85-1] 18 p3137 N85-29428
Variability of short term eddy-correlation estimates of mass exchange
[PB85-172641] 18 p3138 N85-29431
Specification of surface roughness over oceans in the GLAS Fourth Order GCM 18 p3142 N85-29455
Model development highlight for 1984: The GLA Fourth Order GCM 18 p3143 N85-29457
Response of winter forecasts made with the GLA Fourth Order GCM to Changes in the horizontal grid resolution
18 p3143 N85-29458
Comparison of forecast and observed energetics
18 p3143 N85-29459
Mechanistic experiments to determine the origin of Southern Hemisphere stationary waves
18 p3143 N85-29461
Energy sources of the dominant frequency dependent 3-dimensional atmospheric modes
18 p3143 N85-29462
The vertical structure of global rotational normal modes 18 p3144 N85-29464
Quasi stationary states in the Southern Hemisphere
18 p3144 N85-29465
On the global distribution of three-dimensional Eliassen-Palm fluxes by stationary waves
18 p3145 N85-29469
Transient eddies in the UCLA GCM
18 p3145 N85-29470
A new CO2 transmittance parameterization and its impact on the GLA GCM 18 p3146 N85-29476
A GCM study of the atmospheric response to tropical SST anomalies 18 p3146 N85-29477
Influence of land surface processes on the Indian monsoon: A numerical study 18 p3146 N85-29478
Influence of land-surface roughness on atmospheric circulation and rainfall: A sensitivity study with a GCM
18 p3146 N85-29479
The structure and dynamics of an observed moist front 18 p3146 N85-29480
Large-eddy simulation in planetary boundary-layer research 18 p3147 N85-29482
Circulation and transport in the middle atmosphere: Troposphere and lower atmosphere
18 p3148 N85-29491
Circulation and transport in the middle atmosphere: Mesosphere and lower thermosphere
18 p3148 N85-29492

Diagnostic verification of the GLAS (Goddard Laboratory for Atmospheric Sciences) general circulation model as applied to a case of extratropical maritime explosive cyclogenesis
[AD-A153666] 18 p3148 N85-29494
Approximate method for computing wind velocity in atmosphere 19 p3296 N85-30444
Atmospheric planetary wave response to external forcing
[NASA-CR-176000] 19 p3315 N85-30548
On the dynamical climatology of the Amazon Basin and associated rain producing mechanisms
[INPE-3531-RPE/477] 19 p3315 N85-30552
Northeast Brazil droughts and Atlantic SST anomalies
[INPE-3539-PRE/754] 19 p3316 N85-30553
Some studies in filtering of atmospheric turbulence
[AD-A154042] 19 p3316 N85-30557
Experiments using atmospheric forcing from a FGGE analysis to drive an upper ocean model
[INPE-3503-PRE/738] 19 p3319 N85-30576
An examination of the Southern Oscillation in the upper tropospheric tropical and subtropical wind field 20 p3488 N85-31680
Errors and parameterizations of sub-grid scale processes in regional-scale atmospheric models 20 p3488 N85-31682
Structure and energetics of medium-scale atmospheric waves in the Southern Hemisphere 20 p3489 N85-31685
Troposphere-stratosphere (surface-55 km) monthly general circulation statistics for the Northern Hemisphere-four year averages
[NASA-TM-86182] 20 p3495 N85-31730
Carbon dioxide and climate: Potential impacts
[DE85-009473] 20 p3496 N85-31734
Hadley circulation in planetary atmospheres 20 p3546 N85-32067
Middle Atmosphere Program. Handbook for MAP. Volume 14: URSI/SCOSTEP Workshop on Technical Aspects of MST Radar
[NASA-CR-176085] 21 p3615 N85-32466
Tropospheric-stratospheric exchange, part 1.1A 21 p3615 N85-32468
Gravity waves from the stratosphere to the mesosphere, part 1.3B 21 p3616 N85-32471
A numerical analysis of transient planetary waves and the vertical structure in a meso-strato-troposphere model, part 1.4A 21 p3617 N85-32473
General circulation of the middle atmosphere, part 1.4B 21 p3617 N85-32474
Performance of the Colorado wind-profiling network, part 1.5A 21 p3617 N85-32475
Vertical transport in the atmosphere: Measurement capabilities and requirements of VHF radars, part 1.6A 21 p3617 N85-32476
Synoptic-scale dynamics with vertical velocity, part 1.8A 21 p3617 N85-32478
Determination of billows and other turbulent structures, part 4.1A 21 p3621 N85-32500
Spectral measurements of turbulence and gravity waves, part 4.2A 21 p3622 N85-32501
Gravity-wave spectra in the atmosphere observed by MST radar, part 4.2B 21 p3622 N85-32502
Estimation of vertical diffusion from observations of Atmospheric turbulence layers, part 4.4B 21 p3623 N85-32507
Momentum flux measurements: Techniques and needs, part 4.5A 21 p3623 N85-32508
MST radar data management 21 p3627 N85-32532
Data base for the Colorado profiling network 21 p3627 N85-32533
Generation of available potential energy and the energy cycle during the global weather experiment
[NASA-CR-175301] 21 p3634 N85-32572
Circulation analysis of two snowstorms during the SNOW-TWO program
[AD-A155225] 21 p3637 N85-32587
Notes on atmospheric stability, turbulence, and its measurements
[AD-A155230] 21 p3637 N85-32588
Sahara Desert dust transport to the south 21 p3648 N85-32668
Measurements of giant salt nuclei from inland in east China 21 p3648 N85-32669
Observations of cloud droplets, aerosol particles and cloud condensation nuclei in continental air masses 21 p3649 N85-32671
Condensation properties of atmospheric aerosol 21 p3649 N85-32672
Numerical simulations of the response of intense ocean currents to atmospheric forcing
[AD-A155161] 21 p3655 N85-32704
A mixed pseudospectral/finite difference method for a thermally driven fluid in a nonuniform gravitational field
[NASA-TM-87581] 22 p3783 N85-33436
Airborne cloud tracking measurements during the Three Mile Island nuclear station accident, Middletown, Pennsylvania. Date of survey: March - June 1979
[DE85-012060] 22 p3816 N85-33638
Radar wind profilers in the Colorado network
[PB85-185486] 22 p3817 N85-33647
Development of an adjustable buoyancy balloon tracer of atmospheric motion. Phase 1: Systems design and demonstration of feasibility
[PB85-185817] 22 p3817 N85-33648
Subseasonal variability in a two-level atmospheric general circulation model 24 p4114 N85-35504
A strategy for calibrating atmospheric transport models
[CSIRO-DAR-TP-9] 24 p4116 N85-35518
The kinematic structure of cold frontal rainbands 24 p4119 N85-35531
Case studies for flux measurements along a low-flying route to the south of Munich 24 p4121 N85-35548
The determination of lee circulation during the foehn wind 24 p4122 N85-35554
Maintenance of blocking anticyclones in a general circulation model
[PB85-190866] 24 p4124 N85-35567
Airborne Investigations of Mesoscale Convective Systems (AIMCS), 1984: Operational summary and data inventory
[PB85-187904] 24 p4125 N85-35571

ATMOSPHERIC COMPOSITION
NT ATMOSPHERIC MOISTURE
NT IONOSPHERIC COMPOSITION
Effect of hyperoxia and increased gas atmosphere density on contractile function of the right ventricle 01 p0093 N85-10628
Model of atmospheric ozone for middle latitudes 02 p0161 N85-11091
A study of greenhouse effects using zero, 1 and 2 dimensional climate models 02 p0230 N85-11498
Atmospheres of Uranus and Neptune 02 p0298 N85-11929
Aeronomy 02 p0298 N85-11930
Physical properties of the Uranian satellites 02 p0300 N85-11946
STS natural environment analysis
[NASA-CR-171221] 03 p0322 N85-12079
A proposed reference set of scenarios for radiatively active atmospheric constituents
[DOE/NBB-0066] 03 p0388 N85-12483
Measurements of atmospheric carbon disulfide using aircraft platforms and a GC/MS isotopic dilution analysis technique 03 p0391 N85-12500
Carbon dioxide, the greenhouse effect and climate: A primer
[GPO-33-444] 03 p0395 N85-12519
Atmospheric extinction in critical environments
[AD-A146102] 03 p0396 N85-12527
Variations with time of the carbon dioxide partial pressure in central and south Atlantic surface waters
[AD-A145825] 03 p0396 N85-12537
The Jovian atmospheric window at 2.7 microns: A search for H2S
[NASA-TM-86661] 03 p0445 N85-12836
Thermodynamic conditions of the Earth's atmosphere with pollution processes 04 p0523 N85-13345
Trends in ozone and temperature structure: Comparison of theory and measurements
[DE84-016201] 04 p0539 N85-13428
Global carbon - nitrogen - phosphorus cycle interactions: A key to solving the atmospheric CO2 balance problem? 05 p0652 N85-14188
Fundamental equations of the LIF hydroxyl measurements, appendix A 05 p0676 N85-14338
Studies of radiative transfer in planetary atmospheres
[NASA-CR-174194] 05 p0745 N85-14778
Lower atmospheric composition of Jupiter from Voyager infrared measurements
[NASA-CR-174196] 05 p0745 N85-14779
Analysis and characterization of organic carbon compounds in atmospheric particulate matter
[PB84-232636] 06 p0786 N85-14903
Simple formula to estimate carbon dioxide gas effect in radiation balance of underlying surface 06 p0823 N85-15226
The CSIRO (Australia) atmospheric carbon dioxide monitoring program: Surface data
[CSIRO-TP-6] 07 p0996 N85-16324
Middle Atmosphere program. Handbook for MAP. Volume 13: Ground-based techniques
[NASA-CR-174345] 08 p1163 N85-17452
Microwave radiometric studies of composition and structure 08 p1163 N85-17456
Lidar systems for aerosol studies: An outline 08 p1163 N85-17457
Active optical sounding of ozone and minor constituents in the middle atmosphere: A review of ground-based lidar measurements 08 p1163 N85-17458
Lidar studies of the alkali metals 08 p1164 N85-17460
Guidelines for atmospheric measurements in support of electro-optical systems testing
[AD-A148090] 08 p1166 N85-17474
On the importance of light hydrocarbons in multiphase atmospheric systems
[JUEL-1942] 08 p1190 N85-17498
Stratospheric concentration of nitric acid, ozone and carbonyl sulfide: Measurement of nitric acid absorption in the Q branch of the V4 band as a function of temperature
[ESA-TT-864] 09 p1355 N85-18524
Near infrared modeling of the equatorial regions of Jupiter and Saturn 09 p1415 N85-18930
Airborne lidar measurements of El Chichon stratospheric aerosols, October 1982 to November 1982
[NASA-RP-1136] 10 p1514 N85-19550
Development of a low cost electrochemical CO monitor based on stripping voltammetry
[PB85-113470] 11 p1637 N85-20312
UK participation in the Middle Atmosphere Programme 11 p1655 N85-20426
The Middle Atmosphere Program: A special project for the Antarctic Middle Atmosphere (AMA) 11 p1656 N85-20430
Cold Arctic Mesopause Project (CAMP): Scientific objectives 11 p1656 N85-20433
Middle Atmosphere Program. Handbook for MAP, volume 8
[NASA-CR-175478] 11 p1657 N85-20445
MAP/GLOBUS campaign 1983 11 p1658 N85-20447
Carbon dioxide and the greenhouse effect
[GPO-39-043] 11 p1677 N85-20569
Middle atmosphere NO and NO2 observed by means of the Spacelab one grille spectrometer
[AERONOMICA-ACTA-A-293-1984] 11 p1680 N85-20568
The Jovian Stratosphere in the ultraviolet 11 p1760 N85-21069
Atlantic Coast Unique Regional Atmospheric Tracer Experiment (ACURATE)
[PB85-128460] 12 p1866 N85-21839
Multiple element neutron-activation analysis of atmospheric aerosols with X-ray and gamma-spectrometric recording of radionuclides formed 13 p2013 N85-22631
One mechanism of formation of organic fraction in atmospheric aerosol 13 p2014 N85-22632
Possible role of ocean biota in global carbon balance — phytoplankton production 13 p2107 N85-23129
Sulfur oxygen processes on Io 13 p2173 N85-23481
Photometric analysis of Jupiter-illuminated images of Io 13 p2196 N85-23620
Chemical composition of coastal haze aerosol 14 p2338 N85-24456
Spectroscopic study of gas pollutants in atmosphere over large cities: A review 14 p2341 N85-24478
Magnetospheric effects on the upper atmosphere 14 p2365 N85-24616
Extended atmospheres of outer planet satellites and comets
[NASA-CR-175673] 14 p2440 N85-25058
Research on atmospheric dust formations using satellite observation data 15 p2465 N85-25339
Operational methods for calculating atmospheric dispersion
[BLL-CE-TRANS-8040-(9022.09)] 15 p2586 N85-25955
Size distributions of elemental carbon in atmospheric aerosols
[PB85-153534] 15 p2589 N85-25983
Changes in the high-latitude ocean as possible causes of atmosphere CO2 variations 15 p2602 N85-26038
One approach to remote sensing of total ozone content 16 p2725 N85-26822
Comparison of observed and predicted short-term tracer-gas concentrations in the atmosphere
[DE85-007566] 16 p2821 N85-27399
Interactive effects of acid rain and gaseous air pollutants on natural terrestrial vegetation
[DE85-005255] 16 p2821 N85-27401
Acid precipitation in North America: 1980, 1981 and 1982 annual data summaries from acid deposition system data base
[PB85-162477] 16 p2822 N85-27410
Measurement of elements in the stratosphere
[NASA-CR-175891] 16 p2823 N85-27414
Stratospheric ClO: In-situ detection with a new approach 16 p2824 N85-27416
The copper vapor laser 16 p2824 N85-27417
In-situ stratospheric ozone measurements: Recent results and their implications 16 p2824 N85-27419
Water vapor 16 p2824 N85-27420

Role and fate of ozone in the atmosphere
16 p2624 N85-27421
Atmospheric radon measurements in the Antarctic Penninsula: A preliminary report
[INPE-3398-PRE/667] 16 p2627 N85-27436
Elemental analysis of aerosols in Transvaal urban and power-producing areas using time and size-resolved samples 16 p2629 N85-27443
Geophysical monitoring for climatic change, number 12
[PB85-172278] 16 p2637 N85-27496
Cometary atmospheres: Modeling the spatial distribution of observed neutral radicals
[NASA-CR-175852] 16 p2882 N85-27781
Absolute calibrations of SO2 and NO analyzers by photographic methods
[DFVLR-MITT-85-02] 17 p2994 N85-28504
Theoretical basis for the determination of the concentration of radon decay products in air from the activity of a particulate air sample
[IRI-190-83-07] 17 p3035 N85-28774
Improvement of the basic knowledge of the climatology of the vertical ozone layer by enhanced balloon sounding
[BPT-6/84] 18 p3137 N85-29426
Geothermal hydrogen and health in Rotorua, New Zealand
[DE85-901283] 19 p3301 N85-30467
Volatiles in the outer solar system. 1: Thermodynamics of clathrate hydrates. 2: Ethane ocean on Titan. 3: Evolution of primordial Titan atmosphere
19 p3362 N85-30984
Ozone in the 21st century: Increase or decrease
[AERONOMICA-ACTA-A-291-1984]
20 p3489 N85-31687
Concentrations of ice nuclei of different modes of activities 21 p3641 N85-32616
Observations of the atmospheric ice nucleus at northwest China 21 p3641 N85-32618
The investigation of natural and artificial ice nuclei by the improved membrane filter method
21 p3642 N85-32626
A thermal diffusion chamber for the measurement of cloud condensation nuclei 21 p3642 N85-32627
Concentration and source areas of ice nuclei in the Alaskan atmosphere 21 p3643 N85-32634
Eleventh International Conference on Atmospheric Aerosols, Condensation and Ice Nuclei, volume 1
[PB85-182400] 21 p3644 N85-32636
Study of the formation of particles from natural hydrocarbons released by vegetation
21 p3644 N85-32640
Experimental studies of the formation of Aitken nuclei in the atmosphere 21 p3644 N85-32641
Photochemical aerosol formation in polluted atmosphere 21 p3644 N85-32642
The influence of Brownian coagulation on the size distributions of atmospheric aerosols
21 p3645 N85-32643
A study of time transformation of natural photochemical aerosols 21 p3645 N85-32644
Human activity and production rate of secondary nuclei 21 p3645 N85-32645
A new hypothesis for the observed vertical distribution of atmospheric aerosols 21 p3645 N85-32646
On the transformation regularities of time series of solid aerosol concentrations in the surface atmospheric layer
21 p3645 N85-32648
Our knowledge about the atmospheric aerosol
21 p3646 N85-32650
Chemical composition of atmospheric aerosol at Delhi
21 p3646 N85-32653
Aitken particle size distribution in Antarctica
21 p3646 N85-32656
Condensation nuclei and aerosol size distribution measurements in Arctic haze 21 p3647 N85-32658
Aircraft investigations of the distribution of aerosols in the lower troposphere 21 p3647 N85-32659
The variability of aerosol microstructure in continental and oceanic surface layers of the atmosphere in anticyclones 21 p3647 N85-32660
Theoretical studies of structure and stability of hydrates of atmospheric sulfur species 21 p3650 N85-32684
A review on the formation of aerosol particles in the atmosphere 21 p3651 N85-32687
The evolution of complex and higher organisms
[NASA-SP-478] 21 p3656 N85-32708
Origin of life 21 p3657 N85-32713
Evolution of the atmosphere 21 p3658 N85-32725
Participation of singlet oxygen in photodestruction of air-saturated solutions of coumarin dyes
21 p3665 N85-32891
The possibilities of remote analysis of atmospheric gases based on Raman scattering spectroscopy
21 p3665 N85-32892
Constraints on early atmosphere from planetary accretion processes 21 p3717 N85-33064
The composition of the primitive atmosphere and the synthesis of organic compounds on the early Earth
21 p3717 N85-33065
The problem of the Earth's CO2 content and the iron core 21 p3718 N85-33069
Water loss from Venus: Implications for the Earth's early atmosphere 21 p3721 N85-33067
MELSAR: A mesoscale air quality model for complex terrain. Volume 1: Overview, technical description and user's guide
[DE85-010943] 22 p3811 N85-33608
Atmospheric reaction products from hazardous air pollutant degradation
[PB85-185841] 22 p3813 N85-33620
Ozone during sudden stratospheric warming: A three-dimensional simulation
[AERONOMICA-ACTA-A-292-1984]
22 p3813 N85-33621
Acetonitrile in the Earth's atmosphere: An upper limit deduced from infrared solar spectra
[AERONOMICA-ACTA-A-295-1985]
22 p3813 N85-33623
Middle Atmosphere Program. Handbook for MAP, volume 11
[NASA-CR-176107] 22 p3814 N85-33625
Potential spin-offs of the carbon dioxide observational platform system (CO-OPS) for remote sensing opportunities
[NASA-TP-2510] 23 p3899 N85-34149
Agents and effects of ozone trends in the atmosphere
[AERONOMICA-ACTA-A-287-1984]
23 p3948 N85-34466
Climate modeling: A retrospective-prospective view with consideration for the atmospheric carbon dioxide-climate issue
[DE85-011532] 23 p3950 N85-34481

ATMOSPHERIC CONDITIONS
U METEOROLOGY

ATMOSPHERIC CONDUCTIVITY
NT IONOSPHERIC CONDUCTIVITY
An improved rocket-borne electric field meter for the middle atmosphere
[NASA-CR-175510] 12 p1888 N85-21851
Distribution of atmospheric electric current in the global circuit
[CONTRIB-87] 12 p1888 N85-21852
Field validation of 6-particle puff model
[DE85-004073] 15 p2589 N85-25962
The Martian climate: Energy balance models with CO2/H2O atmospheres
[NASA-CR-175722] 15 p2679 N85-26547
Effect of vertical shear on regional-scale trajectories in near-frontal conditions
[DE85-007554] 19 p3317 N85-30561
The electric current densities beneath thunderstorms
20 p3494 N85-31726
Application of Particle Induced X-ray Emission analysis (PIXE) to aerosol long range transport studies
21 p3648 N85-32665

ATMOSPHERIC CORRECTION
Fast Hartmann method for problems in astronomical aseptive optics 02 p0161 N85-11094
Correction for atmospheric refraction in an airborne, operational environment
[AD-A146552] 06 p0835 N85-15314
LANDSAT-4 Thematic Mapper calibration and atmospheric correction 12 p1870 N85-21734
LANDSAT 4 band 6 data evaluation
[E85-10093] 12 p1874 N85-21755
Preliminary investigation into using the sun as a source for G/T (Gain to System Noise Temperature) measurements
[PB85-128148] 12 p1952 N85-22265
Investigating statistical characteristics of atmospheric background brightness and star background density in equatorial region of celestial sphere
15 p2478 N85-25298

ATMOSPHERIC DENSITY
Effect of hyperoxia and increased gas atmosphere density on contractile function of the right ventricle
01 p0093 N85-10628
Global matrix of thermospheric density values for selected solar/geomagnetic conditions and spacecraft orbital attitudes
[NASA-TM-86478] 04 p0533 N85-13409
Continuum absorption by H2O in the 700-1200 cm(-1) and 2400-280 cm(-1) windows
[AD-A147391] 07 p0997 N85-16334
Atmospheric profile imprint in firewall ablation coefficient 11 p1662 N85-20473
Consummative expressions for satellite drag perturbations in a spherically symmetrical atmosphere
[AD-A154230] 19 p3222 N85-29981
Applied research and development for falling-sphere air density measuring systems
[AD-A155227] 21 p3552 N85-32099
Application of satellite accelerometer data to improve density models
[AD-A154904] 21 p3631 N85-32558
Studies of the solar mesosphere explorer: Dynamics and horizon sensor performance. Part A: Spin axis precession and atmospheric drag. Part B: Clouds
[NASA-CR-175306] 24 p4069 N85-35213

ATMOSPHERIC DIFFUSION
Observed rate of tropospheric diffusion
[DE84-016047] 02 p0224 N85-11470
Review of the attributes and performance of six urban diffusion models
[PB84-236850] 04 p0484 N85-13087
A new fast response probe for diffusion studies in atmospheric air — pollution modeling
[IC-AERO-84-01] 08 p1180 N85-17437
Atmospheric wind and diffusion from analysis of an SF6 release at 350 km altitude
[AD-A147965] 08 p1185 N85-17471
Atmospheric diffusion in hilly region on middle reaches of the Chang Jiang 11 p1620 N85-20196
Atmospheric dispersion of hypergolic liquid rocket fuels, volume 1
[AD-A149597] 12 p1817 N85-21399
Adjustment of the national dispersion model for air pollution from elevated sources
[KNMI-TR-57] 14 p2353 N85-24540
The Terrain-Responsive Atmospheric Code (TRAC) for plume growth and dispersion in complex terrain
[DE85-010541] 19 p3309 N85-30513
Modeling of chemical transformations of SO(x) and NO(x) in the polluted atmosphere: An overview of approaches and current status
[PB85-173169] 20 p3487 N85-31677
Impact of fluctuations in optical properties of atmosphere on the ratio of spectral brightness from remote sensing of agricultural land 22 p3734 N85-33149
The first three harmonics of solar daily variation caused by the diffusive propagation of galactic cosmic rays through the heliosphere
[SH-4.5-1] 23 p4035 N85-35019

ATMOSPHERIC EFFECTS
Distribution of atmospheric radio interference
06 p0792 N85-15063
Limits of the propagation medium with respect to digital signal transmission 10 p1469 N85-19270
Propagation of wide bandwidth signals in a tropospheric ducting system 10 p1469 N85-19271
The effect of the arbitrary level assignment of satellite cloud motion wind vectors on wind analyses in the pre-thunderstorm environment
[NASA-TM-86186] 10 p1517 N85-19565
Lake ice occurrence as a possible detector of atmospheric CO2 effects on climate
[DE85-002951] 11 p1687 N85-20606
Proposed preliminary design criteria model environment for the 1990's 12 p1784 N85-21194
Atmospheric environment for Space Shuttle (STS-51A) launch
[NASA-TM-86497] 12 p1892 N85-21675
Thematic Mapper data quality and performance assessment in renewable resources/agriculture/remote sensing 13 p2120 N85-23201
The Terrain-Responsive Atmospheric Code (TRAC) for plume growth and dispersion in complex terrain
[DE85-010541] 19 p3309 N85-30513
Factor analysis of atmospheric pollution by polycyclic aromatic hydrocarbons
[HSE-TRANS-10988] 19 p3311 N85-30528
One-dimensional model hindcasts of warm anomalies in the North Pacific Ocean
[AD-A154128] 19 p3320 N85-30579
Understanding and laboratory prediction of the atmospheric corrosion behavior of steels and of non-ferrous metals and alloys
[AD-A154642] 21 p3566 N85-32179
A review of shock waves around aeroassisted orbital transfer vehicles
[NASA-TM-86769] 22 p3739 N85-33177
Lake ice occurence as a possible detector of atmospheric CO2 effects on climate
[DE85-012987] 23 p3950 N85-34480
Atmospheric effects on the underground muon intensity
[SH-6.1-3] 23 p4044 N85-35078
Determination of characteristic values for fiber reinforced materials 24 p4074 N85-35247

ATMOSPHERIC ELECTRICITY
NT AURORAL ELECTROJETS
NT ELECTROJETS
NT EQUATORIAL ELECTROJET
NT IONOSPHERIC CURRENTS

NASA thunderstorm overflight program: Atmospheric electricity research. An overview report on the optical lightning detection experiment for spring and summer 1983
[NASA-TM-86488] 03 p0363 N85-12330
Measurements of electric fields obtained by stratospheric balloons in the region of the South Atlantic anomaly
[INPE-3218-PRE/571] 05 p0675 N85-14335
Synoptic observations of the radio noise background in the frequency range 150-160 kHz to provide design data for the low frequency communications designer
[AD-A147436] 07 p0941 N85-15965
A study of the effects of triggered lightning
[AD-A148296] 08 p1189 N85-17494
Atmospheric research aircraft --- conductivity/charge measurements
[ONERA-RS-87/7154/PY] 11 p1682 N85-20596
Effects of lightning on aircraft studied at Sheremetyevo 15 p2461 N85-25199
Measuring methods of atmospheric electric elements at the Earth's surface during snowfall and investigation of these relationships 15 p2581 N85-25920
Some considerations about the natural atmospheric radioactive aerosol 21 p3647 N85-32662

ATMOSPHERIC EMISSION
U AIRGLOW

ATMOSPHERIC ENERGY SOURCES
Cage regional energy budgets from the GLAS ATH order model 05 p0685 N85-14402
Comments on the measurements of multiple muon phenomena
[HE-5.2-13] 24 p4203 N85-36089

ATMOSPHERIC ENTRY
NT HYPERSONIC REENTRY
NT REENTRY
NT SPACECRAFT REENTRY
NT UNCONTROLLED REENTRY (SPACECRAFT)
The orbiter air data system 08 p1084 N85-16912
Approximate analytic method of calculating trajectories of movement of a flight vehicle in the atmosphere 14 p2279 N85-24121
Natural reentry of satellites 14 p2397 N85-24774
Results of tests of the SRB aft skirt heat shield curtain in the MSFC Hot Gas Facility
[NASA-CR-170688] 24 p4070 N85-35223

ATMOSPHERIC ENTRY SIMULATION
Method for prompt modeling of quasiperiodic movement of solid near-axisymmetrical body in atmosphere 13 p2043 N85-22790

ATMOSPHERIC GENERAL CIRCULATION EXPERIMENT
Computer studies of baroclinic flow --- Atmospheric General Circulation Experiment
[NASA-CR-171338] 10 p1517 N85-19566

ATMOSPHERIC HEAT BUDGET
Combining Heat Capacity Mapping Mission (HCMM) LANDSAT and thematic map information into a unique high precision merged multichannel system --- climatology 05 p0660 N85-14239
The first winter of MAP-dynamics, 1982-1983: A winter with three different warming periods 11 p1657 N85-20446
Influence of aerosol on formation of outgoing thermal radiation 14 p2342 N85-24483
Partitioning of the vertical turbulent energy transport into positive and negative contributions --- meteorology 24 p4122 N85-35551
Aircraft measurements during the Bonn Experiment (BONEX 1) --- meteorology 24 p4122 N85-35552
Motor glider measurements during the Urban Atmosphere Energy Budget Experiment (EESA 1) 24 p4122 N85-35553

ATMOSPHERIC HEATING
Analysis of diabatic heating during FGGE 05 p0683 N85-14393
Global scale diagnosis of FGGE data 05 p0683 N85-14394
Planetary scale interactions 05 p0684 N85-14397
Atmospheric heating of meteorites: Results from nuclear track studies 05 p0682 N85-15607
The Middle Atmosphere Program: Winter in Northern Europe (MAP/WINE) 11 p1655 N85-20429
Middle Atmosphere Program. Handbook for MAP, volume 8
[NASA-CR-175478] 11 p1657 N85-20445
The first winter of MAP-dynamics, 1982-1983: A winter with three different warming periods 11 p1657 N85-20446
Stratwarm effects in the ionospheric D region wind field 11 p1683 N85-20479
Outer atmospheres of cool stars observed with IUE 11 p1744 N85-20968
Anomalous heating of ionospheric components (thermal e- and He+) via intense Ion Cyclotron Waves (ICW's) 14 p2368 N85-24833
Sensitivity of planetary waves to initial conditions and forcing
[AD-A154111] 19 p3345 N85-30734
Ozone during sudden stratospheric warming: A three-dimensional simulation
[AERONOMICA-ACTA-A-292-1984] 22 p3813 N85-33621

ATMOSPHERIC IMPURITIES
U AIR POLLUTION

ATMOSPHERIC IONIZATION
NT AURORAL IONIZATION
Analysis of ionization sources in D region based on theoretical models 06 p0825 N85-15240
MWR, Meteor Wind Radars 08 p1184 N85-17462
MAP activities in Hungary 11 p1657 N85-20440
Investigation of aeronomic processes on the basis of ionospheric sporadic E 11 p1663 N85-20482
High energy particle effects in the D region during and after geomagnetic storms 11 p1664 N85-20485
Dependence of the high latitude middle atmosphere ionization on structures in interplanetary space 11 p1664 N85-20487
Dependence of equatorial F-region plasma bubble rise velocity and dynamo electric field on solar cycle
[INPE-3439-PRE/896] 16 p2826 N85-27434
X-ray intensification at balloon altitudes of the South Atlantic magnetic anomaly in association with geomagnetic activity
[INPE-3469-PRE/712] 16 p2827 N85-27437
Shuttle Molecular Gun: Smog. Potential experiment for the electrodynamic Tethered Satellite System (TSS) mission
[IFSI-84-17] 20 p3419 N85-31221
Rocket measurements of mesospheric ionization irregularities
[NASA-CR-176056] 20 p3494 N85-31721

ATMOSPHERIC LASERS
Linear absorption and scattering of laser beams
[AD-A156167] 24 p4008 N85-35401

ATMOSPHERIC LOADING
U POLLUTION TRANSPORT

ATMOSPHERIC MODELS
NT REFERENCE ATMOSPHERES
Processing and display of atmospheric phenomenaa data
[NASA-CR-171178] 01 p0072 N85-10475
The mesoscale-beta-scale evolution of mid-latitude meso-alpha-scale convective complexes 01 p0073 N85-10488
Automated analysis and nowcasting of mesoscale convective systems 01 p0074 N85-10492
Three-dimensional mesoscale analysis of serial soundings 01 p0074 N85-10493
Rain bands and symmetric instability 01 p0075 N85-10496
A short-term forecast model for thunderstorm rotation 01 p0081 N85-10542
A system for meteorological satellite, radar, conventional data and model analysis 01 p0082 N85-10551
Interactive computer display systems in nowcasting 01 p0083 N85-10557
Model of atmospheric ozone for middle latitudes 02 p0161 N85-11091
Quasi-stationary atmospheric responses to large-scale forcing 02 p0227 N85-11484
A comparison of 2- and 3-dimensional transport within a stratospheric circulation model 02 p0227 N85-11485
Development of a global model for atmospheric backscatter at CO2 wavelengths
[NASA-CR-174053] 02 p0228 N85-11489
A study of greenhouse effects using zero, 1 and 2 dimensional climate models 02 p0230 N85-11496
Statistical interpretation of NWP model output: An overview of techniques used and results achieved
[REPT-551.509.313] 02 p0231 N85-11503
Report of the Third Session of the International Working Group on Data Management for the International Satellite Cloud Climatology Project (ISCCP)
[WCP-82] 02 p0231 N85-11504
Properties of the upper tropospheres of Uranus and Neptune derived from observations at visible to near-infrared wavelengths 02 p0296 N85-11933
Laboratory evaluation of microwave absorption properties under simulated conditions for planetary atmospheres
[NASA-CR-174060] 02 p0303 N85-11060
A proposed reference set of scenarios for radiatively active atmospheric constituents
[DOE/NBB-0066] 03 p0388 N85-12483
A 2-dimensional description of potential perturbations to the ozone layer due to NOx and H-2-O aircraft emissions
[AD-A146292] 03 p0392 N85-12511
Development of a microcomputer coupled atmospheric and oceanic boundary layer prediction model
[AD-A146334] 03 p0397 N85-12530
The Martian climate: Energy balance models with CO2/H2O atmospheres
[NASA-CR-174073] 03 p0448 N85-12849
Thermodynamic conditions of the Earth's atmosphere with pollution processes 04 p0523 N85-13345
China report: Science and technology
[JPRS-CST-84-001] 04 p0557 N85-13545
Theoretical and observed dispersion of acoustic-gravity waves in atmosphere 04 p0557 N85-13547
The Interaction of Global Biochemical Cycles
[NASA-CR-174184] 05 p0652 N85-14183
Global biogeochemical cycles: Studies of interaction and change, some views on the strategy of approach 05 p0652 N85-14185
Three dimensional global modeling of atmospheric CO2 05 p0652 N85-14189
GLAS fourth order model 05 p0679 N85-14361
Orographic effects in atmospheric circulation 05 p0679 N85-14362
Spectral general circulation model development 05 p0679 N85-14363
Biosphere/atmosphere interactions 05 p0679 N85-14364
A vertically resolved planetary boundary layer 05 p0680 N85-14367
Normal mode initialization 05 p0680 N85-14372
Forecast impact of components of the FGGE observing system 05 p0681 N85-14373
Water vapor profile retrievals from the HIRS/MSU satellite sounder 05 p0681 N85-14378
Jet stream errors and tropospheric-stratospheric interactions in the GLAS general circulation model 05 p0683 N85-14392
Global scale diagnosis of FGGE data 05 p0683 N85-14394
Theoretical modeling for numerical weather prediction 05 p0684 N85-14395
Numerical prediction of the president's day cyclone 05 p0684 N85-14399
Cage regional energy budgets from the GLAS ATH order model 05 p0685 N85-14402
Investigation of cloud feedback in the GLAS model 05 p0685 N85-14404
Application of the bounded derivative initialization method 05 p0686 N85-14407
Implicit numerical methods in meteorology 05 p0686 N85-14408
Linear studies of stationary, extratropical anomalies in the troposphere 05 p0686 N85-14410
The influence of synoptic scales on low-frequency modes of variability 05 p0687 N85-14412
Internal gravity waves in real atmosphere 06 p0825 N85-15236
Analysis of ionization sources in D region based on theoretical models 06 p0825 N85-15240
Modeling influence of three layer cloud cover on outgoing thermal radiation 06 p0825 N85-15242
Indirect estimation of convective boundary layer structure for use in routine dispersion models
[PB84-238260] 06 p0834 N85-15308
Large-eddy simulation. Guidelines for its application to planetary boundary layer research
[AD-A146381] 06 p0880 N85-15651
Fluctuations during observations of extraterrestrial sources from outer space through Earth's atmosphere 07 p0953 N85-16040
Research in geodesy based upon radio interferometric observations of extragalactic radio sources
[AD-A147581] 07 p0988 N85-16280
Atmospheric Modeling And Sensor Simulation (AMASS) study
[NASA-CR-171283] 07 p0996 N85-16325
The role of finite parallel length on the stability of barium clouds
[AD-A146972] 07 p0996 N85-16328
The effects of long-periodic forcing in a zero-dimensional climate model 07 p1002 N85-16363
Index cycles simulated by a low order forced barotropic model 07 p1002 N85-16364
Experiments in forecasting atmospheric marine horizontal visibility using model output statistics with conditional probabilities of discretized parameters
[AD-A147574] 07 p1008 N85-16404
Sensor-atmosphere-target simulation. Computer program SENSAT
[DFVLR-FB-84-32] 08 p1176 N85-17419
Determination of the laws governing the changes in the standard deviations of the distribution of pollution based on observations of the atmospheric turbulence spectrum and the possibility of simulating it in the laboratory
[BLL-TR-T6373/BG/MRS14883/84] 08 p1179 N85-17431

Modeling of turbulent dispersion of neutral and buoyant contaminants released from two dimensional sources — air pollution
[VKI-TN-150] 08 p1180 N85-17438
Plasma and magnetospheric research
[NASA-CR-171293] 08 p1183 N85-17451
Atmospheric photochemical modeling of turbine engine fuels. Phase 1: Experimental studies. Volume 2: Environmental chamber data tabulations
[AD-A147786] 08 p1185 N85-17470
Radiation parameterization programs for use in general circulation models
[AD-A148015] 08 p1188 N85-17488
Development of guidance forecasts at the Royal Netherlands Meteorological Institute (KNMI). Part 1: General information
[KNMI-TR-84-PT-1] 08 p1190 N85-17499
Atmospheric acidification chemistry: A review
[PB84-215490] 09 p1350 N85-18495
A turbulent closure model for the free atmosphere 09 p1351 N85-18502
Atmospheric science and power production
[DE84-005177] 09 p1354 N85-18521
Simulation of entrainment at the top of the atmospheric boundary layer for use in General Circulation Models (GCM)
[DM-42] 09 p1355 N85-18525
Global scale diagnoses of FGGE data
[NASA-CR-174356] 09 p1356 N85-18533
The influence of soil moisture distribution on the severe-storm environment of the southern Great Plains: A numerical study of the SESAME 4 case 09 p1357 N85-18534
Mesoscale storm and dry period parameters from hourly precipitation data: Program documentation
[DE85-001366] 09 p1357 N85-18538
Combined effects of baroclinic and barotropic instability in a nonlinear low order model
[DM-41] 09 p1358 N85-18544
Near infrared modeling of the equatorial regions of Jupiter and Saturn 09 p1415 N85-18930
PMP-1: A coordinated study of the behavior of the middle atmosphere in winter 11 p1654 N85-20421
MAP in Japan: Organization and projects 11 p1655 N85-20425
UK participation in the Middle Atmosphere Programme 11 p1655 N85-20426
Soviet National Middle Atmosphere Program 11 p1655 N85-20428
The global meteor observation system (GLOBMET) 11 p1656 N85-20432
MAP activities in Hungary 11 p1657 N85-20440
Basic features of global circulation in the mesopause lower thermosphere region 11 p1662 N85-20475
Study of pollutant dispersion in an urban street canyon
[DE85-002648] 11 p1677 N85-20571
Comparison of MESOI atmospheric dispersion estimates with data and estimates from other models
[DE85-002372] 11 p1678 N85-20572
Continued research in mesoscale air pollution simulation modeling. Volume 7: Mathematical modeling of urban aerosol dynamics
[PB85-137388] 11 p1679 N85-20584
Atmospheric properties of RU Lupi derived from high- and low-resolution IUE spectra 11 p1754 N85-21031
The physical implications of an isothermal model for the hot intracluster medium
[NASA-TM-86174] 11 p1763 N85-21089
Wind-tunnel research on the mechanics of plumes in the atmospheric surface layer
[AD-A150019] 12 p1846 N85-21584
Spectroradiometric calibration of the Thematic Mapper and Multispectral Scanner system
[E85-10094] 12 p1874 N85-21756
Distribution of atmospheric electric current in the global circuit
[CONTRIB-87] 12 p1888 N85-21852
Substorms in the Earth's atmosphere
[DE85-000654] 12 p1890 N85-21861
Structure and forcing of teleconnection patterns occurring in general circulation model simulations
[DE85-002434] 12 p1890 N85-21862
21 Layer troposphere-stratosphere climate model
[NASA-TM-86183] 12 p1892 N85-21871
Research Reports: 1984 NASA/ASEE Summer Faculty Fellowship Program
[NASA-CR-171317] 12 p1944 N85-22210
New atmospheric sensor analysis study
[NASA-CR-171426] 13 p2094 N85-23069
Modeling of mechanism of positive feedback between mean Earth surface temperature and atmospheric carbon dioxide in geologic time scale 13 p2106 N85-23122
Numerical experiments with simple model of ocean climate 13 p2106 N85-23123
Possibility of determining atmospheric weather parameters by radio and radiooptical measurements of refraction of cosmic sources 13 p2110 N85-23146
Stagnation zone impaction on a simple terrain feature in stable flow 13 p2130 N85-23255
Ground-up-to-Space (GUTS) laser propagation code description and manual
[AD-A150783] 14 p2309 N85-24295
Classification of atmospheric aerosol for evaluation of its effect on climate 14 p2333 N85-24426
Lyapunov stability of very simple steady solutions of prognostic systems 14 p2333 N85-24429
Influence of interaction between ocean and atmosphere on intensity of moving tropical cyclone 14 p2333 N85-24431
Small component spectral model of annual course of zonal atmospheric circulation 14 p2337 N85-24453
Applicability of vertically homogeneous atmospheric models for remote soundings 14 p2341 N85-24477
Influence of aerosol on formation of outgoing thermal radiation 14 p2342 N85-24483
One-dimensional nonstationary model of photochemical transformations of gas impurities in stratosphere 14 p2342 N85-24484
Adjustment of the national dispersion model for air pollution from elevated sources
[KNMI-TR-57] 14 p2353 N85-24540
Ionosphere-magnetosphere coupling and convection 14 p2364 N85-24609
Analysis of atmospheric interferometer data
[AD-A150682] 14 p2372 N85-24663
Characteristics and behavior of atmospheric aerosols; application to prediction of infrared extinction
[AD-A150691] 14 p2372 N85-24665
Statistical/Trend analysis of the marine atmospheric boundary layer model
[AD-A151053] 14 p2374 N85-24673
Sensitivity analysis of a coupled atmospheric-oceanic boundary layer model
[AD-A150760] 14 p2382 N85-24690
Investigation of the daytime lunar atmosphere
[NASA-CR-175636] 14 p2440 N85-25057
A model for the dynamics of the deep photosphere 14 p2450 N85-25129
Linear models of acoustic waves in sunspot umbrae 14 p2450 N85-25130
Use of atmospheric models in predicting artificial Earth satellite motion 15 p2478 N85-25296
One method for constructing model of point masses of planetary gravity field 15 p2479 N85-25300
Evaluating radiation distortions of optical image of Earth's surface in horizontally inhomogeneous atmosphere 15 p2486 N85-25345
Experimental investigation of annular air curtain domes
[UTIAS-288] 15 p2521 N85-25543
Operational methods for calculating atmospheric dispersion
[BLL-CE-TRANS-8040-(9022.09)] 15 p2588 N85-25955
Development of global model for atmospheric backscatter at CO2 wavelengths
[NASA-CR-175679] 15 p2591 N85-25971
The physics of the marine stratocumulus-capped mixed layer 15 p2593 N85-25979
An Earth longwave radiation climate model
[NASA-CR-175749] 15 p2594 N85-25984
Convection modeling and application to severe storms 15 p2595 N85-25991
Modeling of cloud systems 15 p2595 N85-25992
Modeling of midwest severe thunderstorms 15 p2596 N85-25995
Estimation of convective rainfall from visible and infrared satellite data 15 p2596 N85-25999
Mesoscale analysis and modeling group 15 p2596 N85-26001
ILUM code: Solar and lunar flux calculations for multi-cloud layered atmospheres
[DE85-005578] 15 p2600 N85-26025
Studies of electro-optical attenuation in the vicinity of cloud base
[AD-A151745] 15 p2653 N85-26360
Is there more than one steady state for NOx? 15 p2687 N85-26593
Wind modelling for increased aircraft operational efficiency 16 p2697 N85-26652
Modeling plasma mantle of Earth's magnetosphere 16 p2720 N85-26790
Emission inventory applications to regional acid deposition modeling
[PB85-157386] 16 p2760 N85-27033
Theory and modeling of the interaction between subgrid scale orography and large scale flow
[DM-43] 16 p2827 N85-27440
Use of a network of telemetered meteorological stations for prediction of the distribution of an atmospheric tracer 16 p2831 N85-27458
The problem of atmospheric turbulence
[NASA-CR-175783] 16 p2832 N85-27464
Tropical Oceans-Global Atmosphere (TOGA) experiment planning for the Brazilian participation in TOGA global climate program
[INPE-3499-PRE/795] 16 p2834 N85-27477
Simulation of a synchronously coupled atmosphere-ocean prediction model
[AD-A152020] 16 p2835 N85-27482
Circulation statistics from January and July: Simulation with the NCAR (National Center for Atmospheric Research) community climate model (CCMOB)
[PB85-165637] 16 p2837 N85-27497
Test of lidar inversion algorithm sensitivity to atmospheric backscatter and extinction parameters, revision A
[AD-A152082] 16 p2865 N85-27671
Monodeurated methane in the outer solar system. 2. Its detection on Uranus at 1.6 microns
[NASA-CR-175762] 16 p2882 N85-27782
Homogeneous processes of atmospheric interest
[NASA-CR-175770] 17 p2989 N85-28475
Geophysical plasmas and atmospheric modeling
[AD-A152805] 17 p2993 N85-28497
Time-dependence of CO2-induced climate change
[DE85-007568] 17 p2997 N85-28525
Ozone and temperature trends due to the injection of trace species in the atmosphere
[AERONOMICA-ACTA-A-288-1984] 18 p3132 N85-29399
Methods for simulating gas phase SO2 oxidation in atmospheric models
[PB85-173110] 18 p3135 N85-29418
Research Review, 1983
[NASA-TM-86219] 18 p3139 N85-29433
The impact of scatterometer data on limited-area model predictions of the QE 2 storm 18 p3139 N85-29436
Preliminary results from numerical experiments on the summer 1980 heat wave and drought 18 p3140 N85-29438
Experiments on the assimilation of patches of data using a barotropic model 18 p3140 N85-29441
High-latitude filtering in a global grid-point model using model normal modes 18 p3140 N85-29442
On the improvement of satellite temperature retrievals by means of boundary layer models 18 p3140 N85-29443
Development and testing of the variable vertical resolution Fourth Order GCM 18 p3142 N85-29453
Parameterization of surface fluxes in the VVR Fourth Order GCM 18 p3142 N85-29454
Model development highlight for 1984: The GLA Fourth Order GCM 18 p3143 N85-29457
Response of winter forecasts made with the GLA Fourth Order GCM to Changes in the horizontal grid resolution 18 p3143 N85-29458
Energy sources of the dominant frequency dependent 3-dimensional atmospheric modes 18 p3143 N85-29462
A comparison of the bounded derivative and the normal mode initialization methods using real data 18 p3144 N85-29463
The vertical structure of global rotational normal modes 18 p3144 N85-29464
Transient eddies in the UCLA GCM 18 p3145 N85-29470
Analysis of a simulated cloud climatology 18 p3145 N85-29472
A new CO2 transmittance parameterization and its impact on the GLA GCM 18 p3146 N85-29476
A GCM study of the atmospheric response to tropical SST anomalies 18 p3146 N85-29477
Influence of land surface processes on the Indian monsoon: A numerical study 18 p3146 N85-29478
Influence of land-surface roughness on atmospheric circulation and rainfall: A sensitivity study with a GCM 18 p3146 N85-29479
The structure and dynamics of an observed moist front 18 p3146 N85-29480
Some recent developments in numerical modelling at ECMWF 18 p3147 N85-29481
Global model of transport of pollutants in atmosphere 19 p3297 N85-30439
Areal coverage of storm precipitation
[NASA-CR-176013] 19 p3315 N85-30550
Atmospheric Tracer Workshop
[DE85-010573] 20 p3486 N85-31668
Spectral methods for limited area models 20 p3488 N85-31679
Strongly nonlinear dynamics of baroclinic waves 20 p3488 N85-31681

Errors and parameterizations of sub-grid scale processes in regional-scale atmospheric models
20 p3488 N85-31682
A survey of wind and turbulence modeling methods
[AD-A154470] 20 p3496 N85-31733
Carbon dioxide and climate: Potential impacts
[DE85-009473] 20 p3496 N85-31734
Lightcurve CCD spectrophotometry of Pluto
20 p3545 N85-32057
VALMET: A valley air pollution model
[DE85-010820] 21 p3614 N85-32463
A numerical analysis of transient planetary waves and the vertical structure in a meso-strato-troposphere model, part 1.4A 21 p3617 N85-32473
Nuclear thermal transmittance in the atmosphere using LOWTRAN-6 computer code
[AD-A154669] 21 p3630 N85-32553
Application of satellite accelerometer data to improve density models
[AD-A154904] 21 p3631 N85-32556
Generation of available potential energy and the energy cycle during the global weather experiment
[NASA-CR-175301] 21 p3634 N85-32572
Accuracy and operational use of medium and extended range numerical atmospheric forecasts: A review
[AD-A155027] 21 p3635 N85-32579
Mean flow and turbulence in complex terrain
[AD-A155138] 21 p3636 N85-32583
Simulation of the coupled atmospheric and oceanic boundary layer model during MILDEX
[AD-A155166] 21 p3655 N85-32705
A mixed pseudospectral/finite difference method for a thermally driven fluid in a nonuniform gravitational field
[NASA-TM-87561] 22 p3763 N85-33436
Atmospheric modeling of organics for risk assessment: A Chemist's view
[DE85-009770] 23 p3909 N85-34217
User's guide to the MATHEW/ADPIC models
[DE85-012952] 23 p3966 N85-34587
Millimeter-wave propagation in moist air: Model versus path data
[AD-A156040] 24 p4087 N85-35331
Application of a turbulent closure model to the parameterization of the vertical diffusion of heat, momentum, and humidity in the ECMWF model — European Center for Medium Term Weather Forecasting (ECMWF)
[MITT-41] 24 p4095 N85-35387
Subseasonal variability in a two-level atmospheric general circulation model 24 p4114 N85-35504
A strategy for calibrating atmospheric transport models
[CSIRO-DAR-TP-9] 24 p4116 N85-35518
Maintenance of blocking anticyclones in a general circulation model
[PB85-190866] 24 p4124 N85-35567

ATMOSPHERIC MOISTURE
Experiment on nowcasting of heavy rainfall and severe storms in central China in 1979-1981
01 p0081 N85-10545
H2O profile in lower atmosphere of Venus based on effective radiation flux measurements
02 p0163 N85-11102
Effects of atmospheric water vapor and clouds on NOAA (National Oceanic and Atmospheric Administration) AVHRR (Advanced Very High Resolution Radiometer) satellite data
[AD-A145425] 02 p0280 N85-11824
Air-sea heat exchange, an element of the water cycle
05 p0653 N85-14195
A diagnostic approach to obtaining planetary boundary layer winds using satellite-derived thermal data
05 p0674 N85-14330
Conditional symmetric instability and mesoscale rainbands 05 p0678 N85-14358
Studies of atmospheric water in storms with the Nimbus 7 scanning multichannel microwave radiometer
05 p0682 N85-14362
Atmospheric environment for Space Shuttle (STS-41G) launch
[NASA-TM-86486] 07 p0995 N85-16320
Condensational transformation of atmospheric aerosol particle distribution functions 10 p1500 N85-19468
Electrochemical cell to measure corrosion rates in noncondensing environments
[DE85-003148] 12 p1807 N85-21336
TRAJ: Single station trajectory plot
[PB85-135002] 12 p1897 N85-21911
Dependence of combustion of homogeneous kerosene-air mixtures on humidity of air
13 p2051 N85-22835
Possibility of determining atmospheric weather parameters by radio and radiooptical measurements of refraction of cosmic sources 13 p2110 N85-23146
Response of Earth's atmosphere to increases in solar flux and implications for loss of water from Venus
13 p2178 N85-23518
Determination of total moisture content in cloud-free atmosphere by relative radio emission measurements
14 p2340 N85-24472
Determining atmosphere moisture content from differences in two-frequency microwave radiation measurements 14 p2341 N85-24474
Ice multiplication in summertime cumulus clouds in the BEWMEX area 16 p2829 N85-27445
Precipitable water in the atmosphere, determined from surface dewpoint values 16 p2831 N85-27457
Atmospheric frontal zone studies
[NASA-CR-175293] 16 p2833 N85-27469
The moist available energy of a conditionally unstable atmosphere 18 p3145 N85-29473
The structure and dynamics of an observed moist front 18 p3146 N85-29480
Variability of air humidity profiles over ocean determined by lidar sounding 19 p3295 N85-30436
Influence of moisture and elevated temperature on the fatigue properties of WTS-3 glass fiber blade material — wind turbine blade (WTS-3)
[FFA-TN-1984-58] 20 p3470 N85-31558
Water loss from Venus: Implications for the Earth's early atmosphere 21 p3721 N85-33087
Throughfall rate and chemistry studies: Whiteface Mountain
[DE85-012407] 23 p3947 N85-34484
Program for Regional Observing and Forecasting Services (PROFS)
[PB85-188050] 24 p4124 N85-35569

ATMOSPHERIC NOISE
U ATMOSPHERICS

ATMOSPHERIC OPTICS
Fast Hartmann method for problems in astronomical adaptive optics 02 p0161 N85-11094
Some statistical characteristics of atmospheric optical thickness in visible spectral range
02 p0164 N85-11109
Methods for determining atmospheric optical parameters using results of space survey of Earth's surface
02 p0165 N85-11117
Relation between atmospheric scattering and backscattering coefficient
[ESA-TT-837] 05 p0677 N85-14350
Guidelines for atmospheric measurements in support of electro-optical systems testing
[AD-A148090] 08 p1186 N85-17474
Time spectra of intensity fluctuations along reflecting path 13 p2079 N85-22981
Mean free path lenght of photons with broken cloud cover 14 p2338 N85-24455
Error in laser correlation wind speed meters resulting from variable atmospheric transparency
14 p2338 N85-24457
Diffuse reflection of light from turbid conservative medium of finite thickness with incidence of beam on surface of scattering glancing 14 p2342 N85-24481
Visibility of small objects in turbid atmosphere
14 p2342 N85-24482
A brief comparison of Egyptian with West German atmospheric transmission data in the 8 to 11.5 micron waveband
[BAE-BT-12829] 15 p2594 N85-25983
La Recherche Aerospatiale Bimonthly Bulletin Number 1984-3, 220/May-June
[ESA-TT-882] 16 p2695 N85-26636
Airborne measurements of the vertical distribution of Arctic haze 21 p3647 N85-32657

ATMOSPHERIC PHYSICS
NT CLOUD PHYSICS
Research study: Studies in atmospheric processes from Space Platforms
[NASA-CR-171176] 01 p0072 N85-10473
Trapping for Newtonian diffusion processes
[REPT-73] 01 p0130 N85-10893
Seminar on Principal Components Analysis in the Atmospheric and Earth Sciences
[CSIR-S-334] 02 p0211 N85-11388
A review of the millimeter and centimeter observations of Uranus 02 p0290 N85-11935
Atmospheric dynamics of Uranus and Neptune: Theoretical considerations 02 p0290 N85-11936
Report of the Division of Atmospheric Physics, 1980-1983 03 p0391 N85-12501
Millimeter-wave propagation and remote sensing of the atmosphere
[AD-A146339] 03 p0393 N85-12512
Carbon dioxide, the greenhouse effect and climate: A primer
[GPO-33-444] 03 p0395 N85-12519
Proceedings of a Workshop on Atmospheric Research Needs for the Western United States
[DE84-015069] 04 p0534 N85-13412
Structure and energetics of medium-scale atmospheric waves in the southern hemisphere summer
05 p0685 N85-14403
Activities report in Earth and planetary environments physics
[CRPE-NT-134] 05 p0734 N85-14720
USSR report: Earth sciences
[JPRS-UES-84-007] 06 p0819 N85-15196
USSR report: Earth sciences
[JPRS-UES-84-008] 07 p0980 N85-16223
Continuum absorption by H2O in the 700-1200 cm(-1) and 2400-280 cm(-1) windows
[AD-A147391] 07 p0997 N85-16334
Study of infrared atmospheric emission
[AD-A147517] 07 p0998 N85-16336
Electronically excited atomic and molecular oxygen
[AD-A147732] 08 p1121 N85-17064
The use of principal components analysis techniques Nimbus-7 coastal zone color scanner data to define mesoscale ocean features through a warm humid atmosphere
[AD-A148567] 08 p1176 N85-17416
A new fast response probe for diffusion studies in atmospheric air — pollution modeling
[IC-AERO-84-01] 08 p1180 N85-17437
Plasma and magnetospheric research
[NASA-CR-171293] 08 p1183 N85-17451
Atmospheric science and power production
[DE84-005177] 09 p1354 N85-19521
USSR report: Earth sciences
[JPRS-UES-85-003] 10 p1497 N85-19446
Recent investigations at INPE in magnetospheric physics and geomagnetism
[INPE-3260-PRE/603] 10 p1514 N85-19555
Brazil future plans in upper atmosphere research in Antarctica
[INPE-3400-PRE/669] 10 p1515 N85-19559
Science Applications, part 1 11 p1643 N85-20346
PMP-1: A coordinated study of the behavior of the middle atmosphere in winter 11 p1654 N85-20421
French activities relevant to middle atmosphere research 11 p1655 N85-20423
Soviet National Middle Atmosphere Program
11 p1655 N85-20426
Middle Atmosphere Program. Handbook for MAP, volume 10
[NASA-CR-175477] 11 p1658 N85-20450
Atmospheric transmissometer
[AD-D011540] 12 p1932 N85-22140
USSR report: Earth sciences
[JPRS-UES-85-002] 13 p2105 N85-23116
USSR report: Earth sciences
[JPRS-UES-85-004] 14 p2332 N85-24424
Error in laser correlation wind speed meters resulting from variable atmospheric transparency
14 p2338 N85-24457
Observations of auroras and related plasma phenomena by the Kyokko and Jikiken satellite in IMS — EXOS-A and B satellite 14 p2354 N85-24547
The Earth's magnetopause — International Magnetospheric Study 14 p2355 N85-24549
Observations of the magnetospheric boundary layers — International Magnetospheric Study
14 p2355 N85-24551
Magnetospheric effects on the upper atmosphere
14 p2365 N85-24618
Resonance generation of inertial waves (in the atmosphere) by Doppler-shift of inertio-gravity modes
15 p2590 N85-25988
Academician Zuyev notes plans for lasers on spacecraft for atmospheric research 16 p2717 N85-26775
Conceptual Design for a Gulf Coast Oxidant Transport and Transformation Experiment: Workshop proceedings and recommendations
[PB85-173789] 18 p3135 N85-29417
Applied Science Division's Environmental Research Program
[DE85-010637] 19 p3308 N85-30510
Sensitivity of planetary waves to initial conditions and forcing
[AD-A154111] 19 p3345 N85-30734
Comparison of 8 to 12 micrometer and 3 to 5 micrometer CVF transmissometer data with LOWTRAN calculations
[AD-A154218] 19 p3350 N85-30763
Activities report of the Aeronomy Department
[G-774-1984] 21 p3633 N85-32569
Photochemical aerosol formation in polluted atmosphere 21 p3644 N85-32642
Middle Atmosphere Program. Handbook for MAP, volume 11
[NASA-CR-176107] 22 p3814 N85-33625
National Center for Atmospheric Research
[PB85-191237] 22 p3848 N85-33835
Proceedings of Meteorological Motor Glider (MEMO) Workshop '84
[DFVLR-MITT-85-04] 24 p4121 N85-35542

The measurement of nitrogen oxide (NO, NO2) exchange over plant/soil surfaces
[CSIRO-DAR-TP-8] 24 p4127 N85-35587
ATMOSPHERIC PRESSURE
NT CYCLOGENESIS
Numerical forecast of pressure field by considering the mutual influence of orography, thermal nonhomogeneity and surface friction 01 p0060 N85-10534
Effect of hyperoxia and increased gas atmosphere density on contractile function of the right ventricle 01 p0093 N85-10628
Atmospheric environment for Space Shuttle (STS-41G) launch
[NASA-TM-86486] 07 p0995 N85-16320
Revised Uniform Summary of Surface Weather Observations (RUSSWO). Shemya AFB, Alaska, parts A-F
[AD-A146917] 07 p1005 N85-16388
Revised Uniform Summary of Surface Weather Observations (RUSSWO). Pope AFB, Fayetteville, North Carolina, parts A-F
[AD-A146918] 07 p1005 N85-16389
Revised Uniform Summary of Surface Weather Observations (RUSSWO). Sondestrom AB, Greenland, parts A-F
[AD-A146919] 07 p1005 N85-16390
Revised Uniform Summary of Surface Weather Observations (RUSSWO). England AFB, Alexandria, Louisiana, parts A-F
[AD-A146920] 07 p1006 N85-16391
Revised Uniform Summary of Surface Weather Observations (RUSSWO). Parts A-F: Homestead AFB, Florida
[AD-A147203] 07 p1007 N85-16396
Limited surface observations climatic summary (LISOCS). Camp Casey, Tong Du Chon, Korea
[AD-A147204] 07 p1007 N85-16397
Limited surface observation climatic summary (LISOCS). Ansbach AHP, Germany
[AD-A147205] 07 p1007 N85-16398
Revised Uniform Summary of Surface Weather Observations (RUSSWO). O'Hare International Airport, Chicago, parts A-F
[AD-A147206] 07 p1007 N85-16399
Theoretical and experimental analyses of laser altimeters for barometric measurements over the ocean 08 p1165 N85-17351
Isentropic objective analysis
[PB85-112167] 11 p1688 N85-20617
Method of and apparatus for measuring temperature and pressure — atmospheric sounding
[NASA-CASE-GSC-12558-1] 12 p1856 N85-21639
Evaluation of stringtile and related compounds for use in solar energy storage
[PB85-146876] 12 p1883 N85-21816
Seismic observation of infrasonic signals
[AD-A149574] 12 p1889 N85-21853
TRAJ: Single station trajectory plot
[PB85-135002] 12 p1897 N85-21911
A computer controlled mass spectrometer system for investigating the decomposition of non-metallic materials under atmospheric conditions 12 p1948 N85-22237
Portable Automated Mesonet (PAM) data from the 1980 experiment in Anderson Creek Valley
[DE85-004361] 13 p2139 N85-23262
Observations of current pulsations of characteristics in atmosphere with period of about 1.5 hours 14 p2341 N85-24480
Ocean circulation and meteorology off the Georgia coast. Part 1: Real-time telemetry system for data collection
[PB85-155935] 15 p2605 N85-26052
The sea level response to weather along the coast of southern Africa 16 p2629 N85-27446
Summary of Meteorological Observations, Surface (SMOS), Dallas, Texas
[AD-A150599] 16 p2635 N85-27460
Study of synthesis gas conversion over metal oxides
[DE85-010136] 16 p3072 N85-28999
Trends in the Southern Hemisphere 16 p3144 N85-29486
A constant altitude flight survey method for mapping atmospheric ambient pressures and systematic radar errors
[NASA-TM-86733] 19 p3217 N85-29951
Mechanism of the catalytic gasification and reactivity of graphite
[DE85-009932] 19 p3229 N85-30020
The mobile phase in coals: Its nature and modes of release
[DE85-011696] 19 p3230 N85-30026
Approximate method for computing wind velocity in atmosphere 19 p3298 N85-30444
Atmospheric environment for space shuttle (STS-51C) launch
[NASA-TM-86508] 19 p3315 N85-30547
A global low order spectral model designed for climate sensitivity studies
[NASA-CR-175999] 19 p3315 N85-30549
Two-phase flow visualization in a transparent, atmospheric pressure, boiling water loop
[DE84-016857] 21 p3586 N85-32288
Air-sea interaction with SSM/I and altimeter
[NASA-CR-176105] 22 p3816 N85-33650
Electrode erosion in arc discharges at atmospheric pressure
[NASA-TM-87087] 23 p3903 N85-34178
Monitoring dosage of volatile compounds in tests at low barometric pressure 23 p3954 N85-34506
Comparative study of the phase of diurnal anisotropy on quiet and disturbed days on a long term basis up to recent period
[SH-4.5-9] 23 p4037 N85-35027
Atmospheric effects on the underground muon intensity
[SH-6.1-3] 23 p4044 N85-35078
The neutron moderated detector and groundbased cosmic ray modulation studies
[SH-9.1-13] 23 p4052 N85-35128
Air chemistry measurements 2
[AD-A156041] 24 p4117 N85-35520
Maintenance of blocking anticyclones in a general circulation model
[PB85-190866] 24 p4124 N85-35567
ATMOSPHERIC RADIATION
NT AIRGLOW
NT AURORAL ARCS
NT AURORAS
NT DAWN CHORUS
NT GEOCORONAL EMISSIONS
NT IONOSPHERIC NOISE
NT NIGHTGLOW
NT RADIO AURORAS
NT SKY RADIATION
NT TWILIGHT GLOW
NT WHISTLERS
A sphere-scanning radiometer for rapid directional measurements of sky and ground radiance: The PARABOLA field instrument
[NASA-TM-86171] 03 p0363 N85-12329
Investigation of cloud feedback in the GLAS model 05 p0685 N85-14404
Nature of short-period variations of cosmic rays in stratosphere 06 p0823 N85-15224
Simple formula to estimate carbon dioxide gas effect in radiation balance of underlying surface 06 p0823 N85-15226
MAP activities in Hungary 11 p1657 N85-20440
Altitude of auroral scattering observed along auroral electrojets 14 p2339 N85-24465
The keV electrons and 80 keV protons in the vicinity of the high latitude magnetosphere and at the bow shock 14 p2355 N85-24554
Glow of ionospheric F-layer in Line 630 nm determined from photographs taken aboard Salyut-6 orbital station: Interpretation of results 16 p2721 N85-26799
One approach to remote sensing of total ozone content 16 p2725 N85-26822
Analysis of a simulated cloud climatology 16 p3145 N85-29472
Atmospheric X-rays at 11 deg S geomagnetic latitude
[INPE-3539-PRE/755] 19 p3388 N85-31004
Some considerations about the natural atmospheric radioactive aerosol 21 p3647 N85-32662
Determination of altitude of cloud cover top from Meteor satellite data 22 p3734 N85-33150
Propagation and secondary production of low energy antiprotons in the atmosphere
[OG-6.1-3] 22 p3887 N85-34094
Application of imaging to the atmospheric Cherenkov technique
[OG-9.5-4] 23 p4030 N85-34861
Three dimensional calculation of flux of low energy atmospheric neutrinos
[SH-6.1-11] 23 p4050 N85-35116
Nucleon decay and atmospheric neutrinos in the Mont Blanc experiment
[HE-6.2-6] 24 p4211 N85-36142
ATMOSPHERIC REFRACTION
NT RADIO WAVE REFRACTION
A radar sea clutter model for atmospheric ducting conditions
[AD-A145321] 02 p0190 N85-11268
Autonomous navigation of USAF spacecraft 03 p0321 N85-12074
Correction for atmospheric refraction in an airborne, operational environment
[AD-A146552] 06 p0835 N85-15314
Practical application of IREPS (Integrated Refractive Effects Prediction System)
[AD-A146528] 06 p0836 N85-15323
Fluctuations during observations of extraterrestrial sources from outer space through Earth's atmosphere 07 p0953 N85-16040
C2 sub n (optical) studies in the free atmosphere based on rawinsonde data
[AD-A147307] 07 p0997 N85-16332
Statistical/Trend analysis of the marine atmospheric boundary layer model
[AD-A151053] 14 p2374 N85-24673
An assessment of atmospheric refractivity in the northern marginal ice zone
[AD-A152346] 17 p2992 N85-28493
A review of tropospheric refraction effects on Earth-to-satellite systems 18 p3107 N85-29235
Gravity waves from the stratosphere to the mesosphere, part 1.3B 21 p3616 N85-32471
Some recent developments in the interpretation of MST radar returns from clear air (keynote paper), part 2 21 p3618 N85-32480
Mesoscale features and atmospheric refraction conditions of the Arctic marginal ice zone
[AD-A155139] 21 p3636 N85-32584
ATMOSPHERIC SCATTERING
NT TROPOSPHERIC SCATTERING
Characterization of atmospheric conditions along tranamission paths from a remotely piloted vehicle
[AD-A145527] 02 p0232 N85-11511
Mars polar volatiles: Topographic and geologic setting
[NASA-CR-174089] 04 p0581 N85-13708
Relation between atmospheric scattering and backscattering coefficient
[ESA-TT-837] 05 p0677 N85-14350
Multiple scattering effects on transmission through the atmosphere
[AD-A147527] 07 p0941 N85-15969
Middle Atmosphere program. Handbook for MAP. Volume 13: Ground-based techniques
[NASA-CR-174345] 08 p1183 N85-17452
The radiation temperature of a cloud of particles
[FOA-C-30367-E4] 08 p1190 N85-17497
Description of amplitude scintillations on a 11 GHz slant path in terms of forward scattering from turbulent layers
[FI-455-TBR-76] 11 p1625 N85-20232
Prospective investigations with DFVLR radar of possible relevance in the assessment of radio interference due to scattering from precipitations — meteorological radar
[DFVLR-FB 84-42] 12 p1830 N85-21485
Atmospheric handbook: Atmospheric data tables available on computer tape
[PB85-106512] 12 p1891 N85-21867
Radio scintillations observed during atmospheric occultations of Voyager: Internal gravity waves at Titan and magnetic field orientations at Jupiter and Saturn
[NASA-CR-175554] 12 p1961 N85-22327
Mean free path lenght of photons with broken cloud cover 14 p2338 N85-24455
Experimental study of anisotropy of scattering of radar signals by clouds and precipitation 14 p2340 N85-24473
Modeling of radiothermal radiation of rain by Monte-Carlo method 14 p2341 N85-24476
Applicability of vertically homogeneous atmospheric models for remote soundings 14 p2341 N85-24477
Specifics of polarization structure of repeated scattering background in optical laser sounding signals 14 p2342 N85-24485
Test of lidar inversion algorithm sensitivity to atmospheric backscatter and extinction parameters, revision A
[AD-A152082] 16 p2665 N85-27671
Earth observation modeling based on layer scattering matrices
[NLR-MP-84015-U] 17 p2984 N85-28440
Lidar system using polarization discrimination techniques for molecular air pollution monitoring 19 p3306 N85-30504
Meteorological and aeronomical requirements for MST radar networks (keynote paper), part 1 21 p3615 N85-32467
Properties of aerosol particles detected by satellites in coastal regions 21 p3641 N85-32622
Calculation of the diffusion of light by aerosols: Description of the MIELOR software and results obtained
[REPT-80] 24 p4137 N85-35638
Atmospheric interactions detected in both the upper and the lower chambers at Chacaltaya
[HE-3.3-7] 24 p4180 N85-35825
ATMOSPHERIC SHELLS
U ATMOSPHERIC STRATIFICATION
ATMOSPHERIC SOUNDING
Satellite observations 01 p0013 N85-10083
The past, present, and anticipated future contributions of geosynchronous satellites to short range prediction 01 p0076 N85-10503

Use of satellite soundings and imagery for nowcasting and very-short-range forecasting
01 p0076 N85-10504
Remote sensing of atmospheric particulates: Technological innovation and physical limitations in applications to short-range weather prediction
[NSF ATM-82-09684] 01 p0077 N85-10511
Characterization of atmospheric conditions along transmission paths from a remotely piloted vehicle
[AD-A145527] 02 p0232 N85-11511
A case study of a convective outbreak using VAS-derived thermodynamic parameters
[AD-A145560] 02 p0232 N85-11512
Multifrequency lidar based on dye laser
02 p0262 N85-11715
Influence of refraction effects on informativeness of bistatic acoustical atmospheric sounding systems
06 p0825 N85-15237
Actual altitudes of radioacoustic sounding in decimeter wavelength band 06 p0826 N85-15243
Convective scale weather analysis and forecasting
[NASA-CR-174185] 06 p0838 N85-15320
Binary pulse compression techniques for MST radars
08 p1184 N85-17464
The analysis of spaced sensor records by correlation techniques 08 p1184 N85-17465
The MST radar technique 08 p1185 N85-17466
The influence of deep cumulus convection on large-scale flow during AVE/SESAME 1, 10-11 April 1979
09 p1355 N85-18526
Meteorological Sounding System (MSS) standard operating procedures
[AD-A149513] 10 p1519 N85-19578
Space and time variations and turbopause dynamical structure 11 p1663 N85-20483
Middle Atmosphere Program. Handbook for MAP. Volume 12: Coordinated Study of the Behavior of the Middle Atmosphere in Winter (PMP-1) Workshops
[NASA-CR-175475] 11 p1665 N85-20492
Microstructure of Venus cloud layer based on spectrophotometric data from Venera-11 spacecraft
13 p1982 N85-22438
Results of comparison of long-wave radiation fluxes measured by Soviet and Japanese actinometric radiosounds 14 p2333 N85-24427
Experimental results of temperature-wind soundings of the atmosphere by the radio acoustical method
14 p2340 N85-24471
Applicability of vertically homogeneous atmospheric models for remote soundings 14 p2341 N85-24477
Specifics of polarization structure of repeated scattering background in optical laser sounding signals
14 p2342 N85-24485
Results of the Langmuir-probe experiment on board Intercosmos-18 — ionosphere-magnetosphere interaction 14 p2362 N85-24596
Case studies of snow clouds by means of snow crystal sondes 15 p2581 N85-25921
Resonance generation of inertial waves (in the atmosphere) by Doppler-shift of inertio-gravity modes
15 p2590 N85-25968
Mesoscale analysis and modeling group
15 p2596 N85-26001
Review of VAS demonstration
15 p2596 N85-26002
Nowcasting applications of VAS
15 p2597 N85-26003
Recent VAS imaging/sounding research
15 p2597 N85-26004
A simulation experiment on the impact of geostationary temperature retrievals in numerical models
15 p2597 N85-26005
VAS/model impact study 15 p2597 N85-26006
Utilization of satellite data in mesoscale modeling of severe weather 15 p2597 N85-26007
Assessment of VAS soundings in the analysis of a preconvective environment
[NASA-TM-86205] 16 p2625 N85-27427
Improvement of the basic knowledge of the climatology of the vertical ozone layer by enhanced balloon sounding
[BPT-6/84] 18 p3137 N85-29426
Combined catalog of ionosphere vertical soundings data
[PB85-166494] 18 p3138 N85-29430
Small-scale structure of ionospheric F-region
19 p3297 N85-30440
Specifics of laser sounding of atmosphere along horizontal and slightly slanting paths over water surface
19 p3297 N85-30441
Diagnosis of vertical motions from VAS retrievals during a convective outbreak
[NASA-CR-171569] 19 p3316 N85-30554
Atmospheric X-rays at 11 deg S geomagnetic latitude
[INPE-3539-PRE/755] 19 p3366 N85-31004
The role of scientific ballooning for exploration of the magnetosphere
[TRITA-EPP-84-07] 20 p3494 N85-31724
Laser Elektronika-01 for air pollution control lidar
21 p3664 N85-32887
The use of TOMS data in evaluating and improving the total ozone from TOVS measurements
[NOAA-TR-NESDIS-23] 22 p3814 N85-33626

ATMOSPHERIC STRATIFICATION
Layered sloping mesoscale structures and rainbands in atmospheric frontal regions and their relation to symmetric instability 01 p0075 N85-10497
Evaluation of an integrated mixed-layer model for single station prediction in a marine regime
01 p0080 N85-10535
Mixed layers and satellite retrievals
05 p0686 N85-14411
Generation and evolution of diabatic planetary waves in continuously stratified atmosphere with Ekman dissipation 09 p1354 N85-18515
Long nonlinear waves in layers of sudden changes in wind velocity 14 p2340 N85-24470
Coronal structures 14 p2448 N85-25110
Waves in inhomogeneous media — magnetohydrodynamic waves; solar atmosphere
14 p2449 N85-25118
A model for the dynamics of the deep photosphere
14 p2450 N85-25129
Effects of atmospheric stratification on dissipative acoustic and Alfven waves — solar atmosphere
14 p2453 N85-25149
Applications of fuzzy clustering techniques to stratified by tropopause MSU temperature retrievals
18 p3141 N85-29444
Propagation of acoustic pulse in atmospheric waveguide 19 p3297 N85-30443

ATMOSPHERIC TEMPERATURE
NT IONOSPHERIC TEMPERATURE
Use of ground based microwave radiometers for nowcasting 01 p0078 N85-10517
On probability forecasts for temperature
01 p0084 N85-10565
Alpine meteorology: Translations of classic contributions by Wagner, A., Ekhart, E. and Defant, F.
[DE84-014929] 01 p0085 N85-10574
The extremeness of the cold front of December 31, 1978 over the CSR
[REPT-566] 03 p0377 N85-12409
A temperature climatology for New York State
03 p0394 N85-12517
Calibration and use of filter test facility orifice plates
[DE84-016851] 04 p0500 N85-13190
Trends in ozone and temperature structure: Comparison of theory and measurements
[DE84-016201] 04 p0539 N85-13428
NOAA/NASA joint simulation of AMTS and HIRS
05 p0682 N85-14384
Air-sea interaction during cold air outbreaks
05 p0685 N85-14401
Structure of temperature field based on observations of refraction from high meteorological mast
06 p0819 N85-15199
Atmospheric environment for Space Shuttle (STS-41G) launch
[NASA-TM-86486] 07 p0995 N85-18320
The effects of long-periodic forcing in a zero-dimensional climate model 07 p1002 N85-18383
Revised Uniform Summary of Surface Weather Observations (RUSSWO). Alconbury RAF United Kingdom, parts A-F
[AD-A146913] 07 p1004 N85-18384
Revised Uniform Summary of Surface Weather Observations (RUSSWO). McChord AFB, Washington, parts A-F
[AD-A146914] 07 p1005 N85-18385
Revised Uniform Summary of Surface Weather Observations (RUSSWO). Mildenhall RAF, United Kingdom, parts A-F
[AD-A146915] 07 p1005 N85-18386
Revised Uniform Summary of Surface Weather Observations (RUSSWO). Dobbins AFB, Georgia, parts A-F
[AD-A146916] 07 p1005 N85-18387
Revised Uniform Summary of Surface Weather Observations (RUSSWO). Shemya AFB, Alaska, parts A-F
[AD-A146917] 07 p1005 N85-18388
Revised Uniform Summary of Surface Weather Observations (RUSSWO). Pope AFB, Fayetteville, North Carolina, parts A-F
[AD-A146918] 07 p1005 N85-18389
Revised Uniform Summary of Surface Weather Observations (RUSSWO). Sondestrom AB, Greenland, parts A-F
[AD-A146919] 07 p1005 N85-18390
Revised Uniform Summary of Surface Weather Observations (RUSSWO). England AFB, Alexandria, Louisiana, parts A-F
[AD-A146920] 07 p1006 N85-18391
Revised Uniform Summary of Surface Weather Observations (RUSSWO). Parts A-F: Homestead AFB, Florida
[AD-A147203] 07 p1007 N85-18396
Limited surface observations climatic summary (LISOCS). Camp Casey, Tong Du Chon, Korea
[AD-A147204] 07 p1007 N85-18397
Limited surface observations climatic summary (LISOCS). Ansbach AHP, Germany
[AD-A147205] 07 p1007 N85-18398
Revised Uniform Summary of Surface Weather Observations (RUSSWO). O'Hare International Airport, Chicago, parts A-F
[AD-A147206] 07 p1007 N85-18399
Climate at CRREL (Cold Regions Research and Engineering Laboratory) Hanover, New Hampshire
[AD-A148400] 08 p1189 N85-17495
A catalogue of dynamic parameters describing the variability of the middle stratosphere during the northern winters 11 p1656 N85-20435
Middle Atmosphere Program. Handbook for MAP, volume 7
[NASA-CR-175479] 11 p1656 N85-20437
PMP-1 report: The fourth winter of PMP-1, 1981 - 1982: A winter with several interesting features
11 p1657 N85-20441
Workshop on Comparison of Data and Derived Dynamical Quantities During Northern Hemisphere (PMP-1) Winters 11 p1657 N85-20444
The first winter of MAP-dynamics, 1982-1983: A winter with three different warming periods
11 p1657 N85-20446
Variation of derived mesospheric nitric oxide in relation to wind and temperature in winter
11 p1658 N85-20452
Middle atmosphere temperature and dynamics as revealed from D-region observations
11 p1659 N85-20453
Stratwarm effects in the ionospheric D region wind field 11 p1663 N85-20479
Middle Atmosphere Program. Handbook for MAP. Volume 12: Coordinated Study of the Behavior of the Middle Atmosphere in Winter (PMP-1) Workshops
[NASA-CR-175475] 11 p1665 N85-20492
Carbon dioxide and the greenhouse effect
[GPO-39-043] 11 p1677 N85-20569
Method of and apparatus for measuring temperature and pressure — atmospheric sounding
[NASA-CASE-GSC-12558-1] 12 p1856 N85-21639
High time resolution thermospheric temperature and wind studies in the Arctic
[AD-A150114] 12 p1890 N85-21860
On the relationship between maximum surface temperature and various parameters; with reference to objective forecasting
[KNMI-TR-58] 12 p1897 N85-21905
TRAJ: Single station trajectory plot
[PB85-135002] 12 p1897 N85-21911
Monthly and seasonal weather outlook for January 1985, volume 39, number 1
[PB85-148799] 12 p1898 N85-21915
Small component spectral model of annual course of zonal atmospheric circulation 14 p2337 N85-24453
Experimental results of temperature-wind soundings of the atmosphere by the radio acoustical method
14 p2340 N85-24471
Observations of current pulsations of characteristics in atmosphere with period of about 1.5 hours
14 p2341 N85-24480
Fabry-Perot interferometer and skymapping photometer determinations of midlatitude f-region neutral winds and temperatures and airglow enhancement/depletions
[AD-A150730] 14 p2373 N85-24668
Low Temperature Science. Series A: Physical Sciences
[ISSN-0439-3538] 15 p2581 N85-25917
The temperature fluctuation in stable stratification above snow cover 15 p2581 N85-25918
Greenhouse effect in Earth's primordial atmosphere
16 p2807 N85-27310
Regularities in recent changes in surface air temperature and atmospheric precipitation fields
16 p2907 N85-27311
Proper quality of anticorrosion work no matter how bad the atmospheric conditions
[BLL-BISI-TRANS-22080-(6082.06)]
17 p2975 N85-28363
Ozone and temperature trends due to the injection of trace species in the atmosphere
[AERONOMICA-ACTA-A-286-1984]
18 p3132 N85-29309

Objective determination of heat wave patterns
16 p3140 N85-29437
Approximate method for computing wind velocity in atmosphere 19 p3298 N85-30444
Utilization of satellite data and regional scale numerical models in short range weather forecasting
[NASA-CR-175980] 19 p3314 N85-30545
Monthly and seasonal weather outlook for mid-March to mid-April 1985, March 14, 1985, volume 39, no. 6
[PB85-174751] 19 p3317 N85-30585
Influence of moisture and elevated temperature on the fatigue properties of WTS-3 glass fiber blade material — wind turbine blade (WTS-3)
[FFA-TN-1984-58] 20 p3470 N85-31558
Short meridional scale anomalies in the lower stratosphere and upper troposphere
20 p3489 N85-31684
Monthly and seasonal weather outlook for April 1985, March 30, 1985, volume 39, no. 7
[PB85-183804] 22 p3817 N85-33646
Reports from the German Meteorological Service. No. 167: Results of aerological soundings in the model area upper Rhine: Heat release project upper Rhine area, part 3
[ISBN-3-88148-216-4] 23 p3950 N85-34479
Variations of the cosmic ray general component in Antarctica
[SH-4.4-17] 23 p4035 N85-35013
Program for Regional Observing and Forecasting Services (PROFS)
[PB85-186050] 24 p4124 N85-35569
Connection between variations of the atmosphere temperature profile and variations of the meson component intensity
[HE-3.1-12] 24 p4178 N85-35910

ATMOSPHERIC TIDES
The Moon's orbit history and inferences on its origin
04 p0585 N85-13735
Considering zonal wind in semidiurnal tide problem
14 p2335 N85-24440

ATMOSPHERIC TURBULENCE
NT CLEAR AIR TURBULENCE
NT GUSTS
NT LOW LEVEL TURBULENCE
Processing and display of atmospheric phenomenas data
[NASA-CR-171178] 01 p0072 N85-10475
Thermosonde and UHF radar measurements of C2 sub n at Westford, Massachusetts - July 1981
[AD-A145398] 02 p0190 N85-11270
Fluctuations in parameters of light beam along path with reflection in turbulent atmosphere
02 p0263 N85-11722
Stochastic motor blade dynamics
[AD-A146312] 03 p0318 N85-12054
Aircraft accident report Air Canada, Lockheed L-1011, C-FTNJ, near Charleston, South Carolina, November 24, 1983
[PB84-910413] 05 p0594 N85-13790
Variability of short-term eddy-correlation estimates of mass exchange
[DE84-007271] 05 p0677 N85-14349
Air-sea interaction during cold air outbreaks
05 p0695 N85-14401
Field coherence function in layerwise nonhomogeneous troposphere 05 p0714 N85-15012
Lidar measurements of structural characteristics of atmospheric turbulence 06 p0834 N85-15229
Large-eddy simulation. Guidelines for its application to planetary boundary layer research
[AD-A146381] 06 p0870 N85-15651
Determination of the laws governing the changes in the standard deviations of the distribution of pollution based on observations of the atmospheric turbulence spectrum and the possibility of simulating it in the laboratory
[BLL-TR-T6373/BG/MRS14663/84]
08 p1179 N85-17431
Thermosonde C2N measurements in Hawaii–August 1982
[AD-A146016] 08 p1199 N85-17489
Description of amplitude scintillations on a 11 GHz slant path in terms of forward scattering from turbulent layers
[FI-455-TBR-76] 11 p1625 N85-20232
Middle Atmosphere Program. Handbook for MAP, volume 4
[NASA-CR-175462] 11 p1634 N85-20420
Investigation of aeronomic processes on the basis of ionospheric sporadic E 11 p1633 N85-20482
Space and time variations and turbopause dynamical structure 11 p1663 N85-20483
Study of pollutant dispersion in an urban street canyon
[DE85-002648] 11 p1677 N85-20571
Turbulence parameters impacting dispersion in an urban convection boundary layer
[PB85-116036] 11 p1682 N85-20598
Investigations of micro-turbulence in the bottom of the boundary layer
[AD-A149823] 12 p1896 N85-21897
A spatially incoherent and temporally coherent source
[AD-A151261] 13 p2157 N85-23390
Energy structure of atmospheric boundary layer above waves 14 p2335 N85-24442
The effects of atmospheric turbulence on an air-to-air optical communication link
[AD-A151840] 15 p2543 N85-25700
Radar turbulence estimates. Effects of wind shear and reflectivity factor gradients
[AD-A151876] 15 p2599 N85-26023
Mean conditions and turbulence statistics at Vandenberg AFB, California
[AD-A151366] 15 p2665 N85-26449
Response of a wind turbine blade to seismic and turbulent wind excitations 16 p2817 N85-27375
Air flow of the western coastal boundary of South Africa and its influence on the ocean 16 p2831 N85-27459
Analysis of the NASA/MSFC airborne Doppler lidar results from San Gorgonio Pass, California
[NASA-CR-3901] 16 p2832 N85-27463
The problem of atmospheric turbulence
[NASA-CR-175783] 16 p2832 N85-27464
Large-eddy simulation in planetary boundary-layer research 18 p3147 N85-29482
Radio wave scattering and intermittency of turbulence in the atmosphere 19 p3286 N85-30392
Radio wave scattering and turbulence intermittence in atmosphere 19 p3296 N85-30446
Some studies in filtering of atmospheric turbulence
[AD-A154042] 19 p3316 N85-30557
The influence of a turbulent region on the flux of auroral electrons
[KGI-PREPRINT-072] 20 p3494 N85-31723
Comparison of wind and turbulence measurements from Doppler lidar and instrumented aircraft
[NASA-CR-171535] 20 p3495 N85-31729
A survey of wind and turbulence modeling methods
[AD-A154470] 20 p3496 N85-31733
Middle Atmosphere Program. Handbook for MAP. Volume 14: URSI/SCOSTEP Workshop on Technical Aspects of MST Radar
[NASA-CR-176085] 21 p3615 N85-32466
Excerpts from the paper: Research Status and Recommendation from the Alaska Workshop on Gravity Waves and Turbulence in the Middle Atmosphere, part 1.3A 21 p3616 N85-32470
Morphology of the scattering targets: Fresnel and turbulent mechanisms, part 2.1A
21 p3618 N85-32481
Interpretation of radar returns from the mesosphere, part 2.3A 21 p3619 N85-32485
Radar echoes at 2.66 and 40.92 MHz from the mesosphere, part 2.6A 21 p3619 N85-32486
Network ST radar and related measurements at Pennsylvania State University 21 p3629 N85-32544
Notes on atmospheric stability, turbulence, and its measurements
[AD-A155230] 21 p3637 N85-32568
A numerical and analytical investigation of lee cyclogenesis
[AD-A155607] 21 p3638 N85-32594
Size spectra for the source-enhanced coagulation with the turbulent mass transfer 21 p3645 N85-32649
Fog activation and supersaturation
21 p3650 N85-32678
Environmental-physical measurements and determination of atmospheric turbulence with the ASK-16 motor glider 24 p4122 N85-35549

ATMOSPHERIC WINDOWS
Absorption of radiation by water vapor in windows of relative transparency of 95-145 micrometer range
13 p2076 N85-22968
Below-room-temperature water-vapor continuum absorption within the 8- to 10 micron atmospheric transmission window
[TR-0084(4945-09)-1] 13 p2132 N85-23266
Choice of optimum pairs of spectral intervals for IR-range survey of Earth's surface 15 p2486 N85-25344
High-frequency microwave observations of convective precipitation 15 p2596 N85-26000

ATMOSPHERICS
NT DAWN CHORUS
NT HISS
NT WHISTLERS
Tass reports astrophysical, atmospheric studies on Salyut-7 02 p0156 N85-11075
Prospective investigations with DFVLR radar of possible relevance in the assessment of radio interference due to scattering from precipitations — meteorological radar
[DFVLR-FB-84-42] 12 p1830 N85-21485
Comparison of 8 to 12 micrometer and 3 to 5 micrometer CVF transmissometer data with LOWTRAN calculations
[AD-A154218] 19 p3350 N85-30763
A high-speed digital signal processor for atmospheric radar, part 7.3A 21 p3626 N85-32525

ATOLL REEFS
U CORAL REEFS

ATOM CONCENTRATION
Grain boundary structure in NiO
[DE84-016242] 06 p0866 N85-15519
The influence of temperature on the composition density of the transition metals
[BLL-M-35996-(5826.4)] 23 p3915 N85-34262

ATOMIC BATTERIES
U RADIOISOTOPE BATTERIES

ATOMIC BEAMS
Laser cooling and trapping of neutral atoms
[AD-A146048] 03 p0366 N85-12345
Multiphoton ionization of cesium atoms above and below the two-photon ionization threshold
[DE85-000976] 09 p1361 N85-18662
Measurements of integral yields of charged secondary particles using neutral beams simulating a cometary fly-by — Giotto mission 14 p2244 N85-23906
Hydrogen vibrational population distributions and negative ion generation in tandem high-density hydrogen discharges
[DE85-006764] 16 p2863 N85-27657
High efficiency ionizer using a hollow cathode discharge plasma
[DE85-006690] 16 p2868 N85-27693
An examination of the use of wave packets for the calculation of atom diffraction by surface
[AD-A152760] 17 p3029 N85-28735
Cooling high intensity atomic hydrogen beams to liquid helium temperatures
[DE85-012515] 24 p4148 N85-35718

ATOMIC CLOCKS
Clock synchronization by the Symphonie and Laser Synchronization from Stationary Orbit (LASSO) geostationary satellites 14 p2398 N85-24778
Lifetime and reliability of rubidium discharge lamps for use in atomic frequency standards
[AD-A150787] 14 p2417 N85-24915
Recent improvements in the atomic time scales of the National Bureau of Standards 17 p2962 N85-28290
Timing-system design considerations for a mobile astrolabe 17 p2965 N85-28309
Methods for optimal recursive estimation of non-stationary time series, applications to atomic time and frequency metrology 17 p2965 N85-28312
Kalman filtering with a two-state clock model
17 p2965 N85-28314
Kalman filter estimates of the NAVSTAR satellite clock parameters 17 p2965 N85-28315
Physics element design aspects for a tactical rubidium frequency standard 17 p2967 N85-28321
Prospects for atomic frequency standards
18 p3105 N85-29222
On the accuracy of Cs beam primary frequency standards 18 p3105 N85-29224
Methods to recover the narrow Dicke sub-Doppler feature in evacuated wall-coated cells without restrictions on cell size 18 p3105 N85-29225
Diode laser 87Rb optical pumping in an evacuated wall-coated cell 18 p3105 N85-29226
On-orbit frequency stability analysis of the GPS NAVSTAR-1 quartz clock and the NAVSTARs-6 and -8 rubidium clocks 18 p3105 N85-29227
Rubidium and cesium frequency standards status and performance on the GPS program
18 p3106 N85-29228
A low noise synthesizer for autotuning and performance testing of hydrogen masers 18 p3108 N85-29242
Performance data of US Naval Observatory VLG-11 hydrogen masers since September, 1983
18 p3108 N85-29244
Maser and secondary clock in telecommunications networks 18 p3108 N85-29246
The time and frequency comparisons via Loran-C and National TV Network in Yugoslavia
18 p3109 N85-29248
Using GPS and VLBI technology to maintain 14 digit synchronization 18 p3109 N85-29250
Time comparisons using the Global Positioning System (GPS). Method and first results obtained using the DFVLR C/A receiver
[ESA-TT-894] 20 p3460 N85-31490
Elemental technetium as a cosmic-ray clock
[OG-7.1-9] 23 p4013 N85-34870

ATOMIC COLLISIONS
The Berkeley mini-collider
[DE84-014594] 01 p0118 N85-10808
Linac quadrupole connections
[DE84-014694] 01 p0118 N85-10810
Velocity-changing collisional effects in nonlinear atomic spectroscopy and photon echo decay in gases
[NASA-CR-174159] 04 p0559 N85-13559

Energy transfer in atom-molecule scattering experiments in the 1eV region with SF6-Ar, CF4-Ne and Xe-CO2 systems as examples
[REPT-11/1983] 04 p0563 N85-13588
Laboratory studies of atomic collision processes of importance in planetary atmospheres
[NASA-CR-174142] 04 p0589 N85-13758
Scattering experiments on interactions of excited atoms: Differential cross sections of the system Na (3P)+K(4S)
[MPIS-8/1984] 05 p0728 N85-14677
Inclusion of electron transfer in the calculation of K(n)L(v) multiple vacancy production by ion impact
[DE84-016596] 05 p0733 N85-14711
Progress in numerical calculations of ion-atom collisions
[DE84-016598] 06 p0861 N85-15474
Electron capture by multiply charged ions from hydrogen atoms at low energies
[DE84-016560] 06 p0861 N85-15475
Theoretical studies relating to the interaction of radiation with matter: Atomic collision processes occurring in the presence of radiation fields
[AD-A146854] 07 p1040 N85-16602
Theoretical studies of Rydberg atom collisions
[AD-A148558] 08 p1220 N85-17687
ORNL ECR multicharged ion source
[DE85-001283] 09 p1380 N85-18681
Atomic and molecular collision processes
[DE85-001604] 09 p1382 N85-18690
Compilation of atomic data for diagnostics of Tokamak
09 p1390 N85-18744
The coordinated research program at IAEA on atomic collision data for plasma diagnostics
09 p1390 N85-18747
Time dependent Hartree-Fock theory of ion-atom collisions: Application to F(9+) + Ne
[DE85-003063] 11 p1723 N85-20638
Inner shell contribution to multiple ionization in ion-atom collisions
[DE85-003107] 11 p1723 N85-20639
Coincidence techniques to study electron emission in ion-atom collisions
[DE85-003635] 11 p1724 N85-20646
Coincidence studies of secondary electron emission in light ion-atom collisions
[DE85-002373] 11 p1725 N85-20652
Recent advances in forward electron production studies in ion-atom and ion-solid collisions
[DE85-001255] 11 p1726 N85-20653
Atomic processes involving impurities in the plasma edge
[DE85-001277] 11 p1730 N85-20682
Bibliography of atomic and molecular processes, 1983
[DE85-000662] 12 p1929 N85-22121
Mean delta-ray energies in ion molecule collisions
[DE85-005524] 13 p2157 N85-23395
Observation of pure resonance and threshold effects in electron impact experiments in high intensity laser fields
[AD-A150725] 14 p2309 N85-24293
Numerical solution of a first kind Fredholm integral equation arising in electron-atom scattering
[CWI-NM-R8414] 14 p2414 N85-24897
Kinetics and structure of excited states
[AD-A151902] 15 p2648 N85-26334
Atomic physics aspects of a Relativistic Nuclear Collider
[DE85-006867] 15 p2650 N85-26342
Space station as quark matter factory
[DE85-004606] 15 p2685 N85-26585
Ionization coefficient for atomic collisions in meteor trail
16 p2720 N85-26792
Electronically excited alkaline earth oxides: Chemical production and collisional energy transfer processes
[AD-A153172] 17 p3044 N85-28833
Atomic hydrogen maser measurements with wall surfaces of carbon tetrafluoride
18 p3108 N85-29243
Electron-proton collider option for the superconducting super collider
[DE85-010146] 18 p3196 N85-29622
Polarized internal target apparatus
[DE85-011611] 19 p3354 N85-30793
Vibrational energy transfer in benzene-argon collisions
[DE85-009603] 19 p3355 N85-30797
Resonant-transfer-and-excitation for highly charged ions (16 or = Z or = 23) in collisions with helium
[DE85-010550] 19 p3359 N85-30823
A theoretical study of electron capture in ion-ion and ion-atom collisions
[DE85-011154] 19 p3362 N85-30842
Electron-atom collision studies using optically state selected beams
[DE85-010648] 19 p3368 N85-30888
Inelastic Near-Surface Interactions. Proceedings of the Werner Brandt Workshop on Penetration Phenomena
[DE85-010579] 20 p3526 N85-31928
Nuclear data needs for fusion energy development
[DE85-010445] 20 p3536 N85-32000
Multiple vacancy production by high energy heavy ions
[DE85-004428] 24 p4162 N85-35805

ATOMIC ENERGY
U NUCLEAR ENERGY

ATOMIC ENERGY LEVELS
Radiation data and standards for Tokamak diagnostics
09 p1390 N85-18742
Optogalvanic measurement of even parity Rydberg levels in krypton gas
[AD-A152113] 16 p2745 N85-26943
Photophysical studies of triplet exciton processes in pure polymer films
[DE85-006571] 18 p3080 N85-29058

ATOMIC EXCITATIONS
Photoconductivity and emission from the impurity excited states in silicon
[DE84-015563] 04 p0479 N85-13052
Multiphoton ionization of atomic cesium
[DE85-001266] 09 p1380 N85-18678
Laser-induced-fluorescence-spectroscopy of atomic processes under a high magnetic field
09 p1389 N85-18740
Study of light shifts in laser pumped quantum discriminator frequency 11 p1716 N85-20796
Kinetics and structure of excited states
[AD-A151902] 15 p2648 N85-26334
Double photon excitation of high-Rydberg atoms as a long-lived submillimeter detector
[NASA-CASE-NPO-16372-1] 19 p3352 N85-30779
The SLC program
[DE85-011433] 19 p3357 N85-30813
Experimental level-structure determination in odd-odd actinide nuclei
[DE85-010476] 19 p3360 N85-30835
Contributions to the 19th International Cosmic Ray Conference
[NASA-CR-176049] 20 p3543 N85-32044
Energy spectra of elements with 18 less than or equal to Z less than or equal to 28 between 10 and 300 GeV/amu 20 p3543 N85-32045
Elemental abundances of cosmic rays with Z33 as measured on HEAO-3 20 p3543 N85-32046
Abundances of secondary elements among the ultra heavy cosmic rays: Results from HEAO-3
20 p3543 N85-32047
Implications of source abundances of ultraheavy cosmic rays 20 p3543 N85-32049
Study of proton and neutron activation of metal samples in low Earth orbit
[NASA-CR-171596] 21 p3558 N85-32130
Pairing correction of particle-hole state densities for two kinds of fermions
[DE85-011549] 23 p3971 N85-34620

ATOMIC EXPLOSIONS
U NUCLEAR EXPLOSIONS

ATOMIC INTERACTIONS
NT ATOMIC COLLISIONS
Exchange and correlation effects and pair potentials of inter-atomic interaction
[BLL-M-35745-(5828.4)] 02 p0277 N85-11800
Bibliography of atomic and molecular processes, 1983
[DE85-000662] 12 p1929 N85-22121

ATOMIC MASS
U ATOMIC WEIGHTS

ATOMIC PHYSICS
Fundamental molecular physics and chemistry, part 1
[DE84-009127] 04 p0561 N85-13571
Parity and time-reversal non-conversation in atoms
[DE84-016924] 04 p0562 N85-13581
Activities report in nuclear physics
05 p0726 N85-14680
Theoretical issues involving traps for neutral spin-polarized atoms
[AD-A148035] 08 p1220 N85-17682
French activities relevant to middle atmosphere research 11 p1655 N85-20423
Studies of silicon-refractory metal interfaces: Photoemission study of interface formation and compound nucleation
[AD-A150075] 12 p1800 N85-21293
Potential at atomic boundaries in the TF (or TFD) model and equations of states 12 p1820 N85-21419
Laboratory for laser energetics report
[DE85-007235] 15 p2563 N85-25814
Atomic physics aspects of a Relativistic Nuclear Collider
[DE85-006867] 15 p2650 N85-26342
Research activities of the Physics Division
[DE85-006958] 19 p3357 N85-30811
Atomic, Molecular and Solid-State Theory, and Computational Quantum Chemistry, part 1
[DE85-009401] 20 p3526 N85-31929
Activities report in nuclear physics and particle acceleration 20 p3532 N85-31977
Activities of the Physics Division
[DE85-000784] 21 p3702 N85-33002
The 2nd European Conference on Atomic and Molecular Physics
[AD-A155863] 24 p4148 N85-35715

ATOMIC RECOMBINATION
NT OXYGEN RECOMBINATION
Laser-induced-fluorescence-spectroscopy of atomic processes under a high magnetic field
09 p1389 N85-18740
Molecular orbital studies in oxidation: Sulfide formation and metal-metal oxide adhesion
[NASA-CR-176070] 21 p3565 N85-32174

ATOMIC SPECTRA
Velocity-changing collisional effects in nonlinear atomic spectroscopy and photon echo decay in gases
[NASA-CR-174159] 04 p0559 N85-13559
Spectra of highly-ionized atoms for the diagnostics of the new generation of Tokamaks
09 p1388 N85-18730
Impact of atomic data on Tokamak modeling
09 p1390 N85-18743
Sample introduction methods for improving the particle detection capability of the spectrometric oil analysis program
[AD-A150139] 13 p2158 N85-23399
Kinetics and structure of excited states
[AD-A151902] 15 p2648 N85-26334
Optogalvanic measurement of even parity Rydberg levels in krypton gas
[AD-A152113] 16 p2745 N85-26943

ATOMIC STRUCTURE
Relationships between electronic structure and stability of metallic glasses
[AD-A145141] 01 p0028 N85-10176
Influence of 5f electrons on structures and bonding in the actinide-hydrogen intermetallics
[DE84-013893] 01 p0118 N85-10807
Relationships between electronic structure and stability of metallic glasses
[AD-A145506] 02 p0287 N85-11874
Electronic structure and lattice dynamics of solid state substances from gamma nuclear resonance absorption and angular correlation measurements
03 p0427 N85-12728
Paramagnetic impurity effects in NMR determinations of hydrogen diffusion and electronic structure in metal hydrides. Cerium in YH-2 and LaH-2.25
[DE84-014127] 04 p0472 N85-13005
Surface structure determination with ARPEFS
[DE84-016904] 04 p0571 N85-13644
The atomic structure of Si-SiO2 interfaces suggesting a ledge mechanism of silicon oxidation
[DE84-016057] 05 p0731 N85-14703
Theoretical methods for the study of transition metals in crystals
[DE84-015606] 05 p0732 N85-14709
Electronic and magnetic properties of transition-metal surfaces, interfaces and overlayers
[DE84-016886] 05 p0733 N85-14713
Electronic bandstructure of an incommensurate crystal
[DE84-016891] 05 p0733 N85-14714
Structure of adsorbed monolayers. The surface chemical bond
[DE84-016879] 06 p0861 N85-15471
Electron spectrometry experiments with the use of synchrotron radiation
[DE85-001286] 07 p1041 N85-16610
Electronic structure and properties of magnetic defects in Co(1+x)Al(1-x) and Fe(1+x)Al(1-x) alloys
[NASA-TM-77498] 07 p1047 N85-16648
Replacement of Fe-3+ ions in nickel ferrites by nonmagnetic Al-3+ and Sc-3+ ions
[BLL-WH-594-(9091.9F)] 08 p1125 N85-17090
Theoretical research program to study transition metal trimers and embedded clusters
[NASA-CR-174296] 08 p1125 N85-17093
Electronic structure, chemical bonding, and superconductivity of silver films on germanium
[AD-A147720] 08 p1128 N85-17112
Silicon superlattices. 2: Si-Ge heterostructures and MOS systems
[NASA-CR-174287] 08 p1224 N85-17711
Electronic structure of semiconductor interfaces
[AD-A147683] 08 p1225 N85-17715
Electronic structure, chemical bonding, and electron conductivity of thin-film transition-metal silicides
[AD-A147721] 08 p1226 N85-17718
Quantum Monte Carlo for molecules
[AD-A148159] 08 p1227 N85-17727

Electronic structure of liquid metal alloys
[DE85-000904] 09 p1295 N85-18136
Metal atom diffusion in amorphous silica and at the silica surface
[DE84-017351] 09 p1380 N85-18674
Theoretical studies of atomic transition
[DE85-001325] 09 p1381 N85-18687
Compilation of atomic data for diagnostics of Tokamak
09 p1390 N85-18744
Comparative studies on the electronic structures of W2(O2CH)4 and W2(O2CH)4-(CH3)2 by the relativistic X Alpha-SW method: A d3-d3 metal dimer with a quadruple metal-metal bond?
[AD-A148814] 09 p1397 N85-18793
Microscopic determinations of lattice and electronic structures of solids
[DE84-017323] 09 p1399 N85-18806
Surface physics and crystallography
[DE85-003128] 11 p1735 N85-20910
Electronic structure of silicon superlattices
[NASA-CR-175536] 11 p1736 N85-20916
Structural, morphological and optical characteristics of KGd(WO4)2 crystals 14 p2280 N85-24126
Theory and calculations of the electronic structure of solids having directional bonding
[AD-A151082] 14 p2428 N85-24971
Test of the electronic structure of Fe(100) by absorbed current spectroscopy
[DE85-004942] 15 p2661 N85-26422
Experimental studies of the electronic structure of 1-2 and 1-3 intermetallic compounds
[DE85-006978] 15 p2662 N85-26432
Tilt grain boundaries in NiO
[DE85-006839] 16 p2751 N85-26978
Clusters of transition metal atoms
[AD-A153126] 17 p3030 N85-28740
Age hardening and atomic structure of an aluminum-6 at. % silver alloy
[DE85-009677] 18 p3077 N85-29031
Electronic structure calculations for low coverage adlayers
[DE85-007733] 18 p3179 N85-29709
Theoretical studies on the structures of insulating and metallic glasses
[DE85-010022] 18 p3194 N85-29814
VUV synchrotron light as a technique for studying the interface quality and properties of thin overlayers
[DE85-009822] 19 p3262 N85-30227
Many-body processes in atomic and molecular physics
[DE85-009750] 19 p3354 N85-30791
Proceedings of the 1984 Workshop on High-Energy Excitations in Condensed Matter, volume 2
[DE85-007395] 19 p3357 N85-30809
Theoretical investigation of material characteristics of semiconductor superlattices
[AD-A154126] 19 p3375 N85-30938
New adatom model for Si(11) 7X7 and Si(111)Ge 5X5 reconstructed surfaces 20 p3480 N85-31625
Ab initio calculations of materials properties
[DE85-011167] 20 p3531 N85-31964
Experimental studies of the geometric and electronic structure of chemisorption bonding
[PB85-192250] 22 p3747 N85-33228
Standard value for the radiation length in air
[HE-4.4-4] 24 p4193 N85-36013

ATOMIC THEORY
NT HEISENBERG THEORY

ATOMIC WEIGHTS
The inner granulometric density of the tracks in nuclear emulsions and its application to determine the chemical spectrum of primary cosmic ray nuclidi
[OG-4.3-9] 22 p3879 N85-34034

ATOMIZATION
U ATOMIZING

ATOMIZERS
Measurement of drop-size distributions with the aid of a scattered light particle size counting analyser
[BLL-TRANS-WH-620-(8091.9F)]
09 p1317 N85-18278

ATOMIZING
NT GAS ATOMIZATION
NT LIQUID ATOMIZATION
Influence of temperature on wear resistance of detonation coatings of alloy powders
10 p1447 N85-19116
Study of phase composition of Al-B plasma coatings
11 p1598 N85-20050
Liquid fuel spray processes in high-pressure gas flow
[NASA-TM-86944] 12 p1844 N85-21570
Atomization data requirements for rocket combustor modeling 13 p2003 N85-22555
Specifics of fine structure of pressed aluminum alloys manufactured by plasma atomization
19 p3242 N85-30102
Influence of type of processing of AK4 alloy on its surface state and strength of bonding of plasma coatings
19 p3242 N85-30103
Stable generation of highly monodisperse aerosols
21 p3642 N85-32628
Influence of technology of atomization of naturally alloyed iron on grain-size characteristics of powder material
[BLL-M-35810-(5828.4)] 23 p3914 N85-34257

ATOMS
NT HELIUM ATOMS
NT HOT ATOMS
NT HYDROGEN ATOMS
NT METASTABLE ATOMS
NT NEUTRAL ATOMS
NT OXYGEN ATOMS
Diagnostics of ionization in air produced by infrared radiation from A pulse CO2 laser
[AD-A145376] 02 p0201 N85-11342
Dispersion forces of solids under stress. Chemisorption under stress
[AD-A146171] 03 p0373 N85-12380
Deceleration, cooling, and trapping of atoms
[AD-A146234] 03 p0418 N85-12672
Periodic cluster simulation of a disordered impurity system
[INPE-3453-PRE/705] 16 p2858 N85-27628
Studies of collisional and nonlinear radiative process for development of coherent UV and XUV sources
[AD-A152001] 16 p2865 N85-27670
Atom location by electron channeling analysis
[DE85-007549] 16 p2872 N85-27716
The temperature dependence of diffracted beam intensities in atom-surface scattering
[AD-A152762] 17 p3029 N85-28736
Clusters of transition metal atoms
[AD-A153126] 17 p3030 N85-28740
The effect of ion-bombardment-induced atomic mixing on depth-profiling of interfaces
[AD-A153199] 17 p3044 N85-28834
Cavityless optical bistability in systems of two-level atoms 18 p3186 N85-29764
Alkali atom - SbCl(5) reactions: Blue-green chemiluminescence from an inverted population in SbCl
[AD-A154371] 19 p3276 N85-30315
Production of gallium atoms by excimer laser photolysis of trimethyl gallium
[DE85-010742] 19 p3278 N85-30331
Double photon excitation of high-Rydberg atoms as a long-lived submillimeter detector
[NASA-CASE-NPO-16372-1] 19 p3352 N85-30779
Spontaneous emission by two atoms with different resonance frequencies near a metal surface
[AD-A154115] 19 p3353 N85-30781
Many-body processes in atomic and molecular physics
[DE85-009750] 19 p3354 N85-30791
Resonant-transfer-and-excitation for highly charged ions (16 or = Z or = 23) in collisions with helium
[DE85-010550] 19 p3359 N85-30823
New adatom model for Si(11) 7X7 and Si(111)Ge 5X5 reconstructed surfaces 20 p3480 N85-31625
Overlap integrals for atom-metal surface interactions
[AD-A155038] 21 p3702 N85-32998
High-resolution spectroscopy and dynamics of multiphoton processes in atoms and molecules
[AD-A155862] 24 p4147 N85-35714
Exit channels of autoionization resonances in atoms
[DE85-012299] 24 p4149 N85-35726

ATP
U ADENOSINE TRIPHOSPHATE

ATROPHY
Alterations in skeletal muscle with disuse atrophy
[NASA-CR-174195] 08 p0843 N85-15349
Effect of disuse on sarcoplasmic reticulum in fast and slow skeletal muscle
[NASA-CR-174337] 08 p1191 N85-17506
Acid phosphatase and protease activities in immobilized rat skeletal muscles
[NASA-CR-174340] 08 p1192 N85-17509
A comparison of rat myosin from fast and slow skeletal muscle and the effect of disuse
[NASA-CR-174339] 08 p1192 N85-17510
Nutrition in space flight: Some thoughts
14 p2394 N85-24743
Constant fiber number during skeletal muscle atrophy and modified arachidonate metabolism during hypertrophy 15 p2609 N85-26078
Effects of muscle atrophy on motor control: Cage size effects 15 p2609 N85-26080
Responses of skeletal muscle to unloading, a review
[NASA-CR-176177] 24 p4126 N85-35594

ATROPINE
An atropinized heat-stressed rat model: Dose response effects and pharmacokinetics
[AD-A146851] 07 p1011 N85-16423

ATS
Lack of communication 15 p2686 N85-26591

ATTACHMENT
Advanced life analysis methods. Volume 1: Cracking data survey and NDI (nondestructive inspection) assessment for attachment lugs
[AD-A150419] 13 p2103 N85-23108
Advanced life analysis methods. Volume 2: Crack growth analysis methods for attachment lugs
[AD-A150420] 13 p2103 N85-23109

ATTACK AIRCRAFT
NT A-7 AIRCRAFT
NT A-10 AIRCRAFT
NT B-1 AIRCRAFT
NT B-70 AIRCRAFT
NT BOMBER AIRCRAFT
NT CL-41 AIRCRAFT
NT DH 115 AIRCRAFT
NT F-8 AIRCRAFT
NT F-14 AIRCRAFT
NT F-15 AIRCRAFT
NT F-16 AIRCRAFT
NT F-17 AIRCRAFT
NT F-18 AIRCRAFT
NT F-27 AIRCRAFT
NT F-104 AIRCRAFT
NT F-106 AIRCRAFT
NT F-111 AIRCRAFT
NT FIGHTER AIRCRAFT
NT JAGUAR AIRCRAFT
NT JET PROVOST AIRCRAFT
NT MIG AIRCRAFT
NT MIRAGE AIRCRAFT
NT MIRAGE 3 AIRCRAFT
A-5 supersonic attack aircraft described — Qiang-5 aircraft 06 p0747 N85-14792
Details of export A-5 close-support aircraft given — Qiang-5 aircraft 06 p0748 N85-14793
The development of a dynamic model of a generalised combat aircraft with forward wings for the identification of stability and control characteristics
[CAR-84-33] 09 p1280 N85-18050
Details of export A-5 close-support aircraft given
10 p1424 N85-18983
Cost-estimating relationships for tactical combat aircraft
[AD-A151575] 15 p2471 N85-25255
ESP (External-Stores Program): A pilot computer program for determining flutter-critical external-store configurations. Volume 2: Final report on program enhancement and delivery
[AD-A152269] 16 p2711 N85-26726

ATTACKING (ASSAULTING)
NyKINM, a further development of KINM 22 — simulation of a robot attack on an aircraft
[FOA-C-20559-D8(E3)] 07 p0903 N85-15720
Next generation gunship
[AD-A156361] 24 p4065 N85-35193

ATTENTION
Inhibition of return: Neural basis and function
[AD-A145242] 01 p0096 N85-10652
Visual selective attention
[AD-A146220] 03 p0401 N85-12558
Visual attention to radar displays
05 p0704 N85-14514
Selecting one among the many: A simple network implementing shifts in selective visual attention
[AD-A148989] 10 p1530 N85-19644

ATTENUATION
NT ACOUSTIC ATTENUATION
NT ATMOSPHERIC ATTENUATION
NT MANDELSTAM REPRESENTATION
NT MICROWAVE ATTENUATION
NT RADAR ATTENUATION
NT RADIO ATTENUATION
NT SHOCK WAVE ATTENUATION
NT SIDELOBE REDUCTION
NT WAVE ATTENUATION
Transient attenuation in optical fibers
[DE84-016487] 05 p0729 N85-14687
The impact of propagation effects on the design of high capacity digital microwave links in the 18 GHz frequency band 10 p1470 N85-19278
Investigation of bimodal paramagnetic filter
13 p2063 N85-23007
Influence scattering and Q in the lithosphere
[AD-A150939] 14 p2293 N85-24213
Frequency selective signals-to-noise enhancer/limiter apparatus
[AD-D011583] 15 p2548 N85-25724
Multiple scattering of electromagnetic waves in discrete random media
[AD-A151766] 16 p2772 N85-27112
LIGHT: A ray tracing code to simulate light collection in scintillation spectrometers and light pipes
[DE85-007213] 16 p2865 N85-27673

Experimental and analytic characterization of nonlinear seismic attenuation
[AD-A154760] 21 p3631 N85-32556
Normal modes in an overmoded circular waveguide coated with lossy material
[NASA-CR-176186] 24 p4085 N85-35320
Core structure of EAS in 10(15) to 10(17) eV
24 p4189 N85-35989

ATTENUATION COEFFICIENTS
X-ray absorption in perfect crystals
[DE84-016034] 05 p0732 N85-14708
Recommendation on use of series K157UL1 microcircuits 13 p2071 N85-22936
Change of electrical characteristics of radio-frequency cables under thermal effect 13 p2081 N85-22999
Fine structure of vertical distribution of light attenuation index of sea water 13 p2109 N85-23140
Measurement of the attenuation length of an acrylic scintillator --- magnetic monopoles
[NOTA-INTERNA-828] 18 p3097 N85-29175
Precision microwave attenuation measurement by time interval ratio
[RSRE-85005] 22 p3755 N85-33260

ATTENUATORS
NT POTENTIOMETERS (RESISTORS)
NT RESISTORS
NT THERMISTORS
EMC enhanced constant Z modulator
[AD-A147715] 08 p1157 N85-17297
Design of low loss helix circuits for interference fitted and brazed circuits
[NASA-CR-168313] 10 p1478 N85-19328

ATTITUDE (INCLINATION)
NT PITCH (INCLINATION)
NT ROLL
NT SATELLITE ORIENTATION
NT YAW
Theory underlying the peripheral vision horizon device
01 p0008 N85-10048
Stimulus factors in motion perception and spatial orientation 01 p0008 N85-10049
Workload demand and CNS depressant stressor effects on spatial orientation information processing
[AD-A145211] 01 p0098 N85-10651
Maximum normalized rate as a flying qualities parameter 05 p0702 N85-14503
OMEGA: An optronic device to measure the incidence angle of a projectile
[ISL-CO-207/83] 14 p2306 N85-24274
A method of estimating aircraft attitude from fly by wire flight control system data 16 p2697 N85-26653
Space optics
[CNES-84/105/T/CT/DRT/TIT/10]
20 p3533 N85-31985
Typological characteristics of hemodynamic states of healthy subjects in orthostatic position
22 p3821 N85-33673
Cosmic ray intensity and the tilt of the neutral sheet
[SH-4.2-8] 23 p4007 N85-34846

ATTITUDE CONTROL
NT DIRECTIONAL CONTROL
NT LATERAL CONTROL
NT LONGITUDINAL CONTROL
NT SATELLITE ATTITUDE CONTROL
NT THRUST VECTOR CONTROL
Effects of foveal information processing
01 p0009 N85-10052
Peripheral vision horizon display on the single seat night attack A-10 01 p0009 N85-10053
Modular design attitude control system
[NASA-CR-171182] 01 p0016 N85-10098
Autonomous Attitude Determination System (AADS). Volume 1: System description
[NASA-TM-87365] 02 p0240 N85-11559
Analysis and simulation of an inertial system (Strapdown) for auxiliary attitude determination by adaptive drift estimation
[INPE-3257-TDL/177] 04 p0454 N85-12882
Propellant tank resupply system
[AD-D011288] 05 p0603 N85-13848
An Assessment of Integrated Flywheel System Technology
[NASA-CP-2346] 05 p0604 N85-13850
A summary of the 1983 Integrated Flywheel Technology Workshop 05 p0605 N85-13855
Comparative energy storage assessment item
05 p0605 N85-13858
Inertial storage for satellites 05 p0605 N85-13859
Perspectives on energy storage wheels for space station application 05 p0605 N85-13860
Description of a laboratory model Annular Momentum Control Device (AMCD) 05 p0606 N85-13863
Hemispherical antenna pointing mechanism --- satellite antennas 05 p0627 N85-14021
Infrared horizon sensor modeling for attitude determination and control: Analysis and mission experience
[NASA-TM-86181] 10 p1429 N85-19016
Emitted vibration measurement device and method
[NASA-CASE-MFS-25981-1] 11 p1635 N85-20299
Summary presentation of the Constellations Panel
11 p1644 N85-20359
Report of the Constellations Panel
11 p1645 N85-20368
Space station systems technology study (add-on task). Volume 1: Executive summary
[NASA-CR-171415] 13 p1986 N85-22459
Large antenna control methods: Current status and future trends 14 p2234 N85-23645
Space station systems technology study (add-on task). Volume 2: Trade study and technology selection
[NASA-CR-171416] 15 p2475 N85-25279
Programming for Pioneer 12 15 p2688 N85-26606
Controller requirements for uncoupled aircraft motion, volume 2
[AD-A153300] 17 p2900 N85-27879
Operating characteristics of a 0.87 kW-hr flywheel energy storage module
[NASA-TM-87038] 17 p2974 N85-28371
Rationale for an experimental test for flexible space structure attitude control 20 p3411 N85-31167
Numerical and experimental evaluation for single-axis control of an LSS laboratory model
20 p3411 N85-31168
Attitude control tradeoff study between the use of a flexible beam and a tether configuration for the connection of two bodies in orbit 20 p3412 N85-31174
A control concept for large flexible spacecraft using order reduction techniques 20 p3415 N85-31193
Deployable-erectable trade study for space station truss structures
[NASA-TM-87573] 22 p3740 N85-33181
Computer simulation of a cruise missile using brushless dc motor fin control
[AD-A155935] 24 p4089 N85-35349

ATTITUDE GYROS
NT GYRO HORIZONS
Extracts from the test plan for in-flight evaluation of the NT-33A peripheral vision display
01 p0009 N85-10055
Some notes on a tangent plane oriented heading reference --- stabilized platforms
[RAE-TM-IEE-144] 02 p0136 N85-10928
Selection of optimum corrections torque for vertical gyro according to special-purpose program
14 p2273 N85-24082
Optimum parameters of aerogyroscopic satellite orientation system 16 p2718 N85-26782

ATTITUDE INDICATORS
NT GYRO HORIZONS
Peripheral Vision Horizon Display (PVHD)
[NASA-CP-2306] 01 p0008 N85-10044
Effects of foveal information processing
01 p0009 N85-10052
Peripheral vision horizon display testing in RF-4C aircraft 01 p0009 N85-10054
Extracts from the test plan for in-flight evaluation of the NT-33A peripheral vision display
01 p0009 N85-10055
Peripheral vision displays: The future
01 p0009 N85-10058
A production peripheral vision display system
01 p0010 N85-10059
A preliminary flight evaluation of the peripheral vision display using the NT-33A aircraft
[AD-A145123] 01 p0010 N85-10060
Wind tunnel calibration of a hemispherical head angle of attack and angle of sideslip indicator
[FFA-TN-1984-11] 02 p0135 N85-10923
Data analysis techniques for vehicle attitudinal, positional and experimental measurements
[AD-A147752] 08 p1186 N85-17484
Infrared horizon sensor modeling for attitude determination and control: Analysis and mission experience
[NASA-TM-86181] 10 p1429 N85-19016
Wide-field-of-view, helmet-mounted infinity display system development
[AD-A149641] 12 p1777 N85-21159
Attitude data consistence check of rocket payloads
[BMFT-FB-W-84-049] 12 p1790 N85-21239
Studies of the solar mesosphere explorer: Dynamics and horizon sensor performance. Part A: Spin axis precession and atmospheric drag. Part B: Clouds
[NASA-CR-175308] 24 p4089 N85-35213

ATTITUDE STABILITY
NT DIRECTIONAL STABILITY
NT GYROSCOPIC STABILITY
NT LATERAL STABILITY
NT LONGITUDINAL STABILITY
Some aspects of attitude stability of tethered space stations 11 p1648 N85-20069
The design and development of a constant-speed solar array drive 22 p3796 N85-33519

ATTRITION (MATERIALS)
U COMMINUTION

AUDIO EQUIPMENT
NT EARPHONES
NT LOUDSPEAKERS
NT MICROPHONES
Perceptibility of nonlinear distortions in power amplifier
06 p0789 N85-15041
A miniature urethane molded acoustic transducer
[AD-A146459] 06 p0804 N85-15114
Tubes and transistors in audio amplifiers
12 p1837 N85-21532
Robust detection and classification of regional seismic signals using a two mode/two stage cascaded adaptive arma (CAARMA) model
[AD-A154710] 21 p3630 N85-32554

AUDIO FREQUENCIES
Current and current shear effects in the parabolic approximation for underwater sound channels
[AD-A147833] 07 p1039 N85-16587
Application of K176-series microcircuits
13 p2077 N85-22973
Auditory fatigue caused by exposure to different frequency sounds presented at equivalent intensity
[ISL-R-101/84] 20 p3525 N85-31923

AUDIO SIGNALS
Specifics of dynamics of brain biopotentials under the influence of complex audible communicative signals
07 p1014 N85-16440
Processing speech for analysis using optical Fourier techniques
[AD-A151898] 15 p2544 N85-25704
A method and apparatus for operating on companded PCM voice data
[NASA-CASE-KSC-11285-1] 16 p3089 N85-29120
An approach to digital level compression using the zero-crossing points of programme signals
[NHK-LABS-NOTE-308] 18 p3090 N85-29123

AUDIO VISUAL EQUIPMENT
U TRAINING DEVICES
U VISUAL AIDS

AUDIOLOGY
Auditory impairment and the onset of disability and handicap in noise-induced hearing loss
[ISVR-TR-126] 20 p3507 N85-31801

AUDIOMETRY
Second generation USAFSAM (United States Air Force School of Aerospace Medicine) microprocessor audiometer
[AD-A149938] 12 p1905 N85-21983
The audiomat: An automatic audiometer for use in occupational audiometry
[DRIC-T-7138] 13 p2142 N85-23294
Auditory impairment and the onset of disability and handicap in noise-induced hearing loss
[ISVR-TR-126] 20 p3507 N85-31801
Auditory fatigue caused by exposure to different frequency sounds presented at equivalent intensity
[ISL-R-101/84] 20 p3525 N85-31923

AUDITORY DEFECTS
Auditory impairment and the onset of disability and handicap in noise-induced hearing loss
[ISVR-TR-126] 20 p3507 N85-31801

AUDITORY FATIGUE
Comparative assessment of different treatment modalities in miners with vibration- and noise-induced disease 10 p1524 N85-19810
Auditory fatigue caused by exposure to different frequency sounds presented at equivalent intensity
[ISL R-101/84] 20 p3525 N85-31923

AUDITORY PERCEPTION
Evidence for multiple areas in the human auditory cortex
[AD-A146086] 03 p0401 N85-12555
Inner ear characteristics during 7 day antiorthostatic bedrest (6 deg head down tilt) 05 p0695 N85-14470
Human engineer's guide to auditory displays. Volume 2: Elements of signal reception and resolution affecting auditory displays
[AD-A146513] 06 p0859 N85-15482
Human engineer's guide to auditory displays. Volume 1: Elements of perception and memory affecting auditory displays
[AD-A146801] 06 p0860 N85-15484
Specifics of dynamics of brain biopotentials under the influence of complex audible communicative signals
07 p1014 N85-16440
Detection of low frequency impulsive noise from large wind turbine generators
[NASA-CR-172511] 07 p1038 N85-16588

Neurocognitive pattern analysis of an auditory and visual numeric motor control task. Part 1: Development of methods
[AD-A148809] 09 p1364 N85-18578
Quantitative measurement of human auditory acuity
10 p1524 N85-19614
The audiomat: An automatic audiometer for use in occupational audiometry
[DRIC-T-7136] 13 p2142 N85-23294
Dissociation of autonomic and sensory vestibular reactions 23 p3953 N85-34501

AUDITORY SIGNALS
Auditory information systems in military aircraft: Current configurations versus the state of the art
[AD-A145469] 02 p0275 N85-11794
Human engineer's guide to auditory displays. Volume 2: Elements of signal reception and resolution affecting auditory displays
[AD-A146513] 06 p0859 N85-15462
Human engineer's guide to auditory displays. Volume 1: Elements of perception and memory affecting auditory displays
[AD-A146601] 06 p0860 N85-15464
High-frequency acoustic variability in the arctic
[AD-A150550] 13 p2155 N85-23383
An overview of stochastic signal modeling
[AD-A152144] 16 p2855 N85-27605
Rotor blade test apparatus
[AD-D011725] 23 p3934 N85-34381

AUDITORY STIMULI
Evidence for multiple areas in the human auditory cortex
[AD-A146086] 03 p0401 N85-12555
The construction of auditive tests of attention and spatial orientation and their factorial structure
[DFVLR-FB-84-21] 05 p0699 N85-14485

AUDITORY TASKS
Communications skills for CRM training
09 p1276 N85-18017
Neurocognitive pattern analysis of an auditory and visual numeric motor control task. Part 1: Development of methods
[AD-A148809] 09 p1364 N85-18578

AUGER EFFECT
Aspects of silicon bulk lifetimes
20 p3479 N85-31617
Recombination phenomena in high efficiency silicon solar cells 20 p3479 N85-31618
Inter-zone auger recombination in GaSb laser structures 21 p3682 N85-32875
Multiple inner shell vacancies in laser-irradiated Au plasma 23 p3961 N85-34687

AUGER SPECTROSCOPY
Stress-driven solute enrichment of crack-tips during low ductility intergranular fracture of low-alloy steel
[AERE-R-11120] 03 p0333 N85-12150
Oxygen diffusion from anodic surface oxide films on titanium subhydride studies by auger electron spectroscopy and electron energy loss spectroscopy
[DE84-016942] 04 p0572 N85-13648
Photoemission, vibrational and stimulated desorption studies of metal-semiconductor interfaces and of chemisorbed atoms and molecules
[AD-A147709] 08 p1225 N85-17717
Fundamental study of catalysts using laser Raman, infrared, auger electron spectroscopy and low energy electron diffraction
[DE85-001813] 11 p1595 N85-20033
Surface physics instrumentation
[AD-A149304] 11 p1728 N85-20869
Studies of silicon-refractory metal interfaces: Photoemission study of interface formation and compound nucleation
[AD-A150075] 12 p1800 N85-21293
HREELS and Auger studies of conducting polymers
[DE85-004541] 13 p2038 N85-22764
Threshold double photoionization of argon with synchrotron radiation
[AD-A150615] 13 p2157 N85-23389
Bonding information from Auger spectroscopy
[AD-A150864] 14 p2251 N85-23948
Chemical and localization effects in Auger lineshapes of transition metal compounds
[AD-A150865] 14 p2251 N85-23949
Charge transfer, polarization and relaxation effects in the Auger lineshapes of Si
[AD-A150936] 14 p2252 N85-23954
Self-sustaining coatings for fusion applications: Copper lithium alloys
[DE85-009740] 16 p3190 N85-29783
Study of solute segregation at interfaces using Auger electron spectroscopy
[DE85-005709] 20 p3423 N85-31247
The effect of metal overlayers of thermionic dispenser cathodes
[AD-A154795] 21 p3701 N85-32995
Size and shape dependence of CO adsorption sites on sapphire supported Fe microcrystals
[NASA-CR-176171] 24 p4160 N85-35794

AUGMENTATION
NT STABILITY AUGMENTATION
NT THRUST AUGMENTATION
Design of a digital ride quality augmentation system for commuter aircraft
[NASA-CR-172419] 01 p0006 N85-10037
Development and flight evaluation of an augmented stability active controls concept: Executive summary
[NASA-CR-166009] 02 p0149 N85-11006
Helicopter human factors programs and plans
06 p0751 N85-14808
An update of the Canada/USA augmentor-wing project 08 p1070 N85-16781
The enhancement of concurrent processing through functional programming languages
[AD-A150771] 14 p2404 N85-24822
A modern control design methodology with application to the CH-47 helicopter
[AD-A151948] 16 p2710 N85-28723
Visual and part-task manipulations for teaching simulated carrier landings
[AD-A153622] 18 p3154 N85-29529

AURIGA CONSTELLATION
Eclipse observations of Epsilon Aurigae
11 p1755 N85-21037
UV observations of epsilon aurigae during ingress and totality 11 p1755 N85-21038

AURORAL ACTIVITY
U AURORAS

AURORAL ARCS
Circuit transients due to negative bias arcs on a high-voltage solar array in low Earth orbit
[NASA-TP-2407] 06 p0760 N85-14858
Distribution of electric field near westward propagating bend in aurora 06 p0823 N85-15222
Sun-aligned polar cap auroral arcs
[AD-A148052] 08 p1185 N85-17472
One-dimensional model of auroral magnetic force with longitudinal current and cyclotron heating of ions
13 p1960 N85-22424
Characteristics of the electrodynamics of auroral arcs as inferred from rocket and ground-base observations during IMS 14 p2363 N85-24601
Field-aligned currents observed in the vicinity of a moving auroral arc 14 p2363 N85-24603
Two-dimensional quasineutral description of particles and fields above discrete auroral arcs
[NASA-CR-176170] 24 p4116 N85-35517

AURORAL ELECTROJETS
A model for the propagation of the westward traveling surge
[TRITA-EPP-84-03] 03 p0393 N85-12515
Distribution of electric field near westward propagating bend in aurora 06 p0823 N85-15222
Polar orbit electrostatic charging of objects in shuttle wake 13 p1992 N85-22487
Altitude of auroral scattering observed along auroral electrojets 14 p2339 N85-24465
Ground-based and near-Earth observations during the IMS 14 p2359 N85-24575
Auroral X-rays and equatorial electrons in the morning sector — substorm 14 p2361 N85-24590
The GEOS-2 E-field behavior during dynamic auroral development near the satellite footpoint
14 p2362 N85-24598
Three-dimensional current systems and electric fields during active aurora 14 p2362 N85-24599
The relationship between auroral electrojet and visual aurora 14 p2363 N85-24602
Field-aligned currents observed in the vicinity of a moving auroral arc 14 p2363 N85-24603
On the dynamics of the westward traveling surge
14 p2364 N85-24607
Ground magnetic observations of high-latitude Pi2 pulsations: Scandinavian magnetometer array results
14 p2370 N85-24649
Pi2 pulsations and the substorm current wedge - ground observations 14 p2370 N85-24650
Ground-satellite observations of substorm related Pi 2 pulsations and current systems
14 p2370 N85-24651
The influence of a turbulent region on the flux of auroral electrons
[KGI-PREPRINT-072] 20 p3494 N85-31723
Magnetospheric response to solar wind variations
[DE85-010782] 20 p3547 N85-32074

AURORAL IONIZATION
Auroral X-rays and equatorial electrons in the morning sector — substorm 14 p2361 N85-24590
Afternoon radar aurora and polar cap convection pattern 14 p2361 N85-24592
Geophysical plasmas and atmospheric modeling
[AD-A152805] 17 p2993 N85-28497
Characteristics and sources of E-region ionization in the continuous aurora
[AD-A155018] 21 p3632 N85-32562

AURORAL IRRADIATION
The temporal evolution of a small auroral substorm as viewed from high altitudes with Dynamics Explorer 1
[NASA-CR-176064] 20 p3493 N85-31718

AURORAL SPECTROSCOPY
Measurements with an auroral spectrometer in the Energy Budget Campaign
[BMFT-FB-W-84-050] 14 p2374 N85-24677

AURORAL ZONES
Rocket and satellite observations of electric fields and ion convection in the dayside auroral ionosphere
[TRITA-EPP-84-05] 02 p0229 N85-11497
Relation between polarization of artificial low frequency radiation and parameters of auroral ionosphere
06 p0785 N85-15016
Longitudinal current before westward propagating auroral bend 06 p0823 N85-15223
Simultaneous observations of electron spectra in the auroral zone and near the equatorial plane by the DMSP-5D-F2 and GEOS-1 Satellites
[KGI-184] 09 p1355 N85-18522
Experiment for measuring electric fields within the sounding rocket project Energy Budget
[BMFT-FB-W-84-048] 12 p1891 N85-21866
Conjugacy of ELF-VHF emissions near L=6 — chorus phenomenon, hiss 14 p2367 N85-24629
Fast ion polarization jet in subauroral F-layer and its manifestation in structure of high latitude ionosphere
15 p2480 N85-25306
Auroral zone electric fields from DE-1 and -2 at magnetic conjunctions
[NASA-CR-175974] 18 p3136 N85-29421
Preliminary documentation for the polar code
[AD-A154125] 19 p3336 N85-30667

AURORAS
NT AURORAL ARCS
NT RADIO AURORAS
Magnetosphere, rings, and moons of Uranus
02 p0301 N85-11951
Charging of the DMSP F-2 spacecraft in the aurora on 10 January 1983
[AD-A146303] 03 p0324 N85-12066
Magnetospheric plasma studies using data from the dynamics high and low altitude plasma instruments
[AD-A145751] 03 p0392 N85-12505
Temporal and spatial variations in the intensity of ultraviolet emissions from Jupiter and the Io torus
03 p0448 N85-12846
Dayside cusp aurora 04 p0521 N85-13333
Longitudinal current before westward propagating auroral bend 06 p0823 N85-15223
Application of Fabry-Perot spectrometers for measurement of upper atmosphere temperatures and winds 08 p1183 N85-17454
X rays from the aurora
[AD-A146628] 08 p1186 N85-17477
The flow of plasma in the solar terrestrial environment
[NASA-CR-174301] 08 p1224 N85-17707
Simultaneous observations of electron spectra in the auroral zone and near the equatorial plane by the DMSP-5D-F2 and GEOS-1 Satellites
[KGI-184] 09 p1355 N85-18522
Pitch angle scattering and particle precipitation in a pulsating aurora: An experimental study
[KGI-185] 09 p1355 N85-18523
Spatial distribution of auroras and its relationship to geological structure of Norilsk region
10 p1497 N85-19447
Solar system studies with the IUE: 1982 - 1984
11 p1744 N85-20864
The spatial dependence of the Jovian auroral emissions 11 p1759 N85-21068
Description of the SSB/A (Special Sensor B/Aerospace X-ray spectrometer
[AD-A150040] 12 p1790 N85-21236
S3-3 ONR-118 data analysis
[AD-A149725] 12 p1889 N85-21855
Plans for Interbol satellite experiment
13 p1977 N85-22407
Observations of auroras and related plasma phenomena by the Kyokko and Jikiken satellite in IMS — EXOS-A and B satellite 14 p2354 N85-24547
Ground-based and near-Earth observations during the IMS 14 p2359 N85-24575
Electrodynamics of magnetosphere-ionosphere coupling 14 p2359 N85-24579
Electron and proton precipitation in magnetic substorms — auroral substorms
14 p2360 N85-24585
Development of an auroral absorption substorm
14 p2360 N85-24588

The magnetospheric convection electric field at ionospheric altitudes: A case study based on STARE and Saint-Santin data
14 p2362 N85-24594
The GEOS-2 E-field behavior during dynamic auroral development near the satellite footpoint
14 p2362 N85-24598
Three-dimensional current systems and electric fields during active aurora
14 p2362 N85-24599
Testing of some substorm features by multiple balloon observations
14 p2363 N85-24600
The relationship between auroral electrojet and visual aurora
14 p2363 N85-24602
On-off characteristics of auroral pulsations
14 p2363 N85-24604
Multiple correlation between auroral and magnetic pulsations
14 p2363 N85-24605
Multiple correlation between auroral and magnetic pulsations. Part 2: Determination of electric currents and electric fields around a pulsating auroral patch
14 p2363 N85-24606
Contribution of the Scandinavian Twin Auroral Radar Experiment (STARE) radar to the understanding of the physical mechanisms associated with Pc5 pulsations
14 p2364 N85-24613
Theory and computer simulation of auroral kilometric radiation
14 p2365 N85-24617
Observations of the MF-HF plasma wave emissions in active auroras by the sounding rocket experiments at Syowa station
14 p2366 N85-24620
Role of equatorial Electron Cyclotron Harmonic (ECH) waves in the generation of diffuse auroras. Contribution of the GEOS IMS spacecraft
14 p2367 N85-24632
Short-period magnetic pulsations during substorms
14 p2368 N85-24636
The IMS contributions to the understanding of auroral precipitation, transport and particle sources
14 p2372 N85-24660
Measurements with an auroral spectrometer in the Energy Budget Campaign
[BMFT-FB-W-84-050]
14 p2374 N85-24677
Observation of polar aurora from the Salyut-6 space station during the great geomagnetic storm of 11-13 Apr. 1981
15 p2477 N85-25291
Study of spatial distribution of auroras
16 p2806 N85-27315
IMS (International Magnetospheric Study) contributions to the understanding of auroral precipitation, transport, and particle sources
[AD-A152320]
17 p2992 N85-28492
EISCAT electron density studies
[AD-A152820]
17 p2993 N85-28496
Electron and ion distributions at high latitudes as measured by the Air Force polar orbiting satellites
[AD-A153242]
17 p2993 N85-28500
Images of the Earth's aurora and geocorona from the Dynamics Explorer Mission
[NASA-CR-175983]
18 p3136 N85-29423
The temporal evolution of a small auroral substorm as viewed from high altitudes with Dynamics Explorer 1
[NASA-CR-176064]
20 p3493 N85-31718
The influence of a turbulent region on the flux of auroral electrons
[KGI-PREPRINT-072]
20 p3494 N85-31723
Atmospheric Emission Photometric Imaging (AEPI)
23 p3902 N85-34170
Vehicle Charging And Potential (VCAP)
23 p3902 N85-34173
Cosmic rays 10Be biennal data and their relationship to auroras and sunspots
[SH-7.1-1]
23 p4047 N85-35094
Cosmic ray secular variations in terrestrial records and auroras
[SH-7.1-3]
23 p4047 N85-35096
Two-dimensional quasineutral description of particles and fields above discrete auroral arcs
[NASA-CR-176170]
24 p4116 N85-35517

AUSTENITE

Effects of prior austenite and ferrite grain size on fracture properties of a plain carbon steel
[AD-A148276]
03 p0332 N85-12138
Austenite transformation in powder-compacted chromium-nickel-molybdenum steels during continuous cooling
[BLL-M-35981-(5828.4)]
05 p0615 N85-13933
Influence of preliminary cold deformation on fineness of pearlite
[BLL-BISI-TRANS-22409-(9022.06)]
17 p2927 N85-28054
Textural transformations taking place during heat and mechanical treatment in triplex steels
[BLL-BISI-TRANS-22404-(9022.06)]
17 p2927 N85-28063
Influence of structural state and alloy content of austenite on formation of martensitic phases in steels
[BLL-BISI-TRANS-22365-(9022.06)]
17 p2928 N85-28068
Mechanical stabilization of austenite against epsilon martensite and its effect on deformation behavior in high manganese steels
[DE85-007654]
17 p2932 N85-28097
Vacuum pressure welding of commercial titanium with 2Kh13 and 12Kh18N10T steels
19 p3246 N85-30124
Effects of hot deformation on the kinetics of the pearlite transformation in eutectoid steel
[BLL-M-35844-(5828.4)]
23 p3913 N85-34250
Acoustic emission during transformation of austenite in 38KhN3MF steel
[BLL-M-35825-(5828.4)]
23 p3914 N85-34256
Decomposition of martensite in R6M5 and R6AM5 steels after direct immersion in liquid nitrogen
[BLL-M-36305]
24 p4077 N85-35268
Effect of prior warm rolling on the retained austenite content and hardening response of VIM-VAR (vacuum-induction melted-vacuum-arc remelted) AISI M-50 steel
[AD-A156145]
24 p4079 N85-35281

AUSTENITIC STAINLESS STEELS

Influence of nitrogen on the sensitization, corrosion, mechanical, and microstructural properties of austenitic stainless steels
[DE84-015134]
01 p0028 N85-10177
Electro-spark case-hardening of contoured surfaces
01 p0035 N85-10216
Microstructure and deformation aspects of some specialty steels and hard metals
02 p0176 N85-11182
EDS round-robin evaluation of type 308 austenitic stainless steel
[DE84-014574]
02 p0183 N85-11226
Identification of pulse-echo rays in austenitic steels
[AERE-R-11265]
03 p0369 N85-12358
Fractographic study of stress corrosion cracking of SUS 304 stainless steel in various environments
[BLL-RISLEY-TR-4598-(9091.9F)]
05 p0615 N85-13928
Influence of the mechanical and electrochemical characteristics of austenitic and austenoferritic steels on the propagation rate and morphology of stress corrosion cracking
[BLL-RISLEY-TR-4545-(9091.9F)]
06 p0767 N85-14906
Investigations into the fatigue crack growth behaviour of X6CrNi 18 11 (1.4948) austenitic stainless steel
[BLL-RISLEY-TR-4544-(9091.9F)]
06 p0768 N85-14911
Austenitic stainless steel for high temperature and pressure applications
[BLL-RISLEY-TR-4527-(9091.9F)]
07 p0925 N85-15860
Hydrogen trapping, diffusion, and recombination in austenitic stainless steels
[DE85-001871]
09 p1294 N85-18129
Fracture toughness of austenitic stainless steel weld metal at 4 K
[DE84-016638]
09 p1340 N85-18425
Role of nitrogen in improving resistance to localized corrosion in austenitic stainless steels
11 p1609 N85-20115
Partial replacement of chromium in austenitic stainless steels by molybdenum, copper, and vanadium, report of investigations 1984
[PB85-116508]
12 p1809 N85-21348
Hydrogen effects in austenitic stainless steels based on the Fe-Cr-Mn-N system
[DE85-003617]
13 p2023 N85-22672
Swelling behavior of manganese-bearing AISI 216 steel
[DE85-005712]
15 p2512 N85-25495
Swelling behavior of titanium-modified AISI 316 alloys
[DE85-007470]
16 p2752 N85-28982
Method of investigating accumulations of damage to weld joints in the case of low-cycle creep
[BLL-CE-TRANS-8088-(9022.09)]
16 p2792 N85-27219
Stainless steels: Application and welding
[BLL-BISI-TRANS-22357-(9022.06)]
17 p2927 N85-28059
Technical information: Weldability of stainless steel. Part 1: Austenitic stainless steel
[BLL-BISI-TRANS-22458-(9022.06)]
17 p2973 N85-28362
Relaxation properties and fatigue fracture resistance of austenitic spring steel
[BLL-BISI-TRANS-22300-(9022.06)]
17 p2978 N85-28408
Variations in the structure and in the composition of austenitic and carbon steel in spot welds
[BLL-BISI-TRANS-21765-(9022.06)]
18 p3073 N85-29007
Development of reduced activation alloys for fusion service: Draft
[DE85-007464]
18 p3074 N85-29014
Elevated temperature erosion of steels
[DE85-008503]
18 p3075 N85-29018
Corrosion performance of metals and alloys in a tuff geochemical environment
[DE85-009449]
18 p3077 N85-29033
Kinetics of H-induced stress corrosion cracking. Part 1: Important features of cracking in respect of high strength steels
[BLL-BISI-TRANS-(9022.06)]
19 p3282 N85-30350
Hot cracking of austenitic stainless steels: The debut of the Sigmajig
[DE85-010560]
20 p3431 N85-31287
Reactor pressure vessel steels ASME SA533B and SA508 C 1.2
[VTT-340]
22 p3794 N85-33607
Phase transformations taking place in austenitic steel during deformation at different rates
[BLL-M-35875-(5828.4)]
23 p3914 N85-34254
The effect of pre-heating on the structure and properties of chromium-molybdenum steels
[BLL-M-35897-(5828.4)]
23 p3914 N85-34255
Acoustic emission during transformation of austenite in 38KhN3MF steel
[BLL-M-35825-(5828.4)]
23 p3914 N85-34256
The use of austenitic stainless steel versus monel (Ni-cu) alloy in pressurized Gaseous Oxygen (GOX) life support systems
[AD-A156305]
24 p4134 N85-35825

AUSTRALIA

Mineral nutrients in Mediterranean ecosystems
[REPT-71]
01 p0069 N85-10456
Report of the Division of Atmospheric Physics, 1980-1983
03 p0391 N85-12501
Simple prediction of convergence zone propagation in waters around australia
[AD-A145988]
03 p0416 N85-12659
Evaluation of SIR-B imagery for geologic and geomorphic mapping, hydrology, and oceanography in Australia
08 p1148 N85-17229
MAGSAT anomaly field data of the crustal properties of Australia
[E85-10100]
13 p2122 N85-23215
An investigation of the crustal properties of Australia and surrounding regions derived from interpretation of MAGSAT anomaly field data
13 p2122 N85-23216
Data selection techniques in the interpretation of MAGSAT data over Australia
13 p2123 N85-23218
Report of the Hydrographic Service Royal Australian Navy for the year ended 30th June 1984, issue number 20
[AD-A151460]
15 p2583 N85-25932
Australian seismological report, 1980
[REPT-252]
17 p2989 N85-28473

AUSTRIA

Activities report in space research in Austria
11 p1587 N85-19994

AUTOCATALYSIS

Critical analysis of nitramine decomposition data. Preliminary comments on autoacceleration and autoinhibition in HMX and RDX decomposition
[AD-A146570]
06 p0774 N85-14946

AUTOCLAVES

Study of the kinetics of hydrogenation using aged catalysts
[DE85-004373]
12 p1802 N85-21302

AUTOCLAVING

Chemoviscosity modeling for thermosetting resins - I
[NASA-CR-172443]
03 p0326 N85-12096
Chemoviscosity modeling for thermosetting resins, 2
[NASA-CR-177658]
24 p4073 N85-35243

AUTOCOLLIMATORS

U COLLIMATORS

AUTOCORRELATION

Autoregressive nonsteady methods for the analysis and synthesis of the human voice
[FUB-3-1984]
01 p0041 N85-10266
Measures of distance between speech signals in the frequency domain — speech recognition
[FUB-5-1984]
01 p0041 N85-10267
Autoregressive modeling and the classification of land clutter — radar signatures
[ENST-C-84003]
03 p0358 N85-12292
Distributions of extreme values of sequences of autocorrelated random variables
[PB84-240746]
06 p0858 N85-15456
The analysis of spaced sensor records by correlation techniques
08 p1184 N85-17465
Methods and applications of time series analysis. Part 2: Linear stochastic models
[AD-A147292]
08 p1214 N85-17845
Relative-entropy minimization with uncertain constraints--theory and application to spectrum analysis
[AD-A149192]
10 p1548 N85-19752

Asymptotic distributions of the sample mean, autocovariances and autocorrelations of long-memory time series
[AD-A149409] 10 p1551 N85-19781
Method of multivariant intraclass pattern recognition
[AD-D011646] 12 p1818 N85-21405
Method for approximating autocorrelation functions for describing areal photoimage features
13 p1983 N85-22443
Regular synthesis of pairs of phase-keyed binary minimax signals 13 p2069 N85-22923
Parametric coherence estimation via convolved correlations
[DE85-003946] 14 p2416 N85-24909
Higher order residual analysis for nonlinear time series with autoregressive correlation structures
[AD-A149232] 15 p2636 N85-26257
Fast eigenvector methods for digital signal processing
20 p3439 N85-31341
Verification of theoretically computed spectra for a point rotating in a vertical plane
[DE85-011967] 20 p3520 N85-31893

AUTOIONIZATION
Many-electron effects in electron impact ionization of multiply charged ions
[DE85-005570] 15 p2649 N85-26340
Trends in the electric field enhancement of dielectronic recombination cross sections
[DE85-006920] 16 p2871 N85-27711
Experimental approaches to the measurement of dielectronic recombination
[DE85-006927] 17 p3030 N85-28743
Photoelectron studies of autoionizing Rydberg states in HCl
[DE85-011813] 21 p3702 N85-33001
Exit channels of autoionization resonances in atoms
[DE85-012299] 24 p4149 N85-35726

AUTOMATA THEORY
One queue or two pushdown stores take square time on a one-head tape unit
[CWI-CS-R8406] 05 p0717 N85-14601
Advancing automation and robotics technology for the Space Station and for the US economy. Volume 1: Executive overview
[NASA-TM-87566-VOL-1] 13 p1986 N85-22460
Advancing automation and robotics technology for the Space Station and for the US economy, volume 2
[NASA-TM-87566-VOL-2] 13 p1987 N85-22461
The hierarchical database decomposition approach to database concurrency control
[AD-A150612] 13 p2168 N85-23450
USSR report: Machine tools and metalworking equipment
[JPRS-UMM-85-006] 14 p2283 N85-24146
New CNC turning centers described
14 p2284 N85-24148
Large CNC machining center for turbine production
14 p2284 N85-24149
Minister B. V. Balmont on status of automation drive
14 p2284 N85-24151
West Europe report: Science and technology
[JPRS-WST-85-013] 14 p2289 N85-24183
MBB automates aircraft production in many FRG facilities 14 p2289 N85-24188
Robotic deburring. Part 2: Evaluation of cutters and noncompliant tooling
[DE85-006182] 14 p2311 N85-24306
Reliable computation with cellular automata
[AD-A150656] 14 p2399 N85-24790
Space station systems technology study (add-on task). Volume 2: Trade study and technology selection
[NASA-CR-171416] 15 p2475 N85-25279
New stage in robotics development
16 p2762 N85-27045
West Europe report: Science and technology
[JPRS-WST-84-031] 16 p3066 N85-29069
Multinational program to develop intelligent robots
16 p3066 N85-29094
West Europe report: Science and technology
[JPRS-WST-84-035] 16 p3067 N85-29102
Man-machine tradeoff study 16 p3158 N85-29561
Space station automation study. Volume 1: Executive summary. Autonomous systems and assembly
[NASA-CR-171514] 19 p3226 N85-30002
Some examples of the application of automatically guided vehicle systems
[HSE-TRANS-11134] 19 p3281 N85-30348
Computer science: Key to a space program renaissance. The 1981 NASA/ASEE summer study on the use of computer science and technology in NASA. Volume 2: Appendices
[NASA-CR-175295] 22 p3827 N85-33702
Intermittent motion 23 p3925 N85-34323
TRICCS: A proposed teleoperator/robot integrated command and control system for space applications
[NASA-TM-87577] 24 p4136 N85-35637

AUTOMATED EN ROUTE ATC
Start-2 ATC system installation progresses at Leningrad 03 p0311 N85-12007

AUTOMATED GUIDEWAY TRANSIT VEHICLES
Network management simulation of automated guideway transit systems under vehicle-follower control
[PB85-186233] 24 p4166 N85-35830

AUTOMATED TRANSIT VEHICLES
NT AUTOMATED GUIDEWAY TRANSIT VEHICLES
Metrological support for remote transport vehicle speedometers 13 p2076 N85-22983

AUTOMATIC CONTROL
NT ACTIVE CONTROL
NT ADAPTIVE CONTROL
NT AUTOMATIC FLIGHT CONTROL
NT AUTOMATIC FREQUENCY CONTROL
NT AUTOMATIC GAIN CONTROL
NT AUTOMATIC LANDING CONTROL
NT CASCADE CONTROL
NT DYNAMIC CONTROL
NT FEEDBACK CONTROL
NT FEEDFORWARD CONTROL
NT LEARNING MACHINES
NT NUMERICAL CONTROL
NT OFF-ON CONTROL
NT OPTIMAL CONTROL
NT SELF ADAPTIVE CONTROL SYSTEMS
NT SELF ALIGNMENT
NT SEQUENTIAL CONTROL
NT TIME OPTIMAL CONTROL
Development of the Engineering Test Satellite-3 (ETS-3) ion engine system
[NASA-TM-77538] 01 p0017 N85-10101
East Europe report: Science and technology
[JPRS-ESA-84-030] 01 p0101 N85-10670
Automated apparatus for producing gradient gels
[DE84-014507] 01 p0107 N85-10716
Office of Technology Assessment
01 p0127 N85-10872
Technological approach to automation of specialized processing of survey data 02 p0165 N85-11118
Automation of production of semiconductor power devices 03 p0346 N85-12229
New welding equipment for mechanized welding and trends in further development 03 p0352 N85-12264
Individual differences in automatic and controlled information processing
[AD-A146245] 03 p0401 N85-12559
Test-bed for programmable automation research. Phase 1
[AD-A145872] 03 p0409 N85-12614
Developments in Soviet robot technology viewed
04 p0491 N85-13127
Advances of implementing NC machine tools discussed 04 p0491 N85-13131
Fiber optic, Fabry-Perot high temperature sensor
[NASA-CR-174712] 04 p0584 N85-13594
Automated Library Search System (ALSS) user's manual
[DE84-015952] 04 p0576 N85-13672
Self-tuning controller design and implementation
[OUEL-1535/84] 05 p0621 N85-13975
A generalized LQG approach to self-tuning control. Part 1: Aspects of design. Part 2: Implementation and simulation
[OUEL-1536/84] 05 p0622 N85-13976
Measuring and control tasks in OPTIWA
05 p0669 N85-14304
Critical conditions for the automatic control of landing from decision height in variable winds
[UTIAS-284] 06 p0753 N85-14830
A modified unit commitment and generation control for utilities with large wind generation penetrations
[DE84-015362] 06 p0806 N85-15129
Fiat, Peugeot introduce integrated robotized engine: CAD used 07 p0936 N85-15933
Control technology for integrated circuit fabrication at Micro-Circuit Engineering, Incorporated, West Palm Beach, Florida
[PB85-100717/GAR] 07 p0949 N85-16013
Investigation of semiautomatic aircraft control processes employing time redundancy in on-board digital trajectory control computers 07 p0954 N85-16048
Automatic camera tracking for remote manipulators
[DE85-001897] 07 p0974 N85-16187
Interaction of human cognitive models and computer based models in supervisory control
[AD-A142547] 07 p1020 N85-16474
Human factors characteristics of the Joint Tactical Fusion Test Bed: Field test 467 results
[AD-A146856] 07 p1020 N85-16476
Microcomputer control of a residential photovoltaic power conditioning system
[DE84-014774] 07 p1022 N85-16488
Automatic software for controlling cryogenic systems
08 p1097 N85-16932
Managing computer-controlled operations
08 p1097 N85-16934
The effects of manufacturing automation on the surge and mobilization capabilities of the gas turbine engine industry
[AD-A147295] 08 p1137 N85-17162
USSR report: Machine tools and metalworking equipment
[JPRS-UMM-84-021] 08 p1138 N85-17168
Control systems for robotic production lines
08 p1138 N85-17169
Flexible manufacturing system concept features cache memory 08 p1140 N85-17186
Robotics research, integration overview presented. Application objectives cited 08 p1142 N85-17201
Parallel algorithms for robot dynamics
[DE84-016583] 09 p1369 N85-18605
The planning of flexible manufacturing systems
[PNR-90230] 09 p1371 N85-18613
Robotized blanks loader for new forge press
10 p1461 N85-19216
French panel makes specific proposals for robotics research. Current state of French robotics
11 p1616 N85-20160
Linear magnetic bearings
[NASA-CASE-GSC-12582-2] 11 p1641 N85-20337
Control of large collector arrays: The SSPS experience
[DE85-001461] 11 p1675 N85-20553
Operations concept for the advanced automation system man-machine interface
[AD-A149797] 12 p1774 N85-21139
Program for controlling electrical measuring contact instrument on glow-discharge indicator panel
12 p1842 N85-21558
Control of nonlinear objects 12 p1842 N85-21561
Reliability analysis of automatic systems
[VTT-301] 12 p1863 N85-21682
Guidance and control research flight testing with HFB 320 test aircraft 13 p1967 N85-22355
TASS update on unmanned flight of Salyut-7
13 p1977 N85-22404
Automatic charge control system for satellites
13 p1995 N85-22508
Hydraulic brakes for industrial robots
13 p2046 N85-22806
Controllable movements of elastic manipulator with three degrees of freedom 14 p2266 N85-24040
New equipment complex Kaskad 2 for automatic control 14 p2266 N85-24042
Mechanization and automation of production processes in turbine building 14 p2269 N85-24057
Plans, developments in robotics
14 p2289 N85-24191
Computer controlled acquistion of corrosion rate data from multiple sensors
[PB85-157378] 15 p2524 N85-25559
West Europe report: Science and technology
[JPRS-WST-84-007] 15 p2530 N85-25600
West Europe report: Science and technology
[JPRS-WST-84-014] 15 p2536 N85-25647
Calorimeter for measuring high-energy optical pulses
[PB85-160695] 15 p2561 N85-25799
Automation and robotics in welding
15 p2566 N85-25831
A critical review of selected recent advancements in arc welding equipment and processes
15 p2566 N85-25833
Some aspects of nuclear plant fabrication in Japan and the UK relating to automatic and robotic arc welding
15 p2566 N85-25834
Artificial intelligence based control of a sensor-driven machine
[DE85-006972] 15 p2633 N85-26227
Experience of sheet stamping robotic complexes
16 p2761 N85-27041
Automatic manipulators for forging rollers
16 p2762 N85-27042
Updating model RPD-1.25 industrial robot
16 p2762 N85-27043
Industrial robots and automatic manipulators for forging and pressing operations at Second International Exhibition 16 p2762 N85-27044
Status, prospects of computer-aided design discussed
16 p2767 N85-27073
A robotic system for preparing reagent and dilution vials
[DE85-008262] 16 p2793 N85-27231
A Dictionary-Directory System (DDS) for the SPLICE system
[AD-A152223] 16 p2878 N85-27759
Automation and robotics for the National Space Program
[NASA-CR-175681] 17 p2909 N85-27936
Robots, automatic devices inside VW's Wolfsburg plant 17 p2946 N85-28186

Future directions of robotics, automation in Italy
17 p2946 N85-28187
Applications of robots in machine tool industry reviewed 17 p2946 N85-28189
A programming system for a modular flexible multimicrocomputer system for the automatic control of automated test equipment
[JUEL-1962] 17 p3014 N85-28641
West European report: Science and technology
[JPRS-WST-84-036] 18 p3066 N85-28960
Jet pump-drive system for heat removal
[NASA-CASE-NPO-16494-1-CU]
18 p3099 N85-29182
Technical instructions for a control operating system of the gas flow installation for the solid fuel combustion chamber
[VTH-LR-410] 18 p3118 N85-29302
An information theoretical method for automatic noise elimination in digital image processing
18 p3124 N85-29345
Computer program for the control/operating system of the gas flow installation for the solid fuel combustion chamber
[VTH-LR-430] 18 p3165 N85-29605
Space station automation study. Volume 2: Technical report. Autonomous systems and assembly
[NASA-CR-171515] 19 p3226 N85-30001
BREED: A CDC-7600 computer program for the automation of breeder reactor design analysis (LWBR Development Program)
[DE85-010327] 19 p3338 N85-30666
Simulation and operation of the EBR-2 automatic control rod drive system
[DE85-010262] 19 p3360 N85-30832
Space Station man-machine automation trade-off analysis
[NASA-CR-176046] 20 p3408 N85-31147
Automatic assembly of space stations
20 p3409 N85-31153
Automated testing of developmental satellite communications systems and subsystems
[NASA-TM-87070] 20 p3440 N85-31348
Automated FMEA (Failure Modes and Effects Analysis) techniques
[AD-A154161] 20 p3464 N85-31518
Simulation of automatic control of MFTF-B neutral beams
[DE85-010640] 20 p3530 N85-31960
Importance of automation, robotization in economy
21 p3572 N85-32219
Space station automation study. Automation requirements derived from space manufacturing concepts. Volume 1: Executive summary
[NASA-CR-176099] 22 p3738 N85-33170
Space Station automation study. Automation requirements derived from space manufacturing concepts. Volume 2: Technical report
[NASA-CR-176100] 22 p3738 N85-33171
Space station automation and robotics study. Operator-systems interface
[NASA-CR-176095] 22 p3738 N85-33172
Testimony of Robert A. Frosch before the Subcommittee on HUD and Independent Agencies of the Senate Committee on Appropriations
[NASA-TM-87496] 22 p3738 N85-33173
Statement of Aaron Cohen, Director, Research and Engineering, Johnson Space Center and Chairman, Space Station Advanced Technology Advisory Committee, National Aeronautics and Space Administration, before the Subcommittee on Science, Technology, and Space, Committee on Commerce, Science, and Transportation, United States Senate
[NASA-TM-87497] 22 p3739 N85-33174
Space station automation study: Autonomous systems and assembly, volume 2
[NASA-CR-176092] 22 p3739 N85-33175
Utilization of microwave measuring systems for the automation of composite materials manufacturing
[SNIAS-851-430-102] 22 p3742 N85-33197
Probabilistic analysis of automatic control systems for detection systems 22 p3765 N85-33335
Robotic order picking
[AD-D011737] 22 p3792 N85-33493
Automatic rotary valve actuator
[DE85-012797] 22 p3794 N85-33505
Centralized surveillance of flexible workshops for the manufacturing of composite materials
[SNIAS-851-430-103] 23 p3910 N85-34227
Multi-robot assembly of IC's 23 p3964 N85-34577
Maintenance port system
[AD-D011724] 23 p3967 N85-34594
Space Missions for Automation and Robotics Technologies (SMART) Program
[NASA-TM-86620] 24 p4068 N85-35210
Matched filtering of visual evoked potentials to detect acceleration (+Gz) induced blackout
[AD-A155912] 24 p4131 N85-35609
Spreading the control complexity in decentralized control of interconnected systems
[BU-117] 24 p4144 N85-35688

AUTOMATIC CONTROL VALVES
NT PRESSURE REGULATORS
The development of a microprocessor-controlled linearly-actuated valve assembly
[NASA-CR-174437] 10 p1491 N85-19415

AUTOMATIC DATA PROCESSING
U DATA PROCESSING

AUTOMATIC FLIGHT CONTROL
NT AUTOMATIC LANDING CONTROL
Accounting for error stochasticity in terminal homing of aircraft 04 p0489 N85-13115
Investigation of pilot behavior in flight tests with a rate command/attitude hold control system
[DFVLR-FB-84-25] 05 p0699 N85-14486
Flight test of the Open Loop Gust Alleviation (OLGA) system
[BMFT-FB-W-84-036] 06 p1088 N85-16881
Algorithms for automatic four-dimensional aircraft guidance, considering the momentary wind situation
[DFVLR-FB-84-40] 12 p1775 N85-21146
Analytically redundant output feedback scheme for reduction of structural loads of a flexible transport aircraft
[TT-8303] 12 p1777 N85-21154
Automatic control design procedures for restructurable aircraft control
[NASA-CR-172489] 12 p1780 N85-21173
A 320 to have combined automatic pilot, flight control system 14 p2289 N85-24186
Automatic flight control modes for the AFTI/F-111 mission adaptive wing aircraft 17 p2905 N85-27909
Human factors in cockpit automation: A field study of flight crew transition
[NASA-CR-177333] 19 p3215 N85-29937
The integrated manual and automatic control of complex flight systems
[NASA-CR-176166] 24 p4066 N85-35201
Analogies of control mechanisms in flight guidance and medicine 24 p4129 N85-35597

AUTOMATIC FREQUENCY CONTROL
Carrier acquisition and tracking by a COSTAS loop with automatic frequency control
[ESA-TT-836] 04 p0493 N85-13149
High-speed adaptation algorithm for harmonic corrector 22 p3765 N85-33336

AUTOMATIC GAIN CONTROL
Gain restoration after Doppler filtering
[AD-D011425] 08 p1154 N85-17287

AUTOMATIC LANDING CONTROL
Flight tests of the Digital Integrated Automatic Landing System (DIALS)
[NASA-CR-3659] 04 p0457 N85-12900
Research at automated ATC Scientific-Experimental Center 09 p1278 N85-19037

AUTOMATIC PATTERN RECOGNITION
U PATTERN RECOGNITION

AUTOMATIC PILOTS
Polaris guidance system
[AD-D011324] 07 p0900 N85-15704
A digital piloting system for the combat helicopter
08 p1074 N85-16806
A 320 to have combined automatic pilot, flight control system 14 p2289 N85-24186
An approach to planning in the inflight emergency domain
[AD-A151869] 15 p2467 N85-25226
Multi-rate digital autopilot modeling methodology
[AD-A152044] 15 p2474 N85-25272
Development and evaluation of a Fault-Tolerant Multiprocessor (FTMP) computer. Volume 2: FTMP software
[NASA-CR-166072] 19 p3341 N85-30706
Development of control laws for a flight test maneuver autopilot for an F-15 aircraft
[NASA-TM-86736] 22 p3730 N85-33122

AUTOMATIC ROCKET IMPACT PREDICTORS
U COMPUTERIZED SIMULATION
U IMPACT PREDICTION

AUTOMATIC TEST EQUIPMENT
Investigation of the application of the marginal tension technique to test electronic devices, phase 3
[ESD-11-301] 02 p0206 N85-11360
Artificial Intelligence in Maintenance: Proceedings of the Joint Services Workshop
[AD-A145349] 02 p0244 N85-11582
The need for improvements in weapon system maintenance: What can AI (Artificial Intelligence) contribute?
[AD-P003913] 02 p0244 N85-11583
Artificial intelligence applications to maintenance
[AD-P003914] 02 p0244 N85-11584
On applying AI (Artificial Intelligence) to maintenance and troubleshooting
[AD-P003915] 02 p0244 N85-11585
An overview of the Joint Logistics Commanders Automatic Test Equipment Panel
[AD-P003916] 02 p0244 N85-11586
AI (Artificial Intelligence) approaches to troubleshooting
[AD-P003918] 02 p0245 N85-11588
An expert system for representing procedural knowledge
[AD-P003923] 02 p0245 N85-11603
Depot level problems in the testing of printed circuit boards
[AD-P003932] 02 p0247 N85-11612
NAVAIR's (Naval air systems command) AI (Artificial Intelligence) program for ATE (Automated Test Equipment)
[AD-P003935] 02 p0247 N85-11615
Artificial intelligence applications to automatic test equipment
[AD-P003936] 02 p0247 N85-11616
Application of artificial intelligence to equipment maintenance
[AD-P003939] 02 p0248 N85-11619
LES: (Lockheed Expert System): A model-based expert system for electronic maintenance
[AD-P003944] 02 p0248 N85-11624
Accelerated stress facility 1976-1983
[AD-A146101] 03 p0359 N85-12303
DYNA-SIM: A nonstationary queuing simulation with application to the automated test equipment problem
[AD-A146384] 05 p0857 N85-15450
Diagnostic apparatus for radar pulse repetition frequency control circuit card
[AD-D011364] 07 p0937 N85-15938
Design for Tactical Avionics Maintainability
[AGARD-CP-361] 08 p1063 N85-16731
Study and realisation of a 3rd level maintenance center based on ATE systems utilization
08 p1063 N85-16735
ATE user's view on design for maintainability
08 p1064 N85-16737
Built-in-test for first line testing
08 p1064 N85-16739
Functional built-in-test in a pipelined image processor
08 p1064 N85-16740
Built-in test and self repair mechanisms in a digital correlator integrated circuit 08 p1064 N85-16741
Design of a bit-sliced processor array with built-in-self-test
[AD-A149785] 12 p1835 N85-21513
Automation of servicibility of radio-relay station equipment 15 p2527 N85-25582
A programming system for a modular flexible multimicrocomputer system for the automatic control of automated test equipment
[JUEL-1962] 17 p3014 N85-28641
Proceedings of the Electronic Test Equipment Division's Annual Program Review of Electronic Test Equipment Industry Response to Emerging Defense Requirements
[AD-A154455] 20 p3436 N85-31320
F-111 automatic test equipment replacement program
20 p3437 N85-31322
Air Force bid sample testing 20 p3437 N85-31323
An overview of measurement solutions for digital systems 20 p3437 N85-31326
Automated testing of developmental satellite communications systems and subsystems
[NASA-TM-87070] 20 p3440 N85-31348

AUTOMATIC WEATHER STATIONS
Simple methods in very short-range forecasting based on data from a mesoscale network of automatic stations (ANETZ) and from satellite (Meteosat) and radar — Swiss Alps 01 p0082 N85-10548
Operational precipitation observation system using digitized radar and rain gages 01 p0082 N85-10549
An automatic weather station network for low-altitude wind shear investigations
[AD-A148139] 08 p1189 N85-17493
Project PAPA: The integration of drifting buoy data into an operational meteorological service
14 p2238 N85-23674
Applications of ARGOS data collection systems in Arctic regions 14 p2238 N85-23675
Data collection and winter ice dynamics in the Beaufort Sea 14 p2238 N85-23676
Applications of ARGOS data collection system for automatic meteorological observatories in Arctic regions
14 p2240 N85-23693
Automatic weather stations in Antarctica
14 p2324 N85-24360
The development of an automated marine meteorological data system 14 p2324 N85-24382

Meteorological buoys developed at the EERM laboratory 14 p2326 N85-24374
Hydrology and climatic conditions in Greenland 14 p2327 N85-24387
Drifting buoy studies for weather applications 14 p2329 N85-24396
Antarctic automatic weather stations 14 p2329 N85-24397
Collecting meteorological reports with the ARGOS system 14 p2329 N85-24398
Telemetered meteorological and engineering data from a deep sea moored body in the Long Term Upper Ocean Study (LOTUS) 14 p2329 N85-24402
Practical considerations when using water quality and structure monitoring sensors as applied to portable ARGOS satellite transmitter equipment 14 p2330 N85-24405
Applications of ARGOS measurements in equatorial Pacific Ocean-atmosphere interaction studies 14 p2331 N85-24414
Overview of data processing at AES local user terminals — Canadian Atmospheric Environment Service (AES) 14 p2331 N85-24418
The Data Acquisition Control and Telemetry (DACT) system — meteorological buoys 14 p2332 N85-24419
Tactical deployment of satellite-reporting drifting data buoys for environmental data acquisition 14 p2332 N85-24423
DB2 and DB3: The next generation — buoys 16 p2811 N85-27337
An operational buoy network collecting meteorological data 16 p2813 N85-27351
Operational experiences with the ARGOS system in Greenland 16 p2813 N85-27353
Data from BCC-yachts: A significant input to Southern Hemisphere analysis 16 p2814 N85-27356
Automated Weather Observing System (AWOS) demonstration program
[AD-A153463] 18 p3148 N85-29493

AUTOMATION
Automation of coastal engineering modelling facilities
[CSIR-T/SEA-8304] 01 p0035 N85-10219
Automated installation methods for photovoltaic arrays 2
[SAND-84-7035] 02 p0222 N85-11453
Depot modernization at the Defense Logistics Agency
[AD-P004008] 03 p0306 N85-11988
Future robotics program at San Antonio ALC (Air Logistics Center)
[AD-P004011] 03 p0309 N85-11991
Research activities of the Illinois University Coordinated Science Laboratory
[AD-A145589] 03 p0449 N85-12856
Development, new application of Soviet robots 04 p0491 N85-13129
DNC, CNC network for robotized machining cells 04 p0491 N85-13130
Human factors in cockpit automation 06 p0752 N85-14819
Situational planning of production processes in a flexible automated production system 06 p0776 N85-14959
Machine tools at 1984 Leipzig Spring Fair 06 p0815 N85-15177
NC programming, machine tool information 06 p0816 N85-15178
West Europe report: Science and technology
[JPRS-WST-84-039] 07 p0936 N85-15929
Automation of checkout for the shuttle operations era 08 p1092 N85-16900
Technology planning for flexible manufacturing systems 08 p1139 N85-17170
Automated plant, production management system 08 p1139 N85-17171
Design features, applications of new robots 08 p1139 N85-17174
West Europe report: Science and technology
[JPRS-WST-85-001] 08 p1141 N85-17190
Europeans active in magnetic bearing industry 08 p1141 N85-17195
Role of engineering psychology 09 p1361 N85-18581
Problems of psychological support of automated organization control systems 09 p1362 N85-18571
Dialog system of preparation and presentation of visual information 10 p1526 N85-19822
Pilot workload, performance and aircraft control automation 10 p1534 N85-19670
French firm has most advanced continuous-casting machine 11 p1592 N85-20017
East Europe report: Science and technology
[JPRS-ESA-85-009] 11 p1616 N85-20165
Robot production lines in operation 11 p1617 N85-20166
Institute director surveys industrial automation drive 11 p1617 N85-20167
Reliability of DNC system examined 11 p1617 N85-20171
Design of tightening device and calculation of forces in manipulator transmissions with base-drive mounted 13 p2046 N85-22804
USSR report: Machine tools and metalworking equipment
[JPRS-UMM-85-005] 13 p2051 N85-22839
Advances in cutting tool technology surveyed 13 p2051 N85-22840
Motion planning with six degrees of freedom
[AD-A150312] 13 p2165 N85-23432
Mini-Seminar on Non-Destructive Testing
[CSIR-TSD-0009/83] 14 p2316 N85-24308
USSR report: Cybernetics, computers, and automation technology
[JPRS-UCC-85-002] 14 p2400 N85-24794
The retrieval expert model of information retrieval 14 p2433 N85-25003
Experience in automation of data processing in interpretation and defining of linear elements from space photographs 15 p2486 N85-25349
West Europe report: Science and technology
[JPRS-WST-84-012] 15 p2523 N85-25552
French robotics research at Grenoble labs 15 p2523 N85-25555
France develops new continuous vacuum treatment method 15 p2531 N85-25611
USSR report: Cybernetics, computers and automation technology
[JPRS-UCC-85-003] 15 p2625 N85-26174
CAD/CAM (Computer-Aided Design/Computer-Aided Manufacturing) highlights
[AD-A151532] 15 p2629 N85-26201
System design of automated VLSI (Very Large Scale Integrated) test station and implementation of selected system aspects
[AD-A151961] 16 p2778 N85-27147
The introduction of new cockpit technology: A human factors study
[NASA-TM-86659] 16 p2843 N85-27528
Efforts at office automation and information systems utilization at Martin Marietta Energy Systems, Incorporated
[DE85-008154] 17 p3013 N85-28633
DLA: Data/data base administration analysis
[AD-A153031] 17 p3050 N85-28879
West Europe report: Science and technology
[JPRS-WST-84-037] 18 p3088 N85-29106
Automated maintenance system test program increment VI production scheduling
[AD-A153694] 18 p3198 N85-29638
Automatic ac/dc thermal voltage converter and ac voltage calibration system
[PB85-182574] 19 p3274 N85-30304
Implementation of a proposed system for automated microcode generation
[AD-A154235] 19 p3336 N85-30671
Survey of Ada (Trademark)-based PDLs (Program Design Language)
[AD-A154402] 19 p3338 N85-30680
Galileo battery testing and the impact of test automation 20 p3444 N85-31361
NASA space station automation: AI-based technology review
[NASA-CR-176094] 21 p3558 N85-32134
NASA space station automation: AI-based technology review. Executive summary
[NASA-CR-176096] 21 p3558 N85-32135
East Europe report: Science and technology
[JPRS-ESA-85-023] 21 p3572 N85-32217
Robotic order picking
[AD-D011737] 22 p3792 N85-33493

AUTOMOBILE ENGINES
An expert system for representing procedural knowledge
[AD-P003923] 02 p0245 N85-11603
Ceramic technology for advanced heat engines program plan
[DE84-013567] 04 p0479 N85-13055
Advanced concepts for methanol fuel vehicles
[DE84-013612] 04 p0482 N85-13071
Advanced automotive diesel assessment program
[NASA-CR-168285] 04 p0507 N85-13235
Advanced Automotive Diesel Assessment Program, executive summary 04 p0507 N85-13236
A study of the Armstrong Whitworth swing beam engine for automotive application 04 p0508 N85-13239
Advanced automotive diesel engine system study 04 p0508 N85-13240
A.A.D. engine noise evaluation 04 p0508 N85-13241
Long term technology development program 04 p0508 N85-13244
Evaluation of heat engine for hybrid vehicle application
[NASA-CR-174163] 04 p0508 N85-13245
Vibroacoustic control diagnostics of selected machines based on research on the slide bearing of an automobile engine and the alternator
[ISSN-0208-5658] 05 p0841 N85-14112
Fiat, Peugeot introduce integrated robotized engine: CAD used 07 p0936 N85-15933
FRG ceramic engine components (PET) 08 p1141 N85-17193
Development of high temperature ceramic parts for vehicular gas turbines
[PNR-90245] 09 p1282 N85-18062
Advanced Gas Turbine (AGT) powertrain system development for automotive applications
[NASA-CR-174809] 09 p1403 N85-18831
Knock syndrome: Its cures and its victims
[NASA-CR-174395] 10 p1458 N85-19185
West Europe report: Science and technology
[JPRS-WST-85-006] 11 p1618 N85-20183
Fiat introduces 1000-CC engine 11 p1618 N85-20185
Numerical simulation of turbulent reacting flows
[DE84-016777] 11 p1632 N85-20278
Engine wear and cold startability of methanol fueled engines.
[DE85-001208] 11 p1647 N85-20381
Introducing engine innovations: An examination of future markets for Brayton and Stirling automotive engines
[DE84-016319] 11 p1647 N85-20382
PSA, Renault work on all fuel automobile engine 15 p2531 N85-25604
Fiat conducts R and D in ceramic parts for diesel engine 15 p2534 N85-25637
Ceramic technology for advanced heat engines project
[DE85-004796] 16 p2755 N85-27002
Determination of wear intensity and resource of crankshafts and cylinder liners of ZIL-130 and ZMZ-53 engines
[BLL-BISI-TRANS-21393-(9022.06)] 17 p2972 N85-28355
Exhaust systems for passenger vehicles: Test procedure for resistance to internal corrosion of silencers
[BLL-BISI-TRANS-22360-(9022.06)] 17 p2973 N85-28361
Advanced Gas Turbine (AGT) technology project
[NASA-CR-174798] 19 p3219 N85-29961
Durability of oxygen sensors
[PB85-183093] 22 p3789 N85-33477

AUTOMOBILE FUELS
Status of gaseous fuels for use in highway transportation: A 1983 perspective
[DE84-015205] 01 p0034 N85-10211
State of knowledge of environmental concerns related to natural gas-fueled vehicles
[DE84-015894] 01 p0070 N85-10461
Application of the CSRL language to the design of expert diagnosis systems: The Auto-Mech experience
[AD-P003922] 02 p0245 N85-11602
Methane-fueled vehicle RD and D
[GPO-37-926] 04 p0481 N85-13064
Dissociated methanol vehicle test results
[DE84-004507] 04 p0509 N85-13248
Some characteristics of automotive gasolines and their performance in a light aircraft engine
[FAA-CT-84-12] 07 p0934 N85-15919
Dissociated methanol citation
[DE85-000505] 10 p1458 N85-19188
Volatility of in-use gasoline and gasoline-methanol blends
[PB85-117976] 10 p1459 N85-19189
Engine wear and cold startability of methanol fueled engines.
[DE85-001208] 11 p1647 N85-20381
PSA, Renault work on all fuel automobile engine 15 p2531 N85-25604
Low pressure storage of methane on interlayered clays for potential vehicular applications
[DE85-006949] 16 p2758 N85-27017
Auto fuel efficiency standards, part 2
[GPO-41-189] 20 p3435 N85-31309

AUTOMOBILES
NT ELECTRIC AUTOMOBILES
Pavement friction measurements on nontangent sections of roadways, vol. 1
[PB84-219732] 01 p0036 N85-10227
Predictor model for seasonal variations in skid resistance. Volume 2: Comprehensive report
[PB84-226620] 01 p0037 N85-10230
Study of annoyance due to urban automobile traffic
[NASA-TM-77514] 01 p0069 N85-10458

Performance evaluation of automotive wheel bearing greases
[AD-A145948] 03 p0337 N85-12168
Advanced concepts for methanol fuel vehicles
[DE84-013612] 04 p0482 N85-13071
Advanced automotive diesel assessment program
[NASA-CR-168285] 04 p0507 N85-13235
Dissociated methanol vehicle test results
[DE84-004507] 04 p0509 N85-13248
Summary results of the DOE flywheel development effort 05 p0606 N85-13865
ECUT energy data reference series: Lightweight materials for ground transportation
[DE84-015269] 05 p0621 N85-13974
Possibilities of increasing the simulation quality of multiaxial test stands — vehicle testing 05 p0649 N85-14169
Theoretical analysis of the dynamic behavior of structures with a passenger car as example 05 p0649 N85-14170
Evaluation of the crack initiation life behavior of fatigue loaded automotive components made from high strength aluminium alloys
[ESA-TT-733] 05 p0651 N85-14181
West Europe report: Science and technology
[JPRS-WST-84-039] 07 p0936 N85-15929
West Europe report: Science and technology
[JPRS-WST-85-001] 08 p1141 N85-17190
BBC of Switzerland develops electric car 08 p1141 N85-17192
FRG firms jump into market for auto, aircraft ceramics 09 p1309 N85-18225
Evaluation of the particulate levels occurring under 1.0/1.2 g/mi nitrogen oxide standards for light duty diesel vehicles and light duty diesel trucks
[PB85-115939/GAR] 09 p1350 N85-18494
Knock syndrome: Its cures and its victims
[NASA-CR-174395] 10 p1458 N85-19185
Dissociated methanol citation
[DE85-000505] 10 p1458 N85-19188
West Europe report: Science and technology
[JPRS-WST-85-004] 10 p1460 N85-19204
Flexible applications robot used in Moscow training course 10 p1462 N85-19217
Feasibility demonstration of a novel, flat-belt, continuously variable transmission or automotive and electric-hybrid vehicle application
[NASA-CR-174430] 10 p1569 N85-19694
Structural ceramics in transportation: Fuel implications and economic impacts
[DE85-003024] 11 p1611 N85-20130
Robot production lines in operation 11 p1617 N85-20166
Uses of composite materials 13 p2027 N85-22668
Lasers in automobile production 14 p2309 N85-24268
Performance testing and system characterization. DOE hybrid test vehicle, phase 3
[NASA-CR-175668] 14 p2434 N85-25010
Detonation flame spraying extends life of automotive parts 15 p2513 N85-25507
West Europe report: Science and technology
[JPRS-WST-84-007] 15 p2530 N85-25600
Mercedes-Benz auto 2000 achieves low drag coefficient 15 p2530 N85-25602
West Europe report: Science and technology
[JPRS-WST-84-009] 15 p2535 N85-25639
Functional impairment and structureal cervical injuries in human surrogates
[PB85-167436] 15 p2619 N85-26137
Nematic liquid crystals for car dashboards
[BMFT-FB-T-84-298] 16 p2872 N85-27718
Hybrid propulsion technologies for urban bus transit
[PB85-157469] 16 p2880 N85-27773
Robots, automatic devices inside VW's Wolfsburg plant 17 p2946 N85-28186
Exhaust systems for passenger vehicles: Test procedure for resistance to internal corrosion of silencers
[BLL-BISI-TRANS-22380-(9022.06)] 17 p2973 N85-28361
Report to Congress on the Automotive Technology Development Program
[DE85-005840] 17 p3052 N85-28890
West Europe report: Science and technology
[JPRS-WST-84-031] 18 p3086 N85-29089
West Europe report: Science and technology
[JPRS-WST-84-035] 18 p3087 N85-29102
Fuel cell applications literature review
[DE85-011891] 22 p3609 N85-33592

AUTOMORPHISMS
On rotation automorphic functions with descrete rotation groups 10 p1536 N85-19686
On the boundary behaviour of a rotation automorphic function with finite spherical Dirichlet integral 15 p2634 N85-26238

AUTONOMIC NERVOUS SYSTEM
NT SYMPATHETIC NERVOUS SYSTEM
Anatomy of the vestibulo-automatic outflow to the gut 15 p2614 N85-26106
Dissociation of autonomic and sensory vestibular reactions 23 p3953 N85-34501

AUTONOMOUS NAVIGATION
Autonomous navigation of USAF spacecraft 03 p0321 N85-12074
Combinatorial performance/cost analysis of an autonomous navigation system for aircraft 16 p2695 N85-26840
Visual position determination for autonomous vehicle navigation
[AD-A156007] 24 p4063 N85-35181

AUTONOMOUS SPACECRAFT CLOCKS
GPS system field testing 11 p1711 N85-20762
First results of GPS time transfer to Australia 17 p2962 N85-28294
Separating the variances of noise components in the Global Positioning System
[AD-P004578] 17 p2963 N85-28295
On-orbit frequency stability analysis of the GPS NAVSTAR's 3 and 4 rubidium clocks and NAVSTAR's 5 and 6 cesium clocks 17 p2963 N85-28296
Rubidium and cesium frequency standards status and performance on the GPS program 18 p3106 N85-29228

AUTONOMY
Autonomous navigation of USAF spacecraft 03 p0321 N85-12074
Space station systems technology study (add-on task). Volume 1: Executive summary
[NASA-CR-171415] 13 p1986 N85-22459
Autonomous state determination for an Earth orbiting satellite using horizon and star sensors
[AD-A151827] 15 p2493 N85-25379
In orbit infrastructure
[DM-51/CC-FL-044-83] 18 p3066 N85-28966
Standard Generic approach for Spacecraft Autonomy and Automation, phase 2 (SGASA-2). Volume 1: Executive summary
[ESA053-1-VOL-1] 18 p3167 N85-29623
Standard Generic Approach for Spacecraft Autonomy and Automation, phase 2 (SGASA-2). Volume 2: Technical report
[ESA053-1-VOL-2] 18 p3167 N85-29624
Standard Generic Approach for Spacecraft Autonomy and Automation, phase 2 (SGASA-2). Volume 3: Appendices
[ESA053-1-VOL-3] 18 p3167 N85-29625
Development of a temperature-compensated hot-film anemometer system for boundary-layer transition detection on high-performance aircraft
[NASA-TM-86732] 22 p3730 N85-33121

AUTOPILOTS
U AUTOMATIC PILOTS

AUTOPSIES
Head/neck injury: Post mortem procedures, Annex B 12 p1907 N85-21977

AUTORADIOGRAPHY
Electronic autofluorography: Principles, problems and prospects
[DE84-016698] 05 p0639 N85-14097
Development of a recombinant DNA assay system for the detection of genetic change in astronauts cells
[DE85-010103] 20 p3504 N85-31781

AUTOREGRESSIVE PROCESSES
Auto-regressive moving average spectral estimation using modified and least squares modified Yule-Walker estimates
[AD-A145516] 02 p0254 N85-11663
Parametric models for signal processing: Autoregressive (AR), Moving Average (MA) and mixed autoregressive with moving average (ARMA)
[ENST-84D001] 05 p0628 N85-14028
Texture classification using autoregressive filtering 07 p0984 N85-16254
Autoregressive spectral estimation for two dimensional time series 07 p0985 N85-16258
Conditionally heteroscedastic autoregressions
[AD-A147168] 07 p1035 N85-16587
Infinite order autoregressive representations of multivariate stationary stochastic processes
[AD-A147863] 07 p1036 N85-16580
Time series analysis of closed-loop pilot vehicle dynamics 08 p1087 N85-16876
Methods and applications of time series analysis. Part 2: Linear stochastic models
[AD-A147292] 08 p1214 N85-17645
Multivariable Autoregressive Moving Average (ARMA) models: A time approach to antenna processing
[ENST-84E015] 09 p1313 N85-18252
Data-driven choice of a spectrum estimate: Extending the applicability of cross-validation methods
[DE85-001411] 10 p1437 N85-19058
Statistical analysis of autoregressive spectral estimates for noise corrupted autoregressive series
[AD-A149543] 11 p1706 N85-20747
A review of some aspects of robust inference for time series
[AD-A149706] 12 p1923 N85-22082
Higher order residual analysis for nonlinear time series with autoregressive correlation structures
[AD-A149232] 15 p2636 N85-26257
Robust detection and classification of regional seismic signals using a two mode/two stage cascaded adaptive arma (CAARMA) model
[AD-A154710] 21 p3630 N85-32554
Methods and software for cosmic ray scintillation studies
[SH-9.1-17] 23 p4052 N85-35132

AUXILIARY EQUIPMENT (COMPUTERS)
NT PLOTTERS
NT PRINTERS (DATA PROCESSING)

AUXILIARY POWER SOURCES
NT NUCLEAR AUXILIARY POWER UNITS
NT SNAP
NT SOLAR AUXILIARY POWER UNITS
NT SPACE POWER REACTORS
NT SPACE POWER UNIT REACTORS
Ion thruster system (8-cm) cyclic endurance test
[NASA-CR-174745] 04 p0483 N85-12937
SNAP (Space Nuclear Auxiliary Power) reactor overview
[AD-A146831] 07 p1041 N85-16612
Space shuttle orbiter auxiliary power unit development challenges 08 p1099 N85-16945
The solid rocket booster auxiliary power unit: Meeting the challenge 08 p1099 N85-16946
Regenarative fuel cell systems for space station 20 p3443 N85-31372
Multikilowatt hydrogen-nickel oxide battery system 20 p3443 N85-31373

AUXILIARY PROPULSION
Ion thruster system (8-cm) cyclic endurance test
[NASA-CR-174745] 04 p0483 N85-12937

AV-8A AIRCRAFT
U HARRIER AIRCRAFT

AV-8B AIRCRAFT
U HARRIER AIRCRAFT

AVAILABILITY
Availability of transmission systems in continental and intercontinental connections — telecommunication
[FUB-33-1983] 01 p0040 N85-10261
Artificial intelligence approaches to monitoring system integrity
[AD-P003930] 02 p0246 N85-11610
Correlation and reassessment of the OTEC plant power cycle
[DE84-015467] 04 p0529 N85-13382
A practical example of reducing life cycle costs and increased availability 08 p1063 N85-16736
A replication and extension of the inducement of the availability heuristic
[AD-A149755] 12 p1923 N85-22083
Statistical aspects of reliability, maintainability and availability
[AD-A151228] 15 p2640 N85-26282
Solar pond technology for Navy applications
[AD-A155877] 24 p4112 N85-35488

AVALANCHE DIODES
Fine grained hodoscopes based on scintillating optical fibers
[DE84-014849] 01 p0120 N85-10625
The 30 GHz solid state amplifier for low cost low data rate ground terminals
[NASA-CR-174795] 03 p0358 N85-12300
Novel transport and recombination processes in semiconductors
[AD-A145969] 03 p0433 N85-12757
Avalanche photodiode statistics in triggered-avalanche detection mode 05 p0623 N85-13987
The development of a 90 GHz solid state noise source
[CD.8500695] 05 p0733 N85-14715
Millimeter-wave travelling-wave IMPATT diode
[AD-A146545] 06 p0804 N85-15117
Calculations of high-current characteristics of silicon diodes at microwave frequencies
[AD-A147406] 09 p1314 N85-18261
Advanced metal oxide varistor concepts
[DE84-016877] 09 p1316 N85-18276
Image line voltage controlled oscillator with replaceable components
[AD-D011436] 10 p1479 N85-19333
GaAlAs Sb APD optimization
[AD-A149406] 10 p1480 N85-19344

Investigations of the high frequency performance of impact avalanche transit-time diodes
13 p2063 N85-22884
Photon detection with cooled avalanche photodiodes: Theory and preliminary experimental results
16 p2770 N85-27096
Development of photodetectors
[AD-A153773] 18 p3095 N85-29158
Self-detecting optical sensors
[AD-D011657] 18 p3185 N85-29751
Noise characteristics of an avalanche photodiode
[AD-A154096] 19 p3258 N85-30205
Millimetre wave pulse technology — satellite mapping
[ESA-CR(P)-2004] 20 p3478 N85-31611
Sixty GHz IMPATT diode development
[NASA-CR-174969] 22 p3758 N85-33293

AVALANCHES
NT ELECTRON AVALANCHE
Spectral distribution of radiation in n junctions of GaAs during avalanche breakdown 02 p0258 N85-11668
Avalanche photodiode statistics in triggered-avalanche detection mode 05 p0623 N85-13967
Dependence of breakdown voltage for p-n junction on parameters of ion implantation and semiconductor heat treatment 07 p0954 N85-16046
Automated Lavina collects data on snow
07 p0980 N85-16224

AVERAGE
NT MEAN
Limit theory for the sample covariance and correlation functions of moving averages
[AD-A145488] 02 p0251 N85-11642
Auto-regressive moving average spectral estimation using modified and least squares modified Yule-Walker estimates
[AD-A145516] 02 p0254 N85-11663
Model equation for simulating flows in multistage turbomachinery
[NASA-TM-86889] 03 p0315 N85-12036
Distribution of total solar radiation in Spain
04 p0523 N85-13344
Parametric models for signal processing: Autoregressive (AR), Moving Average (MA) and mixed autoregressive with moving average (ARMA)
[ENST-84D001] 05 p0626 N85-14028
Multivariable Autoregressive Moving Average (ARMA) models: A time approach to antenna processing
[ENST-84E015] 09 p1313 N85-18252
The relevance of averaging period to wind power measurements and efficiency of Wind Energy Conversion Systems (WECS)
[GKSS-84-E-35] 11 p1676 N85-20562
Models of the upper atmosphere
12 p1945 N85-22217
Why do noninvertible estimated moving averages occur?
[AD-A150368] 13 p2153 N85-23368
Local likelihood estimation
[DE85-007238] 16 p2857 N85-27620
Method of and apparatus for generating an interstitial point in a data stream having an even number of data points
[NASA-CASE-MFS-25319-1] 22 p3627 N85-33701

AVIATION
U AERONAUTICS

AVIATORS
U AIRCRAFT PILOTS

AVIONICS
The Malcolm horizon: History and future
01 p0006 N85-10046
Avionics integrity program (Avip). Volume 4: Force management. Economic life considerations
[AD-A145582] 02 p0138 N85-10941
Avionics integrity program (Avip). Volume 3: Program cost assessment - environmental stress screening and diagnostic techniques
[AD-A145644] 02 p0139 N85-10942
Avionics integrity program (Avip). Volume 1: Procurement phase issues: Design, manufacturing, and integration
[AD-A145651] 02 p0139 N85-10943
Avionics Integrity Program (Avip). Volume 2: Hardware case studies
[AD-A145669] 02 p0139 N85-10944
Increased joint avionics standardization could result in major economies and operational benefits
[AD-A145730] 02 p0139 N85-10945
Expert systems in maintenance diagnostics for self-repair of digital flight control systems
[AD-P003933] 02 p0247 N85-11613
Army aviation today and tomorrow
06 p0751 N85-14810
HH-65A Dolphin digital integrated avionics
06 p0751 N85-14815
Integrated cockpit design for the Army helicopter improvement program 06 p0751 N85-14816
HH-60D night hawk helicopter
06 p0752 N85-14817
Avionics/crew station integration
06 p0752 N85-14818
Avionics technology - system concepts
06 p0753 N85-14824
Avionics system design for requirements for the United States Coast Guard HH-65A Dolphin
06 p0753 N85-14827
Certification of advanced systems
06 p0753 N85-14829
Integrated Application of Active Controls (IAAC) technology to an advanced subsonic transport project. ACT/Control/Guidance System study, volume 1
[NASA-CR-165963-VOL-1] 06 p0754 N85-14837
The effect of aircraft generated electromagnetic interference (EMI) on future avionics systems: A compendium
[AD-A146360] 06 p0799 N85-15101
Equipment for preflight test of an Electronic Countermeasures (ECM) avionic system
07 p0939 N85-15949
Design for Tactical Avionics Maintainability
[AGARD-CP-361] 08 p1063 N85-16731
Objectives in studying the maintainability of aircraft systems 08 p1063 N85-16732
Joint service design for testability program
08 p1063 N85-16733
The embedded test (BIT): Impact on the total cost of possession 08 p1063 N85-16734
Study and realisation of a 3rd level maintenance center based on ATE systems utilization
08 p1063 N85-16735
ATE user's view on design for maintainability
08 p1064 N85-16737
Built-in-test for first line testing
08 p1064 N85-16739
Maintainability: An ILS effort to manipulate LCC
08 p1064 N85-16743
Documentation and separate test program development is most important for test/maintenance
08 p1065 N85-16745
Effective life cycle software support: A study in discipline and versatility 08 p1065 N85-16746
Experience in using on-aircraft software for testing integrated systems 08 p1065 N85-16747
Investigating version dependence in fault-tolerant software 08 p1065 N85-16749
The effect on software design of testing by symbolic execution 08 p1065 N85-16750
Reliable software design for avionics and space applications 08 p1065 N85-16751
A weapon system design approach to diagnostics
08 p1066 N85-16752
Avionics fault tree analysis and artifical intelligence for future aircraft maintenance 08 p1066 N85-16755
Automatic briefing and mission management systems for battlefield support 08 p1073 N85-16799
Development of a Helicopter integrated navigation system 08 p1073 N85-16802
Standard Attitude Heading Reference System (SAHRS) full scale development program
08 p1073 N85-16804
Evolution toward a multi-bus architecture for Army helicopter avionic systems 08 p1074 N85-16812
Integration of sensor fusion in advanced helicopter cockpit design 08 p1074 N85-16813
Development, production and testing of central control and display unit for helicopters
[BMFT-FB-W-84-039] 08 p1085 N85-16871
Evolution of shuttle avionics redundancy management/fault tolerance 08 p1090 N85-16890
Shuttle avionics software trials, tribulations and success 08 p1090 N85-16891
Shuttle avionics software development trials: Tribulations and successes, the backup flight system
08 p1091 N85-16892
SSME digital control design characteristics
08 p1091 N85-16893
Man-machine interface and control of the shuttle digital flight system 08 p1091 N85-16894
Space shuttle main engine hardware simulation
08 p1091 N85-16895
Development and implementation of the verification process for the shuttle avionics system
08 p1091 N85-16896
Integrated design checkout of shuttle payload avionics interfaces 08 p1092 N85-16899
Automation of checkout for the shuttle operations era
08 p1092 N85-16900
Space Shuttle Technical Conference, part 2
[NASA-CP-2342-PT-2] 08 p1098 N85-16937
Life cycle cost model for very high speed integrated circuits
[AD-A147796] 08 p1157 N85-17298
Human Factors Considerations in High Performance Aircraft
[AGARD-CP-371] 10 p1532 N85-19653
Aircrew and avionics: Friends or Foes?
10 p1532 N85-19654
The evolution of methods of air traffic control
[AD-A149606] 12 p1774 N85-21137
A safety evaluation of the relocation of the ACM (Air Combat Maneuver) panel in the F-14 ( )/AIP (Avionics Integration Program)
[AD-A149598] 12 p1777 N85-21158
Proceedings of the 6th Advanced Aircrew Display Symposium
[AD-A150044] 12 p1778 N85-21160
Development of the F-20 nose radome
[AD-P004374] 12 p1827 N85-21468
Interface specifications for SCR (Software Cost Reduction) (A-7E) extended computer module, revised
[AD-A149948] 12 p1915 N85-22024
Investigation of device and electronic interactions in GaAs device processing
[AD-A149747] 12 p1940 N85-22182
Ground and flight testing for aircraft guidance and control
[AGARD-AG-282] 13 p1966 N85-22350
Civil avionics flight testing with the RAE(B) BAC1-11
13 p1967 N85-22354
Guidance and control research flight testing with HFB 320 test aircraft 13 p1967 N85-22355
Avionics Flight Evaluation System (AFES)
13 p1967 N85-22357
AIRLAB: A laboratory for flight-crucial-electronics system research 13 p1968 N85-22362
Reliability predictions for military avionics. Royal Signals and Radar Establishment reliability prediction method no. 250
[BR69221] 13 p1973 N85-22388
Shuttle flight test of an advanced gamma-ray detection system
[AD-A150316] 13 p1988 N85-22469
Design for tactical avionics maintainability, technical evaluation report
[AGARD-AR-204] 14 p2225 N85-23798
Rotorcraft digital advanced avionics system (RODAAS) functional description
[NASA-CR-166611] 15 p2468 N85-25237
YAV-8B Harrier 15 p2688 N85-26605
Rotorcraft digital advanced avionics system (Rodaas)
15 p2688 N85-26608
Design adequacy: An effectiveness factor
16 p2695 N85-26642
Design-To-Cost (DTC) methodology to achieve affordable avionics 16 p2696 N85-26645
Navigation and flight director guidance for the NASA/FAA helicopter MLS curved approach flight test program
[NASA-CR-177350] 16 p2704 N85-26691
Avionics integrity issues presented during NAECON (National Aerospace and Electronics Convention) 1984
[AD-A151923] 16 p2707 N85-26707
Avionics data base
[AD-A152415] 17 p2897 N85-27863
The Avionics Flight Evaluation System (AFES) of DFVLR
[DFVLR-MITT-85-01] 17 p2897 N85-27864
Air Force technical objective document FY 86
[AD-A152730] 17 p3047 N85-28655
Avionics Data Base users manual
[AD-A153810] 18 p3062 N85-28942
Avionics and civil aircraft systems: The present and the future
[SNIAS-851-111-104] 20 p3392 N85-31038
F-111 automatic test equipment replacement program
20 p3437 N85-31322
Aviation system delays
[S-HRG-98-1241] 21 p3553 N85-32102
HLLM software support
[AD-A154828] 21 p3671 N85-32805

AVOIDANCE
NT COLLISION AVOIDANCE
NT VORTEX AVOIDANCE
Development and certification of a new stall warning and avoidance system 05 p0702 N85-14507

AWARDS
National Science Foundation grants and awards for fiscal year 1983, volume 2
[PB84-212323] 01 p0125 N85-10654
An analysis of production competition and award methodology
[AD-A147775] 08 p1228 N85-17733
1985 Resident research associateships: Postdoctoral and senior research awards
[NASA-TM-87458] 12 p1963 N85-22338

AXAF
U X RAY ASTROPHYSICS FACILITY

AXES (COORDINATES)
U COORDINATES
AXES (REFERENCE LINES)
NT AXES OF ROTATION
NT EARTH AXIS
Acceleration resistant combination of opposite-handed piezoelectric crystals
[AD-D011626] 16 p2778 N85-27143
AXES OF ROTATION
NT EARTH AXIS
Design of two-mirror scanner with axes of rotation not in plane of mirrors 06 p0777 N85-14969
Shoulder and hip joint for hard space suits and the like
[NASA-CASE-ARC-11543-1] 12 p1910 N85-21986
Motion of symmetrical satellite with flexible viscoelastic rods about center of mass in circular orbit 13 p1979 N85-22420
Axial representations of shape
[AD-A150367] 13 p2151 N85-23356
Precise mounting of instruments in universal suspension with skewed axes 14 p2273 N85-24083
Stability of steady modes of motion by axis of rotating wheel in nonlinear bearings 14 p2279 N85-24117
Stability of permanent rotation modes of asymmetric heavy solid body 14 p2279 N85-24118
Structural design of the Sandia 34-meter vertical-axis wind turbine
[DE85-011146] 18 p3118 N85-29300
Wake effects on the aerodynamic performance of horizontal axis wind turbines
[NASA-CR-174920] 18 p3127 N85-29364
Studies of the solar mesosphere explorer: Dynamics and horizon sensor performance. Part A: Spin axis precession and atmospheric drag. Part B: Clouds
[NASA-CR-175308] 24 p4069 N85-35213
AXIAL COMPRESSION LOADS
Fatigue in composite materials 04 p0467 N85-12968
Stability of cylindrical shells with one-way constraints 13 p2048 N85-22820
Dynamic shock studies of PZT 95/5 ferroelectric ceramic
[DE85-006137] 14 p2261 N85-24015
An analysis for axially compressed orthotropic shells with a multimode imperfection representation
[VTH-LR-422] 16 p2803 N85-27281
Optimization of axially compressed carbon fiber reinforced plastic (CFRP) cylinders 18 p3121 N85-29318
Polymer matrix and graphite fiber interface study
[NASA-CR-177357] 19 p3232 N85-30036
Mechanical ratcheting behaviors of a steel pipe under combined cyclic axial load and internal pressure 23 p3904 N85-34184
Monotonous stress-strain properties of structural steel subjected to nonstationary repetitive pre-loading 23 p3904 N85-34185
AXIAL COMPRESSORS
U TURBOCOMPRESSORS
AXIAL FLOW
Development of a Navier-Stokes rotor and stator analysis
[AD-A146967] 07 p0958 N85-16070
Axial flow laser cavity
[AD-D011506] 12 p1855 N85-21633
Flow-induced vibrations of a circular cylinder due to turbulent internal flows
[DE85-002766] 13 p2103 N85-23110
Fluid mechanics and heat transfer spirally fluted tubing
[AD-A150774] 14 p2301 N85-24247
On the structure of the turbulent vortex 15 p2463 N85-25213
Monogroove heat pipe design: Insulated liquid channel with bridging wick
[NASA-CASE-MSC-20497-1] 18 p3098 N85-29180
Classical emission of relativistic charged particles during axial channeling 21 p3681 N85-32871
Second order modelling in non-constant density flows 22 p3744 N85-33206
Wingtip vortex propeller
[NASA-CASE-LAR-13019-1] 24 p4065 N85-35194
AXIAL FLOW COMPRESSORS
U TURBOCOMPRESSORS
AXIAL FLOW PUMPS
NT TURBINE PUMPS
AXIAL LOADS
NT AXIAL COMPRESSION LOADS
Post buckling behavior of a circular rod constrained within a circular cylinder 02 p0207 N85-11385
Flywheel containment and safety considerations 05 p0606 N85-13869
Low cycle fatigue strength for multiaxial loading of ductile materials 05 p0649 N85-14187
Stability of hollow shafts under torsion 06 p0780 N85-14966
Life prediction at high temperature under multiaxial loading 07 p0907 N85-15745
Evaluation of the blind hole drilling method for the measurement of residual stress
[AD-A151459] 15 p2579 N85-25905
Calculation of friction at spherical bearing journals in turbomachines 17 p2940 N85-28150
Improvement of conditions for meshing spiral bevel gears
[NASA-TM-77667] 18 p3117 N85-29294
Multiaxial fatigue and fracture: A literature review
[ARL/STRUC-R-410] 19 p3285 N85-30370
On design of off-axis specimens
[AD-A154328] 19 p3286 N85-30379
Experimental study of collapse of thick-walled tube under external pressure and axial force 23 p3904 N85-34186
AXIAL MODES
The axial velocity spread acceptance of free electron lasers
[AD-A149024] 10 p1489 N85-19403
AXIAL STRAIN
Composite laminate optimization program suitable for microcomputers 01 p0059 N85-10389
The effect of overload on three different kinds of steel 02 p0174 N85-11165
Device for measuring relative axial expansion of turbine rotor employing space-vector tracking method 06 p0776 N85-14962
Strain-controlled creep rupture in non-isothermal materials 09 p1332 N85-18368
Dissipation of energy in composite material 13 p2027 N85-22703
Correlation of uniaxial and biaxial fracture strengths of ceramics
[DE85-003779] 14 p2261 N85-24011
Finite axisymmetric deformation of a thin shell of revolution 16 p2798 N85-27251
Transverse periodic boundary conditions in molecular dynamics with uniaxial strain shock waves
[DE85-006497] 16 p2863 N85-27656
Uniaxial angular accelerometers 17 p2944 N85-28173
Multiaxial fatigue low cycle fatigue testing 20 p3488 N85-31544
Results of an interlaboratory fatigue test program conducted on alloy 800H at room and elevated temperatures
[NASA-CR-174940] 21 p3597 N85-32340
AXIAL STRESS
Improved multiaxial creep-rupture strength criterion
[DE84-014273] 01 p0062 N85-10413
Fatigue limit analysis involving biaxial stress components 03 p0370 N85-12363
Improved beam theory for anisotropic materials 04 p0468 N85-12973
Stress concentration due to axial tension of loaded nonsymmetric-shaped grooves
[AD-A149425] 10 p1496 N85-19442
Multiaxial stress response of ceramics
[DE85-004350] 12 p1814 N85-21379
Dynamic crack curving and branching under biaxial loading
[AD-A151451] 15 p2578 N85-25904
Mechanical properties of high performance carbon fibers 16 p2742 N85-26922
Biaxial buckling of specially orthotropic, symmetric composite rectangular plates
[AD-A152958] 17 p2979 N85-28417
Uniaxial stress induced symmetry breaking for muon sites in Fe 17 p3042 N85-28820
Multiaxial fatigue low cycle fatigue testing 20 p3488 N85-31544
Multiaxial stress analysis taking account of penetration depth of X-rays. A solution by means of polynomial approximation 23 p3907 N85-34204
AXISYMMETRIC BODIES
Method for prompt modeling of quasiperiodic movement of solid near-axisymmetrical body in atmosphere 13 p2043 N85-22790
Flight dynamics of axisymmetrical rotating bodies in air medium 13 p2043 N85-22791
Absolute stability of unsteady movement of axisymmetrical rotating flight vehicle 13 p2044 N85-22793
Steady-state reaction of three-layered cylindrical shell to effect of moving load 13 p2047 N85-22811
Comparison of measured and computed boundary layers at the tail-end of an axisymmetric body in an air-jet
[AMTE(N)-TM-83063] 14 p2209 N85-23700
Flow around axisymmetric bodies with uniform-velocity zones 14 p2276 N85-24103
Some problems in optimally designing shells of revolution 14 p2278 N85-24114
An experimental investigation of confined, multiple, turbulent jet mixing with recirculation — flow distribution in combustors with injection plates 15 p2555 N85-25764
Direct transient analysis of a fuze assembly by axisymmetric solid elements 15 p2576 N85-25890
Stress analysis of axisymmetric sandwich shells of variable thickness 24 p4101 N85-35419
AXISYMMETRIC DEFORMATION
U AXIAL STRAIN
AXISYMMETRIC FLOW
NT ANNULAR FLOW
Mass and momentum transport in a turbulent buoyant vertical axisymmetric jet 05 p0635 N85-14070
Design of swirled axisymmetric turbulent jets 05 p0724 N85-14857
Applications of finite and wave envelope element approximations to acoustic radiation from turbofan engine inlets in flight 05 p0726 N85-14884
A three-dimensional axisymmetric calculation procedure for turbulent flows in a radial vaneless diffuser
[NASA-TM-86903] 06 p0749 N85-14798
Variable loading of elastic-plastic shells of revolution 06 p0779 N85-14981
Analytical modeling of circuit aerodynamics in the new NASA Lewis wind tunnel
[NASA-TM-86912] 07 p0897 N85-15688
A computer program for the performance analysis of scarfed nozzles
[AD-A147370] 07 p0905 N85-15730
Aeroacoustic data for high Reynolds number supersonic axisymmetric jets
[NASA-TM-86296] 07 p1038 N85-16567
Thrust chamber performance using Navier-Stokes solution — space shuttle main engine viscous nozzle calculation
[NASA-CR-171346] 10 p1430 N85-19019
Computer studies of baroclinic flow — Atmospheric General Circulation Experiment
[NASA-CR-171338] 10 p1517 N85-19566
The modelling of latitudinal gradients in the solar wind in the outer solar system 12 p1947 N85-22231
The low frequency behaviour of an immersed structure at a standstill in a high density fluid with free surface
[TP-1983-31] 13 p2103 N85-23105
Analysis of combustion oscillations in heterogeneous systems
[AD-A151999] 16 p2745 N85-26942
Studies of structure and modeling in turbulent shear flows
[AD-A151807] 16 p2782 N85-27170
Computation model of turbulent free flow: Application to axisymmetric jets
[ISL-R-126/83] 16 p2785 N85-27185
Characteristics of steady-state hypersonic flow about blunted bodies with discontinuities in generators 17 p2941 N85-28155
Impact starting of plane nozzles with wide divergence angle 17 p2941 N85-28156
Navier-Stokes computational study of axisymmetric transonic turbulent flows with a two-equation model of turbulence
[AD-A152653] 17 p2958 N85-28265
Modifications to SOLA-VOF for flow dynamics in spinning cylinders
[AD-A154093] 19 p3265 N85-30250
On the evaluation of boundary layer measurements on boattailed bodies of revolution in axisymmetric compressible subsonic flow
[ESA-TT-883] 20 p3457 N85-31471
A panel method study of vortex sheets with special emphasis on sheets of axisymmetric geometry
[NASA-CR-177365] 21 p3552 N85-32095
A numerical study of Taylor-Vortex flow
[AD-A154787] 21 p3584 N85-32277
A mixed pseudospectral/finite difference method for a thermally driven fluid in a nonuniform gravitational field
[NASA-TM-87581] 22 p3783 N85-33436
Studies on effects of boundary conditions in confined turbulent flow predictions
[NASA-CR-3929] 24 p4093 N85-35371
AXISYMMETRY
U SYMMETRY
AXLES
U SHAFTS (MACHINE ELEMENTS)
AZIDES (INORGANIC)
Azido nitramino ether containing solid propellants
[AD-D011511] 12 p1816 N85-21392
Spray pyrolysis as a synthetic tool
[AD-A153891] 19 p3234 N85-30047
AZIDES (ORGANIC)
NT TRIAMINOGUANIDINIUM AZIDE
Spray pyrolysis as a synthetic tool
[AD-A153891] 19 p3234 N85-30047

AZIMUTH
Structural investigation of the Grenville Province by radar and other imaging and nonimaging sensors
08 p1147 N85-17237
The effects of internal waves on acoustic normal modes
[AD-A150235] 13 p2155 N85-23379
The access of energetic charged particles to satellite altitudes
[AD-A150799] 14 p2373 N85-24670
Azimuthal variations in Saturn's A ring
15 p2671 N85-26478
Additional possibilities of radiometeor azimuthal method for measuring wind velocity in lower thermosphere
19 p3296 N85-30438
Terrain illumination conditions when taking scanning photographs from space 22 p3736 N85-33159
Calculating solar highlight and shadeless areas for scanning photographs from space and optimizing lighting conditions 22 p3736 N85-33160
Comprehensive fracture diagnostics experiement. Part 2: Comparison of seven fracture azimuth measurements
[DE85-011707] 23 p3948 N85-34470
A star camera aspect system suitable for use in balloon experiments
[OG-9.3-10] 23 p4026 N85-34965
Azimuthal and meridional asymmetries of the solar wind and quasiperiodic variations of intensity of Galactic Cosmic Rays (GCR)
[SH-4.4-20] 23 p4035 N85-35016
Jets in air-jet family
[HE-3.2-1] 24 p4179 N85-35912
A comparative analysis of gamma and hadron families at the superhigh energies recorded in experiment Pamir
[HE-3.7-1] 24 p4185 N85-35960
AZINES
NT METHYLENE BLUE
Effects of triazine components on physicochemical properties of polybutadiene: urethane block copolymers
13 p2014 N85-22635
The electrochemistry of azine, oxazine and thiazine dyes
[AD-A152394] 17 p2918 N85-27990
AZO COMPOUNDS
NT RDX
Substituent effects on the electrical conductivities of the phenazine derivatives
[NASA-TM-77792] 14 p2249 N85-23938
Electrochemistry of Hexanitroazobenzene (HNAB)
[DE85-010807] 21 p3565 N85-32171
Synthesis of energetic materials
[AD-A154867] 21 p3571 N85-32210
AZOLES
NT CARBAZOLES
NT OXAZOLE
NT PYRROLES
NT TRYPTOPHAN
Development of new and improved polymer matrix resin systems, phase 1
[NASA-CR-166595] 01 p0017 N85-10104
A method for obtaining new cyclical imides of derivative benzimidazoles
[AD-A145042] 01 p0017 N85-10106
Chemically modified electrodes and related solution chemistry
[DE84-017110] 05 p0614 N85-13924
Theoretical studies on N-bonded pyrazole derivatives of boron
[AD-A150036] 12 p1813 N85-21374
Ethylenediamine salt of 5-nitrotetrazole and preparation
[DE85-005738] 23 p3923 N85-34306

B

B STARS
The rotation of B-type stars and processes of star formation 03 p0443 N85-12823
The influence of stellar luminosity and temperature calibration on the determination of the initial mass function 05 p0740 N85-14760
The velocity-age relation for B and A stars
05 p0740 N85-14762
Kinematics of B and A stars 05 p0741 N85-14766
Nonradial pulsation and mass loss in early B stars
06 p1232 N85-17759
Light variations of the B-type star HD 160202
06 p1232 N85-17761
The UV extinction laws in two very young clusters, NGC 6530 in the galaxy and NGC 2100 in the LMC
11 p1748 N85-20894
Interstellar extinction in the nucleus of H PER
11 p1749 N85-21001
Superionized species and winds in low luminosity B and Be stars 11 p1749 N85-21003
Main sequence B stars with strong winds
11 p1750 N85-21005
Analysis of high-depression IUE spectra of subdwarf B stars 11 p1751 N85-21011
Ultraviolet spectroscopy of the interacting binary U Sagittae 11 p1755 N85-21042
Strange F + Be binary star systems
11 p1756 N85-21045
Studies of hot B subdwarfs. Part 2: Energy distributions of three bright sdB/sdOB stars in the 950-5500 angstrom range
[NASA-CR-175854] 16 p2881 N85-27775
B-A-W DEVICES
U BULK ACOUSTIC WAVE DEVICES
B-1 AIRCRAFT
Logistics support costs for the B-1B aircraft can be reduced
[AD-A145846] 03 p0309 N85-11996
B-70 AIRCRAFT
Supersonic cruise technology
[NASA-SP-472] 18 p3057 N85-28912
BABOONS
Functional impairment and structureal cervical injuries in human surrogates
[PB85-167436] 15 p2619 N85-26137
BAC AIRCRAFT
NT JET PROVOST AIRCRAFT
BACILLUS
Differences in susceptibility of inbred mice to bacillus anthracis
[AD-A155646] 21 p3662 N85-32750
Genetic and physiological control of protective antigen synthesis by bacillus anthracis
[AD-A156324] 24 p4133 N85-35617
BACKGROUND NOISE
Sources, paths, and concepts for reduction of noise in the test section of the NASA Langley 4x7m wind tunnel
[NASA-CR-172446-VOL-1] 05 p0726 N85-14666
Comparison of options for reduction of noise in the test section of the NASA Langley 4x7m wind tunnel, including reduction of nozzle area
[NASA-CR-172446-VOL-2] 05 p0726 N85-14667
Synthesis of systems for coherent weighted signal processing against background of correlated interference 06 p0790 N85-15045
Synoptic observations of the radio noise background in the frequency range 150-180 kHz to provide design data for the low frequency communications designer
[AD-A147438] 07 p0941 N85-15965
Microseism level, time variations at Turkmen seismic stations studied 07 p0981 N85-16231
Discriminability of signals from noise in a dynamic stereoscopic space
[AD-A148406] 08 p1196 N85-17535
Extraction of signals from background interference with unknown parameters in quantized sample
13 p2084 N85-23013
Approximate rules for signal detection against background of Gaussian correlated interference
13 p2086 N85-23027
Background noise measurements from jet exit vanes designed to reduced flow pulsations in an open-jet wind tunnel
[NASA-TM-86383] 17 p2906 N85-27916
Fiber optic gyroscope with alternating output signal
[AD-D011689] 19 p3271 N85-30284
Application of adaptive noise cancellation to Coast Guard voice communications
[AD-A154796] 21 p3574 N85-32230
Design of a freestanding noise measurement and recording system to predict the intensity and location of electromagnetic radiation from earthquakes
[AD-A155070] 21 p3632 N85-32563
A real time index of geomagnetic background noise for the MAD (Magnetic Anomaly Detection) frequency band
[AD-A155717] 22 p3814 N85-33627
A comparison of calculated and measured background noise rates in hard X-ray telescopes at balloon altitude
[OG-9.3-7] 23 p4028 N85-34962
BACKGROUND RADIATION
The Belikt experiment 02 p0159 N85-11079
On syntheses of the X-ray background with power-law sources
[NASA-TM-82173] 03 p0446 N85-12840
A large scale height galactic component of the diffuse 2-60 keV background
[NASA-TM-83837] 03 p0446 N85-12841
Search for the radiative decay of a cosmic relic particle with IUE
[PREPRINT-410] 04 p0580 N85-13707
New measurements of the spectrum of the cosmic microwave background
[DE84-016055] 05 p0746 N85-14785
The soft X-ray diffuse background: Implications for the nature of the local interstellar medium
06 p0876 N85-15566
Ultrasoft X-ray background observations of the local interstellar medium 06 p0877 N85-15571
Observations of local ISM emission with the Berkeley EUV/FUV shuttle telescope 06 p0880 N85-15594
Cosmology 07 p1056 N85-16701
The HEAO-1 diffuse component spectrum from 15 to above 500 keV — X and gamma rays
08 p1240 N85-17820
The origin of the X-ray background
08 p1243 N85-17841
Background calculations for the measurement of the ion temperature in a deuterium plasma
[DE84-016546] 09 p1393 N85-18768
An electronically controlled array for simulation of passive target/background signatures at millimeter wavelengths
[AD-D011456] 10 p1468 N85-19263
Elimination of sensor artifacts from infrared data
[AD-A149048] 10 p1556 N85-19614
Galaxy formation 12 p1960 N85-22321
Measurement of the large-scale anisotropy of the cosmic background radiation at 3 MM 13 p2206 N85-23680
A measurement of the intensity of the cosmic background radiation at 3.9 cm
13 p2206 N85-23681
Interplanetary plasma turbulence and the Doppler detection of a gravitational background radiation
[IFSI-85-1] 20 p3546 N85-32066
Visibility and vertical structure measurements in southern Germany
[AD-A154714] 21 p3635 N85-32574
Spectrum of the gamma-ray diffuse component observed from HEAO-1
[OG-3.1-12] 22 p3874 N85-34000
The 1984 biotic studies of Yucca Mountain, Nevada test site, Nye County, Nevada
[DE85-011715] 23 p3951 N85-34487
CYLTRAN calculations of electron effects on XD detectors
[LA-10264-MS] 23 p3969 N85-34601
The design of an experiment to detect low energy antiprotons
[OG-9.1-1] 23 p4022 N85-34928
Neutron-induced 2.2 MeV background in gamma ray telescopes
[OG-9.3-6] 23 p4027 N85-34961
Three dimensional calculation of flux of low energy atmospheric neutrinos
[SH-8.1-11] 23 p4050 N85-35116
The muon content of gamma-ray showers
[HE-4.5-7] 24 p4195 N85-36031
The Nagoya cosmic-ray muon spectrometer 3, part 1: Preliminary observations
[HE-5.2-2] 24 p4202 N85-36080
BACKINGS
U BACKUPS
BACKSCATTERING
Active microwave measurements of sea ice under fall conditions: The RADARSAT/FIREX fall experiment — in the Canadian Arctic
[E85-10019] 02 p0217 N85-11432
Development of a global model for atmospheric backscatter at CO2 wavelengths
[NASA-CR-174053] 02 p0228 N85-11489
Scattering from snow backgrounds at 35, 96, and 140 GHz
[AD-A145798] 03 p0355 N85-12280
Dust properties determined from backscattering in the interplanetary and interstellar medium
03 p0446 N85-12838
Anglo-German millimeter wave backscatter measurements on snow, environmental data report
[REPT-7-84] 04 p0492 N85-13136
Scattering from randomly oriented scatterers of arbitrary shape in the low-frequency limit with application to vegetation 04 p0525 N85-13362
Scattering from randomly oriented circular discs with application to vegetation 04 p0525 N85-13363
Materials characterization using ion, electron, and photon probes
[DE84-004516] 04 p0560 N85-13568
Relation between atmospheric scattering and backscattering coefficient
[ESA-TT-837] 05 p0677 N85-14350
Research on acoustical and optical scattering, optics of bubbles, diffraction catastrophes, laser generation of sound, and shock induced cavitation
[AD-A146703] 06 p0860 N85-15466
Intermediate results of radar backscatter measurements from summer sea ice
[AD-A147212] 07 p0940 N85-15960
Method for non contacting gauging of the wall thickness of tubes by backscattering radiation
[OEFZS-4274] 07 p0968 N85-16144

Simultaneous ocean cross-section and rainfall measurements from space with a nadir-pointing radar
[NASA-TM-86167] 07 p0987 N85-16273
Chemical information from ion scattering spectrometry
[AD-A148287] 08 p1121 N85-17069
The interpretation of SIR-B imagery of surface waves and other oceanographic features using in-situ, meteorological satellite, and infrared satellite data
08 p1143 N85-17212
Quantitative use of multiincidence-angle SAR for geologic mapping 08 p1145 N85-17220
Geologic mapping of Indonesian rain forest with analysis of multiple SIR-B incidence angles
08 p1145 N85-17221
German Radar Observation Shuttle Experiment (ROSE) 08 p1148 N85-17245
Evaluation of the radar response to land surfaces and volumes: Examination of theoretical models, target statistics, and applications 08 p1149 N85-17250
Ground truth for SIR-B images obtained by SIR system 8 impulse radar 08 p1149 N85-17251
Remote sensing of soil moisture
08 p1149 N85-17252
Carbon dioxide laser radar for monitoring atmospheric transmittance and atmospheric aerosol
09 p1354 N85-18516
Specifics of backscattering of sound by bottom of bank in open sea 10 p1499 N85-19460
Cyclone diagnostics — rainfall estimation, backscatter, and lidar
[NASA-CR-171337] 10 p1516 N85-19567
Parametric processes in underdense UV laser-produced plasmas
[DE85-002612] 10 p1559 N85-19630
Nonlinear saturation of stimulated Raman scattering in collisional homogeneous plasma
[DE85-002614] 10 p1559 N85-19631
Applications of the Heavy-Iron Rutherford Backscattering Spectrometry (HIRBS) to the analysis of contact structures on GaAs and Ge
[DE85-000671] 10 p1564 N85-19661
Lidar observations of stratospheric aerosol over Mauna Loa Observatory, 1974 - 1981
[PB85-115061] 11 p1682 N85-20597
Quantitative non-destructive evaluation of damage in composite materials using transmitted and reflected ultrasound
[NASA-CR-175550] 12 p1796 N85-21269
Aerosol multiple-scanning code, ASCAT
[LA-10048-MS] 12 p1823 N85-21440
On the inversion of the lidar equation
[AD-A149853] 12 p1856 N85-21641
Oceanographic and meteorological research based on the data products of SEASAT
[E85-10091] 12 p1874 N85-21753
Phase function, backscatter, extinction, and absorption for standard radiation atmosphere and El Chichon aerosol models at visible and near-infrared wavelengths
[NASA-TM-86379] 12 p1892 N85-21874
Effects of scatterer spacing statistics on ultrasonic backscatter signal spectra
[DE85-003259] 12 p1928 N85-22114
Atmospheric transmissometer
[AD-D011540] 12 p1932 N85-22140
Reaction of amorphous NiNb films with crystalline metal overlayers
[DE85-005483] 13 p2024 N85-22680
Optical reflectometer for multimode fiber lightpipes
13 p2075 N85-22961
The microwave propagation and backscattering characteristics of vegetation — wheat, sorghum, soybeans and corn fields in Kansas
[E85-10088] 13 p2122 N85-23213
Microwave remote sensing of soil moisture
13 p2125 N85-23235
Investigations of ultrasonic wave interactions at boundaries separating anisotropic materials
[DE85-003506] 13 p2155 N85-23364
Influence scattering and Q in the Rhosphere
[AD-A150939] 14 p2293 N85-24213
Afternoon radar aurora and polar cap convection pattern 14 p2361 N85-24592
Secondary fluorescence effects on X-ray microanalysis
[DE85-005585] 15 p2506 N85-25457
Development of global model for atmospheric backscatter at CO2 wavelengths
[NASA-CR-175579] 15 p2591 N85-25971
Modeling the backscattering and transmission properties of vegetation canopies
[E85-10099] 16 p2809 N85-27320
Test of lidar inversion algorithm sensitivity to atmospheric backscatter and extinction parameters, revision A
[AD-A152082] 16 p2865 N85-27671
An experimental investigation of the angular scattering and backscattering behaviors of the simulated clouds of the outer planets
[NASA-CR-175909] 17 p3052 N85-28696
Amorphous alloys of ion-implanted Fe-Ti-C
[DE85-010656] 19 p3360 N85-30834
Broadside scattering of a tubular cylinder for evaluation of target identification
[AD-A155739] 21 p3577 N85-32248
Plating density standards
[DE85-010014] 21 p3591 N85-32318
Meteorological and seronomical requirements for MST radar networks (keynote paper), part 1
21 p3615 N85-32467
A modified Fresnel scattering model for the parameterization of Fresnel returns, part 2.3A
21 p3618 N85-32483
Observations of mesospheric turbulence by rocket probe and VHF radar, part 2.4A 21 p3619 N85-32484
Interpretation of radar returns from the mesosphere, part 2.3A 21 p3619 N85-32485
Usefulness of multifrequency MST radar measurements, part 2.6B 21 p3619 N85-32487
Relationship of spaced antenna and Doppler techniques for velocity measurements (keynote paper), part 3
21 p3619 N85-32488
Anisotropy of the permittivity field inferred from aspect-sensitive radar echoes 21 p3620 N85-32492
Visibility and vertical structure measurements in southern Germany
[AD-A154714] 21 p3635 N85-32574
Fluctuations in light intensity during backscattering in turbulent medium 21 p3695 N85-32956
Data on the backscattering coefficients on light ions from solids: A revision
[IPPJ-AM-41-REV] 23 p3962 N85-34689
Quantitative non-destructive evaluation of composite materials based on ultrasonic wave propagation
[NASA-CR-176176] 24 p4074 N85-35244

BACKSHORES
U BEACHES

BACKUPS
Shuttle avionics software development trials: Tribulations and successes, the backup flight system
08 p1091 N85-16892
SSME digital control design characteristics
08 p1091 N85-16893
Autonomous uninterruptable power supply apparatus
[AD-D011571] 14 p2298 N85-24232

BACKWARD FACING STEPS
Heat transfer and fluid mechanics measurements in the turbulent reattaching flow behind a backward-facing step
15 p2553 N85-25753
A finite element, Navier-Stokes study of the confined, laminar flow over a downstream facing step
15 p2553 N85-25754
An experimental study of compressible turbulent reattaching free shear layers 16 p2781 N85-27161
An implicit finite-difference code for a two-equation turbulence model for three-dimensional flows
[NASA-TM-86752] 20 p3454 N85-31448

BACKWARD WAVE TUBES
NT HELITRONS

BACTERIA
NT BACILLUS
NT CLOSTRIDIUM BOTULINUM
NT ESCHERICHIA
NT PSEUDOMONAS
NT STAPHYLOCOCCUS
An electrochemical approach to the prevention of biofouling phenomena
[PB84-202613] 01 p0025 N85-10155
Proton pumping in purple membrane, appendix 1
[DE84-014601] 01 p0118 N85-10811
Phylogenic distribution of the large 55 rRNA from Halococcus morrhuae
[NASA-CR-174019] 02 p0234 N85-11523
Microbiological method for the desiliconization of high-silica bauxites
[BLL-MINTEK-TR-1168-(5810.5759)]
07 p0925 N85-15864
Respiratory chain of alkalophilic bacteria
[DE84-012558] 09 p1360 N85-18556
Investigation of the initial events in biofouling
[AD-A149695] 12 p1900 N85-21927
Production and turnover of suspended organic detritus in the coastal water of the southeastern continental shelf
[DE85-003977] 13 p2140 N85-23290
Studies of photosynthetic Energy Conversion
[DE85-005973] 15 p2586 N85-25944
The effects of simulated weightlessness on susceptibility to viral and bacterial infections using a murine model
15 p2613 N85-26100
Fatty and aromatic acid catabolizing bacteria from methanogenic ecosystems
[DE85-008133] 17 p2998 N85-28537
A basic study to assess the potential usefulness of resonance Raman spectroscopy as a means of rapidly detecting and identifying bacteria and other microorganisms
[AD-A153549] 18 p3152 N85-29513
Survival of microorganisms and bacterial predation in nature
[AD-A153574] 18 p3152 N85-29514
Genetics in methylotrophic bacteria
[DE85-011460] 19 p3327 N85-30615
Investigation of variation in the concentration of bacteria in outdoor testing, with the use of a detector for aerosols of bacteria
[FOA-C-40201-B2] 20 p3504 N85-31784
Ice active bacteria as condensation nuclei
21 p3639 N85-32609
Aerobic sulfur-oxidizing bacteria: Environmental selection and diversification 21 p3656 N85-32712
Protocyanobacteria: Oxygenic and Anoxygenic photosynthesis in mat-forming bacteria
21 p3657 N85-32714
Sulfur transformations at the hydrogen sulfide/oxygen interface in stratified waters and in cyanobacterial mats
21 p3657 N85-32715
Distribution and abundance of organic thiols
21 p3657 N85-32717
Cytochromes and iron sulfur proteins in sulfur metabolism of phototrophic bacteria
21 p3657 N85-32718
Insights into the phylogenetic positions of photosynthetic bacteria obtained from 5S rRNA and 16S rRNA sequence data 21 p3658 N85-32719
Ecophysiology of phototrophic sulfur bacteria in lakes: Vertical distribution of planktonic populations
21 p3658 N85-32722
Chemolithotrophy and physiology of bacterial nutrient limitation 21 p3659 N85-32730
Structure and physiology of Beggiatoa and Thiothrix
21 p3659 N85-32734
Phototrophic bacteria and their role in the biogeochemical sulfur cycle 21 p3660 N85-32735
Sulfur cycling and metabolism of phototrophic and filamentous sulfur bacteria 21 p3660 N85-32737
Enrichments for phototrophic bacteria and characterization by morphology and pigment analysis
21 p3660 N85-32738
Anaerobic reduction of elemental sulfur by Chromatium vinosum and Beggiatoa alba 21 p3660 N85-32739
Buoyant densities of phototrophic sulfur bacteria and cyanobacteria 21 p3660 N85-32740
Interactions among sulfide-oxidizing bacteria
21 p3661 N85-32741
Cyanobacterial mats: Microanalysis of community metabolism 21 p3661 N85-32743
Microanalysis of dissolved iron and phosphate in pore waters of hypersaline sediment
21 p3661 N85-32744
Glutathione in cyanobacteria
21 p3661 N85-32745
Microbial communities and microprofiles of sulfide and oxygen of alum rock sulfur springs
21 p3661 N85-32748
Composition and dynamics of bacteriocenosis associated with algae in human life-support systems
22 p3823 N85-33684
Legionnaires' disease bacteria in power plant cooling systems: Phase 2
[DE85-011546] 22 p3825 N85-33695
Microbiological and biochemical studies towards optimization of substrate utilization by methanogenic bacteria
[PB85-188332] 24 p4064 N85-35310

BACTERIOLOGY
Growth of soil bacteria in presence of Martian soil analog, carbon dioxide and hydrogen peroxide
09 p1361 N85-18560
Structural-functional changes in bacterial cells under spaceflight conditions 16 p2724 N85-28812
Distinctions in formation of microflora on construction materials used in habitable pressurized compartments
22 p3823 N85-33683

BAFFLES
Internal heat transfer and pressure drop measurements in a variously baffled shell and tube heat exchanger
03 p0360 N85-12310
Optimization of combined convective and film cooling of perforated baffle blades in gas turbines
14 p2270 N85-24067
Shrudless diffuser for gas turbine engine
[AD-D011662] 18 p3082 N85-28943
Failure analysis of fractured capscrews in centrifugal coolant compressor
[DE85-010029] 19 p3287 N85-30384

BAGS
Air bag restraint system
[AD-D011671] 19 p3215 N85-29936
BAILOUT
Study of several factors affecting crew escape trajectories from the Space Shuttle Orbiter at low-subsonic speeds
[NASA-TM-86303] 10 p1428 N85-19008
BAINITE
Development of a high strength isothermally heat-treated nodular iron road wheel arm
[AD-A155755] 24 p4099 N85-35408
BAJA CALIFORNIA
U LOWER CALIFORNIA (MEXICO)
BAKEOUT
U DEGASSING
BALANCE
Force and moment measurements on a 74 deg delta wing with an apex flap
[NASA-CR-166081] 02 p0134 N85-10918
LFMR definition study
[AD-A153691] 18 p3090 N85-29126
Two-plane balance and slip-ring design
22 p3799 N85-33536
All particle energy spectrum of cosmic rays in 10 to the 15th power - 10 to the 20th power eV region
[OG-5.1-15] 22 p3682 N85-34056
BALANCE EQUATIONS
U EQUATIONS
BALANCING
Laser balancing system for high material removal rates
[NASA-CR-174731] 03 p0365 N85-12341
Development of a multiplane multispeed balancing system for turbine systems
[NASA-CR-174750] 13 p1976 N85-22400
Development and application of a unified balancing approach with multiple constraints
16 p2737 N85-26891
Stressed-strained state of tightening buckles in sectional runners of gas turbines 17 p2940 N85-28149
The balancing of complex linkage mechanisms
23 p3924 N85-34313
A versatile computer package for mechanism analysis, part 2: Dynamics and balance
23 p3924 N85-34315
BALL BEARINGS
An evaluation of grease type ball bearing lubricants operating in various environments
[NASA-TM-86460] 02 p0185 N85-11239
Effect of two inner-ring oil-flow distribution schemes on the operating characteristics of a 35 millimeter bore ball bearing to 2.5 million DN
[NASA-TP-2404] 04 p0507 N85-13233
Development of new materials for turbopump bearings
16 p2735 N85-26877
Bearings working group 16 p2735 N85-26878
Hybrid bearings for LH2 and LO2 turbopumps
16 p2736 N85-26880
Rolling contact fatigue life of chromium ion plated 440C bearing steel 16 p2736 N85-26882
Physio-chemical mechanisms of the processes of the formation of globular inclusions in ball-bearing metal
[BLL-BISI-TRANS-22235-(9022.06)]
17 p2924 N85-28030
Operating characteristics of a 0.87 kW-hr flywheel energy storage module
[NASA-TM-87038] 17 p2974 N85-28371
Mechanics of a gaseous film barrier to lubricant wetting of elastohydrodynamically lubricated conjunctions
[NASA-TP-2500] 21 p3595 N85-32330
Friction and wear of solid-lubricated contact in gas turbine engine bearings
[AD-A155042] 21 p3596 N85-32335
The properties of thin-section, four-point-contact ball bearings in space 22 p3797 N85-33521
The use of perfluoroether lubricants in unprotected space environments 22 p3797 N85-33523
Special features of the fracture of ball-bearing steel close to non-metallic inclusion eutectics
[BLL-M-35809-(5828.4)] 23 p3914 N85-34258
BALLASTS (IMPEDANCES)
Determining lamp/ballast system performance with a temperature-controlled integrating chamber
[DE84-014606] 05 p0631 N85-14049
BALLISTIC CAMERAS
Using synchro-ballistic cameras to determine the velocity and spin rate of high-velocity projectiles
[DE85-010829] 19 p3367 N85-30684
BALLISTIC MISSILES
NT INTERCONTINENTAL BALLISTIC MISSILES
NT MINUTEMAN ICBM
NT POLARIS MISSILES
NORAD operational system 12 p1783 N85-21189
BALLISTIC TRAJECTORIES
Tristatic tracking filter used by the multistatic measurement system
[AD-A146885] 07 p0911 N85-15789
A method of calculating the aim point for an unguided projectile fired at a moving target
[BAE-BT-12717] 15 p2489 N85-25365
AN investigation into the control limitations of a bank to turn missile in the terminal homing phase
[AD-A152193] 16 p2704 N85-26896
OMEGA: Optoelectronic measurement of the incidence angle of a projectile
[ISL-CO-223/84] 23 p3974 N85-34634
BALLISTIC VEHICLES
An air-breathing ballistic space transporter for Europe
[NASA-TM-77645] 12 p1792 N85-21244
BALLISTICS
NT INTERIOR BALLISTICS
NT TERMINAL BALLISTICS
ILIR task of digital recoil travel measurement system
[AD-A147102] 07 p0967 N85-16140
Interferometric velocity measurements in ballistics
[ISL-CO-239/83] 14 p2306 N85-24276
Lasers in the domains of ultrashort-time phenomena physics and ballistics
[ISL-CO-236/83] 14 p2310 N85-24299
Effect of low-velocity or ballistic impact damage on the strength of thin composite and aluminum shear panels
[NASA-TP-2441] 16 p2742 N85-26924
Conceptual design and analysis of high-speed electronic imaging
[LA-10072-MS] 22 p3758 N85-33292
BALLISTOCARDIOGRAPHY
Three-dimensional ballistocardiography in weightlessness (experiment 1ES 026) --- Spacelab
05 p0691 N85-14447
Three-dimensional ballistocardiography in microgravity
20 p3510 N85-31818
BALLOON FLIGHT
Space Research in Japan. National report
01 p0013 N85-10062
The de Tifini star pointer characterization and conclusions on the 1982 transmediterranean flight
[CESR-83-1070] 02 p0139 N85-10946
Location and data collection for long stratospheric balloon flights 14 p2326 N85-24377
BALLOON SOUNDING
The BALSAMINE experiment
14 p2238 N85-23876
Coordinated balloon-satellite studies of energetic electron precipitation mechanisms
14 p2360 N85-24587
Testing of some substorm features by multiple balloon observations 14 p2363 N85-24600
The SAMBO-GEOS experiment: A Ps-6 event from ground-satellite observations 14 p2369 N85-24641
Observations of a pulsation event from the ground with balloons and with a geostationary satellite
14 p2369 N85-24643
Upper-air data collection during CAPTEX
[DE85-006300] 16 p2827 N85-27438
Improvement of the basic knowledge of the climatology of the vertical ozone layer by enhanced balloon sounding
[BPT-6/84] 18 p3137 N85-29426
Atmospheric X-rays at 11 deg S geomagnetic latitude
[INPE-3539-PRE/755] 19 p3386 N85-31004
The role of scientific ballooning for exploration of the magnetosphere
[TRITA-EPP-84-07] 20 p3494 N85-31724
Initial results from the Caltech/DRSI balloon-borne isotope experiment
[OG-4.3-8] 22 p3679 N85-34033
Observations of ultraheavy cosmic ray particles at 10 GV cutoff rigidity
[OG-4.4-2] 22 p3679 N85-34035
The dependence of solar modulation on the sign of the cosmic ray particle charge
[SH-4.2-23] 23 p4009 N85-34860
Environmental-physical measurements and determination of atmospheric turbulence with the ASK-16 motor glider 24 p4122 N85-35549
Partitioning of the vertical turbulent energy transport into positive and negative contributions --- meteorology
24 p4122 N85-35551
Aircraft measurements during the Bonn Experiment (BONEX 1) --- meteorology 24 p4122 N85-35552
BALLOON-BORNE INSTRUMENTS
Balloon observations 01 p0014 N85-10086
Study of a coded mask telescope for astronomical measurements in the hard X-ray domain
[MPE-182] 01 p0129 N85-10889
The de Tifini star pointer characterization and conclusions on the 1982 transmediterranean flight
[CESR-83-1070] 02 p0139 N85-10946
Optical studies of nitrogen oxides in the stratosphere
08 p1183 N85-17455
Instrumental background in balloon-borne gamma-ray spectrometers and techniques for its reduction
[NASA-TM-86162] 09 p1413 N85-18911
The Venus Balloon Project 10 p1465 N85-19243
Measurement of nuclear lines with a dual Ge(Li) telescope aboard a stratospheric balloon
[INPE-3380-TDL/185] 11 p1762 N85-21083
Calibration of solar cells outside the atmosphere
13 p2009 N85-22603
Land mobile satellite transmission measurements at 869 MHz: Selected results from the dedicated stratospheric balloon experiment of November 12 and 13, 1984
[NASA-CR-175734] 15 p2541 N85-25685
Free radicals in the stratosphere: A new observational technique 16 p2824 N85-27415
Stratospheric ClO: In-situ detection with a new approach 16 p2824 N85-27416
Balloon-borne, He-cooled Fourier transform spectrometer for far infrared astronomy
[MPE-IR-41] 17 p3053 N85-28899
Damping of suspension oscillations for stratospheric balloon experiments
[MPE-IR-42] 20 p3483 N85-31517
A Cerenkov-delta E-Cerenkov detector for high energy cosmic ray isotopes and an accelerator study of Ar-40 and Fe-56 fragmentation
[NASA-CR-176028] 20 p3549 N85-32086
A balloon-borne imaging gamma-ray telescope
[OG-9.2-2] 21 p3714 N85-33049
Balloon-borne video cassette recorders for digital data storage
[OG-9.3-11] 21 p3715 N85-33050
Development of an adjustable buoyancy balloon tracer of atmospheric motion. Phase 1: Systems design and demonstration of feasibility
[PB85-185817] 22 p3817 N85-33648
A search for solar neutrons on a long duration balloon flight
[SH-1.4-6] 23 p3995 N85-34798
The design of an experiment to detect low energy antiprotons
[OG-9.1-1] 23 p4022 N85-34926
Cherenkov-dE/dx-range measurements on cosmic ray iron group nuclei
[OG-9.1-12] 23 p4024 N85-34937
A balloon-borne imaging gamma-ray telescope
[OG-9.2-2] 23 p4024 N85-34941
The Gamma-Ray Imaging Spectrometer (GRIS): A new balloon-borne experiment for gamma-ray line astronomy
[OG-9.2-4] 23 p4025 N85-34943
An experimental assessment of the imaging quality of the low energy gamma-ray telescope ZEBRA
[OG-9.2-8] 23 p4025 N85-34947
High energy gamma ray balloon instrument
[OG-9.2-12] 23 p4026 N85-34951
Measured performance of the new University of California gamma ray telescope
[OG-9.2-13] 23 p4026 N85-34952
An improved time of flight gamma-ray telescope to monitor diffuse gamma-ray in the energy range 5 MeV - 50 MeV
[OG-9.3-2] 23 p4027 N85-34957
An approach of reducing the background induced by neutrons
[OG-9.3-5] 23 p4027 N85-34960
A star camera aspect system suitable for use in balloon experiments
[OG-9.3-10] 23 p4028 N85-34965
Balloon-borne video cassette recorders for digital data storage
[OG-9.3-11] 23 p4028 N85-34966
Photometric and spectroscopic gamma-ray observations of solar transient phenomena using long duration balloons
[SH-9.1-5] 23 p4051 N85-35120
Some characteristic cosmic ray events and an attempt at their explanation
[HE-3.1-8] 24 p4178 N85-35806
BALLOONING MODES
Theory of resistive ballooning modes in Tokamaks
[DE84-015626] 04 p0566 N85-13606
Fusion plasma theory. Task 1: Magnetic confinement fusion plasma theory
[DE84-014941] 04 p0566 N85-13608
Limits of possible operation of the R-Tokamak due to ideal MHD instabilities
[IPPJ-864] 06 p0863 N85-15486
Theoretical investigations relevant to magnetic fusion research, April 1, 1983 - March 31, 1984
[DE85-001778] 06 p0865 N85-15498
Shear-Alfven dynamics of toroidally confined plasmas, part A
[DE85-001590] 06 p0866 N85-15502

Shear-Alfven dynamics of toroidally confined plasmas, part B
[DE85-001787] 06 p0866 N85-15504
Comments on the paper by F. Pegoraro, L. Sugiyama: Spatial diffusion of charged high-energy fusion products by shear Alfven perturbations
[INPE-3291-PRE/606] 16 p2866 N85-27675
Ballooning beta limits of doe and bean shaped Tokamaks
[IPPJ-713] 16 p2866 N85-27676

BALLOONS
NT HIGH ALTITUDE BALLOONS
NT JIMSPHERE BALLOONS
NT METEOROLOGICAL BALLOONS
NT MICROBALLOONS
NT SUPERPRESSURE BALLOONS
NT TETHERED BALLOONS
Optical pin apparatus for measuring the arrival time and velocity of shock waves and particles
[DE84-014501] 01 p0120 N85-10624
The use of tracers for the study of atmospheric chemical and physical transformation processes
[DE84-015287] 05 p0671 N85-14313
A new physical Lagrangian tracer
[DE84-016212] 05 p0687 N85-14419
Results of the 1984 NASA/JPL balloon flight solar cell calibration program
[NASA-CR-174270] 07 p0991 N85-16294
Balloon observations of hard X-rays from some galactic X-ray sources
[OG-2.5-11] 22 p3870 N85-33966
Gamma-radiation with E gamma 5 MeV detected from Seyfert galaxy 3C120 and region with 1' = 190 deg and b' = 20 deg
[OG-2.8-8] 22 p3871 N85-33981
Lapec: A Phoswich balloon experiment for hard X-ray astronomy
[OG-9.3-1] 23 p4027 N85-34956
A comparison of calculated and measured background noise rates in hard X-ray telescopes at balloon altitude
[OG-9.3-7] 23 p4028 N85-34962
Structure and properties of polyethylene films used in heavy lift balloons
[NASA-CR-176227] 24 p4083 N85-35306

BALLS
Hubble space telescope: Pointing error effects on nonlinear ball joints
[NASA-TM-86511] 20 p3545 N85-32058

BALMER SERIES
Alignment of high Ryberg states in hydrogen
[DE85-000582] 09 p1380 N85-18677
Broad emission features in active galactic nuclei
11 p1746 N85-20979
A model for eclipsing cataclysmic variables
13 p2171 N85-23467
High resolution geocoronal Balmer alpha observations
20 p3489 N85-31686

BALTIC SEA
Intrusion of radioactive industrially polluted water from North Sea into central Baltic Sea
10 p1498 N85-19454

BALTIC SHIELD (EUROPE)
Study of stratigraphy of the Precambrian Soviet Baltic shield 13 p2110 N85-23148

BANACH SPACE
NT SOBOLEV SPACE
Measure determining classes of balls in Banach space
[CTH-MATH-1984-14] 04 p0556 N85-13541
Losb Sobolev spaces with applications to variational integrals and differential equations
[CTH-MATH-1984-19] 04 p0556 N85-13544
Stable monotone variational inequalities
[AD-A147123] 07 p1031 N85-16544
Generalization of Beurling algebras
11 p1698 N85-20675
Using semigroups and the Trotter product formula to solve quasi-linear systems
[DE85-002041] 11 p1706 N85-20736
On stochastic integral representation of stable processes with sample paths in Banach spaces
[AD-A152927] 17 p3025 N85-28703

BAND STRUCTURE OF SOLIDS
Dispersion forces of solids under stress. Chemisorption under stress
[AD-A146171] 03 p0373 N85-12380
Theory of silicon superlattices: Band structure and mobility enhancement 09 p1396 N85-18789
Fermi surface study of CeSb
[DE85-002532] 10 p1564 N85-19662
A mixed-basis band structure interpolation scheme applied to the fluorite structure compounds NiSi2, AuAl2, AuGa2 and AuIn2
[AD-A150131] 12 p1940 N85-22187
Preventing the formation of an anomalous structure in chemically sealed low carbon steel
[BLL-BISI-TRANS-22373-(9022.06)]
17 p2930 N85-28085

BANDGAP
U ENERGY GAPS (SOLID STATE)

BANDPASS FILTERS
NT CRYSTAL FILTERS
NT TRACKING FILTERS
Microstrip directional filters
[INPE-3127-PRE/518] 02 p0194 N85-11293
China report: Science and technology
[JPRS-CST-84-001] 04 p0557 N85-13545
Present status, future prospects of domestic acoustical instruments 04 p0557 N85-13548
Superconducting NbTi and Pb(Cu) bandpass filters
05 p0623 N85-13986
Charge domain filters for enhanced monolithic signal processing
[AD-A147428] 07 p0941 N85-15964
Compensation of skew passband of a SAW filter using predistortion 12 p1821 N85-21422
Detection of angular modulated electromagnetic signals
[AD-D011563] 12 p1823 N85-21437
High-frequency input device for superheterodyne radio receiver with wideband preselector
12 p1839 N85-21540
Method of designing digital band-pass filters with infinite memory 12 p1840 N85-21548
Investigation of bimodal paramagnetic filter
13 p2083 N85-23007
Margin leveling algorithm for fully saturated satellite transponder with CDMA (Code Division Multiple Access) signalling
[AD-A151710] 15 p2543 N85-25699
A short range, high accuracy radar ranging system
[AD-A152195] 16 p2774 N85-27122
Topics in time delay estimation
[AD-A152231] 16 p2855 N85-27607
Reactanceless synthesized impedance bandpass amplifier
[NASA-CASE-GSC-12788-1] 18 p3093 N85-29145
Bandpass filter formed by serial gratings operating in a wood's anomaly region
[AD-D011660] 18 p3093 N85-29148
The seasonal cycle of storminess as measured by band-pass fluctuations 18 p3144 N85-29467
Some studies in filtering of atmospheric turbulence
[AD-A154042] 19 p3316 N85-30557
Optimum filter computation for data transmission
[CNES-83/DRT/TIT/TR/142] 20 p3441 N85-31359
Color evolution in high redshift galaxies
20 p3544 N85-32055
Microwave SAW (Surface Acoustic Wave) monochromator
[AD-D011718] 21 p3590 N85-32311
Design of high-order analog and digital filters with identical sections 22 p3766 N85-33341
Design of digital bandpass filters with finite memory
22 p3775 N85-33392
Miniature two-mode filters 22 p3775 N85-33394
Method of designing digital band-pass filters with pulse response of finite duration 22 p3775 N85-33395
Waveguide dielectric millimeter band filter with enhanced selectivity 22 p3780 N85-33421
A real time index of geomagnetic background noise for the MAD (Magnetic Anomaly Detection) frequency band
[AD-A155717] 22 p3814 N85-33627

BANDWIDTH
NT BROADBAND
NT NARROWBAND
NT SPECTRAL LINE WIDTH
An error analysis for the use of presently available lunar radio flux data in broadbeam antenna-system measurements
[PB84-218361] 01 p0016 N85-10097
Resistance to HF jamming interference in mobile radio networks by an adaptive, distributed reconfiguration technique
[AD-A145117] 01 p0038 N85-10238
Noise jammer discrimination by noise spectral bandwidth
[AD-D011224] 01 p0038 N85-10242
A limbus-sensing eye movement recorder
[AD-A144772] 01 p0049 N85-10323
A high resolution spectroscopic study of the oxygen molecule
[NASA-CR-174061] 02 p0172 N85-11150
Electronic bandwidth compression module
[AD-A145843] 03 p0366 N85-12343
Pulse code modulation telemetry: Properties of various binary modulation types
[AD-A147214] 07 p0913 N85-15780
Array sidelobes, error tolerance, gain, and beamwidth
[AD-A147004] 07 p0940 N85-15956
Multivariable flight control with time-scale separation
[NASA-CR-174320] 08 p1087 N85-16873
An optically coupled sampling system with 4 GHz bandwith
[AD-A148057] 09 p1384 N85-18702
Noise jammer discrimination by noise modulation bandwidth
[AD-D011473] 10 p1488 N85-19284
A technical solution to fadings in tactical satellite digital tranamissions 10 p1473 N85-19297
Heterocontact effects in point contact electron-phonon spectroscopy of the alkali metals
[AD-A149780] 12 p1800 N85-21290
Multichannel digital processing of wideband signals
12 p1840 N85-21548
An asymptotically efficient solution to the bandwidth problem of kernel density estimation, revision
[AD-A149800] 12 p1920 N85-22056
Beamwidth control in pyramidal horns
[R-NIAS-27] 13 p2053 N85-22953
Gyrator frequency selectors with bandwidth independent of input signal level 13 p2083 N85-23009
Infrared nonlinear processes in semiconductors
[AD-A150986] 14 p2427 N85-24968
Linewidth and bandwidth measurements of the q-branch of h2 using CW coherent anti-Stokes Raman spectroscopy
[AD-A151868] 15 p2506 N85-25456
Statistical techniques for signal processing
[AD-A151231] 15 p2541 N85-25660
Wideband fiber optic communications link
[AD-A151704] 15 p2542 N85-25697
Feasibility studies of optical processing of image bandwidth compression schemes
[AD-A151254] 15 p2651 N85-26350
The HURRA, a high resolution experimental radar system broadband receiver
[FOA-C-30375-E1] 18 p3091 N85-29132
Multichannel birefringent filter
18 p3206 N85-29886
Study of a limited band signal transmission chain
[CNES-CT/DRT/TIT/TR-83/221]
20 p3442 N85-31361
Experimental evaluation of a new form of M-ary (M = 8) phase shift keying including design of the transmitter and receiver
[AD-A155103] 21 p3576 N85-32239
Controllable companding in low-frequency FM radio communication systems 22 p3776 N85-33402
Necessary bandwidth and spectral properties of digital modulation
[PB85-185387] 24 p4088 N85-35340
Optical synthetic aperture techniques
[AD-A156151] 24 p4154 N85-35752

BANG-BANG CONTROL
U OFF-ON CONTROL

BANGLADESH
The use of digital spaceborne SAR data for the delineation of surface features indicative of malaria vector breeding habitats 08 p1146 N85-17230

BANKING FLIGHT
U TURNING FLIGHT

BARCHANS
U DUNES

BARDEEN APPROXIMATION
U BARRIER LAYERS
U ELECTRICAL PROPERTIES
U SURFACE PROPERTIES

BARENTS SEA
Eddy detection in the Norwegian, Greenland, and Barents Seas with a radar altimeter
03 p0382 N85-12442
Modern sedimentation in the northern Barents Sea: Input, dispersal and deposition of suspended sediments from glacial meltwater
[AD-A152520] 17 p2997 N85-28530

BARIUM
Search for white dwarf companions of cool stars with peculiar element abundances
[NASA-CR-174030] 02 p0297 N85-11923
The Georges Bank monitoring program 1983: Analysis of trace metals in bottom sediments
[CIRC-915] 05 p0688 N85-14423
The role of finite parallel length on the stability of barium clouds
[AD-A146972] 07 p0996 N85-16328
Experimental research on ionospheric disturbance caused by cumulative barium vapor injection
16 p2719 N85-26787
Environmental surveillance at Los Alamos during 1984
[DE85-011886] 22 p3811 N85-33605

BARIUM ALLOYS
Critical evaluation of binary rare earth phase diagrams
[DE84-015057] 05 p0614 N85-13922

BARIUM COMPOUNDS
NT BARIUM OXIDES
NT BARIUM SULFIDES
NT BARIUM TITANATES
Solid phase reactions among manganese, potassium perchlorate and barium chromate
[HSE-TRANS-11166] 19 p3237 N85-30071

BARIUM ION CLOUDS
Numerical simulation of the effects of radially injected barium plasma in the ionosphere
[NASA-CR-175636] 14 p2354 N85-24542

BARIUM OXIDES
Density and thermal expansion measurements of several mixed oxide glasses in the solid and liquid regions
[DE85-006134] 14 p2261 N85-24014

BARIUM SULFIDES
Application of thermoluminescence for detection of cascade shower 1: Hardware and software of reader system
[HE-7.1-6] 24 p4213 N85-36160
Spatial distribution read-out system for thermoluminescence sheets
[HE-7.1-7] 24 p4213 N85-36161
Application of thermoluminescence for detection of cascade shower 2: Detection of cosmic ray cascade shower at Mount Fuji
[HE-7.1-12] 24 p4214 N85-36162

BARIUM TITANATES
Center for dielectric studies
[AD-A146163] 03 p0434 N85-12761
Degradation mechanisms in ceramic dielectrics
[AD-A149791] 12 p1813 N85-21369
Planar ferroelectric microcapacitors for microwave devices 13 p2087 N85-23032

BARLEY
Multi crop area estimation in Idaho using EDITOR
[E85-10054] 06 p0627 N85-15251

BAROCLINIC INSTABILITY
Layered sloping mesoscale structures and rainbands in atmospheric frontal regions and their relation to symmetric instability 01 p0075 N85-10497
Combined effects of baroclinic and barotropic instability in a nonlinear low order model
[DM-41] 09 p1358 N85-18544
Three-dimensional baroclinic instability of a Hadley cell for small Richardson number
[NASA-TP-2450] 11 p1687 N85-20605
A numerical study of the Pacific polar low
[AD-A153777] 18 p3149 N85-29495

BAROCLINIC WAVES
An improved analytical theory of Rossby wave driven Eulerian and Lagrangian mean flows along non-zonal barriers with application to the Hawaiian Ridge
[AD-A144951] 01 p0068 N85-10503
Structure and energetics of medium-scale atmospheric waves in the southern hemisphere summer
05 p0685 N85-14403
Experiments on the assimilation of patches of data using a barotropic model 18 p3140 N85-29441
Energy sources of the dominant frequency dependent 3-dimensional atmospheric modes
18 p3143 N85-29462
The seasonal cycle of storminess as measured by band-pass fluctuations 18 p3144 N85-29467
Strongly nonlinear dynamics of baroclinic waves
20 p3488 N85-31681
Structure and energetics of medium-scale atmospheric waves in the Southern Hemisphere
20 p3489 N85-31685
On development mechanisms for polar lows
20 p3495 N85-31727
Subseasonal variability in a two-level atmospheric general circulation model 24 p4114 N85-35504

BAROCLINITY
Fully implicit numerical methods for the baroclinic primitive equations 05 p0679 N85-14385
Computer studies of baroclinic flow — Atmospheric General Circulation Experiment
[NASA-CR-171338] 10 p1517 N85-19566
Mountain barrier baroclinity effects on surface winds along the Alaskan Arctic coast 14 p2238 N85-23677
Local mechanism of equatorial countercurrents
14 p2336 N85-24448
Atmospherically forced, coastally trapped, long period gravity waves off the south coast of southern Africa
16 p2832 N85-27461

BAROMETERS
Seismic observation of infrasonic signals
[AD-A149574] 12 p1889 N85-21853
On the solar cycle variation in the barometer coefficients of high latitude neutron monitors
[SH-6.1-2] 23 p4044 N85-35077
The neutron moderated detector and groundbased cosmic ray modulation studies
[SH-9.1-13] 23 p4062 N85-35128

BAROMETRIC PRESSURE
U ATMOSPHERIC PRESSURE

BAROTRAUMA
Hyperbaric physiology (status and prospects)
08 p1194 N85-17521

BAROTROPIC FLOW
Index cycles simulated by a low order forced barotropic model 07 p1002 N85-16984
Spectral modeling of a potential vorticity equation for a barotropic flow on a beta-plane
[CWI-AM-R8408] 08 p1186 N85-17478
High-frequency wind wave spectrum in storm basin
14 p2336 N85-24444
Modeling evolution of unstable geostropic eddies in barotropic ocean 14 p2336 N85-24447
Experiments on the assimilation of patches of data using a barotropic model 18 p3140 N85-29441
A factored implicit scheme for numerical weather prediction with small factorization error
18 p3141 N85-29447
Energy sources of the dominant frequency dependent 3-dimensional atmospheric modes
18 p3143 N85-29462
The contrasting Northern Hemisphere winters of 1980-81 and 1981-82 18 p3144 N85-29466
On Fofonoff's mode 18 p3145 N85-29471
Multiple equilibria of the barotropic vorticity equation on a sphere 18 p3146 N85-29475
Moist barotropic instability in the tropics
20 p3489 N85-31683
A study of the adequacy of quasi-geostrophic dynamics for modeling the effect of frontal cyclones on the larger scale flow
[NASA-CR-176065] 20 p3495 N85-31731

BAROTROPISM
NT PLANETARY WAVES
A comparison of the bounded derivative and the normal mode initialization methods using real data
18 p3144 N85-29463

BARRED GALAXIES
Gas dynamics of the barred spiral galaxy NGC 3359
13 p2170 N85-23465

BARRELS (CONTAINERS)
Conceptual design report for a remotely operated cask handling system, revision 1
[DE85-000348] 08 p1169 N85-17371
Three-dimensional finite element impact analysis of a nuclear waste truck cask
[DE85-010653] 19 p3288 N85-30389
Container for radioactive materials
[DE85-005757] 23 p3972 N85-34626

BARRICADES
U BARRIERS

BARRIER LAYERS
Stochasticity and transport in Hamiltonian systems
02 p0282 N85-11636
Diffusion barrier for long wavelength laser diodes
[AD-D011390] 07 p0970 N85-16157
Rolls-Royce experience with thermal barrier coatings — In aircraft engines
[PNR-90222] 08 p1135 N85-17152
Advanced thermal barrier system bond coatings for use on Ni, Co-, and Fe-base alloy substrates
[NASA-TM-87062] 20 p3431 N85-31283

BARRIERS
Classical free-streamline flow over a polygonal obstacle
[NASA-CR-172448] 01 p0046 N85-10301
Reversible change in parameters of GaAs-based surface-barrier metal-semiconductor diodes induced by hydrogen absorption-desorption
02 p0258 N85-11690
Analysis of waveguide discontinuities by the method of moments
[AD-A151499] 15 p2547 N85-25721

BARRIERS (LANDFORMS)
NT REEFS
Most important geochemical barrier zones in ocean (with example of Atlantic Ocean basin)
14 p2343 N85-24491

BARS
NT ELASTIC BARS
NT PRISMATIC BARS
Thermal-mechanical fatigue crack growth in Inconel X-750
[NASA-CR-174740] 07 p0927 N85-15877
Ultrasonic inspection of alloyed tungsten bars
[AD-A148900] 10 p1495 N85-19435
NDE for heat engine ceramics
[NASA-TM-86949] 11 p1649 N85-20389
Pyrotechnic shock simulation using the controlled response of a resonating bar fixture
[DE85-006537] 16 p2784 N85-27181
Behaviors of stress waves in a conical bar
23 p3904 N85-34182

BARYCENTER
U CENTER OF GRAVITY

BARYON RESONANCE
Proposal for the systematic naming of mesons and baryons
[DE85-008453] 17 p3035 N85-28773

BARYONS
NT HYPERONS
On the nature of the baryon asymmetry
[NASA-TM-86156] 05 p0746 N85-14784
A 1-2 GeV/c beam line for hypernuclear and kaon research
[DE85-007623] 16 p2863 N85-27659
Proposal for the systematic naming of mesons and baryons
[DE85-008453] 17 p3035 N85-28773
On mini-cluster observed by Chacaltaya emulsion chamber experiment
[HE-3.6-12] 24 p4185 N85-35659
An experiment to detect gut monopoles
[HE-6.1-7] 24 p4210 N85-36133

BASALT
The petrology and geochemistry of high cascade volcanics in southern Washington: Mount Saint Helens volcano and the Indian Heaven basalt field
02 p0227 N85-11487
Impact cratering: The process and its effects on planetary evolution — and silicate-carbonate reactions on Venus
[NASA-CR-174016] 02 p0228 N85-11488
Nickel-cobalt systematics and their bearing on lunar origin 04 p0582 N85-13719
Moon 09 p1411 N85-18803
Characteristics of basaltic lava flows on Venus
13 p2177 N85-23508
Magmas as selective filters of volatiles between planetary mantles and surfaces
13 p2185 N85-23557
Basaltic pressure ridges: Formation and relationship to flow emplacement 13 p2186 N85-23567
Basalts of Mars: Constraints on volatile evolution
13 p2194 N85-23610
Mechanisms of basalt-plains ridge formation
13 p2199 N85-23643
Parameters of magnetically active layers of Indian Ocean determined from deep drilling data and magnetic surveys
14 p2337 N85-24451
Identification of the youngest meteorites and a discussion of the possibility that they came from Mars
15 p2681 N85-26559
Sodium concrete reaction: Structural considerations
[DE85-009031] 18 p3081 N85-29083
Chlorine isotopes as environmental tracers in Columbia River basalt groundwaters
[DE85-011392] 19 p3302 N85-30473
The degassing history of the Earth: Noble gas studies of Archaean cherts and zero age glassy submarine basalts 21 p3718 N85-33072
Primordial magmaspheres and their lasting consequences 22 p3857 N85-33882

BASE FLOW
An experimental study of clustered, two-dimensional rocket nozzles
[AD-A151889] 15 p2495 N85-25390

BASE PRESSURE
Empirical formulas for the prediction of the base pressure of missile bodies at subsonic velocities
[DFVLR-FB-84-23] 03 p0316 N85-12044
An experimental study of clustered, two-dimensional rocket nozzles
[AD-A151889] 15 p2495 N85-25390
Empirical formulas for the prediction of the base pressure of missile bodies at subsonic velocities
[ESA-TT-893] 20 p3399 N85-31082

BASES (CHEMICAL)
The conversion of smaller borane fragments to larger structures. Systematics of boron hydride reactions
[AD-A153443] 18 p3070 N85-28985

BASES (FOUNDATIONS)
U FOUNDATIONS

BASIC (PROGRAMMING LANGUAGE)
Convergent Technologies, mega frame CTIX BASIC interpreter version 1.03
[PB84-227776] 03 p0404 N85-12579
Gould Incorporated, Gould PS-3000, Gould PS-3000 BASIC Interpreter Version 1.00
[PB84-229186] 06 p0851 N85-15404
NCR Corporation, NCR 9300, NCR ITX-BASIC Release 2.0
[PB84-229228] 06 p0852 N85-15414
Sperry Corporation, 1100/80, UBASIC/BBASIC Level 9R1
[PB84-229202] 06 p0852 N85-15415
Compter Sciences Corporation, UNIVAC 1100/80, CSTS BASIC Release BAS160
[PB84-229145] 06 p0852 N85-15418

Control Data Corporation, Cyber 835, BASIC Release 3.5 Level 614
[PB84-227990] 06 p0853 N85-15420
Burroughs Corporation B26-CPU, Burroughs B20 BASIC Rel. 4.0
[PB84-216324] 06 p0855 N85-15436
Convergent Technologies NGEN CP001, CT BASIC Version 9.0
[PB84-216332] 06 p0855 N85-15437
Sperry Univac System 80, Model 6, OS/3 BASIC, Version 10.01
[PB85-108066] 10 p1542 N85-19722
Selection and use of general-purpose programming-language: Program examples, volume 2
[PB85-122000] 12 p1917 N85-22039
Selection and use of general-purpose programming language: Overview, volume 1
[PB85-122018] 12 p1917 N85-22040
How a BASIC program works
[DE85-009142] 22 p3831 N85-33727

BASINS
U STRUCTURAL BASINS

BATCH PROCESSING
Computer center introductory reference manual for CDC CYBER
[AD-A145796] 03 p0406 N85-12583
New YeS 1056 unified system computer model described 04 p0485 N85-13092
Method of production of metals by cathodic solution of their compounds in electrolytic cells
[BLL-OA-TRANS-3207-(6196.300)] 20 p3429 N85-31266
Optimize computer throughput using array processors
[AD-A155843] 24 p4135 N85-35628

BATHOLITHS
Stratigraphy, petrology, and tectonic setting of the Alisitos Group, Baja California, Mexico 03 p0389 N85-12488
Geology of selected migmatite zones within the bitterroot lobe of the Idaho batholith, Idaho and Montana 03 p0389 N85-12489

BATHS
NT SALT BATHS
Comparison of simulation of weightlessness by Head Down Tilt (HDT) and Water Immersion (WI) 05 p0692 N85-14454
Hemodynamics and plasma arginine vasopressin during water immersion in normal man 05 p0693 N85-14458
Trace metal determinations in nickel-plating baths by polarographic methods
[DE85-007064] 15 p2511 N85-25488

BATHYMETERS
The investigation of selected oceanographic applications of spaceborne synthetic-aperture radar 08 p1146 N85-17233
Advanced technology for hydrographic mapping
[FOA-C-30371-E1] 08 p1176 N85-17418
Along-track deflection of the vertical from SEASAT: GEBCO (General Bathymetric Chart of the Oceans) overlays
[PB85-129641] 12 p1876 N85-21767
An assessment of the potential role of multispectral imagery in bathymetric charting
[AD-A152460] 17 p2984 N85-28436

BATHYMETRY
U BATHYMETERS

BATHYTHERMOGRAPHS
ADAPS (Airborne Data Acquisition and Processing System) operation and maintenance manual
[AD-A149297] 11 p1585 N85-19983
Preliminary results of the oceanographic cruise of USCGC NORTHWIND to the Greenland Sea
[AD-A149602] 12 p1898 N85-21919
Report of the Hydrographic Service Royal Australian Navy for the year ended 30th June 1984, issue number 20
[AD-A151460] 15 p2583 N85-25932

BATTERIES
U ELECTRIC BATTERIES

BATTERY CHARGERS
Summary of activities pertaining to utilization of grant purchase of batteries for electric van
[DE84-015783] 02 p0195 N85-11305
Performance characteristics of a battery charger and state-of-charge indicator
[NASA-CR-174273] 07 p0946 N85-15992
Battery control and fault detection method
[AD-D011384] 07 p0993 N85-16307
BBC of Switzerland develops electric car 08 p1141 N85-17192
Battery charger
[AD-D011420] 08 p1178 N85-17425
Autonomous uninterruptable power supply apparatus
[AD-D011571] 14 p2298 N85-24232
INEL electric vehicle laboratory qualification: Transition test results and comparisons with JPL ETV1-2 data
[DE85-008006] 16 p2880 N85-27772
Test and evaluation of the Hoppecke Model E240G144/16 electric vehicle battery charger
[DE85-900573] 17 p2955 N85-28253
LEO life testing with different charge control 20 p3446 N85-31393
Deep reconditioning of batteries during DSCS 3 flight operations 20 p3446 N85-31397
Safety characteristics of non-lithium battery systems
[AD-A155733] 22 p3806 N85-33574
Rechargeable lithium-organic electrolyte battery having overcharge protection and method of providing overcharge protection for a lithium-organic electrolyte battery
[AD-D011736] 22 p3806 N85-33575

BATTERY SEPARATORS
U SEPARATORS

BAUXITE
Microbiological method for the desiliconization of high-silica bauxites
[BLL-MINTEK-TR-1168-(5810.5759)] 07 p0925 N85-15884

BAYES THEOREM
Estimation of the threshold in fatigue crack initiation models: A Bayesian approach
[AD-A144847] 01 p0062 N85-10410
Testing of inequality hypotheses in linear models using the Bayes method
[SER-C-292] 01 p0112 N85-10761
Credibility approximations for Bayesian prediction of second moments
[AD-A144996] 01 p0113 N85-10768
Bayesian analysis of item response curves
[AD-A145627] 02 p0254 N85-11665
Maximum likelihood and Bayesian parameter estimation in item response theory
[AD-A145775] 03 p0413 N85-12644
Performance of Bayes-optimal angle-of-arrival estimators
[AD-A146594] 06 p0858 N85-15454
Bayesian estimation of normal mixture parameters 07 p0985 N85-16255
Spatial estimation from remotely sensed data via empirical Bayes models 07 p0985 N85-16256
Multivariate spline methods in surface fitting 07 p0985 N85-16257
Bayesian estimation of undetected errors
[AD-A147198] 07 p1031 N85-16545
Belief structures
[AD-A147526] 07 p1036 N85-16575
A method for automatic water mass classification
[AD-D011405] 08 p1191 N85-17505
A numerical analysis of sampling plans based on prior distribution and costs
[AD-A147718] 08 p1210 N85-17616
An analysis of robust and efficient priors associated with a finite Bayesian model for compliance testing
[AD-A148497] 08 p1213 N85-17635
Empirical Bayes rules for selecting good binomial populations
[AD-A147614] 08 p1214 N85-17646
Improved estimation procedures for item response functions
[AD-A147677] 08 p1215 N85-17648
Minimax multiple t-tests for comparing k normal populations with a control
[AD-A148306] 08 p1215 N85-17656
W.E. Johnson's Sufficientness postulate
[AD-A149014] 10 p1550 N85-19774
Bayesian analysis of time series 1: Householder transformation analyses
[DE85-004449] 11 p1708 N85-20749
Asymptotically optimum multialternative sequential procedures for discernment of processes minimizing average length of observations 13 p2084 N85-23012
Accuracy of approximation of Bayes estimates in presence of noninformative parameters 13 p2084 N85-23015
Spatial acquisition algorithms and systems for intersatellite optical communication links
[AD-A150794] 14 p2292 N85-24207
Bayesian estimation of one dimensional discrete markov random fields
[AD-A151503] 15 p2640 N85-26284
Estimation of launch vehicle performance parameters
[AD-A151927] 16 p2728 N85-26839
Optimal design and use of retry in fault tolerant real-time computer systems
[NASA-CR-175920] 17 p3015 N85-28643
Studies in quality improvement 2. An analysis for unreplicated fractional factorials
[AD-A153539] 18 p3169 N85-29640
Bayesian full rank marginalization for 2-way contingency tables
[AD-A153841] 18 p3171 N85-29649
Bayesian inference and diagnostics for the 3 parameter logistic model
[AD-A153840] 18 p3175 N85-29681
Bayesian factor analysis
[AD-A154184] 19 p3347 N85-30747
A critique of Deming's discussion of acceptance sampling procedures
[AD-A154305] 19 p3348 N85-30751
Reconciling Bayesian and frequentist evidence in the one-sided testing program
[AD-A155603] 21 p3678 N85-32650
Bayesian vs MAP multiple model adaptive estimation for field of view expansion in tracking airborne targets
[AD-A155466] 21 p3679 N85-32655
Optimal Bayesian estimators for image segmentation and surface reconstruction
[AD-A155732] 22 p3827 N85-33704
Model robust response surface designs: Scaling two-level factorials
[AD-A156218] 24 p4143 N85-35686

BAYESIAN STATISTICS
U BAYES THEOREM

BAYOUS
Microseismic monitoring of Chocolate Bayou, Texas: The Pleasant Bayou no. 2 geopressured/geothermal energy test well program
[DE84-014825] 01 p0072 N85-10477

BAYS (STRUCTURAL UNITS)
Investigation of experimental lightweight firewall materials for A/C engine bay applications
[AD-A155765] 24 p4062 N85-35175

BAYS (TOPOGRAPHIC FEATURES)
NT CHESAPEAKE BAY (US)
NT DELAWARE BAY (US)
NT MONTEREY BAY (CA)
NT SAN FRANCISCO BAY (CA)
Geothermal studies in Alaska: Conditions at Prudhoe Bay 04 p0516 N85-13290
Proceedings of the 1st Glacier Bay Science Symposium
[PB85-115913] 11 p1682 N85-20599

BCC LATTICES
U BODY CENTERED CUBIC LATTICES

BCH CODES
Adaptation of bit error rate by coding — spacecraft transmissions
[ESA-CR(P)-1970] 15 p2545 N85-25711

BEACHES
Field studies of run-up generated by wind waves on dissipative beaches
[AD-A148793] 09 p1359 N85-18548
Hurricane storm surge research
[GPO-40-048] 12 p1893 N85-21880
Coastal erosion along Monterey Bay
[AD-A155810] 21 p3655 N85-32707

BEACONS
NT RADAR BEACONS
NT RADIO BEACONS
NT RADIO DIRECTION FINDERS

BEADS
Method for thermal monitoring subcutaneous tissue
[NASA-CASE-LAR-13028-1] 19 p3328 N85-30618

BEAM CURRENTS
Experimental observation of neoclassical currents
[DE84-015113] 01 p0122 N85-10834
In-line beam current monitor
[DE84-014054] 04 p0560 N85-13567
Macroscopic currents and wind perturbations in the frame of the wind and shock model — galactic nuclei 08 p1242 N85-17836
Experimental investigation of certain beam transport issues in a pulsed transmission line linear accelerator
[DE85-002310] 10 p1555 N85-19805
Survey of initial experiments on ATA beam dynamics
[DE85-004410] 10 p1555 N85-19806
SEM (Scanning Electron Microscope) investigation of silicon diodes using the electron beam induced current method
[AD-A150356] 13 p2064 N85-22894
High energy beam experiment 15 p2654 N85-26376
Generalization of the Child-Langmuir relation for 1-dimensional time-dependent diodes
[DE85-007386] 16 p2779 N85-27152
Accelerator column models for low-current beams
[DE85-010722] 19 p3262 N85-30226
Performance of an RF beam monitor on the NBS-Los Alamos racetrack microtron
[DE85-010725] 19 p3262 N85-30232
Beam dynamics in MABE
[DE85-010670] 19 p3358 N85-30819
Beam current sensor
[DE85-011600] 20 p3459 N85-31482

EBIC characterization and hydrogen passivation in silicon sheet
20 p3481 N85-31634
The cw operation of the FMIT RFQ accelerator
[DE85-012667] 22 p3837 N85-33757
RADLAC technology review
[DE85-011995] 23 p3982 N85-34691
Technology of magnetically driven accelerators
[DE85-011657] 23 p3983 N85-34700
ATA upgrade to 150 MeV
[DE85-013174] 24 p4098 N85-35404
Robinson instability and beam loading
[DE85-013301] 24 p4151 N85-35737
Beam intensity increases at the intense pulsed neutron source accelerator
[DE85-012377] 24 p4155 N85-35764
High resolution beam profile monitors in the SLC
[DE85-013375] 24 p4157 N85-35774
Recent advances in remote handling at LAMPF
[DE85-012725] 24 p4157 N85-35775
Kinetic loss experiments on Mite
[DE85-012826] 24 p4158 N85-35780
Numerical studies of high current beam compression in heavy ion fusion
[DE85-011674] 24 p4158 N85-35783

BEAM INJECTION
Use of a first-harmonic RF system in the NSLS booster
[DE84-016432] 02 p0277 N85-11806
ATA gas propagation: 1 foot tank experiment
[DE84-016395] 04 p0561 N85-13575
Mechanism of damping of plasma oscillations in initial stage of injection of electron beams from spacecraft into ionosphere in active experiments
06 p0823 N85-15225
Ion cluster beam deposition research
06 p0831 N85-15283
Sources, densities, and transport of impurities in neutral-beam injected Tokamaks
09 p1388 N85-18731
The plasma assisted modified betatron
[AD-A148726] 09 p1390 N85-18748
Long-pulse beamlines for the mirror fusion test facility
[DE84-017091] 09 p1392 N85-18760
Numerical model for swirl cooling in high-heat-flux particle beam targets and the design of a swirl-flow-based plasma limiter
[DE85-003824] 11 p1732 N85-20894
Neutral beam injector oxygen impurity measurements and concentration reduction via gettering processes
[DE85-000861] 12 p1836 N85-21521
Electric potential of satellite in electron emitting experiments in initial stage of electron beam injection in steady-state mode
15 p2480 N85-25309
MHD fluctuations in ISX-B
[DE85-004800] 15 p2657 N85-26395
Experiments with light ions at CERN super proton synchrotron
[DE85-007625] 17 p3031 N85-28744
Alternating gradient synchrotron
[DE85-005950] 17 p3033 N85-28759
Definition of requirements for injection locking of pulsed UV lasers
[DE85-010126] 18 p3113 N85-29275
Accelerator technology working group summary
[DE85-009547] 18 p3180 N85-29717
Tritium system design for the mirror reactors FPD-1, FPD-2 and FPD-3
[DE85-010400] 19 p3363 N85-30852
Injection of hydrogen macroparticles into T-10 tokamak
21 p3692 N85-32937
The cw operation of the FMIT RFQ accelerator
[DE85-012667] 22 p3837 N85-33757
Transverse emittance of a 2.0-MeV RFQ beam with high brightness
[DE85-012718] 22 p3837 N85-33758
Rf program for LAMPF 2
[DE85-012693] 22 p3837 N85-33760
Acceleration of polarized H(-) in the BNL 200 MeV linac
[DE85-011836] 22 p3840 N85-33777
Ultrahigh vacuum system of the heavy ion transport line at Brookhaven
[DE85-011838] 22 p3840 N85-33778
Commissioning the polarized beam in the AGS
[DE85-010958] 22 p3841 N85-33788
Design status of heavy ion injector program
[DE85-010751] 22 p3842 N85-33793
Considerations on collective ion acceleration as an intense ion injector
[DE85-012706] 24 p4155 N85-35757
Ion source development for the Los Alamos heavy ion fusion injector
[DE85-012682] 24 p4156 N85-35766

BEAM INTERACTIONS
Considerations regarding the choice of beam parameters and IP configuration for the SSC
[DE84-014532] 01 p0118 N85-10803
Neutral beam interactions with materials
[AD-A145836] 02 p0285 N85-11857
Survey of initial experiments on ATA beam dynamics
[DE85-004410] 10 p1555 N85-19806
Statistical phenomena in particle beams
[DE85-001050] 12 p1929 N85-22118
System for forming and focusing high current beam of deuterium ions
13 p2045 N85-22798
Experiments and detectors for high energy heavy ion colliders
[DE85-007927] 17 p3031 N85-28748
Report of the Working Group on Other Acceleration Schemes
[DE85-008447] 17 p3033 N85-28764
Some comments on SSC physics
[DE85-008444] 18 p3179 N85-29712
Phase and amplitude considerations for the 2-beam accelerator
[DE85-008455] 18 p3180 N85-29715
Beam dynamics in MABE
[DE85-010670] 19 p3358 N85-30819
Quantum effects in linear collider scaling laws
[DE85-009846] 19 p3363 N85-30851
Analysis of beam interaction of the electrical thruster RIT 10 (particle emission) with surfaces
[ESA-TT-826] 20 p3421 N85-31231
Nonlinear dynamics: A personal perspective
[DE85-010982] 20 p3521 N85-31899
Studies in mixed species charged particle beam dynamics
[OUEL-1545/84] 20 p3531 N85-31969
Laser beam interactions with vapor plumes during Nd:YAG laser welding on aluminum
[DE85-009793] 21 p3593 N85-32328
Report of working group on detectors for hadrons and event parameters at colliders
24 p4146 N85-35705
A survey of multiplicities and rapidity densities from existing emission data on hadron-nucleus nucleus-nucleus collisions
24 p4146 N85-35706

BEAM LEADS
Yield joint condition for three-dimensional I-beams
[ILR-MITT-137] 12 p1867 N85-21716
Low capacitance e-beam fabricated beam-lead Schottky barrier diodes
[AD-A150238] 13 p2063 N85-22868

BEAM NEUTRALIZATION
Measurement of proton autoneutralization potential
[DE85-001752] 06 p0865 N85-15501

BEAM SPLITTERS
Environmentally independent fiber optic rotation sensor
[AD-D011219] 01 p0119 N85-10818
Precision electrooptical deflector based on corrugated light guide
07 p0950 N85-16020
Matrix-matrix multiplication using an electrooptical systolic-engagement array processing architecture
[AD-D011410] 08 p1223 N85-17704
Multichannel birefringent filter
18 p3206 N85-29688
Applications of holography to X-ray imaging
[DE85-010984] 23 p3934 N85-34384
Polarisation insensitive achromatic cube beamsplitter — binocular microscopes
[NPL-MOM-72] 23 p3973 N85-34630
Differentiating spatial light modulator
[AD-D011727] 23 p3973 N85-34632

BEAM WAVEGUIDES
Improved directional couplers for overmoded waveguide systems
[IPF-84-1] 09 p1394 N85-18775
Design of mode converters from TE circular om modes in circular waveguides to TE rectangular mo modes in rectangular waveguides for high power applications in the frequency range 1 to 30 GHz
[IPF-84-7] 09 p1395 N85-18781
Heavy ion fusion accelerator research in the US
[DE85-006465] 17 p3034 N85-28767
Beam potential measurement of an intense H(-) beam by use of the emissive probe technique
[DE85-012671] 24 p4155 N85-35762
Beam intensity increases at the intense pulsed neutron source accelerator
[DE85-012377] 24 p4155 N85-35764

BEAMS
Coriolis effects on the vibrations of rotating beams, plates and shells
09 p1331 N85-18366
New concepts in deployable beam structures
14 p2232 N85-23832

BEAMS (RADIATION)
NT ATOMIC BEAMS
NT ELECTRON BEAMS
NT GAMMA RAY BEAMS
NT ION BEAMS
NT LIGHT BEAMS
NT MOLECULAR BEAMS
NT NEUTRAL BEAMS
NT NEUTRINO BEAMS
NT NEUTRON BEAMS
NT PARTICLE BEAMS
NT PHOTON BEAMS
NT PION BEAMS
NT PROTON BEAMS
NT RADAR BEAMS
NT RELATIVISTIC ELECTRON BEAMS
Considerations regarding the choice of beam parameters and IP configuration for the SSC
[DE84-014532] 01 p0118 N85-10803
The Berkeley mini-collider
[DE84-014594] 01 p0118 N85-10808
Focusing beam of 1-GeV protons with volumetric capture to the mode of channeling by bent single crystal
02 p0268 N85-11750
Positron flux concentrator: An update
[DE84-016260] 04 p0561 N85-13576
Focussing and confinement
[DE84-016181] 05 p0640 N85-14106
Tracking servo compensator with rate aiding
[AD-D011372] 07 p0942 N85-15971
Design and testing of a refractive laser beam homogenizer
[AD-A146997] 07 p0970 N85-16162
Longer-scalelength plasma perturbations by an intense laser beam
[AD-A147005] 07 p1045 N85-16638
Beam propagation studies at NRL (Naval Research Laboratory) July 1983 to June 1984, volume 2
[AD-A148198] 08 p1152 N85-17270
Beam-foil spectroscopy of highly ionized aluminum atoms
09 p1390 N85-18746
AEM with a convergent beam
[DE85-000667] 11 p1714 N85-20784
Transmission and reflection of laser beams propagating through aerosol clouds in space
[LA-9998-MS] 12 p1856 N85-21638
Atmospheric transmissometer
[AD-D011540] 12 p1932 N85-22140
Beamwidth control in pyramidal horns
[R-NIAS-27] 13 p2053 N85-22853
Experimental verification of beam deflection from hybrid reflector antenna within wide-angle sector
13 p2079 N85-22984
Laser beam shaping system with reduced objective diameter
14 p2275 N85-24095
The measurement of laser beam parameters
14 p2308 N85-24283
Atomic physics aspects of a Relativistic Nuclear Collider
[DE85-006867] 15 p2650 N85-26342
The 10 MWe solar thermal central receiver pilot plant: Beam safety tests and analyses
[SAND-83-8035] 16 p2818 N85-27379
A 1-2 GeV/c beam line for hypernuclear and kaon research
[DE85-007623] 16 p2863 N85-27659
High precision materials characterization in the near millimeter wave-length range
[AD-A153267] 17 p2968 N85-28331
The temperature dependence of diffracted beam intensities in atom-surface scattering
[AD-A152762] 17 p3029 N85-28736
Heavy ion fusion accelerator research in the US
[DE85-006465] 17 p3034 N85-28767
Large, energetic cluster impacts on surfaces
[DE85-008559] 17 p3034 N85-28769
Beam forming network
[NASA-CASE-NPO-15743-1] 18 p3089 N85-29118
Two-degree-of-freedom linear and planar microwave array lenses
[AD-A153701] 18 p3095 N85-29156
Physics of High Energy Particle Accelerators. AIP Conference Proceedings no. 127
[DE85-008891] 18 p3182 N85-29733
Performance of an RF beam monitor on the NBS-Los Alamos racetrack microtron
[DE85-010725] 19 p3262 N85-30232
Clearing of polydisperse aqueous aerosol by laser radiation pulses
19 p3296 N85-30445
Circular-beam ray tracing on a microcomputer
[DE85-010754] 19 p3338 N85-30685
Moments in particle-in-cell simulations
[DE85-010792] 19 p3356 N85-30803
Study of a novel shielding principle for protection against intense gamma-ray beams
[AD-A154374] 19 p3357 N85-30808
Proposed use of the radio-frequency quadrupole structure to funnel high-current ion beams
[DE85-010746] 19 p3364 N85-30857

Grazing incidence beam expander
[DE85-010784] 19 p3366 N85-30889
Hierarchical beamforming with application to a large aperture array system 20 p3439 N85-31345
ECM multiple-target retrodirective antenna
[AD-D011528] 20 p3439 N85-31346
Method to render second order beam optics programs symplectic
[DE85-010631] 20 p3515 N85-31855
Permanent magnets for production and use of high energy particle beams
[DE85-009934] 20 p3522 N85-31905
Propagation and reflection of a finite amplitude ultrasonic beam including harmonic content: A numeric model 20 p3523 N85-31914
Guide to the Main Ring DO overpass
[DE85-011722] 20 p3531 N85-31963
New approximations and findings of theory of nonlinear acoustic beams 21 p3680 N85-32863
Reflection of acoustic beam from inhomogeneous boundary 21 p3680 N85-32864
The problem of brightness enhancement during laser frequency doubling 21 p3686 N85-32897
Design of electrooptical system with annular cathode and electrostatic compressor 22 p3770 N85-33367
Characteristics of optical information-measurement channels with utilization of scattering effects 22 p3781 N85-33429
Method and apparatus for measuring areas of photoelectric cells and photoelectric cell performance parameters
[DE85-011629] 22 p3810 N85-33599
Solar energy meteorological research and training program: Region 4
[DE85-011783] 22 p3816 N85-33640
Materials characterization with intense positron beams
[DE85-011850] 22 p3839 N85-33769
Iris tilting and RF steering in the SLAC Linac
[DE85-011704] 22 p3841 N85-33783
Commissioning the polarized beam in the AGS
[DE85-010958] 22 p3841 N85-33788
Width of nonlinear difference resonances
[DE85-013026] 24 p4148 N85-35719
Use of a minimum-ellipse criterion in the study of ion-beam extraction systems
[DE85-012670] 24 p4148 N85-35721
Time domain reflectometry for SLC BPM system
[DE85-012389] 24 p4155 N85-35758
High resolution beam profile monitors in the SLC
[DE85-013375] 24 p4157 N85-35774

BEAMS (SUPPORTS)
NT CANTILEVER BEAMS
NT CURVED BEAMS
NT I BEAMS
NT RECTANGULAR BEAMS
Interactive buckling of thin-walled structural components under static and dynamic loads 01 p0059 N85-10392
Deformation measurements of composite multi-span beam shear specimens by Moire interferometry
[NASA-CR-3844] 02 p0169 N85-11135
Approximation methods for inverse problems involving the vibration of beams with tip bodies
[NASA-CR-172468] 02 p0209 N85-11379
Static and dynamic characteristics of materials with beam-microstructure 03 p0370 N85-12361
Complex frequency analysis of damped thin-walled beams with open cross sections 03 p0371 N85-12366
Turbine blade damping study
[NASA-CR-171255] 04 p0456 N85-12890
Forced vibrations of friction-damped beam structures in two dimensions
[UDR-TM-82-08] 04 p0456 N85-12892
Contact behavior, impact response and damage in graphite-epoxy laminates subjected to initial stresses 08 p1171 N85-17386
The response of metallic structures to dynamic loading 08 p1172 N85-17389
Durability and behavior of prestressed concrete beams. Posttensioned concrete beam investigation, supplemental laboratory tests of beams exposed from 1961 to 1962
[AD-A148821] 09 p1304 N85-18191
Optimization of vibrating beams including the effects of coupled bending and torsional modes 09 p1331 N85-18364
Reanalysis of continuous dynamic systems with continuous modifications 09 p1337 N85-18411
Determination of shear coefficient of a general beam cross section by finite element method 09 p1338 N85-18413
Swing-arm beam erector (SABER) concept for single astronaut assembly of space structure
[NASA-TP-2379] 10 p1429 N85-19015
A Galerkin method for the estimation of parameters in hybrid systems governing the vibration of flexible beams with tip bodies
[NASA-CR-172537] 10 p1544 N85-19734
Transverse vibration and buckling of a cantilevered beam with tip body under constant axial base acceleration
[NASA-CR-175567] 12 p1864 N85-21694
Control Of Flexible Structures (COFS) flight experiment background and description 14 p2236 N85-23864
Reflection and transmission of flexural waves at discontinuities 15 p2572 N85-25861
Control of a flexible beam
[DE85-007243] 15 p2580 N85-25914
Adaptation of continuous beams and the method of optimizing the flexibility of their elastic supports. Theorem on maximal adaptation loading, supplement
[REPT-10/1984-SUPPL] 16 p2797 N85-27241
Principles of wave formation along web of H-beams
[BLL-M-36041-(5828.4)] 16 p2798 N85-27253
Nonlinear equations for dynamics of pretwisted beams undergoing small strains and large rotations
[NASA-TP-2470] 16 p2799 N85-27258
Deployable controllable geometry truss beam
[NASA-TM-86366] 17 p2909 N85-27934
Numerical solution of one-dimensional nonlinear problems of statics for elastic beams and shells under rigid constraints 17 p2943 N85-28166
Structural dynamics modification of generalized beams using a local eigenvalue modification procedure 19 p3282 N85-30353
Dynamic response of a flexible space beam
[NASA-TM-86441] 19 p3285 N85-30366
Shear deflection in a three-point bend beam of a solid circular cross-section
[AD-A154458] 19 p3287 N85-30381
Attitude control tradeoff study between the use of a flexible beam and a tether configuration for the connection of two bodies in orbit 20 p3412 N85-31174
Stress distribution of fiberglass reinforced plastic beam with a delamination under three-point bending 23 p3908 N85-34210
Design and behavior of coped beams 24 p4100 N85-35417
User's guide: A computer program for strength analysis of non-hydraulic concrete structural elements. Report 1. Concrete General Strength Investigation (CGSI)
[AD-A156392] 24 p4102 N85-35428
User's guide: A computer program for strength analysis of non-hydraulic concrete structural elements. Report 2. Strength design of reinforced concrete column sections (PCAUC)
[AD-A156393] 24 p4102 N85-35429
Static and cyclic behavior of semi-rigid steel beam-column connections
[PB85-194363] 24 p4103 N85-35433

BEAMSHAPING
U COLLIMATION

BEARING
New ferrous metallurgy technology 01 p0019 N85-10114

BEARING (DIRECTION)
Three position estimation procedures
[AD-A148748] 09 p1278 N85-18042
Helium atoms in interstellar and interplanetary space. II: Determination of direction of interstellar gas motion relative to Sun 13 p1980 N85-22425
Wave directional spectra via ARGOS 16 p2812 N85-27343
UTM (Universal Transverse Mercator) determinations from geographical data
[AD-A152293] 16 p2856 N85-27610
Arrival direction distribution of cosmic rays of energy 10 (18) eV
[OG-5.3-7] 22 p3885 N85-34073
Observation of arrival times of EAS with energies or = 6 x 10 (14) eV
[OG-5.3-8] 22 p3885 N85-34074
Angular resolution of air-shower array-telescopes
[OG-9.5-6] 23 p4030 N85-34983

BEARING ALLOYS
Testing the antifriction properties of alloys for heavily loaded bearings 06 p0780 N85-14990
Powder metallurgy bearings for advanced rocket engines 16 p2736 N85-26881
Conservation and substitution technology for critical metals in bearings and related components for industrial equipment and opportunities for improved bearing performance
[PB85-176248] 18 p3082 N85-29089

BEARINGLESS ROTORS
Integrated technology rotor/flight research rotor hub concept definition
[NASA-CR-166447] 09 p1280 N85-18051
Integrated Technology Rotor/Flight Research Rotor (ITR/FRR) concept definition
[NASA-CR-166443] 10 p1423 N85-18978
Integrated Technology Rotor/Flight Research Rotor (ITR/FRR) concept definition
[NASA-CR-166445] 10 p1423 N85-18979
Integrated technology rotor/flight research rotor concept definition study
[NASA-CR-166446] 10 p1424 N85-18980
Integrated Technology Rotor/Flight Research Rotor (ITR/FRR) concept definition study
[NASA-CR-166444] 10 p1424 N85-18981
Electric motors with elastically mounted rotors 16 p2763 N85-27048
An improved servo-controlled inertial clock for laboratory tests of general relativity 19 p3378 N85-30955

BEARINGS
NT ANTIFRICTION BEARINGS
NT BALL BEARINGS
NT FOIL BEARINGS
NT GAS BEARINGS
NT JOURNAL BEARINGS
NT MAGNETIC BEARINGS
NT ROLLER BEARINGS
NT THRUST BEARINGS
Experimental on-stream elimination of resonant whirl in a large centrifugal compressor 05 p0642 N85-14121
Design of electromagnetic bearing for vibration control of flexible transmission shaft 05 p0645 N85-14136
Squeeze-film dampers for turbomachinery stabilization 05 p0645 N85-14136
Dynamic stiffness characteristics of high eccentricity ratio bearings and seals by perturbation testing 05 p0645 N85-14141
Improvement of the corrosion resistance of turbine engine bearings
[AD-A147430] 07 p0905 N85-15731
Thermally isolated structural support link
[AD-D011349] 07 p0972 N85-16176
Bearing tester fit analysis
[NASA-CR-171282] 07 p0973 N85-16181
Assessment of the operating characteristics of the SSME LOX turbopump pump-end bearing
[NASA-CR-171287] 08 p1167 N85-17362
An evaluation of the 64-meter antenna radial bearing for use on the 70-meter antenna 10 p1464 N85-19238
Elevation bearing maximum load, 70-meter antenna 10 p1464 N85-19239
Hydrostatic bearing pad maximum load and overturning conditions for the 70-meter antenna 10 p1465 N85-19241
Low leakage turbine shaft seals for advanced combined cycle systems
[AD-A149372] 10 p1492 N85-19420
Precise bearing support dithering
[AD-D011470] 10 p1493 N85-19426
Emitted vibration measurement device and method
[NASA-CASE-MFS-25981-1] 11 p1635 N85-20299
Characterization of lubricated bearing surfaces operated under high loads
[NASA-TM-86984] 12 p1811 N85-21357
Experimental study of heat transfer from shaft in cooled radial bearing of GNT-25 gas turbine 14 p2270 N85-24068
Selection of bearing type for large steam turbines 14 p2271 N85-24069
Design of piping for oil drain from turbine bearings 14 p2271 N85-24073
Stability of turbine runners in sliding bearings under external circulation forces 14 p2272 N85-24074
Stability of steady modes of motion by axis of rotating wheel in nonlinear bearings 14 p2279 N85-24117
Thermal deformation of flexible rotors in friction bearings 14 p2280 N85-24123
Study of axial bearings without oil bath with radial cooling of blocks 14 p2286 N85-24164
Model of friction bearing hydrodynamics 14 p2288 N85-24178
Computations for segmented radial bearings 14 p2288 N85-24180
Advanced rocket engine cryogenic turbopump bearing thermal model 16 p2735 N85-26879
Effects of bearing deadbands on bearing loads and rotor stability 16 p2737 N85-26889
Reusable rocket engine turbopump condition monitoring 16 p2740 N85-26907
Non-contact hydrostatic bearings 16 p2762 N85-27046
Fatigue life analysis of a turboprop reduction gearbox
[NASA-TM-87014] 16 p2793 N85-27228

BEARS
Polar bear telemetry results from the Nimbus-6 system 14 p2325 N85-24365

BEAT
U SYNCHRONISM

BEAT FREQUENCIES
Optical injection locking of solid-state oscillators by frequency-multiplexed injection-locked, laser diodes
[AD-D011695] 19 p3275 N85-30307
BEAUFORT SEA (NORTH AMERICA)
Analysis and interpretation of current measurements from the Beaufort Sea
[AD-A145197] 01 p0089 N85-10600
Geothermal studies in Alaska: Conditions at Prudhoe Bay 04 p0516 N85-13290
Shore ice ride-up and pile-up features. Part 2. Alaska's Beaufort Sea coast, 1963 - 1984
[AD-A148428] 08 p1190 N85-17501
Atlas of the Beaufort Sea
[AD-A149545] 11 p1689 N85-20619
Data collection and winter ice dynamics in the Beaufort Sea 14 p2238 N85-23878
BED REST
Physical performance capacity after a 7 day head-down tilt (-6 deg) 05 p0692 N85-14451
Leg volume changes. Responses to Lower Body Negative Pressure (LBNP) during 7 days of zero-g simulation (6 deg Head-Down Tilt (HDT))
05 p0692 N85-14452
Heart rate variability during 7 day head-down tilt (6 deg) 05 p0692 N85-14453
Comparison of simulation of weightlessness by Head Down Tilt (HDT) and Water Immersion (WI)
05 p0692 N85-14454
Glucose tolerance in trained and untrained subjects during head-down tilt (6 deg) 05 p0693 N85-14461
Alterations/corrections to the BRASS Program
[NASA-CR-171874] 15 p2616 N85-26121
Effect of 120-day antiorthostatic bedrest on gas exchange and pulmonary circulation in man
19 p3323 N85-30589
Regional circulation during testing on isokinetic dynamometer following 14-day bedrest
19 p3323 N85-30590
BEDROCK
NT BALTIC SHIELD (EUROPE)
NT BATHOLITHS
Geophysical investigations of the central part of Niger State, Nigeria 03 p0390 N85-12496
SIR-B analysis of the Precambrian shield of Sudan and Egypt: Penetration studies and subsurface mapping
08 p1145 N85-17219
Saudi Arabian refraction profile: Crustal structure of the Red Sea-Arabian Shield transition
17 p2990 N85-28484
Saudi Arabian refraction profile: A preliminary interpretation for the Red Sea-Arabian Shield transition
17 p2991 N85-28485
A traveltime interpretation of the 1978 seismic refraction profile in the Kingdom of Saudi Arabia
17 p2991 N85-28486
Interpretation of the data of USGS seismic refraction profile across the Arabian Shield in western Saudi Arabia 17 p2991 N85-28488
One-dimensional velocity-depth functions determined for the Arabian Shield and the southwestern Red Sea: A comparison of models 17 p2992 N85-28490
A comparison of crustal sections: Arabian Shield to the Red Sea 17 p2992 N85-28491
Reduced to pole long-wavelength magnetic anomalies of Africa and Europe 20 p3475 N85-31595
Euro-African MAGSAT anomaly-tectonic observations
20 p3475 N85-31596
Bedrock geology of the Brattleboro Quadrangle, Vermont-New Hampshire
[DE85-011027] 22 p3815 N85-33634
BEDS (GEOLOGY)
NT SALT BEDS
BEDS (PROCESS ENGINEERING)
Influence of inter-layer effect on charge gas-permeability
[BLL-M-35919-(5828.4)] 05 p0616 N85-13940
Influence of size grading of sintering ore on the sintering process
[BLL-M-36004-(5828.4)] 07 p0924 N85-15854
Transition to detonation from rapid-compression (ramp-waves) generated in a burning porous bed
[AD-P004345] 10 p1455 N85-19169
BEER LAW
Aerosol multiple-scanning code, ASCAT
[LA-10046-MS] 12 p1823 N85-21440
BEHAVIOR
NT HUMAN BEHAVIOR
Command control group behaviors. Objective 1: A methodology for and identification of command control group behaviors
[AD-A145690] 02 p0191 N85-11279
Decision process models of contractor behavior: The development of effective contract incentives
[AD-A145524] 02 p0292 N85-11898
USSR report: Life sciences. Biomedical and behavioral sciences
[JPRS-UBB-84-027] 07 p1012 N85-16426
Model of team organization and behavior and team description method
[AD-A147540] 07 p1053 N85-16680
USSR report: Life sciences. Biomedical and behavioral sciences
[JPRS-UBB-85-001] 08 p1193 N85-17515
USSR report: Life sciences. Biomedical and behavioral sciences
[JPRS-UBB-85-007] 09 p1362 N85-18566
Behaviour of soil under a lugged wheel
[AD-P004287] 09 p1407 N85-18864
Turning behaviour of articulated frame steering tractor
[AD-P004304] 09 p1409 N85-18881
USSR report: Life sciences. Biomedical and behavioral sciences
[JPRS-UBB-85-009] 10 p1526 N85-19625
Blackbirds and starlings: Population ecology and habits related to airport environments
[AD-P004190] 11 p1580 N85-19953
Cattle Egret hazard assessment
[AD-P004191] 11 p1580 N85-19954
Learning to search. From weak methods to domain-specific heuristics
[AD-A149949] 12 p1918 N85-22045
Analysis of team performance in a programmed environment
[NASA-CR-175634] 14 p2392 N85-24728
Large-time behavior of viscous surface waves
[AD-A154805] 21 p3584 N85-32278
Experimental and analytic characterization of nonlinear seismic attenuation
[AD-A154760] 21 p3631 N85-32556
Sobolev-Poincare's inequality and the Neumann problem for u sub t = divergence of the absolute value of the gradient u to the p-2 power x the gradient u
[AD-A154786] 21 p3676 N85-32839
BELGIUM
Satellite-determined stresses in the crust of Europe with particular consideration to the Liege earthquake of November 8, 1983 20 p3490 N85-31694
150 years of meteorology in Belgium
22 p3817 N85-33642
BELL AIRCRAFT
NT UH-1 HELICOPTER
BENCHES
U SEATS
BEND TESTS
Yield stress determination from miniaturized disk bend test data
[DE85-009495] 18 p3122 N85-29330
BENDING
NT ELASTIC BENDING
Material degradation in heavy steel plates caused by bending with a laser
[AD-A144784] 01 p0052 N85-10343
Initial sailplane project: The RP-1
04 p0468 N85-12976
Second sailplane project: The RP-2
04 p0468 N85-12977
On a general nonlinear theory of plates and shells: Formulation and applications 08 p1172 N85-17387
Modelling and identification of the structural properties of an astromast
[CRC-1374] 09 p1329 N85-18352
NOAA OTEC CWP (National Oceanic and Atmospheric Administration Ocean Thermal Energy Conversion Cold Water Pipe) at-sea test. Volume 3, part 1: Tabulation of the power spectra for selected channels
[PB84-238955] 09 p1346 N85-18467
Turning behaviour of articulated frame steering tractor
[AD-P004304] 09 p1409 N85-18881
Bending two-layer metal-polymer plates
11 p1604 N85-20085
Simple theoretical models for composite rotor blades
[NASA-CR-175620] 13 p1971 N85-22382
Load carrying capacity of double circular arc gears
14 p2221 N85-23776
Thermomechanically induced pre- and postbuckling of general structure 20 p3467 N85-31540
The effect of abrasive blasting on the fatigue and corrosion of an aluminium-copper alloy
[AD-A154954] 21 p3566 N85-32182
User's guide for computer program CGFAG, Concrete General Flexure Analysis with Graphics
[AD-A155555] 21 p3570 N85-32204
Thin-film reliability and engineering overview
21 p3612 N85-32450
Analysis of long bone and vertebral failure patterns
[AD-A154796] 21 p3663 N85-32758
Stress distribution of fiberglass reinforced plastic beam with a delamination under three-point bending
23 p3908 N85-34210
Stress-intensity factors for circumferential surface cracks in pipes and rods under tension and bending loads
[NASA-TM-87594] 24 p4101 N85-35424
Major facility overhauls at LAMPF
[DE85-012724] 24 p4156 N85-35765
BENDING FATIGUE
Effect of internal pressure on flexibility and stress intensification factors for pipe elbows analyzed by the finite element method
[AD-A151161] 15 p2578 N85-25901
Rotating bending fatigue strength of silicon carbide and alumina-fiber reinforced aluminum
23 p3907 N85-34206
BENDING MOMENTS
Optimum design of nonplanar wings: Minimum induced drag for a given lift and wing root bending moment
[NAL-TR-797] 01 p0002 N85-10011
Three programs for evaluating bending moments, deflections and shear forces in simply-supported uniform bridge decks under South African NA loading: NAB, NAD and NAS. NITRR manual P13
[ISBN-0-7988-2263-X] 01 p0102 N85-10881
Helicopter active control with rotor blades relaxation
08 p1075 N85-16819
Negative flexural behavior of precast composite slabs with steel joint 23 p3904 N85-34183
Nonlinear flap-lag-extensional vibrations of rotating, pretwisted, preconed beams including Coriolis effects
[NASA-TM-87102] 23 p3941 N85-34427
BENDING VIBRATION
Optimization of vibrating beams including the effects of coupled bending and torsional modes
09 p1331 N85-18364
BENDS (PHYSIOLOGY)
U DECOMPRESSION SICKNESS
BENEFICIATION
Novel analytical approaches to coal beneficiation
[DE85-010437] 19 p3229 N85-30021
BENZENE
Effect of toluene on the solubility of biohazardous volatile synthetic organic compounds
[AD-A145188] 01 p0018 N85-10109
Multiphoton ionization of benzene in solution
[DE85-000893] 06 p0766 N85-14899
Vibrational spectroscopy of chemisorption phenomena on model catalyst surfaces
[AD-A146753] 07 p0922 N85-15840
Subtractively normalized interfacial Fourier transform infrared spectroscopy of difluorobenzene adsorbed at polycrystalline platinum electrodes
[AD-A148660] 08 p1123 N85-17080
Supersonic molecular jet study of the liquid state
[AD-A147416] 09 p1379 N85-18671
Improved lithium-intercalation cathode material
[AD-A149319] 10 p1435 N85-19043
Laser schlieren, shock tube studies of high temperature hydrocarbon pyrolysis rates
[DE85-003314] 11 p1636 N85-20303
Synthesis, static and reactive characterization of supported organometallics
[DE85-004285] 12 p1808 N85-21340
Formation of high molecular weight products from benzene during boundary lubrication
[NASA-TM-86966] 13 p2017 N85-22644
Collaborative shock tube studies of benzene pyrolysis
[DE85-006347] 14 p2253 N85-23962
The mobile phase in coals: Its nature and modes of release
[DE85-011696] 19 p3230 N85-30026
Flash pyrolysis of biomass with reactive and non-reactive gases
[DE85-010962] 19 p3306 N85-30496
Vibrational energy transfer in benzene-argon collisions
[DE85-009603] 19 p3355 N85-30797
Fuel-rich catalytic combustion: A soot-free technique for in situ hydrogen-like enrichment
[NASA-TP-2498] 20 p3423 N85-31244
Thermal reactions of aromatics with CaO
[DE85-010688] 22 p3742 N85-33193
Ionization detection of stimulated Raman spectra
[DE85-010672] 22 p3746 N85-33218
Carcinogenesis of nitrated toluenes and benzenes skin and lung tumor assays in mice
[AD-A155723] 22 p3818 N85-33655
BENZOIC ACID
Condensation of anhydrides or dicarboxylic acids with compounds containing active methylene groups. Part 19: Condensation of phthalic and substituted phthalic anhydrides with benzoylacetic ester
[NASA-TM-77885] 19 p3227 N85-30009
BERING SEA
Drift characteristics of northeastern Bering Sea ice during 1982
[PB84-213982] 01 p0089 N85-10604

Recent observations of tides and tidal currents from the northeastern Bering Sea shelf
[PB84-241785] 04 p0543 N85-13452
New data on structure of Shirshov Ridge (Bering Sea) 10 p1498 N85-19456
Seafloor seismic measurements in the southern Bering
[DE85-004908] 14 p2374 N85-24675
Regional meteorology of the Bering Sea during MIZEX-West, February and March 1983
[PB85-173699] 18 p3150 N85-29503
Geological-geophysical and gas-biochemical studies in Bering Sea 19 p3291 N85-30404

BERMUDA
AWS (Air Weather Service) climatic briefs: North America
[AD-A152161] 16 p2835 N85-27483

BERNOULLI EQUATION
U BERNOULLI THEOREM

BERNOULLI THEOREM
The distribution of the number of empty cells in a generalized random allocation scheme
[AD-A154806] 21 p3677 N85-32841

BERYL
Spectroscopic investigation of materials for frequency agile laser systems
[AD-A151731] 16 p2790 N85-27208

BERYLLIUM
NT BERYLLIUM ISOTOPES
NT BERYLLIUM 7
NT BERYLLIUM 9
NT BERYLLIUM 10
Dependence of microplasticity of beryllium on grain size and heat treatment 03 p0353 N85-12273
Narrow absorption components in Be star winds 06 p1232 N85-17760
Mechanical properties of Be-Al composite 10 p1443 N85-19094
Structure-phase state and properties of high-durability VAL8 alloy 11 p1597 N85-20048
Weldability of alloy ABM1 to alloy 1201 11 p1603 N85-20080
Conductivity changes in neutron-irradiated commercial copper alloys at approximately 450(O)C
[DE85-003007] 11 p1606 N85-20100
Effect on work-hardening in dynamic deformation of beryllium
[DE85-002691] 11 p1608 N85-20111
Stability of temporal and energy parameters of picosecond lanthanum beryllate laser 11 p1717 N85-20804
Nondestructive method for detecting machine damage in beryllium
[DE85-001074] 12 p1862 N85-21681
TEM/FIM study of modulated microstructures in the Fe-Be system
[DE85-005379] 13 p2023 N85-22678
Gigantic lithium deposit discovered in France 14 p2289 N85-24184
China report: Science and technology
[JPRS-CST-85-007] 15 p2533 N85-25621
Professional Committee on Solid Propulsion hold conference 15 p2533 N85-25623
Radiation damage experiments and lifetime estimates for beryllium components in fusion systems
[DE85-008038] 17 p3040 N85-28611
Preliminary proposal for a beryllium technology program for fusion applications
[DE85-009815] 18 p3183 N85-29737
Machining of beryllium with the LLNL precision engineering research lathe
[DE85-010832] 19 p3250 N85-30149
The production and destruction of metastable negative ions
[DE85-011056] 19 p3364 N85-30858
Design of a helium-cooled molten salt fusion breeder
[DE85-010474] 20 p3528 N85-31943
Investigation of thick-target neutron emission from Be-9(d,n)B-10 at E(d) = 7 MeV for angles other than zero degrees
[DE85-010254] 20 p3528 N85-31947
Beryllium production
[DE85-013360] 24 p4148 N85-35716

BERYLLIUM ALLOYS
Re-evaluation of phase separation in Ti-Zr-Be metallic glasses
[DE84-015603] 03 p0338 N85-12176
The Al-Be system: The effects of RSP on structure and phase relating
[DE84-015604] 04 p0474 N85-13019
Critical evaluation of binary rare earth phase diagrams
[DE84-015057] 05 p0614 N85-13922
Design and use of nonstandard tensile specimens for irradiated materials testing
[DE85-001071] 11 p1652 N85-20408
Temperature variation of resistivity of certain alloys based on transition and simple metals in amorphous and crystalline states 15 p2496 N85-25399

BERYLLIUM COMPOUNDS
NT BERYL
NT BERYLLIUM FLUORIDES
NT BERYLLIUM OXIDES
Determination of the average neutron activation cross section with an annular-shaped 241 Am/Be neutron source and a NaI(T1) detector for the 27 Al (n,p)27 Mg-reaction
[REPT-4/1984] 20 p3532 N85-31975

BERYLLIUM FLUORIDES
Computer simulations of rare earth sites in glass: Experimental tests and applications to laser materials
[DE85-006156] 14 p2261 N85-24013

BERYLLIUM ISOTOPES
NT BERYLLIUM 7
NT BERYLLIUM 9
NT BERYLLIUM 10
Galactic propagation models consistent with the cosmic ray lifetime derived from Be-10 measurements
[OG-4.3-1] 22 p3878 N85-34026

BERYLLIUM OXIDES
Development of the Cascade inertial-confinement-fusion reactor
[DE85-010933] 19 p3357 N85-30812

BERYLLIUM 7
Proposed solar neutrino experiment using (81)Br(nu,e(-e)) (81)Kr
[DE85-004802] 15 p2684 N85-26579

BERYLLIUM 9
Fast-neutron-spectrum measurements for the thick-target (9)Be(d/ = 7 MeV
[DE85-010481] 18 p3183 N85-29735

BERYLLIUM 10
Cosmic rays 10Be biennal data and their relationship to aurorae and sunspots
[SH-7.1-1] 23 p4047 N85-35094

BESSEL FUNCTIONS
Simplified continued fraction calculation of spherical Bessel functions
[AD-A146844] 06 p0858 N85-15455
Some scientific subroutines in LISP
[AD-A147889] 07 p1026 N85-16515
Calculation of roots of transcendental equations in problems of determining thermal conductivity of cylinder with non-uniform boundary conditions
[BLL-M-35788-(5828.4)] 23 p3929 N85-34349

BETA FACTOR
Elimination of stochasticity in stellarators 02 p0282 N85-11839
Limits of possible operation of the R-Tokamak due to ideal MHD instabilities
[IPPJ-694] 06 p0863 N85-15486
Experimental results on Tokamak beta limits from ISX-B
[DE84-015372] 07 p1046 N85-16644
Effects of q and high beta on Tokamak stability
[DE84-016650] 09 p1393 N85-18767
Finite-(beta) optimization of tandem mirrors
[DE85-002658] 10 p1560 N85-19835
Ballooning beta limits of dee and bean shaped Tokamaks
[IPPJ-713] 16 p2866 N85-27676
System and method of operating toroidal magnetic confinement devices
[DE85-011670] 22 p3845 N85-33814
Simulation studies on stability of hot electron plasma 23 p3978 N85-34684
Confinement and heating of high beta plasmas with emphasis on compact toroids
[DE85-011459] 24 p4155 N85-35761
Generalized reduced fluid model with finite ion-gyroradius effects
[DE85-013123] 24 p4157 N85-35777

BETA INTERACTIONS
U WEAK INTERACTIONS (FIELD THEORY)

BETA PARTICLES
Investigation of internal fields and motions, radiation damages and recovery processes using beta and gamma active probe nuclei 03 p0427 N85-12726
High-Beta Tokamak research
[DE84-016470] 04 p0568 N85-13618
Electronic autofluorography: Principles, problems and prospects
[DE84-016698] 05 p0639 N85-14097
Whist code calculations of ignition margin in an ignition Tokamak
[DE85-009507] 18 p3190 N85-29784
Nuclear structure problems in double beta decay
[DE85-010739] 19 p3364 N85-30859
Beta response of selected instruments
[DE85-013278] 22 p3788 N85-33469
Pulsed-neutron-source models for the astrophysical s-process
[DE85-012927] 24 p4151 N85-35740

BETATRONS
Self potentials of an electron ring in a torus for large ring displacement from the minor axis
[AD-A146088] 03 p0421 N85-12691
Non-linear transverse electron beam dynamics in a modified betatron accelerator
[AD-A148106] 08 p1220 N85-17685
Acceleration of an electron ring in a modified betatron with transverse pressure
[AD-A148626] 08 p1221 N85-17688
The plasma assisted modified betatron
[AD-A148728] 09 p1390 N85-18748
Betatron-synchrotron detrapping in a tapered wiggler free electron laser
[AD-A149686] 12 p1856 N85-21642
Resonance between betatron and synchrotron oscillations in a free electron laser: A 3-D numerical study
[AD-A150059] 12 p1857 N85-21645
Modified betatron accelerator studies
[AD-A151420] 15 p2648 N85-26332

BETHE-SALPETER EQUATION
Notes for lectures in China: The Bethe theory of inelastic collisions of fast charged particles with atoms and molecules
[DE84-017487] 09 p1380 N85-18678

BIAS
Fast envelope detector with bias compensation
[AD-D011226] 01 p0038 N85-10243
Aerosol sampling bias from differential electrostatic charge and particle size 02 p0224 N85-11467
Evaluation of thermocouple junction temperature
[DE84-015159] 04 p0502 N85-13206
Blind zones and aspect ratio bias in acquisition of discontinuity orientation data
[DE84-002718] 04 p0533 N85-13410
Treatment and expression of measurement uncertainties 05 p0630 N85-14042
Circuit transients due to negative bias arcs on a high-voltage solar array in low Earth orbit
[NASA-TP-2407] 06 p0760 N85-14858
Coherent array of Josephson oscillators with external bias leads
[AD-D011367] 08 p1156 N85-17293
Improved magnetic bias and delay linearity in a magnetostatic wave delay line
[AD-D011441] 10 p1479 N85-19337
A replication and extension of the inducement of the availability heuristic
[AD-A149755] 12 p1923 N85-22083
Switching mixer
[AD-D011602] 16 p2777 N85-27139

BIBLIOGRAPHIES
Compilation of data sources for existing chemicals
[GSF-A-2/84] 01 p0017 N85-10103
Publications of Center for Manufacturing Engineering (of the National Bureau of Standards), 1978-1983
[PB84-224526] 01 p0036 N85-10228
Bibliography of data on electrical breakdown in gases
[PB84-218049] 01 p0045 N85-10294
Geology and geomorphology of the southern central Blue Ridge: An indexed bibliography
[PB84-225119] 01 p0072 N85-10480
Space medicine and biology, continuing bibliography (supplement 263)
[NASA-SP-7011(263)] 01 p0094 N85-10636
Publications of the exobiology program for 1981: A special bibliography
[NASA-TM-86653] 01 p0099 N85-10657
Publications of the National Bureau of Standards, 1983 catalog
[PB84-218031] 01 p0126 N85-10869
A bibliography of planetary geology and geophysics principal investigators and their associates, 1983 - 1984
[NASA-TM-87361] 01 p0127 N85-10874
The Shock and Vibration Digest, volume 16, no. 8
[AD-A145653] 02 p0208 N85-11372
Bibliography of climate textbooks and studies
[WCP-94] 02 p0231 N85-11505
Aerospace Medicine and Biology, a continuing bibliography with indexes
[NASA-SP-7011(264)] 02 p0234 N85-11525
Engineering Physics Division
[DE84-007778] 02 p0274 N85-11787
Aeronautical Engineering, A Continuing Bibliography With Indexes
[NASA-SP-7037(179)] 03 p0307 N85-11976
Fire research publications, 1983
[PB84-217066] 03 p0343 N85-12208
Spread-spectrum communications
[AD-A146135] 03 p0355 N85-12285
Center for Electronic and Electrical Engineering Technical Progress Bulletin, January - March 1983, no. 2
[PB84-231224] 03 p0360 N85-12308

Bibliography of Soviet laser developments, number 65, May - June 1983
[AD-A146189] 03 p0366 N85-12347
Penetrator/armour interactions: Background to Australian work
[MRL-R-936] 03 p0367 N85-12353
Earth Resources, A Continuing Bibliography with Indexes
[NASA-SP-7041(43)] 03 p0376 N85-12411
Aeronautical Engineering, a continuing bibliography with indexes
[NASA-SP-7037(180)] 04 p0451 N85-12858
A bibliography of publications on corrosion and oxidation from UK government laboratories at Teddington, 1924 - 1983
[NPL-DMA(A)-82] 04 p0472 N85-13004
Bibliography of US patents on augmentation of convective heat and mass transfer, part 2
[DE84-014865] 04 p0498 N85-13178
Aerospace Medicine and Biology, a continuing bibliography with indexes
[NASA-SP-7011(265)] 04 p0545 N85-13467
Space medicine research publications: 1983-1984
[NASA-CR-3860] 04 p0545 N85-13469
FY 1984 scientific and technical reports, articles, papers and presentations
[NASA-TM-86470] 04 p0575 N85-13670
Economic value of consumer information: A selected, annotated bibliography
[PB84-235795] 04 p0576 N85-13673
Carbon dioxide and climate: Summaries of research in FY 1983 and FY 1984
[DE85-001245] 06 p0839 N85-15327
Publications of the Executive Office of the President: January 20, 1981 - June 30, 1984
[PB84-230671] 06 p0871 N85-15533
A summary of the foundation research program
[AD-A146524] 06 p0891 N85-15656
Circulation control: A bibliography of DTNSRDC research and selected outside references: Update
[AD-A146966] 07 p0893 N85-15661
Loads and Aeroelasticity Division research and technology accomplishments for FY 1984 and plans for FY 1985
[NASA-TM-86356] 07 p0896 N85-15691
Optics of solids (surface related) and effect of surface roughness on MOS
[AD-A146863] 07 p0946 N85-15996
Earth science investigations in the United States Antarctic Research Program (USARP)
[PB84-240508] 07 p0990 N85-16288
Aeronautical Engineering: A continuing bibliography with indexes (supplement 182)
[NASA-SP-7037(182)] 08 p1067 N85-16758
Bibliography update on the California current system and related mesoscale ocean modeling
[AD-A148546] 08 p1190 N85-17503
Bibliography of venomous and poisonous marine animals and their toxins
[AD-A148409] 08 p1192 N85-17514
Aerospace medicine and biology: A continuing bibliography with indexes
[NASA-SP-7011(266)] 08 p1194 N85-17525
Aerospace medicine and biology: A continuing bibliography with indexes, supplement 266
[NASA-SP-7011(268)] 08 p1194 N85-17526
Software test handbook: Software test guidebook, volume 2
[AD-A147269] 08 p1204 N85-17578
Bibliography of adaptive control
[OUEL-1544/84] 08 p1209 N85-17602
Scientific and technical information output of the Langley Research Center for calendar year 1984
[NASA-TM-86336] 08 p1229 N85-17740
Aeronautical engineering, a continuing bibliography with indexes
[NASA-SP-7037(181)] 09 p1263 N85-17932
Brief outline of analytic stability studies of magnetically insulated systems --- bibliolographies
[DE85-000212] 09 p1393 N85-18765
Bibliography of unclassified reports, FY 1984
[AD-A148838] 09 p1401 N85-18819
Aeronautical engineering: A continuing bibliography with indexes
[NASA-SP-7037(184)] 10 p1419 N85-18949
Bibliography of Soviet laser developments, Number 66, July-August 1983
[AD-A149113] 10 p1490 N85-19406
Laser Hazards Bibliography, October 1984
[AD-A149534] 10 p1490 N85-19408
Earth resources: A continuing bibliography with indexes
[NASA-SP-7041(44)] 10 p1503 N85-19484
Aerospace medicine and biology: A continuing bibliography with indexes
[NASA-SP-7011(269)] 10 p1526 N85-19628
Post-processing of bibliographic citations from DOE/Recon, NASA/Recon, and DOD/DROLS
[DE85-000617] 11 p1739 N85-20938
Sourcebook: Gaining access to US government information on the environment and natural resources
[DE84-017419] 11 p1740 N85-20941
Metrology for Electronic Technology: A bibliography of NBS (National Bureau of Standards)
[PB85-112895] 12 p1830 N85-21486
Choice reaction time and color: An annotated bibliography
[AD-A149722] 12 p1908 N85-21979
Cumulative reports and publications through December 31, 1984
[NASA-CR-172569] 12 p1911 N85-21991
Bibliography of atomic and molecular processes, 1983
[DE85-000662] 12 p1929 N85-22121
Compiled and thermodynamic data sources for aqueous and biochemical systems: An annotated bibliography, 1930 - 1983
[PB85-137693] 12 p1944 N85-22208
Bibliography of Lewis Research Center technical publications announced in 1983
[NASA-TM-83693] 12 p1951 N85-22255
List of RAE (Royal Aircraft Establishment) translations issued during the period 1 March 1983 - 31 March 1984
[AD-A149787] 12 p1951 N85-22257
Aeronautical Engineering: A continuing bibliography with indexes, supplement 185
[NASA-SP-7037(185)] 13 p1965 N85-22342
Aeronautical Engineering: A cumulative index to the 1984 issues of the continuing bibliography
[NASA-SP-7037(183)] 13 p1965 N85-22343
Cryogenic wind tunnels: A selected annotated bibliography
[NASA-TM-86346] 13 p1976 N85-22401
Small business innovation research: Abstracts of 1984. Phase 1 awards
[NASA-TM-87427] 13 p2165 N85-23431
NASA Patent Abstracts Bibliography. A continuing bibliography. Section 2: Indexes
[NASA-SP-7039(26)] 13 p2167 N85-23445
Aeronautical engineering, a continuing bibliography with indexes
[NASA-SP-7037(186)] 14 p2207 N85-23682
JP-8 and JP-5 as compression ignition engine fuel
[AD-A150796] 14 p2263 N85-24022
Probalistic analysis of combinatorial algorithms: An annotated bibliography
[CWI-OS-R8411] 14 p2411 N85-24864
Technology for large space systems: A bibliography with indexes, supplement 11
[NASA-SP-7046(11)] 15 p2475 N85-25277
Microwave tubes: Literature survey no. 5 comprising year 1983
[FOA-C-30377-E] 15 p2550 N85-25739
Bibliography of Soviet Laser Developments, Number 67, September-October 1983
[AD-A151199] 15 p2562 N85-25805
Aerospace Medicine and Biology: A continuing bibliography with indexes
[NASA-SP-7011(270)] 15 p2615 N85-26114
Human factors department 1981 publications
[BAE-BT-12685] 15 p2620 N85-26147
Management: A bibliography for NASA managers
[NASA-SP-7500(19)] 15 p2664 N85-26439
List of serials indexed for online users, 1985
[PB85-143220] 15 p2666 N85-26455
The biological effects of radiofrequency radiation
16 p2775 N85-27131
A bibliography of reports of the Sandia solar thermal distributed receiver systems project
[SAND-84-0313] 16 p2817 N85-27378
Review and annotated bibliography of benthic studies in coastal and estuarine areas of Florida with a selected compilation of worldwide benthic methodological references and southeastern United States benthic taxonomic references
[PB85-151041] 16 p2822 N85-27405
Aerospace medicine and biology: A continuing bibliography with indexes, supplement 271, May 1985
[NASA-SP-7011(271)] 16 p2840 N85-27514
Compilation of abstracts of theses submitted by candidates for degrees
[AD-A151722] 16 p2875 N85-27739
Documents of the JPL Photovoltaics Program Analysis and Integration Center: An annotated bibliography
[NASA-CR-175873] 17 p2965 N85-28448
COSMIC Software Catalog, 1985 edition
[NASA-CR-174070] 17 p3010 N85-28608
Design issues in video disc map display
[AD-A153531] 18 p3109 N85-29253
Earth Resources: A continuing bibliography with indexes, issue 45
[NASA-SP-7041(45)] 18 p3123 N85-29336
Data base of all known, published data on trace elements in oil shale and its products
[DE85-003399] 18 p3126 N85-29357
SERI photovoltaic advanced research and development project: FY 1984 accomplishments
[DE85-002939] 18 p3128 N85-29368
Fuel cells: A bibliography
[DE85-004565] 18 p3128 N85-29371
Publications of the Jet Propulsion Laboratory 1983
[NASA-CR-175979] 18 p3199 N85-29648
Aeronautical Engineering: A continuing bibliography with indexes (supplement 188)
[NASA-SP-7037(188)] 19 p3211 N85-29910
Aeronautical Engineering: A continuing bibliography with indexes
[NASA-SP-7037(187)] 19 p3211 N85-29911
Multiaxial fatigue and fracture: A literature review
[ARL/STRUC-R-410] 19 p3285 N85-30370
Publications of the NASA CELSS (Controlled Ecological Life Support Systems) program
[NASA-CR-3911] 19 p3326 N85-30608
Aerospace Medicine and Biology: A continuing bibliography with indexes (supplement 272)
[NASA-SP-7011(272)] 19 p3328 N85-30620
A theoretical study of electron capture in ion-ion and ion-atom collisions
[DE85-011154] 19 p3362 N85-30842
Human factors engineering data sources; an overview
[FOA-C-56044-H2] 20 p3513 N85-31837
Atomic, Molecular and Solid-State Theory, and Computational Quantum Chemistry, part 1
[DE85-009401] 20 p3526 N85-31929
Publications from the Department of Plasma Physics and the Unit of Accelerator Technology, index and abstracts, 1984
[TRITA-EPP-84-13] 20 p3534 N85-31991
Aerospace medicine and biology: A continuing bibliography with indexes, supplement 273
[NASA-SP-7011(273)] 21 p3663 N85-32755
Human performance in continuous/sustained operations and the demands of extended work/rest schedules. An annotated bibliography
[AD-A155819] 21 p3666 N85-32771
A short bibliography of recent developments in selection and ranking procedures
[AD-A155645] 21 p3679 N85-32856
Air Force Office of Scientific Research (AFOSR). Technical report summaries: First quarter (CY)
[AD-A154757] 21 p3713 N85-33041
Aeronautical engineering: A continuing bibliography with indexes (supplement 189)
[NASA-SP-7037(189)] 22 p3727 N85-33104
Military hydrology. Report 9: State-of-the-art review and annotated bibliography of dam-breach flood forecasting
[AD-A155383] 22 p3801 N85-33553
Bibliography and index for nuclear reactions among light charged particles, volume 26
[DE85-011482] 22 p3838 N85-33768
NASA patent abstracts bibliography: A continuing bibliography. Section 1: Abstracts (supplement 27)
[NASA-SP-7039(27)-SECTION-1]
22 p3849 N85-33840
Index of laser program publications and related reports, calendar year 1984
[DE85-011863] 23 p3936 N85-34398
Aerospace Medicine and Biology: A continuing bibliography with indexes (supplement 274)
[NASA-SP-7011(274)] 23 p3952 N85-34491
The next assignment: The state of the literature on space 23 p4057 N85-35146
Aeronautical engineering: A continuing bibliography with indexes, supplement 190
[NASA-SP-7037(190)] 24 p4059 N85-35152
Technology for large space systems: A bibliography with indexes
[NASA-SP-7046(12)] 24 p4068 N85-35209
Bibliography on tidal hydraulics. Report 2. Supplement 9: Supplementary material compiled from June 1980 - June 1983. Tidal flows in rivers and harbors
[AD-A155990] 24 p4125 N85-35574
A research program to reduce the interior noise in general aviation aircraft, index and summary
[NASA-CR-176178] 24 p4145 N85-35695
NASA patent abstracts bibliography, a continuing bibliography. Section 2: Indexes (supplement 27)
[NASA-SP-7039(27)-SECTION-2]
24 p4164 N85-35820
Fire research publications, 1984
[PB85-208502] 24 p4166 N85-35827

BICARBONATES
U CARBONATES

BICRYSTALS

Flux-line pinning by the grain boundary in niobium bicrystals
[DE84-016668] 04 p0570 N85-13638

Characterization of bicrystal grain boundary properties using device structures
[DE84-004509] 08 p0869 N85-15523
BIFURCATION (MATHEMATICS)
U BRANCHING (MATHEMATICS)
BIG BANG COSMOLOGY
Cosmology 07 p1056 N85-16701
Cosmology, galactic astronomy and elementary particle physics 12 p1956 N85-22289
Galaxy formation 12 p1960 N85-22321
Integral constraints on stress energy perturbations in general relativity and applications to cosmology 19 p3383 N85-30985
Charge 4/3 leptons in cosmic rays
[HE-6.2-14] 24 p4212 N85-36150
BIGHORN MOUNTAINS (MT-WY)
Chronologic and climatic control on soil development, northern Bighorn Basin, Wyoming and Montana 08 p1181 N85-17443
BIGHTS
U BAYS (TOPOGRAPHIC FEATURES)
BIHARMONIC EQUATIONS
Numerical treatment of corner singularities of the biharmonic equation
[TUM-M8315] 05 p0717 N85-14602
Multinomial form of the solution of problems of the statistics of elastic rectangular disks
[REPT-17/1984] 16 p2797 N85-27244
BILLETS
The effects of radial yarns, 3-dimensionally reinforced carbon-carbon composite
[AD-A144751] 01 p0022 N85-10134
Modelling temperature changes during hot working operations 06 p0798 N85-15095
Continuous casting of quality steels on billet casters
[BMFT-FB-T-84-262] 18 p3078 N85-29041
BIMETALS
Evaluation of residual stress in laminated metallic composites 11 p1598 N85-20052
Method of constructing diagram of bimetal fatigue failure 11 p1599 N85-20058
Microscopic magnetic structure of multiple bilayers of thin films of Fe and Ge
[DE85-004188] 13 p2024 N85-22682
New process for production of bimetal with corrosion-resistant cladding layer
[BLL-BISI-TRANS-22371-(9022.06)] 17 p2927 N85-28056
Effects of the structural state in thermo-bimetals on their resistance to microscopic plastic deformation
[BLL-BISI-TRANS-22403-(9022.06)] 17 p2979 N85-28412
In situ Moessbauer investigation of bimetallic catalysts on a base: FeRu, FeRh, FePd, FeIr, and FePt on SiO2
[B8563200] 20 p3432 N85-31293
Determination of deformation speed during high-speed deformation of cylindrical shells
[BLL-M-36280-(5828.4)] 20 p3465 N85-31527
Chromium-base powder alloys for welding cladding layer of bimetal
[BLL-M-35776-(5828.4)] 23 p3915 N85-34260
BIMETRIC THEORIES
Fake topological Hilbert spaces and characterizations of dimension in terms of negligibility
[CWI-TRACT-2] 14 p2414 N85-24893
BINARY ALLOYS
Wear properties of rapidly solidified surfaces of a pseudo-binary Fe-TiC alloy 02 p0179 N85-11204
Review: The influence of short circuit diffusion on the oxidation of nickel, chromium and nickel/chromium alloys
[AERE-R-11311] 02 p0185 N85-11237
Low temperature properties of Mo/Mi superlattices
[DE84-014729] 02 p0288 N85-11681
NBS (National Bureau of Standards): Materials measurements
[NASA-CR-174038] 03 p0332 N85-12143
Structure of two-phase titanium alloys with different microstructures 03 p0351 N85-12257
Critical evaluation of binary rare earth phase diagrams
[DE84-015057] 05 p0614 N85-13922
Synergestic sputtering properties of binary alloys 06 p0865 N85-15497
Application of the diffraction model to amorphous magnesium zinc alloys
[AD-A147369] 07 p0928 N85-15883
Phase formation and stability in the pseudobinary Ni3Al-Ni3V alloy system
[DE85-001117] 09 p1296 N85-18143
Synergistic sputtering properties of binary alloys
[DE84-017493] 09 p1297 N85-18148
Research on rapidly solidified al"oys
[AD-A149380] 10 p1441 N85-19080
1984 model of binary alloy solidification
[DE85-002497] 11 p1608 N85-20110
Experimental determination of systems suitable for study as monotectic binary metallic alloy solidification models 12 p1948 N85-22235
Models of long-period superstructure
[DE85-007659] 16 p2751 N85-26981
Glassy metals: New highly resistant material
[BLL-BISI-TRANS-21764-(9022.06)] 17 p2926 N85-28049
The structure of carbon martensite analyzed with Moessbauer spectra
[BLL-BISI-TRANS-22402-(9022.06)] 17 p2927 N85-28062
Use of principle of local equilibrium for assessing diffusional supersaturation during solidification of alloys
[BLL-BISI-TRANS-22487-(9022.06)] 17 p2929 N85-28077
Electrical conductivity and phase diagram of binary alloys. 21: The system palladium-chromium
[NASA-TM-77663] 18 p3073 N85-29009
Process for the epitaxial deposition of 3-5 compounds utilizing a binary alloy as the metallic source
[AD-D011663] 18 p3193 N85-29801
MPS solidification model. Analysis and calculation of macrosegregation in a casting ingot
[NASA-CR-171589] 21 p3566 N85-32178
Thermodynamic properties of alloys in the Fe-Ti system
[NPL-DMA(A)-96] 22 p3748 N85-33229
Anti wear property of two phasic metal composite 23 p3906 N85-34199
Enthalpies of formation of liquid Fe-Ce-Si and Fe-Ce-Al three-component alloys
[BLL-M-36296-(5828.4)] 23 p3913 N85-34247
Calculation of activities of components in liquid alloys of iron with yttrium
[BLL-M-35868-(5828.4)] 23 p3914 N85-34253
BINARY CODES
Linear intersecting codes — error correction
[ENST-C-84002] 03 p0356 N85-12291
A very efficient transfer function bounding technique on bit error rate for Viterbi decoded, rate 1/N convolutional codes 05 p0624 N85-13991
On the binary weight distribution of some Reed-Solomon codes
[NASA-CR-174375] 09 p1373 N85-18628
Codes with parity conditions on subsets of coordinates 10 p1465 N85-19247
The ambiguity function of random binary-phase-coded waveforms
[AD-A148906] 10 p1466 N85-19249
Error probability during optimal noncoherent reception of binary signals in multibeam channel 13 p2069 N85-22922
BINARY DATA
Noise tolerance of digital demodulator for complex signal system employing binary quantization 13 p2070 N85-22929
CRAYCDC
[NASA-CR-177374] 24 p4137 N85-35639
CDCCRAY
[NASA-CR-177375] 24 p4137 N85-35640
BINARY DIGITS
Development of new circuit symbols for binary logic elements
[MBB-Z-39/85-O] 17 p3014 N85-28640
Basic features of personal computers 22 p3766 N85-33344
BINARY MIXTURES
NT EUTECTIC ALLOYS
NT EUTECTICS
Thermodynamic properties of isobutane-isopentane mixtures from -40 to +600(0)F and up to 1000 psia
[DE84-015137] 01 p0124 N85-10850
Thermodynamic study of CO2-organic compound interaction at high pressures and temperatures
[DE84-015777] 04 p0573 N85-13654
Theoretical thermodynamics of mixtures at high pressures 13 p2183 N85-23550
Convective instability of horizontal layer of binary mixture 14 p2338 N85-24458
Ca-Ga, Sr-Ga and Ba-Ga binary systems
[DE85-006454] 16 p2751 N85-26980
Experimental and theoretical study of condensation in multicomponent vapors
[DE85-009357] 17 p2923 N85-28021
Response of steam-water mixtures to pressure transients
[DE85-010798] 19 p3267 N85-30282
Transport and relaxation processes in supercritical fluids
[DE85-010554] 19 p3358 N85-30818
Burn front velocity as a function of pellet density in iron-potassium perchlorate heat powders
[DE85-011448] 21 p3572 N85-32214
Relaxation lens in inhomogeneous binary mixture 21 p3695 N85-32957
BINARY STARS
NT CATACLYSMIC VARIABLES
NT COMPANION STARS
NT DWARF NOVAE
NT ECLIPSING BINARY STARS
NT SYMBIOTIC STARS
NT X RAY BINARIES
Variations of the H and K emission lines of singly ionized calcium in the eclipsing binary star system AR Lacertae 02 p0296 N85-11021
RS CV sub n binary systems
[NASA-CR-174164] 04 p0580 N85-13704
The behaviour of brighter binaries and yellow giants in open clusters 05 p0737 N85-14738
The fate of globular clusters 05 p0739 N85-14751
Nonthermal radio emission and the HR diagram 08 p1232 N85-17763
High precision measurement of stellar radial velocity variations 08 p1250 N85-17886
Combined ultraviolet studies of astronomical sources
[NASA-CR-174361] 09 p1413 N85-18910
Radio emission from RS CVn binary systems 09 p1417 N85-18939
A spectroscopic study of LMC X-4
[NASA-CR-174414] 10 p1571 N85-19905
Contributions of the X-ray astronomy group — conference
[MPE-PREPRINT-28] 11 p1741 N85-20947
Search for millisecond rotational periods in some low-mass X-ray binaries observed by EXOSAT 11 p1741 N85-20948
Optical and X-ray observations of 4U2129+47/V1727 CYG in a quiescent state 11 p1742 N85-20950
EXOSAT observations of the galactic bulge X-ray source GX17+2 — X ray binary star 11 p1742 N85-20951
Contributions of the X-ray astronomy group — conference
[MPE-PREPRINT-29] 11 p1742 N85-20952
EXOSAT observations of the 35d intensity variations of Her X-1 — X ray binary source 11 p1742 N85-20956
Pulse phase spectroscopy of Her X-1 with EXOSAT — X ray binary source 11 p1743 N85-20957
Simultaneous EXOSAT and optical observations of the pulsing X-ray binary H2252-035 / AO Psc 11 p1743 N85-20958
Spectral studies of low-mass X-ray binaries observed by EXOSAT 11 p1743 N85-20959
EXOSAT observations of 4U1705-44 — X ray binary 11 p1743 N85-20960
Interacting binary systems 11 p1744 N85-20967
White dwarf stars at ultraviolet wavelengths 11 p1744 N85-20971
Three short-period binaries seen at high-dispersion UX ARI, IOTA TRI and HA5110 11 p1756 N85-21047
Physical models for the UV continua of symbiotic stars 11 p1756 N85-21048
IUE and optical observations of LMC X-ray binaries 11 p1757 N85-21050
Circumstellar material in Algols and Serpentids 11 p1757 N85-21051
MU Sagittarii and Beta Lyrae: Combined IUE/Voyager observations 11 p1757 N85-21052
A search for the spectroscopic binary companions of Polaris using IUE spectra 11 p1757 N85-21053
LSS 2018: A double-lined spectroscopic binary central star with an extremely large reflection effect
[NASA-CR-175503] 11 p1782 N85-21082
Theoretical and observational studies of stellar activity 13 p2171 N85-23468
Offerings of the Astronomical Institute of Bonn 15 p2667 N85-26459
Photoelectric observations of contact binary stars
[REPT-96] 15 p2667 N85-26460
Photoelectric observations of the dwarf nova VW Hydri during the November 1977 supermaximum
[REPT-97] 15 p2667 N85-26461
Stellar surface phenomena: A spectroscopic study of the RS canum venaticorum binaries 15 p2669 N85-26467
A study of W Serpentis binaries: SX Cassiopeiae, RX Cassiopeiae, and W Serpentis 20 p3544 N85-32053
On gamma and neutrino radiation from Cyg X-3
[OG-2.1-7] 22 p3863 N85-33924
Constraints on cosmic-ray observation of Cygnus X-3
[OG-2.2-3] 22 p3864 N85-33930
Hercules X-1: Pulsed gamma-rays detected above 150 GeV
[OG-2.2-9] 22 p3865 N85-33935
Search for gamma ray lines from SS433
[OG-2.4-11] 22 p3868 N85-33955
Observation of gamma-rays from LMC X-4 above 10(16) eV
[OG-2.8-10] 22 p3870 N85-33972

The 4U 0115+63: Another energetic gamma ray binary pulsar
[OG-2.6-11] 22 p3870 N85-33973
BINARY SUMMATORS
U ADDING CIRCUITS
BINARY SYSTEMS (DIGITAL)
U DIGITAL SYSTEMS
BINARY SYSTEMS (MATERIALS)
NT BINARY ALLOYS
NT BINARY MIXTURES
NT EUTECTIC ALLOYS
NT EUTECTICS
High pressure cosmochemistry applied to major planetary interiors: Experimental studies
[NASA-CR-174032] 02 p0302 N85-11958
Structure of two-phase titanium alloys with different microstructures 03 p0351 N85-12257
Possibilities of conjugating binary solutions for thermal energy storage
[DE84-016704] 04 p0531 N85-13392
Photochemistry and kinetics of the O*2-HI system
[AD-A147433] 07 p0971 N85-16167
Characterization and selection of polymer materials for binary munitions storage. Part 2: Characterization of LLDPE resins
[AD-A148324] 08 p1133 N85-17144
Investigation of foam flotation and phase partitioning techniques 12 p1945 N85-22216
Microstructural characteristics during the controlled solidification of a binary system
[DE85-005200] 15 p2507 N85-25461
BINAURAL HEARING
Psychological and physiological basis of stereophonic effect 15 p2526 N85-25574
BINDERS (ADHESIVES)
U ADHESIVES
BINDERS (MATERIALS)
NT PROPELLANT BINDERS
NT SOLID ROCKET BINDERS
Effects of surface interactions and mechanical properties of PBXs (plastic bonded explosives) on explosive sensitivity
[AD-A146388] 08 p0773 N85-14944
Structure and property formation mechanism in magnetic alloy-binder composite 10 p1444 N85-19103
Polymer blends as high explosive binders
[DE85-001210] 11 p1611 N85-20131
Development and study of two-matrix glass fiber composite with increased transverse deformation 13 p2027 N85-22700
BINDING
Universal binding energy relations in metallic adhesion
[NASA-TM-86889] 03 p0331 N85-12132
CO adsorption on (111) and (100) surfaces of the Pt sub 3 Ti alloy. Evidence for parallel binding and strong activation of CO
[NASA-CR-176077] 21 p3565 N85-32176
Improved flow cytometer measurement of binding assays
[DE85-006407] 23 p3935 N85-34390
BINOCULAR VISION
Binocular overlap in a fiber optic helmet mounted display
[AD-P004331] 09 p1270 N85-17985
BINOMIAL COEFFICIENTS
On the quadratic mean radius of a polynomial in Cz
[AD-A149189] 10 p1546 N85-19751
BINOMIALS
Empirical Bayes rules for selecting good binomial populations
[AD-A147614] 08 p1214 N85-17646
Statistical analysis techniques for small sample sizes
[NASA-CR-171872] 15 p2639 N85-26279
BIOASSAY
Response of algal populations to changes in stream water quality
[PB84-202464] 01 p0070 N85-10465
Molecular interactions of high energy fuels and jet fuels with oncogenic viruses and endogenous viruses
[AD-A145484] 02 p0186 N85-11255
Alterations in skeletal muscle with disuse atrophy
[NASA-CR-174195] 06 p0843 N85-15349
X-ray holography of biological specimens
[DE85-002437] 10 p1489 N85-19398
New techniques for studying calcium gradients 15 p2609 N85-26076
An in vitro method for the screening of trichothecene mycotoxin cytotoxicity and the study of mycotoxin countermeasures
[AD-A153663] 18 p3152 N85-29517
Flow cytometry for health monitoring in space
[DE85-009572] 19 p3329 N85-30625
Development of a recombinant DNA assay system for the detection of genetic change in astronauts cells
[DE85-010103] 20 p3504 N85-31781
Investigation of variation in the concentration of bacteria in outdoor testing, with the use of a detector for aerosols of bacteria
[FOA-C-40201-B2] 20 p3504 N85-31784
Marine environmental quality assessment program, five-year plan (FY 1984 - 1988)
[AD-A154715] 21 p3613 N85-32459
Current internal-dosimetry practices at US Department of Energy facilities
[DE85-011718] 22 p3787 N85-33466
Applications of holography to X-ray imaging
[DE85-010984] 23 p3934 N85-34384
BIOASTRONAUTICS
USSR report: Space Biology and Aerospace Medicine, volume 18, no. 4, July - August 1984
[JPRS-USB-84-006] 01 p0091 N85-10611
USSR report: Space Biology and Aerospace Medicine, volume 18, no. 6, November - December 1984
[JPRS-USB-85-002] 12 p1900 N85-21931
External respiration, gas exchange and energy expenditures of man in weightlessness 12 p1900 N85-21932
Blood amino acids of cosmonauts before and after 211-day spaceflight 12 p1900 N85-21933
Circadian rhythm of human body temperature during spaceflights 12 p1901 N85-21934
Biochemical status of adrenocortical dysfunction following spaceflight 12 p1901 N85-21935
Comparative analysis of effects of weightlessness and its models on velocity and strength properties and tone of human skeletal muscles 12 p1901 N85-21936
Cosmonauts' blood plasma free amino acid levels during preflight training 12 p1901 N85-21937
Plasmodium of myxomycete as research object in gravitational biology 15 p2483 N85-25327
Aerospace Medicine and Biology: A continuing bibliography with indexes
[NASA-SP-7011(270)] 15 p2615 N85-26114
Research opportunities in loss of red blood cell mass in space flight
[NASA-CR-175808] 16 p2841 N85-27517
The cosmic history of the biogenic elements and compounds
[NASA-SP-476] 17 p3003 N85-28562
Spatial orientation in weightlessness and readaptation to Earth's gravity 20 p3509 N85-31811
Study of the cardiovascular system in microgravity: Results and perspectives 20 p3509 N85-31816
Hydroponics developments for spaceship garden 21 p3663 N85-32754
Aerospace medicine and biology: A continuing bibliography with indexes, supplement 273
[NASA-SP-7011(273)] 21 p3663 N85-32755
USSR report: Space Biology and Aerospace Medicine, vol. 19, no. 3, May - June 1985
[JPRS-USB-85-005] 23 p3952 N85-34494
Proceedings of a Scientific Meeting on the Occasion of the Inauguration of New Buildings for the DFVLR Institute for Aerospace Medicine
[ESA-TT-857] 24 p4129 N85-35595
The research programme of the Institute for Aerospace Medicine 24 p4129 N85-35596
BIOCHEMICAL OXYGEN DEMAND
Results of study of hypoxia problems 04 p0544 N85-13462
The effect of an unphysiological oxygen supply on the organism 24 p4130 N85-35605
BIOCHEMISTRY
NT BACTERIOLOGY
NT BIOGEOCHEMISTRY
NT PHYSIOCHEMISTRY
In vivo dermal absorption method and system for laboratory animals
[AD-D011231] 01 p0094 N85-10635
Lagging development of biotechnology described 01 p0115 N85-10787
East Europe report: Science and technology
[JPRS-ESA-84-038] 03 p0343 N85-12210
Architecture of dermatophyte cell Walls: Electron microscopic and biochemical analysis
[NASA-TM-77441] 03 p0390 N85-12548
USSR report: Chemistry
[JPRS-UCH-84-012] 06 p0761 N85-14865
Structure and functions of fungal cell surfaces
[NASA-TM-77439] 06 p0842 N85-15347
The structure and function of fungal cells
[NASA-TM-77443] 06 p0842 N85-15348
Alterations in skeletal muscle with disuse atrophy
[NASA-CR-174195] 06 p0843 N85-15349
Chemistry and metabolism of delayed neurotoxic organophosphorus esters
[AD-P004023] 06 p0844 N85-15357
Biochemistry and pathogenic hypotheses of organophosphorus-induced delayed neurotoxicity
[AD-P004026] 06 p0844 N85-15360
Biocatalyzed processes for production of commodity chemicals: Assessment of future research advances for N-butanol production
[NASA-CR-174264] 07 p0919 N85-15819
USSR report: Life sciences. Biomedical and behavioral sciences
[JPRS-UBB-84-015] 07 p1010 N85-16416
Biochemical evaluation of bodily influence of high and low temperatures 07 p1014 N85-16441
USSR report: Life sciences. Biomedical and behavioral sciences
[JPRS-UBB-85-002] 09 p1360 N85-18559
Aluminum in biogenic cycle and forms of its occurence in ocean 10 p1499 N85-19483
Bioelectrochemistry 2: Membrane phenomena
[AD-A149132] 10 p1522 N85-19602
USSR report: Life sciences. Biomedical and behavioral sciences
[JPRS-UBB-85-010] 11 p1690 N85-20629
Characteristics of human masseter under conditions of hypokinesia 11 p1691 N85-20630
Effects of hypothermia on brain metabolism 11 p1692 N85-20636
A double blind comparative trial of powdered ginger root, hyoscine hydrobromide, and cinnarizine in the prophylaxis of motion sickness induced by cross coupled stimulation 11 p1695 N85-20657
Multiple regression method used to assess animal adaptation to hypoxic hypoxia 12 p1902 N85-21947
Parameters of carbohydrate metabolism and blood serum enzyme activity after short-term spaceflights 12 p1903 N85-21951
Compiled and thermodynamic data sources for aqueous and biochemical systems: An annotated bibliography, 1930 - 1983
[PB85-137693] 12 p1944 N85-22208
International Conference on Coordination Chemistry (23rd) held at Boulder, Colorado on 29 July - 3 August, 1984
[AD-A150980] 14 p2252 N85-23956
NMR imaging and spectroscopy of the mammalian central nervous system after heavy ion radiation
[DE85-004509] 14 p2386 N85-24696
USSR report: Life sciences. Biomedical and behavioral sciences
[JPRS-UBB-85-012] 14 p2386 N85-24697
Abstracts of the 36th Southeastern Regional Meeting of the American Chemical Society
[AD-A151506] 15 p2496 N85-25394
Use and disuse and the control of acetylcholinesterase activity in fast and slow twitch muscle of rat
[NASA-CR-175717] 15 p2614 N85-26109
Experiments in microwave exposure in the rat: Body temperature, serum chemistry and the use of chemical restraint
[PB85-156834] 16 p2840 N85-27512
Academician Ovchinnikov on future of bioorganic chemistry 17 p3049 N85-28874
Diet of first Soviet expedition on Mount Everest 19 p3323 N85-30566
Investigation of biochemical and psychological parameters of air traffic controllers in prestart state before beginning to work 19 p3325 N85-30599
Biocatalysis project
[NASA-CR-176044] 20 p3498 N85-31744
Kidney cell electrophoresis, continuing task 20 p3498 N85-31747
USSR report: Life sciences. Biomedical and behavioral sciences
[JPRS-UBB-85-017] 20 p3504 N85-31785
Marine environmental quality assessment program, five-year plan (FY 1984 - 1988)
[AD-A154715] 21 p3613 N85-32459
Interaction of opiate and phencyclidine derivatives with the acetylcholine receptor
[AD-A155119] 21 p3664 N85-32761
The composition of the primitive atmosphere and the synthesis of organic compounds on the early Earth 21 p3717 N85-33065
USSR report: Life sciences. Biomedical and behavioral sciences
[JPRS-UBB-85-018] 22 p3819 N85-33660
Improved flow cytometer measurement of binding assays
[DE85-006407] 23 p3935 N85-34390
Anaerobic microbial transformations in subsurface environments: Project description
[DE85-012789] 23 p3951 N85-34486
USSR report: Space Biology and Aerospace Medicine, vol. 19, no. 3, May - June 1985
[JPRS-USB-85-005] 23 p3952 N85-34494
Microbiological and biochemical studies towards optimization of substrate utilization by methanogenic bacteria
[PB85-188332] 24 p4084 N85-35310

BIOCLIMATOLOGY
U BIOMETEOROLOGY
BIOCONTROL SYSTEMS
Effects of external loads on human head movement control systems 05 p0707 N85-14534
Factors determining effectiveness of voluntary decrease in ventilation during muscular work using instrumented feedback 08 p1193 N85-17520
Airsickness control using biofeedback to self-regulate psychophysiological responses
[AD-A151167] 15 p2617 N85-26128
BLSS: A contribution to future life support 18 p3155 N85-29534
Advanced regenerative environmental control and life support systems: Air and water regeneration 18 p3155 N85-29535
Atmosphere behavior in gas-closed mouse-algal systems: An experimental and modelling study 18 p3155 N85-29536
CELSS transportation analysis 18 p3156 N85-29538
BIOCONVERSION
Cultivation and conversion of marine macroalgae --- biomass energy production
[DE84-004522] 04 p0544 N85-13464
Current alternative energy research and development in Illinois
[PB85-163137] 16 p2820 N85-27397
Screening Prosopis (mesquite) species for biofuel production on semi-arid lands
[DE85-010048] 19 p3302 N85-30471
Biomass thermochemical conversion program
[DE85-011867] 21 p3572 N85-32213
Aerobic sulfur-oxidizing bacteria: Environmental selection and diversification 21 p3656 N85-32712
Distribution and abundance of organic thiols 21 p3657 N85-32717
Cytochromes and iron sulfur proteins in sulfur metabolism of phototrophic bacteria 21 p3657 N85-32718
Seventh Symposium on Biotechnology for Fuels and Chemicals: Program and abstracts
[DE85-011197] 22 p3742 N85-33192
Pacific Northwest and Alaska bioenergy program glossary
[DE85-011740] 22 p3808 N85-33591
Microbiological and biochemical studies towards optimization of substrate utilization by methanogenic bacteria
[PB85-188332] 24 p4084 N85-35310
BIODEGRADATION
Denitrification-efficiencies of alternate carbon sources
[AD-A148029] 08 p1119 N85-17050
Anaerobic microbial transformations in subsurface environments
[DE85-012790] 22 p3819 N85-33659
Two dimensional CO2-ocean model including the biological processes
[DE85-012341] 23 p3950 N85-34483
Biodegradation of jet fuel by aquatic microbial communities
[PB85-191971] 24 p4084 N85-35311
BIODYNAMICS
Multi-property modeling of the marine biosphere in relation to global climate and carbon cycles 05 p0678 N85-14355
Twentieth Annual Conference on Manual Control, volume 1
[NASA-CP-2341-VOL-1] 05 p0699 N85-14487
New uses for sensitivity analysis: How different movement tasks effect limb model parameter sensitivity 05 p0706 N85-14529
Suppression of biodynamic interference by adaptive filtering 05 p0706 N85-14530
Active sticks: A new dimension in controller design 05 p0706 N85-14531
An analysis of kinetic response variability 05 p0707 N85-14533
Effects of external loads on human head movement control systems 05 p0707 N85-14534
Interaction between lung mechanics and gas exchange by low volume high frequency pulmonary ventilation in patients with respiratory failure
[AD-A146604] 06 p0846 N85-15372
Biodynamic resistant control stick
[AD-D011380] 07 p0904 N85-15721
Unsteady separated flows: Generation and use by insects
[AD-P004168] 09 p1266 N85-17953
Biomechanical studies of impact acceleration research
[AD-A149077] 10 p1522 N85-19601
Biomechanics finds practical applications in aerospace research 11 p1621 N85-20205
Biotechnology in Japan
[PB85-169464] 15 p2615 N85-26113
Stabilizing force feedback in bio-actuated control systems
[AD-D011634] 17 p3002 N85-28560
USSR report: Space Biology and Aerospace Medicine, vol. 19, no. 3, May - June 1985
[JPRS-USB-85-005] 23 p3952 N85-34494
Using dynamic analysis to animate articulated bodies such as humans and robots 23 p3959 N85-34537
BIOELECTRIC POTENTIAL
Change in relationship of biopotentials of brain zones for various levels of working capacity 07 p1013 N85-16438
Specifics of dynamics of brain biopotentials under the influence of complex audible communicative signals 07 p1014 N85-16440
BIOELECTRICITY
Interactions between electromagnetic fields
[AD-A153796] 18 p3091 N85-29129
Changes in the impedance and bioelectrical activity of the cerebral cortex of rats under the action of anaesthetic drugs
[HSE-TRANS-10371] 19 p3327 N85-30617
Physical chemical state of water in living cells
[AD-A154566] 21 p3662 N85-32749
BIOENGINEERING
NT ANTHROPOMETRY
NT BALLISTOCARDIOGRAPHY
NT BIOINSTRUMENTATION
NT BIOMETRICS
NT BODY MEASUREMENT (BIOLOGY)
NT CARDIOGRAPHY
NT ECHOCARDIOGRAPHY
NT ELECTROCARDIOGRAPHY
NT ELECTROENCEPHALOGRAPHY
NT ELECTROMYOGRAPHY
NT PLETHYSMOGRAPHY
China report: Science and technology
[JPRS-CST-84-025] 11 p1620 N85-20197
Research in environmental biology reviewed 11 p1622 N85-20211
A communications link for an implantable electrode array
[AD-A152238] 16 p2840 N85-27510
Bioengineering and rehabilitation: Windows of opportunity past, present and future
[NASA-EP-216] 16 p2841 N85-27516
Applications of aerospace technology in biology and medicine
[NASA-CR-166100] 19 p3328 N85-30619
Seventh Symposium on Biotechnology for Fuels and Chemicals: Program and abstracts
[DE85-011197] 22 p3742 N85-33192
BIOFEEDBACK
NT SENSORY FEEDBACK
Factors determining effectiveness of voluntary decrease in ventilation during muscular work using instrumented feedback 08 p1193 N85-17520
Biofeedback treatment of airsickness: A review 11 p1696 N85-20660
Airsickness control using biofeedback to self-regulate psychophysiological responses
[AD-A151167] 15 p2617 N85-26128
Biofeedback and performance: An update
[AD-A153228] 17 p3001 N85-28553
Stabilizing force feedback in bio-actuated control systems
[AD-D011634] 17 p3002 N85-28560
BIOGENESIS
U BIOLOGICAL EVOLUTION
BIOGENY
Aluminum in biogenic cycle and forms of its occurence in ocean 10 p1499 N85-19483
BIOGEOCHEMISTRY
The Interaction of Global Biochemical Cycles
[NASA-CR-174184] 05 p0652 N85-14183
Biogeochemical cycles: Interactions in global metabolism 05 p0652 N85-14184
Global biogeochemical cycles: Studies of interaction and change, some views on the strategy of approach 05 p0652 N85-14185
Assessment of Techniques for Measuring Tropospheric H sub x O sub y: Summary 05 p0675 N85-14337
Deforestation, floodplain dynamics, and carbon biogeochemistry in the Amazon Basin 08 p1144 N85-17216
Environmental Sciences Division report
[DE85-010452] 19 p3308 N85-30506
Biogeochemical cycling and remote sensing 21 p3659 N85-32733
Phototrophic bacteria and their role in the biogeochemical sulfur cycle 21 p3660 N85-32735
Isotopic Biogeochemistry
[NASA-CR-176128] 22 p3741 N85-33189
BIOGRAPHY
For the sacred air space of our motherland; an interview with our country's famous aircraft designer, Lu Hsiao-Peng
[AD-A146291] 03 p0309 N85-11987
East Europe report: Scientific affairs, no. 791
[JPRS-84624] 03 p0341 N85-12195
Fr. Angelo Secchi, a pioneer in the study of solar-terrestrial relationships 04 p0519 N85-13312
Harold Hazen and the theory and design of servomechanism
[RR-270] 22 p3794 N85-33506
BIOINSTRUMENTATION
NT IMPLANTED ELECTRODES (BIOLOGY)
Clinical measurements using fiber optics and optrodes
[DE84-015043] 05 p0696 N85-14481
A biological sensor for the detection of toxicants
[AD-D011304] 07 p0967 N85-16141
Spirolit-2 instrument used to test pulmonary ventilation 12 p1903 N85-21950
The audiomat: An automatic audiometer for use in occupational audiometry
[DRIC-T-7138] 13 p2142 N85-23294
A communications link for an implantable electrode array
[AD-A152238] 16 p2840 N85-27510
Development of an EM-Based lifeform detector
[AD-A153504] 18 p3151 N85-29512
Chemoreception and detection of micropollutants by means of a telemetric bionic detector
[DRIC-T-7460] 22 p3810 N85-33600
BIOLOGICAL ACTIVITY
U ACTIVITY (BIOLOGY)
BIOLOGICAL ANALYSIS
U BIOASSAY
BIOLOGICAL CELLS
U CELLS (BIOLOGY)
BIOLOGICAL CLOCKS
U RHYTHM (BIOLOGY)
BIOLOGICAL EFFECTS
NT JET LAG
Ecology of estuarine channels of the pacific northwest coast: A community profile
[PB84-209709] 01 p0070 N85-10484
A study of fatigue of shiftworkers in air traffic control and weather service groups in JASDF 01 p0090 N85-10610
Effect of spaceflight factors on rat bone marrow cells 01 p0092 N85-10620
Effect of short-term hypokinesia on rat opioid system reaction 01 p0093 N85-10625
Reaction of cerebral ventricles to anticrthostatic position and occlusion of jugular veins 01 p0093 N85-10626
Effect of maximum physical load on oxygen-transport properties of blood 01 p0093 N85-10627
Effect of hyperoxia and increased gas atmosphere density on contractile function of the right ventricle 01 p0093 N85-10628
Change in energetics of muscular contraction as a result of hyperoxia 01 p0093 N85-10629
Hemodynamics and neurodynamics of the human brain during exposure to moderate hypoxic hypoxia 01 p0094 N85-10630
Space medicine and biology, continuing bibliography (supplement 263)
[NASA-SP-7011(263)] 01 p0094 N85-10636
Proton pumping in purple membrane, appendix 1
[DE84-014601] 01 p0118 N85-10811
Aerospace Medicine and Biology, a continuing bibliography with indexes
[NASA-SP-7011(264)] 02 p0234 N85-11525
The case for concern about very low frequency fields from visual display terminals: The need for further research and shielding of VDTs
[CCOHS-P83-2E] 02 p0234 N85-11526
Electrical parameters in 60-Hz biological exposure systems and their measurement: A primer
[PB84-217793] 03 p0400 N85-12548
Field/cell interaction model
[DE84-011914] 04 p0544 N85-13465
A survey of space biology and space medicine
[ESA-BR-17] 04 p0545 N85-13466
Aerospace Medicine and Biology, a continuing bibliography with indexes
[NASA-SP-7011(265)] 04 p0545 N85-13467
Acid rain and tree physiology: Some hypotheses for observed changes in forest productivity
[DE84-016588] 05 p0672 N85-14318
Report of the Meeting of Experts on Climate and Human Health
[WCP-78] 05 p0687 N85-14413
Organization of the session 05 p0687 N85-14414
Introduction to human biometeorology 05 p0687 N85-14415

Difficulties encountered in determining the potential involvement of consultants on health problems in various climatic zones 05 p0687 N85-14416
Epidemiologic methods applied to the study of the relationship between climate and human health 05 p0687 N85-14418
USSR report: Life sciences. Biomedical and behavioral sciences [JPRS-UBB-84-027] 07 p1012 N85-16426
Distinctions of SPF rats used in experiments aboard biosatellites 07 p1012 N85-16427
Effect of microwave radiation on local blood circulation and oxygenation of brain tissue 07 p1012 N85-16431
Something in the air at Windscale --- radioactive contaminants from the Sellafield nuclear Complex for reprocessing and storing irradiated fuel [BLL-RISLEY-TR-4006-(9091.9F)] 08 p1179 N85-17429
Aerospace medicine and biology: A continuing bibliography with indexes [NASA-SP-7011(268)] 08 p1194 N85-17525
Aerospace medicine and biology: A continuing bibliography with indexes, supplement 268 [NASA-SP-7011(268)] 08 p1194 N85-17526
Genetic effects of microwave exposure on mammalian cells in vitro, volume 2 [AD-A149347] 10 p1523 N85-19603
USSR report: Life sciences. Biomedical and behavioral sciences [JPRS-UBB-85-008] 10 p1523 N85-19605
Aerospace medicine and biology: A continuing bibliography with indexes [NASA-SP-7011(269)] 10 p1526 N85-19628
Effects of electromagnetic fields produced by high voltage transmission lines [DE85-900034] 11 p1625 N85-20230
Laboratory tests of motion sickness susceptibility 11 p1694 N85-20648
Effects of air pollution and acid rain on forest decline [GPO-37-458] 12 p1883 N85-21818
Summary report of the Workshop on Structure Activity Concepts in Environmental Sciences [PB85-137339] 12 p1887 N85-21841
Biological effects on radiofrequency radiation [PB85-120648] 12 p1900 N85-21930
USSR report: Space Biology and Aerospace Medicine, volume 18, no. 6, November - December 1984 [JPRS-USB-85-002] 12 p1900 N85-21931
Biological effects of blast and impact waves [FOA-C-52008-H4-D7] 12 p1906 N85-21968
Interaction of metals and metalloids with biomembranes [DE85-004902] 13 p2141 N85-23293
Nationwide Urban Runoff Project, Champaign, Illinois: The biological impact of urban runoff on the Saline Branch Drainage Ditch and Boneyard Creek [PB85-150274] 14 p2348 N85-24515
Photoreactivation and other ultraviolet/visible light effects on DNA in human skin [DE85-005135] 14 p2390 N85-24719
Psychobiology and food perception 14 p2394 N85-24745
The interaction of calcium and auxin in the gravitropic response of roots 15 p2606 N85-26062
The effects of simulated weightlessness on susceptibility to viral and bacterial infections using a murine model 15 p2613 N85-26100
Aerospace Medicine and Biology: A continuing bibliography with indexes [NASA-SP-7011(270)] 15 p2615 N85-26114
The Impact of Proposed Radio Frequency Radiation Standards on Military Operations [AGARD-LS-138] 16 p2775 N85-27128
The physical interactions of radiofrequency radiation fields and biological systems 16 p2775 N85-27129
The biological effects of radiofrequency radiation 16 p2775 N85-27131
The cumulative effects of long term exposure to low levels of radiofrequency radiation (RFR) 16 p2776 N85-27132
The medical results of human exposures to radio frequency radiation 16 p2776 N85-27133
Review of epidemiological studies of human exposures to radiofrequency radiation 16 p2776 N85-27134
Evaluation of human exposures to low frequency fields 16 p2776 N85-27135
Development and application of new radiofrequency radiation safety standards 16 p2777 N85-27137
Interactive effects of acid rain and gaseous air pollutants on natural terrestrial vegetation [DE85-005255] 16 p2821 N85-27401
Aerospace medicine and biology: A continuing bibliography with indexes, supplement 271, May 1985 [NASA-SP-7011(271)] 16 p2840 N85-27514
Biological influences of low-frequency sinusoidal electromagnetic signals alone and superimposed on RF carrier waves [PB85-161248] 16 p2842 N85-27527
Photosynthetic acclimation of Acer saccharum [DE85-006247] 17 p2998 N85-28536
Biological and human health effects of extremely low frequency electromagnetic fields. Post-1977 literature review [AD-A152731] 17 p2999 N85-28539
The cosmic history of the biogenic elements and compounds [NASA-SP-476] 17 p3003 N85-28562
Investigation of biochemical and psychological parameters of air traffic controllers in prestart state before beginning to work 19 p3325 N85-30599
Metabolic mechanisms of plant growth at low water potentials 19 p3327 N85-30612
Aerospace Medicine and Biology: A continuing bibliography with indexes (supplement 272) [NASA-SP-7011(272)] 19 p3328 N85-30620
A systems analysis of the erythropoietic responses to weightlessness. Volume 1: Mathematical model simulations of the erythropoietic responses to weightlessness [NASA-CR-171890] 20 p3506 N85-31794
Zinc: Biological effects. Facts and fiction [USIP-84-12] 20 p3507 N85-31796
Nordic Association for Aerosol Research (NOSA) Aerosol Symposium: Program and abstracts [FOA-E-40019] 22 p3812 N85-33616
Antihypertensive neutral lipid [DE85-011625] 22 p3819 N85-33656
Microdosimetric spectra measurements of JANUS neutrons [DE85-012108] 22 p3843 N85-33801
Ocean thermal energy conversion [DE85-012291] 23 p3946 N85-34456
Aerospace Medicine and Biology: A continuing bibliography with indexes (supplement 274) [NASA-SP-7011(274)] 23 p3952 N85-34491
Effect of seeds of heavy charged particles of galactic cosmic radiation 23 p3954 N85-34505
Electromagnetic compatibility conference features biological interactions [AD-A155813] 24 p4144 N85-35692

BIOLOGICAL EVOLUTION
NT ABIOGENESIS
Impact phenomena as factors in the evolution of the Earth [NASA-CR-174015] 01 p0072 N85-10474
Influence of simulated weightlessness on the motility of the acellular slime mold Physarum polycephalum 05 p0689 N85-14430
Observation of the contractile vacuolar system of Paramecium caudatum on the fast running clinostat 05 p0689 N85-14431
Development and maturation of the neuromuscular junciton in cell culture under conditions of simulated zero-gravity 15 p2611 N85-26093
Effects of simulated weightlessness on mammalian development. Part 2: Meiotic maturation of mouse oocytes during clinostat rotation 15 p2612 N85-26094
ONR (Office of Naval Research) Far East Scientific Bulletin, Volume 9, Number 4, October-December 1984 [AD-A151274] 15 p2665 N85-26448
Organization of the R region in maize [DE85-011273] 20 p3504 N85-31780
Origin of life 21 p3657 N85-32713
Protocyanobacteria: Oxygenic and Anoxygenic photosynthesis in mat-forming bacteria 21 p3657 N85-32714
Insights into the phylogenetic positions of photosynthetic bacteria obtained from 5S rRNA and 16S rRNA sequence data 21 p3658 N85-32719
Search for the universal ancestors [NASA-SP-477] 21 p3667 N85-32777
Submarine hydrothermal environments as sites for the origin and evolution of life 21 p3719 N85-33074
Biological modulation of planetary atmospheres: The early Earth scenario 22 p3854 N85-33857
NASA Developmental Biology Workshop: A summary [NASA-TM-86756] 24 p4126 N85-35578
Effects of microgravity and hypergravity on invertebrate development 24 p4126 N85-35579
Vertebrate development in space: Gravity is a drag (and has been for eons and eons) 24 p4126 N85-35580
Report of the NASA Mammalian Developmental Biology Working Group 24 p4126 N85-35581
Report of the Avian Development Working Group 24 p4127 N85-35582
Report of Amphibian Development Group 24 p4127 N85-35583
Report of the Insect Development Group 24 p4127 N85-35584
Aquatic Invertebrate Development Working Group 24 p4127 N85-35585
Report of the Microbial Development Working Group 24 p4127 N85-35586

BIOLOGICAL MODELS
U BIONICS

BIOLOGICAL MODELS (MATHEMATICS)
Mathematical Models of the Circadian Sleep-Wake Cycle [AD-A145712] 02 p0235 N85-11532
A mathematical model of visual perception regarding peripheral vision and its application to the Hermann's illusion 04 p0483 N85-13080
Multi-property modeling of the marine biosphere in relation to global climate and carbon cycles 05 p0678 N85-14355
Inverse modelling to obtain head movement controller signal 05 p0705 N85-14525
A control model: Interpretation of Fitts' law 05 p0706 N85-14526
New uses for sensitivity analysis: How different movement tasks effect limb model parameter sensitivity 05 p0706 N85-14529
The growth and composition of supercritical branching populations on general type spaces [CTH-MATH-1984-18] 05 p0721 N85-14631
Hollings hungry mantid model for the invertebrate functional response considered as a Markov process. Part 3: Mathematical elaborations [CWI-AM-R8407-PT-3] 05 p0722 N85-14639
Control and modeling of a CELSS (Controlled Ecological Life Support System) [NASA-CR-177324] 07 p1020 N85-16472
Close air support mission: Development of a unitary measure of pilot performance [AD-A149265] 11 p1697 N85-20685
Artificial Intelligence and Bionics Workshop held at Stowe, Vermont on 11-15 June 1984 [AD-A150433] 13 p2149 N85-23339
The dynamical behavior of the age-size-distribution of a cell population [CWI-AM-R8414] 17 p2998 N85-28538
Stability and feasibility of model ecosystems [PREPRINT-431] 18 p3134 N85-29408
An integrated analysis of the physiological effects of space flight: Executive summary [NASA-CR-171892] 20 p3506 N85-31796
Mathematical analysis of heart rhythm assessment of distinctive features in adaptation to spaceflight conditions 22 p3733 N85-33142
Tritium hazard via the ingestion pathway [DE85-012897] 24 p4133 N85-35618

BIOLOGICAL RHYTHM
U RHYTHM (BIOLOGY)

BIOLOGY
Applications of aerospace technology in biology and medicine [NASA-CR-165872] 02 p0234 N85-11521
East Europe report: Science and technology [JPRS-ESA-84-038] 03 p0343 N85-12210
Achievements in biology outlined 03 p0343 N85-12213
Abstracts of papers submitted in 1983 for publication [PB84-217579] 03 p0396 N85-12543
Overview of German microgravity activities in the field of life science 05 p0696 N85-14476
Aerospace Medicine and Biology: A continuing bibliography with indexes, supplement 267, January 1985 [NASA-SP-7011(267)] 12 p1904 N85-21959
Biology and Medicine Division [DE85-010638] 19 p3327 N85-30613
USSR Space Life Sciences Digest [NASA-CR-3922] 21 p3656 N85-32709

BIOLUMINESCENCE
Bio-optical variability in the Alboran Sea as assessed by Nimbus-7 coastal zone color scanner [AD-A147909] 07 p0989 N85-16281
Luminescence in the ocean [AD-B089136L] 13 p2140 N85-23288
Seasonal variability and spatial non-uniformity of bioluminescence in the Mediterranean Sea [DRIC-T-7545] 24 p4125 N85-35572
Background light measurements at the DUMAND site [HE-5.2-7] 24 p4203 N85-36084
Measurements of light background at large depth in the ocean [HE-5.2-8] 24 p4203 N85-36085

BIOMAGNETISM
Mammalian tissue sensitivity to long-term exposure to high-intensity stationary magnetic fields 22 p3823 N85-33686

BIOMASS
The Marine Resources Experiment Program (MAREX) [NASA-TM-87368] 01 p0086 N85-10580

Modeling effects of toxicants on aquatic systems
[DE84-016594] 04 p0531 N85-13396
Biomass thermochemical conversion program
[DE84-017177] 05 p0621 N85-13972
Ethanol production by enzymatic hydrolysis: Parametric analysis of a base-case process
[DE84-013105] 11 p1614 N85-20147
Alternative anodic reactions in water splitting
[DE85-004159] 12 p1802 N85-21300
Anaerobic digestion of biomass: status summary and research development needs, 1983
[PB85-161925] 13 p2040 N85-22772
Remote sensing of coastal wetlands biomass using Thematic Mapper wavebands — Lewes, Delaware
13 p2119 N85-23196
The impact ejection of living organisms into space
15 p2682 N85-26566
Flash pyrolysis of biomass with reactive and non-reactive gases
[DE85-010962] 19 p3306 N85-30496
Chemical composition of Musca domestica L. larval and pupal biomass when developing in organic waste of biological life-support system for man
22 p3824 N85-33691

BIOMASS ENERGY PRODUCTION
Prospectus of the utilization of leafy spurge (Euphorbia Esula L.) as a source of liquid fuel and biomass
[DE84-015203] 01 p0034 N85-10206
Bench-scale research in biomass direct liquefaction
[DE84-011881] 02 p0223 N85-11460
Construction of a bacterium to convert cellulose to ethanol
[TI84-901639] 04 p0481 N85-13068
Cultivation and conversion of marine macroalgae — biomass energy production
[DE84-004522] 04 p0544 N85-13484
Alcohol fuel from Ohio farms: An introduction
[TI-84-901290] 05 p0621 N85-13970
Versatility of peat emphasized
07 p0994 N85-16316
Developments in the production and use of ethanol fuels
[GPO-40-678] 12 p1817 N85-21398
Alcohol Fuels Program technical review, spring 1984
[DE85-002919] 17 p2938 N85-28134
Renewable technologies program summaries
[DE85-001509] 19 p3307 N85-30500
Uniform cost-estimation method for biomass production and conversion technologies
[DE85-011714] 19 p3360 N85-30970
Biomass thermochemical conversion program
[DE85-011867] 21 p3572 N85-32213
Pacific Northwest and Alaska bioenergy program glossary
[DE85-011740] 22 p3808 N85-33591

BIOMECHANICS
U BIODYNAMICS

BIOMEDICAL DATA
An optically isolated amplifier
[CSIR-SR-ELEK-257] 01 p0049 N85-10321
Potential use of dialogue with computers in biomedical research 01 p0091 N85-10614
Applications of aerospace technology in biology and medicine
[NASA-CR-165872] 02 p0234 N85-11521
USSR report: Life Sciences: Biomedical and behavioral sciences
[JPRS-UBB-84-026] 04 p0543 N85-13457
Space adaptation syndrome: Incidance and operational implications for the space transportation system program
11 p1695 N85-20655
Analysis of head motion during simulated, rough water operation of a 2200 ton surface effect ship
11 p1695 N85-20656
Research and technology activities at Ames Research Center's Biomedical Research Division
[NASA-TM-86692] 12 p1899 N85-21925
Introduction: The clinical and biomedical evaluation for trauma and fatalities associated with aircrew ejection and crash 12 p1906 N85-21970
Development and diffusion of automated clinical chemistry analyzers
[PB85-150696] 15 p2501 N85-25798
Chemicals identified in human biological media, a data base. Volume 6, part 2: Records 7586-8694
[DE85-008767] 18 p3154 N85-29628
Zinc: Biological effects. Facts and fiction
[USIP-84-12] 20 p3507 N85-31798
USSR report: Life sciences. Biomedical and behavioral sciences
[JPRS-UBB-85-021] 23 p3951 N85-34489

BIOMETEOROLOGY
Bibliography of climate textbooks and studies
[WCP-84] 02 p0231 N85-11505
Introduction to human biometeorology
05 p0687 N85-14415
Ecological impacts of hydroelectric projects in Amazonia 07 p1003 N85-16374

BIOMETRICS
NT ANTHROPOMETRY
NT BALLISTOCARDIOGRAPHY
NT BODY MEASUREMENT (BIOLOGY)
NT CARDIOGRAPHY
NT ECHOCARDIOGRAPHY
NT ELECTROCARDIOGRAPHY
NT ELECTROENCEPHALOGRAPHY
NT ELECTROMYOGRAPHY
NT PLETHYSMOGRAPHY
Applications of aerospace technology in biology and medicine
[NASA-CR-165872] 02 p0234 N85-11521

BIONICS
USSR report: Life sciences. Biomedical and behavioral sciences
[JPRS-UBB-84-025] 04 p0543 N85-13453
Applications of connectionist modeling techniques to simulations of motor control systems
05 p0717 N85-14598
Eyes for computers 07 p1012 N85-16428
Artificial Intelligence and Bionics Workshop held at Stowe, Vermont on 11-15 June 1984
[AD-A150463] 13 p2149 N85-23339
A detailed analysis of the erythropoietic control system in the human, squirrel, monkey, rat and mouse
[NASA-CR-171879] 15 p2614 N85-26107
Analysis of head-down tilt as an analog of weightlessness using a mathematical simulation model
[NASA-CR-171870] 15 p2616 N85-26118
Simulation of a G-tolerance curve using the pulsatile cardiovascular model
[NASA-CR-171873] 15 p2616 N85-26120
Description, validation, and modification of the Guyton model for space-flight applications. Part A. Guyton model of circulatory, fluid and electrolyte control. Part B. Modification of the Guyton model for circulatory, fluid and electrolyte control
[NASA-CR-171876] 15 p2616 N85-26122
Distributed memory
[AD-A153364] 17 p3001 N85-28554
Numerical estimation of the curvature of biological surfaces 17 p3006 N85-28588
Verbal information processing paradigms: A review of theory and methods
[AD-A153229] 17 p3050 N85-28880
Organization of the R region in maize
[DE85-011273] 20 p3504 N85-31780
USSR report: Life sciences. Biomedical and behavioral sciences
[JPRS-UBB-85-017] 20 p3504 N85-31785
USSR report: Life sciences. Biomedical and behavioral sciences
[JPRS-UBB-85-020] 21 p3663 N85-32752
Tritium hazard via the ingestion pathway
[DE85-012897] 24 p4133 N85-35618

BIOPHYSICS
NT HEALTH PHYSICS
NT PUBLIC HEALTH
Change in relationship of biopotentials of brain zones for various levels of working capacity
07 p1013 N85-16438
Workshop on membrane biophysics
[AD-A148238] 08 p1192 N85-17512
Radiation physics, biophysics, and radiation biology
[DE84-014885] 09 p1360 N85-18557
Bioelectrochemistry 2: Membrane phenomena
[AD-A149132] 10 p1522 N85-19602
Biophysical evaluation of the wet globe temperature index (Botsball) at high air movements and constant dew point temperature
[AD-A151065] 14 p2378 N85-24683
USSR report: Life sciences. Biomedical and behavioral sciences
[JPRS-UBB-85-012] 14 p2386 N85-24697
Current approaches for the biophysical and physiological evaluation of combat clothing for environmental extremes
[AD-A151012] 14 p2395 N85-24752
Plant growth biophysics: The basis for growth asymmetry induced by gravity 15 p2611 N85-26099
Computerized biophysical data acquisition system for motion sickness studies
[AD-A151691] 15 p2618 N85-26131
Evaluation of human exposures to low frequency fields 16 p2776 N85-27135
Biology and Medicine Division
[DE85-010636] 19 p3327 N85-30613
USSR report: Life sciences. Biomedical and behavioral sciences
[JPRS-UBB-85-017] 20 p3504 N85-31785
Zinc: Biological effects. Facts and fiction
[USIP-84-12] 20 p3507 N85-31798
USSR report: Life sciences. Biomedical and behavioral sciences
[JPRS-UBB-85-018] 22 p3819 N85-33660

BIOPROCESSING
Second Symposium on Space Industrialization — space commercialization
[NASA-CP-2313] 02 p0149 N85-11011
Opportunities for space bioprocessing
02 p0150 N85-11018
Bioprocessing in space 05 p0690 N85-14438
Current concepts and future directions of CELSS
18 p3155 N85-29532

BIOREGENERATION
U REGENERATION (PHYSIOLOGY)

BIOREGENERATIVE LIFE SUPPORT SYSTEMS
U CLOSED ECOLOGICAL SYSTEMS

BIOSATELLITES
Plasmodium of myxomycete as research object in gravitational biology 15 p2483 N85-25327
General description of experiment dealing with rat ontogenesis aboard Cosmos-1514 biosatellite
22 p3822 N85-33679

BIOSENSORS
U BIOINSTRUMENTATION

BIOSIMULATION
U BIONICS

BIOSPHERE
International Geosphere/Biosphere Program: 1984
[GPO-39-222] 04 p0578 N85-13691
Multi-property modeling of the marine biosphere in relation to global climate and carbon cycles
05 p0678 N85-14355
Magmas as selective filters of volatiles between planetary mantles and surfaces
13 p2185 N85-23557
Comet showers and Nemesis, the death star
[DE85-003736] 15 p2683 N85-26575
Mathematical model of global processes in the biosphere 19 p3295 N85-30431
Carbon isotope geochemistry and geobiology
21 p3657 N85-32716

BIOSYNTHESIS
Bioprocessing in space 05 p0690 N85-14438
Nitrogen control of photosynthetic protein synthesis
[DE85-003513] 11 p1690 N85-20623
Effects of hypothermia on brain metabolism
11 p1692 N85-20636
The role of sulfur in osmoregulation and salinity tolerance in cyanobacteria, algae, and plants
21 p3660 N85-32736
Isotopic Biogeochemistry
[NASA-CR-176128] 22 p3741 N85-33189
Production of liquid fuels and chemicals by microalgae
[DE85-006780] 22 p3819 N85-33658
Genetic and physiological control of protective antigen synthesis by bacillus anthracis
[AD-A156324] 24 p4133 N85-35617

BIOTECHNOLOGY
East Europe report: Science and technology
[JPRS-ESA-84-029] 01 p0115 N85-10783
Lagging development of biotechnology described
01 p0115 N85-10787
Opportunities for space bioprocessing
02 p0150 N85-11018
Applications of aerospace technology in biology and medicine
[NASA-CR-165872] 02 p0234 N85-11521
USSR report: Life sciences. Biomedical and behavioral sciences
[JPRS-UBB-84-025] 04 p0543 N85-13453
Outlook for expanding the Federal research in progress system
[AD-A148354] 08 p1229 N85-17737
West Europe report: Science and technology
[JPRS-WST-85-004] 10 p1480 N85-19204
Functional system theory in practice
11 p1690 N85-20629
Laser welding in the manufacture of heart pacemakers
14 p2308 N85-24286
USSR report: Life sciences. Biomedical and behavioral sciences
[JPRS-UBB-85-012] 14 p2386 N85-24697
Complex program of ergonomic studies Pilot described 14 p2388 N85-24698
West Europe report: Science and technology
[JPRS-WST-84-007] 15 p2530 N85-25800
Bioenergy, solar biotech research in France, Europe
15 p2536 N85-25846
Biotechnology in Japan
[PB85-169484] 15 p2615 N85-26113
Progress, goals in biotechnology summarized
17 p2945 N85-28182
Applications of aerospace technology in biology and medicine
[NASA-CR-166100] 19 p3328 N85-30619

West Europe report: Science and technology
[JPRS-WST-85-020] 20 p3438 N85-31333
USSR report: Life sciences. Biomedical and behavioral sciences
[JPRS-UBB-85-017] 20 p3504 N85-31785
East Europe report: Science and technology
[JPRS-ESA-85-023] 21 p3572 N85-32217
USSR report: Life sciences. Biomedical and behavioral sciences
[JPRS-UBB-85-020] 21 p3663 N85-32752
Air force technical objective document, Aerospace Medical Division, Fiscal Year 1986
[AD-A155195] 21 p3664 N85-32762
Seventh Symposium on Biotechnology for Fuels and Chemicals: Program and abstracts
[DE85-011197] 22 p3742 N85-33192

BIOTITE
The mineralogy of global magnetic anomalies
[E85-10061] 07 p0967 N85-16272

BIPLANES
Study of winglets applied to biplanes
[NASA-TM-86350] 08 p1083 N85-16862

BIPOLAR TRANSISTORS
Microwave susceptibility experiments
[DE84-016188] 02 p0192 N85-11281
Trends in development of bipolar power transistors 06 p0793 N85-15072
High-speed power devices with field control 06 p0794 N85-15073
Development of a planar heterojunction bipolar transistor for very high speed logic
[AD-A150374] 13 p2064 N85-22895
Improved, cheaper SIPMOS circuits no. 10, 1983 p 370 15 p2534 N85-25630
High voltage lateral power transisters: Theory and design 19 p3257 N85-30194
Evaluation of semiconductor devices for Electric and Hybrid Vehicle (EHV) ac-drive applications, volume 2
[NASA-CR-176103] 22 p3759 N85-33294
Realization and linearization of a hyperfrequency power amplifier implemented with bipolar transistors in class C polarization --- microwave amplifiers
[CNES-NT-114] 23 p3928 N85-34346

BIPOLARITY
Advanced nickel-hydrogen cell configuration study
[NASA-CR-174775] 01 p0067 N85-10444
Bipolar molecular outflows: T Tauri stars and Herbig-Haro objects 03 p0446 N85-12837
Quasi-three dimensional modeling of functionally-integrated elements of large-scale integrated circuits 04 p0490 N85-13122
Analysis of dynamic characteristics and ways of development of bipolar main memory with miniaturization of integrated circuit elements 04 p0490 N85-13123
Deer control using 7 strand vertical fence 11 p1581 N85-19958
Drift fields and boundary conditions at grain boundaries in bipolar P/N junction silicon devices 13 p2082 N85-22679
Recent developments 15 p2533 N85-25628
Life cycle test results of a bipolar nickel hydrogen battery
[NASA-TM-87046] 19 p3304 N85-30480
Computer simulation of integrated injection logic 22 p3767 N85-33349
Acoustic detection of air shower cores
[HE-7.1-4] 24 p4213 N85-36158

BIPROPELLANTS
U LIQUID ROCKET PROPELLANTS

BIRD-AIRCRAFT COLLISIONS
A study of bird ingestions into large high bypass ratio turbine aircraft engines
[DOE/FAA/CT-84/13] 01 p0005 N85-10028
A bird strike handbook for base-level managers
[AD-A147928] 07 p0948 N85-16008
Evaluation of the birdstrike threat to the F-15 present fleet, rapid deployment force, and dual role fighter transparencies
[AD-A148954] 10 p1421 N85-18886
Wildlife Hazards to Aircraft Conference and Training Workshop: Proceedings
[AD-A148330] 11 p1578 N85-19938
Birds and aviation
[AD-P004177] 11 p1578 N85-19939
Avoiding serious bird strike incidents
[AD-P004178] 11 p1578 N85-19940
Don't fowl out
[AD-P004179] 11 p1578 N85-19941
Accidents and serious incidents to civil aircraft due to birstrikes
[AD-P004180] 11 p1578 N85-19942
Analysis of bird strikes reported by European airlines, 1976 - 1980
[AD-P004181] 11 p1578 N85-19943
1983 Air Force bird strikes
[AD-P004182] 11 p1579 N85-19944
Worldwide birdstrike statistics of Lufthansa German Airlines
[AD-P004183] 11 p1579 N85-19945
Birds and aircraft engine strike rates
[AD-P004184] 11 p1579 N85-19946
Review of engine ingestions to wide body transport aircraft
[AD-P004185] 11 p1579 N85-19947
Aircraft transparency bird impact analysis using the MAGNA computer program
[AD-P004186] 11 p1579 N85-19948
Bird impact evaluation of the F/RF-4 tranaparency system 11 p1579 N85-19949
Microscopic identification of feathers in order to improve birdstrike statistics
[AD-P004187] 11 p1579 N85-19950
The use of small mobile radars to detect, monitor, and quantify bird movements
[AD-P004188] 11 p1580 N85-19951
On the altitudinal distribution of birds and bird strikes in the Netherlands
[AD-P004189] 11 p1580 N85-19952
Blackbirds and starlings: Population ecology and habits related to airport environments
[AD-P004190] 11 p1580 N85-19953
Cattle Egret hazard assessment
[AD-P004191] 11 p1580 N85-19954
Birds on airports: The reason for their presence 11 p1580 N85-19955
The use of falconry as mean to persuade the birds to stay out of the airport vicinity 11 p1580 N85-19956
Landscape management on airports for reduction of bird populations
[AD-P004194] 11 p1581 N85-19960
FAA policy regarding solid waste disposal facilities
[AD-P004196] 11 p1581 N85-19963
Airport bird hazards associated with solid waste disposal facilities
[AD-P004197] 11 p1581 N85-19964
Successful control of gulls and other birds at a sanitary landfill
[AD-P004198] 11 p1582 N85-19965
Bird Strike Committee Europe
[AD-P004207] 11 p1583 N85-19974
Birds and airport agriculture in the conterminous United States: A review of literature
[AD-P004208] 11 p1583 N85-19975

BIRDS
A study of bird ingestions into large high bypass ratio turbine aircraft engines
[DOE/FAA/CT-84/13] 01 p0005 N85-10028
Aircraft transparency bird impact analysis using the MAGNA computer program
[AD-P004186] 11 p1579 N85-19948
Bird impact evaluation of the F/RF-4 transparency system 11 p1579 N85-19949
Microscopic identification of feathers in order to improve birdstrike statistics
[AD-P004187] 11 p1579 N85-19950
The use of small mobile radars to detect, monitor, and quantify bird movements
[AD-P004188] 11 p1580 N85-19951
On the altitudinal distribution of birds and bird strikes in the Netherlands
[AD-P004189] 11 p1580 N85-19952
Blackbirds and starlings: Population ecology and habits related to airport environments
[AD-P004190] 11 p1580 N85-19953
Cattle Egret hazard assessment
[AD-P004191] 11 p1580 N85-19954
Birds on airports: The reason for their presence 11 p1580 N85-19955
The use of falconry as mean to persuade the birds to stay out of the airport vicinity 11 p1580 N85-19956
Airport site selection and design
[AD-P004193] 11 p1581 N85-19959
Reducing gull use of some attractions near airports
[AD-P004195] 11 p1581 N85-19962
Effectiveness of an overhead wire barrier in deterring gulls from feeding at a sanitary landfill
[AD-P004199] 11 p1582 N85-19966
Effectiveness of an overhead wire barrier system in reducing gull use at the BFI Jedburg sanitary landfill, Berkeley and Dorchester counties, South Carolina
[AD-P004200] 11 p1582 N85-19967
Evaluation of effectiveness of bird scaring operations at a sanitary landfill site near CFB Trenton, Ontario, Canada
[AD-P004201] 11 p1582 N85-19968
Development of bird hazard reduction for airport operational safety
[AD-P004202] 11 p1582 N85-19969
The bird strike situation and its ecological background in the Copenhagen Airport, Kastrup
[AD-P004203] 11 p1582 N85-19970
Bird control program Orlando International Airport
[AD-P004204] 11 p1583 N85-19971
Staff assistance to bases for bird hazards
[AD-P004205] 11 p1583 N85-19972
Bird strike avoidance system for Dover AFB, Delaware
[AD-P004206] 11 p1583 N85-19973
Birds and airport agriculture in the conterminous United States: A review of literature
[AD-P004208] 11 p1583 N85-19975
The potential of the NEXRAD radar system for warning of bird hazards
[AD-P004210] 11 p1583 N85-19977
Report of the Avian Development Working Group 24 p4127 N85-35582

BIREFRINGENCE
Investigating compression failure mechanisms in composite laminates with a transparent fiberglass-epoxy birefringent materials
[NASA-TM-86306] 02 p0170 N85-11137
Polarization transformation by single-mode fibers --- optical fibers
[FI-452-TBR-59] 11 p1729 N85-20876
Incident beam polarization for laser Doppler velocimetry employing a sapphire cylindrical window
[NASA-TM-87064] 17 p3037 N85-28786
An evaluation and preparation of ferromagnetic liquid composites for use at millimeter wavelengths
[AD-A153939] 18 p3069 N85-28980
Fiber optic sensors operating at dc
[AD-D011674] 19 p3271 N85-30283
Combustion control with smart sensors
[DE85-009419] 19 p3274 N85-30303

BIREFRINGENT FILTERS
Stokes parameters modulator for birefringent filters 18 p3205 N85-29684
Multichannel birefringent filter 18 p3206 N85-29888

BISMUTH
The growth of metastable peritectic compounds
[NASA-CR-171290] 07 p0920 N85-15825
SPAR X technical report for experiment 76-22 directional solidification of magnetic composites
[NASA-CR-171271] 07 p0927 N85-15880
Use of alternative solvents for low-temperature LPE growth of CdTe films
[AD-A149418] 10 p1562 N85-19853
Electrical resistance measurements of metals to 40 GPa in the diamond cell
[DE85-001009] 11 p1629 N85-20262
Topics in optical materials and device research, 3: Volume 1
[AD-A149726] 12 p1933 N85-22145

BISMUTH ALLOYS
Directional solidification studies of Pb-Bi pertectic alloys
[DE84-015656] 04 p0474 N85-13016
Atomistic studies of grain boundaries with segregated impurities
[DE85-000063] 11 p1737 N85-20924
Directional solidification of an eutectic Bi-MnBi alloy
[BLL-M-36270-(5828.4)] 20 p3430 N85-31275

BISMUTH COMPOUNDS
NT BISMUTH OXIDES
Shuttle flight test of an advanced gamma-ray detection system
[AD-A150316] 13 p1988 N85-22469
Improvements in the energy resolution and high-count-rate performance of bismuth germanate
[DE85-010763] 19 p3240 N85-30092
Bismuth germanate scintillators: Applications in nuclear safeguards and health physics
[DE85-010730] 19 p3365 N85-30865

BISMUTH OXIDES
Recent progress in BGO development for high resolution calorimetry
[MPI-PAE/EXP-E1-129] 01 p0124 N85-10648

BISTABLE AMPLIFIERS
U FLIP-FLOPS

BISTABLE CIRCUITS
Optically bistable devices using semiconductor materials
[AD-A149551] 11 p1628 N85-20253

BISTATIC RADAR
U MULTISTATIC RADAR

BISTATIC REFLECTIVITY
Influence of refraction effects on informativeness of bistatic acoustical atmospheric sounding systems 06 p0825 N85-15237
The effects of soil moisture on bistatic clutter power
[AD-A147638] 08 p1150 N85-17261

BIT ERROR RATE
A very efficient transfer function bounding technique on bit error rate for Viterbi decoded, rate 1/N convolutional codes 05 p0624 N85-13991
TDRSS S-shuttle unique receiver equipment 08 p1100 N85-16951

Modeling techniques used in the communications link analysis and simulation system (CLASS)
08 p1100 N85-16953
Validation of the communications link analysis and simulation system (CLASS) 08 p1100 N85-16954
Further results on rate 1/N convolutional code constructions with minimum required SNR criterion
10 p1464 N85-19235
The impact of propagation effects on the design of high capacity digital microwave links in the 18 GHz frequency band 10 p1470 N85-19278
An error generator to support the trials of the ZODIAC prototype system — raster links
[PHL-1984-71] 14 p2293 N85-24216
Bit error rate of coherent M-ary PSK
16 p2770 N85-27098
Phase locked loop synchronization for direct detection optical PPM communication systems
[NASA-CR-176026] 19 p3254 N85-30178
Study of a limited band signal transmission chain
[CNES-CT/DRT/TIT/TR-83/221]
20 p3442 N85-31361
Necessary bandwidth and spectral properties of digital modulation
[PB85-185387] 24 p4068 N85-35340

BIT SYNCHRONIZATION
Detection and symbol synchronization for multiple-bit per photon optical communications
10 p1463 N85-19228
Design criteria for limited scan antennas at digital microwave line of sight links 10 p1471 N85-19284
Distributed elections in a ring of processors using Archimedean time
[CWI-CS-R8416] 17 p3016 N85-28653

BITERNARY CODE
Converters of sum/difference of codes to frequency
15 p2526 N85-25578
Construction of complementary code sequence sets, part 7.1D 21 p3625 N85-32523

BITS
Floating-point function generation routines for 16-bit microcomputers
[NASA-TM-83783] 01 p0102 N85-10683
Basic features of personal computers
22 p3766 N85-33344

BITUMENS
A study of bituminous pavements to determine a correlation between pavement structure designs and tripping of asphalt cement
[PB84-217751] 01 p0037 N85-10231
Skid resistance of bituminous surfaces in Ohio
[PB84-234491] 04 p0484 N85-13086
Geology and resources of the Tar Sand Triangle, southeastern Utah
[DE84-012017] 05 p0677 N85-14346
Immobilization of toxic waste by embedding it in bitumen
[OEFZS-4277] 07 p0995 N85-16322
Field validation of statistically-based acceptance plan for bituminous airport pavements. Volume 1: Correlation analysis of Marshall properties of laboratory-compacted specimens
[FAA-PM-84-12-VOL-1] 12 p1781 N85-21180
Field validation of statistically-based acceptance plan for bituminous airport pavements. Volume 2: Statistical analysis of Marshall properties of plant-produced bituminous materials
[FAA-PM-84-12-VOL-2] 12 p1781 N85-21181
Field validation of statistically-based acceptance plan for bituminous airport pavements. Volume 3: Statistical analysis of 3 methods for determining maximum specific gravity of bituminous concrete mixtures
[FAA-PM-84-12-VOL-3] 12 p1781 N85-21182
Field validation of statistically-based acceptance plan for bituminous airport pavements. Volume 5: Summary of validation studies
[FAA-PM-84-12-VOL-5] 12 p1782 N85-21184
Stress-relieving interlayers for bituminous resurfacings
[PB85-136885] 12 p1820 N85-21415
Study of acceptance criteria for joint densities in bituminous airport pavements
[FAA-PM-85-5] 16 p2715 N85-26761

BIVARIATE ANALYSIS
Bayesian analysis of item response curves
[AD-A145627] 02 p0254 N85-11685
A variable span smoother
[AD-A148241] 08 p1215 N85-17855
Exact simultaneous confidence intervals for pairwise comparisons of three normal means
[AD-A148751] 09 p1375 N85-18645
Some qualitative properties of bivariate Euler-Frobenius polynomials
[AD-A149408] 10 p1547 N85-19755
Scarsel plots, and letter and blettar stripe
[DE85-001409] 11 p1707 N85-20739
Approximation order from certain spaces of smooth bivariate splines on a 3-direction mesh
[AD-A149633] 12 p1925 N85-22092

BL LACERTAE OBJECTS
Far-infrared photometry of compact extragalactic sources: OJ 187 and BL Lac
[NASA-TM-86022] 04 p0580 N85-13701
X-ray and ultraviolet observations of BL Lacertae objects 05 p0741 N85-14787
X-ray and UV Emission from Active Galactic Nuclei — conference
[MPE-184] 08 p1236 N85-17790
BL Lacertae objects: Multifrequency observations and model applications 08 p1236 N85-17792
The extragalactic nature of H0323+022
08 p1237 N85-17802
Soft X-ray emission from BL Lac objects
08 p1239 N85-17810
X-ray emission from PKS 2155-304 — BL Lac object
08 p1239 N85-17812
One to eight month X-ray light curves for active extragalactic objects 08 p1239 N85-17817
On the surface density of X-ray selected BL Lacertae objects 08 p1240 N85-17822
On the broadband energy spectra of quasars and BL Lac objects 08 p1240 N85-17825
Multifrequency observations of BL LAC objects and violently variable quasars 11 p1746 N85-20961
Very recent IUE observations of 2 BL lacertae objects
11 p1746 N85-20962
Coordinated multifrequency observations of the BL LAC objects MRK 180, MRK 421, and MRK 501
11 p1746 N85-20963
X-ray emission from active galactic nuclei
[NASA-TM-86175] 11 p1783 N85-21068

BLACK AND WHITE PHOTOGRAPHY
Metric camera experiment: Spacelab 1 mission
05 p0658 N85-14229
Some nonatlas work at the European Southern Observatory (ESO) Sky Atlas Laboratory — astronomical photography 07 p0984 N85-16117

BLACK BODY RADIATION
Microwave blackbodies for spaceborne receivers
[NASA-CR-175647] 13 p2094 N85-23068
Measurement of the large-scale anisotropy of the cosmic background radiation at 3 MM 13 p2206 N85-23680
Scaling blackbody laser to high powers
[NASA-TM-86395] 14 p2309 N85-24292
Theoretical studies of solar-pumped lasers
[NASA-CR-175801] 16 p2789 N85-27206
Stable density stratification solar pond
[NASA-CASE-NPO-15419-2] 19 p3303 N85-30474
Self-study manual on optical radiation measurements. Part 1: Concepts. Chapter 12: Blackbodies, blackbody radiation, and temperature scales
[PB85-195303] 24 p4154 N85-35754

BLACK HOLES (ASTRONOMY)
Gravitational vacuum 02 p0265 N85-11734
Topics in black-hole physics: Geometric constraints on noncollapsing, gravitating systems, and tidal distortions of a Schwarzschild black hole 05 p0742 N85-14769
Some aspects of active galactic nuclei
07 p1056 N85-16702
Shock acceleration in active galactic nuclei and quasars 08 p1241 N85-17828
On the hydrodynamical equations of astrophysical jets — active galactic nuclei 08 p1241 N85-17831
Thermal convection and magnetic fields in accretion disks of black holes 12 p1955 N85-22285
Numerical simulation of the effects of radially injected barium plasma in the ionosphere
[NASA-CR-175838] 14 p2354 N85-24542
Gravitational effects in theories with interacting fields: Two studies 15 p2683 N85-26435
A numerical study of nonspherical black hole accretion 16 p2981 N85-27780
Activities report of the Institute of Astronomy
20 p3545 N85-32059
Comments on RS-17 X-ray telescope
22 p3731 N85-33132
Breakdown of helium nuclei in matter processed near black holes
[OG-8.2-20] 23 p4021 N85-34916
High energy cosmic ray signature of quark nuggets
[HE-8.2-11] 24 p4212 N85-36147

BLACK SEA
Black Sea coastal frontogenesis
01 p0075 N85-10500
Manganese in recent sediments of Ukrainian SSR Black Sea shelf 06 p0819 N85-15200
Hydrologic characteristics of the Mediterranean and Black Sea 07 p0981 N85-16228
Electromagnetic field of currents and its use to estimate total conductivity of sedimentary deposits in Western Black Sea 14 p2334 N85-24434
Sea water photoluminescence
19 p3292 N85-30415
Temporal variations of Rn222 concentrations in Black Sea coastal zone 19 p3293 N85-30417

BLACKOUT (PHYSIOLOGY)
Matched filtering of visual evoked potentials to detect acceleration (+Gz) induced blackout
[AD-A155912] 24 p4131 N85-35609
Simulation of high +Gz onset in the dynamic environment simulator
[AD-A155963] 24 p4131 N85-35610

BLACKOUT (PROPAGATION)
NT ATMOSPHERICS
NT DAWN CHORUS
NT ELECTROMAGNETIC NOISE
NT HISS
NT IONOSPHERIC NOISE
NT SHOT NOISE
NT THERMAL NOISE
NT WHISTLERS
NT WHITE NOISE

BLADDER
Spontaneous transitional cell carcinoma in the urinary bladder of a strain 13 guinea pig
[AD-A155845] 21 p3665 N85-32764

BLADDERS (MECHANICS)
U DIAPHRAGMS (MECHANICS)

BLADE SLAP NOISE
Interaction of a turbulent vortex with a lifting surface
15 p2484 N85-25214

BLADE TIPS
Observations from varying the lift and drag inputs to a noise prediction method for supersonic helical tip speed propellers
[NASA-TM-83797] 01 p0115 N85-10788
An experimental investigation and numerical simulation of the thermomechanical phenomena in compressor rotor tip rubbing 03 p0367 N85-12352
Pressure loss due to the tip clearance of impeller blades in centrifugal and axial blowers
05 p0536 N85-14083
Transonic flow of elastic medium past slender solid body 06 p0778 N85-14976
A feasibility study of free-tip rotor application as a passive cyclic control device 09 p1279 N85-18048
Inviscid analysis of unsteady blade tip flow correlation studies
[NASA-CR-172506] 10 p1420 N85-18958
One-piece HPTR blade squealer tip
[AD-D011452] 10 p1425 N85-18989
Cooled turbine blade tip closure
[AD-D011525] 12 p1858 N85-21654
An experimental investigation of the chopping of helicopter main rotor tip vortices by the tail rotor
[NASA-CR-177338] 13 p2154 N85-23378
Unsteady analysis of rotor blade tip flow
[NASA-CR-3868] 15 p2482 N85-25202
Interaction of a turbulent vortex with a lifting surface
15 p2484 N85-25214
Turbine blade-tip clearance excitation forces
[NASA-CR-171534] 19 p3220 N85-29963
Oxidizing seal for a turbine tip gas path
[NASA-CASE-LEW-14053-1] 23 p3937 N85-34402
Optimally designed propellers constrained by noise
24 p4065 N85-35196

BLADES
Post stall airfoil data for wind turbines: Wind tunnel test results
[DE85-004052] 10 p1511 N85-19534

BLADES (CUTTERS)
Device for preventing intrusion of a blade during vibration cutting of intermittent cutting with a lathe
16 p2794 N85-27232

BLANKETS (FISSION REACTORS)
Feasibility study of a fission-suppressed Tokamak fusion breeder
[DE85-009099] 18 p3190 N85-29786

BLANKETS (FUSION REACTORS)
Blanket materials for fusion reactors: Comparisons of thermochemical performance
[DE84-016240] 04 p0568 N85-13622
Special topics reports for the reference tandem mirror fusion breeder: Liquid metal MHD pressure drop effects in the packet bed blanket, volume 1
[DE85-002142] 06 p0865 N85-15500
Magnetic divertor design for the compact reversed-field pinch reactor
[DE85-002031] 09 p1391 N85-18753
Heat transfer and mechanical interactions in fusion nuclear systems
[DE84-016233] 09 p1392 N85-18761
Experimental facility for studying MHD effects in liquid metal cooled blankets
[DE85-000583] 14 p2423 N85-24943

Magneto-fluid-dynamic issues for fusion first wall and blanket systems
[DE85-004022] 14 p2424 N85-24954
Magnetohydrodynamic considerations for the design of self-cooled liquid-metal fusion reactor blankets
[DE85-000242] 14 p2425 N85-24957
Fusion-power-core design of a Compact Reversed-Field Pinch Reactor (CRFPR)
[DE85-007710] 16 p2868 N85-27692
Radiation damage experiments and lifetime estimates for beryllium components in fusion systems
[DE85-008036] 17 p3040 N85-28811
Two-dimensional TBR calculations for conceptual compact reversed-field pinch reactor blanket
[DE85-007636] 17 p3040 N85-28812
Preliminary proposal for a beryllium technology program for fusion applications
[DE85-009815] 18 p3183 N85-29737
Modeling and experiments on tritium permeation in fusion reactor blankets
[DE85-008439] 18 p3183 N85-29741
US blanket technology programs
[DE85-010505] 19 p3358 N85-30817
Test cell modeling and optimization for FPD-2
[DE85-010836] 19 p3358 N85-30821
Molten salt cooling/17Li-83Pb breeding blanket concept
[DE85-010522] 19 p3363 N85-30854
Flow characteristics of the Cascade granular blanket
[DE85-010932] 20 p3420 N85-31227
Neutronics activities for next generation devices
[DE85-010488] 20 p3527 N85-31939
Design of a helium-cooled molten salt fusion breeder
[DE85-010474] 20 p3528 N85-31943
Modeling and optimization of a test-cell upgrade for MFTF-B operating in the high neutron wall loading mode
[DE85-009997] 20 p3528 N85-31946
MFTF-(alpha) + T shield design
[DE85-010496] 20 p3529 N85-31948
Monte Carlo and discrete ordinates calculations of 14-MeV neturons streaming through a stainless-steel duct (L/D = 4.6): Comparison with experiment
[DE85-011423] 22 p3840 N85-33776
Key issues of fusion nuclear technology development (FINESSE)
[DE85-012590] 22 p3845 N85-33817
Blanket optimization studies for Cascade
[DE85-010002] 22 p3846 N85-33824

BLANKS
Correction of engraving stamp for forming blanks of gas turbine engine blades 09 p1307 N85-16213

BLASIUS EQUATION
Existence and non-uniqueness of similarity solutions of a boundary layer problem
[NASA-CR-172503] 07 p0957 N85-16064

BLASIUS FLOW
A mathematical analysis of the effect of free stream turbulence on the Blasius boundary layer
20 p3451 N85-31430

BLAST DEFLECTORS
Wind tunnel tests on a tube-launched missile configuration with a deflectable nose control and a novel wrap-around fin stabiliser
[AR-003-696] 01 p0001 N85-10003
Results of tests of MTA-2 TPS on the SRB hold-down bolt blast container
[NASA-CR-170891] 24 p4070 N85-35224

BLAST LOADS
Model study of the interaction of a blast wave with the superstructure of ships. Part 5: Application of optical measurement methods to the study of blast interaction
[PML-1984-12-PT-5] 01 p0057 N85-10375
Dynamic shear failure of shallow-buried flat-roofed reinforced concrete structures subjected to blast loading
[AD-A145974] 03 p0373 N85-12378
A model of the soft X-ray background as a blast wave viewed from inside 06 p0679 N85-15586
Penetration of short duration airblast into protective structures 09 p1336 N85-18404
Preliminary design criteria and certification test specifications for blast resistant windows
09 p1337 N85-18405
The clinical and biomedical evaluation of trauma and fatalities associated with aircrew ejection and crash. A Working Group report
[AGARD-AR-194] 12 p1906 N85-21969
Introduction: The clinical and biomedical evaluation for trauma and fatalities associated with aircrew ejection and crash 12 p1906 N85-21970
List of head/neck injury on ejection in the German Armed Forces from 1972-1981 12 p1906 N85-21972
Windblast arm protector assembly
[AD-D011512] 12 p1909 N85-21984
Elastic-workhardening SDF (Single-Degree-of-Freedom) system subjected to random blast excitations
[AD-A151866] 15 p2579 N85-25909
The shock desensitization of PBX-9404 and composition B-3
[DE85-009604] 18 p3084 N85-29077
Constitutive modeling for blast-induced wave propagation
[AD-A153576] 18 p3099 N85-29187
Environmental airblast around large shock tubes
[DE85-010654] 20 p3463 N85-31512
Development of an NBS (National Bureau of Standards) polymer gage for dynamic soil stress measurement
[PB85-208494] 24 p4118 N85-35526

BLASTOFF
U ROCKET LAUNCHING

BLASTS
Some of the features of movement of gas through a layer of free-flowing substances
[BLL-M-35732-(5828.4)] 02 p0196 N85-11312

BLEACHING
Hologram bleaching 06 p0789 N85-15038

BLEED-OFF
U PRESSURE REDUCTION

BLENDS
U MIXTURES

BLINDNESS
NT FLASH BLINDNESS
Baffled eye and confounded brain or using visual illusions to train blind pilots
[AD-P004332] 09 p1271 N85-17986
Investigation into the use of the TV magnifier in the Netherlands
[HSE-TRANS-11142] 20 p3533 N85-31986

BLOCH BAND
Electronic bandstructure of an incommensurate crystal
[DE84-016891] 05 p0733 N85-14714
Analysis of solution of Bloch's equations in time domain 22 p3771 N85-33371

BLOCK DIAGRAMS
Dispersion of phase-shift keyed systems with fixed number of blocks 13 p2070 N85-22928

BLOCKING
Experiences with a high-blockage model tested in the NASA Ames 12-foot pressure wind tunnel
03 p0315 N85-12032
Beginner's guide to blocked records on magnetic tape
[DE85-001691] 06 p0855 N85-15433
A simulator for determining the performance of transaction manager and lock manager combinations in a database
[AD-A147827] 07 p1055 N85-16696
Navy tactical applications guide. Volume 4. Part 1. Eastern North Pacific weather analysis and forecast applications
[AD-A150097] 12 p1896 N85-21900
Maintenance of blocking anticyclones in a general circulation model
[PB85-190666] 24 p4124 N85-35567

BLOCKS
Detonator block
[AD-D011248] 06 p0773 N85-14941
Phase diagram of polymer blends containing block copolymers
[AD-A147706] 08 p1132 N85-17134
Lattice actions improved by block-spin renormalisation group and maximally symmetric lattices
[DE85-007416] 17 p3045 N85-28841
Comparison of TT-F-1096 solvent-thinned block fillers with water-thinnable block fillers
[AD-A154207] 19 p3249 N85-30142

BLOOD
NT ERYTHROCYTES
NT LYMPHOCYTES
Effect of maximum physical load on oxygen-transport properties of blood 01 p0093 N85-10627
Measurement of blood and plasma density with the mechanical oscillator technique
05 p0693 N85-14456
Clinical measurements using fiber optics and optrodes
[DE84-015043] 05 p0696 N85-14481
Fatal hemorrhagic shock and acetate solutions
[AD-A146754] 07 p1014 N85-16444
Aviation-related cardiorespiratory effects of blood donation in female pilots
[AD-A146045] 08 p1195 N85-17529
Parameters of carbohydrate metabolism and blood serum enzyme activity after short-term spaceflights
12 p1903 N85-21951
Effect of stationary magnetic field on bleeding time
12 p1904 N85-21956
Blood serum enzyme activity following long term spaceflights 19 p3326 N85-30604
Rat blood serum and liver carbohydrates and lipids in recovery period after 15-day hypokinesia
19 p3328 N85-30606
A system for the assessment of non-thermal effects of ultrasound on cells at liquid nitrogen temperatures
20 p3523 N85-31915
The effect of +Gx acceleration on platelet activation as determined by plasma platelet factor 4 levels
[AD-A155881] 24 p4131 N85-35608

BLOOD CIRCULATION
NT BRAIN CIRCULATION
NT CORONARY CIRCULATION
NT PULMONARY CIRCULATION
Study and realization of a Doppler system with pulsed, directional, multiport (128) emission and sequential signal treatment — ultrasonic echography, blood flow
[ENST-84E006] 05 p0639 N85-14102
Pulmonary blood flow and oxygenation of arterial blood in a healthy subject upon 7 days hypokinesia
07 p1014 N85-16439
Biochemical evaluation of bodily influence of high and low temperatures 07 p1014 N85-16441
Carotid baroreceptor influences on peripheral circulatory and thermal responses during cold exposure
[AD-A146808] 07 p1015 N85-16447
Random pattern tracking acceleration tolerance tester
[AD-D011404] 07 p1017 N85-16459
Blood viscosity responses to acute exercise and aerobic conditioning in women 09 p1363 N85-18573
Hemodynamics responses to upright tilt at sea level and high altitude
[AD-A148848] 10 p1527 N85-19634
China report: Science and technology
[JPRS-CST-84-008] 13 p1972 N85-22384
Exercise-heat strain during hypohydration: Interaction with heat acclimation and aerobic fitness
[AD-A151023] 14 p2389 N85-24717
Regional circulation during testing on isokinetic dynamometer following 14-day bedrest
19 p3323 N85-30590
Long term exposure of animals to antiorthostatis (-90 deg) as a model of critical homeostatic disturbances
19 p3324 N85-30592
Nature of postural changes in human hemodynamics with intake of sydnocarb alone and in combination with obsidan 19 p3325 N85-30597
Effects of blood volume overload on myocardial ultrastructure in relation to adaptation to high altitude hypoxia 22 p3820 N85-33664
Typological characteristics of hemodynamic states of healthy subjects in orthostatic position
22 p3821 N85-33673
Vascular mechanisms of adaptation to antiorthostatic position 22 p3822 N85-33675
Cerebral hemodynamics and ventricular function in -15 deg antiorthostatic position 22 p3822 N85-33676
Effect of short-term antiorthostatic hypokinesia on dynamics of cardiorespiratory parameters during graded physical exercise 22 p3822 N85-33677
Morphological manifestations of hemodynamic changes in lungs of monkeys submitted to antiorthostatic hypokinesia 22 p3824 N85-33686
Effect of hypokinesia and +Gz accelerations on transport function of human blood
23 p3952 N85-34497
Oxygenation and regional circulation in gingival mucosa during exposure to lower body negative pressure
23 p3953 N85-34498

BLOOD FLOW
Circulatory orthostatic instability: Role of deconditioning of resistive vessels 01 p0091 N85-10612
Left heart ventricular function during a 7 day zero-g simulation (6 deg head down tilt)
05 p0691 N85-14446
Distribution of blood flow to brain, kidneys, gut, spleen and posterior extremities in cats in acute hypoxia
07 p1013 N85-16434
Analysis of the transient response of temporal artery blood flow data relative to various anti-G suit pressure schedules 10 p1533 N85-19660
Simultaneous determination of cerebral blood flow and partition coefficient with a freely diffusable tracer
[DE85-001228] 11 p1690 N85-20625
A two phase flow model at the level of a narrowing section — blood flow 20 p3507 N85-31799
Morphological manifestations of hemodynamic changes in lungs of monkeys submitted to antiorthostatic hypokinesia 22 p3824 N85-33686

BLOOD PLASMA
USSR report: Space Biology and Aerospace Medicine, volume 18, no. 6, November - December 1984
[JPRS-USB-85-002] 12 p1900 N85-21931
Research opportunities in loss of red blood cell mass in space flight
[NASA-CR-175806] 16 p2841 N85-27517

Plasma hormonal responses at graded hypohydration levels during exercise/heat stress
[AD-A153681] 18 p3153 N85-29523
Rat plasma hormone levels following flight aboard Cosmos-1129 biosatellite 22 p3823 N85-33681

BLOOD PRESSURE
NT LOWER BODY NEGATIVE PRESSURE
Hemodynamics and plasma arginine vasopressin during water immersion in normal man 05 p0693 N85-14458
Blood pressure levels of active pilots compared with those of air traffic controllers
[AD-A146845] 06 p0846 N85-15373
Effect of microwave radiation on local blood circulation and oxygenation of brain tissue 07 p1012 N85-16431
Carotid baroreceptor influences on peripheral circulatory and thermal responses during cold exposure
[AD-A146808] 07 p1015 N85-16447
Blood pressure responses and mineral ocorticoid levels in the suspended rat model for weightlessness 15 p2609 N85-26079
Effect of 120-day antiorthostatic bedrest on gas exchange and pulmonary circulation in man 19 p3323 N85-30589
Antihypertensive neutral lipid
[DE85-011625] 22 p3819 N85-33656
Cerebral hemodynamics and ventricular function in -15 deg antiorthostatic position 22 p3822 N85-33676
Effect of short-term antiorthostatic hypokinesia on dynamics of cardiorespiratory parameters during graded physical exercise 22 p3822 N85-33677
Effect of water immersion of parameters of central hemodynamics in individuals over 45 years old 23 p3953 N85-34499

BLOOD VESSELS
NT ARTERIES
NT VEINS
Cerebral hemodynamics and ventricular function in -15 deg antiorthostatic position 22 p3822 N85-33676
Development of the osmium-191 yields iridium-191m radionuclide generator
[DE85-011185] 23 p3970 N85-34611

BLOOD VOLUME
A systems analysis of the erythropoietic responses to weightlessness. Volume 1: Mathematical model simulations of the erythropoietic responses to weightlessness
[NASA-CR-171890] 20 p3506 N85-31794
Effects of blood volume overload on myocardial ultrastructure in relation to adaptation to high altitude hypoxia 22 p3820 N85-33664
Thirst and fluid intake following graded hypohydration levels in humans
[AD-A156201] 24 p4132 N85-35615

BLOWDOWN WIND TUNNELS
Experiences with the use of a side-strut model support system for high angles of attack in the Trinsonik wind tunnel TMK
[DFVLR-MITT-84-09] 07 p0910 N85-15763
Transonic Mach number determination in a blow-down wind tunnel with solid walls and a downstream throat
[VTH-LR-402] 17 p2893 N85-27835
Experiences with the use of a side-strut model support system for high angles for attack in the TMK Trinsonik Wind Tunnel
[ESA-TT-895] 20 p3396 N85-31069

BLOWERS
Pressure loss due to the tip clearance of impeller blades in centrifugal and axial blowers 05 p0636 N85-14083
Low solidity cascade diffusers for wide flow range centrifugal blowers 05 p0637 N85-14086
Strong turbulence chemistry interaction in a piloted turbulent jet diffusion flame 20 p3425 N85-31257

BLOWING
Drag reduction due to boundary-layer control by combined blowing and suction 08 p1070 N85-16785

BLUE GREEN ALGAE
Production of hydrogen by cyanobacteria
[PB85-113421/GAR] 07 p0935 N85-15925

BLUE STARS
NT SYMBIOTIC STARS
Blue companions of Cepheids 11 p1754 N85-21033

BLUFF BODIES
Vorticity amplification in viscous flow around a body 03 p0360 N85-12309
Large structure in the far wakes of two-dimensional bluff bodies 05 p0592 N85-13771
Flow Around Bluff Bodies: Numerical and Experimental Approaches — conferences
[VKI-LS-1984-06] 05 p0593 N85-13778
Flow around bluff bodies 05 p0593 N85-13779
Tr.J aerodynamics of bluff bodies in turbulent shear layers 05 p0593 N85-13780
Experimental techniques and instrumentation for bluff body aerodynamics 05 p0593 N85-13781
Numerical methods for bluff body aerodynamics 05 p0593 N85-13782
Wake flow behind bluff bodies 05 p0593 N85-13783
Numerical integrations of the Navier-Stokes equations for flow over surface-mounted obstacles 05 p0593 N85-13784
On the generation of trailing vortices by surface mounted obstacles 05 p0593 N85-13785
Acceleration of bluff bodies through fluids 05 p0593 N85-13786
Numerical calculation of the cold-flow characteristics of a bluff-body flame stabilizer
[CFD/84/14] 08 p1124 N85-17088
Experimental investigation of heat transfer to bluff cylinders and cones in hypersonic rarefied gas flow 11 p1620 N85-20195
The mechanisms of flame holding in the wake of a bluff body
[NASA-CR-3866] 12 p1779 N85-21166
Investigation of the aerodynamic forces on bluff bodies at high Reynolds numbers
[DFVLR-MITT-84-19] 14 p2213 N85-23727
Numerical solutions of 3-dimensional Navier-Stokes equations for closed bluff-bodies
[NASA-CR-175755] 15 p2636 N85-26255
An experimental investigation of a turbulent junction vortex
[NASA-CR-175915] 17 p2957 N85-28259

BLUFFS (LANDFORMS)
U CLIFFS

BLUNT BODIES
Numerical method for computing supersonic flow over wings of flight vehicles 05 p0725 N85-14659
Hypersonic flow of mixture around blunt body 06 p0779 N85-14979
Controllable rotation of system of two solid bodies with elastic elements 06 p0780 N85-14988
On detached shock wave of sphere moving with transonic velocities 11 p1622 N85-20215
A 3-dimensional Navier-Stokes-Euler code for blunt-body flow computations
[NASA-TM-58266] 15 p2483 N85-25211
Navier-Stokes solution of hyperaonic blunt-nosed body flowfields 16 p2693 N85-26624
Bypass transition to turbulence and research Desiderata 20 p3453 N85-31442
Laser Doppler Anemometer (LDA) measurements in the turbulent near-wake of blunt bodies
[ISL-CO-212/84] 22 p3785 N85-33450

BLURRING
New image deblurring method described 16 p2806 N85-27305

BMC
U BONE MINERAL CONTENT

BO-105 HELICOPTER
Flight tests with a new helicopter Force Feel System (FFS) 08 p1075 N85-16818
Flight research on visual aids and navigation equipment for helicopter low-level flight at night 08 p1076 N85-16820

BOATS
NT LIFEBOATS
The 1981 transatlantic boat race contribution for marine meteorological measurements 14 p2324 N85-24361
The transpacific experimental sailing by YASEIGO 3 14 p2327 N85-24380
Miscellaneous ARGOS maritime applications — yacht races 14 p2327 N85-24383
The sinking of the Les Mutuelles du Mans trimaran 14 p2327 N85-24384
The ARGOS contribution to the demonstration of the effectiveness of a satellite-based search and rescue system 14 p2330 N85-24404
Data from BOC-yachts: A significant input to Southern Hemisphere analysis 16 p2614 N85-27956
Some applications of aeronautical engineering in the construction of yachts
[NLR-MP-83042-U] 20 p3394 N85-31052

BOATTAILS
On the evaluation of boundary layer measurements on boattailed bodies of revolution in axisymmetric compressible subsonic flow
[ESA-TT-883] 20 p3457 N85-31471
Laser Doppler Anemometer (LDA) measurements in the turbulent near-wake of blunt bodies
[ISL-CO-212/84] 22 p3785 N85-33450

BOD
U BIOCHEMICAL OXYGEN DEMAND

BODIES OF REVOLUTION
NT CELESTIAL SPHERE
NT CONCENTRIC SPHERES
NT CONICAL BODIES
NT CYLINDRICAL BODIES
NT FALLING SPHERES
NT PARABOLIC BODIES
NT POINCARE SPHERES
NT ROTATING CYLINDERS
NT ROTATING SPHERES
NT SLENDER CONES
NT SPHERES
NT TORUSES
Stability of stellar disk and ratio of halo to disk masses in the galaxy 05 p0740 N85-14783
Numerical modeling of complex interaction of shell of revolution and its filler with allowance for friction 06 p0779 N85-14980
Motion of heavy symmetric body with flexible bars about stationary point 06 p0780 N85-14980
Transient currents of ideally conducting body of revolution with transient diffraction 06 p0785 N85-15019
Effects of body shape on the aerodynamics of a body of revolution at Mach numbers from 1.6 to 4.6
[NASA-TM-86345] 07 p0893 N85-15857
A frozen vorticity approach to the axisymmetric strong interaction problem
[AD-A149101] 10 p1484 N85-19369
Average spacing for rings of individual multi-ring basins is 2.0(0.5)D 13 p2182 N85-23541
Method of solving problems of statics for multilayer shells of revolution 17 p2943 N85-28167
Proceedings of the 9th US Air Force and the Federal Republic of Germany Data Exchange Agreement Meeting, Viscous and Interacting Flow Field Effects
[AD-A153020] 17 p2958 N85-28266

BODY CENTERED CUBIC LATTICES
Lattice defects in body centered cubic transition metals 03 p0427 N85-12727

BODY FLUIDS
NT BLOOD
NT CEREBROSPINAL FLUID
NT ENDOLYMPH
NT ERYTHROCYTES
NT LYMPHOCYTES
NT SWEAT
NT URINE
Intraocular fluid dynamics in microgravity 05 p0693 N85-14455
Fluid metabolism of monkeys during two-week antiorthostatic hypokinesia 12 p1902 N85-21943
Exercise-heat strain during hypohydration: Interaction with heat acclimation and aerobic fitness
[AD-A151023] 14 p2389 N85-24717
Structural development and gravity 15 p2606 N85-26071
Computer simulation studies in fluid and calcium regulation and orthostatic intolerance
[NASA-CR-171869] 15 p2616 N85-26117
The behavior of renal-regulating hormones during hypogravic stress
[NASA-CR-171877] 15 p2616 N85-26123
Fluid-electrolyte responses during prolonged space flight: A review and interpretation of significant findings
[NASA-CR-171878] 15 p2617 N85-26124
Chemicals identified in human biological media, a data base. Volume 6, part 2: Records 7588-8694
[DE85-008767] 18 p3154 N85-29528
Investigation of spectrum of human bile acids during 120-day antiorthostatic hypokinesia 22 p3821 N85-33674
Fluid-electrolyte metabolism and renal function in cosmonauts following 185-day spaceflight 23 p3952 N85-34495

BODY KINEMATICS
Acceleration of bluff bodies through fluids 05 p0593 N85-13786
Electromyographic patterns associated with discrete limb movements 05 p0710 N85-14551
Human body dimensions: Body outlines and envelope curves at different normal positions and movements
[HSE-TRANS-10866] 19 p3332 N85-30640
Effect of body position and immobilization on intensity of spatial illusions in weightlessness 22 p3821 N85-33672
The dynamics of articulated rigid bodies for purposes of animation 23 p3965 N85-34579

BODY MEASUREMENT (BIOLOGY)
NT ANTHROPOMETRY
Human body dimensions: Body outlines and envelope curves at different normal positions and movements
[HSE-TRANS-10866] 19 p3332 N85-30640
Physical dimensions of humans, values, envelope curves in different postures
[HSE-TRANS-10869] 20 p3513 N85-31836

BODY SIZE (BIOLOGY)
Prediction of percent body fat for U.S. Navy women from body circumferences and height
[AD-A146456] 06 p0845 N85-15370

BODY SWAY TEST
Typological characteristics of hemodynamic states of healthy subjects in orthostatic position
22 p3821 N85-33673

BODY TEMPERATURE
Biochemical evaluation of bodily influence of high and low temperatures 07 p1014 N85-16441
Comparison of thermal responses between rest and leg exercise in water
[AD-A146818] 07 p1015 N85-16448
Tolerance endpoint for evaluating the effects of heat stress in dogs
[AD-A148104] 08 p1192 N85-17511
Simultaneous determination of radiation and convection heat transfer 08 p1194 N85-17523
Influence of hyperthermia on body temperature and content of catecholamines in white rat hypothalamus
10 p1524 N85-19615
Heat stress and personal protective equipment
[DE85-009552] 10 p1532 N85-19652
China report: Science and technology
[JPRS-CST-84-030] 13 p2041 N85-22777
Study of effective physiological temperature
13 p2042 N85-22780
Peripheral changes in regional sweating responses to exercise in hypobaric environments
[AD-A150757] 14 p2388 N85-24710
Mathematical models relating to human thermoregulation: Basic assumptions, validation, and application. Parts A and B
[AD-A151556] 15 p2618 N85-26130
Thermal consequences of localized SAR from RFR exposures 16 p2775 N85-27130
Experiments in microwave exposure in the rat: Body temperature, serum chemistry and the use of chemical restraint
[PB85-156834] 16 p2840 N85-27512
Investigation of the requirement for auxiliary heating of Canadian forces personnel
[AD-A151950] 16 p2841 N85-27522
Method for thermal monitoring subcutaneous tissue
[NASA-CASE-LAR-13028-1] 19 p3328 N85-30618
Heat injury: Prevention is the key
[AD-A153734] 19 p3328 N85-30622
Electroanesthesia as a means of controlling cold stress of local hypothermia 22 p3823 N85-33687
Thermal stress suffered by tank crews working in summer heat
[DRIC-T-7492] 22 p3826 N85-33698
Weight loss, rectal temperature and heart rates following the 1984 Boston Marathon
[AD-A155984] 24 p4132 N85-35612

BODY TEMPERATURE (NON-BIOLOGICAL)
U TEMPERATURE

BODY TEMPERATURE REGULATION
U THERMOREGULATION

BODY VOLUME (BIOLOGY)
Leg volume changes. Responses to Lower Body Negative Pressure (LBNP) during 7 days of zero-g simulation (6 deg Head-Down Tilt (HDT))
05 p0692 N85-14452
An analysis of aerobic capacity in a large United States population
[AD-A156200] 24 p4132 N85-35614

BODY WEIGHT
Effects of body mass and morphology on thermal responses in water
[AD-A147556] 07 p1016 N85-16455
The effect of occupational exposure and the body weight to height ratio on exhaled methylene chloride breath concentration in females at one, eighteen and sixty-six hours post exposure 14 p2388 N85-24708
Role of glucocorticoids in the response to unloading of muscle protein and amino acid metabolism
15 p2609 N85-26077
Gravity, body mass and composition, and metabolic rate 15 p2610 N85-26084
Weight loss, rectal temperature and heart rates following the 1984 Boston Marathon
[AD-A155984] 24 p4132 N85-35612
Thirst and fluid intake following graded hypohydration levels in humans
[AD-A156201] 24 p4132 N85-35615

BODY-WING AND TAIL CONFIGURATIONS
The aerodynamics of some guided projectiles
[NASA-TM-86334] 06 p0747 N85-14788
Theoretical study of boundary-layer control
08 p1070 N85-16784
Tail behaviour for supersonic of empirical processes
[AD-A147629] 08 p1210 N85-17613
Supersonic aerodynamic characteristics of canard, tailless, and aft-tail configurations for 2 wing planforms
[NASA-TP-2434] 17 p2691 N85-27822
Experimental and theoretical determination of the wing-induced lateral wind on the tail surfaces in oscillating rolling motion. Part 1: Application of the Mobile Oscillating Derivatives (MOD) on an experimental part
[IFD-1/84-PT-1] 18 p3061 N85-28939
Experimental and theoretical determination of the wing-induced lateral wind on the tail surfaces in oscillating rolling motion. Part 2: Theoretical investigations for calculation of the lateral wind
[IFD-1/84-PT-2] 18 p3061 N85-28940
Transonic and supersonic wind tunnel tests on control effectiveness on schematic missile configurations
[FFA-TN-1983-20] 20 p3389 N85-31020
Transonic and supersonic wind tunnel tests on control effectiveness on schematic missile configurations: Supplement
[FFA-TN-1983-20-SUPPL] 20 p3389 N85-31021

BODY-WING CONFIGURATIONS
An experimental study of the transonic equivalence rule with lift, part 2
[AR-LR-614-PT-2] 01 p0001 N85-10004
A study of aerodynamic characteristics of wing-body combinations. Part 2: Low-wing airplane
[NAL-TR-796] 01 p0002 N85-10010
Drag reduction due to boundary-layer control by combined blowing and suction 08 p1070 N85-16785
Wing rock flow phenomena
[AD-P004154] 09 p1264 N85-17939
Flight mechanics analysis of dynamic derivatives of the Dornier variable wind tunnel model
[ESA-TT-854] 11 p1577 N85-19937
Comparison of computational results of a few representative three-dimensional transonic potential flow analysis programs 16 p2693 N85-26628
The role of computational fluid dynamics in aeronautical engineering 16 p2694 N85-26629
Experimental and theoretical determination of the wing-induced lateral wind on the tail surfaces in oscillating rolling motion. Part 1: Application of the Mobile Oscillating Derivatives (MOD) on an experimental part
[IFD-1/84-PT-1] 18 p3061 N85-28939
Calculation of transonic flows around an aircraft configuration with motorized nacelle
[SNIAS-851-111-106] 20 p3387 N85-31006
Calculation of flow around the SF 310 airplane using a full potential equation method
[FFA-TN-1984-63] 20 p3389 N85-31022

BOEING AIRCRAFT
NT BOEING 727 AIRCRAFT
NT BOEING 737 AIRCRAFT
NT BOEING 747 AIRCRAFT
NT BOEING 767 AIRCRAFT
NT C-135 AIRCRAFT
NT CH-47 HELICOPTER

BOEING MILITARY AIRCRAFT
U MILITARY AIRCRAFT

BOEING 727 AIRCRAFT
Safety recommendation(s), A-84-65
[REPT-3908] 14 p2216 N85-23743

BOEING 737 AIRCRAFT
Full-scale testing, production and cost analysis data for the advanced composite stabilizer for Boeing 737 aircraft. Volume 1: Technical summary
[NASA-CR-3649] 05 p0612 N85-13912
Design, ancillary testing, analysis and fabrication data for the advanced composite stabilizer for Boeing 737 aircraft. Volume 1: Technical summary
[NASA-CR-3648] 05 p0612 N85-13913
Design, ancillary testing, analysis and fabrication data for the advanced composite stabilizer for Boeing 737 aircraft, volume 2
[NASA-CR-166011] 05 p0612 N85-13914
Full-scale testing, production and cost analysis data for the advanced composite stabilizer for Boeing 737 aircraft, volume 2
[NASA-CR-166012] 05 p0613 N85-13915
A preliminary evaluation of a failure detection filter for detecting and identifying control element failures in a transport aircraft
[NASA-TM-87576] 24 p4067 N85-35204

BOEING 747 AIRCRAFT
The orbiter mate/demate device
08 p1103 N85-16972
Simultaneous cabin and ambient ozone measurements on two Boeing 747 airplanes. Volume 3: October 1978 - July 1979
[NASA-TM-86683] 12 p1892 N85-21872

BOEING 767 AIRCRAFT
What pilots like (and don't like) about the new cockpit technology 05 p0710 N85-14554

BOGS
U MARSHLANDS

BOILERS
The effects of microstructure on the temper embrittlement susceptibility of a Cr-2-1/4 1Mo forging
[AERE-R-11110] 03 p0334 N85-12151
Actual versus design performance of solar systems in the National Solar Data Network
[DE85-001190] 09 p1344 N85-18456
Weldability and mechanical property characterization of weld clad alloy 800H tubesheet forging
[DE85-001737] 11 p1609 N85-20116
Carbon granule probe microphone for leak detection — recovery boilers
[NASA-CASE-NPO-16027-1] 12 p1849 N85-21597
Steam generator tube vibration tests
[DE85-003599] 12 p1867 N85-21712
The use of heat pumps in district heat supply
[BLL-OA-TRANS-2728-(6196.3)] 16 p2781 N85-27163
Erosion of corrosion-resistant surface treatments on alloy steels
[DE85-008446] 17 p2932 N85-28100
Current status of TVA's atmospheric fluidized bed combustion development efforts
[DE85-901209] 19 p3308 N85-30507
Control system for fluid heated steam generator
[DE85-005734] 23 p3939 N85-34417
Calculations on the feasibility of ultrasonic inspection of steam generator tubing in pressurized water reactors
[AERE-R-10960] 23 p3940 N85-34419
Computer code calculations of the TMI-2 accident: Initial and boundary conditions
[DE85-012613] 24 p4140 N85-35666

BOILING
NT FILM BOILING
NT NUCLEATE BOILING
Time resolved calorimetry of 30 nm Te-films during laser annealing
[AD-A145047] 01 p0052 N85-10346
Method for making alloy additions to base metals having higher melting points
[AD-D011403] 07 p0928 N85-15884
Review of anode phenomena in vacuum arcs
[DE85-002736] 12 p1926 N85-22101
Effects of temperature variation among droplets in an evaporating fuel spray 13 p2004 N85-22562
Spacecraft, straight-tube evaporator design
[AD-A154462] 19 p3226 N85-30003
An experimental apparatus to study nucleate pool boiling of R-114 and oil mixtures
[AD-A154077] 19 p3265 N85-30249
Two-phase flow visualization in a transparent, atmospheric pressure, boiling water loop
[DE84-016857] 21 p3586 N85-32288
Effects of ambient pressure on the instability of a liquid boiling explosively at the superheat limit
[DE85-009476] 23 p3932 N85-34370

BOILING WATER REACTORS
Stress corrosion of pressure vessel steel A533-B in high temperature water
[BLL-RISLEY-TR-4600-(9091.9F)] 03 p0330 N85-12125
Deterministic sensitivity analysis of two-phase flow systems: Forward and adjoint methods
[DE84-016276] 04 p0499 N85-13185
Steel containment buckling
[DE85-003744] 13 p2103 N85-23111
Inspection evaluation and repair of the flawed feedwater nozzle of the 50 MWe Dodewaard GKN boiling water reactor
[ISBN-90-353-0017-3] 17 p2977 N85-28394
Graphic display development program, volume 1
[DE85-011076] 19 p3333 N85-30649
Advanced ultrasonic imaging of piping in Dresden and Vermont Yankee reactors
[TI85-010049] 20 p3464 N85-31520
Technical assessment of thermal-hydraulics for high heat flux fusion components
[DE85-013178] 23 p3930 N85-34359
Response of a BWR Mark 2 containment vessel head to loads beyond the design basis
[DE85-010524] 24 p4103 N85-35432

BOLIVIA
A silicic shield volcano in Bolivia
13 p2187 N85-23572

BOLKOW AIRCRAFT
NT BO-105 HELICOPTER

BOLOGRAMS
U BOLOMETERS

BOLOMETERS
Thick film radiation detector
[AD-D011211] 01 p0048 N85-10318
Physics and design of advanced infrared bolometers and photoconductors
[DE84-016663] 04 p0503 N85-13213
Imaging polarimeter-interferometer arrays for Tokamak measurements
[DE84-015916] 05 p0730 N85-14693
Fast granular superconducting bolometer
[AD-D011332] 07 p0961 N85-16093

Infrared technology for satellite power conversion --- antenna arrays and bolometers
[NASA-CR-174268] 07 p0991 N85-16293
The mechanical procedures for the 8 channal bolometer — United Kingdom Infrared Telescope
[UKIRT-18] 09 p1414 N85-18916
BIG MAC: A bolometer array for mid-infrared astronomy, Center Director's Discretionary Fund
[NASA-TM-86502] 13 p2170 N85-23483

BOLTS
Measurement of the preloading of bolted joints by the ultrasonic method
[CETIM-1-5H-38-6] 04 p0558 N85-13556
Hydraulic locking boltwork system
[AD-D011299] 06 p0815 N85-15174
Corrosion of aircraft Al and Al-Zn ion plated steel fasteners 13 p2021 N85-22666
Three-dimensional finite element failure model for predicting failure in fibre reinforced bolted joints
[BR94778] 23 p3940 N85-34423
Stresses and strains in a plate resulting from two closely-spaced interference-fit fasteners
[ARL/STRUC-TM-409] 23 p3941 N85-34429
Results of tests of MTA-2 TPS on the SRB hold-down bolt blast container
[NASA-CR-170891] 24 p4070 N85-35224

BOLTZMANN DISTRIBUTION
Loeb solutions of the Boltzmann equation with initial boundary values and external forces
[CTH-MATH-1984-23] 05 p0719 N85-14616
Theoretical foundations of turbulent flows 21 p3683 N85-32880
Time-resolved spectroscopic studies of detonating heterogeneous explosives
[DE85-009760] 23 p3921 N85-34297

BOLTZMANN TRANSPORT EQUATION
Solution of the Boltzmann transport equations for a permeable base transistor
[AD-A144969] 01 p0112 N85-10757
The Boltzmann equation: Global existence for a rare gas in an infinite vacuum
[PREPRINT-78] 01 p0124 N85-10851
Equations of plasma transport in a curved magnetic field
[DE84-015625] 05 p0730 N85-14690
A linear characteristic-nodal transport method for the two-dimensional (X,Y)-geometry multigroup discrete ordinates equations over an arbitrary triangle mesh
[LA-10092-T] 12 p1913 N85-22006
User's guide for TWODANT: A code package for two-dimensional, diffusion-accelerated, neutral-particle transport
[LA-10049-M] 12 p1913 N85-22009
User's guide for TWOHEX: A code package for two-dimensional, neutral-particle transport in equilateral triangular meshes
[DE85-004482] 12 p1930 N85-22125
Semiconductor materials for high frequency solid state sources
[AD-A150020] 12 p1940 N85-22186
The transport of neutral H, D, T and He and O in the boundary layers of a Tokamak plasma
[REPT-84-153] 17 p3041 N85-28817
Direct simulation techniques for the Boltzmann equation
[DFVLR-FB-85-13] 20 p3457 N85-31470

BOLTZMANN-VLASOV EQUATION
Covariant Poisson brackets for classical fields
[DE85-010085] 16 p3171 N85-29654

BOMBER AIRCRAFT
NT B-1 AIRCRAFT
NT B-70 AIRCRAFT
Avionics Integrity Program (AvIp). Volume 2: Hardware case studies
[AD-A145689] 02 p0139 N85-10944
The effect of load factor on aircraft handling qualities
[AD-A152118] 16 p2710 N85-26724
The introduction of new cockpit technology: A human factors study
[NASA-TM-86659] 16 p2843 N85-27528
Electronic reconnaissance aircraft of the Soviet Union Navy
[AD-A154706] 21 p3551 N85-32091
Maintenance and the military environment 22 p3750 N85-33243

BOMBING EQUIPMENT
System for radio remote control of dropping bombs
[CH-639335-A5] 15 p2491 N85-25371

BOMBS (ORDNANCE)
A two-step bomb to determine the inflammability of propellant charge powders
[ISL-CO-211/83] 14 p2264 N85-24026
Components of the combustion gases of propellant charge powders after reaction in the high pressure bomb in the pressure range up to 1000 MPa. Part 1: Nitroglycerine powder GB Pa 125
[ISL-CO-217/83-PT-1] 14 p2264 N85-24027
Optmizing the specifications for an air-surface laser system 16 p2696 N85-26644

BOMBS (PRESSURE GAGES)
U PRESSURE GAGES

BOMBS (SAMPLERS)
U SAMPLERS

BONDING
NT ADHESIVE BONDING
NT AGGLUTINATION
NT CERAMIC BONDING
NT EXPLOSIVE WELDING
NT METAL BONDING
NT METAL-METAL BONDING
NT REACTION BONDING
Optical contacting for gravity probe star tracker
[NASA-TM-86475] 01 p0120 N85-10819
Growth and magnetic investigations of single crystals of intermetallic compounds of rare earths and uranium — magnetic properties 03 p0425 N85-12712
Contamination problems during surface cleaning for thermocompression bonding
[DE84-013066] 04 p0475 N85-13023
Method for bonding insulator to insulator
[AD-D011340] 07 p0929 N85-15891
Insulation bonding test system
[NASA-CASE-MFS-25662-1] 11 p1610 N85-20126
Infrared-thermal wave scanner for NDE of naval thermal spray coatings
[DE85-002237] 11 p1650 N85-20391
Amine salts as bonding agents
[AD-D011543] 12 p1817 N85-21396
Activation of Si-N modes in silicon by pulsed laser annealing
[DE85-003968] 13 p2097 N85-23082
Multiple scattering effects in low energy alkali ion scattering: Application to the analysis of adsorbate ordering and bonding geometry
[DE85-007575] 17 p3032 N85-28757
Method for ultrasonic bonding to soft microelectronic substrates
[NASA-CASE-NPO-16087-1] 18 p3094 N85-29151
Ultrasonic test evaluation of the insert bond on hermetic connectors
[DE85-008394] 18 p3120 N85-29310
X-ray photoelectron spectroscopy study of the compatibility of the explosive PETN with candidate plastic bonding materials
[DE85-010804] 19 p3251 N85-30161
STPI/LARC: A 200 deg C polyimide adhesive
[NASA-TM-86447] 20 p3433 N85-31297
EVA-glass interface bond stability 21 p3608 N85-32408
Non-bonded ultrasonic transducer
[DE85-011006] 22 p3794 N85-33504
Dynamic compaction of a monosized spherical tungsten powder
[DE85-014808] 24 p4080 N85-35289
Ionic crystals
[DE85-009482] 24 p4163 N85-35809

BONE DEMINERALIZATION
Bone structure and microgravity 05 p0694 N85-14463
Loss of bone substance in consequence of amputation as a model for the adaptation to microgravity 05 p0694 N85-14464
Structural development and gravity 15 p2608 N85-26071
Evidence that resorption of bone by rat peritoneal macrophages occurs in an acidic environment 15 p2612 N85-26098
Changes in bone structure and metabolism during simulated weightlessness: Endocrine and dietary factors
[NASA-CR-175961] 18 p3153 N85-29521
The role of 1,25-dihydroxyvitamin D in the inhibition of bone formation induced by skeletal unloading
[NASA-TM-87480] 18 p3153 N85-29522
Rat bone tissue after flight aboard Cosmos-1129 biosatellite 19 p3324 N85-30593

BONE MARROW
Addendum to the STCAL and LTCAL user's guide
[NASA-CR-171880] 15 p2628 N85-26194
Mammalian tissue sensitivity to long-term exposure to high-intensity stationary magnetic fields 22 p3823 N85-33686

BONE MINERAL CONTENT
Actual and simulated weightlessness inhibit osteogenesis in long bone metaphysis by different mechanisms 15 p2608 N85-26074
Evidence that resorption of bone by rat peritoneal macrophages occurs in an acidic environment 15 p2612 N85-26098
Rat bone tissue after flight aboard Cosmos-1129 biosatellite 19 p3324 N85-30593

BONES
NT CEREBRUM
NT FEMUR
NT MARROW
NT PELVIS
NT SCIATIC REGION
NT SKULL
NT VERTEBRAE
Effect of 1,25-dihydroxycholecalciferol and 24,25 dihydroxycholecalciferol on growth and alteration of rat bones during hypokinesa (histomorphometric study) 01 p0092 N85-10622
Vitamin K and the metabolic state of bone 05 p0694 N85-14465
Polyactic-polyglycolic acid copolymer combined with decalcified freeze-dried bone for use as a bone repair material
[AD-D011438] 10 p1451 N85-19142
Distribution of radium and plutonium in human bone
[DE85-005025] 13 p2142 N85-23296
Structural development and gravity 15 p2608 N85-26071
The role of vitamin D in the bone changes associated with simulated weightlessness 15 p2608 N85-26072
The salutary effect of dietary calcium on bone mass in a rat model of simulated weightlessness 15 p2608 N85-26073
Quantitative alterations in the function of bone forming cells due to reduced weight bearing 15 p2609 N85-26075
Evidence that resorption of bone by rat peritoneal macrophages occurs in an acidic environment 15 p2612 N85-26098
Addendum to the STCAL and LTCAL user's guide
[NASA-CR-171880] 15 p2628 N85-26194
Histological and compositional responses of bone to immobilization and other experimental conditions
[NASA-CR-175837] 16 p2841 N85-27518
Changes in bone structure and metabolism during simulated weightlessness: Endocrine and dietary factors
[NASA-CR-175961] 18 p3153 N85-29521
Rat bone tissue after flight aboard Cosmos-1129 biosatellite 19 p3324 N85-30593
Mechanisms of osteodystrophy in weightlessness 22 p3733 N85-33143
Report of the NASA Mammalian Developmental Biology Working Group 24 p4126 N85-35581

BOOLEAN ALGEBRA
NT BOOLEAN FUNCTIONS
Boolean approach to zero-one linear programming
[DE84-016654] 04 p0550 N85-13498
Minimal cut-set methodology for artificial intelligence applications
[DE84-016674] 04 p0553 N85-13518
Investigation of three-dimensional mesh generation with precise controls
[AD-A148759] 09 p1374 N85-18836
Synthesis of tests for programmable logic arrays 22 p3777 N85-33408

BOOLEAN FUNCTIONS
Comparison analysis of algorithm for construction of functional tests for combined large-scale integrated circuits 04 p0490 N85-13121
Priority rewrite systems --- computer programming
[CWI-CS-R8407] 05 p0720 N85-14621
Efficient VLSI (Very Large Scale Integration) fault simulation
[AD-A152661] 17 p2953 N85-28233
An analysis and algorithm for filling propagation 23 p3961 N85-34551
EPALIT: A data management system applied to the control and retrieval of technical reports
[PB85-193068] 24 p4186 N85-35828

BOOMS (EQUIPMENT)
F-8 refueling boom ground vibration test
[NASA-TM-84914] 07 p0902 N85-15713
Extended moment arm anti-spin device
[NASA-CASE-LAR-12979-1] 12 p1776 N85-21147
Modeling and analysis of pinhole occulter experiment: initial study phase
[NASA-CR-175978] 19 p3272 N85-30287
Environmental background measurement program
[AD-A153860] 19 p3319 N85-30577
The Galileo spacecraft magnetometer boom 22 p3796 N85-33513

BOOST
U ACCELERATION (PHYSICS)

BOOSTER RECOVERY
Structural and mechanical design challenges of space shuttle solid rocket boosters separation and recovery subsystems 08 p1095 N85-16917
Solid rocket booster retrieval operations 08 p1096 N85-16928

BOOSTER ROCKET ENGINES
Structural and mechanical design challenges of space shuttle solid rocket boosters separation and recovery subsystems 06 p1095 N85-16917
External tank processing from barge to pad 08 p1096 N85-16927
Solid rocket booster retrieval operations 08 p1096 N85-16928
Thermal design of the space shuttle solid rocket booster 08 p1103 N85-16976
Verification of the SRB motor case pin retainer band lips
[NASA-CR-170882] 24 p4070 N85-35220
Results of tests of MTA-2 TPS on the SRB hold-down bolt blast container
[NASA-CR-170891] 24 p4070 N85-35224
Evaluation of SRB phenolic TPS material made by an alternate vendor
[NASA-CR-170894] 24 p4073 N85-35240
Space shuttle SRB TPS protective paint test and evaluation in NASA Hot Gas Facility and AEDC Tunnel C
[NASA-CR-170884] 24 p4081 N85-35294
Results of tests of Insta-Foam Thermal Protection System (TPS) material for protection of equipment inside the SRB aft skirt
[NASA-CR-170892] 24 p4081 N85-35295
BOOTS (FOOTWEAR)
The energy cost of women walking and running in shoes and boots
[AD-A151022] 14 p2389 N85-24716
BORANES
NT CARBORANE
New synthetic routes to boron cage compounds
[AD-A153554] 18 p3071 N85-28991
BORATES
NT LITHIUM BORATES
Glass corrosion in liquid lithium
[DE85-002086] 09 p1299 N85-18162
Luminescence and absorption of indium-activated potassium-borate glasses subjected to high-power excitation 21 p3681 N85-32868
BORAZON (TRADEMARK)
U BORON NITRIDES
BOREDOM
Study of bodily functional status and quality of controlling action of power unit operators with various intensities of labor 09 p1362 N85-18589
BOREHOLES
The Midway Atoll coral cap: Meteoric diagenesis, amplitude of sea-level fluctuation and dolomitization 09 p1351 N85-18499
On the stress analysis of bonded inserts
[ARL/STRUC-R-407] 12 p1865 N85-21698
The residual strength of cracked specimens representing a section of the mirage into wing main spar
[ARL/STRUC-R-408] 12 p1865 N85-21699
Experimental stiffness of tapered bore seals
[NASA-TM-86978] 15 p2568 N85-25847
Analysis of the elastic and strength properties of Yucca Mountain tuff, Nevada
[DE85-006975] 19 p3300 N85-30460
Preliminary evaluation of alterant geophysical tomography in welded tuff
[DE85-010826] 19 p3302 N85-30469
Physical and chemical changes to rock near electrically heated boreholes at Spent Fuel Test-Climax
[DE85-010834] 19 p3302 N85-30472
Shear wave transducer for boreholes
[DE85-011662] 22 p3787 N85-33461
Generation of round bores in composite structure railguns
[DE85-011872] 22 p3793 N85-33501
Fracture detection and characterization for geothermal reservoir definition
[DE85-006677] 22 p3815 N85-33630
Lithology and stratigraphy of drill holes completed during 1984 in LANL use areas of Yucca Flat, Nevada Test Site, volume 6
[DE85-010695] 22 p3815 N85-33631
Design analysis for a repository in crystalline rock
[DE85-011602] 22 p3839 N85-33771
Iron and manganese in oxide minerals and in glasses: Preliminary consideration of Eh buffering potential at Yucca Mountain, Nevada
[DE85-011892] 23 p3916 N85-34271
BOREL SETS
Measure determining classes of balls in Banach space
[CTH-MATH-1984-14] 04 p0556 N85-13541
Schubert varieties are arithmetically Cohen-Macaulay 16 p2853 N85-27592
BORES
U CAVITIES
BORESIGHT ERROR
Electromagnetic analysis of radomes by the moment method
[AD-P004351] 12 p1824 N85-21445
Generalized radome BSE (radome boresight error) characterization using superposition techniques
[AD-P004354] 12 p1825 N85-21448
A subaperture approach to the calculation of flashlobes introduced by airborne radomes
[AD-P004355] 12 p1825 N85-21449
Near-field effects on radome boresight errors
[AD-P004356] 12 p1825 N85-21450
Automated radome testing
[AD-P004362] 12 p1826 N85-21456
Hot radome boresight error measurements
[AD-P004364] 12 p1826 N85-21458
Ziv-Zakai bound applied to an amplitude-comparison monopulse radar
[AD-A151937] 16 p2773 N85-27118
BORIDES
NT CHROMIUM BORIDES
NT TITANIUM BORIDES
High temperature thermoelectric energy conversion 05 p0610 N85-13894
Vapor pressure and evaporation rate of certain heat-resistant compounds in a vacuum at high temperatures
[NASA-TM-77807] 10 p1434 N85-19036
A program to develop thermite reactions to produce refractory borides and carbides
[AD-A148972] 10 p1434 N85-19037
Pressed boride cathodes
[NASA-TM-77821] 17 p2918 N85-27984
Consortium program for the study of boron-rich borides
[DE85-011378] 22 p3752 N85-33260
Magnitude and range of the RKKy interaction in SmRh4B4
[DE85-012284] 23 p3985 N85-34712
BORING MACHINES
Report on high-precision jig-boring machines 01 p0035 N85-10215
BORN APPROXIMATION
Plane-wave born collision strengths for electron-ion excitation: Comparison with other theoretical methods
[DE85-002348] 10 p1555 N85-19602
Vacancy-rearrangement theory in the first Magnus approximation
[DE85-004435] 12 p1930 N85-22123
Born inversion with a stratified reference velocity
[AD-A149222] 16 p2853 N85-27594
BORN-MAYER EQUATION
U BORN APPROXIMATION
BORON
NT BORON FIBERS
NT BORON 10
Effects of cobalt, boron, and zirconium on the microstructure of Udimet 738
[NASA-CR-174782] 01 p0027 N85-10166
The determination of soluble and insoluble boron in steel by emission spectrometry using an inductively coupled plasma and a scanning monochromator 02 p0180 N85-11211
A study of precipitation and boron distribution in 20 Cr 25Ni base stainless steels
[AERE-M-3353] 03 p0334 N85-12154
Boron cosmochemistry 06 p0688 N85-15642
Fuel-rich solid propellant boron combustion
[AD-A148522] 06 p1136 N85-17157
CVD boron on calcium chromate powder
[DE85-000214] 09 p1299 N85-18158
An infrared study of the hydrogenation of carbon dioxide on supported rhodium catalysts
[AD-A149477] 10 p1436 N85-19049
Study of phase composition of Al-B plasma coatings 11 p1598 N85-20050
Research on the basic understanding of high efficiency in silicon solar cells
[DE85-000507] 11 p1672 N85-20537
Theoretical studies on N-bonded pyrazole derivatives of boron
[AD-A150036] 12 p1813 N85-21374
Status of boron combustion research 13 p1998 N85-22528
Gasification of boron oxide drops and boron slurry agglomerates in combustion gases 13 p1999 N85-22529
Technological process effect on the carrier lifetime degradation of silicon solar cell base layer irradiated by 1 MeV electrons (boron doping case) 13 p2007 N85-22585
Annealing of radiation damage in boron and gallium doped silicon solar cells 13 p2012 N85-22624
Weldability of Ni3Al-type aluminide alloys
[DE85-006932] 15 p2512 N85-25496
Effect of nickel addition on the thermal, magnetic and magnetomechanical properties of Fe(80)B(15)Si(5)
[AD-A152281] 16 p2749 N85-28967
The influence of melting practice and of microalloying, with rare earth metals and with boron, on the quality of low-carbon steel
[BLL-BISI-22467-(9022.06)] 17 p2925 N85-28036
The conversion of smaller borane fragments to larger structures. Systematics of boron hydride reactions
[AD-A153443] 18 p3070 N85-28985
Status of boron combustion research
[AD-A154762] 21 p3563 N85-32160
Consortium program for the study of boron-rich borides
[DE85-011378] 22 p3752 N85-33260
Evaluation of low-temperature geothermal potential in Utah and Goshen Valleys and adjacent areas, Utah. Part 2: Water temperature and chemistry
[DE85-009344] 23 p3943 N85-34438
BORON ALLOYS
Copper-boron low alloy high strength steels 02 p0176 N85-11183
Radiation effects in amorphous metallic alloys
[DE84-014302] 04 p0475 N85-13025
Structural properties of amorphous metals by Raman scattering
[DE84-016947] 04 p0475 N85-13027
Electrical resistivity and structural changes upon relaxation and crystallization of (Mo/sub 0.6/Ru/sub 0.4)sub 100-x/B/sub x/ metallic glasses
[DE84-017281] 09 p1299 N85-18160
Kinetics of the formation of a complex alloyed boride coating on iron and its properties
[BLL-BISI-TRANS-22303-(9022.06)] 17 p2930 N85-28084
Examples of application of machinability tests
[BLL-BISI-TRANS-22346-(9022.06)] 17 p2973 N85-28363
Thermoelectric properties of beta-boron and some boron compounds
[DE85-011976] 21 p3582 N85-32270
BORON CARBIDES
Metallographic evaluation of the reactions between boronated graphite and Fe-Ni-Cr alloys
[DE84-015374] 06 p0769 N85-14922
Anomalous electronic transport in boron carbides
[DE84-015620] 06 p0668 N85-15518
Sintering reactions, structure and properties of a cobalt free nonconventional hard material
[DE85-007704] 18 p3076 N85-29025
TFCX shielding optimization
[DE85-010503] 19 p3359 N85-30626
Shield design for next-generation, low-neutron-fluence, superconducting tokamaks
[DE85-011409] 23 p3982 N85-34695
Elliptical X-ray analyzer spectrograph application to a laser-produced plasma
[DE85-013790] 24 p4097 N85-35396
BORON COMPOUNDS
NT BORANES
NT BORATES
NT BORIDES
NT BORON CARBIDES
NT BORON FLUORIDES
NT BORON HYDRIDES
NT BORON NITRIDES
NT BORON OXIDES
NT CARBORANE
NT CHROMIUM BORIDES
NT LITHIUM BORATES
NT TITANIUM BORIDES
The effect of temperature on the radiation induced losses of large diameter GPS (Germanium phosphosilicate) and GBS core optical fibers
[AD-A145409] 02 p0280 N85-11823
Boron-nitrogen polymers. 1: Mechanistic studies of borazine pyrolyses
[AD-A146470] 06 p0771 N85-14933
Thermoelectric properties of beta-boron and some boron compounds
[DE85-011976] 21 p3582 N85-32270
BORON FIBERS
Chemical modification of the surface of high modulus carbon fibers 04 p0467 N85-12967
Damage to boron fibers during thermal cycling and annealing 10 p1445 N85-19107
Effect of surface state on durability of aluminized boron fibers 19 p3244 N85-30115
BORON FLUORIDES
On the origins of structural defects in BF2(+)-implanted and rapid thermally annealed silicon: Conditions for defect free regrowth
[DE84-016060] 04 p0572 N85-13650
BORON HYDRIDES
NT BORANES
NT CARBORANE

Closed-bomb combustion of Hivelite-based, Very High Burn Rate (VHBR) propellant
[AD-A155740] 21 p3571 N85-32212
BORON ISOTOPES
NT BORON 10
BORON NITRIDES
The current status of diamond and cubic boron nitride composites 02 p0178 N85-11194
Boron-nitrogen polymers. 1: Mechanistic studies of borazine pyrolyses
[AD-A146470] 06 p0771 N85-14933
Tribological properties of boron nitride synthesized by ion beam deposition
[NASA-TM-86962] 12 p1810 N85-21355
BN coating of ceramic fibers for ceramic fiber composites
[AD-D011700] 19 p3249 N85-30145
Thermodynamics of high temperature materials
[AD-A154269] 19 p3378 N85-30958
BORON OXIDES
Method for removing oxide contamination from silicon carbide powders
[DE85-011648] 23 p3919 N85-34287
BORON REINFORCED MATERIALS
Experiences with implanted Back Surface Field (BSF) solar cells 13 p2005 N85-22571
Use of acoustical emission method to study specifics of fracture of boron reinforced plastic structural elements 13 p2026 N85-22696
Effect of operating medium on cyclic durability of AD33-W composite 13 p2029 N85-22716
BORON TRIFLUORIDE
U BORON FLUORIDES
BORON 10
Fast-neutron-spectrum measurements for the thick-target (9)Be(d/ = 7 MeV
[DE85-010481] 18 p3183 N85-29735
Spin dependence of the lamda-nucleus interaction determined by observation of hypernuclear gamma rays
[DE85-011878] 19 p3364 N85-30863
BOROSILICATE GLASS
Sealing ceramic material in low melting point glass
[NASA-TM-77599] 01 p0031 N85-10190
Structural evolution during the gel to glass conversion
[DE84-014954] 06 p0772 N85-14939
Effect of fatigue and thermal loads on silicon carbide fiber reinforced glass matrix composites
[DE85-006069] 15 p2503 N85-25441
Physical-chemical model for the mechanism of glass corrosion with particular consideration of simulated radioactive waste glasses
[DE85-007713] 17 p2935 N85-28121
Slow crack growth in metal reinforced glass composites
[DE85-010094] 18 p3062 N85-29064
Technical and historical overview of the study at Lawrence of porous antireflection coatings
[DE85-010925] 20 p3434 N85-31302
Thermal expansion of selected graphite reinforced polyimide-, epoxy-, and glass-matrix composite
[NASA-TM-87572] 21 p3561 N85-32149
BOSE-CHAUDHURI-HOCQUENGHEM CODES
U BCH CODES
BOSE-EINSTEIN STATISTICS
U QUANTUM STATISTICS
BOSONS
NT ALPHA PARTICLES
NT KAONS
NT LIGHT BEAMS
NT MESONS
NT MUONS
NT PHOTONS
NT PIONS
NT VECTOR MESONS
Sturmian expansion approximation to three-body scattering
[CSIR-TWISK-309] 01 p0109 N85-10731
Thin end of the wedge
[DE84-016439] 09 p1401 N85-18816
Cosmic axions
[DE85-001330] 09 p1418 N85-18944
Theoretical aspects of electroweak and other interactions in medium-energy nuclear physics
[DE85-003821] 13 p2157 N85-23392
Overview of the physics issues at the SSC
[DE85-007074] 16 p2859 N85-27834
Boson degrees of freedom in Fermion many-body systems
[DE85-006897] 16 p2863 N85-27860
Topics in intermediate vector boson physics
[NOTA-INTERNA-841] 18 p3184 N85-29743
Did bosonic sneutrino stars ever exist
[PREPRINT-421] 18 p3202 N85-29867
Boson-fermion symmetries in the W-Pt region
[DE85-009755] 19 p3362 N85-30845
The standard model and beyond
[DE85-010239] 19 p3362 N85-30847
New O(6) region near A = 130 and the interplay of triaxiality and gamma-softness in the IBA
[DE85-010957] 20 p3530 N85-31961
Exotic events of p bar p-collider: Excited quark or excited color boson? 21 p3691 N85-32930
Interacting Boson approximation
[DE85-003016] 22 p3837 N85-33756
Charge 4/3 leptons in cosmic rays
[HE-6.2-14] 24 p4212 N85-36150
BOTANY
NT GEOBOTANY
Botany facility, phase A study. Part 1: Executive summary — EURECA
[BF-DOC-10-VOL-1] 08 p1110 N85-17015
Botany facility phase A study. Core payload number 6 EURECA carrier, volume 1
[ESA-CR(P)-1978-VOL-1] 17 p2908 N85-27918
Botany facility phase A study. Core payload number 6 for EURECA carrier, volume 2
[BF-TD-DRD-03-VOL-2] 17 p2908 N85-27919
BOTTLES
Ten year environmental test of glass fiber/epoxy pressure vessels
[NASA-TM-87058] 19 p3231 N85-30034
BOUGUER LAW
Reduction to outside the atmosphere and statistical tests used in Geneva photometry 06 p1251 N85-17902
Aerosol multiple-scanning code, ASCAT
[LA-10045-MS] 12 p1823 N85-21440
Bouguer images of the North American craton 13 p2200 N85-23648
Optical stability, atmospheric transparency and aerosol absorption 19 p3297 N85-30442
Earth Albedo and the orbit of LAGEOS
[NASA-TM-86210] 21 p3558 N85-32131
BOULES
Ingot slicing machine and method
[NASA-CASE-NPO-15483-1] 12 p1857 N85-21650
BOUNDARIES
NT FLUID BOUNDARIES
NT FREE BOUNDARIES
NT GAS-SOLID INTERFACES
NT GRAIN BOUNDARIES
NT JET BOUNDARIES
NT LIQUID-LIQUID INTERFACES
NT LIQUID-SOLID INTERFACES
NT LIQUID-VAPOR INTERFACES
Metrological consequences of the hard optical boundary assumption
[PB84-223577] 01 p0121 N85-10627
Analysis of accretion and deletion at boundaries in dynamic scenes
[AD-A145944] 03 p0419 N85-12578
Multiple steady states for characteristic initial value problems
[NASA-CR-172486] 06 p0749 N85-14800
Deer control using 7 strand vertical fence 11 p1581 N85-19958
Numerical methods for tracking interfaces
[LA-9917-MS] 12 p1919 N85-22052
Thermal stability of static coronal loops: Part 1: Effects of boundary conditions
[NASA-CR-175495] 12 p1981 N85-22330
On meromorphic functions continuous on the Stollow boundary 15 p2633 N85-26232
On the boundary behaviour of a rotation automorphic function with finite spherical Dirichlet integral 15 p2634 N85-26238
Remarks of the maximal dilatation of the Beurling-Ahlfors extension 15 p2634 N85-26239
An IKBS approach to image understanding
[AD-A151992] 16 p2854 N85-27599
Transverse periodic boundary conditions in molecular dynamics with uniaxial strain shock waves
[DE85-006497] 16 p2863 N85-27656
Boundary to constructive solid geometry mappings: A focus on 2-D issues 17 p3004 N85-28570
Intermediate boundary conditions for LOD, ADI and approximate factorization methods
[NASA-CR-172591] 18 p3167 N85-29626
Mathematics of oil production
[DE85-011235] 19 p3267 N85-30261
Scaling differences between large interplate and intraplate earthquakes
[NASA-CR-176149] 23 p3948 N85-34467
A user-friendly computer-aided construction of boundaries 23 p3962 N85-34584
Dynamics of the penetration boundaries of solar protons during a strong magnetic storm
[SH-6.1-16] 23 p4046 N85-35089
Absorbing boundary conditions for exterior problems
[NASA-CR-177944] 24 p4142 N85-35676
BOUNDARY ELEMENT METHOD
Analysis of in-plane and out-of-plane ground motions using the boundary element method
[AD-A146229] 03 p0355 N85-12287
Boundary element methods in potential theory: Four lectures
[NPL-DITC-46/84] 05 p0718 N85-14804
Integral equation formulations in two dimensions 05 p0718 N85-14805
Applications of the simple-layer logarithmic potential 05 p0718 N85-14806
Applications of Green's boundary formula 05 p0718 N85-14807
Three-dimensional and axisymmetric problems 05 p0718 N85-14808
Element methods for calculation of sound fields
[RUB-IFM-MITT-41] 05 p0726 N85-14865
Transient dynamic solutions of some half space problems by the boundary element method 19 p3283 N85-30360
On the methods to determine the stress intensity factors in boundary element method 23 p3905 N85-34189
BOUNDARY LAYER CONTROL
NT POROUS BOUNDARY LAYER CONTROL
Hybrid laminar flow control study
[NASA-CR-165930] 02 p0137 N85-10933
Effect of upstream sidewall boundary layer removal on an airfoil test — conducted in Langley 0.3-m transonic cryogenic tunnel 03 p0313 N85-12019
Circulation control: A bibliography of DTNSRDC research and selected outside references: Update
[AD-A146966] 07 p0893 N85-15661
Improvement of Aerodynamic Performance Through Boundary Layer Control and High Lift Systems
[AGARD-CP-365] 08 p1068 N85-16771
An update of the Canada/USA augmentor-wing project 08 p1070 N85-16781
Aircraft drag reduction technology 08 p1070 N85-16782
Theoretical study of boundary-layer control 08 p1070 N85-16784
Drag reduction due to boundary-layer control by combined blowing and suction 08 p1070 N85-16785
Technology developments for laminar boundary layer control on subsonic transport aircraft 08 p1071 N85-16787
Shock/turbulent boundary layer interaction and its control 08 p1071 N85-16792
Active and passive shock/boundary layer interaction control on supercritical airfoils 08 p1072 N85-16795
Transonic shock interaction with a tangentially-injected turbulent boundary layer 08 p1072 N85-16796
Re-design of ARL/HLF (Heated Laminar Flow) body nose region
[AD-A150063] 12 p1846 N85-21585
Boundary layer control by transition fixing — conference
[DFVLR-MITT-84-17] 14 p2211 N85-23712
Boundary layer transition control for takeoff and landing configurations 14 p2211 N85-23714
Experiences with transition fixation in the high-speed regime at NLR 14 p2211 N85-23715
Transition fixing in the high speed range for the development of civil aircraft wings 14 p2211 N85-23716
Transition fixing on wings in industrial wind tunnels and associated problems 14 p2212 N85-23717
Transition fixing and simulation of high Reynolds number flow at transonic velocities 14 p2212 N85-23721
Numerical simulation of boundary layer excitation by surface heating/cooling
[NASA-CR-172575] 15 p2554 N85-25756
Three-Dimensional Boundary Layers
[AGARD-R-719] 15 p2558 N85-25784
Investigation to optimize the passive shock wave/boundary layer control for supercritical airfoil drag reduction
[NASA-CR-175788] 16 p2699 N85-26865
Numerical study of porous airfoils in transonic flow
[NASA-TM-86713] 17 p2892 N85-27826
Experiments on the influence of active walls on the initial amplitudes and growths of instability waves
[AD-A154830] 21 p3583 N85-32275
BOUNDARY LAYER EQUATIONS
Finite difference method for solving turbulent boundary layer equations 11 p1619 N85-20193
Low-dimensional behavior of the pattern formation Cahn-Hilliard equation
[DE85-003727] 12 p1922 N85-22072
Significance of the thin-layer Navier-Stokes approximation
[DE85-002630] 13 p2092 N85-23063
Three-Dimensional Boundary Layers
[AGARD-R-719] 15 p2558 N85-25784
Three-dimensional boundary layers: A report on work in Germany 15 p2559 N85-25786

Three-dimensional boundary layer research at NLR
15 p2559 N85-25787

Problems and opportunities with three-dimensional boundary layers — aircraft, missile, and ship components
15 p2559 N85-25789

Computational aerodynamics in designing aircraft
16 p2693 N85-26822

Boundary layer at moving cylinder surface
16 p2785 N85-27064

Boundary layer and parabolic flows
[DFVLR-FB-84-46] 17 p2960 N85-28285

On spectral multigrid methods for the time-dependent Navier-Stokes equations
[NASA-CR-172613] 19 p3344 N85-30725

BOUNDARY LAYER FLOW
NT BOUNDARY LAYER SEPARATION
NT REATTACHED FLOW
NT SECONDARY FLOW
NT SEPARATED FLOW

Measurement of the development of the boundary layer in the annulus walls of a fourstage compressor
[CUED/A-TURBO-TR-121] 01 p0046 N85-10299

Design and wind tunnel evaluation of a symmetric airfoil series for large wind turbine applications
[NASA-CR-174764] 02 p0135 N85-10919

Stability of heated boundary layers
02 p0196 N85-11311

Development in UK of a method for calculating tunnel wall corrections from flow measurements
03 p0314 N85-12026

Wall effects on the slow steady motion of a particle in a viscous incompressible fluid
[PREPRINT-828] 03 p0363 N85-12327

A local slot boundary condition for transonic flow calculations in slotted-wall test sections of wind tunnels
[FFA-TN-1984-34] 04 p0453 N85-12879

Incorporation of viscous-inviscid interactions in turbomachinery design
[PNR-90219] 04 p0457 N85-12897

Modelling viscous flow in turbomachinery
[PNR-90220] 04 p0457 N85-12898

Progress in the development of a two-fluid model of turbulence for near-wall flows, part 1
[CFD/84/7-PT-1] 04 p0501 N85-13196

Progress in the development of a two-fluid model of turbulence for near-wall flows. Part 3: Preliminary investigation of a stably-stratified boundary layer
[CFD/84/9-PT-3] 04 p0501 N85-13197

The resistance and mobility functions of two equal spheres in low Reynolds number flow
[AD-A147301] 07 p0959 N85-16060

Detailed study of the flow around a multi-element airfoil. Comparison with calculations 06 p1069 N85-16775

Application of two and three-dimensional criteria for calculating transitions and boundary layers over swept wings
08 p1070 N85-16783

Numerical modeling of steady, laminar free-convective boundary layer flow beneath heated or combusting horizonal surfaces
08 p1160 N85-17318

Simultaneous flow visualization and unsteady lift measurement on an oscillating lifting surface
[AD-P004157] 09 p1264 N85-17942

Can the singularity be removed in time-dependent flows?
[AD-P004165] 09 p1265 N85-17950

Preliminary results from the unsteady airfoil model USTAR2
[AD-P004171] 09 p1266 N85-17956

Leading edge separation criterion for an oscillating airfoil
[AD-P004175] 09 p1267 N85-17960

Natural unsteadiness of a separation bubble behind a backward-facing step
[AD-P004176] 09 p1267 N85-17961

Averaging effects in models of three-dimensional two-phase flows
[AD-A149313] 10 p1484 N85-19371

A three-dimensional spectral algorithm for simulations of transition and turbulence
[NASA-CR-172561] 12 p1845 N85-21575

Wind-tunnel research on the mechanics of plumes in the atmospheric surface layer
[AD-A150019] 12 p1846 N85-21584

Aerodynamic heating rate distributions induced by trailing edge controls on hypersonic aircraft configurations at Mach 6
[NASA-TM-87453] 13 p1969 N85-22370

Preliminary study of inphase gusts and moment force wind loads over the first 150 meters at KSC, Florida
[NASA-TM-86501] 13 p2137 N85-23273

Calculating isothermal flow in wake beyond injection zone
14 p2267 N85-24175

SAMBO-GEOS: Substorm trapped particle particle boundary movements, particle precipitation and acceleration
14 p2361 N85-24589

Wind tunnel wall interference
[AD-A151212] 15 p2474 N85-25273

Comparison of computational results of a few representative three-dimensional transonic potential flow analysis programs
16 p2693 N85-26828

A curved test section for research on transonic shock wave-boundary layer interaction
[VTH-LR-414] 16 p2701 N85-26682

Numerical solution of transonic normal shock wave-boundary layer interaction using the Bohning-Zierop model — wind tunnel flow
[VTH-LR-416] 16 p2701 N85-26683

Numerical analysis of flow non-uniformity in the hot gas manifold of the Space Shuttle main engine
16 p2736 N85-26899

Vortex studies relating to boundary layer turbulence and noise
[NASA-TM-87475] 16 p2782 N85-27169

A Navier-Stokes capillary free boundary in open boat crystal growth
[REPT-84-34] 17 p2960 N85-28283

Tidal rectification in lateral viscous boundary layers of a semienclosed basin
[CWI-AM-R8415] 17 p2960 N85-28284

Boundary layer and parabolic flows
[DFVLR-FB-84-46] 17 p2960 N85-28285

The transport of neutral H, D, T and He and O in the boundary layers of a Tokamak plasma
[REPT-84-153] 17 p3041 N85-28817

Combined riblet and LEBU drag reduction system
[NASA-CASE-LAR-13286-1] 18 p3058 N85-28922

An experimental investigation of curvature and freestream turbulence effects on heat transfer and fluid mechanics in transitional boundary layer flows
19 p3264 N85-30240

The application of laser anemometry to the study of transonic shock boundary-layer interactions
[ISL-CO-204/84] 20 p3396 N85-31067

Transition in a disturbed environment
20 p3452 N85-31436

On the solution for the sound field in a semi-infinite uniform duct with sheared mean flow
20 p3523 N85-31912

An evaluation of four methods of numerical analysis for two-dimensional airfoil flows
[AD-A155202] 21 p3552 N85-32098

A comparison of laser Doppler anemometry and probe measurements within the boundary layer of an airfoil at subsonic flow
[ISL-CO-219/84] 23 p3895 N85-34127

Adverse pressure gradient and separating turbulent boundary-layer flows: The effect of disequilibrium in initial conditions
24 p4059 N85-35155

Studies on effects of boundary conditions in confined turbulent flow predictions
[NASA-CR-3929] 24 p4093 N85-35371

BOUNDARY LAYER NOISE
U AERODYNAMIC NOISE
U BOUNDARY LAYERS

BOUNDARY LAYER PLASMAS

Some contributions to knowledge of the magnetospheric plasma by ISEE-1 investigators
14 p2354 N85-24546

Hot plasma and energetic particles in the Earth's outer magnetosphere: New understandings during the IMS
14 p2355 N85-24552

Satellite-borne electric field measurements with spherical double probes — ISEE satellites
14 p2356 N85-24558

Structure of the boundary layer for steady-state magnetopause reconnection
14 p2356 N85-24561

Electric fields in the plasma sheet and plasma sheet boundary layer
14 p2357 N85-24562

The ionospheric O+ streams in the magnetotail between 22 RE and 6 RE
14 p2360 N85-24582

SAMBO-GEOS: Substorm trapped particle particle boundary movements, particle precipitation and acceleration
14 p2361 N85-24589

Images of the Earth's aurora and geocorona from the Dynamics Explorer Mission
[NASA-CR-175863] 18 p3136 N85-29423

The temporal evolution of a small auroral substorm as viewed from high altitudes with Dynamics Explorer 1
[NASA-CR-176064] 20 p3493 N85-31718

Wave/particle interactions in the plasma sheet
[NASA-CR-171537] 20 p3547 N85-32072

BOUNDARY LAYER SEPARATION

Prediction of aerodynamic characteristics of fighter wings at high angles of attack
[AD-A145107] 01 p0003 N85-10017

An integral method for analyzing incompressible two dimensional turbulent boundary layers with separation
02 p0196 N85-11309

Approximate solution of a laminar flow over a flat plate with suction and pressure gradient
[AD-A145482] 02 p0198 N85-11321

Geometric characteristics of turbulent boundary layer separation upon action with direct shock wave in conical flows
02 p0269 N85-11755

Laminar and turbulent boundary layers in a plane of symmetry
[AD-A146261] 03 p0362 N85-12323

The role of freestream turbulence scale in subsonic flow separation
[NASA-CR-174172] 04 p0452 N85-12870

Surge and stall in centrifugal compressors
05 p0637 N85-14087

Investigation of phase separation models in RELAP 4/MOD 6
[OEFZS-4286] 05 p0638 N85-14093

Unsteady flow characteristics in the near-wake of a two-dimensional obstacle
[NASA-TM-77762] 07 p0897 N85-15684

Some important problems in unsteady boundary layers including separation. 2: Unsteady boundary layers close to the stagnation region of slender bodies
[AD-A146964] 07 p0958 N85-16069

Some important problems in unsteady boundary layers including separation. 1: Nature of singularity on oscillating airfoils
[AD-A147897] 07 p0960 N85-16067

Drag reduction due to boundary-layer control by combined blowing and suction 08 p1070 N85-16785

Pneumatic turbulators: A device for drag reduction at Reynolds numbers below 5 million
08 p1071 N85-16791

Prediction of dynamic stall characteristics using advanced nonlinear panel methods
[AD-P004160] 09 p1264 N85-17945

Some structural features of unsteady separating turbulent shear flows
[AD-P004164] 09 p1265 N85-17949

On the shedding of vorticity at separation
[AD-P004166] 09 p1265 N85-17951

Genesis of unsteady separation
[AD-P004173] 09 p1266 N85-17958

Flow separation induced by periodic aerodynamic interference
[AD-P004174] 09 p1266 N85-17959

Numerical approach for the aerodynamic analysis if airfoils with laminar separation
[NASA-CR-172496] 09 p1273 N85-18001

Laminar separation bubble with transition: Prediction test with local interaction — airfoils
[PNR-90231] 09 p1274 N85-18008

Experimental studies of Quasi-Two-Dimensional and three-dimensional viscous interaction regions induced by skewed-shock and swept-shock boundary layer interactions
[AD-A150080] 12 p1847 N85-21587

Double and inverse Taylor-Hogg vortices in a stratified ocean
13 p2108 N85-23137

The structure of separated flow regions occurring near the leading edge of airfoils, including transition
[NASA-CR-175670] 14 p2209 N85-23703

Application possibilities of laser Doppler anemometry in the investigation of the transonic interaction between shock wave and boundary layer
[ISL-R-131/83] 14 p2304 N85-24265

Low-speed aerodynamic test of an axisymmetric supersonic inlet with variable cowl slot
[NASA-TM-87039] 16 p2708 N85-26710

Structural stability and bifurcation in conical flow fields
[VTH-LR-424] 16 p2803 N85-27262

An experimental investigation of a turbulent junction vortex
[NASA-CR-175915] 17 p2957 N85-28259

Proceedings of the 9th US Air Force and the Federal Republic of Germany Data Exchange Agreement Meeting, Viscous and Interacting Flow Field Effects
[AD-A153020] 17 p2958 N85-28266

Turbulence structure in the boundary layers of an oscillating airfoil
[AD-A153631] 18 p3059 N85-28926

A study of aerodynamic control in stalled flight long laminar separation bubble analysis
[AD-A153850] 18 p3059 N85-28930

Effect of leading-edge load constraints on the design and performance of supersonic wings
[NASA-TP-2446] 19 p3213 N85-29923

Two approaches for the prediction of plume-induced separation
[AD-A154098] 19 p3215 N85-29935

SANDRAG: A computer code for predicting drag of bodies of revolution at zero angle of attack in incompressible flow
[DE85-011170] 19 p3338 N85-30684

Two-dimensional separation in an incompressible fluid — boundary layer separation
[ONERA-RTS-16/3232-RY-060-R]
20 p3456 N85-31459

An evaluation of four methods of numerical analysis for two-dimensional airfoil flows
[AD-A155202] 21 p3552 N85-32098

Experimental investigations on airfoils with different geometries in the domain of high angles of attack-flow separation
[NASA-TM-77892] 22 p3728 N85-33110

Modelling of unsteady, incompressible separation on an aerofoil using an inviscid flow algorithm
[GU-AERO-8412] 23 p3894 N85-34122

Study of boundary layer separation on a supercritical profile with a spoiler by means of a laser Doppler velocimeter
[ISL-CO-225/84] 23 p3895 N85-34128

Computation of three-dimensional shock wave and boundary-layer interactions
[NASA-TM-86780] 24 p4093 N85-35372

BOUNDARY LAYER STABILITY

Stability of heated boundary layers
02 p0196 N85-11311

On the instability of a 3-dimensional attachment line boundary layer: Weakly nonlinear theory and a numerical approach
[NASA-CR-172504] 07 p0957 N85-16063

Perturbation of a multiple eigenvalue in the Benard problem for two fluid layers
[AD-A149068] 10 p1546 N85-19745

The unsteady boundary layer on an elliptic cylinder following the impulsive onset of translational and rotational motion — dynamic stall 14 p2209 N85-23699

Generation and development of small-amplitude disturbances in a laminar boundary layer in the presence of an acoustic field
[NASA-TM-77826] 14 p2299 N85-24237

Stability of an oscillating boundary layer
[NASA-TM-77827] 14 p2299 N85-24238

Convective instability of horizontal layer of binary mixture 14 p2338 N85-24458

Structural stability and bifurcation in conical flow fields
[VTH-LR-424] 16 p2603 N85-27282

Application of the MHD energy principle to magnetostatic atmospheres
[NASA-CR-175967] 16 p3136 N85-29420

A survey of wind and turbulence modeling methods
[AD-A154470] 20 p3496 N85-31733

Mesoscale features and atmospheric refraction conditions of the Arctic marginal ice zone
[AD-A155139] 21 p3636 N85-32584

Development of artificially produced perturbations in supersonic boundary layer 21 p3683 N85-32879

BOUNDARY LAYER TRANSITION

A review and analysis of boundary layer transition data for turbine application
[NASA-TM-86880] 01 p0047 N85-10306

Natural laminar flow airfoil design considerations for winglets on low-speed airplanes
[NASA-CR-3853] 04 p0452 N85-12863

Experiments on the structure of turbulent reattaching flow 05 p0635 N85-14074

Application of two and three-dimensional criteria for calculating transitions and boundary layers over swept wings 08 p1070 N85-16783

Orbiter entry aerothermodynamics
08 p1104 N85-16978

Aerothermal tests of a 12.5 percent cone at Mach 6.7 for various Reynolds numbers, angles of attack and nose shapes — conducted in Langley 8-foot high temperature tunnel
[NASA-TP-2345] 08 p1161 N85-17322

Research done at DERAT (October 1982 through September 1983); summary of principal results obtained
[NASA-TM-77786] 08 p1228 N85-17730

Laminar separation bubble with transition: Prediction test with local interaction — airfoils
[PNR-90231] 09 p1274 N85-18008

Flight-measured laminar boundary-layer transition phenomena including stability theory analysis
[NASA-TP-2417] 12 p1771 N85-21118

Skin friction measurements for 2 relatively thick airfoil sections at high Reynolds number
[AD-A150021] 12 p1772 N85-21125

Re-design of ARL/HLF (Heated Laminar Flow) body nose region
[AD-A150083] 12 p1846 N85-21585

Hydrodynamic stability problem formulated by numerical solutions of the Navier-Stokes equations
12 p1946 N85-22223

Boundary layer control by transition fixing — conference
[DFVLR-MITT-84-17] 14 p2211 N85-23712

Boundary layer transition control for takeoff and landing configurations 14 p2211 N85-23714

Experiences with transition fixation in the high-speed regime at NLR 14 p2211 N85-23715

Transition fixing in the high speed range for the development of civil aircraft wings
14 p2211 N85-23716

Transition fixing on wings in industrial wind tunnels and associated problems 14 p2212 N85-23717

The influence of transition strips on the pressure distribution on transonic profiles
14 p2212 N85-23718

Development of an artificial boundary layer for different outlet flows 14 p2212 N85-23719

Investigation of the conditions for tripping transition with roughness elements and their influence on boundary layer development 14 p2212 N85-23720

Transition fixing and simulation of high Reynolds number flow at transonic velocities 14 p2212 N85-23721

Transition detection using surface pressure holes
14 p2212 N85-23722

Investigations of the experimental detection of boundary layer transitions 14 p2213 N85-23723

Three-dimensional boundary layers and shear flows activities at ONERA/CERT 15 p2558 N85-25785

Brief review of current work in the UK on three dimensional boundary layers 15 p2559 N85-25788

On the effect of wing taper and sweep direction on leading edge transition
[CA-8435] 17 p2892 N85-27827

An experimental investigation of curvature and freestream turbulence effects on heat transfer and fluid mechanics in transitional boundary layer flows
19 p3264 N85-30240

Transition in Turbines
[NASA-CP-2386] 20 p3452 N85-31433

Experimental observation of transition behavior on a flat plate 20 p3452 N85-31437

Flat-plate transition 20 p3452 N85-31438

Heat transfer and fluid mechanics measurements in transitional boundary layer flows
20 p3453 N85-31439

A review and analysis of boundary layer transition data for turbine application 20 p3453 N85-31440

Bypass transition to turbulence and research Desiderata 20 p3453 N85-31442

Slow tearing modes: Transitions to instability
20 p3534 N85-31989

Development of a temperature-compensated hot-film anemometer system for boundary-layer transition detection on high-performance aircraft
[NASA-TM-86732] 22 p3730 N85-33121

Nozzle wall roughness effects on free-stream noise and transition in the pilot low-disturbance tunnel
[NASA-TM-86389] 23 p3930 N85-34355

BOUNDARY LAYERS

NT ATMOSPHERIC BOUNDARY LAYER
NT COMPRESSIBLE BOUNDARY LAYER
NT HYPERSONIC BOUNDARY LAYER
NT INCOMPRESSIBLE BOUNDARY LAYER
NT LAMINAR BOUNDARY LAYER
NT PLANETARY BOUNDARY LAYER
NT SUPERSONIC BOUNDARY LAYERS
NT THERMAL BOUNDARY LAYER
NT THREE DIMENSIONAL BOUNDARY LAYER
NT TURBULENT BOUNDARY LAYER
NT TWO DIMENSIONAL BOUNDARY LAYER

Prediction of aerodynamic characteristics of fighter wings at high angles of attack
[AD-A145107] 01 p0003 N85-10017

The development of a diode laser Doppler velocimeter for boundary layer measurements under ice: A feasibility investigation
[AD-A145076] 01 p0053 N85-10348

Effect of upstream sidewall boundary layer removal on an airfoil test — conducted in Langley 0.3-m transonic cryogenic tunnel 03 p0313 N85-12019

Effect of boundary layers on solid walls in three-dimensional subsonic wind tunnels
03 p0313 N85-12023

Investigations of boundary layers in the Emmen Federal Aircraft works transonic tunnel, Switzerland
[FW-FO-1641] 04 p0453 N85-12877

Meteorological analysis for clusters of wind turbines
[DE84-013164] 04 p0539 N85-13425

Boundary layer simulator improvement
[NASA-CR-174199] 05 p0597 N85-13802

Influence of inter-layer effect on charge gas-permeability
[BLL-M-35919-(5828.4)] 05 p0616 N85-13940

Atmospheric studies in complex terrain
[DE84-008553] 05 p0676 N85-14345

An investigation of the marine boundary layer during cold air outbreak 05 p0680 N85-14366

Structure and growth of the marine boundary layer
05 p0680 N85-14369

Linear problem of harmonic vibrator acting at supercritical frequencies in subsonic boundary layer
06 p0779 N85-14978

Existence and non-uniqueness of similarity solutions of a boundary layer problem
[NASA-CR-172503] 07 p0957 N85-16064

Aero-optics experimental techniques
[AD-A146755] 07 p0957 N85-16067

Some important problems in unsteady boundary layers including separation. 2: Unsteady boundary layers close to the stagnation region of slender bodies
[AD-A146964] 07 p0958 N85-16069

Bulk cavitation caused by a plane shock wave
[AD-A147031] 07 p0958 N85-16072

Free-surface boundary layer and the origin of bow vortices
[AD-A147427] 07 p0960 N85-16083

Shock/turbulent boundary layer interaction and its control 08 p1071 N85-16792

Active and passive shock/boundary layer interaction control on supercritical airfoils 08 p1072 N85-16795

An experimental study on the instability of a mixing-layer with laminar wake as the initial condition
08 p1078 N85-16824

Corrections for attached sidewall boundary-layer effects in 2-dimensional airfoil testing
[NASA-CR-3873] 09 p1272 N85-17997

Heat-transfer enhancement in natural convection enclosure flow
[DE84-013048] 09 p1319 N85-18297

Benthic boundary layer, IOS observational programme: Discovery Gap measurements, March 1984 — Institute of Oceanographic Sciences (IOS)
[ISO-180] 09 p1350 N85-18552

Efficient self-consistent viscous-inviscid solutions for unsteady transonic flow
[NASA-TM-86335] 10 p1420 N85-18959

Evaluation of inviscid/boundary layer and parabolized Navier-Stokes solutions for design of reentry vehicles
[DE84-014329] 10 p1426 N85-19006

A frozen vorticity approach to the axisymmetric strong interaction problem
[AD-A149101] 10 p1484 N85-19389

Perturbation of a multiple eigenvalue in the Benard problem for two fluid layers
[AD-A149068] 10 p1546 N85-19745

Instrumentation for Application Number 1: Mass spectrometric analysis of the boundary layer associated with the tethered satellite 11 p1646 N85-20372

Turbulence parameters impacting dispersion in an urban convection boundary layer
[PB85-116036] 11 p1682 N85-20598

Pre-turbulence: Transitional Laminar-turbulent flows
11 p1716 N85-20793

Numerical study of large-eddy breakup and its effect on the drag characteristics of boundary layers
[NASA-CR-3884] 12 p1797 N85-21272

Investigations of micro-turbulence in the bottom of the boundary layer
[AD-A149823] 12 p1896 N85-21897

Non-precipitating cumulus cloud study
[DE85-002352] 12 p1896 N85-21902

Investigations of reactive and non reactive acoustic boundary layers in porous walled ducts
13 p2000 N85-22535

The relationship between marine aerosol particles and satellite-detected radiance 13 p2131 N85-23263

H-division materials physics progress
[DE85-004990] 13 p2165 N85-23430

Three-layer generic Ganymedes: Structure and evolution 13 p2202 N85-23657

Comparison of measured and computed boundary layers at the tail-end of an axisymmetric body in an air-jet
[AMTE(N)-TM-83053] 14 p2209 N85-23700

Effect of form and clearance of a piston launched in a tube on the boundary layer and the heat transfer
[ISL-CO-216/83] 14 p2302 N85-24255

Low Reynolds number vehicles
[AGARD-AG-288] 16 p2699 N85-26666

Modeling plasma mantle of Earth's magnetosphere
16 p2720 N85-26790

On the effect of wing taper and sweep direction on leading edge transition
[CA-8435] 17 p2892 N85-27827

Free-surface phenomena under low- and zero-gravity conditions
[NASA-CR-175865] 17 p2907 N85-27922

The boundary layers as the primary transport regions of the Earth's magnetotail
[AD-A152714] 17 p2982 N85-28496

Post-stall wind tunnel data for NACA 44XX series airfoil sections
[DE85-002948] 18 p3080 N85-28931

Development and testing of the variable vertical resolution Fourth Order GCM 18 p3142 N85-29453

Parameterization of surface fluxes in the VVR Fourth Order GCM 18 p3142 N85-29454

Specification of surface roughness over oceans in the GLAS Fourth Order GCM 18 p3142 N85-29455

Modifications to SOLA-VOF for flow dynamics in spinning cylinders
[AD-A154093] 19 p3265 N85-30250
Sidewall boundary-layer effects in two-dimensional airfoil testing
[NASA-CR-176034] 20 p3396 N85-31065
Numerical and experimental investigation of turbomachinery rotor flow fields
20 p3451 N85-31429
Benthic boundary layer modelling studies
[IOS-181] 20 p3497 N85-31742
Mean and large-scale turbulence characteristics of the noise-producing region of an acoustically excited round jet 20 p3523 N85-31911
Applicability of surface CCN measurements
21 p3652 N85-32696
Evaluation of source strength and dispersion model predications with data from large nitrogen tetroxide field experiments
[DE85-011855] 23 p3947 N85-34465
Unsteady flow in a supersonic cascade with two in-passage shocks
[NASA-CR-3925] 24 p4060 N85-35158

BOUNDARY LUBRICATION
Formation of high molecular weight products from benzene during boundary lubrication
[NASA-TM-86966] 13 p2017 N85-22644

BOUNDARY VALUE PROBLEMS
NT CAUCHY PROBLEM
NT DIRICHLET PROBLEM
NT NEUMANN PROBLEM
Wave multiple scattering by a finite number of unclosed circular cylinders
[NASA-TM-77583] 01 p0037 N85-10232
The initialization of mesoscale models
01 p0079 N85-10529
The approximation of nonsmooth solutions of hyperbolic partial differential equations
[CSIR-TWISK-297] 01 p0108 N85-10723
Location of several outliers in multiple regression data using elemental data
[CSIR-TWISK-300] 01 p0108 N85-10724
The convergence of Garlerkin approximation schemes for second-order hyperbolic equations with dissipation
[CSIR-TWISK-325] 01 p0109 N85-10736
On wave propagation in linear viscoelasticity
[AD-A144739] 01 p0111 N85-10750
Boundary behavior of analytic functions, analytic wave front sets and the intersection problem of Ehrenpreis
[PREPRINT-809] 01 p0114 N85-10778
Characteristic boundary conditions for three-dimensional transonic unsteady aerodynamics
[NASA-TM-86292] 02 p0134 N85-10915
Boundary conditions in Chebyshev and Legendre methods
[NASA-CR-172469] 02 p0250 N85-11635
Numerical methods for singularly perturbed differential equations with applications
[AD-A145639] 02 p0252 N85-11650
Theory of radio wave propagation over the ocean
02 p0259 N85-11698
Effects of the oceans on polar motion: Continued investigations
[E85-10037] 03 p0379 N85-12416
Dynamic occlusion analysis in optical flow fields
[AD-A145805] 03 p0406 N85-12594
A comparative study of the finite element and boundary element methods as applied to a boundary value problem of a harmonic function
[AD-A146018] 03 p0411 N85-12627
Free-edge failures of composite laminates
04 p0467 N85-12971
Interval mathematics reports
[REPT-84/1] 04 p0556 N85-13536
Interval-mathematical treatment of initial value problems of ordinary differential equations
04 p0556 N85-13538
Applications of the simple-layer logarithmic potential
05 p0718 N85-14606
Loeb solutions of the Boltzmann equation with initial boundary values and external forces
[CTH-MATH-1984-23] 05 p0719 N85-14616
Step-by-step stability in the numerical solution of partial differential equations
[CWI-NW-161/83] 05 p0720 N85-14623
Mixed defect correction (iteration) for the solution of a singular perturbation problem
[MC-NW-162/83] 05 p0720 N85-14624
Convergence of method of lines approximations to partial differential equations
[CWI-NM-R8404] 05 p0720 N85-14627
Multiple steady states for characteristic initial value problems
[NASA-CR-172486] 06 p0749 N85-14800
Free-surface boundary layer and the origin of bow vortices
[AD-A147427] 07 p0960 N85-16083
Multivariate spline methods in surface fitting
07 p0965 N85-16257
Solution of partial differential equations on vector and parallel computers
[NASA-CR-172500] 07 p1026 N85-16525
An operator method for computing the asymptotics of a collision resolution interval
[AD-A146837] 07 p1028 N85-16528
Viscosity solutions of Hamilton-Jacobi equations at the boundary
[AD-A147444] 07 p1032 N85-16553
Nonlinear wave propagation
[AD-A148114] 08 p1152 N85-17269
Weakly-reflective boundary conditions for two-dimensional shallow water flow problems
[PUBL-322] 08 p1163 N85-17341
Numerical solution of elastodynamic problems in fracture mechanics 08 p1171 N85-17385
An invariant measure for the equation u sub tt - u sub xx + u3 = 0
[AD-A147300] 08 p1210 N85-17612
A finite difference method for inverse mode calculations of a three-dimensional boundary layer
[ESA-TT-863] 09 p1274 N85-18007
A finite element analysis of viscoelastic materials with varying time scales 09 p1330 N85-18355
Mechanical and transient hygrothermal loading of multilayer orthotropic cylinders 09 p1330 N85-18359
Boundary conditions for artificial dissipation operators --- convection
[FFA-TN-1984-53] 09 p1375 N85-18642
Evaluation of inviscid/boundary layer and parabolized Navier-Stokes solutions for design of reentry vehicles
[DE84-014329] 10 p1428 N85-19006
Methodology for stress analysis of heavy metal plate
10 p1460 N85-19203
A program design for an adaptive, non-linear finite element solver
[AD-A148880] 10 p1539 N85-19705
Asymptotic representation of solutions of the basic semiconductor device equations
[AD-A149040] 10 p1545 N85-19741
Recent developments and open problems in the mathematical theory of viscoelasticity
[AD-A149043] 10 p1545 N85-19742
Vectorization and implementation of an efficient multigrid algorithm for the solution of elliptic partial differential equations
[AD-A149049] 10 p1545 N85-19743
Neumann type boundary conditions for Hamilton-Jacobi equations
[AD-A149069] 10 p1546 N85-19746
Numerical solution of semilinear elliptic problems on unbounded domains
[AD-A149559] 10 p1549 N85-19767
Comparison of spherical wave ray tracing and exact boundary value solutions for spherical radomes
[AD-P004353] 12 p1824 N85-21447
A study of coupling the boundary and finite element methods in two-dimensional elastostatics
[AD-A149619] 12 p1865 N85-21702
A convergent series expansion for hyperbolic systems of conservation laws
[NASA-CR-172557] 12 p1910 N85-21990
The performance of a type-insensitive Runge-Kutta code on a personal computer
[TUM-I8410] 12 p1919 N85-22048
Determining conductivity by boundary measurements. Part 2: Interior results
[AD-A149750] 12 p1921 N85-22063
Propagation of three-dimensional turbulent jet from lobar nozzle through surrounding stream
13 p2042 N85-22785
Liquid moment on a filled coning cylinder during spin-up: Ad hoc model
[AD-A150280] 13 p2092 N85-23060
Calculating boundary layer on profile with laminar and turbulent flow zone 14 p2288 N85-24177
On the shift parameter in the backward beam method for parabolic problems for preceding times
[CWI-NM-R8411] 14 p2410 N85-24861
High specific power aircraft turn maneuvers: Tradeoff of time-to-turn versus change in specific energy
[AD-A151701] 15 p2471 N85-25257
Control of a flexible beam
[DE85-007243] 15 p2580 N85-25914
A problem of Burkholder and the existence of harmonic majorants of the absolute value of x sup p in certain domains in R sup d 15 p2634 N85-26236
A new approach to queer differential equations
[AD-A149321] 15 p2636 N85-26272
Propagation of wave packet in a dissipative dielectric medium
[IPPJ-710] 15 p2655 N85-26385
A numerical design method for three-dimensional transonic wings 16 p2694 N85-26831
Three-dimensional wing boundary layer analysis program BLAY and its application
16 p2694 N85-26832
Optimum rotation of solid body with 1 axis of symmetry 16 p2718 N85-26781
Accuracy of the calculated stress field around a craze
[DE85-005520] 16 p2801 N85-27272
An approximation to the problem of a pin-loaded hole in an orthotropic plate
[VTH-LR-386] 16 p2802 N85-27278
Incorporation of an elliptical boundary condition into the program POISSON
[DE85-006820] 16 p2849 N85-27564
The vector potential in a branched Riemann space
[VTH-LR-395] 16 p2856 N85-27614
On the accuracy of the Poincare-Lindstedt method
[REPT-84-37] 17 p3022 N85-28690
On the algebraic equations in implicit Runge-Kutta methods
[CWI-NM-R8413] 17 p3022 N85-28696
Analysis of nonlinear parabolic equations modeling plasma diffusion across a magnetic field
[DE85-007683] 17 p3040 N85-28807
Recent developments in nonlinear normal mode initialization 18 p3142 N85-29451
Singularity solutions for ellipsoids in Low-Reynolds-Number flows: With applications to the calculation of hydrodynamic interactions in suspensions of ellipsoids
[AD-A153503] 18 p3168 N85-29632
Sensitivity analysis of initial value problems with mixed ode's and algebraic equations
[AD-A153528] 18 p3169 N85-29637
On the numerical computation of nonlinear force-free magnetic fields 18 p3203 N85-29871
Numerical methods for the solution of stiff delay differential equations 19 p3334 N85-30653
Well-posedness of one-way wave equations and absorbing boundary conditions
[NASA-CR-172619] 19 p3345 N85-30727
Asymptotic expansions for the finite element approximation of parabolic functions
19 p3345 N85-30731
Superconvergence of finite element approximation for Navier-Stokes equations 19 p3345 N85-30732
On MGR (Upsilon) multigrid methods
[AD-A153887] 19 p3345 N85-30733
Solving Volterra integral equations with ODE codes
[DE85-011216] 19 p3346 N85-30740
Electromagnetic lateral waves in layered media
19 p3369 N85-30894
Approximate solution to the problem of heating massive bodies by radiation
[BLL-M-36272-(5828.4)] 20 p3450 N85-31422
User's manual of the BNDSCO computer program for solving constrained optimal control problems
[DFVLR-MITT-85-05] 20 p3516 N85-31865
Attractors for the Kuramoto-Sivashinsky equations
[DE85-009631] 20 p3520 N85-31892
Scattering from foliage covered terrain
[AD-A154724] 21 p3574 N85-32226
Oscillatory solutions of the Peaceman-Rachford alternating direction implicit method and a comparison of methods for the solution of the two dimensional heat diffusion equation
[AD-A154670] 21 p3675 N85-32833
Sobolev-Poincare's inequality and the Neumann problem for u sub t = divergence of the absolute value of the gradient u to the p-2 power x the gradient u
[AD-A154788] 21 p3676 N85-32839
Exact solutions of singular equations for viscous transonic flows 21 p3683 N85-32882
Comments on two matters related to turbulent combustion 22 p3743 N85-33204
Pressure correlations in turbulent reacting flows
22 p3744 N85-33205
Fundamentals of radio optical theory of resonant and directional quasi-optical devices
22 p3780 N85-33420
Linear boundary detection using pressure buildup tests
[DE85-009926] 22 p3784 N85-33444
A new method for boundary value problems
[AD-A155934] 24 p4143 N85-35683
Some rigorous results concerning spectral theory for ideal MHD
[DE85-013427] 24 p4156 N85-35770

BOUSSINESQ APPROXIMATION
Some approximations of geophysical hydrodynamics
14 p2336 N85-24448

Two-point closure study of covariance budgets for turbulent Rayleigh-Benard convection
[PB85-189108] 24 p4124 N85-35568

BOW SHOCK WAVES
U BOW WAVES
U SHOCK WAVES

BOW WAVES
The propagation and growth of whistler mode waves generated by electron beams in Earth's bow shock
[AD-A145572] 02 p0228 N85-11492
Magnetohydrodynamic and gasdynamic theories for planetary bow waves
[NASA-CR-174132] 03 p0448 N85-12850
Magnetohydrodynamic and gasdynamic theories for planetary bow waves
[NASA-CR-174135] 04 p0589 N85-13760
Waves and instabilities in collisionless shocks
[AD-A146689] 06 p0881 N85-15597
Research study of space plasma boundary processes
[NASA-CR-174351] 10 p1558 N85-19823
Electric field and plasma observations near the magnetopause and bow shock during a rapid compression 14 p2355 N85-24553
The keV electrons and 80 keV protons in the vicinity of the high latitude magnetosphere and at the bow shock 14 p2355 N85-24554
Satellite-borne electric field measurements with spherical double probes — ISEE satellites 14 p2356 N85-24558
Magnetohydrodynamics of Earth's bow shock 15 p2481 N85-25311
Fast and optimal solution to the Rankine-Hugoniot problem
[NASA-TM-86214] 19 p3344 N85-30724
Properties of the reflected beams from the Earth's bow shock: A simple model
[IFSI-84-14] 20 p3549 N85-32068

BOXES (CONTAINERS)
An automatic device for amphibian egg fertilization in space: Technical aspects and biological requirements 05 p0689 N85-14427
Double window viewing chamber assembly
[NASA-CASE-MFS-28057-1] 18 p3063 N85-28951

BRAGG ANGLE
Bragg reflection of surface electroacoustic shear waves 04 p0485 N85-13096
Bragg cell spectrum analyzer specification
[AD-D011320] 07 p1044 N85-16829
Influence of Bragg reflecting lattice groove depth modulation on Rayleigh wave reflection coefficient 10 p1499 N85-19458

BRAGG CURVE
Results from a Bragg curve spectrometer
[DE85-007870] 18 p3176 N85-29691

BRAIN
NT BRAIN STEM
NT CEREBELLUM
NT CEREBRAL CORTEX
NT CEREBRAL VENTRICLES
NT CEREBRUM
Compensatory and adaptive regional hemodynamic reactions to weightlessness during long-term spaceflights 01 p0091 N85-10616
Effect of short-term hypokinesia on rat opioid system reaction 01 p0093 N85-10625
Hemodynamics and neurodynamics of the human brain during exposure to moderate hypoxic hypoxia 01 p0094 N85-10630
Cognitive science program. A framework for relating cognitive to neural systems
[AD-A145185] 01 p0097 N85-10649
Neural control of the direction of covert visual orienting
[AD-A145189] 01 p0097 N85-10650
Mechanisms of oxygen toxicity and methods of protection
[AD-A145830] 03 p0400 N85-12551
Reflection of lateralization of sound stimuli in evoked potentials of human brain 04 p0544 N85-13463
ERPS to monitor non-conscious mentation 05 p0707 N85-14536
Performance enhancements under dual-task conditions 05 p0707 N85-14537
Measurement of workload: Physics, psychophysics, and metaphysics 05 p0708 N85-14539
Distribution of blood flow to brain, kidneys, gut, spleen and posterior extremities in cats in acute hypoxia 07 p1013 N85-16434
Lateral specifics of visual perception 07 p1013 N85-16436
Visual evoked potentials with disrupted functioning of nonspecific cerebral systems 07 p1013 N85-16437
Change in relationship of biopotentials of brain zones for various levels of working capacity 07 p1013 N85-16438
Vision by man and machine: How the brain processes visual information may be suggested by studies in computer vision (and vice versa)
[AD-A147890] 07 p1017 N85-16458
Functional inter-hemisphere asymmetry in recognition of visual stimuli of various classes 08 p1193 N85-17517
Cognitive asymmetry and occupation. Computer programmers, students, and bank personnel, part 1 and part 2
[AD-A147125] 08 p1197 N85-17540
Neurocognitive pattern analysis of an auditory and visual numeric motor control task. Part 1: Development of methods
[AD-A148809] 09 p1364 N85-18578
Electrosleep therapy advanced at medical institute 10 p1526 N85-19823
Multiple resources and brain laterality
[AD-A148912] 10 p1530 N85-19843
Effects of hyperthermia on free amino acids in rat brain and in subcellular fractions 11 p1691 N85-20631
Functional significance of some EEG parameters and dominant principle 11 p1691 N85-20634
Effects of hypothermia on brain metabolism 11 p1692 N85-20636
Rat tissue opioid peptide content during long-term hypokinesia 12 p1904 N85-21954
Effect of long-term repeated exposure to high-intensity stationary magnetic field on adrenomedullary activity 12 p1904 N85-21955
Brain mechanisms underlying individual differences in reaction to stress: An animal model
[AD-A150195] 13 p2143 N85-23301
Biological investigations of adaptive networks. Neuronal control of conditioned responding
[AD-A150969] 14 p2385 N85-24695
Space brain research in China reported 15 p2537 N85-25657
Thermoregulatory and vestibular systems in the rat 15 p2610 N85-26082
A comparison of alternative analytic models for event related potential records
[AD-A151977] 15 p2618 N85-26134
Infinite computing
[AD-A151437] 15 p2628 N85-26197
Does a 50-cycle alternating field have central nervous effects?
[BLL-CE-TRANS-8063-(9022.09)] 16 p2839 N85-27507
Biological influences of low-frequency sinusoidal electromagnetic signals alone and superimposed on RF carrier waves
[PB85-161248] 16 p2842 N85-27527
Distributed memory
[AD-A153364] 17 p3001 N85-28554
Language design, computers and brains
[AD-A152819] 17 p3008 N85-28594
Influence of limboreticular complex on some reactions of rabbits 19 p3326 N85-30607
Changes in pentose and glucuronate pathway dehydrogenases in rat brains following single or multiple hypothermic episodes 20 p3505 N85-31790
Sleep and wake physiology in weightlessness 20 p3510 N85-31819
Resource allocation in cerebral specialization of function: Behavioral and electrophysiological studies
[AD-A155092] 21 p3684 N85-32759

BRAIN CIRCULATION
Reaction of cerebral ventricles to antiorthostatic position and occlusion of jugular veins 01 p0093 N85-10626
Hemodynamics and neurodynamics of the human brain during exposure to moderate hypoxic hypoxia 01 p0094 N85-10630
Effect of microwave radiation on local blood circulation and oxygenation of brain tissue 07 p1012 N85-16431

BRAIN STEM
Visual evoked potentials with disrupted functioning of nonspecific cerebral systems 07 p1013 N85-16437

BRAKES (FOR ARRESTING MOTION)
NT AERODYNAMIC BRAKES
NT DRAG CHUTES
NT LEADING EDGE SLATS
NT TRAILING EDGE FLAPS
NT WHEEL BRAKES
NT WING FLAPS
Investigations on the dynamic loading of wind energy converters with vertical axis and problems of control during starting and overload conditions
[BMFT-FB-T-84-155] 03 p0396 N85-12472
Comparison between cycle ergometers with different mechanical braking systems
[FOA-C-54058-H1] 07 p0975 N85-16193
Space shuttle wheels and brakes 08 p1101 N85-16662
Space shuttle rudder/speedbrake actuation subsystem 08 p1102 N85-16965
Use of braking stages for control of turbine speed 09 p1308 N85-18215
Hydraulic brakes for industrial robots 13 p2046 N85-22806

BRAKING
Testing solution for IL-76 braking system problem 08 p1067 N85-16786
Use of braking stages for control of turbine speed 09 p1308 N85-18215
Expedient runway surfacing with post tensioning system for expeditionary airfields
[AD-D011677] 19 p3222 N85-29976

BRANCHING (MATHEMATICS)
A martingale approach to supercritical (C-M-J) branching processes
[CTH-MATH-1984-25] 05 p0722 N85-14843
On the instability of a 3-dimensional attachment line boundary layer: Weakly nonlinear theory and a numerical approach
[NASA-CR-172504] 07 p0957 N85-16063
Study of mathematical models of mutation and selection in multi-locus systems
[DE85-000873] 09 p1376 N85-18648
Research in nonlinear problems of energy: Informal technical report
[DE85-001529] 11 p1595 N85-20031
Bifurcation theory applied to aircraft motions
[NASA-TM-86704] 14 p2210 N85-23705
Nonlinear problems in flight dynamics involving aerodynamic bifurcations
[NASA-TM-86706] 15 p2462 N85-25206
Solving set covering problems using heuristics with branch and bound
[AD-A151906] 15 p2638 N85-26269
The vector potential in a branched Riemann space
[VTH-LR-306] 16 p2856 N85-27614
Flow through finite collapsible tubes: A branching problem
[REPT-84-29] 17 p2960 N85-28281
Analytical shear buckling investigation of curved composite panels
[AD-A153138] 17 p2980 N85-28421
Chaos and order in an optical ring cavity
[CWI-AM-R8416] 17 p3038 N85-28795
Nonlinear problems in continuum mechanics
[AD-A153387] 17 p3046 N85-28848
Nonlinear global stability analysis of compressor stall phenomena
[NASA-CR-174908] 19 p3219 N85-29960
Nonlinear dynamics: A personal perspective
[DE85-010982] 20 p3521 N85-31699
A note on a theorem of R. Duffin
[AD-A154786] 21 p3676 N85-32838
Diakoptic calculation of characteristics for optimization of linear circuits with respect to parameters of individual branches 22 p3767 N85-33346

BRANCHING (PHYSICS)
Selected topics from J/psi decays
[DE85-010537] 18 p3183 N85-29736
Status of the zeta(8.3)
[DE85-013070] 24 p4149 N85-35724

BRASSES
Corrosion of brass in potable water service
[CETIM-100390] 04 p0477 N85-13037
X-ray diffraction study of changes in stress-strain distributions during fatigue of a 2-phase alloy
[AD-A152367] 17 p2930 N85-28087

BRAYTON CYCLE
Dynamic power systems for power generation 05 p0609 N85-13892
Dynamic conversion working group summary 05 p0611 N85-13904
Active cooling requirements for propellant storage 08 p1108 N85-17004
Introducing engine innovations: An examination of future markets for Brayton and Stirling automotive engines
[DE84-016319] 11 p1647 N85-20382
Some solar dish/heat engine design considerations
[DE85-003479] 12 p1881 N85-21802
Small central receiver Brayton cycle study
[DE85-008882] 18 p3128 N85-29389
Reciprocating Brayton cycle motor
[REPT-84-RR-336] 20 p3462 N85-31507
Comparative evaluation of three alternative power cycles for waste heat recovery from the exhaust of adiabatic diesel engines
[NASA-TM-86953] 20 p3542 N85-32043

BRAZIL
Utilization of LANDSAT orbital imagery in the soil survey processes at Rio Grande do Norte state
[E85-10009] 02 p0216 N85-11422
Remote sensing applied to forest resources
[E85-10012] 02 p0216 N85-11425

Mapping land use changes in the carboniferous region of Santa Catarina, report 2
[E85-10017] 02 p0217 N85-11430
Development and testing of a rural credit supervision system at the level of counties and rural properties utilizing remote sensing techniques
[E85-10018] 02 p0217 N85-11431
Thematic mapping of likely target areas for the occurence of cassiterite in the Serra do Mocambo (GO) granitic massifs using LANDSAT 2 digital imaging
[E85-10027] 02 p0219 N85-11440
Shuttle Experimental Radar for Geological Exploration (SERGE) project: Field work relating to the Shuttle Experimental Radar A (SIR-A) in Brazil (phase 2)
[NASA-CR-174033] 02 p0219 N85-11444
Forecast of the northeastern drought by the method of periodicities: Use and abuses
[INPE-3109-PRE/508] 02 p0230 N85-11502
Evaluation of criteria for selecting the spectral attributes of digital LANDSAT MSS imagery for discriminating lithological units in the lower Curaca River Valley, Bahia — Brazil
[E85-10036] 03 p0379 N85-12415
Contribution to the radiogeology of Sao Roque, SP, granites
[INPE-3079-PRE/492] 03 p0391 N85-12503
Report of the field work performed in the Basins of the Quebra Osso and Tanque Petro Rivers in the Catas Altas quadrangle, Minas Gerais
[INPE-3268-NTE/225] 04 p0525 N85-13359
Heat sources in the tropics and large scale flow anomalies associated with precipitation anomalies in northeast Brazil
[INPE-3211-TDL/175] 04 p0538 N85-13421
Behavior of the ionospheric F region in low latitudes and in the equatorial region of Brazil during strong magnetic storms in the 1978 to 1983 period
[INPE-3231-PRE/581] 05 p0675 N85-14333
Nocturnal increases of ionization in the ionospheric F region in the low latitude of Brazil during magnetic storms
[INPE-3271-PRE/598] 05 p0675 N85-14334
Diagnostics of rainfall anomalies in the nordeste during the global weather experiment 05 p0685 N85-14405
Integrated analysis of remote sensing products from basic geological surveys — Brazil
[E85-10052] 07 p0984 N85-16248
Droughts and floods in South America due to the 1982-83 El Nino-southern oscillation episode
[INPE-3408-PRE/677] 09 p1357 N85-18535
The BRESEX multispectral camera: Preliminary characteristics
[INPE-3357-PRE/635] 10 p1487 N85-19386
Brazilian remote sensing receiving, recording and processing ground systems in the 1980's
[E85-10079] 10 p1504 N85-19493
The sharing of remote sensing techniques in Brazilian geographic research
[INPE-3307-PRE/617] 10 p1506 N85-19502
U, Th, K content, heat production and thermal conductivity of Sao Paulo, Brazil continental shelf sediments: A reconnaissance work
[INPE-3401-PRE/670] 10 p1515 N85-19558
First sodium nightglow results for Natal
[INPE-3397-PRE/666] 10 p1515 N85-19560
Planetary scale circulation anomalies associated with droughts over northeast Brazil
[INPE-3351-PRE/630] 10 p1518 N85-19570
Large scale circulation anomalies and prediction of northeast Brazil droughts
[INPE-3405-PRE/674] 10 p1518 N85-19571
Meridional penetration of frontal systems in South America and its relation to organized convection in the Amazon
[INPE-3407-PRE/676] 10 p1518 N85-19572
Interannual variations of the winter circulation in the Northern Hemisphere and in the southern oscillation (meridian) and their possible connections with the climate of Northeast Brazil
[INPE-3333-TDL/182] 10 p1519 N85-19573
Precursors for Brazilian magnetic anomalies from 1922 to 1969
[INPE-3283-PRE/605] 11 p1681 N85-20590
CNPq/INPE LANDSAT system: Report of activities from October 1, 1983 to September 30, 1984 — Brazil
[E85-10097] 16 p2808 N85-27318
Study of the urban evolution of Brasilia with the use of LANDSAT data
[E85-10101] 16 p2809 N85-27321
The relevance of remote sensing to Brazil
[INPE-3421-PRE/686] 16 p2811 N85-27332
The ARGOS system in Brazil — hydrology
16 p2813 N85-27349
On the 1983 drought in northeast Brazil
[INPE-3412-PRE/678] 16 p2834 N85-27476
An appraisal of the duration of the recent drought in northeast Brazil and a forecast for 1985
[INPE-3477-PRE/720] 16 p2834 N85-27478

BRAZILIAN SPACE PROGRAM
Brazilian Remote Sensing Shuttle Experiment (BRESEX): Characteristics and future utilization on satellites
[INPE-3313-PRE/620] 10 p1487 N85-19385
Remote sensing activities in Latin America
[INPE-3297-PRE/612] 10 p1506 N85-19501
SELPER (Latin American Society of Remote Sensory Specialists)
[INPE-3315-PRE/622] 16 p2810 N85-27328

BRAZING
NT LOW TEMPERATURE BRAZING
Dispersed metal-toughened ceramics and ceramic brazing
[NASA-CR-174284] 07 p0933 N85-15916
Repair welding and brazing procedures for turbine components and investigation of the brazing behavior of thin filler foils
[MTU-TB-908/84] 07 p0974 N85-16190
Design of low loss helix circuits for interference fitted and brazed circuits
[NASA-CR-168313] 10 p1478 N85-19328
Thermodynamics of copper-nickel alloys containing aluminum, silicon, titanium, and chromium relative to their use in ceramic brazing
[DE85-004767] 13 p2023 N85-22674
Indirect brazing of structural ceramics for uncooled diesels
[DE85-005569] 17 p2935 N85-28116
X-ray residual stress analysis on the coarse grain of copper and its application to the brazed copper
23 p3907 N85-34202

BREADBOARD MODELS
Design and analysis report for the RL10-2B breadboard low thrust engine
[NASA-CR-174857] 10 p1430 N85-19020
Firefighters' communication transceiver test plan
[NASA-CR-171419] 13 p2053 N85-22854
Development of a microprocessor controlled communication system for ships
[BMFT-FB-T-84-275] 17 p2950 N85-28216
Research pressure instrumentation for NASA space shuttle main engine
[NASA-CR-176014] 19 p3227 N85-30006
Noiseless coding for the Gamma Ray spectrometer
[NASA-CR-176201] 24 p4069 N85-35219

BREAKAWAY
U BOUNDARY LAYER SEPARATION

BREAKDOWN
Spectral distribution of radiation in n junctions of GaAs during avalanche breakdown 02 p0258 N85-11688

BREAKERS (ELECTRIC)
U CIRCUIT BREAKERS

BREAKING
Electromagnetic braking of a metallic projectile in flight
[AD-A149424] 10 p1480 N85-19345
The investigation of tethered satellite system dynamics
[NASA-CR-176180] 24 p4069 N85-35215

BREATHING
Encephalographic correlates of autogenous change in human functional state 08 p1193 N85-17518

BREATHING APPARATUS
NT UNDERWATER BREATHING APPARATUS
Experiments with hydrox at 1.3 MPa (13 atm) — for divers
[FOA-C-58014-H1] 04 p0545 N85-13471
Operating and maintenance guidelines for the kinergetics (trade name) environmental control system. Carbon dioxide scrubber model DH-10 and heat exchanger model CCU-01
[AD-A148107] 08 p1200 N85-17557
Hazards in welding due to oxygen changes in the workplace atmosphere
[BLL-WI-TRANS-684-(9312.57)]
16 p2792 N85-27224
Ten year environmental test of glass fiber/epoxy pressure vessels
[NASA-TM-87058] 19 p3231 N85-30034
Light-weight oxygen delivery hood assembly for hyperbaric chamber
[AD-D011700] 19 p3331 N85-30634
The use of superoxide mixtures as air-revitalization chemicals in hyperbaric, self-contained, closed-circuit breathing apparatus
[NASA-TM-86709] 20 p3512 N85-31831
Improved oxygen sources for breathing apparatus
[NASA-TM-86671] 24 p4134 N85-35623
The use of austenitic stainless steel versus monel (Ni-cu) alloy in pressurized Gaseous Oxygen (GOX) life support systems
[AD-A156305] 24 p4134 N85-35625

BRECCIA
Mineralogical investigations of lunar samples and meteorites
[NASA-CR-174291] 08 p1258 N85-17918
Moon 09 p1411 N85-18893

BREEDER REACTORS
NT EXPERIMENTAL BREEDER REACTOR 2
NT LIQUID METAL FAST BREEDER REACTORS
Blanket materials for fusion reactors: Comparisons of thermochemical performance
[DE84-016240] 04 p0568 N85-13622
Heat transfer and mechanical interactions in fusion nuclear systems
[DE84-016233] 09 p1392 N85-18761
Radiation damage experiments and lifetime estimates for beryllium components in fusion systems
[DE85-006038] 17 p3040 N85-28811
Two-dimensional TBR calculations for conceptual compact reversed-field pinch reactor blanket
[DE85-007636] 17 p3040 N85-28812
Feasibility study of a fission-suppressed Tokamak fusion breeder
[DE85-009099] 18 p3190 N85-29786
BREED: A CDC-7600 computer program for the automation of breeder reactor design analysis (LWBR Development Program)
[DE85-010327] 19 p3338 N85-30686
Molten salt cooling/17Li-83Pb breeding blanket concept
[DE85-010522] 19 p3363 N85-30854
Consolidated fuel reprocessing program
[DE85-006750] 19 p3366 N85-30871
A review of the SIMMER-2 analyses of liquid-metal-cooled fast breeder reactor core-disruptive accident fuel escape
[DE85-010803] 19 p3366 N85-30876
Tritium technology review
[DE85-010504] 21 p3703 N85-33006
Key issues of fusion nuclear technology development (FINESSE)
[DE85-012599] 22 p3845 N85-33617

BREMSSTRAHLUNG
Bremsstrahlung radiation from longitudinal plasma waves caused by subthermal electrons in plasma
02 p0264 N85-11730
Bremsstrahlung from nuclear scattering at low energy near a resonance
[DE84-014852] 04 p0561 N85-13572
A neutral gas jet in a low velocity shock front at the boundary of the Draco Nebula 06 p0678 N85-15576
Physics of nonmagnetic relativistic thermal plasmas
09 p1386 N85-18715
Lithography radiation effects study
[AD-A149552] 10 p1468 N85-19260
Directivity of Bremsstrahlung radiation from relativistic beams and the Gamma-Rays from solar flares
[NASA-CR-174433] 10 p1572 N85-19913
X-ray intensification at balloon altitudes of the South Atlantic magnetic anomaly in association with geomagnetic activity
[INPE-3469-PRE/712] 16 p2827 N85-27437
Comparison of calculations and measurements of the off-axis radiation dose (SI) in liquid nitrogen as a function of radiation length
[AD-A153676] 18 p3178 N85-29704
Electron temperature measurements from induced toroidal current in ELMO Bumpy Torus scale
[DE85-008549] 18 p3189 N85-29779
Poloidal variations in toroidal fusion reactor wall power loadings
[DE85-009505] 19 p3362 N85-30848
Study of non-thermal photon production under different scenarios in solar flares. 2: The Compton inverse and Bremsstrahlung models and fittings
[SH-1.2-3] 23 p3991 N85-34739
Burst size distributions in the digitized data of the ion chambers t Mt. Norikura and sea level stations
[SH-9.1-9] 23 p4051 N85-35124
LPM effect and primary energy estimations
[HE-3.6-4] 24 p4185 N85-35953
Result of Monte-Carlo simulation of electron-photon cascades in lead and layers of lead-scintillator
[HE-3.6-11] 24 p4185 N85-35958

BRIDGES
The free electron laser variable bridge coupler
[DE85-009630] 18 p3114 N85-29278

BRIDGES (LANDFORMS)
Structure of Reykjanes Ridge rift zone and Icelandic thermal anomaly 19 p3299 N85-30395

BRIDGES (STRUCTURES)
Three programs for evaluating bending moments, deflections and shear forces in simply-supported uniform bridge decks under South African NA loading: NAB, NAD and NAS. NITRR manual P13
[ISBN-0-7988-2283-X] 01 p0102 N85-10681

Exploratory study of shear strength of joints for precast segmental bridges
[PB84-235449] 05 p0651 N85-14182
The Shock and Vibration Digest, volume 16, no. 9
[AD-A146779] 07 p0976 N85-16200
Evaluation of Epoxo 300-C nonskid coating for use on bridge decks
[PB85-108843] 12 p1819 N85-21412
Implementation of polymer impregnation as a bridge deck sealant
[PB85-165716] 22 p3753 N85-33265

BRIDGMAN METHOD
Simulation of solidification in a Bridgman cell
[NASA-CR-3843] 02 p0197 N85-11314
The growth of metastable peritectic compounds
[NASA-CR-171289] 07 p0920 N85-15824
SPAR X technical report for experiment 76-22 directional solidification of magnetic composites
[NASA-CR-171271] 07 p0927 N85-15860
Simulation of solidification in a Bridgman cell
[NASA-CR-175838] 16 p2870 N85-27705

BRIGHTNESS
NT SOLAR GRANULATION
UBV photometry of E region stars: Some intercomparisons 01 p0128 N85-10880
Some statistical characteristics of atmospheric optical thickness in visible spectral range 02 p0164 N85-11109
Holographic subtraction of images by Fourier plane recording and spatial filtration with a narrow beam 02 p0263 N85-11721
Brightness comparison of electroluminescent versus incandescent lighting: A photometric validation
[AD-A145395] 02 p0280 N85-11822
Variability of Neptune 02 p0299 N85-11936
Lyman-Alpha aurora 02 p0302 N85-11953
Infrared images of the Uranian rings 02 p0302 N85-11955
Individual differences in chromatic brightness matching
[AD-A148882] 10 p1529 N85-19641
Brightness limitations in multi-kiloampere electron beam sources
[DE84-017417] 10 p1555 N85-19807
Enhancing the performance of a high-gain free electron laser operating at millimeter wavelengths
[DE85-000862] 12 p1857 N85-21648
The relationship between marine aerosol particles and satellite-detected radiance 13 p2131 N85-23263
Formation of bright terrain bands on Ganymede by unstable lithosphere extension 13 p2173 N85-23485
Remarks on cometary astrometry 14 p2435 N85-25019
Photometric study of Pluto near perihelion. Part 2: Refinement of rotation period: Color indices 15 p2483 N85-25325
The problem of brightness enhancement during laser frequency doubling 21 p3686 N85-32897
Transverse emittance of a 2.0-MeV RFQ beam with high brightness
[DE85-012718] 22 p3837 N85-33758

BRIGHTNESS DISTRIBUTION
Method for interpreting soil cover of flowed fields using spectral brightnesses measured from space photographs 02 p0164 N85-11112
Fiber cable in optical system with brightness amplifier 02 p0263 N85-11724
A review of the millimeter and centimeter observations of Uranus 02 p0299 N85-11935
Brightness distribution in globular clusters derived by the narrow-slit scanning method 05 p0738 N85-14748
Atmospheric limitations in stellar seismology: Should one measure radial velocity or brightness fluctuations? 06 p1251 N85-17899
The physical implications of an isothermal model for the hot intracluster medium
[NASA-TM-86174] 11 p1763 N85-21089
A posteriori increase of resolving power of optical system forming averaged monochromatic images 13 p2082 N85-23003
Relationship between brightness spectrum of photographic image and spectrum of rises on a water surface with waves 13 p2115 N85-23171
Azimuthal variations in Saturn's A ring 15 p2671 N85-26478
Saturn rings: Divisions, gaps and ringlets from ground-based telescopes 15 p2672 N85-26485
Possible period of Jovian activity and possibility of seasons 16 p2723 N85-26810
Effective brightness of zero-point fluctuations of the electromagnetic vacuum accompanying parametric scattering of light 21 p3694 N85-32951
Clusters and cycles in the cosmic ray age distributions of meteorites
[SH-7.1-11] 23 p4048 N85-35103
Longitudinal trial functions and the cosmic ray energy scale 24 p4193 N85-36014
Muon spectrum in air showers initiated by gamma rays
[HE-4.5-4] 24 p4195 N85-36028

BRIGHTNESS TEMPERATURE
An error analysis for the use of presently available lunar radio flux data in broadbeam antenna-system measurements
[PB84-218361] 01 p0016 N85-10097
Multispectral passive microwave correlations with an antecedent precipitation index using the Nimbus 7 SMMR
[AD-A145419] 02 p0200 N85-11334
A review of the millimeter and centimeter observations of Uranus 02 p0299 N85-11935
Mixed layers and satellite retrievals 05 p0686 N85-14411
Mathematical models for the brightness temperature of object and environment in the microwave region
[ESA-TT-829] 05 p0718 N85-14610
A neutral gas jet in a low velocity shock front at the boundary of the Draco Nebula 06 p0878 N85-15576
The Draco Nebula, a molecular cloud associated with a high velocity cloud? 06 p0878 N85-15577
Microwave emissions from snow
[E85-10065] 08 p1174 N85-17403
An alternative to relativistic beaming in AGN — Active Galactic Nuclei (AGN) 08 p1242 N85-17833
On the error of typhoon intensity estimation by means of IR Dvorak technique occurring when the eye is very small 12 p1894 N85-21888
An analysis of the data obtained by a simultaneous observation of GMS and GMS-2: A study of the difference between the brightness temperatures by GMS and those by GMS-2 12 p1894 N85-21888
VISSR infrared calibration by means of calculated radiances 12 p1894 N85-21889
Calculations of microwave brightness temperature of rough soil surfaces: Bare field
[NASA-TM-86200] 13 p2123 N85-23221
General report of the researches of snowpack properties, snowmelt runoff and evapotranspiration in Japan 13 p2124 N85-23225
Microwave radiometer observations of snowpack properties and comparison of U.S. Japanese results — Hokkaido, Japan and Vermont and North Dakota test sites 13 p2125 N85-23230
Studies on physical properties of snow based on multi channel microwave radiometer 13 p2125 N85-23231
Analysis of NIMBUS-7 SMMR data — Hokkaido, Japan snow cover 13 p2125 N85-23232
Estimation of regional evapotranspiration using remotely sensed land surface temperature. Part 1: Measurement of evapotranspiration at the Environmental Research Center and determination of Priestley-Taylor parameter 13 p2125 N85-23233
Venus surface composition from radio/radar measurements 13 p2177 N85-23509
Determination of total moisture content in cloud-free atmosphere by relative radio emission measurements 14 p2340 N85-24472
Digital processing of passive Ka-band microwave images for sea-ice classification
[AD-A150686] 14 p2347 N85-24511
Severe storm detection with passive 37 GHz observations 15 p2596 N85-25997
The validation of sea surface temperatures determined from AVHRR data using in situ data recovered via system ARGOS 16 p2812 N85-27342
Active and passive remote sensing of ice
[AD-A151741] 16 p2815 N85-27369
Atmospheric frontal zone studies
[NASA-CR-175293] 16 p2833 N85-27469
Electron-cyclotron maser emission during solar and stellar flares
[NASA-CR-175883] 17 p3054 N85-28907
Applications of some artificial intelligence methods to satellite soundings 18 p3141 N85-29446
Sea surface radio emission at wavelengths 0.86 and 1.3 cm near Brewster angle 19 p3293 N85-30418
Variations in the small-scale galactic magnetic field and short time-scale intensity variations of extragalactic radio sources 20 p3549 N85-32084
The use of TOMS data in evaluating and improving the total ozone from TOVS measurements
[NOAA-TR-NESDIS-23] 22 p3814 N85-33626

BRILLOUIN EFFECT
Brillouin scattering in underdense UV laser-produced plasmas
[DE84-015184] 04 p0567 N85-13614
Parametric processes in underdense UV laser-produced plasmas
[DE85-002812] 10 p1559 N85-19830
Experimental investigation of wavefront conjugation during Mandelstam-Brillouin scattering of focused laser beams in condensed media 11 p1716 N85-20796
Stimulated Brillouin scattering reflectivity in the presence of various aberrators
[AD-A151750] 15 p2563 N85-25812
Caviton collapse of SRS by SBS
[DE85-009605] 20 p3535 N85-31999
Stimulated Mandelstam-Brillouin scattering with distributed feedback 21 p3696 N85-32961

BRILLOUIN ZONES
A study of structural phase transitions using light scattering techniques
[AD-A147261] 07 p1048 N85-16854
Conducting a thermal conductivity survey
[NASA-CR-175792] 16 p2782 N85-27166

BRINES
Doubly diffusive linear stability with nonconstant gradients
[DE84-013008] 05 p0670 N85-14310
Towing tank studies of stratified flow over ridges and valleys
[DE84-011418] 06 p0839 N85-15329
An experimental study of brine upward migration in thin sea ice 15 p2582 N85-25923
Offshore oceanographic and environmental monitoring services for the Strategic Petroleum Reserve, volume 3
[DE85-009907] 20 p3497 N85-31741
Microbiology of solar salt ponds 21 p3658 N85-32724
Technology transfer report: Feasibility study for the use of geothermal brine in the Ashdod area, Israel
[DE85-013316] 22 p3810 N85-33598
Proposed resource evaluation plan, Salton Sea scientific drilling program
[DE85-011294] 22 p3815 N85-33633
Chemistry of ore-forming fluids 24 p4103 N85-35436
Heat transfer and brine evolution in magma-hydrothermal systems 24 p4104 N85-35441

BRITISH COLUMBIA
The northern coast plutonic-metamorphic complex, southeastern Alaska and northwestern British Columbia 04 p0516 N85-13305

BRITISH GUINEA
U GUYANA

BRITTLE MATERIALS
Evaluation of machining damage in brittle materials
[DE85-001794] 11 p1612 N85-20136
Simulation of brittle fracture via molecular dynamics
[DE85-001061] 11 p1653 N85-20410
Reliability of structural brittle materials 12 p1946 N85-22222
Correlation of uniaxial and biaxial fracture strengths of ceramics
[DE85-003779] 14 p2261 N85-24011
Statistical fracture theories for brittle materials
[AD-A153530] 18 p3121 N85-29324
The shearing contribution in transformation toughening of brittle materials
[AD-A154656] 21 p3568 N85-32195
Mechanics of near tip microcracking in brittle material
[AD-A154684] 21 p3598 N85-32345

BRITTLENESS
Delayed fracture of high-strength steels in spherical tanks for LP gas
[BLL-RISLEY-TR-4926-(9091.9F)] 01 p0026 N85-10162
Mechanism of brittle heat fracture of inhomogeneous solids by high temperature gas jets 02 p0265 N85-11731
Brittleness of ceramics
[NASA-TM-77504] 03 p0335 N85-12156
Effect of crack-tip region constraint on fracture in the ductile-to-brittle transition
[PB84-237395] 06 p0770 N85-14926
Moving nonlocal crack: Anti-plane shear case
[AD-A149996] 12 p1866 N85-21709
Cast-iron technology: Metallographic and mechanical testing results
[DE85-002684] 14 p2257 N85-23984
Study of oxidized surface coating on titanium after annealing 15 p2498 N85-25412
Frangibility of obstacles at airports
[NLR-MP-84002-U] 17 p2981 N85-28431
Fatigue resistance of homogeneous and heterogeneous welded joints of T55 titanium alloy 19 p3246 N85-30126
Indentation fractography: A measure of brittleness
[PB85-179059] 20 p3473 N85-31581
Influence of the resin on interlaminar mixed-mode fracture
[NASA-TM-87571] 21 p3561 N85-32150

Metallurgical origins of fracture toughness and microstructure and fracture toughness of an HSLA (High-Strength/Low-Alloy) steel
[AD-A155530] 21 p3567 N85-32187

BROADBAND
Broadband local distribution networks: Problems and prospects in Italy
[FUB-18-1983] 01 p0040 N85-10255
Free electron lasers
[AD-A145109] 01 p0053 N85-10349
Wideband integrated voice/data technology
[AD-A146054] 03 p0355 N85-12283
Distributed reservation-based code division multiple access
[AD-A147007] 07 p0940 N85-15957
Compact wideband multiple conductor monopole antenna
[AD-D011331] 07 p0944 N85-15981
Lightweight, broadband Rayleigh wave transducer
[AD-D011345] 07 p1037 N85-16584
Determination of crustal and upper mantle structure from analysis of broadband teleseismic P-waveforms
08 p1181 N85-17440
A broadband matching network
[AD-D011406] 08 p1219 N85-17675
On the broadband energy spectra of quasars and BL Lac objects 08 p1240 N85-17825
Broad-band UHF dipole array
[NASA-TM-86373] 10 p1462 N85-19222
HF broadband whip antenna evaluation
[AD-A149527] 10 p1467 N85-19258
Propagation of wide bandwidth signals in a tropospheric ducting system 10 p1469 N85-19271
Wideband line-of-sight channel measurements and simulation: Application to digital radio links
10 p1471 N85-19283
A broadband kevlar radome for shipboard
[AD-P004365] 12 p1826 N85-21459
Multichannel digital processing of wideband signals
12 p1840 N85-21548
Method of measuring sea surface water temperature with a satellite including wideband passive synthetic-aperture multichannel receiver
[NASA-CASE-NPO-15651-1] 12 p1869 N85-21723
Efficiency of digital compensator of strong non-Gaussian interference 13 p2072 N85-22942
Programmable filter with fanned interdigital surface acoustic wave transducer 13 p2083 N85-23008
Design and measured performance of a broadband Archimedes spiral antenna
[R-NIAS-22] 14 p2290 N85-24194
A compact, aperture-matched, balanced transmission line antenna
[R-NIAS-28] 14 p2290 N85-24196
Disturbances in structure of lower ionosphere at terminators based on results of winde-band LW sounding 14 p2339 N85-24467
Wideband integrated voice/data technology
[AD-A152329] 17 p2947 N85-28197
AGS broad band neutrino beam
[DE85-010954] 19 p3366 N85-30875
Wideband disturbance accomodation in precision flexible space structures 20 p3415 N85-31194
Investigation of plasma processes in electronic transition lasers
[AD-A155598] 21 p3593 N85-32327
Cylindrical lens-array antenna for wideband electronic scanning
[AD-A156085] 24 p4090 N85-35350
Scale separation closure and Alfven wave turbulence
[DE85-013124] 24 p4095 N85-35385

BROADBAND AMPLIFIERS
Broadband transverse field interaction continuous beam amplifier
[AD-D011229] 01 p0043 N85-10279
Development of a 30 GHz/1 kW broadband traveling wave tube with suppression of band edge oscillations
[BMFT-FB-W-84-035] 07 p0948 N85-16011
New construction principles for oscillator power summing devices 07 p0949 N85-16016
Development of thin film hybrid IC active filter for video band use
[NHK-LABS-NOTE-312] 18 p3094 N85-29153

BROADCASTING
Subliminal communication technology
[GPO-38-833] 05 p0622 N85-13979
US objectives generally achieved at broadcasting satellite international conference. Improvements can help in future conferences
[PB84-236316] 06 p0800 N85-15109
Measurement of signal separation between radio service and air navigation service
[IRT-TB-B-40/82] 08 p1083 N85-16860
Satellite broadcasting: The performance of C-MAC in a hardware simulation of a DBS transmission chain
[BBC-RD-1984/9] 08 p1143 N85-17206
Subjective evaluation of the effect of noise and interference on frequency modulated NTSC television signals
[CRC-1367] 09 p1310 N85-18230
Star on the horizon: The emergence of the direct broadcast satellite in American mass communications
[AD-A148819] 09 p1312 N85-18242
Study of factors affecting an HF/VHF direct broadcasting satellite service
[PB85-120889/GAR] 09 p1313 N85-18255
Traveling wave tube for broadcast satellites
10 p1475 N85-19310
China's future domestic satellite communications systems 10 p1476 N85-19312
Electronic generation of text for television
[BBC-RD-1984/14] 13 p2053 N85-22856
Alternatives for satellite sound broadcast systems at HF and VHF 14 p2229 N85-23815
The distortion of AM broadcast antenna patterns as caused by nearby towers and highrise buildings
[CRC-1379] 15 p2536 N85-25668
Optimal frequencies for broadcast transmitters in the UHF domain: Report
[TUM-M8404] 16 p2769 N85-27068
SESC (Space Environment Services Center) satellite broadcasting 10-year plan
[PB85-163541] 16 p2775 N85-27126
Generalized graph coloring: A frequency assignment method for VHF broadcasting
[TUM-M8405] 16 p2844 N85-27535
Channel multiplexers for broadcast satellite transponders in the 12 GHz band
[NHK-LABS-NOTE-310] 18 p3090 N85-29122
Preliminary investigation of the performance of repeater technology for satellite sound broadcasting
[SSP/017/82] 18 p3092 N85-29137
Predicting the effects of non-Gaussian interference in HF (High-Frequency) broadcasting. Part 1: A methodology for an analytic approach
[PB85-171544] 18 p3092 N85-29140

BROKEN SYMMETRY
Dynamics of symmetry breaking: Phase coherence in finite and random systems
[NOTA-INTERNA-813] 02 p0253 N85-11658
Cosmic axions
[DE85-001330] 09 p1418 N85-18944
Symmetry breaking for a class of semi-linear elliptic problems
[AD-A149093] 10 p1546 N85-19748
Research in theoretical physics
[DE85-004286] 12 p1944 N85-22207
Standard model and beyond
[DE85-004269] 14 p2418 N85-24919
Activities of the Solid State Physics Research Institute
[NASA-CR-175899] 17 p3042 N85-28618
Uniaxial stress induced symmetry breaking for muon sites in Fe 17 p3042 N85-28620

BROMIDES
NT HYDROBROMIC ACID
Comparison study of analytical methods for the determination of fluoride, chloride, and bromide in plastics
[DE84-015008] 04 p0470 N85-12989
Graphite fiber intercalation: Dynamics of the bromine intercalation process
[NASA-TM-87015] 16 p2742 N85-26921
Determination of organobromide compounds in water by gas chromatography-negative ion chemical ionisation mass spectrometry
[DRIC-T-7411] 22 p3743 N85-33199
Rechargeable lithium-organic electrolyte battery having overcharge protection and method of providing overcharge protection for a lithium-organic electrolyte battery
[AD-D011738] 22 p3806 N85-33575

BROMINE
NT BROMINE ISOTOPES
Stability of bromine intercalated graphite fibers
[NASA-TM-86859] 01 p0031 N85-10187
Investigation of bromine complexed hydrogen/bromine regenerative fuel cells for portable electric power
[AD-A146401] 06 p0833 N85-15300
A study of liquid-vapor equilibria of the bromine-hydrobromic acid-water system
[NASA-TM-77748] 14 p2249 N85-23940
Homogeneity of pristine and bromine intercalated graphite fibers
[NASA-TM-87016] 15 p2517 N85-25521
Environmental stability of intercalated graphite fibers
[NASA-TM-87025] 16 p2753 N85-26992
A micrographic and gravimetric study of intercalation and deintercalation of graphite fibers
[NASA-TM-87026] 17 p2934 N85-28110

BROMINE COMPOUNDS
NT BROMIDES
NT HYDROBROMIC ACID
Study of the liquid vapor equilibrium in the bromine-hydrobromic acid-water system
[NASA-TM-77787] 07 p0921 N85-15836
Crossed molecular beam studies of the reactions of oxygen and fluorine atoms
[AD-A153302] 17 p2921 N85-28008

BROMINE ISOTOPES
Proposed solar neutrino experiment using (81)Br(nu,e(-e)) (81)Kr
[DE85-004802] 15 p2684 N85-26579

BROMINE 82
U BROMINE ISOTOPES

BROMINE 87
U BROMINE ISOTOPES

BRONCHI
Deposition in the human lung during respiration of small particles suspended in the air
[BLL-RISLEY-TR-5021-(9091.9F)]
03 p0400 N85-12549

BRONZES
Testing the antifriction properties of alloys for heavily loaded bearings 06 p0780 N85-14990
Effect of form memory in alloys based on Cu-Al systems 11 p1604 N85-20088
Microstructural study on the processing and properties of high-field A15 superconducting materials
[DE85-004652] 13 p2164 N85-23423
Ferroelectric tungsten bronze bulk crystals and epitaxial thin films for electro-optic device applications
[AD-A151044] 14 p2427 N85-24970
The microstructural state of Nb3Sn in a multifilamentary titanium doped bronze-process wire
[DE85-010979] 19 p3240 N85-30089

BROWNIAN MOVEMENTS
Deuteron NMR (Nuclear Magnetic Resonance) in relation to the glass transition in polymers
[AD-P003910] 01 p0032 N85-10186
A perturbation solution for rigid dumbbell suspensions in steady shear flow
[AD-A144878] 01 p0111 N85-10755
Neutron scattering on polysiloxanes
03 p0432 N85-12751
Study of submicron particle size distributions by laser Doppler measurement of Brownian motion
[AD-A149139] 10 p1487 N85-19388
Brownian motion with a parabolic drift and Airy functions
[CWI-MS-R8413] 12 p1925 N85-22097
A diffusion process and its application to detecting a change in the drift of Brownian motion
[AD-A150096] 12 p1926 N85-22100
Beam loss due to the aperture limitation resulting from intrabeam scattering
[DE85-005136] 12 p1930 N85-22124
Boundary crossing probabilities and statistical applications
[AD-A151027] 14 p2411 N85-24869
Brownian motion with quadratic killing and some implications: Revision
[AD-A151323] 15 p2642 N85-26296
Comments on estimating quantiles for Gaussian functionals by simulation
[AD-A154902] 19 p3348 N85-30750
The influence of Brownian coagulation on the size distributions of atmospheric aerosols
21 p3645 N85-32643
Scavenging of submicron aerosol particles by snow crystals: Theory and experiments
21 p3648 N85-32667
Large deviations for the maxima of some random fields
[AD-A155909] 24 p4143 N85-35681

BRUCETON TEST
U STATISTICAL TESTS

BRUSH (BOTANY)
Determination of low chloride values in Rocky Flats scrub alloy solutions and other complex matrices
[DE85-011506] 23 p3911 N85-34234

BRUSHES
NT BRUSHES (ELECTRICAL CONTACTS)
Investigation of electric and wear phenomena of liquid metal wetted copper fiber brushes under conditions of high slip ring eccentricity
[AD-A147634] 08 p1156 N85-17295

BRUSHES (ELECTRICAL CONTACTS)
Thermal and thermoelastic effects in rolling/sliding contacts
[AD-A150435] 13 p2165 N85-23429
Brush and commutator segment torquer motor
[AD-D011726] 23 p3927 N85-34340

BUBBLE CHAMBERS
Multidimensional analysis of data obtained in experiments with X-ray emulsion chambers and extensive air showers
[HE-3.6-2] 24 p4184 N85-35951

Experimental basis for the models of cascade propagation in atmosphere
[HE-3.6-6] 24 p4185 N85-35954
A comparative analysis of gamma and hadron families at the superhigh energies recorded in experiment Pamir
[HE-3.7-1] 24 p4185 N85-35960
Hadrons registration in emulsion chamber with carbon block
[HE-3.7-3] 24 p4186 N85-35962
New analysis of nuclear interaction observed by Mt. Kanbera emulsion chamber experiment
[HE-3.7-4] 24 p4186 N85-35963
Intensities of high-energy cosmic rays at Mount Kanbela
[HE-3.7-5] 24 p4186 N85-35964
Structured events in Pamir carbon X-ray chambers
[HE-3.7-7] 24 p4186 N85-35965
Ultra high energy events in ECHOS series and primary energy spectrum
[HE-3.7-9] 24 p4186 N85-35966
Search for anomalons using plastic nuclear track detectors
[HE-6.2-12] 24 p4212 N85-36148

BUBBLE MEMORY DEVICES
Integrated circuits, MBM's, form focus of work at French LETI 03 p0341 N85-12194
Feasibility of self-structured current accessed bubble devices in spacecraft recording systems
[NASA-CR-172554] 13 p1998 N85-22525
Advanced detectors and signal processing for bubble memories
[NASA-CR-172534] 14 p2297 N85-24219
SSMIR (Solid State Memory Instrumentation Recorder): A new approach to acquiring data during an aircraft seat/sled ejection sequence
[AD-A154780] 21 p3589 N85-32308
Advanced detectors and signal processing
[NASA-CR-176193] 24 p4086 N85-35343

BUBBLES
Soil tilt measurement: First results of the comparative analysis of the response of two different tiltmeters
[NOTA-INTERNA-818] 02 p0228 N85-11494
Collapse of cavitation bubbles between two walls in ultrasonic field 02 p0266 N85-11739
Characterization of ion implanted deuterium traps in nickel by equilibration with deuterium gas
[DE84-014958] 02 p0288 N85-11879
Laminar separation bubble with transition: Prediction test with local interaction
[BLL-PNR-90231-(8019.3153)] 06 p0808 N85-15132
VORT: A computer code for bubbly two-phase flow
[DE84-017076] 06 p0809 N85-15142
Research on acoustical and optical scattering, optics of bubbles, diffraction catastrophes, laser generation of sound, and shock induced cavitation
[AD-A146703] 06 p0860 N85-15486
Non equilibrium ionization in the local hot bubble 06 p0879 N85-15587
Large-scale bubble structure of the interstellar medium (ISM) and properties of the Local Spiral Arm (LSA) 06 p0879 N85-15588
Turbulent bubbles behind airfoils and wings at high angle of attack 08 p1069 N85-16779
Pneumatic turbulators: A device for drag reduction at Reynolds numbers below 5 million 08 p1071 N85-16791
A theoretical method for selecting space craft and space suit atmospheres
[AD-A148219] 08 p1200 N85-17559
Laminar separation bubble with transition: Prediction test with local interaction — airfoils
[PNR-90231] 09 p1274 N85-18008
Statistical comparison of pooled nitrogen washout data of various altitude decompression response groups
[NASA-TM-58265] 15 p2639 N85-28278
Fluid surface behavior in low gravity. Center discretionary fund no. 83-21
[NASA-TP-2488] 17 p2957 N85-28260
A study of aerodynamic control in stalled flight long laminar separation bubble analysis
[AD-A153650] 18 p3059 N85-28930
Dynamics of thin-film breakup in a constricted pore
[DE85-006442] 18 p3101 N85-29199
The effects of microbubbles on turbulent boundary layer skin friction 20 p3451 N85-31425
Magnetic materials
[AD-A154679] 21 p3580 N85-32256
Experimental studies of glass refining
[NASA-CR-176130] 22 p3751 N85-33248
Features of behavior of gas bubbles in molten oxide films during enamelling: Communication 2
[BLL-M-35781-(5828.4)] 23 p3919 N85-34283
SU(2) x U(1) vacuum and the Centauro events 24 p4175 N85-35885
Exploring results of the possibility on detecting cosmic ray particles by acoustic way
[HE-7.1-3] 24 p4213 N85-36157

BUCKLING
NT CREEP BUCKLING
NT ELASTIC BUCKLING
NT EULER BUCKLING
Design proposals for torsional buckling of stiffeners
[AD-A144783] 01 p0062 N85-10409
A buckling analysis for rectangular orthotropic plates with centrally located cutouts
[NASA-TM-86263] 04 p0513 N85-13268
Formulation and solution methods for classical problems of static buckling
[CETIM-101010] 04 p0514 N85-13280
A review of imperfection sensitivity of stiffened shells
[AD-A147311] 07 p0978 N85-16213
Buckling analysis of cracked, floating ice sheets
[AD-A147390] 07 p0988 N85-16277
Buckling and eccentricity effects on orifice metering accuracy — gas meters
[ERS-E.350] 09 p1324 N85-18321
Transverse vibration and buckling of a cantilevered beam with tip body under constant axial base acceleration
[NASA-CR-175567] 12 p1884 N85-21694
Steel containment buckling
[DE85-003744] 13 p2103 N85-23111
A model for the compressive buckling of extended chain polymers
[AD-A151025] 14 p2260 N85-24008
Solution to eigenvalue problems of antisymmetric cross-ply and antisymmetric angle-ply laminated plates using affine transformations
[AD-A153040] 17 p2917 N85-27980
Continuum modeling of latticed structures 17 p2977 N85-28399
The Shock and Vibration Digest, volume 17, no. 2
[AD-A153129] 17 p2977 N85-28400
Recent progress in the dynamic plastic behaviour of structures, part 4 17 p2978 N85-28402
Buckling and bracing of cantilevers
[CE-42] 17 p2979 N85-28413
Biaxial buckling of specially orthotropic, symmetric composite rectangular plates
[AD-A152958] 17 p2979 N85-28417
Analytical shear buckling investigation of curved composite panels
[AD-A153136] 17 p2980 N85-28421
Buckling and postbuckling behavior of shallow shells 18 p3120 N85-29317
Measurement and calculation of the mechanical response of a highly fractured rock
[DE85-008421] 18 p3127 N85-29362
Buckling and post-buckling behavior of sparsely connected built-up columns 19 p3283 N85-30358
Stress and buckling analysis 21 p3611 N85-32439
Structural analysis of imperfect three-legged truss columns for large space structures applications 24 p4100 N85-35416
Design and behavior of coped beams 24 p4100 N85-35417

BUDGETING
Managing recoverable aircraft components in the PPB and related processes: Executive summary
[AD-A146606] 07 p1050 N85-16667
Activities report of the aerospace industry in West Germany
[ISSN-0722-3838] 07 p1053 N85-16686
Activities report of the aerospace industry in West Germany
[ISSN-0722-3838] 07 p1054 N85-16687
FRG study looks at participation in ESA, US space station 08 p1141 N85-17191
Criteria for qualifying for FRG federal CAD/CAM subsidies 15 p2536 N85-25651
Manufacturing cost analysis of a parabolic dish concentrator (General Electric design) for solar thermal electric power systems in selected production volumes
[NASA-CR-175772] 16 p2818 N85-27380
New ESA director on Ariane, space station, future trends 18 p3066 N85-29096
FRG weighs ESA participation, budget issues 18 p3066 N85-29110
Thermal Energy Storage Program annual operating plan FY 1985
[DE85-008745] 19 p3307 N85-30499
Pricing options for the space shuttle. Special study 21 p3559 N85-32138
Space research in the United Kingdom: An assessment
[AD-A155334] 21 p3712 N85-33038
The 1986 National Aeronautics and Space Administration authorization
[GPO-47-835] 24 p4166 N85-35829

BUDGETS
Non-US approaches to space commercialization 02 p0150 N85-11012
AGARD bulletin technical programme, 1985
[AGARD-BUL-84-2] 02 p0305 N85-11971
Organizations as information processing systems. Toward a strategic contingencies model of budget related influence in municipal government organizations
[AD-A149364] 10 p1567 N85-19883
FRG's DFVLR ready for participation in space station 11 p1818 N85-20178
Academic science and engineering: R and D funds, fiscal year 1982 (detailed statistical tables)
[PB85-154763] 15 p2664 N85-28443

BUFFER STORAGE
A data collection system
[AD-D011266] 05 p0713 N85-14573
Precision digital sampler
[AD-D011265] 06 p0809 N85-15143
The Multimission Image Processing Laboratory's virtual frame buffer interface
[NASA-CR-175655] 14 p2402 N85-24805
Techniques for operating Charge Coupled Devices (CCD's) in very high speed framing mode
[AD-A152878] 17 p2953 N85-28238
Investigation of cosmic rays in very short time scales
[HE-4.6-7] 24 p4197 N85-36044

BUFFERS (CHEMISTRY)
Kinetics of hydrolysis and products of hydrolysis and photolysis of tetryl
[AD-A153144] 17 p2921 N85-28005
Development anmd testing of electrophoresis solutions. Task I.1: Development of optimal buffer system 20 p3500 N85-31755
Electrophoretic mobilities of erythrocytes in various buffers 20 p3500 N85-31756
Electrophoretic mobilities of cultured human embryonic kidney cells in various buffers 20 p3501 N85-31761
Pre-flight report on cultured human embryonic kidney cell handling and cell electrophoresis. Prepared prior to continuous-flow electrophoretic separation experiments aboard space shuttle flight STS-8 20 p3503 N85-31775
Iron and manganese in oxide minerals and in glasses: Preliminary consideration of Eh buffering potential at Yucca Mountain, Nevada
[DE85-011892] 23 p3916 N85-34271

BUFFETING
La Recherche Aerospatiale Bimonthly Bulletin, Number 1984-4, 221/July-August
[ESA-TT-884] 16 p2695 N85-26637
Wing buffeting active control testing on a transport aircraft configuration in a large sonic tunnel 16 p2714 N85-26750
Wing buffeting active control testing on a transport aircraft configuration in a large sonic windtunnel 17 p2904 N85-27903

BUILDING MATERIALS
U CONSTRUCTION MATERIALS

BUILDING STRUCTURES
U BUILDINGS

BUILDINGS
Patterns of behavior in lodgings exposed to traffic noise
[NASA-TM-77750] 03 p0367 N85-12479
Hurricane Alicia, Galveston and Houston, Texas, 17-18 August 1983
[PB84-237056] 04 p0541 N85-13441
The development of fire evaluation system for detention and correctional occupancies
[NBSIR-84-2976] 10 p1459 N85-19192
The 35 kilowatt peak power photovoltaic system
[DE85-000189] 10 p1511 N85-19537
Research on heat-exchanger corrosion
[PB85-126316] 11 p1616 N85-20164
Thermal stress-dependent dilation of concrete
[DE84-014666] 11 p1653 N85-20412
Phase change thermal energy storage and the model building codes
[PB85-111201] 12 p1883 N85-21813
Multiyear plan for experimental systems research passive and hybrid solar energy program
[PB85-146666] 12 p1883 N85-21815
Preliminary investigation of dispersion of pollutants in model building wake flows using bipolar space charge
[IC-AERO-84-04] 20 p3487 N85-31671

BULGARIA
Achievements in biology outlined 03 p0343 N85-12213
Contribution to space program reviewed 16 p2727 N85-26834

BULK ACOUSTIC WAVE DEVICES
Compensation of acoustic wave devices
[AD-D011582] 15 p2648 N85-26322

BULK MODULUS
Research program on the effect of pressure on the mechanical properties of polymers, part 2
[DE85-000995] 13 p2037 N85-22761
Hydrostatic compression of Fe1-chi 0 wustite.
15 p2508 N85-25472

BUMPY TORUSES
N-frequency quasiperiodicity and chaos in dissipative dynamical systems 02 p0282 N85-11840
EBT electron energy confinement experiments
[DE84-015402] 04 p0567 N85-13613
Proceedings of the US-Japan Theory Workshop on 3-D MHD Studies
[DE84-012019] 04 p0568 N85-13620
Elmo Bumpy Torus physics
[DE84-015809] 05 p0730 N85-14694
Theoretical investigations relevant to magnetic fusion research, April 1, 1983 - March 31, 1984
[DE85-001778] 06 p0865 N85-15498
Theoretical investigations relevant to magnetic fusion research
[DE85-001777] 06 p0866 N85-15503
Far-infrared laser diagnostic on EBT and extreme far-forward laser scattering on ISX
[DE85-001788] 07 p1046 N85-16643
Density measurements of atomic hydrogen in NBT-IM by laser-induced fluorescence spectroscopy
09 p1389 N85-18739
Effect of alpha particles on the stability of Elmo Bumpy Torus (EBT) reactor
[DE84-017266] 09 p1392 N85-18750
Electron bounce resonance heating in a bumpy cylinder
[DE85-001732] 10 p1561 N85-19845
Direct reading fast microwave interferometer for EBT
[DE85-000183] 11 p1636 N85-20306
Observations of low frequency plasma fluctuations in ELMC Bumpy Torus
[DE85-003796] 11 p1732 N85-20895
Transient waveform acquisition system for the ELMO Bumpy Torus
[DE85-000154] 11 p1733 N85-20901
Suppression of tilting instability of a compact torus by energetic particle beams
[IPPJ-705] 12 p1935 N85-22157
Electrostatic confinement in a bumpy torus
[DE85-003794] 12 p1936 N85-22164
Nagoya bumpy torus 15 p2655 N85-26377
Heavy ion beam study of potential formation in bumpy torus plasma
[IPPJ-711] 15 p2656 N85-26386
Theoretical studies of Elmo Bumpy Torus
[DE85-007202] 15 p2658 N85-26402
Inherent magnetic field error measurements in ELMO Bumpy Torus
[DE85-005655] 16 p2867 N85-27685
Theoretical and numerical studies of magnetic field line displacements in an Elmo Bumpy Torus
[DE85-006757] 17 p3041 N85-28816
Electron temperature measurements from induced toroidal current in ELMO Bumpy Torus scale
[DE85-006549] 18 p3189 N85-29779
Magnetics calculations for an ELMO Bumpy Square
[DE85-010442] 18 p3191 N85-29792
The effects of alpha particle production on the stability of an Elmo Bumpy Torus (EBT) reactor
19 p3369 N85-30895
Research support for plasma diagnostics on Elmo Bumpy Torus: Diamagnetic measurements and data analysis and development of ring models for realistic representation of fields near the plasma
[DE85-010035] 19 p3371 N85-30912
Thomson scattering on Elmo Bumpy Torus
[DE85-010584] 20 p3527 N85-31941
Magnetics calculations for an ELMO Bumpy Square
[DE85-011436] 21 p3707 N85-33021
Elmo bumpy square plasma confinement device
[DE85-011628] 22 p3845 N85-33816
Assessment of magnetic field asymmetries in ELMO Bumpy square
[DE85-011905] 22 p3846 N85-33819
High-field launch electron cyclotron heating experiments in the ELMO Bumpy Torus
[DE85-012068] 22 p3846 N85-33825
Proceedings of the US-Japan Workshop on Transport in Open-Ended Systems
[IPPJ-727] 23 p3975 N85-34644
Compact DT fusion spherical tori at modest field
[DE85-011568] 23 p3982 N85-34692
Multiple-frequency electron cyclotron heating of hot electron rings in EBT-1
[DE85-011302] 23 p3983 N85-34701
Assessment of magnetic field asymmetries in ELMO Bumpy square
[DE85-011559] 23 p3984 N85-34705

BUNCHING
NT ELECTRON BUNCHING
Considerations regarding the choice of beam parameters and IP configuration for the SSC
[DE84-014532] 01 p0118 N85-10803
Antiproton source beam position system
[DE84-016716] 09 p1380 N85-18679
Bunch coalescing in the main ring to form intense proton and antiproton bunches without RF counterphasing
[DE85-001364] 09 p1382 N85-18682
Adaptive corrector operating in frequency domain
22 p3785 N85-33337
Synchronous timing of multi-energy fast beam extraction during a single AGS cycle
[DE85-011829] 24 p4158 N85-35781

BUNDLES
An efficient algorithm for the computation of the inverse in bundle adjustment systems — photogrammetry
08 p1175 N85-17411
Study of hadron bundles observed in Chacaltaya two-story emulsion chamber
[HE-3.3-4] 24 p4180 N85-35922

BUOYANCY
The properties of plane turbulent buoyant jet
[NAL-TR-798] 01 p0046 N85-10304
Mass and momentum transport in a turbulent buoyant vertical axisymmetric jet 05 p0635 N85-14070
A new physical Lagrangian tracer
[DE84-016212] 05 p0687 N85-14419
The properties of a round turbulent buoyant jet
[NAL-TR-826] 06 p0808 N85-15136
Finite difference calculations of buoyant convection in an enclosure. Part 2: Verification of the nonlinear algorithm
[PB85-104065/GAR] 07 p0961 N85-16089
Primer for mass metrology
[PB85-121424/GAR] 09 p1305 N85-18199
An experimental study of single and multiple turbulent buoyant jets in crossflow 09 p1317 N85-18281
On the flow processes in sharply inclined and stalled airfoils in parallel movement and rotation
[NASA-TM-77509] 10 p1419 N85-18952
Wind-tunnel research on the mechanics of plumes in the atmospheric surface layer
[AD-A150019] 12 p1846 N85-21584
Mechanisms of heat and mass transfer across a double-diffusive interface
[PB85-148468] 12 p1848 N85-21594
Assembly Concept for Construction of Erectible Space Structure (ACCESS) neutral buoyancy testing results
14 p2236 N85-23662
Magnetic buoyancy instabilities in the convective overshoot zone — Sun 14 p2447 N85-25101
Numerical techniques for steady two-dimensional transcritical stratified flow problems, with an application to the intermediate field dynamics of ocean thermal energy conversion plants
[DE85-006347] 18 p3151 N85-29509
Experiences with neutral buoyance testing mockups
18 p3159 N85-29571
Buoyant jet entrainment in stratified fluids
19 p3263 N85-30238
Numerical solutions of turbulent models for flow over a flat plate with angle of attack
[DE85-010380] 21 p3585 N85-32286
Gravity-wave spectra in the atmosphere observed by MST radar, part 4.2B 21 p3622 N85-32502
Buoyant densities of phototrophic sulfur bacteria and cyanobacteria 21 p3660 N85-32740
The calculation of two-dimensional buoyant surface jets with the k-W model of turbulence — kinetic energy-vorticity fluctuations (k-W)
[CFD/84/21] 22 p3785 N85-33448

BUOYS
Sea ice data buoys in the Weddell Sea
[AD-A144953] 01 p0088 N85-10594
High-data-rate wide-angle underwater acoustic telemetry system
[DE84-015696] 02 p0233 N85-11519
Terrestrial locating — of buoys from space
05 p0599 N85-13816
Mariners weather log, volume 28, no. 3, July-August-September 1984
[PB85-107266] 06 p0840 N85-15334
Improvements in linked-spar motion-compensated lifting system
[AD-D011413] 06 p1138 N85-17165
Drifting buoy data from equatorial Pacific Ocean, 31 Aug. 1980 - 30 Apr. 1982
[PB85-120046] 10 p1522 N85-19598
Project PAPA: The integration of drifting buoy data into an operational meteorological service
14 p2238 N85-23674
Automatic buoys to assist the tuna fishery off the Azores 14 p2238 N85-23679
Fourier transform of wave data on ARGOS buoys
14 p2323 N85-24351
The development of Platform Transmitter Terminal (PTT) and its application for drifting buoys
14 p2323 N85-24353
Surface currents in the tropical Pacific during 1979-1980 using drifting buoys 14 p2323 N85-24354
Inferences of future operations drawn from past and present applications of drifting buoys
14 p2323 N85-24356
US program in anchored data buoy and the other fixed observation platforms 14 p2324 N85-24358
One thousand days in the brine — platform transmitter terminals 14 p2324 N85-24359
The development of an automated marine meteorological data system 14 p2324 N85-24362
The ARGOS contribution to the First GARP Global Experiment (FGGE) study of drifting buoys
14 p2325 N85-24371
Meteorological buoys developed at the EERM laboratory 14 p2326 N85-24374
The ARGOS contribution to the successful dredging of a deep moored current meter 14 p2327 N85-24381
Drifting buoy studies for weather applications
14 p2329 N85-24396
Collecting meteorological reports with the ARGOS system 14 p2329 N85-24398
The French Ocean Climate in Equatorial Atlantic (FOCAL) Drifter Program, 1983-1984
14 p2329 N85-24399
The Deep Drifter Program — deep ocean sensors
14 p2329 N85-24400
Telemetered meteorological and engineering data from a deep sea moored body in the Long Term Upper Ocean Study (LOTUS) 14 p2329 N85-24402
Drifting buoy development and future programs — Japanese ARGOS program 14 p2330 N85-24406
Development of a low cost drifting buoy
14 p2330 N85-24408
Arabian gulf circulation — pollution monitoring
14 p2331 N85-24412
A report on the DRIFTERS program — buoys
14 p2331 N85-24413
Drifting buoys on the Labrador shelf
14 p2331 N85-24415
Moored buoy stationkeeping and location system
14 p2331 N85-24416
Overview of data processing at AES local user terminals — Canadian Atmospheric Environment Service (AES) 14 p2331 N85-24418
The Data Acquisition Control and Telemetry (DACT) system — meteorological buoys
14 p2332 N85-24419
An overview of NDBC drifting buoy development programs — NOAA Data Buoy Center (DBC)
14 p2332 N85-24422
Tactical deployment of satellite-reporting drifting data buoys for environmental data acquisition
14 p2332 N85-24423
Studies into location accuracy — ARGOS system
16 p2811 N85-27334
Positioning accuracy of the ARGOS system in operational use 16 p2811 N85-27335
DB2 and DB3: The next generation — buoys
16 p2811 N85-27337
Development of a Lagrangian drifting buoy
16 p2811 N85-27338
Long term drifting float for measuring mean oceanic circulation using ARGOS system
16 p2811 N85-27339
ARGOS-tracked drifters in the Rockall Trough
16 p2812 N85-27340
Monitoring of marine environment
16 p2812 N85-27341
The validation of sea surface temperatures determined from AVHRR data using in situ data recovered via system ARGOS 16 p2812 N85-27342
Wave directional spectra via ARGOS
16 p2812 N85-27343
Routine wave and meteorological measurements in offshore areas using ARGOS data surveillance
16 p2812 N85-27344
Results of an initial trial of a satellite telemetering buoy measuring near surface current
16 p2812 N85-27345
An operational buoy network collecting meteorological data 16 p2813 N85-27351
Checking on the position of navigation marker buoys by the ARGOS system 16 p2813 N85-27354
An inexpensive radar-responding relocation device for drifting oceanographic instruments
[AD-A152170] 16 p2838 N85-27505
A laser slope gauge and a spar buoy wave gauge: Tools for the validation of microwave remote sensors
[AD-A154038] 19 p3272 N85-30290

Free-float Emergency Position Indicating Radio Beacons (EPIRBs) and release mechanism on board Norwegian ships. Main specifications and user experience
20 p3404 N85-31120
Experiments of a LORAN-C aided recovery system and a proposal of its application to rescue system
20 p3404 N85-31121

BURGER EQUATION
On limits of applicability of linear models to dynamics of gas channels in aircraft engines
09 p1308 N85-18219
The stress-strain-time graph of rheological soils and its application
[AD-P004266] 09 p1407 N85-18863
On the relation between upwind-differencing schemes of Godunov, Engquist-Osher and Roe
[NASA-CR-175805] 16 p2852 N85-27583
The Hamiltonian structure of a complex version of the Burgers hierarchy
[PREPRINT-423] 18 p3173 N85-29665

BURNERS
Heat flux sensors for burner liners and turbine blades and vanes
02 p0142 N85-10961
Burner liner thermal/structural load modelling
02 p0143 N85-10970
Burner stabilized flames in fluids
[DE84-017429] 09 p1291 N85-18109
Ribbon burner simulation of T-700 turbine shroud for ceramic lined seals research
[NASA-TM-86940] 10 p1483 N85-19364
Digital temperature and velocity control of mach 0.3 atmospheric pressure durability testing burner rigs in long time, unattended cyclic testing
[NASA-TM-86959] 12 p1805 N85-21321

BURNING
U COMBUSTION

BURNING PROCESS
U COMBUSTION

BURNING RATE
HMX combustion modification
[AD-A145071] 01 p0024 N85-10149
Catalyzed low burning rate propellants for upper-stage solid rocket motor
[NAL-TR-805] 03 p0339 N85-12181
Thrust characterization of very high burning rate propellants
[AD-A145891] 03 p0340 N85-12186
Combustion properties of fuel-rich magnesium propellants with HTPB as binder
[FOA-C-20555-D1] 07 p0935 N85-15924
The pressure deflagration limit of solid rocket propellants
08 p1117 N85-17048
Thermal profiles of thermite reactions
[DE85-003308] 10 p1438 N85-19061
Recovery of damaged solid propellants by interrupting burning and crack-propagation processes
[AD-P004343] 10 p1455 N85-19167
A thermal-mechanical model of deflagration-to-detonation in granular energetic materials
[AD-P004346] 10 p1455 N85-19170
Effects of perforation L/D ratio and slotting on stick propellant combustion
[AD-A146854] 10 p1456 N85-19177
Study of HTPB-based SOFRAM fuels
[FOA-C-20563-D3] 11 p1614 N85-20150
Mechanism of burning rate enhancement by ferric oxide
13 p2002 N85-22546
Effect of variable solid phase thermal properties on propellant combustion
13 p2002 N85-22547
Multiple reflection theory for microwave measurement of solid propellant burning rates
13 p2002 N85-22549
In-situ burning rate determination using flash radiography
13 p2002 N85-22560
Chemical kinetics of gas phase decomposition products of nitramine propellants
13 p2003 N85-22558
A comprehensive review of black powder
[AD-A150455] 13 p2039 N85-22789
A fundamental study of liquid phase particle breakup. Revision
[AD-A150791] 14 p2301 N85-24249
The overall reaction concept in premixed, laminar, steady-state flames. 2: Initial temperatures and pressures
[AD-A152132] 16 p2746 N85-26944
Burn rates of explosives at high pressures
[DE85-010606] 19 p3251 N85-30159
Radiative augmented combustion
[AD-A154137] 20 p3423 N85-31246
The role of aircraft panel materials in cabin fires and their properties
[FAA-CT-84-30] 21 p3553 N85-32104
Closed-bomb combustion of Hivelite-based, Very High Burn Rate (VHBR) propellant
[AD-A155740] 21 p3571 N85-32212
Investigation of the flame speeds of propane/methanol gas mixtures
[DE85-012817] 23 p3912 N85-34239
Modeling heterogeneous high explosive burn with an explicit hot-spot process
[DE85-009593] 23 p3922 N85-34300

BURNOUT
A review of the physics and response models for burnout of semiconductor devices
[AD-A155031] 21 p3709 N85-33028

BURNS (INJURIES)
Man's physical tolerance to heat. Heat storage, burn injury
[FOA-C-54055-H1] 02 p0235 N85-11533

BURSTS
NT GAMMA RAY BURSTS
NT RADIO BURSTS
NT SOLAR RADIO BURSTS
NT TYPE 3 BURSTS
NT TYPE 4 BURSTS
The vertical structure and stability of alpha model accretion disks
09 p1417 N85-18938
X-ray bursts: Observation versus theory
[NASA-CR-174415] 10 p1573 N85-19916
Hydrodynamic simulations of recurrent novae
11 p1753 N85-21025
X-ray spectra of bursting neutron stars
23 p3961 N85-34686
DMSK: A practical 2400-bps receiver for the mobile satellite service: An MSAT-X Report
[NASA-CR-176194] 24 p4086 N85-35324

BUS CONDUCTORS
Fiber optic data bus using Frequency Division Multiplexing (FDM) and an asymmetric coupler
[NASA-TM-86015] 04 p0492 N85-13139
EMI (electromagnetic interference) filter capacitor unit
[AD-D011392] 07 p0937 N85-15941
Analysis of the performance of multiaccess networks of the bus type
[FUB-47-1983] 09 p1313 N85-18249
Survivable local area network
[AD-D011453] 10 p1468 N85-19262
Development of an integrated control unit for the PDV bus concept
[BMFT-FB-T-84-300] 15 p2551 N85-25745
Design of a microprogram control unit with concurrent error detection
[AD-A156447] 24 p4139 N85-35655

BUSHINGS
Damping seal verification setup
16 p2738 N85-26893
Telescoping low vibration pulling mechanism for Czochralski crystal growth
[AD-D011655] 17 p3044 N85-28836
Further investigations to improve the fatigue life of the Mirage 1110 wing main spar
[ARL/STRUC-TM-397] 18 p3061 N85-28938

BUSINESS MANAGEMENT
U INDUSTRIAL MANAGEMENT

BUTADIENE
The effect of pressure on the mechanical properties of polymers. Part 2: Measurement of the time-dependent Poisson's ratio
[DE85-002139] 06 p0772 N85-14938
Reactions of butadiyne. 1: The reaction with hydrogen atoms
[NASA-TM-77805] 07 p0921 N85-15834
Laser schlieren, shock tube studies of high temperature hydrocarbon pyrolysis rates
[DE85-003314] 11 p1636 N85-20303

BUTANES
Thermodynamic properties of isobutane-isopentane mixtures from -40 to +600(0)F and up to 1000 psia
[DE84-015137] 01 p0124 N85-10850
Butene oxidation by molybdenum crystalographic shear compounds
[DE84-013910] 05 p0614 N85-13923
Biocatalyzed processes for production of commodity chemicals: Assessment of future research advances for N-butanol production
[NASA-CR-174264] 07 p0919 N85-15819
Catalytic conversion of C3-C4 paraffins to gasoline
[DE85-004181] 10 p1458 N85-19187
Thermophysical properties of working fluids for binary geothermal cycles
[DE85-000365] 12 p1881 N85-21804
Detailed chemical kinetic study of the effect of molecular structure on autoignition of fuel-air mixtures
[DE85-004424] 17 p2921 N85-28010
On the low temperature chemistry preceding end gas autoignition
[DE85-010471] 19 p3252 N85-30162
Optical waveguide sensor for methane gas
[AD-D011691] 19 p3273 N85-30294
Experimental study of engine knock
[DE85-009851] 22 p3754 N85-33268
Production of butanol by fermentation in the presence of cocultures of clostridium
[NASA-CASE-NPO-16203-1] 24 p4071 N85-35227

BUTENES
Study of vibrational energy transfer at a liquid tin surface
[AD-A145741] 02 p0277 N85-11804

BUTT JOINTS
Radiographic inspection of butt welds described
11 p1620 N85-20198
Evaluation of stress concentration coefficients in butt-welded joints with displaced edges
15 p2501 N85-25425
Differential between crack and pseudo-crack indications by means of objective magnetic flux leakage testing
[BLL-BISI-TRANS-22033-(9022.08)]
17 p2976 N85-28386
Low pressure arc butt welding of dissimilar metals
19 p3248 N85-30126

BUTTERFLY VALVES
NT DAMPERS (VALVES)

BUTYLENE
U BUTENES

BUTYLENE OXIDES
U TETRAHYDROFURAN

BUTYRIC ACID
Production of butanol by fermentation in the presence of cocultures of clostridium
[NASA-CASE-NPO-16203-1] 24 p4071 N85-35227

BY-PRODUCTS
Versatility of peat emphasized
07 p0994 N85-16316
Oil-shale exploration expansion urged
07 p0994 N85-16317
Rockwell Hanford operations defense waste and byproducts management
[DE85-000553] 09 p1382 N85-18694
Current regulatory and licensing status for byproduct sources, facilities and applications
[DE85-010967] 22 p3842 N85-33798

BYPASS RATIO
A study of bird ingestions into large high bypass ratio turbine aircraft engines
[DOE/FAA/CT-84/13] 01 p0005 N85-10028
Effect of combined pressure and temperature distortion orientation on high-bypass-ratio turbofan engine stability
[NASA-TM-83771] 01 p0011 N85-10067
Effect of steady-state temperature distortion on inlet flow to a high-bypass-ration turbofan engine
[NASA-TM-86896] 07 p0904 N85-15725
Planning of air cushion transport vehicles
14 p2285 N85-24190
Energy efficient engine. Fan and quarter-stage component performance report
[NASA-CR-168070] 23 p3897 N85-34141
Energy Efficient Engine Program technology benefit/cost study, volume 1
[NASA-CR-174766-VOL-1] 24 p4086 N85-35197
Energy Efficient Engine Program technology benefit/cost study, volume 2
[NASA-CR-174766-VOL-2] 24 p4086 N85-35198

BYPASSES
Noise isolation system for high-speed circuits
[DE84-014229] 01 p0043 N85-10283
Problems in high temperature thermocouple thermometry
[DE85-000606] 10 p1488 N85-19397
Diodes in photovoltaic modules and arrays
[NASA-CR-175454] 10 p1508 N85-19513
Problems with electrical interference between solar generators and shunt type regulators
13 p2010 N85-22607

C

C BAND
Non-local origin of a substantial portion of the soft X-ray background
06 p0677 N85-15567
The nature of the soft X-ray emitting region in the direction of the North Polar spur
06 p0677 N85-15568
Spectrum resource assessment of the 7125-8500 MHz band
[PB85-127413] 11 p1626 N85-20242
Strongly coupled millimeter-band waveguide directional couplers
22 p3779 N85-33418

C-5 AIRCRAFT
Performance capabilities of the C-5 and C-17 cargo aircraft
[AD-A145518] 02 p0138 N85-10939
Airborne performance measurement system design: C-5 aircraft
[AD-A145436] 02 p0236 N85-11539
The structural finite element model of the C-5A
15 p2576 N85-25885

C-135 AIRCRAFT
Investigation of surface tension phenomena using the KC-135 aircraft
[NASA-TM-82508] 10 p1426 N85-18095
Design of robust controllers for a multiple input-multiple output control system with uncertain parameters application to the lateral and longitudinal modes of the KC-135 transport aircraft
[AD-A153100] 17 p2900 N85-27877
C-141 AIRCRAFT
Far-infrared spectroscopy of interstellar gas
06 p1245 N85-17858
Molecular spectroscopy from the Kuiper Airborne Observatory
[NASA-CR-175748] 16 p2882 N85-27783
CABIN ATMOSPHERES
NT SPACECRAFT CABIN ATMOSPHERES
Airliner cabin air quality
[S-REPT-98-468] 03 p0402 N85-12560
Other challenges in the development of the orbiter environmental control hardware
08 p1096 N85-16824
Simultaneous cabin and ambient ozone measurements on two Boeing 747 airplanes. Volume 3: October 1978 - July 1979
[NASA-TM-86683] 12 p1892 N85-21872
CABLES
Evaluation of the Kerie Cable thermal arc cutting equipment
[AD-A147813] 07 p0974 N85-16186
The dynamics of slack marine cables
[AD-A155022] 21 p3599 N85-32349
Enhanced heat transfer computations for internally cooled cable superconductor
[DE85-011897] 24 p4095 N85-35363
CABLES (ROPES)
Sea water rope batteries
[AD-A144775] 01 p0042 N85-10275
NATFREQ users manual: A FORTRAN 4 program for computing natural frequencies, mode shapes and drag coefficients for taut strumming cables with attached masses and spring-mass combinations
[AD-A146058] 03 p0407 N85-12600
Test methods for cable cars
[CETIM-1-5K-45-1] 04 p0515 N85-13282
Electromagnetic inspection of wire ropes using sensor arrays
[AD-A148317] 06 p1170 N85-17379
Electromagnetic inspection of wire ropes using sensor arrays
[AD-A149016] 10 p1495 N85-19436
Cable-catenary large antenna concept
14 p2231 N85-23629
Apparatus producing constant cable tension for intermittent demand
[DE85-006434] 23 p3938 N85-34412
Study of NSI and related cable performance during tests performed in the NASA Hot Gas Facility
[NASA-CR-170866] 24 p4101 N85-35423
CAD (DESIGN)
U COMPUTER AIDED DESIGN
CADASTRAL MAPPING
Application of the Siemens Computer Aided Computer (Sicad) system to the surveying management in Baden-Wuerttemberg 16 p2814 N85-27951
Automatic engraving of map frames in the revision of the TK 25, 1:25,000 topographical map
16 p2814 N85-27952
The significance of orthophoto maps for developing countries 18 p3124 N85-29341
CADMIUM
Features of laser welding of medium carbon steel through a cadmium coating 01 p0020 N85-10122
Optical bistability in Cd(x)Hg(1-x)Te
18 p3186 N85-29760
Physical and chemical aerosol characteristics in extremely clean air masses at Cape Grim, Tasmania
21 p3646 N85-32655
Environmental surveillance at Los Alamos during 1984
[DE85-011886] 22 p3811 N85-33605
Towards the development of technological processes for the preparation of cadmium plated steel articles
[BLL-M-36315-(5628.4)] 23 p3913 N85-34248
CADMIUM COMPOUNDS
NT CADMIUM FLUORIDES
NT CADMIUM SELENIDES
NT CADMIUM SULFIDES
NT CADMIUM TELLURIDES
An investigation of the role of sintering in gas-solid interactions
[DE84-015491] 02 p0288 N85-11884
The alpha-form of the hydroxides of bivalent metals
[NASA-TM-77508] 04 p0473 N85-13009
CADMIUM FLUORIDES
High temperature laser interferometric studies of solid electrolytes 09 p1396 N85-18785
CADMIUM MERCURY TELLURIDES
U MERCURY CADMIUM TELLURIDES
CADMIUM NICKEL BATTERIES
U NICKEL CADMIUM BATTERIES
CADMIUM SELENIDES
Luminescent properties of graded cadmium sulfoselenide electrodes prepared from cadmium sulfide substrates
[AD-A146710] 06 p0766 N85-14698
Preliminary studies on the low-cost preparation of chalcogenide semiconductors from solution depositions
[DE85-000536] 11 p1736 N85-20918
Development of a CdSe thin film solar cell
12 p1880 N85-21796
The ESFET: Evaporated Sensing Field Effect Transistor 19 p3256 N85-30188
CADMIUM SULFIDES
Development of copper sulfide/cadmium sulfide thin-film solar cells
[DE84-004513] 01 p0044 N85-10287
Preparation and properties of evaporated CdTe films compared with single crystal CdTe
[DE85-000502] 02 p0222 N85-11452
Development of the production technology of Cu2S/CdS solar generators
[BMFT-FB-T-84-137] 03 p0366 N85-12469
Development and utilization of CdS/Cu2S
05 p0662 N85-14256
Luminescent properties of graded cadmium sulfoselenide electrodes prepared from cadmium sulfide substrates
[AD-A146710] 06 p0766 N85-14698
Preliminary studies on the low-cost preparation of chalcogenide semiconductors from solution depositions
[DE85-000536] 11 p1736 N85-20918
Testing and optimization of the production technology of large-surface Cu2S/CdS solar generators
12 p1880 N85-21783
Physical-chemical investigations of copper sulfides for use in CdS/Cu2S solar cells 12 p1880 N85-21794
A study of the stability of cadmium sulfide/copper sulfide and cadmium sulfide copper-indium-diselenide solar cells
[DE85-002902] 15 p2587 N85-25947
Zn3P2 as an improved semiconductor for photovoltaic solar cells
[DE85-006772] 18 p3097 N85-29171
SERI photovoltaic advanced research and development project: FY 1984 accomplishments
[DE85-002939] 18 p3128 N85-29368
Post-deposition heat treatments of CdS/CuInSe2 solar cells
[DE85-002943] 18 p3128 N85-29373
Cadmium sulfide/copper ternary heterojunction cell research
[DE85-006778] 19 p3305 N85-30486
Liquid crystal light valve structures
[NASA-CASE-MSC-20036-1] 22 p3847 N85-33826
Vectorial electron transfer on designed surfaces
[PB85-204600] 24 p4076 N85-35263
CADMIUM TELLURIDES
Preparation and properties of evaporated CdTe films compared with single crystal CdTe
[DE85-000502] 02 p0222 N85-11452
DOE/SERI polycrystalline thin-film photovoltaic research
[DE84-004516] 02 p0223 N85-11464
Liquid-phase epitaxial growth of CdTe on HgCdTe
[AD-D011482] 10 p1561 N85-19846
Investigation of the effect of annealing on the dislocation and sub-grain boundary content of solvent-evaporation-grown CdTe
[AD-A144087] 13 p2162 N85-23415
Investigation of the MBE growth of InSb and novel quantum well structures
[AD-A151014] 14 p2427 N85-24969
Thin film cadmium telluride and zinc phosphide solar cells
[DE85-002904] 15 p2587 N85-25950
Applications of CdTe to nuclear medicine
[DE85-011877] 23 p3952 N85-34492
HgCdTe surface and defect study program
[AD-A156079] 24 p4161 N85-35799
Electron irradiation of N type cadmium telluride
[AD-A156117] 24 p4161 N85-35801
CAI
U COMPUTER ASSISTED INSTRUCTION
CAISSONS
Safe decompression schedules for caisson workers
[PB85-103812/GAR] 07 p1017 N85-16463
CALCIFEROL
The role of vitamin D in the bone changes associated with simulated weightlessness 15 p2606 N85-26072
The role of 1,25-dihydroxyvitamin D in the inhibition of bone formation induced by skeletal unloading
[NASA-TM-87480] 18 p3153 N85-29522
CALCINATION
U ROASTING
CALCITE
Impact cratering: The process and its effects on planetary evolution — and silicate-carbonate reactions on Venus
[NASA-CR-174016] 02 p0228 N85-11488
Shock and release equation of state of calcite
[DE85-013151] 23 p3942 N85-34432
Uranium, thorium isotopic analyses and uranium-series ages of calcite and opal and stable isotopic compositions of calcite from drill cores UE25a no. 1, USR G-2 and USW G-3/GU-3, Yucca Mountain, Nevada
[DE85-013039] 23 p3948 N85-34471
CALCIUM
NT CALCIUM ISOTOPES
Variations of the H and K emission lines of singly ionized calcium in the eclipsing binary star system AR Lacertae
02 p0296 N85-11921
Non-invasive techniques for determining musculoskeleton body composition
[DE84-015718] 04 p0545 N85-13470
Abundancies of Ni, Cr, CO and major elements in the silicate portion of the Moon: Constraints from primary lunar magmas 04 p0582 N85-13720
Effect of disuse on sarcoplasmic reticulum in fast and slow skeletal muscle
[NASA-CR-174337] 08 p1191 N85-17508
Study of superplastic alloys based on Al-Zn-Ca
10 p1442 N85-19092
Evaluation of ettringite and related compounds for use in solar energy storage
[PB85-146876] 12 p1883 N85-21816
Carbonate chemistry of the Weddell Sea
[DOE/EV-110811/4] 12 p1898 N85-21916
Aluminum alloy ATs5K5 (5% Zn + 5% Ca) for superplastic forming 13 p2026 N85-22697
Effect of phase state of TiC-NiTi powder composite materials on nature of failure and mechanical properties
13 p2027 N85-22702
Polyamines as possible modulators of gravity induced calcium transport in plants 15 p2606 N85-26060
Calcium and calmodulin localization in gravitropically-responding plant organs
15 p2606 N85-26061
The interaction of calcium and auxin in the gravitropic response of roots 15 p2606 N85-26062
The role of vitamin D in the bone changes associated with simulated weightlessness 15 p2606 N85-26072
New techniques for studying calcium gradients
15 p2609 N85-26076
Isolation of hybridomas for golgi-associated proteins and a plant calmodulin 15 p2613 N85-26103
Computer simulation studies in fluid and calcium regulation and orthostatic intolerance
[NASA-CR-171869] 15 p2616 N85-26117
Addendum to the STCAL and LTCAL user's guide
[NASA-CR-171880] 15 p2628 N85-26194
The effect of microalloying with calcium and magnesium on the plasticity of Poldi AKN 20 Ni-based alloy
[BLL-BISI-TRANS-2174-(9022.06)]
17 p2929 N85-28075
Examples of application of machinability tests
[BLL-BISI-TRANS-22346-(9022.06)]
17 p2973 N85-28363
Cluster production and entropy
[DE85-007626] 17 p3032 N85-28752
Effect of periodic accelerations on physiochemical properties and Ca2+ reactivity of actomyosin in white rat myocardium and skeletal muscles
19 p3324 N85-30594
Space-flight simulations of calcium metabolism using a mathematical model of calcium regulation
[NASA-CR-171883] 19 p3328 N85-30621
The production and destruction of metastable negative ions
[DE85-011056] 19 p3364 N85-30858
Relative abundances of sub-iron to iron nuclei in low energy (50-250 MeV/N) cosmic rays as observed in the Skylab experiment
[OG-4.1-4] 22 p3876 N85-34010
A new analysis of cosmic ray isotopes at 3 GeV/n from HEAO3-C2 data
[OG-4.3-6] 22 p3879 N85-34031
Effects of acid rain on forest nutrient status
[DE85-012466] 23 p3947 N85-34463
CALCIUM CARBONATES
NT CALCITE
Shock-induced CO2 loss from CaCO3: Implications for early planetary atmospheres
[NASA-CR-174197] 05 p0745 N85-14777
Two dimensional CO2-ocean model including the biological processes
[DE85-012341] 23 p3950 N85-34483

CALCIUM CHLORIDES
Salt action on concrete
[AD-A147812] 07 p0933 N85-15912
Binary phase diagram determinations
[DE85-010656] 19 p3235 N85-30058
CALCIUM COMPOUNDS
NT CALCITE
NT CALCIUM CARBONATES
NT CALCIUM CHLORIDES
NT CALCIUM FLUORIDES
NT CALCIUM OXIDES
NT CALCIUM PHOSPHATES
NT CALCIUM SULFIDES
NT FLUORITE
NT PEROVSKITES
Investigation of the dissolution of CaCrO4 in molten LiCl-KCl eutectic
[DE84-016394] 04 p0469 N85-12985
CVD boron on calcium chromate powder
[DE85-000214] 09 p1299 N85-18158
CALCIUM FLUORIDES
The observation of a single thermoluminescence glow peak described by kinetics more general than the usual 1st and 2nd order kinetics
[DE84-014697] 02 p0173 N85-11160
Spectroscopic investigation of materials for frequency agile laser systems
[AD-A151731] 16 p2790 N85-27208
CALCIUM ISOTOPES
Biological influences of low-frequency sinusoidal electromagnetic signals alone and superimposed on RF carrier waves
[PB85-161248] 16 p2842 N85-27527
The isotopic composition of cosmic ray calcium
[OG-4.3-5] 22 p3879 N85-34030
CALCIUM METABOLISM
Alterations in gut transport of minerals and in binding proteins during simulated weightlessness
[NASA-CR-175637] 14 p2388 N85-24709
Mammalian gravity receptors: Structure and metabolism 15 p2605 N85-26055
The salutary effect of dietary calcium on bone mass in a rat model of simulated weightlessness
15 p2606 N85-26073
The role of 1,25-dihydroxyvitamin D in the inhibition of bone formation induced by skeletal unloading
[NASA-TM-87480] 18 p3153 N85-29522
Space-flight simulations of calcium metabolism using a mathematical model of calcium regulation
[NASA-CR-171683] 19 p3328 N85-30621
Mechanisms of osteodystrophy in weightlessness
22 p3733 N85-33143
CALCIUM OXIDES
Sub-eutectic densification and second phase formation in Al2O3 - CaO
[DE85-002065] 09 p1396 N85-18796
Thermal reactions of aromatics with CaO
[DE85-010688] 22 p3742 N85-33193
Improved oxygen sources for breathing apparatus
[NASA-TM-86671] 24 p4134 N85-35623
CALCIUM PHOSPHATES
Ultramicroscopic study of structure of phosphorites from Sea of Japan floor 19 p3290 N85-30400
CALCIUM SULFIDES
Evaluation of ettringite and related compounds for use in solar energy storage
[DE85-003249] 12 p1882 N85-21809
CALCIUM 45
U CALCIUM ISOTOPES
CALCULATION
U COMPUTATION
CALCULATORS
Digital high speed programmable convolver
[AD-D011455] 10 p1481 N85-19348
Fibre composite laminated plate analysis using a card programmable calculator (HP41C/CV)
[NIAST-83/88] 13 p2103 N85-23106
Art of programming programmable microcalculators, part 4: errors of calculations 22 p3778 N85-33411
Development of NATOPS performance software for the SH-3D and SH-3H helicopters
[AD-A156140] 24 p4065 N85-35192
CALCULUS
NT ASYMPTOTIC SERIES
NT COLLINEARITY
NT CONTINUITY (MATHEMATICS)
NT COPLANARITY
NT DIFFERENTIAL CALCULUS
NT FOURIER SERIES
NT INTEGRAL CALCULUS
NT LIMITS (MATHEMATICS)
NT PADE APPROXIMATION
NT POWER SERIES
NT SERIES (MATHEMATICS)
NT TAYLOR SERIES
NT VECTOR ANALYSIS
NT VORTICITY
Representation and refinement of visual specifications in PegaSys
[AD-A148733] 09 p1368 N85-18598
Analytical foundations of the theory of quasiconformal mappings in Rn 10 p1536 N85-19679
Computable real analysis
[AD-A149079] 10 p1546 N85-19747
A PASCAL interpreter for the functional programming language ELC (Extended lambda calculus)
[AD-A155218] 21 p3672 N85-32810
CALCULUS OF VARIATIONS
Stable monotone variational inequalities
[AD-A147123] 07 p1031 N85-16544
Schubert varieties are arithmetically Cohen-Macaulay
16 p2853 N85-27592
Generalized formulation of a class of explicit and implicit TVD schemes
[NASA-TM-86775] 21 p3675 N85-32830
Edge detection and geometric methods in computer vision
[AD-A155873] 24 p4135 N85-35630
CALDERAS
High-resolution microseismicity study of possible magmatic intrusion in the Long Valley Caldera
[DE85-001076] 11 p1681 N85-20593
Workshop on Recent Research in the Valles Caldera
[DE85-010569] 23 p3949 N85-34472
CALIBRATING
NT WIND TUNNEL CALIBRATION
Single viewpoint self calibration: A contribution to field calibration of recording chambers
[SER-C-289] 01 p0049 N85-10320
Analysis of highly precise gravity measurements
[SER-C-294] 01 p0071 N85-10472
Calibration of hall probes
[CSIR-NAC-83-04] 01 p0116 N85-10794
Photon and electron dosimetry at the Physikalische-Technische Bundesanstalt in Brunswick
[PTB-DOS-9] 01 p0119 N85-10814
Photoelectric photometry of globular cluster giants
01 p0128 N85-10884
A proof-of-principle getaway special free-flying satellite demonstration 02 p0155 N85-11051
Radar, target and ranging
[AD-A145407] 02 p0190 N85-11272
Some considerations on the capacitive calibration used for the 2.3 ton cryogenic antenna at CERN — gravitational antennas
[NOTA-INTERNA-809] 02 p0192 N85-11284
The analysis of tank calibration data from several runs
[DE84-015529] 02 p0200 N85-11337
Evaluation of laser profile and deflection measuring system
[FAA-PM-84-24] 02 p0201 N85-11341
Wall interference measurements for three-dimensional models in transonic wind tunnels: Experimental difficulties 03 p0311 N85-12012
Survey of ONERA activities on adaptive-wall applications and computation of residual corrections
03 p0312 N85-12013
Wind tunnel wall interference in closed, ventilated and adaptive test sections 03 p0312 N85-12014
SEASAT altimeter data over the Mediterranean: Implications for ERS-1 03 p0382 N85-12443
Ice sheets as invariant surfaces for radar altimeter calibration and orbit determination
03 p0383 N85-12449
ERS-1 radar altimeter system performance evaluation and calibration 03 p0383 N85-12451
Calibration and validation areas — satellite altimeters
03 p0384 N85-12456
Self-study manual on optical radiation measurements. Part 1: Concepts. Chapter 11: Linearity considerations and calibrations
[PB84-216346] 03 p0421 N85-12690
Evaluation of thermocouple junction temperature
[DE84-015159] 04 p0502 N85-13206
Special Developments and Methods in High Frequency Measuring Techniques — conference
[PTB-E-24] 05 p0629 N85-14030
Realization of noise power in the microwave range by thermal noise standards 05 p0629 N85-14034
Calibration of noise power transfer standards, measurement uncertainties and long term stability
05 p0630 N85-14035
Coaxial noise measurement circuits
05 p0630 N85-14036
A computer controlled measuring system for the calibration of HF components 05 p0630 N85-14037
Calibrating and measuring systems for electromagnetic fields 05 p0630 N85-14041
Evaluation and results of national and international intercomparison measurements — electromagnetic measurement 05 p0631 N85-14043
LANDSAT instruments characterization
[E85-10030] 05 p0654 N85-14198
Study of the improvement in analyzing passive microwave remote sensing data by integrated use of ground data 05 p0658 N85-14226
Formation of reference signals in laser-type gas analyzers with mechanical switching of optical channels
06 p0787 N85-15027
Experimentation and measurement
[PB84-233659] 06 p0812 N85-15157
Effective use of remote sensing products in litigation
[E85-10048] 06 p0827 N85-15250
Tornado: Structural Usage Monitoring System (SUMS) 07 p0866 N85-15680
Recalibration of the KPNO spot sensitometers — Kitt Peak National Observatory 07 p0963 N85-16103
Extending magnitude standards to faint stars with a sub-beam prism 07 p0965 N85-16124
Sub-beam prism used at the Boscha Schmidt telescope 07 p0965 N85-16125
Astronomers' problems with the calibration of Schmidt plates 07 p0965 N85-16126
Stellar photographic photometry using a double wedge technique with a focal reducer system
07 p0966 N85-16133
Six-component strain gage block scale 167-6B. Part 1: Calibration, September 1983
[F-+W-FO-1699] 07 p0968 N85-16143
NBS (National Bureau of Standards) switching radiometers
[PB84-235894] 07 p0968 N85-16147
Thematic Mapper. Volume 1: Calibration report flight model, LANDSAT 5
[E85-10059] 07 p0987 N85-16270
Research in geodesy based upon radio interferometric observations of extragalactic radio sources
[AD-A147581] 07 p0988 N85-16280
Results of the 1984 I*ASA/JPL balloon flight solar cell calibration program
[NASA-CR-174270] 07 p0991 N85-16294
High accuracy Doppler navigation employing optimum integrated position fix information
08 p1073 N85-16803
Numerical analysis of the first static calibration of the RSRA helicopter active-isolator rotor balance system
[NASA-TM-85975] 08 p1083 N85-16863
Amplitude calibration experiment for SIR-B
08 p1146 N85-17227
Evaluation of the L-band scattering characteristics of volcanic terrain in aid of lithologic identification, assessment of SIR-B calibration, and development of planetary geomorphic analogs 08 p1148 N85-17232
Application and calibration of the subsurface mapping capability of SIR-B in desert regions
08 p1148 N85-17244
German Radar Observation Shuttle Experiment (ROSE) 08 p1148 N85-17245
Multicomponent calibration and quantitation methods
[AD-A148252] 08 p1212 N85-17829
Primer for mass metrology
[PB85-121424/GAR] 09 p1305 N85-18199
Calibration of thermocouples based on two state points of water and BS 4937; part 5, 1974
09 p1324 N85-18317
Flux reconstruction and calibration
09 p1412 N85-18804
Historical cost curves for hydrogen masers and cesium beam frequency and timing standards
10 p1485 N85-19245
High-current measurement techniques
[PB85-100444] 11 p1637 N85-20311
Magnetic measurements, calibrations, and standards: Report on a survey
[PB85-127827] 11 p1638 N85-20317
Generalized method for the calibration of 4-terminal-pair type digital impedance meters
[PB85-128122] 11 p1638 N85-20318
Automated TEM (Transverse electromagnetic) cell calibration system
[PB85-134377] 11 p1638 N85-20319
Report on the Workshop on Intercomparison of Solar UV Irradiance Measurements and Related Instrument Calibration 11 p1658 N85-20448
Radiometric calibration and processing procedure for reflective bands on LANDSAT-4 protoflight Thematic Mapper 11 p1668 N85-20510
Prelaunch absolute radiometric calibration of the reflective bands on the LANDSAT-4 protoflight Thematic Mapper 11 p1669 N85-20515
Characterization of radiometric calibration of LANDSAT-4 reflective bands 11 p1669 N85-20516

Instructor's handbook on meteorological instrumentation
[PB85-105930] 11 p1688 N85-20615
State measurement laboratories: Program description (part 1). Directory (part 2)
[PB85-137651] 11 p1739 N85-20935
Self-consistent recalibration of IUE determination of hot DA white dwarf effective temperatures
11 p1751 N85-21016
IUE observations of faint standard stars for calibration of the space telescope 11 p1761 N85-21076
Calibrations of wavelengths in SWP echelle spectra
11 p1761 N85-21077
Radar calibration using direct measurement equipment and oblique photometry
[AD-D011530] 12 p1822 N85-21433
Method and apparatus for self-calibration and phasing of array antenna
[NASA-CASE-NPO-16820-1] 12 p1832 N85-21493
Thermal band characterization of the LANDSAT-4 Thematic Mapper 12 p1869 N85-21727
Preliminary evaluation of the radiometric calibration of LANDSAT-4 Thematic Mapper data by the Canada Centre for Remote Sensing 12 p1870 N85-21729
VISSR infrared calibration by means of calculated radiances 12 p1894 N85-21869
GMS operational calibration procedure and status
12 p1895 N85-21893
Journal of Research of the National Bureau of Standards, volume 89, number 2, March - April 1984
[PB85-115426] 12 p1926 N85-22103
Fast times at high temperatures
[DE85-003306] 12 p1943 N85-22205
Considerations for upgrading modifications to the Marshall Space Flight Center's X-ray calibration facility
12 p1946 N85-22226
Germanium resistance thermometer calibration at superfluid helium temperatures
12 p1947 N85-22228
Determination of angular resolution of coded aperture gamma-ray telescope 13 p1981 N85-22432
Calibration of solar cells outside the atmosphere
13 p2009 N85-22603
Nonlinearity and spectral mismatch problems of solar cells 13 p2010 N85-22605
A standard aircraft diffusion flame: Spectral characteristics and a feasibility study for developing an alternate calibration source for aircraft optical fire detection systems
[AD-A150231] 13 p2039 N85-22768
Metrological support for remote transport vehicle speedometers 13 p2076 N85-22963
Microwave blackbodies for spaceborne receivers
[NASA-CR-175847] 13 p2094 N85-23068
Low temperature calibration fixture
[DE85-003699] 13 p2094 N85-23071
User's guide to calibration of analog electronic controllers in HVAC systems
[AD-A150803] 14 p2298 N85-24229
Calibration loading of a strain-gauged diverless helicopter weapon recovery system
[AD-A151486] 15 p2471 N85-25253
Detection and location of partial discharges in transformer windings using electrical methods
15 p2551 N85-25750
Space radiation studies for the reporting period, June 1983 - July 1984
[NASA-CR-171411] 15 p2685 N85-26583
Qualification of a wall gage for the SIMA wagon, adapted to the test of half models motorized by compressed air turbines — SIMA wind tunnel
[ONERA-PV-1/6068-GY] 16 p2701 N85-26877
Management of vacuum leak-detection processes, standards and calibration
[DE85-006706] 16 p2788 N85-27202
NBS physical measurement services
[NBSIR-84-2875] 16 p2859 N85-27633
Calibration methods in millimeter-wave radioastronomy
[INPE-3481-PRE/724] 16 p2881 N85-27778
Transonic Mach number determination in a blow-down wind tunnel with solid walls and a downstream throat
[VTH-LR-402] 17 p2893 N85-27835
Simulation of gyrocompassing alignment and calibration of strapdown inertial navigation system in a swaying vehicle
[DFVLR-MITT-84-20] 17 p2895 N85-27850
Construction 1976-1980: Design, manufacturing, calibration of the German-Dutch wind tunnel (DNW)
17 p2905 N85-27913
Heat flux sensor calibrator 17 p2915 N85-27970
Proceedings of the Fifteenth Annual Precise Time and Time Interval (PTTI) Applications and Planning Meeting
[AD-A146163] 17 p2961 N85-28287
New time and frequency services at the National Bureau of Standards 17 p2961 N85-28289
Separating the variances of noise components in the Global Positioning System
[AD-P004578] 17 p2963 N85-28295
Unattended TV time transfer results
17 p2964 N85-28305
Field theory analysis using the finite element method to determine the deliberation curves of three dimensional fracture mechanics specimens with a semicircular surface crack applying the electrical direct current potential method for crack depth measurement
[GKSS-84-E-53] 17 p2982 N85-28434
Comparison of measurement and simulation results of radiation temperatures applied to the thermal mapping of Munich
[DFVLR-FB-85-06] 17 p2984 N85-28442
Absolute calibrations of SO2 and NO analyzers by photographic methods
[DFVLR-MITT-85-02] 17 p2994 N85-28504
Tone calibrated digital radio communication system
[NASA-CASE-NPO-16414-1-CU]
18 p3089 N85-29121
Automatic volume calibration system
[DE85-006955] 18 p3102 N85-29204
Oscillating pressure device for dynamic calibration of pressure transducers
[NASA-CASE-LAR-13094-1] 18 p3104 N85-29217
State Weights and Measures Laboratories: Program handbook
[PB85-183358] 18 p3111 N85-29263
An operational analysis of system calibration
[AD-A153556] 18 p3170 N85-29644
Carbon foil secondary electron emission during ion passage through the 40 to 500 keV energy field
[MPE-190] 18 p3184 N85-29747
Automatic ac/dc thermal voltage converter and ac voltage calibration system
[PB85-182574] 19 p3274 N85-30304
Using regression analysis for determining air data sensor errors by means of an inertial navigation system
[ESA-TT-886] 20 p3392 N85-31041
The 1982 National Measurement Requirements Survey
[NMRC-83-01-SUMM] 20 p3436 N85-31321
Outline of CCVT (Coupling Capacitor Voltage Transformer) calibration procedure, EPRI-NBS (Electric Power Research Institute/National Bureau of Standards) prototype system. Supplement to EPRI report EL-890 (Field Calibration System for CCVTs, April 1978)
[PB85-182566] 20 p3450 N85-31418
Pycnometer shaker
[PB85-174985] 20 p3460 N85-31491
Spectroradiometric calibration of the Thematic Mapper and Multispectral Scanner system
[E85-10104] 20 p3476 N85-31601
TOPEX error budget 20 p3493 N85-31717
An absolute calibration of the solid state detectors in the narrow band neutrino beam at CERN
[NIKHEF-H/84-10] 20 p3536 N85-32017
The response of ionization chambers to relativistic heavy nuclei 20 p3544 N85-32051
Calibration and use of clutter data for simulation
[AD-A154793] 21 p3574 N85-32229
Background equatorial astronomical measurements focal plane assembly (refurbished HI STAR SOUTH)
[AD-A155215] 21 p3590 N85-32313
Improved coordinate measuring machine calibration and control
[DE85-012053] 21 p3590 N85-32315
Reference-cell calibration activities
21 p3613 N85-32453
The 100 years of Aitken Nuclei (AN) study-reminiscence, current and future problems 21 p3641 N85-32621
On-line temperature sensor
[DE85-011641] 22 p3787 N85-33465
Evaluation of coordinate measuring machines
[DE85-011712] 22 p3788 N85-33467
IEA-SSPS CRS calibration report: Calibration of relevant measuring sensors
[DE85-010174] 22 p3788 N85-33468
Beta response of selected instruments
[DE85-013278] 22 p3788 N85-33469
Development of a microorifice uniform deposit cascade impactor
[DE85-006765] 22 p3812 N85-33614
AMI calibration study. Volume 1: SAR calibration. Volume 2: Ground Targets. Volume 3: Scatterometer calibration — Active Microwave Instrument (AMI) ERS-1
[C2248/4/4-VOL-1] 23 p3936 N85-34394
Multi-robot assembly of IC's 23 p3964 N85-34577
Measured performance of the new University of California gamma ray telescope
[OG-9.2-13] 23 p4026 N85-34952
The final COS-B database: In-flight calibration of instrumental parameters
[OG-9.3-9] 23 p4026 N85-34964
Detector calibration of the Indian cosmic ray experiment (ICNS) in Space-Shuttle Spacelab-13
[SH-9.1-2] 23 p4050 N85-35117
Calibrator for displacement gages used in the rock mechanics laboratory
[DE85-013257] 24 p4096 N85-35393
Calibration of a high-level photon irradiation
[DE85-013044] 24 p4151 N85-35738

CALIFORNIA

Mineral nutrients in Mediterranean ecosystems
[REPT-71] 01 p0069 N85-10456
Vertical crustal movements in southern California, 1974 to 1978
[GS-CIRC-905] 02 p0228 N85-11491
Franciscan and related rocks of southern Humboldt County, northern California coast ranges: Analysis of structure, tectonics, sedimentary petrology, paleogeography, depositional history, and thermal maturity 03 p0390 N85-12495
Investigation of several aspects of LANDSAT 4/5 data quality
[E85-10038] 04 p0525 N85-13357
Effects of acid rain on plant microbial associations in California
[PB84-242122] 04 p0532 N85-13404
Models for volcanic processes in Long Valley, California: Testing by continental drilling
[DE84-014943] 04 p0534 N85-13414
Characterizing the scientific potential of satellite sensors — San Francisco, California
[E85-10044] 07 p0983 N85-16244
Characterizing the scientific potential of satellite sensors — San Francisco, California
[E85-10053] 07 p0984 N85-16249
LANDSAT-4 Thematic Mapper Modulation Transfer Function (MFT) evaluation — California and New Mexico
[E85-10055] 07 p0984 N85-16250
Image variance and spatial structure in remotely sensed scenes — South Dakota, California, Missouri, Kentucky, Louisiana, Tennessee, District of Columbia, and Oregon
07 p0986 N85-16265
Image-to-image correspondence: Linear structure matching 07 p0986 N85-16266
Analysis of SIR-B radar illumination of geometry for depth of penetration and surface feature and vegetation detection, Nevada and California
08 p1149 N85-17248
Mesozoic ophiolitic olistostromes and Cenozoic imbricate thrust faulting in the northern California coast ranges: Geology of the Mysterious Valley area, Napa County 08 p1182 N85-17445
Bibliography update on the California current system and related mesoscale ocean modeling
[AD-A148546] 08 p1190 N85-17503
Anaysis of the quality of image data required by the LANDSAT-4 Thematic Mapper and Multispectral Scanner — agricultural and forest cover types in California
[E85-10074] 10 p1504 N85-19488
Vegetation analysis for arid lands geobotany
[NASA-CR-175455] 10 p1506 N85-19500
The 35 kilowatt peak power photovoltaic system
[DE85-000189] 10 p1511 N85-19537
California coastal erosion and storm damage during the winter 1982 - 1983, a reconnaissance report
[PB85-121705] 10 p1521 N85-19591
Investigation of radiometric properties of LANDSAT-4 MSS — California, North Carolina, South Carolina, and New England 11 p1666 N85-20500
Geodetic accuracy of LANDSAT 4 Multispectral Scanner and Thematic Mapper data — Washington, DC, California, Alabama, South Dakota, and Illinois
11 p1667 N85-20504
Impact of LANDSAT MSS sensor differences on change detection analysis — New Mexico, San Francisco, CA, New Hampshire, and Connecticut
11 p1667 N85-20506
High-resolution microseismicity study of possible magmatic intrusion in the Long Valley Caldera
[DE85-001076] 11 p1681 N85-20583
Analysis of the NASA/MSFC Airborne Doppler Lidar results from San Gorgonio Pass, California
[NASA-CR-171355] 12 p1892 N85-21873
USC (University of Southern California) Sea Grant Program Directory, 1984-1985
[PB85-135051] 12 p1899 N85-21922
The future of lightwave technology
[PB85-109759] 12 p1935 N85-22155
Summary of Meteorological Observations, Surface (SMOS) Camp Pendleton, California
[AD-A150482] 13 p2138 N85-23277
Observations of the California countercurrent
[AD-A150781] 14 p2382 N85-24691
Selection of promising sites for magma energy experiments
[DE85-006832] 16 p2820 N85-27363

Air quality benefit analysis for Los Angeles and San Francisco based on housing values and visibility
[PB85-166049] 16 p2822 N85-27409
Application of hierarchical data structures to geographical information systems
[AD-A152169] 16 p2877 N85-27753
Quality assurance for RESOLVE (Research on Operations-Limiting Visual Extinction). A visibility study in the California desert
[AD-A152383] 17 p2992 N85-28494
Formation and fate of toxic chemicals in California's atmosphere
[PB85-172600] 18 p3134 N85-29414
Application of climatological analysis to minimize air pollution impacts in California
[PB85-172963] 18 p3149 N85-29502
Sand dispersion from an ephemeral river delta on the wave-dominated central California coast
[AD-A154352] 19 p3300 N85-30458
Simulated effects of increased recharge on the ground-water flow system of Yucca Mountain and vicinity, Nevada-California
[DE85-012985] 24 p4108 N85-35489
Geology: Structural history and fluvial geomorphology of the southern Death Valley Fault Zone, Inyo and San Bernardino Counties, California
24 p4114 N85-35506
Carbon fiber strainmeter studies in southern California
[PB85-196889] 24 p4118 N85-35526
Sea surface and remotely sensed temperatures off Cape Mendocino, California
[NASA-TM-86712] 24 p4125 N85-35573

CALIFORNIUM
NT CALIFORNIUM ISOTOPES

CALIFORNIUM ISOTOPES
Magnetism of californium metal
[DE85-001141] 09 p1377 N85-18657
Historical review of californium-252 discovery and development
[DE85-010223] 19 p3362 N85-30844
Effects of space radiation on advanced semiconductor devices. Part 3: Further cosmic ray simulation studies of single event upsets and latch-up in CMOS memories
[AERE-G-3368-PT-3] 22 p3848 N85-33833

CALIFORNIUM 252
U CALIFORNIUM ISOTOPES

CALLISTO
Ripple ring basins on Ganymede and Callisto
13 p2183 N85-23547
Tectonics of the Valhalla structure on Callisto
13 p2202 N85-23662
Ganymede and Callisto: Beauty is only skin deep
15 p2680 N85-26552

CALORIC REQUIREMENTS
Nutritional criteria for military rations and effects of prolonged feeding on acceptability
14 p2394 N85-24742
Nutrition in space flight: Some thoughts
14 p2394 N85-24743

CALORIC STIMULI
Caloric stimulation of the vestibular system in microgravity
05 p0695 N85-14469
Inner ear characteristics during 7 day antiorthostatic bedrest (6 deg head down tilt)
05 p0695 N85-14470

CALORIMETERS
A concept for a hadron calorimeter with photodiode readout
[MPI-PAE/EXP-E1-130] 01 p0050 N85-10332
Electromagnetic shower development and applications to sampling calorimeters
[DE84-016355] 04 p0493 N85-13142
Instruments for characterization of carbon black and polymers
[AD-A146475] 06 p0810 N85-15146
Thermal performance testing of passive solar components in NBS (National Bureau of Standards) calorimeter
[PB85-119345/GAR] 09 p1346 N85-18470
Synthesis and thermomechanical properties of new AT-Phenylene R systems
[AD-A149961] 12 p1813 N85-21372
Applications of high pressure differential scanning calorimetry to aviation fuel thermal stability research
[NASA-TM-87002] 14 p2249 N85-23941
Physical chemistry of exothermic gas-aerosol calorimetry
[AD-A150872] 14 p2251 N85-23950
Calorimeter for measuring high-energy optical pulses
[PB85-160695] 15 p2561 N85-25799
A calorimetric approach for measuring emittance and normal spectral absorptance at elevated temperatures
[AD-A151292] 15 p2651 N85-26351
Thermodynamic systematics of oxides of americium, curium and neighboring elements
[DE85-009704] 18 p3197 N85-29831
Cryogenic laser calorimetry for impurity analysis
[NASA-CR-176102] 22 p3743 N85-33201
A lead glass tubing drift calorimeter
24 p4147 N85-35711
X-ray film chamber with carbon target of Tien-Shan complex array
24 p4179 N85-35915
Peculiarities of gamma-quanta distribution at 20 TeV energy
[HE-3.7-10] 24 p4186 N85-35967
Study of muons near shower cores at sea level using the E594 neutrino detector
24 p4191 N85-36000
Measurement of energy muons in EAS at energy region larger thean 10(17) eV
[HE-4.3-8] 24 p4191 N85-36002
Magnetic monopole search by 130 m(2)sr He gas proportional counter
[HE-6.1-2] 24 p4209 N85-36128
Results of a search for monopoles and tachyons in horizontal cosmic ray flux
[HE-6.1-3] 24 p4209 N85-36129
Search for proton decay in the Frejus experiment
[HE-6.2-2] 24 p4210 N85-36136
Results on nucleon life-time from the Kolar gold field experiment
[HE-6.2-3] 24 p4211 N85-36139
Data acquisition system for phase-2 KGF proton decay experiment
[HE-6.2-4] 24 p4211 N85-36140
Construction of the Soudan 2 detector
[HE-6.2-5] 24 p4211 N85-36141
Tien-Shan effect and charmed particles
[HE-6.2-17] 24 p4212 N85-36153
Search for acoustic signals from high energy cascades
[HE-7.1-1] 24 p4213 N85-36155
Spatial distribution read-out system for thermoluminescence sheets
[HE-7.1-7] 24 p4213 N85-36161
Application of thermoluminescence for detection of cascade shower 2: Detection of cosmic ray cascade shower at Mount Fuji
[HE-7.1-12] 24 p4214 N85-36162

CALORIMETRY
U HEAT MEASUREMENT

CALUTRONS
U CYCLOTRONS

CAM (MANUFACTURING)
U COMPUTER AIDED MANUFACTURING

CAMBER
NT WING CAMBER
Effect of a variable camber and twist wing at transonic Mach numbers
[NASA-TM-86281] 04 p0452 N85-12869
Low-speed characteristics of a circulation control airfoil with AFT camber and a spiral trailing edge
[AD-A150651] 14 p2213 N85-23725

CAMBERED WINGS
Extension of the small perturbations method in three-dimensional transonic, unsteady flow to the case of real wings
[ONERA-NT-17/3064-RY-070-R]
20 p3389 N85-31017

CAMERA SHUTTERS
Initial feasibility ground test of a proposed photogrammetric system for measuring the shapes of ice accretions on helicopter rotor blades during forward flight
[NASA-TM-87391] 04 p0455 N85-12887
High-resolution SIT TV tube for subnanosecond image shuttering
[DE85-005189] 13 p2095 N85-23072
Electronic imaging system and technique
[DE85-005740] 23 p3935 N85-34383

CAMERA TUBES
NT IMAGE DISSECTOR TUBES
NT RETURN BEAM VIDICONS
NT THERMICONS
NT VIDICONS
High-resolution SIT TV tube for subnanosecond image shuttering
[DE85-005189] 13 p2095 N85-23072
A new high-resolution pickup tube for live X-ray topography
[NHK-LABS-NOTE-309] 18 p3193 N85-29802

CAMERAS
NT BALLISTIC CAMERAS
NT FRAMING CAMERAS
NT HIGH SPEED CAMERAS
NT MULTISPECTRAL BAND CAMERAS
NT PANORAMIC CAMERAS
NT PINHOLE CAMERAS
NT SCHMIDT CAMERAS
NT STREAK CAMERAS
NT TELEVISION CAMERAS
NASA thunderstorm overflight program: Atmospheric electricity research. An overview report on the optical lightning detection experiment for spring and summer 1983
[NASA-TM-86468] 03 p0363 N85-12330
Developments of optical fast-gated imaging systems
[DE84-016170] 04 p0502 N85-13204
Positron ring system using Anger-type detectors
[DE84-016788] 04 p0503 N85-13212
Improvements in avalanche-transistor sweep circuitry for electrooptic streak cameras
[DE84-016195] 06 p0811 N85-15155
Searching for impact craters using space shuttle photography 06 p0889 N85-15645
Automatic camera tracking for remote manipulators
[DE85-001897] 07 p0974 N85-16187
Improved radiographic viewing system
[AD-A147587] 07 p1016 N85-16456
The ROSAT XUV wide field camera
08 p1243 N85-17844
Time series photometry with a CCD camera
08 p1252 N85-17908
The BRESEX multispectral camera: Preliminary characteristics
[INPE-3357-PRE/635] 10 p1487 N85-19386
Microstrain analysis in bent single crystal silicon by double crystal X-ray topography technique
[DE85-000422] 10 p1584 N85-19863
Preliminary design of an Earth-based debris detection system using current technology and existing installations 12 p1784 N85-21199
Intensified CCD camera system for plasma diagnostics
[DE85-002252] 12 p1853 N85-21620
Electronics Engineering Department EE Technical Review
[UCRL-50025-84-1] 13 p2063 N85-22887
A normal incidence, high resolution X-ray telescope for solar coronal observations
[NASA-CR-175622] 13 p2169 N85-23461
The astrometry programme at Mt. John Observatory
14 p2436 N85-25025
French firm develops new kind of CTD camera for robots 15 p2523 N85-25556
Experimental investigation of the electric breakdown in SF6
[BLL-CE-TRANS-7987-(9022.09)]
15 p2546 N85-25714
Development of robots and application to industrial processes
[NASA-CR-175754] 15 p2567 N85-25840
Errors in compensating for image oscillation by means of a gyroscopic head 16 p2763 N85-27051
The 8.3 and 12.4 micron imaging of the Galactic Center source complex with the Goddard infrared array camera
[NASA-TM-86225] 19 p3382 N85-30982
Large format camera photographs: A new tool for understanding arid environments
21 p3604 N85-32379
Microcomputer controlled image processor
[AD-D011734] 22 p3833 N85-33735
A star camera aspect system suitable for use in balloon experiments
[OG-9.3-10] 23 p4029 N85-34965
Parametric stability of analytical close-range photogrammetry 24 p4107 N85-35481
Application of thermoluminescence for detection of cascade shower 1: Hardware and software of reader system
[HE-7.1-6] 24 p4213 N85-36160
Application of thermoluminescence for detection of cascade shower 2: Detection of cosmic ray cascade shower at Mount Fuji
[HE-7.1-12] 24 p4214 N85-36162

CAMS
Kinematic synthesis of planar cam-link mechanisms for exact path and exact motion generation
03 p0341 N85-12189
Adjustment structure
[AD-D011461] 10 p1459 N85-19193
A rational approach to cam design
23 p3923 N85-34311

CANADA
NT BRITISH COLUMBIA
A summary of operational developments in nowcasting and short-range forecasting techniques on the Canadian West Coast 01 p0062 N85-10547
Canada report to COSPAR 01 p0131 N85-10906
Active microwave measurements of sea ice under fall conditions: The RADARSAT/FIREX fall experiment — in the Canadian Arctic
[E85-10019] 02 p0217 N85-11432
Evaluation of the radar response to land surfaces and volumes: Examination of theoretical models, target statistics, and applications 08 p1149 N85-17250
Birds and aviation
[AD-P004177] 11 p1578 N85-19939

Birds and aircraft engine strike rates
[AD-P004184] 11 p1579 N85-19946
PMP-1 report: The fourth winter of PMP-1, 1981 - 1982: A winter with several interesting features
11 p1657 N85-20441
Canadian plans for Thematic Mapper data
11 p1668 N85-20513
Hydrometric telemetry in Canada
14 p2239 N85-23882
Corrosion problems in the Canadian maritime forces
[AD-A151594] 15 p2509 N85-25481
AWS (Air Weather Service) climatic briefs: North America
[AD-A152161] 16 p2635 N85-27483
Investigation of the requirement for auxiliary heating of Canadian forces personnel
[AD-A151950] 16 p2641 N85-27522
Structural analysis of terrane accretions in the eastern Brooks Range and adjacent areas in central Alaska and Canada
[DE85-006279] 17 p2993 N85-28501
Search and rescue in Canada
20 p3401 N85-31098
COSPAS-SARSAT demonstration and evaluation results in Canada 20 p3405 N85-31129

CANADAIR AIRCRAFT
NT CL-41 AIRCRAFT

CANADAIR CF-104 AIRCRAFT
U F-104 AIRCRAFT

CANADAIR CL-41 AIRCRAFT
U CL-41 AIRCRAFT

CANADIAN SHIELD
Structural investigation of the Grenville Province by radar and other imaging and nonimaging sensors
08 p1147 N85-17237

CANADIAN SPACE PROGRAM
Canada report to COSPAR 01 p0131 N85-10906
Non-US approaches to space commercialization
02 p0150 N85-11012
Tactical military communications by satellite relay at high latitudes 11 p1709 N85-20756

CANADIAN SPACECRAFT
NT ANIK SATELLITES

CANARD CONFIGURATIONS
Aerodynamic-structural study of canard wing, dual wing, and conventional wing systems for general aviation applications
[NASA-CR-172529] 08 p1077 N85-16829
Unsteady transonic flow calculations for two-dimensional canard-wing configurations with aeroelastic applications
[NASA-TM-86375] 10 p1420 N85-18960
Space Shuttle orbiter trimmed center-of-gravity extension study
[NASA-TP-2284] 10 p1428 N85-19003
Wind-tunnel investigation of a full-scale canard-configured general aviation airplane
[NASA-TP-2362] 11 p1575 N85-19925
Parametric study of a canard-configured transport using conceptual design optimization
[NASA-TP-2400] 11 p1584 N85-19979
Approximate neutral point of a subsonic canard aircraft
[NASA-TM-86694] 15 p2462 N85-25205
Description of a computer program treating transonic steady state aeroelastic effects for a canard or tail airplane
[FFA-TN-1983-23] 16 p2700 N85-26674
Supersonic aerodynamic characteristics of canard, tailless, and aft-tail configurations for 2 wing planforms
[NASA-TP-2434] 17 p2891 N85-27822
Real scale test of the Petit Canard aircraft in the number 3 section, 47 sqm, of the SIMA wind tunnel, May 1984
[ONERA-PV-1/0772-GY] 20 p3389 N85-31018
Study of an efficient long-range Mach 2.7 supersonic transport configuration concept
[NASA-TM-86414] 21 p3554 N85-32110
The aerodynamic characteristics of a GU25-5(11)8 aerofoil for low Reynolds numbers
[GU-AERO-8410] 23 p3894 N85-34121
Vortex boundary-layer interactions
[NASA-CR-176192] 24 p4093 N85-35373

CANCELLATION
Research on adaptive antenna techniques 6
[AD-A149341] 11 p1624 N85-20228

CANCELLATION CIRCUITS
Self-adaptive echo cancellation for telephony
[ENST-84E013] 20 p3441 N85-31353

CANCER
NT LEUKEMIAS
Radiation physics, biophysics, and radiation biology
[DE84-014865] 09 p1360 N85-18557
Effects of long-term low-level radiofrequency radiation exposure on rats. Volume 8: Evaluation of longevity, cause of death, and histopathological findings
[AD-A154283] 19 p3327 N85-30610
Spontaneous transitional cell carcinoma in the urinary bladder of a strain 13 guinea pig
[AD-A155645] 21 p3665 N85-32764
Carcinogenesis of nitrated toluenes and benzenes skin and lung tumor assays in mice
[AD-A155723] 22 p3818 N85-33655

CANISTERS
U CANS

CANNING
A scanning laser velocimeter for turbulence research
[NASA-CR-172493] 07 p0897 N85-15686

CANNONS
U GUNS (ORDNANCE)

CANONICAL FORMS
Canonical analysis of the fermion sector in higher-derivative supergravity
[DE85-007828] 16 p2859 N85-27635
Method to render second order beam optics programs symplectic
[DE85-010631] 20 p3515 N85-31855
Design of high-order analog and digital filters with identical sections 22 p3766 N85-33341
Diakoptic calculation of characteristics for optimization of linear circuits with respect to parameters of individual branches 22 p3767 N85-33346

CANOPIES
Deciduous forest radiation regimes: Effects of forest structure, phenology and Earth-Sun geometry upon their spatial, temporal and spectral variability
[AD-A146804] 07 p0996 N85-16327
A theoretical view on the stress analysis of fully inflated parachute canopies
[AD-A148387] 08 p1078 N85-16835
Age life prediction of nylon 66 parachute materials. Part 1: Mechanical properties
[AD-A147698] 08 p1170 N85-17378
Aircraft transparency bird impact analysis using the MAGNA computer program
[AD-P004186] 11 p1579 N85-19948

CANOPIES (VEGETATION)
Space observation of latitudinal changes in vegetation cover 02 p0164 N85-11113
Relationships between grass canopy characteristics and LANDSAT Thematic Mapper bands
02 p0213 N85-11402
Botanical sciences team 02 p0214 N85-11407
Biophysical and spectral modeling for crop identification and assessment
[E85-10006] 02 p0215 N85-11419
Development and testing of a rural credit supervision system at the level of counties and rural properties utilizing remote sensing techniques
[E85-10018] 02 p0217 N85-11431
Remote sensing of plant stress and diseases
05 p0657 N85-14216
Variation in spectral response of soybeans with respect to illumination, view, and canopy geometry
[E85-10040] 07 p0982 N85-16241
Spectral estimators of absorbed photosynthetically active radiation in corn canopies
[E85-10041] 07 p0983 N85-16242
Growth/reflectance model interface for wheat and corresponding model
[E85-10058] 07 p0987 N85-16269
Development and evaluation of techniques for using combined microwave and optical image data for vegetation studies 08 p1148 N85-17240
The extension of an invertible coniferous forest canopy reflectance model using SIR-B and LANDSAT data
08 p1149 N85-17246
Analysis of terrestrial conditions and dynamics
[E85-10063] 08 p1174 N85-17401
Shortwave infrared detection of vegetation
[E85-10064] 08 p1174 N85-17402
Growth and reflectance characteristics of winter wheat canopies
[E85-10080] 10 p1505 N85-19494
Techniques for measuring intercepted and absorbed PAR in corn canopies
[E85-10081] 10 p1505 N85-19495
Influence of the atmosphere on remotely sensed reflection from vegetation surfaces
[DE85-000658] 11 p1670 N85-20521
Investigations of vegetation and soils information contained in LANDSAT Thematic Mapper and Multispectral Scanner data
[E85-10082] 12 p1873 N85-21747
Modeling interception of rainfall by forests and the role of interception in the water balance
[DE85-002822] 12 p1884 N85-21825
Remote sensing of coastal wetlands biomass using Thematic Mapper wavebands — Lewes, Delaware
13 p2119 N85-23198
The microwave propagation and backscattering characteristics of vegetation — wheat, sorghum, soybeans and corn fields in Kansas
[E85-10088] 13 p2122 N85-23213
Testing an energy balance model for estimating actual evapotranspiration using remotely sensed data — Hannover, West Germany barley and wheat fields
13 p2125 N85-23236
Use of space photographic information to map plant cover 15 p2488 N85-25359
Identification of structure of soil-vegetation cover using aerial and space photographs 16 p2726 N85-26826
Radar return from vegetation covered terrains
[INPE-3470-PRE/713] 16 p2770 N85-27093
Modeling the backscattering and transmission properties of vegetation canopies
[E85-10099] 16 p2809 N85-27320
Earth observation modeling based on layer scattering matrices
[NLR-MP-84015-U] 17 p2984 N85-28440
Light scattering by leaf layers with application to canopy reflectance modeling: The Scattering by Arbitrarily Inclined Leaves (SAIL) model
[NLR-MP-84011-U] 17 p3038 N85-28796
Biogeochemical cycling and remote sensing
21 p3659 N85-32733

CANS
Lateral support system for canister-launched missile
[AD-D011389] 08 p1106 N85-16987

CANT
U SLOPES

CANTILEVER BEAMS
Characterization of interlaminar crack growth in composites with the double cantilever beam specimen
04 p0463 N85-12942
Experimental investigation of vibroimpact of two cantilever beams 09 p1336 N85-18399
Comparison of shock-induced displacements with displacements produced by a centrifuge acceleration
[DE85-000467] 12 p1852 N85-21618
Planar dynamics of a uniform beam with rigid bodies affixed to the ends
[NASA-CR-175566] 12 p1864 N85-21693
Stress intensity factor in a tapered specimen
[NASA-CR-175589] 13 p2102 N85-23099
Thermal deformation of flexible rotors in friction bearings 14 p2280 N85-24123
Research and development of subsurface acoustic wave devices for sensor applications
[AD-A152197] 16 p2861 N85-27642
Mathematical modeling and control of a large space structure as applied to a shuttle-antenna configuration
[AD-A153269] 17 p2910 N85-27939
Buckling and bracing of cantilevers
[CE-42] 17 p2979 N85-28413
Large deflections of a cantilever beam under arbitrarily directed tip load
[NASA-TM-86442] 19 p3284 N85-30363
ISAAC (Integrated Structural Analysis and Control) via continuum modeling and distributed frequency domain design techniques 20 p3414 N85-31185
Shear-stress distribution and shear stiffness in the case represented by a non-homogeneous cross-section, of any shape, but composed of an orthotropic material, when subjected to a shear force
[DRIC-T-7430] 20 p3469 N85-31554
Influence of the resin on interlaminar mixed-mode fracture
[NASA-TM-87571] 21 p3561 N85-32150
Nonlinear flap-lag-extensional vibrations of rotating, pretwisted, preconed beams including Coriolis effects
[NASA-TM-87102] 23 p3941 N85-34427
The application of bispectral analyses to aeroelastic phenomena 24 p4060 N85-35157

CANTILEVER MEMBERS
NT CANTILEVER BEAMS
NT CANTILEVER PLATES
Flutter parametric studies of cantilevered twin-engine transport type wing with and without winglet. Volume 2: Transonic and density effect investigations
[NASA-CR-172410-VOL-2] 04 p0513 N85-13270

CANTILEVER PLATES
Deformation of cylindrical shell with cantilevered elastic plates attached 06 p0779 N85-14084

CANTILEVER WINGS
U WINGS

CANYONS
Study of pollutant dispersion in an urban street canyon
[DE85-002648] 11 p1677 N85-20571
Analysis of slope stability, Wilmington to Lindenkohl Canyons, US mid-Atlantic margin
[DE84-012278] 12 p1899 N85-21921
Lithologic and structural control on slope morphology in the Valles Marineris 13 p2201 N85-23651

Valles Marineris basin beds: A complex story
13 p2201 N85-23652

CAP CLOUDS
The physics of the marine stratocumulus-capped mixed layer
15 p2593 N85-25979

CAPACITANCE
Capacitive reactance of compensated semiconductors with deep centers under conditions of transmission of exclusion and double injection currents
02 p0266 N85-11742
Machine computation of delay and capacitance of transistor structures of subnanosecond large integrated circuits
04 p0490 N85-13120
Calculation of transmission line impedances using the ANSYS finite element program
[DE84-016715] 11 p1629 N85-20261
New preamplifier for particle detectors
[DE85-004115] 12 p1836 N85-21524
Low capacitance e-beam fabricated beam-lead Schottky barrier diodes
[AD-A150238] 13 p2063 N85-22888
On filter binary processes
[AD-A150328] 13 p2063 N85-22890
Change of electrical characteristics of radio-frequency cables under thermal effect
13 p2081 N85-22999
New electronic measurement, control devices
14 p2289 N85-24192
Transient voltage oscillations in coils
[DE85-006715] 15 p2550 N85-25738
Studies in electron phenomena in MOS structures: The pulsed C-V method
15 p2659 N85-26407
Germanium detectors with a built-in transverse drift field
[DE85-009944] 18 p3096 N85-29165
A laser slope gauge and a spar buoy wave gauge: Tools for the validation of microwave remote sensors
[AD-A154038] 19 p3272 N85-30290
Sixty GHz IMPATT diode development
[NASA-CR-174969] 22 p3758 N85-33293
Capacitance measuring device
[DE85-011643] 22 p3787 N85-33460

CAPACITANCE SWITCHES
Switched Capacitor (SC) filter and design centering of integrated circuits, part 1
[BMFT-FB-T-84-190-PT-1] 05 p0633 N85-14062

CAPACITORS
Isolated load switching with surge suppression
[AD-D011218] 01 p0042 N85-10274
Some considerations on the capacitive calibration used for the 2.3 ton cryogenic antenna at CERN — gravitational antennas
[NOTA-INTERNA-609] 02 p0192 N85-11284
A high-voltage discharger
[AD-A145659] 02 p0194 N85-11299
Determination of the conservation state of long conservation agricultural products by means of capacitive sensors
[NOTA-INTERNA-799] 02 p0220 N85-11447
Pulse injection on a power cable penetrating a shielding wall by feed-through capacitors
[FOA-C-30372-A3] 04 p0497 N85-13171
Flywheel-powered X-ray generator
05 p0605 N85-13861
Implications of the chiral anomaly for quantum Hall effect devices
[NUB-2662] 05 p0629 N85-14029
EMI (electromagnetic interference) filter capacitor unit
[AD-D011392] 07 p0937 N85-15941
Determination of threshold and maximum operating electric stresses for selected high voltage insulation. Task 3: Investigation of high voltage capacitor insulation
[DE84-017051] 09 p1316 N85-18274
Reliability studies of ceramic capacitors
[AD-A149126] 10 p1479 N85-19338
Technological and economic assessment of advanced ceramic materials. Volume 3: A case study of ceramic capacitors
[PB85-113108] 11 p1613 N85-20141
Rep rated long life capacitor development: Phase 1 and 2
[DE85-000719] 11 p1629 N85-20256
Degradation mechanisms in ceramic dielectrics
[AD-A149791] 12 p1813 N85-21369
Control of cascaded induction generator systems
[AD-A150429] 13 p2065 N85-22897
Planar ferroelectric microcapacitors for microwave devices
13 p2087 N85-23032
Erosion of electrodes due to switching of capacitor-bank discharge circuits
[AD-A151207] 15 p2547 N85-25718
Adjustment of the frequency-temperature characteristics of crystal oscillators
[AD-D011588] 15 p2548 N85-25726
Advanced capacitors
[AD-A151709] 15 p2548 N85-25727
Outline of CCVT (Coupling Capacitor Voltage Transformer) calibration procedure, EPRI-NBS (Electric Power Research Institute/National Bureau of Standards) prototype system. Supplement to EPRI report EL-890 (Field Calibration System for CCVTs, April 1978)
[PB85-182566] 20 p3450 N85-31418
East Europe report: Science and technology
[JPRS-ESA-85-021] 21 p3568 N85-32190
Stress corrosion of ceramic materials
[AD-A155020] 21 p3570 N85-32202
Capacitive energy storage at cryogenic temperatures
[AD-A154508] 21 p3579 N85-32253
A fast discharge excimer laser with symmetric geometry
[AD-A155294] 21 p3592 N85-32322
Batteryless magneto-driven portable radiac
[DE85-011622] 22 p3760 N85-33300
Switching power supply
[DE85-005993] 22 p3761 N85-33312
Capacitance measuring device
[DE85-011643] 22 p3787 N85-33460
Reversing-counterpulse repetitive-pulse inductive storage circuit
[DE85-008409] 23 p3928 N85-34344
Tuning system for capacitively loaded 1/4 accelerating cavity
[DE85-012516] 24 p4091 N85-35358

CAPACITY
Open cycle OTEC thermal-hydraulic systems analysis and parametric studies
[DE84-013011] 04 p0530 N85-13391

CAPE KENNEDY LAUNCH COMPLEX
Chronology of KSC and KSC related events for 1983
[NASA-TM-87400] 08 p1261 N85-17927
Preliminary results of associating cloud-to-ground lightning with surface convergence and radar reflectivity at Kennedy Space Center in 1983
[NASA-CR-175543] 12 p1897 N85-21910
Chronology of KSC and KSC related events for 1983
[NASA-TM-87435] 12 p1963 N85-22339

CAPES (LANDFORMS)
Estuaries of the Cape. Part 2: Synopses of available information on individual systems. Report 12: Buffels (WES) (CSW 1), Elsies (CSW 2), Sir Lowry's Pass (CSW8), Steenbras (CSW 9), and Buffels (OOS) (CSW 11)
[CSIR-RR-411-PT-2] 01 p0086 N85-10581
Estuaries of the Cape. Part 2: Synopses of available information on individual systems. Report 13: Silvermine (CSW 3)
[CSIR-RR-412-PT-2] 01 p0086 N85-10582
Estuaries of the Cape. Part 2: Synopses of available information on individual systems. Report no. 14: Sand (CSW 4)
[CSIR-RR-413-PT-2] 01 p0086 N85-10583
Estuaries of the Cape. Part 2: Synopses of available information on individual systems. Report no. 15: Zeekoe (CSW 5)
[CSIR-RR-414-PT-2] 01 p0087 N85-10584
Estuaries of the Cape. Part 2: Synopses of available information on individual systems. Report no. 16: Eerste (CSW 6)
[CSIR-RR-415-PT-2] 01 p0087 N85-10585

CAPILLARY CIRCULATION
U CAPILLARY FLOW

CAPILLARY FLOW
Capillary Pump Loop (CPL) heat pipe development status report
[NASA-CR-175273] 08 p1161 N85-17323
Special features of the temperature dependence of the capillary constant in the vicinity of the critical point
[BLL-T6438/BG/LRS/LRST750/85]
16 p2859 N85-27632
Generation of capillary instabilities by external disturbances in a liquid jet
[NASA-TM-87041] 19 p3265 N85-30248
Quasi non-intrusive sampling and analysis of gases associated with the boundary layer on the tethered satellite and similar supersonic and hypersonic research vehicles
[NASA-CR-176075] 20 p3407 N85-31140
A two phase flow model at the level of a narrowing section — blood flow
20 p3507 N85-31799

CAPILLARY WAVES
NT BAROCLINIC WAVES
NT GRAVITY WAVES
NT RIPPLES
A laser slope gauge and a spar buoy wave gauge: Tools for the validation of microwave remote sensors
[AD-A154038] 19 p3272 N85-30290

CAPSULES (SPACECRAFT)
U SPACE CAPSULES

CAPTIVE TESTS
NT STATIC FIRING
NT STATIC TESTS

CAPTURE CROSS SECTIONS
U ABSORPTION CROSS SECTIONS

CAPTURE EFFECT
Focusing beam of 1-GeV protons with volumetric capture to the mode of channeling by bent single crystal
02 p0268 N85-11750
Capture of planetesimals into a circumterrestrial swarm
04 p0588 N85-13751
Orbital resonances and planetary accretion in the solar nebula
13 p2179 N85-23523
Capture of liquid hydrogen boiloff with metal hydride absorbers
[NASA-CR-175677] 14 p2249 N85-23939
Computer program for prediction of capture maneuver probability for an on-off reaction controlled upper stage
[NASA-CR-165937] 17 p3010 N85-28611
Capture in the 1.15-keV iron resonance
[DE85-011913] 23 p3970 N85-34612
Electron loss process and cross section of multiply charged ions by neutral atoms
23 p3981 N85-34685

CARBAMATES (TRADENAME)
NT URETHANES

CARBAZOLES
Photophysical studies of triplet exciton processes in pure polymer films
[DE84-016258] 05 p0620 N85-13965
Electrically conducting complexes of poly(3,6-n-methylcarbazolyl methylene)
[AD-A147884] 07 p0933 N85-15914

CARBENES
Transition metal carbene complexes
[AD-A144879] 01 p0026 N85-10173

CARBIDES
NT ALUMINUM CARBIDES
NT BORON CARBIDES
NT CEMENTITE
NT CHROMIUM CARBIDES
NT NIOBIUM CARBIDES
NT SILICON CARBIDES
NT TITANIUM CARBIDES
NT TUNGSTEN CARBIDES
NT URANIUM CARBIDES
NT ZIRCONIUM CARBIDES
Study to optimize Cr-Mo steels to resist hydrogen and temper embrittlement. A study of carbides formed in low alloy Cr-Mo steels
[DE84-015208] 01 p0029 N85-10179
The influence of the carbide distribution on the abrasive wear of ledeburitic chromium steels
01 p0054 N85-10359
Microstructural design and control of sintered hard materials
02 p0176 N85-11180
Some reflections on the competition among different hard materials in industrial applications
02 p0177 N85-11182
Development and performance of CVD-coatings on cutting tools
02 p0178 N85-11193
The adhesion of hard and wear resistant coatings
02 p0179 N85-11203
Wear properties of rapidly solidified surfaces of a pseudo-binary Fe-TiC alloy
02 p0179 N85-11204
Process for producing carbide coatings
[AD-D011295] 06 p0764 N85-14885
The effect of tantalum on the structure/properties of two polycrystalline nickel-base superalloys: B-1900 + Hf MAR-M247
[NASA-CR-174847] 09 p1294 N85-18127
SANS and TEM studies of carbide precipitation and creep damage in type 304 stainless steel
[DE85-000933] 09 p1296 N85-18139
Method of testing carbide inserts for premature fracture by face milling of cylindrical workpieces
09 p1303 N85-18183
Vapor pressure and evaporation rate of certain heat-resistant compounds in a vacuum at high temperatures
[NASA-TM-77807] 10 p1434 N85-19036
A program to develop thermite reactions to produce refractory borides and carbides
[AD-A148972] 10 p1434 N85-19037
Influence of melting conditions on strength of transition zone between steel and composite material
10 p1450 N85-19133
Neutron scattering studies of graphite intercalation compounds
[DE85-003079] 12 p1942 N85-22196
Ordered carbon metal alloys for extraterrestrial power systems
[AD-A150881] 14 p2255 N85-23977
Development of carbon based brake lining materials without asbestos content in the form of carbon-carbon composites and carbon-metal or carbon-carbide composites
[BMFT-FB-T-85-014] 18 p3082 N85-29067
Influence of microstructure on mechanical properties in cemented tungsten-carbides
19 p3230 N85-30029

Method for production of ceramic oxide and carbide bodies by polymer inclusion and decomposition
[DE85-011668] 19 p3250 N85-30152

Thermodynamic data for mineral technology
[PB85-184331] 22 p3803 N85-33560

CARBOHYDRATE METABOLISM

Dynamics of some parameters of carbohydrate and lipid metabolism in recovery period following long-term hypokinesia 01 p0093 N85-10623

Effect of high ammonia content in closed environment on some parameters of human nitrogen and carbohydrate metabolism against background of a controlled diet 12 p1903 N85-21948

Parameters of carbohydrate metabolism and blood serum enzyme activity after short-term spaceflights 12 p1903 N85-21951

Rat blood serum and liver carbohydrates and lipids in recovery period after 15-day hypokinesia 19 p3326 N85-30606

Possible mechanism for changes in glycogen metabolism in unloaded soleus muscle
[NASA-CR-176184] 24 p4127 N85-35588

Muscle protein and glycogen responses to recovery from hypogravity and unloading by tail-cast suspension
[NASA-CR-176181] 24 p4128 N85-35591

CARBOHYDRATES

NT ADENOSINE DIPHOSPHATE
NT ADENOSINE TRIPHOSPHATE
NT ADENOSINES
NT CELLULOSE
NT CHOLINE
NT CITRIC ACID
NT FATS
NT GALACTOSE
NT GLUCOSE
NT GLYCOGENS
NT NUCLEOSIDES
NT PENTOSE
NT RIBOSE
NT STARCHES
NT SUCROSE
NT SUGARS

Pacific Northwest and Alaska bioenergy program glossary
[DE85-011740] 22 p3808 N85-33591

CARBON

NT ACTIVATED CARBON
NT CARBON ISOTOPES
NT CARBON 12
NT CARBON 13
NT CARBON 14
NT CHARCOAL
NT GLASSY CARBON

Electrically conductive rigid polyurethane foam
[DE84-014490] 01 p0033 N85-10203

Plasma deposited diamondlike carbon on GaAs and InP
[NASA-TM-86870] 01 p0123 N85-10844

Microstructural basis of strength and toughness in hardmetals 02 p0177 N85-11185

Magnetic properties of the cobalt matrix in WC-Co compacts 02 p0177 N85-11186

The inter-relation of microstructure, toughness and fatigue crack growth behaviour in WC-Co hardmetals 02 p0177 N85-11188

The effect of tantalum and carbon on the structure/properties of a single crystal nickel-base superalloy
[NASA-CR-174779] 02 p0182 N85-11223

Characterization of amorphous surface layers in Fe implanted with Ti and C
[DE84-014960] 02 p0289 N85-11885

Weld metal solidification cracking in a carbon-manganese steel 03 p0330 N85-12126

Polymer-carbon black interaction in electrically conducting fiber-forming composites 06 p0762 N85-14875

Preparation of polymers of functionalized acetylenes
[AD-D011296] 06 p0771 N85-14935

Instruments for characterization of carbon black and polymers
[AD-A146475] 06 p0810 N85-15146

Arc-evaporated carbon films: Optical properties and electron mean free paths
[DE85-001246] 06 p0867 N85-15510

Reciprocal solubility of phases in multi-component systems
[BLL-M-36003-(5828.4)] 07 p0926 N85-15870

Kinetics of interaction between carbon and iron oxides of metallized materials in solid phase
[BLL-M-36023-(5828.4)] 07 p0926 N85-15873

Electrochemical features of the ferric sulfate leaching of CuFeS2/C aggregates
[AD-A148661] 08 p1123 N85-17081

Deforestation, floodplain dynamics, and carbon biogeochemistry in the Amazon Basin 08 p1144 N85-17216

The 157 micron (C II) luminosity of the galaxy 08 p1248 N85-17877

Far-infrared spectroscopy of galaxies: The 158 micron C(+) line 08 p1249 N85-17882

Implantation of Ti + C for reduced friction and wear of steels
[DE85-001606] 09 p1295 N85-18135

Investigation of vanadium solid solution and zeta phase regions of vanadium-carbon system
[DE85-002678] 11 p1605 N85-20092

Deposition of diamondlike carbon films
[NASA-CASE-LEW-14080-1] 11 p1615 N85-20153

Apparatus for producing diamond-like carbon flakes
[NASA-CASE-LEW-13837-3] 11 p1615 N85-20155

Textured carbon surfaces on copper
[NASA-CASE-LEW-14130-1] 11 p1615 N85-20156

Comments on the origins and variations of carbon and nitrogen in the ISM of galaxies as evident from IUE spectroscopy of H 2 regions 11 p1745 N85-20973

Carbon, silicon, and oxygen in the white dwarf star GD 40 11 p1752 N85-21017

The abundances of the elements -carbon to silicon- in Nova Corona Australa 1981 11 p1753 N85-21024

Carbon filter plates for aluminum filtration at casting
[BMFT-FB-T-84-242] 12 p1808 N85-21343

Carbon granule probe microphone for leak detection — recovery boilers
[NASA-CASE-NPO-16027-1] 12 p1849 N85-21597

Plasma-edge studies using carbon resistance probes
[DE85-005589] 14 p2424 N85-24955

Studies of metal/carbon surface chemistry
[DE85-005513] 15 p2507 N85-25463

Damage development during low cycle fatigue of carbon-black loaded SBR
[DE85-006234] 15 p2519 N85-25533

Aviation turbine fuels from tar sands bitumen and heavy oils. Part 1: Process analysis
[AD-A151319] 15 p2521 N85-25539

West Europe report: Science and technology
[JPRS-WST-84-012] 15 p2523 N85-25552

Size distributions of elemental carbon in atmospheric aerosols
[PB85-153534] 15 p2589 N85-25963

Optical properties of hydrogenated amorphous carbon films grown from methane plasma
[NASA-TM-86995] 15 p2658 N85-26406

Transitional metal activation and functionalization of C-H bonds
[DE85-006816] 16 p2746 N85-26949

Two-d heat transfer through porous media with heat generation
[AD-A151965] 16 p2783 N85-27173

Multi-phase crystallization of ferrous alloys
[BLL-BISI-TRANS-22441-(9022.06)] 17 p2925 N85-28037

The structure of carbon martensite analyzed with Moessbauer spectra
[BLL-BISI-TRANS-22402-(9022.06)] 17 p2927 N85-28062

Influence of manganese and heat treatment on structure and properties of Fe-0.1 percent-C-14 percent Cr-based steels
[BLL-BISI-TRANS-22299-(9022.06)] 17 p2928 N85-28071

Bifunctional oxygen electrodes
[DE85-006871] 17 p2955 N85-28248

Thermodynamic calculations of equilibrium states in metal-carbon-hydrogen-oxygen system
[BLL-BISI-TRANS-22092-(9022.06)] 17 p3045 N85-28844

Development of carbon based brake lining materials without asbestos content in the form of carbon-carbon composites and carbon-metal or carbon-carbide composites
[BMFT-FB-T-85-014] 18 p3062 N85-29067

Role of natural dissolved organic compounds in determining the concentrations of americium in natural waters
[DE85-010266] 19 p3229 N85-30022

New form of graphite 19 p3243 N85-30111

Mechanical protection of DLC films on fused silica slides
[NASA-TM-87056] 19 p3248 N85-30138

Special materials: Carbons
[SNIAS-851-551-104] 20 p3421 N85-31235

Carbon reduction of mixtures of MnO(2) and Fe(2)O(3)
[BLL-M-36260-(5828.4)] 20 p3422 N85-31241

Laminar diffusion flames, carbon gasification, and laser diagnostics applied to combustion systems. 1: Laminar diffusion flames with cylindrical symmetry. 2: Diffusion-controlled gasification of carbon particles. 3: Laser diagnostics applied to combustion systems 20 p3423 N85-31243

Recent measurements in turbulent jet flames at Sandia Combustion Research Facility 20 p3424 N85-31254

Contribution to the modelling of the gas carburizing process for steels
[BLL-OA-TRANS-3205-(6196.300)] 20 p3428 N85-31263

Computer-controlled carburizing
[BLL-OA-TRANS-3204-(6196.300)] 20 p3429 N85-31268

RAY-O-VAC BR2325 lithium carbon monofluoride cell performance 20 p3444 N85-31382

Oxygen and carbon impurities and related defects in silicon 20 p3481 N85-31631

Excitation of some alkaline Earth-like ions
[DE85-010737] 20 p3529 N85-31951

Thermoelectric properties of beta-boron and some boron compounds
[DE85-011978] 21 p3582 N85-32270

Studies of oxygen- and carbon-related defects in high-efficiency silicon solar cells 21 p3609 N85-32420

Physical and chemical aerosol characteristics in extremely clean air masses at Cape Grim, Tasmania 21 p3646 N85-32655

Carbon and nitrogen in the deep Earth 21 p3721 N85-33065

Stress and efficiency studies in EFG
[NASA-CR-176125] 22 p3751 N85-33251

Biological modulation of planetary atmospheres: The early Earth scenario 22 p3854 N85-33967

A measurement of the cosmic ray elements C to Fe in the two energy intervals 0.5-2.0 GeV/n and 20-60 GeV/n
[OG-4.1-6] 22 p3876 N85-34012

Electron photoejection in carbanions
[DE85-011747] 23 p3911 N85-34230

Electron photoejection in carbanions
[DE85-011748] 23 p3912 N85-34237

Diamondlike carbon protective coatings for IR materials
[NASA-TM-87083] 23 p3973 N85-34631

Pressure measurements in a hydrogen combustion environment: Hydrogen-air combustion test series 1 and 2 in the FITS tank, volume 1
[TI85-009899] 24 p4076 N85-35259

Development and characterization of carbon-bonded carbon fiber insulation for radioisotope space power systems
[DE85-013365] 24 p4082 N85-35299

Excessive production of electron pairs by soft photons in low multiplicity ion interactions
[HE-1.4-6] 24 p4176 N85-35894

The effect of the relative nuclear size on the nucleus-nucleus interactions
[HE-1.4-13] 24 p4177 N85-35900

Japan - USSR joint emulsion chamber experiment at Pamir
[HE-3.1-1] 24 p4177 N85-35901

Hadron intensity and energy spectrum at 4360 m above level
[HE-3.1-7] 24 p4178 N85-35905

Scaling violation in fragmentation region at energies above 10-15 eV based on the data on cosmic ray hadron component
[HE-3.1-11] 24 p4178 N85-35909

Hadrons registration in emulsion chamber with carbon block
[HE-3.7-3] 24 p4186 N85-35962

Structured events in Pamir carbon X-ray chambers
[HE-3.7-7] 24 p4186 N85-35965

CARBON ARCS

Diamondlike flakes
[NASA-CASE-LEW-13837-2] 12 p1796 N85-21267

CARBON COMPOUNDS

NT ALUMINUM CARBIDES
NT BORON CARBIDES
NT CALCITE
NT CALCIUM CARBONATES
NT CARBIDES
NT CARBONATES
NT CEMENTITE
NT CHROMIUM CARBIDES
NT DOLOMITE (MINERAL)
NT FLUOROPOLYMERS
NT HALOCARBONS
NT NIOBIUM CARBIDES
NT POLYCARBONATES
NT SIDERITES
NT SILICON CARBIDES
NT TITANIUM CARBIDE3
NT TUNGSTEN CARBIDES
NT URANIUM CARBIDES
NT ZIRCONIUM CARBIDES

Analysis and characterization of organic carbon compounds in atmospheric particulate matter
[PB84-232636] 06 p0766 N85-14903

Critical overview of hexacarbons and organophosphates
[AD-P004027] 06 p0844 N85-15361
Gas cooled fuel cell systems technology development
[NASA-CR-174732] 07 p0991 N85-16291
Denitrification-efficiencies of alternate carbon sources
[AD-A148029] 08 p1119 N85-17050
Gas phase ion-molecule chemistry of carbon, nitrogen and oxygen compounds
[AD-A152876] 17 p2919 N85-27996

CARBON CYCLE

The Marine Resources Experiment Program (MAREX)
[NASA-TM-87368] 01 p0066 N85-10580
Some aspects of understanding changes in the global carbon cycle 05 p0652 N85-14186
Carbon cycle: Terrestrial interactions 05 p0652 N85-14187
Global carbon - nitrogen - phosphorus cycle interactions: A key to solving the atmospheric CO2 balance problem? 05 p0652 N85-14188
Interactions of the marine phosphorus and carbon cycles 05 p0653 N85-14190
Recent studies of the ocean nitrogen cycle 05 p0653 N85-14193
Multi-property modeling of the marine biosphere in relation to global climate and carbon cycles 05 p0678 N85-14355
Carbon dioxide and climate: Summaries of research in FY 1983 and FY 1984
[DE85-001245] 06 p0839 N85-15327
Carbon isotope geochemistry and geobiology 21 p3657 N85-32716
Sulfur and carbon cycling in organic-rich marine sediments 21 p3659 N85-32729
Isotopic Biogeochemistry
[NASA-CR-176128] 22 p3741 N85-33189
Two dimensional CO2-ocean model including the biological processes
[DE85-012341] 23 p3950 N85-34483
Carbon dioxide and climate: A working glossary
[DE85-013535] 24 p4124 N85-35582

CARBON DIOXIDE

The oxidation behaviour of a 20 percent Cr/25 percent Ni/Nb stabilized stainless steel in carbon dioxide at high temperatures and its improvement by cerium and yttrium
[AERE-R-11228] 01 p0029 N85-10182
Response of arctic ecosystems to elevated carbon dioxide regimes, volume 2
[DE84-015236] 01 p0069 N85-10460
Future scenarios and ozone change
[DE84-014781] 01 p0085 N85-10573
The changing pattern of fossil fuel CO2 emissions
[DOE/OR-21400/2] 02 p0224 N85-11469
Impact cratering: The process and its effects on planetary evolution — and silicate-carbonate reactions on Venus
[NASA-CR-174016] 02 p0228 N85-11488
Variations with time of the carbon dioxide partial pressure in central and south Atlantic surface waters
[AD-A145825] 03 p0398 N85-12537
Radiation transport in the Earth atmosphere 04 p0522 N85-13341
CO-2-silica geothermometer for low temperature geothermal resource assessment, with application to resources in the Safford Basin, Arizona
[DE84-013958] 04 p0534 N85-13411
Thermodynamic study of CO2-organic compound interaction at high pressures and temperatures
[DE84-015777] 04 p0573 N85-13654
Quality assurance in the Antares Laser Fusion Construction Project
[DE84-015493] 05 p0640 N85-14104
Some aspects of understanding changes in the global carbon cycle 05 p0652 N85-14186
Three dimensional global modeling of atmospheric CO2 05 p0652 N85-14189
Polar regions and climatic change
[PB84-237023] 05 p0688 N85-14421
Simple formula to estimate carbon dioxide gas effect in radiation balance of underlying surface 06 p0823 N85-15226
Carbon dioxide and climate: Summaries of research in FY 1983 and FY 1984
[DE85-001245] 06 p0839 N85-15327
A biological sensor for the detection of toxicants
[AD-D011304] 07 p0967 N85-16141
Noncontact photo-thermal probe-beam deflection measurement of thermal diffusivity in an confined hot gas
[AD-A147481] 07 p0971 N85-16170
Simulating responses to expected climate change in eastern North America: Applications to decision-making in the forest industry
[DE85-001272] 07 p1008 N85-16406
Manned testing of two closed-circuit oxygen underwater breathing apparatus: US Navy Emerson Rig and Fenzy PO.66
[AD-A148300] 08 p1200 N85-17560
Supercritical fluid chromatography/supersonic jet spectroscopy
[DE85-003310] 09 p1292 N85-18115
Transport and relaxation processes in supercritical fluids
[DE85-002079] 09 p1398 N85-18797
The establishment and experience of the Carbon Dioxide Information Center (CDIC)
[DE85-001934] 09 p1402 N85-18825
An infrared study of isotopic exchange during methanation over supported rhodium catalysts; an inverse spillover effect
[AD-A149390] 10 p1435 N85-19048
An infrared study of the oxidation of carbon monoxide over supported rhodium catalysts
[AD-A149478] 10 p1436 N85-19050
Separation of gas mixtures with coordination complexes
[DE85-000363] 10 p1436 N85-19062
Monte Carlo simulation of gas Cerenkov detectors
[DE85-002422] 10 p1488 N85-19394
Photoelectrochemical reduction of carbon dioxide
[PB85-129054] 11 p1596 N85-20036
Lake ice occurrence as a possible detector of atmospheric CO2 effects on climate
[DE85-002951] 11 p1687 N85-20606
An infrared study of the dissociation of carbon dioxide over supported rhodium catalysts
[AD-A149613] 12 p1800 N85-21291
Pseudo-stationary oblique-shock-wave reflections in a polyatomic gas, sulfur hexafluoride
[UTIAS-TN-253] 12 p1845 N85-21577
Response of unmanaged forests to CO2-induced climate change: Available information, initial tests and data requirements
[DOE/NSB-0053] 12 p1883 N85-21817
Carbonate chemistry of the Weddell Sea
[DOE/EV-110611/4] 12 p1898 N85-21916
Modeling of mechanism of positive feedback between mean Earth surface temperature and atmospheric carbon dioxide in geologic time scale 13 p2106 N85-23122
The evolution of CO2 on Mars 13 p2185 N85-23558
Improvement by cerium and yttrium ion implantation of oxidation behaviour of stabilised stainless steel in carbon dioxide
[AERE-R-11523] 14 p2259 N85-23996
Predischarge parameters of SF6-CO2 determined by laser 15 p2564 N85-25821
North Atlantic Deep Water formation: Information from ice cores 15 p2602 N85-26035
Climatic impact of a change in North Atlantic Deep Water formation 15 p2603 N85-26045
Welding of 11 458.1 steel in shielding atmospheres
[BLL-BISI-TRANS-21763-(8022.06)] 17 p2972 N85-28353
Potential climatic impacts of increasing atmospheric CO2 with emphasis on water availability and hydrology in the United States
[NASA-TM-87479] 17 p2995 N85-28517
Time-dependence of CO2-induced climate change
[DE85-007568] 17 p2997 N85-28525
Photosynthetic acclimation of Acer saccharum
[DE85-006247] 17 p2998 N85-28536
Identification and characterization of watershed models for evaluation of impacts of climate change on hydrology
[DE85-008575] 18 p3125 N85-29348
Reconstruction of past atmospheric CO/sub 2/ contents from the chemistry of the contemporary ocean: An evaluation
[DE85-008426] 18 p3133 N85-29401
A new CO2 transmittance parameterization and its impact on the GLA GCM 18 p3146 N85-29476
Program planning using the GMAP procedure in SAS/GRAPH software
[DE85-008356] 18 p3199 N85-29842
The effect of surface reactions in catalytic combustion
[AD-A154217] 19 p3234 N85-30049
Thermodynamic study of CO2-organic compound interaction at high pressures and temperatures
[DE85-010999] 19 p3268 N85-30266
Mathematical model of global processes in the biosphere 19 p3295 N85-30431
Examination of the time and spatial scales appropriate for the carbon dioxide climate change issue
[DE85-006852] 19 p3317 N85-30563
Transport and relaxation processes in supercritical fluids
[DE85-010554] 19 p3358 N85-30816
Carbon dioxide and climate: Potential impacts
[DE85-009473] 20 p3496 N85-31734
Polymer solution-supercritical fluid behavior
[AD-A154514] 21 p3568 N85-32192
Carbon isotope geochemistry and geobiology 21 p3657 N85-32716
Carbon and sulfur cycling through geologic time 21 p3658 N85-32720
Evolution of the atmosphere 21 p3658 N85-32725
Thermophysical properties of fluids for the gas industry
[PB85-194471] 22 p3747 N85-33227
Model projections of time-dependent response to increasing carbon dioxide
[DE85-013326] 22 p3816 N85-33841
Climatic consequences of very high CO2 levels in Earth's early atmosphere 22 p3854 N85-33865
Potential spin-offs of the carbon dioxide observational platform system (CO-OPS) for remote sensing opportunities
[NASA-TP-2510] 23 p3899 N85-34149
Separation of gas mixtures by supported complexes
[DE85-011998] 23 p3912 N85-34236
Climate modeling: A retrospective-prospective view with consideration for the atmospheric carbon dioxide-climate issue
[DE85-011532] 23 p3950 N85-34481
Increase of total CO2 in the World ocean
[DE85-007756] 23 p3950 N85-34484
Solar modulation of cosmic ray intensity and solar flare events inferred from (14)C contents in dated tree rings
[SH-7.1-2] 23 p4047 N85-35095
Thermodynamics of the corrosion of chromium in molten carbonates
[DE85-011407] 24 p4079 N85-35282
Microbiological and biochemical studies towards optimization of substrate utilization by methanogenic bacteria
[PB85-188332] 24 p4084 N85-35310
Time-dependent response of the climate to increasing atmospheric carbon dioxide 24 p4119 N85-35532
Carbon dioxide and climate: A working glossary
[DE85-013535] 24 p4124 N85-35582
Far-infrared emission lines of CO and OH in the Orion-KL molecular shock
[NASA-TM-86721] 24 p4167 N85-35832

CARBON DIOXIDE CONCENTRATION

Measurement of range-resolved water vapor concentration by coherent CO2 differential absorption lidar
[PB84-236892] 04 p0535 N85-13420
Shock-induced CO2 loss from CaCO3: Implications for early planetary atmospheres
[NASA-CR-174197] 05 p0745 N85-14777
The CSIRO (Australia) atmospheric carbon dioxide monitoring program: Surface data
[CSIRO-TP-6] 07 p0996 N85-16324
The problem of climate and climate variation 07 p1001 N85-16353
Proceedings of a Workshop on Environment of West Antarctica: Potential CO2-induced changes
[PB85-110757] 11 p1671 N85-20527
Carbon dioxide and the greenhouse effect
[GPO-39-043] 11 p1677 N85-20569
Effect of elevated atmospheric CO2 on plant communities
[DE85-001810] 11 p1678 N85-20576
Possible role of ocean biota in global carbon balance — phytoplankton production 13 p2107 N85-23129
Changes in the high-latitude ocean as possible causes of atmosphere CO2 variations 15 p2602 N85-26038
The Martian climate: Energy balance models with CO2/H2O atmospheres
[NASA-CR-175722] 15 p2679 N85-26547
Density and confinement effects on mixing characteristics of an axisymmetrical CO(2) jet
[AD-A154468] 19 p3267 N85-30258
Potential spin-offs of the carbon dioxide observational platform system (CO-OPS) for remote sensing opportunities
[NASA-TP-2510] 23 p3899 N85-34149
Current inventory of anthropogenic carbon dioxide in the North Pacific Subarctic Gyre
[PB85-187938] 24 p4125 N85-35570

CARBON DIOXIDE LASERS

Real time sensing and control of out-of-plane distortion due to line heating by laser
[AD-A144773] 01 p0027 N85-10169
Development of the Antares electron gun
[DE84-014043] 01 p0053 N85-10352
Diagnostics of ionization in air produced by infrared radiation from A pulse CO2 laser
[AD-A145376] 02 p0201 N85-11342
Time variability of directionality properties of pulsed EB-EDL (Electron Beam-Electric Discharge Laser) N2-CO2 lasers
[AD-A145546] 02 p0202 N85-11344

Transient optical nutation in CO2 laser
02 p0261 N85-11709
Optical recording of information on paper by CO2 and YAG-lasers
02 p0261 N85-11710
Optimizing CW CO2 lasers with respect to output power in different bands
02 p0271 N85-11766
Investigation of RF excited CW CO2 waveguide lasers [NASA-CR-174106]
04 p0505 N85-13221
Scattering from multi-scale surface — infrared lasers [RSRE-MEMO-3656]
04 p0505 N85-13222
Laser for determining the ignition conditions of a pyrotechnic mixture [FOA-C-20542-D1]
04 p0506 N85-13230
Silent discharge carbon dioxide gas laser machining facility [BLL-CTO-2267-(9091.9F)]
07 p0969 N85-16150
Remote sensing of atmospheric gases with CO2 lasers. Continuation and conclusion of spectroscopic investigations [BMFT-FB-W-84-030]
07 p0989 N85-16285
Technology for satellite power conversion [NASA-CR-174335]
09 p1343 N85-18451
Carbon dioxide laser radar for monitoring atmospheric transmittance and atmospheric aerosol
09 p1354 N85-18516
Electron-hole plasma formation in semiconductors due to the absorption of pulsed CO2 laser light [DE85-001559]
09 p1392 N85-18757
Experimental investigations of driven Alfven wave resonances in a Tokamak plasma using carbon dioxide laser interferometry [DE85-001049]
09 p1392 N85-18758
Influence of laser hardening on mechanical properties of type 45 steel with vwious preliminary heat treatments
10 p1446 N85-19111
Study of microstructure of aluminum and copper alloys after processing with continuous CO2 laser beam
11 p1601 N85-20066
Chemically amplified laser direct-writing of aluminum [DE85-000306]
11 p1639 N85-20324
Model calculations for a CO2 mixing laser with screen nozzle [ESA-TT-859]
11 p1640 N85-20336
Absorption of ozone molecules in strong field of tea CO2 injection laser
11 p1718 N85-20808
Life study of RF excited Hg arc lamps and CO2 waveguide lasers [AD-A149618]
12 p1856 N85-21640
A 50-kW electric-discharge CO2 laser [AD-A149779]
12 p1857 N85-21644
The effects of atmospheric water vapor on infrared propagation [AD-A150030]
12 p1934 N85-22150
Near Field/Far Field (NF/FF) energy loss in Electric Discharge Lasers (EDL's): A mode-medium interaction [AD-A150290]
13 p2096 N85-23075
Feasibility of alpha particle measurement by CO2 laser Thomson scattering [DE85-004936]
13 p2097 N85-23081
Thresholds of optical breakdown in alkali-halide crystals under pulses from CO2-laser
14 p2262 N85-24134
Laser Welding, Cutting and Surface Treatment
14 p2308 N85-24278
Trends in laser equipment
14 p2308 N85-24280
Laser cutting: A new tool for shipbuilding
14 p2308 N85-24285
Lasers in the nuclear industry
14 p2309 N85-24289
Future trends in the use of lasers in manufacturing
14 p2309 N85-24291
Optimization of the catalytic oxidation of CO for closed-cycle CO2 laser applications [NASA-TM-86421]
15 p2504 N85-25445
Ground slot waveguide laser [AD-D011600]
15 p2563 N85-25813
Development of global model for atmospheric backscatter at CO2 wavelengths [NASA-CR-175679]
15 p2591 N85-25971
Characteristics of laser emission discharge created by pulsed CO2-laser
15 p2643 N85-26305
Theoretical investigation of lasing in 4.3 micron region in CO2 laser
15 p2643 N85-26306
Population inversion in laser-initiated vacuum arcs [AD-A151958]
16 p2790 N85-27210
Europe's primary producers of industrial lasers surveyed
18 p3087 N85-29101
Technology assessment of high pulse energy CO(2) lasers for remote sensing from satellites [NASA-TM-86415]
19 p3275 N85-30309
Summary of research for the Inertial Confinement Fusion Program at Los Alamos National Laboratory [DE85-010330]
19 p3361 N85-30836
Robot, laser tridimensional cutting technology detailed
20 p3438 N85-31335
Simplified analytical model for calculation of population inversion in channels of CW gasdynamic lasers operating at various transitions among levels pertaining to coupled upsilon 1 and upsilon 2 modes of CO2 [STN-2]
20 p3461 N85-31498
Requirements for attaining Treanor's distribution of vibrational energy among CO2 levels in CW gasdynamic laser flows [STN-3]
20 p3461 N85-31499
Identification of vibrational-rotational transitions of Os-192O4 within frequency tuning limits of high pressure CO2 waveguide laser
21 p3689 N85-32917
The possibility of observing and exploiting the generation of high-energy photons by electrons in the field of an intense electromagnetic wave
21 p3691 N85-32931
Investigation of ion-acoustic plasma turbulence in field of powerful electromagnetic wave by CO2-laser radiation scattering
21 p3691 N85-32935
Sliding discharge in CO2 and excimer lasers
22 p3773 N85-33579
Expansion ratio influence on population inversion in CO2/Ar CW gasdynamic lasers operating at various transitions within coupled upsilon 1 and upsilon 2 modes of CO2 [STN-4]
22 p3790 N85-33485
Hole cutting in building frames by laser [FOA-C-20568-D9]
22 p3791 N85-33487

CARBON DIOXIDE TENSION
NT HYPERCAPNIA

CARBON DISULFIDE
Measurements of atmospheric carbon disulfide using aircraft platforms and a GC/MS isotopic dilution analysis technique
03 p0391 N85-12500

CARBON FIBER REINFORCED PLASTICS
Flight simulation fatigue crack propagation in metal/carbon-epoxy laminates [NLR-TR-83006-U]
01 p0063 N85-10416
Thermoplastic-carbon fiber hybrid yarn [NASA-CR-3849]
03 p0325 N85-12093
Modern structural materials. Present situation and evolution prospects — aircraft materials [SNIAS-842-551-101]
04 p0455 N85-12886
Optimization of the injection process for thermostatic polyether-ether-ketone (Peek) thermoplastics reinforced with short carbon fibers [SNIAS-842-422-102]
04 p0480 N85-13062
Mechanical properties of aligned short carbon fiber reinforced PES and PI laminates [DFVLR-FB-84-24]
05 p0613 N85-13918
Influence of thermal cycling on the behavior of CFRP material for space structures
05 p0626 N85-14013
The fourth LBF colloquium [ISSN-0721-5320]
05 p0648 N85-14163
Development of damage in fatigue loaded carbon fiber reinforced plastics
05 p0650 N85-14172
Fatigue behavior of bolted joints made of carbon fiber reinforced epoxy resins
05 p0650 N85-14173
A new generation of sub mm telescopes, made of carbon fiber reinforced plastic
08 p1250 N85-17890
FRG radiotelescope made of carbon fiber-reinforced plastic
09 p1309 N85-18226
Studies of structure and mechanical properties of carbon-reinforced plastic based on spirally reinforced filler
10 p1444 N85-19100
Control technology for fiber reinforced plastics industry at AMF Hatteras Yachts, New Bern Division, New Bern, North Carolina [PB85-109015]
10 p1460 N85-19198
Initial fracture stages of orthogonally reinforced composite material
11 p1599 N85-20055
Strength properties of unidirectionally reinforced hybrid composites
11 p1599 N85-20056
Electrostatic discharge testing on a carbon fiber solar panel structure
13 p2007 N85-22584
Diffusion of water vapor in Carbon Fiber Reinforced Plastics (CFRP). Measurement of the diffusion coefficient under influence of concentration [DFVLR-FB-84-41]
14 p2262 N85-24018
Ultrasonic testing of carbon fiber reinforced plastics (CFRP) using pattern recognition methods [MBB-BB-563/84-0]
16 p2873 N85-27726
Development of a fuselage forward section in Carbon Fiber Reinforced Plastic (CFRP) type of construction [MBB/LFA34/CFK/PUB/006]
17 p2895 N85-27851
Integral profile method for production of carbon fiber sheets [MBB/LFA34/CFK/PUB/006]
17 p2916 N85-27975
Heat resistant Carbon Fiber Reinforced Plastics (CFRP) hardening equipment [MBB/LFA33/CFK/PUB/007]
17 p2916 N85-27976
Optimization of axially compressed carbon fiber reinforced plastic (CFRP) cylinders
18 p3121 N85-29318
Mechanical properties of aligned short carbon fiber reinforced PES and PI laminates [ESA-TT-898]
20 p3422 N85-31240
High reflective surfaces for millimeter RF waves, phase A — satellite antenna reflectors [HRS-FR-01]
20 p3442 N85-31366
Development of fracture mechanics maps for composite materials, volume 1 [ESA-CR(P)-2017-VOL-1]
20 p3471 N85-31573
Development of fracture mechanics maps for composite materials, volume 2 [ESA-CR(P)-2017-VOL-2]
20 p3471 N85-31574
Development of fracture mechanics maps for composite materials. Volume 3: Appendices A-E [ESA-CR(P)-2017-VOL-3]
20 p3472 N85-31575
Development of fracture mechanics maps for composite materials. Volume 4: Appendices F-K [ESA-CR(P)-2017-VOL-4]
20 p3472 N85-31576
Utilization of microwave measuring systems for the automation of composite materials manufacturing [SNIAS-851-490-102]
22 p3742 N85-33197
Filament wound structures in PSP carbon composite [RV10/84424]
22 p3743 N85-33198
Ultrasonic inspection of carbon fiber reinforced plastic by means of sample-recognition methods [NASA-TM-77896]
24 p4074 N85-35245
Contribution to the properties of carbon fiber reinforced composites — structural mechanics [ESA-TT-849]
24 p4074 N85-35246
Methods for nondestructive tests of CFRP laminates
24 p4074 N85-35248
Damage mechanisms in damaged CFRP laminates
24 p4074 N85-35249

CARBON FIBERS
Distributions of fatigue life and fatigue strength in notched specimens of a carbon 8-harness-satin laminate [NAL-TR-809T]
01 p0061 N85-10407
Thermoplastic-carbon fiber hybrid yarn [NASA-CR-3849]
03 p0325 N85-12093
The chemical nature of the fiber/resin interface in composite materials
04 p0465 N85-12953
Newer carbon fibers and their properties
04 p0465 N85-12955
Composite structural materials [NASA-CR-174077]
04 p0467 N85-12966
Chemical modification of the surface of high modulus carbon fibers
04 p0467 N85-12967
Flexible matrix composite laminated disk/ring flywheel
05 p0606 N85-13866
Carbon fibre reinforced aluminum matrix composites: A critical review [AD-A146367]
06 p0764 N85-14883
All-composite Airbus empennage
07 p0936 N85-15931
Composite batteries
07 p0936 N85-15932
Studies of structure and mechanical properties of carbon-reinforced plastic based on spirally reinforced filler
10 p1444 N85-19100
Thermoviscoelastic analysis of dimensionally stable fiber composite space structures [AD-A149275]
11 p1593 N85-20021
Composite structural materials [NASA-CR-175515]
12 p1796 N85-21268
Segregation of silicon in silumin-carbon fiber composites
13 p2028 N85-22706
Environmental effects on the tensile strength of chemically vapor deposited silicon carbide fibers [NASA-TM-86981]
14 p2259 N85-24000
High resistance and raised modulus carbon fibers [NASA-TM-76884]
15 p2502 N85-25436
In-plane shear properties of graphite Fibre/Epoxy composites for aerospace applications: Evaluation of test methods by the decision analysis technique [AD-A151599]
15 p2503 N85-25440
MBB uses new CFC form tool for titanium alloy air intake
15 p2523 N85-25553
Glass, carbon fibers made at Fibre et Mica in France
15 p2534 N85-25634
Graphite fiber intercalation: Dynamics of the bromine intercalation process [NASA-TM-87015]
16 p2742 N85-26921
Mechanical properties of high performance carbon fibers
16 p2742 N85-26922
Environmental stability of intercalated graphite fibers [NASA-TM-87025]
16 p2753 N85-26992
Fiber reinforcement of gun propellant [AD-A152296]
16 p2757 N85-27014
Lightning-safe carbon fiber composite for Airbus tail unit
18 p3087 N85-29100
Mesophase mechanisms in the formation of graphitic microstructures [AD-A154100]
19 p3248 N85-30140
Thermal expansion of selected graphite reinforced polyimide-, epoxy-, and glass-matrix composite [NASA-TM-87572]
21 p3561 N85-32149
Improved materials for composite and adhesive joints [AD-A155065]
21 p3562 N85-32153

Electrical and mechanical properties of intercalated graphite fibers
[AD-A155560] 21 p3570 N85-32205
Crystallization of Polyetheretherketone (PEEK) in carbon fiber composites
[AD-A156316] 24 p4075 N85-35252
Carbon fiber strainmeter studies in southern California
[PB85-196869] 24 p4118 N85-35528

CARBON ISOTOPES
NT CARBON 12
NT CARBON 13
NT CARBON 14
Sixteenth Lunar and Planetary Science Conference. Press abstracts
[NASA-CR-175892] 15 p2680 N85-26548
Carbon isotopes in bulk carbonaceous chondrites 15 p2681 N85-26557
Resonance ionization mass spectrometry of carbon
[DE85-009040] 17 p2923 N85-28018
Isotopic Biogeochemistry
[NASA-CR-176128] 22 p3741 N85-33189
Control technology for radioactive emissions to the atmosphere at US Department of Energy facilities: The Los Alamos Meson Physics Facility
[DE85-011402] 22 p3811 N85-33609
Implications of new measurements of O-16 + p + C-12,13, N-14,15 for the abundances of C, N isotopes at the cosmic ray source
[OG-4.3-2] 22 p3878 N85-34027
Nucleosynthesis in the terrestrial and solar atmospheres
[SH-2.2-2] 23 p4000 N85-34797
Measurements of the fragmentation of (40)Ar, (28)Si and (12)C in CH2C and H targets between 300 and 1500 MeV/nuc at the Bevalac
[OG-7.2-19] 23 p4016 N85-34896

CARBON LASERS
Carbon vaporization/condensation effects
[NASA-TM-87490] 10 p1436 N85-19048

CARBON MONOXIDE
Investigation of the CARS spectrum of carbon monoxide at high pressure and temperature
[AD-A144816] 01 p0024 N85-10146
Mobile source exposure estimation
[PB84-224518] 01 p0095 N85-10643
Review of the NAAQS (National Ambient Air Quality Standards) for carbon monoxide: Reassessment of scientific and technical information
[PB84-231315] 03 p0388 N85-12485
Theoretical studies in molecular fragmentation: Processes, energetics and diagnostics
[AD-A146310] 03 p0418 N85-12673
Carbon monoxide study, Anchorage, Alaska, November 22, 1982 to February 11, 1983
[PB84-236595] 05 p0673 N85-14321
Results of the carbon monoxide study in Washington, D.C. and Denver, Colorado, in the winter of 1982-83
[PB84-230069] 06 p0634 N85-15309
NAAQS (National Ambient Air Quality Standards) Exposure Model (NEM) applied to carbon monoxide
[PB84-242551] 06 p0634 N85-15310
A wide latitude CO survey of molecular clouds in the northern Milky Way 06 p0877 N85-15574
The adsorption of CO and oxygen on Cu layers on a W(110) surface
[AD-A147345] 07 p0923 N85-15847
Bipolar flows and X-ray emission from young stellar object 08 p1234 N85-17779
Far-infrared photometry of low-mass pre-main-sequence stars with broad CO wings 08 p1246 N85-17866
Cation promotion effects in zeolite-supported F-T catalysts
[DE85-001708] 09 p1291 N85-18108
Measurement and analysis of ambient carbon monoxide concentrations for project-level air quality impact studies
[PB85-104602/GAR] 09 p1350 N85-18482
Meteorological factors responsible for high CO (carbon monoxide) levels in Alaskan cities
[PB85-115137/GAR] 09 p1350 N85-18483
New phases and chemical reactions in solid CO under pressure
[DE85-002033] 09 p1377 N85-18655
Experimental determination of the 1 sigma(+) state electron-dipole-moment function of carbon monoxide up to a large internuclear separation
[NASA-TM-85979] 09 p1379 N85-18670
Characterization of CO binding sites on Rh(111) and Rh(331) surfaces by XPS and LEED (Low Energy Electron Diffraction): Comparison to EELS (Electron Energy Loss Spectroscopy) results
[AD-A149331] *0 p1435 N85-19044
An infrared study of the oxidation of carbon monoxide over supported rhodium catalysts
[AD-A149478] 10 p1436 N85-19050
Separation of gas mixtures with coordination complexes
[DE85-000363] 10 p1438 N85-19062
Improved operation of transversely exited N2O lasers
[AD-D011488] 10 p1490 N85-19409
Photoelectrochemical reduction of carbon dioxide
[PB85-129054] 11 p1596 N85-20036
Development of a low cost electrochemical CO monitor based on stripping voltammetry
[PB85-113470] 11 p1637 N85-20312
Development of a low cost electrochemical CO monitor based on anodic scanning voltammetry in nonaqueous electrolyte
[PB85-113488] 11 p1637 N85-20314
Stability evaluation of sulfur dioxide nitric oxide and carbon monoxide gases in cylinders 11 p1648 N85-20387
Carbon monoxide adsorption on a platinum electrode studied by polarization modulated FT-IRRAS (Fourier Transform-IR Reflections Adsorption Spectroscopy). Part 1: CO adsorbed in the double layer potential region and its oxidation in acids
[AD-A149751] 12 p1800 N85-21288
The seasonal cycle of atmospheric CO in the Southern Hemisphere 16 p2830 N85-27447
Hydrogen degradation of pipeline steels
[DE85-006930] 17 p2932 N85-28101
Study of synthesis gas conversion over metal oxides
[DE85-010136] 18 p3072 N85-28999
Heat of mixing experiments for liquified gases
[PB85-183697] 18 p3084 N85-29081
Development of a stationary carbon monoxide detector
[BMFT-FB-T-84-253] 18 p3134 N85-29413
Shock tube measurements of growth constants in the branched-chain ethane-carbon monoxide-oxygen system
[NASA-TM-87068] 21 p3562 N85-32156
Why CO bonds side-on at low coverage and both side-on and upright at high coverage on the Cr(110) surface
[NASA-CR-176071] 21 p3565 N85-32173
CO adsorption on (111) and (100) surfaces of the Pt sub 3 Ti alloy. Evidence for parallel binding and strong activation of CO
[NASA-CR-176077] 21 p3565 N85-32176
The problem of the Earth's CO2 content and the iron core 21 p3718 N85-33089
Effects of low level carbon monoxide (CO) on tracking and monitoring. An attempt to replicate the findings of Putz et al. (1976) protocol 2
[AD-A155722] 22 p3825 N85-33694
Infrared studies of the influence of alkali metals on the C-O bond in chemisorbed carbon monoxide
[DE85-005306] 23 p3911 N85-34232
Separation of gas mixtures by supported complexes
[DE85-011996] 23 p3912 N85-34236
Oxygen analyzer
[DE85-006002] 23 p3935 N85-34392
CO + H2 reaction over nitrogen-modified iron catalysts
[DE85-013791] 24 p4072 N85-35231
Characterization of catalysts with metal-support effects and of the species adsorbed on their surfaces
[DE85-012254] 24 p4096 N85-35394
Size and shape dependance of CO adsorption sites on sapphire supported Fe microcrystals
[NASA-CR-176171] 24 p4160 N85-35794

CARBON MONOXIDE LASERS
Microwave discharge in a supersonic flow for the excitation of a gas dynamic CO laser
[ESA-TT-833] 09 p1326 N85-18337
Developement of a theoretical model to describe the interaction between electric discharge and supersonic flow of a pulsed CO laser
[DFVLR-FB-84-45] 14 p2310 N85-24301
Optically bistable devices using InSb 18 p3186 N85-29758

CARBON MONOXIDE POISONING
Pathophysiological study of poisoning due to thermal degradation of materials — aircraft cabins
[CERMA-84-15] 11 p1692 N85-20640

CARBON STARS
Carbon stars: There is no such thing as a dead leg 08 p1247 N85-17871
Variability of ultraviolet emission lines in the carbon star TX Psc 11 p1753 N85-21027
Neutron-rich nuclei in cosmic rays and Wolf-Rayet stars
[OG-8.2-6] 23 p4019 N85-34906

CARBON STEELS
NT LOW CARBON STEELS
Features of laser welding of medium carbon steel through a cadmium coating 01 p0020 N85-10122
Fretting corrosion and fretting fatigue of medium carbon steels 01 p0054 N85-10958
The effect of overload on three different kinds of steel 02 p0174 N85-11165
Microstructural design in low alloy steels 02 p0176 N85-11179
Effects of prior austenite and ferrite grain size on fracture properties of a plain carbon steel
[AD-A146276] 03 p0332 N85-12138
Study of fatigue fracture in hardened and tempered carbon steel. Report 1: Microscopic observation of the fatigue crack formation process
[BLL-PNR-90242-(8019.3153)] 06 p0767 N85-14909
Ultrahigh carbon steel
[AD-A147762] 08 p1128 N85-17113
Two-dimensional shock response of a mass on energy-absorbing shock mounts 09 p1334 N85-18389
New application possibilities for clad steel by reducing surface treatment expenditure and by using improved welding technology
[BMFT-FB-T-84-236] 12 p1861 N85-21672
Characteristics of polyacrylic acid-complexed zinc phosphate conversion films deposited on metal surfaces
[DE85-004057] 16 p2750 N85-26974
The state of martensite after quenching in a magnetic field
[BLL-BISI-TRANS-22297-(9022.06)] 17 p2926 N85-28051
Variations in the structure and in the composition of austenitic and carbon steel in spot welds
[BLL-BISI-TRANS-21765-(9022.06)] 18 p3073 N85-29007
Corrosion performance of metals and alloys in a tuff geochemical environment
[DE85-009449] 18 p3077 N85-29033
Powder metallurgy forged gear development
[NASA-TM-87483] 18 p3117 N85-29295
Microstructures and mechanical properties of microalloyed medium carbon steels 19 p3238 N85-30074
Corrosion fatigue strength and crack growth in prestrained 0.16% C carbon steel 23 p3905 N85-34192
Effect of microstructure on the fatigue behavior of Fe-C-X alloys
[DE85-011749] 24 p4080 N85-35285

CARBON TETRACHLORIDE
Health assessment document for carbon tetrachloride
[PB85-124196] 10 p1528 N85-19638

CARBON TETRAFLUORIDE
Atomic hydrogen maser measurements with wall surfaces of carbon tetrafluoride 18 p3108 N85-29243

CARBON 12
Spin distributions in heavy ion fusion at and below the Coulomb barrier
[DE85-007817] 17 p3031 N85-28751

CARBON 13
Stable isotope studies
[DE84-016752] 04 p0562 N85-13583
The 13C nuclear magnetic resonance in graphite intercalation compounds
[NASA-CR-174261] 07 p1040 N85-16601
Guest molecules in coal
[DE85-010435] 19 p3228 N85-30018

CARBON 14
Solar modulation of cosmic ray intensity and solar flare events inferred from (14)C contents in dated tree rings
[SH-7.1-2] 23 p4047 N85-35095
High precise measurements of cosmogenic radiocarbon abundance by complex of scintillation equipments
[SH-7.1-14] 23 p4048 N85-35105

CARBON-CARBON COMPOSITES
The effects of radial yarns, 3-dimensionally reinforced carbon-carbon composite
[AD-A144751] 01 p0022 N85-10134
Carbon/carbon rocket motor exit cone reinforcement
[AD-D011360] 07 p0916 N85-15799
Thermophysical property testing using transient techniques
[AD-A147085] 07 p1049 N85-16664
Disclinations in carbon-carbon composites
[AD-A148290] 08 p1119 N85-17052
Glass, carbon fibers made at Fibre et Mica in France 15 p2534 N85-25834
Evaluation of the PSP resin as a precursor of carbon
[ONERA-RT-11/1784-M] 16 p2744 N85-26932
Lightweight piston
[NASA-CASE-LAR-13150-1] 18 p3068 N85-28975
Development of carbon based brake lining materials without asbestos content in the form of carbon-carbon composites and carbon-metal or carbon-carbide composites
[BMFT-FB-T-85-014] 18 p3082 N85-29067
Effects of weak interfaces on thermostructural behavior of carbon-carbon composites
[AD-A155330] 21 p3562 N85-32154

Carbon/carbon combustor external insulation
[AD-D011719] 23 p3910 N85-34224
Oxidation resistant slurry coating for carbon-based materials
[NASA-CASE-LEW-13923-1] 24 p4077 N85-35267

CARBONACEOUS CHONDRITES
NT ALLENDE METEORITE
Bulk compositions of Al-rich chondrules in ordinary and carbonaceous chondrites: Variations and similarities 06 p0881 N85-15801
Hydrothermal alteration of CM carbonaceous chondrites: Implications of the identification of tochilinite as one type of meteoritic PCP 06 p0884 N85-15616
Aqueous alteration of meteorite parent bodies: Possible role of unfrozen water and the Antarctic meteorite analogy 06 p0884 N85-15617
Minor elements and cathodoluminescence of Mg-rich olivines from Murchison and Allende carbonaceous meteorites 06 p0884 N85-15619
Strain analysis of the Leoville chondrite and conditions in asteroidal interiors 06 p0885 N85-15620
Hibonite: Crystal chemistry and origin of blue coloration in meteoritic assemblages 13 p2184 N85-23555
Refractory inclusions in the Omans C30 chondrite 15 p2680 N85-26553

CARBONACEOUS MATERIALS
NT PEAT
Supercritical solvent extraction of lignite to form carbonaceous chars
[DE85-010159] 19 p3229 N85-30019
Ash contents of Costa Rican peat deposits
[DE85-010734] 19 p3301 N85-30462
Development of wide band recording materials
[AD-A154961] 21 p3589 N85-32309
Method of distributing liquefaction catalysts in solid carbonaceous material
[DE85-005759] 23 p3909 N85-34218
Fluidized bed desulfurization
[NASA-CASE-NPO-15924-1] 24 p4075 N85-35253

CARBONACEOUS METEORITES
Minor elements in relict olivine grains of deep-sea spheres: Match with Mg-rich olivines from C2 meteorites 06 p0883 N85-15610

CARBONACEOUS ROCKS
NT COAL
NT LIGNITE

CARBONATES
NT CALCITE
NT CALCIUM CARBONATES
NT DOLOMITE (MINERAL)
NT POLYCARBONATES
NT SIDERITES
Effects of H2S on molten carbonate fuel cells
[DE84-015166] 02 p0195 N85-11307
Syntheses of polyhedranes and polyhedral carboranes
[AD-A146076] 03 p0340 N85-12187
Dynamic compression and volatile release of carbonates
[NASA-CR-174076] 03 p0391 N85-12504
Molten carbonate fuel cell performance model update, draft
[DE85-005423] 13 p2129 N85-23252
Cathode materials for molten carbonate fuel cells
[DE85-004076] 13 p2130 N85-23254
Analysis of SMIRR data for volcanic and sedimentary terrains of the trans-Pecos region, Texas 13 p2197 N85-23626
Chemical weathering of soils from the dry valleys of Antarctica: A terrestrial analog of Martian weathering processes 13 p2197 N85-23628
Exploratory corrosion tests on alloys in molten salts at 900(0)C
[DE85-000511] 14 p2257 N85-23983
Development of molten carbonate fuel cell power plant technology
[DE84-016839] 14 p2352 N85-24536
Carbon isotopes in bulk carbonaceous chondrites 15 p2681 N85-26557
Molten carbonate fuel cell performance model update
[DE85-003356] 17 p2966 N85-28454
Molten carbonate fuel cell cathode material development
[DE85-010268] 18 p3081 N85-29057
Development of molten carbonate fuel cell power plant, volume 1
[DE85-008743] 18 p3131 N85-29394
Advanced fuel cell development
[DE85-009662] 19 p3306 N85-30497
Integrated current collector and catalyst support
[DE85-011616] 22 p3761 N85-33311
Deep-burial diagenesis in carbonates
[DE85-011224] 22 p3802 N85-33554
Thermodynamic data for mineral technology
[PB85-184331] 22 p3803 N85-33560
Molten carbonate fuel cell separator
[DE85-011615] 22 p3806 N85-33577
Effects of H2S on molten carbonate fuel cells. Literature review on the impact of SO2 in the oxidant supplied to molten carbonate fuel cells
[DE85-011698] 22 p3808 N85-33586
Electrolyte reservoir for carbonate fuel cells
[DE85-005738] 23 p3947 N85-34460
Thermodynamics of the corrosion of chromium in molten carbonates
[DE85-011407] 24 p4079 N85-35282

CARBONYL COMPOUNDS
Method of obtaining polychalcones
[AD-A145051] 01 p0018 N85-10107
Development and application of fluorine-containing reagents in the gas chromatography of carbonyl compounds
[BLL-DRIC-TRANS-7205-(3623.66)] 01 p0023 N85-10140
Method for the preparation of poly(carbonyl fluoride) oligomers
[AD-D011207] 01 p0030 N85-10184
Stratospheric concentration of nitric acid, ozone and carbonyl sulfide: Measurement of nitric acid absorption in the Q branch of the V4 band as a function of temperature
[ESA-TT-864] 09 p1355 N85-18524
An infrared study of the hydrogenation of carbon dioxide on supported rhodium catalysts
[AD-A149477] 10 p1436 N85-19049
Analysis of aldehydes and ketones in the gas phase
[PB85-181865] 20 p3426 N85-31261

CARBORANE
Syntheses of polyhedranes and polyhedral carboranes
[AD-A146076] 03 p0340 N85-12187
The synthesis, structural characterization and reactions of closo-Rhodacarborane Anions containing a formal d6 metal vertex 1,2
[AD-A149640] 12 p1799 N85-21285

CARBOXYLATION
Vitamin K and the metabolic state of bone 05 p0694 N85-14485

CARBOXYLIC ACIDS
NT ALANINE
NT ASPARTIC ACID
NT BENZOIC ACID
NT CITRIC ACID
NT DICARBOXYLIC ACIDS
NT TRYPTOPHAN
Method for making heterocyclic block copolymers
[AD-D011446] 10 p1451 N85-19143
Fatty and aromatic acid catabolizing bacteria from methanogenic ecosystems
[DE85-008133] 17 p2998 N85-28537
Alkaline battery containing a separator of a cross-linked copolymer of vinyl alcohol and unsaturated carboxylic acid
[NASA-CASE-LEW-13102-1] 18 p3093 N85-29144

CARBURIZING
Recent developments on the role of molybdenum in irons and steels 02 p0180 N85-11206
Contribution to the modelling of the gas carburizing process for steels
[BLL-OA-TRANS-3205-(6196.300)] 20 p3428 N85-31263
An investigation of cementation and carbonitriding by means of ionic bombardment
[BLL-OA-TRANS-3203-(6196.300)] 20 p3429 N85-31265
Computer-controlled carburizing
[BLL-OA-TRANS-3204-(6196.300)] 20 p3429 N85-31266

CARCINOGENS
Molecular interactions of high energy fuels and jet fuels with oncogenic viruses and endogenous viruses
[AD-A145484] 02 p0188 N85-11255
Toxicology of natural and man-made toxicants in drinking water
[AD-P004035] 06 p0845 N85-15365
Ambient air contamination: Characterization and detection techniques 18 p3157 N85-29546
Use of environmental health-risk analysis for managing toxic substances
[DE85-006964] 18 p3160 N85-29574
Factor analysis of atmospheric pollution by polycyclic aromatic hydrocarbons
[HSE-TRANS-10988] 19 p3311 N85-30528
Repair of DNA treated with lambda-irradiation and chemical carcinogens
[DE85-010298] 19 p3327 N85-30616
Carcinogenesis of nitrated toluenes and benzenes skin and lung tumor assays in mice
[AD-A155723] 22 p3818 N85-33655

CARCINOMA
U CANCER

CARDIAC VENTRICLES
Left heart ventricular function during a 7 day zero-g simulation (6 deg head down tilt) 05 p0691 N85-14446
Changes in cardiovascular function: Weightlessness and ground-based studies 20 p3509 N85-31815

CARDIOGRAPHY
NT BALLISTOCARDIOGRAPHY
NT ECHOCARDIOGRAPHY
NT ELECTROCARDIOGRAPHY
Mapping of mammalian arrhythmias with the cardiac laser scanner 03 p0399 N85-12545
NDE methods for green ceramics
[DE85-004019] 13 p2038 N85-22766
Changes in cardiovascular function: Weightlessness and ground-based studies 20 p3509 N85-31815
Current status of the Os-191 yields Ir-191m generator
[DE85-008306] 23 p3971 N85-34614

CARDIOLOGY
Gravity perception and cardiac function in the spider 15 p2808 N85-26058

CARDIOVASCULAR SYSTEM
NT ARTERIES
NT BLOOD VESSELS
NT CARDIAC VENTRICLES
NT ERYTHROCYTES
NT HEART
NT HEMATOPOIESIS
NT HEMATOPOIETIC SYSTEM
NT LYMPHOCYTES
NT MYOCARDIUM
NT VEINS
Functional capacities of elderly subjects exposed to simulated spaceflight factors 01 p0091 N85-10617
Frequency and nature of electrocardiographic disturbances in dogs during single and repeated exposure to +G sub z accelerations 01 p0092 N85-10619
Cardiovascular disease among U.S. Navy pilots
[AD-A145871] 03 p0400 N85-12552
Impact of space medicine on Earth-based medicine: Academician Ye. I. Chazov comments on the work in orbit of physician O. Atkov 04 p0543 N85-13458
Ultrasonic study of early cardiovascular adaptation to zero gravity 05 p0691 N85-14445
Biochemical evaluation of bodily influence of high and low temperatures 07 p1014 N85-16441
Influence of geomagnetic disturbances on cardiovascular function of athletes 08 p1193 N85-17516
Health examination findings among active civil airmen
[AD-A148325] 08 p1195 N85-17533
Work capacity of heat and electric power plant operations working 12 hour day and night shifts 09 p1362 N85-18567
Morbidity and mortality associated with exposure to Otto Fuel II in the U.S. Navy 1966-1979
[AD-A148726] 09 p1363 N85-18574
Variability of cardiac rhythm during information loading 10 p1525 N85-19619
Medically disqualified airline pilots
[AD-A149454] 10 p1528 N85-19637
Symposium on Military Aviation Medicine summarized 11 p1696 N85-20663
USSR report: Space Biology and Aerospace Medicine, volume 18, no. 6, November - December 1984
[JPRS-USB-85-002] 12 p1900 N85-21931
LBNP training of crew members on main missions aboard Salyut-6 orbital station 12 p1901 N85-21938
Main component method used to study variations of cardiovascular parameters 12 p1901 N85-21939
Morphological study of monkeys submitted to antiorthostatic hypokinesia 12 p1902 N85-21942
Preventive effect of acute heat factors during hypokinesia 12 p1902 N85-21945
Multiple regression method used to assess animal adaptation to hypoxic hypoxia 12 p1902 N85-21947
Computer simulation studies in fluid and calcium regulation and orthostatic intolerance
[NASA-CR-171869] 15 p2616 N85-26117
Analysis of head-down tilt as an analog of weightlessness using a mathematical simulation model
[NASA-CR-171870] 15 p2616 N85-26118
Predictions of cardiovascular responses during STS reentry using mathematical models
[NASA-CR-171871] 15 p2616 N85-26119
Simulation of a G-tolerance curve using the pulsatile cardiovascular model
[NASA-CR-171873] 15 p2616 N85-26120
Cardiovascular effects of weightlessness 15 p2688 N85-26607
Cosmonauts' postural reactions after long-term missions aboard Salyut-6 orbital station 19 p3323 N85-30585
Nature of postural changes in human hemodynamics with intake of sydnocarb alone and in combination with obsidan 19 p3325 N85-30597

Longitudinal study of cardiovascular disease in US Navy pilots
[AD-A154331] 19 p3328 N85-30623
Study of the cardiovascular system in microgravity: Results and perspectives 20 p3509 N85-31816
Cardiovascular research in space: Problems and results 20 p3510 N85-31817
Studies of circulatory and metabolic changes during ketamine narcosis
[AD-A154512] 21 p3663 N85-32758
Intracardiac hemodynamics and human heart function in simulated weightlessness 22 p3733 N85-33140
Cosmonauts' cardiovascular system function during long-term orbital flights aboard Salyut-6 station 22 p3733 N85-33141
Cardiorespiratory function and work performance during adaptation to industrial labor in midalpine conditions 22 p3820 N85-33665
Cerebral hemodynamics and ventricular function in -15 deg anti-orthostatic position 22 p3822 N85-33676
Effect of acute hypoxia on coronary and systemic hemodynamics 23 p3953 N85-34503
Cardiovascular responses to orthostatism and weightlessness 24 p4130 N85-35601

CARDS
Radio frequency probing apparatus for surface acoustic wave devices
[AD-D011230] 01 p0050 N85-10327
Computer center CDC Libraries-PROCFIL (procedures)
[AD-A146633] 08 p1206 N85-17589
Fibre composite laminated plate analysis using a card programmable calculator (HP41C/CV)
[NIAST-83/88] 13 p2103 N85-23106

CARGO
USSR report: Space
[JPRS-USP-84-005] 02 p0156 N85-11060
Features and uses of progress cargo ships 02 p0157 N85-11061
Tass reports launch of Progress-22 02 p0157 N85-11063
Progress-22 docks with Salyut-7 02 p0157 N85-11064
Orbit of Salyut-7 station boosted 02 p0157 N85-11067
Portable pallet weighing apparatus
[NASA-CASE-GSC-12789-1] 11 p1635 N85-20294
Cargo handling system
[AD-D011569] 14 p2219 N85-23762
MI-8 helicopter cargo loading experiment for Arctic shipping 14 p2332 N85-24425
Air traffic: Instruments, airports, companies, post, cargo and passengers 18 p3080 N85-29932
Laboratory vibration schedules
[AD-A155656] 24 p4064 N85-35188

CARGO AIRCRAFT
NT C-5 AIRCRAFT
NT C-135 AIRCRAFT
NT C-141 AIRCRAFT
NT F-27 AIRCRAFT
Performance capabilities of the C-5 and C-17 cargo aircraft
[AD-A145518] 02 p0136 N85-10939
USSR report: Transportation
[JPRS-UTR-84-025] 17 p2894 N85-27841
Test flight of IL-76TD long-range transport variant 17 p2894 N85-27842
OWEMA report: A project study concerning the possibilities and the desirability of a east-west runway for Maastricht Airport (Netherlands) as a Euro-regional air freight center
[B8476490] 18 p3064 N85-29955

CARGO SHIPS
NT TANKER SHIPS

CARIBBEAN SEA
Review of climate problems in Latin America and the Caribbean 07 p1001 N85-16354
Deep source gas
[DE85-001984] 18 p3126 N85-29358

CARNOT CYCLE
Operating experience with potassium systems — thermal power stations
[OEFZS-4275] 03 p0387 N85-12473

CAROTENE
Enrichments for phototrophic bacteria and characterization by morphology and pigment analysis 21 p3660 N85-32736

CARPATHIAN MOUNTAINS (EUROPE)
Earthquake activity in the Bohemian massif and in the western Carpathians
[REPT-547] 03 p0375 N85-12390

CARRIAGES
Small Payload Flight Systems (SPFS)
02 p0152 N85-11030
Dual optical mechanical position tracker
[AD-D011739] 22 p3844 N85-33811

CARRIER DENSITY (SOLID STATE)
Avalanche photodiode statistics in triggered-avalanche detection mode 05 p0623 N85-13987
GaAs material properties and models 05 p0665 N85-14277
Density of states and recombination in amorphous silicon (a-Si:H)
[BMFT-FB-T-84-216] 08 p1135 N85-17151
Investigations of radiation-induced and carrier-enhanced conductivity 13 p1996 N85-22515
Technological process effect on the carrier lifetime degradation of silicon solar cell base layer irradiated by 1 MeV electrons (boron doping case) 13 p2007 N85-22585
Phenomena simulation for heavy doping and surface recombination velocity 20 p3482 N85-31638

CARRIER FREQUENCIES
Carrier acquisition and tracking by a COSTAS loop with automatic frequency control
[ESA-TT-838] 04 p0493 N85-13149
Design and performance of sampled data loops for subcarrier and carrier tracking 05 p0623 N85-13988
Improved carrier tracking by smoothing estimators 05 p0623 N85-13989
Low noise multiple crystal-controlled oscillator
[AD-D011401] 07 p0948 N85-16010
Method and means for providing frequency agile operation of MTI (Moving Target Indicator) radar
[AD-D011561] 12 p1823 N85-21436
Wideband phase keyers 12 p1839 N85-21544
Experimental results on the application of convolutional coding and Viterbi decoding as a frequency diversity technique in HF data transmission
[CRC-1377] 13 p2052 N85-22850
Global positioning system carrier phase: Description and use
[PB85-174126] 19 p3216 N85-29946

CARRIER INJECTION
Capacitive reactance of compensated semiconductors with deep centers under conditions of transmission of exclusion and double injection currents 02 p0296 N85-11742
Surface and allied studies in silicon solar cells
[NASA-CR-175465] 10 p1508 N85-19516

CARRIER LIFETIME
Method and apparatus for measuring minority carrier lifetime in a direct band-gap semiconductor
[NASA-CASE-NPO-16337-1-] 11 p1628 N85-20251
Technological process effect on the carrier lifetime degradation of silicon solar cell base layer irradiated by 1 MeV electrons (boron doping case) 13 p2007 N85-22585
Quantitative analysis of defects in silicon-characterization of UCP, HAMCO, and microcrystalline material
[NASA-CR-175988] 18 p3079 N85-29046
Electrical and structural characterization of web dendrite crystals 20 p3481 N85-31633

CARRIER MOBILITY
NT ELECTRON MOBILITY
NT HOLE MOBILITY
Mobility and trapping time measurements in HgI2
[DE84-015954] 06 p0869 N85-15522
Characterization of high temperature electrically conducting oxides
[DE85-004296] 12 p1803 N85-21307
Heavy doping effects in high efficiency silicon solar cells
[NASA-CR-175687] 15 p2585 N85-25937
Heavy doping effects in high efficiency silicon solar cells
[NASA-CR-175681] 15 p2586 N85-25940
Heavy doping effects in high efficiency silicon solar cells
[NASA-CR-175779] 16 p2816 N85-27383
Quantitative analysis of defects in silicon-characterization of UCP, HAMCO, and microcrystalline material
[NASA-CR-175988] 18 p3079 N85-29046
Quantized Hall conductance as a topological invariant
[DE85-007796] 18 p3193 N85-29608
Drift mobilities by time-of-flight methods and time-dependent phototransport in the nanosecond regime in amorphous semiconductors
[DE85-008729] 18 p3194 N85-29615
Measurement of electrical parameters and current components in the bulk of silicon solar cells 20 p3481 N85-31635
Planar doped barrier semiconductor device
[AD-D011591] 20 p3537 N85-32010

CARRIER MODULATION
U MODULATION

CARRIER ROCKETS
U LAUNCH VEHICLES

CARRIER SYSTEMS
U WIRELESS COMMUNICATION

CARRIER TRANSPORT (SOLID STATE)
Characterization of surface electronic properties of semi-insulating InP
[AD-A146553] 06 p0866 N85-15507
Application of the diffraction model to amorphous magnesium zinc alloys
[AD-A147369] 07 p0928 N85-15883
Development of high efficiency solar cells on silicon web
[NASA-CR-174435] 10 p1509 N85-19521
Heavy doping effects in high efficiency silicon solar cells
[NASA-CR-175681] 15 p2586 N85-25940

CARRIER WAVES
Design and performance of sampled data loops for subcarrier and carrier tracking 05 p0623 N85-13988
Performance of the DSA's subcarrier demodulation digital loop 10 p1465 N85-19242

CARRINGTON ROTATION
U SOLAR ROTATION

CARTESIAN COORDINATES
Development of multigrid algorithms for problems from fluid dynamics
[GMD-111] 09 p1321 N85-18305
Generation of sound by a vortex point in a steady flow of slightly compressible fluid 11 p1715 N85-20799
Location and synchronization — space-time coordinates 14 p2397 N85-24788
Augmented weighted diamond force of the linear nodal scheme for Cartesian coordinate systems
[DE85-005631] 17 p3020 N85-28679
Equations of motion for electromagnetic waves in 4-dimensional Euclidian space 21 p3697 N85-32970
Algorithm for calculation of strain state from measurements of node coordinates of arbitrary curvilinear grid
[BLL-M-36304-(5828.4)] 23 p3940 N85-34422

CARTOGRAPHY
U MAPPING

CARTRIDGE ACTUATED DEVICES
U ACTUATORS
U EXPLOSIVE DEVICES

CARTRIDGES
Flares and photoflash items
[AD-A145442] 02 p0187 N85-11253

CASCADE CONTROL
Multiloop manual control of dynamic systems 05 p0702 N85-14505
FAUST: Introduction and overview — self tuning control
[OUEL-1568/85] 20 p3519 N85-31882

CASCADE FLOW
Characteristics of controlled-oscillating annular cascade test facility with Freon gas
[NAL-TR-812] 01 p0003 N85-10014
Further development of a transonic cascade analysis
[AD-A145410] 02 p0198 N85-11319
Inverse design technique for cascades
[NASA-CR-3836] 03 p0311 N85-12008
Incompressible lifting-surface aerodynamics for a rotor-stator combination
[NASA-TM-83767] 03 p0316 N85-12039
A finite element method for the solution of two-dimensional transonic flows in cascades
[PNR-90216] 03 p0316 N85-12045
Performance deterioration of cascades exposed to solid particles 03 p0319 N85-12057
Unsteady aerodynamic response of cascades and turborotors 03 p0319 N85-12058
Low solidity cascade diffusers for wide flow range centrifugal blowers 05 p0637 N85-14086
Turbine blade test cascade modifications and orations, August 1982 - April 1983
[DE84-009268] 06 p0833 N85-15309
Unsteady pressure measurements on a biconvex airfoil in a transonic oscillating cascade
[NASA-TM-86914] 07 p0898 N85-15689
A method for solving the inverse problem of transonic cascade flow
[AD-A146739] 07 p0899 N85-15690
Results of S5 CH tests with an ARL (Aerospace Research Laboratory) cascade
[NASA-TM-77510] 08 p1089 N85-16882
Secondary flow in cascades
[AD-A148415] 08 p1162 N85-17333
Designing the profile of turbine blades using an iteration technique 09 p1305 N85-18201
Calculating secondary nonviscous gas flows in spatial cascades of turbines 09 p1305 N85-18202
Estimating unsteady aerodynamic forces on a cascade in a three-dimensional turbulence field
[NASA-TM-86701] 14 p2209 N85-23704
An experimental study of aerodynamic damping characteristics of a compressor annular cascade in high speed flow and the visualization of annular cascade flow
[NAL-TR-836] 15 p2564 N85-25759

Gasdynamic evaluation of choking cascade turns
[AD-A151854] 15 p2557 N85-25776
Influence of surface roughness on compressor blades at high reynolds number in a two-dimensional cascade
[AD-A151855] 15 p2557 N85-25777
Proceedings of the NAL Symposium on Aircraft Computational Aerodynamics
[NAL-SP-1] 16 p2691 N85-26611
Two computational methods for cascade flows
16 p2692 N85-26817
Numerical simulation of inviscid compressible flow through three-dimensional cascade
16 p2692 N85-26819
Application of conformal mapping to grid generation
16 p2692 N85-26821
Notes on unsteady transonic cascade flows
[AD-A154829] 21 p3552 N85-32096
Unsteady flow in a supersonic cascade with two in-passage shocks
[NASA-CR-3925] 24 p4060 N85-35158
Analysis of incompressible cascade flows using state-of-the-art computer programs
[AD-A155860] 24 p4062 N85-35173
Experimental basis for the models of cascade propagation in atmosphere
[HE-3.6-6] 24 p4185 N85-35954
A comparative analysis of gamma and hadron families at the superhigh energies recorded in experiment Pamir
[HE-3.7-1] 24 p4185 N85-35960
Hadrons registration in emulsion chamber with carbon block
[HE-3.7-3] 24 p4186 N85-35962
Structured events in Pamir carbon X-ray chambers
[HE-3.7-7] 24 p4186 N85-35965
Peculiarities of gamma-quanta distribution at 20 TeV energy
[HE-3.7-10] 24 p4186 N85-35967

CASCADE RANGE (CA-OR-WA)
The petrology and geochemistry of high cascade volcanics in southern Washington: Mount Saint Helens volcano and the Indian Heaven basalt field
02 p0227 N85-11487
Morphologic evolution of the Mount St. Helens crater area, Washington 13 p2187 N85-23588

CASCADE WIND TUNNELS
Inverse design technique for cascades
[NASA-CR-3838] 03 p0311 N85-12006
Results of S5 CH tests with an ARL (Aerospace Research Laboratory) cascade
[NASA-TM-77510] 08 p1089 N85-16882
Methods for design aerodynamics of modern transport aircraft
[DFVLR-FB-85-05] 17 p2893 N85-27838

CASCADES (FLUID DYNAMICS)
U FLUID DYNAMICS

CASCODE MOSFET
U FIELD EFFECT TRANSISTORS

CASE BONDED PROPELLANTS
Dissected motors-propellants motor number STM-012. Phase 15: Surveillance report, stage 1
[AD-A156088] 24 p4071 N85-35226

CASES (CONTAINERS)
NT ROCKET ENGINE CASES
Gear case vibration isolation in a geared turbine generator 09 p1338 N85-18414
SRB filament wound case material property study
[NASA-CR-171469] 17 p2910 N85-27940
Electrically conductive containment vessel for molten aluminum
[DE85-006518] 23 p3939 N85-34415

CASKS
U BARRELS (CONTAINERS)

CASPIAN SEA
Horizontal coherence of temperature microstructure in upper ocean layer 13 p2109 N85-23139

CASSEGRAIN ANTENNAS
Configuration study for a 30 GHz monolithic receive array: Technical assessment
[NASA-CR-174697] 09 p1311 N85-18238
Configuration study for a 30 GHz monolithic receive array, volume 1
[NASA-CR-174697-VOL-1] 09 p1311 N85-18239
Design procedure for the new 70-meter antenna subreflector positioner 10 p1463 N85-19232
Subreflector focusing techniques applied to new DSS-15 and DSS-45 34-meter antennas
10 p1464 N85-19233
DSN 34-meter antenna optics analysis for wideband SETI investigations 10 p1465 N85-19244

CASSEGRAIN OPTICS
Dual-secondary mirror Cassegrain optical system
[AD-D011273] 06 p0662 N85-15478
Construction of a superheterodyne receiver for 10 micron waves to be put on a Cassegrain optics telescope for spectroscopic research on the Mars and Venus atmospheres
[MPE-183] 06 p0872 N85-15538
Dual mode radio frequency-infrared frequency system
[AD-D011402] 06 p1061 N85-16850
BBC receiving terminal for the European orbital test satellite
[BBC-RD-1984/15] 08 p1142 N85-17205
Innovative solar thermal dish technology development
[DE85-002787] 11 p1673 N85-20539
The astrometry programme at Mt. John Observatory
14 p2436 N85-25026

CASSIOPEIA A
Absolute measurements of radiation intensity from Cassiopeia-A, Cygnus-A and crab nebula in 60-100 cm band 13 p2078 N85-22978

CASSIOPEIA CONSTELLATION
A study of W Serpentis binaries: SX Cassiopeiae, RX Cassiopeiae, and W Serpentis 20 p3544 N85-32053

CAST ALLOYS
Development of rapidly quenched alloys with special physical properties and of processes for their continuous production
[BMFT-FB-T-84-179] 04 p0477 N85-13039
Mechanical properties and microstructure of centrifugally cast alloy 718
[AD-A147800] 08 p1129 N85-17116
Anomalies of aluminum structure and properties
13 p2026 N85-22693
Concept development evaluation for John Deere/UA STS middeck experiment location
[NASA-CR-171541] 20 p3397 N85-31071
Mechanical behavior of Ni-Cr-base superalloys in forms and conditions representative of service
[NPL-DMA(A)-84] 20 p3431 N85-31282

CASTING
NT CENTRIFUGAL CASTING
NT SLIP CASTING
Effect of scandium on the structure and properties of Al-Zn-Mg alloys 01 p0018 N85-10111
New ferrous metallurgy technology
01 p0019 N85-10114
Low-gravity solidification of cast iron and space technology applications 02 p0151 N85-11022
Directional solidification of flake and nodular cast iron during KC-135 low-g maneuvers
02 p0154 N85-11040
Investigation of toughened neat resins and their relations to advanced composite mechanical properties
04 p0464 N85-12949
Development of rapidly quenched alloys with special physical properties and of processes for their continuous production
[BMFT-FB-T-84-179] 04 p0477 N85-13039
Controlled directionally solidified precision casting for superalloys and steels
[BMFT-FB-T-84-198] 05 p0619 N85-13960
Applicability of fatigue strength data obtained from small separately cast specimens on large cast components
05 p0651 N85-14178
Cyclic endurance testing of the RB211-22B cast HP turbine blade 07 p0808 N85-15747
Making high explosive bodies for shaped charges by casting or pressing. Shaped charge research at Research Institute of National Defence (FOA) in 1972 - 1983, part 1
[FOA-C-20554-D4-PT-1] 07 p0935 N85-15923
New applications for robot loaders, unloaders
08 p1139 N85-17175
The effect of tantalum on the structure/properties of two polycrystalline nickel-base superalloys: B-1900 + Hf MAR-M247
[NASA-CR-174847] 09 p1294 N85-18127
Study of superplastic alloys based on Al-Zn-Ca
10 p1442 N85-19092
Method for continuously casting
[AD-D011481] 10 p1459 N85-19195
French firm has most advanced continuous-casting machine 11 p1592 N85-20017
Comparison of the fatigue resistance (initiation, propagation) of cast TA6V with hot rolled TA6V — titanium alloy
[DGT-25369-PT-1] 12 p1808 N85-21341
Carbon filter plates for aluminum filtration at casting
[BMFT-FB-T-84-242] 12 p1808 N85-21343
Nondestructive testing of stainless steel to improve quality and output efficiency of the processing of ingot and continuous casting
[BMFT-FB-T-84-240] 12 p1808 N85-21345
Steel castings by the electroslag casting technique
[DE85-003812] 12 p1819 N85-21409
Development of silicon nitride materials for the casting of solar cell silicon 12 p1878 N85-21779
The influence of melting practice and of microalloying, with rare earth metals and with boron, on the quality of low-carbon steel
[BLL-BISI-22467-(9022.06)] 17 p2925 N85-28036
Influence of temperature in melting and casting on quality of medium-alloy steel
[BLL-BISI-TRANS-22310-(9902.06)]
17 p2938 N85-28137
Precision die forging of blades or gas turbines
17 p2940 N85-28148
Continuous casting of quality steels on billet casters
[BMFT-FB-T-84-262] 18 p3078 N85-29041
Semicrystalline casting process development and verification
[DE85-007695] 18 p3081 N85-29058
Aluminum pressure die casting process for the production of low porosity castings and new casting alloys
[BMFT-FB-T-84-286] 18 p3123 N85-29335
Feasibility of melt casting strontium fluoride to produce high-density heat sources
[DE85-009429] 18 p3130 N85-29381
MPS solidification model. Analysis and calculation of macrosegregation in a casting ingot
[NASA-CR-171589] 21 p3566 N85-32178
Tape casting as an approach to an all-ceramic turbine shroud seal
[NASA-TM-87078] 21 p3596 N85-32333
Method and apparatus for casting conductive and semi-conductive materials
[DE85-011655] 22 p3792 N85-33494
Characterization of modified 9 r-1 Mo steel sand castings
[DE85-012057] 24 p4080 N85-35287
Development of a high strength isothermally heat-treated nodular iron road wheel arm
[AD-A155755] 24 p4099 N85-35408

CASTING SOLVENTS
U PLASTICIZERS

CASTINGS
NT INGOTS
Materials studies for magnetic fusion energy applications at low temperatures, 7
[DE84-013487] 01 p0122 N85-10837
Adaptation of remelting procedures for the use of recycled metal in nickel-base superalloy castings
[PNR-90232] 09 p1297 N85-18149
Robotized blanks loader for new forge press
10 p1461 N85-19216
Method for refining microstructures of cast titanium articles
[AD-D011518] 12 p1804 N85-21318
Fatigue and corrosion fatigue resistance of aluminum casting alloy VAL10 and forging alloy AK6
13 p2025 N85-22690
Cast-iron technology: Metallographic and mechanical testing results
[DE85-002684] 14 p2257 N85-23984
Robotic deburring. Part 2: Evaluation of cutters and noncompliant tooling
[DE85-006182] 14 p2311 N85-24306
Ultrasonic characterization of porosity: Theory
[DE85-005922] 15 p2648 N85-26325
Detection of pores in hot continuously cast rounds
[BMFT-FB-T-85-007] 18 p3072 N85-29000
Continuous casting of quality steels on billet casters
[BMFT-FB-T-84-262] 18 p3078 N85-29041
Aluminum pressure die casting process for the production of low porosity castings and new casting alloys
[BMFT-FB-T-84-286] 18 p3123 N85-29335
Reliability of welds to repair defects in cast components made from CrMoV steel
[BLL-CE-TRANS-8054-(9022.09)]
20 p3461 N85-31501
Centrifugal castings of stainless steel spiked with radioactive tracers
[DE85-012003] 22 p3748 N85-33234

CASUALTIES
Don't fowl out
[AD-P004179] 11 p1578 N85-19941
The clinical and biomedical evaluation of trauma and fatalities associated with aircrew ejection and crash. A Working Group report
[AGARD-AR-194] 12 p1906 N85-21969
Introduction: The clinical and biomedical evaluation for trauma and fatalities associated with aircrew ejection and crash 12 p1906 N85-21970
Statistics of french Armee de l'air ejections 1970 - 1980 12 p1906 N85-21971
List of head/neck injury on ejection in the German Armed Forces from 1972-1981 12 p1906 N85-21972
A review of neck injury and impaired consciousness associated with US Navy ejections 1 January 1969 - 31 December 1979 12 p1906 N85-21973

A review of fatality, impairment of consciousness, and head/neck injury on USAF ejections 1971 - July 1983
12 p1906 N85-21974
A review of fatality, impairment of consciousness and head and neck injury on Royal Air Force ejections 1968-1981 12 p1907 N85-21975
Head/neck injury: Post mortem procedures, Annex B
12 p1907 N85-21977

CAT SCANNER
U COMPUTER AIDED TOMOGRAPHY

CATACLYSMIC VARIABLES
The vertical structure and stability of alpha model accretion disks 09 p1417 N85-18938
Observations of cataclysmic variable star winds
11 p1755 N85-21041
A survey for galactic plane ultraviolet-excess objects: Space densities for white dwarfs, subdwarfs, and cataclysmic variables 13 p2169 N85-23458
A model for eclipsing cataclysmic variables
13 p2171 N85-23467
X-ray emission and the winds of cataclysmic variables
[DE85-007663] 17 p3053 N85-28902

CATALASE
Toxicity, mutagenesis and aging due to endogenous oxygen radicals
[AD-A150121] 12 p1900 N85-21928

CATALOGS
Computer center CDC Libraries-PROCFIL (procedures)
[AD-A148633] 08 p1206 N85-17589
Catalog of completed studies, US Army health care studies and clinical investigation activity
[AD-A149450] 10 p1588 N85-19885

CATALOGS (PUBLICATIONS)
NT ASTRONOMICAL CATALOGS
Sea-level in the world ocean. Part 5: The North-East Pacific and Arctic Oceans, a catalogue of measurements
[CSIR-T/SEA-8303-5] 01 p0087 N85-10589
FSTC (Federal Software Testing Center) software tool catalog
[PB84-212158] 01 p0105 N85-10703
Depository librarians' views on GPO's administration of the depository library program. Report to the Chairman, Joint Committee on Printing
[PB84-212265] 01 p0126 N85-10867
Cries-cross directory of NASA N numbers and DOD AD numbers, 1962-1978 04 p0575 N85-13689
The SPOT data bank system
05 p0659 N85-14236
Orbital maneuvers with finite thrust. Volume 1: Mathematical formulation, numerical methods, catalog concept
[ESA-CR(P)-1910-VOL-1] 06 p0758 N85-14848
Orbit maneuvers with finite thrust. Volume 2: Reference manual, part 1
[ESA-CR(P)-1910-VOL-2-PT-1]
06 p0758 N85-14849
Orbit maneuvers with finite thrust. Volume 3: User's guide, part 2
[ESA-CR(P)-1910-VOL-3-PT-2]
06 p0758 N85-14850
Orbit maneuvers with finite thrust. Volume 3: Reference catalog, parts 1 and 2
[ESA-CR(P)-1910-VOL-3-PT-1/2]
06 p0758 N85-14851
Orbit maneuvers with finite thrust. Volume 3: Reference catalog, part 3
[ESA-CR(P)-1910-VOL-3-PT-3]
06 p0758 N85-14852
Crustal dynamics project: Catalogue of site information
[NASA-TM-87452] 13 p2131 N85-23258
Catalog of the National Energy Software Center
[TI85-900521] 15 p2630 N85-26209
Glossary of landscape and vegetation ecology for Alaska
[PB85-153831] 16 p2816 N85-27372
Catalog of research projects at Lawrence Berkeley Laboratory, 1985
[DE85-006679] 17 p3049 N85-28868
Combined catalog of ionosphere vertical soundings data
[PB85-186494] 18 p3136 N85-29430
Notes for medical catalogers, 1984
[PB85-180206] 18 p3200 N85-29853
CAE tool catalog
[DE85-011290] 19 p3334 N85-30657
Data base management: MSTRAC (keynote paper), part 8
21 p3626 N85-32530

CATALYSIS
NT AUTOCATALYSIS
Liquid hydrocarbon fuels from syngas
[DE84-015942] 04 p0482 N85-13069
USSR report: Chemistry
[JPRS-UCH-84-012] 08 p0761 N85-14865
Catalytic oxidation by transition metal ions in zeolites
[AD-A146828] 07 p0922 N85-15842
Conference on Singlet Molecular Oxygen (COSMO 84), program and abstracts
[AD-A147281] 07 p1040 N85-16605
Catalytic ignition and combustion of lean mixtures
[AD-A148101] 08 p1121 N85-17067
Research in phase transfer catalysis
[AD-A148286] 08 p1121 N85-17068
Multiplex gas chromatography for use in space craft
[NASA-TM-86668] 09 p1290 N85-18097
Dynamics and mechanisms of catalytic processes and hot chemistry
[DE85-002899] 09 p1292 N85-18114
A metal-catalyzed rearrangement of alkene-alkynes and the stereochemistry of metallacyclobutene ring opening
[AD-A149084] 10 p1435 N85-19042
Adsorption thermodynamics and surface transport of metal catalyst poisons
[DE85-002868] 10 p1441 N85-19084
Photosynthesis of ammonia
[DE85-001482] 11 p1595 N85-20029
Studies of the kinetics and mechanisms of ammonia synthesis and hydrodesulfurization on metal single crystal surfaces
[DE85-001650] 11 p1595 N85-20030
Ozone measurements in the mesosphere during a solar proton event 11 p1665 N85-20490
In situ monitoring of electrochemical reactions by surface enhanced Raman scattering
[PB85-149769] 12 p1803 N85-21312
Solar-assisted hydrogen generation by photoelectrocatalysis
[PB85-149706] 12 p1804 N85-21314
The use of hydrazine as an alternate source of energy
[NASA-CR-175535] 12 p1817 N85-21397
Application of modulated hydrodynamic voltammetry to the study of anodic electrocatalysis
[DE85-004182] 13 p2018 N85-22653
International Conference on Coordination Chemistry (23rd) held at Boulder, Colorado on 29 July - 3 August, 1984
[AD-A150980] 14 p2252 N85-23956
A novel polymeric organosilazane precursor to Si3N4/SiC ceramics
[AD-A150748] 14 p2260 N85-24003
The mechanisms of phenylacetylene polymerization by molybdenum and titanium initiators
[AD-A150993] 14 p2260 N85-24007
Electronic structure calculations for low coverage adlayers
[DE85-007733] 18 p3179 N85-29709
Catalytic hydrotreatment studies with model compounds
[DE85-010187] 19 p3236 N85-30064
Molecular toxicology of chromatin: The role of Poly(ADP-Ribose) in gene control
[AD-A154415] 19 p3327 N85-30611
Highly dispersed metal atoms in zeolites
[DE85-010515] 19 p3354 N85-30792
Fuel-rich catalytic combustion: A soot-free technique for in situ hydrogen-like enrichment
[NASA-TP-2498] 20 p3423 N85-31244
Biocatalysis project
[NASA-CR-176044] 20 p3498 N85-31744
Rigid zeolite containing polyurethane foams
[DE85-006406] 23 p3919 N85-34286
Chemistry division report
[DE85-010586] 24 p4071 N85-35228
Vectorial electron transfer on designed surfaces
[PB85-204600] 24 p4076 N85-35263
Review of US NOx abatement technology
[PB85-193522] 24 p4114 N85-35501

CATALYSTS
NT ELECTROCATALYSTS
Study of catalysts and mechanisms in synthesis reactions
[DE84-015025] 04 p0470 N85-12960
Reactive sintering of SiC 04 p0473 N85-13010
Butene oxidation by molybdenum crystalographic shear compounds
[DE84-013910] 05 p0614 N85-13923
Biocatalyzed processes for production of commodity chemicals: Assessment of future research advances for N-butanol production
[NASA-CR-174264] 07 p0919 N85-15819
Vibrational spectroscopy of chemisorption phenomena on model catalyst surfaces
[AD-A146753] 07 p0922 N85-15840
Imide modified epoxy matrix resins
[NASA-CR-174695] 07 p0930 N85-15892
Optimization of technical catalysts with the help of surface analysis
[BMFT-FB-T-84-225] 08 p1124 N85-17066
Electric utility acid fuel cell stack technology advancement
[NASA-CR-174804] 08 p1178 N85-17422
Advanced NMR characterization of zeolite catalysts
[DE85-000456] 09 p1291 N85-18104
Cation promotion effects in zeolite-supported F-T catalysts
[DE85-001708] 09 p1291 N85-18108
Metal-support interactions: The effect of catalyst preparation on catalytic activity
[DE84-017425] 09 p1293 N85-18118
Liquid phase methanol process development unit: Installation, operation, and support studies
[DE85-001311] 09 p1301 N85-18171
ECUT, Energy Conversion and Utilization Technologies program: Technical and economic assessment of processes for the production of butanol and acetone. Phase 2: Analysis of research advances
[NASA-CR-175471] 10 p1434 N85-19034
An infrared study of isotopic exchange during methanation over supported rhodium catalysts; an inverse spillover effect
[AD-A149390] 10 p1435 N85-19046
An infrared study of the oxidation of carbon monoxide over supported rhodium catalysts
[AD-A149478] 10 p1436 N85-19050
Catalytic conversion of C3-C4 paraffins to gasoline
[DE85-004181] 10 p1458 N85-19187
Fundamental study of catalysts using laser Raman, infrared, auger electron spectroscopy and low energy electron diffraction
[DE85-001813] 11 p1595 N85-20033
An infrared study of the dissociation of carbon dioxide over supported rhodium catalysts
[AD-A149813] 12 p1800 N85-21291
Adsorption thermodynamics and surface transport of metal catalyst poisons
[DE85-003750] 12 p1802 N85-21301
Study of the kinetics of hydrogenation using aged catalysts
[DE85-004373] 12 p1802 N85-21302
Properties of supported metal catalysts
[DE85-003927] 12 p1802 N85-21303
Synthesis, static and reactive characterization of supported organometallics
[DE85-004286] 12 p1806 N85-21340
Fluorinated polyurethanes
[AD-D011526] 12 p1810 N85-21353
Tritium catalyzed deuterium Tokamaks
[DE85-004825] 12 p1936 N85-22166
Workshop report: Catalysis of Burn Rate of Energetic Binder propellants 13 p2001 N85-22545
Mechanism of burning rate enhancement by ferric oxide 13 p2002 N85-22546
USSR report: Chemistry
[JPRS-UCH-85-001] 13 p2013 N85-22829
Trifunctional catalysts for conversion of syngas to alcohols
[DE85-004577] 13 p2040 N85-22771
Diagrams of chemical and electrochemical equilibria in the presence of oxygen and sulphur
[AD-A150929] 14 p2251 N85-23953
Characterization of supported metal catalysts by imaging, microdiffraction and microanalysis techniques
[DE85-005567] 14 p2253 N85-23961
Investigation and optimization of fuel production using dye-based transition metal complexes as charge-transfer intermediates
[PB85-161941] 14 p2264 N85-24029
Optimization of the catalytic oxidation of CO for closed-cycle CO2 laser applications
[NASA-TM-86421] 15 p2504 N85-25445
Improved catalysts for liquid hydrocarbon fuels from syngas
[DE85-008589] 16 p2746 N85-26947
The production of copper phthalocyanine and/or its derivatives
[NASA-TM-77629] 17 p2917 N85-27983
Michelle-derived catalysts for extended Schulz-Flory
[DE85-005656] 17 p2922 N85-28012
Correlation of zeolite ZSM-5 acid strength with catalytic activity and selectivity
[DE85-005415] 17 p2922 N85-28013
Catalyst and reactor development for a liquid phase Fischer-Tropsch process
[DE85-005894] 17 p2922 N85-28014
Transition metal catalyzed transformations of unsaturated molecules
[DE85-009531] 18 p3080 N85-29055
Effects of H2S on molten carbonate fuel cells
[DE85-008310] 18 p3130 N85-29386
Liquid hydrocarbon fuels from syngas
[DE85-009813] 19 p3228 N85-30017
Mechanism of the catalytic gasification and reactivity of graphite
[DE85-009932] 19 p3229 N85-30020

Study of the kinetics of hydrogenation using aged catalysts
[DE85-010427] 19 p3230 N85-30025
The mobile phase in coals: Its nature and modes of release
[DE85-011696] 19 p3230 N85-30026
Metallophthalocyanine dimers incorporating five atom covalent bridges
[AD-A154365] 19 p3234 N85-30051
New catalysts and new electrolytes for acid fuel cells
[DE85-009940] 19 p3307 N85-30498
Advanced NMR characterization of zeolite catalysts
[DE85-010143] 19 p3363 N85-30853
Improved catalysts for liquid hydrocarbon fuels from syngas
[DE85-011082] 20 p3421 N85-31234
In situ Mossebauer investigation of bimetallic catalysts on a base: FeRu, FeRh, FePd, FeIr, and FePt on SiO2
[B8563200] 20 p3432 N85-31293
Decomposition of sulfuric acid using solar thermal energy
[DE85-012288] 21 p3564 N85-32170
A safe, high-power-density lithium battery
[AD-A155223] 21 p3613 N85-32454
Experimental studies of the geometric and electronic structure of chemisorption bonding
[PB85-192250] 22 p3747 N85-33228
Integrated current collector and catalyst support
[DE85-011616] 22 p3761 N85-33311
Solids mixing in a three phase fluidized bed containing spherically shaped-porous solid particles
[PB85-187961] 22 p3765 N85-33453
Method of distributing liquefaction catalysts in solid carbonaceous material
[DE85-005759] 23 p3909 N85-34218
FTIR studies of hydrocarbon synthesis on Pd/ZSM5 catalysts
[DE85-012430] 24 p4071 N85-35230
CO + H2 reaction over nitrogn-modified iron catalysts
[DE85-013791] 24 p4072 N85-35231

CATALYTIC ACTIVITY
Radiation/catalytic augmented combustion
[AD-A148758] 09 p1290 N85-18101
Metal-support interactions: The effect of catalyst preparation on catalytic activity
[DE84-017425] 09 p1293 N85-18118
Electrocatalysis research
[NASA-CR-174352] 10 p1437 N85-19054
Catalytic conversion of C3-C4 paraffins to gasoline
[DE85-004181] 10 p1458 N85-19187
Investigation and optimization of fuel production using dye-based transition metal complexes as charge-transfer intermediates
[PB85-161941] 14 p2264 N85-24029
Quantitation of Na+, K+-ATPase enzyme activity in tissues of the mammalian vestibular system
15 p2613 N85-26102
The role of surface generated radicals in catalytic combustion 17 p2898 N85-27889
Oxygen evolution on NiCo2O4 electrodes
17 p2924 N85-28026
Fuel rich catalytic comustion: The first stage of a two-stage combustor
[NASA-TM-87042] 18 p3069 N85-28863
Galactose oxidase in stereospecific oxidation of primary alcohols
[AD-A154059] 19 p3234 N85-30048
Mechanistic and kinetic studies of the elementary processes in catalytic combustion of methane
[PB85-186308] 20 p3436 N85-31314
Elementary processes in the catalytic combustion of methane (mechanism, intermediates, and controlling reactions)
[PB85-186357] 20 p3436 N85-31316
Method for removing chlorine compounds from hydrocarbon mixtures
[DE85-011608] 22 p3742 N85-33191

CATARACTS
Technical support for microwave experiments on the eye lens
[AD-A149702] 12 p1933 N85-22144

CATASTROPHE THEORY
Nonlinear global stability analysis of compressor stall phenomena
[NASA-CR-174908] 19 p3219 N85-29960

CATCHMENT AREAS
U WATERSHEDS

CATECHOLAMINE
NT EPINEPHRINE
Endocrine responses to hypotensive gravitational stress: Catecholamines, pancreatic polypeptide, and vasopressin 05 p0693 N85-14460
Catecholamine excretion and subjective ratings of tension during autogenic training and mental stress
[REPT-172] 05 p0697 N85-14483
Influence of hyperthermia on body temperature and content of catecholamines in white rat hypothalamus
10 p1524 N85-19615

CATENARIES
Cable-catenary large antenna concept
14 p2231 N85-23829
The dynamics of slack marine cables
[AD-A155022] 21 p3599 N85-32349

CATHODE RAY TUBES
NT PICTURE TUBES
Manufacturing Methods and Technology (MM/T) specifications for miniature cathode ray tube
[AD-A145597] 02 p0194 N85-11298
Human engineering data base for design and selection of cathode ray tube and other display systems
[AD-A145704] 02 p0238 N85-11549
Matrix display simulation
[AD-D011371] 07 p1055 N85-16695
Device for controlling operation of lithicon cathode-ray memory tube 12 p1839 N85-21542
A description of the process of elaborating man-machine dialog in an aircraft equipped with cathode tubes: Roles and specifications of piloted simulation methods
16 p2698 N85-26658
Effect of background/foreground color coding on detection in acoustic data displays
[AD-A154105] 19 p3352 N85-30774
Ergonomic problems regarding the interactive touch input via screens in onboard and ground-based flight control
[NASA-TM-77814] 20 p3512 N85-31832
High pressure working mode of hollow cathode arc discharges
[NASA-TM-77880] 20 p3535 N85-31992
The effect of set size on time to recall color coded information
[AD-A155013] 21 p3665 N85-32767
A new large-scale, high-resolution multicolor software display concept
[AD-A155404] 22 p3827 N85-33703
Maintenance port system
[AD-D011724] 23 p3967 N85-34594

CATHODES
NT CELL CATHODES
NT COLD CATHODES
NT HOLLOW CATHODES
NT HOT CATHODES
NT PHOTOCATHODES
NT THERMIONIC CATHODES
NT TUBE CATHODES
Advanced fuel cell development
[DE84-014847] 01 p0044 N85-10289
The driving-force dependence of electrochemical rate parameters: Origins of anodic-cathodic asymmetries for metal aquo redox couples
[AD-A145605] 02 p0172 N85-11153
Method of making a porous carbon cathode: A porous carbon cathode so made, and electrochemical cell including the porous carbon cathode
[AD-D011243] 02 p0195 N85-11301
Properties of cathode materials in alkaline cells
[NASA-CR-174082] 04 p0495 N85-13161
Behaviour of lead-silver anodes in zinc electrodeposition from sulphuric acid baths
[BLL-MINTEK-TR-1180-(5810.5759)]
06 p0764 N85-14887
Synthesis and properties of Hexachloromolybdates(5) and related species
[AD-A139599] 07 p0924 N85-15852
Explosive emission cathode plasmas in intensive relativistic electron beam diodes
[AD-A147917] 07 p1046 N85-16642
Electric utility acid fuel cell stack technology advancement
[NASA-CR-174804] 08 p1178 N85-17422
New liquid cathodes for lithium batteries. Part A: Halocarbons
[AD-A148433] 08 p1178 N85-17423
Improved electron emission by use of a cloth fiber cathode
[AD-A149250] 10 p1480 N85-19340
Virtual cathode oscillator study
[AD-A149268] 10 p1480 N85-19342
Brightness limitations in multi-kiloampere electron beam sources
[DE84-017417] 10 p1555 N85-19607
Approaches to ultrafast neutron detectors
[DE85-001206] 11 p1636 N85-20307
Corrosion and coatings review of specifications and drawings of facilities for the Oman Military Construction Program at Masirah Island, Oman
[AD-A149739] 12 p1812 N85-21366
Molten carbonate fuel cell performance model update, draft
[DE85-005423] 13 p2129 N85-23252
Cathode materials for molten carbonate fuel cells
[DE85-004078] 13 p2130 N85-23254
Diagnostics of a glow discharge used to produce hydrogenated amorphous silicon films
[DE85-002914] 15 p2661 N85-26420
The loss of material from the cathode of metal arcs
[NASA-TM-77845] 17 p2918 N85-27985
Continued development and testing of tungsten controlled porosity dispenser cathodes
[AD-A152595] 17 p2931 N85-28090
Process for making electrodes for discharge tubes
[DE85-006898] 17 p2955 N85-28247
Bifunctional oxygen electrodes
[DE85-006871] 17 p2955 N85-28248
Electrodes for flash discharge lamps
[DE85-006897] 17 p2955 N85-28250
Streak tube characterization
[DE85-009874] 17 p2956 N85-28255
Apparatus for mounting a field emission cathode
[NASA-CASE-LEW-14108-1] 18 p3094 N85-29149
Method for predicting the performance of cathode materials
[AD-D011665] 19 p3257 N85-30198
Advanced fuel cell development
[DE85-009662] 19 p3306 N85-30497
Method of production of metals by cathodic solution of their compounds in electrolytic cells
[BLL-OA-TRANS-3207-(6196.300)]
20 p3429 N85-31266
A safe, high-power-density lithium battery
[AD-A155223] 21 p3613 N85-32454
Electrode erosion in arc discharges at atmospheric pressure
[NASA-TM-87087] 23 p3903 N85-34178
Injector losses on Mite
[DE85-012356] 24 p4090 N85-35355
Considerations on collective ion acceleration as an intense ion injector
[DE85-012706] 24 p4155 N85-35757

CATHODIC COATINGS
Marine corrosion
[AD-A153843] 18 p3074 N85-29012

CATHODOLUMINESCENCE
Minor elements and cathodoluminescence of Mg-rich olivines from Murchison and Allende carbonaceous meteorites 06 p0884 N85-15619
Sedimentary petrology and provenance of the upper Jackforth Sandstone (Morrowan) Quachita Mountains, Arkansas, USA 08 p1182 N85-17447

CATIONS
NT FERRIC IONS
NT METAL IONS
Trivalent ion exchange in beta alumina
[AD-A145373] 02 p0172 N85-11151
Magnetic resonance studies of transient radicals and radical ions
[DE84-011699] 03 p0328 N85-12116
Electronic and redox properties of stacked-ring silicon phthalocyanines from molecular orbital theory
[AD-A147161] 07 p0922 N85-15844
Homogeneous reaction involving components of different redox couples. 1: Theoretical considerations and digital simulation
[AD-A148666] 08 p1124 N85-17084
Homogeneous reaction involving components of different redox couples. 2: Polarographic studies of the interactions of alkali metal cations with anthracene and fluoroanthene dianions in N,N-dimethylformamide and acetonitrile
[AD-A148667] 08 p1124 N85-17085
Cation promotion effects in zeolite-supported F-T catalysts
[DE85-001708] 09 p1291 N85-18108
Ion transporting composite membranes. 1: Nafion impregnated gore-tex
[AD-A151020] 14 p2252 N85-23960
A comparative evaluation of the effects of acid precipitation, natural acid production and harvesting of cation removal from forests
[DE85-005254] 15 p2589 N85-25961
The electronic spectra of phthalocyanine radical anions and cations
[AD-A152328] 17 p2918 N85-27986
The conversion of smaller borane fragments to larger structures. Systematics of boron hydride reactions
[AD-A153443] 18 p3070 N85-28985
Cation promotion effects in zeolite-supported F-T catalysts
[DE85-009869] 19 p3233 N85-30044
Method of reducing impurity and antisite defects in semiconductor crystal materials, and device and apparatus respectively produced from and utilizing same
[AD-D011698] 19 p3260 N85-30216

A comparative evaluation of the effects of acid precipitation, natural acid production and harvesting on cation removal from forests
[DE85-010821] 19 p3309 N85-30511
Low-temperature positron lifetime and Doppler-broadening measurements for single-crystal nickel oxide containing cation vacancies
[DE85-010238] 19 p3376 N85-30944
Throughfall rate and chemistry studies: Whiteface Mountain
[DE85-012407] 23 p3947 N85-34464
Effect of temperature and ionic impurities at very low concentrations on stress corrosion cracking of Type 304 stainless steel
[TI85-003048] 24 p4079 N85-35283

CATS

Susceptibility of cat and squirrel monkey to motion sickness induced by visual stimulation: Correlation with susceptibility to vestibular stimulation
11 p1694 N85-20650
Brain mechanisms underlying individual differences in reaction to stress: An animal model
[AD-A150195] 13 p2143 N85-23301
Percutaneous connectors
[NASA-CR-175627] 16 p2839 N85-27508

CAUCHY PROBLEM

Approximation of discontinuous solutions of hyperbolic partial differential equations
[NRIMS-TWISK-302] 02 p0250 N85-11631
Checking optical-polarization measurements at interfaces
02 p0271 N85-11770
Self similar solutions for a degenerate Cauchy problem
[AD-A147241] 07 p1031 N85-16548
Regularity of the free boundary for the porous medium equation
[AD-A147299] 08 p1210 N85-17611
Multidimensional inverse scattering for first order systems
[AD-A148711] 08 p1214 N85-17642
The Cauchy problem for u sub t = Delta u(m) when O m 1
[AD-A153521] 18 p3169 N85-29635
Art of programming programmable microcalculators: Calculation of response from current values of action
22 p3767 N85-33348
Fundamentals of radio optical theory of resonant and directional quasi-optical devices
22 p3780 N85-33420

CAULKING

Corrosion properties of second-generation conductive materials
07 p1000 N85-16348

CAUSES

Probable cause: A decision making framework
[AD-A147642] 08 p1210 N85-17614

CAUSTIC LINES

The investigation of short wave signal structure in the vicinity of the caustic by means of a high-directed antenna
[PR-194] 03 p0354 N85-12277

CAUSTICS

U ALKALIES

CAVITATION

U CAVITATION FLOW

CAVITATION CORROSION

Characterization of erosion of metallic materials under cavitation attack in a mineral oil
[NASA-TM-86934] 10 p1440 N85-19075
Prediction of the resistance of structural materials to cavitation erosion
[BLL-DRIC-TRANS-7435-(3623.66)]
13 p2020 N85-22659
Marine corrosion
[AD-A153843] 18 p3074 N85-29012

CAVITATION FLOW

Collapse of cavitation bubbles between two walls in ultrasonic field
02 p0266 N85-11739
Diffraction of plane polarized waves by noncircular cylindrical cavity
02 p0269 N85-11754
Potential application of robotics and state-of-the art end effectors at Letterkenny Army Depot
[AD-P004015] 03 p0309 N85-11994
Cavitation phenomenon in superplastic creep
[DE84-015484] 04 p0513 N85-13271
Bulk cavitation caused by a plane shock wave
[AD-A147031] 07 p0958 N85-16072
Study of optical sound generation and amplification
[AD-A147359] 07 p1039 N85-16592
The role of nuclei size in transient cavitation threshold measurements
[AD-A148334] 08 p1162 N85-17332
Cavitation erosion resistant coatings for pumps
[PB85-120210/GAR] 09 p1300 N85-18167
Cavitation phenomenon in superplastic creep
[DE85-001716] 10 p1441 N85-19083
Properties of materials using acoustic waves
[AD-A150465] 13 p2155 N85-23362
Cavitation erosion of plasma sprayed alloys
[DE85-009542] 18 p3077 N85-29036
Effects of annealing treatments on superplasticity in a thermomechanically processed Aluminum-10.2%Mg-0.52%Mn
[AD-A154414] 19 p3239 N85-30080
Bubble dynamics in polymer solutions undergoing shear
[AD-A154575] 21 p3568 N85-32193
Experimental studies of chemical reactivity during shock initiation of hexanitrostilbene
[DE85-011726] 22 p3754 N85-33270

CAVITIES

A finite element method for three dimensional cavity circulation
05 p0635 N85-14071
Analysis of physical-chemical processes governing SSME internal fluid flows
[NASA-CR-174245] 06 p0760 N85-14862
Catalytic oxidation by transition metal ions in zeolites
[AD-A146828] 07 p0922 N85-15842
High Marangoni number convection in a square cavity
[NASA-CR-174283] 07 p0959 N85-16078
Numerical solutions for steady natural convection in a square cavity
[PB84-245752] 07 p0961 N85-16090
Some aspects of the micromechanics of hot spot formation in energetic materials
08 p1116 N85-17036
Effect of air cavity on the vibration analysis of loaded drums
09 p1339 N85-18422
Some aspects of the micromechanics of hot spot formation in energetic materials
[AD-P004348] 10 p1456 N85-19172
An investigation of compressible flows over open cavities including shear layer thickness effects
[AD-A150086] 12 p1847 N85-21588
An investigation of aerowindows for solar receivers
[DE84-010931] 12 p1877 N85-21772
Micromechanical modeling of microstructural damage in creeping alloys
[DE85-003925] 13 p2022 N85-22671
High frequency estimation of 2-dimensional cavity scattering
[AD-A151697] 15 p2542 N85-25696
Transition region for corner cracks at holes
[AD-A151835] 15 p2579 N85-25908
Parametric study of autooscillation upon flow of supersonic jet into cylindrical cavity
16 p2765 N85-27060
The definition and computation of a metric on plane curves. The meaning of a face on a geometric model
17 p3004 N85-28571
Incorporation of Monte Carlo electron interface studies into photon general cavity theory
[DE85-007674] 17 p3034 N85-28772
Maser cavity servo-tuning system
[NASA-CASE-NPO-15890-1-CU]
18 p3093 N85-29143
Hydrogen maser oscillation at 10 K
18 p3108 N85-29241
A collective interaction klystron specification
[AD-D011704] 19 p3255 N85-30188
Fundamentals of radio optical theory of resonant and directional quasi-optical devices
22 p3780 N85-33420
Role of ECRH in potential formation for tandem mirrors
[DE85-011859] 22 p3848 N85-33834
Method of precisely modifying predetermined surface layers of a workpiece by cluster ion impact therewith
[DE85-006519] 23 p3984 N85-34710
Moment-method formulation of the cavity-probe aperture antenna
[DE85-013264] 24 p4088 N85-35338
Experimental study of free and mixed convective flow of air in a heated cavity
[DE85-012538] 24 p4094 N85-35360

CAVITONS

Role of cavitons in laser-plasma interactions
[DE85-001842] 11 p1731 N85-20886

CAVITY RESONATORS

Synchronously pumped mode-locked semiconductor platelet laser
[AD-D011214] 01 p0051 N85-10340
Tunable CW semiconductor platelet laser
[AD-D011215] 01 p0052 N85-10341
Frequency stabilized laser
[AD-D011223] 01 p0053 N85-10351
Time variability of directionality properties of pulsed EB-EDL (Electron Beam-Electric Discharge Laser) N2-CO2 lasers
[AD-A145548] 02 p0202 N85-11344
The S-matrix and acoustic signal structure in simple and compound waveguides
[PP-583] 03 p0415 N85-12652
An 850 J, 150 ns narrow-band krypton fluoride laser
[DE84-013077] 04 p0506 N85-13226
Dual mode directionally coupled band reject filter apparatus
[AD-D011359] 07 p0945 N85-15984
Research relative to the development of a cryogenic microwave cavity gradiometer for orbital use
[NASA-CR-174249] 07 p0962 N85-16095
Halogen mass flow rate detection system
[AD-D011398] 08 p1166 N85-17352
Image line voltage controlled oscillator with replaceable components
[AD-D011436] 10 p1479 N85-19333
A coaxial cavity gunn oscillator using probe coupled microstrip
[AD-D011437] 10 p1479 N85-19334
An integrated varactor tuned coaxial gunn oscillator for 60 GHz operation
[AD-D011439] 10 p1479 N85-19335
Filter reflection image guide oscillator and solid state line scanning device
[AD-D011440] 10 p1479 N85-19336
Integrated circuit tunable cavity oscillator
[AD-D011474] 10 p1481 N85-19351
Single-cavity SLED device
[DE85-002587] 12 p1929 N85-22117
Coupled-cavity gyrotrons with mode conversion
13 p2076 N85-22967
Experimental study of high-stability oscillator with surface-acoustic-wave resonator in feedback loop
13 p2090 N85-23053
Dependence of properties of optical cavity on misalignment
14 p2278 N85-24099
Superconducting traveling wave accelerators
[DE85-006247] 15 p2661 N85-26424
In situ microwave measurements of dielectric properties and moisture in materials
[DE85-003622] 16 p2747 N85-26953
Jinc-trap resonator
[AD-D011650] 17 p2970 N85-28339
Chaos and order in an optical ring cavity
[CWI-AM-R8416] 17 p3038 N85-28795
Maser cavity servo-tuning system
[NASA-CASE-NPO-15890-1-CU]
18 p3093 N85-29143
Atomic hydrogen maser active oscillator cavity and bulb design optimization
18 p3108 N85-29240
Operation of a quasioptical electron cyclotron maser
[DE85-008450] 18 p3113 N85-29276
Cavityless optical bistability in systems of two-level atoms
18 p3166 N85-29764
Performance of an RF beam monitor on the NBS-Los Alamos racetrack microtron
[DE85-010725] 19 p3262 N85-30232
Dye laser traveling wave amplifier
[NASA-CR-175989] 19 p3275 N85-30308
Experimental and theoretical investigations of open resonators — precipitation measurement
[DFVLR-FB-85-12] 20 p3449 N85-31414
Cryogenic system for the University of Washington Superconducting Booster
[DE85-010804] 22 p3754 N85-33274
High-power solid-state rf source for accelerator cavities
[DE85-012672] 22 p3781 N85-33309
Iris tilting and RF steering in the SLAC Linac
[DE85-011704] 22 p3841 N85-33783
New directional couplers for multimode circular waveguides applied to intense pulsed microwave systems
[DE85-011753] 23 p3926 N85-34330
Tuning system for capacitively loaded 1/4 accelerating cavity
[DE85-012516] 24 p4091 N85-35358

CCD

U CHARGE COUPLED DEVICES

CCD STAR TRACKER

Design, manufacture and testing of a medium accuracy star tracker
[REPT-TR/84-048] 20 p3459 N85-31486

CDC COMPUTERS

NT CDC CYBER 170 SERIES COMPUTERS
NT CDC CYBER 205 COMPUTER
Computer center introductory reference manual for CDC CYBER
[AD-A145798] 03 p0406 N85-12593
U: The universal utility controller, revision 1
[DE84-017077] 04 p0547 N85-13481
The CDC: Facilities on offer from the CNES computing center for space mathematics (a look at the capacities of CDC computers)
05 p0599 N85-13818

Computer center CDC Libraries-PROCFIL (procedures)
[AD-A148633] 08 p1206 N85-17589
CDC CYBER 170 SERIES COMPUTERS
The computing facilities of the Toulouse Space Center 14 p2397 N85-24770
CDC CYBER 205 COMPUTER
Developement of an optimum interpolation analysis method for the CYBER 205 16 p3143 N85-29456
CDMA
U CODE DIVISION MULTIPLE ACCESS
CEILING (AIRCRAFT CAPABILITY)
Effect of ground and/or ceiling planes on thrust of rotors in hover
[NASA-TM-86754] 20 p3388 N85-31014
CEILINGS (METEOROLOGY)
Joint probability of selected cloud and visibility thresholds around Koblenz, Germany
[AD-A145294] 02 p0231 N85-11506
Revised Uniform Summary of Surface Weather Observations (RUSSWO). McChord AFB, Washington, parts A-F
[AD-A146914] 07 p1005 N85-16385
Revised Uniform Summary of Surface Weather Observations (RUSSWO). Dobbins AFB, Georgia, parts A-F
[AD-A146916] 07 p1005 N85-16387
Summary of Meteorological Observations, Surface (SMOS), Beaufort, South Carolina
[AD-A150536] 13 p2138 N85-23279
Comparison of some West German cloud height and visibility data — weapon test sites
[BAE-BT-12734] 15 p2593 N85-25982
An evaluation of discretized conditional probability and linear regression threshold techniques in model output statistics forecasting of cloud amount and ceiling over the North Atlantic Ocean
[AD-A155100] 21 p3636 N85-32581
CEILOMETERS
U CLOUD HEIGHT INDICATORS
CELESTIAL BODIES
NT A STARS
NT ALLENDE METEORITE
NT AMOR ASTEROID
NT ANDROMEDA GALAXIES
NT APOLLO ASTEROIDS
NT ARIETID METEOROIDS
NT ASTEROID BELTS
NT ASTEROIDS
NT B STARS
NT BARRED GALAXIES
NT BINARY STARS
NT BL LACERTAE OBJECTS
NT BLUE STARS
NT CALLISTO
NT CARBON STARS
NT CARBONACEOUS CHONDRITES
NT CARBONACEOUS METEORITES
NT CASSIOPEIA A
NT CATACLYSMIC VARIABLES
NT CEPHEID VARIABLES
NT CHARON
NT CHONDRITES
NT COMET NUCLEI
NT COMET TAILS
NT COMETS
NT COMPANION STARS
NT COOL STARS
NT CRAB NEBULA
NT DEIMOS
NT DISK GALAXIES
NT DWARF NOVAE
NT DWARF STARS
NT EARLY STARS
NT EARTH (PLANET)
NT ECLIPSING BINARY STARS
NT ELLIPTICAL GALAXIES
NT ENCKE COMET
NT EUROPA
NT EXTRAGALACTIC RADIO SOURCES
NT FLARE STARS
NT GALACTIC CLUSTERS
NT GALAXIES
NT GALILEAN SATELLITES
NT GANYMEDE
NT GAS GIANT PLANETS
NT GIACOBINI-ZINNER COMET
NT GIANT STARS
NT GLOBULAR CLUSTERS
NT HALLEY'S COMET
NT HERBIG-HARO OBJECTS
NT HERCULES NOVA
NT HOT STARS
NT INFRARED STARS
NT IO
NT IRAS-ARAKI-ALCOCK COMET
NT IRON METEORITES
NT JUPITER (PLANET)
NT JUPITER RINGS
NT JUPITER SATELLITES
NT LATE STARS
NT M STARS
NT MAGNETIC STARS
NT MAIN SEQUENCE STARS
NT MARS (PLANET)
NT MERCURY (PLANET)
NT METALLIC STARS
NT METEORITES
NT METEOROID SHOWERS
NT METEOROIDS
NT MICROMETEORITES
NT MICROMETEOROIDS
NT MILKY WAY GALAXY
NT MOON
NT NATURAL SATELLITES
NT NEBULAE
NT NEPTUNE (PLANET)
NT NEUTRON STARS
NT NOVAE
NT O STARS
NT ORION NEBULA
NT ORIONID METEOROIDS
NT PANTAR CHONDRITES
NT PECULIAR STARS
NT PHOBOS
NT PLANETARY NEBULAE
NT PLANETARY RINGS
NT PLANETS
NT PLUTO (PLANET)
NT PRAESEPE STAR CLUSTERS
NT PRE-MAIN SEQUENCE STARS
NT PROTOPLANETS
NT PROTOSTARS
NT PULSARS
NT QUASARS
NT RADIO GALAXIES
NT RADIO METEORS
NT RADIO SOURCES (ASTRONOMY)
NT RADIO STARS
NT RED DWARF STARS
NT RED GIANT STARS
NT REFERENCE STARS
NT SATURN (PLANET)
NT SATURN RINGS
NT SEYFERT GALAXIES
NT SOLAR SYSTEM
NT SPIRAL GALAXIES
NT STAR CLUSTERS
NT STARS
NT STONY METEORITES
NT SUBDWARF STARS
NT SUBGIANT STARS
NT SUN
NT SUPERGIANT STARS
NT SUPERMASSIVE STARS
NT SUPERNOVAE
NT SYMBIOTIC STARS
NT T TAURI STARS
NT TEKTITES
NT TERRESTRIAL PLANETS
NT TITAN
NT TRITON
NT URANUS (PLANET)
NT URANUS RINGS
NT VARIABLE STARS
NT VENUS (PLANET)
NT VESTA ASTEROID
NT VIRGO GALACTIC CLUSTER
NT WHITE DWARF STARS
NT WOLF-RAYET STARS
NT X RAY BINARIES
NT ZETA AURIGAE STAR
NT ZODIACAL DUST
Dark matter near the sun: Simulated star counts and the Oort limit 06 p0880 N85-15592
Determination of the observation conditions of celestial bodies with the aid of the DISPO system
[NAS 1.15:77632] 14 p2438 N85-25044
Observation of hard X-rays from the Crab pulsar and A0535+26
[OG-2.3-7] 22 p3866 N85-33944
Results of low energy background measurements with the Liquid Scintillation Detector (LSD) of the Mont Blanc Laboratory
[HE-5.3-5] 24 p4205 N85-36099
CELESTIAL GEODESY
Research in geodesy based upon radio interferometric observations of extragalactic radio sources
[AD-A147581] 07 p0988 N85-16280
Recent development in astronomic position determinations
[AD-A148335] 08 p1082 N85-16858
Basic formulae for the computation of the deflection of the vertical from astronomical star observations
[AD-A154912] 21 p3605 N85-32390
CELESTIAL MECHANICS
Some considerations on elliptic heliocentric orbits
[INPE-3217-PRE/570] 02 p0297 N85-11926
Physical properties of Neptune and Triton inferred from the Orbit of Triton 02 p0300 N85-11942
Tidal disruption and the origin of the Moon 04 p0586 N85-13739
Interplanetary trajectories 05 p0800 N85-13827
The restricted problem of 2 + N bodies 09 p1414 N85-18925
Lagrangian solutions in photogravitational restricted circular three-body problem 13 p1979 N85-22416
Computation of elliptical functions in problems of celestial mechanics 13 p1979 N85-22418
Feoktistov argues against U.S. space shuttle design concept 13 p1985 N85-22453
China report: Science and technology
[JPRS-CST-85-006] 13 p2052 N85-22643
Development, prospect of satellite dynamics discussed 13 p2052 N85-22647
Dynamics of gas disks in triaxial galaxies 13 p2171 N85-23469
Elements of celestial mechanics 14 p2396 N85-24762
The solar system: Improving knowledge of the system 14 p2396 N85-24782
Construction of conditionally periodic solutions of problem of reciprocating motion of axially symmetric satellite of triaxial planet 15 p2480 N85-25304
Evolution of collisional systems — planetary disks 15 p2674 N85-26505
The Adiabatic invariant: A tool for the study of the dynamics of the solar system 15 p2676 N85-26519
Instabilities and the fine structure of Saturn's rings 15 p2676 N85-26520
Optimal open loop and nonlinear feedback control for remote orbital capture
[AD-A151967] 16 p2732 N85-26859
The study of the physics of cometary nuclei
[NASA-CR-175917] 17 p3054 N85-28905
CELESTIAL NAVIGATION
NT ASTRONAVIGATION
Optimization of orientation in navigation by two heavenly bodies 07 p0951 N85-16027
CELESTIAL OBSERVATION
U ASTRONOMY
CELESTIAL REFERENCE SYSTEMS
References in space and time 05 p0598 N85-13809
Reference systems — in space mechanics 14 p2399 N85-24784
Materialization of a reference system via a star catalog 14 p2399 N85-24787
Relating the planetary ephemerides and the radio reference frame 16 p2770 N85-27095
CELESTIAL SPHERE
A model of the soft X-ray background as a blast wave viewed from inside 06 p0879 N85-15586
Non equilibrium ionization in the local hot bubble 06 p0879 N85-15587
The stellar wind in the BO V-type eclipsing binary Y Cygni 11 p1755 N85-21040
Investigating statistical characteristics of atmospheric background brightness and star background density in equatorial region of celestial sphere 15 p2478 N85-25298
CELL ANODES
Nickel-cadmium cell design variable program data analysis
[NASA-TM-86198] 19 p3258 N85-30203
CELL CATHODES
Development and testing of TiB2, used as cathode material in Al-electrolysis cells
[BMFT-FB-T-84-176] 05 p0633 N85-14060
The effect of potential on the corrosion fatigue behavior of a precipitation hardened aluminum alloy
[AD-A146537] 06 p0768 N85-14916
Molten carbonate fuel cell cathode material development
[DE85-010268] 18 p3081 N85-29057
Nickel-cadmium cell design variable program data analysis
[NASA-TM-86198] 19 p3258 N85-30203
CELL DIVISION
Chromosome aberrations in Crepis capillaris exposed to gamma radiation and clinostat 19 p3325 N85-30600
Preparative electrophoresis of cultured human cells: Effect of cell cycle phase 20 p3500 N85-31758
CELLS
Lithium battery safety: A fiber-optic application for safe observation of lithium cells under severe tests
[AD-A146646] 06 p0804 N85-15119

Opacity control technique for jet engine test cells
[AD-D011668] 19 p3220 N85-29668
Summary electrophoretic data base on human embryonic kidney cell strain 8514
20 p3501 N85-31766
The Fibrin slide assay for detecting urokinase activity in human fetal kidney cells 20 p3502 N85-31768

CELLS (BIOLOGY)
NT CHROMOSOMES
NT ERYTHROCYTES
NT FIBROBLASTS
NT GAMETOCYTES
NT HEMATOPOIESIS
NT HEMOGLOBIN
NT LYMPHOCYTES
NT MITOCHONDRIA
NT NEURONS
NT OXYHEMOGLOBIN
NT PROTOPLASTS

Effect of spaceflight factors on rat bone marrow cells
01 p0092 N85-10620
Purification of biomaterials by phase partitioning
02 p0154 N85-11043
Architecture of dermatophyte cell Walls: Electron microscopic and biochemical analysis
[NASA-TM-77441] 03 p0399 N85-12546
Field/cell interaction model
[DE84-011914] 04 p0544 N85-13465
Further cell biology experiments with Physarum polycephalum for a reflight of Biorack
05 p0689 N85-14429
Observation of the contractile vacuolar system of Paramecium caudatum on the fast running clinostat
05 p0689 N85-14431
Plant cell cultures in biological space experiments
05 p0690 N85-14434
Structure and functions of fungal cell surfaces
[NASA-TM-77439] 06 p0842 N85-15347
The structure and function of fungal cells
[NASA-TM-77443] 06 p0842 N85-15348
The development of the vestibular apparatus under conditions of weightlessness
[NASA-TM-77517] 07 p1011 N85-18422
Radiation physics, biophysics, and radiation biology
[DE84-014885] 09 p1360 N85-18557
Genetic effects of microwave exposure on mammalian cells in vitro. Volume 2, Appendix A: Cytogenetics and growth kinetics data, 850 MHz
[AD-A148666] 10 p1522 N85-19599
Genetic effects of microwave exposure on mammalian cells in vitro. Volume 2, Appendix B: Cytogenetics and growth kinetics data, 1.2 GHz
[AD-A148667] 10 p152. N85-19600
Genetic effects of microwave exposure on mammalian cells in vitro, volume 2
[AD-A149347] 10 p1523 N85-19603
Purification and cultivation of human pituitary growth hormone secreting cells
[NASA-CR-171846] 12 p1899 N85-21923
Toxicity, mutagenesis and aging due to endogenous oxygen radicals
[AD-A150121] 12 p1900 N85-21928
Morphological study of monkeys submitted to antiorthostatic hypokinesia 12 p1902 N85-21942
Investigation of foam flotation and phase partitioning techniques 12 p1945 N85-22216
Second Soviet-French Symposium on Space Technology 15 p2483 N85-25326
Actual and simulated weightlessness inhibit osteogenesis in long bone metaphysis by different mechanisms 15 p2608 N85-26074
Quantitative alterations in the function of bone forming cells due to reduced weight bearing
15 p2609 N85-26075
Gravitropism in leafy dicot stems
15 p2610 N85-26086
Development and maturation of the neuromuscular junciton in cell culture under conditions of simulated zero-gravity 15 p2611 N85-26093
Differential wall growth in gravistimulated corn roots: Its timing and regulation 15 p2614 N85-26105
Structural-functional changes in bacterial cells under spaceflight conditions 16 p2724 N85-26812
The dynamical behavior of the age-size-distribution of a cell population
[CWI-AM-R8414] 17 p2998 N85-28536
Interactions between electromagnetic fields
[AD-A153796] 18 p3091 N85-29129
Radiation damage and repair in cells and cell components. Part 2: Physical radiations and biological significance
[DE85-006934] 18 p3152 N85-29518
Radiation damage and repair in cells and cell components, part 1
[DE85-006657] 18 p3152 N85-29519
Controlled Ecological Life Support System. Life Support Systems in Space Travel
[NASA-CP-2378] 18 p3155 N85-29531
Current concepts and future directions of CELSS
18 p3155 N85-29532
Molecular toxicology of chromatin: The role of Poly(ADP-Ribose) in gene control
[AD-A154415] 19 p3327 N85-30611
Metabolic mechanisms of plant growth at low water potentials 19 p3327 N85-30612
Mouse oocyte killing by neutrons: Target considerations
[DE85-011382] 19 p3328 N85-30624
Flow cytometry for health monitoring in space
[DE85-009572] 19 p3329 N85-30625
Kidney cell electrophoresis
[NASA-CR-171889] 20 p3498 N85-31745
Task description for the 1983 catalog of tasks for the materials processing in space program
20 p3498 N85-31746
Kidney cell electrophoresis, continuing task
20 p3498 N85-31747
Asymmetric electroosmotic flow and mobility measurements at nonstationary positions in the rectangular chamber 20 p3499 N85-31749
Theoretical prediction of stationary positions in the rectangular chamber during asymmetric electroosmotic flow 20 p3499 N85-31750
A computer program for determining the electrophoretic mobility of cells in a rectangular chamber during asymmetric electroosmotic flow
20 p3499 N85-31751
Operation of the Zeiss cytopherometer with Zn/ZnSO4 electrode system of Tenforde et al
20 p3499 N85-31752
Electrophoretic mobility of cells in a vertical Ficoll gradient 20 p3499 N85-31753
Free-zone electrophoresis of animal cells. 1: Experiments on cell-cell interactions
20 p3499 N85-31754
Development anmd testing of electrophoresis solutions. Task I.1: Development of optimal buffer system
20 p3500 N85-31755
Effects of method of detachment on electrophoretic mobility of mammalian cells grown in monolayer culture
20 p3500 N85-31757
Preparative electrophoresis of cultured human cells: Effect of cell cycle phase 20 p3500 N85-31758
Size and DNA distributions of electrophoretically separated cultured human kidney cells
20 p3500 N85-31759
The role of cell size in density gradient electrophoretic separation of mouse leukemia cells according to position in the cell cycle 20 p3500 N85-31760
Electrophoretic mobilities of cultured human embryonic kidney cells in various buffers 20 p3501 N85-31761
Effect of passage number on electrophoretic mobility distributions of cultured human embryonic kidney cells
20 p3501 N85-31762
Density gradient electrophoresis of cultured human embryonic kidney cells 20 p3501 N85-31763
Identification and quantitation of morphological cell types in electrophoretically separated human embryonic kidney cell cultures 20 p3501 N85-31764
Urokinase production by electrophoretically separated cultured human embryonic kidney cells
20 p3501 N85-31765
A critical synopsis: Continuous growth of proximal tubular kidney epithelial cells in hormone-supplemented serum-free medium 20 p3501 N85-31767
Results of computer calculations for a simulated distribution of kidney cells 20 p3502 N85-31771
Properties of electrophoretic fractions of human embryonic kidney cells separated on space shuttle flight STS-8 20 p3503 N85-31776
Detection of internal structure by scattered light intensity: Application to kidney cell sorting
20 p3503 N85-31777
Flow cytometry of human embryonic kidney cells: A light scattering approach 20 p3503 N85-31778
A cluster analysis method for identification of subpopulations of cells in flow cytometric list-mode arrays 20 p3503 N85-31779
Development of a recombinant DNA assay system for the detection of genetic change in astronauts cells
[DE85-010103] 20 p3504 N85-31781
A system for the assessment of non-thermal effects of ultrasound on cells at liquid nitrogen temperatures
20 p3523 N85-31915
From microbial communities to cells
21 p3659 N85-32726
Physical chemical state of water in living cells
[AD-A154586] 21 p3662 N85-32749
Microorganisms in space flight
23 p3951 N85-34490
Report of Amphibian Development Group
24 p4127 N85-35583
Are living cells generally sensitive to gravity?
24 p4130 N85-35602

CELLULAR MATERIALS (NON BIOLOGICAL)
U FOAMS

CELLULOSE
Fire retardant cellulosehydrate fibers
08 p0761 N85-14570
Effect of polymer matrix on properties of fibers obtained by caking polymer dispersions 08 p0762 N85-14576
Environmental cycling of cellulosic thermal insulation and its influence on fire performance
[DE85-004295] 13 p2041 N85-22778
Effects of coating rectangular microscopic electrophoresis chamber with methylcellulose
20 p3498 N85-31748

CELLULOSE NITRATE
Oxidation resistant slurry coating for carbon-based materials
[NASA-CASE-LEW-13923-1] 24 p4077 N85-35267

CEMENTATION
Some reflections on the competition among different hard materials in industrial applications
02 p0177 N85-11192
Development and performance of CVD-coatings on cutting tools 02 p0178 N85-11193
An investigation of cementation and carbonitriding by means of ionic bombardment
[BLL-OA-TRANS-3203-(6196.300)]
20 p3429 N85-31265

CEMENTITE
Reciprocal solubility of phases in multi-component systems
[BLL-M-38003-(5828.4)] 07 p0926 N85-15870

CEMENTS
Materials for emergency repair of runways
[AD-A146139] 03 p0320 N85-12068
Development of a rapid test method for asphalt concrete content determination in hot-mix paving mixtures
[PB84-218692] 03 p0342 N85-12204
Development of a preliminary ALRS stabilized material pavement analysis system (SPAS)
[AD-A147116] 07 p0910 N85-15760
Development and evaluation of a procedure for the rapid analysis of fresh concrete
[AD-A149741] 12 p1866 N85-21703
Hazardous air pollutants: Dry-deposition phenomena
[PB85-138279] 12 p1887 N85-21843
Pycnometer shaker
[PB85-174985] 20 p3460 N85-31491
Experimental characterization and stability of salt- and nonsalt-containing grouts and mortars (BCT-1F- and BCT-1FF-related)
[DE85-012339] 22 p3753 N85-33263
High temperature polymer concrete
[DE85-005756] 23 p3920 N85-34290

CENSORED DATA (MATHEMATICS)
The EM algorithm for censored data
[AD-A148136] 08 p1212 N85-17626
A power transformation exponential regression model for censored failure time data
[AD-A148377] 08 p1212 N85-17632
Small-sample properties of kernel density estimators from randomly right-censored data
[AD-A148752] 09 p1374 N85-18634
A kernel type estimator of a quantile function from right-censored data
[AD-A148753] 09 p1374 N85-18635
Inference for censored matched pairs using signed ranks
[MATHEMATICS-RESEARCH-162]
12 p1923 N85-22078
On the confidence limits for Weibull reliabilty and quantiles: The case of maximum likelihood estimation from small size censored samples
[REPT-84-RR-345] 20 p3521 N85-31696

CENTAUR LAUNCH VEHICLE
NT ATLAS CENTAUR LAUNCH VEHICLE

Shuttle/Centaur project perspective
08 p1106 N85-16991
Shuttle/Centaur upper stage capability
11 p1712 N85-20773
Linearization of digital derived rate algorithm for use in linear stability analysis
[NASA-TM-87000] 14 p2243 N85-23904

CENTAUR VEHICLE
U CENTAUR LAUNCH VEHICLE

CENTAURUS CONSTELLATION
X-ray emission from Centaurus A — Vela 5B; radio galaxy 08 p1239 N85-17813
X-ray emission from Centaurus A
[DE85-002030] 09 p1417 N85-18943

CENTER OF GRAVITY
Mobility of the small combine (track type) on soft ground-relationship between the position of the center of gravity and the mobility
[AD-P004285] 09 p1407 N85-18662
Space Shuttle Orbiter trimmed center-of-gravity extension study. Volume 9: Effects of configuration modifications on the aerodynamic characteristics of the 140 A/B Orbiter at Mach numbers of 1.5, 2.0, and 2.5 — wind tunnel tests
[NASA-TM-72661-VOL-9] 10 p1420 N85-18958
Space Shuttle orbiter trimmed center-of-gravity extension study
[NASA-TP-2284] 10 p1428 N85-19003
On the quadratic mean radius of a polynomial in Cz
[AD-A149189] 10 p1546 N85-19751

CENTER OF MASS
Spurious center of mass effects in a dynamically determined basis
[CSIR-TWISK-310] 01 p0109 N85-10732
Comment on the validity of an L2 treatment of the center of mass problem
[CSIR-TWISK-324] 01 p0114 N85-10779
Nonlinear oscillations of 2 body system relative to center of mass in elliptical orbit 02 p0159 N85-11082
Motion of symmetrical satellite with flexible viscoelastic rods about center of mass in circular orbit 13 p1979 N85-22420
Rotational motion of a satellite 13 p1981 N85-22426
Evaluating accuracy in determining position of Earth's center of mass and elements of orientation of geodetic coordinate system 13 p1983 N85-22441
Periodic movements of axisymmetrical satellite about center of mass due to gravitational moment 13 p2042 N85-22783
Stability of periodic satellite motions relative to center of mass in circular orbit 16 p2718 N85-26780
Satellite physical and orbital characteristics 16 p2804 N85-27267
Physics of (very) high energy e(+)-e(-) colliders
[DE85-008177] 17 p3036 N85-28780

CENTIMETER WAVES
An Earth-based attempt to detect Saturn Electrostatic Discharge (SED) at 21 centimeters 15 p2674 N85-26501

CENTRAL AMERICA
Climate Conference for Latin America and the Caribbean
[WMO-632] 07 p1000 N85-16352
Review of climate problems in Latin America and the Caribbean 07 p1001 N85-16354
The climate in food production in Latin America 07 p1001 N85-16359
Requirements for training in climate-related subjects 07 p1004 N85-16378
Education and training for the climate related activities in Latin America and the Caribbean 07 p1004 N85-16379

CENTRAL ATLANTIC REGION (US)
East coast snowstorm survey 15 p2598 N85-26013
Model sensitivity studies of major east coast storms 15 p2598 N85-26016
Justification and plan for participation in GALE 15 p2599 N85-26017

CENTRAL EUROPE
Specific phenomena associated with the propagation of seismic waves in central Europe
[REPT-548] 03 p0375 N85-12391
Information relative to cartography and geodesy. Series 2: Translations, Number 42, Volume 2 — maps
[ISSN-0469-4244] 18 p3123 N85-29337
Two satellite image maps of Central Europe 18 p3123 N85-29339

CENTRAL NERVOUS SYSTEM
NT BRAIN
NT BRAIN STEM
NT CEREBELLUM
NT CEREBRAL CORTEX
NT CEREBRAL VENTRICLES
NT CEREBRUM
NT SPINAL CORD
NT SPINE
NT THALAMUS
Nicholet MED-80 (trademark) programs in the Naval Biodynamics Laboratory evoked potential series
[AD-A147105] 07 p1016 N85-16451
Encephalographic correlates of autogenous change in human functional state 08 p1193 N85-17518
Work capacity of heat and electric power plant operations working 12 hour day and night shifts 09 p1362 N85-18567
NMR imaging and spectroscopy of the mammalian central nervous system after heavy ion radiation
[DE85-004509] 14 p2366 N85-24696
Cell death, neuronal plasticity and functional loading in the development of the central nervous system 15 p2612 N85-26096
Circadian rhythm control: Neurophysiological investigations 15 p2612 N85-26099
Does a 50-cycle alternating field have central nervous effects?
[BLL-CE-TRANS-8083-(9022.09)] 16 p2839 N85-27507
Effect of triphthasine and elenium on changes in evoked bioelectrical activity of the brain exposed to stationary magnetic field 19 p3325 N85-30001

CENTRAL PROCESSING UNITS
NT ARITHMETIC AND LOGIC UNITS
Clutter generator for use in radar evaluation
[AD-D011234] 01 p0039 N85-10245
Solution of contaminant transport equations using an orthogonal-upstream finite element scheme
[DE84-014266] 01 p0070 N85-10463
Concurrency in parallel processing systems 05 p0714 N85-14581
Atmospheric Modeling And Sensor Simulation (AMASS) study
[NASA-CR-171263] 07 p0996 N85-16325
Programmable realtime interface between a block floating point processor and memory
[AD-D011431] 08 p1203 N85-17571
Vector computer memory bank contention
[NASA-CR-177342] 09 p1376 N85-18649
Distributing a distributed problem solving network simulator
[AD-A149065] 10 p1537 N85-19693
Relative performance of micro and mainframe computers
[AD-A149261] 10 p1538 N85-19696
Research using a DISCUS based network emulator
[AD-A141294] 13 p2149 N85-23338
Use of function processors in multiprocessor systems 14 p2400 N85-24796
Space-variant optical systems
[AD-A151032] 14 p2421 N85-24939
Use of vector processors in cartographic raster data processing, with special regard to the AP-120B vector processor 16 p2814 N85-27358
A high-accuracy optical linear algebra processor for finite element applications
[NASA-CR-175894] 17 p3017 N85-28658
Optimize computer throughput using array processors
[AD-A155843] 24 p4135 N85-35626

CENTRIFUGAL CASTING
Mechanical properties and microstructure of centrifugally cast alloy 718
[AD-A147800] 08 p1129 N85-17116

CENTRIFUGAL COMPRESSORS
Flow in Centrifugal Compressors — conferences
[VKI-LS-1984-07] 05 p0636 N85-14079
Experimental observation of the flow in impellers and diffusers — centrifugal compressors 05 p0636 N85-14080
Answering thermodynamic questions with three-dimensional viscous flow calculations 05 p0636 N85-14081
Design and off-design performance prediction of high pressure ratio centrifugal compressors 05 p0636 N85-14082
Pressure loss due to the tip clearance of impeller blades in centrifugal and axial blowers 05 p0636 N85-14083
Vaneless diffusers — flow in centrigal compressors 05 p0637 N85-14084
Vaned diffusers — in centrifugal compressors 05 p0637 N85-14085
Low solidity cascade diffusers for wide flow range centrifugal blowers 05 p0637 N85-14086
Surge and stall in centrifugal compressors 05 p0637 N85-14087
Subsynchronous vibrations in a high pressure centrifugal compressor: A case history 05 p0642 N85-14118
Experiences with nonsynchronous forced vibration in centrifugal compressors 05 p0642 N85-14119
Experimental on-stream elimination of resonant whirl in a large centrifugal compressor 05 p0642 N85-14121
Internal hysteresis experienced on a high pressure syn gas compressor 05 p0642 N85-14122
Lateral fluid forces acting on a whirling centrifugal impeller in vaneless and vaned diffuser 05 p0643 N85-14123
Hydraulic forces on a centrifugal impeller undergoing synchronous whirl 05 p0643 N85-14124
Experimental investigation of the oscillation behaviour of a liquid-filled rotor with centrifugal motion
[BLL-DOUNREAY-TR-936-(9091.9F)] 06 p1160 N85-17317
Open-cycle centrifugal vapor-compression heat pump
[PB85-113405/GAR] 09 p1328 N85-18348
Failure analysis of fractured capscrews in centrifugal coolant compressor
[DE85-010029] 19 p3287 N85-30384
R and D activities of the Propulsion Division 20 p3539 N85-32025
A 3-D Euler method for internal transonic flows computation with a multi-domain approach 21 p3587 N85-32298

CENTRIFUGAL FORCE
Two-dimensional unsteady analysis of fluid forces on a whirling centrifugal impeller in a volute 05 p0643 N85-14126
Centrifugally driven magnetohydrodynamic (MHD) winds and the nonthermal emission regions in Active Galactic Nuclei (AGN) 08 p1242 N85-17835
Aerodynamic forces developing in channels between vanes in turbine drive wheels 16 p2765 N85-27062
Modifications to SOLA-VOF for flow dynamics in spinning cylinders
[AD-A154093] 19 p3265 N85-30250
Drying of pulverized material with heated condensible vapor
[DE85-011656] 22 p3783 N85-33438

CENTRIFUGAL PUMPS
A study on dynamic characteristics of liquid oxygen pumps for rocket engines
[NAL-TR-806] 03 p0324 N85-12068
Analysis and testing for rotordynamic coefficients of turbulent annular seals with different, directionally homogeneous surface-roughness treatment for rotor and stator elements 05 p0644 N85-14134
Influence of stationary components on unsteady flow in industrial centrifugal compressors 05 p0645 N85-14140
Effect of apparent fluid masses on natural vibration frequencies of impellers of multistage centrifugal pumps 14 p2277 N85-24108
Two-phase flow in centrifugal pumps
[BLL-CE-TRANS-8065-(9022.09)] 15 p2605 N85-26053
Design and operation of solar thermal heat transfer systems
[DE85-009837] 19 p3267 N85-30263

CENTRIFUGES
NT HUMAN CENTRIFUGES
Investigations into the improvement of processing of Bolivian tin ores
[BMFT-FB-T-84-184] 07 p0917 N85-15807
Unsymmetrical flow in a centrifuge
[DE85-009021] 18 p3103 N85-29206
Method for controlling the viscosity of siloxane oils
[DE85-011586] 23 p3909 N85-34221
Matched filtering of visual evoked potentials to detect acceleration (+Gz) induced blackout
[AD-A155912] 24 p4131 N85-35609
Simulation of high +Gz onset in the dynamic environment simulator
[AD-A155963] 24 p4131 N85-35610

CENTRIFUGING
China report: Science and technology
[JPRS-CST-84-003] 04 p0491 N85-13132
Magnetohydrodynamic flow of two-component gas analyzed 04 p0491 N85-13133
Solution of the h-equation for a single point source excitation of magnitude K
[DE84-017574] 09 p1374 N85-18638
Centrifuge tests to provide closure bounds for switches subjected to random vibration
[DE85-002003] 10 p1482 N85-19357
Comparison of shock-induced displacements with displacements produced by a centrifuge acceleration
[DE85-000467] 12 p1852 N85-21618
Measurement of uranium enrichment for gaseous uranium at low pressure
[DE85-012697] 24 p4150 N85-35733

CENTRIFUGING STRESS
Hydrodynamic impeller stiffness, damping, and inertia in the rotordynamics of centrifugal flow pumps 05 p0643 N85-14125
Centrifuge impact cratering experiments 13 p2181 N85-23533
Positive Gz accelerations tolerance of individuals 41 to 58 years of age 19 p3323 N85-30588

CENTRIPETAL FORCE
Hydraulic forces on a centrifugal impeller undergoing synchronous whirl 05 p0643 N85-14124

CENTROIDS
Quantitative non-destructive evaluation of damage in composite materials using transmitted and reflected ultrasound
[NASA-CR-175550] 12 p1796 N85-21269

CEPHEID VARIABLES
Simultaneous photometry and radial velocities of dwarf cepheids and Delta Scuti stars 01 p0128 N85-10878

Thermal effects in stellar pulsations
02 p0297 N85-11925
Mg 2 emission of Pop. 2 long-period Cepheids
11 p1754 N85-21032
Blue companions of Cepheids
11 p1754 N85-21033
Ultraviolet observations of Population 2 Cepheids
11 p1754 N85-21034
Ultraviolet analysis of the peculiar F supergiant HD 112374
11 p1754 N85-21035
The color excesses of classical cepheids and the structure of our galaxy
13 p2169 N85-23459
The Feinhelt method: A phase-independent formulation of the period-luminosity relation for Cephids
[NASA-CR-175708] 14 p2440 N85-25056

CEPSTRAL ANALYSIS
Classification methods for Italian vowels — speech recognition
[FUB-61-1982] 01 p0039 N85-10248
Autoregressive modeling and the classification of land clutter — radar signatures
[ENST-C-84003] 03 p0356 N85-12292
Radar measurement of thickness of drifting ocean ice employing cepstral signal processing
15 p2644 N85-26313
A classification vocoder: A very low rate speech transmission by vector quantization of the spectrum
[ENST-84D003] 20 p3441 N85-31356

CERAMAL PROTECTIVE COATINGS
U CERMETS
U PROTECTIVE COATINGS

CERAMALS
U CERMETS

CERAMIC BONDING
Ceramic/ceramic seals by microwave heating
[DE84-007486] 04 p0479 N85-13050
BN coating of ceramic fibers for ceramic fiber composites
[AD-D011700] 19 p3249 N85-30145

CERAMIC COATINGS
FRG ceramic engine components (PET)
08 p1141 N85-17193
An investigation of enhanced capability thermal barrier coating systems for diesel engine components
[NASA-CR-174820] 09 p1298 N85-18154
Improved ceramic anodes for corrosion protection
[AD-A149492] 10 p1452 N85-19149
Thermal barrier coating system
[NASA-CASE-LEW-13324-2] 12 p1796 N85-21266
Tribological properties of boron nitride synthesized by ion beam deposition
[NASA-TM-86962] 12 p1810 N85-21355
Metallic and metalloceramic coating by thermal decomposition
[NASA-TM-86892] 13 p2036 N85-22755
Rocket thrust chamber thermal barrier coatings
16 p2734 N85-26867
Simultaneous chemical vapor deposition of SiC-dispersed phase composites
[DE85-007751] 16 p2744 N85-26931
Method for preparing Pb-(beta)-aluminum ceramic
[DE85-011665] 22 p3752 N85-33256

CERAMIC FIBERS
BN coating of ceramic fibers for ceramic fiber composites
[AD-D011700] 19 p3249 N85-30145

CERAMIC MATRIX COMPOSITES
Factors influencing the ball milling of Si3N4 in water
[NASA-TM-86932] 10 p1450 N85-19136
Fabrication of fiber-reinforced ceramic composites by chemical vapor infiltration
[DE85-003809] 11 p1611 N85-20132
Technological and economic assessment of advanced ceramic materials. Volume 3: A case study of ceramic capacitors
[PB85-113108] 11 p1613 N85-20141
Film and interstitial formation of metals in plasma-sprayed ceramics
[NASA-TM-86993] 13 p2036 N85-22756
Evaluation methods of ceramic fiber reinforced metal matrix composite
23 p3907 N85-34206

CERAMIC NUCLEAR FUELS
Inquiry into disintegration control of irradiated low enrichment uranium for high temperature gas cooled reactors
[OEFZS-7281] 07 p1042 N85-16615
Technological apparatus for laser treatment of materials
17 p2944 N85-28174

CERAMICS
NT CERAMIC NUCLEAR FUELS
Silicon nitride sintered body
[NASA-TM-77602] 01 p0021 N85-10131
Silicon nitride powder
[NASA-TM-77731] 01 p0022 N85-10132
Synthesis and characterization of advanced materials
[PB84-215326] 01 p0025 N85-10156
Powder containing 2H-type silicon carbide produced by reacting silicon dioxide and carbon powder in nitrogen atmosphere in the presence of aluminum
[NASA-TM-77597] 01 p0027 N85-10157
Ceramic microstructure and adhesion
[NASA-TM-83804] 01 p0031 N85-10185
Processing ceramics
[NASA-TM-77603] 01 p0031 N85-10188
Fabrication and characterization of Si3N4 ceramics without additives by high pressure hot pressing
[NASA-TM-77724] 01 p0031 N85-10189
Sealing ceramic material in low melting point glass
[NASA-TM-77599] 01 p0031 N85-10190
Milling of Si3N4 with Si3N4 hardware
[NASA-TM-86864] 01 p0031 N85-10191
Selecting the proper ceramic material for a regenerator experiencing large temperature gradients
[AD-A144796] 01 p0032 N85-10199
Fundamental studies of structure property relationship in transformation toughened ceramics
[DE84-015344] 01 p0033 N85-10204
Silicon carbide ceramic production
[NASA-TM-77598] 01 p0035 N85-10220
Single-drop impact damage prediction for low density, coated ceramic materials — rain erosion
01 p0061 N85-10402
Surface protection overview 02 p0144 N85-10978
Energy efficient engine high pressure turbine ceramic shroud support technology report
[NASA-CR-168036] 02 p0147 N85-10996
Inorganic composites for space applications
02 p0155 N85-11047
International Conference on Recent Developments in Specialty Steels and Hard Materials. Conference abstracts
[CSIR-S-256] 02 p0176 N85-11177
Microstructural design and control of sintered hard materials
02 p0176 N85-11180
Some reflections on the competition among different hard materials in industrial applications
02 p0177 N85-11192
The current status of diamond and cubic boron nitride composites
02 p0178 N85-11194
Non-oxide ceramics: A new class of engineering materials
02 p0179 N85-11199
The constitution as the basis for recent and future developments of wear resistant materials
02 p0179 N85-11205
Ceramic materials for MHD electrodes
[DE84-015560] 02 p0187 N85-11250
ONR (Office of Naval Research) Far east Scientific Bulletin, Volume 9, Number 2, April - June 1984
[AD-A145661] 02 p0305 N85-11974
High performance fibers for structurally reliable metal and ceramic composites — advanced gas turbine engine materials
[NASA-TM-86878] 03 p0325 N85-12095
Microstructure and properties of ceramics
[NASA-TM-77416] 03 p0335 N85-12155
Brittleness of ceramics
[NASA-TM-77504] 03 p0335 N85-12156
Microstructure of ceramics fabricated by unidirectional solidification
[NASA-TM-77423] 03 p0336 N85-12157
Ceramic powder for sintering materials
[NASA-TM-77434] 03 p0336 N85-12160
The colloidal chemistry of ceramic clays
[NASA-TM-77734] 03 p0336 N85-12163
Ceramic microstructure development
[AD-A145753] 03 p0337 N85-12166
Time-temperature dependence of the strength of commercial zirconia ceramics
[AD-A146233] 03 p0338 N85-12173
New coatings for high temperature materials protection
[AERE-R-11387] 03 p0339 N85-12180
Center for dielectric studies
[AD-A146183] 03 p0434 N85-12761
Structural changes during milling of aluminum oxide powders
[NASA-TM-77488] 04 p0472 N85-13008
Reactive sintering of SiC 04 p0473 N85-13010
Zeta potential in ceramic industry
[NASA-TM-77478] 04 p0478 N85-13047
Study of the pore structure of ceramics prepared by the slip casting method
[NASA-TM-77495] 04 p0478 N85-13048
Materials for high-temperature fuel cells
[DE84-016316] 04 p0479 N85-13054
Ceramic technology for advanced heat engines program plan
[DE84-013567] 04 p0479 N85-13055
High temperature mechanical properties of ceramics
[DE84-016492] 04 p0480 N85-13058
A study of the Armstrong Whitworth swing beam engine for automotive application 04 p0508 N85-13239
Long term technology development program
04 p0508 N85-13244
Imaging of surfaces and defects of crystals
[DE84-016449] 04 p0570 N85-13632
Controlled directionally solidified precision casting for superalloys and steels
[BMFT-FB-T-84-198] 05 p0619 N85-13960
High temperature corrosion of ceramics
[DE84-017084] 05 p0620 N85-13967
Fundamental tribological properties of ceramics
[NASA-TM-86915] 07 p0930 N85-15893
Oxidation resistance of silicon ceramics
[NASA-TM-77429] 07 p0931 N85-15898
Moisture absorbing anti-arcing coating and method for applying same
[AD-D011310] 07 p0932 N85-15904
Dispersed metal-toughened ceramics and ceramic brazing
[NASA-CR-174284] 07 p0933 N85-15916
Transformation toughened ceramics for the heavy duty diesel engine technology program
[NASA-CR-174889] 07 p1055 N85-16696
Ceramic fabrication process before firing-surface treatment of ceramic powder
[NASA-TM-77437] 08 p1131 N85-17129
Application of computer methods for calculation of multicomponent phase diagrams of high temperature structural ceramics
[AD-A148136] 08 p1133 N85-17140
Experimental and analytical study of ceramic-coated turbine-tip shroud seals for small turbine engines
[NASA-TM-86881] 09 p1281 N85-18057
Development of high temperature ceramic parts for vehicular gas turbines
[PNR-90245] 09 p1282 N85-18062
Fabrication of SiC whiskers and composites
[DE85-002038] 09 p1289 N85-18091
Fabrication of ceramic-ceramic composites by chemical vapor deposition
[DE85-000981] 09 p1296 N85-18155
Mechanisms of elevated temperature rupture in single phase ceramics
[DE85-000697] 09 p1299 N85-18156
High-technology ceramics in Japan
[TI85-900389] 09 p1299 N85-18157
Corrosion of ceramics in heat exchanger applications
[DE84-017459] 09 p1299 N85-18161
Study of charge transport in the thermoelectret state of some ceramics and glasses
[DE85-001763] 09 p1300 N85-18163
Ceramic fabric material testing
[DE84-012014] 09 p1300 N85-18165
West Europe report: Science and technology
[JPRS-WST-85-003] 09 p1309 N85-18224
Advanced latent heat storage media for high-temperature industrial applications
[DE85-000907] 09 p1345 N85-18461
Formation of amorphous layers in Al2O3 by ion implantation
[DE85-001289] 09 p1397 N85-18794
Advanced Gas Turbine (AGT) powertrain system development for automotive applications
[NASA-CR-174809] 09 p1403 N85-18831
Strength and failure of ceramic-metallic material
10 p1448 N85-19112
Effect of powder characteristics on microstructure and properties in alkoxide prepared PZT ceramics
[AD-A149082] 10 p1451 N85-19141
Densification of submicron YSZ (Yttria-Stabilized Zirconia) powders with alumina and borate additives
[AD-A149520] 10 p1452 N85-19150
Hot rolling of ceramics by the use of self propagating synthesis
[AD-D011486] 10 p1453 N85-19154
Evaluating the variability of ceramics with X-ray fluorescence
[DE85-002028] 10 p1453 N85-19155
Amorphization of ceramics by ion beams
[DE85-000936] 10 p1453 N85-19156
Optical studies of dynamical processes in disordered materials
[DE85-002400] 10 p1453 N85-19158
Reliability studies of ceramic capacitors
[AD-A149126] 10 p1479 N85-19338
Experimental study of ceramic coated tip seals for turbojet engines
[NASA-TM-86939] 10 p1483 N85-19363
Ribbon burner simulation of T-700 turbine shroud for ceramic lined seals research
[NASA-TM-86940] 10 p1483 N85-19364
Metals and Ceramics Division Materials Science Program
[DE85-003795] 11 p1592 N85-20012
Kinetics of reaction of metals and non-metals during diffusion welding
11 p1602 N85-20076

Structure of transient zone in diffusion welding of TsTS-19 piezoceramic with AMg6 alloy
11 p1603 N85-20082
Structural ceramics in transportation: Fuel implications and economic impacts
[DE85-003024] 11 p1611 N85-20130
Laser processing of ceramics
[DE85-001184] 11 p1612 N85-20135
Evaluation of machining damage in brittle materials
[DE85-001794] 11 p1612 N85-20136
High temperature corrosion of ceramics
[DE85-002179] 11 p1612 N85-20139
Technological and economic assessment of advanced ceramic materials. Volume 3: A case study of ceramic capacitors
[PB85-113108] 11 p1613 N85-20141
SEP of France manufactures its first silicon carbide fibers 11 p1618 N85-20184
NDE for heat engine ceramics
[NASA-TM-86949] 11 p1649 N85-20389
Slit-ring test for evaluating fracture in tubular cross sections
[DE85-003550] 11 p1654 N85-20416
Oxidation and hot corrosion of hot-pressed Si3N4 at 1000 deg C
[NASA-TM-86977] 12 p1811 N85-21358
Evaluation of corrosion-erosion behavior of various ceramic materials
[AD-A149756] 12 p1812 N85-21367
Degradation mechanisms in ceramic dielectrics
[AD-A149791] 12 p1813 N85-21369
Multiaxial stress response of ceramics
[DE85-004350] 12 p1814 N85-21379
Technological and economic assessment of advanced ceramic materials. Volume 1: Summary and conclusions
[PB85-113082] 12 p1815 N85-21383
Technological and economic assessment of advanced ceramic materials. Volume 2: A case study of ceramics in heat engine applications
[PB85-113090] 12 p1815 N85-21384
Technological and economic assessment of advanced ceramic materials: Volume 4: A case study of integrated optic devices
[PB85-113116] 12 p1815 N85-21385
Technological and economic assessment of advanced ceramic materials. Volume 5: A case study of ceramic toxic and combustible gas sensors
[PB85-113124] 12 p1815 N85-21386
Technological and economic assessment of advanced ceramic materials. Volume 6: A case study of ceramic cutting tools
[PB85-113132] 12 p1815 N85-21387
High-technology ceramics in Japan
[PB85-125029] 12 p1815 N85-21389
Slip casting and nitridation of silicon powder
[NASA-TM-77609] 12 p1816 N85-21406
Silicon carbide-silicon nitride fibers: Preparation and characterization of polycarbosilazane precursors
12 p1945 N85-22214
Thermodynamics of copper-nickel alloys containing aluminum, silicon, titanium, and chromium relative to their use in ceramic brazing
[DE85-004787] 13 p2023 N85-22674
Densification and deformation in the presence of a liquid phase
[DE85-005101] 13 p2038 N85-22763
NDE methods for green ceramics
[DE85-004019] 13 p2038 N85-22766
Cathode materials for molten carbonate fuel cells
[DE85-004078] 13 p2130 N85-23254
Fabrication of ceramic substrate-reinforced and free forms
[NASA-TM-86904] 14 p2247 N85-23926
Exploratory corrosion tests on materials and fluids for advanced high-temperature molten-salt storage
[DE85-002911] 14 p2258 N85-23991
A novel polymeric organosilazane precursor to Si3N4/SiC ceramics
[AD-A150748] 14 p2260 N85-24003
Effect of elevated-temperature neutron irradiation on fracture toughness of ceramics
[DE85-000652] 14 p2261 N85-24010
Correlation of uniaxial and biaxial fracture strengths of ceramics
[DE85-003779] 14 p2261 N85-24011
Pressure-density behavior for AlN, Al2O3, SiO2, TiB2, and TiC powders up to 3.5 GPa
[DE85-006146] 14 p2261 N85-24012
Dynamic shock studies of PZT 95/5 ferroelectric ceramic
[DE85-006137] 14 p2261 N85-24015
Solid state compressor
[AD-A150790] 14 p2311 N85-24302
Special purpose materials for fusion application
[DE85-005346] 14 p2424 N85-24950
Structure and properties of ion-implanted Al sub 2 O sub 3
[DE85-005374] 14 p2430 N85-24987
USSR report: Materials science and metallurgy
[JPRS-UMS-85-001] 15 p2496 N85-25395
Transformation toughened ceramics: A potential material for light diesel engine applications
[AD-A151413] 15 p2518 N85-25525
Transformation toughened ceramics: A potential material for light diesel engine application
[AD-A151421] 15 p2518 N85-25526
Mechanical aspects of interfaces and surfaces in ceramic containing systems
[AD-A151978] 15 p2519 N85-25530
Interfacial and colloidal aspects of aqueous suspension containing oxidic powders
[DE85-005972] 15 p2519 N85-25534
Fabrication of fiber reinforced ceramic composites by chemical vapor infiltration
[DE85-007565] 15 p2520 N85-25536
France develops own aluminum-based composite ceramic 15 p2534 N85-25636
Fiat conducts R and D in ceramic parts for diesel engine 15 p2534 N85-25637
West Europe report: Science and technology
[JPRS-WST-84-010] 15 p2535 N85-25644
Sweden invents new ceramic for more durable cutting tools 15 p2536 N85-25645
Abrasive cutting-off wheel 15 p2568 N85-25843
Nondestructive tests of ceramic components for aircraft turbines 16 p2709 N85-26718
Ceramics for advanced O2/H2 application
16 p2734 N85-26868
Simultaneous chemical vapor deposition of SiC-dispersed phase composites
[DE85-007751] 16 p2744 N85-26931
Material for protection of metal surfaces against corrosion by molten salts
[DE85-007714] 16 p2750 N85-26968
Effects of wear on structure-sensitive magnetic properties of ceramic ferrite in contact with magnetic tape
[NASA-TM-87007] 16 p2753 N85-26991
Breakway friction and dynamic friction/wear measurements of various ceramic materials from 25 C (75 F) to 650 C (1200 F)
[NASA-CR-174803] 16 p2754 N85-26994
Ceramic technology for advanced heat engines project
[DE85-004798] 16 p2755 N85-27002
Screening ceramic materials for intense radiant heat applications
[DE85-006989] 16 p2756 N85-27006
Development of a new faster process for the fabrication of ceramic fiber-reinforced ceramic composites by chemical vapor infiltration
[DE85-007550] 16 p2756 N85-27007
Sintering and properties of metal-ceramic alloys of the Kovar type
[BLL-BISI-TRANS-21822-(9022.06)]
17 p2927 N85-28060
Preparation of silicon carbide-silicon nitride fibers by the pyrolysis of polycarbosilazane precursors
[NASA-TM-86505] 17 p2933 N85-28107
Ceramic applications in turbine engines
[NASA-CR-174715] 17 p2934 N85-28109
Characterization of the fatigue and slow crack growth behavior of partially stabilized zirconia ceramics
[DE85-005240] 17 p2934 N85-28113
Indirect brazing of structural ceramics for uncooled diesels
[DE85-005569] 17 p2935 N85-28116
Microstructure-mechanical property relationships in transformation-toughened ceramics
[DE85-009722] 17 p2935 N85-28117
Ac field-induced order in dense colloidal systems
[DE85-009107] 17 p2935 N85-28119
Investigation of charge transport in the thermoelectret state of some ceramics and glasses
[DE85-000318] 17 p2936 N85-28122
Development of high temperature resistant, noncorrosible, non-metallic ceramic materials, especially silicon nitride in gas turbine application
[BMFT-FB-T-85-015] 17 p2936 N85-28125
Ceramic turbochargers: A case study of a near-term application of high-strength ceramics
[DE85-006495] 17 p2975 N85-28379
Future of ceramic turbochargers: Promises and pitfalls
[DE85-006209] 17 p2975 N85-28380
High temperature composite thermal storage systems
[DE85-005073] 17 p2986 N85-28455
Ceramic Technology for Advanced Heat Engines Project
[DE85-006755] 18 p3080 N85-29052
Ceramic coatings for heat engine materials: Status and future needs
[DE85-006759] 18 p3080 N85-29053
Ceramic coatings for heat engine materials
[DE85-005238] 18 p3080 N85-29054
Predicting microfracture in ceramics via a microcontract model
[DE85-005654] 18 p3081 N85-29060
Synthesis chemistry of ceramics by solid-state combustion processes in micro-gravity
[DE85-009595] 18 p3081 N85-29061
Conservation and substitution technology for critical metals in bearings and related components for industrial equipment and opportunities for improved bearing performance
[PB85-176246] 18 p3082 N85-29069
West Europe report: Science and technology
[JPRS-WST-84-031] 18 p3086 N85-29089
British breakthrough in lightweight lithium batteries
18 p3086 N85-29092
Use of ceramics in internal combustion engines
18 p3088 N85-29114
Burner rig corrosion of SiC at 1000 deg C
[NASA-TM-87061] 19 p3227 N85-30011
USSR report: Materials Science and Metallurgy
[JPRS-UMS-85-005] 19 p3241 N85-30095
Diffusion welding of aluminum with vacuum-tight corundum ceramic 19 p3247 N85-30130
The mechanics of internal stress and microcrack toughening mechanisms in ceramics
[AD-A154049] 19 p3248 N85-30139
BN coating of ceramic fibers for ceramic fiber composites
[AD-D011700] 19 p3249 N85-30145
Study of solute segregation at interfaces using Auger electron spectroscopy
[DE85-005709] 20 p3423 N85-31247
Prediction of lifetime for ceramic materials in the elastic and viscoelastic region by fracture mechanical methods
[ESA-TT-825] 20 p3434 N85-31305
West Europe report: Science and technology
[JPRS-WST-85-020] 20 p3438 N85-31333
Estimation of power-law creep parameters from bend test data
[PB85-183408] 20 p3472 N85-31579
Controlled indentation flaws for the construction of toughness and fatigue master maps
[PB85-179067] 20 p3473 N85-31582
Development of processes for the inclusion of radioactive waste in glass-metal compounds and ceramic materials
[BLL-CE-TRANS-8014-(9022.09)]
20 p3526 N85-31931
The shearing contribution in transformation toughening of brittle materials
[AD-A154656] 21 p3568 N85-32195
Matrix fracture in fiber-reinforced ceramics
[AD-A154704] 21 p3569 N85-32197
Stress corrosion of ceramic materials
[AD-A155020] 21 p3570 N85-32202
Sintering studies project
[AD-A154750] 21 p3572 N85-32216
Capacitive energy storage at cryogenic temperatures
[AD-A154508] 21 p3579 N85-32253
Tape casting as an approach to an all-ceramic turbine shroud seal
[NASA-TM-87078] 21 p3596 N85-32333
Friction and wear of solid-lubricated contact in gas turbine engine bearings
[AD-A155042] 21 p3596 N85-32335
Reliability of void detection in structural ceramics using scanning laser acoustic microscopy
[NASA-TM-87035] 21 p3597 N85-32337
System for electro-optical ceramic recrystallization
21 p3682 N85-32672
Tensile fatigue of glass fibers and composites with conventional and surface compressed fibers
[RR-84-4] 22 p3742 N85-33196
Research study for gel precursors as glass and ceramic starting materials for space processing applications research
[NASA-CR-176113] 22 p3751 N85-33250
Dispersion toughened ceramic composites and method for making same
[DE85-011601] 22 p3751 N85-33252
Sodium nitrate containing mixture for producing ceramic-glass-ceramic seal by microwave heating
[DE85-011610] 22 p3751 N85-33254
Improved process for the preparation of fiber-reinforced ceramic composites by chemical vapor deposition
[DE85-011584] 22 p3752 N85-33255
Microstructure-mechanical property relationships in the transformation-toughened ceramics
[DE85-011946] 22 p3752 N85-33261

Process and device for forming imprints on ceramic tubes
[DE85-013137] 22 p3753 N85-33264
Integrated current collector and catalyst support
[DE85-011618] 22 p3761 N85-33311
Woven heat exchanger
[DE85-011633] 22 p3783 N85-33439
Latch assembly
[DE85-011660] 22 p3792 N85-33492
Technology of off-gas treatment for liquid-fed ceramic melters
[DE85-012467] 22 p3812 N85-33610
Thermal protection systems for reentry vehicles
[CNES-NT-113] 23 p3900 N85-34157
X-ray residual stress analysis on the coarse grain of copper and its application to the brazed copper
23 p3907 N85-34202
High resolution electron microscopic characterization of interfaces in ceramics
[DE85-011207] 23 p3920 N85-34289
High temperature structural insulating material
[DE85-006361] 23 p3920 N85-34291
Synthesis of ultrafine ceramic and metallic powders in a thermal argon rf plasma
[DE85-009634] 23 p3983 N85-34696
Method for measuring surface activity of silicon nitride powder
[NASA-TM-77906] 24 p4073 N85-35242
Noise in silver beta alumina ceramics
[AD-A156135] 24 p4082 N85-35297
Method of preparing thin porous sheets of ceramic material
[DE85-006399] 24 p4082 N85-35300
High temperature corrosion of ceramics
[DE85-013481] 24 p4083 N85-35303
Noise in sodium beta alumina crystals
[AD-A156025] 24 p4161 N85-35798

CEREBELLUM

Visual evoked potentials with disrupted functioning of nonspecific cerebral systems 07 p1013 N85-16437
Specifics of dynamics of brain biopotentials under the influence of complex audible communicative signals
07 p1014 N85-16440
Neurophysiological correlates of motion sickness: Role of vestibulocerebellum and 'vomiting center' reanalyzed
11 p1693 N85-20643
Sensory and motor properties of the cerebellar uvula and modulus 15 p2613 N85-26104

CEREBRAL CORTEX

Visually evoked responses from non-occipital areas of the human cortex
[AD-A146079] 03 p0400 N85-12553
Evidence for multiple areas in the human auditory cortex
[AD-A146086] 03 p0401 N85-12555
Visual selective attention
[AD-A146220] 03 p0401 N85-12558
Electrophysiological correlates of Vernier acuity in human visual cortex
[AD-A146533] 06 p0846 N85-15371
Encephalographic correlates of autogenous change in human functional state 08 p1193 N85-17518
Topography of human brain electric potentials and dominance 11 p1691 N85-20633
Functional significance of some EEG parameters and dominant principle 11 p1691 N85-20634
A communications link for an implantable electrode array
[AD-A152238] 16 p2840 N85-27510
A multipole model of the observed cerebral cortex magnetic field
[AD-A152237] 16 p2842 N85-27526
Encapsulation and packaging of a semiconductor multielectrode array for cortical implantation
[AD-A153180] 17 p2998 N85-28535
Effect of triphthasine and elenium on changes in evoked bioelectrical activity of the brain exposed to stationary magnetic field 19 p3325 N85-30601
Changes in the impedance and bioelectrical activity of the cerebral cortex of rats under the action of anaesthetic drugs
[HSE-TRANS-10371] 19 p3327 N85-30617
Discovery regarding visual neuron adaptation applicable to robot use 20 p3504 N85-31786

CEREBRAL VENTRICLES

Reaction of cerebral ventricles to antiorthostatic position and occlusion of jugular veins 01 p0093 N85-10626

CEREBROSPINAL FLUID

Reaction of cerebral ventricles to antiorthostatic position and occlusion of jugular veins 01 p0093 N85-10626

CEREBRUM

Reaction of cerebral ventricles to antiorthostatic position and occlusion of jugular veins 01 p0093 N85-10626
Pathogenesis and treatment of cerebral air embolism and associated disorders
[AD-A146723] 07 p1014 N85-16443
Simultaneous determination of cerebral blood flow and partition coefficient with a freely diffusable tracer
[DE85-001226] 11 p1690 N85-20625
Resource allocation in cerebral specialization of function: Behavioral and electrophysiological studies
[AD-A155092] 21 p3664 N85-32759
Cerebral hemodynamics and ventricular function in -15 deg antiorthostatic position 22 p3822 N85-33676

CERENKOV COUNTERS

Monte Carlo simulation of gas Cerenkov detectors
[DE85-002422] 10 p1488 N85-19394
Electrons and cosmic ray produced protons in Saturn's inner magnetosphere
[NASA-TM-87469] 15 p2679 N85-26546
A Cerenkov-delta E-Cerenkov detector for high energy cosmic ray isotopes and an accelerator study of Ar-40 and Fe-56 fragmentation
[NASA-CR-176028] 20 p3549 N85-32086
Very high energy gamma rays from the Crab Nebula
[OG-2.3-3] 22 p3866 N85-33940
Search for gamma-rays above 400 GeV from Geminga
[OG-2.4-4] 22 p3867 N85-33951
Energy spectra of elements with 18 or = Z or = 28 between 10 and 300 GeV/amu
[OG-4.1-8] 22 p3876 N85-34014
Results of a search for deuterium at 25-50 GC/c using a magnetic spectrometer
[OG-4.2-4] 22 p3878 N85-34024
EAS spectrum in the primary energy region above 10 to the 15th power eV by the Akeno and Yakutsk array data
[OG-5.1-16] 22 p3882 N85-34057
EAS Cerenkov measurements of the composition of the cosmic ray flux around 10 to the 16th power eV
[OG-5.2-11] 22 p3884 N85-34067
High resolution Cherenkov detectors for cosmic ray isotope experiment
[OG-9.1-4] 23 p4023 N85-34930
Cerenkov counters for high energy nuclei: Some new developments
[OG-9.1-5] 23 p4023 N85-34931
A high resolution gas Cerenkov detector for the superconducting magnet facility
[OG-9.1-6] 23 p4023 N85-34932
Bevalac calibration of the SOFIE range and hodoscope detectors
[OG-9.1-7] 23 p4023 N85-34933
The development of a high energy cosmic ray detector for Spacelab-2
[OG-9.1-8] 23 p4023 N85-34934
Mass resolution optimization in a large isotopic composition experiment
[OG-9.1-9] 23 p4023 N85-34935
Cherenkov-dE/dx-range measurements on cosmic ray iron group nuclei
[OG-9.1-12] 23 p4024 N85-34937
Application of imaging to the atmospheric Cherenkov technique
[OG-9.5-4] 23 p4030 N85-34981
A method to improve observations of gamma-ray sources near 10 (15) eV
[OG-9.5-5] 23 p4030 N85-34982
The response of a scintillation counter below an emulsion chamber to heavy nucleus interactions in the chamber 24 p4175 N85-35889
Study of the energy spectrum of primary cosmic rays: EAS size fluctuations at a fixed primary energy
[HE-4.4-14] 24 p4194 N85-36020
The experimental cascade curves of EAS at E sub 0 10(17) eV obtained by the method of detection of Cherenkov pulse shape
[HE-4.4-18] 24 p4194 N85-36024

CERENKOV EFFECT

U CERENKOV RADIATION

CERENKOV RADIATION

Cerenkov radiation in the neighborhood of the emission threshold, revised
[AD-A145458] 02 p0284 N85-11855
Generation of superpowerful microsecond electromagnetic radiation pulses
03 p0347 N85-12234
Laser-driven particle accelerators
[DE84-015953] 04 p0506 N85-13227
Cerenkov ring imaging detector development at SLAC
[DE84-015883] 04 p0560 N85-13564
Gamma-ray to Cerenkov-light conversion efficiency for pure-silica-core optical fibers
[DE84-015041] 05 p0729 N85-14685
Monte Carlo simulation of gas Cerenkov detectors
[DE85-002422] 10 p1488 N85-19394
Design consideration for the X-ray Cerenkov experiment
[AD-A153636] 18 p3189 N85-29777
Abundances of secondary elements among the ultra heavy cosmic rays: Results from HEAO-3
20 p3543 N85-32047
Lead, platinum, and other heavy elements in the primary cosmic radiation: HEAO-3 results sec wg032961 cb553097 20 p3543 N85-32048
Cerenkov maser and Cerenkov laser devices
[AD-A155443] 21 p3592 N85-32324
Predictive model of electron beam induced flashblindness
[AD-A155260] 21 p3664 N85-32783
Form factor effects on microwave Cerenkov radiation
[AD-A154577] 21 p3701 N85-32993
1000 GeV gamma rays from Cygnus X-3: An update
[OG-2.1-8] 22 p3863 N85-33925
Evidence for long-term variability in the ultra high energy photon flux from Cygnus X-3
[OG-2.1-10] 22 p3863 N85-33926
Pulsed emission of TeV gamma rays from Vela pulsar
22 p3867 N85-33947
Periodic gamma-ray emissions from Geminga at or = 10(12) eV
[OG-2.4-2] 22 p3867 N85-33949
Search for TeV gamma rays from extragalactic sources and the Galactic Center
[OG-2.7-1] 22 p3871 N85-33976
Absolute rigidity spectrum of protons and helium nuclei above 10 GV/c
[OG-4.1-1] 22 p3875 N85-34007
Cosmic ray charge and energy spectrum measurements using a new large area Cerenkov x dE/dx telescope
[OG-4.1-5] 22 p3876 N85-34011
Cosmic ray isotope measurements with a new Cerenkov X total energy telescope
[OG-4.3-4] 22 p3878 N85-34029
Initial results from the Caltech/DRSI balloon-borne isotope experiment
[OG-4.3-8] 22 p3879 N85-34030
Ariel 6 measurements of ultra-heavy cosmic ray fluxes in the region 34 or = Z or = 48
[OG-4.4-3] 22 p3879 N85-34036
Ariel 6 measurements of ultra-heavy cosmic ray fluxes in the region Z or = 48
[OG-4.4-4] 22 p3880 N85-34037
Elemental abundances of cosmic rays with Z 33 as measured on HEAO-3
[OG-4.4-5] 22 p3880 N85-34038
Abundances of secondary elements among the ultra heavy cosmic rays: Results from HEAO-3
[OG-4.4-6] 22 p3880 N85-34039
A new measurement of the cosmic ray energy spectrum between 3 x 10 to the 15th power eV and 3 x 10 to the 16th power eV
[OG-5.1-6] 22 p3881 N85-34048
Fluctuations of development maximum depth and nuclear composition of primary cosmic radiation
[OG-5.1-13] 22 p3882 N85-34054
Estimation of composition of cosmic rays with E sub zero approximately equals 10(17) - 10(18) eV
[OG-5.1-14] 22 p3882 N85-34055
Cosmic ray spectra measurements at the Yakutsk EAS array
[OG-5.1-17] 22 p3882 N85-34058
Observation of cosmic ray positrons from 5 to 25 GeV
[OG-6.2-5] 22 p3889 N85-34104
A high resolution gas Cerenkov detector for the superconducting magnet facility
[OG-9.1-6] 23 p4023 N85-34932
A Cerenkov imaging telescope for high energy gamma rays
[OG-9.3-13] 23 p4028 N85-34968
The University of Durham Mark 3 very high energy gamma ray telescope
[OG-9.4-2] 23 p4028 N85-34969
Cerenkov light images of EAS produced by primary gamma
[OG-9.5-3] 23 p4030 N85-34979
Angular resolution of an EAS array for gamma ray astronomy energies 5 x 10 (13) eV
[OG-9.5-8] 23 p4031 N85-34985
Cerenkov radiation from periodic electron bunches for finite emission length in air
[AD-A156156] 24 p4090 N85-35352
Simulation of EAS properties on the basis of high energy interaction model deduced from the accelerator data
24 p4187 N85-35973
Sensitivity of depth of maximum and absorption depth of EAS to hadron production mechanism
24 p4188 N85-35982
Muon fluctuation studies of EAS 10(17) eV
[HE-4.3-9] 24 p4191 N85-36003
EAS development curve at energy of 10(16) - 10(18) eV measured by optical Cerenkov light
[HE-4.4-7] 24 p4193 N85-36015
On the determination of the depth of EAS development maximum using the lateral distribution of Cerenkov light at distances 150 m from EAS axis
[HE-4.4-13] 24 p4194 N85-36019

Study of the shower maximum depth by the method of detection of the EAS Cerenkov light pulse shape
[HE-4.4-15] 24 p4194 N85-36021
Analysis of Cerenkov pulses recorded simultaneously at two sites
[HE-4.4-16] 24 p4194 N85-36022
Preliminary results of the Cerenkov EAS flashes the Crimean Astrophysical Observatory
[HE-4.4-17] 24 p4194 N85-36023
Lateral-angular and temporal characteristics of EAS optical radiation
[HE-4.4-19] 24 p4194 N85-36025
The hump in the Cerenkov lateral distribution of gamma ray showers
[HE-4.5-9] 24 p4195 N85-36032
A new study on the emission of EM waves from large EAS
[HE-4.6-5] 24 p4197 N85-36042
Radio wave emitted by an extensive air showers in 10KHz to 1MHz region
[HE-4.6-15] 24 p4198 N85-36051
Longitudinal development of muons in large air showers studies from the arrival time distributions measured at 900m above sea level
[HE-4.7-4] 24 p4199 N85-36055
The thickness of the shower disc as observed in showers produced by primaries above 10 (19)eV
[HE-4.7-6] 24 p4199 N85-36057
Measurements of light background at large depth in the ocean
[HE-5.2-8] 24 p4203 N85-36065
Measurement of muon intensity by Cerenkov method
[HE-5.2-15] 24 p4204 N85-36091
A transient digitiser for fast air shower events
[HE-5.2-21] 24 p4204 N85-36097

CERIUM
NT CERIUM 144
Low temperature properties of CeOe2 in the C14 and C15 crystallographic Laves phases
[DE85-003754] 10 p1564 N85-19666
Improvement by cerium and yttrium ion implantation of oxidation behaviour of stabilised stainless steel in carbon dioxide
[AERE-R-11523] 14 p2259 N85-23966
Long range ordered alloys modified by addition of niobium and cerium
[DE85-011661] 20 p3431 N85-31285
Trivalent cerium doped crystals as tunable laser systems: Two bad apples
[DE85-008168] 22 p3790 N85-33482
Enthalpies of formation of liquid Fe-Ce-Si and Fe-Ce-Al three-component alloys
[BLL-M-36296-(5626.4)] 23 p3913 N85-34247

CERIUM COMPOUNDS
NT CERIUM OXIDES
Cerium compounds in the fashion of the light actinides
[DE84-014642] 04 p0475 N85-13024
Supercell band structure calculations of the two peak photo-and inverse photoemission spectra in Ce and Pr compounds
[DE84-017485] 06 p0867 N85-15513
Fermi surface study of CeSb
[DE85-002532] 10 p1564 N85-19662
The UFe4P12 and CeFe4P12: Non-metallic isotopes of superconducting LaFe4P12
[DE85-003724] 12 p1942 N85-22195
Anomalous magnetism of CeRh3B2 under pressure
[DE85-003089] 13 p2164 N85-23425

CERIUM ISOTOPES
NT CERIUM 144

CERIUM OXIDES
Defect interactions at high concentrations in solid oxide electrolytes
[DE85-011824] 22 p3807 N85-33580

CERIUM 144
High altitude sampling program: Radioactivity in the stratosphere
[DE85-005924] 14 p2374 N85-24676

CERMETS
Strength and failure of ceramic-metallic material
10 p1446 N85-19112
Effect of zero-wear in friction pairs operating in abrasive media
13 p2045 N85-22801
Thin film phase transition materials development program
[AD-A154280] 19 p3259 N85-30209

CERTIFICATION
Certification of advanced systems
08 p0753 N85-14829
Orbiter wheel and tire certification
08 p1101 N85-16959
Preliminary design criteria and certification test specifications for blast resistant windows
09 p1337 N85-18405
GPS system field testing 11 p1711 N85-20762
State measurement laboratories: Program description (part 1). Directory (part 2)
[PB85-137651] 11 p1739 N85-20935
Glider Nimbus 3-24.5. Partial certification test results for importation in the U category
[REPT-CEV/IS/SE/AV/84] 14 p2220 N85-23763
Interactive design of specifications for airborne software set (GISELE)
16 p2714 N85-26753
The certification of airborne complex digital systems
16 p2714 N85-26754
Statistical study of the dynamic analysis of the workload in the A310 certification campaign
16 p2844 N85-27531
Certifying complex digital systems on civil aviation aircraft
17 p2904 N85-27907
A systematic determination of skill and simulator requirements for airline transport pilot certification
[AD-A154135] 19 p3330 N85-30630
Standardization of helicopter certification requirements in the western world
[SNIAS-851-210-103] 20 p3393 N85-31048

CESIUM
NT CESIUM ISOTOPES
NT CESIUM 134
NT CESIUM 137
Multiphoton ionization of atomic cesium
[DE85-001266] 09 p1380 N85-18678
Multiphoton ionization of cesium atoms above and below the two-photon ionization threshold
[DE85-000976] 09 p1381 N85-18682
Effects of dc electric fields on multiphoton ionization spectra in cesium
[DE85-001542] 09 p1381 N85-18684
Calorimetric investigation into the possibility of a charge density wave ground state in alkali metals
[DE85-002006] 09 p1397 N85-18795
Historical cost curves for hydrogen masers and cesium beam frequency and timing standards
10 p1465 N85-19245
Frequency and time standards based on stored ions
18 p3105 N85-29223
On the accuracy of Cs beam primary frequency standards
18 p3105 N85-29224
Diode laser 87Rb optical pumping in an evacuated wall-coated cell
18 p3105 N85-29226
On-orbit frequency stability analysis of the GPS NAVSTAR-1 quartz clock and the NAVSTARs-6 and -8 rubidium clocks
18 p3105 N85-29227
The time and frequency comparisons via Loran-C and National TV Network in Yugoslavia
18 p3109 N85-29248
The 1984 environmental monitoring program report for Idaho National Engineering Laboratory site
[DE85-011209] 22 p3812 N85-33611
Infrared generation and wave-mixing studies in cesium
[DE85-012883] 24 p4063 N85-35304

CESIUM ALLOYS
Mossbauer spectrometry: Testing of a new computer based system and its application to a study of an aluminum-iron-cerium alloy
[AD-A151826] 15 p2510 N85-25483

CESIUM COMPOUNDS
NT CESIUM IODIDES

CESIUM HALIDES
NT CESIUM IODIDES

CESIUM IODIDES
Improvements in photodiode readout for small CsI (T1) crystals
[MPI-PAE/EXP-E1-131] 01 p0051 N85-10333
Downstream behavior of volatile fission product species
[DE85-012124] 23 p3971 N85-34617

CESIUM IONS
Intense non-relativistic cesium ion beam
[DE84-012575] 04 p0560 N85-13566
Collision-induced dipole moments
[AD-A147682] 08 p1121 N85-17063

CESIUM ISOTOPES
NT CESIUM 134
NT CESIUM 137
Portable real-time clock
[AD-A146218] 03 p0364 N85-12336

CESIUM 134
Intrusion of radioactive industrially polluted water from North Sea into central Baltic Sea
10 p1498 N85-19454

CESIUM 137
WESF (173)Cs gamma ray sources
[DE85-000676] 11 p1727 N85-20859
High altitude sampling program: Radioactivity in the stratosphere
[DE85-005924] 14 p2374 N85-24676
Environmental surveillance at Los Alamos during 1984
[DE85-011886] 22 p3811 N85-33605
The 1984 environmental monitoring report, Sandia National Laboratories, Albuquerque, New Mexico
[DE85-011175] 22 p3811 N85-33607
Estimation of Sr90 and Cs137 activity introduced and accumulation in the Po basin until 1983
[CISE-2515] 22 p3813 N85-33617

CESSNA AIRCRAFT
NT CESSNA 402B AIRCRAFT

CESSNA MILITARY AIRCRAFT
U MILITARY AIRCRAFT

CESSNA 402B AIRCRAFT
Design of a digital ride quality augmentation system for commuter aircraft
[AD-A148233] 08 p1086 N85-16879

CF-104 AIRCRAFT
U F-104 AIRCRAFT

CFRP
U CARBON FIBER REINFORCED PLASTICS

CH-47 HELICOPTER
A mathematical simulation model of the CH-47B helicopter, volume 1
[NASA-TM-84351-VOL-1] 01 p0006 N85-10033
Noise measurement flight test for Boeing Vertol 234/CH 47-d helicopter: Data/analyses
[AD-A148172] 08 p1218 N85-17670
A modern control design methodology with application to the CH-47 helicopter
[AD-A151946] 16 p2710 N85-26723

CHAFF
An empirical self-protection chaff model
[AD-A151928] 16 p2773 N85-27115

CHAINS
Kinematic synthesis of planar cam-link mechanisms for exact path and exact motion generation
03 p0341 N85-12189
Safing and arming mechanism
[AD-D011261] 05 p0621 N85-13989
Chain dynamics and structure property relation in high impact strength polycarbonate plastic
[AD-A152011] 15 p2519 N85-25531

CHAIRS
U SEATS

CHALCOGENIDES
NT ALKALINE EARTH OXIDES
NT ALUMINUM OXIDES
NT ANHYDRIDES
NT BARIUM OXIDES
NT BARIUM SULFIDES
NT BERYLLIUM OXIDES
NT BISMUTH OXIDES
NT BORON OXIDES
NT CADMIUM SELENIDES
NT CADMIUM SULFIDES
NT CADMIUM TELLURIDES
NT CALCIUM OXIDES
NT CALCIUM SULFIDES
NT CARBON DIOXIDE
NT CARBON DISULFIDE
NT CARBON MONOXIDE
NT CHLORINE OXIDES
NT CHROMITES
NT CHROMIUM OXIDES
NT COBALT OXIDES
NT COPPER OXIDES
NT COPPER SELENIDES
NT COPPER SULFIDES
NT DIOXIDES
NT DISULFIDES
NT ENSTATITE
NT GERMANIUM OXIDES
NT HYDROGEN PEROXIDE
NT HYDROGEN SULFIDE
NT INDIUM TELLURIDES
NT INORGANIC PEROXIDES
NT IRON OXIDES
NT LEAD OXIDES
NT LEAD TELLURIDES
NT LITHIUM OXIDES
NT MAGNESIUM OXIDES
NT MAGNETITE
NT MANGANESE OXIDES
NT MERCURY TELLURIDES
NT METAL OXIDES
NT MOLYBDENUM DISULFIDES
NT MOLYBDENUM OXIDES
NT NICKEL OXIDES
NT NIOBIUM OXIDES
NT NITRIC OXIDE
NT NITROGEN DIOXIDE
NT NITROGEN OXIDES
NT NITROGEN TETROXIDE
NT NITROUS OXIDES
NT ORGANIC PEROXIDES
NT OXIDES
NT PEROXIDES
NT PLUTONIUM OXIDES

NT POLYSULFIDES
NT POTASSIUM OXIDES
NT PYRITES
NT PYROXENES
NT QUARTZ
NT RUTILE
NT SAPPHIRE
NT SELENIDES
NT SILICON DIOXIDE
NT SILICON OXIDES
NT SULFIDES
NT SULFUR DIOXIDES
NT SULFUR OXIDES
NT TIN OXIDES
NT TIN TELLURIDES
NT TITANIUM OXIDES
NT TROILITE
NT VANADIUM OXIDES
NT YTTRIUM OXIDES
NT ZINC OXIDES
NT ZINC SELENIDES
NT ZINC SULFIDES
NT ZIRCONIUM OXIDES
Effect of light pulses on film of chalcogenide vitreous semiconductors 02 p0258 N85-11687
Neutron scattering for the investigation of solid state materials, utilization in chemical structures 03 p0432 N85-12752
High temperature thermoelectric energy conversion 05 p0610 N85-13894
Preliminary studies on the low-cost preparation of chalcogenide semiconductors from solution depositions [DE85-000538] 11 p1736 N85-20918
Multilayer reflecting systems based on glassy chalcogenides for infrared lasers 14 p2274 N85-24089

CHALLENGER (ORBITER)
National Space Transportation Systems Program mission report [NASA-TM-87455] 14 p2242 N85-23900

CHAMBERS
Heat exchanger [DE84-014299] 01 p0047 N85-10309

CHANCE-VOUGHT MILITARY AIRCRAFT
U MILITARY AIRCRAFT

CHANDLER MOTION
U POLAR WANDERING (GEOLOGY)

CHANDRASEKHAR EQUATION
Chandrasekhar equations and computational algorithms for distributed parameter systems [NASA-CR-172467] 03 p0402 N85-12564
Chandrasekhar equations for infinite dimensional systems [NASA-CR-172515] 09 p1376 N85-18651

CHANGE DETECTION
An amplitude correlation and differencing method for the monitoring of flaws in repeat ultrasonic inspections [AERE-R-11416] 15 p2571 N85-25854

CHANNEL CAPACITY
A system for measuring the characteristics of the ionospheric channel by digital transmissions 10 p1472 N85-19287
Serial data transmission with large output on the HF channel 10 p1475 N85-19305
The coding capacity of mismatched Gaussian channels [AD-A149453] 10 p1551 N85-19782

CHANNEL FLOW
NT OPEN CHANNEL FLOW
The effect of channel convergence on heat transfer in a passage with short pin fins [NASA-TM-83801] 01 p0046 N85-10303
Vertical channel free convection for a power law fluid with a constant heat flux [DE84-014551] 01 p0047 N85-10311
Direct numerical simulation of curved turbulent channel flow [NASA-TM-86074] 02 p0197 N85-11316
The structure of the vorticity field in turbulent channel flow. Part 2: Study of ensemble-averaged fields [NASA-TM-86657] 03 p0361 N85-12317
Modelling the aerodynamics in a system of continuous channels and experimentation procedure [BLL-M-35923-(5828.4)] 05 p0634 N85-14067
Direct numerical simulation of curved turbulent channel flow 05 p0835 N85-14072
Channel constructed to provide well defined boundary layers for vorticity optical probe measurements [AD-A146679] 06 p0809 N85-15140
Shock waves in transonic flows at moderate Reynolds Number 08 p1076 N85-16823
A study of Reynolds-stress closure model [NASA-CR-174342] 08 p1161 N85-17324
On limits of applicability of linear models to dynamics of gas channels in aircraft engines 09 p1308 N85-18219
Application of large eddy interaction model to channel flow [NASA-TM-86691] 12 p1844 N85-21572
A three-dimensional spectral algorithm for simulations of transition and turbulence [NASA-CR-172561] 12 p1845 N85-21575
Turbulent wake of a submerged flat plate [AD-A153776] 16 p3100 N85-29190
Finite amplitude stability of a Rossby wave in a channel 19 p3314 N85-30543
Finite analytic solutions of supersonic flows in two-dimensional non-symmetrical channels 24 p4059 N85-35154

CHANNEL MULTIPLIERS
Analysis of a coded, M-ary orthogonal input optical channel with random-gain photomultiplier detection 05 p0624 N85-13990
Correlation of intensities of different scattering channels 21 p3694 N85-32952

CHANNEL NOISE
SVKD and SVKM-3 seismographs with a low-sensitivity channel [REPT-553] 03 p0376 N85-12396
Synthesis of systems for coherent weighted signal processing against background of correlated interference 06 p0790 N85-15045

CHANNELS
Novel applications of the NASA/GSFC Viterbi decoder hardware simulator 08 p1101 N85-16957
The effect of jamming/deception on decision making [AD-A149740] 12 p1828 N85-21472
Study of fatigue strength of shafts with segmented channels 14 p2282 N85-24136
Receiver optimization for detection in doubly spread communication channels [AD-A151226] 15 p2541 N85-25689
Current enhancement in a conducting channel [AD-A155418] 22 p3845 N85-33812
Recombination and ionization in a nitrogen plasma [AD-A155426] 22 p3845 N85-33813

CHANNELS (DATA TRANSMISSION)
Gaussian Wide Sense Stationary Uncorrelated Scattering (GWSSUS) channel simulation program to be used for mobile radio systems [FUB-40-1963] 01 p0041 N85-10265
Atmospheric channel performance measurements at 10 to 100 GHz [PB84-211325] 01 p0042 N85-10271
Evaluation of criteria for selecting the spectral attributes of digital LANDSAT MSS imagery for discriminating lithological units in the lower Curaca River Valley, Bahia — Brazil [E85-10036] 03 p0379 N85-12415
Formation of reference signals in laser-type gas analyzers with mechanical switching of optical channels 06 p0787 N85-15027
A perspective on multiaccess channels [AD-A146606] 06 p0799 N85-15105
Systems study for an Integrated Digital-Electric Aircraft (IDEA) [NASA-CR-3840] 07 p0902 N85-15714
Evolution toward a multi-bus architecture for Army helicopter avionic systems 08 p1074 N85-16812
Integration of sensor fusion in advanced helicopter cockpit design 08 p1074 N85-16813
Multidimensional digital signal processing [AD-A148055] 08 p1205 N85-17585
Reed-Solomon code synchronization revisited 10 p1464 N85-19234
Propagation Influences on Digital Transmission Systems: Problems and Solutions [AGARD-CP-363] 10 p1469 N85-19269
Digital data communications over microwave radio channels 10 p1469 N85-19272
A review of atmospheric multipath measurements and digital system performance 10 p1470 N85-19279
An ionospheric mode detection system for HF communications application 10 p1471 N85-19282
Time and space domain filtering for improved HF communication 10 p1473 N85-19298
Extracting digital data from a bus and multiplexing it with a video signal [AD-D011491] 11 p1636 N85-20302
Prelaunch absolute radiometric calibration of the reflective bands on the LANDSAT-4 protoflight Thematic Mapper 11 p1669 N85-20515
The 20:16 block code for digital recording and transmission channels [BBC-RD-1985/1] 12 p1824 N85-21443
Digital channel efficiency model [AD-A150084] 12 p1829 N85-21479
Data compression for noiseless channels 13 p2053 N85-22651
Horizontal deflection TS-257 13 p2069 N85-22926
Dynamics of adaptive signal corrector 13 p2071 N85-22940
Interactive communication channel [AD-D011580] 15 p2542 N85-25695
Multi-access fiber optic data bus using FDM/FSK [NASA-CR-175739] 15 p2621 N85-26152
On the throughput of channel access algorithms with limited sensing [AD-A151984] 15 p2630 N85-26208
A study of topologies and protocols for fiber optic local area network [NASA-CR-175771] 16 p2864 N85-27669
Introduction to the IEEE-488 bus [INPE-3316-NTE/227] 17 p3010 N85-29813
High performance asynchronous limited sensing algorithms for CSMA and CSMA-CD channels [AD-A153919] 18 p3171 N85-29650
Adaptive corrector operating in frequency domain 22 p3765 N85-33337
Optimum predistortion of digital signals for transmission over parallel channels 22 p3776 N85-33397
Estimate of signal-to-interference energy ratio in discrete-data transmission 22 p3776 N85-33398
Operations considerations in designing a high speed multi-channel data acquisition system [DE85-012840] 24 p4154 N85-35756

CHANNELTRONS
U CHANNEL MULTIPLIERS

CHAOS
Chaos near the Coulomb Barrier: Nuclear molecules [DE85-001280] 07 p1041 N85-16608
Synchrotron emission from chaotic stellar winds 08 p1234 N85-17774
Chaotic dynamics of instabilities in solids [DE85-004909] 14 p2429 N85-24978
Chaos and order in an optical ring cavity [CWI-AM-R8416] 17 p3038 N85-28795

CHAOTIC CLOUD PATTERNS
U CLOUDS (METEOROLOGY)

CHAPMAN SHEAR LAYER
U SHEAR LAYERS

CHAPMAN-ENSKOG THEORY
Surface-slip equations for multicomponent nonequilibrium air flow [NASA-TM-85820] 12 p1845 N85-21573

CHAPMAN-JOUGET FLAME
U CHEMICAL EQUILIBRIUM
U DETONATION
U FLAME PROPAGATION

CHARACTER RECOGNITION
Comparative review of single-line and multiline optical character readers used in mail processing [PB84-234824] 04 p0548 N85-13489
The combinatorics of local constraints in model-based recognition and localization [AD-A148338] 08 p1230 N85-17746
ONR (Office of Naval Research) Far East Scientific Bulletin, volume 9, number 3, July to September 1984 [AD-A147282] 08 p1262 N85-17930
Character recognition using correlation techniques [AD-A152006] 16 p2847 N85-27549

CHARACTERISTIC EQUATIONS
U EIGENVALUES
U EIGENVECTORS

CHARACTERISTIC FUNCTIONS
U EIGENVALUES
U EIGENVECTORS

CHARACTERISTIC METHOD
U METHOD OF CHARACTERISTICS

CHARACTERIZATION
Synthesis and characterization of advanced materials [PB84-215326] 01 p0025 N85-10156
Novel techniques for the fabricating and characterization of GaAs MIS (Metal Insulator Semiconductor) structures [AD-A145766] 03 p0358 N85-12301
The TA6Zr5D (IMI 685) characterization in strain controlled tests. (Specimens obtained from a forged spinning wheel) no. M4-45870 [M4-45870] 03 p0373 N85-12384
Quality assurance of composite materials, test report no. 45-849/F 04 p0489 N85-12981
Characterization of aluminum alloy 7010 in moderate width plate and T651 and T7651 metallurgical states [REPT-44-606/F] 05 p0619 N85-13961
The synthesis, structural characterization and reactions of closo-Rhodacarborane Anions containing a formal d8 metal vertex 1,2 [AD-A149640] 12 p1799 N85-21285
Production and characterization of amorphous silicon (a-Si:H) as base material for solar cells 12 p1879 N85-21791
Electrical characterization of analog microprocessors [AD-A149629] 12 p1911 N85-21985
Crack propation in unidirectional laminates by the stress intensity factors 18 p3121 N85-29320

Loss-of-flow transient characterization in carbide-fueled LMFBRs
[DE85-009552] 19 p3289 N85-30270
CHARACTERS
U SYMBOLS
CHARCOAL
NT ACTIVATED CARBON
A comprehensive review of black powder
[AD-A150455] 13 p2039 N85-22769
Remarks on preparation of indandione detection reagents
[NASA-TM-77905] 21 p3580 N85-32146
CHARGE CARRIERS
NT FREE ELECTRONS
NT HOLES (ELECTRON DEFICIENCIES)
NT MINORITY CARRIERS
Lifetime of excess charge carriers in weakly doped epitaxial GaAs layers 04 p0487 N85-13108
Determination of parameters of doped thin semiconductor layers from plasmatic minimum of reflection coefficient for infrared radiation 07 p0954 N85-16047
Current carriers for the field-aligned current system
[NASA-TM-86161] 06 p1260 N85-17925
A picosecond population modulation study of near interband resonances in semiconductors 09 p1396 N85-18787
Determination of the mobility profile in GaAs-MESFETs
[NASA-TM-77818] 11 p1734 N85-20905
Characterization of high purity Si-doped molecular beam epitaxial GaAs
[AD-A149651] 12 p1939 N85-22181
A scanning optical microprobe for infrared detector measurement
[AD-A151748] 15 p2653 N85-26381
Carrier loss in dispersive transport in amorphous semiconductors
[DE85-009122] 18 p3194 N85-29811
Influence of coherent light beams on free carriers in semiconductors 21 p3681 N85-32867
Hermetic chip carrier compliant soldering pads
[AD-D011722] 23 p3938 N85-34410
CHARGE COUPLED DEVICES
Multiple object spectroscopy: The MX spectrometer design 02 p0296 N85-11920
Electronic bandwidth compression module
[AD-A145843] 03 p0366 N85-12343
Characterization of electronic streak tubes including one with internal CCD readout
[DE84-016823] 05 p0639 N85-14096
Electronic satellite imaging system MOMS-ESA
[BMFT-FB-W-84-033] 05 p0661 N85-14248
Electrooptical sensor for automatic detection of objects 06 p0789 N85-15040
Numerical estimation of charge transfer time in charge-coupled device employing latent gallium arsenide channel 06 p0793 N85-15069
Oblique focus ICCD laboratory evaluation
[NASA-CR-174205] 06 p0862 N85-15480
Study of alternate optical and fine guidance sensor designs for the space infrared telescope facility (SIRTF)
[NASA-CR-166814] 07 p0915 N85-15794
Design and fabrication of a CCD camera for use with relay optics in solar X-ray astronomy
[NASA-CR-174334] 08 p1164 N85-17344
A CCD system for photometry of direct and spectroscopic images 08 p1252 N85-17904
CCDs: Their cause and cure 08 p1252 N85-17905
Time series photometry with a CCD camera 08 p1252 N85-17906
Airborne remote sensing CCD imaging system 11 p1623 N85-20220
Intensified CCD camera system for plasma diagnostics
[DE85-002252] 12 p1853 N85-21620
Monolithic short wave infrared (SWIR) detector array
[NASA-CR-175284] 12 p1874 N85-21759
Development of high resolution imaging detectors for X-ray astronomy
[NASA-CR-175505] 12 p1953 N85-22286
French firm develops new kind of CTD camera for robots 15 p2523 N85-25556
Parallel programmable charge domain device
[AD-D011599] 15 p2549 N85-25733
Summary of optical groundbased E ring observations at the University of Arizona 15 p2671 N85-26482
INPE's line imaging camera: Preliminary results
[INPE-3476-PRE/719] 16 p2767 N85-27194
Self-scanning MOS-integrated photosensor strip 17 p2940 N85-28151
Pipelined programmable charge domain device
[AD-D011598] 17 p2951 N85-28225
Techniques for operating Charge Coupled Devices (CCD's) in very high speed framing mode
[AD-A152878] 17 p2953 N85-28238
Energizing arrangement for charge coupled device control electrodes
[AD-D011712] 19 p3261 N85-30220
The Extended Range X-Ray Telescope center director's discretionary fund report
[NASA-TM-86507] 19 p3362 N85-30983
CCD-based X-ray spectrometry for on-line determination of laser plasma electron temperature 21 p3692 N85-32938
Solid state research
[AD-A154783] 21 p3709 N85-33025
Microcomputer controlled image processor
[AD-D011734] 22 p3833 N85-33735
The nature and origin of outer solar system asteroids from reflectance spectrophotometry 24 p4168 N85-35838
Application of thermoluminescence for detection of cascade shower 1: Hardware and software of reader system
[HE-7.1-6] 24 p4213 N85-36160
Spatial distribution read-out system for thermoluminescence sheets
[HE-7.1-7] 24 p4213 N85-36161
Application of thermoluminescence for detection of cascade shower 2: Detection of cosmic ray cascade shower at Mount Fuji
[HE-7.1-12] 24 p4214 N85-36162
CHARGE DISTRIBUTION
Minimizing the energy spread within a single bunch by shaping its charge distribution
[DE84-016172] 05 p0727 N85-14676
Mathematical physics approaches to lightning discharge problems
[NASA-TM-86349] 08 p1187 N85-17482
Accelerator column models for low-current beams
[DE85-010722] 19 p3262 N85-30226
Form factor effects on microwave Cerenkov radiation
[AD-A154577] 21 p3701 N85-32993
Charge composition and energy spectral of cosmic ray primary particles for energies higher than 1 TeV
[OG-4.1-14] 22 p3877 N85-34020
Electron photoejection in carbanions
[DE85-011747] 23 p3911 N85-34230
Electron photoejection in carbanions
[DE85-011748] 23 p3912 N85-34237
Calculations of heavy ion charge state distributions for nonequilibrium conditions
[SH-2.1-12] 23 p3999 N85-34793
On the influence of the heliomagnetospheric periphery on the galactic cosmic rays
[SH-4.2-19] 23 p4009 N85-34856
Lateral distribution on charged particles in EAS
[HE-4.3-15] 24 p4192 N85-36009
Lateral distribution of high energy muons in EAS of sizes Ne approximately equals 10(5) and Ne approximately equals 10(6)
[HE-4.3-16] 24 p4192 N85-36010
Properties of 10 (18)-10 (19)eV EAS at far core distance
[HE-4.7-3] 24 p4198 N85-36054
CHARGE EFFICIENCY
Electrical and thermal performance during charging and discharging a Phase 1 gel cell battery
[PB85-114312] 11 p1677 N85-20565
State-of-charge coulometer
[NASA-CASE-NPO-15759-1] 12 p1849 N85-21596
Kapton charging characteristics: Effects of material thickness and electron-energy distribution 13 p1996 N85-22513
An improved battery state-of-charge indicator
[NASA-CR-175701] 14 p2298 N85-24227
Method for determining the point of zero zeta potential of semiconductor
[NASA-CASE-LAR-12893-1] 19 p3373 N85-30923
Modeling taper charge with a non-linear equation 20 p3445 N85-31390
A 34 ampere-hour nickel-cadmium minimum trickle charge testing 20 p3446 N85-31394
Two-dimensional inversion of resistivity monitoring data from the Cerro Prieto geothermal field
[DE85-012554] 24 p4113 N85-35494
CHARGE EXCHANGE
Twisted domain wall in very thin magnetic films with perpendicular anisotropy 03 p0350 N85-12252
Experimental investigations in particle physics at intermediate energies
[DE85-001481] 11 p1722 N85-20832
Time dependent Hartree-Fock theory of ion-atom collisions: Application to F(9+) + Ne
[DE85-003083] 11 p1723 N85-20838
Atomic processes involving impurities in the plasma edge
[DE85-001277] 11 p1730 N85-20882
Theoretical study of near-threshold electron-molecule scattering
[DE85-004530] 12 p1930 N85-22126
Development of an apparatus for obtaining molecular beams in the energy range from 2 to 200 eV
[NASA-TM-77835] 15 p2647 N85-26326
Germanium detectors with a built-in transverse drift field
[DE85-009944] 18 p3096 N85-29165
Excited state populations and charge-exchange of fast ions in solids
[DE85-009382] 18 p3180 N85-29714
An alpha particle diagnostic beam line system to generate an intense Li(O) beam with an ORNL SITEX source
[DE85-010564] 18 p3182 N85-29730
Resonant-transfer-and-excitation for highly charged ions (16 or = Z or = 23) in collisions with helium
[DE85-010550] 19 p3359 N85-30623
The production and destruction of metastable negative ions
[DE85-011056] 19 p3364 N85-30658
Discussion session: Nucleon- and antinucleon-nucleus inelastic scattering and charge exchange
[DE85-010723] 19 p3364 N85-30660
Evaluated nuclear-data file for niobium
[DE85-012095] 21 p3704 N85-33009
Calculated neutron-induced cross sections for /sup 63,65/Cu/sup 58,60/Ni and (52) Cr from 1 to 20 MeV and comparisons with experiments
[DE85-011926] 22 p3844 N85-33808
Propagation and secondary production of low energy antiprotons in the atmosphere
[OG-6.1-3] 22 p3887 N85-34094
Noble metals as incipient transition metals
[DE85-013263] 24 p4080 N85-35286
Is the inelastic charge-exchange contribution constant at the large X and superhigh energies? Qaut 01Kuchin, I. A. 24 p4173 N85-35871
A study of gamma-families generated in nucleon-nucleus (NA) and pion-nucleus (pi A) interactions
[HE-3.7-2] 24 p4186 N85-35961
CHARGE INJECTION DEVICES
Photometry with Multi-Anode Microchannel Arrays (MAMAs) and Charge Injection Devices (CIDs) 08 p1252 N85-17909
Performance of charge-injection-device infrared detector arrays at low and moderate backgrounds
[NASA-TM-86667] 15 p2560 N85-25793
CHARGE SEPARATION
U POLARIZATION (CHARGE SEPARATION)
CHARGE TRANSFER
Study of application of organic semiconductors to electronic components
[BMFT-FB-T-84-142] 02 p0289 N85-11890
Theoretical studies of highly ionized species
[DE84-016797] 04 p0561 N85-13574
Laboratory studies of atomic collision processes of importance in planetary atmospheres
[NASA-CR-174142] 04 p0589 N85-13758
Numerical estimation of charge transfer time in charge-coupled device employing latent gallium arsenide channel 06 p0793 N85-15069
Recent development in astronomic position determinations
[AD-A148335] 08 p1082 N85-16858
Correlation of electronic charge transfer transitions and electrochemical potentials. The Bipyrazine(Tetracarbonyl)Molybdenum(O) system in various solvents
[AD-A147660] 08 p1120 N85-17062
Study of charge transport in the thermoelectret state of some ceramics and glasses
[DE85-001763] 09 p1300 N85-18163
Battery response to pulse loads: A mathematical model
[DE85-001149] 09 p1316 N85-18277
Process for preparing highly optically transparent-colorless armomatic polyimide film
[NASA-CASE-LAR-13351-1] 12 p1811 N85-21360
Observation of a novel low-lying excited state in zinc complexes
[AD-A150188] 13 p2156 N85-23385
Charge transfer, polarization and relaxation effects in the Auger lineshapes of Si
[AD-A150938] 14 p2252 N85-23054
Charge isolation in a spatial light modulator
[AD-D011581] 15 p2652 N85-26356
Neutralization and excitation in low-energy ion-surface collisions
[AD-A151568] 15 p2660 N85-26414
Theory of electron-impact atomic ionization cross sections
[AD-A151763] 16 p2861 N85-27648
Investigation of charge transport in the thermoelectret state of some ceramics and glasses
[DE85-009318] 17 p2936 N85-28122

The mean trajectory approximation for charge and energy transfer processes at surfaces
[AD-A152708] 17 p3043 N85-29830
Characteristics of charge transfer in the dispersed phase of electrorheological suspensions
[RAE-TRANS-2125] 19 p3233 N85-30040
Photoeffects of semiconductor electrolyte interfaces
[AD-A154163] 20 p3449 N85-31411
Polymer-water interaction studies
21 p3609 N85-32411

CHARGE TRANSFER DEVICES
NT CHARGE COUPLED DEVICES
NT CHARGE INJECTION DEVICES
Charge Injection Device (CID) used as a photodector: Implementation and performance. Application to light source tracking (stars, lasers)
[CNES-83/CT/DRT/TIT/OE/148] 20 p3533 N85-31983

CHARGED PARTICLES
NT ALPHA PARTICLES
NT ANIONS
NT ANTIPROTONS
NT ARGON PLASMA
NT BETA PARTICLES
NT BOUNDARY LAYER PLASMAS
NT CATIONS
NT COLD PLASMAS
NT COLLISIONAL PLASMAS
NT COLLISIONLESS PLASMAS
NT CONDUCTION ELECTRONS
NT COSMIC PLASMA
NT CYLINDRICAL PLASMAS
NT DENSE PLASMAS
NT DEUTERIUM PLASMA
NT DEUTERONS
NT ELECTRON PLASMA
NT ELECTRONS
NT ELLIPTICAL PLASMAS
NT ENERGETIC PARTICLES
NT EVEN-EVEN NUCLEI
NT FERRIC IONS
NT FREE ELECTRONS
NT HEAVY NUCLEI
NT HELIUM PLASMA
NT HIGH ENERGY ELECTRONS
NT HIGH TEMPERATURE PLASMAS
NT HOT ELECTRONS
NT HYDROGEN PLASMA
NT HYPERNUCLEI
NT INNER RADIATION BELT
NT LASER PLASMAS
NT MAGNETICALLY TRAPPED PARTICLES
NT METAL IONS
NT METALLIC PLASMAS
NT NEGATIVE IONS
NT NEGATRONS
NT NITROGEN PLASMA
NT NONEQUILIBRIUM PLASMAS
NT NONUNIFORM PLASMAS
NT NUCLEI (NUCLEAR PHYSICS)
NT ODD-EVEN NUCLEI
NT ODD-ODD NUCLEI
NT OUTER RADIATION BELT
NT PHOTOELECTRONS
NT PLASMA CLOUDS
NT PLASMA FOCUS
NT PLASMA LAYERS
NT PLASMA SHEATHS
NT PLASMAS (PHYSICS)
NT POLARONS
NT POSITIVE IONS
NT POSITRONS
NT PROTON BELTS
NT PROTONS
NT RADIATION BELTS
NT RELATIVISTIC ELECTRON BEAMS
NT RELATIVISTIC PLASMAS
NT ROTATING PLASMAS
NT SEMICONDUCTOR PLASMAS
NT SOLAR ELECTRONS
NT SOLAR PROTONS
NT SOLAR WIND
NT SPACE PLASMAS
NT SPHERICAL PLASMAS
NT STELLAR WINDS
NT STRONGLY COUPLED PLASMAS
NT THERMAL PLASMAS
NT TOROIDAL PLASMAS
Behavior of charged particles in lower ionosphere with acoustical effects 02 p0161 N85-11089
Charged particle erosion of icy satellites: Coronal atmospheres and surface redistribution
03 p0448 N85-12845
Cerankov ring imaging detector development at SLAC
[DE84-015883] 04 p0560 N85-13564
Charge trapping in low temperature MOS (Metal-Oxide-Silicon) oxides
[AD-A146450] 06 p0860 N85-15467
Fermilab research program workbook
[DE84-012568] 06 p0862 N85-15476
Earth's radiation belts
[AD-A147927] 07 p0998 N85-16339
Beam propagation studies at NRL (Naval Research Laboratory) July 1983 to June 1984, volume 2
[AD-A148198] 08 p1152 N85-17270
Force balance limiting current for charged particle beams
[DE84-016976] 09 p1381 N85-18685
One-electron capture processes by highly charged ions from helium: Present status of HICE-IPP
09 p1389 N85-18736
Diffusion of particles in a slowly modulated wave
[DE85-000729] 09 p1391 N85-18756
Ozone measurements in the mesosphere during a solar proton event 11 p1665 N85-20490
Self-Optimized Sector (SOS) model of self-consistent energy loss and scattering for an electron beam propagating in air
[DE85-003161] 11 p1722 N85-20831
Covariant lie-transformed plasma action principle
[DE85-000295] 11 p1732 N85-20891
SCATHA (spacecraft charging at high altitudes) plasma interaction experiment: SC-3 high energy particle spectrometer; SC-6 energetic ion composition experiment
[AD-A149728] 12 p1793 N85-21252
S3-3 ONR-118 data analysis
[AD-A149725] 12 p1889 N85-21855
Characteristics of latitude effect on cosmic ray charged component in atmosphere at altitudes 3-5 KM
13 p1978 N85-22413
Observation of cosmic ray flux variations in stratosphere 13 p1981 N85-22430
Suprathermal plasma observed on STS-3 Mission by plasma diagnostics package 13 p1988 N85-22472
Discharges on a negatively biased solar cell array in a charged-particle environment 13 p1994 N85-22499
EMI characteristics of a potential control system
13 p1994 N85-22502
Spacecraft environmental interactions: A joint Air Force and NASA research and technology program
13 p1997 N85-22517
Variable flexing device for targets in internal beams of charged particle accelerators 13 p2044 N85-22797
Scattering of electromagnetic waves by charged particles 13 p2067 N85-22913
Nonrelativistic Kapitza-Dirac scattering
[AD-A150822] 13 p2159 N85-23405
Local phase transformation in alloys during charged-particle irradiation
[DE85-005012] 14 p2258 N85-23990
The access of energetic charged particles to satellite altitudes
[AD-A150799] 14 p2373 N85-24670
Active Magnetospheric Particle Tracing Explorers (AMPTE)
[AD-A151072] 14 p2374 N85-24674
Nonrelativistic Kapitza-Dirac scattering
[AD-A150649] 14 p2417 N85-24911
First- and second-order charged particle optics
[DE85-006310] 14 p2421 N85-24940
Space radiation monitor observations from Salyut-4 orbital station 15 p2482 N85-25317
Beam trapping in high current cyclic accelerators with strong focusing fields
[AD-A151392] 15 p2648 N85-26331
Gravitational effects in theories with interacting fields: Two studies 15 p2663 N85-26435
Implications for supersymmetry of the CERN monojets
[DE85-008178] 17 p3030 N85-29741
Conversion efficiencies of charged particle beam driven free electron lasers
[AD-A154404] 19 p3276 N85-30316
Circular-beam ray tracing on a microcomputer
[DE85-010754] 19 p3336 N85-30685
LINE: A code which simulates spectral line shapes for fusion reaction products generated by various speed distributions
[DE85-010633] 19 p3341 N85-30702
Present and future directions of atomic physics research with multiply-charged ions at Brookhaven National Laboratory
[DE85-010980] 19 p3354 N85-30788
Surface effects on sputtered atoms and their angular and energy dependence
[DE85-010506] 19 p3354 N85-30790
Radiation interactions for tomography
[DE85-008961] 19 p3355 N85-30799
High-energy particle Monte Carlo at Los Alamos
[DE85-010716] 19 p3363 N85-30856
Energy-advanced nuclear data: Measurements and physical interpretations
[DE85-006196] 19 p3366 N85-30872
Schottky theory of three component plasmas
[AD-A154461] 19 p3371 N85-30907
Monte-Carlo treatment of nonlinear collisional effects in charged-particle transport
[DE85-010755] 20 p3521 N85-31897
Studies in mixed species charged particle beam dynamics
[OUEL-1545/84] 20 p3531 N85-31969
Trapping of ion conics by downward parallel electric fields
[AD-A155306] 21 p3633 N85-32568
Classical emission of relativistic charged particles during axial channeling 21 p3681 N85-32871
Transformation of charged particle beams by concentrating electro-optical systems
21 p3690 N85-32925
Mirror reflection of charged particles from amorphous and polycrystalline surfaces 21 p3690 N85-32927
Possibility of developing charged-particle energy analyzer based on hyperboloidal axisymmetrical lens
21 p3691 N85-32933
Multistage spent particle collector and a method for making same
[NASA-CASE-LEW-13914-1] 22 p3791 N85-33489
Bibliography and index for nuclear reactions among light charged particles, volume 26
[DE85-011482] 22 p3838 N85-33768
Heavy quarks and CP: Moriond 1985
[DE85-010553] 22 p3841 N85-33790
High-energy multiple muons and heavy primary cosmic-rays
[OG-5.2-9] 22 p3883 N85-34065
Effect of seeds of heavy charged particles of galactic cosmic radiation 23 p3954 N85-34505
Theoretical and computational research on the focused transport of intense charged particle beams
[DE85-012960] 23 p3972 N85-34821
Guiding center distribution function and longitudinal invariant 23 p3978 N85-34883
Acceleration of ions and electrons to near-cosmic ray energies in a perpendicular shock: The January 6, 1978 event
[SH-1.5-4] 23 p3996 N85-34773
The Jovian electron spectrum: 1978-1984
[SH-1.5-19] 23 p3998 N85-34782
Silicon to iron abundances in solar cosmic rays and in the sun
[SH-2.1-6] 23 p3998 N85-34787
The mean ionic charges of N, Na, MG, SI and S in solar energetic particle events
[SH-2.1-11] 23 p3999 N85-34792
On the connection between the 3HE-enrichment and spectral index of solar energetic particles
[SH-2.2-9] 23 p4001 N85-34804
The dispersive evolution of charged-particle bunches in random magnetic fields
[SH-4.1-2] 23 p4004 N85-34828
Spatial distribution of cosmic rays in magnetic cycles of the Sun
[SH-4.2-20] 23 p4009 N85-34857
The dependence of solar modulation on the sign of the cosmic ray particle charge
[SH-4.2-23] 23 p4009 N85-34860
Observation of energy spectrum of electron albedo in low latitude region at Hyderabad, India
[SH-6.1-7] 23 p4045 N85-35081
The influence of quiet asymmetric magnetosphere on the cutoff rigidities of the main cone
[SH-6.1-10] 23 p4045 N85-35083
A bi-directional charged particle telescope to observe flux, energy spectrum and angular distribution of relativistic and non-relativistic particles
[SH-9.1-4] 23 p4050 N85-35119
Burst size distributions in the digitized data of the ion chambers t Mt. Norikura and sea level stations
[SH-9.1-9] 23 p4051 N85-35124
Plastic scintillators in coincidence for the study of multi-particle production of sea level cosmic rays in dense medium
[SH-9.1-11] 23 p4052 N85-35126
Observation of nuclei with energies 8-30 MeV per nucleon in the Earth's magnetosphere at the altitudes 350 KM
[SH-10.1-5] 23 p4053 N85-35136
The effect of the relative nuclear size on the nucleus-nucleus interactions
[HE-1.4-13] 24 p4177 N85-35900
Experimental basis for the models of cascade propagation in atmosphere
[HE-3.6-6] 24 p4185 N85-35954

The lateral distributions of charged particles of energy greater than 0.3 E sub crit in electron-photon cascades in lead and air
[HE-3.6-10] 24 p4185 N85-35957
A study of gamma-families generated in nucleon-nucleus (NA) and pion-nucleus (pi A) interactions
[HE-3.7-2] 24 p4186 N85-35961
Lateral distribution on charged particles in EAS
[HE-4.3-15] 24 p4192 N85-36009
Muon spectrum in air showers initiated by gamma rays
[HE-4.5-4] 24 p4195 N85-36026
High energy cosmic ray signature of quark nuggets
[HE-6.2-11] 24 p4212 N85-36147
Experimental investigation of radiative-acoustic effects in the water by the thermodynamical conditions of Dumand
[HE-7.1-2] 24 p4213 N85-36156

CHARM (PARTICLE PHYSICS)
Anomalies in cosmic rays: New particles versus charm?
[HE-5.4-9] 24 p4206 N85-36120
Collimated groups of particles as possible manifestation of heavy meson production
[HE-5.4-14] 24 p4206 N85-36124
Tien-Shan effect and charmed particles
[HE-6.2-17] 24 p4212 N85-36153

CHARON
Research in planetary studies and operation of Mauna Kea Observatory
[NASA-CR-175618] 13 p2169 N85-23460

CHARPY IMPACT TEST
The influence of rare Earth elements on the temper embrittlement behaviour and mechanical properties of a low alloy steel 02 p0180 N85-11210
Instrumented impact testing machine with reduced specimen oscillation effects
[VTT-290] 04 p0504 N85-13218
Statistical aspects of shear fracture propagation
[ERS-E.368] 09 p1341 N85-18434
Development of an automated miniature Charpy test method
[DE85-003011] 11 p1652 N85-20405
The Hopkinson pressure bar: An alternative to the instrumented pendulum for Charpy tests
[OUEL-1566/85] 20 p3471 N85-31569
Inertial analysis of the Charpy test
[OUEL-1571/85] 20 p3471 N85-31570

CHARTS
NT FLOW CHARTS
NT GRAPHS (CHARTS)
NT METEOROLOGICAL CHARTS
NT NAUTICAL CHARTS
A program to produce standard shewhart control charts for the statistics X-bar and R or S, P, NP, C, or U
[AD-A146971] 07 p1024 N85-16501
Commercial data base management system for geonames data base
[AD-A150835] 14 p2433 N85-25007
Dialog system with minicomputer for plotting performance charts 22 p3768 N85-33355

CHASSIS
The guidelines to design the lever turning gears in articulated vehicles
[AD-P004301] 09 p1409 N85-18878

CHEBYSHEV APPROXIMATION
Calibration of hail probes
[CSIR-NAC-83-04] 01 p0116 N85-10794
Minimax optimal control in the reentry of a space glider 02 p0167 N85-11124
Boundary conditions in Chebyshev and Legendre methods
[NASA-CR-172469] 02 p0250 N85-11635
Optimized response functions for 2-dimensional observations of solar oscillations 14 p2443 N85-25075
H-sets, convex programming and constrained approximation
[TRITA-NA-8306] 16 p2953 N85-27587
To the theory of approximation of experimental curves by smooth functions
[PREPRINT-438] 18 p3173 N85-29671
Spectral methods for limited area models 20 p3486 N85-31679

CHECKOUT
Debug testing and confidence testing
[AD-A147104] 07 p1025 N85-16504
Joint service design for testability program 08 p1063 N85-16733
Launch processing system concept to reality 08 p1097 N85-16931
Mathematical models for space shuttle ground systems 08 p1097 N85-16933
PASLIB programmer's guide for the finite element machine, revision 2.1-A
[NASA-CR-172281] 11 p1705 N85-20727
Definition of ground test for Large Space Structure (LSS) control verification
[NASA-TM-86495] 12 p1792 N85-21249
Two-phase flow in geothermal systems
[DE85-004692] 12 p1848 N85-21591
Equipment for the ARGOS system from Eidsvoll Electronics A.S. 14 p2239 N85-23685
Automation of development of software for switching units that are implemented in the form of multiprocessor systems on a microcomputer base 14 p2401 N85-24802
Using a logic analyser and trigger unit to de-bug a program
[BAE-881/ELO/1487] 15 p2626 N85-26180
Reentrancy and multitasking on CRAY computers
[DE85-007256] 15 p2630 N85-26211
Debugging distributed computations in a nested atomic action system
[AD-A153617] 16 p3162 N85-29585
International flight planning handbook
[AD-A156330] 24 p4062 N85-35177

CHECKOUT EQUIPMENT
U TEST EQUIPMENT

CHELATE COMPOUNDS
U CHELATES

CHELATES
Polymers and macromolecules
[DE85-003178] 10 p1454 N85-19160
A soluble linear Schiff-base coordination polymer containing eight-coordinate zirconium(4)
[AD-A151446] 15 p2518 N85-25527
Nuclear magnetic resonance study of the intramolecular rearrangement of 2-(5-cyanotetrazolato)pentaammine cobalt (III) perchlorate
[DE85-010810] 22 p3839 N85-33772

CHEMICAL ANALYSIS
NT ELECTROPHOTOMETRY
NT GAS ANALYSIS
NT LASER SPECTROSCOPY
NT MICROANALYSIS
NT NEUTRON ACTIVATION ANALYSIS
NT OZONOMETRY
NT QUALITATIVE ANALYSIS
NT QUANTITATIVE ANALYSIS
NT SPECTROSCOPIC ANALYSIS
NT URINALYSIS
NT VOLUMETRIC ANALYSIS
Development and application of fluorine-containing reagents in the gas chromatography of carbonyl compounds
[BLL-DRIC-TRANS-7205-(3623.66)] 01 p0023 N85-10140
Synthesis and characterization of advanced materials
[PB84-215326] 01 p0025 N85-10156
Water resources data for Michigan, water year 1983
[PB84-225176] 01 p0066 N85-10442
Ecology of estuarine channels of the pacific northwest coast: A community profile
[PB84-209709] 01 p0070 N85-10464
Inorganic composites for space applications 02 p0155 N85-11047
Fluids Experiment Apparatus (FEA) 02 p0155 N85-11048
Surface chemistry of palladium
[DE84-014572] 02 p0173 N85-11163
The oxidation of transition-metal ions by molecular oxygen
[BLL-M-29593-(5828.4)] 02 p0175 N85-11172
EDS round-robin evaluation of type 308 austenitic stainless steel
[DE84-014574] 02 p0183 N85-11226
Optical detection of alkali compounds
[DE84-015505] 03 p0328 N85-12117
The colloidal chemistry of ceramic clays
[NASA-TM-77734] 03 p0336 N85-12163
Compound class quantitation of JP-5 jet fuels by high performance liquid chromatography-differential refractive index detection
[AD-A145754] 03 p0340 N85-12185
Crystal chemistry and real structure of crystals 03 p0423 N85-12703
Matrix resin characterization in cured graphite composites using diffuse reflectance-FTIR 04 p0466 N85-12959
Comparison study of analytical methods for the determination of fluoride, chloride, and bromide in plastics
[DE84-015008] 04 p0470 N85-12989
Official journey to USA, November 1983. Symposium on the Compatibility of Explosives; Mound Laboratory; Naval Surface Weapons Center
[FOA-C-20548-D1] 04 p0482 N85-13072
Measuring system with ion selective electrodes
[BMFT-FB-T-84-170] 05 p0639 N85-14100
Geothermal assessment of a portion of the Escalante Valley, Utah
[DE84-015964] 06 p0828 N85-15257
The toxicity of complex mixtures
[AD-P004033] 06 p0844 N85-15363
The influence of sample collection and methods of analysis on chemical concentrations measured in rainwater
[KNMI-TR-55] 07 p0924 N85-15853
Coso Monitoring Program, January 1981 through December 1983
[AD-A147894] 07 p0998 N85-16338
Analysis of Nonvolatile Residue (NVR) from spacecraft systems
[NASA-TM-86184] 08 p1113 N85-17019
Comparative usefulness of flue gas oxygen and carbon dioxide analysis
[BLL-TRANS-T8356/BG/WH783/84] 08 p1179 N85-17430
Advanced NMR characterization of zeolite catalysts
[DE85-000456] 09 p1291 N85-18104
Geothermal assessment of part of the east shore area, Davis and Weber Counties, Utah
[DE84-016817] 09 p1342 N85-18448
Location of volatile buried wastes by field portable instrumentation
[AD-P004147] 09 p1348 N85-18483
Quality assurance for environmental analytical chemistry, 1983
[DE84-016045] 09 p1349 N85-18489
Correlation and petrological interpretation of abyssal and terrestrial tephra layers 09 p1353 N85-18512
Metal atom diffusion in amorphous silica and at the silica surface
[DE84-017351] 09 p1380 N85-18674
Microstructural analysis of ion containing polymers
[DE85-001594] 10 p1453 N85-19157
SANS studies of polymers
[DE85-002471] 11 p1612 N85-20134
Chemical and photographic evaluation of rigid explosive transfer lines
[AD-A149303] 11 p1613 N85-20145
China report: Science and technology
[JPRS-CST-84-040] 11 p1623 N85-20219
Theta pinch discharges for solids vaporization and elemental chemical analysis
[DE85-002968] 11 p1733 N85-20899
Method and apparatus for mapping the distribution of chemical elements in an extended medium
[NASA-CASE-GSC-12808-1] 12 p1798 N85-21279
Microprocessor-controlled anodic stripping voltammeter for trace metal analysis in tap water
[DE85-002781] 12 p1852 N85-21619
Stability of organic audit materials and results of source test analysis audits
[PB85-116184] 12 p1885 N85-21832
Standard analytical procedures of the NOAA National Analytical Facility, 1984-85: Extractable toxic organic compounds
[PB85-126282] 12 p1887 N85-21840
Characterization of material surfaces exposed to atomic oxygen on space shuttle missions 12 p1946 N85-22220
Analyses via automated mass spectrometry (MS/DS) 12 p1947 N85-22227
Structural distortions of ultra-dispersed titanium nitride powders 13 p2029 N85-22717
Compositional and structural analysis of Air Force materials
[AD-A150992] 14 p2252 N85-23957
Literature review for development of the master analytical scheme for organic compounds in water
[PB85-152874] 15 p2507 N85-25468
Development and diffusion of automated clinical chemistry analyzers
[PB85-150696] 15 p2561 N85-25798
Infinite computing
[AD-A151437] 15 p2628 N85-26197
Development of a persistent chemical agent simulation system
[NASA-CR-175780] 16 p2745 N85-26937
Development of a Persistent Chemical Agent Simulator System (PCASS)
[NASA-CR-175776] 16 p2745 N85-26938
Design of a Mobile Combustion Diagnostic Fixture (MCDF)
[AD-A151814] 16 p2745 N85-26941
Photoionization mass spectrometry with VUV hydrogen laser source
[AD-A153362] 17 p2921 N85-28009
Examination of steels by chemical analysis for quality assurance
[BLL-BISI-TRANS-22068-(9022.06)] 17 p2929 N85-28074
Proton induced X-ray emission method, its application in analytics 17 p2945 N85-28178

Voltammetric analysis of ordnance materials. Part 2: A portable digital voltammeter for use with a silver wire working electrode
[AD-A152460] 17 p2967 N85-28325
Analytical Chemistry Division
[DE85-010585] 18 p3068 N85-28974
Chemical, biological, and physical measurements from the subtropical western North Atlantic Ocean. Summer 1982, USNS Lynch, cruise 710-82
[AD-A153823] 18 p3201 N85-29657
Study of the chemical mechanism in lubrication
[DE85-010768] 19 p3228 N85-30013
Guest molecules in coal
[DE85-010435] 19 p3228 N85-30016
Technical and administrative activities of the Analytical Chemistry Laboratory (ACL)
[DE85-010150] 19 p3236 N85-30063
Advanced NMR characterization of zeolite catalysts
[DE85-010143] 19 p3363 N85-30653
Differential optical absorption techniques for diagnostics of coal gasification
[DE85-010177] 19 p3368 N85-30690
Quasi non-intrusive sampling and analysis of gases associated with the boundary layer on the tethered satellite and similar supersonic and hypersonic research vehicles
[NASA-CR-176075] 20 p3407 N85-31140
Development anmd testing of electrophoresis solutions. Task I.1: Development of optimal buffer system
20 p3500 N85-31755
Toxic hazards tests for vehicles and other equipment
[AD-A149164] 20 p3506 N85-31797
Remarks on preparation of indandione detection reagents
[NASA-TM-77905] 21 p3560 N85-32146
A manual of methods for the continuous flow determination of ammonia, nitrate-nitrite, phosphate and silicate in seawater
[IOS-177] 23 p3913 N85-34243
Uranium, thorium isotopic analyses and uranium-series ages of calcite and opal and stable isotopic compositions of calcite from drill cores UE25a no. 1, USR G-2 and USW G-3/GU-3, Yucca Mountain, Nevada
[DE85-013039] 23 p3948 N85-34471
Aspects of high-resolution gas chromatography as applied to the analysis of hydrocarbon fuels and other complex organic mixtures. Volume 1
[AD-A156154] 24 p4076 N85-35257
Experimental technique for measuring the isentrope of hydrogen to several megabars
[DE85-014332] 24 p4095 N85-35386
Measurement control for plutonium isotopic measurements using gamma-ray spectrometry
[DE85-013394] 24 p4097 N85-35397

CHEMICAL ATTACK
NT INTERGRANULAR CORROSION
The effect of replacing molybdenum with vanadium on the corrosion resistant properties of stainless steels
02 p0178 N85-11197
Hydrogen attack of steel
[DE85-002645] 11 p1608 N85-20113
Study of Kapton under simulated shuttle environment
[NASA-CR-176003] 19 p3225 N85-29997
Burner rig corrosion of SiC at 1000 deg C
[NASA-TM-87061] 19 p3227 N85-30011
On compounding nickel alloys as defense against sulfide-oxide corrosion 19 p3243 N85-30109
Magnetically-localizable, polymerized lipid vesicles and method of disrupting same
[AD-D011686] 19 p3249 N85-30144

CHEMICAL BONDS
NT COVALENT BONDS
NT HYDROGEN BONDS
Chemically modified electrodes and related solution chemistry
[DE84-017110] 05 p0614 N85-13924
Neutron diffraction studies of the hydrogen bonding and water molecules in zeolites
[DE84-016431] 06 p0766 N85-14900
Structure of adsorbed monolayers. The surface chemical bond
[DE84-016679] 06 p0861 N85-15471
(Vinyloxy)fluorocyclotriphosphazenes
[AD-A147448] 07 p0924 N85-15850
Electronic structure, chemical bonding, and superconductivity of silver films on germanium
[AD-A147720] 08 p1126 N85-17112
Electronic structure, chemical bonding, and electron conductivity of thin-film transition-metal silicides
[AD-A147721] 08 p1226 N85-17718
Characterization of CO binding sites on Rh(111) and Rh(331) surfaces by XPS and LEED (Low Energy Electron Diffraction): Comparison to EELS (Electron Energy Loss Spectroscopy) results
[AD-A149331] 10 p1435 N85-19044
(Vinyloxy)chlorocyclotriphosphazenes
[AD-D011471] 10 p1453 N85-19152
Theoretical studies on N-bonded pyrazole derivatives of boron
[AD-A150036] 12 p1813 N85-21374
Bonding information from Auger spectroscopy
[AD-A150864] 14 p2251 N85-23948
Chemical and localization effects in Auger lineshapes of transition metal compounds
[AD-A150865] 14 p2251 N85-23949
C2H(n) fragments on metal surfaces
[AD-A151474] 15 p2505 N85-25449
Nitrolysis of the CN single bond and related chemistry of nitro and nitroso groups
[AD-A151753] 15 p2505 N85-25453
System for NDH of thermal spray coating bonds
[DE85-007463] 15 p2572 N85-25858
Molecular dynamics studies of energy transfer processes in crystal systems
[DE85-007247] 15 p2662 N85-26426
Compensation of dangling bonds in A-Si, Ge:H alloys
[DE85-002905] 15 p2662 N85-26433
Transitional metal activation and functionalization of C-H bonds
[DE85-006816] 16 p2746 N85-26949
New examples of clusters, extended metal-metal bonding and interstitial derivatives
[DE85-005926] 17 p3044 N85-28837
Exploratory study of coal conversion chemistry
[DE85-010393] 19 p3229 N85-30018
Diffusion welding of incompatible materials
19 p3245 N85-30121
Producing titanium-sapphire items by solid-phase bonding through aluminum gasket
19 p3246 N85-30127
Diffusion welding of aluminum with vacuum-tight corundum ceramic 19 p3247 N85-30130
Threshold effects and cellular recognition
[DE85-010816] 19 p3327 N85-30614
Why CO bonds side-on at low coverage and both side-on and upright at high coverage on the Cr(110) surface
[NASA-CR-176071] 21 p3565 N85-32173
Defects in tetrahedrally coordinated amorphous semiconductors
[AD-A155150] 21 p3581 N85-32283
Interfacial bonding stability 21 p3608 N85-32409
Infrared studies of the influence of alkali metals on the C-O bond in chemisorbed carbon monoxide
[DE85-005306] 23 p3911 N85-34232
Separation of gas mixtures by supported complexes
[DE85-011996] 23 p3912 N85-34236
The photodissociation of acetylene at 193.3 NM
[AD-A155775] 24 p4075 N85-35255
Dangling bonds and sub-gap optical absorption in silicon
[DE85-011752] 24 p4082 N85-35302

CHEMICAL CLEANING
NT PICKLING (METALLURGY)
Composition and method for cleaning embedded soil from surfaces having low gloss coatings
[AD-D011465] 10 p1459 N85-19194
Chemical cleaning of 304 and 304-L stainless steel surfaces by the nitradd passivation process
[DE85-003714] 11 p1615 N85-20158

CHEMICAL CLOUDS
NT BARIUM ION CLOUDS

CHEMICAL COMPOSITION
NT CARBON DIOXIDE CONCENTRATION
NT STELLAR COMPOSITION
Compilation of elemental concentration data for NBS (National Bureau of Standards) biological, geological and environmental standard reference materials, 1982
[PB84-218398] 01 p0025 N85-10158
Milling of Si3N4 with Si3N4 hardware
[NASA-TM-86864] 01 p0031 N85-10191
Microtektite discovered in Beijing
[NASA-TM-77765] 01 p0130 N85-10895
Solidification and crystal growth of solid solution semiconducting alloys 02 p0155 N85-11046
Factor analysis applied to a silane coupling agent on E-glass fiber system
[AD-A145687] 02 p0187 N85-11249
Variability of major organic components in aircraft fuels. Volume 3: Sample data package for the reference JP-4 fuel
[AD-A145483] 02 p0188 N85-11254
Variability of major organic components in aircraft fuels. Volume 1: Technical discussion
[AD-A145574] 02 p0188 N85-11256
Mechanical properties of a leaded, resulfurized, rephosphorized steel in various thermo/mechanical conditions
[PB84-216464] 03 p0333 N85-12144
Effect of oxidizing medium and heat treatment on stoichiometry of ZnSe crystal surface
03 p0353 N85-12272
Nutritional models for space travel from chemically defined diets
[NASA-CR-3850] 03 p0402 N85-12581
CVD parameter study using strategy of experimentation
[DE84-015900] 04 p0473 N85-13011
Variability of major organic components in aircraft fuels. Volume 2: Illustrations
[AD-A145831] 04 p0481 N85-13067
Development and evaluation of cloud water collectors
[PB84-232529] 04 p0540 N85-13437
Non-invasive techniques for determining musculoskeleton body composition
[DE84-015718] 04 p0545 N85-13470
Testing of production of silicon-titanium-magnesium alloying composition
[BLL-M-35904-(5828.4)] 05 p0616 N85-13937
In vivo neutron activation analysis: Body composition studies in health and disease
[DE84-014092] 05 p0696 N85-14480
Clinical measurements using fiber optics and optrodes
[DE84-015043] 05 p0696 N85-14481
In situ analysis of corroeive and passive surfaces by laser-excited Raman spectroscopy --- lead, galvanized iron, and asbestos-cement pipes
[PB84-229756] 06 p0767 N85-14904
Method for predicting the creep rupture life of nickel-base precipitation-hardened superalloys from their chemical composition
[BLL-PNR-90241-(8019.3153)]
06 p0768 N85-14910
Bulk compositions of Al-rich chondrules in ordinary and carbonaceous chondrites: Variations and similarities
06 p0881 N85-15601
Major element chemical compositions of chondrules in unequilibrated chondrites 06 p0881 N85-15602
Chondrule rims and interchondrule matrix in UOC
06 p0882 N85-15604
The Colony meteorite and the possible existence of a new chemical subgroup of CO3 chondrites
06 p0885 N85-15821
Where is the Earth's missing xenon?
06 p0888 N85-15841
The chemistry of rare earth elements in the solar nebula 06 p0889 N85-15843
Optimization of the NiCrAl-Y/ZrO-Y2O3 thermal barrier system
[NASA-TM-86905] 07 p0927 N85-15878
Gradient polymers
[AD-A148636] 07 p0931 N85-15900
General theory and design considerations for optical waveguide chemical vapor sensors
[AD-A148505] 08 p1223 N85-17702
Variation of oxygen and nitrogen abundances in the galaxy 08 p1248 N85-17878
Aromatics determination in middle distillate petroleum fractions by spectrophotometric titration
[PNR-90239] 09 p1293 N85-18123
CVD boron on calcium chromate powder
[DE85-000214] 09 p1299 N85-18158
Corrosion of ceramics in heat exchanger applications
[DE84-017459] 09 p1299 N85-18161
Compositional, structural, and physical studies of some graphite hexafluoroarsenates and their relatives
[DE85-000855] 10 p1432 N85-19030
Composition and method for cleaning embedded soil from surfaces having low gloss coatings
[AD-D011465] 10 p1459 N85-19194
Interaction of large meteoroids with the atmosphere
11 p1656 N85-20431
Microalgae culture collection, 1984-1985
[DE84-013035] 11 p1690 N85-20626
Carbon, silicon, and oxygen in the white dwarf star GD 40 11 p1752 N85-21017
Plasticizer system for propellant compositions
[AD-D011514] 12 p1817 N85-21393
Summary report of the Workshop on Structure Activity Concepts in Environmental Sciences
[PB85-137339] 12 p1887 N85-21841
Chemical characterization and toxicologic evaluation of airborne mixtures. Inhalation toxicology of diesel fuel obscurant aerosol in Sprague-Dawley rats. Phase 3. Subchronic exposures
[AD-A150100] 12 p1905 N85-21966
Characterization of high purity Si-doped molecular beam epitaxial GaAs
[AD-A149851] 12 p1939 N85-22181
Silicon carbide-silicon nitride fibers: Preparation and characterization of polycarbosilazane precursors
12 p1945 N85-22214
Cosmic ray composition and origin
12 p1955 N85-22287
The influence of fuel quality upon flame-tube temperature and flame radiation in a model gas-turbine primary zone
[K233] 13 p1974 N85-22396

Structural distortions of ultra-dispersed titanium nitride powders 13 p2029 N85-22717
Composition and thickness of oxide coatings on granule surfaces of aluminum alloys 13 p2030 N85-22719
Impurities in Kevlar 49 fibers
[DE85-004996] 13 p2038 N85-22767
Composition and photochemical reactivity of turbine engine exhaust
[AD-A150559] 13 p2130 N85-23256
Chemical composition of coastal haze aerosol 14 p2338 N85-24456
Long-term exposure of pressed plutonium oxide heat sources to aquatic environments
[DE85-007385] 15 p2495 N85-25392
Resonant coherent anti-Stokes Raman scattering
[ESA-TT-876] 15 p2507 N85-25466
Studies of photosynthetic Energy Conversion
[DE85-005973] 15 p2586 N85-25944
A review of radar observations of Saturn's rings 15 p2670 N85-26474
Physical properties of Saturn's rings 15 p2672 N85-26493
Technical and economic analysis of liquid fuel production from microalgae
[DE85-002926] 16 p2758 N85-27018
High resolution spectroscopy of C13O16 in gas mixtures
[AD-A152625] 17 p2919 N85-27991
Influence of structural state and alloy content of austenite on formation of martensitic phases in steels
[BLL-BISI-TRANS-22385-(9022.06)] 17 p2928 N85-28068
The effect of microalloying with calcium and magnesium on the plasticity of Poldi AKN 20 Ni-based alloy
[BLL-BISI-TRANS-2174-(9022.06)] 17 p2929 N85-28075
In situ HVEM studies of electron beam-driven composition changes in thin film alloys: Displacement-rate gradient effects
[DE85-007992] 17 p2931 N85-28092
Application of scattering methods to the studies of the structure of polymer blends
[IFPR-13/1984] 17 p2933 N85-28104
Chemicals identified in human biological media, a data base, volume 6, part 1
[DE85-006766] 17 p2999 N85-28542
Adsorption of Hg on lunar samples
[DE85-007948] 17 p3054 N85-28906
The distribution of higher n-alkanes in partially frozen middle distillate fuels
[AD-A153940] 18 p3063 N85-29074
Measurement of radical species concentrations and polycyclic aromatic hydrocarbons in flames by fluorescence and absorption using a tunable dye laser
[DE85-008624] 18 p3113 N85-29274
Chemicals identified in human biological media, a data base. Volume 6, part 2: Records 7568-8694
[DE85-008767] 18 p3154 N85-29528
Combustion characterization of coals for industrial applications
[DE85-010673] 19 p3228 N85-30014
Adherence of ash particles from the combustion of micronized coal
[DE85-008800] 19 p3229 N85-30023
The mobile phase in coals: Its nature and modes of release
[DE85-011696] 19 p3230 N85-30026
Chemical composition and kinetics of libration of gases upon welding of aluminum alloys 19 p3247 N85-30131
The origin and evolution of the Earth's atmosphere and hydrosphere 19 p3312 N85-30533
Debye temperature and static displacements in LuH sub x single crystals from energy dispersive X-ray diffraction
[DE85-010961] 19 p3376 N85-30946
Solar photospheric and coronal abundances from solar energetic particle measurements
[NASA-CR-176029] 20 p3547 N85-32073
The effect of diffusive hydrogen segregation on fracture of polycrystalline nickel
[AD-A155236] 21 p3567 N85-32186
Chemical composition of atmospheric aerosol at Delhi 21 p3646 N85-32653
Investigation of the formation of cloud particle spectrum on natural condensation nuclei 21 p3649 N85-32674
Variations of particulate sulfur concentrations in a coastal atmospheric environment in connection with the change of air masses origin 21 p3652 N85-32692
Liquid-phase compositions from vapor-phase analyses 2: Adaptation of the Prausnitz program to UF6 and some of its potential impurities
[DE85-011521] 21 p3673 N85-32819
Evaluation of pilot ESP used with a spray dryer FGD system at Pittsburgh Energy Technology Center, Bruceton, Pennsylvania
[DE85-011151] 22 p3746 N85-33217
Experimental studies of glass refining
[NASA-CR-176130] 22 p3751 N85-33248
Metallic glass composition
[DE85-011594] 22 p3751 N85-33253
Technology of off-gas treatment for liquid-fed ceramic melters
[DE85-012467] 22 p3812 N85-33610
Venus, Earth and Mars: Present bounds on similarities and differences in bulk composition 22 p3856 N85-33876
A new method to determine the chemical composition of the cosmic rays beyond 10 to the 15th power eV
[OG-5.1-11] 22 p3882 N85-34052
Cosmic ray composition between 10 to the 15th power - 10 to the 17th power eV obtained by air shower experiments
[OG-5.1-12] 22 p3882 N85-34053
The primary composition beyond 10 to the 5th power GeV as deduced from high energy hadrons and muons in air showers
[OG-5.2-6] 22 p3883 N85-34063
Determination of low chloride values in Rocky Flats scrub alloy solutions and other complex matrices
[DE85-011506] 23 p3911 N85-34234
The influence of temperature on the composition density of the transition metals
[BLL-M-35896-(5826.4)] 23 p3915 N85-34262
Throughfall rate and chemistry studies: Whiteface Mountain
[DE85-012407] 23 p3947 N85-34464
Thermally induced chemical migration: A natural analog approach
[DE85-012308] 23 p3949 N85-34474
Energetic particle observations of the solar-gamma ray/neutron flare events of 3 Jun 1982 and 21 June 1980 isotopic and chemical composition
[SH-2.1-3] 23 p3998 N85-34784
Precision measurements of solar energetic particle elemental composition
[SH-2.1-4] 23 p3998 N85-34785
Variations in elemental composition of several MEV/nucleon ions observed in interplanetary space
[SH-2.1-7] 23 p3998 N85-34788
The cosmic ray composition as viewed from the chemical abundances of the solar system
[OG-7.1-8] 23 p4013 N85-34869
The 4He1H ratios in the chemical compositions of solar flare particles and the primordial solar nebula
[SH-7.1-12] 23 p4048 N85-35104
Measurement of low energy cosmic rays aboard Spacelab-1
[SH-10.1-6] 23 p4053 N85-35137
Ion composition measurements of the disturbed and quiet D-region in 1980 - 1981
[AD-A156055] 24 p4117 N85-35521
Energy spectra of proton and nuclei of primary cosmic rays in energy region 10 TeV/particle
[HE-3.1-10] 24 p4178 N85-35908
A comparative analysis of gamma and hadron families at the superhigh energies recorded in experiment Pamir
[HE-3.7-1] 24 p4185 N85-35960
Correlation of high energy muons with primary composition in extensive air shower
[HE-4.3-7] 24 p4191 N85-36001
A large area cosmic muon detector located at Ohya stone mine
[HE-5.1-7] 24 p4201 N85-36072
On muon energy spectrum in muon groups underground
[HE-5.1-14] 24 p4201 N85-36076
Multiple muons in MACRO
[HE-5.2-1] 24 p4202 N85-36079

CHEMICAL COMPOUNDS
Compilation of data sources for existing chemicals
[GSF-A-2/84] 01 p0017 N85-10103
Method for fluorination of actinide fluorides and oxyfluorides using O2F2
[DE85-011646] 22 p3743 N85-33202

CHEMICAL DEFENSE
Anthropometric cockpit compatibility assessment of US Army aircraft for large and small personnel wearing A cold weather, armored vest, chemical defense protective clothing configuration
[AD-A145472] 02 p0238 N85-11547

CHEMICAL EFFECTS
Chemical-mechanical interaction in gears 14 p2223 N85-23785
Detailed chemical kinetic study of the effect of molecular structure on autoignition of fuel-air mixtures
[DE85-004424] 17 p2921 N85-28010

CHEMICAL ELEMENTS
NT ACTINIDE SERIES
NT ACTIVATED CARBON
NT ALKALI METALS
NT ALKALINE EARTH METALS
NT ALUMINUM
NT ALUMINUM ISOTOPES
NT ALUMINUM 26
NT AMERICIUM
NT AMERICIUM ISOTOPES
NT AMERICIUM 241
NT ANTIMONY
NT ARGON
NT ARGON ISOTOPES
NT ARSENIC
NT BARIUM
NT BERYLLIUM
NT BERYLLIUM ISOTOPES
NT BERYLLIUM 7
NT BERYLLIUM 9
NT BERYLLIUM 10
NT BISMUTH
NT BORON
NT BORON 10
NT BROMINE
NT BROMINE ISOTOPES
NT CADMIUM
NT CALCIUM
NT CALCIUM ISOTOPES
NT CALIFORNIUM ISOTOPES
NT CARBON
NT CARBON ISOTOPES
NT CARBON 12
NT CARBON 13
NT CARBON 14
NT CERIUM
NT CERIUM 144
NT CESIUM
NT CESIUM ISOTOPES
NT CESIUM 134
NT CESIUM 137
NT CHARCOAL
NT CHLORINE
NT CHROMIUM
NT CHROMIUM ISOTOPES
NT COBALT
NT COBALT 60
NT COPPER
NT CURIUM
NT CURIUM 244
NT DEUTERIUM
NT DEUTERIUM PLASMA
NT ERBIUM
NT FLUORINE
NT GADOLINIUM
NT GALLIUM
NT GERMANIUM
NT GERMANIUM ISOTOPES
NT GOLD
NT HAFNIUM
NT HALOGENS
NT HELIUM
NT HELIUM ATOMS
NT HELIUM ISOTOPES
NT HOLMIUM
NT HYDROGEN
NT HYDROGEN ATOMS
NT HYDROGEN IONS
NT HYDROGEN ISOTOPES
NT HYDROGEN PLASMA
NT INDIUM
NT IODINE
NT IODINE ISOTOPES
NT IRIDIUM
NT IRON
NT IRON ISOTOPES
NT IRON 59
NT ISOTOPES
NT KRYPTON
NT KRYPTON ISOTOPES
NT KRYPTON 85
NT LANTHANUM
NT LEAD (METAL)
NT LIGHT ELEMENTS
NT LIQUID HELIUM
NT LIQUID HELIUM 2
NT LIQUID HYDROGEN
NT LIQUID LITHIUM
NT LIQUID NITROGEN
NT LIQUID POTASSIUM
NT LIQUID SODIUM
NT LITHIUM
NT LUTETIUM
NT MAGNESIUM
NT MAGNESIUM ISOTOPES
NT MANGANESE

NT MANGANESE ISOTOPES
NT MERCURY (METAL)
NT METALLIC HYDROGEN
NT METALLOIDS
NT MOLYBDENUM
NT NEODYMIUM
NT NEODYMIUM ISOTOPES
NT NEON
NT NEON ISOTOPES
NT NICKEL
NT NICKEL ISOTOPES
NT NIOBIUM
NT NITROGEN
NT NITROGEN IONS
NT NITROGEN ISOTOPES
NT NITROGEN 15
NT NUCLIDES
NT OSMIUM
NT OSMIUM ISOTOPES
NT OXYGEN
NT OXYGEN ATOMS
NT OXYGEN IONS
NT OXYGEN ISOTOPES
NT OXYGEN PLASMA
NT PALLADIUM
NT PHOSPHORUS
NT PLATINUM
NT PLUTONIUM
NT PLUTONIUM ISOTOPES
NT PLUTONIUM 238
NT PLUTONIUM 239
NT POTASSIUM
NT POTASSIUM 40
NT POWDERED ALUMINUM
NT PRASEODYMIUM
NT RADIOACTIVE ISOTOPES
NT RADIUM
NT RADON
NT RADON ISOTOPES
NT RARE EARTH ELEMENTS
NT RARE GASES
NT REFRACTORY METALS
NT RHODIUM
NT RUBIDIUM
NT RUBIDIUM ISOTOPES
NT RUTHENIUM
NT SAMARIUM
NT SCANDIUM
NT SCANDIUM ISOTOPES
NT SELENIUM
NT SILICON
NT SILICON ISOTOPES
NT SILVER
NT SINTERED ALUMINUM POWDER
NT SODIUM
NT SODIUM ISOTOPES
NT SODIUM VAPOR
NT STRONTIUM 90
NT SULFUR
NT TANTALUM
NT TECHNETIUM
NT TELLURIUM
NT THALLIUM
NT THORIUM
NT THORIUM ISOTOPES
NT TIN
NT TITANIUM
NT TRACE ELEMENTS
NT TRANSURANIUM ELEMENTS
NT TRITIUM
NT TUNGSTEN
NT URANIUM
NT URANIUM ISOTOPES
NT URANIUM 235
NT VANADIUM
NT XENON
NT XENON ISOTOPES
NT XENON 129
NT YTTERBIUM
NT YTTRIUM
NT ZINC
NT ZIRCONIUM

User's manual for GRIZZLY
[DE85-001405] 11 p1702 N85-20702

The cosmic ray composition as viewed from the chemical abundances of the solar system
[OG-7.1-8] 23 p4013 N85-34869

CHEMICAL ENERGY
NT ENERGY OF FORMATION

Phase equilibria of stored chemical energy reactants
[AD-A146527] 06 p0765 N85-14896

Sensitization and quenching in the conversion of light energy into chemical energy
[DE85-006301] 14 p2351 N85-24535

Modeling heterogeneous high explosive burn with an explicit hot-spot process
[DE85-009593] 23 p3922 N85-34300

CHEMICAL ENGINEERING
Experimental and theoretical study of a solar thermochemical receiver module
[NASA-CR-174107] 04 p0528 N85-13374

Chemical engineering principles of constant temperature-constant supersaturation growth of potassium dihydrogen phosphate (KDP) crystals
[DE84-017081] 04 p0571 N85-13645

Activities report in technology
[ISBN-951-38-1998-1] 04 p0577 N85-13681

USSR report: Chemistry
[JPRS-UCH-85-001] 13 p2013 N85-22629

Current plans for development of chemical industry 13 p2014 N85-22633

Failure mechanisms in metal-sheathed thermocouples
[DE85-011929] 21 p3590 N85-32317

CHEMICAL EQUILIBRIUM
NT ACID BASE EQUILIBRIUM

Catalyzed low burning rate propellants for upper-stage solid rocket motor
[NAL-TR-805] 03 p0339 N85-12181

Computer calculation of chemical equilibrium in multi-component systems
[BLL-M-35973-(5828.4)] 05 p0614 N85-13919

Effect of water on hydrogen permeability --- Stirling engines
[NASA-TM-86904] 06 p0761 N85-14864

Phase equilibria of stored chemical energy reactants
[AD-A146527] 06 p0765 N85-14896

Vaporization behavior, phase equilibria, and thermodynamic stabilities of nickel phosphides
[AD-A146683] 06 p0765 N85-14897

Computer program for calculation of complex chemical equilibrium compositions and applications. Supplement 1: Transport properties
[NASA-TM-86885] 07 p1049 N85-16663

Carbon vaporization/condensation effects
[NASA-TM-87430] 10 p1436 N85-10048

French activities relevant to middle atmosphere research 11 p1655 N85-20423

Diagrams of chemical and electrochemical equilibria in the presence of oxygen and sulphur
[AD-A150929] 14 p2251 N85-23953

The origin and evolution of the Earth's atmosphere and hydrosphere 19 p3312 N85-30533

Combustion gas properties. Part 3: Hydrogen gas fuel and dry air
[NASA-TP-2477] 20 p3395 N85-31058

Nonequilibrium chemistry in an isothermal turbulent flow 22 p3745 N85-33211

Comparison of experimental data on detonation velocity and Chapman-Jouget pressure vs initial HE density with predictions from Ree's model equation of state
[DE85-007266] 23 p3922 N85-34304

Aqueous volatile weak electrolyte equilibria to 300 C
[DE85-013840] 24 p4076 N85-35261

CHEMICAL EVOLUTION
Chemical evolution of the solar nebula: A new model 06 p0687 N85-15631

Origin of life 21 p3657 N85-32713

Insights into the phylogenetic positions of photosynthetic bacteria obtained from 5S rRNA and 16S rRNA sequence data 21 p3658 N85-32719

Search for the universal ancestors
[NASA-SP-477] 21 p3667 N85-32777

Submarine hydrothermal environments as sites for the origin and evolution of life 21 p3719 N85-33074

CHEMICAL EXPLOSIONS
NT GAS EXPLOSIONS

Measurements of two-phase exhaust flow parameters of a small caliber gun associated with muzzle flash phenomena
[ISL-CO-212/83] 16 p2784 N85-27182

Detonation behavior of LX-14 and PBX-9404: Theoretical aspect
[DE85-010038] 18 p3084 N85-29076

The shock desensitization of PBX-9404 and composition B-3
[DE85-009604] 18 p3084 N85-29077

Explosibility of ammonium nitrate
[HSE-TRANS-11111] 19 p3252 N85-30164

Combustion-deflagration-detonation transition in a confined spherical powder
[ISL-R-108/84] 22 p3747 N85-33223

Behavior of the porous bed in a combustion-deflagration-detonation transition
[ISL-CO-220/84] 22 p3747 N85-33224

Nuclear magnetic resonance study of the intramolecular rearrangement of 2-(5-cyanotetrazolato)pentaammine cobalt (III) perchlorate
[DE85-010810] 22 p3839 N85-33772

Time-resolved spectroscopic studies of detonating heterogeneous explosives
[DE85-009760] 23 p3921 N85-34297

Pressure-shear loading of PBX-9404
[DE85-009982] 23 p3921 N85-34298

Modeling heterogeneous high explosive burn with an explicit hot-spot process
[DE85-009593] 23 p3922 N85-34300

Three-dimensional hydrodynamic hot-spot model
[DE85-009587] 23 p3922 N85-34301

Effect of precipitation variables on the specific surface and explosion characteristics of pentaerythritol tetranitrate
[DE85-009620] 23 p3922 N85-34302

Comparison of experimental data on detonation velocity and Chapman-Jouget pressure vs initial HE density with predictions from Ree's model equation of state
[DE85-007266] 23 p3922 N85-34304

Friction, impact, and electrostatic discharge sensitivities of energetic materials
[DE85-013321] 24 p4083 N85-35309

CHEMICAL EXTINGUISHERS
U FIRE EXTINGUISHERS

CHEMICAL FRACTIONATION
Effects of method of detachment on electrophoretic mobility of mammalian cells grown in monolayer culture 20 p3500 N85-31757

Isotopic Biogeochemistry
[NASA-CR-176128] 22 p3741 N85-33189

CHEMICAL FUELS
NT AIRCRAFT FUELS
NT AUTOMOBILE FUELS
NT DIESEL FUELS
NT GASOHOL (FUEL)
NT GASOLINE
NT HYDROCARBON FUELS
NT HYDROGEN FUELS
NT JET ENGINE FUELS
NT JP-4 JET FUEL
NT JP-5 JET FUEL
NT JP-8 JET FUEL
NT KEROSENE
NT LIQUID FUELS
NT SLURRY PROPELLANTS
NT SYNTHETIC FUELS

Technical instructions for a control operating system of the gas flow installation for the solid fuel combustion chamber
[VTH-LR-410] 18 p3118 N85-29302

CHEMICAL INDICATORS
Electrochromic display device
[AD-D011733] 22 p3759 N85-33299

CHEMICAL KINETICS
U REACTION KINETICS

CHEMICAL LASERS
Influence of translational and hyperfine relaxation on energy characteristics of oxygen-iodine laser 02 p0261 N85-11707

Delta wing nozzle assembly for chemical lasers
[AD-D011396] 07 p0970 N85-16158

Conference on Singlet Molecular Oxygen (COSMO 84), program and abstracts
[AD-A147281] 07 p1040 N85-16805

Halogen mass flow rate detection system
[AD-D011398] 08 p1166 N85-17352

Bibliography of Soviet laser developments, Number 66, July-August 1983
[AD-A149113] 10 p1490 N85-19406

Chemically amplified laser direct-writing of aluminum
[DE85-000308] 11 p1639 N85-20324

Saturation kinetics of active medium of oxygen-iodine laser 11 p1718 N85-20807

Waveguide phenomena in dense relaxing gases and their use in chemical and gas-dynamic lasers 15 p2644 N85-26308

Short Wavelength Chemical Laser (SWCL) Workshop
[AD-A151959] 16 p2790 N85-27211

Rotational relaxation studies of hydrogen fluoride
[AD-A152711] 17 p3029 N85-28734

Review of short wavelength lasers
[DE85-009858] 18 p3114 N85-29277

Chemical lasers
[ISL-R-107/84] 23 p3936 N85-34400

CHEMICAL MACHINING
NT ELECTROCHEMICAL MACHINING

Electropulse chemical machining
[DE84-016693] 04 p0484 N85-13084

CHEMICAL MILLING
U CHEMICAL MACHINING

CHEMICAL PROPERTIES
NT ACIDITY
NT HEAT OF FORMATION
NT HEAT OF FUSION
NT HEAT OF VAPORIZATION
NT SALINITY
NT THERMOCHEMICAL PROPERTIES

Development of new and improved polymer matrix resin systems, phase 1
[NASA-CR-166505] 01 p0017 N85-10104
Synthesis and characterization of advanced materials
[PB84-215328] 01 p0025 N85-10156
Guide to the selection of rubbers
[AMTE(N)-TM-84301] 03 p0336 N85-12164
Online directory of databases for material properties
[DE84-016511] 09 p1402 N85-18824
Monitoring approaches for assessing quality of high altitude lakes: Colorado Flat Tops Wilderness Area
[PB85-117232] 11 p1679 N85-20579
A brief review of the technology of microemulsions and other micellar systems
[AD-A149759] 12 p1800 N85-21289
Sequential excitation preparation of molecular energy levels with special structural and chemical properties
[AD-A150301] 13 p2156 N85-23386
Resistance of optical coatings to alkali solutions and sea water 14 p2281 N85-24129
Water-resistance and some other properties of polyalkali fluorophosphate glasses 14 p2281 N85-24133
Electrochemical behavior of amorphous alloys based on iron, cobalt and nickel in H3PO4 solutions alone and mixed with HF 15 p2513 N85-25505
Liquid propellants for use in guns: A review
[AD-A153051] 17 p2937 N85-28131
Operation guiding light-scientific program and field plan. The pilot field experiment for NORDA project chemical dynamics in ocean frontal areas
[AD-A153765] 18 p3150 N85-29507
Chemical spectroscopy
[DE85-009594] 18 p3191 N85-29790
Chemical, biological, and physical measurements from the subtropical western North Atlantic Ocean. Summer 1982, USNS Lynch, cruise 710-82
[AD-A153823] 18 p3201 N85-29857
Chemical-acoustic interactions in combustion systems
[AD-A153857] 19 p3233 N85-30046
Optical 3-D signature device for detecting chemical agents
[AD-D011669] 19 p3272 N85-30293
Numerical simulation of chemical and physical properties of cumulus clouds
[DE85-009744] 19 p3317 N85-30564
Chromophores with auxochrome-like function
[NASA-TM-77849] 20 p3421 N85-31233
Electrochemistry of Hexanitroazobenzene (HNAB)
[DE85-010807] 21 p3565 N85-32171
Physical chemical state of water in living cells
[AD-A154566] 21 p3662 N85-32749
Experimental studies of chemical reactivity during shock initiation of hexanitrostilbene
[DE85-011726] 22 p3754 N85-33270
Hydrazine nitrate based explosives
[ISL-CO-229/84] 22 p3754 N85-33272
The effect of liquid-liquid phase separation of glass on the properties and crystallization behavior
[NASA-TM-77690] 23 p3919 N85-34285
Chemical lasers
[ISL-R-107/84] 23 p3936 N85-34400
Chemoviscosity modeling for thermosetting resins, 2
[NASA-CR-177958] 24 p4073 N85-35243

CHEMICAL PROPULSION
NT HYBRID PROPULSION
Preliminary assessment of power-generating tethers in space and of propulsion for their orbit maintenance 13 p1997 N85-22520
Primary propulsion of electrothermal, ion and chemical systems for space-based radar orbit transfer
[NASA-TM-87043] 17 p2916 N85-27972

CHEMICAL REACTION CONTROL
China report: Science and technology
[JPRS-CST-85-011] 15 p2551 N85-25746

CHEMICAL REACTIONS
NT ALKYLATION
NT ATOMIC RECOMBINATION
NT CARBOXYLATION
NT CHLORINATION
NT COPOLYMERIZATION
NT CRACKING (CHEMICAL ENGINEERING)
NT DECARBONATION
NT DEHYDROGENATION
NT DENITROGENATION
NT DEOXIDIZING
NT DESULFURIZING
NT DIELS-ALDER REACTIONS
NT ELECTROCHEMICAL OXIDATION
NT EXOTHERMIC REACTIONS
NT FERMENTATION
NT FLUORINATION
NT HALOGENATION
NT HYDROGENATION
NT HYDROGENOLYSIS
NT HYDROLYSIS
NT ION RECOMBINATION
NT METHANATION
NT NITRATION
NT NITRIDING
NT NITROGENATION
NT NITROLYSIS
NT OXIDATION
NT OXIDATION-REDUCTION REACTIONS
NT OXYGEN RECOMBINATION
NT OXYGENATION
NT PHOSPHORYLATION
NT PHOTOCHEMICAL REACTIONS
NT PHOTOCHROMISM
NT PHOTODECOMPOSITION
NT PHOTOLYSIS
NT PHOTOOXIDATION
NT PHOTOSYNTHESIS
NT PYROLYSIS
NT RADIOLYSIS
NT REDUCTION (CHEMISTRY)
NT RUSTING
NT SULFATION
NT SULFIDATION
NT THERMAL DECOMPOSITION
NT THERMAL DISSOCIATION
NT TITRATION
Treating silicon carbide sinter by heating in nitrogen
[NASA-TM-77601] 01 p0021 N85-10130
Lagging development of biotechnology described 01 p0115 N85-10787
Kinetics of simple inner- and outer-sphere electrochemical reactions at rotating silver electrodes as examined using surface-enhanced Raman spectroscopy
[AD-A145606] 02 p0172 N85-11154
Surface environmental effects in electrochemical kinetics: Outer-sphere chromium (3) reductions at mercury, gallium, lead, and thallium surfaces
[AD-A145607] 02 p0172 N85-11155
Alloying effects of reactive elements in ferritic stainless steels 02 p0178 N85-11196
The reactions of cobalt, iron and nickel in SO-2 atmospheres: Similarities and differences
[NASA-TM-86868] 02 p0181 N85-11217
The 7-Amino-4,6-Dinitrobenzofuroxan, an insensitive high explosive
[AD-A145665] 02 p0188 N85-11257
Impact cratering: The process and its effects on planetary evolution — and silicate-carbonate reactions on Venus
[NASA-CR-174016] 02 p0228 N85-11488
Study of singlet oxygen-pentavalent phosphorus reactions
[AD-A145896] 03 p0327 N85-12107
Experimental and theoretical study of a solar thermochemical receiver module
[NASA-CR-174107] 04 p0528 N85-13374
Mononitration of durene
[NASA-TM-77774] 06 p0765 N85-14892
Integrating chemical kinetic rate equations by selective use of stiff and nonstiff methods
[NASA-TM-86923] 07 p0904 N85-15726
Influence of temperatures of reactants on nature of product of solid-phase reactions
[BLL-M-36019-(5826.4)] 07 p0921 N85-15832
Laser spectroscopy of alkali atom-tetrahaloethylene reactions
[AD-A147431] 07 p0923 N85-15848
(Vinyloxy)fluorocyclotriphosphazenes
[AD-A147448] 07 p0924 N85-15850
Thio and seleno compounds of the transition metals with the d (o) configuration
[BLL-MINTEK-TR-1177-(5810.5759)] 07 p0925 N85-15863
Imide modified epoxy matrix resins
[NASA-CR-174695] 07 p0930 N85-15892
Performance and cost of energy transport and storage systems for dish applications using reversible chemical reactions
[NASA-CR-174263] 07 p0992 N85-16298
Method for introducing fluorine into an aromatic ring
[AD-D011397] 08 p1120 N85-17061
Basic instability mechanisms in chemically reacting subsonic and supersonic flows
[AD-A148408] 08 p1122 N85-17071
Homogeneous reaction involving components of different redox couples. 1: Theoretical considerations and digital simulation
[AD-A148666] 08 p1124 N85-17084
Ground-based measurements of mesosphere temperatures by optical means 08 p1183 N85-17453
Effects of heteroatom substituents on the properties of 1,2-dioxetanes
[AD-A148727] 09 p1290 N85-18100
Behavior of pressurized tubes of candidate alloys in a simulated low-Btu environment
[DE85-003403] 09 p1296 N85-18141
Time-resolved studies of free radicals and laser-initiated chain reactions
[DE85-002100] 09 p1326 N85-18332
New phases and chemical reactions in solid CO under pressure
[DE85-002033] 09 p1377 N85-18655
Reactivity of ion implanted silicon carbide
[DE85-001543] 09 p1399 N85-18802
Effects of a periodic disturbance on structure and mixing in turbulent shear layers and wakes
[AD-A149278] 10 p1484 N85-19370
Bibliography of Soviet laser developments, Number 86, July-August 1983
[AD-A149113] 10 p1490 N85-19406
Mixing chemical reaction and flow field development in ducted rockets
[DE85-002710] 11 p1591 N85-20009
Dynamical studies of molecular systems
[DE85-003053] 11 p1594 N85-20028
Analysis of the natural initiation of vapor explosions
[DE85-000188] 11 p1632 N85-20279
A study of organic chemical reactions in microemulsions
[AD-A150063] 12 p1796 N85-21265
Process for producing tris(n-methylamino) methylsilane
[NASA-CASE-MFS-25721-1] 12 p1799 N85-21280
Ionic mechanisms of soot formation in flames
[AD-A150119] 12 p1801 N85-21297
Electrostatic potentials: A new method for interpreting and predicting molecular reactivities and for designing synthetic pathways. Applications to nitroaromatics, nitramines and nitrated
[AD-A150120] 12 p1801 N85-21298
Alternative anodic reactions in water splitting
[DE85-004159] 12 p1802 N85-21300
Low temperature deposition of nickel films
[AD-D011568] 12 p1805 N85-21319
Chemical approach for controlling nadimide cure temperature and rate
[NASA-CASE-LEW-13770-5] 12 p1810 N85-21352
Amine salts as bonding agents
[AD-D011543] 12 p1817 N85-21396
Sulfur oxygen processes on Io 13 p2173 N85-23481
Evaluation of unimolecular rate constants for some outer-sphere electrochemical reactions
[AD-A150758] 14 p2250 N85-23946
Diagrams of chemical and electrochemical equilibria in the presence of oxygen and sulphur
[AD-A150929] 14 p2251 N85-23953
Spectral methods for modeling supersonic chemically reacting flow fields
[NASA-CR-172578] 14 p2300 N85-24240
Modelling of photodegradation in solar cell modules of substrate and superstrate design made with ethylene-vinyl acetate as pottant material
[NASA-CR-175690] 14 p2350 N85-24527
Shock tube study of the fuel structure effects on the chemical kinetic mechanisms responsible for soot formation, part 2
[NASA-CR-174880] 15 p2504 N85-25444
Scattering properties of a moving dielectric object
[AD-A151974] 15 p2544 N85-25706
Transduction of the root gravitropic stimulus: Can apical calcium regulate auxin distribution? 15 p2606 N85-26063
Development of a persistent chemical agent simulation system
[NASA-CR-175780] 16 p2745 N85-26937
Development of a Persistent Chemical Agent Simulator System (PCASS)
[NASA-CR-175776] 16 p2745 N85-26938
Fluorinated polyesters
[AD-D011611] 16 p2753 N85-26988
Dual electrochemical system
[AD-D011616] 16 p2817 N85-27376
Evaluation of chemical reaction mechanisms for photochemical smog. Part 2: Quantitative evaluation of the mechanisms, revised
[PB85-166060] 16 p2822 N85-27408
Atmospheric chemistry
[INPE-3190-PRE/554] 16 p2826 N85-27430
The production of copper phthalocyanine and/or its derivatives
[NASA-TM-77629] 17 p2917 N85-27983
Investigation of reaction layer formation in high-load capacity lubricating oils
[MPA-83-01] 17 p2975 N85-28361
Average collisional vibrational energy transfer quantities and the inversion temperature
[AD-A152674] 17 p3029 N85-28733
The conversion of smaller borane fragments to larger structures. Systematics of boron hydride reactions
[AD-A153443] 18 p3070 N85-28985

Continous chemical reaction chromatography
[DE85-009612] 18 p3072 N85-28998
Effects of H2S on molten carbonate fuel cells
[DE85-006310] 18 p3130 N85-29386
Expected behavior of plutonium in the IFR fuel cycle
[DE85-006225] 18 p3181 N85-29725
Study of the chemical mechanism in lubrication
[DE85-010768] 19 p3228 N85-30013
Chemical-acoustic interactions in combustion systems
[AD-A153857] 19 p3233 N85-30046
Selective detection of species in complex matrices by SIMS (Secondary Ion Mass Spectrometry)
[AD-D011685] 19 p3235 N85-30053
Determination of the association constant for pertechnetic acid
[DE85-010224] 19 p3235 N85-30057
Variational transition state theory
[DE85-010685] 19 p3235 N85-30059
Thermodynamic study of CO2-organic compound interaction at high pressures and temperatures
[DE85-010999] 19 p3268 N85-30266
Production of gallium atoms by excimer laser photolysis of trimethyl gallium
[DE85-010742] 19 p3278 N85-30331
Lithium cell reactions
[AD-A154429] 19 p3305 N85-30484
KIVA: A computer program for two- and three-dimensional fluid flows with chemical reactions and fuel sprays
[DE85-010334] 19 p3339 N85-30693
Reactions of metal ions and their clusters in the gas phase using laser ionization-ion cyclotron resonance spectroscopy
[DE85-009478] 19 p3361 N85-30838
Slow chemistry effects in a turbulent mixing layer
20 p3424 N85-31252
Strong turbulence chemistry interaction in a piloted turbulent jet diffusion flame 20 p3425 N85-31257
Remarks on preparation of indandione detection reagents
[NASA-TM-77905] 21 p3560 N85-32146
Interface chemistry of Hg(1-x)Cd(x)Te
[AD-A154876] 21 p3563 N85-32161
Design of micelles as dephosphorylating agents
[AD-A155589] 21 p3564 N85-32166
EVA-glass interface bond stability
21 p3606 N85-32408
Experimental studies of the formation of Aitken nuclei in the atmosphere 21 p3644 N85-32641
In-cavity laser IR spectrum analyzer for investigating non-steady-state processes 21 p3685 N85-32894
Prospects for a new kind of synthesis: Assembly of molecular components to achieve functions
[AD-A155023] 21 p3702 N85-32997
Pulsed hydrojet propulsion
[DE85-010771] 22 p3784 N85-33446
Separation of gas mixtures by supported complexes
[DE85-011996] 23 p3912 N85-34236
Experimental evaluation of the thermodynamic properties of concentrated aqueous potassium hydroxide solutions
[DE85-010628] 23 p3912 N85-34238
Metal alkoxides: Models for metal oxides. Alkoxide ligands in early transition metal organometallic chemistry
[DE85-011366] 23 p3916 N85-34269
Fire-resistant phosphorus containing polyimides and copolyimides
[NASA-CASE-ARC-11522-2] 23 p3918 N85-34280
Real time analysis of PETN detonation products
[DE85-009581] 23 p3922 N85-34303
Chemical lasers
[ISL-R-107/84] 23 p3936 N85-34400
Studies in thermo-hydro-chemical transport in porous and fractured media
[DE85-012555] 23 p3949 N85-34473
Thermally induced chemical migration: A natural analog approach
[DE85-012308] 23 p3949 N85-34474
Multi-solute subsurface transfer modeling for energy solid wastes: Highlights FY 1984
[DE85-012789] 23 p3966 N85-34591
CO + H2 reaction over nitrogn-modified iron catalysts
[DE85-013791] 24 p4072 N85-35231

CHEMICAL REACTORS

Development of a polysilicon process based on chemical vapor deposition of dichlorosilane in an advanced Siemen's reactor
[NASA-CR-174148] 04 p0483 N85-13083
Aerosol reactor for silicon processing
06 p0832 N85-15292
Assessment of the need for an advanced high-strength chromium-molybdenum steel for construction of third-generation gasifier pressure vessels
[DE85-002965] 11 p1606 N85-20097
Development of a polysilicon process based on chemical vapor deposition of dichlorosilane in an advanced Siemen's reactor
[NASA-CR-174445] 11 p1672 N85-20532
Monodisperse Latex Reactor (MLR): A materials processing space shuttle mid-deck payload
[NASA-TM-86487] 12 p1782 N85-21187
Apparatus and method to keep the walls of a free-space reactor free from deposits of solid materials
[NASA-CASE-NPO-15851-1] 12 p1858 N85-21652
Preparation of polystryene latex particles in a rotating reactor
[NASA-CR-171475] 17 p2933 N85-28108
Continous chemical reaction chromatography
[DE85-009612] 18 p3072 N85-28998
Comparison of isothermal kerogen decomposition results using reactors with different heat-up rates
[DE85-006563] 19 p3237 N85-30068
Flash pyrolysis of biomass with reactive and non-reactive gases
[DE85-010962] 19 p3306 N85-30496
Decomposition of sulfuric acid using solar thermal energy
[DE85-012288] 21 p3564 N85-32170
Silicon production in an aerosol reactor
21 p3609 N85-32416

CHEMICAL RELAXATION

U MOLECULAR RELAXATION

CHEMICAL RELEASE MODULES

Environmental effects of space activities
11 p1678 N85-20577

CHEMICAL SHIFT

U CHEMICAL EQUILIBRIUM

CHEMICAL TESTS

NT CHEMICAL ANALYSIS
NT ELECTROPHOTOMETRY
NT GAS ANALYSIS
NT MICROANALYSIS
NT NEUTRON ACTIVATION ANALYSIS
NT OZONOMETRY
NT QUALITATIVE ANALYSIS
NT QUANTITATIVE ANALYSIS
NT SALT SPRAY TESTS
NT SPECTROSCOPIC ANALYSIS
NT URINALYSIS
NT VOLUMETRIC ANALYSIS
Chemical approach for controlling nadimide cure temperature and rate
[NASA-CASE-LEW-13770-6] 19 p3232 N85-30039
Soil extraction kit
[AD-D011736] 22 p3742 N85-33190
Quantitative determination of mineral composition by powder X-ray diffraction
[DE85-011654] 22 p3760 N85-33301

CHEMICAL WARFARE

Effects of pyridostigmine on psychomotor and visual performance
[AD-A149553] 08 p1196 N85-17539
Development of a persistent chemical agent simulation system
[NASA-CR-175780] 16 p2745 N85-26937
Development of a Persistent Chemical Agent Simulator System (PCASS)
[NASA-CR-175776] 16 p2745 N85-26938
Design of micelles as dephosphorylating agents
[AD-A155589] 21 p3564 N85-32166
The identification of compounds in mustard hydrolysate
[AD-A156381] 24 p4076 N85-35258

CHEMILUMINESCENCE

Two silicon phthalocyanines and a silicon naphthalocyanine: Synthesis, electrochemistry and electrogenerated chemiluminescence
[AD-A144760] 01 p0023 N85-10145
NaK chemiluminescence
[AD-A146077] 03 p0328 N85-12110
A silicon phthalocyanine and a silicon naphthalocyanine: Synthesis, electrochemistry, and electrogenerated chemiluminescence
[AD-A146441] 06 p0785 N85-14895
Laser spectroscopy of alkali atom-tetrahaloethylene reactions
[AD-A147431] 07 p0923 N85-15848
An investigation of chemiluminescent reactions
[AD-A148460] 08 p1122 N85-17073
Mg 2 emission of Pop. 2 long-period Cepheids
11 p1754 N85-21032
Magnetically-induced luminescence of (tr(2=phos)(2)C10(4)
[AD-A149659] 12 p1799 N85-21286
Luminescence in the ocean
[AD-B089136L] 13 p2140 N85-23286
Thermolysis of 4-methyl-4-(1-propenyl)malonyl peroxide: Mechanistic limits to chemiluminescence efficiency
[AD-A151567] 15 p2505 N85-25452
Spectroscopic studies of lead oxide in a flow tube
[AD-A151849] 15 p2505 N85-25455
Electrogenerated chemiluminescence
[AD-A153547] 18 p3070 N85-28990
Equipment development for rapid detection of microorganisms in air and water
[FOA-A-40048-B2] 18 p3134 N85-29410
Alkali atom - SbCl(5) reactions: Blue-green chemiluminescence from an inverted population in SbCl
[AD-A154371] 19 p3276 N85-30315
Function of a device for detection of biological aerosols in field testing
[FOA-C-40194-B2] 20 p3504 N85-31782
Investigation of variation in the concentration of bacteria in outdoor testing, with the use of a detector for aerosols of bacteria
[FOA-C-40201-B2] 20 p3504 N85-31784
Calculation of molecular constants potential energy curves and Franck-Condon factors for lead oxide
[AD-A154521] 21 p3562 N85-32158
Nitrogen analysis by chemiluminescence
[AD-A156197] 24 p4083 N85-35308

CHEMISORPTION

Surface chemistry of palladium
[DE84-014572] 02 p0173 N85-11183
Dispersion forces of solids under stress. Chemisorption under stress
[AD-A146171] 03 p0373 N85-12390
Vibrational spectroscopy of chemisorption phenomena on model catalyst surfaces
[AD-A146753] 07 p0922 N85-15840
A study of the chemical interaction of gases with activated carbon
[AD-A147342] 07 p0923 N85-15846
The reaction of oxygen-nitrogen mixtures with granular activated carbons below the spontaneous ignition temperature
[AD-A149041] 10 p1434 N85-19039
Characterization of CO binding sites on Rh(111) and Rh(331) surfaces by XPS and LEED (Low Energy Electron Diffraction): Comparison to EELS (Electron Energy Loss Spectroscopy) results
[AD-A149331] 10 p1435 N85-19044
Adsorption thermodynamics and surface transport of metal catalyst poisons
[DE85-003750] 12 p1802 N85-21301
Chemisorption theory: Adsorption on copper-nickel alloys and titanium surface embrittlement
[DE85-001815] 12 p1807 N85-21334
Dipole active surface vibrational resonances on clean and hydrogen covered Ni(110)
[AD-A150548] 13 p2163 N85-23420
C2H(n) fragments on metal surfaces
[AD-A151474] 15 p2505 N85-25449
Experimental and theoretical study of the infrared reflectance of thin oxide films on metals
[DE85-005799] 15 p2653 N85-26366
Coadsorption studies on transition metals
[PB85-183713] 16 p3072 N85-29003
Pseudopotentials and total energy calculations: Applications to crystal stability, vibrational properties, phase transformations, and surface structures
[DE85-007657] 16 p3194 N85-29810
Cation promotion effects in zeolite-supported F-T catalysts
[DE85-009969] 19 p3233 N85-30044
Why CO bonds side-on at low coverage and both side-on and upright at high coverage on the Cr(110) surface
[NASA-CR-176071] 21 p3585 N85-32173
Experimental studies of the geometric and electronic structure of chemisorption bonding
[PB85-192250] 22 p3747 N85-33228
Infrared studies of the influence of alkali metals on the C-O bond in chemisorbed carbon monoxide
[DE85-005306] 23 p3911 N85-34232

CHEMISTRY

Abstracts of papers submitted in 1983 for publication
[PB84-217579] 03 p0396 N85-12543
Neutron scattering for the investigation of solid state materials, utilization in chemical structures
03 p0432 N85-12752
On the relationship between electronics and chemistry
[DRIC-T-7480] 22 p3743 N85-33200
Solar energy education: Renewable energy activities for chemistry and physics
[DE85-010371] 23 p3946 N85-34455

CHEMONUCLEAR PROPULSION

U CHEMICAL PROPULSION

CHEMORECEPTORS

Chemoreception and detection of micropollutants by means of a telemetric bionic detector
[DRIC-T-7480] 22 p3810 N85-33600

CHEMOTHERAPY

Magnetically-localizable, polymerized lipid vesicles and method of disrupting same
[AD-D011686] 19 p3249 N85-30144

CHESAPEAKE BAY (US)
Spectral model for subtidal variability in the Chesapeake Bay
[PB84-228679] 06 p0842 N85-15345
Comparison of MSS and TM data for landcover classification in the Chesapeake Bay area: A preliminary report — Taylor's Island, Maryland
13 p2121 N85-23210
Reverification of the Chesapeake Bay model
[AD-A155466] 21 p3655 N85-32706
CHEWING
U MASTICATION
CHILD-LANGMUIR LAW
Quenching of the beam-plasma instability by 3-D spectra of large scale density fluctuations
[NASA-CR-175969] 19 p3389 N85-30897
CHILDREN
Respiratory protection for children 3 - 6 years of age
[FOA-C-40197-C2] 02 p0238 N85-11550
Test and evaluation of the 2.4-micron photorefractor ocular screening system
[NASA-TM-86492] 15 p2615 N85-26115
Oral discussion, group-to-individual transfer and achievement in cooperative learning groups
[AD-A153209] 17 p3001 N85-28552
CHILE
Mineral nutrients in Mediterranean ecosystems
[REPT-71] 01 p0069 N85-10456
CHILLING
U COOLING
CHIMES
U AUDITORY SIGNALS
CHIMNEYS
Leakage-flow induced vibrations of a chimney structure suspended in a liquid flow — nuclear reactors
09 p1339 N85-18420
CHINA
Development of nowcasting in China
01 p0083 N85-10554
Microtektite discovered in Beijing
[NASA-TM-77765] 01 p0130 N85-10895
China report: Science and technology
[JPRS-CST-84-003] 04 p0491 N85-13132
Development of robot technology in Shanghai surveyed
04 p0492 N85-13134
China report: Science and technology
[JPRS-CST-84-001] 04 p0557 N85-13545
Present status, future prospects of domestic acoustical instruments
04 p0557 N85-13548
The characteristics of generation and the rate of distribution for science and technology information in our country (China)
[AD-A141037] 04 p0575 N85-13671
China report: Science and technology
[JPRS-CST-84-042] 06 p0747 N85-14789
New fighter aircraft reported — Jian-8 aircraft
06 p0747 N85-14790
F-7 supersonic day fighter viewed — Jian-7 aircraft
06 p0747 N85-14791
A-5 supersonic attack aircraft described — Qiang-5 aircraft
06 p0747 N85-14792
Details of export A-5 close-support aircraft given — Qiang-5 aircraft
06 p0748 N85-14793
China report: Science and technology
[JPRS-CST-84-037] 10 p1424 N85-18982
Details of export A-5 close-support aircraft given
10 p1424 N85-18983
China's future domestic satellite communications systems
10 p1476 N85-19312
China's domestic satellite communications
10 p1476 N85-19313
China report: Science and technology
[JPRS-CST-84-026] 11 p1619 N85-20189
Remote sensing technology now playing practical roles
11 p1619 N85-20190
China report: Science and technology
[JPRS-CST-84-025] 11 p1620 N85-20197
Thermophysical properties of matter
11 p1620 N85-20199
China report: Science and technology
[JPRS-CST-84-032] 11 p1621 N85-20202
China report: Science and technology
[JPRS-CST-84-039] 11 p1621 N85-20206
China report: Science and technology
[JPRS-CST-84-036] 11 p1666 N85-20661
China report: Science and technology
[JPRS-CST-85-006] 12 p1820 N85-21416
Systems research on China in year 2000
12 p1820 N85-21418
Studies of the development of cyclones over Southern China coastal areas and adjacent seas
[AD-A150108] 12 p1896 N85-21901
China report: Science and technology
[JPRS-CST-84-030] 13 p2041 N85-22777
China report: Science and technology
[JPRS-CST-85-003] 13 p2166 N85-23433
The astrometry network of observers in China
14 p2436 N85-25027
China report: Science and technology
[JPRS-CST-85-009] 15 p2530 N85-25596
Future prospects of China's microwave semiconductor technology
15 p2530 N85-25598
China report: Science and technology
[JPRS-CST-85-007] 15 p2533 N85-25621
China report: Science and technology
[JPRS-CST-85-011] 15 p2551 N85-25746
China report: Science and technology
[JPRS-CST-85-010] 15 p2564 N85-25819
China report: Science and Technology
[JPRS-CST-85-012] 16 p2806 N85-27300
China has developed a new version of fighter aircraft
[AD-A155293] 21 p3555 N85-32118
Geology and petroleum resources of basins in western China
[DE85-013038] 23 p3948 N85-34469
Space activities in the Soviet Union, Japan, and the People's Republic of China
23 p4057 N85-35149
CHINA (COMMUNIST) MAINLAND
U CHINA
CHINESE PEOPLES REPUBLIC
U CHINA
CHINOOK HELICOPTER
U CH-47 HELICOPTER
CHIPS (ELECTRONICS)
Routing the power and ground wires on a VLSI chip
[AD-A145356] 02 p0194 N85-11296
NMOS test chip for a course in semiconductor parameter measurements
[PB84-216506] 04 p0497 N85-13174
VLSI architectures for the multiplication of integers modulo a Fermat number
05 p0624 N85-13993
Specialized silicon compilers for language recognition
[AD-A146526] 06 p0853 N85-15425
Charge domain filters for enhanced monolithic signal processing
[AD-A147428] 07 p0941 N85-15964
Built-in test and self repair mechanisms in a digital correlator integrated circuit
08 p1084 N85-16741
Life cycle cost model for very high speed integrated circuits
[AD-A147798] 08 p1157 N85-17298
Design of a bit-sliced processor array with built-in-self-test
[AD-A149785] 12 p1835 N85-21513
Built-in tests for VLSI (Very Large Scale Integration) finite-state machines
[AD-A149784] 12 p1911 N85-21997
UW/NW (University of Washington/Northwest) VLSI Consortium
[AD-A150740] 14 p2404 N85-24818
Developments in microelectronics: Past and future
15 p2530 N85-25597
Improved, cheaper SIPMOS circuits no. 10, 1983 p 370
15 p2534 N85-25630
An integrated UNIX-based CAD system for the design and testing of custom VLSI chips
16 p2771 N85-27102
Goals, achievements of microelectronics program
17 p2945 N85-28179
Modern equipment for manufacture of IC's in Hungary
17 p2945 N85-28181
Measurement methods for accurate microwave characterization and modeling of MESFET chips
[AD-A152360] 17 p2952 N85-28227
Encapsulation and packaging of a semiconductor multielectrode array for cortical implantation
[AD-A153180] 17 p2998 N85-28535
Random access memory technologies
[AD-A153089] 17 p3008 N85-28597
Speed-up techniques for complementary metal oxide semiconductor very large scale integration
[AD-A152466] 17 p3043 N85-28829
Evaluation of VLSI technology — space applications
[CD.6501702] 18 p3098 N85-29177
Basic development of one-chip control circuitry for commutatorless dc motors
[BMFT-FB-T-84-305] 18 p3098 N85-29178
Electro-optic techniques for VLSI interconnect
18 p3186 N85-29774
A single chip VLSI architecture for radar signal processing
19 p3257 N85-30195
Leading-edge microelectronics research at Sweden's Chalmers
20 p3438 N85-31337
Digital integrated circuits
21 p3669 N85-32787
Hermetic chip carrier compliant soldering pads
[AD-D011722] 23 p3938 N85-34410
CHIPS (MEMORY DEVICES)
Compository speech output (KOSA) with a very large scale integration speech synthesis chip
[FI-13-TBR-18] 07 p0942 N85-15974
Vector computer memory bank contention
[NASA-CR-177342] 09 p1376 N85-18649
Siemens, Philips megaproject to yield superchip in 5 years
11 p1592 N85-20018
The design of an adaptive predictive coder using a single-chip digital signal processor
[AD-A152461] 17 p2952 N85-28231
Evaluation of VLSI technology — space applications
[CD.6501702] 18 p3098 N85-29177
Fault-tolerant computing research
[AD-A154062] 19 p3342 N85-30710
CHIRAL DYNAMICS
Skyrmions and vector mesons: A symmetric approach
[DE84-015297] 04 p0563 N85-13584
Implications of the chiral anomaly for quantum Hall effect devices
[NUB-2662] 05 p0629 N85-14029
Comment on quantum effects on 4-dimensional space-time symmetries
[DE85-007780] 16 p2872 N85-27722
Modern test of chiral anomalies
[DE85-005892] 17 p3020 N85-28680
Lattice actions improved by block-spin renormalisation group and maximally symmetric lattices
[DE85-007416] 17 p3045 N85-28841
On the definition of topological susceptibility via lattice anomalous Ward identities and its perturbative tail
[PREPRINT-416] 18 p3184 N85-29744
CHLORIDES
NT ALUMINUM CHLORIDES
NT CALCIUM CHLORIDES
NT CARBON TETRACHLORIDE
NT COPPER CHLORIDES
NT DICHLORIDES
NT HYDROCHLORIC ACID
NT HYDROGEN CHLORIDES
NT IRON CHLORIDES
NT LITHIUM CHLORIDES
NT MAGNESIUM CHLORIDES
NT POTASSIUM CHLORIDES
NT SILVER CHLORIDES
NT SODIUM CHLORIDES
NT TITANIUM CHLORIDES
NT ZINC CHLORIDES
Dynamics of graphite fiber intercalation: In situ resistivity measurements with a four point probe
[NASA-TM-86858] 01 p0017 N85-10105
Comparison study of analytical methods for the determination of fluoride, chloride, and bromide in plastics
[DE84-015008] 04 p0470 N85-12989
Development and evaluation of a procedure for the rapid analysis of fresh concrete
[AD-A149741] 12 p1866 N85-21703
Exploratory corrosion tests on alloys in molten salts at 900(0)C
[DE85-000511] 14 p2257 N85-23983
The effect of occupational exposure and the body weight to height ratio on exhaled methylene chloride breath concentration in females at one, eighteen and sixty-six hours post exposure
14 p2368 N85-24708
Radiation-induced degradation of trichloroethylene and tetrachloroethylene in drinking water
[OEFZS-4298] 18 p3134 N85-29409
Alkali atom - SbCl(5) reactions: Blue-green chemiluminescence from an inverted population in SbCl
[AD-A154371] 19 p3276 N85-30315
Lithium cell reactions
[AD-A154429] 19 p3305 N85-30484
Safety of Li-SOCl2 cells
20 p3444 N85-31383
Environmental surveillance at Los Alamos during 1984
[DE85-011866] 22 p3811 N85-33605
CHLORINATION
Biofouling and corrosion studies at the Seacoast Test Facility in Hawaii
[DE84-014643] 01 p0029 N85-10180
The development of titanium production in the USSR
[BLL-OA-TRANS-3226-(6196.3)]
23 p3913 N85-34244
CHLORINE
Chlorine isotopes as environmental tracers in Columbia River basalt groundwaters
[DE85-011392] 19 p3302 N85-30473
Facility for large-scale hazardous gas testing
[DE85-011852] 21 p3564 N85-32169
Characteristics of aerosol composition in a nonurban area, north China
21 p3646 N85-32651
Precision measurements of solar energetic particle elemental composition
[PAPER-SH-2.1-4] 21 p3715 N85-33052
Method for removing chlorine compounds from hydrocarbon mixtures
[DE85-011608] 22 p3742 N85-33191
The isotopic composition of cosmic ray chlorine
[OG-4.3-3] 22 p3878 N85-34026

Results of ultra-low level 71ge counting for application in the Gallex-solar neutrino experiment at the Gran Sasso Underground Physics Laboratory
[SH-8.1-2] 23 p4049 N85-35108
Correlation between solar neutrino flux and other solar phenomena 23 p4049 N85-35109
Fluidized bed desulfurization
[NASA-CASE-NPO-15924-1] 24 p4075 N85-35253

CHLORINE COMPOUNDS
NT ALUMINUM CHLORIDES
NT AMMONIUM PERCHLORATES
NT CALCIUM CHLORIDES
NT CARBON TETRACHLORIDE
NT CHLORIDES
NT CHLORINE OXIDES
NT CHLOROSILANES
NT COPPER CHLORIDES
NT DDT
NT DICHLORIDES
NT HYDROCHLORIC ACID
NT IRON CHLORIDES
NT LITHIUM CHLORIDES
NT MAGNESIUM CHLORIDES
NT PERCHLORATES
NT POTASSIUM CHLORIDES
NT POTASSIUM PERCHLORATES
NT SILVER CHLORIDES
NT SODIUM CHLORIDES
NT TITANIUM CHLORIDES
NT ZINC CHLORIDES
Study of effectiveness of fire-resistant activity of antipyrenes for fibers of aromatic polyamides 06 p0762 N85-14874
Working medium for sorption heat pumps
[BLL-T6360/BG/WH785/84] 06 p0807 N85-15131
Thermally modulated electron affinity detector for priority pollutant analysis
[PB85-158145] 15 p2508 N85-25469
Atmospheric chlorofluromethanes as tracers of ocean circulation and mixing: Measurement and calibration techniques and studies in the Greenland and Norwegian Seas 19 p3319 N85-30573
Throughfall rate and chemistry studies: Whiteface Mountain
[DE85-012407] 23 p3947 N85-34464

CHLORINE OXIDES
Stratospheric ClO: In-situ detection with a new approach 16 p2824 N85-27416
Investigation of the reaction system NOX/ClOX/HOX under tropospheric and stratospheric conditions
[BPT-11/84] 18 p3137 N85-29427

CHLOROAROMATICS
Sensitization and quenching in the conversion of light energy into chemical energy
[DE85-006301] 14 p2351 N85-24535

CHLOROETHYLENE
Fate and disposition of trichloroethylene in surface soils
[AD-A147918] 07 p0995 N85-16321
Search for acoustic signals from high energy cascades
[HE-7.1-1] 24 p4213 N85-36155

CHLOROFORM
The mobile phase in coals: Its nature and modes of release
[DE85-011686] 19 p3230 N85-30026

CHLOROPHYLLS
Characteristic vector analysis of inflection ratio spectra: New technique for analysis of ocean color data
[NASA-TP-2428] 13 p2126 N85-23237
Eight DOE Solar Photochemistry Research Conference: Proceedings
[DE85-005094] 15 p2587 N85-25948
Chemical, biological, and physical measurements from the subtropical western North Atlantic Ocean. Summer 1982, USNS Lynch, cruise 710-82
[AD-A153623] 18 p3201 N85-29857

CHLOROPRENE RESINS
Design, manufacture, and testing of compliant coatings for reduction of turbulent drag
[AD-A145510] 02 p0196 N85-11323
The effect of pressure on the mechanical properties of polymers. Part 2: Measurement of the time-dependent Poisson's ratio
[DE85-002139] 06 p0772 N85-14938

CHLOROSILANES
Silazane precursors to silicon nitride
[AD-A146791] 07 p0931 N85-15899
A novel polymeric organosilazane precursor to Si3N4/SiC ceramics
[AD-A150748] 14 p2260 N85-24003
An analysis of the feasibility of producing silicon for solar cells by a dichlorosilane/fluidized-bed reactor process
[NASA-CR-176036] 20 p3478 N85-31614

CHOICE
U SELECTION

CHOKES
Investigation of the choking effect of an inert granular bed on an ignition gas jet charged with particles
[ISL-CO-235/83] 14 p2264 N85-24028

CHOLESKY FACTORIZATION
Internal variables in the lattice for cholesky factorization. Kalman filtering and model identification
[AD-A149431] 10 p1547 N85-19757
Parallel Cholesky factorization on a multiprocessor
[DE85-006762] 17 p3021 N85-26662
Parallel Cholesky factorization in message-passing multiprocessor environments
[DE85-012079] 22 p3830 N85-33717

CHOLINE
Induced changes in the cholinergic system of sciatic nerve and slow and fast twitch muscle of rats 15 p2609 N85-26081
Changes in the cholinergic system of rat sciatic nerve and skeletal muscle following suspension induced disuse
[NASA-CR-175718] 15 p2615 N85-26111

CHOLINERGIC BLOCKING AGENTS
U ANTICHOLINERGICS

CHOLINERGICS
NT ANTICHOLINERGICS

CHOLINESTERASE
Effects of pyridostigmine on psychomotor and visual performance
[AD-A148553] 08 p1196 N85-17539
Is fast fiber innervation responsible for increased acetylcholinesterase activity in reinnervating soleus muscles?
[NASA-CR-175716] 15 p2614 N85-26108
Use and disuse and the control of acetylcholinesterase activity in fast and slow twitch muscle of rat
[NASA-CR-175717] 15 p2614 N85-26109
Changes in the cholinergic system of rat sciatic nerve and skeletal muscle following suspension induced disuse
[NASA-CR-175718] 15 p2615 N85-26111

CHONDRITES
NT ALLENDE METEORITE
NT CARBONACEOUS CHONDRITES
NT CARBONACEOUS METEORITES
NT PANTAR CHONDRITES
The asteroidal source region of ordinary chondrites 06 p0881 N85-15600
Major element chemical compositions of chondrules in unequilibrated chondrites 06 p0881 N85-15602
Fine-grained millimeter-sized objects in type 3 ordinary chondrites and their relation to chondrules and matrix 06 p0882 N85-15603
Chondrules in the bishunpur L13 chondrite 06 p0882 N85-15605
Size dependence of chondrule textural types 06 p0882 N85-15606
Neutron activation analysis of stoney spherules from a marine sediment sample 06 p0883 N85-15608
Oxygen isotopes in deep sea spherules 06 p0883 N85-15609
Evolutionary history of CI and CM chondrites 06 p0884 N85-15615
Unexplained Fe, Ni and S anomalies in CV chondrite components 06 p0884 N85-15618
The Colony meteorite and the possible existence of a new chemical subgroup of CO3 chondrites 06 p0885 N85-15621
Meteoritic constraints on processes in the solar nebula 06 p0887 N85-15630
Chemical evolution of the solar nebula: A new model 06 p0887 N85-15631
Where is the Earth's missing xenon? 06 p0888 N85-15641
Boron cosmochemistry 06 p0888 N85-15642
The chemistry of rare earth elements in the solar nebula 06 p0889 N85-15643
Differentiated meteorites and the components of chondrites
[NASA-CR-174201] 06 p0890 N85-15649
Origin and evolution of ordinary chondrite meteorites 15 p2683 N85-26571
A model for core formation in the early Earth 21 p3719 N85-33078
Noble gases in meteorites and terrestrial planets 22 p3851 N85-33850
Relationships between chondritic meteorites and planets 22 p3851 N85-33851
Nebular volatile fractionations associated with chondrule formation 22 p3852 N85-33855
The cosmic ray composition as viewed from the chemical abundances of the solar system
[OG-7.1-8] 23 p4013 N85-34869
Cosmogenic Mn-53 in meteorites
[SH-7.1-17] 23 p4049 N85-35107

CHONDRULE
Dynamic crystallization of silicate melts
[NASA-CR-174103] 05 p0743 N85-14774
Bulk compositions of Al-rich chondrules in ordinary and carbonaceous chondrites: Variations and similarities 06 p0881 N85-15601
Major element chemical compositions of chondrules in unequilibrated chondrites 06 p0881 N85-15602
Fine-grained millimeter-sized objects in type 3 ordinary chondrites and their relation to chondrules and matrix 06 p0882 N85-15603
Chondrule rims and interchondrule matrix in UOC 06 p0882 N85-15604
Chondrules in the bishunpur L13 chondrite 06 p0882 N85-15605
Size dependence of chondrule textural types 06 p0882 N85-15606
The influence of gravitational body force in meteoritic chondrule and lunar glass formation 06 p0884 N85-15614
Meteoritic constraints on processes in the solar nebula 06 p0887 N85-15630
Chemical evolution of the solar nebula: A new model 06 p0887 N85-15631
Chondrule-like particles provide evidence of early Archean meteorite impacts, South Africa and western Australia 15 p2682 N85-26562

CHORUS (DAWN PHENOMENON)
U DAWN CHORUS

CHORUS PHENOMENON
U DAWN CHORUS

CHROMATES
Investigation of the dissolution of CaCrO4 in molten LiCl-KCl eutectic
[DE84-016394] 04 p0469 N85-12985
Determination of Faradaic current through a bipolar electrode in acidic bichromate 04 p0483 N85-13077
CVD boron on calcium chromate powder
[DE85-000214] 09 p1299 N85-18158
Solid phase reactions among manganese, potassium perchlorate and barium chromate
[HSE-TRANS-11166] 19 p3237 N85-30071

CHROMATOGRAPHY
NT GAS CHROMATOGRAPHY
NT LIQUID CHROMATOGRAPHY
Ion chromatographic determination of gold in plating baths
[DE84-016187] 02 p0184 N85-11230
Comparison study of analytical methods for the determination of fluoride, chloride, and bromide in plastics
[DE84-015008] 04 p0470 N85-12989
Determination of halogens and sulfur in organic compounds and polymers by combustion-ion chromatography
[DE84-016186] 05 p0614 N85-13921
ECUT, Energy Conversion and Utilization Technologies program: Isothermal separation processes update
[NASA-CR-175463] 10 p1433 N85-19033
High performance size exclusion chromatography (IX) bulk and component analysis of silanol groups in polydimethylsiloxanes: Process development endeavor
[DE85-006853] 15 p2506 N85-25458
Experiments on sorption characteristics of solid desiccant materials for solar desiccant cooling systems
[DE85-000542] 17 p2923 N85-26019
Continous chemical reaction chromatography
[DE85-009812] 18 p3072 N85-28998
Multidimensional luminescence measurements
[AD-A154950] 21 p3563 N85-32162
Size exclusion chromatography-low angle laser light scattering photometry of lignite macromolecules
[DE85-012017] 22 p3745 N85-33215
Supercritical fluid chromatography/supersonic jet spectroscopy
[DE85-007005] 22 p3746 N85-33221
Electrochromic display device
[AD-D011733] 22 p3759 N85-33299
Modulated voltage metastable ionization detector
[NASA-CASE-ARC-11503-1] 23 p3933 N85-34374

CHROME
U CHROMIUM

CHROMIC ACID
Electrolytic deposition of chromium from aqueous chromium solutions containing foreign anions
[BLL-MINTEK-TR-1170-(5810.5750)] 06 p0764 N85-14889

CHROMITES
Some recent deposit modeling efforts 24 p4106 N85-35453

CHROMIUM
NT CHROMIUM ISOTOPES
An investigation of the solubility and diffusivity of chromium in gallium arsenide
[AD-A144949] 01 p0024 N85-10148

Thermodynamic properties and environmental chemistry of chromium
[DE84-015123] 01 p0025 N85-10152
The oxidation behaviour of a 20 percent Cr/25 percent Ni/Nb stabilized stainless steel in carbon dioxide at high temperatures and its improvement by cerium and yttrium
[AERE-R-11228] 01 p0029 N85-10182
EDS round-robin evaluation of type 308 austenitic stainless steel
[DE84-014574] 02 p0183 N85-11226
Review: The influence of short circuit diffusion on the oxidation of nickel, chromium and nickel/chromium alloys
[AERE-R-11311] 02 p0185 N85-11237
EXAFS and Mossebauer study of small metal clusters isolated in rare-gas solids
[DE84-015976] 04 p0470 N85-12994
Abundancies of Ni, Cr, CO and major elements in the silicate portion of the Moon: Constraints from primary lunar magmas 04 p0582 N85-13720
Studies on copper alloys containing chromium on the copper side phase diagram
[NASA-TM-77752] 07 p0927 N85-15876
Optimization of the NiCrAl-Y/ZrO-Y2O3 thermal barrier system
[NASA-TM-86905] 07 p0927 N85-15878
Influence of plastic deformation on structural stability of nichrome-tungsten composite materials 11 p1599 N85-20080
Transverse microstructure of an oxide scale formed on a 20 % Cr/25 % Ni niobium stabilized stainless steel
[AERE-R-11034] 12 p1804 N85-21315
Effects of chromium and aluminum on mechanical and oxidation properties of iron-nickel-base superalloys based on CG-27
[NASA-TP-2443] 12 p1805 N85-21323
Dispersed-metal-toughened alumina
[NASA-CR-174667] 13 p2037 N85-22758
Microstructure and properties of ferrous alloy weldments
[DE85-005582] 14 p2257 N85-23987
Positron annihilation studies of vacancy formation in tungsten, chromium, and niobium
[DE85-006837] 16 p2671 N85-27710
Influence of manganese and heat treatment on structure and properties of Fe-0.1 percent-C-14 percent Cr-based steels
[BLL-BISI-TRANS-22299-(9022.06)] 17 p2928 N85-28071
Determination of the vacancy formation enthalpy in chromium by positron annihilation
[DE85-010286] 19 p3230 N85-30084
Why CO bonds side-on at low coverage and both side-on and upright at high coverage on the Cr(110) surface
[NASA-CR-176071] 21 p3585 N85-32173
Electrodeposition of chromium and copper in magnetic fields
[AD-A154648] 21 p3566 N85-32180
Microscopic control of semiconductor surface oxidation
[AD-A154799] 21 p3709 N85-33026
Measurements of Fe and Ar fragmentation cross sections
[PAPER-OG-7.2-20] 21 p3714 N85-33047
Environmental surveillance at Los Alamos during 1984
[DE85-011866] 22 p3811 N85-33605
Calculated neutron-induced cross sections for /sup 63,65/Cu/sup 58,60/Ni and (52) Cr from 1 to 20 MeV and comparisons with experiments
[DE85-011928] 22 p3844 N85-33808
The effect of pre-heating on the structure and properties of chromium-molybdenum steels
[BLL-M-35697-(5828.4)] 23 p3914 N85-34255
Special features of the fracture of ball-bearing steel close to non-metallic inclusion eutectics
[BLL-M-35809-(5828.4)] 23 p3914 N85-34258
Process for improving moisture resistance of epoxy resins by addition of chromium ions
[NASA-CASE-LAR-13228-1] 23 p3919 N85-34282
Thermodynamics of the corrosion of chromium in molten carbonates
[DE85-011407] 24 p4079 N85-35282
X-ray fluorescence analysis of 304L stainless steel
[DE85-013254] 24 p4080 N85-35288
Applications of the mineral resources data system and the international strategic minerals inventory in mineral-resource assessments by region and commodity 24 p4105 N85-35451
The Conterminous United States Mineral Assessment Program 24 p4106 N85-35458
The Alaska Mineral Resources Assessment Program 24 p4107 N85-35460
Development of electrodes for the NASA iron/chromium
[NASA-CR-174724] 24 p4109 N85-35471

CHROMIUM ALLOYS
NT CHROMIUM STEELS
NT RENE 95
Thermodynamics of decarburization of niobium-bearing high-alloy melts
[BLL-M-35726-(5828.4)] 02 p0175 N85-11169
Review: The influence of short circuit diffusion on the oxidation of nickel, chromium and nickel/chromium alloys
[AERE-R-11311] 02 p0185 N85-11237
Study of the reactive-element effect in oxidation of Fe-Cr alloys using transverse section analytical electron microscopy
[DE84-016237] 04 p0571 N85-13641
Experimental determination of the critical cavity radius in Fe-10% Cr for ion irradiation
[DE84-016570] 04 p0571 N85-13646
Thermal diffusivity and conductivity of chromium-manganese alloying compositions
[BLL-M-35925-(5828.4)] 05 p0616 N85-13938
The effect of trace elements on the properties at high temperature of a Ni-Cr-base alloy 05 p0617 N85-13944
Metallographic evaluation of the reactions between boronated graphite and Fe-Ni-Cr alloys
[DE84-015374] 06 p0769 N85-14922
The formation of isolated phase precipitates during the decomposition of high-coercive force Fe-Cr-Co alloys
[BLL-M-36028-(5828.4)] 07 p0924 N85-15855
On heat-treatable copper-chromium alloy, 1
[NASA-TM-77753] 07 p0927 N85-15879
On reversion phenomena in Cu-Zr-Cr alloys
[NASA-TM-77791] 08 p1125 N85-17092
Reversion phenomena of Cu-Cr alloys
[NASA-TM-77780] 08 p1125 N85-17094
Recommendations for the use of Ni-Cr-base alloy extensometers for measurement of creep strain
[NPL-DMA(A)-81] 06 p1184 N85-17342
Low and moderate temperature oxidation of atomically clean nickel, chromium and Ni-Cr alloys
[DE84-017350] 09 p1295 N85-18131
Initial aging phenomena in copper-chromium alloys
[NASA-TM-77790] 10 p1439 N85-19070
Influence of volumetric fiber content on some matrix damage factors during thermal cycling of tungsten-EI 765 composite 10 p1443 N85-19097
Stress relief of transition zones
[DE85-000234] 11 p1653 N85-20411
Partial replacement of chromium in austenitic stainless steels by molybdenum, copper, and vanadium, report of investigations 1984
[PB85-116508] 12 p1809 N85-21346
Performance of Chromel versus Alumel and Nicrosil versus Nisil thermocouple assemblies in vacuum and argon between 1000 deg C and 1200 deg C
[DE85-000810] 12 p1853 N85-21624
Orientation and temperature dependence of some mechanical properties of the single-crystal nickel-base superalloy Rene N4. 3: Tension-compression anisotropy
[NASA-TM-86982] 13 p2021 N85-22680
Study of the effects of implantation on the high Fe-Ni-Cr and Ni-Cr-Al alloys
[NASA-CR-175625] 13 p2021 N85-22681
Structure and aging of amorphous chromium-germanium alloys 15 p2497 N85-25401
Reduced-chromium stainless steel substitutes containing silicon and aluminum
[PB85-160786] 15 p2513 N85-25502
Electrical conductivity and phase diagram of binary alloys. 21: The system palladium-chromium
[NASA-TM-77863] 18 p3073 N85-29009
Changes of structure of EP648-VI alloy as a result of high-temperature gas corrosion 19 p3243 N85-30110
Optimisation of MCr Al coating compositions for marine gas turbines
[BR91159] 20 p3394 N85-31056
Mechanical behavior of Ni-Cr-base superalloys in forms and conditions representative of service
[NPL-DMA(A)-94] 20 p3431 N85-31282
A systematic plan for the continued study of dimensional stability of metallic alloys considered for the fabrication of cryogenic wind tunnel models
[NASA-CR-172449] 21 p3565 N85-32172
Dynamics of the melting of chromium-manganese alloys in molten steel
[BLL-M-35850-(5828.4)] 23 p3914 N85-34252
Chromium-base powder alloys for welding cladding layer of bimetal
[BLL-M-35776-(5828.4)] 23 p3915 N85-34260
Deposition of nickel-cobalt alloys by controlled-potential electrolysis
[PB85-196562] 24 p4081 N85-35291

CHROMIUM BORIDES
The use of moments of momentum to account for crystal habits
[NASA-CR-3907] 20 p3421 N85-31232
CHROMIUM CARBIDES
Effects of silver and group 2 fluorides addition to plasma sprayed chromium carbide high temperature solid lubricant for foil gas bearing to 650 deg C
[NASA-TM-86895] 08 p0770 N85-14928
Antifriction properties of gas thermal coatings of clad carbine powders 10 p1447 N85-19115
CHROMIUM COMPOUNDS
NT CHROMATES
NT CHROMIC ACID
NT CHROMITES
NT CHROMIUM BORIDES
NT CHROMIUM CARBIDES
NT CHROMIUM OXIDES
Vaporization behavior of chromium phosphides. The solid 2-phase regions CrP-Cr12P7, Cr12P7-Cr3P, and Cr3P-Cr
[AD-A145481] 02 p0172 N85-11152
Properties of chromate coatings formed on electrolytic zinc substrates
[BLL-BISI-TRANS-22349-(9022.06)] 17 p2926 N85-28052
Electrical conductivity and phase diagram of binary alloys. 21: The system palladium-chromium
[NASA-TM-77863] 18 p3073 N85-29009
CHROMIUM ISOTOPES
Experimental test for interpreting the increase in sensibility of doped CR-39
[OG-4.4-11] 22 p3880 N85-34042
CHROMIUM OXIDES
NT CHROMITES
Review: The influence of short circuit diffusion on the oxidation of nickel, chromium and nickel/chromium alloys
[AERE-R-11311] 02 p0185 N85-11237
Diffusion of Cr-51 tracer in Cr-2O-3 and the growth of Cr-2O-3 films
[AERE-R-11314] 03 p0333 N85-12146
Interaction between chromium oxide and carbon
[BLL-M-36002-(5828.4)] 07 p0926 N85-15867
Strength and failure of ceramic-metallic material 10 p1446 N85-19112
Test and modeling for sintering theory
[DE85-007761] 16 p2755 N85-27004
CHROMIUM STEELS
Study to optimize Cr-Mo steels to resist hydrogen and temper embrittlement. A study of carbides formed in low alloy Cr-Mo steels
[DE84-015208] 01 p0029 N85-10179
Structure and wear workshop colloquium 01 p0054 N85-10356
The influence of the carbide distribution on the abrasive wear of ledeburitic chromium steels 01 p0054 N85-10359
Metalurgy of a 12 percent chromium stainless steel 02 p0178 N85-11195
Thermal ageing studies of 9%Cr 1%Mo steel
[AERE-R-11109] 03 p0333 N85-12149
The effects of microstructure on the temper embrittlement susceptibility of a Cr-2-1/4 1Mo forging
[AERE-R-11110] 03 p0334 N85-12151
A study of precipitation and boron distribution in 20 Cr 25Ni base stainless steels
[AERE-M-3353] 03 p0334 N85-12154
Stress relief cracking studies of 2 1/4Cr1Mo steel
[AERE-R-11111] 03 p0374 N85-12368
Autenite transformation in powder-compacted chromium-nickel-molybdenum steels during continuous cooling
[BLL-M-35981-(5828.4)] 05 p0615 N85-13933
Susceptibility of 2 1/4 Cr-1Mo steel to liquid metal induced embrittlement by lithium-lead solutions
[DE85-000997] 09 p1294 N85-18130
Effect of tempering on the strength and toughness of 2 1/4 Cr-1 Mo steel weldments
[DE85-003818] 09 p1296 N85-18140
Assessment of the need for an advanced high-strength chromium-molybdenum steel for construction of third-generation gasifier pressure vessels
[DE85-002865] 11 p1606 N85-20097
The role of void nucleation in the swelling resistance of ferritic steel
[AERE-R-11525] 11 p1610 N85-20122
Frictional and structural characterization of ion-nitrided low and high chromium steels
[NASA-TM-86991] 13 p2098 N85-23085
Radiation effects on structural materials
[DE85-007032] 15 p2649 N85-26338
The corrosion resistance of chromium-nickel steel containing rare-earth metals
[BLL-BISI-TRANS-22477-(9022.06)] 17 p2925 N85-28041

Influence of heat treatment parameters on the properties of induction hardened Ni-Cr-Mo steels
[BLL-BISI-TRANS-2499-(9022.06)] 17 p2926 N85-28053

Obtaining oxide films on surface of tubes of chromium-nickel steels
[BLL-BISI-TRANS-22478-(9022.06)] 17 p2929 N85-28076

Dispersion-strengthened powder-metallurgical chromium steels
[BLL-BISI-TRANS-22323-(9022.06)] 17 p2929 N85-28081

Study to optimize Cr-Mo steels to resist hydrogen and temper embrittlement
[DE85-005492] 17 p2932 N85-28096

Influence of temperature in melting and casting on quality of medium-alloy steel
[BLL-BISI-TRANS-22310-(9902.06)] 17 p2938 N85-28137

Study of a simulated test for assessing the machinability of steels
[BLL-BISI-TRANS-22344-(9022.06)] 17 p2972 N85-28357

Fracture mechanics analysis of cold drawn SI-Cr valve steel
[BLL-BISI-TRANS-22216-(9022.06)] 17 p2978 N85-28405

Fatigue and chromium-ferritic steels at elevated temperatures
[DE85-007735] 18 p3074 N85-29015

Elevated temperature erosion corrosion of 9Cr1Mo steel
[DE85-008445] 18 p3074 N85-29016

Surface degradation of ductile metal in elevated temperature gas-particle streams
[DE85-008426] 18 p3074 N85-29017

Corrosion-erosion rates/mechanisms of 9Cr1Mo steel
[DE85-008506] 18 p3076 N85-29029

The effect of temperature on the corrosion-erosion of 9Cr1Mo steel
[DE85-008507] 18 p3076 N85-29030

Conservation and substitution technology for critical metals in bearings and related components for industrial equipment and opportunities for improved bearing performance
[PB85-176246] 18 p3082 N85-29069

Effects of heat treatment and tracer element impurities on the impact properties of the 12Cr steels
[DE85-010676] 19 p3240 N85-30088

Vacuum pressure welding of commercial titanium with 2Kh13 and 12Kh18N10T steels
19 p3246 N85-30124

Structural transformation of a 9% Cr - 2%Mo steel (type Z10CDNbV 09-02) for use in steam generators for fast neutron reactors
[BLL-CE-TRANS-7943-(9022.09)] 20 p3430 N85-31271

Fatigue-crack growth and ductile fracture toughness behavior of ASTM A387 Grade 91 steel
[DE85-008495] 20 p3431 N85-31296

Reliability of welds to repair defects in cast components made from CrMoV steel
[BLL-CE-TRANS-8054-(9022.09)] 20 p3461 N85-31501

Application of the unloading compliance methods in fracture toughness measurements of a quenched and tempered steel
[BLL-CE-TRANS-7953-(9022.09)] 20 p3465 N85-31523

Fatigue behavior of chromium-containing ferritic steels at elevated temperature
[DE85-012309] 22 p3748 N85-33231

Characterization of modified 9 Cr Mo steel extruded pipe
[DE85-012056] 23 p3941 N85-34430

Characterization of modified 9 r-1 Mo steel sand castings
[DE85-012057] 24 p4060 N85-35287

CHROMOSOMES

Chromosome aberrations in Crepis capillaris exposed to gamma radiation and clinostat
19 p3325 N85-30600

Three-dimensional reconstruction and data display of chromosome structure studied by electron microscope tomography
[DE85-011562] 22 p3825 N85-33697

CHROMOSPHERE

Vector magnetic field analysis of Lorentz forces acting in the solar atmosphere
[AD-A145941] 03 p0449 N85-12852

Time dependent effects at the foot of the chromosphere
[NASA-CR-174143] 04 p0589 N85-13762

Theoretical studies of chromospheres and winds in cool stars
[NASA-CR-174204] 06 p0860 N85-15596

Spicules and surges
[AD-A146785] 07 p1061 N85-16727

Heating in the solar mantle 06 p1233 N85-17769

Extreme limb profiles of the Sun at far infrared and submillimeter wavelengths 06 p1244 N85-17852

Coronal and chromospheric physics — Sun, sunspots, and solar limb
[NASA-CR-174290] 08 p1259 N85-17921

The calculation of theoretical chromospheric models and the interpretation of solar spectra from rockets and spacecraft
[NASA-CR-174289] 08 p1259 N85-17922

A search for young stellar chromospheres in NGC 2264 11 p1748 N85-20993

Chromospheric activity in M giants 11 p1757 N85-21056

Chromospheric emission lines in high-resolution LWR spectra (220 - 3000 alpha) of gamma CRU (M3 3) and alpha ORI (M2 lab) 11 p1758 N85-21058

Betegeuse at maximum luminosity 11 p1758 N85-21061

Rotational modulation of chromospheric emission in cool giants and hybrid stars 11 p1759 N85-21064

Thermal stability of static coronal loops: Part 1: Effects of boundary conditions
[NASA-CR-175495] 12 p1961 N85-22330

Application of the MHD energy principle to magnetostatic atmospheres
[NASA-CR-175967] 18 p3136 N85-29420

Heating of the deep chromosphere during solar flares
[AD-A155256] 21 p3723 N85-33100

Study of photon emission by electron capture during solar nuclei acceleration. 3: Photon production evaluations
[SH-1.1-10] 23 p3990 N85-34737

Onset of solar flares as predicted by two-dimensional MHD-models of quiescent prominences
[SH-1.3-1] 23 p3992 N85-34750

On the detectability of key-MeV solar protons through their nonthermal Lyman-alpha emission
[SH-1.3-5] 23 p3993 N85-34752

Diffusion in the chromosphere and the composition of the solar corona and energetic particles
[SH-2.1-9] 23 p3999 N85-34790

Sporadic radio emission connected with a definite manifestation of solar activity in the near Earth space
[SH-10.1-8] 23 p4053 N85-35139

Near Earth space sporadic radio emission bursts occurring during sunrise
[SH-10.1-9] 23 p4054 N85-35140

CHRONIC CONDITIONS

Estimating risks of lead-induced hemoglobin decrements under conditions of uncertainty: Methodology, pilot judgments and illustrative calculations
[DE85-012293] 23 p3952 N85-34493

CHRONOGRAPHS

U CHRONOMETERS

CHRONOLOGY

NT GEOCHRONOLOGY

Open star clusters and the evolution of the galactic disk 05 p0736 N85-14734

Chronologic and climatic control on soil development, northern Bighorn Basin, Wyoming and Montana 08 p1181 N85-17443

Chronology of KSC and KSC related events for 1983
[NASA-TM-87400] 08 p1261 N85-17927

Chronology of KSC and KSC related events for 1983
[NASA-TM-87435] 12 p1963 N85-22339

Relative time-scale for channeling events within chaotic terrains, Margaritifer Sinus, Mars 13 p2190 N85-23589

Heat flow through ocean floor and its relationship to lithosphere structure and thickness 19 p3294 N85-30422

A new global geomorphology? 21 p3601 N85-32358

Why do leaky-box models work so fine?
[OG-7.2-8] 23 p4014 N85-34877

CHRONOMETERS

Timing-system design considerations for a mobile astrolabe 17 p2965 N85-28309

CHRONOTRONS

U PULSE RATE

U TIME LAG

CHUGGING

U COMBUSTION STABILITY

CHUTES

Air carrier overwater emergency equipment and procedures
[PB85-917006] 21 p3553 N85-32105

CID

U CHARGE INJECTION DEVICES

CINDER CONES

U CONES (VOLCANOES)

CINEFLUOROGRAPHY

U MOTION PICTURES

U RADIOGRAPHY

CINEMATOGRAPHY

Sub-nanosecond cinematography in laser fusion research: Current techniques and applications at the Lawrence Livermore Laboratory
[DE85-007252] 17 p2968 N85-28334

Holographic cinematography with the help of a pulse YAG laser
[ISL-CO-213/84] 22 p3788 N85-33472

Cineholography
[ISL-CO-214/84] 22 p3788 N85-33473

CINERADIOGRAPHY

U MOTION PICTURES

U RADIOGRAPHY

CIRCADIAN RHYTHMS

Jet lag prevention: Physiological mechanisms and pharmacological therapy
[AD-A145444] 02 p0235 N85-11529

Mathematical Models of the Circadian Sleep-Wake Cycle
[AD-A145712] 02 p0235 N85-11532

Spontaneous motility of goldfish in absence of terrestrial zeitgebers: Space flight simulation in a mine 05 p0689 N85-14432

Heart rate variability during 7 day head-down tilt (6 deg) 05 p0692 N85-14453

Circadian rhythm of human body temperature during spaceflights 12 p1901 N85-21934

Annals of the New York Academy of Sciences, Volume 423 — timing and time perception
[AD-A150031] 12 p1909 N85-21981

Homeostasis in primates in the hyperdynamic environment — circadian timekeeping and effects of lower body positive pressure on sleep 15 p2610 N85-26085

Circadian rhythm control: Neurophysiological investigations 15 p2612 N85-26099

Circadian dynamics of potassium excretion in urine as related to working on one and two shifts 19 p3325 N85-30598

Human performance in continuous/sustained operations and the demands of extended work/rest schedules. An annotated bibliography
[AD-A155619] 21 p3666 N85-32771

CIRCLES (GEOMETRY)

On the turning lozange of constant side whose vertices alternate between two fixed circles of a ring
[AD-A154803] 21 p3677 N85-32840

CIRCUIT BOARDS

Extractor for spring-lock pin connectors
[AD-D011235] 01 p0043 N85-10260

Depot level problems in the testing of printed circuit boards
[AD-P003932] 02 p0247 N85-11612

Mechanical locking between multi-layer printed wiring board conductors and through-hole plating
[AD-D011477] 10 p1481 N85-19352

The state of the art in printed wiring board inspection
[AD-A149871] 12 p1862 N85-21679

Applications, specifications of Robotron CAD-CAM work stations 15 p2537 N85-25681

Design and swept-frequency measurement of printed circuit board log-periodic dipole arrays
[R-NIAS-23] 15 p2539 N85-25671

Voltammetric analysis of ordnance materials. Part 2: A portable digital voltammeter for use with a silver wire working electrode
[AD-A152480] 17 p2967 N85-28325

Beam forming network
[NASA-CASE-NPO-15743-1] 18 p3089 N85-29118

A comparison and analysis of Vintr's global routing algorithm with the Lee routing algorithm in two-layer printed circuit boards
[AD-A155600] 21 p3673 N85-32816

Heat sinking for printed circuitry
[DE85-011585] 22 p3783 N85-33440

CIRCUIT BREAKERS

Improvement of lightning arresters energy capability
[SNIAS-842-422-104] 04 p0497 N85-13172

High-voltage, high-power, solid-state remote power controllers for aerospace applications
[NASA-TP-2437] 12 p1795 N85-21263

Optimization of overall dimensions of enclosures for low-voltage devices and equipment 13 p2087 N85-23033

Derated application of parts for (Electronic Systems Division) systems development. Revision
[AD-A153299] 17 p2955 N85-28246

CIRCUIT DIAGRAMS

Measured noise performance of a new method of frequency hopping
[AD-A152679] 17 p2953 N85-28234

Development of new circuit symbols for binary logic elements
[MBB-Z-39/85-O] 17 p3014 N85-28640
Recognition and clear representation of handwritten electronic diagrams 23 p3960 N85-34541

CIRCUIT PROTECTION
Improvement of lightning arresters energy capability
[SNIAS-842-422-104] 04 p0497 N85-13172
Circuit transients due to negative bias arcs on a high-voltage solar array in low Earth orbit
[NASA-TP-2407] 06 p0760 N85-14858
The ac power line protection for an IEEE 587 Class B environment 07 p1000 N85-16347
Intermediate load modules for test and evaluation: Flat-Plate Solar Array Project
[NASA-CR-174450] 10 p1508 N85-19512
Electrical overstress protection of submicron devices
[AD-A150334] 13 p2064 N85-22692
Requirements placed on information processing equipment
[BLL-CE-TRANS-7983-(9022.09)] 13 p2144 N85-23307
Aspects of CSSR CMOS integrated circuits discussed 15 p2533 N85-25627

CIRCUIT RELIABILITY
Procedures for precap visual inspection
[NASA-RP-1122] 04 p0495 N85-13156
Qualification of a thick film hybrid
[BMFT-FB-W-84-024] 04 p0497 N85-13170
Design of self-checking N-MOS (H-MOS) integrated circuits 08 p1084 N85-16742
Circuit topology, signal propagation delay and the efficiency of VLSI circuits
[CWI-CS-R8414] 11 p1630 N85-20267
Transistor-transistor logic microcircuit tester 12 p1842 N85-21556
Designing VLSI (Very Large Scale Integrated) circuits for testability
[AD-A151834] 15 p2549 N85-25729
Improved Gonda's circuit described 15 p2551 N85-25748
Efficient VLSI (Very Large Scale Integration) fault simulation
[AD-A152661] 17 p2953 N85-28233
Derated application of parts for (Electronic Systems Division) systems development. Revision
[AD-A153290] 17 p2955 N85-28246
Split-cross-bridge resistor for testing for proper fabrication of integrated circuits
[NASA-CASE-NPO-16021-1] 19 p3256 N85-30187

CIRCUITS
NT ADDING CIRCUITS
NT ANALOG CIRCUITS
NT BISTABLE CIRCUITS
NT CANCELLATION CIRCUITS
NT CIRCULATORS (PHASE SHIFT CIRCUITS)
NT COINCIDENCE CIRCUITS
NT COMPARATOR CIRCUITS
NT COUNTING CIRCUITS
NT COUPLING CIRCUITS
NT DELAY CIRCUITS
NT DIGITAL INTEGRATORS
NT DIPLEXERS
NT DISCRIMINATORS
NT ECHO SUPPRESSORS
NT ELECTRIC BRIDGES
NT EQUIVALENT CIRCUITS
NT FEEDBACK CIRCUITS
NT FLIP-FLOPS
NT FLUID SWITCHING ELEMENTS
NT FLUIDIC CIRCUITS
NT FREQUENCY DISCRIMINATORS
NT GATES (CIRCUITS)
NT HYBRID CIRCUITS
NT INTEGRATED CIRCUITS
NT ITERATIVE NETWORKS
NT LARGE SCALE INTEGRATION
NT LIMITER CIRCUITS
NT LINEAR CIRCUITS
NT LOGIC CIRCUITS
NT MAGNETIC CIRCUITS
NT MATRICES (CIRCUITS)
NT MICROWAVE CIRCUITS
NT MIXING CIRCUITS
NT OHMS LAW
NT PHASE DETECTORS
NT PHASE SHIFT CIRCUITS
NT POWER SUPPLY CIRCUITS
NT PRINTED CIRCUITS
NT RC CIRCUITS
NT SCALERS
NT SWEEP CIRCUITS
NT SWITCHING CIRCUITS
NT THRESHOLD GATES
NT TRANSISTOR CIRCUITS
NT TRANSMISSION CIRCUITS
NT TRIGGER CIRCUITS
NT TTL INTEGRATED CIRCUITS
NT VERY LARGE SCALE INTEGRATION
NT VHSIC (CIRCUITS)
NT WHEATSTONE BRIDGES
NT WIRE BRIDGE CIRCUITS
Electrical system technology Working Group (WG) report 05 p0611 N85-13907
USSR report: Electronics and electrical engineering
[JPRS-UEE-84-011] 06 p0789 N85-15042
The replacement of precious metal thick film inks using conductive polymer technology. Phase 1: Feasibility study
[AD-A147814] 07 p0933 N85-15913
Characterization of CNRS Fizeau wedge laser tuner
[NASA-CR-174357] 09 p1325 N85-18328
Low voltage two wire to four wire telephone circuit converter apparatus
[AD-D011449] 10 p1468 N85-19261
Design of low loss helix circuits for interference fitted and brazed circuits
[NASA-CR-168313] 10 p1478 N85-19326
A circuit grammar for operational amplifier design
[AD-A149566] 10 p1481 N85-19346
Problems in high temperature thermocouple thermometry
[DE85-000808] 10 p1488 N85-19397
Processing circuit with asymmetry corrector and convolutional encoder for digital data
[NASA-CASE-MSC-20187-1] 11 p1628 N85-20249
Digital channel efficiency model
[AD-A150084] 12 p1829 N85-21479
Electromagnetic rail launcher as a circuit element
[AD-A150067] 12 p1835 N85-21516
Summator of radio pulse signals 12 p1839 N85-21539
Problems with electrical interference between solar generators and shunt type regulators 13 p2010 N85-22607
Repetitive energy transfers from an inductive energy store 13 p2062 N85-22861
USSR report: Electronics and electrical engineering
[JPRS-UEE-85-001] 13 p2078 N85-22976
Design, fabrication and testing of a multibeam forming network
[NASA-CR-175695] 14 p2298 N85-24228
Distributed control of circuits in multiuser communication networks with circuit precedence and path suitability criteria using failsafe routing concepts
[AD-A151825] 16 p2772 N85-27113
Numerical methods for stiff ordinary and elliptic partial differential equations
[AD-A153247] 17 p3020 N85-28675
High voltage power supply
[NASA-CASE-GSC-12818-1] 18 p3093 N85-29147
Temperature sensitive oscillator
[NASA-CASE-GSC-12958-1] 19 p3258 N85-30201
Parallel simulation of digital LSI circuits
[AD-A154745] 21 p3580 N85-32258
State of art and development problems in computer-aided design of electronic circuits 22 p3765 N85-33342
Algorithms and organization of software for computer-aided circuit design 22 p3767 N85-33347
System for computer-aided design of analog electronic circuits 22 p3768 N85-33353
Optimization of radioelectronic circuits with software for modeling of integrated circuits on unified system computer 22 p3768 N85-33354
Dislog system with minicomputer for plotting performance charts 22 p3768 N85-33355
Algorithms for constructing models of circuit elements in input language of computer-aided design software 22 p3768 N85-33356
Electronic temperature equalizer
[PB85-181485] 22 p3789 N85-33475
Method and apparatus for transfer function simulator for testing complex systems
[NASA-CASE-NPO-15696-1] 23 p3926 N85-34333
Interfacing interactive circuit simulation with standard graphics facilities 23 p3958 N85-34529

CIRCULAR CYLINDERS
Wave multiple scattering by a finite number of unclosed circular cylinders
[NASA-TM-77593] 01 p0037 N85-10232
An experimental study of jet impingement on a circular cylinder
[AD-A145583] 02 p0196 N85-11326
Post buckling behavior of a circular rod constrained within a circular cylinder 02 p0207 N85-11365
Stress intensity factors for a circular ring with uniform array of radial cracks of unequal depth
[AD-A145893] 03 p0372 N85-12377
Acoustic radiation from single and double ribbed circular cylindrical shells
[AD-A148771] 08 p1219 N85-17676
Numerical predictions for unsteady viscous flow past an array of cylinders 09 p1318 N85-18284
Turbulent bouyant flow and pressure variations around a circular cylinder in a cross uniform flow near the ground 09 p1318 N85-18287
Stability evaluation of sulfur dioxide nitric oxide and carbon monoxide gases in cylinders 11 p1648 N85-20387
Generation of sound by a vortex point in a steady flow of slightly compressible fluid 11 p1715 N85-20789
Electromagnetic analysis of radomes by the moment method
[AD-P004351] 12 p1824 N85-21445
Behavior of buried flexible cylinders under the influence of nonuniform hoop compression
[PB85-116523] 12 p1868 N85-21718
Turbulent flow around circular cylinder uniformly rotating in infinite incompressible fluid 14 p2277 N85-24109
Measurements in the flow field of a cylinder with a laser transit anemometer and a drag rake in the Langley 0.3 m transonic cryogenic tunnel
[NASA-TM-86399] 14 p2305 N85-24270
The influence of jet-grid turbulence on heat transfer from the stagnation region of a cylinder in crossflow
[NASA-TM-87011] 15 p2554 N85-25760
Natural convection in cylindrical containers 15 p2555 N85-25763
Flow around rotating and nonmoving circular cylinder near flat screen. Report 1: Aerodynamic forces in cylinder 16 p2765 N85-27059
Boundary layer at moving cylinder surface 16 p2765 N85-27064
On residual stress in an elastic body 16 p2798 N85-27248
Solution of problem of equilibrium confinement of plasma by magnetic field in an infinite circular cylinder 21 p3692 N85-32936
Vibrations of free hollow circular cylindrical bodies 24 p4100 N85-35418

CIRCULAR ORBITS
NT STATIONARY ORBITS
Stability of periodic satellite motions relative to center of mass in circular orbit 16 p2718 N85-26760
Maximizing the semi-major axis for a freely coning solar sailcraft
[AD-A153175] 17 p2909 N85-27938

CIRCULAR PLATES
Large transverse deflections of circular plates loaded symmetrically
[NPL-DMA(A)-86] 04 p0512 N85-13262

CIRCULAR POLARIZATION
Characteristics of circular-polarized printed radiators in planar phased antenna array 06 p0790 N85-15049
Modern problems in polarimetry of solid surfaces of cosmic bodies 13 p1977 N85-22409
Design and measured performance of a broadband Archimedes spiral antenna
[R-NIAS-22] 14 p2290 N85-24194
Design and performance of etched polarisation transformers for microwave frequencies
[R-NIAS-26] 14 p2297 N85-24218
Dual sense, circularly polarized helical antenna
[AD-D011680] 19 p3254 N85-30175
A special antenna for SARSAT EPIRBs providing circular polarization and hemispheric coverage for reliable transmission to satellites --- Emergency Position Indicating Radio Beacon (EPIRB) 20 p3404 N85-31122

CIRCULAR SHELLS
Stability of circular cylindrical shell with piecewise constant thickness subjected to radial pressure 06 p0779 N85-14862

CIRCULAR TUBES
Estimating defectiveness buildup during service in metal of welded runner in low-pressure cylinder of turbine 14 p2271 N85-24070
Steel Tubes
[BLL-BISI-TRANS-22064-(9022.06)] 17 p2973 N85-28369

CIRCULAR WAVEGUIDES
Scattering of waves by axisymmetrical edge 13 p2080 N85-22987
New directional couplers for multimode circular waveguides applied to intense pulsed microwave systems
[DE85-011753] 23 p3926 N85-34330

CIRCULATION
NT ATMOSPHERIC CIRCULATION
NT BLOOD CIRCULATION
NT BRAIN CIRCULATION
NT COASTAL CURRENTS
NT CORONARY CIRCULATION
NT EL NINO
NT GULF STREAM
NT OCEAN CURRENTS

NT PULMONARY CIRCULATION
NT WATER CIRCULATION
NT WATER CURRENTS
Urban aerosol modeling
[PB84-233469] 04 p0532 N85-13401
Circulation control: A bibliography of DTNSRDC research and selected outside references: Update
[AD-A146966] 07 p0893 N85-15681
Heat and mass exchange in a partially stratified fluid
[DE85-000528] 10 p1486 N85-19364
Some preliminary results concerning deep northern-boundary currents in the North Pacific
[AD-A151021] 14 p2382 N85-24692
Heat management system for aircraft
[AD-D011658] 18 p3061 N85-28936
Lost circulation in geothermal wells: Research and development status
[DE85-009836] 19 p3268 N85-30267

CIRCULATION CONTROL AIRFOILS
Modelling circulation control by blowing — airfoils
08 p1069 N85-16778
Low-speed characteristics of a circulation control airfoil with AFT camber and a spiral trailing edge
[AD-A150851] 14 p2213 N85-23725
Basic consideration of the lifting capability of stoppable rotors
[AD-A150850] 14 p2219 N85-23759
Circulation control propellers for general aviation, including a BASIC computer program
[NASA-CR-165968] 19 p3219 N85-29950
Circulation control lift generation experiment: Hardware development 22 p3799 N85-33535

CIRCULATION DISTRIBUTION
Structure and energetics of medium-scale atmospheric waves in the Southern Hemisphere
20 p3489 N85-31685

CIRCULATORS (PHASE SHIFT CIRCUITS)
Basic development of one-chip control circuitry for commutatorless dc motors
[BMFT-FB-T-84-305] 18 p3098 N85-29178

CIRCULATORY SYSTEM
NT ARTERIES
NT BLOOD VESSELS
NT VASCULAR SYSTEM
NT VEINS
Circulatory orthostatic instability: Role of deconditioning of resistive vessels 01 p0001 N85-10612
Management of microcirculatory disorders in vibration sickness 10 p1524 N85-19611
Cosmonauts' postural reactions after long-term missions aboard Salyut-6 orbital station 19 p3323 N85-30585

CIRCUMFERENCES
Prediction of percent body fat for U.S. Navy women from body circumferences and height
[AD-A146456] 06 p0845 N85-15370
Circumferential cracks in cylindrical shells
09 p1330 N85-18354

CIRCUMSOLAR RADIATION
Neutron and gamma-ray signatures for particle acceleration in solar flares 12 p1954 N85-22278

CIRCUMSTELLAR MATTER
U STELLAR ENVELOPES

CIRRUS CLOUDS
Investigation of cloud feedback in the GLAS model
05 p0685 N85-14404
Ice crystal nucleation on hygroscopic aerosols
21 p3639 N85-32605

CITIES
NT MOSCOW
NT SAN FRANCISCO (CA)
Review of the attributes and performance of six urban diffusion models
[PB84-236850] 04 p0484 N85-13087
Impact of alcohol fuels on urban air pollution: Methanol photochemistry study
[DE84-012950] 04 p0531 N85-13397
Urban aerosol modeling
[PB84-233469] 04 p0532 N85-13401
Transformation processes and wet deposition on the urban scale
[DE84-015294] 04 p0539 N85-13432
Detecting agricultural to urban land use change from multi-temporal MSS digital data — Salt Lake County, Utah
[E85-10049] 07 p0993 N85-16245
Image variance and spatial structure in remotely sensed scenes — South Dakota, California, Missouri, Kentucky, Louisiana, Tennessee, District of Columbia, and Oregon
07 p0996 N85-16265
Meteorological factors responsible for high CO (carbon monoxide) levels in Alaskan cities
[PB85-115137/GAR] 09 p1350 N85-18493
Weather data for simplified energy calculation methods. Volume 4: United States, WYEC data
[DE85-000491] 09 p1357 N85-18539
Measurements of propagation at 900 MHz in an urban zone for establishing a digital radiomobile system
10 p1472 N85-19288
Statistical study of anthropogenic seismic noise with IVK-7 computer system 10 p1503 N85-19483
Nationwide urban runoff program. Relationship of urban runoff to land use and groundwater resources
[PB85-114692] 10 p1506 N85-19505
Organizations as information processing systems. Toward a strategic contingencies model of budget related influence in municipal government organizations
[AD-A149364] 10 p1567 N85-19883
The use of image registration technique in Brasilia's urban growth monitoring
[INPE-3302-PRE/614] 10 p1569 N85-19896
Study of pollutant dispersion in an urban street canyon
[DE85-002648] 11 p1677 N85-20571
Turbulence parameters impacting dispersion in an urban convection boundary layer
[PB85-116036] 11 p1682 N85-20598
A comparison of metropolitan and non-metropolitan employment characteristics: Indications of the size of non-metropolitan mobile communication services user classes
[NASA-CR-175648] 13 p2053 N85-22855
The use of Thematic Mapper data for land cover discrimination: Preliminary results from the UK SATMaP programme 13 p2121 N85-23207
Technology and Economics, Inc. Technology Application Team
[NASA-CR-175630] 13 p2168 N85-23454
Spectroscopic study of gas pollutants in atmosphere over large cities: A review 14 p2341 N85-24478
Nationwide Urban Runoff Project, Champaign, Illinois: The biological impact of urban runoff on the Saline Branch Drainage Ditch and Boneyard Creek
[PB85-150274] 14 p2348 N85-24515
Experience of the Institute of Space Research with the use of remote sensing in urban planning studies
[INPE-3159-PRE/533] 16 p2880 N85-27770
Impact of alcohol fuels on urban air pollution: Methanol photochemistry study
[DE85-009539] 18 p3133 N85-29403
Urban climate and air hygiene before, during, and after the lifework of Helmut Berg. Overview of a branch of applied meteorology 18 p3147 N85-29487
The timing of noise-sensitive activities in residential areas
[NASA-CR-177937] 20 p3524 N85-31918
On the transformation regularities of time series of solid aerosol concentrations in the surface atmospheric layer
21 p3645 N85-32648
An electron microscopic study of urban aerosol
21 p3651 N85-32689
Helicopter noise survey for selected cities in the contiguous US
[AD-A154893] 21 p3699 N85-32985
Department of Housing and Urban Development Independent Agencies Appropriation Bill, 1986
[S-REPT-99-129] 23 p3967 N85-34720
Motor glider measurements during the Urban Atmosphere Energy Budget Experiment (EESA 1)
24 p4122 N85-35553

CITRIC ACID
Vinyl citrates from citric acid as new monomers
[BMFT-FB-T-83-256] 03 p0338 N85-12178

CIVIL AVIATION
Development trends and requirements of propulsion system technology for civil aircraft
01 p0011 N85-10066
Foreign civil aviation competition: 1976 summary and implications
[NASA-TM-X-73907] 02 p0133 N85-10907
Energy efficient engine. Volume 2. Appendix A: Component development and integration program
[NASA-CR-173085] 02 p0146 N85-10991
USSR report: Transportation
[JPRS-UTR-84-028] 03 p0310 N85-12002
Ministry wants better commo facilities for agroaviation
03 p0310 N85-12003
Editorial urges improved aviation repair work quality
03 p0310 N85-12004
Activities report of the aerospace industry in West Germany
[ISSN-0176-5086] 05 p0734 N85-14718
Design study of technology requirements for high performance single-propeller-driven business airplanes
[NASA-CR-3863] 07 p0898 N85-15692
West Europe report: Science and technology
[JPRS-WST-84-039] 07 p0936 N85-15829
Activities report of the aerospace industry in West Germany
[ISSN-0722-3838] 07 p1053 N85-16686
Activities report of the aerospace industry in West Germany
[ISSN-0722-3838] 07 p1054 N85-16687
FAA (Federal Aviation Administration) statistical handbook of aviation, calendar year 1983
[AD-A148171] 08 p1067 N85-16760
USSR report: Transportation
[JPRS-UTR-85-001] 08 p1067 N85-16763
Director on institute's civil aviation projects
08 p1067 N85-16764
Designer on Aeroflot automated COMMO system development 08 p1067 N85-16765
Testing solution for IL-76 braking system problem
08 p1067 N85-16766
International projects, other work of Aeroproyekt Institute 08 p1068 N85-16767
Designer on civil aircraft design trends in USSR
08 p1068 N85-16768
Improved sprayer for AN-2 cropdusting work
08 p1068 N85-16769
Airport activity statistics of certificated route air carriers
[AD-A148472] 08 p1081 N85-16846
Directions of the West German Ministry of Transport for education and control of airline personnel (section 3, chapters 2 and 12) 08 p1081 N85-16848
Directions of the West German Ministry of Transport for education and control or airline personnel, Report 6; chapters 3/A and 3/B 08 p1081 N85-16849
Satellite navigation
[S-HRG-98-856] 08 p1082 N85-16851
Activities report on West German civil airports. Part 1: Text
[ISBN-3-87977-055-7-PT-1] 08 p1090 N85-16887
Activities report for the West German Civil Airports. Part 2: Tables
[ISBN-3-87977-055-7-PT-2] 08 p1090 N85-16888
West Europe report: Science and technology
[JPRS-WST-85-001] 08 p1141 N85-17190
Flight Training Technology for Regional/Commuter Airline Operations: Regional Airline Association/NASA Workshop Proceedings
[NASA-CP-2348] 09 p1275 N85-18009
Captain development training at US Air
09 p1275 N85-18012
Management training for cockpit crews at Piedmont flight 09 p1276 N85-18013
Integrated approach to flight crew training
09 p1276 N85-18014
Video concepts in CRM training
09 p1276 N85-18015
Use of simplifier scenarios for CRM training
09 p1276 N85-18016
First deputy minister on 1984 civil aviation performance 09 p1277 N85-18033
Collegium on aviation fuel conservation efforts
09 p1278 N85-18034
Finnair, LOT, SAS reps in USSR on present operations, plans 09 p1278 N85-18035
Activities at Mil Experimental Design Bureau
09 p1278 N85-18036
Research at automated ATC Scientific-Experimental Center 09 p1278 N85-18037
Airport ground equipment under development at Riga
09 p1278 N85-18038
Improvements in Kazan airport equipment, facilities
09 p1278 N85-18039
Improvements under way at Gorkiy airport
09 p1278 N85-18040
New discovery in supersonic flight research
09 p1278 N85-18041
Sunset of the Civil Aeronautics Board
[S-HRG-98-940] 09 p1403 N85-18829
Digest of the Deutsche Lufthansa report, 1983
[ISSN-0415-603X] 09 p1418 N85-18948
Semiannual report to Congress on the effectiveness of the civil aviation security program
[AD-A149522] 10 p1421 N85-18967
Medically disqualified airline pilots
[AD-A149454] 10 p1528 N85-19637
Wildlife Hazards to Aircraft Conference and Training Workshop: Proceedings
[AD-A148330] 11 p1578 N85-19938
Accidents and serious incidents to civil aircraft due to birdstrikes
[AD-P004180] 11 p1578 N85-19942
Analysis of bird strikes reported by European airlines, 1976 - 1980
[AD-P004181] 11 p1578 N85-19943
West Europe report: Science and technology
[JPRS-WST-85-008] 11 p1617 N85-20174
General aviation activity and avionics survey
[AD-A149572] 12 p1769 N85-21103
Transportation
[JPRS-UTR-85-004] 12 p1769 N85-21105

Aviation repair plant directors on quality control measures 12 p1769 N85-21106
New flight simulators at Vnukovo permit less in-flight training 12 p1769 N85-21107
Annual review of aircraft accident data: US air carrier operations calendar year 1981 [NTSB/ARC-85/01] 12 p1774 N85-21134
Ground and flight testing for aircraft guidance and control [AGARD-AG-262] 13 p1966 N85-22350
Civil avionics flight testing with the RAE(B) BAC1-11 13 p1967 N85-22354
USSR report: Transportation [JPRS-UTR-85-005] 14 p2207 N85-23688
Minister Bugayev on civil aviation in 1984, plans for 1985 14 p2208 N85-23689
1st deputy minister on civil aviation support of economy 14 p2208 N85-23690
Deputy minister on civil aviation fuel conservation efforts 14 p2208 N85-23691
Deputy minister on civil aviation construction projects 14 p2208 N85-23692
Improvements in personnel needed for better flight safety 14 p2208 N85-23693
USSR report: Transportation [JPRS-UTR-84-008] 14 p2208 N85-23694
Minister Bugayev reviews 1983 civil aviation work, sets course for 1984 14 p2208 N85-23695
Bugayev on civil aviation ministry's 1983 achievements 14 p2208 N85-23696
Riga Institute seeking faster introduction of new technology 14 p2208 N85-23698
Safety recommendation(s), A84-111 through -115 [REPT-4011C/27] 14 p2216 N85-23744
Safety recommendation(s), A-84-103 [REPT-3909B/101B] 14 p2216 N85-23745
FAA aviation forecasts: Fiscal years 1985-1996 [AD-A151050] 14 p2216 N85-23747
Safety recommendation(s), A-84-82 through -84 [REPT-3957] 14 p2217 N85-23748
West Europe report: Science and technology [JPRS-WST-85-013] 14 p2289 N85-24183
USSR report: Transportation [JPRS-UTR-85-008] 15 p2460 N85-25189
Roundtable on effective use of flight simulators 15 p2460 N85-25190
Official on Soviet research in deicing techniques 15 p2460 N85-25191
USSR report: Transportation [JPRS-UTR-84-015] 15 p2460 N85-25192
Administration chief on air traffic control improvements 15 p2460 N85-25193
Civil air code international flights section explained 15 p2460 N85-25194
USSR report: Transportation [JPRS-UTR-84-017] 15 p2461 N85-25196
Chronic fuel shortages in Volga civil aviation administration 15 p2461 N85-25198
Safety recommendation(s), A-84-128 through -133 [REPT-3996C/41] 15 p2466 N85-25221
Safety recommendation(s), A-84-123 and -124 [REPT-3894B/93] 15 p2466 N85-25222
USSR report: Transportation [JPRS-UTR-84-014] 15 p2467 N85-25229
Ilyushin bureau designer on fuel conservation research 15 p2467 N85-25231
Calculation and display of stack departure times for aircraft inbound to Heathrow Airport [AD-A151991] 15 p2469 N85-25241
West Europe report: Science and technology [JPRS-WST-84-003] 15 p2534 N85-25635
FRG journal analyzes state, prospects of airbus programs: General analysis 15 p2535 N85-25638
West Europe report: Science and technology [JPRS-WST-84-009] 15 p2535 N85-25639
West Europe report: Science and technology [JPRS-WST-84-014] 15 p2536 N85-25647
Certifying complex digital systems on civil aviation aircraft 17 p2904 N85-27907
Operations research [B8561897] 17 p3026 N85-28712
West Europe report: Science and technology [JPRS-WST-84-037] 18 p3088 N85-29108
A systematic determination of skill and simulator requirements for airline transport pilot certification [AD-A154135] 19 p3330 N85-30630
FAA regulation of 9-seat and under passenger aircraft [GPO-42-703] 20 p3391 N85-31032
Search and rescue services for international civil aviation 20 p3400 N85-31090
West Europe report: Science and technology [JPRS-WST-85-020] 20 p3438 N85-31333
MBB demonstrates new research aircraft ATTAS 20 p3438 N85-31334
NASA authorization, 1986, volume 1 [GPO-46-385] 20 p3541 N85-32039
An error-dependent model of instrument-scanning behavior in commercial airline pilots [NASA-CR-3908] 21 p3665 N85-32765
U.S. Civil airmen statistics for calendar year 1984 [AD-A156326] 24 p4059 N85-35153
The contribution made by flight mechanics to civil aviation 24 p4061 N85-35169
Introduction to European air traffic control [AD-A156328] 24 p4062 N85-35176

CL-41 AIRCRAFT
TUTOR (CL-41A) tail flight load survey 07 p0896 N85-15678

CLADDING
Microfluorescence studies of zirconium oxide [DE84-016116] 03 p0329 N85-12118
Effect of iron on the performance of IN 625 weld deposits [BR91456] 08 p1169 N85-17376
Elevated temperature creep behavior of inconel alloy 625 [DE84-015836] 09 p1297 N85-18144
Antifriction properties of gas thermal coatings of clad carbine powders 10 p1447 N85-19115
Fracture resistance of surface layer with technological defects under cyclical loading 10 p1448 N85-19126
Lightweight cladding for magnetic circuits [AD-D011469] 10 p1481 N85-19350
New application possibilities for clad steel by reducing surface treatment expenditure and by using improved welding technology [BMFT-FB-T-84-236] 12 p1861 N85-21672
Ring-on-ring tests and load capacity of cladding glass [PB85-106391] 12 p1868 N85-21717
Fatigue of clad aluminum materials D16T and 2024-T3 with stepped loading 15 p2496 N85-25397
Investigation of the influence of some paint systems and water displacing corrosion inhibitors on anodic undermining corrosion of aluminum 2024 clad alloy --- aircraft structures [VTH-LR-443] 16 p2756 N85-27009
New process for production of bimetal with corrosion-resistant cladding layer [BLL-BISI-TRANS-22371-(9022.06)] 17 p2927 N85-28056
Fiber optic moisture sensor [DE85-011651] 22 p3787 N85-33462
Chromium-base powder alloys for welding cladding layer of bimetal [BLL-M-35776-(5828.4)] 23 p3915 N85-34260
Manufacturing process to reduce large grain growth in zirconium alloys [DE85-011649] 23 p3915 N85-34267
Effect of stainless steel weld overlay cladding on the structural integrity of flawed steel plates in bending, series 1 [TI85-010349] 23 p3939 N85-34418

CLAMPS
A metallographic investigation of rotating bands for 7.5 cm artillery projectiles [FOA-C-20551-D2] 07 p0929 N85-15888
Reusable thermal cycling clamp [NASA-CASE-LAR-12868-1] 12 p1858 N85-21651
Pneumatic clamping device [AD-D011544] 12 p1858 N85-21656
Effectiveness of use of heat-dissipating clamps to reduce deformation during argon arc welding of thin sheets of AMg6 alloy 15 p2501 N85-25427

CLARK Y AIRFOIL
U AIRFOIL PROFILES

CLASSES
The rate of convergence of a class of block Jacobi schemes [AD-A144736] 01 p0111 N85-10749

CLASSICAL MECHANICS
NT ASTRODYNAMICS
NT CELESTIAL MECHANICS
NT KEPLER LAWS
NT MINIMUM VARIANCE ORBIT DETERMINATION
NT ORBITAL MECHANICS
NT SPACE MECHANICS
Semiclassical theory of resonances [REPT-67] 01 p0114 N85-10777
Study on controllability and stability of high speed tracked vehicles [AD-P004302] 09 p1409 N85-18879
How a swing behaves [DE85-006280] 17 p3027 N85-28720

CLASSIFICATIONS
NT HIERARCHIES
NT INDEXES (DOCUMENTATION)
NT SUBJECTS
Direction dependent radiation behavior in the classification of multispectral aircraft remote sensing data [SER-C-290] 01 p0063 N85-10419
An investigation into fuzzy clustering and classification [AD-A145571] 02 p0251 N85-11645
Interdisciplinary structure of information science 03 p0436 N85-12779
Comparability and accuracy of industry codes in different data systems [PB84-215607] 04 p0548 N85-13482
Documentation for the machine-readable version of the MK classification extension catalogue Morris-Kennedy (1983) [NASA-TM-87372] 04 p0549 N85-13491
Generic composite flywheel designs 05 p0806 N85-13864
Estimating location parameters in a mixture 07 p0964 N85-16252
Texture classification using autoregressive filtering 07 p0964 N85-16254
A method for automatic water mass classification [AD-D011405] 08 p1191 N85-17505
Assessment of LANDSAT for rangeland mapping, Rush Valley, Utah [E85-10072] 10 p1503 N85-19486
An IUE high-resolution atlas of O-type spectra 11 p1760 N85-21074
Multiple resolution representation and probabilistic matching of 2-D gray-scale shape [AD-A149861] 12 p1933 N85-22147
On the morphology of spiral modes --- disk galaxies 12 p1955 N85-22283
Impact of Thematic Mapper sensor characteristics on classification accuracy --- suburban Washington, D.C., Maryland, and the Chesapeake Bay 13 p2117 N85-23188
Quick look analysis of TM data of the Washington, District of Columbia, area 13 p2119 N85-23197
Microcomputer: Controlled statistics analyzer [BLL-CE-TRANS-7971-(9022.09)] 13 p2144 N85-23306
Geomorphic classification of lava flows on Io 13 p2173 N85-23480
Classification of circular features on Venus 13 p2177 N85-23511
Digital processing of passive Ka-band microwave images for sea-ice classification [AD-A150686] 14 p2347 N85-24511
A structural classification of geomagnetic pulsations 14 p2371 N85-24857
Classification and multiple regression through projection pursuit [AD-A150797] 14 p2411 N85-24867
Efficient contextual measures for classification of multispectral image data 14 p2433 N85-25005
Low-resolution target classification from a staring infrared sensor [AD-A151690] 15 p2652 N85-26358
Criteria for the classification of hydrographic positioning data [AD-A152283] 16 p2705 N85-26697
Comparative study of the digital analysis of areas of the Earth's surface prepared for planting using different classification algorithms [INPE-3359-PRE/637] 16 p2846 N85-27545
New method of calculating the economic effects of corrosion [BLL-BISI-TRANS-22348-(9022.06)] 17 p2929 N85-28079
Air photo analysis, photo interpretation logic, and feature extraction [AD-A153926] 18 p3124 N85-29347
Geomorphic classification of Icelandic and Martian volcanoes: Limitations of comparative planetology research from LANDSAT and Viking orbiter images 21 p3603 N85-32372
Source hierarchy list. Volume 1: A through H [AD-A156300] 24 p4165 N85-35825

CLASSIFYING
Efficient sorting routines in FORTRAN 77 [OUEL-1529/84] 05 p0716 N85-14590
Diamonds and diamond sorting [PB85-128502] 10 p1542 N85-19726
Generation and termination of binary decision trees for nonparametric multiclass classification [AD-A151361] 15 p2640 N85-26283

CLATHRATES
Volatiles in the outer solar system. 1: Thermodynamics of clathrate hydrates. 2: Ethane ocean on Titan. 3: Evolution of primordial Titan atmosphere 19 p3382 N85-30084

CLAYS
The colloidal chemistry of ceramic clays [NASA-TM-77734] 03 p0336 N85-12163
Site-specific research conducted in support of the Salton Sea Solar Pond Project, FY 1982 report [NASA-CR-174182] 05 p0666 N85-14260
Laboratory investigations 05 p0666 N85-14261

Solar pond research at Argonne National Laboratory
05 p0667 N85-14291
Interactions of hydrazine and of hydrazine derivatives with soil constituents and with soils
[AD-A148475] 08 p1122 N85-17074
Evaluating the variability of ceramics with X-ray fluorescence
[DE85-002028] 10 p1453 N85-19155
Response of earth-covered slabs in clay and sand backfills
[AD-A149296] 11 p1615 N85-20157
First direct detection of clay minerals on Mars
13 p2194 N85-23612
Analysis of SMIRR data for volcanic and sedimentary terrains of the trans-Pecos region, Texas
13 p2197 N85-23626
Chemical weathering of soils from the dry valleys of Antarctica: A terrestrial analog of Martian weathering processes
13 p2197 N85-23628
Low pressure storage of methane on interlayered clays for potential vehicular applications
[DE85-006949] 16 p2758 N85-27017
Clay identification and amount measured by laboratory techniques compared to well log responses: Application to tight gas sands and shales
[DE85-010411] 19 p3362 N85-30843

CLEAN FUELS
NT FUEL OILS

CLEAN ROOMS
Particle size distribution on surfaces in clean rooms
[AD-A146057] 03 p0328 N85-12109
MATRA has Europe's largest white room for satellites
10 p1477 N85-19320
Particulate contamination control in clean rooms by particle fallout (PFO) measurements
[ESA-PSS-01-204-ISSUE-1] 20 p3487 N85-31673

CLEANERS
NT AIR FILTERS
Apparatus and method to keep the walls of a free-space reactor free from deposits of solid materials
[NASA-CASE-NPO-15851-1] 12 p1858 N85-21652

CLEANING
NT ULTRASONIC CLEANING
Hot-gas cleanup for molten carbonate fuel cells-dechlorination and soot formation
[DE84-003072] 01 p0068 N85-10450
Potential application of robotics and state-of-the art end effectors at Letterkenny Army Depot
[AD-P004015] 03 p0309 N85-11994
Contamination problems during surface cleaning for thermocompression bonding
[DE84-013066] 04 p0475 N85-13023
Certain optimal parameters of high-velocity Venturi ejection tubes
[BLL-M-35924-(5828.4)] 05 p0634 N85-14066
Anticoiling technology: Theories of surface coiling and performance of anticoiling surface coatings
[NASA-CR-174274] 07 p0991 N85-16296
Community relations activities at Department of Defense sites
[AD-P004150] 09 p1349 N85-18486
Protocol for aquifer cleanup decision making at military installations
[AD-P004151] 09 p1349 N85-18487
Improved techniques for removal of sediments contaminated with hazardous materials
[PB85-116093] 11 p1679 N85-20580
Control of surface composition and hydrogen recycling by plasma conditioning
[DE85-001859] 11 p1731 N85-20889
Apparatus and method to keep the walls of a free-space reactor free from deposits of solid materials
[NASA-CASE-NPO-15851-1] 12 p1858 N85-21652
Steam generator tube vibration tests
[DE85-003599] 12 p1867 N85-21712
The effect of abrasive blasting on the fatigue and corrosion of an aluminium-copper alloy
[AD-A154954] 21 p3566 N85-32182
Review of hazardous waste cleanup and disposal efforts at Tinker Air Force Base
[GPO-43-294] 21 p3613 N85-32457

CLEAR AIR TURBULENCE
Safety recommendation(s), A84-111 through -115
[REPT-4011C/27] 14 p2216 N85-23744
Millstone Hill radar: Capabilities for S/T observations
21 p3629 N85-32548
Millimeter-wave propagation in moist air: Model versus path data
[AD-A156040] 24 p4067 N85-35331
The physical and empirical basis for a specific clear-air turbulence risk index
[NASA-CR-178522] 24 p4120 N85-35540

CLEARANCES
Pressure loss due to the tip clearance of impeller blades in centrifugal and axial blowers
05 p0636 N85-14063
Effect of form and clearance of a piston launched in a tube on the boundary layer and the heat transfer
[ISL-CO-216/83] 14 p2302 N85-24255
Effects of bearing deadbands on bearing loads and rotor stability 16 p2737 N85-26889

CLEARINGS (OPENINGS)
Relationship between forest clearing and biophysical factors in tropical environments: Implications for the design of a forest change monitoring approach — Costa Rica
[E85-10051] 07 p0983 N85-16247

CLEBSCH-GORDAN COEFFICIENTS
A packed storage program for angular momentum coupling coefficients
[TWISK-316] 01 p0102 N85-10680
Interacting Boson approximation
[DE85-003016] 22 p3837 N85-33756

CLIFFS
Coastal erosion along Monterey Bay
[AD-A155610] 21 p3655 N85-32707

CLIMATE
Illinois Climate: Trends, Impacts and Issues
[PB84-211966] 01 p0086 N85-10577
Bibliography of climate textbooks and studies
[WCP-84] 02 p0231 N85-11505
The Martian climate: Energy balance models with CO2/H2O atmospheres
[NASA-CR-174073] 03 p0448 N85-12849
Research activities of the Illinois University Coordinated Science Laboratory
[AD-A145589] 03 p0449 N85-12856
Climate of the Northern Hemisphere, 1851 - 1900 compared to contemporary climate
[DE84-016368] 04 p0539 N85-13426
Climate-chamber experiments to improve pilots' work conditions 04 p0543 N85-13454
Massively parallel processor 05 p0680 N85-14366
Spectral energetics diagnoses and FGGE spectral observing periods and energetics analyses of forecast experiments with GLAS GCM 05 p0683 N85-14391
Report of the Meeting of Experts on Climate and Human Health
[WCP-78] 05 p0687 N85-14413
Organization of the session 05 p0687 N85-14414
Difficulties encountered in determining the potential involvement of consultants on health problems in various climatic zones 05 p0687 N85-14416
Review on physiological and medical problems related to climates ranging from altitude to sub-tropics
05 p0687 N85-14417
Epidemiologic methods applied to the study of the relationship between climate and human health
05 p0687 N85-14418
Polar regions and climatic change
[PB84-237023] 05 p0688 N85-14421
Paleoclimatologists use past to predict weather patterns 06 p0819 N85-15197
Monthly and seasonal climatology over the global tropics and subtropics for the decade 1973 to 1983. Volume 1: 200 mb winds
[AD-A146521] 06 p0838 N85-15322
Carbon dioxide and climate: Summaries of research in FY 1983 and FY 1984
[DE85-001245] 06 p0839 N85-15327
Climate Conference for Latin America and the Caribbean
[WMO-632] 07 p1000 N85-16352
The problem of climate and climate variation
07 p1001 N85-16353
Review of climate problems in Latin America and the Caribbean 07 p1001 N85-16354
Climate applications: General
07 p1001 N85-16355
Meteorological aspects of the 1982-83 El Nino/southern oscillation episode 07 p1001 N85-16356
Climate and climate data. Report on the workshop held in Brasilia (Argentina) from 11-15 April 1983
07 p1001 N85-16357
The climate in food production in Latin America
07 p1001 N85-16359
The challenge of food production: The importance of climate 07 p1001 N85-16361
Ocean and climate, an example. The interannual variability of the tropical Pacific Ocean
07 p1002 N85-16365
Climate and water quality 07 p1002 N85-16368
The water balance and climate — Amazon region
07 p1003 N85-16370
The potential contributions of the World Climate Program (WCP) to the economies of developing countries
07 p1003 N85-16371
Socio-economic impact of climate — Mexico
07 p1003 N85-16372
Climate and fisheries: A Peruvian case study
07 p1003 N85-16373
Energy and climate: Problems in Latin America
07 p1003 N85-16375
Requirements for training in climate-related subjects
07 p1004 N85-16378
Education and training for the climate related activities in Latin America and the Caribbean
07 p1004 N85-16379
Revised Uniform Summary of Surface Weather Observations (RUSSWO). Alconbury RAF United Kingdom, parts A-F
[AD-A146913] 07 p1004 N85-16384
Revised Uniform Summary of Surface Weather Observations (RUSSWO). Mildenhall RAF, United Kingdom, parts A-F
[AD-A146915] 07 p1005 N85-16386
Revised Uniform Summary of Surface Weather Observations (RUSSWO). Dobbins AFB, Georgia, parts A-F
[AD-A146916] 07 p1005 N85-16387
Limited surface observations climatic summary (LISOCS). Hohenfels, AAF, West Germany
[AD-A147167] 07 p1006 N85-16393
Revised Uniform Summary of Surface Weather Observations (RUSSWO). Offutt AFB, Nebraska, parts A-F
[AD-A147183] 07 p1006 N85-16394
Revised Uniform Summary of Surface Weather Observations (RUSSWO). Hill AFB, Utah, parts A-F
[AD-A147184] 07 p1006 N85-16395
Interrelationship of atmospheric parameters in Honduras
[AD-A147371] 07 p1007 N85-16401
Simulating responses to expected climate change in eastern North America: Applications to decision-making in the forest industry
[DE85-001272] 07 p1008 N85-16406
Chronologic and climatic control on soil development, northern Bighorn Basin, Wyoming and Montana
08 p1181 N85-17443
Revised Uniform Summary of Surface Weather Observations (RUSSWO). Parts A-F Zweibrucken AB, Germany
[AD-A147165] 09 p1357 N85-18536
A model for the climatic behavior of water on Mars
09 p1415 N85-19031
Natural environment analysis
[NASA-CR-171333] 10 p1428 N85-19010
Atlas of snow and ice resources
10 p1497 N85-19449
Climate of Salt Lake City, Utah
[PB85-123875] 10 p1521 N85-19589
Carbon dioxide and the greenhouse effect
[GPO-39-043] 11 p1677 N85-20569
Lake ice occurrence as a possible detector of atmospheric CO2 effects on climate
[DE85-002951] 11 p1687 N85-20606
Oceanic role in terrestrial climate
[DE85-004422] 12 p1896 N85-21904
Impact of aerosols on visibility and climate: A report prepared for Panel 3, Environmental Impact, of the NATO/CCMS Air Pollution Pilot Study on Air Pollution Control Strategies and Impact Modelling
[PB85-106744] 12 p1897 N85-21906
Environmental cycling of cellulosic thermal insulation and its influence on fire performance
[DE85-004295] 13 p2041 N85-22776
Global paleoclimatic data base for 6000 years BP
[DE85-006828] 15 p2600 N85-26024
North Atlantic Deep Water formation: Information from ice cores 15 p2602 N85-26035
Sea ice, climate and Fram Strait
15 p2603 N85-26042
The Martian climate: Energy balance models with CO2/H2O atmospheres
[NASA-CR-175722] 15 p2679 N85-26547
Regularities in recent changes in surface air temperature and atmospheric precipitation fields
16 p2807 N85-27311
Ecology of Pamlico River, North Carolina: An estuarine profile
[PB85-155703] 16 p2822 N85-27404
AWS (Air Weather Service) climatic briefs: Asia
[AD-A151944] 16 p2835 N85-27481
AWS (Air Weather Service) climatic briefs: North America
[AD-A152161] 16 p2835 N85-27483
A climatic data bank for Northern Hemisphere land areas, 1851-1980
[DE85-007863] 16 p2835 N85-27486
Intercomparison of Radiation Codes in Climate Models (ICRCCM)
[DE85-007251] 16 p2835 N85-27487
Preliminary assessment of climatic change during late Wisconsin time, southwest Great Basin and vicinity, Arizona, California and Nevada
[DE85-006343] 16 p2836 N85-27488
Time-dependence of CO2-induced climate change
[DE85-007568] 17 p2997 N85-28525

Identification and characterization of watershed models for evaluation of impacts of climate change on hydrology
[DE85-009575] 18 p3125 N85-29348

Humidity/cloud-radiation feedback on possible climate perturbation due to fossil fuel utilization
[DE85-008686] 18 p3133 N85-29402

Helmut Berg issue — meteorology
[MITT-39] 18 p3147 N85-29483

Environmental Research Laboratories (of the National Oceanic and Atmospheric Administration) programs and plans: FY 1984 programs and FY 1985 plans
[PB85-171494] 18 p3149 N85-29501

Summary of archived Atlantic coast wave information study pressure, wind, wave, and water level data
[AD-A153782] 18 p3151 N85-29508

Examination of the time and spatial scales appropriate for the carbon dioxide climate change issue
[DE85-009852] 19 p3317 N85-30563

Carbon dioxide and climate: Potential impacts
[DE85-009473] 20 p3496 N85-31734

Acclimatization to far north 20 p3506 N85-31792

Quantitative analysis in megageomorphology
21 p3603 N85-32376

Meteorological weapons
[AD-A154735] 21 p3635 N85-32575

Model projections of time-dependent response to increasing carbon dioxide
[DE85-013326] 22 p3816 N85-33641

Climatic consequences of very high CO2 levels in Earth's early atmosphere 22 p3854 N85-33865

The polar caps and the climatic evolution of Mars
22 p3854 N85-33866

Simulated effects of increased recharge on the ground-water flow system of Yucca Mountain and vicinity, Nevada-California
[DE85-012965] 24 p4106 N85-35468

Time-dependent response of the climate to increasing atmospheric carbon dioxide 24 p4119 N85-35532

Carbon dioxide and climate: A working glossary
[DE85-013535] 24 p4124 N85-35562

CLIMATOLOGY
NT AGROCLIMATOLOGY
NT MICROCLIMATOLOGY

The climate of Denmark. Summaries of observations from light vessels. 3: Sea temperature
[ISBN-87-7478-215-0] 01 p0073 N85-10481

Report of the First Session of the International Working Group on Data Management for the International Satellite Cloud Climatology Project (ISCCP)
[WCP-42] 01 p0073 N85-10483

Cloud cover sampling capability of various satellite combinations for ISCCP 01 p0073 N85-10484

ISCCP Cloud Algorithm Intercomparison Workshop
01 p0073 N85-10485

ISSCP Cloud Algorithm Intercomparison Workshop
01 p0073 N85-10486

Spatial relationships in stream flow residuals
02 p0212 N85-11397

A study of greenhouse effects using zero, 1 and 2 dimensional climate models 02 p0230 N85-11498

Report of the Third Session of the International Working Group on Data Management for the International Satellite Cloud Climatology Project (ISCCP)
[WCP-82] 02 p0231 N85-11504

Bibliography of climate textbooks and studies
[WCP-84] 02 p0231 N85-11505

A temperature climatology for New York State
03 p0394 N85-12517

Carbon dioxide, the greenhouse effect and climate: A primer
[GPO-33-444] 03 p0395 N85-12519

Plans for the NRL/NORDA (Naval Research Laboratory-Naval Ocean Research and Development Activity) fine-scale variability experiment - 1984 (FVX-84)
[AD-A146041] 03 p0398 N85-12540

Homogeneous macroclimatic zones of the lake states
[PB84-215821] 04 p0540 N85-13496

Global biogeochemical cycles: Studies of interaction and change, some views on the strategy of approach
05 p0652 N85-14185

Modeling long-term changes in forested landscapes and their relation to the Earth's energy balance
05 p0653 N85-14194

Combining Heat Capacity Mapping Mission (HCMM) LANDSAT and thematic map information into a unique high precision merged multichannel system — climatology 05 p0660 N85-14239

Numerical modeling of the atmosphere
05 p0680 N85-14370

Some new mathematical methods for variational objective analysis 05 p0681 N85-14375

Extended range forecasting 05 p0681 N85-14376

Weather and climate parameters from Tiros-N
05 p0681 N85-14377

Monthly and seasonal climatology over the global tropics and subtropics for the decade 1973 to 1983. Volume 1: 200 mb winds
[AD-A146521] 06 p0836 N85-15322

Diurnal and seasonal patterns of temperature and wind flow in the planetary boundary layer for ten locations in complex terrain
[PB85-106698/GAR] 06 p0840 N85-15333

Climatological information and water resources
07 p1002 N85-16367

Water and climate, study of one case
07 p1002 N85-16369

The Amazon and climate 07 p1003 N85-16376

A microprocessor data system for developing countries — climatology 07 p1003 N85-16377

Revised Uniform Summary of Surface Weather Observations (RUSSWO). Spangdahlem AB, Germany, parts A-F
[AD-A147166] 07 p1006 N85-16392

Polar research in Earth sciences described
08 p1142 N85-17204

Natural environment analysis
[NASA-CR-174330] 08 p1180 N85-17433

Pilot climate data system
[NASA-CR-174321] 08 p1187 N85-17481

The visibility climatology of McMurdo Sound-Williams Field, Antarctica
[AD-A148108] 08 p1189 N85-17482

Consideration of future climatic changes in three geologic settings
[DE85-001704] 09 p1357 N85-18537

The establishment and experience of the Carbon Dioxide Information Center (CDIC)
[DE85-001934] 09 p1402 N85-18825

Optimization of a ground coupled heat pump
[DE85-000273] 10 p1486 N85-19380

Polar regions and climatic change: Appendix
[PB85-122679] 10 p1521 N85-19580

Soviet National Middle Atmosphere Program
11 p1655 N85-20428

Lidar observations of stratospheric aerosol over Mauna Loa Observatory, 1974 - 1981
[PB85-115081] 11 p1682 N85-20597

A study of eddy-mean flow interactions using Eliassen-Palm diagnostics: FGGE SOP-1 data and the NASA GLAS general circulation model compared
[NASA-CR-175506] 11 p1686 N85-20604

Performance evaluation of an active solar cooling system utilizing low cost plastic collectors and an evaporatively-cooled absorption chiller
[DE84-010813] 12 p1880 N85-21798

NBS solar collector durability/reliability test program
[DE85-003489] 12 p1881 N85-21801

Response of unmanaged forests to CO2-induced climate change: Available information, initial tests and data requirements
[DOE/NSB-0053] 12 p1883 N85-21817

Rationale and basic design for experimental acidification of a lake ecosystem in Northern Wisconsin
[PB85-116077] 12 p1885 N85-21829

The effect of stochastic surface heat fluxes on the climatology of the seasonal thermocline
[AD-A149957] 12 p1889 N85-21857

21 Layer troposphere-stratosphere climate model
[NASA-TM-86183] 12 p1892 N85-21871

A new NASA/MSFC mission analysis global cloud cover data base
[NASA-TP-2448] 12 p1893 N85-21878

Los Alamos MINI-Review: Tracking Antarctic winds
[DE85-004597] 12 p1896 N85-21903

Earth radiation budget experiment software development
[NASA-CR-172567] 12 p1912 N85-22002

Relationship of Indian monsoon intensity to time of onset 13 p2106 N85-23120

Numerical experiments with simple model of ocean climate 13 p2106 N85-23123

Summary of Meteorological Observations, Surface (SMOS), Fallon, Nevada
[AD-A150481] 13 p2138 N85-23276

Summary of Meteorological Observations, Surface (SMOS) Camp Pendleton, California
[AD-A150482] 13 p2138 N85-23277

Summary of Meteorological Observations, Surface (SMOS), Alameda, California
[AD-A150609] 13 p2138 N85-23281

Classification of atmospheric aerosol for evaluation of its effect on climate 14 p2333 N85-24428

Absolute movement of Pacific Ocean plate based on paleoclimatic and paleomagnetic data and trajectory of hot spots during last 120 million years
14 p2334 N85-24435

Atlas of archived vegetation, land-use and seasonal Albedo data sets
[NASA-TM-86199] 14 p2348 N85-24508

Geophysical Fluid Dynamics Laboratory activities, FY84, plans, FY85
[PB85-147601] 15 p2558 N85-25783

SAM 2 measurements of the polar stratospheric aerosol, volume 5
[NASA-RP-1140] 15 p2590 N85-25970

An Earth longwave radiation climate model
[NASA-CR-175749] 15 p2594 N85-25984

Characteristics of precipitation regimes during first global atmospheric research project global experiments
[AD-A151572] 15 p2599 N85-26021

Possible sea ice impacts on oceanic deep convection
15 p2603 N85-26041

Climatic impact of a change in North Atlantic Deep Water formation 15 p2603 N85-26045

Origin of the Greenland ice sheet
15 p2604 N85-26048

Real-time enhancement of a climatology or forecast of ocean thermal structure using observed ocean temperatures
[AD-A151118] 15 p2604 N85-26049

Evaluation of the area and severity of last night's frosts
[REPT-109] 16 p2833 N85-27473

Geophysical monitoring for climatic change, number 12
[PB85-172278] 16 p2837 N85-27496

NASA Oceanic Processes Program annual review
[NASA-TM-87565] 16 p2838 N85-27503

Centralized Storm Information System (CSIS)
[NASA-CR-175898] 17 p2994 N85-28506

A report from the Space Science and Engineering Center, the University of Wisconsin-Madison, Madison, Wisconsin 17 p2994 N85-28507

CSIS test and evaluation 17 p2994 N85-28509

Potential climatic impacts of increasing atmospheric CO2 with emphasis on water availability and hydrology in the United States
[NASA-TM-87479] 17 p2995 N85-28517

Air Weather Service (AWS) climatic briefs: Europe
[AD-A152528] 17 p2996 N85-28519

Characteristics of North Indian Ocean tropical cyclone activity
[AD-A153085] 17 p2997 N85-28524

Mathematical modeling and simulation of climate and climatic change
[DE85-008974] 17 p2997 N85-28526

Improvement of the basic knowledge of the climatology of the vertical ozone layer by enhanced balloon sounding
[BPT-6/84] 18 p3137 N85-29426

Research Review, 1983
[NASA-TM-86219] 18 p3139 N85-29433

Analysis of a simulated cloud climatology
18 p3145 N85-29472

Helmut Berg issue — meteorology
[MITT-39] 18 p3147 N85-29483

Applied climatology — regional planning
18 p3147 N85-29486

Climatological data of stations in the Netherlands No. 11: Frequency tables and tables with runs according to measurements at principal climatological stations 1961-1980, sunshine stations 1956-1960, precipitation stations 1951-1980
[KNMI-150-11] 18 p3149 N85-29499

A global low order spectral model designed for climate sensitivity studies
[NASA-CR-175099] 19 p3315 N85-30549

On the dynamical climatology of the Amazon Basin and associated rain producing mechanisms
[INPE-3531-RPE/477] 19 p3315 N85-30552

A modified Fresnel scattering model for the parameterization of Fresnel returns, part 2.3A
21 p3618 N85-32483

Activities report of the Aeronomy Department
[G-774-1984] 21 p3633 N85-32569

Paleoenvironmental investigations at seed cave (Windust cave H-45FR46), Franklin County, Washington
[AD-A154777] 21 p3635 N85-32576

A simulation of weather in 3D space
[AD-A155221] 21 p3636 N85-32586

Airborne measurements of the vertical distribution of Arctic haze 21 p3647 N85-32657

Middle Atmosphere Program. Handbook for MAP, volume 11
[NASA-CR-176107] 22 p3814 N85-33625

Reports from the German Meteorological Service. No. 166: The optimal spectral density of climatological station networks
[ISBN-3-88148-214-8] 23 p3950 N85-34478

Lake ice occurence as a possible detector of atmospheric CO2 effects on climate
[DE85-012987] 23 p3950 N85-34480

Current inventory of anthropogenic carbon dioxide in the North Pacific Subarctic Gyre
[PB85-187938] 24 p4125 N85-35570

CLIMBING FLIGHT
Wind tunnel results of advanced high speed propellers in the takeoff, climb and landing operating regimes
[NASA-TM-87054] 19 p3213 N85-29925
CLINICAL MEDICINE
Review on physiological and medical problems related to climates ranging from altitude to sub-tropics
05 p0687 N85-14417
In vivo neutron activation analysis: Body composition studies in health and disease
[DE84-014092] 05 p0696 N85-14480
Comparative assessment of different treatment modalities in miners with vibration- and noise-induced disease 10 p1524 N85-19610
Management of microcirculatory disorders in vibration sickness 10 p1524 N85-19611
Catalog of completed studies, US Army health care studies and clinical investigation activity
[AD-A149450] 10 p1568 N85-19885
A double blind comparative trial of powdered ginger root, hyoscine hydrobromide, and cinnarizine in the prophylaxis of motion sickness induced by cross coupled stimulation
11 p1695 N85-20657
Review of US manual of clinical aviation medicine
12 p1904 N85-21957
The clinical and radiological assessment of cervical injury, Annex A 12 p1907 N85-21976
Oversight review of the five-year outlook report on science and technology
[GPO-41-058] 12 p1949 N85-22243
Medical subject headings, tree structures, 1985
[PB84-216092] 12 p1952 N85-22261
Permuted medical subject headings, 1985
[PB84-216100] 12 p1952 N85-22262
Technology transfer to the Middle East
[PB85-127744] 12 p1952 N85-22264
Medical planning criteria for implementation of clinical hyperbaric facilities
[AD-A151001] 14 p2389 N85-24715
Development and diffusion of automated clinical chemistry analyzers
[PB85-150696] 15 p2561 N85-25798
List of serials indexed for online users, 1985
[PB85-143220] 15 p2666 N85-26455
Thermal consequences of localized SAR from RFR exposures 16 p2775 N85-27130
Diagnostic system
[INPE-3350-PRE/659] 16 p2841 N85-27519
New technologies to improve laboratory testing
[DE85-008151] 18 p3110 N85-29257
Effect of spironolactone on acute mountain sickness
[AD-A153780] 18 p3153 N85-29525
Accepting error to make less error
[AD-A153949] 18 p3171 N85-29651
Test and Evaluation Master Plan (TEMP) for the Navy Occupational Health Information Management System (NOHIMS). Phase 1: Appendix A through appendix U
[AD-A154179] 19 p3380 N85-30967
USSR report: Life sciences. Biomedical and behavioral sciences
[JPRS-UBB-85-018] 22 p3819 N85-33660
Heavy ion medical accelerator options
[DE85-011204] 22 p3841 N85-33784
USSR report: Life sciences. Biomedical and behavioral sciences
[JPRS-UBB-85-021] 23 p3951 N85-34489
Effect of water immersion of parameters of central hemodynamics in individuals over 45 years old
23 p3953 N85-34499
Effect of dibazol on parameters of nonspecific resistance of subjects in pressurized cabins
23 p3954 N85-34504
Analogies of control mechanisms in flight guidance and medicine 24 p4129 N85-35507
CLOCKS
NT ATOMIC CLOCKS
NT AUTONOMOUS SPACECRAFT CLOCKS
NT CHRONOMETERS
Portable real-time clock
[AD-A146218] 03 p0364 N85-12336
Precision digital sampler
[AD-D011285] 06 p0809 N85-15143
Laser clock
[AD-D011513] 12 p1855 N85-21634
Application of K176-series microcircuits
13 p2077 N85-22973
Active dispersion control for a Doppler broadened laser
[AD-D011570] 14 p2310 N85-24297
Maintenance of time and frequency in the DSN using the global positioning system 16 p2771 N85-27105
Proceedings of the Fifteenth Annual Precise Time and Time Interval (PTTI) Applications and Planning Meeting
[AD-A149163] 17 p2961 N85-28287
Unattended TV time transfer results
17 p2964 N85-28305
Clock characterization tutorial
17 p2965 N85-28311
A plan for the development of inertial reconstruction of initial state clock (IRIS) 17 p2966 N85-28317
Atmospheric limitations to clock synchronization at microwave frequencies 18 p3107 N85-29236
Development of hydrogen masers for K-3 VLBI system
18 p3108 N85-29239
Numerical optical computing at the Ohio State University 18 p3188 N85-29775
A new fault-tolerant algorithm for clock synchronization
[AD-A154771] 21 p3676 N85-32836
Method of characterizing critical timing paths and analyzing timing related failure modes in very large scale integrated circuits
[AD-D011731] 22 p3759 N85-33296
Recording system for the solar neutron monitoring at Mt. Norikura
[SH-9.1-8] 23 p4051 N85-35123
CLOSED BASINS
U STRUCTURAL BASINS
CLOSED CYCLES
Advanced technology cogeneration system conceptual design study: Closed cycle gas turbines
[NASA-CR-168222] 07 p0982 N85-16300
Manned testing of two closed-circuit oxygen underwater breathing apparatus: US Navy Emerson Rig and Fenzy PO.68
[AD-A148300] 08 p1200 N85-17560
Closed cycle versus open cycle gas turbines. A review of A.D. Little's ICOP report, vol. 3
[DE85-000564] 12 p1861 N85-21671
Solid state compressor
[AD-A150790] 14 p2311 N85-24302
Optimization of the catalytic oxidation of CO for closed-cycle CO2 laser applications
[NASA-TM-86421] 15 p2504 N85-25445
CLOSED ECOLOGICAL SYSTEMS
Problems associated with the utilization of algae in bioregenerative life support systems
[NASA-CR-166615] 07 p1019 N85-16469
Algal culture studies related to a Closed Ecological Life Support System (CELSS)
[NASA-CR-177322] 07 p1019 N85-16470
Controlled ecological life support system higher plant flight experiments
[NASA-CR-177323] 07 p1020 N85-16471
Control and modeling of a CELSS (Controlled Ecological Life Support System)
[NASA-CR-177324] 07 p1020 N85-16472
Feasibility of producing a range of food products from a limited range of undifferentiated major food components
[NASA-CR-177329] 07 p1020 N85-16473
Effect of high ammonia content in closed environment on some parameters of human nitrogen and carbohydrate metabolism against background of a controlled diet
12 p1903 N85-21948
Controlled Ecological Life Support System. Life Support Systems in Space Travel
[NASA-CP-2378] 18 p3155 N85-29531
Current concepts and future directions of CELSS
18 p3155 N85-29532
Survey of CELSS concepts and preliminary research in Japan 18 p3155 N85-29533
Dynamic considerations for control of closed life support systems 18 p3155 N85-29537
CELSS transportation analysis
18 p3156 N85-29538
Extended mission life support systems
18 p3157 N85-29547
Space shuttle revitalization system
18 p3157 N85-29548
Internal contamination in the space station
18 p3157 N85-29549
Space station trace contaminant control
18 p3157 N85-29550
Publications of the NASA CELSS (Controlled Ecological Life Support Systems) program
[NASA-CR-3911] 19 p3326 N85-30608
CLOSED FAULTS
U GEOLOGICAL FAULTS
CLOSED LOOP SYSTEMS
U FEEDBACK CONTROL
CLOSTRIDIUM BOTULINUM
Production of butanol by fermentation in the presence of cocultures of clostridium
[NASA-CASE-NPO-16203-1] 24 p4071 N85-35227
CLOSURE LAW
A study of Reynolds-stress closure model
[NASA-CR-174342] 08 p1161 N85-17324
A 2-dimensional second order closure model of the upper atmosphere 08 p1182 N85-17450
A turbulent closure model for the free atmosphere
09 p1351 N85-16502
Centrifuge tests to provide closure bounds for switches subjected to random vibration
[DE85-002003] 10 p1482 N85-19357
A study of the second and third order closure models of turbulence for prediction of separated shear flows
[NASA-CR-176127] 23 p3929 N85-34353
Application of a turbulent closure model to the parameterization of the vertical diffusion of heat, momentum, and humidity in the ECMWF model — European Center for Medium Term Weather Forecasting (ECMWF)
[MITT-41] 24 p4095 N85-35367
CLOSURES
Cooled turbine blade tip closure
[AD-D011525] 12 p1858 N85-21654
Synthesis of tree-structured computing systems through use of closures
[AD-A150502] 13 p2147 N85-23329
Scale separation closure and Alfven wave turbulence
[DE85-013124] 24 p4095 N85-35365
CLOTH
U FABRICS
CLOTHING
NT BOOTS (FOOTWEAR)
NT COVERALLS
NT FLIGHT CLOTHING
NT GOGGLES
NT HELMETS
NT PRESSURE SUITS
NT PROTECTIVE CLOTHING
NT SHOES
NT SPACE SUITS
Measurement of stress in clothing: A literature review and methods selected
[AD-A147674] 08 p1132 N85-17132
Current approaches for the biophysical and physiological evaluation of combat clothing for environmental extremes
[AD-A151012] 14 p2395 N85-24752
The location of stress in clothing
[AD-A154423] 19 p3331 N85-30633
Physical dimensions of humans; values; the effect of clothing, working clothes and protective equipment on the design of work places
[HSE-TRANS-10888] 19 p3331 N85-30636
Human body dimensions: Body outlines and envelope curves at different normal positions and movements
[HSE-TRANS-10886] 19 p3332 N85-30640
CLOUD CHAMBERS
An experimental investigation of the angular scattering and backscattering behaviors of the simulated clouds of the outer planets
[NASA-CR-175909] 17 p3052 N85-28896
Construction of University of Missouri, Rolla's full scale cloud simulation chamber and applied research
[AD-A154682] 21 p3557 N85-32128
Missing energies at pair creation
[HE-4.4-8] 24 p4193 N85-36016
Progress report on a new search for free e/3 quarks in the cores of 10(15) - 10(16) eV air showers
[HE-6.2-15] 24 p4212 N85-36151
CLOUD COVER
Shipboard measurement of cloud bases and average surface visibility with an eye-safe lidar
[AD-A144889] 01 p0052 N85-10345
Report of the First Session of the International Working Group on Data Management for the International Satellite Cloud Climatology Project (ISCCP)
[WCP-42] 01 p0073 N85-10483
ISSCP Cloud Algorithm Intercomparison Workshop
01 p0073 N85-10486
Combining radar and satellite data for the localization and identification of summer convection
01 p0077 N85-10509
The possibility of detection and measurement of cloud structure in the atmosphere of Uranus
02 p0290 N85-11937
Investigations of severe/tornadic thunderstorm development and evolution based on satellite and AVE/SESAME/VAS data
[NASA-CR-174154] 04 p0538 N85-13424
Investigation of satellite measurements in the presence of clouds, forcing influences on clouds and feedback to the large scale following convection
05 p0682 N85-14381
NOAA/NASA joint simulation of AMTS and HIRS
05 p0682 N85-14384
Modeling influence of three layer cloud cover on outgoing thermal radiation 06 p0825 N85-15242
Conditions governing the formation of stratocumulus clouds over the western Atlantic during cold air outbreaks
[AD-A146760] 07 p1004 N85-16383
First sodium nightglow results for Natal
[INPE-3397-PRE/686] 10 p1515 N85-19580

Military applications of meteorological satellite (METSAT) data 11 p1711 N85-20767
A new NASA/MSFC mission analysis global cloud cover data base
[NASA-TP-2448] 12 p1693 N85-21878
Summary of Meteorological Observations, Surface (SMOS), Alameda, California
[AD-A150609] 13 p2138 N85-23281
Variation of Arctic cloud cover in summer
[DE85-004507] 13 p2139 N85-23285
Mean free path lenght of photons with broken cloud cover 14 p2336 N85-24455
Methods for cloud cover estimation
14 p2444 N85-25081
ILUM code: Solar and lunar flux calculations for multi-cloud layered atmospheres
[DE85-005578] 15 p2600 N85-26025
Symposium on Atmospheric Sciences in South Africa
[CSIR-S-331] 16 p2829 N85-27442
A modeling analysis program for the JPL table mountain lo sodium cloud
[NASA-CR-175851] 16 p2833 N85-27468
AWS (Air Weather Service) climatic briefs: Asia
[AD-A151944] 16 p2835 N85-27481
Space photographs confirm 40-year-old hydrodynamics discovery 19 p3269 N85-30393
Issue of sky conditions
[DE85-010590] 19 p3317 N85-30562
A simulation of weather in 3D space
[AD-A155221] 21 p3636 N85-32586
Enhancing precision of remote temperature sensing data from satellites under cloudy atmospheric conditions
22 p3734 N85-33148
Determination of altitude of cloud cover top from Meteor satellite data 22 p3734 N85-33150
Repetition of dense cloud cover above Indian Ocean from generalized satellite data 22 p3737 N85-33165
Mean cloudiness over the global tropics from satellite observations
[AD-A156188] 24 p4123 N85-35561

CLOUD DISPERSAL

The effect of the arbitrary level assignment of satellite cloud motion wind vectors on wind analyses in the pre-thunderstorm environment
[NASA-TM-86186] 10 p1517 N85-19585

CLOUD HEIGHT INDICATORS

Shipboard measurement of cloud bases and average surface visibility with an eye-safe lidar
[AD-A144889] 01 p0052 N85-10345
Improved cloud and surface fields derived from HIRS2/MSU 18 p3140 N85-29439

CLOUD PHOTOGRAPHY

Geostationary satellite cloud and precipitation analysis using an interactive computer system
01 p0076 N85-10506
Technique that uses satellite, radar, and conventional data for analyzing and short-range forecasting of precipitation from extratropical cyclones
[PB85-164994] 16 p2837 N85-27499
Radio-frequency radiation of storm clouds
21 p3692 N85-32939
Determination of altitude of cloud cover top from Meteor satellite data 22 p3734 N85-33150

CLOUD PHYSICS

Processing and display of atmospheric phenomenas data
[NASA-CR-171178] 01 p0072 N85-10475
Cloud cover sampling capability of various satellite combinations for ISCCP 01 p0073 N85-10484
A tropical cyclone precipitation estimation technique using geostationary satellite data
[PB84-226703] 01 p0086 N85-10579
Observed rate of tropospheric diffusion
[DE84-016047] 02 p0224 N85-11470
Theoretical development of Monte Carlo codes for modeling cumulus cloud fields
[NASA-CR-174063] 02 p0230 N85-11500
Report of the Third Session of the International Working Group on Data Management for the International Satellite Cloud Climatology Project (ISCCP)
[WCP-82] 02 p0231 N85-11504
Aircraft flow effects on cloud droplet images and concentrations
[AD-A146176] 03 p0396 N85-12529
Operational test of three instruments for measuring liquid water content in laboratory and from aircraft
[DFVLR-MITT-84-08] 03 p0397 N85-12531
International Conference on Physics of Clouds
06 p0619 N85-15196
First stage of equipping a Do 28 as a research aircraft for icing, and first research results
[ESA-TT-855] 11 p1584 N85-19982
Case studies of snow clouds by means of snow crystal sondes 15 p2581 N85-25921
The physics of the marine stratocumulus-capped mixed layer 15 p2593 N85-25979
Convection modeling and application to severe storms
15 p2595 N85-25991
Modeling of cloud systems 15 p2595 N85-25992
Anvil structure of severe thunderstorms
15 p2595 N85-25993
The use of radar in determining precipitation processes in the BEWMEX area 16 p2831 N85-27455
Effects of cloud seeding on precipitation development in cumulus clouds 16 p2831 N85-27456
Cloud physics studies in the SCPP (Sierra Cooperative Pilot Project)
[PB85-163095] 16 p2837 N85-27501
An experimental investigation of the angular scattering and backscattering behaviors of the simulated clouds of the outer planets
[NASA-CR-175909] 17 p3052 N85-28896
Atmospheric probing by active millimeter wave system
[AD-A153550] 18 p3136 N85-29422
Cloud physics 18 p3147 N85-29485
On the state of knowledge on meteorologically caused icing of aircraft in clouds
[ESA-TT-861] 20 p3496 N85-31736
Eleventh International Conference on Atmospheric Aerosols, Condensation and Ice Nuclei, volume 2
[PB85-182418] 21 p3638 N85-32596
Experimental studies of the kinetics of deposition nucleation on an ice nucleant used in weather modification 21 p3638 N85-32598
Inactivation of silver iodide by atmospheric nucleation inhibitors 21 p3638 N85-32599
Ice active bacteria as condensation nuclei
21 p3639 N85-32603
The effect of supersaturation, temperature and particle size on ice-nucleating ability of atmospheric aerosol
21 p3639 N85-32604
On the efficiency of the mechanism of ice particles formation in the vapor supersaturation field around a freezing droplet 21 p3639 N85-32606
The nucleation of ice crystals during the freezing of large supercooled drops 21 p3640 N85-32608
On the problem of possible mechanism of ice nuclei formation in convective clouds 21 p3640 N85-32610
Bacterial ice nuclei of marine origin: Some recent observations 21 p3640 N85-32611
Airborne measurements of atmospheric ice nuclei
21 p3640 N85-32612
Aircraft observations of condensation and ice nuclei at a tropical station 21 p3640 N85-32613
The nucleation of ice at very low temperatures and pressures 21 p3641 N85-32617
The 100 years of Aitken Nuclei (AN) study-reminiscence, current and future problems 21 p3641 N85-32621
A thermal diffusion chamber for the measurement of cloud condensation nuclei 21 p3642 N85-32627
Stable generation of highly monodisperse aerosols
21 p3642 N85-32628
Monte Carlo studies of H2O layers adsorbed on a model basal face of AgI 21 p3643 N85-32633
Eleventh International Conference on Atmospheric Aerosols, Condensation and Ice Nuclei, volume 1
[PB85-182400] 21 p3644 N85-32636
The first condensation nucleus conference
21 p3644 N85-32637
Cloud condensation on insoluble particles
21 p3648 N85-32670
Measurements of the critical supersaturation of 0.029 to 0.035 micron radius particles at Washington, District of Columbia 21 p3649 N85-32676
A relationship between cloud droplet size and CCN critical supersaturation 21 p3649 N85-32677
Fog activation and supersaturation
21 p3650 N85-32678
On the question to the effect of surfactants on the spectrum of cloud drops in the process of their condensation growth 21 p3650 N85-32679
Aircraft observations of cloud condensation nuclei in maritime and continental environments
21 p3650 N85-32680
The distribution of giant salt nuclei inside and outside cloud over the basin of Xin and Jiang
21 p3650 N85-32681
Characterization of insoluble particles associated with cloud droplets 21 p3652 N85-32693
Applicability of surface CCN measurements
21 p3652 N85-32696
Effect of ions on cloud formation and its role in solar terrestrial relationship 21 p3653 N85-32697
on the transport of large condensation nuclei in the atmosphere at various altitudes over the territory of the USSR 21 p3653 N85-32698
Study of the parameters affecting the collapse of a rotating protostellar cloud 24 p4168 N85-35837

CLOUD SEEDING

NOAA/NASA joint simulation of AMTS and HIRS
05 p0682 N85-14384
Ground-based snow and ice crystal observation system used in Sierra Nevada winter orographic storms
[PB85-115343] 10 p1520 N85-19584
Methods for cloud cover estimation
14 p2444 N85-25081
Cloud-seeding for regulating precipitation in Moscow area 16 p2807 N85-27308
Effects of cloud seeding on precipitation development in cumulus clouds 16 p2831 N85-27458
SCPP (Sierra Cooperative Pilot Project) Forecasting Support 16 p2837 N85-27493
Cloud physics studies in the SCPP (Sierra Cooperative Pilot Project)
[PB85-163095] 16 p2837 N85-27501
Observations of cloud droplets, aerosol particles and cloud condensation nuclei in continental air masses
21 p3649 N85-32671
Project Skywater, 1983-84 SCPP (Sierra Cooperative Pilot Project) data inventory
[PB85-187052] 24 p4124 N85-35565

CLOUDS

NT ANVIL CLOUDS
NT ARC CLOUDS
NT BARIUM ION CLOUDS
NT CAP CLOUDS
NT CIRRUS CLOUDS
NT CLOUDS (METEOROLOGY)
NT CONVECTION CLOUDS
NT CUMULUS CLOUDS
NT ELECTRON CLOUDS
NT HYDROGEN CLOUDS
NT MAGELLANIC CLOUDS
NT MOLECULAR CLOUDS
NT NOCTILUCENT CLOUDS
NT PLASMA CLOUDS
NT STRATOCUMULUS CLOUDS
NT STRATUS CLOUDS
NT VENUS CLOUDS

Clouds above the Martin Limb: Viking observations
[NASA-CR-174027] 02 p0296 N85-11922
Aircraft flow effects on cloud droplet images and concentrations
[AD-A146176] 03 p0396 N85-12529
The Jovian atmospheric window at 2.7 microns: A search for H2S
[NASA-TM-86661] 03 p0445 N85-12836
Optical observations of nearby interstellar gas
06 p0875 N85-15557
Distances of local clouds from optical line observations 06 p0875 N85-15558
Dark cloud and globule distribution for galactic longitudes 230 to 360 degrees 06 p0878 N85-15575
The smallest sizes of diffuse interstellar clouds
06 p0878 N85-15578
Polarization of radio molecular lines and mapping of magnetic field direction 06 p0878 N85-15581
Fuel-rich solid propellant boron combustion
[AD-A148522] 08 p1136 N85-17157
The radiation temperature of a cloud of particles
[FOA-C-30367-E4] 08 p1190 N85-17497
A modeling analysis program for the JPL table mountain lo sodium cloud data
[NASA-CR-175474] 10 p1572 N85-19910
Fragmentation and turbulence in collapsing gas clouds
[DE85-003745] 11 p1633 N85-20282
A modeling analysis program for the JPL Table Mountain lo sodium cloud data
[NASA-CR-175493] 11 p1681 N85-20589
Transmission and reflection of laser beams propagating through aerosol clouds in space
[LA-9998-MS] 12 p1856 N85-21638
The orientation distribution of nonspherical aerosol particles within a cloud
[AD-A150600] 13 p2092 N85-23061
Snow reflectance from Thematic Mapper
13 p2120 N85-23205
Water-ice clouds on Mars: Location and seasonal variation 13 p2194 N85-23611
Participation in the Mars Data Analysis Program: Analysis of cloud forms in Viking and Mariner 9 images
[NASA-CR-175604] 13 p2204 N85-23673
PLUVIUS: A generalized 1-dimensional model of reactive pollutant behavior, including dry deposition, precipitation formation, and wet removal, 2nd edition
[DE85-005542] 14 p2353 N85-24538
The structure and angular momentum content of dark clouds 14 p2439 N85-25054
SAM II measurements of the polar stratospheric aerosol. Volume 6: April to October 1981
[NASA-RP-1141] 16 p2825 N85-27422
Evolution of stratospheric aerosol size distribution from ground-based radiometric measurements: A study of El Chichon aerosol
[DE85-007555] 16 p2827 N85-27439

Humidity/cloud-radiation feedback on possible climate perturbation due to fossil fuel utilization
[DE85-008886] 18 p3133 N85-29402
Environmental Research Division report: Atmospheric physics
[DE85-009659] 18 p3133 N85-29404
Stable generation of highly monodisperse aerosols 21 p3642 N85-32628
Cloud droplet nucleation and initial growth derived from lidar depolarization studies 21 p3644 N85-32635
A simple model to investigate the activation process in waterclouds 21 p3649 N85-32675
A relationship between cloud droplet size and CCN critical supersaturation 21 p3649 N85-32677
Properties of forest derived cloud condensation nuclei 21 p3650 N85-32682
Influence on an industrial site on the characteristics of CCN supersaturation with air masses of different origin 21 p3650 N85-32683
Airborne cloud tracking measurements during the Three Mile Island nuclear station accident, Middletown, Pennsylvania. Data of survey: March - June 1979
[DE85-012060] 22 p3816 N85-33638
Electrons and positrons from expanding supernova envelopes in dense clouds
[OG-6.2-9] 22 p3889 N85-34108
Far-infrared observations of young clusters embedded in the R Coronae Austrinae and RHO Ophiuchi dark clouds
[NASA-TM-86681] 24 p4167 N85-35834

CLOUDS (METEOROLOGY)
NT ANVIL CLOUDS
NT ARC CLOUDS
NT BARIUM ION CLOUDS
NT CAP CLOUDS
NT CIRRUS CLOUDS
NT CONVECTION CLOUDS
NT CUMULUS CLOUDS
NT NOCTILUCENT CLOUDS
NT STRATOCUMULUS CLOUDS
NT STRATUS CLOUDS
ISCCP Cloud Algorithm Intercomparison Workshop 01 p0073 N85-10485
Boundary layer-cloud interactions as potential storm predictors 01 p0081 N85-10543
The identification of rain-bearing synoptic systems through principal component analysis 02 p0212 N85-11394
Joint probability of selected cloud and visibility thresholds around Koblenz, Germany
[AD-A145294] 02 p0231 N85-11506
Development and evaluation of cloud water collectors
[PB84-232529] 04 p0540 N85-13437
Planetary scale interactions 05 p0684 N85-14397
Atmospheric environment for Space Shuttle (STS-41G) launch
[NASA-TM-86486] 07 p0995 N85-16320
Radiation parameterization programs for use in general circulation models
[AD-A148015] 08 p1188 N85-17488
The concentration of sulfate in broken cloud layers
[DE85-000228] 11 p1678 N85-20574
Accuracy of typhoon center determined by GMS imagery 12 p1894 N85-21887
A supplement study on the subsynoptic cloud system off the south coast of Japan 12 p1895 N85-21892
Studies of the mechanisms and rates with which nitrogen species are incorporated into cloud water and precipitation
[PB85-144350] 12 p1898 N85-21914
Empirical and modeled synoptic cloud climatology of the Arctic Ocean
[NASA-CR-175628] 13 p2137 N85-23272
Sea surface temperatures from VAS MSI data
[NASA-CR-175706] 14 p2382 N85-24689
Observation of precipitating clouds by a vertically pointing radar at Morino in the Iburi District, Hokkaido, Japan 15 p2582 N85-25922
Mesoscale Atmospheric Processes Research Program Science Review
[NASA-TM-87485] 15 p2594 N85-25987
Hurricane structure and dynamics from stereoscopic and infrared satellite observations and radar data 15 p2594 N85-25988
Modeling of cloud systems 15 p2595 N85-25992
Lidar and radiometer observations of thunderstorm tops 15 p2595 N85-25994
Modeling of midwest severe thunderstorms 15 p2596 N85-25995
Estimation of convective rainfall from visible and infrared satellite data 15 p2596 N85-25999
Studies of electro-optical attenuation in the vicinity of cloud base
[AD-A151745] 15 p2653 N85-26360
The development and application of volume scan and cell tracking capabilities for the analysis of convective cloud systems 16 p2830 N85-27451
Cloud physics studies in the SCPP (Sierra Cooperative Pilot Project)
[PB85-163095] 16 p2837 N85-27501
Presentations at the Tri-Service Cloud Modeling Workshop (2nd), held at the Naval Surface Weapons Center, White Oak, Maryland, 26-27 June 1984, volume 1
[AD-A152735] 17 p2996 N85-28522
Improved cloud and surface fields derived from HIRS2/MSU 18 p3140 N85-29439
Analysis of a simulated cloud climatology 18 p3145 N85-29472
Cloud physics 18 p3147 N85-29485
Satellite measurements of atmospheric aerosols
[AD-A153807] 19 p3316 N85-30556
An evaluation of discretized conditional probability and linear regression threshold techniques in model output statistics forecasting of cloud amount and ceiling over the North Atlantic Ocean
[AD-A155100] 21 p3636 N85-32581
A simulation of weather in 3D space
[AD-A155221] 21 p3636 N85-32586
Circulation analysis of two snowstorms during the SNOW-TWO program
[AD-A155225] 21 p3637 N85-32587
A thermal diffusion chamber for the measurement of cloud condensation nuclei 21 p3642 N85-32627
Measurements of giant salt nuclei from inland in east China 21 p3648 N85-32668
Investigation of the formation of cloud particle spectrum on natural condensation nuclei 21 p3649 N85-32674
The nuclei of cloud formation 21 p3651 N85-32685
The measured rate of condensation nucleation to droplets using the techniques of chemical kinetics 21 p3652 N85-32694
Applicability of surface CCN measurements 21 p3652 N85-32695
Mean cloudiness over the global tropics from satellite observations
[AD-A156188] 24 p4123 N85-35581

CLUMPS
Comparative analysis of the clustering of the LPC coefficients in phoneme recognition
[FUB-39-1983] 01 p0041 N85-10264
Open cluster formation — stellar evolution 03 p0442 N85-12815
Meteorological analysis for clusters of wind turbines
[DE84-013164] 04 p0539 N85-13425
Large-scale bubble structure of the interstellar medium (ISM) and properties of the Local Spiral Arm (LSA) 06 p0879 N85-15588
Direct assessment of synaptic modification rules
[AD-A148376] 08 p1196 N85-17534
Data reduction 09 p1412 N85-18903
Integrating non-semantic knowledge into image segmentation processes
[AD-A149571] 12 p1851 N85-21612
The chemistry of RDX and HMX cluster ions 13 p2004 N85-22561
Relationship between topological and magnetic order in small metal clusters
[AD-A150547] 13 p2018 N85-22651
Clustering and ordering in 3-5 alloys
[AD-A150604] 13 p2022 N85-22670
Clusters of transition metal atoms
[AD-A153126] 17 p3030 N85-28740
Large, energetic cluster impacts on surfaces
[DE85-006559] 17 p3034 N85-28769
Applications of fuzzy clustering techniques to stratified by tropopause MSU temperature retrievals 18 p3141 N85-29444
Applications of some artificial intelligence methods to satellite soundings 18 p3141 N85-29446
Two-point theory of current-driven ion-cyclotron turbulence
[DE85-010114] 19 p3372 N85-30918
A cluster analysis method for identification of subpopulations of cells in flow cytometric list-mode arrays 20 p3503 N85-31779
Clusters and cycles in the cosmic ray age distributions of meteorites
[SH-7.1-11] 23 p4048 N85-35103
Cluster variation study of coherent ordering in FCC and BCC solid solutions
[AD-A156039] 24 p4079 N85-35280

CLUSTER ANALYSIS
An investigation into fuzzy clustering and classification
[AD-A145571] 02 p0251 N85-11645
Homogeneous macroclimatic zones of the lake states
[PB84-215821] 04 p0540 N85-13436
Calibration or inverse regression: Which is appropriate for crop surveys using LANDSAT data? 07 p0985 N85-16260
Local dependence and point processes of exceedances in stationary sequences
[AD-A147859] 07 p1036 N85-16578
Asteroid taxonomy from cluster analysis of Photometry 09 p1411 N85-18897
Technical support for creating an artificial intelligence system for feature extraction and experimental design
[NASA-CR-175286] 12 p1918 N85-22044
Multi-sample cluster analysis as an alternative to multiple comparison procedures
[AD-A149960] 12 p1923 N85-22064
Decomposing the joint distribution of several linear combinations of uniform spacings
[AD-A155056] 21 p3677 N85-32845

CLUSTERS
U CLUMPS

CLUTCHES
Clutchless mechanism for engagement of forging press 14 p2268 N85-24051
Non-backdriveable free wheeling coupling
[NASA-CASE-MSC-20475-1] 18 p3116 N85-29290

CLUTTER
Clutter generator for use in radar evaluation
[AD-D011234] 01 p0039 N85-10245
A radar sea clutter model for atmospheric ducting conditions
[AD-A145321] 02 p0190 N85-11268
Autoregressive modeling and the classification of land clutter — radar signatures
[ENST-C-84003] 03 p0356 N85-12292
Rivista Tecnica Selenia, volume 9, number 1 07 p0938 N85-15945
Reference oscillator stability effect on clutter cancellation in a radar system 07 p0938 N85-15948
Support for the Naval Research Laboratory Passive Microwave Clutter Analysis Program
[AD-A146771] 07 p0939 N85-15951
The effects of soil moisture on bistatic clutter power
[AD-A147636] 08 p1150 N85-17261
Loop radiating elements
[AD-D011409] 08 p1158 N85-17308
MTI system simulation and clutter output statistics
[AD-A149193] 10 p1467 N85-19255
A short range, high accuracy radar ranging system
[AD-A152195] 16 p2774 N85-27122
Phase synchronizing large antenna arrays using the spatial correlation properties of radar clutter 20 p3439 N85-31344
The use of the glistening surface concept in rough surface scattering
[AD-A154922] 21 p3575 N85-32234
Most desirable terrain, e.g., flat vs valley location, part 5.1B 21 p3624 N85-32513
Nonlinear filtration of clutter 22 p3777 N85-33404

CMOS
Switched Capacitor (SC) filter and design centering of integrated circuits, part 1
[BMFT-FB-T-84-190-PT-1] 05 p0633 N85-14062
Development of a 2 micrometer silicon-gate-CMOS-technology for microcomputer oriented VLSI circuits with a supply voltage range between 1.5 and 5 V
[BMFT-FB-T-84-203] 07 p0949 N85-16012
High quality super-large circuits developed 11 p1622 N85-20209
Tally cell circuit
[AD-D011492] 11 p1629 N85-20254
Aspects of CSSR CMOS integrated circuits discussed 15 p2533 N85-25627
Recent developments 15 p2533 N85-25628
MHB4046 phase-lock circuit 15 p2533 N85-25629
Phase-locked loop design with MHB4046 15 p2534 N85-25631
Additional PLL designs 15 p2534 N85-25632
Analysis of the capability to effectively design complementary metal oxide semiconductor integrated circuits
[AD-A151832] 15 p2548 N85-25728
Speed-up techniques for complementary metal oxide semiconductor very large scale integration
[AD-A152466] 17 p3043 N85-28829
Silicide conductors reliability research
[AD-A153768] 18 p3095 N85-29157
Design of a sixteen-bit pipelined adder using CMOS bulk P-well technology
[AD-A155043] 21 p3580 N85-32260
East Europe report: Science and technology. Selections on CSSR computer technology
[JPRS-ESA-84-017] 21 p3668 N85-32781
Selections on CSSR computer technology 21 p3668 N85-32782

Effects of space radiation on advanced semiconductor devices. Part 3: Further cosmic ray simulation studies of single event upsets and latch-up in CMOS memories
[AERE-G-3368-PT-3] 22 p3848 N85-33833
Transient two-dimensional simulation of SEU in a CMOS SRAM cell
[DE85-008419] 22 p3890 N85-34111
Total integrated dose testing of solid-state scientific CD4011, CD4013, and CD4060 devices by irradiation with CO-60 gamma rays
[NASA-CR-176196] 24 p4161 N85-35795

CN EMISSION
The fluorescence of cometary OH and CN
09 p1411 N85-18896

CNOIDAL WAVES
An analytical model of periodic waves in shallow water
[AD-A147501] 07 p0960 N85-16085
An analytical model of periodic waves in shallow water
[AD-A147502] 07 p0960 N85-16086

COAGULATION
Evolution of grains in a turbulent solar nebula
13 p2179 N85-23525
The influence of Brownian coagulation on the size distributions of atmospheric aerosols
21 p3645 N85-32643
Size spectra for the source-enhanced coagulation with the turbulent mass transfer 21 p3645 N85-32649

COAL
NT LIGNITE
Compilation of elemental concentration data for NBS (National Bureau of Standards) biological, geological and environmental standard reference materials, 1982
[PB84-218336] 01 p0025 N85-10158
The feasibility of satellite remote sensing as a technique for evaluating coal mine surface features
02 p0213 N85-11401
Mapping land use changes in the carboniferous region of Santa Catarina, report 2
[E85-10017] 02 p0217 N85-11430
Interactive system for the interpretation of coal deposit data as a basis of future mine planning systems
[BMFT-FB-T-83-115] 02 p0220 N85-11449
Dynamics of burnout of solid fuel in fluidized bed of finely divided inert particles 02 p0273 N85-11782
The status of synthetic fuels and cost-shared energy R and D facilities
[GPO-36-903] 03 p0339 N85-12182
Fabric filter system study
[PB84-229749] 03 p0342 N85-12206
Estimation of dynamic stresses around the shot point by scale model experiment 04 p0462 N85-13076
US energy for the rest of the century, 1984 edition
[PB84-207406] 04 p0531 N85-13393
Additives for heat engine coal slurry fuels
[DE84-016434] 05 p0621 N85-13971
Ceramic fabric material testing
[DE84-012014] 09 p1300 N85-18165
Combustion characterization of coals for industrial applications
[DE85-010673] 19 p3228 N85-30014
Application of the reference intensity method to coal analysis
[DE85-009526] 19 p3228 N85-30015
Guest molecules in coal
[DE85-010435] 19 p3228 N85-30016
Novel analytical approaches to coal beneficiation
[DE85-010437] 19 p3229 N85-30021
Adherence of ash particles from the combustion of micronized coal
[DE85-008600] 19 p3229 N85-30023
The mobile phase in coals: Its nature and modes of release
[DE85-011686] 19 p3230 N85-30026
Development of a coal-water slurry-fueled diesel engine for industrial cogeneration. Task 1.0 topical report: Thermodynamic analysis
[DE85-010455] 19 p3236 N85-30062
Current status of TVA's atmospheric fluidized bed combustion development efforts
[DE85-001209] 19 p3306 N85-30507
Technical guide for estimating fugitive dust impacts from coal handling operations, volume 2
[DE85-010939] 19 p3309 N85-30514
Coal slurry ignition in a diesel engine simulator
[DE85-010987] 20 p3463 N85-31513
Ames Laboratory measurements of alkali levels in the Curtiss-Wright PFBC gas stream
[DE85-011357] 22 p3745 N85-33214
Drying of pulverized material with heated condensible vapor
[DE85-011656] 22 p3783 N85-33436
Shuttle car loading system
[NASA-CASE-NPO-15949-1] 23 p3987 N85-34722
Fluidized bed desulfurization
[NASA-CASE-NPO-15924-1] 24 p4075 N85-35253
Depositional systems and coal occurrence in the Fort Union Formation (Paleocene), Powder River Basin, Wyoming and Montana 24 p4114 N85-35505

COAL DERIVED LIQUIDS
Superheated fuel injection for combustion of liquid-solid slurries
[DE85-011624] 22 p3753 N85-33266

COAL GASIFICATION
Optical detection of alkali compounds
[DE84-015505] 03 p0328 N85-12117
USSR report: Chemistry
[JPRS-UCH-84-012] 06 p0761 N85-14865
Behavior of pressurized tubes of candidate alloys in a simulated low-Btu environment
[DE85-003403] 09 p1296 N85-18141
Corrosion of ceramics in heat exchanger applications
[DE84-017459] 09 p1299 N85-18161
Assessment of the need for an advanced high-strength chromium-molybdenum steel for construction of third-generation gasifier pressure vessels
[DE85-002865] 11 p1606 N85-20097
USSR report: Chemistry
[JPRS-UCH-85-001] 13 p2013 N85-22629
Electricity production from coal through molten-carbonate fuel cells
[TI85-005072] 14 p2351 N85-24534
Studies of metal/carbon surface chemistry
[DE85-005513] 15 p2507 N85-25463
Commercial feasibility of underground gasification of Texas lignite to produce synthetic gas
[DE85-001998] 18 p3127 N85-29361
Differential optical absorption techniques for diagnostics of coal gasification
[DE85-010177] 19 p3368 N85-30890
Energy and Technology Review
[DE85-011767] 21 p3716 N85-33061
Photofragment fluorescence as a sensitive probe for gas-phase alkali compounds and their photochemistry
[DE85-010707] 22 p3746 N85-33219

COAL LIQUEFACTION
Developing a flowmeter for streams with high solids content
[DE84-016643] 09 p1323 N85-18316
Integration of advanced preparation with coal liquefaction
[DE85-010432] 19 p3228 N85-30012
Exploratory study of coal conversion chemistry
[DE85-010393] 19 p3229 N85-30018
Method of distributing liquefaction catalysts in solid carbonaceous material
[DE85-005759] 23 p3909 N85-34218

COAL UTILIZATION
USSR report: Energy
[JPRS-UEN-84-038] 07 p0994 N85-16312
Closed cycle versus open cycle gas turbines. A review of A.D. Little's ICOP report, vol. 3
[DE85-000564] 12 p1861 N85-21671
Development of molten carbonate fuel cell power plant, volume 1
[DE85-008743] 18 p3131 N85-29394
Magnetohydrodynamics and the National Coal Science, Technology, and Engineering Development Acts
[S-HRG-98-1179] 20 p3535 N85-31994
Superheated fuel injection for combustion of liquid-solid slurries
[DE85-011624] 22 p3753 N85-33266
Chemistry division report
[DE85-010586] 24 p4071 N85-35228

COALESCENCE
U COALESCING

COALESCING
Bunch coalescing in the main ring to form intense proton and antiproton bunches without RF counterphasing
[DE85-001364] 09 p1382 N85-18692
Signatures of the coalescence instability in solar flares
12 p1956 N85-22293

COANDA EFFECT
Circulation control propellers for general aviation, including a BASIC computer program
[NASA-CR-165968] 19 p3219 N85-29959

COARSENESS
X-ray residual stress analysis on the coarse grain of copper and its application to the brazed copper
23 p3907 N85-34202

COASTAL CURRENTS
Satellite definition of the bio-optical and thermal variation of coastal eddies associated with the African current
[AD-A147910] 07 p0969 N85-16282
Studies of coastal mesoscale winds using SIR-B
08 p1147 N85-17238
California coastal erosion and storm damage during the winter 1982 - 1983, a reconnaissance report
[PB85-121705] 10 p1521 N85-19591
Two-cycle mechanism of dissipation of tidal energy in ocean 14 p2335 N85-24438
The sea level response to weather along the coast of southern Africa 16 p2829 N85-27446
Atmospherically forced, coastally trapped, long period gravity waves off the south coast of southern Africa
16 p2832 N85-27401
Comparison of a diffusion model with dye dispersion measurements to study turbulence in coastal waters
[INPE-3492-PRE/729] 16 p2838 N85-27504

COASTAL DUNES
U DUNES

COASTAL ECOLOGY
Environmental geologic atlas of the North Carolina coastal zone: Dare, Hyde, Tyrrell and Washington Counties
[PB84-222975] 01 p0066 N85-10439
The SANCOR programme on coastal processes, April 1982 - March 1988
[REPT-68] 01 p0069 N85-10455
Ecology of estuarine channels of the pacific northwest coast: A community profile
[PB84-209709] 01 p0070 N85-10464
The ecology of tundra ponds of the Arctic coastal plain: A community profile
[TI85-900650] 15 p2589 N85-25958
Review and annotated bibliography of benthic studies in coastal and estuarine areas of Florida with a selected compilation of worldwide benthic methodological references and southeastern United States benthic taxonomic references
[PB85-151041] 16 p2822 N85-27405

COASTAL MARSHLANDS
U MARSHLANDS

COASTAL PLAINS
Potential geological natural landmarks of the East Gulf Coastal Plain
[PB84-230317] 06 p0835 N85-15316
Soil formation on tertiary landsurfaces of the New Jersey coastal plain 08 p1181 N85-17441
The ecology of tundra ponds of the Arctic coastal plain: A community profile
[TI85-900650] 15 p2589 N85-25958

COASTAL RANGES (CA)
Franciscan and related rocks of southern Humbolt County, northern California coast ranges: Analysis of structure, tectonics, sedimentary petrology, paleogeography, depositional histroy, and thermal maturity 03 p0390 N85-12495
Mesozoic ophiolitic olistostromes and Cenozoic imbricate thrust faulting in the northern California coast ranges: Geology of the Mysterious Valley area, Napa County 08 p1182 N85-17445

COASTAL WATER
The SANCOR estuaries programme, 1982-1986
[ISBN-0-7988-2662-2] 01 p0068 N85-10454
The SANCOR programme on coastal processes, April 1982 - March 1988
[REPT-68] 01 p0069 N85-10455
Ecology of estuarine channels of the pacific northwest coast: A community profile
[PB84-209709] 01 p0070 N85-10464
Estuaries of the Cape. Part 2: Synopses of available information on individual systems. Report 12: Buffels (WES) (CSW 1), Elsies (CSW 2), Sir Lowry's Pass (CSW8), Steenbras (CSW 9), and Buffels (OOS) (CSW 11)
[CSIR-RR-411-PT-2] 01 p0086 N85-10581
Estuaries of the Cape. Part 2: Synopses of available information on individual systems. Report no. 14: Sand (CSW 4)
[CSIR-RR-413-PT-2] 01 p0086 N85-10583
Estuaries of the Cape. Part 2: Synopses of available information on individual systems. Report no. 15: Zeekoe (CSW 5)
[CSIR-RR-414-PT-2] 01 p0087 N85-10584
The altimeter as a support to the scatterometer in the representation of winds and derived wave fields in coastal waters and enclosed seas: A research at its onset
03 p0383 N85-12453
Use of SIR-B multiincidence-angle imagery to study iceberg detectability and offshore ocean feature extraction 08 p1145 N85-17225
Analysis of flow within the coastal boundary layer off Long Island, New York
[DE85-001384] 09 p1359 N85-18550
Mesoscale studies of flow regimes and fluxes of particulate matter in coastal waters
[DE85-003825] 11 p1689 N85-20620
USC (University of Southern California) Sea Grant Program Directory, 1984-1985
[PB85-135051] 12 p1899 N85-21922
Production and turnover of suspended organic detritus in the coastal water of the southeastern continental shelf
[DE85-003977] 13 p2140 N85-23290
Evaluation of wave energy resources on the French Atlantic seaboard 14 p2325 N85-24369

Chemical composition of coastal haze aerosol
14 p2336 N85-24458
Analysis of hydrometeorological conditions in Antarctic coastal waters according to data from hydrological and satellite observations
15 p2487 N85-25354
Analysis of suspended sediment distributions in the surface waters of Delaware Bay using remote sensing of optical properties
15 p2582 N85-25926
Deepwater wind wave growth with fetch and duration
[AD-A151604] 15 p2604 N85-26051
Diffusion coefficients for coastal water determined from aerial photographs
[INPE-3413-PRE/679] 16 p2810 N85-27331
The sea level response to weather along the coast of southern Africa
16 p2829 N85-27446
Comparison of a diffusion model with dye dispersion measurements to study turbulence in coastal waters
[INPE-3492-PRE/729] 16 p2838 N85-27504
Properties of aerosol particles detected by satellites in coastal regions
21 p3641 N85-32622
Coastal erosion along Monterey Bay
[AD-A155610] 21 p3655 N85-32707
Arctic and offshore research
[DE85-001995] 22 p3818 N85-33653
Sea surface and remotely sensed temperatures off Cape Mendocino, California
[NASA-TM-86712] 24 p4125 N85-35573

COASTAL ZONE COLOR SCANNER
Coastal Zone Color Scanner (CZCS): Imagery of near-surface phytoplankton pigment concentrations from the first coastal ocean dynamics experiment (CODE-1), March - July 1981
[NASA-CR-174169] 04 p0542 N85-13447
Bio-optical variability in the Alboran Sea as assessed by Nimbus-7 coastal zone color scanner
[AD-A147909] 07 p0989 N85-16281
The use of principal components analysis techniques Nimbus-7 coastal zone color scanner data to define mesoscale ocean features through a warm humid atmosphere
[AD-A148567] 08 p1176 N85-17416
Nimbus 7 Coastal Zone Color Scanner (CZCS). Level 2 data product users' guide
[NASA-TM-86202] 19 p3299 N85-30452
Nimbus 7 Coastal Zone Color Scanner (CZCS). Level 1 data product users' guide
[NASA-TM-86203] 19 p3299 N85-30453

COASTS
Environmental geologic atlas of the North Carolina coastal zone: Dare, Hyde, Tyrrell and Washington Counties
[PB84-222975] 01 p0066 N85-10439
The SANCOR estuaries programme, 1982-1986
[ISBN-0-7968-2662-2] 01 p0068 N85-10454
The SANCOR programme on coastal processes, April 1982 - March 1986
[REPT-88] 01 p0069 N85-10455
Black Sea coastal frontogenesis
01 p0075 N85-10500
Some aspects of post-frontal convective areas along the west coast of the united states
[AD-A144895] 01 p0085 N85-10572
Estuaries of the Cape. Part 2: Synopses of available information on individual systems. Report 12: Buffels (WES) (CSW 1), Elsies (CSW 2), Sir Lowry's Pass (CSW8), Steenbras (CSW 9), and Buffels (OOS) (CSW 11)
[CSIR-RR-411-PT-2] 01 p0086 N85-10581
Estuaries of the Cape. Part 2: Synopses of available information on individual systems. Report no. 14: Sand (CSW 4)
[CSIR-RR-413-PT-2] 01 p0086 N85-10583
Estuaries of the Cape. Part 2: Synopses of available information on individual systems. Report no. 15: Zeekoe (CSW 5)
[CSIR-RR-414-PT-2] 01 p0087 N85-10584
Evaluation of an aerosol prediction model for coastal regions using marine aerosol generation and transport data
[AD-A145443] 02 p0231 N85-11510
Plotting TDL coastal wind forecasts
[PB84-220789] 03 p0397 N85-12533
Prediction of wave height of wind-generated seas in finite water depth
[AD-A145996] 03 p0398 N85-12539
Numerical prediction of the president's day cyclone
05 p0684 N85-14399
Avionics system design for requirements for the United States Coast Guard HH-65A Dolphin
06 p0753 N85-14827
Conditions governing the formation of stratocumulus clouds over the western Atlantic during cold air outbreaks
[AD-A146780] 07 p1004 N85-16383
On the formation of the nocturnal coastal surface wind speed maximum
09 p1356 N85-18526
Nautical charting with remotely sensed imagery, volume 1
[AD-A149361] 10 p1506 N85-19503
Nautical charting with remotely sensed imagery. Volume 2: Case studies
[AD-A149362] 10 p1506 N85-19504
Hurricane experience levels of coastal county populations: Texas to Maine
[PB85-111383] 10 p1520 N85-19581
Atlantic Coast Unique Regional Atmospheric Tracer Experiment (ACURATE)
[PB85-128460] 12 p1886 N85-21839
Studies of the development of cyclones over Southern China coastal areas and adjacent seas
[AD-A150108] 12 p1896 N85-21901
Observations of the California countercurrent
[AD-A150781] 14 p2382 N85-24691
Research on atmospheric dust formations using satellite observation data
15 p2485 N85-25339
Meso-8 scale numerical simulations of the jet streak adjustments which organized the Carolina tornado outbreak and the subsequent explosive coastal cyclogenesis
15 p2598 N85-26011
Contamination of the fetch-limited directional wave spectrum by waves emanating from an embayment
[NASA-TM-84441] 15 p2604 N85-26048
Review and annotated bibliography of benthic studies in coastal and estuarine areas of Florida with a selected compilation of worldwide benthic methodological references and southeastern United States benthic taxonomic references
[PB85-151041] 16 p2822 N85-27405
Operation guiding light-scientific program and field plan. The pilot field experiment for NORDA project chemical dynamics in ocean frontal areas
[AD-A153785] 18 p3150 N85-29507
Summary of archived Atlantic coast wave information study pressure, wind, wave, and water level data
[AD-A153782] 18 p3151 N85-29508
Geoacoustic models: Washington state continental margin
[AD-A153781] 18 p3177 N85-29699
Temporal variations of Rn222 concentrations in Black Sea coastal zone
19 p3293 N85-30417
Sand dispersion from an ephemeral river delta on the wave-dominated central California coast
[AD-A154352] 19 p3300 N85-30458
Properties of aerosol particles detected by satellites in coastal regions
21 p3641 N85-32622
Aircraft observations of cloud condensation nuclei in maritime and continental environments
21 p3650 N85-32680
Marine phosphorite deposits model for exploration, with emphasis on deposits in the US Atlantic coastal plain
24 p4104 N85-35439
USGS coastal research, studies and maps: A source of information for coastal decision making
[USGS-CIRC-883] 24 p4108 N85-35465
Atlantic coast hindcast. Phase 2: Wave information, additional extremal estimates
[AD-A156137] 24 p4125 N85-35575

COATING
NT ANODIZING
NT ELECTROPLATING
NT ENCAPSULATING
NT METALLIZING
Thermodynamic calculations and the chemical vapour deposition of hard materials
02 p0179 N85-11200
Textured carbon surfaces on copper
[NASA-CASE-LEW-14130-1] 11 p1615 N85-20156
Corrosion resistant coating
[NASA-CASE-NPO-15928-1] 18 p3073 N85-29005
New metal coating method developed
21 p3508 N85-32191

COATINGS
NT ALUMINUM COATINGS
NT ANODIC COATINGS
NT ANTIREFLECTION COATINGS
NT CATHODIC COATINGS
NT CERAMIC COATINGS
NT ELECTROPLATING
NT ENAMELS
NT ENCAPSULATING
NT GLASS COATINGS
NT GLAZES
NT GOLD COATINGS
NT LACQUERS
NT MAGNETIC FILMS
NT METAL COATINGS
NT METALLIZING
NT NICKEL COATINGS
NT PAINTS
NT PLASTIC COATINGS
NT PRIMERS (COATINGS)
NT PROTECTIVE COATINGS
NT REFRACTORY COATINGS
NT RUBBER COATINGS
NT SPRAYED COATINGS
NT THERMAL CONTROL COATINGS
NT ZINC COATINGS
USSR report: Materials science and metallurgy, no. 93
[JPRS-84810] 01 p0018 N85-10110
Aircraft surface coatings
[NASA-CR-3681] 02 p0137 N85-10935
Turbine Engine Hot Section Technology (HOST)
[NASA-TM-83022] 02 p0140 N85-10951
The adhesion of hard and wear resistant coatings
02 p0179 N85-11203
Plasma variables and tribological properties of coatings in low pressure (0.1 - 10.0 torr) plasma systems
[NASA-TM-83798] 02 p0189 N85-11281
Simulation of vibration processes in damped structures with allowance for temperature-frequency characteristics of vibration absorbing materials
02 p0257 N85-11680
The effect of heat treatment on wear resistance of gas-plasma eutectic coatings
[BLL-M-35756-(5828.4)] 03 p0329 N85-12122
Surface coatings for low emittance in the thermal surveillance band
[MRL-R-937] 03 p0336 N85-12158
Effects of monolayer coverages on substrate sputtering yields
[DE84-016312] 04 p0478 N85-13033
Effect of oxide coated thickness on thermal ignition of titanium-based pyrotechnics
[DE84-013061] 04 p0481 N85-13065
Effect of water on hydrogen permeability --- Stirling engines
[NASA-TM-86904] 06 p0761 N85-14864
Process for producing carbide coatings
[AD-D011295] 06 p0764 N85-14885
Surface studies of Nb, its compounds, and coatings
[DE84-017353] 06 p0868 N85-15516
Deposition of titanium nitride coatings by reactive evaporation and electrically activated reactive evaporation
[BLL-TRANS-5043-(9091.9F)] 07 p0925 N85-15858
Experimental test program for evaluation of solid lubricant coating as applied to compliant foil gas bearings to 315 deg C
[NASA-CR-174837] 07 p0930 N85-15895
Moisture absorbing anti-arcing coating and method for applying same
[AD-D011310] 07 p0932 N85-15904
Damping capacity of multilayer tube during torsion
[BLL-M-36011-(5828.4)] 07 p0977 N85-16202
Anticoiling technology: Theories of surface soiling and performance of anticoiling surface coatings
[NASA-CR-174274] 07 p0991 N85-16296
Corrosion properties of second-generation conductive materials
07 p1000 N85-16348
Optical fibers with reduced pressure sensitivity to high frequency acoustic field
[AD-D011306] 07 p1043 N85-16627
Construction tolerances for low loss, dielectric coated, metallic waveguide for transmission optical radiation
[DE85-004056] 10 p1558 N85-19822
Study of phase composition of Al-B plasma coatings
11 p1598 N85-20050
Improving operational properties of titanium alloys by diffusion siliciding
11 p1602 N85-20075
Status of specific FRG high tech research funded by BMFT
11 p1618 N85-20181
Time resolved Raman studies of laser induced damage in TiO2 optical coatings
[DE85-003166] 11 p1640 N85-20332
Evaluation of infrared reflectance as a technique for measuring absorber materials degradation
[DE85-002171] 11 p1729 N85-20874
Diamondlike flakes
[NASA-CASE-LEW-13837-2] 12 p1796 N85-21267
Corrosion and coatings review of specifications and drawings of facilities for the Oman Military Construction Program at Masirah Island, Oman
[AD-A149739] 12 p1812 N85-21366
Evaluation of Epoxo 300-C nonskid coating for use on bridge decks
[PB85-108843] 12 p1819 N85-21412
Numerical methods for analyzing electromagnetic scattering
[NASA-CR-175507] 12 p1823 N85-21436
Advanced thin film thermocouples
[NASA-CR-175541] 12 p1850 N85-21607
Experimental studies of low temperature surface interactions of atomic hydrogen using maser technique
[AD-A150216] 13 p2017 N85-22647
USSR report: Materials science and metallurgy
[JPRS-UMS-85-002] 13 p2025 N85-22688

Research directed advanced high temperature coating system beyond current state-of-the art systems
[AD-A150696] 14 p2255 N85-23974
High-temperature X-ray diffraction study of coating-substrate compatibility in yttria-coated graphite
[DE85-005916] 14 p2262 N85-24016
Multilayer reflecting systems based on glassy chalcogenides for infrared lasers
14 p2274 N85-24089
Color-selective coating for viewfinder in optical instruments 14 p2276 N85-24098
Selective coatings for solar-to-thermal energy converters 14 p2280 N85-24127
Corrosion control through a better understanding of the metallic substrate-organic coating-interface
[AD-A151238] 15 p2509 N85-25479
USSR report: Materials science and metallurgy
[JPRS-UMS-85-004] 15 p2513 N85-25503
Surface composition, properties and thermal stability of massive and fine metallic glasses
15 p2513 N85-25506
Procedure for certifying quantity of volatile organic compounds emitted by paint, ink and other coatings
[PB85-159044] 15 p2520 N85-25537
Investigation of silicon surface passivation by silicon nitride film deposition
[NASA-CR-175663] 15 p2585 N85-25936
Performance of a copper-lithium alloy as an impurity control system surface material for a fusion reactor
[DE85-006494] 15 p2657 N85-26398
In situ thin film measurement
[AD-A151365] 15 p2659 N85-26411
Tooth wear in worm gears in vacuum
16 p2766 N85-27070
Development of a polystyrene insulation system
[DE85-006950] 16 p2784 N85-27180
High-altitude testing of selective optical coatings for solar radiators and collectors 17 p2939 N85-28143
Heat pipe and method of making same
[AD-D011654] 17 p2959 N85-28273
Raman studies of laser damaged single and multi-layer optical coatings
[DE85-009431] 17 p2971 N85-28351
Absorber coatings degradation
[DE85-008628] 18 p3128 N85-29367
Self-sustaining coatings for fusion applications: Copper lithium alloys
[DE85-009740] 18 p3190 N85-29783
Influence of type of processing of AK4 alloy on its surface state and strength of bonding of plasma coatings
19 p3242 N85-30103
Effect of protective method on cyclic durability and nature of failure of titanium alloy welded joints
19 p3245 N85-30122
Effect of heating temperature in a vacuum on state of surface layers of welded OT4 titanium alloy
19 p3245 N85-30123
BN coating of ceramic fibers for ceramic fiber composites
[AD-D011700] 19 p3249 N85-30145
Mutual coupling analysis for conformal microstrip antennas
[AD-A154292] 19 p3259 N85-30210
Stress concentration in the elastoplastic state and residual stress after unloading
[AD-A155628] 21 p3600 N85-32356
Dielectric mirror with ferromagnetic substrate
21 p3696 N85-32966
Management of Corrosion
[AGARD-LS-141] 22 p3749 N85-33238
Land vehicle corrosion management
22 p3750 N85-33246
Electrically conductive containment vessel for molten aluminum
[DE85-006518] 23 p3939 N85-34415

COAXIAL CABLES
Microminiature coaxial cable and methods of manufacture
[DE84-014228] 01 p0044 N85-10284
Coaxial noise measurement circuits
05 p0630 N85-14036
A coaxial probe for measuring the current density profile of intense electron beams
[AD-D011407] 08 p1164 N85-17347
High voltage RF coaxial cable
[AD-D011493] 11 p1629 N85-20255
A moment solution for an arbitrary configuration of partly shielded wires above a ground plane
[AD-A149762] 12 p1828 N85-21473
Change of electrical characteristics of radio-frequency cables under thermal effect 13 p2081 N85-22999
Spectral evaluation of irregularity of superconducting coaxial cables 13 p2082 N85-23000
Basic EMC technology advancement for C3 systems. Volume 4F: Prediction of crosstalk in flatpack coaxial cables
[AD-A153111] 17 p2954 N85-28242
Predicting electrical performance parameters of underwater cables 22 p3775 N85-33391

COAXIAL FLOW
Stability of fluid flow in a cylindrical annulus
[NASA-TM-77720] 01 p0046 N85-10300
Turbulent transport and length scale measurement experiments with confined coaxial jets
[NASA-CR-174831] 19 p3265 N85-30245

COAXIAL PLASMA ACCELERATORS
Steady-state spheromak reactor studies
[DE85-009595] 19 p3372 N85-30916
Intercomparison of the calculated absolute efficiency values between true coaxial and true closed-end coaxial Ge (Li) and NaI detectors
[REPT-5-1984] 20 p3532 N85-31976

COAXIAL TRANSMISSION
U COAXIAL CABLES
U TRANSMISSION

COBALT
NT COBALT 60
Effects of cobalt, boron, and zirconium on the microstructure of Udimet 738
[NASA-CR-174762] 01 p0027 N85-10166
Microstructural basis of strength and toughness in hardmetals 02 p0177 N85-11185
Magnetic properties of the cobalt matrix in WC-Co compacts 02 p0177 N85-11186
The inter-relation of microstructure, toughness and fatigue crack growth behaviour in WC-Co hardmetals
02 p0177 N85-11188
Erosion of sintered WC-Co alloys
02 p0179 N85-11201
The reactions of cobalt, iron and nickel in SO-2 atmospheres: Similarities and differences
[NASA-TM-86868] 02 p0181 N85-11217
Nickel-cobalt systematics and their bearing on lunar origin 04 p0582 N85-13719
Abundancies of Ni, Cr, CO and major elements in the silicate portion of the Moon: Constraints from primary lunar magmas 04 p0582 N85-13720
Anisotropy and relaxation effects of Co2+ ions in LiTi ferrite
[AD-A146550] 06 p0861 N85-15469
Preparation and electronic properties of MoS(2) and WS(2) single crystals grown in the presence of cobalt
[AD-A146508] 06 p0866 N85-15506
The growth of metastable peritectic compounds
[NASA-CR-171289] 07 p0920 N85-15824
Metal-support interactions: Their effects upon adsorption, electronics, and activity/selectivity properties of cobalt in hydrogenation
[DE85-003316] 09 p1292 N85-18113
Improved lithium-intercalation cathode material
[AD-A149319] 10 p1435 N85-19043
Antifriction properties of gas thermal coatings of clad carbine powders 10 p1447 N85-19115
The response of cobalt-free Udimet 700 type alloy to modified heat treatments
[NASA-TM-86842] 11 p1597 N85-20043
Ligand structural influences upon electrochemical reactivity: Organic substituent effects upon Carboxylatopentaammminecobalt(3) reductions at mercury and gold electrodes
[AD-A150685] 14 p2250 N85-23944
Neutron scattering and reactions on 59Co from 1 to 20 MeV
[AERE-R-11439] 17 p3028 N85-28729
Improved catalysts for liquid hydrocarbon fuels from syngas
[DE85-011062] 20 p3421 N85-31234
Analysis of ferrates and ferrites of three transition metals using Moessbauer effects
[BLL-CE-TRANS-8019-(9022.09)] 20 p3430 N85-31273
Measurements of Fe and Ar fragmentation cross sections
[PAPER-OG-7.2-20] 21 p3714 N85-33047
Metal (2) 4,4',4',4'' phthalocyanine tetraamines as curing agents for epoxy resins
[NASA-CASE-ARC-11424-1] 23 p3919 N85-34281
Cobalt-rich ferromanganese crusts in the oceans
24 p4104 N85-35444
Applications of the mineral resources data system and the international strategic minerals inventory in mineral-resource assessments by region and commodity
24 p4105 N85-35451
The Conterminous United States Mineral Assessment Program 24 p4106 N85-35458
The Alaska Mineral Resources Assessment Program
24 p4107 N85-35460

COBALT ALLOYS
NT RENE 95
The Palmqvist test and its applications in WC-Co alloys 02 p0177 N85-11187
Erosion of multiphase materials
[DE84-015816] 04 p0474 N85-13018
Laser-initiated combustion studies on metallic alloys in pressurized oxygen
[PB85-128114] 10 p1438 N85-19066
Production method of nickel electrode
[NASA-TM-76946] 10 p1439 N85-19069
Method of producing nickel electrode
[NASA-TM-76944] 10 p1440 N85-19077
Creep-rupture behavior of iron superalloys in high-pressure hydrogen
[NASA-CR-174411] 10 p1441 N85-19078
Proton NMR and susceptibility measurements in TiCoH/sub x
[DE85-003309] 12 p1807 N85-21336
Corrosion-resistant amorphous alloys
13 p2035 N85-22748
Determination of symmetry of immediate surroundings in amorphous Co-P alloys 15 p2496 N85-25398
Erosion of multiphase materials
[DE85-008895] 18 p3068 N85-28978
Slow crack growth in metal reinforced glass composites
[DE85-010094] 18 p3082 N85-29064
Long range ordered alloys modified by addition of niobium and cerium
[DE85-011661] 20 p3431 N85-31285
Nonequilibrium kinetics of growth of oxide layer grains during laser heating of metals in air
21 p3689 N85-32919
Deposition of nickel-cobalt alloys by controlled-potential electrolysis
[PB85-198582] 24 p4081 N85-35291

COBALT COMPOUNDS
NT COBALT OXIDES
The alpha-form of the hydroxides of bivalent metals
[NASA-TM-77508] 04 p0473 N85-13009
Chemically modified electrodes and related solution chemistry
[DE84-017110] 05 p0614 N85-13924
Phase size distribution in WC/Co hardmetal
[NPL-DMA(A)-93] 20 p3431 N85-31281
Nuclear magnetic resonance study of the intramolecular rearrangement of 2-(5-cyanotetrazolato)pentaammine cobalt (III) perchlorate
[DE85-010810] 22 p3839 N85-33772

COBALT ISOTOPES
NT COBALT 60

COBALT OXIDES
Mechanisms of elevated temperature rupture in single phase ceramics
[DE85-000697] 09 p1299 N85-18156

COBALT 60
Mechanisms of impurity diffusion in rutile
[DE84-014741] 06 p0766 N85-14902

COBOL
Digital equipment Corporation, professional 350, COBOL-81 Version 2.1
[PB84-227602] 03 p0403 N85-12572
Digital Equipment Corporation, Professional 350, COBOL-81 Version 2.1 (COBOL technical report)
[PB84-227719] 03 p0403 N85-12573
Northern Telecom, Incorporated, NTI-585/565, ACOBOL/3 Release 4.1 Version H(01)
[PB84-228022] 03 p0404 N85-12574
Northern Telecom, Incorporated NTI-585/565, ACOBOL/3 Release 4.1 Version H(01) (COBOL technical report)
[PB84-228030] 03 p0404 N85-12575
Digital Equipment Corporation, DECSYSTEM-10, model 1090-SMP, COBOL-74 V12B
[PB84-227941] 03 p0404 N85-12576
Data General Corporation, Eclipse C350, AOS COBOL Release 3.51
[PB84-227883] 03 p0404 N85-12577
Convergent Technologies, NGEN CP001, CT COBOL version 9.0
[PB84-227784] 03 p0404 N85-12578
Digital Equipment Corp., VAX/750, VAX COBOL version 3.0
[PB84-227693] 03 p0405 N85-12583
IBM Corporation, IBM 5361 model 5, system/38 COBOL release 6
[PB84-227677] 03 p0405 N85-12584
Gould Incorporated, GOULD Concept 32/87, COBOL release 1.4
[PB84-227669] 04 p0548 N85-13484
Digital Equipment Corp., VAX/750, VAX COBOL version 3.0
[PB84-227651] 04 p0548 N85-13485
Digital Equipment Corp., MICRO/PDP-11, COBOL-81 version 2.2
[PB84-227644] 04 p0548 N85-13486

C3, Incorporated, C50 System, C3 COBOL/75 version 2.00
[PB84-226006] 04 p0548 N85-13488
Burroughs Corporation B26-CPU, B20 COBOL, Release 4.0
[PB84-216241] 04 p0551 N85-13505
Burroughs Corporation B26-CPU, B20 COBOL Version 4.0 (COBOL technical report)
[PB84-216258] 04 p0551 N85-13506
Convergent technologies NGEN CP001, CT COBOL Version 9.0
[PB84-216266] 04 p0551 N85-13507
Convergent Technologies, Incorporated, NGEN CP001, CT COBOL Version 9.0 (COBOL technical report)
[PB84-216274] 04 p0551 N85-13508
Computer Sciences Corporation UNIVAC 1100/80, CSTS COBOL Release COB250
[PB84-216282] 04 p0551 N85-13509
C3, Incorporated NGEN CP001, COBOL Version 9.0
[PB84-216308] 04 p0552 N85-13511
NECIS Incorporated, NEC ASTRA model 270, COBOL 74 version 8.3 (COBOL technical report)
[PB84-227933] 06 p0848 N85-15381
Data general Corporation, Eclipse C150, Interactive COBOL Revision 1.30 (COBOL technical report)
[PB84-227834] 06 p0849 N85-15391
Data General Corporation, Eclipse C150, interactive COBOL Revision 1.30
[PB84-227691] 06 p0849 N85-15392
IBM Corporation, IBM Series/1 4955, IBM Series/1 host COBOL Release 1.1 EDX (COBOL technical report)
[PB84-227909] 06 p0849 N85-15393
IBM Corporation, IBM Series/1 4955, IBM Series/1 host COBOL Release 1.1 EDX
[PB84-227818] 06 p0849 N85-15394
IBM Corporation, IBM Series/1 4955, IBM Series/1 host COBOL Release 1.1 RPS
[PB84-227917] 06 p0850 N85-15395
IBM Corporation, IBM Series/1 4955, IBM Series/1 host COBOL Release 1.1 RPS (COBOL technical report)
[PB84-227925] 06 p0850 N85-15396
NECIS, Incorporated, NEC ASTRA model 270 COBOL 74 Version 8.3
[PB84-227636] 06 p0850 N85-15397
Digital Equipment Corporation, DECSYSTEM-20, model 2060, COBOL V13
[PB84-227958] 06 p0850 N85-15398
Digital Equipment Corporation, DECSYSTEM-20, model 2060, COBOL V13 (COBOL technical report)
[PB84-227966] 06 p0850 N85-15399
Northern Telecom, Incorporated, IBM 3033 (compilation), NTI-585/565 (execution), XCOBOL Release 4.1 Version H(01)
[PB84-227875] 06 p0850 N85-15400
NCR Corporation, NCR I9300, NCR ITX Cobol Release 3.0
[PB84-228055] 06 p0850 N85-15401
NCR Corporation, NCR I9300, NCR ITX COBOL Release 3.0 (COBOL technical report)
[PB84-228063] 06 p0850 N85-15402
Gould Incorporated, Gould PS-3000, Gould PS-3000 COBOL V2.0
[PB84-229160] 06 p0850 N85-15403
Control Data Corporation, CYBER 835, COBOL Release 5.3 Level 614
[PB84-227842] 06 p0851 N85-15408
Prime Computer, Inc., PRIME 750, COBOL-74 Revision 19.3.2
[PB84-227826] 06 p0851 N85-15409
Sperry Univac, System 80 Model 6, OS/3 COBOL, Version 08.00/06
[PB84-227800] 06 p0851 N85-15410
Digital Equipment Corporation, MICRO/PDP-11, COBOL-61 Version 2.2
[PB84-229236] 06 p0852 N85-15413
Computer Sciences Corporation, UNIVAC 1100/80, CSTS COBOL Release COB250
[PB84-229154] 06 p0852 N85-15417
Data General Corporation, Eclipse C350, AOS COBOL Release 3.51
[PB84-227982] 06 p0853 N85-15421
C3, Incorporated NGEN CP001, C3 COBOL Version 9.0 (COBOL Technical Report)
[PB84-216316] 06 p0855 N85-15435
Microsoft Corporation, Sun Microsystems, Microsoft COBOL Version 2.0
[PB84-243401] 06 p0856 N85-15443
Microsoft Corporation, IBM PC XT, Microsoft COBOL, Version 2.0
[PB84-243419] 06 p0856 N85-15444
Four Phase Systems, Incorporated, Four Phase Series 5000, COBOL 1974 version BE06.8
[PB85-108017] 10 p1541 N85-19717
Four Phase Systems, Incorporated, Mini-Frame Series 6300, COBOL Series 6000
[PB85-108025] 10 p1541 N85-19718
Micro focus DEC Rainbow 100 + compact level 2 COBOL; V2.5
[PB85-108975] 10 p1542 N85-19719
Micro focus DEC Rainbow 100 + high performance level 2 COBOL; V2.5
[PB85-108983] 10 p1542 N85-19720
DTSS, Incorporated, DPS 8/44, DTSS COBOL Release 12
[PB85-108058] 10 p1542 N85-19721
Micro Focus, Intel Microprocessor Development System MDS221 CIS COBOL; V4.5
[PB85-110823] 11 p1699 N85-20682
Validation Summary Report (VSR), Ryan-McFarland Corporation, AT and T 385, RM/COBOL Version 2.0
[PB85-102093] 11 p1703 N85-20709
Micro focus Cifer 2687 high performance level 2 COBOL; V2.5
[PB85-108859] 11 p1703 N85-20714
Micro focus Cifer 2687 compact level 2 COBOL; V2.5
[PB85-108967] 11 p1703 N85-20715
Micro focus Fortune 32:16 compact level 2 COBOL; V2.5
[PB85-108864] 11 p1704 N85-20718
Micro focus Fortune 32:16 high performance level 2 COBOL; V2.5
[PB85-108882] 11 p1704 N85-20719
Micro Focus IBM personal computer XT CIS COBOL; V4.5
[PB85-108868] 11 p1704 N85-20720
ICL, ICL 2988 COBOL C2COB. 1321
[PB85-108876] 11 p1704 N85-20721
MICRO FOCUS Intel Microprocessor Development System MDS221 Compact Level 2 COBOL; V2.5
[PB85-108900] 11 p1704 N85-20722
Selection and use of general-purpose programming-language: Program examples, volume 2
[PB85-122000] 12 p1917 N85-22039
Selection and use of general-purpose programming language: Overview, volume 1
[PB85-122018] 12 p1917 N85-22040

COCHLEA

Measurement of cochlear acoustic pressure in guinea pigs
[ISL-CO-234/83] 16 p2861 N85-27644
Design of a physical model of the cochlea. Displacement sensor for small amplitudes in a highly viscous liquid
[STN-6] 20 p3507 N85-31802

COCKPIT SIMULATORS

Psychophysical research in development of a fiber-optic helmet mounted display 05 p0701 N85-14501
Predictions of cockpit simulator experimental outcome using system models 05 p0702 N85-14504
Advanced flight simulation for helicopter development 08 p1075 N85-16815
Dynamic training devices in CRM training 09 p1276 N85-18018
Cockpit resources management and the theory of the situation 09 p1276 N85-18022
Cockpit resource management training 09 p1276 N85-18023
Research Flight Simulator for Helicopters (RFSH): Description and application to fire control system design
[SNIAS-851-210-106] 20 p3393 N85-31050

COCKPITS

Effects of foveal information processing 01 p0009 N85-10052
LED multifunction keyboard engineering study
[AD-A145199] 01 p0010 N85-10061
Training effectiveness evaluation and utilization demonstration of a low cost cockpit procedures trainer
[AD-A145179] 01 p0013 N85-10078
Anthropometric cockpit compatibility assessment of US Army aircraft for large and small personnel wearing a training, warm-weather clothing configuration
[AD-A145208] 01 p0099 N85-10656
Anthropometric cockpit compatibility assessment of US Army aircraft for large and small personnel wearing A cold weather, armored vest, chemical defense protective clothing configuration
[AD-A145472] 02 p0238 N85-11547
Psychophysical research in development of a fiber-optic helmet mounted display 05 p0701 N85-14501
Cockpit window edge proximity effects on judgements of horizon vertical displacement 05 p0704 N85-14518
What pilots like (and don't like) about the new cockpit technology 05 p0710 N85-14554
Technical Workshop: Advanced Helicopter Cockpit Design
[NASA-CP-2351] 06 p0750 N85-14806
Superaugmented rotorcraft program 06 p0750 N85-14807
Helicopter human factors programs and plans 06 p0751 N85-14808
Civil law enforcement missions 06 p0751 N85-14812
HH-65A Dolphin digital integrated avionics 06 p0751 N85-14815
Integrated cockpit design for the Army helicopter improvement program 06 p0751 N85-14816
HH-60D night hawk helicopter 06 p0752 N85-14817
Avionics/crew station integration 06 p0752 N85-14818
Human factors in cockpit automation 06 p0752 N85-14819
Human factors of visual displays 06 p0752 N85-14821
Operational requirements - system concepts 06 p0752 N85-14823
Avionics technology - system concepts 06 p0753 N85-14824
Attack helicopter (AH-1T) cockpit systems integration 06 p0753 N85-14826
Integration of sensor fusion in advanced helicopter cockpit design 08 p1074 N85-16813
A cockpit-display concept for executing a multiple glide-slope approach for wake-vortex avoidance
[NASA-TP-2386] 08 p1085 N85-16869
Simulation 09 p1277 N85-18024
Crewstation assessment of reach as applied to the OH-58A helicopter
[AD-A149413] 10 p1531 N85-19650
Impact of future aircombat characteristics on pilot performance and cockpit design 10 p1533 N85-19661
Electronic displays: Their strengths and weaknesses for advanced high performance aircraft 10 p1533 N85-19664
Changing system and display concepts and their impact on aircrew performance 10 p1533 N85-19665
The cockpit of the year 2000: How big a step? 10 p1534 N85-19667
Influence of a perspective cockpit traffic display format on pilot avoidance maneuvers 10 p1534 N85-19668
The F-18: A new era for human factors 10 p1534 N85-19671
Aviation medicine's role in modern airforce discussed 11 p1696 N85-20662
A safety evaluation of the relocation of the ACM (Air Combat Maneuver) panel in the F-14 ( )/AIP (Avionics Integration Program)
[AD-A149566] 12 p1777 N85-21158
Analysis of estimation algorithms for CDTI and CAS applications
[NASA-CR-172444] 13 p1973 N85-22387
Dual-task timesharing using a projected attitude display (Malcolm horizon)
[AD-A150789] 14 p2395 N85-24750
YAV-8B Harrier 15 p2688 N85-26805
A comparison of pictorial and speech warning messages in the modern cockpit
[AD-A151917] 16 p2707 N85-26706
The introduction of new cockpit technology: A human factors study
[NASA-TM-86659] 16 p2843 N85-27528
Trends shaping advanced aircrew training capabilities through the 1990s
[AD-A152277] 18 p2843 N85-27530
Human factors in cockpit automation: A field study of flight crew transition
[NASA-CR-177333] 19 p3215 N85-29637
Crew systems and flight station concepts for a 1995 transport aircraft
[NASA-CR-166068] 19 p3221 N85-29673

COCKS

Tap noise-pressure fluctuations. Study of the acoustic behavior of hydraulic equipment in buildings as a function of the temperature
[CETIM-11-H-337] 04 p0502 N85-13201

CODE DIVISION MULTIPLE ACCESS

Distributed reservation-based code division multiple access
[AD-A147007] 07 p0940 N85-15957
Margin leveling algorithm for fully saturated satellite transponder with CDMA (Code Division Multiple Access) signalling
[AD-A151710] 15 p2543 N85-25899

CODERS

Improvement of the narrowband linear predictive coder. Part 2: Synthesis improvements
[AD-A145031] 01 p0038 N85-10237
Digital raster timing encoder-decoder
[AD-D011279] 06 p0904 N85-15120
ILIR task of digital recoil travel measurement system
[AD-A147102] 07 p0967 N85-16140
The removal, mechanical handling and installation procedures for declination tachometer and flak encoder — United Kingdom Infrared Telescope
[UKIRT-17] 09 p1414 N85-18915

The removal, mechanical handling and installation procedures for the RA itek encoder
[UKIRT-21] 09 p1414 N85-18919
Extracting digital data from a bus and multiplexing it with a video signal
[AD-D011491] 11 p1636 N85-20302
Low-bit rate speech encoders based on Line-Spectrum Frequencies (LSF)
[AD-A150518] 13 p2056 N85-22871
A software simulation study of a (255,223) Reed-Solomon encoder-decoder
[NASA-CR-175872] 17 p2947 N85-28192
Filtration of higher harmonic components in two-level digital computing synthesizers 22 p3778 N85-33410
Noiseless coding for the Gamma Ray spectrometer
[NASA-CR-176201] 24 p4069 N85-35219

CODES
The POK project; studies of information handling problems with a new kind of communication device — precoded signals
[FOA-A-53001-H2] 18 p3091 N85-29131

CODING
NT DECODING
NT REDUNDANCY ENCODING
NT SIGNAL ENCODING
Digital correlator speed improvement by multiplexing
[AD-A145207] 01 p0100 N85-10662
A comparative evaluation of algorithms for generalized network problems
[TWISK-269] 01 p0107 N85-10721
Study of a coded mask telescope for astronomical measurements in the hard X-ray domain
[MPE-182] 01 p0129 N85-10889
Gas flow environment and heat transfer nonrotating 3D program 02 p0142 N85-10966
Dynamical models for radio jets 03 p0449 N85-12854
Comparability and accuracy of industry codes in different data systems
[PB84-215607] 04 p0548 N85-13482
Electrooptical matrix multiplication using the twos complement arithmetic for improved accuracy
[AD-D011252] 05 p0728 N85-14682
Wavelength coded image transmission and holographic optical elements
[AD-A146490] 06 p0810 N85-15147
Techniques for vector quantization
[AD-A147052] 07 p1030 N85-16539
Data stimulated on-line-checking (IROLD) 08 p1066 N85-16754
The ambiguity function of random binary-phase-coded waveforms
[AD-A148606] 10 p1466 N85-19249
A modem with pseudo-orthogonal codes: Experimental results 10 p1474 N85-19302
The coding capacity of mismatched Gaussian channels
[AD-A149453] 10 p1551 N85-19782
Extracting digital data from a bus and multiplexing it with a video signal
[AD-D011491] 11 p1636 N85-20302
Object-oriented algebraic specification: Proposal for a notation and 12 examples
[CWI-CS-R8411] 11 p1707 N85-20744
ITS: The Integrated TIGER Series of coupled electron/photon Monte Carlo transport codes
[DE85-003719] 11 p1725 N85-20847
Integrated control system engineering support
[AD-A149742] 12 p1760 N85-21177
Automatic multi-banking of memory for microprocessors
[NASA-CASE-NPO-15295-1] 12 p1911 N85-21992
Determination of angular resolution of coded aperture gamma-ray telescope 13 p1961 N85-22432
Experimental results on the application of convolutional coding and Viterbi decoding as a frequency diversity technique in HF data transmission
[CRC-1377] 13 p2052 N85-22850
Code lock with microcircuit 13 p2071 N85-22935
A perspective on multiaccess channels
[AD-A150183] 13 p2146 N85-23322
ANTENA user guide
[DE85-004961] 14 p2424 N85-24953
Recent trends in software technology for vector processors 16 p2691 N85-26615
DOD manual for standard data elements, part 1
[AD-A152201] 16 p2878 N85-27754
Alphabet-constrained data compression
[AD-A152887] 17 p3019 N85-28667
Fourier coding and reconstruction of complicated contours
[REPT-84-39] 17 p3022 N85-28691
System of white-light density pseudocolor encoding with three primary colors
[AD-D011651] 17 p3037 N85-28791
ZOG-Vinson technology demonstration project. Volume 2: System description
[AD-A153871] 19 p3333 N85-30645
Comparison of 8 to 12 micrometer and 3 to 5 micrometer CVF transmissometer data with LOWTRAN calculations
[AD-A154218] 19 p3350 N85-30763
Construction of complementary code sequence sets, part 7.1D 21 p3625 N85-32523
Colour coding scales and computer graphics 23 p3963 N85-34568
Hexagonal uniformly redundant arrays for coded-aperture imaging
[OG-9.2-1] 23 p4024 N85-34940
A coded aperture imaging system optimized for hard X-ray and gamma ray astronomy
[OG-9.2-3] 23 p4024 N85-34942
SONTRAC: A solar neutron track chamber detector
[SH-9.1-12] 23 p4052 N85-35127
X-ray fluorescence analysis of 304L stainless steel
[DE85-013254] 24 p4080 N85-35288

COEFFICIENT OF FRICTION
Proposal for wall function for friction and heat transfer in the presence of roughness and mass transfer
[CFD/84/12] 04 p0501 N85-13198
Effects of B, Ti and Ta implantation on the wear resistance of Fe and Ni-plated Fe
[AD-A149947] 12 p1806 N85-21330
Interaction of cylindrical shell with concentrated mass moving along its inner surface 13 p2047 N85-22810
Experimental study of heat transfer from shaft in cooled radial bearing of GNT-25 gas turbine 14 p2270 N85-24068
Studies on surface processes during friction and wear
[AD-A153509] 18 p3117 N85-29296
Friction and wear of solid-lubricated contact in gas turbine engine bearings
[AD-A155042] 21 p3596 N85-32335
Kinetic friction coefficient of ice
[AD-A155035] 21 p3680 N85-32859
Action of wear-inhibiting Al2O3-coatings when applied to hard metal cutting tools
[BLL-RISLEY-TR-5041-(9091.9F)] 24 p4081 N85-35292

COEFFICIENTS
NT AERODYNAMIC COEFFICIENTS
NT ATTENUATION COEFFICIENTS
NT BINOMIAL COEFFICIENTS
NT CLEBSCH-GORDAN COEFFICIENTS
NT COEFFICIENT OF FRICTION
NT COHERENCE COEFFICIENT
NT CORRELATION COEFFICIENTS
NT COUPLING COEFFICIENTS
NT DIFFUSION COEFFICIENT
NT FLOW COEFFICIENTS
NT HEAT TRANSFER COEFFICIENTS
NT INFLUENCE COEFFICIENT
NT IONIZATION COEFFICIENTS
NT NOZZLE THRUST COEFFICIENTS
NT RECOMBINATION COEFFICIENT
NT REGRESSION COEFFICIENTS
NT SCATTERING COEFFICIENTS
NT VIRIAL COEFFICIENTS
NT WIGNER COEFFICIENT
Some statistical characteristics of atmospheric optical thickness in visible spectral range 02 p0164 N85-11109
Individual geopotential coefficients of order 15 and 30, from resonant satellite orbits
[AD-A146687] 06 p0828 N85-15256
Determination of shear coefficient of a general beam cross section by finite element method 09 p1338 N85-18413
On the local behaviour of solutions of degenerate parabolic equations with measurable coefficients
[AD-A147412] 09 p1373 N85-18631
Fourier-Stieltjes coefficients and continuation of functions 15 p2633 N85-26231
An incremental multigrid strategy for the fluid dynamics equations
[AD-A151953] 16 p2783 N85-27172
GAMPHI: A database of activity and osmotic coefficients for aqueous electrolyte solutions
[PB85-183390] 18 p3072 N85-29002
Evaluation of densities and distributions via hermite and generalized laguerre series employing high-order expansion coefficients determined recursively via moments or cumulants
[AD-A153950] 18 p3175 N85-29682
Thermal expansion coefficients of a 30% glass fiber filled PEEK pyrotechnic charge holder
[DE85-010805] 19 p3251 N85-30155
Visibility and vertical structure measurements in southern Germany
[AD-A154714] 21 p3635 N85-32574
Hardware realization of digital filters without multipliers 22 p3768 N85-33340

COENZYMES
NT CYTOCHROMES
NT GLUTATHIONE

COERCIVITY
Cobalt-free permanent magnet alloys
[AD-A149272] 10 p1441 N85-19079
Investigation for low-cost permanent magnets
[AD-A154387] 19 p3260 N85-30212

COGENERATION
Free-piston Stirling engine development
[PB84-237767] 01 p0056 N85-10369
Control and performance of a photovoltaic-thermal energy system 03 p0387 N85-12475
Advanced technology cogeneration system conceptual design study: Closed cycle gas turbines
[NASA-CR-168222] 07 p0992 N85-16300
Closed cycle versus open cycle gas turbines. A review of A.D. Little's ICOP report, vol. 3
[DE85-000564] 12 p1861 N85-21671
Development of a coal-water slurry-fueled diesel engine for industrial cogeneration. Task 1.0 topical report: Thermodynamic analysis
[DE85-010455] 19 p3236 N85-30062

COGNITION
Cognitive science program. A framework for relating cognitive to neural systems
[AD-A145185] 01 p0097 N85-10649
Inhibition of return: Neural basis and function
[AD-A145242] 01 p0098 N85-10652
Cognitive coordinate systems: Accounts of mental rotation and individual differences in spatial ability
[AD-A146149] 03 p0401 N85-12557
The impact of pictorial display on operator learning and performance 05 p0706 N85-14527
ERPS to monitor non-conscious mentation 05 p0707 N85-14536
Performance enhancements under dual-task conditions 05 p0707 N85-14537
Interaction of human cognitive models and computer based models in supervisory control
[AD-A142547] 07 p1020 N85-16474
Cognitive performance during successive sustained physical work episodes
[AD-A148061] 08 p1200 N85-17558
Neurocognitive pattern analysis of an auditory and visual numeric motor control task. Part 1: Development of methods
[AD-A148809] 09 p1364 N85-18578
Study of cognitive styles of students in automated teaching system 10 p1525 N85-19620
Military pilot ergonomics 10 p1532 N85-19655
Some effects of display format variables on the perception of aircraft spatial orientation 10 p1534 N85-19666
Research needs on the interaction between information systems and their users: Report of a workshop
[PB85-121523] 10 p1568 N85-19891
Human cognition and intelligence: Towards an integrated theoretical perspective
[CSIR-SR-PERS-350] 13 p2143 N85-23300
Stereotype traits can be processed automatically
[AD-A150947] 14 p2391 N85-24725
The acquisition of procedures from text. A production-system analysis of transfer of training
[AD-A151029] 14 p2392 N85-24732
Mental workload measurement: Event-related potentials and ratings of workload and fatigue
[NASA-CR-177354] 15 p2619 N85-26139
Effects of dehydration or cold exposure and restricted fluid intake upon cognitive performance
[AD-A151973] 16 p2842 N85-27525
Verbal information processing paradigms: A review of theory and methods
[AD-A153229] 17 p3050 N85-28880
Individual differences in online search behavior: The effect of learning styles and cognitive abilities on process and outcome 20 p3541 N85-32037
Resource allocation in cerebral specialization of function: Behavioral and electrophysiological studies
[AD-A155092] 21 p3664 N85-32759
Review of the psychological issues relating to the effectiveness of structured programming
[AD-A154593] 21 p3665 N85-32766

COGNITIVE PSYCHOLOGY
Cognitive science program. A framework for relating cognitive to neural systems
[AD-A145185] 01 p0097 N85-10649
Toward a computational neuropsychology of high-level vision
[AD-A145711] 02 p0236 N85-11540
The psychology of technical devices and technical discourse
[AD-P003929] 02 p0246 N85-11609
The construction of auditive tests of attention and spatial orientation and their factorial structure
[DFVLR-FB-84-21] 05 p0699 N85-14485

On looking into the black box: Prospects and limits in the search for mental models 05 p0709 N85-14546
Issues in developing a normative descriptive model for dyadic decision making 05 p0709 N85-14547
The design and use of subtasks in part training and their relationship to the whole task 05 p0711 N85-14559
Human cognition and intelligence: Towards an integrated theoretical perspective [CSIR-SR-PERS-350] 13 p2143 N85-23300
Stereotype traits can be processed automatically [AD-A150947] 14 p2391 N85-24725
Skilled memory [AD-A152063] 15 p2620 N85-26143
The levels of processing conceptualization of human memory: Some empirical and theoretical issues [AD-A152321] 17 p3000 N85-28544
Identifying solution paths in cognitive diagnosis [AD-A152463] 17 p3000 N85-28549
Conceptualizing in assembly tasks [AD-A155564] 21 p3665 N85-32770

COHERENCE
Singular perturbations, coherency and aggregation of dynamic systems [DE84-014166] 01 p0114 N85-10772
Field coherence function in layerwise nonhomogeneous troposphere 06 p0784 N85-15012

COHERENCE COEFFICIENT
Proust radar: Decoding hardware and coherent integration, part 7.2A 21 p3626 N85-32524

COHERENT ACOUSTIC RADIATION
LANDSAT-4/5 image data quality analysis [E85-10105] 24 p4107 N85-35463

COHERENT ANTI-STOKES RAMAN SPECTROSCOPY
U RAMAN SPECTROSCOPY

COHERENT ELECTROMAGNETIC RADIATION
NT COHERENT LIGHT
Device for measuring average power of laser radiation 06 p0786 N85-15026
Transmission line biased coherent array of Josephson oscillators [AD-D011323] 07 p0944 N85-15979
A new free electron laser using a relativistic beam with spiralling electron [AD-D011318] 07 p0971 N85-16185
High energy particle acceleration by coherent electromagnetic waves propagating across the magnetic field [IPPJ-717] 16 p2866 N85-27679
Solvability of some inverse problems in laser radiation focusing 21 p3696 N85-32965
The 2nd European Conference on Atomic and Molecular Physics [AD-A155863] 24 p4148 N85-35715

COHERENT LIGHT
Effect of aberration in optical system on illuminance distribution over image of strip in semicoherent light 06 p0777 N85-14970
Two-photon coherent state light - its generation and potential applications [AD-A148245] 08 p1166 N85-17356
A posteriori increase of resolving power of optical system forming averaged monochromatic images 13 p2082 N85-23003
Influence of coherent light beams on free carriers in semiconductors 21 p3681 N85-32867

COHERENT RADAR
Test and evaluation of a coherent 35 gigahertz radar repeater [AD-A145714] 02 p0191 N85-11280
Test signal generator for coherent air-to-ground radars [AD-D011278] 05 p0628 N85-14025
Activities report in Earth and planetary environments physics [CRPE-NT-134] 05 p0734 N85-14720
The MST radar technique 08 p1185 N85-17466
Bistatic coherent radar receiving system [AD-D011447] 10 p1466 N85-19252
Digital coherent detector [AD-D011560] 12 p1833 N85-21501
The magnetospheric convection electric field at ionospheric altitudes: A case study based on STARE and Saint-Santin data 14 p2362 N85-24594
A brief summary of results derived from Scandinavian Twin Auroral Radar Experiment (STARE) observations during IMS — ionospheric electric fields 14 p2362 N85-24595
Contribution of the Scandinavian Twin Auroral Radar Experiment (STARE) radar to the understanding of the physical mechanisms associated with Pc5 pulsations 14 p2364 N85-24613
Satellite, auroral radar and ground magnometer observations of transient ULF pulsations 14 p2369 N85-24645
Forth system for coherent-scatter radar data acquisition and processing [NASA-CR-176055] 20 p3494 N85-31720
Observations of frontal zone structures with a VHF Doppler radar and radiosondes, part 1.2A 21 p3616 N85-32469
Potential advantages of the spaced antenna method for operational wind profiling, part 3.1B 21 p3620 N85-32490
Proust radar: Decoding hardware and coherent integration, part 7.2A 21 p3626 N85-32524
Potential coordinate estimate accuracy estimation accuracy by multiposition radar systems 22 p3763 N85-33322
Detection of signals from coherent pulsed radars with random variation in parameters of sounding signals from pulse to pulse against background of worst-case Gaussian noise 22 p3763 N85-33324

COHERENT RADIATION
NT COHERENT ACOUSTIC RADIATION
NT COHERENT ELECTROMAGNETIC RADIATION
NT COHERENT LIGHT
Diffusion and intermittency in an extended one-dimensional maps 02 p0282 N85-11834
Influence of propagation in digital wireless beam, microwave links 10 p1470 N85-19277
Exploration of new methods to produce efficient sources of coherent near millimeter wave radiation [AD-A150094] 12 p1829 N85-21481
A spatially incoherent and temporally coherent source [AD-A151281] 13 p2157 N85-23390
Parametric coherence estimation via convolved correlations [DE85-003946] 14 p2416 N85-24909
Principle and design of a medium-enhanced free-electron laser 15 p2561 N85-25802
Studies of collisional and nonlinear radiative process for development of coherent UV and XUV sources [AD-A152001] 16 p2665 N85-27670
Coherent X-rays and vacuum-ultraviolet radiation from storage-ring-based undulators and free electron lasers [DE85-009968] 18 p3183 N85-29738
Method of reducing impurity and antisite defects in semiconductor crystal materials, and device and apparatus respectively produced from and utilizing same [AD-D011698] 19 p3260 N85-30216
Laser radiation propagation in inertialess nonlinear medium 21 p3686 N85-32898
Mean intensity of wave reflected by wavefront reversing mirror in turbulent medium 22 p3782 N85-33432
A theoretical and empirical analysis of coherent ray-tracing 23 p3957 N85-34524

COHERENT SCATTERING
Measurement of scattering cross sections of liquid and solid hydrogen deuterium and deuterium hydride for thermal neutrons [DE84-014814] 05 p0727 N85-14671
A spatially incoherent and temporally coherent source [AD-A151281] 13 p2157 N85-23390
The Hanle effect applied to magnetic field measurements 18 p3204 N85-29878
Grain structure identification by ultrasound frequency averaging and deconvolution [AD-A154332] 19 p3352 N85-30777
Forth system for coherent-scatter radar data acquisition and processing [NASA-CR-176055] 20 p3494 N85-31720
Morphology of the scattering targets: Fresnel and turbulent mechanisms, part 2.1A 21 p3618 N85-32481
Numerical and analytic descriptions of cosmic-ray transport [SH-4.1-4] 23 p4005 N85-34830

COHERENT SOURCES
U COHERENT RADIATION
U RADIATION SOURCES

COHERENT TRANSMISSION
U COHERENT RADIATION

COHESION
Experimental AC (Asphalt Concrete) overlays of PCC pavement [PB84-218171] 03 p0342 N85-12203

COHOMOLOGY
U HOMOLOGY

COILS
Induction voidmeter [DE84-014321] 01 p0050 N85-10329

COINCIDENCE CIRCUITS
A theoretical basis for the analysis of redundant software subject to coincident errors [NASA-TM-86369] 13 p2145 N85-23317

COLD ACCLIMATIZATION
Effects of restricted water intake on performance in a cold environment [AD-A146904] 07 p1015 N85-16450
Predictors of cold weather health behaviors [AD-A151910] 16 p2643 N85-27529
Acclimatization to far north 20 p3508 N85-31782

COLD CATHODE TUBES
NT PHOTOMULTIPLIER TUBES
Process for making electrodes for discharge tubes [DE85-008898] 17 p2955 N85-28247

COLD CATHODES
High power pulsed accelerators with potential industrial applications [DE85-001710] 11 p1720 N85-20821

COLD DRAWING
Impact toughness of wire after cold deformation and annealing [BLL-M-35941-(5828.4)] 05 p0615 N85-13930
Uniaxial orientation of linear low density polyethylene [AD-A151037] 14 p2261 N85-24009
Fracture mechanics analysis of cold drawn Si-Cr valve steel [BLL-BISI-TRANS-22216-(9022.06)] 17 p2978 N85-28405
A new drawing technique for nylon 6 by reversible plasticization with iodine [AD-A156272] 24 p4162 N85-35803

COLD FLOW TESTS
An experimental study of clustered, two-dimensional rocket nozzles [AD-A151889] 15 p2495 N85-25390
Contribution to the study of equivalent noise source identification in fast cold jets [ISL-R-114/83] 16 p2661 N85-27645

COLD FORMING
U COLD WORKING

COLD FRONTS
Frontal motion in mountainous terrain: Analysis and implications for 0 to 12 hour forecasts 01 p0076 N85-10502
The extremeness of the cold front of December 31, 1978 over the CSR [REPT-566] 03 p0377 N85-12409
Conditions governing the formation of stratocumulus clouds over the western Atlantic during cold air outbreaks [AD-A146780] 07 p1004 N85-16383
The structure and dynamics of an observed moist front 18 p3146 N85-29480
The kinematic structure of cold frontal rainbands 24 p4119 N85-35531

COLD GAS
Study of the velocity-acoustic pressure correlation in a cold jet, centered on the sign and the amplitude of the velocity fluctuations [ISL-R-124/83] 04 p0501 N85-13193
Experiment on triggered fragmentation on a molten copper droplet in water [BLL-WH-602-(9091.9F)] 08 p1125 N85-17091
Localization of sources of equivalent noise in fast cold jets, excited and nonexcited [ISL-CO-201/83] 14 p2416 N85-24910
Preliminary wind tunnel experiments to investigate the effect of heat transfer on the dispersion of cold dense gases [OUEL-1546/84] 20 p3456 N85-31467

COLD NEUTRONS
Construction of a cold neutron source at FRM, Munich 03 p0427 N85-12722
Breakthrough in container confinement of ultracold neutrons 15 p2644 N85-26311

COLD PLASMAS
Direct measurements of severe spacecraft charging in auroral ionosphere 13 p1991 N85-22480
Charging of DMSP/F6 spacecraft in aurora on 10 January 1983 13 p1991 N85-22481
Double layer formation due to contact of different temperature plasmas [IPPJ-722] 19 p3370 N85-30900

COLD PRESSING
Fatigue resistance of VT3-1 titanium alloy related to surface cold working 19 p3245 N85-30120
Establishment of a Computer-Aided Design (CAD)-Computer-Aided Manufacturing (CAM) process for the production of cold forged gears [AD-A155756] 24 p4137 N85-35644

COLD ROLLING
Effect of texture in steel on the susceptibility of hydrogen embrittlement [BLL-BISI-TRANS-22026-(9022.06)] 17 p2926 N85-28048
Influence of preliminary thermomechanical treatment on depth and hardness of nitrided layers [BLL-BISI-TRANS-22488-(9022.06)] 17 p2929 N85-28078
Fatigue resistance of VT3-1 titanium alloy related to surface cold working 19 p3245 N85-30120

COLD SURFACES
Low temperature deposition of nickel films
[AD-D011568] 12 p1805 N85-21319
Experimental aerodynamic heating to simulated space shuttle tiles in laminar and turbulent boundary layers with variable flow angles at a nominal Mach number of 7
[NASA-TP-2307] 23 p3929 N85-34351
COLD TOLERANCE
Advances in study of cold injury in Army
14 p2283 N85-24145
COLD WALLS
U COLD SURFACES
U WALLS
COLD WATER
Comparison of thermal responses between rest and leg exercise in water
[AD-A146818] 07 p1015 N85-16448
NOAA OTEC CWP (National Oceanic and Atmospheric Administration Ocean Thermal Energy Conversion Cold Water Pipe) at-sea test. Volume 3: Additional tabulation of the power spectra, part 2
[PB84-236997] 09 p1346 N85-18468
SCPP (Sierra Cooperative Pilot Project) data collection and analysis. Volume 1: Executive summary
[PB85-156065] 16 p2837 N85-27494
COLD WEATHER
Anthropometric cockpit compatibility assessment of US Army aircraft for large and small personnel wearing A cold weather, armored vest, chemical defense protective clothing configuration
[AD-A145472] 02 p0238 N85-11547
Behavior and characteristics of storm cold outflows
09 p1356 N85-18529
A systems analysis of alternative concepts for aircrew cold weather clothing
[AD-A148805] 09 p1365 N85-18580
Investigation of the requirement for auxiliary heating of Canadian forces personnel
[AD-A151950] 16 p2841 N85-27522
Predictors of cold weather health behaviors
[AD-A151910] 16 p2843 N85-275.9
Land vehicle corrosion management
22 p3750 N85-33246
COLD WELDING
Method of calculating strength of joint produced by cold welding of aluminum under discrete loading
13 p2034 N85-22743
Diffusion vacuum welding 15 p2499 N85-25416
COLD WORKING
NT COLD ROLLING
NT ELECTROHYDRAULIC FORMING
NT EXPLOSIVE FORMING
Mechanical properties of a leaded, resulfurized, rephosphorized steel in various thermo/mechanical conditions
[PB84-216464] 03 p0333 N85-12144
Defining effect of hardening on mean yield strength in deformation zone
[BLL-M-35934-(5828.4)] 05 p0847 N85-14154
On heat-treatable copper-chromium alloy, 1
[NASA-TM-77753] 07 p0927 N85-15879
Role of residual stresses in stress corrosion cracking in alloy 600 tubes. Part 1: Determination of throughwall residual stresses and their modification by transient heat treatment
[DE85-004648] 14 p2257 N85-23988
Modular design, versatility of robots viewed
14 p2284 N85-24155
Calculating reliability and productivity of cold stamping robot complex as queuing system
16 p2761 N85-27039
Preparation of metal for cold upsetting
[BLL-BISI-TRANS-22383-(9022.09)]
17 p2926 N85-28043
The fabrication, microstructure, and strengthening behavior of heavily cold-worked in situ composites
19 p3231 N85-30091
The effect of prior parent phase cold work on martensite transformation in Cu-Zn-Al shape memory alloys
[AD-A155140] 21 p3566 N85-32163
Wear-resistant coatings for tools intended for cold working
[BLL-RISLEY-TR-5040-(9091.9F)]
24 p4081 N85-35293
COLLAPSE
Collapse of cavitation bubbles between two walls in ultrasonic field 02 p0266 N85-11739
Some aspects of the micromechanics of hot spot formation in energetic materials
[AD-P004348] 10 p1456 N85-19172
Neutrino-antineutrino annihilation around collapsing star
[OG-1.1-10] 22 p3881 N85-33911
Experimental study of collapse of thick-walled tube under external pressure and axial force
23 p3904 N85-34186
The capability of the existing network of installations for detecting the antineutrino burst from collapsing stars
[HE-5.3-13] 24 p4206 N85-36107
COLLATING
Design of a scientific information collation and dissemination system, volumes 1 thru 3
[AD-A146002] 03 p0436 N85-12791
COLLECTION
Acid rain: Towards automated monitoring
16 p2829 N85-27444
Evaluation of a field expedient technique for sweat sample collection
[AD-A151916] 16 p2841 N85-27521
COLLECTORS
U ACCUMULATORS
COLLEGES
U UNIVERSITIES
COLLIMATION
Collimation techniques for dense object flash radiography
[DE84-016461] 05 p0647 N85-14152
On the hydrodynamical equations of astrophysical jets — active galactic nuclei 08 p1241 N85-17831
Collimated winds from active galactic nuclei
08 p1241 N85-17832
Intensity fluctuations of focused laser beam during reflection in turbulent atmosphere
13 p2078 N85-22975
Distortion functions
[DE85-007511] 16 p2862 N85-27655
Laser Schlieren crystal monitor
[NASA-CASE-MFS-28060-1] 19 p3374 N85-30932
COLLIMATORS
Study of a coded mask telescope for astronomical measurements in the hard X-ray domain
[MPE-162] 01 p0129 N85-10869
Collimation techniques for dense object flash radiography
[DE84-016461] 05 p0647 N85-14152
Apparatus for determining the liquid water content of a gas
[AD-D011297] 07 p0922 N85-15839
A cometary ion mass spectrometer
[NASA-CR-174328] 08 p1164 N85-17343
Measurement of sensitivity of shadowgraphic instruments with spherical autocollimating mirror
14 p2274 N85-24067
Muon spin rotation studies 17 p3042 N85-28819
Soft X-ray polychromator for the Solar Maximum Mission
[NASA-CR-175297] 21 p3723 N85-33096
COLLINEARITY
The information in the minor principal components
[CSIR-TWISK-320] 01 p0109 N85-10735
COLLISION AVOIDANCE
Enhanced TCAS 2/CDTI traffic Sensor digital simulation model and program description
[NASA-CR-172445] 02 p0136 N85-10927
Air-to-air visual acquisition performance with TCAS 2
[FAA-PM-84-17] 02 p0236 N85-11537
TCAS 2 logic performance during phase one operational evaluation
[DOT/FAA/PM-84/20] 05 p0595 N85-13793
A bird strike handbook for base-level managers
[AD-A147928] 07 p0948 N85-16008
Influence of a perspective cockpit traffic display format on pilot avoidance maneuvers 10 p1534 N85-19668
Collision avoidance for Naval training aircraft
[FAA-PM-84-4] 12 p1774 N85-21136
TCAS II: Design and validation of the high-traffic-density surveillance subsystem
[DOT/FAA/PM-84/5] 13 p1970 N85-22375
Analysis of estimation algorithms for CDTI and CAS applications
[NASA-CR-172444] 13 p1973 N85-22387
An analysis of the impacts of the Airport Radar Service Area (ARSA)
[AD-A150954] 14 p2217 N85-23749
Helicopter user survey: Traffic alert and collision avoidance system (TCAS)
[FAA-PM-85-6] 15 p2468 N85-25236
Aircraft accident report: United Airlines Flight 663, Boeing 727-222, N7647U, Denver, Colorado, May 31, 1984
[PB85-910405] 16 p2703 N85-26686
Traffic alert and collision avoidance system: Operational simulation
[FAA-PM-85-10] 19 p3216 N85-29941
System safety study of minimum TCAS 2 for instrument weather conditions
[FAA-PM-85-12] 22 p3728 N85-33113
COLLISION PARAMETERS
NT COLLISION RATES
The coordinated research program at IAEA on atomic collision data for plasma diagnostics
09 p1390 N85-18747
Collision detection for moving polyhedra
[AD-A148981] 10 p1544 N85-19735
Plane-wave born collision strengths for electron-ion excitation: Comparison with other theoretical methods
[DE85-002348] 10 p1555 N85-19802
Beam loss due to the aperture limitation resulting from intrabeam scattering
[DE85-005138] 12 p1930 N85-22124
Workshop on Nuclear Dynamics 3
[INC-40007-24] 12 p1931 N85-22130
Statistical theory of planet growth
15 p2678 N85-26534
Experiments and detectors for high energy heavy ion colliders
[DE85-007927] 17 p3031 N85-28748
Polarization of fast particle beams by collisional pumping
[DE85-011621] 22 p3838 N85-33764
Fokker-Planck calculation of hot electron formation in the thermal barrier region of tandem mirror Gamma-10
[IPPJ-726] 23 p3979 N85-34669
Electron loss process and cross section of multiply charged ions by neutral atoms 23 p3981 N85-34685
Observations of accelerated high current low emittance beams in the SLC Linac
[DE85-013073] 24 p4088 N85-35211
Relation between gamma-ray family and EAS core: Monte-Carlo simulation of EAS core
[HE-3.6-7] 24 p4185 N85-35955
On mini-cluster observed by Chacaltaya emulsion chamber experiment
[HE-3.6-12] 24 p4185 N85-35959
Observation of genetic relation among new phenomena Geminion, Chiron and mini-Centauro
[HE-6.2-16] 24 p4212 N85-36152
COLLISION RATES
Dense but collisionless orbiting rings — Saturn rings
15 p2675 N85-26517
Multiple collision solutions for time-dependent neutron transport in slabs of finite thickness
[OEFZS-4312] 22 p3838 N85-33762
Breakdown of intrinsic ambipolarity for the radial diffusion due to a rotating RF field 23 p3977 N85-34660
COLLISION WARNING DEVICES
U COLLISION AVOIDANCE
U WARNING SYSTEMS
COLLISIONAL PLASMAS
NT STRONGLY COUPLED PLASMAS
Report of the reference designs study group on the superconducting super collider
[DE84-015567] 04 p0569 N85-13630
Equations of plasma transport in a curved magnetic field
[DE84-015625] 05 p0730 N85-14690
A propagator expansion method for solving linearized plasma kinetic equations with collisions
[AD-A147524] 07 p1045 N85-16840
Hydrodynamic response of a radiating Al plasma excited by a proton beam
[AD-A148904] 10 p1558 N85-19824
Nonlinear saturation of stimulated Raman scattering in collisional homogeneous plasma
[DE85-002814] 10 p1559 N85-19831
Atomic processes involving impurities in the plasma edge
[DE85-001277] 11 p1730 N85-20882
Analysis and computations of microwave-atmospheric interactions
[AD-A149666] 12 p1889 N85-21854
Fluid modeling of magnetized plasmas
[DE85-007679] 17 p3039 N85-28604
Time-implicit Monte-Carlo collision algorithm for particle-in-cell electron transport models
[DE85-010758] 20 p3521 N85-31900
Investigation of space-time structure of glow of laser plasma colliding with flat screen
21 p3693 N85-32947
Recombination and ionization in a nitrogen plasma
[AD-A155426] 22 p3845 N85-33813
Collisional transport for a superthermal ion species in a plasma
[DE85-011943] 22 p3845 N85-33816
COLLISIONLESS PLASMAS
Review of simulation of quasiparallel collisionless shocks
[DE84-015489] 02 p0304 N85-11967
Preliminary user's guide for BIGONE on the Cray
[DE84-017075] 04 p0568 N85-13623
Collective processes and formation of star clusters
05 p0736 N85-14743
Strong iron accelerating by collisionless magnetosonic shock wave propagating perpendicular to a magnetic field
[IPPJ-709] 12 p1935 N85-22161

Resonant ion acceleration by oblique magnetosonic shock wave in a collisionless plasma
[IPPJ-735] 23 p3975 N85-34643
Numerical solutions of the Vlasov equation
23 p3979 N85-34672
Current interruption by density depression
[DE85-013120] 24 p4169 N85-35846

COLLISIONS
NT ATOMIC COLLISIONS
NT BIRD-AIRCRAFT COLLISIONS
NT COULOMB COLLISIONS
NT INELASTIC COLLISIONS
NT IONIC COLLISIONS
NT METEORITE COLLISIONS
NT MIDAIR COLLISIONS
NT MOLECULAR COLLISIONS
NT PARTICLE COLLISIONS

Throughput characteristics of Carrier Sense Multiple Access (CSMA) networks
[FUB-25-1983] 01 p0106 N85-10713
Mechanical models of close approaches and collisions of large protoplanets 04 p0588 N85-13756
Aircraft accident report, Scandinavian Airlines System, Flight 901, McDonnell Douglas DC-10-30, John F. Kennedy International Airport, Jamaica, New York, February 28, 1984
[PB84-910415] 05 p0594 N85-13768
An operator method for computing the asymptotics of a collision resolution interval
[AD-A146837] 07 p1026 N85-16529
Orbital Debris
[NASA-CP-2360] 12 p1783 N85-21188
NASA/JSC orbital debris study: Debris model
12 p1783 N85-21193
Assessment of satellite collision hazards by simulated sampling in space 12 p1784 N85-21195
A model for the evolution of on-orbit manmade debris environment 12 p1784 N85-21196
Geosynchronous satellite collision avoidance
12 p1784 N85-21197
Preliminary design of an Earth-based debris detection system using current technology and existing installations 12 p1784 N85-21199
Debris impact on Earth-orbiting spacecraft
12 p1948 N85-22234
Experimental studies of low temperature surface interactions of atomic hydrogen using maser technique
[AD-A150216] 13 p2017 N85-22647
Asteroid collisional evolution studies
13 p2176 N85-23501
A circum-terrestrial compositional filter
13 p2179 N85-23520
Neutralization and excitation in low-energy ion-surface collisions
[AD-A151568] 15 p2660 N85-26414
Collisional outcomes in the asteroid belt
15 p2676 N85-26538
Comet showers and Nemesis, the death star
[DE85-003736] 15 p2683 N85-26575
Refinements in the computation of collision probabilities
[DE85-006118] 16 p2864 N85-27863
Average collisional vibrational energy transfer quantities and the inversion temperature
[AD-A152674] 17 p3029 N85-28733
Theory of high energy collision processes
[DE85-010163] 19 p3382 N85-30846

COLLOIDING
The colloidal chemistry of ceramic clays
[NASA-TM-77734] 03 p0336 N85-12163

COLLOIDS
NT AEROSOLS
NT FOG

Electrokinetic potential and stability of SiC suspensions in electrolyte solutions
[NASA-TM-77492] 04 p0469 N85-12984
Combustion waves in dispersed-2-phase mixtures
[CFD/84/13] 04 p0472 N85-13003
Zeta potential in ceramic industry
[NASA-TM-77476] 04 p0478 N85-13047
Light scattering studies of lower dimensional colloidal particle and critical fluid systems
[DE85-002087] 09 p1377 N85-18654
Solar fuel synthesis based on colloidal and particulate semiconductors
[PB85-129104] 11 p1614 N85-20152
Ac field-induced order in dense colloidal systems
[DE85-009107] 17 p2935 N85-28119
An evaluation and preparation of ferromagnetic liquid composites for use at millimeter wavelengths
[AD-A153939] 18 p3089 N85-29980
Colloidal particle transport with simultaneous birth, growth and capture
[DE85-010986] 19 p3235 N85-30065

COLOMBIA
Characteristics of a recent Columbian earthquake, December 12, 1979 04 p0523 N85-13347
Use of minicomputers for the formation of hydrological data banks 07 p1001 N85-16358

COLONIES
Cyanobacterial mats: Microanalysis of community metabolism 21 p3661 N85-32743
Microbial communities and microprofiles of sulfide and oxygen of alum rock sulfur springs
21 p3661 N85-32746
Microbial colonization and growth on metal sulfides and other mineral surfaces 21 p3662 N85-32747

COLOR
NT WATER COLOR

Peripheral vision displays: The future
01 p0009 N85-10058
Effects of alternative chromatic mixed graphics displays in decision support systems
[AD-A145561] 02 p0242 N85-11578
Visibility of various target-background color combinations under different chromatic ambient illuminations
[AD-A146348] 03 p0420 N85-12684
Analysis of data entry performance: Chromatic versus monochromatic
[AD-A145568] 03 p0438 N85-12789
Coastal Zone Color Scanner (CZCS): Imagery of near-surface phytoplankton pigment concentrations from the first coastal ocean dynamics experiment (CODE-1), March - July 1981
[NASA-CR-174169] 04 p0542 N85-13447
Color and grey scale in sonar displays
05 p0710 N85-14552
Human factors of visual displays
06 p0752 N85-14821
Local interstellar extinction with an emphasis on uvby beta results 06 p0875 N85-15559
Do the arching HI filaments show in local reddening data?
06 p0876 N85-15561
Inverse relations between 0.25 keV counts and local interstellar dust 06 p0877 N85-15572
New technology high efficiency and high stability color motion video compression system
[AD-A147523] 07 p0941 N85-15968
A comparative study of dust and young stars in three small galaxies 09 p1415 N85-18928
Pictorial format display evaluation
[AD-A149252] 10 p1425 N85-18966
Individual differences in chromatic brightness matching
[AD-A148882] 10 p1529 N85-19641
The relative effectiveness of red and white light for subsequent dark-adaptation
[AD-A148883] 10 p1530 N85-19642
Electronic displays: Their strengths and weaknesses for advanced high performance aircraft
10 p1533 N85-19664
Proceedings of the 6th Advanced Aircrew Display Symposium
[AD-A150044] 12 p1778 N85-21160
Television animation store: Digital chroma, key and mixer units
[BBC-RD-1984/16] 12 p1824 N85-21442
A concept for the processing and display of Thematic Mapper data 13 p2119 N85-23196
Color-selective coating for viewfinder in optical instruments 14 p2276 N85-24068
Using color to separate reflection components
[AD-A150999] 14 p2405 N85-24828
The Feinheit method: A phase-independent formulation of the period-luminosity relation for Cephids
[NASA-CR-175708] 14 p2440 N85-25056
The Mars ancient cratered terrain, smooth plains boundary: Implications of Viking color data for evolution of the Amenthes Region 15 p2682 N85-26564
System of white-light density pseudocolor encoding with three primary colors
[AD-D011651] 17 p3037 N85-28791
A general area air traffic controller simulation using colour graphics
[AD-A153634] 18 p3060 N85-28933
Effect of background/foreground color coding on detection in acoustic data displays
[AD-A154105] 19 p3352 N85-30774
Chromophores with auxochrome-like function
[NASA-TM-77849] 20 p3421 N85-31233
Color evolution in high redshift galaxies
20 p3544 N85-32055
Passive Q-modulation of optical cavities by KCl crystals containing OH(-) -ions 21 p3688 N85-32915
Pulsed lasers for filming color holographic film images
22 p3781 N85-33426
The development and evaluation of color display systems for airborne applications. Phase 1: Fundamental visual, perceptual, and display system considerations
[FAA/PM-85-19] 22 p3826 N85-33700
Electrolytic synthesis of colored eta alumina film
23 p3906 N85-34201
Theoretical and experimental analyses of the performance of two-color laser ranging systems
[NASA-CR-176159] 23 p3936 N85-34397
Graph-theoretical exorcism
[DE85-011916] 23 p3955 N85-34512
An analysis and algorithm for filling propagation
23 p3961 N85-34551
Design and implementation of an interactive route editor 23 p3962 N85-34559
Colour spaces and colour contrast
23 p3963 N85-34567
Colour coding scales and computer graphics
23 p3963 N85-34568
Low cost geometric modelling system for CAM
23 p3964 N85-34578
Radiation measurements on magnesium flames
[BLL-CE-TRANS-8110-(9022.09)]
24 p4075 N85-35254
Edge information in color images based on histograms of differences
[AD-A156002] 24 p4154 N85-35751

COLOR (PARTICLE PHYSICS)
U QUANTUM CHROMODYNAMICS

COLOR CENTERS
Polarimetric image recorder
[AD-D011605] 16 p2787 N85-27192

COLOR CODING
Choice reaction time and color: An annotated bibliography
[AD-A149722] 12 p1908 N85-21979
The effect of set size on color matching
[AD-A150899] 14 p2388 N85-24713
Effect of background/foreground color coding on detection in acoustic data displays
[AD-A154105] 19 p3352 N85-30774
The effect of set size on time to recall color coded information
[AD-A155013] 21 p3685 N85-32767

COLOR INFRARED PHOTOGRAPHY
Metric camera experiment: Spacelab 1 mission
05 p0558 N85-14229

COLOR PERCEPTION
U COLOR VISION

COLOR PHOTOGRAPHY
Some nonstellar work at the European Southern Observatory (ESO) Sky Atlas Laboratory — astronomical photography 07 p0964 N85-16117
Bio-optical variability in the Alboran Sea as assessed by Nimbus-7 coastal zone color scanner
[AD-A147909] 07 p0969 N85-16281

COLOR TELEVISION
Problems relevant to town incoming radio TV links
[NASA-TM-77623] 08 p1150 N85-17255
Electronic detection and concealment of film dirt
[BBC-RD-1985/4] 15 p2536 N85-25867
LI481 and LI482 vidicons for two-tube color TV cameras with improved image quality 22 p3764 N85-33333
Theoretical principles of vertical subsampling of color difference signals at half the sampling rate — television
[FI-447-TBR-18] 23 p3926 N85-34332

COLOR VISION
Color visual simulation applications at the Defense Mapping Agency
[AD-P004315] 09 p1268 N85-17969
Color measurement and discrimination
[NASA-CR-3824] 09 p1365 N85-18579
Individual observer data for the 1955 Stiles-Burch 2 deg pilot investigation — color vision
[NPL-CU-68] 20 p3512 N85-31630
Theoretical principles of vertical subsampling of color difference signals at half the sampling rate — television
[FI-447-TBR-18] 23 p3926 N85-34332
Edge information in color images based on histograms of differences
[AD-A156002] 24 p4154 N85-35751

COLORADO
Green River air quality model development: Meteorological and tracer data, July/August 1982. Field study in Brush Valley, Colorado
[DE84-014975] 02 p0225 N85-11474
Atmospheric tracer experiments in a deep narrow valley
[PB84-234590] 04 p0532 N85-13402
Effect of lithology and climate on the morphology of drainage basins in northwestern Colorado
[PB84-228238] 06 p0826 N85-15258
Results of the carbon monoxide study in Washington, D.C. and Denver, Colorado, in the winter of 1982-83
[PB84-230089] 06 p0834 N85-15309

Water resources data for Colorado, water year 1983. Volume 1: Missouri River Basin, Arkansas River Basin and Rio Grande Basin
[PB85-123859] 11 p1671 N85-20528
Water resources data for Colorado, water year 1983. Volume 2: River Basin above Dolores River
[PB85-123867] 11 p1671 N85-20529
Monitoring approaches for assessing quality of high altitude lakes: Colorado Flat Tops Wilderness Area
[PB85-117232] 11 p1679 N85-20579
Measurements of the surface energy budget in the southern Gobi Desert of China, and in the Rocky Mountains of Colorado
[NASA-CR-175506] 12 p1888 N85-21847
Volcanism of the Colorado Plateau (basin and range transition): Implications for crustal processes
13 p2187 N85-23569
Evaluation of the PROFS (Program for Regional Observing and Forecasting Services) 1982, real-time forecast experiment
[PB85-159747] 16 p2837 N85-27495
Categorization of nocturnal drainage flows within the Brush Creek valley in western Colorado and the variability of sigma theta in complex terrain
[DE85-011291] 19 p3300 N85-30461
Aeromagnetic and gravity models of the pluton below the Lake City caldera, Colorado
24 p4104 N85-35442

COLORADO RIVER (NORTH AMERICA)
Water resources data for Colorado, water year 1983. Volume 2: River Basin above Dolores River
[PB85-123867] 11 p1671 N85-20529

COLORATION
U COLOR

COLORIMETRY
NUTSATSEA: An on line data reduction program linking a Chemlab continuous flow analyser to a Commodore PET microcomputer
[IOS-176] 03 p0403 N85-12570
Comparison study of analytical methods for the determination of fluoride, chloride, and bromide in plastics
[DE84-015008] 04 p0470 N85-12989
A comparison of some photometric parameters of active and normal spiral galaxies 08 p1238 N85-17806
Photometric study of Pluto near perihelion. Part 2: Refinement of rotation period: Color indices
15 p2483 N85-25325
System of white-light density pseudocolor encoding with three primary colors
[AD-D011651] 17 p3037 N85-28791
Chromophores with auxochrome-like function
[NASA-TM-77849] 20 p3421 N85-31233
A manual of methods for the continuous flow determination of ammonia, nitrate-nitrite, phosphate and silicate in seawater
[IOS-177] 23 p3913 N85-34243

COLS
U GAPS (GEOLOGY)

COLUMBIA (ORBITER)
National Space Transportation Systems Program mission report
[NASA-TM-87456] 14 p2241 N85-23698
Correlation of predicted and measured sonic boom characteristics from the reentry of STS-1 orbiter
[NASA-TP-2475] 18 p3177 N85-29694

COLUMBIUM
U NIOBIUM

COLUMNS (PROCESS ENGINEERING)
Free zone electrophoresis simulation of static column electrophoresis in microgravity on shuttle flight STS-3
20 p3502 N85-31773

COLUMNS (SUPPORTS)
Interactive buckling of thin-walled structural components under static and dynamic loads
01 p0059 N85-10392
Refined modeling of reinforced concrete columns of seismic analysis
[PB84-234384] 04 p0484 N85-13089
Support structures for optical components in the Laser Demonstration Facility
[DE85-008879] 17 p2971 N85-26349
Buckling and post-buckling behavior of sparsely connected built-up columns 19 p3283 N85-30358
Structural analysis of imperfect three-legged truss columns for large space structures applications
24 p4100 N85-35416
User's guide: A computer program for strength analysis of non-hydraulic concrete structural elements. Report 1, Concrete General Strength Investigation (CGSI)
[AD-A156392] 24 p4102 N85-35428
Static and cyclic behavior of semi-rigid steel beam-column connections
[PB85-194363] 24 p4103 N85-35433

COMBAT
Air Force Human Resources Laboratory report: Fiscal year, 1983
[AD-A145847] 02 p0236 N85-11548
Quantification of cross-coupling and motion feedthrough for multiaxis controllers used in an air combat flying task
05 p0700 N85-14491
HH-60D night hawk helicopter
06 p0752 N85-14817
Computer sizing of fighter aircraft
[NASA-TM-86351] 08 p1067 N85-16759
Evaluation of nose, roof, and mast mounted sensor platforms for piloting and sighting, integrated in future combat helicopters 08 p1074 N85-16808
The design and development of an integrated core system for battlefield helicopters
08 p1074 N85-16811
Air combat visual simulation using a head slaved projector
[AD-P004327] 09 p1270 N85-17981
Binocular overlap in a fiber optic helmet mounted display
[AD-P004331] 09 p1270 N85-17985
Combat capable space systems for tactical support
11 p1713 N85-20775
Air combat simulation: Methods, models, trends
13 p1967 N85-22359
Equilibrium solutions, stabilities and dynamics of Lanchester's equations with optimization of initial force commitments
[AD-A151510] 15 p2637 N85-26266
Piloted simulation of one-on-one helicopter air combat at NOE flight levels
[NASA-TM-86686] 16 p2710 N85-26720
The STOL and maneuver technology program integrated control system 16 p2715 N85-26757
An extended two-target differential game model for medium-range air combat game analysis
[NASA-CR-175968] 18 p3175 N85-29687
Design and implementation of input signals for identification of pilot/aircraft models
[ESA-TT-880] 20 p3394 N85-31055
A formulation and analysis of combat games
[NASA-TP-2487] 22 p3835 N85-33745
Air university commander's and supervisor's guide on substance abuse
[AD-A156336] 24 p4133 N85-35622

COMBINATIONS (MATHEMATICS)
Some facets of the tri-index assignment polytope
[AD-A149195] 10 p1547 N85-19753
On large matchings and cycles in sparse random graphs
[AD-A149194] 10 p1550 N85-19778

COMBINATORIAL ANALYSIS
NT BINOMIAL COEFFICIENTS
NT COMBINATIONS (MATHEMATICS)
NT FACTORIALS
NT PARTITIONS (MATHEMATICS)
COM-GEOM Interactive Display Debugger (CIDD)
[AD-A145001] 01 p0104 N85-10692
Heuristics based on spacefilling curves for combinatorial problems in the plane
[AD-A149320] 10 p1552 N85-19788
Multi-sample cluster analysis as an alternative to multiple comparison procedures
[AD-A149960] 12 p1923 N85-22084
Introduction to combinatorial geometry
[DE85-003266] 13 p2152 N85-23364
Probalistic analysis of combinatorial algorithms: An annotated bibliography
[CWI-OS-RB411] 14 p2411 N85-24864
Signal flow model for sequential logic built from combinational logic elements and its implementation in Prolog
[DE85-005792] 15 p2549 N85-25734
Combinatorial performance/cost analysis of an autonomous navigation system for aircraft
16 p2695 N85-26640
Routing algorithms and stochastic analysis for large communications networks
[AD-A154654] 21 p3573 N85-32225

COMBINED CYCLE POWER GENERATION
High pressure combustion test facility for gas turbine research
[NAL-TR-801] 06 p0757 N85-14845
Low leakage turbine shaft seals for advanced combined cycle systems
[AD-A149372] 10 p1492 N85-19420

COMBINED STRESS
Fatigue strength of alpha-titanium alloys under cophasal action of variable normal and tangential stresses
15 p2498 N85-25407

COMBUSTIBILITY
U FLAMMABILITY

COMBUSTIBLE FLOW
Combustion hot section technology
02 p0145 N85-10981
Aerothermal modeling 02 p0145 N85-10982
Aerothermal modeling program
02 p0145 N85-10983
Dilution zone mixing studies 02 p0145 N85-10984
Linear long-wave stability of cylindrical steady laminar flame in rotating medium 02 p0266 N85-11752
Fundamental study of three dimensional two phase flow in combustion systems
[AD-A142886] 04 p0498 N85-13177
Basic instability mechanisms in chemically reacting subsonic and supersonic flows
[AD-A148408] 08 p1122 N85-17071
Burner stabilized flames in fluids
[DE84-017429] 09 p1291 N85-18109
1984 AFOSR Research Meeting on Diagnostics of Reacting Flow held at New Haven, Connecticut on 21-22 March 1984
[AD-A149023] 10 p1484 N85-19367
Mixing chemical reaction and flow field development in ducted rockets
[DE85-002710] 11 p1591 N85-20009
The mechanisms of flame holding in the wake of a bluff body
[NASA-CR-3866] 12 p1779 N85-21166
Investigation of flowfields found in typical combustor geometries
[NASA-CR-3869] 12 p1779 N85-21167
Development of a three-phrase combustion code for modeling liquid rocket engines 13 p2003 N85-22554
Fundamental study of three dimensional two phase flow in combustion systems
[AD-A150739] 14 p2250 N85-23945
Investigation of the choking effect of an inert granular bed on an ignition gas jet charged with particles
[ISL-CO-235/83] 14 p2284 N85-24028
Unsteady flows in a tube with combustion reaction
[ISL-R-118/83] 14 p2303 N85-24261
Error reduction program — combustor performance evaluation codes
[NASA-CR-174776] 16 p2852 N85-27584
Mechanisms of exhaust pollutants and plume formation in continuous combustion
[AD-A154169] 20 p3435 N85-31310
Sandia Cooperative Group on the Aerothermochemistry of Turbulent Combustion. Discussion record of the second meeting
[DE85-007493] 22 p3743 N85-33203
Pressure correlations in turbulent reacting flows
22 p3744 N85-33205
Nonequilibrium chemistry in an isothermal turbulent flow 22 p3745 N85-33211
Modeling of turbulent recirculating combusting flows
22 p3745 N85-33212

COMBUSTION
NT AFTERBURNING
NT DEFLAGRATION
NT EROSIVE BURNING
NT FUEL COMBUSTION
NT HYDROCARBON COMBUSTION
NT METAL COMBUSTION
NT PROPELLANT COMBUSTION
NT SOLID PROPELLANT COMBUSTION
NT SOLID PROPELLANT IGNITION
NT SPONTANEOUS COMBUSTION
Variable inlet vane assembly for a gas turbine combustion
[AD-D011220] 01 p0010 N85-10063
CREKID: A computer code for transient, gas-phase combustion of kinetics
[NASA-TM-83606] 01 p0011 N85-10068
Investigation of the CARS spectrum of carbon monoxide at high pressure and temperature
[AD-A144816] 01 p0024 N85-10146
Turbine Engine Hot Section Technology (HOST)
[NASA-TM-83022] 02 p0140 N85-10951
Laser spectroscopy of combustion intermediates
[DE84-016101] 02 p0173 N85-11161
Gas dynamics of combustion of gas-air mixture in semi-closed space with relief of pressure into gasless adjacent space 02 p0260 N85-11699
Analysis and simulation of the I C engine Otto cycle using the second law of thermodynamics
02 p0291 N85-11891
Thrust characterization of very high burning rate propellants
[AD-A145891] 03 p0340 N85-12186
Studies of ignition and combustion wave propagation in exothermic systems using high-speed photography
[DE84-016482] 04 p0471 N85-12995
Study of combustion and flame processes initiated by laser-induced multiple-photon absorption
[DE84-017095] 04 p0471 N85-12996

New integration techniques for chemical kinetic rate equations. 2: Accuracy comparison
[NASA-TM-86893] 05 p0596 N85-13798
Biomass thermochemical conversion program
[DE84-017177] 05 p0621 N85-13972
Procedural aspects of testing aerodynamic models with combustion in high-enthalpy transient-mode installations 05 p0725 N85-14658
High pressure combustion test facility for gas turbine research
[NAL-TR-801] 06 p0757 N85-14845
Analysis of physical-chemical processes governing SSME internal fluid flows
[NASA-CR-174245] 06 p0760 N85-14862
USSR report: Chemistry
[JPRS-UCH-84-012] 06 p0761 N85-14865
Integrating chemical kinetic rate equations by selective use of stiff and nonstiff methods
[NASA-TM-86923] 07 p0904 N85-15726
The structure of dilute combusting sprays
[NASA-CR-174838] 07 p0905 N85-15728
The two-fluid model of turbulence applied to combustion phenomena
[CFD/84/15] 08 p1124 N85-17089
Closed vessel combustion of stick propellant
[AD-A147602] 08 p1135 N85-17154
Comparative usefulness of flue gas oxygen and carbon dioxide analysis
[BLL-TRANS-T6358/BG/WH783/84] 08 p1179 N85-17430
High pressure combustion test facility for gas turbine research
[NAL-TR-801] 09 p1283 N85-18065
Combustion driven oscillation of ducted diffusion flame 09 p1289 N85-18094
Swirling turbulent spray group combustion 09 p1289 N85-18095
Pressure measurements in a hydrogen combustion environment: An evaluation of 3 pressure transducers
[TI85-003645] 09 p1323 N85-18312
Theoretical studies of the ignition and combustion of silane-hydrogen-air mixtures
[NASA-CR-3876] 10 p1433 N85-19032
Investigation on the burning of unpulverized coal in a self excited acoustic field
[INPE-3295-PRE/610] 10 p1434 N85-19035
Infrared thermography of burn front propagation in heat powders
[DE85-003307] 10 p1436 N85-19060
Thermal profiles of thermite reactions
[DE85-003308] 10 p1436 N85-19061
Capabilities of laser diagnostics for combustion and flow fields
[DE85-002661] 10 p1438 N85-19064
Laser-initiated combustion studies on metallic alloys in pressurized oxygen
[PB85-128114] 10 p1438 N85-19066
Recovery of damaged solid propellants by interrupting burning and crack-propagation processes
[AD-P004343] 10 p1455 N85-19167
Dynamical studies of molecular systems
[DE85-003053] 11 p1594 N85-20028
Research in nonlinear problems of energy: Informal technical report
[DE85-001529] 11 p1595 N85-20031
Combustion gas properties. 2: Natural gas fuel and dry air
[NASA-TP-2435] 12 p1779 N85-21168
Atmospheric dispersion of hypergolic liquid rocket fuels, volume 1
[AD-A149597] 12 p1817 N85-21399
Size and velocity distributions of particles and droplets in spray combustion systems
[AD-A150355] 13 p2017 N85-22648
A comprehensive review of black powder
[AD-A150455] 13 p2039 N85-22769
Fundamental study of three dimensional two phase flow in combustion systems
[AD-A150739] 14 p2250 N85-23945
Non-steady combustion of composite solid propellants
[AD-A150827] 14 p2250 N85-23947
Model of normal and erosive burning of composite propellants
[ONERA-NT-1984-3] 14 p2263 N85-24024
Ignition of metals in high pressure oxygen 16 p2735 N85-26874
Ignition/combustion processes 16 p2740 N85-26909
Laser Schlieren and ultraviolet diagnostics of rocket combustion 16 p2740 N85-26911
Combustion and micro-explosion of water/oil emulsions in high pressure environments
[AD-A152960] 17 p2919 N85-27997
Photochemical ignition studies. 1: Laser ignition of flowing premixed gases
[AD-A153048] 17 p2920 N85-28002
Elementary reactions of importance in oxidation, combustion ignition and flame inhibitions
[AD-A153139] 17 p2921 N85-28004
Fuel rich catalytic comustion: The first stage of a two-stage combustor
[NASA-TM-87042] 18 p3069 N85-28983
Synthesis chemistry of ceramics by solid-state combustion processes in micro-gravity
[DE85-009595] 18 p3081 N85-29081
Measurement of radical species concentrations and polycyclic aromatic hydrocarbons in flames by fluorescence and absorption using a tunable dye laser
[DE85-006624] 18 p3113 N85-29274
Chemical-acoustic interactions in combustion systems
[AD-A153857] 19 p3233 N85-30046
Measurement of combustion species by electron impact fluorescence
[DE85-011163] 19 p3236 N85-30065
The acoustic mode in numerical calculations of subsonic combustion
[DE85-010788] 19 p3237 N85-30066
Theoretical studies of combustion chemistry
[DE85-010284] 19 p3237 N85-30069
Study of the explosive combustion of drops of sulphur at high temperatures
[HSE-TRANS-11182] 19 p3252 N85-30163
Explosibility of ammonium nitrate
[HSE-TRANS-11111] 19 p3252 N85-30164
LDA study of the unburned gas motion induced by nonsteady flame propagation in a constant volume duct
[DE85-009938] 19 p3270 N85-30277
Experimental determination of the mixing frequency parameter for coalescence/dispersion modeling of turbulent combustion
[DE85-011468] 19 p3270 N85-30280
Applied Science Division's Environmental Research Program
[DE85-010637] 19 p3308 N85-30510
Combustion gas properties. Part 3: Hydrogen gas fuel and dry air
[NASA-TP-2477] 20 p3395 N85-31058
Laminar diffusion flames, carbon gasification, and laser diagnostics applied to combustion systems. 1: Laminar diffusion flames with cylindrical symmetry. 2: Diffusion-controlled gasification of carbon particles. 3: Laser diagnostics applied to combustion systems 20 p3423 N85-31243
Radiative augmented combustion
[AD-A154137] 20 p3423 N85-31246
Sandia Cooperative Group on the Aerothermochemistry of Turbulent Combustion. Discussion record of fourth meeting
[DE85-004720] 20 p3423 N85-31248
Intermittency, conditional sampling and turbulent combustion 20 p3424 N85-31249
Mechanisms of exhaust pollutants and plume formation in continuous combustion
[AD-A154169] 20 p3435 N85-31310
Mechanistic and kinetic studies of the elementary processes in catalytic combustion of methane
[PB85-188308] 20 p3435 N85-31314
Elementary processes in the catalytic combustion of methane (mechanism, intermediates, and controlling reactions)
[PB85-188357] 20 p3436 N85-31316
Sandia Cooperative Group on the Aerothermochemistry of Turbulent Combustion
[DE85-004720] 20 p3455 N85-31453
Sandia Cooperative Group on the Aerothermochemistry of Turbulent Combustion
[DE85-007493] 20 p3455 N85-31454
PHOENICS 84: A multi-dimensional multi-phase general-purpose computer simulator for fluid flow, heat transfer and combustion: 36 lecture panels
[CFD/84/18] 20 p3457 N85-31468
Aerosol analysis and emission spectrometry with free jets
[DE85-010576] 21 p3564 N85-32168
Biomass thermochemical conversion program
[DE85-011867] 21 p3572 N85-32213
In-cavity laser IR spectrum analyzer for investigating non-steady-state processes 21 p3685 N85-32894
Comments on two matters related to turbulent combustion 22 p3743 N85-33204
Turbulent mixing and combustion 22 p3744 N85-33207
Jet flows: Modelling and experiments 22 p3744 N85-33208
Simultaneous measurement of velocity and density in a turbulent nonpremixed flame 22 p3744 N85-33209
Vortex dynamics simulation of conserved scalar dissipation 22 p3745 N85-33210
Combustion-deflagration-detonation transition in a confined spherical powder
[ISL-R-108/84] 22 p3747 N85-33223
Superheated fuel injection for combustion of liquid-solid slurries
[DE85-011624] 22 p3753 N85-33266
Development of a prototype energy meter
[PB85-198430] 22 p3789 N85-33476
Multiparameter conditionally sampled laser velocimetry measurements during flame propagation in a spark ignition engine
[DE85-009850] 22 p3793 N85-33502
Description of a test site for large-scale heavy gas dispersion and combustion experiments
[DE85-004987] 23 p3911 N85-34231
The application of models to the assessment of fire hazard from consumer products
[NBSIR-85-3219] 23 p3925 N85-34325
Upgrading auxiliary facility outleakage and combustion detection
[DE85-012796] 23 p3934 N85-34366
Pressure measurements in a hydrogen combustion environment: Hydrogen-air combustion test series 1 and 2 in the FITS tank, volume 1
[TI85-009899] 24 p4076 N85-35259
Laser probes of natural gas ignition chemistry
[PB85-200210] 24 p4077 N85-35264
An analytical and numerical model of radiation heat transfer in direct injection-type diesel combustion 24 p4092 N85-35368
Review of US NOx abatement technology
[PB85-193522] 24 p4114 N85-35501

COMBUSTION CHAMBERS

Variable inlet vane assembly for a gas turbine combustion
[AD-D011220] 01 p0010 N85-10063
Columbium chamber fabrication study
[AD-A145230] 01 p0017 N85-10102
Turbine Engine Hot Section Technology (HOST)
[NASA-TM-83022] 02 p0140 N85-10951
Nonlinear structural and life analyses of a combustor liner 02 p0141 N85-10955
Dynamic gas temperature measurement system 02 p0141 N85-10958
Effects of surface chemistry on hot corrosion life: Overview 02 p0145 N85-10980
Combustion hot section technology 02 p0145 N85-10981
Aerothermal modeling 02 p0145 N85-10982
Aerothermal modeling program 02 p0145 N85-10983
Dilution zone mixing studies 02 p0145 N85-10984
Combustion system for radiation investigations 02 p0145 N85-10986
Validation of structural analysis methods using the in-house liner cyclic rig 02 p0146 N85-10987
Energy efficient engine component development and integration program
[NASA-CR-170034] 02 p0146 N85-10990
Alternate fuels combustion research
[AD-A145691] 02 p0188 N85-11258
Methane heat transfer investigation
[NASA-CR-171199] 03 p0382 N85-12318
Back end valves: History and modifications
[DE84-009272] 05 p0648 N85-14145
Design of swirled axisymmetric turbulent jets 05 p0724 N85-14657
Combined cycle ramjet engine
[AD-D011247] 06 p0760 N85-14859
The structure of dilute combusting sprays
[NASA-CR-174838] 07 p0905 N85-15728
Verification of life prediction through component testing 07 p0908 N85-15748
Integral boost, heat protection, port covers and transition 07 p0918 N85-15813
Combustion chamber floatwall panel attachment arrangement
[AD-D011358] 07 p1047 N85-16847
Design evolution of the orbiter reaction control subsystem 08 p1099 N85-16944
Advanced OTV engine concepts 08 p1108 N85-17001
Rayleigh and Raman scattering for density in a swirling flow combustor 08 p1120 N85-17060
A study of air breathing rockets. Part 4: Direct fuel injection into a secondary combustor
[NAL-TR-832] 09 p1287 N85-18083
Analysis of sudden expansion flow in a two-dimensional duct with and without side-wall injection using the k-epsilon turbulence model 09 p1317 N85-18282
SSME thrust chamber simulation using Navier-Stokes equations
[NASA-CR-171349] 10 p1430 N85-19017
Investigation on the burning of unpulverized coal in a self excited acoustic field
[INPE-3295-PRE/610] 10 p1434 N85-19035
Analytical fuel property effects: Small combustors, phase 2
[NASA-CR-174848] 10 p1456 N85-19175

Preliminary analysis of selected gas dynamic problems — space shuttle main engine main combustion transients and IUS nozzle flow
[NASA-CR-171343] 10 p1483 N85-19361
Low loss injector for liquid propellant rocket engines
[NASA-CASE-MFG-25869-1] 11 p1591 N85-20008
A new method for calculating the flow field in a dump combustor
[AD-A149305] 11 p1631 N85-20271
Experimental investigation of a pulse combustor: Flow visualization by Schlieren photography
[DE85-002862] 11 p1636 N85-20304
Advanced liner-cooling techniques for gas turbine combustors
[NASA-TM-86952] 12 p1770 N85-21115
Combustion research for gas turbine engines
[NASA-TM-86983] 12 p1778 N85-21164
Investigation of flowfields found in typical combustor geometries
[NASA-CR-3869] 12 p1779 N85-21167
On the coupling of an anchored flame with an acoustic field
[COLL-AERON-8434] 12 p1799 N85-21282
Deflected jet experiments in a turbulent combustor flowfield
[NASA-CR-174863] 13 p1973 N85-22390
Dilution jet configurations in a reverse flow combustor
[NASA-CR-174868] 13 p1974 N85-22392
Nonlinear interactions between vortices and acoustic waves in a rocket combustion chamber
13 p1999 N85-22533
Exergetical analysis of turbojet engine cycle
13 p2049 N85-22825
Fundamental study of three dimensional two phase flow in combustion systems
[AD-A150739] 14 p2250 N85-23945
Application of laser anemometry to jets in combustion chambers
[ISL-CO-210/83] 14 p2302 N85-24253
Hypergolic combustion demonstration in a reciprocating internal combustion engine
[AD-A150848] 14 p2311 N85-24303
Small gas turbine combustor study: Fuel injector performance in a transpiration-cooled liner
[NASA-TM-86999] 15 p2473 N85-25264
Experiments in dilution jet mixing effects of multiple rows and non-circular orifices
[NASA-TM-86996] 15 p2473 N85-25266
The effect of air holes on combustor liner wall temperature profile: Experiments
[NAL-TR-840] 15 p2504 N85-25443
An experimental investigation of confined, multiple, turbulent jet mixing with recirculation — flow distribution in combustors with injection plates
15 p2555 N85-25764
Large-scale commercial combustion systems for producing energy from municipal solid waste
[DE85-007097] 15 p2587 N85-25946
Analytical fuel property effects–small combustors
[NASA-CR-174736] 16 p2708 N85-26709
Turbulence characteristics of swirling flowfields
[NASA-CR-174918] 16 p2709 N85-26717
Study of the primary zone of gas turbine hearths
[ONERA-RTS-22/3256-EY] 16 p2709 N85-26719
Advanced High Pressure O2/H2 Technology
[NASA-CP-2372] 16 p2733 N85-26862
Thrust chamber life prediction
16 p2733 N85-26865
Rocket thrust chamber thermal barrier coatings
16 p2734 N85-26867
Liquid rocket combustor computer code development
16 p2740 N85-26910
Laser Schlieren and ultraviolet diagnostics of rocket combustion
16 p2740 N85-26911
Solid fuel combustion chamber
[VTH-LR-415] 16 p2741 N85-26918
Solid fuel combustion chamber
[VTH-LR-436] 16 p2741 N85-26919
Solid fuel combustion chamber research in the Netherlands
[VTH-LR-444] 16 p2742 N85-26920
Design of a Mobile Combustion Diagnostic Fixture (MCDF)
[AD-A151814] 16 p2745 N85-26941
Error reduction program — combustor performance evaluation codes
[NASA-CR-174776] 16 p2852 N85-27584
Segmented zoned fuel injection system for use with a combustor
[AD-D011640] 17 p2897 N85-27865
Predictions and measurements of isothermal flowfields in axisymmetric combustor geometries
[NASA-CR-174916] 17 p2896 N85-27867
The role of surface generated radicals in catalytic combustion 17 p2896 N85-27869
Future fundamental combustion research for aeropropulsion systems
[NASA-TM-87049] 17 p2898 N85-27870
Reaction-bonded and fiber-reinforced SiC static and dynamic gas turbine components
[BMFT-FB-T-84-302] 17 p2899 N85-27874
Polynomial approaches for the characteristic velocity and flame temperature as a function of mixing compounding and pressure for the systems PMMA/O2, PMMA/air, PE/O2, PE/air, PS/O2 and PS/air
[VTH-LR-421] 17 p2924 N85-28024
Multi-ducted inlet combustor research and development
[AD-A153753] 18 p3063 N85-28946
Fuel rich catalytic comustion: The first stage of a two-stage combustor
[NASA-TM-87042] 18 p3069 N85-28983
Research test facility for evaporation and combustion of alternative jet fuels at high air temperatures
[AD-A153830] 18 p3063 N85-29073
Time-averaged and time-dependent computations of isothermal flowfields in a centerbody combustor
[AD-A153682] 18 p3100 N85-29189
Technical instructions for a control operating system of the gas flow installation for the solid fuel combustion chamber
[VTH-LR-410] 18 p3118 N85-29302
Computer program for the control/operating system of the gas flow installation for the solid fuel combustion chamber
[VTH-LR-430] 18 p3165 N85-29605
A model for the combustion of polymethyl methacrylate in air in a laminar diffusion flame
[VTH-LR-439] 18 p3165 N85-29606
The effect of surface reactions in catalytic combustion
[AD-A154217] 19 p3234 N85-30049
Radiative augmented combustion
[AD-A154137] 20 p3423 N85-31246
Application of the Diffusion Raman Anti-Stokes Coherent (DRASC) method to a SNECMA combustion chamber
[YKC-3066/84] 20 p3425 N85-31260
Mechanisms of exhaust pollutants and plume formation in continuous combustion
[AD-A154169] 20 p3435 N85-31310
An experimental investigation of confined, multiple, turbulent jet mixing with recirculation
20 p3451 N85-31426
Combustor turbulence 20 p3452 N85-31434
R and D activities of the Propulsion Division
20 p3539 N85-32025
Carbon/carbon combustor external insulation
[AD-D011719] 23 p3910 N85-34224
Numerical model of a pulse combustor
[DE85-011717] 23 p3912 N85-34240
Investigation of non-intrusive radiometers for entrained gasifier temperature measurement, revision 3
[DE85-011795] 23 p3934 N85-34385
Flow modifying device
[NASA-CASE-LEW-13562-2] 24 p4065 N85-35195
Basic research on pulse-combustion phenomena
[PB85-200226] 24 p4077 N85-35265
Development of advanced high-temperature heat flux sensors. Phase 2: Verification testing
[NASA-CR-174973] 24 p4096 N85-35391

COMBUSTION CONTROL
Energy efficient engine combustor test hardware detailed design report
[NASA-CR-167945] 02 p0140 N85-10950
The mechanisms of flame holding in the wake of a bluff body
[NASA-CR-174058] 02 p0172 N85-11149
The detonation of aerosols and vapors of combustible substances under controlled conditions. Part 1: Construction of a test installation
[ISL-R-109/83-PT-1] 14 p2254 N85-23966
Nonintrusive shaft speed sensor
16 p2740 N85-26908
On the low temperature chemistry preceding end gas autoignition
[DE85-010471] 19 p3252 N85-30162
Combustion control with smart sensors
[DE85-009419] 19 p3274 N85-30303
Reduction of pollutant formation in combustion processes
[DE85-010181] 19 p3309 N85-30512

COMBUSTION EFFICIENCY
Comparison of numerical techniques for integration of stiff ordinary differential equations arising in combustion chemistry
[NASA-TP-2372] 01 p0011 N85-10065
Combustion modeling of a 2 cylinder cycle reciprocating engine
[AD-A144782] 01 p0055 N85-10364
An interactive computer code for calculation of gas-phase chemical equilibrium (EQLBRM)
[NASA-CR-168337] 02 p0140 N85-10948
The mechanisms of flame holding in the wake of a bluff body
[NASA-CR-174058] 02 p0172 N85-11149
Speed governor for diesel engine
09 p1307 N85-18214
Investigation on the burning of unpulverized coal in a self excited acoustic field
[INPE-3295-PRE/610] 10 p1434 N85-19035
Study of HTPB-based SOFRAM fuels
[FOA-C-20583-D3] 11 p1614 N85-20150
The influence of fuel quality upon flame-tube temperature and flame radiation in a model gas-turbine primary zone
[K233] 13 p1974 N85-22396
Dependence of combustion of homogeneous kerosene-air mixtures on humidity of air
13 p2051 N85-22835
A fundamental study of liquid phase particle breakup. Revision
[AD-A150791] 14 p2301 N85-24249
Shock tube study of the fuel structure effects on the chemical kinetic mechanisms responsible for soot formation, part 2
[NASA-CR-174880] 15 p2504 N85-25444
Influence of fuel properties on gas turbine combustion performance
[AD-A151464] 15 p2504 N85-25448
PSA, Renault work on all fuel automobile engine
15 p2531 N85-25604
The role of surface generated radicals in catalytic combustion 17 p2896 N85-27869
SSME fuel preburner two-dimensional analysis
17 p2911 N85-27943
Coal-Fired MHD Combustor Development Project, Phase 3D
[DE85-008822] 18 p3192 N85-29795
Combustion characterization of coals for industrial applications
[DE85-010673] 19 p3228 N85-30014
A mathematical model of reciprocating combustion engine dynamics for the diagnosis of deficient energy conversion 19 p3280 N85-30339
Closed-bomb combustion of Hivelite-based, Very High Burn Rate (VHBR) propellant
[AD-A155740] 21 p3571 N85-32212
Effect of precipitation variables on the specific surface and explosion characteristics of pentaerythritol tetranitrate
[DE85-009620] 23 p3922 N85-34302

COMBUSTION INSTABILITY
U COMBUSTION STABILITY

COMBUSTION PHYSICS
Combustion hot section technology
02 p0145 N85-10961
Aerothermal modeling 02 p0145 N85-10962
Aerothermal modeling program
02 p0145 N85-10963
Gravitational effects on premixed particle cloud flames
02 p0171 N85-11144
The mechanisms of flame holding in the wake of a bluff body
[NASA-CR-174058] 02 p0172 N85-11149
Dynamics of burnout of solid fuel in fluidized bed of finely divided inert particles 02 p0273 N85-11782
Combustion and detonation of hydrogen-air mixture in free spaces 02 p0274 N85-11783
Limiting effects during turbulent combustion
02 p0274 N85-11784
Diffusive combustion of fluids with free surface
02 p0274 N85-11785
Combustion kinetics of metal oxide and halide radicals
[AD-A148521] 08 p1122 N85-17076
The two-fluid model of turbulence applied to combustion phenomena
[CFD/84/15] 08 p1124 N85-17089
Investigation on the burning of unpulverized coal in a self excited acoustic field
[INPE-3295-PRE/610] 10 p1434 N85-19035
Mixing chemical reaction and flow field development in ducted rockets
[DE85-002710] 11 p1591 N85-20009
A comparison of the efficiency of numerical methods for integrating chemical kinetic rate equations
[NASA-TM-83590] 12 p1778 N85-21162
Gasification of boron oxide drops and boron slurry agglomerates in combustion gases
13 p1999 N85-22529
Comprehensive mechanisms for combustion chemistry: An experimental and numerical study with emphasis on applied sensitivity analysis
[DE85-000173] 13 p2018 N85-22656
Combustion kinetics of metal oxide and halide radicals
[AD-A150924] 14 p2251 N85-23952
Asymptotic methods especially in combustion
[AD-A151505] 15 p2505 N85-25450

Solid fuel combustion chamber
[VTH-LR-415] 16 p2741 N85-26918
Solid fuel combustion chamber
[VTH-LR-438] 16 p2741 N85-26919
A model for the combustion of polymethyl methacrylate in air in a laminar diffusion flame
[VTH-LR-439] 16 p3165 N85-29606
Measurement of combustion species by electron impact fluorescence
[DE85-011163] 19 p3236 N85-30065
Sandia Cooperative Group on the Aerothermochemistry of Turbulent Combustion. Discussion record of the second meeting
[DE85-007493] 22 p3743 N85-33203
Second order modelling in non-constant density flows
22 p3744 N85-33206
Behavior of the porous bed in a combustion-deflagration-detonation transition
[ISL-CO-220/84] 22 p3747 N85-33224
Combustion-deflagration-detonation transition
[ISL-CO-221/84] 22 p3747 N85-33225

COMBUSTION PRODUCTS
Combustion gas properties I-ASTM jet A fuel and dry air
[NASA-TP-2359] 01 p0010 N85-10064
HMX combustion modification
[AD-A145071] 01 p0024 N85-10149
Size specific total particulate emission factors for mobile sources
[PB84-226653] 01 p0071 N85-10471
Clean-burning diesel engines
[AD-A145515] 02 p0205 N85-11349
Dissociated methanol vehicle test results
[DE84-004507] 04 p0509 N85-13248
Mechanism of soot formation
[AD-A146817] 07 p0922 N85-15841
Heater block assembly for use in thermal oxidation testing of jet fuel
[AD-D011430] 08 p1123 N85-17077
Ceramic fabric material testing
[DE84-012014] 09 p1300 N85-18165
Atmospheric science and power production
[DE84-005177] 09 p1354 N85-18521
Study of deposition control using transpiration
[DE85-002339] 10 p1485 N85-19378
Study of deposition control using transpiration
[DE85-003463] 11 p1585 N85-19984
Combustion gas properties. 2: Natural gas fuel and dry air
[NASA-TP-2435] 12 p1779 N85-21166
Kinetics of nitric oxide formation in laminar and turbulent methane combustion
[PB85-149698] 12 p1804 N85-21313
Digital temperature and velocity control of mach 0.3 atmospheric pressure durability testing burner rigs in long time, unattended cyclic testing
[NASA-TM-86959] 12 p1805 N85-21321
Determination of toxicity of combustion products of habitability foams concurrently with flammability studies of these materials
[AD-A149647] 12 p1905 N85-21961
Experimental investigations of thermal radiation from potassium atoms in magnetohydrodynamic system: Preliminary report
[DE85-003715] 12 p1936 N85-22169
Solid propellant combustion diagnostics and automated data retrieval from holograms 13 p1998 N85-22527
Picosecond lidar techniques in laboratory and field diagnostics
[AD-A150755] 14 p2309 N85-24294
Transformation of nitrogen oxides while sampling combustion products
[AD-A152184] 16 p2746 N85-26945
Analytical methods for determination of POHC (Principal Organic Hazardous Constituents) in combustion products
[PB85-161578] 16 p2747 N85-26955
The remote detection of polynuclear aromatic hydrocarbons using laser-induced fluorescence
[AD-A152294] 16 p2757 N85-27013
Jet fuel instability mechanisms
[NASA-CR-175856] 17 p2936 N85-28127
Equation of state for detonation products
[DE85-009608] 18 p3084 N85-29079
Changes of structure of EP648-VI alloy as a result of high-temperature gas corrosion
19 p3243 N85-30110
Flow field effects on nucleation in a reacting mixing layer
[ARL/AERO-R-165] 19 p3263 N85-30237
Fuel-rich catalytic combustion: A soot-free technique for in situ hydrogen-like enrichment
[NASA-TP-2498] 20 p3423 N85-31244
Polyesters: A review of the literature on products of combustion and toxicity
[NBSIR-85-3139] 20 p3433 N85-31298
Toxic hazards tests for vehicles and other equipment
[AD-A149164] 20 p3506 N85-31797
Ice nucleating characteristics of Capparis Aphylla, an Indian herb 21 p3641 N85-32619
System for the continuous generation of phosphorous aerosols from red phosphorus-butyl rubber
[DE85-013527] 24 p4072 N85-35232
Proceedings of the 7th Joint Panel Meeting of the UJNR Panel on Fire Research and Safety
[PB85-190545] 24 p4085 N85-35317
Fire research publications, 1984
[PB85-206502] 24 p4166 N85-35827

COMBUSTION STABILITY
NT FLAME STABILITY
An experimental investigation of combustion pressure oscillations in solid fuel ramjets
[AD-A144870] 01 p0024 N85-10147
Chemistry of fuel deposits and sediments and their precursors
[NASA-CR-174778] 01 p0034 N85-10209
Combustion dynamics in rockets
[AD-A148478] 08 p1114 N85-17024
Basic instability mechanisms in chemically reacting subsonic and supersonic flows
[AD-A148408] 08 p1122 N85-17071
Proceedings of the AFOSR/AFRPL Rocket Propulsion Research Meeting: Abstracts and Agenda
[AD-A148818] 09 p1286 N85-18085
Radiation/catalytic augmented combustion
[AD-A148758] 09 p1290 N85-18101
Burner stabilized flames in fluids
[DE84-017429] 09 p1291 N85-18109
Numerical simulations of liquid propellant combustion instability: Onset and growth
[DE85-000743] 10 p1458 N85-19186
An investigation of space shuttle main engine shutdown chugging instability 12 p1946 N85-22221
Twenty-first JANNAF Combustion Meeting, volume 1
[AD-A150981] 13 p1998 N85-22526
Coupling between velocity oscillations and solid propellant combustion 13 p2000 N85-22536
Acoustic energy balance method
13 p2000 N85-22537
Coupled acoustic and hydrodynamic wave instabilities
13 p2000 N85-22538
Characterization of heterogeneity of composite propellants and its effects on combustion behavior
13 p2000 N85-22539
Investigation of the characteristics of the velocity-coupled response functions of solid propellants
13 p2001 N85-22540
Comparisons of solid propellant with instability predictions and motor firing experience
13 p2001 N85-22541
Measurements of distributed combustion
13 p2001 N85-22542
Distributed combustion: A mechanism of acoustic suppression 13 p2001 N85-22543
Workshop report: Catalysis of Burn Rate of Energetic Binder propellants 13 p2001 N85-22545
An integral closed loop combustion stability model-status and review 13 p2003 N85-22553
Transient combustion dynamics
[AD-A154430] 19 p3235 N85-30052
The acoustic mode in numerical calculations of subsonic combustion
[DE85-010788] 19 p3237 N85-30066
Combustor turbulence 20 p3452 N85-31434
Status of boron combustion research
[AD-A154782] 21 p3563 N85-32160
Closed-bomb combustion of Hivelite-based, Very High Burn Rate (VHBR) propellant
[AD-A155740] 21 p3571 N85-32212

COMBUSTION TEMPERATURE
Application of atomic fluorescence to measurement of combustion temperature in solid propellants
[AD-A150733] 14 p2263 N85-24021
Nonintrusive shaft speed sensor
16 p2740 N85-26908
Combustion characterization of coals for industrial applications
[DE85-010673] 19 p3228 N85-30014

COMBUSTION VIBRATION
An investigation of space shuttle main engine shutdown chugging instability 12 p1946 N85-22221

COMBUSTION WAVES
U FLAME PROPAGATION

COMBUSTORS
U COMBUSTION CHAMBERS

COMET NUCLEI
Giacobini-Zinner comet: Polarimetric and physical observations
[NASA-TM-77771] 01 p0130 N85-10894
Implications of the presence of S2 in cometary ice
11 p1760 N85-21072
The International VEGA 'Venus-Halley' (1984-1986 experiment: Description and scientific objectives
[NASA-TM-77536] 12 p1960 N85-22324
Studies of icy bodies: Uranian satellites and cometary nuclei 13 p2175 N85-23496
Surfaces of asteroids and cometary nuclei
13 p2176 N85-23503
An idealized short period comet model: Surface insolation, H2O flux, dust flux and mantle evolution
13 p2176 N85-23504
Comet thermal modeling 13 p2176 N85-23505
Dynamics of long-period comets
13 p2176 N85-23506
Halley's Comet, a bibliography
[LC-84-600109] 13 p2204 N85-23674
Current ideas on the nature of comets
14 p2435 N85-25017
Dust emission of Comet Halley at large heliocentric distances 15 p2661 N85-26556

COMET TAILS
Halley's Comet, a bibliography
[LC-84-600109] 13 p2204 N85-23674
Current ideas on the nature of comets
14 p2435 N85-25017
Occultations of stars and radio sources by comets: Predictions and observing prospects
14 p2437 N85-25034
Dust emission of Comet Halley at large heliocentric distances 15 p2661 N85-26556
Comet Halley returns: A teachers' guide 1985-1986
[NASA-EP-197] 24 p4188 N85-35839

COMETARY ATMOSPHERES
Outer satellite atmospheres: Their nature and planetary interactions
[NASA-CR-174146] 04 p0589 N85-13759
Studies of radiative transfer in planetary atmospheres
[NASA-CR-174194] 05 p0745 N85-14778
Extended atmospheres of outer planet satellites and comets
[NASA-CR-174338] 08 p1258 N85-17916
The fluorescence of cometary OH and CN
09 p1411 N85-18898
Extended atmospheres of outer planet satellites and comets
[NASA-CR-174398] 09 p1416 N85-18933
The essence of binary star coalescence: A coordinated ground-based photometric and IUE ultraviolet study of FK Comae 11 p1756 N85-21044
Observations of comets: Radio and otherwise — conference
[TB-84] 11 p1782 N85-21086
Cometary atmospheres: Modeling the spatial distribution of observed neutral radicals
[NASA-CR-175491] 11 p1785 N85-21097
Cometary atmospheres: Modeling the spatial distribution of observed neutral radicals
[NASA-CR-175485] 11 p1785 N85-21098
Averaging of equations of cometary orbital motion with allowance for nongravitational effects
13 p1978 N85-22411
An idealized short period comet model: Surface insolation, H2O flux, dust flux and mantle evolution
13 p2176 N85-23504
Comet thermal modeling 13 p2176 N85-23505
Dynamics of long-period comets
13 p2176 N85-23506
Halley's Comet, a bibliography
[LC-84-600109] 13 p2204 N85-23674
Current ideas on the nature of comets
14 p2435 N85-25017
Occultations of stars and radio sources by comets: Predictions and observing prospects
14 p2437 N85-25034
Astrometric needs for the ISEE-3/ICE mission to Comet Giacobini-Zinner 14 p2438 N85-25043
Extended atmospheres of outer planet satellites and comets
[NASA-CR-175673] 14 p2440 N85-25058
Magnetic field penetration into cometary ionosphere
15 p2477 N85-25290
Development of a global 3-D magnetohydrodynamic computational model for solar wind/cometary and planetary studies
[NASA-CR-175724] 15 p2664 N85-26577
Cometary atmospheres: Modeling the spatial distribution of observed neutral radicals
[NASA-CR-175852] 16 p2882 N85-27781
Cometary atmospheres: Modeling the spatial distribution of observed neutral radicals
[NASA-CR-175882] 17 p3054 N85-28904
The study of the physics of cometary nuclei
[NASA-CR-175917] 17 p3054 N85-28905
Extended atmospheres of outer planet satellites and comets
[NASA-CR-176137] 22 p3851 N85-33848

Comet Halley returns: A teachers' guide 1985-1986
[NASA-EP-197] 24 p4168 N85-35839
COMETS
NT COMET NUCLEI
NT COMET TAILS
NT ENCKE COMET
NT GIACOBINI-ZINNER COMET
NT HALLEY'S COMET
NT IRAS-ARAKI-ALCOCK COMET
Forbidden lines of oxygen in comet spectra
02 p0163 N85-11105
The significance of comets for star formation
03 p0443 N85-12824
Dust properties determined from backscattering in the interplanetary and interstellar medium
03 p0446 N85-12836
Sample return from a comet flyby
06 p0869 N85-15646
Airborne observations of comets
08 p1244 N85-17853
The geology of the terrestrial planets
[NASA-SP-469] 09 p1410 N85-18888
Asteroids, comets and planet formation
09 p1410 N85-18889
Solar system studies with the IUE: 1982 - 1984
11 p1744 N85-20984
Observations of comets: Radio and otherwise — conference
[TB-84] 11 p1762 N85-21086
Magnetospheres in the solar system
12 p1954 N85-22274
Study and estimation of planet-crossing asteroid populations: Discoveries and analysis
13 p2175 N85-23498
Cometary Astrometry
[NASA-CR-175660] 14 p2435 N85-25015
Remarks on cometary astrometry
14 p2435 N85-25019
Cometary astrometry with Schmidt cameras
14 p2435 N85-25020
Astrometry of comets using hypersensitized type 2415 film
14 p2435 N85-25021
Astrometric plates obtained at the primary focus of large aperture reflectors
14 p2436 N85-25022
Problems and procedures of cometary astrometry
14 p2436 N85-25024
Astrometry at La Silla
14 p2436 N85-25025
Desired characteristics of catalogs for cometary astrometry
14 p2436 N85-25030
Comets and nongravitational forces
14 p2437 N85-25038
On the orbit improvement results obtained by referring old cometary observations to the SAO Star Catalog
14 p2438 N85-25042
Systematic and random deformations of orbits of long-period comets
15 p2479 N85-25299
Periodic cometary showers: Real or imaginary?
15 p2680 N85-26555
Mining cosmic dust from the blue ice lakes of Greenland
15 p2682 N85-26563
A search for evidence of large body Earth impacts associated with biological crisis zones in the fossil record
15 p2682 N85-26567
Comet showers and Nemesis, the death star
[DE85-003736] 15 p2683 N85-26575
Radio observations of comet P/Crommelin
[INPE-3480-PRE/723] 16 p2881 N85-27777
Study of the accuracy of astrometric observations of comets
[ESA-CR(P)-1964] 17 p3054 N85-28803
Cometary atmospheres: Modeling the spatial distribution of observed neutral radicals
[NASA-CR-175882] 17 p3054 N85-28804
The study of the physics of cometary nuclei
[NASA-CR-175917] 17 p3054 N85-28805
COMFORT
Ride comfort of off-road vehicles
[AD-P004279] 09 p1406 N85-18855
Comparison of measured and simulated ride comfort for an agricultural tractor and influence of travel speed and tyre-inflation pressure on dynamic response
[AD-P004281] 09 p1407 N85-18857
Operator's functional comfort zone when controlling moving object
22 p3621 N85-33670
COMMAND AND CONTROL
Command control group behaviors. Objective 1: A methodology for and identification of command control group behaviors
[AD-A145890] 02 p0191 N85-11279
Air Force Human Resources Laboratory report: Fiscal year, 1983
[AD-A145647] 02 p0239 N85-11548
A mathematical theory of command and control structures
[AD-A145808] 02 p0256 N85-11675
An approach to interfacing data bases in WWMCCS ADP
[AD-A146350] 03 p0439 N85-12793
A framework for research on adaptive decision aids
[AD-A138331] 05 p0734 N85-14719
Human factors characteristics of the Joint Tactical Fusion Test Bed: Field test 467 results
[AD-A146856] 07 p1020 N85-16476
Acquisition planning at the Defense Communications Agency
[AD-A146877] 07 p1051 N85-16669
A simulator for determining the performance of transaction manager and lock manager combinations in a database
[AD-A147827] 07 p1055 N85-16696
Defense Meteorological Satellite Program (DMSP)
11 p1711 N85-20766
Optimization of guidance and control using function minimization and NAVSTAR/GPS
[AD-A148956] 12 p1775 N85-21141
The effect of jamming/deception on decision making
[AD-A149740] 12 p1828 N85-21472
Space station systems technology study (add-on task). Volume 1: Executive summary
[NASA-CR-171415] 13 p1986 N85-22459
Basic EMC (electromagnetic interference) technology advancement for c3 systems. Volume 3A: Probabilistic analysis of combinational circuits with random delays
[AD-A150349] 13 p2055 N85-22866
Remote control of an impact demonstration vehicle
[NASA-TM-85925] 14 p2225 N85-23797
Interference effects of vocalization on dual task performance
[AD-A150687] 14 p2291 N85-24203
Basic EMC (Electromagnetic Compatibility) technology advancement for C3 systems: Model revision for IEMCAP (Intrasystem Electromagnetic Compatibility Analysis Program)
[AD-A150795] 14 p2292 N85-24208
Research needs for artificial intelligence applications in support of C3 (Command, Control, and Communication)
[AD-A150867] 14 p2292 N85-24210
Automated CPX support system preliminary design phase
[NASA-CR-175784] 16 p2769 N85-27091
A study of error rates in voice recognition
[AD-A153282] 17 p2949 N85-28211
Rome Development Center Air Force technical objective document C3I FY-86
[AD-A152476] 17 p3047 N85-28851
LAN (Local Area Network) interoperability study of protocols needed for distributed command and control
[AD-A154033] 19 p3255 N85-30182
Study and realization of a command system adapted to space robotics
[SNIAS-851-440-106] 22 p3740 N85-33183
Assured information flow capping architecture
[AD-A155392] 22 p3756 N85-33283
TRICCS: A proposed teleoperator/robot integrated command and control system for space applications
[NASA-TM-87577] 24 p4136 N85-35637
COMMAND GUIDANCE
Determining functional requirements for NASA Goddard's command management system software design using expert systems
20 p3539 N85-32020
COMMAND LANGUAGES
NT QUERY LANGUAGES
Construction of a menu-based system
[NASA-CR-172560] 13 p2146 N85-23321
COMMAND SYSTEMS
U COMMAND GUIDANCE
COMMAND-CONTROL
U COMMAND AND CONTROL
COMMERCE
Foreign civil aviation competition: 1976 summary and implications
[NASA-TM-X-73907] 02 p0133 N85-10907
Commercial space services 02 p0153 N85-11039
The Expendable Launch Vehicle Commercialization Act
[GPO-30-838] 04 p0480 N85-12919
Power for commercial space applications
05 p0606 N85-13684
International airport study: How to improve the effect of airports on trade and on export-related industries
[PB85-124923] 11 p1586 N85-19992
The 1981 transatlantic boat race contribution for marine meteorological measurements 14 p2324 N85-24361
Miscellaneous ARGOS maritime applications — yacht races 14 p2327 N85-24383
RESO: Expert system applied to company computer networks
[ENST-84E016] 20 p3518 N85-31874
Spin-offs from technical commercial infrastructures, no. 2 20 p3540 N85-32035
New innovative businesses from industry. Experiences in the Netherlands in the successful transfer of technology from university to industry 22 p3849 N85-33843
COMMERCE LAB
Commerce Lab: Mission analysis payload integration study. Appendix A: Data bases
[NASA-CR-176016] 19 p3224 N85-29988
COMMERCIAL AIRCRAFT
NT A-310 AIRCRAFT
NT A-320 AIRCRAFT
NT BOEING 727 AIRCRAFT
NT BOEING 737 AIRCRAFT
NT BOEING 747 AIRCRAFT
NT BOEING 767 AIRCRAFT
NT CV-990 AIRCRAFT
NT DC 8 AIRCRAFT
NT DC 9 AIRCRAFT
NT DC 10 AIRCRAFT
NT EUROPEAN AIRBUS
NT L-1011 AIRCRAFT
NT LEAR JET AIRCRAFT
Energy efficient engine component development and integration program
[NASA-CR-170034] 02 p0146 N85-10990
USSR report: Transportation
[JPRS-UTR-84-028] 03 p0310 N85-12002
Commercial aircraft noise
[PNR-90206] 03 p0417 N85-12665
Aircraft navigation and landing technology: Status of implementation
[GPO-38-615] 04 p0454 N85-12683
Airport activity statistics of certificated route air carriers
[AD-A148472] 06 p1081 N85-16646
Design of a digital ride quality augmentation system for commuter aircraft
[AD-A148233] 08 p1088 N85-16879
Use of airplanes for loft training
09 p1276 N85-18019
Study of advanced fuel system concepts for commercial aircraft and engines
[NASA-CR-174752] 10 p1458 N85-19176
Study of advanced fuel system concepts for commercial aircraft
[NASA-CR-174751] 11 p1584 N85-19978
Minister Bugayev on civil aviation in 1984, plans for 1985 14 p2208 N85-23689
Minister Bugayev reviews 1983 civil aviation work, sets course for 1984 14 p2208 N85-23695
Bugayev on civil aviation ministry's 1983 achievements 14 p2208 N85-23696
Ilyushin bureau designer on fuel conservation research
15 p2467 N85-25231
Calculation and display of stack departure times for aircraft inbound to Heathrow Airport
[AD-A151991] 15 p2469 N85-25241
Demonstration of relaxed stability on a commercial transport 16 p2713 N85-26745
Realisation of relaxed static stability on a commercial transport 16 p2713 N85-26746
Demonstration of relaxed static stability on a commercial transport 17 p2903 N85-27899
Realisation of relaxed static stability on a commercial transport 17 p2903 N85-27899
Aircraft accident report: World Airways Inc., Flight 30H, McDonnell Douglas DC-10-30CF, N113WA, Boston-Logan International Airport, Boston, Massachusetts, January 23, 1982
[PB85-910406] 22 p3728 N85-33114
U.S. Civil airmen statistics for calendar year 1984
[AD-A156326] 24 p4059 N85-35153
COMMERCIAL AVIATION
U CIVIL AVIATION
U COMMERCIAL AIRCRAFT
COMMERCIAL ENERGY
Solar-gas systems impact analysis study
[PB85-129068] 11 p1618 N85-20163
COMMERCIAL SPACECRAFT
The Ariane launch vehicle is the key of the Europeans to the space market 17 p2908 N85-27931
Commerce Lab: Mission analysis payload integration study. Appendix A: Data bases
[NASA-CR-176016] 19 p3224 N85-29988
Insurance and the commercialization of space
[S-PRT-99-16] 20 p3397 N85-31074
COMMINUTION
NT CRUSHING
NT GRINDING (COMMINUTION)
Grainsize evolution and differential comminution in an experimental regolith 06 p0888 N85-15838
COMMITTEE ON SPACE RESEARCH
Space research in Spain 08 p1231 N85-17751
Space research in Denmark 08 p1231 N85-17753
Space activities in Finland 08 p1231 N85-17754
Space research in the Federal Republic of Germany
09 p1265 N85-18074

Activities report in space research in Austria
11 p1587 N85-19994
The French space program 22 p3731 N85-33127
COMMODITIES
Biocatalyzed processes for production of commodity chemicals: Assessment of future research advances for N-butanol production
[NASA-CR-174264] 07 p0919 N85-15819
Intermediate term forecasting techniques for management
[AD-A151370] 15 p2637 N85-26262
COMMUNICATING
NT AIRCRAFT COMMUNICATION
NT CONVERSATION
NT GROUND-AIR-GROUND COMMUNICATION
NT INFORMATION DISSEMINATION
NT INTERSTELLAR COMMUNICATION
NT MESSAGES
NT SELECTIVE DISSEMINATION OF INFORMATION
NT VERBAL COMMUNICATION
Communications skills for CRM training
09 p1276 N85-18017
The multiple resources model of human performance: Implications for display design 10 p1534 N85-19689
Lack of communication 15 p2686 N85-26591
COMMUNICATION
NT FACSIMILE COMMUNICATION
NT INFORMATION DISSEMINATION
NT LINE OF SIGHT COMMUNICATION
NT OPTICAL COMMUNICATION
NT SHIP TO SHORE COMMUNICATION
NT VERBAL COMMUNICATION
Second Symposium on Space Industrialization — space commercialization
[NASA-CP-2313] 02 p0149 N85-11011
The real world: The user 02 p0150 N85-11017
Inclusion of audiovisual media in information services for the special subjects journalism and communication science (pilot study)
[BMFT-FB-ID-83-004] 02 p0294 N85-11909
Research activities of the Illinois University Coordinated Science Laboratory
[AD-A145589] 03 p0449 N85-12856
Equivocation limits in Gaussian additive channels
[INPE-2828-PRE/380] 04 p0492 N85-13137
Scientific communications and national security
[GPO-36-093] 04 p0492 N85-13138
Subliminal communication technology
[GPO-38-833] 05 p0622 N85-13979
A comparative study of alternative controls and displays for by the severely physically handicapped
05 p0709 N85-14549
USSR report: Electronics and electrical engineering
[JPRS-UEE-84-012] 06 p0761 N85-14991
Space infrastructure 07 p0914 N85-15783
An analysis of constraints to coordinated tactical crew interaction in the P-3C aircraft
[AD-A147220] 07 p1021 N85-16478
Space Shuttle Technical Conference, part 2
[NASA-CP-2342-PT-2] 08 p1096 N85-16937
Commission operation. National Low-Level Radioactive Waste Management Program
[DOE/LLW-33T] 09 p1383 N85-18689
Space System Applications to Tactical Operations
[AGARD-CP-344] 11 p1709 N85-20751
Civil weather satellite systems
11 p1711 N85-20788
Application of the Hardman methodology to the Single Channel Ground-Airborne Radio System (SINCGARS)
[NASA-CR-175894] 14 p2218 N85-23758
China report: Science and technology
[JPRS-CST-85-013] 15 p2536 N85-25652
Management communication and financial modeling
15 p2627 N85-26190
White paper on new international satellite systems
[PB85-162501] 16 p2775 N85-27127
Numerical modeling of subsurface communication
[DE85-012818] 21 p3577 N85-32249
Adaptive corrector operating in frequency domain
22 p3765 N85-33337
A new description of combined trellis coding with asymmetric modulation
[NASA-CR-176197] 24 p4066 N85-35323
DMSK: A practical 2400-bps receiver for the mobile satellite service: An MSAT-X Report
[NASA-CR-176194] 24 p4066 N85-35324
COMMUNICATION CABLES
NT BEAM WAVEGUIDES
NT CIRCULAR WAVEGUIDES
NT COAXIAL CABLES
NT OPTICAL WAVEGUIDES
NT PLASMAGUIDES
NT RECTANGULAR WAVEGUIDES
NT WAVEGUIDES
Regenerators of binary pulses for optical communication systems 04 p0485 N85-13099
Metallized synthetic cable
[AD-D011263] 05 p0628 N85-14023
Characterization of fiber optic cables under large tensile loads
[DE84-016816] 05 p0651 N85-14180
Siemens-Corning plant to manufacture optical fibers
11 p1617 N85-20175
Optical fiber communications link design in compliance with systems performance standards
[PB85-111037] 12 p1630 N85-21489
Surge strength of symmetric cable with monolithic polyethylene insulation of quads
13 p2082 N85-23001
Frequency selection for dispersion signal in satellite communication lines 15 p2528 N85-25584
Instrument for measuring dispersional distortions in optical fibers and cables 15 p2530 N85-25595
COMMUNICATION EQUIPMENT
NT DIPLEXERS
NT RADIO RECEIVERS
NT SATELLITE TELEVISION
NT SPACECRAFT TELEVISION
NT SUPERHETERODYNE RECEIVERS
NT TRANSMITTER RECEIVERS
The ACE (Automated Cable Expert) experiment: Initial evaluation of an expert system for preventive maintenance
[AD-P003943] 02 p0248 N85-11623
Spread-spectrum communications
[AD-A146135] 03 p0355 N85-12285
Problems of development of space communication
06 p0793 N85-15067
The Western Aeronautical Test Range of NASA Ames Research Center
[NASA-TM-85924] 07 p0909 N85-15758
Electronics systems test laboratory testing of shuttle communications systems 08 p1101 N85-16958
NTT unveils satellite communications equipment
10 p1476 N85-19315
Automation of servicibility of radio-relay station equipment 15 p2527 N85-25582
System of light protection of antenna-mast structures of radio-relay lines 15 p2527 N85-25583
Survey of developments in tropospheric communication apparatus 15 p2528 N85-25587
Quality control of radioelectronic apparatus components on basis of external characteristics in frequency domain
15 p2529 N85-25590
ADCCP (Advanced Data Communication Control Procedure) communication processor
[AD-D011595] 15 p2544 N85-25709
The POK project; studies of information handling problems with a new kind of communication device — precoded signals
[FOA-A-53001-H2] 18 p3091 N85-29131
US Coast Guard High Frequency Emergency Network (HFEN) implementation plan
[PB85-174167] 18 p3092 N85-29141
Time transfer techniques: Historical overview, current practices and future capabilities
18 p3108 N85-29245
Transmission Monitoring and Control (TRAMCON) segmentation plan for the DCS (Defense Communications System) digital transmission network
[AD-A154175] 20 p3440 N85-31351
Design of a jamming simulator for a binary communication system
[AD-A154617] 21 p3573 N85-32221
Globally-asynchronous locally-synchronous systems
[AD-A154624] 21 p3573 N85-32222
COMMUNICATION NETWORKS
Broadband local distribution networks: Problems and prospects in Italy
[FUB-18-1983] 01 p0040 N85-10255
Voice communication handling in X 25 packet switching networks
[FUB-30-1983] 01 p0040 N85-10260
Availability of transmission systems in continental and intercontinental connections — telecommunication
[FUB-33-1983] 01 p0040 N85-10261
Reserve and authentication in Integrated Services Distributed Networks (ISDN) networks
[FUB-37-1983] 01 p0041 N85-10262
Communications protocols for a fault tolerant, integrated local area network for Space Station applications
[NASA-TM-86304] 01 p0106 N85-10711
Agribusiness and space: No limits to growth
02 p0152 N85-11029
Pluribus satellite IMP (Interface Message Provision) development mobile access terminal network
[AD-A145348] 02 p0190 N85-11269
Distributed hypothesis testing in distributed sensor networks
[AD-A145434] 02 p0294 N85-11905
Wideband integrated voice/data technology
[AD-A146054] 03 p0355 N85-12283
Distributed sensor networks
[AD-A146209] 03 p0355 N85-12286
DCS (Defense Communications System) network synchronization design criteria
[AD-A146251] 03 p0356 N85-12289
The design and performance analysis of an arbiter for a multi-processor shared-memory system
[AD-A146074] 03 p0403 N85-12566
Computer center introductory reference manual for CDC CYBER
[AD-A145796] 03 p0406 N85-12593
Ongoing activities in the field of communication at DFVLR 04 p0459 N85-12913
The application of queueing theory to communications networks: A review
[AD-A146660] 04 p0492 N85-13140
The Telecom 1 satellite telecommunication system
04 p0493 N85-13147
APOLLO system requirements specification — electronic document delivery
[ESA-SP-1068] 04 p0494 N85-13150
Test experience on an ultrareliable computer communication network
[NASA-TM-85915] 04 p0552 N85-13514
Implementation assessment of a network service. The test responder exerciser specification
[NPL-DITC-44/84] 05 p0716 N85-14594
The transient behavior of networks with infinite server nodes
[CWI-OS-R8408] 05 p0722 N85-14640
Problems of development of space communication
06 p0793 N85-15067
Hardwire missile receiver coupler
[AD-D011350] 07 p0937 N85-15936
Distributed reservation-based code division multiple access
[AD-A147007] 07 p0940 N85-15957
Synoptic observations of the radio noise background in the frequency range 150-180 kHz to provide design data for the low frequency communications designer
[AD-A147438] 07 p0941 N85-15965
Shuttle S-band communications technical concepts
08 p1099 N85-16948
The Communications link analysis and simulation system (CLASS) 08 p1100 N85-16952
Architecture for a demonstration radar-communication link
[AD-A147635] 08 p1150 N85-17260
Distributed sensor networks
[AD-A147638] 08 p1151 N85-17262
Extremely Low Frequency (ELF) Communications System Ecological Monitoring Program: Summary of 1983 progress
[AD-A147704] 08 p1151 N85-17265
Transmission scheduling to reduce convex delay costs in packet networks
[AD-A148451] 08 p1153 N85-17278
Performance evaluation and control of distributed computer communication networks
[AD-A148103] 08 p1208 N85-17556
DDN directory
[AD-A148213] 08 p1230 N85-17744
Voice data processing in packet switching modes
[FUB-44-1983] 09 p1312 N85-18248
Analysis of the performance of multiaccess networks of the bus type
[FUB-47-1983] 09 p1313 N85-18249
Dissemination of ERS-1 low bit rate data and the use of L-band receiving stations
[NLR-TR-83049-U] 09 p1358 N85-18542
Asymptotic analysis of Markovian access control computer communication networks
09 p1372 N85-18619
An ultra reliable computer communication network: The dispersed sensor processing mesh
09 p1372 N85-18620
Survivable local area network
[AD-D011453] 10 p1468 N85-19262
Commentary on start of scientific data transmissions with USSR 10 p1476 N85-19319
Selected NBSNET software
[PB85-109148] 10 p1542 N85-19723
Process algebra with asynchronous communication mechanisms
[CWI-CS-R8410] 11 p1625 N85-20235
Communications software for Olympics Micromation Computer System
[PB85-109510] 11 p1704 N85-20723
Minimization of system vulnerability in Naval satellite communication networks 11 p1710 N85-20758
Defense Meteorological Satellite Program (DMSP)
11 p1711 N85-20766
Base communications issues for the 1980s
[AD-A149764] 12 p1828 N85-21474

Space Shuttle interactive meteorological data system study
[NASA-CR-171418] 12 p1692 N85-21876
System dynamics and network control
[AD-A149420] 13 p2054 N85-22863
Integrated digital networks
[AD-A150605] 13 p2056 N85-22873
Satellite channels in packet-switching networks 13 p2067 N85-22909
Satellite bridges in communications networks 13 p2067 N85-22910
Introduction to the Space Physics Analysis Network (SPAN)
[NASA-TM-86499] 14 p2290 N85-24196
Research needs for artificial intelligence applications in support of C3 (Command, Control, and Communication)
[AD-A150867] 14 p2292 N85-24210
Data-link alternatives for the NASA pilot data systems
[NASA-TM-85999] 14 p2412 N85-24873
Survey of developments in tropospheric communication apparatus 15 p2528 N85-25587
Pluribus Satellite IMP (Interface Message Provision) development mobile access terminal network
[AD-A151312] 15 p2542 N85-25692
Evaluating computer-communication networks with simulation techniques
[AD-A151852] 15 p2632 N85-26222
Thin Route Project 15 p2687 N85-26596
Communications 15 p2687 N85-26600
Design and specification of a local area network architecture for use in real-time flight simulation
[AD-A152242] 16 p2716 N85-26762
Distributed control of circuits in multiuser communication networks with circuit precedence and path suitability criteria using failsafe routing concepts
[AD-A151825] 16 p2772 N85-27113
Evaluation of Ada (trademark) as a communications programming language, volume 1
[AD-A152314] 16 p2848 N85-27559
Evaluation of Ada (trademark) as a communications programming language. Volume 2: Communications protocols application
[AD-A152315] 16 p2848 N85-27560
Evaluation of Ada (trademark) as a communications programming language. Volume 3: Trusted software application
[AD-A152316] 16 p2848 N85-27561
A study of topologies and protocols for fiber optic local area network
[NASA-CR-175771] 16 p2864 N85-27669
Future information technology, 1984: Telecommunications
[NBS/SP-500/119] 16 p2878 N85-27762
Wideband integrated voice/data technology
[AD-A152329] 17 p2947 N85-28197
Logical design of a decision support system to forecast technology, prices and costs for the national communications system
[AD-A152330] 17 p2948 N85-28198
A real-time executive for multiple-computer clusters
[AD-A152961] 17 p3015 N85-28646
Reliability report for communication networks
[AD-A153764] 18 p3090 N85-29127
US Coast Guard High Frequency Emergency Network (HFEN) implementation plan
[PB85-174167] 18 p3092 N85-29141
Maser and secondary clock in telecommunications networks 18 p3108 N85-29246
High performance asynchronous limited sensing algorithms for CSMA and CSMA-CD channels
[AD-A153919] 18 p3171 N85-29650
LAN (Local Area Network) interoperability study of protocols needed for distributed command and control
[AD-A154033] 19 p3255 N85-30182
INMARSAT: An overview 20 p3400 N85-31091
Existing and potential INMARSAT capabilities for the Future Global Maritime Distress and Safety System 20 p3402 N85-31110
INMARSAT distress and safety communication 20 p3406 N85-31134
Future prospects for a combined INMARSAT polar communication and search and rescue satellite system 20 p3406 N85-31137
Scientific report of the Department of Systems and Communications
[ENST-84D002] 20 p3441 N85-31355
A comparison of millimeter wave, direct detect and heterodyne laser intersatellite links
[AD-A151964] 20 p3461 N85-31496
Routing algorithms and stochastic analysis for large communications networks
[AD-A154654] 21 p3573 N85-32225
Broadcasting topology and routing information in computer networks
[AD-A155668] 21 p3674 N85-32827
Assured information flow capping architecture
[AD-A155392] 22 p3756 N85-33283
Petcom: A software instrument for the analysis of Petri networks, oriented towards communication protocols
[FUB-50-1983] 22 p3756 N85-33286
Research on distributed artificial intelligence
[AD-A155356] 22 p3833 N85-33733
Performance interface document for the S-band diplexer for space users of NASA networks
[NASA-TM-86224] 23 p3900 N85-34155
A graphics interface for interactive simulation of packet-switched networks 23 p3962 N85-34558
Communication complexity of distributed shortest path algorithms
[AD-A156049] 24 p4087 N85-35332
A ray trace program for line-of-sight microwave communication links
[AD-A156168] 24 p4087 N85-35336

COMMUNICATION SATELLITES
NT AERONAUTICAL SATELLITES
NT COMMUNICATIONS TECHNOLOGY SATELLITE
NT EUROPEAN COMMUNICATIONS SATELLITE
NT INTELSAT SATELLITES
NT L-SAT
NT SYMPHONIE SATELLITES

The Telecom 1 satellite telecommunication system 04 p0493 N85-13147
Space power for communication satellites beyond 1995 05 p0606 N85-13883
Evaluating NASA technology programs in terms of private sector impacts 05 p0608 N85-13885
Offset unfurlable antenna concepts 05 p0625 N85-14002
Technology and performances of structural thermal mechanical equipment used for antenna of TV.SAT-TDF 1 program 05 p0626 N85-14012
Demand for satellite-provided domestic communications services up to the year 2000
[NASA-TM-86894] 06 p0798 N85-15099
US objectives generally achieved at broadcasting satellite international conference. Improvements can help in future conferences
[PB84-235316] 06 p0800 N85-15109
NOAA (National Oceanic and Atmospheric Administration) Aircraft Satellite Data Link (ASDL)
[PB84-243773] 07 p0942 N85-15976
A modified Monte-Carlo technique for the simulation of satellite communication systems
[AD-A148669] 08 p1214 N85-17641
Propagation measurements for land-mobile satellite services in the 800 MHz band
[CRC-TN-724] 09 p1310 N85-18231
Propagation measurements for land-mobile satellite systems at 1541 MHz
[CRC-TN-723] 09 p1310 N85-18232
Star on the horizon: The emergence of the direct broadcast satellite in American mass communications
[AD-A148819] 09 p1312 N85-18242
Technical evaluation report on the 46th Symposium of the Avionics Panel on Space System Applications to Tactical Operations
[AGARD-AR-203] 10 p1425 N85-18986
Commercial space: Europe should have independent strategy 10 p1460 N85-19205
Worldwide report: Telecommunications policy, research and development
[JPRS-TTP-85-002] 10 p1475 N85-19309
Traveling wave tube for broadcast satellites 10 p1475 N85-19310
Worldwide report: Telecommunications policy, research and development
[JPRS-TTP-85-006] 10 p1476 N85-19314
NTT unveils satellite communications equipment 10 p1476 N85-19315
Ex-minister urges communications satellite development 10 p1476 N85-19316
Communications satellite needs examined 10 p1476 N85-19317
MATRA has Europe's largest white room for satellites 10 p1477 N85-19320
US MILSATCOM: Present and future 11 p1709 N85-20753
Tactical military communications by satellite relay at high latitudes 11 p1709 N85-20756
The Ferranti Tactical SHF SATCOM station (MANSAT) 11 p1710 N85-20759
The international environment UNISPACE '82 and the ITU: A relationship between orbit-spectrum resource allocation and orbital debris 12 p1787 N85-21215
Transmission and orbital constraints in space-related programs: Briefing summary 12 p1787 N85-21216
Engineering calculations for communications satellite systems planning
[NASA-CR-175552] 12 p1789 N85-21233
Radioelectronics and space exploration 12 p1838 N85-21533
Satellite communications and amateur radio 12 p1838 N85-21534
NASA mobile satellite program 14 p2229 N85-23814
Alternatives for satellite sound broadcast systems at HF and VHF 14 p2229 N85-23815
Damping models for flexible communications satellites by substructural damping synthesis
[UTIAS-287] 14 p2237 N85-23868
Spatial acquisition algorithms and systems for intersatellite optical communication links
[AD-A150794] 14 p2292 N85-24207
Satellite reception of reentry vehicle telemetry
[AD-A151851] 15 p2492 N85-25372
Frequency selection for dispersion signal in satellite communication lines 15 p2528 N85-25584
Preliminary estimation of mutual interference between fixed satellite service systems 15 p2528 N85-25586
Trade-off between land vehicle antenna cost and gain for satellite mobile communications
[NASA-CR-175732] 15 p2540 N85-25681
Measurement results from a balloon experiment simulating land mobile satellite transmissions
[NASA-CR-175740] 15 p2540 N85-25683
Pluribus Satellite IMP (Interface Message Provision) development mobile access terminal network
[AD-A151201] 15 p2541 N85-25688
Pluribus Satellite IMP (Interface Message Provision) development mobile access terminal network
[AD-A151312] 15 p2542 N85-25692
Lack of communication 15 p2686 N85-26591
Thin Route Project 15 p2687 N85-26596
Communications 15 p2687 N85-26600
Satellite provided customer promises services, a forecast of potential domestic demand through the year 2000. Volume 4: Sensitivity analysis
[NASA-CR-174662] 16 p2769 N85-27092
FAA (Federal aviation administration) assessment of satellite concepts and aviation spectrum requirements
[AD-A152338] 17 p2948 N85-28199
Spread spectrum time transfer experiment via INTELSAT 17 p2964 N85-28304
Channel multiplexers for broadcast satellite transponders in the 12 GHz band
[NHK-LABS-NOTE-310] 18 p3090 N85-29122
International space research perspectives of commercialization for German industry
[NASA-TM-77657] 19 p3222 N85-29979
Design and evaluation of control systems for large communications satellites 20 p3409 N85-31157
Analysis of beam interaction of the electrical thruster RIT 10 (particle emission) with surfaces
[ESA-TT-826] 20 p3421 N85-31231
Combined trellis coding with asymmetric MPSK modulation: An MSAT-X report
[NASA-CR-176039] 20 p3440 N85-31347
A comparison of millimeter wave, direct detect and heterodyne laser intersatellite links
[AD-A151964] 20 p3461 N85-31496
A model for predicting propagation-related DSCS (Defense Communications Engineering Center) margin requirements
[AD-A155355] 22 p3756 N85-33281
International prototype network in Dubna experimental satellite communications system 22 p3773 N85-33383
Telecommunications forecast for ITU Region 2 to the year 1995
[NASA-TM-87077] 23 p3899 N85-34150
Spacecraft (Mobile Satellite) configuration design study
[NASA-CR-176153] 23 p3899 N85-34152
Satellites and politics: Weather, communications, and earth resources 23 p4057 N85-35144
Second-generation mobile satellite system. A conceptual design and trade-off study
[NASA-CR-176195] 24 p4086 N85-35325

COMMUNICATION SYSTEMS
U TELECOMMUNICATION

COMMUNICATION THEORY
NT WORDS (LANGUAGE)

Research activities of the Illinois University Coordinated Science Laboratory
[AD-A145589] 03 p0449 N85-12856
Knowledge-based communication and management support in a system development environment 05 p0717 N85-14596
Process algebra for communication and mutual excitation
[CWI-CS-R8409] 05 p0720 N85-14622
Process algebra with asynchronous communication mechanisms
[CWI-CS-R8410] 11 p1625 N85-20235
The study of certain aspects of probability with applications in communications theory
[AD-A149820] 12 p1829 N85-21476

Algebra of communicating processes
[CWI-CS-R8421] 17 p2950 N85-28214
Expressiveness and language choice
[AD-A153280] 17 p3012 N85-28623
COMMUNICATIONS TECHNOLOGY SATELLITE
Damping synthesis for a spacecraft using substructure and component data
[CRC-1365] 03 p0323 N85-12082
COMMUNITIES
Test of dispersal of turbojet aircraft departure tracks at washington National Airport (1983-84), volume 1 report
[AD-A148111] 08 p1218 N85-17669
Air quality benefit analysis for Los Angeles and San Francisco based on housing values and visibility
[PB85-166049] 16 p2822 N85-27409
COMMUTATION
Finite products of commutators in C* algebras 11 p1696 N85-20676
Positioning errors of commutating lenses and their influence on characteristics of high speed movie cameras 14 p2273 N85-24085
COMMUTATORS
Summator of radio pulse signals 12 p1839 N85-21539
Brush and commutator segment torquer motor
[AD-D011726] 23 p3927 N85-34340
COMPACTING
Solid-phase sintering of tantalum carbide
[BLL-M-36013-(5828.4)] 07 p0926 N85-15872
No-slump Roller-Compacted Concrete (RCC) for use in mass concrete construction
[AD-A148564] 08 p1138 N85-17164
Traction forces of drive tyre on the compacted soil
[AD-P004264] 09 p1404 N85-18840
Quality control in soil compaction by behaviours of exciter
[AD-P004295] 09 p1408 N85-18872
Compaction of sand using ordinary off-road vehicles
[AD-P004297] 09 p1409 N85-18874
Flotation tires and subsurface compaction
[AD-P004299] 09 p1409 N85-18876
Tractor power selection with compaction constraints
[AD-P004300] 09 p1409 N85-18877
Dynamic compaction of powders
[DE85-001062] 11 p1612 N85-20137
Pressure-density behavior for AlN, Al2O3, SiO2, TiB2, and TiC powders up to 3.5 GPa
[DE85-006146] 14 p2261 N85-24012
Rapid solidification of candidate ferritic steels
[DE85-006596] 16 p2750 N85-26971
Ac field-induced order in dense colloidal systems
[DE85-009107] 17 p2935 N85-28119
Hot Isostatic Pressing (HIP): Techniques, applications and economical use
[JUEL-SPEZ-288] 17 p2939 N85-28141
Feasibility of melt casting strontium fluoride to produce high-density heat sources
[DE85-009429] 18 p3130 N85-29381
Deep-burial diagenesis in carbonates
[DE85-011224] 22 p3902 N85-33554
Dynamic compaction of a monosized spherical tungsten powder
[DE85-014808] 24 p4060 N85-35289
Computational methods for the explosive and impact compaction of powders
[AD-A156219] 24 p4139 N85-35653
COMPACTNESS
U VOID RATIO
COMPANDING
Digital sound: Programme-modulated noise levels in sound signals subjected to a number of digital companding processes
[BBC-RD-1984/11] 09 p1310 N85-18233
Controllable companding in low-frequency FM radio communication systems 22 p3776 N85-33402
COMPANION STARS
Search for white dwarf companions of cool stars with peculiar element abundances
[NASA-CR-174030] 02 p0297 N85-11923
Evidence for a solar companion star
[DE85-002069] 10 p1571 N85-19907
A search for white-dwarf companions of subgiant CH stars 11 p1752 N85-21019
The white dwarf companion of the mild BA star Xi1 Cet 11 p1752 N85-21020
The outburst and long term behavior of the triple period cataclysmic variable TV Col 11 p1752 N85-21021
Blue companions of Cepheids 11 p1754 N85-21033
Comet showers and Nemesis, the death star
[DE85-003736] 15 p2683 N85-26575
COMPARATOR CIRCUITS
Qualification of a thick film hybrid
[BMFT-FB-W-84-024] 04 p0497 N85-13170
COMPARATORS
Comparator with noise suppression
[NASA-CASE-LAR-13151-1] 11 p1627 N85-20247
MHB4046 phase-lock circuit 15 p2533 N85-25629
COMPARISON
Observations of four Beta Cephei stars in NGC6231 01 p0128 N85-10877
Atmospheric and pressurized low speed wind tunnel performance and cost comparisons
[ARL/AERO-R-160] 02 p0149 N85-11008
Comparison of the multigrid and ICCG methods in solving the diffusion equation
[DE84-014409] 02 p0253 N85-11657
A comparison of methods for predicting ductile crack growth instability
[AERE-R-11199] 03 p0374 N85-12387
Comparative energy storage assessment item 05 p0605 N85-13858
Evaluation and results of national and international intercomparison measurements — electromagnetic measurement 05 p0631 N85-14043
Comparison of optimum interpolation and Cressman analyses 05 p0660 N85-14371
Comparison of uniform perturbation solutions and numerical solutions for some potential flows past slender bodies
[NASA-CR-172485] 06 p0749 N85-14799
Analysis of the flow field about a T-45 using PANAIR
[AD-A146811] 07 p0899 N85-15699
Comparison measurements on optical particle counters
[BLL-DOUNREAY-TR-934-(9091.9F)] 07 p0961 N85-16092
Comparative investigation of three commercial radiocrde systems
[KNMI-TR-53] 07 p1009 N85-16409
Can the Aggressors continue to be effective in the F-5E?
[AD-A146861] 07 p1019 N85-16485
A computer package for ranking, selection and multiple comparisons with the best
[AD-A147617] 08 p1204 N85-17579
Models for mixture experiments when the response depends on the total amount
[DE85-000370] 09 p1374 N85-18637
Comparison of methods for predicting fiber stresses in a cracked Kevlar/epoxy monolayer
[DE84-016118] 11 p1593 N85-20022
Cost comparison of small gas turbines versus electric motors in a variable load industrial application
[PB85-149763] 12 p1837 N85-21530
A diffusion process and its application to detecting a change in the drift of Brownian motion
[AD-A150096] 12 p1926 N85-22100
Optimal designs for comparisons between two sets of treatments
[AD-A150821] 13 p2152 N85-23360
Costs, payload of Ariane, US Space Shuttle compared 15 p2530 N85-25601
Self-scanning MDS-integrated photosensor strip 17 p2940 N85-28151
Generic data entry quality assurance tool
[DE85-008359] 18 p3200 N85-29852
Inherent angular tracking error in an amplitude comparison monopulse radar
[AD-A154212] 19 p3255 N85-30185
Comparison of 8 to 12 micrometer and 3 to 5 micrometer CVF transmissometer data with LOWTRAN calculations
[AD-A154218] 19 p3350 N85-30763
Multiaxial fatigue low cycle fatigue testing 20 p3468 N85-31544
Fuel cell applications literature review
[DE85-011891] 22 p3809 N85-33592
Large-scale sea surface temperature variability from satellite and shipboard measurements
[NASA-CR-176123] 22 p3818 N85-33651
Comparison of experimental data on detonation velocity and Chapman-Jouget pressure vs initial HE density with predictions from Ree's model equation of state
[DE85-007266] 23 p3922 N85-34304
COMPARTMENTATION
U COMPARTMENTS
COMPARTMENTS
NT AIR LOCKS
NT AIRCRAFT COMPARTMENTS
NT ANECHOIC CHAMBERS
NT HYPERBARIC CHAMBERS
NT PRESSURE CHAMBERS
NT PRESSURIZED CABINS
NT SPACECRAFT CABINS
NT TEST CHAMBERS
NT VACUUM CHAMBERS
The distribution of the number of empty cells in a generalized random allocation scheme
[AD-A154806] 21 p3677 N85-32841
COMPASSES
NT GYROCOMPASSES
NT MAGNETIC COMPASSES
Determining an azimuth with a north seeking gyro
[AD-A155880] 24 p4063 N85-35180
COMPATIBILITY
NT ELECTROMAGNETIC COMPATIBILITY
NT SYSTEMS COMPATIBILITY
Anthropometric cockpit compatibility assessment of US Army aircraft for large and small personnel wearing A cold weather, armored vest, chemical defense protective clothing configuration
[AD-A145472] 02 p0238 N85-11547
Official journey to USA, November 1983. Symposium on the Compatibility of Explosives; Mound Laboratory; Naval Surface Weapons Center
[FOA-C-20548-D1] 04 p0482 N85-13072
Metallographic evaluation of the reactions between boronated graphite and Fe-Ni-Cr alloys
[DE84-015374] 06 p0769 N85-14922
Deuterium isotope effect on the compatibility between polystyrene and polybutadiene
[AD-A148551] 08 p1134 N85-17145
Implementation of an Intel 8086 microprocessor-based realization library for the control system design language
[AD-A148506] 08 p1202 N85-17569
Quantitative estimate of compatibility of fiber composite material components 10 p1444 N85-19099
High-temperature X-ray diffraction study of coating-substrate compatibility in yttria-coated graphite
[DE85-005916] 14 p2262 N85-24016
Deployable Core Automated Maintenance System (DCAMS)
[AD-A153695] 18 p3198 N85-29839
Compatibility, contamination and IR microspectrophotometry
[DE85-010809] 19 p3273 N85-30297
A study of the effect of a mismatch in gamma and gamma prime phase lattice spacings on the high temperature strength characteristics of dispersion-hardened nickel alloys
[BLL-CE-TRANS-6048-(9022.09)] 20 p3430 N85-31279
Determination of instrument errors by compatibility checking: Results from dynamic flight test data
[ARL/AERO-R-162] 23 p3896 N85-34137
Parallel processing on the Livermore VAX 11/780-4 parallel processor system with compatability to Cray Research, Inc. (CRI) multitasking, version 1
[DE85-011856] 23 p3967 N85-34595
COMPENSATORS
Robust rate control system designs for a submersible
[AD-A144792] 01 p0111 N85-10753
Tracking servo compensator with rate aiding
[AD-D011372] 07 p0942 N85-15971
Dynamic polymer pressure transducer with temperature compensation
[AD-D011373] 07 p0967 N85-16142
Multivariable flight control with time-scale separation
[NASA-CR-174320] 08 p1087 N85-16873
Compensator development and examination of performance and robustness
[NASA-CR-175470] 11 p1627 N85-20244
Dynamic visual servo control of robots: An adaptive image-based approach
[AD-A150057] 12 p1860 N85-21667
Efficiency of digital compensator of strong non-Gaussian interference 13 p2072 N85-22942
Aberration characteristics of plane-parallel compensator plate 14 p2276 N85-24100
Compensator development and examination of performance and robustness
[NASA-CR-175703] 15 p2540 N85-25678
Flight control system reconfiguration design using quantitative feedback theory
[AD-A151771] 16 p2710 N85-26722
Principles of designing digital compensating accelerometers 17 p2944 N85-28172
Interactive computer program for the analysis and design of linear time invariant systems
[AD-A154078] 19 p3335 N85-30664
Approximation of optimal infinite dimensional compensators for flexible structures 20 p3413 N85-31181
Control of a flexible space antenna: A finite dimensional perspective based on distributed parameter theory 20 p3413 N85-31182
Selectivity of weight compensator of passive interference to unknown velocities of detectable targets 22 p3762 N85-33317
Magnetic field and equivalent circuit of induction motors with shielded poles 22 p3772 N85-33378
Design of dynamic compensators of prescribed pattern
[BU-109] 24 p4142 N85-35674

COMPETITION
An analysis of production competition and award methodology
[AD-A147775] 06 p1226 N85-17733
International cooperation and competition in civilian space activities
[OTA-ISC-240] 06 p1231 N85-17750
Competitive assessment of the US manufacturing automation equipment industries
[PB85-103927] 10 p1569 N85-19693
COMPILATION (COMPUTERS)
U COMPILERS
COMPILER PROGRAMS
U COMPILERS
COMPILERS
THLL (TRIDENT Higher Level Language) reference manual
[AD-A145116] 01 p0104 N85-10696
PASCAL-MP algebraic and numerical manipulator for polynomials
[INPE-3229-TDL/176] 02 p0240 N85-11562
SMILE user's guide: A macro preprocessor for extending FORTRAN
[DE84-015984] 02 p0243 N85-11584
Application of a silicon compiler to VLSI (Very Large Scale Integrated circuits) design of digital pipelined multipliers
[AD-A146328] 03 p0403 N85-12569
Digital equipment Corporation, professional 350, COBOL-81 Version 2.1
[PB84-227602] 03 p0403 N85-12572
Digital Equipment Corporation, Professional 350, COBOL-81 Version 2.1 (COBOL technical report)
[PB84-227719] 03 p0403 N85-12573
Northern Telecom, Incorporated, NTI-585/565, ACOBOL/3 Release 4.1 Version H(01)
[PB84-228022] 03 p0404 N85-12574
Northern Telecom, Incorporated NTI-585/565, ACOBOL/3 Release 4.1 Version H(01) (COBOL technical report)
[PB84-228030] 03 p0404 N85-12575
Digital Equipment Corporation, DECSYSTEM-10, model 1090-SMP, COBOL-74 V12B
[PB84-227941] 03 p0404 N85-12576
Data General Corporation, Eclipse C350, AOS COBOL Release 3.51
[PB84-227883] 03 p0404 N85-12577
Convergent Technologies, NGEN CP001, CT COBOL version 9.0
[PB84-227784] 03 p0404 N85-12578
Convergent Technologies, mega frame CTIX BASIC interpreter version 1.03
[PB84-227776] 03 p0404 N85-12579
Convergent Technologies, mega frame, CTIX FORTRAN 77 version 2.1
[PB84-227768] 03 p0404 N85-12580
Convergent Technologies, mega frame, CTIX COBOL version 2.0
[PB84-227750] 03 p0404 N85-12581
Digital Equipment Corp., VAX-11/782, VAX FORTRAN version 4.0
[PB84-227701] 03 p0405 N85-12582
Digital Equipment Corp., VAX/750, VAX COBOL version 3.0
[PB84-227693] 03 p0405 N85-12583
IBM Corporation, IBM 5381 model 5, system/36 COBOL release 6
[PB84-227677] 03 p0405 N85-12584
Gould Incorporated, GOULD Concept 32/87, COBOL release 1.4
[PB84-227669] 04 p0548 N85-13484
Digital Equipment Corp., VAX/750, VAX COBOL version 3.0
[PB84-227651] 04 p0548 N85-13485
Digital Equipment Corp., MICRO/PDP-11, COBOL-81 version 2.2
[PB84-227644] 04 p0548 N85-13486
Prime Computer, Inc., PRIME 750, FORTRAN-77 revision 19.4
[PB84-227628] 04 p0548 N85-13487
C3, Incorporated, C50 System, C3 COBOL/75 version 2.00
[PB84-228006] 04 p0548 N85-13488
Burroughs Corporation B26-CPU, B20 COBOL, Release 4.0
[PB84-216241] 04 p0551 N85-13505
Burroughs Corporation B26-CPU, B20 COBOL Version 4.0 (COBOL technical report)
[PB84-216258] 04 p0551 N85-13506
Convergent technologies NGEN CP001, CT COBOL Version 9.0
[PB84-216266] 04 p0551 N85-13507
Convergent Technologies, Incorporated, NGEN CP001, CT COBOL Version 9.0 (COBOL technical report)
[PB84-216274] 04 p0551 N85-13508
Computer Sciences Corporation UNIVAC 1100/80, CSTS COBOL Release COB250
[PB84-216282] 04 p0551 N85-13509
Control Data Corporation CYBER 205 model 442, FORTRAN 200 (G201-25)
[PB84-216290] 04 p0551 N85-13510
C3, Incorporated NGEN CP001, COBOL Version 9.0
[PB84-216308] 04 p0552 N85-13511
United Information Services, Inc., CRAY 1-S/2000, FORTRAN CFT 1.10
[PB84-227685] 04 p0552 N85-13512
Datapoint Corporation Datapoint 6600, 8600, DOS COBOL Version 3.6
[PB84-242973] 04 p0552 N85-13513
Northern Telecom, Inc., IBM 3033 (compilation), NTI-585/565 (execution), XCOBOL, release 4.1, version H(01) (COBOL technical report)
[PB84-228048] 05 p0714 N85-14578
NECIS Incorporated, NEC ASTRA model 270, COBOL 74 version 8.3 (COBOL technical report)
[PB84-227933] 06 p0848 N85-15381
Digital Research Incorporated, IBM PC XT, FORTRAN-77 V4.0
[PB84-243633] 06 p0849 N85-15388
Perkin-Elmer, Perkin-Elmer 3230, FORTRAN 7 D R00-00
[PB84-243682] 06 p0849 N85-15389
Gould Incorporated, Gould PS-3000, Gould PS-3000 FORTRAN 77 V2.1
[PB84-229178] 06 p0849 N85-15390
Data general Corporation, Eclipse C150, interactive COBOL Revision 1.30 (COBOL technical report)
[PB84-227834] 06 p0849 N85-15391
Data General Corporation, Eclipse C150, interactive COBOL Revision 1.30
[PB84-227891] 06 p0849 N85-15392
IBM Corporation, IBM Series/1 4955, IBM Series/1 host COBOL Release 1.1 EDX (COBOL technical report)
[PB84-227909] 06 p0849 N85-15393
IBM Corporation, IBM Series/1 4955, IBM Series/1 host COBOL Release 1.1 EDX
[PB84-227818] 06 p0849 N85-15394
IBM Corporation, IBM Series/1 4955, IBM Series/1 host COBOL Release 1.1 RPS
[PB84-227917] 06 p0850 N85-15395
IBM Corporation, IBM Series/1 4955, IBM Series/1 host COBOL Release 1.1 RPS (COBOL technical report)
[PB84-227925] 06 p0850 N85-15396
NECIS, Incorporated, NEC ASTRA model 270 COBOL 74 Version 8.3
[PB84-227636] 06 p0850 N85-15397
Digital Equipment Corporation, DECSYSTEM-20, model 2060, COBOL V13
[PB84-227958] 06 p0850 N85-15398
Digital Equipment Corporation, DECSYSTEM-20, model 2080, COBOL V13 (COBOL technical report)
[PB84-227966] 06 p0850 N85-15399
Northern Telecom, Incorporated, IBM 3033 (compilation), NTI-585/565 (execution), XCOBOL Release 4.1 Version H(01)
[PB84-227875] 06 p0850 N85-15400
NCR Corporation, NCR I9300, NCR ITX Cobol Release 3.0
[PB84-228055] 06 p0850 N85-15401
NCR Corporation, NCR I9300, NCR ITX COBOL Release 3.0 (COBOL technical report)
[PB84-228063] 06 p0850 N85-15402
Gould Incorporated, Gould PS-3000, Gould PS-3000 COBOL V2.0
[PB84-229160] 06 p0850 N85-15403
Gould Incorporated, Gould PS-3000, Gould PS-3000 BASIC Interpreter Version 1.00
[PB84-229186] 06 p0851 N85-15404
Digital Equipment Corporation, PDP-11/23-PLUS PDP-11 FORTRAN-77 V5.0
[PB84-227610] 06 p0851 N85-15405
Computervision Corporation, CDS-4000 32-Bit processor, CV FORTRAN Version 2.84
[PB84-227867] 06 p0851 N85-15406
Plexus Computers, Inc., Plexus P/60, Plexus FORTRAN 77 Version 1.1
[PB84-227859] 06 p0851 N85-15407
Control Data Corporation, CYBER 835, COBOL Release 5.3 Level 614
[PB84-227842] 06 p0851 N85-15408
Prime Computer, Inc., PRIME 750, COBOL-74 Revision 19.3.2
[PB84-227826] 06 p0851 N85-15409
Sperry Univac, System 80 Model 6, OS/3 COBOL, Version 08.00/08
[PB84-227800] 06 p0851 N85-15410
Modular Computer Systems, Incorporated, MODCOMP CLASSIC 7860, MODCOMP FORTRAN 77/16 Version A.0
[PB84-230556] 06 p0852 N85-15411
Modular Computer Systems, Incorporated, MODCOMP CLASSIC 7860, MODCOMP NASA EXTENDED FORTRAN 78 Version A.40
[PB84-230549] 06 p0852 N85-15412
Digital Equipment Corporation, MICRO/PDP-11, COBOL-81 Version 2.2
[PB84-229236] 06 p0852 N85-15413
NCR Corporation, NCR 9300, NCR ITX-BASIC Release 2.0
[PB84-229228] 06 p0852 N85-15414
Sperry Corporation, 1100/80, UBASIC/BBASIC Level 9R1
[PB84-229202] 06 p0852 N85-15415
Sperry Corporation, 1100/80 ASC2 FORTRAN Level 11R1
[PB84-229194] 06 p0852 N85-15416
Computer Sciences Corporation, UNIVAC 1100/80, CSTS COBOL Release COB250
[PB84-229154] 06 p0852 N85-15417
Compter Sciences Corporation, UNIVAC 1100/80, CSTS BASIC Release BAS180
[PB84-229145] 06 p0852 N85-15418
Wang Laboratories, Incorporated, Wang VS100, FORTRAN 77 Version 01.00.02
[PB84-228014] 06 p0852 N85-15419
Control Data Corporation, Cyber 835, BASIC Release 3.5 Level 614
[PB84-227990] 06 p0853 N85-15420
Data General Corporation, Eclipse C350, AOS COBOL Release 3.51
[PB84-227982] 06 p0853 N85-15421
Digital Equipment Corporation, DECSYSTEM-20 2060 Model B, FORTRAN-20 Version 10
[PB84-227974] 06 p0853 N85-15422
Specialized silicon compilers for language recognition
[AD-A146526] 06 p0853 N85-15425
C3, Incorporated NGEN CP001, C3 COBOL Version 9.0 (COBOL Technical Report)
[PB84-216316] 06 p0855 N85-15435
Burroughs Corporation B26-CPU, Burroughs B20 BASIC Rel. 4.0
[PB84-216324] 06 p0855 N85-15436
Convergent Technologies NGEN CP001, CT BASIC Version 9.0
[PB84-216332] 06 p0855 N85-15437
Convergent Technologies, NGEN CP001, CT FORTRAN Version 9.0
[PB84-229210] 06 p0856 N85-15442
Microsoft Corporation, Sun Microsystems, Microsoft COBOL Version 2.0
[PB84-243401] 06 p0856 N85-15443
Microsoft Corporation, IBM PC XT, Microsoft COBOL, Version 2.0
[PB84-243419] 06 p0856 N85-15444
Research on introspective systems
[AD-A146406] 06 p0870 N85-15530
Ada compiler validation summary report: New York University (NYU Ada/Ed) compiler, version 1.4 for VAX 11/780, using VMS 3.5
[AD-A146924] 07 p1022 N85-16483
Ada compiler validation summary report: TeleSoft (TeleSoft Ada) compiler, version 2.0a for Sun 120 Motorola M68010, using 4.2 BSD UNIX-Sun Version 1.1
[AD-A146925] 07 p1022 N85-16484
NYU Ada/Ed user's guide: Version 1.4 for VAX/VMS systems
[AD-A146759] 07 p1024 N85-16495
Ada compiler validation summary report: TeleSoft (TeleSoft Ada) compiler, version 2.0a2 for Callan Unistar 300, using System V, version 4.1a
[AD-A147115] 07 p1025 N85-16505
The production of maintainable, trustworthy, and portable software 08 p1064 N85-16744
FLAD user's manual: FLAD file contents
[AD-A148700] 09 p1368 N85-18594
Digital Equipment Corporation VAX Ada Compiler Version T0.6-2 VAX-11/785, 11/750, 11/730, using VMS, Version 4.0 and MicroVAX 1, using MicroVMS Version 1.0
[AD-A149375] 10 p1538 N85-19696
Ada in mission critical system acquisition: A guidebook
[AD-A149271] 10 p1540 N85-19710
Four Phase Systems, Incorporated, Four Phase Series 5000, COBOL 1974 version BE08.8
[PB85-108017] 10 p1541 N85-19717
Four Phase Systems, Incorporated, Mini-Frame Series 6300, COBOL Series 6000
[PB85-108025] 10 p1541 N85-19718
Micro focus DEC Rainbow 100 + compact level 2 COBOL; V2.5
[PB85-108975] 10 p1542 N85-19719
Micro focus DEC Rainbow 100 + high performance level 2 COBOL; V2.5
[PB85-108983] 10 p1542 N85-19720

DTSS, Incorporated, DPS 8/44, DTSS COBOL Release 12
[PB85-108058] 10 p1542 N85-19721
Sperry Univac System 80, Model 6, OS/3 BASIC, Version 10.01
[PB85-108066] 10 p1542 N85-19722
Ada compiler validation summary report, Dansk Datamatik Center, VAX 11 compiler version 1.1
[AD-A149340] 11 p1699 N85-20681
Micro Focus, Intel Microprocessor Development System MDS221 CIS COBOL; V4.5
[PB85-110823] 11 p1699 N85-20682
Prime Computer, Incorporated, PRIME 750, BASICV revision 19.4
[PB85-108074] 11 p1699 N85-20683
Validation Summary Report (VSR), Ryan-McFarland Corporation, AT and T 385, RM/COBOL Version 2.0
[PB85-102093] 11 p1703 N85-20709
Burroughs Corporation, Burroughs B3955 COBOL9 Version 6.8
[PB85-103110] 11 p1703 N85-20710
Burroughs Corporation, Burroughs B3955 FORT77 Version 6.8
[PB85-110328] 11 p1703 N85-20711
Micro Focus Plessy Micro Systems 68/50 Compact Level 2 COBOL; V2.5
[PB85-108934] 11 p1703 N85-20712
Micro Focus Plessy Micro Systems 68/50 High Performance Level 2 Cobol; V2.5
[PB85-108942] 11 p1703 N85-20713
Micro focus Cifer 2687 high performance level 2 COBOL; V2.5
[PB85-108959] 11 p1703 N85-20714
Micro focus Cifer 2687 compact level 2 COBOL; V2.5
[PB85-108967] 11 p1703 N85-20715
Micro Focus IBM personal computer XT Compact Level 2 COBOL; V2.5
[PB85-108918] 11 p1703 N85-20716
Micro Focus IBM personal computer XT High Performance Level 2 COBOL; V2.5
[PB85-108926] 11 p1704 N85-20717
Micro focus Fortune 32:16 compact level 2 COBOL; V2.5
[PB85-108884] 11 p1704 N85-20718
Micro focus Fortune 32:16 high performance level 2 COBOL; V2.5
[PB85-108892] 11 p1704 N85-20719
Micro Focus IBM personal computer XT CIS COBOL; V4.5
[PB85-108868] 11 p1704 N85-20720
ICL, ICL 2988 COBOL C2COB. 1321
[PB85-108876] 11 p1704 N85-20721
MICRO FOCUS Intel Microprocessor Development System MDS221 Compact Level 2 COBOL; V2.5
[PB85-108900] 11 p1704 N85-20722
Micro focus IBM personal computer XT, high performance level, 2 COBOL, IBM PC tailored; V2.6
[PB85-110815] 11 p1705 N85-20725
An algorithm for generating abstract syntax trees
[NASA-CR-172541] 12 p1912 N85-22003
A Gypsy-to-Ada program compiler
[TR-39] 12 p1913 N85-22005
Programs for dynamic loading of precompiled subroutine packages, especially for applications with the Watfiv compiler
[DFVLR-MITT-84-18] 12 p1917 N85-22035
Ryan-McFarland Corporation, IBM PC model XT, RM/FORTRAN, version 2.0.0
[PB85-107993] 12 p1917 N85-22037
Ryan-McFarland Corporation, sun microsystem with sky fast floating point processor, RM/FORTRAN version 1.5.0
[PB85-108009] 12 p1917 N85-22038
Validation summary report, Burroughs Corporation, B20 FORTRAN release 4.0
[PB84-227792] 13 p2145 N85-23316
Prada language environment: Distribution package description, revision 1
[DE85-008699] 15 p2630 N85-26212
Ada validation summary report. ALS AdaVAX version 1.1 VAX-11/780 using VAX/VMS release 3.6
[AD-A153684] 18 p3162 N85-29588
Ada (trademark) compiler validation summary report. Honeywell information systems GCOS6 Ada version 1.1
[AD-A153746] 18 p3162 N85-29590
Ada compiler validation summary report, University of Karlsruhe-GMD/German MOD Siemens - BS 2000 version 7.30
[AD-A153747] 18 p3163 N85-29591
Ada (trademark) compiler validation summary report: ALSYS ALSYCOMP-0001
[AD-A153750] 18 p3163 N85-29592
Development and analysis of a global compaction technique of microprograms 19 p3334 N85-30654
BP (Basic Processor) TRICOMP user's guide
[AD-A154340] 19 p3337 N85-30674
VAX TRICOMP user's guide
[AD-A154341] 19 p3337 N85-30675
Ada compiler validation summary report: University of Karlsruhe-GMD/German MOD VAX 11 compiler, version v1.0
[AD-A154370] 19 p3337 N85-30678
Resource management for the tagged token dataflow architecture
[AD-A154773] 21 p3667 N85-32779
Integrated Support Software System (ISSS)
[AD-A155715] 22 p3829 N85-33710
The parser generator as a general purpose tool
[NASA-CR-177955] 23 p3957 N85-34521

COMPLEMENTARY METAL OXIDE SEMICONDUCTORS
U CMOS

COMPLETENESS
Sky coverage, confusion, completeness and reliability 09 p1412 N85-16906

COMPLEX COMPOUNDS
Transition metal carbene complexes
[AD-A144879] 01 p0028 N85-10173
Surface environmental effects in electrochemical kinetics: Outer-sphere chromium (3) reductions at mercury, gallium, lead, and thallium surfaces
[AD-A145607] 02 p0172 N85-11155
Macrocyclic poly(tertiary) phosphines for the attachment of metals to surfaces of photodevices
[DE84-015552] 05 p0617 N85-13946
Polyphosphazene solid electrolytes
[AD-A147008] 07 p0931 N85-15902
Separation of gas mixtures with coordination complexes
[DE85-000363] 10 p1438 N85-19062
Observation of a novel low-lying excited state in zinc complexes
[AD-A150168] 13 p2156 N85-23385
Selective detection of species in complex matrices by SIMS (Secondary Ion Mass Spectrometry)
[AD-D011685] 19 p3235 N85-30053

COMPLEX SYSTEMS
Grasp of information by the pilot in future combat aircraft 10 p1533 N85-19662
Improving engineering system design by formal decomposition, sensitivity analysis, and optimization
[NASA-TM-86377] 10 p1551 N85-19785
Mean flow and turbulence in complex terrain NPS (Naval Postgraduate School)/Vandenberg measurement system
[AD-A150184] 13 p2136 N85-23274
Automatic symbolic solution of Markov chains
[AD-A150476] 13 p2153 N85-23369

COMPLEX VARIABLES
NT AIRY FUNCTION
NT ANALYTIC FUNCTIONS
NT BESSEL FUNCTIONS
NT CONFORMAL MAPPING
NT CONJUGATE POINTS
NT ELLIPTIC FUNCTIONS
NT ENTIRE FUNCTIONS
NT EXPONENTIAL FUNCTIONS
NT GAMMA FUNCTION
NT HARMONIC FUNCTIONS
NT HYPERBOLIC FUNCTIONS
NT HYPERGEOMETRIC FUNCTIONS
NT LAGUERRE FUNCTIONS
NT LEGENDRE FUNCTIONS
NT LOGARITHMS
NT MEROMORPHIC FUNCTIONS
NT ORTHOGONAL FUNCTIONS
NT SINGULARITY (MATHEMATICS)
NT SPHERICAL HARMONICS
Simultaneous rational approximation of a function and its derivatives in the complex plane
[CSIR-TWISK-311] 01 p0109 N85-10733
Existence and non-uniqueness of similarity solutions of a boundary layer problem
[NASA-CR-172503] 07 p0957 N85-16064
Bootstrap confidence intervals
[AD-A147572] 07 p1033 N85-16559
Complex symmetric matrices with strongly stable iterates
[NASA-CR-172542] 11 p1706 N85-20731
Computation of elliptical functions in problems of celestial mechanics 13 p1979 N85-22418
Applicability of log-normal model to probabilitistic description of quasi-pulse interference 13 p2084 N85-23014
Pade tables of a class of entire functions
[CSIR-TWISK-337] 14 p2413 N85-24877
Fourier-Stieltjes coefficients and continuation of functions 15 p2633 N85-26231

COMPLEXITY
NT TASK COMPLEXITY
Atmospheric studies in complex terrain
[DE84-008553] 05 p0676 N85-14345
Recognition of complex 3-dimensional objects using 3-dimensional moment invariants
[AD-A148119] 08 p1212 N85-17825
Categorization of nocturnal drainage flows within the Brush Creek valley in western Colorado and the variability of sigma theta in complex terrain
[DE85-011291] 19 p3300 N85-30461
Determination of low chloride values in Rocky Flats scrub alloy solutions and other complex matrices
[DE85-011506] 23 p3911 N85-34234
Communication complexity of distributed shortest path algorithms
[AD-A156049] 24 p4087 N85-35332

COMPLIANCE (ELASTICITY)
U MODULUS OF ELASTICITY

COMPLICATION
U COMPLEXITY

COMPONENT RELIABILITY
Procedures for precap visual inspection
[NASA-RP-1122] 04 p0495 N85-13158
Electronic components for space applications
[CNES-NT-109] 04 p0496 N85-13169
Component reliability and assembling technologies
[CNES-NT-108] 04 p0511 N85-13258
Evaluation of the crack initiation life behavior of fatigue loaded automotive components made from high strength aluminium alloys
[ESA-TT-733] 05 p0651 N85-14181
Engine cyclic durability by analysis and material testing 07 p0907 N85-15744
Bearing tester fit analysis
[NASA-CR-171282] 07 p0973 N85-16181
A practical example of reducing life cycle costs and increased availability 08 p1053 N85-16738
Investigation of accelerated stress factors and failure/degradation mechanisms in terrestrial solar cells
[NASA-CR-175469] 10 p1510 N85-19524
Reliability predictions for military avionics. Royal Signals and Radar Establishment reliability prediction method no. 250
[BR69221] 13 p1973 N85-22388
Reliability bounds for fault-tolerant systems with competing responses to component failures
[NASA-TP-2409] 13 p2100 N85-23090
Automatic symbolic solution of Markov chains
[AD-A150476] 13 p2153 N85-23369
Current transmission systems 14 p2220 N85-23767
The observation and interpretation of gear tooth failures 14 p2224 N85-23792
Establishment and maintenance of certification standards for helicopter and turboprop power transmission systems 14 p2224 N85-23796
Experimental development of a failure detection scheme for large space structures 14 p2234 N85-23846
Estimate of fatigue stability of gas-turbine engine compressor vanes in probabilistic aspect 14 p2287 N85-24169
Detonation flame spraying extends life of automotive parts 15 p2513 N85-25507
Creep ratcheting simplified methods experience from structural design of elevated temperature components
[DE85-007433] 15 p2580 N85-25915
Cost prediction model for various payloads and instruments for the Space Shuttle Orbiter
[NASA-CR-175781] 16 p2729 N85-28842
Component-specific modeling
[NASA-CR-174765] 16 p2799 N85-27261
Experimental measurements and analysis of heat transfer and gas dynamics in a rotating turbine stage 17 p2911 N85-27949
Flow-induced vibration of SSME main injector liquid-oxygen posts 17 p2912 N85-27951
Composite loads spectra for select space propulsion structural components 17 p2912 N85-27953
Development of high temperature resistant, noncorrosible, non-metallic ceramic materials, especially silicon nitride in gas turbine application
[BMFT-FB-T-85-015] 17 p2936 N85-28125
Atomic hydrogen maser active oscillator cavity and bulb design optimization 18 p3108 N85-29240
High level radioactive waste vitrification process equipment component testing
[DE85-011143] 19 p3273 N85-30296
A modular docking mechanism for in-orbit assembly and spacecraft servicing 22 p3796 N85-33516
Failure testing of active solar energy system components
[DE84-013024] 22 p3804 N85-33561
High pressure compressor component performance report
[NASA-CR-168245] 23 p3897 N85-34138

COMPOSITE FUNCTIONS
The nonlinear analysis of thick composite plates using a cubic spline function
[AD-A152115] 16 p2801 N85-27268

COMPOSITE MATERIALS
NT ALUMINUM BORON COMPOSITES
NT ALUMINUM GRAPHITE COMPOSITES
NT BORON REINFORCED MATERIALS
NT CARBON FIBER REINFORCED PLASTICS
NT CARBON-CARBON COMPOSITES
NT CERAMIC MATRIX COMPOSITES
NT CERMETS
NT COMPOSITE PROPELLANTS
NT EPOXY MATRIX COMPOSITES
NT FIBER COMPOSITES
NT FIBER REINFORCED COMPOSITES
NT GLASS FIBER REINFORCED PLASTICS
NT GLASSY CARBON
NT GRAPHITE-EPOXY COMPOSITES
NT GRAPHITE-POLYIMIDE COMPOSITES
NT LAMINATES
NT METAL MATRIX COMPOSITES
NT PLYWOOD
NT POLYMER MATRIX COMPOSITES
NT REINFORCED PLASTICS
NT RESIN MATRIX COMPOSITES
NT SUPERHYBRID MATERIALS
NT WHISKER COMPOSITES

Development of powder metallurgy in various sections of USSR 01 p0019 N85-10116

The theory of elastic modulus of fabric composites and its examination by experiments
[NAL-TR-808] 01 p0022 N85-10133

Piezoelectric and electrostrictive materials for transducer applications
[AD-A145115] 01 p0043 N85-10277

Development of advanced constitutive model for reinforced concrete
[AD-A145050] 01 p0062 N85-10411

Materials studies for magnetic fusion energy applications at low temperatures, 7
[DE84-013487] 01 p0122 N85-10837

Advanced blade tip seal system, volume 2
[NASA-CR-167851] 02 p0147 N85-10999

Advanced manufacturing development of a composite empennage component for L-1011 aircraft
[NASA-CR-165885] 02 p0170 N85-11141

Cumulative damage model for advanced composite materials
[AD-A145441] 02 p0171 N85-11142

Determination of nonlinear viscoelasticity parameters for polymeric and composite materials by numerical methods
[AD-A145311] 02 p0185 N85-11240

Metallography of Kovar/glass/thermite interfaces
[DE84-015247] 02 p0195 N85-11302

Thermal deformation measurements of heat-resistant structural materials for aircraft by electro optical displacement transducer
[NAL-TR-810] 03 p0325 N85-12092

Fatigue-impact studies in laminated composites
[AD-A142841] 03 p0326 N85-12097

A digital algorithm for composite laminate analysis: FORTRAN, Revised
[AD-A145833] 03 p0326 N85-12098

General studies on composite materials. Evaluation of auxiliary products of national origin
[SNIAS-2500/DCI-PR/84] 03 p0326 N85-12101

Modeling the stress field in laminated composite plates near discontinuities
[PB84-219237] 03 p0327 N85-12103

Research in quantitative NDE techniques
[AD-A145000] 03 p0369 N85-12358

Matrix synthesis and characterization 04 p0467 N85-12965

Numerical investigation of the micromechanics of composite fracture 04 p0467 N85-12970

Work hardening of simple two phase composites
[DE84-014629] 04 p0468 N85-12978

Quality assurance of composite materials, test report no. 45-649/F 04 p0469 N85-12981

Erosion of multiphase materials
[DE84-015816] 04 p0474 N85-13018

Insulating polymer concrete
[DE84-017239] 04 p0480 N85-13057

Rotating assembly working group summary 05 p0604 N85-13851

Investigation of the relations between neat resin and advanced composite mechanical properties. Volume 1: Results
[NASA-CR-172303] 05 p0612 N85-13911

Synthesis of reinforced composite threads based on polymer mixtures 06 p0761 N85-14869

Carbon fibre reinforced aluminum matrix composites: A critical review
[AD-A146367] 06 p0764 N85-14883

Optical properties of composite materials
[AD-A146768] 07 p0920 N85-15828

All-composite Airbus empennage 07 p0936 N85-15931

Composite batteries 07 p0936 N85-15932

Advances in composites technology
[NASA-TM-86359] 08 p1118 N85-17048

Model for prediction of the elastic response of composite materials over wide ranges of concentration
[AD-A146186] 08 p1119 N85-17051

Composites with a periodic structure, mathematical analysis and numerical treatment
[AD-A148301] 08 p1119 N85-17053

Composite structure repair, addendum
[AGARD-R-716-ADD] 08 p1120 N85-17057

Repair of composites 08 p1120 N85-17058

Composite repair of aircraft structures 08 p1120 N85-17059

High pressure physics research focusing on composite materials 08 p1140 N85-17185

Nonlinear analysis of composite laminates 09 p1288 N85-18087

Fabrication of ceramic-ceramic composites by chemical vapor deposition
[DE85-000981] 09 p1298 N85-18155

West Europe report: Science and technology
[JPRS-WST-85-003] 09 p1309 N85-18224

Electromagnetic processing of materials
[AD-A148804] 09 p1311 N85-18241

European Scientific Notes, volume 38, number 12
[AD-A148713] 09 p1418 N85-18946

Resistance foil strain gage technology as applied to composite materials
[NASA-CR-3872] 10 p1431 N85-19024

Mechanics of composite materials
[DE85-003611] 10 p1432 N85-19031

Mechanical properties of Be-Al composite 10 p1443 N85-19094

Influence of volumetric fiber content on some matrix damage factors during thermal cycling of tungsten-EI 765 composite 10 p1443 N85-19097

Study of surface damage in cathode composite materials in a high flux CO2 laser 10 p1444 N85-19098

Laser rupture of composite materials 10 p1444 N85-19102

Influence of melting conditions on strength of transition zone between steel and composite material 10 p1450 N85-19133

Ultrasonic analysis of Kevlar-epoxy filament wound spherical test specimens
[DE85-005196] 11 p1593 N85-20024

USSR report: Materials science and metallurgy
[JPRS-UMS-84-005] 11 p1597 N85-20044

Evaluation of residual stress in laminated metallic composites 11 p1598 N85-20052

Predicting stability of full-scale composite constructions of the basis of stiffness 11 p1599 N85-20054

High-strength composite materials for aircraft, body armor 11 p1599 N85-20057

Influence of plastic deformation on structural stability of nichromo-tungsten composite materials 11 p1599 N85-20060

Structure and properties of copper-titanium-aluminum composites obtained by thermoreactive sintering 11 p1600 N85-20061

Stability of superconducting composites in a magnetic field
[DE85-002731] 11 p1734 N85-20907

Magnetization measurements on multifilamentary Nb3Sn and NbTi conductors
[DE85-001237] 11 p1737 N85-20923

Composite structural materials
[NASA-CR-175515] 12 p1795 N85-21268

Temperature responses of composite panels
[AD-A150053] 12 p1798 N85-21277

Chemical approach for controlling nadimide cure temperature and rate with maleimide
[NASA-CASE-LEW-13770-3] 12 p1809 N85-21350

Chemical approach for controlling nadimide cure temperature and rate with maleimide
[NASA-CASE-LEW-13770-4] 12 p1810 N85-21351

Finger materials for air cushion vehicles. Volume 2: Base fabrics for finger materials
[AD-A149701] 12 p1819 N85-21408

Fiber reinforced fused silica for hypersonic radome applications
[AD-P004366] 12 p1826 N85-21460

Proceedings of the 9th Biennial Army Symposium on Solid Mechanics. Advances in Solid Mechanics for Design and Analysis
[AD-A150042] 12 p1867 N85-21710

Nonlinear analysis of layered composite plates and shells
[PB85-127181] 12 p1868 N85-21719

Research Reports: 1984 NASA/ASEE Summer Faculty Fellowship Program
[NASA-CR-171317] 12 p1944 N85-22210

Investigation of the effects of NaOH dopant level on the physical and mechanical properties of carbon/phenolic composite material 12 p1945 N85-22213

Silicon carbide-silicon nitride fibers: Preparation and characterization of polycarboallazane precursors 12 p1945 N85-22214

Solid Rocket Motor Case (SRMC) dynamic sensitivity to changes in composite properties 12 p1948 N85-22238

Simple theoretical models for composite rotor blades
[NASA-CR-175620] 13 p1971 N85-22382

Mechanism of strengthening plastics with rubbers 13 p2014 N85-22636

USSR report: Materials science and metallurgy
[JPRS-UMS-85-002] 13 p2025 N85-22688

Uses of composite materials 13 p2027 N85-22698

Dissipation of energy in composite material 13 p2027 N85-22703

Possibility of producing monolithic composite materials based on niobium carbide 13 p2028 N85-22707

Theoretical and experimental investigation of mechanically fastened composites
[AD-A150961] 14 p2248 N85-23935

Some optimization problems in static aeroelasticity for wings made of composite materials 14 p2277 N85-24104

Recent developments in the dynamics of advanced rotor systems
[NASA-TM-86669] 14 p2317 N85-24320

USSR report: Materials science and metallurgy
[JPRS-UMS-85-001] 15 p2496 N85-25395

West Europe report: Science and technology
[JPRS-WST-84-012] 15 p2523 N85-25552

MBB uses new CFC form tool for titanium alloy air intake 15 p2523 N85-25553

West Europe report: Science and technology
[JPRS-WST-84-008] 15 p2531 N85-25606

Pechiney strategy includes development of new materials 15 p2531 N85-25607

Glass, carbon fibers made at Fibre et Mica in France 15 p2534 N85-25634

West Europe report: Science and technology
[JPRS-WST-84-003] 15 p2534 N85-25635

France develops own aluminum-based composite ceramic 15 p2534 N85-25636

A study of the time dependence in fracture processes relating to service prediction of adhesive joints and advanced composites
[AD-A152064] 15 p2579 N85-25910

Simultaneous chemical vapor deposition of SiC-dispersed phase composites
[DE85-007751] 16 p2744 N85-26931

The nonlinear analysis of thick composite plates using a cubic spline function 16 p2798 N85-27252

The nonlinear analysis of thick composite plates using a cubic spline function
[AD-A152115] 16 p2801 N85-27268

Friction and wear behavior of aluminum and composite I-beam stiffened airplane skins
[NASA-TM-86418] 17 p2895 N85-27852

Gordon Research Conference on Composites
[AD-A152688] 17 p2917 N85-27979

Solution to eigenvalue problems of antisymmetric cross-ply and antisymmetric angle-ply laminated plates using affine transformations
[AD-A153040] 17 p2917 N85-27980

Interaction among inhomogeneities and inclusions
[AD-A153114] 17 p2979 N85-28419

Analytical shear buckling investigation of curved composite panels
[AD-A153136] 17 p2980 N85-28421

High temperature composite thermal storage systems
[DE85-005073] 17 p2986 N85-28455

Erosion of multiphase materials
[DE85-006895] 18 p3068 N85-28978

An evaluation and preparation of ferromagnetic liquid composites for use at millimeter wavelengths
[AD-A153939] 18 p3069 N85-28980

Application of lightweight composite materials to naval weapons systems
[PB85-173607] 18 p3069 N85-28981

British breakthrough in lightweight lithium batteries 18 p3086 N85-29092

West Europe report: Science and technology
[JPRS-WST-84-032] 18 p3086 N85-29095

West Europe report: Science and technology
[JPRS-WST-84-037] 18 p3088 N85-29108

Structural Analysis
[DFVLR-MITT-84-21] 18 p3120 N85-29313

Mechanics of composite materials, theory and application
[VTH-LR-431] 18 p3123 N85-29334

Influence of microstructure on mechanical properties in cemented tungsten-carbides 19 p3230 N85-30029

The fabrication, microstructure, and strengthening behavior of heavily cold-worked in situ composites 19 p3231 N85-30031

A study of the stress wave factor technique for the characterization of composite materials
[NASA-CR-174870] 19 p3231 N85-30035
USSR report: Materials Science and Metallurgy
[JPRS-UMS-85-005] 19 p3241 N85-30095
Thermo-mechanical and thermal behavior of high-temperature structural materials
[AD-A154154] 19 p3266 N85-30251
Impact dynamics research on composite transport structures
[NASA-TM-86391] 19 p3284 N85-30967
Some asymptotic problems in the optimal control of distributed systems 20 p3412 N85-31175
Long-term thermal aging of Celion/V378A composite materials
[NASA-TM-86362] 20 p3421 N85-31236
Design and fabrication of durable owner-built wind turbine blades
[DE85-009200] 20 p3484 N85-31650
R and D programmes at the National Aeronautical Laboratory
[AR-22] 20 p3539 N85-32022
R and D activities of the Materials Science Division 20 p3539 N85-32024
A cracked orthotropic sheet stiffened by a semi-infinite orthotropic sheet
[NASA-TP-2455] 21 p3597 N85-32339
New materials needs in aeronautics
[SNIAS-851-502-101] 22 p3729 N85-33120
Dispersion toughened ceramic composites and method for making same
[DE85-011601] 22 p3751 N85-33252
Proceedings of the Twentyseventh Japan Congress on Materials Research
[ISSN-0368-3141] 23 p3903 N85-34180
Negative flexural behavior of precase composite slabs with steel joint 23 p3904 N85-34183
Composite desiccant structure
[DE85-006400] 23 p3910 N85-34226
Centralized surveillance of flexible workshops for the manufacturing of composite materials
[SNIAS-851-430-103] 23 p3910 N85-34227
Product definition: Technical specification of needs
[SNIAS-851-430-104] 23 p3910 N85-34228
Process for improving moisture resistance of epoxy resins by addition of chromium ions
[NASA-CASE-LAR-13226-1] 23 p3919 N85-34282
Development and demonstration of a spiral-wound thin-film composite membrane system for the economical production of oxygen-enriched air, phase 4
[DE85-012380] 23 p3920 N85-34296
SRB TPS closeout materials characterization
[NASA-CR-170885] 24 p4070 N85-35222

COMPOSITE PROPELLANTS
Catalyzed low burning rate propellants for upper-stage solid rocket motor
[NAL-TR-805] 03 p0339 N85-12181
Study of the transition from deflagration to detonation of previously fragmented propellants 08 p1115 N85-17032
The heat sensitivity of solid propellants 08 p1117 N85-17043
Plasticizer system for propellant compositions
[AD-D011502] 12 p1816 N85-21390
Characterization of heterogeneity of composite propellants and its effects on combustion behavior 13 p2000 N85-22539
Mechanism of burning rate enhancement by ferric oxide 13 p2002 N85-22546
Non-steady combustion of composite solid propellants
[AD-A150627] 14 p2250 N85-23947
Model of normal and erosive burning of composite propellants
[ONERA-NT-1984-3] 14 p2263 N85-24024
PSA, Renault work on all fuel automobile engine 15 p2531 N85-25604
Propellant plasticizer
[AD-D011501] 20 p3434 N85-31306

COMPOSITE STRUCTURES
NT LAMINATES
NT PLYWOOD
Lightweight composite launcher pod
[AD-D011236] 01 p0015 N85-10092
Effect of stress concentrations in composite structures
[NASA-CR-173976] 02 p0170 N85-11140
Solvent resistant thermoplastic composite matrices 04 p0466 N85-12960
Composite fracture toughness and impact characterization 04 p0466 N85-12963
Full-scale testing, production and cost analysis data for the advanced composite stabilizer for Boeing 737 aircraft. Volume 1: Technical summary
[NASA-CR-3649] 05 p0612 N85-13912
Design, ancillary testing, analysis and fabrication data for the advanced composite stabilizer for Boeing 737 aircraft. Volume 1: Technical summary
[NASA-CR-3648] 05 p0612 N85-13913
Design, ancillary testing, analysis and fabrication data for the advanced composite stabilizer for Boeing 737 aircraft, volume 2
[NASA-CR-166011] 05 p0612 N85-13914
Full-scale testing, production and cost analysis data for the advanced composite stabilizer for Boeing 737 aircraft, volume 2
[NASA-CR-166012] 05 p0613 N85-13915
Verification of a computer program for vibration analysis of composite wing cores
[NAL-TR-825] 06 p0817 N85-15187
Evaluation of the alkaline peroxide pre-bond surface treatment for titanium
[AD-A147352] 07 p0928 N85-15881
Modeling localized stress fields in composite laminates
[AD-A148830] 08 p1120 N85-17056
Composite structure repair, addendum
[AGARD-R-716-ADD] 08 p1120 N85-17057
Wave propagation in periodic, composite structures 09 p1332 N85-18370
Proceedings of Colloquium/Workshop on Composite Materials and Structures, Standardization, Qualification, Certification held at washington, D.C. on 8-10 May 1984
[AD-A149039] 10 p1432 N85-19029
Thermoviscoelastic analysis of dimensionally stable fiber composite space structures
[AD-A149275] 11 p1593 N85-20021
Ultrasonic characterization of advanced composite flywheels
[DE85-000158] 11 p1593 N85-20026
Characterization of mode 1 and mixed-mode failure of adhesive bonds between composite adherends
[NASA-TM-86355] 12 p1797 N85-21270
Temperature responses of composite panels
[AD-A150053] 12 p1798 N85-21277
Use of acoustical emission method to study specifics of fracture of boron reinforced plastic structural elements 13 p2026 N85-22696
Axisymmetrical oscillations of shell systems subjected to impulse loads 13 p2047 N85-22814
Finite element model for creep in composite masonry
[PB85-150324] 14 p2322 N85-24347
Design, fabrication and test of composite curved frames for helicopter fuselage structure
[NASA-CR-172438] 15 p2470 N85-25247
A preliminary investigation into transverse fracture of unidirectional fiber composites
[AERE-R-11494] 15 p2503 N85-25438
Directional thermal conductivities of graphite-epoxy composites: 0/90 and 0/+ or - 45/90
[AD-A152209] 16 p2743 N85-28929
Effects of the phase compositions of cast low-pearlite steels micro-alloyed with vanadium and titanium of their structure and properties
[BLL-BISI-TRANS-22301-(9022.06)] 17 p2928 N85-28067
Initial imperfection surveys on conical shells at Hoechst AG
[VTH-LR-407] 17 p2981 N85-28429
Light weight fire resistant graphite composites
[NASA-CASE-ARC-11615-1-SB] 18 p3068 N85-29976
The effect of center delamination on the instability of composite cylindrical panels
[AD-A153494] 18 p3069 N85-29979
Expedient runway surfacing with post tensioning system for expeditionary airfields
[AD-D011677] 19 p3222 N85-29976
Thermo-mechanical and thermal behavior of high-temperature structural materials
[AD-A154154] 19 p3266 N85-30251
Automated fabrication of composite structures for helicopters
[SNIAS-851-210-104] 20 p3393 N85-31049
Generation of round bores in composite structure railguns
[DE85-011872] 22 p3793 N85-33501

COMPOSITE WRAPPING
Testing of wound materials for strength with loading in the reinforcement plane 13 p2027 N85-22701

COMPOSITES
U COMPOSITE MATERIALS

COMPOSITION (PROPERTY)
NT ATMOSPHERIC COMPOSITION
NT ATMOSPHERIC MOISTURE
NT ATOM CONCENTRATION
NT CARBON DIOXIDE CONCENTRATION
NT CHEMICAL COMPOSITION
NT CONCENTRATION (COMPOSITION)
NT GAS COMPOSITION
NT IONOSPHERIC COMPOSITION
NT LOW CONCENTRATIONS
NT LUNAR COMPOSITION
NT MASCONS
NT METEORITIC COMPOSITION
NT MOISTURE CONTENT
NT PLANETARY COMPOSITION
NT PLASMA COMPOSITION
NT STELLAR COMPOSITION
The constitution as the basis for recent and future developments of wear resistant materials 02 p0179 N85-11205
The effects of Cr, Co, Al, Mo and Ta on the cyclic oxidation behavior of a prototype cast Ni-base superalloy based on a 2(5) composite statistically designed experiment
[NASA-TM-83784] 03 p0331 N85-12131
The influence of inert particulate material on the properties of RDX/polyethylene wax compositions
[MRL-R-929] 03 p0336 N85-12159
Compound class quantitation of JP-5 jet fuels by high performance liquid chromatography-differential refractive index detection
[AD-A145754] 03 p0340 N85-12185
The growth of metastable peritectic compounds
[NASA-CR-171289] 07 p0920 N85-15824
Properties of miscible polymer blends
[AD-A147090] 07 p0931 N85-15903
Clustering and ordering in 3-5 alloys
[AD-A150604] 13 p2022 N85-22670
Synthesis and properties of elevated temperature P/M aluminum alloys
[AD-A151031] 14 p2256 N85-23981
Ion kinetics, small neutral and excited components in D-region with elevated ionization level. Part 2: Variations in small neutral and excited components 15 p2480 N85-25307
Self-sustaining coatings for fusion applications: Copper lithium alloys
[DE85-009740] 18 p3190 N85-29783
Application of the Diffusion Raman Anti-Stokes Coherent (DRASC) method to a SNECMA combustion chamber
[YKC-3096/84] 20 p3425 N85-31260
Chemical structure of interfaces 20 p3480 N85-31629
Quantitative determination of mineral composition by powder X-ray diffraction
[DE85-011654] 22 p3760 N85-33301
Energy dependence of cosmic ray composition above 10(15) GeV/nucleus
[OG-5.4-4] 22 p3886 N85-34081
The primary cosmic ray mass composition at energies above 10(14) eV
[OG-5.4-6] 22 p3886 N85-34083
Uranium, thorium isotopic analyses and uranium-series ages of calcite and opal and stable isotopic compositions of calcite from drill cores UE25a no. 1, USR G-2 and USW G-3/GU-3, Yucca Mountain, Nevada
[DE85-013039] 23 p3948 N85-34471
Screening and characterizing oleaginous microalgal species from the southeastern United States
[DE85-008787] 23 p3951 N85-34488

COMPOUNDING
Milling of Si3N4 with Si3N4 hardware
[NASA-TM-86884] 01 p0031 N85-10191

COMPRESSED AIR
Dynamic and other secondary benefits of compressed air energy storage
[DE84-015571] 03 p0386 N85-12488
Qualification of a wall gage for the SIMA wagon, adapted to the test of half models motorized by compressed air turbines — SIMA wind tunnel
[ONERA-PV-1/6068-GY] 16 p2701 N85-26877

COMPRESSED GAS
Experiments with phase transitions at very high pressure
[NASA-CR-174029] 02 p0172 N85-11148
Internal hysteresis experienced on a high pressure syn gas compressor 05 p0642 N85-14122
Development of improved capabilities for computation of gas supercompressibility factors and other properties
[PB85-166316] 20 p3436 N85-31315

COMPRESSIBILITY
Design proposals for torsional buckling of stiffeners
[AD-A144783] 01 p0082 N85-10409
Methods to increase linac efficiency
[DE84-014692] 01 p0118 N85-10809
Volume compressibilities of transuranium elements compounds, especially of neptunium compounds 03 p0431 N85-12744
Influence of pressure on compaction during compression of powders of iron and 40Kh and 10R6M5 steels
[BLL-M-35995-(5826.4)] 07 p0926 N85-15866
Investigations into the effects of scale and compressibility on lift and drag in the RAE 5m pressurized low-speed wind tunnel 08 p1068 N85-16773

New discovery in supersonic flight research
09 p1278 N85-16041
Measurement of gas compressibility factor data for natural gas and synthetic gas components and their mixtures
[PB85-129047] 11 p1614 N85-20151
Development and evaluation of a procedure for the rapid analysis of fresh concrete
[AD-A149741] 12 p1866 N85-21703
Pion production and the nuclear equation of state
[DE85-009941] 19 p3365 N85-30870
Development of improved capabilities for computation of gas supercompressibility factors and other properties
[PB85-186316] 20 p3436 N85-31315
Analysis of long bone and vertebral failure patterns
[AD-A154796] 21 p3663 N85-32758
Characteristics of central collision events in Fe-nucleus interactions for 20 - 60 GeV/nucleon
[HE-1.4-3] 24 p4176 N85-35691

COMPRESSIBILITY EFFECTS
Flutter parametric studies of cantilevered twin-engine-transport type wing with and without winglet. Volume 1: Low-speed investigations
[NASA-CR-172410-VOL-1] 04 p0513 N85-13269
Investigations into the effects of scale and compressibility on lift and drag in the RAE 5m pressurised low-speed wind tunnel
[RAE-TM-AERO-2006] 13 p1969 N85-22372
Deceleration of a supersonic flow behind a curved shock wave with isentropic precompression
[NASA-TM-77920] 24 p4061 N85-35164

COMPRESSIBLE BOUNDARY LAYER
Measurement of the development of the boundary layer in the annulus walls of a fourstage compressor
[CUED/A-TURBO-TR-121] 01 p0046 N85-10299

COMPRESSIBLE FLOW
NT TRANSONIC FLOW
Measurement of the development of the boundary layer in the annulus walls of a fourstage compressor
[CUED/A-TURBO-TR-121] 01 p0046 N85-10299
Review of some vortex relations
[NASA-CR-172452] 01 p0046 N85-10302
Particle entrainment in a compressible vortex
[ISL-CO-230/83] 04 p0500 N85-13182
An Iwatsubo-based solution for labyrinth seals - comparison with experimental results
05 p0644 N85-14131
A simple extension to multidimensional problems of the artificial viscosity due to Lapidus
06 p0808 N85-15134
Inviscid compressible flow past a multi-element aerofoil
08 p1069 N85-16776
A Van Leer shock capturing algorithm for the Euler equations
[AD-A148761] 08 p1163 N85-17335
Front tracking for gas dynamics
[DE85-000571] 08 p1163 N85-17336
Notes on compressible flow equations for thermodynamics of hot jets
[BAE-KRS-N-GEN-273] 09 p1318 N85-18269
Development of multigrid algorithms for problems from fluid dynamics
[GMD-111] 09 p1321 N85-18305
A 3-dimensional mass conserving element for compressible flows
[NASA-CR-172513] 09 p1373 N85-18626
Efficient self-consistent viscous-inviscid solutions for unsteady transonic flow
[NASA-TM-86335] 10 p1420 N85-18959
SSME thrust chamber simulation using Navier-Stokes equations
[NASA-CR-171349] 10 p1430 N85-19017
Algorithms for the Euler and Navier-Stokes equations for supercomputers
[NASA-CR-172543] 10 p1539 N85-19701
Modeling turbulent flow in compressible fluids: Metrological aspects --- conferences
11 p1575 N85-19926
An investigation of compressible flows over open cavities including shear layer thickness effects
[AD-A150086] 12 p1847 N85-21588
Computations of two-dimensional airfoil-vortex interactions --- helicopter rotor flowfields
[NASA-CR-3885] 14 p2210 N85-23700
Experimental and theoretical investigation of the motion of particles in a compressible vortex
[ISL-R-129/83] 14 p2303 N85-24264
Gasdynamic evaluation of choking cascade turns
[AD-A151854] 15 p2557 N85-25776
Pseudo-unsteady systems for steady inviscid flows
[ESA-TT-877] 15 p2558 N85-25782
Waveguide phenomena in dense relaxing gases and their use in chemical and gas-dynamic lasers
15 p2644 N85-26308
Numerical simulation of inviscid compressible flow through three-dimensional cascade
16 p2692 N85-26619
Recent progress in computational aerodynamics
16 p2693 N85-26626
LU methods for the compressible Navier-Stokes equations
16 p2781 N85-27160
An experimental study of compressible turbulent reattaching free shear layers
16 p2781 N85-27161
Solution of Onsager's equation for a rotating compressible fluid in a multiply-connected domain
[DE85-007048] 16 p2784 N85-27178
A four-field model for Tokamak plasma dynamics
[DE85-007111] 16 p2866 N85-27694
Calculation of viscous compressible flows in small gas turbines
17 p2912 N85-27950
Supersonic flow around blunt wedge
17 p2942 N85-28158
The method of residual minimization in compressible steady flows
[AD-A153924] 18 p3100 N85-29193
Application of computational fluid dynamics to complex inlet ducts
[NASA-TM-87060] 19 p3265 N85-30247
An implicit finite-difference code for a two-equation turbulence model for three-dimensional flows
[NASA-TM-86752] 20 p3454 N85-31448
On the evaluation of boundary layer measurements on boattailed bodies of revolution in axisymmetric compressible subsonic flow
[ESA-TT-863] 20 p3457 N85-31471
Two-dimensional simulation of instability growth due to shocks
[DE85-011869] 22 p3784 N85-33442
Scalar/Vector potential formulation for compressible viscous unsteady flows
[NASA-CR-3921] 23 p3893 N85-34113
Compressible two-phase flow instabilities simulated with a hybrid Lagrange-Euler pseudospectral method
[DE85-009904] 23 p3931 N85-34361
Calculation of compressible flow about three-dimensional inlets with auxiliary inlets, slats and vanes by means of a panel method
[NASA-CR-174975] 24 p4060 N85-35162
Acoustic resonances in cylinder bundles oscillating in a compressible fluid
[DE85-004066] 24 p4145 N85-35699

COMPRESSIBLE FLUIDS
Rayleigh-Taylor instability in compressible media
[AD-A145491] 02 p0198 N85-11322
Nonsteady motion of solid sphere in compressible viscous fluid
02 p0269 N85-11753
Analysis of the surface load and radiated sound of a vibrating airfoil with application to the experiment of Brooks
[NASA-CR-3864] 07 p1038 N85-16590
Generation of sound by a vortex point in a steady flow of slightly compressible fluid
11 p1715 N85-20789
Some approximations of geophysical hydrodynamics
14 p2336 N85-24448
An analysis of flow models: From Navier-Stokes to potential flow equations
21 p3587 N85-32295

COMPRESSING
NT PLASMA COMPRESSION
Light scattering studies of lower dimensional colloidal particle and critical fluid systems
[DE85-002087] 09 p1377 N85-18654
Simplified theory for the behaviour of buried flexible cylinders under the influence of uniform hoop compression
[PB85-116531] 11 p1654 N85-20419
Thermocompression welding of parts made from AMIs and VT1 alloys
15 p2501 N85-25430
Design of electrooptical system with annular cathode and electrostatic compressor
22 p3770 N85-33367
Preliminary considerations for the gasdynamic precompression of solid molecular hydrogen
[DE85-013256] 22 p3784 N85-33445

COMPRESSION LOADS
NT AXIAL COMPRESSION LOADS
NT IMPACT LOADS
Method and apparatus for determining pressure-induced frequency-shifts in shock-compressed materials
[DE84-014313] 01 p0024 N85-10151
Force standard machines of the National Institutes for Metrology, vol. 2
[PTB-ME-62-VOL-2] 01 p0036 N85-10224
Interactive buckling of thin-walled structural components under static and dynamic loads
01 p0059 N85-10392
Locomotion research for the analysis of the human gait and for the determination of the maximum loads of the pelvis-leg skeleton. Volume 2: Three-dimensional analysis
[BMFT-FB-T-83-168-VOL-2] 02 p0236 N85-11536
A buckling analysis for rectangular orthotropic plates with centrally located cutouts
[NASA-TM-86263] 04 p0513 N85-13268
Fatigue life improvement due to mechanically induced compressive residual stresses 05 p0650 N85-14175
Computer program for determining induced stresses and consolidation settlements (CSETT)
[AD-A146730] 07 p1023 N85-16493
Delamination growth in graphite epoxy laminates under compressive loads 09 p1288 N85-18088
Slit-ring test for evaluating fracture in tubular cross sections
[DE85-003550] 11 p1654 N85-20416
Simplified theory for the behaviour of buried flexible cylinders under the influence of uniform hoop compression
[PB85-116531] 11 p1654 N85-20419
Stability of viscoelastic constructions subjected to steady random compressing loads 11 p1720 N85-20819
Behavior of buried flexible cylinders under the influence of nonuniform hoop compression
[PB85-116523] 12 p1868 N85-21718
Orientation and temperature dependence of some mechanical properties of the single-crystal nickel-base superalloy Rene N4. 3: Tension-compression anisotropy
[NASA-TM-86982] 13 p2021 N85-22660
Testing of wound materials for strength with loading in the reinforcement plane 13 p2027 N85-22701
Impacts in ice: Commissions of solar system crater population 13 p2181 N85-23538
Design of transversely stiffened FRP panels under compressive load --- fiber reinforced plastic (FRP) ships
[AMTE(S)-R-84104] 23 p3940 N85-34424
User's guide: A computer program for strength analysis of non-hydraulic concrete structural elements. Report 2. Strength design of reinforced concrete column sections (PCAUC)
[AD-A156393] 24 p4102 N85-35429

COMPRESSION RATIO
Converting gasoline farm tractors to run efficiently on farm-produced alcohol
[DE84-015796] 02 p0205 N85-11350

COMPRESSION TESTERS
U COMPRESSION TESTS

COMPRESSION TESTS
Effects of constituent properties on compression failure mechanisms 04 p0464 N85-12946
Compression of a band made of elastic, ideally Coulomb plastic material
[ISSN-0208-5658] 05 p0648 N85-14157
Strength properties of unidirectionally reinforced hybrid composites 11 p1599 N85-20056
Experimental investigation of crippling strength of Chinese aluminum alloy (LY12CZ) sections
13 p2041 N85-22779
Hydrostatic compression of Fe1-chi 0 wustite.
15 p2508 N85-25472
System expectations for Pioneer 1 foil implosion experiments
[DE85-014129] 24 p4091 N85-35359

COMPRESSION WAVES
Dynamic compression and volatile release of carbonates
[NASA-CR-174076] 03 p0391 N85-12504
Shock compression of liquid helium to 56 GPa (560) kbar
13 p2184 N85-23551
Compression waves in front of and behind a piston launched in a shock tube
[ISL-R-101/83] 14 p2303 N85-24260
Crosswell acoustic surveying in gas sands: Travel-time pattern recognition, seismic Q and channel waves
[DE85-010777] 19 p3352 N85-30778

COMPRESSIVE STRENGTH
Effect of impact damage and open holes on the compression strength of tough resin/high strain fiber laminates 04 p0464 N85-12945
Effects of constituent properties on compression failure mechanisms 04 p0464 N85-12946
Mechanical property data 7050-t736511 alloy
[AD-A147365] 07 p0928 N85-15882
Laboratory investigation on adhesives for Naval facilities construction
[AD-A147453] 07 p0932 N85-15909
Compressive strength-maturity relationships of mortar containing fly ash
[AD-A148705] 09 p1339 N85-18423
Studies of structure and mechanical properties of carbon-reinforced plastic based on spirally reinforced filler 10 p1444 N85-19100
A model for the compressive buckling of extended chain polymers
[AD-A151025] 14 p2260 N85-24008
Compressive strength of epoxy resin chocks subjected to elevated temperatures
[AD-A152018] 15 p2519 N85-25532

Experimental study of the effect of moist environments on epoxy resin chocks
[AD-A152052] 15 p2568 N85-25849
User's guide for concrete strength investigation and design (CSTR)
[AD-A151617] 15 p2579 N85-25906
Buckling and post-buckling behavior of sparsely connected built-up columns 19 p3283 N85-30358
Analysis of the elastic and strength properties of Yucca Mountain tuff, Nevada
[DE85-006975] 19 p3300 N85-30460
Geothermal COMPAX drill bit development
[DE85-011353] 20 p3469 N85-31556
The effect of mould size on the exothermic reaction and compressive strength of epoxy resin chocks
[AD-A155102] 21 p3570 N85-32203

COMPRESSOR BLADES
Jet engine blade repair at the Oklahoma Air Logistics Center, Propulsion Division
[AD-P004003] 03 p0307 N85-11983
An experimental investigation and numerical simulation of the thermomechanical phenomena in compressor rotor tip rubbing 03 p0367 N85-12352
Users manual for a computer program for dynamic response analysis of bladed systems
[UDR-TR-84-38] 04 p0456 N85-12893
Vaned diffusers — in centrifugal compressors 05 p0637 N85-14085
Annular groove in compressor casing as device for control of air stream 13 p2050 N85-22832
Influence of surface roughness on compressor blades at high reynolds number in a two-dimensional cascade
[AD-A151855] 15 p2557 N85-25777
Precision die forging of blades or gas turbines 17 p2940 N85-28148
Design, development and operation of a high simultaneous capacity digital telemetry system — turbomachine blade flutter
[PNR-90261] 23 p3899 N85-34151
Unsteady flow in a supersonic cascade with two in-passage shocks
[NASA-CR-3925] 24 p4060 N85-35158

COMPRESSOR EFFICIENCY
Vaneless diffusers — flow in centrigal compressors 05 p0637 N85-14084
Experimental study of influence of size of upper and lower laps on operational efficiency of centripetal full-inlet air driven microturbines 09 p1307 N85-18211

COMPRESSOR ROTORS
Energy efficient engine component development and integration program
[NASA-CR-170034] 02 p0146 N85-10990
An experimental investigation and numerical simulation of the thermomechanical phenomena in compressor rotor tip rubbing 03 p0367 N85-12352
Experimental on-stream elimination of resonant whirl in a large centrifugal compressor 05 p0642 N85-14121
Problems and possibilities for life extension in gas turbine components 07 p0907 N85-15742
Study of dynamic characteristics of prefabricated gas turbine compressor rotor 14 p2272 N85-24078
Investigation of gas-turbine engine blower impeller vibrations with change in engine intake conditions 14 p2287 N85-24170
Ceramic turbochargers: A case study of a near-term application of high-strength ceramics
[DE85-006495] 17 p2975 N85-28379
Numerical and experimental investigation of turbomachinery rotor flow fields 20 p3451 N85-31429

COMPRESSORS
NT CENTRIFUGAL COMPRESSORS
NT SUPERCHARGERS
NT TRANSONIC COMPRESSORS
NT TURBOCOMPRESSORS
Measurement of the development of the boundary layer in the annulus walls of a fourstage compressor
[CUED/A-TURBO-TR-121] 01 p0046 N85-10299
Energy efficient engine. High pressure compressor detail design report
[NASA-CR-165558] 02 p0147 N85-10998
Development of a Brsun linear engine-driven, heat-actuated heat pump
[DE84-016647] 04 p0500 N85-13188
Screw expander for light duty diesel engines 04 p0508 N85-13242
Noise in small portable motocompressors. Experiments on limited-cost acoustic treatments to obtain progressive improvements
[CETIM-11-H-445] 04 p0558 N85-13557
Measurements of satellite refrigeration compressor power consumption and efficiency
[DE84-016724] 05 p0632 N85-14056
Open-cycle vapor compression heat pump
[PB85-101475/GAR] 06 p0775 N85-14951
Verification of life prediction through component testing 07 p0908 N85-15748
Turbo fluid machinery and diffusers
[NASA-TM-77467] 08 p1167 N85-17363
On one design principle of surge protector for gas turbine engine compressor 09 p1306 N85-18206
New air supply-prime mover facility for engine tests detailed 11 p1621 N85-20204
Magentically actuated compressor
[NASA-CASE-GSC-12799-1] 12 p1818 N85-21404
Annular groove in compressor casing as device for control of air stream 13 p2050 N85-22832
Automating the study of error in discrete aerodynamic fairing design 14 p2288 N85-24176
Solid state compressor
[AD-A150790] 14 p2311 N85-24302
An experimental study of aerodynamic damping characteristics of a compressor annular cascade in high speed flow and the visualization of annular cascade flow
[NAL-TR-838] 15 p2554 N85-25759
Testing of materials and coatings for jet engine components under simulated operational conditions
[B8580073] 17 p2899 N85-27873
Strutless diffuser for gas turbine engine
[AD-D011662] 18 p3062 N85-28943
Compressor and turbine models - numerical stability and other aspects
[AD-A153811] 18 p3063 N85-28948
Nonlinear global stability analysis of compressor stall phenomena
[NASA-CR-174908] 19 p3219 N85-29960
High pressure compressor component performance report
[NASA-CR-168245] 23 p3897 N85-34136
Combined cold compressor/ejector helium refrigerator
[DE85-006408] 23 p3925 N85-34326

COMPTON EFFECT
Neutron activation analysis of stoney spherules from a marine sediment sample 06 p0883 N85-15608
An inverse Compton model of the X-ray emission in Seyfert galaxies 08 p1241 N85-17827
Power law X- and gamma-ray emission from relativistic thermal plasmas 08 p1241 N85-17829
Consequences of hot gas in the broad line region of active galactic nuclei
[NASA-TM-86176] 11 p1763 N85-21090
X-ray polarimetry: The measurement of the polarization of solar flare X-rays and the design of a Compton polarimeter 14 p2441 N85-25059
A synchrotron/inverse Compton interpretation of a solar burst producing fast pulses at lambda 3 mm and hard X-rays 16 p2887 N85-27815
Angle averaged Compton cross sections for degenerate electron gases
[AD-A154464] 19 p3371 N85-30908
Variations in the small-scale galactic magnetic field and short time-scale intensity variations of extragalactic radio sources 20 p3549 N85-32084
The possibility of observing and exploiting the generation of high-energy photons by electrons in the field of an intense electromagnetic wave 21 p3691 N85-32931
Inverse-Compton gamma rays in the galaxy
[OG-3.1-2] 22 p3873 N85-33990
Multicomponent analysis of total COS-B gamma-ray data at intermediate latitudes
[OG-3.1-3] 22 p3873 N85-33991
X-ray spectra of bursting neutron stars 23 p3981 N85-34886
Study of non-thermal photon production under different scenarios in solar flares. 2: The Compton inverse and Bremsstrahlung models and fittings
[SH-1.2-3] 23 p3991 N85-34739
Solar flare gamma-ray line spectroscopy
[SH-2.1-14] 23 p3999 N85-34795
Breeding new light into old machines (and new)
[DE85-013055] 24 p4155 N85-35763
Result of Monte-Carlo simulation of electron-photon cascades in lead and layers of lead-scintillator
[HE-3.6-11] 24 p4185 N85-35958

COMPUTATION
NT MINIMUM VARIANCE ORBIT DETERMINATION
NT ORBIT CALCULATION
Interpolation formulas for viscosity of six gases: Air, nitrogen, carbon dioxide, helium, argon and oxygen
[PB84-217801] 01 p0026 N85-10161
Research in Structures and Dynamics, 1984
[NASA-CP-2335] 01 p0057 N85-10377
Numerical algorithms and parallel tasking
[AD-A145090] 01 p0104 N85-10663
Fast Fourier transform for unequally spaced data 01 p0128 N85-10676
Calculations of optical properties of transition metals
[BLL-M-35744-(5828.4)] 02 p0175 N85-11175
Criteria for the optimization of processing flow in a model of an incremental computer with multiprocessing resources
[INPE-3046-TDL/158] 02 p0240 N85-11560
Parallel triangularization of substructured finite element problems
[NASA-CR-172466] 02 p0241 N85-11569
Concurrent processing and the decomposition of problems
[DE84-015285] 02 p0242 N85-11581
Research topics: Multiprocessing algorithms for computational logic
[DE84-015500] 02 p0242 N85-11583
Shuffle-exchanges on augmented meshes
[NASA-CR-172476] 02 p0243 N85-11587
Comparison of the multigrid and ICCG methods in solving the diffusion equation
[DE84-014409] 02 p0253 N85-11657
Survey of ONERA activities on adaptive-wall applications and computation of residual corrections 03 p0312 N85-12013
An inviscid computational method for supersonic inlets
[AD-A145997] 03 p0316 N85-12042
Verification of a class of deadlock-free, self-timed, computational arrays
[AD-A146272] 03 p0412 N85-12638
Computational models of crystals
[DE84-016631] 04 p0572 N85-13647
Numerical method for computing supersonic flow over wings of flight vehicles 05 p0725 N85-14659
Advanced cube processor
[AD-D011262] 05 p0729 N85-14683
Current status of blast wave theory and computations. Volume 2: The quasi-similar solution
[AD-A146536] 06 p0808 N85-15138
Progress in numerical calculations of ion-atom collisions
[DE84-016598] 06 p0861 N85-15474
Research in applied mathematics, numerical analysis, and computer science
[NASA-CR-172505] 07 p1021 N85-16480
Sequential and parallel matrix computations
[AD-A147871] 07 p1034 N85-16562
Structural optimization and other large-scale processes
[AD-A147895] 07 p1034 N85-16564
Efficient computation of optimal time for transaction processing in a database system
[AD-A147568] 07 p1054 N85-16693
Automated plant, production management system 08 p1139 N85-17171
Computing worldwide sunrise, sunset, moonrise, moonset and twilight times using 5 WWPs 105-3 and 105-4
[AD-A148049] 08 p1189 N85-17490
Resistivity of alloys
[DE85-000906] 09 p1296 N85-18138
Computing environments for data analysis. Part 1. Introduction
[AD-A148677] 09 p1373 N85-18632
Computing environments for data analysis. Part 2. Hardware
[AD-A148678] 09 p1374 N85-18633
Computation of thermal shock-free straightening conditions for aluminum-magnesium alloy welded structures 10 p1449 N85-19131
A circuit grammar for operational amplifier design
[AD-A149566] 10 p1481 N85-19348
Digital high speed programmable convolver
[AD-D011455] 10 p1481 N85-19348
Domain decomposition techniques for solving elliptic partial differential equations on multiprocessors
[DE85-004448] 10 p1549 N85-19769
Application of Monte Carlo and molecular dynamics methods to the calculation of thermodynamic properties of molten salts
[AD-A148897] 10 p1565 N85-19869
Applied mathematics of transport theory
[DE85-000848] 11 p1633 N85-20283
Parallel processing experiences on the Denelcor HEP computer
[DE85-000653] 11 p1702 N85-20703
Polylith and environments for mathematical computation
[DE85-002967] 11 p1702 N85-20704
Solving partial differential equations on multiprocessors
[DE85-000745] 11 p1706 N85-20734
Numerical model for swirl cooling in high-heat-flux particle beam targets and the design of a swirl-flow-based plasma limiter
[DE85-003824] 11 p1732 N85-20894
Instrumentation award
[AD-A150081] 12 p1912 N85-21999

PISCES: An environment for parallel scientific computation
[NASA-CR-172544] 12 p1913 N85-22004
Surface forward scattering and reflection
[AD-A150115] 12 p1926 N85-22112
Development of a Global 3-D magnetohydrodynamic computational model for solar wind-cometary and planetary studies
[NASA-CR-175490] 12 p1962 N85-22331
Rejection of anomalous observations when determining spacecraft trajectories 13 p1979 N85-22421
Second thoughts on the mathematical software effort: A perspective
[DE85-004831] 13 p2148 N85-23333
Sparse matrix computations
[DE85-004780] 13 p2152 N85-23362
Some recent developments in systems reliability
[AD-A150661] 14 p2317 N85-24318
Perceptual organization and visual recognition
[AD-A150828] 14 p2391 N85-24723
Propagation of numerical errors in computers and numerical quality 14 p2396 N85-24760
Arithmetic and elementary functions on mini and microcomputers 14 p2396 N85-24761
Practical methods for the compensation and control of multivariable systems
[AD-A151047] 14 p2407 N85-24841
Properties of systems which lead to efficient computation of reliability
[AD-A151033] 14 p2409 N85-24853
Mathematical modeling of the AEDC (Arnold Engineering Development Center) propulsion wind tunnel (16T)
[AD-A151293] 15 p2475 N85-25275
Infinite computing
[AD-A151437] 15 p2628 N85-26197
BLAS (Basic Linear Algebra Subroutines), linear algebra modules and supercomputers
[AD-A151504] 15 p2628 N85-26199
Recent progress in computational aerodynamics 16 p2693 N85-26626
Techniques for computing the DFT using the residue Fermat number systems and VLSI 16 p2770 N85-27097
Management of vacuum leak-detection processes, standards and calibration
[DE85-006705] 16 p2788 N85-27202
Error reduction program — combustor performance evaluation codes
[NASA-CR-174776] 16 p2852 N85-27584
Nonlinear DSA difference schemes for radiative transfer applications
[DE85-005729] 16 p2856 N85-27611
Optimizing computational efficiency and user convenience in plasma simulation codes
[DE85-007681] 16 p2866 N85-27662
Heating parameter estimation using coaxial thermocouple gages in wind tunnel test articles
[AD-A153039] 17 p2968 N85-28328
The definition and computation of a metric on plane curves. The meaning of a face on a geometric model 17 p3004 N85-28571
Software environment for conducting interactive statistical analysis
[AD-A153378] 17 p3012 N85-28626
Projected discrete ordinates methods for numerical transport problems
[DE85-005632] 17 p3020 N85-28678
Augmented weighted diamond force of the linear nodal scheme for Cartesian coordinate systems
[DE85-005631] 17 p3020 N85-28679
An examination of the use of wave packets for the calculation of atom diffraction by surface
[AD-A152760] 17 p3029 N85-28735
Debugging distributed computations in a nested atomic action system
[AD-A153617] 18 p3162 N85-29585
Computable numerical bounds for Lagrange multipliers of stationary points of nonconvex differentiable nonlinear programs
[AD-A153513] 18 p3169 N85-29633
A comparison of methods of least squares adjustment of traverses
[AD-A153612] 18 p3170 N85-29645
Electronic structure calculations for low coverage adlayers
[DE85-007733] 18 p3179 N85-29709
Numerical optical computing at the Ohio State University 18 p3188 N85-29775
A method for computing the core flow in three-dimensional leading-edge vortices
[NASA-TM-87489] 19 p3214 N85-29932
Research on optimal control, stabilization and computational algorithms for aerospace applications
[NASA-CR-172526] 19 p3221 N85-29970
Approximate factorization method for computation of nonhydrostatic mesoscale flows
[DE85-007259] 19 p3313 N85-30537
SHAPS-2: A three-dimensional computer program for linear/non-linear, static/dynamic analyses of piping systems
[DE85-010500] 19 p3335 N85-30658
An algorithm to test for confluence in a system of left to right rewrite rules
[AD-A154066] 19 p3335 N85-30662
MCNP variance reduction overview
[DE85-010765] 19 p3346 N85-30741
Development of improved capabilities for computation of gas supercompressibility factors and other properties
[PB85-188316] 20 p3436 N85-31315
Optimum filter computation for data transmission
[CNES-83/DRT/TIT/TR/142] 20 p3441 N85-31359
Global mean sea surface based upon a combination of the GEOS-3 and SEASAT altimeter data 20 p3492 N85-31710
Symposium on Computational Mathematics-State-of-the-Art: Informal Proceedings
[DE85-006122] 20 p3516 N85-31858
Intersatellite optical links: The point ahead angle
[CNES-83/DRT/TIT/TR/150] 20 p3533 N85-31964
Survival function of hypo-exponential distributions
[AD-A155518] 21 p3672 N85-32814
On the dependence of the convergence of Gummel's algorithm on the regularity of the solution
[AD-A154628] 21 p3675 N85-32832
Ice fog as an electro-optical obscurant
[AD-A155059] 21 p3705 N85-33015
Magnetics calculations for an ELMO Bumpy Square
[DE85-011438] 21 p3707 N85-33021
System of microprocessor instructions 22 p3770 N85-33362
Finite element methods for viscoelastic flow
[AD-A154877] 22 p3783 N85-33437
Report of Workshop on Computational Geometry and summary of related research
[AD-A155399] 22 p3833 N85-33734
Calculated neutron-induced cross sections for /sup 63,65/Cu/sup 58,60/Ni and (52) Cr from 1 to 20 MeV and comparisons with experiments
[DE85-011928] 22 p3844 N85-33806
Reordering computations for parallel execution
[NASA-CR-177961] 23 p3957 N85-34522
On the statistical significance of excess events: Remarks of caution and the need for a standard method of calculation
[OG-9.5-10] 23 p4031 N85-34987
Adaptive rezoner in a two-dimensional Lagrangian hydrodynamic code
[DE85-010108] 24 p4094 N85-35381
DEPTH-CHARGE static and time-dependent perturbation/sensitivity system for nuclear reactor core analysis, revision 1
[DE85-013103] 24 p4139 N85-35659

COMPUTATIONAL ASTROPHYSICS
Development of a global 3-D magnetohydrodynamic computational model for solar wind/cometary and planetary studies
[NASA-CR-175724] 15 p2684 N85-26577

COMPUTATIONAL CHEMISTRY
Computer calculation of chemical equilibrium in multi-component systems
[BLL-M-35973-(5828.4)] 05 p0614 N85-13919
Integrating chemical kinetic rate equations by selective use of stiff and nonstiff methods
[NASA-TM-86923] 07 p0904 N85-15726

COMPUTATIONAL FLUID DYNAMICS
Computational methods for complex flowfields
[AD-A145219] 01 p0004 N85-10019
Experimental data base for computers program assessment. Report of the Fluid Dynamics Panel Working Group 04: Addendum
[AGARD-AR-138-ADD] 01 p0004 N85-10020
Transonic wing and far field test data on a high aspect ratio transport wing for three dimensional computational method evaluation 01 p0004 N85-10021
Transonic wing and far field test data on a moderate aspect ratio wing for three dimensional computational method evaluation 01 p0004 N85-10022
Computational thermo-fluid dynamics contributions to advanced gas turbine engine design
[NASA-TM-86865] 01 p0011 N85-10089
Aerothermal modeling 02 p0145 N85-10982
Aerothermal modeling program 02 p0145 N85-10983
Numerical simulation of natural convection in porous media — heat transfer
[CFD/84/10] 02 p0199 N85-11330
Computer simulation techniques for turbulent flows
[CFD/84/11] 02 p0199 N85-11331
Inverse design technique for cascades
[NASA-CR-3836] 03 p0311 N85-12008
Model equation for simulating flows in multistage turbomachinery
[NASA-TM-86869] 03 p0315 N85-12036
Status and prospects of computational fluid dynamics for unsteady transonic viscous flows
[NASA-TM-86016] 03 p0315 N85-12037
Vorticity amplification in viscous flow around a body 03 p0360 N85-12309
Second order modeling of scalar turbulent flows 03 p0360 N85-12311
Numerical studies of unsteady transonic flow over an oscillating airfoil
[NASA-TM-86011] 03 p0361 N85-12316
Study of the structure of turbulent shear flows at supersonic speeds and high Reynolds number
[NASA-CR-174144] 04 p0452 N85-12865
Development of computational fluid dynamics at NASA Ames Research Center
[NASA-TM-86021] 04 p0452 N85-12866
Fundamental study of three dimensional two phase flow in combustion systems
[AD-A142896] 04 p0496 N85-13177
Numerical calculations of stratified Ekman layer flow over ridges with a finite element model
[DE84-014482] 04 p0499 N85-13179
Numerical calculation of steady turbulent flows in adverse pressure gradients
[CFD/83/9] 04 p0501 N85-13195
Simulation of separated transonic airfoil flow by finite-difference viscous-inviscid interaction 05 p0591 N85-13768
Transition and mixing in axisymmetric jets and vortex rings 05 p0591 N85-13769
The numerical simulation of steady transonic rotational flow using a dual potential formulation 05 p0591 N85-13770
Transonic jets: A numerical approach in the hodograph plane 05 p0592 N85-13774
Flow calculation on a thin wing, with specific attention to separation point at the trailing edge
[FTW-FO-1721] 05 p0594 N85-13787
A finite element method for three dimensional cavity circulation 05 p0635 N85-14071
Numerical investigations into the paraboilzed Navier-Stokes equations 05 p0635 N85-14075
Theoretical description of film boiling in a two phase flow calculation
[IKE-2-86] 05 p0638 N85-14092
Review of requirements and status of simulation and scaling of transonic, viscous flows
[AD-A146357] 06 p0808 N85-15137
Supersonic nonlinear potential analysis
[NASA-CR-172456] 07 p0897 N85-15685
Analysis of the flow field about a T-45 using PANAIR
[AD-A146811] 07 p0899 N85-15699
Current problems in turbomachinery fluid dynamics
[AD-A147127] 07 p0958 N85-16074
Detailed study of the flow around a multi-element airfoil. Comparison with calculations 08 p1069 N85-16775
Vectorizable multigrid algorithms for transonic flow calculations
[NASA-CR-174326] 08 p1077 N85-16827
The NYU inverse swept wing code
[NASA-CR-3662] 08 p1077 N85-16830
Numerical calculation of the cold-flow characteristics of a bluff-body flame stabilizer
[CFD/84/14] 08 p1124 N85-17068
Analysis of a penalty finite element approximation of the Navier Stokes equations 08 p1161 N85-17321
Computational fluid mechanics utilizing the variational principle of modeling damping seals
[NASA-CR-174332] 08 p1161 N85-17325
Front tracking for gas dynamics
[DE85-000571] 08 p1163 N85-17336
Numerical experiments and theoretical analysis of the flow of an elastic liquid of the Maxwell-Oldroyd type in the presence of geometrical singularities
[WTHD-164] 08 p1163 N85-17340
A numerical study of several supersonic flows 09 p1272 N85-17995
Numerical approach for the aerodynamic analysis if airfoils with laminar separation
[NASA-CR-172496] 09 p1273 N85-18001
Calculating heat transfer coefficients for turbine profiles taking surface curvature and elevated flow turbulence into account 09 p1307 N85-18212
Turbulent jet flow in a channel with a circulation region 09 p1308 N85-18218
Long range effect of turbulent pressure pulsations in plane-parallel flows at different velocities with various flame fronts 09 p1308 N85-18220
Microscopic study of fluid flow 09 p1317 N85-18280
Numerical predictions for unsteady viscous flow past an array of cylinders 09 p1318 N85-18284

An implicit, conservative, zonal-boundary scheme for Euler equation calculations
[NASA-CR-3865] 09 p1318 N85-18290
Researched applied to transonic compressors in numerical fluid mechanics of inviscid flow and viscous flow
[NASA-CR-174353] 09 p1319 N85-18291
Three-dimensional vortex methods
[DE85-000391] 09 p1320 N85-18299
Accuracy of the finite analytic method for scalar transport calculations
[DE85-001474] 09 p1320 N85-18300
Development of multigrid algorithms for problems from fluid dynamics
[GMD-111] 09 p1321 N85-18305
Large deformations of a nonlinear elastic solid and the diffusion of an ideal fluid treated as interacting continua
09 p1330 N85-18356
NASA Lewis Research Center/University Graduate Research Program on Engine Structures
[NASA-TM-86916] 09 p1333 N85-18375
Verification of a model of the Eastern Scheldt
[RAND/R-3108-NETH] 09 p1354 N85-18518
Effects of airfoil shape, thickness, camber, and angle of attack on calculated transonic unsteady airloads
[NASA-TM-86320] 10 p1420 N85-18957
Unsteady transonic flow calculations for two-dimensional canard-wing configurations with aeroelastic applications
[NASA-TM-86375] 10 p1420 N85-18960
Viscous effects on transonic airfoil stability and response
[NASA-TM-86374] 10 p1421 N85-18961
Thrust chamber performance using Navier-Stokes solution — space shuttle main engine viscous nozzle calculation
[NASA-CR-171346] 10 p1430 N85-19019
Preliminary analysis of selected gas dynamic problems — space shuttle main engine main combustion transients and RS nozzle flow
[NASA-CR-171343] 10 p1483 N85-19361
Calculation of flow about posts and powerhead model — space shuttle main engine
[NASA-CR-171344] 10 p1483 N85-19362
Computer studies of baroclinic flow — Atmospheric General Circulation Experiment
[NASA-CR-171338] 10 p1517 N85-19566
Contribution to the study of a numerical implicit method for solving the Euler equations
[ESA-TT-872] 10 p1549 N85-19771
Developments in the simulation of compressible inviscid and viscous flow on supercomputers
[NASA-TM-86674] 11 p1575 N85-19924
A fast algorithm of the finite difference method for computation of the transonic flow past an arbitrary airfoil with the conservative full-potential equation
11 p1619 N85-20191
A mixed finite difference analysis of the internal and external transonic flow fields of inlets with centerbody
11 p1619 N85-20192
Finite difference method for solving turbulent boundary layer equations 11 p1619 N85-20193
A study for calculating rotor loads using free vortex concept 11 p1620 N85-20194
Triple layer system for numerical integration of equations of gas dynamics and nonlinear heat conduction equation
[DE85-000297] 11 p1632 N85-20277
Three-dimensional unsteady lifting surface theory in the subsonic range
[NASA-TM-77812] 12 p1770 N85-21111
Transonic interactions of unsteady vortical flows
[NASA-TM-86656] 12 p1770 N85-21113
Combustion research for gas turbine engines
[NASA-TM-86963] 12 p1778 N85-21164
China report: Science and technology
[JPRS-CST-85-008] 12 p1820 N85-21416
Application of large eddy interaction model to channel flow
[NASA-TM-86691] 12 p1844 N85-21572
Algorithm for the simulation of transient viscoelastic flows with free surfaces
[DE85-002713] 12 p1848 N85-21590
Robust calculation of three-dimensional transonic potential flow based on the nonlinear gas multigrid method and a mixed incomplete lower upper decomposition/strongly implicit procedure (ILU/SIP) algorithm
[NLR-MP-84003-U] 12 p1848 N85-21593
High-pressure rocket engine turnaround duct computational fluid dynamics analysis
13 p2003 N85-22556
Grid generation for a pump collector
[AD-A150217] 13 p2092 N85-23059
F-14A aircraft high-speed flow simulations
[NASA-CR-172559] 14 p2209 N85-23702
Calculating isothermal flow in wake beyond injection zone 14 p2257 N85-24175
Discrete models for the numerical analysis of time-dependent multidimensional gas dynamics
[NASA-CR-172574] 14 p2300 N85-24239
Spectral methods for modeling supersonic chemically reacting flow fields
[NASA-CR-172578] 14 p2300 N85-24240
Transonic Unsteady Aerodynamics and its Aeroelastic Applications
[AGARD-CP-374] 15 p2457 N85-25171
Trends in computational capabilities for fluid dynamics
15 p2457 N85-25172
Numerical studies of unsteady transonic flow over oscillating airfoil 15 p2458 N85-25174
Calculation of harmonic aerodynamic forces of aerofoils and wings from the Euler equations
15 p2458 N85-25177
Calculation of unsteady transonic separated flows by viscous-inviscid interaction 15 p2458 N85-25178
A semi-empirical unsteady transonic method with supersonic free stream 15 p2458 N85-25179
Status and prospects of computational fluid dynamics for unsteady transonic flow 15 p2459 N85-25180
Improvement and extension of a numerical procedure for the three dimensional unsteady transonic flows
15 p2459 N85-25181
Application of time-linearized methods to oscillating wings in transonic flow and flutter
15 p2459 N85-25182
Computation of unsteady transonic flows about two-dimensional and three-dimensional AGARD standard configurations 15 p2459 N85-25183
Calculation of unsteady transonic flow around a high swept wing 15 p2459 N85-25184
Unsteady transonic aerodynamic and aeroelastic calculations about airfoils and wings
15 p2459 N85-25185
The application of transonic unsteady methods for calculation of flutter airloads 15 p2460 N85-25186
The development of unsteady transonic 3-D full potential code and its aeroelastic applications
15 p2460 N85-25187
Transonic aerodynamic and aeroelastic characteristics of a variable sweep wing
[NASA-TM-86677] 15 p2462 N85-25203
A critical evaluation of various turbulence models as applied to internal fluid flows
[NASA-TP-2474] 15 p2554 N85-25757
Flow over a biconic configuration with an afterbody compression flap
[AD-A151882] 15 p2557 N85-25778
Application of the Van Leer method to the solution of one-dimensional volume fraction equations
[CFD/84/17] 15 p2558 N85-25781
Three-dimensional boundary layers and shear flows activities at ONERA/CERT 15 p2558 N85-25785
Three-dimensional boundary layers: A report on work in Germany 15 p2559 N85-25786
Three-dimensional boundary layer research at NLR
15 p2559 N85-25787
Brief review of current work in the UK on three dimensional boundary layers 15 p2559 N85-25788
Problems and opportunities with three-dimensional boundary layers — aircraft, missile, and ship components 15 p2559 N85-25789
Inviscid upwind finite difference model for two dimensional vertical axis wind turbines
15 p2585 N85-25933
Stream dynamics between 1 AU and 2 AU: A detailed comparison of observations and theory
[NASA-TM-86086] 15 p2684 N85-28578
Proceedings of the NAL Symposium on Aircraft Computational Aerodynamics
[NAL-SP-1] 16 p2691 N85-26611
Some numerical analyses of flows with separation
16 p2692 N85-26616
Two computational methods for cascade flows
16 p2692 N85-26617
The role of computational fluid dynamics in aeronautical engineering 16 p2694 N85-26629
A method for simulating 3-D aircraft flow fields with jet plume effects
[NASA-CR-175802] 16 p2699 N85-26664
Low Reynolds number vehicles
[AGARD-AG-288] 16 p2699 N85-26666
Application of CFD techniques toward the validation of nonlinear aerodynamic models
[NASA-TM-86715] 16 p2700 N85-26671
A numerical simulation of the NFAC (National Full-scale Aerodynamics Complex) open-return wind tunnel inlet flow
[NASA-TM-86724] 16 p2700 N85-26672
Numerical solution of transonic normal shock wave-boundary layer interaction using the Bohning-Zierop model — wind tunnel flow
[VTH-LR-416] 16 p2701 N85-26683
Solid fuel combustion chamber
[VTH-LR-415] 16 p2741 N85-26918
Solid fuel combustion chamber
[VTH-LR-438] 16 p2741 N85-26919
Turbulent flow of fluid near trailing edge of plate in stream at zero angle of attack 16 p2764 N85-27067
LU methods for the compressible Navier-Stokes equations 16 p2781 N85-27160
Theoretical investigation of three-dimensional shock wave turbulent boundary layer interactions. Part 3
[AD-A152251] 16 p2783 N85-27177
The development of a computational model for a two-dimensional turbulent flow. Part 1: Mathematical background — solid fuel combustion
[VTH-LR-436-PT-1] 16 p2785 N85-27188
Adaptive grid generation for numerical solution of Burger's equation
[AD-A152217] 16 p2855 N85-27606
Future fundamental combustion research for aeropropulsion systems
[NASA-TM-87049] 17 p2898 N85-27870
CALTECH-DOE program on numerical analysis, computing and fundamental studies of motion, energy and mass transfer in fluids
[DE85-008106] 17 p2959 N85-28274
A second-order pressure-correction method for viscous incompressible flow
[REPT-84-15] 17 p2960 N85-28280
Numerical simulation of unsteady motion in a turbulent mixing layer
[NAL-TR-849T] 18 p3099 N85-29183
Two approaches for the prediction of plume-induced separation
[AD-A154098] 19 p3215 N85-29935
Study of second order upwind differencing in a recirculating flow
[NASA-CR-174939] 19 p3264 N85-30243
Decay of a coherent scalar disturbance in a turbulent flow
[NASA-TM-86700] 19 p3264 N85-30244
Application of computational fluid dynamics to complex inlet ducts
[NASA-TM-87060] 19 p3265 N85-30247
On spectral multigrid methods for the time-dependent Navier-Stokes equations
[NASA-CR-172613] 19 p3344 N85-30725
Calculation of transonic flows around an aircraft configuration with motorized nacelle
[SNIAS-851-111-106] 20 p3387 N85-31008
Transonic calculations for a flexible supercritical wing and comparison with experiment
[NASA-TM-86439] 20 p3388 N85-31012
Calculation of flow around the SF 310 airplane using a full potential equation method
[FFA-TN-1984-63] 20 p3389 N85-31022
A theory of quasi-conical solutions of noninteger degree — flow fields on supersonic wings
[UTH-LR-420] 20 p3390 N85-31024
A supersonic potential gradient method for the calculation of unsteady aerodynamic pressures on harmonically oscillating wings
[DFVLR-FB-85-11] 20 p3390 N85-31026
Verification of calculation methods for unsteady airloads in the precipitation of transonic flutter
[NLR-MP-84016-U] 20 p3390 N85-31027
Numerical and experimental investigation of turbomachinery rotor flow fields
20 p3451 N85-31429
A new finite element approach: Progress in inviscid flow computations
[NASA-TM-86434] 20 p3454 N85-31450
Three-Dimensional Techniques Applied to Internal Flows in Propulsion Systems
[AGARD-LS-140] 21 p3586 N85-32293
The calculation of fully three dimensional flow through any type of turbomachine blade row
21 p3587 N85-32294
An analysis of flow models: From Navier-Stokes to potential flow equations 21 p3587 N85-32295
Computation of three-dimensional, inviscid, rotational flows 21 p3587 N85-32296
An elliptic calculation procedure for 3-D viscous flow
21 p3587 N85-32297
A 3-D Euler method for internal transonic flows computation with a multi-domain approach
21 p3587 N85-32298
Performance evaluation of flow in turbomachinery blade rows 21 p3587 N85-32299
Numerical solution of the Navier-Stokes equations for 3-D internal flows: An emerging capability
21 p3588 N85-32300

Calculation of 3-D flow without numerical mixing
21 p3588 N85-32301
Gradient scaling for nonuniform meshes
[DE85-009625] 22 p3784 N85-33443
Tabular and graphical solutions of regular and Mach reflections in pseudo-stationary frozen and vibrational-equilibrium flows, part 1
[UTIAS-283-PT-1] 23 p3893 N85-34117
Tabular and graphical solutions of regular and Mach reflections in pseudo-stationary frozen and vibrational-equilibrium flows, part 2
[UTIAS-283-PT-2] 23 p3894 N85-34118
A study of the second and third order closure models of turbulence for prediction of separated shear flows
[NASA-CR-176127] 23 p3929 N85-34953
Studies on effects of boundary conditions in confined turbulent flow predictions
[NASA-CR-3929] 24 p4083 N85-35371

COMPUTATIONAL GRIDS

Embedded-grid generation with complete continuity across interfaces for multi-element airfoils
02 p0133 N85-10911
Discretization formulas on an arbitrary grid
[FFA-MEMO-127] 02 p0253 N85-11659
Comprehensive silicon solar cell computer modeling
[NASA-CR-174151] 04 p0530 N85-13386
Analytical construction of flight vehicle surfaces
06 p0775 N85-14957
Vectorizable multigrid algorithms for transonic flow calculations
[NASA-CR-174326] 06 p1077 N85-16827
Front tracking for gas dynamics
[DE85-000571] 06 p1163 N85-17336
Numerical generation of orthogonal and nonorthogonal coordinates in two dimensional simply and doubly connected regions
[VKI-TN-151] 08 p1216 N85-17662
An implicit, conservative, zonal-boundary scheme for Euler equation calculations
[NASA-CR-3965] 09 p1318 N85-18290
Development of multigrid algorithms for problems from fluid dynamics
[GMD-111] 09 p1321 N85-18305
On the connection between multigrid and cyclic reduction
[NASA-TM-86020] 09 p1373 N85-18629
The implementation of irregular grid systems for the finite difference solution of partial differential equations
[LU-MATH-RES-181] 09 p1373 N85-18630
Experimental approach to terms within grids — turbulent flow calculations
11 p1576 N85-19930
Computation of the inviscid velocity potential for general ellipsoids on a nearly quadratic surface grid
[REPT-25/84] 11 p1633 N85-20287
Solution of the three-dimensional Navier-Stokes equations for a steady laminar horseshoe vortex flow
[AD-A149851] 12 p1846 N85-21582
Robust calculation of three-dimensional transonic potential flow based on the nonlinear gas multigrid method and a mixed incomplete lower upper decomposition/strongly implicit procedure (ILU/SIP) algorithm
[NLR-MP-84003-U] 12 p1848 N85-21593
Mesh effects on the computation of non-linear gravity waves of arbitrary discharge
[COLL-AERON-8501] 12 p1888 N85-21848
Differentiating matrices for arbitrarily spaced grid points
[NASA-CR-172556] 12 p1919 N85-22051
Numerical methods for tracking interfaces
[LA-9917-MS] 12 p1919 N85-22052
Approximation order from certain spaces of smooth bivariate splines on a 3-direction mesh
[AD-A149833] 12 p1925 N85-22092
Correcting depth line on nonlongitudinal seismic profile
13 p2117 N85-23184
The complexity of reliability computations in planar and acyclic graphs
[AD-A150750] 14 p2408 N85-24845
A fast ray tracing routine for laterally inhomogeneous media
[AD-A150984] 14 p2421 N85-24938
Communication complexity of the Gaussian elimination algorithm on multiprocessors
[AD-A151891] 15 p2638 N85-26267
Mathematical software for hyperbolic equations and two point boundary value problems
[AD-A151982] 15 p2638 N85-26270
Solution of coupled system of PDE by the transistorized multigrid method
[DE85-006377] 15 p2639 N85-26276
Application of conformal mapping to grid generation
16 p2692 N85-26621
Local uniform mesh refinement on loosely-coupled parallel processors
[AD-A152199] 16 p2850 N85-27571
Adaptive grid generation for numerical solution of Burger's equation
[AD-A152217] 16 p2855 N85-27606
Computational Geometry and Computer-Aided Design
[NASA-CP-2379] 17 p3003 N85-28563
Examination of the circle spline routine
17 p3004 N85-28573
Parameterization in grid generation
17 p3005 N85-28581
Contouring trivariate data 17 p3005 N85-28582
Generation of surface coordinates by elliptic partial differential equations 17 p3006 N85-28583
A survey of composite grid generation for general three-dimensional sections 17 p3006 N85-28584
A discussion of adaptive grids and their applicability in numerical hydrodynamic modeling
[AD-A151843] 17 p3017 N85-28659
Developement of an optimum interpolation analysis method for the CYBER 205 18 p3143 N85-29456
Response of winter forecasts made with the GLA Fourth Order GCM to Changes in the horizontal grid resolution
18 p3143 N85-29458
Tradeoffs among portability, complexity, and efficiency in multiprocessing environments
[DE85-007899] 18 p3161 N85-29580
Embedding graphs in lines, trees and grids
19 p3334 N85-30652
On spectral multigrid methods for the time-dependent Navier-Stokes equations
[NASA-CR-172613] 19 p3344 N85-30725
On MGR (Upsilon) multigrid methods
[AD-A153887] 19 p3345 N85-30733
Computer program for plotting and fairing wind-tunnel data
[NASA-TM-85648] 20 p3387 N85-31009
Application of closed-form solutions to a mesh point field in silicon solar cells 20 p3482 N85-31637
Generation of three-dimensional body-fitted coordinates using hyperbolic partial differential equations
[NASA-TM-86753] 20 p3519 N85-31887
Calculation of transonic steady and oscillatory pressures on a low aspect ratio model and comparison with experiment
[NASA-TM-86449] 21 p3551 N85-32092
Simulation of complex three-dimensional flows
[NASA-TM-86773] 21 p3675 N85-32831
A vectorized nearest-neighbors algorithm of order N using a monotonic logical grid
[AD-A155169] 21 p3679 N85-32853
Generation by conformal mappings of aerofoil sections and of certain other simple shapes suitable for both aerodynamic and stress-concentration problems
[AD-A154901] 22 p3728 N85-33112
Use of a hyperbolic grid generation scheme in simulating supersonic viscous flow about three-dimensional winged configuration
[NASA-TM-85344] 23 p3893 N85-34116
Box truss analysis and technology development. Task 1: Mesh analysis and control
[NASA-CR-172570] 23 p3900 N85-34156

COMPUTER AIDED DESIGN

Applications of numerical optimization methods to helicopter design problems: A survey
[NASA-TM-86010] 01 p0006 N85-10036
The Influence of Large Scale Computing on Aircraft Structural Design
[AGARD-R-706] 01 p0007 N85-10040
Aerospatiale's experimentations of vectorization on supercomputers for aircraft structural problems
01 p0007 N85-10041
Large scale computing in aeronautical design
01 p0007 N85-10043
AGS-880 menu system user guide
[DE84-014338] 01 p0104 N85-10699
Interactive system for the interpretation of coal deposit data as a basis of future mine planning systems
[BMFT-FB-T-83-115] 02 p0220 N85-11449
Air Force Human Resources Laboratory report: Fiscal year, 1983
[AD-A145647] 02 p0238 N85-11548
Air Force honeycomb shaping at SM-ALC (Sacramento Air Logistics Center)
[AD-P004005] 03 p0306 N85-11985
Kinematic synthesis of planar cam-link mechanisms for exact path and exact motion generation
03 p0341 N85-12189
VLSI (Very Large Scale Integration) design tools reference manual, release 1.0
[AD-A148273] 03 p0408 N85-12604
An input translator for a computer-aided design system
[AD-A146337] 03 p0408 N85-12605
CONTROL: A suite of interactive transfer-function analysis programs
[OUEL-1527/84] 03 p0408 N85-12609
Turbomachinery blade design using advanced calculation methods
[PNR-90218] 04 p0458 N85-12896
Conceptual design for scaled truss antenna flight experiment
[NASA-TM-85804] 04 p0462 N85-12932
High-temperature steam electrolysis: Technical and economic evaluation of alternative process designs
[DE84-015702] 04 p0469 N85-12986
Computerized circuit designs: Realization of masks to manufacture microwave circuits
[CNES-NT-107] 04 p0496 N85-13168
Standard cell initial placement strategy
[DE84-016921] 05 p0632 N85-14051
User-oriented development and production of integrated circuits in small and medium quantities
[BMFT-FB-T-84-171] 05 p0633 N85-14059
Increase in the economy of design and process planning by integrated and graphic data processing, phase 2 — aircraft design
[BMFT-FB-W-84-028] 05 p0716 N85-14589
Computer-aided design of extrusion dies by metal-flow simulation 06 p0797 N85-15094
VLSI design tools, reference manual, release 2.0
[AD-A146444] 06 p0803 N85-15112
Specialized silicon compilers for language recognition
[AD-A146526] 06 p0853 N85-15425
Recent advances in data compression
[DE85-001133] 06 p0854 N85-15432
Control system design language implementation of a gas turbine starting controller
[AD-A147896] 07 p0905 N85-15732
The design of high order active RC-filters
[DRIC-T-7147] 07 p0945 N85-15987
Trends in development of software for computer-aided analysis of large-scale integrated circuits
07 p0955 N85-16055
Program visualization: Graphics support for software development
[AD-A146887] 07 p1024 N85-16499
The reactor dynamic code RETRANS: Structure and users guide
[OEFZS-4287] 07 p1041 N85-16614
Hardware/software codesign for maintainable systems
08 p1066 N85-16753
Design of an airfoil leading edge slat using an inverse aerodynamic calculation method
08 p1069 N85-16777
Design of a digital ride quality augmentation system for commuter aircraft
[AD-A148233] 08 p1088 N85-16879
Challenges of developing an electro-optical system for measuring man's operational envelope
08 p1095 N85-16921
East Europe report: Science and technology
[JPRS-ESA-84-047] 08 p1140 N85-17163
A computer aided Multi-Man-Machine Work Area Design and Evaluation System (MAWADES)
[AD-A147950] 08 p1199 N85-17554
Adapting logistics models to a microcomputer for interface with computer-aided design systems
[AD-A147666] 08 p1202 N85-17566
Extraction of feature information from 3-dimensional CAD data 08 p1203 N85-17573
COPES/ADS (Control Program for Engineering Synthesis) (Automated Design Synthesis) using the ADS optimization program
[AD-A148576] 08 p1206 N85-17586
Correction of engraving stamp for forming blanks of gas turbine engine blades 09 p1307 N85-18213
Generation of radiation transport geometry from computer-generated design data — monte carlo solution of the neutron transport equation
[DE84-017380] 09 p1370 N85-18606
Siemens' CAD system designs VLSI circuits
10 p1461 N85-19209
Productivity gains through CAD of CNC programs
10 p1462 N85-19219
Research into self-timed VLSI circuits
[AD-A149140] 10 p1479 N85-19339
SUBOPT: A CAD program for suboptimal linear regulators
[NASA-CR-172536] 10 p1539 N85-19702
Graphics translators for computer-aided drafting and design: Interface alternatives for the A/E community
[AD-A148892] 10 p1540 N85-19706
Management challenges encountered in CAD implementation
[DE85-002072] 10 p1541 N85-19716
Design of explosive logic elements
[DE84-009811] 11 p1614 N85-20146
Overview of leading-edge research at French CNRS lab 11 p1618 N85-20179
CAD/CAM systems for printed circuit design, manufacture 11 p1619 N85-20188

Console I/O routines
[DE85-002644] 11 p1702 N85-20700
Computer aided of maintainability design: A feasibility study
[AD-A149293] 11 p1738 N85-20932
ACOSS 17 (Active Control of Space Structures)
[AD-A150007] 12 p1793 N85-21253
Computer integration of engineering design and production: A national opportunity
[NASA-CR-175483] 12 p1820 N85-21414
Structural sensitivity analysis: Methods, applications and needs
[NASA-TM-85827] 12 p1865 N85-21695
A survey of the project CIP: Computer aided, intuition-guided programming. Wide spectrum language and program transformations
[TUM-I8406] 12 p1912 N85-22000
Evaluation of PHOENICS as a design analysis tool for SSME 12 p1949 N85-22240
Study for the optimization of a transport aircraft wing for maximum fuel efficiency. Volume 1: Methodology, criteria, aeroelastic model definition and results
[NASA-CR-172551] 13 p1971 N85-22378
A description of the Langley wireframe geometry standard (LaWGS) format
[NASA-TM-85767] 13 p1971 N85-22380
Preliminary development of an approximation procedure for supercritical wing design optimization applications
[AD-A150177] 13 p1972 N85-22383
Computer aided engineering applied to the design and verification of the generic Advanced Rigid Array (ARA) — solar array 13 p2008 N85-22593
Redesign of fuselage compartments by method of special contours 13 p2042 N85-22784
Computer aided antenna design and frequency selection for HF communications
[AD-A150485] 13 p2055 N85-22869
Optimum design of electrical motors for multilink manipulators and automated manufacturing systems 13 p2062 N85-22880
Algorithm in Walsh function basis for analysis of integrated microcircuits on MOS-structures 13 p2083 N85-23006
Grid generation for a pump collector
[AD-A150217] 13 p2092 N85-23059
Development of a single-family absorption chiller for use in a solar heating and cooling system, phase 3, volume 2
[DE85-003218] 13 p2130 N85-23253
Motion planning with six degrees of freedom
[AD-A150312] 13 p2165 N85-23432
Software for designing teeth for reduction gears and transmissions 14 p2221 N85-23773
Cable-catenary large antenna concept 14 p2231 N85-23829
Construction of profiles of intermediate blade sections from master profiles given on conical surfaces 14 p2272 N85-24075
French work toward flexible software workshops 14 p2289 N85-24187
East Europe report: Science and technology
[JPRS-ESA-85-015] 14 p2289 N85-24189
Research on CAD/CAM support for microprocessor development surveyed 14 p2290 N85-24193
Integration of solid modeling and database management for CAD/CAM 14 p2402 N85-24804
An expert system for choosing the best combination of options in a general-purpose program for automated design synthesis
[NASA-TM-86329] 14 p2402 N85-24807
Mini-Seminar on CAD/CAM
[CSIR-TSD-0007/83] 14 p2402 N85-24809
Selection criteria for a CAD/CM system 14 p2402 N85-24810
The use of a 3-D system for a civil engineering project 14 p2402 N85-24811
EDIPAS: A multidiscipline and integrated facility for management and evaluation of engineering data
[NLR-MP-83062-U] 14 p2405 N85-24832
Selection criteria and computer aided design (CAD) systems
[NLR-MP-84037-U] 14 p2406 N85-24834
Executive control systems in the engineering design environment
[NASA-CR-172582] 14 p2406 N85-24835
Preliminary helicopter design decision making based on flight performance factors
[AD-A151468] 15 p2471 N85-25254
Resources for robotics research in Europe, by country 15 p2489 N85-25364
An analysis of grid-based line drawing quantization methods
[AD-A151847] 15 p2522 N85-25547
French firm plans recapture of domestic CAD/CAM market 15 p2535 N85-25641
Criteria for qualifying for FRG federal CAD/CAM subsidies 15 p2536 N85-25651
East Europe report: Science and technology
[JPRS-ESA-85-018] 15 p2537 N85-25658
Process control systems for largely automated manufacturing 15 p2537 N85-25659
CaD systems for electronic component design reviewed 15 p2537 N85-25660
Applications, specifications of Robotron CAD-CAM work stations 15 p2537 N85-25661
Mathematical aspect of welding technology research discussed 15 p2538 N85-25663
Conversion of algorithms to custom integrated circuit devices
[AD-A151288] 15 p2547 N85-25720
Analysis of the capability to effectively design complementary metal oxide semiconductor integrated circuits
[AD-A151832] 15 p2548 N85-25728
Use of computer-aided design in large-computer development described 15 p2564 N85-25822
Isoparametric 3-D finite element mesh generation using interactive computer graphics 15 p2574 N85-25873
CADS: A Computer Aided Design System 15 p2574 N85-25876
Use of COSMIC NASTRAN in a design department 15 p2575 N85-25881
The structural finite element model of the C-5A 15 p2576 N85-25885
User's guide for concrete strength investigation and design (CSTR)
[AD-A151617] 15 p2579 N85-25906
Symposium on Computers in Civil Engineering 1983
[CSIR-S-298] 15 p2626 N85-26182
Future directions in computers 15 p2626 N85-26183
Computers and the consulting engineer 15 p2626 N85-26184
Programme development: A state of the art 15 p2626 N85-26185
CAD/CAM (Computer-Aided Design/Computer-Aided Manufacturing) highlights
[AD-A151532] 15 p2629 N85-26201
A microcomputer-based program for printing check plots of integrated circuits specified in Caltech intermediate form
[AD-A151715] 15 p2629 N85-26205
SPRING: Helical spring design software for microcomputers
[DE85-006200] 15 p2631 N85-26217
IPAD: Integrated Programs for Aerospace-vehicle Design
[NASA-CR-3890] 15 p2632 N85-26221
Design of a variable-focal-length optical system
[NASA-CR-175710] 15 p2651 N85-26349
Computational aerodynamics for aircraft wing design 16 p2693 N85-26627
A numerical design method for three-dimensional transonic wings 16 p2694 N85-26631
Three-dimensional wing boundary layer analysis program BLAY and its application 16 p2694 N85-26632
Design-To-Cost (DTC) methodology to achieve affordable avionics 16 p2696 N85-26645
A modern control design methodology with application to the CH-47 helicopter
[AD-A151946] 16 p2710 N85-26723
Status, prospects of computer-aided design discussed 16 p2767 N85-27073
An integrated UNIX-based CAD system for the design and testing of custom VLSI chips 16 p2771 N85-27102
Development and application of optimum sensitivity analysis of structures
[NASA-CR-175857] 16 p2799 N85-27257
China report: Science and Technology
[JPRS-CST-85-012] 16 p2806 N85-27300
Fujian forges ahead in electronic production 16 p2806 N85-27301
The systematic integration of very large scale integrated circuit computer-aided design tools into a toolkit optimized for academic applications
[AD-A151813] 16 p2845 N85-27538
Further development of an Interactive Control Engineering Computer Analysis Package (ICECAP) for discrete and continuous systems
[AD-A151783] 16 p2846 N85-27546
Manufacturing methods and technology CAD/CAM (Computer-Aided Design/Computer-Aided Manufacturing) related efforts (FY 1980 - 1986)
[AD-A151817] 16 p2846 N85-27547
Numerical optimization algorithm for engineering problems using microcomputer
[AD-A152135] 16 p2847 N85-27554
Mathematical programming in computer network design
[AD-A152275] 16 p2848 N85-27556
Mapping principles for the standards interface for computer aided design
[PB85-177905] 16 p2849 N85-27566
The application of computer aided structural optimization to the design of aircraft components
[MBB-UT-21/84-O] 16 p2873 N85-27728
NBS (National Bureau of Standards) research reports
[PB85-127421] 16 p2879 N85-27764
Aerodynamic research in preparation for a new Dutch transport aircraft with supercritical wings
[B8580077] 17 p2893 N85-27836
Methods for design aerodynamics of modern transport aircraft
[DFVLR-FB-85-05] 17 p2893 N85-27838
USAF damage tolerant design handbook: Guidelines for the analysis and design of damage tolerant aircraft structures, revision B
[AD-A153161] 17 p2896 N85-27858
Engineering robot actions in a computer integrated manufacturing environment
[CWI-CS-R8415] 17 p2938 N85-28139
Future directions of robotics, automation in Italy 17 p2946 N85-28187
Report on high intensity solar cells
[DE85-006396] 17 p2987 N85-28462
Computational Geometry and Computer-Aided Design
[NASA-CP-2379] 17 p3003 N85-28563
Multivariate spline algorithms for CAGD 17 p3003 N85-28566
A survey of patch methods 17 p3003 N85-28567
Boundary to constructive solid geometry mappings: A focus on 2-D issues 17 p3004 N85-28570
Adapting shape parameters for cubic Bezier curves 17 p3004 N85-28576
Triangular Berstein-Bezier patches, a survey and new results 17 p3005 N85-28577
A uniform subdivision method for triangular Bezier patches 17 p3005 N85-28578
An intuitive approach to geometric continuity for parametric curves and surfaces (extended abstract) 17 p3005 N85-28579
Urn models and beta-splines 17 p3005 N85-28580
A unified representation scheme for solid geometric objects using B-splines (extended abstract) 17 p3006 N85-28585
Improving the effectiveness of integral property calculation in a CSG solid modeling system by exploiting predictability 17 p3006 N85-28586
Spline curves, wire frames and B-value 17 p3006 N85-28587
A new technique for system-to-system transfer of surface data 17 p3007 N85-28589
Curved finite elements and curve approximation 17 p3007 N85-28590
Comparison of two algebraic methods for curve/curve intersection 17 p3007 N85-28591
Manufacturing information system
[AD-A152715] 17 p3011 N85-28616
A modern control theory enhancement to an Interactive Control Engineering Computer Analysis Package (ICECAP)
[AD-A153249] 17 p3012 N85-28622
Advanced secondary power system for transport aircraft
[NASA-TP-2463] 18 p3062 N85-28944
West Europe report: Science and technology
[JPRS-WST-84-032] 18 p3086 N85-29095
MBB expands CADAM system for a 320 program 18 p3087 N85-29099
An interactive computer aid for the design and analysis of linear, single input/single output digital and continuous control systems
[AD-A153704] 18 p3162 N85-29589
Two-dimensional/speed/couple/data base management system
[A-1] 18 p3165 N85-29606
Three-dimensional/integration two and three dimensional/numerical control/communication
[A-2] 18 p3165 N85-29609
The CEADS-CADD system
[A-4] 18 p3165 N85-29610
System test CALMA DDM (Design Drafting Manufacturing)
[A-5] 18 p3165 N85-29611
The International Computers Limited (ICL) PERQ 1/Engineering Architectural Graphics Language Environment (EAGLE) Computer Aided Design system (CAD)
[A-7] 18 p3165 N85-29612
System test: Hewlett-Packard draft
[A-9] 18 p3166 N85-29613

Test Drawing Office Graphics System (DOGS)/APOLLO
[A-10] 18 p3166 N85-29614
Some examples of the application of automatically guided vehicle systems
[HSE-TRANS-11134] 19 p3281 N85-30348
CAE tool catalog
[DE85-011290] 19 p3334 N85-30657
Demonstration project: Putting the bioastronautics data book on line
[NASA-CR-178424] 19 p3335 N85-30659
Interactive computer program for the analysis and design of linear time invariant systems
[AD-A154076] 19 p3335 N85-30664
Design of the nacelle for the A-320 aircraft
[SNIAS-851-111-111] 20 p3393 N85-31048
Design and evaluation of control systems for large communications satellites 20 p3409 N85-31157
Intersection of three-dimensional geometric surfaces
[NASA-TP-2454] 20 p3513 N85-31839
System test Oce 5200
[A-3] 20 p3515 N85-31850
The General Drafting System (GDS) design system
[A-6] 20 p3517 N85-31869
The IGOS design system
[A-8] 20 p3517 N85-31870
FAUST: Introduction and overview — self tuning control
[OUEL-1568/85] 20 p3519 N85-31882
R and D activities of the Aerodynamics Division 20 p3539 N85-32023
R and D activities of the Propulsion Division 20 p3539 N85-32025
NASA space station automation: AI-based technology review. Executive summary
[NASA-CR-176096] 21 p3558 N85-32135
Importance of automation, robotization in economy 21 p3572 N85-32219
Design of a sixteen-bit pipelined adder using CMOS bulk P-well technology
[AD-A155043] 21 p3580 N85-32260
Design of a generator for near-tangential transonic swirling outflow
[AD-A155163] 21 p3584 N85-32280
Research and development activities in unified control-structure modeling and design
[NASA-CR-176129] 22 p3740 N85-33179
State of art and development problems in computer-aided design of electronic circuits 22 p3766 N85-33342
Modeling of electronic circuits with high degree of component integration 22 p3766 N85-33343
Adaptive modeling of electronic circuits 22 p3766 N85-33345
Algorithms and organization of software for computer-aided circuit design 22 p3767 N85-33347
System for computer-aided design of analog electronic circuits 22 p3768 N85-33353
Algorithms for constructing models of circuit elements in input language of computer-aided design software 22 p3768 N85-33356
IGES/RIM Parser/Converter users guide
[DE85-011965] 22 p3829 N85-33716
User commands for product design and system management
[DE85-011706] 22 p3830 N85-33721
A strategy planner for NASA robotics applications
[NASA-CR-175319] 22 p3834 N85-33738
Proceedings of the Mechanisms Conference, volume 1 23 p3923 N85-34309
Proceedings of the Mechanisms Conference, volume 2 23 p3924 N85-34318
Optimisation in the computer aided design of mechanisms 23 p3924 N85-34321
Design and lubrication of high-speed rolling-element bearings
[NASA-TM-87107] 23 p3938 N85-34409
A model for graphics interface tool development 23 p3960 N85-34545
An analysis and algorithm for filling propagation 23 p3961 N85-34551
The CADME approach to the interface of solid modellers 23 p3961 N85-34554
An innovative user interface for microcomputer-based computer-aided design 23 p3961 N85-34555
A geometric modeller for turbomachinery applications 23 p3962 N85-34556
Architecture of languages for large CAD systems development 23 p3962 N85-34557
Design and implementation of an interactive route editor 23 p3962 N85-34559
A user-friendly computer-aided construction of boundaries 23 p3962 N85-34564
A simple but systematic CSG system 23 p3963 N85-34569
Geometric continuity with interpolating Bezier curves 23 p3963 N85-34570
An intuitive approach to geometric continuity for parametric curves and surfaces 23 p3963 N85-34571
Developing graphical tools with minimal GKS 23 p3964 N85-34573
Designing a graphics application interface 23 p3964 N85-34574
Low cost geometric modelling system for CAM 23 p3964 N85-34578
Computer animation in distance teaching 23 p3965 N85-34581
Generative design in architecture using an expert system 23 p3965 N85-34582
Design and construction of an advanced power conditioning subsystem for small photovoltaic applications
[DE85-013940] 24 p4113 N85-35495
VLSI (Very Large Scale Integrated) tutorials through the video-computer courseware implementation system
[AD-A155889] 24 p4135 N85-35631
Establishment of a Computer-Aided Design (CAD)-Computer-Aided Manufacturing (CAM) process for the production of cold forged gears
[AD-A155756] 24 p4137 N85-35644
Software maintenance relating to the input translator and z-80 realization volume of the computer systems design environment
[AD-A155849] 24 p4138 N85-35646
Computer Aided Design (CAD) methods for very large scale integration systems
[BMFT-FB-T-85-029] 24 p4141 N85-35668

COMPUTER AIDED MANUFACTURING

ICAM (Integrated Computer Aided Manufacturing) conceptual design for computer-integrated manufacturing. Volume 4, part 6: Task d. Quality assurance/quality control/technical requirement/tasks, quality assurance modeling and analysis, quality assurance program management standard recommendations (ISP)
[AD-A144891] 01 p0056 N85-10372
Integrated computer-aided manufacturing (ICAM) architecture. Part 3, volume 8: Technology transfer
[AD-A144732] 01 p0103 N85-10689
Computer aided process planning of machined metal parts
[AD-A145628] 02 p0189 N85-11283
DoD Robotics Application Workshop Proceedings
[AD-A145867] 03 p0307 N85-11978
Sensor technology for second, third generation industrial robots. Optical sensor applications 03 p0342 N85-12198
East Europe report: Science and technology
[JPRS-ESA-84-041] 04 p0484 N85-13090
Use of robotics in heavy machinery, equipment construction industry 04 p0485 N85-13093
Robotics technology application assessed, statistics 04 p0485 N85-13094
Computerized circuit designs: Realization of masks to manufacture microwave circuits
[CNES-NT-107] 04 p0496 N85-13168
Manufacturing Sciences and Robotics Research and Development Act of 1984
[H-REPT-98-1078] 04 p0578 N85-13688
Design and construction of a mode converter from rectangular TE 10 to circular TE 11
[REPT-84-158] 05 p0633 N85-14064
Specialized silicon compilers for language recognition
[AD-A146526] 06 p0853 N85-15425
Manufacturing methods and technology project summary reports
[AD-A148209] 06 p1138 N85-17163
Automated plant, production management system 06 p1139 N85-17171
Coordinated research in robotics and integrated manufacturing
[AD-A148204] 06 p1168 N85-17365
Cognitive asymmetry and occupation. Computer programmers, students, and bank personnel, part 1 and part 2
[AD-A147125] 06 p1197 N85-17540
Extraction of feature information from 3-dimensional CAD data 06 p1203 N85-17573
Flexible manufacturing system for machining axially symmetric workpieces
[PNR-90229] 09 p1305 N85-18196
The planning of flexible manufacturing systems
[PNR-90230] 09 p1371 N85-18613
The use of simulation for the technical and economic evaluation of flexible manufacturing systems. Part 2: Results of the simulation
[PNR-90233-PT-2] 09 p1371 N85-18614
Control of the manufacturing process and material flow in flexible manufacturing systems
[PNR-90234] 09 p1371 N85-18615
The control of manufacturing systems for varying medium-batch production
[PNR-90235] 09 p1371 N85-18616
State and development of the machine-tool industry in Japan. Part 2: Flexible manufacturing systems
[PNR-90236-PT-2] 09 p1371 N85-18617
Material flow in the manufacturing system: Fault-diagnosis systems as support for the maintenance of highly automated manufacturing systems
[PNR-90238] 09 p1371 N85-18618
European Scientific Notes, volume 38, number 12
[AD-A148713] 09 p1418 N85-18946
Competitive assessment of the US manufacturing automation equipment industries
[PB85-103827] 10 p1563 N85-19893
West Europe report: Science and technology
[JPRS-WST-85-006] 11 p1618 N85-20183
CAD/CAM systems for printed circuit design, manufacture 11 p1619 N85-20188
Computer integration of engineering design and production: A national opportunity
[NASA-CR-175483] 12 p1820 N85-21414
Impacts of robotic and flexible manufacturing technologies on manufacturing costs and employment
[AD-A150060] 12 p1860 N85-21668
The EEC's information technology program: An update
[AD-A150022] 12 p1951 N85-22258
Flexible manufacturing system for the production of aircraft parts
[PNR-90237] 14 p2207 N85-23687
MBB automates aircraft production in many FRG facilities 14 p2289 N85-24188
East Europe report: Science and technology
[JPRS-ESA-85-015] 14 p2289 N85-24189
Research on CAD/CAM support for microprocessor development surveyed 14 p2290 N85-24193
Integration of solid modeling and database management for CAD/CAM 14 p2402 N85-24804
Mini-Seminar on CAD/CAM
[CSIR-TSD-0007/83] 14 p2402 N85-24809
EDIPAS: A multidiscipline and integrated facility for management and evaluation of engineering data
[NLR-MP-83062-U] 14 p2405 N85-24832
Executive control systems in the engineering design environment
[NASA-CR-172582] 14 p2406 N85-24835
Resources for robotics research in Europe, by country 15 p2489 N85-25364
East European report: Science and technology
[JPRS-ESA-85-010] 15 p2524 N85-25560
Electrical features of new DNC, CNC system viewed — direct numerical control 15 p2524 N85-25562
Flexible machining systems described 15 p2524 N85-25563
Operation of Prisma flexible manufacturing system 15 p2524 N85-25564
West Europe report: Science and technology
[JPRS-WST-84-009] 15 p2535 N85-25639
French firm plans recapture of domestic CAD/CAM market 15 p2535 N85-25641
French consulting firm develops own robotics 15 p2535 N85-25642
Italy invents robot to compete with Asea, Hitachi 15 p2535 N85-25643
Criteria for qualifying for FRG federal CAD/CAM subsidies 15 p2536 N85-25651
East Europe report: Science and technology
[JPRS-ESA-85-018] 15 p2537 N85-25658
Process control systems for largely automated manufacturing 15 p2537 N85-25659
Applications, specifications of Robotron CAD-CAM work stations 15 p2537 N85-25661
Automation and robotics in welding 15 p2566 N85-25831
Recent advances in arc welding equipment and their application 15 p2566 N85-25832
A critical review of selected recent advancements in arc welding equipment and processes 15 p2566 N85-25833
Some aspects of nuclear plant fabrication in Japan and the UK relating to automatic and robotic arc welding 15 p2566 N85-25834
Welding techniques in pressure part technology 15 p2566 N85-25835
SHAFT: Interactive shaft design program
[DE85-007333] 15 p2568 N85-25850
CAD/CAM (Computer-Aided Design/Computer-Aided Manufacturing) highlights
[AD-A151532] 15 p2629 N85-26201
IPAD: Integrated Programs for Aerospace-vehicle Design
[NASA-CR-3690] 15 p2632 N85-26221
Method of selecting robotized system design for pressing process 16 p2761 N85-27040

Experience of sheet stamping robotic complexes
16 p2761 N85-27041
Robotic thermal battery pellet fabrication
[DE85-007755] 16 p2779 N85-27154
Fujian forges ahead in electronic production
16 p2806 N85-27301
Manufacturing methods and technology CAD/CAM (Computer-Aided Design/Computer-Aided Manufacturing) related efforts (FY 1980 - 1986)
[AD-A151817] 16 p2846 N85-27547
Engineering robot actions in a computer integrated manufacturing environment
[CWI-CS-R8415] 17 p2938 N85-28139
The application of numerical control (NC) in manufacturing wind tunnel models
[B8580078] 17 p2939 N85-28140
A new technique for system-to-system transfer of surface data 17 p3007 N85-28589
Comparison of two algebraic methods for curve/curve intersection 17 p3007 N85-28591
Manufacturing information system
[AD-A152715] 17 p3011 N85-28616
Automated fabrication of composite structures for helicopters
[SNIAS-851-210-104] 20 p3393 N85-31049
Robot, laser tridimensional cutting technology detailed
20 p3438 N85-31335
NASA space station automation: AI-based technology review
[NASA-CR-176094] 21 p3558 N85-32134
Importance of automation, robotization in economy
21 p3572 N85-32219
IGES/RIM Parser/Converter users guide
[DE85-011965] 22 p3829 N85-33716
Low cost geometric modelling system for CAM
23 p3964 N85-34578
Establishment of a Computer-Aided Design (CAD)-Computer-Aided Manufacturing (CAM) process for the production of cold forged gears
[AD-A155756] 24 p4137 N85-35844

COMPUTER AIDED MAPPING

Specification and preliminary design of the CARTA system for satellite cartography
[E85-10035] 03 p0378 N85-12414
The integrated use of digital cartographic data and remotely sensed imagery 05 p0655 N85-14206
Statistics and mapping of land uses by means of LANDSAT MSS imagery 05 p0657 N85-14219
A geoinformation expert system for synergetic use of map and image data 05 p0659 N85-14233
A methodology for an integrated spatial data model and its application to image classification
05 p0659 N85-14234
Contour line generalization using digital image processing methods
[SER-C-291] 11 p1700 N85-20688
Assessment of computer based geologic mapping of rock units in the LANDSAT-4 scene of northern Death Valley, California 13 p2119 N85-23195
An investigation of the crustal properties of Australia and surrounding regions derived from interpretation of MAGSAT anomaly field data 13 p2122 N85-23216
Data structure considerations in automatic cartography
15 p2583 N85-25930
Reports on cartography and geodesy. Series 1: Original reports, no. 94
[ISSN-0469-4236] 16 p2814 N85-27357
Use of vector processors in cartographic raster data processing, with special regard to the AP-120B vector processor 16 p2814 N85-27358
Testing of scanner-assisted revision of the topographic map 1:25,000 (TK 25) 16 p2814 N85-27359
Realization of cartographic tasks on the multiprocessor system EGPA --- image processing
16 p2814 N85-27360
Application of the Siemens Computer Aided Computer (Sicad) system to the surveying management in Baden-Wuerttemberg 16 p2814 N85-27361
Automatic engraving of map frames in the revision of the TK 25, 1:25,000 topographical map
16 p2814 N85-27362
Application of interactive graphic systems in land consolidation. Processing of planning maps
16 p2815 N85-27363
A concept for map updating using digital image processing methods 16 p2815 N85-27364
Raster or vector processing. Experience with the application of programs for the construction of thematic maps with boundary design in the Lower Saxony (West Germany) Land Administration for ground research
16 p2815 N85-27365
Status of computer aided mapping in hydrographic services 16 p2815 N85-27366
Contour line generalization using digital image processing methods 16 p2815 N85-27367
What does digital image processing perform in the production of orthophotomaps 16 p2815 N85-27368
A graphic system for drawing synoptic maps by computer
[INPE-3215-PRE/568] 16 p2834 N85-27474
Information relative to cartography and geodesy. Series 2: Translations, number 42, volume 1
[ISSN-0469-4244] 18 p3123 N85-29338
Two satellite image maps of Central Europe
18 p3123 N85-29339
Digital image mapping of Antarctica using NOAA-7 AVHRR imagery 18 p3124 N85-29340
Interactive procedures for discriminating and restoring contour line networks 22 p3736 N85-33158
A model for graphics interface tool development
23 p3960 N85-34545
The scientific and technical issues in integrating remotely sensed imagery with geocoded data bases
23 p3960 N85-34547
A new approach to linear quadtrees
23 p3961 N85-34550
The automatic labeling of geographic maps: A problem in computer aesthetics 23 p3962 N85-34561
How map designers can represent their ideas in thematic maps: Effective user interfaces for thematic map design
23 p3962 N85-34562
Applied computer graphics in a geographic information system: Problems and successes
23 p3962 N85-34563

COMPUTER AIDED TOMOGRAPHY

Three-dimensional reconstruction and data display of chromosome structure studied by electron microscope tomography
[DE85-011562] 22 p3825 N85-33697

COMPUTER ASSISTED INSTRUCTION

Self-paced instruction. Factors critical to implementation in Air Force technical training: A preliminary inquiry
[AD-A145098] 01 p0097 N85-10647
Factors critical to the implementation of self-paced instruction: A background review
[AD-A145143] 01 p0097 N85-10648
Command control group behaviors. Objective 1: A methodology for and identification of command control group behaviors
[AD-A145690] 02 p0191 N85-11279
GUIDON
[AD-P003925] 02 p0248 N85-11605
Air Force honeycomb shaping at SM-ALC (Sacramento Air Logistics Center)
[AD-P004005] 03 p0308 N85-11985
Training capabilities test of Electronics Equipment Maintenance Trainer (EEMT): Findings and conclusions
[AD-A146075] 03 p0359 N85-12302
Experience with a sophisticated computer based authoring system
[DE84-014644] 05 p0713 N85-14575
Computer-managed instruction: Theory, application, and some key implementation issues
[AD-A146564] 06 p0854 N85-15426
Producing high scene content with perspective validity
[AD-P004314] 09 p1268 N85-17968
Study of cognitive styles of students in automated teaching system 10 p1525 N85-19620
Micro-CAE mechanical engineering software development at Lawrence Livermore National Laboratory and participating universities and technology transfer
[DE85-008680] 18 p3163 N85-29597
Air Force Human Resources Laboratory research and development summary
[AD-A154310] 19 p3331 N85-30832
Engineering education based on computer simulation
[CFD/85/1] 20 p3512 N85-31829
The Naval Postgraduate School Flight Mechanics Laboratory: A feasibility study
[AD-A154578] 21 p3557 N85-32127
A microcomputer tutorial on spreadsheets and databases with a simulated budget preparation
[AD-A155516] 21 p3672 N85-32813
Designing a graphics application interface
23 p3964 N85-34574
VLSI (Very Large Scale Integrated) tutorials through the video-computer courseware implementation system
[AD-A155889] 24 p4135 N85-35831

COMPUTER COMPATIBLE TAPES

Standardization of data formats for radar altimeter data 03 p0384 N85-12455
TM digital image products for applications
11 p1668 N85-20512
Cabauw (Netherlands) meteorological data tapes 1973-1984: Description of instrumentation and data processing for continuous measurements
[KNMI-WR-84-6] 14 p2379 N85-24685

COMPUTER COMPONENTS

Hardware multiplier processor
[DE84-006174] 05 p0713 N85-14574
Distributed database components in a DBMS (Database Management System) component architecture
[PB84-217546] 06 p0848 N85-15382
Microcomputers in transit: A hardware handbook
[PB85-113660] 10 p1538 N85-19700
Image processing instrumentation for speckle interferometry and imaging
[AD-A149308] 11 p1762 N85-21084
Bipolar nonswitching logic arrays: Universal components of function expanders for computation of elementary functions 14 p2400 N85-24797
Preliminary assessment of the Heuristics H2000 speechlink - speech recognition device --- voice data input for Apple 2 computer
[BAE-BT-12276] 15 p2539 N85-25674

COMPUTER DESIGN

Description of MBB computerized design techniques for A320 08 p1141 N85-17194
Design and analysis of an access control system for a multi-backend database system
[AD-A148750] 09 p1367 N85-18586
Automatic multi-banking of memory for microprocessors
[NASA-CASE-NPO-15295-1] 12 p1911 N85-21992
UW/NW (University of Washington/Northwest) VLSI Consortium
[AD-A150740] 14 p2404 N85-24818
Czech institute develops microcomputer for satellites
15 p2484 N85-25331
Use of computer-aided design in large-computer development described 15 p2564 N85-25822
Recent advances in supercomputers
16 p2693 N85-26625
East Europe report: Science and technology
[JPRS-ESA-85-021] 21 p3568 N85-32190
Globally-asynchronous locally-synchronous systems
[AD-A154624] 21 p3573 N85-32222
A methodology for the design of testable custom large-scale integrated circuits
[AD-A156098] 24 p4090 N85-35351

COMPUTER GRAPHICS

Analysis of on-board CIG (Computer Image Generator) applications for aircrew training
[AD-A145214] 01 p0013 N85-10079
Interactive graphics nonlinear constrained optimization
01 p0058 N85-10387
FRONTIERS: Progress with a system for nowcasting rain --- Forecasting Rain Optimized using New Techniques of Interactively Enhanced Radar and Satellite (FRONTIERS) 01 p0082 N85-10552
A subjective evaluation of the PROFS operational workstation based upon a real-time forecasting experiment in summer 1983 --- Program for Regional Observing and Forecasting Services (PROFS) 01 p0083 N85-10556
Interactive computer display systems in nowcasting
01 p0083 N85-10557
COM-GEOM Interactive Display Debugger (CIDD)
[AD-A145001] 01 p0104 N85-10692
RSCORS graphics system
[DE84-015693] 01 p0104 N85-10698
Halfspace representations of extrusions, solids of revolution and pyramids
[DE84-015005] 01 p0104 N85-10700
DATAPLOT: Introduction and overview
[PB84-214055] 01 p0105 N85-10708
A modular data acquisition and display software system for a laboratory environment
[PB84-217992] 01 p0105 N85-10709
EG and G Idaho's response to a request for a graphic data base support package
[DE84-015171] 01 p0126 N85-10862
Interactive system for the interpretation of coal deposit data as a basis of future mine planning systems
[BMFT-FB-T-83-115] 02 p0220 N85-11449
Effects of alternative chromatic mixed graphics displays in decision support systems
[AD-A145561] 02 p0242 N85-11578
An effective graphics user interface for rules and inference mechanisms
[AD-P003942] 02 p0248 N85-11622
Use of prototyping for man-machine interface requirements definition on the AWDS (Automated Weather Distribution System) program
[AD-A146033] 03 p0396 N85-12526
Plotting TDL coastal wind forecasts
[PB84-220789] 03 p0397 N85-12533
CONTROL: A suite of interactive transfer-function analysis programs
[OUEL-1527/84] 03 p0408 N85-12609
DATAPLOT: Implementation tapes guide
[PB84-214063] 03 p0408 N85-12610
Graphics software for the display of body deformation motion
[FW-FO-1640] 04 p0455 N85-12888

Computerized circuit designs: Realization of masks to manufacture microwave circuits
[CNES-NT-107] 04 p0486 N85-13168
Documentation for DIGLIB: Device independent graphics library
[DE84-017385] 04 p0550 N85-13500
International information networks for material properties
[DE84-013836] 04 p0576 N85-13676
A method for measuring the effective throughput time delay in simulated displays involving manual control
05 p0701 N85-14497
The impact of pictorial display on operator learning and performance 05 p0706 N85-14527
Increase in the economy of design and process planning by integrated and graphic data processing, phase 2 — aircraft design
[BMFT-FB-W-84-028] 05 p0716 N85-14589
AFOS (Automation of Field Operations and Services) display of MDR (Manually Digitized Radar) data on local map backgrounds
[PB84-220797] 06 p0840 N85-15338
Nonparametric analysis of Minnesota spruce and aspen tree data and LANDSAT data 07 p0964 N85-16253
Research activities of the Norwegian seismic array (NORSAR)
[AD-A146778] 07 p0998 N85-16326
Interactive Signal Analysis Software (ISAS). User's manual
[AD-A146999] 07 p1022 N85-16485
Program visualization: Graphics support for software development
[AD-A146887] 07 p1024 N85-16499
A program to produce standard shewhart control charts for the statistics X-bar and R or S, P, NP, C, or U
[AD-A146971] 07 p1024 N85-16501
Interactive color-graphics interface for energy monitoring and control systems
[AD-A147538] 07 p1025 N85-16509
PLOT3D: An interactive graphics code for 3-dimensional plots
[AD-A147887] 07 p1026 N85-16514
Local area network evaluation by MICROSS extensions
[AD-A146773] 07 p1027 N85-16521
A Computer-generated topographic display system for navigation and mission planning in helicopters
08 p1073 N85-16800
Computer aided processing using laser measurements
08 p1103 N85-16973
Description of MBB computerized design techniques for A320 08 p1141 N85-17194
Two-dimensional modeling for lineal and areal probabilities of weather conditions
[AD-A147970] 08 p1188 N85-17488
A FORTRAN plotting package for graphic VDUs
[AD-A148489] 08 p1204 N85-17577
The IMAGE 3 Conference Proceedings
[AD-A148636] 09 p1267 N85-17962
Color visual simulation applications at the Defense Mapping Agency
[AD-P004315] 09 p1268 N85-17969
Raster graphics extensions to the core system
[NASA-CR-174348] 09 p1367 N85-18590
SPADE: Serise-parallel directed acyclic graph evaluator
[AD-A148458] 09 p1368 N85-18592
Representation and refinement of visual specifications in PegaSys
[AD-A148733] 09 p1368 N85-18598
Introduction to LBL graphics
[DE85-000389] 09 p1369 N85-18600
Organizational tools for data analysis environments
[DE85-000396] 09 p1369 N85-18601
Role of environments in managing data analysis
[DE85-000397] 09 p1369 N85-18602
User/programmer guide for UCMD 108 multi-vertex polyarc/path integrity verifier
[DE84-017173] 09 p1369 N85-18604
User's manual: Menu-driven data graphing program for the Tektronix 7912AD and 7612D transient digitizer system
[DE85-002151] 09 p1370 N85-18610
Computing environments for data analysis. Part 1. Introduction
[AD-A148677] 09 p1373 N85-18632
Computing environments for data analysis. Part 2. Hardware
[AD-A148678] 09 p1374 N85-18633
Application of SIMCA (Soft Independent Modeling of Class Analogy) pattern recognition to air pollutant analytical data
[PB85-124683] 10 p1513 N85-19549
Hurricane plotting program
[PB85-121432] 10 p1521 N85-19592
Graphics translators for computer-aided drafting and design: Interface alternatives for the A/E community
[AD-A148692] 10 p1540 N85-19706
Design of a pictorial program reference language
[AD-A148323] 10 p1540 N85-19711
Interactive Graphics Simulator: Design, development and effectiveness/cost evaluation
[AD-A149417] 10 p1540 N85-19712
Research study of space plasma boundary processes
[NASA-CR-174351] 10 p1558 N85-19823
Digital and color energy maps for graphic display of hourly data
[DE85-000526] 11 p1673 N85-20543
Computer-generated display system guidelines. Volume 1: Display design
[DE85-000679] 11 p1701 N85-20699
Looking at multivariate data through fuzzy sets
[DE85-000684] 11 p1702 N85-20706
Data and information systems and decision making in large public organizations: Research agenda
[DE85-003639] 11 p1736 N85-20931
Tests of low-frequency geometric distortions in LANDSAT 4 images 12 p1872 N85-21744
Review of computer mapping and display techniques applicable to regional analysis
[DE85-003545] 12 p1875 N85-21764
HGRAPH: A subroutine package for the IBM personal computer to support the Hercules Graphic Card
[LA-10144-MS] 12 p1914 N85-22013
Tekedit: An enhanced editor for Direct View Storage Tube (DVST) graphics display devices
[AD-A149715] 12 p1915 N85-22021
Design of graphic displays in computerized systems
[AD-A150071] 12 p1916 N85-22027
EZPIX: A tablet entry method for computer-generated slides, drawings, and graphs
[DE85-005234] 12 p1916 N85-22030
A description of the Langley wireframe geometry standard (LaWGS) format
[NASA-TM-85767] 13 p1971 N85-22380
MAGSAT anomaly field data of the crustal properties of Australia
[E85-10100] 13 p2122 N85-23215
Data selection techniques in the interpretation of MAGSAT data over Australia 13 p2123 N85-23218
Low altitude texture comparison data base and smooth shaded texture
[AD-A150342] 13 p2146 N85-23323
ROSS: An object-oriented language for constructing simulations
[AD-A150556] 13 p2147 N85-23330
Introduction to CHART: A graphic analysis and display system, revision
[DE85-004612] 13 p2148 N85-23335
An error generator to support the trials of the ZODIAC prototype system — raster links
[PHL-1984-71] 14 p2293 N85-24216
The use of a 3-D system for a civil engineering project
14 p2402 N85-24811
The integration of information from an analog-visual display: The role of dimensional integrality
[AD-A150756] 14 p2404 N85-24820
Easyplot: An interactive, user-friendly graphics program
[AD-A150779] 14 p2404 N85-24824
Video animation system
[DE85-005494] 14 p2405 N85-24831
EDIPAS: A multidiscipline and integrated facility for management and evaluation of engineering data
[NLR-MP-83062-U] 14 p2405 N85-24832
Computer Visual System (CVS) reference manual
[DE85-006328] 14 p2407 N85-24837
Determination of the observation conditions of celestial bodies with the aid of the DISPO system
[NAS 1.15:77632] 14 p2438 N85-25044
Using SM-4 Omega system in checking and editing digital terrain information 15 p2487 N85-25350
NPLOT: An interactive plotting program for NASTRAN finite element models 15 p2573 N85-25869
COSMIC/NASTRAN-PATRAN interface
15 p2574 N85-25870
Two interactive graphics postprocessors for NASTRAN 15 p2574 N85-25871
An unusual application of NASTRAN contour plotting capability 15 p2574 N85-25872
Isoparametric 3-D finite element mesh generation using interactive computer graphics 15 p2574 N85-25873
CADS: A Computer Aided Design System
15 p2574 N85-25876
An experimental investigation into the dynamic response of a stiffened flat plate loaded impulsively by an underwater shockwave
[AD-A151321] 15 p2578 N85-25903
Three-dimensional/perspective display techniques for meteorological data sets 15 p2599 N85-26018
Activities report for FOA 53: Laboratory for man and information systems
[FOA-C-53019-H] 15 p2621 N85-26150
The interactive plotting program: GRAPH
[AD-A151371] 15 p2623 N85-26165
An extension of a microcomputer based system for analysis of line drawing quantization schemes
[AD-A152008] 15 p2624 N85-26171
Programme development: A state of the art
15 p2626 N85-26185
Computer aided draughting in a civil engineering consulting practice 15 p2627 N85-26189
A microcomputer-based program for printing check plots of integrated circuits specified in Caltech intermediate form
[AD-A151715] 15 p2629 N85-26205
VAX-based graphics mail system
[DE85-007231] 15 p2630 N85-26214
Interactive graphical data analysis
[DE85-005945] 15 p2631 N85-26215
Graphic simulation of a machine-repairman model
[AD-A151761] 16 p2694 N85-26633
Criteria for the classification of hydrographic positioning data
[AD-A152283] 16 p2705 N85-26697
Development of a graphic system: Example using the outline of synoptic charts
[INPE-3296-PRE/611] 16 p2810 N85-27327
Application of interactive graphic systems in land consolidation. Processing of planning maps
16 p2815 N85-27363
SINOGRAFO: A system for influencing and forecasting weather
[INPE-3349-PRE/628] 16 p2834 N85-27475
Development of computer aided database design and maintenance tools
[AD-A151782] 16 p2845 N85-27537
Span graphics display utilities handbook, first edition
[NASA-TM-86500] 16 p2849 N85-27567
A fast hidden line algorithm with contour option
[NASA-CR-175803] 16 p2852 N85-27582
An interpolation method with the possibility of first derivative correction
[INPE-3352-PRE/631] 16 p2853 N85-27590
Surface interpolation using weighted splines
[INPE-3387-PRE/658] 16 p2853 N85-27591
The interactive generation of specifications for an onboard software series (GISELE)
17 p2904 N85-27906
FLOWPLOT 2: A fluid dynamics and heat transfer plotting package
[DE85-009802] 17 p2959 N85-28277
Free-form design in solid modelling
17 p3004 N85-28569
Boundary to constructive solid geometry mappings: A focus on 2-D issues 17 p3004 N85-28570
Examination of the circle spline routine
17 p3004 N85-28573
A natural bias approach to cardinal spline curves
17 p3004 N85-28575
Adapting shape parameters for cubic Bezier curves
17 p3004 N85-28576
Triangular Berstein-Bezier patches, a survey and new results 17 p3005 N85-28577
A uniform subdivision method for triangular Bezier patches 17 p3005 N85-28578
An intuitive approach to geometric continuity for parametric curves and surfaces (extended abstract)
17 p3005 N85-28579
Um models and beta-splines
17 p3005 N85-28580
Parameterization in grid generation
17 p3005 N85-28581
Contouring trivariate data 17 p3005 N85-28582
Generation of surface coordinates by elliptic partial differential equations 17 p3006 N85-28583
A survey of composite grid generation for general three-dimensional sections 17 p3006 N85-28584
A unified representation scheme for solid geometric objects using B-splines (extended abstract)
17 p3006 N85-28585
Improving the effectiveness of integral property calculation in a CSG solid modeling system by exploiting predictability 17 p3006 N85-28586
Looking at more than three dimensions
[DE85-007764] 17 p3009 N85-28600
Tracking algorithm performance analysis program (TRAPP)
[DE85-007304] 17 p3009 N85-28601
Computing environments for data analysis. Part 1: Introduction
[DE85-007919] 17 p3009 N85-28603
Computing environments for data analysis. Part 2: Hardware
[DE85-008320] 17 p3009 N85-28604

Research in computer science
[NASA-CR-175922] 17 p3010 N85-28612
AFIT GKS: A GKS implementation in the Ada programming language
[AD-A152954] 17 p3012 N85-28620
Study of raster metafile formats
[AD-A153322] 17 p3012 N85-28624
The addition of advanced scene rendering techniques to a general purpose graphics package
[AD-A153323] 17 p3012 N85-28625
Software environment for conducting interactive statistical analysis
[AD-A153378] 17 p3012 N85-28626
Introduction to LINE: A Feynman diagram graphic operator
[DE85-009299] 17 p3013 N85-28632
Ray tracing general sweep defined objects
[REPT-84-36] 17 p3014 N85-28636
Fourier coding and reconstruction of complicated contours
[REPT-84-39] 17 p3022 N85-28691
Visual simulation of radiographs
[DE85-010213] 18 p3110 N85-29255
Two satellite image maps of Central Europe
18 p3123 N85-29339
The use of VLSI technology for the real-time generation of graphics displays: A proposal
[AD-A153766] 18 p3160 N85-29578
Program DISAS: A computer program to obtain hard-copy plots of an image displayed on a vector graphics device in a local-area-network
[AD-A153643] 18 p3162 N85-29586
Graphics package, version 4: User reference manual
[DE85-007894] 18 p3163 N85-29596
Two-dimensional/speed/couple/data base management system
[A-1] 18 p3165 N85-29606
Three-dimensional/integration two and three dimensional/numerical control/communication
[A-2] 18 p3165 N85-29609
The CEADS-CADD system
[A-4] 18 p3165 N85-29610
System test CALMA DDM (Design Drafting Manufacturing)
[A-5] 18 p3165 N85-29611
System test: Hewlett-Packard draft
[A-9] 18 p3166 N85-29613
Test Drawing Office Graphics System (DOGS)/APOLLO
[A-10] 18 p3166 N85-29614
Solar physics applications of computer graphics and image processing 18 p3208 N85-29903
Graphic displays of vector magnetograph data
18 p3209 N85-29904
AEV local verification for aviation, precipitation, and temperature programs: AV, REL, TEM
[PB85-179125] 19 p3318 N85-30568
Cultural data base implementation study and computer-aided scene modeling system users manual
[AD-A154232] 19 p3333 N85-30646
Graphic display development program. Volume 2, revision 0: Appendices
[DE85-011078] 19 p3333 N85-30648
Interactive graphics for a data analysis management system
[DE85-010977] 19 p3334 N85-30651
Demonstration project: Putting the bioastronautics data book on line
[NASA-CR-178424] 19 p3335 N85-30659
Defense Mapping Agency (DMA) raster-to-Vector analysis
[AD-A154153] 19 p3336 N85-30668
Defense Mapping Agency (DMA) raster-to-Vector benchmark testing
[AD-A154152] 19 p3338 N85-30683
A Lotus 1-2-3 based system reliability program
[DE85-010533] 19 p3340 N85-30701
MANHIST user's guide
[DE85-010684] 19 p3346 N85-30754
Radiation interactions for tomography
[DE85-006961] 19 p3355 N85-30799
User's guide for the Mk-3 D-coronameter data system
[PB85-181204] 19 p3385 N85-31002
A feasibility study for the use of electronic flight strips in ATC controller workstations
[DFVLR-FB-85-08] 20 p3392 N85-31039
The application of computer imaging techniques to ocean topography and geophysical data
20 p3492 N85-31711
Intersection of three-dimensional geometric surfaces
[NASA-TP-2454] 20 p3513 N85-31839
Visualization of computation results. Definition of a graphics satellite computer
[ONERA-RT-2/3587-CY] 20 p3514 N85-31845
A set of subroutines for masked three-dimensional plotting with rotations
[MEAH-33] 20 p3514 N85-31846
System test Oce 5200
[A-3] 20 p3515 N85-31850
The General Drafting System (GDS) design system
[A-6] 20 p3517 N85-31869
The IGOS design system
[A-8] 20 p3517 N85-31870
R and D activities of the Computer Centre
20 p3540 N85-32029
User's guide for computer program CGFAG, Concrete General Flexure Analysis with Graphics
[AD-A155555] 21 p3570 N85-32204
Flexible satellite communications systems simulator, phase 3
[AD-A155647] 21 p3577 N85-32247
Realizing the full potential of the video disc for mapping applications
[AD-A154966] 21 p3606 N85-32391
Real-time contour surface display generation
[AD-A155232] 21 p3668 N85-32780
DYNA3D, INGRID, and TAURUS: An integrated, interactive software system for crashworthiness engineering
[DE85-010928] 21 p3677 N85-32846
Interactive procedures for discriminating and restoring contour line networks 22 p3736 N85-33158
Dislog system with minicomputer for plotting performance charts 22 p3766 N85-33355
A new large-scale, high-resolution multicolor software display concept
[AD-A155404] 22 p3827 N85-33703
QKPLT users guide, version 2.0
[L-10094-M] 22 p3828 N85-33707
IGES/RIM Parser/Converter users guide
[DE85-011965] 22 p3829 N85-33716
MORSE-CGA: A Monte Carlo radiation transport code with array geometry capability
[DE85-012063] 22 p3830 N85-33718
An introduction to finite elements
23 p3924 N85-34319
A device-independent 2D plotting package written in FORTRAN
[RSRE-MEMO-3776] 23 p3956 N85-34514
Graphics Interface 1985: Proceedings
[ISSN-0713-5424] 23 p3957 N85-34523
A theoretical and empirical analysis of coherent ray-tracing 23 p3957 N85-34524
Frame buffer algorithms for stochastic models
23 p3957 N85-34525
Specifying stochastic objects in a hierarchical graphics system 23 p3957 N85-34526
The interactive planning work station: A graphics-based UNIX (trademark) tool for application users and developers 23 p3957 N85-34527
Computer graphics for multivariate data
23 p3958 N85-34528
Interfacing interactive circuit simulation with standard graphics facilities 23 p3958 N85-34529
Computer analysis techniques for the temporal evaluation of cardiac wall motion
23 p3958 N85-34530
A computerized system for spot detection and analysis of two-dimensional electrophoresis images
23 p3958 N85-34531
An image management kernel for the design of relational and pictorial data bases 23 p3958 N85-34532
Spatial trees: A fast access method for unstructured graphical data 23 p3958 N85-34533
Graphics interaction in databases
23 p3958 N85-34534
Animengine: An engineering animation system
23 p3959 N85-34535
3D computer animation: More an evolution problem than a motion problem 23 p3959 N85-34536
Using dynamic analysis to animate articulated bodies such as humans and robots 23 p3959 N85-34537
Towards an integrated view of 3-D computer character animation 23 p3959 N85-34538
Research issues in generating graphical explanations
23 p3959 N85-34539
An integrated system for printing and publishing applications 23 p3959 N85-34540
Recognition and clear representation of handwritten electronic diagrams 23 p3960 N85-34541
A model for a document maintenance system
23 p3960 N85-34542
Efficient recovery and reversal in graphical user interfaces generated by the Higgens system
23 p3960 N85-34544
A model for graphics interface tool development
23 p3960 N85-34545
Using percent-done program indicators to enhance user interfaces 23 p3960 N85-34546
Selection of segment similarity measures for hierarchical picture segmentation 23 p3960 N85-34548
A general purpose image processing package
23 p3961 N85-34549
A new approach to linear quadtrees
23 p3961 N85-34550
An analysis and algorithm for filling propagation
23 p3961 N85-34551
The CADME approach to the interface of solid modellers 23 p3961 N85-34554
A graphics interface for interactive simulation of packet-switched networks 23 p3962 N85-34558
Design and implementation of an interactive route editor 23 p3962 N85-34559
Project management using graphics
23 p3962 N85-34560
The automatic labeling of geographic maps: A problem in computer aesthetics 23 p3962 N85-34561
How map designers can represent their ideas in thematic maps: Effective user interfaces for thematic map design
23 p3962 N85-34562
Applied computer graphics in a geographic information system: Problems and successes
23 p3962 N85-34563
Image synthesis: Optical identity or pictorial communication? 23 p3963 N85-34565
Strategic use of business graphics: A stakeholder approach 23 p3963 N85-34566
Colour spaces and colour contrast
23 p3963 N85-34567
Colour coding scales and computer graphics
23 p3963 N85-34568
Geometric continuity with interpolating Bezier curves
23 p3963 N85-34570
An intuitive approach to geometric continuity for parametric curves and surfaces
23 p3963 N85-34571
Building an octree from a set of parallelepipeds
23 p3964 N85-34572
Developing graphical tools with minimal GKS
23 p3964 N85-34573
Designing a graphics application interface
23 p3964 N85-34574
NAPGEN: Automatic NAPLPS page generator
23 p3964 N85-34575
Low cost geometric modelling system for CAM
23 p3964 N85-34578
The dynamics of articulated rigid bodies for purposes of animation 23 p3965 N85-34579
Shadow volumes for non-planar polygons
23 p3965 N85-34580
Computer animation in distance teaching
23 p3965 N85-34581
Generative design in architecture using an expert system 23 p3965 N85-34582
Heuristic rules for visualization
23 p3965 N85-34584
Using LINE as an interactive graphics package. Interfacing line and Topdraw in 43 and 24 VM
[DE85-012007] 23 p3965 N85-34585
Raster functionality for a VDI
[DE85-006734] 24 p4097 N85-35396
Edge detection and geometric methods in computer vision
[AD-A155873] 24 p4135 N85-35630
An exploratory study of the effect of screen size and resolution on the legibility of graphics in automated job performance aids
[AD-A155989] 24 p4136 N85-35632
Selected publications in image understanding and computer vision from 1974 to 1983
[AD-A156196] 24 p4136 N85-35634
Master Fit users' guide, version 1.0
[DE85-014199] 24 p4140 N85-35667

COMPUTER INFORMATION SECURITY

Reserve and authentication in Integrated Services Distributed Networks (ISDN) networks
[FUB-37-1983] 01 p0041 N85-10262
Computer science and technology: Overview of computer security certification and accreditation
[PB84-217819] 06 p0848 N85-15384
Digital signatures: An update
[NPL-CITC-51/84] 09 p1367 N85-18589
French commentary on Soviet industrial espionage
10 p1481 N85-19210
Computer crime
[GPO-30-544] 10 p1537 N85-19691
Computer and communications security and privacy
[GPO-39-741] 12 p1911 N85-21994
Security of personal computer systems: A management guide
[PB85-161040] 14 p2400 N85-24793
Commercial data base management system for geonames data base
[AD-A150835] 14 p2433 N85-25007

Future information technology, 1984 telecommunications
[PB85-165850] 15 p2624 N85-26173
Future Information technology, 1984: Telecommunications
[NBS/SP-500/119] 16 p2876 N85-27762
NASA guidelines for assuring the adequacy and appropriateness of security safeguards in sensitive applications
[NASA-CR-175489] 17 p3007 N85-28593
A secure high-speed transaction protocol
[CWI-CS-R8417] 17 p3009 N85-28605
Computer center policy
[AD-A154416] 19 p3338 N85-30681
Security controls in the Stockpoint Logistics Integrated Communications Environment (SPLICE)
[AD-A155536] 21 p3576 N85-32244
Design guidelines for user-system interface software
[AD-A154907] 21 p3671 N85-32607
An approach to determining computer security requirements for Navy systems
[AD-A155750] 24 p4135 N85-35627

COMPUTER METHODS
U COMPUTER PROGRAMS

COMPUTER NETWORKS
Tendencies in the development of utilization protocols, seminar report — communication networks
[FUB-11-1983] 01 p0039 N85-10252
Interactive graphics nonlinear constrained optimization
01 p0058 N85-10387
Nowcasting with Doppler radar: The forecaster-computer relationship
01 p0077 N85-10514
Evaluating a scientific workstation computer
[DE84-014764] 01 p0100 N85-10663
REMOTE: Modem Communicator Program for the IBM personal computer
[DE84-015047] 01 p0100 N85-10665
Assessing the reliability of computer software and computing networks: An opportunity for partnership with computer scientists
[AD-A145131] 01 p0104 N85-10697
Storage in the LLNL Octopus network: An overview and reflections
[DE84-014711] 01 p0106 N85-10712
Throughput characteristics of Carrier Sense Multiple Access (CSMA) networks
[FUB-25-1983] 01 p0106 N85-10713
End-to-end performance in local area networks of interconnected token rings
[FUB-42-1983] 01 p0107 N85-10714
Proceedings of the 5th LAN-Transport Workshop
[PB84-232667] 01 p0107 N85-10715
The computer-communication link for the innovative use of Space Station
02 p0150 N85-11016
Shuffle-exchanges on augmented meshes
[NASA-CR-172476] 02 p0243 N85-11587
Fault tolerant computing research
[AD-A145640] 02 p0244 N85-11590
Study on the conversion and test of protocols
[ENST-84E005] 03 p0356 N85-12293
On a program for solution of BCMP queueing network model
[NAL-TR-813] 03 p0405 N85-12585
Regenerative simulation methods for local area computer networks
[AD-A146197] 03 p0409 N85-12612
Verification of a class of deadlock-free, self-timed, computational arrays
[AD-A146272] 03 p0412 N85-12638
Test experience on an ultrareliable computer communication network
[NASA-TM-85915] 04 p0552 N85-13514
User behavior upon introduction of a network help system
[DE84-016466] 04 p0552 N85-13515
International information networks for material properties
[DE84-013836] 04 p0576 N85-13676
Development of the NLTSS operating system
[DE84-013702] 05 p0714 N85-14576
Requirements and overview of the LINCS distributed operating system architecture
[DE84-013721] 05 p0714 N85-14577
Contribution to the study and realization of the CARTHAGE multiservice local network
[ENST-84E006] 05 p0716 N85-14595
Specification of a transport protocol for computer communications. Volume 1: Overview and Services. Volume 2: Class 2 protocol. Volume 3: Class 4 protocol
[PB84-222850] 06 p0848 N85-15380
Distributed database components in a DBMS (Database Management System) component architecture
[PB84-217548] 06 p0848 N85-15382
Specification of a transport protocol for computer communications. Volume 4: Service specifications. Volume 5: Guidance for the implementor. Volume 6: Guidance for implementation selection
[PB84-222868] 06 p0848 N85-15385
Specification of a transport protocol for computer communications. Volume 7: Testing OSI protocols, a compendium of papers. Volume 8: User's guide to the testing system for implementations of the ICST transport protocol. Volume 9: A test suite for implementations of the ICST transport protocol. Volume 10: Specification of a remote scenario interpreter for implementations of the ICST transport protocol
[PB84-222876] 06 p0848 N85-15386
Selecting a leader in a clique in O(N log N) messages
[AD-A146561] 06 p0857 N85-15453
Stuttgart Interconnection Network Project from PIX to NICS
[NASA-TM-77802] 06 p0870 N85-15528
Upper Atmosphere Research Satellite (UARS) trade analysis
[NASA-CR-175269] 07 p0912 N85-15774
Support for distributed transactions in the TABS (Transaction based systems) prototype
[AD-A147213] 07 p1022 N85-16486
NSW (National Software Works) lessons learned
[AD-A146737] 07 p1023 N85-16494
Reliability analysis of local area networks, intermediate report
[BLL-WH-610-(9091.9F)] 07 p1027 N85-16520
Local area network evaluation by MICROSS extensions
[AD-A146773] 07 p1027 N85-16521
NSWC-NADC interactive communication links for AN/UYS-1 loadtape creation and retrieval
[AD-A148418] 08 p1153 N85-17277
Performance evaluation and control of distributed computer communication networks
[AD-A148103] 08 p1208 N85-17598
DDN directory
[AD-A148213] 08 p1230 N85-17744
Identification of emerging designer needs and high payoff CAE tools
[DE85-000755] 09 p1369 N85-18599
Software for event oriented processing on multiprocessor systems
[DE84-016720] 09 p1370 N85-18607
Asymptotic analysis of Markovian access control computer communication networks
09 p1372 N85-18619
Gateway testing techniques — computer system interconnection
[NPL-DITC-49/84] 09 p1372 N85-18621
Concepts and tools for the software life cycle
10 p1464 N85-19236
A validated methodology for determination of laboratory instrument computer interface efficacy
[AD-A149338] 10 p1487 N85-19391
Distributing a distributed problem solving network simulator
[AD-A149065] 10 p1537 N85-19693
Guidepost routing algorithm for distributed computer networks
11 p1622 N85-20210
Development of computer centers, equipment described: Problems of computer centers
11 p1700 N85-20686
Personal desktop computing in a research and development laboratory
[DE85-002765] 11 p1705 N85-20728
Post-processing of bibliographic citations from DOE/Recon, NASA/Recon, and DOD/DROLS
[DE85-000617] 11 p1739 N85-20938
Multicomputer communication system
[NASA-CASE-NPO-15433-1] 12 p1822 N85-21428
Collection and use of lightning strike data in the western US during summer 1983
[PB85-110534] 12 p1897 N85-21907
Computing Division two-year operational plan, FY 1984 - 1985
[LA-9978-MS] 12 p1913 N85-22006
Satellite channels in packet-switching networks
13 p2067 N85-22909
Exploiting parallel computing with limited program changes using a network of microcomputers
[NASA-TM-86387] 13 p2146 N85-23318
Introduction to CHART: A graphic analysis and display system, revision
[DE85-004612] 13 p2148 N85-23335
Research using a DISCUS based network emulator
[AD-A141294] 13 p2149 N85-23338
Introduction to the Space Physics Analysis Network (SPAN)
[NASA-TM-86499] 14 p2290 N85-24198
The problem of creating a standardized series of personal computers 14 p2400 N85-24795
LINCS
[DE85-006151] 14 p2407 N85-24836
Pluribus Satellite IMP (Interface Message Provision) development mobile access terminal network
[AD-A151201] 15 p2541 N85-25688
Pluribus Satellite IMP (interface Message Provision) development mobile access terminal network
[AD-A151312] 15 p2542 N85-25692
Standards in process: Foundation and profiles of ISDN (Integrated Services Digital Network) and OSI (Open Systems Interconnection) studies
[PB85-165041/GAR] 15 p2545 N85-25712
Mini- and microcomputer local control network architecture and design principles
15 p2625 N85-26179
Backbone network simulations: A comparative study
[DE85-006674] 15 p2632 N85-26224
Maintaining consistency and accommodating network repair in a self-regenerative distributed database management system (a discussion of the means and cost)
16 p2696 N85-26656
East Europe report: Science and technology
[JPRS-ESA-84-032] 16 p2727 N85-26833
Network information management subsystem
16 p2771 N85-27106
Standards and specifications for geodetic control networks
[PB85-166478] 16 p2816 N85-27374
Mathematical programming in computer network design
[AD-A152275] 16 p2848 N85-27558
Span graphics display utilities handbook, first edition
[NASA-TM-86500] 16 p2849 N85-27567
Continued development and implementation of the Universal Network Interface Device (UNID) 2, Digital Engineering Laboratory Network (DELNET), volume 1
[AD-A151935] 16 p2850 N85-27569
Continued development and implementation of the Universal Network Interface Device (UNID) 2 in the Digital Engineering Laboratory Network (DELNET), volume 2
[AD-A151947] 16 p2850 N85-27570
Internation information networks for material properties: Revision 1
[DE85-007412] 16 p2850 N85-27572
Access path optimization for network database retrieval
16 p2877 N85-27749
Design of an interface to an information retrieval network
16 p2877 N85-27750
There is no I/O like no I/O
[DE85-009115] 17 p3014 N85-28634
System Analysis for the Huntsville Operation Support Center, Distributed Computer System
[NASA-CR-171506] 17 p3015 N85-28642
Interfacing the VAX 11/780 using Berkeley Unix 4.2.BSD and Ethernet based Xerox network systems, volume 1
[AD-A152953] 17 p3015 N85-28645
Distributed systems management in wide area networks
[CWI-CS-R8419] 17 p3016 N85-28651
Distributed matchmaking for processes in computer networks
[CWI-CS-R8421] 17 p3016 N85-28652
Distributed elections in a ring of processors using Archimedean time
[CWI-CS-R8416] 17 p3016 N85-28653
Performance measurement of OSI (Open System Interconnection) class 4 transport implementations
[PB85-177657] 18 p3161 N85-29582
INEL User Network Exchange, volume 1-85, Jan./Feb. 1985
[DE85-006108] 18 p3166 N85-29615
Distribution of mathematical software via electronic mail
[DE85-009664] 18 p3166 N85-29617
Graceful fault tolerance in large networks of microcomputers
19 p3332 N85-30643
A new taxonomy for distributed computer systems based upon operating system structure
[NASA-TM-86436] 19 p3342 N85-30709
ZOG/VINSON technology demonstration project system description. Volume 1
[AD-A154211] 19 p3342 N85-30713
Apollo multiplexer operations manual
[DE85-011293] 19 p3343 N85-30719
The application of artificial intelligence techniques to large distributed networks
[NASA-CR-177346] 19 p3344 N85-30721
Computerized Laboratory Analytical and Diagnostic Services (CLADS)
[DE85-010854] 20 p3518 N85-31871
RESO: Expert system applied to company computer networks
[ENST-84E016] 20 p3518 N85-31874
Interactive on-line conferences
[AD-A154723] 21 p3574 N85-32227

A high-speed digital signal processor for atmospheric radar, part 7.3A 21 p3626 N85-32525
Microcomputer network: Investigation and implementation
[AD-A155631] 21 p3674 N85-32826
Broadcasting topology and routing information in computer networks
[AD-A155668] 21 p3674 N85-32827
Some plant location problems — computer networks
[FUB-14-1984] 22 p3835 N85-33746
An innovative user interface for microcomputer-based computer-aided design 23 p3961 N85-34555

COMPUTER PROGRAM INTEGRITY
Assessing the reliability of computer software and computing networks: An opportunity for partnership with computer scientists
[AD-A145131] 01 p0104 N85-10697
NECIS incorporated, NEC ASTRA model 270, COBOL 74 version 8.3 (COBOL technical report)
[PB84-227933] 06 p0848 N85-15381
Computer science and technology: Overview of computer security certification and accreditation
[PB84-217819] 06 p0848 N85-15384
Digital Research Incorporated, IBM PC XT, FORTRAN-77 V4.0
[PB84-243633] 06 p0849 N85-15388
Perkin-Elmer, Perkin-Elmer 3230, FORTRAN 7 D R00-00
[PB84-243682] 06 p0849 N85-15389
Gould Incorporated, Gould PS-3000, Gould PS-3000 FORTRAN 77 V2.1
[PB84-229178] 06 p0849 N85-15390
NECIS, Incorporated, NEC ASTRA model 270 COBOL 74 Version 8.3
[PB84-227636] 06 p0850 N85-15397
Digital Equipment Corporation, DECSYSTEM-20, model 2060, COBOL V13
[PB84-227958] 06 p0850 N85-15398
Digital Equipment Corporation, DECSYSTEM-20, model 2080, COBOL V13 (COBOL technical report)
[PB84-227966] 06 p0850 N85-15399
Northern Telecom, Incorporated, IBM 3033 (compilation), NTI-585/585 (execution), XCOBOL Release 4.1 Version H(01)
[PB84-227875] 06 p0850 N85-15400
NCR Corporation, NCR I9300, NCR ITX Cobol Release 3.0
[PB84-228055] 06 p0850 N85-15401
NCR Corporation, NCR I9300, NCR ITX COBOL Release 3.0 (COBOL technical report)
[PB84-228063] 06 p0850 N85-15402
Computervision Corporation, CDS-4000 32-Bit processor, CV FORTRAN Version 2.84
[PB84-227867] 06 p0851 N85-15406
Sperry Univac, System 80 Model 6, OS/3 COBOL, Version 08.00/08
[PB84-227800] 06 p0851 N85-15410
Modular Computer Systems, Incorporated, MODCOMP CLASSIC 7860, MODCOMP FORTRAN 77/16 Version A.0
[PB84-230556] 06 p0852 N85-15411
Modular Computer Systems, Incorporated, MODCOMP CLASSIC 7860, MODCOMP NASA EXTENDED FORTRAN 78 Version A.40
[PB84-230549] 06 p0852 N85-15412
Digital Equipment Corporation, MICRO/PDP-11, COBOL-81 Version 2.2
[PB84-229236] 06 p0852 N85-15413
NCR Corporation, NCR 9300, NCR ITX-BASIC Release 2.0
[PB84-229228] 06 p0852 N85-15414
Sperry Corporation, 1100/80, UBASIC/BBASIC Level 9R1
[PB84-229202] 06 p0852 N85-15415
Sperry Corporation, 1100/80 ASC2 FORTRAN Level 11R1
[PB84-229194] 06 p0852 N85-15416
Computer Sciences Corporation, UNIVAC 1100/80, CSTS COBOL Release COB250
[PB84-229154] 06 p0852 N85-15417
Compter Sciences Corporation, UNIVAC 1100/80, CSTS BASIC Release BAS180
[PB84-229145] 06 p0852 N85-15418
Wang Laboratories, Incorporated, Wang VS100, FORTRAN 77 Version 01.00.02
[PB84-228014] 06 p0852 N85-15419
Control Data Corporation, Cyber 835, BASIC Release 3.5 Level 614
[PB84-227990] 06 p0853 N85-15420
Data General Corporation, Eclipse C350, AOS COBOL Release 3.51
[PB84-227982] 06 p0853 N85-15421
Digital Equipment Corporation, DECSYSTEM-20 2060 Model B, FORTRAN-20 Version 10
[PB84-227974] 06 p0853 N85-15422
Convergent Technologies, NGEN CP001, CT FORTRAN Version 9.0
[PB84-229210] 06 p0856 N85-15442
Formal verification of mathematical software
[NASA-CR-172407] 07 p1023 N85-16489
Completely monotone regression estimates of software failure rates
[NASA-CR-174319] 08 p1204 N85-17575
Ada (trademark) Joint Program Office objectives and progress through 1983
[AD-A149436] 10 p1541 N85-19713
Sperry Univac System 80, Model 6, OS/3 BASIC, Version 10.01
[PB85-108066] 10 p1542 N85-19722
FORTRAN 66 analyser: User's manual
[PB85-111748] 10 p1542 N85-19724
Ada compiler validation summary report, Dansk Datamatik Center, VAX 11 compiler version 1.1
[AD-A149340] 11 p1699 N85-20681
Micro Focus IBM personal computer XT Compact Level 2 COBOL; V2.5
[PB85-108918] 11 p1703 N85-20716
Micro Focus IBM personal computer XT High Performance Level 2 COBOL; V2.5
[PB85-108926] 11 p1704 N85-20717
Micro focus IBM personal computer XT, high performance level, 2 COBOL, IBM PC tailored; V2.6
[PB85-110815] 11 p1705 N85-20725
A theoretical basis for the analysis of redundant software subject to coincident errors
[NASA-TM-86369] 13 p2145 N85-23317
Security of personal computer systems: A management guide
[PB85-161040] 14 p2400 N85-24793
Management aspects of software maintenance
[AD-A152035] 16 p2847 N85-27550
Integrated software engineering system (SIGL)
[DT/GL/7254/Z482/G-C./MJ] 20 p3516 N85-31863

COMPUTER PROGRAMMING
NT ASSEMBLER ROUTINES
NT LANGUAGE PROGRAMMING
NT LOGIC PROGRAMMING
NT MICROPROGRAMMING
NT MULTIPROGRAMMING
NT PARALLEL PROGRAMMING
NT SYMBOLIC PROGRAMMING
Applications of numerical optimization methods to helicopter design problems: A survey
[NASA-TM-86010] 01 p0006 N85-10036
Research in Structures and Dynamics, 1984
[NASA-CP-2335] 01 p0057 N85-10377
Digital correlator speed improvement by multiplexing
[AD-A145207] 01 p0100 N85-10662
Ada (trademark) training curriculum. Basic Ada programming I202 teacher's guide. Laboratory manual and exercises
[AD-A143583] 01 p0103 N85-10687
THLL (TRIDENT Higher Level Language) reference manual
[AD-A145116] 01 p0104 N85-10696
Mathmatics and Computer Science Division activities
[DE84-014842] 01 p0104 N85-10701
Establishing a Software Engineering Technology (SET)
[PB84-212141] 01 p0105 N85-10702
FSTC (Federal Software Testing Center) software tool catalog
[PB84-212158] 01 p0105 N85-10703
DATAPLOT: Introduction and overview
[PB84-214055] 01 p0105 N85-10708
Software engineering environments for mission critical applications: STARS alternative programmatic approaches
[AD-A145285] 02 p0241 N85-11571
DOD related software technology requirements, practices, and prospects for the future
[AD-A145493] 02 p0242 N85-11575
Yearly report for programming productivity enhancement by the use of application generators
[AD-A145623] 02 p0242 N85-11579
Research on distributed languages and algorithms
[AD-A145661] 02 p0242 N85-11580
GUIDON
[AD-P003925] 02 p0246 N85-11605
Artificial intelligence applications to automatic test equipment
[AD-P003936] 02 p0247 N85-11616
Memory-based expert systems
[AD-A145812] 02 p0249 N85-11628
Pointwise iterations of finite element modeling of advection-diffusion equations
[DE84-015284] 02 p0253 N85-11656
Programmable optical sensor
[AD-D011244] 02 p0261 N85-11829
Air Force Materials Laboratory plans/projects
[AD-P004010] 03 p0306 N85-11990
An inviscid computational method for supersonic inlets
[AD-A145997] 03 p0316 N85-12042
Power subsystem automation study
[NASA-CR-171213] 03 p0358 N85-12299
A methodology for the analysis of programmer productivity and effort estimation within the framework of software conversion
[AD-A145757] 03 p0406 N85-12592
Computer center introductory reference manual for CDC CYBER
[AD-A145798] 03 p0406 N85-12593
Programming effort estimation
[AD-A145839] 03 p0406 N85-12595
Configuration management for mission-critical software: The Los Alamos solution
[DE84-015515] 03 p0408 N85-12606
Experimenting with the Rolm Ada language workshop for specifying and designing 03 p0408 N85-12607
Definition of technology development missions for early Space Station satellite servicing. Volume 1: Executive summary
[NASA-CR-171228] 04 p0460 N85-12922
DNC, CNC network for robotized machining cells 04 p0491 N85-13130
Concentrator optical characterization using computer mathematical modelling and point source testing
[NASA-CR-174109] 04 p0528 N85-13375
Minimal cut-set methodology for artificial intelligence applications
[DE84-016574] 04 p0553 N85-13518
An electronic documentation system
[SNIAS-842-111-101] 04 p0577 N85-13683
Research in computer science
[NASA-CR-174088] 05 p0713 N85-14572
Experience with a sophisticated computer based authoring system
[DE84-014644] 05 p0713 N85-14575
Control of walking: Local control and real time systems 05 p0715 N85-14583
A proposal for standard basic functions in Ada
[NPL-DITC-45/84] 05 p0715 N85-14584
How to implement the welcome program in compatible microcomputers such as Apple 2
[INPE-3114-PRE/511] 05 p0715 N85-14586
Use of monitors in FORTRAN: A tutorial on the barrier, self-scheduling DO-loop and Askfor monitors
[DE84-016506] 05 p0715 N85-14587
Experimental techniques of formal specifications for the design of tested and reliable computer programs
[ENST-84E007] 05 p0716 N85-14591
Towards a specification of the B programming environment
[CWI-CS-R8408] 05 p0716 N85-14593
Programming and application of numerical controlled measuring machines (NCMES)
[BMFT-FB-T-84-153] 05 p0717 N85-14599
Priority rewrite systems — computer programming
[CWI-CS-R8407] 05 p0720 N85-14621
Setting time standards at NISTARS (Naval Integrated Storage and Retrieval System)
[AD-A148371] 06 p0870 N85-15529
Art of programming programmable microcalculators. Part 12: Solution of differential equations 07 p0953 N85-16043
RATFOR user's guide version 2.0
[NASA-CR-166601] 07 p1023 N85-16480
Program visualization: Graphics support for software development
[AD-A146867] 07 p1024 N85-16499
Functional semantics of modules
[AD-A146923] 07 p1024 N85-16500
The electronic typesetting program programmer's manual
[AD-A147500] 07 p1025 N85-16508
Implementation of a constraint machine for prism - A parallel problem solver
[AD-A147844] 07 p1026 N85-16512
Operating system versus programming environment, for example the UNIX
[SWA-84/037] 07 p1027 N85-16516
Trust region methods for minimization
[AD-A147073] 07 p1030 N85-16540
The production of maintainable, trustworthy, and portable software 08 p1054 N85-16744
On the validation of computer science theories
[AD-A148637] 08 p1203 N85-17572
Fundamentals of computer programming for engineers
[AD-A147964] 08 p1205 N85-17583
Computer center CDC Libraries-PROCFIL (procedures)
[AD-A148633] 08 p1206 N85-17589
Concept paper for the development of a DOD Ada (trademark) software engineering education and training plan
[AD-A148774] 08 p1206 N85-17592

Computer center CDC libraries/NSRD (subprograms)
[AD-A148792] 08 p1206 N85-17593
Solutions to structural dynamics problems
09 p1334 N85-18384
Automatic map name placement system
09 p1341 N85-18438
Computer center CDC libraries/utility (programs)
[AD-A148680] 09 p1368 N85-18593
FLAD user's manual: FLAD file contents
[AD-A148700] 09 p1368 N85-18594
Partial evaluation as a means of language extensibility
[AD-A146730] 09 p1368 N85-18596
Organizational tools for data analysis environments
[DE85-000396] 09 p1369 N85-18601
Role of environments in managing data analysis
[DE85-000397] 09 p1369 N85-18602
Software for event oriented processing on multiprocessor systems
[DE84-016720] 09 p1370 N85-18607
Multitasking kernel for the C and FORTRAN programming languages
[DE85-001799] 09 p1370 N85-18609
Computing environments for data analysis. Part 2. Hardware
[AD-A148678] 09 p1374 N85-18633
MACSYMA usage at Langley
[NASA-CR-172518] 10 p1537 N85-19688
Managing permanent objects
[AD-A149007] 10 p1540 N85-19708
SOLIDGEN: A solid finite element data generator. User's manual
[AD-A149490] 10 p1541 N85-19715
East Europe report: Science and technology
[JPRS-ESA-85-009] 11 p1616 N85-20165
Space Station Software Issues
[NASA-CP-2361] 11 p1700 N85-20689
Software development environment issues — space station software development 11 p1700 N85-20691
Software technology within NASA
11 p1701 N85-20695
A computer system for generating single and double sampling plans for attributes data
[AD-A149548] 11 p1701 N85-20696
Polyith and environments for mathematical computation
[DE85-002967] 11 p1702 N85-20704
User's guide for the computer program response fuctor (REFAC)
[PB85-136600] 11 p1705 N85-20726
Integrated control system engineering support
[AD-A149742] 12 p1780 N85-21177
Universal file processing program for field programmable integrated circuits
[DE85-004384] 12 p1837 N85-21526
A survey of the project CIP: Computer aided, intuition-guided programming. Wide spectrum language and program transformations
[TUM-I8406] 12 p1912 N85-22000
PISCES: An environment for parallel scientific computation
[NASA-CR-172544] 12 p1913 N85-22004
Towards the generation of efficient code from verified programs
[TR-40] 12 p1914 N85-22017
Very-high level concurrent programming
[AD-A150009] 12 p1916 N85-22026
METC VAX-IBM guide to ASPEN
[DE85-001974] 12 p1916 N85-22031
VAX-ASPEN installation guide
[DE85-001973] 12 p1916 N85-22032
Programs for dynamic loading of precompiled subroutine packages, especially for applications with the Watfiv compiler
[DFVLR-MITT-84-18] 12 p1917 N85-22035
A formal method for specifying computer resources in an implementation independent manner
[AD-A149955] 12 p1918 N85-22043
Research Reports: 1984 NASA/ASEE Summer Faculty Fellowship Program
[NASA-CR-171317] 12 p1944 N85-22210
Requirements for a database management system
[DE85-004661] 12 p1951 N85-22259
Optimal allocation of components in parallel-series and series-parallel systems
[AD-A150169] 13 p2144 N85-23309
FORTRAN in the 90's
[DE85-006154] 13 p2148 N85-23332
The hierarchical database decomposition approach to database concurrency control
[AD-A150612] 13 p2168 N85-23450
Design for tactical avionics maintainability, technical evaluation report
[AGARD-AR-204] 14 p2225 N85-23798
Ground-up-to-Space (GUTS) laser propagation code description and manual
[AD-A150783] 14 p2309 N85-24295
Propagation of numerical errors in computers and numerical quality 14 p2396 N85-24760
Flowcharting with D-charts
[NASA-CR-175641] 14 p2402 N85-24806
Guidelines for development structured FORTRAN programs
[NASA-TM-86407] 14 p2402 N85-24808
Functional analysis of programs
[AD-A150742] 14 p2404 N85-24819
The HORNE reasoning system, revision
[AD-A150963] 14 p2405 N85-24827
Software and its relationship to methods
[DE85-004784] 14 p2405 N85-24829
Unsteady transonic aerodynamic and aeroelastic calculations about airfoils and wings
15 p2459 N85-25185
Study of experimental robotized system for arc welding based on Universal-15 manipulator
15 p2500 N85-25423
The design and implementation of a syntax directed editor for a space constrained microcomputer
[AD-A151313] 15 p2623 N85-26163
Continued development of a data base management system performance monitor, volume 2
[AD-A151714] 15 p2623 N85-26167
Computer program TRAMP: Inclusion of state space facilities and the analysis of non-linear elements
[BAE-BT-12643] 15 p2626 N85-26181
Efficient implementation of real-time programs under the VAX/VMS operating system
[NASA-TM-86354] 15 p2627 N85-26193
GRID: A FORTRAN program for using a digitizing table to enter a finite element GRID
[AD-A151317] 15 p2628 N85-26196
A learning strategy approach for teaching novice computer programmers
[AD-A151523] 15 p2628 N85-26200
The development of a programming support system for rapid prototyping. Tasks 2 and 3
[AD-A151549] 15 p2629 N85-26202
Preliminary design of the Ada programming support environment configuration manager
[AD-A151845] 15 p2629 N85-26206
Extension of the software development workbench to include microcomputer workstations
[AD-A151903] 15 p2630 N85-26207
Praxis language environment: Distribution package description, revision 1
[DE85-006699] 15 p2630 N85-26212
Harnessing computional power: Distributed combinator reduction
[DE85-005967] 15 p2631 N85-26216
Numerical solutions of 3-dimensional Navier-Stokes equations for closed bluff-bodies
[NASA-CR-175755] 15 p2636 N85-26255
Programming for Pioneer 12 15 p2688 N85-26606
Rotorcraft digital advanced avionics system (Rodass)
15 p2688 N85-26608
Automatic manipulators for forging rollers
16 p2762 N85-27042
A heuristic solution to the spacing problem: Maximizing the minimum Euclidean distance among N points in a convex region
[AD-A152116] 16 p2855 N85-27603
Management considerations for an information center
[AD-A151774] 16 p2875 N85-27742
A method to calculate the parameters of wings of arbitrary planform
[AD-A152689] 17 p2892 N85-27831
Investigation and implementation of a tree transformation system for user friendly programming
[AD-A152716] 17 p3011 N85-28617
Sample problems for STAGSC-1
[AD-A153142] 17 p3012 N85-28621
A modern control theory enhancement to an Interactive Control Engineering Computer Analysis Package (ICECAP)
[AD-A153249] 17 p3012 N85-28622
Software for estimating sparse Hessian matrices
[DE85-008121] 17 p3013 N85-28629
Introduction to LINE: A Feynman diagram graphic operator
[DE85-009299] 17 p3013 N85-28632
Towards a uniform topological treatment of streams and functions on streams
[CWI-CS-R8422] 17 p3014 N85-28639
Parallel Cholesky factorization on a multiprocessor
[DE85-008762] 17 p3021 N85-28682
Evaluation and Validation (E/V) team public report, volume 1
[AD-A153609] 18 p3161 N85-29584
Graphics package, version 4: User reference manual
[DE85-007894] 18 p3163 N85-29596
Ada developments
[REPT-84-26] 18 p3164 N85-29604
Hybrid uncertainty theory
[DE85-008357] 18 p3167 N85-29622
Activities of the Institute for Computer Applications in Science and Engineering (ICASE)
[NASA-CR-172610] 19 p3332 N85-30641
Proceedings of the Argonne Workshop on Programming the Next Generation of Supercomputers
[DE85-008348] 19 p3343 N85-30718
Perspectives of nonlinear dynamics
[IPPJ-723] 19 p3370 N85-30902
Modified dynamic hashing
[DE85-011166] 19 p3381 N85-30974
Synthetic aperture radar data processing — satellite-borne radar
[CNES-196-T-CT/DRT/TIT/RL]
20 p3442 N85-31363
Informatics Division 20 p3449 N85-31416
Study of new computing algorithms for supercomputers. Application to parallel processing computation
[SNIAS-440-070/84] 20 p3516 N85-31860
Coordinate transformations and programming for small revolute coordinate robots
[RR-273] 20 p3519 N85-31881
Determining functional requirements for NASA Goddard's command management system software design using expert systems 20 p3539 N85-32020
Review of the psychological issues relating to the effectiveness of structured programming
[AD-A154583] 21 p3665 N85-32766
Ada (trademark) training curriculum. Advanced Ada topics L305 teacher's guide exercises
[AD-A154621] 21 p3670 N85-32798
SIGMA - A stochastic-integration global minimization algorithm
[AD-A154878] 21 p3671 N85-32806
Design guidelines for user-system interface software
[AD-A154907] 21 p3671 N85-32807
Experience with omega: Implementation of a prototype programming environment: Part 1
[AD-A155436] 21 p3672 N85-32811
Evaluation of a software design approach: Develop a threat resolution module in Ada (trademark)
[AD-A155599] 21 p3672 N85-32815
A simple software environment based on objects and relations
[AD-A155704] 21 p3673 N85-32817
Microcomputer network: Investigation and implementation
[AD-A155631] 21 p3674 N85-32826
New developments on the core function for efficient implementation of the difficult residue number system operations
[AD-A154678] 21 p3676 N85-32834
Continued development of a data base management system performance monitor: Volume 1
[AD-A154635] 21 p3713 N85-33040
Art of programming programmable microcalculators: Calculation of response from current values of action
22 p3767 N85-33348
Method of estimating convergence of Haar coefficients in message compression problems
22 p3769 N85-33358
USSR report: Electronics and electrical engineering
[JPRS-UEE-84-003] 22 p3773 N85-33381
Art of programming programmable microcalculators, part 4: errors of calculations 22 p3778 N85-33411
Use of monitors in Pascal on the Lemur: A tutorial on the barrier, self-scheduling FOR-loop, and askfor monitors
[ANL-84-53] 22 p3826 N85-33706
Integrated Support Software System (ISSS)
[AD-A155715] 22 p3829 N85-33710
AUTSKED: An addendum
[DE85-010410] 22 p3829 N85-33712
Portable database driven control system for SPEAR
[DE85-010465] 22 p3830 N85-33720
Flat is not necessarily good
[DE85-012819] 22 p3830 N85-33723
How a BASIC program works
[DE85-009142] 22 p3831 N85-33727
Microcomputer controlled image processor
[AD-D011734] 22 p3833 N85-33735
Logical and physical modeling and design of scientific and statistical databases for energy research
[DE85-006081] 22 p3833 N85-33737
The interactive planning work station: A graphics-based UNIX (trademark) tool for application users and developers 23 p3957 N85-34527
Graphics interaction in databases
23 p3958 N85-34534
Parallel processing on the Livermore VAX 11/780-4 parallel processor system with compatability to Cray Research, Inc. (CRI) multitasking, version 1
[DE85-011856] 23 p3967 N85-34595

Development of NATOPS (Naval Air Training and Operating Procedure Standardization) performance software for the H-46D helicopter
[AD-A156089] 24 p4064 N85-35190
AUTOSIM: An automated repetitive software testing tool
[NASA-CR-177930] 24 p4137 N85-35643
Polylith: The early goals
[DE85-012534] 24 p4139 N85-35658

COMPUTER PROGRAMS

NT APPLICATIONS PROGRAMS (COMPUTERS)
NT ASSEMBLER ROUTINES
NT COMPILERS
NT COMPUTER SYSTEMS PROGRAMS
NT EDITING ROUTINES (COMPUTERS)
NT INPUT/OUTPUT ROUTINES
NT MACHINE-INDEPENDENT PROGRAMS
NT NASTRAN
NT OPERATING SYSTEMS (COMPUTERS)
NT SUBROUTINE LIBRARIES (COMPUTERS)
NT SUBROUTINES
Three degree of freedom steady state point performance program: Updated version 1
[CSIR-NIAST-83/48] 01 p0001 N85-10005
Implementation of the supersonic triplet singularity into the USTORE computer code
[CSIR-NIAST-83/47] 01 p0001 N85-10006
Experimental data base for computers program assessment. Report of the Fluid Dynamics Panel Working Group 04: Addendum
[AGARD-AR-138-ADD] 01 p0004 N85-10020
Impact of new computing systems on computational mechanics and flight-vehicle structures technology
01 p0007 N85-10042
CREKID: A computer code for transient, gas-phase combustion of kinetics
[NASA-TM-83806] 01 p0011 N85-10068
High frequency radar software reference manual for Product Two
[PB84-210079] 01 p0041 N85-10270
Battery optimization considerations
[DE84-014759] 01 p0044 N85-10288
ICARUS: A general one-dimensional heat conduction code
[DE84-016125] 01 p0047 N85-10310
Combustion modeling of a 2 cylinder cycle reciprocating engine
[AD-A144782] 01 p0055 N85-10364
Application guide for Hydrological Simulation Program FORTRAN (HSPF)
[PB84-215763] 01 p0064 N85-10427
Manual of phosphoric acid fuel cell stack three-dimensional model and computer program
[NASA-CR-174722] 01 p0067 N85-10447
Processing and display of atmospheric phenomenas data
[NASA-CR-171178] 01 p0072 N85-10475
Severe weather statistics STADTS decoder (SXW) and plotter (SWY)
[PB84-213993] 01 p0086 N85-10576
Psychological testing on the computer
[R/PERS-618] 01 p0097 N85-10645
REMOTE: Modem Communicator Program for the IBM personal computer
[DE84-015047] 01 p0100 N85-10665
IAC user manual
[NASA-CR-175300] 01 p0102 N85-10677
A packed storage program for angular momentum coupling coefficients
[TWISK-316] 01 p0102 N85-10680
Three programs for evaluating bending moments, deflections and shear forces in simply-supported uniform bridge decks under South African NA loading: NAB, NAD and NAS. NITRR manual P13
[ISBN-0-7988-2283-X] 01 p0102 N85-10681
Floating-point function generation routines for 16-bit microcomputers
[NASA-TM-83783] 01 p0102 N85-10683
RSCORS graphics system
[DE84-015693] 01 p0104 N85-10698
A modular data acquisition and display software system for a laboratory environment
[PB84-217892] 01 p0105 N85-10709
Methods, applications of image processing
01 p0115 N85-10785
SANDYL radiation transport code at the Naval Research Laboratory
[AD-A144890] 01 p0117 N85-10799
Automated Data Systems (ADS) documentation standards
[AD-A144867] 01 p0125 N85-10857
Fast Fourier transform for unequally spaced data
01 p0128 N85-10876
Transonic flow analysis for rotors. Part 1: Three-dimensional quasi-steady, full-potential calculation
[NASA-TP-2375-PT-1] 02 p0134 N85-10914
VORCOR: A computer program for calculating characteristics of wings with edge vortex separation by using a vortex-filament and-core model
[NASA-CR-165902] 02 p0135 N85-10921
PAN AIR: A computer program for predicting subsonic or supersonic linear potential flows about arbitrary configurations using a higher order panel method. Volume 3: Case manual (version 1.0)
[NASA-CR-3253] 02 p0135 N85-10922
Enhanced TCAS 2/CDTI traffic Sensor digital simulation model and program description
[NASA-CR-172445] 02 p0136 N85-10927
An interactive computer code for calculation of gas-phase chemical equilibrium (EQLBRM)
[NASA-CR-168337] 02 p0140 N85-10948
Burner liner thermal/structural load modelling
02 p0143 N85-10970
Computations for the 16-foot transonic tunnel, NASA, Langley Research Center
[NASA-TM-86319] 02 p0149 N85-11009
Resistance and inductance calculations for helical flux compression generators
[DE84-015068] 02 p0195 N85-11306
The CMC/3DPNS computer program for prediction of three-dimensional, subsonic, turbulent aerodynamic juncture region flow. Volume 3: Programmers' manual
[NASA-CR-165998] 02 p0197 N85-11318
Efficient methods for mechanical and structural reliability analysis and design 02 p0205 N85-11355
STARS: A general-purpose finite element computer program for analysis of engineering structures
[NASA-RP-1129] 02 p0209 N85-11378
Phosphoric acid fuel cell power plant system performance model and computer program
[NASA-CR-174638] 02 p0222 N85-11456
Generalized linear inversion of 2.5 - dimensional gravity and magnetic anomalies 02 p0226 N85-11480
Proposal for a semiautomatic program testing system
[INPE-3262-TDL/178] 02 p0240 N85-11561
Description of the logical support for an image processing system
[INPE-2783-PRE/349] 02 p0240 N85-11563
SITIM system: Object manager module
[INPE-3284-NTE/226] 02 p0240 N85-11564
SITIM system: Supervisor utilization
[INPE-3267-NTE/224] 02 p0240 N85-11565
Contracting for computer software development: Serious problems require management attention to avoid wasting additional millions
[FGMSD-80-4] 02 p0241 N85-11567
SMP: A solid modeling program
[NASA-CR-172473] 02 p0241 N85-11570
Program flow analyzer, volume 1
[AD-A145320] 02 p0241 N85-11572
DOD related software technology requirements, practices, and prospects for the future
[AD-A145493] 02 p0242 N85-11575
Parametric analysis for generalized network flow problems
[AD-A145558] 02 p0243 N85-11589
GUIDON
[AD-P003925] 02 p0248 N85-11605
Modeling holographic recognition system by using number-theory convolution transformation
02 p0272 N85-11774
Turbofan noise generation. Volume 2: Computer programs
[NASA-CR-167952] 02 p0275 N85-11791
Archiving and exchange of a computerized marine seismic database: The ROSE (Rivera Ocean Seismic Experiment) data archive system
[AD-A145658] 02 p0294 N85-11908
A data base for three-dimensional all-interference code evaluation 03 p0312 N85-12017
An inerference assessment approach for a three-dimensional slotted tunnel with sparse wall pressure data 03 p0314 N85-12030
Estimation of helicopter performance using a program based on blade element analysis
[AD-A146341] 03 p0318 N85-12055
A digital algorithm for composite laminate analysis: FORTRAN, Revised
[AD-A145633] 03 p0326 N85-12098
Ballpark reliability estimation techniques
[AD-A145971] 03 p0369 N85-12357
A research program in computer technology
[AD-A145776] 03 p0402 N85-12565
On line digitizer software
[AD-A146249] 03 p0403 N85-12568
NUTSATSEA: An on line data reduction program linking a Chemlab continuous flow analyser to a Commodore PET microcomputer
[IOS-176] 03 p0403 N85-12570
On a program for solution of BCMP queueing network model
[NAL-TR-813] 03 p0405 N85-12585
A user's guide to the Flexible Spacecraft Dynamics and Control Program
[NASA-TM-87389] 03 p0405 N85-12586
Conversion of FEB (Fast and Easy Binary) utilities to ASCII FORTRAN
[AD-A145840] 03 p0406 N85-12596
A sequential quadratic programming algorithm for solving large, sparse nonlinear programs
[AD-A145854] 03 p0407 N85-12597
Automating software design metrics
[AD-A145869] 03 p0407 N85-12598
An input translator for a computer-aided design system
[AD-A146337] 03 p0408 N85-12605
Designing optimal AOQL sampling plans a computerized approach
[AD-A146288] 03 p0413 N85-12639
Analysis of piezoelectric disks and cylinders using finite element method
[AD-A146323] 03 p0414 N85-12650
Free-space propagation of light pulses
[PB84-217108] 03 p0421 N85-12689
Information Center handbook
[PB84-211341] 03 p0439 N85-12795
Development of gas-lubricated pistons for heavy duty diesel engine technology program
[NASA-CR-174746] 03 p0441 N85-12808
Algorithm for astronomical, extended source, signal-to-noise radio calculations
[NASA-TP-2396] 03 p0445 N85-12833
Algorithm for astronomical, point source, signal to noise ratio calculations
[NASA-TP-2397] 03 p0445 N85-12834
NIKE3D: An implicit, finite-deformation, finite element code for analyzing the static and dynamic response of three-dimensional solids, revision 1
[DE84-017161] 04 p0514 N85-13277
Concentrator optical characterization using computer mathematical modelling and point source testing
[NASA-CR-174109] 04 p0528 N85-13375
Software used with the flux mapper at the solar parabolic dish test site
[NASA-CR-174108] 04 p0528 N85-13376
Open cycle OTEC thermal-hydraulic systems analysis and parametric studies
[DE84-013011] 04 p0530 N85-13391
WXR (hydrologic weather wire and PLT product software package)
[PB84-237221] 04 p0541 N85-13442
U: The universal utility controller, revision 1
[DE84-017077] 04 p0547 N85-13481
Expert systems in design and manufacture
[DE84-005522] 04 p0550 N85-13496
Design and implementation of a modular program system for statistical analyses
[IKE-4-114] 04 p0551 N85-13503
Multigrid iteration solution procedure for solving two-dimensional sets of coupled equations
[DE84-016554] 04 p0555 N85-13533
Preliminary user's guide for BIGONE on the Cray
[DE84-017075] 04 p0568 N85-13623
Real space solution to the phase problem in X-ray crystallography: ALCAMPS (Ames Laboratory Computer-aided Analysis of Multi-solution Patterson Superpositions)
[DE84-015476] 04 p0572 N85-13651
Archiving and exchange of a computerized marine seismic database: The ROSE data archive system
[DE84-901453] 04 p0576 N85-13677
Certain optimal parameters of high-velocity Venturi ejection tubes
[BLL-M-35624-(5828.4)] 05 p0634 N85-14068
Navier-Stokes computational study of axisymmetric transonic turbulent flows with a two-equation model of turbulence 05 p0634 N85-14068
Comparison of SCAPID/GaAs to experiment
05 p0665 N85-14279
A summary description of a computer program concept for the design and simulation of solar pond electric power generation systems 05 p0666 N85-14285
Implicit numerical methods in meteorology
05 p0666 N85-14406
Improving the Spacelab mass memory unit tape layout with a simulation model
[NASA-TM-86483] 05 p0713 N85-14571
How to implement the welcome program in compatible microcomputers such as Apple 2
[INPE-3114-PRE/511] 05 p0715 N85-14586
Use of monitors in FORTRAN: A tutorial on the barrier, self-scheduling DO-loop and Askfor monitors
[DE84-016506] 05 p0715 N85-14587
Maximum likelihood estimation of parameters in linear systems from flight test data: A FORTRAN program
[AD-B087198L] 05 p0715 N85-14588

Knowledge-based communication and management support in a system development environment
05 p0717 N85-14596

Use of artificial intelligence and simple mathematics to analyze a physiological model 05 p0717 N85-14597

Development of the code NSFOIL for analyzing high Reynolds number transonic flow around an airfoil
[NAL-TR-816] 06 p0749 N85-14801

PROGRAM VSAERO: A computer program for calculating the non-linear aerodynamic characteristics of arbitrary configurations: User's manual
[NASA-CR-166476] 06 p0749 N85-14802

HH-60D night hawk helicopter
06 p0752 N85-14817

Certification of advanced systems
06 p0753 N85-14829

Software for Crimea-Pushchino radiointerferometer
06 p0783 N85-15007

Computer-aided design of extrusion dies by metal-flow simulation 06 p0797 N85-15094

Summary of photovoltaic performance models
06 p0832 N85-15296

Probable maximum flood estimation - Eastern United States
[AD-A146536] 06 p0839 N85-15324

AFOS (Automation of Field Operations and Services) display of MDR (Manually Digitized Radar) data on local map backgrounds
[PB84-220797] 06 p0840 N85-15338

Two-dimensional lake wave prediction system
[PB84-231094] 06 p0841 N85-15342

Reusable software
[AD-A146575] 06 p0854 N85-15427

Time series analysis programs for stratigraphic data
[AD-A146627] 06 p0854 N85-15429

Two programs for the HP9836C computer to acquire frequency or voltage data from a source
[AD-A146632] 06 p0854 N85-15430

Introduction to software packages
[PB84-217843] 06 p0856 N85-15441

Intercomparison between West Germany and US thermodynamic codes
[AD-A146622] 06 p0869 N85-15525

Research on introspective systems
[AD-A146406] 06 p0870 N85-15530

Analysis of the flow field about a T-45 using PANAIR
[AD-A146811] 07 p0899 N85-15699

NyKINM, a further development of KINM 22 — simulation of a robot attack on an aircraft
[FOA-C-20559-D8(E3)] 07 p0903 N85-15720

Integrating chemical kinetic rate equations by selective use of stiff and nonstiff methods
[NASA-TM-86923] 07 p0904 N85-15726

A computer program for the performance analysis of scarfed nozzles
[AD-A147370] 07 p0905 N85-15730

High altitude chemically reacting gas particle mixtures. Volume 3: Computer code user's and applications manual — rocket nozzle and orbital plume flow fields
[NASA-CR-171828] 07 p0917 N85-15803

A study of interply layer effects on the free-edge stress field of angleplied laminates
[NASA-TM-86924] 07 p0919 N85-15822

Bearing tester fit analysis
[NASA-CR-171262] 07 p0973 N85-16181

Research activities of the Norwegian seismic array (NORSAR)
[AD-A146778] 07 p0996 N85-16326

Computer program to compute soil thermal conductivity from transient temperature measurements
[PB85-100550] 07 p0996 N85-16341

Upset susceptibility study employing circuit analysis and digital simulation — digital systems and electromagnetic interference 07 p0999 N85-16344

Random pattern tracking acceleration tolerance tester
[AD-D011404] 07 p1017 N85-16459

Formal verification of mathematical software
[NASA-CR-172407] 07 p1023 N85-16469

Computer program for determining induced stresses and consolidation settlements (CSETT)
[AD-A146730] 07 p1023 N85-16493

A program to produce standard shewhart control charts for the statistics X-bar and R or S, P, NP, C, or U
[AD-A146971] 07 p1024 N85-16501

The effects of software quality control and baseline management on the acquisition of computer programs
[AD-A147051] 07 p1024 N85-16502

NOISEMAP 4.4 computer program update, operator's manual, addendum 1
[AD-A147091] 07 p1025 N85-16503

Debug testing and confidence testing
[AD-A147104] 07 p1025 N85-16504

A virial equation of state option for the TIGER computer program
[AD-A147490] 07 p1025 N85-16507

A survey and evaluation of software quality assurance
[AD-A147552] 07 p1026 N85-16510

On the structure of information in software
[AD-A147580] 07 p1026 N85-16511

PLOT3D: An interactive graphics code for 3-dimensional plots
[AD-A147887] 07 p1026 N85-16514

FORTRAN version of the quantitative energy-dispersive electron beam X-ray analysis program FRAME C
[PB84-240936] 07 p1027 N85-16519

Extracting embedded generalized networks from linear programming problems
[AD-A147565] 07 p1033 N85-16556

Arctic marine acoustics
[AD-A147492] 07 p1039 N85-16594

Computer program for calculation of complex chemical equilibrium compositions and applications. Supplement 1: Transport properties
[NASA-TM-86885] 07 p1049 N85-16663

Data base support for SIO (System Integration Office)
[AD-A147487] 07 p1054 N85-16692

ATE user's view on design for maintainability
08 p1064 N85-16737

Built-in-test for first line testing
08 p1064 N85-16739

Development of a Helicopter integrated navigation system 08 p1073 N85-16802

A Generalized Escape System Simulation (GESS) computer program. Volume 2: GESS programmer's manual, version 2
[AD-A148363] 08 p1081 N85-16845

Shuttle avionics software trials, tribulations and success 08 p1090 N85-16891

Shuttle avionics software development trials: Tribulations and successes, the backup flight system
08 p1091 N85-16892

SSME digital control design characteristics
08 p1091 N85-16893

Automatic software for controlling cryogenic systems
08 p1097 N85-16932

Managing computer-controlled operations
08 p1097 N85-16934

The Communications link analysis and simulation system (CLASS) 08 p1100 N85-16952

Modeling techniques used in the communications link analysis and simulation system (CLASS)
08 p1100 N85-16953

Validation of the communications link analysis and simulation system (CLASS) 08 p1100 N85-16954

Performance assessment of aero-assisted orbital transfer vehicles 08 p1106 N85-16993

Computer subroutines for estimation of human exposure to radiation in low Earth orbit
[NASA-TM-86324] 08 p1199 N85-17550

Performance management system enhancement and maintenance
[NASA-CR-175271] 08 p1202 N85-17564

On the validation of computer science theories
[AD-A148637] 08 p1203 N85-17572

A FORTRAN plotting package for graphic VDUs
[AD-A148489] 08 p1204 N85-17577

A computer package for ranking, selection and multiple comparisons with the best
[AD-A147617] 08 p1204 N85-17579

Developing double sampling plans for attributes to meet sample size criteria
[AD-A148144] 08 p1205 N85-17587

COPES/ADS (Control Program for Engineering Synthesis) (Automated Design Synthesis) using the ADS optimization program
[AD-A148576] 08 p1206 N85-17588

Algorithm for space-time analysis of data on geomagnetic field
[NASA-TM-77804] 08 p1209 N85-17609

Numerical generation of orthogonal and nonorthogonal coordinates in two dimensional simply and doubly connected regions
[VKI-TN-151] 08 p1216 N85-17662

SIMM1: A linearized particle code
[AD-A148627] 08 p1221 N85-17689

A voice-actuated wind tunnel model leak checking system
[NASA-TM-86359] 09 p1263 N85-17936

Preliminary results from the unsteady airfoil model USTAR2
[AD-P004171] 09 p1266 N85-17956

Automatic land vehicle navigation using road map data
[DE84-017178] 09 p1278 N85-18043

FORTRAN 77 computer program for test procedure calculations of vented heaters
[PB85-109627/GAR] 09 p1305 N85-18198

Mesoscale storm and dry period parameters from hourly precipitation data: Program documentation
[DE85-001368] 09 p1357 N85-18538

JOVIAL J73 automated verification system: Implementation phase
[AD-A148732] 09 p1368 N85-18597

Introduction to LBL graphics
[DE85-000389] 09 p1369 N85-18600

User/programmer guide for UCMD 108 multi-vertex polyarc/path integrity verifier
[DE84-017173] 09 p1369 N85-18604

Beyond fault trees to fault graphs
[DE84-017022] 09 p1370 N85-18608

User's manual: Menu-driven data graphing program for the Tektronix 7912AD and 7612D transient digitizer system
[DE85-002151] 09 p1370 N85-18610

Computer programs for the adjustment of indirect observation with condition equations between the unknowns
[SER-B-268-MITT-170] 09 p1370 N85-18612

System software for the finite element machine
[NASA-CR-3870] 09 p1372 N85-18622

Fixed vs. variable order Runge-Kutta
[DE85-001320] 09 p1374 N85-18639

Theoretical studies of atomic transition
[DE85-001325] 09 p1381 N85-18687

Documentation for an instrument database system
[DE84-017392] 09 p1402 N85-18826

UKIRT spectro-photometry system — United Kingdom Infrared Telescope (UKIRT)
[UKIRT-23] 09 p1414 N85-18921

Analysis of inviscid transonic flow around an airfoil by diagonal form of IAF scheme
[NAL-TR-831] 10 p1420 N85-18955

Inviscid analysis of unsteady blade tip flow correlation studies
[NASA-CR-172506] 10 p1420 N85-18958

Efficient self-consistent viscous-inviscid solutions for unsteady transonic flow
[NASA-TM-86335] 10 p1420 N85-18959

Directory of range data conversion and processing systems
[AD-A148996] 10 p1427 N85-19001

A shock wave capability for the improved Two-Dimensional Kinetics (TDK) computer program
[NASA-CR-171302] 10 p1483 N85-19360

PATHFINDER: A trajectory prediction system for the Great Lakes
[PB85-115335] 10 p1506 N85-19506

Application of SIMCA (Soft Independent Modeling of Class Analogy) pattern recognition to air pollutant analytical data
[PB85-124683] 10 p1513 N85-19549

OBLOG: Designed to create and maintain a 49 hour observation log file
[PB85-109528] 10 p1519 N85-19579

Hurricane plotting program
[PB85-121432] 10 p1521 N85-19582

Crewstation assessment of reach as applied to the OH-58A helicopter
[AD-A149413] 10 p1531 N85-19650

Microprocessor-based monitoring and control project, phase 1
[DE84-901974] 10 p1536 N85-19699

A program design for an adaptive, non-linear finite element solver
[AD-A148880] 10 p1539 N85-19705

RELTIM: A library of routines used in real time machine control applications
[PB85-116507] 10 p1542 N85-19725

Modeling the internal combustion engine
[NASA-RP-1094] 10 p1544 N85-19733

LOVEL-84: A LOw-VELocity aerodynamic heating code for flat plates, wedges, and cones
[DE85-002604] 11 p1576 N85-19933

Aircraft transparency bird impact analysis using the MAGNA computer program
[AD-P004186] 11 p1579 N85-19948

Reliability of DNC system examined
11 p1617 N85-20171

CAD/CAM systems for printed circuit design, manufacture 11 p1619 N85-20188

Computation of the inviscid velocity potential for general ellipsoids on a nearly quadratic surface grid
[REPT-25/84] 11 p1633 N85-20287

Vertical solar louver project
[DE84-017335] 11 p1676 N85-20558

Plotfile appender
[PB85-109502] 11 p1688 N85-20616

Isentropic objective analysis
[PB85-112167] 11 p1688 N85-20617

User's manual for GRIZZLY
[DE85-001405] 11 p1702 N85-20702

MCNP code
[DE85-002565] 11 p1702 N85-20705

Standardized format for computer series
[PB85-109668] 11 p1705 N85-20724

Needs, opportunities, and options for large scale systems research
[DE85-002664] 11 p1709 N85-20750
GPS system field testing 11 p1711 N85-20762
Self-Optimized Sector (SOS) model of self-consistent energy loss and scattering for an electron beam propagating in air
[DE85-003161] 11 p1722 N85-20631
AID: Access to Informal Documentation
[DE85-000418] 11 p1740 N85-20939
Sample size and precision in communication performance measurements
[PB85-1143270] 12 p1830 N85-21488
Program for controlling electrical measuring contact instrument on glow-discharge indicator panel
12 p1842 N85-21558
Method of calculating cooldown process in cryostat of cryogenic electric machine 12 p1843 N85-21567
TRACR3D: A model of flow and transport in porous/fractured media
[LA-9657-MS] 12 p1845 N85-21576
3-D inelastic analysis methods for hot section components (base program) — turbine blades, turbine vanes, and combustor liners
[NASA-CR-174700] 12 p1863 N85-21686
Time marching numerical solution of the dynamic response of nonlinear systems
[NAF-AN-25] 12 p1865 N85-21696
An analysis of the high frequency vibrations in early Thematic Mapper scenes 12 p1872 N85-21742
User's manual for the University of Houston individual heliostat layout and performance code
[DE85-004643] 12 p1882 N85-21808
Investigations of micro-turbulence in the bottom of the boundary layer
[AD-A149823] 12 p1896 N85-21897
FTASUM: Aviation forecast summaries
[PB85-112977] 12 p1897 N85-21908
SAOSUM: A short summary of observations
[PB85-120364] 12 p1897 N85-21909
TRAJ: Single station trajectory plot
[PB85-135002] 12 p1897 N85-21911
AFOS (Automation of Field Operations and Service) surface observation decoding
[PB85-137566] 12 p1898 N85-21913
Topics in optical materials and device research, 3. Volume 2
[AD-A149727] 12 p1911 N85-21996
Computing Division two-year operational plan, FY 1984 - 1985
[LA-9978-MS] 12 p1913 N85-22006
The liner package: An incipient MHD capability for CCUBE
[LA-9969-MS] 12 p1913 N85-22007
User's guide for TWODANT: A code package for two-dimensional, diffusion-accelerated, neutral-particle transport
[LA-10049-M] 12 p1913 N85-22009
Adaptive meshes in the 2DL code
[LA-9938-MS] 12 p1914 N85-22011
The automated reasoning system ITP
[ANL-84-27] 12 p1914 N85-22016
A user's guide to sensitivity testing on computer models at Los Alamos National Laboratory
[LA-10104-M] 12 p1914 N85-22018
The portable LISP translation tool
[AD-A149765] 12 p1915 N85-22023
Interface specifications for SCR (Software Cost Reduction) (A-7E) extended computer module, revised
[AD-A149948] 12 p1915 N85-22024
MFTF sensor verification computer program
[DE85-004452] 12 p1916 N85-22029
EZPIX: A tablet entry method for computer-generated slides, drawings, and graphs
[DE85-005234] 12 p1916 N85-22030
VAX-ASPEN installation guide
[DE85-001973] 12 p1916 N85-22032
Software for special functions
[DE85-004684] 12 p1917 N85-22033
Parallel linear algebra library for the Denelcor HEP
[DE85-004685] 12 p1917 N85-22034
SIMULA: Digital controller simulation package
[PB85-134492] 12 p1917 N85-22041
Experimental mathematics
[CWI-PM-R8411] 12 p1925 N85-22096
User's guide for TWOHEX: A code package for two-dimensional, neutral-particle transport in equilateral triangular meshes
[DE85-004482] 12 p1930 N85-22125
Strong iron accelerating by collisionless magnetosonic shock wave propagating perpendicular to a magnetic field
[IPPJ-709] 12 p1935 N85-22161
Models of the upper atmosphere
12 p1945 N85-22217
A study of the compatibility of an existing CFD package with a broader class of material constitutions
12 p1945 N85-22219
Analyses via automated mass spectrometry (MS/DS)
12 p1947 N85-22227
Evaluation of expert systems
12 p1947 N85-22229
Method for the prediction of the installation aerodynamics of a propfan at subsonic speeds
[NASA-CR-3887] 13 p1969 N85-22369
Two degree-of-freedom flutter solution for a personal computer
[NASA-TM-86381] 13 p1971 N85-22379
Three-dimensional calculation of shuttle charging in polar orbit 13 p1992 N85-22486
NASCAP simulation of PIX 2 experiments
13 p1993 N85-22497
Investigations of radiation-induced and carrier-enhanced conductivity 13 p1996 N85-22515
Development of a three-phrase combustion code for modeling liquid rocket engines 13 p2003 N85-22554
Numerical/Electromagnetics Code (NEC)
[DE85-004999] 13 p2056 N85-22874
Pre- and post-processing for stream-function eddy current calculations
[AD-A150417] 13 p2065 N85-22896
New atmospheric sensor analysis study
[NASA-CR-171426] 13 p2094 N85-23069
Use of three omega radionavigation system position lines for solving problems in marine geodesy
13 p2107 N85-23131
ROSA: A computer model for optical power ratio calculations
[DE85-005174] 13 p2129 N85-23251
A design analysis and implementation of a user-friendly interface for the UNIX operating system
[AD-A150558] 13 p2145 N85-23312
Principles of software engineering environment design
[AD-A150352] 13 p2147 N85-23324
ROSS: An object-oriented language for constructing simulations
[AD-A150556] 13 p2147 N85-23330
Second thoughts on the mathematical software effort: A perspective
[DE85-004831] 13 p2148 N85-23333
On a mathematical structure for an image algebra
[AD-A150228] 13 p2150 N85-23348
Hexagonal data base study
[AD-A150176] 13 p2167 N85-23448
Copyright law, computer software, and government acquisition
[AD-A150347] 13 p2168 N85-23453
Comet thermal modeling 13 p2176 N85-23505
Model for high rate gas flows in deformable and reactive porous beds
[DE85-006140] 14 p2253 N85-23964
Analysis of slabs-on-grade for a variety of loading and support conditions
[AD-A150965] 14 p2264 N85-24030
Investigation of doubly-fed machine in variable speed application
[DE85-004378] 14 p2299 N85-24234
Effect of flight sequences in complex load histories on crack front marking 14 p2318 N85-24326
Observation model and parameter partials for the JPL VLBI parameter estimation software MASTERFIT-F 2.0
[NASA-CR-175640] 14 p2347 N85-24509
Modelling of photodegradation in solar cell modules of substrate and superstrate design made with ethylene-vinyl acetate as pottant material
[NASA-CR-175690] 14 p2350 N85-24527
Streamlined Test Reporting And Planning (STRAP): Computerized human factors questionnaire
[AD-A150811] 14 p2395 N85-24751
Security of personal computer systems: A management guide
[PB85-161040] 14 p2400 N85-24793
GRAFIT language for simulating two-dimensional geometric entities and sketches
14 p2401 N85-24801
Automation of development of software for switching units that are implemented in the form of multiprocessor systems on a microcomputer base
14 p2401 N85-24802
The Multimission Image Processing Laboratory's virtual frame buffer interface
[NASA-CR-175655] 14 p2402 N85-24805
The use of a 3-D system for a civil engineering project
14 p2402 N85-24811
Runstreams for using ASKA
[NIAST-84/27] 14 p2403 N85-24812
An experiment in software reliability
[NASA-CR-172553] 14 p2403 N85-24813
TAPTRN: A tape utility program
[AD-A150644] 14 p2403 N85-24814
Software library: A reusable software issue
[AD-A150722] 14 p2403 N85-24816
Functional analysis of programs
[AD-A150742] 14 p2404 N85-24819
The enhancement of concurrent processing through functional programming languages
[AD-A150771] 14 p2404 N85-24822
Integration of an Apple 2 Plus computer into an existing dual axis sun tracker system
[AD-A150778] 14 p2404 N85-24823
Implementation of a C1 triangular element based on the p-version of the finite element method
[AD-A150904] 14 p2404 N85-24825
Dataflow computation
[CWI-TRACT-6] 14 p2406 N85-24833
LINCS
[DE85-006151] 14 p2407 N85-24836
Computer Visual System (CVS) reference manual
[DE85-006328] 14 p2407 N85-24837
A fast ray tracing routine for laterally inhomogeneous media
[AD-A150884] 14 p2421 N85-24938
Thermodynamic calculations and the chemical vapour deposition of hard materials 14 p2431 N85-24981
Documentation for the machine-readable version of the Revised S210 Catalog of Far-Ultraviolet Objects (Page, Carruthers and Heckathorn 1982)
[NASA-TM-87439] 14 p2438 N85-25047
Cosmic ray environment model for Earth orbit
[NASA-CR-175668] 14 p2455 N85-25165
Trends in computational capabilities for fluid dynamics
15 p2457 N85-25172
Unsteady analysis of rotor blade tip flow
[NASA-CR-3868] 15 p2482 N85-25202
A computer program to calculate the supersonic flow over a solid cone in air or water
[AD-A151102] 15 p2484 N85-25217
Global positioning system: A modification to the baseline satellite constellation for improved geometric performance
[AD-A151602] 15 p2489 N85-25239
The development of a performance and mission planning program for the A-7E aircraft
[AD-A151717] 15 p2471 N85-25258
A user's manual for AMEER flight path trajectory simulation code
[DE85-006580] 15 p2472 N85-25260
Mathematical modeling of the AEDC (Arnold Engineering Development Center) propulsion wind tunnel (16T)
[AD-A151293] 15 p2475 N85-25275
A decision support methodology for space technology advocacy
[AD-A151695] 15 p2478 N85-25283
Selection of optimal control program for solar cell panels of Earth satellites 15 p2484 N85-25335
Computing parameters characterizing possibility of planets falling in star camera field of view during space survey 15 p2487 N85-25351
A FORTRAN program for deep space sensor analysis
[AD-A151700] 15 p2489 N85-25366
The investigation of tethered satellite system dynamics
[NASA-CR-171433] 15 p2492 N85-25375
Computer-assisted Gran titration procedure for strong acid determination
[DE85-006801] 15 p2507 N85-25462
CON1D: A computer program for calculating spherically symmetric droplet combustion
[DE85-005604] 15 p2507 N85-25464
The design and validation of software for dimensional metrology
[NPL-DITC-50/84] 15 p2521 N85-25542
An analysis of grid-based line drawing quantization methods
[AD-A151847] 15 p2522 N85-25547
Computer-aided identification of complete constitution model of transistor structure for design of subnanosecond large-scale-integrated circuits 15 p2529 N85-25594
West Europe report: Science and technology
[JPRS-WST-84-026] 15 p2532 N85-25617
Applications, specifications of Robotron CAD-CAM work stations 15 p2537 N85-25661
New sensor for industrial metrology developed
15 p2538 N85-25665
Design and swept-frequency measurement of printed circuit board log-periodic dipole arrays
[R-NIAS-23] 15 p2539 N85-25671
Null generation using dace on a reflector
[AD-A151697] 15 p2544 N85-25703
On the interconnection of incompatible solid finite element meshes using multipoint constraints
15 p2575 N85-25879
Use of COSMIC NASTRAN in a design department
15 p2575 N85-25881
An elastic analysis of a plated bone to determine fracture gap motion 15 p2575 N85-25882

An experimental investigation into the dynamic response of a stiffened flat plate loaded impulsively by an underwater shockwave
[AD-A151321] 15 p2576 N85-25903
Crack closure characteristics considering center cracked and compact tension specimens
[AD-A151702] 15 p2579 N85-25907
Elastic-workhardening SDF (Single-Degree-of-Freedom) system subjected to random blast excitations
[AD-A151866] 15 p2579 N85-25909
Technical development to improve satellite sounding over radiatively complex terrain
[NASA-CR-175746] 15 p2583 N85-25929
Plasma and magnetospheric research
[NASA-CR-171447] 15 p2591 N85-25976
ILUM code: Solar and lunar flux calculations for multi-cloud layered atmospheres
[DE85-005578] 15 p2600 N85-26025
Alterations/corrections to the BRASS Program
[NASA-CR-171874] 15 p2616 N85-26121
Interactive data analysis. Development of an interactive data manipulation system
[AD-A151359] 15 p2623 N85-26164
Development of a user support package for CPESIM 2 (a computer simulation for CPE (Computer Performance Evaluation) use
[AD-A151699] 15 p2624 N85-26170
Role of supercomputers in energy research programs
[DE85-006865] 15 p2624 N85-26172
USSR report: Cybernetics, computers and automation technology
[JPRS-UCC-85-003] 15 p2625 N85-26174
Computer technology advances exhibited
15 p2625 N85-26175
Effective microinstruction pipeline organization in a high-capacity microprocessor 15 p2625 N85-26176
Principles of organizing a real-time control system
15 p2625 N85-26177
Care 3 model overview and user's guide, first revision
[NASA-TM-86404] 15 p2627 N85-26192
Efficient implementation of real-time programs under the VAX/VMS operating system
[NASA-TM-86354] 15 p2627 N85-26193
GRID: A FORTRAN program for using a digitizing table to enter a finite element GRID
[AD-A151317] 15 p2628 N85-26196
A microcomputer-based program for printing check plots of integrated circuits specified in Caltech intermediate form
[AD-A151715] 15 p2629 N85-26205
Preliminary design of the Ada programming support environment configuration manager
[AD-A151845] 15 p2629 N85-26206
Catalog of the National Energy Software Center
[TI85-900521] 15 p2630 N85-26209
MATRIX: A program that shows how row and column orderings affect matrix fill-in
[DE85-007522] 15 p2630 N85-26213
VAX-based graphics mail system
[DE85-007231] 15 p2630 N85-26214
SPRING: Helical spring design software for microcomputers
[DE85-006200] 15 p2631 N85-26217
GEMINI: A computer program for two and three dimensional linear elastic and seismic structural analysis, CDC 7600 version
[DE85-007496] 15 p2631 N85-26218
Mathematical software for hyperbolic equations and two point boundary value problems
[AD-A151982] 15 p2638 N85-26270
SPLOT: A plot program for finite element data, function versus distance
[DE85-007129] 15 p2638 N85-26273
Implementation of Weeks' method for the inverse Laplace transform problem
[DE85-005919] 15 p2639 N85-26275
Time dependent and steady-state solutions of the electron energy distribution in a weakly ionized gas subject to an ac or dc electric field
[AD-A151829] 15 p2656 N85-26391
A database design for the Brazilian Air Force Flying Unit Operational Control System
[AD-A151848] 15 p2666 N85-26452
The controlled ecological life support system
15 p2668 N85-26603
Proceedings of the NAL Symposium on Aircraft Computational Aerodynamics
[NAL-SP-1] 16 p2691 N85-26611
Computer software for aerodynamic design of aircraft developed within the National Aerospace Laboratory
16 p2691 N85-26613
Recent trends in software technology for vector processors 16 p2691 N85-26615
A computer program for the drag prediction of subsonic, turbine powered aircraft in the en-route configuration
[VTH-LR-412] 16 p2701 N85-26681
Generation of flight paths using heuristic search
[AD-A151949] 16 p2704 N85-26694
ESP (External-Stores Program): A pilot computer program for determining flutter-critical external-store configurations. Volume 3, part 2. Program compilation
[AD-A152271] 16 p2706 N85-26703
Confined turbulent swirling recirculating flow predictions
[NASA-CR-174917] 16 p2709 N85-26716
The effect of load factor on aircraft handling qualities
[AD-A152118] 16 p2710 N85-26724
ESP (External-Stores Program): A pilot computer program for determining flutter-critical external-store configurations. Volume 3, part 1: Program compilation
[AD-A152270] 16 p2711 N85-26727
A modular dissimilar redundant computer designed for high integrity control 16 p2714 N85-26751
Interactive design of specifications for airborne software set (GISELE) 16 p2714 N85-26753
The flight control system for the Experimental Aircraft Programme (EAP) demonstrator aircraft
16 p2714 N85-26755
Flight Experiment Demonstration System (FEDS) functional description and interface document
[NASA-CR-175290] 16 p2717 N85-26769
The effect of inaccuracies in structural models on the control of large space structures
[AD-A151794] 16 p2732 N85-26856
Application of the hydraulic system frequency response program to propellant feed systems
[AD-A151824] 16 p2741 N85-26914
Paramagnetic form factors from itinerant electron theory
[DE85-005272] 16 p2750 N85-26973
The design of an English word-processor for scientific and technical use in which superscripts, subscripts and Greek characters are operated by screen-edit. 3
16 p2759 N85-27025
East Europe report: Science and technology
[JPRS-ESA-85-019] 16 p2767 N85-27077
Evaluating syntactic constraints to speech recognition in a fighter aircraft environment
[AD-A152117] 16 p2773 N85-27119
An analysis of data dictionaries and their role in information resource management
[AD-A152134] 16 p2774 N85-27121
A study of computational techniques for noncanonical microstrip antennas and arrays
[AD-A152216] 16 p2774 N85-27123
Computer program for the calculation of multicomponent convective diffusion deposition rates from chemically frozen boundary layer theory
[NASA-CR-166329] 16 p2781 N85-27164
A general simulation program for robot manipulator arm dynamics
[AD-A152121] 16 p2793 N85-27230
Automatic tracking of crack growth via finite elements
16 p2797 N85-27246
Development and application of optimum sensitivity analysis of structures
[NASA-CR-175857] 16 p2799 N85-27257
Component-specific modeling
[NASA-CR-174765] 16 p2799 N85-27261
Stress analysis of the space telescope focal plane structure joint
[NASA-CR-175797] 16 p2803 N85-27284
Gravity model development software status
16 p2804 N85-27289
Development of computer aided database design and maintenance tools
[AD-A151782] 16 p2845 N85-27537
The systematic integration of very large scale integrated circuit computer-aided design tools into a toolkit optimized for academic applications
[AD-A151813] 16 p2845 N85-27538
Forward library searching of previously-quantitated peaks, using a scan list created from a quantitation list by a novel FORTRAN program for the INCOS data system
[PB85-165535] 16 p2845 N85-27541
Further development of an Interactive Control Engineering Computer Analysis Package (ICECAP) for discrete and continuous systems
[AD-A151783] 16 p2846 N85-27546
Numerical optimization algorithm for engineering problems using microcomputer
[AD-A152135] 16 p2847 N85-27554
Development of graphical pole-zero, root-locus, Bode, Nyquist, and Nichols responses using the OPTSYSX program
[AD-A152148] 16 p2847 N85-27555
Development of graphical time response using the OPTSYSX program
[AD-A152221] 16 p2848 N85-27557
Evaluation of Ada (trademark) as a communications programming language, volume 1
[AD-A152314] 16 p2848 N85-27559
Evaluation of Ada (trademark) as a communications programming language. Volume 2: Communications protocols application
[AD-A152315] 16 p2848 N85-27560
Evaluation of Ada (trademark) as a communications programming language. Volume 3: Trusted software application
[AD-A152316] 16 p2848 N85-27561
Incorporation of an elliptical boundary condition into the program POISSON
[DE85-006820] 16 p2849 N85-27564
Continued development and implementation of the Universal Network Interface Device (UNID) 2 in the Digital Engineering Laboratory Network (DELNET), volume 2
[AD-A151947] 16 p2850 N85-27570
Error reduction program — combustor performance evaluation codes
[NASA-CR-174778] 16 p2852 N85-27584
A decomposition procedure for convex quadratic programs
[AD-A151732] 16 p2854 N85-27595
UTM (Universal Transverse Mercator) determinations from geographical data
[AD-A152293] 16 p2856 N85-27610
Computer assisted flight schedule optimization
[AD-A151689] 16 p2858 N85-27623
Optimizing computational efficiency and user convenience in plasma simulation codes
[DE85-007661] 16 p2866 N85-27682
Tokamak systems code
[DE85-008147] 16 p2869 N85-27696
Management considerations for an information center
[AD-A151774] 16 p2875 N85-27742
Users manual for coordinate generation code CRDSRA
[NASA-CR-172584] 17 p2891 N85-27824
User's manual for airfoil flow field computer code SRAIR
[NASA-CR-172585] 17 p2891 N85-27825
Addition of flexible body option to the TOLA computer program, part 1
[NASA-CR-132732-1] 17 p2896 N85-27855
Addition of flexible body option to the TOLA computer program. Part 2: User and programmer documentation
[NASA-CR-132732-2] 17 p2896 N85-27856
Predictions and measurements of isothermal flowfields in axisymmetric combustor geometries
[NASA-CR-174916] 17 p2898 N85-27867
Operational and developmental experience with the F/A-18A digital flight control system
17 p2902 N85-27895
Certifying complex digital systems on civil aviation aircraft 17 p2904 N85-27907
SRB filament wound case material property study
[NASA-CR-171469] 17 p2910 N85-27940
Composite loads spectra for select space propulsion structural components: Probabilistic load model development 17 p2912 N85-27954
Probabilistic finite element development
17 p2913 N85-27956
Structural tailoring of SSME blades (vanes)
17 p2913 N85-27960
Electromagnetic transmission through a slot in a perfectly conducting plane
[AD-A153224] 17 p2949 N85-28210
Restructurable VLSI (Very large scale integration) program
[AD-A152340] 17 p2951 N85-28226
Analysis of physical-chemical processes governing SSME internal fluid flows
[NASA-CR-175893] 17 p2957 N85-28261
FLOWPLOT 2: A fluid dynamics and heat transfer plotting package
[DE85-009802] 17 p2959 N85-28277
Voltammetric analysis of ordnance materials. Part 2: A portable digital voltammeter for use with a silver wire working electrode
[AD-A152480] 17 p2967 N85-28325
Documentation of PHOTO: A user's manual for the analysis of photographic and X-ray negatives
[AD-A152988] 17 p2967 N85-28327
Heating parameter estimation using coaxial thermocouple gages in wind tunnel test articles
[AD-A153039] 17 p2968 N85-28328
Multi-mesh gear dynamics program evaluation and enhancements
[NASA-CR-174747] 17 p2974 N85-28372
System analysis of a field Army Topographic Support System
[AD-A153318] 17 p2984 N85-28439

A program for the calculation of paraboloidal-dish solar thermal power plant performance
[NASA-CR-175874] 17 p2985 N85-28449
Report on high intensity solar cells
[DE85-006396] 17 p2987 N85-28462
Two-dimensional inverse kinematic problem: Application to the Saudi Arabian refraction profile
17 p2990 N85-28478
Crustal structure of the Red Sea-Arabian Shield transition 17 p2990 N85-28479
Centralized Storm Information System (CSIS)
[NASA-CR-175898] 17 p2994 N85-28506
A survey of composite grid generation for general three-dimensional sections 17 p3006 N85-28584
A new technique for system-to-system transfer of surface data 17 p3007 N85-28589
Language design, computers and brains
[AD-A152619] 17 p3008 N85-28594
Optical phenomena in computer vision
[AD-A152970] 17 p3008 N85-28595
Tracking algorithm performance analysis program (TRAPP)
[DE85-007304] 17 p3009 N85-28601
COSMIC Software Catalog, 1985 edition
[NASA-CR-174070] 17 p3010 N85-28608
Automatic distribution of programs in MASCOT and Ada (trademark) environments: A feasibility study
[AD-A152665] 17 p3010 N85-28614
Implementation of a general finite element code on an IBM PC compatible microcomputer
[AD-A152681] 17 p3011 N85-28615
CLEANROOM software development: An empirical evaluation
[AD-A152924] 17 p3011 N85-28619
The addition of advanced scene rendering techniques to a general purpose graphics package
[AD-A153323] 17 p3012 N85-28625
Evidential reasoning in expert systems for image analysis
[AD-A153379] 17 p3013 N85-28627
TRINITY: A pre- and post-processing program for 2-dimensional finite element data
[DE85-008029] 17 p3013 N85-28628
Numerical benchmark study for the finite element computer code NEPTUNE
[DE85-008400] 17 p3013 N85-28630
VULTURE manual
[DE85-006873] 17 p3013 N85-28631
CAMAC 488 module: 68000 based GPIB interface module
[DE85-009367] 17 p3014 N85-28635
Analytical generation of satellite orbits at the RAE (Royal Aircraft Establishment)
[AD-A152655] 17 p3053 N85-28901
Flight testing for performance and flying qualities
18 p3058 N85-28920
DEAN: A program for dynamic engine analysis
[NASA-TM-87033] 18 p3062 N85-28945
Computer-aided thermohydraulic design of TEMA type E shell and tube heat exchangers for use in low pressure, liquid-to-liquid, single phase applications
[AD-A153779] 18 p3100 N85-29191
KIVA: A comprehensive model for 2D and 3D engine simulations
[DE85-005562] 18 p3118 N85-29296
Buckling and postbuckling behavior of shallow shells
18 p3120 N85-29317
Description and illustration of the use of CRACKS IV
[AD-A153543] 18 p3121 N85-29325
Program RNTHR/2: An HP-41 C program for the calculation of RaA, RaB, and RaC concentrations in air based on three measurements of an air-dust sample
[IRI-190-83-10] 18 p3134 N85-29412
Comparison of two orographical data sets for the GLAS Fourth Order GCM 18 p3142 N85-29452
Model development highlight for 1984: The GLA Fourth Order GCM 18 p3143 N85-29457
Isotropic plotter
[PB85-175651] 18 p3150 N85-29504
A task battery for applied human performance assessment research
[AD-A153677] 18 p3154 N85-29530
Program DiSAS: A computer program to obtain hard-copy plots of an image displayed on a vector graphics device in a local-area-network
[AD-A153643] 18 p3162 N85-29586
Specification of software quality attributes, volume 1
[AD-A153988] 18 p3163 N85-29593
Specification of software quality attributes. Volume 2: Software quality specification guidebook
[AD-A153989] 18 p3163 N85-29594
Specification of software quality attributes. Volume 3: Software quality evaluation guidebook
[AD-A153990] 18 p3163 N85-29595
Graphics package, version 4: User reference manual
[DE85-007894] 18 p3163 N85-29598
Micro-CAE mechanical engineering software development at Lawrence Livermore National Laboratory and participating universities and technology transfer
[DE85-008680] 18 p3163 N85-29597
Scattered data interpolation codes
[DE85-007337] 18 p3164 N85-29601
Computer program for the control/operating system of the gas flow installation for the solid fuel combustion chamber
[VTH-LR-430] 18 p3165 N85-29605
Annotated bibliography of recent papers on software engineering environments
[PB85-191385] 18 p3165 N85-29607
Distribution of mathematical software via electronic mail
[DE85-009664] 18 p3166 N85-29617
A quadratic programming algorithm
[AD-A153476] 18 p3168 N85-29631
A comparison of methods of least squares adjustment of traverses
[AD-A153612] 18 p3170 N85-29645
Further studies of the NRL collective particle accelerator via numerical modeling with the MAGIC code
[AD-A153583] 18 p3178 N85-29703
Comparison of calculations and measurements of the off-axis radiation dose (SI) in liquid nitrogen as a function of radiation length
[AD-A153676] 18 p3178 N85-29704
Program planning using the GMAP procedure in SAS/GRAPH software
[DE85-006356] 18 p3199 N85-29842
Distributed database design tool
[AD-A153760] 18 p3200 N85-29850
Generic data entry quality assurance tool
[DE85-008359] 18 p3200 N85-29852
Solar physics applications of computer graphics and image processing 18 p3208 N85-29903
Application of two-dimensional unsteady aerodynamic to a free-tip rotor response analysis
[NASA-CR-177348] 19 p3215 N85-29933
A computation of fin-line impedance
[AD-A154080] 19 p3258 N85-30204
Fast approach for calculating film thicknesses and pressures in elastohydrodynamically lubricated contacts at high loads
[NASA-TM-87032] 19 p3264 N85-30242
Modifications to SOLA-VOF for flow dynamics in spinning cylinders
[AD-A154093] 19 p3265 N85-30250
Structural dynamics modification of generalized beams using a local eigenvalue modification procedure
19 p3282 N85-30353
Large deflections of a cantilever beam under arbitrarily directed tip load
[NASA-TM-86442] 19 p3284 N85-30363
Application of the ADAMS program to deployable space truss structures
[NASA-CR-177927] 19 p3284 N85-30366
Nimbus 7 Coastal Zone Color Scanner (CZCS). Level 2 data product users' guide
[NASA-TM-86202] 19 p3299 N85-30452
Flood-runoff forecasting with HEC1F
[AD-A154286] 19 p3300 N85-30458
Modeling water resources systems for water quality
[AD-A154288] 19 p3300 N85-30457
MELSAR: A mesoscale air quality model for complex terrain. Volume 2: Appendices
[DE85-010991] 19 p3310 N85-30519
VIDTEX
[PB85-175669] 19 p3318 N85-30567
AEV local verification for aviation, precipitation, and temperature programs: AV, REL, TEM
[PB85-179125] 19 p3318 N85-30568
An interim user's manual for the advanced scavenging module version 1.2
[PB85-173904] 19 p3318 N85-30572
Environmental background measurement program
[AD-A153860] 19 p3319 N85-30577
Activities of the Institute for Computer Applications in Science and Engineering (ICASE)
[NASA-CR-172610] 19 p3332 N85-30641
CAE tool catalog
[DE85-011290] 19 p3334 N85-30657
SHAPS-2: A three-dimensional computer program for linear/non-linear, static/dynamic analyses of piping systems
[DE85-010500] 19 p3335 N85-30658
Demonstration project: Putting the bioastronautics data book on line
[NASA-CR-178424] 19 p3335 N85-30659
Interactive computer program for the analysis and design of linear time invariant systems
[AD-A154076] 19 p3335 N85-30664
Defense Mapping Agency (DMA) raster-to-Vector analysis
[AD-A154153] 19 p3336 N85-30668
The design, implementation and application of a table-driven syntax-directed editor
[AD-A154234] 19 p3336 N85-30670
Implementation of a proposed system for automated microcode generation
[AD-A154235] 19 p3336 N85-30671
The origin of the binary-search paradigm
[AD-A154367] 19 p3337 N85-30677
A parallelized point successive over-relaxation method on a multiple instruction multiple data stream computer
[AD-A154377] 19 p3337 N85-30679
Survey of Ada (Trademark)-based PDLs (Program Design Language)
[AD-A154402] 19 p3338 N85-30680
Computer center policy
[AD-A154416] 19 p3338 N85-30681
Computer Performance Modeling Tool (CPMT)
[AD-A154438] 19 p3338 N85-30682
Defense Mapping Agency (DMA) raster-to-Vector benchmark testing
[AD-A154152] 19 p3338 N85-30683
SANDRAG: A computer code for predicting drag of bodies of revolution at zero angle of attack in incompressible flow
[DE85-011170] 19 p3338 N85-30684
Circular-beam ray tracing on a microcomputer
[DE85-010754] 19 p3338 N85-30685
BREED: A CDC-7600 computer program for the automation of breeder reactor design analysis (LWBR Development Program)
[DE85-010327] 19 p3338 N85-30686
MELCOR Accident Consequence Code System (MACCS)
[DE85-009712] 19 p3339 N85-30689
Performance and library issues for mathematical software on high performance computers
[DE85-010263] 19 p3339 N85-30690
Touch-off: A method to determine the position of an object by means of a sensor-driven robot
[DE85-011178] 19 p3339 N85-30691
SABRINA: An interactive solid geometry modeling program for Monte Carlo
[DE85-010796] 19 p3339 N85-30692
Energy accounting software
[DE85-010612] 19 p3340 N85-30694
Using MATHLIB on the IBM computer and sundry plotting examples with a taste of IMSL
[DE85-011395] 19 p3340 N85-30695
Combined finite element meshing techniques using SUPERTAB
[DE85-011393] 19 p3340 N85-30696
CMP: Code Maintenance Package reference manual, version 2.0
[DE85-011396] 19 p3340 N85-30697
EDS operator and control software
[DE85-010470] 19 p3340 N85-30698
A dynamic programming approach to time-staged convex programs
[DE85-010616] 19 p3340 N85-30700
A Lotus 1-2-3 based system reliability program
[DE85-010533] 19 p3340 N85-30701
System enhancements of Mesoscale Analysis and Space Sensor (MASS) computer system
[NASA-CR-171483] 19 p3342 N85-30708
MCNP: A general Monte Carlo code for neutron and photon transport
[DE85-010764] 19 p3348 N85-30753
MANHIST user's guide
[DE85-010684] 19 p3348 N85-30754
Nonequilibrium air radiation (Nequair) program: User's manual
[NASA-TM-86707] 19 p3353 N85-30780
Surface effects on sputtered atoms and their angular and energy dependence
[DE85-010506] 19 p3354 N85-30790
Measurement problem in PROGRAM UNIVERSE
[DE85-008179] 19 p3378 N85-30959
Description and operation of CHISQMO, INVRTS, VOIGEN, VOIGTV, SMEAR, RUFF, AND POSCAR in the Stokes Analysis Program
[PB85-180628] 19 p3384 N85-30991
Computer program for plotting and fairing wind-tunnel data
[NASA-TM-85848] 20 p3387 N85-31009
Computer programs for smoothing and scaling airfoil coordinates
[NASA-TM-84666] 20 p3388 N85-31011
Combustion gas properties. Part 3: Hydrogen gas fuel and dry air
[NASA-TP-2477] 20 p3395 N85-31058
Design of multivariable controllers using the Integrated Analysis Capability (IAC) 20 p3412 N85-31172
A structural dynamics approach to the simulation of spacecraft control/structure interaction
20 p3412 N85-31173

SPAR improved structural-fluid dynamic analysis capability
[NASA-CR-171549] 20 p3454 N85-31449
A comparison of smooth specimen and analytical simulation techniques for notched members at elevated temperatures 20 p3466 N85-31546
Nonlinear analysis of an axisymmetric structure subjected to non-axisymmetric loading 20 p3466 N85-31549
Geodyn systems development 20 p3492 N85-31706
The application of computer imaging techniques to ocean topography and geophysical data 20 p3492 N85-31711
A computer program for determining the electrophoretic mobility of cells in a rectangular chamber during asymmetric electroosmotic flow 20 p3499 N85-31751
A cluster analysis method for identification of subpopulations of cells in flow cytometric list-mode arrays 20 p3503 N85-31779
Distributed implementation of functional program evaluation
[DE85-009573] 20 p3514 N85-31844
PIPE-1000: An implementation of piping on an HP-1000 minicomputer
[PB85-191955] 20 p3514 N85-31847
Methods for design and evaluation of integrated hardware-software systems for concurrent computation
[NASA-CR-176086] 20 p3515 N85-31851
Exponential order statistic models of software reliability growth
[NASA-CR-3909] 20 p3515 N85-31852
Proceedings of the 1st Workshop for the Design of Expert System Partial Differential Equation Solvers
[AD-A154192] 20 p3515 N85-31853
SCAP: A Shaped Charge Analysis Program. User's manual for SCAP 1.0
[DE85-011182] 20 p3515 N85-31854
Model documentation of the gas analysis modeling system. Volume 1: Model overview
[DE85-010952] 20 p3515 N85-31856
Microcomputers in transportation: Software and source book, February 1985
[PB85-181022] 20 p3517 N85-31866
Monte Carlo: In the beginning and some great expectations
[DE85-010789] 20 p3518 N85-31872
Nonlinear dynamics: A personal perspective
[DE85-010982] 20 p3521 N85-31899
Calculation of transonic steady and oscillatory pressures on a low aspect ratio model and comparison with experiment
[NASA-TM-86449] 21 p3551 N85-32092
Tip vortex computer code SRATIP. User's guide
[NASA-CR-172603] 21 p3551 N85-32093
Preliminary sizing and performance of aircraft
[NASA-TM-86357] 21 p3554 N85-32111
Component-specific modeling
[NASA-CR-174925] 21 p3556 N85-32119
Microprocessor control design for a low-head crossflow turbine
[AD-A155477] 21 p3556 N85-32121
Development and validation of a general purpose linearization program for rigid aircraft models
[NASA-TM-86737] 21 p3556 N85-32122
Development of reduced order models for control system design using the OPTSYSX program
[AD-A154552] 21 p3556 N85-32124
Myoelectric control of a computer based expert system for flight control
[AD-A154981] 21 p3557 N85-32126
MPS solidification model. Analysis and calculation of macrosegregation in a casting ingot
[NASA-CR-171589] 21 p3566 N85-32178
User's guide for computer program CGFAG, Concrete General Flexure Analysis with Graphics
[AD-A155555] 21 p3570 N85-32204
Fin line filters technology and electronic warfare
[AD-A154975] 21 p3576 N85-32237
Calculation of 3-D flow without numerical mixing 21 p3588 N85-32301
SSMIR (Solid State Memory Instrumentation Recorder): A new approach to acquiring data during an aircraft seat/sled ejection sequence
[AD-A154760] 21 p3589 N85-32308
Plating density standards
[DE85-010014] 21 p3591 N85-32318
An investigation into the comparisons of the underwater shock effects on a stiffened flat plate to the predictive nature of a computer model
[AD-A155612] 21 p3600 N85-32355
Analysis of inclined growth of silicon sheet 21 p3612 N85-32442
Assessment of the performance of an in-field Gaussian plume/puff model for overwater use
[AD-A155435] 21 p3614 N85-32460
Nuclear thermal transmittance in the atmosphere using LOWTRAN-6 computer code
[AD-A154669] 21 p3630 N85-32553
An evaluation of discretized conditional probability and linear regression threshold techniques in model output statistics forecasting of cloud amount and ceiling over the North Atlantic Ocean
[AD-A155100] 21 p3636 N85-32581
Analysis of spacecraft data
[NASA-CR-171587] 21 p3669 N85-32789
Analysis of spacecraft data
[NASA-CR-171597] 21 p3669 N85-32790
CARE 3 user friendly interface user's guide
[NASA-CR-172608] 21 p3669 N85-32791
Design of an expert-system flight status monitor
[NASA-TM-86739] 21 p3669 N85-32794
The NAS kernel benchmark program
[NASA-TM-86711] 21 p3670 N85-32795
Development of computer programs using the method of images to predict the sound field in a wedge overlaying a fast fluid and comparison with laboratory experiments
[AD-A154580] 21 p3670 N85-32797
An automated quality assurance surveillance plan for ADP (Automated Data Processing) operations under the Navy's commercial activities program
[AD-A154767] 21 p3671 N85-32802
The design and implementation of an object-oriented, production-rule interpreter
[AD-A154769] 21 p3671 N85-32803
Qualitative analysis of sign-bit processing
[AD-A154776] 21 p3671 N85-32804
The formal specification of an abstract machine: Design and implementation
[AD-A155167] 21 p3672 N85-32808
A comprehensive study of the AFIT (Air Force Institute of Technology) software development environment
[AD-A155450] 21 p3672 N85-32812
Survival function of hypo-exponential distributions
[AD-A155518] 21 p3672 N85-32814
A practical approach to Karmarkar's algorithm
[AD-A155714] 21 p3673 N85-32818
Praxis release notes, version 7.3
[DE85-011662] 21 p3673 N85-32820
Discrete-element acoustic analysis of submerged structures using doubly asymptotic approximations
[AD-A154959] 21 p3700 N85-32987
Speech understanding research
[AD-A155462] 21 p3700 N85-32990
An EPR (Electron-Paramagnetic-Resonance) and ENDOR (Electron-Nuclear-Double-Resonance) study of ferroelectric ammonium sulfate
[AD-A155580] 21 p3710 N85-33033
Continued development of a data base management system performance monitor: Volume 1
[AD-A154635] 21 p3713 N85-33040
Use of the computer programs PARA 80 to study results from firing the railgun ERGS-1M
[MRL-R-900] 22 p3738 N85-33167
SHELTER: Description of a program code — indoor climate
[FOA-C-58002-H1] 22 p3755 N85-33278
Petcom: A software instrument for the analysis of Petri networks, oriented towards communication protocols
[FUB-50-1983] 22 p3756 N85-33286
Introduction to adaptive techniques for voice signal processing
[FUB-52-1983] 22 p3758 N85-33287
Algorithms and organization of software for computer-aided circuit design 22 p3767 N85-33347
Software for frequency analysis of microwave circuits 22 p3768 N85-33352
Optimization of radioelectronic circuits with software for modeling of integrated circuits on unified system computer 22 p3768 N85-33354
Dialog system with minicomputer for plotting performance charts 22 p3768 N85-33355
Algorithms for constructing models of circuit elements in input language of computer-aided design software 22 p3768 N85-33356
Algorithm for determination of isomorphic graphs 22 p3769 N85-33357
Analysis of crosstalk in nonhomogeneous multiconductor lines 22 p3769 N85-33360
Developmental trends in radio receiver design 22 p3777 N85-33407
KRAK: A computer program for two-phase two-component porous flow and fracture
[LA-9703] 22 p3782 N85-33434
Machine intelligence for robotics applications
[DE85-011430] 22 p3793 N85-33503
Electromagnetic inspection of wire ropes using sensor arrays
[AD-A155412] 22 p3795 N85-33509
A new large-scale, high-resolution multicolor software display concept
[AD-A155404] 22 p3827 N85-33703
Electronic file system on an SM 90 minicomputer: The SARDE project
[ENST-84E018] 22 p3828 N85-33705
QKPLT users guide, version 2.0
[L-10094-M] 22 p3828 N85-33707
DECODE: A software manual for use with the Serial ASCII Instrumentation Loop (SAIL) system
[AD-A155358] 22 p3828 N85-33709
AUTSKED: An addendum
[DE85-010410] 22 p3829 N85-33712
Data Base Workshop: Availability-Reliability Modeling
[DE85-011570] 22 p3829 N85-33713
SANCHO: A finite element computer program for the quasistatic, large deformation, inelastic response of two-dimensional solids
[DE85-011456] 22 p3829 N85-33714
MORSE-CGA: A Monte Carlo radiation transport code with array geometry capability
[DE85-012063] 22 p3830 N85-33718
KIVA computer program for multidimensional chemically reactive fluid flows with fuel sprays
[DE85-012730] 22 p3830 N85-33722
PMEXA: Diagnostic filtering program for the PBFA-1 performance monitoring and evaluation system
[DE85-013179] 22 p3831 N85-33725
How a BASIC program works
[DE85-009142] 22 p3831 N85-33727
Search of the VAXintosh customizing VMS V4.0 for DCL windows
[DE85-011306] 22 p3831 N85-33729
A strategy planner for NASA robotics applications
[NASA-CR-175319] 22 p3834 N85-33738
Electron and ion cyclotron heating calculations in the tandem-mirror
[DE85-011858] 22 p3842 N85-33797
A hierarchy of knowledge levels implemented in a rule-based production system to calculate bounds on the size of intersections and unions of simple sets
[AD-A155291] 22 p3848 N85-33836
Component-specific modeling
[NASA-CR-174765] 23 p3897 N85-34140
Box truss analysis and technology development. Task 1: Mesh analysis and control
[NASA-CR-172570] 23 p3900 N85-34156
An introduction to finite elements 23 p3924 N85-34319
Detailed validation of a liquid and heat flow code against field performance
[DE85-009901] 23 p3932 N85-34366
Modular digital holographic fringe data processing system
[NASA-CR-177952] 23 p3933 N85-34376
Hardware math for the 6502 microprocessor
[NASA-TM-86517] 23 p3955 N85-34511
DISPL1: A software package for one and two spatially dimensioned kinetics-diffusion problems
[ANL-84-56] 23 p3956 N85-34516
User's operating procedures. Volume 3: Projects directorate information programs
[NASA-CR-177950] 23 p3956 N85-34520
Computer graphics for multivariate data 23 p3958 N85-34528
Interfacing interactive circuit simulation with standard graphics facilities 23 p3958 N85-34529
Research issues in generating graphical explanations 23 p3959 N85-34539
An integrated system for printing and publishing applications 23 p3959 N85-34540
Using percent-done program indicators to enhance user interfaces 23 p3960 N85-34546
Knowledge engineering application in image processing 23 p3965 N85-34583
Using LINE as an interactive graphics package. Interfacing line and Topdraw in 43 and 24 VM
[DE85-012007] 23 p3965 N85-34585
Analysis of transient radiation upset in a 16K SRAM
[DE85-009442] 23 p3965 N85-34586
Real-time multiparameter pulse processing with decision tables
[DE85-011683] 23 p3966 N85-34589
User's manual for the FLORA equilibrium and stability code
[DE85-013182] 23 p3966 N85-34590
Maintenance port system
[AD-D011724] 23 p3967 N85-34594
CYLTRAN calculations of electron effects on XD detectors
[LA-10264-MS] 23 p3969 N85-34601
Modeling a high energy gamma-ray telescope
[OG-9.2-5] 23 p4025 N85-34944
The final COS-B database now publicly available
[OG-9.3-8] 23 p4028 N85-34963

General design method for 3-dimensional, potential flow fields. Part 2: Computer program DIN3D1 for simple, unbranched ducts
[NASA-CR-3926] 24 p4060 N85-35159
Analysis of incompressible cascade flows using state-of-the-art computer programs
[AD-A155850] 24 p4062 N85-35173
Development of NATOPS performance software for the SH-3D and SH-3H helicopters
[AD-A156140] 24 p4065 N85-35192
The investigation of tethered satellite system dynamics
[NASA-CR-176180] 24 p4069 N85-35215
Cluster variation study of coherent ordering in FCC and BCC solid solutions
[AD-A156039] 24 p4079 N85-35280
X-ray fluorescence analysis of 304L stainless steel
[DE85-013254] 24 p4080 N85-35288
Millimeter-wave propagation in moist air: Model versus path data
[AD-A156040] 24 p4087 N85-35331
Solid state high power amplifier for driving the SLC injector klystron
[DE85-013063] 24 p4090 N85-35356
Studies on effects of boundary conditions in confined turbulent flow predictions
[NASA-CR-3929] 24 p4093 N85-35371
Design and behavior of coped beams
24 p4100 N85-35417
Justified generalization: Acquiring procedures from examples
[AD-A156408] 24 p4135 N85-35626
DSS/MIS (Decision Support Systems/Management Information Systems) design and implementation for LAMPS Mk 3 utilizing a microcomputer and a maintenance personnel assignment program
[AD-A155852] 24 p4135 N85-35629
Users guide for optimum interpolation method of global data assimilation
[AD-A155929] 24 p4138 N85-35648
Specifying and verifying concurrent programs
[AD-A156190] 24 p4138 N85-35652
Using an LSI-11/23 and RT-11 to digitize analog tapes
[DE85-012736] 24 p4139 N85-35656
SASSYS-1 computer code verification with EBR-2 test data
[DE85-012119] 24 p4139 N85-35657
DEPTH-CHARGE static and time-dependent perturbation/sensitivity system for nuclear reactor core analysis, revision 1
[DE85-013103] 24 p4139 N85-35659
RFQ modeling computer program
[DE85-012665] 24 p4140 N85-35661
Error message recording and reporting in the SLC control system
[DE85-013057] 24 p4140 N85-35664
Toolpack
[DE85-013135] 24 p4140 N85-35665
Computer code calculations of the TMI-2 accident: Initial and boundary conditions
[DE85-012613] 24 p4140 N85-35666
Master Fit users' guide, version 1.0
[DE85-014199] 24 p4140 N85-35667

COMPUTER SIMULATION
U COMPUTERIZED SIMULATION

COMPUTER STORAGE DEVICES
NT BUBBLE MEMORY DEVICES
NT BUFFER STORAGE
NT COMPUTER COMPATIBLE TAPES
NT FLIP-FLOPS
NT MAGNETIC DISKS
NT MAGNETIC TAPES
NT OPTICAL DISKS
NT RANDOM ACCESS MEMORY
NT READ-ONLY MEMORY DEVICES
NT REGISTERS (COMPUTERS)
Storage in the LLNL Octopus network: An overview and reflections
[DE84-014711] 01 p0106 N85-10712
Reducing spectral dimension of remotely sensed data using principal components analysis and a Peano scanning
02 p0212 N85-11399
Parallel searching and merging on ZMOB
[AD-A145424] 02 p0241 N85-11574
The design and performance analysis of an arbiter for a multi-processor shared-memory system
[AD-A146074] 03 p0403 N85-12586
Electromechanical switch
[AD-D011400] 07 p0948 N85-16009
An algorithm for assembly of stiffness matrices into a compacted data structure
[AD-A146727] 07 p1023 N85-16492
Vector computer memory bank contention
[NASA-CR-177342] 09 p1376 N85-18649
Redundancy of codes for detection and correction of unidirectional errors 12 p1842 N85-21557
Variable data base generator apparatus
[AD-D011515] 12 p1911 N85-21993
Problems in decentralized decision making and computation
[AD-A150025] 12 p1950 N85-22251
Fibre composite laminated plate analysis using a card programmable calculator (HP41C/CV)
[NIAST-83/88] 13 p2103 N85-23106
A general purpose scatter storage subsystem and a comparison of hashing methods
[NASA-CR-175814] 16 p2845 N85-27542
A stored data acquisition system: Update
[DE85-010534] 18 p3166 N85-29816
Memory effects in dynamical many-body systems: The isomneaic (constant-memory) approximation
[AD-A154160] 20 p3520 N85-31889
SSMIR (Solid State Memory Instrumentation Recorder): A new approach to acquiring data during an aircraft seat/sled ejection sequence
[AD-A154780] 21 p3589 N85-32308
Development of a dedicated speech work station
[AD-A155485] 21 p3674 N85-32824
Method of and apparatus for generating an interstitial point in a data stream having an even number of data points
[NASA-CASE-MFS-25319-1] 22 p3827 N85-33701
Spatial trees: A fast access method for unstructured graphical data 23 p3958 N85-34533
L-step sequential decoding
[AD-A156121] 24 p4138 N85-35649

COMPUTER SYSTEMS DESIGN
TEQUEL: The query language of SADDLE
01 p0058 N85-10382
SAGA: A project to automate the management of software production systems
[NASA-CR-174017] 01 p0103 N85-10685
Microcomputer management guidelines
[PB84-212174] 01 p0105 N85-10704
Logical database processor interface specifications
[PB84-216456] 01 p0105 N85-10705
The development of an optoelectronic assembly applied to computer systems
[AD-A145028] 01 p0120 N85-10821
The computer-communication link for the innovative use of Space Station 02 p0150 N85-11016
DISCUS multiprocessor enhancements — Distributed Control Microprocessor System (DISCUS)
[RSRE-MEMO-3691] 02 p0239 N85-11554
Systems analysis for microcomputer acquisitions
[AD-A145447] 02 p0239 N85-11556
Design and descriptive tools for systolic architectures
[DE84-015521] 02 p0239 N85-11557
East Europe report, science and technology. Czechoslovakia: System of small electronic computers
[JPRS-ESA-84-040] 02 p0239 N85-11558
Autonomous Attitude Determination System (AADS). Volume 1: System description
[NASA-TM-87385] 02 p0240 N85-11559
Concurrent processing and the decomposition of problems
[DE84-015285] 02 p0242 N85-11581
Telemetry (TM)/telecommand (TC) processor study
[ESA-CR(P)-1915] 03 p0323 N85-12061
An introduction to the MIAS conversion system
[IOS-184] 03 p0403 N85-12571
A control scheme for microcomputers being used in multiprocessor arrays
[DE84-014590] 04 p0547 N85-13479
The facilities of the Calculation Center and Real Time Room for satellite positioning 05 p0599 N85-13819
A geoinformation expert system for synergetic use of map and image data 05 p0659 N85-14233
Integrated resource management algorithms for computer systems 05 p0715 N85-14582
S-MICRO: A system for simulating a microprogrammed control unit
[INPE-3224-PRE/575] 05 p0715 N85-14585
Heterogeneous data base access
05 p0735 N85-14724
Role of DESIGNMANAGER in information engineering
[DE84-016807] 05 p0736 N85-14730
NC programming, machine tool information
06 p0816 N85-15178
Implementation of a Zilog Z-80 base realization library for the computer systems design environment
[AD-A146359] 06 p0853 N85-15423
The Torun measuring system for astronomical spectra
07 p0966 N85-16130
Support for distributed transactions in the TABS (Transaction based systems) prototype
[AD-A147213] 07 p1022 N85-16486
Integration of ground and on-board system for terminal count 08 p1092 N85-16898
Kernel Ada Programming Support Environment (KAPSE) interface team public report, volume 4
[AD-A147648] 08 p1205 N85-17581
Computer equipment at 1984 Leipzig Spring Fair
09 p1378 N85-18662
Dialog system of preparation and presentation of visual information 10 p1526 N85-19622
ESOP expert system model described
11 p1619 N85-20187
Needs, opportunities, and options for large scale systems research
[DE85-002664] 11 p1709 N85-20750
AID: Access to Informal Documentation
[DE85-000418] 11 p1740 N85-20939
A survey of the project CIP: Computer aided, intuition-guided programming. Wide spectrum language and program transformations
[TUM-I8406] 12 p1912 N85-22000
Construction of a menu-based system
[NASA-CR-172560] 13 p2146 N85-23321
Measurement of SIFT operating system overhead
[NASA-TM-86322] 13 p2149 N85-23337
The hierarchical database decomposition approach to database concurrency control
[AD-A150612] 13 p2168 N85-23450
Design for tactical avionics maintainability, technical evaluation report
[AGARD-AR-204] 14 p2225 N85-23798
The Edmonton data collection platform processing and locating facility 14 p2323 N85-24352
Systems design and application of computers with flexible architecture 14 p2401 N85-24800
Integration of solid modeling and database management for CAD/CAM 14 p2402 N85-24804
LINCS
[DE85-006151] 14 p2407 N85-24836
Properties of systems which lead to efficient computation of reliability
[AD-A151033] 14 p2409 N85-24853
Design and analysis of ordering and join for a multi-backed database system
[AD-A150711] 14 p2433 N85-25006
Microprocessor controlled storage sampling oscilloscope 15 p2533 N85-25622
CaD systems for electronic component design reviewed 15 p2537 N85-25660
A review of speech systems
[BAE-BT-12285] 15 p2539 N85-25676
General meteorological package (GEMPAK)
15 p2599 N85-26019
Activities report for FOA 53: Laboratory for man and information systems
[FOA-C-53019-H] 15 p2621 N85-26150
Logic analyzer survey and reviews
[BAE-881/ELO/1645] 15 p2621 N85-26151
Research in the design of high-performance reconfigurable systems
[NASA-CR-175706] 15 p2621 N85-26153
Workshop on Parallel Computer Architectures in Pattern Recognition and Image Processing
[BMFT-FB-DV-84-006] 15 p2622 N85-26154
High-capacity real-time computer system for processing hydrophysical data 15 p2625 N85-26178
Mini- and microcomputer local control network architecture and design principles
15 p2625 N85-26179
Design and analysis of a complete relational interface for a multi-backend database system
[AD-A151501] 15 p2628 N85-26198
The development of a programming support system for rapid prototyping. Tasks 2 and 3
[AD-A151549] 15 p2629 N85-26202
Procedures for use in compiling requirements specifications for computerized library systems
[CSTI-76] 15 p2665 N85-26446
Reusable software: A concept for cost reduction
16 p2697 N85-26955
Active control technology: Past, present, future
16 p2711 N85-26731
Automated CPX support system preliminary design phase
[NASA-CR-175784] 16 p2769 N85-27091
Use of vector processors in cartographic raster data processing, with special regard to the AP-120B vector processor 16 p2814 N85-27358
Detailed design of an object oriented, multiprogramming, multitasking operating system for sixteen-bit microcomputers
[AD-A152086] 16 p2847 N85-27552
Continued development and implementation of the Universal Network Interface Device (UNID) 2, Digital Engineering Laboratory Network (DELNET), volume 1
[AD-A151935] 16 p2850 N85-27569
Development of a microprocessor controlled communication system for ships
[BMFT-FB-T-84-275] 17 p2950 N85-28216

VLSI workshop and project: February - November 1982
[WSRL-0374-TR] 17 p2951 N85-28223
CAMAC 488 module: 68000 based GPIB interface module
[DE85-009367] 17 p3014 N85-28635
A programming system for a modular flexible multimicrocomputer system for the automatic control of automated test equipment
[JUEL-1962] 17 p3014 N85-28641
System Analysis for the Huntsville Operation Support Center, Distributed Computer System
[NASA-CR-171506] 17 p3015 N85-28642
The design of a capability-based distributed operating system
[CWI-CS-R8418] 17 p3016 N85-28650
The IRAS end-to-end data system
[NLR-MP-83056-U] 17 p3051 N85-28683
The development of information systems at NLR
[B8580079] 17 p3051 N85-28684
An interactive computer aid for the design and analysis of linear, single input/single output digital and continuous control systems
[AD-A153704] 18 p3162 N85-29589
The multiple processor machine for image processing, volume 5
[ESA-CR(P)-1976-VOL-5] 18 p3164 N85-29603
Investigation and construction of the Mini Remote Terminal Unit (mRTU-M) Analog Processor Module (AP-M), volume 1
[MR-DS-01-VOL-1] 18 p3166 N85-29619
Investigation and construction of the Mini Remote Terminal Unit (mRTU-M), Analog Processor Module (AP-M), volume 2
[MR-DS-01-VOL-2] 18 p3166 N85-29620
Statistical estimation of software reliability
[AD-A154097] 19 p3335 N85-30665
A micro/PDP-11 system for 406 MHz COSPAS/SARSAT processing 20 p3403 N85-31117
Fault tolerant multiprocessor SARSAT-COSPAS 406 MHz local user terminal 20 p3404 N85-31123
Visualization of computation results. Definition of a graphics satellite computer
[ONERA-RT-2/3587-CY] 20 p3514 N85-31845
Work in Amsterdam on local intelligence — artificial intelligence
[NIKHEF-H/84-9] 20 p3518 N85-31877
Determining functional requirements for NASA Goddard's command management system software design using expert systems 20 p3539 N85-32020
A high-speed digital signal processor for atmospheric radar, part 7.3A 21 p3626 N85-32525
Comparative study on data system architectures — spacecraft data processing
[ESA-CR(P)-2015] 21 p3675 N85-32826
Hardware realization of digital filters without multipliers 22 p3766 N85-33340
Basic features of personal computers 22 p3766 N85-33344
Algorithms and organization of software for computer-aided circuit design 22 p3767 N85-33347
Software for frequency analysis of microwave circuits 22 p3768 N85-33952
Re-designing a mechanism for higher speed: A case history from textile machinery 23 p3923 N85-34310
An integrated system for printing and publishing applications 23 p3959 N85-34540
Efficient recovery and reversal in graphical user interfaces generated by the Higgens system 23 p3960 N85-34544
A model for graphics interface tool development 23 p3960 N85-34545
Using percent-done program indicators to enhance user interfaces 23 p3960 N85-34546
Selection of segment similarity measures for hierarchical picture segmentation 23 p3960 N85-34548
A graphics interface for interactive simulation of packet-switched networks 23 p3962 N85-34558
A Programmable Automatic Noise Data and Other Related parameter Acquisition system (PANDORA) — wind energy converters 24 p4111 N85-35479
Software maintenance relating to the input translator and z-80 realization volume of the computer systems design environment
[AD-A155849] 24 p4138 N85-35646
Toolpack
[DE85-013135] 24 p4140 N85-35665

COMPUTER SYSTEMS PERFORMANCE

Finite element computation on nearest neighbor connected machines 01 p0057 N85-10379
Application of concurrent processing to structural dynamic response computations 01 p0057 N85-10380
Performance evaluation of database systems: A benchmark methodology
[PB84-217504] 01 p0105 N85-10707
Throughput characteristics of Carrier Sense Multiple Access (CSMA) networks
[FUB-25-1983] 01 p0106 N85-10713
Systems analysis for microcomputer acquisitions
[AD-A145447] 02 p0239 N85-11556
Autonomous Attitude Determination System (AADS). Volume 1: System description
[NASA-TM-87385] 02 p0240 N85-11559
A unified method for evaluating real-time computer controllers: A case study — aircraft control
[NASA-CR-174168] 04 p0547 N85-13478
Integrated resource management algorithms for computer systems 05 p0715 N85-14582
Human factors characteristics of the Joint Tactical Fusion Test Bed: Field test 467 results
[AD-A146856] 07 p1020 N85-16476
Performance evaluation and control of distributed computer communication networks
[AD-A148103] 08 p1208 N85-17598
A unified model for performance and reliability of Fault-Tolerant/Multi-Mode systems
[AD-A148789] 08 p1208 N85-17601
Results of data base management system parameterized performance testing related to GSFC scientific applications
[NASA-CR-170615] 08 p1229 N85-17741
Vector computer memory bank contention
[NASA-CR-177342] 09 p1376 N85-18649
Man-machine interaction: Operator
[AD-A149075] 10 p1531 N85-19648
Bottleneckology: Evaluating supercomputers
[DE85-005574] 13 p2145 N85-23315
Service ARGOS technical report and improvement 14 p2328 N85-24395
Plasma and magnetospheric research
[NASA-CR-175675] 14 p2354 N85-24543
Selection criteria for a CAD/CM system 14 p2402 N85-24810
Continued development of a data base management system performance monitor, volume 2
[AD-A151714] 15 p2623 N85-26167
Development of a user support package for CPESIM 2 (a computer simulation for CPE (Computer Performance Evaluation) use
[AD-A151899] 15 p2624 N85-26170
Future information technology, 1984 telecommunications
[PB85-165850] 15 p2624 N85-26173
There is no I/O like no I/O
[DE85-009115] 17 p3014 N85-28634
Tradeoffs among portability, complexity, and efficiency in multiprocessing environments
[DE85-007899] 18 p3161 N85-29580
Two-dimensional/speed/couple/data base management system
[A-1] 18 p3165 N85-29608
Three-dimensional/integration two and three dimensional/numerical control/communication
[A-2] 18 p3165 N85-29609
The CEADS-CADD system
[A-4] 18 p3165 N85-29610
System test CALMA DDM (Design Drafting Manufacturing)
[A-5] 18 p3165 N85-29611
The International Computers Limited (ICL) PERQ 1/Engineering Architectural Graphics Language Environment (EAGLE) Computer Aided Design system (CAD)
[A-7] 18 p3165 N85-29612
Test Drawing Office Graphics System (DOGS)/APOLLO
[A-10] 18 p3166 N85-29614
INEL User Network Exchange, volume 1-85, Jan./Feb. 1985
[DE85-006108] 18 p3166 N85-29615
Instrument Systems Analysis and Verification Facility (ISAVF) users guide
[NASA-TM-86226] 19 p3223 N85-29982
An approach to modeling database activity 19 p3332 N85-30642
Development and analysis of a global compaction technique of microprograms 19 p3334 N85-30654
The completion time of a job on multi-mode systems
[AD-A154113] 19 p3336 N85-30666
Computer Performance Modeling Tool (CPMT)
[AD-A154436] 19 p3338 N85-30682
Performance and library issues for mathematical software on high performance computers
[DE85-010263] 19 p3339 N85-30690
Development and evaluation of a Fault-Tolerant Multiprocessor (FTMP) computer. Volume 3: FTMP test and evaluation
[NASA-CR-166073] 19 p3341 N85-30707
SPAR improved structural-fluid dynamic analysis capability
[NASA-CR-171549] 20 p3454 N85-31449
System test Oce 5200
[A-3] 20 p3515 N85-31860
The General Drafting System (GDS) design system
[A-6] 20 p3517 N85-31869
The IGOS design system
[A-8] 20 p3517 N85-31870
The 6060 emulator 21 p3668 N85-32783
The NAS kernel benchmark program
[NASA-TM-86711] 21 p3670 N85-32795
An image compression survey and algorithm switching based on scene activity
[NASA-TP-2458] 22 p3727 N85-33106
Some ideas for decomposing the domain of elliptic partial differential equations in the Schwarz process
[DE85-011844] 22 p3834 N85-33739
Raster functionality for a VDI
[DE85-006734] 24 p4097 N85-35396

COMPUTER SYSTEMS PROGRAMS

NT ASSEMBLER ROUTINES
NT INPUT/OUTPUT ROUTINES
NT OPERATING SYSTEMS (COMPUTERS)
NT SUBROUTINE LIBRARIES (COMPUTERS)

DYNKIN: A computer program for the description of detailed gas reactions in interaction with gas dynamics
[AD-B085364] 01 p0046 N85-10298
Three-dimensional mesoscale analysis of serial soundings 01 p0074 N85-10493
Geostationary satellite cloud and precipitation analysis using an interactive computer system 01 p0076 N85-10506
Operational use of shipboard numerical aid programs 01 p0082 N85-10546
East Europe report: Science and technology
[JPRS-ESA-84-030] 01 p0101 N85-10670
Remote data processing system software in Hungary 01 p0101 N85-10673
SAGA: A project to automate the management of software production systems
[NASA-CR-174017] 01 p0103 N85-10685
MICROSCOPE: A software system for multivariate analysis
[AD-A144720] 01 p0103 N85-10688
Normal approximation for response time in a processor-shared computer system model
[AD-A144997] 01 p0103 N85-10690
Autonomous Attitude Determination System (AADS). Volume 1: System description
[NASA-TM-87385] 02 p0240 N85-11559
Software engineering environments for mission critical applications: STARS alternative programmatic approaches
[AD-A145285] 02 p0241 N85-11571
ADAM: An abstract database machine
[RSRE-84007] 02 p0293 N85-11904
Specification and preliminary design of the CARTA system for satellite cartography
[E85-10035] 03 p0378 N85-12414
Simulation of wavefronts returned by realistic surfaces 03 p0383 N85-12448
CONTROL: A suite of interactive transfer-function analysis programs
[OUEL-1527/84] 03 p0408 N85-12609
PRIAMUS, a computer program for the calculation of thermophysical properties of gas mixtures containing O2, N2, CO, CO2, He, H2O, H2, CH4
[JUEL-1916] 04 p0472 N85-13002
Simulation of a transmission circuit composed of slightly nonlinear elements. Computation of the intermodulation on signals composed of N carriers
[CNES-NT-105] 04 p0496 N85-13167
An organ-pipe oscillation — PHOENICS code
[PDR/CFDU-IC/14] 04 p0501 N85-13199
Laminar jet issuing into stagnant surroundings — PHOENICS code
[PDR/CFDU-IC/15] 04 p0501 N85-13200
New directions in software for advanced computer architectures
[DE84-017435] 04 p0550 N85-13502
The CDC: Facilities on offer from the CNES computing center for space mathematics (a look at the capacities of CDC computers) 05 p0599 N85-13818
The Search And Rescue Satellite Aided Tracking (SARSAT) experiment. Presentation of CNES processing for the SARGOS project: Context and orbit processing 05 p0600 N85-13830
Loss of bone substance in consequence of amputation as a model for the adaptation to microgravity 06 p0694 N85-14464
SENSIT.FOR: A program for sensitometric reduction 07 p0963 N85-16105
Characterizing the scientific potential of satellite sensors — San Francisco, California
[E85-10044] 07 p0983 N85-16244
On the structure of information in software
[AD-A147580] 07 p1026 N85-16511

Operating system versus programming environment, for example the UNIX
[SWA-84/037] 07 p1027 N85-16516
Austrian contributions to fuel rod failure models shown at the International Standard Problem (ISP)-14
[OEFZS-4276] 07 p1041 N85-16613
Investigating version dependence in fault-tolerant software 08 p1065 N85-16749
The effect on software design of testing by symbolic execution 08 p1065 N85-16750
Reliable software design for avionics and space applications 08 p1065 N85-16751
Hardware/software codesign for maintainable systems 08 p1066 N85-16753
Sensor-atmosphere-target simulation. Computer program SENSAT
[DFVLR-FB-84-32] 08 p1176 N85-17419
MINDS: A microcomputer interactive data system for 8086-based controllers
[NASA-TP-2378] 08 p1204 N85-17576
Software test handbook: Software test guidebook, volume 2
[AD-A147289] 08 p1204 N85-17578
An application of discriminant analysis to the selection of software cost estimating models
[AD-A147632] 08 p1204 N85-17580
Approaches to structuring the software development process
[AD-A147694] 08 p1205 N85-17582
The description of large systems
[AD-A148072] 08 p1205 N85-17586
Results of data base management system parameterized performance testing related to GSFC scientific applications
[NASA-CR-170615] 08 p1229 N85-17741
Four-fluid description of turbulent plasma focus dynamics
[IPF-84-4] 09 p1395 N85-18778
Computer-assisted data processing and analysis system for ground-based meteorological data collection, report on the Sierra Cooperative Pilot Project
[PB85-115350] 10 p1520 N85-19587
Digital Equipment Corporation VAX Ada Compiler Version T0.6-2 VAX-11/785, 11/750, 11/730, using VMS, Version 4.0 and MicroVAX 1, using MicroVMS Version 1.0
[AD-A149375] 10 p1538 N85-19696
SUBOPT: A CAD program for suboptimal linear regulators
[NASA-CR-172536] 10 p1539 N85-19702
Methodology investigation software testing of multiprocessor systems
[AD-A149446] 10 p1541 N85-19714
SOLIDGEN: A solid finite element data generator. User's manual
[AD-A149490] 10 p1541 N85-19715
French work toward flexible software workshops 11 p1592 N85-20015
Crack growth geometry in aluminum alloy sheet material under flight simulation loading. 1: A comparison between TWIST and miniTWIST FALSTAFF and short FALSTAFF. 2: Effect of truncating high loads
[VTH-LR-441] 11 p1609 N85-20119
Application of model following control and estimation techniques to attitude control of maneuvering spacecraft. Part 2: Simulation software description
[NLR-TR-82116-U-PT-2] 12 p1793 N85-21254
Interface specifications for SCR (Software Cost Reduction) (A-7E) extended computer module, revised
[AD-A149948] 12 p1915 N85-22024
Computer aided engineering applied to the design and verification of the generic Advanced Rigid Array (ARA) — solar array 13 p2008 N85-22593
Contribution of instrumentation and control software to system reliability
[DE85-004693] 13 p2149 N85-23340
Numerical algorithms and software for matrix Riccati equations
[AD-A150148] 13 p2150 N85-23344
French work toward flexible software workshops 14 p2269 N85-24187
Plasma and magnetospheric research
[NASA-CR-175675] 14 p2354 N85-24543
Finite element methods in space mathematics 14 p2396 N85-24757
The computing facilities of the Toulouse Space Center 14 p2397 N85-24770
Organization of conveyor processing of vector commands in multiprocessor computer systems with a reorganizable structure 14 p2401 N85-24799
ESABASE extension to spacecraft charging analysis. Phase 1: NASCAP software (VAX version)
[ESA-CR(P)-1968] 15 p2493 N85-25381
The design and validation of software for dimensional metrology
[NPL-DITC-50/84] 15 p2521 N85-25542
Computer program TRAMP: Inclusion of state space facilities and the analysis of non-linear elements
[BAE-BT-12643] 15 p2626 N85-26181
Design and analysis of a complete relational interface for a multi-backend database system
[AD-A151501] 15 p2628 N85-26198
Mathematical software for hyperbolic equations and two point boundary value problems
[AD-A151982] 15 p2638 N85-26270
Reusable software: A concept for cost reduction 16 p2697 N85-26855
Description of a computer program treating transonic steady state aeroelastic effects for a canard or tail airplane
[FFA-TN-1983-23] 16 p2700 N85-26674
Computation model of turbulent free flow: Application to axisymmetric jets
[ISL-R-126/83] 16 p2785 N85-27185
Raster or vector processing. Experience with the application of programs for the construction of thematic maps with boundary design in the Lower Saxony (West Germany) Land Administration for ground research 16 p2815 N85-27365
Generalized graph coloring: A frequency assignment method for VHF broadcasting
[TUM-M8405] 16 p2844 N85-27535
Management aspects of software maintenance
[AD-A152035] 16 p2847 N85-27550
Proposal for an extended set of FORTRAN Basic Linear Algebra subprograms
[DE85-007241] 16 p2848 N85-27562
Formulation of a coherent light-sheet by means of a cylindrical-spherical optical system
[ISL-R-116/83] 16 p2865 N85-27674
Software for reflectivity calculations of X-ray mirrors, revision 1
[DE85-006642] 16 p2867 N85-27688
A secure high-speed transaction protocol
[CWI-CS-R8417] 17 p3009 N85-28605
Research in computer science
[NASA-CR-175922] 17 p3010 N85-28612
CLEANROOM software development: An empirical evaluation
[AD-A152924] 17 p3011 N85-28619
Software environment for conducting interactive statistical analysis
[AD-A153378] 17 p3012 N85-28626
Software for estimating sparse Hessian matrices
[DE85-008121] 17 p3013 N85-28629
Optimal design and use of retry in fault tolerant real-time computer systems
[NASA-CR-175920] 17 p3015 N85-28643
A program for solving first kind Fredholm integral equations by means of regularization
[CWI-NM-R8416] 17 p3022 N85-28697
Specification of software quality attributes, volume 1
[AD-A153988] 18 p3163 N85-29583
Specification of software quality attributes. Volume 2: Software quality specification guidebook
[AD-A153989] 18 p3163 N85-29584
Specification of software quality attributes. Volume 3: Software quality evaluation guidebook
[AD-A153990] 18 p3163 N85-29585
ODIN: An extensible software environment. Report and user's reference manual
[DE85-003459] 18 p3164 N85-29600
A computer code IB-KB for interior ballistics of recoiling and recoilless guns
[FOA-C-20566-D2] 18 p3164 N85-29602
Fracture mechanics formulas on microcomputers
[NASA-TM-77850] 19 p3284 N85-30362
ZOG-Vinson technology demonstration project. Volume 2: System description
[AD-A153671] 19 p3333 N85-30645
Local automation model software benchmarking: Test plan
[AD-A154349] 19 p3337 N85-30676
Development and evaluation of a Fault-Tolerant Multiprocessor (FTMP) computer. Volume 2: FTMP software
[NASA-CR-166072] 19 p3341 N85-30706
Definition and layout of a traffic generator for an air traffic control simulation
[ESA-TT-886] 20 p3391 N85-31034
PHOENICS 84: A multi-dimensional multi-phase general-purpose computer simulator for fluid flow, heat transfer and combustion: 36 lecture panels
[CFD/84/18] 20 p3457 N85-31468
Visualization of computation results. Definition of a graphics satellite computer
[ONERA-RT-2/3587-CY] 20 p3514 N85-31845
Evaluative report on the Institute for Computer Sciences and Technology, National Bureau of Standards, fiscal year 1984
[PB85-176097] 20 p3514 N85-31848
A system identification package for VAX and LSI 11
[OUEL-1569/85] 20 p3518 N85-31862
Monte Carlo: In the beginning and some great expectations
[DE85-010789] 20 p3518 N85-31872
FAUST: Introduction and overview — self tuning control
[OUEL-1568/85] 20 p3519 N85-31882
A guide to the statistical analysis of the results of linear and nonlinear least-squares data fitting
[NPL-DITC-53/84] 20 p3521 N85-31895
HLLM software support
[AD-A154828] 21 p3671 N85-32805
Design guidelines for user-system interface software
[AD-A154907] 21 p3671 N85-32807
The effect of communication-language designs on software specifications
[AD-A155173] 21 p3672 N85-32809
Evaluation of a software design approach: Develop a threat resolution module in Ada (trademark)
[AD-A155599] 21 p3672 N85-32815
A simple software environment based on objects and relations
[AD-A155704] 21 p3673 N85-32817
DYNA3D, INGRID, and TAURUS: An integrated, interactive software system for crashworthiness engineering
[DE85-010928] 21 p3677 N85-32846
SHELTER: Description of a program code — indoor climate
[FOA-C-58002-H1] 22 p3755 N85-33278
State of art and development problems in computer-aided design of electronic circuits 22 p3766 N85-33342
Integrated Support Software System (ISSS)
[AD-A155715] 22 p3829 N85-33710
Proceedings of the Mechanisms Conference, volume 1 23 p3923 N85-34309
A versatile computer package for mechanism analysis, part 2: Dynamics and balance 23 p3924 N85-34315
Proceedings of the Mechanisms Conference, volume 2 23 p3924 N85-34318
Software for mechanism design 23 p3925 N85-34324
An innovative user interface for microcomputer-based computer-aided design 23 p3961 N85-34555
A geometric modeller for turbomachinery applications 23 p3962 N85-34556
Architecture of languages for large CAD systems development 23 p3962 N85-34557
The automatic labeling of geographic maps: A problem in computer aesthetics 23 p3962 N85-34561
Calculation of the diffusion of light by aerosols: Description of the MIELOR software and results obtained
[REPT-80] 24 p4137 N85-35638
AUTOSIM: An automated repetitive software testing tool
[NASA-CR-177930] 24 p4137 N85-35643
Attacking software crisis: A macro approach
[AD-A155846] 24 p4138 N85-35645
Software maintenance relating to the input translator and z-80 realization volume of the computer systems design environment
[AD-A155849] 24 p4138 N85-35648

COMPUTER SYSTEMS SIMULATION

Hardware for a real-time multiprocessor simulator
[NASA-TM-83805] 01 p0099 N85-10659
S-MICRO: A system for simulating a microprogrammed control unit
[INPE-3224-PRE/575] 05 p0715 N85-14585
Research using a DISCUS based network emulator
[AD-A141294] 13 p2149 N85-23338
Use of computer-aided design in large-computer development described 15 p2564 N85-25822
Distributed database design tool
[AD-A153760] 18 p3200 N85-29850
Development and evaluation of a Fault-Tolerant Multiprocessor (FTMP) computer. Volume 3: FTMP test and evaluation
[NASA-CR-166073] 19 p3341 N85-30707
Comments on estimating quantiles for Gaussian functionals by simulation
[AD-A154302] 19 p3348 N85-30750
Construction of University of Missouri, Rolla's full scale cloud simulation chamber and applied research
[AD-A154682] 21 p3557 N85-32128

COMPUTER TECHNIQUES

NT COMPUTER AIDED DESIGN
NT COMPUTER AIDED MANUFACTURING
NT COMPUTER AIDED MAPPING
NT COMPUTER AIDED TOMOGRAPHY
NT COMPUTER ASSISTED INSTRUCTION

The Influence of Large Scale Computing on Aircraft Structural Design
[AGARD-R-706] 01 p0007 N85-10040
Impact of new computing systems on computational mechanics and flight-vehicle structures technology 01 p0007 N85-10042
Large scale computing in aeronautical design 01 p0007 N85-10043
Analysis of on-board CIG (Computer Image Generator) applications for aircrew training
[AD-A145214] 01 p0013 N85-10079
A thermodynamic surface for the critical region of ethylene
[PB84-217850] 01 p0025 N85-10159
A review of selected studies of computerized speech recognition conducted at the Naval Postgraduate School
[AD-A144841] 01 p0037 N85-10235
Electronics Engineering Department: EE technical review
[DE84-016124] 01 p0044 N85-10286
Research in Structures and Dynamics, 1984
[NASA-CP-2335] 01 p0057 N85-10377
Finite element computation on nearest neighbor connected machines 01 p0057 N85-10379
Application of concurrent processing to structural dynamic response computations 01 p0057 N85-10380
USSR report: Space Biology and Aerospace Medicine, volume 18, no. 4, July - August 1984
[JPRS-USB-84-006] 01 p0091 N85-10611
Potential use of dialogue with computers in biomedical research 01 p0091 N85-10614
Analysis of computer and communication information processing and system development
[AD-A144986] 01 p0100 N85-10660
Activities of the MIT Laboratory for Computer Science
[AD-A145134] 01 p0100 N85-10661
REMOTE: Modem Communicator Program for the IBM personal computer
[DE84-015047] 01 p0100 N85-10665
On the formal description and derivation of temporal proof rules for program properties
[TUM-I8405] 01 p0101 N85-10675
Construction of approximate confidence intervals for probability-of-kill via the bootstrap
[AD-A144761] 01 p0113 N85-10784
Microcomputers in Hungary 01 p0115 N85-10786
LANDSAT data and interactive computer mapping 02 p0152 N85-11028
Computer aided process planning of machined metal parts
[AD-A145628] 02 p0189 N85-11263
Hardware and software selection for experimental modal analysis 02 p0206 N85-11373
A system for the management of requests at an image data bank
[E85-10014] 02 p0216 N85-11427
Visual representations subserving texture perception
[AD-A145412] 02 p0236 N85-11538
East Europe report, science and technology. Czechoslovakia: System of small electronic computers
[JPRS-ESA-84-040] 02 p0239 N85-11558
Criteria for the optimization of processing flow in a model of an incremental computer with multiprocessing resources
[INPE-3046-TDL/158] 02 p0240 N85-11560
Software engineering environments for mission critical applications: STARS alternative programmatic approaches
[AD-A145285] 02 p0241 N85-11571
Description of the software acquisition process (SWAP) model
[AD-A145413] 02 p0241 N85-11573
Yearly report for programming productivity enhancement by the use of application generators
[AD-A145623] 02 p0242 N85-11579
Concurrent processing and the decomposition of problems
[DE84-015285] 02 p0242 N85-11581
Shuffle-exchanges on augmented meshes
[NASA-CR-172476] 02 p0243 N85-11587
AI (Artificial Intelligence) approaches to troubleshooting
[AD-P003918] 02 p0245 N85-11598
Diagnosis based on description of structure and function
[AD-P003919] 02 p0245 N85-11599
Artificial intelligence approaches to monitoring system integrity
[AD-P003930] 02 p0246 N85-11610
NAVAIR's (Naval air systems command) AI (Artificial Intelligence) program for ATE (Automated Test Equipment)
[AD-P003935] 02 p0247 N85-11615
DELTA: An expert system for diesel electric locomotive repair
[AD-P003941] 02 p0248 N85-11621
On the requirements of expert systems for fault isolation
[AD-P003947] 02 p0249 N85-11627
Memory-based expert systems
[AD-A145612] 02 p0249 N85-11628
Tomographic reconstruction of neutron radiograph images
[AD-A145682] 02 p0260 N85-11826
Decision Support System (DSS): A survey
[NRIMS-TWISK-317] 02 p0292 N85-11896
An operational system for subject switching between controlled vocabularies: A computational linguistics approach
[NASA-CR-3838] 02 p0293 N85-11903
A management workstation concept
[AD-A145617] 02 p0294 N85-11906
AGARD Highlights
[AGARD-HIGHLIGHTS-84/2] 02 p0305 N85-11972
ONR (Office of Naval Research) Far east Scientific Bulletin, Volume 9, Number 2, April - June 1984
[AD-A145681] 02 p0305 N85-11974
European Scientific Notes, Number 38-9
[AD-A145683] 02 p0306 N85-11975
DoD Robotics Application Workshop Proceedings
[AD-A145867] 03 p0307 N85-11976
Air force plasma spray at SA-ALC (San Antonio Air Logistics Center)
[AD-P004004] 03 p0308 N85-11984
NEO robotic application development at Letterkenny Army Depot: The application of robotics to agricultural blast cleaning
[AD-P004007] 03 p0308 N85-11987
Expert systems: The application of new computer methods to corrosion problems
[AERE-M-3395] 03 p0334 N85-12153
Assessment of computer techniques for processing digital LANDSAT MSS data for lithological discrimination of Serra do Ramalho, State of Bahia
[E85-10033] 03 p0378 N85-12412
A research program in computer technology
[AD-A145776] 03 p0402 N85-12565
Computer equipment for research in statistics
[AD-A145755] 03 p0406 N85-12591
Test-bed for programmable automation research. Phase 1
[AD-A145872] 03 p0409 N85-12614
Psychological issues in the design of expert systems
[AD-A146081] 03 p0438 N85-12792
USSR report: Electronics and electrical engineering
[JPRS-UEE-84-010] 04 p0485 N85-13095
Architecture of adaptive space-frequency-time signal processing system 04 p0486 N85-13103
Microprocessor implementation of algorithms of nonlinear filtration 04 p0486 N85-13104
Revision of signal and interference space-time processing algorithms for implementation by microprocessors 04 p0487 N85-13105
Efficiency of computer system digital processing of signals 04 p0487 N85-13106
Computer-generated latitude and longitude templates for rapid determination of geographic positions in Alaska 04 p0516 N85-13288
The 1984 ASEE-NASA summer faculty fellowship program (aeronautics and research)
[NASA-TM-87393] 04 p0575 N85-13664
A refined computer program for the transient simulation of ground coupled heat pump systems
[DE84-014098] 05 p0637 N85-14088
Simulation experiments on the relative accuracy of inferred atmospheric states from idealized wind and temperature profiling systems 05 p0682 N85-14386
Integrated navigation systems: Where are we headed?
[AD-A146425] 06 p0753 N85-14832
Computer investigation of effects of high injection in transistor large integrated circuit structures 06 p0793 N85-15068
Computer vision research and its applications to automated cartography
[AD-A146668] 06 p0828 N85-15255
Standard SHEF (Standard Hydrometeorologic Exchange Format) decoder Version 1.1
[PB85-106506/GAR] 06 p0840 N85-15332
Architecture, design, and system; performance assessment and development methodology for computer-based systems. Volume 1: Methodology description, discussion, and assessment
[AD-A146577] 06 p0847 N85-15379
A framework for the development of Navy computer-based systems: Combat system architecture and combat system engineering put into perspective
[AD-A146460] 06 p0856 N85-15445
Methodology investigation. Streamlined Test Reporting and Planning (STRAP): Data flow procedures
[AD-A146463] 06 p0871 N85-15531
Automated Lavina collects data on snow 07 p0980 N85-16224
Alabama Tin Belt: Metallogenesis and mineral resource evaluation. Year-end report
[DE84-901335] 07 p0989 N85-16283
Research in applied mathematics, numerical analysis, and computer science
[NASA-CR-172505] 07 p1021 N85-16480
NSW (National Software Works) lessons learned
[AD-A146737] 07 p1023 N85-16494
Ada training curriculum. Real-time systems in Ada 1401 teacher's guide, volume 1
[AD-A146782] 07 p1024 N85-16496
Ada training curriculum. Real-time systems in Ada 1401 teacher's guide, volume 2
[AD-A146783] 07 p1024 N85-16497
Local area network evaluation by MICROSS extensions
[AD-A146773] 07 p1027 N85-16521
Ion microscopy of metals and semiconductors
[AD-A147118] 07 p1043 N85-16626
Manual and automated line generalization and feature displacement: Appendixes
[AD-A143251] 07 p1054 N85-16689
Distributed knowledge base systems for diagnosis and information retrieval
[AD-A146890] 07 p1054 N85-16690
Computer sizing of fighter aircraft
[NASA-TM-86351] 08 p1067 N85-16759
Automation of checkout for the shuttle operations era 08 p1092 N85-16900
Modeling techniques used in the communications link analysis and simulation system (CLASS) 08 p1100 N85-16953
Validation of the communications link analysis and simulation system (CLASS) 08 p1100 N85-16954
Computer aided processing using laser measurements 08 p1103 N85-16973
Application of computer methods for calculation of multicomponent phase diagrams of high temperature structural ceramics
[AD-A148138] 08 p1133 N85-17140
Description of MBB computerized design techniques for A320 08 p1141 N85-17194
Beam propagation studies at NRL (Naval Research Laboratory) July 1983 to June 1984, volume 2
[AD-A148198] 08 p1152 N85-17270
Performance management system enhancement and maintenance
[NASA-CR-175271] 08 p1202 N85-17564
Steps towards parsing of query sequences to a database
[AD-A148769] 08 p1206 N85-17590
Guide to personal desktop computing at ANL
[DE85-001438] 08 p1206 N85-17594
A unified model for performance and reliability of Fault-Tolerant/Multi-Mode systems
[AD-A148789] 08 p1208 N85-17601
Reduction to outside the atmosphere and statistical tests used in Geneva photometry 08 p1251 N85-17902
Integrated approach to flight crew training 09 p1276 N85-18014
Electrical resistivity technique to assess the integrity of geomembrane liners
[PB85-122414/GAR] 09 p1325 N85-18327
Shock response analysis by personal computer using the extended IFT algorithm 09 p1335 N85-18397
SPADE: Series-parallel directed acyclic graph evaluator
[AD-A148458] 09 p1368 N85-18592
An object-oriented signal processing environment: The knowledge-based signal processing package
[AD-A148963] 10 p1466 N85-19251
A circuit grammar for operational amplifier design
[AD-A149566] 10 p1481 N85-19346
Electromagnetic inspection of wire ropes using sensor arrays
[AD-A149016] 10 p1495 N85-19436
Equations and algorithms for meteorological applications in air weather service
[AD-A148894] 10 p1519 N85-19575
Methods of computer-aided analysis of non-Gaussian noise and application to robust adaptive detection, part 2
[AD-A148879] 10 p1539 N85-19704
Ada in mission critical system acquisition: A guidebook
[AD-A149271] 10 p1540 N85-19710
French plans for fifth generation computer systems
[AD-A149435] 10 p1544 N85-19732
Computable real analysis
[AD-A149079] 10 p1546 N85-19747

Image Understanding: Proceedings of the 15th Workshop
[AD-A149496] 10 p1557 N85-19616
Optical implementation of the synthetic discriminant function
[AD-A149562] 10 p1557 N85-19817
The integrated library system design concepts for a complete serials control subsystem
[AD-A149379] 10 p1568 N85-19684
East Europe report: Science and technology
[JPRS-ESA-85-009] 11 p1616 N85-20165
ESOP expert system model described
11 p1619 N85-20187
Computer aided of maintainability design: A feasibility study
[AD-A149293] 11 p1738 N85-20932
A computer analysis of the RF performance of a ground-mounted, air-supported radome
[AD-P004352] 12 p1824 N85-21446
Radioelectronics and space exploration
12 p1836 N85-21533
The man-machine interface
[AD-A149971] 12 p1910 N85-21989
A computer-based gaming system for assessing recognition performance (RECOG)
[AD-A149752] 12 p1915 N85-22022
Very-high level concurrent programming
[AD-A150009] 12 p1916 N85-22026
Experimental mathematics
[CWI-PM-R8411] 12 p1925 N85-22096
Evaluation of PHOENICS as a design analysis tool for SSME 12 p1949 N85-22240
Theoretical interpretation of thermal arrest data from differential thermal analysis measurements
12 p1949 N85-22241
The EEC's information technology program: An update
[AD-A150022] 12 p1951 N85-22258
Aviation maintenance computerized management information systems: Perspective for the future
[AD-A150637] 13 p1966 N85-22349
Avionics Flight Evaluation System (AFES)
13 p1967 N85-22357
The potential for advanced computerized aids for comprehensible writing of technical documents
[AD-A150501] 13 p2055 N85-22870
Orphan detection in the Argus system
[AD-A150562] 13 p2148 N85-23331
Map design for computer processing: Literature review and DMA product critique
[AD-A151061] 14 p2347 N85-24513
Evaluating the appropriateness of microcomputers for litigation document management using the analytic hierarchy process 14 p2399 N85-24788
A two-cycle shift register with error detection
[AD-A150768] 14 p2400 N85-24791
The problem of creating a standardized series of personal computers 14 p2400 N85-24795
ANTENA user guide
[DE85-004961] 14 p2424 N85-24953
Microcomputer application of aerospace asset surface search planning
[AD-A151833] 15 p2467 N85-25227
Calculation and display of stack departure times for aircraft inbound to Heathrow Airport
[AD-A151991] 15 p2469 N85-25241
Microcomputer controlled automatic peak locking of laser circuit 15 p2537 N85-25655
Applicability of modular versus universal robots discussed 15 p2538 N85-25664
Using a single-board computer to maintain constant voltage, current sources 15 p2551 N85-25749
Calorimeter for measuring high-energy optical pulses
[PB85-160695] 15 p2561 N85-25799
Eye movement in response to single and multiple targets
[AD-A151115] 15 p2617 N85-26126
USSR report: Cybernetics, computers and automation technology
[JPRS-UCC-85-003] 15 p2625 N85-26174
Progress through cooperation and exchange of ideas and experiences 15 p2626 N85-26186
Computers in the determination of rainfall septh-duration-frequencies in Natal
15 p2627 N85-26188
Computer aided draughting in a civil engineering consulting practice 15 p2627 N85-26189
Interactive graphical data analysis
[DE85-005946] 15 p2631 N85-26215
Developing an automated technique for translating a relational database into an equivalent network one
[AD-A151844] 15 p2666 N85-26451
Information technology applications in voluntary sector transport operations. SP1: Objectives and programme of work
[TT-8501] 15 p2667 N85-26457
Computer software for aerodynamic design of aircraft developed within the National Aerospace Laboratory
16 p2691 N85-26613
Planning fuel-conservative descents in an airline environmental using a small programmable calculator: Algorithm development and flight test results
[NASA-TP-2393] 16 p2707 N85-26705
The design of an English word-processor for scientific and technical use in which superscripts, subscripts and Greek characters are operated by screen-edit. 3
16 p2759 N85-27025
China report: Science and Technology
[JPRS-CST-85-012] 16 p2806 N85-27300
New image deblurring method described
16 p2806 N85-27305
A wind-bivane/microprocessor system for on-line prediction and display of pollutant distributions
16 p2830 N85-27449
The development and application of volume scan and cell tracking capabilities for the analysis of convective cloud systems 16 p2830 N85-27451
Incorporation of an elliptical boundary condition into the program POISSON
[DE85-006820] 16 p2849 N85-27564
Finite elements and the method of conjugate gradients on a concurrent processor
[NASA-CR-175812] 16 p2853 N85-27588
Adaptive grid generation for numerical solution of Burger's equation
[AD-A152217] 16 p2855 N85-27606
ACT applied to helicopter flight control
17 p2902 N85-27891
Some flight test results with redundant digital flight control systems 17 p2902 N85-27892
Evaluation of used crankcase oils using computerized infrared spectrometry
[AD-A152993] 17 p2920 N85-27999
Evaluation of used crankcase oils using computerized infrared spectrometry. Appendices
[AD-A152994] 17 p2920 N85-28000
Automation of Precise Time Reference Stations (PTRS) 17 p2962 N85-28291
US Naval Observatory collection and utilization of time comparison data 17 p2962 N85-28292
Documentation of PHOTO: A user's manual for the analysis of photographic and X-ray negatives
[AD-A152968] 17 p2967 N85-28327
Generation and display apparatus
[AD-D011639] 17 p3008 N85-28599
Microprocessor controlled temperature chassis
[DE85-008392] 17 p3009 N85-28602
Computer program for prediction of capture maneuver probability for an on-off reaction controlled upper stage
[NASA-CR-165937] 17 p3010 N85-28611
Interfacing the VAX 11/780 using Berkeley Unix 4.2.BSD and Ethernet based Xerox network systems, volume 1
[AD-A152953] 17 p3015 N85-28645
Computing in the Soviet general economy: An introductory overview
[AD-P004563] 17 p3047 N85-28858
Turbulence structure in the boundary layers of an oscillating airfoil
[AD-A153831] 18 p3059 N85-28926
MBB expands CADAM system for a 320 program
18 p3087 N85-29099
Automatic volume calibration system
[DE85-008956] 18 p3102 N85-29204
Improved model for fluid-driven cracks in jointed rock
[DE85-008963] 18 p3125 N85-29349
Deployable Core Automated Maintenance System (DCAMS)
[AD-A153695] 18 p3198 N85-29839
Projects of the Computer Center of the academy's Siberian branch 19 p3295 N85-30425
Activities of the Institute for Computer Applications in Science and Engineering (ICASE)
[NASA-CR-172610] 19 p3332 N85-30641
Multigrid method for multiprocessors
[DE85-007929] 19 p3333 N85-30647
Local automation model software benchmarking: Test plan
[AD-A154349] 19 p3337 N85-30676
Survey of Ada (Trademark)-based PDLs (Program Design Language)
[AD-A154402] 19 p3338 N85-30680
T sub EX font tables
[DE85-011394] 19 p3339 N85-30687
Identification of a mathematical model 1: Goodness of fit criterion
[HSE-TRANS-11109] 19 p3341 N85-30709
Development and evaluation of a fault-tolerant multiprocessor (FTMP) computer. Volume 1: FTMP principles of operation
[NASA-CR-166071] 19 p3341 N85-30705
Computer studies of the quench behavior of an SSC model dipole
[DE85-010633] 19 p3360 N85-30829
Galileo battery testing and the impact of test automation 20 p3444 N85-31381
Computer methods in manipulator kinematics, dynamics and control: A comparative study
20 p3462 N85-31506
Electrophoretic mobility of cells in a vertical Ficoll gradient 20 p3499 N85-31753
Activities report of the Laboratory for Computer Science (FOA 32)
[FOA-C-30364-E1] 20 p3516 N85-31861
Mathematical programming in the Netherlands
[REPT-ARW-03-THE-BDK/ORS/83/10]
20 p3517 N85-31868
USAFSAM review and analysis of radiofrequency radiation bioeffects literature
[AD-A155113] 21 p3664 N85-32760
Design guidelines for user-system interface software
[AD-A154907] 21 p3671 N85-32807
New developments on the core function for efficient implementation of the difficult residue number system operations
[AD-A154678] 21 p3676 N85-32834
Distributed name management
[AD-A154785] 21 p3712 N85-33037
Interactive procedures for discriminating and restoring contour line networks 22 p3736 N85-33156
Discrimination of linear contour elements of space photographs based on visual perception model
22 p3736 N85-33161
Signal processing in quasi-holographic system as an inverse problem 22 p3762 N85-33315
Synthesis of tests for programmable logic arrays
22 p3777 N85-33408
Detection of and search for faults in programmable logic arrays 22 p3778 N85-33409
Computer science: Key to a space program renaissance. The 1981 NASA/ASEE summer study on the use of computer science and technology in NASA. Volume 2: Appendices
[NASA-CR-175295] 22 p3827 N85-33702
Microcomputer controlled image processor
[AD-D011734] 22 p3833 N85-33735
Proceedings of the Mechanisms Conference, volume 1 23 p3923 N85-34309
A versatile computer package for mechanism analysis
23 p3924 N85-34314
A versatile computer package for mechanism analysis, part 2: Dynamics and balance
23 p3924 N85-34315
Optimisation in the computer aided design of mechanisms 23 p3924 N85-34321
Method and apparatus for transfer function simulator for testing complex systems
[NASA-CASE-NPO-15896-1] 23 p3926 N85-34333
Animengine: An engineering animation system
23 p3959 N85-34535
Efficient recovery and reversal in graphical user interfaces generated by the Higgens system
23 p3960 N85-34544
Numerical and analytic descriptions of cosmic-ray transport
[SH-4.1-4] 23 p4005 N85-34830
Computational techniques for fiber reinforced components 24 p4075 N85-35250
Wholebody radiation counting system
[AD-A155842] 24 p4131 N85-35807
TRICCS: A proposed teleoperator/robot integrated command and control system for space applications
[NASA-TM-87577] 24 p4136 N85-35837
Design of a microprogram control unit with concurrent error detection
[AD-A156447] 24 p4139 N85-35855
Toolpack
[DE85-013135] 24 p4140 N85-35865
Edge information in color images based on histograms of differences
[AD-A156002] 24 p4154 N85-35751

COMPUTER VISION
Computer vision research and its applications to automated cartography
[AD-A146668] 06 p0828 N85-15255
Vision by man and machine: How the brain processes visual information may be suggested by studies in computer vision (and vice versa)
[AD-A147880] 07 p1017 N85-16458
JPL Robotics Laboratory computer vision software library
[NASA-CR-174272] 07 p1023 N85-16481
Dutch institutes do research in tactile visual robot sensors 09 p1310 N85-18228
French firm develops 2D, 3D computer vision system
10 p1461 N85-19208

Fourth International Conference on Robot Vision and Sensory Controls
[AD-A149524] 10 p1492 N85-19422
A method for reduction of ambiguity in segmentation of images
[INPE-3394-TDL/186] 11 p1667 N85-20664
3D (Three-Dimensional) sensor for adaptive suspension vehicle
[AD-A150921] 14 p2311 N85-24305
Positioning of a robotic manipulator through the use of visual feedback
[AD-A151933] 16 p2651 N85-27577
Optical phenomena in computer vision
[AD-A152970] 17 p3008 N85-28595
Activities report of the Laboratory for Computer Science (FOA 32)
[FOA-C-30384-E1] 20 p3516 N85-31861
Edge detection and geometric methods in computer vision
[AD-A155873] 24 p4135 N85-35630
Selected publications in image understanding and computer vision from 1974 to 1983
[AD-A156196] 24 p4136 N85-35634

COMPUTERIZED CONTROL
U NUMERICAL CONTROL

COMPUTERIZED DESIGN
U COMPUTER AIDED DESIGN

COMPUTERIZED SIMULATION
NT ANALOG SIMULATION
NT DIGITAL SIMULATION
Computer simulation of the shock initiation of detonation in solid explosives
[PML-1984-23] 01 p0033 N85-10207
Clutter generator for use in radar evaluation
[AD-D011234] 01 p0039 N85-10245
Availability of transmission systems in continental and intercontinental connections --- telecommunication
[FUB-33-1983] 01 p0040 N85-10261
Gaussian Wide Sense Stationary Uncorrelated Scattering (GWSSUS) channel simulation program to be used for mobile radio systems
[FUB-40-1983] 01 p0041 N85-10265
DYNKIN: A computer program for the description of detailed gas reactions in interaction with gas dynamics
[AD-B085364] 01 p0046 N85-10298
Application guide for Hydrological Simulation Program FORTRAN (HSPF)
[PB84-215763] 01 p0064 N85-10427
Variable geometry Darrieus wind machine
[PB84-207261] 01 p0068 N85-10453
Processing and display of atmospheric phenomenaa data
[NASA-CR-171178] 01 p0072 N85-10475
Feature discovery by competitive learning
[AD-A145052] 01 p0097 N85-10646
A relational approach to the development of expert diagnostic systems
[NASA-TM-86296] 01 p0099 N85-10658
Three programs for evaluating bending moments, deflections and shear forces in simply-supported uniform bridge decks under South African NA loading: NAB, NAD and NAS. NITRR manual P13
[ISBN-0-7988-2283-X] 01 p0102 N85-10681
PDSS/IMC CIS user's guide
[NASA-CR-171179] 01 p0102 N85-10682
Robust rate control system designs for a submersible
[AD-A144792] 01 p0111 N85-10753
KrCl lasers for fusion
[DE84-012210] 01 p0122 N85-10835
VORCOR: A computer program for calculating characteristics of wings with edge vortex separation by using a vortex-filament and-core model
[NASA-CR-165902] 02 p0135 N85-10921
Enhanced TCAS 2/CDTI traffic Sensor digital simulation model and program description
[NASA-CR-172445] 02 p0136 N85-10927
Command control group behaviors. Objective 1: A methodology for and identification of command control group behaviors
[AD-A145690] 02 p0191 N85-11279
Simulation study of a new inverse-pinch high Coulomb transfer switch
[NASA-CR-172420] 02 p0194 N85-11294
Robotics investment decision model user's manual
[AD-A145467] 02 p0204 N85-11347
A constitutive modeling technique based on a generalized rheological model to predict the response of materials 02 p0207 N85-11368
Computer models and output, Spartan REM: Appendix B
[NASA-CR-171093] 02 p0208 N85-11376
Basic research for the geodynamics program
[NASA-CR-174055] 02 p0226 N85-11490
Description of the software acquisition process (SWAP) model
[AD-A145413] 02 p0241 N85-11573
Parallel searching and merging on ZMOB
[AD-A145424] 02 p0241 N85-11574
Diagnosis via causal reasoning: Paths of interaction and the locality principle
[AD-P003920] 02 p0245 N85-11600
A generalized model of fault-isolation performance
[AD-P003928] 02 p0246 N85-11608
Experimental study with parameter variations on a hydraulic positioning servo with computer implemented observer
[FOA-C-20545-E3] 02 p0256 N85-11673
Modeling holographic recognition system by using number-theory convolution transformation 02 p0272 N85-11774
Decision process models of contractor behavior: The development of effective contract incentives
[AD-A145524] 02 p0292 N85-11898
Review of simulation of quasiparallel collisionless shocks
[DE84-015489] 02 p0304 N85-11967
Numerical simulation of the subsonic wing-rock phenomenon 03 p0320 N85-12064
Liquid payload moment equations
[AD-A145977] 03 p0362 N85-12319
Numerical simulations of fuel droplet flows using a Lagrangian triangular mesh
[AD-A146087] 03 p0362 N85-12320
Simulation of wavefronts returned by realistic surfaces 03 p0383 N85-12448
A user's guide to the Flexible Spacecraft Dynamics and Control Program
[NASA-TM-87369] 03 p0405 N85-12586
Regenerative simulation methods for local area computer networks
[AD-A146197] 03 p0409 N85-12612
Rotary-wing aircraft noise measurements: Analysis of variations and proposed measurement standard
[AD-A146207] 03 p0416 N85-12662
Ways to improve management of Federal funded computerized models
[LCD-75-111] 03 p0435 N85-12771
A comparison of Wortmann airfoil computer-generated lift and drag polars with flight and wind tunnel results
[NASA-TM-86035] 04 p0452 N85-12866
A transmission analysis for the use of 2-4 PSK modulation in satellite broadcasting
[ESA-STM-231] 04 p0494 N85-13151
Simulation of a transmission circuit composed of slightly nonlinear elements. Computation of the intermodulation on signals composed of N carriers
[CNES-NT-105] 04 p0496 N85-13167
Comprehensive silicon solar cell computer modeling
[NASA-CR-174151] 04 p0530 N85-13386
Regional-scale (1000 KM) model of photochemical air pollution. Part 2: Input processor network design
[PB84-232651] 04 p0532 N85-13400
Measurement of range-resolved water vapor concentration by coherent CO2 differential absorption lidar
[PB84-236892] 04 p0535 N85-13420
Development and verification of MCD-2 and MOD-OA simulation models
[DE84-017389] 04 p0550 N85-13499
Evaluation of automated decisionmaking methodologies and development of an integrated robotic system simulation
[NASA-CR-172401] 04 p0552 N85-13516
Preliminary user's guide for BIGONE on the Cray
[DE84-017075] 04 p0568 N85-13623
Dynamic decision making --- and programming
[FOA-C-53015-H2] 04 p0575 N85-13668
Numerical simulations of fission 04 p0585 N85-13737
Simulation of separated transonic airfoil flow by finite-difference viscous-inviscid interaction 05 p0591 N85-13768
Boundary layer simulator improvement
[NASA-CR-174199] 05 p0597 N85-13802
Level of effort 05 p0602 N85-13839
Elimination of uncontrollable rigid body mode, appendix C 05 p0603 N85-13842
Simulation of the interaction of single-pulsed optical lasers with targets in a vacuum
[DE84-016476] 05 p0640 N85-14107
MC2969 escapement study
[DE84-014542] 05 p0645 N85-14143
Improving the Spacelab mass memory unit tape layout with a simulation model
[NASA-TM-86483] 05 p0713 N85-14571
High-efficiency solar-cell design modeling 06 p0829 N85-15262
Probable maximum flood estimation - Eastern United States
[AD-A146536] 06 p0839 N85-15324
Sigma code testing
[AD-A146548] 06 p0841 N85-15340
Translational control of a graphically simulated robot arm by kinematic rate equations that overcome elbow joint singularity
[NASA-TP-2376] 06 p0856 N85-15446
Large-eddy simulation. Guidelines for its application to planetary boundary layer research
[AD-A146381] 06 p0890 N85-15651
A Q-GERT network simulation model for examining pipeline time in the Navy's J-52 intermediate level jet engine repair cycle
[AD-A147269] 07 p0894 N85-15663
On the generation of random variables for radar simulation purposes 07 p0938 N85-15947
An interactive FORTRAN program for determining reliability of pseudo-range geodetic point positioning using the global positioning system
[AD-A147133] 07 p0988 N85-16275
Experiments in forecasting atmospheric marine horizontal visibility using model output statistics with conditional probabilities of discretized parameters
[AD-A147574] 07 p1008 N85-16404
Interaction of human cognitive models and computer based models in supervisory control
[AD-A142547] 07 p1020 N85-16474
Convection schemes for use with curvilinear coordinate systems: A survey
[AD-A147093] 07 p1031 N85-16543
A simulation model for Air Launched Cruise Missile engine management
[AD-A147018] 07 p1051 N85-16672
Computer sizing of fighter aircraft
[NASA-TM-86351] 08 p1067 N85-16759
Development of a Helicopter integrated navigation system 08 p1073 N85-16802
A Generalized Escape System Simulation (GESS) computer program. Volume 2: GESS programmer's manual, version 2
[AD-A148363] 08 p1081 N85-16845
Space shuttle main engine hardware simulation 08 p1091 N85-16895
Managing computer-controlled operations 08 p1097 N85-16934
The Communications link analysis and simulation system (CLASS) 08 p1100 N85-16952
Modeling techniques used in the communications link analysis and simulation system (CLASS) 08 p1100 N85-16953
Numerical simulation of the shock detonation transition 08 p1116 N85-17039
Satellite broadcasting: The performance of C-MAC in a hardware simulation of a DBS transmission chain
[BBC-RD-1984/9] 08 p1143 N85-17206
The extension of an invertible coniferous forest canopy reflectance model using SIR-B and LANDSAT data 08 p1149 N85-17246
Characterization of jet-contaminant interaction flow in chemical decontamination
[AD-A147298] 08 p1161 N85-17327
The value and utility of inflight onboard simulation
[AD-A148033] 08 p1198 N85-17543
Exposure modelling of particle beam lithography
[AD-A147849] 08 p1219 N85-17678
SIMM1: A linearized particle code
[AD-A148627] 08 p1221 N85-17689
Supermaneuverability
[AD-P004153] 09 p1263 N85-17938
The IMAGE 3 Conference Proceedings
[AD-A148636] 09 p1267 N85-17962
Geographic subdivision and top level data structures, Columbus, Magellan, and expanding CIG (Computer Image Generation) horizons
[AD-P004317] 09 p1268 N85-17971
CIG (Computer image generation) data bases in an instance: Bits and pieces
[AD-P004318] 09 p1269 N85-17972
The generation of three-dimensional data bases using a building block approach
[AD-P004319] 09 p1269 N85-17973
Control systems analysis program: A tool for analysis of the GE-VSCDP (General Electric-Visual System Component Display Program) image display system
[AD-P004325] 09 p1270 N85-17979
Air combat visual simulation using a head slaved projector
[AD-P004327] 09 p1270 N85-17981
The fiber-optic helmet-mounted display
[AD-P004330] 09 p1270 N85-17984
Baffled eye and confounded brain or using visual illusions to train blind pilots
[AD-P004332] 09 p1271 N85-17986
On-board Computer Image Generator (CIG) applications
[AD-P004335] 09 p1271 N85-17989
CIG (Computer Image Generator) goes to war: The tactical illusion
[AD-P004336] 09 p1271 N85-17990

AVTS (Advanced Visual Technology System): A high fidelity visual simulator
[AD-P004338] 09 p1271 N85-17992
An analytic model of gas turbine engine installations
[AD-A148708] 09 p1281 N85-18059
Study of bridgewire size and pyrotechnic density relationships on all-fire levels
[DE84-016946] 09 p1302 N85-18177
Simulation in the design of gas pressure control equipment
[ERS-E.352] 09 p1324 N85-18322
Simulation of repetitively-pulsed laser irradiation of graphite-epoxy composite
[AD-A148698] 09 p1325 N85-18329
Comparing computing formulas for estimating concentration ratios
[DE84-006844] 09 p1349 N85-18480
Identification of emerging designer needs and high payoff CAE tools
[DE85-000755] 09 p1369 N85-18599
The use of simulation for the technical and economic evaluation of flexible manufacturing systems. Part 2: Results of the simulation
[PNR-90233-PT-2] 09 p1371 N85-18614
Issues in sensitivity and statistical analysis of large-scale, computer-based models
[PB85-116317/GAR] 09 p1376 N85-18650
Calculation and computer simulation of the Paraboloidal Mirror Analyzer (PMA)
[DE85-001417] 09 p1384 N85-18705
Simulation of bent crystal spectrometers
[DE85-002042] 09 p1385 N85-18709
Computational plasma physics and supercomputers
[DE85-001739] 09 p1393 N85-18766
Computer simulation of multiple stability regions in an internally cooled superconducting conductor and of helium replenishment in a bath-cooled conductor
[DE85-002112] 09 p1399 N85-18805
Dynamic simulation of track laying vehicles
[AD-P004266] 09 p1405 N85-18842
Numerical simulations of liquid propellant combustion instability: Onset and growth
[DE85-000743] 10 p1458 N85-19186
Simulation of the performance of adaptively controlled Navstar antennas in battlefield scenarios
10 p1472 N85-19292
A shock wave capability for the improved Two-Dimensional Kinetics (TDK) computer program
[NASA-CR-171302] 10 p1483 N85-19360
Mechanical interactions of rough surfaces
[DE85-000814] 10 p1494 N85-19434
Distributing a distributed problem solving network simulator
[AD-A149065] 10 p1537 N85-19693
Microprocessor-based monitoring and control project, phase 1
[DE84-901974] 10 p1538 N85-19699
Interactive Graphics Simulator: Design, development and effectiveness/cost evaluation
[AD-A149417] 10 p1540 N85-19712
Regenerative structure of Markov chains simulated via common random numbers
[AD-A149092] 10 p1550 N85-19777
Optical implementation of the synthetic discriminant function
[AD-A149562] 10 p1557 N85-19817
Some investigations of molecular beam epitaxial growth of 3-5 semiconductor films via Monte-Carlo computer simulations, carrier tunneling and spectroscopic ellipsometry
[AD-A149465] 10 p1563 N85-19854
Application of Monte Carlo and molecular dynamics methods to the calculation of thermodynamic properties of molten salts
[AD-A148897] 10 p1565 N85-19869
Wildlife Hazards to Aircraft Conference and Training Workshop: Proceedings
[AD-A148330] 11 p1578 N85-19936
Shock propagation in the exhaust gas handling system of the proposed large altitude rocket cell: Methods and preliminary analysis
[DE85-003055] 11 p1591 N85-20010
Distribution of hydrogen in multi-layer welded joints of alloyed steels 11 p1603 N85-20079
Effect on work-hardening in dynamic deformation of beryllium
[DE85-002691] 11 p1608 N85-20111
Acta Electronica Sinica (selected articles)
[AD-A148829] 11 p1628 N85-20252
Three-dimensional analysis of heat transfer and gas flow in a radiant furnace
[DE84-011732] 11 p1633 N85-20284
Neutron streak camera electron gun design
[DE85-000620] 11 p1637 N85-20315
A computerized study of rigid cones penetrating aluminum targets
[FOA-C-20561-D4] 11 p1648 N85-20384
Simulation of brittle fracture via molecular dynamics
[DE85-001061] 11 p1653 N85-20410
Influence of the atmosphere on remotely sensed reflection from vegetation surfaces
[DE85-000658] 11 p1670 N85-20521
Performance of the SERI parallel-passage dehumidifier
[DE85-000509] 11 p1672 N85-20536
Digital and color energy maps for graphic display of hourly data
[DE85-000526] 11 p1673 N85-20543
Envelope thermal test unit: Technical description
[DE84-012254] 11 p1674 N85-20548
Continued research in mesoscale air pollution simulation modeling. Volume 5: Refinements in numerical analysis, transport, chemistry, and pollutant removal
[PB85-137362] 11 p1680 N85-20585
Evaluation of two numerical integrator schemes
[PB85-138196] 11 p1683 N85-20603
BIT/BITE tradeoff analysis model
[AD-A149345] 11 p1701 N85-20697
Advanced concepts in systems analysis and simulation
[DE85-002728] 11 p1702 N85-20701
Computerized study of several electrostatic, surface-ionization ion-source configurations
[DE85-001512] 11 p1721 N85-20823
Self-Optimized Sector (SOS) model of self-consistent energy loss and scattering for an electron beam propagating in air
[DE85-003161] 11 p1722 N85-20831
Aperture studies with PATRICIA and RACETRACK on simple attices containing SSC dipoles
[DE85-004163] 11 p1724 N85-20842
Computer simulation of grain-boundary properties in ionic crystals and metals
[DE85-000577] 11 p1734 N85-20908
Simulating supersymmetry at the SSC
[DE85-000699] 11 p1736 N85-20917
Hydrodynamic simulations of recurrent novae
11 p1753 N85-21025
Deflection model of a CT4-A undercarriage
[AD-A149778] 12 p1777 N85-21156
A safety evaluation of the relocation of the ACM (Air Combat Maneuver) panel in the F-14 ( )/AIP (Avionics Integration Program)
[AD-A149596] 12 p1777 N85-21158
Field validation of statistically-based acceptance plan for bituminous airport pavements. Volume 4: Computer simulation of multiple acceptance criteria
[FAA-PM-84-12-VOL-4] 12 p1782 N85-21183
Field validation of statistically-based acceptance plan for bituminous airport pavements. Volume 5: Summary of validation studies
[FAA-PM-84-12-VOL-5] 12 p1782 N85-21184
Impacts of Space Shuttle thermal protection system tile on F-15 aircraft vertical tile
[NASA-TM-85904] 12 p1792 N85-21245
A computer simulation of thin film nucleation and growth: The Volmer-Weber case
[NASA-TM-86966] 12 p1796 N85-21264
Near-field effects on radome boresight errors
[AD-P004356] 12 p1825 N85-21450
Nickel-cadmium battery cell reversal from resistive network effects
[AD-A149626] 12 p1834 N85-21505
Concurrent simulation techniques exploiting hierarchy
[AD-A149783] 12 p1835 N85-21512
Distributed Gunn effect devices; a numerical analysis of microstrip circuits on thin active GaAs substrates
[FOA-C-30383-E] 12 p1837 N85-21527
Computer simulation of equipment and processes involved in high-frequency heating of dielectrics
12 p1841 N85-21555
Modeling of transient heat pipe operation
[NASA-CR-175496] 12 p1844 N85-21571
Experimental test of the three subaperture method for estimating largst elevation angle
[AD-A149687] 12 p1851 N85-21614
On local total strain redistribution using a simplified cyclic inelastic analysis based on an elastic solution
[NASA-TM-86913] 12 p1864 N85-21690
Computer analysis of wind turbine blade dynamic loads
[DE85-000530] 12 p1867 N85-21714
Numerical simulation of static and dynamic shadow patterns using an atomistic description of crack initiation and propagation
[DE85-003226] 12 p1867 N85-21715
A linear characteristic-nodal transport method for the two-dimensional (X,Y)-geometry multigroup discrete ordinates equations over an arbitrary triangle mesh
[LA-10092-T] 12 p1913 N85-22008
The automated reasoning system ITP
[ANL-84-27] 12 p1914 N85-22016
A user's guide to sensitivity testing on computer models at Los Alamos National Laboratory
[LA-10104-M] 12 p1914 N85-22018
SIMULA: Digital controller simulation package
[PB85-134492] 12 p1917 N85-22041
Theoretical study of collective ion acceleration in the Luce diode
[AD-A150107] 12 p1929 N85-22116
Simulation of space charge effects in particle accelerators
[DE85-001828] 12 p1929 N85-22120
Electron image simulation: A complementary processing technique
[DE85-000685] 12 p1941 N85-22190
Computational mechanics: A perspective on problems and opportunities for increasing productivity and quality of engineering
[PB85-128106] 12 p1950 N85-22252
Space shuttle pilot-induced-oscillation research testing
13 p1966 N85-22351
Dynamic wind tunnel testing for active control research 13 p1966 N85-22352
Algorithm for determining optimal three impulse point-to-orbit transfer with limited transfer time
13 p1979 N85-22419
Three-dimensional calculation of shuttle charging in polar orbit 13 p1992 N85-22486
Self-consistent simulation of plasma interactions with secondary-emitting insulators 13 p1993 N85-22492
NASCAP simulation of PIX 2 experiments
13 p1993 N85-22497
Development of a three-phrase combustion code for modeling liquid rocket engines 13 p2003 N85-22554
Method for prompt modeling of quasiperiodic movement of solid near-axisymmetrical body in atmosphere
13 p2043 N85-22790
Research efforts in support of resonance extraction studies. Volume 1: Improvement and validation of TWFD (Thin-Wire Frequency-Domain): A thin-wire frequency-domain scattering code
[AD-A150296] 13 p2054 N85-22864
Advanced mixed-mode simulation techniques
13 p2062 N85-22883
Investigations of the high frequency performance of impact avalanche transit-time diodes
13 p2063 N85-22884
Numerical simulation of inverters with I2L elements including effects of high doping level
13 p2068 N85-23039
T700 cutter life improvement program
[AD-A150450] 13 p2089 N85-23089
Effects of assuming independent component failure times, if they are actually dependent, in a series system
[AD-A150582] 13 p2101 N85-23062
Structural design of the Sandia 34-M Vertical Axis Wind Turbine
[DE85-002831] 13 p2129 N85-23247
ROSA: A computer model for optical power ratio calculations
[DE85-005174] 13 p2129 N85-23251
Molten carbonate fuel cell performance model update, draft
[DE85-005423] 13 p2129 N85-23252
ROSS: An object-oriented language for constructing simulations
[AD-A150556] 13 p2147 N85-23330
SIGPI: A user's manual for the fast computation of the probabilistic performance of a complex system
[DE85-005447] 13 p2148 N85-23336
Regenerative simulation of non-Markovian stochastic systems
[AD-A150344] 13 p2153 N85-23367
Accumulation of the terrestrial planets
13 p2179 N85-23524
A parmetric study of crater-saturation simulation
13 p2182 N85-23540
Load capacity of cages of roller bearings for planet wheels 14 p2221 N85-23775
Shuttle attached antenna Flight Experiment Definition Study (FEDS) 14 p2237 N85-23985
Diesel combustion: Advances in analysis and simulation 14 p2253 N85-23995
Computer simulations of rare earth sites in glass: Experimental tests and applications to laser materials
[DE85-006158] 14 p2261 N85-24013
Multidimensional digital signal processing
[AD-A150833] 14 p2292 N85-24209
Ground-up-to-Space (GUTS) laser propagation code description and manual
[AD-A150783] 14 p2309 N85-24295
Modeling of photodegradation in solar cell modules of substrate and superstrate design made with ethylene-vinyl acetate as pottant material
[NASA-CR-175690] 14 p2350 N85-24527

Theory and computer simulation of auroral kilometric radiation 14 p2365 N85-24617
Characteristics and behavior of atmospheric aerosols; application to prediction of infrared extinction
[AD-A150691] 14 p2372 N85-24665
GRAFIT language for simulating two-dimensional geometric entities and sketches
14 p2401 N85-24801
A numerical simulation of the formation of solar prominences 14 p2448 N85-25112
Automatic Dynamic Aircraft Modeler (ADAM), volume 1
[AD-A151410] 15 p2471 N85-25252
A user's manual for AMEER flight path trajectory simulation code
[DE85-006580] 15 p2472 N85-25260
Shuttle fleet operations: A simulation analysis
[AD-A151383] 15 p2491 N85-25370
The investigation of tethered satellite system dynamics
[NASA-CR-171433] 15 p2492 N85-25375
Analysis of space station operations in the space debris environment
[AD-A151872] 15 p2493 N85-25380
Numerical experiments on flexible spacecraft with the aid of the Dynamic Control and Analysis Package (DCAP)
[ESA-STM-229] 15 p2493 N85-25382
The effects of atmospheric turbulence on an air-to-air optical communication link
[AD-A151840] 15 p2543 N85-25700
CSMP (Continuous System Modeling Program) modeling of brushless DC motors
[AD-A152043] 15 p2549 N85-25731
Development of simulation procedures for VLSI systems (timing simulation)
[BMFT-FB-T-84-297] 15 p2550 N85-25743
Modeling and optimization of a multiple-cell photovoltaic converter system 15 p2585 N85-25934
Impact of soil moisture in organizing a severe storm outbreak 15 p2597 N85-26009
General meteorological package (GEMPAK)
15 p2599 N85-26019
Computer simulation studies in fluid and calcium regulation and orthostatic intolerance
[NASA-CR-171869] 15 p2616 N85-26117
Analysis of head-down tilt as an analog of weightlessness using a mathematical simulation model
[NASA-CR-171870] 15 p2616 N85-26118
Simulation of a G-tolerance curve using the pulsatile cardiovascular model
[NASA-CR-171873] 15 p2616 N85-26120
Mathematical models relating to human thermoregulation: Basic assumptions, validation, and application. Parts A and B
[AD-A151556] 15 p2618 N85-26130
Research in the design of high-performance reconfigurable systems
[NASA-CR-175705] 15 p2621 N85-26153
Development of a user support package for CPESIM 2 (a computer simulation for CPE (Computer Performance Evaluation) use
[AD-A151899] 15 p2624 N85-26170
CAD/CAM (Computer-Aided Design/Computer-Aided Manufacturing) highlights
[AD-A151532] 15 p2629 N85-26201
Catalog of the National Energy Software Center
[TI85-900521] 15 p2630 N85-26209
Backbone network simulations: A comparative study
[DE85-006874] 15 p2632 N85-26224
The modeling and simulation of feedback control systems
[NASA-CR-171875] 15 p2632 N85-26225
High current beam hollowing instability study
[AD-A151301] 15 p2648 N85-26329
Low-resolution target classification from a staring infrared sensor
[AD-A151690] 15 p2652 N85-26356
Lattice overview
[DE85-007282] 15 p2662 N85-26427
The formation of the terrestrial planets from lunar sized planetesimals 15 p2678 N85-26533
Galileo 15 p2688 N85-26601
Numerical simulation of inviscid compressible flow through three-dimensional cascade
16 p2692 N85-26619
Numerical simulation of transonic flutter of a high-aspect ratio transport wing 16 p2694 N85-26630
Graphic simulation of a machine-repairman model
[AD-A151761] 16 p2694 N85-26633
Simulation: A tool for cost-effective systems design and live test reduction 16 p2696 N85-26657
Generalized escape system simulation: Its purpose, recent modifications and potential
[DE85-005571] 16 p2703 N85-26689
Study of the primary zone of gas turbine hearths
[ONERA-RTS-22/3256-EY] 16 p2709 N85-26719
The effect of load factor on aircraft handling qualities
[AD-A152118] 16 p2710 N85-26724
Probabilistic computer model of optimal runway turnoffs
[NASA-CR-172549] 16 p2715 N85-26760
A SLAM II simulation model for analyzing space station mission processing requirements
[NASA-CR-175664] 16 p2731 N85-26853
Ignition/combustion processes
16 p2740 N85-26909
Liquid rocket combustor computer code development
16 p2740 N85-26910
Laser Schlieren and ultraviolet diagnostics of rocket combustion 16 p2740 N85-26911
Influence of behavior laws in the explosive deformation of metal plates
[ISL-R-122/83] 16 p2760 N85-27032
Automated CPX support system preliminary design phase
[NASA-CR-175784] 16 p2769 N85-27091
A software simulation study of a sequential decoder using the Fano algorithm 16 p2771 N85-27100
An empirical self-protection chaff model
[AD-A151928] 16 p2773 N85-27115
Radiation and scattering of spiral antennas
[AD-A151929] 16 p2773 N85-27116
Pulsewidth modulated speed control of brushless dc motors
[AD-A151966] 16 p2778 N85-27148
Electrical resistivity in amorphous metals: Consequences of phonon ineffectiveness in the diffraction model
[AD-A152130] 16 p2779 N85-27150
Computer modeling of vibrational energy levels of potential laser candidates (diatomic molecules)
[AD-A151785] 16 p2790 N85-27209
A general simulation program for robot manipulator arm dynamics
[AD-A152121] 16 p2793 N85-27230
Numerical resolution calculation for elastic-plastic impact problems
[AD-A152292] 16 p2801 N85-27270
Hopkinson bar simulation using DYNA2D
[DE85-006766] 16 p2802 N85-27275
Diagnostic system
[INPE-3950-PRE/659] 16 p2841 N85-27519
A multipole model of the observed cerebral cortex magnetic field
[AD-A152237] 16 p2842 N85-27526
Parallel time 0(log N) acceptance of deterministic CFLs
[AD-A152255] 16 p2845 N85-27539
An interactive computer package for use with simulation models which performs multidimensional sensitivity analysis by employing the techniques of response surface methodology
[AD-A151956] 16 p2846 N85-27548
Development of graphical pole-zero, root-locus, Bode, Nyquist, and Nichols responses using the OPTSYSX program
[AD-A152148] 16 p2847 N85-27555
Kinematic rate control of simulated robot hand at or near wrist singularity
[NASA-TP-2440] 16 p2851 N85-27575
The NAVTAG (Naval Tactical Game) system and its modification to include the SH-60B helicopter
[AD-A152004] 16 p2858 N85-27624
LIGHT: A ray tracing code to simulate light collection in scintillation spectrometers and light pipes
[DE85-007213] 16 p2865 N85-27673
Optimizing computational efficiency and user convenience in plasma simulation codes
[DE85-007661] 16 p2866 N85-27682
Fundamentals of plasma simulation
[DE85-007699] 16 p2867 N85-27683
Tokamak systems code
[DE85-008147] 16 p2869 N85-27696
Electronic density of states for the double donor system Si:P, As
[INPE-3447-PRE/700] 16 p2869 N85-27700
Addition of flexible body option to the TOLA computer program. Part 2: User and programmer documentation
[NASA-CR-132732-2] 17 p2896 N85-27856
OLGA: An open loop gust alleviation system
17 p2903 N85-27897
Simulation of multistage turbine flows
17 p2911 N85-27945
Calculation of viscous compressible flows in small gas turbines 17 p2912 N85-27950
Stressed-strained state of tightening buckles in sectional runners of gas turbines 17 p2940 N85-28149
Performance evaluation of fiber-optic converters
17 p2941 N85-28154
A software simulation study of a (255,223) Reed-Solomon encoder-decoder
[NASA-CR-175872] 17 p2947 N85-28192
Analysis and modeling for thermal focal plane arrays
[AD-A153156] 17 p2968 N85-28329
System analysis of a field Army Topographic Support System
[AD-A153318] 17 p2984 N85-28439
Comparison of measurement and simulation results of radiation temperatures applied to the thermal mapping of Munich
[DFVLR-FB-85-06] 17 p2984 N85-28442
Simplified analysis of Stirling engines and heat pumps
[DE85-008753] 17 p2986 N85-28457
Comprehensive silicon solar cell computer modeling
[NASA-CR-175950] 17 p2987 N85-28461
Performance of an active/passive hybrid solar system utilizing vapor transport
[DE85-008627] 17 p2988 N85-28466
A crustal section for the Arabian Shield and adjacent Red Sea margin derived from first-arrival data
17 p2990 N85-28480
A seismic refraction profile across the Arabian Shield
17 p2990 N85-28481
Technical evaluation of the Naval Automated Pilot Aptitude Measurement System (NAPAMS)
[AD-A152361] 17 p3000 N85-28547
Computer program for prediction of capture maneuver probability for an on-off reaction controlled upper stage
[NASA-CR-165937] 17 p3010 N85-28611
Manufacturing information system
[AD-A152715] 17 p3011 N85-28616
VULTURE manual
[DE85-008873] 17 p3013 N85-28631
Adding computationally efficient realism to Monte Carlo turbulence simulation
[NASA-TP-2469] 17 p3025 N85-28708
Operations research
[B8561897] 17 p3026 N85-28712
Theoretical studies of heavy ion scattering processes
[DE85-008823] 17 p3032 N85-28753
Multiple time-scale methods in particle simulations of plasmas
[DE85-007519] 17 p3040 N85-28808
Experimental and theoretical determination of the wing-induced lateral wind on the tail surfaces in oscillating rolling motion. Part 2: Theoretical investigations for calculation of the lateral wind
[IFD-1/84-PT-2] 18 p3061 N85-28940
DEAN: A program for dynamic engine analysis
[NASA-TM-87033] 18 p3062 N85-28945
Compressor and turbine models - numerical stability and other aspects
[AD-A153611] 18 p3063 N85-28946
Piloted simulation of an algorithm for onboard control of time-optimal intercept
[NASA-TP-2445] 18 p3063 N85-28949
An approach to digital level compression using the zero-crossing points of programme signals
[NHK-LABS-NOTE-308] 18 p3090 N85-29123
A simulation study of jammer nulling trade-offs in a reactively steered adaptive array
[AD-A153461] 18 p3090 N85-29124
Electrical line source and point source interactions with anomalies in the ground
[DE85-009777] 18 p3095 N85-29161
Visual simulation of radiographs
[DE85-010213] 18 p3110 N85-29255
KIVA: A comprehensive model for 2D and 3D engine simulations
[DE85-005562] 18 p3118 N85-29298
Establishment of a methodology for predicting lifetimes in active solar systems
[DE85-008629] 18 p3130 N85-29383
F-cell: The Aspen fuel cell model
[DE85-001975] 18 p3131 N85-29393
Materials research for passive solar systems: Solid-state phase-change materials
[DE85-008779] 18 p3132 N85-29395
On the improvement of satellite temperature retrievals by means of boundary layer models
18 p3140 N85-29443
Transient eddies in the UCLA GCM
18 p3145 N85-29470
Analysis of a simulated cloud climatology
18 p3145 N85-29472
An operational analysis of system calibration
[AD-A153556] 18 p3170 N85-29644
Fast electromagnetic (EM) shower simulation
[NOTA-INTERNA-831] 18 p3175 N85-29663
An experimental study of the pressure in a fast bottom beneath the apex of an overlying fluid wedge
[AD-A153618] 18 p3177 N85-29696
Calculations of beam dynamics in Sandia linear electron accelerators, 1984
[DE85-010417] 18 p3180 N85-29719

Circulation control propellers for general aviation, including a BASIC computer program
[NASA-CR-165968] 19 p3219 N85-29959
Computer simulation of the effects of a distributed array antenna on synthetic aperture radar images
[NASA-CR-171868] 19 p3254 N85-30176
Approaches to digital image registration and recognition 19 p3257 N85-30197
Dynamic simulation of dispersed, grid-connected photovoltaic power systems: System studies
[DE85-011179] 19 p3262 N85-30231
An investigation of hydraulic transients in combination free surface and pressurized flows 19 p3264 N85-30239
Seismic analysis of liquid-filled tanks with an eccentric core barrel
[DE85-010249] 19 p3269 N85-30272
Modeling and analysis of pinhole occulter experiment: Initial study phase
[NASA-CR-175978] 19 p3272 N85-30287
Flood-runoff forecasting with HEC1F
[AD-A154286] 19 p3300 N85-30456
Modeling water resources systems for water quality
[AD-A154288] 19 p3300 N85-30457
A multiphase continuum model to describe dynamic loading effects in nonlinear porous media
[DE85-010102] 19 p3301 N85-30483
Reference data source documentation for performance assessment studies, Basalt Waste Isolation Project, Hanford Site, Washington
[DE85-010543] 19 p3301 N85-30488
Using PVFORM, a systems performance model, to determine optimum mounting configurations for flat-plate photovoltaic modules
[DE85-011191] 19 p3306 N85-30495
F-CAP documentation
[DE85-003369] 19 p3307 N85-30503
Qualitative and quantitative examination of the performance of regional air quality models representing different modeling approaches
[DE85-010508] 19 p3310 N85-30518
Synthetic rainfall and its use in hydrologic modeling 19 p3314 N85-30542
Arctic acoustic tomography MIZEX 84
[AD-A154428] 19 p3320 N85-30580
Activities of the Institute for Computer Applications in Science and Engineering (ICASE)
[NASA-CR-172610] 19 p3332 N85-30641
CAE tool catalog
[DE85-011290] 19 p3334 N85-30657
Preliminary documentation for the polar code
[AD-A154125] 19 p3336 N85-30667
Computer Performance Modeling Tool (CPMT)
[AD-A154438] 19 p3338 N85-30682
Circular-beam ray tracing on a microcomputer
[DE85-010754] 19 p3338 N85-30685
SABRINA: An interactive solid geometry modeling program for Monte Carlo
[DE85-010796] 19 p3339 N85-30692
A Lotus 1-2-3 based system reliability program
[DE85-010533] 19 p3340 N85-30701
LINE: A code which simulates spectral line shapes for fusion reaction products generated by various speed distributions
[DE85-010633] 19 p3341 N85-30702
Development and evaluation of a Fault-Tolerant Multiprocessor (FTMP) computer. Volume 3: FTMP test and evaluation
[NASA-CR-166073] 19 p3341 N85-30707
Expanding expertise by use of an expert system
[DE85-010759] 19 p3344 N85-30723
Comparison of simulation with experiment in an RFQ
[DE85-010770] 19 p3349 N85-30757
Comparison of 8 to 12 micrometer and 3 to 5 micrometer CVF transmissometer data with LOWTRAN calculations
[AD-A154218] 19 p3350 N85-30763
Moments in particle-in-cell simulations
[DE85-010792] 19 p3356 N85-30803
A model for the economic assessment of solar power plants
[DE85-009355] 19 p3381 N85-30977
Description and operation of CHISQMO, INVRTS, VOIGEN, VOIGTV, SMEAR, RUFF, AND POSCAR in the Stokes Analysis Program
[PB85-180628] 19 p3384 N85-30991
Numerical simulation of potential flow in transonic steady regimes 20 p3389 N85-31016
Analysis of rotorcraft crash dynamics for development of improved crashworthiness design criteria
[FAA-CT-85-11] 20 p3391 N85-31031
Definition and layout of a traffic generator for an air traffic control simulation
[ESA-TT-868] 20 p3391 N85-31034
Search and rescue satellite (SARSAT) error analysis of the 406 MHz system 20 p3403 N85-31118
Docking simulation analysis of range data requirements for the orbital maneuvering vehicle
[NASA-TM-86510] 20 p3407 N85-31143
Large space structure flight experiment 20 p3410 N85-31163
A structural dynamics approach to the simulation of spacecraft control/structure interaction 20 p3412 N85-31173
Solid state altimeter model: Simulation description; analysis of first results (narrow band filters, weighting) --- satellite-borne instruments
[CNES-DRT/TIT/RL-160-T] 20 p3419 N85-31220
Comparison of ERS-1 scatterometer Monte Carlo performance simulations using a weighted nonlinear least squares and a maximum likelihood estimation method 20 p3420 N85-31224
Flow modeling at the base region of missiles
[SNIAS-851-320-101] 20 p3420 N85-31226
The use of moments of momentum to account for crystal habits
[NASA-CR-3907] 20 p3421 N85-31232
Fundamental algorithms of the Goddard battery model 20 p3445 N85-31389
Nickel-cadmium battery cell reversal from resistive network effects 20 p3446 N85-31392
High Re separated flow solutions using the Navier-Stokes and approximate equations
[AD-A152252] 20 p3454 N85-31451
Environmental airblast around large shock tubes
[DE85-010654] 20 p3483 N85-31512
Investigation of dynamic noise affecting geodynamics information in a tethered subsatellite
[NASA-CR-176031] 20 p3476 N85-31602
Comparative study of fracture planes computed from topography and lineaments from imagery with structures and mineralization in the magnetic belt of Washington State
[DE85-010972] 20 p3477 N85-31608
Application of closed-form solutions to a mesh point field in silicon solar cells 20 p3482 N85-31637
Phenomena simulation for heavy doping and surface recombination velocity 20 p3482 N85-31638
Design and fabrication of durable owner-built wind turbine blades
[DE85-009200] 20 p3484 N85-31650
Results of computer calculations for a simulated distribution of kidney cells 20 p3502 N85-31771
A systems analysis of the erythropoietic responses to weightlessness. Volume 2: Description of the model of erythropoiesis regulation. Part A: Model for regulation of erythropoiesis. Part B: Detailed description of the model for regulation of erythropoiesis
[NASA-CR-171891] 20 p3506 N85-31795
An integrated analysis of the physiological effects of space flight: Executive summary
[NASA-CR-171892] 20 p3506 N85-31796
Learning and self adaptation applied to the simulation of a human pilot
[ONERA-RT-24/5122-SY] 20 p3511 N85-31828
SCAP: A Shaped Charge Analysis Program. User's manual for SCAP 1.0
[DE85-011182] 20 p3515 N85-31854
Model documentation of the gas analysis modeling system. Volume 1: Model overview
[DE85-010952] 20 p3515 N85-31856
MIG: MCNP Input Generator for EFFI magnet geometries
[DE85-010494] 20 p3515 N85-31857
Monte Carlo: In the beginning and some great expectations
[DE85-010789] 20 p3518 N85-31872
FAUST: Introduction and overview --- self tuning control
[OUEL-1568/85] 20 p3519 N85-31882
Methods of Monte Carlo electron transport in particle-in-cell codes
[DE85-010702] 20 p3521 N85-31898
Simulation studies of time-control procedures for the advanced air traffic control system
[NASA-TP-2493] 21 p3553 N85-32101
Development and validation of a general purpose linearization program for rigid aircraft models
[NASA-TM-86737] 21 p3556 N85-32122
Numerical modeling of subsurface communication
[DE85-012818] 21 p3577 N85-32249
Parallel simulation of digital LSI circuits
[AD-A154745] 21 p3580 N85-32258
BLAF: A blast field reconstruction program from pressure histories
[AD-A155300] 21 p3585 N85-32283
Characteristics of a numerical fluid dynamics simulator
[DE85-009802] 21 p3586 N85-32290
An investigation into the comparisons of the underwater shock effects on a stiffened flat plate to the predictive nature of a computer model
[AD-A155612] 21 p3600 N85-32355
Micromolecular modeling 21 p3608 N85-32405
Comprehensive silicon solar-cell computer modeling 21 p3609 N85-32421
Emergency modeling of hazardous air pollutants
[AD-A155441] 21 p3614 N85-32461
Simulation of complex three-dimensional flows
[NASA-TM-86773] 21 p3675 N85-32831
SHELTER: Description of a program code --- indoor climate
[FOA-C-58002-H1] 22 p3755 N85-33278
Modeling of electronic circuits with high degree of component integration 22 p3766 N85-33343
Adaptive modeling of electronic circuits 22 p3766 N85-33345
Computer simulation of integrated injection logic 22 p3767 N85-33349
Numerical simulation of nonisothermal transient processes in GaAs diode structures 22 p3767 N85-33350
Determination of sensitivity functions for discrete dynamic systems from results of function modeling on digital computer 22 p3769 N85-33359
Analysis of crosstalk in nonhomogeneous multiconductor lines 22 p3769 N85-33360
Calculation of external magnetic field of a shielded transformer 22 p3771 N85-33373
Computer and water-model simulation of flow through poppet valves
[CFD/85/2] 22 p3785 N85-33449
Lasertron simulation with a two-gap output cavity
[DE85-011213] 22 p3790 N85-33480
Development of a chemical kinetic mechanism for the US EPA (Environmental Protection Agency) regional oxidant model
[PB85-185858] 22 p3813 N85-33618
Surface wave modes of a multilayered medium backed by a perfectly conducting ground plane: Computation of propagation constants
[DE85-011454] 22 p3829 N85-33715
Determination of DTL configurations
[DE85-010714] 22 p3830 N85-33719
PMEXA: Diagnostic filtering program for the PBFA-1 performance monitoring and evaluation system
[DE85-013179] 22 p3831 N85-33725
Numerical simulation of interior and terminal ballistics phenomena. Investigation of the effects of the parameters and application examples
[ISL-R-112/84] 22 p3831 N85-33731
Some ideas for decomposing the domain of elliptic partial differential equations in the Schwarz process
[DE85-011844] 22 p3834 N85-33739
Presentation of numerical simulation work in terminal ballistics using a few examples. Applications of the calculation model Program for Elastoplastic Simulation of Impacts (PEPSI) of the Franco-German Research Institute Saint Louis (ISL)
[ISL-CO-209/84] 22 p3834 N85-33741
Transverse emittance of a 2.0-MeV RFQ beam with high brightness
[DE85-012718] 22 p3837 N85-33758
Long term variability of the cosmic ray intensity
[OG-3.1-11] 22 p3874 N85-33999
Transient two-dimensional simulation of SEU in a CMOS SRAM cell
[DE85-008419] 22 p3890 N85-34111
Time-resolved spectroscopic studies of detonating heterogeneous explosives
[DE85-009760] 23 p3921 N85-34297
Method and apparatus for transfer function simulator for testing complex systems
[NASA-CASE-NPO-15696-1] 23 p3926 N85-34333
Compressible two-phase flow instabilities simulated with a hybrid Lagrange-Euler pseudospectral method
[DE85-009904] 23 p3931 N85-34361
The impact of supercomputers on experimentation: A view from a national laboratory
[NASA-TM-86822] 23 p3955 N85-34510
System maintenance manual for master modeling of aerodynamic surfaces by three-dimensional explicit representation
[NASA-CR-178224] 23 p3956 N85-34517
Frame buffer algorithms for stochastic models 23 p3957 N85-34525
Specifying stochastic objects in a hierarchical graphics system 23 p3957 N85-34526
Interfacing interactive circuit simulation with standard graphics facilities 23 p3958 N85-34529
A computerized system for spot detection and analysis of two-dimensional electrophoresis images 23 p3958 N85-34531
Animengine: An engineering animation system 23 p3959 N85-34535
3D computer animation: More an evolution problem than a motion problem 23 p3959 N85-34536
Using dynamic analysis to animate articulated bodies such as humans and robots 23 p3959 N85-34537

Towards an integrated view of 3-D computer character animation 23 p3959 N85-34538
The CADME approach to the interface of solid modellers 23 p3961 N85-34554
An innovative user interface for microcomputer-based computer-aided design 23 p3961 N85-34555
Analysis of transient radiation upset in a 16K SRAM [DE85-009442] 23 p3965 N85-34586
Circuit approaches to increasing SRAM performance in total dose environments [DE85-009441] 23 p3966 N85-34588
Workshop report on Simulation Techniques for Shock Wave Phenomena and Characteristics of Plasmas in Inertial Confinement Fusion [IPPJ-725] 23 p3979 N85-34670
Vector calculation of particle code 23 p3981 N85-34688
Data on the backscattering coefficients on light ions from solids: A revision [IPPJ-AM-41-REV] 23 p3982 N85-34689
Perspective on the next ten years in plasma physics [DE85-011849] 23 p3984 N85-34706
Acceleration of ions and electrons to near-cosmic ray energies in a perpendicular shock: The January 6, 1978 event [SH-1.5-4] 23 p3996 N85-34773
Particle accelevation due to shocks in the interplanetary field: High time resolution data and simulation results [SH-1.5-5] 23 p3996 N85-34774
Energy management of three-dimensional minimum-time intercept [NASA-CR-176174] 24 p4084 N85-35186
The investigation of tethered satellite system dynamics [NASA-CR-176180] 24 p4089 N85-35215
Actuator rigging test set electromagnetic interference test (CE03) [AD-A155819] 24 p4086 N85-35327
Investment justification of robotic technology in aerospace manufacturing. User's manual [AD-A156193] 24 p4099 N85-35410
Expert systems research in regional resource evaluation: Experiences in the application of microcomputer technologies 24 p4105 N85-35450
The NORDA/FNOC (Naval Ocean Research and Development Activity's/Fleet Numerical Oceanography Center) Polar Ice Prediction System (PIPS)-Arctic: A technical description [AD-A156332] 24 p4126 N85-35577
Enhancement of the flexible spacecraft dynamics program for open spacecraft [NASA-CR-175309] 24 p4137 N85-35641
Benchmark evaluation of PC simscript [AD-A156133] 24 p4138 N85-35651
Computational methods for the explosive and impact compaction of powders [AD-A156219] 24 p4139 N85-35653
SASSYS-1 computer code verification with EBR-2 test data [DE85-012119] 24 p4139 N85-35657
RFQ modeling computer program [DE85-012665] 24 p4140 N85-35661
TOSCA calculations and measurements for the SLAC SLC damping ring dipole magnet [DE85-014366] 24 p4160 N85-35793
Investigations of the molecular beam epitaxial growth and characteristics of external excitation induced non-equilibrium phases of immiscible 3-5 compound semiconductors [AD-A156325] 24 p4162 N85-35804
Simulation of lattice damage due to dynamic loading [DE85-008468] 24 p4162 N85-35806
Network management simulation of automated guideway transit systems under vehicle-follower control [PB85-186233] 24 p4166 N85-35830
Preliminary results on underground muon bundles observed in the Frejus proton-decay detector [HE-5.1-1] 24 p4200 N85-36067
A transient digitiser for fast air shower events [HE-5.2-21] 24 p4204 N85-36097

COMPUTERS

NT AIRBORNE/SPACEBORNE COMPUTERS
NT ANALOG COMPUTERS
NT CDC COMPUTERS
NT CDC CYBER 170 SERIES COMPUTERS
NT CDC CYBER 205 COMPUTER
NT DIGITAL COMPUTERS
NT EMBEDDED COMPUTER SYSTEMS
NT HEWLETT-PACKARD COMPUTERS
NT HYBRID COMPUTERS
NT IBM COMPUTERS
NT MICROCOMPUTERS
NT MINICOMPUTERS
NT OPTICAL COMPUTERS
NT PARALLEL COMPUTERS
NT PDP 11 COMPUTER
NT PDP 11/70 COMPUTER
NT PERSONAL COMPUTERS
NT SEQUENTIAL COMPUTERS
NT UNIVAC COMPUTERS
NT UNIVAC 1100 SERIES COMPUTERS
NT VAX COMPUTERS
NT VAX-11 SERIES COMPUTERS
NT VAX-11/780 COMPUTER

Storage in the LLNL Octopus network: An overview and reflections [DE84-014711] 01 p0106 N85-10712
Diagnosis via causal reasoning: Paths of interaction and the locality principle [AD-P003920] 02 p0245 N85-11600
Technological institute director views artificial intelligence 03 p0341 N85-12197
A research program in computer technology [AD-A145776] 03 p0402 N85-12565
Research activities of the Illinois University Coordinated Science Laboratory [AD-A145589] 03 p0449 N85-12856
Computer Literacy Act of 1983, part 2 [H-REPT-98-752-PT-2] 04 p0578 N85-13687
USSR report: Electronics and electrical engineering [JPRS-UEE-84-011] 06 p0789 N85-15042
FCC (Federal Communication Commission) methods of measurement of radio noise emissions from computing devices [PB84-243591] 06 p0849 N85-15387
A summary of the foundation research program [AD-A146524] 06 p0891 N85-15656
West Europe report: Science and technology [JPRS-WST-84-039] 07 p0936 N85-15929
Eyes for computers 07 p1012 N85-16428
Computer science research in Europe [AD-A146905] 07 p1022 N85-16482
Research and technology, 1984 report [NASA-TM-83096] 07 p1061 N85-16730
Hardware/software codesign for maintainable systems 08 p1066 N85-16753
East Europe report: Science and technology [JPRS-ESA-84-047] 08 p1140 N85-17183
ES devices at fair 08 p1141 N85-17187
MOM peripherals 08 p1141 N85-17189
West Europe report: Science and technology [JPRS-WST-85-001] 08 p1141 N85-17190
Performance management system enhancement and maintenance [NASA-CR-175271] 08 p1202 N85-17564
On the validation of computer science theories [AD-A148637] 08 p1203 N85-17572
Technology development for unmanned untethered submersible vehicle systems [AD-A148794] 09 p1304 N85-18190
East Europe report: Science and technology [JPRS-ESA-85-005] 09 p1377 N85-18659
Computer equipment at 1984 Leipzig Spring Fair 09 p1378 N85-18662
West Europe report: Science and technology [JPRS-WST-85-004] 10 p1460 N85-19204
Computers and education [GPO-28-378] 10 p1537 N85-19689
Computer crime [GPO-30-544] 10 p1537 N85-19691
Computer center CDC libraries [AD-A149005] 10 p1540 N85-19707
China report: Science and technology [JPRS-CST-84-025] 11 p1620 N85-20197
Development of computer centers, equipment described: Problems of computer centers 11 p1700 N85-20686
Long-range electronics program outlined 11 p1700 N85-20687
USSR report: Electronics and electrical engineering [JPRS-UEE-85-004] 12 p1837 N85-21531
Cumulative reports and publications through December 31, 1984 [NASA-CR-172569] 12 p1911 N85-21991
Computing Division two-year operational plan, FY 1984 - 1985 [LA-9978-MS] 12 p1913 N85-22006
Oversight review of the five-year outlook report on science and technology [GPO-41-058] 12 p1949 N85-22243
Research and Modeling of Supervisory Control Behavior, report of a workshop [AD-A149621] 12 p1950 N85-22248
Liquid mass flow rate computer 13 p2075 N85-22962
China report: Science and technology [JPRS-CST-85-003] 13 p2166 N85-23433
West Europe report: Science and technology [JPRS-WST-85-013] 14 p2289 N85-24183
The Effect of Computers on the Generation and Use of Technical Data [NBSIR-84-2907] 14 p2400 N85-24792
Integration of an Apple 2 Plus computer into an existing dual axis sun tracker system [AD-A150778] 14 p2404 N85-24823
Gordon Conference on Fundamentals of Cybernetics [AD-A151074] 14 p2408 N85-24842
Our future in the cosmos: Computers 14 p2432 N85-24997
Computer controlled acquistion of corrosion rate data from multiple sensors [PB85-157378] 15 p2524 N85-25559
East Europe report: Science and technology [JPRS-ESA-84-016] 15 p2533 N85-25624
West Europe report: Science and technology [JPRS-WST-84-009] 15 p2535 N85-25639
West Europe report: Science and technology [JPRS-WST-84-014] 15 p2536 N85-25647
China report: Science and technology [JPRS-CST-85-013] 15 p2536 N85-25652
Microcomputer controlled image acquisition system 15 p2537 N85-25654
China report: Science and technology [JPRS-CST-85-011] 15 p2551 N85-25748
Computerized biophysical data acquisition system for motion sickness studies [AD-A151691] 15 p2618 N85-26131
Future directions in computers 15 p2626 N85-26183
Computers and the consulting engineer 15 p2626 N85-26184
Physics, Computer Science and Mathematics Div. [DE85-006868] 15 p2642 N85-26298
Computer software for aerodynamic design of aircraft developed within the National Aerospace Laboratory 16 p2691 N85-26613
Design of computer-related workstations in relation to job functions and productivity [AD-A151938] 16 p2844 N85-27534
Squeezing the most out of Eigenvalue solvers on high-performance computers [DE85-007569] 16 p2849 N85-27565
East Europe report: Science and technology [JPRS-ESA-85-017] 17 p2945 N85-28177
The touch panel system: Design and development [AD-A153014] 17 p3008 N85-28596
Efforts at office automation and information systems utilization at Martin Marietta Energy Systems, Incorporated [DE85-008154] 17 p3013 N85-28633
Synchronization and fault-masking in redundant real-time systems [NASA-TM-87478] 17 p3015 N85-28644
European Science Notes, Volume 39, Number 3 [AD-A152446] 17 p3027 N85-28717
Computing in the Soviet general economy: An introductory overview [AD-P004563] 17 p3047 N85-28858
A study of user-defined searching requirements for the on-line version of the directory of DOD-sponsored R and D data bases on the Defense Gateway computer system [AD-A153000] 17 p3050 N85-28878
West Europe report: Science and technology [JPRS-WST-84-031] 18 p3066 N85-29089
France's use of Cray 1, plans for national supercomputer 18 p3066 N85-29093
West Europe report: Science and technology [JPRS-WST-84-035] 18 p3067 N85-29102
West Europe report: Science and technology [JPRS-WST-84-037] 18 p3068 N85-29106
Coping with computer terminology [DE85-006076] 18 p3161 N85-29579
Projects of the Computer Center of the academy's Siberian branch 19 p3295 N85-30425
A parallelized point successive over-relaxation method on a multiple instruction multiple data stream computer [AD-A154377] 19 p3337 N85-30679
High accuracy digital accousto-optic matrix computer [AD-D011692] 19 p3343 N85-30716
Simulation and operation of the EBR-2 automatic control rod drive system [DE85-010262] 19 p3360 N85-30832
Proust radar: Decoding hardware and coherent integration, part 7.2A 21 p3626 N85-32524
East Europe report: Science and technology. Selections on CSSR computer technology [JPRS-ESA-84-017] 21 p3668 N85-32781
Machine intelligence for robotics applications [DE85-011430] 22 p3793 N85-33503
Computer science: Key to a space program renaissance. The 1981 NASA/ASEE summer study on the use of computer science and technology in NASA. Volume 2: Appendices [NASA-CR-175295] 22 p3827 N85-33702
Integration of office automation within computing [DE85-010021] 22 p3833 N85-33736
Issues and techniques in touch-sensitive tablet input (executive summary) 23 p3960 N85-34543

Ranging system which compares an object reflected component of a light beam to a reference component of the light beam
[NASA-CASE-NPO-15865-1] 23 p3973 N85-34629
CONCATENATED CODES
Reed-Solomon code synchronization revisited
10 p1464 N85-19234
A concatenated coding scheme for error control
[NASA-CR-175504] 12 p1912 N85-22001
A concatenated coding scheme for error control
[NASA-CR-176006] 19 p3334 N85-30655
CONCAVITY
Equivocation limits in Gaussian additive channels
[INPE-2828-PRE/380] 04 p0492 N85-13137
Measurement of the configuration of a concave surface by the interference of reflected light
[NASA-TM-77796] 11 p1726 N85-20867
CONCENTRATION
Measuring methods of atmospheric electric elements at the Earth's surface during snowfall and investigation of these relationships 15 p2581 N85-25920
CONCENTRATION (COMPOSITION)
NT ATMOSPHERIC MOISTURE
NT ATOM CONCENTRATION
NT CARBON DIOXIDE CONCENTRATION
NT LOW CONCENTRATIONS
NT MASCONS
NT MOISTURE CONTENT
Factor analysis applied to a silane coupling agent on E-glass fiber system
[AD-A145667] 02 p0187 N85-11249
Evaluation of an aerosol prediction model for coastal regions using marine aerosol generation and transport data
[AD-A145443] 02 p0231 N85-11510
Effect of liquid phase composition on thickness of epitaxial Ga sub (1-x) Al sub x As films
02 p0257 N85-11683
The influence of aluminum on the qualities of low and medium carbon steel
[BLL-M-35754-(5828.4)] 03 p0330 N85-12123
Feasibility of the electrochemical method of determining nitrogen content in metallic melts
[BLL-M-35730-(5828.4)] 03 p0330 N85-12124
Development of a rapid test method for asphalt concrete content determination in hot-mix paving mixtures
[PB84-216692] 03 p0342 N85-12204
Aircraft flow effects on cloud droplet images and concentrations
[AD-A146176] 03 p0396 N85-12529
The effect of temperature and pressure on the composition density of alkaline metals
[BLL-M-35940-(5828.4)] 05 p0616 N85-13934
Reproducibility of readings from oxygen concentration elements
[BLL-M-35920-(5828.4)] 05 p0616 N85-13941
Fundamental equations of the LIF hydroxyl measurements, appendix A 05 p0676 N85-14338
Detailed performance calculations: Harvard Group, appendix G 05 p0676 N85-14344
Meteorite concentrations in Antarctica: How complete is the picture? 06 p0869 N85-15844
The influence of sample collection and methods of analysis on chemical concentrations measured in rainwater
[KNMI-TR-55] 07 p0924 N85-15853
Fluid temperature and concentration gradient measurement study — for spaceborne experiments
[CISE-R/FL/1/04] 11 p1637 N85-20309
Saturation kinetics of active medium of oxygen-iodine laser 11 p1718 N85-20807
Simultaneous cabin and ambient ozone measurements on two Boeing 747 airplanes. Volume 3: October 1978 - July 1979
[NASA-TM-86683] 12 p1892 N85-21872
The body burden of organic vapors in artificial air trial measurements aboard a moored submarine
[AD-A149698] 12 p1910 N85-21988
Spectroscopic study of sources and control of impurities in TMX-U: Revision 1
[DE85-004423] 12 p1937 N85-22170
Characterization of high purity Si-doped molecular beam epitaxial GaAs
[AD-A149851] 12 p1939 N85-22181
Progress on studies of early intense cratering
13 p2181 N85-23535
A parmetric study of crater-saturation simulation
13 p2182 N85-23540
Influence of phosphorus content and heat treatment on the machinability of electroless nickel deposits
[DE85-007250] 15 p2522 N85-25548
Compositional control of plate steels
15 p2565 N85-25826
On the analytic calculation of premixed flames
[VTH-LR-417] 16 p2747 N85-26954
Comparison of observed and predicted short-term tracer-gas concentrations in the atmosphere
[DE85-007566] 16 p2821 N85-27399
Evaluation of chemical reaction mechanisms for photochemical smog. Part 2: Quantitative evaluation of the mechanisms, revised
[PB85-166080] 16 p2822 N85-27408
Radon concentration inversion in the troposphere: Still unexplained
[INPE-3360-PRE/838] 16 p2826 N85-27431
The distribution of higher n-alkanes in partially frozen middle distillate fuels
[AD-A153940] 18 p3083 N85-29074
Compact L-edge densitometer for uranium concentration assay
[DE85-010344] 18 p3110 N85-29261
The effect of surface reactions in catalytic combustion
[AD-A154217] 19 p3234 N85-30049
concentration variation of work function of alloys in the system nickel-titanium-aluminum
19 p3247 N85-30134
Temporal variations of Rn222 concentrations in Black Sea coastal zone 19 p3293 N85-30417
Toxic hazards tests for vehicles and other equipment
[AD-A149164] 20 p3506 N85-31797
Concentrations of ice nuclei of different modes of activities 21 p3641 N85-32616
Observations of the atmospheric ice nucleus at northwest China 21 p3641 N85-32618
Concentration and source areas of ice nuclei in the Alaskan atmosphere 21 p3643 N85-32634
Human activity and production rate of secondary nuclei 21 p3645 N85-32645
On the transformation regularities of time series of solid aerosol concentrations in the surface atmospheric layer
21 p3645 N85-32648
Variability of rural aerosols under stable weather conditions 21 p3647 N85-32663
Marine aerosols at the Dutch North Sea coast: Size distributions and fractionation of trace elements
21 p3648 N85-32664
A statistical study of CCN concentration in subequatorial climate: The particular case of the tropical wet forest
21 p3649 N85-32673
Sulfur Cycle 21 p3662 N85-32748
Measurement of velocity and concentration in free jets
[ISL-CO-215/84] 22 p3785 N85-33451
The heavy ion composition in 3HE-rich solar flares
[SH-2-2-7] 23 p4000 N85-34602
The effect of +Gx acceleration on platelet activation as determined by plasma platelet factor 4 levels
[AD-A155881] 24 p4131 N85-35608
CONCENTRATORS
Liquid cooled, linear focus solar cell receiver
[DE84-014446] 01 p0067 N85-10448
Evaluation of some photovoltaic concentrator solar cell-heat sink coupling materials
[DE84-016027] 04 p0529 N85-13376
Positron flux concentrator: An update
[DE84-016260] 04 p0561 N85-13576
Trends in concentrator, receiver, and storage development for terrestrial applications
05 p0609 N85-13891
Joint Indo-German program on solar energy: Parabolic dish program, step 1
[BMFT-FB-T-84-175] 05 p0670 N85-14312
Advanced high-efficiency concentrator cells
[DE84-013020] 09 p1344 N85-18459
Nebulization reflux concentrator
[NASA-CASE-LAR-13254-1] 11 p1615 N85-20154
Innovative solar thermal dish technology development
[DE85-002787] 11 p1673 N85-20539
Photovoltaic Systems Development and Evaluation Projects Integration Meeting
[DE84-006530] 11 p1673 N85-20542
Phase 2 fabrication and construction of the Sky Harbor Airport, solar photovoltaic concentrator project
[DE85-000019] 11 p1676 N85-20561
Concentrator technologies evaluation for large solar arrays and their application for space stations/platforms
13 p2010 N85-22609
Study of concentration for space photovoltaic generators 13 p2011 N85-22618
Power plants of modular construction with quasi-paraboloidal concentrators of solar energy
14 p2266 N85-24038
Development and testing of Parabolic Dish Concentrator No. 1
[NASA-CR-175651] 14 p2350 N85-24522
Development of an Organic Rankine-Cycle power module for a small community solar thermal power experiment
[NASA-CR-175650] 14 p2350 N85-24523
Development of mass-producible line-focus tracking concentrating solar collectors. Category 2: Control systems
[DE85-007873] 17 p2987 N85-28459
Development of a second-generation linear Fresnel Photovoltaic and Thermal (PVT) concentrator array, including fabrication and installation of a 200 square meter collector field
[DE85-008473] 17 p2988 N85-28485
DOE/Sandia point-focus concentrator program, draft
[DE85-008209] 17 p3038 N85-28793
Airport solar photovoltaic concentrator phase 3
[DE85-006773] 18 p3128 N85-29370
Nomographs for estimating the levelized cost of energy from flat-plate and concentrator photovoltaic systems
[NASA-CR-176048] 20 p3483 N85-31645
Photovoltaic concentrator research status
[DE85-010119] 20 p3483 N85-31647
Study of concentration for space photovoltaic generators
[SNIAS-851-440-105] 20 p3485 N85-31658
Photovoltaics technology program summary
[DE85-013098] 24 p4112 N85-35493
CONCENTRIC CYLINDERS
Stability of fluid flow in a cylindrical annulus
[NASA-TM-77720] 01 p0048 N85-10300
Unsteady free-convection heat transfer inside an annular cavity
[CFD/84/16] 08 p1163 N85-17339
On spectral multigrid methods for the time-dependent Navier-Stokes equations
[NASA-CR-172613] 19 p3344 N85-30725
Acoustic radiation from concentric shells containing an inner fluid
[AD-A155476] 21 p3700 N85-32991
Couette flow of two fluids between concentric cylinders
[AD-A155827] 24 p4093 N85-35376
CONCENTRIC SPHERES
Average spacing for rings of individual multi-ring basins is 2.0(0.5)D 13 p2182 N85-23541
Ring-diameter ratios for multi-ring basins average 2.0(0.5)D 13 p2182 N85-23542
CONCORDE AIRCRAFT
Avionics and civil aircraft systems: The present and the future
[SNIAS-851-111-104] 20 p3392 N85-31038
CONCRETE STRUCTURES
A rigid body mechanism in structural dynamics
02 p0206 N85-11361
Related studies to cathodic protection of reinforced concrete structures
[PB84-218114] 03 p0333 N85-12145
Dynamic shear failure of shallow-buried flat-roofed reinforced concrete structures subjected to blast loading
[AD-A145974] 03 p0373 N85-12378
Refined modeling of reinforced concrete columns of seismic analysis
[PB84-234384] 04 p0484 N85-13089
Measuring the corrosion rate of reinforcing steel in concrete
[PB84-244532] 06 p0770 N85-14925
Finite element procedures applicable to nonlinear analysis of reinforced concrete shell structures
[AD-A146796] 07 p0978 N85-16209
User's guide for concrete strength investigation and design (CSTR)
[AD-A151617] 15 p2579 N85-25906
An approach for user controlled reinforced concrete design optimization 15 p2627 N85-26167
In-service supervision of a pressurized concrete pressure vessel
[OEFZS-4308] 20 p3470 N85-31564
Implementation of polymer impregnation as a bridge deck sealant
[PB85-165718] 22 p3753 N85-33265
Prestressed concrete vessel according to the hot liner concept: A critical evaluation of experimental results with a prototype vessel
[OEFZS-4313] 22 p3801 N85-33550
Negative flexural behavior of precase composite slabs with steel joint 23 p3904 N85-34183
Membrane reinforcement in concrete shells: Design versus nonlinear behavior 24 p4084 N85-35312
CONCRETES
Development of advanced constitutive model for reinforced concrete
[AD-A145050] 01 p0082 N85-10411
Experimental AC (Asphalt Concrete) overlays of PCC pavement
[PB84-216171] 03 p0342 N85-12203
Evaluation of moduli and thicknesses of pavement systems by spectral-analysis-of-surface-waves method
[PB84-219112] 03 p0342 N85-12205
Improved reinforcement metal
03 p0353 N85-12271

Insulating polymer concrete
[DE84-017239] 04 p0480 N85-13057
Underground engineering (selected articles)
[AD-A141053] 04 p0483 N85-13082
Pulse-echo method for flaw detection in concrete
[PB84-234509] 06 p0775 N85-14953
Tests of the load-bearing and deformation behaviour of reinforced concrete spherical shells under point loading
[BLL-RISLEY-TR-4550-8091.9F)] 06 p0816 N85-15182
Salt action on concrete
[AD-A147812] 07 p0933 N85-15912
Thermal and mechanical properties of polyurethane foams and a survey of insulating concretes at cryogenic temperatures
[PB85-100949/GAR] 07 p0934 N85-15918
No-slump Roller-Compacted Concrete (RCC) for use in mass concrete construction
[AD-A148564] 08 p1138 N85-17164
Durability and behavior of prestressed concrete beams. Posttensioned concrete beam investigation, supplemental laboratory tests of beams exposed from 1961 to 1982
[AD-A148821] 09 p1304 N85-18191
Fracture toughness of fiber reinforced concrete
[AD-A149403] 10 p1496 N85-19441
Response of earth-covered slabs in clay and sand backfills
[AD-A148296] 11 p1615 N85-20157
Thermal stress-dependent dilation of concrete
[DE84-014688] 11 p1653 N85-20412
A new rheological model for concrete structural analysis
[DE84-014743] 11 p1653 N85-20413
Field validation of statistically-based acceptance plan for bituminous airport pavements. Volume 3: Statistical analysis of 3 methods for determining maximum specific gravity of bituminous concrete mixtures
[FAA-PM-84-12-VOL-3] 12 p1781 N85-21182
Development and evaluation of a procedure for the rapid analysis of fresh concrete
[AD-A149741] 12 p1866 N85-21703
Electrically conductive polymer concrete overlays
[DE85-006728] 15 p2522 N85-25549
Overlays for plain jointed concrete pavements
[PB85-156297] 15 p2523 N85-25557
Repair of the DSS-14 pedestal concrete
16 p2772 N85-27108
Hopkinson bar simulation using DYNA2D
[DE85-006766] 16 p2802 N85-27275
Development of concrete polymer materials
[DE85-005957] 17 p2934 N85-28114
Sodium concrete reaction: Structural considerations
[DE85-009031] 18 p3081 N85-29063
Behavior of reinforced concrete at elevated temperatures
[DE85-009032] 18 p3123 N85-29332
Effect of matrix composition on steel fiber reinforced concrete properties 19 p3230 N85-30028
Effects of humidity cycles on the corrosion of galvanised reinforcements in carbonated and uncarbonated mortars
[BLL-CE-TRANS-8039-(9022.09)] 20 p3430 N85-31272
Pycnometer shaker
[PB85-174985] 20 p3460 N85-31491
User's guide for computer program CGFAG, Concrete General Flexure Analysis with Graphics
[AD-A155555] 21 p3570 N85-32204
Dynamic fracture of concrete and other heterogeneous materials
[AD-A154513] 21 p3598 N85-32343
Hole cutting in building frames by laser
[FOA-C-20569-D9] 22 p3791 N85-33487
Monte Carlo and discrete ordinates calculations of 14-MeV neturons streaming through a stainless-steel duct (L/D = 4.6): Comparison with experiment
[DE85-011423] 22 p3840 N85-33776
High temperature polymer concrete
[DE85-005756] 23 p3920 N85-34290
User's guide: A computer program for strength analysis of non-hydraulic concrete structural elements. Report 1. Concrete General Strength Investigation (CGSI)
[AD-A156392] 24 p4102 N85-35428
User's guide: A computer program for strength analysis of non-hydraulic concrete structural elements. Report 2. Strength design of reinforced concrete column sections (PCAUC)
[AD-A156393] 24 p4102 N85-35429

CONCURRENT PROCESSING
Concurrent processing and the decomposition of problems
[DE84-015265] 02 p0242 N85-11581
Concurrency in parallel processing systems
05 p0714 N85-14581
Concurrency in a data flow database machine
09 p1366 N85-18582
The enhancement of concurrent processing through functional programming languages
[AD-A150771] 14 p2404 N85-24822
Performance evaluation of stochastic timed decision-free Petri Nets
[AD-A153987] 18 p3171 N85-29652
Methods for design and evaluation of integrated hardware-software systems for concurrent computation
[NASA-CR-176066] 20 p3515 N85-31851
Concurrent implementation of the Crank-Nicolson method for heat transfer analysis
[NASA-TM-86448] 21 p3674 N85-32822
Simulation of complex three-dimensional flows
[NASA-TM-86773] 21 p3675 N85-32831
Specifying and verifying concurrent programs
[AD-A156190] 24 p4138 N85-35652

CONDENSATES
Neutron interferometry and double diffractometer for condensed matter 03 p0424 N85-12705
Experimental and theoretical study of condensation in multicomponent vapors
[DE85-000843] 10 p1485 N85-19376
Continued research in mesoscale air pollution simulation modeling. Volume 7. Mathematical modeling of urban aerosol dynamics
[PB85-137388] 11 p1679 N85-20584
Proper quality of anticorrosion work no matter how bad the atmospheric conditions
[BLL-BISI-TRANS-22060-(9022.06)] 17 p2975 N85-28383
Aitken particle size distribution in Antarctica
21 p3646 N85-32656
Properties of forest derived cloud condensation nuclei
21 p3650 N85-32682
Influence on an industrial site on the characteristics of CCN supersaturation with air masses of different origin
21 p3650 N85-32683

CONDENSATION
The lifting condensation level and its relation to convective cloud base
[AD-A145654] 02 p0232 N85-11513
Chemical evolution of the solar nebula: A new model
06 p0687 N85-15631
Homogeneous condensation of gaseous mixtures of Si, Fe, O, N, and C in relative cosmic abundance and implications for astronomical condensation
06 p0687 N85-15632
Theoretical analysis of condensation in the presence of noncondensable gases as applied to open cycle OTEC condensers
[DE84-015809] 11 p1675 N85-20556
An examination of the Southern Oscillation in the upper troposheric tropical and subtopical wind field
20 p3488 N85-31680
Remarks on preparation of indandione detection reagents
[NASA-TM-77905] 21 p3560 N85-32146
Eleventh International Conference on Atmospheric Aerosols, Condensation and Ice Nuclei, volume 2
[PB85-182418] 21 p3638 N85-32596
Ice active bacteria as condensation nuclei
21 p3639 N85-32603
Generation of lead, lead iodide and iodide aerosols and their ice nucleation 21 p3639 N85-32607
Ice nucleus measurements 21 p3640 N85-32609
Airborne measurements of atmospheric ice nuclei
21 p3640 N85-32612
Aircraft observations of condensation and ice nuclei at a tropical station 21 p3640 N85-32613
Supersaturation spect A of Ice Nuclei at different locations in Europe and over the North-Atlantic
21 p3640 N85-32615
The nuclei of cloud formation
21 p3651 N85-32685
Transport and formation of summertime cloud condensation nuclei over the Arctic Ocean
21 p3651 N85-32686
A review on the formation of aerosol particles in the atmosphere 21 p3651 N85-32687
The measured rate of condensation nucleation to droplets using the techniques of chemical kinetics
21 p3652 N85-32694
The interaction of polynuclear aromatic hydrocarbons PAH's with water vapor and their role as condensation nuclei in the formation of haze and fog
21 p3652 N85-32695
Applicability of surface CCN measurements
21 p3652 N85-32696
on the transport of large condensation nuclei in the atmosphere at various altitudes over the territory of the USSR 21 p3653 N85-32698

CONDENSATION NUCLEI
NT AITKEN NUCLEI
Condensational transformation of atmospheric aerosol particle distribution functions 10 p1500 N85-19468
Test results from a comparative evaluation of a condensation nuclei fire detector
[NASA-CR-3874] 12 p1862 N85-21675
Measurements of giant salt nuclei from inland in east China 21 p3648 N85-32666
Cloud condensation on insoluble particles
21 p3648 N85-32670
Observations of cloud droplets, aerosol particles and cloud condensation nuclei in continental air masses
21 p3649 N85-32671
A statistical study of CCN concentration in subequatorial climate: The particular case of the tropical wet forest
21 p3649 N85-32673
Investigation of the formation of cloud particle spectrum on natural condensation nuclei
21 p3649 N85-32674
A simple model to investigate the activation process in waterclouds 21 p3649 N85-32675
A relationship between cloud droplet size and CCN critical supersaturation 21 p3649 N85-32677
On the question to the effect of surfactants on the spectrum of cloud drops in the process of their condensation growth 21 p3650 N85-32679
Aircraft observations of cloud condensation nuclei in maritime and continental environments
21 p3650 N85-32680
The distribution of giant salt nuclei inside and outside cloud over the basin of Xin and Jiang
21 p3650 N85-32681

CONDENSER RADIATORS
U CONDENSERS (LIQUEFIERS)
U HEAT RADIATORS

CONDENSERS
Modeling of a second-generation solar-driven Rankine air conditioner
[DE84-015132] 01 p0036 N85-10223

CONDENSERS (LIQUEFIERS)
Heat transfer due to film condensation on vertical fluted tubes
[AD-A147258] 07 p0959 N85-16079
Theoretical analysis of condensation in the presence of noncondensable gases as applied to open cycle OTEC condensers
[DE84-015809] 11 p1675 N85-20556
Direct-contact condensers for solar pond power production
[DE84-004510] 12 p1876 N85-21771
Mass and heat transfer in reflux condensers of absorption heat pumps
[DFVLR-FB-83-43] 14 p2304 N85-24266
Filmwise condensation of steam on low integral-finned tubes
[AD-A152220] 16 p2783 N85-27176

CONDENSING
NT FILM CONDENSATION
Method of obtaining polychalcones
[AD-A145051] 01 p0018 N85-10107
Experimental and theoretical study of condensation in multicomponent vapors
[DE84-015610] 02 p0174 N85-11164
Carbon vaporization/condensation effects
[NASA-TM-87430] 10 p1436 N85-19048
Isentropic objective analysis
[PB85-112167] 11 p1688 N85-20617
Experimental and theoretical study of condensation in multicomponent vapors
[DE85-009357] 17 p2923 N85-28021
Condensation of anhydrides or dicarboxylic acids with compounds containing active methylene groups. Part 19: Condensation of phthalic and substituted phthalic anhydrides with benzoylacetic ester
[NASA-TM-77885] 19 p3227 N85-30009
Condensation of anhydrides or dicarboxylic acids with compounds containing active methylene groups. Part 1: Condensation of phthalic anhydride with acetoacetic and malonic ester
[NASA-TM-77886] 19 p3227 N85-30010
Flow field effects on nucleation in a reacting mixing layer
[ARL/AERO-R-165] 19 p3263 N85-30237
Construction of University of Missouri, Rolla's full scale cloud simulation chamber and applied research
[AD-A154682] 21 p3557 N85-32128
The 100 years of Aitken Nuclei (AN) study-reminiscence, current and future problems 21 p3641 N85-32621
Supersaturation obtained in a condensation nucleus counter 21 p3642 N85-32624
Analysis of performance of dynamic thermal diffusion chamber 21 p3642 N85-32625
A thermal diffusion chamber for the measurement of cloud condensation nuclei 21 p3642 N85-32627
Critical supersaturations with respect to water for fast condensation-freezing ice nucleation
21 p3643 N85-32632

Eleventh International Conference on Atmospheric Aerosols, Condensation and Ice Nuclei, volume 1
[PB85-162400] 21 p3644 N85-32636
The first condensation nucleus conference
21 p3644 N85-32637
Cloud condensation on insoluble particles
21 p3646 N85-32670
Condensation properties of atmospheric aerosol
21 p3649 N85-32672

CONDITIONED RESPONSES
U CONDITIONING (LEARNING)

CONDITIONING (LEARNING)
Control of mammals at airports
[AD-P004192] 11 p1580 N85-19957
Psychological components in the development and prevention of air sickness 11 p1695 N85-20659
Biofeedback treatment of airsickness: A review
11 p1696 N85-20660
M-BLASER: A device to study pursuit tracking in the rhesus monkey
[AD-A152986] 17 p2998 N85-28534

CONDITIONS
NT ADIABATIC CONDITIONS
NT CHRONIC CONDITIONS
NT FLIGHT CONDITIONS
NT LIPSCHITZ CONDITION
NT NONEQUILIBRIUM CONDITIONS
NT RUNWAY CONDITIONS
Setting hurricane conditions of readiness with high confidence
[AD-A144785] 01 p0065 N85-10570
Computer programs for the adjustment of indirect observation with condition equations between the unknowns
[SER-B-266-MITT-170] 09 p1370 N85-18612
Estimating risks of lead-induced hemoglobin decrements under conditions of uncertainty: Methodology, pilot judgments and illustrative calculations
[DE85-012293] 23 p3952 N85-34493

CONDUCTANCE
U RESISTANCE

CONDUCTING FLUIDS
Magnetic inductive flowmeter for low conducting liquids
[BMFT-FB-T-84-136] 04 p0504 N85-13216

CONDUCTING MEDIA
U CONDUCTORS

CONDUCTION BANDS
Electron and hole effective masses for two-dimensional transport in strained-layer superlattices
[DE84-016222] 04 p0570 N85-13637
The Valence- and conduction-band structure of the sapphire (1102) surface
[AD-A150001] 12 p1940 N85-22184
Modulation doped GaAs/Al(x)Ga(1-x)As layered structures with applications to field effect transistors
[AD-A155360] 22 p3759 N85-33256

CONDUCTION ELECTRONS
Very low temperature studies of hyperfine effects in metals
[DE85-013367] 22 p3749 N85-33236

CONDUCTIVE HEAT TRANSFER
Self-similar expansion of dense matter due to heat transfer by nonlinear conduction
[MPQ-81] 01 p0046 N85-10297
ICARUS: A general one-dimensional heat conduction code
[DE84-016125] 01 p0047 N85-10310
A similarity analysis of phase change heat conduction in corners 05 p0634 N85-14069
Wave propagation in compliant tubes containing a heat-conducting viscous fluid
[WTHD-163] 05 p0638 N85-14094
Intensification of convective heat transfer by means of artificial surface roughness 06 p0778 N85-14975
New aspects of thermoelastic contact
[AD-A147554] 07 p0979 N85-16217
Two-dimensional modeling of conduction-mode laser welding
[DE85-001804] 09 p1327 N85-18341
Measurements of sediment temperatures, conductivity and heat flow in the North Atlantic and their relevance to radioactive waste disposal
[IOS-172] 09 p1359 N85-18651
Triple layer system for numerical integration of equations of gas dynamics and nonlinear heat conduction equation
[DE85-000297] 11 p1632 N85-20277
Temperature responses of composite panels
[AD-A150053] 12 p1798 N85-21277
Models of the upper atmosphere
12 p1945 N85-22217
Conducting a thermal conductivity survey
[NASA-CR-175792] 16 p2782 N85-27166
Evaluation of the eigenvalue method in the solution of transient heat conduction problems
[AD-A154434] 19 p3268 N85-30256
Sequential regularization solution of the inverse heat conduction problem
[DE85-010657] 23 p3931 N85-34362
Analytic solutions of inverse heat conduction problems
24 p4092 N85-35367

CONDUCTIVITY
Conductivity changes in neutron-irradiated commercial copper alloys at approximately 450(0)C
[DE85-003007] 11 p1606 N85-20100
The replacement of precious metal thick film inks using conductive polymer technology
[AD-A152002] 16 p2749 N85-28965
Gyrotron traveling-wave device including quarter wavelength anti-reflective dielectric layer to enhance microwave absorption
[AD-D011690] 19 p3271 N85-30285

CONDUCTIVITY METERS
NT ELECTRICAL CONDUCTIVITY METERS

CONDUCTORS
NT BUS CONDUCTORS
NT ELECTRIC CONDUCTORS
NT ELECTRIC WIRE
NT ELECTROLYTES
NT ION EXCHANGE MEMBRANE ELECTROLYTES
NT MOLTEN SALT ELECTROLYTES
NT NONAQUEOUS ELECTROLYTES
NT PHOTOCONDUCTORS
NT SOLID ELECTROLYTES
NT SUPERCONDUCTORS
Diffraction of plane electromagnetic waves on semiinfinite grid of parallel conductors arranged at angle to its edge 03 p0344 N85-12217
Magnetic field calculation for ideal conductors by method of equivalent currents 06 p0788 N85-15035
Corrosion properties of second-generation conductive materials 07 p1000 N85-16348
Control of electronic, magnetic and optical properties of doped polyacetylene conductors
[AD-A150117] 12 p1814 N85-21375
Performance ranges of helical antenna made of conductor with extra bends 12 p1838 N85-21536
Study of amorphous strips and microconductors by ferromagnetic resonance method
15 p2497 N85-25402
Electronic properties of new organic conductors
[DE85-005590] 15 p2549 N85-25736
Nuclear responses in INTOR plasma stabilization elements
[DE85-010489] 20 p3535 N85-31995
Method for determining depth and shape of a sub-surface conductive object
[DE85-006502] 23 p3935 N85-34389

CONES
NT CONICAL BODIES
NT NOSE CONES
NT SLENDER CONES
Aerothermal tests of a 12.5 percent cone at Mach 6.7 for various Reynolds numbers, angles of attack and nose shapes — conducted in Langley 8-foot high temperature tunnel
[NASA-TP-2345] 08 p1161 N85-17322
LOVEL-84: A LOw-VELocity aerodynamic heating code for flat plates, wedges, and cones
[DE85-002604] 11 p1576 N85-19933
Experimental investigation of heat transfer to bluff cylinders and cones in hypersonic rarefied gas flow
11 p1620 N85-20195

CONES (VOLCANOES)
The geology of Mt. Hope, a silicic volcanic center in West Central Arizona 13 p2187 N85-23571

CONFERENCES
Aeronautics Technology Possibilities for 2000: Report of a workshop
[NASA-CR-174018] 01 p0001 N85-10001
Experimental data base for computers program assessment. Report of the Fluid Dynamics Panel Working Group 04: Addendum
[AGARD-AR-138-ADD] 01 p0004 N85-10020
Proceedings of the Aviation Accident Investigation Symposium
[PB84-917004] 01 p0005 N85-10029
Peripheral Vision Horizon Display (PVHD)
[NASA-CP-2306] 01 p0008 N85-10044
Nuclear Magnetic Resonance of Polymeric Materials
[AD-A145078] 01 p0032 N85-10192
Tendencies in the development of utilization protocols, seminar report — communication networks
[FUB-11-1983] 01 p0039 N85-10252
Voice phonetic coding and decoding processes
[FUB-29-1983] 01 p0040 N85-10259
Second All-Union Seminar on Hydromechanics and Heat and Mass Exchange in Weightlessness, summaries of reports
[NASA-TM-77580] 01 p0047 N85-10305
Structure and wear workshop colloquium
01 p0054 N85-10356
NASA Geodynamics Program
[NASA-TM-87359] 01 p0063 N85-10418
Technical Review of the Solid Particle Receiver Program
[DE84-015181] 01 p0068 N85-10451
Report of the First Session of the International Working Group on Data Management for the International Satellite Cloud Climatology Project (ISCCP)
[WCP-42] 01 p0073 N85-10483
Nowcasting 2. Mesoscale Observations and Very-Short-Range Weather Forecasting — conference
[ESA-SP-208] 01 p0073 N85-10487
Illinois Climate: Trends, Impacts and Issues
[PB84-211986] 01 p0086 N85-10577
Office of Technology Assessment
01 p0127 N85-10872
Workshop on Automated Space Station
01 p0127 N85-10873
Turbine Engine Hot Section Technology (HOST)
[NASA-TM-83022] 02 p0140 N85-10951
Second Symposium on Space Industrialization — space commercialization
[NASA-CP-2313] 02 p0149 N85-11011
Seminar on Principal Components Analysis in the Atmospheric and Earth Sciences
[CSIR-S-334] 02 p0211 N85-11388
The Multispectral Imaging Science Working Group. Volume 2: Working group reports
[E85-10002] 02 p0213 N85-11405
MIZEX. A program for mesoscale air-ice-ocean interaction experiments in arctic marginal ice zones. III: Modeling the marginal ice zone
[AD-A145351] 02 p0233 N85-11517
Mathematical Models of the Circadian Sleep-Wake Cycle
[AD-A145712] 02 p0235 N85-11532
Statistical Plasma Physics. Proceedings of the Workshop of the US-Japan Joint Institute for Fusion Theory Program
[IPPJ-669] 02 p0282 N85-11832
Gauge Theory on a Lattice, 1984: Proceedings
[DE84-014856] 02 p0291 N85-11992
Uranus and Neptune
[NASA-CP-2330] 02 p0298 N85-11927
Wind Tunnel Wall Interference Assessment and Correction, 1983
[NASA-CP-2319] 03 p0311 N85-12011
Proceedings of a Workshop on Applications of Tethers in Space, Executive Summary
[NASA-CR-171195] 03 p0322 N85-12075
Proceedings of a Workshop on the Applications of Tethers in Space, Volume 1
[NASA-CR-171196] 03 p0322 N85-12076
Proceedings of a Workshop on Applications of Tethers in Space, Volume 2
[NASA-CR-171197] 03 p0322 N85-12077
ERS-1 radar altimeter data products — conference
[ESA-SP-221] 03 p0379 N85-12419
Star Formation Workshop
[ROE-OR-13] 03 p0441 N85-12809
Colloquium about Joint Projects within DFVLR/ISRO Cooperation
[DFVLR-MITT-84-12] 04 p0458 N85-12907
Tough Composite Materials
[NASA-CP-2334] 04 p0483 N85-12941
Official journey to USA, November 1983. Symposium on the Compatibility of Explosives; Mound Laboratory; Naval Surface Weapons Center
[FOA-C-20548-D1] 04 p0482 N85-13072
Digital image processing; report from a conference and study trip to the USA and Canada, summer 1984
[FOA-C-30369-E1] 04 p0494 N85-13153
Scientific contributions in commemoration of Ebro Observatory's 75th anniversary — conference
[ISBN-84-00-05380-X] 04 p0518 N85-13308
National Photovoltaics Program Annual Review Meeting, abstracts
[DE84-013003] 04 p0530 N85-13390
Proceedings of a Workshop on Atmospheric Research Needs for the Western United States
[DE84-015005] 04 p0534 N85-13412
Proceedings of the US-Japan Theory Workshop on 3-D MHD Studies
[DE84-012019] 04 p0568 N85-13620
The 1984 ASEE-NASA summer faculty fellowship program (aeronautics and research)
[NASA-TM-87393] 04 p0575 N85-13664
FY 1984 scientific and technical reports, articles, papers and presentations
[NASA-TM-86470] 04 p0575 N85-13670
Energy information exchange, 1983
[DE84-901446] 04 p0577 N85-13680
Conference on the Origin of the Moon
[NASA-CR-174068] 04 p0581 N85-13709

Flow Around Bluff Bodies: Numerical and Experimental Approaches — conferences
[VKI-LS-1984-06] 05 p0593 N85-13778
An Assessment of Integrated Flywheel System Technology
[NASA-CP-2346] 05 p0604 N85-13850
Space Power
[NASA-CP-2352] 05 p0608 N85-13880
Workshop on Mechanical Technology for Antennas — conferences; satellite antennas
[ESA-SP-225] 05 p0625 N85-13999
Special Developments and Methods in High Frequency Measuring Techniques — conferences
[PTB-E-24] 05 p0629 N85-14030
Flow in Centrifugal Compressors — conferences
[VKI-LS-1984-07] 05 p0636 N85-14079
Rotordynamic Instability Problems in High-Performance Turbomachinery
[NASA-CP-2338] 05 p0642 N85-14116
The fourth LBF colloquium
[ISSN-0721-5320] 05 p0648 N85-14163
The Interaction of Global Biochemical Cycles
[NASA-CR-174184] 05 p0652 N85-14183
EARSeL/ESA Symposium on Integrative Approaches in Remote Sensing
[ESA-SP-214] 05 p0655 N85-14202
Assessment of Techniques for Measuring Tropospheric H sub x O sub y
[NASA-CP-2332] 05 p0675 N85-14336
Report of the Meeting of Experts on Climate and Human Health
[WCP-78] 05 p0687 N85-14413
Life Sciences Research in Space — conference
[ESA-SP-212] 05 p0689 N85-14425
Twentieth Annual Conference on Manual Control, volume 1
[NASA-CP-2341-VOL-1] 05 p0699 N85-14487
Twentieth Annual Conference on Manual Control, volume 2
[NASA-CP-2341-VOL-2] 05 p0707 N85-14535
Fifth Conference on Star Clusters and Associations and Their Relation to the Evolution of the Galaxy
[PUBL-56] 05 p0736 N85-14732
Technical Workshop: Advanced Helicopter Cockpit Design
[NASA-CP-2351] 06 p0750 N85-14806
US objectives generally achieved at broadcasting satellite international conference. Improvements can help in future conferences
[PB84-235316] 06 p0800 N85-15109
International Conference on Physics of Clouds 06 p0819 N85-15198
Proceedings of the 23rd Project Integration Meeting
[NASA-CR-174186] 06 p0829 N85-15260
Miniworkshop on effects of stress and strain in high-speed-growth silicon ribbons 06 p0831 N85-15284
Proceedings of the 22nd Project Integration Meeting
[DE85-000334] 06 p0833 N85-15302
Recent developments in photovoltaics
[DE84-004528] 06 p0833 N85-15305
Proceedings of the 14th Conference on Environmental Toxicology
[AD-A146400] 06 p0843 N85-15350
Proceedings of the National Bureau of Standards and National Security Agency Workshop on Standardization Issues for Optical Data Disk (OD3) Technology
[PB84-217785] 06 p0848 N85-15383
Proceedings of Workshop on Synergistic Effects in Surface Phenomena Related to Plasma-Wall Interactions
[IPPJ-AM-35] 06 p0864 N85-15486
ASC 1984 Applied Superconductivity Conference
[DE84-016204] 06 p0868 N85-15521
Local Interstellar Medium. International Astronomical Union Colloquium No. 81
[NASA-CP-2345] 06 p0872 N85-15539
The 47th Annual Meteoritical Society Meeting
[NASA-CR-174071] 06 p0881 N85-15599
Proceedings of the International Conference and Exposition on Structural Impact and Crashworthiness
[AD-A147845] 07 p0900 N85-15703
Engine Cyclic Durability by Analysis and Testing
[AGARD-CP-368] 07 p0905 N85-15733
Modern signal processing and reconnaissance — conferences
[FOA-C-30374-E1] 07 p0942 N85-15975
Astronomical photography 1984 — conferences
[ROE-OR-14] 07 p0962 N85-16102
Proceedings of the Second Annual Symposium on Mathematical Pattern Recognition and Image Analysis Program
[E85-10056] 07 p0984 N85-16251
International Aerospace and Ground Conference on Lightning and Static Electricity. 1984 technical papers. Supplement
[NASA-CP-2356] 07 p0999 N85-16343
Climate Conference for Latin America and the Caribbean
[WMO-632] 07 p1000 N85-16352
QUASAT: A VLBI observatory in space — conferences
[ESA-SP-213] 07 p1056 N85-16700
Helicopter Guidance and Control Systems for Battlefield Support
[AGARD-CP-359] 08 p1072 N85-16797
Space Shuttle Technical Conference, part 2
[NASA-CP-2342-PT-2] 08 p1098 N85-16937
OTV Propulsion Issues
[NASA-CP-2347] 08 p1106 N85-16989
Hazard Studies for Solid Propellant Rocket Motors
[AGARD-CP-367] 08 p1114 N85-17025
Proceedings of the 2nd Workshop on Nondestructive Evaluation (NDE) of Titanium Alloys
[AD-A147626] 08 p1125 N85-17095
Papers of the 15th International Society for Photogrammetry and Remote Sensing (ISPRS) Congress — conferences
[TRITA-FMI-9] 08 p1175 N85-17406
Proceedings of a Workshop on Research Issues in Simulator Sickness
[AD-A148543] 08 p1196 N85-17538
International Conference on Luminescence
[AD-A148470] 08 p1223 N85-17701
The Origin of Nonradiative Heating/Momentum in Hot Stars
[NASA-CP-2358] 08 p1231 N85-17755
X-ray and UV Emission from Active Galactic Nuclei — conference
[MPE-184] 08 p1236 N85-17790
Airborne Astronomy Symposium. A symposium commemorating the tenth anniversary of operations of the Kuiper Airborne Observatory
[NASA-CP-2353] 08 p1244 N85-17848
Proceedings of the Workshop on Improvements to Photometry
[NASA-CP-2350] 08 p1250 N85-17892
Proceedings of the workshop on unsteady separated flow held at the United States Air Force Academy on August 10-11, 1983
[AD-A148249] 09 p1263 N85-17937
The IMAGE 3 Conference Proceedings
[AD-A148636] 09 p1267 N85-17962
Simulating speed and height cues in the C-130 weapon system trainer
[AD-P004313] 09 p1268 N85-17967
Producing high scene content with perspective validity
[AD-P004314] 09 p1268 N85-17968
Geographic subdivision and top level data structures, Columbus, Magellan, and expanding CIG (Computer Image Generation) horizons
[AD-P004317] 09 p1268 N85-17971
An overview of the research program at the visual technology research simulator
[AD-P004321] 09 p1269 N85-17975
Considerations in an optical variable acuity display system
[AD-P004323] 09 p1269 N85-17977
Control systems analysis program: A tool for analysis of the GE-VSCDP (General Electric-Visual System Component Display Program) image display system
[AD-P004325] 09 p1270 N85-17979
The effects of time delay in man-machine control systems: Implications for design of flight simulator Visual-Display-Delay compensation
[AD-P004329] 09 p1270 N85-17983
The fiber-optic helmet-mounted display
[AD-P004330] 09 p1270 N85-17984
Binocular overlap in a fiber optic helmet mounted display
[AD-P004331] 09 p1270 N85-17985
Baffled eye and confounded brain or using visual illusions to train blind pilots
[AD-P004332] 09 p1271 N85-17986
Simulator sickness: Sensorimotor disturbances induced in flight simulators
[AD-P004334] 09 p1271 N85-17988
On-board Computer Image Generator (CIG) applications
[AD-P004335] 09 p1271 N85-17989
CIG (Computer Image Generator) goes to war: The tactical illusion
[AD-P004336] 09 p1271 N85-17990
Military applications of the Singer Link-Miles IMAGE visual system
[AD-P004337] 09 p1271 N85-17991
Flight Training Technology for Regional/Commuter Airline Operations: Regional Airline Association/NASA Workshop Proceedings
[NASA-CP-2348] 09 p1275 N85-18009
Proceedings of the AFOSR/AFRPL Rocket Propulsion Research Meeting: Abstracts and Agenda
[AD-A148618] 09 p1288 N85-18085
The Shock and Vibration Bulletin 54. Part 1: Welcome, keynote address, invited papers MIL-STD-810D, MIL-STD-810D panel session
[AD-A148131] 09 p1333 N85-18377
Proceedings of the Environmental Systems Symposium (13th) held at Bethesda, Md., 20-22 March 1984
[AD-A148194] 09 p1346 N85-18471
Proceedings of the International Conference on the Performance of Off-Road Vehicles and Machines, (8th), volume 1
[AD-A148634] 09 p1403 N85-18633
Proceedings of the 8th International Conference on the Performance of Off-Road Vehicles and Machines, volume 2
[AD-A148635] 09 p1407 N85-18859
Proceedings of Colloquium/Workshop on Composite Materials and Structures, Standardization, Qualification, Certification held at washington, D.C. on 8-10 May 1984
[AD-A149039] 10 p1432 N85-19029
The 1984 JANNAF Propulsion Systems Hazards Subcommittee Meeting, volume 1
[AD-A148865] 10 p1454 N85-19162
Report on AGARD Meeting: Hazards Studies for Solid Propellant Rocket Motors
[AD-P004340] 10 p1454 N85-19164
National Machine Tools Conference slated for 1985: Conference agenda, papers 10 p1460 N85-19202
Proceedings of the 17th Symposium on Electromagnetic Windows, part 1
[AD-A149185] 10 p1466 N85-19253
Propagation Influences on Digital Transmission Systems: Problems and Solutions
[AGARD-CP-363] 10 p1469 N85-19269
1984 AFOSR Research Meeting on Diagnostics of Reacting Flow held at New Haven, Connecticut on 21-22 March 1984
[AD-A149023] 10 p1484 N85-19367
Fourth International Conference on Robot Vision and Sensory Controls
[AD-A149524] 10 p1492 N85-19422
Summer study program in geophysical fluid dynamics, the Woods Hole Oceanographic Institution, dynamic differentiation
[AD-A149366] 10 p1521 N85-19595
Image Understanding: Proceedings of the 15th Workshop
[AD-A149496] 10 p1557 N85-19816
Calendar of selected aeronautical and space meetings
[AGARD-CAL-84/2] 10 p1573 N85-19917
Proceedings of the 14th Army Science Conference. Volume 1: Principal Authors A through H
[AD-A149200] 10 p1573 N85-19920
Modeling turbulent flow in compressible fluids: Metrological aspects — conferences 11 p1575 N85-19926
Wildlife Hazards to Aircraft Conference and Training Workshop: Proceedings
[AD-A148330] 11 p1578 N85-19936
Applications of Tethers in Space, volume 1
[NASA-CP-2364] 11 p1642 N85-20339
Applications of Tethers in Space, volume 2
[NASA-CP-2365] 11 p1644 N85-20361
Middle Atmosphere Program. Handbook for MAP, volume 4
[NASA-CR-175482] 11 p1654 N85-20420
Middle Atmosphere Program. Handbook for MAP, volume 10
[NASA-CR-175477] 11 p1658 N85-20450
LANDSAT-4 Science Characterization Early Results. Volume 2, part 1: Thematic Mapper (TM)
[E85-10068] 11 p1668 N85-20508
Proceedings of a Workshop on Environment of West Antarctica: Potential CO2-induced changes
[PB85-110757] 11 p1671 N85-20527
Photovoltaic Systems Development and Evaluation Projects Integration Meeting
[DE84-006530] 11 p1673 N85-20542
Proceedings of the 1st Glacier Bay Science Symposium
[PB85-115913] 11 p1682 N85-20599
Symposium on Military Aviation Medicine summarized 11 p1696 N85-20663
Contributions of the X-ray astronomy group — conference
[MPE-PREPRINT-28] 11 p1741 N85-20947
Contributions of the X-ray astronomy group — conference
[MPE-PREPRINT-29] 11 p1742 N85-20952
Observations of comets: Radio and otherwise — conference
[TB-64] 11 p1762 N85-21086
Proceedings of the 6th Advanced Aircrew Display Symposium
[AD-A150044] 12 p1776 N85-21160
Orbital Debris
[NASA-CP-2360] 12 p1783 N85-21188

Proceedings of the Symposium on Electromagnetic Windows (17th) held at Georgia Inst. of Technology, Engineering Experiment Station, Atlanta, Georgia on 25-27 July 1984. Part 2
[AD-A149125] 12 p1824 N85-21444
International Congress Centrum Berlin report on photovoltaics 12 p1877 N85-21773
Gas-liquid chemistry of natural waters, volume 2
[DE85-002457] 12 p1884 N85-21823
Biological effects of blast and impact waves
[FOA-C-52006-H4-D7] 12 p1905 N85-21968
Proceedings of the 1984 DOE Nuclear Reactor and Facility Safety Conference, volume 1
[DE84-012130] 12 p1931 N85-22132
Proceedings of the DOE Nuclear Reactor and Facility Safety Conference, volume 2
[DE84-012694] 12 p1931 N85-22133
The future of lightwave technology
[PB85-109759] 12 p1935 N85-22155
International Conference on Defects in Insulating Crystals
[AD-A149611] 12 p1939 N85-22180
Research and Modeling of Supervisory Control Behavior, report of a workshop
[AD-A149821] 12 p1950 N85-22248
Plasma Astrophysics — conference
[ESA-SP-207] 12 p1953 N85-22270
All-Union conference of radio astronomers 13 p1977 N85-22408
Spacecraft Environmental Interactions Technology, 1983
[NASA-CP-2359] 13 p1989 N85-22470
Twenty-first JANNAF Combustion Meeting, volume 1
[AD-A150981] 13 p1998 N85-22526
Workshop report: Swirl Enhanced Combustion 13 p2005 N85-22564
Photovoltaic Generators in Space — conferences
[ESA-SP-210] 13 p2005 N85-22565
LANDSAT-4 Science Characterization Early Results. Volume 4: Applications — agriculture, soils land use, geology, hydrology, wetlands, water quality, biomass identification, and snow mapping
[E85-10070] 13 p2117 N85-23186
Remote Sensing of Snow and Evapotranspiration
[NASA-CP-2363] 13 p2123 N85-23223
Abstracts of 6th Annual Review Meeting on Photovoltaic Advanced Research and Development
[DE84-013047] 13 p2128 N85-23246
Proceedings of the Geoscience Instrumentation Workshop
[DE85-004359] 13 p2132 N85-23268
The ASCOT Data Analysis Workshop
[DE85-004407] 13 p2139 N85-23283
Modulation of light energy transduction in photosynthesis
[DE85-004711] 13 p2141 N85-23292
Technical Digest: Symposium on Optical Fiber measurements, 1984
[PB85-114700] 13 p2160 N85-23407
Gears and Power Transmission Systems for Helicopters and Turboprops
[AGARD-CP-369] 14 p2220 N85-23765
Large Space Antenna Systems Technology, 1984
[NASA-CP-2368-PT-1] 14 p2229 N85-23813
Large Space Antenna Systems Technology, 1984
[NASA-CP-2368-PT-2] 14 p2233 N85-23840
Data Collection and Platform Location by Satellite: ARGOS Users' Conference 14 p2237 N85-23869
Report on the panel discussion of the Workshop on Data Collection Platform Networks 14 p2239 N85-23880
Data Collection and Platform Location by Satellite: ARGOS Users' Conference 14 p2239 N85-23883
The Giotto spacecraft impact-induced plasma environment
[ESA-SP-224] 14 p2243 N85-23905
Proceedings of the ARGOS Users Conference on Data Collection and Location by Satellite 14 p2322 N85-24348
Data Collection and Platform Location by Satellite: ARGOS Users' Conference 14 p2325 N85-24366
Data Collection and Platform Location by Satellite: ARGOS users' Conference 14 p2328 N85-24391
Data Collection and Platform Location by Satellite: ARGOS Users' Conference 14 p2330 N85-24409
Achievements of the International Magnetospheric Study (IMS) — conference
[ESA-SP-217] 14 p2354 N85-24544
Second Soviet-French Symposium on Space Cytology 14 p2386 N85-24699
Mini-Seminar on CAD/CAM
[CSIR-TSD-0007/83] 14 p2402 N85-24809
Finite Element Methods in South Africa 1983 — conference
[S-332] 14 p2410 N85-24863
Investigations carried out under the Director's Discretionary Fund
[NASA-CR-175676] 14 p2432 N85-24999
Cometary Astrometry
[NASA-CR-175660] 14 p2435 N85-25015
The hydromagnetics of the Sun — conferences
[ESA-SP-220] 14 p2445 N85-25091
Solar magnetohydrodynamics: Symposium review 14 p2455 N85-25162
Transonic Unsteady Aerodynamics and its Aeroelastic Applications
[AGARD-CP-374] 15 p2457 N85-25171
Roundtable on effective use of flight simulators 15 p2460 N85-25190
NASA R and T aerospace plane vehicles: Progress and plans
[NASA-TM-88429] 15 p2491 N85-25368
Three-Dimensional Boundary Layers
[AGARD-R-719] 15 p2558 N85-25784
Welding technology: Japan — Conference
[ISBN-0-85300177-4] 15 p2565 N85-25823
Thirteenth NASTRAN Users' Colloquium
[NASA-CP-2373] 15 p2573 N85-25863
Eight DOE Solar Photochemistry Research Conference: Proceedings
[DE85-005094] 15 p2587 N85-25948
Papers from the Symposium on Emissions: The Value of Incentives and Guidelines for Control
[S-336] 15 p2590 N85-25967
NASA Space Biology Program: 9th Annual Symposium
[NASA-CP-2336] 15 p2605 N85-26054
Proceedings of the BAe human factors seminar
[BAE-BT-11873] 15 p2620 N85-26145
Workshop on Parallel Computer Architectures in Pattern Recognition and Image Processing
[BMFT-FB-DV-84-006] 15 p2622 N85-26154
Very large least squares problems and supercomputers
[AD-A151270] 15 p2623 N85-26162
Supercomputers and symbolic computation
[AD-A151376] 15 p2623 N85-26166
Symposium on Computers in Civil Engineering 1983
[CSIR-S-298] 15 p2626 N85-26182
ONR (Office of Naval Research) Far East Scientific Bulletin, Volume 9, Number 4, October-December 1984
[AD-A151274] 15 p2665 N85-26448
Planetary Rings. Colloquium 75 — conferences
[ISBN-2-85428-100-4] 15 p2670 N85-26473
Proceedings of the NAL Symposium on Aircraft Computational Aerodynamics
[NAL-SP-1] 16 p2691 N85-26611
Technical evaluation report on the Flight Mechanics Symposium on Active Control Systems: Review, Evaluation and Projections
[AGARD-AR-220] 16 p2711 N85-26730
Tenth Conference of Working Group of Socialist Countries on Remote Sensing of Earth under Intercosmos Program 16 p2725 N85-26820
Advanced High Pressure O2/H2 Technology
[NASA-CP-2372] 16 p2733 N85-26862
Sixth DOE Electrochemical Contractor's Review. Extended abstracts
[DE84-013679] 16 p2779 N85-27151
Short Wavelength Chemical Laser (SWCL) Workshop
[AD-A151959] 16 p2790 N85-27211
Data Collection and Platform Location by Satellite: ARGOS Users' Conference 16 p2811 N85-27333
Proceedings of the Workshop on Polarized Targets in Storage Rings
[DE85-002704] 16 p2862 N85-27653
Active Control Systems: Review, Evaluation and Projections
[AGARD-CP-384] 17 p2901 N85-27883
Adaptive wall wind tunnels and wall interference correction methods
[DFVLR-IB-222-84-A-37] 17 p2905 N85-27912
Structural Integrity and Durability of Reusable Space Propulsion Systems
[NASA-CP-2381] 17 p2910 N85-27941
Systematic nomenclature of the nitrogen, oxygen and sulfur functional polycyclic aromatic hydrocarbons
[DE85-007426] 17 p2916 N85-27974
Gordon Research Conference on Composites
[AD-A152888] 17 p2917 N85-27979
Proceedings of the 9th US Air Force and the Federal Republic of Germany Data Exchange Agreement Meeting. Viscous and Interacting Flow Field Effects
[AD-A153020] 17 p2958 N85-28266
Airphoto interpretation of vegetation and landforms for soil mapping 17 p2983 N85-28436
Presentations at the Tri-Service Cloud Modeling Workshop (2nd), held at the Naval Surface Weapons Center, White Oak, Maryland, 26-27 June 1984, volume 1
[AD-A152735] 17 p2996 N85-28522
Peer Review of a Formal Verification/Design Proof Methodology
[NASA-CP-2377] 17 p3010 N85-28609
Science and Technology in the Soviet Union
[AD-A152826] 17 p3047 N85-28858
Proceedings of the Sixteenth Annual Precise Time and Time Interval (PTTI) Applications and Planning Meeting
[NASA-TM-87561] 18 p3105 N85-29221
Environmental management needs
[DE85-007859] 18 p3133 N85-29405
Controlled Ecological Life Support System. Life Support Systems in Space Travel
[NASA-CP-2378] 18 p3155 N85-29531
Proceedings of the Seminar on Space Station Human Productivity
[NASA-TM-86673] 18 p3158 N85-29539
Report of the 11th Regional IRPA Congress on Recent Developments and New Trends in Radiation Protection
[IRI-190-83-13] 18 p3160 N85-29575
Proceedings of the 14th European Solid State Device Research Conference Including Solid State Device Technology, ESSDERC 84
[AD-A153409] 18 p3193 N85-29804
Space methods for geological research 19 p3295 N85-30429
Symposium on Luminescent Radiation Receivers and Converters 19 p3295 N85-30430
Proceedings of the Distributed Receiver Solar Thermal Technology Conference
[DE85-010551] 19 p3306 N85-30493
Third US/USSR Symposium on Particulate Control
[PB85-190890] 19 p3310 N85-30522
Proceedings of the Argonne Workshop on Programming the Next Generation of Supercomputers
[DE85-008348] 19 p3343 N85-30718
MCNP variance reduction overview
[DE85-010765] 19 p3346 N85-30741
Proceedings of the 1984 Workshop on High-Energy Excitations in Condensed Matter, volume 2
[DE85-007395] 19 p3357 N85-30809
Possibilities for studying short-lived nuclei produced at LAMPF
[DE85-010740] 19 p3365 N85-30864
U.S.-China conference on science policy
[PB85-176345] 19 p3380 N85-30971
Satellite aided search and rescue. Experimental results and operational prospects — conference
[ISBN-2-85428-120-9] 20 p3400 N85-31088
Proceedings of the Workshop on Identification and Control of Flexible Space Structures, volume 1
[NASA-CR-176051] 20 p3408 N85-31148
Sandia Cooperative Group on the Aerothermochemistry of Turbulent Combustion. Discussion record of fourth meeting
[DE85-004720] 20 p3423 N85-31248
Cryogenics for the Superconducting Super Collider: Workshop Proceedings
[DE85-010951] 20 p3437 N85-31327
The 1984 Goddard Space Flight Center Battery Workshop
[NASA-CP-2382] 20 p3443 N85-31371
Nonlinear Constitutive Relations for High Temperature Application, 1984
[NASA-CP-2389] 20 p3465 N85-31530
Remote Sensing Technology: Symposium Proceedings
[DE85-010212] 20 p3477 N85-31606
Proceedings of the Flat-Plate Solar Array Project Research Forum on High-Efficiency Crystalline Silicon Solar Cells
[NASA-CR-176047] 20 p3478 N85-31615
Commission for Marine Meteorology
[WMO-640] 20 p3496 N85-31735
Results of Space Experiments in Physiology and Medicine and Informal Briefings by the F-16 Medical Working Group
[AGARD-CP-377] 20 p3507 N85-31805
Spectral Theory of Sturm-Liouville Differential Operators: Proceedings of the 1984 Workshop
[DE85-009893] 20 p3520 N85-31890
Proceedings of the 19th Annual Conference of the Finnish Physical Society
[REPT-104] 20 p3532 N85-31974
VLF (Very low frequency) workshop held at San Diego California, 24-25 January 1985
[AD-A154652] 21 p3573 N85-32224
Middle Atmosphere Program. Handbook for MAP. Volume 14: URSI/SCOSTEP Workshop on Technical Aspects of MST Radar
[NASA-CR-176065] 21 p3615 N85-32486
Data base management: MSTRAC (keynote paper), part 8 21 p3626 N85-32530
Eleventh International Conference on Atmospheric Aerosols, Condensation and Ice Nuclei, volume 2
[PB85-182418] 21 p3636 N85-32596

Eleventh International Conference on Atmospheric Aerosols, Condensation and Ice Nuclei, volume 1
[PB85-162400] 21 p3644 N85-32636
Software for interactive on-line conferences
[AD-A154742] 21 p3670 N85-32801
Workshop on the Early Earth: The Interval from Accretion to the Older Archean
[NASA-CR-176037] 21 p3717 N85-33062
Management of Corrosion
[AGARD-LS-141] 22 p3749 N85-33236
Nineteenth Aerospace Mechanisms Symposium
[NASA-CP-2371] 22 p3795 N85-33512
Nordic Association for Aerosol Research (NOSA) Aerosol Symposium: Program and abstracts
[FOA-E-40019] 22 p3812 N85-33616
Proceedings of the 18th LAMPF Users Group Meeting
[DE85-011886] 22 p3839 N85-33773
Terrestrial Planets: Comparative Planetology
[NASA-CR-176093] 22 p3851 N85-33849
Nineteenth International Cosmic Ray Conference. Conference program and author index
[NASA-CP-2376] 22 p3860 N85-33901
Nineteenth International Cosmic Ray Conference. OG sessions, volume 1
[NASA-CP-2376-VOL-1] 22 p3860 N85-33902
Nineteenth International Cosmic Ray Conference. OG sessions, volume 2
[NASA-CP-2376-VOL-2] 22 p3875 N85-34006
Space Station Engineering and Technology Development: Proceedings of the Panel on In-Space Engineering Research and Technology Development
[NASA-CR-176110] 23 p3899 N85-34153
Coordinated study of solar-terrestrial payloads on space station
[NASA-CR-176160] 23 p3900 N85-34158
Proceedings of the Twentyseventh Japan Congress on Materials Research
[ISSN-0368-3141] 23 p3903 N85-34180
Proceedings of the Mechanisms Conference, volume 1 23 p3923 N85-34309
Proceedings of the Mechanisms Conference, volume 2 23 p3924 N85-34318
Problems of aviation and space medicine and psychology discussed at 14th Gagarin lectures 23 p3954 N85-34509
Graphics Interface 1985: Proceedings
[ISSN-0713-5424] 23 p3957 N85-34523
Nineteenth International Cosmic Ray Conference. SH sessions, volume 4
[NASA-CP-2376-VOL-4] 23 p3989 N85-34729
Nineteenth International Cosmic Ray Conference. OG sessions, volume 3
[NASA-CP-2376-VOL-3] 23 p4012 N85-34862
Nineteenth International Cosmic Ray Conference. SH sessions, volume 5
[NASA-CP-2376-VOL-5] 23 p4031 N85-34991
Lectures of a Flight Mechanics Conference --- conferences
[ESA-TT-831] 24 p4061 N85-35165
Proceedings of the 7th Joint Panel Meeting of the UJNR Panel on Fire Research and Safety
[PB85-196545] 24 p4085 N85-35317
USGS research on mineral resources, 1985
[CIRC-949] 24 p4103 N85-35435
Implementing agreement for cooperation in the development of large scale wind energy conversion systems
[JUEL-SPEZ-276] 24 p4110 N85-35473
Land Disposal of Hazardous Waste
[PB85-196376] 24 p4113 N85-35500
Workshop Proceedings: Interpretation of Seismic Wave Propagation in Laterally Heterogeneous Structures
[BMR-258] 24 p4118 N85-35530
Proceedings of Meteorological Motor Glider (MEMO) Workshop '84
[DFVLR-MITT-85-04] 24 p4121 N85-35542
Proceedings of a Scientic Meeting on the Occasion of the Inauguration of New Buildings for the DFVLR Institute for Aerospace Medicine
[ESA-TT-857] 24 p4129 N85-35595
Proceedings of the 14th Army Science Conference. Volume 2: Principal authors I through O
[AD-A149201] 24 p4144 N85-35690
Proceedings of the 14th Army Science Conference. Volume 3: Principal authors P through Z
[AD-A149202] 24 p4144 N85-35691
Proceedings of the Workshop on Detectors for Relativistic Nuclear Collisions
[LBL-18225] 24 p4146 N85-35700
The 2nd European Conference on Atomic and Molecular Physics
[AD-A155663] 24 p4148 N85-35715
Nineteenth International Cosmic Ray Conference. HE Sessions, volume 6
[NASA-CP-2376-VOL-6] 24 p4170 N85-35848
Nineteenth International Cosmic Ray Conference. HE Sessions, volume 7
[NASA-CP-2376-VOL-7] 24 p4186 N85-35868
Nineteenth International Cosmic Ray Conference. HE sessions, volume 8
[NASA-CP-2376-VOL-8] 24 p4200 N85-36066

CONFIDENCE
Setting hurricane conditions of readiness with high confidence
[AD-A144785] 01 p0085 N85-10570
Bootstrap confidence intervals
[AD-A147572] 07 p1033 N85-16559
Exact simultaneous confidence intervals for pairwise comparisons of three normal means
[AD-A148751] 09 p1375 N85-18645

CONFIDENCE LIMITS
Construction of approximate confidence intervals for probability-of-kill via the bootstrap
[AD-A144761] 01 p0113 N85-10764
Construction of a confidence region for linear functions with unknown parameters
[CTH-MATH-1984-17] 05 p0721 N85-14630
The theory of optimal confidence limits for systems reliability with counterexamples for results on optimal confidence limits for series systems
[AD-A147236] 07 p1031 N85-16546
Bootstrap confidence intervals
[AD-A147572] 07 p1033 N85-16559
Exact simultaneous confidence intervals for pairwise comparisons of three normal means
[AD-A148751] 09 p1375 N85-18645
An asymptotically optimal subclass of BTIB designs for comparisons with a control
[AD-A149819] 12 p1921 N85-22066
Confidence intervals using the regenerative method for simulation output analysis
[AD-A150147] 13 p2149 N85-23343
Better bootstrap confidence intervals
[AD-A150798] 14 p2408 N85-24846
Shuttle fleet operations: A simulation analysis
[AD-A151383] 15 p2491 N85-25370
Criteria for the classification of hydrographic positioning data
[AD-A152283] 16 p2705 N85-26697
Confidence intervals based on interpolated order statistics
[AD-A152607] 17 p3025 N85-28701
Limit theorems for the method of replication
[AD-A153541] 18 p3170 N85-29642
On the confidence limits for Weibull reliability and quantiles: The case of maximum likelihood estimation from small size censored samples
[REPT-84-RR-345] 20 p3521 N85-31896
The optimality of lower confidence limits for the reliability of series systems obtained by the method of key test results or other related techniques
[AD-A154880] 21 p3597 N85-32338

CONFIGURATION MANAGEMENT
Configuration management for mission-critical software: The Los Alamos solution
[DE84-015515] 03 p0408 N85-12606
Software configuration management across project boundaries and in distributed development environments
[RSRE-MEMO-3704] 04 p0549 N85-13494
Managing computer-controlled operations 06 p1097 N85-16934
Space Station Software Issues
[NASA-CP-2361] 11 p1700 N85-20689
Space Station reference configuration description
[NASA-TM-87493] 20 p3408 N85-31148
Integrated Support Software System (ISSS)
[AD-A155715] 22 p3629 N85-33710

CONFIGURATIONS
Changes in spectral properties of detached leaves
[E85-10042] 07 p0963 N85-16243

CONFINEMENT
Focusing and confinement
[DE84-016181] 05 p0640 N85-14106
Confinement of low-energy electrons near metallic surfaces for plasmon generation
[DE85-001119] 09 p1381 N85-18688
Efficient heating and confinement of ions in an axisymmetric magnetic mirror supplemented with dc electric field
[IPPJ-707] 12 p1935 N85-22160
Behavior of turbulent gas jets in an axisymmetric confinement
[NASA-CR-174829] 15 p2473 N85-25265
Effects of muscle atrophy on motor control: Cage size effects 15 p2609 N85-26080
Breakthrough in container confinement of ultracold neutrons 15 p2644 N85-26311
Effect of confinement on failure in 95 TATB/5 KEL-F
[DE85-010790] 19 p3251 N85-30158
Density and confinement effects on mixing characteristics of an axisymmetrical CO(2) jet
[AD-A154468] 19 p3267 N85-30258
Los Alamos Spheromak Program
[DE85-010748] 20 p3398 N85-31077
Magnetics calculations for an ELMO Bumpy Square
[DE85-011438] 21 p3707 N85-33021
Behavior of the porous bed in a combustion-deflagration-detonation transition
[ISL-CO-220/84] 22 p3747 N85-33224
Combustion-deflagration-detonation transition
[ISL-CO-221/84] 22 p3747 N85-33225

CONFIRMATION
U PROVING

CONFLUENCE
U CONVERGENCE

CONFORMAL MAPPING
Deformations of two-dimensional dissipative maps --- orbit perturbation
[REPT-69] 01 p0129 N85-10891
What formulas are good for representing dipole and generalized oscillator-strength spectra
[DE84-014641] 02 p0276 N85-11809
Nicolai maps and stochastic observables from a coupling constant flow
[BONN-HE-84-26] 09 p1376 N85-18653
Annuals of the Finnish Academy of Sciences, series A. 1: Mathematics, volume 8, part 2
[ISSN-0066-1953] 10 p1535 N85-19673
Domains with Lipschitz mapping functions 10 p1535 N85-19675
Simplified proofs of some basic theorems for quasiregular mappings 10 p1535 N85-19677
Diffeomorphic approximation of quasiconformal and quasisymmetric homeomorphisms 10 p1536 N85-19678
Analytical foundations of the theory of quasiconformal mappings in Rn 10 p1536 N85-19679
A conformal mapping suitable for problems involving interaction between given geometries and known far fields
[AD-A149050] 10 p1545 N85-19744
Applications of the conformal mapping method to the solution of mechanical vibrations problems 13 p2102 N85-23103
Investigation of potential and viscous flow effects contributing to dynamic stall
[AD-A151696] 15 p2557 N85-25773
Annals of the Scientific Academy of Finland, series A. 1: Mathematics, volume 9
[ISSN-0066-1953] 15 p2633 N85-26229
Harmonic univalent functions 15 p2633 N85-26230
Old and new in Moebius groups 15 p2634 N85-26235
Remarks of the maximal dilatation of the Beurling-Ahlfors extension 15 p2634 N85-26239
A remark on the conformal capacity of Groetzsch's condenser in space 15 p2634 N85-26240
Extension of embeddings close to isometries or similarities 15 p2634 N85-26242
Application of conformal mapping to grid generation 16 p2692 N85-26621
Conditions for the possibility of conformal sewing
[ST-AASF-IMD-58] 16 p2858 N85-27625
Chaos and order in an optical ring cavity
[CWI-AM-R8416] 17 p3038 N85-28795
Generation by conformal mappings of aerofoil sections and of certain other simple shapes suitable for both aerodynamic and stress-concentration problems
[AD-A154901] 22 p3728 N85-33112
Adaptive rezoner in a two-dimensional Lagrangian hydrodynamic code
[DE85-010108] 24 p4094 N85-35381

CONFORMAL TRANSFORMATIONS
U CONFORMAL MAPPING

CONGRESSIONAL REPORTS
Soviet space programs, 1976-1980, with supplementary data through 1983. Part 2: Manned space programs and space life sciences
[S-REPT-98-235-PT-2] 01 p0014 N85-10088
Department of Housing and Urban Development, and certain independent agencies appropriations for fiscal year 1985, part 2
[S-REPT-98-869-PT-2] 01 p0127 N85-10870
National Aeronautics and Space Administration 01 p0127 N85-10871
Office of Technology Assessment 01 p0127 N85-10872
Workshop on Automated Space Station 01 p0127 N85-10873
Initiatives to promote space commercialization
[GPO-37-551] 02 p0156 N85-11058
Statement of Hon. James M. Beggs, Administrator, NASA, Washington, DC 02 p0156 N85-11059

Civilian space stations and the US future in space: Summary
[OTA-STI-242] 03 p0323 N85-12083
The status of synthetic fuels and cost-shared energy R and D facilities
[GPO-36-903] 03 p0339 N85-12182
Carbon dioxide, the greenhouse effect and climate: A primer
[GPO-33-444] 03 p0395 N85-12519
Airliner cabin air quality
[S-REPT-98-458] 03 p0402 N85-12560
Emergency Mathematics and Science Education Act
[GPO-29-561] 03 p0435 N85-12770
Ways to improve management of Federal funded computerized models
[LCD-75-111] 03 p0435 N85-12771
Federal Telecommunications Privacy Act of 1984
[H-REPT-98-815] 03 p0441 N85-12807
Aircraft navigation and landing technology: Status of implementation
[GPO-38-615] 04 p0454 N85-12883
The Expendable Launch Vehicle Commercialization Act
[GPO-30-838] 04 p0460 N85-12919
Review of Space Shuttle requirements, operations, and future plans
[GPO-39-101] 04 p0461 N85-12927
Results of Space Shuttle Flight 41-C
[GPO-36-092] 04 p0461 N85-12928
Statement of Captain Robert L. Crippen, USN, Commander of Space Shuttle Flight 41-C; Francis R. Scobee, pilot; Doctor George D. Nelson, Mission Specialist; Terry J. Hart, Mission Specialist; and Doctor James D. Van Hoften, Mission Specialist; accompanied by Frank Capollina, Solar Maximum Repair Mission Project Manager, Goddard Space Flight Center 04 p0461 N85-12929
Guayule research
[GPO-29-562] 04 p0477 N85-13042
Methane-fueled vehicle RD and D
[GPO-37-926] 04 p0481 N85-13064
Fire prevention and control
[GPO-30-743] 04 p0482 N85-13074
Scientific communications and national security
[GPO-36-093] 04 p0492 N85-13138
Summary and analysis of hearing on improving the research infrastructure at US universities and colleges
[GPO-36-854] 04 p0574 N85-13660
Improving the research infrastructure at US universities and colleges
[GPO-35-290] 04 p0574 N85-13661
The Uniform Science and Technology Research and Development Utilization Act
[GPO-36-327] 04 p0577 N85-13685
Uniform Science and Technology Research and Development Utilization Act
[H-REPT-98-983-PT-1] 04 p0577 N85-13686
Computer Literacy Act of 1983, part 2
[H-REPT-98-752-PT-2] 04 p0578 N85-13687
Manufacturing Sciences and Robotics Research and Development Act of 1984
[H-REPT-98-1078] 04 p0578 N85-13688
Commercial Space Launch Act
[GPO-39-613] 04 p0578 N85-13690
International Geosphere/Biosphere Program: 1984
[GPO-39-222] 04 p0578 N85-13691
Space telescope cost, schedule, and performance review, 1984
[GPO-39-065] 04 p0579 N85-13606
Vandenberg space shuttle launch complex
[S-HRG-98-1075] 05 p0601 N85-13833
Statement of Edward C. Aldridge, Jr., Under Secretary of the Air Force, Department of the Air Force, accompanied by Lieutenant General Robert W. Bazley, Inspector General and Brigadier General Donald J. Kutyna, Director of Space Systems and Command, Control and Communications, Deputy Chief of Staff, Research, Development and Acquisition 05 p0601 N85-13834
Statement of Honorable James M. Beggs, Administrator, National Aeronautics and Space Administration 05 p0601 N85-13835
Subliminal communication technology
[GPO-38-833] 05 p0622 N85-13979
Land Remote-Sensing Commercialization Act
[S-REPT-98-458] 05 p0654 N85-14201
The availability of Japanese scientific and technical information in the United States
[GPO-35-241] 05 p0735 N85-14726
Man in Space: National Historic Landmark Theme Study
[PB85-107233/GAR] 07 p0911 N85-15768
Civilian space stations and the US future in space
[OTA-STI-241] 07 p0914 N85-15781
Satellite navigation
[S-HRG-98-858] 08 p1082 N85-16851
International cooperation and competition in civilian space activites
[OTA-ISC-240] 08 p1231 N85-17750
Sunset of the Civil Aeronautics Board
[S-HRG-98-940] 09 p1403 N85-18829
Semiannual report to Congress on the effectiveness of the civil aviation security program
[AD-A149522] 10 p1421 N85-18967
Computers and education
[GPO-28-378] 10 p1537 N85-19689
Computer crime
[GPO-30-544] 10 p1537 N85-19691
Department of defense, office of inspector general semiannual report to the Congress, 1 April - 30 September 1984
[AD-A149560] 10 p1567 N85-19879
Provision of Federal government publication in electronic format to depository libraries
[S-PRT-98-260] 10 p1567 N85-19880
High-speed intercity rail passenger service
[GPO-35-896] 10 p1570 N85-19897
Synthetic fuels policy
[GPO-34-227] 11 p1613 N85-20143
Environmental Monitoring Improvement Act
[GPO-39-742] 11 p1677 N85-20568
Carbon dioxide and the greenhouse effect
[GPO-39-043] 11 p1677 N85-20569
National Acid Precipitation Assessment Program. Report to the President and Congress (1963)
[PB85-116713] 11 p1679 N85-20581
Ultralight aircraft technology and public safety
[GPO-38-948] 12 p1773 N85-21131
Legislation to improve airline safety
[GPO-36-222] 12 p1773 N85-21132
Commercial space launches
[S-REPT-98-656] 12 p1788 N85-21225
Brussels Satellite Convention
[S-EXEC-REPT-98-52] 12 p1790 N85-21234
Results of Space Shuttle flight 41-D
[GPO-39-481] 12 p1791 N85-21243
Developments in the production and use of ethanol fuels
[GPO-40-678] 12 p1817 N85-21396
Effects of air pollution and acid rain on forest decline
[GPO-37-459] 12 p1883 N85-21818
Wind shear detection technology
[GPO-38-920] 12 p1893 N85-21879
Hurricane storm surge research
[GPO-40-048] 12 p1893 N85-21880
Computer and communications security and privacy
[GPO-39-741] 12 p1911 N85-21994
Oversight review of the five-year outlook report on science and technology
[GPO-41-058] 12 p1949 N85-22243
1984 science and technology posture hearing with the director of the Office of Science and Technology Policy
[GPO-41-060] 12 p1949 N85-22244
An agenda for a study of government science policy
[GPO-40-860] 12 p1949 N85-22245
Transfer of technology
[S-REPT-98-664] 12 p1949 N85-22246
Transfer of technology
[S-HRG-98-986] 12 p1949 N85-22247
The availability of Japanese scientific and technical information in the United States
[GPO-39-478] 12 p1951 N85-22254
Summary of activities of the Committee on Science and Technology
[H-REPT-98-1169] 12 p1964 N85-22341
The impact of weather on aviation safety
[GPO-35-520] 16 p2703 N85-26685
Recent failures of weather satellites
[S-HRG-98-1070] 16 p2731 N85-26855
Soviet space programs, 1976-1980 (with supplementary data through 1983). Part 3: Unmanned space activities
[S-PRT-98-235-PT-3] 16 p2879 N85-27765
National Telecommunications and Information Administration authorization
[GPO-38-660] 16 p2879 N85-27766
East-West cooperation in outer space
[S-HRG-98-1064] 16 p2879 N85-27767
Department of Housing and Urban Development-independent agencies appropriations for 1986. Part 6: National Aeronautics and Space Administration
[GPO-47-235] 16 p2879 N85-27768
The Department of Defense statement on the Science and Technology Program by Colonel Donald I. Carter, USAF Acting Deputy Under Secretary of Defense for Research and Advanced Technology before the Subcommittee on Research and Development of the Committee on Armed Services of the United States House of Representatives, 99th Congress, first session
[AD-A152467] 17 p3048 N85-28850
National Aeronautics and Space Administration Authorization Act, 1986
[S-REPT-99-91] 17 p3051 N85-28885
Report to Congress on the Automotive Technology Development Program
[DE85-005640] 17 p3052 N85-28890
Electric and hybrid vehicle program
[DE85-010025] 19 p3282 N85-30230
National Aeronautics and Space Administration Authorization Act, 1986
[S-REPT-99-91] 19 p3381 N85-30978
Department of Housing and Urban Development-Independent Agencies Appropriation Bill, 1986
[H-REPT-99-212] 19 p3382 N85-30979
National Aeronautics and Space Administration 19 p3382 N85-30980
FAA regulation of 9-seat and under passenger aircraft
[GPO-42-703] 20 p3391 N85-31032
Status of air traffic control system
[S-HRG-98-1197] 20 p3391 N85-31036
Insurance and the commercialization of space
[S-PRT-99-16] 20 p3397 N85-31074
Auto fuel efficiency standards, part 2
[GPO-41-189] 20 p3435 N85-31309
Antarctica
[S-HRG-98-1161] 20 p3473 N85-31584
Magnetohydrodynamics and the National Coal Science, Technology, and Engineering Development Acts
[S-HRG-98-1179] 20 p3535 N85-31994
NASA authorization, 1986, volume 1
[GPO-46-385] 20 p3541 N85-32039
United States-Soviet satellite accord: SARSAT/Cospas search-and-rescue program
[GPO-41-113] 20 p3541 N85-32040
Department of Housing and Urban Development-Independent Agencies Appropriation Act, 1986 20 p3542 N85-32041
National Aeronautics and Space Administration research and development 20 p3542 N85-32042
Aviation system delays
[S-HRG-98-1241] 21 p3553 N85-32102
Status of the air traffic control system
[GPO-40-343] 21 p3554 N85-32107
Review of hazardous waste cleanup and disposal efforts at Tinker Air Force Base
[GPO-43-294] 21 p3613 N85-32457
Hazardous air pollutants
[GPO-43-064] 21 p3613 N85-32458
Acid rain in Europe
[COMMITTEE-PRINT-99-F] 22 p3810 N85-33601
Aviation safety (aircraft passenger survivability and cabin safety)
[GPO-39-847] 23 p3895 N85-34130
Department of Housing and Urban Development Independent Agencies Appropriation Bill, 1986
[S-REPT-99-129] 23 p3987 N85-34720
National Aeronautics and Space Administration research and development: Program description 23 p3987 N85-34721
The 1986 National Aeronautics and Space Administration authorization
[GPO-47-835] 24 p4166 N85-35829

CONGRUENCES
Algebra of communicating processes
[CWI-CS-R8421] 17 p2950 N85-28214
A complete inference system for regular processes with silent moves
[CWI-CS-R8420] 17 p3014 N85-28638

CONICAL BODIES
NT SLENDER CONES
An algorithm for least squares projections onto the intersection of shifted, convex cones
[AD-A145428] 02 p0251 N85-11640
Experimental and predicted heating distributions for biconics at incidence in air at Mach 10
[NASA-TP-2334] 03 p0361 N85-12313
A computer program to calculate the supersonic flow over a solid cone in air or water
[AD-A151102] 15 p2484 N85-25217
Flow over a biconic configuration with an afterbody compression flap
[AD-A151882] 15 p2557 N85-25778
Cone drag in the transition from continuum to free molecular flow
[OUEL-1536/84] 20 p3390 N85-31023
Aerodynamic characteristics of the standard dynamics model in coning motion at Mach 0.6
[NASA-TM-86717] 21 p3552 N85-32094
Behavior of stress waves in a conical bar 23 p3904 N85-34182

CONICAL FLARE
U CONES

CONICAL FLOW
Geometric characteristics of turbulent boundary layer separation upon action with direct shock wave in conical flows 02 p0269 N85-11755
Conical stagnation points in the flow around an external corner — delta wings [VTH-LR-396] 16 p2701 N85-26680
CONICAL NOZZLES
Density distribution in supersonic jet discharged into vacuum from nozzle with bevel tip 02 p0269 N85-11757
Carbon/carbon rocket motor exit cone reinforcement [AD-D011360] 07 p0916 N85-15799
Nozzle wall roughness effects on free-stream noise and transition in the pilot low-disturbance tunnel [NASA-TM-86389] 23 p3930 N85-34355
CONICAL SCANNING
Integrated dual beam line scanning antenna and negative resistance diode oscillator [AD-D011717] 19 p3261 N85-30223
CONICAL SHELLS
Determination of stresses and deformations in linearly elastic conical shell subjected to aerodynamic loading and heating 13 p2047 N85-22812
Initial imperfection surveys on conical shells at Hoechst AG [VTH-LR-407] 17 p2981 N85-28429
CONICS
NT ELLIPSES
NT HYPERBOLAS
NT PARABOLAS
Precursors for Brazilian magnetic anomalies from 1922 to 1969 [INPE-3283-PRE/605] 11 p1681 N85-20590
Trapping of ion conics by downward parallel electric fields [AD-A155306] 21 p3633 N85-32568
CONIFERS
The 1984 NASA/ASEE summer faculty fellowship program [NASA-CR-174138] 04 p0574 N85-13663
Microwave model prediction and verifications for vegetated terrain [E85-10102] 16 p2809 N85-27322
Study of the formation of particles from natural hydrocarbons released by vegetation 21 p3644 N85-32640
CONJUGATE GRADIENT METHOD
Comparison of the multigrid and ICCG methods in solving the diffusion equation [DE84-014409] 02 p0253 N85-11657
Solution of finite element problems by preconditioned conjugate gradient and Lanczos methods [AD-A146921] 07 p1029 N85-16532
Solving large linear systems 14 p2396 N85-24759
CONJUGATE POINTS
Conjugacy of ELF-VHF emissions near L=6 — chorus phenomenon, hiss 14 p2367 N85-24629
Conjugated symmetrical coupler curves, produced by 4-bar linkages having the same transmission angles 23 p3924 N85-34322
CONJUGATES
NT CONJUGATE POINTS
CONJUGATION
NT PHASE CONJUGATION
Experimental investigation of wavefront conjugation during Mandel'shtam-Brillouin scattering of focused laser beams in condensed media 11 p1716 N85-20796
Four-wave hypersonic reversing mirrors in saturated mode 11 p1719 N85-20812
CONNECTICUT
Impact of LANDSAT MSS sensor differences on change detection analysis — New Mexico, San Francisco, CA, New Hampshire, and Connecticut 11 p1667 N85-20506
CONNECTIONS
U JOINTS (JUNCTIONS)
CONNECTIVE TISSUE
NT MARROW
CONNECTORS
NT ELECTRIC CONNECTORS
Extractor for spring-lock pin connectors [AD-D011235] 01 p0043 N85-10260
Vehicle-to-vehicle connection mechanism [AD-D011267] 05 p0645 N85-14142
Safety requirements for wiring systems and connectors for photovoltaic systems [NASA-CR-174211] 06 p0803 N85-15110
Connection system — insuring against loss of a tool component without using multiple tethers [NASA-CASE-MSC-20319-1] 12 p1857 N85-21649
Releasable cable connector assembly for use between a mobile and stationary object [AD-D011536] 12 p1858 N85-21655
Fiber optics applications for MIL-STD-1760 [AD-A151113] 15 p2470 N85-25251
Wideband fiber optic communications link [AD-A151704] 15 p2542 N85-25697
Ultrasonic test evaluation of the insert bond on hermetic connectors [DE85-008394] 18 p3120 N85-29310
Fiber optic expanded beam connector [AD-A154057] 19 p3367 N85-30680
Attitude control tradeoff study between the use of a flexible beam and a tether configuration for the connection of two bodies in orbit 20 p3412 N85-31174
Static and cyclic behavior of semi-rigid steel beam-column connections [PB85-194363] 24 p4103 N85-35433
CONNECTORS (ELECTRIC)
U ELECTRIC CONNECTORS
CONOIDS
U CONICAL BODIES
CONSCIOUSNESS
G-induced Loss of Consciousness (GLC) 20 p3510 N85-31823
Centrifuge operations and training in the Royal Netherlands Air Force 20 p3511 N85-31825
CONSERVATION
NT ENERGY CONSERVATION
Research and development requirements for ion implantation [AD-P003951] 02 p0286 N85-11867
Use of ion implantation to modify the corrosion behavior of metals [AD-P003953] 02 p0286 N85-11869
Closed-loop concepts for the Army: Water conservation, recycle, and reuse [AD-A148839] 09 p1365 N85-18581
Basic cryogenics and materials. Phase 1 [NASA-CR-177932] 21 p3572 N85-32215
CONSERVATION EQUATIONS
Further developments of a nongradient theory of premixed turbulent flames [NAL-TR-802T] 01 p0023 N85-10143
Numerical analysis of flow and heat transfer in the VAFB LOX storage Dewar tank [NASA-CR-171203] 02 p0197 N85-11315
Statistical Plasma Physics. Proceedings of the Workshop of the US-Japan Joint Institute for Fusion Theory Program [IPPJ-689] 02 p0282 N85-11832
Conservative and nonconservative schemes for the solution of the nonlinear Schroedinger equation [CWI-NM-R8405] 05 p0720 N85-14628
High altitude chemically reacting gas particle mixtures. Volume 1: A theoretical analysis and development of the numerical solution — rocket nozzle and orbital plume flow fields [NASA-CR-171826] 07 p0916 N85-15801
The omni-transform in single-channel queues [AD-A151019] 14 p2409 N85-24852
On coupling factors of explosion 15 p2551 N85-25747
Progress of computational fluid dynamics in the world 16 p2691 N85-26612
Approximate factorization method for computation of nonhydrostatic mesoscale flows [DE85-007259] 19 p3313 N85-30537
On the convergence of difference approximations to scalar conservation laws [NASA-CR-172614] 19 p3344 N85-30726
CONSERVATION LAWS
Conservation laws and the numerical solution of ODEs [DE84-016206] 04 p0555 N85-13531
Parity and time-reversal non-conversation in atoms [DE84-016924] 04 p0562 N85-13561
A geometric approach to high resolution TVD schemes [NASA-CR-172484] 06 p0857 N85-15449
Isolated systems in general relativity 09 p1400 N85-18813
A convergent series expansion for hyperbolic systems of conservation laws [NASA-CR-172557] 12 p1910 N85-21990
An approximation theory for nonlinear evolution equations and single conservation laws 16 p2691 N85-26614
New semi-implicit method for solving the time-dependent conservation equations for incompressible flow [DE85-010926] 23 p3931 N85-34367
Generalized reduced fluid model with finite ion-gyroradius effects [DE85-013123] 24 p4157 N85-35777
Phase space factors in multiparticle processes 24 p4175 N85-35888
CONSISTENCY
Precedency control and other semantic integrity issues in a workbench database 13 p2123 N85-23220
Consistency of smoothing with running linear fits [AD-A150232] 13 p2150 N85-23349
CONSOLIDATION
Computer program for determining induced stresses and consolidation settlements (CSETT) [AD-A146730] 07 p1023 N85-16493
Consolidation of thermites by pressing and sintering [DE84-016943] 09 p1297 N85-18146
Consolidation around a point heat source [PB85-116549] 11 p1682 N85-20601
Metallurgical characterization of aluminum powder consolidation [AD-A151990] 15 p2510 N85-25484
CONSTANT SPEED PROPELLERS
U VARIABLE PITCH PROPELLERS
CONSTANT VOLUME BALLOONS
U SUPERPRESSURE BALLOONS
CONSTANTS
NT GRUNEISEN CONSTANT
NT HUBBLE CONSTANT
NT PLANCKS CONSTANT
NT SOLAR CONSTANT
NT TIME CONSTANT
One-dimensional two-phase constant lag flow in combustion chamber of solid propellant rocket motors [AD-A145679] 02 p0173 N85-11157
Quark models of hadronic interactions [DE84-013787] 04 p0561 N85-13570
Chemical kinetics and photochemical data for use in stratospheric modeling. Evaluation number 6 [NASA-CR-175564] 12 p1888 N85-21849
Conserved quantities and radiative aspects of asymptotically anti-de Sitter space-times 12 p1958 N85-22303
An integral representation of the generalized Euler-Mascheroni constants [NASA-TP-2456] 13 p2144 N85-23305
Attenuated total reflection method for obtaining optical constants of powders [AD-A154094] 19 p3367 N85-30881
Large-time behavior of viscous surface waves [AD-A154805] 21 p3584 N85-32278
On the turning lozange of constant aide whose vertices alternate between two fixed circles of a ring [AD-A154803] 21 p3677 N85-32840
CONSTELLATIONS
NT AURIGA CONSTELLATION
NT CASSIOPEIA CONSTELLATION
NT CENTAURUS CONSTELLATION
NT CORONA BOREALIS CONSTELLATION
NT CYGNUS CONSTELLATION
NT LYRA CONSTELLATION
NT ORION CONSTELLATION
Proceedings of a Workshop on Applications of Tethers in Space, Executive Summary [NASA-CR-171195] 03 p0322 N85-12075
Proceedings of a Workshop on Applications of Tethers in Space, Volume 2 [NASA-CR-171197] 03 p0322 N85-12077
CONSTITUTIONAL DIAGRAMS
U PHASE DIAGRAMS
CONSTITUTIVE EQUATIONS
Biaxial constitutive equation development for single crystals [NASA-CR-174056] 02 p0266 N85-11862
Dynamics of coupled ice-ocean system in the marginal ice zone: Study of the mesoscale processes and of constitutive equations for sea ice [NASA-CR-174171] 04 p0542 N85-13448
Single integral constitutive equations for viscoelastic fluids [AD-A149410] 10 p1547 N85-19758
Viscoplastic constitutive relationships with dependence on thermomechanical history [NASA-CR-174836] 12 p1864 N85-21691
Unified constitutive material models for nonlinear finite-element structural analysis — gas turbine engine blades and vanes [NASA-TM-86885] 14 p2320 N85-24338
On thermomechanical testing in support of constitutive equation development for high temperature alloys [NASA-CR-174879] 15 p2577 N85-25894
Some remarks on the constitutive equations of stratified gas-liquid flow [EME-137] 20 p3456 N85-31466
Nonlinear Constitutive Relations for High Temperature Application, 1984 [NASA-CP-2369] 20 p3465 N85-31530
A survey of unified constitutive theories 20 p3466 N85-31531
Physical concepts in the development of constitutive equations 20 p3467 N85-31537
Numerical considerations in the development and implementation of constitutive models 20 p3467 N85-31541
On numerical integration and computer implementation of viscoplastic models 20 p3467 N85-31542

Finite element analysis of notch behavior using a state variable constitutive equation 20 p3468 N85-31548
Analytical simulation of weld effects in creep range 20 p3468 N85-31550
Creep crack growth predictions in INCO 718 using a continuum damage model 20 p3469 N85-31551
CONSTRAINTS
NT METEOROLOGICAL PARAMETERS
Simple nonrestrictive arm restraint system [AD-D011216] 01 p0005 N85-10026
Aircraft chocks [AD-A145135] 01 p0012 N85-10077
Resistance to HF jamming interference in mobile radio networks by an adaptive, distributed reconfiguration technique [AD-A145117] 01 p0038 N85-10238
Constraint-based scheduling in an intelligent logistics support system: An artificial intelligence approach [AD-A145613] 02 p0293 N85-11900
Barriers to achieving high efficiency 06 p0629 N85-15264
Implementation of a constraint machine for prism - A parallel problem solver [AD-A147844] 07 p1026 N85-16512
Trust region methods for minimization [AD-A147073] 07 p1030 N85-16540
The analysis of kinematic restraint and freedom using point contacts [RR-154/03/75/02] 08 p1169 N85-17372
The synthesis of kinematic restraint and freedom using point contacts [RR-154/03/75/03] 08 p1169 N85-17373
The combinatorics of local constraints in model-based recognition and localization [AD-A148338] 08 p1230 N85-17746
The IRAS mission 09 p1412 N85-18901
A generalized ordering constraint for stereo correspondence [AD-A149182] 10 p1487 N85-19390
Brightness limitations in multi-kiloampere electron beam sources [DE84-017417] 10 p1555 N85-19807
A FORTRAN program for deep space sensor analysis [AD-A151700] 15 p2489 N85-25366
Orbiter middeck/payload standard interfaces control document [NASA-TM-87473] 16 p2729 N85-26840
On the exceedance point process for a stationary sequence [AD-A152827] 17 p3018 N85-28665
Construction of constraint equation for stresses and strains [BLL-M-36239-(5828.4)] 20 p3485 N85-31524
On the limiting configuration of interfacial gravity waves [AD-A154821] 21 p3631 N85-32557
Detector problems at the SSC [DE85-010217] 21 p3703 N85-33007
Design and testing of an energy-absorbing crewseat for the F/FB-111 aircraft. Volume 2: Data from seat testing [NASA-CR-3917] 24 p4064 N85-35184
CONSTRICTIONS
Test your contacts by measuring their constriction resistance [BLL-WH-611-(9091.9F)] 07 p0944 N85-15978
A two phase flow model at the level of a narrowing section --- blood flow 20 p3507 N85-31799
CONSTRUCTION
Modelling the demand for construction [CSIR-TWISK-322] 01 p0035 N85-10218
Copper-boron low alloy high strength steels 02 p0178 N85-11183
Construction of a cold neutron source at FRM, Munich 03 p0427 N85-12722
Construction of a neutron single crystal diffractometer 03 p0427 N85-12723
Field testing of a lightweight relocatable structure in a desert environment [AD-A148841] 09 p1304 N85-18192
Increase in performance and improvement of ride comfort of self-propelled construction machinery by reducing pitch and vertical vibration [AD-P004269] 09 p1405 N85-18845
Airport site selection and design [AD-P004193] 11 p1581 N85-19959
Landscape management on airports for reduction of bird populations [AD-P004194] 11 p1581 N85-19960
Inexpensive multipurpose landscaping 11 p1581 N85-19961
Institute director surveys industrial automation drive 11 p1617 N85-20167
Laser-Electron-Gamma-Source (LEGS) [DE85-003204] 11 p1638 N85-20322
New runway enables IL-76 flights to Tenkeli in far north 12 p1769 N85-21108
Stress-relieving interlayers for bituminous resurfacings [PB85-136865] 12 p1820 N85-21415
Phase change thermal energy storage and the model building codes [PB85-111201] 12 p1883 N85-21813
The space station as a construction base for large space structures 14 p2235 N85-23856
Microwave methods for paving [DE85-004194] 14 p2265 N85-24032
Construction in space 15 p2484 N85-25328
Evidential reasoning in expert systems for image analysis [AD-A153379] 17 p3013 N85-28627
A bilaterally deterministic rho-mixing stationary random sequence [AD-A152856] 17 p3019 N85-28666
US restrictions on technology transfer reviewed 18 p3088 N85-29115
Fire performance of interstitial space construction system [NBSIR-85-3158] 20 p3436 N85-31318
Airborne sound transmission loss characteristics of wood-frame construction [AD-A154174] 20 p3524 N85-31919
Construction of University of Missouri, Rolla's full scale cloud simulation chamber and applied research [AD-A154682] 21 p3557 N85-32128
Field testing of a lightweight relocatable structure in a temperate environment [AD-A155171] 21 p3599 N85-32350
Literature survey of underground construction methods for application to hardened facilities [AD-A155212] 21 p3599 N85-32351
Deployable-erectable trade study for space station truss structures [NASA-TM-87573] 22 p3740 N85-33181
Low-head hydroelectric power demonstration project: City of Gonzales, Texas [DE85-010403] 22 p3809 N85-33595
A 1984 environmental summary: Sandia National Laboratories Tonopah Test Range, Tonopah, Nevada [DE85-011145] 22 p3812 N85-33612
Nuclear physics in the 10 to 300 MeV energy range using a pulsed white neutron source [DE85-003713] 22 p3839 N85-33775
Space Station Engineering and Technology Development: Proceedings of the Panel on In-Space Engineering Research and Technology Development [NASA-CR-176110] 23 p3899 N85-34153
Small Hydroelectric Power Plan Demonstration Project [DE85-011343] 23 p3946 N85-34454
Design and construction of an advanced power conditioning subsystem for small photovoltaic applications [DE85-013940] 24 p4113 N85-35495
Reachable grasps on a polygon: The convex rope algorithm [AD-A155913] 24 p4138 N85-35647
The 1986 National Aeronautics and Space Administration authorization [GPO-47-635] 24 p4166 N85-35829
CONSTRUCTION IN SPACE
U ORBITAL ASSEMBLY
CONSTRUCTION INDUSTRY
Use of short-range weather forecasts at construction sites: Some results from a user and a market test 01 p0084 N85-10583
Activities report in technology [ISBN-951-38-1998-1] 04 p0577 N85-13681
Robotics application in construction industry assessed 06 p1139 N85-17178
Deputy minister on civil aviation construction projects 14 p2208 N85-23692
CONSTRUCTION MATERIALS
Models for shock damage to marine structural materials 09 p1336 N85-18400
Hazardous air pollutants: Dry-deposition phenomena [PB85-138279] 12 p1887 N85-21843
Expedient runway surfacing with post tensioning system for expeditionary airfields [AD-D011677] 19 p3222 N85-29976
Field testing of a lightweight relocatable structure in a temperate environment [AD-A155171] 21 p3599 N85-32350
CONSUMABLES (SPACECRAFT)
NT CONSUMABLES (SPACECREW SUPPLIES)
NT PROPELLANT STORAGE
NT SPACE LOGISTICS
NT SPACE RATIONS
NT STORABLE PROPELLANTS
NT WORKING FLUIDS
CONSUMABLES (SPACECREW SUPPLIES)
NT POTABLE WATER
NT SPACE RATIONS
Food Service and Nutrition for the Space Station [NASA-CP-2370] 14 p2393 N85-24733
Food acquisition: Food ingredients, raw materials and supply 14 p2393 N85-24737
Preparation methods: Past and potential methods of food preparation for space 14 p2393 N85-24738
Alternative food preservation techniques, new technology in food preparation and appropriateness of food supply for the permanently manned space station 14 p2393 N85-24739
Use of irradiated foods 14 p2393 N85-24740
Equipment for hot-to-serve foods 14 p2393 N85-24741
Food service and nutritional needs 14 p2394 N85-24744
Packaging's contribution for the effectiveness of the space station's food service operation 14 p2394 N85-24746
Packaging for food service 14 p2394 N85-24747
A life-saving device for ships [NASA-TM-77670] 23 p3895 N85-34129
CONSUMERS
Economic value of consumer information: A selected, annotated bibliography [PB84-235795] 04 p0576 N85-13673
Sunset of the Civil Aeronautics Board [S-HRG-98-940] 09 p1403 N85-18829
CONSUMPTION
NT ENERGY CONSUMPTION
NT FUEL CONSUMPTION
NT OXYGEN CONSUMPTION
NT WATER CONSUMPTION
Cosmonauts' blood plasma free amino acid levels during preflight training 12 p1901 N85-21937
CONTACT RESISTANCE
Test your contacts by measuring their constriction resistance [BLL-WH-611-(9091.9F)] 07 p0944 N85-15978
Oil resistant silicone elastomers [AD-131523] 16 p2753 N85-26987
CONTACTORS
Free-surface phenomena under low- and zero-gravity conditions [NASA-CR-175835] 16 p2782 N85-27168
CONTACTS (ELECTRIC)
U ELECTRIC CONTACTS
CONTACTS (GEOLOGY)
Contact properties of rare-earth silicides and germanides on Si and Ge 19 p3374 N85-30931
The 3.5 b.y. old Onverwacht Group: A remnant of ancient oceanic crust 21 p3718 N85-33073
CONTAINERLESS MELTS
Microgravity containerless processing in long drop tubes 02 p0153 N85-11037
Containerless drop tube solidification and grain refinement of NiAl3 02 p0154 N85-11042
NBS (National Bureau of Standards): Materials measurements [NASA-CR-174038] 03 p0332 N85-12143
CONTAINERS
Inert atmosphere transfer vessel [AD-D011433] 08 p1169 N85-17370
Vibrational loading mechanism of unitized corrugated containers with cushions and non-load-bearing contents 09 p1339 N85-18419
Single crystal silicon as a low-temperature structural material [DE84-017469] 09 p1400 N85-18810
Latch assembly [DE85-011660] 22 p3792 N85-33492
CONTAINMENT
Flywheel containment and safety considerations 05 p0606 N85-13669
Polymeric liner selection for military waste impoundments [AD-P004143] 09 p1348 N85-18479
Thermal stress-dependent dilation of concrete [DE84-014688] 11 p1653 N85-20412
Hemispherical latching apparatus [NASA-CASE-MFS-25837-1] 19 p3224 N85-29991
Counter current extraction system for tritium recovery from 17Li-83Pb [DE85-010519] 19 p3240 N85-30090
Explosive containment study [DE85-011719] 22 p3753 N85-33267
Corrosion resistant storage container for radioactive material [DE85-011666] 22 p3836 N85-33765
Measurement of radionuclides in waste packages [DE85-011674] 22 p3836 N85-33766
MATADOR (Methods for the Analysis of Transport And Deposition Of Radionuclides) code description and user's manual [TI85-901402] 23 p3966 N85-34592

Fuel containment and damage tolerance for large composite primary aircraft structures. Phase 1: Testing
[NASA-CR-166091] 24 p4073 N85-35241
Response of a BWR Mark 2 containment vessel head to loads beyond the design basis
[DE85-010524] 24 p4103 N85-35432

CONTAMINANTS
NT RADIOACTIVE CONTAMINANTS
NT TRACE CONTAMINANTS
The use of fixed-bed adsorber models to predict the fluxes of toxic substances in groundwaters and soil environments
[PB84-202563] 01 p0071 N85-10468
Reverse osmosis treatment to control inorganic and volatile organic contamination
[PB84-223528] 01 p0071 N85-10470
Toxicological evaluation of Columbia spacecraft
01 p0094 N85-10631
Clean-burning diesel engines
[AD-A145515] 02 p0205 N85-11349
VOC emissions from volatile organic liquid storage tanks: Background information for proposed standards
[PB84-237320] 04 p0532 N85-13403
Climatological variability in modeling of long-term regional transport and deposition of air pollutants
[DE84-014726] 04 p0539 N85-13430
Portable instrument for the detection and identification of air pollutants
[DE84-014767] 05 p0672 N85-14316
Fate and disposition of trichloroethylene in surface soils
[AD-A147918] 07 p0995 N85-16321
Evaluation of test equipment for the detection of contamination on electronic circuits — spacecraft electronics
[ESA-STM-234] 08 p1159 N85-17316
A new fast response probe for diffusion studies in atmospheric air — pollution modeling
[IC-AERO-84-01] 08 p1180 N85-17437
Applying an innovative approach to field investigations at a remedial action site
[AD-P004145] 09 p1348 N85-18481
Measurement and analysis of ambient carbon monoxide concentrations for project-level air quality impact studies
[PB85-104602/GAR] 09 p1350 N85-18492
Meteorological factors responsible for high CO (carbon monoxide) levels in Alaskan cities
[PB85-115137/GAR] 09 p1350 N85-18493
Improved techniques for removal of sediments contaminated with hazardous materials
[PB85-116093] 11 p1679 N85-20580
Method and apparatus for mapping the distribution of chemical elements in an extended medium
[NASA-CASE-GSC-12808-1] 12 p1798 N85-21279
The body burden of organic vapors in artificial air trial measurements aboard a moored submarine
[AD-A149898] 12 p1910 N85-21988
Spectroscopic study of gas pollutants in atmosphere over large cities: A review 14 p2341 N85-24478
Thermally modulated electron affinity detector for priority pollutant analysis
[PB85-158145] 15 p2508 N85-25469
Density of impurity states associated to inversion layers
[INPE-3406-PRE/675] 16 p2869 N85-27702
A study of gas solid reactions using coated piezoelectric detectors
[AD-A153047] 17 p2920 N85-28001
Elemental tracers of source regions of contaminants in precipitation
[DE85-007366] 18 p3133 N85-29407
Internal contamination issues
18 p3156 N85-29543
Reduction of pollutant formation in combustion processes
[DE85-010181] 19 p3309 N85-30512
Mechanisms of exhaust pollutants and plume formation in continuous combustion
[AD-A154169] 20 p3435 N85-31310
Toxic hazards tests for vehicles and other equipment
[AD-A149164] 20 p3506 N85-31797
New estimating procedures for surface runoff, sediment yield, and contaminant transport in Los Alamos County, New Mexico
[DE85-011690] 21 p3606 N85-32393
Atmospheric modeling of organics for risk assessment: A Chemist's view
[DE85-009770] 23 p3909 N85-34217

CONTAMINATION
NT FUEL CONTAMINATION
NT SPACECRAFT CONTAMINATION
Contamination problems during surface cleaning for thermocompression bonding
[DE84-013066] 04 p0475 N85-13023
Gas contamination detection device
[AD-D011368] 07 p0921 N85-15833
Contamination and distortion of steady flow field induced by discrete frequency in aircraft gas turbines
[AD-A147092] 07 p0958 N85-16073
Assessment of radiation dosages obtained by intake of radioactive fallout contaminated food
[VTT-292] 07 p1017 N85-16460
Other challenges in the development of the orbiter environmental control hardware
08 p1096 N85-16924
Proceedings of the 2nd Workshop on Nondestructive Evaluation (NDE) of Titanium Alloys
[AD-A147626] 08 p1125 N85-17095
Acoustical characterization of Ti-6211 weldments and oxygen contamination Ti-6211 plate
[AD-P004125] 08 p1126 N85-17100
Ultrasonic evaluation of titanium contamination with correlation techniques
[AD-P004126] 08 p1126 N85-17101
Photoacoustic microscopy of oxygen contaminated titanium alloys
[AD-P004127] 08 p1127 N85-17102
High resolution acoustic microstructural characterization of titanium with interstitial contamination
[AD-P004128] 08 p1127 N85-17103
Feasibility study to demonstrate detection of low levels of oxygen contaminant in titanium using eddy current and ultrasonic NDE (Nondestructive Evaluation) techniques
[AD-P004129] 08 p1127 N85-17104
Evaluation of interstitial gas contamination in titanium alloys using induced magnetic field analysis
[AD-P004130] 08 p1127 N85-17105
Neutron activation analysis of titanium with oxygen contamination
[AD-P004134] 08 p1128 N85-17109
Location of volatile buried wastes by field portable instrumentation
[AD-P004147] 09 p1348 N85-18483
Practical application of earth resistivity methods in phase 2 of the installation restoration program
[AD-P004148] 09 p1348 N85-18484
Ventilation flow: Submerged
18 p3156 N85-29545
Compatibility, contamination and IR microspectrophotometry
[DE85-010809] 19 p3273 N85-30297
Occurrence of uranium in ground water in the vicinity of the US Department of Energy Feed Materials Production Center, Fernald, Ohio
[DE85-010340] 19 p3364 N85-30862
The influence of oil contamination on the nucleate pool-boiling behavior of R-114 from a structured surface
[AD-A155609] 21 p3585 N85-32284
JPL in-house fluidized-bed reactor research
21 p3609 N85-32414
Soil extraction kit
[AD-D011736] 22 p3742 N85-33190
The 1984 environmental monitoring report, Sandia National Laboratories, Albuquerque, New Mexico
[DE85-011175] 22 p3811 N85-33607
Method for removing oxide contamination from silicon carbide powders
[DE85-011648] 23 p3919 N85-34287
Radiation safety problems in handling highly active tritium targets
[DE85-014268] 24 p4151 N85-35742

CONTENT
NT BONE MINERAL CONTENT

CONTEXT
Efficient contextual measures for classification of multispectral image data 14 p2433 N85-25005

CONTINENTAL DRIFT
Antarctic glaciation, or what are catastrophes in Earth's history 13 p2105 N85-23118

CONTINENTAL MARGINS
U CONTINENTAL SHELVES

CONTINENTAL SHELVES
Marine geological and geophysical investigations of the Antarctic Continental Margin, 1984
[GS-CIRC-935] 02 p0212 N85-11400
Submarine sand ridges: Geology and development, New Jersey, USA 02 p0227 N85-11482
Recent observations of tides and tidal currents from the northeastern Bering Sea shelf
[PB84-241785] 04 p0543 N85-13452
Maritime prospecting, mining discussed
07 p0990 N85-16226
Types of placer formation of eastern Arctic shelf
10 p1498 N85-19452
Calculation of optical characteristics of shelf ecological system based on its mathematical model
10 p1498 N85-19453
U, Th, K content, heat production and thermal conductivity of Sao Paulo, Brazil continental shelf sediments: A reconnaissance work
[INPE-3401-PRE/670] 10 p1515 N85-19558
Preliminary results of the oceanographic cruise of USCGC NORTHWIND to the Greenland Sea
[AD-A149802] 12 p1898 N85-21919
Biological processes in the water column of the South Atlantic Bight. Volume 1: Published manuscripts
[DE85-004610] 12 p1900 N85-21929
Twenty-five sound propagation tests on the continental shelf between Long Island, New York and Cape Canaveral, Florida
[AD-A149869] 12 p1928 N85-22111
A tectonic model of an incipient spreading center and its margins: The Northern Red Sea and the Dead Sea rift 13 p2140 N85-23286
Two-cycle mechanism of dissipation of tidal energy in ocean 14 p2335 N85-24438
MARMAP survey of the continental shelf from Cape Hatteras, North Carolina to Cape Sable, Nova Scotia (1977 - 1983). Atlas 1: Summary of operations
[PB85-150985] 16 p2839 N85-27506
An assessment of the potential role of multispectral imagery in bathymetric charting
[AD-A152460] 17 p2984 N85-28438
Geoacoustic models: Washington state continental margin
[AD-A153781] 18 p3177 N85-29689
Pacific Index, April 1983 - October 1984
[TI85-901335] 19 p3320 N85-30582

CONTINENTS
NT AFRICA
NT ASIA
NT AUSTRALIA
NT EUROPE
NT NORTH AMERICA
NT SOUTH AMERICA
Some methodological aspects of study of layer associations in continents and oceans
06 p0820 N85-15205
Continental and oceanic magnetic anomalies: Enhancement through GRM 20 p3476 N85-31598
Continental magnetic anomaly constraints on continental reconstruction 20 p3476 N85-31599
Regional magnetic anomaly constraints on continental rifting 20 p3476 N85-31600
The origin of continental crust: Outlines of a general theory 21 p3720 N85-33083
Crustal radiogenic heat production and the selective survival of ancient continental crust
21 p3721 N85-33086

CONTINGENCY
Log linear model applications
[AD-A146620] 06 p0858 N85-15457
A model for large sparse contingency tables
[AD-A150320] 13 p2151 N85-23350
An examination of alternative forms of fit in contingency theory
[AD-A152602] 17 p3047 N85-28853
The concept of fit in contingency theory
[AD-A152603] 17 p3047 N85-28854
Bayesian full rank marginalization for 2-way contingency tables
[AD-A153841] 18 p3171 N85-29649

CONTINUITY
Viscosity solutions of Hamilton-Jacobi equations at the boundary
[AD-A147444] 07 p1032 N85-16553
On existence and uniqueness of solutions of Hamilton-Jacobi equations
[AD-A147597] 07 p1033 N85-16560

CONTINUITY (MATHEMATICS)
Shear deformation plate continua of large double-layered space structures
01 p0059 N85-10391
Continuity of the null space basis and constrained optimization
[AD-A147038] 07 p1030 N85-16538
Domains with Lipschitz mapping functions
10 p1535 N85-19675
Topology and Order Structures, part 2
[MCT-169-PT-2] 14 p2413 N85-24879
Twenty questions on ordered spaces
14 p2413 N85-24880
A note on perfect normality in generalized ordered spaces 14 p2413 N85-24881
Metrization theorems for continuous images of compact ordered spaces 14 p2413 N85-24882
A pathological homogeneous subspace of the real line
14 p2413 N85-24883
A note on topological groups with dense orderable subspaces 14 p2413 N85-24884
The Kappa sub n property in small Omega sub 1 trees
14 p2413 N85-24885
On compactifications of generalized order GO-spaces
14 p2413 N85-24886
The orderability of compact scattered spaces
14 p2413 N85-24887

Submetrizable topologies on the ordinals
14 p2414 N85-24888
When is a GO-space JO(2)? 14 p2414 N85-24889
Local bases and product partial order II
14 p2414 N85-24890
Mappings of finite oscillations at local separating points 14 p2414 N85-24891
Orderable subspaces of compact F-spaces
14 p2414 N85-24892
Extension of embeddings close to isometries or similarities 15 p2634 N85-26242
On functions with a finite or locally bounded Dirichlet integral 15 p2635 N85-26243

CONTINUITY EQUATION
New approach for solving large residual nonlinear least squares problems
[DE85-002555] 11 p1707 N85-20742
Theory of oriented nucleation with asymmetric single elements. 2: Effects of rotational diffusion
[IFTR-32/1984] 12 p1939 N85-22179

CONTINUOUS RADIATION
NT MODULATED CONTINUOUS RADIATION
The IMS advances in understanding terrestrial myriametric radiation 14 p2365 N85-24618
Terrestrial continuum radiation study during the IMS
14 p2365 N85-24619
A sampling phasemeter design for pulsed continuous wave signals
[AD-A155237] 21 p3581 N85-32264
Optimal complex nonlinear processing of continuous and pulsed signals 22 p3763 N85-33323
The cw operation of the FMIT RFQ accelerator
[DE85-012667] 22 p3837 N85-33757
Search for positron annihilation line and continuum radiation from the Galactic Center
[OG-2.5-5] 22 p3869 N85-33962

CONTINUOUS SPECTRA
The continuous spectrum of an axisymmetric, self-gravitating equilibrium in the presence of a poloidal magnetic field 12 p1959 N85-22315
The continuous spectrum of an axisymmetric equilibrium with a mixed poloidal and toroidal magnetic field with gravity included 14 p2450 N85-25128

CONTINUOUS WAVE LASERS
Tunable CW semiconductor platelet laser
[AD-D011215] 01 p0052 N85-10341
Study of CW injection laser with a dispersive external cavity 02 p0270 N85-11760
Optimizing CW CO2 lasers with respect to output power in different bands 02 p0271 N85-11766
Transformation of energy spread of laser pumping via phase conjugation 05 p0725 N85-14661
Instrumentation for particle-beams research using laser excited merging beams
[AD-A147966] 06 p1220 N85-17681
A 50-kW electric-discharge CO2 laser
[AD-A149779] 12 p1857 N85-21644
Laser Welding, Cutting and Surface Treatment
14 p2308 N85-24278
The measurement of laser beam parameters
14 p2308 N85-24283
A plasma initiation-flow chamber to study CW laser beamed energy absorption in light gases
[AD-A151225] 15 p2562 N85-25806
Design and construction of a CW Nd:YAG laser using a single elliptical cavity and water cooled krypton arc lamp pumping
[AD-A152657] 17 p2970 N85-28340
Simplified analytical model for calculation of population inversion in channels of CW gasdynamic lasers operating at various transitions among levels pertaining to coupled upsilon 1 and upsilon 2 modes of CO2
[STN-2] 20 p3461 N85-31498
High-power two-frequency CW dye laser
21 p3696 N85-32900
Expansion ratio influence on population inversion in CO2/Ar CW gasdynamic lasers operating at various transitions within coupled upsilon 1 and upsilon 2 modes of CO2
[STN-4] 22 p3790 N85-33485
Laser and electron beam processing of semiconductors
[AD-A155914] 24 p4161 N85-35796

CONTINUOUS WAVE RADAR
Design of an analog spectrum analyzer for probing experiments
[AD-A147384] 07 p0941 N85-15863
Signal processing and range spreading in the FM-CW radar
[PB85-106256] 11 p1626 N85-20239
Use of radar with frequency modulation for studying atmospheric boundary layer 19 p3296 N85-30437

CONTINUOUS WAVES
U CONTINUOUS RADIATION

CONTINUUM FLOW
Modeling of transient heat pipe operation
[NASA-CR-175496] 12 p1844 N85-21571

CONTINUUM MECHANICS
Acceleration waves 02 p0207 N85-11367
Free-edge failures of composite laminates
04 p0467 N85-12971
Continuum distributions of active galactic nuclei
05 p0742 N85-14770
Physical conditions in low-luminosity active galactic nuclei 05 p0742 N85-14771
Theoretical studies relating to the interaction of radiation with matter: Atomic collision processes occurring in the presence of radiation fields
[AD-A146854] 07 p1040 N85-16602
Computational methods for nonlinear dynamics problems in solid and structural mechanics
[AD-A148352] 08 p1172 N85-17392
The principle of virtual work and associated variational principles
[ESA-TT-673] 09 p1340 N85-18428
Axiomatic characterizations of continuum structure functions
[AD-A149617] 12 p1866 N85-21706
A solution method for nonlinear dynamic analysis of shell structures
[AD-A149846] 12 p1866 N85-21708
Adaptive meshes in the 2DL code
[LA-9938-MS] 12 p1914 N85-22011
Parallel processing for computational continuum dynamics
[AD-A150513] 13 p2147 N85-23327
The Shock and Vibration Digest, volume 17, no. 1
[AD-A151051] 17 p2977 N85-28397
Continuum modeling of latticed structures
17 p2977 N85-28399
Nonlinear problems in continuum mechanics
[AD-A153387] 17 p3046 N85-28846
A high energy X-ray study of the galactic center
[AD-A153852] 18 p3202 N85-29662
Efficient solution methods for nonlinear finite element analysis 20 p3519 N85-31696
Mechanics of near tip microcracking in brittle material
[AD-A154684] 21 p3598 N85-32346

CONTINUUM MODELING
Spline-based Rayleigh-Ritz methods for the approximation of the natural modes of vibration for flexible beams with tip bodies
[NASA-CR-172566] 13 p2102 N85-23100

CONTINUUMS
Modules of continuum structures, revised
[AD-A148620] 06 p1213 N85-17639
Bounding the stochastic performance of continuum structure functions 1
[AD-A148621] 06 p1213 N85-17640
An extension of the multiconfiguration Hartree-Fock program for continuum functions
[DE85-002060] 09 p1379 N85-18672
Bounding the stochastic performance of continuum structure functions 2
[AD-A149458] 10 p1548 N85-19762
Mappings of finite oscillations at local separating points 14 p2414 N85-24891
On the definition of topological susceptibility via lattice anomalous Ward identities and its perturbative tail
[PREPRINT-416] 18 p3184 N85-29744
Low-excitation Herbig-Haro objects and interstellar extinction
[NASA-CR-176142] 23 p3968 N85-34726

CONTOUR SENSORS
A digital contour-corrector for a high-definition TV camera
[NHK-LABS-NOTE-311] 19 p3254 N85-30179
LANDSAT-4/5 image data quality analysis
[E85-10105] 24 p4107 N85-35463

CONTOURS
Detection and coding techniques of contours in image signals
[FUB-8-1983] 01 p0039 N85-10251
Image signals encoding techniques oriented towards the reduction of perceptive redundance
[FUB-23-1983] 01 p0040 N85-10256
A human visual system investigation applicable to image contour coding
[FUB-36-1983] 01 p0095 N85-10640
Detection and estimation of image contours
[FUB-35-1983] 01 p0112 N85-10760
A decomposable algorithm for contour surface display generation
[AD-A145783] 03 p0410 N85-12619
Free-surface boundary layer and the origin of bow vortices
[AD-A147427] 07 p0960 N85-16083
Transonic shock interaction with a tangentially-injected turbulent boundary layer 08 p1072 N85-16796
Critical flashing flow of subcooled fluids in nozzles with contour discontinuities
[DE84-017229] 09 p1319 N85-18296
The feasibility of a multiprocessor architecture for real-time contour surface display generation
[AD-A149427] 10 p1538 N85-19697
Experimental investigation of a turbulent incompressible boundary layer on a curved wall
11 p1577 N85-19936
Contour line generalization using digital image processing methods
[SER-C-291] 11 p1700 N85-20688
An unusual application of NASTRAN contour plotting capability 15 p2574 N85-25872
Contamination of the fetch-limited directional wave spectrum by waves emanating from an embayment
[NASA-TM-84441] 15 p2604 N85-26048
Acceleration sensitivity reduction method
[AD-D011631] 16 p2778 N85-27148
Contour line generalization using digital image processing methods 16 p2815 N85-27367
A fast hidden line algorithm with contour option
[NASA-CR-175803] 16 p2852 N85-27582
Application of hierarchical data structures to geographical information systems
[AD-A152169] 16 p2877 N85-27753
Contouring trivariate data 17 p3005 N85-28582
Fourier coding and reconstruction of complicated contours
[REPT-84-39] 17 p3022 N85-28691
SEASAT altimetry for surface height of inland seas
20 p3493 N85-31714
Real-time contour surface display generation
[AD-A155232] 21 p3668 N85-32780
Interactive procedures for discriminating and restoring contour line networks 22 p3736 N85-33158
Discrimination of linear contour elements of space photographs based on visual perception model
22 p3736 N85-33161
Block-implicit calculations of three-dimensional laminar flow in strongly curved ducts
[DE85-003047] 23 p3931 N85-34363
Evaluation: Close-range photogrammetry for slope inventory and monitoring
[PB85-192755] 24 p4108 N85-35470
Invariant tests and likelihood ratio tests for multivariate elliptically contoured distributions
[AD-A155844] 24 p4142 N85-35679

CONTRACT INCENTIVES
Decision process models of contractor behavior: The development of effective contract incentives
[AD-A145524] 02 p0292 N85-11898
Using incentives to improve maintainability
[AD-A153792] 18 p3199 N85-29841

CONTRACT MANAGEMENT
Contracting for computer software development: Serious problems require management attention to avoid wasting additional millions
[FGMSD-80-4] 02 p0241 N85-11567
Benefit value to the Air Force of the GIDEP (Government Industry Data Exchange Program) alert
[AD-A145470] 02 p0292 N85-11897
Decision process models of contractor behavior: The development of effective contract incentives
[AD-A145524] 02 p0292 N85-11898
The application of artificial intelligence to contract management
[AD-A146881] 06 p0857 N85-15448
Technical performance measurement handbook
[AD-A147314] 07 p1052 N85-16675
An appraisal of the USAF Technology Modernization Program
[AD-A147344] 07 p1052 N85-16677
Evaluation of the effectiveness of the weighted guidelines to induce contractor's investment in cost reducing facilities equipment
[AD-A147586] 07 p1053 N85-16681
Government contract contingent liabilities. The anti-deficiency act, and the hobgoblin of little minds
[AD-A147919] 07 p1053 N85-16684
Ground test article for deployable space structure systems
[NASA-CR-171301] 10 p1429 N85-19011
Expert systems in contract management: A pilot study
[AD-A149363] 10 p1566 N85-19873
Department of defense, office of inspector general semiannual report to the Congress, 1 April - 30 September 1984
[AD-A149560] 10 p1567 N85-19879
Program manager: The Journal of the Defense Systems Management College. Volume 13, Number 6, November-December 1984
[AD-A149548] 11 p1739 N85-20933
Life cycle costing in government procurement
[AD-A151878] 15 p2666 N85-26456

Automation of the reporting and tracking requirements of architect-engineering type contracts
[AD-A152218] 16 p2876 N85-27745
R/D contracts in the Soviet Union
[AD-P004569] 17 p3048 N85-28865
Cost savings from multiyear contracting
[AD-A153564] 18 p3197 N85-29834
Capital investment motivational techniques used by prime contractors on subcontractors
[AD-A153660] 18 p3198 N85-29837
Using incentives to improve maintainability
[AD-A153792] 18 p3199 N85-29841
Analyzing performance of small projects using URS and PMAS, information pamphlet
[DE85-011984] 23 p3966 N85-34716
DoD Value Engineering conference report. Value Engineering (VE): A tool that benefits line management. Part 4, Workshop B: VE on spare parts
[AD-A156070] 24 p4163 N85-35813
DoD Value Engineering conference report. Value Engineering (VE): A tool that benefits line management. Part 7, Workshop E: VE in construction and architect engineer contracts
[AD-A156073] 24 p4164 N85-35815

CONTRACT NEGOTIATION
Using incentives to improve maintainability
[AD-A153792] 18 p3199 N85-29841

CONTRACTION
Effect of hyperoxia and increased gas atmosphere density on contractile function of the right ventricle
01 p0093 N85-10628
Change in energetics of muscular contraction as a result of hyperoxia 01 p0093 N85-10629
On the convergence of an iterative formulation of the electromagnetic scattering from an infinite grating of thin wires 24 p4085 N85-35319

CONTRACTORS
Decision process models of contractor behavior: The development of effective contract incentives
[AD-A145524] 02 p0292 N85-11868
Contractor productivity measurement
[AD-A146756] 07 p1050 N85-16666
An appraisal of the USAF Technology Modernization Program
[AD-A147344] 07 p1052 N85-16677
Evaluation of the effectiveness of the weighted guidelines to induce contractor's investment in cost reducing facilities equipment
[AD-A147586] 07 p1053 N85-16681
Integrated control system engineering support
[AD-A149742] 12 p1780 N85-21177
Capital investment motivational techniques used by prime contractors on subcontractors
[AD-A153660] 18 p3198 N85-29837
The evolution of the U.S. helicopter industry
[AD-A154290] 19 p3211 N85-29913
The flow of scientific and technical information in the US Army Research Laboratories
[AD-A155050] 21 p3713 N85-33043

CONTRACTS
Contracting for computer software development: Serious problems require management attention to avoid wasting additional millions
[FGMSD-80-4] 02 p0241 N85-11567
Companies participating in the Department of Defense Subcontracting Program, first three quarters fiscal year 1984
[AD-A146137] 03 p0436 N85-12775
Contractor productivity measurement
[AD-A146756] 07 p1050 N85-16666
Government contract contingent liabilities. The anti-deficiency act, and the hobgoblin of little minds
[AD-A147919] 07 p1053 N85-16684
Cost-plus-percentage-of-costs in government contracts
[AD-A147779] 08 p1228 N85-17735
R/D contracts in the Soviet Union
[AD-P004569] 17 p3048 N85-28865
Cost savings from multiyear contracting
[AD-A153564] 18 p3197 N85-29834
The evolution of the U.S. helicopter industry
[AD-A154290] 19 p3211 N85-29913
Progress report on implementing the recommendations of the White House Science Council's Federal Laboratory Review Panel, volume 1
[PB85-165072] 24 p4164 N85-35819

CONTRAST
NT IMAGE CONTRAST
NT PHASE CONTRAST
Reconciling Bayesian and frequentist evidence in the one-sided testing program
[AD-A155603] 21 p3678 N85-32850

CONTROL
Real time sensing and control of out-of-plane distortion due to line heating by laser
[AD-A144773] 01 p0027 N85-10169
Turnaround control for mechanically scanned radar antennas
[AD-D011238] 01 p0039 N85-10246
Research activities of the Illinois University Coordinated Science Laboratory
[AD-A145589] 03 p0449 N85-12656
A control model: Interpretation of Fitts' law
05 p0706 N85-14526
Decentralized control of scheduling in distributed systems
[AD-A147446] 07 p1022 N85-16487
NASA three-laser airborne differential absorption lidar system electronics
[NASA-CR-174293] 08 p1166 N85-17353
Problems of psychological support of automated organization control systems 09 p1362 N85-18571
Operational effectiveness of a Multiple Aquila Control System (MACS)
[NASA-CR-174436] 10 p1427 N85-19000
Active control of large space structures: An introduction and overview
[NASA-TM-86490] 10 p1429 N85-19014
Successful control of gulls and other birds at a sanitary landfill
[AD-P004198] 11 p1582 N85-19985
Control technology for integrated circuit fabrication at Honeywell Optoelectronics Division, Richardson, Texas
[PB85-109023] 11 p1616 N85-20162
Design of a semi-custom integrated circuit for the SLAC SLC timing control system
[DE85-003091] 11 p1629 N85-20258
Television camera video level control system
[NASA-CASE-MSC-18578-1] 12 p1821 N85-21427
Transfer of technology
[S-REPT-98-664] 12 p1949 N85-22246
The performance of an alternating-current thyristor-controlled motor 15 p2546 N85-25716
Airsickness control using biofeedback to self-regulate psychophysiological responses
[AD-A151167] 15 p2617 N85-26128
Ultrareliable, fault-tolerant control systems: A conceptual description
[NASA-TM-86017] 19 p3221 N85-29972
Control and regulation of generalized linear systems
19 p3257 N85-30193
Frequency domain control design of large space structures: A practical approach
20 p3415 N85-31192
Solid state high power amplifier for driving the SLC injector klystron
[DE85-013053] 24 p4090 N85-35356

CONTROL BOARDS
LED multifunction keyboard engineering study
[AD-A145199] 01 p0010 N85-10061
New control design principles based on measured performance and energy analysis of HVAC (Heating, Ventilating, and Air-Conditioning) systems
[AD-A151708] 15 p2522 N85-25546
Information presentation in power plant control rooms
[VTT-320] 16 p2864 N85-27668
The touch panel system: Design and development
[AD-A153014] 17 p3008 N85-28596
Crew systems and flight station concepts for a 1995 transport aircraft
[NASA-CR-166068] 19 p3221 N85-29973

CONTROL CONFIGURED VEHICLES
A 320 to have combined automatic pilot, flight control system 14 p2269 N85-24186
Multivariable control of a soft coupled space station
20 p3408 N85-31151

CONTROL DATA (COMPUTERS)
Design and analysis of an access control system for a multi-backend database system
[AD-A148750] 09 p1367 N85-18586
Meta-level control through fault detection and diagnosis
[AD-A149064] 10 p1540 N85-19709

CONTROL DEVICES
U CONTROL EQUIPMENT

CONTROL EQUIPMENT
NT CONTROL STICKS
NT CRYOSTATS
NT PRESSURE REGULATORS
NT SPEED REGULATORS
NT TELEOPERATORS
NT THERMOSTATS
Potential application of robotics and state-of-the art end effectors at Letterkenny Army Depot
[AD-P004015] 03 p0309 N85-11994
Torque sensor
[AD-D011276] 05 p0639 N85-14096
Back end valves: History and modifications
[DE84-009272] 05 p0646 N85-14145
S-MICRO: A system for simulating a microprogrammed control unit
[INPE-3224-PRE/575] 05 p0715 N85-14585
Lighting controls: The role of advanced technology; past, present and future
[DE84-015977] 09 p1384 N85-18706
Electromagnetic compatibility of measurement and control equipment in nuclear installations
[BLL-WH-607-(9091.9F)] 11 p1623 N85-20222
Electronics Engineering Department EE Technical Review
[UCRL-50025-84-1] 13 p2063 N85-22887
Experimental development of a failure detection scheme for large space structures 14 p2234 N85-23646
Controllable movements of elastic manipulator with three degrees of freedom 14 p2266 N85-24040
New equipment complex Kaskad 2 for automatic control 14 p2266 N85-24042
Investigation of transport operations of ergatic robot
14 p2266 N85-24166
New electronic measurement, control devices
14 p2269 N85-24192
New control design principles based on measured performance and energy analysis of HVAC (Heating, Ventilating, and Air-Conditioning) systems
[AD-A151708] 15 p2522 N85-25546
Italy's Fiat uses Sweden's Asea seeing robot
15 p2536 N85-25650
Development of an integrated control unit for the PDV bus concept
[BMFT-FB-T-84-300] 15 p2551 N85-25745
Superfine laser position control using statistically enhanced resolution in real time
[DE85-005643] 15 p2564 N85-25817
Development of a multiprocessor system, using the MOTORLA microprocessor 6809, with the aim of providing maximum flexibility in the design of individual control devices
[BMFT-FB-T-84-270] 17 p3010 N85-28607
Control system design for lightly coupled large space structures 20 p3399 N85-31086
Computer methods in manipulator kinematics, dynamics and control: A comparative study
20 p3462 N85-31506
Improved coordinate measuring machine calibration and control
[DE85-012053] 21 p3590 N85-32315
Robots, Manipulators 21 p3668 N85-32786
Dual optical mechanical position tracker
[AD-D011739] 22 p3844 N85-33611
Method for controlling the viscosity of siloxane oils
[DE85-011586] 23 p3909 N85-34221
The compliance of end effector force sensors for robot manipulator control 24 p4098 N85-35406
On-line model driven control of the SLC electron Damping Ring
[DE85-013377] 24 p4157 N85-35772

CONTROL MOMENT GYROSCOPES
Torque command steering law for double-gimbaled control moment gyros applied to rotor energy storage
05 p0608 N85-13879
Active nutation control of spacecraft using a magnetic bearing momentum wheel with Vernier gimballing capability
[NAL-TR-8201] 06 p0759 N85-14857
A Gimbal sizing analysis for an IPACS rotating assembly
[NASA-CR-172524] 16 p2741 N85-26913
Space station automation and robotics study. Operator-systems interface
[NASA-CR-176095] 22 p3738 N85-33172
Application of traction drives as servo mechanisms
22 p3797 N85-33520

CONTROL PANELS
U CONTROL BOARDS

CONTROL RODS
Simulation and operation of the EBR-2 automatic control rod drive system
[DE85-010262] 19 p3360 N85-30632
Source Term Experiments Project (STEP): Aerosol characterization system
[DE85-010248] 19 p3361 N85-30639

CONTROL SIMULATION
Control aspects of the Schuchuli Village stand-alone photovoltaic power system
[NASA-TM-83790] 04 p0495 N85-13157
Elimination of uncontrollable rigid body mode, appendix C 05 p0603 N85-13842
Application of model following control and estimation techniques to attitude control of maneuvering spacecraft. Part 2: Simulation software description
[NLR-TR-82116-U-PT-2] 12 p1793 N85-21254
Construction of high speed guaranteed regulators
14 p2270 N85-24063
Modal synthesis of multidimensional PI-regulators for objects with inertial sections 14 p2270 N85-24064
The modeling and simulation of feedback control systems
[NASA-CR-171875] 15 p2632 N85-26225

In-flight investigation of the influence of pitch damping and pitch control effectiveness on landing approach flying qualities of statically unstable transport aircraft
[DFVLR-FB-84-12] 17 p2900 N85-27980
Application of model following control and estimation techniques to attitude control of maneuvering spacecraft. Part 1: Theory and simulation results
[NLR-TR-82116-U-PT-1] 18 p3065 N85-28957
Adaptive filtering for large space structures: A closed-form solution 20 p3417 N85-31206
Reduced order models and simulation data in control systems design
[RR-267] 20 p3463 N85-31516
Learning and self adaptation applied to the simulation of a human pilot
[ONERA-RT-24/5122-SY] 20 p3511 N85-31828
Power density and threshold control strategies for radar track initiation
[AD-A155357] 22 p3756 N85-33282
A preliminary evaluation of a failure detection filter for detecting and identifying control element failures in a transport aircraft
[NASA-TM-87576] 24 p4067 N85-35204
Enhancement of the flexible spacecraft dynamics program for open spacecraft
[NASA-CR-175309] 24 p4137 N85-35841
Network management simulation of automated guideway transit systems under vehicle-follower control
[PB85-186233] 24 p4166 N85-35830

CONTROL STABILITY

The numerical range: A tool for robust stability studies — multivariable feedback systems
[RR-255] 02 p0253 N85-11660
On the relationship between Lehtomaki's robustness test and an inverse Nyquist based test
[OUEL-1526/84] 03 p0409 N85-12616
Space Shuttle Orbiter trimmed center-of-gravity extension study. Volume 8: Effects of configuration modifications on the aerodynamic characteristics of the 140 A/B Orbiter at a Mach number of 5.97
[NASA-TM-72661-VOL-8] 04 p0452 N85-12867
Self-tuning control of offset: A unified approach
[OUEL-1539/84] 04 p0553 N85-13520
An H-infinity-minimax approach to the design of robust control systems
[OUEL-1537/84] 05 p0717 N85-14600
On the global asymptotic stabilization of nonlinear systems
[PREPRINT-938] 08 p1209 N85-17604
Improved stability and performance bounds using approximate models — control system design
[RR-260] 08 p1209 N85-17606
Some stability and control problems with trailed farm tankers on slopes
[AD-P004291] 09 p1408 N85-18868
Control of tractors on sloping ground
[AD-P004292] 09 p1408 N85-18869
Wind-tunnel investigation of a full-scale canard-configured general aviation airplane
[NASA-TP-2382] 11 p1575 N85-19925
Contribution to the study of perturbational stabilization
[ONERA-NT-1984-1] 11 p1714 N85-20781
Structural dynamics analysis 14 p2233 N85-23838
Static longitudinal stability and control characteristics of the Fokker F27 Friendship calculated by simple handbook methods
[VTH-LR-394] 16 p2711 N85-26728
Matrix transfer function design for flexible structures: An application 20 p3416 N85-31199
Maximum likelihood estimation with emphasis on aircraft flight data 20 p3417 N85-31208
Extensions of the small-mu test for robust stability — control stability
[OUEL-1573/85-REV] 20 p3519 N85-31884
Decentralized control of dynamically interconnected systems
[BU-111] 22 p3835 N85-33744

CONTROL STICKS

Level of effort 05 p0602 N85-13839
Effects of control stick parameters on human controller response 05 p0701 N85-14496
Active sticks: A new dimension in controller design 05 p0706 N85-14531
Biodynamic resistant control stick
[AD-D011380] 07 p0904 N85-15721

CONTROL SURFACES

NT AERIAL RUDDERS
NT AILERONS
NT ELEVATORS (CONTROL SURFACES)
NT ELEVONS
NT FLAPERONS
NT FLAPS (CONTROL SURFACES)
NT GUIDE VANES
NT HORIZONTAL TAIL SURFACES
NT JET FLAPS
NT JET VANES
NT LEADING EDGE FLAPS
NT LEADING EDGE SLATS
NT RUDDERS
NT SPOILERS
NT TABS (CONTROL SURFACES)
NT TRAILING EDGE FLAPS
NT WING FLAPS
Integral equation of lifting surfaces in Laplace domain and analytic continuation of its pressure kernel
[NAL-TR-795T] 01 p0002 N85-10009
Advanced composite stabilizer for Boeing 737 aircraft
[NASA-CR-168451] 02 p0137 N85-10934
Improvement of Aerodynamic Performance Through Boundary Layer Control and High Lift Systems
[AGARD-CP-365] 08 p1066 N85-16771
Steady- and unsteady-pressure measurements on a supercritical-wing model with oscillating control surfaces at subsonic and transonic speeds
[NASA-TM-84543] 08 p1077 N85-16831
Transonic steady- and unsteady-pressure measurements on a high-aspect-ratio supercritical-wing model with oscillating control surfaces
[NASA-TM-81868] 09 p1273 N85-18003
Subsonic and transonic pressure measurements on a high-aspect-ratio supercritical-wing model with oscillating control surfaces
[NASA-TM-83201] 09 p1273 N85-18004
Wind-tunnel investigation of a full-scale canard-configured general aviation airplane
[NASA-TP-2382] 11 p1575 N85-19925
Multivariable control law design for the AFTI/F-16 with a failed control surface
[AD-A151908] 15 p2474 N85-25271
Harrier 15 p2887 N85-28595
Flight control system reconfiguration design using quantitative feedback theory
[AD-A151771] 16 p2710 N85-26722
The aerodynamics of controls 16 p2713 N85-26748
X-29 digital flight control system design 17 p2901 N85-27889
The aerodynamics of control 17 p2903 N85-27901
Method of calculating separation flow of subsonic gas stream around wings 17 p2942 N85-28161
A study of aerodynamic control in stalled flight leading-edge vortex formation analysis
[AD-A153758] 18 p3069 N85-28928
Gust load alleviation of a cantilevered rectangular elastic wing. Wind tunnel experiment and analysis
[NAK-TR-86] 18 p3083 N85-28950
Mathematics of surfaces
[DE85-010439] 19 p3346 N85-30742

CONTROL SYSTEMS

U CONTROL

CONTROL SYSTEMS DESIGN

Return difference feedback design for robust uncertainty tolerance in stochastic multivariable control systems
[AD-A145861] 03 p0411 N85-12624
Development and demonstration of a vertical axis wind turbine POWERHOUSE
[DE84-901449] 04 p0527 N85-13369
Frequency response design methods for large scale systems
[DE84-014161] 04 p0553 N85-13517
Model reduction for control system design 05 p0596 N85-13799
Level of effort 05 p0602 N85-13839
Oral presentation of first year final report, appendix A 05 p0602 N85-13840
An apparatus for and a method of controlling multiple time-varying processes
[AD-D011253] 05 p0631 N85-14045
Using the control system design environment in the design of a data link receiver unit for the Coast Guard HH-65A helicopter
[AD-A148624] 08 p1088 N85-16880
Man-machine interface and control of the shuttle digital flight system 09 p1091 N85-16894
Implementation of an Intel 8086 microprocessor-based realization library for the control system design language
[AD-A148506] 08 p1202 N85-17589
Improved stability and performance bounds using approximate models — control system design
[RR-260] 08 p1209 N85-17606
Design of mismatched Smith predictors using plant step data
[RR-263] 08 p1217 N85-17664
Simulation in the design of gas pressure control equipment
[ERS-E.352] 09 p1324 N85-18322
The influence of modern control techniques on the gas industry
[ERS-E.396] 09 p1325 N85-18326
NASA-VCOSS dynamic test facility
[NASA-TM-86491] 10 p1427 N85-18898
Development of mass-producible line-focus tracking concentrating solar collectors. Category 2: Trackers
[DE85-002673] 10 p1512 N85-19543
Personnel protection concepts for advance escape system design 10 p1532 N85-19658
Microprocessor-based monitoring and control project, phase 1
[DE84-001974] 10 p1538 N85-19699
Robustness of continuous multivariable flight controls
[ONERA-RT-12/7224-SY] 11 p1586 N85-19967
Robustness of continuous multivariable flight controls
[ONERA-RT-11/7224-SY] 11 p1586 N85-19968
Compensator development and examination of performance and robustness
[NASA-CR-175470] 11 p1627 N85-20244
Automatic control design procedures for restructurable aircraft control
[NASA-CR-172489] 12 p1760 N85-21173
Some aspects of the design of a fly-by-wire flying control system for a supersonic V/STOL fighter aircraft
[COLL-AERON-8413] 12 p1780 N85-21175
Application of model following control and estimation techniques to attitude control of maneuvering spacecraft. Part 2: Simulation software description
[NLR-TR-82116-U-PT-2] 12 p1793 N85-21254
System dynamics and network control
[AD-A149420] 13 p2054 N85-22863
Activities in flight mechanics and flight control
[ISSN-0720-7808] 14 p2227 N85-23603
Application of the maximum entropy/optimal projection control design approach for large space structures 14 p2234 N85-23849
Synthesis of hyperstable control system with adaptive model 14 p2273 N85-24084
Modeling needed for the design and definition of spacecraft attitude and orbit control systems 14 p2397 N85-24766
Modeling and control of large flexible structures, phase 1
[AD-A150736] 14 p2403 N85-24817
Multivariable control law design for the AFTI/F-16 with a failed control surface
[AD-A151908] 15 p2474 N85-25271
Definition of ground test for verification of large space structure control
[NASA-CR-171438] 15 p2492 N85-25377
Process control systems for largely automated manufacturing 15 p2537 N85-25659
Cost Effective and Affordable Guidance and Control Systems
[AGARD-CP-360] 16 p2695 N85-26638
Some aspects of how to design cost-effective flight control systems 16 p2695 N85-26639
Design adequacy: An effectiveness factor 16 p2695 N85-26642
A modern control design methodology with application to the CH-47 helicopter
[AD-A151946] 16 p2710 N85-26723
Application of linear optimal control theory to the design of the elevator control system of the DHC-2 Beaver experimental aircraft
[VTH-LR-411] 16 p2711 N85-26729
The flight control system for the Experimental Aircraft Programme (EAP) demonstrator aircraft 16 p2714 N85-26755
The STOL and maneuver technology program integrated control system 16 p2715 N85-26757
Corrective-predictive systems
[BLL-M-36063-(5828.4)] 16 p2851 N85-27573
Some aspects of how to design cost-effective flight control systems
[MBB-LKE-32/S/PUB/143] 16 p2873 N85-27729
The state-of-the-art and future of flight control systems 17 p2901 N85-27885
Aspects of application of ACT systems for pilot workload alleviation 17 p2901 N85-27887
Application of AFTI/F-16 task-tailored control modes in advanced multirole fighters 17 p2901 N85-27888
X-29 digital flight control system design 17 p2901 N85-27889
The evolution of ACS for helicopters: Conceptual simulation studies to preliminary design 17 p2902 N85-27890
ACT applied to helicopter flight control 17 p2902 N85-27891
An update of experience on the fly by wire Jaguar equipped with a full-time digital flight control system 17 p2902 N85-27893
ACT flight research experience 17 p2902 N85-27894
Operational and developmental experience with the F/A-18A digital flight control system 17 p2902 N85-27895
Flight testing and development of the F/A-18A digital flight control system 17 p2902 N85-27896

OLGA: An open loop gust alleviation system
17 p2903 N85-27807
A modular dissimilar redundant computer designed for high integrity control
17 p2904 N85-27904
The flight control system for the Experimental Aircraft Programme (EAP) demonstration aircraft
17 p2904 N85-27908
Automatic flight control modes for the AFTI/F-111 mission adaptive wing aircraft
17 p2905 N85-27909
The STOL and maneuver technology program integrated control system development
17 p2905 N85-27910
Development of a multiprocessor system, using the MOTORLA microprocessor 6809, with the aim of providing maximum flexibility in the design of individual control devices
[BMFT-FB-T-84-270]
17 p3010 N85-28607
A modern control theory enhancement to an Interactive Control Engineering Computer Analysis Package (ICECAP)
[AD-A153249]
17 p3012 N85-28622
Technical instructions for a control operating system of the gas flow installation for the solid fuel combustion chamber
[VTH-LR-410]
18 p3118 N85-29302
Research Flight Simulator for Helicopters (RFSH): Description and application to fire control system design
[SNIAS-851-210-106]
20 p3393 N85-31050
A study of the ESA-NAVSAT control segment
[ESA-CR(P)-2000]
20 p3398 N85-31079
Control system design for lightly coupled large space structures
20 p3399 N85-31086
Multivariable control of a soft coupled space station
20 p3408 N85-31151
A hardware demonstration of distributed control for a flexible offset-feed antenna
20 p3410 N85-31160
Control of flexible structures
20 p3410 N85-31161
Time-optimal bang-bang slew of rigidized SCOLE configuration
20 p3410 N85-31164
Numerical and experimental evaluation for single-axis control of an LSS laboratory model
20 p3411 N85-31168
Self-tuning adaptive-controller using online frequency identification
20 p3417 N85-31205
Robust adaptive control
20 p3417 N85-31207
Experimental verification of identification algorithms for control of flexible structures
20 p3418 N85-31211
Feedforward-feedback control logic for robust target-tracking
20 p3436 N85-31317
Control system for parabolic dish concentrator No. 1
[NASA-CR-176045]
20 p3463 N85-31510
Reduced order models and simulation data in control systems design
[RR-267]
20 p3463 N85-31516
On the equivalent bilinearization of nonlinear controlled delay systems
[RR-272]
20 p3519 N85-31880
FAUST: Introduction and overview — self tuning control
[OUEL-1568/85]
20 p3519 N85-31882
Models for describing active noise control in ducts
[ISVR-TR-127]
20 p3525 N85-31922
Performance improvements of a highly integrated digital electronic control system for an F-15 airplane
[NASA-TM-86748]
21 p3556 N85-32120
A preliminary investigation of handling qualities requirements for helicopter instrument flight during decelerating approach manuevers and overshoot
[AD-A154650]
21 p3557 N85-32125
Research on an expert system for database operation of simulation-emulation math models. Volume 1, Phase 1: Results
[NASA-CR-176087]
21 p3669 N85-32792
Flight test experience and controlled impact of a large, four-engine, remotely piloted airplane
[NASA-TM-86738]
22 p3730 N85-33123
Application of frequency domain handling qualities criteria to the longitudinal landing task
[NASA-TM-86728]
22 p3730 N85-33124
The interpretation of flying qualities requirements for flight control system design
[NASA-CR-177942]
22 p3730 N85-33125
Research and development activities in unified control-structure modeling and design
[NASA-CR-176129]
22 p3740 N85-33179
Portable database driven control system for SPEAR
[DE85-010465]
22 p3830 N85-33720
Reactant pressure differential control for fuel cell gases
[NASA-CASE-MSC-20127-2]
23 p3937 N85-34403
Robot environment expert system
[NASA-CR-3915]
23 p3967 N85-34593
Discrete simulation models - their role in the design, development and management of inventory control systems
[PNR-90249]
23 p3966 N85-34719
Report on the SLC control system
[DE85-013076]
24 p4148 N85-35722

CONTROL THEORY
Research in Structures and Dynamics, 1984
[NASA-CP-2335]
01 p0057 N85-10377
Control of the dynamic response of a damped membrane by distributed forces
[CSIR-TWISK-312]
01 p0061 N85-10406
Markovian control problems: Functional equations and algorithms
[MCTH-97]
01 p0107 N85-10717
Robust rate control system designs for a submersible
[AD-A144792]
01 p0111 N85-10753
Model simplification of flight control systems
02 p0147 N85-11000
A research program in active control/aeroelasticity in the JIAFS at NASA Langley Research Center
[NASA-CR-174052]
02 p0148 N85-11001
Application of modern guidance control theory to a bank-to-turn missile
[AD-A145646]
02 p0166 N85-11123
Asynchronous discrete control of continuous processes
[AD-A145570]
02 p0189 N85-11262
Asymptotically optimal adaptive control
[AD-A145666]
02 p0249 N85-11629
On a class of suboptimal controls for infinite-dimensional bilinear systems
[RR-258]
02 p0249 N85-11630
The numerical range: A tool for robust stability studies — multivariable feedback systems
[RR-255]
02 p0253 N85-11660
Linear and bilinear infinite-dimensional representations of finite-dimensional nonlinear systems
[RR-259]
02 p0254 N85-11661
Gain-phase structures for linear multivariable systems
[RR-256]
02 p0256 N85-11674
Theory of information, automation in Czechoslovakia
04 p0485 N85-13091
Self-tuning control of offset: A unified approach
[OUEL-1539/84]
04 p0553 N85-13520
Dynamic decision making — and programming
[FOA-C-53015-H2]
04 p0575 N85-13668
Definition of ground test for verification of large space structure control
[NASA-CR-171208]
05 p0602 N85-13838
Definition of ground test for Large Space Structure (LSS) control verification, appendix G
05 p0603 N85-13845
Review of technical papers, appendix H
05 p0603 N85-13846
Ground test experiment for large space structures, appendix I
05 p0603 N85-13847
Self-tuning controller design and implementation
[OUEL-1535/84]
05 p0621 N85-13975
A generalized LQG approach to self-tuning control. Part 1: Aspects of design. Part 2: Implementation and simulation
[OUEL-1536/84]
05 p0622 N85-13976
Getting mental models and computer models to cooperate
05 p0709 N85-14548
Manual-control analysis applied to the money-supply control task
05 p0710 N85-14553
Determination of row-and-column control principle of phase antenna array from amplitude-phase distribution of field in aperture
07 p0952 N85-16033
Precise control of flexible manipulators
[NASA-CR-174210]
07 p0973 N85-16178
Control and modeling of a CELSS (Controlled Ecological Life Support System)
[NASA-CR-177324]
07 p1020 N85-16472
Numerical methods and approximation and modelling problems in stochastic control theory
[AD-A146927]
07 p1029 N85-16533
Bibliography of adaptive control
[OUEL-1544/84]
08 p1209 N85-17602
Research on optimal control, stabilization and computational algorithms for aerospace applications
[NASA-CR-174318]
08 p1209 N85-17603
On the global asymptotic stabilization of nonlinear systems
[PREPRINT-838]
08 p1209 N85-17604
Optimal stochastic LQ control with measurements displaced in time
[OUEL-1547/84]
08 p1209 N85-17605
Improved stability and performance bounds using approximate models — control system design
[RR-260]
08 p1209 N85-17606
The practical identification of systems with nonlinearities
[RR-264]
08 p1209 N85-17607
Approximate models in multivariable process control: An inverse Nyquist array and robust tuning regulator interpretation
[RR-261]
08 p1216 N85-17663
Design of mismatched Smith predictors using plant step data
[RR-263]
08 p1217 N85-17664
Ground test experiment for large space structures
[NASA-TM-86480]
10 p1429 N85-19013
A note on the disturbance decoupling problem for retarded systems
[AD-A149045]
10 p1543 N85-19730
Advanced industrial robot control systems
[PB85-110773]
11 p1648 N85-20385
Advanced industrial robot control systems
[PB85-110781]
11 p1648 N85-20386
Needs, opportunities, and options for large scale systems research
[DE85-004642]
12 p1825 N85-22091
Testing of the digital flight control system of the German CCV fighter experimental aircraft
13 p1968 N85-22361
Model reduction for control system design
[NASA-CR-170417]
13 p1975 N85-22398
AFWAL space control technology program
14 p2233 N85-23839
Large antenna control methods: Current status and future trends
14 p2234 N85-23845
A mathematical formulation of the Scole control problem, part 1
[NASA-CR-172581]
14 p2243 N85-23903
Adaptive techniques for control of large space structures
[AD-A150957]
14 p2246 N85-23923
Construction of high speed guaranteed regulators
14 p2270 N85-24063
Modal synthesis of multidimensional PI-regulators for objects with inertial sections
14 p2270 N85-24064
Synthesis of hyperstable control system with adaptive model
14 p2273 N85-24084
Optimal control and optimization
14 p2395 N85-24755
High specific power aircraft turn maneuvers: Tradeoff of time-to-turn versus change in specific energy
[AD-A151701]
15 p2471 N85-25257
Multivariable control law design for the AFTI/F-16 with a failed control surface
[AD-A151908]
15 p2474 N85-25271
Frequency/period estimation and adaptive rejection of periodic disturbances
[AD-A149229]
15 p2632 N85-26226
Fundamental equivalence of generalised state space systems
[MATHEMATICS-RESEARCH-182]
15 p2642 N85-26293
Optimal control theory applied to fusion plasma thermal stabilization
[DE85-007599]
15 p2658 N85-26405
AN investigation into the control limitations of a bank to turn missile in the terminal homing phase
[AD-A152193]
16 p2704 N85-26696
Flight control system reconfiguration design using quantitative feedback theory
[AD-A151771]
16 p2710 N85-26722
Application of linear optimal control theory to the design of the elevator control system of the DHC-2 Beaver experimental aircraft
[VTH-LR-411]
16 p2711 N85-26729
Technical evaluation report on the Flight Mechanics Symposium on Active Control Systems: Review, Evaluation and Projections
[AGARD-AR-220]
16 p2711 N85-26730
ACT applied to helicopter flight control
16 p2712 N85-26738
The flight control system for the Experimental Aircraft Programme (EAP) demonstrator aircraft
16 p2714 N85-26755
The investigation of tethered satellite system dynamics
[NASA-CR-175855]
16 p2731 N85-26854
Optimal open loop and nonlinear feedback control for remote orbital capture
[AD-A151967]
16 p2732 N85-26859
Control of motion of manipulator robots on basis of first-order kinematic algorithms
16 p2762 N85-27047
Design of robust controllers for a multiple input-multiple output control system with uncertain parameters application to the lateral and longitudinal modes of the KC-135 transport aircraft
[AD-A153100]
17 p2900 N85-27877
Controller requirements for uncoupled aircraft motion, volume 1
[AD-A153173]
17 p2900 N85-27878
Controller requirements for uncoupled aircraft motion, volume 2
[AD-A153300]
17 p2900 N85-27879
Active Control Systems: Review, Evaluation and Projections
[AGARD-CP-384]
17 p2901 N85-27883

Hand controllers for teleoperation. A state-of-the-art technology survey and evaluation
[NASA-CR-175890] 17 p3002 N85-28559
A modern control theory enhancement to an Interactive Control Engineering Computer Analysis Package (ICECAP)
[AD-A153249] 17 p3012 N85-28622
Scalar model control of a nonlinear system using time varying gain
[AD-A153252] 17 p3020 N85-28676
Nonlinear global stability analysis of compressor stall phenomena
[NASA-CR-174908] 19 p3219 N85-29960
Research on optimal control, stabilization and computational algorithms for aerospace applications
[NASA-CR-172528] 19 p3221 N85-29970
Proceedings of the Workshop on Identification and Control of Flexible Space Structures, volume 1
[NASA-CR-176051] 20 p3408 N85-31148
AFWAL control technology programs
20 p3408 N85-31150
Time-optimal bang-bang slew of rigidized SCOLE configuration 20 p3410 N85-31164
Experiments in structural dynamics and control using a grid 20 p3410 N85-31165
Rationale for an experimental test for flexible space structure attitude control 20 p3411 N85-31167
Proceedings of the Workshop on Identification and Control of Flexible Space Structures, volume 2
[NASA-CR-176052] 20 p3411 N85-31170
Finite control in underdamped distributed parameter systems 20 p3412 N85-31176
Control of a flexible space antenna: A finite dimensional perspective based on distributed parameter theory
20 p3413 N85-31182
Sensor/actuator selection for the constrained variance control problem 20 p3415 N85-31197
Decentralized control synthesis method for large-scale interconnected systems
[DE85-000748] 20 p3518 N85-31678
Linear system structure and cone containment for bilinear systems
[RR-268] 20 p3519 N85-31679
Multivariable model-following self-tuning control with offset rejection
[OUEL-1572/85] 20 p3519 N85-31683
Extensions of the small-mu test for robust stability — control stability
[OUEL-1573/85-REV] 20 p3519 N85-31684
Robust control of multivariable and large space systems
[AD-A155117] 21 p3559 N85-32140
Development of control laws for a flight test maneuver autopilot for an F-15 aircraft
[NASA-TM-86736] 22 p3730 N85-33122
Research and development activities in unified control-structure modeling and design
[NASA-CR-176129] 22 p3740 N85-33179
Decentralized control of dynamically interconnected systems
[BU-111] 22 p3835 N85-33744
Analogies of control mechanisms in flight guidance and medicine 24 p4129 N85-35597
Network management simulation of automated guideway transit systems under vehicle-follower control
[PB85-186233] 24 p4166 N85-35830

CONTROL UNITS (COMPUTERS)
Direct digital control study
[AD-A153685] 18 p3167 N85-29621

CONTROL VALVES
Slow opening valve — valve design for shuttle portable oxygen system
[NASA-CASE-MSC-20112-1] 11 p1642 N85-20338
Voyager 0.2-lbf thruster valve assembly short pulse test report
[NASA-CR-176121] 22 p3741 N85-33185
Computer and water-model simulation of flow through poppet valves
[CFD/85/2] 22 p3785 N85-33449

CONTROLLABILITY
Integrated Application of Active Controls (IAAC) technology to an advanced subsonic transport project-longitudinal handling qualities study of a relaxed-stability airplane
[NASA-CR-3660] 02 p0148 N85-11005
Simulation evaluation of two VTOL control/display systems in IMC approach and shipboard landing
[NASA-TM-85996] 06 p0756 N85-14841
Controllable rotation of system of two solid bodies with elastic elements 06 p0780 N85-14988
Electric and hybrid vehicle demonstration project
[DE84-014622] 06 p0871 N85-15535
Operational requirements versus technological capabilities 06 p1072 N85-16798
Space shuttle handling qualities
06 p1092 N85-16804
The development of a dynamic model of a generalised combat aircraft with forward wings for the identification of stability and control characteristics
[CAR-84-33] 09 p1280 N85-18050
Dynamics and control of general linear lumped-parameter systems 09 p1372 N85-18623
Study on controllability and stability of high speed tracked vehicles
[AD-P004302] 09 p1409 N85-18879
A functional vehicle for autonomous mobile robot research
[AD-A150052] 12 p1860 N85-21666
Simulation of aircraft behaviour on and close to the ground
[NASA-TM-87460] 14 p2218 N85-23754
A preliminary investigation of handling qualities requirements for helicopter instrument flight during decelerating approach maneuvers and overshoot
[NRC-24173] 17 p2896 N85-27857
ACT flight research experience
17 p2902 N85-27864
How to handle failures in advanced flight control systems of future transport aircraft 17 p2904 N85-27905
Mission requirements and handling qualities
18 p3057 N85-28918
Development of control laws for a flight test maneuver autopilot for an F-15 aircraft
[NASA-TM-86736] 22 p3730 N85-33122
Application of frequency domain handling qualities criteria to the longitudinal landing task
[NASA-TM-86728] 22 p3730 N85-33124
Ground-based and in-flight simulator studies of flight characteristics of a twin-fuselage passenger transport airplane during approach and landing
[NASA-TP-2451] 23 p3898 N85-34144
Analysis of flexible aircraft longitudinal dynamics and handling qualities. Volume 1: Analysis methods
[NASA-CR-177943-VOL-1] 24 p4066 N85-35202
Analysis of flexible aircraft longitudinal dynamics and handling qualities. Volume 2: Data
[NASA-CR-177943-VOL-2] 24 p4067 N85-35203

CONTROLLED ATMOSPHERES
NT CABIN ATMOSPHERES
NT INERT ATMOSPHERE
NT SPACECRAFT CABIN ATMOSPHERES
Stability of several substituted ferrites in a reducing atmosphere
[AD-A146106] 03 p0328 N85-12112
Inert atmosphere transfer vessel
[AD-D011433] 08 p1169 N85-17370
A theoretical method for selecting space craft and space suit atmospheres
[AD-A148219] 08 p1200 N85-17559
The body burden of organic vapors in artificial air trial measurements aboard a moored submarine
[AD-A149696] 12 p1910 N85-21988
Effect of protective atmosphere composition on durability of welded joints of niobium alloys
15 p2502 N85-25432
Preparation of heavy metal fluoride glasses in the bulk form
[AD-A153784] 18 p3079 N85-29049
Controlled Ecological Life Support System. Life Support Systems in Space Travel
[NASA-CP-2378] 18 p3155 N85-29531
Survey of CELSS concepts and preliminary research in Japan 18 p3155 N85-29533
Advanced regenerative environmental control and life support systems: Air and water regeneration
18 p3155 N85-29535
Atmosphere behavior in gas-closed mouse-algal systems: An experimental and modelling study
18 p3155 N85-29536
Ventilation flow: Submerged
18 p3156 N85-29545
An environmentally-controlled extended-use small animal hypobaric chamber
[AD-A153735] 19 p3221 N85-29974
Development of growth techniques for electromagnetic crystals
[AD-A154089] 19 p3375 N85-30937
Hydroponics developments for spaceship garden
21 p3663 N85-32754

CONTROLLED FUSION
Progress in inertial confinement fusion at Lawrence Livermore National Laboratory
[DE84-016227] 04 p0568 N85-13621
Lidar-Thomson scattering — nuclear fusion
[IPP-1/299] 08 p1221 N85-17693
Atomic data for controlled fusion research. Volume 4: Spectroscopic data for iron
[DE85-009658] 19 p3354 N85-30787
Research activities of the Physics Division
[DE85-006958] 19 p3357 N85-30811
Report to the Working Group on Technology, Growth and Employment
[DE85-010320] 19 p3372 N85-30920

CONTROLLED STABILITY
U CONTROL

CONTROLLERS
NT POWER FACTOR CONTROLLERS
NT SERVOMECHANISMS
NT SERVOMOTORS
Aircraft cabin pressurization control system tester
[AD-D011225] 01 p0013 N85-10081
Programmable digital temperature controller apparatus
[AD-D011221] 01 p0049 N85-10319
Robust rate control system designs for a submersible
[AD-A144792] 01 p0111 N85-10753
An input translator for a computer-aided design system
[AD-A146337] 03 p0408 N85-12605
A unified method for evaluating real-time computer controllers: A case study — aircraft control
[NASA-CR-174166] 04 p0547 N85-13478
Microcomputer control of a residential photovoltaic power conditioning system
[DE84-013867] 04 p0547 N85-13480
Level of effort 05 p0602 N85-13839
Speed test results and hardware/software study of computational speed problem, appendix D
05 p0603 N85-13843
Self-tuning controller design and implementation
[OUEL-1535/84] 05 p0621 N85-13975
Quantification of cross-coupling and motion feedthrough for multiaxis controllers used in an air combat flying task
05 p0700 N85-14491
Model estimation and identification of manual controller objectives in complex tracking tasks
05 p0700 N85-14494
Effects of control stick parameters on human controller response 05 p0701 N85-14496
Measurements of pilot time delay as influenced by controller characteristics and vehicles time delays
05 p0701 N85-14500
Active sticks: A new dimension in controller design
05 p0706 N85-14531
Implementation of a Zilog Z-80 base realization library for the computer systems design environment
[AD-A146359] 06 p0853 N85-15423
Control system design language implementation of a gas turbine starting controller
[AD-A147896] 07 p0905 N85-15732
Flutter control with unsteady aerodynamic models
[AD-A147858] 07 p0909 N85-15753
Battery control and fault detection method
[AD-D011364] 07 p0983 N85-16307
Interactive color-graphics interface for energy monitoring and control systems
[AD-A147538] 07 p1025 N85-16509
Mirror actuator control system
[AD-D011383] 07 p1042 N85-16819
Experience of one UK electronic equipment supplier with bite on engine/flight control systems over the past ten years 08 p1084 N85-16736
Mission-oriented requirements for updating MIL-H-8501. Volume 1: STI proposed structure — military rotorcraft
[NASA-CR-177331-VOL-1] 08 p1088 N85-16877
Implementation of an Intel 8086 microprocessor-based realization library for the control system design language
[AD-A148506] 08 p1202 N85-17569
Dual arm master controller concept
[DE85-001901] 09 p1327 N85-18344
An ultra reliable computer communication network: The dispersed sensor processing mesh
09 p1372 N85-18620
Dynamics and control of general linear lumped-parameter systems 09 p1372 N85-18623
RELTIM: A library of routines used in real time machine control applications
[PB85-116507] 10 p1542 N85-19725
Solar optical telescope primary mirror controller
[NASA-CR-174416] 10 p1570 N85-19903
Digital controller for the Wave Propagation Laboratory's VHF and UHF wind-profiling radars
[PB85-112142] 11 p1626 N85-20238
Microprocessor-controlled rotating shadowband radiometer
[DE85-003633] 12 p1854 N85-21630
Model reduction for control system design
[NASA-CR-170417] 13 p1975 N85-22398
Large antenna control methods: Current status and future trends 14 p2234 N85-23845
Model and controller reduction of uncertain systems using covariance equivalent realizations
14 p2243 N85-23902
Modal synthesis of multidimensional PI-regulators for objects with inertial sections 14 p2270 N85-24064

Some problems in improving reliability and accuracy of regulators with hydraulic amplifiers in main channel of power turbine
[AD-A155477] 14 p2271 N85-24071

Investigation of transport operations of ergatic robot
[AD-A154677] 14 p2286 N85-24166

User's guide to calibration of analog electronic controllers in HVAC systems
[AD-A150803] 14 p2286 N85-24229

Effects of side-stick controllers on rotorcraft handling qualities for terrain flight
[NASA-TM-86688] 15 p2473 N85-25267

Space station systems technology study (add-on task). Volume 3: Technology advancement program plan
[NASA-CR-171417] 15 p2475 N85-25280

Czech institute develops microcomputer for satellites
15 p2484 N85-25331

Development of robots and application to industrial processes
[NASA-CR-175754] 15 p2567 N85-25840

Feasibility analysis of moving bank multiple model adaptive estimation and control algorithms
[AD-A152015] 15 p2641 N85-26292

Model reduction techniques applied to the control of large space structures
[AD-A151784] 16 p2731 N85-26857

Further development of an interactive Control Engineering Computer Analysis Package (ICECAP) for discrete and continuous systems
[AD-A151783] 16 p2846 N85-27546

Design of robust controllers for a multiple input-multiple output control system with uncertain parameters application to the lateral and longitudinal modes of the KC-135 transport aircraft
[AD-A153100] 17 p2900 N85-27877

Controller requirements for uncoupled aircraft motion, volume 2
[AD-A153300] 17 p2900 N85-27879

ACT applied to helicopter flight control
17 p2902 N85-27891

A ten channel temperature controller
[AD-A152664] 17 p2967 N85-28326

Scalar modal control of a nonlinear system using time varying gain
[AD-A153252] 17 p3020 N85-28676

A proportional-plus-integral controller for a particle beam weapon
[AD-A153213] 17 p3035 N85-28778

Ultrareliable, fault-tolerant control systems: A conceptual description
[NASA-TM-86017] 19 p3221 N85-29972

Thrust vectoring apparatus for maneuvering missile in flight
[AD-D011693] 19 p3226 N85-30004

A variable frequency control for three-phase induction motors
19 p3256 N85-30190

Spillover minimization: An approach for actuators and sensors placement in distributed parameter study
[INPE-3525-PRE/746] 19 p3272 N85-30289

Physiochemically controlled scour jet array system
[AD-D011688] 19 p3308 N85-30505

The experimental computer control of a two-dimensional hyperbolic system
20 p3411 N85-31166

Rationale for an experimental test for flexible space structure attitude control
20 p3411 N85-31167

Proceedings of the Workshop on Identification and Control of Flexible Space Structures, volume 2
[NASA-CR-176052] 20 p3411 N85-31170

Design of multivariable controllers using the Integrated Analysis Capability (IAC)
20 p3412 N85-31172

ISAAC (Integrated Structural Analysis and Control) via continuum modeling and distributed frequency domain design techniques
20 p3414 N85-31185

Frequency domain control design of large space structures: A practical approach
20 p3415 N85-31192

A control concept for large flexible spacecraft using order reduction techniques
20 p3415 N85-31193

Wideband disturbance accomodation in precision flexible space structures
20 p3415 N85-31194

Proceedings of the Workshop on Identification and Control of Flexible Space Structures, volume 3
[NASA-CR-176053] 20 p3415 N85-31195

Sensor/actuator selection for the constrained variance control problem
20 p3415 N85-31197

Eigenvalue placement and stabilization by constrained optimization
20 p3416 N85-31198

Adaptive control: Actual status and trends
20 p3416 N85-31202

Stable direct adaptive control of linear infinite-dimensional systems using a command generator tracker approach
20 p3416 N85-31204

Multivariable model-following self-tuning control with offset rejection
[OUEL-1572/85] 20 p3519 N85-31883

Microprocessor control design for a low-head crossflow turbine
[AD-A155477] 21 p3556 N85-32121

Secure digital voice communications in the Defense Data Network (DDN)
[AD-A154677] 21 p3574 N85-32226

An analysis of the effects of active solar energy system control sensor degradation on system performance
[DE84-013023] 22 p3804 N85-33562

Feedback regulated induction heater for a flowing fluid
[DE85-006508] 23 p3939 N85-34414

Neutral particle beam intensity controller
[DE85-006411] 23 p3969 N85-34604

State-of-the-art of solid-state motor controllers
[TI85-008674] 24 p4162 N85-35806

CONVAIR MILITARY AIRCRAFT
U MILITARY AIRCRAFT

CONVAIR 990 AIRCRAFT
U CV-990 AIRCRAFT

CONVECTION
NT FORCED CONVECTION
NT FREE CONVECTION
NT MARANGONI CONVECTION

Second All-Union Seminar on Hydromechanics and Heat and Mass Exchange in Weightlessness, summaries of reports
[NASA-TM-77580] 01 p0047 N85-10305

Preparation steps for the use of one-dimensional interpretation models for nowcasting purposes in the German weather net
01 p0081 N85-10540

Some aspects of post-frontal convective areas along the west coast of the united states
[AD-A144895] 01 p0085 N85-10572

Investigation of summertime convection over the upper Current River valley of southeast Missouri
[PB84-222389] 01 p0086 N85-10578

Analytical modeling of random thermal fluctuations in the NORDA high-frequency sound scattering facility
[AD-A145024] 01 p0116 N85-10790

The absence of convective stability in incongruent crystal growth on Earth
02 p0150 N85-11019

Finite element analysis of thermoelasticity problems
02 p0206 N85-11369

The arc cloud complex: A case study
[AD-A145384] 02 p0231 N85-11507

NBS (National Bureau of Standards): Materials measurements
[NASA-CR-174038] 03 p0332 N85-12143

Mesoscale and convective-scale characteristics of mature hurricanes
03 p0394 N85-12516

On the cause of X-line formation in the near-Earth plasma sheet: Results of adiabatic convection of Plasma-Sheet-Plasma
[AD-A145835] 03 p0396 N85-12525

Study of plasma convection and wall interactions in magnetic confinement systems
[DE84-013959] 03 p0421 N85-12692

A preliminary study of numerical simulation of thermosolutal convection of interest to crystal growth
[NASA-TP-2394] 04 p0498 N85-13175

Planetary scale interactions
05 p0684 N85-14397

Stresses and strains in lithosphere caused by Earth's thermoconvective oscillations
06 p0822 N85-15217

Convective scale weather analysis and forecasting
[NASA-CR-174185] 06 p0838 N85-15320

Precipitation characteristics of a dual mesoscale convective complex
[PB84-226711] 06 p0840 N85-15337

Studies of the ocean surface and the coupling between the sea and the atmosphere
[AD-A146546] 06 p0841 N85-15339

The growth of metastable peritectic compounds
[NASA-CR-171290] 07 p0920 N85-15825

Finite difference calculations of buoyant convection in an enclosure. Part 2: Verification of the nonlinear algorithm
[PB85-104065/GAR] 07 p0961 N85-16089

Numerical solutions for steady natural convection in a square cavity
[PB84-245752] 07 p0961 N85-16090

Convection schemes for use with curvilinear coordinate systems: A survey
[AD-A147083] 07 p1031 N85-16543

Sea breeze-induced mesoscale systems and severe weather
[NASA-CR-174317] 08 p1187 N85-17480

Heat-transfer enhancement in natural convection enclosure flow
[DE84-013048] 09 p1319 N85-18297

The influence of deep cumulus convection on large-scale flow during AVE/SESAME 1, 10-11 April 1979
09 p1355 N85-18526

Behavior and characteristics of storm cold outflows
09 p1356 N85-18529

Meridional penetration of frontal systems in South America and its relation to organized convection in the Amazon
[INPE-3407-PRE/676] 10 p1518 N85-19572

Stochastic convective-dispersive transport model for wastes disposed at the 106-mile ocean disposal site
[PB85-116176] 12 p1885 N85-21831

Observational study of transport in the free troposphere
[PB85-144145] 12 p1887 N85-21845

Thermal convection and magnetic fields in accretion disks of black holes
12 p1955 N85-22285

The role of convective perturbations in supercritical inlet oscillations
13 p2004 N85-22563

Contribution to theory of ocean-atmosphere gas exchange
13 p2108 N85-23134

Cumulus effects on the large-scale vorticity and momentum fields in the tropical atmosphere
13 p2137 N85-23270

Implications of convection in the Moon and the terrestrial planets
13 p2183 N85-23548

Solar wind control of magnetospheric convection
14 p2365 N85-24615

Implications of observed frequencies of solar P modes
14 p2443 N85-25073

Numerical simulations of convectively excited gravity waves
14 p2444 N85-25082

On the influence of turbulent motions on non-radial oscillations
14 p2444 N85-25083

Magnetoconvection: The interaction of convection and small scale magnetic fields --- photosphere
14 p2446 N85-25098

Oscillatory convection in sunspots
14 p2446 N85-25099

Amplification and maintenance of thin magnetic flux tubes by compressible convection --- solar magnetism
14 p2447 N85-25104

Nonlinear time-evolution of kink-unstable magnetic flux tubes in the convection zone of the Sun
14 p2447 N85-25105

Linear incompressible magnetoconvection in a planar layer with a nonuniform horizontal magnetic field
14 p2450 N85-25127

Convective collapse and overstable oscillations in solar flux tubes
14 p2452 N85-25138

Modeling longitudinal motions of thermal O+ and H+ ions in magnetic field tube convective through daytime polar cusp
15 p2481 N85-25314

Natural convection in cylindrical containers
15 p2555 N85-25763

VAS/model impact study
15 p2597 N85-26006

Role of jet streaks and boundary layer processes in organizing a pre-convective environment
15 p2597 N85-26008

Possible sea ice impacts on oceanic deep convection
15 p2603 N85-26041

Optimum convection conditions for Czochralski growth of semiconductors
[INPE-3395-PRE/665] 16 p2870 N85-27703

Centralized Storm Information System (CSIS)
[NASA-CR-175898] 17 p2994 N85-28506

Natural convection in square partitioned enclosures
[AD-A153707] 18 p3197 N85-29828

Coolant mixing in LMFBR rod bundles and outlet plenum mixing transients
[DE85-010336] 19 p3268 N85-30268

Diagnosis of vertical motions from VAS retrievals during a convective outbreak
[NASA-CR-171569] 19 p3316 N85-30554

Natural convection experiments in a stratified liquid-saturated porous medium
[DE85-009003] 20 p3455 N85-31457

Automated cell detection as a mesocyclone precursor tool
[AD-A154952] 21 p3635 N85-32577

On the problem of possible mechanism of ice nuclei formation in convective clouds
21 p3640 N85-32610

Magnetic fields in laser heated plasmas
[DE85-010715] 21 p3707 N85-33022

Solar convection
[AD-A155214] 21 p3723 N85-33098

Forced convective, nonequilibrium, post-CHF heat transfer experiment data and correlation comparison report
[TI85-009331] 23 p3932 N85-34371

Diffusion-convection function of cosmic rays
[SH-3.2-10] 23 p4004 N85-34825

IMF-sense-dependent cosmic ray anisotropy produced from diffusion-convection in heliosphere
[SH-4.3-9] 23 p4032 N85-34994

Diurnal anisotropy during solar activity cycle twenty and diffusion-convection model
[SH-4.5-7] 23 p4036 N85-35025

Experimental study of free and mixed convective flow of air in a heated cavity
[DE85-012538] 24 p4094 N85-35380

Airborne investigations of Mesoscale Convective Systems (AIMCS), 1984: Operational summary and data inventory
[PB85-187904] 24 p4125 N85-35571

CONVECTION CLOUDS
NT ARC CLOUDS
NT CIRRUS CLOUDS
NT STRATOCUMULUS CLOUDS
NT STRATUS CLOUDS

Generation of deep convective clouds along mesoscale storm outflow boundaries 01 p0074 N85-10490
Automated analysis and nowcasting of mesoscale convective systems 01 p0074 N85-10492
Combining radar and satellite data for the localization and identification of summer convection 01 p0077 N85-10509
The use of dual polarisation radar for observing and predicting convective activity 01 p0077 N85-10512
Doppler radar analysis of a frontal zone prior to convective development 01 p0077 N85-10515
The lifting condensation level and its relation to convective cloud base
[AD-A145654] 02 p0232 N85-11513
Experimental study of anisotropy of scattering of radar signals by clouds and precipitation 14 p2340 N85-24473
Case studies of snow clouds by means of snow crystal sondes 15 p2581 N85-25921
Assessment of VAS soundings in the analysis of a preconvective environment
[NASA-TM-86205] 16 p2825 N85-27427
Statistical comparison of radar echoes of convective precipitation between the northern Alps and its foreland
[DFVLR-FB-85-07] 17 p2950 N85-29215
Vertical redistribution of a pollutant tracer due to cumulus convection
[PB85-172971] 18 p3134 N85-29415
Mesoscale features and atmospheric refraction conditions of the Arctic marginal ice zone
[AD-A155139] 21 p3636 N85-32584

CONVECTION CURRENTS
Theoretical and observational studies of stellar activity 13 p2171 N85-23468
Atmosphere ice-ocean interactions in the Antarctic (IAGO) 14 p2326 N85-24375
Afternoon radar aurora and polar cap convection pattern 14 p2361 N85-24592
Disturbance of midlatitude electrodynamic parameters due to the magnetospheric convection 14 p2362 N85-24593
The magnetospheric convection electric field at ionospheric altitudes: A case study based on STARE and Saint-Santin data 14 p2362 N85-24594
Ionosphere-magnetosphere coupling and convection 14 p2364 N85-24609
On the structure of magnetic fields in the solar convection zone 14 p2447 N85-25103
Convection modeling and application to severe storms 15 p2595 N85-25991
Modeling of cloud systems 15 p2595 N85-25992
The sensitivity of mesoscale cyclogenesis forecasts to detailed three-dimensional isentropic initial analyses and varied vertical model resolution 15 p2598 N85-26015
Assessment of VAS soundings in the analysis of a preconvective environment
[NASA-TM-86205] 16 p2825 N85-27427
Diagnostics of severe convection and subsynoptic scale ageostrophic circulations
[NASA-CR-171581] 21 p3634 N85-32571
Dynamics of Mesoscale Weather Systems: 1984 Summer Colloquium
[PB85-188266] 22 p3817 N85-33649
Measurements for the determination of the vertical structure of the convective boundary layer — atmospheric boundary layer 24 p4122 N85-35550
Two-point closure study of covariance budgets for turbulent Rayleigh-Benard convection
[PB85-189106] 24 p4124 N85-35568

CONVECTIVE FLOW
Vertical channel free convection for a power law fluid with a constant heat flux
[DE84-014551] 01 p0047 N85-10311
The mesoscale-beta-scale evolution of mid-latitude meso-alpha-scale convective complexes 01 p0073 N85-10488
Convection of plasma in polar ionosphere, comparison of measurements from Cosmos-184 with model dependent on interplanetary magnetic field vector 02 p0180 N85-11086
Stresses and strains in lithosphere caused by Earth's thermoconvective oscillations 06 p0822 N85-15217
High Marangoni number convection in a square cavity
[NASA-CR-174283] 07 p0959 N85-16078
Numerical investigation of phase change heat transfer in a horizontal cylinder including effects of natural convection 09 p1318 N85-18266
A 3-D treatment of convective flow in the Earth's mantle
[DE85-003734] 12 p1890 N85-21863
Convective instability of horizontal layer of binary mixture 14 p2338 N85-24458
What would a dynamo theorist like to know about the dynamics of the solar convection zone? 14 p2441 N85-25062
North Atlantic Deep Water Formation
[NASA-CP-2367] 15 p2601 N85-26028
Deep water formation 15 p2601 N85-26030
Temporal and spatial scales of Labrador Sea water formation 15 p2601 N85-26031
Possible sea ice impacts on oceanic deep convection 15 p2603 N85-26041
Large-eddy simulation in planetary boundary-layer research 18 p3147 N85-29482
Spacecraft, straight-tube evaporator design
[AD-A154462] 19 p3226 N85-30003
Development of thermoconvective instabilities in porous media. Influence of boundary conditions 20 p3456 N85-31461
Effects of solar magnetic field on cosmic rays
[SH-4.2-12] 23 p4008 N85-34850
Difference between even and odd 11-year cycles in cosmic ray intensity
[SH-4.2-22] 23 p4009 N85-34859

CONVECTIVE HEAT TRANSFER
About the influence of nonadiabatic processes on frontogenesis near the ground 01 p0075 N85-10498
Investigation of crisis phenomena in thermosyphons with internal heat-dissipation
[BLL-M-35765-(5826.4)] 02 p0197 N85-11313
Numerical simulation of natural convection in porous media — heat transfer
[CFD/84/10] 02 p0199 N85-11330
Methane heat transfer investigation
[NASA-CR-171199] 03 p0362 N85-12318
Bibliography of US patents on augmentation of convective heat and mass transfer, part 2
[DE84-014865] 04 p0498 N85-13178
Influence of Prandtl number on natural convection heat transfer correlations
[DE84-013006] 05 p0637 N85-14089
Convection heat transfer in the critical region of fluid mixtures
[DE85-002118] 07 p0961 N85-16088
Methods for heat transfer and temperature field analysis of the insulated diesel
[NASA-CR-174783] 07 p1056 N85-16699
Numerical modeling of steady, laminar free-convective boundary layer flow beneath heated or combusting horizonal surfaces 08 p1160 N85-17318
Unsteady free-convection heat transfer inside an annular cavity
[CFD/84/16] 08 p1163 N85-17339
Simultaneous determination of radiation and convection heat transfer 08 p1194 N85-17523
Natural convection experiments about a finite-length cylindrical heat source in a liquid-saturated porous medium
[DE84-012657] 09 p1320 N85-18298
Natural convection heat transfer between arrays of horizontal cylinders and their enclosure
[DE85-003773] 11 p1632 N85-20280
Convection heat transfer in the critical region of fluid mixtures
[DE85-001282] 11 p1633 N85-20285
Theoretical and empirical studies of the basic structure of turbulent shear flows, including separated flows and effects of wall curvature
[AD-A149657] 12 p1848 N85-21580
Turbulent convecting flow in a square duct with a 180 deg bend: An experimental and numerical study
[AD-A149969] 12 p1848 N85-21583
A 3-D treatment of convective flow in the Earth's mantle
[DE85-003734] 12 p1890 N85-21863
Theory of relaxation processes in decomposing polymer materials during high-intensity convective heating 13 p2028 N85-22710
Natural convection during heat accumulation by substances with change of aggregate state 13 p2043 N85-22787
A theoretical analysis of solar-driven natural convection energy conversion systems
[DE84-004431] 13 p2128 N85-23245
Cumulus cloud venting of mixed layer ozone
[NASA-TM-87429] 13 p2132 N85-23269
Optimization of combined convective and film cooling of perforated baffle blades in gas turbines 14 p2270 N85-24067
Convective instability of horizontal layer of binary mixture 14 p2338 N85-24458
Models of solar differential rotation 14 p2446 N85-25097
North Atlantic Deep Water and the world ocean 15 p2602 N85-26033
Unsteady heat transfer due to time-dependent free stream velocity 17 p2911 N85-27947
Effects of the corona wind on the cooling of a horizontal cylinder
[AD-A153101] 17 p2954 N85-28241
Heat transfer in pipes
[NASA-TM-77838] 17 p2957 N85-28262
Solar pond research at the Los Alamos National Laboratory
[DE85-008631] 18 p3128 N85-29366
Natural convection in square partitioned enclosures
[AD-A153707] 18 p3197 N85-29828
Spacecraft, straight-tube evaporator design
[AD-A154462] 19 p3226 N85-30003
Selective radiative cooling with MgO and/or LiF layers
[DE85-011595] 19 p3262 N85-30228
Experimental investigation of turbulent heat transfer in straight and curved rectangular ducts
[AD-A154413] 19 p3266 N85-30255
A numerical solution of a nonisothermal wall using the two-dimensional Navier-Stokes equations
[AD-A154467] 19 p3266 N85-30257
Enhanced thermal coupling by a repetitively pulsed laser
[AD-A154435] 19 p3276 N85-30317
Parametric description of cold film on ocean surface 19 p3292 N85-30410
Natural convection experiments in a stratified liquid-saturated porous medium
[DE85-009003] 20 p3455 N85-31457
Evaluation of the effects of roll angle on the natural convection heat transfer from an array of cylindrical spines
[AD-A154594] 21 p3583 N85-32273

CONVERGENCE
The effect of channel convergence on heat transfer in a passage with short pin fins
[NASA-TM-83801] 01 p0046 N85-10303
The convergence of Garlerkin approximation schemes for second-order hyperbolic equations with dissipation
[CSIR-TWISK-325] 01 p0109 N85-10736
Legendre-Tau approximation for functional differential equations. Part 3: Eigenvalue approximations and uniform stability
[NASA-CR-172447] 01 p0110 N85-10744
The rate of convergence of a class of block Jacobi schemes
[AD-A144738] 01 p0111 N85-10749
Accelerated convergence for incompressible flow calculations
[NASA-TM-86863] 02 p0140 N85-10949
Qualitative results for distributed systems with discrete damping and stiffness with application to control
[AD-A145525] 02 p0209 N85-11382
An iterative procedure for obtaining I-projections onto the intersection of convex sets
[AD-A145402] 02 p0251 N85-11639
Rapidly convergent algorithms for nonsmooth optimization
[AD-A145556] 02 p0251 N85-11643
Comparison of the multigrid and ICCG methods in solving the diffusion equation
[DE84-014409] 02 p0253 N85-11657
On the rate of mean convergence of finite linear predictors of multivariate stationary stochastic processes
[AD-A145609] 02 p0254 N85-11664
Convergence of SIP (Strongly Implicit Procedure)
[AD-A145810] 03 p0410 N85-12021
Sinc method of solution of singular integral equations
[AD-A146155] 03 p0411 N85-12031
Oceanic plateaus, anomalous subduction, and the accretion of buoyant features at convergent margins 05 p0688 N85-14422
On an algorithm for Pythagorean sums and its connection with continued fractions
[NPL-DITC-42/84] 05 p0718 N85-14803
Random equations in aerodynamics
[NASA-CR-174279] 08 p1077 N85-16825
Convergence of quasi-stationary to stationary distributions for stochastically monotone Markov processes
[AD-A146041] 08 p1215 N85-17852
New methods for numerical solution of one class of strongly nonlinear partial differential equations with applications in hydrodynamics
[AD-A149026] 10 p1545 N85-19739
On the modified likelihood for density estimation
[AD-A149437] 10 p1547 N85-19758

A method of calculating periodic solutions of second order dynamical systems
[AD-A149634] 12 p1920 N85-22058
Determining conductivity by boundary measurements. Part 2: Interior results
[AD-A149750] 12 p1921 N85-22063
Distributed asynchronous deterministic and stochastic gradient optimization algorithms: Revision
[AD-A149997] 12 p1921 N85-22068
Convergence rates in the strong law for bounded mixing sequences
[GWI-MS-R8412] 12 p1922 N85-22076
Rates of convergence of semistochastic approximation procedures for solving stochastic optimization problems
12 p1924 N85-22088
A note about the strong convergence of the nonparametric estimation of a regression function
[AD-A150325] 13 p2151 N85-23353
Attainable rates of convergence of maxima
[AD-A150636] 14 p2406 N85-24847
Weak convergence of a sequence of queueing and storage processes to a singular diffusion
[AD-A150655] 14 p2411 N85-24866
The South Pacific convergence zone and energy balance of the southern hemisphere
15 p2593 N85-25980
An incremental multigrid strategy for the fluid dynamics equations
[AD-A151953] 16 p2783 N85-27172
Analysis of the convergence of mixed finite element methods
[HTKK-MAT-A227] 16 p2856 N85-27613
Convergence of Newton's method for a single real equation
[NASA-TP-2489] 17 p3017 N85-28656
About product formulas with variable step-size
[AD-A153527] 18 p3169 N85-29636
Control of a flexible space antenna: A finite dimensional perspective based on distributed parameter theory
20 p3413 N85-31182
On the dependence of the convergence of Gummel's algorithm on the regularity of the solution
[AD-A154628] 21 p3675 N85-32832
Method of estimating convergence of Haar coefficients in message compression problems
22 p3769 N85-33358
Design of electrooptical system with annular cathode and electrostatic compressor 22 p3770 N85-33367
Admissible convergence of Poisson integrals in symmetric spaces
[CTH-MATH-1985-04] 22 p3836 N85-33750
Reordering computations for parallel execution
[NASA-CR-177961] 23 p3957 N85-34522
On the convergence of an iterative formulation of the electromagnetic scattering from an infinite grating of thin wires 24 p4085 N85-35319
Characterizations of generalized hyperexponential distributions
[AD-A155855] 24 p4142 N85-35680

CONVERGENT NOZZLES
Experimental investigation of shock-cell noise reduction for dual-stream nozzles in simulated flight
[NASA-CR-3846] 04 p0557 N85-13549
Experimental investigation of shock-cell noise reduction for single stream nozzles in simulated flight
[NASA-CR-3845] 04 p0557 N85-13550
Static internal performance of a two-dimensional convergent nozzle with thrust-vectoring capability up to 60 deg
[NASA-TP-2391] 10 p1419 N85-18951
Modifications to the nozzle test chamber to extend nozzle static-test capability
[NASA-TM-86368] 15 p2464 N85-25216

CONVERGENT-DIVERGENT NOZZLES
Experimental investigation of shock-cell noise reduction for dual-stream nozzles in simulated flight
[NASA-CR-3846] 04 p0557 N85-13549
Experimental investigation of shock-cell noise reduction for single stream nozzles in simulated flight
[NASA-CR-3845] 04 p0557 N85-13550
A computer program for the performance analysis of scarfed nozzles
[AD-A147370] 07 p0905 N85-15730
Vacuum chamber pressure effects on thrust measurements of low Reynolds number nozzles
[NASA-TM-86955] 12 p1794 N85-21259
An experimental study of clustered, two-dimensional rocket nozzles
[AD-A151869] 15 p2495 N85-25390
Characteristics of heat exchange in the region of injection into a supersonic high-temperature flow
[NASA-TM-77833] 15 p2555 N85-25762
Static investigation of several yaw vectoring concepts on nonaxisymmetric nozzles
[NASA-TP-2432] 18 p3058 N85-28924

CONVERSATION
Communications skills for CRM training
09 p1276 N85-18017

CONVERSION
Conversion of FEB (Fast and Easy Binary) utilities to ASCII FORTRAN
[AD-A145840] 03 p0406 N85-12596
Conversion efficiencies of charged particle beam driven free electron lasers
[AD-A154404] 19 p3276 N85-30316

CONVERTAPLANES
U V/STOL AIRCRAFT

CONVERTERS
Symposium on Luminescent Radiation Receivers and Converters 19 p3295 N85-30430

CONVEXITY
Generalized convex functions: Properties, optimality and duality
[DE85-001553] 09 p1376 N85-18652
Close-to-convex functions and linear-invariant families
10 p1536 N85-19683
An extension of the Gleason problem in pseudoconvex domains 11 p1698 N85-20871
Intertwining functions on compact Lie groups
[GWI-TRACT-5] 14 p2414 N85-24895
On positive vectors, positive matrices and the specialization ordering
[GWI-PM-R8407] 14 p2414 N85-24899
A convexity theorem for semisimple symmetric spaces
[GWI-PM-R8414] 14 p2415 N85-24900
An experimental investigation of the interaction between a shock wave and a turbulent boundary layer on a convex wall
[VTH-LR-428] 16 p2785 N85-27187
The essence of invexity
[CSIR-TWISK-321] 16 p2858 N85-27626
Convex interpolating splines of arbitrary degree
17 p3004 N85-28574
A quadratic programming algorithm
[AD-A153476] 18 p3168 N85-29631
An experimental investigation of curvature and freestream turbulence effects on heat transfer and fluid mechanics in transitional boundary layer flows
19 p3264 N85-30240
A dynamic programming approach to time-staged convex programs
[DE85-010616] 19 p3340 N85-30700
Reachable grasps on a polygon: The convex rope algorithm
[AD-A155913] 24 p4138 N85-35647

CONVEYORS
Automated parts storage and retrieval system positioning device and method
[AD-D011494] 11 p1647 N85-20379
Shuttle car loading system
[NASA-CASE-NPO-15949-1] 23 p3967 N85-34722

CONVOLUTION INTEGRALS
Modeling holographic recognition system by using number-theory convolution transformation
02 p0272 N85-11774
A very efficient transfer function bounding technique on bit error rate for Viterbi decoded, rate 1/N convolutional codes 05 p0624 N85-13991
Sequential syndrome decoding of convolutional codes
05 p0624 N85-13992
Linear autonomous retarded functional differential equations; a sharp version of Henry's theorem
[GWI-AM-R8405] 05 p0720 N85-14825
FLAD user's manual: FLAD file contents
[AD-A148700] 09 p1368 N85-18594
Digital high speed programmable convolver
[AD-D011455] 10 p1481 N85-19348
A remark on regularization in Hilbert spaces
[AD-A149046] 10 p1552 N85-19787
Generalization of Beurling algebras
11 p1698 N85-20675
New convolution and discrete Fourier transformation algorithms based on rectangular transformations over field of roots of unity 13 p2085 N85-23022
Convolution of the IFRA (Increasing Failure Rate Average) scaled-mins class
[AD-A151070] 14 p2411 N85-24870
Generalised translation invariance and systems theory
[CRM-8501] 17 p3017 N85-28657
Deconvolution methods for multi-sensors
[AD-A152351] 17 p3018 N85-28660
A convolution integral equation solved by Laplace transformation
[GWI-AM-R8409] 17 p3022 N85-28692
Convoluted nozzle design for the RL10 derivative 2B engine
[NASA-CR-174953] 19 p3220 N85-29965

CONVOLUTIONS (MATHEMATICS)
U CONVOLUTION INTEGRALS

CONVULSIONS
Mechanisms of oxygen toxicity and methods of protection
[AD-A145830] 03 p0400 N85-12551

COOL STARS
Search for white dwarf companions of cool stars with peculiar element abundances
[NASA-CR-174030] 02 p0297 N85-11923
Theoretical studies of chromospheres and winds in cool stars
[NASA-CR-174204] 06 p0880 N85-15596
Spectrophotometry of cool stars from objective prism spectra 07 p0966 N85-16134

COOLANTS
NT ENGINE COOLANTS
Coolant passage heat transfer with rotation
02 p0143 N85-10966
Electrochemical pitting evaluation of aluminum alloy 7075 in machining coolant
[DE84-016844] 04 p0475 N85-13026
Drop of coolant temperature in individual components of solar heating system 14 p2265 N85-24035
Role of fluid lubricant-coolant in fine grinding of optical glass by diamond tool 14 p2280 N85-24125
Jet pump-drive system for heat removal
[NASA-CASE-NPO-16494-1-CU]
18 p3099 N85-29182
Modeling and experiments on tritium permeation in fusion reactor blankets
[DE85-006439] 18 p3183 N85-29741
Coolant mixing in LMFBR rod bundles and outlet plenum mixing transients
[DE85-010336] 19 p3268 N85-30268
Resolution of thermal striping issue downstream of a horizontal pipe elbow in stratified pipe flow
[DE85-006195] 21 p3586 N85-32292
Cooling of pulverized material with heated condensible vapor
[DE85-011656] 22 p3783 N85-33438
Reaction of uranium and the fluorocarbon FC-75
[DE85-012322] 22 p3843 N85-33802
Computer code calculations of the TMI-2 accident: Initial and boundary conditions
[DE85-012613] 24 p4140 N85-35666

COOLERS
Modeling of a second-generation solar-driven Rankine air conditioner
[DE84-015132] 01 p0036 N85-10223

COOLING
NT ABSORPTION COOLING
NT AIR COOLING
NT CRYOGENIC COOLING
NT EVAPORATIVE COOLING
NT FILM COOLING
NT GAS COOLING
NT LIQUID COOLING
NT MAGNETIC COOLING
NT QUENCHING (COOLING)
NT RADIANT COOLING
NT SOLAR COOLING
NT SPACE COOLING (BUILDINGS)
NT SUPERCOOLING
NT SURFACE COOLING
NT SWEAT COOLING
The effect of channel convergence on heat transfer in a passage with short pin fins
[NASA-TM-83801] 01 p0046 N85-10303
Investigation of crisis phenomena in thermosyphons with internal heat-dissipation
[BLL-M-35765-(5828.4)] 02 p0197 N85-11313
Producing semiconductor materials by superfast cooling of melt 03 p0354 N85-12274
Heat transfer and pressure drop in blade cooling channels with turbulence promoters
[NASA-CR-3837] 03 p0361 N85-12315
Austenite transformation in powder-compacted chromium-nickel-molybdenum steels during continuous cooling
[BLL-M-35961-(5828.4)] 05 p0615 N85-13933
Thermal characterization of photovoltaic modules in natural environments 06 p0832 N85-15296
Low temperature diffusion coefficients in the Fe-Ni and FeNiP systems: Application to meteorite cooling rates
06 p0886 N85-15826
Dynamic thermal episodes in the protosolar nebula: Development of models from observations on CAI's
06 p0887 N85-15833
The feasibility of low-G grey solidification of nodular iron in the F-104 experimental furnace package
[NASA-TM-82527] 10 p1426 N85-18996
Vibration isolated cold plate assembly
[AD-D011444] 10 p1484 N85-19368
An evaluation of liquid and two-phase cooling techniques for use in electrical machinery
[AD-A149528] 10 p1484 N85-19372

Evaluation of residual stress in laminated metallic composites 11 p1598 N85-20052
Residual stress after laser processing 11 p1600 N85-20065
Proposal for hollow cathode electron gun for electron cooling
[DE85-002721] 11 p1630 N85-20263
The Middle Atmosphere Program: Winter in Northern Europe (MAP/WINE) 11 p1655 N85-20429
Numerical model for swirl cooling in high-heat-flux particle beam targets and the design of a swirl-flow-based plasma limiter
[DE85-003824] 11 p1732 N85-20894
Improvements in glazings: SERI materials research in progress
[DE84-013049] 12 p1814 N85-21378
Heat pipe cooled probe
[NASA-CASE-LAR-12588-1] 12 p1844 N85-21568
Cooled turbine blade tip closure
[AD-D011525] 12 p1858 N85-21654
Energy losses at leading edge of turbine blade during multirow jet cooling 13 p2049 N85-22826
Pressure drop and coefficients of internal heat transfer necessary for transpiration cooling 13 p2050 N85-22831
Cooling performance improvement of a horizontal ground coupled heat pump
[DE85-002470] 13 p2093 N85-23065
Cooling of neutron stars with hyperons
[DE85-004641] 13 p2171 N85-23472
A measurement of the intensity of the cosmic background radiation at 3.9 cm 13 p2206 N85-23681
Fabrication of ceramic substrate-reinforced and free forms
[NASA-TM-86994] 14 p2247 N85-23926
Experimental study of heat transfer from shaft in cooled radial bearing of GNT-25 gas turbine 14 p2270 N85-24068
Computations for segmented radial bearings 14 p2268 N85-24180
The effects of cooling on delay-time limits in IC's 14 p2297 N85-24224
Experimental facility for studying MHD effects in liquid metal cooled blankets
[DE85-000583] 14 p2423 N85-24943
Small gas turbine combustor study: Fuel injector performance in a transpiration-cooled liner
[NASA-TM-86989] 15 p2473 N85-25264
Effectiveness of use of heat-dissipating clamps to reduce deformation during argon arc welding of thin sheets of AMg6 alloy 15 p2501 N85-25427
Sweden develops new rapid solidification process 15 p2531 N85-25610
Numerical simulation of boundary layer excitation by surface heating/cooling
[NASA-CR-172575] 15 p2554 N85-25756
Experimental and theoretical studies of laser cooling and emittance control of neutral beams
[AD-A149215] 15 p2562 N85-25804
Development of high strength ship hull steel for high heat input welding --- controlled rolling and accelerated cooling 15 p2565 N85-25827
Mechanism of formation of low temperatures in nighttime Venusian thermosphere 16 p2723 N85-26807
The use of heat pumps in district heat supply
[BLL-OA-TRANS-2728-(6196.3)] 16 p2781 N85-27163
Multi-phase crystallization of ferrous alloys
[BLL-BISI-TRANS-22441-(9022.06)] 17 p2925 N85-28037
Production and compaction of amorphous metal powders
[BLL-BISI-TRANS-22387-(9022.06)] 17 p2929 N85-28080
Performance analysis of radiation cooled dc transmission lines for high power space systems
[NASA-TM-87040] 17 p2951 N85-28222
Effects of the corona wind on the cooling of a horizontal cylinder
[AD-A153101] 17 p2954 N85-28241
Opacity control technique for jet engine test cells
[AD-D011688] 19 p3220 N85-29968
Heat injury: Prevention is the key
[AD-A153734] 19 p3328 N85-30622
Experiments with stored heavy ions
[DE85-009976] 19 p3356 N85-30802
Molten salt cooling/17Li-83Pb breeding blanket concept
[DE85-010522] 19 p3383 N85-30854
Design of aggressive superconducting TFCX magnet systems
[DE85-010003] 19 p3376 N85-30943
The nature of the anomalies on the polytherms of the properties of molten metallic alloys
[BLL-M-36265-(5828.4)] 20 p3430 N85-31277
Design principles for nickel-hydrogen cells and batteries
[NASA-TM-87037] 20 p3483 N85-31646
Design of a helium-cooled molten salt fusion breeder
[DE85-010474] 20 p3526 N85-31943
Temperature field around a spherical, cylindrical, and needle-shaped crystal, growing in a pre-cooled melt
[NASA-TM-77889] 20 p3537 N85-32011
Observations of the use of the setapoint detector
[AD-A154533] 21 p3571 N85-32206
Design and lubrication of high-speed rolling-element bearings
[NASA-TM-87107] 23 p3938 N85-34409
Enhanced heat transfer computations for internally cooled cable superconductor
[DE85-011897] 24 p4095 N85-35383

COOLING FINS
Optimization of combined convective and film cooling of perforated baffle blades in gas turbines 14 p2270 N85-24067
Welding of steel-aluminum cooling panels for the holds of refrigerator vessels 19 p3248 N85-30129

COOLING SYSTEMS
Heat rejection working group synopsis 05 p0611 N85-13906
Phosphoric and electric utility fuel cell technology development
[NASA-CR-174215] 06 p0805 N85-15124
Cooling system investigation of the 3-kW MEP models 016A, 021A, and 026A (60Hz, 400-Hz and 28-V dc) gasoline-engine-driven generator sets
[AD-A147571] 07 p0974 N85-16185
Hybrid system for producing and storing ice
[DE84-017474] 09 p1304 N85-18195
Thermal energy storage
[DE85-001492] 09 p1344 N85-18454
15KW power supply development
[DE85-001057] 11 p1629 N85-20260
Performance of the SERI parallel-passage dehumidifier
[DE85-000509] 11 p1672 N85-20536
Transmissive Dewar cooling chamber for optically pumped semiconductor ring lasers
[AD-D011550] 12 p1855 N85-21636
Latent heat storage in cooling systems
[DE85-005355] 13 p2129 N85-23248
Thermal state of cooled thin-walled nozzle blade 14 p2270 N85-24066
High thermal power density heat transfer apparatus providing electrical isolation at high temperature using heat pipes
[NASA-CASE-LEW-12950-2] 18 p3098 N85-29179
Jet pump-drive system for heat removal
[NASA-CASE-NPO-16494-1-CU] 18 p3099 N85-29182
Precision manipulator heating and cooling apparatus for use in UHV systems with sample transfer capability
[NASA-CASE-LAR-13040-1] 18 p3118 N85-29286
Spacecraft, straight-tube evaporator design
[AD-A154462] 19 p3226 N85-30003
Vortex generating flow passage design for increased film cooling effectiveness
[NASA-CASE-LEW-14039-1] 22 p3782 N85-33433
On-line temperature sensor
[DE85-011641] 22 p3787 N85-33465
Legionnaires' disease bacteria in power plant cooling systems: Phase 2
[DE85-011548] 22 p3825 N85-33695
Mathematical modeling of ultimate heat sink cooling ponds
[TI85-009747] 23 p3932 N85-34369
A two-phase flow and heat transfer model for zero gravity
[AD-A156097] 24 p4094 N85-35377
Transient three-phase three-component systems. Part 1: Formulation of the system of differential equations
[DE85-013267] 24 p4095 N85-35384

COOPERATION
The effects of controversy and concurrence seeking on effective decision making
[AD-A153370] 17 p3002 N85-28555

COORDINATE SYSTEMS
U COORDINATES

COORDINATE TRANSFORMATIONS
Automatic camera tracking for remote manipulators
[DE85-001697] 07 p0974 N85-16187
The Gauss-Krueger projection of the Earth ellipsoid with direct calculation of elliptic integrals through Landen transformations
[SER-C-296] 11 p1666 N85-20495
Distance-inertial guidance of launch vehicle described 12 p1820 N85-21417
Reduction of astrographic catalogues 14 p2437 N85-25033
Least squares reduction technique 14 p2437 N85-25036
Reduction of astrometric plates 14 p2437 N85-25037
Allowance for differences in ellipsoids and geodetic control coordinate systems in determining ship's position using radio navigation systems 19 p3292 N85-30413
Coordinate transformations and programming for small revolute coordinate robots
[RR-273] 20 p3519 N85-31881
Second-order Compton-Getting effect on arbitrary intensity distribution
[SH-3.1-10] 23 p4002 N85-34814

COORDINATES
NT ASTRONOMICAL COORDINATES
NT CARTESIAN COORDINATES
NT GEOCENTRIC COORDINATES
NT GEODETIC COORDINATES
NT HYPERBOLIC COORDINATES
NT LAGRANGE COORDINATES
NT SPHERICAL COORDINATES
Cognitive coordinate systems: Accounts of mental rotation and individual differences in spatial ability
[AD-A146149] 03 p0401 N85-12557
Development of a modular multicoordinate measuring system with continuous-path microprocessor control
[BMFT-FB-T-84-158] 03 p0408 N85-12608
Analysis of frequency-selective integrated circuits in system of normal coordinates 04 p0489 N85-13119
References in space and time 05 p0596 N85-13809
Use of coordinate functions to calculate deformation fields
[BLL-M-36010-(5828.4)] 07 p1028 N85-16524
Numerical generation of orthogonal and nonorthogonal coordinates in two dimensional simply and doubly connected regions
[VKI-TN-151] 08 p1216 N85-17682
Generation of 3-dimensional body fitted coordinates using hyperbolic partial differential equations
[AD-A148059] 09 p1274 N85-18006
Codes with parity conditions on subsets of coordinates 10 p1485 N85-19247
Geodetic accuracy of LANDSAT 4 Multispectral Scanner and Thematic Mapper data 12 p1873 N85-21746
Motion of symmetrical satellite with flexible viscoelastic rods about center of mass in circular orbit 13 p1979 N85-22420
Analysis of systematic errors in systems of selenodetic coordinates 13 p1982 N85-22435
Coordinate determination errors in measuring characteristics of radiation field of airborne antennas 13 p2068 N85-22919
Zero-crossings on lines of curvature
[AD-A150171] 13 p2150 N85-23345
A unified lunar control network 13 p2203 N85-23669
The control network of Mars: October 1984 13 p2203 N85-23670
The control networks of the satellites of Jupiter and Saturn 13 p2204 N85-23671
Shape of Io 13 p2204 N85-23672
An analysis of grid-based line drawing quantization methods
[AD-A151847] 15 p2522 N85-25547
Electromagnetic scattering by arbitrarily shaped reflectors: Subreflector efficiency
[AD-A149224] 15 p2541 N85-25687
Analysis of elastoplastic grids under conditions of variable loads
[REPT-16/1984] 16 p2797 N85-27242
When is a Bernstein-Bezier curve the graph of a function? 17 p3003 N85-28568
Generation of surface coordinates by elliptic partial differential equations 17 p3006 N85-28583
A survey of composite grid generation for general three-dimensional sections 17 p3006 N85-28584
A discussion of adaptive grids and their applicability in numerical hydrodynamic modeling
[AD-A151843] 17 p3017 N85-28659
Monotonicity preserving bicubic interpolation, revision 1
[DE85-007976] 17 p3021 N85-28683
Derivation of model topography 18 p3141 N85-29449
Three-dimensional data display on the two-dimensional screen
[AD-A153699] 18 p3160 N85-29577
A comparison of methods of least squares adjustment of traverses
[AD-A153612] 18 p3170 N85-29645
Computer programs for smoothing and scaling airfoil coordinates
[NASA-TM-84666] 20 p3388 N85-31011
A note on a theorem of R. Duffin
[AD-A154786] 21 p3676 N85-32838

Potential coordinate estimate accuracy estimation accuracy by multiposition radar systems
22 p3763 N85-33322
Production of initial estimates of photogrammetric variables
[NPL-MOM-66] 23 p3943 N85-34434
Second-order Compton-Getting effect on arbitrary intensity distribution
[SH-3.1-10] 23 p4002 N85-34814

COORDINATION
Collection overlap and coordinated collection development 02 p0293 N85-11902
A full mission simulator study of aircrew performances: The measurement of crew coordination and decisionmaking factors and their relationships to flight task performances 05 p0710 N85-14556
Communication on the flight deck
05 p0711 N85-14557
Instrument for determining spatial coordination of hand movements 14 p2387 N85-24702
Photochemistry of coordination complexes: The phthalocyanines
[DE85-007693] 17 p2923 N85-28022
Improved coordinate measuring machine calibration and control
[DE85-012053] 21 p3590 N85-32315
United States Army welding research and development topical and coordination meeting
[AD-A155834] 24 p4099 N85-35409

COORDINATION POLYMERS
A soluble linear Schiff-base coordination polymer containing eight-coordinate zirconium(4)
[AD-A151446] 15 p2518 N85-25527

COPERNICUS SPACECRAFT
U OAO 3

COPILOTS
U AIRCRAFT PILOTS

COPLANARITY
Experiment Pamir-3. Coplaner emission of high energy gamma-quanta at interaction of hadrons with nuclei of air atoms at energies above 10 to the 7th power GeV
[HE-1.4-12] 24 p4177 N85-35899

COPOLYMERIZATION
Vinyl citrates from citric acid as new monomers
[BMFT-FB-T-83-256] 03 p0336 N85-12178
Chemical control of nadimide cure temperature and rate
[NASA-CASE-LEW-13770-2] 18 p3069 N85-28982
Transition metal catalyzed transformations of unsaturated molecules
[DE85-009531] 18 p3080 N85-29055
High performance mixed bisimide resins and composites based thereon
[NASA-CASE-ARC-11538-1-SB]
19 p3231 N85-30033

COPOLYMERS
Nuclear Magnetic Resonance of Polymeric Materials
[AD-A145078] 01 p0032 N85-10192
13C and 1H NMR (Nuclear Magnetic Resonance) studies of solid polyolefines
[AD-P003909] 01 p0032 N85-10195
Diblock copolymers of polystyrene/1,2 polybutadiene and polystyrene/polybutene-1: Molecular structure, morphology and mechanical properties
[AD-A144980] 01 p0033 N85-10201
Physical-chemical properties of articulated rodlike polymers
[AD-A145549] 02 p0186 N85-11244
Low temperature synthesis of polycaproamide copolymers grafted with polydimethylaminothylmethacrylate
06 p0761 N85-14868
Forming fluorine-containing threads from vinylidene fluoride-tetrafluoroethylene copolymer by dry method
06 p0762 N85-14873
Polymer-carbon black interaction in electrically conducting fiber-forming composites
06 p0762 N85-14875
Properties of miscible polymer blends
[AD-A147080] 07 p0931 N85-15903
Synthesis and characterization of unique liquid crystalline block copolyesters. A proposal for a polymer research center at the Atlanta University
[AD-A147280] 07 p0932 N85-15907
New synthesis of phosphazene polymers
[AD-A147567] 07 p0933 N85-15910
Phase diagram of polymer blends containing block copolymers
[AD-A147706] 08 p1132 N85-17134
Synthesis and characterization of a 1,4 Polybutadiene/Isotactic polypropylene block copolymer
[AD-A148199] 08 p1133 N85-17142
The synthesis and characterization of Poly(Oxy(2-Methyl-1,3-Phenylene) Methyl-1,3 -Phenylene) Oxyterephthaloyl)Oxy
[AD-A148269] 08 p1133 N85-17143
Poly(dimethylsiloxane)-polyurethane elastomers: Synthesis and properties of segmented copolymers and related zwitterionomers
[AD-A148571] 08 p1134 N85-17147
GC-FTIR (Fourier Transform Infrared Spectrometry) of jet fuels
[AD-A148272] 08 p1135 N85-17155
Crystallization behavior of poly(3,3-bis(Ethoxymethyl) oxentane) and poly(3,3-bis(Azidomethyl) oxetane)
[AD-A148271] 08 p1226 N85-17720
Characterization of novel binders based on energetic thermoplastic elastomers
[AD-A148993] 10 p1451 N85-19139
Polyactic-polyglycolic acid copolymer combined with decalcified freeze-dried bone for use as a bone repair material
[AD-D011438] 10 p1451 N85-19142
Method for making heterocyclic block copolymers
[AD-D011446] 10 p1451 N85-19143
Chemical approach for controlling nadimide cure temperature and rate with maleimide
[NASA-CASE-LEW-13770-3] 12 p1809 N85-21350
Chemical approach for controlling nadimide cure temperature and rate with maleimide
[NASA-CASE-LEW-13770-4] 12 p1810 N85-21351
Effects of triazine components on physicochemical properties of polybutadiene: urethane block copolymers
13 p2014 N85-22635
Influence of hydrogen bonding in block copolymers and their blends 13 p2035 N85-22752
Exploratory development of foams from liquid crystal polymers
[NASA-CR-172510] 13 p2036 N85-22754
Chiral polymers
[AD-A150366] 13 p2037 N85-22760
An investigation of molecular structure of copolymers using positron annihilation spectroscopy
[NASA-TM-86431] 17 p2916 N85-27977
Thermally stable elastomers: Review of silarylene-siloxane polymers and polysilmethylenes
[AD-A152323] 17 p2934 N85-28111
Alkaline battery containing a separator of a cross-linked copolymer of vinyl alcohol and unsaturated carboxylic acid
[NASA-CASE-LEW-13102-1] 18 p3093 N85-29144
High performance mixed bisimide resins and composites based thereon
[NASA-CASE-ARC-11538-1-SB]
19 p3231 N85-30033
Self-developing polysilane deep-UV resists: Photochemistry, photophysics and submicron lithography
[DE85-007608] 19 p3237 N85-30067
STPI/LARC: A 200 deg C polyimide adhesive
[NASA-TM-86447] 20 p3433 N85-31297
Structure-property relationships in thermoplastic elastomers. Part 3: Segmented polyacetal-polyurethanes
[AD-A154897] 21 p3569 N85-32200
Electrically conductive doped block copolymer of polyacetylene and polyisoprene
[DE85-006500] 24 p4082 N85-35301

COPPER
Numerical analysis of parameters of self-heating copper vapor lasers 02 p0260 N85-11704
Polycyclic aromatic hydrocarbons on the inner surfaces of copper tubing
[AD-A145979] 03 p0337 N85-12169
Fast and precise processing of material by means of an intensive electron beam
[BMFT-FB-T-84-123] 03 p0342 N85-12201
The metallurgical processes during the soft soldering of copper and copper alloys and the strength characteristics of soldered joints
[BLL-T6388/BG/WH803/84] 06 p0767 N85-14908
Thermal conductivity of aluminum, copper, iron and tungsten for temperature from 1 K to the melting point
[PB84-235676] 06 p0770 N85-14924
The adsorption of CO and oxygen on Cu layers on a W(110) surface
[AD-A147345] 07 p0923 N85-15847
Investigation of electric and wear phenomena of liquid metal wetted copper fiber brushes under conditions of high slip ring eccentricity
[AD-A147634] 08 p1156 N85-17295
Antifriction properties of gas thermal coatings of clad carbine powders 10 p1447 N85-19115
Behavior and specifics of fracture of porous fiber materials in extension 10 p1447 N85-19118
Magnetization of very thin Ni films in epitaxial metal film sandwiches of Cu
[DE85-001840] 10 p1563 N85-19860
Structure and properties of copper-titanium-aluminum composites obtained by thermoreactive sintering
11 p1600 N85-20061
Effect of temperature and deformation rate on hardness of copper 11 p1605 N85-20090
Effect of rhodamine-B on the electrodeposition of lead on copper, revision
[DE85-000674] 11 p1606 N85-20101
Effect of interfacial characteristics of metal clad polymeric substrates on electrical high frequency interconnection performance
[NASA-TM-86948] 11 p1624 N85-20223
Mechanical properties of electrodeposited nickel and copper
[DE85-005321] 13 p2023 N85-22677
Effects of neutron irradiation at 450(0)C and 16 dpa on the properties of various commercial copper alloys
[DE85-005716] 13 p2024 N85-22684
Structural strenght of strip D16T aluminum alloy with low copper and magnesium content
13 p2025 N85-22691
New deformable secondary aluminum alloys
13 p2026 N85-22694
Possibility of producing monolithic composite materials based on niobium carbide 13 p2028 N85-22707
Observation of surface vibrational resonances on (110) surfaces of FCC metals
[AD-A150469] 13 p2163 N85-23419
Nd-isotopic evidence for the origin of the Sudbury complex by meteoritic impact 15 p2680 N85-26554
Measurement of elements in the stratosphere
[NASA-CR-175891] 16 p2823 N85-27414
The production of copper phthalocyanine and/or its derivatives
[NASA-TM-77629] 17 p2917 N85-27983
The loss of material from the cathode of metal arcs
[NASA-TM-77845] 17 p2918 N85-27985
Improving the properties of copper and copper alloys through heat treatment and alloying
[BLL-BISI-TRANS-21939-(9022.06)]
17 p2926 N85-28047
Localized ionic currents from a corroding iron-copper galvanic couple
[AD-A153627] 18 p3074 N85-29011
Establishment of a methodology for predicting lifetimes in active solar systems
[DE85-008629] 18 p3130 N85-29383
Preliminary results on open accelerating structures
[DE85-010231] 18 p3191 N85-29793
Effect of confinement on failure in 95 TATB/5 KEL-F
[DE85-010790] 19 p3251 N85-30158
Investigation for low-cost permanent magnets
[AD-A154387] 19 p3260 N85-30212
Sources of copper air emissions
[PB85-191138] 19 p3310 N85-30523
Defect production and recovery in FCC metals irradiated at 4.2 K
[DE85-010477] 20 p3538 N85-32014
Electrodeposition of chromium and copper in magnetic fields
[AD-A154648] 21 p3566 N85-32180
The effect of abrasive blasting on the fatigue and corrosion of an aluminium-copper alloy
[AD-A154954] 21 p3566 N85-32182
Modification of the grain size of sputtered copper with additions of oxygen, krypton, silver, or yttrium
[DE85-010975] 21 p3567 N85-32189
Plasma mass and effective inductance in a small railgun
[AD-A154644] 21 p3589 N85-32304
Management of Corrosion
[AGARD-LS-141] 22 p3749 N85-33238
Corrosion management strategies for aircraft and related systems 22 p3749 N85-33239
Metal vapor lasers and their applications
[ISL-CO-218/84] 22 p3791 N85-33488
Environmental surveillance at Los Alamos during 1984
[DE85-011886] 22 p3811 N85-33605
Calculated neutron-induced cross sections for /sup 63,65/Cu/sup 58,60/Ni and (52) Cr from 1 to 20 MeV and comparisons with experiments
[DE85-011926] 22 p3844 N85-33906
X-ray residual stress analysis on the coarse grain of copper and its application to the brazed copper
23 p3907 N85-34202
Metal (2) 4,4',4',4'' phthalocyanine tetraamines as curing agents for epoxy resins
[NASA-CASE-ARC-11424-1] 23 p3919 N85-34281
Some recent deposit modeling efforts
24 p4106 N85-35453
The Conterminous United States Mineral Assessment Program 24 p4106 N85-35458
The Alaska Mineral Resources Assessment Program
24 p4107 N85-35460
Ore genesis at the Monterrosas deposit in the Coastal Batholith, Ica, Peru 24 p4115 N85-35510
Few-particles generation channels in inelastic hadron-nuclear interactions at energy approximately equals 400 GeV
[HE-3.2-9] 24 p4179 N85-35917

COPPER ALLOYS
NT BRASSES
NT BRONZES
Copper-boron low alloy high strength steels
02 p0176 N85-11183
Calculation of critical temperature for Nb-Cu multilayer film superconductor
[AD-A144321] 02 p0274 N85-11786
The metallurgical processes during the soft soldering of copper and copper alloys and the strength characteristics of soldered joints
[BLL-T6368/BG/WH803/84] 06 p0767 N85-14908
Application of solidification theory to rapid solidification processing
[AD-A146619] 06 p0769 N85-14917
Studies on copper alloys containing chromium on the copper side phase diagram
[NASA-TM-77752] 07 p0927 N85-15876
On heat-treatable copper-chromium alloy, 1
[NASA-TM-77753] 07 p0927 N85-15879
On reversion phenomena in Cu-Zr-Cr alloys
[NASA-TM-77791] 08 p1125 N85-17092
Reversion phenomena of Cu-Cr alloys
[NASA-TM-77780] 08 p1125 N85-17094
Synergistic sputtering properties of binary alloys
[DE84-017493] 09 p1297 N85-18148
Initial aging phenomena in copper-chromium alloys
[NASA-TM-77790] 10 p1439 N85-19070
Magnetic excitation in CuMn spin glass alloy
[DE85-002564] 10 p1453 N85-19159
Study of microstructure of aluminum and copper alloys after processing with continuous CO2 laser beam
11 p1601 N85-20066
Conductivity changes in neutron-irradiated commercial copper alloys at approximately 450(0)C
[DE85-003007] 11 p1606 N85-20100
Surface physics and crystallography
[DE85-003128] 11 p1735 N85-20910
Chemisorption theory: Adsorption on copper-nickel alloys and titanium surface embrittlement
[DE85-001815] 12 p1607 N85-21334
Partial replacement of chromium in austenitic stainless steels by molybdenum, copper, and vanadium, report of investigations 1984
[PB85-116508] 12 p1609 N85-21346
Structures of ordered linear dislocation multipoles in Cu-Al alloys
[ISSN-0379-6906] 13 p2021 N85-22664
Thermodynamics of copper-nickel alloys containing aluminum, silicon, titanium, and chromium relative to their use in ceramic brazing
[DE85-004787] 13 p2023 N85-22674
First principles theory of Fermi-surface driven concentration waves in Cu/sub c/Pd/sub 1-c/ alloys
[DE85-005367] 13 p2024 N85-22681
Effects of neutron irradiation at 450(0)C and 16 dpa on the properties of various commercial copper alloys
[DE85-005716] 13 p2024 N85-22684
Application of solidification theory to rapid solidification processing
[AD-A151251] 15 p2509 N85-25480
Performance of a copper-lithium alloy as an impurity control system surface material for a fusion reactor
[DE85-006494] 15 p2857 N85-26398
Self-sustaining low-Z coatings for fusion applications 2 - copper-lithium
[DE85-002553] 15 p2858 N85-26403
Improving the properties of copper and copper alloys through heat treatment and alloying
[BLL-BISI-TRANS-21939-(9022.06)]
17 p2926 N85-28047
Aging study of copper alloy 172
[DE85-009848] 16 p3075 N85-29023
The precipitation mechanism in a metallic solid solution crystal: Case of the aluminum-copper and aluminum-silver systems
[DE85-009861] 16 p3077 N85-29032
Self-sustaining coatings for fusion applications: Copper lithium alloys
[DE85-009740] 16 p3190 N85-29783
Current state of development and expected performance of copper-lithium alloys as an impurity control system in fusion applications
[DE85-009673] 19 p3372 N85-30917
Critical current density and microstructural state of an internal tin multifilamentary superconducting wire
[DE85-009906] 22 p3761 N85-33308

COPPER CHLORIDES
Environmental stability of intercalated graphite fibers
[NASA-TM-87025] 16 p2753 N85-26992
Stationary properties and switching characteristics of dispersive optical bistability in CuCl
16 p3186 N85-29763

COPPER COMPOUNDS
NT COPPER CHLORIDES
NT COPPER OXIDES
NT COPPER SELENIDES
NT COPPER SULFIDES
The X-ray Absorption Coefficient Fine Structure (EXAFS) study on precipitates in AlCu
[DESY-SR-84-15] 01 p0025 N85-10153
Electrochemical features of the ferric sulfate leaching of CuFeS2/C aggregates
[AD-A146661] 06 p1123 N85-17081
Sources of copper air emissions
[PB85-191138] 19 p3310 N85-30523

COPPER OXIDES
Textured carbon surfaces on copper
[NASA-CASE-LEW-14130-1] 11 p1615 N85-20156
Time-resolved and infrared spectroscopy of excitons
[DE85-011679] 23 p3912 N85-34235

COPPER SELENIDES
CuInSe2-based photoelectrochemical cells: Their use in characterization of thin CuInSe2 films, and as photovoltaic cells per se
[DE84-004514] 04 p0529 N85-13379
Preliminary studies on the low-cost preparation of chalcogenide semiconductors from solution depositions
[DE85-000538] 11 p1736 N85-20918
Low cost, sprayed CuInSe2 solar cell research
[DE85-003467] 12 p1881 N85-21799
A study of the stability of cadmium sulfide/copper sulfide and cadmium sulfide copper-indium-diselenide solar cells
[DE85-002902] 15 p2587 N85-25947
Post-deposition heat treatments of CdS/CuInSe2 solar cells
[DE85-002943] 18 p3128 N85-29373
Cadmium sulfide/copper ternary heterojunction cell research
[DE85-006778] 19 p3305 N85-30486
Stable n-CuInSe/sub 2/iodide-iodine photoelectrochemical cell
[DE85-011597] 22 p3806 N85-33576

COPPER SULFIDES
Development of copper sulfide/cadmium sulfide thin-film solar cells
[DE84-004513] 01 p0044 N85-10287
Development of the production technology of Cu2S/CdS solar generators
[BMFT-FB-T-84-137] 03 p0386 N85-12469
Development and utilization of CdS/Cu2S
05 p0962 N85-14256
Testing and optimization of the production technology of large-surface Cu2S/CdS solar generators
12 p1880 N85-21793
Physical-chemical investigations of copper sulfides for use in CdS/Cu2S solar cells 12 p1880 N85-21794
A study of the stability of cadmium sulfide/copper sulfide and cadmium sulfide copper-indium-diselenide solar cells
[DE85-002902] 15 p2587 N85-25947

COPYRIGHTS
Copyright law, computer software, and government acquisition
[AD-A150347] 13 p2168 N85-23453

CORAL HEADS
U CORAL REEFS

CORAL REEFS
The Midway Atoll coral cap: Meteoric diagenesis, amplitude of sea-level fluctuation and dolomitization
09 p1351 N85-18499

CORDITE
U DOUBLE BASE PROPELLANTS

CORE FLOW
Transports studies of ECH and ICRH-heated bumpy torus plasma in NBT-1M 23 p3978 N85-34662
Simulation studies on stability of hot electron plasma
23 p3978 N85-34664

CORE SAMPLING
Cosmogenic Na-22 and Al-26 in Luna-24 lunar drill core soil samples 13 p1981 N85-22427
Characteristics of fast sea ice collected near Barrow, Alaska 15 p2582 N85-25925
Deep-burial diagenesis in carbonates
[DE85-011224] 22 p3802 N85-33554
Uranium, thorium isotopic analyses and uranium-series ages of calcite and opal and stable isotopic compositions of calcite from drill cores UE25a no. 1, USR G-2 and USW G-3/GU-3, Yucca Mountain, Nevada
[DE85-013039] 23 p3948 N85-34471

CORES
NT EARTH CORE
NT HONEYCOMB CORES
NT LUNAR CORE
NT PLANETARY CORES
NT REACTOR CORES
NT STELLAR CORES
Iron core collapse models of Type 2 supernovae
[DE84-013909] 05 p0743 N85-14775
Induction motors with minimum waste of magnetic iron
22 p3772 N85-33377
Monte Carlo simulations of electron lateral distributions in the core region of 10(13) - 10(16) eV air showers
24 p4190 N85-35992
A new study of shower age distribution in near vertical showers by EAS air shower array
24 p4190 N85-35996
Lateral distribution of electrons of air showers
24 p4191 N85-35998
Properties of 10 (18)-10 (19)eV EAS at far core distance
[HE-4.7-3] 24 p4198 N85-36054
Longitudinal development of muons in large air showers studies from the arrival time distributions measured at 900m above sea level
[HE-4.7-4] 24 p4199 N85-36055
Arrival time distributions of electrons in air showers with primary energies above 10 (18)eV observed at 900m above sea level
[HE-4.7-5] 24 p4199 N85-36056
The thickness of the shower disc as observed in showers produced by primaries above 10 (19)eV
[HE-4.7-6] 24 p4199 N85-36057
Sub-luminal pulses from cosmic ray air showers
[HE-4.7-13] 24 p4200 N85-36063
Progress report on a new search for free e/3 quarks in the cores of 10(15) - 10(16) eV air showers
[HE-6.2-15] 24 p4212 N85-36151
Acoustic detection of air shower cores
[HE-7.1-4] 24 p4213 N85-36158

CORIOLIS EFFECT
Effects of the oceans on polar motion: Continued investigations
[E85-10037] 03 p0379 N85-12416
Hydraulic forces on a centrifugal impeller undergoing synchronous whirl 05 p0643 N85-14124
Coriolis effects on the vibrations of rotating beams, plates and shells 09 p1331 N85-18366
Influence of gravitoinertial force level on apparent magnitude of coriolis cross-coupled angular accelerations and motion sickness 11 p1693 N85-20644
Susceptability to kinetoses and the amplitude perceived from sensory illusions 11 p1694 N85-20651
Space adaptation syndrome: Incidence and operational implications for the space transportation system program
11 p1695 N85-20655
Biofeedback treatment of airsickness: A review
11 p1696 N85-20660
Vibration and buckling of rotating, pretwisted, preconed beams including Coriolis effects
[NASA-TM-87004] 15 p2577 N85-25893
What is being done to control motion sickness?
15 p2687 N85-26599
Elastic wave gyrometer
[REPT-26/4924/HF] 20 p3459 N85-31484
Nonlinear flap-lag-extensional vibrations of rotating, pretwisted, preconed beams including Coriolis effects
[NASA-TM-87102] 23 p3941 N85-34427
Applications of the Galerkin formalism in the coupling of the earth's free oscillations 24 p4116 N85-35514

CORK (MATERIALS)
Verification of the SRB motor case pin retainer band tips
[NASA-CR-170882] 24 p4070 N85-35220
SRB TPS closeout materials characterization
[NASA-CR-170885] 24 p4070 N85-35222

CORN
Multi crop area estimation in Idaho using EDITOR
[E85-10054] 06 p0827 N85-15251
Spectral estimators of absorbed photosynthetically active radiation in corn canopies
[E85-10041] 07 p0963 N85-16242
Shortwave infrared detection of vegetation
[E85-10064] 08 p1174 N85-17402
Comparative effects of auxin and abscisic acid on growth, hydrogen ion efflux and gravitropism in primary roots of maize
[NASA-CR-174355] 09 p1342 N85-18444
Techniques for measuring intercepted and absorbed PAR in corn canopies
[E85-10081] 10 p1505 N85-19495
NOAA-AISC user's guide for implementing CERES maize model for large area yield estimation
[E85-10083] 12 p1873 N85-21748
Amyloplast sedimentation kinetics in corn roots
15 p2606 N85-26059
Calcium and calmodulin localization in gravitropically-responding plant organs
15 p2606 N85-26061
Gravistimulus production in roots of corn
15 p2607 N85-26066
Differential wall growth in gravistimulated corn roots: Its timing and regulation 15 p2614 N85-26105

Modeling the backscattering and transmission properties of vegetation canopies
[E85-10099] 16 p2609 N85-27320
Organization of the R region in maize
[DE85-011273] 20 p3504 N85-31780
CORNER FLOW
First derivatives of flow quantities behind two-dimensional, nonuniform supersonic flow over a convex corner
[NASA-TM-86272] 08 p1077 N85-16828
Three-dimensional boundary layers and shear flows activities at ONERA/CERT 15 p2558 N85-25785
Conical stagnation points in the flow around an external corner — delta wings
[VTH-LR-396] 16 p2701 N85-26880
CORNERS
Stress intensity factors for corner cracks at holes located near an edge
[FFA-TN-1984-20] 04 p0514 N85-13279
A similarity analysis of phase change heat conduction in corners 05 p0634 N85-14069
On the corner singularity of a 3-D Griffith crack
[AD-A150989] 14 p2321 N85-24342
Transition region for corner cracks at holes
[AD-A151835] 15 p2579 N85-25906
Free-surface phenomena under low- and zero-gravity conditions
[NASA-CR-175835] 16 p2762 N85-27168
CORONA BOREALIS CONSTELLATION
The fading of R coronae borealis 11 p1753 N85-21029
CORONA DISCHARGES
U ELECTRIC CORONA
CORONAGRAPHS
Lyman alpha coronagraph research sounding rocket program
[NASA-CR-174376] 09 p1354 N85-18517
User's guide for the Mk-3 D-coronameter data system
[PB85-181204] 19 p3385 N85-31002
CORONAL HOLES
A leaky waveguide model for MHD wave driven winds from coronal holes 08 p1235 N85-17761
Correlation of interplanetary medium parameters in transition region of high-velocity solar wind streams 13 p1978 N85-22412
Solar cycle variation of ephemeral regions
[AD-A154987] 21 p3723 N85-33097
A study of the cyclical variations of coronal holes and their relation to open magnetic fields
[AD-A155251] 21 p3723 N85-33099
White Light Coronograph (WLC) and Ultra-Violet Coronal Spectrometer (UVCS) 23 p3901 N85-34161
The expected cosmic ray density and stream distributions at the heliolatitudinal asymmetry of solar wind
[SH-4.2-14] 23 p4008 N85-34852
Study of dominating parameters of high speed solar plasma streams in relation to cosmic ray and geomagnetic storms
[SH-5.1-11] 23 p4042 N85-35064
CORONAL LOOPS
Studies of solar flares and coronal loops
[AD-A145009] 01 p0130 N85-10868
Active late-type stars and the applicability of coronal loop models 11 p1758 N85-21059
Thermal stability of static coronal loops: Part 1: Effects of boundary conditions
[NASA-CR-175495] 12 p1961 N85-22330
Heating of coronal loops by tearing turbulence 14 p2448 N85-25114
Axisymmetric magnetofluidstatic (MFS) equilibria of solar coronal loops: An integral equation approach 14 p2449 N85-25118
Prominences, two-ribbon flares and coronal transients 14 p2454 N85-25158
Very large array observations of coronal loops and related observations of solar type stars
[AD-A152027] 16 p2668 N85-27617
Simultaneous Solar Maximum Mission and Very Large Array (VLA) observations of solar active regions
[NASA-CR-176090] 22 p3859 N85-33897
The propagation of solar flare particles in a turbulent coronal loop
[SH-1.1-3] 23 p3999 N85-34730
Ion energy storage for post-flare loops
[SH-1.2-10] 23 p3992 N85-34745
Helios 1 energetic particle observations of the solar gamma ray flare events of 7, 21 June 1980 and 3 June 1982
[SH-1.3-8] 23 p3993 N85-34755
CORONARY ARTERY DISEASE
The effect of propranolol on the training response to endurance exercise in normal human adults 05 p0696 N85-14479
CORONARY CIRCULATION
Natural electrical activity of human sympathetic nerve fibers, recorded from body surface 07 p1013 N85-16433
Effect of acute hypoxia on coronary and systemic hemodynamics 23 p3953 N85-34503
CORONAS
NT CORONAL HOLES
NT CORONAL LOOPS
NT ELECTRIC CORONA
NT SOLAR CORONA
NT STELLAR CORONAS
Coronal spectroscopy in laser plasmas
[DE85-002817] 11 p1730 N85-20880
Images of the Earth's aurora and geocorona from the Dynamics Explorer Mission
[NASA-CR-175983] 18 p3136 N85-29423
Magnetic probing of the solar interior
[NASA-CR-176025] 19 p3385 N85-30998
Helios 1 energetic particle observations of the solar gamma ray flare events of 7, 21 June 1980 and 3 June 1982
[SH-1.3-8] 23 p3993 N85-34755
Source energy spectra from demodulation of solar particle data by interplanetary and coronal transport
[SH-1.3-13] 23 p3994 N85-34758
Far-infrared observations of young clusters embedded in the R Coronae Australnae and RHO Ophiuchi dark clouds
[NASA-TM-86681] 24 p4167 N85-35834
CORPUSCULAR RADIATION
NT BETA PARTICLES
NT CYCLOTRON RADIATION
NT ELECTRON BEAMS
NT ELECTRON PRECIPITATION
NT ELECTRON RADIATION
NT ENERGETIC PARTICLES
NT ION CYCLOTRON RADIATION
NT PRIMARY COSMIC RAYS
NT RADIATION BELTS
NT RELATIVISTIC ELECTRON BEAMS
NT SOLAR CORPUSCULAR RADIATION
NT SOLAR COSMIC RAYS
NT SOLAR ELECTRONS
NT SOLAR PROTONS
Search for neutral, penetrating, metastable particles produced in the SLAC beam dump
[DE84-012468] 04 p0560 N85-13589
Standing of industrial radiography in South Africa 14 p2316 N85-24311
Limits on deeply penetrating particles in the 10(17) eV cosmic ray flux
[HE-5.3-1] 24 p4205 N85-36098
CORRECTION
NT ATMOSPHERIC CORRECTION
NT OPTICAL CORRECTION PROCEDURE
Wall influence corrections in wind tunnels: Blockage correction according to the wall pressure signature method
[FW-FO-1613] 04 p0453 N85-12875
Automatic correction of static characteristics of measurement channel of digital oscillograph 06 p0795 N85-15083
Wind sheltering correction — anemometry
[KNMI-TR-52] 07 p1009 N85-16408
Determination of corrections to flow direction measurements obtained with a wing-tip mounted sensor
[NASA-CR-174412] 10 p1421 N85-18962
Dynamics of adaptive signal corrector 13 p2071 N85-22940
Design of single-wheel gyrocompass with correction 14 p2272 N85-24079
Selection of optimum corrections torque for vertical gyro according to special-purpose program 14 p2273 N85-24082
A digital contour-corrector for a high-definition TV camera
[NHK-LABS-NOTE-311] 19 p3254 N85-30179
Computation of three-dimensional, inviscid, rotational flows 21 p3587 N85-32296
Microcomputer controlled image processor
[AD-D011734] 22 p3833 N85-33735
CORRELATION
NT ANGULAR CORRELATION
NT AUTOCORRELATION
NT CORRELATION COEFFICIENTS
NT CORRELATION DETECTION
NT CROSS CORRELATION
NT DATA CORRELATION
NT SIGNAL ANALYSIS
NT STATISTICAL CORRELATION
An investigation of the effect of correlated abilities on observed test characteristics
[AD-A144869] 01 p0113 N85-10765
Limit theory for the sample covariance and correlation functions of moving averages
[AD-A145488] 02 p0251 N85-11642
Many-body correlations in strongly-coupled plasmas 02 p0264 N85-11650
Study of the velocity-acoustic pressure correlation in a cold jet, centered on the sign and the amplitude of the velocity fluctuations
[ISL-R-124/83] 04 p0501 N85-13193
Correlation and reassessment of the OTEC plant power cycle
[DE84-015467] 04 p0529 N85-13382
Variability of short-term eddy-correlation estimates of mass exchange
[DE84-007271] 05 p0677 N85-14349
Advanced cube processor
[AD-D011262] 05 p0729 N85-14683
Energy correlation between natural extra-low-frequency noises at various frequencies 06 p0784 N85-15010
Correlation radius of gravitational and magnetic anomalies and methods of its determination 06 p0821 N85-15213
Correlations of solar irradiance and daylight illuminance for building energy analysis
[DE85-001736] 06 p0839 N85-15326
Non-local origin of a substantial portion of the soft X-ray background 06 p0877 N85-15567
Analysis of subpixel registration 07 p0986 N85-16267
Built-in test and self repair mechanisms in a digital correlator integrated circuit 08 p1064 N85-16741
Analysis of pressure gradient-velocity correlation in turbulent, premixed flames 09 p1272 N85-17994
Inviscid analysis of unsteady blade tip flow correlation studies
[NASA-CR-172506] 10 p1420 N85-18958
Internal forced convection to low Prandtl number gas mixtures
[AD-A148932] 10 p1484 N85-19366
Estimating deformability upon pressing of aluminum alloys based on results of mechanical testing 11 p1598 N85-20049
Double pinhole spatial phase correlator apparatus
[AD-D011495] 11 p1729 N85-20872
Response time correlations for platinum resistance thermometers in flowing fluids
[NASA-CR-172523] 12 p1850 N85-21606
Method for determining the number of correlative measurements required to validate the SBUV/2 ozone retrievals 13 p2105 N85-23114
Calculations of microwave brightness temperature of rough soil surfaces: Bare field
[NASA-TM-86200] 13 p2123 N85-23221
Surface units on Venus derived from Pioneer-Venus altimetry, roughness, and reflectivity measurements 13 p2177 N85-23510
Venus gravity: Global field results 13 p2177 N85-23512
Localization of sources of equivalent noise in fast cold jets, excited and nonexcited
[ISL-CO-201/83] 14 p2416 N85-24910
The Feinhelt method: A phase-independent formulation of the period-luminosity relation for Cephids
[NASA-CR-175708] 14 p2440 N85-25056
An amplitude correlation and differencing method for the monitoring of flaws in repeat ultrasonic inspections
[AERE-R-11416] 15 p2571 N85-25854
Analysis of motions of Jupiter's great red spot and white ovals 15 p2670 N85-26472
Elevated temperature biaxial fatigue
[NASA-CR-175795] 16 p2800 N85-27283
Correlation of zeolite ZSM-5 acid strength with catalytic activity and selectivity
[DE85-005415] 17 p2922 N85-28013
A bilaterally deterministic rho-mixing stationary random sequence
[AD-A152856] 17 p3019 N85-28666
Study of the equilibrium vacancy ensemble in aluminum using 1D- and 2D-angular correlation of annihilation radiation
[DE85-008987] 18 p3194 N85-29613
Thermophysical properties correlations and pseudocomponent characterization parameter estimation for fossil fluids
[DE85-009297] 19 p3230 N85-30024
Orthogonalizer for inphase and quadrature digital data
[AD-D011679] 19 p3254 N85-30174
A comparison of four Monte Carlo methods for estimating the probability OF S=T connectedness
[AD-A154264] 19 p3348 N85-30749
Development of improved capabilities for computation of gas supercompressibility factors and other properties
[PB85-186316] 20 p3436 N85-31315
Bivariate Rayleigh distribution: Formulas and curves, for correlation computing using the distribution function
[FOA-C-30360-E2] 20 p3521 N85-31901

Correlation analysis of 1 to 30 MeV celestial gamma rays 20 p3549 N85-32083
Effect of ions on cloud formation and its role in solar terrestrial relationship 21 p3653 N85-32697
Digital matched filter 22 p3765 N85-33339
Comparison of experimental data on detonation velocity and Chapman-Jouget pressure vs initial HE density with predictions from Ree's model equation of state [DE85-007268] 23 p3922 N85-34304
An update on the correlation between the cosmic radiation intensity and the geomagnetic AA index [SH-4.2-24] 23 p4009 N85-34861
Implications of source abundances of ultraheavy cosmic rays [OG-7.1-4] 23 p4013 N85-34866
On the solar cycle variation in the barometer coefficients of high latitude neutron monitors [SH-6.1-2] 23 p4044 N85-35077
Correlation between solar neutrino flux and other solar phenomena 23 p4049 N85-35109
A search for mini-clusters in Japan-USSR Joint Experiment at Pamir [HE-3.5-2] 24 p4183 N85-35941
Takhra-Takaro complex intended for the investigations of EAS spatial characteristics near axis 24 p4190 N85-35995
Correlation of high energy muons with primary composition in extensive air shower [HE-4.3-7] 24 p4191 N85-36001

CORRELATION COEFFICIENTS
Flame propagation and stabilization studies using Rayleigh scattering and laser Doppler velocimetry [AD-A148802] 09 p1290 N85-18102
An HF communications frequency-management procedure for forecasting the frequency of optimum transmission [AD-A149191] 10 p1467 N85-19254
Formation of galaxies [DE85-009537] 18 p3202 N85-29863
The corotating variation of the north-south anisotropy of cosmic rays [SH-4.3-15] 23 p4033 N85-34899

CORRELATION DETECTION
The ambiguity function of random binary-phase-coded waveforms [AD-A148906] 10 p1466 N85-19249
Theory of optimum M-filtration of signals against background of correlated interference 13 p2069 N85-22927
On the 1983 drought in northeast Brazil [INPE-3412-PRE/678] 16 p2834 N85-27476
On the probability density of signal-to-noise ratio in an improved detector [AD-A152529] 17 p2952 N85-28232

CORRELATION FUNCTIONS
U CORRELATION

CORRELATORS
NT IMAGE CORRELATORS
Digital correlator speed improvement by multiplexing [AD-A145207] 01 p0100 N85-10662
An automatic pattern recognition apparatus [AD-D011319] 07 p1043 N85-16628
Correlator and data processing requirements for QUASAT 07 p1057 N85-16709
Processing system for space VLBI 07 p1057 N85-16711
Built-in test and self repair mechanisms in a digital correlator integrated circuit 08 p1064 N85-16741
Double pinhole spatial phase correlator apparatus [AD-D011495] 11 p1729 N85-20872
Study of phase radiogeodetic systems with phase-locked loops 13 p2115 N85-23172
Fatigue damage detection in steels by optical correlation [AD-A155830] 24 p4079 N85-35277

CORRIDORS
NT GREAT PLAINS CORRIDOR (NORTH AMERICA)

CORROSION
NT CAVITATION CORROSION
NT ELECTROCHEMICAL CORROSION
NT FRETTING CORROSION
NT HOT CORROSION
NT INTERGRANULAR CORROSION
NT RUSTING
NT SCALE (CORROSION)
NT STRESS CORROSION
USSR report: Materials science and metallurgy, no. 93 [JPRS-84810] 01 p0018 N85-10110
Biofouling and corrosion studies at the Seacoast Test Facility in Hawaii [DE84-014643] 01 p0029 N85-10180
User experience of existing corrosion monitoring techniques and the development of Thin Layer Activation (TLA) for corrosion monitoring [AERE-R-11248] 01 p0029 N85-10183
Sea water rope batteries [AD-A144775] 01 p0042 N85-10275
The reactions of cobalt, iron and nickel in SO-2 atmospheres: Similarities and differences [NASA-TM-86868] 02 p0181 N85-11217
Investigation of chemical durability mechanisms in fluoride glasses [AD-A145420] 02 p0186 N85-11241
Proceedings of the Ion Implantation for Army Needs Workshop [AD-A145474] 02 p0286 N85-11863
Expert systems: The application of new computer methods to corrosion problems [AERE-M-3395] 03 p0334 N85-12153
Wear and corrosion of components under stress and subjected to motion [AD-A145781] 03 p0372 N85-12372
A bibliography of publications on corrosion and oxidation from UK government laboratories at Teddington, 1924 - 1983 [NPL-DMA(A)-82] 04 p0472 N85-13004
Materials characterization using ion, electron, and photon probes [DE84-004518] 04 p0560 N85-13568
Current and potential transients during localized corrosion of stainless steel [DE84-014100] 05 p0618 N85-13954
High temperature corrosion of ceramics [DE84-017084] 05 p0820 N85-13967
Titanium-potassium heat pipe corrosion studies [DE84-015526] 05 p0637 N85-14090
Back end valves: History and modifications [DE84-009272] 05 p0646 N85-14145
In situ analysis of corrosive and passive surfaces by laser-excited Raman spectroscopy — lead, galvanized iron, and asbestos-cement pipes [PB84-229756] 06 p0767 N85-14904
The effect of potential on the corrosion fatigue behavior of a precipitation hardened aluminum alloy [AD-A146537] 06 p0768 N85-14916
Measuring the corrosion rate of reinforcing steel in concrete [PB84-244532] 06 p0770 N85-14925
Encapsulation materials and processing 06 p0830 N85-15269
Turbine blade test cascade modifications and orations, August 1982 - April 1983 [DE84-009268] 06 p0833 N85-15303
Mechanical aspects of high temperature coatings 07 p0906 N85-15749
Corrosion study on zirconium refractory coatings. 1: Oxidation of zirconium nitride coatings by oxygen [BLL-RISLEY-TR-5044-(9091.9F)] 07 p0925 N85-15857
Surface effects of corrosive media on hardness, friction, and wear of materials [NASA-TM-83711] 07 p0930 N85-15896
Salt action on concrete [AD-A147812] 07 p0933 N85-15912
Application of electrochemical engineering methods and theory to solving corrosion and adhesion problems with organic coatings [AD-A147799] 08 p1129 N85-17115
Fluctuation phenomena studies in chemically sensitive field effect transistor. Part 1: Corrosion of aluminum [AD-A148240] 08 p1129 N85-17118
Fluctuation phenomena studies in chemically sensitive field effect transistors. Part 2: Corrosion of silicon oxynitride [AD-A148227] 08 p1157 N85-17302
Photoacoustic spectroscopy at electrode-solution interface [DE85-001872] 09 p1292 N85-18111
Replaceable blade turbine and stationary specimen corrosion testing facility [NASA-TM-86931] 09 p1294 N85-18126
Behavior of pressurized tubes of candidate alloys in a simulated low-Btu environment [DE85-003403] 09 p1296 N85-18141
Corrosion of ceramics in heat exchanger applications [DE84-017459] 09 p1299 N85-18161
Glass corrosion in liquid lithium [DE85-002066] 09 p1299 N85-18162
Study of surface damage in cathode composite materials in a high flux CO2 laser 10 p1444 N85-19098
USSR report: Materials science and metallurgy [JPRS-UMS-84-005] 11 p1597 N85-20044
Application of Raman, TEM and other ion based techniques to oxidation problems [AERE-R-11447] 11 p1610 N85-20121
Research on heat-exchanger corrosion [PB85-126316] 11 p1616 N85-20164
The application of expert systems to corrosion problems [AERE-M-3445] 12 p1604 N85-21316
Electrochemical cell to measure corrosion rates in noncondensing environments [DE85-003148] 12 p1807 N85-21338
Corrosion and coatings review of specifications and drawings of facilities for the Oman Military Construction Program at Masirah Island, Oman [AD-A149739] 12 p1812 N85-21366
Evaluation of corrosion-erosion behavior of various ceramic materials [AD-A149756] 12 p1812 N85-21367
Steam generator tube vibration tests [DE85-003599] 12 p1867 N85-21712
Local electrochemistry of pitting corrosion in stainless steels [DE85-005207] 13 p2023 N85-22673
Applications of the vibration probe to localized current measurements [DE85-004702] 13 p2023 N85-22675
The effect of water chemistry on the rates of hydrogen generation for galvanized steel corrosion at post-loca conditions [NUREG/CR-3361] 14 p2253 N85-23963
Studies of the initiation of pitting corrosion on stainless steels [AERE-M-3400] 14 p2254 N85-23967
Role of passive surface films on corrosion fatigue crack initiation [DE85-000438] 14 p2257 N85-23985
Corrosion problems in the Canadian maritime forces [AD-A151594] 15 p2509 N85-25481
Corrosion inhibitor formulation for molybdenum, tungsten and other metals [AD-D011593] 15 p2510 N85-25486
Computer controlled acquisition of corrosion rate data from multiple sensors [PB85-157376] 15 p2524 N85-25559
Sodium and lithium corrosion in molybedenum heat pipes [DE85-005561] 16 p2784 N85-27179
NBS (National Bureau of Standards) research reports [PB85-127421] 16 p2879 N85-27764
Thermomechanical treatment aimed at the protection of type 316 stainless steel from IGC and IGSCC [BLL-BISI-TRANS-22496-(9022.06)] 17 p2925 N85-28040
Effect of the agressive action of soil on metallic pipelines. New possibilities for the passive and active corrosion protection [BLL-BISI-TRANS-21630-(9022.06)] 17 p2926 N85-28070
New method of calculating the economic effects of corrosion [BLL-BISI-TRANS-22348-(9022.06)] 17 p2929 N85-28079
Metallurgical means of preventing the corrosion of metal [BLL-BISI-TRANS-22320-(9022.06)] 17 p2929 N85-28082
Physical-chemical model for the mechanism of glass corrosion with particular consideration of simulated radioactive waste glasses [DE85-007713] 17 p2935 N85-28121
Exhaust systems for passenger vehicles: Test procedure for resistance to internal corrosion of silencers [BLL-BISI-TRANS-22360-(9022.06)] 17 p2973 N85-28361
Surface degradation of ductile metal in elevated temperature gas-particle streams [DE85-008429] 18 p3074 N85-29017
Long-Term Materials Test Program [DE85-003248] 18 p3077 N85-29034
High-temperature oxidation of alloys in mixed oxidants [DE85-009706] 18 p3077 N85-29035
Protection products for the conductors of high voltage overhead lines [BLL-OA-TRANS-3219-(9190.300)] 20 p3429 N85-31269
Effects of humidity cycles on the corrosion of galvanised reinforcements in carbonated and uncarbonated mortars [BLL-CE-TRANS-8039-(9022.09)] 20 p3430 N85-31272
Corrosion in civil aircraft structures [SNIAS-851-111-105] 20 p3432 N85-31291
Decomposition of sulfuric acid using solar thermal energy [DE85-012288] 21 p3564 N85-32170
Understanding and laboratory prediction of the atmospheric corrosion behavior of steels and of non-ferrous metals and alloys [AD-A154842] 21 p3566 N85-32179
The effect of abrasive blasting on the fatigue and corrosion of an aluminum-copper alloy [AD-A154954] 21 p3566 N85-32182
Polymer-water interaction studies 21 p3609 N85-32411

Theoretical aspects of corrosion and practical implications for aircraft and related systems
22 p3749 N85-33240
Maintenance and the military environment
22 p3750 N85-33243
Current requirements for the design and maintenance against corrosion of UK military aircraft
22 p3750 N85-33244
Ocean thermal energy conversion
[DE85-012291] 23 p3946 N85-34458
Thermodynamics of the corrosion of chromium in molten carbonates
[DE85-011407] 24 p4079 N85-35262
Experimental lithium system
[DE85-013252] 24 p4094 N85-35382

CORROSION PREVENTION
Implantation of ionized monomer into aluminum alloy 6061 for marine corrosion protection
[AD-A144874] 01 p0028 N85-10172
Aircraft surface coatings
[NASA-CR-3861] 02 p0137 N85-10935
Research and development requirements for ion implantation
[AD-P003951] 02 p0286 N85-11867
Use of ion implantation to modify the corrosion behavior of metals
[AD-P003953] 02 p0286 N85-11869
The modification of metallic corrosion by ion implantation: Engineering applications and fundamentals studies
[AD-P003954] 02 p0286 N85-11870
Effects of introduction of alkyl groups into aluminium anodized coatings
[DRIC-T-7244] 03 p0331 N85-12133
Related studies to cathodic protection of reinforced concrete structures
[PB84-216114] 03 p0333 N85-12145
Improved reinforcement metal
03 p0353 N85-12271
A review of metallic surface treatments for corrosion mitigation
[AD-A146701] 06 p0769 N85-14918
Improved ceramic anodes for corrosion protection
[AD-A149492] 10 p1452 N85-19149
Oxidation protection coatings for polymers
[NASA-CASE-LEW-14072-1] 11 p1611 N85-20129
Formation of alumina layers on iron-base alloys
[BLL-T6418/BG/LRS/LRST737/84] 13 p2020 N85-22657
Chemical-mechanical interaction in gears
14 p2223 N85-23785
Corrosion control through a better understanding of the metallic substrate-organic coating-interface
[AD-A151238] 15 p2509 N85-25479
Corrosion inhibitor formulation for molybdenum, tungsten and other metals
[AD-D011593] 15 p2510 N85-25486
Electrical research on solar cells and photovoltaic materials
[NASA-CR-175699] 15 p2585 N85-25035
Protective coatings for aircraft structures: A review
[VTH-LR-413] 16 p2706 N85-26704
Material for protection of metal surfaces against corrosion by molten salts
[DE85-007714] 16 p2750 N85-26968
Forming of coating protection system: Mechanism of paint-coating anti-corrosion protection of steel
[BLL-BISI-TRANS-22061-(9022.06)]
17 p2925 N85-28033
Anticorrosion protection of reinforcing steel in prestressed gypsum and anhydrite concrete
[BLL-BISI-TRANS-22079-(9022.06)]
17 p2926 N85-28044
Properties of chromate coatings formed on electrolytic zinc substrates
[BLL-BISI-TRANS-22349-(9022.06)]
17 p2926 N85-28052
Effect of the agressive action of soil on metallic pipelines. New possibilities for the passive and active corrosion protection
[BLL-BISI-TRANS-21630-(9022.06)]
17 p2928 N85-28070
Marine corrosion
[AD-A153843] 18 p3074 N85-29012
Effect of multi-functional inhibitors on the electrochemistry within corrosion crack
19 p3238 N85-30075
On compounding nickel alloys as defense against sulfide-oxide corrosion 19 p3243 N85-30109
Atomized magnetism-aluminum protective coatings
19 p3244 N85-30116
Concretization of high level radioactive source in marine sediment
[AD-D011709] 19 p3249 N85-30146
Protection products for the conductors of high voltage overhead lines
[BLL-OA-TRANS-3219-(6196.300)]
20 p3429 N85-31269
New corrosion protection concept for very high voltage line towers
[BLL-OA-TRANS-2691-(6196.300)]
20 p3429 N85-31270
Inhibited anticorrosion protection of automotive steel strip in the NLMK
[BLL-M-36250-(5828.4)] 20 p3430 N85-31274
Corrosion in civil aircraft structures
[SNIAS-851-111-105] 20 p3432 N85-31291
Management of Corrosion
[AGARD-LS-141] 22 p3749 N85-33238
Corrosion management strategies for aircraft and related systems 22 p3749 N85-33239
Environmental factors in corrosion and deterioration of materials 22 p3750 N85-33241
Rationale in the selection of corrosion protective coating systems 22 p3750 N85-33242
Maintenance and the military environment
22 p3750 N85-33243
Current requirements for the design and maintenance against corrosion of UK military aircraft
22 p3750 N85-33244
Protective systems and maintenance policies for marine environments 22 p3750 N85-33245
Land vehicle corrosion management
22 p3750 N85-33246
Relating corrosion maintenance to environmental factors 22 p3750 N85-33247

CORROSION RESISTANCE
NT OXIDATION RESISTANCE
Effect of scandium on the structure and properties of Al-Zn-Mg alloys 01 p0018 N85-10111
Effect of welding method on corrosion resistance of welded compositions made of 1201 alloy
01 p0020 N85-10124
Methods for producing platinum-group metal coatings from molten alkali cyanides
[PB84-225994] 01 p0029 N85-10181
International Conference on Recent Developments in Specialty Steels and Hard Materials. Conference abstracts
[CSIR-S-256] 02 p0176 N85-11177
Metalurgy of a 12 percent chromium stainless steel
02 p0178 N85-11195
The effect of replacing molybdenum with vanadium on the corrosion resistant properties of stainless steels
02 p0178 N85-11197
Non-oxide ceramics: A new class of engineering materials 02 p0179 N85-11199
The influence of metallurgical aspects on the pitting corrosion behaviour of high alloy stainless steels
02 p0179 N85-11202
Recent developments on the role of molybdenum in irons and steels 02 p0180 N85-11206
The transient oxidation of single crystal NiAl+Zr
[NASA-CR-174756] 02 p0182 N85-11221
Optimization of mechanical/corrosion properties of Ticode-12 plate and sheet. Part 1: Compositional effects, stage 1
[DE84-015935] 02 p0184 N85-11231
Corrosion in alkali metal/molybdenum heat pipes
[DE84-014039] 02 p0184 N85-11233
Investigation of chemical durability mechanisms in fluoride glasses
[AD-A145420] 02 p0186 N85-11241
Localized corrosion and stress corrosion cracking behavior of stainless steel weldments
[DE84-016095] 04 p0474 N85-13017
Corrosion of brass in potable water service
[CETIM-100390] 04 p0477 N85-13037
Corrosion resistance of nitrided low-alloy steels
[PB84-235027] 04 p0477 N85-13040
Galvanized wire protected against corrosion by chromate passivization
[BLL-M-35908-(5828.4)] 05 p0616 N85-13936
Material selection consideration for solar ponds
05 p0666 N85-14284
Characterization of newly developed conductive composites
[AD-A146652] 06 p0764 N85-14884
A review of metallic surface treatments for corrosion mitigation
[AD-A146701] 06 p0769 N85-14918
Copper-nickel sheathing study, phase 2. Two-year service performance of test panels on the ARCO TEXAS
[PB84-242411] 06 p0775 N85-14952
Improvement of the corrosion resistance of turbine engine bearings
[AD-A147490] 07 p0905 N85-15731
Corrosion properties of second-generation conductive materials 07 p1000 N85-16348
Effect of iron on the performance of IN 625 weld deposits
[BR91456] 08 p1169 N85-17376
Development of materials for open-cycle MHD
[DE84-017293] 09 p1393 N85-18770
Evaluation of 7010 aluminium alloy extruded tube in the T76 condition
[BR92019] 11 p1596 N85-20039
Initial development of nickel and nickel-iron aluminides for structural uses
[DE84-016641] 11 p1606 N85-20108
Role of nitrogen in improving resistance to localized corrosion in austenitic stainless steels
11 p1609 N85-20115
Research on heat-exchanger corrosion
[PB85-126316] 11 p1616 N85-20164
Progress on transparent yttria
[AD-P004370] 12 p1827 N85-21464
Carbon granule probe microphone for leak detection — recovery boilers
[NASA-CASE-NPO-16027-1] 12 p1849 N85-21597
Delayed cracking strength of experimental grades of 42 CD 4 steel in aqueous H2S surroundings
[BLL-T6419/BG/LRS/LRST736/84]
13 p2020 N85-22658
Study of the effects of implantation on the high Fe-Ni-Cr and Ni-Cr-Al alloys
[NASA-CR-175625] 13 p2021 N85-22661
Corrosion of aircraft Al and Al-Zn ion plated steel fasteners 13 p2021 N85-22666
Influence of 3% NaCl solution on rate of accumulation of damage and residual strength of aluminum-boron composite 13 p2027 N85-22699
Corrosion-resistant amorphous alloys
13 p2035 N85-22748
Exploratory corrosion tests on materials and fluids for advanced high-temperature molten-salt storage
[DE85-002911] 14 p2258 N85-23991
Conservation of turbines by inhibited air
14 p2268 N85-24054
Development of molten carbonate fuel cell power plant technology
[DE84-016839] 14 p2352 N85-24536
Resistance of hydrogenated alpha-titanium alloys to corrosion-fatigue fracture 15 p2499 N85-25413
Mechanisms of corrosion fatigue in high strength I/M (Ingot Metallurgy) and P/M (Powder Metallurgy) aluminum alloys
[AD-A151177] 15 p2509 N85-25478
Corrosion control through a better understanding of the metallic substrate-organic coating-interface
[AD-A151238] 15 p2509 N85-25479
The corrosion resistance of zinc coatings on depleted uranium and uranium alloys
[DE85-007216] 15 p2510 N85-25487
Oxidation of nickel-aluminum and iron-aluminum alloys
[DE85-006930] 15 p2512 N85-25497
Surface composition, properties and thermal stability of massive and fine metallic glasses
15 p2513 N85-25506
Modified aluminosilicide coating for heat-resistant nickel alloys 15 p2514 N85-25509
Titanium diffusion method prevents metal corrosion
15 p2514 N85-25510
Inhibiting titanium corrosion in hot nitrogen nitrate solutions using sulfate ions 15 p2514 N85-25511
Corrosion behavior of Al4 aluminum alloy hardened by CO2 laser radiation 15 p2514 N85-25512
The influence of abrasive blast cleaning and corrosion inhibitors on protective paint coatings
15 p2517 N85-25522
Electrically conductive polymer concrete overlays
[DE85-006726] 15 p2522 N85-25549
Powder metallurgy bearings for advanced rocket engines 16 p2736 N85-26881
Evaluation of the corrosion properties of aluminum alloy 5083 weldments
[DE85-007729] 16 p2751 N85-26977
Investigation of the pitting potential of rapidly solidified aluminum-lithium alloys
[VTH-LR-434] 16 p2752 N85-26986
Investigation of the influence of some paint systems and water displacing corrosion inhibitors on anodic undermining corrosion of aluminum 2024 clad alloy — aircraft structures
[VTH-LR-443] 16 p2756 N85-27009
Material for electrodes of pulsed and arc sources of light
[DE85-007453] 16 p2780 N85-27156
Properties of corrosion resistant stabilized ferritic steels
[BLL-BISI-TRANS-22519-(9022.06)]
17 p2925 N85-28039

The corrosion resistance of chromium-nickel steel containing rare-earth metals
[BLL-BISI-TRANS-22477-(9022.06)] 17 p2925 N85-28041
Anticorrosion protection of reinforcing steel in prestressed gypsum and anhydrite concrete
[BLL-BISI-TRANS-22079-(9022.06)] 17 p2926 N85-28044
Properties of chromate coatings formed on electrolytic zinc substrates
[BLL-BISI-TRANS-22349-(9022.06)] 17 p2926 N85-28052
New process for production of bimetal with corrosion-resistant cladding layer
[BLL-BISI-TRANS-22371-(9022.06)] 17 p2927 N85-28056
Obtaining oxide films on surface of tubes of chromium-nickel steels
[BLL-BISI-TRANS-22478-(9022.06)] 17 p2929 N85-28076
Dispersion-strengthened powder-metallurgical chromium steels
[BLL-BISI-TRANS-22323-(9022.06)] 17 p2929 N85-28081
Metallurgical means of preventing the corrosion of metal
[BLL-BISI-TRANS-22320-(9022.06)] 17 p2929 N85-28082
Properties of nitrogen containing stainless alloy designed for high resistance to pitting
[DE85-008282] 17 p2931 N85-28095
Development of high temperature resistant, noncorrosible, non-metallic ceramic materials, especially silicon nitride in gas turbine application
[BMFT-FB-T-85-015] 17 p2936 N85-28125
Development of high temperature resistant noncorrodible silicon carbide components for gas turbine applications, follow-up report
[BMFT-FB-T-85-016] 17 p2936 N85-28126
Exhaust systems for passenger vehicles: Test procedure for resistance to internal corrosion of silencers
[BLL-BISI-TRANS-22360-(9022.06)] 17 p2973 N85-28361
Proper quality of anticorrosion work no matter how bad the atmospheric conditions
[BLL-BISI-TRANS-22080-(9022.06)] 17 p2975 N85-28383
Corrosion resistant coating
[NASA-CASE-NPO-15928-1] 18 p3073 N85-29005
Variations in the structure and in the composition of austenitic and carbon steel in spot welds
[BLL-BISI-TRANS-21765-(9022.06)] 18 p3073 N85-29007
Development of reduced activation alloys for fusion service: Draft
[DE85-007464] 18 p3074 N85-29014
Long-Term Materials Test Program
[DE85-003248] 18 p3077 N85-29034
Development of corrosion resistant heat exchangers for flue gas desulfurization
[BMFT-FB-T-84-281] 18 p3103 N85-29211
SERI Solar Energy Storage Program: FY 1984
[DE85-002936] 18 p3130 N85-29385
USSR report: Materials Science and Metallurgy
[JPRS-UMS-85-005] 19 p3241 N85-30095
On compounding nickel alloys as defense against sulfide-oxide corrosion 19 p3243 N85-30109
Vacuum pressure welding of commercial titanium with 2Kh13 and 12Kh18N10T steels 19 p3246 N85-30124
Mechanism of strength degradation for hot corrosion of alpha-SiC
[NASA-TM-87052] 19 p3248 N85-30135
Concretization of high level radioactive source in marine sediment
[AD-D011703] 19 p3249 N85-30146
Optimisation of MCr Al coating compositions for marine gas turbines
[BR91159] 20 p3394 N85-31056
Corrosion in civil aircraft structures
[SNIAS-851-111-105] 20 p3432 N85-31291
Management of Corrosion
[AGARD-LS-141] 22 p3749 N85-33238
Theoretical aspects of corrosion and practical implications for aircraft and related systems 22 p3749 N85-33240
Rationale in the selection of corrosion protective coating systems 22 p3750 N85-33242
Current requirements for the design and maintenance against corrosion of UK military aircraft 22 p3750 N85-33244
Corrosion resistant storage container for radioactive material
[DE85-011666] 22 p3838 N85-33765
Nitriding of super alloys for enhancing physical properties
[DE85-005762] 23 p3917 N85-34275
The development and evaluation of the creep and corrosion resistant alloy IN6201
[PNR-90253] 23 p3917 N85-34278
Electrically conductive containment vessel for molten aluminum
[DE85-006518] 23 p3939 N85-34415
Electrochemical method for investigation of the susceptibility of corrosion-resistant steels to intercrystalline corrosion
[BLL-CE-TRANS-8082-(9022.09)] 24 p4077 N85-35269
X-ray fluorescence analysis of 304L stainless steel
[DE85-013254] 24 p4080 N85-35288
Development of a mathematical model for predicting the percentage fatigue life increase resulting from shot peened components
[AD-A155774] 24 p4101 N85-35425

CORROSION TESTS
NT SALT SPRAY TESTS
Interactions between corrosion and creep of uncoated and coated superalloys in sulfate melts 04 p0477 N85-13038
Method for evaluating petrol products corroeivity using piezoelectric crystals. Part 2: Instruction manual — jet engine corrosion tests
[FOA-C-40198-B4] 04 p0482 N85-13073
A simple, low cost potentiostat for corrosion studies
[NPL-DMA(A)-47] 04 p0502 N85-13203
Testing of non-alloyed and low-alloyed steels for their behaviour with respect to intercrystalline stress corrosion cracking
[BLL-RISLEY-TR-4546-(9091.9F)] 07 p0925 N85-15861
Replaceable blade turbine and stationary specimen corrosion testing facility
[NASA-TM-86931] 09 p1294 N85-18126
Forced corrosion tests of construction components of passenger aircraft fuselages 11 p1600 N85-20062
Compatibility experiments of facilities, materials, and propellants for electrothermal thrusters
[NASA-TM-86956] 12 p1795 N85-21260
An electrochemical study of the corrosion behavior of primer coated 2219-T87 aluminum
[NASA-TP-2459] 13 p2021 N85-22662
Change in microstructure of heat-resistant nickel alloys upon thermal cycling in a current of gas 13 p2031 N85-22725
Variability in constant-load-amplitude fatigue crack growth rates in marine environments
[AD-A150786] 14 p2255 N85-23975
Exploratory corrosion tests on alloys in molten salts at 900(0)C
[DE85-000511] 14 p2257 N85-23983
Exploratory corrosion tests on materials and fluids for advanced high-temperature molten-salt storage
[DE85-002911] 14 p2258 N85-23991
The design and construction of a flow channel and rig for corrosion studies
[AERE-M-3455] 15 p2508 N85-25474
Influence of pretreatment, environment and strain rate on stress corrosion cracking of the aluminum alloy 7075-T6
[VTH-LR-433] 16 p2752 N85-26985
Corrosion characteristics of some steels produced through a self-cleaning rotating electrode
[BLL-BISI-TRANS-22046-(9022.06)] 17 p2925 N85-28034
Corrosion test on high-alloy steels
[BLL-BISI-TRANS-21627-(9022.06)] 17 p2926 N85-28046
Exhaust systems for passenger vehicles: Test procedure for resistance to internal corrosion of silencers
[BLL-BISI-TRANS-22360-(9022.06)] 17 p2973 N85-28361
Tendency of selected low-carbon steels to corrosion cracking in nitrates
[BLL-BISI-TRANS-22262-(9022.06)] 18 p3073 N85-29006
Burner rig corrosion of SiC at 1000 deg C
[NASA-TM-87061] 19 p3227 N85-30011
Corrosion fatigue cooperative testing program statistical analysis
[AD-A153686] 19 p3238 N85-30077
Management of Corrosion
[AGARD-LS-141] 22 p3749 N85-33238
Protective systems and maintenance policies for marine environments 22 p3750 N85-33245
Corrosion fatigue strength and crack growth in prestrained 0.16% C carbon steel 23 p3905 N85-34192

CORRUGATED SHELLS
Vibrational loading mechanism of unitized corrugated containers with cushions and non-load-bearing contents 09 p1339 N85-18419
Stressed state of multilayer thick-walled longitudinally corrugated cylinders 16 p2766 N85-27069

CORRUGATING
Microwave SAW (Surface Acoustic Wave) monochromator
[AD-D011718] 21 p3590 N85-32311

CORSAIR AIRCRAFT
U A-7 AIRCRAFT

CORTICOSTEROIDS
NT ALDOSTERONE
NT CORTISONE
NT HYDROXYCORTICOSTEROID
Role of glucocorticoids in the response to unloading of muscle protein and amino acid metabolism 15 p2609 N85-26077
Blood pressure responses and mineral ocorticoid levels in the suspended rat model for weightlessness 15 p2609 N85-26079

CORTISONE
Skeletal muscle metabolism in hypokinetic rats
[NASA-CR-174059] 02 p0233 N85-11520

CORUNDUM
U ALUMINUM OXIDES

COS-B SATELLITE
The galactic gamma-ray distribution: Implications for galactic structure and the radial cosmic ray gradient
[NASA-TM-86173] 07 p1061 N85-16729
Multicomponent analysis of total COS-B gamma-ray data at intermediate latitudes
[OG-3.1-3] 22 p3873 N85-33991

COSMIC DUST
NT INTERPLANETARY DUST
NT ZODIACAL DUST
The distribution of dust in the region of the Rosette Nebula and MON OB2 association 05 p0739 N85-14753
Local interstellar extinction with an emphasis on uvby beta results 06 p0875 N85-15559
The unidentified emission features: A study of the Orion Bar and planetary nebulae 06 p1246 N85-17862
Circumstellar dust disks around young stars 06 p1247 N85-17870
Spectral characteristics of dust in planetary nebulae 06 p1247 N85-17873
Interstellar grain mantles 06 p1247 N85-17874
Dust irradiation from NGC 6946 06 p1248 N85-17880
A comparative study of dust and young stars in three small galaxies 09 p1415 N85-18928
Dust in the region of Herbig-Haro objects: The case of NGC 1999 11 p1747 N85-20991
Survey of probable micrometer-sized Earth-orbital debris fragments in the NASA-JSC cosmic dust sample collection 12 p1785 N85-21203
In-situ detection of micron-sized dust particles in near-Earth space 12 p1785 N85-21205
Research in planetary studies and operation of Mauna Kea Observatory
[NASA-CR-175618] 13 p2189 N85-23460
Sixteenth Lunar and Planetary Science Conference. Press abstracts
[NASA-CR-175892] 15 p2680 N85-26548
Dust emission of Comet Halley at large heliocentric distances 15 p2681 N85-26556
Mining cosmic dust from the blue ice lakes of Greenland 15 p2682 N85-26563
A comprehensive investigation of the dynamics of micron and submicron lunar ejecta in heliocentric space 19 p3384 N85-30994

COSMIC GAMMA RAY BURSTS
U GAMMA RAY BURSTS

COSMIC GASES
NT INTERSTELLAR GAS
NT NEUTRAL GASES
Measuring EUV line emission from the hot interstellar medium 06 p0680 N85-15595
Constraints on the galactic distribution of cosmic rays from the COS-B gamma-ray data
[OG-3.1-6] 22 p3873 N85-33994
Relevance of cosmic gamma rays to the mass of gas in the galaxy
[OG-3.1-8] 22 p3874 N85-33996
COS-B gamma-ray sources and interstellar gas
[OG-3.1-9] 22 p3874 N85-33997
Excess gamma rays from the Loop I supernova remnant
[OG-3.1-10] 22 p3874 N85-33998
Breakdown of helium nuclei in matter processed near black holes
[OG-8.2-20] 23 p4021 N85-34916

COSMIC PLASMA
Space research and the new approach to the mechanics of fluid media in cosmos
[TRITA-EPP-84-04] 03 p0447 N85-12844
Physical processes in relativistic plasmas — active galactic nuclei 08 p1240 N85-17824
Plasma Astrophysics — conference
[ESA-SP-207] 12 p1953 N85-22270
Space research and the new approach to the mechanics of fluid media in cosmos 12 p1953 N85-22271
X-ray astronomy and plasma astrophysics 12 p1958 N85-22288
Explosive transverse electric field and particle acceleration during magnetic collapse — cosmic plasma 12 p1956 N85-22292
Nonlinear evolution of astrophysical Alfven waves 12 p1956 N85-22294
Plasma in the clusters of galaxies 12 p1957 N85-22299
Plasma processes in Herbig-Haro objects 12 p1957 N85-22301
Hydromagnetic precursors of interplanetary plasma burst 13 p1978 N85-22414
Solar wind and cosmic rain 15 p2644 N85-26312
On planetary rings as sources and sinks of magnetospheric plasmas 15 p2677 N85-26526
Prognoz-10 intercosmos' station launched to study shock waves 19 p3298 N85-30434
Implications of source abundances of ultraheavy cosmic rays 20 p3543 N85-32049
Interstellar turbulence, random density variations, and scintillation measurements
[OG-7.2-13] 23 p4015 N85-34880
The role of cosmic rays in magnetic hydrodynamics of interstellar medium
[OG-7.2-15] 23 p4015 N85-34882

COSMIC RADIATION
U COSMIC RAYS

COSMIC RADIO WAVES
U EXTRATERRESTRIAL RADIO WAVES

COSMIC RAY ALBEDO
Longitude and pitch-angle distributions of streams of high-energy electrons under Earth's radiation belts 13 p1978 N85-22415

COSMIC RAY SHOWERS
Electromagnetic shower development and applications to sampling calorimeters
[DE84-016355] 04 p0493 N85-13142
Characteristics of latitude effect on cosmic ray charged component in atmosphere at altitudes 3-5 KM 13 p1978 N85-22413
Longitude and pitch-angle distributions of streams of high-energy electrons under Earth's radiation belts 13 p1978 N85-22415
Solar wind and cosmic rain 15 p2644 N85-26312
Yakutsk Institute's cosmic ray research facility 22 p3732 N85-33135
Search for gamma rays of energy 10(15) eV from Cygnus X-3
[OG-2.1-1] 22 p3862 N85-33919
Observation of an excess of cosmic ray muons of energies 2 TeV from the direction of Cygnus X-3
[OG-2.1-3] 22 p3863 N85-33920
Muon content of gamma ray induced EAS from Cygnus X-3
[OG-2.1-4] 22 p3863 N85-33921
Gamma rays of energy or = 10(15) eV from Cyg X-3
[OG-2.1-5] 22 p3863 N85-33922
1000 GeV gamma rays from Cygnus X-3: An update
[OG-2.1-8] 22 p3863 N85-33925
Evidence for long-term variability in the ultra high energy photon flux from Cygnus X-3
[OG-2.1-10] 22 p3863 N85-33926
Variability in the high energy gamma ray emission from Cyg X-3 over a two-year period (1983 - 1984) at E 4 x 10(11) eV
[OG-2.1-11] 22 p3864 N85-33927
A search for gamma-ray point sources with the Carpet shower array
[OG-2.1-12] 22 p3864 N85-33928
Cyg X-3: Not seen in high-energy gamma rays by COS-B
[OG-2.2-2] 22 p3864 N85-33929
Constraints on cosmic-ray observation of Cygnus X-3
[OG-2.2-3] 22 p3864 N85-33930
Ultra high energy gamma rays, cosmic rays and neutrinos from accreting degenerate stars
[OG-2.2-5] 22 p3864 N85-33931
Relevance of the observation of UHE gammas to hard X-ray astronomy
[OG-2.2-6] 22 p3865 N85-33932
500 TeV gamma rays from Hercules X-1
[OG-2.2-7] 22 p3865 N85-33933
A model for the UHE gamma-rays from Hercules X-1
[OG-2.2-8] 22 p3865 N85-33934
Hercules X-1: Pulsed gamma-rays detected above 150 GeV
[OG-2.2-9] 22 p3865 N85-33935
Experimental results on gamma-ray sources at E sub 0 = 10(13) - 10(14) eV
[OG-2.2-12] 22 p3865 N85-33937
Search for excess showers from Crab Nebula
[OG-2.3-2] 22 p3866 N85-33939
All sky Northern Hemisphere 10(15) EV gamma-ray survey
[OG-2.6-3] 22 p3870 N85-33968
Search for ultra high energy gamma-rays from various sources
[OG-2.6-7] 22 p3870 N85-33969
A search for sources of ultra high energy gamma rays at air shower energies with Ooty EAS array
[OG-2.6-8] 22 p3870 N85-33970
Observations of potential ultra high energy gamma-ray sources above 10(15) eV
[OG-2.6-9] 22 p3870 N85-33971
Observation of gamma-rays from LMC X-4 above 10(16) eV
[OG-2.6-10] 22 p3870 N85-33972
The 4U 0115+63: Another energetic gamma ray binary pulsar
[OG-2.6-11] 22 p3870 N85-33973
Primary gamma-rays with E gamma or = to 10(15) eV: Evidence for ultrahigh energy particle acceleration in galactic sources
[OG-2.6-13] 22 p3871 N85-33974
Search for the gamma-ray fluxes with energies above 10915) eV from various objects
[OG-2.6-14] 22 p3871 N85-33975
Search for gamma-rays from M31 and other extragalactic objects
[OG-2.7-3] 22 p3871 N85-33977
Some evidence for high energy gamma-ray sources at large galactic latitudes
[OG-2.7-5] 22 p3871 N85-33978
Energy spectrum and arrival direction of primary cosmic rays of energy above 10 to the 18th power eV
[OG-5.1-1] 22 p3880 N85-34043
Ultra high energy cosmic ray spectrum
[OG-5.1-2] 22 p3881 N85-34044
The primary cosmic ray spectrum above 10 to the 19th power eV
[OG-5.1-3] 22 p3881 N85-34045
New calorimetric all-particle energy spectrum
[OG-5.1-4] 22 p3881 N85-34046
The muon content of EAS as a function of primary energy
[OG-5.1-8] 22 p3881 N85-34050
On the possibility of the determining the average mass composition near 10 to the 14th power eV through the solar magnetic field
[OG-5.1-9] 22 p3882 N85-34051
Cosmic ray composition between 10 to the 15th power - 10 to the 17th power eV obtained by air shower experiments
[OG-5.1-12] 22 p3882 N85-34053
Estimation of composition of cosmic rays with E sub zero approximately equals 10(17) - 10(18) eV
[OG-5.1-14] 22 p3882 N85-34055
All particle energy spectrum of cosmic rays in 10 to the 15th power - 10 to the 20th power eV region
[OG-5.1-15] 22 p3882 N85-34056
Cosmic ray spectra measurements at the Yakutsk EAS array
[OG-5.1-17] 22 p3882 N85-34058
Composition of primary cosmic rays near the bend from a study of hadrons in air showers at sea level
[OG-5.2-2] 22 p3883 N85-34059
The composition of cosmic rays near the Bend (10 to the 15th power eV) from a study of muons in air showers at sea level
[OG-5.2-3] 22 p3883 N85-34060
Composition of primary cosmic rays at energies 10(15) to approximately 10(16) eV
[OG-5.2-4] 22 p3883 N85-34061
EAS fluctuation approach to primary mass composition investigation
[OG-5.2-5] 22 p3883 N85-34062
The primary composition beyond 10 to the 5th power GeV as deduced from high energy hadrons and muons in air showers
[OG-5.2-6] 22 p3883 N85-34063
Implication of EAS data for the study of primary cosmic rays above 10 to the 5th power GeV
[OG-5.2-7] 22 p3883 N85-34064
Composition of primary cosmic rays near the knee
[OG-5.2-10] 22 p3884 N85-34066
EAS Cerenkov measurements of the composition of the cosmic ray flux around 10 to the 16th power eV
[OG-5.2-11] 22 p3884 N85-34067
Electron and muon parameters of EAS and the composition of primary cosmic rays in 10(15) to approximately 10(16) eV
[OG-5.2-12] 22 p3884 N85-34068
Arrival directions of large air showers, low-mu showers and old-age low-mu air showers observed at SL Chacaltaya
[OG-5.3-2] 22 p3884 N85-34069
Anisotropy of cosmic rays of energy 10 (15) eV to 10 (17) eV observed at Akeno
[OG-5.3-3] 22 p3884 N85-34070
Arrival directions of cosmic rays of E .4 EeV
[OG-5.3-4] 22 p3884 N85-34071
The sidereal anisotropy of cosmic rays around 3 x 10 (15) eV observed at a middle north latitude
[OG-5.3-6] 22 p3884 N85-34072
Arrival direction distribution of cosmic rays of energy 10 (18) eV
[OG-5.3-7] 22 p3885 N85-34073
Observation of arrival times of EAS with energies or = 8 x 10 (14) eV
[OG-5.3-8] 22 p3885 N85-34074
Cosmic ray intensity variations at primary rigidities near 1900 GV
[OG-5.3-0] 22 p3885 N85-34075
Search for bursts in air shower data
[OG-5.3-10] 22 p3885 N85-34076
Air shower arrival directions measured at Buckland Park
[OG-5.3-11] 22 p3885 N85-34077
A simulation of high energy cosmic ray propagation 1
[OG-5.4-1] 22 p3885 N85-34078
A simulation of high energy cosmic ray propagation 2
[OG-5.4-2] 22 p3885 N85-34079
Cosmic rays in the 10(16) to 10(19) eV range from pulsars
[OG-5.4-3] 22 p3886 N85-34080
Energy dependence of cosmic ray composition above 10(15) GeV/nucleus
[OG-5.4-4] 22 p3886 N85-34081
Implications of the experimental results on high energy cosmic rays with regard to their origin
[OG-5.4-5] 22 p3886 N85-34082
The primary cosmic ray mass composition at energies above 10(14) eV
[OG-5.4-6] 22 p3886 N85-34083
UHE particle production in close binary systems
[OG-5.4-7] 22 p3886 N85-34084
Virgo cluster as a high energy cosmic rays source
[OG-5.4-8] 22 p3886 N85-34085
Modeling cosmic ray anisotropies near 10(18) eV
[OG-5.4-9] 22 p3886 N85-34086
Anisotropy and the knee of the energy spectrum
[OG-5.4-10] 22 p3887 N85-34087
Anisotropy of cosmic rays above 10(14) eV
[OG-5.4-11] 22 p3887 N85-34088
A model for the proton spectrum and cosmic ray anisotropy
[OG-5.4-12] 22 p3887 N85-34089
Interpretation of cosmic-ray anisotropy below 10(14) eV
[OG-5.4-13] 22 p3887 N85-34090
Injection of energetic particles following the gamma-ray flares on June 7, 1980, as observed on Helios 1
[SH-1.3-9] 23 p3993 N85-34756
Spectra of solar proton ground level events using neutron monitor and neutron moderated detector recordings
[SH-1.3-14] 23 p3994 N85-34759
Ground increase of cosmic ray intensity on February 16, 1984
[SH-1.3-15] 23 p3994 N85-34760
The SCR flare of 16 February 1984 as recorded by the Sayan spectrograph
[SH-1.3-17] 23 p3994 N85-34761
Energetic solar particle events
[SH-3.2-2] 23 p4003 N85-34818
Cosmic ray intensity and the tilt of the neutral sheet
[SH-4.2-6] 23 p4007 N85-34846
Differential measurement of cosmic-ray gradient with respect to interplanetary current sheet
[SH-4.2-9] 23 p4007 N85-34847
Effects of a wavy neutral sheet on cosmic ray anisotropies
[SH-4.2-11] 23 p4008 N85-34849
Implications of cross section errors for cosmic ray propagation
[OG-7.2-3] 23 p4014 N85-34875
Cosmic ray secondary nuclei and the structure of the galaxy
[OG-7.2-4] 23 p4014 N85-34876
Why do leaky-box models work so fine?
[OG-7.2-8] 23 p4014 N85-34877
Alfven wave scattering and the secondary to primary ratio
[OG-7.2-9] 23 p4015 N85-34878

On the cosmic ray diffusion in a violent interstellar medium
[OG-7.2-14] 23 p4015 N85-34881
The role of cosmic rays in magnetic hydrodynamics of interstellar medium
[OG-7.2-15] 23 p4015 N85-34882
A new ultra high energy gamma ray telescope at Ohya mine
[OG-9.4-3] 23 p4029 N85-34970
The Buckland Park air shower array
[OG-9.4-4] 23 p4029 N85-34971
An EAS experiment at mountain altitude for the detection of gamma-ray sources
[OG-9.4-5] 23 p4029 N85-34972
An observatory to study 10 (10) to 10 (17) by EV gamma rays
[OG-9.4-6] 23 p4029 N85-34973
A new array for the study of ultra high energy gamma-ray sources
[OG-9.4-7] 23 p4029 N85-34974
Akeno 20 km (2) air shower array (Akeno Branch)
[OG-9.4-8] 23 p4029 N85-34975
Mini and super mini arrays for the study of highest energy cosmic rays
[OG-9.4-9] 23 p4029 N85-34976
Detection of 10 (1) GeV cosmic neutrinos with a space station
[OG-9.4-10] 23 p4030 N85-34977
The longitudinal thickness of air-shower fronts
[OG-9.5-1] 23 p4030 N85-34978
Cerenkov light images of EAS produced by primary gamma
[OG-9.5-3] 23 p4030 N85-34979
Shower disc sampling and the angular resolution of gamma-ray shower detectors
[OG-9.5-2] 23 p4030 N85-34980
A method to improve observations of gamma-ray sources near 10 (15) eV
[OG-9.5-5] 23 p4030 N85-34982
Angular resolution of air-shower array-telescopes
[OG-9.5-6] 23 p4030 N85-34983
Astrophysical applications of high angular resolution array-telescopes
[OG-9.5-7] 23 p4031 N85-34984
Angular resolution of an EAS array for gamma ray astronomy energies 5 x 10 (13) eV
[OG-9.5-8] 23 p4031 N85-34985
Note on the detection of high energy primary cosmic gamma rays by air shower observation
[OG-9.5-9] 23 p4031 N85-34986
On the statistical significance of excess events: Remarks of caution and the need for a standard method of calculation
[OG-9.5-10] 23 p4031 N85-34987
A new statistic for the analysis of circular data in gamma-ray astronomy
[OG-9.5-13] 23 p4031 N85-34989
The angular resolution of air shower gamma ray telescopes
[OG-9.5-14] 23 p4031 N85-34990
Accelerator experiments on the contribution of secondary particles to the production of cosmogenic nuclides in meteorites
[SH-7.1-8] 23 p4048 N85-35100
Depth and size effects on cosmogenic nuclide production in meteorites
[SH-7.1-9] 23 p4048 N85-35101
A suggested standardized format for cosmic ray ground-level event data
[SH-9.1-15] 23 p4052 N85-35130
Using the information of cosmic rays to predict influence epidemic
[SH-10.1-2] 23 p4053 N85-35134
Strong earthquakes, novae and cosmic ray environment
[SH-10.1-3] 23 p4053 N85-35135
Proton-air and proton-proton cross sections from air shower data
[HE-1.1-1] 24 p4170 N85-35849
Proton-air inelastic cross section at S(1/2) = 30 TeV
[HE-1.1-2] 24 p4170 N85-35850
Hadron cross sections at ultra high energies and unitarity bounds on diffraction dissociation
[HE-1.1-3] 24 p4170 N85-35851
P(P bar)P elastic scattering and cosmic ray data
[HE-1.1-6] 24 p4170 N85-35854
Estimation of the total inelasticity coefficient in interaction of greater than or equal to 20 TeV hadrons with lead
[HE-1.1-9] 24 p4171 N85-35857
The method for the study of the inelastic cross-section for high energy protons by means of shower arrays with the large calorimetric area
[HE-1.1-11] 24 p4171 N85-35858
Multiplicity distributions in interaction models used for cascade simulations
[HE-1.2-5] 24 p4172 N85-35863
Some remarks about simulation of cosmic ray phenomena with use of nuclear interaction models based on the current SPS proton-antiproton data
[HE-1.2-6] 24 p4172 N85-35864
Anuglar distribution of shower particles produced in the collisions of 20-GeV/c and 300-GeV negative pions with emulsion nuclei 24 p4172 N85-35866
Scaling violation in the fragmentation region of inclusive nucleon spektrum 24 p4173 N85-35874
The response of a scintillation counter below an emulsion chamber to heavy nucleus interactions in the chamber 24 p4175 N85-35889
Japan - USSR joint emulsion chamber experiment at Pamir
[HE-3.1-1] 24 p4177 N85-35901
Energy spectra of proton and nuclei of primary cosmic rays in energy region 10 TeV/particle
[HE-3.1-10] 24 p4178 N85-35908
Scaling violation in fragmentation region at energies above 10-15 eV based on the data on cosmic ray hadron component
[HE-3.1-11] 24 p4178 N85-35909
High sensitive X-ray films to detect electron showers in 100 GeV region
[HE-3.1-13] 24 p4178 N85-35911
Exotic interactions among C-jets and Pb-jets
[HE-3.2-6] 24 p4179 N85-35914
X-ray film chamber with carbon target of Tien-Shan complex array 24 p4179 N85-35915
Penetrative nature of high energy showers observed in Chacaltaya emulsion chamber
[HE-3.3-5] 24 p4180 N85-35923
Anomalous correlation between hadron and electromagnetic particles in hadron and gamma-ray families
[HE-3.3-6] 24 p4180 N85-35924
Atmospheric interactions detected in both the upper and the lower chambers at Chacaltaya
[HE-3.3-7] 24 p4180 N85-35925
Lateral distribution of high energy hadrons and gamma ray in air shower cores observed with emulsion chambers
[HE-3.3-8] 24 p4180 N85-35926
Size distributions of air showers accompanied with high energy gamma ray bundles observed at Mt. Chacaltaya
[HE-3.3-9] 24 p4181 N85-35927
EAS accompanied by gamma-families at Mt. Norikura and comparison with Monte Carlo simulation
[HE-3.3-10] 24 p4181 N85-35928
Comparison of absolute intensity between EAS with gamma-families and general EAS at Mount Norikura
[HE-3.3-11] 24 p4181 N85-35929
Analytical-numerical methods of calculations of energy and three-dimensional particle distributions in electromagnetic cascades
[HE-3.5-13] 24 p4184 N85-35950
Multidimensional analysis of data obtained in experiments with X-ray emulsion chambers and extensive air showers
[HE-3.6-2] 24 p4184 N85-35951
LPM effect and primary energy estimations
[HE-3.6-4] 24 p4185 N85-35953
Experimental basis for the models of cascade propagation in atmosphere
[HE-3.6-6] 24 p4185 N85-35954
Relation between gamma-ray family and EAS core: Monte-Carlo simulation of EAS core
[HE-3.6-7] 24 p4185 N85-35955
Comparison of big event with calculations of the air shower development
[HE-3.6-8] 24 p4185 N85-35956
The lateral distributions of charged particles of energy greater than 0.3 E sub crit in electron-photon cascades in lead and air
[HE-3.6-10] 24 p4185 N85-35957
Result of Monte-Carlo simulation of electron-photon cascades in lead and layers of lead-scintillator
[HE-3.6-11] 24 p4185 N85-35958
On mini-cluster observed by Chacaltaya emulsion chamber experiment
[HE-3.6-12] 24 p4185 N85-35959
A comparative analysis of gamma and hadron families at the superhigh energies recorded in experiment Pamir
[HE-3.7-1] 24 p4185 N85-35960
A study of gamma-families generated in nucleon-nucleus (NA) and pion-nucleus (pi A) interactions
[HE-3.7-2] 24 p4186 N85-35961
New analysis of nuclear interaction observed by Mt. Kanbara emulsion chamber experiment
[HE-3.7-4] 24 p4186 N85-35963
Intensities of high-energy cosmic rays at Mount Kanbala
[HE-3.7-5] 24 p4186 N85-35964
Structured events in Pamir carbon X-ray chambers
[HE-3.7-7] 24 p4186 N85-35965
Ultra high energy events in ECHOS series and primary energy spectrum
[HE-3.7-9] 24 p4186 N85-35966
Peculiarities of gamma-quanta distribution at 20 TeV energy
[HE-3.7-10] 24 p4186 N85-35967
Nineteenth International Cosmic Ray Conference. HE Sessions, volume 7
[NASA-CP-2378-VOL-7] 24 p4186 N85-35968
Electrons, muons and hadrons in extensive air showers and how do they depend on nuclear interaction model, part 2 24 p4187 N85-35969
Analysis of equi-intensity curves and NU distribution of EAS 24 p4187 N85-35970
Analysis of the hadron component in E.A.S. 24 p4187 N85-35971
Electrons, muons and hadrons in extensive air showers and how do they depend on nuclear interaction model, part 1 24 p4187 N85-35972
Simulation of EAS properties on the basis of high energy interaction model deduced from the accelerator data 24 p4187 N85-35973
New aspects in nucleon-nucleus collisions and EAS properties around 10(8) GeV 24 p4187 N85-35974
Small air showers and collider physics
[HE-4.1-9] 24 p4187 N85-35975
High energy hadrons in extensive air showers 24 p4187 N85-35976
Dependence of the average spatial and energy characteristics of the hadron-lepton cascade on the strong interaction parameters at superhigh energies 24 p4188 N85-35977
Hadronic components of EAS by rigorous saddle point method in the energy range between 10(5) and 10(8) GeV 24 p4188 N85-35978
About increase of the large transvere momentum processes fraction in hA interactions at energies 5.10(14) - 10(16) eV according to the data on E.A.S. hadrons 24 p4188 N85-35979
Phenomenology of soft hadron interactions and the relevant EAS data 24 p4188 N85-35980
The maximum depth of shower with E sub 0 larger than 10(17) eV on average characteristics of EAS different components 24 p4188 N85-35981
Sensitivity of depth of maximum and absorption depth of EAS to hadron production mechanism 24 p4188 N85-35982
A critical analysis of air shower structure functions and size spectrum measurements with the NBU air shower array 24 p4188 N85-35983
Character of energy flow in air shower core 24 p4189 N85-35985
Observation of EAS using a large water tank 24 p4189 N85-35986
The development of air shower in the iron absorber 24 p4189 N85-35987
Application of photodiodes to the detection of electromagnetic bursts 24 p4189 N85-35988
Core structure of EAS in 10(15) to 10(17) eV 24 p4189 N85-35989
Particle distributions in approximately 10(14) 10(16) eV air shower cores at sea level 24 p4189 N85-35990
Theoretical study of EAS hadronic structure 24 p4189 N85-35991
Monte Carlo simulations of electron lateral distributions in the core region of 10(13) - 10(16) eV air showers 24 p4190 N85-35992
Comparison of simulation results with sea-level experimental data on 10(14) - 10(16) air shower cores 24 p4190 N85-35993
Particle distributions in approximately 10(13) - 10(16) eV air shower cores at mountain altitude and comparison with Monte Carlo simulations
[HE-4.2-18] 24 p4190 N85-35994
Takhra-Takaro complex intended for the investigations of EAS spatial characteristics near axis 24 p4190 N85-35995
A new study of shower age distribution in near vertical showers by EAS air shower array 24 p4190 N85-35996
A new study of muons in air showers by NBU air shower array 24 p4190 N85-35997
Lateral distribution of electrons of air showers 24 p4191 N85-35998
Detailed studies of the electron lateral distribution in extensive air showers with energies around 10(16) eV 24 p4191 N85-35999
Study of muons near shower cores at sea level using the E594 neutrino detector 24 p4191 N85-36000
Correlation of high energy muons with primary composition in extensive air shower
[HE-4.3-7] 24 p4191 N85-36001

Measurement of energy muons in EAS at energy region larger thean 10(17) eV
[HE-4.3-8] 24 p4191 N85-36002
Muon fluctuation studies of EAS 10(17) eV
[HE-4.3-9] 24 p4191 N85-36003
Average features of the muon component of EAS or = 10(17) eV
[HE-4.3-10] 24 p4191 N85-36004
Measurement of shower electrons and muons using a small air shower array
[HE-4.3-11] 24 p4192 N85-36005
The longitudinal development of muons in cosmic ray air showers at energies 10(15) - 10(17) eV
[HE-4.3-12] 24 p4192 N85-36006
Topological aspects of age parameter
[HE-4.3-13] 24 p4192 N85-36007
Monte Carlo simulation of EAS generated by 10(14) - 10(16) eV protons
[HE-4.3-14] 24 p4192 N85-36008
Lateral distribution on charged particles in EAS
[HE-4.3-15] 24 p4192 N85-36009
Lateral distribution of high energy muons in EAS of sizes Ne approximately equals 10(5) and Ne approximately equals 10(6)
[HE-4.3-16] 24 p4192 N85-36010
Energy calibration of the fly's eye detector
[HE-4.4-1] 24 p4192 N85-36011
The structure of EAS at E 0.1 EeV
[HE-4.4-2] 24 p4193 N85-36012
Standard value for the radiation length in air
[HE-4.4-4] 24 p4193 N85-36013
Longitudinal trial functions and the cosmic ray energy scale 24 p4193 N85-36014
EAS development curve at energy of 10(16) - 10(18) eV measured by optical Cerenkov light
[HE-4.4-7] 24 p4193 N85-36015
Transition effect of air shower particles in plastic scintillators
[HE-4.4-9] 24 p4193 N85-36017
The system of EAS time analysis
[HE-4.4-10] 24 p4193 N85-36018
On the determination of the depth of EAS development maximum using the lateral distribution of Cerenkov light at distances 150 m from EAS axis
[HE-4.4-13] 24 p4194 N85-36019
Study of the energy spectrum of primary cosmic rays: EAS size fluctuations at a fixed primary energy
[HE-4.4-14] 24 p4194 N85-36020
Study of the shower maximum depth by the method of detection of the EAS Cerenkov light pulse shape
[HE-4.4-15] 24 p4194 N85-36021
Analysis of Cerenkov pulses recorded simultaneously at two sites
[HE-4.4-16] 24 p4194 N85-36022
Preliminary results of the Cerenkov EAS flashes the Crimean Astrophysical Observatory
[HE-4.4-17] 24 p4194 N85-36023
The experimental cascade curves of EAS at E sub 0 10(17) eV obtained by the method of detection of Cherenkov pulse shape
[HE-4.4-18] 24 p4194 N85-36024
Lateral-angular and temporal characteristics of EAS optical radiation
[HE-4.4-19] 24 p4194 N85-36025
The identification of gamma ray induced EAS
[HE-4.5-1] 24 p4195 N85-36026
Muons in gamma showers
[HE-4.5-3] 24 p4195 N85-36027
Muon spectrum in air showers initiated by gamma rays
[HE-4.5-4] 24 p4195 N85-36028
Electromagnetic and muonic structure of showers initiated by gamma-rays and by hadrons
[HE-4.5-6] 24 p4195 N85-36030
The muon content of gamma-ray showers
[HE-4.5-7] 24 p4195 N85-36031
Simulation of gamma-initiated showers
[HE-4.5-10] 24 p4195 N85-36033
Phenomenological characteristic of the electron component in gamma-quanta initiated showers
[HE-4.5-11] 24 p4196 N85-36034
A three-dimensional Monte Carlo calculation of the photon initiated showers and Kiel result
[HE-4.5-13] 24 p4196 N85-36035
Construction of a cosmic ray air shower telescope
[HE-4.5-14] 24 p4196 N85-36036
On the possibilities of large-scale radio and fiber optics detectors in cosmic rays
[HE-4.6-2] 24 p4196 N85-36039
Radio signals from very large showers
[HE-4.6-3] 24 p4196 N85-36040
On the production mechanism of radio-pulses from large extensive air showers
[HE-4.6-4] 24 p4196 N85-36041
A new study on the emission of EM waves from large EAS
[HE-4.6-5] 24 p4197 N85-36042
Air fluorescence detection of large air showers below the horizon
[HE-4.6-6] 24 p4197 N85-36043
A facility for investigation of multiple hadrons at cosmic-ray energies
[HE-4.6-8] 24 p4197 N85-36045
A possible EAS array above the Soudan 2 detector
[HE-4.6-9] 24 p4197 N85-36046
Fast scintillation counter system and performance
[HE-4.6-10] 24 p4197 N85-36047
Performance of a local electron density trigger to select extensive air showers at sea level
[HE-4.6-11] 24 p4198 N85-36048
Microprocessor-based single particle calibration of scintillation counter
[HE-4.6-13] 24 p4198 N85-36049
Samarkand complex setup for investigation of cosmic ray variation in the energy range of 7 10 (9) - 10 (15) eV
[HE-4.6-14] 24 p4198 N85-36050
Radio wave emitted by an extensive air showers in 10KHz to 1MHz region
[HE-4.6-15] 24 p4198 N85-36051
The structure of the shower disk observed at Mt. Norikura
[HE-4.7-1] 24 p4198 N85-36052
Structure of air shower disc near the core
[HE-4.7-2] 24 p4198 N85-36053
Properties of 10 (18)-10 (19)eV EAS at far core distance
[HE-4.7-3] 24 p4198 N85-36054
Longitudinal development of muons in large air showers studies from the arrival time distributions measured at 900m above sea level
[HE-4.7-4] 24 p4199 N85-36055
Arrival time distributions of electrons in air showers with primary energies above 10 (16)eV observed at 900m above sea level
[HE-4.7-5] 24 p4199 N85-36056
The thickness of the shower disc as observed in showers produced by primaries above 10 (19)eV
[HE-4.7-6] 24 p4199 N85-36057
Methods for roof-top mini-arrays
[HE-4.7-7] 24 p4199 N85-36058
Expected rates with mini-arrays for air showers
[HE-4.7-8] 24 p4199 N85-36059
Fast scintillation counter preamplifier for the observation of Linsley effect
[HE-4.7-9] 24 p4199 N85-36060
A mini-array for large air showers
[HE-4.7-10] 24 p4199 N85-36061
A note on some statistical properties of rise time parameters used in muon arrival time measurements
[HE-4.7-12] 24 p4199 N85-36062
Sub-luminal pulses from cosmic ray air showers
[HE-4.7-13] 24 p4200 N85-36063
Thickness of the particle swarm in cosmic ray air showers
[HE-4.7-14] 24 p4200 N85-36064
Study of the time-differentiated particle flux density at various distances from EAS axis
[HE-4.7-15] 24 p4200 N85-36065
Muon and neutrino results from KGF experiment at a depth of 7000 hg/square cm
[HE-5.1-2] 24 p4200 N85-36066
A large area cosmic muon detector located at Ohya stone mine
[HE-5.1-7] 24 p4201 N85-36072
The Nagoya cosmic-ray muon spectrometer 3, part 2: Track detector
[HE-5.2-3] 24 p4202 N85-36081
An upper limit of muon flux of energies above 100 TeV determined from horizontal air showers observed at Akeno
[HE-5.2-12] 24 p4203 N85-36088
Comments on the measurements of multiple muon phenomena
[HE-5.2-13] 24 p4203 N85-36089
Energy spectrum of cascade showers induced by cosmic ray muons in the range from 50 GeV to 5 TeV
[HE-5.2-14] 24 p4203 N85-36090
Measurement of muon intensity by Cerenkov method
[HE-5.2-15] 24 p4204 N85-36091
Photo nuclear energy loss term for muon-nucleus interactions based on xi scaling model of QCD
[HE-5.2-17] 24 p4204 N85-36093
On method of muon spectrum measurements by the scintillation detectors of a large thickness T4t sub o
[HE-5.2-18] 24 p4204 N85-36094
A transient digitiser for fast air shower events
[HE-5.2-21] 24 p4204 N85-36097
A study of atmospheric neutrinos with the IMB detector
[HE-5.3-7] 24 p4205 N85-36101
Atmospheric neutrinos observed in underground detectors
[HE-5.3-8] 24 p4205 N85-36102
Analysis of the electron component of EAS at observational level 700 g x cm(-2) with a scale breaking interaction model and gammaisation hypothesis
[HE-5.4-8] 24 p4208 N85-36119
Calculation of intensity of high energy muon groups observed deep underground
[HE-5.4-13] 24 p4208 N85-36123
A search for heavy long lived particles in high energy cosmic rays
[HE-6.2-7] 24 p4211 N85-36143
Delayed particles in EAS at Akeno
[HE-6.2-8] 24 p4211 N85-36144
Energetic delayed hadrons in large air showers observed at 5200m above sea level
[HE-6.2-9] 24 p4211 N85-36145
Search for long-lived massive particles in extensive air showers
[HE-6.2-10] 24 p4212 N85-36146
High energy cosmic ray signature of quark nuggets
[HE-6.2-11] 24 p4212 N85-36147
Search for tachyons associated with extensive air showers in the ground level cosmic radiation
[HE-6.2-13] 24 p4212 N85-36149
Charge 4/3 leptons in cosmic rays
[HE-6.2-14] 24 p4212 N85-36150
Progress report on a new search for free e/3 quarks in the cores of 10(15) - 10(16) eV air showers
[HE-6.2-15] 24 p4212 N85-36151
Observation of genetic relation among new phenomena Geminion, Chiron and mini-Centauro
[HE-6.2-16] 24 p4212 N85-36152
Tien-Shan effect and charmed particles
[HE-6.2-17] 24 p4212 N85-36153
Search for acoustic signals from high energy cascades
[HE-7.1-1] 24 p4213 N85-36155
Experimental investigation of radiative-acoustic effects in the water by the thermodynamical conditions of Dumand
[HE-7.1-2] 24 p4213 N85-36156
Exploring results of the possibility on detecting cosmic ray particles by acoustic way
[HE-7.1-3] 24 p4213 N85-36157
Acoustic detection of air shower cores
[HE-7.1-4] 24 p4213 N85-36158
Detection threshold energy of high energy cascade showers using thermoluminescence PTFE-sheet and hot-gas reader
[HE-7.1-5] 24 p4213 N85-36159
Application of thermoluminescence for detection of cascade shower 1: Hardware and software of reader system
[HE-7.1-6] 24 p4213 N85-36160
Spatial distribution read-out system for thermoluminescence sheets
[HE-7.1-7] 24 p4213 N85-36161
Application of thermoluminescence for detection of cascade shower 2: Detection of cosmic ray cascade shower at Mount Fuji
[HE-7.1-12] 24 p4214 N85-36162

COSMIC RAYS
NT COSMIC RAY SHOWERS
NT GALACTIC COSMIC RAYS
NT GAMMA RAY BURSTS
NT PRIMARY COSMIC RAYS
NT SECONDARY COSMIC RAYS
NT SOLAR COSMIC RAYS
Cosmic ray effects on microelectronics. Part 3: Propagation of cosmic rays in the atmosphere
[AD-A145026] 01 p0131 N85-10902
Interplanetary cosmic ray intensity: 1972-1984 and out to 32 AU
[AD-A145130] 01 p0131 N85-10903
Cosmic ray propagation in the local superbubble
[NASA-TM-85030] 03 p0449 N85-12855
Supernova envelope shock origin of cosmic rays: A review
[DE84-016479] 04 p0590 N85-13783
New measurements of the spectrum of the cosmic microwave background
[DE84-016055] 05 p0746 N85-14785
Nature of short-period variations of cosmic rays in stratosphere 06 p0823 N85-15224
Diurnal variation harmonics and spatial change in cosmic ray flux 06 p0824 N85-15230
On the record of galactic cosmic ray flux and traffic break-ups in iron meteorites 06 p0887 N85-15634
The low-energy secondary cosmic ray flux: Detectors in iron meteorites 06 p0887 N85-15635
Solar wind and cosmic ray irradiation of grains and ices - application to erosion and synthesis of organic compounds in the solar system 06 p0888 N85-15637

Solar-geophysical data number 478, June 1984. Part 1 (prompt reports): Data for May 1984, Apr. 1984, and late data
[PB84-243153] 06 p0690 N85-15653
The calibration of photographic and spectroscopic films: A densitometric analysis of IIaO film flown aboard the Space Shuttle 3
[NASA-CR-174278] 07 p0962 N85-16101
The galactic gamma-ray distribution: Implications for galactic structure and the radial cosmic ray gradient
[NASA-TM-86173] 07 p1061 N85-16729
A T-matrix theory of galactic heavy-ion fragmentation
[NASA-TP-2363] 08 p1221 N85-17690
Extragalactic cosmic rays from active galaxies
08 p1238 N85-17805
SU(2) x U(1) vacuum and the Centauro events
[NASA-TM-86082] 08 p1260 N85-17926
High energy physics study
[DE84-015803] 09 p1383 N85-18700
Radiation safety of crew and passengers of air transportation in civil aviation. Provisional standards
[NASA-TM-77610] 11 p1692 N85-20638
Charge-to-mass dispersion methods for abrasion-ablation fragmentation models
[NASA-TM-86340] 11 p1726 N85-20857
Cosmic ray generation by plasma turbulence: Development of a new paradigm in physics
12 p1955 N85-22286
Cosmic ray composition and origin
12 p1955 N85-22287
Self-similar modified shock structures — cosmic rays
12 p1956 N85-22290
Solar-geophysical data number 483. November 1984. Part 1: (Prompt reports). Data for October 1984, September 1984 and late data
[PB85-147692] 12 p1962 N85-22335
Research in particles and fields
[NASA-CR-175472] 12 p1963 N85-22337
Correlation of interplanetary medium parameters in transition region of high-velocity solar wind streams
13 p1978 N85-22412
Observation of cosmic ray flux variations in stratosphere 13 p1981 N85-22430
Dielectric detector device for registering heavy cosmic radiation particles 13 p2045 N85-22799
Measurement of the large-scale anisotropy of the cosmic background radiation at 3 MM 13 p2206 N85-23680
A measurement of the intensity of the cosmic background radiation at 3.9 cm
13 p2206 N85-23681
The access of energetic charged particles to satellite altitudes
[AD-A150799] 14 p2373 N85-24670
Cosmic ray environment model for Earth orbit
[NASA-CR-175666] 14 p2455 N85-25165
Pulsations of cosmic ray intensities before increasing flux of relativistic particles from solar flares
15 p2477 N85-25292
Cyclic changes in barometric coefficient of cosmic ray neutron component 15 p2478 N85-25293
Space-time features of solar cosmic ray penetration into high latitude regions of Earth's magnetosphere based on Intercosmos-19 satellite data 15 p2481 N85-25310
Electron flux with electron energies above 40 MeV at altitudes of about 500 km in region where capture is possible and outside it when L is 3 or greater
15 p2481 N85-25315
Professional Committee on Solid Propulsion hold conference 15 p2533 N85-25823
Interstellar Al-26 and excess Mg-26
15 p2680 N85-26551
Identification of the youngest meteorites and a discussion of the possibility that they came from Mars
15 p2681 N85-26559
The propagation of ultraheavy cosmic rays
15 p2685 N85-26582
Measurements of fluxes of high-energy protons and electrons by 2 oppositely oriented spectrometers aboard Cosmos-368 artificial Earth satellite
16 p2722 N85-26800
The fast individualists in the solar system: Cosmic rays 16 p2866 N85-27806
Results from the Helios galactic and solar cosmic ray experiment (E7) 16 p2866 N85-27807
Cosmic ray modulation and turbulent interaction regions near 11 AU
[NASA-TM-86193] 18 p3209 N85-29909
A comparison of the radiation hardness of various VLSI technologies for defense applications
[DE85-006973] 19 p3263 N85-30236
Biostack experiments on STS-flights and the impact for man in space 20 p3510 N85-31821
Contributions to the 19th International Cosmic Ray Conference
[NASA-CR-176049] 20 p3543 N85-32044
Abundances of secondary elements among the ultra heavy cosmic rays: Results from HEAO-3
20 p3543 N85-32047
Lead, platinum, and other heavy elements in the primary cosmic radiation: HEAO-3 results sac wg032961 cb553097 20 p3543 N85-32048
Implications of source abundances of ultraheavy cosmic rays 20 p3543 N85-32049
Interactions of heavy nuclei, Kr, Xe and Ho, in light targets 20 p3544 N85-32050
Solar-geophysical data no. 485, January 1985. Part 1 (prompt reports): Data for December 1984, November 1984 and late data
[PB85-181360] 20 p3548 N85-32079
A Cerenkov-delta E-Cerenkov detector for high energy cosmic ray isotopes and an accelerator study of Ar-40 and Fe-56 fragmentation
[NASA-CR-176028] 20 p3549 N85-32086
Contributions to the 19th International Cosmic Ray Conference
[NASA-CR-176060] 21 p3714 N85-33044
Cosmic ray He3 measurements
[OG-4.2-3] 21 p3714 N85-33045
Initial results from the Caltech/DSRI balloon-borne isotope experiment
[OG-4.3-6] 21 p3714 N85-33046
Measurements of Fe and Ar fragmentation cross sections
[PAPER-OG-7.2-20] 21 p3714 N85-33047
Precision measurements of solar energetic particle elemental composition
[PAPER-SH-2.1-4] 21 p3715 N85-33052
Research in extreme ultraviolet and far ultraviolet astronomy
[NASA-CR-176068] 21 p3716 N85-33060
Research in particles and fields
[NASA-CR-176069] 21 p3724 N85-33103
Effects of space radiation on advanced semiconductor devices. Part 3: Further cosmic ray simulation studies of single event upsets and latch-up in CMOS memories
[AERE-G-3368-PT-3] 22 p3848 N85-33833
Nineteenth International Cosmic Ray Conference. Conference program and author index
[NASA-CP-2376] 22 p3860 N85-33901
Nineteenth International Cosmic Ray Conference. OG sessions, volume 1
[NASA-CP-2376-VOL-1] 22 p3860 N85-33902
Excess gamma-rays in the direction of the rho Ophiuchi cloud: An exotic object?
[OG-2.5-1] 22 p3868 N85-33958
Spectral evolution of gamma-rays from adiabatically expanding sources in dense clouds
[OG-2.5-2] 22 p3869 N85-33959
Search for positron annihilation line and continuum radiation from the Galactic Center
[OG-2.5-5] 22 p3869 N85-33962
Cosmic gamma rays from quasars
[OG-2.7-10] 22 p3872 N85-33983
Ultrahigh energy gamma rays: Carriers of cosmological information
[OG-2.7-14] 22 p3872 N85-33987
Local interstellar medium and gamma-ray astronomy
[OG-3.1-1] 22 p3873 N85-33989
The galactic gamma-ray distribution and the radial cosmic ray gradient
[OG-3.1-4] 22 p3873 N85-33992
Radial distribution of cosmic ray intensity in the galaxy from gamma-ray data
[OG-3.1-5] 22 p3873 N85-33993
Constraints on the galactic distribution of cosmic rays from the COS-B gamma-ray data
[OG-3.1-6] 22 p3873 N85-33994
Relevance of cosmic gamma rays to the mass of gas in the galaxy
[OG-3.1-8] 22 p3874 N85-33996
Excess gamma rays from the Loop I supernova remnant
[OG-3.1-10] 22 p3874 N85-33998
Long term variability of the cosmic ray intensity
[OG-3.1-11] 22 p3874 N85-33999
SMM detection of interstellar Al-26 gamma radiation
[OG-3.2-1] 22 p3874 N85-34001
Galactic distribution of interstellar Al-26
[OG-3.2-3] 22 p3874 N85-34002
Gamma ray line production from cosmic ray spallation reactions 22 p3875 N85-34005
Nineteenth International Cosmic Ray Conference. OG sessions, volume 2
[NASA-CP-2376-VOL-2] 22 p3875 N85-34006
Source spectral index of heavy cosmic ray nuclei
[OG-4.1-2] 22 p3875 N85-34008
Charge and energy dependence of the residence time of cosmic ray nuclei below 15 GeV/nucleon
[OG-4.1-3] 22 p3876 N85-34009
Relative abundances of sub-iron to iron nuclei in low energy (50-250 MeV/N) cosmic rays as observed in the Skylab experiment
[OG-4.1-4] 22 p3876 N85-34010
Cosmic ray charge and energy spectrum measurements using a new large area Cerenkov x dE/dx telescope
[OG-4.1-5] 22 p3876 N85-34011
A measurement of the cosmic ray elements C to Fe in the two energy intervals 0.5-2.0 GeV/n and 20-60 GeV/n
[OG-4.1-6] 22 p3876 N85-34012
Relative abundances of elements (20 or = Z or = 28) at energies up to 70 GeV/amu using relativistic rise in ion chambers
[OG-4.1-7] 22 p3876 N85-34013
Primary cosmic ray spectra in the range 20-60 GeV/n
[OG-4.1-9] 22 p3877 N85-34015
Energy spectrum of cosmic-ray iron nucleus observed with emulsion chamber
[OG-4.1-10] 22 p3877 N85-34016
Measurement of the iron spectrum from 60 to 200 GeV per nucleon
[OG-4.1-11] 22 p3877 N85-34017
Cosmic ray nuclei of energy 50 GeV/NUC
[OG-4.1-12] 22 p3877 N85-34018
Composition and energy spectra of cosmic ray nuclei above 500 GeV/nucleon from the JACEE emulsion chambers
[OG-4.1-13] 22 p3877 N85-34019
Charge composition and energy spectral of cosmic ray primary particles for energies higher than 1 TeV
[OG-4.1-14] 22 p3877 N85-34020
Interstellar propagation and the isotopic composition of hydrogen in the galactic cosmic rays
[OG-4.2-1] 22 p3877 N85-34021
Measurements of galactic hydrogen and helium isotopes from 1978 through 1983
[OG-4.2-2] 22 p3877 N85-34022
Cosmic ray He-3 measurements
[OG-4.2-3] 22 p3878 N85-34023
Parametrized energy spectrum of cosmic-ray protons with kinetic energies down to 1 GeV
[OG-4.2-11] 22 p3878 N85-34025
Galactic propagation models consistent with the cosmic ray lifetime derived from Be-10 measurements
[OG-4.3-1] 22 p3878 N85-34026
Implications of new measurements of O-16 + p + C-12,13, N-14,15 for the abundances of C, N isotopes at the cosmic ray source
[OG-4.3-2] 22 p3878 N85-34027
Cosmic ray isotope measurements with a new Cerenkov X total energy telescope
[OG-4.3-4] 22 p3878 N85-34029
The isotopic composition of cosmic ray calcium
[OG-4.3-5] 22 p3879 N85-34030
A new analysis of cosmic ray isotopes at 3 GeV/n from HEA03-C2 data
[OG-4.3-6] 22 p3879 N85-34031
The energy dependence of the neon-22 excess in the cosmic radiation
[OG-4.3-7] 22 p3879 N85-34032
Initial results from the Caltech/DRSI balloon-borne isotope experiment
[OG-4.3-8] 22 p3879 N85-34033
Ariel 6 measurements of ultra-heavy cosmic ray fluxes in the region 34 or = Z or = 48
[OG-4.4-3] 22 p3879 N85-34036
Ariel 6 measurements of ultra-heavy cosmic ray fluxes in the region Z or = 48
[OG-4.4-4] 22 p3880 N85-34037
Elemental abundances of cosmic rays with Z 33 as measured on HEAO-3
[OG-4.4-5] 22 p3880 N85-34038
Abundances of secondary elements among the ultra heavy cosmic rays: Results from HEAO-3
[OG-4.4-6] 22 p3880 N85-34039
Capabilities of the LDEF-2 heavy nuclei collection
[OG-4.4-8] 22 p3880 N85-34040
Ultraheavy cosmic ray tracks in meteorites: A reappraisal, based on calibrations with relativistic ions
[OG-4.4-10] 22 p3880 N85-34041
Energy spectrum and arrival direction of primary cosmic rays of energy above 10 to the 19th power eV
[OG-5.1-1] 22 p3880 N85-34043
Ultra high energy cosmic ray spectrum
[OG-5.1-2] 22 p3881 N85-34044
The primary cosmic ray spectrum above 10 to the 19th power eV
[OG-5.1-3] 22 p3881 N85-34045
A new measurement of the cosmic ray energy spectrum between 3 x 10 to the 15th power eV and 3 x 10 to the 18th power eV
[OG-5.1-6] 22 p3881 N85-34048
Study of composition of cosmic rays with energy .7 E 3 Ee
[OG-5.1-7] 22 p3881 N85-34049

The muon content of EAS as a function of primary energy
[OG-5.1-8] 22 p3881 N85-34050
EAS fluctuation approach to primary mass composition investigation
[OG-5.2-5] 22 p3883 N85-34062
On galactic origin of cosmic rays with energy up to 10(19) eV
[OG-5.4-15] 22 p3887 N85-34091
Abundance of low energy (50-150 MeV) antiprotons in cosmic rays
[OG-6.1-1] 22 p3887 N85-34092
Search for heavy antinuclei in the cosmic radiation
[OG-6.1-2] 22 p3887 N85-34093
The flux of secondary anti-deuterons and antihelium produced in the interstellar medium
[OG-6.1-5] 22 p3888 N85-34096
Observed antiprotons and energy dependent confinement of cosmic rays: A conflict?
[OG-6.1-7] 22 p3888 N85-34098
Antiparticles in the extragalactic cosmic radiation
[OG-6.1-8] 22 p3888 N85-34099
Galactic cosmic ray antiprotons and supersymmetry
[OG-6.1-9] 22 p3888 N85-34100
Galactic antiprotons of 0.2-2 GeV energy
[OG-6.1-11] 22 p3888 N85-34101
Evidence for a dynamical halo around the edge-on galaxy NGC 4631
[OG-6.2-1] 22 p3889 N85-34102
Halo of NGC 4631 and models of cosmic-ray transport
[OG-6.2-3] 22 p3889 N85-34103
Observation of cosmic ray positrons from 5 to 25 GeV
[OG-6.2-5] 22 p3889 N85-34104
An observation of cosmic ray positrons from 10-20 GeV
[OG-6.2-6] 22 p3889 N85-34105
Electrons and positrons from expanding supernova envelopes in dense clouds
[OG-6.2-9] 22 p3889 N85-34108
The electron spectra in the synchrotron nebula of the supernova remnant G 29.7-0.3
[OG-6.2-10] 22 p3889 N85-34109
Relativistic electron in curved magnetic fields
[OG-6.2-11] 22 p3890 N85-34110
Transient two-dimensional simulation of SEU in a CMOS SRAM cell
[DE85-008419] 22 p3890 N85-34111
Effect of seeds of heavy charged particles of galactic cosmic radiation 23 p3954 N85-34505
Nineteenth International Cosmic Ray Conference. SH sessions, volume 4
[NASA-CP-2376-VOL-4] 23 p3969 N85-34729
Acceleration of ions and electrons to near-cosmic ray energies in a perpendicular shock: The January 6, 1978 event
[SH-1.5-4] 23 p3996 N85-34773
Cosmic ray acceleration by stellar wind. Simulation for heliosphere
[SH-1.5-17] 23 p3997 N85-34780
The energy spectrum of Jovian electrons in interplanetary space
[SH-1.5-18] 23 p3997 N85-34781
Observation of the fluxes of nuclei with energies 10-20 MEV per nucleon during the solar flare of April 26, 1984
[SH-2.1-1] 23 p3998 N85-34783
On the retention of high-energy protons and nuclei with charges Z or equal to 2 in large solar flares after the process of their acceleration
[SH-2.1-8] 23 p3998 N85-34789
Type 3 solar radio bursts and 3HE-rich events
[SH-2.2-3] 23 p4000 N85-34798
Numerical descriptions of cosmic-ray transport
[SH-4.1-3] 23 p4004 N85-34829
Numerical and analytic descriptions of cosmic-ray transport
[SH-4.1-4] 23 p4005 N85-34830
the role of shock waves in modulation of galactic cosmic rays
[SH-4.1-7] 23 p4005 N85-34831
The intensity recovery of Forbush-type decreases as a function of heliocentric distance and its relationship to the 11-year variation
[SH-4.1-9] 23 p4005 N85-34832
Cumulative effect of Forbush decreases in the heliospheric modulation during the present solar cycle
[SH-4.1-10] 23 p4005 N85-34833
Cosmic ray modulatin and merged interaction regions
[SH-4.1-11] 23 p4005 N85-34834
Longitudinal distribuion of cosmic rays in the heliosphere
[SH-4.1-14] 23 p4006 N85-34837
The 1973-1984 solar modulation of cosmic ray nuclei
[SH-4.1-16] 23 p4006 N85-34838
Cosmic ray modulation in a random anisotropic magnetic field
[SH-4.1-20] 23 p4006 N85-34839
Evidence for regions of negligible cosmic-ray modulation in the inner heliosphere (10 AU)
[SH-4.1-21] 23 p4006 N85-34840
Notes on drift theory
[SH-4.2-3] 23 p4006 N85-34841
Drift and observations in cosmic-ray modulation, 1
[SH-4.2-4] 23 p4007 N85-34842
Drift and observations in cosmic-ray modulation, 2
[SH-4.2-5] 23 p4007 N85-34843
Cosmic ray north-south anisotropy 1961 - 1983
[SH-4.2-6] 23 p4007 N85-34844
Nineteenth International Cosmic Ray Conference. OG sessions, volume 3
[NASA-CP-2376-VOL-3] 23 p4012 N85-34862
Germanium and lead: Significant differences between meteoritic and photospheric abundances?
[OG-7.1-2] 23 p4012 N85-34864
Lead and uranium group abundances in cosmic rays
[OG-7.1-3] 23 p4013 N85-34865
Implications of source abundances of ultraheavy cosmic rays
[OG-7.1-4] 23 p4013 N85-34866
Propagation and nucleosynthesis of ultraheavy cosmic rays
[OG-7.1-5] 23 p4013 N85-34867
Sources of the ultraheavy cosmic rays
[OG-7.1-7] 23 p4013 N85-34868
The cosmic ray composition as viewed from the chemical abundances of the solar system
[OG-7.1-8] 23 p4013 N85-34869
Elemental technetium as a cosmic-ray clock
[OG-7.1-9] 23 p4013 N85-34870
Electron capture decay of cosmic rays: A model of the inhomogeneous interstellar medium
[OG-7.1-10] 23 p4014 N85-34871
The model-independence of cosmic ray source determinations
[OG-7.2-1] 23 p4014 N85-34873
Interstellar turbulence, random density variations, and scintillation measurements
[OG-7.2-13] 23 p4015 N85-34880
Diffusion of strongly magnetized cosmic ray particles in a turbulent medium
[OG-7.2-16] 23 p4015 N85-34883
Cosmic-ray transport in the galactic magnetosphere
[OG-7.2-17] 23 p4016 N85-34884
The role of cosmic rays and Alfven waves in the structure of the galactic halo
[OG-7.2-18] 23 p4016 N85-34885
Measurements of Fe and Ar fragmentation cross sections
[OG-7.2-20] 23 p4016 N85-34887
Interactions of heavy nuclei, Kr, Xe and Ho, in light targets
[OG-7.2-21] 23 p4016 N85-34888
The cosmic-ray shock structure problem for relativistic shocks
[OG-8.1-1] 23 p4017 N85-34891
Instabilities in decelerating supersonic flows with applications to cosmic ray shocks
[OG-8.1-2] 23 p4017 N85-34892
Time-dependent nonlinear cosmic ray shocks confirming abstract
[OG-8.1-3] 23 p4017 N85-34893
A cosmic ray driven instability
[OG-8.1-5] 23 p4018 N85-34895
Relativistic cosmic ray spectra in the full non-linear theory of shock acceleration
[OG-8.1-6] 23 p4018 N85-34896
Acceleration of cosmic rays in supernova-remnants
[OG-8.1-9] 23 p4018 N85-34899
Onion-shell model for cosmic ray electrons and radio synchrotron emission in supernova remnants
[OG-8.1-10] 23 p4018 N85-34900
Approximate supernova remnant dynamics with cosmic ray production
[OG-8.1-12] 23 p4019 N85-34901
A numerical study of diffusive shock acceleration of cosmic rays in supernova shocks
[OG-8.2-2] 23 p4019 N85-34903
Scaling from Jupiter to pulsars and the acceleration of cosmic ray particles by pulsars, 3
[OG-8.2-3] 23 p4019 N85-34904
Do supernovae of type 1 paly a role in cosmic-ray production?
[OG-8.2-5] 23 p4019 N85-34905
Neutron-rich nuclei in cosmic rays and Wolf-Rayet stars
[OG-8.2-6] 23 p4019 N85-34906
Interstellar (Na-22) as a possible source of the excess (Ne-22) in the galactic cosmic ray
[OG-8.2-12] 23 p4020 N85-34908
The electromagnetic ram action of the plasma focus as a paradigm for the generation of cosmic rays and the gigantic jets in active galaxies
[OG-8.2-14] 23 p4020 N85-34910
The origins of cosmic rays and quantum effects on gravity
[OG-8.2-15] 23 p4020 N85-34911
Evaluation of parameters for particles acceleration by the zero-point field of quantum electrodynamics
[OG-8.2-16] 23 p4020 N85-34912
Giant molecular clouds as regions of particle acceleration 23 p4020 N85-34913
The nucleosynthesis of deterium and helium-3
[OG-8.2-18] 23 p4020 N85-34914
Pulsars as cosmic ray particle accelerators: Proton orbits
[OG-8.2-21] 23 p4021 N85-34917
Pulsars as cosmic ray accelerators: Energy development of protons
[OG-8.2-22] 23 p4021 N85-34918
Pulsars as cosmic ray particle accelerators: Dynamics of electrons
[OG-8.2-23] 23 p4021 N85-34919
Propagation of injected cosmic rays under distributed reacceleration
[OG-8.3-3] 23 p4021 N85-34922
Propagation of cosmic rays and new evidence for distributed acceleration
[OG-8.3-5] 23 p4022 N85-34924
Exact solutions for sporadic acceleration of cosmic rays
[OG-8.3-7] 23 p4022 N85-34925
Relativistic transport theory for cosmic-rays
[OG-8.3-8] 23 p4022 N85-34926
The design of an experiment to detect low energy antiprotons
[OG-9.1-1] 23 p4022 N85-34928
An experiment to measure the energy spectrum of cosmic ray antiprotons from 100 to 1000 MeV
[OG-9.1-3] 23 p4022 N85-34929
High resolution Cherenkov detectors for cosmic ray isotope experiment
[OG-9.1-4] 23 p4023 N85-34930
A high resolution gas Cerenkov detector for the superconducting magnet facility
[OG-9.1-6] 23 p4023 N85-34932
Bevalac calibration of the SOFIE range and hodoscope detectors
[OG-9.1-7] 23 p4023 N85-34933
The development of a high energy cosmic ray detector for Spacelab-2
[OG-9.1-8] 23 p4023 N85-34934
Mass resolution optimization in a large isotopic composition experiment
[OG-9.1-9] 23 p4023 N85-34935
The heavy ions in space experiment
[OG-9.1-10] 23 p4023 N85-34936
Cherenkov-dE/dx-range measurements on cosmic ray iron group nuclei
[OG-9.1-12] 23 p4024 N85-34937
The response of ionization chambers to relativistic heavy nuclei
[OG-9.1-13] 23 p4024 N85-34939
A balloon-borne imaging gamma-ray telescope
[OG-9.2-2] 23 p4024 N85-34941
A coded aperture imaging system optimized for hard X-ray and gamma ray astronomy
[OG-9.2-3] 23 p4024 N85-34942
The final COS-B database: In-flight calibration of instrumental parameters
[OG-9.3-9] 23 p4028 N85-34964
Nineteenth International Cosmic Ray Conference. SH sessions, volume 5
[NASA-CP-2376-VOL-5] 23 p4031 N85-34991
Isotropic intensity waves and features of their occurrence
[SH-4.3-8] 23 p4032 N85-34993
Cosmic ray sidereal diurnal variation of galactic origin observed by neutron monitors
[SH-4.4-2] 23 p4033 N85-35000
Sidereal anisotropies in the median rigidity range 60-600GV in 1978-1983
[SH-4.4-3] 23 p4033 N85-35001
Sidereal variations deep underground in Tasmania
[SH-4.4-4] 23 p4033 N85-35002
The effect of the interplanetary magnetic field on sidereal variations observed at medium depth underground detectors
[SH-4.4-5] 23 p4033 N85-35003
Corrected sidereal anisotropy for underground moons
[SH-4.4-7] 23 p4033 N85-35005
A study of periodicities and recurrences in solar activity and cosmic ray modulation
[SH-4.4-14] 23 p4034 N85-35010
Cosmic ray biannual variation
[SH-4.4-15] 23 p4034 N85-35011
Cosmic ray power spectral variations. 3: Solar rotation periodicities
[SH-4.4-16] 23 p4034 N85-35012

Variations of the cosmic ray general component in Antarctica
[SH-4.4-17] 23 p4035 N85-35013

The difference in the energy spectra of galactic cosmic rays at the minima of the 19th and 20th solar activity cycles
[SH-4.4-18] 23 p4035 N85-35014

Cosmic ray variations with the period close to 27 days and their connection with solar activity longitudinal distribution
[SH-4.4-19] 23 p4035 N85-35015

Long-term modulation of galactic cosmic rays in high-energy region
[SH-4.4-22] 23 p4035 N85-35018

The first three harmonics of solar daily variation caused by the diffusive propagation of galactic cosmic rays through the heliosphere
[SH-4.5-1] 23 p4035 N85-35019

Formulation of cosmic-ray solar daily variation and its seasonal variation, produced from generalized stationary anisotropy of solar origin
[SH-4.5-2] 23 p4036 N85-35020

Diurnal effect in cosmic rays at middle latitudes according to stratospheric measurements
[SH-4.5-8] 23 p4036 N85-35026

Comparative study of the phase of diurnal anisotropy on quiet and disturbed days on a long term basis up to recent period
[SH-4.5-9] 23 p4037 N85-35027

Study of spectral exponent on quiet and disturbed days
[SH-4.5-10] 23 p4037 N85-35028

Diurnal variation of galactic cosmic ray intensity on quiet days
[SH-4.5-11] 23 p4037 N85-35029

Diurnal variations from muon data at Takeyama underground station
[SH-4.5-13] 23 p4037 N85-35030

Long term changes in cosmic ray diurnal variations observed by ion chambers in Hong Kong and Japan
[SH-4.5-14] 23 p4037 N85-35031

The modulation features of the long-period cosmic ray variations in connection with the sign change of the general magnetic field of the Sun
[SH-4.5-15] 23 p4037 N85-35032

The cosmic ray differential diurnal variation dependences on the zenith angle and the geomagnetic disturbance
[SH-4.5-16] 23 p4038 N85-35033

Cosmic ray density gradient and its dependence on the north-south asymmetry in solar activity
[SH-4.5-17] 23 p4038 N85-35034

Anomalous increase of solar anisotropy above 150GV in 1981-1983
[SH-4.5-18] 23 p4038 N85-35035

Diagnostic of electromagnetic conditions in space using cosmic rays
[SH-4.5-19] 23 p4038 N85-35036

Change of cosmic ray anisotropy with solar activity
[SH-4.5-20] 23 p4038 N85-35037

Magnetic fluctuation and cosmic ray diurnal variations
[SH-4.5-21] 23 p4038 N85-35038

Changes in the energy spectrum of anomalous oxygen and helium during 1977-1985
[SH-4.6-1] 23 p4039 N85-35039

Solar cycle variations of the anaomalous cosmic ray component
[SH-4.6-2] 23 p4039 N85-35040

Radial and latitudinal gradients of anomalous oxygen during 1977 - 1985
[SH-4.6-4] 23 p4039 N85-35042

Observation of pick-up ions in the solar wind: Evidence for the source of the anomalous cosmic ray component?
[SH-4.6-5] 23 p4039 N85-35043

On the anomalous component
[SH-4.6-6] 23 p4039 N85-35044

Possible origin of the anomalous component of cosmic rays
[SH-4.6-7] 23 p4039 N85-35045

The cosmic ray interplanetary radial gradient from 1972 - 1985
[SH-4.7-1] 23 p4040 N85-35046

The large scale dynamics of the outer heliosphere and the long-term modulation of galactic cosmic rays
[SH-4.7-3] 23 p4040 N85-35048

Solar modulation and interplanetary gradients of the galactic electrons flux, 1977 - 1984
[SH-4.7-4] 23 p4040 N85-35049

Galactic cosmic ray radial gradients and the anomalous He component near maximum solar modulation and to radii beyond 34 AU from the Sun
[SH-4.7-5] 23 p4040 N85-35050

Voyager 1 and 2 measurements of radial and latitudinal cosmic ray gradients during 1981 - 1984
[SH-4.7-6] 23 p4041 N85-35051

The recovery of the cosmic ray flux from maximum solar modulation at IMP-8 (1 AU) and at Pioneer (R 30 AU)
[SH-4.7-7] 23 p4041 N85-35052

The large-scale modulation of cosmic rays in mid-1982: Its dependence on heliospheric longitude and radius
[SH-4.7-9] 23 p4041 N85-35053

Nonstationary modulation of galactic cosmic rays in a nonlinear model
[SH-4.7-10] 23 p4041 N85-35054

Dimensions of the solar wind cavity and of the region of interplanetary cosmic ray modulation
[SH-4.7-11] 23 p4041 N85-35055

Drift and Forbush decreases
[SH-5.1-2] 23 p4041 N85-35056

Anomalous short-term increase in the galactic cosmic ray intensity: Are they related to the interplanetary magnetic cloud-like structures?
[SH-5.1-3] 23 p4041 N85-35057

The flare origin of Forbush decreases not associated with solar flares on the visible hemisphere of the Sun
[SH-5.1-4] 23 p4041 N85-35058

Longitudinal dependence of the interplanetary perturbation produced by energetic type 4 solar flares and of the associated cosmic ray modulation
[SH-5.1-5] 23 p4042 N85-35059

Rigidity spectrum of Forbush decrease
[SH-5.1-6] 23 p4042 N85-35060

Spectral analysis of the Forbush decrease of 13 July 1982
[SH-5.1-7] 23 p4042 N85-35061

Transient cosmic ray increase associated with a geomagnetic storm
[SH-5.1-8] 23 p4042 N85-35062

Galactic cosmic ray currents and magnetic field irregularity degree in high-speed solar wind streams
[SH-5.1-9] 23 p4042 N85-35063

Study of dominating parameters of high speed solar plasma streams in relation to cosmic ray and geomagnetic storms
[SH-5.1-11] 23 p4042 N85-35064

Influence of magnetic clouds on cosmic ray intensity variations
[SH-5.1-12] 23 p4042 N85-35065

The solar wind effect on cosmic rays and solar activity
[SH-5.1-13] 23 p4043 N85-35066

A relation between the short time variations of cosmic rays and geomagnetic field change
[SH-5.1-14] 23 p4043 N85-35067

Anomalous low level of cosmic ray intensity decreases observed during 1980
[SH-5.1-15] 23 p4043 N85-35068

Observations of cosmic-ray modulations in the fall, 1984
[SH-5.1-16] 23 p4043 N85-35069

Study of cosmic ray scintillations from 5-minute data of the scintillations telescope Izmiran and world-wide network stations
[SH-5.1-18] 23 p4043 N85-35071

The theoretical and experimental investigation of cosmic ray Forbush-effects
[SH-5.1-20] 23 p4044 N85-35072

Peculiarities of Galactic Cosmic Ray (GCR) anisotropy variation in connection with the recurrent and sporadic Forbush effects
[SH-5.1-21] 23 p4044 N85-35073

Cosmic ray modulation by high-speed solar wind fluxes
[SH-5.1-22] 23 p4044 N85-35074

Solar activity beyond the disk and variations of the cosmic ray gradient
[SH-5.1-23] 23 p4044 N85-35075

Coupling functions for lead and lead-free neutron monitors from the latitudinal measurements performed in 1982 in the research station Academician Kurchatov
[SH-6.1-1] 23 p4044 N85-35076

On the solar cycle variation in the barometer coefficients of high latitude neutron monitors
[SH-6.1-2] 23 p4044 N85-35077

Altitude variations of cosmic-ray soft and hard components observed by airborne detectors
[SH-6.1-5] 23 p4045 N85-35079

Additional flux of particles and albedo-electrons in upper atmosphere
[SH-6.1-6] 23 p4045 N85-35080

Observation of energy spectrum of electron albedo in low latitude region at Hyderabad, India
[SH-6.1-7] 23 p4045 N85-35081

Proton albedo spectrum observation in low latitude region at Hyderabad, India
[SH-6.1-8] 23 p4045 N85-35082

The influence of quiet asymmetric magnetosphere on the cutoff rigidities of the main cone
[SH-6.1-10] 23 p4045 N85-35083

Re-evaluation of cosmic ray cutoff terminology
[SH-6.1-11] 23 p4045 N85-35084

The use of the McIlwain L-parameter to estimate cosmic ray vertical cutoff rigidities for different epochs of the geomagnetic field
[SH-6.1-12] 23 p4045 N85-35085

Estimating the change in asymptotic direction due to secular changes in the geomagnetic field
[SH-6.1-13] 23 p4045 N85-35086

Short perturbations of cosmic ray intensity and electric field in atmosphere
[SH-6.1-18] 23 p4046 N85-35090

Long-period cosmic ray variations and their altitude dependence
[SH-6.1-19] 23 p4046 N85-35091

Diurnal variations of cosmic ray geomagnetic cut-off threshold rigidities
[SH-6.1-21] 23 p4046 N85-35092

The influence of the Earth's magnetosphere on the high-energy solar protons
[SH-6.1-22] 23 p4046 N85-35093

Cosmic rays 10Be biennal data and their relationship to aurorae and sunspots
[SH-7.1-1] 23 p4047 N85-35094

Solar modulation of cosmic ray intensity and solar flare events inferred from (14)C contents in dated tree rings
[SH-7.1-2] 23 p4047 N85-35095

Cosmic ray secular variations in terrestrial records and aurorae
[SH-7.1-3] 23 p4047 N85-35096

When did the average cosmic ray flux increase?
[SH-7.1-4] 23 p4047 N85-35097

Cosmic-ray exposure records and origins of meteorites
[SH-7.1-7] 23 p4047 N85-35099

Accelerator experiments on the contribution of secondary particles to the production of cosmogenic nuclides in meteorites
[SH-7.1-8] 23 p4048 N85-35100

Depth and size effects on cosmogenic nuclide production in meteorites
[SH-7.1-9] 23 p4048 N85-35101

Spallogenic origin of nuclei in meteorites
[SH-7.1-10] 23 p4048 N85-35102

Clusters and cycles in the cosmic ray age distributions of meteorites
[SH-7.1-11] 23 p4048 N85-35103

High precise measurements of cosmogenic radiocarbon abundance by complex of scintillation equipments
[SH-7.1-14] 23 p4048 N85-35105

Radiocarbon content in the annual tree rings during last 150 years and time variation of cosmic rays
[SH-7.1-15] 23 p4048 N85-35106

Cosmogenic Mn-53 in meteorites
[SH-7.1-17] 23 p4049 N85-35107

Solar neutrinos, solar flares, solar activity cycle and the proton decay
[SH-8.1-8] 23 p4049 N85-35113

Neutrino production from the solar atmosphere
[SH-8.1-9] 23 p4050 N85-35114

Three dimensional calculation of flux of low energy atmospheric neutrinos
[SH-8.1-11] 23 p4050 N85-35116

Detector calibration of the Indian cosmic ray experiment (ICONS) in Space-Shuttle Spacelab-13
[SH-9.1-2] 23 p4050 N85-35117

Biophysical research in space — radiation effects
24 p4130 N85-35603

Gamma-ray production cross sections for alpha-particle induced reactions on F-19 and Na-23
[DE85-012603] 24 p4150 N85-35732

Nineteenth International Cosmic Ray Conference. HE Sessions, volume 6
[NASA-CP-2376-VOL-6] 24 p4170 N85-35848

Measurement of interaction cross section of cosmic ray Fe nuclei (E4 GeV/N) with Al target
[HE-1.1-7] 24 p4170 N85-35855

QCD-motivated description of very high energy particle interactions
[HE-1.2-2] 24 p4171 N85-35861

Nucleon-nucleus interactions from JACEE
24 p4173 N85-35869

General consequences of the violated Feynman scaling 24 p4173 N85-35872

Propagation of cosmic rays through the atmosphere in the quark-gluon strings model 24 p4173 N85-35873

Determination of primary energy in nucleus-nucleus collisions and the high P(sub)T tail of alpha-particles
24 p4173 N85-35875

SU(2) x U(1) vacuum and the Centauro events
24 p4175 N85-35885

Ringlike inelastic events in cosmic rays and accelerators 24 p4175 N85-35887

Heavy nucleus collisions between 20 and 60 GeV/nucleon
[HE-1.4-2] 24 p4175 N85-35890

Characteristics of central collision events in Fe-nucleus interactions for 20 - 60 GeV/nucleon
[HE-1.4-3] 24 p4176 N85-35891
Nucleus-nucleus interaction above several hundred GeV/n
[HE-1.4-4] 24 p4176 N85-35892
Excessive production of electron pairs by soft photons in low multiplicity ion interactions
[HE-1.4-6] 24 p4176 N85-35894
Forward particle production in inelastic Ne-22 inteVractions in emulsion at 4.1 A Ge/c
[HE-1.4-7] 24 p4176 N85-35895
On the mechanism of anomalous nucleus-nucleus interactions at energies above 1 TeV/nucleon
[HE-1.4-8] 24 p4177 N85-35896
Meson multiplicity in nucleus-nucleus collisions above 4 GeV/amu
[HE-1.4-10] 24 p4177 N85-35897
Inclusive angular distribution of alpha and Li fragments produced in the Fe-C and Fe-Pb collisions at 1.88 GeV/u
[HE-1.4-11] 24 p4177 N85-35898
The effect of the relative nuclear size on the nucleus-nucleus interactions
[HE-1.4-13] 24 p4177 N85-35900
Intensities of high-energy cosmic rays at Mount Kanbala
[HE-3.1-2] 24 p4177 N85-35902
On the characteristics of emulsion chamber family events produced in low heights
[HE-3.1-6] 24 p4178 N85-35904
Hadron intensity and energy spectrum at 4380 m above level
[HE-3.1-7] 24 p4178 N85-35905
The nucleon intensity in the atmosphere and the Pt distribution
[HE-3.1-9] 24 p4178 N85-35907
Connection between variations of the atmosphere temperature profile and variations of the meson component intensity
[HE-3.1-12] 24 p4178 N85-35910
Search for anomalous C-jets in Chacaltaya emulsion chamber experiment
[HE-3.2-5] 24 p4179 N85-35913
Scaling violation in hadron-nucleus interaction
[HE-3.2-8] 24 p4179 N85-35916
Few-particles generation channels in inelastic hadron-nuclear interactions at energy approximately equals 400 GeV
[HE-3.2-9] 24 p4179 N85-35917
A cosmic ray super high multicore family event. 1: Experiment and general features
[HE-3.4-1] 24 p4181 N85-35930
A cosmic ray super high energy multicore family event. 2: Structure and fragmentation characteristics of the jets
[HE-3.4-2] 24 p4181 N85-35931
Observation of super high energy big family with large scale Fe emulsion chambers
[HE-3.4-3] 24 p4182 N85-35932
A halo event created at 200 m above the Chacaltaya emulsion chamber
[HE-3.4-5] 24 p4182 N85-35933
A binocular-type atmospheric interaction generating sequential exotic features
[HE-3.4-6] 24 p4182 N85-35934
Gamma-hadron families and scaling violation
[HE-3.4-7] 24 p4182 N85-35935
Super-family P2 C-96-125 observed by Japan-URSS Joint Emulsion Chamber Experiment
[HE-3.4-8] 24 p4182 N85-35936
On the halo events observed by Mount Fuji and Mount Kanbala Emulsion Chamber Experiments
[HE-3.4-9] 24 p4182 N85-35937
Experiment Pamir-2. Fianit: A giant super-family with halo (Epsilon sub 0 at approximately 10(17) eV)
[HE-3.4-10] 24 p4182 N85-35938
Experiment Pamir-4: Analysis of superfamily with halo of electromagnetic nature detected in deep XEC
[HE-3.4-11] 24 p4183 N85-35939
Particle interactions at energies over 1000 TeV inferred from gamma-families observed at Mount Fuji
[HE-3.5-1] 24 p4183 N85-35940
A search for mini-clusters in Japan-USSR Joint Experiment at Pamir
[HE-3.5-2] 24 p4183 N85-35941
Mini-clusters
[HE-3.5-3] 24 p4183 N85-35942
Giant mini-clusters as possible origin of halo phenomena observed in super-families
[HE-3.5-4] 24 p4183 N85-35943
Structure of super-families
[HE-3.5-7] 24 p4183 N85-35944
Extremely high energy hadron and gamma-ray families(3). Core structure of the halo of superfamily
[HE-3.5-8] 24 p4183 N85-35945
Numerical analysis of electromagnetic cascades in emulsion chambers
[HE-3.5-9] 24 p4184 N85-35946
An experimental study of correlations in the development of the electron-photon cascades
[HE-3.5-10] 24 p4184 N85-35947
The electromagnetic component of albedo from superhigh energy cascades in dense media
[HE-3.5-11] 24 p4184 N85-35948
Integral functions of electron lateral distribution and their fluctuations in electron-photon cascades
[HE-3.5-12] 24 p4184 N85-35949
Nineteenth International Cosmic Ray Conference. HE Sessions, volume 7
[NASA-CP-2376-VOL-7] 24 p4186 N85-35968
Measurement of the local density spectrum
24 p4189 N85-35984
An underground cosmic ray muon telescope for observation of cosmic ray anisotropy
24 p4196 N85-36037
Investigation of cosmic rays in very short time scales
[HE-4.6-7] 24 p4197 N85-36044
Nineteenth International Cosmic Ray Conference. HE sessions, volume 8
[NASA-CP-2376-VOL-8] 24 p4200 N85-36066
Preliminary results on underground muon bundles observed in the Frejus proton-decay detector
[HE-5.1-1] 24 p4200 N85-36067
The spectrum of cosmic ray muons obtained with 100-ton scintillation detector underground and the analysis of recent experimental data
[HE-5.1-6] 24 p4201 N85-36071
A new world survey expression for cosmic ray vertical intensity vs. depth in standard rock
[HE-5.1-10] 24 p4201 N85-36073
On muon energy spectrum in muon groups underground
[HE-5.1-14] 24 p4201 N85-36076
Energy spectrum of cascades generated by muons in Baksan underground scintillation telescope
[HE-5.1-15] 24 p4202 N85-36077
Underwater measurements of muon intensity
[HE-5.1-16] 24 p4202 N85-36078
The Nagoya cosmic-ray muon spectrometer 3, part 1: Preliminary observations
[HE-5.2-2] 24 p4202 N85-36080
The Nagoya cosmic-ray muon spectrometer 3, part 3: Automatic film scanning equipment
[HE-5.2-4] 24 p4202 N85-36082
The Nagoya cosmic-ray muon spectrometer 3, part 4: Track reconstruction method
[HE-5.2-5] 24 p4202 N85-36083
Background light measurements at the DUMAND site
[HE-5.2-7] 24 p4203 N85-36084
Measurements of light background at large depth in the ocean
[HE-5.2-8] 24 p4203 N85-36085
Hybrid TLC-pair meter for the Sphinx Project
[HE-5.2-10] 24 p4203 N85-36086
Proportional drift tubes for large area muon detectors
[HE-5.2-11] 24 p4203 N85-36087
Analytical calculation of muon intensities under deep sea-water
[HE-5.2-16] 24 p4204 N85-36092
The spectrum of neutrons at 60 hg m(-2)
[HE-5.2-20] 24 p4204 N85-36096
Limits on deeply penetrating particles in the 10(17) eV cosmic ray flux
[HE-5.3-1] 24 p4205 N85-36098
Results of low energy background measurements with the Liquid Scintillation Detector (LSD) of the Mont Blanc Laboratory
[HE-5.3-5] 24 p4205 N85-36099
Geophysical searches for three-neutrino oscillations
[HE-5.3-9] 24 p4205 N85-36103
Measurement of neutrino oscillations in MACRO experiment
[HE-5.3-10] 24 p4206 N85-36104
Energy spectra of high energy atmospheric neutrinos
[HE-5.3-14] 24 p4206 N85-36108
A search for cosmic sources of high energy neutrinos with small underground detectors
[HE-5.3-16] 24 p4206 N85-36110
Neutrino astronomy and the atmospheric background
[HE-5.3-17] 24 p4207 N85-36111
High-energy neutrinos from a lunar observatory
[HE-5.3-21] 24 p4207 N85-36112
Angular distribution of muons produced by cosmic ray neutrinos in rock
[HE-5.3-24] 24 p4207 N85-36115
Underground measurements on secondary cosmic rays
[HE-5.4-1] 24 p4207 N85-36116
Atmospheric muons and neutrinos, and the neutrino-induced muon flux underground
[HE-5.4-7] 24 p4207 N85-36118
Anomalies in cosmic rays: New particles versus charm?
[HE-5.4-9] 24 p4208 N85-36120
Results of investigation of muon fluxes of superhigh energy cosmic rays with X-ray emulsion chambers
[HE-5.4-16] 24 p4208 N85-36126
Search for magnetic monopoles using proportional counters filled with helium gas
[HE-6.1-1] 24 p4209 N85-36127
Magnetic monopole search by 130 m(2)sr He gas proportional counter
[HE-6.1-2] 24 p4209 N85-36128
Results of a search for monopoles and tachyons in horizontal cosmic ray flux
[HE-6.1-3] 24 p4209 N85-36129
Monopole, astrophysics and cosmic ray observatory at Gran Sasso
[HE-6.1-4] 24 p4209 N85-36130

COSMIC X RAYS
The HEAO-1 diffuse component spectrum from 15 to above 500 keV --- X and gamma rays
08 p1240 N85-17820
The origin of the X-ray background
08 p1243 N85-17841
X-ray emission from Centaurus A
[DE85-002030] 09 p1417 N85-18943
High resolution hard X-ray spectra of solar and cosmic sources 14 p2455 N85-25163
Long-term observations of Cyg X-3 with Vela 5B
[DE85-005556] 15 p2686 N85-26586
Observation of the Crab nebula in the hard X-ray
[MPE-186] 17 p3053 N85-28897
Cosmic X-ray physics
[NASA-CR-175908] 17 p3055 N85-28910
Atmospheric X-rays at 11 deg S geomagnetic latitude
[INPE-3539-PRE/755] 19 p3386 N85-31004
Balloon observations of hard X-rays from NGC 4151 and an X-ray transient source
[OG-2.7-6] 22 p3871 N85-33979
CEN A observation at MeV-energies
[OG-2.7-7] 22 p3871 N85-33980

COSMOCHEMISTRY
High pressure cosmochemistry applied to major planetary interiors: Experimental studies
[NASA-CR-174032] 02 p0302 N85-11958
Decaying particles do not heat up the Universe
[DE85-002191] 11 p1763 N85-21091
Implications of convection in the Moon and the terrestrial planets 13 p2183 N85-23548
High pressure cosmochemistry of major planetary interiors: Laboratory studies of the water-rich region of the system ammonia-water 13 p2183 N85-23549
High pressure cosmochemistry applied to major planetary interiors: Experimental studies
[NASA-CR-175715] 15 p2679 N85-26544
The cosmic ray composition as viewed from the chemical abundances of the solar system
[OG-7.1-8] 23 p4013 N85-34869

COSMOGONY
U COSMOLOGY

COSMOLOGY
NT BIG BANG COSMOLOGY
NT HUBBLE DIAGRAM
The origin and evolution of Uranus and Neptune
02 p0296 N85-11926
Future theoretical needs in studies of star formation
03 p0444 N85-12829
Space research and the new approach to the mechanics of fluid media in cosmos
[TRITA-EPP-84-04] 03 p0447 N85-12844
Toward unification of elementary particle physics and cosmology in 10-dimensions
[DE84-013950] 05 p0727 N85-14674
On collective effects in the rotation of stars in clusters and associations 05 p0737 N85-14739
On the nature of the baryon asymmetry
[NASA-TM-86156] 05 p0746 N85-14784
Local Interstellar Medium. International Astronomical Union Colloquium No. 81
[NASA-CP-2345] 06 p0872 N85-15539
Supersymmetric inflationary cosmology
[DE85-001331] 06 p0881 N85-15598
Supersymmetric inflationary cosmology
[DE85-001332] 09 p1415 N85-18929
Axions in astrophysics and cosmology
[DE85-002720] 11 p1763 N85-21094
Recent heavy particle decay in a matter dominated universe
[NASA-CR-175501] 11 p1764 N85-21095
Space research and the new approach to the mechanics of fluid media in cosmos 12 p1953 N85-22271
University of Cambridge Institute of Astronomy report of activities 13 p2170 N85-23464
Measurement of the large-scale anisotropy of the cosmic background radiation at 3 MM 13 p2206 N85-23680

Formation of the solar system
15 p2577 N85-26532
Superheavy magnetic monopoles and the standard cosmology
[DE85-003922] 15 p2686 N85-26587
Dark matter, galaxies, and large scale structure in the universe
[DE85-008053] 16 p2882 N85-27766
Inflation from extra dimensions
[DE85-007834] 16 p2883 N85-27767
Formation of galaxies
[DE85-009537] 18 p3202 N85-29663
Cosmology in theories with extra dimensions
18 p3202 N85-29664
Did bosonic sneutrino stars ever exist
[PREPRINT-421] 18 p3202 N85-29667
Primordial inflation and supergravity
[DE85-009538] 19 p3383 N85-30989
The dimensional reduction transition
[DE85-003948] 19 p3383 N85-30990
Activities report of the Institute of Astronomy
20 p3545 N85-32059
Activities report of the Department of Astrophysics
20 p3548 N85-32064
Cosmogenic-nuclide production by primary cosmic-ray protons
[SH-7.1-8] 23 p4047 N85-35098

COSMONAUTS
Vitamin metabolism in cosmonauts following short-term flights 01 p0091 N85-10615
Compensatory and adaptive regional hemodynamic reactions to weightlessness during long-term spaceflights 01 p0091 N85-10616
Cosmonauts complete 4th month aboard Salyut-7
02 p0157 N85-11065
Orbit of Salyut-7 station boosted
02 p0157 N85-11067
Commentary on cosmonauts geological mapping, photography 02 p0158 N85-11069
Tass reports launch of Soyuz T-12
02 p0158 N85-11070
25th anniversary of the Gagarin Cosmonaut Training Center
[NASA-TM-77644] 09 p1286 N85-18076
Feoktistov recalls period leading to Gagarin spaceflight 13 p1985 N85-22451
Feoktistov says manned lunar, Mars flights lack justification 13 p1985 N85-22452
Cosmonaut Savitskaya says many women in cosmonaut training 16 p2717 N85-26774
Cosmonauts' postural reactions after long-term missions aboard Salyut-6 orbital station 19 p3329 N85-30585
USSR report: Space
[JPRS-USP-84-006] 22 p3731 N85-33128
Results and prospects of physiological research during spaceflights 22 p3732 N85-33139

COSMOS SATELLITES
NT COSMOS 1129 SATELLITE
NT INTERCOSMOS SATELLITES
Hemopoiesis in rats submitted to weightlessness
01 p0091 N85-10613
Geopotential harmonics of order 15 and 30, from analysis of the orbit of satellite 1971-10B
[RAE-TR-84008] 02 p0165 N85-11121
Plasmodium of myxomycete as research object in gravitational biology 15 p2483 N85-25327
International conference on COSPAS-SARSAT system
15 p2484 N85-25336
The COSPAS-SARSAT space segment: Present status and evolution 20 p3401 N85-31102
Rescue satellite COSPAS 20 p3401 N85-31103
The 406 MHz ELT/EPIRBs — Emergency Locator Transmitters/Emergency Position Indicating Radio Beacons (ELT/EPIRB) 20 p3402 N85-31106
Soviet Emergency Locator Transmitter/Emergency Position Indicating Radio Beacon (ELT/EPIRBs) at 121.5 and 406 MHz 20 p3402 N85-31107
Ground segment of COSPAS system
20 p3402 N85-31108
The COSPAS system tests. Technical results
20 p3404 N85-31125
COSPAS-SARSAT demonstration and evaluation phase: COSPAS tests in the USSR and their results
20 p3405 N85-31130
General description of experiment dealing with rat ontogenesis aboard Cosmos-1514 biosatellite
22 p3822 N85-33679
Charge composition and energy spectral of cosmic ray primary particles for energies higher than 1 TeV
[OG-4.1-14] 22 p3877 N85-34020

COSMOS 936 SATELLITE
Results of sanitary-microbiological studies aboard Cosmos-1129 biosatellites 12 p1903 N85-21952

COSMOS 1129 SATELLITE
Results of sanitary-microbiological studies aboard Cosmos-1129 biosatellites 12 p1903 N85-21952
Lipogenesis in rat liver after flight aboard Cosmos-1129 biosatellite 23 p3954 N85-34508

COSPAR (COMMITTEE)
U COMMITTEE ON SPACE RESEARCH

COSPAS
COSPAS-SARSAT satellite orbit predictor, volume 5
[NASA-TM-86015-VOL-5] 14 p2439 N85-25052
United States-Soviet satellite accord: SARSAT/Cospas search-and-rescue program
[GPO-41-113] 20 p3541 N85-32040

COST ANALYSIS
Battery optimization considerations
[DE84-014759] 01 p0044 N85-10288
Standards for commercially emerging technologies: A preliminary cost-benefit assessment for the Optical Digital data disk (OD3) technology for mass data storage applications
[PB84-223593] 01 p010f N85-10669
Shuttle-exchanges on augmented meshes
[NASA-CR-172476] 02 p0243 N85-11587
Artificial intelligence applications to maintenance
[AD-P003914] 02 p0244 N85-11594
Use and value of a geodetic reference system
[PB84-216167] 03 p0379 N85-12418
A methodology for comparing the variable costs of the continuous and periodic review models
[AD-A146351] 03 p0436 N85-12776
Economic analysis handbook
[AD-A146263] 03 p0441 N85-12805
Full-scale testing, production and cost analysis data for the advanced composite stabilizer for Boeing 737 aircraft. Volume 1: Technical summary
[NASA-CR-3649] 05 p0612 N85-13912
Full-scale testing, production and cost analysis data for the advanced composite stabilizer for Boeing 737 aircraft, volume 2
[NASA-CR-166012] 05 p0613 N85-13915
Integrated technology wing study (oral presentation)
[NASA-CR-169497] 07 p0902 N85-15716
More than you want to know about maximum likelihood estimation
[NASA-TM-85905] 07 p0909 N85-15752
The effect of assumptions about cost element probability distributions on operating and support cost risk analysis
[AD-A147553] 07 p1036 N85-16576
Evaluation of the effectiveness of the weighted guidelines to induce contractor's investment in cost reducing facilities equipment
[AD-A147586] 07 p1053 N85-16681
On estimating the cost growth of weapon systems
[AD-A147297] 08 p1230 N85-17749
Assessment of environmental costs at ordnance activities
[AD-P004140] 09 p1347 N85-18476
Electrocatalysis research
[NASA-CR-174352] 10 p1437 N85-19054
Interactive Graphics Simulator: Design, development and effectiveness/cost evaluation
[AD-A149417] 10 p1540 N85-19712
Space Transportation System (STS) propellant scavenging system study. Volume 3: Cost and work breakdown structure-dictionary
[NASA-CR-171850-VOL-3] 11 p1560 N85-20002
Impacts of robotic and flexible manufacturing technologies on manufacturing costs and employment
[AD-A150060] 12 p1960 N85-21668
An analysis of a dynamic project cost problem
[CSIR-TWISK-336] 13 p2149 N85-23341
Sensitivities of projected 1980 photovoltaic system costs to major system cost drivers
[NASA-CR-175669] 14 p2349 N85-24519
Investigations carried out under the Director's Discretionary Fund
[NASA-CR-175676] 14 p2432 N85-24999
Minimal cost flow in processing networks: A primal approach
[CWI-TRACT-4] 14 p2432 N85-25001
Space station propulsion: The advanced development program at Lewis
[NASA-TM-86999] 15 p2494 N85-25386
Pavement-marking materials: New York's experience
[PB85-153294] 15 p2523 N85-25558
An application of the Rayleigh distribution to contract cost data
[AD-A151551] 15 p2684 N85-26441
Combinatorial performance/cost analysis of an autonomous navigation system for aircraft
16 p2695 N85-26540
Design-To-Cost (DTC) methodology to achieve affordable avionics 16 p2696 N85-26545
Cost prediction model for various payloads and instruments for the Space Shuttle Orbiter
[NASA-CR-175781] 16 p2729 N85-26842
Model reduction techniques applied to the control of large space structures
[AD-A151764] 16 p2731 N85-26857
Manufacturing cost analysis of a parabolic dish concentrator (General Electric design) for solar thermal electric power systems in selected production volumes
[NASA-CR-175772] 16 p2818 N85-27360
Logical design of a decision support system to forecast technology, prices and costs for the national communications system
[AD-A152330] 17 p2948 N85-28198
Space insurance firms view shuttle, Ariane reliability
18 p3066 N85-29090
Conceptual design of a fixed-pitch wind turbine generator system rated at 400 kilowatts
[NASA-CR-174877] 18 p3127 N85-29383
Plastic heliostat enclosure analysis
[DE85-009112] 18 p3130 N85-29387
Solar Thermal Research Program
[DE85-000514] 18 p3131 N85-29388
10 MWe Solar Thermal Central Receiver Pilot Plant total capital costs
[DE85-009113] 18 p3131 N85-29390
KrF laser cost/performance model for ICF commercial applications
[DE85-009589] 18 p3182 N85-29728
Megajoule-class single-pulse KrF laser test facility as a logical step toward inertial fusion commercialization
[DE85-009590] 18 p3191 N85-29794
Cost savings from multiyear contracting
[AD-A153564] 18 p3197 N85-29834
Overhead management guide for aerospace procurements
[AD-A153626] 18 p3198 N85-29835
Advanced evacuated tube collectors
[DE85-010271] 19 p3274 N85-30302
Steady-state spheromak reactor studies
[DE85-009585] 19 p3372 N85-30916
Test and Evaluation Master Plan (TEMP) for the Navy Occupational Health Information Management System (NOHIMS). Phase 1: Appendix A through appendix U
[AD-A154179] 19 p3380 N85-30967
Cost and schedule implications of multinational coproduction
[AD-A154358] 19 p3380 N85-30969
An overview of latest model reduction and control methods of large flexible space structures
20 p3414 N85-31191
Hidden costs of robotized production systems revealed 20 p3438 N85-31332
Pricing options for the space shuttle. Special study
21 p3559 N85-32138
High-efficiency crystalline silicon technology development 21 p3607 N85-32395
Flat-plate module efficiency versus cost tradeoffs
21 p3607 N85-32396
Los Alamos optical materials reliability, maintainability, and exposure testing program
[DE85-011894] 21 p3613 N85-32456
Tritium technology review
[DE85-010504] 21 p3703 N85-33006
Feasibility of applications of Competition Decision Assist Package (CDAP) to spare parts
[AD-A154716] 21 p3712 N85-33036
The Human Resource Management Information Network (HRMIN): A cost comparison in accordance with Office of Management and Budget (OMB) Circular no. A-76, 5 April 1979
[AD-A154583] 21 p3713 N85-33039
Spacecraft (Mobile Satellite) configuration design study
[NASA-CR-176153] 23 p3899 N85-34152
Energy Efficient Engine Program technology benefit/cost study, volume 1
[NASA-CR-174766-VOL-1] 24 p4086 N85-35187
Energy Efficient Engine Program technology benefit/cost study, volume 2
[NASA-CR-174766-VOL-2] 24 p4086 N85-35188
Assessment of metal heating technologies for ferrous forging: A pilot study of the form value of natural gas
[PB85-204394] 24 p4084 N85-35314
Investment justification of robotic technology in aerospace manufacturing. User's manual
[AD-A158193] 24 p4099 N85-35410
DoD Value Engineering conference report. Value Engineering (VE): A tool that benefits line management. Part 3, Workshop A: VE in the program office
[AD-A158069] 24 p4163 N85-35812
DoD Value Engineering conference report. Value Engineering (VE): A tool that benefits line management. Part 5, Workshop C: VEP/VECP administration, negotiation, and implementation
[AD-A158071] 24 p4163 N85-35814
DoD Value Engineering conference report. Value Engineering (VE): A tool that benefits line management. Part 6, Workshop D: VE training-orientation
[AD-A158072] 24 p4164 N85-35815

COST EFFECTIVENESS

Increased joint avionics standardization could result in major economies and operational benefits
[AD-A145730] 02 p0139 N85-10945

Atmospheric and pressurized low speed wind tunnel performance and cost comparisons
[ARL/AERO-R-160] 02 p0149 N85-11008

Economic evaluation of space survey materials use in land improvement engineering field work
02 p0165 N85-11115

Modular photovoltaic array field
[SAND-83-7028] 02 p0222 N85-11454

Benefit value to the Air Force of the GIDEP (Government Industry Data Exchange Program) alert
[AD-A145470] 02 p0292 N85-11897

Continuing issues (FY 1983) concerning military use of the space transportation system
[AD-A146091] 03 p0323 N85-12080

The human role in space. Volume 3: Generalizations on human roles in space
[NASA-CR-171225] 04 p0546 N85-13475

Toward an improved FIPS cost-benefit methodology. Phase 2: Descriptive models, general purpose application software development and maintenance
[PB84-226943] 06 p0870 N85-15527

Integrated technology wing study (oral presentation)
[NASA-CR-169497] 07 p0902 N85-15718

Europeans active in magnetic bearing industry
08 p1141 N85-17195

Low cost training aids and devices
09 p1277 N85-18025

A validated methodology for determination of laboratory instrument computer interface efficacy
[AD-A149398] 10 p1487 N85-19391

A low-cost, general purpose image processing system
[INPE-3292-PRE/607] 10 p1537 N85-19690

Department of defense, office of inspector general semiannual report to the Congress, 1 April - 30 September 1984
[AD-A149560] 10 p1567 N85-19879

Polymer intermediates from limonene (follow-up project)
[BMFT-FB-T-84-243] 12 p1814 N85-21380

RAPIDbus: Design of an extensible multiprocessor structure
[AD-A150061] 12 p1912 N85-21998

Comprehensive evaluation of cost effectiveness of solar electric power plants 14 p2265 N85-24036

Pulsed excimer laser processing for cost-effective solar cells
[NASA-CR-175700] 14 p2351 N85-24530

Electricity production from coal through molten-carbonate fuel cells
[TI85-006072] 14 p2351 N85-24534

Artificial intelligence applications to testability
[AD-A150894] 14 p2407 N85-24839

Financial, economic commentary on Airbus, European aviation 15 p2536 N85-25849

Cost Effective and Affordable Guidance and Control Systems
[AGARD-CP-360] 16 p2695 N85-26638

The series 2000: A miniature gas bearing DTG for low cost strapdown guidance and control
16 p2696 N85-26648

A cost-efficient control procedure for the benefit of all airspace users 16 p2697 N85-26651

Simulation: A tool for cost-effective systems design and live test reduction 16 p2698 N85-26657

New stage in robotics development
16 p2762 N85-27045

Paton Institute expert on GDR-USSR welding research
16 p2768 N85-27078

Parametric study of potential early commercial power plants Task 3-A MHD cost analysis
[NASA-CR-175839] 16 p2817 N85-27377

Trends shaping advanced aircrew training capabilities through the 1990s
[AD-A152277] 16 p2843 N85-27530

Some aspects of how to design cost-effective flight control systems
[MBB-LKE-32/S/PUB/143] 16 p2873 N85-27729

Plasma processing of materials
[AD-A152398] 17 p3039 N85-28800

Some Europeans voice opposition to space station participation 18 p3066 N85-28961

Space insurance firms view shuttle, Ariane reliability
18 p3066 N85-29090

Time transfer techniques: Historical overview, current practices and future capabilities
18 p3108 N85-29245

The human role in space (THURIS)
18 p3158 N85-29557

Energy efficient engine component development and integration program
[NASA-CR-172846] 19 p3219 N85-29958

Operational results for the experimental DOE/NASA Mod-OA wind turbine project
[NASA-TM-83517] 19 p3304 N85-30479

EOQ (Economic Order Quantity) range model
[AD-A153709] 19 p3379 N85-30965

Multi-kW solar arrays for Earth orbit applications
[NASA-CR-171536] 20 p3406 N85-31139

Historical perspective of barriers to achieving high-efficiency silicon solar cells
20 p3479 N85-31616

The future of crystalline silicon technology in the US Department of Energy program
21 p3607 N85-32399

Advanced module development overview
21 p3612 N85-32445

The effect of communication-language designs on software specifications
[AD-A155173] 21 p3672 N85-32809

Feasibility of applications of Competition Decision Assist Package (CDAP) to spare parts
[AD-A154716] 21 p3712 N85-33036

The Human Resource Management Information Network (HRMIN): A cost comparison in accordance with Office of Management and Budget (OMB) Circular no. A-76, 5 April 1979
[AD-A154583] 21 p3713 N85-33039

Estimating optimum technical and economic indicators of data transmission systems 22 p3777 N85-33406

A modular docking mechanism for in-orbit assembly and spacecraft servicing 22 p3796 N85-33516

Development of an adjustable buoyancy balloon tracer of atmospheric motion. Phase 1: Systems design and demonstration of feasibility
[PB85-185817] 22 p3817 N85-33648

Cost effective single crystals: The Rolls Royce approach — gas turbine components
[PNR-90262] 23 p3985 N85-34717

Solar pond technology for Navy applications
[AD-A155877] 24 p4112 N85-35468

Design for MISP: A multiple instruction stream shared pipeline processor
[AD-A156314] 24 p4136 N85-35635

COST ESTIMATES

Microcomputers in Hungary 01 p0115 N85-10786

Atmospheric and pressurized low speed wind tunnel performance and cost comparisons
[ARL/AERO-R-160] 02 p0149 N85-11008

Description of the software acquisition process (SWAP) model
[AD-A145413] 02 p0241 N85-11573

Economic analysis handbook
[AD-A146263] 03 p0441 N85-12605

Parametric estimates of propulsion system maintenance manhours
[AD-A147120] 07 p0894 N85-15662

A buyer's guide to space infrastructure
07 p0914 N85-15784

Performance and cost of energy transport and storage systems for dish applications using reversible chemical reactions
[NASA-CR-174263] 07 p0992 N85-16296

The effect of assumptions about cost element probability distributions on operating and support cost risk analysis
[AD-A147553] 07 p1036 N85-16576

The application of a technology index to aircraft turbine engine cost estimating relationships
[AD-A147701] 08 p1087 N85-16874

An application of discriminant analysis to the selection of software cost estimating models
[AD-A147632] 08 p1204 N85-17580

On estimating the cost growth of weapon systems
[AD-A147297] 08 p1230 N85-17749

An agenda for a study of government science policy
[GPO-40-860] 12 p1949 N85-22245

Feasibility study for an AFGL fiber optic data link at WSMR sounding rocket launch area
[AD-A150852] 14 p2240 N85-23894

Sensitivities of projected 1980 photovoltaic system costs to major system cost drivers
[NASA-CR-175869] 14 p2349 N85-24519

Cost-estimating relationships for tactical combat aircraft
[AD-A151575] 15 p2471 N85-25255

Intermediate term forecasting techniques for management
[AD-A151370] 15 p2637 N85-26262

Cost prediction model for various payloads and instruments for the Space Shuttle Orbiter
[NASA-CR-175761] 16 p2729 N85-26842

Manufacturing cost analysis of a parabolic dish concentrator (General Electric design) for solar thermal electric power systems in selected production volumes
[NASA-CR-175772] 16 p2818 N85-27380

Airport and airway system cost allocation model. Volume 7: User's manual
[AD-A152677] 17 p2906 N85-27917

Structural analysis and cost estimate of an eight-leg space frame as a support structure for horizontal axis wind turbines
[NASA-TM-83470] 19 p3284 N85-30361

Regression diagnostics in practice: Experiences from modelling jet engine costs
[AD-A154199] 19 p3347 N85-30748

Uniform cost-estimation method for biomass production and conversion technologies
[DE85-011714] 19 p3380 N85-30970

Methodology for assessing benefits and costs of government information collection
[DE85-010594] 19 p3381 N85-30975

Wind energy in the north Netherlands region
20 p3485 N85-31661

Pricing options for the space shuttle. Special study
21 p3559 N85-32138

Clarke Stations and mercurian mass-drivers: Energy for large-scale transportation systems
[DE85-009607] 21 p3560 N85-32145

Low-head hydroelectric power demonstration project: City of Gonzales, Texas
[DE85-010403] 22 p3809 N85-33595

Control technology for radioactive emissions to the atmosphere at US Department of Energy facilities: The Los Alamos Meson Physics Facility
[DE85-011402] 22 p3811 N85-33609

Attacking software crisis: A macro approach
[AD-A155846] 24 p4138 N85-35645

Progress report on implementing the recommendations of the White House Science Council's Federal Laboratory Review Panel, volume 1
[PB85-185072] 24 p4164 N85-35819

COST INCENTIVES

DoD Value Engineering conference report. Value Engineering (VE): A tool that benefits line management. Part 3, Workshop A: VE in the program office
[AD-A156069] 24 p4163 N85-35812

COST REDUCTION

Energy efficient engine. Volume 1: Component development and integration program
[NASA-CR-173084] 02 p0146 N85-10992

Energy-saving technological methods of obtaining controlled atmospheres
[BLL-M-35724-(5828.4)] 02 p0171 N85-11145

Logistics support costs for the B-1B aircraft can be reduced
[AD-A145846] 03 p0309 N85-11996

Modern structural materials. Present situation and evolution prospects — aircraft materials
[SNIAS-842-551-101] 04 p0455 N85-12886

A practical example of reducing life cycle costs and increased availability 08 p1063 N85-16736

Conceptual design of a 10 MW shore-based OTEC plant
[DE84-015808] 10 p1511 N85-19532

MBB uses superplastic forming, diffusion bonding for alloys 11 p1618 N85-20177

Photovoltaic solar components
12 p1878 N85-21782

President's private sector survey on cost control, report on research and development
[PB84-173269] 12 p1951 N85-22253

A low cost approach with larger diameter silicon wafer — solar cells 13 p2006 N85-22572

MBB cost-reduction plan for Airbus construction described 15 p2532 N85-25618

Reusable software: A concept for cost reduction
16 p2697 N85-26655

A simplified GPS C/A reciever front end with low noise performance 18 p3109 N85-29251

Cost savings from multiyear contracting
[AD-A153564] 18 p3197 N85-29634

Evaluation of radio navigation systems and their configuration with respect to minimum cost
[ESA-TT-847] 20 p3392 N85-31043

High-efficiency cell concepts on low-cost silicon sheets 20 p3479 N85-31621

Design improvements and cost reductions for a 5000 MWh superconducting Magnetic Energy Storage plant
[DE85-010572] 22 p3847 N85-33830

DoD Value Engineering conference report. Value Engineering (VE): A tool that benefits line management. Part 3, Workshop A: VE in the program office
[AD-A156069] 24 p4163 N85-35812

DoD Value Engineering conference report. Value Engineering (VE): A tool that benefits line management. Part 5, Workshop C: VEP/VECP administration, negotiation, and implementation
[AD-A156071] 24 p4163 N85-35814

DoD Value Engineering conference report. Value Engineering (VE): A tool that benefits line management. Part 6, Workshop D: VE training-orientation
[AD-A156072] 24 p4164 N85-35815

DoD Value Engineering conference report. Value Engineering (VE): A tool that benefits line management. Part 7, Workshop E: VE in construction and architect engineer contracts
[AD-A156073] 24 p4164 N85-35816

COSTA RICA
Relationship between forest clearing and biophysical factors in tropical environments: Implications for the design of a forest change monitoring approach — Costa Rica
[E85-10051] 07 p0983 N85-16247
Ash contents of Costa Rican peat deposits
[DE85-010734] 19 p3301 N85-30462

COSTS
NT AIRCRAFT PRODUCTION COSTS
NT LIFE CYCLE COSTS
NT LOW COST
NT OPERATING COSTS
A methodology for comparing the variable costs of the continuous and periodic review models
[AD-A146351] 03 p0436 N85-12776
Space telescope cost, schedule, and performance review, 1984
[GPO-39-065] 04 p0579 N85-13698
Determining training device requirements in Army aviation systems 05 p0711 N85-14558
Analyses to develop models to project failure rates and repair costs of electronic modules and subassemblies
[AD-A146509] 06 p0816 N85-15180
Synopsis of the OTA Workshop on Cost Containment of Civilian Infrastructure (Civilian Space Station) Elements 07 p0915 N85-15790
An analysis of the effect of process controls on productivity and weapon system costs in DoD procurement
[AD-A147496] 07 p1052 N85-16676
The embedded test (BIT): Impact on the total cost of possession 08 p1083 N85-16734
Transmission scheduling to reduce convex delay costs in packet networks
[AD-A148451] 08 p1153 N85-17278
A numerical analysis of sampling plans based on prior distribution and costs
[AD-A147718] 08 p1210 N85-17816
Cost-plus-percentage-of-costs in government contracts
[AD-A147779] 08 p1228 N85-17735
Assessment of environmental costs at ordnance activities
[AD-P004140] 09 p1347 N85-18476
Historical cost curves for hydrogen masers and cesium beam frequency and timing standards 10 p1485 N85-19245
Electric-Hybrid Vehicle (E-HV) demonstration-test project
[DE85-002370] 10 p1570 N85-19899
Worldwide birdstrike statistics of Lufthansa German Airlines
[AD-P004183] 11 p1579 N85-19945
Inexpensive multipurpose landscaping 11 p1581 N85-19961
Advanced mixed-mode simulation techniques 13 p2062 N85-22883
Status of the U.K. N.D.T. industry today 14 p2316 N85-24309
The energy cost of women walking and running in shoes and boots
[AD-A151022] 14 p2389 N85-24716
Costs, payload of Ariane, US Space Shuttle compared 15 p2530 N85-25601
Jet fuel property changes and their effect on producibility and cost in the U.S., Canada, and Europe
[NASA-CR-174840] 16 p2757 N85-27012
Flying in spite of the weather
[NLR-MP-84021-U] 17 p2895 N85-27847
10 MWe Solar Thermal Central Receiver Pilot Plant total capital costs
[DE85-009113] 18 p3131 N85-29390
Cost savings from multiyear contracting
[AD-A153584] 18 p3197 N85-29834
Overhead management guide for aerospace procurements
[AD-A153826] 18 p3198 N85-29835
Hidden costs of robotized production systems revealed 20 p3438 N85-31332
Nomographs for estimating the levelized cost of energy from flat-plate and concentrator photovoltaic systems
[NASA-CR-176048] 20 p3483 N85-31645

COUETTE FLOW
Couette flow of two fluids between concentric cylinders
[AD-A155827] 24 p4093 N85-35376

COULEES
U CANYONS

COULOMB COLLISIONS
Chaos near the Coulomb Barrier: Nuclear molecules
[DE85-001280] 07 p1041 N85-16808
Plane-wave born collision strengths for electron-ion excitation: Comparison with other theoretical methods
[DE85-002345] 10 p1555 N85-19802
Monte-Carlo treatment of nonlinear collisional effects in charged-particle transport
[DE85-010755] 20 p3521 N85-31897
Collisional relaxation of electron tail distribution
[IPPJ-729] 23 p3974 N85-34635
LPM effect and primary energy estimations
[HE-3.6-4] 24 p4185 N85-35953
Result of Monte-Carlo simulation of electron-photon cascades in lead and layers of lead-scintillator
[HE-3.6-11] 24 p4185 N85-35958
Structure of air shower disc near the core
[HE-4.7-2] 24 p4196 N85-36053

COULOMB POTENTIAL
Memory function for cyclotron resonance of two-dimensional electron systems
[AD-A152632] 17 p3029 N85-28731
Spin distributions in heavy ion fusion at and below the Coulomb barrier
[DE85-007817] 17 p3031 N85-28751
Screening phase transitions in two-dimensional Coulomb gas
[NOTA-INTERNA-830] 18 p3192 N85-29798
K(-) hydrogen bound and continuum states in momentum space
[DE85-010429] 22 p3841 N85-33789
Electron loss process and cross section of multiply charged ions by neutral atoms 23 p3981 N85-34685
Anomalous abundances of solar energetic particles and coronal gas: Coulomb effects and First Ionization Potential (FIP) ordering
[SH-2.1-10] 23 p3999 N85-34791

COULOMETERS
State-of-charge coulometer
[NASA-CASE-NPO-15759-1] 12 p1849 N85-21596
Portable electrochemical cell interrogator
[DE85-005186] 13 p2065 N85-22901

COULOMETRY
Voltammetry and coulometry with immersed thin layer electrodes. Part 1: Model for effects of solution resistivity in linear sweep voltammetry
[AD-A148655] 08 p1159 N85-17313
Voltammetry and coulometry with immersed thin layer electrodes. Part 2: Practical considerations and experimental results
[AD-A148656] 08 p1159 N85-17314
Computer-assisted Gran titration procedure for strong acid determination
[DE85-006801] 15 p2507 N85-25462
Electrochemistry of Hexanitroazobenzene (HNAB)
[DE85-010807] 21 p3585 N85-32171

COUNTDOWN
West Europe report: Science and technology
[JPRS-WST-84-004] 03 p0309 N85-11998
View of Ariane countdown procedures, Kourou launch facilities 03 p0310 N85-12001

COUNTER-ROTATING WHEELS
Perspectives on energy storage wheels for space station application 05 p0605 N85-13860
An improved servo-controlled inertial clock for laboratory tests of general relativity 19 p3378 N85-30955

COUNTERFLOW
Local mechanism of equatorial countercurrents 14 p2336 N85-24446

COUNTERMEASURES
NT CHAFF
NT ELECTRONIC COUNTERMEASURES
NT JAMMING
Resistance to HF jamming interference in mobile radio networks by an adaptive, distributed reconfiguration technique
[AD-A145117] 01 p0036 N85-10236
Minimization of system vulnerability in Naval satellite communication networks 11 p1710 N85-20758
Dual band radome wall design
[AD-P004357] 12 p1825 N85-21451

COUNTERS
NT CERENKOV COUNTERS
NT NEUTRON COUNTERS
NT NEUTRON SPECTROMETERS
NT PARTICLE TELESCOPES
NT PROPORTIONAL COUNTERS
NT QUANTUM COUNTERS
NT RADIATION COUNTERS
NT SCINTILLATION COUNTERS
NT SPARK CHAMBERS
Methods for the design of quantizers for image signals
[FUB-38-1983] 01 p0041 N85-10263
Safety evaluation of an electronic totalizer containing a Li/(CF)x cell
[AD-A147306] 07 p0993 N85-16305
Charge depletion meter
[AD-D011484] 10 p1488 N85-19393
Extraction of signals from background interference with unknown parameters in quantized sample 13 p2084 N85-23013
The 100 years of Aitken Nuclei (AN) study-reminiscence, current and future problems 21 p3641 N85-32621
Supersaturation obtained in a condensation nucleus counter 21 p3642 N85-32624
Observations on (3)He neutron spectrometry
[DE85-010731] 23 p3970 N85-34808

COUNTING
Estimating number, time and length; a baseline study 05 p0695 N85-14473
Counting is easy — Turing machines
[CWI-CS-R8423] 17 p3009 N85-28606

COUNTING CIRCUITS
NT SCALERS
Tally cell circuit
[AD-D011492] 11 p1829 N85-20254

COUPLED MODES
Behavior orbits of two coupled oscillators 02 p0262 N85-11633
Quark models of hadronic interactions
[DE84-013767] 04 p0581 N85-13570
Coupled-cavity gyrotrons with mode conversion 13 p2076 N85-22967
Techniques for operating Charge Coupled Devices (CCD's) in very high speed framing mode
[AD-A152878] 17 p2953 N85-28238
Simplified analytical model for calculation of population inversion in channels of CW gasdynamic lasers operating at various transitions among levels pertaining to coupled upsilon 1 and upsilon 2 modes of CO2
[STN-2] 20 p3481 N85-31498
Expansion ratio influence on population inversion in CO2/Ar CW gasdynamic lasers operating at various transitions within coupled upsilon 1 and upsilon 2 modes of CO2
[STN-4] 22 p3790 N85-33485
Mechanical ratcheting behaviors of a steel pipe under combined cyclic axial load and internal pressure 23 p3904 N85-34184
Nonlinear flap-lag-extensional vibrations of rotating, pretwisted, preconed beams including Coriolis effects
[NASA-TM-87102] 23 p3941 N85-34427

COUPLERS
NT ANTENNA COUPLERS
NT COUPLING CIRCUITS
NT DIPLEXERS
NT DIRECTIONAL COUPLERS
Fiber optic data bus using Frequency Division Multiplexing (FDM) and an asymmetric coupler
[NASA-TM-86015] 04 p0492 N85-13139
Application of commercial star couplers to increase signal dynamic range
[DE84-014769] 04 p0565 N85-13600
Vehicle-to-vehicle connection mechanism
[AD-D011267] 05 p0645 N85-14142
Multihole couplers for overmoded waveguide systems
[IPF-83-8] 09 p1394 N85-18773
Short mode selective directional couplers
[IPF-83-9] 09 p1394 N85-18774
Improved directional couplers for overmoded waveguide systems
[IPF-84-1] 09 p1394 N85-18775
A coaxial cavity gunn oscillator using probe coupled microstrip
[AD-D011437] 10 p1479 N85-19334
Multi-access fiber optic data bus using FDM/FSK
[NASA-CR-175739] 15 p2621 N85-26152
The free electron laser variable bridge coupler
[DE85-009630] 18 p3114 N85-29278
The 3lambda/4 post coupler for drift-tube linacs
[DE85-010753] 20 p3531 N85-31682
Conjugated symmetrical coupler curves, produced by 4-bar linkages having the same transmission angles 23 p3924 N85-34322

COUPLES
Localized ionic currents from a corroding iron-copper galvanic couple
[AD-A153627] 18 p3074 N85-29011
Additional experiments relative to the shelf life of Li(Si)/FeS2 thermal batteries
[DE85-009482] 18 p3095 N85-29182

COUPLING
NT COUPLES
NT CROSS COUPLING
NT MICROWAVE COUPLING
NT OPTICAL COUPLING
NT SPIN-SPIN COUPLING
NT THERMODYNAMIC COUPLING
Factor analysis applied to a silane coupling agent on E-glass fiber system
[AD-A145687] 02 p0187 N85-11249
Using fiber-optics light guides in diagnosing intense shock waves 02 p0272 N85-11773

Structure of silane coupling agents adsorbed on silicon powder
[AD-A145803] 03 p0327 N85-12105
Evaluation of some photovoltaic concentrator solar cell-heat sink coupling materials
[DE84-016027] 04 p0529 N85-13378
Coupling of multidirectional diffusions by reflection
[CTH-MATH-1984-20] 05 p0719 N85-14613
Wavelength scaling of laser plasma coupling
[DE84-014637] 06 p0866 N85-15505
Application of quantum chemistry of atmospheric chemistry
[AD-A147035] 07 p0922 N85-15843
Photoacoustic spectroscopy at electrode-solution interface
[DE85-001872] 09 p1292 N85-18111
Electromagnetic processing of materials
[AD-A148804] 09 p1311 N85-18241
Modal analysis of structural systems involving nonlinear coupling 09 p1337 N85-18409
Effect of coupled torsional-flexural vibration of a geared shaft system on the dynamic tooth load
09 p1338 N85-18415
Nicolai maps and stochastic observables from a coupling constant flow
[BONN-HE-84-26] 09 p1376 N85-18653
An optically coupled sampling system with 4 GHz bandwith
[AD-A148057] 09 p1384 N85-18702
Nonlocal and nonlinear effects on solar oscillations
09 p1416 N85-18934
A coaxial cavity gunn oscillator using probe coupled microstrip
[AD-D011437] 10 p1479 N85-19334
Parametric processes in underdense UV laser-produced plasmas
[DE85-002812] 10 p1559 N85-19830
Nonlinear saturation of stimulated Raman scattering in collisional homogeneous plasma
[DE85-002814] 10 p1559 N85-19831
Comparison of measured and calculated mutual coupling in the near field between microwave antennas
[PB85-105963] 11 p1625 N85-20237
Coupling between the thermosphere and the stratosphere: The role of nitric oxide
11 p1662 N85-20472
Application of dimensional analysis to the problem of solar wind-magnetosphere energy coupling
[DE85-002414] 11 p1674 N85-20551
Magnetically-induced luminescence of (Ir(2-phoe)(2)C10(4)
[AD-A149659] 12 p1799 N85-21286
A study of coupling the boundary and finite element methods in two-dimensional elastostatics
[AD-A149619] 12 p1865 N85-21702
Coupling between velocity oscillations and solid propellant combustion 13 p2000 N85-22536
Characterization of heterogeneity of composite propellants and its effects on combustion behavior
13 p2000 N85-22539
Impacts in ice: Commissions of solar system crater population 13 p2181 N85-23538
ICRF antenna coupling theory for a cylindrically stratified plasma
[DE85-004960] 14 p2424 N85-24952
Effect of nickel addition on the thermal, magnetic and magnetomechanical properties of Fe(80)B(15)Si(5)
[AD-A152281] 16 p2749 N85-26967
Study of the coupling between average, coherent and turbulent fields in a circular excited free jet
[ISL-R-115/83] 16 p2785 N85-27184
An analytical investigation of dynamic coupling in nonlinear, geared rotor systems
16 p2792 N85-27218
Laser plasma LINAC
[DE85-006294] 17 p2971 N85-28348
Basic EMC (Electromagnetic compatibility) technology advancement for C3 systems. Volume 4D: Modeling crosstalk in balanced twisted pairs
[AD-A153678] 18 p3090 N85-29125
The free electron laser variable bridge coupler
[DE85-009830] 18 p3114 N85-29278
Torsion-tension coupling in rods
18 p3120 N85-29315
Chemical-acoustic interactions in combustion systems
[AD-A153857] 19 p3233 N85-30046
Mutual coupling analysis for conformal microstrip antennas
[AD-A154292] 19 p3259 N85-30210
Seismic analysis of liquid-filled tanks with an eccentric core barrel
[DE85-010249] 19 p3269 N85-30272
Progress in inertial fusion at LLNL
[DE85-010931] 19 p3277 N85-30321
Strong-coupling approximations
[DE85-007829] 19 p3353 N85-30785
ICRF antenna coupling and wave propagation in a tokamak plasma 19 p3369 N85-30893
Control system design for lightly coupled large space structures 20 p3399 N85-31086
The 3lambda/4 post coupler for drift-tube linacs
[DE85-010753] 20 p3531 N85-31962
Ab initio calculations of materials properties
[DE85-011167] 20 p3531 N85-31964
A substructure coupling procedure applicable to general linear time-invariant dynamic systems
[NASA-CR-176144] 22 p3600 N85-33542
Substructure coupling in the frequency domain
[NASA-CR-176140] 22 p3600 N85-33543
Experimental measurements of the ion cyclotron antennas' coupling and RF characteristics
[DE85-011569] 23 p3962 N85-34694
Generation of stimulated emission in the soft X-ray range by nonlinear processes with excimer lasers
[DE85-012465] 24 p4096 N85-35403
Applications of the Galerkin formalism in the coupling of the earth's free oscillations 24 p4116 N85-35514
Study to assess the effects of magnetohydrodynamic electromagnetic pulse on electric power systems, phase 1, volume 3
[DE85-011301] 24 p4156 N85-35771

COUPLING CIRCUITS

Cascode and differential amplifier using field-effect transistors 15 p2529 N85-25591
Outline of CCVT (Coupling Capacitor Voltage Transformer) calibration procedure, EPRI-NBS (Electric Power Research Institute/National Bureau of Standards) prototype system. Supplement to EPRI report EL-890 (Field Calibration System for CCVTs, April 1978)
[PB85-182566] 20 p3450 N85-31418

COUPLING COEFFICIENTS

A packed storage program for angular momentum coupling coefficients
[TWISK-316] 01 p0102 N85-10680
The application of dimensional analysis to the problem of solar wind-magnetosphere energy coupling
14 p2357 N85-24564
Coupling of the solar wind to measures of magnetic activity 14 p2357 N85-24565
On coupling factors of explosion
15 p2551 N85-25747
Finite-perturbation intermediate neglect of differential overlap molecular orbital calculations of nuclear magnetic resonance spin-spin coupling constants for polycyclic aromatic hydrocarbons and aromatic nitrogen heterocyclics
[NASA-TM-87486] 20 p3525 N85-31927
Noise in stages and in interstage couplings of various transistor circuits 22 p3765 N85-33334
Statistical analyses in the study of solar wind-magnetosphere coupling
[DE85-009596] 22 p3859 N85-33898

COUPLINGS

Nonlinear oscillations of 2 body system relative to center of mass in elliptical orbit 02 p0159 N85-11082
Stress analysis of pin-loaded orthotropic plates using orthotropic photoelasticity 02 p0207 N85-11366
Improvement of gas-tightness of OTTG and TBO-5 threaded pipe couplings
[BLL-M-35993-(5828.4)] 07 p0972 N85-16175
Flexible line support assembly
[AD-D011391] 07 p0972 N85-16177
Tube coupling device
[NASA-CASE-MFS-25984-1] 11 p1647 N85-20378
Connection system — insuring against loss of a tool component without using multiple tethers
[NASA-CASE-MSC-20319-1] 12 p1857 N85-21649
Normal coordinate monolithic crystal filter
[AD-D011496] 12 p1941 N85-22188
Cooling performance improvement of a horizontal ground coupled heat pump
[DE85-002470] 13 p2093 N85-23065
Clutchless mechanism for engagement of forging press 14 p2268 N85-24051
Vibrations of rotors connected through couplings with backlash 17 p2940 N85-28147
Non-backdriveable free wheeling coupling
[NASA-CASE-MSC-20475-1] 18 p3116 N85-29290
Mechanical ratcheting behaviors of a steel pipe under combined cyclic axial load and internal pressure
23 p3904 N85-34184
The balancing of complex linkage mechanisms
23 p3924 N85-34313

COVALENT BONDS

Metallophthalocyanine dimers incorporating five atom covalent bridges
[AD-A154365] 19 p3234 N85-30051

COVARIANCE

Principal components: A review
02 p0211 N85-11390
Limit theory for the sample covariance and correlation functions of moving averages
[AD-A145488] 02 p0251 N85-11642
Filtering and prediction performance for a class of systems with uncertain parameters
[AD-A146145] 03 p0411 N85-12630
Construction of a confidence region for linear functions with unknown parameters
[CTH-MATH-1984-17] 05 p0721 N85-14630
Methodology for economic evaluation of process technologies in the early research and development stages
[DE84-015863] 05 p0736 N85-14731
An interactive FORTRAN program for determining reliability of pseudo-range geodetic point positioning using the global positioning system
[AD-A147133] 07 p0988 N85-16275
Estimation for a semimartingale regression model using the method of sieves
[AD-A146809] 07 p1028 N85-16527
Local likelihood estimation
[AD-A147317] 07 p1035 N85-16571
A factor analysis for time series
[AD-A147495] 07 p1036 N85-16574
Generating positively correlated random variables from a sequence of independent random variables with symmetric logarithmically concave densities
[AD-A148438] 08 p1216 N85-17658
Initialization of Thompson-Pisarenko's algorithm — sinusoidal signal parameter estimation
[FUB-46-1983] 09 p1375 N85-18641
Data-driven choice of a spectrum estimate: Extending the applicability of cross-validation methods
[DE85-001411] 10 p1437 N85-19058
On the probability density of signal-to-noise ratio in an improved adaptive detector, part 1
[AD-A148856] 10 p1550 N85-19772
Asymptotic distributions of the sample mean, autocovariances and autocorrelations of long-memory time series
[AD-A149409] 10 p1551 N85-19781
Tests of fit based on normalized spacings
[AD-A149749] 12 p1921 N85-22062
Asymptotics for configural estimators
[AD-A150108] 12 p1924 N85-22067
On limit of the largest eigenvalue of the large dimensional sample covariance matrix
[AD-A150589] 13 p2151 N85-23358
Model and controller reduction of uncertain systems using covariance equivalent realizations
14 p2243 N85-23902
Local covariance functions and density distributions
[AD-A150792] 14 p2373 N85-24669
Statistical analysis techniques for small sample sizes
[NASA-CR-171872] 15 p2639 N85-26279
Optimal relative data weights
16 p2805 N85-27296
Robust regression through robust covariances
[AD-A153301] 17 p3020 N85-28677
Hybrid uncertainty theory
[DE85-008357] 18 p3167 N85-29622
Two-point closure study of covariance budgets for turbulent Rayleigh-Benard convection
[PB85-189108] 24 p4124 N85-35588

COVERALLS

The new Navy flier's fire-resistant blue coverall
[AD-A146611] 06 p0846 N85-15375
Fire pit tests of blue flight coverall program
[AD-A151884] 15 p2620 N85-26149

COVERINGS

Protective coverings for fiber reinforced epoxy composites
[PB84-231059] 04 p0480 N85-13063
Solar cell coverslide extraction method and apparatus
[AD-D011275] 05 p0669 N85-14306
Integral boost, heat protection, port covers and transition 07 p0918 N85-15813
NBS solar collector durability/reliability test program
[DE85-003489] 12 p1881 N85-21801
Analysis of optimum front cover thickness for lightweight solar arrays 13 p2010 N85-22606

COVES

U BAYS (TOPOGRAPHIC FEATURES)

COWELL METHOD

U NUMERICAL INTEGRATION

COWLINGS

Low-speed aerodynamic test of an axisymmetric supersonic inlet with variable cowl slot
[NASA-TM-87039] 16 p2708 N85-26710

CRAB NEBULA

Observation of gamma radiation from crab nebula in 5-100 MeV range 02 p0162 N85-11098
The X-ray structure of the Crab Nebula
11 p1741 N85-20948
The X-ray structure of the Crab Nebula
11 p1742 N85-20954

Recent results on the Crab Pulsar X-ray light curve
11 p1742 N85-20955
Old and new neutron stars
[DE85-002716] 11 p1762 N85-21085
Absolute measurements of radiation intensity from Cassiopeia-A, Cygnus-A and crab nebula in 60-100 cm band 13 p2078 N85-22978
High resolution hard X-ray spectra of solar and cosmic sources 14 p2455 N85-25163
Optical pulsar in the Large Magellanic Cloud remnant 0540-69.3
[DE85-006707] 16 p2883 N85-27788
Observation of the Crab nebula in the hard X-ray
[MPE-186] 17 p3053 N85-28897
Salyut-7 cosmonauts work with RS-17 and GSPS X-ray telescopes 22 p3731 N85-33131
Observations of the Crab Nebula at energies 4.10(11)
[OG-2.3-1] 22 p3865 N85-33938
Search for excess showers from Crab Nebula
[OG-2.3-2] 22 p3866 N85-33939
Very high energy gamma rays from the Crab Nebula
[OG-2.3-3] 22 p3866 N85-33940
Detection of gamma-ray lines from the direction of the Crab Nebula 22 p3866 N85-33943
Observation of hard X-rays from the Crab pulsar and A0535+26
[OG-2.3-7] 22 p3866 N85-33944
Gamma rays of 0.3 to 30 MeV from PSR 0531+21
[OG-2.3-8] 22 p3866 N85-33945
The 1000 GeV gamma ray emission from radio pulsars 22 p3867 N85-33946
High energy radiation from neutron stars
[DE85-014353] 24 p4169 N85-35843

CRACK ARREST
Retardation analytical model to extend service life
[NASA-CR-171177] 01 p0057 N85-10376

CRACK CLOSURE
Near-threshold fatigue crack growth and crack closure in 17-4 precipitation hardening steel and 2043-T3 aluminum alloy
[FFA-TN-1984-16] 02 p0210 N85-11385
Short cracks and crack closure in AL 2024-T3
[FFA-TN-1984-40] 02 p0210 N85-11387
Ultrasound interaction with partially closed fatigue cracks
[DE84-016360] 04 p0514 N85-13276
The effect of overload cycles on fatigue crack propagation in structural steels
15 p2577 N85-25897
Crack closure characteristics considering center cracked and compact tension specimens
[AD-A151702] 15 p2579 N85-25907
Fatigue crack retardation phenomenon caused by single-multiple overloads in 2017-T3 aluminum alloy
23 p3906 N85-34196

CRACK FORMATION
U CRACK INITIATION

CRACK GEOMETRY
NT CRACK TIPS
Short cracks and crack closure in AL 2024-T3
[FFA-TN-1984-40] 02 p0210 N85-11387
The effect of orientation on fatigue growth in a nickel-based single crystal superalloy
[PNR-90207] 03 p0332 N85-12141
Correlation of stable crack growth with the J-integral and the crack tip opening displacement, effects of geometry, size and material: Report on an investigation of the elastic-plastic R-curve methodology
[GKSS-84-E-37] 08 p1173 N85-17395
Measurement of fracture macro-geometry in evaluating fracture toughness
[BLL-BISI-TRANS-22241-(9022.06)]
17 p2978 N85-28403
A clamped rectangular plate containing a crack
[NASA-CR-177925] 20 p3469 N85-31552

CRACK INITIATION
Estimation of the threshold in fatigue crack initiation models: A Bayesian approach
[AD-A144847] 01 p0082 N85-10410
Nonlinear structural and life analyses of a combustor liner 02 p0141 N85-10955
Pre-HOST high temperature crack propagation
02 p0141 N85-10956
Life prediction and constitutive behavior: Overview
02 p0143 N85-10973
Creep-fatigue life prediction for engine hot section materials (isotropic) 02 p0144 N85-10974
Constitutive model development for isotropic materials
02 p0144 N85-10975
Life prediction and constitutive models for anisotropic materials 02 p0144 N85-10976
The inter-relation of microstructure, toughness and fatigue crack growth behaviour in WC-Co hardmetals
02 p0177 N85-11188
Detection of hydrogen assisted crack growth by measurement of modulus changes and acoustic emission
[DE84-015752] 02 p0184 N85-11236
The influence of sublaminate cracks on the tension fatigue behavior of a graphite epoxy laminate
[FFA-TN-1984-32] 02 p0210 N85-11386
Stress-driven solute enrichment of crack-tips during low ductility intergranular fracture of low-alloy steel
[AERE-R-11120] 03 p0333 N85-12150
Sequence of effects in the crack initiation and crack propagation phase 05 p0649 N85-14168
Evaluation of the crack initiation life behavior of fatigue loaded automotive components made from high strength aluminium alloys
[ESA-TT-733] 05 p0651 N85-14181
Study of fatigue fracture in hardened and tempered carbon steel. Report 1: Microscopic observation of the fatigue crack formation process
[BLL-PNR-90242-(8019.3153)]
06 p0767 N85-14909
Comparative investigation of testing methods to determine hot crack susceptibility during welding
[BAM-ERP-2415] 07 p0979 N85-16218
Influence of constant amplitude and variable amplitude loading on crack initiation and micro crack propagation in Al 2024-T3
[DFVLR-FB-84-29] 07 p0979 N85-16220
The effect of the test atmosphere on the formation and propagation of creep cracks in commercial high temperature alloys
[JUEL-1939] 07 p0980 N85-16221
Hydrogen induced cracking in pipeline steels
[ERS-E.327] 09 p1340 N85-18429
Mechanism of hydrogen induced cracking in pipeline steels
[ERS-E.349] 09 p1340 N85-18430
Fracture resistance of surface layer with technological defects under cyclical loading 10 p1448 N85-19126
Mechanism and pattern of fatigue crack growth in aluminum alloys 11 p1597 N85-20047
New method for studying surface crack growth in laminated polymer composite materials
11 p1598 N85-20051
Theoretical and experimental study of crack resistance and macrocrack growth rate in organic fiber reinforced plastic under pure shear condition
11 p1598 N85-20053
Initial fracture stages of orthogonally reinforced composite material 11 p1599 N85-20055
Distribution of hydrogen in multi-layer welded joints of alloyed steels 11 p1603 N85-20079
Comparison of the fatigue resistance (initiation, propagation) of cast TA5V with hot rolled TA5V — titanium alloy
[DGT-25369-PT-1] 12 p1808 N85-21341
Fatigue life, crack initiation, and propagation of 304 stainless steel with non-proportional axial/torsional strain-paths 13 p2101 N85-23094
An investigation of elevated temperature fatigue crack initiation in 2 and 1/4 cR-1 MO low alloy steel
[AD-A150870] 14 p2255 N85-23973
Role of passive surface films on corrosion fatigue crack initiation
[DE85-000438] 14 p2257 N85-23985
On the use of marker loads and replicas for measuring growth rates for small cracks 14 p2319 N85-24331
Study of oxidized surface coating on titanium after annealing 15 p2498 N85-25412
Fatigue damage and small crack growth during biaxial loading 16 p2797 N85-27247
The practical and theoretical significance of small cracks: An evaluation
[VTH-LR-432] 16 p2803 N85-27283
Engineering significance of fatigue thresholds and short fatigue cracks for structural design
[NLR-MP-84001-U] 17 p2961 N85-28430
High temperature fracture mechanics of silicon nitride
[BMFT-FB-T-84-285] 17 p2961 N85-28433
Method of assessment of start of slow crack growth by acoustic emission technique
[BLL-BISI-TRANS-21762-(9022.06)]
17 p3027 N85-28722
An effective substructure technique applied to crack problems 18 p3121 N85-29319
Experimental and theoretical study of fatigue crack initiation in metals 19 p3283 N85-30357
Creep fatigue life prediction for engine hot section materials (isotropic)
[NASA-CR-168228] 20 p3394 N85-31057
Long-term thermal aging of Celion/V378A composite materials
[NASA-TM-86362] 20 p3421 N85-31236
Finite element modeling of cracked bodies using the Bodner-Partom flow law 20 p3468 N85-31547
Creep crack growth predictions in INCO 718 using a continuum damage model 20 p3469 N85-31551
The three-dimensional J-integral. An investigation into its use for post-yield fracture safety assessment
[WTHD-167] 20 p3472 N85-31578
A cracked orthotropic sheet stiffened by a semi-infinite orthotropic sheet
[NASA-TP-2455] 21 p3597 N85-32399
Short-time creep of ice
[NRC/CNR-TT-2111] 23 p3941 N85-34428
Computational techniques for fiber reinforced components 24 p4075 N85-35250
Evaluation of the crack plane equilibrium model for predicting plastic fractures
[DE85-005558] 24 p4102 N85-35431

CRACK PROPAGATION
Influence of annealing on properties of AT3 alloy welded joints 01 p0019 N85-10118
Cumulative damage model for advanced composite materials
[AD-A144840] 01 p0022 N85-10135
Acoustic emission linear pulse holography
[DE84-014519] 01 p0050 N85-10330
Fracture, failure, and fragmentation
01 p0059 N85-10390
Crack tip opening displacement for work hardening materials
[GKSS-84-E-26] 01 p0083 N85-10415
Flight simulation fatigue crack propagation in metal/carbon-epoxy laminates
[NLR-TR-83006-U] 01 p0083 N85-10416
Pre-HOST high temperature crack propagation
02 p0141 N85-10956
HOST high temperature crack propagation
02 p0144 N85-10977
Tensile strength of composite sheets with unidirectional stringers and crack-like damage: A brief report
[NASA-TM-86310] 02 p0170 N85-11139
The inter-relation of microstructure, toughness and fatigue crack growth behaviour in WC-Co hardmetals
02 p0177 N85-11188
Detection of hydrogen assisted crack growth
[DE84-015920] 02 p0183 N85-11228
Environment-induced embrittlement: Effect of impurity segregation and state of stress
[DE84-015436] 02 p0184 N85-11235
Detection of hydrogen assisted crack growth by measurement of modulus changes and acoustic emission
[DE84-015752] 02 p0184 N85-11236
Model for non-linear crack growth prediction, taking load sequence (LOSEQ) effects into consideration
[BLL-RAE-TRANS-2114-(5207)]
02 p0208 N85-11371
Near-threshold fatigue crack growth and crack closure in 17-4 precipitation hardening steel and 2043-T3 aluminum alloy
[FFA-TN-1984-16] 02 p0210 N85-11385
Short cracks and crack closure in AL 2024-T3
[FFA-TN-1984-40] 02 p0210 N85-11387
Wedge with crack in bielastic medium
02 p0273 N85-11780
Weld metal solidification cracking in a carbon-manganese steel 03 p0330 N85-12126
The effect of orientation on fatigue growth in a nickel-based single crystal superalloy
[PNR-90207] 03 p0332 N85-12141
Sour-gas cracking in ferritic steels
[AERE-R-10908] 03 p0333 N85-12148
Acoustic emission monitoring of fatigue in 7010 aluminum alloys
[AERE-R-11167] 03 p0334 N85-12152
Crack resistance of pressed and rolled semifinished goods of aluminum alloys used in load-bearing aircraft wing structures 03 p0348 N85-12245
Kinetics of fatigue factor of AT3 titanium alloys in air, distilled water and 3.5% aqueous NaCl solution
03 p0350 N85-12255
Viscoplastic finite element analysis of rapid fracture
03 p0370 N85-12365
Applications of integral equations with strong singularities in fracture mechanics
03 p0371 N85-12367
Bending strength studies on hot-pressed silicon carbide
[NASA-TM-77512] 03 p0371 N85-12369
Fatigue crack propagation in metastable titanium alloys
[AD-A145824] 03 p0372 N85-12376
Influence of cyclic tangential loading on indentation fracture
[DE84-015969] 03 p0373 N85-12382
Tensile and crack propagation tests on aluminum alloys of the 2000 and 7000 series in laminated plate and forged products
[M2-878300] 03 p0373 N85-12383

A comparison of methods for predicting ductile crack growth instability
[AERE-R-11199] 03 p0374 N85-12387
Stress relief cracking studies of 2 1/4Cr1Mo steel
[AERE-R-11111] 03 p0374 N85-12388
Characterization of interlaminar crack growth in composites with the double cantilever beam specimen
04 p0463 N85-12942
Numerical investigation of the micromechanics of composite fracture 04 p0467 N85-12970
Ultrasound interaction with partially closed fatigue cracks
[DE84-016360] 04 p0514 N85-13276
Mechanical properties of aligned short carbon fiber reinforced PES and PI laminates
[DFVLR-FB-84-24] 05 p0613 N85-13918
Fractographic study of stress corrosion cracking of SUS 304 stainless steel in various environments
[BLL-RISLEY-TR-4566-(9091.9F)]
05 p0615 N85-13928
The fourth LBF colloquium
[ISSN-0721-5320] 05 p0648 N85-14163
Sequence of effects in the crack initiation and crack propagation phase 05 p0649 N85-14168
Processes to increase the fatigue life of constructions with already initiated cracks 05 p0650 N85-14176
Influence of the mechanical and electrochemical characteristics of austenitic and austenoferritic steels on the propagation rate and morphology of stress corrosion cracking
[BLL-RISLEY-TR-4545-(9091.9F)]
06 p0767 N85-14906
Study of fatigue fracture in hardened and tempered carbon steel. Report 1: Microscopic observation of the fatigue crack formation process
[BLL-PNR-90242-(8019.3153)]
06 p0767 N85-14909
Investigations into the fatigue crack growth behaviour of X8CrNi 18 11 (1.4948) austenitic stainless steel
[BLL-RISLEY-TR-4544-(9091.9F)]
06 p0768 N85-14911
Fractographic observation and estimation of crack growth curve of aluminum alloy under ramdom flight simulation loading
[NAL-TR-824] 06 p0768 N85-14913
Development and characterization of ductile Long-Range-Ordered (LRO) alloys (Fe,Co, Ni)3V for high-temperature structural use
[DE84-016750] 06 p0769 N85-14921
Constitutive modeling of engine materials
[AD-A146630] 06 p0817 N85-15189
Inclined dislocation emission at a shielded crack tip
[DE84-016703] 06 p0818 N85-15192
Inconel 718 alloy resistance to crack propagation
07 p0907 N85-15740
Cumulative damage modeling of fatigue crack growth
07 p0907 N85-15741
Thermal-mechanical fatigue crack growth in inconel X-750
[NASA-CR-174740] 07 p0927 N85-15877
Possibilities for a more accurate life prediction of components — gas turbine disks
07 p0976 N85-16198
Investigation of the HPFTP first stage impeller crack
[NASA-CR-171281] 07 p0977 N85-16206
A hydrogen partitioning model for hydrogen assisted crack growth
[AD-A147365] 07 p0978 N85-16214
Influence of constant amplitude and variable amplitude loading on crack initiation and micro crack propagation in Al 2024-T3
[DFVLR-FB-84-29] 07 p0979 N85-16220
The effect of the test atmosphere on the formation and propagation of creep cracks in commercial high temperature alloys
[JUEL-1939] 07 p0980 N85-16221
Crack growth in propellants 08 p1116 N85-17034
Mechanical properties of adhesively bonded aluminum structures protected with hydration inhibitors
[AD-A148123] 08 p1133 N85-17139
Electrodes for repairing power engineering equipment made from creep resisting steel
[BLL-CE-TRANS-8084-(9022.09)]
08 p1167 N85-17360
Correlation of stable crack growth with the J-integral and the crack tip opening displacement, effects of geometry, size and material: Report on an investigation of the elastic-plastic R-curve methodology
[GKSS-84-E-37] 08 p1173 N85-17395
A simple engineering treatment of center cracked tension panels in the regime of nonlinear fracture mechanics under plane stress conditions
[GKSS-84-E-38] 08 p1173 N85-17396
Engineering property comparisons of PM and IM aluminum alloy forgings
[AD-B098146L] 08 p1173 N85-17398
Delamination growth in graphite epoxy laminates under compressive loads 09 p1288 N85-18088
A study of spectrum fatigue crack propagation in two aluminum alloys. 1: Spectrum simplification
[NASA-TM-86929] 09 p1293 N85-18124
A study of spectrum fatigue crack propagation in two aluminum alloys. 2: Influence of microstructures
[NASA-TM-86930] 09 p1294 N85-18125
Applicability of linear elastic fracture mechanics to fatigue in polymers and short-fiber composites
09 p1298 N85-18152
Circumferential cracks in cylindrical shells
09 p1330 N85-18354
Assessing expired fatigue life in large turbine shafts
[DE84-016676] 09 p1340 N85-18427
Statistical aspects of shear fracture propagation
[ERS-E.368] 09 p1341 N85-18434
A comprehensive study on subliminate crack growth stability and its effects on the load-carrying capacity
[AD-A149037] 10 p1432 N85-19028
Development of surface cracks in AMg6 alloy under low-cycle loading conditions 10 p1442 N85-19089
K sub 1° -n diagram of cyclical crack resistance of aluminum alloys 10 p1442 N85-19090
Impact toughness of composites with layered microstructure of OT4 titanium alloy
10 p1445 N85-19104
Fracture resistance of surface layer with technological defects under cyclical loading 10 p1448 N85-19126
Recovery of damaged solid propellants by interrupting burning and crack-propagation processes
[AD-P004343] 10 p1455 N85-19167
Antiplane cracks in solid propellants
[AD-P004344] 10 p1455 N85-19168
Interaction between a crack and a soft inclusion
[NASA-CR-172533] 10 p1495 N85-19439
Fracture toughness of fiber reinforced concrete
[AD-A149403] 10 p1496 N85-19441
Rock mechanics: Issues and research needs in the disposal of wastes in hydraulic fractures
[DE85-001399] 10 p1556 N85-19809
Fracture analysis of notched composites
[NASA-CR-172583] 11 p1593 N85-20020
Mechanism and pattern of fatigue crack growth in aluminum alloys 11 p1597 N85-20047
Estimating deformability upon pressing of aluminum alloys based on results of mechanical testing
11 p1598 N85-20049
Theoretical and experimental study of crack resistance and macrocrack growth rate in organic fiber reinforced plastic under pure shear condition
11 p1598 N85-20053
Contributions of segregated phosphorus to the intergranular stress corrosion cracking of nickel
[DE85-003112] 11 p1606 N85-20099
Fatigue crack growth in Aramid Reinforced Aluminum Laminates (ARALL): Mechanisms and predictions
[DFVLR-FB-84-37] 11 p1609 N85-20118
Crack growth geometry in aluminum alloy sheet material under flight simulation loading. 1: A comparison between TWIST and minTWIST FALSTAFF and short FALSTAFF. 2: Effect of truncating high loads
[VTH-LR-441] 11 p1609 N85-20119
Direct comparison of unloading compliance and potential drop techniques in J-integral testing
[DE85-001550] 11 p1650 N85-20392
Statistical theory of fragmentation processes
[DE85-002208] 11 p1653 N85-20414
Fatigue crack propagation in mirage 1110 wing main spar specimens and the effects of spectrum truncation on life
[ARL/STRUC-R-405] 12 p1776 N85-21152
Defect characterisation and monitoring by acoustic emission
[AERE-R-11409] 12 p1863 N85-21683
Translational and extensional energy release rates (the J- and M-integrals) for a crack layer in thermoelasticity
[NASA-CR-174872] 12 p1863 N85-21685
Interaction of part-through cracks in a flat plate
[NASA-CR-175586] 12 p1864 N85-21692
The residual strength of cracked specimens representing a section of the mirage into wing main spar
[ARL/STRUC-R-408] 12 p1865 N85-21699
Fracture analysis of cracks in complete cylindrical shells
[AD-A150091] 12 p1867 N85-21711
Fracture toughness of materials
[DE85-004306] 12 p1867 N85-21713
Numerical simulation of static and dynamic shadow patterns using an atomistic description of crack initiation and propagation
[DE85-003226] 12 p1867 N85-21715
Characterisation of fatigue crack extension by quantitative acoustic emission
[AERE-R-11289] 12 p1868 N85-21721
Longitudinal splitting in unidirectional composites, analysis and experiments
[NASA-CR-3881] 13 p2015 N85-22639
Delayed cracking strength of experimental grades of 42 CD 4 steel in aqueous H2S surroundings
[BLL-T6419/BG/LRS/LRST738/84]
13 p2020 N85-22658
Micromechanical modeling of microstructural damage in creeping alloys
[DE85-003925] 13 p2022 N85-22671
Creep crack growth in ductile alloys
[DE85-003937] 13 p2023 N85-22676
Characteristics of surface crack development in AlTiaS aluminum alloy during slow-cycle loading
13 p2034 N85-22745
Fatigue life, crack initiation, and propagation of 304 stainless steel with non-proportional axialtorsional strain-paths 13 p2101 N85-23094
Elastic wave scattering from an interface crack in a layered half space 13 p2101 N85-23095
Fracture mechanics evaluation of GaAs
[NASA-CR-175657] 13 p2102 N85-23101
Advanced life analysis methods. Volume 1: Cracking data survey and NDI (nondestructive inspection) assessment for attachment lugs
[AD-A150419] 13 p2103 N85-23108
Advanced life analysis methods. Volume 2: Crack growth analysis methods for attachment lugs
[AD-A150420] 13 p2103 N85-23109
Advanced life analysis methods. Volume 5: Executive summary and damage tolerance criteria recommendations for attachment lugs
[AD-A151017] 14 p2219 N85-23781
Variability in constant-load-amplitude fatigue crack growth rates in marine environments
[AD-A150786] 14 p2255 N85-23975
Role of passive surface films on corrosion fatigue crack initiation
[DE85-000436] 14 p2257 N85-23985
A study of fatigue crack growth in 2 1/4 Cr1Mo steel. Part 1: The influences of environment and material condition
[AERE-R-11472] 14 p2258 N85-23993
Effect of elevated-temperature neutron irradiation on fracture toughness of ceramics
[DE85-000852] 14 p2261 N85-24010
Advanced life analysis methods. Volume 3: Experimental evaluation of crack growth analysis methods for attachment lugs
[AD-A151058] 14 p2317 N85-24319
Fatigue Crack Topography
[AGARD-CP-376] 14 p2318 N85-24321
Essential features in fatigue fractures and remarkable phenomena in fatigue crack growth
14 p2318 N85-24322
Fatigue crack propagation and fracture in 7050 and 7091 aluminum alloy forgings 14 p2318 N85-24324
Two recent cases of marker load applications on cargo/fighter aircraft fatigue tests
14 p2318 N85-24325
Effect of flight sequences in complex load histories on crack front marking 14 p2318 N85-24326
Periodic loading sequences for the systematic marking of fatigue crack fracture surfaces
14 p2319 N85-24329
On the use of marker loads and replicas for measuring growth rates for small cracks 14 p2319 N85-24331
On the use of marker loads for fatigue crack growth measurements 14 p2319 N85-24332
Fatigue crack topography and crack growth analysis — wrought and cast aluminum 14 p2319 N85-24333
Application of optical and electron microscopic techniques in the fractographic determination of fatigue crack growth rates 14 p2320 N85-24334
New analysis aspects of the fatigue crack propagation behavior by SEM in situ microscopy
14 p2320 N85-24335
Crack propagation under constant and variable stress amplitudes: A comparison of calculations based on the Striation spacing and tests 14 p2320 N85-24336
Crack growth direction in unidirectional off-axis graphite epoxy
[NASA-CR-175752] 15 p2502 N85-25433
Finger materials for air cushion vehicles. Volume 1: Flexible coatings for finger materials
[AD-A151438] 15 p2522 N85-25545
On Rayleigh waves and Rayleigh wave extension of surface micro-cracks 15 p2572 N85-25860
Fatigue life, fatigue crack propagation and fracture toughness study of 7075 aluminum alloy subjected to thermomechanical processing 15 p2573 N85-25862
The effect of overload cycles on fatigue crack propagation in structural steels
15 p2577 N85-25867

The effect of frictional forces on fatigue crack growth in lugs
[AD-A151994] 15 p2578 N85-25898
Fracture problems in power law viscoelastic materials
[AD-A149221] 15 p2578 N85-25900
Entropy production during fatigue as a criterion for failure. A local theory of fracture in engineering materials
[AD-A151289] 15 p2578 N85-25902
Dynamic crack curving and branching under biaxial loading
[AD-A151451] 15 p2578 N85-25904
Transition region for corner cracks at holes
[AD-A151835] 15 p2579 N85-25906
A study of the time dependence in fracture processes relating to service prediction of adhesive joints and advanced composites
[AD-A152064] 15 p2579 N85-25910
Degradation phenomena in solid electrolytes
[DE85-007066] 15 p2587 N85-25949
Advanced life analysis methods. Volume 6: User's manual for LUGRO computer program to predict crack growth in attachment lugs
[AD-A151235] 15 p2626 N85-26195
A review of fracture mechanics life technology
16 p2733 N85-26863
Hydrogen induced crack growth in Grade-12 Titanium
[BNL-NUREG-35598] 16 p2751 N85-26976
Initial quality of advanced joining concepts
[AD-A152241] 16 p2759 N85-27027
Automatic tracking of crack growth via finite elements
16 p2797 N85-27246
Predicting fully plastic mode 2 crack growth from an asymmetric defect
[AD-A152227] 16 p2801 N85-27269
On the use of marker loads for fatigue crack growth measurements
[FFA-TN-1984-52] 16 p2802 N85-27277
The practical and theoretical significance of small cracks: An evaluation
[VTH-LR-432] 16 p2803 N85-27283
USAF damage tolerant design handbook: Guidelines for the analysis and design of damage tolerant aircraft structures, revision B
[AD-A153161] 17 p2898 N85-27858
The synergistic actions of stress corrosion cracking and corrosion fatigue
[BLL-BISI-TRANS-22334-(9022.06)] 17 p2926 N85-28045
Study on mechanism of surface deformation induced by stress corrosion cracking
[BLL-BISI-TRANS-21806-(9022.06)] 17 p2928 N85-28066
Overload effects on sustained load crack growth at elevated temperature
[AD-A153223] 17 p2931 N85-28091
Hydrogen degradation of pipeline steels
[DE85-006930] 17 p2932 N85-28101
Characterization of the fatigue and slow crack growth behavior of partially stabilized zirconia ceramics
[DE85-005240] 17 p2934 N85-28113
Differential between crack and pseudo-crack indications by means of objective magnetic flux leakage testing
[BLL-BISI-TRANS-22033-(9022.06)] 17 p2976 N85-28386
On validity of threshold values of fatigue strength of steel structures
[BLL-BISI-TRANS-22192-(9022.06)] 17 p2978 N85-28408
The fatigue properties of welds at low temperature, according to the type of steel
[BLL-BISI-TRANS-22455-(9022.06)] 17 p2978 N85-28410
Fatigue crack propagation characteristics and fatigue fracture toughness in 780 MPa grade high strength steel weldments at low temperature
[BLL-BISI-TRANS-22369-(9022.06)] 17 p2979 N85-28411
Interaction among inhomogeneities and inclusions
[AD-A153114] 17 p2979 N85-28419
Evaluation of interpolative modeling concepts for fatigue crack growth at elevated temperature
[AD-A153222] 17 p2980 N85-28422
Method of assessment of start of slow crack growth by acoustic emission technique
[BLL-BISI-TRANS-21782-(9022.06)] 17 p3027 N85-28722
Fatigue and chromium-ferritic steels at elevated temperatures
[DE85-007735] 18 p3074 N85-29015
Slow crack growth in metal reinforced glass composites
[DE85-010084] 18 p3082 N85-29064
Ultrasonic testing of plates containing edge cracks
[NASA-CR-3904] 18 p3119 N85-29307
Structural Analysis
[DFVLR-MITT-84-21] 18 p3120 N85-29313
An effective substructure technique applied to crack problems
18 p3121 N85-29319
Crack propation in unidirectional laminates by the stress intensity factors
18 p3121 N85-29320
Description and illustration of the use of CRACKS IV
[AD-A153543] 18 p3121 N85-29325
Study of the influence of metallurgical factors on fatigue and fracture of aerospace structural materials
[AD-A153913] 18 p3122 N85-29328
Fracture of laminated composite materials
19 p3230 N85-30030
Effect of multi-functional inhibitors on the electrochemistry within corrosion crack
19 p3238 N85-30075
Thermo-mechanical and thermal behavior of high-temperature structural materials
[AD-A154154] 19 p3266 N85-30251
Kinetics of H-induced stress corrosion cracking. Part 1: Important features of cracking in respect of high strength steels
[BLL-BISI-TRANS-(9022.06)] 19 p3282 N85-30350
Acoustic emission study of fatigue crack extension position in a stress cycle
19 p3283 N85-30355
Hold-time effects in elevated temperature fatigue crack propagation
[AD-A154146] 19 p3286 N85-30376
Micromechanism of fracture for stage 1 hydrogen-induced crack growth
[DE85-010027] 19 p3288 N85-30390
Fatigue-crack propagation behavior of alloy A-286
[DE85-007460] 19 p3288 N85-30391
Fatigue-crack growth and ductile fracture toughness behavior of ASTM A387 Grade 91 steel
[DE85-008495] 20 p3431 N85-31286
Hot cracking of austenitic stainless steels: The debut of the Sigmajig
[DE85-010560] 20 p3431 N85-31287
Crack growth data for two aluminum alloys 7050-T73651 and 2024-T3
[FFA-TN-1984-51] 20 p3432 N85-31290
Finite element modeling of cracked bodies using the Bodner-Partom flow law
20 p3468 N85-31547
Creep crack growth predictions in INCO 718 using a continuum damage model
20 p3469 N85-31551
A clamped rectangular plate containing a crack
[NASA-CR-177925] 20 p3469 N85-31552
R and D activities of the Materials Science Division
20 p3539 N85-32024
Metallurgical origins of fracture toughness and microstructure and fracture toughness of an HSLA (High-Strength/Low-Alloy) steel
[AD-A155530] 21 p3587 N85-32187
Stress corrosion of ceramic materials
[AD-A155020] 21 p3570 N85-32202
A cracked orthotropic sheet stiffened by a semi-infinite orthotropic sheet
[NASA-TP-2455] 21 p3597 N85-32339
Measurement and analysis of critical crack tip processes during fatigue crack growth
[NASA-CR-172597] 21 p3598 N85-32342
KRAK: A computer program for two-phase two-component porous flow and fracture
[LA-9703] 22 p3782 N85-33434
The influence of temperature on static and dynamic SCC crack growth behavior in aluminum alloy
23 p3905 N85-34190
A fractographic study on mode 2 and mode 3 SCC crack growth in an Al-Zn-Mg alloy
23 p3905 N85-34191
Corrosion fatigue strength and crack growth in prestrained 0.16% C carbon steel
23 p3905 N85-34192
Experimental study on time and temperature dependent behavior of crack growth in viscoelastic strip
23 p3905 N85-34193
Fractographic analysis for nonpropagating conditions of fatigue crack at high stress ratios in mild steel
23 p3905 N85-34194
Crystallographic orientation dependence of fatigue crack propagation in extremely low carbon steel
23 p3906 N85-34195
Influence of cyclic thermal loading on internal stress in casted epoxy resin
23 p3908 N85-34211
Near-threshold fatigue: An overview of the role of microstructure and environment
[DE85-009903] 23 p3941 N85-34431
Fatigue lives of specimens representing critical locations in Mirage 3 spars under Australian and Swiss test spectra
[ARL-STRUC-R-415] 24 p4084 N85-35187
Effect of microstructure on the fatigue behavior of Fe-C-X alloys
[DE85-011749] 24 p4080 N85-35285
Stress-intensity factors for circumferential surface cracks in pipes and rods under tension and bending loads
[NASA-TM-87584] 24 p4101 N85-35424
On size effects in plane stress crack-growth resistance
[AD-A155926] 24 p4102 N85-35426
Evaluation of the crack plane equilibrium model for predicting plastic fractures
[DE85-005558] 24 p4102 N85-35431
Subcritical fracture propagation in rocks: An examination using the methods of fracture mechanics and non-destructive testing
24 p4116 N85-35516

CRACK TIPS

Stress-driven solute enrichment of crack-tips during low ductility intergranular fracture of low-alloy steel
[AERE-R-11120] 03 p0333 N85-12150
Viscoplastic finite element analysis of rapid fracture
03 p0370 N85-12365
Stress intensity factors for corner cracks at holes located near an edge
[FFA-TN-1984-20] 04 p0514 N85-13279
Correlation of stable crack growth with the J-integral and the crack tip opening displacement, effects of geometry, size and material: Report on an investigation of the elastic-plastic R-curve methodology
[GKSS-84-E-37] 08 p1173 N85-17395
The fracture mechanics of a slit crack with crack-tip dual zones
09 p1332 N85-18371
Creep crack growth in ductile alloys
[DE85-003937] 13 p2023 N85-22676
Detecting and analyzing crack defects
[BLL-BISI-TRANS-22062-(9022.06)]
17 p3027 N85-28723
Ultrasonic crack tip method for the determination of crack depth
17 p3028 N85-28725
Crack tip chemistry modeling of intergranular stress corrosion cracks of nickel containing segregated phosphorus and sulphur
[DE85-010059] 18 p3076 N85-29028
A cracked orthotropic sheet stiffened by a semi-infinite orthotropic sheet
[NASA-TP-2455] 21 p3587 N85-32339

CRACKING (CHEMICAL ENGINEERING)

NT PYROLYSIS

Jet fuel property changes and their effect on producibility and cost in the U.S., Canada, and Europe
[NASA-CR-174840] 16 p2757 N85-27012
Crack tip chemistry modeling of intergranular stress corrosion cracks of nickel containing segregated phosphorus and sulphur
[DE85-010059] 18 p3076 N85-29028
The effect of surface reactions in catalytic combustion
[AD-A154217] 19 p3234 N85-30049

CRACKING (FRACTURING)

NT STRESS CORROSION CRACKING

Delayed fracture of high-strength steels in spherical tanks for LP gas
[BLL-RISLEY-TR-4926-(9091.9F)]
01 p0026 N85-10162
Research on high-strength steels with an improved resistance against weld cracking
[AD-A144830] 01 p0027 N85-10170
Thermomechanical cracking due to moving frictional loads
[AD-A146271] 03 p0373 N85-12381
Effect of crack-tip region constraint on fracture in the ductile-to-brittle transition
[PB84-237395] 06 p0770 N85-14926
Research on nondestructive testing
[AD-A148375] 08 p1171 N85-17380
Stress-relieving interlayers for bituminous resurfacings
[PB85-136865] 12 p1820 N85-21415
Advanced life analysis methods. Volume 2: Crack growth analysis methods for attachment lugs
[AD-A150420] 13 p2103 N85-23109
Terrestrial analog studies for Martian patterned ground
13 p2190 N85-23590
An investigation of elevated temperature fatigue crack initiation in 2 and 1/4 cR-1 MO low alloy steel
[AD-A150870] 14 p2255 N85-23973
Fracture toughness of HY-130 steel weld metals
[AD-A150841] 14 p2255 N85-23976
Periodic loading sequences for the systematic marking of fatigue crack fracture surfaces
14 p2319 N85-24329
Mechanical aspects of interfaces and surfaces in ceramic containing systems
[AD-A151978] 15 p2519 N85-25530
Creep ratcheting simplified methods experience from structural design of elevated temperature components
[DE85-007433] 15 p2580 N85-25915
Echo-response from crack-like two-dimensional reflectors in focused ultrasonic fields. Ultrasonic crack tip method for the determination of crack depth
[BLL-BISI-22062-(9022.06)] 16 p2796 N85-27238
Initiation, growth and coalescence of small fatigue cracks
[AD-A151799] 16 p2800 N85-27265

Technical information: Weldability of stainless steel. Part 1: Austenitic stainless steel
[BLL-BISI-TRANS-22456-(9022.06)] 17 p2973 N85-28362
On validity of threshold values of fatigue strength of steel structures
[BLL-BISI-TRANS-22192-(9022.06)] 17 p2978 N85-28408
Interaction among inhomogeneities and inclusions
[AD-A153114] 17 p2979 N85-28419
Detecting and analyzing crack defects
[BLL-BISI-TRANS-22062-(9022.06)] 17 p3027 N85-28723
Echo-response from crack-like two-dimensional reflectors in focused ultrasonic fields 17 p3027 N85-28724
Fatigue and chromium-ferritic steels at elevated temperatures
[DE85-007735] 18 p3074 N85-29015
Fatigue characterization of fabricated ship details for design
[SSC-318] 19 p3285 N85-30371
Study on fracture behavior of epoxy resin 23 p3909 N85-34216

CRACKS
NT CRACK TIPS
NT MICROCRACKS
NT SURFACE CRACKS
Cumulative damage model for advanced composite materials
[AD-A144840] 01 p0022 N85-10135
Wedge with crack in bilastic medium 02 p0273 N85-11780
Study of delamination cracking under static and cyclic loads of carbon-epoxy composite materials
[REPT-42-727/F] 03 p0327 N85-12102
Stress intensity factors for a circular ring with uniform array of radial cracks of unequal depth
[AD-A145893] 03 p0372 N85-12377
Ultrasound interaction with partially closed fatigue cracks
[DE84-016360] 04 p0514 N85-13276
Stress intensity factors for corner cracks at holes located near an edge
[FFA-TN-1984-20] 04 p0514 N85-13279
Processes to increase the fatigue life of constructions with already initiated cracks 05 p0650 N85-14176
Pulse-echo method for flaw detection in concrete
[PB84-234509] 06 p0775 N85-14953
Elastodynamic stress intensity factors of an interface finite-width crack
[DE84-016908] 06 p0817 N85-15190
Cumulative damage modeling of fatigue crack growth 07 p0907 N85-15741
Problems and possibilities for life extension in gas turbine components 07 p0907 N85-15742
Disc fatigue life predictions for gas turbine engines 07 p0907 N85-15743
A general theory of circuit analogy in fracture diagnosis
[AD-A147177] 07 p0978 N85-16212
Buckling analysis of cracked, floating ice sheets
[AD-A147330] 07 p0988 N85-16277
Modeling of real UT transducer field/flaw interactions
[DE85-000941] 09 p1329 N85-18351
The fracture mechanics of a slit crack with crack-tip dual zones 09 p1332 N85-18371
Antiplane cracks in solid propellants
[AD-P004344] 10 p1455 N85-19168
Statistical theory of fragmentation processes
[DE85-002208] 11 p1653 N85-20414
Finger materials for air cushion vehicles. Volume 2: Base fabrics for finger materials
[AD-A149701] 12 p1819 N85-21408
Eddy current test probe with circumferential segments and method of testing material surrounding fastener holes
[AD-D011554] 12 p1850 N85-21609
Defect characterisation and monitoring by acoustic emission
[AERE-R-11409] 12 p1863 N85-21683
Interaction of part-through cracks in a flat plate
[NASA-CR-175588] 12 p1864 N85-21692
Moving nonlocal crack: Anti-plane shear case
[AD-A149996] 12 p1866 N85-21709
Characterisation of fatigue crack extension by quantitative acoustic emission
[AERE-R-11280] 12 p1868 N85-21721
Experimental and numerical analysis of electric currents and electromagnetic blunting of cracks in thin plates
[AD-A150418] 13 p2022 N85-22980
Effects of fracture roughness on fluid flow through a single deformable fracture
[DE85-004593] 13 p2092 N85-23062
Stress intensity factor in a tapered specimen
[NASA-CR-175589] 13 p2102 N85-23099
Fatigue fracture topography 14 p2318 N85-24323
On the corner singularity of a 3-D Griffith crack
[AD-A150980] 14 p2321 N85-24342
Weldability of Ni3Al-type aluminide alloys
[DE85-006932] 15 p2512 N85-25496
Crack elements for COSMIC/NASTRAN 15 p2573 N85-25866
Fracture problems in power law viscoelastic materials
[AD-A149221] 15 p2578 N85-25900
Dynamic crack curving and branching under biaxial loading
[AD-A151451] 15 p2578 N85-25904
Fatigue life extension 16 p2733 N85-26864
The practical and theoretical significance of small cracks: An evaluation
[VTH-LR-432] 16 p2803 N85-27263
Measurement of fracture macro-geometry in evaluating fracture toughness
[BLL-BISI-TRANS-22241-(9022.06)] 17 p2978 N85-28403
On validity of threshold values of fatigue strength of steel structures
[BLL-BISI-TRANS-22192-(9022.06)] 17 p2978 N85-28408
Ultrasonic testing of plates containing edge cracks
[NASA-CR-3904] 18 p3119 N85-29307
Study of the influence of metallurgical factors on fatigue and fracture of aerospace structural materials
[AD-A153913] 18 p3122 N85-29328
Improved model for fluid-driven cracks in jointed rock
[DE85-006963] 18 p3125 N85-29349
Hold-time effects in elevated temperature fatigue crack propagation
[AD-A154146] 19 p3286 N85-30376
Physical and chemical changes to rock near electrically heated boreholes at Spent Fuel Test-Climax
[DE85-010634] 19 p3302 N85-30472
Reliability of welds to repair defects in cast components made from CrMoV steel
[BLL-CE-TRANS-8054-(9022.06)] 20 p3461 N85-31501
Source characterization of point-like and distributed sources of acoustic emission 20 p3523 N85-31910
Automatic capability to store and retrieve component data and to calculate structural integrity of these components
[DE85-012429] 22 p3631 N85-33728
Damage induced stress redistribution in composite laminates 24 p4072 N85-35235
On size effects in plane stress crack-growth resistance
[AD-A156926] 24 p4102 N85-35426

CRANES
NT GANTRY CRANES
Increase in performance and improvement of ride comfort of self-propelled construction machinery by reducing pitch and vertical vibration
[AD-P004269] 09 p1405 N85-18845
Modernization of running gear of crane 14 p2286 N85-24163

CRANKED WINGS
U SWEPT WINGS

CRASH INJURIES
Functional impairment and structureal cervical injuries in human surrogates
[PB85-167436] 15 p2619 N85-26137
Design and testing of an energy-absorbing crewseat for the F/FB-111 aircraft. Volume 3: Data from crew module testing
[NASA-CR-3918] 23 p3896 N85-34134

CRASH LANDING
NT DITCHING (LANDING)
Safety recommendation(s), A-84-65
[REPT-3908] 14 p2216 N85-23743
Safety recommendation(s), A-84-93 through -95
[REPT-3983/33] 14 p2216 N85-23746
Air carrier overwater emergency equipment and procedures
[PB85-917006] 21 p3553 N85-32105
Aircraft accident report: World Airways Inc., Flight 30H, McDonnell Douglas DC-10-30CF, N113WA, Boston-Logan International Airport, Boston, Massachusetts, January 23, 1982
[PB85-910406] 22 p3728 N85-33114

CRASHES
NT CRASH LANDING
NT DITCHING (LANDING)
Establishment of posture and working movements of pilot in air crash enquiries 07 p1010 N85-16417
Annual review of aircraft accident data: US air carrier operations calendar year 1981
[NTSB/ARC-85/01] 12 p1774 N85-21134
The clinical and biomedical evaluation of trauma and fatalities associated with aircrew ejection and crash. A Working Group report
[AGARD-AR-194] 12 p1906 N85-21969
Introduction: The clinical and biomedical evaluation for trauma and fatalities associated with aircrew ejection and crash 12 p1906 N85-21970
Safety recommendation(s), A-84-93 through -95
[REPT-3983/33] 14 p2216 N85-23746
Structures and Dynamics Division research and technology plans for FY 1985 and accomplishments for FY 1984
[NASA-TM-86417] 15 p2577 N85-25865
General Aviation Crashworthiness Project. Phase 2: Impact severity and potential injury prevention in general aviation accidents
[PB85-917002] 19 p3215 N85-29938
Analysis of rotorcraft crash dynamics for development of improved crashworthiness design criteria
[FAA-CT-85-11] 20 p3391 N85-31031

CRASHWORTHINESS
Crashworthiness of light aircraft fuselage structures: A numerical and experimental investigation 01 p0080 N85-10399
Full-scale crash-test evaluation of two load-limiting subfloors for general aviation airframes
[NASA-TP-2380] 04 p0512 N85-13267
A study of crashworthiness of light aircraft fuselage structures: A numerical and experimental investigation
[UTIAS-286] 06 p0750 N85-14803
Proceedings of the International Conference and Exposition on Structural Impact and Crashworthiness
[AD-A147845] 07 p0900 N85-15703
Recommended improvements for second generation 121.5/243 MHz ELT's
[NASA-CR-175274] 08 p1080 N85-16841
The Shock and Vibration Digest, volume 17, no. 2
[AD-A153129] 17 p2977 N85-28400
Recent progress in the dynamic plastic behaviour of structures, part 4 17 p2978 N85-28402
General Aviation Crashworthiness Project. Phase 2: Impact severity and potential injury prevention in general aviation accidents
[PB85-917002] 19 p3215 N85-29938
Impact dynamics research on composite transport structures
[NASA-TM-86391] 19 p3284 N85-30367
The role of aircraft panel materials in cabin fires and their properties
[FAA-CT-84-30] 21 p3553 N85-32104
Seat experiments for the full-scale transport aircraft controlled impact demonstration
[AD-A155024] 21 p3553 N85-32106
DYNA3D, INGRID, and TAURUS: An integrated, interactive software system for crashworthiness engineering
[DE85-010928] 21 p3677 N85-32846
Flight test experience and controlled impact of a large, four-engine, remotely piloted airplane
[NASA-TM-86736] 22 p3730 N85-33123
Aviation safety (aircraft passenger survivability and cabin safety)
[GPO-39-847] 23 p3895 N85-34130
Design and testing of an energy-absorbing crewseat for the F/FB-111 aircraft. Volume 3: Data from crew module testing
[NASA-CR-3918] 23 p3896 N85-34134
Design and testing of an energy-absorbing crewseat for the F/FB-111 aircraft. Volume 2: Data from seat testing
[NASA-CR-3917] 24 p4084 N85-35184

CRATERING
NT PROJECTILE CRATERING
Impact cratering: The process and its effects on planetary evolution — and silicate-carbonate reactions on Venus
[NASA-CR-174016] 02 p0228 N85-11488
Impact and collisional processes in the solar system
[NASA-CR-174297] 08 p1255 N85-17914
Reports of the Planetary Geology and Geophysics Program, 1984
[NASA-TM-87563] 13 p2172 N85-23474
Study and estimation of planet-crossing asteroid populations: Discoveries and analysis 13 p2175 N85-23486
Impact and collisional processes in the solar system 13 p2180 N85-23530
Centrifuge impact cratering experiments 13 p2181 N85-23533
Progress on Experimental impact studies 13 p2181 N85-23534
Progress on studies of early intense cratering 13 p2181 N85-23535
Martian terrain ages 13 p2181 N85-23537
Impacts in ice: Commissions of solar system crater population 13 p2181 N85-23538
Problems in recovering crater production functions 13 p2182 N85-23539
A parmetric study of crater-saturation simulation 13 p2182 N85-23540

Ring-diameter ratios for multi-ring basins average 2.0(0.5)D 13 p2182 N85-23542
Morphology and mechanics of terraces in lunar craters 13 p2182 N85-23543
The nature of Martian flow ejecta craters 13 p2183 N85-23545
Periodic cometary showers: Real or imaginary? 15 p2680 N85-26555
Planetary surface processes: A review 22 p3855 N85-33869

CRATERS
NT LUNAR CRATERS
NT MARS CRATERS
NT METEORITE CRATERS
NT PLANETARY CRATERS
NASA-Ames vertical gun 04 p0579 N85-13696
Searching for impact craters using space shuttle photography 06 p0889 N85-15645
Shuttle navigation status 08 p1092 N85-16901
Dark halo craters and the thickness of grooved terrain on Ganymede 13 p2173 N85-23484
Average spacing for rings of individual multi-ring basins is 2.0(0.5)D 13 p2182 N85-23541
Ring-diameter ratios for multi-ring basins average 2.0(0.5)D 13 p2182 N85-23542
Ridged plains of Lunae Planum: Thickness distribution revised 13 p2185 N85-23559
Planetary analogs in Antarctica: Icy satellites 13 p2193 N85-23605
Analyses of radar images of small craters 13 p2199 N85-23642
Impact processes and their implications for planetary formation and early evolution 22 p3853 N85-33860

CRATONS
The mineralogy of global magnetic anomalies [E85-10061] 07 p0987 N85-16272
Synthesis of proterozoic data as a prerequisite for tectonic and thermal modeling [NASA-CR-174252] 07 p0995 N85-16323

CRAY COMPUTERS
U: The universal utility controller, revision 1 [DE84-017077] 04 p0547 N85-13481
Preliminary user's guide for BIGONE on the Cray [DE84-017075] 04 p0568 N85-13623
Reentrancy and multitasking on CRAY computers [DE85-007256] 15 p2630 N85-26211
Introduction to programming multiple-processor computers [DE85-010274] 18 p3164 N85-29599
Performance and library issues for mathematical software on high performance computers [DE85-010263] 19 p3339 N85-30690
Experiments and improvements of the ordinary differential equation solvers DEPAC on the CRAY computer [DE85-013260] 22 p3831 N85-33726
Parallel processing on the Livermore VAX 11/780-4 parallel processor system with compatability to Cray Research, Inc. (CRI) multitasking, version 1 [DE85-011856] 23 p3967 N85-34595

CRAZING
U SURFACE CRACKS

CREATION
U CREATIVITY

CREATIVITY
Central problems in the management of innovation [AD-A152598] 17 p3047 N85-28852

CREEP ANALYSIS
Strength analysis of fan-shaped wing considering temperature deformation and creep deformations 06 p0779 N85-14963
Recommendations for the use of Ni-Cr-base alloy extensometers for measurement of creep strain [NPL-DMA(A)-81] 08 p1164 N85-17342
Stress studies in EFG [NASA-CR-175464] 10 p1509 N85-19522
Low dose irradiation creep of pure nickel [DE85-006320] 16 p2751 N85-26975
Interferometric creep testing [AD-A154249] 19 p3266 N85-30378

CREEP BUCKLING
A new rheological model for concrete structural analysis [DE84-014743] 11 p1653 N85-20413
Dynamic creep buckling: Analysis of shell structures subjected to time-dependent mechanical and thermal loading 17 p2913 N85-27959
A state variable approach to transient creep deformation in stress reduction experiments [DE85-009492] 18 p3122 N85-29331

CREEP PROPERTIES
NT SHEAR CREEP
NT STEADY STATE CREEP
NT TENSILE CREEP
Evaluation of the role of diffusion creep in superplastic deformation 01 p0021 N85-10127
Nonlinear structural and life analyses of a combustor liner 02 p0141 N85-10955
Creep-fatigue life prediction for engine hot section materials (isotropic) 02 p0144 N85-10974
Life prediction and constitutive models for anisotropic materials 02 p0144 N85-10976
Swaged Mo-5 percent W alloy and recrystallized commercially pure molybdenum 02 p0160 N85-11208
Microstructure and creep behaviour at elevated temperature of unidirectionally solidified eutectic nickel base superalloys 02 p0181 N85-11216
Critical assessment of low fluence irradiation creep mechanisms [DE84-015578] 02 p0184 N85-11232
Determination of nonlinear viscoelasticity parameters for polymeric and composite materials by numerical methods [AD-A145311] 02 p0185 N85-11240
Reliability considerations for the total strain range version of strainrange partitioning [NASA-CR-174757] 02 p0209 N85-11380
High temperature deformation of hot-pressed polycrystalline orthoenstatite [NASA-CR-174026] 02 p0285 N85-11861
The rheology of icy satellites [NASA-CR-174024] 02 p0302 N85-11959
Accelerated viscoelastic characterization of T300/5208 graphite-epoxy laminates 03 p0325 N85-12091
Evaluation of ferritic alloy Fe-2 1/4Cr-1Mo after neutron irradiation: Irradiation creep and swelling [DE84-014647] 04 p0474 N85-13022
Cavitation phenomenon in superplastic creep [DE84-015484] 04 p0513 N85-13271
The effect of trace elements on the properties at high temperature of a Ni-Cr-base alloy 05 p0617 N85-13944
Influence of the mechanical and electrochemical characteristics of austenitic and austenoferritic steels on the propagation rate and morphology of stress corrosion cracking [BLL-RISLEY-TR-4545-(9091.9F)] 06 p0767 N85-14906
Longevity of thin-walled engine parts subjected to transient stresses under creep conditions 06 p0777 N85-14966
Irradiation creep induced anisotropy in a/2110 dislocation populations [DE84-016523] 05 p0868 N85-15520
Study of residual stresses introduced into TA6ZrD (685) cylinders by quenching [BLL-PNR-90240-(8019.3153)] 07 p0925 N85-15859
Investigation of the creep behaviour of soft soldered joints with solder L-SnAg5 at ambient temperature [BLL-T6363/BG/WH798/84] 07 p0926 N85-15865
Back stress in dislocation creep. Part 1: Basic concepts and measuring techniques [NASA-TM-77773] 07 p0977 N85-16206
Electrodes for repairing power engineering equipment made from creep resisting steel [BLL-CE-TRANS-8064-(9022.09)] 08 p1167 N85-17360
Elevated temperature creep behavior of Inconel alloy 625 [DE84-015836] 09 p1297 N85-18144
Creep deformation of compacted decomposed granite soils 09 p1303 N85-18187
Comparison of property regeneration techniques and life prediction procedures applied to laboratory tested and service exposed Ni-Cr alloys [NPL-DMA(A)-91] 09 p1333 N85-18374
Cavitation phenomenon in superplastic creep [DE85-001716] 10 p1441 N85-19083
Stress studies in EFG [NASA-CR-175488] 10 p1503 N85-19856
Non-isothermal irradiation creep of nickel alloys Inconel 706 and PE-16 [DE85-000842] 11 p1607 N85-20102
Accelerated viscoelastic characterization of T300-5208 graphite-epoxy laminates [NASA-CR-3871] 12 p1797 N85-21271
Multiaxial stress response of ceramics [DE85-004350] 12 p1814 N85-21379
Steel castings by the electroslag casting technique [DE85-003812] 12 p1819 N85-21409
Creep crack growth in ductile alloys [DE85-003937] 13 p2023 N85-22676
Some specifics of development of fatigue and creep in heat-resistant alloys with asymmetrical multicycle loading 13 p2031 N85-22724
Densification and deformation in the presence of a liquid phase [DE85-005101] 13 p2038 N85-22763
Microstructure and properties of ferrous alloy weldments [DE85-005582] 14 p2257 N85-23987
Variation in the spacing of dislocations in subgrain boundaries with creep strain in Type 304 stainless steel [DE85-006184] 15 p2511 N85-25493
Creep ratcheting simplified methods experience from structural design of elevated temperature components [DE85-007433] 15 p2580 N85-25915
Method of investigating accumulations of damage to weld joints in the case of low-cycle creep [BLL-CE-TRANS-8088-(9022.09)] 16 p2792 N85-27219
Liquid-metal transducers for strain measurement during in-pile materials testing 17 p2945 N85-28176
Influence of materials creep on rotor dynamics [DE85-008545] 17 p2961 N85-28426
Interferometric creep testing [AD-A154249] 19 p3266 N85-30378
Creep fatigue life prediction for engine hot section materials (isotropic) [NASA-CR-168228] 20 p3394 N85-31057
Long range ordered alloys modified by addition of niobium and cerium [DE85-011661] 20 p3431 N85-31285
A comparison of two contemporary creep-fatigue life prediction methods 20 p3467 N85-31538
Estimation of power-law creep parameters from bend test data [PB85-183406] 20 p3472 N85-31579
The effect of stress and hot corrosion on nickel-base superalloys [AD-A154722] 21 p3566 N85-32181
SANCHO: A finite element computer program for the quasistatic, large deformation, inelastic response of two-dimensional solids [DE85-011456] 22 p3829 N85-33714
Short-time creep of ice [NRC/CNR-TT-2111] 23 p3941 N85-34428

CREEP RESISTANCE
U CREEP STRENGTH

CREEP RUPTURE STRENGTH
The effects of seven alloying elements on the microstructure and stress-rupture behavior of nickle-base superalloys [NASA-TM-83791] 01 p0027 N85-10168
Improved multiaxial creep-rupture strength criterion [DE84-014273] 01 p0062 N85-10413
Effects of tin on microstructure and mechanical behavior of Inconel 718 [NASA-TM-86866] 03 p0330 N85-12129
Stirling material technology [NASA-TM-86888] 04 p0472 N85-13007
Non-linear data fitting for the analysis of creep rupture data on GRP materials in aggressive environments — glass reinforced plastics (GRP) [NPL-DMA(A)-79] 04 p0512 N85-13261
The effect of trace elements on the properties at high temperature of a Ni-Cr-base alloy 05 p0617 N85-13944
Method for predicting the creep rupture life of nickel-base precipitation-hardened superalloys from their chemical composition [BLL-PNR-90241-(8019.3153)] 06 p0768 N85-14910
Inconel 718 alloy resistance to crack propagation 07 p0907 N85-15740
Strain-controlled creep rupture in non-isothermal materials 09 p1332 N85-18368
Creep-rupture behavior of iron superalloys in high-pressure hydrogen [NASA-CR-174411] 10 p1441 N85-19078
High-thermal-gradient superalloy crystal growth 17 p2914 N85-27966
Experiments and micromechanical models for creep-rupture in polymer matrix composites [DE85-009533] 17 p2935 N85-28118
Fatigue behavior of synthetic fibers, yarns and ropes 17 p2979 N85-28415
Long-term strength of glass fibre/phenolic resin composites [NPL-DMA(A)-98] 22 p3742 N85-33195

CREEP STRENGTH
The metallurgical processes during the soft soldering of copper and copper alloys and the strength characteristics of soldered joints [BLL-T6388/BG/WH803/84] 06 p0767 N85-14908
Advanced stress analysis methods applicable to turbine engine structures [NASA-CR-175573] 12 p1778 N85-21165
Alloys based on NiAl for high temperature applications [NASA-TM-86976] 12 p1805 N85-21322
Investigation of the development possibilities of a ferritic creep and oxidation-resistant steel for application under creep conditions above 650 deg C [BMFT-FB-T-84-244] 12 p1808 N85-21344

Finite element model for creep in composite masonry
[PB85-150324] 14 p2322 N85-24947
An investigation of the structure and high temperature mechanical properties of oxide dispersion strengthened alloys
[AD-A151107] 15 p2509 N85-25477
Mechanical properties of polycrystalline alpa titanium
[BLL-BISI-TRANS-21923-(9022.06)] 17 p2924 N85-28029
Load-carrying capabilities of refractory alloys for space reactor power applications
[DE85-010566] 19 p3240 N85-30087
The effect of stress and hot corrosion on nickel-base superalloys
[AD-A154722] 21 p3566 N85-32181
The development and evaluation of the creep and corrosion resistant alloy IN6201
[PNR-90253] 23 p3917 N85-34278

CREEP TESTS
Interactions between corrosion and creep of uncoated and coated superalloys in sulfate melts 04 p0477 N85-13038
The creep and creep rupture of SMC-R50 under different thermomechanical conditions 05 p0648 N85-14160
The effect of the test atmosphere on the formation and propagation of creep cracks in commercial high temperature alloys
[JUEL-1939] 07 p0980 N85-16221
Creep-fatigue interaction of notched 304 stainless steel bars 16 p2798 N85-27249
Design and fabrication of durable owner-built wind turbine blades
[DE85-009200] 20 p3484 N85-31650
The effect of stress and hot corrosion on nickel-base superalloys
[AD-A154722] 21 p3566 N85-32181
A continuous damage model based on stepwise-stress creep rupture tests
[NASA-CR-174941] 21 p3597 N85-32341
Tensile testing apparatus
[NASA-CASE-LAR-13243-1] 23 p3933 N85-34375

CRESTATRONS
U TRAVELING WAVE TUBES

CRESTS
U WAVES

CREVASSES
NT GLACIERS

CREVICES
U CRACKS

CREW PROCEDURES (INFLIGHT)
A comparative evaluation of EMADS (Engine Monitoring and Display System) and conventional engine instruments
[AD-A145901] 03 p0319 N85-12060
Aircraft accident report, Scandinavian Airlines System, Flight 901, McDonnell Douglas DC-10-30, John F. Kennedy International Airport, Jamaica, New York, February 28, 1984
[PB84-910415] 05 p0594 N85-13788
A full mission simulator study of aircrew performances: The measurement of crew coordination and decisionmaking factors and their relationships to flight task performances 05 p0710 N85-14556
Multi-crew model analytic assessment of landing performance and decision-making demands 05 p0712 N85-14567
Influence of a perspective cockpit traffic display format on pilot avoidance maneuvers 10 p1534 N85-19668
Contamination control for increased crew productivity 18 p3158 N85-29555

CREW STATIONS
NT CREW WORKSTATIONS
The human role in space. Volume 3: Generalizations on human roles in space
[NASA-CR-171225] 04 p0546 N85-13475
Avionics/crew station integration 06 p0752 N85-14818
Crewstation design and validation 06 p0752 N85-14822
Display Techniques for Advanced Crew Stations (DTACS). Phase 1: Display technique study
[AD-A146922] 07 p0904 N85-15722
Proceedings of the 6th Advanced Aircrew Display Symposium
[AD-A150044] 12 p1778 N85-21160
Habitability sleep accommodations 18 p3159 N85-29566
Crew systems and flight station concepts for a 1995 transport aircraft
[NASA-CR-166068] 19 p3221 N85-29973

CREW WORKSTATIONS
An analysis of constraints to coordinated tactical crew interaction in the P-3C aircraft
[AD-A147220] 07 p1021 N85-16478
A computer aided Multi-Man-Machine Work Area Design and Evaluation System (MAWADES)
[AD-A147950] 08 p1199 N85-17554

CREWS
NT FLIGHT CREWS
NT SPACECREWS
The human role in space. Volume 2: Research analysis and technology report
[NASA-CR-171224] 04 p0546 N85-13474
Crew communication as a factor in aviation accidents 05 p0710 N85-14555
Communication on the flight deck 05 p0711 N85-14557
A crew exposure study. Volume 1: Offshore
[AD-A146884] 07 p1015 N85-16449
The sinking of the Les Mutuelles du Mans trimaran 14 p2327 N85-24384
The ARGOS contribution to the demonstration of the effectiveness of a satellite-based search and rescue system 14 p2330 N85-24404
Space station crew safety alternatives study, volume 1
[NASA-CR-3854] 19 p3223 N85-29985
A crew exposure study. Phase II. Volume 2. At sea. Part A
[AD-A155233] 21 p3666 N85-32774
Design and testing of an energy-absorbing crewseat for the F/FB-111 aircraft. Volume 3: Data from crew module testing
[NASA-CR-3918] 23 p3896 N85-34134

CRIME
Computer crime
[GPO-30-544] 10 p1537 N85-19691

CRITERIA
NT STRUCTURAL DESIGN CRITERIA
The identification of the scientific community's choice criteria in the history of scientific research: The case of quantum mechanics
[NOTA-INTERNA-797] 02 p0291 N85-11893
Measurement procedures for the radar spectrum engineering criteria
[PB85-119022/GAR] 09 p1313 N85-18254
Transient vibration test criteria for spacecraft hardware — galileo spacecraft 09 p1336 N85-18418
Experimental investigation of a breakdown criterion for a vortex in an incompressible flow — delta wing
[ONERA-RT-27/1147-AY] 11 p1577 N85-19935
Stability results for discrete Volterra equations: Numerical experiments
[CWI-NM-R8409] 11 p1707 N85-20743
Stochastic runaway of dynamical systems
[IPP-6/244] 11 p1708 N85-20745
Air quality criteria for ozone and other photochemical oxidants. External review draft, volume 4
[PB85-126068] 12 p1886 N85-21838
Personal decision making: The influence of perceived locus of control and degree of rationality on information seeking strategies 13 p2167 N85-23446
Discovery refutation and verification refutation: The proposals of Von Neumann and Wiener in the development of 20th century physics
[NOTA-INTERNA-840] 14 p2431 N85-24993
Selection of promising sites for magma energy experiments
[DE85-006832] 16 p2820 N85-27393

CRITICAL EXPERIMENTS
Drag-free satellite simulator
[REPT-615] 12 p1789 N85-21229

CRITICAL FLOW
Investigation of phase separation models in RELAP 4/MOD 6
[OEFZS-4286] 05 p0638 N85-14093
Critical flashing flow of subcooled fluids in nozzles with contour discontinuities
[DE84-017229] 09 p1319 N85-18296
Flow-induced vibration of the SSME LOX posts: Additional issues
[DE85-007339] 16 p2741 N85-26916

CRITICAL FREQUENCIES
Global maps of foF2 derived from observations and theoretical values
[AD-A145866] 03 p0392 N85-12509
Dispersion curves for normal waves in cylindrical shell and conditions for spatial coincidence in vicinity of critical frequencies 08 p0778 N85-14973
Linear problem of harmonic vibrator acting at supercritical frequencies in subsonic boundary layer 08 p0779 N85-14978
Domain of applicability of asymptotic description of radio pulse fields near critical frequency 13 p2073 N85-22949

CRITICAL LOADING
Design oriented identification of critical points in transient response 09 p1330 N85-18357
An evaluation of the 64-meter antenna radial bearing for use on the 70-meter antenna 10 p1464 N85-19238
Spectral frequency of eigenvalues in optimal problems of stability of cylindrical shells of variable thickness 13 p2047 N85-22815

CRITICAL MACH NUMBER
U CRITICAL VELOCITY
U MACH NUMBER

CRITICAL MASS
A very important process of nucleosynthesis in stars
[OG-7.1-11] 23 p4014 N85-34872

CRITICAL PATH METHOD
On stochastic integral representation of stable processes with sample paths in Banach spaces
[AD-A152927] 17 p3025 N85-28703
Method of characterizing critical timing paths and analyzing timing related failure modes in very large scale integrated circuits
[AD-D011731] 22 p3759 N85-33298

CRITICAL POINT
Critical point wetting drop tower experiment 02 p0155 N85-11045
The isochoric heat capacity of fluid substances in the critical region. Pre-examinations for a Spacelab experiment
[BMFT-FB-W-84-034] 05 p0723 N85-14650
A study of degenerate and nondegenerate critical points in three-dimensional flow fields
[DFVLR-FB-84-36] 11 p1633 N85-20288
Explorations into thermodynamics analogies and critical points in reference to gas-solid transport
[DE85-000616] 11 p1738 N85-20929
Special features of the temperature dependence of the capillary constant in the vicinity of the critical point
[BLL-T6436/BG/LRS/LRST750/85] 16 p2859 N85-27632

CRITICAL PRESSURE
Liquid-phase compositions from vapor-phase analyses 2: Adaptation of the Prausnitz program to UF6 and some of its potential impurities
[DE85-011521] 21 p3673 N85-32819

CRITICAL REYNOLDS NUMBER
U CRITICAL VELOCITY
U REYNOLDS NUMBER

CRITICAL SPEED
U CRITICAL VELOCITY

CRITICAL STRESS
U CRITICAL LOADING

CRITICAL TEMPERATURE
Critical point wetting drop tower experiment 02 p0155 N85-11045
External fuel vaporization study, phase 2
[NASA-CR-174079] 02 p0187 N85-11252
Calculation of critical temperature for Nb-Cu multilayer film superconductor
[AD-A144321] 02 p0274 N85-11786
Storage life of thermal detents
[DE84-016934] 04 p0476 N85-13030
Modeling the thermal explosion phenomenon in solid propellants: The case of fixed and variable temperatures 08 p1117 N85-17044
Convection heat transfer in the critical region of fluid mixtures
[DE85-001282] 11 p1633 N85-20285
Examination of the contact wetting angle in the vicinity of critical temperature
[BLL-T6416/BG/CRS/LR-ST735/84] 13 p2091 N85-23054
Lattice Monte Carlo calculations of finite temperature QCD
[DE86-004035] 14 p2431 N85-24992
Self-heating to ignition measurements and computation of critical size for solar energy collector materials
[PB85-163374] 20 p3485 N85-31663

CRITICAL VELOCITY
Critical velocities in He II for independently varied superfluid and normal fluid velocities 09 p1396 N85-18784
Shuttle Molecular Gun: Smog. Potential experiment for the electrodynamic Tethered Satellite System (TSS) mission
[IFSI-84-17] 20 p3419 N85-31221
Improved turbopump dynamics
[NASA-TM-86514] 20 p3462 N85-31509
On the role of the magnetic field strength in critical ionization velocity interaction
[TRITA-EPP-85-01] 20 p3536 N85-32003

CROCCO METHOD
Existence and non-uniqueness of similarity solutions of a boundary layer problem
[NASA-CR-172503] 07 p0957 N85-16064

CROP DUSTING
Effectiveness of agricultural aviation 04 p0544 N85-13460
Operation of aviation support bases 04 p0544 N85-13461
Director on institute's civil aviation projects 08 p1057 N85-16764

Improved sprayer for AN-2 cropdusting work
08 p1068 N85-16769
CROP GROWTH
Remote sensing of plant stress and diseases
05 p0657 N85-14216
Timing in dry seeds 05 p0690 N85-14437
Spectral estimators of absorbed photosynthetically active radiation in corn canopies
[E85-10041] 07 p0983 N85-16242
Growth/reflectance model interface for wheat and corresponding model
[E85-10058] 07 p0987 N85-16269
Controlled ecological life support system higher plant flight experiments
[NASA-CR-177323] 07 p1020 N85-16471
Growth and reflectance characteristics of winter wheat canopies
[E85-10080] 10 p1505 N85-19494
NOAA-AISC user's guide for implementing CERES maize model for large area yield estimation
[E85-10083] 12 p1873 N85-21748
Research on zero-gravity botany apparatus
16 p2723 N85-26811
Evaluation of the area and severity of last night's frosts
[REPT-109] 16 p2833 N85-27473
Publications of the NASA CELSS (Controlled Ecological Life Support Systems) program
[NASA-CR-3911] 19 p3326 N85-30608
Deficit irrigation feasibility study and demonstration project
[DE85-011531] 22 p3802 N85-33555
CROP IDENTIFICATION
Biophysical and spectral modeling for crop identification and assessment
[E85-10006] 02 p0215 N85-11419
Basic principles, methodology, and applications of remote sensing in agriculture
[E85-10016] 02 p0217 N85-11429
Application of digital analysis of MSS to agro-environmental studies
[E85-10024] 02 p0218 N85-11437
Characterization of LANDSAT-4 TM and MSS image quality for the interpretation of California's agricultural resources — Central Valley 13 p2118 N85-23190
An initial analysis of LANDSAT-4 Thematic Mapper data for the discrimination of agricultural, forested wetlands, and urban land cover — Poinsett County, Arkansas; and Reelfoot Lake and Union City, Tennessee
13 p2118 N85-23193
Preliminary evaluation of Thematic Mapper image data quality 13 p2118 N85-23194
Interpretation of multiband photographs made during Telefoto-80 experiment for the purpose of discriminating agricultural crops 22 p3735 N85-33152
Direct regression analysis of remote sensing data (using example of grass cover) 22 p3738 N85-33157
CROP INVENTORIES
Executive report: Results of the IRGA-CNPq/INPE experimental project
[E85-10011] 02 p0216 N85-11424
Basic principles, methodology, and applications of remote sensing in agriculture
[E85-10016] 02 p0217 N85-11429
Multispectral (X and C band) crop classification with synthetic aperture radar (SAR-580) optical data
05 p0657 N85-14217
Multi crop area estimation in Idaho using EDITOR
[E85-10054] 06 p0827 N85-15251
Calibration or inverse regression: Which is appropriate for crop surveys using LANDSAT data?
07 p0985 N85-16260
Remote sensing research for agricultural applications — San Joaquin County, California and Snake River Plain and Twin Falls area, Idaho
[E85-10090] 12 p1873 N85-21752
Thematic Mapper data quality and performance assessment in renewable resources/agriculture/remote sensing 13 p2120 N85-23201
CROP INVENTORIES BY REMOTE SENSING
U AGRISTARS PROJECT
CROPLANDS
U FARMLANDS
CROPS
Research activities of the Illinois University Coordinated Science Laboratory
[AD-A145589] 03 p0449 N85-12856
Thematic Mapper spectral dimensionality and data structure 12 p1871 N85-21736
CROSS CORRELATION
Optimum parameters for determining the motion of radar field by cross-correlation method
01 p0079 N85-10524
Electrostatic wave observation during a space simulation Beam-Plasma-Discharge (BPD)
[NASA-CR-174286] 07 p1045 N85-16639
The analysis of spaced sensor records by correlation techniques 08 p1184 N85-17465
Method and apparatus for calibrating the ionosphere and application to surveillance of geophysical events
[NASA-CASE-NPO-15430-1] 12 p1887 N85-21846
Regular synthesis of pairs of phase-keyed binary minimax signals 13 p2069 N85-22923
Parametric coherence estimation via convolved correlations
[DE85-003946] 14 p2416 N85-24909
Higher order residual analysis for nonlinear time series with autoregressive correlation structures
[AD-A149232] 15 p2636 N85-26257
Scene analysis using recursive frequency domain correlation with energy normalization
[AD-A151777] 16 p2954 N85-27596
Optical 3-D signature device for detecting chemical agents
[AD-D011669] 19 p3272 N85-30293
CROSS COUPLING
Quantification of cross-coupling and motion feedthrough for multiaxis controllers used in an air combat flying task
05 p0700 N85-14491
Particle sources, transport, storage and precipitation — magnetosphere 14 p2359 N85-24576
Electrodynamics of magnetosphere-ionosphere coupling 14 p2359 N85-24579
Ionosphere-magnetosphere coupling and convection
14 p2364 N85-24609
Magnetosphere-ionosphere interaction through hydromagnetic waves 14 p2364 N85-24610
CROSS FAULTS
U GEOLOGICAL FAULTS
CROSS FLOW
Jet array impingement flow distributions and heat transfer characteristics: Effects of initial crossflow and nonuniform array geometry 02 p0142 N85-10967
Dilution zone mixing studies 02 p0145 N85-10984
Dilution jet mixing 02 p0145 N85-10985
Tunnel constraint for a jet in crossflow
03 p0314 N85-12027
A study of flow past an airfoil with a jet issuing from its lower surface
[NASA-CR-166810] 04 p0451 N85-12660
Computer programs to predict induced effects of jets exhausting into a crossflow
[NASA-CR-166591] 05 p0592 N85-13776
An experimental study of single and multiple turbulent buoyant jets in crossflow 09 p1317 N85-18281
Turbulent bouyant flow and pressure variations around a circular cylinder in a cross uniform flow near the ground 09 p1318 N85-18287
Effect of inclination, transverse intertip spacing, and logitudinal pitch on crossflow heat transfer from an array of finned tubes 10 p1482 N85-19359
Flow visualization study of the effect of injection hole geometry on an inclined jet in crossflow
[NASA-TM-86936] 11 p1631 N85-20269
Non-steady combustion of composite solid propellants
[AD-A150827] 14 p2250 N85-23947
Development of a temperature measurement system with application to a jet in a cross flow experiment
[NASA-CR-174896] 15 p2472 N85-25262
Numerical calculation of subsonic jets in crossflow with reduced numerical diffusion
[NASA-TM-87003] 15 p2472 N85-25263
The influence of jet-grid turbulence on heat transfer from the stagnation region of a cylinder in crossflow
[NASA-TM-87011] 15 p2554 N85-25760
Design and construction of a computer controlled mirothermocouple probe for the study of buoyant jets
[AD-A152224] 16 p2788 N85-27199
A study of aerodynamic control in stalled flight leading-edge vortex formation analysis
[AD-A153758] 18 p3059 N85-28928
Acroswind response of towers and stacks of circular cross-section 19 p3282 N85-30354
Microprocessor control design for a low-head crossflow turbine
[AD-A155477] 21 p3556 N85-32121
Wingtip vortex propeller
[NASA-CASE-LAR-13019-1] 24 p4065 N85-35194
CROSS POLARIZATION
Environmentally independent fiber optic rotation sensor
[AD-D011219] 01 p0119 N85-10818
Scattering from snow backgrounds at 35, 98, and 140 GHz
[AD-A145798] 03 p0355 N85-12280
Mechanical/thermal design of a polarization sensitive reflector — communication satellites
05 p0626 N85-14009
The impact of propagation effects on the design of high capacity digital microwave links in the 18 GHz frequency band 10 p1470 N85-19278
CROSS RELAXATION
Contribution of relaxation sounding experiments to the understanding of magnetospheric processes
14 p2371 N85-24655
CROSS SECTIONS
Experimental studies of atomic inner shell ionization phenomena
[DE84-013448] 01 p0118 N85-10805
Stark broadening of H(-) resonances in large electric fields
[DE84-016974] 04 p0496 N85-13164
Focusing effects of a laser beam in the nonresonant multiphoton ionization (MPI) of gases
[LP-207] 04 p0506 N85-13231
Theoretical studies of highly ionized species
[DE84-016797] 04 p0561 N85-13574
On the importance of interstellar helium for the propagation of heavy cosmic rays
[OG-7.2-11] 23 p4015 N85-34879
CROSSBEDDING (GEOLOGY)
The U.S. Geological Survey in Alaska: Accomplishments during 1982
[US-GEOL-SURV-CIRC-939] 20 p3493 N85-31719
CROSSED FIELDS
Improved negative ion source
[DE85-006445] 23 p3912 N85-34241
CROSSINGS
Some studies in filtering of atmospheric turbulence
[AD-A154042] 19 p3316 N85-30557
CROSSLINKING
Method of obtaining heterocyclic polymers
[AD-A145127] 01 p0033 N85-10202
The effect of cross-link density on the toughening mechanism of elastomer-modified epoxies
04 p0485 N85-12951
Gradient polymers
[AD-A146836] 07 p0931 N85-15900
Thermoset-thermoplastic aromatic polyamide containing N-propargyl groups
[NASA-CASE-LAR-12723-1] 11 p1610 N85-20123
Status of specific FRG high tech research funded by BMFT 11 p1618 N85-20181
Chemical approach for controlling nadimide cure temperature and rate
[NASA-CASE-LEW-13770-5] 12 p1810 N85-21352
Synthesis of hydrophobic, crosslinkable resins
[AD-A150658] 14 p2260 N85-24002
Polyaromatic ether-sulfone-keytones with fluoro-substituted-p-cyclophane units as cross-linking sites
[AD-D011649] 17 p2933 N85-28105
Chemical control of nadimide cure temperature and rate
[NASA-CASE-LEW-13770-2] 18 p3069 N85-28982
Orientation and strength of semi-crystalline polymers
20 p3432 N85-31294
Development of a lithium secondary battery separator
20 p3444 N85-31378
CROSSOVERS
Interference immunity of fiber-optic communication lines with spectral multiplexing of channels
13 p2069 N85-22924
CROSSTALK
A gyro sensor block suspension
[AD-D011411] 08 p1154 N85-17284
In-flight tests 09 p1412 N85-18902
Basic EMC technology advancement for C3 systems. Volume 4F: Prediction of crosstalk in flatpack coaxial cables
[AD-A153111] 17 p2954 N85-28242
Basic EMC (Electromagnetic compatibility) technology advancement for C3 systems. Volume 4D: Modeling crosstalk in balanced twisted pairs
[AD-A153678] 18 p3090 N85-29125
Analysis of crosstalk in nonhomogeneous multiconductor lines 22 p3769 N85-33360
On the principle of uniformity of satellite communications systems 22 p3773 N85-33382
CRUCIBLES
High-temperature X-ray diffraction study of coating-substrate compatibility in yttria-coated graphite
[DE85-005916] 14 p2262 N85-24016
Power control of induction equipment for founding optical glass in array of platinum crucibles
14 p2267 N85-24044
Structure and properties of VT20L titanium alloy with 0.1-0.3 percent content 15 p2515 N85-25517
CRUDE OIL
USSR report: Chemistry
[JPRS-UCH-84-012] 06 p0761 N85-14865
Aromatics determination in middle distillate petroleum fractions by spectrophotometric titration
[PNR-90239] 09 p1293 N85-18123
Diesel fuel alternatives for engines in civil works prime movers
[AD-A149738] 12 p1817 N85-21400

Hydrocarbon pool and vapor fire data analysis
[DE85-005857] 15 p2523 N85-25550
Analysis of mesoflesuring on space photographs: New technique for study of petroleum and gas deposits
16 p2726 N85-26628
Fracture detection and mapping for geothermal reservoir definition: An assessment of current technology, research, and research needs
[DE85-010627] 19 p3301 N85-30464
Subsurface petroleum geology of Santa Rosa sandstone (Triassic), northeast New Mexico
[TI85-901364] 19 p3313 N85-30538
Petroleum and mineral resources of Antarctica
[US-GEOL-SURV-CIRC-909] 20 p3477 N85-31605
A crew exposure study. Phase II. Volume 2. At sea. Part A
[AD-A155233] 21 p3666 N85-32774
AUTSKED: An addendum
[DE85-010410] 22 p3829 N85-33712
Preliminary SPR thermal model description and results for WH-11 and BM-4
[DE85-013171] 23 p3931 N85-34360
Geology and petroleum resources of basins in western China
[DE85-013038] 23 p3948 N85-34469

CRUISE MISSILES
A simulation model for Air Launched Cruise Missile engine management
[AD-A147018] 07 p1051 N85-16672
Evaluation of air and ground launched cruise missile navigational element containers
[AD-A149654] 12 p1774 N85-21136
AN investigation into the control limitations of a bank to turn missile in the terminal homing phase
[AD-A152193] 16 p2704 N85-26696
An artificial intelligence based framework for planning air launched cruise missile missions
[AD-A154466] 19 p3344 N85-30722
Computer simulation of a cruise missile using brushless dc motor fin control
[AD-A155935] 24 p4089 N85-35349
Application of pulsed power in the simulation of severe natural lightning
[DE85-012866] 24 p4124 N85-35564

CRUISING FLIGHT
Insight. Background information for multipurpose pilots: Flight phenomena
02 p0138 N85-10940

CRUSADER AIRCRAFT
U F-8 AIRCRAFT

CRUSHING
Single-point diamond crushing of Zerodur with in-situ polishing and metrology on a diamond turning machine
[DE85-012918] 24 p4083 N85-35305

CRUSTAL FRACTURES
Localization of destruction process
10 p1500 N85-19470
On the absence of strike-slip faults from the planets and satellites
13 p2200 N85-23645
Lunar mascon loading: An example of the importance of fault initiation depth on fault type predictions from stresses on planetary surfaces
13 p2200 N85-23646
Fault offsets and lateral crustal movement on Europa
13 p2201 N85-23656
Basic research for the geodynamics program
[NASA-CR-175751] 16 p2825 N85-27424
Fracture detection and mapping for geothermal reservoir definition: An assessment of current technology, research, and research needs
[DE85-010627] 19 p3301 N85-30464
Geodynamics Branch research program
[NASA-TM-86223] 20 p3489 N85-31688
The global VLBI fiducial network
20 p3490 N85-31690
First epoch measurements by Mark III VLBI of the San Andreas Fault experiment baseline
20 p3490 N85-31691
Geophysical interpretation of satellite laser ranging measurements
20 p3490 N85-31692
Satellite-determined stresses in the crust of Europe with particular consideration to the Liege earthquake of November 8, 1983
20 p3490 N85-31694
Mega-geomorphology and neotectonics
21 p3602 N85-32366
Use of space photographs for analysis of structural and dynamic conditions of formation of ancient phlogopite and apatite deposits
22 p3735 N85-33153
Subcritical fracture propagation in rocks: An examination using the methods of fracture mechanics and non-destructive testing
24 p4116 N85-35516
Groundwater radon studies for earthquake precursors in southern California
[PB85-196871] 24 p4118 N85-35529

CRUSTS
NT EARTH CRUST
NT LUNAR CRUST
More precise curve of dependence between density and velocity of longitudinal waves in consolidated crust and top of mantle in oceanic structures
13 p2110 N85-23143
Crustal and upper mantle density model of Owen fault zone
13 p2110 N85-23144
Interrelationship of earthquake magnitude and lithospheric-asthenospheric thermodynamic parameters in seismically active zones
13 p2116 N85-23163
Crustal development in the terrestrial planets
22 p3856 N85-33879
Cobalt-rich ferromanganese crusts in the oceans
24 p4104 N85-35444

CRYOGENIC COOLING
Active cooling requirements for propellant storage
08 p1106 N85-17004
Computer simulation of multiple stability regions in an internally cooled superconducting conductor and of helium replenishment in a bath-cooled conductor
[DE85-002112] 09 p1399 N85-18805
Experimental studies of low temperature surface interactions of atomic hydrogen using maser technique
[AD-A150216] 13 p2017 N85-22647
Effect of deep cooling on crack resistance and low-temperature hardening of aluminum alloys
15 p2496 N85-25396
A liquid nitrogen cooled composite wall hollow cathode — molecular spectroscopy
[USIP-85-07] 20 p3526 N85-31930

CRYOGENIC EQUIPMENT
Exothermic processes in solids under low temperatures, their physics and their cryogenic implications
[JUEL-1919] 03 p0414 N85-12651
Passive Orbital Disconnect Strut (PODS 3) structural test program
[NASA-CR-177325] 06 p1113 N85-17020
Magentically actuated compressor
[NASA-CASE-GSC-12799-1] 12 p1818 N85-21404
Transmissive Dewar cooling chamber for optically pumped semiconductor ring lasers
[AD-D011550] 12 p1855 N85-21636
France officially proposes development of Ariane 5 to ESA
15 p2532 N85-25613
SEP of France to make Ariane HM-60 cryogenic engine
15 p2532 N85-25614
Infrared telescope
[NASA-CR-171392] 15 p2668 N85-26465
Cryogenic test technology, 1984
[AGARD-AR-212] 18 p3088 N85-29116
Vapor-liquid phase separator studies
[NASA-CR-166545] 21 p3583 N85-32272
Results of variable enthalpy tests of CPR-488 TIP panels in MSFC Hot Gas Facility
[NASA-CR-170889] 24 p4072 N85-35237

CRYOGENIC FLUID STORAGE
Shock testing of a nitrogen tank (Cryo diffusion type 220 VLR) on the middle weight shock stand
[NASA-TM-77747] 06 p0617 N85-15183
Risks in the transport and storage of liquefied natural gas. Sub-project 5-2: Investigation into building damage [BLL-RISLEY-TR-4608-(9091.9F)]
07 p0935 N85-15926
Space shuttle electrical power generation and reactant supply system
08 p1099 N85-16947
Passive storage technologies
08 p1108 N85-17003
Propellant transfer: Attached depot
08 p1108 N85-17005
OTV fluid mangement systems
08 p1108 N85-17007
Passive Orbital Disconnect Strut (PODS 3) structural test program
[NASA-CR-177325] 06 p1113 N85-17020
Technology requirements to be addressed by the NASA Lewis Research Center Cryogenic Fluid Management Facility program
[NASA-TM-87048] 19 p3224 N85-29987
Vapor-liquid phase separator studies
[NASA-CR-166545] 21 p3583 N85-32272

CRYOGENIC FLUIDS
NT FERMI LIQUIDS
NT LIQUID HELIUM
NT LIQUID HELIUM 2
NT LIQUID HYDROGEN
NT LIQUID NITROGEN
NT LIQUID OXYGEN
NT SOLIDIFIED GASES
OTV Propulsion Issues
[NASA-CP-2347] 08 p1106 N85-16989
Ignition characterization of LOX/hydrocarbon propellants
[NASA-CR-171884] 18 p3083 N85-29070
Ignition characterization of LOX/hydrocarbon propellants
[NASA-CR-171882] 18 p3083 N85-29071
Technology requirements to be addressed by the NASA Lewis Research Center Cryogenic Fluid Management Facility program
[NASA-TM-87048] 19 p3224 N85-29987
Basic cryogenics and materials. Phase 1
[NASA-CR-177932] 21 p3572 N85-32215

CRYOGENIC MAGNETS
MFTF sensor verification computer program
[DE85-004452] 12 p1916 N85-22029

CRYOGENIC ROCKET PROPELLANTS
History, design and performance of the space shuttle hazardous gas detection system
08 p1098 N85-16936
Earth-to-orbit propellant transportation overview
08 p1108 N85-17002
Assessment study of liquid content measurement methods applicable to space missions — Infrared Space Observatory
[TU-HH-TRI-ESA-84-2] 17 p2938 N85-28135
Investigation, development, and certification of a burst disk for cryogenic fuel tanks
[GCP-3/MT-CM-21-2548] 18 p3067 N85-29972

CRYOGENIC WIND TUNNELS
Review of the advanced technology airfoil test program in the 0.3-meter transonic cryogenic tunnel
03 p0315 N85-12033
Some experience with Barnwell-Sewall type correction to two-dimensional airfoil data
03 p0315 N85-12034
Adaptation of a four-wall interference assessment/correction procedure for airfoil tests in the 0.3-m TCT
03 p0315 N85-12035
First cryogenic test of the CAST 7 profile in the T2 wind tunnel. Comparison with calculations — airfoils
[ONERA-RTS-58/1685-AY-035-D]
04 p0577 N85-13682
Description of the insulation system for the Langley 0.3-Meter Transonic Cryogenic Tunnel
[NASA-TM-86274] 07 p0909 N85-15755
Initial investigation of cryogenic wind tunnel model filler materials
[NASA-TM-86363] 09 p1283 N85-18069
Exploratory flutter test in a cryogenic wind tunnel
[NASA-TM-86380] 12 p1663 N85-21689
Cryogenic wind tunnels: A selected annotated bibliography
[NASA-TM-86346] 13 p1976 N85-22401
Qualification of the T2 wind tunnel in cryogenic operation. A: Thermal field, preliminary study of a schematic model
[NASA-TM-77781] 14 p2227 N85-23805
Qualification of the T2 wind tunnel in cryogenic operation. B: Flow fluctuations, particle detection and qualification
[NASA-TM-77782] 14 p2227 N85-23806
Measurements in the flow field of a cylinder with a laser transit anemometer and a drag rake in the Langley 0.3 m transonic cryogenic tunnel
[NASA-TM-86399] 14 p2305 N85-24270
Cryogenic test technology, 1984
[AGARD-AR-212] 18 p3088 N85-29116
High Reynolds number tests of a NASA SC(3)-0712(B) airfoil in the Langley 0.3-meter transonic cryogenic tunnel
[NASA-TM-86371] 19 p3213 N85-29926
Pressure distribution from high Reynolds number tests of a NASA SC(3)-0712(B) airfoil in the Langley 0.3-meter transonic cryogenic tunnel
[NASA-TM-86370] 19 p3213 N85-29927
Sidewall boundary-layer effects in two-dimensional airfoil testing
[NASA-CR-176034] 20 p3392 N85-31065
Materials and techniques for model construction
[NASA-CR-172620] 20 p3396 N85-31066
A systematic plan for the continued study of dimensional stability of metallic alloys considered for the fabrication of cryogenic wind tunnel models
[NASA-CR-172449] 21 p3565 N85-32172
A theoretical study of non-adiabatic surface effects for a model in the NTF cryogenic wind tunnel
[NASA-CR-3924] 23 p3929 N85-34352

CRYOGENICS
Conversion of microwave signals by superconducting films in the resistive state
[NASA-TM-77595] 01 p0123 N85-10843
Formation of superconductive Al(GeSi) alloys by low temperature laser quenching methods
[DE84-016667] 04 p0474 N85-13021
Thermal and cryogenic design study for space infrared telescope facility (SIRTF)
[NASA-CR-166613] 07 p0915 N85-15793
Cryogenic glass-to-metal seal
[AD-D011370] 07 p0933 N85-15911
Study of infrared atmospheric emission
[AD-A147517] 07 p0998 N85-16336
Research and technology, 1984 report
[NASA-TM-83096] 07 p1061 N85-16730

Automatic software for controlling cryogenic systems
08 p1097 N85-16932
Cryogenic propellant management: Integration of design, performance and operational requirements
08 p1098 N85-16939
Advanced OTV engines and issues
08 p1108 N85-17000
Acoustic microscopy at cryogenic temperatures
[AD-A148755] 09 p1384 N85-18704
Analysis of compact heat exchanger performance
[DE84-012824] 10 p1485 N85-19377
Emergency Locator Transmitter (ELT) batteries guidance and recommendations
[NASA-TM-87436] 11 p1624 N85-20225
Method of calculating cooldown process in cryostat of cryogenic electric machine 12 p1843 N85-21567
Electrical performance of semiconductor devices at cryogenic temperatures 12 p1948 N85-22239
Survey of the state-of-the-art of miniature cryocoolers for superconductive devices
[AD-A150319] 13 p2041 N85-22774
Manrating orbital transfer vehicle propulsion
[NASA-TM-87019] 15 p2494 N85-25385
Electronic transport in Mo/Ni superlattice
[DE85-006835] 15 p2661 N85-26425
Bearings working group 16 p2735 N85-26878
Advanced rocket engine cryogenic turbopump bearing thermal model 16 p2735 N85-26879
Hybrid bearings for LH2 and LO2 turbopumps
16 p2736 N85-26880
Rolling contact fatigue life of chromium ion plated 440C bearing steel 16 p2736 N85-26882
Research on design of cryotransformers and its prospects for the future
[AD-A152400] 17 p2952 N85-28230
Experience with oepration of a large magnet system in the international fusion superconducting magnet test facility
[DE85-009288] 17 p3027 N85-28721
Technique to reduce scattered light in optical systems
[AD-D011597] 18 p3185 N85-29752
E-beam-induced fluorescence of excimers in cryogenic solutions
[DE85-010703] 19 p3278 N85-30328
Cryogenics for the Superconducting Super Collider: Workshop Proceedings
[DE85-010951] 20 p3437 N85-31327
Capacitive energy storage at cryogenic temperatures
[AD-A154508] 21 p3579 N85-32253
SCRIBE data of October 23, 1983 flight
[AD-A154864] 21 p3705 N85-33012
Cryogenic system for the University of Washington Superconducting Booster
[DE85-010804] 22 p3754 N85-33274
Evaluation study of mechanical refrigeration systems for application to space missions — infrared astronomy
[SNIAS-1029ACA/LL/V] 22 p3755 N85-33277
Partial discharges in and electric strength of high-voltage polymer insulation at cryogenic temperatures
22 p3770 N85-33364
Separation of gas mixtures by supported complexes
[DE85-011996] 23 p3912 N85-34236
Cryogenic laser calorimetry for impurity analysis
[NASA-CR-176179] 24 p4097 N85-35395
Solid neon sources for plasma and X-ray lasers
[DE85-011347] 24 p4098 N85-35402

CRYOSORPTION
U SORPTION

CRYOSTATS
Method of calculating cooldown process in cryostat of cryogenic electric machine 12 p1843 N85-21567
Superconducting magnet technology for accelerators
[DE85-004192] 12 p1926 N85-22102
Germanium resistance thermometer calibration at superfluid helium temperatures
12 p1947 N85-22228
Infrared telescope
[NASA-CR-171392] 15 p2668 N85-26485
Cryostat and electronic development associated with multi-detector spectrometer systems
[DE85-007624] 16 p2788 N85-27203
Operation of HFTF to test the MIT 12 T coil
[DE85-010409] 18 p3195 N85-29821
Cryogenic system for the University of Washington Superconducting Booster
[DE85-010804] 22 p3754 N85-33274

CRYPTOGRAPHY
Reserve and authentication in Integrated Services Distributed Networks (ISDN) networks
[FUB-37-1983] 01 p0041 N85-10262
Most wanted factorizations usinq the quadratic sieve
[DE84-016208] 05 p0718 N85-14609
A public key cryptographic algorithm based on a generalization of the knapsack problem
[FUB-7-1984] 09 p1313 N85-18250
Digital signatures: An update
[NPL-DITC-51/84] 09 p1367 N85-18589
Security controls in the Stockpoint Logistics Integrated Communications Environment (SPLICE)
[AD-A155536] 21 p3576 N85-32244
An algorithm for the generation of primitive polynomials
[FUB-17-1984] 22 p3831 N85-33730

CRYSTAL DEFECTS
NT CRYSTAL DISLOCATIONS
NT EDGE DISLOCATIONS
NT POINT DEFECTS
NT SCREW DISLOCATIONS
NT VACANCIES (CRYSTAL DEFECTS)
Process Research of Polycrystalline Silicon Material (PROPSM)
[NASA-CR-173838] 01 p0067 N85-10446
Toughness in high speed steels and hard metals
02 p0176 N85-11181
Formation of lattice defects by nitrogen laser exposure in A2B6 semiconductors with wide forbidden band
02 p0258 N85-11692
Internal friction, microstructure and radiation effects
[DE84-013905] 02 p0288 N85-11880
Annealing of implanted Al-2O-3 in a reducing environment
[DE84-015370] 03 p0332 N85-12140
Microstructure of ceramics fabricated by unidirectional solidification
[NASA-TM-77423] 03 p0336 N85-12157
Study of structure of sponge titanium varieties
03 p0350 N85-12256
Energy of stacking fault and dislocation structure of titanium alloys 03 p0351 N85-12259
Lattice defects in body centered cubic transition metals 03 p0427 N85-12727
Neutron irradiation of semiconductors — lattice defects, electron irradiation 03 p0428 N85-12732
Radiation induced defects in superconductors of type 2 03 p0429 N85-12734
Determination of depth profiles and lattice positions with (n, p)- and (n, alpha) reactions (n, alpha) and channeling-blocking method) 03 p0429 N85-12735
Mossbauer spectroscopic investigations of the diffusion and correlation of lattice defects (complementary to neutron spectroscopic investigations)
03 p0429 N85-12736
Investigation of the production and properties of lattice defects induced by low temperature reactor irradiation
03 p0430 N85-12739
X-ray and neutron scattering and X-ray spectroscopy for the study of defects in solid state materials
03 p0430 N85-12741
Spectroscopic investigations on neutron induced impurity atoms and radiation defects
03 p0430 N85-12742
Studies of grown-in defects versus growth parameters in 3-4 compound semiconductors
[AD-A145864] 03 p0433 N85-12755
Interaction of hydrogen with defects in metals
[DE84-016781] 04 p0476 N85-13032
Imaging of surfaces and defects of crystals
[DE84-016449] 04 p0570 N85-13632
EPR linewidth studies of unpaired electrons at the Si-SiO2
[DE84-016727] 05 p0733 N85-14712
Investigation of structural and electrical properties of low-angle silicon sheet 06 p0831 N85-15288
Semicrystalline casting process development and verification 06 p0832 N85-15289
Defective nature of the crystalline lattice of nickel ferrite-based solid solutions
[BLL-WH-595-(9091.9F)] 07 p1048 N85-16645
Ferromagnetism in metals at finite temperatures
[DE85-000696] 09 p1377 N85-18656
Fundamental aspects on ion-beam surface modification: Defect production and migration processes
[DE85-000093] 09 p1399 N85-18804
Stress studies in EFG
[NASA-CR-175486] 10 p1563 N85-19656
International Conference on Defects in Insulating Crystals
[AD-A149611] 12 p1939 N85-22180
Fracture mechanics evaluation of GaAs
[NASA-CR-175657] 13 p2102 N85-23101
Recent developments in semiconductor research
14 p2297 N85-24222
Influences of thermal spikes in ion beam mixing
[DE85-006130] 14 p2419 N85-24924
Energy trapping, release, and transport in three-dimensional energetic solids and molecular crystals: Theory of defects and impurities
[AD-A151071] 14 p2428 N85-24973
High resolution Z-contrast imaging and lattice location analysis of dopants in ion-implanted silicon
[DE85-005261] 14 p2429 N85-24980
Electrochemical behavior of amorphous alloys based on iron, cobalt and nickel in H3PO4 solutions alone and mixed with HF 15 p2513 N85-25505
Process Research on Polycrystalline Silicon Material (PROPSM)
[NASA-CR-175761] 15 p2587 N85-25851
Compensation of dangling bonds in A-Si, Ge:H alloys
[DE85-002905] 15 p2662 N85-26433
Simulation of solidification in a Bridgman cell
[NASA-CR-175838] 16 p2870 N85-27705
TEM investigation of polar-on-nonpolar epitaxy: GaAs-AlGaAs on (100) Ge
[DE85-007613] 16 p2871 N85-27714
Quantitative analysis of defects in silicon-characterization of UCP, HAMCO, and microcrystalline material
[NASA-CR-175988] 18 p3079 N85-29046
Method of reducing impurity and antisite defects in semiconductor crystal materials, and device and apparatus respectively produced from and utilizing same
[AD-D011698] 19 p3260 N85-30218
Method for growing low defect, high purity crystalline layers
[NASA-CASE-NPO-15813-2] 19 p3374 N85-30933
Solid State Division report on its mission-oriented basic research
[DE85-008766] 19 p3376 N85-30941
Surface passivation and junction formation using low energy hydrogen implants 20 p3480 N85-31626
Structural defects in crystalline silicon
20 p3481 N85-31630
Oxygen and carbon impurities and related defects in silicon 20 p3481 N85-31631
EBIC characterization and hydrogen passivation in silicon sheet 20 p3481 N85-31634
Defect production and recovery in FCC metals irradiated at 4.2 K
[DE85-010477] 20 p3538 N85-32014
Studies of oxygen- and carbon-related defects in high-efficiency silicon solar cells
21 p3609 N85-32420
High-purity silicon crystal growth
21 p3612 N85-32444
Defect formation in amorphous hydrated silicon subjected to laser radiation 21 p3682 N85-32873
An EPR (Electron-Paramagnetic-Resonance) and ENDOR (Electron-Nuclear-Double-Resonance) study of ferroelectric ammonium sulfate
[AD-A155580] 21 p3710 N85-33033
Solid-melt interface studies of high-speed silicon sheet growth
[NASA-CR-176112] 22 p3751 N85-33249
Simulation of lattice damage due to dynamic loading
[DE85-008468] 24 p4162 N85-35808

CRYSTAL DISLOCATIONS
NT EDGE DISLOCATIONS
NT SCREW DISLOCATIONS
Plastic deformation and microstructural transformations of metals under shock waves 02 p0272 N85-11775
Energy of stacking fault and dislocation structure of titanium alloys 03 p0351 N85-12259
Irradiation creep induced anisotropy in a/2110 dislocation populations
[DE84-016623] 06 p0868 N85-15520
Strain analysis of the Leoville chondrite and conditions in asteroidal interiors 06 p0885 N85-15620
Back stress in dislocation creep. Part 1: Basic concepts and measuring techniques
[NASA-TM-77773] 07 p0977 N85-16206
The fundamentals of dislocation transport of hydrogen in bcc iron
[AD-A148143] 08 p1129 N85-17117
Influence of the amorphous-crystalline interface morphology on dislocation nucleation in pre-amorphized silicon
[DE85-002088] 09 p1396 N85-18800
Comparisons between computed and observed grain boundary structures and properties in metals
[DE85-002596] 10 p1442 N85-19085
Role of hydrogen in processes of deformation and fracture of metals 10 p1449 N85-19132
Stress studies in EFG
[NASA-CR-175464] 10 p1509 N85-19522
The role of dislocations in ultrasonic attenuation
[AERE-R-11384] 12 p1804 N85-21317
Investigation of the effect of annealing on the dislocation and sub-grain boundary content of solvent-evaporation-grown CdTe
[AD-A144067] 13 p2182 N85-23415
Solid/melt interface studies of high-speed silicon sheet growth
[NASA-CR-175696] 14 p2350 N85-24525
Stress and efficiency studies
[NASA-CR-175688] 14 p2351 N85-24531

Studies of deformation in niobium by X-ray topographic methods
[AD-A150726] 14 p2427 N85-24965
Structural unit/grain boundary dislocation model for twist boundaries in cubic crystals
[DE85-000425] 14 p2430 N85-24985
Effects of gamma-ray irradiation on dislocations in sodium nitrate single crystals
[DE85-006291] 18 p3195 N85-29818
Electrical and structural characterization of web dendrite crystals 20 p3481 N85-31633
Solid-melt interface studies of high-speed silicon sheet growth
[NASA-CR-176112] 22 p3751 N85-33249
An enhanced photoresponse at dislocation subgrain boundaries revealed by X-ray topography of polysilicon solar cells 22 p3806 N85-33572

CRYSTAL FILTERS
Single crystal semiconductor multilayers for electrically active optical interference filters
[DE84-015814] 04 p0571 N85-13640
Quartz filter transceiver 12 p1838 N85-21538
Normal coordinate monolithic crystal filter
[AD-D011496] 12 p1941 N85-22188

CRYSTAL GROWTH
NT CZOCHRALSKI METHOD
NT DIRECTIONAL SOLIDIFICATION (CRYSTALS)
NT ELECTROEPITAXY
NT EPITAXY
NT HYDROTHERMAL CRYSTAL GROWTH
NT LIQUID PHASE EPITAXY
NT MOLECULAR BEAM EPITAXY
NT TRAVELING SOLVENT METHOD
NT VAPOR PHASE EPITAXY
Critical conditions for the growth of SiC, Si3N4, and SiO2
[DE84-014824] 01 p0030 N85-10185
The absence of convective stability in incongruent crystal growth on Earth 02 p0150 N85-11019
Solidification and crystal growth of solid solution semiconducting alloys 02 p0155 N85-11046
Microstructural design in low alloy steels 02 p0176 N85-11179
The growth of twins and twin lamellae in synthetic diamond crystals 02 p0181 N85-11213
Simulation of solidification in a Bridgman cell
[NASA-CR-3843] 02 p0197 N85-11314
Silicon sheet with molecular beam epitaxy for high efficiency solar cells
[NASA-CR-174022] 02 p0222 N85-11459
Large-area sheet task advanced dendritic web growth development
[NASA-CR-174021] 02 p0223 N85-11463
Low-threshold injection lasers on grown GaInPAs/InP heterostructures (1.2-1.6 micrometers wavelengths) 02 p0258 N85-11693
Transport phenomena in the boundary layer during solution solidification under microgravity. Ice growth from a water-salt solution
[BMFT-FB-W-84-031] 03 p0329 N85-12121
Bibliography of Soviet laser developments, number 65, May - June 1983
[AD-A146169] 03 p0366 N85-12347
Measurements on the triple axis spectrometer UNIDAS for the investigation of dynamic processes in crystals using inelastic neutron scattering 03 p0426 N85-12716
Structure and kinetics of physisorption, properties of helium during reduction of the dimension 03 p0432 N85-12749
Studies of grown-in defects versus growth parameters in 3-4 compound semiconductors
[AD-A145864] 03 p0433 N85-12755
The effect of thin-film growth mode on XPS/UPS/AES intensities
[AD-A146284] 03 p0434 N85-12763
A preliminary study of numerical simulation of thermoceutal convection of interest to crystal growth
[NASA-TP-2394] 04 p0498 N85-13175
Silicon for solar cells
[DE84-004503] 04 p0529 N85-13381
Chemical engineering principles of constant temperature-constant supersaturation growth of potassium dihydrogen phosphate (KDP) crystals
[DE84-017081] 04 p0571 N85-13645
Electron channeling and EBIC studies of polycrystalline silicon sheets
[DE84-004515] 05 p0670 N85-14309
Minisworkshop on effects of stress and strain in high-speed-growth silicon ribbons 06 p0831 N85-15284
Advanced dendritic web growth development 06 p0831 N85-15286
Preparation and electronic properties of MoS(2) and WS(2) single crystals grown in the presence of cobalt
[AD-A146508] 06 p0866 N85-15506
Research on submicrometer structures
[AD-A146578] 06 p0867 N85-15508
The growth and properties of semiconductor strained-layer superlattices
[DE84-012979] 06 p0868 N85-15515
Float zone experiments in space
[NASA-CR-171284] 07 p0911 N85-15766
Crystal growth and characterization of BaMgF4
[AD-A146805] 07 p1047 N85-16650
Improved solid-state laser sources, volume 2
[DE85-000759] 09 p1325 N85-18330
Advanced high-efficiency concentrator cells
[DE84-013020] 09 p1344 N85-18459
The growth of large diameter single crystals by vertical solidification of the melt
[AD-A148756] 09 p1397 N85-18792
Silicon film solar cell process
[NASA-CR-174446] 10 p1508 N85-19514
Material growth and characterization for solid state devices
[NASA-CR-174410] 10 p1561 N85-19847
Quaternary narrow-band semiconductors (HgTe)x (InSb)1-x for far-infrared detectors
[AD-A149350] 10 p1562 N85-19852
Development of a polysilicon process based on chemical vapor deposition of dichlorosilane in an advanced Siemen's reactor
[NASA-CR-174445] 11 p1672 N85-20532
A computer simulation of thin film nucleation and growth: The Volmer-Weber case
[NASA-TM-86968] 12 p1796 N85-21264
Topics in optical materials and device research, 3: Volume 1
[AD-A149726] 12 p1933 N85-22145
Nucleation of phase transitions in the vicinity of phase boundary. Part 1: Comparison of various idolated mechanisms. Part 2: Coupled cluster growth processes
[N-0208-5658] 12 p1938 N85-22174
Method for the preparation of epitaxial films of mercury cadmium telluride
[AD-D011532] 12 p1938 N85-22175
Total immersion crystal growth
[NASA-CASE-NPO-15800-2] 12 p1939 N85-22178
Basis and pyramidal slipping in single crystals of alpha-alloy Ti-Al-Sn 13 p2032 N85-22730
Hibonite: Crystal chemistry and origin of blue coloration in meteoritic assemblages 13 p2184 N85-23555
Material research in microgravity
[NASA-TM-77628] 14 p2228 N85-23811
Proceedings of the Cold Electronics Workshop
[NASA-CR-175662] 14 p2297 N85-24220
Recent developments in semiconductor research 14 p2297 N85-24222
Stress and efficiency studies
[NASA-CR-175688] 14 p2351 N85-24531
Development of solid state infrared emitters for gas detection applications
[PB85-148450] 15 p2561 N85-25800
Fundamental studies of growth, doping and transformation in beta silicon carbide
[AD-A152047] 15 p2680 N85-26416
Optimum convection conditions for Czochralski growth of semiconductors
[INPE-3395-PRE/665] 16 p2870 N85-27703
Simulation of solidification in a Bridgman cell
[NASA-CR-175838] 16 p2870 N85-27705
Dendritic growth from amorphous matrix
[DE85-007630] 16 p2871 N85-27712
High-thermal-gradient superalloy crystal growth 17 p2914 N85-27966
Research on the kinetics of phase changes in solids
[AD-A152387] 17 p2918 N85-27989
Model for the growth of fractal silica polymers
[DE85-007884] 17 p2935 N85-28115
Heat pipe and method of making same
[AD-D011654] 17 p2959 N85-28273
InP materials
[AD-A152341] 17 p3043 N85-28828
Telescoping low vibration pulling mechanism for Czochralski crystal growth
[AD-D011655] 17 p3044 N85-28836
Rapid growth of potassium dihydrogen phosphate crystals
[DE85-007261] 17 p3045 N85-28839
Morphology of GaAs/sub 1-x/P/sub x/ superlattices grown by MOCVD and chloride VPE
[DE85-002044] 17 p3045 N85-28842
Method for growth of crystals by pressure reduction of supercritical or subcritical solution
[NASA-CASE-NPO-15772-1] 18 p3192 N85-29800
Growth mechanism and properties of the thermal and anodic oxides of the 3-5 compound semiconductors
[AD-A153406] 18 p3193 N85-29803
TEM combined with Al/sub x/Ga/sub 1-x/ as marker layers as a technique for the study of GaAs MBE growth
[DE85-008451] 18 p3194 N85-29809
Crystal growth from the vapor in low gravity environments
[DE85-009628] 18 p3195 N85-29816
Method of reducing impurity and antisite defects in semiconductor crystal materials, and device and apparatus respectively produced from and utilizing same
[AD-D011698] 19 p3260 N85-30216
Electrohydrodynamic process for the production of large area polycrystalline silicon sheet
[DE85-006781] 19 p3261 N85-30225
Method for the preparation of photochromic insulating crystals
[DE85-011606] 19 p3262 N85-30229
Spectroscopic investigation of materials for tunable infrared lasers
[AD-A154124] 19 p3272 N85-30291
Low defect, high purity crystalline layers grown by selective deposition
[NASA-CASE-NPO-15813-1] 19 p3373 N85-30922
Method for growing low defect, high purity crystalline layers
[NASA-CASE-NPO-15813-2] 19 p3374 N85-30933
Crystal growth of device quality GaAs in space
[NASA-CR-176024] 19 p3375 N85-30935
Development of growth techniques for electromagnetic crystals
[AD-A154089] 19 p3375 N85-30937
The use of moments of momentum to account for crystal habits
[NASA-CR-3907] 20 p3421 N85-31232
High-efficiency cell concepts on low-cost silicon sheets 20 p3479 N85-31621
Temperature field around a spherical, cylindrical, and needle-shaped crystal, growing in a pre-cooled melt
[NASA-TM-77889] 20 p3537 N85-32011
The EURECA solution growth facility conceptual design study. Executive summary
[ESA-CR(P)-2007] 20 p3538 N85-32016
High-frequency furnace
[DE85-011210] 21 p3586 N85-32291
Silicon production in an aerosol reactor 21 p3609 N85-32416
Silicon dendritic web growth 21 p3611 N85-32435
Temperature-stress modeling 21 p3611 N85-32436
Silicon ribbon stress-strain activities 21 p3611 N85-32437
Analysis of stress-strain relationships in silicon ribbon 21 p3611 N85-32438
Stress and buckling analysis 21 p3611 N85-32439
Stress and efficiency studies in EFG 21 p3611 N85-32440
Silicon sheet surface studies 21 p3611 N85-32441
Analysis of inclined growth of silicon sheet 21 p3612 N85-32442
Edge-defined film-fed growth of thin silicon sheets 21 p3612 N85-32443
High-purity silicon crystal growth 21 p3612 N85-32444
Failure analysis of thin-film amorphous-silicon solar-cell modules 21 p3613 N85-32452
Ice crystal nucleation on hygroscopic aerosols 21 p3639 N85-32605
The nucleation of ice crystals during the freezing of large supercooled drops 21 p3640 N85-32608
X-ray diffractometric measurements and calculations of limiting values of discrepancy between lattices and layer thicknesses, preventing generation of dislocations during growth of multilayer heterostructures 21 p3681 N85-32866
Nonequilibrium kinetics of growth of oxide layer grains during laser heating of metals in air 21 p3689 N85-32919
The development and evaluation of point defect models for the growth of passive films on single crystal, polycrystalline, and amorphous metal surfaces
[AD-A154685] 21 p3709 N85-33023
Chemical constraints on the evolution of Archean continental crust 21 p3722 N85-33093
New and revised methods of purifying mercuric iodide
[DE85-011684] 22 p3749 N85-33237
Solid-melt interface studies of high-speed silicon sheet growth
[NASA-CR-176112] 22 p3751 N85-33249
Stress and efficiency studies in EFG
[NASA-CR-176125] 22 p3751 N85-33251
Striation free doped silicon
[AD-A155730] 22 p3847 N85-33827
Apparatus and method for the horizontal, crucible-free growth of silicon sheet crystals
[DE85-011588] 22 p3847 N85-33829
Manufacturing process to reduce large grain growth in zirconium alloys
[DE85-011649] 23 p3915 N85-34267

Crystallization of Polyetheretherketone (PEEK) in carbon fiber composites
[AD-A156316] 24 p4075 N85-35252
Investigations of the molecular beam epitaxial growth and characteristics of external excitation induced non-equilibrium phases of immiscible 3-5 compound semiconductors
[AD-A156325] 24 p4162 N85-35804

CRYSTAL LATTICES
NT BODY CENTERED CUBIC LATTICES
NT CUBIC LATTICES
NT FACE CENTERED CUBIC LATTICES
NT SUPERLATTICES
Structure and wear workshop colloquium 01 p0054 N85-10358
Structure and abrasive resistance of iron based alloys rich in hardening components 01 p0054 N85-10360
Friction, wear and structure of heterogeneous materials 01 p0055 N85-10362
Kinetics of short-range ordering in metallic glasses: Analysis of the crossover effect
[DE84-015524] 02 p0187 N85-11251
Microfluorescence studies of zirconium oxide
[DE84-016116] 03 p0329 N85-12118
Annealing of implanted Al-2O-3 in a reducing environment
[DE84-015370] 03 p0332 N85-12140
Neutron scattering on the FRM double crystal spectrometer 03 p0423 N85-12704
Anharmonic lattice effects in molecular crystals 03 p0424 N85-12709
Phonon anomalies in superconducting transition metal compounds — lanthanum and niobium compounds 03 p0426 N85-12718
Electronic structure and lattice dynamics of solid state substances from gamma nuclear resonance absorption and angular correlation measurements 03 p0427 N85-12728
Determination of depth profiles and lattice positions with (n, p)- and (n, alpha) reactions (n, alpha) and channeling-blocking method) 03 p0429 N85-12735
Reaction mechanisms in the formation of intercalation complexes, and properties of intercalated molecules 03 p0431 N85-12745
Structural changes during milling of aluminum oxide powders
[NASA-TM-77488] 04 p0472 N85-13008
The alpha-form of the hydroxides of bivalent metals
[NASA-TM-77508] 04 p0473 N85-13009
The disordering process in an L1sub2 ordered alloy
[DE84-016599] 04 p0475 N85-13025
Interaction of hydrogen with defects in metals
[DE84-016781] 04 p0476 N85-13032
Coherent amplification of ultrasonic pulses in activated crystals 05 p0724 N85-14653
The atomic structure of Si-SiO2 interfaces suggesting a ledge mechanism of silicon oxidation
[DE84-016057] 05 p0731 N85-14703
Electronic bandstructure of an incommensurate crystal
[DE84-016891] 05 p0733 N85-14714
Theoretical investigation of device aspects of semiconductor superlattices
[AD-A146841] 06 p0867 N85-15509
Superlattice ultrasonic wave generator
[AD-D011383] 07 p1036 N85-16585
Defective nature of the crystalline lattice of nickel ferrite-based solid solutions
[BLL-WH-595-(9091.9F)] 07 p1046 N85-16645
Microscopic determinations of lattice and electronic structures of solids
[DE84-017323] 09 p1399 N85-18806
Defective nature of the crystalline lattice of nickel ferrite-based solid solutions
[BLL-TRANS-WH-595-(9091.9F)] 10 p1439 N85-19068
Comparisons between computed and observed grain boundary structures and properties in metals
[DE85-002596] 10 p1442 N85-19085
Study of influence of cold plastic deformation on aging of VT30 alloy 10 p1448 N85-19124
Solid electrolytes: Mechanisms for achieving optimal conductivity
[AD-A150116] 12 p1801 N85-21296
The crystal and molecular structure of a new propellant compound: Triaminoguanidium Azide Nitrate (TAZN) 13 p2002 N85-22551
Molecular dynamics studies of energy transfer processes in crystal systems
[AD-A150161] 13 p2163 N85-23416
Peculiarities of MgF2 film formation and optimization of MgF2 film deposition process 14 p2261 N85-24132
Recent developments in semiconductor research 14 p2297 N85-24222
Monte Carlo lattice models for adsorbed polymer conformation
[NASA-TP-2453] 14 p2426 N85-24961
Interaction of low energy electrons with surface lattice vibrations
[DE85-005475] 14 p2428 N85-24975
Relationship between symmetrical tilt, twist, special, and favored grain boundaries
[DE85-004024] 14 p2429 N85-24982
Novel materials properties of strained-layer superlattices
[DE85-003676] 14 p2430 N85-24989
Raman scattering of light in epitaxial films of solid phosphide-gallium arsenide solutions 15 p2643 N85-26301
Electronic transport in Mo/Ni superlattice
[DE85-006835] 15 p2661 N85-26425
Molecular dynamics studies of energy transfer processes in crystal systems
[DE85-007247] 15 p2662 N85-26426
On the feasibility of Ab Initio calculations of ordering alloy phase diagrams
[DE85-007073] 16 p2751 N85-26979
Thermal annealing of Fe implanted Al2O3 in oxidizing and reducing environment: Revised version
[DE85-007546] 16 p2752 N85-26983
Atom location by electron channeling analysis
[DE85-007549] 16 p2672 N85-27716
Investigation of superlattice device structures
[NASA-CR-3903] 18 p3094 N85-29152
Structural and physical studies on a new class of low-dimensional conducting material: FeOCl intercalated with TTF and related molecules
[DE85-009701] 18 p3196 N85-29824
Quasiparticle excitations in valence-fluctuation materials: Effects of band structure and crystal fields
[DE85-010783] 19 p3359 N85-30824
Solid State Division report on its mission-oriented basic research
[DE85-008766] 19 p3376 N85-30941
A study of the effect of a mismatch in gamma and gamma prime phase lattice spacings on the high temperature strength characteristics of dispersion-hardened nickel alloys
[BLL-CE-TRANS-8048-(9022.09)] 20 p3430 N85-31279
Structural defects in crystalline silicon 20 p3481 N85-31630
Interfacial bonding stability 21 p3608 N85-32409
Raman scattering studies in solids
[AD-A155528] 21 p3710 N85-33032
On the potential link equation of a spot centre with relative deformation for a semi-infinite molecular crystal
[BLL-M-35795-(5828.4)] 23 p3985 N85-34711
Flux-line lattice anisotropy in V3Si: Observation and interpretation
[DE85-011935] 23 p3985 N85-34713
Simulation of lattice damage due to dynamic loading
[DE85-008466] 24 p4162 N85-35806

CRYSTAL OPTICS
Coherent amplification of ultrasonic pulses in activated crystals 05 p0724 N85-14653
Research progress on laser crystals in China 13 p2166 N85-23440
Lidar ER2 (ozone). Crystal characterization for harmonic conversion — laser systems
[CERT-2/6129-00] 16 p2672 N85-27717
Generation and amplification of radiation during stimulated Raman scattering in crystals 21 p3681 N85-32869

CRYSTAL OSCILLATORS
NT PIEZOELECTRIC CRYSTALS
Method of heating quartz resonators
[AD-D011454] 10 p1481 N85-19347
SAW oscillator with digital compensation for the temperature related frequency changes
[AD-D011537] 12 p1833 N85-21500
Externally compensated crystal oscillator (ECXO) study
[AD-A150335] 13 p2064 N85-22863
Adjustment of the frequency-temperature characteristics of crystal oscillators
[AD-D011588] 15 p2548 N85-25726
Development of a Digitally Compensated SAW Oscillator (DCSO) to provide temperature stable frequency
[AD-A151907] 15 p2549 N85-25730
Cut angles for quartz crystal resonators
[AD-D011652] 17 p2951 N85-28220
Acceleration insensitive oscillator
[AD-D011621] 17 p2953 N85-28236
Proceedings of the Fifteenth Annual Precise Time and Time Interval (PTTI) Applications and Planning Meeting
[AD-A149163] 17 p2961 N85-28287
A new precision time and frequency source for stationary PTTI applications 17 p2963 N85-28297
A plan for the development of inertial reconstruction of initial state clock (IRIS) 17 p2966 N85-28317
High performances from a new design of crystal oscillator 17 p2966 N85-28318
Design of SC cut 10 MHZ H.Q. crystals with G. sensitivity better than 2.10(-10)/G 17 p2966 N85-28319
Crystal resonator/oscillator test facility and test results 17 p2967 N85-28322
The Rubidium-Crystal Oscillator Hybrid Development Program 18 p3106 N85-29230
New features of different frequency generating systems due to the use of electrodeless rigidly mounted VBA quartz crystal resonator 18 p3106 N85-29231

CRYSTAL STRUCTURE
13C and 1H NMR (Nuclear Magnetic Resonance) studies of solid polyolefines
[AD-P003909] 01 p0032 N85-10195
Fundamental studies of structure property relationship in transformation toughened ceramics
[DE84-015344] 01 p0033 N85-10204
Rapid solidification processing and the control of structure/property relationships 02 p0176 N85-11178
Photoelectric effect in liquid crystals 02 p0259 N85-11695
Determining composition in surface region of semiconductor crystals by method of sudden changes in X-ray photoelectric effect 02 p0267 N85-11748
Low temperature properties of Mo/Ni superlattices
[DE84-014729] 02 p0288 N85-11881
Fundamental electronic properties of donor-type graphite intercalated compounds
[AD-A146148] 03 p0326 N85-12099
Effect of heat treatment on phase composition and crystal structure of thin WSi2 films on silicon substrates 03 p0350 N85-12253
One-dimensional model of thin films. Analysis of aluminum surface 03 p0350 N85-12254
Report on research results in solid state nuclear physics, 1980-1982
[JUEL-SPEZ-250] 03 p0422 N85-12696
Fine structure analysis with thermal neutrons and development and construction of a multidetector system 03 p0422 N85-12698
Crystal chemistry and real structure of crystals 03 p0423 N85-12703
Diffuse elastic and inelastic neutron scattering of disorder transitions and boundaries. Phase determination of structure factors 03 p0424 N85-12708
Anharmonic lattice effects in molecular crystals 03 p0424 N85-12709
Phase transformations of AlPO4 with SiO2 structures 03 p0425 N85-12713
Inelastic neutron scattering on crystals for the clarification of structure and semiconductor properties 03 p0425 N85-12714
Magnetic interaction in low-dimensional systems 03 p0426 N85-12717
Investigations on low-dimensional solid state substances — solitons 03 p0426 N85-12720
Structural phase transitions in doped hexahalogen metallates 03 p0426 N85-12721
Structure and kinetics of physisorption, properties of helium during reduction of the dimension 03 p0432 N85-12749
Neutron scattering for the investigation of solid state materials, utilization in chemical structures 03 p0432 N85-12752
Static and quasielastic neutron scattering for the investigation of structure, dynamics and transport properties of lipid layers and lipid/protein compounds 03 p0432 N85-12753
A physical interpretation of the structure and electron-optical data for spinel (MgAl2O4)
[AERE-R-11278] 03 p0434 N85-12767
Critical evaluation of binary rare Earth diagrams
[DE84-014880] 04 p0470 N85-12991
Structural changes during milling of aluminum oxide powders
[NASA-TM-77488] 04 p0472 N85-13008
Cerium compounds in the fashion of the light actinides
[DE84-014642] 04 p0475 N85-13024
Nonthermal mechanism for laser annealing of semiconductors and formation of super structure 04 p0487 N85-13109
Improved apparatus and techniques for high temperature and pressure deformation of crystalline materials
[DE84-016049] 04 p0569 N85-13829
Computational models of crystals
[DE84-016631] 04 p0572 N85-13847
Real space solution to the phase problem in X-ray crystallography: ALCAMPS (Ames Laboratory Computer-aided Analysis of Multi-solution Patterson Superpositions)
[DE84-015476] 04 p0572 N85-13851
Critical evaluation of binary rare earth phase diagrams
[DE84-015057] 05 p0614 N85-13922
Structural studies on lead dioxides
[DE84-015837] 06 p0805 N85-15127

Structural development in the Santa Catharina meteorite 06 p0886 N85-15625
Snow characterization measurements from SNOW-TWO/Smoke Week 6 [AD-A147423] 07 p1008 N85-16402
Clusters of defects in semiconductors [AD-A147426] 07 p1048 N85-16655
Temperature dependence of the crystal structures of Nylon 11 [AD-A147563] 07 p1049 N85-16661
Depositional modeling of tetrahedrite in the Coeur d'Alene district, Idaho 08 p1162 N85-17448
Structure-property relationships in intercalated graphite [AD-A147949] 08 p1219 N85-17680
Crystalline structure of urea ice sheets used in modeling experiments in the CRREL test basin [AD-A148434] 08 p1226 N85-17722
The growth of large diameter single crystals by vertical solidification of the melt [AD-A148756] 09 p1397 N85-18792
Characterization of erosion of metallic materials under cavitation attack in a mineral oil [NASA-TM-86934] 10 p1440 N85-19075
Characterization of novel binders based on energetic thermoplastic elastomers [AD-A148993] 10 p1451 N85-19139
Fundamental studies of growth, doping and transformation in beta silicon carbide [AD-A149339] 10 p1562 N85-19851
Electronic structure of silicon superlattices [NASA-CR-175536] 11 p1736 N85-20916
A mixed-basis band structure interpolation scheme applied to the fluorite structure compounds NiS2, AuAl2, AuGa2 and AuIn2 [AD-A150131] 12 p1940 N85-22187
Specifics of structure and mechanical properties of metastable beta-titanium alloys after deformation and aging 13 p2032 N85-22731
H-division materials physics progress [DE85-004990] 13 p2165 N85-23430
Solid/melt interface studies of high-speed silicon sheet growth [NASA-CR-175698] 14 p2350 N85-24525
Structural unit/grain boundary dislocation model for twist boundaries in cubic crystals [DE85-000425] 14 p2430 N85-24985
Determination of symmetry of immediate surroundings in amorphous Co-P alloys 15 p2496 N85-25398
Structure and aging of amorphous chromium-germanium alloys 15 p2497 N85-25401
Study of structural changes of dual-phase titanium alloy during shock wave loading 15 p2498 N85-25406
Superplasticity in a thermo-mechanically processed Aluminum-10.2%Mg-0.52%Mn alloy [AD-A152016] 15 p2510 N85-25485
Influence of solidification parameters on the formation of the gamma-M7C3 eutectic structure of 2% C-12%Cr steel 15 p2512 N85-25500
Crystallinity determination by curvefit procedure for a semi-crystalline polymer [NASA-TM-86412] 15 p2517 N85-25520
Applications of piezoelectric and pyroelectric thin films: Opportunities for Langmuir-Blodgett technology [AD-A149239] 15 p2659 N85-26406
On the feasibility of Ab Initio calculations of ordering alloy phase diagrams [DE85-007073] 16 p2751 N85-26979
Conducting a thermal conductivity survey [NASA-CR-175792] 16 p2762 N85-27166
Simulation studies for surfaces and materials strength [NASA-CR-175766] 16 p2800 N85-27262
Effects of the cooling rate on the structure of the graphite in inoculated irons [BLL-BISI-TRANS-22305-(9022.06)] 17 p2930 N85-28083
Pseudopotentials and total energy calculations: Applications to crystal stability, vibrational properties, phase transformations, and surface structures [DE85-007657] 18 p3194 N85-29810
Fundamental studies of beta phase decomposition modes in titanium alloys [AD-A154122] 19 p3238 N85-30078
Effects of annealing treatments on superplasticity in a thermomechanically processed Aluminum-10.2%Mg-0.52%Mn [AD-A154414] 19 p3239 N85-30080
Grain structure identification by ultrasound frequency averaging and deconvolution [AD-A154332] 19 p3352 N85-30777
Journal of Research of the National Bureau of Standards, volume 89, no. 6, November - December 1984 [PB85-179042] 20 p3472 N85-31580
The interactions of composition and stress in crystalline solids [PB85-179075] 20 p3473 N85-31583
Proceedings of the Flat-Plate Solar Array Project Research Forum on High-Efficiency Crystalline Silicon Solar Cells [NASA-CR-176047] 20 p3478 N85-31615
Aspects of silicon bulk lifetimes 20 p3479 N85-31617
Structural defects in crystalline silicon 20 p3481 N85-31630
NBS (National Bureau of Standards) reactor: Summary of activities Jul. 1983 through Jun. 1984 [PB85-184836] 20 p3522 N85-31907
Z-contrast imaging and electron channeling analysis of dopants in semiconductors [DE85-011410] 21 p3582 N85-32269
Silicon dendritic web growth 21 p3611 N85-32435
Temperature-stress modeling 21 p3611 N85-32436
Silicon ribbon stress-strain activities 21 p3611 N85-32437
Analysis of stress-strain relationships in silicon ribbon 21 p3611 N85-32438
Stress and buckling analysis 21 p3611 N85-32439
Stress and efficiency studies in EFG 21 p3611 N85-32440
Silicon sheet surface studies 21 p3611 N85-32441
Analysis of inclined growth of silicon sheet 21 p3612 N85-32442
Edge-defined film-fed growth of thin silicon sheets 21 p3612 N85-32443
High-purity silicon crystal growth 21 p3612 N85-32444
Influence on bi-phonon states on Raman scattering of light in molecular crystals 21 p3680 N85-32865
X-ray diffractometric measurements and calculations of limiting values of discrepancy between lattices and layer thicknesses, preventing generation of dislocations during growth of multilayer heterostructures 21 p3681 N85-32866
Classical emission of relativistic charged particles during axial channeling 21 p3681 N85-32871
Influence of background electrically neutral argon admixture on mechanical strength of silicon crystals 21 p3683 N85-32878
Low-threshold injection InGaAsP/GaAs double heterostructure lasers with separate limiting obtained by liquid-phase epitaxy (lambda = 0.78 divided by 0.87 microns, I sub thr = 460 A/cm 2, T = 300 K) 21 p3687 N85-32906
An EPR (Electron-Paramagnetic-Resonance) and ENDOR (Electron-Nuclear-Double-Resonance) study of ferroelectric ammonium sulfate [AD-A155580] 21 p3710 N85-33033
Striation free doped silicon [AD-A155730] 22 p3847 N85-33827
Electrolytic synthesis of colored eta alumina film 23 p3906 N85-34201
High resolution electron microscopic characterization of interfaces in ceramics [DE85-011207] 23 p3920 N85-34289
On the potential link equation of a spot centre with relative deformation for a semi-infinite molecular crystal [BLL-M-35795-(5828.4)] 23 p3985 N85-34711
Cluster variation study of coherent ordering in FCC and BCC solid solutions [AD-A156039] 24 p4079 N85-35280
Ionic crystals [DE85-009482] 24 p4163 N85-35809

CRYSTAL SURFACES

Effect of oxidizing medium and heat treatment on stoichiometry of ZnSe crystal surface 03 p0353 N85-12272
Dispersion forces of solids under stress. Chemisorption under stress [AD-A146171] 03 p0373 N85-12380
USSR report: Physics and mathematics [JPRS-UPM-84-007] 05 p0723 N85-14651
Laser excitation of coupled surface electromagnetic and acoustic waves and of static structures in solids 05 p0723 N85-14652
Amorphization of ceramics by ion beams [DE85-000936] 10 p1453 N85-19156
Studies of the kinetics and mechanisms of ammonia synthesis and hydrodesulfurization on metal single crystal surfaces [DE85-001650] 11 p1595 N85-20030
Low-energy, high-intensity positron beam experiments with a linac [DE85-001048] 11 p1723 N85-20835
The use of moments of momentum to account for crystal habits [NASA-CR-3907] 20 p3421 N85-31232
The development and evaluation of point defect models for the growth of passive films on single crystal, polycrystalline, and amorphous metal surfaces [AD-A154685] 21 p3709 N85-33023
Characterization of catalysts with metal-support effects and of the species adsorbed on their surfaces [DE85-012254] 24 p4096 N85-35394

CRYSTALLINITY

Symmetry of exchange interaction in crystalline magnetic films 02 p0259 N85-11694
Newer carbon fibers and their properties 04 p0465 N85-12955
Study of the physical properties of crystalline rocks in the southeast Voronezh anteclise [NASA-TM-77823] 10 p1514 N85-19551
Characterization and adhesive bonding of poly(etheretherketone) resins and composites [DE85-002526] 11 p1593 N85-20023
Development of AK18 alloy production technology based on electrothermic silumin 11 p1598 N85-20048
Theory of oriented nucleation with asymmetric single elements. 2: Effects of rotational diffusion [IFTR-32/1984] 12 p1939 N85-22179
Influence of substrate heating and thermal annealing on the surface crystallinity in single Si crystals implanted with high doses of (16)O [DE85-005264] 13 p2184 N85-23428
Silicon-sheet and thin-film cell and module technology potential: Issue study [NASA-CR-175654] 14 p2349 N85-24520
Excimer laser annealing to fabricate low cost solar cells [NASA-CR-175702] 14 p2351 N85-24529
Crystallinity determination by curvefit procedure for a semi-crystalline polymer [NASA-TM-86412] 15 p2517 N85-25520
Application of the reference intensity method to coal analysis [DE85-009526] 19 p3228 N85-30015
NMR investigation of crystalline electric field effect on spin-spin relaxation in (Y(1-x)RE(x))Rh4B4 [DE85-010512] 19 p3357 N85-30814
Method for growing low defect, high purity crystalline layers [NASA-CASE-NPO-15813-2] 19 p3374 N85-30933
Use of low energy hydrogen ion implants in high efficiency crystalline silicon solar cells [NASA-CR-176109] 22 p3806 N85-33571
Investigation of the microstructure and photovoltaic properties of semicrystalline silicon 22 p3806 N85-33573

CRYSTALLITES

Structural changes during milling of aluminum oxide powders [NASA-TM-77488] 04 p0472 N85-13008
Study of energy versus misorientation for grain boundaries in gold by crystallite rotation method. 1: 001 twist boundaries [DE85-004598] 12 p1943 N85-22201
Plastic deformation of crystalline polymers [AD-A152090] 16 p2755 N85-26999

CRYSTALLIZATION

NT DIRECTIONAL SOLIDIFICATION (CRYSTALS)
NT MELT SPINNING
NT RECRYSTALLIZATION

New metallurgical processes based on high-speed crystallization and diffusion of metals 01 p0021 N85-10126
Second All-Union Seminar on Hydromechanics and Heat and Mass Exchange in Weightlessness, summaries of reports [NASA-TM-77590] 01 p0047 N85-10305
International Conference on Recent Developments in Specialty Steels and Hard Materials. Conference abstracts [CSIR-S-256] 02 p0176 N85-11177
Rapid solidification processing and the control of structure/property relationships 02 p0176 N85-11178
Microstructural design in low alloy steels 02 p0176 N85-11179
Transport phenomena in the boundary layer during solution solidification under microgravity. Ice growth from a water-salt solution [BMFT-FB-W-84-031] 03 p0329 N85-12121
Microstructure development in polymers [AD-A145980] 03 p0337 N85-12170
Magnetic properties of and superfine interactions in amorphous Fe-Cr-Co-Si-B alloys 03 p0349 N85-12248
Producing semiconductor materials by superfast cooling of melt 03 p0354 N85-12274
Nickel-cobalt systematics and their bearing on lunar origin 04 p0582 N85-13719
Ge abundances in the lunar mantle and implications for the origin of the Moon 04 p0582 N85-13721
Dynamic crystallization of silicate melts [NASA-CR-174103] 05 p0743 N85-14774

Low temperature diffusion coefficients in the Fe-Ni and FeNiP systems: Application to meteorite cooling rates
06 p0886 N85-15626
Extreme incompatibility of Pb during the crystallization of magmatic iron meteorites 06 p0886 N85-15627
Experimental and theoretical study of the formation of the 2AB, 3AB, and 9A meteorite chemical groups from the parent liquid 06 p0886 N85-15628
Method of preparing single crystalline cubic silicon carbide layers
[AD-D011305] 07 p1048 N85-16653
Temperature dependence of the crystal structures of Nylon 11
[AD-A147563] 07 p1049 N85-16661
Crystallization behavior of poly(3,3-bis(Ethoxymethyl) oxentane) and poly(3,3-bis(Azidomethyl) oxetane)
[AD-A148271] 08 p1226 N85-17720
Electrical resistivity and structural changes upon relaxation and crystallization of (Mo/sub 0.6/Ru/sub 0.4)sub 100-x/B/sub x/ metallic glasses
[DE84-017281] 09 p1299 N85-18160
Light scattering studies of lower dimensional colloidal particle and critical fluid systems
[DE85-002087] 09 p1377 N85-18654
Influence of excess phases on fracture toughness of cast alumiun-magnesium-zinc alloy
10 p1442 N85-19091
Conduction in polymerized polyfunctional diacetylenes
[AD-A149104] 10 p1451 N85-19145
Heavy ion induced crystallization in amorphous phases
[DE85-003114] 11 p1606 N85-20098
Total immersion crystal growth
[NASA-CASE-NPO-15800-2] 12 p1939 N85-22178
Reaction of amorphous NiNb films with crystalline metal overlayers
[DE85-005483] 13 p2024 N85-22680
Study of processes of modification of Al-Si alloys
13 p2026 N85-22695
Composition and thickness of oxide coatings on granule surfaces of aluminum alloys 13 p2030 N85-22719
Thermodynamic and kinetic studies of pulsed laser annealing from transient conductivity measurements
[DE85-003677] 13 p2096 N85-23078
Modelling equilibrium and fractional crystallization in the system MgO-FeO-CaO-Al2O3-SiO2
13 p2184 N85-23552
Effect of zirconium on forming ultrafine-grained structure in Al-Mg-Zr alloy 15 p2513 N85-25504
Development of solid state infrared emitters for gas detection applications
[PB85-148450] 15 p2561 N85-25800
An analysis of the economics of turning titanium alloys with polycrystalline diamond tools
15 p2567 N85-25841
Plastic deformation of crystalline polymers
[AD-A152080] 16 p2755 N85-26990
Dendritic growth from amorphous matrix
[DE85-007630] 16 p2871 N85-27712
Multi-phase crystallization of ferrous alloys
[BLL-BISI-TRANS-22441-(9022.06)]
17 p2925 N85-28037
The synthesis and structure of polyphosphazenes
[AD-A153134] 17 p2934 N85-28112
Microstructure-mechanical property relationships in transformation-toughened ceramics
[DE85-009722] 17 p2935 N85-28117
The distribution of higher n-alkanes in partially frozen middle distillate fuels
[AD-A153940] 18 p3083 N85-29074
Aluminum-air power cell: The M3-3 experiment
[DE85-008678] 18 p3096 N85-29168
Study of phase equilibria and crystallization processes in Al-Zn-Mg alloy systems 19 p3241 N85-30098
Crystallization of aluminum-based alloys in weightlessness 19 p3242 N85-30101
The use of moments of momentum to account for crystal habits
[NASA-CR-3907] 20 p3421 N85-31232
Interaction of solutes with stretched polymers
[AD-A154662] 21 p3569 N85-32196
Introduction of structural variations into oxide polymers and their effect on sintering and crystallization
[AD-A155597] 21 p3570 N85-32206
A fluidized-bed reactor for silane pyrolysis
21 p3609 N85-32413
The effect of liquid-liquid phase separation of glass on the properties and crystallization behavior
[NASA-TM-77690] 23 p3919 N85-34285
Crystallization of Polyetheretherketone (PEEK) in carbon fiber composites
[AD-A156316] 24 p4075 N85-35252
High temperature corrosion of ceramics
[DE85-013481] 24 p4083 N85-35303
A new drawing technique for nylon 6 by reversible plasticization with iodine
[AD-A156272] 24 p4162 N85-35803

CRYSTALLOGRAPHY
Report on research results in solid state nuclear physics, 1980-1982
[JUEL-SPEZ-250] 03 p0422 N85-12696
Investigation of solid state problems using the hyperfine interaction between static and dynamic internal fields with short live excited probe nuclei 03 p0428 N85-12729
Measurement of static and dynamic solid state properties in nonmetals using excited probe nuclei on the Erlanger 12 MeV tandem accelerator 03 p0428 N85-12730
Solid state investigations with nuclear physics methods 03 p0428 N85-12731
Utilization of a tandem accelerator for the investigation of solid state properties by means of heavy ions
03 p0429 N85-12733
Investigation of the interaction of atoms with lattice defects using probe methods 03 p0429 N85-12737
Fast ions as probes in solid state research
03 p0430 N85-12740
X-ray and neutron scattering and X-ray spectroscopy for the study of defects in solid state materials
03 p0430 N85-12741
Real space solution to the phase problem in X-ray crystallography: ALCAMPS (Ames Laboratory Computer-aided Analysis of Multi-solution Patterson Superpositions)
[DE84-015476] 04 p0572 N85-13651
Butene oxidation by molybdenum crystalographic shear compounds
[DE84-013910] 05 p0614 N85-13923
Investigation of structural and electrical properties of low-angle silicon sheet 06 p0831 N85-15288
Semicrystalline casting process development and verification 06 p0832 N85-15289
AEM with a convergent beam
[DE85-000667] 11 p1714 N85-20784
Influence of individual reflections on the precision of parameter estimates in least squares refinement
[DE85-000830] 11 p1735 N85-20909
Surface physics and crystallography
[DE85-003128] 11 p1735 N85-20910
New high resolution scanning ion microprobe and focused ion beam applications
[AD-A149992] 12 p1852 N85-21616
Crystal chemistry of meteoritic hibonites
13 p2185 N85-23558
Structural, morphological and optical characteristics of KGd(WO4)2 crystals 14 p2280 N85-24126
Case studies of snow clouds by means of snow crystal sondes 15 p2581 N85-25921
Characteristics of fast sea ice collected near Barrow, Alaska 15 p2582 N85-25925
Atom location by electron channeling analysis
[DE85-007549] 16 p2872 N85-27716
X-ray crystallography of steel U8 after pulsed laser hardening
[BLL-BISI-22444-(9022.06)] 17 p2925 N85-28038
A new high-resolution pickup tube for live X-ray topography
[NHK-LABS-NOTE-309] 18 p3193 N85-29802
Low-energy electron diffraction experiment and theory
[DE85-009967] 18 p3195 N85-29820
X-ray diffractometric measurements and calculations of limiting values of discrepancy between lattices and layer thicknesses, preventing generation of dislocations during growth of multilayer heterostructures
21 p3681 N85-32866
Crystallographic orientation dependence of fatigue crack propagation in extremely low carbon steel
23 p3908 N85-34195

CRYSTALS
NT BICRYSTALS
NT BOULES
NT CRYSTAL OSCILLATORS
NT CRYSTALLITES
NT DENDRITIC CRYSTALS
NT DOPED CRYSTALS
NT IONIC CRYSTALS
NT LIQUID CRYSTALS
NT METAL CRYSTALS
NT MICROCRYSTALS
NT MIXED CRYSTALS
NT PIEZOELECTRIC CRYSTALS
NT POLYCRYSTALS
NT QUARTZ CRYSTALS
NT SINGLE CRYSTALS
NT WHISKERS (CRYSTALS)
Current controlled LPE (Liquid Phase Epitaxy) growth of semiconductors
[AD-A145536] 02 p0297 N85-11875
Static and dynamic disordering in amorphous magnets and crystals 03 p0422 N85-12699
Computational models of crystals
[DE84-016831] 04 p0572 N85-13647
X-ray absorption in perfect crystals
[DE84-016034] 05 p0732 N85-14708
Theoretical methods for the study of transition metals in crystals
[DE84-015606] 05 p0732 N85-14709
Microstructural origins of hot spots in RDX explosive and a reference inert material
[AD-A146685] 06 p0774 N85-14947
Semicrystalline casting process development and verification 06 p0832 N85-15289
Simulation of bent crystal spectrometers
[DE85-002042] 09 p1385 N85-18709
International Conference on Defects in Insulating Crystals
[AD-A149611] 12 p1939 N85-22180
Electron image simulation: A complementary processing technique
[DE85-000685] 12 p1941 N85-22190
Molecular dynamics studies of energy transfer processes in crystal systems
[AD-A150161] 13 p2163 N85-23416
Thresholds of optical breakdown in alkali-halide crystals under pulses from CO2-laser 14 p2282 N85-24134
Energy trapping, release, and transport in three-dimensional energetic solids and molecular crystals: Theory of defects and impurities
[AD-A151071] 14 p2428 N85-24973
Method of fabricating acceleration resistant crystal resonators and acceleration resistant crystal resonators so formed
[AD-D011630] 16 p2778 N85-27145
Ac field-induced order in dense colloidal systems
[DE85-009107] 17 p2935 N85-28119
Central limit theorems in the area of large deviations for some dependent random variables
[AD-A153125] 17 p3043 N85-28831
Method of reducing impurity and antisite defects in semiconductor crystal materials, and device and apparatus respectively produced from and utilizing same
[AD-D011698] 19 p3260 N85-30216
A method to estimate the self-consistency effects on electronic structure calculations
[INPE-3536-PRE/752] 19 p3375 N85-30936
Leading-edge microelectronics research at Sweden's Chalmers 20 p3438 N85-31337
High temperature electronics technology: Life test report
[AD-A154681] 21 p3580 N85-32257
Monte Carlo studies of H2O layers adsorbed on a model basal face of AgI 21 p3643 N85-32633
USSR report: Physics and mathematics
[JPRS-UPM-85-004] 21 p3680 N85-32660
Lasing on LiF:F(-)2 - dye centers with transverse pumping 21 p3684 N85-32690
The problem of brightness enhancement during laser frequency doubling 21 p3686 N85-32697
Transparent electrode for optical switch
[DE85-011618] 22 p3761 N85-33310
Striation free doped silicon
[AD-A155730] 22 p3847 N85-33827
Refractive indices and thermo-optic coefficients of nonlinear crystals isomorphic to KH2PO4
[DE85-012968] 22 p3847 N85-33831
Lead and uranium group abundances in cosmic rays
[OG-7.1-3] 23 p4013 N85-34865
Characterization of catalysts with metal-support effects and of the species adsorbed on their surfaces
[DE85-012254] 24 p4096 N85-35394
Search for supermassive magnetic monopoles using mica crystals
[HE-6.1-8] 24 p4210 N85-36134

CT-114 AIRCRAFT
U CL-41 AIRCRAFT

CTD
U CHARGE TRANSFER DEVICES

CUBA
Evaluation of the climatic resources of Cuba applied to agricultural work 07 p1004 N85-16380

CUBIC LATTICES
NT BODY CENTERED CUBIC LATTICES
NT FACE CENTERED CUBIC LATTICES
Monotonicity preserving bicubic interpolation
[DE85-004206] 18 p3172 N85-29657
On the group-theoretical approach to the energy spectra problem of charge carriers in cubic solids
[PREPRINT-435] 18 p3196 N85-29827

CUES
An in-flight investigation of a twin fuselage configuration in approach and landing
[NASA-CR-172366] 05 p0598 N85-13801
Use of linear perspective scene cues in a simulated height regulation task 05 p0704 N85-14517

Cockpit window edge proximity effects on judgements of horizon vertical displacement
05 p0704 N85-14518
Mean and random errors of visual roll rate perception from central and peripheral visual displays
05 p0704 N85-14519
Direction judgement errors in perspective displays
05 p0705 N85-14520
The interaction of focused attention with flow-field sensitivity
05 p0705 N85-14521
Accuracy of system step response roll magnitude estimation from central and peripheral visual displays and simulator cockpit motion
05 p0705 N85-14522
Models for the effects of G-seat cuing on roll-axis tracking performance
05 p0707 N85-14532
Low altitude texture comparison data base and smooth shaded texture
[AD-A150342] 13 p2146 N85-23323

CUESTAS
U RIDGES

CULTIVATION
NT PLOWING
Assessing erosion on US cropland: Land management and physical features
[PB84-219252] 04 p0526 N85-13366
Cultivation and conversion of marine macroalgae --- biomass energy production
[DE84-004522] 04 p0544 N85-13464
Screening Prosopis (mesquite) species for biofuel production on semi-arid lands
[DE85-010048] 19 p3302 N85-30471

CULTURE (SOCIAL SCIENCES)
The legacy of science
14 p2432 N85-24995

CULTURE TECHNIQUES
Bioprocessing in space
05 p0690 N85-14439
Problems associated with the utilization of algae in bioregenerative life support systems
[NASA-CR-166615] 07 p1019 N85-16469
Algal culture studies related to a Closed Ecological Life Support System (CELSS)
[NASA-CR-177322] 07 p1019 N85-16470
Research and development of shallow algal mass culture systems for the production of oils
[DE85-000518] 11 p1690 N85-20624
Microalgae culture collection, 1984-1985
[DE84-013035] 11 p1690 N85-20626
Flow through bacteria detection system
[NASA-CASE-LAR-12871-1] 18 p3104 N85-29218
Effects of method of detachment on electrophoretic mobility of mammalian cells grown in monolayer culture
20 p3500 N85-31757
Preparative electrophoresis of cultured human cells: Effect of cell cycle phase
20 p3500 N85-31758
Size and DNA distributions of electrophoretically separated cultured human kidney cells
20 p3500 N85-31759
The role of cell size in density gradient electrophoretic separation of mouse leukemia cells according to position in the cell cycle
20 p3500 N85-31760
Electrophoretic mobilities of cultured human embryonic kidney cells in various buffers
20 p3501 N85-31761
Flow cytometry of human embryonic kidney cells: A light scattering approach
20 p3503 N85-31778
Chemolithotrophy and physiology of bacterial nutrient limitation
21 p3659 N85-32730
Microbial colonization and growth on metal sulfides and other mineral surfaces
21 p3662 N85-32747
Production of liquid fuels and chemicals by microalgae
[DE85-009780] 22 p3819 N85-33658
Production of butanol by fermentation in the presence of cocultures of clostridium
[NASA-CASE-NPO-16203-1] 24 p4071 N85-35227

CUMULATIVE DAMAGE
Cumulative damage model for advanced composite materials
[AD-A144840] 01 p0022 N85-10135
Equivalent damage: A critical assessment
02 p0140 N85-10952
Cumulative damage model for advanced composite materials
[AD-A145441] 02 p0171 N85-11142
The influence of mechanical damage on transmission pipeline integrity
[ERS-E.351] 09 p1340 N85-18431
Recent studies of the significance of mechanical damage in pipelines
[ERS-E.367] 09 p1341 N85-18433
Influence of 3% NaCl solution on rate of accumulation of damage and residual strength of aluminum-boron composite
13 p2027 N85-22899
The cumulative effects of long term exposure to low levels of radiofrequency radiation (RFR)
16 p2776 N85-27132
Modifications of flight-by-flight load sequences to provide for good fracture surface readability
[NLR-MP-84012-U] 20 p3472 N85-31577
Damage mechanisms in damaged CFRP laminates
24 p4074 N85-35249

CUMULONIMBUS CLOUDS
NT ANVIL CLOUDS
NT ARC CLOUDS

CUMULUS CLOUDS
NT ANVIL CLOUDS
Theoretical development of Monte Carlo codes for modeling cumulus cloud fields
[NASA-CR-174063] 02 p0230 N85-11500
Non-precipitating cumulus cloud study
[DE85-002352] 12 p1896 N85-21902
Cumulus cloud venting of mixed layer ozone
[NASA-TM-87429] 13 p2132 N85-23269
Cumulus effects on the large-scale vorticity and momentum fields in the tropical atmosphere
13 p2137 N85-23270
Convection modeling and application to severe storms
15 p2595 N85-25991
Ice multiplication in summertime cumulus clouds in the BEWMEX area
16 p2829 N85-27445
The use of radar in determining precipitation processes in the BEWMEX area
16 p2831 N85-27455
Effects of cloud seeding on precipitation development in cumulus clouds
16 p2831 N85-27456
Vertical redistribution of a pollutant tracer due to cumulus convection
[PB85-172971] 18 p3134 N85-29415
Numerical simulation of chemical and physical properties of cumulus clouds
[DE85-009744] 19 p3317 N85-30564
Aircraft investigations of the distribution of aerosols in the lower troposphere
21 p3647 N85-32659

CURIE TEMPERATURE
Determination of optimum Curie point as a function of source and sink temperatures for magnetic heat pumps
[DE84-016995] 04 p0499 N85-13182
Magnetic studies of Ni3Al(Fe) compounds
[DE85-005262] 13 p2025 N85-22686

CURIE-WEISS LAW
Magnetism of californium metal
[DE85-001141] 09 p1377 N85-18657

CURING
Development of new and improved polymer matrix resin systems, phase 1
[NASA-CR-166595] 01 p0017 N85-10104
Infrared spectroscopy study of the SP-250 epoxy resin system
[AD-A145860] 03 p0337 N85-12167
Morphology and dynamic mechanical properties of diglycidyl ether of bisphenol-A toughened with carboxyl-terminated butadiene-acrylonitrile
04 p0466 N85-12958
Matrix resin characterization in cured graphite composites using diffuse reflectance-FTIR
04 p0466 N85-12959
Solvent resistant thermoplastic composite matrices
04 p0466 N85-12960
Aliphatic-aromatic heterocyclics as potential thermoplastics for composite matrices
04 p0466 N85-12962
Variation of resin properties through the thickness of cured samples
04 p0468 N85-12974
Rubber-modified epoxies. 1: Cure, transitions, and morphology
[AD-A147377] 07 p0932 N85-15908
Monitoring cure of epoxy resins using a microdielectrometer
[AD-A148618] 08 p1119 N85-17054
The use of microdielectrometry in monitoring the cure of resins and composites
[AD-A148619] 08 p1119 N85-17055
Characterization of a thermoplastic polyimidesulfone
[NASA-TM-86358] 10 p1450 N85-19135
Characterization of acetylene-terminated resin cure states
[AD-A149463] 10 p1452 N85-19148
Chemical approach for controlling nadimide cure temperature and rate with maleimide
[NASA-CASE-LEW-13770-3] 12 p1809 N85-21350
Chemical approach for controlling nadimide cure temperature and rate with maleimide
[NASA-CASE-LEW-13770-4] 12 p1810 N85-21351
SRM filament wound case resin characterization studies
12 p1944 N85-22212
Monitoring of laminate cure with microdielectrometry
[AD-A150863] 14 p2248 N85-23934
Chemical interpretation of the relaxed permittivity during epoxy resin cure
[AD-A150955] 14 p2260 N85-24005
Characterization-curing-property studies of HBRF 55A resin formulations
[NASA-CR-175836] 16 p2753 N85-26989
Formulation/cure technology for ultrahigh molecular weight silphenylene-siloxane polymers
[NASA-TP-2476] 16 p2753 N85-26990
Evaluation of experimental epoxy monomers
[NASA-TM-87476] 16 p2754 N85-26996
Chemical control of nadimide cure temperature and rate
[NASA-CASE-LEW-13770-2] 18 p3069 N85-28962
Metal (2) 4,4',4',4'' phthalocyanine tetraamines as curing agents for epoxy resins
[NASA-CASE-ARC-11424-1] 23 p3919 N85-34281
Chemoviscosity modeling for thermosetting resins, 2
[NASA-CR-177958] 24 p4073 N85-35243

CURIUM
NT CURIUM 244
Thermodynamic systematics of oxides of americium, curium and neighboring elements
[DE85-009704] 18 p3197 N85-29831

CURIUM ISOTOPES
NT CURIUM 244

CURIUM 244
Historical review of californium-252 discovery and development
[DE85-010223] 19 p3362 N85-30844

CURL (VECTORS)
NT VORTICITY

CURRENT ALGEBRA
Modern test of chiral anomalies
[DE85-005892] 17 p3020 N85-28680

CURRENT AMPLIFIERS
NT PHOTOMULTIPLIER TUBES
Multi-channel pulser for the SLC thermionic electron source
[DE85-014222] 24 p4160 N85-35792

CURRENT CONVERTERS (AC TO DC)
Design and operating experience of an ac-dc power converter for a superconducting magnetic energy storage unit
[DE84-014041] 09 p1316 N85-18275

CURRENT DENSITY
Manual of phosphoric acid fuel cell stack three-dimensional model and computer program
[NASA-CR-174722] 01 p0067 N85-10447
Theory of the double critical state in type-2 superconductors
[DE84-015461] 02 p0289 N85-11886
Westinghouse programs in pulsed homopolar power supplies
05 p0606 N85-13862
Transient currents of ideally conducting body of revolution with transient diffraction
06 p0785 N85-15019
Current-voltage characteristics of semiconductor power devices operating at high current densities
06 p0795 N85-15079
Semiconductor submicrosecond power commutator switches
06 p0795 N85-15081
A coaxial probe for measuring the current density profile of intense electron beams
[AD-D011407] 08 p1164 N85-17347
A superconducting quantum current standard
[NPL-QU-67] 08 p1224 N85-17710
Contributions of segregated phosphorus to the intergranular stress corrosion cracking of nickel
[DE85-003112] 11 p1606 N85-20099
Hydrogen vibrational population distributions and negative ion generation in tandem high density hydrogen discharges
[DE85-001207] 11 p1722 N85-20834
Pre- and post-processing for stream-function eddy current calculations
[AD-A150417] 13 p2065 N85-22896
New high-efficiency silicon solar cells
[NASA-CR-175643] 13 p2128 N85-23244
Degradation phenomena in solid electrolytes
[DE85-007066] 15 p2587 N85-25949
Investigation of pseudo bi-polar nickel cadmium batteries as filter elements for pulsed power loads
[AD-A152112] 16 p2819 N85-27389
Maximum current densities from tandem high density systems
[DE85-008966] 18 p3180 N85-29720
Development of power system measurements
[PB85-182582] 20 p3450 N85-31420
The electric current densities beneath thunderstorms
20 p3494 N85-31726
Superconducting toroidal field coil current densities for the TFCX
[DE85-010285] 20 p3530 N85-31959
Detection of excited states by laser-induced fluorescence
[AD-A155558] 21 p3592 N85-32326
Influence of technological factors on luminescence characteristics of InGaAsP/InP heterolasers (lambda = 1.55 microns)
21 p3688 N85-32910
Critical current density and microstructural state of an internal tin multifilamentary superconducting wire
[DE85-009966] 22 p3761 N85-33308

Electrochemical method for investigation of the susceptibility of corrosion-resistant steels to intercrystalline corrosion
[BLL-CE-TRANS-8082-(9022.09)] 24 p4077 N85-35269
Effect of Cu4Ti compound formation on the characteristics of NbTi accelerator magnet wire
[DE85-014226] 24 p4159 N85-35788
Current interruption by density depression
[DE85-013120] 24 p4169 N85-35848

CURRENT DISTRIBUTION
A generalized solution to a class of printed circuit antennas
[AD-A145626] 02 p0191 N85-11278
Magnetic field calculation for ideal conductors by method of equivalent currents 06 p0788 N85-15035
Radiation patterns of a pyramidal horn antenna 09 p1311 N85-18236
Mathematical simulation of thermal prrocesses involved in electron-beam treatment 12 p1843 N85-21585
Solar cells with distributed parameters: Current-voltage characteristics under uniform and nonuniform illumination 14 p2275 N85-24093
IMS advances in studies of field-aligned currents and their related electrodynamics 14 p2359 N85-24578
Current distribution in a plasma erosion opening switch
[AD-A150967] 14 p2424 N85-24949
Acoustic emission of semiconductor devices 15 p2529 N85-25593

CURRENT REGULATORS
Optimization of design parameters for alternating current stabilizer based on magnetic suspension 22 p3772 N85-33374

CURRENT SHEETS
Solar flares and laboratory experiments on magnetic reconnection in current sheaths 02 p0162 N85-11099
Structure and evolution of the large scale solar and heliospheric magnetic fields 05 p0746 N85-14782
Birkeland currents correlated with dc-electric fields observed during the CENTAUR BBX rocket experiments
[DRI-6-84] 06 p0834 N85-15311
Partial penetration of IMF B(sub y) into the magnetosphere
[DRI-5-84] 10 p1514 N85-19554
Magnetotail current sheet and energetic particles observed on ISEE-1 14 p2357 N85-24566
Entry of solar energetic protons into the distant plasma sheet dependence on distance from the neutral sheet 14 p2357 N85-24567
Estimate of the amplitude of transient electric fields in the magnetotail 14 p2358 N85-24568
Plasma sheet dynamics deduced from ISEE-1 and -2 energetic particle flux data 14 p2358 N85-24570
Plasma waves at and near the neutral sheet 14 p2358 N85-24572
The near Earth current sheet: ISEE-1 and -2 case studies 14 p2358 N85-24573
Ring current dynamics and plasma sheet sources — magnetic storms 14 p2359 N85-24577
Pi2 pulsations and the substorm current wedge - ground observations 14 p2370 N85-24650
Ground-satellite observations of substorm related Pi 2 pulsations and current systems 14 p2370 N85-24651
The influence of the heliospheric current sheet and angular separation on flare accelerated solar wind
[NASA-CR-175962] 18 p3209 N85-29907
Contributions to the 19th International Cosmic Ray Conference
[NASA-CR-176060] 21 p3714 N85-33044
Differential measurement of cosmic-ray gradient with respect to interplanetary current sheet
[PAPER-SH-4.2-9] 21 p3715 N85-33055
Cosmic ray intensity and the tilt of the neutral sheet
[SH-4.2-8] 23 p4007 N85-34846
Differential measurement of cosmic-ray gradient with respect to interplanetary current sheet
[SH-4.2-9] 23 p4007 N85-34847
Spatial variation of cosmic rays near the heliospheric current sheet
[SH-4.2-10] 23 p4007 N85-34848
Determination of galactic cosmic ray latitudinal gradient using Earth based detectors
[SH-4.2-13] 23 p4008 N85-34851
Latitudinal gradients of cosmic rays and the polarity reversal of the heliospheric magnetic field: A preliminary evaluation
[SH-4.2-16] 23 p4008 N85-34853
The effect of the neutral sheet structure of the interplanetary magnetic field on cosmic ray distribution in space
[SH-4.2-18] 23 p4008 N85-34855
Difference between even and odd 11-year cycles in cosmic ray intensity
[SH-4.2-22] 23 p4009 N85-34859
The dependence of solar modulation on the sign of the cosmic ray particle charge
[SH-4.2-23] 23 p4009 N85-34860

CURRENT STABILIZERS
U CURRENT REGULATORS

CURRENTS
An optically isolated amplifier
[CSIR-SR-ELEK-257] 01 p0049 N85-10321

CURRENTS (OCEANOGRAPHY)
U WATER CURRENTS

CURTAINS
Experimental investigation of annular air curtain domes
[UTIAS-288] 15 p2521 N85-25543
Particle curtain generator for optical property measurements of solid particles
[DE85-005784] 15 p2560 N85-25797
Results of tests on a specimen of the SRB aft skirt heat shield curtain in the MSFC LRLF
[NASA-CR-170883] 24 p4070 N85-35221
Results of tests of the SRB aft skirt heat shield curtain in the MSFC Hot Gas Facility
[NASA-CR-170888] 24 p4070 N85-35223

CURTISS-WRIGHT MILITARY AIRCRAFT
U MILITARY AIRCRAFT

CURVATURE
Direct numerical simulation of curved turbulent channel flow
[NASA-TM-85974] 02 p0197 N85-11316
First derivatives of flow quantities behind two-dimensional, nonuniform supersonic flow over a convex corner
[NASA-TM-86272] 08 p1077 N85-16828
Convective heat transfer coefficients for pipe flow with curvature induced secondary motion 09 p1318 N85-18285
Theoretical and empirical studies of the basic structure of turbulent shear flows, including separated flows and effects of wall curvature
[AD-A149657] 12 p1846 N85-21580
Zero-crossings on lines of curvature
[AD-A150171] 13 p2150 N85-23345
Gravity perception and response in shoot of cereal grasses 15 p2611 N85-26091
Temperature: Curvature relationships for unsymmetric graphite-epoxy laminates
[VPI-E-85-06] 16 p2743 N85-26926
Formulas for updating the generalized inverse of a symmetric matrix perturbed by a symmetric rank 2 matrix composed of 2 nonsymmetric DYADS
[AD-A151736] 16 p2858 N85-27629
Examination of the circle spline routine 17 p3004 N85-28573
Convex interpolating splines of arbitrary degree 17 p3004 N85-28574
Effects of solar magnetic field on cosmic rays
[SH-4.2-12] 23 p4008 N85-34850
The effect of the neutral sheet structure of the interplanetary magnetic field on cosmic ray distribution in space
[SH-4.2-18] 23 p4008 N85-34855
The dependence of solar modulation on the sign of the cosmic ray particle charge
[SH-4.2-23] 23 p4009 N85-34860
RF stabilization of interchange-ballooning modes
[DE85-012080] 24 p4090 N85-35353

CURVE FITTING
A method for evaluating the contamination of steel in relation to the solidification curve
[BLL-M-35735-(5828.4)] 02 p0175 N85-11171
Non-linear data fitting for the analysis of creep rupture data on GRP materials in aggressive environments — glass reinforced plastics (GRP)
[NPL-DMA(A)-79] 04 p0512 N85-13261
Response surface designs
[AD-A147202] 07 p1035 N85-16569
A variable span smoother
[AD-A146241] 08 p1215 N85-17655
Smoothing with split linear fits
[AD-A149032] 10 p1545 N85-19740
Determination of quantitative relationships between selected critical helicopter design parameters
[AD-A152034] 16 p2706 N85-26700
Locally-weighted-regression scatter-plot smoothing (LOWESS): A graphical exploratory data analysis technique
[AD-A152239] 16 p2855 N85-27609
A new world survey expression for cosmic ray vertical intensity vs. depth in standard rock
[HE-5.1-10] 24 p4201 N85-36073

CURVED BEAMS
Design, fabrication and test of composite curved frames for helicopter fuselage structure
[NASA-CR-172498] 15 p2470 N85-25347

CURVED PANELS
Vortex sheet modeling with higher order curved panels 20 p3451 N85-31428

CURVED SURFACES
U CONTOURS
U SHAPES
U SURFACES

CURVES
Principal curves and surfaces
[AD-A148833] 09 p1375 N85-18846

CURVES (GEOMETRY)
NT CATENARIES
NT EPICYCLOIDS
An integral equation formulation for a boundary value problem of elasticity in the domain exterior to an arc
[PREPRINT-833] 03 p0413 N85-12643
Spacefilling curves and the planar travelling salesman problem
[AD-A149337] 10 p1551 N85-19786
Reflected wave travel-time curves in stratified media with vertically heterogeneous layers and slightly sloping curved boundaries 13 p2114 N85-23167
Constrained parabolic approximation of curves in the finite element method
[CSIR-TWISK-340] 14 p2408 N85-24843
Entire functions with spiral limits 15 p2634 N85-26241
On the role of mother-planet magnetic field in spiral structure explanation of formation of spokes — Saturn rings 15 p2676 N85-26525
Shape preserving spline interpolation 17 p3003 N85-28564
The construction of curves and surfaces using numerical optimization techniques 17 p3003 N85-28565
A survey of patch methods 17 p3003 N85-28567
When is a Bernstein-Bezier curve the graph of a function? 17 p3003 N85-28568
Boundary to constructive solid geometry mappings: A focus on 2-D issues 17 p3004 N85-28570
The definition and computation of a metric on plane curves. The meaning of a face on a geometric model 17 p3004 N85-28571
A natural bias approach to cardinal spline curves 17 p3004 N85-28575
Adapting shape parameters for cubic Bezier curves 17 p3004 N85-28576
A uniform subdivision method for triangular Bezier patches 17 p3005 N85-28578
An intuitive approach to geometric continuity for parametric curves and surfaces (extended abstract) 17 p3005 N85-28579
Spline curves, wire frames and B-value 17 p3006 N85-28587
Numerical estimation of the curvature of biological surfaces 17 p3006 N85-28588
Curved finite elements and curve approximation 17 p3007 N85-28590
Comparison of two algebraic methods for curve/curve intersection 17 p3007 N85-28591
A comparison of three curve intersection algorithms 17 p3007 N85-28592
Some relations among directions of curves at an invariant point on a thermodynamic phase diagram 19 p3312 N85-30530
Conjugated symmetrical coupler curves, produced by 4-bar linkages having the same transmission angles 23 p3924 N85-34322
Geometric continuity with interpolating Bezier curves 23 p3983 N85-34570
An intuitive approach to geometric continuity for parametric curves and surfaces 23 p3983 N85-34571
The dynamics of articulated rigid bodies for purposes of animation 23 p3985 N85-34579

CURVILINEAR COORDINATES
U SPHERICAL COORDINATES

CUSHIONCRAFT GROUND EFFECT MACHINE
Planning of air cushion transport vehicles 14 p2285 N85-24160

CUSHIONS
Vibrational loading mechanism of unitized corrugated containers with cushions and non-load-bearing contents 09 p1339 N85-18419
Blanket integrated cushioning of foldable and retractable solar arrays 13 p2011 N85-22612

CUSPS
Dayside cusp aurora 04 p0521 N85-13333

CUT-OUTS
U OPENINGS

CUTANEOUS PERCEPTION
U TOUCH

CUTTERS
NT BLADES (CUTTERS)
NT DRILL BITS
NT DRILLS
NT SAWS
Portable slotting device
[AD-D011213] 01 p0033 N85-10206
Development and performance of CVD-coatings on cutting tools 02 p0178 N85-11193
Evaluation of the Kerie Cable thermal arc cutting equipment
[AD-A147813] 07 p0974 N85-16186
Technological and economic assessment of advanced ceramic materials: Volume 4: A case study of integrated optic devices
[PB85-113116] 12 p1815 N85-21385
Technological and economic assessment of advanced ceramic materials. Volume 6: A case study of ceramic cutting tools
[PB85-113132] 12 p1815 N85-21387
Diamond cutters' grinders 13 p2051 N85-22841
T700 cutter life improvement program
[AD-A150450] 13 p2099 N85-23089
New technology of finish cutting teeth in large gear blanks 14 p2267 N85-24047
Milling machine with numerical programmed control for cutting teeth 14 p2268 N85-24052
Cutting structural materials in vacuum
14 p2286 N85-24165
An analysis of machine tool systems suitable for laser profiling 14 p2308 N85-24282
Sweden invents new ceramic for more durable cutting tools 15 p2536 N85-25645
Classification and types of diamond wear in honing
15 p2567 N85-25842
Abrasive cutting-off wheel 15 p2568 N85-25843
Removal of longitudinal internal flash from electrically welded tubes
[BLL-BISI-TRANS-22360-(9022.06)]
17 p2938 N85-28136
Portable cutting apparatus
[DE85-011635] 22 p3792 N85-33496
Properties of tungsten-free steel for cutting tools
[BLL-M-35808-(5828.4)] 23 p3915 N85-34259
Action of wear-inhibiting Al2O3-coatings when applied to hard metal cutting tools
[BLL-RISLEY-TR-5041-(8091.9F)]
24 p4081 N85-35292

CUTTING
NT LASER CUTTING
NT METAL CUTTING
NT MILLING (MACHINING)
NT SCARFING
NT SHEARING
NT SLICING
NT SPARK MACHINING
Portable slotting device
[AD-D011213] 01 p0033 N85-10206
Thermal shock as a carbide grade development tool
[DE84-016839] 04 p0509 N85-13251
Evaluation of the Kerie Cable thermal arc cutting equipment
[AD-A147813] 07 p0974 N85-16186
New method for heat treatment of metals
10 p1446 N85-19110
Specifics of laser heat treatment of high steel tools
13 p2029 N85-22714
USSR report: Machine tools and metalworking equipment
[JPRS-UMM-85-005] 13 p2051 N85-22839
T700 cutter life improvement program
[AD-A150450] 13 p2099 N85-23089
Cutting structural materials in vacuum
14 p2286 N85-24165
Device for preventing intrusion of a blade during vibration cutting of intermittent cutting with a lathe
16 p2794 N85-27232
Semicrystalline casting process development and verification
[DE85-007695] 16 p3081 N85-29058
Geothermal COMPAX drill bit development
[DE85-011353] 20 p3469 N85-31556
Hole cutting in building frames by laser
[FOA-C-20569-D9] 22 p3791 N85-33487
Portable cutting apparatus
[DE85-011635] 22 p3792 N85-33496

CV-990 AIRCRAFT
MIZEX, 1984, NASA CV-990 flight report
[NASA-TM-86216] 19 p3299 N85-30451

CW RADAR
U CONTINUOUS WAVE RADAR

CYANIDE EMISSION
U CN EMISSION

CYANIDES
NT CYANOGEN
NT IRON CYANIDES
Ion chromatographic determination of gold in plating baths
[DE84-016187] 02 p0184 N85-11230
Acetonitrile in the Earth's atmosphere: An upper limit deduced from infrared solar spectra
[AERONOMICA-ACTA-A-295-1985]
22 p3813 N85-33623

CYANO COMPOUNDS
NT DIISOCYANATES
NT ISOCYANATES
Protocyanobacteria: Oxygenic and Anoxygenic photosynthesis in mat-forming bacteria
21 p3657 N85-32714
Sulfur transformations at the hydrogen sulfide/oxygen interface in stratified waters and in cyanobacterial mats
21 p3657 N85-32715

CYANOGEN
Adiabatic approach in the theory of polyatomic photodissociation: Application to C2N2
[DE85-008515] 18 p3071 N85-28996
Cyanobacterial mats: Microanalysis of community metabolism 21 p3661 N85-32743
Microanalysis of dissolved iron and phosphate in pore waters of hypersaline sediment
21 p3661 N85-32744
Glutathione in cyanobacteria
21 p3661 N85-32745

CYANOPHYTA
U BLUE GREEN ALGAE

CYBERNETICS
Asynchronous discrete control of continuous processes
[AD-A145570] 02 p0189 N85-11262
The application of basic control laws to human medicine
[DFVLR-MITT-84-13] 05 p0697 N85-14482
Applications of connectionist modeling techniques to simulations of motor control systems
05 p0717 N85-14596
Functional system theory in practice
11 p1690 N85-20629
USSR report: Cybernetics, computers, and automation technology
[JPRS-UCC-85-002] 14 p2400 N85-24794
Gordon Conference on Fundamentals of Cybernetics
[AD-A151074] 14 p2408 N85-24842
Development of robots, robotics discussed
15 p2530 N85-25599
New sensor for industrial metrology developed
15 p2538 N85-25665
USSR report: Cybernetics, computers and automation technology
[JPRS-UCC-85-003] 15 p2625 N85-26174
Mathematical analysis of heart rhythm assessment of distinctive features in adaptation to spaceflight conditions 22 p3733 N85-33142

CYCLES
NT ACTIVITY CYCLES (BIOLOGY)
NT BRAYTON CYCLE
NT CARBON CYCLE
NT CARNOT CYCLE
NT OTTO CYCLE
NT RANKINE CYCLE
NT SOLAR CYCLES
NT STIRLING CYCLE
NT STRESS CYCLES
NT SUNSPOT CYCLE
NT THERMODYNAMIC CYCLES
NT WORK-REST CYCLE
The nitrogen cycle: Atmosphere interactions
05 p0653 N85-14191
Terrestrial nitrogen cycles: Some unanswered questions 05 p0653 N85-14192
Recent studies of the ocean nitrogen cycle
05 p0653 N85-14193
Cyclic endurance testing of the RB211-22B cast HP turbine blade 07 p0908 N85-15747
View of future requirements for engine cyclic durability by analysis and testing 07 p0908 N85-15751
Investigation of welded interconnection of large area wraparound contacted silicon solar cells
[NASA-CR-174438] 10 p1509 N85-19519
Exergetical analysis of turbojet engine cycle
13 p2049 N85-22825
Mathematical model of the nitrogen cycle in a nonsaturated area of cultivated soil
20 p3478 N85-31610
Possible roles of manganese redox chemistry in the sulfur cycle 21 p3659 N85-32731
Biogeochemical cycling and remote sensing
21 p3659 N85-32733
Phototrophic bacteria and their role in the biogeochemical sulfur cycle 21 p3660 N85-32735
Sulfur cycling and metabolism of phototrophic and filamentous sulfur bacteria 21 p3660 N85-32737

CYCLIC ACCELERATORS
NT BETATRONS
NT STORAGE RINGS (PARTICLE ACCELERATORS)
NT SYNCHROTRONS
A low perturbation electron injector for cyclic accelerators
[AD-D011312] 07 p1040 N85-16604
Stability in dynamical systems
[DE85-008696] 17 p3034 N85-28766
Physics of High Energy Particle Accelerators. AIP Conference Proceedings no. 127
[DE85-008891] 18 p3182 N85-29733
High-power solid-state rf source for accelerator cavities
[DE85-012672] 22 p3761 N85-33309

CYCLIC COMPOUNDS
NT CYCLIC HYDROCARBONS
A method for obtaining new cyclical imides of derivative benzimidazoles
[AD-A145042] 01 p0017 N85-10106
Infrared spectroscopy study of the SP-250 epoxy resin system
[AD-A145860] 03 p0337 N85-12167
Pseudo-p-1,2,2,9,9,10,10-octofluoro (2,2)-p-cyclophane bis-acid chloride
[AD-D011393] 07 p0919 N85-15818
Research on microemulsions for storage and conversion of solar energy
[DE85-000181] 12 p1882 N85-21807
Polyaromatic ether-sulfone-ketones with fluoro-substituted-p-cyclophane units as cross-linking sites
[AD-D011649] 17 p2933 N85-28105
Synthesis of energetic materials
[AD-A154887] 21 p3571 N85-32210
Influence of particle arrangement on sintering
[AD-A155337] 21 p3599 N85-32352

CYCLIC HYDROCARBONS
NT ANTHRACENE
NT CYCLOPROPANE
Study of vibrational energy transfer at a liquid tin surface
[AD-A145741] 02 p0277 N85-11804
A metal-catalyzed rearrangement of alkene-alkynes and the stereochemistry of metallacyclobutene ring opening
[AD-A149084] 10 p1435 N85-19042
Synthesis of energetic materials
[AD-A154887] 21 p3571 N85-32210
Synthesis of 2,4,8,10-tetroxaspiro5,5undecane
[NASA-CASE-ARC-11243-2] 22 p3741 N85-33187

CYCLIC LOADS
Benchmark notch test for life prediction
02 p0140 N85-10953
Nonlinear structural and life analyses of a combustor liner 02 p0141 N85-10955
Strain distribution in a type 316/16-8-2 stainless steel weldment during cyclic loading
[DE84-015644] 02 p0210 N85-11384
Study of delamination cracking under static and cyclic loads of carbon-epoxy composite materials
[REPT-42-727/F] 03 p0327 N85-12102
Structure of two-phase titanium alloys with different microstructures 03 p0351 N85-12257
Influence of cyclic tangential loading on indentation fracture
[DE84-015969] 03 p0373 N85-12382
Autonomous momentum management for space station
[NASA-CR-174065] 04 p0462 N85-12931
Possibilities of fatigue life estimation in the higher cycle range 05 p0649 N85-14166
Low cycle fatigue strength for multiaxial loading of ductile materials 05 p0649 N85-14167
Design procedures for fiber composite structural components: Panels subjected to combined in-plane loads
[NASA-TM-86909] 07 p0919 N85-15823
Low cycle fatigue of MAR-M 200 single crystals at 760 and 870 deg C
[NASA-TM-86933] 10 p1440 N85-19074
Mechanisms of damage accumulation in time-dependent cyclic deformation
[DE85-001004] 10 p1496 N85-19443
Effect of stress concentration fatigue resistance of refractory nickel alloys under asymmetrical multicycle loading, communication 1 11 p1604 N85-20086
Local strain redistribution corrections for a simplified inelastic analysis procedure based on an elastic finite-element analysis
[NASA-TP-2421] 11 p1651 N85-20396
On local total strain redistribution using a simplified cyclic inelastic analysis based on an elastic solution
[NASA-TM-86913] 12 p1864 N85-21690
Fatigue and corrosion fatigue resistance of aluminum casting alloy VAL10 and forging alloy AK6
13 p2025 N85-22690

Dissipation of energy in composite material
13 p2027 N85-22703
Effect of operating medium on cyclic durability of AD33-W composite
13 p2029 N85-22716
Cyclic industrial robots with mechanical energy storing devices: Multipositional system with one or several degrees of freedom
13 p2045 N85-22803
Cyclic industrial robots with mechanical energy storing devices: Principles of drive design
13 p2046 N85-22807
Cyclic structural analyses of anisotropic turbine blades for reusable space propulsion systems — same fuel turbopump
[NASA-TM-86990] 14 p2320 N85-24339
Elastic-plastic analysis for cyclic loading using a linearized yield condition
[PB85-149607] 14 p2322 N85-24346
Long-life high performance fuel cell program
[NASA-CR-174874] 15 p2494 N85-25384
Effect of fatigue and thermal loads on silicon carbide fiber reinforced glass matrix composites
[DE85-006069] 15 p2503 N85-25441
Analysis of shell type structures subjected to time dependent mechanical and thermal loading
[NASA-CR-175747] 15 p2577 N85-25896
A review of fracture mechanics life technology
16 p2733 N85-26863
Analysis of elastoplastic grids under conditions of variable loads
[REPT-16/1984] 16 p2797 N85-27242
On the use of marker loads for fatigue crack growth measurements
[FFA-TN-1984-52] 16 p2802 N85-27277
Structural tailoring of SSME blades (vanes)
17 p2913 N85-27960
Interaction of high-cycle and low-cycle fatigue of Haynes 188 alloy at 1400 F deg
17 p2913 N85-27961
Effects of high mean stress on high-cycle fatigue behavior of PWA 1480
17 p2914 N85-27964
Constitutive cyclic deformation behavior in single-crystal and directionally solidified SSME high-pressure fuel turbopump airfoil materials
17 p2914 N85-27965
Fatigue behavior of synthetic fibers, yarns and ropes
17 p2979 N85-28415
Effect of protective method on cyclic durability and nature of failure of titanium alloy welded joints
19 p3245 N85-30122
Thermomechanical deformation in the presence of metallurgical changes
20 p3466 N85-31533
Micromechanics of high temperature deformation and failure
20 p346d N85-31534
Results of an interlaboratory fatigue test program conducted on alloy 800H at room and elevated temperatures
[NASA-CR-174940] 21 p3597 N85-32340
Influence of cyclic thermal loading on internal stress in casted epoxy resin
23 p3908 N85-34211
Static and cyclic behavior of semi-rigid steel beam-column connections
[PB85-194363] 24 p4103 N85-35433

CYCLING
U CYCLES

CYCLOGENESIS
NT ARC CLOUDS
A simulation experiment of a rapidly developed medium scale cyclone
01 p0079 N85-10530
Mesoscale lee cyclogenesis
09 p1355 N85-18527
Meso-S scale numerical simulations of the jet streak adjustments which organized the Carolina tornado outbreak and the subsequent explosive coastal cyclogenesis
15 p2596 N85-26011
The sensitivity of mesoscale cyclogenesis forecasts to detailed three-dimensional isentropic initial analyses and varied vertical model resolution
15 p2598 N85-26015
Justification and plan for participation in GALE
15 p2599 N85-26017
A survey of major east coast snowstorms, 1900-1983. Part 2. Summary of surface and upperlevel characteristics
[NASA-TM-86195] 16 p2833 N85-27471
A survey of major east coast snowstorms, 1900-1983. Part 2: Case studies of eighteen storms
[NASA-TM-86196] 16 p2833 N85-27472
Diagnostic verification of the GLAS (Goddard Laboratory for Atmospheric Sciences) general circulation model as applied to a case of extratropical maritime explosive cyclogenesis
[AD-A153686] 18 p3148 N85-29494
A numerical and analytical investigation of lee cyclogenesis
[AD-A155607] 21 p3636 N85-32594
Surface cyclogenesis as indicated by satellite imagery
[PB85-191815] 24 p4124 N85-35566

CYCLOHEXANE
Influence of pressure on speed of sound in single-phase region of stratifying mixtures
11 p1715 N85-20788

CYCLONES
NT CYCLOGENESIS
NT HURRICANES
NT TYPHOONS
Statistical tropical cyclone forecasting techniques for the Southern Hemisphere
[AD-A144752] 01 p0085 N85-10569
Summary of 1984 Atlantic seasonal tropical cyclone activity and verification of author's forecast
03 p0395 N85-12520
Energy diagnostics and impact studies of FGGE global data sets and GLAS GCM simulations
05 p0683 N85-14390
A study of the adequacy of quasi-geostrophic dynamics for modeling the effect of frontal cyclones on the larger scale flow
05 p0684 N85-14398
Numerical prediction of the president's day cyclone
05 p0684 N85-14399
Observational-numerical study of maritime extratropical cyclones using FGGE data
05 p0685 N85-14400
Frequency and motion of western North Pacific tropical cyclones
[PB85-106486/GAR] 06 p0839 N85-15331
Estimations of diabatic heating for an explosively-developing maritime cyclone
[AD-A147678] 08 p1188 N85-17483
A possible mechanism for the diurnal oscillations of tropical cyclones
09 p1356 N85-18530
Annual data and verification tabulation for Eastern North Pacific tropical storms and hurricanes, 1983
[PB85-109635] 10 p1520 N85-19580
Tropical cyclone data tape for the Eastern and Central North Pacific Basins, 1949-1983: Contents, limitations and uses
[PB85-110054] 10 p1520 N85-19585
Varying structure and intensity change characteristics of 4 Western North Pacific tropical cyclones
[AD-A149828] 12 p1895 N85-21895
Studies of the development of cyclones over Southern China coastal areas and adjacent seas
[AD-A150108] 12 p1896 N85-21901
Influence of interaction between ocean and atmosphere on intensity of moving tropical cyclone
14 p2333 N85-24431
Mesoscale Atmospheric Processes Research Program Science Review
[NASA-TM-87465] 15 p2594 N85-25987
Monitoring tropical cyclone growth using GOES VISSR/VAS and Nimbus-7 TOMS data
15 p2595 N85-25989
Model sensitivity studies of major east coast storms
15 p2598 N85-26016
Technique that uses satellite, radar, and conventional data for analyzing and short-range forecasting of precipitation from extratropical cyclones
[PB85-164964] 16 p2837 N85-27499
Kinetic energy and vorticity of lee cyclones
[MITT-40] 17 p2963 N85-28502
Characteristics of North Indian Ocean tropical cyclone activity
[AD-A153065] 17 p2997 N85-28524
A study of the adequacy of quasi-geostrophic dynamics for modeling the effect of frontal cyclones on the larger scale flow
[NASA-CR-176085] 20 p3495 N85-31731
Real-time automated detection of mesocyclones and tornado vortex signatures
[AD-A154968] 21 p3635 N85-32578
Forecasting of tropical cyclone motion using an EOF (Empirical Orthogonal Function) representation of wind forcing
[AD-A155034] 21 p3636 N85-32580

CYCLONES (EQUIPMENT)
U CENTRIFUGES

CYCLOPROPANE
Cation promotion effects in zeolite-supported F-T catalysts
[DE85-001706] 09 p1291 N85-18108

CYCLOTETRAMETHYLENE TETRANITRAMINE
U HMX

CYCLOTRIMETHYLENE TRINITRAMINE
U RDX

CYCLOTRON FREQUENCY
Two-point theory of current-driven ion-cyclotron turbulence
[DE85-010114] 19 p3372 N85-30918
Analysis of Jovian decametric data: Study of radio emission mechanisms
[NASA-CR-176057] 22 p3851 N85-33848
Generalized reduced fluid model with finite ion-gyroradius effects
[DE85-013123] 24 p4157 N85-35777

Proposed FRX-D experiment
[DE85-012766] 24 p4158 N85-35778

CYCLOTRON RADIATION
NT ION CYCLOTRON RADIATION
Polarized electron cyclotron emission in the Tokapole 2 Tokamak
[DE84-014953] 01 p0122 N85-10838
Generation and propagation of electron cyclotron harmonic waves
14 p2367 N85-24830
Theoretical studies of electric cyclotron harmonic (ECH) waves based on experimental data from GEOS 1
14 p2367 N85-24831
Role of equatorial Electron Cyclotron Harmonic (ECH) waves in the generation of diffuse auroras. Contribution of the GEOS IMS spacecraft
14 p2367 N85-24832
Heating of electrons in a high density tokamak by a micro-wave near second harmonic frequency
[DE85-010662] 19 p3359 N85-30822
Poloidal variations in toroidal fusion reactor wall power loadings
[DE85-009505] 19 p3362 N85-30848
Activation analysis of natural water using neutrons of various energies
21 p3690 N85-32924
Diamagnetic instability of cyclotron waves in plasma
21 p3693 N85-32948
Electrostatic ion cyclotron instability due to a nonuniform electric field perpendicular to the external magnetic field
[AD-A155474] 21 p3707 N85-33019
Research on gyrotrons
[AD-A154032] 23 p3934 N85-34360
Multiple-frequency electron cyclotron heating of hot electron rings in EBT-1
[DE85-011302] 23 p3963 N85-34701

CYCLOTRON RESONANCE
Fine structure of Alfven maser radiation
06 p0824 N85-15232
Effect of resonant microwave power on a PIG ion source
[DE85-001396] 09 p1379 N85-18573
ORNL ECR multicharged ion acurce
[DE85-001283] 09 p1380 N85-18681
Recent activities on JIPP T-IIU Tokamak
09 p1387 N85-18724
Memory function for cyclotron resonance of two-dimensional electron systems
[AD-A152632] 17 p3029 N85-28731
Millimeter wave generation by relativistic electron beams
[AD-A153980] 18 p3179 N85-29708
Reactions of metal ions and their clusters in the gas phase using laser ionization-ion cyclotron resonance spectroscopy
[DE85-009478] 19 p3361 N85-30836
Electromagnetic wave amplification during cyclotron resonance in a medium
21 p3693 N85-32942
Influence of ECR-heating on MHD activity of plasma in tokamak-10 installation
21 p3694 N85-32949
Cyclotron resonance in a nonneutral plasma
[AD-A155248] 21 p3707 N85-33017
Investigations of the cyclotron resonance effects in the X ray spectrum of the neutron star Hercules X-1
[MPE-191] 22 p3890 N85-34112
Transport issues in Phaedrus-type plasmas
23 p3976 N85-34653

CYCLOTRON RESONANCE DEVICES
A nonlinear theory for gyro-devices
[AD-A145297] 02 p0200 N85-11333
Harmonic emission from high power gyrotron oscillators
[AD-A145821] 02 p0200 N85-11335
Gyrotron beam generation with helical magnetic fields
[AD-A145987] 03 p0417 N85-12570
Buildup of oscillations in two-mode gyrotron
06 p0788 N85-15037
Quasi-optical harmonic gyrotron and gyroklystron
[AD-D011306] 07 p0947 N85-16001
Analytical and numerical modeling of gyrotrons
[AD-A148100] 08 p1157 N85-17300
Electron cyclotron resonance heating system for the stellarator W 7-AS
[IPF-84-5] 09 p1395 N85-18779
High power millimeter-wave mode converters in overmoded circular waveguides using periodic wall perturbations
[IPF-84-6] 09 p1395 N85-18780
The use of synthesis method in the design of gyrotron electron guns
[INPE-3305-PRE/616] 10 p1478 N85-19329
Activities report of the Institute of Plasma Research
11 p1733 N85-20903
Millimeter wave dielectric property measurement of gyrotron window materials
[DE85-004430] 12 p1802 N85-21304
The 60 GHz gyrotron development program
[DE85-000599] 12 p1836 N85-21522

Design considerations for a 100 kW CW, 140 GHz gyrotron oscillator
[DE85-005262] 13 p2066 N85-22904
A 60 GHz 200 kW CW gyrotron with high output mode purity
[DE85-005263] 13 p2066 N85-22905
Coupled-cavity gyrotrons with mode conversion 13 p2076 N85-22907
Design and testing of gyroklystron amplifiers
[AD-A151026] 14 p2296 N85-24231
Design and testing of a high power quasi-optical gyrotron
[AD-A153212] 17 p2968 N85-28330
The design of megawatt gyrotrons
[DE85-007892] 17 p3032 N85-28754
Proposal for continuation of research on megawatt gyrotrons for the period January 1, 1985 through December 31, 1986
[DE85-009862] 18 p3110 N85-29260
Operation of a quasioptical electron cyclotron maser
[DE85-008450] 18 p3113 N85-29276
High harmonic rectangular gyrotron 19 p3256 N85-30189
140 GHz gyrotron development program
[DE85-010348] 20 p3537 N85-32013
Research on gyrotrons
[AD-A154032] 23 p3934 N85-34380

CYCLOTRONS
NT MICROTRONS
Notes on NAC report NAC-83-05: Beam Pulse Length Determination by Spectral Analysis
[CSIR-NAC-83-06] 01 p0119 N85-10616
Operation of a quasioptical electron cyclotron maser
[DE85-008450] 18 p3113 N85-29276
Summary of the discussion of the theory of radiative processes
[DE85-007812] 19 p3371 N85-30914
Cyclotron absorption of fast magnetosonic wave in stellerator 21 p3693 N85-32945
Low frequency instabilities driven by an ion temperature anisotropy
[AD-A154902] 21 p3707 N85-33016
Experimental measurements of the ion cyclotron antennas' coupling and RF characteristics
[DE85-011569] 23 p3962 N85-34694

CYGNUS CONSTELLATION
Optical and X-ray observations of 4U2129+47/V1727 CYG in a quiescent state 11 p1742 N85-20850
Accretion in the zeta Aurigae and 32 Cygni shock cones 11 p1754 N85-21036
Long-term observations of Cyg X-3 with Vela 5B
[DE85-005556] 15 p2686 N85-26586
Salyut-7 cosmonauts work with RS-17 and GSPS X-ray telescopes 22 p3731 N85-33131
Search for gamma rays of energy 10(15) eV from Cygnus X-3
[OG-2.1-1] 22 p3862 N85-33919
1000 GeV gamma rays from Cygnus X-3: An update
[OG-2.1-8] 22 p3863 N85-33925
Variability in the high energy gamma ray emission from Cyg X-3 over a two-year period (1983 - 1984) at E 4 x 10(11) eV
[OG-2.1-11] 22 p3864 N85-33927
A search for gamma-ray point sources with the Carpet shower array
[OG-2.1-12] 22 p3864 N85-33928
Cyg X-3: Not seen in high-energy gamma rays by COS-B
[OG-2.2-2] 22 p3864 N85-33929
Constraints on cosmic-ray observation of Cygnus X-3
[OG-2.2-3] 22 p3864 N85-33930
Ultra high energy gamma rays, cosmic rays and neutrinos from accreting degenerate stars
[OG-2.2-5] 22 p3864 N85-33931
Relevance of the observation of UHE gammas to hard X-ray astronomy
[OG-2.2-6] 22 p3865 N85-33932
Low-energy gamma rays from Cygnus X-1
[OG-2.4-13] 22 p3868 N85-33957
UHE particle production in close binary systems
[OG-5.4-7] 22 p3886 N85-34084
The identification of gamma ray induced EAS
[HE-4.5-1] 24 p4195 N85-36026

CYLINDERS
Experimental study on the glow plug aided alcohol driven diesel engine 04 p0483 N85-13078
Electromagnetic resonances of cylinders and aircraft model with resistive wires
[NASA-CR-174203] 06 p0838 N85-15319
Temperature prediction in mechanical components, an analytical approach 09 p1327 N85-16339
Large deformations of a nonlinear elastic solid and the diffusion of an ideal fluid treated as interacting continua 09 p1330 N85-16358
A remote source system for measuring relative positron annihilation line widths in individual slab cylindrical samples
[AERE-R-10549] 12 p1936 N85-22173
Alignment and assembly tool for very large diameter cylinders
[NASA-CASE-MFS-28001-1] 18 p3116 N85-29269

CYLINDRICAL AFTERBODIES
U AFTERBODIES
U CYLINDRICAL BODIES

CYLINDRICAL ANTENNAS
Transient analysis of loaded thin-wire antennas and transmission lines 13 p2053 N85-22852
Experimental verification of beam deflection from hybrid reflector antenna within wide-angle sector 13 p2079 N85-22984
Digital holographic synthesis of pattern-forming transparencies for ring antenna arrays 22 p3763 N85-33326
Cylindrical lens-array antenna for wideband electronic scanning
[AD-A156085] 24 p4090 N85-35350

CYLINDRICAL BODIES
NT ROTATING CYLINDERS
Influence of aluminum metallization coatings on corrosion fatigue properties of steel 01 p0018 N85-10112
Overall heat transfer coefficients for a horizontal cylinder in a fluidized bed
[AD-A144878] 01 p0124 N85-10849
Scattering by a parabolic cylinder: A uniform asymptotic expansion
[AD-A145688] 02 p0252 N85-11652
Analysis of piezoelectric disks and cylinders using finite element method
[AD-A146323] 03 p0414 N85-12650
Allowing for the temperature field in the wall thickness of checkerwork in thermal calculation
[BLL-M-36015-(5828.4)] 07 p0956 N85-16058
Stability of rigid motions and rollers in bicomponent flows of immiscible liquids
[AD-A147302] 07 p0980 N85-16061
Shock and impact response of solid rocket propellants: Experimental and theoretical 08 p1116 N85-17040
Method of testing carbide inserts for premature fracture by face milling of cylindrical workpieces 09 p1303 N85-18183
Numerical investigation of phase change heat transfer in a horizontal cylinder including effects of natural convection 09 p1318 N85-18286
Natural convection experiments about a finite-length cylindrical heat source in a liquid-saturated porous medium
[DE84-012657] 09 p1320 N85-18298
Study of residual stresses introduced into TA6ZrD (685) cylinders by quenching — compressor disk alloy
[PNR-90240] 09 p1341 N85-18435
Experimental investigation of heat transfer to bluff cylinders and cones in hypersonic rarefied gas flow 11 p1620 N85-20195
Natural convection heat transfer between arrays of horizontal cylinders and their enclosure
[DE85-003773] 11 p1632 N85-20280
Determining distribution of complex dielectric permittivity over cylindrical body of intricate cross section from electromagnetic field measurement 12 p1842 N85-21559
Pneumatic clamping device
[AD-D011544] 12 p1858 N85-21656
Transonic merging separated flows
[AD-A150667] 14 p2213 N85-23724
Measurement of damping of graphite epoxy materials
[NASA-CR-175663] 14 p2246 N85-23931
One physical mechanism of formation of fine structure of ocean waters 14 p2334 N85-24436
Investigation of potential and viscous flow effects contributing to dynamic stall
[AD-A151696] 15 p2557 N85-25773
Measurements of the symmetric aerodynamic coefficients for flat faced cylinders in the angle of attack regime 0 to 90 deg for transonic and supersonic speeds
[FFA-TN-1984-04] 16 p2700 N85-26875
Buildup of oscillation of bodies in stratified fluid 17 p2941 N85-28157
Effects of the corona wind on the cooling of a horizontal cylinder
[AD-A153101] 17 p2954 N85-28241
Unsymmetrical flow in a centrifuge
[DE85-009021] 18 p3103 N85-29208
Mutual coupling analysis for conformal microstrip antennas
[AD-A154292] 19 p3259 N85-30210
Seismic analysis of liquid-filled tanks with an eccentric core barrel
[DE85-010249] 19 p3269 N85-30272
Solid-state resistance welding cylinders and spheres
[DE85-010084] 20 p3469 N85-31555
The effect of stress and hot corrosion on nickel-base superalloys
[AD-A154722] 21 p3566 N85-32181
TNT equivalency of EAK explosive
[AD-A155737] 21 p3571 N85-32211
Evaluation of the effects of roll angle on the natural convection heat transfer from an array of cylindrical spines
[AD-A154594] 21 p3583 N85-32273
Nonlinear response and failure characteristics of internally pressurized composite cylindrical panels
[NASA-CR-176148] 22 p3800 N85-33546
Calculation of roots of transcendental equations in problems of determining thermal conductivity of cylinder with non-uniform boundary conditions
[BLL-M-35788-(5828.4)] 23 p3929 N85-34349
Vibrations of free hollow circular cylindrical bodies 24 p4100 N85-35418
A towed instrument vehicle for deep ocean sampling
[AD-A156322] 24 p4125 N85-35576
Acoustic resonances in cylinder bundles oscillating in a compressible fluid
[DE85-004066] 24 p4145 N85-35699

CYLINDRICAL PLASMAS
ICRF antenna coupling theory for a cylindrically stratified plasma
[DE85-004960] 14 p2424 N85-24952

CYLINDRICAL SHELLS
Oil flow patterns of separated flow on a hemispherical cylinder at incidence
[DFVLR-FB-84-20] 01 p0048 N85-10313
Initial postbuckling analysis of elastoplastic thin-shear structures 01 p0059 N85-10393
Resonant frequencies and mode shapes for single and double cylindrical shells
[AD-A144778] 01 p0062 N85-10408
Three dimensional separation and vortex formation 02 p0196 N85-11306
Scattering of plane wave on cylindrical shell in low-frequency region 02 p0256 N85-11677
Dispersion curves for normal waves in cylindrical shell and conditions for spatial coincidence in vicinity of critical frequencies 06 p0778 N85-14973
Stability of circular cylindrical shell with piecewise constant thickness subjected to radial pressure 06 p0779 N85-14982
Deformation of cylindrical shell with cantilevered elastic plates attached 06 p0779 N85-14984
Stability of hollow shafts under torsion 06 p0780 N85-14986
Saint Venant conditions in theory of piezoelastic shells 06 p0780 N85-14987
Acoustic radiation from single and double ribbed circular cylindrical shells
[AD-A148771] 08 p1219 N85-17676
Circumferential cracks in cylindrical shells 09 p1330 N85-18354
Direct energy minimization approach to whipping analysis of pressure hulls 09 p1335 N85-18393
Simplified theory for the behaviour of buried flexible cylinders under the influence of uniform hoop compression
[PB85-116531] 11 p1654 N85-20419
Fracture analysis of cracks in complete cylindrical shells
[AD-A150091] 12 p1867 N85-21711
Behavior of buried flexible cylinders under the influence of nonuniform hoop compression
[PB85-116523] 12 p1868 N85-21718
Solid Rocket Motor Case (SRMC) dynamic sensitivity to changes in composite properties 12 p1948 N85-22238
Automatic multi-layer welding of thick cylindrical structures under flux 13 p2035 N85-22746
Interaction of cylindrical shell with concentrated mass moving along its inner surface 13 p2047 N85-22810
Steady-state reaction of three-layered cylindrical shell to effect of moving load 13 p2047 N85-22811
Spectral frequency of eigenvalues in optimal problems of stability of cylindrical shells of variable thickness 13 p2047 N85-22815
Stability of cylindrical shells with one-way constraints 13 p2048 N85-22820
Parametric study of autooscillation upon flow of supersonic jet into cylindrical cavity 16 p2765 N85-27060
Stability of anisotropic cylindrical sandwich shells 16 p2766 N85-27065
Study of oscillations of composite cylindrical shells using a dynamic stiffness technique 16 p2766 N85-27066
Stressed state of multilayer thick-walled longitudinally corrugated cylinders 16 p2766 N85-27069

An analysis for axially compressed orthotropic shells with a multimode imperfection representation
[VTH-LR-422] 16 p2803 N85-27281
Stability of cylindrical shells with variable thickness under external pressure 17 p2943 N85-28164
Scattering of sounds by piezoceramic cylindrical shell near rigid surface 17 p2943 N85-28166
The effect of center delamination on the instability of composite cylindrical panels
[AD-A153494] 18 p3069 N85-28979
Optimization of axially compressed carbon fiber reinforced plastic (CFRP) cylinders 18 p3121 N85-29318
Determination of deformation speed during high-speed deformation of cylindrical shells
[BLL-M-36280-(5826.4)] 20 p3465 N85-31527
Finite elastic deformations of cylindrical and spherical shells under pressure
[OUEL-1549/84] 20 p3470 N85-31559
Acoustic wave scattering by round cylindrical shell reinforced with stringers 21 p3688 N85-32916
Iteration solution for a submerged force-driven finite cylinder
[AD-A154587] 21 p3699 N85-32982
Acoustic radiation from concentric shells containing an inner fluid
[AD-A155476] 21 p3700 N85-32991

CYLINDRICAL TANKS
SRB filament wound case material property study
[NASA-CR-171469] 17 p2910 N85-27940
Local heat treatment of welded joints of pipes and rotary vessels 17 p2924 N85-28026

CYLINDRICAL WAVES
Parameters of detonation waves excited in gas during concentrated release of energy 02 p0268 N85-11751
Propagation of non-axisymmetric elastic waves through shell with filler under radial load at one end 17 p2943 N85-28169
A dual spin space station design 20 p3408 N85-31152

CYLINDROIDS
U CYLINDRICAL BODIES

CYTOCHROMES
Respiratory chain of alkalophilic bacteria
[DE84-012558] 09 p1360 N85-18556
Cytochromes and iron sulfur proteins in sulfur metabolism of phototrophic bacteria 21 p3657 N85-32718

CYTOLOGY
Second Soviet-French Symposium on Space Cytology 14 p2396 N85-24699
Second Soviet-French Symposium on Space Technology 15 p2483 N85-25326
Flow cytometry for health monitoring in space
[DE85-009572] 19 p3329 N85-30625
Operation of the Zeiss cytopharometer with Zn/ZnSO4 electrode system of Tenforde et al 20 p3499 N85-31752
Detection of internal structure by scattered light intensity: Application to kidney cell sorting 20 p3503 N85-31777
Flow cytometry of human embryonic kidney cells: A light scattering approach 20 p3503 N85-31778
A cluster analysis method for identification of subpopulations of cells in flow cytometric list-mode arrays 20 p3503 N85-31779
Improved flow cytometer measurement of binding assays
[DE85-006407] 23 p3935 N85-34390

CYTOPLASM
Further cell biology experiments with Physarum polycephalum for a reflight of Biorack 05 p0689 N85-14429
Influence of simulated weightlessness on the motility of the acellular slime mold Physarum polycephalum 05 p0689 N85-14430
Physical chemical state of water in living cells
[AD-A154566] 21 p3662 N85-32749

CZECHOSLOVAKIA
Earthquake activity in the Bohemian massif and in the western Carpathians
[REPT-547] 03 p0375 N85-12390
Hole shots along refraction profile R4/78 recorded at the temporary seismic station near Stary Plzenec (west Bohemia)
[REPT-549] 03 p0375 N85-12392
Catalogue of earthquakes for the territory of Czechoslovakia for the period 1957 - 1980
[REPT-555] 03 p0376 N85-12398
The extremeness of the cold front of December 31, 1978 over the CSR
[REPT-566] 03 p0377 N85-12409
Aspects of CSSR CMOS integrated circuits discussed 15 p2533 N85-25627
Recent developments 15 p2533 N85-25628
MHB4046 phase-lock circuit 15 p2533 N85-25629
Improved, cheaper SIPMOS circuits no. 10, 1983 p 370 15 p2534 N85-25630
Phase-locked loop design with MHB4046 15 p2534 N85-25631
Additional PLL designs 15 p2534 N85-25632

CZOCHRALSKI METHOD
Recent progress in BGO development for high resolution calorimetry
[MPI-PAE/EXP-E1-129] 01 p0124 N85-10848
Research on gallium arsenide diffused junction solar cells
[NASA-CR-174057] 02 p0222 N85-11457
Investigation of liquid encapsulation Chochralski growth of InP
[AD-A146096] 03 p0433 N85-12760
Stress studies of EFG
[NASA-CR-174078] 05 p0651 N85-14179
Crystal growth and characterization of BaMgF4
[AD-A146805] 07 p1047 N85-16650
Clusters of defects in semiconductors
[AD-A147426] 07 p1048 N85-16655
Stress studies in EFG
[NASA-CR-175488] 10 p1583 N85-19856
Research on the basic understanding of high efficiency in silicon solar cells
[DE85-000507] 11 p1672 N85-20537
Thermally stimulated conductivity in semi-insulating gallium arsenide 13 p2088 N85-23036
InP materials
[AD-A152341] 17 p3043 N85-28828
Telescoping low vibration pulling mechanism for Czochralski crystal growth
[AD-D011655] 17 p3044 N85-28836
Current status of silicon materials research for photovoltaic applications
[DE85-008799] 19 p3304 N85-30482
Oxygen and carbon impurities and related defects in silicon 20 p3481 N85-31631

D

D LAYER
U D REGION

D LINES
Distances of local clouds from optical line observations 06 p0675 N85-15558

D REGION
Experience with proposed improvements of the International Reference Ionosphere (IRI)
[PB84-235670] 05 p0678 N85-14353
Analysis of ionization sources in D region based on theoretical models 06 p0825 N85-15240
Partial reflection D-region electron densities 06 p1184 N85-17461
D1 LF wind measurements in the 90 to 100 km height range 08 p1185 N85-17468
Middle Atmosphere Program. Handbook for MAP, volume 10
[NASA-CR-175477] 11 p1658 N85-20450
Neutral atmosphere properties determining D-region electron densities 11 p1658 N85-20451
Variation of derived mesospheric nitric oxide in relation to wind and temperature in winter 11 p1658 N85-20452
Middle atmosphere temperature and dynamics as revealed from D-region observations 11 p1659 N85-20453
Indirect phase height measurements in central and eastern Europe for monitoring D region plasma 11 p1659 N85-20456
Abnormal circulation changes in the winter stratosphere, detected through variations of D region ionospheric absorption 11 p1659 N85-20458
A model of the influence of neutral air dynamics on the seasonal variation in the low ionosphere 11 p1660 N85-20462
Seasonal characteristics of mesospheric plasma and their transitions 11 p1660 N85-20464
The dynamics of ionospheric D region over East Siberia 11 p1662 N85-20477
Stratwarm effects in the ionospheric D region wind field 11 p1663 N85-20479
The high latitude D region during electron precipitation events 11 p1664 N85-20484
High energy particle effects in the D region during and after geomagnetic storms 11 p1664 N85-20485
Solar terrestrial influences on the D region as shown by the level of atmospheric radio noise 11 p1664 N85-20488
Ion kinetics, small neutral and excited components in D-region with elevated ionization level. Part 2: Variations in small neutral and excited components 15 p2480 N85-25307
Ion composition measurements of the disturbed and quiet D-region in 1980 - 1981
[AD-A156055] 24 p4117 N85-35521

DAEMO (DATA ANALYSIS)
U DATA PROCESSING
U DATA REDUCTION
U DATA TRANSMISSION

DAMA
U DEMAND ASSIGNMENT MULTIPLE ACCESS

DAMAGE
NT CUMULATIVE DAMAGE
NT EARTHQUAKE DAMAGE
NT FIRE DAMAGE
NT FROST DAMAGE
NT IMPACT DAMAGE
NT LASER DAMAGE
NT METEORITIC DAMAGE
NT RADIATION DAMAGE
NT STORM DAMAGE
Material degradation in heavy steel plates caused by bending with a laser
[AD-A144784] 01 p0052 N85-10343
Deformation measurements of composite multi-span beam shear specimens by Moire interferometry
[NASA-CR-3844] 02 p0169 N85-11135
Development of powder metallurgy 2XXX series Al alloys for high temperature aircraft structural applications
[NASA-CR-172408] 02 p0182 N85-11220
Influence of cyclic tangential loading on indentation fracture
[DE84-015969] 03 p0373 N85-12382
Selection, procurement and description of Salem Limestone samples used to study the effects of acid rain
[PB84-231067] 04 p0484 N85-13088
Development of damage in fatigue loaded carbon fiber reinforced plastics 05 p0650 N85-14172
The F-15 flight loads tracking program 07 p0894 N85-15666
Cumulative damage modeling of fatigue crack growth 07 p0907 N85-15741
Advances in composites technology
[NASA-TM-86353] 08 p1118 N85-17048
Repair of composites 08 p1120 N85-17058
Life assessment and damage tolerance of wind turbines
[AD-B088148L] 08 p1179 N85-17427
Models for shock damage to marine structural materials 09 p1336 N85-18400
Influence of volumetric fiber content on some matrix damage factors during thermal cycling of tungsten-El 765 composite 10 p1443 N85-19097
Applications of vibration analysis to the condition monitoring of rolling element bearings
[ARL/AERO-R-163] 12 p1859 N85-21663
Nondestructive method for detecting machine damage in beryllium
[DE85-001074] 12 p1862 N85-21681
Advanced life analysis methods. Volume 1: Cracking data survey and NDI (nondestructive inspection) assessment for attachment lugs
[AD-A150419] 13 p2103 N85-23108
Advanced life analysis methods. Volume 2: Crack growth analysis methods for attachment lugs
[AD-A150420] 13 p2103 N85-23109
Advanced life analysis methods. Volume 5: Executive summary and damage tolerance criteria recommendations for attachment lugs
[AD-A151017] 14 p2219 N85-23761
Significant parameters of the behavior and of the surface damage of the lubricated Hertzian contact: An application to gears 14 p2222 N85-23783
Estimating defectiveness buildup during service in metal of welded runner in low-pressure cylinder of turbine 14 p2271 N85-24070
Experimental report on a fiber optic light guide made by Galileo Electro-Optics Corporation
[DE85-006161] 14 p2421 N85-24941
Damage development during low cycle fatigue of carbon-black loaded SBR
[DE85-006234] 15 p2519 N85-25533
Differential effect of denervation on free radical scavenging enzymes in slow and fast muscle of rat
[NASA-CR-175719] 15 p2614 N85-26110
Thermal annealing of Fe implanted Al2O3 in oxidizing and reducing environment: Revised version
[DE85-007546] 16 p2752 N85-29983
Damage caused to polyurethane foams by aging, simulated sunlight exposure, heat and fire
[AD-A152040] 16 p2754 N85-28998
Method of investigating accumulations of damage to weld joints in the case of low-cycle creep
[BLL-CE-TRANS-6088-(9022.09)] 16 p2792 N85-27219
Impact of ozone on vegetation
[PB85-159937] 16 p2821 N85-27403

Reexamination of cumulative fatigue damage laws
17 p2914 N85-27962
Laboratory investigation of formation damage of an artificial fracture at simulated geothermal conditions
[DE85-010301] 18 p3102 N85-29201
Description and illustration of the use of CRACKS IV
[AD-A153543] 18 p3121 N85-29325
Fuel containment and damage tolerance in large composite primary aircraft structures
[NASA-CR-156083] 19 p3231 N85-30032
Temperature and surface damage under lubricated sliding-rolling contacts 19 p3260 N85-30338
A continuous damage model based on stepwise-stress creep rupture tests
[NASA-CR-174941] 21 p3597 N85-32341
Damage induced stress redistribution in composite laminates 24 p4072 N85-35235
Fuel containment and damage tolerance for large composite primary aircraft structures. Phase 1: Testing
[NASA-CR-166091] 24 p4073 N85-35241
Fatigue damage detection in steels by optical correlation
[AD-A155830] 24 p4079 N85-35277
Static and cyclic behavior of semi-rigid steel beam-column connections
[PB85-194363] 24 p4103 N85-35433
Three-dimensional finite deformation viscoelastic model accounting for damage effects
[DE85-012951] 24 p4139 N85-35860
Thermal hydraulic features of the TMI accident
[DE85-014569] 24 p4152 N85-35747

DAMAGE ASSESSMENT
Review of aircraft accident data: US General Aviation
[PB84-230980] 01 p0005 N85-10027
Results of tests of advanced flexible insulation vortex and flow environments in the North American Aerodynamics Laboratory lowspeed wind tunnel using 0.0405-scale Space Shuttle Orbiter model 16-0 (test OA-309)
[NASA-CR-167892] 01 p0015 N85-10096
Construction of approximate confidence intervals for probability-of-kill via the bootstrap
[AD-A144761] 01 p0113 N85-10764
Integrative investigation on forest damage detection based on airborne Multispectral Scanner data
05 p0656 N85-14215
Mechanisms of damage accumulation in time-dependent cyclic deformation
[DE85-001004] 10 p1496 N85-19443
History of satellite break-ups in space
12 p1783 N85-21190
Systems vulnerability and lethality in the development phase
[AD-A149737] 12 p1924 N85-22089
USAF damage tolerant design handbook: Guidelines for the analysis and design of damage tolerant aircraft structures, revision B
[AD-A153161] 17 p2896 N85-27858
Theoretical modeling of laser induced optical degradation
[AD-A155302] 21 p3592 N85-32323
Maintenance and the military environment
22 p3750 N85-33243
Protective systems and maintenance policies for marine environments 22 p3750 N85-33245
Relating corrosion maintenance to environmental factors 22 p3750 N85-33247

DAMAGE THRESHOLD
U YIELD POINT

DAMKOHLER NUMBER
Flow field effects on nucleation in a reacting mixing layer
[ARL/AERO-R-165] 19 p3283 N85-30237

DAMPERS (VALVES)
Multiple rate shock isolator damping valve
[AD-D011429] 08 p1168 N85-17368
Dual clearance squeeze film damper
[NASA-CASE-LEW-13506-1] 22 p3791 N85-33490

DAMPING
NT ELASTIC DAMPING
NT LANDAU DAMPING
NT VIBRATION DAMPING
NT VISCOELASTIC DAMPING
NT VISCOUS DAMPING
Review of some vortex relations
[NASA-CR-172452] 01 p0048 N85-10302
Power flow between non-conservatively coupled oscillators
[ISVR-TR-125] 02 p0209 N85-11377
Dynamics of the Uranian rings
02 p0302 N85-11956
Damping synthesis for a spacecraft using substructure and component data
[CRC-1365] 03 p0323 N85-12082
Complex frequency analysis of damped thin-walled beams with open cross sections
03 p0371 N85-12366
Experimental on-stream elimination of resonant whirl in a large centrifugal compressor 05 p0642 N85-14121
Hydrodynamic impeller stiffness, damping, and inertia in the rotordynamics of centrifugal flow pumps
05 p0643 N85-14125
Effects of fluid inertia and turbulence on force coefficients for squeeze film dampers
05 p0645 N85-14137
Squeeze-film dampers for turbomachinery stabilization
05 p0645 N85-14138
Status of beam transport with the ETA and ATA accelerators
[DE84-013205] 05 p0726 N85-14670
Mechanism of damping of plasma oscillations in initial stage of injection of electron beams from spacecraft into ionosphere in active experiments
06 p0823 N85-15225
Computational fluid mechanics utilizing the variational principle of modeling damping seals
[NASA-CR-174332] 08 p1161 N85-17325
Identification of vibration parameters of flexible structures 09 p1331 N85-18360
Integrated Technology Rotor/Flight Research Rotor (ITR/FRR) concept definition
[NASA-CR-166445] 10 p1423 N85-18979
Model testing and analysis of NOVA laser structures
[DE84-017569] 11 p1636 N85-20321
A study of transonic flutter of a two-dimensional airfoil using the U-g and p-k methods
[LR-615] 12 p1771 N85-21121
Stability analysis of flexible spacecraft with PID controller
[CRC-1372] 12 p1792 N85-21247
Workshop on Nuclear Dynamics 3
[INC-40007-24] 12 p1931 N85-22130
Distributed combustion: A mechanism of acoustic suppression 13 p2001 N85-22543
Damping models for flexible communications satellites by substructural damping synthesis
[UTIAS-287] 14 p2237 N85-23868
An experimental study of aerodynamic damping characteristics of a compressor annular cascade in high speed flow and the visualization of annular cascade flow
[NAL-TR-838] 15 p2554 N85-25759
Energy dependence of the emittance of damping ring beams
[DE85-007080] 15 p2649 N85-26341
Model reduction techniques applied to the control of large space structures
[AD-A151784] 16 p2731 N85-26857
Turbine blade friction damping study
16 p2736 N85-26886
Measurement of damping of graphite epoxy materials
[NASA-CR-175793] 16 p2743 N85-26925
Non-contact hydrostatic bearings
16 p2762 N85-27046
Influence of materials creep on rotor dynamics
[DE85-008545] 17 p2981 N85-28426
Hyperbolic phenomena in the flow of viscoelastic fluids
[AD-A153533] 18 p3099 N85-29186
The effect of line damping, magneto-optics and parasitic light on the derivation of sunspot vector magnetic fields
18 p3207 N85-29895
Arrangement for damping the resonance in a laser diode
[NASA-CASE-NPO-15980-1] 19 p3274 N85-30305
Damping seal for turbomachinary
[NASA-CASE-MFS-25842-2] 19 p3280 N85-30341
SSME seal test program: Test results for hole-pattern damper seals
[NASA-CR-171595] 20 p3395 N85-31059
Measurement of material damping in a simulated space environment 20 p3397 N85-31070
On the measurement of material damping in a simulated space environment 20 p3411 N85-31169
Finite control in underdamped distributed parameter systems 20 p3412 N85-31176
An overview of latest model reduction and control methods of large flexible space structures
20 p3414 N85-31191
Report of near field group
[DE85-010536] 20 p3527 N85-31940
Measurement of damping of graphite epoxy materials
[NASA-CR-176073] 21 p3596 N85-32334
Nonradiative damping of molecular electronic excited states by metal surfaces
[AD-A154619] 21 p3701 N85-32994
A research program to reduce the interior noise in general aviation aircraft, index and summary
[NASA-CR-176178] 24 p4145 N85-35695
Accelerator physics measurements at the damping ring
[DE85-013373] 24 p4159 N85-35785
TOSCA calculations and measurements for the SLAC SLC damping ring dipole magnet
[DE85-014366] 24 p4160 N85-35793

DAMPING FACTOR
U DAMPING

DAMPING IN PITCH
U DAMPING
U PITCH (INCLINATION)

DAMPING IN ROLL
U DAMPING
U ROLL

DAMPING IN YAW
U DAMPING
U YAW

DAMPING TESTS
Measurement of damping of graphite epoxy materials
[NASA-CR-176073] 21 p3596 N85-32334

DAMPNESS
U MOISTURE CONTENT

DAMS
Military hydrology. Report 9: State-of-the-art review and annotated bibliography of dam-breach flood forecasting
[AD-A155383] 22 p3801 N85-33553
National program for inspection of non-federal dams. Woodward reservoir dam (VT 00209), Connecticut River Basin, Plymouth, Vermont. Phase 1 inspection report
[AD-A156256] 24 p4144 N85-35693

DANGER
U HAZARDS

DARK ADAPTATION
Effect of extreme peripheral light on dark adaptation
[AD-A148923] 10 p1526 N85-19636
The relative effectiveness of red and white light for subsequent dark-adaptation
[AD-A148883] 10 p1530 N85-19642
Glutathione in cyanobacteria
21 p3661 N85-32745

DARKNESS
Dark focus: Intersubject variation, intrasubject stability, and relationship to near retinoscopy
[AD-A145489] 02 p0235 N85-11530
Long-term light induced changes in dark conductivity of kapton
[AD-A148791] 08 p1224 N85-17706

DART TURBOPROP ENGINES
U TURBOPROP ENGINES

DASSAULT AIRCRAFT
NT MIRAGE AIRCRAFT
NT MIRAGE 3 AIRCRAFT

DASSAULT MIRAGE 3 AIRCRAFT
U MIRAGE 3 AIRCRAFT

DATA
Quality of scientific and engineering data
[DE85-000294] 11 p1739 N85-20936
A study of frequency effects and damage accumulation during the fatigue of graphite/epoxy and glass/epoxy composite materials 14 p2247 N85-23930

DATA ACQUISITION
User experience of existing corrosion monitoring techniques and the development of Thin Layer Activation (TLA) for corrosion monitoring
[AERE-R-11248] 01 p0029 N85-10183
Automation of coastal engineering modelling facilities
[CSIR-T/SEA-8304] 01 p0035 N85-10219
Flight demonstration of new NRL real-time data acquisition system and laser video waveform sampler
[AD-A145126] 01 p0053 N85-10350
Analysis strategies for field dependent estimation and network design — mesoscale modeling
01 p0078 N85-10520
East Europe report: Science and technology
[JPRS-ESA-84-030] 01 p0101 N85-10670
Decentralized data acquisition to remedy EDP bottleneck 01 p0101 N85-10671
A modular data acquisition and display software system for a laboratory environment
[PB84-217892] 01 p0105 N85-10709
Field tests of the real-data acquisiton system for the NASA-LaRC differential absorption lidar
[NASA-CR-174020] 01 p0108 N85-10710
Data input, processing and presentation — helicopter rotor balance measurement
[NASA-TM-77739] 01 p0125 N85-10856
EG and G Idaho's response to a request for a graphic data base support package
[DE84-015171] 01 p0126 N85-10862
Airborne performance measurement system design: C-5 aircraft
[AD-A145436] 02 p0236 N85-11539
NESDIS international activities, appendix 2
02 p0295 N85-11917

Satellite, airborne remote sensing development outlined 03 p0342 N85-12199
The current formal status of the ERS-1 ground segment 03 p0360 N85-12423
An inexpensive microcomputer for laboratory data acquisition and test equipment control [AD-A146095] 03 p0403 N85-12567
Noise analysis of the Coarse Optical Power Spectrum Estimator (COPSE) data acquisition system [AD-A145918] 03 p0419 N85-12677
Heavy duty precision pan and tilt head [AD-A146669] 04 p0509 N85-13246
Solar energy resource assessment in Eastern New Mexico and solar and wind energy resource assessment in Eastern New Mexico [DE84-901511] 04 p0527 N85-13370
FSA field test [NASA-CR-174114] 04 p0528 N85-13373
Testing of production of silicon-titanium-magnesium alloying composition [BLL-M-35904-(5828.4)] 05 p0616 N85-13937
ECUT energy data reference series: Lightweight materials for ground transportation [DE84-015269] 05 p0621 N85-13974
The Telecommunications and Data Acquisition Report [NASA-CR-174149] 05 p0622 N85-13980
Programmable digital baud integrators for the radar high-speed data acquisition system 05 p0624 N85-13994
The acquisition, processing, and use of tactile sensor data in robot control 05 p0641 N85-14114
Measurement data acquisition and processing system for wind rotor measurements in the wind channel of Bremen University 05 p0668 N85-14296
Measuring-technical investigation of wind energy units from the control-technical, electrical and energetic point of view 05 p0668 N85-14301
Measuring techniques in the measuring program for the windpowered unit GROWIAN 05 p0669 N85-14303
Water vapor profile retrievals from the HIRS/MSU satellite sounder 05 p0681 N85-14378
Miniature personal physiological tape recorder (experiment 1ES 30) — Spacelab 05 p0692 N85-14448
A data collection system [AD-D011266] 05 p0713 N85-14573
Statistical analysis of visual wave observations and gage/radar measurements [AD-A146358] 06 p0796 N85-15100
Spring program summary, 1983 [PB84-222223] 06 p0839 N85-15330
The chemistry of rare earth elements in the solar nebula 06 p0869 N85-15643
Operational Loads Data [AGARD-CP-375] 07 p0894 N85-15664
Operational loads measurement: A philosophy and its implementation 07 p0894 N85-15665
Navy operational loads data sources and systems 07 p0895 N85-15668
Advanced fatigue monitoring on service aircraft 07 p0895 N85-15671
Helicopter data acquisition in WHL 07 p0896 N85-15676
USAF approach to airborne structural data recording: Airborne Data Acquisition Multifunction System (ADAMS) 07 p0897 N85-15683
Support for the Naval Research Laboratory Passive Microwave Clutter Analysis Program [AD-A146771] 07 p0939 N85-15951
National Bureau of Standards passive solar test facility: Instrumentation and site handbook [PB85-100451/GAR] 07 p0968 N85-16148
Rule-based evidence accrual system for image understanding [AD-A147835] 07 p1044 N85-16634
Data acquisition channel apparatus [AD-D011428] 08 p1159 N85-17311
Sequential data processing for photogrammetric acquisition of digital elevation models 08 p1176 N85-17413
Guidelines for atmospheric measurements in support of electro-optical systems testing [AD-A148090] 08 p1186 N85-17474
Noise measurement flight test: Data-analyses, Sikorsky S-76A helicopter [AD-A148525] 08 p1218 N85-17673
Survey of remote data monitoring systems [DE85-001385] 09 p1323 N85-18313
Medium speed computer interface (digitizer) for general purpose data acquisition [DE85-001585] 09 p1367 N85-18587
East Europe report: Science and technology [JPRS-ESA-85-005] 09 p1377 N85-18659
D"ta acquisition, measurement devices at 1984 Leipzig Spring Fair 09 p1378 N85-18661
The Telecommunications and Data Acquisition Report [NASA-CR-174366] 10 p1462 N85-19224
Nationwide urban runoff program. Relationship of urban runoff to land use and groundwater resources [PB85-114692] 10 p1506 N85-19505
OBLOG: Designed to create and maintain a 49 hour observation log file [PB85-109528] 10 p1519 N85-19579
Tropical cyclone data tape for the Eastern and Central North Pacific Basins, 1949-1983: Contents, limitations and uses [PB85-110054] 10 p1520 N85-19585
Computer-assisted data processing and analysis system for ground-based meteorological data collection, report on the Sierra Cooperative Pilot Project [PB85-115350] 10 p1520 N85-19587
Drifting buoy data from equatorial Pacific Ocean, 31 Aug. 1980 - 30 Apr. 1982 [PB85-120046] 10 p1522 N85-19598
Characteristics of quality data [DE85-001203] 10 p1568 N85-19889
Research needs on the interaction between information systems and their users: Report of a workshop [PB85-121523] 10 p1568 N85-19891
ADAPS (Airborne Data Acquisition and Processing System) operation and maintenance manual [AD-A149297] 11 p1585 N85-19983
Extracting digital data from a bus and multiplexing it with a video signal [AD-D011491] 11 p1636 N85-20302
An overview of LANDSAT-4 and the Thematic Mapper 11 p1668 N85-20509
Image processing instrumentation for speckle interferometry and imaging [AD-A149308] 11 p1762 N85-21084
In-situ detection of micron-sized dust particles in near-Earth space 12 p1785 N85-21205
Research in image understanding as applied to 3-D tomographic imaging with near optical resolution [AD-A150098] 12 p1829 N85-21483
Building a functional, integrated GIS/remote sensing resource analysis and planning system — Utah [E85-10092] 12 p1874 N85-21754
Atmospheric handbook: Atmospheric data tables available on computer tape [PB85-106512] 12 p1891 N85-21867
Catalog of submarine volcanoes and hydrological phenomena associated with volcanic events: 1500 BC to 31 Dec. 1899 [PB85-117984] 12 p1891 N85-21869
Collection and use of lightning strike data in the western US during summer 1983 [PB85-110534] 12 p1897 N85-21907
Topics in optical materials and device research, 3: Volume 1 [AD-A149726] 12 p1933 N85-22145
Analyses via automated mass spectrometry (MS/DS) 12 p1947 N85-22227
Development of a multiplane multispeed balancing system for turbine systems [NASA-CR-174750] 13 p1976 N85-22400
Measurement requirements for the detection of ozone trends 13 p2105 N85-23115
Analysis of the inflow layer and air-sea interactions in Hurricane Frederic (1979) [NASA-CR-175616] 13 p2137 N85-23271
Mean flow and turbulence in complex terrain NPS (Naval Postgraduate School)/Vandenberg measurement system [AD-A150184] 13 p2138 N85-23274
Operational loads measurement: A philosophy and its implementation — aircraft structures [AD-A149445] 13 p2144 N85-23306
The experience of the Swedish Meteorological and Hydrological Institute (SMHI) with the ARGOS system [PM-U1/81] 14 p2240 N85-23892
Fatigue crack topography and crack growth analysis — wrought and cast aluminum 14 p2319 N85-24333
Automatic hydrological data collection facility using ARGOS 14 p2324 N85-24363
Hydrological data collection from Swedish mountain areas 14 p2327 N85-24366
Geostationary Operational Environmental Satellite Data Collection System 14 p2328 N85-24393
The Data Acquisition Control and Telemetry (DACT) system — meteorological buoys 14 p2332 N85-24419
Seafloor seismic measurements in the southern Bering [DE85-004908] 14 p2374 N85-24675
Variational mesoscale satellite data assimilation and initialization [NASA-CR-175704] 14 p2378 N85-24680
Kitt Peak measurements of P/Halley positions 14 p2436 N85-25023
Shuttle imaging radar-B (SIR-B) data analysis for identifying rainfall event occurrence and intensity [NASA-CR-175712] 15 p2594 N85-25986
Space methods in oceanology [NASA-TM-77652] 15 p2604 N85-26047
Computerized biophysical data acquisition system for motion sickness studies [AD-A151691] 15 p2618 N85-26131
A practical system for collecting reliable data on the space-time behavior of people [AD-A151174] 15 p2619 N85-26140
The human engineering of laboratory data acquisition and control systems [AD-A151576] 15 p2620 N85-26148
Computer use in research for data analysis [PB85-153567] 15 p2631 N85-26220
The Telecommunications and Data Acquisition Report [NASA-CR-175842] 16 p2770 N85-27094
Infrared presensitization photography 16 p2786 N85-27189
Design and construction of a computer controlled mirothermocouple probe for the study of buoyant jets [AD-A152224] 16 p2788 N85-27199
CNPq/INPE LANDSAT system: Report of activities from October 1, 1983 to September 30, 1984 — Brazil [E85-10097] 16 p2808 N85-27318
Present stage of utilization of the ARGOS system by the ORSTOM hydrological service for hydrometric data collection 16 p2813 N85-27348
Use of a network of telemetered meteorological stations for prediction of the distribution of an atmospheric tracer 16 p2831 N85-27458
A climatic data bank for Northern Hemisphere land areas, 1851-1980 [DE85-007863] 16 p2835 N85-27486
Data processing on the rotor test stand at DFVLR in Brunswick: Microprogrammable interfaces and array processor as key components in a PDP 11 real time data acquisition and processing system [DFVLR-MITT-85-03] 17 p2906 N85-27921
Automation of Precise Time Reference Stations (PTRS) 17 p2962 N85-28291
US Naval Observatory collection and utilization of time comparison data 17 p2962 N85-28292
Laser measurement techniques: Laser spectroscopy in semiconductors [DE85-007887] 17 p2971 N85-28350
DOE/ANL/HTRI heat exchanger tube vibration data bank: Addendum 5 [DE85-007730] 17 p2980 N85-28425
Microcomputer-controlled system for measuring atmospheric particle fluxes [DE85-007910] 17 p2988 N85-28489
Centralized Storm Information System (CSIS) [NASA-CR-175888] 17 p2994 N85-28506
Test and evaluation plan for the Centralized Storm Information System 17 p2994 N85-28508
CSIS test and evaluation 17 p2994 N85-28509
Functional and performance requirements of the next NOAA-Kansas City computer system 17 p2994 N85-28510
Axial topography from digitized real time radiography [DE85-006767] 18 p3091 N85-29130
Some further aspects of the influence of raindrop-size distributions on millimeter-wave propagation [PB85-198334] 18 p3092 N85-29138
Reliability derating procedures [AD-A153744] 18 p3119 N85-29309
Revised draft: Southeastern regional geologic characterization report [DE85-006285] 18 p3125 N85-29351
Pacific Northwest solar radiation data [DE85-009773] 18 p3149 N85-29496
A stored data acquisition system: Update [DE85-010534] 18 p3166 N85-29616
Deployment of a regional array in Norway [AD-A154120] 19 p3313 N85-30596
Workshop on objective analysis: Analysis strategies for field-dependent estimation [PB85-179901] 19 p3318 N85-30569
EDS operator and control software [DE85-010470] 19 p3340 N85-30698
ASME performance test on TVA Sequoyah unit 1 [DE85-901316] 19 p3358 N85-30815
TMI-2 technical information and examination program [DE85-010614] 19 p3359 N85-30827
Methodology for assessing benefits and costs of government information collection [DE85-010594] 19 p3381 N85-30975
Remote Sensing Technology: Symposium Proceedings [DE85-010212] 20 p3477 N85-31606
New stations supporting crustal dynamics project VLBI measurements 20 p3491 N85-31701
New VLBI technology developments 20 p3491 N85-31702

Forth system for coherent-scatter radar data acquisition and processing
[NASA-CR-176055] 20 p3494 N85-31720
Tropical Ocean and Global Atmosphere (TOGA) heat exchange project: A summary report
[NASA-CR-176038] 20 p3496 N85-31735
A cluster analysis method for identification of subpopulations of cells in flow cytometric list-mode arrays 20 p3503 N85-31779
Microprocessor AirborneData Acquisition and Replay (MADAR) system
[AD-A151728] 20 p3514 N85-31843
A microprocessor based multiscaling data acquisition system for Mossbauer spectroscopy
[USIP-85-01] 20 p3518 N85-31875
SSMIR (Solid State Memory Instrumentation Recorder): A new approach to acquiring data during an aircraft seat/sled ejection sequence
[AD-A154780] 21 p3589 N85-32308
Microcomputer processing of LANDSAT Thematic Mapper data for the acquisition of military tactical terrain data
[AD-A154781] 21 p3605 N85-32389
Problems and solutions in analyzing partial-reflection drift data by correlation techniques 21 p3626 N85-32529
Continued development of a data base management system performance monitor: Volume 1
[AD-A154635] 21 p3713 N85-33040
Sensitivity and performance characterization of DINGU
[DE85-010750] 22 p3754 N85-33269
Conceptual design and analysis of high-speed electronic imaging
[LA-10072-MS] 22 p3758 N85-33292
Control technology for radioactive emissions to the atmosphere at US Department of Energy facilities: The Los Alamos Meson Physics Facility
[DE85-011402] 22 p3811 N85-33609
Technology of off-gas treatment for liquid-fed ceramic melters
[DE85-012467] 22 p3812 N85-33610
The 1984 environmental monitoring program report for Idaho National Engineering Laboratory site
[DE85-011209] 22 p3812 N85-33611
Hit-size effectiveness theory applied to high doses of low LET radiation for pink mutations in Tradescantia
[DE85-011835] 22 p3819 N85-33657
Determination of instrument errors by compatibility checking: Results from dynamic flight test data
[ARL/AERO-R-162] 23 p3896 N85-34137
Separation of gas mixtures by supported complexes
[DE85-011996] 23 p3912 N85-34236
Throughfall rate and chemistry studies: Whiteface Mountain
[DE85-012407] 23 p3947 N85-34464
The 1984 biotic studies of Yucca Mountain, Nevada test site, Nye County, Nevada
[DE85-011715] 23 p3951 N85-34487
Akeno 20 km (2) air shower array (Akeno Branch)
[OG-9.4-8] 23 p4029 N85-34975
Miniature infra-red data acquisition and telemetry system
[NASA-CR-177953] 24 p4096 N85-35390
Federal Mineral Land Information System 24 p4106 N85-35459
A Programmable Automatic Noise Data and Other Related parameter Acquisition system (PANDORA) — wind energy converters 24 p4111 N85-35479
Incorporating meteorological data into receptor analysis: RAPS (Regional Air Pollution Study) revisited
[PB85-186944] 24 p4114 N85-35503
Development and operation of a measuring data acquisition system for use in light airplanes 24 p4123 N85-35556
Airborne Investigations of Mesoscale Convective Systems (AIMCS), 1984: Operational summary and data inventory
[PB85-187904] 24 p4125 N85-35571
Users guide for optimum interpolation method of global data assimilation
[AD-A155929] 24 p4138 N85-35648
Operations considerations in designing a high speed multi-channel data acquisition system
[DE85-012640] 24 p4154 N85-35756
Data acquisition system for phase-2 KGF proton decay experiment
[HE-6.2-4] 24 p4211 N85-36140

DATA ADAPTIVE EVALUATOR/MONITOR

U DATA PROCESSING
U DATA REDUCTION
U DATA TRANSMISSION

DATA ANALYSIS

U DATA PROCESSING
U DATA REDUCTION

DATA BASE MANAGEMENT SYSTEMS

TEQUEL: The query language of SADDLE
01 p0058 N85-10382
Logical database processor interface specifications
[PB84-216456] 01 p0105 N85-10705
Analysis of three database system architectures using benchmarks
[PB84-217512] 01 p0105 N85-10706
Performance evaluation of database systems: A benchmark methodology
[PB84-217504] 01 p0105 N85-10707
EG and G Idaho's response to a request for a graphic data base support package
[DE84-015171] 01 p0126 N85-10862
A technique to model and design physical database systems
[DE84-015337] 01 p0126 N85-10863
Vertical compression algorithms
[DE84-015040] 01 p0126 N85-10864
Attenuation experimental data bank in the COST 205 project. Structure and management of the final supports
[FUB-5-1983] 01 p0126 N85-10865
Information Science Panel joint meeting with Imaging Science Panel 02 p0214 N85-11415
ADAM: An abstract database machine
[RSRE-84007] 02 p0293 N85-11904
On update semantics and relational views
[AD-A145622] 02 p0294 N85-11907
Business planning for information services under special consideration of German management information systems
[BMFT-FB-ID-83-007] 02 p0294 N85-11910
A building blocks approach to statistical databases 03 p0437 N85-12782
A methodology for supporting views in relational databases 03 p0437 N85-12783
Preserving the time dimension in information systems 03 p0437 N85-12784
Competitive assessment of the US information services industry
[PB84-174804] 03 p0440 N85-12803
Climate of the Northern Hemisphere, 1851 - 1900 compared to contemporary climate
[DE84-016366] 04 p0539 N85-13426
NODC/1983: National Oceanographic Data Center report
[PB84-222231] 04 p0542 N85-13449
The human role in space. Volume 3: Generalizations on human roles in space
[NASA-CR-171225] 04 p0546 N85-13475
Archiving and exchange of a computerized marine seismic database: The ROSE data archive system
[DE84-901453] 04 p0576 N85-13677
Nuclear criticality information system: Database examples
[DE84-014462] 04 p0576 N85-13678
Research in computer science
[NASA-CR-174068] 05 p0713 N85-14572
Optimal query processing in distributed data base management systems with data redundancy 05 p0734 N85-14722
Lower level inference control in statistical database systems
[DE84-016005] 05 p0735 N85-14729
Role of DESIGNMANAGER in information engineering
[DE84-015807] 05 p0736 N85-14730
Distributed database components in a DBMS (Database Management System) component architecture
[PB84-217546] 06 p0848 N85-15382
Design and analysis of an SQL (Structured Query Language) interface for a multi-backend database system
[AD-A146534] 06 p0856 N85-15447
Future database machine architectures
[AD-A146786] 07 p1022 N85-16481
The effects of software quality control and baseline management on the acquisition of computer programs
[AD-A147051] 07 p1024 N85-16502
Model-model mappings and conversion in a family of data model specifications
[PB84-217124] 07 p1027 N85-16518
Data base support for SIO (System Integration Office)
[AD-A147487] 07 p1054 N85-16692
A simulator for determining the performance of transaction manager and lock manager combinations in a database
[AD-A147827] 07 p1055 N85-16696
The space shuttle ascent vehicle aerodynamic challenges configuration design and data base development 08 p1093 N85-16906
Flexible manufacturing system for the production of aircraft parts
[BLL-PNR-90237-(8019.3153)] 08 p1137 N85-17159
Data user's manual 08 p1150 N85-17254
Kernel Ada Programming Support Environment (KAPSE) interface team public report, volume 4
[AD-A147648] 08 p1205 N85-17581
Steps towards parsing of query sequences to a database
[AD-A148769] 08 p1206 N85-17590
Results of data base management system parameterized performance testing related to GSFC scientific applications
[NASA-CR-176815] 08 p1229 N85-17741
Towards an ideal database server for office automation environments
[AD-A148184] 08 p1229 N85-17742
Boring information and subsurface data base package user's guide
[AD-A148623] 08 p1230 N85-17747
Automated and interactive data base generation
[AD-P004316] 09 p1268 N85-17970
Geographic subdivision and top level data structures, Columbus, Magellan, and expanding CIG (Computer Image Generation) horizons
[AD-P004317] 09 p1268 N85-17971
CIG (Computer image generation) data bases in an instance: Bits and pieces
[AD-P004318] 09 p1269 N85-17972
Design and analysis of an access control system for a multi-backend database system
[AD-A148750] 09 p1367 N85-18586
Integrating heterogeneous non-geometric information systems using RIM
[DE84-017600] 09 p1402 N85-18823
Online directory of databases for material properties
[DE84-016511] 09 p1402 N85-18824
Sector suite man-machine functional capabilities and performance requirements
[AD-A148881] 10 p1531 N85-19647
Managing permanent objects
[AD-A149007] 10 p1540 N85-19706
Structure and application of extremely large geophysical data bases
[DE85-003527] 10 p1588 N85-19888
Data and information systems and decision making in large public organizations: Research agenda
[DE85-003639] 11 p1738 N85-20931
Requirements formulation subtask 1.A of the Major Item System Mapping (MISM) project
[DE85-000978] 11 p1740 N85-20940
Use of the ORACLE DEMS in determining the response of complex scientific instrumentation
[DE85-001742] 12 p1853 N85-21621
Computer and communications security and privacy
[GPO-39-741] 12 p1911 N85-21994
Research Reports: 1984 NASA/ASEE Summer Faculty Fellowship Program
[NASA-CR-171317] 12 p1944 N85-22210
Using a data base management system for modelling SSME test history data 12 p1944 N85-22211
The intelligent database machine 12 p1949 N85-22242
Requirements for a database management system
[DE85-004661] 12 p1951 N85-22259
New atmospheric sensor analysis study
[NASA-CR-171426] 13 p2094 N85-23069
GADB: A database facility for modelling naturally occurring geophysical fields 13 p2122 N85-23217
Precedency control and other semantic integrity issues in a workbench database 13 p2123 N85-23220
Presentation based user interfaces
[AD-A150311] 13 p2144 N85-23311
Digital processing of mesoscale analysis and space sensor data
[NASA-CR-171429] 13 p2146 N85-23319
Hexagonal data base study
[AD-A150176] 13 p2167 N85-23448
The hierarchical database decomposition approach to database concurrency control
[AD-A150612] 13 p2168 N85-23450
Integration of solid modeling and database management for CAD/CAM 14 p2402 N85-24804
EDIPAS: A multidiscipline and integrated facility for management and evaluation of engineering data
[NLR-MP-83062-U] 14 p2405 N85-24832
Design and analysis of ordering and join for a multi-backed database system
[AD-A150711] 14 p2433 N85-25006
Commercial data base management system for geonames data base
[AD-A150835] 14 p2433 N85-25007
Continued development of a data base management system performance monitor, volume 2
[AD-A151714] 15 p2623 N85-26167
Backend control processor for a multi-processor relational database computer system
[AD-A151692] 15 p2624 N85-26169
Symposium on Computers in Civil Engineering 1983
[CSIR-S-298] 15 p2626 N85-26182

Design and analysis of a complete relational interface for a multi-backend database system
[AD-A151501] 15 p2628 N85-26196
CAD/CAM (Computer-Aided Design/Computer-Aided Manufacturing) highlights
[AD-A151532] 15 p2629 N85-26201
The design and analysis of a complete hierarchical interface for the multi-backend database system
[AD-A151550] 15 p2629 N85-26203
Document retrieval from a relational database management system: An investigation of multiple-line query formulation using SEQUEL
15 p2665 N85-26447
Design and implementation of the digital engineering laboratory distributed database management system
[AD-A151694] 15 p2665 N85-26450
Developing an automated technique for translating a relational database into an equivalent network one
[AD-A151844] 15 p2666 N85-26451
A database design for the Brazilian Air Force Flying Unit Operational Control System
[AD-A151848] 15 p2666 N85-26452
Analysis and specification of a universal data model for distributed data base systems
[AD-A151856] 15 p2666 N85-26453
Maintaining consistency and accommodating network repair in a self-regenerative distributed database management system (a discussion of the means and cost)
16 p2698 N85-26656
Flow dynamic environment data base development for the SSME
16 p2736 N85-26885
Network information management subsystem
16 p2771 N85-27106
Implementation and analysis of a microcomputer based relational database system
[AD-A151770] 16 p2845 N85-27536
An adaptive technique and its application in database design
16 p2877 N85-27748
Internal and external performance measurement methodologies for database systems
[AD-A152025] 16 p2877 N85-27751
Data dictionary design as a stepping-stone to DBMS (Data Base Management System) implementation in the Indonesian Army Data Collecting and Processing Service
[AD-A152101] 16 p2877 N85-27752
Application of hierarchical data structures to geographical information systems
[AD-A152169] 16 p2877 N85-27753
DOD manual for standard data elements, part 1
[AD-A152201] 16 p2878 N85-27754
Scientific data bases on a VAX-11/780 running VMS
[DE85-007925] 16 p2878 N85-27760
Data management issues of statistical databases
[DE85-007616] 16 p2879 N85-27763
Defense data network support concept analysis
[AD-A153214] 17 p3016 N85-28649
Complete development and implement AFIT/ENG database management system, volume 1
[AD-A153043] 17 p3048 N85-28866
DLA: Data/data base administration analysis
[AD-A153031] 17 p3050 N85-28879
Avionics Data Base users manual
[AD-A153810] 18 p3062 N85-28942
Distributed database design tool
[AD-A153760] 18 p3200 N85-29850
Generic data entry quality assurance tool
[DE85-008359] 18 p3200 N85-29852
Cultural data base implementation study and computer-aided scene modeling system users manual
[AD-A154232] 19 p3333 N85-30646
System enhancements of Mesoscale Analysis and Space Sensor (MASS) computer system
[NASA-CR-171463] 19 p3342 N85-30708
CODA: A concept organization and development aid for the research environment
[AD-A154240] 19 p3343 N85-30715
Test and Evaluation Master Plan (TEMP) for the Navy Occupational Health Information Management System (NOHIMS). Phase 1: Appendix A through appendix U
[AD-A154179] 19 p3360 N85-30967
Design and implementation of an intelligence database
[AD-A154095] 19 p3381 N85-30973
Guide on logical database design
[PB85-177970] 19 p3381 N85-30976
Data base management: MSTRAC (keynote paper), part 8
21 p3628 N85-32530
Analysis of spacecraft data
[NASA-CR-171587] 21 p3669 N85-32789
The architectural requirements and integration analysis of a database server for office automation
[AD-A155517] 21 p3674 N85-32825
Continued development of a data base management system performance monitor: Volume 1
[AD-A154635] 21 p3713 N85-33040
Investigation of DBMS (Data Base Management Systems) for use in a research environment
[AD-A154662] 21 p3713 N85-33042
IGES/RIM Parser/Converter users guide
[DE85-011965] 22 p3829 N85-33716
Automatic capability to store and retrieve component data and to calculate structural integrity of these components
[DE85-012429] 22 p3831 N85-33728
Technology transfer system automation implementation
[PB85-177335] 22 p3849 N85-33838
User's operating procedures. Volume 1: Scout project financial analysis program
[NASA-CR-177949] 23 p3956 N85-34519
The interactive planning work station: A graphics-based UNIX (trademark) tool for application users and developers
23 p3957 N85-34527
An image management kernel for the design of relational and pictorial data bases
23 p3958 N85-34532
DSS/MIS (Decision Support Systems/Management Information Systems) design and implementation for LAMPS Mk 3 utilizing a microcomputer and a maintenance personnel assignment program
[AD-A155652] 24 p4135 N85-35629
Prototyping with data dictionaries for requirements analysis
[AD-A156303] 24 p4139 N85-35654
EPALIT: A data management system applied to the control and retrieval of technical reports
[PB85-193068] 24 p4166 N85-35829

DATA BASES

Pressure distribution on a swept wing aircraft in flight
01 p0004 N85-10025
TEQUEL: The query language of SADDLE
01 p0058 N85-10382
A relational approach to the development of expert diagnostic systems
[NASA-TM-86288] 01 p0099 N85-10658
Logical database processor interface specifications
[PB84-216456] 01 p0105 N85-10705
Performance evaluation of database systems: A benchmark methodology
[PB84-217504] 01 p0105 N85-10707
Updating logical databases
[AD-A144937] 01 p0125 N85-10860
Set-theoretic problems of null completion in relational databases
[AD-A145045] 01 p0125 N85-10861
EG and G Idaho's response to a request for a graphic data base support package
[DE84-015171] 01 p0126 N85-10862
EPA (Environmental Protection Agency) environmental data base and model directory, volume 1
[PB84-207562] 01 p0126 N85-10866
Royal Signals and Radar Establishment speech database recordings 1983: Part 2: Recordings made for automatic speech recognition assessment and research
[RSRE-84008-PT-2] 02 p0190 N85-11267
A system for the management of requests at an image data bank
[E85-10014] 02 p0216 N85-11427
Human engineering data base for design and selection of cathode ray tube and other display systems
[AD-A145704] 02 p0238 N85-11549
Research on distributed languages and algorithms
[AD-A145661] 02 p0242 N85-11560
Failure detection processes by pattern recognition and expert systems
[AD-P003924] 02 p0246 N85-11604
On update semantics and relational views
[AD-A145622] 02 p0294 N85-11907
Archiving and exchange of a computerized marine seismic database: The ROSE (Rivera Ocean Seismic Experiment) data archive system
[AD-A145658] 02 p0294 N85-11908
Inclusion of audiovisual media in information services for the special subjects journalism and communication science (pilot study)
[BMFT-FB-ID-83-004] 02 p0294 N85-11909
A data base for three-dimensional all-interference code evaluation
03 p0312 N85-12017
Expert systems: The application of new computer methods to corrosion problems
[AERE-M-3395] 03 p0334 N85-12153
International banking of satellite and in-situ wave data by the Marine Information and Advisory Services (MIAS)
03 p0381 N85-12434
An introduction to the MIAS conversion system
[IOS-184] 03 p0403 N85-12571
Knowledge representation and natural-language semantics
[AD-A146025] 03 p0409 N85-12615
A topological approach to database theory
03 p0437 N85-12781
On complementary and independent mappings on databases
[AD-A145557] 03 p0438 N85-12788
An approach to interfacing data bases in WWMCCS ADP
[AD-A146350] 03 p0439 N85-12793
Evaluation of the National Library of Medicine's programs in the medical behavior sciences. Coverage of the Medical Behavioral Sciences (MBS) literature in monographic databases, study 5
[PB84-230531] 03 p0439 N85-12797
Evaluation of the National Library of Medicine's programs in the medical behavior sciences. Online searchers' reactions to database and vendor capabilities in the Medical Behavioral Sciences (MBS), study 4
[PB84-230523] 03 p0439 N85-12798
Evaluation of the National Library of Medicine's programs in the medical behavior sciences. Quality of indexing: The development and testing of a methodology comparing databases covering the Medical Behavioral Sciences (MBS) literature, study 3
[PB84-230515] 03 p0439 N85-12799
Evaluation of the National Library of Medicine's programs in the medical behavior sciences. Test retrievals in five major databases covering the Medical Behavioral Sciences (MBS) literature, study 2
[PB84-230507] 03 p0440 N85-12800
Evaluation of the National Library of Medicine's programs in the medical behavior sciences. Coverage, overlaps and gaps in bibliographic databases dealing with the Medical Behavioral Sciences (MBS) literature, study 1
[PB84-230499] 03 p0440 N85-12801
Evaluation of the National Library of Medicine's program in the medical behavior sciences. An analysis of the National Library of Medicine's (NLM) handling of Medical Behavioral Sciences (MBS) literatures: Some research tests of methods for evaluating bibliographic databases, executive summary
[PB84-230481] 03 p0440 N85-12802
Experimental and theoretical study of a solar thermochemical receiver module
[NASA-CR-174107] 04 p0528 N85-13374
Relationship between model complexity and data base quality for complex terrain tracer experiments
[DE84-015022] 04 p0539 N85-13429
Comparability and accuracy of industry codes in different data systems
[PB84-215807] 04 p0548 N85-13482
Physical database processor preliminary interface specifications
[PB84-217581] 04 p0548 N85-13483
The 1984 NASA/ASEE summer faculty fellowship program
[NASA-CR-174138] 04 p0574 N85-13683
Energy information exchange, 1983
[DE84-901446] 04 p0577 N85-13680
The SPOT data bank system
05 p0659 N85-14236
Combinations of remote sensing data with a digital map data base — regional planning 05 p0660 N85-14240
Helicopter pilot performance for discrete-maneuver flight tasks 05 p0702 N85-14502
Optimal query processing in distributed data base management systems with data redundancy
05 p0734 N85-14722
Interpretation of natural language database queries using optimization methods 05 p0735 N85-14723
Heterogeneous data base access
05 p0735 N85-14724
A self-organizing database system: A different approach to query optimization 05 p0735 N85-14725
Integrated data base program: A status report
[DE84-013604] 05 p0735 N85-14727
Spring program summary, 1983
[PB84-222223] 06 p0839 N85-15330
Tree Query Language Flat (TQLF) specifications
[PB84-217116] 06 p0855 N85-15438
Relational Query Language Flat (RQLF) specifications
[PB84-217406] 06 p0855 N85-15439
Network Query Language Flat (NQLF) specifications
[PB84-217538] 06 p0855 N85-15440
Commerce Laboratory: Mission analysis payload integration study
[NASA-CR-171298] 07 p0911 N85-15784
Climatological information and water resources
07 p1002 N85-16367
Water and climate, study of one case
07 p1002 N85-16369
The potential contributions of the World Climate Program (WCP) to the economies of developing countries
07 p1003 N85-16371
An algorithm for assembly of stiffness matrices into a compacted data structure
[AD-A146727] 07 p1023 N85-16492

Model-model mappings and conversion in a family of data model specifications
[PB84-217124] 07 p1027 N85-16518
Managing recoverable aircraft components in the PPB and related processes: Executive summary
[AD-A146908] 07 p1050 N85-16687
NBS (National Bureau of Standards) daylight availability database
[PB84-245745] 07 p1054 N85-16688
Distributed knowledge base systems for diagnosis and information retrieval
[AD-A146890] 07 p1054 N85-16690
Efficient computation of optimal time for transaction processing in a database system
[AD-A147566] 07 p1054 N85-16693
Mission-oriented requirements for updating MIL-H-8501, Volume 2: STI background and rationale — military rotorcraft
[NASA-CR-177331-VOL-2] 08 p1068 N85-16878
The orbiter air data system 08 p1094 N85-16912
Managing computer-controlled operations 08 p1097 N85-16934
Computer aided processing using laser measurements 08 p1103 N85-16973
Commerce Lab: Mission analysis. Payload integration study
[NASA-CR-171265] 08 p1104 N85-16982
Distributed sensor networks
[AD-A147638] 08 p1151 N85-17262
Hierarchical data structures and algorithms for digital stereoscopical mensuration 08 p1175 N85-17410
Pilot climate data system
[NASA-CR-174321] 08 p1187 N85-17481
Benchmarking database systems in multiple backend configurations
[AD-A148191] 08 p1202 N85-17568
A single server queue with mixed types of interruptions
[AD-A148538] 08 p1213 N85-17637
Antisampling for estimation: An overview
[AD-A148545] 08 p1216 N85-17659
Performance evaluation of a database system in multiple backend configurations
[AD-A148192] 08 p1229 N85-17743
The combinatorics of local constraints in model-based recognition and localization
[AD-A148338] 08 p1230 N85-17746
A description of the NRL oblique-incidence-ionogram data base
[AD-A148625] 08 p1230 N85-17748
Color visual simulation applications at the Defense Mapping Agency
[AD-P004315] 09 p1268 N85-17969
The generation of three-dimensional data bases using a building block approach
[AD-P004319] 09 p1269 N85-17973
Calculation of the area covered by mobile radio systems using geographic data stored in a computer
[FUB-43-1983] 09 p1312 N85-18247
Organizational tools for data analysis environments
[DE85-000396] 09 p1369 N85-18601
Methodology for evaluating related databases and a computerized algorithm for merging their output 09 p1401 N85-18821
Online database search strategies and thesaural relationship models 09 p1402 N85-18822
Documentation for an instrument database system
[DE84-017362] 09 p1402 N85-18826
Automation of information services furnished by documentation centers and specialized libraries
[FUB-6-1984] 09 p1402 N85-18827
Guide to human factors information sources
[AD-A149102] 10 p1531 N85-19649
SOLIDGEN: A solid finite element data generator. User's manual
[AD-A149490] 10 p1541 N85-19715
Air quality criteria for ozone and other photochemical oxidants. External review draft, volume 5
[PB86-126076-VOL-5] 11 p1679 N85-20583
A DOE directory of databases for material properties
[UCAR-10124] 11 p1739 N85-20937
Sourcebook: Gaining access to US government information on the environment and natural resources
[DE84-017419] 11 p1740 N85-20941
Conclusion of Viking Lander Imaging Investigation: Picture catalog of experiment data record
[NASA-RP-1137] 11 p1765 N85-21099
Transmission and orbital constraints in space-related programs: Briefing summary 12 p1787 N85-21216
Base communications issues for the 1980s
[AD-A149764] 12 p1828 N85-21474
Theoretical and empirical studies of the basic structure of turbulent shear flows, including separated flows and effects of wall curvature
[AD-A149657] 12 p1846 N85-21580
An analysis of short-to-medium-range seismic attenuation tests using a multilayered viscoelastic seismic propagation model
[AD-A149771] 12 p1889 N85-21856
Atlas of relectance patterns for uniform earth and cloud surfaces (NIMBUS-7ERB-61 days)
[PB85-116382] 12 p1891 N85-21870
A new NASA/MSFC mission analysis global cloud cover data base
[NASA-TP-2448] 12 p1893 N85-21878
A review of fatality, impairment of consciousness, and head/neck injury on USAF ejections 1971 - July 1983 12 p1906 N85-21974
Variable data base generator apparatus
[AD-D011515] 12 p1911 N85-21993
Evaluation of the vocabulary switching systems
[PB85-127157] 12 p1951 N85-22260
Precedency control and other semantic integrity issues in a workbench database 13 p2123 N85-23220
Low altitude texture comparison data base and smooth shaded texture
[AD-A150342] 13 p2148 N85-23323
General design considerations of an Air Force information system
[AD-A150611] 13 p2168 N85-23449
The hierarchical database decomposition approach to database concurrency control
[AD-A150612] 13 p2168 N85-23450
Intel iDIS evaluation
[DE85-003748] 13 p2168 N85-23451
Unsupervised classification of global radar units on Venus 13 p2198 N85-23632
Space Shuttle aerothermodynamic data report, phase C
[NASA-CR-171858] 14 p2241 N85-23897
An introduction to USAFETAC (USAF Environmental Technical Applications Center)
[AD-A150971] 14 p2378 N85-24682
Programmer/analyst workstation evaluation report
[NASA-CR-175289] 14 p2394 N85-24749
The Effect of Computers on the Generation and Use of Technical Data
[NBSIR-84-2907] 14 p2400 N85-24792
The identification of semantics for the file/database problem domain and their use in a template-based software environment 14 p2401 N85-24803
Integration of solid modeling and database management for CAD/CAM 14 p2402 N85-24804
Design and analysis of ordering and join for a multi-backed database system
[AD-A150711] 14 p2433 N85-25006
CADS: A Computer Aided Design System 15 p2574 N85-25876
Global paleoclimatic data base for 6000 years BP
[DE85-006626] 15 p2600 N85-26024
Alterations/corrections to the BRASS Program
[NASA-CR-171874] 15 p2616 N85-26121
Backend control processor for a multi-processor relational database computer system
[AD-A151892] 15 p2624 N85-26169
Computers in the determination of rainfall depth-duration-frequencies in Natal 15 p2627 N85-26188
Computer science and technology: A guide to performance evaluation of database systems
[PB85-155794] 15 p2631 N85-26219
Computer use in research for data analysis
[PB85-153567] 15 p2631 N85-26220
Procedures for use in compiling requirements specifications for computerized library systems
[CSTI-76] 15 p2665 N85-26446
Developing an automated technique for translating a relational database into an equivalent network one
[AD-A151844] 15 p2666 N85-26451
A database design for the Brazilian Air Force Flying Unit Operational Control System
[AD-A151848] 15 p2666 N85-26452
Analysis and specification of a universal data model for distributed data base systems
[AD-A151856] 15 p2666 N85-26453
List of serials indexed for online users, 1985
[PB85-143220] 15 p2666 N85-26455
Flow dynamic environment data base development for the SSME 16 p2736 N85-26885
An analysis of data dictionaries and their role in information resource management
[AD-A152134] 16 p2774 N85-27121
Status of the observational data sets — TOPEX 16 p2804 N85-27286
Acid precipitation in North America: 1980, 1981 and 1982 annual data summaries from acid deposition system data base
[PB85-162477] 16 p2822 N85-27410
Implementation and analysis of a microcomputer based relational database system
[AD-A151770] 16 p2845 N85-27536
Diagnosis: Using automatic test equipment and an artificial intelligence expert system
[AD-A151918] 16 p2851 N85-27576
Software for reflectivity calculations of X-ray mirrors, revision 1
[DE85-006642] 16 p2867 N85-27688
Retrieval performance in a full text journal article database 16 p2877 N85-27747
Access path optimization for network database retrieval 16 p2877 N85-27749
Design of an interface to an information retrieval network 16 p2877 N85-27750
Internal and external performance measurement methodologies for database systems
[AD-A152025] 16 p2877 N85-27751
Data management issues of statistical databases
[DE85-007616] 16 p2879 N85-27763
Evaluation of Defense Mapping Agency level 1 second edition digital data for training simulator applications
[AD-A152444] 17 p2983 N85-28437
Chemicals identified in human biological media, a data base, volume 6, part 1
[DE85-008788] 17 p2999 N85-28542
A test methodology for an automated and interactive software development environment
[AD-A152857] 17 p3011 N85-28618
Distributed systems management in wide area networks
[CWI-CS-R8419] 17 p3016 N85-28651
Experimental philosophy leading to a small scale digital data base of the conterminous United States for designing experiments with remotely sensed data
[NASA-TM-85009] 17 p3049 N85-28677
A study of user-defined searching requirements for the on-line version of the directory of DOD-sponsored R and D data bases on the Defense Gateway computer system
[AD-A153000] 17 p3050 N85-28878
Energy data base: Subject categories and scope
[DE84-017376] 17 p3050 N85-28881
Avionics Data Base users manual.
[AD-A153810] 18 p3062 N85-28942
GAMPHI: A database of activity and osmotic coefficients for aqueous electrolyte solutions
[PB85-183390] 18 p3072 N85-29002
Data base of all known, published data on trace elements in oil shale and its products
[DE85-003399] 18 p3126 N85-29357
Error growth in operational 10-day forecasts 18 p3143 N85-29460
Summary of archived Atlantic coast wave information study pressure, wind, wave, and water level data
[AD-A153782] 18 p3151 N85-29508
Chemicals identified in human biological media, a data base. Volume 6, part 2: Records 7588-8694
[DE85-008787] 18 p3154 N85-29528
Bayesian full rank marginalization for 2-way contingency tables
[AD-A153841] 18 p3171 N85-29649
Notes for medical catalogers, 1984
[PB85-180206] 18 p3200 N85-29853
CSIN (Chemical Substances Information Network) workbook: US Geological Survey training course for Chemical Substances Information Network
[PB85-170058] 18 p3200 N85-29855
North American acid deposition data base system (ADS) and its use in spatial analysis
[PB85-173235] 18 p3201 N85-29856
Analysis of the elastic and strength properties of Yucca Mountain tuff, Nevada
[DE85-006975] 19 p3300 N85-30460
VIDTEX
[PB85-175669] 19 p3318 N85-30567
An approach to modeling database activity 19 p3332 N85-30642
Cultural data base implementation study and computer-aided scene modeling system users manual
[AD-A154232] 19 p3333 N85-30646
EDS operator and control software
[DE85-010470] 19 p3340 N85-30668
CODA: A concept organization and development aid for the research environment
[AD-A154240] 19 p3343 N85-30715
SAFEORD: Safety of explosive ordnance databank
[AD-A154058] 19 p3360 N85-30972
Design and implementation of an intelligence database
[AD-A154095] 19 p3381 N85-30973
Transmission Monitoring and Control (TRAMCON) segmentation plan for the DCS (Defense Communications System) digital transmission network
[AD-A154175] 20 p3440 N85-31351
An industry and government survey: A nickel-hydrogen testing data base 20 p3448 N85-31409
Remote Sensing Technology: Symposium Proceedings
[DE85-010212] 20 p3477 N85-31606

Human factors engineering data sources; an overview
[FOA-C-56044-H2] 20 p3513 N85-31837
Inference in hierarchic classification — data bases
[ENST-84E014] 20 p3518 N85-31873
Realizing the full potential of the video disc for mapping applications
[AD-A154966] 21 p3606 N85-32391
A transportable, machine oriented library of european sky and terrain radiance distributions with contemporary radiometric and meteorological profiles
[AD-A155254] 21 p3637 N85-32590
USAFSAM review and analysis of radiofrequency radiation bioeffects literature
[AD-A155113] 21 p3664 N85-32760
Research on an expert system for database operation of simulation-emulation math models. Volume 1, Phase 1: Results
[NASA-CR-176067] 21 p3669 N85-32792
The architectural requirements and integration analysis of a database server for office automation
[AD-A155517] 21 p3674 N85-32825
Investigation of DBMS (Data Base Management Systems) for use in a research environment
[AD-A154662] 21 p3713 N85-33042
Evaluation of the 2DFLOW and hybrid complex-terrain dispersion models with the 1980 ASCOT data base from the Geysers
[DE85-012960] 22 p3812 N85-33613
Portable database driven control system for SPEAR
[DE85-010465] 22 p3830 N85-33720
Logical and physical modeling and design of scientific and statistical databases for energy research
[DE85-006061] 22 p3833 N85-33737
A hierarchy of knowledge levels implemented in a rule-based production system to calculate bounds on the size of intersections and unions of simple sets
[AD-A155291] 22 p3848 N85-33836
Novelis diagnostic support
[DE85-012987] 23 p3934 N85-34363
User's operating procedures. Volume 3: Projects directorate information programs
[NASA-CR-177950] 23 p3956 N85-34520
Graphics interaction in databases
23 p3958 N85-34534
NAPGEN: Automatic NAPLPS page generator
23 p3964 N85-34575
The final COS-B database now publicly available
[OG-9.3-8] 23 p4028 N85-34963
The final COS-B database: In-flight calibration of instrumental parameters
[OG-9.3-9] 23 p4028 N85-34964
Applications of the mineral resources data system and the international strategic minerals inventory in mineral-resource assessments by region and commodity
24 p4105 N85-35451
The NORDA/FNOC (Naval Ocean Research and Development Activity's/Fleet Numerical Oceanography Center) Polar Ice Prediction System (PIPS)-Arctic: A technical description
[AD-A156332] 24 p4126 N85-35577
LOCAT: A data retrieval program
[AD-A156004] 24 p4165 N85-35822
Source header list, supplement 3
[AD-A156100] 24 p4165 N85-35824

DATA BUSSES
U CHANNELS (DATA TRANSMISSION)

DATA COLLECTION PLATFORMS
Data Collection and Platform Location by Satellite: ARGOS Users' Conference 14 p2237 N85-23869
The ARGOS Platform Transmitter Terminals (PTTs)
14 p2237 N85-23872
The ARGOS VHF direct readout mini-station and CML-80-MP data collection Platform Transmitter Terminals (PTTs)
14 p2238 N85-23873
Project PAPA: The integration of drifting buoy data into an operational meteorological service
14 p2238 N85-23874
Applications of ARGOS data collection systems in Arctic regions 14 p2238 N85-23875
Data collection and winter ice dynamics in the Beaufort Sea 14 p2238 N85-23876
Report on the panel discussion of the Workshop on Data Collection Platform Networks
14 p2239 N85-23880
Data Collection and Platform Location by Satellite: ARGOS Users' Conference 14 p2239 N85-23883
Equipment for the ARGOS system from Eidsvoll Electronics A.S. 14 p2239 N85-23885
ARGOS VHF direct readout mini-station
14 p2239 N85-23886
Applications of ARGOS data collection system for automatic meteorological observatories in Arctic regions
14 p2240 N85-23893
Proceedings of the ARGOS Users Conference on Data Collection and Location by Satellite
14 p2322 N85-24348
Improvements brought about to the system since 1978 and statements on future development
14 p2323 N85-24349
New directions in ARGOS instrumentation at Polar Research Lab (PRL) 14 p2323 N85-24350
The Edmonton data collection platform processing and locating facility 14 p2323 N85-24352
The development of Platform Transmitter Terminal (PTT) and its application for drifting buoys
14 p2323 N85-24353
US programs using the ARGOS data collection and platform location system 14 p2323 N85-24355
US program in anchored data buoy and the other fixed observation platforms 14 p2324 N85-24358
One thousand days in the brine — platform transmitter terminals 14 p2324 N85-24359
Data Collection and Platform Location by Satellite: ARGOS Users' Conference 14 p2325 N85-24366
Data Collection and Platform Location by Satellite: ARGOS users' Conference 14 p2326 N85-24391
Collecting meteorological reports with the ARGOS system 14 p2329 N85-24398
US programs using the ARGOS data collection and platform location system 14 p2329 N85-24401
Data Collection and Platform Location by Satellite: ARGOS Users' Conference 14 p2330 N85-24409
US program using the ARGOS data collection and platform location system 14 p2330 N85-24410
A new versatile ARGOS PTT for oceanographic applications — Platform Transmit Terminal (PTT)
14 p2331 N85-24417
Data Collection and Platform Location by Satellite: ARGOS Users' Conference 16 p2811 N85-27333
DB2 and DB3: The next generation — buoys
16 p2811 N85-27337
A seismic ARGOS data collection platform
16 p2813 N85-27350
An operational buoy network collecting meteorological data 16 p2813 N85-27351
Operational experiences with the ARGOS system in Greenland 16 p2813 N85-27353

DATA COMPACTION
U DATA COMPRESSION

DATA COMPRESSION
Vertical compression algorithms
[DE84-015040] 01 p0126 N85-10864
Utilization of interpolation and transformation for the compression of digital image data
[INPE-3061-PRE/479] 02 p0240 N85-11566
Electronic bandwidth compression module
[AD-A145843] 03 p0368 N85-12343
Vector quantization of digital images
05 p0714 N85-14580
Recent advances in data compression
[DE85-001133] 06 p0854 N85-15432
Information extraction and transmission technique for spaceborne synthetic aperture radar images
[NASA-CR-174341] 06 p1150 N85-17256
Data compression for noiseless channels
13 p2053 N85-22851
Image data compression using uneven knots selection
[AD-A150602] 13 p2152 N85-23359
Feasibility studies of optical processing of image bandwidth compression schemes
[AD-A151254] 15 p2651 N85-26350
Alphabet-constrained data compression
[AD-A152667] 17 p3019 N85-28667
Research on signal detection and block truncation coding for image compression
[AD-A153444] 18 p3168 N85-29628
Development and analysis of a global compaction technique of microprograms 19 p3334 N85-30654
An image compression survey and algorithm switching based on scene activity
[NASA-TP-2458] 22 p3727 N85-33106
Electronic file system on an SM 90 minicomputer: The SARDE project
[ENST-84E018] 22 p3828 N85-33705
Noiseless coding for the Gamma Ray spectrometer
[NASA-CR-176201] 24 p4069 N85-35219
Raster functionality for a VDI
[DE85-006734] 24 p4097 N85-35396

DATA CONVERSION ROUTINES
NT SUBROUTINES
An introduction to the MIAS conversion system
[IOS-184] 03 p0403 N85-12571
A methodology for the analysis of programmer productivity and effort estimation within the framework of software conversion
[AD-A145757] 03 p0406 N85-12592
Data handling for the Spectral Radiometer (SPERAD)
[FOA-C-30368-E1,E4] 07 p0968 N85-16145
Defense Mapping Agency (DMA) raster-to-Vector analysis
[AD-A154153] 19 p3336 N85-30668
CRAYCDC
[NASA-CR-177374] 24 p4137 N85-35639
CDCCRAY
[NASA-CR-177375] 24 p4137 N85-35640
Two methods of global data assimilation
[AD-A155981] 24 p4143 N85-35684

DATA CONVERTERS
NT ANALOG TO DIGITAL CONVERTERS
NT DIGITAL TO ANALOG CONVERTERS

DATA CORRELATION
NT SIGNAL ANALYSIS
Numerical studies of mesoscale eddies using quasigeostrophic and primitive equation ocean models
[PB84-214048] 01 p0089 N85-10602
KrCl lasers for fusion
[DE84-012210] 01 p0122 N85-10635
Simulator study of flight characteristics of several large, dissimilar, cargo transport airplanes during approach and landing
[NASA-TP-2357] 02 p0148 N85-11002
Multispectral passive microwave correlations with an antecedent precipitation index using the Nimbus 7 SMMR
[AD-A145419] 02 p0200 N85-11334
A constitutive modeling technique based on a generalized rheological model to predict the response of materials 02 p0207 N85-11388
A principal component analysis of eastern Transvaal seasonal rainfall, 1950 to 1981
02 p0212 N85-11395
Study on spectral/radiometric characteristics of the Thematic Mapper for land use applications
[E85-10021] 02 p0218 N85-11434
Report of the Third Session of the International Working Group on Data Management for the International Satellite Cloud Climatology Project (ISCCP)
[WCP-82] 02 p0231 N85-11504
A study of highly energetic near-bottom ocean flow at the base of the Scotian Rise 02 p0233 N85-11515
Fluctuations in parameters of light beam along path with reflection in turbulent atmosphere
02 p0263 N85-11722
Optical constant determination of thin polymer films in the infrared
[AD-A145669] 02 p0287 N85-11877
Laboratory evaluation of microwave absorption properties under simulated conditions for planetary atmospheres
[NASA-CR-174060] 02 p0303 N85-11980
Methods for correlating geological, geochemical and geophysical data with satellite imagery in central Ireland
05 p0655 N85-14208
Selection of spacing of modular and gradient measurement surveys based on statistical characteristics of measured geomagnetic field
06 p0821 N85-15214
Characterization of radiometric calibration of LANDSAT-4 reflective bands 11 p1669 N85-20516
Looking at multivariate data through fuzzy sets
[DE85-000684] 11 p1702 N85-20706
TM geometric performance: Line to Line Displacement Analysis (LLDA) — New Mexico
12 p1870 N85-21732
Investigation of TM band-to-band registration using the JSC registration processor 12 p1872 N85-21745
Ozone Correlative Measurements Workshop
[NASA-CP-2362] 13 p2105 N85-23112
Lectures on probability and statistics
[DE85-007079] 15 p2641 N85-26291
A suggested standardized format for cosmic ray ground-level event data
[SH-9.1-15] 23 p4052 N85-35130

DATA FLOW ANALYSIS
Innovative image processing architectures
15 p2822 N85-26159

DATA HANDLING SYSTEMS
U DATA SYSTEMS

DATA INTEGRATION
Use and value of a geodetic reference system
[PB84-216167] 03 p0379 N85-12418
An integrated remote sensing approach for identifying ecological range sites — parker mountain
[E85-10050] 07 p0983 N85-16246
Global scale diagnoses of FGGE data
[NASA-CR-174358] 09 p1358 N85-18533
LANDSAT 4 investigation of Thematic Mapper and Multispectral Scanner applications
[E85-10076] 10 p1504 N85-19490
Spectroradiometric calibration of the Thematic Mapper and Multispectral Scanner system
[E85-10077] 10 p1504 N85-19491

DATA LINKS

Hardware implementation of a support system for the 2501 Western digital LSI, complete controller of the second level, first version of the CCITT 25 (CAP) recommendations
[FUB-60-1982] 01 p0100 N85-10666

Photo-reconnaissance system
[AD-D011287] 06 p0826 N85-15245

National airspace system configuration management interface control document. Maintenance processor subsystem to remote monitoring subsystems and remote monitoring subsystem concentrators
[NAS-MD-790] 07 p0900 N85-15705

NOAA (National Oceanic and Atmospheric Administration) Aircraft Satellite Data Link (ASDL)
[PB84-243773] 07 p0942 N85-15976

Using the control system design environment in the design of a data link receiver unit for the Coast Guard HH-65A helicopter
[AD-A148624] 08 p1088 N85-16880

TDRSS S-shuttle unique receiver equipment
08 p1100 N85-16951

The Communications link analysis and simulation system (CLASS)
08 p1100 N85-16952

Modeling techniques used in the communications link analysis and simulation system (CLASS)
08 p1100 N85-16953

Validation of the communications link analysis and simulation system (CLASS) 08 p1100 N85-16954

Digital scrambling for shuttle communication links: Do drawbacks outweigh advantages?
08 p1101 N85-16956

Novel applications of the NASA/GSFC Viterbi decoder hardware simulator 08 p1101 N85-16957

NSWC-NADC interactive communication links for AN/UYS-1 loadtape creation and retrieval
[AD-A148418] 08 p1153 N85-17277

The impact of propagation effects on the design of high capacity digital microwave links in the 18 GHz frequency band 10 p1470 N85-19278

Graphics translators for computer-aided drafting and design: Interface alternatives for the A/E community
[AD-A146892] 10 p1540 N85-19706

The evolution of methods of air traffic control
[AD-A149606] 12 p1774 N85-21137

Satellite bridges in communications networks
13 p2067 N85-22910

Optimum path selection in automated radio relay link design 13 p2073 N85-22947

Investigation of influence of communications link and synchronization error on noise tolerance of group transmission of binary information based on orthogonal Walsh function 13 p2086 N85-23026

Feasibility study for an AFGL fiber optic data link at WSMR sounding rocket launch area
[AD-A150852] 14 p2240 N85-23894

Geostationary Operational Environmental Satellite Data Collection System 14 p2328 N85-24393

NOAA'S role in support of service ARGOS
14 p2328 N85-24394

Data-link alternatives for the NASA pilot data systems
[NASA-TM-85999] 14 p2412 N85-24873

Satellite reception of reentry vehicle telemetry
[AD-A151851] 15 p2492 N85-25372

Consultative Committee for Space Data Systems. Panel 1: Support
[NASA-CR-175786] 16 p2769 N85-27090

Continued development and implementation of the Universal Network Interface Device (UNID) 2 in the Digital Engineering Laboratory Network (DELNET), volume 2
[AD-A151947] 16 p2850 N85-27570

Performance measurement of OSI (Open System Interconnection) class 4 transport implementations
[PB85-177657] 18 p3161 N85-29582

Phase-locked loops for optical homodyne detection, volume 1 — spaceborne receivers
[ESA-CR(P)-2029-VOL-1] 20 p3442 N85-31367

Phase locked loops for optical homodyne detection, volume 2 — spaceborne receivers
[ESA-CR(P)-2029-VOL-2] 20 p3442 N85-31368

Space optics
[CNES-84/105/T/CT/DRT/TIT/10]
20 p3533 N85-31985

Broadcasting topology and routing information in computer networks
[AD-A155668] 21 p3674 N85-32827

Satellite links in the ISO architecture: Models and performance evaluation
[ENST-84E017] 22 p3756 N85-33284

Performance interface document for the S-band diplexer for space users of NASA networks
[NASA-TM-86224] 23 p3900 N85-34155

DATA MANAGEMENT

Facsimile transmission of microforms
[AD-A144855] 01 p0038 N85-10236

MERIT: A man/computer data management and enhancement system for upper air nowcasting/forecasting in the United States — Minimum Energy Routes using Interactive Techniques (MERIT)
01 p0083 N85-10558

Hardware implementation of a support system for the 2501 Western digital LSI, complete controller of the second level, first version of the CCITT 25 (CAP) recommendations
[FUB-60-1982] 01 p0100 N85-10666

Telemetry (TM)/telecommand (TC) processor study
[ESA-CR(P)-1915] 03 p0323 N85-12061

The current formal status of the ERS-1 ground segment 03 p0380 N85-12423

International banking of satellite and in-situ wave data by the Marine Information and Advisory Services (MIAS)
03 p0381 N85-12434

Lessons from the SEASAT and GEOS-3 altimeters data projects 03 p0384 N85-12457

Research in data management and system reliability
[AD-A145498] 03 p0436 N85-12773

Primer on the registration of technical information in industry 03 p0438 N85-12786

Archiving and exchange of a computerized marine seismic database: The ROSE data archive system
[DE84-901453] 04 p0576 N85-13677

Integrated resource management algorithms for computer systems 05 p0715 N85-14582

Recent advances in data compression
[DE85-001133] 06 p0854 N85-15432

Methodology investigation. Streamlined Test Reporting and Planning (STRAP): Data flow procedures
[AD-A146463] 06 p0871 N85-15531

Climate and climate data. Report on the workshop held in Brasilia (Argentina) from 11-15 April 1983
07 p1001 N85-16357

Decentralized control of scheduling in distributed systems
[AD-A147446] 07 p1022 N85-16487

Pilot climate data system
[NASA-CR-174321] 08 p1187 N85-17481

DDN directory
[AD-A148213] 08 p1230 N85-17744

Concurrency in a data flow database machine
09 p1366 N85-18582

Role of environments in managing data analysis
[DE85-000397] 09 p1369 N85-18602

Elimination of sensor artifacts from infrared data
[AD-A149048] 10 p1556 N85-19614

A proposed integration among organizational information requirements, media richness and structural design
[AD-A149317] 10 p1567 N85-19681

Some data manipulation requirements for the exploratory analysis of large data sets
[DE85-002541] 10 p1568 N85-19687

A DOE directory of databases for material properties
[UCAR-10124] 11 p1739 N85-20937

A GC/MS (Gas Chromatograph/Mass Spectrometer) data management process. Part 1: User's guide, version 1.0
[PB85-116051] 12 p1803 N85-21309

A GC/MS (Gas Chromatograph/Mass Spectrometer) data management process. Part 2: Program documentation, version 1.0
[PB85-116069] 12 p1803 N85-21310

Introduction to the Space Physics Analysis Network (SPAN)
[NASA-TM-86499] 14 p2290 N85-24198

Integration of solid modeling and database management for CAD/CAM 14 p2402 N85-24804

Interactive data analysis. Development of an interactive data manipulation system
[AD-A151359] 15 p2623 N85-26164

Implementation and analysis of a microcomputer based relational database system
[AD-A151770] 16 p2845 N85-27536

Data dictionary design as a stepping-stone to DBMS (Data Base Management System) implementation in the Indonesian Army Data Collecting and Processing Service
[AD-A152101] 16 p2877 N85-27752

Replication methods for abstract data types
[AD-A153648] 18 p3162 N85-29587

CSIN (Chemical Substances Information Network) workbook: US Geological Survey training course for Chemical Substances Information Network
[PB85-170058] 18 p3200 N85-29855

The international scope of data evaluation
[DE85-005653] 19 p3349 N85-30760

Guide on logical database design
[PB85-177970] 19 p3361 N85-30976

Distributed name management
[AD-A154765] 21 p3712 N85-33037

Report of Workshop on Computational Geometry and summary of related research
[AD-A155399] 22 p3833 N85-33734

DATA PROCESSING

NT ASSOCIATIVE PROCESSING (COMPUTERS)
NT ATMOSPHERIC & OCEANOGRAPHIC INFORM SYS
NT BATCH PROCESSING
NT CENSORED DATA (MATHEMATICS)
NT CONCURRENT PROCESSING
NT DATA CORRELATION
NT DATA REDUCTION
NT DATA RETRIEVAL
NT DATA SMOOTHING
NT DATA STORAGE
NT DISTRIBUTED PROCESSING
NT KARHUNEN-LOEVE EXPANSION
NT MULTIPROCESSING (COMPUTERS)
NT OPTICAL DATA PROCESSING
NT PARALLEL PROCESSING (COMPUTERS)
NT PIPELINING (COMPUTERS)
NT SCENE ANALYSIS
NT SIGNAL ANALYSIS
NT SIGNAL PROCESSING
NT VOICE DATA PROCESSING

The data processing system of the NAL 2m x 2m transonic wind tunnel
[NAL-TR-811] 01 p0012 N85-10075

TEQUEL: The query language of SADDLE
01 p0058 N85-10362

Seismic discrimination of a geothermal field: Cerro Prieto
[DE84-014581] 01 p0064 N85-10425

Analysis of highly precise gravity measurements
[SER-C-294] 01 p0071 N85-10472

Data flow computer architecture
[DE84-014362] 01 p0100 N85-10664

East Europe report: Science and technology
[JPRS-ESA-84-030] 01 p0101 N85-10670

Decentralized data acquisition to remedy EDP bottleneck 01 p0101 N85-10671

Remote data processing system software in Hungary
01 p0101 N85-10673

Normal approximation for response time in a processor-shared computer system model
[AD-A144997] 01 p0103 N85-10690

A modular data acquisition and display software system for a laboratory environment
[PB84-217892] 01 p0105 N85-10709

Construction of approximate confidence intervals for probability-of-kill via the bootstrap
[AD-A144761] 01 p0113 N85-10764

Hardware and software selection for experimental modal analysis 02 p0208 N85-11373

A mathematical theory of command and control structures
[AD-A145606] 02 p0256 N85-11675

On update semantics and relational views
[AD-A145622] 02 p0294 N85-11907

Nonlinear system identification methodology development based on F-4S flight test data analysis
[AD-A146289] 03 p0318 N85-12053

Satellite, airborne remote sensing development outlined 03 p0342 N85-12199

The current formal status of the ERS-1 ground segment 03 p0380 N85-12423

Factors affecting the archiving, processing and dissemination of ERS-1 altimeter data
03 p0381 N85-12435

Individual differences in automatic and controlled information processing
[AD-A146245] 03 p0401 N85-12559

On line digitizer software
[AD-A146249] 03 p0403 N85-12568

Vibration data analysis system for SNLA area 3 reference manual
[DE84-016207] 04 p0514 N85-13275

Advantages and limitations of spherical harmonic analyses of geomagnetic data 04 p0519 N85-13318

Human reliability data bank: Feasibility study
[DE84-015215] 04 p0546 N85-13476

Toward a non-bureaucratic approach to quality assurance in data processing
[DE84-007484] 04 p0550 N85-13497

Formats for numerical and textual data in data processing
[DFVLR-MITT-84-07] 04 p0551 N85-13504

Measurement of infrasonic waves from remotely detonated artificial explosion 04 p0557 N85-13546

Nuclear criticality information system: Database examples
[DE84-014462] 04 p0576 N85-13678

Speed test results and hardware/software study of computational speed problem, appendix D
05 p0603 N85-13843

Treatment and expression of measurement uncertainties 05 p0630 N85-14042
The acquisition, processing, and use of tactile sensor data in robot control 05 p0641 N85-14114
LANDSAT instruments characterization [E85-10030] 05 p0654 N85-14199
Measurement data acquisition and processing system for wind rotor measurements in the wind channel of Bremen University 05 p0668 N85-14298
Measuring techniques in the measuring program for the windpowered unit GROWIAN 05 p0669 N85-14303
Weather and climate parameters from Tiros-N 05 p0681 N85-14377
Global scale diagnosis of FGGE data 05 p0683 N85-14394
Application of the bounded derivative initialization method 05 p0686 N85-14407
Increase in the economy of design and process planning by integrated and graphic data processing, phase 2 — aircraft design [BMFT-FB-W-84-028] 05 p0716 N85-14589
Integrated navigation systems: Where are we headed? [AD-A146425] 06 p0753 N85-14832
Geological effectiveness of automated processing of highly precise aeromagnetic surveys in Caspian region 06 p0821 N85-15216
Standard SHEF (Standard Hydrometeorologic Exchange Format) decoder Version 1.1 [PB85-106506/GAR] 06 p0840 N85-15332
Investigative findings of image enhancement techniques [AD-A146392] 06 p0853 N85-15424
Recent advances in data compression [DE85-001133] 06 p0854 N85-15432
Beginner's guide to blocked records on magnetic tape [DE85-001691] 06 p0855 N85-15433
Recommended documentation for computer users at ANL [DE84-016265] 06 p0855 N85-15434
Research on introspective systems [AD-A146406] 06 p0870 N85-15530
Methodology investigation. Streamlined Test Reporting and Planning (STRAP): Data flow procedures [AD-A146463] 06 p0871 N85-15531
Adaptive preprocessing system [AD-D011327] 07 p0937 N85-15935
Literature review of voice recognition and generation technology for Army helicopter applications [AD-A146878] 07 p0939 N85-15954
Efficient computation of optimal time for transaction processing in a database system [AD-A147568] 07 p1054 N85-16693
Correlator and data processing requirements for QUASAT 07 p1057 N85-16709
TDRSS S-shuttle unique receiver equipment 08 p1100 N85-16951
EDP computer tapes described 08 p1142 N85-17203
A scanning alarm electronic processor [AD-D011419] 08 p1156 N85-17309
An efficient algorithm for the computation of the inverse in bundle adjustment systems — photogrammetry 08 p1175 N85-17411
Plasma and magnetospheric research [NASA-CR-171293] 08 p1183 N85-17451
Data analysis techniques for vehicle attitudinal, positional and experimental measurements [AD-A147752] 08 p1186 N85-17484
Hybrid data processing research facility [AD-A148092] 08 p1202 N85-17567
A nonlinear technique for high-resolution data processing [AD-D011415] 08 p1203 N85-17570
Approaches to structuring the software development process [AD-A147694] 08 p1205 N85-17582
On edge detection [AD-A148573] 08 p1223 N85-17703
Survey of remote data monitoring systems [DE85-001385] 09 p1323 N85-18313
Data report on variations in the composition of sea ice during MIZEX/East'83 with the Nimbus-7 SMMR [NASA-TM-86170] 09 p1342 N85-18443
NOAA OTEC CWP (National Oceanic and Atmospheric Administration Ocean Thermal Energy Conversion Cold Water Pipe) at-sea test. Volume 3: Additional tabulation of the power spectra, part 2 [PB84-236997] 09 p1346 N85-18468
Analysis of geohydrologic data by kriging [AD-F004152] 09 p1349 N85-18488
Velocity stack and slant stack inversion methods 09 p1351 N85-18497
Proposal for a small scheme implementation [AD-A148707] 09 p1368 N85-18595
JOVIAL J73 automated verification system: Implementation phase [AD-A148732] 09 p1368 N85-18597
Organizational tools for data analysis environments [DE85-000396] 09 p1369 N85-18601
Role of environments in managing data analysis [DE85-000397] 09 p1369 N85-18602
Software for event oriented processing on multiprocessor systems [DE84-016720] 09 p1370 N85-18607
User's manual: Menu-driven data graphing program for the Tektronix 7912AD and 7612D transient digitizer system [DE85-002151] 09 p1370 N85-18610
Computing environments for data analysis. Part 1. Introduction [AD-A148677] 09 p1373 N85-18632
Computing environments for data analysis. Part 2. Hardware [AD-A148678] 09 p1374 N85-18633
Principal curves and surfaces [AD-A148833] 09 p1375 N85-18646
Data reduction 09 p1412 N85-18903
Analysis of processing 09 p1412 N85-18905
Prospects and means for development of theory and practice of interpretation of gravitational and magnetic anomalies 10 p1501 N85-19474
Brazilian remote sensing receiving, recording and processing ground systems in the 1980's [E85-10079] 10 p1504 N85-19483
Processing of Global Area Coverage (GAC) data of the TIROS-N/NOAA series polar orbiters [AD-A148992] 10 p1519 N85-19576
Computer-assisted data processing and analysis system for ground-based meteorological data collection, report on the Sierra Cooperative Pilot Project [PB85-115350] 10 p1520 N85-19587
Ada (trademark) primer [AD-A148855] 10 p1539 N85-19703
Diamonds and diamond sorting [PB85-128502] 10 p1542 N85-19726
The evolution from data processing to information resource management [AD-A149429] 10 p1567 N85-19878
Some data manipulation requirements for the exploratory analysis of large data sets [DE85-002541] 10 p1568 N85-19887
Characteristics of quality data [DE85-001203] 10 p1568 N85-19889
A modeling analysis program for the JPL table mountain Io sodium cloud data [NASA-CR-175474] 10 p1572 N85-19910
European Scientific Notes. Volume 39, number 2 [AD-A148994] 10 p1573 N85-19919
Comparative evaluation of GC/MS (Gas Chromatography/Mass Spectrometry) data analysis processing [PB85-125664] 11 p1596 N85-20037
Processing circuit with asymmetry corrector and convolutional encoder for digital data [NASA-CASE-MSC-20187-1] 11 p1628 N85-20249
Photonic methods of high speed analog data recording [DE84-016723] 11 p1637 N85-20308
Middle Atmosphere Program. Handbook for MAP. Volume 12: Coordinated Study of the Behavior of the Middle Atmosphere in Winter (PMP-1) Workshops [NASA-CR-175475] 11 p1665 N85-20492
An overview of the Thematic Mapper geometric correction system 11 p1668 N85-20511
Canadian plans for Thematic Mapper data 11 p1668 N85-20513
A DOE directory of databases for material properties [UCAR-10124] 11 p1739 N85-20937
Post-processing of bibliographic citations from DOE/Recon, NASA/Recon, and DOD/DROLS [DE85-000617] 11 p1739 N85-20938
Base communications issues for the 1980s [AD-A149764] 12 p1828 N85-21474
Universal file processing program for field programmable integrated circuits [DE85-004384] 12 p1837 N85-21526
GSFC specification electronic data processing magnetic recording tape [NASA-TM-80599] 12 p1851 N85-21609
Use of the ORACLE DEMS in determining the response of complex scientific instrumentation [DE85-001742] 12 p1853 N85-21621
An analysis of the high frequency vibrations in early Thematic Mapper scenes 12 p1872 N85-21742
Draftsman displays: A graphical technique for exploratory data analysis [AD-A150515] 13 p2041 N85-22775
Laser applications in last 10 years reviewed 13 p2052 N85-22844
Liquid mass flow rate computer 13 p2075 N85-22982
Efficiency of multitarget signal detection by digital radar data processing devices 13 p2080 N85-22991
Application of field X-ray: Radiometric analysis in exploratory geology and means for its improvement 13 p2115 N85-23176
Analysis and evaluation of the LANDSAT-4 MSS and TM sensors and ground data processing systems: Early results 13 p2117 N85-23189
Geologic utility of LANSDAT-4 TM data — Death Valley, California and the Silver Bell area of southern Arizona 13 p2118 N85-23192
Microcomputer: Controlled statistics analyzer [BLL-CE-TRANS-7971-(9022.09)] 13 p2144 N85-23306
Presentation based user interfaces [AD-A150311] 13 p2144 N85-23311
Measurement of SIFT operating system overhead [NASA-TM-86322] 13 p2149 N85-23337
Map design for computer processing: Literature review and DMA product critique [AD-A151061] 14 p2347 N85-24513
Evaluation of carrying capacity and landscape damage in northern Kenya by multistage remote sensing [DFVLR-FB-84-47] 14 p2347 N85-24514
Cabauw (Netherlands) meteorological data tapes 1973-1984: Description of instrumentation and data processing for continuous measurements [KNMI-WR-84-6] 14 p2379 N85-24685
Scientific experiments. Preprocessing of scientific data — spaceborne experiments 14 p2398 N85-24779
The problem of creating a standardized series of personal computers 14 p2400 N85-24795
TAPTRN: A tape utility program [AD-A150644] 14 p2403 N85-24814
CHIL: A comprehensive histogramming language [DE85-005356] 14 p2405 N85-24830
Dataflow computation [CWI-TRACT-6] 14 p2406 N85-24833
Experience in automation of data processing in interpretation and defining of linear elements from space photographs 15 p2486 N85-25349
Data structure considerations in automatic cartography 15 p2583 N85-25930
General meteorological package (GEMPAK) 15 p2599 N85-26019
Interactive data analysis. Development of an interactive data manipulation system [AD-A151359] 15 p2623 N85-26164
USSR report: Cybernetics, computers and automation technology [JPRS-UCC-85-003] 15 p2625 N85-26174
GRID: A FORTRAN program for using a digitizing table to enter a finite element GRID [AD-A151317] 15 p2628 N85-26196
Constructing unifying frameworks for the study of distributed system and algorithms [AD-A151287] 15 p2637 N85-26281
Scattered data interpolation and approximation [DE85-007495] 15 p2641 N85-26290
An application of the Rayleigh distribution to contract cost data [AD-A151551] 15 p2964 N85-26441
Space radiation studies — Spacelab 2 Payload [NASA-CR-171410] 15 p2665 N85-26584
Consultative Committee for Space Data Systems. Panel 1: Support [NASA-CR-175786] 16 p2769 N85-27090
Gravity model development software status 16 p2804 N85-27289
The relevance of remote sensing to Brazil [INPE-3421-PRE/666] 16 p2811 N85-27332
Comparison of circulation statistics based on FGGE (First GARP Global Experiment) level 3-B analyses produced by GFDL (Geophysics Fluid Dynamics Laboratory) and ECMWF (European Centre for Medium Range Weather Forecasts) for special observing periods [PB85-153948] 16 p2836 N85-27492
Algorithms for determining the relative complexity of dynamic signals [BLL-M-36111-(5828.4)] 16 p2851 N85-27574
Management considerations for an information center [AD-A151774] 16 p2875 N85-27742
DOD manual for standard data elements, part 1 [AD-A152201] 16 p2876 N85-27754
A Dictionary-Directory System (DDS) for the SPLICE system [AD-A152223] 16 p2878 N85-27759
A study of error rates in voice recognition [AD-A153282] 17 p2949 N85-28211
Restructurable VLSI (Very large scale integration) program [AD-A152340] 17 p2951 N85-28226

Developments in remote sensing
[B8580069] 17 p2984 N85-26441
A comparison of numeric data entry with touch-sensitive and conventional numeric keypads
[AD-A153276] 17 p3008 N85-28596
Computing environments for data analysis. Part 1: Introduction
[DE85-007919] 17 p3009 N85-28603
Computing environments for data analysis. Part 2: Hardware
[DE85-008320] 17 p3009 N85-28604
Interfacing the VAX 11/780 using Berkeley Unix 4.2.BSD and Ethernet based Xerox network systems, volume 1
[AD-A152953] 17 p3015 N85-28645
Estimating random integrals from noisy observations: Sampling designs and their performance
[AD-A152926] 17 p3025 N85-28702
Complete development and implement AFIT/ENG database management system, volume 1
[AD-A153043] 17 p3048 N85-28866
Processing methods of rawinsonde measurements at the descent by parachute
[KNMI-WR-84-7] 18 p3149 N85-29496
Scattered data interpolation codes
[DE85-007337] 18 p3164 N85-29601
Annotated bibliography of recent papers on software engineering environments
[PB85-191365] 18 p3165 N85-29607
Transform domain adaptive filtering using a recursive DFT
[DE85-008965] 18 p3172 N85-29656
Activities report in energy technology
[OEFZS-4302] 18 p3199 N85-29846
LDV multiplexer interface
[NASA-CASE-ARC-11536-1] 19 p3258 N85-30202
An approach to modeling database activity
19 p3332 N85-30642
Cultural data base implementation study and computer-aided scene modeling system users manual
[AD-A154232] 19 p3333 N85-30646
Recovery of lost files from VAX/VMS disk structures: A case study
[DE85-010652] 19 p3333 N85-30650
Interactive graphics for a data analysis management system
[DE85-010977] 19 p3334 N85-30651
Local automation model software benchmarking: Test plan
[AD-A154349] 19 p3337 N85-30676
Ada compiler validation summary report: University of Karlsruhe-GMD/German MOD VAX 11 compiler, version v1.0
[AD-A154370] 19 p3337 N85-30678
Computer Performance Modeling Tool (CPMT)
[AD-A154438] 19 p3338 N85-30682
Defense Mapping Agency (DMA) raster-to-Vector benchmark testing
[AD-A154152] 19 p3338 N85-30683
CMP: Code Maintenance Package reference manual, version 2.0
[DE85-011396] 19 p3340 N85-30697
EDS operator and control software
[DE85-010470] 19 p3340 N85-30698
Guide on workload forecasting
[PB85-177632] 19 p3341 N85-30704
System enhancements of Mesoscale Analysis and Space Sensor (MASS) computer system
[NASA-CR-171463] 19 p3342 N85-30708
TMI-2 technical information and examination program
[DE85-010614] 19 p3359 N85-30827
Modified dynamic hashing
[DE85-011166] 19 p3361 N85-30974
France's LETI reports 1983 electronic components research 20 p3436 N85-31336
Scientific report of the Department of Systems and Communications
[ENST-84D002] 20 p3441 N85-31355
Informatics Division 20 p3449 N85-31416
Microprocessor AirborneData Acquisition and Replay (MADAR) system
[AD-A151728] 20 p3514 N85-31843
Symposium on Computational Mathematics-State-of-the-Art: Informal Proceedings
[DE85-008122] 20 p3516 N85-31858
Overview of on-line data processing for MST radars (keynote paper), part 7 21 p3625 N85-32519
The Norwegian seismic array (NORSAR)
[AD-A154751] 21 p3631 N85-32555
Analysis of spacecraft data
[NASA-CR-171507] 21 p3669 N85-32790
An automated quality assurance surveillance plan for ADP (Automated Data Processing) operations under the Navy's commercial activities program
[AD-A154767] 21 p3671 N85-32802
Design guidelines for user-system interface software
[AD-A154907] 21 p3671 N85-32807
Environmental surveillance at Los Alamos during 1984
[DE85-011886] 22 p3811 N85-33605
Solar energy meteorological research and training program: Region 4
[DE85-011783] 22 p3816 N85-33640
DECODE: A software manual for use with the Serial ASCII Instrumentation Loop (SAIL) system
[AD-A155358] 22 p3826 N85-33709
Automatic capability to store and retrieve component data and to calculate structural integrity of these components
[DE85-012429] 22 p3831 N85-33728
Report of Workshop on Computational Geometry and summary of related research
[AD-A155399] 22 p3833 N85-33734
Comparison of experimental data on detonation velocity and Chapman-Jouget pressure vs initial HE density with predictions from Ree's model equation of state
[DE85-007266] 23 p3922 N85-34304
Modular digital holographic fringe data processing system
[NASA-CR-177952] 23 p3933 N85-34376
Evaluation of low-temperature geothermal potential in Utah and Goshen Valleys and adjacent areas, Utah. Part 2: Water temperature and chemistry
[DE85-009344] 23 p3943 N85-34438
Real-time multiparameter pulse processing with decision tables
[DE85-011683] 23 p3966 N85-34589
Vector calculation of particle code
23 p3981 N85-34688
On the statistical significance of excess events: Remarks of caution and the need for a standard method of calculation
[OG-9.5-10] 23 p4031 N85-34987
Aspects of input signal design for order and parameter estimation in linear dynamical systems
[ER-83/05] 24 p4091 N85-35362
Adaptive rezoner in a two-dimensional Lagrangian hydrodynamic code
[DE85-010108] 24 p4094 N85-35381
Federal Mineral Land Information System
24 p4106 N85-35459
Gravity gradiometer survey data processing
[AD-A156165] 24 p4117 N85-35522
An approach to determining computer security requirements for Navy systems
[AD-A155750] 24 p4135 N85-35627
Optimize computer throughput using array processors
[AD-A155843] 24 p4135 N85-35628
Using an LSI-11/23 and RT-11 to digitize analog tapes
[DE85-012736] 24 p4139 N85-35656
Analysis of two-parameter constant background born inversion for acoustic synthetic data
[AD-A156394] 24 p4145 N85-35698
Data processing professionals and DP application users' perceptions and expectations of operational roles of persons working in a DP/application user interface group 24 p4165 N85-35821
Investigation of cosmic rays in very short time scales
[HE-4.6-7] 24 p4197 N85-36044

DATA PROCESSING EQUIPMENT
NT AIRBORNE/SPACEBORNE COMPUTERS
NT ANALOG COMPUTERS
NT CDC COMPUTERS
NT CDC CYBER 170 SERIES COMPUTERS
NT CDC CYBER 205 COMPUTER
NT COMPUTERS
NT DATA PROCESSING TERMINALS
NT DIGITAL COMPUTERS
NT EMBEDDED COMPUTER SYSTEMS
NT HEWLETT-PACKARD COMPUTERS
NT HYBRID COMPUTERS
NT IBM COMPUTERS
NT MICROCOMPUTERS
NT MICROPROCESSORS
NT MINICOMPUTERS
NT OPTICAL COMPUTERS
NT PARALLEL COMPUTERS
NT PDP 11 COMPUTER
NT PDP 11/70 COMPUTER
NT PERSONAL COMPUTERS
NT PRINTERS (DATA PROCESSING)
NT SEQUENTIAL COMPUTERS
NT UNIVAC COMPUTERS
NT UNIVAC 1100 SERIES COMPUTERS
NT VAX COMPUTERS
NT VAX-11 SERIES COMPUTERS
NT VAX-11/780 COMPUTER
The FLEX/32 multicomputing environment
01 p0057 N85-10378
On line digitizer software
[AD-A146249] 03 p0403 N85-12568
Intelligent interfaces for tactical airborne platforms
C6 p0752 N85-14820
Papers of the 15th International Society for Photogrammetry and Remote Sensing (ISPRS) Congress — conferences
[TRITA-FMI-9] 08 p1175 N85-17406
Hybrid data processing research facility
[AD-A148092] 08 p1202 N85-17567
Dual adaptive control based upon sensitivity functions
[NASA-CR-169331] 10 p1543 N85-19727
New types of power supplies for ultrasonic processing equipment 12 p1843 N85-21566
RAPIDbus: Design of an extensible multiprocessor structure
[AD-A150061] 12 p1912 N85-21998
Instrumentation award
[AD-A150081] 12 p1912 N85-21999
Requirements placed on information processing equipment
[BLL-CE-TRANS-7983-(9022.09)] 13 p2144 N85-23307
Parallel test method for LSI (Large Scale Integration) microprocessors
[AD-A150237] 13 p2144 N85-23310
Research on CAD/CAM support for microprocessor development surveyed 14 p2290 N85-24193
Microprocessor controlled storage sampling oscilloscope 15 p2533 N85-25622
ADCCP (Advanced Data Communication Control Procedure) communication processor
[AD-D011595] 15 p2544 N85-25709
Computer use in research for data analysis
[PB85-153567] 15 p2631 N85-26220
A procedure for communications with PDP-10 and PDP-11 (IS/1 UNIX) type computers through use of CPT word processing equipment, revision 1
[DE85-007596] 16 p2845 N85-27540
The touch panel system: Design and development
[AD-A153014] 17 p3008 N85-28596
A study of user-defined searching requirements for the on-line version of the directory of DOD-sponsored R and D data bases on the Defense Gateway computer system
[AD-A153000] 17 p3050 N85-28878
User's guide for the Mk-3 D-coronameter data system
[PB85-181204] 19 p3385 N85-31002

DATA PROCESSING TERMINALS
Analysis of data entry performance: Chromatic versus monochromatic
[AD-A145568] 03 p0436 N85-12789
Selected NBSNET software
[PB85-109146] 10 p1542 N85-19723
Optical processor for synthetic aperture radar
11 p1621 N85-20203
The ARGOS Platform Transmitter Terminals (PTTs)
14 p2237 N85-23872
The ARGOS VHF direct readout mini-station and CML-80-MP data collection Platform Transmitter Terminals (PTTs) 14 p2238 N85-23873
Direct readout and dissemination of results using ARGOS keypad terminals 14 p2328 N85-24390
Data transmission using ARGOS keypad platform transmitter terminals (PTT) 14 p2330 N85-24407
A new versatile ARGOS PTT for oceanographic applications — Platform Transmit Terminal (PTT)
14 p2331 N85-24417
Overview of data processing at AES local user terminals — Canadian Atmospheric Environment Service (AES) 14 p2331 N85-24418
Investigation and construction of the Mini Remote Terminal Unit (mRTU-M) Analog Processor Module (AP-M), volume 1
[MR-DS-01-VOL-1] 18 p3166 N85-29619
Investigation and construction of the Mini Remote Terminal Unit (mRTU-M), Analog Processor Module (AP-M), volume 2
[MR-DS-01-VOL-2] 18 p3166 N85-29620
Canadian Astronautics Limited's SARSAT ground stations 20 p3401 N85-31104
A 406 MHz ELT processor for geostationary satellites — Emergency Locator Transmitter (ELT)
20 p3403 N85-31114
Evolution of 406 MHz Search and Rescue (SAR) processor 20 p3403 N85-31116
A micro/PDP-11 system for 406 MHz COSPAS/SARSAT processing 20 p3403 N85-31117
Fault tolerant multiprocessor SARSAT-COSPAS 406 MHz local user terminal 20 p3404 N85-31123
Secure digital voice communications in the Defense Data Network (DDN)
[AD-A154677] 21 p3574 N85-32226

DATA PROCESSORS
U DATA PROCESSING EQUIPMENT

DATA READOUT SYSTEMS
U DATA SYSTEMS
U DISPLAY DEVICES

DATA RECORDERS
Analog disc recorder system: Operator's reference manual
[DE84-016926] 04 p0503 N85-13209
System for automatic recording of vibration parameters 14 p2262 N85-24135
Balloon-borne video cassette recorders for digital data storage
[OG-9.3-11] 23 p4028 N85-34966
Mini and super mini arrays for the study of highest energy cosmic rays
[OG-9.4-9] 23 p4029 N85-34976
DATA RECORDING
Requirements and specifications for cartographic video discs
[AD-A144906] 01 p0049 N85-10325
Existing measuring systems for wind energy units 05 p0669 N85-14302
Operational loads measurement: A philosophy and its implementation 07 p0894 N85-15665
The F-15 flight loads tracking program 07 p0894 N85-15666
Flight parameters recording for structure fatigue life monitoring 07 p0896 N85-15682
USAF approach to airborne structural data recording: Airborne Data Acquisition Multifunction System (ADAMS) 07 p0897 N85-15683
Extracting digital data from a bus and multiplexing it with a video signal
[AD-D011491] 11 p1636 N85-20302
Quarter-inch streaming tape drive application with the Serial ASCII Instrumentation Loop (SAIL) system
[AD-A155354] 22 p3759 N85-33295
Error message recording and reporting in the SLC control system
[DE85-013057] 24 p4140 N85-35664
DATA REDUCTION
NT DATA SMOOTHING
Analysis of highly precise gravity measurements
[SER-C-294] 01 p0071 N85-10472
Computations for the 16-foot transonic tunnel, NASA, Langley Research Center
[NASA-TM-86319] 02 p0149 N85-11009
Reducing spectral dimension of remotely sensed data using principal components analysis and a Peano scanning 02 p0212 N85-11399
Command flight path display. Phase I and II: Appendix F
[AD-A145858] 03 p0318 N85-12056
Physical oceanography report. Helicopter-based STD data from MIZEX 83 (Marginal ice zone experiment)
[AD-A145843] 03 p0398 N85-12538
NUTSATSEA: An on line data reduction program linking a Chemlab continuous flow analyser to a Commodore PET microcomputer
[IOS-176] 03 p0403 N85-12570
Reduction and analysis of data from the plasma wave instruments on the IMP-6 and IMP-8 spacecraft
[NASA-CR-175127] 04 p0460 N85-12918
The human role in space. Volume 2: Research analysis and technology report
[NASA-CR-171224] 04 p0548 N85-13474
TCAS 2 logic performance during phase one operational evaluation
[DOT/FAA/PM-84/20] 05 p0595 N85-13793
Measuring system and data evaluation methods of the test field for wind energy units at Pellworm 05 p0668 N85-14296
Utilization of SAGE aerosol profiles in the analysis of Mauna Loa stratospheric lidar data
[NASA-CR-174198] 05 p0675 N85-14332
Forecast impact of components of the FGGE observing system 05 p0681 N85-14373
Some new mathematical methods for variational objective analysis 05 p0681 N85-14375
The use of available potential energy to evaluate two GLAS FGGE data sets 05 p0682 N85-14387
Keeping up with operational loads in the French Air Force: Defining new equipment 07 p0896 N85-15681
Support for the Naval Research Laboratory Passive Microwave Clutter Analysis Program
[AD-A146771] 07 p0939 N85-15951
Results of the 1984 NASA/JPL balloon flight solar cell calibration program
[NASA-CR-174270] 07 p0991 N85-16294
Human factors characteristics of the Joint Tactical Fusion Test Bed: Field test 467 results
[AD-A146858] 07 p1020 N85-16476
Processing system for space VLBI 07 p1057 N85-16711
Reduction to outside the atmosphere and statistical tests used in Geneva photometry 08 p1251 N85-17902
Flux reconstruction and calibration 09 p1412 N85-18904
Analysis of a visual performance experiment
[DE85-000710] 10 p1530 N85-19645
Looking at multivariate data through fuzzy sets
[DE85-000684] 11 p1702 N85-20706
Image processing instrumentation for speckle interferometry and imaging
[AD-A149308] 11 p1762 N85-21084
A GC/MS (Gas Chromatograph/Mass Spectrometer) data management process. Part 1: User's guide, version 1.0
[PB85-116051] 12 p1803 N85-21309
Main component method used to study variations of cardiovascular parameters 12 p1901 N85-21939
Draftsman displays: A graphical technique for exploratory data analysis
[AD-A150515] 13 p2041 N85-22775
MAGSAT anomaly field data of the crustal properties of Australia
[E85-10100] 13 p2122 N85-23215
An investigation of the crustal properties of Australia and surrounding regions derived from interpretation of MAGSAT anomaly field data 13 p2122 N85-23216
Data selection techniques in the interpretation of MAGSAT data over Australia 13 p2123 N85-23218
Variational mesoscale satellite data assimilation and initialization
[NASA-CR-175704] 14 p2378 N85-24680
Scientific experiments. Preprocessing of scientific data — spaceborne experiments 14 p2398 N85-24779
Nonparametric estimation of density and hazard rate functions when samples are censored
[AD-A150946] 14 p2411 N85-24868
Kitt Peak measurements of P/Halley positions 14 p2436 N85-25023
On the orbit improvement results obtained by referring old cometary observations to the SAO Star Catalog 14 p2438 N85-25042
A new NASTRAN capability for data reduction 15 p2574 N85-25874
Plasma and magnetospheric research
[NASA-CR-171447] 15 p2591 N85-25976
VAS/model impact study 15 p2597 N85-26008
Interactive graphical data analysis
[DE85-005946] 15 p2631 N85-26215
Computer use in research for data analysis
[PB85-153567] 15 p2631 N85-26220
Jupiter/Voyager data analysis
[NASA-CR-175723] 15 p2679 N85-26545
Status of the observational data sets — TOPEX 16 p2804 N85-27286
Shuttle imaging radar-A (SIR-A) data analysis — geology of the Ozark Plateau of southern Missouri, land use in western Illinois, and vegetation types at Koonamore Station, Australia
[NASA-CR-175785] 16 p2809 N85-27324
Digital filters for application to data analysis in electron energy loss spectroscopy
[DE85-007932] 17 p2923 N85-28020
US Naval Observatory collection and utilization of time comparison data 17 p2962 N85-28292
Heating parameter estimation using coaxial thermocouple gages in wind tunnel test articles
[AD-A153039] 17 p2966 N85-28328
Flight testing for performance and flying qualities 18 p3058 N85-28920
Measurements of Solar Vector Magnetic Fields
[NASA-CP-2374] 18 p3203 N85-29669
Interactive graphics for a data analysis management system
[DE85-010977] 19 p3334 N85-30651
The application of artificial intelligence techniques to large distributed networks
[NASA-CR-177346] 19 p3344 N85-30721
Foundations of data envelopment analysis for Pareto-Koopmans efficient empirical productions functions
[AD-A154244] 19 p3346 N85-30735
User's guide for the Mk-3 D-coronameter data system
[PB85-181204] 19 p3385 N85-31002
Use of MIMLE3 to determine lower order equivalent systems in the time domain
[AD-A154700] 21 p3554 N85-32112
In-situ measurement of wall thermal performance: Data interpretation and apparatus design recommendations
[DE85-011979] 21 p3566 N85-32289
SSMIR (Solid State Memory Instrumentation Recorder): A new approach to acquiring data during an aircraft seat/sled ejection sequence
[AD-A154780] 21 p3589 N85-32308
A modified Fresnel scattering model for the parameterization of Fresnel returns, part 2.3A 21 p3618 N85-32483
Overview of on-line data processing for MST radars (keynote paper), part 7 21 p3625 N85-32519
Analysis of spacecraft data
[NASA-CR-171597] 21 p3669 N85-32790
Search for bursts in air shower data
[OG-5.3-10] 22 p3885 N85-34076
Time-resolved spectroscopic studies of detonating heterogeneous explosives
[DE85-009760] 23 p3921 N85-34297
Computer graphics for multivariate data 23 p3958 N85-34528
An image management kernel for the design of relational and pictorial data bases 23 p3958 N85-34532
Spatial trees: A fast access method for unstructured graphical data 23 p3958 N85-34533
New Matsushiro underground cosmic ray station (220 M.W.E. in depth)
[SH-9.1-14] 23 p4052 N85-35129
A suggested standardized format for cosmic ray ground-level event data
[SH-9.1-15] 23 p4052 N85-35130
Three-dimensional gravity ideal body studies in rough terrain
[DE85-014097] 24 p4118 N85-35525
Users guide for optimum interpolation method of global data assimilation
[AD-A155929] 24 p4138 N85-35648
DATA RETRIEVAL
Facsimile transmission of microforms
[AD-A144655] 01 p0038 N85-10236
SITIM system: Object manager module
[INPE-3284-NTE/226] 02 p0240 N85-11564
NSSDC and WDC-A-R and S document availability and distribution services
[NASA-TM-87374] 03 p0436 N85-12767
Human reliability data bank: Feasibility study
[DE84-015215] 04 p0546 N85-13476
International information networks for material properties
[DE84-013836] 04 p0576 N85-13676
Optimal query processing in distributed data base management systems with data redundancy 05 p0734 N85-14722
Retrieval procedures for hydrologic data from ARS (Agricultural Research Service) experimental watersheds in the US (REPHLEX)
[PB85-111326/GAR] 09 p1402 N85-18828
Solid propellant combustion diagnostics and automated data retrieval from holograms 13 p1998 N85-22527
Notes for medical catalogers, 1984
[PB85-180206] 18 p3200 N85-29853
CODA: A concept organization and development aid for the research environment
[AD-A154240] 19 p3343 N85-30715
MANHIST user's guide
[DE85-010884] 19 p3348 N85-30754
The international scope of data evaluation
[DE85-005953] 19 p3349 N85-30760
Sample interchange of MST radar data from the Urbana radar 21 p3627 N85-32531
Technology transfer system automation implementation
[PB85-177335] 22 p3849 N85-33838
NAPGEN: Automatic NAPLPS page generator 23 p3964 N85-34575
Federal Mineral Land Information System 24 p4106 N85-35459
EPALIT: A data management system applied to the control and retrieval of technical reports
[PB85-193068] 24 p4166 N85-35826
DATA SAMPLING
Adaptive preprocessing system
[AD-D011327] 07 p0937 N85-15935
Diamonds and diamond sorting
[PB85-128502] 10 p1542 N85-19726
Main component method used to study variations of cardiovascular parameters 12 p1901 N85-21939
Measurement requirements for the detection of ozone trends 13 p2105 N85-23115
Application of model following control and estimation techniques to attitude control of maneuvering spacecraft. Part 1: Theory and simulation results
[NLR-TR-82116-U-PT-1] 18 p3065 N85-28957
The HURRA high resolution experimental radar system sampling unit
[FOA-C-30376-E1] 18 p3091 N85-29133
The Mk.1 NPL digital sampling ac wattmeter
[NPL-DES-82] 22 p3758 N85-33290
Theoretical principles of vertical subsampling of color difference signals at half the sampling rate — television
[FI-447-TBR-18] 23 p3926 N85-34332
DATA SIMULATION
Comparison of land cover information from LANDSAT Multispectral Scanner (MSS) and airborne Thematic Mapper simulator (TMS) data for hydrologic applications — Clinton River Basin, Michigan 13 p2122 N85-23211

Calibration and use of clutter data for simulation
[AD-A154793] 21 p3574 N85-32229

DATA SMOOTHING

The approximation of nonsmooth solutions of hyperbolic partial differential equations
[CSIR-TWISK-297] 01 p0108 N85-10723
A variable span smoother
[AD-A148241] 08 p1215 N85-17655
Smoothing with split linear fits
[AD-A149032] 10 p1545 N85-19740
Locally-weighted-regression scatter-plot smoothing (LOWESS): A graphical exploratory data analysis technique
[AD-A152239] 16 p2855 N85-27609
Fast moving average recursive least mean square fit
[DE85-010036] 19 p3348 N85-30752
Smoothing surface data by spline functions
[AD-A155829] 24 p4142 N85-35678
Two methods of global data assimilation
[AD-A155961] 24 p4143 N85-35684

DATA STORAGE

Requirements and specifications for cartographic video discs
[AD-A144906] 01 p0049 N85-10325
A modular data acquisition and display software system for a laboratory environment
[PB84-217892] 01 p0105 N85-10709
Storage in the LLNL Octopus network: An overview and reflections
[DE84-014711] 01 p0106 N85-10712
SITIM system: Object manager module
[INPE-3284-NTE/226] 02 p0240 N85-11584
ADAM: An abstract database machine
[RSRE-84007] 02 p0293 N85-11904
Archiving and exchange of a computerized marine seismic database: The ROSE (Rivera Ocean Seismic Experiment) data archive system
[AD-A145658] 02 p0294 N85-11908
Factors affecting the archiving, processing and dissemination of ERS-1 altimeter data
03 p0361 N85-12435
Standardization of data formats for radar altimeter data
03 p0384 N85-12455
Human reliability data bank: Feasibility study
[DE84-015215] 04 p0546 N85-13476
Multichannel electrooptical modulators for digital information storage and processing systems
07 p0950 N85-19021
Data handling for the Spectral Radiometer (SPERAD)
[FOA-C-30368-E1,E4] 07 p0968 N85-16145
Data stimulated on-line-checking (IROLD)
08 p1066 N85-16754
Benchmarking database systems in multiple backend configurations
[AD-A148191] 08 p1202 N85-17568
Computer center CDC Libraries-PROCFIL (procedures)
[AD-A148633] 08 p1206 N85-17589
Performance evaluation of a database system in multiple backend configurations
[AD-A148192] 08 p1229 N85-17743
Boring information and subsurface data base package user's guide
[AD-A148623] 08 p1230 N85-17747
Computer center CDC libraries/utility (programs)
[AD-A148680] 09 p1366 N85-18593
FLAD user's manual: FLAD file contents
[AD-A148700] 09 p1368 N85-18594
Satellite-computer interface 10 p1476 N85-19318
Computer center CDC libraries
[AD-A149005] 10 p1540 N85-19707
ADAPS (Airborne Data Acquisition and Processing System) operation and maintenance manual
[AD-A149297] 11 p1585 N85-19983
RAPIDbus: Design of an extensible multiprocessor structure
[AD-A150061] 12 p1912 N85-21908
The intelligent database machine
12 p1949 N85-22242
Role of optical disk at computing centers
[DE85-005124] 13 p2145 N85-23314
Performance evaluation of distributed systems with unbalanced flows: An analysis of the INFOPLEX data storage hierarchy
[AD-A150528] 13 p2147 N85-23328
General design considerations of an Air Force information system
[AD-A150811] 13 p2168 N85-23449
West Europe report: Science and technology
[JPRS-WST-84-026] 15 p2532 N85-25617
Philips tested new materials for optical data storage
15 p2532 N85-25620
China report: Science and technology
[JPRS-CST-85-007] 15 p2533 N85-25621
Microprocessor controlled storage sampling oscilloscope
15 p2533 N85-25622
Use of a network of telemetered meteorological stations for prediction of the distribution of an atmospheric tracer
16 p2831 N85-27458
A climatic data bank for Northern Hemisphere land areas, 1851-1980
[DE85-007663] 16 p2835 N85-27486
Study of raster metafile formats
[AD-A153322] 17 p3012 N85-28624
Replication methods for abstract data types
[AD-A153648] 18 p3162 N85-29587
A stored data acquisition system: Update
[DE85-010534] 18 p3166 N85-29616
ZOG-Vinson technology demonstration project. Volume 2: System description
[AD-A153871] 19 p3333 N85-30645
ZOG/VINSON technology demonstration project system description. Volume 1
[AD-A154211] 19 p3342 N85-30713
CODA: A concept organization and development aid for the research environment
[AD-A154240] 19 p3343 N85-30715
Characteristics of a numerical fluid dynamics simulator
[DE85-009602] 21 p3586 N85-32290
Problems and solutions in analyzing partial-reflection drift data by correlation techniques
21 p3626 N85-32529
Sample interchange of MST radar data from the Urbana radar
21 p3627 N85-32531
Development of a dedicated speech work station
[AD-A155465] 21 p3674 N85-32824
The automatic labeling of geographic maps: A problem in computer aesthetics
23 p3962 N85-34561
Building an octree from a set of parallelepipeds
23 p3964 N85-34572
Balloon-borne video cassette recorders for digital data storage
[OG-9.3-11] 23 p4028 N85-34966
A suggested standardized format for cosmic ray ground-level event data
[SH-9.1-15] 23 p4052 N85-35130

DATA STRUCTURES

An algorithm for assembly of stiffness matrices into a compacted data structure
[AD-A146727] 07 p1023 N85-16492
GADB: A database facility for modelling naturally occurring geophysical fields 13 p2122 N85-23217
Synthesis of tree-structured computing systems through use of closures
[AD-A150502] 13 p2147 N85-23326
Invariant system of technological preparation of production 14 p2268 N85-24056
Data structure considerations in automatic cartography
15 p2583 N85-25930

DATA SYSTEMS

Field tests of the real-data acquisiton system for the NASA-LaRC differential absorption lidar
[NASA-CR-174020] 01 p0106 N85-10710
Time invariant memoryless nonlinear systems identification method
[FUB-9-1983] 01 p0114 N85-10773
Automated Data Systems (ADS) documentation standards
[AD-A144867] 01 p0125 N85-10857
Data dictionary systems and their role in information resource management
[AD-A144905] 01 p0125 N85-10859
Business planning for information services under special consideration of German management information systems
[BMFT-FB-ID-83-007] 02 p0294 N85-11910
Factors affecting the archiving, processing and dissemination of ERS-1 altimeter data
03 p0361 N85-12435
A microprocessor data system for developing countries — climatology 07 p1003 N85-16377
Shuttle payload S-band communications system
08 p1100 N85-16950
Survey of remote data monitoring systems
[DE85-001385] 09 p1323 N85-18313
General design considerations of an Air Force information system
[AD-A150611] 13 p2168 N85-23449
Applications of ARGOS data collection systems in Arctic regions 14 p2238 N85-23875
Applications of ARGOS data collection system for automatic meteorological observatories in Arctic regions
14 p2240 N85-23893
Geostationary Operational Environmental Satellite Data Collection System 14 p2328 N85-24393
NOAA'S role in support of service ARGOS
14 p2328 N85-24394
Service ARGOS technical report and improvement
14 p2328 N85-24395
Data-link alternatives for the NASA pilot data systems
[NASA-TM-85999] 14 p2412 N85-24873
NOAA satellite operations: Programs briefing — Environmental satellites, LANDSAT, and space station polar platform 15 p2599 N85-26020
Computer use in research for data analysis
[PB85-153567] 15 p2631 N85-26220
Determining availability characteristics of DSN data systems using discrepancy report data
16 p2772 N85-27100
US Naval Observatory collection and utilization of time comparison data 17 p2962 N85-28292
A comparison of numeric data entry with touch-sensitive and conventional numeric keypads
[AD-A153276] 17 p3008 N85-28598
The IRAS end-to-end data system
[NLR-MP-83056-U] 17 p3051 N85-28883
CSIN (Chemical Substances Information Network) workbook: US Geological Survey training course for Chemical Substances Information Network
[PB85-170058] 18 p3200 N85-29855
The international scope of data evaluation
[DE85-005953] 19 p3349 N85-30760

DATA TRANSMISSION

NT CODE DIVISION MULTIPLE ACCESS
NT FREQUENCY DIVISION MULTIPLE ACCESS
NT MULTIPLE ACCESS
NT SINGLE CHANNEL PER CARRIER TRANSMISSION

Facsimile transmission of microforms
[AD-A144855] 01 p0038 N85-10236
Interaction of voice and data traffic in a packet switching communication network and virtual circuit
[FUB-83-1982] 01 p0039 N85-10249
The average power density spectra of additive scrambler signals and their versions in AMI code
[FUB-27-1983] 01 p0040 N85-10258
Center for Electronics and Electrical Engineering Technical Bulletin covering center programs
[PB84-219716] 01 p0045 N85-10295
REMOTE: Modem Communicator Program for the IBM personal computer
[DE84-015047] 01 p0100 N85-10665
High-data-rate wide-angle underwater acoustic telemetry system
[DE84-015696] 02 p0233 N85-11519
Shuffle-exchanges on augmented meshes
[NASA-CR-172476] 02 p0243 N85-11587
Mission science value-cost savings from the Advanced Imaging Communication System (AICS)
[NASA-CR-174170] 04 p0458 N85-12905
Regenerators of binary pulses for optical communication systems 04 p0485 N85-13099
Digital raster timing encoder-decoder
[AD-D011279] 06 p0804 N85-15120
Wavelength coded image transmission and holographic optical elements
[AD-A146490] 06 p0810 N85-15147
Recent advances in data compression
[DE85-001133] 06 p0854 N85-15432
Methodology investigation. Streamlined Test Reporting and Planning (STRAP): Data flow procedures
[AD-A146463] 06 p0871 N85-15531
National airspace system configuration management interface control document. Maintenance processor subsystem to remote monitoring subsystems and remote monitoring subsystem concentrators
[NAS-MD-790] 07 p0900 N85-15705
A modified Monte-Carlo technique for the simulation of satellite communication systems
[AD-A148689] 08 p1214 N85-17641
Dissemination of ERS-1 low bit rate data and the use of L-band receiving stations
[NLR-TR-83049-U] 09 p1358 N85-18542
Directory of range data conversion and processing systems
[AD-A148996] 10 p1427 N85-19001
An ionospheric mode detection system for HF communications application 10 p1471 N85-19282
Time and space domain filtering for improved HF communication 10 p1473 N85-19298
Serial data transmission with large output on the HF channel 10 p1475 N85-19305
Worldwide report: Telecommunications policy, research and development
[JPRS-TTP-85-006] 10 p1476 N85-19314
Commentary on start of scientific data transmissions with USSR 10 p1476 N85-19319
L.F. RADIO-DATA: Specification of BBC phase-modulated transmissions on long-wave
[BBC-RD-1984/19] 12 p1822 N85-21431
The 20:16 block code for digital recording and transmission channels
[BBC-RD-1985/1] 12 p1824 N85-21443
The intelligent database machine
12 p1949 N85-22242

Experimental results on the application of convolutional coding and Viterbi decoding as a frequency diversity technique in HF data transmission
[CRC-1377] 13 p2052 N85-22850
Data compression for noiseless channels
13 p2053 N85-22851
Integrated digital networks
[AD-A150605] 13 p2056 N85-22873
Noise immunity of information transmission system with pseudorandom frequency switching under worst-case interference conditions 13 p2066 N85-23029
Authorizing appropriations to the National Aeronautics and Space Administration for fiscal year 1986
[H-REPT-99-32] 13 p2166 N85-23452
The ARGOS system and hydrology. Results obtained by ORSTROM and benefits of a degree of standardization 14 p2239 N85-23881
Accurate baseline determination by radio interferometry on NAVSTAR GPS satellite transmissions
[AD-A150681] 14 p2291 N85-24202
The ARGOS communications performance trials
14 p2326 N85-24376
Location and data collection for long stratospheric balloon flights 14 p2326 N85-24377
Measurement of water equivalent of mountain snow cover — ARGOS system 14 p2327 N85-24386
Hydrology and climatic conditions in Greenland
14 p2327 N85-24387
The ARGOS system and hydrology: The use of Platform Terminal Transmitter (PTT) with built-in memory and direct reception by the Seine basin hydrology service
14 p2328 N85-24389
Direct readout and dissemination of results using ARGOS keypad terminals 14 p2328 N85-24390
NOAA'S role in support of service ARGOS
14 p2328 N85-24394
Data transmission using ARGOS keypad platform transmitter terminals (PTT) 14 p2330 N85-24407
Analysis of atmospheric interferometer data
[AD-A150682] 14 p2372 N85-24683
ADCCP (Advanced Data Communication Control Procedure) communication processor
[AD-D011595] 15 p2544 N85-25709
Computer use in research for data analysis
[PB85-153567] 15 p2631 N85-26220
A method of estimating aircraft attitude from fly by wire flight control system data 16 p2697 N85-26853
The Record of Electrical and Communication Engineering Conversazione, volume 53, no. 2, November 1984
[ISSN-0385-7719] 16 p2758 N85-27022
Historical perspectives on information transmission engineering 16 p2759 N85-27023
Optical non-line-of-sight covert, secure high data communication system
[AD-D011607] 16 p2769 N85-27067
Meteorological factors in Earth-Satellite propagation
[NASA-CR-175764] 16 p2769 N85-27069
Evaluation of Ada (trademark) as a communications programming language, volume 1
[AD-A152314] 16 p2848 N85-27559
Evaluation of Ada (trademark) as a communications programming language. Volume 2: Communications protocols application
[AD-A152315] 16 p2848 N85-27560
Rational pulse-shaping filters for almost MSK-like modulation
[AD-A153065] 17 p2949 N85-28208
Automation of Precise Time Reference Stations (PTRS) 17 p2962 N85-28291
UHF IRIG G distribution system
17 p2965 N85-28308
A new technique for system-to-system transfer of surface data 17 p3007 N85-28589
Interfacing the VAX 11/780 using berkeley UNIX 4.2BSD and Ethernet based Xerox Network Systems
[AD-A153174] 17 p3016 N85-28647
Torus data flow for parallel computation of missized matrix problems
[DE85-006761] 17 p3026 N85-28715
A concatenated coding scheme for error control
[NASA-CR-178006] 19 p3334 N85-30655
The application of artificial intelligence techniques to large distributed networks
[NASA-CR-177346] 19 p3344 N85-30721
Fiber optics in transient radiation fields
[DE85-010721] 19 p3368 N85-30896
Navigation data for Emergency Position Indicating Radio Beacons (EPIRBs) 20 p3403 N85-31115
Transmission Monitoring and Control (TRAMCON) segmentation plan for the DCS (Defense Communications System) digital transmission network
[AD-A154175] 20 p3440 N85-31351
Microprocessor AirborneData Acquisition and Replay (MADAR) system
[AD-A151728] 20 p3514 N85-31843
Determining functional requirements for NASA Goddard's command management system software design using expert systems 20 p3539 N85-32020
Proust radar: Decoding hardware and coherent integration, part 7.2A 21 p3626 N85-32524
Design guidelines for user-system interface software
[AD-A154907] 21 p3671 N85-32807
An image compression survey and algorithm switching based on scene activity
[NASA-TP-2458] 22 p3727 N85-33106
Telemetry system for the transmission of data from projectiles during the acceleration phase in the gun barrel
[ISL-CO-207/84] 22 p3739 N85-33178
A model for predicting propagation-related DSCS (Defense Communications Engineering Center) margin requirements
[AD-A155355] 22 p3756 N85-33281
Estimating optimum technical and economic indicators of data transmission systems 22 p3777 N85-33406
Developmental trends in radio receiver design
22 p3777 N85-33407
Characteristics of optical information-measurement channels with utilization of scattering effects
22 p3781 N85-33429
IGES/RIM Parser/Converter users guide
[DE85-011965] 22 p3829 N85-33716
Optimizing data access in the LAMPF control system
[DE85-012653] 24 p4140 N85-35683
Investigation of cosmic rays in very short time scales
[HE-4.6-7] 24 p4197 N85-36044

DATING
U CHRONOLOGY
U TIME MEASUREMENT

DAWN CHORUS
ELF chorus in the Earth's outer magnetosphere
14 p2366 N85-24624
Conjugacy of ELF-VHF emissions near L=6 — chorus phenomenon, hiss 14 p2367 N85-24629

DAYTIME
On some new features of semiannual variation of the geomagnetic field 04 p0520 N85-13327
Dayside cusp aurora 04 p0521 N85-13333
Correlations of solar irradiance and daylight illuminance for building energy analysis
[DE85-001736] 06 p0839 N85-15328

DC (CURRENT)
U DIRECT CURRENT

DC 8 AIRCRAFT
Aircraft accident report: Flying Tigers, Inc., Flight 2468, McDonell Douglas DC8-63, N797FT, Chambers Field, Naval Air Station, Norfolk, Virginia, October 25, 1983
[PB84-910408] 02 p0136 N85-10925

DC 9 AIRCRAFT
Safety recommendation(s), A-84-76 through -78
[REPT-3751E] 15 p2466 N85-25224

DC 10 AIRCRAFT
Results of winglet development studies for DC-10 derivatives
[NASA-CR-3677] 02 p0138 N85-10936
Safety recommendation(s), A-84-123 and -124
[REPT-3694B/93] 15 p2466 N85-25222
DC-10 winglet flight evaluation
[NASA-CR-3704] 19 p3217 N85-29949
Flight-service program for advanced composite rudders on transport aircraft
[NASA-CR-174537] 19 p3217 N85-29950
Aircraft accident report: World Airways Inc., Flight 30H, McDonnell Douglas DC-10-30CF, N113WA, Boston-Logan International Airport, Boston, Massachusetts, January 23, 1982
[PB85-910406] 22 p3728 N85-33114

DDT
Development of a PETN DDT detonator
[DE84-016944] 09 p1302 N85-18178
CP DDT detonators. Part 1: Design sensitivity study
[DE84-017255] 09 p1302 N85-18180

DE HAVILLAND AIRCRAFT
NT DH 115 AIRCRAFT
NT DHC 2 AIRCRAFT

DE HAVILLAND DH 115 AIRCRAFT
U DH 115 AIRCRAFT

DE LAVAL NOZZLES
U CONVERGENT-DIVERGENT NOZZLES

DEACCLIMATIZATION
U ACCLIMATIZATION

DEACTIVATION
Adsorption thermodynamics and surface transport of metal catalyst poisons
[DE85-002868] 10 p1441 N85-19084
Elementary processes of electronically excited particles. Part 5: Deactivation of CHF (A1a' (O, V'2, O) after excitation by a pulsed dye laser
[MPIS-13/1984] 14 p2420 N85-24930

DEAD RECKONING
Reference systems for the evaluation of dead-reckoning navigation equipment 13 p1967 N85-22358

DEADWEIGHT
U STATIC LOADS

DEAFNESS
U AUDITORY DEFECTS

DEATH
Fatal hemorrhagic shock and acetate solutions
[AD-A146754] 07 p1014 N85-16444
Effects of long-term low-level radiofrequency radiation exposure on rats. Volume 8: Evaluation of longevity, cause of death, and histopathological findings
[AD-A154283] 19 p3327 N85-30610

DEATH VALLEY (CA)
Assessment of computer based geologic mapping of rock units in the LANDSAT-4 scene of northern Death Valley, California 13 p2119 N85-23195
Geology: Structural history and fluvial geomorphology of the southern Death Valley Fault Zone, Inyo and San Bernardino Counties, California
24 p4114 N85-35506

DEBRIS
NT SPACE DEBRIS
Microfluorescence studies of zirconium oxide
[DE84-016116] 03 p0329 N85-12116
Debris control design achievements of the booster separation motors 08 p1096 N85-16942
On the latitudinal distribution of debris in the Northern Hemisphere of Mars 13 p2188 N85-23579
Marine Sample Exploitation Project: Estimates regarding the sensitivity and technology for the detection of nuclear explosion debris in the marine environment
[DE85-013176] 23 p3947 N85-34462

DEBUGGING
U CHECKOUT

DEBYE TEMPERATURE
U SPECIFIC HEAT

DECAMETRIC WAVES
The catalogue of the discrete sources in the declination range from -13 deg to -2 deg
[NASA-TM-77594] 01 p0129 N85-10887
Interferometry with decametric waves (review)
06 p0761 N85-14996
Analysis of Jovian decametric data: Study of radio emission mechanisms
[NASA-CR-174206] 08 p1258 N85-17917
Standing wave pattern of HF radio waves in the ionospheric reflection region. Part 1: General formulas
[UIO-SR-84-05-PT-1] 09 p1313 N85-18253
Three dimensional ray tracing of the Jovian magnetosphere in the low frequency range
[NASA-CR-175462] 10 p1571 N85-19909
Analysis of Jovian decametric data: Study of radio emission mechanisms
[NASA-CR-176057] 22 p3851 N85-33846

DECARBONATION
Shock-induced CO2 loss from CaCO3: Implications for early planetary atmospheres
[NASA-CR-174197] 05 p0745 N85-14777

DECARBURIZATION
Thermodynamics of decarburization of niobium-bearing high-alloy melts
[BLL-M-35728-(5828.4)] 02 p0175 N85-11169
Production process for steel with decarburized surface adapted for single coating enameling
[BMFT-FB-T-85-022] 20 p3432 N85-31292

DECAY
NT ACOUSTIC EMISSION
NT ALPHA DECAY
NT BIOLUMINESCENCE
NT CATHODOLUMINESCENCE
NT CHEMILUMINESCENCE
NT CN EMISSION
NT ELECTROLUMINESCENCE
NT ELECTRON EMISSION
NT EMISSION
NT EXHAUST EMISSION
NT FIELD EMISSION
NT FLUORESCENCE
NT HALF LIFE
NT HYDROXYL EMISSION
NT INCANDESCENCE
NT ION EMISSION
NT LIGHT EMISSION
NT LUMINESCENCE
NT MICROWAVE EMISSION
NT NEUTRON DECAY
NT NEUTRON EMISSION
NT NUCLEAR FISSION
NT OPTICAL RESONANCE
NT PARTICLE EMISSION
NT PHOSPHORESCENCE
NT PHOTOELECTRIC EFFECT
NT PHOTOELECTRIC EMISSION
NT PHOTOIONIZATION

NT PHOTOLUMINESCENCE
NT PHOTOPRODUCTION
NT RADIO EMISSION
NT RADIOACTIVE DECAY
NT RESONANCE FLUORESCENCE
NT SECONDARY EMISSION
NT SHOCK WAVE LUMINESCENCE
NT SOLAR RADIO BURSTS
NT SOLAR RADIO EMISSION
NT SPECTRAL EMISSION
NT SPONTANEOUS EMISSION
NT STIMULATED EMISSION
NT STRANGENESS
NT THERMAL EMISSION
NT THERMIONIC EMISSION
NT THERMOLUMINESCENCE
NT TYPE 3 BURSTS
NT TYPE 4 BURSTS
NT WATER MASERS
NT WEAK ENERGY INTERACTIONS
NT X RAY FLUORESCENCE

Searching for top, Higgs, and supersymmetry: The minimum invariant mass technique
[DE84-014539] 01 p0119 N85-10813

The search for proton decay: Introduction
[DE84-014349] 01 p0131 N85-10904

Experimental medium energy physics
[DE84-014825] 02 p0273 N85-11807

Irregularity decay in an isolated plasma bubble
[AD-A145782] 03 p0392 N85-12506

Surface and allied studies in silicon solar cells
[NASA-CR-174447] 11 p1671 N85-20531

Simulating supersymmetry at the SSC
[DE85-000699] 11 p1736 N85-20917

Decaying particles do not heat up the Universe
[DE85-002191] 11 p1763 N85-21091

Nuclear structure problems in double beta decay
[DE85-010739] 19 p3364 N85-30859

Aircraft investigations of the distribution of aerosols in the lower troposphere 21 p3647 N85-32859

Application of evaluated fission-product delayed-neutron precursor data in reactor kinetics calculations
[DE85-012726] 23 p3972 N85-34624

Pulsed-neutron-source models for the astrophysical s-process
[DE85-012927] 24 p4151 N85-35740

High energy physics at Tufts University
[DOE/ER-40085/7] 24 p4152 N85-35744

On mini-cluster observed by Chacaltaya emulsion chamber experiment
[HE-3.8-12] 24 p4185 N85-35959

A study of atmospheric neutrinos with the IMB detector
[HE-5.3-7] 24 p4205 N85-36101

Energy spectra of high energy atmospheric neutrinos
[HE-5.3-14] 24 p4206 N85-36108

A standard source for high energy neutrino astronomy
[HE-5.3-15] 24 p4206 N85-36109

DECAY RATES

Velocity-changing collisional effects in nonlinear atomic spectroscopy and photon echo decay in gases
[NASA-CR-174159] 04 p0559 N85-13559

The stability of the low-degree 5-minute solar oscillations 14 p2444 N85-25084

Some nuclear data needs in astrophysics
[DE85-012916] 24 p4188 N85-35842

DECELERATION

NT SPIN REDUCTION

Laser cooling and trapping of neutral atoms
[AD-A146048] 03 p0366 N85-12345

Deceleration, cooling, and trapping of atoms
[AD-A146234] 03 p0416 N85-12572

Nondestructive deceleration of a rocket sled — target penetration tests
[FOA-C-20549-D3] 07 p0912 N85-15771

Optical flow and texture variables useful in detecting decelerating and accelerating self-motion
[AD-A146718] 09 p1384 N85-18703

Improving inflight negative Gz restraint for aircrewmen
[AD-A151909] 16 p2703 N85-26686

Why do leaky-box models work so fine?
[OG-7.2-8] 23 p4014 N85-34677

Instabilities in decelerating supersonic flows with applications to cosmic ray shocks
[OG-8.1-2] 23 p4017 N85-34892

Deceleration of a supersonic flow behind a curved shock wave with isentropic precompression
[NASA-TM-77920] 24 p4061 N85-35164

Applications of decelerated ions
[DE85-011832] 24 p4156 N85-35787

DECELERATORS

U BRAKES (FOR ARRESTING MOTION)

DECIDUOUS TREES

Changes in spectral properties of detached leaves
[E85-10042] 07 p0983 N85-16243

Effect of elevated atmospheric CO2 on plant communities
[DE85-001810] 11 p1678 N85-20576

Microwave model prediction and verifications for vegetated terrain
[E85-10102] 16 p2809 N85-27322

DECIMETER WAVES

Metric-wave and decimetric-wave aperture synthesis systems (review) 06 p0782 N85-14998

Decimetric-wave aperture synthesis system at Scientific Research Institute of Radiophysics 06 p0782 N85-15000

DECISION ELEMENTS

U LOGICAL ELEMENTS

DECISION MAKING

Hydrologic and economic models for watershed evaluation and research
[PB84-222371] 01 p0066 N85-10436

Some concepts in multi-criteria optimization
[CSIR-TWISK-299] 01 p0106 N85-10722

The inferring of preferences from indifferences in multicriteria decision analysis
[CSIR-TWISK-306] 01 p0108 N85-10729

Command control group behaviors. Objective 1: A methodology for and identification of command control group behaviors
[AD-A145690] 02 p0191 N85-11279

Robotics investment decision model user's manual
[AD-A145467] 02 p0204 N85-11347

Eyelid motion sequences predictive of decision errors
[AD-A145702] 02 p0235 N85-11531

Effects of alternative chromatic mixed graphics displays in decision support systems
[AD-A145561] 02 p0242 N85-11578

Artificial intelligence applications to automatic test equipment
[AD-P003936] 02 p0247 N85-11616

A mathematical theory of command and control structures
[AD-A145608] 02 p0256 N85-11675

Decision Support System (DSS): A survey
[NRIMS-TWISK-317] 02 p0292 N85-11896

Decision process models of contractor behavior: The development of effective contract incentives
[AD-A145524] 02 p0292 N85-11898

Research in knowledge representation for natural language understanding
[AD-A145807] 03 p0409 N85-12613

Psychological issues in the design of expert systems
[AD-A146081] 03 p0438 N85-12792

System status display information
[NASA-CR-172347] 04 p0455 N85-12889

Ocean services user needs assessment. Volume 1: Survey results, conclusions and recommendations
[NASA-CR-174104] 04 p0541 N85-13445

Analysis of the impact of error detection on computer performance
[NASA-CR-174167] 04 p0547 N85-13477

Evaluation of automated decisionmaking methodologies and development of an integrated robotic system simulation
[NASA-CR-172401] 04 p0552 N85-13516

Real-time planning by an intelligent robot
[DE84-016669] 04 p0553 N85-13519

Induction of fuzzy decision rules
[INPE-3053-PRE/474] 04 p0554 N85-13525

R and D project selection with nonnumerical returns
[INPE-2760-PRE/335] 04 p0575 N85-13665

Dynamic decision making — and programming
[FOA-C-53015-H2] 04 p0575 N85-13668

Utilization of historic information in an optimization task 05 p0700 N85-14490

A model for the effectiveness of aircraft alerting and warning systems 05 p0702 N85-14506

On looking into the black box: Prospects and limits in the search for mental models 05 p0709 N85-14546

Issues in developing a normative descriptive model for dyadic decision making 05 p0709 N85-14547

Getting mental models and computer models to cooperate 05 p0709 N85-14548

A full mission simulator study of aircrew performances: The measurement of crew coordination and decisionmaking factors and their relationships to flight task performances 05 p0710 N85-14556

Communication on the flight deck 05 p0711 N85-14557

On choosing between two probabilistic choice sub-models in a dynamic multitask environment 05 p0711 N85-14563

Multi-crew model analytic assessment of landing performance and decision-making demands 05 p0712 N85-14567

A framework for research on adaptive decision aids
[AD-A136331] 05 p0734 N85-14719

Man-machine interface requirements - advanced technology 06 p0753 N85-14825

Critical conditions for the automatic control of landing from decision height in variable winds
[UTIAS-284] 06 p0753 N85-14830

The application of artificial intelligence to contract management
[AD-A146661] 06 p0857 N85-15448

Survey relating to the implementation of cost/schedule control systems criteria within the Department of Defense and industry
[AD-A146664] 06 p0870 N85-15526

Performance evaluation of A-10 aircraft maintenance units and aircraft using constrained facet analysis
[AD-A146955] 07 p0893 N85-15660

Broadening the debate 07 p0914 N85-15785

Distribution and storage of aviation turbine fuel for military operations in northern Australia
[AD-A147180] 07 p0935 N85-15921

Ambiguity and uncertainty in probabilistic inference
[AD-A147378] 07 p1035 N85-16572

Development of a mixed scanning interactive system for decision support
[AD-A146895] 07 p1051 N85-16670

On the complexity of distributed decision problems
[AD-A147174] 07 p1052 N85-16674

Principles of multiobjective optimization
[AD-A147520] 07 p1052 N85-16679

Compatibility effects and preference reversals
[AD-A148399] 08 p1198 N85-17544

An application of discriminant analysis to the selection of software cost estimating models
[AD-A147632] 08 p1204 N85-17580

Probable cause: A decision making framework
[AD-A147842] 08 p1210 N85-17614

A theory of preference reversals
[AD-A147952] 08 p1216 N85-17661

An analysis of production competition and award methodology
[AD-A147775] 08 p1228 N85-17733

Decision making in stressful conditions: A model based on the coping perspective
[FOA-C-55064-H3] 08 p1229 N85-17738

Protocol for aquifer cleanup decision making at military installations
[AD-P004151] 09 p1349 N85-18487

Communications satellite needs examined 10 p1476 N85-19317

A validated methodology for determination of laboratory instrument computer interface efficacy
[AD-A149338] 10 p1487 N85-19391

Some effects of display format variables on the perception of aircraft spatial orientation 10 p1534 N85-19666

A decision model for selection of microcomputers and operating systems
[AD-A149076] 10 p1538 N85-19694

Efficient algorithm for fuzzy linear programming with multiple objectives
[AD-A149012] 10 p1544 N85-19736

The R and D project selection problem with fuzzy coefficients
[INPE-3329-PRE/626] 10 p1565 N85-19871

Research needs on the interaction between information systems and their users: Report of a workshop
[PB85-121523] 10 p1566 N85-19891

Development of computer centers, equipment described: Problems of computer centers 11 p1700 N85-20686

Meteorological and oceanographic support during the Falklands conflict 11 p1712 N85-20769

Data and information systems and decision making in large public organizations: Research agenda
[DE85-003639] 11 p1738 N85-20931

Computer aided of maintainability design: A feasibility study
[AD-A149293] 11 p1738 N85-20932

The effect of jamming/deception on decision making
[AD-A149740] 12 p1828 N85-21472

Automatic pickup of trajectory by method of sequential analysis taking into account deviation of radar markers from center of strobe 12 p1838 N85-21535

Report on the Second Annual Review Meeting of the National Acid Precipitation Assessment Program. Research to assist decisionmaking: Summary
[DE85-003003] 12 p1884 N85-21820

Choice reaction time and color: An annotated bibliography
[AD-A149722] 12 p1908 N85-21979

A replication and extension of the inducement of the availability heuristic
[AD-A149755] 12 p1923 N85-22083

A statistical approach to vendor selection
[AD-A149781] 12 p1950 N85-22249

Task influences in the analytic-intuitive approach to decision making
[AD-A149870] 12 p1950 N85-22250

Problems in decentralized decision making and computation
[AD-A150025] 12 p1950 N85-22251
Rejection of anomalous observations when determining spacecraft trajectories 13 p1979 N85-22421
Personal decision making: The influence of perceived locus of control and degree of rationality on information seeking strategies 13 p2167 N85-23446
Spaceborne power systems preference analyses. Volume 1: Summary
[NASA-CR-175644] 14 p2349 N85-24517
Spaceborne power systems preference analyses. Volume 2: Decision analysis
[NASA-CR-175645] 14 p2349 N85-24518
The integration of information from an analog-visual display: The role of dimensional integrality
[AD-A150756] 14 p2404 N85-24820
Gordon Conference on Fundamentals of Cybernetics
[AD-A151074] 14 p2408 N85-24842
Some applications of fuzzy sets and the analytical hierarchy process to decision making
[AD-A150720] 14 p2412 N85-24876
Preliminary helicopter design decision making based on flight performance factors
[AD-A151488] 15 p2471 N85-25254
A decision support methodology for space technology advocacy
[AD-A151885] 15 p2476 N85-25283
Computers and the consulting engineer 15 p2626 N85-26184
Equilibrium solutions, stabilities and dynamics of Lanchester's equations with optimization of initial force commitments
[AD-A151510] 15 p2637 N85-26266
Feasibility analysis of moving bank multiple model adaptive estimation and control algorithms
[AD-A152015] 15 p2641 N85-26292
Management: A bibliography for NASA managers
[NASA-SP-7500(19)] 15 p2664 N85-26439
Design adequacy: An effectiveness factor 16 p2695 N85-26642
Method of selecting robotized system design for pressing process 16 p2761 N85-27040
Diagnostic system
[INPE-3350-PRE/659] 16 p2841 N85-27519
Research in knowledge representation for natural language understanding
[AD-A152260] 16 p2851 N85-27579
Personal computer aided decision analysis
[AD-A151911] 16 p2875 N85-27743
Logical design of a decision support system to forecast technology, prices and costs for the national communications system
[AD-A152330] 17 p2948 N85-28196
The effects of controversy and concurrence seeking on effective decision making
[AD-A153370] 17 p3002 N85-28555
The interface with decision makers in interactive multiobjective linear programming
[REPT-84-38] 17 p3014 N85-28637
On estimating transition intensities of a Markov process with aggregate data of a certain type
[CWI-MS-R8411] 17 p3025 N85-28707
Multicriteria decision analysis as an aid to strategic planning of energy research and development
[REPT-84-02] 17 p3049 N85-28870
Hybrid uncertainty theory
[DE85-008357] 18 p3167 N85-29622
Accepting error to make less error
[AD-A153949] 18 p3171 N85-29651
The economics of private sector R and D decisionmaking in aeronautics
[NASA-CR-176007] 19 p3379 N85-30962
Interactive on-line conferences
[AD-A154723] 21 p3574 N85-32227
Search of the VAXintosh customizing VMS V4.0 for DCL windows
[DE85-011306] 22 p3831 N85-33729
Real-time multiparameter pulse processing with decision tables
[DE85-011683] 23 p3966 N85-34589
Opportunities for policy historians: The evolution of the US civilian space program 23 p4057 N85-35147
Manual and computer-aided sequential diagnostic inference
[AD-A156229] 24 p4133 N85-35620
DSS/MIS (Decision Support Systems/Management Information Systems) design and implementation for LAMPS Mk 3 utilizing a microcomputer and a maintenance personnel assignment program
[AD-A155652] 24 p4135 N85-35629

DECISION THEORY
NT STATISTICAL DECISION THEORY
A combined logistic regression and Zionts-Wallenius methodology for multiple criteria linear programming
[TWISK-314] 01 p0102 N85-10679
Research activities of the Illinois University Coordinated Science Laboratory
[AD-A145589] 03 p0449 N85-12856
Theory of information, automation in Czechoslovakia 04 p0485 N85-13091
Interaction of human cognitive models and computer based models in supervisory control
[AD-A142547] 07 p1020 N85-16474
Principles of multiobjective optimization
[AD-A147520] 07 p1052 N85-16679
A method for automatic water mass classification
[AD-D011405] 08 p1191 N85-17505
Compatibility effects and preference reversals
[AD-A148399] 08 p1196 N85-17544
Decentralized control of scheduling in distributed systems
[AD-A147688] 08 p1228 N85-17731
Strategic use of business graphics: A stakeholder approach 23 p3963 N85-34566

DECISIONS
Eyelid motion sequences predictive of decision errors
[AD-A145702] 02 p0235 N85-11531

DECKS (FLOORS)
U FLOORS

DECLINATION
The catalogue of the discrete sources in the declination range from -13 deg to -2 deg
[NASA-TM-77594] 01 p0129 N85-10887
Absolute measurement of Declination (D) by means of a proton magnetometer
[DMI-GEOPHYS-PAPERS-R-68] 22 p3836 N85-33751

DECODERS
Digital raster timing encoder-decoder
[AD-D011279] 06 p0804 N85-15120
Precision digital sampler
[AD-D011285] 06 p0809 N85-15143
Novel applications of the NASA/GSFC Viterbi decoder hardware simulator 08 p1101 N85-16957
Reed-Solomon decoder — applicable to Galileo Project requirements
[NASA-CASE-NPO-15562-1] 11 p1699 N85-20680
Stereo decoder without subcarrier restoration 13 p2068 N85-22921
A software simulation study of a sequential decoder using the Fano algorithm 16 p2771 N85-27100
A software simulation study of a (255,223) Reed-Solomon encoder-decoder
[NASA-CR-175872] 17 p2947 N85-28192
Noiseless coding for the Gamma Ray spectrometer
[NASA-CR-176201] 24 p4089 N85-35219

DECODING
Severe weather statistics STADTS decoder (SXW) and plotter (SWY)
[PB84-213693] 01 p0086 N85-10576
Sequential syndrome decoding of convolutional codes 05 p0624 N85-13992
Standard SHEF (Standard Hydrometeorologic Exchange Format) decoder Version 1.1
[PB85-108508/GAR] 06 p0840 N85-15332
Coding for reliable satellite communications
[NASA-CR-174315] 08 p1150 N85-17257
The algebraic structure of convolutional codes with application to code construction and decoding
[AD-A148770] 08 p1206 N85-17591
FLAD user's manual: FLAD file contents
[AD-A148700] 09 p1368 N85-18584
Further results on rate 1/N convolutional code constructions with minimum required SNR criterion 10 p1464 N85-19235
Fundamental limits to synchronization and tracking
[AD-A149623] 12 p1833 N85-21504
Experimental results on the application of convolutional coding and Viterbi decoding as a frequency diversity technique in HF data transmission
[CRC-1377] 13 p2052 N85-22850
A perspective on multiaccess channels
[AD-A150183] 13 p2148 N85-23322
Symbol stream combining in a convolutionally coded system 16 p2771 N85-27101
Proust radar: Decoding hardware and coherent integration, part 7.2A 21 p3626 N85-32524
L-step sequential decoding
[AD-A156121] 24 p4138 N85-35649
Pruned error-trails decoding of certain non-systematic convolutional codes
[AD-A156122] 24 p4138 N85-35650

DECOMPOSITION
NT CRACKING (CHEMICAL ENGINEERING)
NT HYDROGENOLYSIS
NT NITROLYSIS
NT PHOTODECOMPOSITION
NT PHOTODISSOCIATION
NT PHOTOLYSIS
NT RADIOLYSIS
NT THERMAL DECOMPOSITION
HMX combustion modification
[AD-A145071] 01 p0024 N85-10149
Theoretical studies in molecular fragmentation: Processes, energetics and diagnostics
[AD-A146310] 03 p0418 N85-12673
Deformation, fracture and explosive properties of reactive materials
[AD-A146396] 06 p0774 N85-14945
Metallo-Organic Decomposition (MOD) silver metallization for photovoltaics 06 p0830 N85-15278
Electrochemical production of silicon 06 p0832 N85-15290
The formation of isolated phase precipitates during the decomposition of high-coercive force Fe-Cr-Co alloys
[BLL-M-36028-(5826.4)] 07 p0924 N85-15855
Multiplex gas chromatography for use in space craft
[NASA-TM-86668] 09 p1290 N85-18097
Development of a polysilicon process based on chemical vapor deposition of dichlorosilane in an advanced Siemen's reactor
[NASA-CR-174445] 11 p1672 N85-20532
TEM/FIM study of modulated microstructures in the Fe-Be system
[DE85-005379] 13 p2023 N85-22678
Decomposition of VTAN alloy solid solution upon irradiation and thermal aging 13 p2029 N85-22712
Algorithm for singular decomposition
[DE85-016488] 13 p2152 N85-23361
Decomposition in problem of correcting inertial navigation systems 14 p2287 N85-24172
Solving large linear systems 14 p2396 N85-24759
Photovoltaic cell reliability research: Investigation of accelerated stress factors and failure-degradation mechanisms in terrestrial solar cells
[NASA-CR-175815] 16 p2819 N85-27388
A decomposition procedure for convex quadratic programs
[AD-A151732] 16 p2854 N85-27595
The decomposition of gas phase formaldehyde by plasma discharge
[AD-A153202] 17 p2921 N85-28007
Methanol adsorption on Pt(111)
[DE85-006802] 17 p2923 N85-28017
Powder-metallurgy alloys and steels
[BLL-BISI-TRANS-22239-(0022.06)] 17 p2926 N85-28050
Comparison of isothermal kerogen decomposition results using reactors with different heat-up rates
[DE85-006563] 19 p3237 N85-30068
Fundamental studies of beta phase decomposition modes in titanium alloys
[AD-A154122] 19 p3238 N85-30078
Method for production of ceramic oxide and carbide bodies by polymer inclusion and decomposition
[DE85-011668] 19 p3250 N85-30152
Decomposition of sulfuric acid using solar thermal energy
[DE85-012268] 21 p3564 N85-32170
Decomposing the joint distribution of several linear combinations of uniform spacings
[AD-A155056] 21 p3677 N85-32845

DECOMPRESSION
U PRESSURE REDUCTION

DECOMPRESSION SICKNESS
Hyperbaric physiology (status and prospects) 08 p1194 N85-17521
A theoretical method for selecting space craft and space suit atmospheres
[AD-A148219] 08 p1200 N85-17559
Assessing the short- and long-term health effects of decompression sickness among US Navy divers
[AD-A151687] 15 p2618 N85-26132

DECONTAMINATION
Characterization of jet-contaminant interaction flow in chemical decontamination
[AD-A147298] 08 p1161 N85-17327
Remedial action of hazardous waste US Army Corps of Engineers, Anniston, Alabama
[AD-P004141] 09 p1347 N85-18477
Incineration of explosives contaminated soils
[AD-P004142] 09 p1347 N85-18478
Stabilization of contaminated soils by in situ vitrification
[AD-P004144] 09 p1348 N85-18480
Community relations activities at Department of Defense sites
[AD-P004150] 09 p1349 N85-18486
Protocol for aquifer cleanup decision making at military installations
[AD-P004151] 09 p1349 N85-18487
Development of a Persistent Chemical Agent Simulator System (PCASS)
[NASA-CR-175778] 16 p2745 N85-26838
Ventilation flow: Submerged 18 p3156 N85-29545

TRU decontamination of high-level PUREX waste by solvent extraction using a mixed octyl(phenyl)-N,N-diisobutyl-carbamoyl methylphosphine oxide/TBP/NPH (TRUEX) solvent
[DE85-010251] 19 p3235 N85-30054
Method for removing chlorine compounds from hydrocarbon mixtures
[DE85-011608] 22 p3742 N85-33191

DECOUPLING
Practical considerations for noninteracting control synthesis
[AD-A150130] 12 p1918 N85-22046
Frequency/period estimation and adaptive rejection of periodic disturbances
[AD-A149229] 15 p2632 N85-26226
A modern control design methodology with application to the CH-47 helicopter
[AD-A151946] 16 p2710 N85-26723
On the choice of coordinates for semiconductor simulation
[AD-A152214] 16 p2870 N85-27708
On the dependence of the convergence of Gummel's algorithm on the regularity of the solution
[AD-A154628] 21 p3875 N85-32832

DECOYS
Pyrophoric alkylaluminum compounds in decoy flares
[FOA-C-20562-E4] 18 p3078 N85-29039

DECREMENTING
U REDUCTION

DEEP SPACE
NT INTERPLANETARY SPACE
NT INTERSTELLAR SPACE
A FORTRAN program for deep space sensor analysis
[AD-A151700] 15 p2488 N85-25366

DEEP SPACE NETWORK
The Telecommunications and Data Acquisition Report
[NASA-CR-174149] 05 p0622 N85-13980
Submilliarcsecond VLBI using compact close pairs of radio sources: Error analysis 05 p0622 N85-13981
VLBI solutions for the time variation of DSN baselines: 1978 - 1983 05 p0623 N85-13983
The performance of differential VLBI delay during interplanetary cruise 05 p0623 N85-13984
Development and testing of a 20-kW X-band transmitter with high phase stability 05 p0623 N85-13985
Superconducting NbTi and Pb(Cu) bandpass filters 05 p0623 N85-13986
Mark IVA DSN 26-meter subnet 05 p0624 N85-13995
64-meter to 70-meter antenna extension 05 p0624 N85-13996
Antenna microwave subsystem 05 p0625 N85-13997
VLBI system (BLK I) IF-video down conversion design 05 p0625 N85-13998
The Telecommunications and Data Acquisition Report
[NASA-CR-174306] 10 p1462 N85-19224
Arcsecond positions for milliarcsecond VLBI nuclei of extragalactic radio sources. Part 3: 74 sources 10 p1463 N85-19225
Microwave surface resistivity of several materials at ambient temperature 10 p1463 N85-19226
Subreflector focusing techniques applied to new DSS-15 and DSS-45 34-meter antennas 10 p1464 N85-19233
The Venus Balloon Project 10 p1465 N85-19243
DSN 34-meter antenna optics analysis for wideband SETI investigations 10 p1465 N85-19244
Activities of the Jet Propulsion Laboratory, 1 January - 31 December 1983
[NASA-CR-175555] 13 p2167 N85-23447
Consultative Committee for Space Data Systems. Panel 1: Support
[NASA-CR-175786] 16 p2769 N85-27090
The Telecommunications and Data Acquisition Report
[NASA-CR-175642] 16 p2770 N85-27094
Maintenance of time and frequency in the DSN using the global positioning system 16 p2771 N85-27105
Network information management subsystem 16 p2771 N85-27106
Determining availability characteristics of DSN data systems using discrepancy report data 16 p2772 N85-27109
Performance analysis of the DSN baseband assembly (Bba) Real-Time Combiner (RTC)
[NASA-CR-175676] 17 p2946 N85-28190
Performance analysis of the DSN baseband assembly (Bba) Real-Time Combiner (RTC)
[NASA-CR-175677] 17 p2947 N85-28193
Maintenance of time and frequency in the Jet Propulsion Laboratory's Deep Space Network using the Global Positioning System 18 p3109 N85-29249
Using GPS and VLBI technology to maintain 14 digit synchronization 18 p3109 N85-29250
Publications of the Jet Propulsion Laboratory 1983
[NASA-CR-175979] 18 p3190 N85-29848

DEEP WELL INJECTION (WASTES)
Rock mechanics: Issues and research needs in the disposal of wastes in hydraulic fractures
[DE85-001399] 10 p1556 N85-19809
Office of Civilian Radioactive Waste Management
[DE85-012585] 22 p3839 N85-33774

DEER
Deer control using 7 strand vertical fence 11 p1581 N85-19958

DEFECTS
NT AUDITORY DEFECTS
NT CRYSTAL DEFECTS
NT CRYSTAL DISLOCATIONS
NT EDGE DISLOCATIONS
NT INCLUSIONS
NT POINT DEFECTS
NT SCREW DISLOCATIONS
NT SURFACE DEFECTS
NT VACANCIES (CRYSTAL DEFECTS)
Effects of member imperfections on the behavior of space trusses 02 p0207 N85-11383
Hydrogen passivation of electrically active defects in crystalline silicon solar cells
[DE84-004590] 02 p0223 N85-11461
Application of positron annihilation in materials science
[DE84-014733] 02 p0288 N85-11883
Weld metal solidification cracking in a carbon-manganese steel 03 p0330 N85-12126
Identification of pulse-echo rays in austenitic steels
[AERE-R-11265] 03 p0360 N85-12356
A comparison of methods for predicting ductile crack growth instability
[AERE-R-11199] 03 p0374 N85-12387
Newer carbon fibers and their properties 04 p0465 N85-12955
On the origins of structural defects in BF2(+)-implanted and rapid thermally annealed silicon: Conditions for defect free regrowth
[DE84-016060] 04 p0572 N85-13650
Vandenberg space shuttle launch complex
[S-HRG-98-1075] 05 p0601 N85-13833
Statement of Edward C. Aldridge, Jr., Under Secretary of the Air Force, Department of the Air Force, accompanied by Lieutenant General Robert W. Bazley, Inspector General and Brigadier General Donald J. Kutyna, Director of Space Systems and Command, Control and Communications, Deputy Chief of Staff, Research, Development and Acquisition 05 p0601 N85-13834
The detection and assessment of defects in automatic ultrasonic inspection
[BLL-RISLEY-TR-4597-(9091.9F)] 05 p0647 N85-14150
Impact of NDE unreliability on pressure vessel fracture predictions
[DE84-015586] 05 p0647 N85-14151
A review of imperfection sensitivity of stiffened shells
[AD-A147311] 07 p0978 N85-16213
Ultrasonic measurements, X-ray photographs and image processing
[BLL-RISLEY-TR-4586-(9091.9F)] 07 p1037 N85-16583
Built-in-test for first line testing 08 p1064 N85-16739
Holographic FLI for detection of defects
[AD-A148330] 08 p1164 N85-17345
Experimental verification of eddy-current flaw theory
[DE85-001288] 09 p1329 N85-18350
Modeling of real UT transducer field/flaw interactions
[DE85-000341] 09 p1329 N85-18351
Interaction between a crack and a soft inclusion
[NASA-CR-172533] 10 p1495 N85-19439
Stress studies in EFG
[NASA-CR-174441] 10 p1508 N85-19515
Estimating deformability upon pressing of aluminum alloys based on results of mechanical testing 11 p1598 N85-20049
Collapse and removal of discontinuities in joint zone during diffusion welding 11 p1602 N85-20077
Effect of macrostructure on durability of polycrystalline graphite 11 p1605 N85-20091
Infrared-thermal wave scanner for NDE of naval thermal spray coatings
[DE85-002237] 11 p1650 N85-20391
Effect of input distributions on the probabilistic fracture mechanics analysis of reactor pressure vessels
[DE85-000832] 11 p1652 N85-20403
Requirements of quantitative NDE in developing fracture control plans
[DE85-003147] 11 p1654 N85-20415
Aerostructure nondestructive evaluation by thermal field detection. Phase 2: Technique refinement and quantitative determination of flaw detection capabilities
[AD-A149622] 12 p1777 N85-21155
Reliability of structural brittle materials 12 p1946 N85-22222
Influence of welding defects at melting boundary on static strength of welded joint in large-diameter pipe 13 p2033 N85-22735
NDE methods for green ceramics
[DE85-004019] 13 p2038 N85-22766
Shape optimization for minimal stress concentration 13 p2101 N85-23083
Estimating defectiveness buildup during service in metal of welded runner in low-pressure cylinder of turbine 14 p2271 N85-24070
Effects of primary recoil energy on the production rate of mobile defects during elevated temperature irradiation
[DE85-006210] 15 p2511 N85-25489
Echo-response from crack-like two-dimensional reflectors in focused ultrasonic fields. Ultrasonic crack tip method for the determination of crack depth
[BLL-BISI-22062-(9022.06)] 16 p2796 N85-27236
Predicting fully plastic mode 2 crack growth from an asymmetric defect
[AD-A152227] 16 p2801 N85-27269
An analysis for axially compressed orthotropic shells with a multimode imperfection representation
[VTH-LR-422] 16 p2803 N85-27281
The statistical analysis of initial imperfection measurements — shell profiles
[VTH-LR-442] 16 p2857 N85-27622
Interaction among inhomogeneities and inclusions
[AD-A153114] 17 p2979 N85-28419
Specifics of fine structure of pressed aluminum alloys manufactured by plasma atomization 19 p3242 N85-30102
Reliability of welds to repair defects in cast components made from CrMoV steel
[BLL-CE-TRANS-8054-(9022.09)] 20 p3461 N85-31501
Experimental and theoretical assessment of a new technique for the non-destructive evaluation of laminated panels
[AD-A155622] 21 p3562 N85-32155
Defects in tetrahedrally coordinated amorphous semiconductors
[AD-A155150] 21 p3581 N85-32263
Reliability of void detection in structural ceramics using scanning laser acoustic microscopy
[NASA-TM-87035] 21 p3597 N85-32337

DEFENSE COMMUNICATIONS SATELLITE SYSTEM
US MILSATCOM: Present and future 11 p1709 N85-20753
Integrated support of tactical operations by satellite communications 11 p1709 N85-20754
EHF MILSATCOM systems for tactical users 11 p1709 N85-20755

DEFENSE COMMUNICATIONS SYSTEM (DCS)
DCS (Defense Communications System) network synchronization design criteria
[AD-A146251] 03 p0356 N85-12289
Integrated defense communications system antijamming antenna system
[AD-D011423] 08 p1154 N85-17285
Transmission Monitoring and Control (TRAMCON) segmentation plan for the DCS (Defense Communications System) digital transmission network
[AD-A154175] 20 p3440 N85-31351
Deep reconditioning of batteries during DSCS 3 flight operations 20 p3446 N85-31397

DEFENSE INDUSTRY
The US machine tool industry and the defense industrial base
[PB84-216628] 01 p0036 N85-10225
Companies participating in the Department of Defense Subcontracting Program, first three quarters fiscal year 1984
[AD-A146137] 03 p0436 N85-12775
Survey relating to the implementation of cost/schedule control systems criteria within the Department of Defense and industry
[AD-A146864] 06 p0870 N85-15526
The evolution of the U.S. helicopter industry
[AD-A154290] 19 p3211 N85-29913

DEFENSE METEOROLOGICAL SATELLITE PROGRAM
U DMSP SATELLITES

DEFENSE PROGRAM
DOD related software technology requirements, practices, and prospects for the future
[AD-A145493] 02 p0242 N85-11575
Companies participating in the Department of Defense Subcontracting Program, first three quarters fiscal year 1984
[AD-A146137] 03 p0436 N85-12775
On estimating the cost growth of weapon systems
[AD-A147297] 06 p1230 N85-17749
Proceedings of the Environmental Systems Symposium (13th) held at Bethesda, Md., 20-22 March 1984
[AD-A148194] 09 p1346 N85-18471

Community relations activities at Department of Defense sites
[AD-P004150] 09 p1349 N85-18486
Department of defense, office of inspector general semiannual report to the Congress, 1 April - 30 September 1984
[AD-A149560] 10 p1567 N85-19879
Air Force Office of Scientific Research (AFOSR) technical report summaries. Third quarter (CY)
[AD-A148965] 10 p1573 N85-19918
PRC journal discusses 'Star Wars' space program
11 p1621 N85-20207
Military applications of meteorological satellite (METSAT) data 11 p1711 N85-20767
Program manager: The Journal of the Defense Systems Management College. Volume 13, Number 6, November-December 1984
[AD-A149546] 11 p1739 N85-20933
Fiscal year 1986 technical objective document
[AD-A151039] 14 p2432 N85-25000
Militarization of space activity in United States
15 p2488 N85-25360
Defense data network support concept analysis
[AD-A153214] 17 p3016 N85-28649
The Department of Defense statement on the Science and Technology Program by Colonel Donald I. Carter, USAF Acting Deputy Under Secretary of Defense for Research and Advanced Technology before the Subcommittee on Research and Development of the Committee on Armed Services of the United States House of Representatives, 99th Congress, first session
[AD-A152467] 17 p3046 N85-28850
Rome Development Center Air Force technical objective document C3I FY-86
[AD-A152476] 17 p3047 N85-28851
The revolution in military affairs and the Soviet system
[AD-P004568] 17 p3048 N85-28863
Selected university laboratory needs in support of national security
[AD-A153511] 18 p3197 N85-29633
Improving the defense energy information system (DEIS)
[AD-A153524] 18 p3200 N85-29649
Proceedings of the Electronic Test Equipment Division's Annual Program Review of Electronic Test Equipment Industry Response to Emerging Defense Requirements
[AD-A154455] 20 p3436 N85-31320
Evaluation of a software design approach: Develop a threat resolution module in Ada (trademark)
[AD-A155599] 21 p3672 N85-32815
The flow of scientific and technical information in the US Army Research Laboratories
[AD-A155060] 21 p3713 N85-33043
DoD Value Engineering conference report. Value Engineering (VE): A tool that benefits line management. Part 4, Workshop B: VE on spare parts
[AD-A156070] 24 p4163 N85-35813
DoD Value Engineering conference report. Value Engineering (VE): A tool that benefits line management. Part 7, Workshop E: VE in construction and architect engineer contracts
[AD-A156073] 24 p4164 N85-35816

DEFINITION
Fracture detection and characterization for geothermal reservoir definition
[DE85-006677] 22 p3815 N85-33630

DEFLAGRATION
Hazard Studies for Solid Propellant Rocket Motors
[AGARD-CP-367] 08 p1114 N85-17025
Review of USAF treatment of solid propellant rocket motor hazards 08 p1114 N85-17027
Analysis of Deflagration to Shock to Detonation Transition (DSDT) in porous energetic solid propellants
08 p1115 N85-17030
Penguin warhead safety tests
08 p1115 N85-17031
Study of the transition from deflagration to detonation of previously fragmented propellants
08 p1115 N85-17032
Transient combustion: An important consideration in deflagration-to-detonation transition
08 p1116 N85-17037
The DDT process for high energy propellants
08 p1116 N85-17038
Shock and impact response of solid rocket propellants: Experimental and theoretical 08 p1116 N85-17040
The pressure deflagration limit of solid rocket propellants 08 p1117 N85-17046
Analysis of deflagration to detonation transition in high-energy solid propellants
[AD-A148302] 08 p1135 N85-17156
Transition to detonation from rapid-compression (ramp-waves) generated in a burning porous bed
[AD-P004345] 10 p1455 N85-19169
A thermal-mechanical model of deflagration-to-detonation in granular energetic materials
[AD-P004346] 10 p1455 N85-19170
A summary of the mechanism of delayed detonation
[AD-P004347] 10 p1455 N85-19171
Analysis of Shock to Detonation Transition (SDT) of porous high energy propellant from ramp-wave compression loading
[AD-A149333] 10 p1457 N85-19180
Analysis of deflagration to detonation transition in high-energy solid propellants 16 p2757 N85-27010
Combustion-deflagration-detonation transition in a confined spherical powder
[ISL-R-106/84] 22 p3747 N85-33223
Behavior of the porous bed in a combustion-deflagration-detonation transition
[ISL-CO-220/84] 22 p3747 N85-33224
Combustion-deflagration-detonation transition
[ISL-CO-221/84] 22 p3747 N85-33225

DEFLATING
U INFLATABLE STRUCTURES
U PRESSURE REDUCTION

DEFLECTION
Three programs for evaluating bending moments, deflections and shear forces in simply-supported uniform bridge decks under South African NA loading: NAB, NAD and NAS. NITRR manual P13
[ISBN-0-7988-2283-X] 01 p0102 N85-10681
Initial sailplane project: The RP-1
04 p0468 N85-12976
Second sailplane project: The RP-2
04 p0468 N85-12977
Influence of relaxation on the mechanical characteristics of a carbon-epoxy composite. Report no. 45.427/1
04 p0468 N85-12980
Large transverse deflections of circular plates loaded symmetrically
[NPL-DMA(A)-86] 04 p0512 N85-13282
Encapsulation design analysis
06 p0829 N85-15268
Determination of shear coefficient of a general beam cross section by finite element method
09 p1338 N85-18413
Advanced ion thruster research
[NASA-CR-174862] 10 p1430 N85-19021
Deflection model of a CT4-A undercarriage
[AD-A149778] 12 p1777 N85-21156
Photo-thermal detection of the onset of photo-chemical nucleation (laser-snow) in vapor
[AD-A150111] 12 p1801 N85-21295
Along-track deflection of the vertical from SEASAT: GEBCO (General Bathymetric Chart of the Oceans) overlays
[PB85-129641] 12 p1876 N85-21767
Horizontal deflection TS-257
13 p2069 N85-22926
Load carrying capacity of double circular arc gears
14 p2221 N85-23776
A feasibility study for using low boiling point fluids to change aircraft tire deflection
[AD-A152096] 16 p2706 N85-26701
Analysis of elastoplastic grids under conditions of variable loads
[REPT-16/1984] 16 p2797 N85-27242
Quasi-steady vibrations of a rotating shaft grazing an obstacle: Spiral vibration
[BLL-CE-TRANS-7962-(9022.09)]
16 p2799 N85-27256
Finite element thermal-structural analysis of cable-stiffened space structures
[AD-A153622] 18 p3066 N85-28963
Yield stress determination from miniaturized disk bend test data
[DE85-009495] 18 p3122 N85-29330
Large deflections of a cantilever beam under arbitrarily directed tip load
[NASA-TM-86442] 19 p3284 N85-30363
Shear deflection in a three-point bend beam of a solid circular cross-section
[AD-A154458] 19 p3287 N85-30381
Optical beam deflection detection of thermal waves in opaque solids 19 p3374 N85-30927
A comparison of electronic heterodyne moire deflectometry and electronic heterodyne holographic interferometry for flow measurements
[NASA-TM-87071] 21 p3568 N85-32302
Basic formulae for the computation of the deflection of the vertical from astronomical star observations
[AD-A154912] 21 p3605 N85-32390
Galactic antiprotons of 0.2-2 GeV energy
[OG-6.1-11] 22 p3868 N85-34101

DEFLECTORS
NT BLAST DEFLECTORS
Precision electrooptical deflector based on corrugated light guide 07 p0950 N85-16020
Optimization of piezoceramic optical deflector
11 p1719 N85-20813
Flameholder with integrated air mixer
[AD-D011549] 12 p1778 N85-21161

DEFOCUSING
Artificial defocusing lens in ionosphere
05 p0724 N85-14654
Defocusing losses in a log periodic-fed reflector
[AD-A151616] 15 p2547 N85-25722

DEFORESTATION
Relationship between forest clearing and biophysical factors in tropical environments: Implications for the design of a forest change monitoring approach — Costa Rica
[E85-10051] 07 p0963 N85-16247
The water balance and climate — Amazon region
07 p1003 N85-16370
The Amazon and climate 07 p1003 N85-16376
Deforestation, floodplain dynamics, and carbon biogeochemistry in the Amazon Basin
08 p1144 N85-17216

DEFORMATION
NT AXIAL STRAIN
NT ELASTIC BENDING
NT ELASTIC BUCKLING
NT ELASTIC DEFORMATION
NT NUCLEAR DEFORMATION
NT PLASTIC DEFORMATION
NT STATIC DEFORMATION
NT TENSILE DEFORMATION
NT WAVE FRONT DEFORMATION
Deformation measurements of composite multi-span beam shear specimens by Moire interferometry
[NASA-CR-3844] 02 p0169 N85-11135
Microstructure and deformation aspects of some specialty steels and hard metals
02 p0176 N85-11182
Deformations and strains in adhesive joints by moire interferometry
[NASA-CR-172474] 02 p0185 N85-11238
Vertical crustal movements in southern California, 1974 to 1978
[GS-CIRC-905] 02 p0228 N85-11491
High temperature deformation of hot-pressed polycrystalline orthoenstatite
[NASA-CR-174026] 02 p0285 N85-11861
Study of deformation and fracture of AMg6N weldable aluminum alloy by method of acoustic emission
03 p0352 N85-12266
Penetrator/armour interactions: Background to Australian work
[MRL-R-936] 03 p0367 N85-12353
Deformation mechanisms associated with mesoscopic kinkbands, Jura Mountains (Switzerland) and Chaines Subalpines (France) 03 p0389 N85-12492
Cavitation phenomenon in superplastic creep
[DE84-015484] 04 p0513 N85-13271
Structural observations in the Circle quadrangle, Yukon-Tanana Upland, Alaska 04 p0517 N85-13298
Improved apparatus and techniques for high temperature and pressure deformation of crystalline materials
[DE84-016049] 04 p0569 N85-13629
Multiaxial yield behavior of 1100 aluminum following various magnitudes of prestrain
[DE84-013904] 05 p0617 N85-13949
Experimental investigation and analysis of oscillations of thin-walled spherical shell during pulse loading
05 p0725 N85-14662
Creep of chemically vapor deposited SiC fibers
[NASA-TM-86697] 06 p0763 N85-14878
Deformation, fracture and explosive properties of reactive materials
[AD-A146396] 06 p0774 N85-14945
Process Modeling Applied to Metal Forming and Thermomechanical Processing
[AGARD-LS-137] 06 p0796 N85-15086
Flow-based analyses of metal deformation processes: An overview 06 p0796 N85-15087
Prediction of forming limit diagrams for deep drawing
06 p0796 N85-15089
The role of microstructure in the modelling of plastic flow in P/M superalloys at forging temperatures and strain rate 06 p0796 N85-15090
Control of microstructure during hot working of Ti-6242 06 p0797 N85-15091
Numerical methods in metalforming
06 p0797 N85-15092
Modeling microstructural changes during hot rolling of steels 06 p0798 N85-15096
Tests of the load-bearing and deformation behaviour of reinforced concrete spherical shells under point loading
[BLL-RISLEY-TR-4550-9091.9F)]
06 p0816 N85-15182
Modeling of deformation and fracture in high-temperature structural materials
[DE84-016006] 06 p0818 N85-15181

Analysis of the impact of a deformable missile model on a deformable obstruction
[BLL-RISLEY-TR-8534-(9091.9F)] 06 p0859 N85-15459
Strain analysis of the Leoville chondrite and conditions in asteroidal interiors 06 p0885 N85-15620
Special features of the deformation of molybdenum at high temperatures
[BLL-M-36027-(5828.4)] 07 p0924 N85-15856
Stereo Electro-optical Tracking System (SETS)
[NASA-CR-172471] 07 p0962 N85-16098
The influence of strain rate and porosity on the deformation and fracture of titanium and nickel
[AD-A148670] 08 p1130 N85-17123
On a general nonlinear theory of plates and shells: Formulation and applications 08 p1172 N85-17367
The response of metallic structures to dynamic loading 08 p1172 N85-17369
Modeling of large-scale accretionary wedge and thin-skinned trust-and-fold belt mechanics 08 p1181 N85-17442
Nonlinear analysis of composite laminates 09 p1288 N85-18087
Deformation and fracture of P/M (Powder/Metallurgy) titanium alloys
[AD-A148672] 09 p1294 N85-18128
Large deformations of a nonlinear elastic solid and the diffusion of an ideal fluid treated as interacting continua 09 p1330 N85-18356
Direct energy minimization approach to whipping analysis of pressure hulls 09 p1335 N85-18393
Light scattering studies of lower dimensional colloidal particle and critical fluid systems
[DE85-002087] 09 p1377 N85-18654
Cavitation phenomenon in superplastic creep
[DE85-001716] 10 p1441 N85-19083
Study of superplastic alloys based on Al-Zn-Ca 10 p1442 N85-19092
Mechanical properties of Be-Al composite 10 p1443 N85-19094
Spreading upon compacting of fiber composite materials with porous metal matrix 10 p1443 N85-19096
Behavior and specifics of fracture of porous fiber materials in extension 10 p1447 N85-19118
Influence of extension rate on strength and deformation characteristics of titanium alloys over a broad temperature range 10 p1448 N85-19121
Mechanisms of damage accumulation in time-dependent cyclic deformation
[DE85-001004] 10 p1496 N85-19443
Simple higher-order theory for laminated composite plates
[NASA-CR-174421] 10 p1496 N85-19445
Study of tectonic earthquake precursors by geodetic methods 10 p1502 N85-19479
Estimating deformability upon pressing of aluminum alloys based on results of mechanical testing 11 p1598 N85-20049
Evaluation of features of reinforcing fibers by testing bundles 11 p1599 N85-20059
Effect on work-hardening in dynamic deformation of beryllium
[DE85-002691] 11 p1608 N85-20111
China report: Science and technology
[JPRS-CST-84-025] 11 p1620 N85-20197
Micro-deformation of quartz under dynamic action and its applications 11 p1620 N85-20201
A new rheological model for concrete structural analysis
[DE84-014743] 11 p1653 N85-20413
A three-dimensional geometric-physical model for conventional geodetic observations-observables, parameter estimation, and deformation analysis
[SER-C-298] 11 p1665 N85-20493
Advanced stress analysis methods applicable to turbine engine structures
[NASA-CR-175573] 12 p1778 N85-21165
Algorithm for the simulation of transient viscoelastic flows with free surfaces
[DE85-002713] 12 p1848 N85-21590
An orthogonal grid technique for studying internal deformation and energy absorption in target penetration
[AD-A149989] 12 p1860 N85-21665
Fracture toughness of materials
[DE85-004306] 12 p1867 N85-21713
Summary of recent research on mechanical behavior of polycrystalline solids
[DE85-004601] 12 p1942 N85-22199
Structures of ordered linear dislocation multipoles in Cu-Al alloys
[ISSN-0379-6906] 13 p2021 N85-22684
Temperature effects of heterogenized annealing on structure and properties of V95 aluminum alloy 13 p2025 N85-22692
High temperature antifriction properties of Ti sub 1-sub xNb sub x C sub 0.5N sub 0.5 alloys 13 p2029 N85-22715
Specifics of structure and mechanical properties of metastable beta-titanium alloys after deformation and aging 13 p2032 N85-22731
Densification and deformation in the presence of a liquid phase
[DE85-005101] 13 p2038 N85-22763
On Hybrid and mixed finite element methods
[NASA-CR-175551] 13 p2101 N85-23096
Normal-fault and fold development in sedimentary rocks above a pre-existing basement normal fault 13 p2131 N85-23259
Theoretical and experimental investigation of mechanically fastened composites
[AD-A150961] 14 p2248 N85-23935
Cast-iron technology: Metallographic and mechanical testing results
[DE85-002684] 14 p2257 N85-23984
Influence of short-range order on deformation mechanisms in solid solutions
[DE85-006374] 14 p2258 N85-23989
Thermal deformation of flexible rotors in friction bearings 14 p2280 N85-24123
Cutting structural materials in vacuum 14 p2286 N85-24165
Systematic and random deformations of orbits of long-period comets 15 p2479 N85-25299
Study of structural changes of dual-phase titanium alloy during shock wave loading 15 p2498 N85-25408
Possible use of rapid heating for improving mechanical properties of titanium alloys 15 p2498 N85-25409
Effect of aluminum on nature of titanium alloy failure 15 p2498 N85-25411
Structure and mechanical properties of dispersion-hardened nickel alloy joints welded by diffusion 15 p2500 N85-25422
Effectiveness of use of heat-dissipating clamps to reduce deformation during argon arc welding of thin sheets of AMg6 alloy 15 p2501 N85-25427
Summary of recent investigations of the mechanical properties of polycrystalline solids
[DE85-006776] 15 p2511 N85-25492
Reflection and transmission of flexural waves at discontinuities 15 p2572 N85-25861
Design of shear deformable antisymmetric angle-ply laminates to maximize the fundamental frequency and frequency separation
[CSIR-TWISK-333] 15 p2577 N85-25892
Estimation of the depth of a spherical cap in an hydraulic drawing test for some simple conditions of loss of stability
[REPT-4/1984] 16 p2748 N85-26956
Tooth wear in worm gears in vacuum 16 p2766 N85-27070
Optimal modeling with a minimum of local distortion
[REPT-18/1984] 16 p2797 N85-27243
Finite axisymmetric deformation of a thin shell of revolution 16 p2798 N85-27251
Principles of wave formation along web of H-beams
[BLL-M-36041-(5828.4)] 16 p2798 N85-27253
Full statistical characteristics of microdeformation
[BLL-M-36076-(5828.4)] 16 p2798 N85-27254
Nonlinear equations for dynamics of pretwisted beams undergoing small strains and large rotations
[NASA-TP-2470] 16 p2799 N85-27258
Constitutive cyclic deformation behavior in single-crystal and directionally solidified SSME high-pressure fuel turbopump airfoil materials 17 p2914 N85-27985
Preparation of metal for cold upsetting
[BLL-BISI-TRANS-22383-(9022.06)] 17 p2926 N85-28043
Study on mechanism of surface deformation induced by stress corroion cracking
[BLL-BISI-TRANS-21866-(9022.06)] 17 p2928 N85-28066
Temperature and manganese content dependences of tensile deformation in iron-high manganese binary alloys
[DE85-007656] 17 p2932 N85-28098
Investigations of the material factors in the adiabatic shearing of steels
[AD-A153084] 17 p2979 N85-28418
Interfacial segregation and fracture
[DE85-009779] 18 p3075 N85-29019
Studies of strain rate effects in the deformation of solids by means of stress pulses and ultrasonic methods
[DE85-009463] 18 p3122 N85-29329
A state variable approach to transient creep deformation in stress reduction experiments
[DE85-009492] 18 p3122 N85-29331
Measurement and calculation of the mechanical response of a highly fractured rock
[DE85-006421] 18 p3127 N85-29362
Deformable mirror nearest neighbor optical computer 18 p3188 N85-29772
Effect of matrix composition on steel fiber reinforced concrete properties 19 p3230 N85-30028
Deformation, fracture and explosive properties of reactive materials
[AD-A154073] 19 p3251 N85-30157
Residual stress distributions in (plastically) surface deformed two-phase materials 19 p3263 N85-30356
Fundamental studies related to failure of adhesively bonded structures
[AD-A154072] 19 p3285 N85-30374
Interferometric creep testing
[AD-A154249] 19 p3288 N85-30378
Influence of error of determination of moire isotach orders on the stability of their approximation
[BLL-M-36277-(5828.4)] 20 p3450 N85-31423
Determination of local deformation during explosive welding
[BLL-M-36279-(5828.4)] 20 p3462 N85-31503
Determination of deformation speed during high-speed deformation of cylindrical shells
[BLL-M-36280-(5828.4)] 20 p3465 N85-31527
Indentation fractography: A measure of brittleness
[PB85-179059] 20 p3473 N85-31581
Machining-induced deformation in stepped specimens of PH 13-8 Mo, 18 nickel maraging steel grade 200T1 and grain-refined HP 9-4-20
[NASA-CR-172450] 21 p3565 N85-32177
Bubble dynamics in polymer solutions undergoing shear
[AD-A154575] 21 p3568 N85-32193
The effect of mould size on the exothermic reaction and compressive strength of epoxy resin chocks
[AD-A155102] 21 p3570 N85-32203
A comparison of electronic heterodyne moire deflectometry and electronic heterodyne holographic interferometry for flow measurements
[NASA-TM-87071] 21 p3588 N85-32302
Development of improved dynamic failure models
[AD-A155586] 21 p3600 N85-32354
Local epi-continuity and local optimization
[AD-A154812] 21 p3677 N85-32843
Microstructure-mechanical property relationships in the transformation-toughened ceramics
[DE85-011946] 22 p3752 N85-33261
Stresses and deformations in cross-ply composite tubes subjected to a uniform temperature change: Elasticity and Approximate Solutions
[NASA-CR-176147] 22 p3800 N85-33545
Crustal Dynamics Project: Catalogue of site information
[NASA-TM-86218] 22 p3801 N85-33552
Deep-burial diagenesis in carbonates
[DE85-011224] 22 p3802 N85-33554
Discontinuous deformation analysis
[DE85-011208] 22 p3814 N85-33628
SANCHO: A finite element computer program for the quasistatic, large deformation, inelastic response of two-dimensional solids
[DE85-011456] 22 p3829 N85-33714
Effects of hot deformation on the kinetics of the pearlite transformation in eutectoid steel
[BLL-M-35844-(5828.4)] 23 p3913 N85-34250
Phase transformations taking place in austenitic steel during deformation at different rates
[BLL-M-35875-(5828.4)] 23 p3914 N85-34254
Inertial stresses and deformations in mechanisms 23 p3924 N85-34320
Scaling differences between large interplate and intraplate earthquakes
[NASA-CR-176149] 23 p3948 N85-34467
On the potential link equation of a spot centre with relative deformation for a semi-infinite molecular crystal
[BLL-M-35795-(5828.4)] 23 p3965 N85-34711
Solid-state co-extrusion of nylon 6 gel
[AD-A158187] 24 p4062 N85-35296
Strain measurement using point recognition picture processing
[DRIC-T-7407] 24 p4101 N85-35421
Response of a BWR Mark 2 containment vessel head to loads beyond the design basis
[DE85-010524] 24 p4103 N85-35432
Geology: Structural history and fluvial geomorphology of the southern Death Valley Fault Zone, Inyo and San Bernardino Counties, California 24 p4114 N85-35506
Structural development of the west-central Grant Range, Nye County, Nevada 24 p4115 N85-35508
Three-dimensional finite deformation viscoelastic model accounting for damage effects
[DE85-012951] 24 p4139 N85-35660

DEGASSING
NT DEOXYGENATION
Working medium for sorption heat pumps
[BLL-T6360/BG/WH785/84] 06 p0807 N85-15131
Degassification of silicon nitride powders of various origins 13 p2030 N85-22718

Chemical composition and kinetics of libration of gases upon welding of aluminum alloys
19 p3247 N85-30131
The degassing history of the Earth: Noble gas studies of Archaean cherts and zero age glassy submarine basalts
21 p3718 N85-33072
Terrestrial Xe isotopic contraints on the early history of the Earth
22 p3852 N85-33852
Evacuate and backfill apparatus and method
[DE85-006018] 23 p3938 N85-34411

DEGENERATION
A study of degenerate and nondegenerate critical points in three-dimensional flow fields
[DFVLR-FB-84-36] 11 p1633 N85-20288
On some physical impurity properties of doped-indirect gap semiconductors at low and intermediate concentrations
[INPE-3452-PRE/704] 16 p2689 N85-27701

DEGENERATIVE FEEDBACK
U NEGATIVE FEEDBACK

DEGRADATION
NT BIODEGRADATION
NT THERMAL DEGRADATION
Mechanisms of syncrude-synfuel degradation
[DE84-015206] 01 p0034 N85-10212
Material degradation in heavy steel plates caused by bending with a laser
[AD-A144784] 01 p0052 N85-10343
Theoretical analysis of physical processes of lasing medium degradation in semiconductor lasers
02 p0269 N85-11759
Boron-nitrogen polymers. 1: Mechanistic studies of borazine pyrolyses
[AD-A146470] 06 p0771 N85-14933
Storage stability of jet fuels
[AD-A146360] 06 p0773 N85-14943
Investigation of accelerated stress factors and failure/degradation mechanisms
06 p0832 N85-15295
Interactions of hydrazine and of hydrazine derivatives with soil constituents and with soils
[AD-A148475] 06 p1122 N85-17074
Design of an evaluation system to measure performance degradation due to continuous operations
[AD-A148188] 08 p1200 N85-17558
Reliability studies of ceramic capacitors
[AD-A149126] 10 p1479 N85-19338
Investigation of accelerated stress factors and failure/degradation mechanisms in terrestrial solar cells
[NASA-CR-175469] 10 p1510 N85-19524
Evaluation of infrared reflectance as a technique for measuring absorber materials degradation
[PB85-106488] 11 p1677 N85-20567
Degradation mechanisms in ceramic dielectrics
[AD-A149791] 12 p1813 N85-21369
Radiation effects induced in pin photodiodes by 40- and 85-MeV protons
[NASA-CR-175678] 14 p2426 N85-24960
Surface degradation of ductile metal in elevated temperature gas-particle streams
[DE85-006426] 18 p3074 N85-29017
Study of Kapton under simulated shuttle environment
[NASA-CR-176003] 19 p3225 N85-29997
Theoretical modeling of laser induced optical degradation
[AD-A155302] 21 p3592 N85-32323
Topics in electrochemical degradation of photovoltaic modules
21 p3608 N85-32410
Accelerated stress factors and failure/degradation mechanisms in terrestrial solar cells
21 p3613 N85-32451
Induction motors with minimum waste of magnetic iron
22 p3772 N85-33377
Solar maximum: Solar array degradation
[NASA-TM-86194] 23 p3903 N85-34175
Degradation mechanisms and accelerated aging test design
[TI85-003251] 23 p3940 N85-34420

DEGREES OF FREEDOM
Three degree of freedom steady state point performance program: Updated version 1
[CSIR-NIAST-83/48] 01 p0001 N85-10005
Direct numerical simulation of curved turbulent channel flow
[NASA-TM-85974] 02 p0197 N85-11316
Autonomous momentum management for space station
[NASA-CR-174085] 04 p0462 N85-12931
Direct numerical simulation of curved turbulent channel flow
05 p0635 N85-14072
Effect of aerodynamic and angle-of-attack uncertainties on the May 1979 entry flight control system of the Space Shuttle from Mach 8 to 1.5
[NASA-TP-2365] 07 p0913 N85-15778
Optimum design for nonlinear shock mounts for transient inputs
09 p1334 N85-18390
Modal analysis of structural systems involving nonlinear coupling
09 p1337 N85-18409
Discrete modifications to continuous dynamic structural systems
09 p1337 N85-18410
An alignment fixture for a 2-Degree-of-Freedom (TDF) gyroscope
[AD-A148885] 10 p1422 N85-18969
Condensed antenna structural models for dynamics analysis
10 p1483 N85-19230
A numerical approach for the vibration analysis of an axiaymmetric shell structure with a nonuniform edge constraint
[AD-A149286] 11 p1651 N85-20402
Time marching numerical solution of the dynamic response of nonlinear systems
[NAF-AN-25] 12 p1865 N85-21696
Two degree-of-freedom flutter solution for a personal computer
[NASA-TM-86381] 13 p1971 N85-22379
Cyclic industrial robots with mechanical energy storing devices: Multipositional system with one or several degrees of freedom
13 p2045 N85-22803
Design of tightening device and calculation of forces in manipulator transmissions with base-drive mounted
13 p2046 N85-22804
Approximate rules for signal detection against background of Gaussian correlated interference
13 p2066 N85-23027
Motion planning with six degrees of freedom
[AD-A150312] 13 p2165 N85-23432
Controllable movements of elastic manipulator with three degrees of freedom
14 p2266 N85-24040
Investigation of the time history and modal responses of some simple linear and nonlinear systems
[DE85-002027] 14 p2321 N85-24344
Simulator study of the stall departure characteristics of a light general aviation airplane with and without a wing-leading-edge modification
[NASA-TM-86309] 15 p2470 N85-25250
Manipulation and simulation of general robots using the zero-position description
15 p2567 N85-25838
Ritz procedure for COSMIC/NASTRAN
15 p2575 N85-25877
On the interconnection of incompatible solid finite element meshes using multipoint constraints
15 p2575 N85-25879
Elastic-workhardening SDF (Single-Degree-of-Freedom) system subjected to random blast excitations
[AD-A151866] 15 p2579 N85-25909
Dispersion sensitivity of the eight inch advanced ramjet munitions technology projectile due to wind and minor thrust errors
[AD-A152145] 16 p2727 N85-26835
Boson degrees of freedom in Fermion many-body systems
[DE85-006997] 16 p2863 N85-27660
Electroweak interactions in nuclei
[DE85-007811] 17 p3033 N85-28762
Quantum model of dephasing-enhanced laser desorption: Master equation approach
[AD-A153769] 18 p3112 N85-29269
Ground-based and in-flight simulator studies of flight characteristics of a twin-fuselage passenger transport airplane during approach and landing
[NASA-TP-2451] 23 p3898 N85-34144
Identification and control of structures in space
[NASA-CR-176175] 24 p4069 N85-35214
On mini-cluster observed by Chacaltaya emulsion chamber experiment
[HE-3.6-12] 24 p4185 N85-35959

DEHUMIDIFICATION
Performance of the SERI parallel-passage dehumidifier
[DE85-000509] 11 p1672 N85-20536
High performance solar desiccant cooling system: Performance evaluation and research recommendations
[DE85-000508] 11 p1676 N85-20559
Solid desiccant dehumidification systems for residential applications
[PB85-196489] 22 p3755 N85-33279

DEHYDRATION
Voluntary dehydration and electrolyte losses during prolonged exercise in the heat
[AD-A145157] 01 p0095 N85-10639
Effects of restricted water intake on performance in a cold environment
[AD-A146904] 07 p1015 N85-16450
Thermoregulatory responses during exercise at graded hypohydration levels
[AD-A147733] 08 p1195 N85-17528
Preparing Alberto Salazar for the heat of the 1984 Olympic Marathon
[AD-A150942] 14 p2389 N85-24714
Exercise-heat strain during hypohydration: Interaction with heat acclimation and aerobic fitness
[AD-A151023] 14 p2389 N85-24717
Effects of dehydration or cold exposure and restricted fluid intake upon cognitive performance
[AD-A151973] 16 p2842 N85-27525
Plasma hormonal responses at graded hypohydration levels during exercise/heat stress
[AD-A153681] 18 p3153 N85-29623
Transport properties of Topopah Spring tuff
[DE85-010448] 19 p3270 N85-30278
Heat injury: Prevention is the key
[AD-A153734] 19 p3328 N85-30622
Thirst and fluid intake following graded hypohydration levels in humans
[AD-A156201] 24 p4132 N85-35615

DEHYDROGENATION
Biochemical evaluation of bodily influence of high and low temperatures
07 p1014 N85-16441
Catalytic conversion of C3-C4 paraffins to gasoline
[DE85-004181] 10 p1458 N85-19187
Mechanistic and kinetic studies of the elementary processes in catalytic combustion of methane
[PB85-188308] 20 p3435 N85-31314

DEICERS
To take off and to land safely, Hoechst 1678 for ice and snow free runways
05 p0595 N85-13791
Salt action on concrete
[AD-A147812] 07 p0933 N85-15912
Electro-expulsive separation system
[NASA-CASE-ARC-11613-1] 18 p3094 N85-29150
Land vehicle corrosion management
22 p3750 N85-33246

DEICING
To take off and to land safely, Hoechst 1678 for ice and snow free runways
05 p0595 N85-13791
Analytical and physical modeling program for the NASA Lewis Research Center's Altitude Wind Tunnel (AWT)
[NASA-TM-86919] 07 p0909 N85-15757
Official on Soviet research in deicing techniques
15 p2460 N85-25191

DEICING SYSTEMS
U DEICERS

DEIMOS
Structure and origin of Martian satellites
15 p2483 N85-25323

DEKATRONS
U COUNTERS

DELAMINATING
Study of delamination cracking under static and cyclic loads of carbon-epoxy composite materials
[REPT-42-727/F] 03 p0327 N85-12102
Characterization of interlaminar crack growth in composites with the double cantilever beam specimen
04 p0463 N85-12942
Characterizing delamination resistance of toughened resin composites
04 p0464 N85-12943
Composite materials characterization and development at AFWAL
04 p0464 N85-12944
Free-edge failures of composite laminates
04 p0467 N85-12971
On the effects of delamination damage in fibre composite laminates
[ARL/STRUC-R-403] 06 p0763 N85-14881
Delamination growth in graphite epoxy laminates under compressive loads
09 p1288 N85-18068
Fracture mechanics analysis and prediction of delamination growth in composite structures
[FFA-TN-1984-45] 09 p1289 N85-18092
Forced corrosion tests of construction components of passenger aircraft fuselages
11 p1600 N85-20062
Stress distribution of fiberglass reinforced plastic beam with a delamination under three-point bending
23 p3908 N85-34210
Damage induced stress redistribution in composite laminates
24 p4072 N85-35235
Damage mechanisms in damaged CFRP laminates
24 p4074 N85-35249
Computational techniques for fiber reinforced components
24 p4075 N85-35250

DELAWARE
Contamination of the fetch-limited directional wave spectrum by waves emanating from an embayment
[NASA-TM-84441] 15 p2604 N85-26048

DELAWARE BAY (US)
Analysis of suspended sediment distributions in the surface waters of Delaware Bay using remote sensing of optical properties
15 p2582 N85-25926

DELAY
One-dimensional two-phase constant lag flow in combustion chamber of solid propellant rocket motors
[AD-A145679] 02 p0173 N85-11157
Machine computation of delay and capacitance of transistor structures of subnanosecond large integrated circuits
04 p0490 N85-13120

A group delay standard for the MHz frequency range
05 p0630 N85-14040
Measurements of pilot time delay as influenced by controller characteristics and vehicles time delays
05 p0701 N85-14500
Transmission scheduling to reduce convex delay costs in packet networks
[AD-A148451] 06 p1153 N85-17278
Analysis of the performance of multiaccess networks of the bus type
[FUB-47-1983] 09 p1313 N85-18249
The effects of cooling on delay-time limits in IC's
14 p2297 N85-24224
On the equivalent bilinearization of nonlinear controlled delay systems
[RR-272] 20 p3519 N85-31860
Aviation system delays
[S-HRG-98-1241] 21 p3553 N85-32102
FAA requirements for model to support capacity, delay, noise and energy programs
[AD-A155815] 24 p4063 N85-35179

DELAY CIRCUITS
Programmable synchronous digital delay line
[AD-D011382] 07 p0945 N85-15985
Probabilistic analysis of combinational circuits with random delays
19 p3257 N85-30192

DELAY LINES
Radio frequency probing apparatus for surface acoustic wave devices
[AD-D011230] 01 p0050 N85-10327
Magnetostatic wave frequency analyzer apparatus
[AD-D011249] 05 p0631 N85-14044
Analog to digital converter
[AD-D011338] 07 p0945 N85-15983
Programmable synchronous digital delay line
[AD-D011382] 07 p0945 N85-15985
Improved magnetic bias and delay linearity in a magnetostatic wave delay line
[AD-D011441] 10 p1479 N85-19337
Dynamics of adaptive signal corrector
13 p2071 N85-22940
Diffraction of periodic grounding system of finite length
13 p2081 N85-22994
A digital contour-corrector for a high-definition TV camera
[NHK-LABS-NOTE-311] 19 p3254 N85-30179
Energizing arrangement for charge coupled device control electrodes
[AD-D011712] 19 p3261 N85-30220
Optical 3-D signature device for detecting chemical agents
[AD-D011669] 19 p3272 N85-30293

DELETION
Analysis of accretion and deletion at boundaries in dynamic scenes
[AD-A145944] 03 p0419 N85-12678

DELIVERY
NT PAYLOAD DELIVERY (STS)
NT WEAPONS DELIVERY
Research on knowledge delivery
[AD-A149565] 10 p1538 N85-19698

DELPHI METHOD (FORECASTING)
A description of a logistically ideal aircraft
[AD-A148425] 08 p1084 N85-16866

DELTA DART AIRCRAFT
U F-106 AIRCRAFT

DELTA FUNCTION
Wake fields and wake field acceleration
[DE85-006054] 17 p3031 N85-26750

DELTA WINGS
On vortex bursting
[NASA-TM-77587] 01 p0002 N85-10008
Prediction of aerodynamic characteristics of fighter wings at high angles of attack
[AD-A145107] 01 p0003 N85-10017
Force and moment measurements on a 74 deg delta wing with an apex flap
[NASA-CR-166081] 02 p0134 N85-10918
The lateral-directional characteristics of a 74-degree Delta wing employing gothic planform vortex flaps
[NASA-CR-3648] 03 p0311 N85-12009
Flow calculation on a thin wing, with specific attention to separation point at the trailing edge
[FTW-FO-1721] 05 p0594 N85-13787
Exploratory investigation of the aerodynamic characteristics of a biwing vehicle at Mach 20.3
[NASA-TM-86314] 08 p1113 N85-17021
A visual study of a delta wing in steady and unsteady motion
[AD-P004158] 09 p1264 N85-17943
Experimental investigation of a breakdown criterion for a vortex in an incompressible flow — delta wing
[ONERA-RT-27/1147-AY] 11 p1577 N85-19935
Unsteady flows around 3-dimensional wings
[AD-A149993] 12 p1772 N85-21124
A calculation of slender delta wing with leading-edge separation by quasi-vortex-lattice method
12 p1821 N85-21423
Stability of vortex structures during separation flow past array of wings
14 p2278 N85-24110
An exploratory study of apex fence flaps on a 74 deg delta wing
[NASA-CR-172463] 15 p2463 N85-25208
Investigation of the Vortex Tab
[NASA-CR-172586] 15 p2463 N85-25209
Flow past a flat plat with a vortex/sink combination
[JIAA-TR-58] 15 p2464 N85-25215
Conical stagnation points in the flow around an external corner — delta wings
[VTH-LR-396] 16 p2701 N85-26680
Lee-side flow over delta wings at supersonic speeds
[NASA-TP-2430] 19 p3212 N85-29921
Experimental and theoretical study of the longitudinal aerodynamic characteristics of delta and double-delta wings at Mach numbers of 1.60, 1.90, and 2.16
[NASA-TP-2433] 19 p3213 N85-29922
China has developed a new version of fighter aircraft
[AD-A155293] 21 p3555 N85-32118
Vortex boundary-layer interactions
[NASA-CR-176192] 24 p4093 N85-35373

DELTAS
NT MISSISSIPPI DELTA (LA)
Study of Volga river delta using space photosurvey materials
15 p2485 N85-25340
Sand dispersion from an ephemeral river delta on the wave-dominated central California coast
[AD-A154352] 19 p3300 N85-30458
Mapping of dynamics of deltas by space photography
22 p3737 N85-33163
Depositional systems and coal occurrence in the Fort Union Formation (Paleocene), Powder River Basin, Wyoming and Montana
24 p4114 N85-35505

DEMAGNETIZATION
Magnetic method of inspecting mechanical properties of general purpose tubes
[BLL-M-36084-(5826.4)] 16 p2796 N85-27235

DEMAND (ECONOMICS)
Demand for satellite-provided domestic communications services up to the year 2000
[NASA-TM-86894] 06 p0796 N85-15099
Satellite provided customer promises services, a forecast of potential domestic demand through the year 2000. Volume 4: Sensitivity analysis
[NASA-CR-174662] 16 p2769 N85-27092

DEMAND ASSIGNMENT MULTIPLE ACCESS
Integrated support of tactical operations by satellite communications
11 p1709 N85-20754

DEMINERALIZING
NT BONE DEMINERALIZATION

DEMODULATION
Carrier acquisition and tracking by a COSTAS loop with automatic frequency control
[ESA-TT-838] 04 p0493 N85-13149
Acoustooptic demodulation of frequency-modulated signals
13 p2090 N85-23050
Source energy spectra from demodulation of solar particle data by interplanetary and coronal transport
[SH-1.3-13] 23 p3994 N85-34758

DEMODULATORS
NT MODEMS
NT PHASE DEMODULATORS
NT PHASE LOCK DEMODULATORS
Digital signal demodulators with single-sideband
07 p0950 N85-16019
Performance of the DSA's subcarrier demodulation digital loop
10 p1485 N85-19242
Noise tolerance of digital demodulator for complex signal system employing binary quantization
13 p2070 N85-22929
Digital Optical Circuit Technology
[AGARD-CP-362] 18 p3185 N85-29757

DEMOGRAPHY
Characteristics of recent science/engineering graduates, 1982: Detailed statistical tables
[PB85-149060] 15 p2663 N85-26437
Experience of the Institute of Space Research with the use of remote sensing in urban planning studies
[INPE-3159-PRE/533] 16 p2880 N85-27770
An empirical comparison of the accuracy of univariate and multivariate corrections for range restriction
[AD-A153071] 17 p3019 N85-28670
On estimating transition intensities of a Markov process with aggregate data of a certain type
[CWI-MS-R8411] 17 p3025 N85-28707

DEMONSTRATION
U PROVING

DEMULTIPLEXING
Interference immunity of fiber-optic communication lines with spectral multiplexing of channels
13 p2069 N85-22924

DENDRITIC CRYSTALS
New metallurgical processes based on high-speed crystallization and diffusion of metals
01 p0021 N85-10126
Hydrogen passivation of electrically active defects in crystalline silicon solar cells
[DE84-004590] 02 p0223 N85-11461
Large-area sheet task advanced dendritic web growth development
[NASA-CR-174021] 02 p0223 N85-11463
Microstructure development in polymers
[AD-A145980] 03 p0337 N85-12170
Dynamic crystallization of silicate melts
[NASA-CR-174103] 05 p0743 N85-14774
Development of high-efficiency solar cells on silicon web
[NASA-CR-174212] 06 p0828 N85-15259
Advanced dendritic web growth development
06 p0831 N85-15286
The growth of metastable peritectic compounds
[NASA-CR-171289] 07 p0920 N85-15824
Characterization of terrestrial solar cells for space applications: Electrical characteristics of thin Westinghouse dendritic web cells as a function of solar intensity, temperature, and incidence angle
[NASA-CR-175642] 14 p2349 N85-24516
Solid/melt interface studies of high-speed silicon sheet growth
[NASA-CR-175898] 14 p2350 N85-24525
Influence of solidification parameters on the formation of the gamma-M7C3 eutectic structure of 2% C-12%Cr steel
15 p2512 N85-25500
Dendritic growth from amorphous matrix
[DE85-007630] 16 p2871 N85-27712
Role of hydrogen and structure on CMSX-2
17 p2915 N85-27967
Electrical and structural characterization of web dendrite crystals
20 p3481 N85-31633
Silicon dendritic web growth
21 p3611 N85-32435
Temperature-stress modeling
21 p3611 N85-32436
Silicon ribbon stress-strain activities
21 p3611 N85-32437
Analysis of stress-strain relationships in silicon ribbon
21 p3611 N85-32438
Advanced module development overview
21 p3612 N85-32445

DENDRITIC DRAINAGE
U DRAINAGE PATTERNS

DENDROCHRONOLOGY
Solar modulation of cosmic ray intensity and solar flare events inferred from (14)C contents in dated tree rings
[SH-7.1-2] 23 p4047 N85-35095
High precise measurements of cosmogenic radiocarbon abundance by complex of scintillation equipments
[SH-7.1-14] 23 p4048 N85-35105
Radiocarbon content in the annual tree rings during last 150 years and time variation of cosmic rays
[SH-7.1-15] 23 p4048 N85-35106

DENITROGENATION
Denitrification-efficiencies of alternate carbon sources
[AD-A148029] 08 p1119 N85-17050

DENMARK
The climate of Denmark. Summaries of observations from light vessels. 3: Sea temperature
[ISBN-87-7478-215-0] 01 p0073 N85-10481
Space research in Denmark
08 p1231 N85-17753
Finnair, LOT, SAS reps in USSR on present operations, plans
09 p1278 N85-18035
Siting of large scale wind turbines in Denmark
24 p4111 N85-35483

DENSE PLASMAS
NT PLASMA FOCUS
NT STRONGLY COUPLED PLASMAS
Ion-density correlations and enhancement of thermonuclear reaction rate in dense, inertially confined fusion plasmas
02 p0284 N85-11849
Many-body correlations in strongly-coupled plasmas
02 p0284 N85-11850
Compact toroid development, activity plan for spheromaks
[DE84-016736] 04 p0567 N85-13617
A research proposal for the theoretical study of the thermodynamic and transport properties of dense plasmas
[AD-A148040] 08 p1224 N85-17708
X-ray spectroscopy of high-Z and high-density plasmas
09 p1387 N85-18728
Extended abstract: Ergodic magnetic limiter experiments on TEXT with a 7/3 resonance
[DE85-001390] 09 p1391 N85-18754
X-ray line broadening of a diagnostic in laser produced plasma
[DE85-001179] 10 p1560 N85-19841
Numerical analysis of thermonuclear detonation in dense plasma
11 p1719 N85-20614

Adequacy of metal ablation process with laser radiation and a shock-compressed plasma
13 p2028 N85-22708
Basic studies. 1: Basic experiments in plasma physics
15 p2655 N85-26378
Basic experiments in plasma physics (TPL)
15 p2655 N85-26379
Direct electron and ion fluid computation of high electrostatic fields in dense inhomogeneous plasma with subsequent nonlinear optical and dynamical laser interaction
15 p2656 N85-26388
Restrike particle beam experiments on a dense plasma focus. Opening switch research on a dense plasma focus
[AD-A152991] 17 p3039 N85-28602
Slow tearing modes: Transitions to instability
20 p3534 N85-31989

DENSIFICATION

A strategy for the adjustment and analysis of densification networks — geodetic networks
[SER-C-295] 01 p0063 N85-10420
Sub-eutectic densification and second phase formation in Al2O3 - CaO
[DE85-002065] 09 p1398 N85-18796
Densification of submicron YSZ (Yttria-Stabilized Zirconia) powders with alumina and borate additives
[AD-A149520] 10 p1452 N85-19150
Densification and deformation in the presence of a liquid phase
[DE85-005101] 13 p2038 N85-22763
Computational methods for the explosive and impact compaction of powders
[AD-A156219] 24 p4139 N85-35853

DENSIMETERS

X-ray gauge measures areal density variations as small as 0.1%
[DE85-003774] 12 p1854 N85-21629

DENSITOMETERS

NT MICRODENSITOMETERS
Compact L-edge densitometer for uranium concentration assay
[DE85-010344] 18 p3110 N85-29261
Applied research and development for falling-sphere air density measuring systems
[AD-A155227] 21 p3552 N85-32099

DENSITY

On the modified likelihood for density estimation
[AD-A149437] 10 p1547 N85-19758
Profile of a relativistic electron beam propagated through a linear wiggler and an axial guide field
[AD-A154403] 19 p3353 N85-30783

DENSITY (MASS/VOLUME)

NT ATMOSPHERIC DENSITY
NT GAS DENSITY
NT SPACE DENSITY
Study of bridgewire size and pyrotechnic density relationships on all-fire levels
[DE84-016946] 09 p1302 N85-18177
Compaction of sand using ordinary off-road vehicles
[AD-P004297] 09 p1409 N85-18874
Investigation of structure-permeability relationships of silicone polymer membranes
[PB85-148476] 11 p1596 N85-20038
Field validation of statistically-based acceptance plan for bituminous airport pavements. Volume 3: Statistical analysis of 3 methods for determining maximum specific gravity of bituminous concrete mixtures
[FAA-PM-84-12-VOL-3] 12 p1781 N85-21182
Field validation of statistically-based acceptance plan for bituminous airport pavements. Volume 4: Computer simulation of multiple acceptance criteria
[FAA-PM-84-12-VOL-4] 12 p1782 N85-21183
Simple EOS for the silicone rubber Sylgard 184
[DE85-001394] 12 p1814 N85-21376
Models of the upper atmosphere
12 p1945 N85-22217
More precise curve of dependence between density and velocity of longitudinal waves in consolidated crust and top of mantle in oceanic structures
13 p2110 N85-23143
Crustal and upper mantle density model of Owen fault zone
13 p2110 N85-23144
Determination of density of the crust and upper mantle from deep seismic sounding and gravimetry, 2
13 p2111 N85-23153
The effect of particle density on aeolian transport
13 p2189 N85-23581
Pressure-density behavior for AlN, Al2O3, SiO2, TiB2, and TiC powders up to 3.5 GPa
[DE85-006146] 14 p2261 N85-24012
Density and thermal expansion measurements of several mixed oxide glasses in the solid and liquid regions
[DE85-006134] 14 p2261 N85-24014
Trends of petroleum fuels
[DE85-000116] 14 p2263 N85-24023
Characterization-curing-property studies of HBRF 55A resin formulations
[NASA-CR-175836] 16 p2753 N85-26980
Distribution of density in closed-impression die forging of axisymmetrical products from metal powders
19 p3245 N85-30118
Density characteristics of asthenosphere in Atlantic Ocean
19 p3294 N85-30423
Haze over eastern North America. Part 1: Haze properties
[PB85-181857] 19 p3311 N85-30526
Pycnometer shaker
[PB85-174965] 20 p3460 N85-31491
An investigation into the fluidization and heat transfer of low density particles in a fluidized bed with applications
[AD-A155259] 21 p3584 N85-32282
A safe, high-power-density lithium battery
[AD-A155223] 21 p3613 N85-32454
Buoyant densities of phototrophic sulfur bacteria and cyanobacteria
21 p3660 N85-32740
Optimization of design parameters for alternating current stabilizer based on magnetic suspension
22 p3772 N85-33374
The influence of temperature on the composition density of the transition metals
[BLL-M-35896-(5828.4)] 23 p3915 N85-34262
Comparison of experimental data on detonation velocity and Chapman-Jouget pressure vs initial HE density with predictions from Ree's model equation of state
[DE85-007266] 23 p3922 N85-34304
Transports studies of ECH and ICRH-heated bumpy torus plasma in NBT-1M
23 p3978 N85-34662

DENSITY (NUMBER/VOLUME)

NT CARRIER DENSITY (SOLID STATE)
NT ELECTRON DENSITY (CONCENTRATION)
NT ELECTRON DENSITY PROFILES
NT ELECTRON DISTRIBUTION
NT ION DENSITY (CONCENTRATION)
NT IONOSPHERIC ELECTRON DENSITY
NT IONOSPHERIC ION DENSITY
NT MAGNETOSPHERIC ELECTRON DENSITY
NT MAGNETOSPHERIC ION DENSITY
NT MAGNETOSPHERIC PROTON DENSITY
NT PACKING DENSITY
NT PARTICLE DENSITY (CONCENTRATION)
NT PLASMA DENSITY
NT PROTON DENSITY (CONCENTRATION)
NT SPACE DENSITY
SIMM1: A linearized particle code
[AD-A148827] 08 p1221 N85-17689
Electronic structure of liquid metal alloys
[DE85-000904] 09 p1295 N85-18136
An equation of profile of snow drift density during snowfall
15 p2581 N85-25919
Rayleigh scattering for density measurements in premixed flames: One point, time series data
20 p3424 N85-31253
Solar flare gamma-ray line spectroscopy
[SH-2.1-14] 23 p3999 N85-34795
Gradients and anisotropies of high energy cosmic rays in the outer heliosphere
[SH-4.3-7] 23 p4032 N85-34992

DENSITY (RATE/AREA)

U FLUX DENSITY

DENSITY DISTRIBUTION

Estimating a monotone density
[CWI-MS-R8403] 05 p0721 N85-14833
Dark matter near the sun: Simulated star counts and the Oort limit
06 p0880 N85-15592
The Malin effect in stellar photography
07 p0966 N85-16131
Feasibility of alpha particle measurement by CO2 laser Thomson scattering
[DE85-001764] 09 p1326 N85-18334
Small-sample properties of kernel density estimators from randomly right-censored data
[AD-A148752] 09 p1374 N85-18634
Gas dynamics of the barred spiral galaxy NGC 3359
13 p2170 N85-23465
Problems in recovering crater production functions
13 p2182 N85-23539
A parmetric study of crater-saturation simulation
13 p2182 N85-23540
Local covariance functions and density distributions
[AD-A150792] 14 p2373 N85-24869
Research on thermionic plasmas
[AD-A150683] 14 p2423 N85-24944
A model containing blobs for the A ring of Saturn
15 p2671 N85-26479
Measurements in low pressure flow using an electronic beam detector — wind tunnel tests
16 p2701 N85-26676
Altimetry data and the elastic stress tensor of subduction zones
[NASA-CR-175796] 16 p2825 N85-27425
The transport of neutral H, D, T and He and O in the boundary layers of a Tokamak plasma
[REPT-84-153] 17 p3041 N85-28617
Anisotropic electron-impurity scattering in dilute AlLi: (Small) corrections to the local density approximation
[DE85-002948] 19 p3238 N85-30076
The electric current densities beneath thunderstorms
20 p3494 N85-31726
Electron density distribution analysis for nitroguanidine
[DE85-009598] 23 p3969 N85-34603
Breakdown of intrinsic ambipolarity for the radial diffusion due to a rotating RF field
23 p3977 N85-34660
Transports studies of ECH and ICRH-heated bumpy torus plasma in NBT-1M
23 p3978 N85-34662
Guiding center distribution function and longitudinal invariant
23 p3978 N85-34663
Cosmic ray density gradient and its dependence on the north-south asymmetry in solar activity
[SH-4.5-17] 23 p4038 N85-35034
Observation of pick-up ions in the solar wind: Evidence for the source of the anomalous cosmic ray component?
[SH-4.6-5] 23 p4039 N85-35043
Average features of the muon component of EAS or = 10(17) eV
[HE-4.3-10] 24 p4191 N85-36004
Transition effect of air shower particles in plastic scintillators
[HE-4.4-9] 24 p4193 N85-36017

DENSITY MEASUREMENT

NT GAMMA RAY ABSORPTIOMETRY
NT PHOTON ABSORPTIOMETRY
NT X RAY DENSITY MEASUREMENT
Measurement of blood and plasma density with the mechanical oscillator technique
05 p0693 N85-14456
A wind-tunnel study of the saltation of heterogeneous (size, density) sands
08 p1182 N85-17449
Density measurements of atomic hydrogen in NBT-IM by laser-induced fluorescence spectroscopy
09 p1389 N85-18739
Fourier densitometry: A new optical method for measuring density fluctuations by Rayleigh scattering — turbulent jets
11 p1578 N85-19932
Field validation of statistically-based acceptance plan for bituminous airport pavements. Volume 3: Statistical analysis of 3 methods for determining maximum specific gravity of bituminous concrete mixtures
[FAA-PM-84-12-VOL-3] 12 p1781 N85-21182
Field validation of statistically-based acceptance plan for bituminous airport pavements. Volume 4: Computer simulation of multiple acceptance criteria
[FAA-PM-84-12-VOL-4] 12 p1782 N85-21183
Determination of permissible heating rate of metal
[BLL-M-36107-(5828.4)] 18 p2748 N85-29957
A study of freezing and melting with eutectic interactions
19 p3378 N85-30956
Applied research and development for falling-sphere air density measuring systems
[AD-A155227] 21 p3552 N85-32099
Application of satellite accelerometer data to improve density models
[AD-A154904] 21 p3831 N85-32558
Second order modelling in non-constant density flows
22 p3744 N85-33206
Simultaneous measurement of velocity and density in a turbulent nonpremixed flame
22 p3744 N85-33209
Calculation of flow kinetics of composite media
[BLL-M-35819-(5828.4)] 23 p3929 N85-34348
The lateral distributions of charged particles of energy greater than 0.3 E sub crit in electron-photon cascades in lead and air
[HE-3.6-10] 24 p4185 N85-35957
Properties of 10 (18)-10 (19)eV EAS at far core distance
[HE-4.7-3] 24 p4198 N85-36054

DENSITY WAVE MODEL

The lunar angular momentum problem
04 p0588 N85-13752
Excitation of spiral patterns in responsible density wave theory
05 p0740 N85-14784
Studies of planetary rings
13 p2174 N85-23488
Structure and dynamics of Saturn's rings as seen by the Voyager stellar occultation
15 p2673 N85-26494
Excitation of turbulence by density waves
[NASA-CR-3905] 19 p3314 N85-30546

DENTISTRY

Catalog of completed studies, US Army health care studies and clinical investigation activity
[AD-A149450] 10 p1568 N85-19885
Applications of CdTe to nuclear medicine
[DE85-011677] 23 p3952 N85-34492
Dental multi-purpose slowspeed handpieces test and evaluation
[AD-A155764] 24 p4130 N85-35606

DEOXIDIZING
Thermodynamics of reactions of deoxidation of nickel melts
[BLL-M-35729-(5828.4)] 02 p0175 N85-11168
Metallurgy Institute's developments for alloy and aircraft producers 03 p0353 N85-12268
The electrochemical deoxidation of molten oxide substances
[BLL-M-35982-(5828.4)] 05 p0614 N85-13920
Improvement of the ladle deoxidizing of Al-killed steel
[BMFT-FB-T-84-172] 06 p0769 N85-14923

DEOXYGENATION
Primary light harvesting system: The relationship of phycobiliesomes to photosystem 1 and 2
[DE85-103075] 11 p1689 N85-20622
Noble gases and the early history of the Earth: Inappropriate paradigms and assumptions inhibit research and communication 21 p3719 N85-33075

DEOXYRIBONUCLEIC ACID
Genetic effects of microwave exposure on mammalian cells in vitro. Volume 2, Appendix A: Cytogenetics and growth kinetics data, 850 MHz
[AD-A148866] 10 p1522 N85-19599
Genetic effects of microwave exposure on mammalian cells in vitro. Volume 2, Appendix B: Cytogenetics and growth kinetics data, 1.2 GHz
[AD-A148867] 10 p1522 N85-19600
Genetic effects of microwave exposure on mammalian cells in vitro, volume 2
[AD-A149347] 10 p1523 N85-19603
Photoreactivation and other ultraviolet/visible light effects on DNA in human skin
[DE85-005135] 14 p2390 N85-24719
Molecular toxicology of chromatin: The role of Poly(ADP-Ribose) in gene control
[AD-A154415] 19 p3327 N85-30611
Repair of DNA treated with lambda-irradiation and chemical carcinogens
[DE85-010298] 19 p3327 N85-30616
Size and DNA distributions of electrophoretically separated cultured human kidney cells
20 p3500 N85-31759
Development of a recombinant DNA assay system for the detection of genetic change in astronauts cells
[DE85-010103] 20 p3504 N85-31781
The DNA metabolism and poly-(ADP-ribose) synthesis in lymphocytes of persons exposed to low doses of ionizing radiation
[OEFZS-4307] 20 p3507 N85-31800
Molecular biology of environmental aromatic hydrocarbons
[DE85-015036] 24 p4128 N85-35593

DEPENDENCE
NT SPATIAL DEPENDENCIES
NT TEMPERATURE DEPENDENCE
NT TIME DEPENDENCE
Potential dependence of electrical conductivity and chemical charge storage of poly(pyrrole) films on electrodes
[AD-A148513] 08 p1122 N85-17075
A modified Fresnel scattering model for the parameterization of Fresnel returns, part 2.3A
21 p3618 N85-32483
Observations of mesospheric turbulence by rocket probe and VHF radar, part 2.4A 21 p3619 N85-32484
On the dependence of the convergence of Gummel's algorithm on the regularity of the solution
[AD-A154628] 21 p3675 N85-32832

DEPENDENCY
U DEPENDENCE

DEPENDENT VARIABLES
Development factors and field dependence-independence
[AD-A152337] 17 p3000 N85-26545
On the interpretation of variables — simulation and regression models
[FEW-136] 20 p3522 N85-31903

DEPLETION
The dependence of interstellar element depletions on mean space density 11 p1749 N85-20998
Depletion modeling of liquid dominated geothermal reservoirs
[DE85-009923] 23 p3943 N85-34437

DEPLOYMENT
In-orbit performance of INTELSAT V communications antennae deployment systems 05 p0627 N85-14018
ARABSAT spacecraft: Rx and Tx antenna mechanisms 05 p0628 N85-14022
Deployment of a regional array in Norway
[AD-A147032] 07 p0997 N85-16330
Deployment sequence mode selection system for aircraft ejection seat
[AD-D011464] 10 p1422 N85-18968
Integrated paratroop door
[AD-D011507] 12 p1776 N85-21148
Concept for controlled fold by fold deployment and retraction of flexible, foldable solar generators
13 p2011 N85-22613
Deployment analysis of the Olympus Astromast and comparison with test measurements — solar arrays
13 p2011 N85-22616
Developments in deployable masts to support flexible solar arrays 13 p2012 N85-22620
New concepts in deployable beam structures
14 p2232 N85-23632
Utilization of space station by the large deployment reflector 14 p2235 N85-23857
Deployable controllable geometry truss beam
[NASA-TM-86366] 17 p2909 N85-27934
Solar array flight experiment
[NASA-TM-86506] 17 p2909 N85-27935
Deployable Core Automated Maintenance System (DCAMS)
[AD-A153665] 18 p3198 N85-29839
Application of the ADAMS program to deployable space truss structures
[NASA-CR-177927] 19 p3284 N85-30366
Vibration/libration interaction dynamics during the orbiter based deployment of flexible members
20 p3411 N85-31171
The Galelso spacecraft magnetometer boom
22 p3796 N85-33513
Hoop/column antenna deployment mechanism overview 22 p3796 N85-33514
Structural dynamics model and response of the deployable reference configuration space station
[NASA-TM-86386] 22 p3799 N85-33539

DEPOLARIZATION
Alternative anodic reactions in water splitting
[DE85-004159] 12 p1802 N85-21300
Using fuel cells or anode depolarization to reduce electrowinning energy consumption
[DE85-006167] 13 p2129 N85-23250
Influence of depolarization of linear polarized radiation on the heterodyne detection in laser range finders
[ESA-TT-903] 20 p3461 N85-31500

DEPOLARIZERS
U DEPOLARIZATION

DEPOSITION
NT ANODIZING
NT ELECTRODEPOSITION
NT ELECTROLESS DEPOSITION
NT ELECTROPLATING
NT VACUUM DEPOSITION
NT VAPOR DEPOSITION
Analysis of glow discharges for understanding the process of film formation
[NASA-TM-83750] 01 p0022 N85-10138
MOD silver metallization for photovoltaics
[NASA-CR-174011] 01 p0026 N85-10163
Acoustic resonator and method of making same
[DE84-014655] 01 p0116 N85-10782
Plasma deposited diamondlike carbon on GaAs and InP
[NASA-TM-86870] 01 p0123 N85-10844
Energy deposition in microvolumes of silicon from high energy proton reactions
[AD-A144713] 01 p0123 N85-10845
Estimation of the potential and probable source regions for acid precipitation
[DE84-015119] 02 p0225 N85-11472
Interaction of UV-laser radiation with molecular surface-films
[AD-A146311] 03 p0366 N85-12349
Analysis of accretion and deletion at boundaries in dynamic scenes
[AD-A145944] 03 p0419 N85-12678
Structural studies of sputtered MOS(2) films by angle-resolved photoelectron spectroscopy
[AD-A146052] 03 p0433 N85-12759
The effect of thin-film growth mode on XPS/UPS/AES intensities
[AD-A146264] 03 p0434 N85-12763
Initial feasibility ground test of a proposed photogrammetric system for measuring the shapes of ice accretions on helicopter rotor blades during forward flight
[NASA-TM-87391] 04 p0455 N85-12887
Liquid phase products and solid deposit formation from thermally stressed model jet fuels
[NASA-TM-86874] 04 p0481 N85-13066
Newly recognized sedimentary environments in the Shelikof Formation, Alaska 04 p0516 N85-13292
Climatological variability in modeling of long-term regional transport and deposition of air pollutants
[DE84-014726] 04 p0539 N85-13430
Transformation processes and wet deposition on the urban scale
[DE84-015294] 04 p0539 N85-13432
Lunar magma ocean and its implication for origin of the Moon 04 p0581 N85-13711
The initial thermal state of the Moon
04 p0581 N85-13712
Origin of the Moon 04 p0587 N85-13745
Lunar origin: role of giant impacts
04 p0587 N85-13749
Oceanic plateaus, anomalous subduction, and the accretion of buoyant features at convergent margins
05 p0688 N85-14422
LPE (Liquid phase epitaxy) semiconductor material transfer method
[AD-D011250] 05 p0731 N85-14896
Contamination analysis of Ti-O2 thin films deposited using ion assisted deposition
[DE84-014944] 05 p0732 N85-14705
Substrate preparation for thin film deposition: A survey
[DE84-016119] 06 p0868 N85-15514
Meteoritic constraints on processes in the solar nebula 06 p0887 N85-15830
The adsorption of CO and oxygen on Cu layers on a W(110) surface
[AD-A147345] 07 p0923 N85-15847
Evaluation of jet fuel deposit kinetics. Lot 4
[AD-A147196] 07 p0935 N85-15922
French research on gallium arsenide devices
08 p1141 N85-17196
Impact and collisional processes in the solar system
[NASA-CR-174297] 08 p1255 N85-17914
Plasma deposition of amorphous metal alloys
[DE85-000768] 09 p1295 N85-18132
Quaternary stratigraphy of the lower Iowa and Cedar River Valleys, southeast Iowa 09 p1352 N85-18504
Non-photochemical interactions of sulfur and nitrogen compounds in acid deposition
[DE84-016141] 10 p1513 N85-19546
Study of deposition control using transpiration
[DE85-003463] 11 p1585 N85-19984
Deposition of diamondlike carbon films
[NASA-CASE-LEW-14080-1] 11 p1615 N85-20153
Laser-plasma interactions for the deposition and etching of semiconductor materials
[DE85-000458] 11 p1731 N85-20685
Low temperature deposition of nickel films
[AD-D011568] 12 p1805 N85-21319
Combined effects of atmospheric deposition, internal acid production, and harvesting on nutrient gains and losses from forest ecosystems
[DE85-002325] 12 p1884 N85-21621
Hazardous air pollutants: Wet removal rates and mechanisms
[PB85-138626] 12 p1887 N85-21842
Hazardous air pollutants: Dry-deposition phenomena
[PB85-138279] 12 p1887 N85-21843
A simple model of electron beam initiated dielectric breakdown 13 p1996 N85-22516
Diffusion deposition in fibrous filters for parallel and transverse flow models
[DE85-006149] 13 p2093 N85-23066
Non-linear optical techniques for visible and UV lasers and thin film deposition
[AD-A150489] 13 p2096 N85-23077
Electronic transport in hydrogenated amorphous silicon films
[DE85-002901] 13 p2164 N85-23426
Lunar origin: Role of giant impacts
13 p2179 N85-23519
Impact and collisional processes in the solar system
13 p2180 N85-23530
Eolian erosion on Mars: Three scales
13 p2188 N85-23577
The origin of regional dust deposits on Mars
13 p2188 N85-23578
On the latitudinal distribution of debris in the Northern Hemisphere of Mars 13 p2188 N85-23579
PLUVIUS: A generalized 1-dimensional model of reactive pollutant behavior, including dry deposition, precipitation formation, and wet removal, 2nd edition
[DE85-005542] 14 p2353 N85-24538
Aerosol deposition along the respiratory tract at zero gravity: A theoretical study
[DE85-006703] 15 p2619 N85-26136
Optical properties of hydrogenated amorphous carbon films grown from methane plasma
[NASA-TM-86995] 15 p2658 N85-26406
In situ thin film measurement
[AD-A151365] 15 p2659 N85-26411
LPCVD tungsten deposition on Si-Ge alloy
[DE85-005588] 16 p2750 N85-26970
Emission inventory applications to regional acid deposition modeling
[PB85-157386] 16 p2760 N85-27033
Energy deposition from particle beams
[DE85-007362] 16 p2662 N85-27654
Jet fuel instability mechanisms
[NASA-CR-175856] 17 p2936 N85-28127

Heat pipe and method of making same
[AD-D011654] 17 p2959 N85-28273
The structure of ion plated films in relation to coating properties
[NASA-TM-87055] 18 p3085 N85-29085
Energy deposition and its effects on the E+ capture section at Sector 20
[DE85-010964] 18 p3182 N85-29727
Process for the epitaxial deposition of 3-5 compounds utilizing a binary alloy as the metallic source
[AD-D011663] 18 p3193 N85-29801
Micro-reactions of metal contacts on various types of GaAs surfaces
[AD-A153650] 18 p3193 N85-29806
A comparative evaluation of the effects of acid precipitation, natural acid production and harvesting on cation removal from forests
[DE85-010821] 19 p3309 N85-30511
Technical guide for estimating fugitive dust impacts from coal handling operations. Volume 1: Project summary
[DE85-010948] 19 p3309 N85-30515
An interim user's manual for the advanced scavenging module version 1.2
[PB85-173904] 19 p3318 N85-30572
Droplet deposition in vertical two-phase flow
[CFD/84/22] 20 p3456 N85-31460
Design of the National Trends Network for monitoring the chemistry of atmospheric precipitation
[GS-CIRC-984] 20 p3486 N85-31664
Experimental method for measuring positronium reflection from surfaces
[DE85-010949] 20 p3531 N85-31967
Modification of the grain size of sputtered copper with additions of oxygen, krypton, silver, or yttrium
[DE85-010975] 21 p3567 N85-32189
Laser-assisted solar-cell metallization processing
21 p3610 N85-32429
Microwave-enhanced thin-film deposition
21 p3611 N85-32431
Experimental studies of the kinetics of deposition nucleation on an ice nucleant used in weather modification
21 p3638 N85-32598
Ice nucleus measurements 21 p3640 N85-32600
Geology and geochemistry of sulfide and sulfate deposition 21 p3658 N85-32723
Archean sedimentary systems and crustal evolution
21 p3720 N85-33082
Method of bonding silver to glass and mirrors produced according to this method
[DE85-011642] 22 p3792 N85-33495
1985 Amorphous Silicon Review Meeting
[DE85-006794] 22 p3807 N85-33582
Development of a microorifice uniform deposit cascade impactor
[DE85-006765] 22 p3812 N85-33614
Liquid crystal light valve structures
[NASA-CASE-MSC-20036-1] 22 p3847 N85-33826
Oxidation states of iron in the terrestrial planets: Evidence and implications for accretion models
22 p3852 N85-33854
Late-stage planetesimals: How big?
22 p3852 N85-33857
Dual-chamber plasma deposition of A-Si:H solar cells at high rates using disilane
[DE85-011828] 23 p3946 N85-34451
Throughfall rate and chemistry studies: Whiteface Mountain
[DE85-012407] 23 p3947 N85-34464
User's guide to the MATHEW/ADPIC models
[DE85-012952] 23 p3966 N85-34587
MATADOR (Methods for the Analysis of Transport And Deposition Of Radionuclides) code description and user's manual
[TI85-901402] 23 p3966 N85-34592
Diamondlike carbon protective coatings for IR materials
[NASA-TM-87063] 23 p3973 N85-34631
Depositional systems and coal occurrence in the Fort Union Formation (Paleocene), Powder River Basin, Wyoming and Montana 24 p4114 N85-35505

DEPOSITS
Evaluation of jet fuel deposit kinetics. Lot 4
[AD-A147196] 07 p0935 N85-15922
Study of deposition control using transpiration
[DE85-002339] 10 p1485 N85-19378
Study of deposition control using transpiration
[DE85-003483] 11 p1585 N85-19984
Apparatus and method to keep the walls of a free-space reactor free from deposits of solid materials
[NASA-CASE-NPO-15851-1] 12 p1858 N85-21652
Fracture detection and mapping f.r geothermal reservoir definition: An assessment of current technology, research, and research needs
[DE85-010827] 19 p3301 N85-30464

DEPRESSANTS
Workload demand and CNS depressant stressor effects on spatial orientation information processing
[AD-A145211] 01 p0098 N85-10651

DEPRESSIONS (TOPOGRAPHY)
U STRUCTURAL BASINS

DEPRESSURIZATION
U PRESSURE REDUCTION

DEPRIVATION
NT SENSORY DEPRIVATION
NT SLEEP DEPRIVATION

DEPTH
Nonlinear propagation in a depth-dependent ocean
[AD-A145079] 01 p0116 N85-10791
Active remote sensing of ocean parameters, an engineering study 02 p0213 N85-11403
Determination of depth profiles and lattice positions with (n, p)- and (n, alpha) reactions (n, alpha) and channeling-blocking method) 03 p0429 N85-12735
Subsurface temperatures in northeastern Wyoming measured by bottom hole temperature records
[TI84-901610] 04 p0534 N85-13413
An extension of the Born inversion method to a depth dependent reference profile
[AD-A146469] 06 p0859 N85-15461
Microwave radiometer observations of snowpack properties and comparison of U.S. Japanese results — Hokkaido, Japan and Vermont and North Dakota test sites 13 p2125 N85-23230
Studies on physical properties of snow based on multi channel microwave radiometer
13 p2125 N85-23231
Analysis of NIMBUS-7 SMMR data — Hokkaido, Japan snow cover 13 p2125 N85-23232
The effects of internal waves on acoustic normal modes
[AD-A150235] 13 p2155 N85-23379
Regional seismic wave propagation
[AD-A150801] 14 p2373 N85-24671
Estimation of the depth of a spherical cap in an hydraulic drawing test for some simple conditions of loss of stability
[REPT-4/1984] 16 p2748 N85-26956
The effect of ion-bombardment-induced atomic mixing on depth-profiling of interfaces
[AD-A153199] 17 p3044 N85-28834
Altitude variations of cosmic-ray soft and hard components observed by airborne detectors
[SH-6.1-5] 23 p4045 N85-35079

DEPTH MEASUREMENT
Variations in resistivity of upper crustal layer
13 p2113 N85-23164
An assessment of the potential role of multispectral imagery in bathymetric charting
[AD-A152400] 17 p2984 N85-28438
Detecting and analyzing crack defects
[BLL-BISI-TRANS-22062-(9022.06)]
17 p3027 N85-28723
Ultrasonic crack tip method for the determination of crack depth 17 p3028 N85-28725
Fluctuations of development maximum depth and nuclear composition of primary cosmic radiation
[OG-5.1-13] 22 p3862 N85-34054
Estimation of composition of cosmic rays with E sub zero approximately equals 10(17) - 10(18) eV
[OG-5.1-14] 22 p3862 N85-34055
Method for determining depth and shape of a sub-surface conductive object
[DE85-006502] 23 p3935 N85-34369
The transient electromagnetic depth sounding technique applied to hydrocarbons and geothermal exploration
[MITT-42] 23 p3949 N85-34476
Analysis of Cerenkov pulses recorded simultaneously at two sites
[HE-4.4-16] 24 p4194 N85-36022

DEPTH PERCEPTION
U SPACE PERCEPTION

DERIVATION CALCULUS
U DIFFERENTIAL CALCULUS

DESALINIZATION
An evaluation of the electrodialysis reversal process (Edr) for the desalination of brackish water from the Omaruru delta (SWA/Namibia)
01 p0023 N85-10141
Evaluation of hollow fiber ultrafiltration as a pretreatment for reverse osmosis desalination of seawater
[PB84-212408] 01 p0026 N85-10160
Feasibility study for small group water desalination equipment
[AD-A155106] 21 p3563 N85-32164
Oxidation of formaldehyde solutions used for the preservation of reverse osmosis membranes
[PB85-185585] 22 p3742 N85-33194

DESCENT
NT PARACHUTE DESCENT
Error analysis of wind determined using a VLF Omega sonde
[WSRL-0361-TM] 06 p0838 N85-15321
Effects of aircraft and flight parameters on energy-efficient profile descents in time-based metered traffic
[NASA-CR-172338-ADD] 07 p0901 N85-15708
Reference energy-altitude descent guidance: Simulator evaluation — aircraft descent and fuel conservation
[NASA-TP-2383] 08 p1085 N85-16868
Planning fuel-conservative descents in an airline environmental using a small programmable calculator: Algorithm development and flight test results
[NASA-TP-2393] 16 p2707 N85-26705

DESCENT PROPULSION SYSTEMS
Descent vehicles
[NASA-TM-77654] 17 p2909 N85-27933

DESCENT TRAJECTORIES
NT REENTRY TRAJECTORIES
Descent guidance and mission planning for space shuttle 08 p1092 N85-16902
Some effects of digital sampling on orbiter flight control system operation 08 p1092 N85-16903
Descent vehicles
[NASA-TM-77654] 17 p2909 N85-27933

DESCRIPTIONS
Glossary of landscape and vegetation ecology for Alaska
[PB85-153831] 16 p2816 N85-27372
DoD manual for standard data elements, part 2
[AD-A152202] 16 p2878 N85-27755
DoD manual for standard data elements, part 3
[AD-A152203] 16 p2878 N85-27756
Systematic nomenclature of the nitrogen, oxygen and sulfur functional polycyclic aromatic hydrocarbons
[DE85-007426] 17 p2916 N85-27974

DESCRIPTIVE GEOMETRY
Generation of radiation transport geometry from computer-generated design data — monte carlo solution of the neutron transport equation
[DE84-017380] 09 p1370 N85-18606
X-ray satellite
[NASA-TM-77898] 20 p3407 N85-31144

DESENSITIZING
The current status of the RAF programme of desensitisation for motion sick aircrew
11 p1685 N85-20658
The shock desensitization of PBX-9404 and composition B-3
[DE85-009604] 18 p3084 N85-29077
Manufacturing process to reduce large grain growth in zirconium alloys
[DE85-011649] 23 p3915 N85-34257

DESERTS
NT GOBI DESERT
NT MOJAVE DESERT (CA)
NT SAHARA DESERT (AFRICA)
An integrated LANDSAT/ancillary data classification of desert rangeland
[E85-10046] 06 p0826 N85-15248
Application of SIR-B data for groundwater exploration in the Arabian shield and sand-drift monitoring in the AN Nafud and Al Jafurah fringe areas, Kingdom of Saudi Arabia 08 p1144 N85-17214
Application and calibration of the subsurface mapping capability of SIR-B in desert regions
08 p1148 N85-17244
Field testing of a lightweight relocatable structure in a desert environment
[AD-A148841] 09 p1304 N85-18192
Analysis of SMIRR data for volcanic and sedimentary terrains of the trans-Pecos region, Texas
13 p2197 N85-23626
Meteorological conditions affecting electromagnetic propagation on the Arabian Peninsula
[AD-A152019] 15 p2544 N85-25708
The behavior of the atmosphere in the desert planetary boundary layer
[AD-A151266] 15 p2592 N85-25877
Utilization of remote sensing data in the evaluation of air pollution characteristics in the south coast/Southeast Desert Air Basin
[PB85-162063] 16 p2822 N85-27407
Quality assurance for RESOLVE (Research on Operations-Limiting Visual Extinction). A visibility study in the California desert
[AD-A152363] 17 p2992 N85-29494
Microbial ecology of extreme environments: Antarctic yeasts and growth in substrate-limited habitats
[NASA-CR-176005] 19 p3326 N85-30809

DESICCANTS
High performance solar desiccant cooling system: Performance evaluation and research recommendations
[DE85-000608] 11 p1678 N85-20559

Investigation of manganese dioxide as an improved solid desiccant
[DE85-004034] 13 p2018 N85-22654
Experiments on sorption characteristics of solid desiccant materials for solar desiccant cooling systems
[DE85-000542] 17 p2923 N85-26019
Solid desiccant dehumidification systems for residential applications
[PB85-199469] 22 p3755 N85-33279
Advances in open-cycle solid desiccant cooling
[DE85-008797] 22 p3808 N85-33590
Rigid zeolite containing polyurethane foams
[DE85-008406] 23 p3919 N85-34286

DESICCATION
U DRYING

DESIGN
CCDs: Their cause and cure
08 p1252 N85-17905
Ultrareliable, fault-tolerant control systems: A conceptual description
[NASA-TM-86017] 19 p3221 N85-29972

DESIGN ANALYSIS
Applications of numerical optimization methods to helicopter design problems: A survey
[NASA-TM-86010] 01 p0006 N85-10036
Development trends and requirements of propulsion system technology for civil aircraft
01 p0011 N85-10066
Natural environment design criteria for the Advanced X-ray Astrophysics Facility (AXAF) definition and preliminary design
[NASA-TM-86481] 01 p0014 N85-10069
Design sensitivity analysis of an antisymmetric angle-ply laminate
[CSIR-TWISK-318] 01 p0021 N85-10128
Methods for the design of quantizers for image signals
[FUB-38-1983] 01 p0041 N85-10283
Development of the Antares electron gun
[DE84-014043] 01 p0053 N85-10352
Achievements in laser development
01 p0115 N85-10784
Means of varying conditions in the expanded boundary divertor without affecting energy confinement
[DE84-013640] 01 p0122 N85-10836
Energy efficient engine flight propulsion system preliminary analysis and design report
[NASA-CR-174701] 02 p0140 N85-10947
Energy efficient engine high pressure turbine test hardware detailed design report
[NASA-CR-167955] 02 p0147 N85-10995
Conceptual design and evaluation of selected Space Station concepts: Executive summary
[NASA-TM-87382] 02 p0167 N85-11128
Conceptual design and evaluation of selected Space Station concepts, volume 1
[NASA-TM-87383] 02 p0168 N85-11129
Conceptual design and evaluation of selected Space Station concepts, volume 2
[NASA-TM-87384] 02 p0168 N85-11130
Simulation study of a new inverse-pinch high Coulomb transfer switch
[NASA-CR-172420] 02 p0194 N85-11294
Laser source of neutral atoms for collective-field particle accelerator 02 p0263 N85-11719
Optical waveguide spatial filters
[AD-A145674] 02 p0280 N85-11825
Inverse design technique for cascades
[NASA-CR-3836] 03 p0311 N85-12008
Modular electromechanical industrial robots
03 p0345 N85-12223
Burmester theory for 4 precision positions: An extended discourse with application to the dimensional synthesis of arbitrary planar linkages 03 p0367 N85-12351
Accelerator development in support of the NRL (Naval research laboratory) beam dynamic program
[AD-A145976] 03 p0417 N85-12669
A topological approach to database theory
03 p0437 N85-12781
Design, construction, and operational results of an 800-A, 10-kV hot deck amplifier
[DE84-014044] 04 p0496 N85-13162
Westinghouse programs in pulsed homopolar power supplies 05 p0606 N85-13862
Generic composite flywheel designs
05 p0606 N85-13864
Design, ancillary testing, analysis and fabrication data for the advanced composite stabilizer for Boeing 737 aircraft, volume 2
[NASA-CR-166011] 05 p0612 N85-13914
A summary description of a computer program concept for the design and simulation of solar pond electric power generation systems 05 p0666 N85-14285
Salt-gradient solar ponds: Summary of US Department of Energy sponsored research
[NASA-CR-174183] 05 p0667 N85-14286
Salton Sea solar pond power plant design study and regional applicability 05 p0667 N85-14290
Crewstation design and validation
06 p0752 N85-14822
Avionics technology - system concepts
06 p0753 N85-14824
Avionics system design for requirements for the United States Coast Guard HH-65A Dolphin
06 p0753 N85-14827
The need for a dedicated public service helicopter design 06 p0753 N85-14828
A theoretical design method for 3-dimensional transonic wings
[NAL-TR-830] 06 p0754 N85-14834
Efficiency estimation and sensitivity modeling
06 p0829 N85-15263
Computational analysis of scramjet dual mode operation
[NASA-CR-174250] 07 p0956 N85-16060
Development of large wind energy power generation system
[NASA-TM-77779] 07 p0992 N85-16301
Development of a preprototype times wastewater recovery subsystem, addendum
[NASA-CR-171823] 07 p1019 N85-16468
Design of self-checking N-MOS (H-MOS) integrated circuits 08 p1084 N85-16742
A description of a logistically ideal aircraft
[AD-A148425] 08 p1084 N85-16866
Design concept definition study for an improved shuttle waste collection subsystem
[NASA-CR-171834] 08 p1198 N85-17546
MHD performance demonstration experiment, FY 1974 to FY 1984
[DE85-000854] 08 p1224 N85-17709
Finite element computation of structural design sensitivity analysis 09 p1330 N85-18353
Treatment of general boundary conditions and point-wise state variable constraints in optimum design for static and dynamic response
09 p1330 N85-18358
DDL system: Design synthesis of digital systems
[NASA-CR-170759] 09 p1366 N85-18584
Design and analysis of an access control system for a multi-backend database system
[AD-A148750] 09 p1367 N85-18586
Antiproton source beam position system
[DE84-016716] 09 p1380 N85-18679
Cookbook for determining essential transmission characteristics of spherical section electrostatic analyzers
[DE85-001404] 09 p1391 N85-18751
Hybrid vehicle program
[DE85-000326] 09 p1410 N85-18886
Integrated Technology Rotor/Flight Research Rotor (ITR/FRR) concept definition study
[NASA-CR-166444] 10 p1424 N85-18981
Control system of complex CNC machining cell
10 p1462 N85-19218
Proceedings of the 17th Symposium on Electromagnetic Windows, part 1
[AD-A149185] 10 p1466 N85-19253
The use of synthesis method in the design of gyrotron electron guns
[INPE-3305-PRE/616] 10 p1478 N85-19329
Experience highlights from the design and manufacture of US LCT coils
[DE84-017504] 10 p1482 N85-19354
Performance of the 10 KSI Wilson valve breech
[DE85-000258] 10 p1493 N85-19430
Intermediate load modules for test and evaluation: Flat-Plate Solar Array Project
[NASA-CR-174450] 10 p1508 N85-19512
Conceptual design of a 10 MW shore-based OTEC plant
[DE84-015808] 10 p1511 N85-19532
Microstrain analysis in bent single crystal silicon by double crystal X-ray topography technique
[DE85-000422] 10 p1584 N85-19863
Design and analysis of airborne scanning optical systems 11 p1623 N85-20218
Mini-modal testing of wind turbines using novel excitation
[DE85-000666] 11 p1654 N85-20417
Computerized study of several electrostatic, surface-ionization ion-source configurations
[DE85-001512] 11 p1721 N85-20823
Stability analysis of flexible spacecraft with PID controller
[CRC-1372] 12 p1792 N85-21247
A radome for air traffic control SSR radar systems
[AD-P004373] 12 p1827 N85-21467
The 13.9 GHz radiometer design
[AD-A149637] 12 p1851 N85-21613
Reliability of structural brittle materials
12 p1946 N85-22222
Dynamic wind-tunnel testing of active controls by the NASA Langley Research Center
13 p1966 N85-22353
Rational use of tatanium in nonferrous metallurgy
13 p2031 N85-22728
Experimental determination of optimum ratio of runner blade height at exit to runner blade height at entrance of radial inward-flow microturbines
13 p2049 N85-22827
Reluctance and doubly-excited reluctance motors
[DE85-003585] 13 p2065 N85-22900
A 60 GHz 200 kW CW gyrotron with high output mode purity
[DE85-005283] 13 p2066 N85-22905
Analysis and design of linear microwave transistor amplifiers 13 p2068 N85-23038
Magnetic refrigeration and heat pumping design options
[DE85-003405] 13 p2092 N85-23064
Optimum design and automated dynamic analysis of flexible mechanisms
[AD-A150152] 13 p2099 N85-23068
A design analysis and implementation of a user-friendly interface for the UNIX operating system
[AD-A150558] 13 p2145 N85-23312
Manufacturing perspective in the design of bevel gearing 14 p2221 N85-23777
Manufacturing considerations related to aircraft gearboxes 14 p2222 N85-23778
Possible technological answers to new design requirements for power tranamission systems
14 p2222 N85-23779
Design of single-wheel gyrocompass with correction
14 p2272 N85-24079
Determining optimum service conditions for concentrator mirrors by methods of mathematically planned experiment 14 p2274 N85-24090
Module performance and failure analysis area: Flat-plate solar array project
[NASA-CR-175689] 15 p2585 N85-25936
SPRING: Helical spring design software for microcomputers
[DE85-006200] 15 p2631 N85-26217
Outline of alternative design of R-Tokamak
15 p2654 N85-26371
Metal armatures for railguns
[AD-A152129] 16 p2728 N85-26838
Fuel and oxidizer turbine loss analysis
16 p2739 N85-26900
Cryostat and electronic development associated with multi-detector spectrometer systems
[DE85-007624] 16 p2788 N85-27203
Numerical optimization algorithm for engineering problems using microcomputer
[AD-A152135] 16 p2847 N85-27554
Radiometer integrated into a communication terminal
[AD-A151746] 17 p2947 N85-28195
SC filters and design centering of integrated circuits. Part 2: Design centering of integrated circuits
[BMFT-FB-T-84-265-PT-2] 17 p2956 N85-28257
A ten channel temperature controller
[AD-A152664] 17 p2967 N85-28326
Design and construction of a CW ND:YAG laser using a single elliptical cavity and water cooled krypton arc lamp pumping
[AD-A152657] 17 p2970 N85-28340
Resonator optical designs for free electron lasers
[DE85-007678] 17 p2971 N85-28347
Silica problem in the design of geothermal power plants
[DE85-006245] 17 p2986 N85-28453
Peer Review of a Formal Verification/Design Proof Methodology
[NASA-CP-2377] 17 p3010 N85-28609
Optimum dimensions of power solenoids for magnetic suspension
[NASA-TM-77864] 17 p3026 N85-28716
Impurity control and vacuum pumping system design and analysis for next-generation Tokamaks
[DE85-009291] 17 p3041 N85-28815
A simulation study of jammer nulling trade-offs in a reactively steered adaptive array
[AD-A153461] 18 p3090 N85-29124
Development of hydrogen masers for K-3 VLBI system
18 p3106 N85-29239
Atomic hydrogen maser active oscillator cavity and bulb design optimization 18 p3108 N85-29240
High temperature sensible heat storage options
[DE85-000534] 18 p3129 N85-29375
Atmosphere monitoring requirements
18 p3158 N85-29553
Analysis of remote operating systems for space-based servicing operations, volume 1
[NASA-CR-171885] 19 p3225 N85-29993

Analysis of remote operating systems for space-based servicing operations. Volume 2: Study results
[NASA-CR-171686] 19 p3225 N85-29994
Space station automation study-satellite servicing, volume 2
[NASA-CR-171513] 19 p3226 N85-30000
Liquid sampling system
[DE85-011673] 19 p3265 N85-30248
A numerical method for the solution of the inverse problem in external aerodynamics
[STN-7] 20 p3390 N85-31025
Design of a basic airfoil for a slightly swept wing. Part 1: Theoretical transonic airfoil design
[ESA-TT-892] 20 p3394 N85-31054
Proceedings of the Workshop on Identification and Control of Flexible Space Structures, volume 3
[NASA-CR-176053] 20 p3415 N85-31195
Optimum filter computation for data transmission
[CNES-83/DRT/TIT/TR/142] 20 p3441 N85-31359
Nickel cadmium cell design variable program data analysis 20 p3445 N85-31387
A small-scale self-excited rotor electrostatic generator
[AD-A155264] 21 p3581 N85-32265
Sensitivity analysis of high-efficiency silicon solar-cell design parameters 21 p3610 N85-32422
Land vehicle corrosion management 22 p3750 N85-33246
Optimization of radioelectronic circuits with software for modeling of integrated circuits on unified system computer 22 p3768 N85-33354
Design of inductive shift transducers 22 p3771 N85-33368
Design analysis for a repository in crystalline rock
[DE85-011802] 22 p3839 N85-33771
Optimization in the computer aided design of mechanisms 23 p3924 N85-34321
Realization and linearization of a hyperfrequency power amplifier implemented with bipolar transistors in class C polarization — microwave amplifiers
[CNES-NT-114] 23 p3928 N85-34348
SLC arc transport system: Magnet design and construction
[DE85-014289] 24 p4159 N85-35789
SLC Energy Upgrade Program at SLAC
[DE85-014290] 24 p4160 N85-35790

DESIGN OF EXPERIMENTS
U EXPERIMENT DESIGN

DESIGN TO COST
Evaluation of the measured energy performance of four solar systems
[AD-A147912] 07 p0993 N85-16306
Manufacturing considerations related to aircraft gearboxes 14 p2222 N85-23778
Design-To-Cost (DTC) methodology to achieve affordable avionics 16 p2696 N85-26645
The series 2000: A miniature gas bearing DTG for low cost strapdown guidance and control 16 p2696 N85-26648
Reusable software: A concept for cost reduction 16 p2697 N85-26655
A towed instrument vehicle for deep ocean sampling
[AD-A156322] 24 p4125 N85-35576

DESORPTION
Reversible change in parameters of GaAs-based surface-barrier metal-semiconductor diodes induced by hydrogen absorption-desorption 02 p0258 N85-11690
Synergistic effects related to surface composition, session summary 06 p0865 N85-15495
The adsorption of CO and oxygen on Cu layers on a W(110) surface
[AD-A147345] 07 p0923 N85-15847
Phase-dissipative mechanisms for laser-induced surface desorption-dissociation processes
[AD-A147961] 08 p1121 N85-17065
Modulated surface vibrational spectroscopies at electrode/electrolyte interfaces
[AD-A148685] 08 p1123 N85-17083
Photoemission, vibrational and stimulated desorption studies of metal-semiconductor interfaces and of chemisorbed atoms and molecules
[AD-A147709] 08 p1225 N85-17717
Multiplex gas chromatography for use in space craft
[NASA-TM-86668] 09 p1290 N85-18097
Characterization of CO binding sites on Rh(111) and Rh(331) surfaces by XPS and LEED (Low Energy Electron Diffraction): Comparison to EELS (Electron Energy Loss Spectroscopy) results
[AD-A149331] 10 p1435 N85-19044
Desorption efficiences of vapor phase polynuclear aromatic compounds on solid adsorbents
[DE85-001303] 10 p1436 N85-19052
Separation of gas mixtures with coordination complexes
[DE85-000363] 10 p1438 N85-19062
Quasi-thermodynamic prediction of hydrogen reemission behavior from titanium films
[DE85-003667] 10 p1564 N85-19864
Laser studies of chemical dynamics at the gas-solid interface
[DE84-017590] 11 p1736 N85-20920
Study of outgassing and decomposition of space shuttle heat protection tiles, fillers and adhesive
[NASA-CR-175565] 12 p1791 N85-21242
Electron stimulated desorption and the role of secondary electrons
[AD-A150974] 14 p2252 N85-23955
Studies of metal/carbon surface chemistry
[DE85-005513] 15 p2507 N85-25463
The physical effects of different stress situations on graphite/epoxy compounds 15 p2687 N85-26594
Quantum statistical theory of vibrational dynamics in a laser-driven admolecule-surface system
[AD-A152022] 16 p2872 N85-27719
The development of laser analytical methods for the characterization of solid-liquid and solid-high pressure gas interfaces
[AD-A152382] 17 p2918 N85-27968
Theory of laser-stimulated surface process. 2: A generalized-master-equation approach to energy transfer between an IR laser, an aspecties and phonons
[AD-A153083] 17 p2970 N85-28344
Quantum model of dephasing-enhanced laser desorption: Master equation approach
[AD-A153769] 18 p3112 N85-29269
Selective detection of species in complex matrices by SIMS (Secondary Ion Mass Spectrometry)
[AD-D011665] 19 p3235 N85-30053
Method for measuring surface activity of silicon nitride powder
[NASA-TM-77906] 24 p4073 N85-35242
Evaluation: Close-range photogrammetry for slope inventory and monitoring
[PB85-192755] 24 p4108 N85-35470

DESPINNING
U SPIN REDUCTION

DESTRUCTION
Interaction among inhomogeneities and inclusions
[AD-A153114] 17 p2979 N85-28419

DESTRUCTIVE TESTS
The adhesion of hard and wear resistant coatings 02 p0179 N85-11203
Lithium battery safety: A fiber-optic application for safe observation of lithium cells under severe tests
[AD-A146846] 06 p0804 N85-15119
Comparison of the sensitivities of ultrasonic, radiographic and acoustic emission test methods for the examination of a thick weld
[BLL-RISLEY-TR-4547-(9091.9F)] 07 p0975 N85-16194
Nondestructive tests and fracture mechanics investigations in the Component Integrity Research Programme
[BLL-RISLEY-TR-4541-(9091.9F)] 07 p0976 N85-16199
Quantitative acoustic emission techniques
[AERE-R-11262] 07 p0977 N85-16203
Evaluation of laterally loaded laminated glass units by theory and experiment
[PB85-111532/GAR] 09 p1300 N85-18166
Laser induced damage of zinc sulphide
[BAE-BT-13363] 15 p2562 N85-25803
An improved torsional method for determining the fracture toughness of stiff materials and of adhesive joints
[AD-A152091] 16 p2900 N85-27267
Qualitative and quantitative determination of aging by mechanical tests — plastics 17 p2977 N85-28393
Seat experiments for the full-scale transport aircraft controlled impact demonstration
[AD-A155024] 21 p3553 N85-32106

DESULFURIZING
Studies of the kinetics and mechanisms of ammonia synthesis and hydrodesulfurization on metal single crystal surfaces
[DE85-001650] 11 p1595 N85-20030
Development of corrosion resistant heat exchangers for flue gas desulfurization
[BMFT-FB-T-84-281] 18 p3103 N85-29211
Evaluation of the Santee limestone for use in flue-gas desulfurization systems
[DE85-001277] 19 p3249 N85-30148
Fluidized bed desulfurization
[NASA-CASE-NPO-15924-1] 24 p4075 N85-35253

DESYNCHRONIZED SLEEP
U RAPID EYE MOVEMENT STATE

DETECTION
NT AIRCRAFT DETECTION
NT CHANGE DETECTION
NT CORRELATION DETECTION
NT FOREST FIRE DETECTION
NT HAZE DETECTION
NT RADAR DETECTION
NT REMOTE SENSING
NT SIGNAL DETECTION
NT TARGET RECOGNITION
NT ULTRASONIC FLAW DETECTION
The perceptual quality of smoke screens: An analysis of the Oldsbrook 2 trials, May 1981
[IZF-1984-20] 01 p0095 N85-10641
Visual representations subserving texture perception
[AD-A145412] 02 p0236 N85-11538
Failure detection processes by pattern recognition and expert systems
[AD-P003924] 02 p0246 N85-11604
Compound class quantitation of JP-5 jet fuels by high performance liquid chromatography-differential refractive index detection
[AD-A145754] 03 p0340 N85-12185
Visibility of various target-background color combinations under different chromatic ambient illuminations
[AD-A146348] 03 p0420 N85-12684
Early detection of environmental exposure
[AD-P004039] 06 p0845 N85-15369
Performance of Bayes-optimal angle-of-arrival estimators
[AD-A146594] 06 p0858 N85-15454
Detection of narrow C 4 and Si 4 absorption features in spectra of stars within 200 pc f the Sun 06 p0876 N85-15564
Electronics research at the University of Texas at Austin
[AD-A146900] 07 p0947 N85-15998
A biological sensor for the detection of toxicants
[AD-D011304] 07 p0987 N85-16141
Battery control and fault detection method
[AD-D011384] 07 p0993 N85-16307
Electro-optical target detection
[AD-D011366] 07 p1042 N85-16617
Holographic FLI for detection of defects
[AD-A148339] 08 p1164 N85-17345
Halogen mass flow rate detection system
[AD-D011398] 08 p1166 N85-17352
Spatio-temporal characteristics of visual localization
[AD-A148013] 08 p1200 N85-17555
Background detection and correction in multicomponent analysis
[AD-A148251] 08 p1212 N85-17628
Calculation of cumulative distributions and detection probabilities in communications and optics
[AD-A147781] 08 p1215 N85-17650
On edge detection
[AD-A148573] 08 p1223 N85-17703
Photometric precision needed for planetary detection 08 p1250 N85-17894
Mass spectrometry/mass spectrometry as a screening method for detecting explosive vapors
[DE85-001276] 09 p1292 N85-18110
The use of synthetic aperture radar imagery to detect hazards to navigation
[AD-A149324] 10 p1422 N85-18971
Detection and symbol synchronization for multiple-bit per photon optical communications 10 p1463 N85-19228
Calculation of Si(Li) X-ray detector efficiencies
[DE85-002732] 10 p1489 N85-19400
Infrared-thermal wave scanner for NDE of naval thermal spray coatings
[DE85-002237] 11 p1650 N85-20391
Lake ice occurrence as a possible detector of atmospheric CO2 effects on climate
[DE85-002951] 11 p1687 N85-20808
Double pinhole spatial phase correlator apparatus
[AD-D011495] 11 p1729 N85-20872
In-situ detection of micron-sized dust particles in near-Earth space 12 p1785 N85-21205
Photo-thermal detection of the onset of photo-chemical nucleation (laser-snow) in vapor
[AD-A150111] 12 p1801 N85-21295
Detection of angular modulated electromagnetic signals
[AD-D011583] 12 p1823 N85-21437
Inelastic scattering in condensed matter with high intensity Moessbauer radiation
[DE85-003531] 12 p1854 N85-21627
Radiographic detectability limits for seeded voids in sintered silicon carbide and silicon nitride
[NASA-TM-86945] 12 p1861 N85-21674
Characterisation of fatigue crack extension by quantitative acoustic emission
[AERE-R-11289] 12 p1868 N85-21721
A diffusion process and its application to detecting a change in the drift of Brownian motion
[AD-A150096] 12 p1926 N85-22100
Focal plane array optical proximity sensor
[NASA-CASE-NPO-15155-1] 12 p1932 N85-22139

Operational experience with ion concentration sensors in orientation systems 13 p1980 N85-22422
Optimization of number of pulses in detection of fluctuating optical signals 13 p2081 N85-22993
Orphan detection in the Argus system [AD-A150562] 13 p2148 N85-23331
Sample introduction methods for improving the particle detection capability of the spectrometric oil analysis program [AD-A150139] 13 p2158 N85-23399
Electronic detection and concealment of film dirt [BBC-RD-1985/4] 15 p2536 N85-25667
Receiver optimization for detection in doubly spread communication channels [AD-A151226] 15 p2541 N85-25689
Skywave radar detectability of volcanic aerosols [AD-A151448] 15 p2542 N85-25694
Attempts to localize and identify the gravity sensing device of plant seedlings 15 p2607 N85-26064
Ion sensor signal fluctuations during operation of spacecraft reaction engines 16 p2724 N85-26815
New focal plane detector system for the broad range spectrometer [DE85-005370] 16 p2788 N85-27201
A mathematical model for calculating detection probability of a diffusion target [AD-A152026] 16 p2854 N85-27601
Optimally robust redundancy relations for failure in uncertain systems [NASA-CR-175953] 17 p2976 N85-28391
Automatic detection of gust fronts [FAA-PM-85-11] 17 p2995 N85-28516
Evaluation of a fault tolerant system for an integrated avionics sensor configuration with TSRV flight data [NASA-CR-172589] 18 p3062 N85-28941
Resonant CARS detection of OH radicals [AD-A153842] 18 p3071 N85-28995
Visual simulation of radiographs [DE85-010213] 18 p3110 N85-29255
Dual differential interferometer [NASA-CASE-LAR-12966-1] 19 p3271 N85-30282
Evaluation of a high pressure proportional counter for the detection of radioactive noble gases [AD-A154436] 19 p3272 N85-30292
Optical 3-D signature device for detecting chemical agents [AD-D011669] 19 p3272 N85-30293
Optical waveguide sensor for methane gas [AD-D011691] 19 p3273 N85-30294
Development of a technique for in situ detection of stratospheric nitrogen dioxide 19 p3312 N85-30634
An empirical technique to measure X-ray production and detection efficiencies in the analytical electron microscope [DE85-010270] 19 p3361 N85-30837
Detection of internal structure by scattered light intensity: Application to kidney cell sorting 20 p3503 N85-31777
A cluster analysis method for identification of subpopulations of cells in flow cytometric list-mode arrays 20 p3503 N85-31779
Function of a device for detection of biological aerosols in field testing [FOA-C-40194-B2] 20 p3504 N85-31782
Investigation of variation in the concentration of bacteria in outdoor testing, with the use of a detector for aerosols of bacteria [FOA-C-40201-B2] 20 p3504 N85-31784
Gas sensing with surface acoustic wave devices [DE85-009125] 20 p3524 N85-31921
Experimental and theoretical assessment of a new technique for the non-destructive evaluation of laminated panels [AD-A155622] 21 p3562 N85-32155
A microprocessor-controlled, multichannel fluorimeter for analysis of sea water [AD-A154966] 21 p3590 N85-32310
Detection of excited states by laser-induced fluorescence [AD-A155558] 21 p3592 N85-32326
Automated cell detection as a mesocyclone precursor tool [AD-A154952] 21 p3635 N85-32577
Real-time automated detection of mesocyclones and tornado vortex signatures [AD-A154966] 21 p3635 N85-32578
Resource management for the tagged token dataflow architecture [AD-A154773] 21 p3667 N85-32779
Analysis of unreplicated factorials allowing for possibly faulty observations [AD-A154813] 21 p3678 N85-32948
An attempt to detect induced neutron capture in laser radiation field 21 p3690 N85-32928
Fire protection review revisit no. 2, Argonne National Laboratory, Argonne, Illinois [DE85-013245] 22 p3755 N85-33276
Probabilistic analysis of automatic control systems for detection systems 22 p3765 N85-33335
Linear boundary detection using pressure buildup tests [DE85-009926] 22 p3784 N85-33444
Fiber optic moisture sensor [DE85-011651] 22 p3787 N85-33462
Fracture detection and characterization for geothermal reservoir definition [DE85-006677] 22 p3815 N85-33630
Effects of low level carbon monoxide (CO) on tracking and monitoring. An attempt to replicate the findings of Putz et al. (1976) protocol 2 [AD-A155722] 22 p3825 N85-33694
Dual optical mechanical position tracker [AD-D011739] 22 p3844 N85-33811
Search for infrared counterparts of gamma-ray bursters [OG-1.1-9] 22 p3861 N85-33910
Gamma ray burst size-frequency distributions: Spectral selection effects [OG-1.2-3] 22 p3862 N85-33913
Direct determination of metals in organic matrices by Inductively Coupled Plasma-Atomic Emission Spectrometry (ICP-AES) [DE85-012015] 23 p3911 N85-34233
Instrumentation for sensing moisture content of material using a transient thermal pulse [NASA-CASE-NPO-15493-2] 23 p3933 N85-34373
Modulated voltage metastable ionization detector [NASA-CASE-ARC-11503-1] 23 p3933 N85-34374
Upgrading auxiliary facility outleakage and combustion detection [DE85-012798] 23 p3934 N85-34386
Solar system fault detection [DE85-005987] 23 p3946 N85-34458
Marine Sample Exploitation Project: Estimates regarding the sensitivity and technology for the detection of nuclear explosion debris in the marine environment [DE85-013176] 23 p3947 N85-34462
Magnetic search system [PB85-185108] 23 p3949 N85-34477
Applications of CdTe to nuclear medicine [DE85-011877] 23 p3952 N85-34492
Issues and techniques in touch-sensitive tablet input (executive summary) 23 p3960 N85-34543
On the detectability of key-MeV solar protons through their nonthermal Lyman-alpha emission [SH-1.3-5] 23 p3993 N85-34752
Measurement of low energy cosmic rays aboard Spacelab-1 [SH-10.1-6] 23 p4053 N85-35137
Heavy cosmic ray measurement aboard Spacelab-1 [SH-10.1-7] 23 p4053 N85-35138
A preliminary evaluation of a failure detection filter for detecting and identifying control element failures in a transport aircraft [NASA-TM-87576] 24 p4067 N85-35204
The detection and study of molecular species using time resolved laser spectroscopy [AD-A155910] 24 p4075 N85-35256
Fatigue damage detection in steels by optical correlation [AD-A155830] 24 p4079 N85-35277
LANDSAT-4/5 image data quality analysis [E85-10105] 24 p4107 N85-35463
Literature search for new physical methods for biological aerosol detection [AD-A155883] 24 p4128 N85-35592
Edge detection and geometric methods in computer vision [AD-A155873] 24 p4135 N85-35630
Proceedings of the Workshop on Detectors for Relativistic Nuclear Collisions [LBL-18225] 24 p4146 N85-35700
Detectors for relativistic nuclear collisions (report from the Fixed-Target Hadron Group) 24 p4145 N85-35701
Event parameters: Fixed targets 24 p4146 N85-35702
Working group on penetrating probes at fixed target facilities 24 p4146 N85-35703
Summary of the working group on penetrating probes in collider experiments. 1: The collider environment 24 p4146 N85-35704
Report of working group on detectors for hadrons and event parameters at colliders 24 p4146 N85-35705
Detector requirements for intensity interferometry measurements 24 p4147 N85-35709
A holographic streamer chamber for relativistic nucleus-nucleus collision experiments 24 p4147 N85-35710
A lead glass tubing drift calorimeter 24 p4147 N85-35711
X-ray fluorescence analysis of uranium concentrates [DE85-013189] 24 p4148 N85-35717
Observation of super high energy big family with large scale Fe emulsion chambers [HE-3.4-3] 24 p4182 N85-35932
A halo event created at 200 m above the Chacaltaya emulsion chamber [HE-3.4-5] 24 p4182 N85-35933
A critical analysis of air shower structure functions and size spectrum measurements with the NBU air shower array 24 p4186 N85-35983
Measurement of the local density spectrum 24 p4189 N85-35984
Character of energy flow in air shower core 24 p4189 N85-35985
Observation of EAS using a large water tank 24 p4189 N85-35986
The development of air shower in the iron absorber 24 p4189 N85-35987
Application of photodiodes to the detection of electromagnetic bursts 24 p4189 N85-35988
High-energy neutrinos from a lunar observatory [HE-5.3-21] 24 p4207 N85-36112
Underground measurements on secondary cosmic rays [HE-5.4-1] 24 p4207 N85-36116
Modular detector for deep underwater registration of muons and muon groups [HE-5.4-15] 24 p4208 N85-36125
Application of thermoluminescence for detection of cascade shower 2: Detection of cosmic ray cascade shower at Mount Fuji [HE-7.1-12] 24 p4214 N85-36162

DETECTORS
A limbus-sensing eye movement recorder [AD-A144772] 01 p0049 N85-10323
Induction voidmeter [DE84-014321] 01 p0050 N85-10329
The development and test of ultra-large-format multi-anode microchannel array detector systems [NASA-CR-174247] 07 p1043 N85-16622
Leak detectors for organic Rankine cycle power plants: On-line and manual methods [DE85-002792] 12 p1852 N85-21617
Development of high resolution imaging detectors for X-ray astronomy [NASA-CR-175505] 12 p1953 N85-22266
Estimation of optimum scores for partition detectors using stochastic approximation techniques 14 p2411 N85-24865
Germanium detectors with a built-in transverse drift field [DE85-009944] 18 p3096 N85-29165
New concept for a wall detector for alpha particles [DE85-006037] 18 p3183 N85-29740
Kalman filter time series analysis of gamma-ray data from NaI(T1) detectors for the ND6620 computer [AD-A154995] 21 p3705 N85-33014
The sidereal anisotropy of cosmic rays around 3 x 10 (15) eV observed at a middle north latitude [OG-5.3-6] 22 p3884 N85-34072
The ISAVF opto-mechanical test bed [NASA-TM-87505] 24 p4067 N85-35206
Preliminary results on underground muon bundles observed in the Frejus proton-decay detector [HE-5.1-1] 24 p4200 N85-36067

DETERIORATION
Life distribution properties of devices subject to deterioration [AD-A145554] 02 p0206 N85-11358
Design of alternate launch and recovery surfaces for environmental effects [AD-A145800] 03 p0320 N85-12066
Bridge erosion in electrical contacts 04 p0486 N85-13102
Microspots on spectroscopic plates — astronomical photography 07 p0964 N85-16113
Applications of vibration analysis to the condition monitoring of rolling element bearings [ARL/AERO-R-163] 12 p1859 N85-21663
Management of Corrosion [AGARD-LS-141] 22 p3749 N85-33236
Environmental factors in corrosion and deterioration of materials 22 p3750 N85-33241
Current requirements for the design and maintenance against corrosion of UK military aircraft 22 p3750 N85-33244
Dissected motors-propellants motor number STM-012. Phase 15: Surveillance report, stage 1 [AD-A156088] 24 p4071 N85-35226

DETERMINANTS
Computing the Kac determinant using dual mode techniques and more about the No-ghost theorem [DE85-001329] 09 p1375 N85-18640

DETERMINATION
U MEASUREMENT

DETONATION
Computer simulation of the shock initiation of detonation in solid explosives
[PML-1984-23] 01 p0033 N85-10207
Combustion and detonation of hydrogen-air mixture in free spaces 02 p0274 N85-11783
The influence of inert particulate material on the properties of RDX/polyethylene wax compositions
[MRL-R-929] 03 p0336 N85-12159
Detonator block
[AD-D011248] 06 p0773 N85-14941
Hazard Studies for Solid Propellant Rocket Motors
[AGARD-CP-367] 08 p1114 N85-17025
Review of USAF treatment of solid propellant rocket motor hazards 08 p1114 N85-17027
Analysis of Deflagration to Shock to Detonation Transition (DSDT) in porous energetic solid propellants 08 p1115 N85-17030
Penguin warhead safety tests 08 p1115 N85-17031
Study of the transition from deflagration to detonation of previously fragmented propellants 08 p1115 N85-17032
Transient combustion: An important consideration in deflagration-to-detonation transition 08 p1116 N85-17037
The DDT process for high energy propellants 08 p1116 N85-17038
Numerical simulation of the shock detonation transition 08 p1116 N85-17039
Influence of temperature on wear resistance of detonation coatings of alloy powders 10 p1447 N85-19116
Transition to detonation from rapid-compression (ramp-waves) generated in a burning porous bed
[AD-P004345] 10 p1455 N85-19169
A thermal-mechanical model of deflagration-to-detonation in granular energetic materials
[AD-P004346] 10 p1455 N85-19170
A summary of the mechanism of delayed detonation
[AD-P004347] 10 p1455 N85-19171
Analysis of Shock to Detonation Transition (SDT) of porous high energy propellant from ramp-wave compression loading
[AD-A149333] 10 p1457 N85-19180
Shock propagation in the exhaust gas handling system of the proposed large altitude rocket cell: Methods and preliminary analysis
[DE85-003055] 11 p1591 N85-20010
Numerical analysis of thermonuclear detonation in dense plasma 11 p1719 N85-20814
Hydrogen flame acceleration and transition to detonation
[DE85-000611] 12 p1802 N85-21290
The detonation of aerosols and vapors of combustible substances under controlled conditions. Part 1: Construction of a test installation
[ISL-R-109/83-PT-1] 14 p2254 N85-23966
Stress in axially symmetrical heavy metal projectiles during discharge — numerical simulation
[ISL-CO-219/83] 14 p2321 N85-24345
Vapor explosions in superheated liquids and fundamental studies of the physics of detonation
[AD-A151382] 15 p2504 N85-25447
Detonations of solid explosives
[AD-A152012] 15 p2521 N85-25540
Analysis of deflagration to detonation transition in high-energy solid propellants 16 p2757 N85-27010
Model for computing late detonations initiated in propellants by impact (XDT reactions)
[DE85-007377] 16 p2758 N85-27019
Generation of detonation waves of given spatial and temporal characteristics
[ISL-R-103/83] 16 p2758 N85-27021
Detonation behavior of LX-14 and PBX-9404: Theoretical aspect
[DE85-010038] 18 p3084 N85-29076
Equation of state for detonation products
[DE85-009808] 18 p3084 N85-29079
Chemical-acoustic interactions in combustion systems
[AD-A153857] 19 p3233 N85-30046
Effect of confinement on failure in 95 TATB/5 KEL-F
[DE85-010790] 19 p3251 N85-30158
Static high pressure study of nitric oxide chemistry: Proposed mechanism for nitric oxide detonation
[DE85-010795] 22 p3746 N85-33220
Combustion-deflagration-detonation transition in a confined spherical powder
[ISL-R-108/84] 22 p3747 N85-33223
Behavior of the porous bed in a combustion-deflagration-detonation transition
[ISL-CO-220/84] 22 p3747 N85-33224
Combustion-deflagration-detonation transition
[ISL-CO-221/84] 22 p3747 N85-33225
Gas composition and molecule velocity in the detonation products of pentaerythritol tetranitrate (PETN) in expansion in a high vacuum container. Analysis by mass spectroscopy and time of flight spectrometry
[ISL-R-109/84] 22 p3747 N85-33226
Explosive containment study
[DE85-011719] 22 p3753 N85-33267
A model of hypersonic two-dimensional oblique detonation wave ramjet
[UTIAS-TN-257] 23 p3897 N85-34139
Intermolecular explosives
[DE85-009609] 23 p3921 N85-34296
Time-resolved spectroscopic studies of detonating heterogeneous explosives
[DE85-009760] 23 p3921 N85-34297
Pressure-shear loading of PBX-9404
[DE85-009982] 23 p3921 N85-34298
Detonation in tungsten-loaded HMX
[DE85-009606] 23 p3922 N85-34299
Modeling heterogeneous high explosive burn with an explicit hot-spot process
[DE85-009593] 23 p3922 N85-34300
Three-dimensional hydrodynamic hot-spot model
[DE85-009587] 23 p3922 N85-34301
Real time analysis of PETN detonation products
[DE85-009581] 23 p3922 N85-34303
Comparison of experimental data on detonation velocity and Chapman-Jouget pressure vs initial HE density with predictions from Ree's model equation of state
[DE85-007266] 23 p3922 N85-34304
Detonation of condensed explosives: Evolution of knowledge in the last 40 years
[ISL-CO-226/84] 23 p3923 N85-34307
Investigation of the lightning vulnerability of nuclear explosive test systems at the Nevada Test Site
[DE85-011761] 24 p4124 N85-35563
Evaluation of nuclear detonation location capability under high attack scenario
[AD-A155761] 24 p4149 N85-35729
DETONATION WAVES
Model study of the interaction of a blast wave with the superstructure of ships. Part 5: Application of optical measurement methods to the study of blast interaction
[PML-1984-12-PT-5] 01 p0057 N85-10375
Parameters of detonation waves excited in gas during concentrated release of energy 02 p0268 N85-11751
Flash radiography as a quantitative tool
[DE84-016465] 04 p0503 N85-13211
Current status of blast wave theory and computations. Volume 2: The quasi-similar solution
[AD-A146538] 06 p0808 N85-15138
Thermal evaporation in blast waves: A model for aneurism formation in the NRL (Naval Research Laboratory) LASER-HANE simulation experiment
[AD-A147006] 07 p0978 N85-16210
Analysis of deflagration to detonation transition in high-energy solid propellants
[AD-A148302] 08 p1135 N85-17156
Dynamic compaction of powders
[DE85-001062] 11 p1612 N85-20137
Waveform control and application of detonation wave in explosives 12 p1820 N85-21420
The behaviour of detonation waves in single phase heterogeneous systems
[AD-A149825] 12 p1846 N85-21581
Vapor explosions in superheated liquids and fundamental studies of the physics of detonation
[AD-A151382] 15 p2504 N85-25447
Viscous effects on blast wave flowfields
[AD-A152013] 15 p2558 N85-25779
NASTRAN analysis comparison to shock tube tests used to simulate nuclear overpressures 15 p2576 N85-25888
The 2-D simulations of the NRL (Naval Research Laboratory) laser experiment
[AD-A154915] 21 p3592 N85-32321
A model of hypersonic two-dimensional oblique detonation wave ramjet
[UTIAS-TN-257] 23 p3897 N85-34139
DETONATORS
Modular detonator device
[AD-D011232] 03 p0340 N85-12184
Detonator block
[AD-D011248] 06 p0773 N85-14941
Parameters affecting hot wire ignition of thermite mixtures
[DE84-016941] 09 p1301 N85-18176
Development of a PETN DDT detonator
[DE84-016944] 09 p1302 N85-18178
CP DDT detonators. Part 1: Design sensitivity study
[DE84-017255] 09 p1302 N85-18180
High-temperature-stable detonators
[DE85-005188] 12 p1818 N85-21402
Nonprimary-explosive, hot-wire detonator
[DE85-005195] 12 p1818 N85-21403
Surveillance program for the dissection and analysis of explosive and pyrotechnic components
[DE85-006105] 16 p2757 N85-27016
CP DDT detonators. 4: Thermal aging
[DE85-011172] 19 p3251 N85-30160
DEUTERIUM
Characterization of ion implanted deuterium traps in nickel by equilibration with deuterium gas
[DE84-014958] 02 p0288 N85-11879
Measurement of scattering cross sections of liquid and solid hydrogen deuterium and deuterium hydride for thermal neutrons
[DE84-014814] 05 p0727 N85-14671
Deuterium abundance in the local interstellar medium 06 p0874 N85-15552
The abundance of deuterium in the outer solar system from ground-based measurements of monodeuterated methane 07 p1060 N85-16725
Deuterium isotope effect on the compatibility between polystyrene and polybutadiene
[AD-A148551] 08 p1134 N85-17145
Deuterium diffusion in a soil-water-ice mixture
[AD-A148457] 08 p1178 N85-17415
NMR study on rotational fluctuation in solid hydrogen and deuterium 09 p1289 N85-18093
Direct measurement of the temperature dependence of the velocity of the reaction of deuterium atoms with vibration-excited hydrogen molecules
[MPIS-12/1984] 11 p1726 N85-20856
Neutral beam injector oxygen impurity measurements and concentration reduction via gettering processes
[DE85-000661] 12 p1836 N85-21521
Tritium catalyzed deuterium Tokamaks
[DE85-004825] 12 p1936 N85-22166
System for forming and focusing high current beam of deuterium ions 13 p2045 N85-22796
Calculations of collision-induced optical gain in high-density mixtures of D2 or HD with a buffer gas
[AD-A151372] 15 p2648 N85-26330
Monodeurated methane in the outer solar system. 2. Its detection on Uranus at 1.6 microns
[NASA-CR-175762] 16 p2682 N85-27782
Possible indication of an A-dependence of R in deep-inelastic electron scattering from nuclei
[DE85-008174] 17 p3033 N85-28763
Trajectories of charged particles traversing a plasma sheath in an oblique magnetic field
[DE85-011070] 19 p3371 N85-30911
Tables of generalized hydrogen diffusion profiles and permeating fluxes for fusion applications
[DE85-006876] 19 p3372 N85-30919
Preparation and use of very pure o-D2
[DE85-009415] 22 p3843 N85-33600
Ultraviolet radiation-damage absorption peak in solid deuterium-tritium, revision 1
[DE85-012969] 22 p3844 N85-33806
Results of a search for deuterium at 25-50 GC/c using a magnetic spectrometer
[OG-4.2-4] 22 p3878 N85-34024
Measuring method and confirmation of H- (D-) ion current by sheet plasma 1
[IPPJ-730] 23 p3974 N85-34638
Size effects of vacuum chamber for H- (D-) ion volume production by sheet plasma 1
[IPPJ-731] 23 p3974 N85-34639
Data on the backscattering coefficients on light ions from solids: A revision
[IPPJ-AM-41-REV] 23 p3982 N85-34689
DEUTERIUM COMPOUNDS
NT DEUTERIUM FLUORIDES
Monodeurated methane in the outer solar system. 2. Its detection on Uranus at 1.6 microns
[NASA-CR-175762] 16 p2682 N85-27782
Nuclear magnetic resonance study of the intramolecular rearrangement of 2-(5-cyanotetrazolato)pentaammine cobalt (III) perchlorate
[DE85-010610] 22 p3839 N85-33772
DEUTERIUM FLUORIDE LASERS
U DF LASERS
DEUTERIUM FLUORIDES
Rotational energy transfer in highly vibrationally excited hydrogen fluoride and deuterium fluoride
[AD-A152003] 16 p2662 N85-27650
DEUTERIUM PLASMA
Background calculations for the measurement of the ion temperature in a deuterium plasma
[DE84-016546] 09 p1393 N85-18768
Scientific activities. A: Reacting plasma physics. 1: Introduction and overview 15 p2654 N85-26370
Plasma heating 15 p2654 N85-26372
Measuring method and confirmation of H- (D-) ion current by sheet plasma 1
[IPPJ-730] 23 p3974 N85-34638

DEUTERON IRRADIATION
Investigation of thick-target neutron emission from Be-9(d,n)B-10 at E(d) = 7 MeV for angles other than zero degrees
[DE85-010254] 20 p3528 N85-31847

DEUTERONS
Performing (p vector,)c)n), (d vector, n) and (n vector, n) measurements with a rotating magnet beam swinger
[DE84-017003] 04 p0562 N85-13582
Deuteron whistlers at low latitudes in the low altitude topside ionosphere 14 p2366 N85-24625
Cluster production and entropy
[DE85-007626] 17 p3032 N85-28752
Time-resolved energy spectrum of the ion beam generated in the plasma focus 19 p3360 N85-30892
The flux of secondary anti-deuterons and antihelium produced in the interstellar medium
[OG-8.1-5] 22 p3886 N85-34096
The electromagnetic ram action of the plasma focus as a paradigm for the generation of cosmic rays and the gigantic jets in active galaxies
[OG-8.2-14] 23 p4020 N85-34910

DEVELOPING NATIONS
The changing pattern of fossil fuel CO2 emissions
[DOE/OR-21400/2] 02 p0224 N85-11469
Solar energy supplied mobile water purification unit 05 p0664 N85-14270
Realized field tests — solar generators 05 p0664 N85-14271
The potential contributions of the World Climate Program (WCP) to the economies of developing countries 07 p1003 N85-16371
A microprocessor data system for developing countries — climatology 07 p1003 N85-16377
Competitive assessment of the US manufacturing automation equipment industries
[PB85-103027] 10 p1589 N85-19893
The significance of orthophoto maps for developing countries 18 p3124 N85-29341

DEVELOPMENT
Achievements in laser development 01 p0115 N85-10784
Global aspects of stream evolution in the solar wind
[DE85-002207] 11 p1766 N85-21101

DEVIATION
Large deviations for processes with independent increments
[AD-A147293] 08 p1210 N85-17810
Design of single-wheel gyrocompass with correction 14 p2272 N85-24079

DEVICES
Topics in optical materials and device research, 3. Volume 2
[AD-A149727] 12 p1911 N85-21998

DEVITRIFICATION
U CRYSTALLIZATION

DEW POINT
Climate at CRREL (Cold Regions Research and Engineering Laboratory) Hanover, New Hampshire
[AD-A148400] 08 p1169 N85-17495
Precipitable water in the atmosphere, determined from surface dewpoint values 16 p2831 N85-27457
AWS (Air Weather Service) climatic briefs: Asia
[AD-A151944] 16 p2835 N85-27481
Instrumentation for sensing moisture content of material using a transient thermal pulse
[NASA-CASE-NPO-15493-2] 23 p3933 N85-34373

DEWAR SYSTEMS
U CRYOGENIC EQUIPMENT

DEWETTING
U DRYING

DF
U DEUTERIUM FLUORIDES

DF LASERS
Operating characteristics, absorptivity/reflectivity measurements, and pulse system design of the NPS (Naval Postgraduate School) hydrogen fluoride/deuterium fluoride laser
[AD-A152712] 17 p2970 N85-28341
Ship-to-ship propagation: Maritime data analyses
[AD-A155484] 21 p3592 N85-32325
Chemical lasers
[ISL-R-107/84] 23 p3836 N85-34400

DH 115 AIRCRAFT
Long term durability of urea formaldehyde glued joints removed from Vampire aircraft
[AD-A149053] 10 p1424 N85-18985

DHC BEAVER AIRCRAFT
U DHC 2 AIRCRAFT

DHC 2 AIRCRAFT
Application of linear optimal control theory to the design of the elevator control system of the DHC-2 Beaver experimental aircraft
[VTH-LR-411] 16 p2711 N85-26729

DIAGNOSIS
Atmospheric channel performance measurements at 10 to 100 GHz
[PB84-211325] 01 p0042 N85-10271
Application of the CSRL language to the design of expert diagnosis systems: The Auto-Mech experience
[AD-P003922] 02 p0245 N85-11602
Models of natural intelligence in fault diagnosis tasks: Implications for training and aiding of maintenance personnel
[AD-P003927] 02 p0246 N85-11607
Artificial intelligence approaches to monitoring system integrity
[AD-P003930] 02 p0246 N85-11610
The application of basic control laws to human medicine
[DFVLR-MITT-84-13] 05 p0697 N85-14482
A general theory of circuit analogy in fracture diagnosis
[AD-A147177] 07 p0978 N85-16212
Distributed knowledge base systems for diagnosis and information retrieval
[AD-A146890] 07 p1054 N85-16890
Electromagnetic inspection of wire ropes using sensor arrays
[AD-A149016] 10 p1495 N85-19436
Meta-level control through fault detection and diagnosis
[AD-A149064] 10 p1540 N85-19709
Diagnostic system
[INPE-3350-PRE/659] 16 p2841 N85-27519
H1-NMR studies on lymphocyte membranes in human lymphoproliferative diseases 20 p3505 N85-31787
Remote medical diagnosis 21 p3663 N85-32753
Applications of CdTe to nuclear medicine
[DE85-011877] 23 p3952 N85-34492

DIAGRAMS
NT BLOCK DIAGRAMS
NT CIRCUIT DIAGRAMS
NT FEYNMAN DIAGRAMS
NT HERTZSPRUNG-RUSSELL DIAGRAM
NT NYQUIST DIAGRAM
NT PHASE DIAGRAMS
NT S-N DIAGRAMS
NT STRESS-STRAIN DIAGRAMS
The resonant count diagram and solar g mode oscillations 14 p2445 N85-25088
A model for a document maintenance system 23 p3960 N85-34542

DIALYSIS
NT ELECTRODIALYSIS
Synthesis and characterization of novel polymers from non-petroleum sources for use in enhanced oil recovery
[DE85-010922] 19 p3250 N85-30151

DIAMAGNETISM
The plasma assisted modified betatron
[AD-A146728] 09 p1390 N85-18748
Finite-(beta) optimization of tandem mirrors
[DE85-002858] 10 p1560 N85-19835
Diamagnetic instability of cyclotron waves in plasma 21 p3693 N85-32948

DIAMETERS
A low cost approach with larger diameter silicon wafer — solar cells 13 p2008 N85-22572
Spectral evaluation of irregularity of superconducting coaxial cables 13 p2082 N85-23000
Alignment and assembly tool for very large diameter cylinders
[NASA-CASE-MFS-28001-1] 18 p3116 N85-29289
A gel-halo sample pellet: The best of both worlds? Stubby zones without a constricted sample gate 20 p3502 N85-31770

DIAMINES
NT ETHYLENEDIAMINE
NT TRIAMINOGUANIDINIUM AZIDE
A new heat-resistant polymer from dimer diamine bismaleimide. Part 1: Preparation and free radical cure of dimer diamine bismaleimide
[AD-A145684] 02 p0186 N85-11247
Process for preparing highly optically transparent-colorless aromatic polyimide film
[NASA-CASE-LAR-13351-1] 12 p1811 N85-21360
Fire resistant polymers based on 1-(diorgano oxyphosphonyl)methyl-2,4- and 2,6-diamino benzenes
[NASA-CASE-ARC-11512-2] 12 p1811 N85-21362
Polymer intermediates from limonene (follow-up project)
[BMFT-FB-T-84-243] 12 p1814 N85-21380
Remarks on preparation of indandione detection reagents
[NASA-TM-77905] 21 p3560 N85-32146
Preparation of ethylenediamine dinitrate
[DE85-006423] 23 p3922 N85-34305

DIAMOND WINGS
U LOW ASPECT RATIO WINGS
U SWEPT WINGS

DIAMONDS
Fluorinated diamond particles bonded in a filled fluorocarbon resin matrix
[DE84-014444] 01 p0022 N85-10136
The current status of diamond and cubic boron nitride composites 02 p0178 N85-11194
The growth of twins and twin lamellae in synthetic diamond crystals 02 p0181 N85-11213
Process development for the production of technically high quality monocrystalline diamond grits
[BMFT-FB-T-84-204] 08 p1138 N85-17166
Optimization of production of composite diamond-containing materials using titanium carbide-steel alloys 10 p1446 N85-19113
Apparatus for producing diamond-like carbon flakes
[NASA-CASE-LEW-13837-3] 11 p1615 N85-20155
Electrical resistance measurements of metals to 40 GPa in the diamond cell
[DE85-001009] 11 p1629 N85-20262
Diamondlike flakes
[NASA-CASE-LEW-13837-2] 12 p1798 N85-21267
Sound velocity of carbon at high pressures
[DE85-002016] 12 p1928 N85-22113
Diamond cutters' grinders 13 p2051 N85-22841
Role of fluid lubricant-coolant in fine grinding of optical glass by diamond tool 14 p2280 N85-24125
An analysis of the economics of turning titanium alloys with polycrystalline diamond tools 15 p2567 N85-25841
Classification and types of diamond wear in honing 15 p2567 N85-25842
Geothermal COMPAX drill bit development
[DE85-011353] 20 p3469 N85-31558
Ab initio calculations of materials properties
[DE85-011167] 20 p3531 N85-31964
Single-point diamond crushing of Zerodur with in-situ polishing and metrology on a diamond turning machine
[DE85-012918] 24 p4083 N85-35305

DIAPHRAGM (ANATOMY)
Change in energetics of muscular contraction as a result of hyperoxia 01 p0093 N85-10629
Effects of posture and water immersion on diaphragmatic function 16 p2840 N85-27515

DIAPHRAGMS (MECHANICS)
Scattering of electromagnetic waves in flat waveguide with bilateral diaphragms 03 p0347 N85-12235
Variable friction secondary seal for face seals
[NASA-CASE-LEW-14170-1] 11 p1647 N85-20377
Experimentally determined characteristics of vortex heaters 13 p2050 N85-22833
Theory of diaphragm light modulators with electrical input signal 13 p2082 N85-23002
Effect of diaphragm leakage on turbine stage characteristics 14 p2288 N85-24168
Tuning system for capacitively loaded 1/4 accelerating cavity
[DE85-012516] 24 p4091 N85-35358
Hadrons registration in emulsion chamber with carbon block
[HE-3.7-3] 24 p4186 N85-35962

DIATOMIC GASES
Molecular hydrogen and thermal phases in astrophysics 09 p1414 N85-18922

DIATOMIC MOLECULES
Polarization of radio molecular lines and mapping of magnetic field direction 06 p0678 N85-15581
Spectroscopic studies of lasing transitions in the diatomic mercury halides
[AD-A151553] 15 p2563 N85-25809
Equation of state and two-body correlations for fluids of non-spherical molecules
[AD-A151985] 16 p2783 N85-27174
Computer modeling of vibrational energy levels of potential laser candidates (diatomic molecules)
[AD-A151765] 16 p2790 N85-27209
Calculation of Franck-Condon factors for diatomic molecules
[AD-A154463] 19 p3353 N85-30784
A liquid nitrogen cooled composite wall hollow cathode — molecular spectroscopy
[USIP-85-07] 20 p3526 N85-31930
Vibrationally enhanced dissociation of diatomic molecules
[AD-A154827] 21 p3701 N85-32996

DICARBOXYLIC ACIDS
Condensation of anhydrides or dicarboxylic acids with compounds containing active methylene groups. Part 1: Condensation of phthalic anhydride with acetoacetic and malonic ester
[NASA-TM-77886] 19 p3227 N85-30010

DICHLORIDES
Development of a polysilicon process based on chemical vapor deposition of dichlorosilane in an advanced Siemen's reactor
[NASA-CR-174445] 11 p1672 N85-20532

DICHLORODIPHENYLTRICHLOROETHANE
U DDT
DICHROISM
Multidimensional luminescence measurements
[AD-A154950] 21 p3563 N85-32162
DICHROMATES
U CHROMATES
DICTIONARIES
An operational system for subject switching between controlled vocabularies: A computational linguistics approach
[NASA-CR-3838] 02 p0293 N85-11903
Space Transportation System and associated payloads: Glossary, acronyms, and abbreviations
[NASA-RP-1059-REV] 10 p1428 N85-19007
Glossary of the soil sciences
[PB85-133452] 12 p1952 N85-22263
Glossary of fusion energy
[DE84-017180] 14 p2425 N85-24958
An analysis of data dictionaries and their role in information resource management
[AD-A152134] 16 p2774 N85-27121
Spanish language equivalents for a glossary of terms used in the field of space exploration
[NASA-TM-86211] 19 p3379 N85-30981
Pacific Northwest and Alaska bioenergy program glossary
[DE85-011740] 22 p3808 N85-33501
DIELECTRIC CONSTANT
U PERMITTIVITY
DIELECTRIC MATERIALS
U DIELECTRICS
DIELECTRIC PERMEABILITY
Dielectric measurements in intralow-frequency band
13 p2087 N85-23034
DIELECTRIC POLARIZATION
Center for dielectric studies
[AD-A146183] 03 p0434 N85-12761
Interaction of solutes with stretched polymers
[AD-A154662] 21 p3569 N85-32196
Transient analysis of electromagnetic reflection from dispersive materials
[PB85-200186] 24 p4154 N85-35753
DIELECTRIC PROPERTIES
NT PERMITTIVITY
Recent advances in gaseous dielectrics
[DE84-014279] 02 p0195 N85-11304
Determination of bound water in biological tissue and energy dissipated in bound water by low level microwaves
[AD-A143101] 03 p0399 N85-12547
Extinction by dielectric particles at optical and infrared wavelengths
[AD-A146305] 03 p0413 N85-12640
Dielectric and optical properties of sputtered thin films
[AD-A146210] 03 p0420 N85-12661
Theory of non-linear index of refraction of compound semiconductors
[DE84-013660] 04 p0569 N85-13626
Low frequency electrical properties of selected dielectrics
[DE84-016220] 05 p0832 N85-14052
The HEMP (High-altitude Electromagnetic Pulse) response of a long transmission line buried in the earth
[AD-A146517] 06 p0800 N85-15106
Pulse transmission through frozen silt
[AD-A147108] 07 p0940 N85-15958
A quasi-optical method for measuring the complex permittivity of materials
[AD-A147463] 07 p0941 N85-15966
Monitoring cure of epoxy resins using a microdielectrometer
[AD-A148618] 08 p1119 N85-17054
The use of microdielectrometry in monitoring the cure of resins and composites
[AD-A148619] 08 p1119 N85-17055
Characterization of III-V compound semiconductor device materials
[AD-A148203] 08 p1225 N85-17719
Advanced artificial dielectric materials for millimeter wavelength applications
[AD-A148960] 10 p1431 N85-19027
UHF radiowave propagation through forests
[AD-A149518] 10 p1467 N85-19256
Millimeter wave dielectric property measurement of gyrotron window materials
[DE85-004430] 12 p1802 N85-21304
Method for the fabrication of dielectric isolated junction field effect transistor and PNP transistor
[AD-D011500] 12 p1832 N85-21484
Investigations of radiation-induced and carrier-enhanced conductivity 13 p1996 N85-22515
A simple model of electron beam initiated dielectric breakdown 13 p1996 N85-22516
Monitoring of laminate cure with microdielectrometry
[AD-A150863] 14 p2248 N85-23834
Proceedings of the Cold Electronics Workshop
[NASA-CR-175662] 14 p2297 N85-24220
Design and swept-frequency measurement of printed circuit board log-periodic dipole arrays
[R-NIAS-23] 15 p2539 N85-25671
Scattering properties of a moving dielectric object
[AD-A151974] 15 p2544 N85-25708
In situ microwave measurements of dielectric properties and moisture in materials
[DE85-003822] 16 p2747 N85-26953
Design of the waveguide for microwave heating of solid lithium ceramic blankets
[DE85-009776] 17 p2935 N85-28120
Application of single and multiple scattering techniques to optical properties of dielectric media
19 p3366 N85-30877
Strong coupling effects on bound states in plasmas
[AD-A154353] 19 p3370 N85-30905
Vibrational properties of disordered solids: Far infrared studies
[DE85-010400] 19 p3377 N85-30951
Buildup of electric charge in foil dielectrics during gamma irradiation 22 p3770 N85-33363
Application of field similitude theory to calculation of stripline heating 22 p3780 N85-33419
Waveguide dielectric millimeter band filter with enhanced selectivity 22 p3780 N85-33421
Multidiode integrated-circuit protective device
22 p3781 N85-33425
DIELECTRICS
NT LOSSLESS MATERIALS
NT RADOME MATERIALS
Interaction of a stream of dielectric spheres in an electric field in a high vacuum
[DE84-014714] 01 p0115 N85-10782
Recent advances in gaseous dielectrics
[DE84-014279] 02 p0195 N85-11304
Transformation of heterogeneous surface waves by skewed streams 02 p0259 N85-11897
Center for dielectric studies
[AD-A146183] 03 p0434 N85-12761
Investigation of effect of photocurrent amplification in meta-dielectric-semiconductor structures based on silicon 04 p0488 N85-13110
Microwave measurement of the complex dielectric tensor at anisotropic slab materials
[DE84-017050] 04 p0493 N85-13144
Scattering from thin dielectric disks
[NASA-TM-86155] 06 p0798 N85-15098
Low-loss flexible dielectric waveguide for millimeter-wave transmission and its application to devices
[AD-A147848] 07 p0948 N85-16006
Method of producing a buried long period grating
[AD-D011351] 07 p0969 N85-16153
High specific heat dielectrics and Kapitza resistance at dielectric boundaries
[AD-A148476] 08 p1217 N85-17886
Surface and interfacial properties of Ga(0.47) In(0.53)As alloys
[AD-A148891] 10 p1562 N85-19949
A 10/sup 11/W high current pulse electron beam accelerator described 11 p1620 N85-20200
Adaptation of an air-dielectric RF cable for use as an oil-filled high voltage pulse transmission line
[DE84-017414] 11 p1630 N85-20285
Degradation mechanisms in ceramic dielectrics
[AD-A149791] 12 p1813 N85-21369
Design and calibration of a 35GHz dielectrometer
[AD-P004383] 12 p1826 N85-21457
Program plan for research and development of dielectric materials for electric power systems
[DE85-001327] 12 p1836 N85-21520
Evaluation of resonant modes in isolated dielectric resonators using a surface integral equation formulation
[PB85-110891] 12 p1837 N85-21528
Computer simulation of equipment and processes involved in high-frequency heating of dielectrics
12 p1841 N85-21555
Determining distribution of complex dielectric permittivity over cylindrical body of intricate cross section from electromagnetic field measurement
12 p1842 N85-21559
Electric field effects on ion currents in satellite wakes
13 p1991 N85-22485
Self-consistent simulation of plasma interactions with secondary-emitting insulators 13 p1993 N85-22492
An investigation of arc discharging on negatively biased dielectric conductor samples in a plasma
13 p1994 N85-22498
Characteristics of EMI generated by negative metal-positive dielectric voltage stresses due to spacecraft charging 13 p1995 N85-22505
Discharge pulse phenomenology
13 p1995 N85-22509
Discharge characteristics of dielectric materials examined in mono-, dual-, and spectral energy electron charging environments 13 p1995 N85-22510
Electrical conduction in polymer dielectrics
13 p1996 N85-22514
A simple model of electron beam initiated dielectric breakdown 13 p1996 N85-22516
Dielectric detector device for registering heavy cosmic radiation particles 13 p2045 N85-22799
Scattering of electromagnetic waves by charged particles 13 p2057 N85-22913
Surge strength of symmetric cable with monolithic polyethylene insulation of quads
13 p2082 N85-23001
Chemical interpretation of the relaxed permittivity during epoxy resin cure
[AD-A150955] 14 p2260 N85-24006
Dielectric resonator
[AD-D011573] 14 p2299 N85-24233
Special purpose materials for fusion application
[DE85-005346] 14 p2424 N85-24950
Field-induced phenomena in electrical insulation
[AD-A151234] 15 p2547 N85-25719
Monolithic planar doped barrier limiter
[AD-D011578] 15 p2548 N85-25723
Advanced capacitors
[AD-A151709] 15 p2548 N85-25727
Trends in the electric field enhancement of dielectronic recombination cross sections
[DE85-006920] 16 p2671 N85-27711
Completely consumed carbide: A new process for dielectric isolation
[AD-A152379] 17 p2918 N85-27987
Self-scanning MDS-integrated photosensor strip
17 p2940 N85-28151
Analysis of time dependent dielectric failures
[AD-A153200] 17 p2954 N85-28243
Experimental approaches to the measurement of dielectronic recombination
[DE85-006927] 17 p3030 N85-28743
Integrated electrooptical components using dielectric substrates 18 p3187 N85-29767
Separation of Drude and band-to-band spectra in polyvalent metals
[DE85-010247] 19 p3240 N85-30083
Guided and radiation wave interactions in periodic dielectric waveguides 19 p3253 N85-30173
Dielectric resonator oscillators with digital temperature compensation
[AD-D011715] 19 p3261 N85-30221
High temperature Raman studies of phase transitions in thin film dielectrics
[DE85-010873] 19 p3263 N85-30234
Gyrotron traveling-wave device including quarter wavelength anti-reflective dielectric layer to enhance microwave absorption
[AD-D011690] 19 p3271 N85-30285
A concept for the intrinsic dielectric strength of electrical insulation materials
[NASA-CR-176040] 20 p3448 N85-31410
Chemical structure of interfaces
20 p3480 N85-31629
Guided-mode launching in a slab waveguide by way of diffraction at the edge of a conducting screen residing on one surface of the slab
[AD-A154886] 21 p3575 N85-32232
Radiation-hardened polymeric films
[DE85-011636] 22 p3752 N85-33259
Effect of polymer additives on characteristics of direct-current motor with liquid dielectric filler
22 p3772 N85-33376
Effects of laser radiation on surfaces and coatings
[DE85-010475] 22 p3790 N85-33484
Supermite vacuum interface design
[DE85-012861] 22 p3837 N85-33759
An experimental study of dielectric rod antennas for millimeter-wave imaging applications
[AD-A155832] 24 p4088 N85-35328
DIELECTRONIC SATELLITE LINES
U RESONANCE LINES
DIELS-ALDER REACTIONS
Chemical approach for controlling nadimide cure temperature and rate
[NASA-CASE-LEW-13770-6] 19 p3232 N85-30039
DIENES
NT BUTADIENE
Structural and synthetic organosilicon chemistry
[AD-A147101] 07 p0919 N85-15820
Field test results of experimental EPDM (Ethylene Propylene Diene Monomer) and PUF (Polyurethane Foam) roofing
[AD-A147667] 08 p1132 N85-17133
DIES
Radio frequency probing apparatus for surface acoustic wave devices
[AD-D011230] 01 p0060 N85-10327

Conditions for assembling dies for drawing under hydrodynamic friction conditions
[BLL-M-35954-(5826.4)] 05 p0647 N85-14153
Optimization of the die entrance shape for polymeric extrusion
[DE85-001588] 06 p0772 N85-14937
Computer-aided design of extrusion dies by metal-flow simulation 06 p0797 N85-15094
Correction of engraving stamp for forming blanks of gas turbine engine blades 09 p1307 N85-16213
Precision die forging of blades or gas turbines 17 p2940 N85-28148

DIESEL ENGINES
Cylinder power fault diagnosis in military diesel engines
[TT-8406] 01 p0053 N85-10054
Combustion modeling of a 2 cylinder cycle reciprocating engine
[AD-A144782] 01 p0055 N85-10064
Clean-burning diesel engines
[AD-A145515] 02 p0205 N85-11349
Cooperative program evaluation of NATO multigraded diesel engine oils
[AD-A146072] 03 p0337 N85-12171
Time-temperature dependence of the strength of commercial zirconia ceramics
[AD-A146233] 03 p0338 N85-12173
Development of gas-lubricated pistons for heavy duty diesel engine technology program
[NASA-CR-174746] 03 p0441 N85-12808
Ceramic technology for advanced heat engines program plan
[DE84-013567] 04 p0479 N85-13055
Bulletin of the Faculty of Engineering, Hokkaido University, no. 123
[ISSN-0385-802-X] 04 p0482 N85-13075
Experimental study on the glow plug aided alcohol driven diesel engine 04 p0483 N85-13076
Advanced automotive diesel assessment program
[NASA-CR-168285] 04 p0507 N85-13235
Advanced Automotive Diesel Assessment Program, executive summary 04 p0507 N85-13236
Advanced automotive diesel engine system study 04 p0508 N85-13240
Screw expander for light duty diesel engines 04 p0508 N85-13242
Thermal and mechanical analysis of major components for the advanced adiabatic diesel engine 04 p0508 N85-13243
Overview of waste heat utilization systems
[NASA-TM-86901] 04 p0576 N85-13692
Transformation toughened ceramics for the heavy duty diesel engine technology program
[NASA-CR-174669] 07 p1055 N85-16698
Methods for heat transfer and temperature field analysis of the insulated diesel
[NASA-CR-174763] 07 p1056 N85-16699
FRG ceramic engine components (PET) 08 p1141 N85-17193
An investigation of enhanced capability thermal barrier coating systems for diesel engine components
[NASA-CR-174820] 09 p1298 N85-18154
Natural gas the new locomotive fuel
[DE84-901624] 09 p1302 N85-18179
Speed governor for diesel engine 09 p1307 N85-18214
Structural ceramics in transportation: Fuel implications and economic impacts
[DE85-003024] 11 p1611 N85-20130
Diesel fuel alternatives for engines in civil works prime movers
[AD-A149738] 12 p1617 N85-21400
Sliding seal materials for adiabatic engines
[NASA-CR-174693] 13 p2087 N85-22757
Diesel combustion: Advances in analysis and simulation 14 p2253 N85-23965
JP-8 and JP-5 as compression ignition engine fuel
[AD-A150796] 14 p2263 N85-24022
Transformation toughened ceramics: A potential material for light diesel engine applications
[AD-A151413] 15 p2518 N85-25525
Transformation toughened ceramics: A potential material for light diesel engine application
[AD-A151421] 15 p2518 N85-25526
Flat conducts R and D in ceramic parts for diesel engine 15 p2534 N85-25637
Diesel engine emissions of particulates and associated organic matter
[PB85-154425] 15 p2560 N85-25964
Breakway friction and dynamic friction/wear measurements of various ceramic materials from 25 C (75 F) to 650 C (1200 F)
[NASA-CR-174803] 16 p2754 N85-26994
Effect of traffic and meteorology on air pollution 16 p2930 N85-27452
Clean-burning diesel engines
[AD-A152606] 17 p2974 N85-28374
Future of ceramic turbochargers: Promises and pitfalls
[DE85-006209] 17 p2975 N85-28380
Ceramic Technology for Advanced Heat Engines Project
[DE85-008755] 18 p3060 N85-29052
Ceramic coatings for heat engine materials: Status and future needs
[DE85-008759] 18 p3060 N85-29053
Ceramic coatings for heat engine materials
[DE85-005238] 18 p3060 N85-29054
Development of a high-temperature coolant for advanced diesel engines
[AD-A153680] 18 p3117 N85-29297
Development of a coal-water slurry-fueled diesel engine for industrial cogeneration. Task 1.0 topical report: Thermodynamic analysis
[DE85-010455] 19 p3236 N85-30062
A device to detect Top Dead Center (TDC) position in motored engines
[REPT-84-RR-347] 20 p3458 N85-31475
The design of Direct Injection (DI) diesel engines. Injection system by a numerical optimization technique
[REPT-84-RR-346] 20 p3462 N85-31508
Coal slurry ignition in a diesel engine simulator
[DE85-010987] 20 p3463 N85-31513
Noise reduction in the automotive test cell of the Motor Institute of Naples
[REPT-85-RR-361] 20 p3524 N85-31917
An analytical and numerical model of radiation heat transfer in direct injection-type diesel combustion 24 p4092 N85-35368

DIESEL FUELS
Synthesis of transit practice: Diesel fuel quality and effects of fuel additives
[PB84-235668] 05 p0621 N85-13973
Diesel fuel alternatives for engines in civil works prime movers
[AD-A149738] 12 p1617 N85-21400
Chemical characterization and toxicologic evaluation of airborne mixtures. Inhalation toxicology of diesel fuel obscurant aerosol in Sprague-Dawley rats. Phase 3. Subchronic exposure
[AD-A150100] 12 p1905 N85-21968
JP-8 and JP-5 as compression ignition engine fuel
[AD-A150796] 14 p2263 N85-24022
Trends of petroleum fuels
[DE85-000116] 14 p2263 N85-24023
Catalyst and reactor development for a liquid phase Fischer-Tropsch process
[DE85-005694] 17 p2922 N85-28014
The distribution of higher n-alkanes in partially frozen middle distillate fuels
[AD-A153940] 18 p3083 N85-29074
Particle sizing from forward scattered light at two angles using a Variable-Focal-Length optical system
[AD-A154164] 20 p3533 N85-31980

DIETS
Effect of fluid and salt supplements to food allowance on endurance of head-to-pelvis accelerations following 7-day dry immersion and under ordinary motor activity conditions 01 p0092 N85-10618
Nutritional models for space travel from chemically defined diets
[NASA-CR-3850] 03 p0402 N85-12561
Food acquisition: Food ingredients, raw materials and supply 14 p2393 N85-24737
Diet of first Soviet expedition on Mount Everest 18 p3323 N85-30586

DIFFERENCE EQUATIONS
On explicit difference schemes for hyperbolic systems with variable coefficient 2
[PREPRINT-806] 03 p0413 N85-12541
Numerical treatment of corner singularities of the biharmonic equation
[TUM-M8315] 05 p0717 N85-14602
On a random difference equation for matrices and a characterization of the gamma distribution
[AD-A146858] 07 p1029 N85-16529
High order difference schemes with reduced dispersion for hyperbolic differential equations
[CWI-NM-R8408] 11 p1634 N85-20293
Upwind-difference methods for aerodynamic problems governed by the Euler equations
[REPT-84-23] 17 p2893 N85-27834
Intermediate boundary conditions for LOD, ADI and approximate factorization methods
[NASA-CR-172591] 18 p3167 N85-29626
Study of second order upwind differencing in a recirculating flow
[NASA-CR-174939] 19 p3264 N85-30243
Non-model based estimation with applications to sensor calibration using multiple sensors
[AD-A154736] 21 p3589 N85-32306

DIFFERENCES
Individual differences in chromatic brightness matching
[AD-A148882] 10 p1529 N85-19641
An amplitude correlation and differencing method for the monitoring of flaws in repeat ultrasonic inspections
[AERE-R-11416] 15 p2571 N85-25854
Basic research for the geodynamics program
[NASA-CR-175751] 16 p2825 N85-27424
On the relation between upwind-differencing schemes of Godunov, Engquist-Osher and Roe
[NASA-CR-175805] 16 p2852 N85-27583
Retinally stabilized differential resolution television display
[NASA-CASE-NPO-15432-1] 18 p3089 N85-29117
Width of nonlinear difference resonances
[DE85-013026] 24 p4148 N85-35719

DIFFERENTIAL ALGEBRA
U DIFFERENTIAL CALCULUS
U MATRICES (MATHEMATICS)

DIFFERENTIAL AMPLIFIERS
Cascode and differential amplifier using field-effect transistors 15 p2529 N85-25691
High temperature position sensors based on monolithic GaAs Hall IC
[BMFT-FB-T-84-266] 17 p2989 N85-28337

DIFFERENTIAL CALCULUS
A comment on Rosen's comments on activation and inhibition
[CTH-MATH-1984-24] 05 p0719 N85-14617
A geometric approach to high resolution TVD schemes
[NASA-CR-172484] 06 p0857 N85-15449

DIFFERENTIAL EQUATIONS
NT BIHARMONIC EQUATIONS
NT BLASIUS EQUATION
NT BURGER EQUATION
NT CHANDRASEKHAR EQUATION
NT ELLIPTIC DIFFERENTIAL EQUATIONS
NT EULER-CAUCHY EQUATIONS
NT FALKNER-SKAN EQUATION
NT FOKKER-PLANCK EQUATION
NT GAUSS EQUATION
NT HELMHOLTZ VORTICITY EQUATION
NT HYPERBOLIC DIFFERENTIAL EQUATIONS
NT LAME WAVE EQUATIONS
NT LIOUVILLE EQUATIONS
NT MONGE-AMPEPE EQUATION
NT PARABOLIC DIFFERENTIAL EQUATIONS
NT PARTIAL DIFFERENTIAL EQUATIONS
NT POISSON EQUATION
NT VLASOV EQUATIONS
NT VORTICITY EQUATIONS
Singular asymptotic expansions in nonlinear roiordynamics
[NASA-CR-174012] 01 p0017 N85-10100
HULL users' manual
[AD-A145000] 01 p0103 N85-10891
Legendre-Tau approximation for functional differential equations. Part 3: Eigenvalue approximations and uniform stability
[NASA-CR-172447] 01 p0110 N85-10744
Quasi-Newton algorithms for large scale nonlinear systems 02 p0208 N85-11370
Boundary conditions in Chebyshev and Legendre methods
[NASA-CR-172469] 02 p0250 N85-11635
Inverse problems, optimization and algorithms
[AD-A145397] 02 p0250 N85-11636
Numerical methods for singularly perturbed differential equations with applications
[AD-A145639] 02 p0252 N85-11650
United States Air Force on research on algebraic manipulation
[AD-A145737] 02 p0253 N85-11655
Discretization formulas on an arbitrary grid
[FFA-MEMO-127] 02 p0253 N85-11659
Forced oscillations theory for resonant extended interaction electron devices
[PR-206] 03 p0356 N85-12298
Control of linear stationary objects subject to external actions by means of various types of feedback 04 p0488 N85-13114
Quasi-three dimensional modeling of functionally-integrated elements of large-scale integrated circuits 04 p0490 N85-13122
Conservation laws and the numerical solution of ODEs
[DE84-016206] 04 p0555 N85-13531
Interval mathematics reports
[REPT-84/1] 04 p0556 N85-13536
Interval-mathematical treatment of initial value problems of ordinary differential equations 04 p0556 N85-13538
Supersymmetric Yang-Mills fields as an integrable system and connections with other non-linear systems
[DE84-013231] 04 p0556 N85-13539

New integration techniques for chemical kinetic rate equations. 2: Accuracy comparison
[NASA-TM-86693] 05 p0596 N85-13798
USSR report: Physics and mathematics
[JPRS-UPM-84-007] 05 p0723 N85-14651
Design of swirled axisymmetric turbulent jets
05 p0724 N85-14657
Iterative method of calculating strength of airframe members using finite element method
06 p0775 N85-14955
Controllable rotation of system of two solid bodies with elastic elements 06 p0780 N85-14988
Integrating chemical kinetic rate equations by selective use of stiff and nonstiff methods
[NASA-TM-86923] 07 p0904 N85-15726
An asymptotic analysis of a transient p-n junction model
[AD-A147270] 07 p0947 N85-16004
Art of programming programmable microcalculators. Part 12: Solution of differential equations
07 p0953 N85-16043
Dynamical characteristics of weak turbulence
[AD-A147186] 07 p0959 N85-16075
Strain-controlled creep rupture in non-isothermal materials 09 p1332 N85-18368
Fixed vs. variable order Runge-Kutta
[DE85-001320] 09 p1374 N85-18639
Magnetostatic problems in nonlinear media with hysteresis
[DE85-003701] 10 p1482 N85-19358
Locally univalent functions in the unit disk
10 p1535 N85-19680
A note on the disturbance decoupling problem for retarded systems
[AD-A149045] 10 p1543 N85-19730
Modeling the internal combustion engine
[NASA-RP-1094] 10 p1544 N85-19733
Asymptotic representation of solutions of the basic semiconductor device equations
[AD-A149040] 10 p1545 N85-19741
Periodic solutions of prescribed energy for a class of Hamiltonian systems
[AD-A149487] 10 p1548 N85-19764
Numerical solution of semilinear elliptic problems on unbounded domains
[AD-A149559] 10 p1549 N85-19767
Using semigroups and the Trotter product formula to solve quasi-linear systems
[DE85-002041] 11 p1706 N85-20736
Solution of structured non-stiff ODEs
[DE85-004137] 11 p1707 N85-20741
A comparison of the efficiency of numerical methods for integrating chemical kinetic rate equations
[NASA-TM-83580] 12 p1778 N85-21162
The performance of a type-insensitive Runge-Kutta code on a personal computer
[TUM-I8410] 12 p1919 N85-22046
Differentiating matrices for arbitrarily spaced grid points
[NASA-CR-172556] 12 p1919 N85-22051
Nonlinear partial differential equations and related problems of Pade approximations
[AD-A149650] 12 p1920 N85-22059
Low-dimensional behavior of the pattern formation Cahn-Hilliard equation
[DE85-003727] 12 p1922 N85-22072
Singular asymptotic expansions in nonlinear rotordynamics 12 p1945 N85-22218
New results on the PLL false lock phenomenon
12 p1948 N85-22236
Nonlinear rotordynamics analysis
[NASA-CR-171425] 13 p1988 N85-22364
Controlled movement of elastic manipulator with distributed parameters 13 p2048 N85-22818
Mathematical modeling of transient performance of gas turbine engine 13 p2050 N85-22834
Flow around axisymmetric bodies with uniform-velocity zones 14 p2276 N85-24103
Solving large linear systems 14 p2396 N85-24759
Maintaining solution invariants in the numerical solution of ODEs
[DE85-005916] 14 p2410 N85-24857
Simple-motion pursuit-evasion differential games in the plane
[CSIR-TWISK-336] 14 p2412 N85-24874
Kinematic dynamo theory for an arbitrary mean flow
14 p2446 N85-25106
One method for constructing model of point masses of planetary gravity field 15 p2479 N85-25300
Resonant rotations of satellite in polar orbit in magnetic and gravitational fields 15 p2479 N85-25302
Equilibrium solutions, stabilities and dynamics of Lanchester's equations with optimization of initial force commitments
[AD-A151510] 15 p2837 N85-26286
A new approach to queer differential equations
[AD-A149321] 15 p2838 N85-26272
Fundamental equivalence of generalised state space systems
[MATHEMATICS-RESEARCH-182]
15 p2842 N85-26293
Finite axisymmetric deformation of a thin shell of revolution 15 p2798 N85-27251
Use of REDUCE 2 for symbolic programming
[INPE-3355-PRE/833] 16 p2846 N85-27544
Explicit construction of contractivity matrices
[TRITA-NA-8309] 16 p2852 N85-27586
Evaluation of an algorithm for the solution of the time-dependent Euler equations
[AD-A151993] 16 p2854 N85-27600
Projected discrete ordinates methods for numerical transport problems
[DE85-005632] 17 p3020 N85-28678
Spatial differencing for finite difference codes
[DE85-006902] 17 p3021 N85-28684
Dynamical systems and numerical integration
[CWI-AM-R8413] 17 p3022 N85-28695
Symmetric linear multistep methods for second-order differential equations with periodic solutions
[CWI-NM-R8501] 17 p3022 N85-28696
Unsymmetrical flow in a centrifuge
[DE85-009021] 18 p3103 N85-29208
A global optimization algorithm using stochastic differential equations
[AD-A153526] 18 p3161 N85-29583
Shock capturing
[NASA-CR-172592] 18 p3168 N85-29627
Sensitivity analysis of initial value problems with mixed ode's and algebraic equations
[AD-A153528] 18 p3169 N85-29637
Determinal representations of polynomials satisfying linear Ordinary Differential Equations (ODEs) or linear recurrence relations
[PREPRINT-417] 18 p3172 N85-29660
Some applications of a convenient finite-dimensional matrix representation of the differential operator
[PREPRINT-416] 18 p3172 N85-29661
Interpolation and differentiation for periodic functions
[PREPRINT-419] 18 p3172 N85-29662
An introductory view of Raman-Nath type equations
[PREPRINT-422] 18 p3172 N85-29664
Numerical tests of a novel technique to compute the eigenvalues of differential operators
[PREPRINT-427] 18 p3173 N85-29667
Application of Floquet theory to helicopter blade flapping stability
[AD-A154460] 19 p3218 N85-29952
Control and regulation of generalized linear systems
19 p3257 N85-30193
Quantized Hall effect in two-dimensional electron systems
[AD-A154347] 19 p3259 N85-30211
Multigrid method for multiprocessors
[DE85-007929] 19 p3333 N85-30647
Numerical methods for the solution of stiff delay differential equations 19 p3334 N85-30653
MECA: A multiprocessor concept specialized to Monte Carlo
[DE85-010791] 19 p3348 N85-30737
Solving Volterra integral equations with ODE codes
[DE85-011216] 19 p3346 N85-30740
Computer-controlled carburizing
[BLL-OA-TRANS-3204-(6196.300)]
20 p3429 N85-31266
An analysis of multi-fingered hands
20 p3462 N85-31504
A theoretical model for the study of nonlinear dynamics of magnetic bearings 20 p3462 N85-31505
Spectral Theory of Sturm-Liouville Differential Operators: Proceedings of the 1984 Workshop
[DE85-009893] 20 p3520 N85-31890
Attractors for the Kuramoto-Sivashinsky equations
[DE85-009831] 20 p3520 N85-31892
Development of reduced order models for control system design using the OPTSYSX program
[AD-A154552] 21 p3556 N85-32124
Size spectra for the source-enhanced coagulation with the turbulent mass transfer 21 p3645 N85-32849
SIGMA - A stochastic-integration global minimization algorithm
[AD-A154878] 21 p3671 N85-32906
Identification of unsteady aerodynamics and aeroelastic integro-differential systems
[NASA-TM-86749] 21 p3679 N85-32951
Exact solutions of singular equations for viscous transonic flows 21 p3683 N85-32982
One method of solving the problem of unsteady heat exchange of a body and its ablation
22 p3733 N85-33146
Gradient scaling for nonuniform meshes
[DE85-009825] 22 p3784 N85-33443
Stochastic groundwater flow modeling using the second-order method
[DE85-011250] 22 p3802 N85-33586
Experiments and improvements of the ordinary differential equation solvers DEPAC on the CRAY computer
[DE85-013280] 22 p3831 N85-33726
Implementing linear multistep formulas for solving DAES
[DE85-012400] 22 p3834 N85-33740
Nonlinear flap-lag-extensional vibrations of rotating, pretwisted, preconed beams including Coriolis effects
[NASA-TM-87102] 23 p3941 N85-34427
DISPL1: A software package for one and two spatially dimensioned kinetics-diffusion problems
[ANL-84-56] 23 p3958 N85-34518
A geometric modeller for turbomachinery applications
23 p3962 N85-34556
Second-order Compton-Getting effect on arbitrary intensity distribution
[SH-3.1-10] 23 p4002 N85-34814
The application of bispectral analyses to aeroelastic phenomena 24 p4060 N85-35157
Identification and control of structures in space
[NASA-CR-176175] 24 p4069 N85-35214
Noise-sustained structure, intermittency and the Ginzburg-Landau equation
[DE85-009626] 24 p4094 N85-35379
A new theory for multistep discretizations of stiff ordinary differential equations: Stability with large step sizes
[NASA-CR-177941] 24 p4142 N85-35675
A new method for boundary value problems
[AD-A155934] 24 p4143 N85-35683

DIFFERENTIAL GEOMETRY
NT LIE GROUPS
NT RIEMANN MANIFOLD
NT SPINOR GROUPS
NT TENSOR ANALYSIS
Analytical foundations of the theory of quasiconformal mappings in Rn 10 p1536 N85-19679
On rotation automorphic functions with discrete rotation groups 10 p1536 N85-19688
Supermanifolds and Berezin's new integral
[DE85-001833] 11 p1706 N85-20732
A deformation analysis of flat flexible gear and its equation of original curved surfaces
[NASA-TM-77493] 12 p1859 N85-21680
Zero-crossings on lines of curvature
[AD-A150171] 13 p2150 N85-23345

DIFFERENTIAL INTERFEROMETRY
Measurement of ultrasonic fields in transparent media using a scanning differential interferometer
[NASA-CR-175921] 17 p3028 N85-28726

DIFFERENTIAL OPERATORS
U DIFFERENTIAL EQUATIONS
U OPERATORS (MATHEMATICS)

DIFFERENTIAL THERMAL ANALYSIS
U THERMAL ANALYSIS

DIFFERENTIATION
Differentiating spatial light modulator
[AD-D011727] 23 p3973 N85-34832

DIFFERENTIATION (BIOLOGY)
Gravity and cell differentiation in lentil roots
05 p0690 N85-14433

DIFFRACTION
NT ELECTRON DIFFRACTION
NT FRESNEL DIFFRACTION
NT NEUTRON DIFFRACTION
NT WAVE DIFFRACTION
NT X RAY DIFFRACTION
A determination of the photochemical quantum yields from 2 excited triplet states of biacetyl using holography
[AD-A145091] 01 p0050 N85-10326
Cerenkov radiation in the neighborhood of the emission threshold, revised
[AD-A145458] 02 p0284 N85-11655
Characteristics of light diffraction by two acoustic waves, one with complex frequency composition
03 p0348 N85-12343
DRG theory on the basis of a discrete interaction model
[PR-215] 03 p0358 N85-12357
Transient currents of ideally conducting body of revolution with transient diffraction
06 p0785 N85-15019
Unstable optical resonator with cancelling edge waves
[AD-D011379] 07 p1042 N85-16618
Switchable zero order diffraction gratings as light valves
[AD-A147575] 07 p1044 N85-16633
The evaluation of a deformable diffraction grating for a stigmatic EUV spectrohelioimeter
[NASA-CR-174350] 09 p1322 N85-18309
Field implementation of geophysical diffraction tomography
[DE84-017594] 09 p1343 N85-18449

Diffraction diffusion screen with holographically-suppressed zero-order beam
[AD-D011445] 10 p1497 N85-19387
Diffraction-limited imaging of space objects 2
[AD-A149344] 11 p1726 N85-20870
High resolution diffraction grating
[AD-D011541] 12 p1933 N85-22141
Switchable zero order diffraction gratings as light valves
[AD-A150129] 12 p1934 N85-22163
Reflex attachment for line alignment in spectral diffraction devices 13 p2044 N85-22794
Integrated optical components utilizing acoustooptic and electrooptic diffraction in micro-waveguides 13 p2089 N85-23044
Acoustooptic cell as space-frequency filter 13 p2090 N85-23051
Application of modern Aperture Integration (AI) and Geometrical Theory of Diffraction (GTD) techniques for analysis of large reflector antennas 14 p2234 N85-23651
Millimeter-wave diffraction devices and materials
[AD-A150876] 14 p2416 N85-24917
Sizing capability of automated ultrasonic time-of-flight diffraction in thick section steel and aspects of reliable inspection in practice
[AERE-R-11548] 15 p2571 N85-25856
An X-ray study of residual stresses in narrow groove TIG weldments
[DE85-006495] 16 p2602 N85-27274
The problem of atmospheric turbulence
[NASA-CR-175763] 16 p2632 N85-27464
Experimental studies of diffractive phenomena
[DE85-006812] 17 p3031 N85-28749
Investigation of superlattice device structures
[NASA-CR-3903] 18 p3094 N85-29152
NBS (National Bureau of Standards) reactor: Summary of activities Jul. 1983 through Jun. 1984
[PB85-184836] 20 p3522 N85-31907
Switchable zero order diffraction gratings as light valves
[AD-A154471] 20 p3539 N85-31981
Guided-mode launching in a slab waveguide by way of diffraction at the edge of a conducting screen residing on one surface of the slab
[AD-A154696] 21 p3575 N85-32232
Optical image of bounded objects 21 p3697 N85-32968
Picosecond-pulse damage studies of diffraction gratings
[DE85-010786] 22 p3790 N85-33461
Optical receivers using rough reflectors
[NASA-CR-176200] 24 p4164 N85-35750

DIFFRACTION GRATINGS
U GRATINGS (SPECTRA)

DIFFRACTION PATTERNS
NT RAINBOWS
A physical interpretation of the structure and electron-optical data for spinel (MgAl2O4)
[AERE-R-11278] 03 p0434 N85-12767
A short note on the high precision navigation of QUASAT 07 p1069 N85-16722
Structural characterization by intensity measurements of electron diffraction patterns
[DE85-004803] 13 p2164 N85-23427
Diffraction analysis of mesh deployable reflector antennas 14 p2235 N85-23654
Image formation in terms of the transport equation
[DE85-004883] 15 p2653 N85-25365
The development and implementation of an optical communications laboratory
[AD-A151682] 18 p2772 N85-27111

DIFFRACTION PROPAGATION
Problems on the diffraction and propagation of waves (selected articles)
[AD-A145139] 01 p0036 N85-10240
Intensity fluctuations of focused laser beam during reflection in turbulent atmosphere 13 p2078 N85-22975

DIFFRACTION TELESCOPES
U SPECTROSCOPIC TELESCOPES

DIFFRACTOMETERS
Neutron interferometry and double diffractometer for condensed matter 03 p0424 N85-12705
Construction of a neutron single crystal diffractometer 03 p0427 N85-12723

DIFFUSE RADIATION
The soft X-ray diffuse background: Implications for the nature of the local interstellar medium 06 p0876 N85-15586
Local contributions to the 0.6 keV diffuse X-ray background 06 p0877 N85-15589
HEAO-1 diffuse soft X-ray sky maps 06 p0877 N85-15570
Observations of local ISM emission with the Berkeley EUV/FUV shuttle telescope 06 p0880 N85-15594
The HEAO-1 diffuse component spectrum from 15 to above 500 keV — X and gamma rays 08 p1240 N85-17820
Weather data for simplified energy calculation methods. Volume 1. Eastern United States: TRY data
[DE85-000493] 09 p1358 N85-18541
Diffuse reflection of light from turbid conservative medium of finite thickness with incidence of beam on surface of scattering glancing 14 p2342 N85-24481
Nineteenth International Cosmic Ray Conference. OG sessions, volume 1
[NASA-CP-2376-VOL-1] 22 p3860 N85-33902
Cosmic gamma rays from quasars
[OG-2.7-10] 22 p3872 N85-33963
Relevance of cosmic gamma rays to the mass of gas in the galaxy
[OG-3.1-8] 22 p3874 N85-33996
COS-B gamma-ray sources and interstellar gas
[OG-3.1-9] 22 p3874 N85-33997
Spectrum of the gamma-ray diffuse component observed from HEAO-1
[OG-3.1-12] 22 p3874 N85-34000
Diffuse galactic annihilation radiation from supernova nucleosynthesis
[OG-3.2-6] 22 p3875 N85-34004
Literature search for new physical methods for biological aerosol detection
[AD-A155683] 24 p4128 N85-35592

DIFFUSERS
Turbo fluid machinery and diffusers
[NASA-TM-77467] 08 p1167 N85-17363
Determination of total pressure losses in stepped annular diffusers with curvilinear outer walls and uniform velocity field at inlet 09 p1306 N85-18203
A diffuser heat transfer code
[AD-A149270] 10 p1430 N85-19022
Mathematical modeling of the AEDC (Arnold Engineering Development Center) propulsion wind tunnel (16T)
[AD-A151293] 15 p2475 N85-25275

DIFFUSION
NT AMBIPOLAR DIFFUSION
NT ATMOSPHERIC DIFFUSION
NT ELECTRON DIFFUSION
NT GASEOUS DIFFUSION
NT GASEOUS SELF-DIFFUSION
NT IONIC DIFFUSION
NT MOLECULAR DIFFUSION
NT PARTICLE DIFFUSION
NT PLASMA DIFFUSION
NT SELF DIFFUSION (SOLID STATE)
NT SELF PROPAGATION
NT SURFACE DIFFUSION
NT THERMAL DIFFUSION
NT TURBULENT DIFFUSION
An investigation of the solubility and diffusivity of chromium in gallium arsenide
[AD-A144949] 01 p0024 N85-10148
Nuclear Magnetic Resonance of Polymeric Materials
[AD-A145078] 01 p0032 N85-10192
NMR (Nuclear Magnetic Resonance) and macromolecular migration in a melt or in concentrated solutions
[AD-P003908] 01 p0032 N85-10194
Sea water rope batteries
[AD-A144775] 01 p0042 N85-10275
Solution of the Boltzmann transport equations for a permeable base transistor
[AD-A144999] 01 p0112 N85-10757
Trapping for Newtonian diffusion processes
[REPT-73] 01 p0130 N85-10893
Review: The influence of short circuit diffusion on the oxidation of nickel, chromium and nickel/chromium alloys
[AERE-R-11311] 02 p0185 N85-11237
A dispersion model for airborne particulates inside a building
[DE84-014961] 02 p0225 N85-11473
Green River air quality model development: Meteorological and tracer data, July/August 1982. Field study in Brush Valley, Colorado
[DE84-014975] 02 p0225 N85-11474
Pointwise iterations of finite element modeling of advection-diffusion equations
[DE84-015284] 02 p0253 N85-11656
Comparison of the multigrid and ICCG methods in solving the diffusion equation
[DE84-014409] 02 p0253 N85-11657
Method of splitting for solution of problems in semiconductor physics 02 p0265 N85-11736
Problems in theory of diffusion under shock wave 02 p0272 N85-11776
Transport phenomena in the boundary layer during solution solidification under microgravity. Ice growth from a water-salt solution
[BMFT-FB-W-84-031] 03 p0329 N85-12121
Diffusion of Cr-51 tracer in Cr-2O-3 and the growth of Cr-2O-3 films
[AERE-R-11314] 03 p0333 N85-12146
Analysis techniques for tracer studies of oxidation
[NASA-CR-174796] 03 p0336 N85-12162
Effects of core mixing on solar oscillation frequencies
[DE84-015540] 03 p0449 N85-12653
Diffusion of gases in porous solids: Simulation and measurements
[DE84-016292] 04 p0500 N85-13191
Diffusion mechanisms and point defects in transition-metal oxides
[DE84-016238] 04 p0571 N85-13639
Oxygen diffusion from anodic surface oxide films on titanium subhydride studies by auger electron spectroscopy and electron energy loss spectroscopy
[DE84-016942] 04 p0572 N85-13648
Zero-flux planes and flux reversals in multicomponent diffusion
[DE84-015212] 05 p0616 N85-13950
Parallel flow diffusion battery
[DE84-005984] 05 p0631 N85-14047
Coupling of multidirectional diffusions by reflection
[CTH-MATH-1984-20] 05 p0719 N85-14613
Transport and relaxation processes in supercritical fluids
[DE84-006591] 05 p0731 N85-14698
Reducing numerical diffusion for incompressible flow calculations
[NASA-TM-83621] 06 p0756 N85-14840
Mechanisms of impurity diffusion in rutile
[DE84-014741] 06 p0766 N85-14902
The structure of dilute combusting sprays
[NASA-CR-174838] 07 p0905 N85-15726
Diffusion in metals under high mechanical strain and acceleration
[JUEL-1913] 07 p0926 N85-15887
Dependence of breakdown voltage for p-n junction on parameters of ion implantation and semiconductor heat treatment 07 p0954 N85-16046
Hydrologic characteristics of the Mediterranean and Black Sea 07 p0981 N85-16226
Estimation for a semimartingale regression model using the method of sieves
[AD-A146809] 07 p1028 N85-16527
Hydrogen embrittlement of nickel
[AD-A148322] 08 p1129 N85-17119
Deuterium diffusion in a soil-water-ice mixture
[AD-A148457] 08 p1176 N85-17415
Study of controlled diffusion stator blading
[NASA-CR-167995] 09 p1281 N85-18058
Hydrogen trapping, diffusion, and recombination in austenitic stainless steels
[DE85-001871] 09 p1294 N85-18129
Stability of amorphous metals on semiconductor substrates
[DE84-017256] 09 p1295 N85-18134
Battery response to pulse loads: A mathematical model
[DE85-001149] 09 p1318 N85-18277
Large deformations of a nonlinear elastic solid and the diffusion of an ideal fluid treated as interacting continua 09 p1330 N85-18356
Metal atom diffusion in amorphous silica and at the silica surface
[DE84-017351] 09 p1360 N85-18674
Cavitation phenomenon in superplastic creep
[DE85-001716] 10 p1441 N85-19063
Diffraction diffusion screen with holographically-suppressed zero-order beam
[AD-D011445] 10 p1497 N85-19387
A study of interdiffusion in beta + gamma/gamma + gamma prime Ni-Cr-Al
[NASA-CR-174852] 11 p1597 N85-20041
Improving operational properties of titanium alloys by diffusion siliciding 11 p1602 N85-20075
Distribution of hydrogen in multi-layer welded joints of alloyed steels 11 p1603 N85-20079
Analysis of diffusion in an ion-implanted alloy using a phenomenological model
[AERE-R-11527] 11 p1609 N85-20120
Comparison of MESOI atmospheric dispersion estimates with data and estimates from other models
[DE85-002372] 11 p1678 N85-20572
Evaluation of two numerical integrator schemes
[PB85-136196] 11 p1683 N85-20603
Solid electrolytes: Mechanisms for achieving optimal conductivity
[AD-A150116] 12 p1801 N85-21296
The behaviour of detonation waves in single phase heterogeneous systems
[AD-A149825] 12 p1846 N85-21581
Time and space variability of turbulent concentration fluctuations
[AD-A149963] 12 p1896 N85-21896

A diffusion process and its application to detecting a change in the drift of Brownian motion
[AD-A150096] 12 p1926 N85-22100
Enhanced diffusion from interstitial trapping during solid-phase-epitaxial growth of silicon alloys
[DE85-001285] 12 p1941 N85-22193
Diffusion deposition in fibrous filters for parallel and transverse flow models
[DE85-006149] 13 p2093 N85-23068
Cathode materials for molten carbonate fuel cells
[DE85-004076] 13 p2130 N85-23254
The ASCOT Data Analysis Workshop
[DE85-004407] 13 p2139 N85-23263
Material research in microgravity
[NASA-TM-77628] 14 p2228 N85-23811
The effect of water chemistry on the rates of hydrogen generation for galvanized steel corrosion at post-loca conditions
[NUREG/CR-3361] 14 p2253 N85-23963
Tracer diffusion in an ordered alloy: Application of the path probability and Monte Carlo methods
[DE85-002768] 14 p2257 N85-23966
Synthetic acceleration of coarse-mesh S/sub n/ transport calculations
[DE84-014721] 14 p2409 N85-24855
Weak convergence of a sequence of queueing and storage processes to a singular diffusion
[AD-A150855] 14 p2411 N85-24866
Steady state solution of the Fokker-Planck equation combined with unidirectional quasilinear diffusion under detailed balance conditions
[DE85-004917] 14 p2425 N85-24959
Experimental check of ion transport mechanism in Earth's radiation belt with exposure to nonsteady-state electric fields 15 p2480 N85-25308
Ways of improving level and stability of mechanical characteristics of diffusion-welded joints of OT4 titanium alloy 15 p2499 N85-25417
Structure and mechanical properties of dispersion-hardened nickel alloy joints welded by diffusion 15 p2500 N85-25422
Titanium diffusion method prevents metal corrosion 15 p2514 N85-25510
Development and diffusion of automated clinical chemistry analyzers
[PB85-150696] 15 p2561 N85-25798
Ionic conduction and water diffusion in Li (BETA)-alumina
[DE85-007548] 16 p2755 N85-27005
The seasonal cycle of atmospheric CO in the Southern Hemisphere 16 p2830 N85-27447
Comparison of a diffusion model with dye dispersion measurements to study turbulence in coastal waters
[INPE-3492-PRE/729] 16 p2836 N85-27504
A mathematical model for calculating detection probability of a diffusion target
[AD-A152026] 16 p2854 N85-27601
Polycrystalline semiconductor heterojunction modelling (CdS/CuInSe(sub)2)
[DE85-002913] 16 p2871 N85-27713
The development of laser analytical methods for the characterization of solid-liquid and solid-high pressure gas interfaces
[AD-A152362] 17 p2916 N85-27958
Use of principle of local equilibrium for assessing diffusional supersaturation during solidification of alloys
[BLL-BISI-TRANS-22487-(9022.09)] 17 p2929 N85-28077
Metallurgical means of preventing the corrosion of metal
[BLL-BISI-TRANS-22320-(9022.09)] 17 p2929 N85-28082
The effect of ion-bombardment-induced atomic mixing on depth-profiling of interfaces
[AD-A153199] 17 p3044 N85-28834
Strutless diffuser for gas turbine engine
[AD-D011662] 18 p3092 N85-28943
In situ Tuff water migration/heater experiment
[DE85-010415] 18 p3101 N85-29200
Analysis and model/data comparisons of large-scale releases of nitrogen tetroxide
[DE85-009899] 18 p3133 N85-29406
International space research perspectives of commercialization for German industry
[NASA-TM-77657] 19 p3222 N85-29979
Study of phase equilibria and crystallization processes in Al-Zn-Mg alloy systems 19 p3241 N85-30096
Technical guide for estimating fugitive dust impacts from coal handling operations. Volume 1: Project summary
[DE85-010948] 19 p3309 N85-30515
On MGR (Upelion) multigrid methods
[AD-A153667] 19 p3345 N85-30733
Tables of generalized hydrogen diffusion profiles and permeating fluxes for fusion applications
[DE85-008876] 19 p3372 N85-30919
Application of the Diffusion Raman Anti-Stokes Coherent (DRASC) method to a SNECMA combustion chamber
[YKC-9086/84] 20 p3425 N85-31260
Measurement of electrical parameters and current components in the bulk of silicon solar cells 20 p3481 N85-31635
High efficiency large area polysilicon solar cells 20 p3482 N85-31639
A positron annihilation Doppler broadening study of niobium
[DE85-010287] 20 p3527 N85-31936
Permeation of mixed penetrants through glassy polymer membranes
[AD-A155605] 21 p3570 N85-32207
A multilevel-multigrid method for recirculating flows 21 p3583 N85-32271
Simultaneous junction formation 21 p3610 N85-32426
Notes on atmospheric stability, turbulence, and its measurements
[AD-A155230] 21 p3637 N85-32588
Scavenging of submicron aerosol particles by snow crystals: Theory and experiments 21 p3648 N85-32667
Evaluation of the 2DFLOW and hybrid complex-terrain dispersion models with the 1980 ASCOT data base from the Geysers
[DE85-012960] 22 p3812 N85-33613
Airborne cloud tracking measurements during the Three Mile Island nuclear station accident, Middletown, Pennsylvania. Date of survey: March - June 1979
[DE85-012060] 22 p3816 N85-33638
A model for the proton spectrum and cosmic ray anisotropy
[OG-5.4-12] 22 p3887 N85-34089
New semi-implicit method for solving the time-dependent conservation equations for incompressible flow
[DE85-010926] 23 p3931 N85-34367
Evaluation of source strength and dispersion model predications with data from large nitrogen tetroxide field experiments
[DE85-011855] 23 p3947 N85-34485
User's guide to the MATHEW/ADPIC models
[DE85-012952] 23 p3966 N85-34587
Grain boundary and surface diffusion in oxide systems
[DE85-007291] 23 p3985 N85-34715
The model-independence of cosmic ray source determinations
[OG-7.2-1] 23 p4014 N85-34873
The role of cosmic rays in magnetic hydrodynamics of interstellar medium
[OG-7.2-15] 23 p4015 N85-34882
IMF-sense-dependent cosmic ray anisotropy produced from diffusion-convection in heliosphere
[SH-4.3-9] 23 p4032 N85-34994
Diurnal anisotropy during solar activity cycle twenty and diffusion-convection model
[SH-4.5-7] 23 p4036 N85-35025
Noise in sodium beta alumina crystals
[AD-A156025] 24 p4161 N85-35798
The nucleon intensity in the atmosphere and the Pt distribution
[HE-3.1-9] 24 p4178 N85-35007
Development of electromagnetic cascades in the atmosphere including the Landau-Pomeranchuk-Migdal effect
[HE-4.5-5] 24 p4195 N85-36029
Search for tachyons associated with extensive air showers in the ground level cosmic radiation
[HE-6.2-13] 24 p4212 N85-36149

DIFFUSION BONDING
U DIFFUSION WELDING

DIFFUSION COEFFICIENT
Definition of global dispersion coefficients — aquifers
[PSE-83/4-B] 01 p0064 N85-10426
Radiotracer studies of the dispersion of solid pollutants in marine and estuarial environment: Measurement of diffusion coefficients and the phenomenon of dispersion by currents
[BLL-DRIC-TRANS-7104-(3623.68)] 02 p0224 N85-11468
Diffusion and intermittency in an extended one-dimensional maps 02 p0282 N85-11834
Long time correlation and stochastic diffusion in the standard map 02 p0282 N85-11835
Diffusion of Fe-55 in Fe-20-3 single crystals
[AERE-R-11266] 03 p0333 N85-12147
Monte Carlo studies of transport in stellarators
[DE84-017633] 04 p0566 N85-13625
Low temperature diffusion coefficients in the Fe-Ni and FeNiP systems: Application to meteorite cooling rates 05 p0866 N85-15626
Diffusion in metals under high mechanical strain and acceleration
[JUEL-1913] 07 p0828 N85-15867
Adsorption thermodynamics and surface transport of metal catalyst poisons
[DE85-003750] 12 p1802 N85-21301
Measurements of radiation-induced segregation and diffusion in ion irradiated alloy using implanted manganese
[AERE-R-11528] 14 p2258 N85-23994
Diffusion of water vapor in Carbon Fiber Reinforced Plastics (CFRP). Measurement of the diffusion coefficient under influence of concentration
[DFVLR-FB-84-41] 14 p2262 N85-24018
Diffusion coefficients for coastal water determined from aerial photographs
[INPE-3413-PRE/679] 16 p2810 N85-27331
Transport in aqueous battery systems
[DE85-007246] 17 p2955 N85-28251
Computer-controlled carburizing
[BLL-OA-TRANS-3204-(6196.300)] 20 p3429 N85-31268
Relaxation lens in inhomogeneous binary mixture 21 p3695 N85-32957
Breakdown of intrinsic ambipolarity for the radial diffusion due to a rotating RF field 23 p3977 N85-34880
Effect of ECH and ICH on ambipolar potential in NBT-1M 23 p3978 N85-34881
Neoclassical diffusion including ellipticity in a heliotron-like configuration 23 p3978 N85-34887
Spatial dependence of the local diffusion coefficient measured upstream of the November 12, 1978 interplanetary traveling shock
[SH-1.5-12] 23 p3998 N85-34776
The Jovian electron spectrum: 1978-1984
[SH-1.5-19] 23 p3998 N85-34782
Cosmic ray modulatin and merged interaction regions
[SH-4.1-11] 23 p4005 N85-34834
Cosmic ray modulation in a random anisotropic magnetic field
[SH-4.1-20] 23 p4006 N85-34839
Spatial variation of cosmic rays near the heliospheric current sheet
[SH-4.2-10] 23 p4007 N85-34848
Effects of a wavy neutral sheet on cosmic ray anisotropies
[SH-4.2-11] 23 p4008 N85-34849
Effects of solar magnetic field on cosmic rays
[SH-4.2-12] 23 p4008 N85-34850
The expected cosmic ray density and stream distributions at the heliolatitudinal asymmetry of solar wind
[SH-4.2-14] 23 p4008 N85-34852
The influence of nonstationarity of the solar activity and general solar field on modulation of cosmic rays
[SH-4.2-17] 23 p4008 N85-34854
The effect of the neutral sheet structure of the interplanetary magnetic field on cosmic ray distribution in space
[SH-4.2-18] 23 p4008 N85-34855
Spatial distribution of cosmic rays in magnetic cycles of the Sun
[SH-4.2-20] 23 p4009 N85-34857
Difference between even and odd 11-year cycles in cosmic ray intensity
[SH-4.2-22] 23 p4009 N85-34859
Nonstationary modulation of galactic cosmic rays in a nonlinear model
[SH-4.7-10] 23 p4041 N85-35054

DIFFUSION EFFECT
U DIFFUSION

DIFFUSION FLAMES
Engineering method of calculating a turbulent diffusion flame
[BLL-M-35761-(5828.4)] 02 p0171 N85-11147
Ionization and time structure of flames
[LE-484/1-2] 05 p0614 N85-13925
Combustion driven oscillation of ducted diffusion flame 09 p1289 N85-18084
Core temperature measurements in sooting, laminar diffusion flames
[AD-A148801] 09 p1319 N85-18294
Fuels combustion research
[AD-A149108] 10 p1457 N85-19178
Investigation of fuel additive effects on sooting flames
[AD-A149154] 10 p1457 N85-19179
Laser diagnostic analyses of sooting flames
[AD-A150478] 13 p2017 N85-22849
A standard aircraft diffusion flame: Spectral characteristics and a feasibility study for developing an alternate calibration source for aircraft optical fire detection systems
[AD-A150231] 13 p2039 N85-22768
Asymptotic methods especially in combustion
[AD-A151505] 15 p2505 N85-25450

Laminar diffusion flames, carbon gasification, and laser diagnostics applied to combustion systems. 1: Laminar diffusion flames with cylindrical symmetry. 2: Diffusion-controlled gasification of carbon particles. 3: Laser diagnostics applied to combustion systems
20 p3423 N85-31243
Assessment of superlayer contribution to the conserved scalar PDF in a hydrogen turbulent jet diffusion flame
20 p3425 N85-31255
Blowout of turbulent diffusion flames
20 p3425 N85-31256
Strong turbulence chemistry interaction in a piloted turbulent jet diffusion flame 20 p3425 N85-31257
Non-equilibrium effects in turbulent diffusion flames
20 p3425 N85-31258
Sandia Cooperative Group on the Aerothermochemistry of Turbulent Combustion. Discussion record of the second meeting
[DE85-007493] 22 p3743 N85-33203
Pressure correlations in turbulent reacting flows
22 p3744 N85-33205
Vortex dynamics simulation of conserved scalar dissipation 22 p3745 N85-33210

DIFFUSION THEORY
Definition of global dispersion coefficients — aquifers
[PSE-83/4-B] 01 p0064 N85-10426
Problems in theory of diffusion under shock wave
02 p0272 N85-11776
Beam loss due to the aperture limitation resulting from intrabeam scattering
[DE85-005138] 12 p1930 N85-22124
Projected discrete ordinates methods for numerical transport problems
[DE85-005632] 17 p3020 N85-28678
Augmented weighted diamond force of the linear nodal scheme for Cartesian coordinate systems
[DE85-005631] 17 p3020 N85-28679
Nonlinear problems in continuum mechanics
[AD-A153367] 17 p3046 N85-28846
The Cauchy problem for u sub t = Delta u(m) when O m 1
[AD-A153521] 18 p3169 N85-29635
Oscillatory solutions of the Peaceman-Rachford alternating direction implicit method and a comparison of methods for the solution of the two dimensional heat diffusion equation
[AD-A154670] 21 p3675 N85-32633

DIFFUSION WAVES
Diffusion of particles in a slowly modulated wave
[DE85-000729] 09 p1391 N85-18756

DIFFUSION WELDING
New metallurgical processes based on high-speed crystallization and diffusion of metals
01 p0021 N85-10126
Causes of strength reduction in welded titanium-steel joints 03 p0352 N85-12262
Laser and diffusion welding equipment R and D
03 p0352 N85-12265
Residual stresses at small diffusion welds
[DE84-014982] 07 p0974 N85-16189
Application of diffusion welding of nickel based metals and application of electron beam welding of hot isostatically pressed nickel based powdered metals
08 p1169 N85-17375
Kinetics of joint formation during diffusion welding of VT5 titanium alloys 10 p1448 N85-19125
Diffusion welding with forced deformation of heat-resistant nickel-based dispersion hardened alloy
10 p1449 N85-19130
Kinetics of reaction of metals and non-metals during diffusion welding 11 p1602 N85-20076
Collapse and removal of discontinuities in joint zone during diffusion welding 11 p1602 N85-20077
Structure of transient zone in diffusion welding of TsTS-19 piezoceramic with AMg6 alloy
11 p1603 N85-20082
MDB uses superplastic forming, diffusion bonding for alloys 11 p1618 N85-20177
Mechanical properties and brittle fracture resistance of welded multilayer elements for high pressure vessels
13 p2033 N85-22736
Effect of protective medium on durability and fracture structure on seam zones of thin-walled titanium articles produced by diffusion welding 13 p2033 N85-22738
Technological parameters of diffusion welding processes in honeycomb titanium alloy structures
13 p2033 N85-22739
Durability of VT16 alloy compounds obtained by diffusion welding 13 p2034 N85-22740
Diffusion vacuum welding 15 p2499 N85-25416
Residual oxygen pressure in contact gap upon diffusion welding of titanium 15 p2499 N85-25418
Durability of joints of 30KhGSA and 12Kh18N10T steels made by diffusion welding 15 p2501 N85-25426
Diffusion welding of incompatible materials
19 p3245 N85-30121
Effect of heating temperature in a vacuum on state of surface layers of welded OT4 titanium alloy
19 p3245 N85-30123
Producing titanium-sapphire items by solid-phase bonding through aluminum gasket
19 p3246 N85-30127
Diffusion welding of aluminum with vacuum-tight corundum ceramic 19 p3247 N85-30130
Prospective uses for diffusion welding in vacuum
22 p3733 N85-33145
Welding methods for high melting metals
22 p3794 N85-33508
Joint design for improved fatigue life of diffusion-bonded box-stiffened panels
[NASA-TP-2480] 22 p3799 N85-33537
Diffusion welding of Cassegrainian concentrator cell stack assemblies
[NASA-CR-176104] 22 p3805 N85-33566

DIFFUSIVITY
The reactions of cobalt, iron and nickel in SO-2 atmospheres: Similarities and differences
[NASA-TM-86868] 02 p0181 N85-11217
Mixing in the solar interior 14 p2446 N85-25095
Heavy doping effects in high efficiency silicon solar cells
[NASA-CR-175687] 15 p2585 N85-25937
Diffusely reflecting paints including polytetrafluoroethylene and method of manufacture
[NASA-CASE-GSC-12683-1] 18 p3079 N85-29044
Turbulent wake of a submerged flat plate
[AD-A153776] 18 p3100 N85-29190
Study of molecular diffusivity influence on mass transfer rate at a water-atmosphere interface
22 p3747 N85-33222

DIFLUORIDES
NT CALCIUM FLUORIDES
Method for fluorination of actinide fluorides and oxyfluorides using O2F2
[DE85-011646] 22 p3743 N85-33202

DIFLUORO COMPOUNDS
NT PERFLUOROALKANE
NT POLYTETRAFLUOROETHYLENE
Subtractively normalized interfacial Fourier transform infrared spectroscopy of difluorobenzene adsorbed at polycrystalline platinum electrodes
[AD-A148660] 08 p1123 N85-17060

DIGESTING
Anaerobic digestion of biomass: status summary and research development needs, 1983
[PB85-161925] 13 p2040 N85-22772
Lipid hydrolysis in man during antiorthostatic hypokinesia 23 p3953 N85-34500

DIGESTIVE SYSTEM
NT GASTROINTESTINAL SYSTEM
NT INTESTINES
NT PANCREAS
NT RECTUM
NT TEETH

DIGITAL COMMAND SYSTEMS
Basic EMC (Electromagnetic Compatibility) technology advancement for C3 systems, macromodeling of digital circuits, volume 2B
[AD-A146333] 03 p0359 N85-12306
Speed test results and hardware/software study of computational speed problem, appendix D
05 p0603 N85-13843
Closing the design loop on HiMAT (highly maneuverable aircraft technology)
[NASA-TM-85923] 06 p0754 N85-14836
Some effects of digital sampling on orbiter flight control system operation 08 p1092 N85-16903
Robustness of discrete-time dynamical systems: Application to the multivariable digital control of combat aircraft
[ONERA-NT-1984-2] 11 p1585 N85-19986
Application of AFTI/F-16 task-tailored control modes in advanced multirole fighters 17 p2901 N85-27888
X-29 digital flight control system design
17 p2901 N85-27889
Some flight test results with redundant digital flight control systems 17 p2902 N85-27892

DIGITAL COMMUNICATION
U PULSE COMMUNICATION

DIGITAL COMPUTERS
NT CDC CYBER 170 SERIES COMPUTERS
NT CDC CYBER 205 COMPUTER
NT HEWLETT-PACKARD COMPUTERS
NT MICROCOMPUTERS
NT MINICOMPUTERS
NT PARALLEL COMPUTERS
NT PDP 11 COMPUTER
NT PDP 11/70 COMPUTER
NT PERSONAL COMPUTERS
NT SEQUENTIAL COMPUTERS
NT UNIVAC 1100 SERIES COMPUTERS
NT VAX COMPUTERS
NT VAX-11 SERIES COMPUTERS
NT VAX-11/780 COMPUTER
Data flow computer architecture
[DE84-014362] 01 p0100 N85-10864
THLL (TRIDENT Higher Level Language) reference manual
[AD-A145116] 01 p0104 N85-10896
Development and flight evaluation of an augmented stability active controls concept: Executive summary
[NASA-CR-166009] 02 p0149 N85-11006
International exhibition: Industrial Robots, 1982
03 p0345 N85-12224
Digital equipment Corporation, professional 350, COBOL-81 Version 2.1
[PB84-227602] 03 p0403 N85-12572
Digital Equipment Corporation, Professional 350, COBOL-81 Version 2.1 (COBOL technical report)
[PB84-227719] 03 p0403 N85-12573
Digital Equipment Corporation, DECSYSTEM-10, model 1090-SMP, COBOL-74 V129
[PB84-227941] 03 p0404 N85-12576
Data General Corporation, Eclipse C350, AOS COBOL Release 3.51
[PB84-227883] 03 p0404 N85-12577
Convergent Technologies, mega frame, CTIX COBOL version 2.0
[PB84-227750] 03 p0404 N85-12581
Digital Equipment Corp., VAX/750, VAX COBOL version 3.0
[PB84-227693] 03 p0405 N85-12583
Turbine blade damping study, introduction
04 p0456 N85-12891
New directions in software for advanced computer architectures
[DE84-017435] 04 p0550 N85-13502
Psychological issues in online adaptive task allocation
05 p0704 N85-14516
Experience with a sophisticated computer based authoring system
[DE84-014644] 05 p0713 N85-14575
Investigation of semiautomatic aircraft control processes employing time redundancy in on-board digital trajectory control computers 07 p0954 N85-16048
Reliability analysis of local area networks, intermediate report
[BLL-WH-610-(9091.9F)] 07 p1027 N85-16520
Automatic land vehicle navigation using road map data
[DE84-017178] 09 p1278 N85-18043
Digital high speed programmable convolver
[AD-D011455] 10 p1481 N85-19348
Man-machine interaction: Operator
[AD-A149075] 10 p1531 N85-19648
New CNC systems described
11 p1617 N85-20172
A modern approach of a synthetic aperture radar processor and its technological aspects
11 p1713 N85-20778
Multicomputer communication system
[NASA-CASE-NPO-15433-1] 12 p1822 N85-21428
Interface specifications for SCR (Software Cost Reduction) (A-7E) extended computer module, revised
[AD-A149948] 12 p1915 N85-22024
Signal flow model for sequential logic built from combinational logic elements and its implementation in Prolog
[DE85-005792] 15 p2549 N85-25734
Programming the digital computer ODRA-1204 in MOST-2 language
[NASA-TM-87462] 15 p2627 N85-26191
GRID: A FORTRAN program for using a digitizing table to enter a finite element GRID
[AD-A151317] 15 p2628 N85-26196
A concept for map updating using digital image processing methods 16 p2815 N85-27364
Contour line generalization using digital image processing methods 16 p2815 N85-27367
An update of experience on the fly by wire Jaguar equipped with a full-time digital flight control system
17 p2902 N85-27893
Operational and developmental experience with the F/A-18A digital flight control system
17 p2902 N85-27895
Flight testing and development of the F/A-18A digital flight control system 17 p2902 N85-27896
Language design, computers and brains
[AD-A152818] 17 p3008 N85-28594
An approach to digital level compression using the zero-crossing points of programme signals
[NHK-LABS-NOTE-308] 18 p3090 N85-29123
Tenth-order expansion formulae for the orbital eccentricity function K (sub lpq)(e) obtained using a symbolic algebraic manipulation system
[AD-A153754] 18 p3170 N85-29647

The prospects of the digital optical computer
18 p3188 N85-29771
A single chip VLSI architecture for radar signal processing 19 p3257 N85-30195
BP (Basic Processor) TRICOMP user's guide
[AD-A154340] 19 p3337 N85-30674
Filtration of higher harmonic components in two-level digital computing synthesizers 22 p3778 N85-33410
CARE 3 MENU maintenance manual
[NASA-CR-172609] 22 p3826 N85-33708
Re-designing a mechanism for higher speed: A case history from textile machinery 23 p3923 N85-34310
Method and apparatus for transfer function simulator for testing complex systems
[NASA-CASE-NPO-15696-1] 23 p3926 N85-34333

DIGITAL DATA
Ultrasonic synthetic aperture focusing using unfocused pulse-echo transducers
[AERE-R-11230] 01 p0057 N85-10374
A preliminary study of the feasibility of detecting the floating macrophytes by means of digital processing of MSS/LANDSAT data
[E85-10005] 02 p0215 N85-11418
Digital Terrain Elevation Data (DTED) anomaly removal through the use of an interactive Fourier frequency filtering process
[AD-A145433] 02 p0219 N85-11445
Description of the logical support for an image processing system
[INPE-2783-PRE/349] 02 p0240 N85-11563
Utilization of interpolation and transformation for the compression of digital image data
[INPE-3081-PRE/479] 02 p0240 N85-11566
Assessment of computer techniques for processing digital LANDSAT MSS data for lithological discrimination of Serra do Ramalho, State of Bahia
[E85-10033] 03 p0378 N85-12412
Digital image processing; report from a conference and study trip to the USA and Canada, summer 1984
[FOA-C-30369-E1] 04 p0494 N85-13153
Digital elevation models improve processing of Alaskan gravity data 04 p0515 N85-13285
Automatic correction of static characteristics of measurement channel of digital oscillograph
06 p0795 N85-15083
Classification of vegetation communities in the Battle Mountain SE quadrangle, Nevada with MSS digital data
[E85-10043] 06 p0826 N85-15246
Multi crop area estimation in Idaho using EDITOR
[E85-10054] 06 p0827 N85-15251
Characterizing the scientific potential of satellite sensors — San Francisco, California
[E85-10044] 07 p0983 N85-16244
Detecting agricultural to urban land use change from multi-temporal MSS digital data — Salt Lake County, Utah
[E85-10049] 07 p0983 N85-16245
Image variance and spatial structure in remotely sensed scenes — South Dakota, California, Missouri, Kentucky, Louisiana, Tennessee, District of Columbia, and Oregon
07 p0986 N85-16265
Analysis of subpixel registration
07 p0986 N85-16267
Interactive digital image processing for terrain data extraction
[AD-A148580] 08 p1176 N85-17417
A system for measuring the characteristics of the ionospheric channel by digital transmissions
10 p1472 N85-19287
Satellite-computer interface 10 p1476 N85-19318
Satellite support to the Sierra Cooperative Pilot Project: 1979/80 and 1980/81
[PB85-115079] 10 p1520 N85-19583
Application of SLF (Standard Linear Format) to digital hydrographic products
[AD-A149509] 10 p1522 N85-19586
Extracting digital data from a bus and multiplexing it with a video signal
[AD-D011491] 11 p1636 N85-20302
Radiometric accuracy assessment of LANDSAT 4 Multispectral Scanner data 11 p1666 N85-20498
LANDSAT scene-to-scene registration accuracy assessment 11 p1667 N85-20502
Geometric accuracy assessment of LANDSAT-4 Multispectral Scanner (MSS) data
11 p1667 N85-20505
TM digital image products for applications
11 p1668 N85-20512
Digital and color energy maps for graphic display of hourly data
[DE85-000526] 11 p1673 N85-20543
Digital channel efficiency model
[AD-A150084] 12 p1829 N85-21479
A preliminary assessment of LANDSAT-4 Thematic Mapper data — Windsor, Ontario and Medicine Hat areas, Canada 12 p1869 N85-21728
Preliminary evaluation of the radiometric calibration of LANDSAT-4 Thematic Mapper data by the Canada Centre for Remote Sensing 12 p1870 N85-21729
A preliminary analysis of LANDSAT-4 Thematic Mapper radiometric performance 12 p1870 N85-21730
Dynamics of adaptive signal corrector
13 p2071 N85-22940
Ionospheric distortions of digital signals with wideband modulation 13 p2072 N85-22945
Synthesis of quasi-optimum two-level signal discriminator with level changing at unknown point
13 p2083 N85-23010
LANDSAT-4 Science Characterization Early Results. Volume 4: Applications — agriculture, soils land use, geology, hydrology, wetlands, water quality, biomass identification, and snow mapping
[E85-10070] 13 p2117 N85-23186
Overview of TM applications research reports
13 p2117 N85-23187
A preliminary comparison of the information content of data from the LANDSAT 4 Thematic Mapper and Multispectral Scanner — Arkansas
13 p2119 N85-23199
Early results of investigations of LANDSAT 4 Thematic Mapper and Multispectral Scanner applications — Washington, D.C.
13 p2119 N85-23200
Relative accuracy assessment of LANDSAT-4 MSS and TM data for level 1 land cover inventory — Washington, D.C.
13 p2122 N85-23212
Using SM-4 Omega system in checking and editing digital terrain information 15 p2487 N85-25350
An amplitude correlation and differencing method for the monitoring of flaws in repeat ultrasonic inspections
[AERE-R-11416] 15 p2571 N85-25854
Shuttle imaging radar-B (SIR-B) data analysis for identifying rainfall event occurrence and intensity
[NASA-CR-175712] 15 p2594 N85-25966
Three-dimensional/perspective display techniques for meteorological data sets 15 p2599 N85-26018
CNPq/INPE LANDSAT system: Report of activities from October 1, 1983 to September 30, 1984 — Brazil
[E85-10097] 16 p2808 N85-27318
A concept for map updating using digital image processing methods 16 p2815 N85-27364
Contour line generalization using digital image processing methods 16 p2815 N85-27367
What does digital image processing perform in the production of orthophotomaps 16 p2815 N85-27368
Evaluation of Defense Mapping Agency level 1 second edition digital data for training simulator applications
[AD-A152444] 17 p2983 N85-28437
Experimental philosophy leading to a small scale digital data base of the conterminous United States for designing experiments with remotely sensed data
[NASA-TM-85009] 17 p3049 N85-29877
Defense Mapping Agency (DMA) raster-to-Vector benchmark testing
[AD-A154152] 19 p3338 N85-30683
A high-speed digital signal processor for atmospheric radar, part 7.3A 21 p3626 N85-32525
Estimate of signal-to-interference energy ratio in discrete-data transmission 22 p3776 N85-33396
Digital tachometer 22 p3779 N85-33416

DIGITAL FILTERS
NT FIR FILTERS
Nonlinear regression with emphasis on spline methods
[AD-A146192] 03 p0412 N85-12633
Application of high frequency 2-D digital filtering to remote sensing image processing
05 p0660 N85-14242
Derivation of recursive digital filters by the step-invariant and the ramp-invariant transformations
[AD-A146500] 06 p0857 N85-15452
Enhancement of multispectral scanner images by digital filtering
[ESA-TT-824] 07 p0969 N85-18284
Digital coherent detector
[AD-D011560] 12 p1833 N85-21501
Estimating algorithmic error of digital recursive filters
12 p1839 N85-21543
Synthesis of digital nonrecursive band-elimination filters for moving-target selectors 12 p1840 N85-21545
Method of designing digital band-pass filters with infinite memory 12 p1840 N85-21546
Digital detector of harmonic signals
12 p1840 N85-21549
Optimal design efforts in Shanghai described
13 p1972 N85-22986
Two-dimensional signal processing and storage and theory and applications of electromagnetic measurements
[AD-A150590] 13 p2065 N85-22999
Optimal synthesis of surface acoustic wave filters
13 p2070 N85-22933
Efficiency of digital compensator of strong non-Gaussian interference 13 p2072 N85-22942
Methods of digital correction for channels of multichannel radar receivers 13 p2082 N85-23005
Use of Walsh functions for calculating characteristics of digital filters with impulse response of finite duration
13 p2083 N85-23011
Linearization of digital derived rate algorithm for use in linear stability analysis
[NASA-TM-87000] 14 p2243 N85-23904
Digital computer applications of Kalman filter in target tracking
[AD-A150770] 14 p2404 N85-24821
Correlating and adaptive digital filters
[BMFT-FB-T-84-299] 15 p2551 N85-25744
High-speed digital baseband mixer
16 p2771 N85-27103
Digital filters for digital phase-locked loops
16 p2771 N85-27104
Digital filters for application to data analysis in electron energy loss spectroscopy
[DE85-007932] 17 p2923 N85-29020
Application of adaptive noise cancellation to Coast Guard voice communications
[AD-A154798] 21 p3574 N85-32230
Digital matched filter 22 p3765 N85-33339
Hardware realization of digital filters without multipliers
22 p3766 N85-33340
Design of high-order analog and digital filters with identical sections 22 p3766 N85-33341
Design of digital bandpass filters with finite memory
22 p3775 N85-33392
Maximally flat approximation of attenuation characteristics of coupled-line filters
22 p3775 N85-33393
Miniature two-mode filters 22 p3775 N85-33394
Method of designing digital band-pass filters with pulse response of finite duration 22 p3775 N85-33395

DIGITAL INTEGRATORS
Programmable digital baud integrators for the radar high-speed data acquisition system
05 p0624 N85-13994
Rotorcraft digital advanced avionics system (RODAAS) functional description
[NASA-CR-166611] 15 p2468 N85-25237
Digital filters for digital phase-locked loops
16 p2771 N85-27104
Probabilistic analysis of combinational circuits with random delays 19 p3257 N85-30192

DIGITAL NAVIGATION
Implementation of the SITAN algorithm in the digital terrain management and display system
[DE85-010659] 22 p3729 N85-33115

DIGITAL RADAR SYSTEMS
Digital rader data as an aid in nowcasting in Hong Kong 01 p0079 N85-10525
AFOS (Automation of Field Operations and Services) display of MDR (Manually Digitized Radar) data on local map backgrounds
[PB84-220797] 08 p0840 N85-15338
Digital controller for the Wave Propagation Laboratory's VHF and UHF wind-profiling radars
[PB85-112142] 11 p1626 N85-20236
Mathematical model of discriminator for signals with fluctuations and thermal noise 13 p2072 N85-22943
Efficiency of multitarget signal detection by digital radar data processing devices 13 p2080 N85-22991
Factorized algorithms for combined spatial and temporal processing of radar signals 13 p2081 N85-22997
Digital signal processing for spaceborne synthetic aperture radar
[FOA-C-30381-E1] 20 p3442 N85-31364

DIGITAL SIMULATION
A simulation experiment of a rapidly developed medium scale cyclone 01 p0079 N85-10530
Numerical simulation of natural convection in porous media — heat transfer
[CFD/84/10] 02 p0199 N85-11330
Computer simulation techniques for turbulent flows
[CFD/84/11] 02 p0199 N85-11331
Operational behavior of wind energy converters. Control and dynamic and types of generators, volume 1
[BMFT-FB-T-84-154-VOL-1] 03 p0386 N85-12470
Operational behavior of wind energy converters: Control and dynamic and types of generators, volume 2
[BMFT-FB-T-84-154-VOL-2] 03 p0386 N85-12471
Geographic subdivision and top level data structures, Columbus, Magellan, and expanding CIG (Computer Image Generation) horizons
[AD-P004317] 09 p1268 N85-17971
Digital simulation of communications channels: An overview 10 p1472 N85-19290
Application of model following control and estimation techniques to attitude control of maneuvering spacecraft. Part 2: Simulation software description
[NLR-TR-82116-U-PT-2] 12 p1793 N85-21254
Evolution of collisional systems — planetary disks
15 p2674 N85-26505

A numerical simulation of the NFAC (National Full-scale Aerodynamics Complex) open-return wind tunnel inlet flow
[NASA-TM-86724] 16 p2700 N85-26672
Dispersion sensitivity of the eight inch advanced ramjet munitions technology projectile due to wind and minor thrust errors
[AD-A152145] 16 p2727 N85-26935
Digital image mapping of Antarctica using NOAA-7 AVHRR imagery 18 p3124 N85-29340
Computer simulation of elastic waves by a new mass-point system with potentials
[DRIC-T-7274] 20 p3469 N85-31553
Flexible satellite communications systems simulator, phase 3
[AD-A155647] 21 p3577 N85-32247
Research on an expert system for database operation of simulation-emulation math models. Volume 1, Phase 1: Results
[NASA-CR-176067] 21 p3669 N85-32792
Research on an expert system for database operation of simulation-emulation math models. Volume 2, Phase 1: Results
[NASA-CR-176068] 21 p3669 N85-32793
A preliminary evaluation of a failure detection filter for detecting and identifying control element failures in a transport aircraft
[NASA-TM-87576] 24 p4067 N85-35204
Computer simulation of a cruise missile using brushless dc motor fin control
[AD-A155935] 24 p4089 N85-35349

DIGITAL SYSTEMS
NT DIGITAL NAVIGATION
NT DIGITAL RADAR SYSTEMS
Design of a digital ride quality augmentation system for commuter aircraft
[NASA-CR-172419] 01 p0006 N85-10037
Clutter generator for use in radar evaluation
[AD-D011234] 01 p0039 N85-10245
Digital correlator speed improvement by multiplexing
[AD-A145207] 01 p0100 N85-10662
Expert systems in maintenance diagnostics for self-repair of digital flight control systems
[AD-P003933] 02 p0247 N85-11613
Minimization of anomalous errors in measuring systems employing search and testing devices
03 p0344 N85-12219
On line digitizer software
[AD-A146249] 03 p0403 N85-12568
Application of a silicon compiler to VLSI (Very Large Scale Integrated circuits) design of digital pipelined multipliers
[AD-A146328] 03 p0403 N85-12569
High-temperature optically activated GaAs power switching for aircraft digital electronic control
[NASA-CR-174711] 04 p0457 N85-12901
Interference immunity of digital equipment for coherent processing of wideband signals
04 p0486 N85-13100
Digital radio receivers and problems of analog-to-digital conversion of narrow-band signals
04 p0486 N85-13101
Architecture of adaptive space-frequency-time signal processing system 04 p0486 N85-13103
Efficiency of computer system digital processing of signals 04 p0487 N85-13106
Test experience on an ultrareliable computer communication network
[NASA-TM-85915] 04 p0552 N85-13514
Primary data processing in very long baseline radiointerferometer 06 p0783 N85-15008
Intralow-frequency digital phase meter
06 p0787 N85-15031
A noise-suppressing digital frequency meter
06 p0796 N85-15084
The effect of aircraft generated electromagnetic interference (EMI) on future avionics systems: A compendium
[AD-A146380] 06 p0799 N85-15101
Digital raster timing encoder-decoder
[AD-D011279] 06 p0804 N85-15120
Precision digital sampler
[AD-D011285] 06 p0809 N85-15143
Systems study for an Integrated Digital-Electric Aircraft (IDEA)
[NASA-CR-3840] 07 p0902 N85-15714
Predicted performance benefits of an adaptive digital engine control system of an F-15 airplane
[NASA-TM-85916] 07 p0905 N85-15729
Programmable synchronous digital delay line
[AD-D011382] 07 p0945 N85-15985
Digital signal demodulators with single-sideband
07 p0950 N85-16019
Digital thermometer with linearizer on slide wire
07 p0954 N85-16049
ILIR task of digital recoil travel measurement system
[AD-A147102] 07 p0967 N85-16140
Metric aspects of digital images and digital image processing
[AD-A147211] 07 p0988 N85-16276
Upset susceptibility study employing circuit analysis and digital simulation --- digital systems and electromagnetic interference 07 p0999 N85-16344
Data and results of a laboratory investigation of microprocessor upset caused by simulated lightning-induced analog transients
07 p0999 N85-16345
Experience of one UK electronic equipment supplier with bite on engine/flight control systems over the past ten years 08 p1064 N85-16738
Built-in test and self repair mechanisms in a digital correlator integrated circuit 08 p1064 N85-16741
A digital piloting system for the combat helicopter
08 p1074 N85-16806
Integrated digital/electric aircraft concepts study
[NASA-CR-3841] 08 p1083 N85-16861
Design of a digital ride quality augmentation system for commuter aircraft
[AD-A148233] 08 p1088 N85-16879
Interactive digital image processing for terrain data extraction
[AD-A148580] 08 p1176 N85-17417
VICOM technical description
[REPT-611-0012-REV-A] 08 p1202 N85-17563
Multidimensional digital signal processing
[AD-A148055] 08 p1205 N85-17585
Complexity, testability, and fault analysis of digital, analog and hybrid systems
[AD-A148465] 08 p1213 N85-17634
A modified Monte-Carlo technique for the simulation of satellite communication systems
[AD-A146689] 08 p1214 N85-17641
A description of the NRL oblique-incidence-ionogram data base
[AD-A148625] 08 p1230 N85-17748
Transdigitizer for relaying signals from Global Positioning System (GPS) satellites
[AD-D011442] 10 p1422 N85-18970
French firm develops 2D, 3D computer vision system
10 p1461 N85-19208
Television animation store: Recording pictures on a parallel transfer magnetic disc
[BBC-RD-1984/17] 10 p1462 N85-19220
Limits of the propagation medium with respect to digital signal transmission 10 p1469 N85-19270
Propagation influences on the performance of a reduced bandwidth quadrature phase shift keyed digital radio system 10 p1470 N85-19274
Equatorial transionospheric propagation conditions affecting digital communications
10 p1470 N85-19275
The impact of propagation effects on the design of high capacity digital microwave links in the 18 GHz frequency band 10 p1470 N85-19278
A review of atmospheric multipath measurements and digital system performance 10 p1470 N85-19279
Wideband line-of-sight channel measurements and simulation: Application to digital radio links
10 p1471 N85-19283
Some propagation experimental results on protection techniques for line-of-sight digital systems
10 p1472 N85-19286
LOS microwave channel simulation: A survey of models, realizations and new concepts 10 p1472 N85-19291
A review of transmission and channel evaluation techniques for digital communication systems
10 p1474 N85-19301
Application of SLF (Standard Linear Format) to digital hydrographic products
[AD-A149509] 10 p1522 N85-19596
Telemetry systems of Interkosmos satellites
11 p1617 N85-20173
Extracting digital data from a bus and multiplexing it with a video signal
[AD-D011491] 11 p1636 N85-20302
Digital imaging processing
[INPE-3325-PRE/624] 11 p1701 N85-20696
Integrated support of tactical operations by satellite communications 11 p1709 N85-20754
Integrated control system engineering support
[AD-A149742] 12 p1780 N85-21177
Low sidelobe phased array antenna system
[AD-D011558] 12 p1823 N85-21435
Television animation store: Digital chroma, key and mixer units
[BBC-RD-1984/16] 12 p1824 N85-21442
The study of certain aspects of probability with applications in communications theory
[AD-A149820] 12 p1829 N85-21476
Digital coherent detector
[AD-D011560] 12 p1833 N85-21501
Digital detector of harmonic signals
12 p1840 N85-21549
Synthesis of digital control for object with lag
12 p1843 N85-21562
SIMULA: Digital controller simulation package
[PB85-134492] 12 p1917 N85-22041
Testing of the digital flight control system of the German CCV fighter experimental aircraft
13 p1988 N85-22361
The use of a high-speed 12-bit A/D converter for digital sampling of communication signal carriers
[AD-A150578] 13 p2056 N85-22672
Noise tolerance of digital demodulator for complex signal system employing binary quantization
13 p2070 N85-22929
Analysis of characteristics of digital discriminators for phase-shift keyed signals 13 p2070 N85-22930
Interference immunity of binary systems with second-order phase-difference modulation in various reception modes 13 p2072 N85-22944
Noise tolerance of diversity reception in frequency-adaptive digital transmission systems
13 p2086 N85-23024
Use of importance sampling to investigate signal detection systems by simulated method
13 p2086 N85-23028
Digital laser platemaker modifications
[AD-A150190] 13 p2095 N85-23074
Optical memory research and its application to digital optical processing 13 p2158 N85-23397
Synthesis of optimal controls for real-time linear digital systems 14 p2270 N85-24062
Digital processing of passive Ka-band microwave images for sea-ice classification
[AD-A150686] 14 p2347 N85-24511
Map design for computer processing: Literature review and DMA product critique
[AD-A151061] 14 p2347 N85-24513
Factors affecting dwell times on digital displaying
[NASA-TM-86406] 14 p2390 N85-24722
Multi-rate digital autopilot modeling methodology
[AD-A152044] 15 p2474 N85-25272
Converters of sum/difference of codes to frequency
15 p2526 N85-25578
Analysis of spectral characteristics of multilevel digital computing synthesis 15 p2527 N85-25579
Interactive communication channel
[AD-D011580] 15 p2542 N85-25695
Standards in process: Foundation and profiles of ISDN (Integrated Services Digital Network) and OSI (Open Systems Interconnection) studies
[PB85-165041/GAR] 15 p2545 N85-25712
Superfine laser position control using statistically enhanced resolution in real time
[DE85-005643] 15 p2564 N85-25817
Data structure considerations in automatic cartography
15 p2583 N85-25930
Design specifications for IMAGER: The DREO (Defence Research Establishment Ottawa) image processing system
[AD-A151752] 15 p2624 N85-26168
User manual for IMAGER: The DREO (Defence Research Establishment Ottawa) image processing system
[AD-A151754] 15 p2653 N85-26362
Technical evaluation report on Avionics Panel Specialists' Meeting on Digital Optical Circuit Technology
[AGARD-AR-202] 15 p2653 N85-26367
Design and implementation of the digital engineering laboratory distributed database management system
[AD-A151694] 15 p2665 N85-26450
Rotorcraft digital advanced avionics system (Rodasa)
15 p2688 N85-26608
Application of AFTI/F-16 task-tailored control modes in advanced multirole fighters 16 p2712 N85-26735
X-29A digital flight control system design
16 p2712 N85-26736
Some flight test results with redundant digital flight control systems 16 p2712 N85-26739
An update on experience on the fly by wire Jaguar equipped with a full-time digital flight control system
16 p2712 N85-26740
Operational and developmental experience with the F/A-18A digital flight control system
16 p2713 N85-26742
Flight testing and development of the F/A-18A digital flight control system 16 p2713 N85-26743
The certification of airborne complex digital systems
16 p2714 N85-26754
Automatic flight control modes for the AFTI/F-111 mission adaptive wing aircraft 16 p2714 N85-26756
High-speed digital baseband mixer
16 p2771 N85-27103
Certifying complex digital systems on civil aviation aircraft 17 p2904 N85-27907

The design of an adaptive predictive coder using a single-chip digital signal processor
[AD-A152461] 17 p2952 N85-28231
Evaluation of Defense Mapping Agency level 1 second edition digital data for training simulator applications
[AD-A152444] 17 p2963 N85-28437
Further study of digital matching of dissimilar images
[AD-A153112] 17 p3019 N85-28672
Tone calibrated digital radio communication system
[NASA-CASE-NPO-16414-1-CU] 18 p3089 N85-29121
A possible digital circuit able to recognize magnetic monopoles crossing a thick scintillator counter
[NOTA-INTERNA-826] 18 p3097 N85-29173
Experimental performance of a digital circuit able to recognize magnetic monopole events
[NOTA-INTERNA-838] 18 p3037 N85-29176
Maser and secondary clock in telecommunications networks 18 p3108 N85-29248
Digital control of diode laser for atmospheric spectroscopy
[NASA-CASE-NPO-16000-1] 18 p3112 N85-29264
An interactive computer aid for the design and analysis of linear, single input/single output digital and continuous control systems
[AD-A153704] 18 p3162 N85-29589
Direct digital control study
[AD-A153685] 18 p3167 N85-29621
Energy Efficient Engine (E3) controls and accessories detail design report
[NASA-CR-168017] 19 p3218 N85-29957
Dielectric resonator oscillators with digital temperature compensation
[AD-D011715] 19 p3261 N85-30221
Environmental background measurement program
[AD-A153860] 19 p3319 N85-30577
Defense Mapping Agency (DMA) raster-to-Vector analysis
[AD-A154153] 19 p3336 N85-30668
High accuracy digital acousto-optic matrix computer
[AD-D011692] 19 p3343 N85-30716
An overview of measurement solutions for digital systems 20 p3437 N85-31326
Performance improvements of a highly integrated digital electronic control system for an F-15 airplane
[NASA-TM-86748] 21 p3556 N85-32120
Myoelectric control of a computer based expert system for flight control
[AD-A154981] 21 p3557 N85-32126
Design of a jamming simulator for a binary communication system
[AD-A154617] 21 p3573 N85-32221
Globally-asynchronous locally-synchronous systems
[AD-A154624] 21 p3573 N85-32222
Secure digital voice communications in the Defense Data Network (DDN)
[AD-A154677] 21 p3574 N85-32226
Experimental evaluation of a new form of M-ary (M = 8) phase shift keying including design of the transmitter and receiver
[AD-A155103] 21 p3576 N85-32239
Microcomputer processing of LANDSAT Thematic Mapper data for the acquisition of military tactical terrain data
[AD-A154781] 21 p3605 N85-32389
Realizing the full potential of the video disc for mapping applications
[AD-A154986] 21 p3606 N85-32391
Bayesian vs MAP multiple model adaptive estimation for field of view expansion in tracking airborne targets
[AD-A155466] 21 p3679 N85-32955
Implementation of the SITAN algorithm in the digital terrain management and display system
[DE85-010859] 22 p3729 N85-33115
Quarter-inch streaming tape drive application with the Serial ASCII Instrumentation Loop (SAIL) system
[AD-A155364] 22 p3759 N85-33295
Characteristics of digital range finder with stroboscopic discretization 22 p3762 N85-33319
Amplitude stabilization of pulse signals 22 p3762 N85-33320
Digital holographic synthesis of pattern-forming transparencies for ring antenna arrays 22 p3763 N85-33326
Design of digital bandpass filters with finite memory 22 p3775 N85-33362
Binary signal detection in acoustooptic receivers 22 p3782 N85-33430
Transceiver test device
[AD-D011728] 22 p3786 N85-33458
Digital characterization of particle tracks for microdosimetry
[DE85-012866] 22 p3846 N85-33822
Modular digital holographic fringe data processing system
[NASA-CR-177952] 23 p3933 N85-34376
Balloon-borne video cassette recorders for digital data storage
[OG-9.3-11] 23 p4028 N85-34966
Burst size distributions in the digitized data of the ion chambers t Mt. Norikura and sea level stations
[SH-9.1-9] 23 p4051 N85-35124
Microprocessor-based single particle calibration of scintillation counter
[HE-4.6-13] 24 p4198 N85-36049

DIGITAL TECHNIQUES
Range-reeldusted mappings
[AD-A145148] 01 p0112 N85-10759
Research activities of the Illinois University Coordinated Science Laboratory
[AD-A145589] 03 p0449 N85-12856
Interference immunity of digital equipment for coherent processing of wideband signals 04 p0486 N85-13100
Digital radio link: Wave propagation measurements using narrow band technique
[FOA-C-30364-E2] 04 p0494 N85-13152
Digital image processing; report from a conference and study trip to the USA and Canada, summer 1984
[FOA-C-30369-E1] 04 p0494 N85-13153
Digital comparison and correlation techniques of remote sensing images with differing spatial resolutions 05 p0655 N85-14204
Multi-disciplinary techniques for understanding time-varying space-based imagery
[AD-A144357] 05 p0728 N85-14681
Infralow-frequency digital phase meter 06 p0767 N85-15031
Telstrack: A special effect
[BBC-RD-1984/10] 06 p0796 N85-15097
Experiences with digital processing of images at INPE
[E85-10045] 06 p0826 N85-15247
Detecting agricultural to urban land use change from multi-temporal MSS digital data — Salt Lake County, Utah
[E85-10049] 07 p0983 N85-16245
Some effects of digital sampling on orbiter flight control system operation 08 p1092 N85-16903
Information extraction and transmission techniques for spaceborne synthetic aperture radar images
[NASA-CR-174341] 08 p1150 N85-17256
Data acquisition channel apparatus
[AD-D011428] 08 p1159 N85-17311
Mathematical aspects of digital terrain information; Report from International Society for Photogrammetry and Remote Sensing (ISPRS) working group 3:3, 1980 - 1984 — photogrammetry 08 p1175 N85-17407
A comparative test of photogrammetrically sampled digital elevation models 08 p1175 N85-17408
Digital elevation model computation using fast Poisson solutions 08 p1175 N85-17412
Digital sound: Programme-modulated noise levels in sound signals subjected to a number of digital companding processes
[BBC-RD-1984/11] 09 p1310 N85-18233
Multipath and Doppler observations during transatlantic digital HF propagation experiments 10 p1471 N85-19281
Fast synchronization model for UHF spread-spectrum communication system 10 p1473 N85-19296
A technical solution to fadings in tactical satellite digital transmissions 10 p1473 N85-19297
Overview of RADC adaptive antenna developments for communications 10 p1474 N85-19299
The development of a microprocessor-controlled linearly-actuated valve assembly
[NASA-CR-174437] 10 p1491 N85-19415
Solar optical telescope primary mirror controller
[NASA-CR-174416] 10 p1570 N85-19903
Telemetry systems of Interkosmos satellites 11 p1617 N85-20173
Contour line generalization using digital image processing methods
[SER-C-291] 11 p1700 N85-20688
Conclusion of Viking Lander Imaging Investigation: Picture catalog of experiment data record
[NASA-RP-1137] 11 p1765 N85-21099
Semianalytic modeling of aerodynamic shapes
[NASA-TP-2413] 12 p1771 N85-21120
Estimation of the impulse response of television channels from digitized waveforms
[CRC-1378] 12 p1822 N85-21429
Fundamental limits to synchronization and tracking
[AD-A149623] 12 p1833 N85-21504
GSFC specification electronic data processing magnetic recording tape
[NASA-TM-80599] 12 p1851 N85-21609
Assessment of computer based geologic mapping of rock units in the LANDSAT-4 scene of northern Death Valley, California 13 p2119 N85-23195
Comparative techniques used to evaluate Thematic Mapper data for land cover classification in Logan County, West Virginia 13 p2121 N85-23209
Bouguer images of the North American craton 13 p2200 N85-23648
Near-nucleus studies of Comet Halley 14 p2435 N85-25018
Microcomputer controlled image acquisition system 15 p2537 N85-25654
Scene analysis using recursive frequency domain correlation with energy normalization
[AD-A151777] 16 p2854 N85-27596
Digital methods of the optimum processing of radar signals
[AD-A152469] 17 p2948 N85-28202
Image processing: Mathematics, engineering or art
[DE85-007666] 18 p3154 N85-29527
Approaches to digital image registration and recognition 19 p3257 N85-30197
Spectral reflectances of natural targets for use in remote sensing studies
[NASA-RP-1139] 19 p3299 N85-30450
Fast eigenvector methods for digital signal processing 20 p3439 N85-31341
Electron lithography STAR design guidelines. Part 1: The STAR user design manual
[NASA-CR-170765] 20 p3513 N85-31840
Electron lithography STAR design guidelines. Part 2: The design of a STAR for space applications
[NASA-CR-170766] 20 p3513 N85-31841
Electron lithography STAR design guidelines. Part 3: The mosaic transistor array applied to custom microprocessors. Part 4: Stores logic arrays, SLAs implemented with clocked CMOS
[NASA-CR-170767] 20 p3514 N85-31842
Interactive procedures for discriminating and restoring contour line networks 22 p3738 N85-33158
The Mk.1 NPL digital sampling ac wattmeter
[NPL-DES-62] 22 p3758 N85-33290
Design of digital bandpass filters with finite memory 22 p3775 N85-33362
Hierarchical chamfer matching
[FOA-C-30387-E1] 22 p3802 N85-33558
Design, development and operation of a high simultaneous capacity digital telemetry system — turbomachine blade flutter
[PNR-90261] 23 p3899 N85-34151
Computer analysis techniques for the temporal evaluation of cardiac wall motion 23 p3958 N85-34530
The scientific and technical issues in integrating remotely sensed imagery with geocoded data bases 23 p3960 N85-34547
A general purpose image processing package 23 p3961 N85-34549
Hologram-like transmission of pictures 23 p3961 N85-34552
Processing of LANDSAT imagery to map surface mineral alteration on the Alaska Peninsula, Alaska 24 p4106 N85-35455
Remote sensing of hydrologic transport processes using spot simulation data
[DE85-012412] 24 p4108 N85-35467

DIGITAL TO ANALOG CONVERTERS
Clutter generator for use in radar evaluation
[AD-D011234] 01 p0029 N85-10245
Programmable digital temperature controller apparatus
[AD-D011221] 01 p0049 N85-10319
Optical waveguide spatial filters
[AD-A145674] 02 p0260 N85-11825
Formation of reference signals in laser-type gas analyzers with mechanical switching of optical channels 06 p0787 N85-15027
RELTIM: A library of routines used in real time machine control applications
[PB85-116507] 10 p1542 N85-18725
Electrical characterization of analog microprocessors
[AD-A149629] 12 p1911 N85-21995
A method and apparatus for operating on companded PCM voice data
[NASA-CASE-KSC-11295-1] 18 p3089 N85-29120

DIGITIZERS
U ANALOG TO DIGITAL CONVERTERS

DIGITS
NT BINARY DIGITS

DIHEDRAL EFFECT
U LATERAL STABILITY

DIISOCYANATES
Structure-property relationships in thermoplastic elastomers. Part 1: Segmented polyether-polyurethanes
[AD-A148043] 06 p1133 N85-17138
Polymer intermediates from limonene (follow-up project)
[BMFT-FB-T-84-243] 12 p1814 N85-21380

DIKES (GEOLOGY)
U ROCK INTRUSIONS
DILATATION
U STRETCHING
DILATOMETERS
U EXTENSOMETERS
DILUENTS
New air-curing lacquer systems with high solids content
[BMFT-FB-T-85-005] 17 p2936 N85-28124
DILUTION
Dilution zone mixing studies 02 p0145 N85-10984
Dilution jet mixing 02 p0145 N85-10985
Measurements of atmospheric carbon disulfide using aircraft platforms and a GC/MS isotopic dilution analysis technique 03 p0391 N85-12500
Development of a temperature measurement system with application to a jet in a cross flow experiment
[NASA-CR-174696] 15 p2472 N85-25262
Dual electrochemical system
[AD-D011616] 16 p2817 N85-27376
DIMENSIONAL ANALYSIS
Development of structured regression hypotheses/interactive descriptive geometry through five dimensions
[INT-324] 04 p0554 N85-13524
Application of dimensional analysis to the problem of solar wind-magnetosphere energy coupling
[DE85-002414] 11 p1674 N85-20551
The application of dimensional analysis to the problem of solar wind-magnetosphere energy coupling
14 p2357 N85-24584
Applications of fuzzy set theory to satellite soundings
18 p3141 N85-29445
Diffusion-convection function of cosmic rays
[SH-3.2-10] 23 p4004 N85-34625
Computation of three-dimensional shock wave and boundary-layer interactions
[NASA-TM-85760] 24 p4083 N85-35372
DIMENSIONAL MEASUREMENT
Publications of Center for Manufacturing Engineering (of the National Bureau of Standards), 1976-1983
[PB84-224526] 01 p0036 N85-10228
Development of a measuring procedure for the automatic evaluation of the flatness of reflective surfaces
[BMFT-FB-T-84-168] 03 p0421 N85-12686
Programming and application of numerical controlled measuring machines (NCMES)
[BMFT-FB-T-84-153] 05 p0717 N85-14690
Method for non contacting gauging of the wall thickness of tubes by backscattering radiation
[OEFZS-4274] 07 p0968 N85-16144
The design and validation of software for dimensional metrology
[NPL-DITC-50/84] 15 p2521 N85-25542
Interferometric creep testing
[AD-A154249] 19 p3286 N85-30378
A simple optical extensometer achieving high accuracy
[NPL-DMA(A)-95] 20 p3458 N85-31474
DIMENSIONAL STABILITY
NT SHELL STABILITY
NT STRUCTURAL STABILITY
Parameters of geometric stability of laser mirror optical surface 02 p0273 N85-11777
Interferometric creep testing
[AD-A154249] 19 p3286 N85-30378
Materials and techniques for model construction
[NASA-CR-172820] 20 p3396 N85-31066
A systematic plan for the continued study of dimensional stability of metallic alloys considered for the fabrication of cryogenic wind tunnel models
[NASA-CR-172449] 21 p3565 N85-32172
DIMENSIONLESS NUMBERS
NT GRASHOF NUMBER
NT HIGH REYNOLDS NUMBER
NT LOW REYNOLDS NUMBER
NT MACH NUMBER
NT NUSSELT NUMBER
NT PRANDTL NUMBER
NT RAYLEIGH NUMBER
NT REYNOLDS NUMBER
NT RICHARDSON NUMBER
NT SIMILARITY NUMBERS
NT STROUHAL NUMBER
Ohmic potential drop and gas bubble radius distribution in alkaline water electrolysis 17 p2924 N85-28025
Linear boundary detection using pressure buildup tests
[DE85-009926] 22 p3784 N85-33444
DIMENSIONS
NT DEPTH
NT DIAMETERS
NT FILM THICKNESS
NT FRACTALS
NT HEIGHT
NT LARMOR RADIUS
NT LENGTH
NT RADII
NT TARGET THICKNESS
Shift-variant multidimensional systems
[AD-A144756] 01 p0111 N85-10752
Fractals: From snow flakes to galactic clusters
[NOTA-INTERNA-796] 02 p0206 N85-11918
Thermomechanical cracking in layered media from moving friction load
[AD-A146022] 03 p0373 N85-12379
Optimum dimensions of power solenoids for magnetic suspension 04 p0489 N85-13116
Considerations on the dimensioning of photovoltaic supply systems in the low power range
05 p0665 N85-14273
Coupling of multidirectional diffusions by reflection
[CTH-MATH-1984-20] 05 p0719 N85-14613
Challenges in the development of the shuttle extravehicular mobility unit 08 p1095 N85-16922
Cosmology in theories with extra dimensions
18 p3202 N85-29664
Physical dimensions of humans; values; the effect of clothing, working clothes and protective equipment on the design of work places
[HSE-TRANS-10868] 19 p3331 N85-30638
Physical dimensions of humans, values, envelope curves in different postures
[HSE-TRANS-10869] 20 p3513 N85-31838
A simulation study of Sylvester's problem in three dimensions
[AD-A155266] 21 p3679 N85-32854
Photo-acoustic effect in finite-dimensional semiconductors 21 p3682 N85-32876
DIMERS
A new heat-resistant polymer from dimer diamine bismaleimide. Part 1: Preparation and free radical cure of dimer diamine bismaleimide
[AD-A145864] 02 p0186 N85-11247
Theoretical research program to study transition metal trimers and embedded clusters
[NASA-CR-174296] 08 p1125 N85-17093
Comparative studies on the electronic structures of W2(O2CH)4 and W2(O2CH)4-(CH3)2 by the relativistic X Alpha-SW method: A d3-d3 metal dimer with a quadruple metal-metal bond?
[AD-A148814] 09 p1397 N85-18793
Conduction in polymerized polyfunctional diacetylenes
[AD-A148104] 10 p1451 N85-19145
Below-room-temperature water-vapor continuum absorption within the 8- to 10 micron atmospheric transmission window
[TR-0084(4945-09)-1] 13 p2132 N85-23266
Photoreactivation and other ultraviolet/visible light effects on DNA in human skin
[DE85-005135] 14 p2390 N85-24719
Investigation of the structure and dynamics of electrolytes in solvents used for primary and secondary Li-batteries
[AD-A153099] 17 p2954 N85-28240
Metallophthalocyanine dimers incorporating five atom covalent bridges
[AD-A154365] 19 p3234 N85-30051
Method of reducing impurity and antisite defects in semiconductor crystal materials, and device and apparatus respectively produced from and utilizing same
[AD-D011698] 19 p3260 N85-30216
DIMINUTION
U REDUCTION
DINITRATES
Preparation of ethylenediamine dinitrate
[DE85-006423] 23 p3922 N85-34305
DIODES
NT AVALANCHE DIODES
NT GERMANIUM DIODES
NT GUNN DIODES
NT JUNCTION DIODES
NT LIGHT EMITTING DIODES
NT MIM DIODES
NT PHOTODIODES
NT PLASMA DIODES
NT SCHOTTKY DIODES
NT SEMICONDUCTOR DIODES
NT TUNNEL DIODES
NT VARACTOR DIODES
The development of a diode laser Doppler velocimeter for boundary layer measurements under ice: A feasibility investigation
[AD-A145076] 01 p0063 N85-10348
Reversible change in parameters of GaAs-based surface-barrier metal-semiconductor diodes induced by hydrogen absorption-desorption
02 p0258 N85-11690
Gallium-arsenide power devices
06 p0794 N85-15076
Current-voltage characteristics of semiconductor power devices operating at high current densities
06 p0795 N85-15079
External cavity diode laser sensor
[AD-D011341] 07 p0969 N85-16152
Diffusion barrier for long wavelength laser diodes
[AD-D011390] 07 p0970 N85-16157
EMC enhanced constant Z modulator
[AD-A147715] 08 p1157 N85-17297
Effect of neutron irradiation on the high temperature operation of injection laser diodes
[DE85-000068] 09 p1326 N85-18333
Radiation effects induced in pin photodiodes by 40- and 85-MeV protons
[NASA-CR-175678] 14 p2426 N85-24960
Development of solid state infrared emitters for gas detection applications
[PB85-148450] 15 p2561 N85-25800
Generalization of the Child-Langmuir relation for 1-dimensional time-dependent diodes
[DE85-007386] 16 p2779 N85-27152
Diode laser 87Rb optical pumping in an evacuated wall-coated cell 18 p3105 N85-29226
Digital control of diode laser for atmospheric spectroscopy
[NASA-CASE-NPO-16000-1] 18 p3112 N85-29264
Intense ion beam diode diagnostics using a tunable dye laser
[DE85-008079] 18 p3113 N85-29272
Measurements of vector fields with diode array
18 p3204 N85-29680
Integrated dual beam line scanning antenna and negative resistance diode oscillator
[AD-D011717] 19 p3261 N85-30223
Arrangement for damping the resonance in a laser diode
[NASA-CASE-NPO-15960-1] 19 p3274 N85-30305
Optical injection locking of solid-state oscillators by frequency-multiplexed injection-locked, laser diodes
[AD-D011695] 19 p3275 N85-30307
Resistance of polyaniline films as a function of electrochemical potential and the fabrication of polyaniline-based microelectronic devices
[AD-A154999] 21 p3569 N85-32201
A microprocessor-controlled, multichannel fluorimeter for analysis of sea water
[AD-A154986] 21 p3590 N85-32310
T/R switch design for short-range measurements, part 6.1A 21 p3624 N85-32515
Magnetically insulated diode for generating pulsed neutron and gamma ray emissions
[DE85-011658] 22 p3760 N85-33306
Multidiode integrated-circuit protective device
22 p3761 N85-33425
Power flow evaluations for HERMES 3
[DE85-013116] 24 p4156 N85-35769
Surface discharges as intense photon sources in the extreme ultraviolet
[DE85-012593] 24 p4158 N85-35782
DIOXIDES
NT CARBON DIOXIDE
NT HYDROGEN PEROXIDE
NT QUARTZ
NT SILICON DIOXIDE
NT SULFUR DIOXIDES
Structural studies on lead dioxides
[DE84-015837] 06 p0805 N85-15127
Investigation of manganese dioxide as an improved solid desiccant
[DE85-004034] 13 p2018 N85-22854
DIPHOSPHATES
NT ADENOSINE DIPHOSPHATE
DIPLEXERS
Performance interface document for the S-band diplexer for space users of NASA networks
[NASA-TM-86224] 23 p3900 N85-34155
DIPOLE ANTENNAS
Characteristics of two-frequency combined dipole antenna arrays 06 p0791 N85-15055
Infrared technology for satellite power conversion --- antenna arrays and bolometers
[NASA-CR-174266] 07 p0991 N85-16293
Tactical HF communication for military helicopters using the NVIS mode 08 p1074 N85-16807
Broad-band UHF dipole array
[NASA-TM-86373] 10 p1462 N85-19222
Printed circuit balun with a dipole antenna
[AD-D011534] 12 p1833 N85-21498
Surface wave excitation study
[DE85-005301] 13 p2056 N85-22875
Exact design formulas for field intensity of dipole deployed above flat homogeneous Earth with finite conductivity 13 p2081 N85-22998

A special antenna for SARSAT EPIRBs providing circular polarization and hemispheric coverage for reliable transmission to satellites — Emergency Position Indicating Radio Beacon (EPIRB) 20 p3404 N85-31122
Artificial and natural icing tests YEH-60A quick fix helicopter
[AD-A155147] 21 p3555 N85-32116
Minimizing field scattered by slender dipoles 22 p3774 N85-33388

DIPOLE MOMENTS
NT ELECTRIC MOMENTS
NT MAGNETIC MOMENTS
Studies of the chemistry of vibrationally and electronically excited species in planetary upper atmospheres
[NASA-CR-174134] 03 p0449 N85-12851
Collision-induced dipole moments
[AD-A147682] 06 p1121 N85-17063
Experimental determination of the 1 sigma(+) state electron-dipole-moment function of carbon monoxide up to a large internuclear separation
[NASA-TM-86979] 09 p1379 N85-18670
Development of high field Nb-Ti accelerator dipoles
[DE85-000621] 11 p1714 N85-20782
Charge-to-mass dispersion methods for abrasion-ablation fragmentation models
[NASA-TM-86340] 11 p1726 N85-20857
Applications of piezoelectric and pyroelectric thin films: Opportunities for Langmuir-Blodgett technology
[AD-A149239] 15 p2659 N85-26408
Electroweak interactions in nuclei
[DE85-007811] 17 p3033 N85-28762
Scattering by distributions of small thin particles 19 p3253 N85-30172
Mutual coupling analysis for conformal microstrip antennas
[AD-A154292] 19 p3259 N85-30210
Effects of CP violation in SU(2) sub L x SU(2) sub R x U(1) electroweak models
[DE85-010801] 20 p3531 N85-31865

DIPOLES
Theory of nuclear magnetic relaxation
[AD-P003911] 01 p0032 N85-10197
A generalized solution to a class of printed circuit antennas
[AD-A145628] 02 p0191 N85-11278
Computer studies of the quench behavior of an SSC model dipole
[DE85-010633] 19 p3360 N85-30829
Testing and optimizing MST coaxial collinear arrays, part 6.4A 21 p3625 N85-32518
The magnetic field of planets 22 p3858 N85-33881
What we have learned about the magnetic field of Mars 22 p3858 N85-33882
Magnetic field generation in the cores of terrestrial bodies 22 p3859 N85-33884

DIRAC EQUATION
Scattering theory by Enss' method for operator valued matrices: Dirac operator in an electric field
[REPT-84] 01 p0045 N85-10290
Solutions of field equations in General Relativity with spinor connection 15 p2663 N85-26436
Interpretation of 119 Sn isomer shifts and 3d 5/2-core-level shifts based on Dirac-Slater calculations on a number of ionic states
[USIP-85-06] 20 p3532 N85-31973

DIRECT CURRENT
Isolated load switching with surge suppression
[AD-D011218] 01 p0042 N85-10274
DC switching regulated power supply for driving an inductive load
[DE84-014238] 01 p0044 N85-10285
Nitriding of titanium and its alloys by N2, NH3 or mixtures of N2 + H2 in a dc arc plasma at low pressures (or = to torr)
[NASA-TM-83803] 06 p0814 N85-15168
Calculations of high-current characteristics of silicon diodes at microwave frequencies
[AD-A147408] 09 p1314 N85-18261
Variable speed generator technology options for wind turbine generators
[RFI-84-4] 10 p1478 N85-19331
Study of electric field and ion effects on HVDC lines
[DE85-002975] 12 p1833 N85-21503
Ultrasensitive measuring devices
[DE85-000672] 12 p1853 N85-21622
Efficient heating and confinement of ions in an axisymmetric magnetic mirror supplemented with dc electric field
[IPPJ-707] 12 p1935 N85-22160
Outlook for realization of proximity effect and Josephson direct current in helium-2 13 p2074 N85-22956
Method of improving dynamic characteristics of DC voltage stabilizers with compound regulation 15 p2526 N85-25589
CSMP (Continuous System Modeling Program) modeling of brushless DC motors
[AD-A152043] 15 p2549 N85-25731
Pulsewidth modulated speed control of brushless dc motors
[AD-A151966] 16 p2778 N85-27148
Performance analysis of radiation cooled dc transmission lines for high power space systems
[NASA-TM-87040] 17 p2951 N85-28222
A small-scale self-excited rotor electrostatic generator
[AD-A155264] 21 p3581 N85-32265
Optical output stabilization method for direct current arc lamps
[AD-A154987] 21 p3705 N85-33013
Standard series of direct-current motors for regulated electric drives 22 p3772 N85-33375
Effect of polymer additives on characteristics of direct-current motor with liquid dielectric filler 22 p3772 N85-33376
Computer simulation of a cruise missile using brushless dc motor fin control
[AD-A155935] 24 p4089 N85-35349

DIRECT LIFT CONTROLS
Low-speed characteristics of a circulation control airfoil with AFT camber and a spiral trailing edge
[AD-A150851] 14 p2213 N85-23725
Basic consideration of the lifting capability of stoppable rotors
[AD-A150650] 14 p2219 N85-23759

DIRECT POWER GENERATORS
NT ALKALINE BATTERIES
NT ELECTROSTATIC GENERATORS
NT FUEL CELLS
NT HOMOJUNCTIONS
NT MAGNETOHYDRODYNAMIC GENERATORS
NT NICKEL ZINC BATTERIES
NT PHOSPHORIC ACID FUEL CELLS
NT PHOTOELECTRIC GENERATORS
NT PRIMARY BATTERIES
NT RADIOISOTOPE BATTERIES
NT REGENERATIVE FUEL CELLS
NT SOLAR BLANKETS
NT SOLAR CELLS
NT SOLAR SEA POWER PLANTS
NT THERMAL BATTERIES
NT THERMIONIC CONVERTERS
NT THERMOELECTRIC GENERATORS
NT VERTICAL JUNCTION SOLAR CELLS
Measurement-Technical investigations of Wind Energy Units
[JUEL-SPEZ-244] 05 p0667 N85-14293
Measuring methods to determine the static and dynamic behavior of wind energy converters 05 p0668 N85-14297
VOITH: Wind energy converter WEC 520 05 p0668 N85-14299
Measuring and control tasks in OPTIWA 05 p0669 N85-14304
Operational performance of the photovoltaic-powered grain mill and water pump at Tengaye, Burkina Faso (formerly Upper Volta)
[NASA-TM-86970] 13 p2128 N85-23243
Space power plants 16 p2724 N85-26813

DIRECTION FINDERS (RADIO)
U RADIO DIRECTION FINDERS

DIRECTION FINDING
Radiation and scattering of spiral antennas
[AD-A151929] 16 p2773 N85-27116
The moving thermoacoustic array: A theoretical feasibility study
[AD-A154510] 21 p3699 N85-32980

DIRECTIONAL ANTENNAS
NT DIPOLE ANTENNAS
NT HELICAL ANTENNAS
NT HORN ANTENNAS
NT LENS ANTENNAS
NT LOG PERIODIC ANTENNAS
NT LOOP ANTENNAS
NT PARABOLIC ANTENNAS
NT RADAR ANTENNAS
NT RHOMBIC ANTENNAS
NT SLOT ANTENNAS
NT STEERABLE ANTENNAS
NT TWO REFLECTOR ANTENNAS
Reflector antenna having sidelobe suppression elements
[AD-D011227] 01 p0039 N85-10244
Possibility of realization of highly-directional antenna arrays 03 p0344 N85-12220
A sphere-scanning radiometer for rapid directional measurements of sky and ground radiance: The PARABOLA field instrument
[NASA-TM-86171] 03 p0363 N85-12329
System of equations for finding antenna radiation pattern from near-field samples 06 p0781 N85-15054
Dual band, low sidelobe, high efficiency mirror antenna
[AD-D011329] 07 p0944 N85-15960
Contamination of the fetch-limited directional wave spectrum by waves emanating from an embayment
[NASA-TM-84441] 15 p2604 N85-26048

DIRECTIONAL CONTROL
NT THRUST VECTOR CONTROL
Relative control effectiveness technique with application to airplane control coordination
[NASA-TP-2416] 14 p2218 N85-23753
Controller requirements for uncoupled aircraft motion, volume 1
[AD-A153173] 17 p2900 N85-27878
New Matsushiro underground cosmic ray station (220 M.W.E. in depth)
[SH-9.1-14] 23 p4052 N85-35129

DIRECTIONAL COUPLERS
Synthesis of multistep directional couplers with nonminimum-phase characteristics 13 p2079 N85-22986
Strongly coupled millimeter-band waveguide directional couplers 22 p3779 N85-33418
New directional couplers for multimode circular waveguides applied to intense pulsed microwave systems
[DE85-011753] 23 p3926 N85-34330

DIRECTIONAL SOLIDIFICATION (CRYSTALS)
Materials for advanced turbine engines. Project 2: Rene 150 directionally solidified superalloy turbine blades, volume 2
[NASA-CR-167993] 03 p0319 N85-12059
Directional solidification studies of Pb-Bi peritectic alloys
[DE84-015656] 04 p0474 N85-13016
Controlled directionally solidified precision casting for superalloys and steels
[BMFT-FB-T-84-198] 05 p0619 N85-13980
Crystallization methods for solar cell silicon 12 p1877 N85-21774
Influence of solidification parameters on the formation of the gamma-M7C3 eutectic structure of 2% C-12%Cr steel 15 p2512 N85-25500
Properties of heat resistant Ni-Al-Nb alloys with unidirectional eutectic structure 19 p3247 N85-30133
Mechanical behavior of Ni-Cr-base superalloys in forms and conditions representative of service
[NPL-DMA(A)-84] 20 p3431 N85-31282
MPS solidification model. Analysis and calculation of macrosegregation in a casting ingot
[NASA-CR-171598] 21 p3588 N85-32178
Directionally solidified gas turbine alloys
[PNR-90264] 23 p3917 N85-34279

DIRECTIONAL STABILITY
NT GYROSCOPIC STABILITY
Determining characteristics of optical radiation reflectors based on results of remote sensing 15 p2488 N85-25358

DIRECTIVITY
Direction dependent radiation behavior in the classification of multispectral aircraft remote sensing data
[SER-C-290] 01 p0063 N85-10419
Short mode selective directional couplers
[IPF-83-9] 09 p1384 N85-18774
Improved directional couplers for overmoded waveguide systems
[IPF-84-1] 09 p1384 N85-18775
Directivity of Bremsstrahlung radiation from relativistic beams and the Gamma-Rays from solar flares
[NASA-CR-174433] 10 p1572 N85-19913
Effect of axisymmetric vibration modes on sensitivity and directivity characteristics of piezoceramic sphere — hydrophones 15 p2525 N85-25589
Study on the correlation between grinding conditions and residual stresses in ground surface of steel by the X-ray method 23 p3807 N85-34203
Properties of 10 (18)-10 (19)eV EAS at far core distance
[HE-4.7-3] 24 p4198 N85-36054
Fast scintillation counter preamplifier for the observation of Linsley effect
[HE-4.7-9] 24 p4199 N85-36060
Acoustic detection of air shower cores
[HE-7.1-4] 24 p4213 N85-36158

DIRECTORIES
EPA (Environmental Protection Agency) environmental data base and model directory, volume 1
[PB84-207582] 01 p0128 N85-10868
DDN directory
[AD-A148219] 08 p1230 N85-17744
Middle Atmosphere Program. Handbook for MAP, volume 6
[NASA-CR-175480] 11 p1656 N85-20436

State measurement laboratories: Program description (part 1). Directory (part 2)
[PB85-137851] 11 p1739 N85-20935
A DOE directory of databases for material properties
[UCAR-10124] 11 p1739 N85-20937
Current alternative energy research and development in Illinois
[PB85-163137] 16 p2620 N85-27397
A study of user-defined searching requirements for the on-line version of the directory of DOD-sponsored R and D data bases on the Defense Gateway computer system
[AD-A153000] 17 p3050 N85-28878
Worldwide directory of national Earth-science agencies and related international organizations
[GS-CIRC-934] 21 p3605 N85-32366
DIRICHLET PROBLEM
An integral equation formulation for a boundary value problem of elasticity in the domain exterior to an arc
[PREPRINT-833] 03 p0413 N85-12843
Integral equation formulations in two dimensions
05 p0716 N85-14605
Three-dimensional and axisymmetric problems
05 p0716 N85-14606
Lectures on generalized solutions to the minimal surface equation
[DE84-016882] 05 p0722 N85-14642
Orthogonal polynomials and a Dirichlet problem related to the Hilbert transform
[CWI-PM-R8406] 05 p0723 N85-14647
Three-dimensional, direct and vectorized elliptic solvers for various boundary conditions
[AD-B088266L] 08 p1206 N85-17595
A non-hypoelliptic Dirichlet problem from stochastics
10 p1537 N85-19667
W.E. Johnson's Sufficientness postulate
[AD-A149014] 10 p1550 N85-19774
Some estimates of harmonic majorants
15 p2634 N85-26237
On functions with a finite or locally bounded Dirichlet integral
15 p2635 N85-26243
DIRIGIBLES
U AIRSHIPS
DIRT
Anticoiling technology: Theories of surface coiling and performance of anticoiling surface coatings
[NASA-CR-174274] 07 p0991 N85-16296
Electronic detection and concealment of film dirt
[BBC-RD-1985/4] 15 p2536 N85-25687
DISARMAMENT
The structures and the role of an international agency for the control of satellites
[NASA-TM-76765] 03 p0441 N85-12806
Arms control and The President's Strategic Defense Initiative
[AD-A155334] 24 p4068 N85-35212
DISASTERS
Meteorological aspects of the 1982-83 El Nino/southern oscillation episode 07 p1001 N85-16356
Climate and fisheries: A Peruvian case study
07 p1003 N85-16373
The El Nino phenomenon and its agrometeorological implications 07 p1004 N85-16382
Hurricane experience levels of coastal county populations: Texas to Maine
[PB85-111383] 10 p1520 N85-19581
Large natural geophysical events: Planetary planning
[DE85-000859] 11 p1763 N85-21092
Hurricane storm surge research
[GPO-40-048] 12 p1893 N85-21880
Comet showers and Nemesis, the death star
[DE85-003736] 15 p2663 N85-26575
Hazardous air pollutants
[GPO-43-064] 21 p3613 N85-32458
DISCHARGE
Statistical analysis of partial discharge inception in high voltage 15 p2546 N85-25715
Detection and location of partial discharges in transformer windings using electrical methods
15 p2551 N85-25750
DISCHARGE TUBES
U GAS DISCHARGE TUBES
DISCHARGERS
A high-voltage discharger
[AD-A145659] 02 p0194 N85-11299
Extended performance technology study 30-cm thruster
[NASA-CR-168259] 07 p0917 N85-15606
DISCIPLINING
Rapid determination of cadet discipline by projective tests 22 p3821 N85-33671
DISCONNECT DEVICES
High voltage disconnect protection
[AD-D011480] 10 p1481 N85-19353
Releasable cable connector assembly for use between a mobile and stationary object
[AD-D011536] 12 p1858 N85-21655
Torsc restraint system
[AD-D011609] 16 p2702 N85-26684
Slide release mechanism --- for space shuttle orbiter/external tank connection device
[NASA-CASE-MSC-20060-1] 19 p3279 N85-30334
DISCONNECTORS
U DISCONNECT DEVICES
DISCONTINUITY
NT SHOCK DISCONTINUITY
Visual representations subserving texture perception
[AD-A145412] 02 p0236 N85-11538
Blind zones and aspect ratio bias in acquisition of discontinuity orientation data
[DE84-002718] 04 p0533 N85-13410
MMIC devices for active phased array antennas
[NASA-CR-174281] 07 p0938 N85-15943
Deep structure of Western Siberia
07 p0981 N85-16235
Surface reconstruction preserving discontinuities
[AD-A146741] 07 p1029 N85-16528
Critical flashing flow of subcooled fluids in nozzles with contour discontinuities
[DE84-017229] 09 p1319 N85-18296
Recovering pointwise values of discontinuous data within spectral accuracy
[NASA-CR-172535] 12 p1919 N85-22049
Lateral inhomogeneity of mantle surface in western Eurasia 14 p2344 N85-24497
The GEOS-2 electric field observations at times of solar wind discontinuities 14 p2360 N85-24584
Studies on the interference of wings and propeller slipstreams
[NASA-CR-175753] 15 p2463 N85-25210
Reflection and transmission of flexural waves at discontinuities 15 p2572 N85-25861
Analysis of systems of waveguide discontinuities by the method of moments 19 p3253 N85-30171
MMIC devices for active phased array antennas
[NASA-CR-176015] 19 p3254 N85-30177
Characterization of microstrip discontinuities in the time and frequency domains
[NASA-CR-176190] 24 p4088 N85-35342
DISCOVERING
U EXPLORATION
DISCOVERY (ORBITER)
Results of Space Shuttle flight 41-D
[GPO-39-481] 12 p1791 N85-21243
DISCRETE FUNCTIONS
Long time correlation and stochastic diffusion in the standard map 02 p0282 N85-11835
Some scientific subroutines in LISP
[AD-A147869] 07 p1026 N85-16515
Discrete modifications to continuous dynamic structural systems 09 p1337 N85-18410
Computing convolution of multifrequency signal employing truncated fast Fourier transform algorithms
13 p2065 N85-23019
An incremental multigrid strategy for the fluid dynamics equations
[AD-A151953] 16 p2783 N85-27172
Quadratic spaces over discrete Hodge algebras
16 p2853 N85-27593
On the choice of coordinates for semiconductor simulation
[AD-A152214] 16 p2870 N85-27708
Discrete mathematics for communications systems
[AD-A152814] 17 p3018 N85-28664
Modeling of discrete devices with use of multivalued logic and nemograms 22 p3768 N85-33351
Generalization of discrete Fourier transform for interpolation in time domain 22 p3775 N85-33396
Generalization of discrete Fourier transformation for interpolation in time domain 22 p3776 N85-33400
Monte Carlo techniques for analyzing deep penetration problems
[DE85-011426] 23 p3968 N85-34508
DISCRIMINANT ANALYSIS (STATISTICS)
Statistical tropical cyclone forecasting techniques for the Southern Hemisphere
[AD-A144752] 01 p0085 N85-10569
Asymptotic distributions of estimators for posterior probabilities in a classification model with both continuous and discrete variables
[CWI-MS-R8409] 05 p0722 N85-14637
Discriminant analysis of pulsar groups in the diagram P versus P 12 p1960 N85-22319
Forecasting atmospheric viability over the summer north Atlantic using the principal discriminant method
[AD-A155537] 21 p3637 N85-32593
Efficiency of discrimination in some invariant signal transformations 22 p3776 N85-33399
DISCRIMINANT FUNCTIONS
U DISCRIMINANT ANALYSIS (STATISTICS)
DISCRIMINATION
NT SENSORY DISCRIMINATION
NT TACTILE DISCRIMINATION
NT VISUAL DISCRIMINATION
Noise jammer discrimination by noise modulation bandwidth
[AD-D011473] 10 p1488 N85-19264
Performance of time-position discriminator of composite signal 13 p2072 N85-22941
Vertical discrimination in the sound channel
[AD-A150254] 13 p2155 N85-23380
Psychophysiological studies. 1: Performance and physiological response in learning, short-term memory and discrimination tasks
[AD-A151018] 14 p2392 N85-24731
Rayleigh criteria resolution of optical correlations
[AD-A151711] 15 p2652 N85-26359
Seismic discrimination
[AD-A154167] 20 p3494 N85-31722
Mass-discrimination during prolonged weightlessness
20 p3509 N85-31814
Efficiency of discrimination in some invariant signal transformations 22 p3776 N85-33399
DISCRIMINATORS
NT FREQUENCY DISCRIMINATORS
Mathematical model of discriminator for signals with fluctuations and thermal noise 13 p2072 N85-22943
DISEASES
NT ANEMIAS
NT ARTERIOSCLEROSIS
NT ASTHMA
NT BONE DEMINERALIZATION
NT CANCER
NT CARBON MONOXIDE POISONING
NT CATARACTS
NT CORONARY ARTERY DISEASE
NT EYE DISEASES
NT HEART DISEASES
NT INFECTIOUS DISEASES
NT INFLUENZA
NT LEAD POISONING
NT LEUKEMIAS
NT MYOCARDIAL INFARCTION
NT OSTEOPOROSIS
NT PARKINSON DISEASE
NT PULMONARY LESIONS
NT RESPIRATORY DISEASES
NT TOXIC DISEASES
NT TUMORS
Evaluation of the musculoskeletal diseases program
[PB84-230648] 07 p1017 N85-16461
The physiology of ultradian rhythms and their role in affecting disease resistance
[AD-A148842] 09 p1383 N85-18575
Review of US manual of clinical aviation medicine
12 p1904 N85-21957
DISHES
U PARABOLIC REFLECTORS
DISILICIDES
Reinforcement of molybdenum disilicide with nematic crystals of aluminum oxide 03 p0353 N85-12269
DISINFECTANTS
U ANTISEPTICS
DISINTEGRATION
Inquiry into disintegration control of irradiated low enrichment uranium for high temperature gas cooled reactors
[OEFZS-7281] 07 p1042 N85-16615
DISK GALAXIES
Excitation of spiral patterns in responsible density wave theory 05 p0740 N85-14764
Dark matter near the sun: Simulated star counts and the Oort limit 06 p0860 N85-15592
On the morphology of spiral modes --- disk galaxies
12 p1955 N85-22283
Drift-accretion theory of the spiral structure of galaxies
12 p1957 N85-22296
Dynamics of gas disks in triaxial galaxies
13 p2171 N85-23469
The Formation of preplanetary disks from the collapse of rotating molecular cloud cores
13 p2180 N85-23526
Limits on the Doppler factor in relativistic jets by means of gamma-ray observations
[OG-2.7-12] 22 p3872 N85-33985
Interpretation of cosmic-ray anisotropy below 10(14) eV
[OG-5.4-13] 22 p3887 N85-34090
Evidence for a dynamical halo around the edge-on galaxy NGC 4631
[OG-6.2-1] 22 p3889 N85-34102
Solar activity beyond the disk and variations of the cosmic ray gradient
[SH-5.1-23] 23 p4044 N85-36075

DISKS
Flexible matrix composite laminated disk/ring flywheel
05 p0806 N85-13866
Proceedings of the National Bureau of Standards and National Security Agency Workshop on Standardization Issues for Optical Data Disk (OD3) Technology
[PB84-217785] 06 p0848 N85-15383
Yield stress determination from miniaturized disk bend test data
[DE85-009495] 18 p3122 N85-29330
DISKS (SHAPES)
NT ACTUATOR DISKS
NT ROTATING DISKS
Hot isostatically pressed manufacture of high strength MERL 76 disk and seal shapes
[NASA-CR-165550] 02 p0183 N85-11225
Basic study of bladed disk structural response
[AD-A146228] 03 p0319 N85-12061
Analysis of piezoelectric disks and cylinders using finite element method
[AD-A146323] 03 p0414 N85-12650
Scattering from thin dielectric disks
[NASA-TM-86155] 06 p0798 N85-15098
Locally univalent functions in the unit disk
10 p1536 N85-19680
The definition and computation of a metric on plane curves. The meaning of a face on a geometric model
17 p3004 N85-28571
DISLOCATIONS (MATERIALS)
NT CRYSTAL DISLOCATIONS
NT EDGE DISLOCATIONS
NT SCREW DISLOCATIONS
Subgrains, dislocations and the elevated-temperature strength of type 304 stainless steel
[DE84-001233] 04 p0473 N85-13014
Inclined dislocation emission at a shielded crack tip
[DE84-016703] 06 p0818 N85-15192
Stress-strain analysis of silicon ribbon
[NASA-CR-175459] 10 p1510 N85-19525
Electron-plastic effect in metals
11 p1605 N85-20089
Structures of ordered linear dislocation multipoles in Cu-Al alloys
[ISSN-0379-6906] 13 p2021 N85-22684
Influence of short-range order on deformation mechanisms in solid solutions
[DE85-006374] 14 p2258 N85-23969
Hydrogen embrittlement testing
[DE85-007352] 23 p3916 N85-34273
HgCdTe surface and defect study program
[AD-A156079] 24 p4161 N85-35799
DISORDERS
Interactions in localization
[NOTA-INTERNA-815] 02 p0279 N85-11818
Comparative analysis of effects of weightlessness and its models on velocity and strength properties and tone of human skeletal muscles 12 p1901 N85-21936
DISORIENTATION
NT DISORDERS
NT JET LAG
Theory underlying the peripheral vision horizon device
01 p0008 N85-10048
DISPENSERS
Improved materials and processes of dispenser cathodes
[AD-A148810] 09 p1314 N85-18262
Continued development and testing of tungsten controlled porosity dispenser cathodes
[AD-A152585] 17 p2931 N85-28090
The effect of metal overlayers of thermionic dispenser cathodes
[AD-A154795] 21 p3701 N85-32995
DISPERSING
Urban aerosol modeling
[PB84-233469] 04 p0532 N85-13401
Determination of the laws governing the changes in the standard deviations of the distribution of pollution based on observations of the atmospheric turbulence spectrum and the possibility of simulating it in the laboratory
[BLL-TR-T6373/BG/MRS14683/84]
08 p1179 N85-17431
Analyzing two-level fractional factorial experiments for possible dispersion effects
[AD-A149455] 10 p1548 N85-19760
Atmospheric dispersion of hypergolic liquid rocket fuels, volume 1
[AD-A149587] 12 p1817 N85-21399
Effect of ScAl3 phase dispersion on hardening of alloy Al-6.3 percent Mg-0.21 percent Sc
19 p3241 N85-30096
Preliminary wind tunnel experiments to investigate the effect of heat transfer on the dispersion of cold dense gases
[OUEL-1548/84] 20 p3456 N85-31467
Benthic boundary layer modelling studies
[IOS-181] 20 p3497 N85-31742
Assessment of the performance of an in-field Gaussian plume/puff model for overwater use
[AD-A155435] 21 p3614 N85-32460
Investigation of the formation of cloud particle spectrum on natural condensation nuclei
21 p3649 N85-32674
DISPERSION
An experimental investigation of microstrip properties on soft substrates from 2 to 40 GHz
[NASA-TM-86961] 11 p1624 N85-20224
Dispersion characteristics of small-mode gradient optical fibers 13 p2062 N85-23004
An investigation of the structure and high temperature mechanical properties of oxide dispersion strengthened alloys
[AD-A151107] 15 p2509 N85-25477
Results of recent large-scale NH3 and N2O4 dispersion experiments
[DE85-004988] 15 p2589 N85-25960
Evaluation of source strength and dispersion model predications with data from large nitrogen tetroxide field experiments
[DE85-011855] 23 p3947 N85-34465
DISPERSION PRECIPITATION HARDENING
U PRECIPITATION HARDENING
DISPERSIONS
NT AEROSOLS
NT COLLOIDS
NT EMULSIONS
NT FOG
NT LIQUID-GAS MIXTURES
NT NUCLEAR EMULSIONS
NT PHOTOGRAPHIC EMULSIONS
NT SMOKE
A perturbation solution for rigid dumbbell suspensions in steady shear flow
[AD-A144878] 01 p0111 N85-10755
Transport properties of multiphase systems
[DE84-015580] 02 p0173 N85-11159
Radiotracer studies of the dispersion of solid pollutants in marine and estuarial environment: Measurement of diffusion coefficients and the phenomenon of dispersion by currents
[BLL-DRIC-TRANS-7104-(3823.66)]
02 p0224 N85-11468
A dispersion model for airborne particulates inside a building
[DE84-014961] 02 p0225 N85-11473
Carbon monoxide study, Anchorage, Alaska, November 22, 1982 to February 11, 1983
[PB84-236595] 05 p0673 N85-14321
Turbulent shear fields for dispersion of aqueous drops in organic liquids and application to gel-sphere processes
[DE84-016562] 06 p0809 N85-15141
Influence of turbulence on erosion by a particle-laden fluid jet
[DE84-014365] 09 p1320 N85-18301
Dispersion of phase-shift keyed systems with fixed number of blocks 13 p2070 N85-22928
Ultrasonic dispersion of soils for routine particle size analysis: Recommended procedures
[DE85-005530] 16 p2861 N85-27643
Transmission of light by disperse medium of densely packed optically soft particles 21 p3697 N85-32969
Calculating dominant (quasi-t) mode group velocity in shielded microstrip line 22 p3780 N85-33422
DISPLACEMENT
Metrological consequences of the hard optical boundary assumption
[PB84-223577] 01 p0121 N85-10827
Predicting optical image displacement velocity in survey of Earth's surface 02 p0165 N85-11116
Deformation measurements of composite multi-span beam shear specimens by Moire interferometry
[NASA-CR-3844] 02 p0169 N85-11135
Deformations and strains in adhesive joints by moire interferometry
[NASA-CR-172474] 02 p0185 N85-11238
An experimental evaluation of the J integral in 50% sidegrooved compact geometry specimens
[AERE-R-11202] 03 p0374 N85-12366
Holographic displacement analysis with fiber optics
[AD-A146185] 03 p0420 N85-12680
Quantification of Saint-Venant's principle for a general prismatic member 04 p0467 N85-12972
Improved beam theory for anisotropic materials
04 p0468 N85-12973
A study of crashworthiness of light aircraft fuselage structures: A numerical and experimental investigation
[UTIAS-286] 06 p0750 N85-14803
Bearing tester fit analysis
[NASA-CR-171282] 07 p0973 N85-16181
Experimental compliance calibration of the NASA Lewis Research Center Mode 2 fatigue specimen
[NASA-TM-86908] 07 p0977 N85-16205
Use of coordinate functions to calculate deformation fields
[BLL-M-36010-(5828.4)] 07 p1028 N85-16524
On some exact solutions in elastostatics in terms of harmonic functions 09 p1332 N85-18367
The fracture mechanics of a slit crack with crack-tip dual zones 09 p1332 N85-18371
Ground shock effect on soil field inclusions
09 p1336 N85-18403
NOAA OTEC CWP (National Oceanic and Atmospheric Administration Ocean Thermal Energy Conversion Cold Water Pipe) at-sea test. Volume 3, part 1: Tabulation of the power spectra for selected channels
[PB84-236955] 09 p1346 N85-18467
Nonlocal and nonlinear effects on solar oscillations
09 p1416 N85-18934
Ice segregation and frost heaving
[PB85-122430] 10 p1460 N85-19199
The likelihood displacement: A unifying principle for influence measures
[AD-A149456] 10 p1551 N85-19783
Elastic compliance of imperfect interfaces: Review and relationship to ultrasonic scattering
[DE85-003068] 11 p1652 N85-20404
Comparison of shock-induced displacements with displacements produced by a centrifuge acceleration
[DE85-000467] 12 p1852 N85-21618
Recent advances in hybrid/mixed finite elements
[NASA-CR-175574] 12 p1883 N85-21687
Elastic response of a half-plane to a bonded interference-fit disc of the same material
[ARL/STRUC-R-406] 12 p1885 N85-21701
On the relative motion of typhoons: In the case of Typhoon 8305 and Typhoons 8306 and 8307
12 p1894 N85-21885
Fault offsets and lateral crustal movement on Europa
13 p2201 N85-23658
Importance of the tectonic motions on Ganymede
13 p2202 N85-23661
Transducer of linear displacements
14 p2281 N85-24130
Evaluation of stress concentration coefficients in butt-welded joints with displaced edges
15 p2501 N85-25425
On the interconnection of incompatible solid finite element meshes using multipoint constraints
15 p2575 N85-25879
Empirical development of ground acceleration, velocity and displacement for accidental explosions at J5 or the proposed large altitude rocket cell at Arnold Engineering Development Center
[DE85-008324] 16 p2758 N85-27020
The nonlinear analysis of thick composite plates using a cubic spline function 16 p2798 N85-27252
Improvement of conditions for meshing spiral bevel gears
[NASA-TM-77867] 18 p3117 N85-29294
Debye temperature and static displacements in LuH sub x single crystals from energy dispersive X-ray diffraction
[DE85-010961] 19 p3376 N85-30946
Finite element modeling of crashed bodies using the Bodner-Partom flow law 20 p3466 N85-31547
Estimation of power-law creep parameters from bend test data
[PB85-183408] 20 p3472 N85-31579
Efficient solution methods for nonlinear finite element analysis 20 p3519 N85-31886
Effects of contact area of an interface on acoustic wave transmission characteristics
[DE85-009936] 20 p3524 N85-31920
Hubble space telescope: Pointing error effects on nonlinear ball joints
[NASA-TM-86511] 20 p3545 N85-32058
The collected data for ramp function tests on a NACA 23012 aerofoil. Volume 1: Description and pressure data
[GU-AERO-8413-VOL-1] 23 p3894 N85-34123
Calibrator for displacement gages used in the rock mechanics laboratory
[DE85-013257] 24 p4096 N85-35393
DISPLACEMENT MEASUREMENT
Development of a modular multicoordinate measuring system with continuous-path microprocessor control
[BMFT-FB-T-84-158] 03 p0408 N85-12508
Instantaneous kinematics and joint displacement analysis of fully-parallel robotic devices
05 p0841 N85-14113
High speed electric field and voltage measurements with field coupled sensors
[DE85-009637] 15 p2642 N85-26299
Improved coordinate measuring machine calibration and control
[DE85-012053] 21 p3590 N85-32315
Possibility of measurement of small displacements by ring laser 21 p3667 N85-32904

New method for compensating and measuring any motion of three-dimensional objects in holographic interferometry
[ISL-CO-216/84] 22 p3789 N85-33474
DISPLAY DEVICES
NT ANEMOMETERS
NT APPROACH INDICATORS
NT FLOW DIRECTION INDICATORS
NT GYRO HORIZONS
NT HEAD-UP DISPLAYS
NT HELMET MOUNTED DISPLAYS
NT HOT-FILM ANEMOMETERS
NT HOT-WIRE ANEMOMETERS
NT PLAN POSITION INDICATORS
NT PLASMA DISPLAY DEVICES
NT POSITION INDICATORS
NT RADARSCOPES
NT RADIO DIRECTION FINDERS
NT SPACECRAFT POSITION INDICATORS
NT SPEED INDICATORS
NT TACHOMETERS
NT WIND VANES
Peripheral Vision Horizon Display (PVHD)
[NASA-CP-2306] 01 p0008 N85-10044
Personal experience with the PVHD and opinion of situations in which a wide Field Of View (FOV) PVHD might be helpful 01 p0008 N85-10045
Effects of foveal information processing 01 p0009 N85-10052
Peripheral vision horizon display on the single seat night attack A-10 01 p0009 N85-10053
Extracts from the test plan for in-flight evaluation of the NT-33A peripheral vision display 01 p0009 N85-10055
NASA Ames-Dryden T-37 demonstration comments 01 p0009 N85-10056
Early Air Force Flight Test Center (AFFTC) experience with Peripheral Vision Horizon Displays (PVHD) 01 p0009 N85-10057
Peripheral vision displays: The future 01 p0009 N85-10058
A production peripheral vision display system 01 p0010 N85-10059
A preliminary flight evaluation of the peripheral vision display using the NT-33A aircraft
[AD-A145123] 01 p0010 N85-10060
LED multifunction keyboard engineering study
[AD-A145199] 01 p0010 N85-10061
Content, variety, and augmentation of simulated visual scenes for teaching air-to-ground attack
[AD-A145218] 01 p0013 N85-10080
A subjective evaluation of the PROFS operational workstation based upon a real-time forecasting experiment in summer 1983 — Program for Regional Observing and Forecasting Services (PROFS) 01 p0083 N85-10556
Interactive computer display systems in nowcasting 01 p0083 N85-10557
Field tests of the real-data acquisition system for the NASA-LaRC differential absorption lidar
[NASA-CR-174020] 01 p0106 N85-10710
The case for concern about very low frequency fields from visual display terminals: The need for further research and shielding of VDTs
[CCOHS-P83-2E] 02 p0234 N85-11526
Human engineering data base for design and selection of cathode ray tube and other display systems
[AD-A145704] 02 p0238 N85-11549
Implications of artificial intelligence for a user defined technical information system
[AD-P003938] 02 p0248 N85-11618
Command flight path display. Phase I and II: Appendix F
[AD-A145858] 03 p0318 N85-12056
A comparative evaluation of EMADS (Engine Monitoring and Display System) and conventional engine instruments
[AD-A145901] 03 p0319 N85-12060
Analysis of data entry performance: Chromatic versus monochromatic
[AD-A145568] 03 p0436 N85-12789
System status display information
[NASA-CR-172347] 04 p0455 N85-12869
Vibration data analysis system for SNLA area 3 reference manual
[DE84-016207] 04 p0514 N85-13275
Investigation and development of multicolored liquid crystal display systems for automotive dashboard application and large format information boards
[BMFT-FB-T-84-187] 04 p0572 N85-13652
Visual systems for remotely controlled vehicles 05 p0703 N85-14512
A comparative study of alternative controls and displays for by the severely physically handicapped 05 p0709 N85-14549
Color and grey scale in sonar displays 05 p0710 N85-14552
Representing multidimensional systems using visual displays 05 p0711 N85-14560
Experience with a sophisticated computer based authoring system
[DE84-014344] 05 p0713 N85-14575
Human factors of visual displays 06 p0752 N85-14821
Crewstation design and validation 06 p0752 N85-14822
Avionics technology - system concepts 06 p0753 N85-14824
Weather satellite products in the Flight Service Automation System (FSAS)
[AD-A146520] 06 p0759 N85-14855
Human engineer's guide to auditory displays. Volume 2: Elements of signal reception and resolution affecting auditory displays
[AD-A146513] 06 p0859 N85-15462
Human engineer's guide to auditory displays. Volume 1. Elements of perception and memory affecting auditory displays
[AD-A146601] 06 p0860 N85-15464
Display Techniques for Advanced Crew Stations (DTACS). Phase 1: Display techniques study
[AD-A146922] 07 p0904 N85-15722
Interactive Signal Analysis Software (ISAS). User's manual
[AD-A146999] 07 p1022 N85-16485
Program visualization: Graphics support for software development
[AD-A146887] 07 p1024 N85-16499
Matrix display simulation
[AD-D011371] 07 p1055 N85-16695
Built-in-test for first line testing 08 p1064 N85-16739
A Computer-generated topographic display system for navigation and mission planning in helicopters 08 p1073 N85-16800
Map display for helicopters 08 p1073 N85-16801
Integration of sensor fusion in advanced helicopter cockpit design 08 p1074 N85-16813
Flight research on visual aids and navigation equipment for helicopter low-level flight at night 08 p1076 N85-16820
A cockpit-display concept for executing a multiple glide-slope approach for wake-vortex avoidance
[NASA-TP-2386] 08 p1085 N85-16889
Realization and testing of an experimental color display system for general aviation helicopters and aircraft
[BMFT-FB-W-84-042] 08 p1086 N85-16872
Pilot climate data system
[NASA-CR-174321] 08 p1187 N85-17481
A FORTRAN plotting package for graphic VDUs
[AD-A148489] 08 p1204 N85-17577
Improved real-time ultra-high resolution image projection display using laser-addressed liquid crystal light valve
[AD-D011414] 08 p1223 N85-17705
Thin film transistors for addressing flat panel displays
[BMFT-FB-T-84-210] 08 p1227 N85-17726
Producing high scene content with perspective validity
[AD-P004314] 09 p1268 N85-17966
Geographic subdivision and top level data structures, Columbus, Magellan, and expanding CIG (Computer Image Generation) horizons
[AD-P004317] 09 p1268 N85-17971
The use of lasers in wide-angle visual systems
[AD-P004322] 09 p1269 N85-17976
Considerations in an optical variable acuity display system
[AD-P004323] 09 p1269 N85-17977
Design considerations for an eye tracked AOI (Area of Interest) display system
[AD-P004324] 09 p1269 N85-17978
Control systems analysis program: A tool for analysis of the GE-VSCDP (General Electric-Visual System Component Display Program) image display system
[AD-P004325] 09 p1270 N85-17979
Progress report on an eye-slaved area-of-interest visual display
[AD-P004326] 09 p1270 N85-17980
Air combat visual simulation using a head slaved projector
[AD-P004327] 09 p1270 N85-17981
A second generation WAVIDS (Wide Angle Virtual Image Display System)
[AD-P004328] 09 p1270 N85-17982
The effects of time delay in man-machine control systems: Implications for design of flight simulator Visual-Display-Delay compensation
[AD-P004329] 09 p1270 N85-17983
Baffled eye and confounded brain or using visual illusions to train blind pilots
[AD-P004332] 09 p1271 N85-17986
Pictorial format display evaluation
[AD-A149252] 10 p1425 N85-18986
Dialog system of preparation and presentation of visual information 10 p1526 N85-19622
Sector suite man-machine functional capabilities and performance requirements
[AD-A148881] 10 p1531 N85-19647
Human Factors Considerations in High Performance Aircraft
[AGARD-CP-371] 10 p1532 N85-19653
Aircrew and avionics: Friends or Foes? 10 p1532 N85-19654
Observations of physiological and psychological effects of terrain following flight based on in-flight test experience 10 p1532 N85-19657
Electronic displays: Their strengths and weaknesses for advanced high performance aircraft 10 p1533 N85-19664
Changing system and display concepts and their impact on aircrew performance 10 p1533 N85-19665
The cockpit of the year 2000: How big a step? 10 p1534 N85-19667
Influence of a perspective cockpit traffic display format on pilot avoidance maneuvers 10 p1534 N85-19668
The multiple resources model of human performance: Implications for display design 10 p1534 N85-19669
The F-16: A new era for human factors 10 p1534 N85-19671
Aircrew-aircraft integration issues in future US Army helicopters 10 p1535 N85-19672
A low-cost, general purpose image processing system
[INPE-3292-PRE/607] 10 p1537 N85-19690
Digital and color energy maps for graphic display of hourly data
[DE85-000526] 11 p1673 N85-20543
Computer-generated display system guidelines. Volume 1: Display design
[DE85-000679] 11 p1701 N85-20699
Proceedings of the 6th Advanced Aircrew Display Symposium
[AD-A150044] 12 p1778 N85-21160
Program for controlling electrical measuring contact instrument on glow-discharge indicator panel 12 p1842 N85-21568
Choice reaction time and color: An annotated bibliography
[AD-A149722] 12 p1908 N85-21979
Implementation of the computer program-system MOSS (Map Overlay and Statistical System) on a VAX-11 series computer under VMS
[AD-A149812] 12 p1914 N85-22019
Design of graphic displays in computerized systems
[AD-A150071] 12 p1916 N85-22027
An airborne infrared thermal scanning system for easy use on Navy P-3 aircraft
[AD-A149690] 12 p1933 N85-22143
Analysis of estimation algorithms for CDTI and CAS applications
[NASA-CR-172444] 13 p1973 N85-22387
Draftsman displays: A graphical technique for exploratory data analysis
[AD-A150515] 13 p2041 N85-22775
Introduction to CHART: A graphic analysis and display system, revision
[DE85-004612] 13 p2148 N85-23335
Multiple resources and display formatting: The implications of task integration in a simulated air traffic control task
[AD-A150713] 14 p2292 N85-24205
The effect of set size on color matching
[AD-A150899] 14 p2388 N85-24713
Factors affecting dwell times on digital displaying
[NASA-TM-86408] 14 p2390 N85-24722
Dual-task timesharing using a projected attitude display (Malcolm horizon)
[AD-A150789] 14 p2395 N85-24750
Investigation of absorptive electrochemical systems for display applications
[BMFT-FB-T-84-301] 15 p2507 N85-25467
Three-dimensional/perspective display techniques for meteorological data sets 15 p2599 N85-26018
Eye movement in response to single and multiple targets
[AD-A151115] 15 p2617 N85-26126
The measurement of human time estimating ability using a modified jerison device
[AD-A151870] 15 p2620 N85-26141
Infinite computing
[AD-A151437] 15 p2628 N85-26197
A comparison of pictorial and speech warning messages in the modern cockpit
[AD-A151917] 16 p2707 N85-26706
Spatial and temporal visual masking and visibility
[AD-A151968] 16 p2842 N85-27524
Trends shaping advanced aircrew training capabilities through the 1990s
[AD-A152277] 16 p2843 N85-27530

A heuristic solution to the spacing problem: Maximizing the minimum Euclidean distance among N points in a convex region
[AD-A152116] 16 p2855 N85-27603
Nematic liquid crystals for car dashboards
[BMFT-FB-T-84-296] 16 p2872 N85-27718
Centralized Storm Information System (CSIS)
[NASA-CR-175898] 17 p2994 N85-28506
A report from the Space Science and Engineering Center, the University of Wisconsin-Madison, Madison, Wisconsin 17 p2994 N85-28507
CSIS test and evaluation 17 p2994 N85-28509
Generation and display apparatus
[AD-D011639] 17 p3008 N85-28599
Study of raster metafile formats
[AD-A153322] 17 p3012 N85-28624
Spatial light modulator having a capacitively coupled photoconductor
[AD-D011648] 17 p3037 N85-28790
A general area air traffic controller simulation using colour graphics
[AD-A153634] 18 p3060 N85-28933
Retinally stabilized differential resolution television display
[NASA-CASE-NPO-15432-1] 18 p3069 N85-29117
Beam tests of phosphorescent screens
[DE85-009843] 18 p3097 N85-29170
Design issues in video disc map display
[AD-A153531] 18 p3109 N85-29253
Three-dimensional data display on the two-dimensional screen
[AD-A153699] 18 p3160 N85-29577
The use of VLSI technology for the real-time generation of graphics displays: A proposal
[AD-A153766] 18 p3160 N85-29578
Measurements of Solar Vector Magnetic Fields
[NASA-CP-2374] 18 p3203 N85-29869
Solar physics applications of computer graphics and image processing 18 p3206 N85-29903
Graphic displays of vector magnetograph data 18 p3209 N85-29904
Graphic display development program. Volume 2, revision 0: Appendices
[DE85-011078] 19 p3333 N85-30648
Graphic display development program, volume 1
[DE85-011076] 19 p3333 N85-30649
ZOG/VINSON technology demonstration project system description. Volume 1
[AD-A154211] 19 p3342 N85-30713
Effect of background/foreground color coding on detection in acoustic data displays
[AD-A154105] 19 p3352 N85-30774
Avionics and civil aircraft systems: The present and the future
[SNIAS-851-111-104] 20 p3392 N85-31038
Ergonomic problems regarding the interactive touch input via screens in onboard and ground-based flight control
[NASA-TM-77814] 20 p3512 N85-31832
Microprocessor AirborneData Acquisition and Replay (MADAR) system
[AD-A151728] 20 p3514 N85-31843
Switchable zero order diffraction gratings as light valves
[AD-A154471] 20 p3533 N85-31981
Advanced simulator for pilot training and helmet-mounted visual display configuration comparisons
[AD-A155326] 21 p3667 N85-32776
Design guidelines for user-system interface software
[AD-A154907] 21 p3671 N85-32807
Implementation of the SITAN algorithm in the digital terrain management and display system
[DE85-010859] 22 p3729 N85-33115
Electrochromic display device
[AD-D011733] 22 p3759 N85-33299
Batteryless magneto-driven portable radiac
[DE85-011622] 22 p3760 N85-33300
Basic features of personal computers 22 p3766 N85-33344
The development and evaluation of color display systems for airborne applications. Phase 1: Fundamental visual, perceptual, and display system considerations
[FAA/PM-85-19] 22 p3826 N85-33700
A new large-scale, high-resolution multicolor software display concept
[AD-A155404] 22 p3827 N85-33703
The improved display of 525-line television pictures: Adaptive interpolation
[BBC-RD-1985/5] 23 p3925 N85-34328
Instrumentation for sensing moisture content of material using a transient thermal pulse
[NASA-CASE-NPO-15493-2] 23 p3933 N85-34373
An integrated system for printing and publishing applications 23 p3959 N85-34540
Colour coding scales and computer graphics 23 p3963 N85-34568
Developing graphical tools with minimal GKS 23 p3964 N85-34573
NAPGEN: Automatic NAPLPS page generator 23 p3964 N85-34575
Using LINE as an interactive graphics package. Interfacing line and Topdraw in 43 and 24 VM
[DE85-012007] 23 p3965 N85-34585
Maintenance port system
[AD-D011724] 23 p3967 N85-34594
Raster functionality for a VDI
[DE85-006734] 24 p4097 N85-35396
The human engineering eye movement measurement research facility
[AD-A156099] 24 p4132 N85-35613
An exploratory study of the effect of screen size and resolution on the legibility of graphics in automated job performance aids
[AD-A155969] 24 p4136 N85-35632

DISPLAY SYSTEMS
U DISPLAY DEVICES

DISPOSAL
NT HAZARDOUS MATERIAL DISPOSAL (IN SPACE)
NT WASTE DISPOSAL
Records Disposal: A guidebook for laboratory offices
[AD-A156064] 24 p4165 N85-35823

DISRUPTING
Simulating the effects of plasma disruption with a 1 MA current pulse in a coaxial test fixture
[DE85-010491] 20 p3535 N85-31996

DISSIPATION
NT ENERGY DISSIPATION
NT OHMIC DISSIPATION
Deformations of two-dimensional dissipative maps — orbit perturbation
[REPT-69] 01 p0129 N85-10691
Statistical Plasma Physics. Proceedings of the Workshop of the US-Japan Joint Institute for Fusion Theory Program
[IPPJ-669] 02 p0282 N85-11832
Tidal dissipation in the Earth and Moon from lunar laser ranging 04 p0585 N85-13733
Phase-dissipative mechanisms for laser-induced surface desorption-dissociation processes
[AD-A147961] 08 p1121 N85-17085
Generation and evolution of diabatic planetary waves in continuously stratified atmosphere with Ekman dissipation 09 p1354 N85-18515
Analysis of the dissipation mechanism within an instationary cathode spot of metal vapor arcs
[AD-A149258] 10 p1558 N85-19625
Mixing, chemical reaction and flow field development in ducted rockets
[DE85-004083] 14 p2247 N85-23928
Evaluation of the effects of roll angle on the natural convection heat transfer from an array of cylindrical spines
[AD-A154594] 21 p3583 N85-32273
Vortex dynamics simulation of conserved scalar dissipation 22 p3745 N85-33210
On the importance of viscous dissipation in Io 22 p3855 N85-33873

DISSIPATORS
U DISSIPATION

DISSOCIATION
NT AUTOIONIZATION
NT GAS DISSOCIATION
NT PHOTODISSOCIATION
NT THERMAL DISSOCIATION
Effect of maximum physical load on oxygen-transport properties of blood 01 p0093 N85-10627
Computer molecular dynamics of 2-D water (ice) structures under shock
[AD-A145818] 03 p0372 N85-12375
Detailed performance calculations: Wayne State University and Ford Motor Company, appendix C 05 p0676 N85-14340
Ionic reactions of atmospheric importance
[AD-A147354] 07 p0997 N85-16333
Phase-dissipative mechanisms for laser-induced surface desorption-dissociation processes
[AD-A147961] 08 p1121 N85-17085
Time-of-flight spectroscopy of ionic and metastable fragments from dissociating molecules
[AD-A148068] 08 p1220 N85-17683
An infrared study of the hydrogenation of carbon dioxide on supported rhodium catalysts
[AD-A149477] 10 p1436 N85-19049
An infrared study of the dissociation of carbon dioxide over supported rhodium catalysts
[AD-A149813] 12 p1800 N85-21291
Kinetic energies of fragment ions produced by dissociative photoionization of NO
[NASA-CR-175721] 15 p2647 N85-26327
Identification and properties of molecular systems of potential use in solar-pumped lasers
[NASA-CR-175804] 16 p2789 N85-27207
Experimental study of dissociative attachment in optically-pumped lithium molecules
[AD-A152800] 17 p3030 N85-28738
Experimental studies of diffractive phenomena
[DE85-008812] 17 p3031 N85-28749
Vibrationally enhanced dissociation of diatomic molecules
[AD-A154827] 21 p3701 N85-32986

DISSOLUTION
U DISSOLVING

DISSOLVED GASES
North Atlantic Deep Water Formation
[NASA-CP-2367] 15 p2601 N85-26028
Chemical signatures associated with the freshening of Northern Atlantic waters between 1972 and 1981 15 p2601 N85-26032

DISSOLVING
Effects of additives and KOH electrolyte concentration on dissolution of iron electrodes
[DE84-014840] 02 p0173 N85-11182
Investigation of the dissolution of CaCrO4 in molten LiCl-KCl eutectic
[DE84-016394] 04 p0469 N85-12985
Effect of host-rock dissolution and precipitation on permeability in a nuclear waste repository in tuff
[DE85-000675] 11 p1727 N85-20680
Dissolution of solid solutions in absence of internal mass transfer
[BLL-M-36092-(5828.4)] 16 p2748 N85-26959
Sol-gel processing of lead zirconate titanate films
[ATR-85(8343)-2] 18 p3073 N85-29010

DISSYMMETRY
U ASYMMETRY

DISTANCE
NT MISS DISTANCE
NT RADAR RANGE
NT RANGE AND RANGE RATE TRACKING
Distances of local clouds from optical line observations 06 p0875 N85-15558
Long range effect of turbulent pressure pulsations in plane-parallel flows at different velocities with various flame fronts 09 p1308 N85-18220
FAA policy regarding solid waste disposal facilities
[AD-P004196] 11 p1581 N85-19963
Distance-inertial guidance of launch vehicle described 12 p1820 N85-21417
Visual simulation requirements for aircraft aspect recognition at real world distances
[AD-A151040] 14 p2228 N85-23810
Laser measurements of distances from the ORELA neutron target to experiment stations along flight paths 1 and 8
[DE85-009457] 17 p2971 N85-28352
Particle distributions in approximately 10(14) 10(16) eV air shower cores at sea level 24 p4189 N85-35990

DISTANCE MEASURING EQUIPMENT
NT ALTIMETERS
NT LASER RANGE FINDERS
NT OPTICAL RANGE FINDERS
NT RADIO ALTIMETERS
NT RANGE FINDERS
Modular laser distance measurement system for multiaxis machine tools
[BMFT-FB-T-84-156] 05 p0641 N85-14110
Development of a capacitive sensor system for high temperature application
[BMFT-FB-HA-84-027] 05 p0648 N85-14147
Water masers and distance measurements: The impact of QUASAT 07 p1059 N85-16721
Error of distance measurement by phase-type optical range finders with photoreceivers of various types 14 p2276 N85-24101
The integration of information from an analog-visual display: The role of dimensional integrality
[AD-A150756] 14 p2404 N85-24820
Distance Measuring Equipment (DME), general
[AD-A152585] 17 p2895 N85-27846
Evaluation of radio navigation systems and their configuration with respect to minimum cost
[ESA-TT-847] 20 p3392 N85-31043
Comparison of survey and photogrammetry methods to position gravity data, Yucca Mountain, Nevada
[DE85-011665] 21 p3590 N85-32316
Analysis of Cerenkov pulses recorded simultaneously at two sites
[HE-4.4-16] 24 p4194 N85-36022

DISTANCE PERCEPTION
U SPACE PERCEPTION

DISTILLATION
DOE supported research in alcohol fuel technology development
[DE84-007686] 06 p0774 N85-14948

Analysis of middle distillate fuels by high resolution field ionization mass spectrometry
[AD-A147724] 08 p1135 N85-17153
Ethanol production by enzymatic hydrolysis: Parametric analysis of a base-case process
[DE84-013105] 11 p1614 N85-20147
Trends of petroleum fuels
[DE85-000116] 14 p2263 N85-24023
Nitrogen analysis by chemiluminescence
[AD-A158197] 24 p4083 N85-35308

DISTILLATION EQUIPMENT
Alcohol: An alternate energy resource for community use
[DE85-007731] 16 p3084 N85-29075

DISTORTION
NT FLOW DISTORTION
NT SIGNAL DISTORTION
NT SURFACE DISTORTION
Effect of combined pressure and temperature distortion orientation on high-bypass-ratio turbofan engine stability
[NASA-TM-83771] 01 p0011 N85-10057
Real time sensing and control of out-of-plane distortion due to line heating by laser
[AD-A144773] 01 p0027 N85-10189
Iterative method for determining the distortion of elastic-plastic frames
[ISSN-0208-5658] 05 p0647 N85-14156
Effect of aberration in optical system on illuminance distribution over image of strip in semicoherent light
06 p0777 N85-14970
Perceptibility of nonlinear distortions in power amplifier
06 p0789 N85-15041
Characteristics of two-frequency combined dipole antenna arrays 06 p0791 N85-15055
Temperature distortion generator for turboshaft engine testing
[NASA-TM-83748] 07 p0893 N85-15658
Effect of steady-state temperature distortion on inlet flow to a high-bypass-ratio turbofan engine
[NASA-TM-86896] 07 p0904 N85-15725
Contamination and distortion of steady flow field induced by discrete frequency in aircraft gas turbines
[AD-A147092] 07 p0958 N85-16073
New aspects of thermoelastic contact
[AD-A147654] 07 p0979 N85-16217
Real-time estimation of amplitude and group delay distortion in a PSK line-of-sight communications channel
[AD-A147735] 08 p1151 N85-17288
Distortion of temporal characteristics during parametric up-conversion of ultrashort laser pulses
11 p1717 N85-20803
Tests of low-frequency geometric distortions in LANDSAT 4 images 12 p1872 N85-21744
Reflex attachment for fine alignment in spectral diffraction devices 13 p2044 N85-22794
Optimal modeling with a minimum of local distortion
[REPT-18/1984] 16 p2767 N85-27243
Distortion functions
[DE86-007511] 16 p2862 N85-27655
Improved statistical analysis method for prediction of maximum inlet distortion
[AD-A153767] 16 p3063 N85-28947
One mechanism for generation of wave disturbances in spectra of turbulent flows near ocean surface
19 p3289 N85-30397
Method of measuring spherical aberration and apparatus therefor
[AD-D011706] 19 p3367 N85-30882
Effects of residual stresses and distortion on the nickel 200 and stainless steel 304 weldments
[DE85-011868] 22 p3748 N85-33233
On the importance of viscous dissipation in Io
22 p3855 N85-33873

DISTRIBUTED PARAMETER SYSTEMS
Qualitative results for distributed systems with discrete damping and stiffness with application to control
[AD-A145525] 02 p0209 N85-11382
Chandrasekhar equations and computational algorithms for distributed parameter systems
[NASA-CR-172467] 03 p0402 N85-12584
Non-linear systems in infinite dimensional state spaces
[AD-A145628] 03 p0410 N85-12623
Effect of space-charge field on output characteristics of O-type oscillators with distributed interaction
13 p2089 N85-23043
LINCS
[DE85-006151] 14 p2407 N85-24836
Proceedings of the Workshop on Identification and Control of Flexible Space Structures, volume 2
[NASA-CR-176052] 20 p3411 N85-31170
Some asymptotic problems in the optimal control of distributed systems 20 p3412 N85-31175
Finite control in underdamped distributed parameter systems 20 p3412 N85-31176
New directions in asymptotically stable finite-dimensional adaptive control of linear distributed parameter systems 20 p3412 N85-31177
Space station parametric models
20 p3413 N85-31180
Approximation of optimal infinite dimensional compensators for flexible structures
20 p3413 N85-31181
Control of a flexible space antenna: A finite dimensional perspective based on distributed parameter theory
20 p3413 N85-31182
Sub-optimal control of nonlinear flexible space structures 20 p3414 N85-31190
A residuals approach to filtering, smoothing and identification for static distributed systems
20 p3418 N85-31213
Numerical experimentation with maximum likelihood identification in static distributed systems
20 p3418 N85-31214

DISTRIBUTED PROCESSING
Research on distributed languages and algorithms
[AD-A145861] 02 p0242 N85-11580
Distributed sensor networks
[AD-A146209] 03 p0355 N85-12286
Advanced Ada (trademark)
[AD-A146257] 03 p0407 N85-12602
Requirements and overview of the LINCS distributed operating system architecture
[DE84-013721] 05 p0714 N85-14577
Distributed database components in a DBMS (Database Management System) component architecture
[PB84-217546] 06 p0848 N85-15382
Logic elements for systems with variable structure
07 p0955 N85-16054
Support for distributed transactions in the TABS (Transaction based systems) prototype
[AD-A147213] 07 p1022 N85-16488
Decentralized control of scheduling in distributed systems
[AD-A147446] 07 p1022 N85-16487
On modeling the performance and reliability of multi-mode computer systems
[AD-A148444] 08 p1208 N85-17599
Decentralized control of scheduling in distributed systems
[AD-A147668] 08 p1228 N85-17731
SPADE: Series-parallel directed acyclic graph evaluator
[AD-A148458] 09 p1368 N85-18592
Distributed data processing design methodology
[AD-A148868] 10 p1537 N85-19692
Distributing a distributed problem solving network simulator
[AD-A149065] 10 p1537 N85-19693
Predicting the performance of distributed knowledge-based systems: A modeling approach
[AD-A149021] 10 p1545 N85-19736
Guidepost routing algorithm for distributed computer networks 11 p1622 N85-20210
Distributed asynchronous deterministic and stochastic gradient optimization algorithms: Revision
[AD-A149907] 12 p1921 N85-22068
Orphan detection in the Argus system
[AD-A150582] 13 p2148 N85-23331
Constructing unifying frameworks for the study of distributed system and algorithms
[AD-A151267] 15 p2637 N85-26261
Analysis and specification of a universal data model for distributed data base systems
[AD-A151656] 15 p2666 N85-26453
Real-Time Multiprocessor Programming Language (RTMPL) user's manual
[NASA-TP-2422] 17 p3010 N85-28610
Automatic distribution of programs in MASCOT and Ada (trademark) environments: A feasibility study
[AD-A152665] 17 p3010 N85-28614
Investigation and implementation of a tree transformation system for user friendly programming
[AD-A152716] 17 p3011 N85-28617
CLEANROOM software development: An empirical evaluation
[AD-A152924] 17 p3011 N85-28619
System Analysis for the Huntsville Operation Support Center, Distributed Computer System
[NASA-CR-171506] 17 p3015 N85-28642
A real-time executive for multiple-computer clusters
[AD-A152961] 17 p3015 N85-28648
Multicomputer operating systems and applications
[AD-A153205] 17 p3016 N85-28648
The design of a capability-based distributed operating system
[CWI-CS-R8418] 17 p3016 N85-28650
Distributed systems management in wide area networks
[CWI-CS-R8419] 17 p3016 N85-28651
Distributed matchmaking for processes in computer networks
[CWI-CS-R8421] 17 p3016 N85-28652
Distributed elections in a ring of processors using Archimedean time
[CWI-CS-R8416] 17 p3016 N85-28653
Debugging distributed computations in a nested atomic action system
[AD-A153617] 18 p3162 N85-29585
Replication methods for abstract data types
[AD-A153648] 18 p3162 N85-29587
LAN (Local Area Network) interoperability study of protocols needed for distributed command and control
[AD-A154033] 19 p3255 N85-30182
Graceful fault tolerance in large networks of microcomputers 19 p3332 N85-30843
A new taxonomy for distributed computer systems based upon operating system structure
[NASA-TM-86438] 19 p3342 N85-30709
Distributed implementation of functional program evaluation
[DE85-009573] 20 p3514 N85-31844
A distributed real-time operating system
[NIKHEF-H/84-8] 20 p3518 N85-31876
Consensus in the presence of partial synchrony (Preliminary version)
[AD-A154705] 21 p3670 N85-32799
Comparative study on data system architectures — spacecraft data processing
[ESA-CR(P)-2015] 21 p3675 N85-32826
A new fault-tolerant algorithm for clock synchronization
[AD-A154771] 21 p3676 N85-32836

DISTRIBUTION
Manganese in recent sediments of Ukrainian SSR Black Sea shelf 06 p0819 N85-15200
Decentralized control of scheduling in distributed systems
[AD-A147445] 07 p1026 N85-16523
On the altitudinal distribution of birds and bird strikes in the Netherlands
[AD-P004189] 11 p1580 N85-19952
Classic Fourier microdistributions in the real analytic case 11 p1698 N85-20673
Consistency of smoothing with running linear fits
[AD-A150232] 13 p2150 N85-23349
Limits on deeply penetrating particles in the 10(17) eV cosmic ray flux
[HE-5.3-1] 24 p4205 N85-36096

DISTRIBUTION (PROPERTY)
NT ANGULAR DISTRIBUTION
NT ANTENNA RADIATION PATTERNS
NT BOLTZMANN DISTRIBUTION
NT BRIGHTNESS DISTRIBUTION
NT CHARGE DISTRIBUTION
NT CURRENT DISTRIBUTION
NT DIFFRACTION PATTERNS
NT ELECTRON DENSITY PROFILES
NT ELECTRON DISTRIBUTION
NT ENERGY DISTRIBUTION
NT FLOW DISTRIBUTION
NT FORCE DISTRIBUTION
NT FREQUENCY DISTRIBUTION
NT HOLE DISTRIBUTION (ELECTRONICS)
NT HOLE DISTRIBUTION (MECHANICS)
NT INTERFERENCE LIFT
NT ION DISTRIBUTION
NT LOAD DISTRIBUTION (FORCES)
NT MASS DISTRIBUTION
NT MOMENT DISTRIBUTION
NT PRESSURE DISTRIBUTION
NT RADIAL DISTRIBUTION
NT RADIATION DISTRIBUTION
NT RAINBOWS
NT SIDELOBES
NT SPATIAL DISTRIBUTION
NT SPECTRAL ENERGY DISTRIBUTION
NT STAR DISTRIBUTION
NT STRESS CONCENTRATION
NT TEMPERATURE DISTRIBUTION
NT VELOCITY DISTRIBUTION
NT VERTICAL DISTRIBUTION
Determination of depth profiles and lattice positions with (n, p)- and (n, alpha) reactions (n, alpha) and channeling-blocking method) 03 p0429 N85-12735
Studies of the chemistry of vibrationally and electronically excited species in planetary upper atmospheres
[NASA-CR-174134] 03 p0449 N85-12951
Determining distribution of complex dielectric permittivity over cylindrical body of intricate cross section from electromagnetic field measurement
12 p1842 N85-21559
Distribution of radium and plutonium in human bone
[DE85-005025] 13 p2142 N85-23298

On the latitudinal distribution of debris in the Northern Hemisphere of Mars 13 p2188 N85-23579
Maintaining consistency and accommodating network repair in a self-regenerative distributed database management system (a discussion of the means and cost) 16 p2898 N85-26656
Hydrogen vibrational population distributions and negative ion generation in tandem high-density hydrogen discharges
[DE85-006784] 16 p2863 N85-27857
Influence of underwater volcanic mountains of Atlantic on microplankton distribution 19 p3284 N85-30424
NASA Space controls research and technology program 20 p3408 N85-31149
Results of computer calculations for a simulated distribution of kidney cells 20 p3502 N85-31771
Subduction zone tectonic studies to develop concepts for the occurrence of sediment subduction
[DE85-011794] 22 p3815 N85-33632
The distribution of compositional classes in the asteroid belt: A cosmochemical fingerprint?
22 p3852 N85-33656
Relationships between log N-log S and celestial distribution of gamma-ray bursts
[OG-1.2-10] 22 p3862 N85-33918
A simulation of high energy cosmic ray propagation 2
[OG-5.4-2] 22 p3885 N85-34079
Pitch angle distributions of solar energetic particles and the local scattering properties of the interplanetary magnetic field
[SH-9.1-13] 23 p4002 N85-34816
Cosmic ray intensity distribution perpendicular to solar equatorial plane at 1 A.U. during 1976-83
[SH-4.3-14] 23 p4032 N85-34996
Cosmogenic Mn-53 in meteorites
[SH-7.1-17] 23 p4049 N85-35107
Distribution of computer functionality for accelerator control at the Brookhaven AGS
[DE85-012520] 24 p4141 N85-35669
Resonance localization in tokamaks excited with ICRF waves
[DE85-014550] 24 p4160 N85-35791
Integral functions of electron lateral distribution and their fluctuations in electron-photon cascades
[HE-9.5-12] 24 p4184 N85-35949
Analysis of equi-intensity curves and NU distribution of EAS 24 p4187 N85-35970
About increase of the large transvers momentum processes fraction in hA interactions at energies 5.10(14) - 10(16) eV according to the data on E.A.S. hadrons 24 p4188 N85-35979

DISTRIBUTION FUNCTIONS
Approximating hierarchical normal priors using a vague component
[CSIR-TWISK-284] 01 p0107 N85-10720
An integral inequality with applications to order statistics
[AD-A145081] 01 p0113 N85-10770
Weighted distributions arising out of methods of ascertainment
[AD-A145615] 02 p0252 N85-11648
Likelihood estimation for generalized mixed exponential distributions
[AD-A145875] 02 p0252 N85-11651
Equations of plasma transport in a curved magnetic field
[DE84-015825] 05 p0730 N85-14690
Limiting distributions of functionals of Markov chains
[AD-A147832] 07 p1036 N85-16577
Electron distribution function and mobility in 3-5 compounds for high and low fields
[AD-A147447] 07 p1048 N85-16658
Transport properties and distribution functions in 3-5 semiconductors
[AD-A147525] 07 p1049 N85-16660
Tail behaviour for suprema of empirical processes
[AD-A147829] 08 p1210 N85-17613
Convergence of quasi-stationary to stationary distributions for stochastically monotone Markov processes
[AD-A148041] 08 p1215 N85-17652
Optical frequency domain reflectometry
08 p1222 N85-17695
User's guide to MIX: A computer code for fitting mixture distributions to data
[DE85-001451] 09 p1369 N85-18603
Estimating the scale parameter of an exponential distribution from a sample of time-censored r-th order statistics
[AD-A148060] 09 p1375 N85-18644
Condensational transformation of atmospheric aerosol particle distribution functions 10 p1500 N85-19466
Inequalities for the M/G/Infinity queue and related shot noise processes
[AD-A149015] 10 p1545 N85-19737
More limit theory for the sample correlation function of moving averages
[AD-A148975] 10 p1550 N85-19773
Asymptotic distributions of the sample mean, autocovariances and autocorrelations of long-memory time series
[AD-A149409] 10 p1551 N85-19781
Checking the shape of discrete distributions
[DE85-000177] 11 p1706 N85-20733
Scrawl plots, and letter and blotter strips
[DE85-001409] 11 p1707 N85-20739
The ambiguity function and the Wigner distribution
[AD-A150095] 12 p1829 N85-21482
On the limiting empirical distribution function of the eigenvalues of a multivariate F matrix
[AD-A149818] 12 p1921 N85-22065
The orientation distribution of nonspherical aerosol particles within a cloud
[AD-A150800] 13 p2092 N85-23061
Attainable rates of convergence of maxima
[AD-A150838] 14 p2408 N85-24847
On limiting empirical distribution function of the eigenvalues of a multivariate F matrix, revised
[AD-A151685] 15 p2641 N85-26288
Asymptotic expansions of the distribution of test statistics associated with several two parameter exponential distributions
[AD-A151906] 15 p2641 N85-26289
Nonermouth analysis and Frechet differentiability of M-functionals
[AD-A152932] 17 p3019 N85-28668
Determination of the association constant for pertechnetic acid
[DE85-010224] 19 p3235 N85-30057
Acoustic emission study of fatigue crack extension position in a stress cycle 19 p3283 N85-30355
Comments on estimating quantiles for Gaussian functionals by simulation
[AD-A154302] 19 p3348 N85-30750
Bivariate Rayleigh distribution: Formulas and curves, for correlation computing using the distribution function
[FOA-C-30380-E2] 20 p3521 N85-31901
Antistarshapedness, dispersiveness and mixtures
[AD-A155583] 21 p3676 N85-32849
A graphics interface for interactive simulation of packet-switched networks 23 p3962 N85-34558
Numerical solutions of the Vlasov equation
23 p3979 N85-34672
Pitch angle distributions of 35-1000 keV protons at quasi-perpendicular interplanetary shocks
[SH-1.5-6] 23 p3996 N85-34775
The dispersive evolution of charged-particle bunches in random magnetic fields
[SH-4.1-2] 23 p4004 N85-34826
On the determination of the depth of EAS development maximum using the lateral distribution of Cerenkov light at distances 150 m from EAS axis
[HE-4.4-13] 24 p4194 N85-36019

DISTRIBUTION MOMENTS
NT MEAN
NT ORTHOGONALITY
NT STANDARD DEVIATION
Long time correlation and stochastic diffusion in the standard map 02 p0262 N85-11835
A martingale approach to supercritical (C-M-J) branching processes
[CTH-MATH-1984-25] 05 p0722 N85-14643
Annual cycle. Part 2: The annual variation of precipitation over the United States and Canada
[PB85-147684] 15 p2600 N85-26027
Derivation of model topography
18 p3141 N85-29449
Evaluation of densities and distributions via hermite and generalized laguerre series employing high-order expansion coefficients determined recursively via moments or cumulants
[AD-A153950] 18 p3175 N85-29682

DISTRICT OF COLUMBIA
Results of the carbon monoxide study in Washington, D.C. and Denver, Colorado, in the winter of 1982-83
[PB84-230069] 06 p0834 N85-15309
Image variance and spatial structure in remotely sensed scenes — South Dakota, California, Missouri, Kentucky, Louisiana, Tennessee, District of Columbia, and Oregon
07 p0986 N85-16285
Test of dispersal of turbojet aircraft departure tracks at washington National Airport (1983-84), volume 1 report
[AD-A148111] 08 p1218 N85-17669
Geodetic accuracy of LANDSAT 4 Multispectral Scanner and Thematic Mapper data — Washington, DC, California, Alabama, South Dakota, and Illinois
11 p1667 N85-20604
Geometric accuracy assessment of LANDSAT-4 Multispectral Scanner (MSS) data
11 p1667 N85-20605
Intraband radiometric performance of the LANDSAT 4 Thematic Mapper — Washington, DC, Arkansas, Massachusetts, Virginia, and Arizona
12 p1671 N85-21736

DISTURBANCE THEORY
U PERTURBATION THEORY

DISTURBANCES
Wideband disturbance accomodation in precision flexible space structures 20 p3415 N85-31194

DISULFIDES
NT CARBON DISULFIDE
The violet absorber on Io: Dieulfur monoxide derivatives 13 p2173 N85-23482
Geosynchronous performance of a lithium-titanium disulfide battery 20 p3444 N85-31377

DITCHING (EXCAVATION)
U EXCAVATION

DITCHING (LANDING)
Air carrier overwater emergency equipment and procedures
[PB85-917006] 21 p3553 N85-32106

DITHERS
Precise bearing support dithere
[AD-D011470] 10 p1483 N85-19439

DITHIOLS
U THIOLS

DIURNAL RHYTHMS
U CIRCADIAN RHYTHMS

DIURNAL VARIATIONS
Green River air quality model development: Meteorological and tracer data, July/August 1982. Field study in Brush Valley, Colorado
[DE84-014875] 02 p0225 N85-11474
Analysis of the daily geomagnetic variation with the use of MAGSAT data — MAGSAT satellites
04 p0520 N85-13319
Daily magnetic variations at Ebro, Spain
04 p0520 N85-13325
The need for integrating ground thermal measurements with thermal aircraft imagery 05 p0690 N85-14243
Diurnal variation harmonics and spatial change in cosmic ray flux 06 p0824 N85-15230
Diurnal freeze-thaw frequencies in selected regions of the high latitudes
[AD-A147276] 07 p1007 N85-16400
Interrelationship of atmospheric parameters in Honduras
[AD-A147371] 07 p1007 N85-16401
A possible mechanism for the diurnal oscillations of tropical cyclones 09 p1356 N85-18530
Considering zonal wind in semidiurnal tide problem
14 p2335 N85-24440
Ionspheric effects of seasonal and diurnal variations of electric fields in equatorial F-region
14 p2336 N85-24459
The dawn-dusk asymmetry of particles near the neutral sheet of geomagnetotail 14 p2358 N85-24574
Afternoon radar aurora and polar cap convection pattern 14 p2361 N85-24582
Spectral analysis of diurnal nonuniformity of Earth's rotation 15 p2477 N85-25289
Spectral characteristics of protons at low and high altitudes during geomagnetic storm of 29 July 1977
16 p2719 N85-26786
Precipitation and snow cover data, 1977
[ISBN-951-997-215-2] 17 p2966 N85-28514
Measurements of VHF/UHF radio propagation in a maritime temperate climate
[CRC-1380] 18 p3089 N85-29119
The determination of daily usage or occupancy in the land-mobile band 138-174 MHz at Montreal
[CRC-1383] 19 p3283 N85-30167
Qualitative and quantitative examination of the performance of regional air quality models representing different modeling approaches
[DE85-010508] 19 p3310 N85-30519
Soil temperature extrema recovery rates after precipitation cooling 20 p3481 N85-31697
The diurnal variation of the neutral sodium species in the upper atmosphere: A model study
[AD-A154998] 21 p3631 N85-32561
A study of time transformation of natural photochemical aerosols 21 p3645 N85-32644
Drift and observations in cosmic-ray modulation, 2
[SH-4.2-5] 23 p4007 N85-34843
Cosmic ray sidereal diurnal variation of galactic origin observed by neutron monitors
[SH-4.4-2] 23 p4033 N85-35000
Sidereal anisotropies in the median rigidity range 60-600GV in 1976-1983
[SH-4.4-3] 23 p4033 N85-35001
The sidereal semi-diurnal variation observed at high zenith angles at Mawson, 1968-1984, and the polarity of the solar main field
[SH-4.4-6] 23 p4033 N85-35004

Cosmic ray intensity variations observed at Matsushiro (220 M.W.E. in depth)
[SH-4.4-9] 23 p4034 N85-35007
Solar tri-diurnal variation of cosmic rays in a wide range of rigidity
[SH-4.5-3] 23 p4036 N85-35021
Upper cut-off rigidity for corotation anisotropy during solar activity cycles 20 and 21
[SH-4.5-4] 23 p4036 N85-35022
Twenty-two-year cycle of the upper limiting rigidity of Daily waves
[SH-4.5-5] 23 p4036 N85-35023
Solar wind velocity and daily variation of cosmic rays
[SH-4.5-6] 23 p4036 N85-35024
Diurnal anisotropy during solar activity cycle twenty and diffusion-convection model
[SH-4.5-7] 23 p4036 N85-35025
Diurnal effect in cosmic rays at middle latitudes according to stratospheric measurements
[SH-4.5-8] 23 p4036 N85-35026
Comparative study of the phase of diurnal anisotropy on quiet and disturbed days on a long term basis up to recent period
[SH-4.5-9] 23 p4037 N85-35027
Study of spectral exponent on quiet and disturbed days
[SH-4.5-10] 23 p4037 N85-35028
Diurnal variation of galactic cosmic ray intensity on quiet days
[SH-4.5-11] 23 p4037 N85-35029
Diurnal variations from muon data at Takeyama underground station
[SH-4.5-13] 23 p4037 N85-35030
Long term changes in cosmic ray diurnal variations observed by ion chambers in Hong Kong and Japan
[SH-4.5-14] 23 p4037 N85-35031
The cosmic ray differential diurnal variation dependences on the zenith angle and the geomagnetic disturbance
[SH-4.5-16] 23 p4038 N85-35033
Anomalous increase of solar anisotropy above 150GV in 1951-1953
[SH-4.5-18] 23 p4038 N85-35035
Magnetic fluctuation and cosmic ray diurnal variations
[SH-4.5-21] 23 p4038 N85-35038
Transient cosmic ray increase associated with a geomagnetic storm
[SH-5.1-8] 23 p4042 N85-35062
Long-period cosmic ray variations and their altitude dependence
[SH-6.1-19] 23 p4048 N85-35091
Diurnal variations of cosmic ray geomagnetic cut-off threshold rigidities
[SH-6.1-21] 23 p4048 N85-35092

DIVERGENCE
NT MAGNETIC CHARGE DENSITY
Spatial and temporal interpolation of NEROS radiosonde winds
[PB84-232545] 04 p0540 N85-13438
Active control of forward swept wings with divergence and flutter aeroelastic instabilities
09 p1282 N85-18063
An analysis of the seasonal variations in the water vapor transport fields over the Southern Hemisphere
09 p1356 N85-18531
Advanced ion thruster research
[NASA-CR-174662] 10 p1430 N85-19021
Determining geometrical divergence using seismic observation data 14 p2343 N85-24489

DIVERTERS
A nonnoble front metallization process
06 p0830 N85-15279
Versator divertor experiment: Preliminary designs
[DE84-017159] 09 p1393 N85-18769
HPFTP flow diverter analysis
[NASA-CR-171424] 13 p2091 N85-23057
Coupled plasma-neutral transport model for the scrape-off region
[DE85-007559] 16 p2868 N85-27695
Electrolytic cell
[DE85-011586] 22 p3607 N85-33576
Neutral pumping rates for a next step tokamak ignition device
[DE85-012780] 24 p4157 N85-35776

DIVIDES (LANDFORMS)
Physiography of the Martian west equatorial uplift
12 p1961 N85-22325

DIVIDING (MATHEMATICS)
On the distribution of integral and prime divisors with equal norms 11 p1698 N85-20669

DIVING (UNDERWATER)
Experiments with hydrox at 1.3 MPa (13 atm) — for divers
[FOA-C-56014-H1] 04 p0545 N85-13471
Evaluation of the Kerls Cable thermal arc cutting equipment
[AD-A147813] 07 p0974 N85-16186
Vityaz specialists study human adaptability to ocean depths 07 p0980 N85-16225
Manned testing of two closed-circuit oxygen underwater breathing apparatus: US Navy Emerson Rig and Fenzy PO.66
[AD-A148300] 08 p1200 N85-17560
Hydrogen-oxygen (hydrox) breathing at 1.3MPa
[FOA-C-56015-H1] 09 p1364 N85-18577
High pressure environmental conditioning systems and chamber rehabilitation
[AD-A150039] 12 p1905 N85-21964
Assessing the short- and long-term health effects of decompression sickness among US Navy divers
[AD-A151887] 15 p2618 N85-26132
A comprehensive strategy for saturation decompression with nitrogen-oxygen
[AD-A151800] 16 p2841 N85-27520
Pressure chamber simulation of 450-meter dive
20 p3505 N85-31788
Diving simulation experiment with pressure chambers
20 p3506 N85-31793
Preliminary results of an ALVIN dive program on active hydrothermal vents at the southern Juan de Fuca Ridge
24 p4106 N85-35454
The research programme of the Institute for Aerospace Medicine 24 p4129 N85-35596
The deep diving simulator TITAN: Physiological problems associated with staying in great depths of water 24 p4130 N85-35604

DMSP SATELLITES
Fluxgate magnetometer (SSM) for the defense meteorological satellite program (DMSP) block 5D-2, flight 7
[AD-A155229] 21 p3560 N85-32143

DNA
U DEOXYRIBONUCLEIC ACID

DO-28 AIRCRAFT
First stage of equipping a Do 28 as a research aircraft for icing, and first research results
[ESA-TT-856] 11 p1584 N85-19982
Identification of gust input and gust response characteristics from Do 28 TNT flight test data
[DFVLR-FB-84-48] 17 p2900 N85-27881

DOCKING
U SPACECRAFT DOCKING

DOCUMENT STORAGE
Depository librarians' views on GPO's administration of the depository library program. Report to the Chairman, Joint Committee on Printing
[PB84-212265] 01 p0126 N85-10867
An electronic documentation system
[SNIAS-842-111-101] 04 p0577 N85-13683
Managing permanent objects
[AD-A149007] 10 p1540 N85-19708
Tekedit: An enhanced editor for Direct View Storage Tube (DVST) graphics display devices
[AD-A149715] 12 p1915 N85-22021
The conservation and utilization of scientific research documents: Practical aspects and organization
[NOTA-INTERNA-834] 14 p2433 N85-25008
ZOG-Vinson technology demonstration project. Volume 2: System description
[AD-A153871] 19 p3333 N85-30645
Electronic file system on an SM 90 minicomputer: The SARDE project
[ENST-84E018] 22 p3626 N85-33705
Records Disposal: A guidebook for laboratory offices
[AD-A156064] 24 p4165 N85-35823

DOCUMENTATION
Water resources data for Maine, water year 1983
[PB84-225143] 01 p0066 N85-10440
Water resources data for Ohio, water year 1983. Volume 1: Ohio River basin
[PB84-224690] 01 p0066 N85-10441
AGS-880 menu system user guide
[DE84-014338] 01 p0104 N85-10699
Automated Data Systems (ADS) documentation standards
[AD-A144867] 01 p0125 N85-10857
Improving technical documents
[AD-B084855] 01 p0126 N85-10866
Publications of the National Bureau of Standards, 1983 catalog
[PB84-218031] 01 p0126 N85-10869
Inclusion of audiovisual media in information services for the special subjects journalism and communication science (pilot study)
[BMFT-FB-ID-83-004] 02 p0294 N85-11909
Effective date (E-DATE) model documentation. Changes to reflect model enhancement
[AD-A148050] 03 p0407 N85-12589
NSSDC and WDC-A-R and S document availability and distribution services
[NASA-TM-87374] 03 p0436 N85-12767
Criss-cross directory of NASA N numbers and DOD AD numbers, 1962-1978 04 p0575 N85-13669
FY 1984 scientific and technical reports, articles, papers and presentations
[NASA-TM-86470] 04 p0575 N85-13670
An electronic documentation system
[SNIAS-842-111-101] 04 p0577 N85-13683
Recommended documentation for computer users at ANL
[DE84-016285] 06 p0855 N85-15434
Built-in-test for first line testing
08 p1064 N85-16739
Computer center CDC libraries/NSRD (subprograms)
[AD-A148792] 08 p1206 N85-17593
Documentation for an instrument database system
[DE84-017392] 09 p1402 N85-18826
Preserve the sense of Earth from space — achieves of remote sensing data
[PB85-124121] 11 p1740 N85-20942
Integrated control system engineering support
[AD-A149742] 12 p1760 N85-21177
The availability of Japanese scientific and technical information in the United States
[GPO-30-478] 12 p1951 N85-22254
The conservation and utilization of scientific research documents: Practical aspects and organization
[NOTA-INTERNA-834] 14 p2433 N85-25008
Documentation for the machine-readable version of A Library of Stellar Spectra (Jacoby, Hunter and Christian 1984)
[NASA-TM-87438] 14 p2438 N85-25046
Documentation for the machine-readable version of the Revised S210 Catalog of Far-Ultraviolet Objects (Page, Carruthers and Heckathorn 1982)
[NASA-TM-87439] 14 p2438 N85-25047
Documentation for the machine-readable version of A Finding List for the Multiplet Tables of NSRDS-NBS 3, Sections 1-10 (Adelman, Adelman, Fischel and Warren 1984)
[NASA-TM-87440] 14 p2438 N85-25048
Documentation for the machine-readable version of the Cordoba Durchmusterung (CD)
[NASA-TM-87441] 14 p2439 N85-25049
A modern control theory enhancement to an Interactive Control Engineering Computer Analysis Package (ICECAP)
[AD-A153249] 17 p3012 N85-28622
Bibliography of Lewis Research Center technical publications announced in 1984
[NASA-TM-87012] 17 p3049 N85-29876
National Archives and Records Service (NARS) twenty year preservation plan
[PB85-177640] 18 p3200 N85-29854
Guide on logical database design
[PB85-177970] 19 p3381 N85-30976
The documentation assistant: An intelligent system for documentation
[AD-A154709] 21 p3670 N85-32900
EPALIT: A data management system applied to the control and retrieval of technical reports
[PB85-193068] 24 p4166 N85-35828

DOCUMENTS
NT ABSTRACTS
NT ASTRONOMICAL CATALOGS
NT BIBLIOGRAPHIES
NT CATALOGS (PUBLICATIONS)
NT ENGINEERING DRAWINGS
NT HANDBOOKS
NT INSTALLATION MANUALS
NT MANUALS
NT PERIODICALS
NT PRESIDENTIAL REPORTS
NT RECORDS
NT SUPPLEMENTS
NT TEXTS
NT USER MANUALS (COMPUTER PROGRAMS)
NT VIDEO DISKS
Improving technical documents
[AD-B084855] 01 p0126 N85-10866
AGARD bulletin technical programme, 1985
[AGARD-BUL-84-2] 02 p0305 N85-11971
Energy information exchange, 1983
[DE84-901446] 04 p0577 N85-13680
Document interchange format
[PB84-217033] 07 p1027 N85-16517
Technical order managers handbook: Utilization assessment
[AD-A147579] 07 p1055 N85-16894
Provision of Federal government publication in electronic format to depository libraries
[S-PRT-98-280] 10 p1567 N85-19680
M68000 RNF text formatter user's manual
[NASA-TM-86327] 13 p2146 N85-23320

Recent Naval Postgraduate School publications
[AD-A151723] 16 p2875 N85-27740
Electrochemical Energy Storage Branch
[DE85-007592] 18 p3131 N85-29391
Technology transfer system automation implementation
[PB85-177395] 22 p3849 N85-33838
Recognition and clear representation of handwritten electronic diagrams 23 p3960 N85-34541
A model for a document maintenance system 23 p3960 N85-34542

DOGS
Tolerance endpoint for evaluating the effects of heat stress in dogs
[AD-A148104] 08 p1192 N85-17511
Long term exposure of animals to antiorthostatic (-90 deg) as a model of critical homeostatic disturbances 19 p3324 N85-30592

DOLOMITE (MINERAL)
The Midway Atoll coral cap: Meteoric diagenesis, amplitude of sea-level fluctuation and dolomitization 09 p1351 N85-18499
Diagenesis of niagaran (middle silurian) pinnacle reefs, northwest Michigan 09 p1352 N85-18508
Deep-burial diagenesis in carbonates
[DE85-011224] 22 p3802 N85-33554

DOLPHINS
Tracking pelagic dolphins by satellite 14 p2324 N85-24364

DOMAIN WALL
Twisted domain wall in very thin magnetic films with perpendicular anisotropy 03 p0350 N85-12252
Investigation of domain structures and walls using neutron diffraction 03 p0423 N85-12702
Monitoring the execution of plans in SIPE (System for Interactive Planning and Execution) monitoring
[AD-A149138] 10 p1544 N85-19731

DOMAINS
NT MAGNETIC DOMAINS
On Bezout domains, elementary divisor rings, and pole assignability
[CSIR-TWISK-330] 01 p0110 N85-10740
The disordering process in an L1sub2 ordered alloy
[DE84-016599] 04 p0475 N85-13028
Domains with Lipschitz mapping functions 10 p1535 N85-19675
Domain decomposition techniques for solving elliptic partial differential equations on multiprocessors
[DE85-004448] 10 p1549 N85-19769
An extension of the Gleason problem in pseudoconvex domains 11 p1696 N85-20671
On the solution for the sound field in a semi-infinite uniform duct with sheared mean flow 20 p3523 N85-31912
Use of MMLE3 to determine lower order equivalent systems in the time domain
[AD-A154700] 21 p3554 N85-32112

DOMES
Wide angle phased array dome lens antenna with a reflection/transmission switch
[AD-D011582] 12 p1833 N85-21502

DOMES (GEOLOGY)
New data on presence of ores in salt dome structures of Dnieper-Donets Basin 07 p0981 N85-16234
Ridged plains of Lunae Planum: Thickness distribution revised 13 p2186 N85-23559
Preliminary SPR thermal model description and results for WH-11 and BM-4
[DE85-013171] 23 p3931 N85-34360

DOMES (STRUCTURAL FORMS)
NT RADOMES

DOMESTIC ENERGY
Solar house, Freiburg
[BMFT-FB-T-84-249] 15 p2588 N85-25853
Solar energy for highway uses
[DE84-015653] 18 p3130 N85-29382
Operational results for the experimental DOE/NASA Mod-OA wind turbine project
[NASA-TM-83517] 19 p3304 N85-30479

DOMESTIC SATELLITE COMMUNICATIONS SYSTEMS
Methodology for the implementation of a domestic satellite communications network 04 p0493 N85-13148
China's future domestic satellite communications systems 10 p1476 N85-19312
China's domestic satellite communications 10 p1476 N85-19313

DOMINANCE
Functional significance of some EEG parameters and dominant principle 11 p1691 N85-20634

DONOR MATERIALS
Fundamental electronic properties of donor-type graphite intercalated compounds
[AD-A146148] 03 p0326 N85-12099
Electronic density of states for the double donor system SiP, As
[INPE-3447-PRE/700] 16 p2869 N85-27700
Electron-donor dopant, method of improving conductivity of polymers by doping therewith, and a polymer so treated
[DE85-011640] 22 p3752 N85-33257

DOORS
Hydraulic locking boltwork system
[AD-D011299] 06 p0815 N85-15174
Challenges in the development of the orbiter radiator system 08 p1096 N85-16925
Integrated paratroop door
[AD-D011607] 12 p1776 N85-21148
Get Away Special (GAS) thermal design summary
[X-732-83-8] 15 p2475 N85-25278
Application of lightweight composite materials to naval weapons systems
[PB85-173807] 18 p3089 N85-28981
Airborne sound transmission loss characteristics of wood-frame construction
[AD-A154174] 20 p3524 N85-31919

DOPED CRYSTALS
The transient oxidation of single crystal NiAl+Zr
[NASA-CR-174756] 02 p0182 N85-11221
Silicon sheet with molecular beam epitaxy for high efficiency solar cells
[NASA-CR-174022] 02 p0222 N85-11459
Structural phase transitions in doped hexahalogen metallates 03 p0426 N85-12721
Effect of doping on the voltage holdoff performance of alumina insulators in vacuum
[DE84-017163] 04 p0480 N85-13060
Lifetime of excess charge carriers in weakly doped epitaxial GaAs layers 04 p0487 N85-13108
Development of high responsitivity Ge:Ga photoconductors
[DE84-016902] 04 p0571 N85-13643
Gallium arsenide/AlGaAs multilayer structures with special doping profiles for microwave and optoelectronic devices
[BMFT-FB-T-84-207] 08 p1227 N85-17725
Optical studies of dynamical processes in disordered materials
[DE85-002400] 10 p1453 N85-19158
Modern solid state laser materials
[DE85-003665] 10 p1490 N85-19410
Metal-nonmetal transitions in N-doped many-valley Si and Ge
[INPE-3358-PRE/636] 10 p1562 N85-19648
Use of alternative solvents for low-temperature LPE growth of CdTe films
[AD-A149418] 10 p1562 N85-19653
Research on the basic understanding of high efficiency in silicon solar cells
[DE85-000507] 11 p1672 N85-20537
Preparation of crystal growth experiments in Spacelab: SI (FSLP), CdTe (D1), ZnS (D1)
[BMFT-FB-W-84-045] 12 p1788 N85-21227
Enhanced diffusion from interstitial trapping during solid-phase-epitaxial growth of silicon alloys
[DE85-001285] 12 p1941 N85-22193
Technological process effect on the carrier lifetime degradation of silicon solar cell base layer irradiated by 1 MeV electrons (boron doping case) 13 p2007 N85-22585
Annealing of radiation damage in boron and gallium doped silicon solar cells 13 p2012 N85-22624
High sheet resistance, arsenic implanted polycrystalline silicon for integrated circuit resistors
[DE85-004355] 13 p2065 N85-22902
Noise characteristics of sulfur-doped silicon diodes 13 p2073 N85-22952
Numerical simulation of inverters with I2L elements including effects of high doping level 13 p2088 N85-23039
Structural, morphological and optical characteristics of KGd(WO4)2 crystals 14 p2280 N85-24126
High resolution Z-contrast imaging and lattice location analysis of dopants in ion-implanted silicon
[DE85-005261] 14 p2429 N85-24360
Heavy doping effects in high efficiency silicon solar cells
[NASA-CR-175687] 15 p2585 N85-25837
Fundamental studies of growth, doping and transformation in beta silicon carbide
[AD-A152047] 15 p2660 N85-26416
Flat-plate solar array project process development area: Process research of non-CZ silicon material
[NASA-CR-175777] 16 p2818 N85-27382
Heavy doping effects in high efficiency silicon solar cells
[NASA-CR-175779] 16 p2818 N85-27383
On some physical impurity properties of doped-indirect gap semiconductors at low and intermediate concentrations
[INPE-3452-PRE/704] 16 p2869 N85-27701
Effect of dislocations on gallium arsenide FETs
[AD-A152249] 16 p2870 N85-27709
TEM investigation of polar-on-nonpolar epitaxy: GaAs-AlGaAs on (100) Ge
[DE85-007613] 16 p2871 N85-27714
GaAs MESFET with lateral non-uniform doping 17 p3043 N85-28827
Zn3P2 as an improved semiconductor for photovoltaic solar cells
[DE85-008772] 18 p3087 N85-29171
Chemistry and physics of silicon-based amorphous semiconductors
[DE85-001931] 19 p3377 N85-30949
Aspects of silicon bulk lifetimes 20 p3479 N85-31617
Z-contrast imaging and electron channeling analysis of dopants in semiconductors
[DE85-011410] 21 p3582 N85-32269
Physics of heavily doped silicon and solar-cell parameter measurement 21 p3609 N85-32418
Influence of background electrically neutral argon admixture on mechanical strength of silicon crystals 21 p3663 N85-32678
Doping superlattices in organometallic VPE InP
[AD-A155151] 21 p3710 N85-33029
Modulation doped GaAs/Al(x)Ga(1-x)As layered structures with applications to field effect transistors
[AD-A155360] 22 p3759 N85-33296
Trivalent cerium doped crystals as tunable laser systems: Two bad apples
[DE85-008168] 22 p3790 N85-33482

DOPES
Polarization in chemically doped hydrogen-rich glasses
[DE84-017486] 06 p0771 N85-14936
Lithium counterdoped silicon solar cell
[NASA-CASE-LEW-14177-1] 11 p1672 N85-20535
Status of French research in plastic batteries 15 p2530 N85-25603
Flat-plate solar array project process development area: Process research of non-CZ silicon material
[NASA-CR-175777] 16 p2818 N85-27382
Molecular orbital studies in oxidation: Sulfate formation and metal-metal oxide adhesion
[NASA-CR-176070] 21 p3565 N85-32174
Electron-donor dopant, method of improving conductivity of polymers by doping therewith, and a polymer so treated
[DE85-011640] 22 p3752 N85-33257
Radiation-hardened polymeric films
[DE85-011636] 22 p3752 N85-33259
Experimental test for interpreting the increase in sensibility of doped CR-39
[OG-4.4-11] 22 p3880 N85-34042
Flat-plate solar array project process development area process research of non-CZ silicon material
[NASA-CR-176117] 23 p3945 N85-34445

DOPING (ADDITIVES)
U ADDITIVES

DOPPLER EFFECT
NT DOPPLER-FIZEAU EFFECT
The development of a diode laser Doppler velocimeter for boundary layer measurements under ice: A feasibility investigation
[AD-A145076] 01 p0053 N85-10348
The investigation of short wave signal structure in the vicinity of the caustic by means of a high-directed antenna
[PR-194] 03 p0354 N85-12277
Using measured variance of skywave radar sea-echo power spectra to estimate ionospheric Doppler broadening of mean spectra
[PB84-214071] 03 p0399 N85-12544
Methodology improvement program for the second generation mid-distance radar (MIDI 2)
[AD-A148467] 08 p1153 N85-17281
Tropospheric and ionospheric phase perturbations and Doppler frequency shift effects
[AD-A148579] 08 p1154 N85-17283
Five-minute P modes detected in Doppler shift measurement on Alpha Centauri 08 p1250 N85-17895
Atmospheric limitations in stellar seismology: Should one measure radial velocity or brightness fluctuations? 08 p1251 N85-17899
Propagation effects on the Doppler frequency shift of satellite transmissions 10 p1470 N85-19276
Multipath and Doppler observations during transatlantic digital HF propagation experiments 10 p1471 N85-19281
Study of submicron particle size distributions by laser Doppler measurement of Brownian motion
[AD-A149139] 10 p1487 N85-19388

An evaluation of wind measurements by four Doppler sodars
[PB86-116301] 10 p1520 N86-19586
Flow measurement by laser Doppler anemometry in a nuclear fuel assembly
[DE85-003280] 12 p1848 N85-21592
Investigation of generation of oscillations using anomalous Doppler effect 13 p2078 N85-22980
Synthetic aperture radar simulation study
[AD-A151000] 14 p2293 N85-24214
Establishment of hydrographic shore control by Doppler satellite techniques
[AD-A150709] 14 p2347 N85-24512
Optimized response functions for 2-dimensional observations of solar oscillations
14 p2443 N85-25075
Resonance generation of inertial waves (in the atmosphere) by Doppler-shift of inertio-gravity modes
15 p2590 N85-25966
Simulation of a low orbit restitution. Covariance analysis of the position-velocity by Doppler and accelerometer measurements
[CNES-CT/DTI/MS/AE/166] 16 p2728 N85-26836
DORIS: Prediction in Doppler measurement — satellite onboard measurement
[CNES-CT/DTI/MS/AE/170] 16 p2729 N85-26843
LDA study of non-steady flame propagation in a constant volume duct
[DE85-007233] 16 p2746 N85-26948
Thermospheric winds observed by OI6300A Doppler shifts at 23 deg S in the Brazilian sector
[INPE-3384-RPE/470] 16 p2834 N85-27479
A comprehensive strategy for saturation decompression with nitrogen-oxygen
[AD-A151800] 16 p2841 N85-27520
Positron annihilation studies of vacancy formation in tungsten, chromium, and niobium
[DE85-006837] 16 p2671 N85-27710
Vibration-free Raman Doppler velocimeter
[NASA-CASE-LAR-13268-1] 16 p3104 N85-29216
On the accuracy of Ca beam primary frequency standards 16 p3105 N85-29224
Determination of the vacancy formation enthalpy in chromium by positron annihilation
[DE85-010286] 19 p3239 N85-30084
LDA study of the unburned gas motion induced by nonsteady flame propagation in a constant volume duct
[DE85-009936] 19 p3270 N85-30277
Filter induced errors in laser anemometer measurements using counter processors
[NASA-TM-87047] 19 p3272 N85-30299
Accuracy in determining velocity of fluid movement by Doppler method 19 p3293 N85-30419
Velocity visualization in gaseous flows
[NASA-CR-174954] 20 p3453 N85-31445
A derivation of relativistic effects in satellite tracking
[AD-A154620] 21 p3558 N85-32132
Accuracy of velocity and power determination by the Doppler method 21 p3620 N85-32493
Coding schemes for improving MST radar performance, part 7.1A 21 p3625 N85-32520
The moving thermoacoustic array: A theoretical feasibility study
[AD-A154510] 21 p3699 N85-32980
HEAO 3 upper limits to the expected 1634 KeV line from SS 433
[OG-2.4-9] 22 p3868 N85-33954
Search for gamma ray lines from SS433
[OG-2.4-11] 22 p3868 N85-33955
Limits on the Doppler factor in relativistic jets by means of gamma-ray observations
[OG-2.7-12] 22 p3872 N85-33985
Wide Angle Michelson Doppler Imaging Interferometer (WAMDI)
23 p3902 N85-34172
On the detectability of key-MeV solar protons through their nonthermal Lyman-alpha emission
[SH-1.3-5] 23 p3993 N85-34752
DMSK: A practical 2400-bps receiver for the mobile satellite service: An MSAT-X Report
[NASA-CR-176194] 24 p4086 N85-35324

DOPPLER NAVIGATION
Use of microprocessor techniques and new antenna systems to improve the navigation aids very high frequency omnidirectional radar (VOR), Doppler VOR and Instrument Landing System (ILS)
[BMFT-FB-W-84-026] 02 p0137 N85-10930
Observations of lightweight Doppler system accuracy
[AD-A145966] 03 p0317 N85-12049
Flight research on visual aids and navigation equipment for helicopter low-level flight at night
08 p1076 N85-16820
Interplanetary navigation 14 p2398 N85-24781

DOPPLER RADAR
NT MULTISTATIC RADAR
Diagnosis and therapy of geodetic satellite networks of Doppler type — error analysis
[SER-C-293] 01 p0015 N85-10090
Operational evaluation of 5 cm Doppler radar. Two contributions: Review of WSR-74C Doppler radar operations at WSO Montgomery, Alabama (April 1982 - August 1983). The Johnson-Effect resolving ambiguous Doppler velocities
[PB84-207521] 01 p0041 N85-10269
High frequency radar software reference manual for Product Two
[PB84-210079] 01 p0041 N85-10270
The PROMIS Doppler radar system; design and operational experience 01 p0077 N85-10515
Nowcasting with Doppler radar: The forecaster-computer relationship
01 p0077 N85-10514
Doppler radar analysis of a frontal zone prior to convective development 01 p0077 N85-10515
The potential use of atmospheric profilers in short-range prediction 01 p0078 N85-10516
Microburst wind structure and evaluation of Doppler radar for wind shear detection
[DOT/FAA/PM-84/29] 02 p0230 N85-11501
Terrestrial locating — of buoys from space
05 p0599 N85-13816
The motion of the Earth by Doppler observing campaign (MEDOC) 05 p0601 N85-13831
Spring program summary, 1983
[PB84-222223] 06 p0839 N85-15330
High accuracy Doppler navigation employing optimum integrated position fix information
08 p1073 N85-16803
The MST radar technique 08 p1185 N85-17488
Multiple channel adaptive filtering using a fast orthogonalization network: An application to efficient pulsed Doppler radar processing
[AD-A147929] 08 p1211 N85-17619
The potential of the NEXRAD radar system for warning of bird hazards
[AD-P004210] 11 p1583 N85-19977
Analysis of the NASA/MSFC Airborne Doppler Lidar results from San Gorgonio Pass, California
[NASA-CR-171355] 12 p1892 N85-21673
Geophysical interpretation of Venus gravity data
13 p2178 N85-23513
A brief summary of results derived from Scandinavian Twin Auroral Radar Experiment (STARE) observations during IMS — ionospheric electric fields
14 p2382 N85-24595
Interplanetary navigation 14 p2398 N85-24781
Injection controlled laser transmitter with twin local oscillators
[AD-D011577] 15 p2583 N85-25810
Radar turbulence estimates. Effects of wind shear and reflectivity factor gradients
[AD-A151876] 15 p2599 N85-26023
Comparison of wind velocity in thunderstorms determined from measurements by a ground-based Doppler radar and an F-106B airplane
[NASA-TM-86348] 16 p2703 N85-26687
Analysis of the NASA/MSFC airborne Doppler lidar results from San Gorgonio Pass, California
[NASA-CR-3901] 16 p2832 N85-27463
Influence of coherent mesoscale structures on satellite-based Doppler lidar wind measurements
[NASA-CR-175853] 16 p2833 N85-27467
Weather radar studies
[AD-A152563] 17 p2996 N85-28521
Atmospheric probing by active millimeter wave system
[AD-A153550] 18 p3136 N85-29422
Use of radar with frequency modulation for studying atmospheric boundary layer 19 p3296 N85-30437
Comparison of wind and turbulence measurements from Doppler lidar and instrumented aircraft
[NASA-CR-171535] 20 p3495 N85-31729
Middle Atmosphere Program. Handbook for MAP. Volume 14: URSI/SCOSTEP Workshop on Technical Aspects of MST Radar
[NASA-CR-176085] 21 p3615 N85-32466
Observations of frontal zone structures with a VHF Doppler radar and radiosondes, part 1.2A
21 p3616 N85-32469
Performance of the Colorado wind-profiling network, part 1.5A 21 p3617 N85-32475
Relationship of spaced antenna and Doppler techniques for velocity measurements (keynote paper), part 3
21 p3619 N85-32486
On the spectrum of atmospheric velocity fluctuations seen by MST/ST radar and their interpretation
21 p3622 N85-32504
Coding schemes for improving MST radar performance, part 7.1A 21 p3625 N85-32520
Real-time automated detection of mesocyclones and tornado vortex signatures
[AD-A154988] 21 p3635 N85-32578
A multi-channel radar receiver
[AD-A156058] 24 p4087 N85-35333
Polarization diversity addition to the 10 centimeter Doppler weather radar
[AD-A156062] 24 p4087 N85-35334

DOPPLER-FIZEAU EFFECT
The solar vector magnetograph of the Okayama Astrophysical Observatory 18 p3205 N85-29882

DORNIER AIRCRAFT
NT DO-28 AIRCRAFT

DORNIER DO-28 AIRCRAFT
U DO-28 AIRCRAFT

DOSAGE
NT RADIATION DOSAGE
SANDYL radiation transport code at the Naval Research Laboratory
[AD-A144890] 01 p0117 N85-10799
Acute oral toxicity (LD50) of 4-nitrophenyl monochloromethyl (Phenyl) phosphinate (TA009) in male rats
[AD-A148337] 08 p1192 N85-17513
Study of a novel shielding principle for protection against intense gamma-ray beams
[AD-A154374] 19 p3357 N85-30808
Beta response of selected instruments
[DE85-013278] 22 p3788 N85-33469
Environmental surveillance at Los Alamos during 1984
[DE85-011866] 22 p3811 N85-33605
The 1984 environmental monitoring report, Sandia National Laboratories, Albuquerque, New Mexico
[DE85-011175] 22 p3811 N85-33607
The 1984 environmental monitoring program report for Idaho National Engineering Laboratory site
[DE85-011209] 22 p3812 N85-33611
Hit-size effectiveness theory applied to high doses of low LET radiation for pink mutations in Tradescantia
[DE85-011835] 22 p3819 N85-33857
The 1983 International intercomparison of nuclear accident dosimetry systems at Oak Ridge National Laboratory
[DE85-011303] 23 p3934 N85-34362
The 1984 biotic studies of Yucca Mountain, Nevada test site, Nye County, Nevada
[DE85-011715] 23 p3951 N85-34487
Estimating risks of lead-induced hemoglobin decrements under conditions of uncertainty: Methodology, pilot judgments and illustrative calculations
[DE85-012293] 23 p3952 N85-34493
Analysis of transient radiation upset in a 16K SRAM
[DE85-009442] 23 p3965 N85-34586

DOSE
U DOSAGE

DOSIMETERS
NT THRESHOLD DETECTORS (DOSIMETERS)
Radiation measuring system using transistor flux sensors
[AD-D011239] 01 p0050 N85-10326
Photon and electron dosimetry at the Physikalische-Technische Bundesanstalt in Brunswick
[PTB-DOS-9] 01 p0119 N85-10814
Specific absorption rate in a sitting rhesus model at 225, 1290, and 5950 MHz for E, H, and K polarizations
[AD-A145435] 02 p0234 N85-11524
The effect of the choice or response matrix on unfolded bonner sphere spectra
[AD-A150482] 13 p2159 N85-23404
The physical interactions of radiofrequency radiation fields and biological systems 16 p2775 N85-27129
Radio Frequency Radiation (RFR) measurements in operational settings 16 p2777 N85-27136
Results from radiation monitoring equipment experiment on STS-11
[AD-A152531] 17 p2908 N85-27932
Energy and Technology Review
[DE85-004358] 17 p3049 N85-28868
Results from radiation monitoring equipment experiment on STS-8
[AD-A153241] 17 p3055 N85-28911
Dosimeasurements with thermoluminescence dosimeters at a Febetron 701, 600 kV in room 022 of the Interuniversity Reactor Institute (IRI)
[IRI-190-84-02] 18 p3111 N85-29262
Safety system with microcomputer
[OEFZS-4294] 18 p3166 N85-29618
Comparison of calculations and measurements of the off-axis radiation dose (SI) in liquid nitrogen as a function of radiation length
[AD-A153676] 18 p3178 N85-29704
Safety report, 1982 18 p3184 N85-29748
Symposium on Luminescent Radiation Receivers and Converters 19 p3295 N85-30430
Research on the experimental verification of dosimetry calculations
[DE85-011282] 19 p3331 N85-30637

MELCOR Accident Consequence Code System (MACCS)
[DE85-009712] 19 p3339 N85-30689
Dosimetry and limit values for internal contamination with radionuclides: From (International Commission on Radioactive Protection) ICRP-2 to ICRP-30
[IRI-190-84-03] 20 p3507 N85-31804
Solid-state track recorder neutron dosimetry in the Three-Mile Island Unit-2 reactor cavity
[DE85-011360] 20 p3531 N85-31986
Results from radiation monitoring equipment experiments on STS-41C, 41D, 41G and 51A
[AD-A154676] 21 p3560 N85-32142
A crew exposure study. Phase II. Volume 2. At sea. Part A
[AD-A155233] 21 p3666 N85-32774
Paired ion chamber constants for fission gamma-neutron fields
[AD-A155069] 21 p3702 N85-32999
A practical guide to ionization chamber dosimetry at the AFRRI reactor
[AD-A155185] 21 p3703 N85-33003
Current internal-dosimetry practices at US Department of Energy facilities
[DE85-011718] 22 p3787 N85-33466
Error evaluation in measurements with thermoluminescent dosimeters
[ISS-T-84/6] 22 p3788 N85-33471
Hit-size effectiveness theory applied to high doses of low LET radiation for pink mutations in Tradescantia
[DE85-011835] 22 p3819 N85-33657
Digital characterization of particle tracks for microdosimetry
[DE85-012698] 22 p3846 N85-33822
The 1983 international intercomparison of nuclear accident dosimetry systems at Oak Ridge National Laboratory
[DE85-011303] 23 p3934 N85-34382

DOSIMETRY
U DOSIMETERS

DOUBLE BASE PROPELLANTS
NT DOUBLE BASE ROCKET PROPELLANTS
Study of the transition from deflagration to detonation of previously fragmented propellants 08 p1115 N85-17032
Effects of perforation L/D ratio and slotting on stick propellant combustion
[AD-A148854] 10 p1456 N85-19177

DOUBLE BASE ROCKET PROPELLANTS
Embedment system for ultrahigh-burning rate propellants of solid propulsion subsystems
[AD-D011257] 06 p0773 N85-14942
The vulnerability of cast double base rocket motors to thermomechanical attack 08 p1115 N85-17033
Crack growth in propellants 08 p1116 N85-17034
Determination of the decomposition behavior of double base propellants at low temperatures 08 p1117 N85-17045

DOUBLE STARS
NT BINARY STARS
NT COMPANION STARS
NT DWARF NOVAE
NT ECLIPSING BINARY STARS

DOUGLAS AIRCRAFT
NT DC 8 AIRCRAFT
NT DC 9 AIRCRAFT
NT DC 10 AIRCRAFT

DOUGLAS DC-8 AIRCRAFT
U DC 8 AIRCRAFT

DOUGLAS DC-9 AIRCRAFT
U DC 9 AIRCRAFT

DOUGLAS MILITARY AIRCRAFT
U MILITARY AIRCRAFT

DOVAP
U DOPPLER EFFECT

DOWN-CONVERTERS
Optical RF downconverter
[AD-D011336] 07 p1042 N85-16616

DOWNLINKING
BBC receiving terminal for the European orbital test satellite
[BBC-RD-1984/15] 08 p1142 N85-17205
Polarization angles of linearly polarized antennas and radio waves in satellite communications
[PB85-131613] 11 p1626 N85-20240
Remote control of an impact demonstration vehicle
[NASA-TM-85925] 14 p2225 N85-23797
Analysis of space diversity techniques for EHF (Extremely High Frequency) satellite downlinks
[AD-A151900] 15 p2544 N85-25705
The IRAS end-to-end data system
[NLR-MP-83056-U] 17 p3051 N85-28883

DOWNWASH
Downwash in the plane of symmetry of an elliptically loaded wing
[NASA-TP-2414] 07 p0898 N85-15893

DRAFTING (DRAWING)
Accomplishments of Institute of Cartography summarized 13 p2166 N85-23435
Computer aided draughting in a civil engineering consulting practice 15 p2627 N85-26189

DRAFTING MACHINES
Two-dimensional/speed/couple/data base management system
[A-1] 18 p3165 N85-29608
The CEADS-CADD system
[A-4] 18 p3165 N85-29610
System test CALMA DDM (Design Drafting Manufacturing)
[A-5] 18 p3165 N85-29611
The International Computers Limited (ICL) PERQ 1/Engineering Architectural Graphics Language Environment (EAGLE) Computer Aided Design system (CAD)
[A-7] 18 p3165 N85-29612
System test: Hewlett-Packard draft
[A-9] 18 p3166 N85-29613
Test Drawing Office Graphics System (DOGS)/APOLLO
[A-10] 18 p3166 N85-29614
System test Oce 5200
[A-3] 20 p3515 N85-31850
The General Drafting System (GDS) design system
[A-6] 20 p3517 N85-31869
The IGOS design system
[A-8] 20 p3517 N85-31870

DRAG
NT AERODYNAMIC DRAG
NT FRICTION DRAG
NT INTERFERENCE DRAG
NT SATELLITE DRAG
NT VISCOUS DRAG
NT WAVE DRAG
Observations from varying the lift and drag inputs to a noise prediction method for supersonic helical tip speed propellers
[NASA-TM-83797] 01 p0115 N85-10788
UH-60A external stores support system fixed provision fairings drag determination
[AD-A147188] 07 p0902 N85-15719
The NYU inverse swept wing code
[NASA-CR-3662] 08 p1077 N85-16830
Icing flight research: Aerodynamic effects of ice and ice shape documentation with stereo photography
[NASA-TM-86906] 09 p1279 N85-18049
Report of the Constellations Panel 11 p1645 N85-20368
Evaluating wind flow around buildings on heliport placement
[FAA-PM-84-25] 12 p1893 N85-21881
Effect of drag behind nozzle array on its force and energy characteristics 14 p2277 N85-24107
Hydraulic drag of rod with artificial microroughness in longitudinal flow 14 p2278 N85-24111

DRAG BALANCE
U AERODYNAMIC BALANCE
U LIFT DRAG RATIO

DRAG CHUTES
Extended moment arm anti-spin device
[NASA-CASE-LAR-12979-1] 12 p1776 N85-21147
Parachute extraction device for ultralight gliders
[CH-643499-A5] 16 p2690 N85-26683

DRAG DEVICES
NT AERODYNAMIC BRAKES
NT DRAG CHUTES
NT LEADING EDGE SLATS
NT SPOILERS
NT TRAILING EDGE FLAPS
NT WING FLAPS
Measurements in the flow field of a cylinder with a laser transit anemometer and a drag rake in the Langley 0.3 m transonic cryogenic tunnel
[NASA-TM-86399] 14 p2305 N85-24270

DRAG EFFECT
U DRAG

DRAG MEASUREMENT
Flow through very porous screens
[NASA-TP-2436] 11 p1631 N85-20270
Determination of the drag of free flying particles in supersonic flow with a pulsed laser 12 p1773 N85-21129
Cone drag in the transition from continuum to free molecular flow
[OUEL-1538/84] 20 p3390 N85-31023

DRAG REDUCTION
Force and moment measurements on a 74 deg delta wing with an apex flap
[NASA-CR-166081] 02 p0134 N85-10918
Aircraft surface coatings
[NASA-CR-3661] 02 p0137 N85-10935
Design, manufacture, and testing of compliant coatings for reduction of turbulent drag
[AD-A145510] 02 p0186 N85-11323
Numerical simulations of compliant material response to turbulent flow, revision 1
[AD-A145801] 03 p0372 N85-12373
Installed nacelle drag-improvement tests of an M = 0.8 turboprop transport configuration
[NASA-TM-84302] 07 p0902 N85-15718
Aircraft drag reduction technology 08 p1070 N85-16782
Drag reduction due to boundary-layer control by combined blowing and suction 08 p1070 N85-16785
Turbulent drag reduction research 08 p1071 N85-16788
On the relaxation of a turbulent boundary layer after an encounter with a forward facing step 08 p1071 N85-16789
Full scale experiments into the use of large eddy breakup devices for drag reduction on aircraft 08 p1071 N85-16790
Pneumatic turbulators: A device for drag reduction at Reynolds numbers below 5 million 08 p1071 N85-16791
Study of winglets applied to biplanes
[NASA-TM-86350] 08 p1083 N85-16862
A survey of the turbulent drag reduction using passive devices
[NMI-R-193] 11 p1630 N85-20268
Drag-free satellite simulator
[REPT-815] 12 p1789 N85-21229
Numerical study of large-eddy breakup and its effect on the drag characteristics of boundary layers
[NASA-CR-3984] 12 p1797 N85-21272
Investigation of the initial events in biofouling
[AD-A149995] 12 p1900 N85-21927
Mercedes-Benz auto 2000 achieves low drag coefficient 15 p2530 N85-25602
Exploratory wind-tunnel investigation of a wingtip-mounted vortex turbine for vortex energy recovery
[NASA-TP-2468] 16 p2699 N85-26867
Demonstration of relaxed stability on a commercial transport 16 p2713 N85-26745
Realisation of relaxed static stability on a commercial transport 16 p2713 N85-26746
Numerical study of porous airfoils in transonic flow
[NASA-TM-86713] 17 p2892 N85-27828
Combined riblet and LEBU drag reduction system
[NASA-CASE-LAR-13266-1] 18 p3058 N85-28922
A method for predicting additive drag reduction from small-diameter pipe flows
[AD-A154411] 19 p3266 N85-30254
Injection of drag reducing additives into turbulent water flows: Two-component velocity measurements and mixing length model predictions
[AD-A154604] 21 p3583 N85-32274
Experiments on the influence of active walls on the initial amplitudes and growths of instability waves
[AD-A154830] 21 p3583 N85-32275
An automated technique for encasing specific payloads with low-drag fairings 24 p4063 N85-35183
Wingtip vortex propeller
[NASA-CASE-LAR-13019-1] 24 p4065 N85-35194

DRAGULATORS
U BRAKES (FOR ARRESTING MOTION)
U DRAG DEVICES

DRAINAGE
Systematic data interpretation of remote sensing in the reception of hydrocarbons, volume 1
[E85-10008] 02 p0215 N85-11421
Geothermal assessment of the lower Bear River drainage and northern East Shore ground-water areas, Box Elder County, Utah
[DE84-017358] 04 p0526 N85-13368
Comparison between tracer measurements and model calculations for nighttime drainage flows in complex terrain
[DE84-014709] 04 p0539 N85-13431
Effect of lithology and climate on the morphology of drainage basins in northwestern Colorado
[PB84-228238] 06 p0828 N85-15258
Statistical relationships between meteorological data stations and implications to diagnostic models in complex terrain
[DE84-014360] 06 p0839 N85-15328
Retrieval procedures for hydrologic data from ARS (Agricultural Research Service) experimental watersheds in the US (REPHLEX)
[PB85-111326/GAR] 09 p1402 N85-18828
Nationwide urban runoff program. Relationship of urban runoff to land use and groundwater resources
[PB85-114692] 10 p1506 N85-19505
The ASCOT Data Analysis Workshop
[DE85-004407] 13 p2139 N85-23283

A comparison of terrestrial saltation flux in the laboratory and the field 13 p2189 N85-23582
Fluvial drainage basins and valley networks: Eastern Margaritifer Sinus, Mars 13 p2190 N85-23586
Surface hydrologic characteristics of proposed repository locations in the Palo Duro Basin of the Texas Panhandle
[DE85-010530] 18 p3126 N85-29355
Flood-runoff forecasting with HEC1F
[AD-A154286] 19 p3300 N85-30456
Categorization of nocturnal drainage flows within the Brush Creek valley in western Colorado and the variability of sigma theta in complex terrain
[DE85-011291] 19 p3300 N85-30461
Synthetic rainfall and its use in hydrologic modeling 19 p3314 N85-30542
Geomorphic analyses from space imagery 21 p3603 N85-32374
New estimating procedures for surface runoff, sediment yield, and contaminant transport in Los Alamos County, New Mexico
[DE85-011890] 21 p3606 N85-32393
Long-term exposure of (238) PuO2 to a terrestrial environment, volume 3
[DE85-011696] 22 p3840 N85-33781
Hydrology
[PB85-182954] 23 p3944 N85-34440

DRAINAGE PATTERNS
Utilization of LANDSAT orbital imagery in the soil survey processes at Rio Grande do Norte state
[E85-10009] 02 p0216 N85-11422
Geologic utility of LANSDAT-4 TM data — Death Valley, California and the Silver Bell area of southern Arizona 13 p2118 N85-23192
Nationwide Urban Runoff Project, Champaign, Illinois: The biological impact of urban runoff on the Saline Branch Drainage Ditch and Boneyard Creek
[PB85-150274] 14 p2348 N85-24515
Example of joint use of data from surface studies and space photographs in investigating dynamics of zone of North Zeravshan seismogenic faults 15 p2485 N85-25342

DRAINING
U DRAINAGE

DRAWINGS
NT ENGINEERING DRAWINGS
Intersection of three-dimensional geometric surfaces
[NASA-TP-2454] 20 p3513 N85-31639

DREDGED MATERIALS
Improved techniques for removal of sediments contaminated with hazardous materials
[PB85-116093] 11 p1679 N85-20580

DRIFT
Drift characteristics of northeastern Bering Sea ice during 1982
[PB84-213682] 01 p0089 N85-10604
Acceleration of an electron ring in a modified betatron with transverse pressure
[AD-A148626] 08 p1221 N85-17688
Simulation of the ion-beam-driven drift instability in a magnetic trap, 1
[AD-A149451] 10 p1452 N85-19147
Simulation of the ion-beam-driven drift instability in a magnetic trap, 2
[AD-A149452] 10 p1554 N85-19798
A diffusion process and its application to detecting a change in the drift of Brownian motion
[AD-A150096] 12 p1926 N85-22100
Interpreting refracted waves method data on basis of automated determination of seismic drift 14 p2343 N85-24486

DRIFT (INSTRUMENTATION)
Evaluation of the stochastic drift of rate-integrating gyros as preparation for the analysis of laser gyro drift measurements
[ESA-TT-827] 05 p0630 N85-14099
ATA probe beam experiment
[DE84-016017] 06 p0862 N85-15477
First tests on the astrometric performance of the new PDS1010G at Hamburg Observatory — granite microdensitometer 07 p0955 N85-16135
Drift fields and boundary conditions at grain boundaries in bipolar P/N junction silicon devices 13 p2062 N85-22879
An investigation of tropospheric ions 16 p2823 N85-27412
An inexpensive radar-responding relocation device for drifting oceanographic instruments
[AD-A152170] 16 p2836 N85-27505
Measurements of laser gyro errors as a function of the beam path
[DFVLR-FB-85-02] 17 p2969 N85-28336
Technology development for thin-film-trace humidity sensors
[BMFT-FB-T-84-268] 17 p2969 N85-28338
Relationship between Allan variances and Kalman Filter parameters 18 p3107 N85-29236
Performance data of US Naval Observatory VLG-11 hydrogen masers since September, 1983 18 p3108 N85-29244
Criteria for optimum spacing of spaced antenna, part 3.2A 21 p3620 N85-32491
Problems and solutions in analyzing partial-reflection drift data by correlation techniques 21 p3626 N85-32529
Recording small frequency drifts of microwave oscillators 22 p3771 N85-33372
Improved method for the stabilization of NaI-photomultiplier gamma detectors against thermal and other drift
[DE85-011830] 23 p3970 N85-34613

DRIFT RATE
Evaluation of the stochastic drift of rate-integrating gyros as preparation for the analysis of laser gyro drift measurements
[ESA-TT-827] 05 p0639 N85-14099
Transport properties and distribution functions in 3-5 semiconductors
[AD-A147525] 07 p1049 N85-16660
MIZEX. A program for mesoscale Air-Ice-Ocean interaction experiments in arctic marginal ice zones. 4: Initial results and analysis from MIZEX 83
[AD-A148255] 08 p1173 N85-17399
The analysis of spaced sensor records by correlation techniques 08 p1184 N85-17485
New instabilities in line driven winds 08 p1235 N85-17785
Suspension torques on a gimballed electrostatically supported gyroscope and requirements on the gyroscope and spacecraft for the relativity gyroscope experiment 12 p1851 N85-21606
The use of the ARGOS system for the study of the drift of Antarctic icebergs 14 p2240 N85-23690
Drift mobilities by time-of-flight methods and time-dependent photoltransport in the nanosecond regime in amorphous semiconductors
[DE85-008729] 18 p3194 N85-29815
Moving random surfaces and correlation analysis
[CRC-1384] 19 p3253 N85-30168
Test evaluation of the Honeywell GG1111 Single-Degree-of-Freedom (SDF) strapdown gyroscope
[AD-A154768] 21 p3589 N85-32307
Guiding center distribution function and longitudinal invariant 23 p3978 N85-34663
Notes on drift theory
[SH-4.2-3] 23 p4006 N85-34841
Drift and observations in cosmic-ray modulation, 1
[SH-4.2-4] 23 p4007 N85-34842
Drift and observations in cosmic-ray modulation, 2
[SH-4.2-5] 23 p4007 N85-34843
The influence of nonstationarity of the solar activity and general solar field on modulation of cosmic rays
[SH-4.2-17] 23 p4008 N85-34854
Changes in the energy spectrum of anomalous oxygen and helium during 1977-1985
[SH-4.6-1] 23 p4039 N85-35039
On the anomalous component
[SH-4.6-6] 23 p4039 N85-35044
Fractional charge resolution in music 24 p4147 N85-35712
Proportional drift tubes for large area muon detectors
[HE-5.2-11] 24 p4203 N85-36087

DRILL BITS
Geothermal COMPAX drill bit development
[DE85-011353] 20 p3469 N85-31558

DRILLING
NT LASER DRILLING
Priorities for a national program of continental drilling for scientific purposes 04 p0534 N85-13418
The Georges Bank monitoring program 1983: Analysis of trace metals in bottom sediments
[CIRC-915] 05 p0688 N85-14423
Organogenic structures (submerged reefs) in Silhetian limestone of west Bengal basin 10 p1500 N85-19484
Shallow magma targets in the western US
[DE85-003274] 12 p1881 N85-21803
Evaluation of the blind hole drilling method for the measurement of residual stress
[AD-A151450] 15 p2579 N85-25905
Lost circulation in geothermal wells: Research and development status
[DE85-009836] 19 p3268 N85-30267
Geologic, technical, and economic sensitivity analysis in support of the GRI (Gase Research Institute) tight gas reservoirs project area
[PB85-192276] 22 p3802 N85-33559
Lithology and stratigraphy of drill holes completed during 1984 in LANL use areas of Yucca Flat, Nevada Test Site, volume 6
[DE85-010695] 22 p3815 N85-33631
Proposed resource evaluation plan, Salton Sea scientific drilling program
[DE85-011294] 22 p3815 N85-33633

DRILLS
Novel drives for machine tools 14 p2268 N85-24053

DROGUE PARACHUTES
U DRAG CHUTES

DROGUES
U TOWED BODIES

DRONE HELICOPTERS
U HELICOPTERS

DROP SIZE
Atmospheric extinction in critical environments
[AD-A146102] 03 p0396 N85-12527
Liquid fuel spray processes in high-pressure gas flow
[NASA-TM-86944] 12 p1844 N85-21570
Research study of droplet sizing technology leading to the development of an advanced droplet sizing system
[NASA-CR-174839] 12 p1850 N85-21604
Effects of temperature variation among droplets in an evaporating fuel spray 13 p2004 N85-22562
Experimental study of anisotropy of scattering of radar signals by clouds and precipitation 14 p2340 N85-24473
Limiting factor of flame propagation in mono-sized sprays of low-volatility fuels
[NAL-TR-839T] 15 p2521 N85-25536
Some further aspects of the influence of raindrop-size distributions on millimeter-wave propagation
[PB85-168334] 18 p3092 N85-29138
Particle sizing from forward scattered light at two angles using a Variable-Focal-Length optical system
[AD-A154164] 20 p3533 N85-31980
A relationship between cloud droplet size and CCN critical supersaturation 21 p3649 N85-32677
Fog activation and supersaturation 21 p3650 N85-32678
On the question to the effect of surfactants on the spectrum of cloud drops in the process of their condensation growth 21 p3650 N85-32679
The distribution of giant salt nuclei inside and outside cloud over the basin of Xin and Jiang 21 p3650 N85-32681

DROP TESTS
Analysis of a transport fuselage section drop test 01 p0060 N85-10400
Research relative to the development of a cryogenic microwave cavity gradiometer for orbital use
[NASA-CR-174249] 07 p0962 N85-16095
Results of an EPRG round robin test programme with DWTT specimens — drop weight test (DWTT);pipe steels
[ERS-E.365] 09 p1341 N85-18432
Direct comparison of unloading compliance and potential drop techniques in J-integral testing
[DE85-001550] 11 p1650 N85-20392
Impact studies of a 1/3-scale model of an air cushion vehicle
[NASA-TM-86360] 14 p2218 N85-23757
B-52B/DTV (Drop Test Vehicle) flight test results: Drop test missions
[NASA-CR-171530] 19 p3215 N85-29834
Graphite/PMR polyimide composites with improved toughness
[NASA-TM-87081] 21 p3561 N85-32148

DROP TOWERS
Results of the technical exchange agreement between NASA and DuPont on the containerless drop tube solidification of NiAl3
[NASA-TM-86473] 01 p0014 N85-10087
Microgravity containerless processing in long drop tubes 02 p0153 N85-11037
Containerless drop tube solidification and grain refinement of NiAl3 02 p0154 N85-11042
Critical point wetting drop tower experiment 02 p0155 N85-11045

DROP TUBES
U DROP TOWERS

DROP WEIGHT TESTS
U DROP TESTS

DROPS (LIQUIDS)
Single-drop impact damage prediction for low density, coated ceramic materials — rain erosion 01 p0061 N85-10402
Interaction of a stream of dielectric spheres in an electric field in a high vacuum
[DE84-014714] 01 p0115 N85-10782
Numerical simulations of fuel droplet flows using a Lagrangian triangular mesh
[AD-A146067] 03 p0362 N85-12320
Aircraft flow effects on cloud droplet images and concentrations
[AD-A146176] 03 p0396 N85-12529

Turbulent shear fields for dispersion of aqueous drops in organic liquids and application to gel-sphere processes
[DE84-016582] 06 p0809 N85-15141
Experimental study of the spray characteristics of a research airblast atomizer
[NASA-TM-86911] 07 p0904 N85-15727
The structure of dilute combusting sprays
[NASA-CR-174838] 07 p0905 N85-15728
Swirling turbulent spray group combustion
09 p1289 N85-18095
Measurement of drop-size distributions with the aid of a scattered light particle size counting analyser
[BLL-TRANS-WH-620-(9091.9F)] 09 p1317 N85-18278
Application of scattered light particle size counting analysis to the determination of wide drop size distributions
[BLL-TRANS-WH-619-(9091.9F)] 09 p1317 N85-18279
Effect of water vapor and water droplets on the RAM-1 (Real-Time Aerosol Monitor): Preliminary results
[PB85-109429] 11 p1637 N85-20313
Gasification of boron oxide drops and boron slurry agglomerates in combustion gases
13 p1999 N85-22529
Effects of temperature variation among droplets in an evaporating fuel spray 13 p2004 N85-22582
Size and velocity distributions of particles and droplets in spray combustion systems
[AD-A150355] 13 p2017 N85-22648
Advanced radiator concepts
[NASA-TM-87008] 14 p2300 N85-24245
CON1D: A computer program for calculating spherically symmetric droplet combustion
[DE85-005604] 15 p2507 N85-25464
Experimental investigation of annular air curtain domes
[UTIAS-288] 15 p2521 N85-25543
Study of the explosive combustion of drops of sulphur at high temperatures
[HSE-TRANS-11182] 19 p3252 N85-30163
Laser-induced fluorescence measurement of vapor concentration surrounding evaporating droplets
[DE85-009409] 19 p3277 N85-30320
Droplet deposition in vertical two-phase flow
[CFD/84/22] 20 p3456 N85-31460
Instability and chaotic behavior in a free-surface flow
[AD-A154879] 21 p3584 N85-32279
Ice nucleation of single water droplet by silver iodide: A laboratory observation 21 p3643 N85-32630
Cloud droplet nucleation and initial growth derived from lidar depolarization studies 21 p3644 N85-32635
Characterization of insoluble particles associated with cloud droplets 21 p3652 N85-32693
The measured rate of condensation nucleation to droplets using the techniques of chemical kinetics
21 p3652 N85-32694

DROUGHT
Forecast of the northeastern drought by the method of periodicities: Use and abuses
[INPE-3109-PRE/508] 02 p0230 N85-11502
Droughts and floods in South America due to the 1982-83 El Nino-southern oscillation episode
[INPE-3408-PRE/677] 09 p1357 N85-18535
Planetary scale circulation anomalies associated with droughts over northeast Brazil
[INPE-3351-PRE/630] 10 p1518 N85-19570
Large scale circulation anomalies and prediction of northeast Brazil droughts
[INPE-3405-PRE/674] 10 p1518 N85-19571
On the 1983 drought in northeast Brazil
[INPE-3412-PRE/678] 16 p2834 N85-27476
An appraisal of the duration of the recent drought in northeast Brazil and a forecast for 1985
[INPE-3477-PRE/720] 16 p2834 N85-27478
Preliminary results from numerical experiments on the summer 1980 heat wave and drought
16 p3140 N85-29438
Northeast Brazil droughts and Atlantic SST anomalies
[INPE-3538-PRE/754] 19 p3316 N85-30583

DROUGHT CONDITIONS
U DROUGHT

DROWSINESS
U SLEEP

DRUG THERAPY
U CHEMOTHERAPY

DRUGS
NT ADRENERGICS
NT ANESTHETICS
NT ANTIADRENERGICS
NT ANTICHOLINERGICS
NT ANTIEMETICS AND ANTINAUSEANTS
NT ANTIRADIATION DRUGS
NT ATROPINE
NT CHLOROFORM
NT CORTISONE
NT CYCLOPROPANE
NT EPINEPHRINE
NT INSULIN
NT METHYL CHLORIDE
NT MOTION SICKNESS DRUGS
NT MUSCLE RELAXANTS
NT NOREPINEPHRINE
NT TRANQUILIZERS
China report: Science and technology
[JPRS-CST-84-025] 11 p1620 N85-20197
Review of US guide on medication and flying
12 p1904 N85-21958
Progress, goals in biotechnology summarized
17 p2945 N85-28182
Chemicals identified in human biological media, a data base, volume 6, part 1
[DE85-006768] 17 p2999 N85-28542
Effect of spironolactone on acute mountain sickness
[AD-A153760] 18 p3153 N85-29525
Interaction of opiate and phencyclidine derivatives with the acetylcholine receptor
[AD-A155119] 21 p3664 N85-32761
Effect of dibazol on parameters of nonspecific resistance of subjects in pressurized cabins
23 p3954 N85-34504

DRUMLINS
U GLACIAL DRIFT

DRUMS
Effect of air cavity on the vibration analysis of loaded drums 09 p1339 N85-18422

DRUMS (CONTAINERS)
Centrifugal castings of stainless steel spiked with radioactive tracers
[DE85-012003] 22 p3748 N85-33234
Drying of pulverized material with heated condensible vapor
[DE85-011656] 22 p3783 N85-33438

DRY CELLS
NT NICKEL ZINC BATTERIES

DRY FRICTION
Interactions among system stiffness, wear and vibrations 03 p0370 N85-12364
Thermomechanical cracking due to moving frictional loads
[AD-A146271] 03 p0373 N85-12381

DRYERS (EQUIPMENT)
U DRYING APPARATUS

DRYING
NT DEHUMIDIFICATION
NT DEHYDRATION
NT FREEZE DRYING
Numerical modelling of the drying of porous materials
[DE84-013056] 04 p0499 N85-13181
Improved uniformity of viscous textile fibers obtained by altering drying procedures 06 p0762 N85-14871
Modeling of transient heat pipe operation
[NASA-CR-175496] 12 p1844 N85-21571
New air-curing lacquer systems with high solids content
[BMFT-FB-T-85-005] 17 p2936 N85-28124
Thermomigration in porous media. Study of the development of a drying zone 20 p3456 N85-31462
The design and development of a spacecraft appendage tie down mechanism 22 p3797 N85-33522
Composite desiccant structure
[DE85-006400] 23 p3910 N85-34226
Nonsaturable microdryer
[DE85-005760] 23 p3946 N85-34457
Method of preparing thin porous sheets of ceramic material
[DE85-006399] 24 p4062 N85-35300

DRYING APPARATUS
Performance of the SERI parallel-passage dehumidifier
[DE85-000509] 11 p1672 N85-20536
Evaluation of pilot ESP used with a spray dryer FGD system at Pittsburgh Energy Technology Center, Bruceton, Pennsylvania
[DE85-011151] 22 p3748 N85-33217
Drying of pulverized material with heated condensible vapor
[DE85-011656] 22 p3783 N85-33438

DTA (ANALYSIS)
U THERMAL ANALYSIS

DTMB-111 GROUND EFFECT MACHINE
U GROUND EFFECT MACHINES

DTMB-430 GROUND EFFECT MACHINE
U GROUND EFFECT MACHINES

DUAL MODE PROPULSION
U HYBRID PROPULSION

DUAL SPIN SPACECRAFT
A dual spin space station design
20 p3408 N85-31152

DUALITY THEOREM
The role of duality in optimization problems involving entropy functionals, with applications to information theory
[AD-A152336] 17 p3026 N85-28713

DUCT GEOMETRY
Calculation of flow about posts and powerhead model — space shuttle main engine
[NASA-CR-171344] 10 p1483 N85-19362
Determination of boundary line between reverse jet and surrounding stream 13 p2043 N85-22789
An analytical and numerical study of the interaction of rarefaction waves with area changes in ducts. Part 2: Area enlargements
[UTIAS-273] 14 p2300 N85-24242
Analytical study of flow phenomena in SSME turnaround duct geometries 16 p2739 N85-29902

DUCTED BODIES
Time-averaged and time-dependent computations of isothermal flowfields in a centerbody combustor
[AD-A153682] 18 p3100 N85-29189

DUCTED FANS
Numerical analyses in aerodynamic design of aero-engine fan 16 p2682 N85-26618

DUCTED FLOW
NT KNUDSEN FLOW
Vertical channel free convection for a power law fluid with a constant heat flux
[DE84-014551] 01 p0047 N85-10311
A comparison of evaporation duct models for IREPS (Integrated Refractive Effects Prediction System)
[AD-A146471] 06 p0799 N85-15103
Shock waves in transonic flows at moderate Reynolds Number 08 p1076 N85-16823
Computation of flow and heat transfer in flow around a 180 deg bend
[AD-A148065] 08 p1162 N85-17330
Secondary flow in cascades
[AD-A148415] 08 p1162 N85-17333
Combustion driven oscillation of ducted diffusion flame
09 p1289 N85-18094
Turbulent jet flow in a channel with a circulation region
09 p1306 N85-18218
An experimental investigation of confined, multiple, turbulent jet mixing with recirculation — flow distribution in combustors with injection plates
15 p2555 N85-25784
Application of computational fluid dynamics to complex inlet ducts
[NASA-TM-87060] 19 p3265 N85-30247

DUCTED ROCKET ENGINES
Integral boost, heat protection, port covers and transition 07 p0918 N85-15813
Mixing chemical reaction and flow field development in ducted rockets
[DE85-002710] 11 p1591 N85-20009

DUCTILITY
Material degradation in heavy steel plates caused by bending with a laser
[AD-A144784] 01 p0052 N85-10343
Design of strong, ductile, duplex low alloy steels
02 p0177 N85-11189
Structural uses for ductile ordered alloys. Report of the committee on application potential for ductile ordered alloys
[AD-A146313] 03 p0332 N85-12139
Stress-driven solute enrichment of crack-tips during low ductility intergranular fracture of low-alloy steel
[AERE-R-11120] 03 p0333 N85-12150
Structure and ductility of fracture of joints produced by electron-beam welding of VT6ch titanium alloy parts
03 p0351 N85-12261
A comparison of methods for predicting ductile crack growth instability
[AERE-R-11199] 03 p0374 N85-12387
The effect of cross-link density on the toughening mechanism of elastomer-modified epoxies
04 p0465 N85-12951
Toughening mechanism in elastomer-modified epoxy resins, part 2
[NASA-CR-3852] 04 p0478 N85-13048
Tensile properties and swelling of 20%-cold-worked Type 316 stainless steel irradiated in HFIR
[DE84-014080] 05 p0617 N85-13048
Low cycle fatigue strength for multiaxial loading of ductile materials 05 p0649 N85-14167
Development and characterization of ductile Long-Range-Ordered (LRO) alloys (Fe,Co, Ni)3V for high-temperature structural use
[DE84-016750] 06 p0769 N85-14921
Effect of crack-tip region constraint on fracture in the ductile-to-brittle transition
[PB84-237395] 06 p0770 N85-14926
Effect of input distributions on the probabilistic fracture mechanics analysis of reactor pressure vessels
[DE85-000832] 11 p1652 N85-20403

Creep crack growth in ductile alloys
[DE85-003937] 13 p2023 N85-22676
Analysis of strength and ductility of welded joints in AMts5 and AMg5 aluminum alloys
13 p2033 N85-22737
Effect of oxygen on mechanical properties of Nb-V alloy
[DE85-002661] 14 p2256 N85-23982
Mechanical properties of welded joints of 1201 aluminum alloy 15 p2502 N85-25431
Design of ductile polycrystaline NiAl alloys
[DE85-005572] 15 p2511 N85-25491
Weldability of NiAl-type aluminide alloys
[DE85-006932] 15 p2512 N85-25496
Ductility equation for porous metals and its linearization
[BLL-M-36118-(5826.4)] 16 p2748 N85-26958
On the accurate representation of large strain non-proportional plastic flow in ductile materials
[DE85-007106] 16 p2801 N85-27273
High-strength weldable steel 03G4N2MAF Sh with improved ductility
[BLL-BISI-TRANS-22233-(9022.06)]
17 p2924 N85-28031
Preparation of metal for cold upsetting
[BLL-BISI-TRANS-22383-(9022.06)]
17 p2926 N85-28043
Assessing the machinability of gearwheel steels during manufacture
[BLL-BISI-TRANS-22343-(9002.06)]
17 p2973 N85-28365
Surface degradation of ductile metal in elevated temperature gas-particle streams
[DE85-008428] 18 p3074 N85-29017
Load-carrying capabilities of refractory alloys for space reactor power applications
[DE85-010566] 19 p3240 N85-30067
Comparative analysis of laboratory and fullscale experimental data for metal flow displacements and speeds
[BLL-M-36288-(5826.4)] 20 p3430 N85-31276
Fatigue-crack growth and ductile fracture toughness behavior of ASTM A387 Grade 91 steel
[DE85-008495] 20 p3431 N85-31286
Numerical study of ductile rupture in plane deformations
[ONERA-RT-23/7169-RY-072-R]
20 p3469 N85-31557
Numerical study of tensile fracture in plane stress
[ONERA-RT-22/7169-RY-070-R]
20 p3470 N85-31563
Metallurgical origins of fracture toughness and microstructure and fracture toughness of an HSLA (High-Strength/Low-Alloy) steel
[AD-A155530] 21 p3567 N85-32187
Development of improved dynamic failure models
[AD-A155586] 21 p3600 N85-32354
Metallic glass composition
[DE85-011504] 22 p3751 N85-33253

DUCTS
NT ACOUSTIC DUCTS
NT AIR DUCTS
NT ANNULAR DUCTS
Vortex-generating coolant-flow-passage design for increased film-cooling effectiveness and surface coverage
[NASA-TP-2388] 03 p0361 N85-12314
Laminar flame propagation/quench for a parallel-wall duct
[DE84-009773] 04 p0470 N85-12993
Modeling the aerodynamics in a system of continuous channels and experimentation procedure
[BLL-M-35923-(5826.4)] 05 p0634 N85-14067
The Shock and Vibration Digest, volume 16, no. 10
[AD-A147588] 09 p1331 N85-18361
Sound transmission in ducts 09 p1331 N85-18362
Basic studies of multiple free and confined jets
[AD-A149556] 10 p1485 N85-19374
An experimental investigation of an underexpanded rectangular jet ejector
[AD-A149656] 12 p1779 N85-21170
Turbulent convecting flow in a square duct with a 180 deg bend: An experimental and numerical study
[AD-A149669] 12 p1846 N85-21583
High frequency estimation of 2-dimensional cavity scattering
[AD-A151697] 15 p2542 N85-25696
Vortex shedding flowmeters for liquids at high flow velocities 16 p2740 N85-26906
LDA study of non-steady flame propagation in a constant volume duct
[DE85-007233] 16 p2745 N85-26948
The hydrosynclastic infundibulum
[AD-A153849] 18 p3100 N85-29192
Experimental investigation of turbulent heat transfer in straight and curved rectangular ducts
[AD-A154413] 19 p3266 N85-30255
Mechanical connection for a tubular assembly
[DE85-011580] 22 p3792 N85-33497
Monte Carlo and discrete ordinates calculations of 14-MeV neturons streaming through a stainless-steel duct (L/D = 4.6): Comparison with experiment
[DE85-011423] 22 p3840 N85-33776
Block-implicit calculations of three-dimensional laminar flow in strongly curved ducts
[DE85-003047] 23 p3931 N85-34363

DUMMY LOADS
U IMPEDANCE
U LOADING
U OUTPUT

DUNES
Surface soil moisture measurements of the White Sands, New Mexico
[NOAA-TM-NESDIS-7] 02 p0219 N85-11441
Application of SIR-B data for groundwater exploration in the Arabian shield and sand-drift monitoring in the AN Nafud and Al Jafurah fringe areas, Kingdom of Saudi Arabia 08 p1144 N85-17214
Microdunes and other aeolian bedforms on Venus: Wind tunnel simulations 13 p2189 N85-23584
Planetary analogs in Antarctica: Mars
13 p2193 N85-23604

DUNGEYS WIND SHEAR MECHANISM
U WIND SHEAR

DUPLEX OPERATION
Design of strong, ductile, duplex low alloy steels
02 p0177 N85-11189
Evalustion of 7010 aluminium alloy extruded tube in the T76 condition
[BR92019] 11 p1596 N85-20039
Combined processing method and matched filter for discrete composite frequency phase-shift keyed signal
13 p2070 N85-22931

DUPLICATING
U REPRODUCTION (COPYING)

DURABILITY
Investigation of chemical durability mechanisms in fluoride glasses
[AD-A145420] 02 p0186 N85-11241
F-16 force management, yesterday, today and tomorrow 07 p0895 N85-15674
Design and test requirements for development of today's engines 07 p0906 N85-15737
Overview of the AGARD SMP activities on turbine engine materials technology in the 1972 - 1982 period
07 p0906 N85-15738
Cyclic endurance testing of the RB211-22B cast HP turbine blade 07 p0908 N85-15747
Experimental test program for evaluation of solid lubricant coating as applied to compliant foil gas bearings to 315 deg C
[NASA-CR-174837] 07 p0930 N85-15895
NBS (National Bureau of Standards) solar collector durability-reliability test program
[PB85-113603/GAR] 09 p1346 N85-18469
Long term durability of urea formaldehyde glued joints removed from Vampire aircraft
[AD-A149053] 10 p1424 N85-18985
Influence of volumetric fiber content on some matrix damage factors during thermal cycling of tungsten-El 765 composite 10 p1443 N85-19097
USSR report: Materials science and metallurgy
[JPRS-UMS-84-006] 11 p1597 N85-20044
Structure-phase state and properties of high-durability VAL8 alloy 11 p1597 N85-20046
New method for studying surface crack growth in laminated polymer composite materials
11 p1598 N85-20051
Predicting stability of full-scale composite constructions of the basis of stiffness 11 p1599 N85-20054
Evaluation of features of reinforcing fibers by testing bundles 11 p1599 N85-20059
Kinetics of reaction of metals and non-metals during diffusion welding 11 p1602 N85-20076
Effect of macrostructure on durability of polycrystalline graphite 11 p1605 N85-20091
Prediction of the resistance of structural materials to cavitation erosion
[BLL-DRIC-TRANS-7435-(3623.66)]
13 p2020 N85-22659
Temperature effects of heterogenized annealing on structure and properties of V95 aluminum alloy
13 p2025 N85-22692
Estimate of fatigue stability of gas-turbine engine compressor vanes in probabilistic aspect
14 p2287 N85-24169
Generation of marker lines on fatigue fracture surfaces 14 p2319 N85-24328
Possible use of rapid heating for improving mechanical properties of titanium alloys 15 p2498 N85-25409
Effect of annealing procedures on structure and properties of VT6 alloy with initial large-grained structure
15 p2498 N85-25410
Effect of aluminum on nature of titanium alloy failure
15 p2498 N85-25411
Effect of protective atmosphere composition on durability of welded joints of niobium alloys
15 p2502 N85-25432
Durability of Aramid reinforced aluminum laminate (ARALL)
[VTH-LR-423] 16 p2744 N85-26933
Documentation and solar cell modules
[NASA-CR-175769] 16 p2818 N85-27384
Properties of polyethylene gas piping materials
[PB85-187045] 18 p3082 N85-29068
Effect of thermochemical processing on fatigue resistance of titanium alloys 19 p3244 N85-30112
Effect of heating temperature in a vacuum on state of surface layers of welded OT4 titanium alloy
19 p3245 N85-30123
Vacuum pressure welding of commercial titanium with 2Kh13 and 12Kh18N10T steels
19 p3246 N85-30124
Computational methods in advanced stress and durability analyses
[AD-A154119] 19 p3286 N85-30375
Durability of reinforced hard-alloy draw plates
[BLL-M-36278-(5826.4)] 20 p3465 N85-31526
Thin-film reliability and engineering overview
21 p3612 N85-32450
Durability of oxygen sensors
[PB85-183093] 22 p3789 N85-33477

DURATION
U TIME

DURENE
Mononitration of durene
[NASA-TM-77774] 06 p0765 N85-14892

DUST
NT COSMIC DUST
NT INTERPLANETARY DUST
NT ZODIACAL DUST
Dust properties determined from backscattering in the interplanetary and interstellar medium
03 p0446 N85-12838
A method of making the gas-electric removal of highly dispersed particles more effective
[BLL-M-36030-(5826.4)] 06 p0765 N85-14890
Antisoiling technology: Theories of surface soiling and performance of antisoiling surface coatings
[NASA-CR-174274] 07 p0991 N85-16296
Interaction of large meteoroids with the atmosphere
11 p1656 N85-20431
Theoretical and experimental investigations of dust loaded flow fields in industrial halls
[BMFT-FB-HA-84-044] 12 p1819 N85-21411
Seasonal and secular variation of the Solis Lacus albedo feature: Relation to the Martian dust-transport cycle
13 p2188 N85-23576
Transformation of polar ice sublimate residue into Martian circumpolar sand 13 p2189 N85-23580
Near-nucleus studies of Comet Halley
14 p2435 N85-25018
Research on atmospheric dust formations using satellite observation data 15 p2485 N85-25339
Skywave radar detectability of volcanic aerosols
[AD-A151448] 15 p2542 N85-25694
The behavior of the atmosphere in the desert planetary boundary layer
[AD-A151266] 15 p2592 N85-25977
Multivalued electrostatic potentials; chance or necessity for the charge of solid particles near Saturn?
15 p2677 N85-26529
The gravito-electrodynamics of charged dust in planetary ring systems 15 p2677 N85-26531
Program RNTHR/2: An HP-41 C program for the calculation of RaA, RaB, and RaC concentrations in air based on three measurements of an air-dust sample
[IRI-190-83-10] 18 p3134 N85-29412
Technical guide for estimating fugitive dust impacts from coal handling operations, volume 2
[DE85-010939] 19 p3309 N85-30514
Technical guide for estimating fugitive dust impacts from coal handling operations. Volume 1: Project summary
[DE85-010948] 19 p3309 N85-30515
Ice-forming efficiency of the soluble and insoluble portions of dust contained in snow
21 p3643 N85-32631
Sahara Desert dust transport to the south
21 p3648 N85-32668
Distinctions in formation of microflora on construction materials used in habitable pressurized compartments
22 p3823 N85-33683

DUST COLLECTORS
A Mars dust sample return mission
[CNES-CT/PMF/APS/EMS-177]
04 p0459 N85-12915

Acoustic agglomeration methods and apparatus
[NASA-CASE-NPO-15466-1] 12 p1927 N85-22104
DUST STORMS
A Mars dust sample return mission
[CNES-CT/PMF/APS/EMS-177] 04 p0459 N85-12915
Observed changes at Viking Lander 1 13 p2188 N85-23575
Seasonal and secular variation of the Solis Lacus albedo feature: Relation to the Martian dust-transport cycle 13 p2188 N85-23576
The origin of regional dust deposits on Mars 13 p2188 N85-23578
Dust devils on Mars 15 p2683 N85-26573
The influence of global dust storms on the mean seasonal daily insolations at the Martian surface
[AERONOMICA-ACTA-A-269-1984] 18 p3203 N85-29868
Hadley circulation in planetary atmospheres 20 p3546 N85-32067
DWARF NOVAE
Combined ultraviolet studies of astronomical sources
[NASA-CR-174361] 09 p1413 N85-18910
FP Cygni profiles in HL CMa 11 p1752 N85-21022
Photoelectric observations of the dwarf nova VW Hydri during the November 1977 supermaximum
[REPT-97] 15 p2667 N85-26481
Winds in cataclysmic variable stars
[DE85-006708] 15 p2669 N85-26470
DWARF STARS
NT DWARF NOVAE
NT FLARE STARS
NT RED DWARF STARS
NT SUBDWARF STARS
NT WHITE DWARF STARS
Simultaneous photometry and radial velocities of dwarf cepheids and Delta Scuti stars 01 p0128 N85-10878
A spectroscopic survey of 113 nearby red dwarf stars 01 p0129 N85-10886
Detection of narrow C 4 and Si 4 absorption features in spectra of stars within 200 pc f the Sun 06 p0676 N85-15584
Theoretical studies of chromospheres and winds in cool stars
[NASA-CR-174204] 06 p0680 N85-15596
Evidence for non-radiative activity in stars with T sub eff 10000 K 08 p1231 N85-17757
Theory tested by means of the stars — viability of the alpha-omega dynamo model 08 p1233 N85-17770
Stellar granulation 14 p2451 N85-25132
DWELL
An investigation of elevated temperature fatigue crack initiation in 2 and 1/4 cR-1 MO low alloy steel
[AD-A150670] 14 p2255 N85-23973
DYE LASERS
Manual for Raman cells
[NASA-TM-77756] 01 p0052 N85-10342
A high resolution spectroscopic study of the oxygen molecule
[NASA-CR-174061] 02 p0172 N85-11150
Multifrequency lidar based on dye laser 02 p0262 N85-11715
Narrowband tunable dye laser with amplifier pumped by powerful nitrogen laser 02 p0262 N85-11716
Study in molecular lasers
[AD-A148248] 08 p1166 N85-17357
Influence of structure of thiopyrilocyanic dyes on output characteristics of passive mode-locked laser 11 p1717 N85-20801
Investigation of dye lasers pumped by high-power KrF laser radiation 11 p1718 N85-20806
Chemical stabilization of laser dyes
[AD-A150451] 13 p2066 N85-23076
Elementary processes of electronically excited particles. Part 5: Deactivation of CHF (A1a' (O, V'2, O) after excitation by a pulsed dye laser
[MPIS-13/1984] 14 p2420 N85-24930
Experimental report on a fiber optic light guide made by Galileo Electro-Optics Corporation
[DE85-006161] 14 p2421 N85-24941
Linewidth and bandwidth measurements of the q-branch of h2 using CW coherent anti-Stokes Raman spectroscopy
[AD-A151888] 15 p2506 N85-25458
Electric discharge excitation and energy source integration
[AD-A151502] 15 p2562 N85-25808
Raman studies of surface temperature in laser-heated semiconductors
[AD-A151377] 15 p2659 N85-26412
A study of mode-locked argon ion-dye laser systems 16 p2789 N85-27205
Study on a prismatic dye vat — laser systems
[CERT-2/6124-04-RO] 18 p2791 N85-27217
Intense excitation source for high power laser
[AD-A153424] 18 p3112 N85-29267
Intense ion beam diode diagnostics using a tunable dye laser
[DE85-006079] 18 p3113 N85-29272
Measurement of radical species concentrations and polycyclic aromatic hydrocarbons in flames by fluorescence and absorption using a tunable dye laser
[DE85-006524] 18 p3113 N85-29274
Dye laser traveling wave amplifier
[NASA-CR-175089] 19 p3275 N85-30308
Instrumentation for particle-beams research using excited merging beams
[AD-A154155] 19 p3356 N85-30607
Spectral evolution of the pulse of a dual frequency dye laser
[CNES-83/168/T/CT/DRT/TIT/10] 20 p3461 N85-31497
Lasing on LIF:F(-)2 - dye centers with transverse pumping 21 p3684 N85-32690
Dynamics of emission from dye lasers employing synchronous pumping by limited picosecond pulse train 21 p3686 N85-32899
High-power two-frequency CW dye laser 21 p3686 N85-32900
Self Q-modulation and generation of short pulses in distributed-feedback lasers 21 p3687 N85-32907
Doppler spectrometer for measuring narrow photochemical gaps in inhomogeneously broadened spectra 21 p3689 N85-32921
Pulsed lasers for filming color holographic film images 22 p3781 N85-33426
Picosecond-pulse damage studies of diffraction gratings
[DE85-010785] 22 p3790 N85-33481
Fiber optics interface for a dye laser oscillator and method
[DE85-005765] 23 p3973 N85-34633
Infrared generation and wave-mixing studies in cesium
[DE85-012683] 24 p4083 N85-35304
DYES
NT METHYLENE BLUE
NT THIAZINE (TRADEMARK)
Efficiency of lasing dye media in pumping high-power radiation with nanosecond pulses 02 p0270 N85-11763
Fluorescent dyes for luminescent solar concentrators
[BMFT-FB-T-84-164] 04 p0480 N85-13061
Influence of structure of thiopyrilocyanic dyes on output characteristics of passive mode-locked laser 11 p1717 N85-20801
Investigation of dye lasers pumped by high-power KrF laser radiation 11 p1718 N85-20806
Spontaneous diffraction of sequence of supershort light pulses in dye solution 11 p1718 N85-20811
Practical surface methods 14 p2316 N85-24314
Comparison of a diffusion model with dye dispersion measurements to study turbulence in coastal waters
[INPE-3492-PRE/729] 16 p2836 N85-27504
The production of copper phthalocyanine and/or its derivatives
[NASA-TM-77629] 17 p2917 N85-27983
Chromophores with auxochrome-like function
[NASA-TM-77849] 20 p3421 N85-31233
Lasing on LIF:F(-)2 - dye centers with transverse pumping 21 p3684 N85-32690
Choice of optimum saturating absorber for YAG passive mode-locking laser 21 p3685 N85-32893
DYNAMIC CHARACTERISTICS
NT AERODYNAMIC DRAG
NT AERODYNAMIC STABILITY
NT AIRCRAFT STABILITY
NT ATTITUDE STABILITY
NT BOUNDARY LAYER STABILITY
NT COMBUSTION STABILITY
NT CONTROL STABILITY
NT DIRECTIONAL STABILITY
NT DRAG
NT DYNAMIC PRESSURE
NT DYNAMIC STABILITY
NT FLAME STABILITY
NT FLOW CHARACTERISTICS
NT FLOW DISTRIBUTION
NT FLOW STABILITY
NT FLOW VELOCITY
NT FREQUENCY STABILITY
NT FRICTION DRAG
NT GYROSCOPIC STABILITY
NT INTERFERENCE DRAG
NT INTERFERENCE LIFT
NT LATERAL STABILITY
NT LIFT
NT LONGITUDINAL STABILITY
NT LOW SPEED STABILITY
NT MAGNETOHYDRODYNAMIC STABILITY
NT MOTION STABILITY
NT ROTARY STABILITY
NT SATELLITE DRAG
NT SPACECRAFT STABILITY
NT TRANSIENT RESPONSE
NT VISCOUS DRAG
NT WAVE DRAG
NT WEIBEL INSTABILITY
NT ZERO LIFT
Structural analysis of the Space Shuttle Orbiter 01 p0061 N85-10401
Determination of the input-output characteristics of time-invariant memoryless nonlinear devices
[FUB-41-1983] 01 p0100 N85-10867
Singular perturbations, coherency and aggregation of dynamic systems
[DE84-014186] 01 p0114 N85-10772
High temperature static strain sensor development program 02 p0141 N85-10959
Control of lateral conjectory motion of spacecraft in atmosphere 02 p0160 N85-11085
Transfer function of multilayered magnetooptical space-time modulator 02 p0264 N85-11726
Static and dynamic characteristics of materials with beam-microstructure 03 p0370 N85-12361
Dynamic shear failure of shallow-buried flat-roofed reinforced concrete structures subjected to blast loading
[AD-A145974] 03 p0373 N85-12378
Analysis of dynamic characteristics and ways of development of bipolar main memory with miniaturization of integrated circuit elements 04 p0490 N85-13123
Hydrodynamic impeller stiffness, damping, and inertia in the rotordynamics of centrifugal flow pumps 05 p0643 N85-14125
Does McKuer's law hold for heart rate control via biofeedback display? 05 p0706 N85-14528
Power of deterministic thinking in machine tool accuracy
[DE85-001751] 07 p0974 N85-16186
Ice dynamics
[AD-A147376] 07 p0988 N85-16278
Prediction of dynamic stall characteristics using advanced non-linear panel methods
[AD-A148453] 08 p1078 N85-16836
Low cost gyrocompass
[AD-A148295] 08 p1082 N85-16857
Applications of molecular dynamics to the study of shock-induced chemistry
[AD-A148017] 08 p1121 N85-17066
International Conference on Luminescence
[AD-A148470] 08 p1223 N85-17701
The dynamic interaction between track and soil
[AD-P004274] 09 p1406 N85-18850
The research of driving wheel with movable lugs of the paddy field floating tractor
[AD-P004283] 09 p1407 N85-18860
The analysis on the dynamic performance of a single lug
[AD-P004289] 09 p1408 N85-18868
A tracked vehicle test plant for the simulation of dynamic operation
[AD-P004305] 09 p1410 N85-18882
Integrated Technology Rotor/Flight Research Rotor (ITR/FRR) concept definition
[NASA-CR-166445] 10 p1423 N85-18979
Oscillator development
[AD-A149699] 12 p1834 N85-21509
State-selected ion-molecule reaction dynamics
[AD-A150068] 12 p1926 N85-22115
Dynamics of space charge waves in the laser beat wave accelerator
[AD-A149688] 12 p1936 N85-22183
Dynamics of elliptical galaxies and the r sup 1/4 luminosity law 12 p1965 N85-22282
Comparison of dynamic-tension and constant-load strength characteristics of heat-resistant materials 13 p2030 N85-22722
A parmatric study of crater-saturation simulation 13 p2182 N85-23540
Solar Array Experiment (SAE) flight experience 14 p2236 N85-23861
Determining characteristics of optical radiation reflectors based on results of remote sensing 15 p2480 N85-25358
Dynamic characteristics of ac arc in welding aluminum alloys 15 p2500 N85-25424
Investigation of potential and viscous flow effects contributing to dynamic stall
[AD-A151698] 15 p2557 N85-25773
Ritz procedure for COSMIC/NASTRAN 15 p2575 N85-25877
Active control landing gear for ground loads alleviation 16 p2714 N85-26749
Rotordynamics 16 p2737 N85-26868
LFMR definition study
[AD-A153691] 18 p3090 N85-29126

Operation guiding light-scientific program and field plan. The pilot field experiment for NORDA project chemical dynamics in ocean frontal areas
[AD-A153765] 18 p3150 N85-29607
One- and two-electron transfer processes in ion-surface scattering
[AD-A154208] 19 p3353 N85-30782
Design of helicopter rotor blades for optimum dynamic characteristics
[NASA-CR-176078] 20 p3393 N85-31044
Flight-mechanics test with a restricted flying aircraft model in a wind tunnel
[ESA-TT-885] 20 p3394 N85-31053
Dynamic performance of several large antenna concepts 20 p3409 N85-31155
Space station configuration and flight dynamics identification 20 p3410 N85-31162
Sub-optimal control of nonlinear flexible space structures 20 p3414 N85-31190
Frequency domain control design of large space structures: A practical approach
20 p3415 N85-31192
Design of a physical model of the cochlea. Displacement sensor for small amplitudes in a highly viscous liquid
[STN-6] 20 p3507 N85-31602
Dynamic fracture behavior of structural materials
[AD-A154566] 21 p3596 N85-32345
The dynamics of slack marine cables
[AD-A155022] 21 p3599 N85-32349
Ductile fracture of dynamically loaded naval structures-compact tension specimen tests and analyses
[AD-A155472] 21 p3600 N85-32353
Hydrographic data from the OPTOMA (Ocean Prediction Through Observations, Modeling and Analysis) program: OPTOMA15, 24 January to 23 February 1985
[AD-A155012] 21 p3655 N85-32703
Analysis of flexible aircraft longitudinal dynamics and handling qualities. Volume 1: Analysis methods
[NASA-CR-177943-VOL-1] 24 p4086 N85-35202
Analysis of flexible aircraft longitudinal dynamics and handling qualities. Volume 2: Data
[NASA-CR-177943-VOL-2] 24 p4087 N85-35203
A new drawing technique for nylon 6 by reversible plasticization with iodine
[AD-A156272] 24 p4162 N85-35803

DYNAMIC CONTROL
Qualitative results for distributed systems with discrete damping and stiffness with application to control
[AD-A145525] 02 p0209 N85-11382
Experiments in control of flexible structures with uncertain parameters 05 p0602 N85-13837
Review of technical papers, appendix H
05 p0603 N85-13846
Dynamics and controls working group summary
05 p0604 N85-13854
Efficiency of programmed motion control systems
06 p0776 N85-14961
Aileron effectiveness for a subsonic transport model with a high-aspect-ratio supercritical wing
[NASA-TM-85674] 07 p0896 N85-15695
Power of deterministic thinking in machine tool accuracy
[DE85-001751] 07 p0974 N85-16188
The development of a microprocessor-controlled linearly-actuated valve assembly
[NASA-CR-174437] 10 p1491 N85-19415
Automatic speech recognition in severe environments
[PB85-121697] 12 p1830 N85-21490
Alternatives for jet engine control
[NASA-CR-175831] 16 p2709 N85-26713
Alternatives for jet engine control
[NASA-CR-175832] 16 p2709 N85-26714
Alternatives for jet engine control
[NASA-CR-175833] 16 p2709 N85-26715
A perspective on supersugmented flight control advantages and problems 16 p2712 N85-26733
The investigation of tethered satellite system dynamics
[NASA-CR-175855] 16 p2731 N85-26854
Dynamic considerations for control of closed life support systems 16 p3155 N85-29537
Dynamics and control of tethers in elliptical orbits
20 p3399 N85-31087
Experimental verification of identification algorithms for control of flexible structures 20 p3418 N85-31211
Numerical experimentation with maximum likelihood identification in static distributed systems
20 p3418 N85-31214
Bayesian vs MAP multiple model adaptive estimation for field of view expansion in tracking airborne targets
[AD-A155486] 21 p3679 N85-32855
Design of dynamic compensators of prescribed pattern
[BU-109] 24 p4142 N85-35674
Spreading the control complexity in decentralized control of interconnected systems
[BU-117] 24 p4144 N85-35688
Decentralized stabilization by high gain feedback
[BU-115] 24 p4144 N85-35689

DYNAMIC LOADS
NT AERODYNAMIC LOADS
NT BLAST LOADS
NT CYCLIC LOADS
NT GUST LOADS
NT IMPACT LOADS
NT LANDING LOADS
NT ROLLING CONTACT LOADS
NT SHOCK LOADS
NT THRUST LOADS
NT TRANSIENT LOADS
NT VIBRATORY LOADS
NT WING LOADING
Theoretical analysis of the dynamic behavior of structures with a passenger car as example
05 p0649 N85-14170
Characterization of fiber optic cables under large tensile loads
[DE84-016616] 05 p0651 N85-14180
Evaluation of operational loads to verify structural design 07 p0896 N85-15677
TUTOR (CL-41A) tail flight load survey
07 p0896 N85-15678
Tornado: Structural Usage Monitoring System (SUMS) 07 p0896 N85-15680
Flight parameters recording for structure fatigue life monitoring 07 p0896 N85-15682
USAF approach to airborne structural data recording: Airborne Data Acquisition Multifunction System (ADAMS)
07 p0897 N85-15683
Bearing tester fit analysis
[NASA-CR-171282] 07 p0973 N85-16181
Improvements in linked-spar motion-compensated lifting system
[AD-D011413] 08 p1136 N85-17165
The response of metallic structures to dynamic loading 08 p1172 N85-17389
Response of saturated porous nonlinear materials to dynamic loadings
[AD-A148528] 08 p1173 N85-17394
A discussion of problems encountered in the dynamic fracture toughness testing of materials
[OUEL-1524/84] 08 p1173 N85-17397
Some dynamical aspects of Army missile systems
09 p1333 N85-18380
Effect of coupled torsional-flexural vibration of a geared shaft system on the dynamic tooth load
09 p1338 N85-18415
Vibrational loading mechanism of unitized corrugated containers with cushions and non-load-bearing contents
09 p1339 N85-18419
A tracked vehicle test plant for the simulation of dynamic operation
[AD-P004305] 09 p1410 N85-18882
Analytically redundant output feedback scheme for reduction of structural loads of a flexible transport aircraft
[TT-8303] 12 p1777 N85-21154
Wavecode constitutive models: Nonhomogeneous mixtures
[DE85-000836] 12 p1798 N85-21278
Computer analysis of wind turbine blade dynamic loads
[DE85-000530] 12 p1867 N85-21714
Using NASTRAN to model missile inertia loads
15 p2576 N85-25886
Dynamic crack curving and branching under biaxial loading
[AD-A151451] 15 p2578 N85-25904
An assessment of the suitability of the BHGA structural test rig for aerodynamic testing of hang gliders
[CA-8505] 17 p2896 N85-27853
Critical conditions for failure in materials subjected to high rates of loading
[AD-A153135] 17 p2980 N85-28420
Expedient runway surfacing with post tensioning system for expeditionary airfields
[AD-D011677] 19 p3222 N85-29976
SHAPS-2: A three-dimensional computer program for linear/non-linear, static/dynamic analyses of piping systems
[DE85-010500] 19 p3335 N85-30658
Load transfer by analytical methods
[SNIAS-851-111-109] 20 p3470 N85-31561
In-situ measurement of wall thermal performance: Data interpretation and apparatus design recommendations
[DE85-011979] 21 p3586 N85-32289
The dynamics of slack marine cables
[AD-A155022] 21 p3599 N85-32349
Shock and release equation of state of calcite
[DE85-013151] 23 p3942 N85-34432

DYNAMIC MODELS
Analysis strategies for field dependent estimation and network design — mesoscale modeling
01 p0078 N85-10520
Application of automatic pattern methods in very-short-range forecasting 01 p0078 N85-10521
The development of objective forecast techniques based on advection of surface weather parameters
01 p0078 N85-10522
Predicability of mesoscale phenomena
01 p0079 N85-10528
The initialization of mesoscale models
01 p0079 N85-10529
Applications of a finite-element regional model to very-short-range forecasting 01 p0080 N85-10531
Application of mesoscale numerical model to local weather prediction 01 p0080 N85-10532
The United Kingdom Meteorological Office mesoscale forecasting system 01 p0080 N85-10533
A local dynamical interpretation method of numerical weather forecasting 01 p0080 N85-10536
An operational numerical model for prediction of fog and stratus 01 p0080 N85-10537
A 1-dimensional model with a sub-grid scale condensation scheme for stratiform clouds and fog
01 p0080 N85-10538
A one-level mesoscale model suitable for nowcasting and short-term forecasting in regions of complex terrain
01 p0081 N85-10541
Development of an operational system for Very-Short-Range Forecasting (VSRF) at Swedish Meteorological and Hydrological Institute (SMHI)
01 p0083 N85-10559
The structure of the Uranian rings and the search for rings around Neptune 02 p0302 N85-11954
Dynamics of the Uranian rings
02 p0302 N85-11958
A model for the propagation of the westward traveling surge
[TRITA-EPP-84-03] 03 p0393 N85-12515
Modeling of aircraft cabin fires
[NBS-GCR-84-473] 04 p0454 N85-12860
Users manual for a computer program for dynamic response analysis of bladed systems
[UDR-TR-84-38] 04 p0456 N85-12893
Superconducting magnet for probing eddy currents in dynamic models 04 p0489 N85-13117
Quark models of hadronic interactions
[DE84-013787] 04 p0561 N85-13570
Satellite attitude determination
05 p0599 N85-13814
Analytical modeling of circuit aerodynamics in the new NASA Lewis wind tunnel
[NASA-TM-86912] 07 p0897 N85-15688
Dynamical characteristics of weak turbulence
[AD-A147186] 07 p0959 N85-16075
Combustion dynamics in rockets
[AD-A148478] 08 p1114 N85-17024
Rapid solidification processing and powder metallurgy of Al alloys
[AD-A148427] 08 p1130 N85-17120
The development of a dynamic model of a generalised combat aircraft with forward wings for the identification of stability and control characteristics
[CAR-84-33] 09 p1280 N85-18050
The optimal control and design of a flexible manipulator arm 09 p1327 N85-18340
Reanalysis of continuous dynamic systems with continuous modifications 09 p1337 N85-18411
A one dimensional dynamical model of ocean/atmosphere interactions
09 p1358 N85-18545
Condensed antenna structural models for dynamics analysis 10 p1463 N85-19230
Experimental determination of systems suitable for study as monotectic binary metallic alloy solidification models
12 p1948 N85-22235
Dynamic stochastic model of long-period variability of ocean surface temperature 14 p2334 N85-24437
Considering zonal wind in semidiurnal tide problem
14 p2335 N85-24440
Electrodynamics of magnetosphere-ionosphere coupling 14 p2359 N85-24579
On the dynamics of the westward traveling surge
14 p2364 N85-24607
Observations, theoretical ideas and modeling of turbulent flows: Past, present and future
[NASA-TM-86679] 16 p2782 N85-27167
Dynamic models of flux tubes in the interpretation of polarization measurements 18 p3206 N85-29891
Three-dimensional finite element impact analysis of a nuclear waste truck cask
[DE85-010653] 19 p3288 N85-30389
Use of adjoint equations in problems of evaluating state of random hydrodynamic fields
19 p3289 N85-30396

Space station dynamic modeling, disturbance accommodation, and adaptive control
20 p3409 N85-31154
Antenna pointing of large flexible telecommunications spacecraft
20 p3409 N85-31156
An overview of latest model reduction and control methods of large flexible space structures
20 p3414 N85-31191
An examination of the Southern Oscillation in the upper tropospheric tropical and subtropical wind field
20 p3488 N85-31660
Mechanics of a gaseous film barrier to lubricant wetting of elastohydrodynamically lubricated conjunctions
[NASA-TP-2500] 21 p3595 N85-32330
Development of improved dynamic failure models
[AD-A155586] 21 p3600 N85-32354
Numerical modeling of sea ice dynamics and ice thickness characteristics
[AD-A154600] 21 p3654 N85-32700
Space robot simulator vehicle
[NASA-CR-176133] 22 p3739 N85-33176

DYNAMIC MODULUS OF ELASTICITY
Elastic dispersion effects on dynamics and control of large modular antennas — spacecraft antennas
05 p0627 N85-14019

DYNAMIC PRESSURE
The gulf stream deflection and meander energetics experiment. Current meter and bottom pressure gauge data report for the September, 1981 to April, 1982 mooring period
[AD-A144977] 01 p0088 N85-10595
One-year records of current and bottom pressure in the strait between Nordaustlandet and Kvitoeya and Svalbard, 1980 - 1981
[AD-A145594] 02 p0233 N85-11518
A study of wear characteristics due to pressure for hydraulic fixed displacement vane pumps
[AD-A146023] 06 p0814 N85-15169
Dynamic pressure test unit-ratio method
[AD-D011466] 10 p1488 N85-19392
TMX-U neutral pressure measurement diagnostic systems
[DE85-000748] 11 p1730 N85-20681
Strain rate sensitivity estimation from high velocity impact data
[AD-A154703] 21 p3599 N85-32347
Development of a temperature-compensated hot-film anemometer system for boundary-layer transition detection on high-performance aircraft
[NASA-TM-86732] 22 p3730 N85-33121
Pressure-shear loading of PBX-9404
[DE85-009962] 23 p3921 N85-34296

DYNAMIC PROGRAMMING
Dynamic decision making — and programming
[FOA-C-53015-H2] 04 p0575 N85-13668
Programs for dynamic loading of precompiled subroutine packages, especially for applications with the Watfiv compiler
[DFVLR-MITT-84-18] 12 p1917 N85-22035
Normal mode calculations for fuselage type intricate structures by regarding them as systems with superposed constraints
13 p2048 N85-22617
A dynamic programming approach to time-staged convex programs
[DE85-010616] 19 p3340 N85-30700

DYNAMIC PROPERTIES
U DYNAMIC CHARACTERISTICS

DYNAMIC RESPONSE
NT TRANSIENT RESPONSE
Rotordynamic analysis of the SSME turbopumps using reduced models
[NASA-CR-171170] 01 p0054 N85-10355
Nonlinear dynamic analysis of sandwich panels
01 p0080 N85-10394
Non-Gaussian approach for parametric random vibration of non-linear structures
01 p0080 N85-10395
Response and characteristics of structures subjected to S-H waves
01 p0080 N85-10396
The Shock and Vibration Digest, volume 16, no. 8
[AD-A145853] 02 p0206 N85-11372
Hardware and software selection for experimental modal analysis
02 p0206 N85-11373
Analysis of turbomachine blades: A review
02 p0206 N85-11374
Basic study of bladed disk structural response
[AD-A146226] 03 p0319 N85-12061
Users manual for a computer program for dynamic response analysis of bladed systems
[UDR-TR-84-39] 04 p0456 N85-12883
Bulletin of the Faculty of Engineering, Hokkaido University, no. 123
[ISSN-0385-602-X] 04 p0482 N85-13075
Estimation of dynamic stresses around the shot point by scale model experiment
04 p0482 N85-13076
Mathematical modeling of assembly processes involving use of sensitized robots
04 p0488 N85-13111
NIKE3D: An implicit, finite-deformation, finite element code for analyzing the static and dynamic response of three-dimensional solids, revision 1
[DE84-017161] 04 p0514 N85-13277
Dynamic stiffness characteristics of high eccentricity ratio bearings and seals by perturbation testing
05 p0645 N85-14141
Effects of control stick parameters on human controller response
05 p0701 N85-14496
Does McKuer's law hold for heart rate control via biofeedback display?
05 p0706 N85-14528
An analysis of kinetic response variability
05 p0707 N85-14533
Dynamic response of electromagnetic current meters
[PB84-229731] 06 p0842 N85-15344
Flutter control with unsteady aerodynamic models
[AD-A147858] 07 p0909 N85-15753
The investigation of tethered satellite system dynamics
[NASA-CR-171278] 07 p0912 N85-15772
Sensitivity tests for solid propellants in Germany
08 p1115 N85-17028
Transient combustion: An important consideration in deflagration-to-detonation transition
08 p1116 N85-17037
Computational methods for nonlinear dynamics problems in solid and structural mechanics
[AD-A148352] 08 p1172 N85-17392
An investigation of spinal injury potential from the use of the ACES 2 ejection seat by lower weight female pilots
[AD-A148449] 08 p1196 N85-17537
Theoretical investigation of dynamic stall using a momentum integral method
[AD-P004170] 09 p1268 N85-17955
Nonlinear analysis of composite laminates
09 p1268 N85-18067
Investigation of the pressure-and velocity-coupled responses of solid propellants using impedance tube method
09 p1300 N85-18168
Pressure measurements in a hydrogen combustion environment: An evaluation of 3 pressure transducers
[TI85-003645] 09 p1323 N85-18312
Modelling and identification of the structural properties of an astromast
[CRC-1374] 09 p1329 N85-18352
Design oriented identification of critical points in transient response
09 p1330 N85-18357
Treatment of general boundary conditions and point-wise state variable constraints in optimum design for static and dynamic response
09 p1330 N85-18358
Keynote address
09 p1333 N85-18376
Ellas Klein memorial lecture: Modal testing, a critical review
09 p1334 N85-18383
Least favorable response of inelastic structures
09 p1336 N85-18398
Models for shock damage to marine structural materials
09 p1336 N85-18400
The Shock and Vibration Bulletin 54. Part 3: Structural dynamics, machinery dynamics and vibration problems
[AD-A148133] 09 p1337 N85-18405
Modal analysis of structural systems involving nonlinear coupling
09 p1337 N85-18409
Reanalysis of continuous dynamic systems with continuous modifications
09 p1337 N85-18411
Precision measurement of torsional oscillations induced by gear errors
09 p1338 N85-18416
Dynamic simulation of track laying vehicles
[AD-P004266] 09 p1405 N85-18842
Designing off-road vehicles with good ride behaviour
[AD-P004267] 09 p1405 N85-18843
Operational fitness of box truss antennae in response to dynamic slewing
[NASA-CR-172470] 10 p1429 N85-19012
Response of earth-covered slabs in clay and sand backfills
[AD-A149296] 11 p1615 N85-20157
Multiaxial stress response of ceramics
[DE85-004350] 12 p1814 N85-21379
Method of designing digital band-pass filters with infinite memory
12 p1840 N85-21546
Symmetric primal-dual variational formulations of coupled dynamic systems: Three-dimensional elasticity, shells, fluid-structure interaction
[ONERA-1983-91] 12 p1863 N85-21684
The effect of an elastic foundation and of dissipative forces on the stability of fluid conveying pipes
[TAE-563] 12 p1863 N85-21688
Structural sensitivity analysis: Methods, applications and needs
[NASA-TM-86827] 12 p1865 N85-21695
Time marching numerical solution of the dynamic response of nonlinear systems
[NAF-AN-25] 12 p1865 N85-21696
A solution method for nonlinear dynamic analysis of shell structures
[AD-A149646] 12 p1866 N85-21706
Intraband radiometric performance of the LANDSAT 4 Thematic Mapper — Washington, DC, Arkansas, Massachusetts, Virginia, and Arizona
12 p1871 N85-21736
Vibroacoustic study of the NASA Goddard Space Flight Center OSS-1 payload
[NASA-CR-175320] 13 p1988 N85-22466
Use of importance sampling to investigate signal detection systems by simulated method
13 p2066 N85-23028
Noise immunity of information transmission system with pseudorandom frequency switching under worst-case interference conditions
13 p2066 N85-23029
A research program in active control/aeroelasticity
[NASA-CR-175874] 14 p2218 N85-23752
Dynamic verification of large space structures
14 p2234 N85-23847
Control Of Flexible Structures (COFS) flight experiment background and description
14 p2236 N85-23864
Shuttle payload bay dynamic environments: Summary and conclusion report for STS flights 1-5 and 9
[NASA-CR-175656] 14 p2241 N85-23886
Study of dynamic characteristics of prefabricated gas turbine compressor rotor
14 p2272 N85-24078
Acoustic radiation from bilaminar plates
14 p2415 N85-24903
An experimental investigation into the dynamic response of a stiffened flat plate loaded impulsively by an underwater shockwave
[AD-A151321] 15 p2578 N85-25909
NASTRAN-based software for the structural dynamic analysis of vertical and horizontal axis wind turbines
[DE85-001712] 15 p2580 N85-25911
Mechanical stress regulation of plant growth and development
15 p2610 N85-26067
Ion sensor signal fluctuations during operation of spacecraft reaction engines
16 p2724 N85-26815
Proposal of a method for evaluating accuracy of estimated impulse response of a system
16 p2759 N85-27024
Dynamic response of fluid transmission lines
[AD-A151926] 16 p2782 N85-27171
An analytical investigation of dynamic coupling in nonlinear, geared rotor systems
16 p2792 N85-27218
Dynamic response of shells and plates subjected to variable magnitude traveling loads
16 p2796 N85-27250
Hopkinson bar simulation using DYNA2D
[DE85-006766] 16 p2802 N85-27275
Controller requirements for uncoupled aircraft motion, volume 1
[AD-A153173] 17 p2900 N85-27878
On the accuracy of modelling the dynamics of large space structures
19 p3225 N85-29995
The dynamics and control of large flexible space structures, 8
[NASA-CR-175986] 19 p3225 N85-29996
Underwater shock-induced responses of stiffened flat plates: An investigation into the predictive capabilities of the USA-STAGS code
[AD-A154245] 19 p3286 N85-30377
Forced structural response using component mode synthesis
[DE85-008479] 19 p3287 N85-30383
Flight-mechanics test with a restricted flying aircraft model in a wind tunnel
[ESA-TT-885] 20 p3394 N85-31053
A model parameter extraction procedure applicable to linear time-invariant dynamic systems
[NASA-CR-176120] 22 p3635 N85-33747
Automated dynamic analytical model improvement for damped structures
[NASA-CR-177945] 23 p3941 N85-34425
A multi-touch three dimensional touch-sensitive tablet (executive summary)
23 p3961 N85-34553
The investigation of tethered satellite system dynamics
[NASA-CR-176180] 24 p4069 N85-36215

DYNAMIC STABILITY
NT AERODYNAMIC STABILITY
NT AIRCRAFT STABILITY
NT ATTITUDE STABILITY
NT BOUNDARY LAYER STABILITY
NT COMBUSTION STABILITY
NT CONTROL STABILITY
NT DIRECTIONAL STABILITY
NT FLAME STABILITY
NT FLOW STABILITY
NT FREQUENCY STABILITY
NT GYROSCOPIC STABILITY
NT LATERAL STABILITY
NT LONGITUDINAL STABILITY

NT LOW SPEED STABILITY
NT MAGNETOHYDRODYNAMIC STABILITY
NT MOTION STABILITY
NT ROTARY STABILITY
NT SPACECRAFT STABILITY
NT WEIBEL INSTABILITY
Index cycles simulated by a low order forced barotropic model 07 p1002 N85-16364
Effect of scattering on instabilities in line-driven stellar winds 08 p1235 N85-17784
Optimum design and automated dynamic analysis of flexible mechanisms [AD-A150152] 13 p2099 N85-23088
Bifurcation theory applied to aircraft motions [NASA-TM-86704] 14 p2210 N85-23705
Adaptive techniques for control of large space structures [AD-A150957] 14 p2246 N85-23923
Method of improving dynamic characteristics of DC voltage stabilizers with compound regulation 15 p2528 N85-25589
Effects of bearing deadbands on bearing loads and rotor stability 16 p2737 N85-26889
Solar array flight experiment [NASA-TM-86506] 17 p2909 N85-27935
Dynamic stability of a spinning tube conveying a flowing fluid [DE85-007583] 18 p3102 N85-29207
Newton's method as a dynamical system: Global convergence and predictability [AD-A155170] 21 p3632 N85-32564
Experimental characterization and stability of salt- and nonsalt-containing grouts and mortars (BCT-1F- and BCT-1FF-related) [DE85-012339] 22 p3753 N85-33263

DYNAMIC STRUCTURAL ANALYSIS
Helicopter rotor blade design for minimum vibration [NASA-CR-3825] 01 p0008 N85-10032
The NBS tri-directional test facility [PB84-217462] 01 p0051 N85-10334
Rotordynamic analysis of the SSME turbopumps using reduced models [NASA-CR-171170] 01 p0054 N85-10355
Effect of penetrant on fatigue of aluminum alloy lap joints [NLR-TR-82104-U] 01 p0056 N85-10373
Research in Structures and Dynamics, 1984 [NASA-CP-2335] 01 p0057 N85-10377
Augmented weak forms and element-by-element preconditioners: Efficient iterative strategies for structural finite elements. A preliminary study 01 p0058 N85-10384
Stress-derivative control of keystoning deformation in finite element codes 01 p0058 N85-10385
Interactive buckling of thin-walled structural components under static and dynamic loads 01 p0059 N85-10392
Initial postbuckling analysis of elastoplastic thin-shear structures 01 p0059 N85-10393
Nonlinear dynamic analysis of sandwich panels 01 p0060 N85-10394
Non-Gaussian approach for parametric random vibration of non-linear structures 01 p0060 N85-10395
Response and characteristics of structures subjected to S-H waves 01 p0060 N85-10396
Crashworthiness of light aircraft fuselage structures: A numerical and experimental investigation 01 p0060 N85-10399
Analysis of a transport fuselage section drop test 01 p0060 N85-10400
IAC user manual [NASA-CR-175300] 01 p0102 N85-10677
A rigid body mechanism in structural dynamics 02 p0206 N85-11361
Aeroelastic stability analysis with interacting structural nonlinearities 02 p0207 N85-11364
Post buckling behavior of a circular rod constrained within a circular cylinder 02 p0207 N85-11365
A constitutive modeling technique based on a generalized rheological model to predict the response of materials 02 p0207 N85-11368
The Shock and Vibration Digest, volume 16, no. 8 [AD-A145653] 02 p0208 N85-11372
STARS: A general-purpose finite element computer program for analysis of engineering structures [NASA-RP-1129] 02 p0209 N85-11378
Status and prospects of computational fluid dynamics for unsteady transonic viscous flows [NASA-TM-86016] 03 p0315 N85-12037
Complex frequency analysis of damped thin-walled beams with open cross sections 03 p0371 N85-12366
Theoretical and experimental modal analysis of a rotor test rig — shipboard equipment [AMTE(N)-TM-83079] 03 p0371 N85-12370
Refined modeling of reinforced concrete columns of seismic analysis [PB84-234364] 04 p0484 N85-13089
Spacecraft structural acoustic studies: Development of structural acoustic design guides [ESA-CR(P)-1916] 05 p0604 N85-13849
Elastic dispersion effects on dynamics and control of large modular antennas — spacecraft antennas 05 p0627 N85-14019
Study of structure control dynamic interaction for radio frequency antenna control systems — satellite antennas 05 p0627 N85-14020
Aeroelastic analysis and the identification of flight loads — Mirage 2000 aircraft 07 p0896 N85-15579
Shuttle structural dynamics characteristics: The analysis and verification 08 p1094 N85-16913
Keynote address 09 p1333 N85-18378
Some dynamical aspects of Army missile systems 09 p1333 N85-18390
Elias Klein memorial lecture: Modal testing, a critical review 09 p1334 N85-18393
Solutions to structural dynamics problems 09 p1334 N85-18394
Least favorable response of inelastic structures 09 p1336 N85-18398
The Shock and Vibration Bulletin 54, Part 3: Structural dynamics, machinery dynamics and vibration problems [AD-A148133] 09 p1337 N85-18406
Discrete modifications to continuous dynamic structural systems 09 p1337 N85-18410
Reanalysis of continuous dynamic systems with continuous modifications 09 p1337 N85-18411
The UKIRT centre section structural investigation — United Kingdom Infrared Telescope (UKIRT) [UKIRT-22] 09 p1414 N85-18920
The use of analytical models to interpret data properly [ERS-E.341] 11 p1651 N85-20399
The use of analytical models to interpret measured data properly. 2. The application to modal analysis of structures 11 p1651 N85-20401
Dynamic investigations of a spherical tank structure filled with liquid using ANSYS three-dimensional fluid elements [MBB-UR-E-737-83-O] 11 p1654 N85-20418
The effect of an elastic foundation and of dissipative forces on the stability of fluid conveying pipes [TAE-583] 12 p1863 N85-21688
Structural sensitivity analysis: Methods, applications and needs [NASA-TM-85827] 12 p1865 N85-21695
Deployment analysis of the Olympus Astromast and comparison with test measurements — solar arrays 13 p2011 N85-22616
Investigation of dynamics of manipulator with elastic sections 13 p2048 N85-22819
Large Space Antenna Systems Technology, 1984 [NASA-CP-2368-PT-1] 14 p2229 N85-23813
Structural dynamics analysis 14 p2233 N85-23838
AFWAL space control technology program 14 p2233 N85-23839
Large Space Antenna Systems Technology, 1984 [NASA-CP-2368-PT-2] 14 p2233 N85-23840
On-orbit systems identification of flexible spacecraft Technol., 1984, Pt. 2 p 465-481 14 p2233 N85-23841
Dynamic verification of large space structures 14 p2234 N85-23847
Space Technology Experiments Platform (STEP) status: An in-space test facility 14 p2236 N85-23863
Seismic analysis of rotating mechanical systems [PB85-149599] 14 p2311 N85-24307
Runstreams for using ASKA [NIAST-84/27] 14 p2403 N85-24812
Modeling and control of large flexible structures, phase 1 [AD-A150736] 14 p2403 N85-24817
Experience with transonic unsteady aerodynamic calculations 15 p2456 N85-25176
Status and prospects of computational fluid dynamics for unsteady transonic flow 15 p2456 N85-25180
Numerical experiments on flexible spacecraft with the aid of the Dynamic Control and Analysis Package (DCAP) [ESA-STM-229] 15 p2493 N85-25382
NASTRAN-based software for the structural dynamic analysis of vertical and horizontal axis wind turbines [DE85-001712] 15 p2580 N85-25911
Estimation theory applied to improving dynamic structural models [DE85-004148] 15 p2630 N85-26210
Impact of magnetic isolation on pointing system performance in the presence of structural flexibility [NASA-CR-172481] 16 p2732 N85-26861
Technical overview structural dynamics 16 p2736 N85-26883
USSR report: Engineering and equipment [JPRS-UEQ-84-006] 16 p2760 N85-27035
Nonlinear equations for dynamics of pretwisted beams undergoing small strains and large rotations [NASA-TP-2470] 16 p2799 N85-27256
Wind energy technology program summary [DE85-007349] 16 p2820 N85-27392
On various Fourier series utilized for solution of structural mechanics problems [VTH-LR-429] 16 p2856 N85-27615
Overview of structural response: Probabilistic structural analysis 17 p2912 N85-27952
Probabilistic finite element development 17 p2913 N85-27956
Dynamic creep buckling: Analysis of shell structures subjected to time-dependent mechanical and thermal loading 17 p2913 N85-27959
Turbulence structure in the boundary layers of an oscillating airfoil [AD-A153631] 18 p3059 N85-29926
A natural modes formulation and modal identities for structures with linear viscous damping [CRC-1382] 18 p3120 N85-29312
Spillover minimization: An approach for actuators and sensors placement in distributed parameter study [INPE-3525-PRE/746] 19 p3272 N85-30269
Structural dynamics modification of generalized beams using a local eigenvalue modification procedure 19 p3282 N85-30353
Adaptive identification and control of structural dynamics systems using recursive lattice filters [NASA-TP-2371] 20 p3407 N85-31142
AFWAL control technology programs 20 p3408 N85-31150
Proceedings of the Workshop on Identification and Control of Flexible Space Structures, volume 2 [NASA-CR-176052] 20 p3411 N85-31170
Vibration/libration interaction dynamics during the orbiter based deployment of flexible members 20 p3411 N85-31171
Design of multivariable controllers using the Integrated Analysis Capability (IAC) 20 p3412 N85-31172
A structural dynamics approach to the simulation of spacecraft control/structure interaction 20 p3412 N85-31173
Finite control in underdamped distributed parameter systems 20 p3412 N85-31176
An integrated control and minimum mass structural optimization algorithm for large space structures 20 p3413 N85-31183
ISAAC (Integrated Structural Analysis and Control) via continuum modeling and distributed frequency domain design techniques 20 p3414 N85-31185
Optimization of controlled structures 20 p3414 N85-31186
Parametric stiffness control of flexible structures 20 p3414 N85-31187
Vibrational stabilization of flexible structures 20 p3414 N85-31188
Optimal sensor locations for structural identification 20 p3417 N85-31209
SPAR improved structural-fluid dynamic analysis capability [NASA-CR-171549] 20 p3454 N85-31449
Load transfer by analytical methods [SNIAS-851-111-109] 20 p3470 N85-31561
Inertial analysis of the Charpy test [OUEL-1571/85] 20 p3471 N85-31570
Dynamical study of flat plates by nonlinear elasticity theory [STN-8] 20 p3471 N85-31572
User's guide for computer program CGFAG, Concrete General Flexure Analysis with Graphics [AD-A155555] 21 p3570 N85-32204
Dynamic fracture behavior of structural materials [AD-A154568] 21 p3598 N85-32345
Structural dynamics model and response of the deployable reference configuration space station [NASA-TM-86386] 22 p3799 N85-33539
A substructure coupling procedure applicable to general linear time-invariant dynamic systems [NASA-CR-176144] 22 p3800 N85-33542
Substructure coupling in the frequency domain [NASA-CR-176140] 22 p3800 N85-33543
Negative flexural behavior of precase composite slabs with steel joint 23 p3904 N85-34163
Mechanical ratcheting behaviors of a steel pipe under combined cyclic axial load and internal pressure 23 p3904 N85-34164
Automated dynamic analytical model improvement for damped structures [NASA-CR-177945] 23 p3941 N85-34425
Structural analysis of imperfect three-legged truss columns for large space structures applications 24 p4100 N85-35416

An evaluation of a class of practical optimization techniques for structural dynamics applications
[PB85-195766] 24 p4103 N85-35434
DYNAMIC TESTS
Measuring methods to determine the static and dynamic behavior of wind energy converters
05 p0668 N85-14297
Response of earth-covered slabs in clay and sand backfills
[AD-A149296] 11 p1615 N85-20157
Assessment of dynamic test methods for the measurement of fracture toughness — steels
[OUEL-1561/85] 20 p3470 N85-31565
The Hopkinson pressure bar: An alternative to the instrumented pendulum for Charpy tests
[OUEL-1566/85] 20 p3471 N85-31569
Seat experiments for the full-scale transport aircraft controlled impact demonstration
[AD-A155024] 21 p3553 N85-32106
DYNAMICAL SYSTEMS
Control of rotordynamic instability in a typical gas turbine's power system 05 p0642 N85-14120
Multiloop manual control of dynamic systems
05 p0702 N85-14505
Four-fluid description of turbulent plasma focus dynamics
[IPF-84-4] 09 p1395 N85-18778
Robustness of discrete-time dynamical systems: Application to the multivariable digital control of combat aircraft
[ONERA-NT-1984-2] 11 p1585 N85-19986
Dynamical studies of molecular systems
[DE85-003053] 11 p1594 N85-20028
Stochastic runaway of dynamical systems
[IPP-6/244] 11 p1706 N85-20745
Solar array dynamical simulation for illumination and temperature variation 13 p2011 N85-22611
Parameter estimation in stochastic dynamic systems
14 p2395 N85-24754
Optimal control and optimization
14 p2395 N85-24755
System theoretic description of physical systems
[CWI-TRACT-3] 14 p2414 N85-24894
The dynamical behavior of the age-size-distribution of a cell population
[CWI-AM-R8414] 17 p2998 N85-28538
Dynamical systems and numerical integration
[CWI-AM-R8413] 17 p3022 N85-28695
Stability in dynamical systems
[DE85-006696] 17 p3034 N85-28766
Characterization of intermittency in chaotic systems
[PREPRINT-429] 18 p3173 N85-29669
Stochastic resonance in the Landau-Ginzburg equation
[PREPRINT-430] 18 p3175 N85-29685
Solar dynamic systems 20 p3443 N85-31374
On the multifractal nature of fully developed turbulence and chaotic systems
[PREPRINT-413] 20 p3455 N85-31458
Decentralized control of dynamically interconnected systems
[BU-111] 22 p3835 N85-33744
The investigation of tethered satellite system dynamics
[NASA-CR-176160] 24 p4069 N85-35215
Aspects of input signal design for order and parameter estimation in linear dynamical systems
[ER-83/05] 24 p4091 N85-35362
DYNAMICS
A mathematical simulation model of the CH-47B helicopter, volume 1
[NASA-TM-84351-VOL-1] 01 p0006 N85-10033
Images of the Earth's aurora and geocorona from the Dynamics Explorer Mission
[NASA-CR-175963] 18 p3136 N85-29423
DYNAMICS EXPLORER SATELLITES
NT DYNAMICS EXPLORER 1 SATELLITE
DYNAMICS EXPLORER 1 SATELLITE
A retarding ion mass spectrometer for the Dynamics Explorer-1
[NASA-CR-171586] 21 p3589 N85-32303
DYNAMO THEORY
Models of nonkeplerian accretion disks based on dynamo magnetic field: Application to Active Galactic Nuclei (AGN) 08 p1242 N85-17834
Nonlinear dynamos — solar activity
14 p2447 N85-25106
The solar dynamo and the complex Lorenz equations
14 p2447 N85-25107
Kinematic dynamo theory for an arbitrary mean flow
14 p2448 N85-25108
The generation of magnetic fields by a flow with chaotic streamlines 14 p2451 N85-25135
Dynamo action of magnetostrophic waves — solar atmosphere 14 p2451 N85-25136
Cyclic flows in the solar convection zone due to the dynamo reaction 14 p2451 N85-25137
Modeling 22-year solar activity cycle within framework of dynamo theory with allowance for primary field
15 p2477 N85-25288
Planetary Dynamos
[NASA-CR-176001] 21 p3679 N85-32857
Magnetic field generation in the cores of terrestrial bodies 22 p3859 N85-33894
DYNAMOMETERS
Water brake convertor: A simple device to convert mechanical energy into heat energy
[DE85-008021] 16 p2716 N85-26766
Regional circulation during testing on isokinetic dynamometer following 14-day bedrest
19 p3323 N85-30590
Durability of oxygen sensors
[PB85-183093] 22 p3789 N85-33477
DYNAMOS
U ROTATING GENERATORS

E

E GLASS
NT S GLASS
E LAYERS
U E REGION
E REGION
NT SPORADIC E LAYER
UBV photometry of E region standard stars of intermediate brightness 01 p0128 N85-10879
UBV photometry of E region stars: Some intercomparisons 01 p0128 N85-10880
Occurrences of the polar slant E condition (SEC) at Narssarssuaq, Godhavn, Thule 1982
03 p0393 N85-12514
Experience with proposed improvements of the International Reference Ionosphere (IRI)
[PB84-235670] 05 p0678 N85-14353
Dynamics of the low-latitude thermosphere and ionosphere 09 p1351 N85-18501
Seasonal characteristics of mesospheric plasma and their transitions 11 p1660 N85-20484
Investigation of aeronomic processes on the basis of ionospheric sporadic E 11 p1663 N85-20482
Space and time variations and turbopause dynamical structure 11 p1663 N85-20483
Protons with energies above 30 KeV in Earth's radiation belt at low altitudes during magnetically quiet time close to geomagnetic equator 13 p1980 N85-22423
A brief summary of results derived from Scandinavian Twin Auroral Radar Experiment (STARE) observations during IMS — ionospheric electric fields
14 p2362 N85-24595
Characteristics and sources of E-region ionization in the continuous aurora
[AD-A155018] 21 p3632 N85-32562
EAR
NT COCHLEA
NT LABYRINTH
NT VESTIBULES
The European vestibular experiments of the Spacelab-1 mission 20 p3508 N85-31808
EARLY STARS
NT PROTOSTARS
NT T TAURI STARS
The Origin of Nonradiative Heating/Momentum in Hot Stars
[NASA-CP-2358] 08 p1231 N85-17755
Evidence for non-radiative activity in hot stars
08 p1231 N85-17756
Observations of nonthermal radio emission from early-type stars 08 p1232 N85-17758
Nonradial pulsation and mass loss in early B stars
08 p1232 N85-17759
Is the ratio of observed X-ray luminosity to bolometric luminosity in early-type stars really a constant?
08 p1234 N85-17777
Multi-spectral observations of the star formation: The role of far infrared photometry 08 p1245 N85-17859
Circumstellar dust disks around young stars
08 p1247 N85-17870
The variation of galactic interstellar extinction in the ultraviolet 11 p1749 N85-21000
Interstellar extinction in the nucleus of H PER
11 p1749 N85-21001
Coronal effects of the winds of early-type stars
11 p1749 N85-21002
The spectroscopic antics of S 18/SMC
11 p1750 N85-21006
EARPHONES
Hearing protection and speech intelligibility of two nonstandard inflight communication headsets
[AD-A146110] 03 p0355 N85-12284
EARTH (PLANET)
Impact phenomena as factors in the evolution of the Earth
[NASA-CR-174015] 01 p0072 N85-10474
Orbit of Salyut-7 station boosted
02 p0157 N85-11067
Lithospheric structure in the Pacific geoid
[NASA-CR-174155] 04 p0526 N85-13365
The problem of iron partition between Earth and Moon during simultaneous formation as a double planet system 04 p0587 N85-13744
Formation of the preluner accretion disk
04 p0588 N85-13755
Lunar origin from impact on the Earth
04 p0588 N85-13757
Biogeochemical cycles: Interactions in global metabolism 05 p0652 N85-14184
Global biogeochemical cycles: Studies of interaction and change, some views on the strategy of approach
05 p0652 N85-14185
Some aspects of understanding changes in the global carbon cycle 05 p0652 N85-14186
Investigating phase structure of electromagnetic field in local inhomogeneities by modeling method
06 p0822 N85-15220
Where is the Earth's missing xenon?
06 p0688 N85-15641
Sample return from a comet flyby
06 p0689 N85-15648
Research of inverse methods to describe the structure of the earth and ocean bottom
[AD-A147082] 07 p1030 N85-16541
Algorithm for space-time analysis of data on geomagnetic field
[NASA-TM-77804] 08 p1209 N85-17809
The discovery circumstances of Earth-approaching asteroids
[NASA-CR-174327] 08 p1258 N85-17920
The geology of the terrestrial planets
[NASA-SP-469] 09 p1410 N85-18888
Earth 09 p1411 N85-18892
Evolution of sedimentation basins in Earth's history
10 p1497 N85-19451
Recent investigations at INPE in magnetospheric physics and geomagnetism
[INPE-3280-PRE/603] 10 p1514 N85-19555
Multiple parallel wires above a finitely conducting plane earth in the presence of a plane wave (EMP)
[DE85-001116] 11 p1625 N85-20231
Large natural geophysical events: Planetary planning
[DE85-000959] 11 p1763 N85-21092
Evaluating accuracy in determining position of Earth's center of mass and elements of orientation of geodetic coordinate system 13 p1983 N85-22441
Nature of seismic images with amplitude and time fluctuations of recorded oscillations
13 p2112 N85-23156
Gravity field of Venus and comparison with Earth
13 p2178 N85-23514
A circum-terrestrial compositional filter
13 p2179 N85-23520
Models of angular momentum input to a circum-terrestrial swarm from encounters with heliocentric planetesimals 13 p2179 N85-23521
Terrestrial analogs for planetary wrinkle ridges
13 p2199 N85-23644
Motion of satellite with total dynamic symmetry around rotating aspherical Earth 14 p2287 N85-24174
Relationship between seismic status of Earth and relative position of bodies in sun-earth-moon system
14 p2345 N85-24489
Local covariance functions and density distributions
[AD-A150792] 14 p2373 N85-24669
Resonant rotations of satellite in polar orbit in magnetic and gravitational fields 15 p2479 N85-25302
Space-time features of solar cosmic ray penetration into high latitude regions of Earth's magnetosphere based on Intercosmos-19 satellite data 15 p2481 N85-25310
Magnetohydrodynamics of Earth's bow shock
15 p2481 N85-25311
Selection of a model of Earth's albedo radiation, practical calculation of its effect on the trajectory of a satellite
[NASA-TM-77670] 15 p2591 N85-25972
Apparent thickness of Saturn's rings from the observations of the ring plane crossing
15 p2671 N85-26477
Comet showers and Nemesis, the death star
[DE85-003736] 15 p2693 N85-26575
Studies related to the deep Earth gas: 1983
[PB85-171114] 16 p2816 N85-27373
General continuous formulations of atmospheric energy laws 16 p2830 N85-27448
Moon bounce communications to small terminals
[AD-A153297] 17 p2950 N85-28212
Parameterization of surface fluxes in the VVR Fourth Order GCM 18 p3142 N85-29454

Analysis and modeling of variations in length of day
19 p3349 N85-30761
Properties of the reflected beams from the Earth's bow shock: A simple model
[IFSI-84-14] 20 p3549 N85-32068
Earth Albedo and the orbit of LAGEOS
[NASA-TM-86210] 21 p3558 N85-32131
Mega-geomorphology: Mars vis a vis Earth
21 p3801 N85-32360
Workshop on the Early Earth: The Interval from Accretion to the Older Archean
[NASA-CR-176037] 21 p3717 N85-33062
Permafrost features on Earth and Mars: Similarities, differences 22 p3855 N85-33870
Venus, Earth and Mars: Present bounds on similarities and differences in bulk composition
22 p3856 N85-33876
Mineralogy and chemistry of the Earth
22 p3856 N85-33877
Contrasts in evolution of Venus and Earth
22 p3857 N85-33880
Planning for VRM: Radar and sonar studies of volcanic terrains on Earth, Venus and Mars
22 p3857 N85-33884
Comparisons of the North Polar Cap of Mars and the Earth's Northern Hemisphere snow cover
[NASA-TM-86191] 23 p3969 N85-34726
Applications of the Galerkin formalism in the coupling of the earth's free oscillations 24 p4116 N85-35514

EARTH ALBEDO

Modeling influence of three layer cloud cover on outgoing thermal radiation 06 p0825 N85-15242
The effects of long-periodic forcing in a zero-dimensional climate model 07 p1002 N85-16363
Bifacial light sensitive space solar cell
13 p2006 N85-22573
Effect of diffusely-reflected sunlight on the orbit of LAGEOS 20 p3491 N85-31700
The electromagnetic component of albedo from superhigh energy cascades in dense media
[HE-3.5-11] 24 p4184 N85-35948

EARTH ATMOSPHERE

NT BIOSPHERE
NT D REGION
NT E REGION
NT EXOSPHERE
NT F REGION
NT F 2 REGION
NT FREE ATMOSPHERE
NT GEOMAGNETIC TAIL
NT INNER RADIATION BELT
NT IONOSPHERE
NT LOWER ATMOSPHERE
NT LOWER IONOSPHERE
NT MAGNETOPAUSE
NT MAGNETOSPHERE
NT MESOPAUSE
NT MESOSPHERE
NT MIDDLE ATMOSPHERE
NT MIDLATITUDE ATMOSPHERE
NT OUTER RADIATION BELT
NT OZONOSPHERE
NT PRIMITIVE EARTH ATMOSPHERE
NT PROTON BELTS
NT RADIATION BELTS
NT SPORADIC E LAYER
NT STRATOPAUSE
NT STRATOSPHERE
NT THERMOSPHERE
NT TROPOPAUSE
NT TROPOSPHERE
NT TURBOPAUSE
NT UPPER ATMOSPHERE
NT UPPER IONOSPHERE

Alpine meteorology: Translations of classic contributions by Wagner, A., Ekhart, E. and Defant, F.
[DE84-014929] 01 p0065 N85-10574
Green River air quality model development: Meteorological and tracer data, July/August 1982. Field study in Brush Valley, Colorado
[DE84-014975] 02 p0225 N85-11474
Achievements in development of space meteorology
03 p0343 N85-12212
A proposed reference set of scenarios for radiatively active atmospheric constituents
[DOE/NBB-0086] 03 p0368 N85-12483
Millimeter-wave propagation and remote sensing of the atmosphere
[AD-A146339] 03 p0393 N85-12512
Atmospheric extinction in critical environments
[AD-A146102] 03 p0396 N85-12527
Atlas of polar cap energetic particle observations. Volume 1: TIROS-N, 1 January 1979 - 28 February 1981
[PB84-233402] 04 p0535 N85-13419
Atmospheric studies in complex terrain
[DE84-008553] 05 p0676 N85-14345
Chemical kinetics and Earth's atmosphere
06 p0822 N85-15218
Attempted measurement of gaseous H-2O-2 in the ambient atmosphere
[DE85-001937] 06 p0834 N85-15306
Fractionation of siderophiles in cosmic spherules and its implications 06 p0884 N85-15613
Fluctuations during observations of extraterrestrial sources from outer space through Earth's atmosphere
07 p0953 N85-16040
Research in geodesy based upon radio interferometric observations of extragalactic radio sources
[AD-A147581] 07 p0988 N85-16280
Remote sensing of atmospheric gases with CO2 lasers. Continuation and conclusion of spectroscopic investigations
[BMFT-FB-W-84-030] 07 p0989 N85-16285
Development of an airborne measuring system for remote sensing of Earth surface and atmosphere, spectroscopic investigations
[BMFT-FB-W-84-029] 08 p1176 N85-17420
Earth 09 p1411 N85-18892
Study proposal for the possible use of ISS as an aerodynamic facility for aerospace applications
11 p1646 N85-20374
Environmental effects of space activities
11 p1678 N85-20577
Substorms in the Earth's atmosphere
[DE85-000654] 12 p1890 N85-21861
Atmospheric handbook: Atmospheric data tables available on computer tape
[PB85-106512] 12 p1891 N85-21867
Characterization of material surfaces exposed to atomic oxygen on space shuttle missions
12 p1946 N85-22220
Response of Earth's atmosphere to increases in solar flux and implications for loss of water from Venus
13 p2178 N85-23518
The Earth's magnetopause — International Magnetospheric Study 14 p2355 N85-24549
Hot plasma and energetic particles in the Earth's outer magnetosphere: New understandings during the IMS
14 p2355 N85-24552
Magnetic field in the Earth's outer magnetosphere: Prognoz-3, -7 data 14 p2356 N85-24556
Analysis of atmospheric interferometer data
[AD-A150682] 14 p2372 N85-24663
The behavior of the atmosphere in the desert planetary boundary layer
[AD-A151288] 15 p2592 N85-25977
ILUM code: Solar and lunar flux calculations for multi-cloud layered atmospheres
[DE85-005578] 15 p2600 N85-26025
Modeling plasma mantle of Earth's magnetosphere
16 p2720 N85-26790
The problem of atmospheric turbulence
[NASA-CR-175783] 16 p2832 N85-27464
Intercomparison of Radiation Codes in Climate Models (ICRCCM)
[DE85-007251] 16 p2835 N85-27487
The role of thermal motions of air particles for fireballs
[PUBL-59] 17 p3053 N85-28900
Identification and characterization of watershed models for evaluation of impacts of climate change on hydrology
[DE85-000575] 18 p3125 N85-29348
Formation and fate of toxic chemicals in California's atmosphere
[PB85-172609] 18 p3134 N85-29414
The moist available energy of a conditionally unstable atmosphere 18 p3145 N85-29473
Preliminary GCM results with a new radiation parameterization 18 p3145 N85-29474
Environmental Research Laboratories (of the National Oceanic and Atmospheric Administration) programs and plans: FY 1984 programs and FY 1985 plans
[PB85-171494] 18 p3149 N85-29501
Study of Kapton under simulated shuttle environment
[NASA-CR-176003] 19 p3225 N85-29997
Density characteristics of asthenosphere in Atlantic Ocean 19 p3294 N85-30423
Optical stability, atmospheric transparency and aerosol absorption 19 p3297 N85-30442
Approximate method for computing wind velocity in atmosphere 19 p3298 N85-30444
The origin and evolution of the Earth's atmosphere and hydrosphere 19 p3312 N85-30533
Effects of relative humidity gradients on the evaluation of submicron aerosol flux measurements in the atmospheric surface layer
[DE85-010510] 19 p3316 N85-30555
Intraplate crustal deformation due to continental collisions 20 p3490 N85-31693
A survey of wind and turbulence modeling methods
[AD-A154470] 20 p3496 N85-31733
Medium range atmospheric forecast system: Evaluation plan
[AD-A155623] 21 p3638 N85-32595
Production of stable embryo particles in dense ion tracks of alpha particle emissions in the atmosphere
21 p3644 N85-32638
Photochemical aerosol formation in polluted atmosphere 21 p3644 N85-32642
Evolution of the atmosphere 21 p3658 N85-32725
Constraints on early atmosphere from planetary accretion processes 21 p3717 N85-33064
The composition of the primitive atmosphere and the synthesis of organic compounds on the early Earth
21 p3717 N85-33065
The degassing history of the Earth: Noble gas studies of Archaean cherts and zero age glassy submarine basalts 21 p3718 N85-33072
Water loss from Venus: Implications for the Earth's early atmosphere 21 p3721 N85-33087
Impact of fluctuations in optical properties of atmosphere on the ratio of spectral brightness from remote sensing of agricultural land 22 p3734 N85-33149
Determination of altitude of cloud cover top from Meteor satellite data 22 p3734 N85-33150
A review of shock waves around aeroassisted orbital transfer vehicles
[NASA-TM-86769] 22 p3739 N85-33177
Evaluation of the 2DFLOW and hybrid complex-terrain dispersion models with the 1980 ASCOT data base from the Geysers
[DE85-012960] 22 p3812 N85-33613
Terrestrial Planets: Comparative Planetology
[NASA-CR-176093] 22 p3851 N85-33849
Terrestrial Xe isotopic contraints on the early history of the Earth 22 p3852 N85-33852
Noble gas patterns in the atmospheres of Mars and Earth: A comparison via the SNC meteorites
22 p3852 N85-33853
Biological modulation of planetary atmospheres: The early Earth scenario 22 p3854 N85-33867
Imaging Spectrometric Observatory (ISO)
23 p3902 N85-34169
Evaluation of source strength and dispersion model predications with data from large nitrogen tetroxide field experiments
[DE85-011855] 23 p3947 N85-34485
Nucleosynthesis in the terrestrial and solar atmospheres
[SH-2.2-2] 23 p4000 N85-34797
The influences of the galactic cosmic ray on the atmospheric ozone
[SH-10.1-1] 23 p4053 N85-35133
Propagation of cosmic rays through the atmosphere in the quark-gluon strings model 24 p4173 N85-35873
Experimental basis for the models of cascade propagation in atmosphere
[HE-3.6-6] 24 p4185 N85-35954
The lateral distributions of charged particles of energy greater than 0.3 E sub crit in electron-photon cascades in lead and air
[HE-3.6-10] 24 p4185 N85-35957
Longitudinal trial functions and the cosmic ray energy scale 24 p4193 N85-36014
Nuclear cascades in electromagnetic showers produced by primary gamma-quanta in the atmosphere
[HE-4.5-16] 24 p4196 N85-36038
Air fluorescence detection of large air showers below the horizon
[HE-4.6-6] 24 p4197 N85-36043

EARTH AXIS

The MEDOC 2: Experimental Doppler measurement of Earth kinematics 14 p2399 N85-24786
Global coordinate system
[AD-A153878] 19 p3299 N85-30454

EARTH CORE

Is phosphorus predictably incompatible in igneous processes? 04 p0583 N85-13722
Magnetic location of Earth's core-mantle boundary and estimates of the adjacent fluid motion
13 p2131 N85-23260
Origin of life 21 p3657 N85-32713
Was core formation violent enough to homogenize the early mantle? 21 p3718 N85-33068
The problem of the Earth's CO2 content and the iron core 21 p3718 N85-33069
A model for core formation in the early Earth
21 p3719 N85-33078
Implications for the Earth of the early dynamical environment 21 p3719 N85-33079
Chemical evolution of the Earth: Equilibrium or disequilibrium process? 21 p3721 N85-33088
Thermal, dynamic and compositional aspects of the core-forming Earth 21 p3722 N85-33091

EARTH CRUST
Marine geological and geophysical investigations of the Antarctic Continental Margin, 1984
[GS-CIRC-935] 02 p0212 N85-11400
The south-central United States magnetic anomaly
[E85-10025] 02 p0218 N85-11438
A comparison of seismic properties of young and mature oceanic crust 02 p0226 N85-11479
Heat flow map of Europe: Brief summary of the geophysical implications
[REPT-562] 03 p0377 N85-12405
Continental and oceanic crustal magnetization modelling
[E85-10034] 03 p0378 N85-12413
Horizontal-strain observations in the Shumagin Island and Yakataga seismic gaps, Alaska
04 p0515 N85-13287
Structure of the crust and upper mantle of the Iberian continental platform 04 p0523 N85-13350
Deep structure and seismicity in the Catalonia-Pyrenees region 04 p0524 N85-13352
Priorities for a national program of continental drilling for scientific purposes 04 p0534 N85-13418
Geophysical investigation of precambrian crustal structure and Laramide effects across a precambrian suture in southeastern Wyoming
05 p0674 N85-14328
Oceanic plateaus, anomalous subduction, and the accretion of buoyant features at convergent margins
05 p0688 N85-14422
Some trends in the modern Earth sciences --- plate tectonics and Earth's crust 06 p0820 N85-15207
Deep structure of terrestrial crust and upper mantle in southeastern Siberia and Far East according geological-geophysical data 06 p0821 N85-15212
Deep structure of Western Siberia
07 p0981 N85-16235
Model of earthquake mechanism
07 p0982 N85-16236
Statistical filtering as method for detecting transcrustal acoustic anomalies 07 p0982 N85-16237
The mineralogy of global magnetic anomalies
[E85-10061] 07 p0987 N85-16272
Analysis of gases in the Earth's crust
[PB85-113307/GAR] 07 p0990 N85-16287
High pressure physics research focusing on composite materials 08 p1140 N85-17185
Determination of crustal and upper mantle structure from analysis of broadband teleseismic P-waveforms
08 p1181 N85-17440
Detailed oceanic crustal modeling
[AD-A148589] 08 p1191 N85-17507
Utilization of mobile VLBI for geodetic measurements
10 p1466 N85-19248
New data on structure of Shirshov Ridge (Bering Sea)
10 p1466 N85-19456
Crustal stretching and subsidence in sedimentary eastern Switzerland and permo-carboniferous basins in the continental United States
[DE85-000622] 11 p1661 N85-20592
Determination of density of the crust and upper mantle from deep seismic sounding and gravimetry, 2
13 p2111 N85-23153
Induction excitation of deep conducting zones
13 p2111 N85-23154
Study of resolution of deep MT soundings by means of physical model 13 p2112 N85-23155
Structure of Iceland and ocean floor spreading
13 p2112 N85-23159
Variations in resistivity of upper crustal layer
13 p2113 N85-23164
Boundary velocities of longitudinal seismic waves and lateral inhomogeneities of upper ocean mantle
13 p2113 N85-23165
Solution of direct magnetometric problem on spherical Earth 13 p2116 N85-23179
MAGSAT anomaly field data of the crustal properties of Australia
[E85-10100] 13 p2122 N85-23215
An investigation of the crustal properties of Australia and surrounding regions derived from interpretation of MAGSAT anomaly field data 13 p2122 N85-23216
Remanent magnetization model for the broken ridge satellite magnetic anomaly 13 p2123 N85-23219
Crustal dynamics project: Catalogue of site information
[NASA-TM-87452] 13 p2131 N85-23258
Volcanism of the Colorado Plateau (basin and range transition): Implications for crustal processes
13 p2187 N85-23569
Bouguer images of the North American craton
13 p2200 N85-23648
Determination of crust and upper mantle density based on deep seismic sounding and gravimetry data, part 1
14 p2345 N85-24498
Polar motions measurement study
[AD-A150690] 14 p2372 N85-24664
Study of spatial distribution of aurorae
16 p2808 N85-27315
Altimetry data and the elastic stress tensor of subduction zones
[NASA-CR-175796] 16 p2825 N85-27425
Proceedings of the 1980 Workshop of the International Association of Seismology and Physics of the Earth's Interior on the Seismic Modeling of Laterally Varying Structures: Contributions based on data from the 1978 Saudi Arabian refraction profile
[GS-CIRC-937] 17 p2969 N85-28476
A crustal section for the Arabian Shield and adjacent Red Sea margin derived from first-arrival data
17 p2990 N85-28480
The rifted margin of Saudi Arabia
17 p2990 N85-28483
Density characteristics of asthenosphere in Atlantic Ocean 19 p3294 N85-30423
Discovery in earthquake forecasting and seismic zoning recorded 19 p3295 N85-30426
Improving the geological interpretation of magnetic and gravity satellite anomalies
[E85-10103] 20 p3473 N85-31585
The south-central United States magnetic anomaly
20 p3474 N85-31591
The south-central United States magnetic anomaly
20 p3475 N85-31592
Continental and oceanic magnetic anomalies: Enhancement through GRM 20 p3476 N85-31598
Continental magnetic anomaly constraints on continental reconstruction 20 p3476 N85-31599
Regional magnetic anomaly constraints on continental rifting 20 p3476 N85-31600
The global VLBI fiducial network
20 p3490 N85-31690
Mega-geomorphology: Mars vis a vis Earth
21 p3601 N85-32360
Crustal dynamics project data analysis fixed station VLBI geodetic results
[NASA-TM-86229] 21 p3615 N85-32465
Development of ultrasonic modeling techniques for the study of crustal inhomogeneities
[AD-A155206] 21 p3632 N85-32585
Origin of life 21 p3657 N85-32713
Workshop on the Early Earth: The Interval from Accretion to the Older Archean
[NASA-CR-176037] 21 p3717 N85-33062
Early evolution of the crust-mantle system
21 p3717 N85-33067
Considerations of large scale impact and the early Earth 21 p3718 N85-33070
The 3.5 b.y. old Onverwacht Group: A remnant of ancient oceanic crust 21 p3718 N85-33073
Constraints on the development of the early continental crust from isotopic data 21 p3719 N85-33076
Anorthositic oceanic crust in the Archean Earth
21 p3719 N85-33077
Archean sedimentary systems and crustal evolution
21 p3720 N85-33082
The origin of continental crust: Outlines of a general theory 21 p3720 N85-33083
Crustal radiogenic heat production and the selective survival of ancient continental crust
21 p3721 N85-33086
Large arcuate scars: A geological legacy of the Earth's accretionary past 21 p3721 N85-33089
Spacecraft-aided research discussed at geology Congress 22 p3734 N85-33147
Noble gases in meteorites and terrestrial planets
22 p3851 N85-33850
Crustal structure in southern California from array data
24 p4115 N85-35512
Groundwater radon studies for earthquake precursors in southern California
[PB85-196871] 24 p4118 N85-35529

EARTH CURRENTS
U TELLURIC CURRENTS

EARTH ENVIRONMENT
International Geosphere/Biosphere Program: 1984
[GPO-39-222] 04 p0578 N85-13691
Sourcebook: Gaining access to US government information on the environment and natural resources
[DE84-017419] 11 p1740 N85-20941

EARTH FIGURE
U GEODESY

EARTH HYDROSPHERE
Earth 09 p1411 N85-18892
Drifting ice as mechanical factor in purifying and polluting hydrosphere 13 p2108 N85-23132
World ocean level oscillations and their relationship to change in inflow of continental waters
13 p2108 N85-23133
The origin and evolution of the Earth's atmosphere and hydrosphere 19 p3312 N85-30533
Origin of the atmosphere and hydrosphere of the terrestrial planets 22 p3863 N85-33863

EARTH MANTLE
Structure of the crust and upper mantle of the Iberian continental platform 04 p0523 N85-13350
Constraints on the origin of the Moon from molybdenum and other siderophile elements
04 p0582 N85-13718
Origin of the Moon 04 p0587 N85-13745
Earthquakes and tectonics of Pacific Ocean margins
06 p0820 N85-15206
Boundary velocities of mohorovicic discontinuity and upper mantle structure of Pacific Ocean bed
06 p0821 N85-15211
Deep structure of terrestrial crust and upper mantle in southeastern Siberia and Far East according geological-geophysical data 06 p0821 N85-15212
The mineralogy of global magnetic anomalies
[E85-10061] 07 p0987 N85-16272
Determination of crustal and upper mantle structure from analysis of broadband teleseismic P-waveforms
08 p1181 N85-17440
Detailed oceanic crustal modeling
[AD-A148589] 08 p1191 N85-17507
Vertical movements and structure formation within island systems of northeast Asia 10 p1501 N85-19471
A 3-D treatment of convective flow in the Earth's mantle
[DE85-003734] 12 p1890 N85-21863
Determining degree of partial melting of asthenosphere from seismic data 13 p2107 N85-23127
Determination of density of the crust and upper mantle from deep seismic sounding and gravimetry, 2
13 p2111 N85-23153
Induction excitation of deep conducting zones
13 p2111 N85-23154
Study of resolution of deep MT soundings by means of physical model 13 p2112 N85-23155
Boundary velocities of longitudinal seismic waves and lateral inhomogeneities of upper ocean mantle
13 p2113 N85-23165
Magnetic location of Earth's core-mantle boundary and estimates of the adjacent fluid motion
13 p2131 N85-23260
Bouguer images of the North American craton
13 p2200 N85-23648
Lateral inhomogeneity of mantle surface in western Eurasia 14 p2344 N85-24497
Determination of crust and upper mantle density based on deep seismic sounding and gravimetry data, part 1
14 p2345 N85-24498
Frequency dependence of Q in the mantle underlying the shield areas of eurasia
[AD-A151367] 15 p2592 N85-25978
Internal waves in layers of Earth's upper mantle
16 p2807 N85-27312
Proceedings of the 1980 Workshop of the International Association of Seismology and Physics of the Earth's Interior on the Seismic Modeling of Laterally Varying Structures: Contributions based on data from the 1978 Saudi Arabian refraction profile
[GS-CIRC-937] 17 p2969 N85-28476
Density characteristics of asthenosphere in Atlantic Ocean 19 p3294 N85-30423
Evolution of the oceanic upper mantle and effects on sea floor subsidence geoid height and heat flow
19 p3319 N85-30575
Origin of life 21 p3657 N85-32713
Workshop on the Early Earth: The Interval from Accretion to the Older Archean
[NASA-CR-176037] 21 p3717 N85-33062
The relation between the age of the subconducting slab and the recycling of sediments into the mantle
21 p3717 N85-33063
Constraints on early atmosphere from planetary accretion processes 21 p3717 N85-33064
Early evolution of the crust-mantle system
21 p3717 N85-33067
Was core formation violent enough to homogenize the early mantle? 21 p3718 N85-33068
Constraints on the development of the early continental crust from isotopic data 21 p3719 N85-33076
A model for core formation in the early Earth
21 p3719 N85-33078
Carbon and nitrogen in the deep Earth
21 p3721 N85-33085
Chemical evolution of the Earth: Equilibrium or disequilibrium process? 21 p3721 N85-33088
Thermal, dynamic and compositional aspects of the core-forming Earth 21 p3722 N85-33091
Landscape interpretation capabilities using space photographs of regions of a multistage platform mantle structure 22 p3734 N85-33151
Noble gases in meteorites and terrestrial planets
22 p3851 N85-33850

Terrestrial Xe isotopic contraints on the early history of the Earth 22 p3852 N85-33852
A dynamic model of Venus's gravity field [NASA-CR-176173] 24 p4169 N85-35845

EARTH MOVEMENTS
NT EARTHQUAKES
Vertical crustal movements in southern California, 1974 to 1978 [GS-CIRC-806] 02 p0228 N85-11491
Soil tilt measurement: First results of the comparative analysis of the response of two different tiltmeters [NOTA-INTERNA-618] 02 p0228 N85-11494
Analysis of in-plane and out-of-plane ground motions using the boundary element method [AD-A146229] 03 p0355 N85-12287
The motion of the Earth by Doppler observing campaign (MEDOC) 05 p0801 N85-13631
On seismic waves 06 p1171 N85-17383
Absolute movement of Pacific Ocean plate during last 120 million years 13 p2107 N85-23126
Numerical modeling of plane stick-slip fault 13 p2111 N85-23150
Crustal dynamics project: Catalogue of site information [NASA-TM-87452] 13 p2131 N85-23258
Inversion of Rayleigh wave group velocities from high-explosive tests [AD-A152172] 16 p2783 N85-27175
The effects of seismic waves 17 p2978 N85-28401
The global VLBI fiducial network 20 p3490 N85-31690
New stations supporting crustal dynamics project VLBI measurements 20 p3491 N85-31701
Mapping of dynamics of deltas by space photography 22 p3737 N85-33163
Crustal Dynamics Project: Catalogue of site information [NASA-TM-86218] 22 p3801 N85-33552
Seismic stratigraphic analysis of the Mississippi Fan 24 p4115 N85-35507

EARTH OBSERVATIONS (FROM SPACE)
NT PHOTORECONNAISSANCE
NT SATELLITE OBSERVATION
NT SPOT (FRENCH SATELLITE)
Satellite reconnaissance [AD-B085034] 01 p0015 N85-10084
NASA's SESAC report on research and analysis in space and Earth science 04 p0579 N85-13607
Basic investigation concerning the applicability of multispectral radiation data from microwave radiometry measurements to geoscientific objectives of remote sensing [ESA-TT-846] 05 p0628 N85-14027
EARSeL/ESA Symposium on Integrative Approaches in Remote Sensing [ESA-SP-214] 05 p0655 N85-14202
Perspectives of remote sensing at the end of the decade 05 p0659 N85-14236
Electronic satellite imaging system MOMS-ESA [BMFT-FB-W-84-033] 05 p0661 N85-14248
Simulation experiments on the relative accuracy of inferred atmospheric states from idealized wind and temperature profiling systems 05 p0662 N85-14366
Upper Atmosphere Research Satellite (UARS) trade analysis [NASA-CR-175269] 07 p0912 N85-15774
Brazilian Remote Sensing Shuttle Experiment (BRESEX): Characteristics and future utilization on satellites [INPE-3313-PRE/620] 10 p1487 N85-19365
Summary presentation of the Science Applications Panel 11 p1644 N85-20355
Solar flare and IMF sector structure effects in the lower ionosphere 11 p1664 N85-20486
The spot operational remote sensing satellite system: Current status and perspectives 11 p1713 N85-20776
The ESA remote sensing satellite system (ERS-1) 11 p1713 N85-20777
Earth resources research using the Shuttle Imaging Radar system 11 p1713 N85-20779
JPL highlights [NASA-CR-175517] 11 p1767 N85-21102
NASA's land remote sensing plans for the 1980's 13 p2124 N85-23224
A silicic shield volcano in Bolivia 13 p2187 N85-23572
Utilization of the polar platform of NASA's Space Station Program for operational Earth observations [PB85-152502] 14 p2240 N85-23895
Environmental satellites 14 p2328 N85-24362
Observation of polar aurora from the Salyut-6 space station during the great geomagnetic storm of 11-13 Apr. 1981 15 p2477 N85-25291
Determining characteristics of optical radiation reflectors based on results of remote sensing 15 p2488 N85-25358
Use of space photographic information to map plant cover 15 p2488 N85-25359
Selection of a model of Earth's albedo radiation, practical calculation of its effect on the trajectory of a satellite [NASA-TM-77870] 15 p2591 N85-25972
Satellite detection of severe thunderstorms 15 p2596 N85-25998
NOAA satellite operations: Programs briefing — Environmental satellites, LANDSAT, and space station polar platform 15 p2599 N85-26020
Space methods in oceanology [NASA-TM-77652] 15 p2604 N85-26047
Application of space methods in geodesy 16 p2724 N85-26817
Tenth Conference of Working Group of Socialist Countries on Remote Sensing of Earth under Intercosmos Program 16 p2725 N85-26820
Contribution to space program reviewed 16 p2727 N85-26834
Status of the observational data sets — TOPEX 16 p2804 N85-27286
Shuttle imaging radar-A (SIR-A) data analysis — geology of the Ozark Plateau of southern Missouri, land use in western Illinois, and vegetation types at Koonamore Station, Australia [NASA-CR-175785] 16 p2809 N85-27324
Modular Optoelectronic Multispectral Scanner (MOMS) for Earth observation. First results of STS-7 mission [MBB-UR-717/83-O] 16 p2874 N85-27732
Experimental philosophy leading to a small scale digital data base of the conterminous United States for designing experiments with remotely sensed data [NASA-TM-85009] 17 p3049 N85-28677
Looking down looking forward: Earth observation, sciences and applications, a perspective [ESA-SP-1073] 18 p3149 N85-29497
Space optics [CNES-84/105/T/CT/DRT/TIT/10] 20 p3533 N85-31965
Large format camera photographs: A new tool for understanding arid environments 21 p3604 N85-32379
Quantitative geomorphologic studies from spaceborne platforms 21 p3604 N85-32381
Process thresholds: Report of Working Group Number 3 21 p3604 N85-32384
Planetary perspective. Report of Working Group Number 4 21 p3605 N85-32385
Properties of aerosol particles detected by satellites in coastal regions 21 p3641 N85-32622
Cosmonauts participate in multilevel remote sensing experiment 22 p3731 N85-33130
Physico-geographical regionalization of Caspian lowland based on space survey materials 22 p3736 N85-33162

EARTH ORBITING SPACE STATIONS
U EOSS

EARTH ORBITS
NT PERIGEES
Study of proton and neutron activation of metal samples in low Earth orbit [NASA-CR-171183] 01 p0026 N85-10164
Winged first stages of space transport appliances [TUM-RT-TB-84/3] 02 p0167 N85-11125
Capture of planetesimals into a circumterrestrial swarm 04 p0568 N85-13751
Contributions to the error analysis in the relativity gyroscope experiment 05 p0638 N85-14095
Theory of the orbital motion of an artificial Earth satellite [NAL-TR-807] 06 p0758 N85-14847
Electric fields in Earth orbital space [AD-A146448] 06 p0835 N85-15313
Broadening the debate 07 p0914 N85-15785
OTV propulsion tecnology programmatic overview 08 p1107 N85-16997
Computer subroutines for estimation of human exposure to radiation in low Earth orbit [NASA-TM-86324] 08 p1199 N85-17550
Report of the Constellations Panel 11 p1645 N85-20368
A model for the evolution of on-orbit manmade debris environment 12 p1784 N85-21196
Debris in the geostationary orbit ring, the endless shooting gallery: The necessity for a disposal policy 12 p1786 N85-21214
Considerations for policy on man-made debris propagation control 12 p1787 N85-21219
Environment definition, large particles 12 p1787 N85-21220
Modeling 12 p1787 N85-21221
Measurements 12 p1787 N85-21222
Environment definition, small particles, diameter less than or equal to 1 MM 12 p1786 N85-21223
Spacecraft hazard and shielding requirements 12 p1786 N85-21224
Radiation exposure and performance of multiple burn LEO-GEO orbit transfer trajectories [NASA-TM-86946] 12 p1788 N85-21228
Characterization of material surfaces exposed to atomic oxygen on space shuttle missions 12 p1946 N85-22220
Nontraditional method for determining unperturbed orbits of unknown space objects using incomplete optical observational data 13 p1979 N85-22417
Spacecraft Environmental Interactions Technology, 1983 [NASA-CP-2359] 13 p1989 N85-22470
Argon ion pollution of the magnetosphere 13 p1996 N85-22523
Nation said to rank high with 15 satellites 13 p2041 N85-22778
Mission analysis and orbit control of the hallosynchronous satellite SPOT 14 p2397 N85-24773
Cosmic ray environment model for Earth orbit [NASA-CR-175666] 14 p2455 N85-25165
Some numerical estimates of perturbation of orbital elements of artificial Earth satellite with total dynamic symmetry about rotating aspherical Earth 15 p2478 N85-25294
Autonomous state determination for an Earth orbiting satellite using horizon and star sensors [AD-A151827] 15 p2493 N85-25379
Nondestructive equipment study [NASA-CR-171865] 15 p2571 N85-25853
Examination of returned solar-max surfaces for impacting orbital debris and meteoroids 15 p2681 N85-26560
Simultaneous Earth observations from 2 satellites [NASA-TM-86204] 16 p2810 N85-27325
Maximizing the semi-major axis for a freely coning solar sailcraft [AD-A153175] 17 p2909 N85-27938
Study of Kapton under simulated shuttle environment [NASA-CR-176003] 19 p3225 N85-29997
LEO life testing with different charge control 20 p3446 N85-31393
Flight experience of Solar Mesosphere Explorer's two nickel-cadmium batteries 20 p3446 N85-31396
Design principles for nickel hydrogen cells and batteries 20 p3447 N85-31398
Life cycle test results of a bipolar nickel hydrogen battery 20 p3448 N85-31406
Procedure for estimating orbital debris risks [NASA-TP-2507] 22 p3738 N85-33169

EARTH PLANETARY STRUCTURE
Stratigraphy, sedimentology and tectonic significance of the Upper Cretaceous Virginian Ridge formation, Method Basin, Washington: Implications for tectonic history of the North Cascades 03 p0390 N85-12494
Individual geopotential coefficients of order 15 and 30, from resonant satellite orbits [AD-A146867] 06 p0628 N85-15256
Khibiny experiment described 07 p0961 N85-16230
Earth 09 p1411 N85-18892
Crustal dynamics studies in China [NASA-CR-175817] 13 p2132 N85-23265
Submarine volcanic eruptions and potential analogs for Venus 13 p2187 N85-23573
Altimetry data and the elastic stress tensor of subduction zones [NASA-CR-175796] 16 p2825 N85-27425
Highly important features of regional tectonics of Earth's Arctic sector 19 p3298 N85-30449
Development of ultrasonic modeling techniques for the study of crustal inhomogeneities [AD-A155206] 21 p3632 N85-32585
Conditions during formation of the Earth 21 p3717 N85-33066
Constraints on the development of the early continental crust from isotopic data 21 p3719 N85-33076
Anorthositic oceanic crust in the Archean Earth 21 p3719 N85-33077
A model for core formation in the early Earth 21 p3719 N85-33078
Implications for the Earth of the early dynamical environment 21 p3719 N85-33079
Chemical evolution of the Earth: Equilibrium or disequilibrium process? 21 p3721 N85-33088
Earth's primordial differentiation, and its after-effects 21 p3722 N85-33092
Landscape interpretation capabilities using space photographs of regions of a multistage platform mantle structure 22 p3734 N85-33151

EARTH RADIATION
U TERRESTRIAL RADIATION

EARTH RADIATION BUDGET EXPERIMENT
Earth radiation budget experiment software development
[NASA-CR-172567] 12 p1912 N85-22002
An Earth longwave radiation climate model
[NASA-CR-175740] 15 p2504 N85-25984
Origin of the Greenland ice sheet
15 p2604 N85-26046
Year-to-year variability of components of Earth's radiation budget according to satellite measurement data 16 p2725 N85-26821
Validation of the ERBE scanner scene identification methodology: Analysis with Nimbus-7 ERB data
[NASA-CR-172586] 16 p2832 N85-27466
Solar radiance models for determination of ERBE scanner filter factor
[NASA-CR-172585] 17 p2995 N85-28513
Space Station Polar Platform: integrating research and operational missions
[PB85-195279] 24 p4069 N85-35218
The 1986 National Aeronautics and Space Administration authorization
[GPO-47-635] 24 p4166 N85-35829

EARTH RESOURCES
NT AQUIFERS
NT COAL
NT CRUDE OIL
NT FORESTS
NT FOSSIL FUELS
NT GEOTHERMAL RESOURCES
NT GEYSERS
NT GLACIERS
NT ICEBERGS
NT LAND ICE
NT LIGNITE
NT MARINE RESOURCES
NT OIL FIELDS
NT PEAT
NT RAIN FORESTS
NT SPRINGS (WATER)
NT TAR SANDS
NT THERMAL RESOURCES
NT UNDERWATER RESOURCES
NT WATER RESOURCES
Geophysical experiments, photography aboard Salyut-7 02 p0157 N85-11066
Salyut-7 crew in orbit 150 days
02 p0157 N85-11068
Choice of cartographic projection for space system data bank used in studying natural resources
02 p0165 N85-11119
Seismology 1983: Nuclear test ban verification, earthquake and Earth resource investigation
[FOA-C-20537-T1] 02 p0229 N85-11495
Satellite, airborne remote sensing development outlined 03 p0342 N85-12190
Corporate use of information regarding natural resources and environmental quality
[PB84-222736] 03 p0439 N85-12794
Deep seabed stable reference areas
[PB84-241470] 09 p1360 N85-18555
Reducing gull use of some attractions near airports
[AD-P004195] 11 p1581 N85-19982
Remote sensing technology now playing practical roles 11 p1619 N85-20190
Monitoring approaches for assessing quality of high altitude lakes: Colorado Flat Tops Wilderness Area
[PB85-117232] 11 p1679 N85-20579
Sourcebook: Gaining access to US government information on the environment and natural resources
[DE84-017419] 11 p1740 N85-20941
Process development for commercial production of natural rubber from Guayule
[PB85-124958] 12 p1815 N85-21388
Remote sensing used for study of forest resources
13 p1983 N85-22440
Characteristics of alumyte deposits discussed
13 p2166 N85-23438
An analysis of issues concerning acid rain, report to the Congress of the United States
[TI85-001070] 15 p2589 N85-25959
Comparative study of the digital analysis of areas of the Earth's surface prepared for planting using different classification algorithms
[INPE-3359-PRE/637] 16 p2846 N85-27545
Thermal Infrared Multispectral Scanner (TIMS): An investigator's guide to TIMS data
[NASA-CR-175875] 17 p2961 N85-28288
Yearbook of the Bureau of Mineral Resources, Geology and Physics: Geoscientific research, resource assessment, and database development, 1 Jul. 1983 to 30 Jun. 1984
[BMR-84] 17 p2999 N85-28474
Earth Resources: A continuing bibliography with indexes, issue 45
[NASA-SP-7041(45)] 18 p3123 N85-29336
Remote Sensing Technology: Symposium Proceedings
[DE85-010212] 20 p3477 N85-31606
Gas hydrates
[DE85-001988] 20 p3477 N85-31607
The U.S. Geological Survey in Alaska: Accomplishments during 1982
[US-GEOL-SURV-CIRC-939] 20 p3483 N85-31719
Geologic and hydrologic characterization and evaluation of the basin and range province relative to the disposal of high-level radioactive waste. Part 1: Introduction and guidelines
[GS-CIRC-904-A] 20 p3526 N85-31932
Handbook for obtaining and using aerial photography to map aquatic plant distribution
[AD-A154584] 21 p3605 N85-32366
Cosmonauts participate in multilevel remote sensing experiment 22 p3731 N85-33130
Indications of mineral zoning in a fossil hydrothermal system at the Meager Creek geothermal prospect, British Columbia, Canada from induced polarization studies
[DE85-011962] 22 p3815 N85-33636
Geology and petroleum resources of basins in western China
[DE85-013098] 23 p3948 N85-34469
The scientific and technical issues in integrating remotely sensed imagery with geocoded data bases
23 p3960 N85-34547
Selection of segment similarity measures for hierarchical picture segmentation 23 p3960 N85-34548
Satellites and politics: Weather, communications, and earth resources 23 p4057 N85-35144
Microwave properties of a quiet sea
[NASA-CR-176199] 24 p4065 N85-35322
USGS coastal research, studies and maps: A source of information for coastal decision making
[USGS-CIRC-883] 24 p4108 N85-35465
Remote sensing of hydrologic transport processes using spot simulation data
[DE85-012412] 24 p4108 N85-35467

EARTH RESOURCES PROGRAM
Earth Resources, A Continuing Bibliography with Indexes
[NASA-SP-7041(43)] 03 p0378 N85-12411
Earth resources: A continuing bibliography with indexes
[NASA-SP-7041(44)] 10 p1503 N85-19484

EARTH RESOURCES SHUTTLE IMAGING RADAR
Earth resources research using the Shuttle Imaging Radar system 11 p1713 N85-20779

EARTH RESOURCES TECHNOLOGY SATELLITE D
U LANDSAT 4

EARTH RESOURCES TECHNOLOGY SATELLITE 1
U LANDSAT 1

EARTH RESOURCES TECHNOLOGY SATELLITES
U LANDSAT SATELLITES

EARTH ROTATION
Basic research for the geodynamics program
[NASA-CR-174055] 02 p0228 N85-11490
Development of optical techniques for Earth rotational measurements
[AD-A145850] 03 p0364 N85-12333
The Moon's orbit history and inferences on its origin
04 p0585 N85-13735
A reappraisal of Darwin's fission hypothesis and a possible limit to the primordial angular momentum of the Earth 04 p0585 N85-13736
The motion of the Earth by Doppler observing campaign (MEDOC) 05 p0601 N85-13831
Research in geodesy based upon radio interferometric observations of extragalactic radio sources
[AD-A147561] 07 p0958 N85-16260
The wobble of the Earth and the low frequency dynamics of the ocean 09 p1358 N85-18546
The accuracy of radio interferometric measurements of Earth rotation 10 p1465 N85-19246
Earth rotation and polar wandering
14 p2399 N85-24785
The MEDOC 2: Experimental Doppler measurement of Earth kinematics 14 p2399 N85-24786
Spectral analysis of diurnal nonuniformity of Earth's rotation 15 p2477 N85-25280
Some numerical estimates of perturbation of orbital elements of artificial Earth satellite with total dynamic symmetry about rotating aspherical Earth
15 p2478 N85-25294
Full shadow phenomenon in Earth's upper atmosphere 16 p2908 N85-27316
New stations supporting crustal dynamics project VLBI measurements 20 p3491 N85-31701
Crustal dynamics project data analysis fixed station VLBI geodetic results
[NASA-TM-86229] 21 p3615 N85-32465

EARTH SHAPE
U GEODESY

EARTH SURFACE
The development of objective forecast techniques based on advection of surface weather parameters
01 p0078 N85-10622
Evaluation of surface sensible heat flux effects on the generation and modification of mesoscale circulations
01 p0079 N85-10627
Predicting optical image displacement velocity in survey of Earth's surface 02 p0165 N85-11118
Plane wave (EMP) incidence on a finitely conducting plane Earth with the magnetic field intensity parallel to the Earth's surface
[DE84-015364] 02 p0229 N85-11493
Mars-Earth geographical comparisons: A pictorial view
[NASA-TM-86166] 02 p0302 N85-11957
Long-distance propagation of infrasound in atmosphere near Earth's surface 06 p0625 N85-15238
Sensor-atmosphere-target simulation. Computer program SENSAT
[DFVLR-FB-84-32] 08 p1178 N85-17419
Earth 09 p1411 N85-18892
Polar regions and climatic change: Appendix
[PB85-122679] 10 p1521 N85-19580
Evaluation of the radiometric quality of the TM data using clustering, linear transformations and multispectral distance measures — Illinois 12 p1870 N85-21731
The origin and evolution of terrestrial and Martian rock labyrinths
[NASA-CR-175511] 12 p1981 N85-22328
Choice of optimum pairs of spectral intervals for IR-range survey of Earth's surface 15 p2486 N85-25944
Evaluating radiation distortions of optical image of Earth's surface in horizontally inhomogeneous atmosphere 15 p2488 N85-25945
Measuring methods of atmospheric electric elements at the Earth's surface during snowfall and investigation of these relationships 15 p2581 N85-25920
Selection of a model of Earth's albedo radiation, practical calculation of its effect on the trajectory of a satellite
[NASA-TM-77870] 15 p2591 N85-25972
Preliminary interpretation of Saudi Arabian seismic refraction data 17 p2969 N85-28477
Expedient runway surfacing with post tensioning system for expeditionary airfields
[AD-D011677] 19 p3222 N85-29978
HANDTC: A FORTRAN program to calculate inner-zone terrain corrections
[DE85-011196] 19 p3340 N85-30699
Geomorphological similarity and uniqueness
21 p3601 N85-32361
Quantitative analysis of geomorphic processes using satellite image data at different scales
21 p3604 N85-32380
Quantitative geomorphologic studies from spaceborne platforms 21 p3604 N85-32381
Global geomorphology: Report of Working Group Number 1 21 p3604 N85-32382
Landscape inheritance: Report of Working Group Number 2 21 p3604 N85-32383
Planetary perspective. Report of Working Group Number 4 21 p3605 N85-32385
Upward continuation of surface gravity anomalies
[AD-A154973] 21 p3631 N85-32560
Large arcuate scars: A geological legacy of the Earth's accretionary past 21 p3721 N85-33089
Landscape interpretation capabilities using space photographs of regions of a multistage platform mantle structure 22 p3734 N85-33151
Cataloging the spectral brightness coefficients of the forested region of the European territory of the USSR
22 p3735 N85-33155
Gravity gradiometer survey data processing
[AD-A156165] 24 p4117 N85-35522

EARTH TERMINALS
The Ferranti Tactical SHF SATCOM station (MANSAT) 11 p1710 N85-20759
Tactical satellite terminals for land and airborne C3 applications 11 p1710 N85-20760
Moon bounce communications to small terminals
[AD-A153297] 17 p2950 N85-28212

EARTH TIDES
Effects of the oceans on polar motion: Continued investigations
[E85-10037] 03 p0379 N85-12418
Constraints on the origin of viscoelastic bodies
04 p0584 N85-13732
Tidal dissipation in the Earth and Moon from lunar laser ranging 04 p0585 N85-13733
Ocean tide models for Topex analysis
16 p2905 N85-27291
Analysis and modeling of variations in length of day
19 p3349 N85-30781
Interpolation problems in meteor radar analysis, part 7.6A 21 p3626 N85-32528

EARTH-MOON SYSTEM
Two lunar global asymmetries
04 p0585 N85-13734
The Moon's orbit history and inferences on its origin
04 p0585 N85-13735
A reappraisal of Darwin's fission hypothesis and a possible limit to the primordial angular momentum of the Earth 04 p0585 N85-13736
Numerical simulations of fission
04 p0585 N85-13737
The dynamic fission instability and the origin of the Moon 04 p0586 N85-13738
A testable gravitational capture model for the origin of the Earth's Moon 04 p0586 N85-13742
The problem of iron partition between Earth and Moon during simultaneous formation as a double planet system 04 p0587 N85-13744
The evolution of complex and higher organisms
[NASA-SP-478] 21 p3856 N85-32708
The coorbital hypothesis 22 p3858 N85-33690
The magnetic field of planets
22 p3858 N85-33691

EARTH-VENUS TRAJECTORIES
Kovtunenko discusses Vega Project
16 p2722 N85-26804

EARTHQUAKE DAMAGE
Characteristics of a recent Columbian earthquake, December 12, 1979 04 p0523 N85-13347

EARTHQUAKE RESISTANCE
Refined modeling of reinforced concrete columns of seismic analysis
[PB84-234364] 04 p0484 N85-13090
Assessment of seismic survivability
09 p1336 N85-18402

EARTHQUAKE RESISTANT STRUCTURES
Earthquake engineering facilities and instrumentation
[PB84-231661] 04 p0504 N85-13220
Assessment of seismic survivability
09 p1336 N85-18402
Seismic analysis of rotating mechanical systems
[PB85-149599] 14 p2311 N85-24307

EARTHQUAKES
NASA Geodynamics Program
[NASA-TM-87359] 01 p0063 N85-10418
Seismology 1983: Nuclear test ban verification, earthquake and Earth resource investigation
[FOA-C-20537-T1] 02 p0229 N85-11495
Earthquake activity in the Bohemian massif and in the western Carpathians
[REPT-547] 03 p0375 N85-12390
Specific phenomena associated with the propagation of seismic waves in central Europe
[REPT-548] 03 p0375 N85-12391
Catalogue of earthquakes for the territory of Czechoslovakia for the period 1957 - 1980
[REPT-555] 03 p0376 N85-12398
Finite-difference synthetic seismograms for SH waves
[AD-A145834] 03 p0392 N85-12508
Horizontal-strain observations in the Shumagin Island and Yakataga seismic gaps, Alaska
04 p0515 N85-13257
Seismology today 04 p0523 N85-13346
Characteristics of a recent Columbian earthquake, December 12, 1979 04 p0523 N85-13347
A review of seismicity in peninsular Spain
04 p0523 N85-13349
Models for volcanic processes in Long Valley, California: Testing by continental drilling
[DE84-014943] 04 p0534 N85-13414
Earthquake catalog for northern New Mexico
[DE84-016684] 04 p0534 N85-13416
A computational study of two possible intraplate earthquake triggering mechanisms
05 p0674 N85-14329
Documentation of earthquake algorithms
[PB84-235324] 05 p0677 N85-14351
Earthquakes and tectonics of Pacific Ocean margins
06 p0820 N85-15206
Statistical relationship of strong earthquakes with planetary geomagnetic field activity
06 p0820 N85-15209
Possible effects of interaction of electric seismic fields with the ionosphere 06 p0823 N85-15228
Evaluation of the RSTN (Regional Seismic Test Network) network and further improvement to automatic association
[AD-A146306] 06 p0835 N85-15312
General model of earthquakes and the place of warnings in it 07 p0981 N85-16232
Earthquake forecasting research in the Ukraine
07 p0981 N85-16233
Model of earthquake mechanism
07 p0982 N85-16236
Research activities of the Norwegian seismic array (NORSAR)
[AD-A146778] 07 p0996 N85-16326
Seismicity of southern Sweden
[FOA-C-20543-T1] 07 p0998 N85-16340
The Shock and Vibration Digest, volume 16, no. 11
[AD-A148466] 08 p1171 N85-17382
Seismic performance of low-rise light-framed wood buildings 08 p1171 N85-17384
Earthquake-modeling experiment using unique press
10 p1500 N85-19469
Localization of destruction process
10 p1500 N85-19470
Study of tectonic earthquake precursors by geodetic methods 10 p1502 N85-19479
Influence of scattering on Q in the lithosphere
[AD-A149318] 10 p1515 N85-19583
High-resolution microseismicity study of possible magmatic intrusion in the Long Valley Caldera
[DE85-001076] 11 p1681 N85-20583
Catalog of submarine volcanoes and hydrological phenomena associated with volcanic events: 1500 BC to 31 Dec. 1899
[PB85-117984] 12 p1891 N85-21869
Observation of long-period oscillations of Earth
13 p2110 N85-23149
Space and time distribution of aftershocks
13 p2112 N85-23157
Magmatism in continent-ocean transition zone (development of ideas of A. N. Zavaritskiy)
13 p2113 N85-23161
Study of geological media based on scattered earthquake waves 13 p2114 N85-23168
Geomagnetic precursors of intensive earthquakes in the 1-0.-2 Hz frequency range of geomagnetic pulsations
13 p2116 N85-23178
Attenuation of seismic waves at regional distances
[AD-A150198] 13 p2132 N85-23267
Study of earthquake preparation processes from distribution of weak tremor epicenters
14 p2345 N85-24501
Seafloor seismic measurements in the southern Bering
[DE85-004908] 14 p2374 N85-24675
Innovation in earthquake and natural hazards research: Determining soil liquefaction potential
[PB85-149573] 14 p2374 N85-24678
A seismic ARGOS data collection platform
16 p2813 N85-27350
Response of a wind turbine blade to seismic and turbulent wind excitations 16 p2817 N85-27375
The Shock and Vibration Digest, volume 17, no. 2
[AD-A153129] 17 p2977 N85-28400
The effects of seismic waves
17 p2978 N85-28401
Australian seismological report, 1980
[REPT-252] 17 p2989 N85-28473
Revised draft: Southeastern regional geologic characterization report
[DE85-008265] 18 p3125 N85-29351
Kuril-Aleutian subduction 19 p3290 N85-30402
Discovery in earthquake forecasting and seismic zoning recorded 19 p3295 N85-30426
Satellite-determined stresses in the crust of Europe with particular consideration to the Liege earthquake of November 8, 1983 20 p3490 N85-31694
Seismic discrimination
[AD-A154167] 20 p3494 N85-31722
Design of a freestanding noise measurement and recording system to predict the intensity and location of electromagnetic radiation from earthquakes
[AD-A155070] 21 p3632 N85-32563
Tectonic stability and expected ground motion at Yucca Mountain
[DE85-012004] 22 p3814 N85-33629
Compressional environment in the location and orientation of planetary dorsa and terrestrial earthquake fault structures 22 p3857 N85-33665
Scaling differences between large interplate and intraplate earthquakes
[NASA-CR-176149] 23 p3948 N85-34467
Geophysical-geological studies of possible extensions of the New Madrid fault zone
[TI85-901341] 23 p3949 N85-34475
Crustal structure in southern California from array data
24 p4115 N85-35512
Attenuation properties of the Petatlan region, Mexico, and a local magnitude scale for microearthquakes in this area 24 p4116 N85-35513
Simplified procedures for the evaluation of settlements in sands due to earthquake shaking
[PB85-197887] 24 p4116 N85-35527
Carbon fiber strainmeter studies in southern California
[PB85-196889] 24 p4116 N85-35528
Groundwater radon studies for earthquake precursors in southern California
[PB85-196871] 24 p4116 N85-35529

EAST GERMANY
Limited surface observations climatic summary (LISCOS). Hohenfels, AAF, West Germany
[AD-A147167] 07 p1006 N85-16383
Revised Uniform Summary of Surface Weather Observations (RUSSWO). Parts A-F Zweibrucken AB, Germany
[AD-A147165] 09 p1357 N85-18538
East Europe report: Science and technology
[JPRS-ESA-85-005] 09 p1377 N85-18659
East European report: Science and technology
[JPRS-ESA-85-010] 15 p2524 N85-25580

EATING
Characteristics of human masseter under conditions of hypokinesia 11 p1691 N85-20630
Psychobiology and food perception
14 p2394 N85-24745
The effects of prolonged feeding meal, ready-to-eat (MRE) operational rations
[AD-A154763] 21 p3666 N85-32773

EBR-2 REACTOR
U EXPERIMENTAL BREEDER REACTOR 2

EBULLITION
U BOILING

ECCENTRIC ORBITS
Galactic orbits of globular clusters
05 p0739 N85-14750
Stability of the Galilean satellites in deep orbital resonance 13 p2172 N85-23477
Studies of planetary rings 13 p2174 N85-23488
Dynamical studies of Saturn's rings
13 p2174 N85-23489
The eccentric ringlet at 1.29 R sub S — Saturn radius (RS) 15 p2673 N85-26496

ECCENTRICITY
The structure of the Uranian rings and the search for rings around Neptune 02 p0302 N85-11954
Buckling and eccentricity effects on orifice metering accuracy — gas meters
[ERS-E.350] 09 p1324 N85-18321
An experimental investigation into the effects of plate eccentricity and elastic deformation on orifice meter accuracy
[ERS-E.391] 09 p1325 N85-18325
Studies of icy bodies: Uranian satellites and cometary nuclei 13 p2175 N85-23496
Global positioning system: A modification to the baseline satellite constellation for improved geometric performance
[AD-A151692] 15 p2469 N85-25239

ECHELETTE GRATINGS
Calibrations of wavelengths in SWP echelle spectra
11 p1761 N85-21077
A new generation of spectrometer designs for ultraviolet astronomy 11 p1761 N85-21079

ECHELON FAULTS
U GEOLOGICAL FAULTS

ECHO SOUNDING
High-frequency asymptotic behavior of reflected and transmitted waves during scattering of sound by hollow elastic sphere filled with fluid 02 p0266 N85-11736
Technical data on new engineering products
10 p1460 N85-19201
Acoustooptic pulse-echo transducer system
[NASA-CR-175919] 17 p2951 N85-28224

ECHO SUPPRESSORS
Interference suppressor for radar MTI
[AD-D011606] 16 p2769 N85-27086

ECHOCARDIOGRAPHY
Study and realization of a Doppler system with pulsed, directional, multiport (128) emission and sequential signal treatment — ultrasonic echography, blood flow
[ENST-84E008] 05 p0639 N85-14102

ECHOES
NT CLUTTER
NT LUNAR RADAR ECHOES
NT RADAR ECHOES
NT RADIO ECHOES
NT SIGNAL REFLECTION
NT VENUS RADAR ECHOES
Resonant scattering of acoustic waves by elastic spherical shell in fluid 06 p0778 N85-14972
Self-adaptive echo cancellation for telephony
[ENST-84E013] 20 p3441 N85-31353

ECLIPSES
NT SOLAR ECLIPSES
A model for eclipsing cataclysmic variables
13 p2171 N85-23467

ECLIPSING BINARY STARS
NT DWARF NOVAE
Observations of the O-type subdwarf eclipsing binary system LB 3459 (AA Dor) 01 p0128 N85-10681
Accretion in the zeta Aurigae and 32 Cygni shock cones 11 p1754 N85-21036
Eclipse observations of Epsilon Aurigae
11 p1755 N85-21037

UV observations of epsilon aurigae during ingress and totality 11 p1755 N85-21036
Egress spectra of the new eclipsing supergiant 22 Vulpeculae 11 p1755 N85-21039
The stellar wind in the BO V-type eclipsing binary Y Cygni 11 p1755 N85-21040
Ultraviolet spectroscopy of the interacting binary U Sagittae 11 p1755 N85-21042
The eclipsing binary U Sagittae: Evidence for CNO processing and mass exchange in the past 11 p1757 N85-21049
Tasks for observations of close binary systems in the extreme ultraviolet 11 p1757 N85-21054
Photoelectric observations of the eclipsing binary V 836 Cygni
[REPT-98] 15 p2668 N85-26482

ECLIPTIC
Electric field in plasma layer of magnetosphere during preliminary substorm phase 06 p0824 N85-15231
An update on the correlation between the cosmic radiation intensity and the geomagnetic AA index
[SH-4.2-24] 23 p4009 N85-34861

ECLOGITE
Anorthositic oceanic crust in the Archean Earth 21 p3719 N85-33077

ECOLOGICAL SYSTEMS
U ECOLOGY

ECOLOGY
NT COASTAL ECOLOGY
Mineral nutrients in Mediterranean ecosystems
[REPT-71] 01 p0069 N85-10456
Future scenarios and ozone change
[DE84-014781] 01 p0085 N85-10573
Fungi of Mt. Babia Gora. 2: Indicative value of macromycetes in forest associations. A: Initial considerations
[NASA-TM-77485] 01 p0094 N85-10632
Fungi of Mount Babia Gora. 3: The indicating value of macromycetes in the forest associations
[NASA-TM-77486] 01 p0094 N85-10633
East Europe report: Science and technology
[JPRS-ESA-84-030] 01 p0101 N85-10670
East Europe report: Science and technology
[JPRS-ESA-84-038] 03 p0343 N85-12210
An integrated remote sensing approach for identifying ecological range sites — parker mountain
[E85-10050] 07 p0983 N85-16246
Relationship between forest clearing and biophysical factors in tropical environments: Implications for the design of a forest change monitoring approach — Costa Rica
[E85-10051] 07 p0983 N85-16247
Ecological impacts of hydroelectric projects in Amazonia 07 p1003 N85-16374
Analysis of terrestrial conditions and dynamics
[E85-10063] 08 p1174 N85-17401
Comparing computing formulas for estimating concentration ratios
[DE84-006644] 09 p1349 N85-18490
Calculation of optical characteristics of shelf ecological system based on its mathematical model 10 p1498 N85-19453
Blackbirds and starlings: Population ecology and habits related to airport environments
[AD-P004190] 11 p1580 N85-19953
The bird strike situation and its ecological background in the Copenhagen Airport, Kastrup
[AD-P004203] 11 p1582 N85-19970
Effect of elevated atmospheric CO2 on plant communities
[DE85-001810] 11 p1678 N85-20576
Large natural geophysical events: Planetary planning
[DE85-000859] 11 p1763 N85-21092
Rationale and basic design for experimental acidification of a lake ecosystem in Northern Wisconsin
[PB85-116077] 12 p1885 N85-21829
Evaluation of carrying capacity and landscape damage in northern Kenya by multistage remote sensing
[DFVLR-FB-84-47] 14 p2347 N85-24514
Controlled Ecological Life Support Systems (CELSS) 15 p2666 N85-26604
ELF (Extremely Low Frequency) communications system ecological monitoring program: Measurements of ELF electromagnetic fields for site selection and characterization, 1983
[AD-A153120] 17 p2949 N85-29209
USSR report: Life sciences. Biomedical and behavioral sciences
[JPRS-UBB-85-017] 20 p3504 N85-31785
The global sulfur cycle
[NASA-TM-87570] 21 p3666 N85-32710
Sulfur cycling and metabolism of phototrophic and filamentous sulfur bacteria 21 p3680 N85-32737
Environmental summary for calendar year 1984
[DE85-012020] 22 p3810 N85-33604
Environmental surveillance at Los Alamos during 1984
[DE85-011886] 22 p3811 N85-33605
A 1984 environmental summary: Sandia National Laboratories Tonopah Test Range, Tonopah, Nevada
[DE85-011145] 22 p3812 N85-33612
Model projections of time-dependent response to increasing carbon dioxide
[DE85-013326] 22 p3816 N85-33641
USSR report: Life sciences. Biomedical and behavioral sciences
[JPRS-UBB-85-016] 22 p3819 N85-33660
Climate modeling: A retrospective-prospective view with consideration for the atmospheric carbon dioxide-climate issue
[DE85-011532] 23 p3950 N85-34481
The 1984 biotic studies of Yucca Mountain, Nevada test site, Nye County, Nevada
[DE85-011715] 23 p3951 N85-34487

ECONOMETRICS
Hydrologic and economic models for watershed evaluation and research
[PB84-222371] 01 p0066 N85-10436
A stochastic model for optimizing the consumption and exploration of nonrenewable natural resources
[INPE-2770-PRE/343] 03 p0440 N85-12804
Scientific, technical progress as factor of intensification of economy 13 p2167 N85-23444

ECONOMIC ANALYSIS
Economic model of calibration improvements for automatic test equipment
[PB84-217827] 01 p0051 N85-10335
Uncertainty in water resource planning: An economic evaluation of a water use reduction alternative
[PB84-202605] 01 p0065 N85-10430
Benefits resulting from tailored very-short-range forecasts in Sweden 01 p0084 N85-10564
Foreign civil aviation competition: 1976 summary and implications
[NASA-TM-X-73907] 02 p0133 N85-10907
Satellite servicing: A business opportunity? 02 p0156 N85-11056
Doing business in space: How to get there from here 02 p0156 N85-11057
Space research benefits national economy 02 p0163 N85-11107
Evaluating effectiveness of using space information in specialized hydrogeological research 02 p0164 N85-11114
Robotics investment decision model user's manual
[AD-A145467] 02 p0204 N85-11347
Economic analysis handbook
[AD-A146263] 03 p0441 N85-12805
Report of the reference designs study group on the superconducting super collider
[DE84-015567] 04 p0569 N85-13630
Evaluating NASA technology programs in terms of private sector impacts 05 p0608 N85-13865
Manual-control analysis applied to the money-supply control task 05 p0710 N85-14553
cost and benefits optimization model for fault-tolerant aircraft electronic systems
[NASA-CR-166043] 07 p0946 N85-15993
Development of design and economic parameters for passive solar systems
[AD-A147161] 07 p0993 N85-16303
Life cycle cost management master plan for the Defense Communications Agency
[AD-A146876] 07 p1050 N85-16668
Planning for the on-orbit servicing of military spacecraft
[AD-A148447] 08 p1104 N85-16983
The use of simulation for the technical and economic evaluation of flexible manufacturing systems. Part 2: Results of the simulation
[PNR-90233-PT-2] 09 p1371 N85-18614
Digest of the Deutsche Lufthansa report, 1983
[ISSN-0415-603X] 09 p1418 N85-18948
An assessment of ground-coil heat-pump technology
[DE85-002567] 10 p1486 N85-19362
A decision model for selection of microcomputers and operating systems
[AD-A149076] 10 p1538 N85-19694
Technological and economic assessment of advanced ceramic materials. Volume 2: A case study of ceramic capacitors
[PB85-113108] 11 p1813 N85-20141
Ethanol production by enzymatic hydrolysis: Parametric analysis of a base-case process
[DE84-013105] 11 p1814 N85-20147
Transportation
[JPRS-UTR-85-004] 12 p1789 N85-21105
Current development, applications of airships in USSR 12 p1790 N85-21109
Feasibility of producing commodities and electricity for space shuttle operations at Vandenberg Air Force Base
[DCN-84-203-001-80-21] 12 p1799 N85-21230
Polymer intermediates from limonene (follow-up project)
[BMFT-FB-T-84-243] 12 p1814 N85-21380
Technological and economic assessment of advanced ceramic materials. Volume 1: Summary and conclusions
[PB85-113082] 12 p1815 N85-21383
Closed cycle versus open cycle gas turbines. A review of A.D. Little's ICOP report, vol. 3
[DE85-000584] 12 p1881 N85-21671
FAA aviation forecasts: Fiscal years 1985-1996
[AD-A151080] 14 p2216 N85-23747
MBB/Erno's views, future plans in aerospace activities 15 p2531 N85-25609
Financial, economic commentary on Airbus, European aviation 15 p2536 N85-25648
Kalman filtering and exponential smoothing in economics 15 p2635 N85-26248
Intermediate term forecasting techniques for management
[AD-A151370] 15 p2637 N85-26262
Technical and economic analysis of liquid fuel production from microalgae
[DE85-002926] 16 p2758 N85-27016
New method of calculating the economic effects of corrosion
[BLL-BISI-TRANS-22348-(9022.06)] 17 p2929 N85-29079
An analysis of the economic impact of the AN/APS-134 FLAR (Forward Looking Airborne Radar) retrofit on Coast Guard HC-130 aircraft
[AD-A152619] 17 p2949 N85-29204
Technology and technical efficiency in the Soviet Union: Dominant patterns of constrained optimization in a noncompetitive economic regime
[AD-P004587] 17 p3048 N85-29862
Semicrystalline casting process development and verification
[DE85-007695] 18 p3081 N85-29058
ERS economic impace study
[ESA-CR(P)-1979] 18 p3199 N85-29847
A model for the economic assessment of solar power plants
[DE85-009355] 19 p3381 N85-30977
The helicopter, instrument of choice for health evacuation
[SNIAS-851-220-101] 20 p3393 N85-31051
Improved catalysts for liquid hydrocarbon fuels from syngas
[DE85-011082] 20 p3421 N85-31234
Hidden costs of robotized production systems revealed 20 p3438 N85-31332
Renewable energy research and development outlook, volume 1
[DE85-011577] 20 p3540 N85-32033
Quality analysis 21 p3668 N85-32785
New materials needs in aeronautics
[SNIAS-851-502-101] 22 p3729 N85-33120
Geologic, technical, and economic sensitivity analysis in support of the GRI (Gase Research Institute) tight gas reservoirs project area
[PB85-192276] 22 p3802 N85-33559
Small-hydropower development: The process, pitfalls, and experience. Volume 1: Feasibility studies summary and analysis
[DE85-010639] 22 p3806 N85-33580
Investment justification of robotic technology in aerospace manufacturing. User's manual
[AD-A158193] 24 p4099 N85-35410
Solar pond technology for Navy applications
[AD-A155877] 24 p4112 N85-35488

ECONOMIC DEVELOPMENT
Fusion and its future in Illinois
[DE84-014696] 01 p0122 N85-10833
Methodology for economic evaluation of process technologies in the early research and development stages
[DE84-015863] 05 p0736 N85-14731
Systems research on China in year 2000 12 p1820 N85-21418
China report: Science and technology
[JPRS-CST-85-011] 15 p2551 N85-25748
Spin-offs from technical scientific infrastructures, no. 1 20 p3540 N85-32034
Spin-offs from technical commercial infrastructures, no. 2 20 p3540 N85-32035
Spin-offs from technical scientific research organizations, no. 5 20 p3540 N85-32036
Testimony of Robert A. Frosch before the Subcommittee on HUD and Independent Agencies of the Senate Committee on Appropriations
[NASA-TM-87406] 22 p3738 N85-33173
Federal export assistance programs applicable to the US photovoltaic industry
[NASA-CR-176114] 22 p3849 N85-33641

ECONOMIC FACTORS
Second Symposium on Space Industrialization — space commercialization
[NASA-CP-2313] 02 p0149 N85-11011
Satellite servicing: A business opportunity?
02 p0156 N85-11056
ERS-1 and its potential for industrial utilization
05 p0659 N85-14235
Area handbook series. Honduras: A country study
[AD-A146510] 06 p0927 N85-15253
Socio-economic impact of climate — Mexico
07 p1003 N85-16372
The El Nino phenomenon and its agrometeorological implications 07 p1004 N85-16382
Development of high-efficiency economic systems for photovoltaics 12 p1880 N85-21795
USSR report: Science and technology policy
[JPRS-UST-85-002] 13 p2167 N85-23442
Economic mechanism of integration of science, production 13 p2167 N85-23443
Ecology of Pamlico River, North Carolina: An estuarine profile
[PB85-155703] 16 p2822 N85-27404
Foundations of data envelopment analysis for Pareto-Koopmans efficient empirical productions functions
[AD-A154244] 19 p3346 N85-30735
A model for the economic assessment of solar power plants
[DE85-009055] 19 p3381 N85-30977
Nomographs for estimating the levelized cost of energy from flat-plate and concentrator photovoltaic systems
[NASA-CR-176048] 20 p3483 N85-31645

ECONOMIC IMPACT
Increased joint avionics standardization could result in major economies and operational benefits
[AD-A145730] 02 p0139 N85-10945
The embedded test (BIT): Impact on the total cost of possession 06 p1063 N85-16734
International airport study: How to improve the effect of airports on trade and on export-related industries
[PB85-124923] 11 p1586 N85-19992
Technological and economic assessment of advanced ceramic materials. Volume 2: A case study of ceramics in heat engine applications
[PB85-113090] 12 p1815 N85-21384
Technological and economic assessment of advanced ceramic materials. Volume 5: A case study of ceramic toxic and combustible gas sensors
[PB85-113124] 12 p1815 N85-21386
Industrial laser use expanding in the USSR
15 p2644 N85-26310
New method of calculating the economic effects of corrosion
[BLL-BISI-TRANS-22348-(6022.06)] 17 p2929 N85-29079
An analysis of the economic impact of the AN/APS-134 FLAR (Forward Looking Airborne Radar) retrofit on Coast Guard HC-130 aircraft
[AD-A152619] 17 p2949 N85-29204
ERS economic impace study
[ESA-CR(P)-1979] 18 p3199 N85-29647
Foundations of data envelopment analysis for Pareto-Koopmans efficient empirical productions functions
[AD-A154244] 19 p3346 N85-30735
Aviation noise effects
[AD-A154319] 19 p3352 N85-30776

ECONOMICS
NT DEMAND (ECONOMICS)
International cooperation and competition in space. Introduction 02 p0295 N85-11912
Problems in CEMA microelectronic cooperation noted
03 p0341 N85-12196
High-temperature steam electrolysis: Technical and economic evaluation of alternative process designs
[DE84-015702] 04 p0469 N85-12986
USSR report: Machine tools and metalworking equipment
[JPRS-UMM-84-020] 04 p0491 N85-13126
Economic value of consumer information: A selected, annotated bibliography
[PB84-235795] 04 p0576 N85-13673
Manual-control analysis applied to the money-supply control task 05 p0710 N85-14553
Review of climate problems in Latin America and the Caribbean 07 p1001 N85-16354
Oceanographic data for development of the US exclusive economic zone
[PB85-106458/GAR] 07 p1010 N85-16415
An evaluation of the effect of establishing a minimum Economic Order Quantity (EOQ) on the Air Force EOQ item management system
[AD-A147121] 07 p1051 N85-16673
USSR report: Machine tools and metalworking equipment
[JPRS-UMM-85-001] 08 p1139 N85-17172
Summaries of press automation conference presented
08 p1139 N85-17173
FRG study looks at participation in ESA, US space station 08 p1141 N85-17191
Safety awareness, pilot education, and incident reporting programs 09 p1276 N85-18020
Issues in air transport
[PB85-121374/GAR] 09 p1277 N85-18030
National Machine Tools Conference slated for 1985: Conference agenda, papers 10 p1480 N85-19202
USSR report: Machine tools and metalworking equipment
[JPRS-UMM-85-003] 10 p1481 N85-19211
Long-range electronics program outlined
11 p1700 N85-20687
Latent heat storage technology and application workshop. Summary report: Session 6
[DE85-001097] 12 p1882 N85-21806
USSR report: Science and technology policy
[JPRS-UST-85-002] 13 p2167 N85-23442
Scientific, technical progress as factor of intensification of economy 13 p2167 N85-23444
Clutchless mechanism for engagement of forging press 14 p2266 N85-24051
Liquid membranes for the production of oxygen-enriched air
[DE85-006056] 15 p2506 N85-25460
Prospects for developing attractive magnetic fusion concepts
[DE85-006925] 16 p2867 N85-27684
USSR report: Machine tools and metalworking equipment
[JPRS-UMM-84-014] 17 p2946 N85-28188
Foundations of data envelopment analysis for Pareto-Koopmans efficient empirical productions functions
[AD-A154244] 19 p3346 N85-30735
EOQ (Economic Order Quantity) range model
[AD-A153709] 19 p3379 N85-30965
CEMA venture to develop FMS, robot technology
20 p3436 N85-31330
Photovoltaics technical information guide
[DE85-002924] 22 p3806 N85-33585

ECONOMY
1st deputy minister on civil aviation support of economy 14 p2208 N85-23690
Minister Bugayev reviews 1983 civil aviation work, sets course for 1984 14 p2208 N85-23695
Computing in the Soviet general economy: An introductory overview
[AD-P004563] 17 p3047 N85-28858
Quality analysis 21 p3668 N85-32785

ECOSYSTEMS
Response of arctic ecosystems to elevated carbon dioxide regimes, volume 2
[DE84-015236] 01 p0069 N85-10460
The 1984 NASA/ASEE summer faculty fellowship program
[NASA-CR-174138] 04 p0574 N85-13663
Terrestrial nitrogen cycles: Some unanswered questions 05 p0853 N85-14192
Classification of vegetation communities in the Battle Mountain SE quadrangle, Nevada with MSS digital data
[E85-10043] 06 p0826 N85-15246
Ecological impacts of hydroelectric projects in Amazonia 07 p1003 N85-16374
Extremely Low Frequency (ELF) Communications System Ecological Monitoring Program: Summary of 1983 progress
[AD-A147704] 08 p1151 N85-17265
Compilation of annual reports of the Navy ELF (Extremely Low Frequency) communications system ecological monitoring program. Volume 1: Tabs A-E
[AD-A148326] 08 p1152 N85-17272
Compilation of annual reports of the Navy ELF (Extremely Low Frequency) communications system ecological monitoring program (1983). Volume 2: Tabs F-J
[AD-A148327] 08 p1152 N85-17273
Comparing computing formulas for estimating concentration ratios
[DE84-006644] 09 p1349 N85-18490
Air quality criteria for ozone and other photochemical oxidants. External review draft, volume 5
[PB85-126076-VOL-5] 11 p1679 N85-20583
Proceedings of the 1st Glacier Bay Science Symposium
[PB85-115913] 11 p1682 N85-20599
Combined effects of atmospheric deposition, internal acid production, and harvesting on nutrient gains and losses from forest ecosystems
[DE85-002325] 12 p1884 N85-21821
Ecological observations at the site of the 10 MWe solar thermal power system (1978-1984)
[DE85-004572] 12 p1885 N85-21827
Rationale and basic design for experimental acidification of a lake ecosystem in Northern Wisconsin
[PB85-116077] 12 p1885 N85-21829
Air quality criteria for ozone and other photochemical oxidants. External review draft, volume 2
[PB85-126043] 12 p1886 N85-21836
Combined analysis of the dynamics of complex ecosystems based on repeated remote measurements
13 p1965 N85-22450
Technologies to sustain tropical forest resources
[TI85-901085] 13 p2126 N85-23241
Areas with forest soils sensitive to acidic deposition under alternative damage hypotheses
[DE85-005257] 13 p2130 N85-23257
The ecology of tundra ponds of the Arctic coastal plain: A community profile
[TI85-900650] 15 p2589 N85-25958
An analysis of issues concerning acid rain, report to the Congress of the United States
[TI85-901070] 15 p2589 N85-25959
Ecology of Pamlico River, North Carolina: An estuarine profile
[PB85-155703] 16 p2822 N85-27404
MARMAP survey of the continental shelf from Cape Hatteras, North Carolina to Cape Sable, Nova Scotia (1977 - 1983). Atlas 1: Summary of operations
[PB85-150985] 16 p2839 N85-27506
ELF (Extremely Low Frequency) communications system ecological monitoring program: Measurements of ELF electromagnetic fields for site selection and characterization, 1983
[AD-A153120] 17 p2949 N85-28209
Fatty and aromatic acid catabolizing bacteria from methanogenic ecosystems
[DE85-006133] 17 p2998 N85-28537
Stability and feasibility of model ecosystems
[PREPRINT-431] 18 p3134 N85-29406
Use of a two-dimensional flow model to quantify aquatic habitat
[AD-A154287] 19 p3266 N85-30253
Microbial ecology of extreme environments: Antarctic yeasts and growth in substrate-limited habitats
[NASA-CR-176005] 19 p3326 N85-30609
Global geomorphology 21 p3601 N85-32359
Biogeochemical cycling and remote sensing
21 p3659 N85-32733

ECS
U EUROPEAN COMMUNICATIONS SATELLITE

EDDIES
U VORTICES

EDDINGTON APPROXIMATION
Energy relations on the small oscillations excitation in the stars 14 p2450 N85-25125
Ultra high energy gamma rays, cosmic rays and neutrinos from accreting degenerate stars
[OG-2.2-5] 22 p3864 N85-33931
X-ray spectra of bursting neutron stars
23 p3981 N85-34686

EDDY CURRENTS
Technical activities 1983, Office of Nondestructive Evaluation
[PB84-217074] 03 p0370 N85-12380
Superconducting magnet for probing eddy currents in dynamic models 04 p0480 N85-13117
The determination of eddy current losses in electrical equipment
[DE84-016340] 05 p0632 N85-14050
A narrow band pulsed eddy current instrument for materials testing
[AERE-R-11229] 07 p0968 N85-16149
Feasibility study to demonstrate detection of low levels of oxygen contaminant in titanium using eddy current and ultrasonic NDE (Nondestructive Evaluation) techniques
[AD-P004129] 08 p1127 N85-17104
Experimental verification of eddy-current flaw theory
[DE85-001288] 09 p1329 N85-18350
Behavior of small ferromagnetic particles in traveling magnetic field 12 p1843 N85-21564
Eddy current test probe with circumferential segments and method of testing material surrounding fastener holes
[AD-D011554] 12 p1850 N85-21603
Pre- and post-processing for stream-function eddy current calculations
[AD-A150417] 13 p2065 N85-22896
Magnetic field interactions with material discontinuities
[AD-A150197] 13 p2154 N85-23373
Applications of eddy currents
14 p2316 N85-24315
Preliminary results on passive eddy current damper technology for SSME turbomachinery
16 p2737 N85-26690

Investigation on the application of the pulsed eddy current method of non-destructive testing using controlled signals (CS-technique)
[BLL-BISI-TRANS-22249-(9022.06)] 18 p3119 N85-29303
Plating density standards
[DE85-010014] 21 p3501 N85-32318
Development of contactless sensors for industrial and automative applications
[BMFT-FB-T-85-031] 24 p4097 N85-35400

EDDY DIFFUSION
U TURBULENT DIFFUSION

EDDY VISCOSITY
Model equations describing unsteady fluid motion
[ESA-TT-850] 04 p0501 N85-13194
Application of large eddy interaction model to channel flow
[NASA-TM-86691] 12 p1844 N85-21572
Modeling evolution of unstable geostropic eddies in barotropic ocean 14 p2336 N85-24447
SSME fuel preburner two-dimensional analysis 17 p2911 N85-27943
SSME turbopump turbine computations 17 p2911 N85-27944
MST radar data management 21 p3627 N85-32532

EDGE DISLOCATIONS
Fracture toughness of materials
[DE85-004306] 12 p1867 N85-21713
Determination of edge and screw dislocation density in single crystals of high-purity iron
[DE85-010237] 20 p3537 N85-32012
Stress and efficiency studies in EFG
[NASA-CR-176125] 22 p3751 N85-33251
Influence of edge effects on performance of electrooptical lens 22 p3770 N85-33366
Crystallographic orientation dependence of fatigue crack propagation in extremely low carbon steel 23 p3906 N85-34195

EDGE LOADING
Checking optical-polarization measurements at interfaces 02 p0271 N85-11770
Large transverse deflections of circular plates loaded symmetrically
[NPL-DMA(A)-86] 04 p0512 N85-13262
Stress intensity factors for corner cracks at holes located near an edge
[FFA-TN-1984-20] 04 p0514 N85-13279
Effect of edge distance on yield initiation in a remotely loaded half-plane containing interference-fit disc of the same material
[ARL/STRUC-R-413] 19 p3285 N85-30369

EDGES
NT LEADING EDGES
NT TRAILING EDGES
Design of edge detectors for reduced images
[AD-A145700] 02 p0252 N85-11653
Analysis of accretion and deletion at boundaries in dynamic scenes
[AD-A145944] 03 p0419 N85-12676
A study of interply layer effects on the free-edge stress field of angleplied laminates
[NASA-TM-86924] 07 p0919 N85-15822
On edge detection
[AD-A146573] 08 p1223 N85-17703
On large matchings and cycles in sparse random graphs
[AD-A149194] 10 p1550 N85-19778
Edge diagnostics for tandem mirror machines
[DE85-001209] 11 p1733 N85-20902
Edge detection in SAR imagery using gradient operators --- synthetic aperture radar (SAR)
[AD-A149411] 13 p2054 N85-22662
Stress intensity factor in a tapered specimen
[NASA-CR-175589] 13 p2102 N86-23099
Feasibility of optical instruments based on multiaperture optics
[AD-A150668] 14 p2421 N85-24836
Evaluation of stress concentration coefficients in butt-welded joints with displaced edges 15 p2501 N85-25425
Mechanical aspects of interfaces and surfaces in ceramic containing systems
[AD-A151978] 15 p2519 N85-25530
Chemical applications of topology and group theory. 17: An information theoretical approach to polyhedral symmetry
[AD-A152821] 17 p2919 N85-27935
Ultrasonic testing of plates containing edge cracks
[NASA-CR-3904] 18 p3119 N85-29307
Experimental and theoretical assessment of a new technique for the non-destructive evaluation of laminated panels
[AD-A155622] 21 p3582 N85-32155
Hierarchical chamfer matching
[FOA-C-30367-E1] 22 p3802 N85-33558
Mechanical properties of plasma arc cut steel 23 p3905 N85-34188
Anti wear property of two phasic metal composite 23 p3906 N85-34199
Edge detection and geometric methods in computer vision
[AD-A155873] 24 p4135 N85-35630
Edge information in color images based on histograms of differences
[AD-A156002] 24 p4154 N85-35751

EDITING
Ada (trademark) training curriculum. Basic Ada programming I202 teacher's guide. Laboratory manual and exercises
[AD-A143583] 01 p0103 N85-10687
Tekedit: An enhanced editor for Direct View Storage Tube (DVST) graphics display devices
[AD-A149715] 12 p1915 N85-22021
The potential for advanced computerized aids for comprehensible writing of technical documents
[AD-A150501] 13 p2055 N85-22670
Computer program for plotting and fairing wind-tunnel data
[NASA-TM-85648] 20 p3387 N85-31009
An integrated system for printing and publishing applications 23 p3959 N85-34540
A model for a document maintenance system 23 p3960 N85-34542

EDITING ROUTINES (COMPUTERS)
SAGA: A project to automate the management of software production systems
[NASA-CR-174017] 01 p0103 N85-10685
PROGEN: An incremental programming environment
[NRIMS-TWISK-315] 02 p0241 N85-11568
SMILE user's guide: A macro preprocessor for extending FORTRAN
[DE84-015894] 02 p0243 N85-11584
DATAPLOT: Implementation tapes guide
[PB84-214063] 03 p0408 N85-12610
MACSYMA usage at Langley
[NASA-CR-172518] 10 p1537 N85-19668
The design and implementation of a syntax directed editor for a space constrained microcomputer
[AD-A151313] 15 p2623 N85-26183
The design, implementation and application of a table-driven syntax-directed editor
[AD-A154234] 19 p3336 N85-30670
Experience with omega: Implementation of a prototype programming environment: Part 1
[AD-A155438] 21 p3672 N85-32811
Design and implementation of an interactive route editor 23 p3962 N85-34559
Procedure for editing the fluxgate magnetometer data of the AFGL (Air Force Geophysics Laboratory) magnetometer network
[AD-A156331] 24 p4117 N85-35523

EDUCATION
NT ASTRONAUT TRAINING
NT FLIGHT TRAINING
NT MAINTENANCE TRAINING
NT PILOT TRAINING
NT SPACE FLIGHT TRAINING
Self-paced instruction. Factors critical to implementation in Air Force technical training: A preliminary inquiry
[AD-A145098] 01 p0097 N85-10647
Comprehension of instructions for operating devices
[AD-A145263] 01 p0098 N85-10653
IAC user manual
[NASA-CR-175300] 01 p0102 N85-10677
Ada (trademark) training curriculum. Using the Ada language reference manual I402 teacher's guide
[AD-A143582] 01 p0103 N85-10686
Ada (trademark) training curriculum. Basic Ada programming I202 teacher's guide. Laboratory manual and exercises
[AD-A143583] 01 p0103 N85-10687
Integrated computer-aided manufacturing (ICAM) architecture. Part 3, volume 8: Technology transfer
[AD-A144732] 01 p0103 N85-10689
National Science Foundation grants and awards for fiscal year 1983, volume 2
[PB84-212323] 01 p0125 N85-10854
A report on the training course at Fortaleza (Ceara)
[E85-10013] 02 p0216 N85-11426
Designing an expert system for training automotive electrical troubleshooting
[AD-P003926] 02 p0246 N85-11606
Emergency Mathematics and Science Education Act
[GPO-29-561] 03 p0435 N85-12770
The 1984 ASEE-NASA summer faculty fellowship program (aeronautics and research)
[NASA-TM-87393] 04 p0575 N85-13664
Computer Literacy Act of 1983, part 2
[H-REPT-98-752-PT-2] 04 p0578 N85-13687
East Europe report: Science and technology
[JPRS-ESA-84-045] 06 p0815 N85-15175
Computer-managed instruction: Theory, application, and some key implementation issues
[AD-A146564] 06 p0854 N85-15428
Requirements for training in climate-related subjects 07 p1004 N85-16378
Education and training for the climate related activities in Latin America and the Caribbean 07 p1004 N85-16379
Human factors and training research in military organizations and systems
[AD-A146832] 07 p1020 N85-16475
Ada training curriculum. Real-time systems in Ada I401 teacher's guide, volume 1
[AD-A146782] 07 p1024 N85-16496
Ada training curriculum. Real-time systems in Ada I401 teacher's guide, volume 2
[AD-A146783] 07 p1024 N85-16497
A study of Air Force Quality Circle program effectiveness as viewed through facilitator's perceptions
[AD-A147833] 08 p1170 N85-17377
Efforts to improve aviation medical examiner performance through continuing medical education and annual performance reports
[AD-A148078] 08 p1195 N85-17531
Training guide for scientific and engineering trainees 1984
[AD-A147963] 08 p1198 N85-17542
Training high performance skills: Fallacies and guidelines
[AD-A148574] 08 p1198 N85-17545
Concept paper for the development of a DOD Ada (trademark) software engineering education and training plan
[AD-A148774] 08 p1206 N85-17562
Pilot education and safety awareness programs 09 p1277 N85-18026
Innovative approaches to recurrent training 09 p1277 N85-18028
NASA Lewis Research Center/University Graduate Research Program on Engine Structures
[NASA-TM-86916] 09 p1333 N85-18375
Bibliography of unclassified reports, FY 1984
[AD-A148636] 09 p1401 N85-18819
Application of the HARDMAN methodology to the single channel ground-airborne radio system (SINCGARS)
[NASA-CR-175486] 10 p1467 N85-19259
USSR report: Life sciences. Biomedical and behavioral sciences
[JPRS-UBB-85-011] 10 p1525 N85-19616
Study of cognitive styles of students in automated teaching system 10 p1525 N85-19620
Computers and education
[GPO-28-378] 10 p1537 N85-19689
Topics in optical materials and device research, 3. Volume 2
[AD-A149727] 12 p1911 N85-21996
Application of the Hardman methodology to the Single Channel Ground-Airborne Radio System (SINCGARS)
[NASA-CR-175694] 14 p2218 N85-23756
The role of prior knowledge in operating equipment from written instructions
[AD-A151007] 14 p2392 N85-24730
The acquisition of procedures from text. A production-system analysis of transfer of training
[AD-A151029] 14 p2392 N85-24732
Administration chief on air traffic control improvements 15 p2460 N85-25193
China report: Science and technology
[JPRS-CST-85-011] 15 p2551 N85-25746
A learning strategy approach for teaching novice computer programmers
[AD-A151523] 15 p2628 N85-26200
Academic science and engineering: Graduate enrollment and support, fall 1982 (detailed statistical tables)
[PB85-154730] 15 p2664 N85-26438
Programming for Pioneer 12 15 p2688 N85-26606
Rotorcraft digital advanced avionics system (Rodasa) 15 p2688 N85-26608
The search for extraterrestrial intelligence 15 p2689 N85-26609
A review of safety practices and safety training for the explosives field
[AD-A152295] 16 p2759 N85-27028
Automated CPX support system preliminary design phase
[NASA-CR-175784] 16 p2769 N85-27091
The impact of group processing on achievement in cooperative learning groups
[AD-A153166] 17 p3001 N85-28551
Oral discussion, group-to-individual transfer and achievement in cooperative learning groups
[AD-A153209] 17 p3001 N85-28552

Summer High School Apprenticeship Research Program (SHARP) of the National Aeronautics and Space Administration
[NASA-CR-175791] 17 p3046 N85-28849
Engineering education based on computer simulation
[CFD/85/1] 20 p3512 N85-31829
The Naval Postgraduate School Flight Mechanics Laboratory: A feasibility study
[AD-A154578] 21 p3557 N85-32127
One application of mega-geomorphology in education 21 p3602 N85-32370
Ada (trademark) training curriculum. Advanced Ada topics L305 teacher's guide exercises
[AD-A154621] 21 p3670 N85-32798
Solar energy meteorological research and training program: Region 4
[DE85-011783] 22 p3816 N85-33840
Solar energy education. Renewable energy: A background text
[DE85-010365] 23 p3946 N85-34452
Development of NATOPS (Naval Air Training and Operating Procedure Standardization) performance software for the H-46D helicopter
[AD-A156089] 24 p4064 N85-35190
Benchmark evaluation of PC simscript
[AD-A156133] 24 p4136 N85-35651
Comet Halley returns: A teachers' guide 1985-1986
[NASA-EP-197] 24 p4168 N85-35939

EEG (ELECTROENCEPHALOGRAMS)
U ELECTROENCEPHALOGRAPHY

EFFECTIVE PERCEIVED NOISE LEVELS
Contribution of tonal components to the overall loudness, annoyance and noisiness of noise: Relation between single tones and noise spectral shape
[NASA-CR-3892] 15 p2645 N85-26317
Noise reduction in the automotive test cell of the Motor Institute of Naples
[REPT-85-RR-361] 20 p3524 N85-31917
The timing of noise-sensitive activities in residential areas
[NASA-CR-177937] 20 p3524 N85-31918

EFFECTIVENESS
NT COST EFFECTIVENESS
NT SYSTEM EFFECTIVENESS

EFFECTORS
U CONTROL EQUIPMENT

EFFECTS
The effect of modified spectacles on the field of view of the helmet display unit of the integrated helmet and display sighting system
[AD-A149693] 09 p1281 N85-18055
Analyzing two-level fractional factorial experiments for possible dispersion effects
[AD-A149455] 10 p1548 N85-19760
The effects of internal waves on acoustic normal modes
[AD-A150235] 13 p2155 N85-23379
The effects of controversy and concurrence seeking on effective decision making
[AD-A153370] 17 p3002 N85-28555

EFFERENT NERVOUS SYSTEMS
Development and evaluation of a performance-based test of saccadic and vestibulo-ocular control
[AD-A145367] 02 p0237 N85-11545
Applications of connectionist modeling techniques to simulations of motor control systems 05 p0717 N85-14598
Advanced development of an active neuromusculature response to mechanical stress
[AD-A148436] 08 p1196 N85-17536
Effects of tasks on responses of human skin mechanoreceptors 11 p1691 N85-20635
Comparative analysis of effects of weightlessness and its models on velocity and strength properties and tone of human skeletal muscles 12 p1901 N85-21936
Effects of muscle atrophy on motor control: Cage size effects 15 p2609 N85-26080
Eye movement in response to single and multiple targets
[AD-A151115] 15 p2617 N85-26126

EFFICIENCY
NT CHARGE EFFICIENCY
NT COMBUSTION EFFICIENCY
NT COMPRESSOR EFFICIENCY
NT ENERGY CONVERSION EFFICIENCY
NT NOZZLE EFFICIENCY
NT POWER EFFICIENCY
NT PROPELLER EFFICIENCY
NT PROPULSIVE EFFICIENCY
NT THERMODYNAMIC EFFICIENCY
NT TRANSMISSION EFFICIENCY
A determination of the photochemical quantum yields from 2 excited triplet states of biacetyl using holography
[AD-A145091] 01 p0050 N85-10326
Oscillatory integrals by Hermite interpolatory rules
[CSIR-TWISK-301] 01 p0108 N85-10725
Fuel efficiency through new airframe technology
[NASA-TM-84548] 02 p0133 N85-10909
Component-specific modeling 02 p0143 N85-10971
Energy efficient engine. High pressure compressor detail design report
[NASA-CR-165558] 02 p0147 N85-10998
Standardized efficiency terms: Comparison of some Stirling engine performance figures
[DE84-015407] 02 p0205 N85-11352
Efficiency of lasing dye media in pumping high-power radiation with nanosecond pulses 02 p0270 N85-11763
Maintenance Management Information and Control System (MMICS): Administrative boon or burden
[AD-A145762] 03 p0438 N85-12790
Comparability and accuracy of industry codes in different data systems
[PB84-215607] 04 p0548 N85-13482
Analyses of energy extraction efficiency of unstable resonators
[AD-A146391] 06 p0813 N85-15161
Recent developments in photovoltaics
[DE84-004528] 06 p0833 N85-15305
Comparison measurements on optical particle counters
[BLL-DOUNREAY-TR-934-(9091.9F)] 07 p0961 N85-16092
Overview od STS ground operations/orbiter turnaround STS-1 through STS-7 08 p1096 N85-16926
USSR report: Machine tools and metalworking equipment
[JPRS-UMM-84-021] 08 p1138 N85-17168
Control systems for robotic production lines 08 p1138 N85-17169
Metallographic grinding efficiency
[DE85-001520] 09 p1304 N85-18194
Available energy method for evaluating thermodynamic performance of heat pump systems
[DE84-017223] 09 p1400 N85-18614
Calculation of Si(Li) X-ray detector efficiencies
[DE85-002732] 10 p1489 N85-19400
Electric-Hybrid Vehicle (E-HV) demonstration-test project
[DE85-002370] 10 p1570 N85-19699
Assessment of effectiveness of electron beam welding of titanium alloys up to 40 mm in thickness by vertical or horizontal beam 11 p1603 N85-20078
Some solar dish/heat engine design considerations
[DE85-003479] 12 p1881 N85-21802
Characterizing the parallelism in rule-based expert systems
[DE85-002432] 12 p1919 N85-22047
Methods of digital correction for channels of multichannel radar receivers 13 p2082 N85-23005
Proceedings of the Cold Electronics Workshop
[NASA-CR-175662] 14 p2297 N85-24220
Cold electronics: An overview 14 p2297 N85-24221
Electromagnetic scattering by arbitrarily shaped reflectors: Subreflector efficiency
[AD-A149224] 15 p2541 N85-25687
Efficiency analysis of the electronic mail system (INFOMAIL) on the defense data network
[AD-A151694] 15 p2632 N85-26223
Optimal control of electric drive with simultaneous control inputs for motor current and flux 16 p2763 N85-27049
High efficiency ionizer using a hollow cathode discharge plasma
[DE85-00cd90] 16 p2868 N85-27693
Flow characteristics of a partially submerged liquid pickup
[DE85-006744] 17 p2959 N85-28276
Small central receiver Brayton cycle study
[DE85-006862] 18 p3128 N85-29369
Megajoule-class single-pulse KrF laser test facility as a logical step toward inertial fusion commercialization
[DE85-009590] 18 p3191 N85-29794
Receiver loss study of optimized solar central receiver systems as a function of receiver thermal loss per unit area
[DE85-010831] 19 p3268 N85-30265
Design and operation of epitaxial reactor
[DE85-011089] 19 p3306 N85-30491
Foundations of data envelopment analysis for Pareto-Koopmans efficient empirical productions functions
[AD-A154244] 19 p3346 N85-30735
An empirical technique to measure X-ray production and detection efficiencies in the analytical electron microscope
[DE85-010270] 19 p3361 N85-30837
Auto fuel efficiency standards, part 2
[GPO-41-189] 20 p3435 N85-31309
High efficiency large area polysilicon solar cells 20 p3482 N85-31639
High efficiency solar cell processing 20 p3482 N85-31640
Efficiency tests of samplers for microbiological aerosols, a review
[FOA-C-40199-B1] 20 p3504 N85-31783
The use of superoxide mixtures as air-revitalization chemicals in hyperbaric, self-contained, closed-circuit breathing apparatus
[NASA-TM-86709] 20 p3512 N85-31831
Application of adaptive noise cancellation to Coast Guard voice communications
[AD-A154798] 21 p3574 N85-32230
Physics of heavily doped silicon and solar-cell parameter measurement 21 p3609 N85-32418
Sensitivity analysis of high-efficiency silicon solar-cell design parameters 21 p3610 N85-32422
Silicon surface passivation by silicon nitride deposition 21 p3610 N85-32423
Important loss mechanisms in high-efficiency solar cells 21 p3610 N85-32424
Stress and efficiency studies in EFG 21 p3611 N85-32440
Sixty GHz IMPATT diode development
[NASA-CR-174969] 22 p3758 N85-33293
Experiments and improvements of the ordinary differential equation solvers DEPAC on the CRAY computer
[DE85-013260] 22 p3831 N85-33726
Lubrication and cooling for high speed gears
[NASA-TM-87096] 23 p3938 N85-34407
Development of a high-efficiency, gas-fired, heat pipe, warm-air heating system
[PB85-199636] 24 p4085 N85-35318
The NORDA/FNOC (Naval Ocean Research and Development Activity's/Fleet Numerical Oceanography Center) Polar Ice Prediction System (PIPS)-Arctic: A technical description
[AD-A156332] 24 p4126 N85-35577

EFFLUENTS
Supercritical fluid chromatography/supersonic jet spectroscopy
[DE84-016199] 04 p0471 N85-12998
The Georges Bank monitoring program 1983: Analysis of trace metals in bottom sediments
[CIRC-915] 05 p0688 N85-14423
Investigation of internal friction of free-flowing material during discharge
[BLL-M-36141-(5828.4)] 15 p2553 N85-25752
Influence on an industrial site on the characteristics of CCN supersaturation with air masses of different origin 21 p3650 N85-32683
The 1984 effluent and environmental monitoring report for the Bettis Atomic Power Laboratory
[DE85-011533] 22 p3810 N85-33602
Environmental summary for calendar year 1984
[DE85-012020] 22 p3810 N85-33604
Environmental monitoring at Lawrence Livermore National Laboratory: 1984 report
[DE85-011593] 22 p3811 N85-33606
The 1984 environmental monitoring report, Sandia National Laboratories, Albuquerque, New Mexico
[DE85-011175] 22 p3811 N85-33607
Control technology for radioactive emissions to the atmosphere at US Department of Energy facilities: The Los Alamos Meson Physics Facility
[DE85-011402] 22 p3811 N85-33609

EFFORT
A theorem on the optimal allocation of effort
[AD-A148028] 08 p1211 N85-17823

EFFUSIVES
NT LAVA
Changes in the organic material in lakes in the blast zone of Mount St. Helens, Washington: Hydrologic effects of the eruptions
[GS-CIRC-850-1] 21 p3630 N85-32551

EGGS
An automatic device for amphibian egg fertilization in space: Technical aspects and biological requirements 05 p0689 N85-14427
Radiobiological studies on egg systems exposed to heavy nuclei of cosmic galactic radiation -- insects 05 p0690 N85-14440
Simulated microgravity as a probe for understanding the mechanisms of early pattern specification 15 p2611 N85-26092
Report of Amphibian Development Group 24 p4127 N85-35583

EGRESS
Egress spectra of the new eclipsing supergiant 22 Vulpeculae 11 p1755 N85-21039
Fire research publications, 1984
[PB85-208502] 24 p4166 N85-35827

EGYPT
SIR-B analysis of the Precambrian shield of Sudan and Egypt: Penetration studies and subsurface mapping
08 p1145 N85-17219
A brief comparison of Egyptian with West German atmospheric transmission data in the 8 to 11.5 micron waveband
[BAE-BT-12829] 15 p2594 N85-25983
EIGENFUNCTIONS
U EIGENVECTORS
EIGENSTATES
U EIGENVECTORS
EIGENVALUES
Problems on the diffraction and propagation of waves (selected articles)
[AD-A145139] 01 p0038 N85-10240
Rotordynamic analysis of the SSME turbopumps using reduced models
[NASA-CR-171170] 01 p0054 N85-10355
Legendre-Tau approximation for functional differential equations. Part 3: Eigenvalue approximations and uniform stability
[NASA-CR-172447] 01 p0110 N85-10744
Moment induced by liquid payload during spin-up without a critical layer
[AD-A145716] 02 p0199 N85-11327
The application of principal components analysis to LANDSAT MSS data 02 p0212 N85-11398
Gain-phase structures for linear multivariable systems
[RR-256] 02 p0256 N85-11674
A study of the critical layer in a rotating liquid payload
[AD-A146094] 03 p0362 N85-12321
Effects of changing the signs of rows and columns of a matrix and the hyperbolic transpose
[DE84-014651] 04 p0555 N85-13530
A routine to find the lowest few eigenvalues and vectors for the generalised sparse symmetric eigenproblem
[NPL-DITC-43/84] 05 p0722 N85-14641
Splitting methods for the numerical solution of the incompressible Navier-Stokes equations
[AD-A147463] 07 p1032 N85-16554
Eigenvalues of rotating machinery
08 p1167 N85-17361
Experimental investigations of driven Alfven wave resonances in a Tokamak plasma using carbon dioxide laser interferometry
[DE85-001049] 09 p1392 N85-18758
Perturbation of a multiple eigenvalue in the Benard problem for two fluid layers
[AD-A149068] 10 p1548 N85-19745
Applied mathematics of transport theory
[DE85-000848] 11 p1633 N85-20283
A numerical approach for the vibration analysis of an axisymmetric shell structure with a nonuniform edge constraint
[AD-A149286] 11 p1651 N85-20402
The eigenvalues of the pseudospectral Fourier approximation to the operator sin (2x) d/dx
[NASA-CR-172538] 11 p1706 N85-20729
Optical eigenvector
[AD-A149550] 11 p1729 N85-20671
Normal mode analysis for linear resistive magnetohydrodynamics
[IPP-6/235] 11 p1730 N85-20878
Role of cavitons in laser-plasma interactions
[DE85-001842] 11 p1731 N85-20886
Modal control of structural systems
[AD-A149734] 12 p1790 N85-21235
Planar dynamics of a uniform beam with rigid bodies affixed to the ends
[NASA-CR-175566] 12 p1864 N85-21683
Practical considerations for noninteracting control synthesis
[AD-A150130] 12 p1918 N85-22046
On the limiting empirical distribution function of the eigenvalues of a multivariate F matrix
[AD-A149818] 12 p1921 N85-22065
Spectral frequency of eigenvalues in optimal problems of stability of cylindrical shells of variable thickness
13 p2047 N85-22815
On limit of the largest eigenvalue of the large dimensional sample covariance matrix
[AD-A150569] 13 p2151 N85-23358
Design of multivariable feedback control systems via spectral assignment using reduced-order models and reduced-order observers
[NASA-CR-3869] 14 p2226 N85-23800
Representation of temperature and salinity fields using statistically orthogonal functions (in example of polymode data) 14 p2337 N85-24449
On limiting empirical distribution function of the eigenvalues of a multivariate F matrix, revised
[AD-A151865] 15 p2641 N85-26288
On asymptotic joint distribution of the eigenvalues of the noncentral manova matrix for nonnormal populations
[AD-A151866] 15 p2642 N85-26294
Squeezing the most out of Eigenvalue solvers on high-performance computers
[DE85-007569] 16 p2849 N85-27585
Eigenvalue approximation methods for quantum lattice Hamiltonians 16 p2858 N85-27627
Incorporating control into the optimal structural design of large flexible space structures
[AD-A152858] 17 p2909 N85-27937
Solution to eigenvalue problems of antisymmetric cross-ply and antisymmetric angle-ply laminated plates using affine transformations
[AD-A153040] 17 p2917 N85-27980
Continuum modeling of latticed structures
17 p2977 N85-28399
Some applications of a convenient finite-dimensional matrix representation of the differential operator
[PREPRINT-418] 18 p3172 N85-29661
Numerical tests of a novel technique to compute the eigenvalues of differential operators
[PREPRINT-427] 18 p3173 N85-29667
Evaluation of the eigenvalue method in the solution of transient heat conduction problems
[AD-A154434] 19 p3266 N85-30256
Structural dynamics modification of generalized beams using a local eigenvalue modification procedure
19 p3282 N85-30353
Asymptotic expansions for finite element eigenvalues and finite element solution 19 p3345 N85-30730
Monte Carlo alpha calculation
[DE85-010720] 19 p3349 N85-30758
Eigenvalue placement and stabilization by constrained optimization 20 p3416 N85-31198
An Eigensystem Realization Algorithm (ERA) for modal parameter identification and model reduction
20 p3418 N85-31212
Spectral Theory of Sturm-Liouville Differential Operators: Proceedings of the 1984 Workshop
[DE85-009693] 20 p3520 N85-31890
On the solution for the sound field in a semi-infinite uniform duct with sheared mean flow
20 p3523 N85-31912
Systematics of quark mass matrices in the Standard Electroweak Model
[USIP-85-05] 20 p3532 N85-31972
Finding the roots of the transcendental equations in problems in determining the thermal conductivity of spheres with heterogeneous boundary conditions
[BLL-M-35878-(5828.4)] 23 p3929 N85-34347
Vibrations of free hollow circular cylindrical bodies
24 p4100 N85-35418
EIGENVECTORS
A subspace iteration method for determining a dominant span of eigenvectors
[TWISK-329] 01 p0109 N85-10739
The application of principal components analysis to LANDSAT MSS data 02 p0212 N85-11398
Linear autonomous retarded functional differential equations; a sharp version of Henry's theorem
[CWI-AM-R8405] 05 p0720 N85-14625
A routine to find the lowest few eigenvalues and vectors for the generalised sparse symmetric eigenproblem
[NPL-DITC-43/84] 05 p0722 N85-14641
Lax-pair operators for squared-sum and squared-difference eigenfunctions
[AD-B089063L] 09 p1386 N85-18718
A numerical approach for the vibration analysis of an axisymmetric shell structure with a nonuniform edge constraint
[AD-A149286] 11 p1651 N85-20402
The eigenstructure assignment of deadbeat control systems
[AD-A149761] 12 p1834 N85-21510
Practical considerations for noninteracting control synthesis
[AD-A150130] 12 p1918 N85-22046
Analysis of interaction of dynamically adjustable gyroscopes on elastic platform by finite-element method
13 p2048 N85-22822
Design of multivariable feedback control systems via spectral assignment using reduced-order models and reduced-order observers
[NASA-CR-3869] 14 p2226 N85-23800
Observed spatial properties of the solar eigenfunctions and the implications for the existence of resolved multiplets 14 p2443 N85-25074
Squeezing the most out of Eigenvalue solvers on high-performance computers
[DE85-007569] 16 p2849 N85-27585
Mutual coupling analysis for conformal microstrip antennas
[AD-A154292] 19 p3259 N85-30210
Spectral Theory of Sturm-Liouville Differential Operators: Proceedings of the 1984 Workshop
[DE85-009693] 20 p3520 N85-31890
Interacting Boson approximation
[DE85-003016] 22 p3837 N85-33756
EIKONAL EQUATION
A theoretical study of electron capture in ion-ion and ion-atom collisions
[DE85-011154] 19 p3362 N85-30842
EINSTEIN EQUATIONS
Solution generating technique for the Einstein equations 03 p0435 N85-12766
Conserved quantities and radiative aspects of asymptotically anti-de Sitter space-times
12 p1958 N85-22303
Solutions of field equations in General Relativity with spinor connection 15 p2663 N85-26436
EINSTEIN OBSERVATORY
U HEAO 2
EJECTA
Capture of planetesimals into a circumterrestrial swarm 13 p2179 N85-23522
Impact cratering calculation 13 p2180 N85-23531
Progress on Experimental impact studies
13 p2181 N85-23534
The nature of Martian flow ejecta craters
13 p2183 N85-23545
Interaction of Martian flow ejecta blankets with pre-existing impact craters: Morphological observations
13 p2183 N85-23546
Geomorphology and geology of the Southwestern Margaritifer Sinus and Argyre regions of Mars. Part 4: Flow ejecta crater distribution 13 p2193 N85-23603
Magnetic instabilities in solar filaments: Models of twisting motions and ejecta 14 p2454 N85-25156
Identification of the youngest meteorites and a discussion of the possibility that they came from Mars
15 p2681 N85-26559
Examination of returned solar-max surfaces for impacting orbital debris and meteoroids
15 p2681 N85-26560
A comprehensive investigation of the dynamics of micron and submicron lunar ejecta in heliocentric space
19 p3364 N85-30994
EJECTION
NT STELLAR MASS EJECTION
Low-profile fastener
[AD-D011667] 19 p3280 N85-30343
EJECTION INJURIES
The clinical and biomedical evaluation of trauma and fatalities associated with aircrew ejection and crash. A Working Group report
[AGARD-AR-194] 12 p1906 N85-21969
Introduction: The clinical and biomedical evaluation for trauma and fatalities associated with aircrew ejection and crash 12 p1906 N85-21970
Statistics of french Armee de l'air ejections 1970 - 1980 12 p1906 N85-21971
List of head/neck injury on ejection in the German Armed Forces from 1972-1981 12 p1906 N85-21972
A review of neck injury and impaired consciousness associated with US Navy ejections 1 January 1969 - 31 December 1979 12 p1906 N85-21973
A review of fatality, impairment of consciousness, and head/neck injury on USAF ejections 1971 - July 1983
12 p1906 N85-21974
A review of fatality, impairment of consciousness and head and neck injury on Royal Air Force ejections 1968-1981 12 p1907 N85-21975
The clinical and radiological assessment of cervical injury, Annex A 12 p1907 N85-21976
Head/neck injury: Post mortem procedures, Annex B
12 p1907 N85-21977
Tight Ribbon Arm Protection (TRAP) for aircrewman ejection
[AD-A150464] 13 p2143 N85-23303
EJECTION SEATS
Simple nonrestrictive arm restraint system
[AD-D011216] 01 p0005 N85-10026
Windblast leg protector assembly
[AD-D011376] 07 p0899 N85-15700
Powered articulated headrest system
[AD-D011353] 07 p0901 N85-15710
S-3A ballast block final design and engineering tests
[AD-A147685] 08 p1080 N85-16842
A Generalized Escape System Simulation (GESS) computer program. Volume 2: GESS programmer's manual, version 2
[AD-A148383] 08 p1081 N85-16845
An investigation of spinal injury potential from the use of the ACES 2 ejection seat by lower weight female pilots
[AD-A148449] 08 p1196 N85-17537
Deployment sequence mode selection system for aircraft ejection seat
[AD-D011464] 10 p1422 N85-18988
Airspeed sensing pressure valve system
[AD-D011472] 10 p1425 N85-18987
Personnel protection concepts for advance escape system design 10 p1532 N85-19658

A safety evaluation of the relocation of the ACM (Air Combat Maneuver) panel in the F-14 ( )/AIP (Avionics Integration Program)
[AD-A149596] 12 p1777 N85-21158
The clinical and biomedical evaluation of trauma and fatalities associated with aircrew ejection and crash. A Working Group report
[AGARD-AR-194] 12 p1906 N85-21969
Introduction: The clinical and biomedical evaluation for trauma and fatalities associated with aircrew ejection and crash 12 p1906 N85-21970
Statistics of french Armee de l'air ejections 1970 - 1980 12 p1906 N85-21971
List of head/neck injury on ejection in the German Armed Forces from 1972-1981 12 p1906 N85-21972
Windblast arm protector assembly
[AD-D011512] 12 p1909 N85-21984
Tight Ribbon Arm Protection (TRAP) for aircrewman ejection
[AD-A150464] 13 p2143 N85-23303
Preliminary design of a limb restraint evaluator
[AD-A151749] 15 p2486 N85-25226
Air bag restraint system
[AD-D011671] 19 p3215 N85-29936
SSMIR (Solid State Memory Instrumentation Recorder): A new approach to acquiring data during an aircraft seat/sled ejection sequence
[AD-A154760] 21 p3589 N85-32308
Design and testing of an energy-absorbing crewseat for the F/FB-111 aircraft. Volume 2: Data from seat testing
[NASA-CR-3917] 24 p4064 N85-35184

EJECTORS
An engine trade study for a supersonic STOVL fighter-attack aircraft, volume 1
[NASA-CR-168304] 02 p0133 N85-10910
Viscous-Inviscid aerodynamic analysis of two-dimensional thrust augmentors
[NASA-CR-177321] 04 p0451 N85-12861
An experimental investigation of two-dimensional thrust augmenting ejectors, part 1
[NASA-CR-174111] 04 p0456 N85-12894
An experimental investigation of two-dimensional thrust augmenting ejectors, part 2
[NASA-CR-174110] 04 p0456 N85-12895
Basic studies of multiple free and confined jets
[AD-A149556] 10 p1485 N85-19374
Mixing characteristics of an underexpanded multiple jet ejector
[AD-A149557] 10 p1485 N85-19375
An experimental investigation of an underexpanded rectangular jet ejector
[AD-A149656] 12 p1779 N85-21170
A theoretical study of two stage thrust augmenting ejectors
[ARL/AERO-R-166] 19 p3218 N85-29054
Applied research and development for falling-sphere air density measuring systems
[AD-A155227] 21 p3552 N85-32099
Combined cold compressor/ejector helium refrigerator
[DE85-006406] 23 p3925 N85-34326

EKMAN LAYER
Numerical calculations of stratified Ekman layer flow over ridges with a finite element model
[DE84-014482] 04 p0499 N85-13179
Strongly nonlinear dynamics of baroclinic waves 20 p3498 N85-31681

EL NINO
Meteorological aspects of the 1982-83 El Nino/southern oscillation episode 07 p1001 N85-16356
Ocean and climate, an example. The interannual variability of the tropical Pacific Ocean 07 p1002 N85-16365
Climate and fisheries: A Peruvian case study 07 p1003 N85-16373
The El Nino phenomenon and its agrometeorological implications 07 p1004 N85-16382
Droughts and floods in South America due to the 1982-83 El Nino-southern oscillation episode
[INPE-3408-PRE/677] 09 p1357 N85-18535
El Nino, the capricious child 13 p2106 N85-23121
Forecast of Atlantic seasonal hurricane activity for 1985 16 p2833 N85-27470
Southern oscillation/El Nino excitation of the Earth's Chandler wobble 20 p3490 N85-31695

ELASTIC BARS
On the asymptotic analysis of travelling shocks and phase boundaries in elastic bars
[AD-A147239] 07 p0959 N85-16076
Hopkinson bar simulation using DYNA2D
[DE85-006706] 16 p2802 N85-27275

ELASTIC BENDING
A model for the compressive buckling of extended chain polymers
[AD-A151025] 14 p2260 N85-24008
An experimental study of the magnetoelastic bending of thin plates made of soft ferromagnetic material 19 p3282 N85-30352
A refinement of the transverse shear deformation theory for multilayered anisotropic plates
[STN-5] 20 p3471 N85-31571

ELASTIC BODIES
Controlling rotation of elastic manipulator link 04 p0488 N85-13113
A compact finite element method for elastic bodies
[NASA-CR-172487] 06 p0817 N85-15185
Stability of viscoelastic constructions subjected to steady random compressing loads 11 p1720 N85-20819
Experience with free bodies 15 p2576 N85-25687
Finite element prediction of loss factors for structures with frequency-dependent damping treatments 15 p2576 N85-25689
A natural modes formulation and modal identities for structures with linear viscous damping
[CRC-1382] 18 p3120 N85-29312
The role of ellipticity and normality assumptions in formulating live-boundary conditions in elasticity
[AD-A153475] 18 p3168 N85-29630
Application of deformable body mean-axis to dynamics of flexible mechanical systems 19 p3283 N85-30359
Approximation techniques for parameter estimation and feedback control for distributed models of large flexible structures 20 p3413 N85-31179
Characteristic elastic systems of time-limited optimal maneuvers 20 p3413 N85-31184

ELASTIC BUCKLING
Initial postbuckling analysis of elastoplastic thin-shear structures 01 p0059 N85-10393
Thermomechanically induced pre- and postbuckling of general structure 20 p3467 N85-31540

ELASTIC COLLISIONS
U ELASTIC SCATTERING

ELASTIC CONSTANTS
U ELASTIC PROPERTIES

ELASTIC CYLINDERS
Second Colloquim on the Scattering of Ultrasonic Waves
[AD-A156295] 24 p4145 N85-35697

ELASTIC DAMPING
NT VISCOELASTIC DAMPING
Controlled movement of elastic manipulator with distributed parameters 13 p2048 N85-22818
Stability of steady modes of motion by axis of rotating wheel in nonlinear bearings 14 p2279 N85-24117

ELASTIC DEFORMATION
NT ELASTIC BENDING
NT ELASTIC BUCKLING
Weak shocks and steady waves in a nonlinear elastic rod or granular material
[AD-A145715] 02 p0209 N85-11383
Symmetry of exchange interaction in crystalline magnetic films 02 p0250 N85-11694
Seismology in rockburst research
[REPT-551] 03 p0375 N85-12394
Iterative method for determining the distortion of elastic-plastic frames
[ISSN-0208-5658] 05 p0647 N85-14158
Deformation of cylindrical shell with cantilevered elastic plates attached 06 p0779 N85-14984
Fundamental tribological properties of ceramics
[NASA-TM-86915] 07 p0930 N85-15893
An experimental investigation into the effects of plate eccentricity and elastic deformation on orifice meter accuracy
[ERS-E.391] 09 p1325 N85-18325
Existence, uniqueness and stability conditions for general finite element methods in linear elasticity 09 p1332 N85-18372
Modal analysis of structural systems involving nonlinear coupling 09 p1337 N85-18409
Localization of destruction process 10 p1500 N85-19470
A deformation analysis of flat flexible gear and its equation of original curved surfaces
[NASA-TM-77493] 12 p1859 N85-21660
On local total strain redistribution using a simplified cyclic inelastic analysis based on an elastic solution
[NASA-TM-86913] 12 p1864 N85-21690
Planar dynamics of a uniform beam with rigid bodies affixed to the ends
[NASA-CR-175586] 12 p1864 N85-21693
Deployment analysis of the Olympus Astromast and comparison with test measurements — solar arrays 13 p2011 N85-22816
Time dependent interaction of internal pressure wave with system of two spherical shells 13 p2046 N85-22809
Determination of stresses and deformations in linearly elastic conical shell subjected to aerodynamic loading and heating 13 p2047 N85-22812
Gear noise origins 14 p2224 N85-23791
Determination of parameters of elastically strained mirror facets of rapidly rotating prisms 14 p2282 N85-24137
Development of a dynamic finite element model for unrestrained flexible structures
[AD-A151176] 15 p2636 N85-26259
Identification and control of structures in space
[NASA-CR-175790] 16 p2731 N85-26850
Simulation studies for surfaces and materials strength
[NASA-CR-175766] 16 p2800 N85-27282
Influence of preliminary cold deformation on fineness of pearlite
[BLL-BISI-TRANS-22409-(9022.06)] 17 p2927 N85-28054
The role of ellipticity and normality assumptions in formulating live-boundary conditions in elasticity
[AD-A153475] 18 p3168 N85-29630
Application of deformable body mean-axis to dynamics of flexible mechanical systems 19 p3283 N85-30359
Shear deflection in a three-point bend beam of a solid circular cross-section
[AD-A154458] 19 p3287 N85-30361
On elastic-plastic fracture criterion 20 p3485 N85-31526
Finite elastic deformations of cylindrical and spherical shells under pressure
[OUEL-1549/84] 20 p3470 N85-31559
Hertzian contact in two and three dimensions
[NASA-TP-2473] 21 p3596 N85-32331
Identification and control of structures in space
[NASA-CR-176175] 24 p4069 N85-35214

ELASTIC MEDIA
Propagation of longitudinal elastic waves in multilayered half-space 02 p0273 N85-11779
Wedge with crack in bielastic medium 02 p0273 N85-11780
An inverse source problem for elastic waves 03 p0371 N85-12368
Transonic flow of elastic medium past slender solid body 06 p0778 N85-14976
Numerical experiments and theoretical analysis of the flow of an elastic liquid of the Maxwell-Oldroyd type in the presence of geometrical singularities
[WTHD-164] 08 p1183 N85-17340
Numerical evaluation of low frequency sound propagation in layered media
[AD-A152690] 17 p3028 N85-28728

ELASTIC MODULUS
U MODULUS OF ELASTICITY

ELASTIC PLATES
Stress intensity factors for corner cracks at holes located near an edge
[FFA-TN-1984-20] 04 p0514 N85-13279
Numerical treatment of corner singularities of the biharmonic equation
[TUM-M8315] 05 p0717 N85-14602
Investigation of dynamics of manipulator with elastic sections 13 p2048 N85-22819
Load transfer by analytical methods
[SNIAS-851-111-109] 20 p3470 N85-31561
Generation by conformal mappings of aerofoil sections and of certain other simple shapes suitable for both aerodynamic and stress-concentration problems
[AD-A154901] 22 p3728 N85-33112

ELASTIC PROPERTIES
NT AEROELASTICITY
NT DYNAMIC MODULUS OF ELASTICITY
NT ELASTOPLASTICITY
NT HYDROELASTICITY
NT MAGNETOSTRICTION
NT MODULUS OF ELASTICITY
NT PHOTOELASTICITY
NT PHOTOVISCOELASTICITY
NT PROPORTIONAL LIMIT
NT THERMOELASTICITY
NT THERMOVISCOELASTICITY
NT VISCOELASTICITY
Theory of nonlocal elasticity and some applications
[AD-A145201] 01 p0062 N85-10412
Wedge with crack in bielastic medium 02 p0273 N85-11780
Eta values for compact geometry specimens to calculate the J integral
[AERE-R-11126] 03 p0374 N85-12385
In situ experiment on shear waves generation and determination of elastic properties of soils
[REPT-550] 03 p0375 N85-12393
An integral equation formulation for a boundary value problem of elasticity in the domain exterior to an arc
[PREPRINT-833] 03 p0413 N85-12643
Nondestructive evaluation of residual stress in low-carbon steel
[NASA-CR-174157] 04 p0512 N85-13264
Nondestructive determination of mechanical properties — aluminum alloys 04 p0512 N85-13266

Influence of the mechanical and electrochemical characteristics of austenitic and austenoferritic steels on the propagation rate and morphology of stress corrosion cracking
[BLL-RISLEY-TR-4545-(9091.9F)] 06 p0767 N85-14906
Saint Venant conditions in theory of piezoelastic shells 06 p0780 N85-14987
Controllable rotation of system of two solid bodies with elastic elements 06 p0780 N85-14988
Elastic fields under a spherical indenter
[AD-A146519] 06 p0817 N85-15186
Theoretical and experimental study of hydro-elastic instability on the line of shafting of a rotating machine
[BLL-DOUNREAY-TR-937-(9091.9F)] 07 p0972 N85-16174
Nonlinear waves in a rod. Results for incompressible elastic materials
[AD-A147485] 07 p0979 N85-16216
Model for prediction of the elastic response of composite materials over wide ranges of concentration
[AD-A148186] 08 p1119 N85-17051
Study of reaction kinetics and development of elastic properties in network polymerization systems by the impulse technique
[AD-A148187] 08 p1133 N85-17141
Determination of the elastic constants of inhomogeneous materials with X-ray diffraction
[AD-A148469] 08 p1173 N85-17393
Nonlinear finite element analysis of elastic and elastic-plastic buckling of cylinders under complex combined loads 09 p1332 N85-18373
Earthquake-modeling experiment using unique press 10 p1500 N85-19469
Simplified theory for the behaviour of buried flexible cylinders under the influence of uniform hoop compression
[PB85-116531] 11 p1654 N85-20419
Parachute inflation dynamics 11 p1715 N85-20792
Rheology of dissemination
[AD-A150006] 12 p1813 N85-21373
Elastic response of a half-plane to a bonded interference-fit disc of the same material
[ARL/STRUC-R-406] 12 p1865 N85-21701
Moving nonlocal crack: Anti-plane shear case
[AD-A149996] 12 p1866 N85-21709
Elasticity formulas for thin-walled shells with piezoceramic layers 13 p2047 N85-22816
Controlled movement of elastic manipulator with distributed parameters 13 p2048 N85-22818
Attenuation of seismic waves at regional distances
[AD-A150198] 13 p2132 N85-23267
Influence of short-range order on deformation mechanisms in solid solutions
[DE85-006374] 14 p2258 N85-23999
Research on composite materials for structural design
[AD-A150602] 14 p2260 N85-24004
Uniaxial orientation of linear low density polyethylene
[AD-A151037] 14 p2261 N85-24009
Analysis of slabs-on-grade for a variety of loading and support conditions
[AD-A150965] 14 p2264 N85-24030
The application of transonic unsteady methods for calculation of flutter airloads 15 p2480 N85-25186
An experimental investigation into the dynamic response of a stiffened flat plate loaded impulsively by an underwater shockwave
[AD-A151321] 15 p2578 N85-25903
Control of a flexible beam
[DE85-007243] 15 p2580 N85-25914
Mechanical properties of high performance carbon fibers 16 p2742 N85-26922
The effects of pin elasticity, clearance, and friction on the stresses in a pin-loaded orthotropic plate
[NASA-CR-175816] 16 p2743 N85-26927
Solution softening in molybdenum-rhenium alloys
[DE85-006708] 16 p2750 N85-26972
On residual stress in an elastic body 16 p2798 N85-27248
Numerical solution of one-dimensional nonlinear problems of statics for elastic beams and shells under rigid constraints 17 p2943 N85-28166
Electronically excited alkaline earth oxides: Chemical production and collisional energy transfer processes
[AD-A153172] 17 p3044 N85-28833
Gust load alleviation of a cantilevered rectangular elastic wing. Wind tunnel experiment and analysis
[NAK-TR-86] 18 p3063 N85-28950
Interaction of large amplitude stress waves in layered elastic-plastic materials
[AD-A153519] 18 p3121 N85-29323
Mechanics of composite materials, theory and application
[VTH-LR-431] 18 p3123 N85-29334
Shear deflection in a three-point bend beam of a solid circular cross-section
[AD-A154458] 19 p3287 N85-30381
Analysis of the elastic and strength properties of Yucca Mountain tuff, Nevada
[DE85-006975] 19 p3300 N85-30460
A survey of unified constitutive theories 20 p3466 N85-31531
Viscoplasticity based on overstress with a differential growth law for the equilibrium stress 20 p3466 N85-31532
On the use of internal state variables in thermoviscoplastic constitutive equations 20 p3466 N85-31536
Dynamical study of flat plates by nonlinear elasticity theory
[STN-8] 20 p3471 N85-31572
Stresses and deformations in cross-ply composite tubes subjected to a uniform temperature change: Elasticity and Approximate Solutions
[NASA-CR-176147] 22 p3800 N85-33545
SANCHO: A finite element computer program for the quasistatic, large deformation, inelastic response of two-dimensional solids
[DE85-011456] 22 p3829 N85-33714
Viscoelastic behavior of short-fiber composite materials
[DE85-011233] 23 p3910 N85-34225
The study of the effect of residual microimpurities on the fatigue strength of 55S2 steel
[BLL-M-36317-(5828.4)] 23 p3913 N85-34246
An introduction to finite elements 23 p3924 N85-34319
Stresses and strains in a plate resulting from two closely-spaced interference-fit fasteners
[ARL/STRUC-TM-409] 23 p3941 N85-34429
Analysis of the nonlinear equations describing the elastic, thermal, and electromagnetic behavior of solids: Existence of solutions of semi-inverse problems 24 p4100 N85-35415
Vibrations of free hollow circular cylindrical bodies 24 p4100 N85-35418
(NAT)Fe(n,n'x) spectra at 65.5 MeV
[AD-A155776] 24 p4150 N85-35730
Ionic crystals
[DE85-009482] 24 p4163 N85-35809

ELASTIC SCATTERING
Sturmian expansion approximation to three-body scattering
[CSIR-TWiSK-309] 01 p0109 N85-10731
Monte Carlo simulation of thermalization of subexcitation electrons in molecular hydrogen
[NAL-TR-815T] 01 p0117 N85-10798
Study of structure of nuclei with neutrons and nuclear data measurements for MFE
[DE84-015126] 01 p0117 N85-10802
Molecular beam scattering 03 p0417 N85-12668
Diffuse elastic and inelastic neutron scattering of disorder transitions and boundaries. Phase determination of structure factors 03 p0424 N85-12708
Quasielastic neutron scattering on single crystals of solid ionic conductor 03 p0426 N85-12719
Fundamentals of microcrack nucleation mechanics
[NASA-CR-3851] 07 p0975 N85-16195
High energy physics study
[DE84-015803] 09 p1383 N85-18700
Instrumental background in balloon-borne gamma-ray spectrometers and techniques for its reduction
[NASA-TM-86162] 09 p1413 N85-18911
Low energy antiproton interaction studies at Brookhaven
[DE85-001228] 11 p1720 N85-20820
Recent progress in electron scattering at SLAC
[DE85-002718] 11 p1723 N85-20840
Cometary atmospheres: Modeling the spatial distribution of observed neutral radicals
[NASA-CR-175485] 11 p1765 N85-21098
A remote source system for measuring relative positron annihilation line widths in individual slab cylindrical samples
[AERE-R-10549] 12 p1938 N85-22173
Elastic wave scattering from an interface crack in a layered half space 13 p2101 N85-23095
Intensity vectors of sound scattering by a spherical shell
[AD-A147847] 13 p2103 N85-23107
Elastic wave scattering from cavities and sound inclusions analyzed by the resonance method
[AD-A150315] 13 p2155 N85-23361
Theoretical aspects of the nucleon-nucleon workshop
[DE85-003740] 14 p2420 N85-24933
Interaction of low energy electrons with surface lattice vibrations
[DE85-005475] 14 p2428 N85-24975
Energy deposition from particle beams
[DE85-007382] 16 p2862 N85-27654
Stefan-Maxwell relations for plasma diffusion currents in magnetic field 17 p2942 N85-28160
Experimental studies of diffractive phenomena
[DE85-006612] 17 p3031 N85-28749
Development of the relativistic impulse approximation
[DE85-008505] 18 p3179 N85-29711
Intermediate energy nuclear theory
[DE85-010440] 18 p3182 N85-29731
Theory of high energy collision processes
[DE85-010183] 19 p3362 N85-30646
Energy-advanced nuclear data: Measurements and physical interpretations
[DE85-006198] 19 p3366 N85-30672
Methods of Monte Carlo electron transport in particle-in-cell codes
[DE85-010702] 20 p3521 N85-31866
Spin physics at BNL
[DE85-009768] 20 p3529 N85-31955
Remarks on nucleon-nucleon hard scattering
[NIKHEF-H/84-14] 20 p3532 N85-31979
Spatial parity violation in elastic neutron-nuclei interaction channel 21 p3691 N85-32932
Evaluated nuclear-data file for niobium
[DE85-012095] 21 p3704 N85-33009
P(P bar)P elastic scattering and cosmic ray data
[HE-1.1-6] 24 p4170 N85-35854
General consequences of the violated Feynman scaling 24 p4173 N85-35872

ELASTIC SHELLS
High-frequency asymptotic behavior of reflected and transmitted waves during scattering of sound by hollow elastic sphere filled with fluid 02 p0266 N85-11736
Selective observation of elastic-body resonances via their ringing in transient acoustic scattering
[AD-A145868] 03 p0416 N85-12658
Resonant scattering of acoustic waves by elastic spherical shell in fluid 06 p0778 N85-14972
Some problems in optimally designing shells of revolution 14 p2278 N85-24114
Elastic equilibrium of composite shells with finite shear rigidity 17 p2942 N85-28163
Numerical solution of one-dimensional nonlinear problems of statics for elastic beams and shells under rigid constraints 17 p2943 N85-28166
Scattering of sounds by piezoceramic cylindrical shell near rigid surface 17 p2943 N85-28168

ELASTIC STABILITY
U DAMPING

ELASTIC STRENGTH
U PROPORTIONAL LIMIT

ELASTIC WAVES
NT AERODYNAMIC NOISE
NT AIRCRAFT NOISE
NT BAROCLINIC WAVES
NT CAPILLARY WAVES
NT COHERENT ACOUSTIC RADIATION
NT COMPRESSION WAVES
NT DETONATION WAVES
NT ELECTROACOUSTIC WAVES
NT ELECTROSTATIC WAVES
NT ENGINE NOISE
NT GRAVITY WAVES
NT ION ACOUSTIC WAVES
NT IONIC WAVES
NT JET AIRCRAFT NOISE
NT LAMB WAVES
NT LOVE WAVES
NT MAGNETOACOUSTIC WAVES
NT MAGNETOELASTIC WAVES
NT MAGNETOHYDRODYNAMIC WAVES
NT MICROSEISMS
NT NOISE (SOUND)
NT NORMAL SHOCK WAVES
NT OBLIQUE SHOCK WAVES
NT P WAVES
NT PHONONS
NT PLASMA WAVES
NT RAYLEIGH WAVES
NT RIPPLES
NT S WAVES
NT SEISMIC WAVES
NT SHOCK WAVES
NT SONIC BOOMS
NT SOUND WAVES
NT STRESS WAVES
NT THERMAL NOISE
NT TOLLMIEN-SCHLICHTING WAVES
NT ULTRASONIC RADIATION
Influence of radiation wavelength on elastic pulse shape during laser excitation 02 p0257 N85-11681
Propagation of longitudinal elastic waves in multilayered half-space 02 p0273 N85-11779
Elastic wave propagation through polycrystals
[DE84-016772] 04 p0558 N85-13554

A geometric approach to high resolution TVD schemes
[NASA-CR-172484] 06 p0657 N85-15449
Fundamentals of microcrack nucleation mechanics
[NASA-CR-3851] 07 p0975 N85-16195
Quantitative acoustic emission techniques
[AERE-R-11262] 07 p0977 N85-16203
On seismic waves 08 p1171 N85-17383
Characterisation of fatigue crack extension by quantitative acoustic emission
[AERE-R-11269] 12 p1866 N85-21721
Scattering of elastic waves on fractures randomly distributed in a three-dimensional medium
13 p2111 N85-23151
Elastic wave scattering from cavities and sound inclusions analyzed by the resonance method
[AD-A150315] 13 p2155 N85-23381
An analytical and numerical study of the interaction of rarefaction waves with area changes in ducts. Part 2: Area enlargements
[UTIAS-273] 14 p2300 N85-24242
Propagation of non-axisymmetric elastic waves through shell with filler under radial load at one end
17 p2943 N85-28169
Theoretical and experimental studies of the mechanics of viscoelastic liquids
[AD-A153505] 18 p3070 N85-29987
Computer simulation of elastic waves by a new mass-point system with potentials
[DRIC-T-7274] 20 p3469 N85-31553
Source characterization of point-like and distributed sources of acoustic emission 20 p3523 N85-31910
Numerical experiment of elastic wave propagation by framework model
[DRIC-T-7462] 22 p3795 N85-33511

ELASTICITY
U ELASTIC PROPERTIES

ELASTICIZERS
U PLASTICIZERS

ELASTODYNAMICS
NT ELASTIC DAMPING
NT ELASTOHYDRODYNAMICS
Acoustic emission waveforms in a half space
[AD-A146322] 03 p0417 N85-12684
Transonic flow of elastic medium past slender solid body 06 p0778 N85-14978
Numerical modeling of complex interaction of shell of revolution and its filler with allowance for friction
06 p0779 N85-14980
Deformation of cylindrical shell with cantilevered elastic plates attached 06 p0779 N85-14984
Numerical solution of elastodynamic problems in fracture mechanics 06 p1171 N85-17385
A numerical method for interface problems in elastodynamics
[NASA-TM-86458] 08 p1172 N85-17391
Symmetric primal-dual variational formulations of coupled dynamic systems: Three-dimensional elasticity, shells, fluid-structure interaction
[ONERA-1983-91] 12 p1863 N85-21684
Controllable movements of elastic manipulator with three degrees of freedom 14 p2296 N85-24040
Application of deformable body mean-axis to dynamics of flexible mechanical systems 19 p3283 N85-30359
Transient dynamic solutions of some half space problems by the boundary element method
19 p3283 N85-30360

ELASTOHYDRODYNAMICS
Normal mode method of solving problem forced oscillations of rib-reinforced shell of revolution in liquid
02 p0273 N85-11781
Fluidelastic instability in shell and tube heat exchangers: A framework for a prediction method
[DE84-006518] 10 p1498 N85-19444
Problems of elastic hydrodynamic lubrication of helicopter transmission gears 14 p2222 N85-23784
Wear reduction by lubricants in confined contacts
14 p2223 N85-23786
Fast approach for calculating film thicknesses and pressures in elastohydrodynamically lubricated contacts at high loads
[NASA-TM-87032] 19 p3264 N85-30242
Surface roughness effects in elastohydrodynamic contacts
[NASA-TP-2486] 21 p3595 N85-32329
Mechanics of a gaseous film barrier to lubricant wetting of elastohydrodynamically lubricated conjunctions
[NASA-TP-2500] 21 p3595 N85-32330

ELASTOMERS
NT CHLOROPRENE RESINS
NT VULCANIZED ELASTOMERS
Electricaly conductive rigid polyurethane foam
[DE84-014460] 01 p0033 N85-10203
Aircraft surface coatings
[NASA-CR-3661] 02 p0137 N85-10935
The role of molecular diffusion in the adhesion of elastomers
[AD-A145576] 02 p0186 N85-11245
Mechanochemical reactions of elastomers with metals
[AD-A145657] 02 p0186 N85-11246
Description and characterization of deuterated polymers for the analysis with neutron scattering
03 p0431 N85-12748
The effect of cross-link density on the toughening mechanism of elastomer-modified epoxies
04 p0485 N85-12951
Toughening mechanism in elastomer-modified epoxy resins, part 2
[NASA-CR-3852] 04 p0478 N85-13046
Flexible matrix composite laminated disk/ring flywheel
05 p0606 N85-13866
Structure-property relationships in thermoplastic elastomers. Part 1: Segmented polyether-polyurethanes
[AD-A148043] 08 p1133 N85-17138
Poly(dimethylsiloxane)-polyurethane elastomers: Synthesis and properties of segmented copolymers and related zwitterionomers
[AD-A148571] 08 p1134 N85-17147
Development of a heterogeneous laminating resin system
[NASA-CR-172459] 09 p1288 N85-18089
Mechanisms of gas permeation through polymer membranes
[DE84-017423] 09 p1293 N85-18117
Characterization of novel binders based on energetic thermoplastic elastomers
[AD-A148993] 10 p1451 N85-19139
Elastomer toughened polyimide adhesives — bonding metal and composite material structures for aircraft and spacecraft
[NASA-CASE-LAR-12775-2] 12 p1809 N85-21349
Effect of alternative aging and accident simulations on polymer properties
[DE85-002642] 13 p2037 N85-22762
Oil resistant silicone elastomers
[AD-131523] 16 p2753 N85-26987
Formulation/cure technology for ultrahigh molecular weight silphenylene-siloxane polymers
[NASA-TP-2476] 16 p2753 N85-26990
Thermally stable elastomers: Review of silarylene-siloxane polymers and polysilmethylenes
[AD-A152323] 17 p2934 N85-28111
Electro-expulsive separation system
[NASA-CASE-ARC-11613-1] 18 p3094 N85-29150
Elastomers used in aeronautics industry
[SNIAS-851-551-103] 20 p3434 N85-31304
Structure-property relationships in thermoplastic elastomers. Part 3: Segmented polyacetal-polyurethanes
[AD-A154897] 21 p3569 N85-32200

ELASTOPLASTICITY
Initial postbuckling analysis of elastoplastic thin-shear structures 01 p0059 N85-10393
HOST high temperature crack propegation
02 p0144 N85-10977
Acceleration waves 02 p0207 N85-11357
Analysis based on Reissner theory for rectangular plates with all edges built-in 04 p0483 N85-13081
Compression of a band made of elastic, ideally Coulomb plastic material
[ISSN-0208-5658] 05 p0648 N85-14157
Variable loading of elastic-plastic shells of revolution
06 p0779 N85-14981
Correlation of stable crack growth with the J-integral and the crack tip opening displacement, effects of geometry, size and material: Report on an investigation of the elastic-plastic R-curve methodology
[GKSS-84-E-37] 06 p1173 N85-17395
Elastic-plastic analysis for cyclic loading using a linearized yield condition
[PB85-149607] 14 p2322 N85-24346
Local elastoplastic fracture of fibrous composite materials 15 p2497 N85-25405
Influence of behavior laws in the explosive deformation of metal plates
[ISL-R-122/83] 16 p2760 N85-27032
Consolidation theory with consideration of frame plasticity
[REPT-9/1984] 16 p2796 N85-27240
Adaptation of continuous beams and the method of optimizing the flexibility of their elastic supports. Theorem on maximal adaptation loading, supplement
[REPT-10/1984-SUPPL] 16 p2797 N85-27241
Analysis of elastoplastic grids under conditions of variable loads
[REPT-16/1984] 16 p2797 N85-27242
Multinomial form of the solution of problems of the statistics of elastic rectangular disks
[REPT-17/1984] 16 p2797 N85-27244
Specimen thickness effects for elastic-plastic CTOD toughness of A36 steel
[DE85-006992] 18 p3077 N85-29038
Micromechanics of high temperature deformation and failure 20 p3486 N85-31534
Numerical study of ductile rupture in plane deformations
[ONERA-RT-23/7169-RY-072-R] 20 p3469 N85-31557
A review of path-independent integrals in elastic-plastic fracture mechanics, task 4
[NASA-CR-174956] 22 p3799 N85-33541

ELASTOSTATICS
On some exact solutions in elastostatics in terms of harmonic functions 09 p1332 N85-18367
A study of coupling the boundary and finite element methods in two-dimensional elastostatics
[AD-A149619] 12 p1865 N85-21702
Numerical solution of one-dimensional nonlinear problems of statics for elastic beams and shells under rigid constraints 17 p2943 N85-28166
The role of ellipticity and normality assumptions in formulating live-boundary conditions in elasticity
[AD-A153475] 18 p3168 N85-29630
Ductile fracture of dynamically loaded naval structures-compact tension specimen tests and analyses
[AD-A155472] 21 p3600 N85-32353

ELBOW (ANATOMY)
Elbow and knee joint for hard space suits and the like
[NASA-CASE-ARC-11610-1] 11 p1697 N85-20666

ELECTRETS
Study of charge transport in the thermoelectret state of some ceramics and glasses
[DE85-001763] 09 p1300 N85-18163
Investigation of charge transport in the thermoelectret state of some ceramics and glasses
[DE85-009318] 17 p2936 N85-28122

ELECTRIC AIRCRAFT
U FLY BY WIRE CONTROL

ELECTRIC APPLIANCES
U ELECTRIC EQUIPMENT

ELECTRIC ARCS
NT CARBON ARCS
NT MERCURY ARCS
The anode mechanism of a thermal argon arc
[NASA-TM-77754] 07 p0921 N85-15835
The discharge mechanism of the high-temperature arc
[NASA-TM-77794] 07 p0922 N85-15837
Arc erosion of metal in current interval of 1-10 amperes 07 p0953 N85-16042
Evaluation of the Kerle Cable thermal arc cutting equipment
[AD-A147813] 07 p0974 N85-16186
Metal vapor arc switch electromagnetic accelerator technology
[NASA-CR-174360] 09 p1314 N85-18259
Flashover failures from wet-wire arcing and tracking
[AD-A149055] 10 p1478 N85-19332
Improved operation of transversely exited N2O lasers
[AD-D011488] 10 p1490 N85-19409
Analysis of the dissipation mechanism within an instationary cathode spot of metal vapor arcs
[AD-A149258] 10 p1558 N85-19825
Apparatus for producing diamond-like carbon flakes
[NASA-CASE-LEW-13837-3] 11 p1615 N85-20155
Thermal investigation of an electrical high-current arc with porous gas-cooled anode
[NASA-TM-77789] 11 p1627 N85-20245
Neutral beam injector oxygen impurity measurements and concentration reduction via gettering processes
[DE85-000861] 12 p1836 N85-21521
Characteristics of multiarc plasma devices
12 p1841 N85-21554
Review of anode phenomena in vacuum arcs
[DE85-002736] 12 p1926 N85-22101
Study of a constricted electric arc cooled by transpiration
[NASA-TM-77846] 17 p3038 N85-28798
Examination of a method for predicting the properties of railgun plasmas
[AR-004-322] 17 p3039 N85-28799
Experimental research on electrical propulsion
[NASA-TM-77876] 18 p3067 N85-29969
An alpha particle diagnostic beam line system to generate an intense Li(O) beam with an ORNL SITEX source
[DE85-010564] 18 p3182 N85-29730

ELECTRIC AUTOMOBILES
Summary of activities pertaining to utilization of grant purchase of batteries for electric van
[DE84-015793] 02 p0195 N85-11305
ElectriFleet Project
[DE85-001598] 10 p1570 N85-19888
Electric vehicle demonstration project
[DE85-003124] 11 p1741 N85-20944

West Europe report: Science and technology
[JPRS-WST-84-027] 15 p2532 N85-25612
Nickel-iron battery to be used in Peugeot electric car
15 p2532 N85-25615
AC powertrain for an electric vehicle, phase 2 and phase 3
[NASA-CR-175760] 16 p2880 N85-27771
Advanced vehicle systems assessment. Volume 1: Executive summary
[NASA-CR-175676] 17 p3051 N85-28867
West Europe report: Science and technology
[JPRS-WST-84-032] 18 p3086 N85-29095
Electric Peugeot to have new nickel-iron batteries
18 p3086 N85-29096
Electric and hybrid vehicle program: FY 1985 program plan
[DE85-008933] 18 p3201 N85-29856
Test plan for performance testing of the Eaton AC-3 electric vehicle
[DE85-011954] 23 p3927 N85-34341

ELECTRIC BATTERIES
NT ALKALINE BATTERIES
NT LEAD ACID BATTERIES
NT NICKEL CADMIUM BATTERIES
NT NICKEL HYDROGEN BATTERIES
NT NICKEL ZINC BATTERIES
NT PRIMARY BATTERIES
NT REDOX CELLS
NT SILVER HYDROGEN BATTERIES
NT SODIUM SULFUR BATTERIES
NT STORAGE BATTERIES
NT THERMAL BATTERIES
NT ZINC-BROMIDE BATTERIES
NT ZINC-CHLORINE BATTERIES
Sea water rope batteries
[AD-A144775] 01 p0042 N85-10275
Battery optimization considerations
[DE84-014750] 01 p0044 N85-10288
Summary of activities pertaining to utilization of grant purchase of batteries for electric van
[DE84-015793] 02 p0195 N85-11305
Properties of cathode materials in alkaline cells
[NASA-CR-174082] 04 p0495 N85-13161
Lithium battery safety: A fiber-optic application for safe observation of lithium cells under severe tests
[AD-A146846] 06 p0804 N85-15119
Composite batteries 07 p0936 N85-15932
Safety evaluation of an electronic totalizer containing a Li/(CF)x cell
[AD-A147306] 07 p0993 N85-16305
Battery control and fault detection method
[AD-D011384] 07 p0993 N85-16307
New liquid cathodes for lithium batteries. Part A: Halocarbons
[AD-A148493] 08 p1178 N85-17423
Status of the Li-Al/FeS battery manufacturing technology. An evaluation for the US Army, Belvoir R and D Center
[DE85-000776] 09 p1315 N85-18264
Battery response to pulse loads: A mathematical model
[DE85-001149] 09 p1316 N85-18277
The development of a method for the shock-resistant securing of large batteries in submarines
09 p1335 N85-18391
Hybrid vehicle program
[DE85-000326] 09 p1410 N85-18886
Electric vehicle battery test plan and results
[DE84-901972] 09 p1410 N85-18887
Polymer electrolytes: An investigation of some poly (N-propylaziridine)/lithium salt compositions
[AD-A149444] 10 p1452 N85-19146
Charge depletion meter
[AD-D011484] 10 p1488 N85-19393
Emergency Locator Transmitter (ELT) batteries guidance and recommendations
[NASA-TM-87436] 11 p1624 N85-20225
Emergency Locator Transmitter (ELT) batteries guidance and recommendations
[NASA-TM-87415] 11 p1672 N85-20533
Electric vehicle demonstration project
[DE85-002167] 11 p1741 N85-20943
Nickel-cadmium battery cell reversal from resistive network effects
[AD-A149626] 12 p1834 N85-21505
Polymeric electrolytes for ambient temperature lithium batteries
[DE85-001032] 12 p1835 N85-21518
Research to explore the feasibility of sulfolanes as electrolytic solvents for rechargeable lithium batteries
[DE85-004345] 12 p1837 N85-21525
State-of-charge coulometer
[NASA-CASE-NPO-15759-1] 12 p1849 N85-21586
An improved battery state-of-charge indicator
[NASA-CR-175701] 14 p2298 N85-24227
Status of French research in plastic batteries
15 p2530 N85-25603
A portable battery for objective, non-obstrusive measures of human performances
[NASA-CR-171666] 15 p2586 N85-25942
Calcium/thionyl chloride battery technology
[AD-A151975] 15 p2586 N85-25945
INEL electric vehicle laboratory qualification: Transition test results and comparisons with JPL ETV1-2 data
[DE85-008006] 16 p2880 N85-27772
Investigation of the structure and dynamics of electrolytes in solvents used for primary and secondary Li-batteries
[AD-A153099] 17 p2954 N85-28240
Aluminum-air power cell research and development
[DE85-008117] 17 p2966 N85-28456
British breakthrough in lightweight lithium batteries
18 p3086 N85-29092
West Europe report: Science and technology
[JPRS-WST-84-035] 18 p3087 N85-29102
Low-rate discharge of various electrochemical batteries for use with oceanographic instruments
[AD-A153965] 18 p3095 N85-29159
Lithium-alloy/iron sulfide battery design studies
[DE85-007991] 18 p3131 N85-29389
Electric and hybrid vehicle program
[DE85-010025] 19 p3262 N85-30230
Lithium cell reactions
[AD-A154429] 19 p3305 N85-30484
Polyethylene imine-metal salt solid electrolyte
[AD-D011678] 19 p3305 N85-30485
Galileo battery testing and the impact of test automation
20 p3444 N85-31381
An update of the JPL program to develop Li-SOCl2 cells
20 p3445 N85-31384
Nickel-cadmium battery cell reversal from resistive network effects
20 p3446 N85-31392
A 34 ampere-hour nickel-cadmium minimum trickle charge testing
20 p3448 N85-31394
A safe, high-power-density lithium battery
[AD-A155223] 21 p3613 N85-32454
Rechargeable lithium-organic electrolyte battery having overcharge protection and method of providing overcharge protection for a lithium-organic electrolyte battery
[AD-D011738] 22 p3806 N85-33575
Transfer of battery technology developed by the US Department of Energy
[DE85-009666] 22 p3808 N85-33586
Electric vehicle operations by the City of Huntsville, Alabama, March 1983 - May 1984
[DE85-005913] 22 p3849 N85-33842
Test plan for performance testing of the Eaton AC-3 electric vehicle
[DE85-011954] 23 p3927 N85-34341
Wind energy battery storage, phase 2
[DE85-009753] 23 p3945 N85-34450
Development and evaluation of sulfonated polysulfone membranes for the zinc-ferricyanide battery
[DE85-009104] 24 p4090 N85-35357
Cationic exchange membrane for the zinc-ferricyanide battery
[DE85-013152] 24 p4112 N85-35489

ELECTRIC BRIDGES
NT WHEATSTONE BRIDGES
NT WIRE BRIDGE CIRCUITS
Bridge erosion in electrical contacts
04 p0486 N85-13102
Piezoelectric filter with low-Q inductances
13 p2070 N85-22932
Adjustment of the frequency-temperature characteristics of crystal oscillators
[AD-D011688] 15 p2548 N85-25726
Simultaneous phase and frequency control of a three-phase inductor-convertor bridge
[DE85-006197] 18 p3096 N85-29164
Temperature sensors for OTEC applications
[DE85-009807] 18 p3110 N85-29254
R, L, C, G measurement 21 p3668 N85-32784
State of art and development problems in computer-aided design of electronic circuits
22 p3766 N85-33342
Modeling of electronic circuits with high degree of component integration 22 p3766 N85-33343
System for computer-aided design of analog electronic circuits 22 p3766 N85-33353

ELECTRIC CHARGE
NT ELECTRIC DIPOLES
NT ELECTROSTATIC CHARGE
NT ION CHARGE
NT SPACE CHARGE
Performance characteristics of a battery charger and state-of-charge indicator
[NASA-CR-174273] 07 p0948 N85-15892
A comparison of lightning and nuclear electromagnetic pulse response of a helicopter 07 p1000 N85-16349
Potential dependence of electrical conductivity and chemical charge storage of poly(pyrrole) films on electrodes
[AD-A148513] 08 p1122 N85-17075
SIMM1: A linearized particle code
[AD-A148627] 08 p1221 N85-17889
Charge depletion meter
[AD-D011484] 10 p1488 N85-19393
Atmospheric research aircraft — conductivity/charge measurements
[ONERA-RS-87/7154/PY] 11 p1682 N85-20596
Interfacial and colloidal aspects of aqueous suspension containing oxidic powders
[DE85-005972] 15 p2519 N85-25534
Investigation of charge transport in the thermoelectret state of some ceramics and glasses
[DE85-009318] 17 p2936 N85-28122
Preliminary documentation for the polar code
[AD-A154125] 19 p3336 N85-30667
Buildup of electric charge in foil dielectrics during gamma irradiation 22 p3770 N85-33363
Friction, impact, and electrostatic discharge sensitivities of energetic materials
[DE85-013321] 24 p4083 N85-35309

ELECTRIC CIRCUITS
U CIRCUITS

ELECTRIC COILS
NT MAGNETIC COILS
Superconducting rotor dynamics
[AD-A147176] 07 p0947 N85-16000
Fast switching driver for inductive load, such as a phase shifter
[AD-D011368] 08 p1143 N85-17207
High-current measurement techniques
[PB85-100444] 11 p1637 N85-20311
Eddy current test probe with circumferential segments and method of testing material surrounding fastener holes
[AD-D011554] 12 p1850 N85-21603
Detection and location of partial discharges in transformer windings using electrical methods
15 p2551 N85-25750
Outline of alternative design of R-Tokamak
15 p2654 N85-26371

ELECTRIC CONDUCTORS
Conductor structure for thick film electrical device
[AD-D011240] 01 p0043 N85-10281
Resistance and inductance calculations for helical flux compression generators
[DE84-015068] 02 p0195 N85-11306
Plasma drift towards a plane equipotential surface
[TRITA-EPP-84-01] 02 p0285 N85-11860
Mechanical locking between multi-layer printed wiring board conductors and through-hole plating
[AD-D011477] 10 p1481 N85-19352
Characterization of high temperature electrically conducting oxides
[DE85-004296] 12 p1803 N85-21307
The liner package: An incipient MHD capability for CCUBE
[LA-9969-MS] 12 p1913 N85-22007
Properties of Ti alloyed multifilamentary Nb3Sn wires by internal tin process
[DE85-003212] 12 p1941 N85-22191
An investigation of arc discharging on negatively biased dielectric conductor samples in a plasma
13 p1994 N85-22496
Electrical conduction in polymer dielectrics
13 p1996 N85-22514
Transport studies of several novel organic conductors
[DE85-003950] 14 p2429 N85-24979
Heat resistant sheathed insulated electrical conductors
[AD-D011644] 17 p2951 N85-28219
Silicide conductors reliability research
[AD-A153768] 18 p3095 N85-29157
Quantized Hall conductance as a topological invariant
[DE85-007796] 18 p3193 N85-29808
Structural and physical studies on a new class of low-dimensional conducting material: FeOCl intercalated with TTF and related molecules
[DE85-009701] 18 p3196 N85-29824
Tailored vacuum chambers for ac magnets
[DE85-010767] 21 p3591 N85-32319
Method and apparatus for casting conductive and semi-conductive materials
[DE85-011655] 22 p3792 N85-33494
Feasibility study of radar-transmitting materials
[AD-A155639] 24 p4087 N85-35329

ELECTRIC CONNECTORS
Advanced high-power transfer through rotary interfaces 05 p0607 N85-13875
Power quality and protection of electric distribution systems with small, dispersed generation devices
[DE85-000980] 09 p1344 N85-18453

Safety requirements for wiring systems and connectors for photovoltaic systems
[NASA-CR-174431] 10 p1477 N85-19324
Connector/nitinol delta contact force device
[AD-D011467] 10 p1481 N85-19349
Magnetic field interactions with material discontinuities
[AD-A150197] 13 p2154 N85-23373
Characterization of solderless minimrapping connections
[CNES-NT-112] 16 p2796 N85-27236
Derated application of parts for (Electronic Systems Division) systems development. Revision
[AD-A153299] 17 p2955 N85-28246

ELECTRIC CONTACTS
MOD silver metallization for photovoltaics
[NASA-CR-174011] 01 p0026 N85-10163
Surface segregation of sulfur during oscillatory pin-on-plate wear studies of precious metal electrical contact alloys. 1: Friction and electrical contact resistance
[DE84-008862] 02 p0195 N85-11303
Bridge erosion in electrical contacts
04 p0496 N85-13102
Advanced high-power transfer through rotary interfaces 05 p0607 N85-13875
Thermal contact conductance measurements on Doublet 3 armor tile trophite
[DE84-013554] 05 p0613 N85-13916
Laser-assisted solar cell metallization processing
[NASA-CR-174213] 06 p0613 N85-15160
Electromechanical switch
[AD-D011400] 07 p0948 N85-16009
Arc erosion of metal in current interval of 1-10 amperes 07 p0953 N85-16042
Screen printed interdigitated back contact solar cell
[NASA-CASE-LEW-13414-1] 11 p1671 N85-20530
A solution method for large deformation contact problems
[AD-A149842] 12 p1866 N85-21707
Control of cascaded induction generator systems
[AD-A150429] 13 p2065 N85-22997
Thermal and thermoelastic effects in rolling/sliding contacts
[AD-A150435] 13 p2165 N85-23429
Some observations of heated gallium arsenide heteroface solar cells
[NASA-TM-86386] 14 p2248 N85-23925
Erosion of electrodes due to switching of capacitor-bank discharge circuits
[AD-A151207] 15 p2547 N85-25718
Thin-film polycrystalline silicon research
[DE85-002908] 15 p2663 N85-26434
LPCVD tungsten deposition on Si-Ge alloy
[DE85-005588] 16 p2750 N85-26970
Comprehensive silicon solar cell computer modeling
[NASA-CR-175959] 17 p2967 N85-28461
Temperature and surface damage under lubricated sliding-rolling contacts 19 p3280 N85-30338
Design and operation of epitaxial reactor
[DE85-011089] 19 p3306 N85-30491
Ink jet printing of silver metallization for photovoltaics
[NASA-CR-176019] 19 p3343 N85-30720
Silicon MINP solar cells 20 p3480 N85-31623
A rotating electrical transfer device
22 p3798 N85-33529
Noise in silver beta alumina ceramics
[AD-A156135] 24 p4082 N85-35297
Computer simulation of a cruise missile using brushless dc motor fin control
[AD-A156935] 24 p4089 N85-35349
Development of contactless sensors for industrial and automotive applications
[BMFT-FB-T-85-031] 24 p4097 N85-35400

ELECTRIC CONTROL
Adjustable indicating device for load position
[NASA-CASE-MFS-28008-1] 11 p1635 N85-20300
Robotized system for treating gear wheels
14 p2285 N85-24162

ELECTRIC CORONA
Bibliography of data on electrical breakdown in gases
[PB84-216049] 01 p0045 N85-10294
Electrical parameters in 60-Hz biological exposure systems and their measurement: A primer
[PB84-217793] 03 p0400 N85-12548
Development of power system management
[PB84-216530] 04 p0497 N85-13173
Effects of the corona wind on the cooling of a horizontal cylinder
[AD-A153101] 17 p2954 N85-28241
Third US/USSR Symposium on Particulate Control
[PB85-190690] 19 p3310 N85-30522
Development of power system measurements
[PB85-162582] 20 p3450 N85-31420

ELECTRIC CURRENT
NT ALTERNATING CURRENT
NT ARC DISCHARGES
NT AURORAL ELECTROJETS
NT BEAM CURRENTS
NT CARBON ARCS
NT DIRECT CURRENT
NT EDDY CURRENTS
NT ELECTRIC ARCS
NT ELECTRIC CORONA
NT ELECTRIC DISCHARGES
NT ELECTRIC SPARKS
NT ELECTRODELESS DISCHARGES
NT ELECTROJETS
NT EQUATORIAL ELECTROJET
NT FLASHOVER
NT GAS DISCHARGES
NT GLOW DISCHARGES
NT HIGH CURRENT
NT IONOSPHERIC CURRENTS
NT LIGHTNING
NT MERCURY ARCS
NT PLASMA CURRENTS
NT RADIO FREQUENCY DISCHARGE
NT RING CURRENTS
NT SHORT CIRCUIT CURRENTS
NT TELLURIC CURRENTS
NT THRESHOLD CURRENTS
Excitation of quasi-static magnetic fields with axial structure 02 p0259 N85-11696
Photocurrent oscillations in Bi12GeO20 metal-semiconductor-metal structures
02 p0266 N85-11741
Theory of the double critical state in type-2 superconductors
[DE84-015461] 02 p0269 N85-11886
Related studies to cathodic protection of reinforced concrete structures
[PB84-218114] 03 p0333 N85-12145
Bulletin of the Faculty of Engineering, Hokkaido University, no. 123
[ISSN-0385-602-X] 04 p0482 N85-13075
Determination of Faradaic current through a bipolar electrode in acidic bichromate 04 p0483 N85-13077
Electropulse chemical machining
[DE84-016693] 04 p0484 N85-13084
Investigation of effect of photocurrent amplification in meta-dielectric-semiconductor structures based on silicon 04 p0488 N85-13110
Preliminary evaluation of RCA C83036E prototype photomultiplier
[DE84-016894] 04 p0496 N85-13165
Experimental observation of plasma neoclassical currents
[DE84-015706] 04 p0566 N85-13805
Oscillating field current drive for reversed field pinch discharges
[DE84-015090] 04 p0567 N85-13810
Current and potential transients during localized corrosion of stainless steel
[DE84-014100] 05 p0618 N85-13954
Behaviour of lead-silver anodes in zinc electrodeposition from sulphuric acid baths
[BLL-MINTEK-TR-1180-(5810.5759)]
06 p0764 N85-14887
Transient currents of ideally conducting body of revolution with transient diffraction
06 p0785 N85-15019
Current-voltage characteristics of semiconductor power devices operating at high current densities
06 p0795 N85-15079
Human reactions to transient electric currents, volume 12
[PB84-231463] 06 p0846 N85-15374
Arc erosion of metal in current interval of 1-10 amperes 07 p0953 N85-16042
Region 1 birkeland currents from a global MHD simulation of the magnetosphere
[AD-A147435] 07 p0997 N85-16335
Data and results of a laboratory investigation of microprocessor upset caused by simulated lightning-induced analog transients
07 p0999 N85-16345
A comparison of lightning and nuclear electromagnetic pulse response of a helicopter 07 p1000 N85-16349
Electromagnetic fields from the generation and absorption of discontinuous linear current fronts
[AD-A148076] 08 p1151 N85-17268
Fluctuation phenomena studies in chemically sensitive field effect transistors. Part 2: Corrosion of silicon oxynitride
[AD-A148227] 08 p1157 N85-17302
Studies on organic semiconductors. 15: Effects of the substituents on the photoconductivities of substituted anthracenes
[NASA-TM-77788] 08 p1225 N85-17712
Exploratory development of advanced surface flaw detection methods
[AD-A148757] 09 p1261 N85-18060
IREB (Intense Relativistic Electron Beam) converter to ac pulses
[AD-D011479] 10 p1554 N85-19800
Thermal investigation of an electrical high-current arc with porous gas-cooled anode
[NASA-TM-77789] 11 p1627 N85-20245
The liner package: An incipient MHD capability for CCUBE
[LA-9969-MS] 12 p1913 N85-22007
Calculation of secondary-electron escape currents from inclined-spacecraft surfaces in a magnetic field
13 p1992 N85-22491
Experimental and numerical analysis of electric currents and electromagnetic blunting of cracks in thin plates
[AD-A150418] 13 p2022 N85-22669
Critical current measurements on an NbTi superconducting wire standard reference material
[PB85-116594] 13 p2066 N85-22906
Noise characteristics of sulfur-doped silicon diodes
13 p2073 N85-22952
Localized corrosion currents from graphite/aluminum and welded SiC/Al metal matrix composites
[AD-A150988] 14 p2256 N85-23980
New electronic measurement, control devices
14 p2289 N85-24192
Investigation of electron attachment and dissociation rates in C2F6/CH4 electric gas discharges
[AD-A151796] 16 p2862 N85-27649
Electro-expulsive separation system
[NASA-CASE-ARC-11613-1] 18 p3094 N85-29150
Development of photodetectors
[AD-A153773] 18 p3095 N85-29158
Trace water sensor
[NASA-CASE-NPO-15722-1] 18 p3103 N85-29212
Theoretical approach to evolution of solar magnetic field 18 p3204 N85-29874
Inferred flows of electric currents in solar active regions 18 p3208 N85-29899
Design and testing of a pulsed current transformer
[AD-A154228] 19 p3259 N85-30208
The electric current densities beneath thunderstorms
20 p3494 N85-31726
Runaway electrons and plasma turbulence in current ramping by lower hybrid waves in tokamak plasmas
[DE85-011390] 20 p3535 N85-31997
Method of characterizing critical timing paths and analyzing timing related failure modes in very large scale integrated circuits
[AD-D011731] 22 p3759 N85-33298
Photothyristor optrons and optron microcircuits, part 1
22 p3781 N85-33424
Current enhancement in a conducting channel
[AD-A155418] 22 p3845 N85-33612
System expectations for Pioneer 1 foil implosion experiments
[DE85-014129] 24 p4091 N85-35359
Current interruption by density depression
[DE85-013120] 24 p4169 N85-35846

ELECTRIC DIPOLES
Image theory for a vertical electric dipole above a wire grid with square cells
[REPT-S-150] 02 p0192 N85-11286
Impedance of vertical dipoles above a dissipative ground
[REPT-S-152] 02 p0192 N85-11287
General image theory for the Sommerfeld problem
[REPT-S-154] 02 p0193 N85-11289
Experimental determination of the 1 sigma(+) state electron-dipole-moment function of carbon monoxide up to a large internuclear separation
[NASA-TM-85979] 09 p1379 N85-18670
The ULF/ELF/VLF electromagnetic fields generated in a sea of finite depth by elevated dipole sources
[AD-A149636] 12 p1828 N85-21470
Piezoelectric transducer using electrically poled gamma-phase Nylon 11
[AD-D011552] 12 p1850 N85-21602
High-field dipoles for future accelerators
[DE85-002315] 13 p2157 N85-23391
Ac field-induced order in dense colloidal systems
[DE85-009107] 17 p2935 N85-28119
Atomic data for controlled fusion research. Volume 4: Spectroscopic data for iron
[DE85-009658] 19 p3354 N85-30787
Effects of CP violation in SU(2) sub L x SU(2) sub R x U(1) electroweak models
[DE85-010601] 20 p3531 N85-31965
Numerical modeling of subsurface communication
[DE85-012818] 21 p3577 N85-32249

ELECTRIC DISCHARGES
NT ARC DISCHARGES
NT CARBON ARCS
NT ELECTRIC ARCS

NT ELECTRIC CORONA
NT ELECTRIC SPARKS
NT ELECTRODELESS DISCHARGES
NT FLASHOVER
NT GAS DISCHARGES
NT GLOW DISCHARGES
NT LIGHTNING
NT MERCURY ARCS
NT RADIO FREQUENCY DISCHARGE

A high-voltage discharger
[AD-A145859] 02 p0194 N85-11299

Time variability of directionality properties of pulsed EB-EDL (Electron Beam-Electric Discharge Laser) N2-CO2 lasers
[AD-A145546] 02 p0202 N85-11344

Electron collision processes in molecular gases
[AD-A146078] 03 p0418 N85-12671

Glow spots and breakdown in GaAs transistor structure 04 p0487 N85-13107

Physico-chemical investigations on the electronic partial conductivity of molten electrolytes, especially of the eutectic mixture LiCl-KCl
[BMFT-FB-T-84-205] 05 p0633 N85-14063

Pulsed electric discharge laser technology. Electron beam window foil material
[AD-A146420] 06 p0813 N85-15162

Galileo internal electrostatic discharge program 13 p1995 N85-22504

Laboratory studies of spacecraft response to transient discharge pulses 13 p1995 N85-22506

Discharge pulse phenomenology 13 p1995 N85-22509

Discharge characteristics of dielectric materials examined in mono-, dual-, and spectral energy electron charging environments 13 p1995 N85-22510

Mass spectra of neutral particles released during electrical breakdown of thin polymer films 13 p1996 N85-22511

EOS (electrical overstress) protection for VLSI (Very Large Scale Integration) devices
[AD-A150333] 13 p2064 N85-22691

Non-self-maintained high-voltage low-pressure discharge 13 p2068 N85-23037

Near Field/Far Field (NF/FF) energy loss in Electric Discharge Lasers (EDL's): A mode-medium interaction
[AD-A150299] 13 p2096 N85-23075

Developement of a theoretical model to describe the interaction between electric discharge and supersonic flow of a pulsed CO laser
[DFVLR-FB-84-45] 14 p2310 N85-24301

Experimental investigation of the electric breakdown in SF6
[BLL-CE-TRANS-7987-(9022.09)] 15 p2548 N85-25714

Erosion of electrodes due to switching of capacitor-bank discharge circuits
[AD-A151207] 15 p2547 N85-25718

Field-induced phenomena in electrical insulation
[AD-A151234] 15 p2547 N85-25719

On the electric charge carried by dust grain excitation of violent discharge — planetary rings 15 p2677 N85-26530

Investigation of electron attachment and dissociation rates in C2F6/CH4 electric gas discharges
[AD-A151796] 16 p2862 N85-27649

Electrode for flash discharge lamps
[DE85-006896] 17 p2955 N85-28252

Design and testing of a pulsed current transformer
[AD-A154228] 19 p3259 N85-30206

Coordinated research program in pulsed power physics
[AD-A154629] 21 p3679 N85-32858

Powerful XeCl excimer electric discharge laser with good temporal stability and fast response time 21 p3688 N85-32911

Model that predicts pulse charged gas switching breakdown phenomena
[DE85-013119] 22 p3761 N85-33313

Safety characteristics of non-lithium battery systems
[AD-A155733] 22 p3806 N85-33574

Surface discharges as intense photon sources in the extreme ultraviolet
[DE85-012593] 24 p4158 N85-35782

ELECTRIC ENERGY STORAGE

Battery optimization considerations
[DE84-014759] 01 p0044 N85-10288

Trends in concentrator, receiver, and storage development for terrestrial applications 05 p0609 N85-13891

Electrodynamic tethers. 1: Power generator in LEO. 2: Thrust for propulsion and power storage 05 p0611 N85-13901

Energy storage with lead acid batteries in photovoltaic systems 05 p0663 N85-14260

Energy storage for stationary and mobile operation as a buffer of power supply from additive energy sources 05 p0663 N85-14261

Design and operating experience of an ac-dc power converter for a superconducting magnetic energy storage unit
[DE84-014041] 09 p1316 N85-18275

Thermal design requirements of a 50-kW zinc/redox flow battery for solar electrical energy storage
[DE84-017086] 09 p1345 N85-18463

Cycling performance of the iron-chromium redox energy storage system
[NASA-TM-87034] 16 p2819 N85-27387

ELECTRIC EQUIPMENT

Electrical/electronics working group summary 05 p0604 N85-13853

The determination of eddy current losses in electrical equipment
[DE84-016340] 05 p0632 N85-14050

DOE/ORNL electric systems program overview
[DE85-003334] 10 p1459 N85-19197

The touch panel system: Design and development
[AD-A153014] 17 p3008 N85-28596

High Temperature Heating System (HTHS)
[PB85-188340] 24 p4084 N85-35316

ELECTRIC EQUIPMENT TESTS

Choice of criteria for rejection of insulating components in high-voltage surge equipment 06 p0785 N85-15021

Evaluation of adequacy pf JP54 protection level for large electric machines 15 p2528 N85-25588

Module Hipot and ground continuity test results 21 p3612 N85-32447

ELECTRIC FIELD STRENGTH

Choice of criteria for rejection of insulating components in high-voltage surge equipment 06 p0785 N85-15021

Electric field in plasma layer of magnetosphere during preliminary substorm phase 06 p0824 N85-15231

Method of separately determining electrophysical properties of bulky conductor 13 p2073 N85-22951

Measuring intensity of electric field produced by electromagnetic pulse with aid of active probes 13 p2075 N85-22958

Satellite-borne electric field measurements with spherical double probes — ISEE satellites 14 p2356 N85-24558

Estimate of the amplitude of transient electric fields in the magnetotail 14 p2358 N85-24568

The GEOS-2 electric field observations at times of solar wind discontinuities 14 p2360 N85-24584

Multiple correlation between auroral and magnetic pulsations. Part 2: Determination of electric currents and electric fields around a pulsating auroral patch 14 p2363 N85-24606

Measuring electrical field fluctuations by Langmuir Double Probe Method 16 p2720 N85-26789

Measurement of RF fields associated with ISM equipment as it relates to aeronautical services
[FAA-ES-84-2] 19 p3254 N85-30180

Experimental and theoretical investigations of open resonators — precipitation measurement
[DFVLR-FB-85-12] 20 p3449 N85-31414

Development of power system measurements
[PB85-162582] 20 p3450 N85-31420

ELECTRIC FIELDS

NT EXTERNAL SURFACE CURRENTS

Scattering theory by Enss' method for operator valued matrices: Dirac operator in an electric field
[REPT-84] 01 p0045 N85-10290

Interaction of a stream of dielectric spheres in an electric field in a high vacuum
[DE84-014714] 01 p0115 N85-10782

Methods to increase linac efficiency
[DE84-014692] 01 p0118 N85-10809

Rocket and satellite observations of electric fields and ion convection in the dayside auroral ionosphere
[TRITA-EPP-84-05] 02 p0229 N85-11497

Method of splitting for solution of problems in semiconductor physics 02 p0265 N85-11736

Electric field and plasma energization in computer simulations of magnetotail reconnection
[DE84-014023] 02 p0285 N85-11859

Electrical parameters in 60-Hz biological exposure systems and their measurement: A primer
[PB84-217793] 03 p0400 N85-12548

Investigation of solid state problems using the hyperfine interaction between static and dynamic internal fields with short live excited probe nuclei 03 p0428 N85-12729

Stark broadening of H(-) resonances in large electric fields
[DE84-016974] 04 p0496 N85-13184

Development of power system management
[PB84-216530] 04 p0497 N85-13173

Human reactions to ELF (Extremely Low Frequency) electric and magnetic fields. An annotated bibliography of current literature, fourth edition
[PB84-230358] 04 p0545 N85-13472

Local fields in strongly coupled plasmas
[DE84-013375] 04 p0567 N85-13611

Monte Carlo studies of transport in stellarators
[DE84-017633] 04 p0568 N85-13625

Measurements of electric fields obtained by stratospheric balloons in the region of the South Atlantic anomaly
[INPE-3218-PRE/571] 05 p0675 N85-14335

Motion of electrons in non polar classical liquids
[DE84-013809] 05 p0727 N85-14672

Stabilization of the hot electron precessional mode in a symmetric tandem mirror by the axial variation of radial electric field
[DE84-016388] 05 p0730 N85-14692

Optimization of energy conversion during locking of electron bunches by electromagnetic wave in longitudinal electrostatic field 06 p0786 N85-15025

An indirect measure of below-ground electric field, conductivity, and dielectric constant
[AD-A146518] 06 p0804 N85-15115

Distribution of electric field near westward propagating bend in aurora 06 p0823 N85-15222

Electric fields in Earth orbital space
[AD-A146448] 06 p0835 N85-15313

High voltage effects measured on dummy mannequin 07 p1012 N85-16432

Research relative to plasma transport across the magnetopause
[NASA-CR-174300] 07 p1045 N85-16636

Electron distribution function and mobility in 3-5 compounds for high and low fields
[AD-A147447] 07 p1048 N85-16658

Transport properties and distribution functions in 3-5 semiconductors
[AD-A147525] 07 p1049 N85-16660

In-situ formation of a grain boundary in field ion microscopy using a laser
[AD-A148225] 08 p1166 N85-17355

Plasma and magnetospheric research
[NASA-CR-171293] 08 p1183 N85-17451

Theoretical studies of Rydberg atom collisions
[AD-A148558] 08 p1220 N85-17687

The flow of plasma in the solar terrestrial environment
[NASA-CR-174301] 08 p1224 N85-17707

Development of photoconductive power switch technology
[DE85-001514] 09 p1315 N85-18270

Multimode harmonic power measurement of 40 MW pulsed S-band klystrons
[DE85-001560] 09 p1316 N85-18272

Effects of dc electric fields on multiphoton ionization spectra in cesium
[DE85-001542] 09 p1381 N85-18684

Calculation and computer simulation of the Paraboloidal Mirror Analyzer (PMA)
[DE85-001417] 09 p1384 N85-18705

Measurements of electric fields in plasmas by using beam probe and laser fluorescence techniques 09 p1389 N85-18737

Ionospheric research at INPE
[INPE-3279-PRE/602] 10 p1514 N85-19656

Electron acceleration by laser fields in a gas
[DE85-000575] 11 p1639 N85-20323

Study of electric field and ion effects on HVDC lines
[DE85-002975] 12 p1833 N85-21503

An improved rocket-borne electric field meter for the middle atmosphere
[NASA-CR-175510] 12 p1888 N85-21851

Reconsideration of sheath related to negative ion extraction
[IPPJ-706] 12 p1935 N85-22159

Efficient heating and confinement of ions in an axisymmetric magnetic mirror supplemented with dc electric field
[IPPJ-707] 12 p1935 N85-22160

Dynamics of space charge waves in the laser beat wave accelerator
[AD-A149666] 12 p1936 N85-22163

Explosive transverse electric field and particle acceleration during magnetic collapse — cosmic plasma 12 p1956 N85-22292

Galileo internal electrostatic discharge program 13 p1995 N85-22504

Influence of external electric field on structural-mechanical properties of powdered materials 13 p2013 N85-22630

Elasticity formulas for thin-walled shells with piezoceramic layers 13 p2047 N85-22816

Analysis and optimization of parameters of tanned surface acoustic wave transducers 13 p2070 N85-22934

Measuring intensity of electric field produced by electromagnetic pulse with aid of active probes
13 p2075 N85-22958
Theory of diaphragm light modulators with electrical input signal 13 p2082 N85-23002
Discrimination of normal and anomalous magnetic and electric fields in geoelectromagnetic variations
13 p2114 N85-23166
1981 wC-130 airborne lightning characterization program data review
[AD-A150230] 13 p2136 N85-23275
Electric field and plasma observations near the magnetopause and bow shock during a rapid compression 14 p2355 N85-24553
Efficiency of electric field transfer at Earth's magnetopause and flow amplitudes related to reconnection 14 p2356 N85-24557
Electric fields in the plasma sheet and plasma sheet boundary layer 14 p2357 N85-24562
The magnetospheric convection electric field at ionospheric altitudes: A case study based on STARE and Saint-Santin data 14 p2362 N85-24594
A brief summary of results derived from Scandinavian Twin Auroral Radar Experiment (STARE) observations during IMS -- ionospheric electric fields
14 p2362 N85-24595
Comparison of magnetospheric and ionospheric electric fields using different empirical mapping factors
14 p2362 N85-24597
The GEOS-2 E-field behavior during dynamic auroral development near the satellite footpoint
14 p2362 N85-24598
Three-dimensional current systems and electric fields during active aurora 14 p2362 N85-24599
Solar wind control of electric fields and currents in the magnetosphere and ionosphere
14 p2364 N85-24606
Long-period magnetospheric pulsations observed with an electric field experiment in the magnetosphere
14 p2369 N85-24639
Electroreflectance spectroscopy as a probe of the electronic structure at the metal-electronic interface
[DE85-003541] 14 p2426 N85-24976
Experimental check of ion transport mechanism in Earth's radiation belt with exposure to nonsteady-state electric fields 15 p2480 N85-25306
Measuring methods of atmospheric electric elements at the Earth's surface during snowfall and investigation of these relationships 15 p2581 N85-25920
High speed electric field and voltage measurements with field coupled sensors
[DE85-006637] 15 p2642 N85-26299
Compensation of acoustic wave devices
[AD-D011582] 15 p2646 N85-26322
Time dependent and steady-state solutions of the electron energy distribution in a weakly ionized gas subject to an ac or dc electric field
[AD-A151829] 15 p2656 N85-26391
The physical interactions of radiofrequency radiation fields and biological systems 16 p2775 N85-27129
Evaluation of human exposures to low frequency fields 16 p2776 N85-27135
Theoretical and experimental comparisons of nearfield electrogalvanic fields due to nonlinear polarization layers
[AD-A152085] 16 p2779 N85-27149
Equatorial F-region irregularity latitudinal extension and dynamo electric field
[INPE-3494-PRE/731] 16 p2826 N85-27433
Trends in the electric field enhancement of dielectronic recombination cross sections
[DE85-006920] 16 p2871 N85-27711
Ac field-induced order in dense colloidal systems
[DE85-009107] 17 p2935 N85-28119
Dependence of characteristics of centrifugal magnetohydrodynamic conduction pump on electrical conductance of end walls. Part 1: Experiment
17 p2939 N85-28146
Electromagnetic transmission through a slot in a perfectly conducting plane
[AD-A153224] 17 p2949 N85-28210
Laser plasma LINAC
[DE85-006294] 17 p2971 N85-28348
Wake fields and wake field acceleration
[DE85-008054] 17 p3031 N85-28750
Maser cavity servo-tuning system
[NASA-CASE-NPO-15890-1-CU]
18 p3083 N85-29143
Germanium detectors with a built-in transverse drift field
[DE85-009944] 18 p3096 N85-29165
Upgrade of the LLNL EM transient range monocone antenna
[DE85-006839] 18 p3097 N85-29172
Intense ion beam diode diagnostics using a tunable dye laser
[DE85-008079] 18 p3113 N85-29272
Auroral zone electric fields from DE-1 and -2 at magnetic conjunctions
[NASA-CR-175874] 18 p3136 N85-29421
Preliminary results on open accelerating structures
[DE85-010231] 18 p3191 N85-29793
Characteristics of charge transfer in the dispersed phase of electrorheological suspensions
[RAE-TRANS-2125] 19 p3233 N85-30040
Accelerator column models for low-current beams
[DE85-010722] 19 p3262 N85-30226
Many-body processes in atomic and molecular physics
[DE85-009750] 19 p3354 N85-30791
Toroidal viscosity and ambipolarity in the neoclassical transport theory of axisymmetric tori
[DE85-010622] 19 p3358 N85-30820
Emittance growth caused by current variation in a beam-transport channel
[DE85-010743] 19 p3363 N85-30849
Effects of a radial electric field on tokamak edge turbulence
[DE85-010401] 19 p3371 N85-30910
Development of power system measurements
[PB85-182582] 20 p3450 N85-31420
Performance and electric field limitations in inflow disk MHD generators 20 p3534 N85-31987
A theory of electromagnetic shielding with applications to MIL-STD-285, IEEE-299, and EMP simulation
[AD-A154905] 21 p3575 N85-32233
Trapping of ion conics by downward parallel electric fields
[AD-A155306] 21 p3633 N85-32568
Electrostatic ion cyclotron instability due to a nonuniform electric field perpendicular to the external magnetic field
[AD-A155474] 21 p3707 N85-33019
Vacuum interface flashover with bipolar electric fields
[DE85-012027] 22 p3755 N85-33275
New formulation for linear accelerator design
[DE85-011171] 22 p3842 N85-33792
Role of ECRH in potential formation for tandem mirrors
[DE85-011859] 22 p3848 N85-33834
Interplanetary magnetic field control of high-latitude electric fields and currents determined from Greenland magnetometer data
[DMI-GEOPHYS-PAPERS-R-69]
22 p3850 N85-33845
Theoretical and Experimental Beam Plasma Physics (TEBPP) 23 p3901 N85-34166
Improved negative ion source
[DE85-006445] 23 p3912 N85-34241
Negative ion sources equipped with continuous annular and spherical geometry surface ionizers
[DE85-011939] 23 p3971 N85-34619
Potential effect in transport due to non-axisymmetric confining field 23 p3975 N85-34645
Activities of the RF Section 23 p3975 N85-34646
Radial transport phenomena for TMX-upgrade
23 p3976 N85-34647
RF induced radial diffusion in tandem mirrors
23 p3976 N85-34649
Induced azimuthal electric field effects on tandem transport and ambipolarity 23 p3976 N85-34650
Breakdown of intrinsic ambipolarity for the radial diffusion due to a rotating RF field 23 p3977 N85-34660
Transports studies of ECH and ICRH-heated bumpy torus plasma in NBT-1M 23 p3978 N85-34662
Guiding center distribution function and longitudinal invariant 23 p3978 N85-34663
Analytic and numerical calculations of the ambipolar electric field in a stellarator 23 p3978 N85-34665
Confinement experiments on ISX-B
[DE85-012346] 23 p3984 N85-34709
The role of cosmic rays in magnetic hydrodynamics of interstellar medium
[OG-7.2-15] 23 p4015 N85-34882
Short perturbations of cosmic ray intensity and electric field in atmosphere
[SH-6.1-18] 23 p4046 N85-35090
Moment-method formulation of the cavity-probe aperture antenna
[DE85-013264] 24 p4088 N85-35336
Injector losses on Mite
[DE85-012356] 24 p4090 N85-35355
A lead glass tubing drift calorimeter
24 p4147 N85-35711
High energy plasma accelerators
[DE85-013121] 24 p4155 N85-35760

ELECTRIC FILTERS
NT CRYSTAL FILTERS
NT DIGITAL FILTERS
NT FIR FILTERS
NT MICROWAVE FILTERS
NT RADAR FILTERS
NT RADIO FILTERS
NT TRACKING FILTERS
NT WAVEGUIDE FILTERS

Microstrip directional filters
[INPE-3127-PRE/518] 02 p0194 N85-11293
EMI (electromagnetic interference) filter capacitor unit
[AD-D011392] 07 p0937 N85-15941
Analog to digital converter
[AD-D011338] 07 p0945 N85-15983
The design of high order active RC-filters
[DRIC-T-7147] 07 p0945 N85-15987
Optimal discrete filtration of intricate phase-keyed signals 12 p1840 N85-21550
On filter binary processes
[AD-A150328] 13 p2063 N85-22890
Dynamics of adaptive signal corrector
13 p2071 N85-22940
Synthesis of optimum single-channel discrete signals and filters 13 p2080 N85-22990
Pseudo bipolar nickel-cadmium batteries used as filter elements to pulsed current loads
[AD-A151192] 15 p2547 N85-25717
Length dependent, optical time delay/filter device for electrical signals
[AD-D011594] 15 p2549 N85-25732
Development of thin film hybrid IC active filter for video band use
[NHK-LABS-NOTE-312] 18 p3094 N85-29153
High discharge rate characteristics of nickel-cadmium batteries for pulse load filtering
20 p3446 N85-31391
Stripe filters on multispectral linear arrays
[NASA-CR-175305] 21 p3579 N85-32252

ELECTRIC FURNACES
New ferrous metallurgy technology
01 p0019 N85-10114
High Temperature Heating System (HTHS)
[PB85-188340] 24 p4084 N85-35316

ELECTRIC FUSES
Fuse status indicator system
[AD-D011294] 06 p0804 N85-15121

ELECTRIC GENERATORS
NT AC GENERATORS
NT ALKALINE BATTERIES
NT DIRECT POWER GENERATORS
NT DYNAMOMETERS
NT ELECTROSTATIC GENERATORS
NT FUEL CELLS
NT HOMOJUNCTIONS
NT HOMOPOLAR GENERATORS
NT MAGNETOHYDRODYNAMIC GENERATORS
NT NICKEL ZINC BATTERIES
NT PHOSPHORIC ACID FUEL CELLS
NT PHOTOELECTRIC GENERATORS
NT PRIMARY BATTERIES
NT RADIOISOTOPE BATTERIES
NT REGENERATIVE FUEL CELLS
NT ROTATING GENERATORS
NT SOLAR AUXILIARY POWER UNITS
NT SOLAR BLANKETS
NT SOLAR CELLS
NT SOLAR GENERATORS
NT SOLAR SEA POWER PLANTS
NT THERMAL BATTERIES
NT THERMIONIC CONVERTERS
NT THERMOELECTRIC GENERATORS
NT TURBOGENERATORS
NT VERTICAL JUNCTION SOLAR CELLS
Motor/generator and electronic control considerations for energy storage flywheels 05 p0808 N85-13878
Superconducting rotor dynamics
[AD-A147176] 07 p0947 N85-16000
Power quality and protection of electric distribution systems with small, dispersed generation devices
[DE85-000990] 09 p1344 N85-18453
Variable speed generator technology options for wind turbine generators
[RR-84-4] 10 p1478 N85-19331
Rocky Flats Wind Energy Research Center FY 1983 report
[DE85-004500] 10 p1511 N85-19535
15KW power supply development
[DE85-001057] 11 p1629 N85-20260
Solar powered actuator with continuously variable auxiliary power control
[NASA-CASE-MFS-25637-1] 12 p1876 N85-21769
Preliminary assessment of power-generating tethers in space and of propulsion for their orbit maintenance
13 p1997 N85-22520
Control of cascaded induction generator systems
[AD-A150429] 13 p2065 N85-22897
Basic research on inertial confinement fusion by LIMAY-I 15 p2655 N85-26383
Test flight of IL-76TD long-range transport variant
17 p2894 N85-27842
Principles of designing digital compensating accelerometers 17 p2944 N85-28172

Activity and accomplishments of dish/Stirling electric power system development
[NASA-CR-175841] 17 p2985 N85-28445
Control of acid deposition precursors through dry scrubbing
[DE85-010281] 19 p3235 N85-30056
Free-piston Stirling engine/linear alternator 1000-hour endurance test
[NASA-CR-174771] 19 p3304 N85-30481
Experimental investigation of a variable speed constant frequency electric generating system from a utility perspective
[NASA-CR-174950] 21 p3579 N85-32251
Operational window for a plasma erosion opening switch used for voltage multiplication on pulsed power generators
[AD-A155482] 21 p3707 N85-33020
Long-term research in Japan: Amorphous metals, metal oxide varistors, high-power semiconductors and superconducting generators
[DE85-010627] 22 p3748 N85-33230
Study to assess the effects of magnetohydrodynamic electromagnetic pulse on electric power systems, phase 1, volume 3
[DE85-011301] 24 p4156 N85-35771

ELECTRIC HYBRID VEHICLES
Evaluation of heat engine for hybrid vehicle application
[NASA-CR-174163] 04 p0508 N85-13245
Electric and hybrid vehicle demonstration project
[DE84-014622] 06 p0871 N85-15535
Feasibility demonstration of a novel, flat-belt, continuously variable transmission or automotive and electric-hybrid vehicle application
[NASA-CR-174430] 10 p1569 N85-19894
ElectriFleet Project
[DE85-001598] 10 p1570 N85-19898
Electric vehicle demonstration project
[DE85-002167] 11 p1741 N85-20943
Electric and hybrid vehicle demonstration project
[DE85-003939] 13 p2169 N85-23455
A system-level mathematical model for evaluation of power train performance of load-leveled electric-vehicles
[NASA-CR-175652] 14 p2434 N85-25009
Performance testing and system characterization. DOE hybrid test vehicle, phase 3
[NASA-CR-175668] 14 p2434 N85-25010
Advanced vehicle systems assessment. Volume 1: Executive summary
[NASA-CR-175876] 17 p3051 N85-28887
Urban vehicle research project
[DE85-005444] 17 p3052 N85-28889
Electric and hybrid vehicle program
[DE85-010025] 19 p3262 N85-30230
Evaluation of semiconductor devices for Electric and Hybrid Vehicle (EHV) ac-drive applications, volume 1
[NASA-CR-176118] 23 p3927 N85-34335

ELECTRIC IMPULSES
U ELECTRIC PULSES

ELECTRIC MOMENTS
Particle physics
[DE84-013834] 05 p0727 N85-14873

ELECTRIC MOTOR VEHICLES
Performance of improved lead acid batteries for electric vehicles
[DE84-015845] 04 p0495 N85-13160
Electric vehicle maintenance
[PB84-233352] 04 p0579 N85-13693
Research, development, and demonstration of nickel-iron batteries for electric vehicle propulsion
[DE84-017430] 05 p0632 N85-14054
Research, development, and demonstration of lead-acid batteries for electric vehicle propulsion
[DE84-017442] 05 p0632 N85-14055
Performance characteristics of a battery charger and state-of-charge indicator
[NASA-CR-174273] 07 p0946 N85-15892
BBC of Switzerland develops electric car
08 p1141 N85-17192
Hybrid vehicle program
[DE85-000326] 09 p1410 N85-18886
Electric vehicle battery test plan and results
[DE84-901972] 09 p1410 N85-18887
Electric-Hybrid Vehicle (E-HV) demonstration-test project
[DE85-002370] 10 p1570 N85-19899
High-strength composite materials for aircraft, body armor 11 p1599 N85-20057
Electric vehicle demonstration project
[DE85-003124] 11 p1741 N85-20944
Electric vehicle test program: INEL transition qualification test plan
[DE85-005171] 13 p2169 N85-23456
In-vehicle evaluation of the Globe EV 2300 lead-acid, Delco Remy 150 nickel-zinc, and Eagle-Picher NIF 270 nickel-iron battery systems
[NASA-CR-175653] 14 p2349 N85-24521
Field use of electric vehicles compared to prototype tests
[DE85-006867] 15 p2667 N85-26458
INEL electric vehicle laboratory qualification: Transition test results and comparisons with JPL ETV1-2 data
[DE85-008006] 16 p2880 N85-27772
Test and evaluation of the Hoppecke Model E240G144/16 electric vehicle battery charger
[DE85-900573] 17 p2955 N85-28253
Test plan for acceptance, verification and performance testing of the Bedford Lucas Chloride Electric Van. Part 1: Acceptance and verification testing at EG and G Automotive Research. Part 2: INEL performance testing, revision 1
[DE85-005157] 17 p3051 N85-28888
Environmental concerns related to natural gas vehicles
[DE85-010246] 20 p3486 N85-31666
State of knowledge of environmental concerns related to natural-gas-fueled vehicles
[DE85-009746] 20 p3486 N85-31667
Electric vehicle operations by the City of Huntsville, Alabama, March 1983 - May 1984
[DE85-005913] 22 p3849 N85-33842
Evaluation of half wave induction motor drive for use in passenger vehicles
[NASA-CR-176119] 23 p3926 N85-34334
Evaluation of semiconductor devices for Electric and Hybrid Vehicle (EHV) ac-drive applications, volume 1
[NASA-CR-176118] 23 p3927 N85-34335
Test plan for performance testing of the Eaton AC-3 electric vehicle
[DE85-011954] 23 p3927 N85-34341

ELECTRIC MOTORS
NT ASYNCHRONOUS MOTORS
NT INDUCTION MOTORS
NT MICROMOTORS
NT SYNCHRONOUS MOTORS
NT TORQUE MOTORS
Vibrational power transmission of an idealised gearbox
[ISVR-TR-124] 02 p0204 N85-11346
Description of a laboratory model Annular Momentum Control Device (AMCD) 05 p0606 N85-13663
Motor/generator and electronic control considerations for energy storage flywheels 05 p0608 N85-13678
Measurements of satellite refrigeration compressor power consumption and efficiency
[DE84-016724] 05 p0632 N85-14056
Design and test of a four channel motor for electromechanical flight control actuation
[NASA-CR-171838] 08 p1156 N85-17294
Armenia markets new drive motors for machine tools
10 p1461 N85-19212
Permanent magnet motors
[DE85-000660] 10 p1482 N85-19355
An evaluation of liquid and two-phase cooling techniques for use in electrical machinery
[AD-A149528] 10 p1484 N85-19372
Cost comparison of small gas turbines versus electric motors in a variable load industrial application
[PB85-149763] 12 p1837 N85-21530
Optimum design of electrical motors for multilink manipulators and automated manufacturing systems
13 p2062 N85-22880
Reluctance and doubly-excited reluctance motors
[DE85-003585] 13 p2065 N85-22900
Nickel-iron battery to be used in Peugeot electric car
15 p2532 N85-25615
CSMP (Continuous System Modeling Program) modeling of brushless DC motors
[AD-A152043] 15 p2549 N85-25731
Electric motors with elastically mounted rotors
16 p2763 N85-27048
Optimal control of electric drive with simultaneous control inputs for motor current and flux
16 p2763 N85-27049
AC powertrain for an electric vehicle, phase 2 and phase 3
[NASA-CR-175760] 16 p2880 N85-27771
Standard series of direct-current motors for regulated electric drives 22 p3772 N85-33375
Evaluation of half wave induction motor drive for use in passenger vehicles
[NASA-CR-176119] 23 p3926 N85-34334
Computer simulation of a cruise missile using brushless dc motor fin control
[AD-A155935] 24 p4089 N85-35349

ELECTRIC NETWORKS
Diagnosis of insulation defects in 1000+ V distribution networks with insulated neutral
07 p0954 N85-16044
A Monte Carlo sampling plan for estimating network reliability
[AD-A150511] 13 p2065 N85-22898
Numerical methods for stiff ordinary and elliptic partial differential equations
[AD-A153247] 17 p3020 N85-28675
Microcomputer network: Investigation and implementation
[AD-A155631] 21 p3674 N85-32826

ELECTRIC POTENTIAL
NT BIOELECTRIC POTENTIAL
NT COULOMB POTENTIAL
NT LOW VOLTAGE
NT OPEN CIRCUIT VOLTAGE
NT PHOTOVOLTAGES
NT QUANTUM WELLS
Effects of H2S on molten carbonate fuel cells
[DE84-015166] 02 p0195 N85-11307
Method of splitting for solution of problems in semiconductor physics 02 p0265 N85-11736
Efficiency of photoelectric conversion of short radiation pulses 03 p0348 N85-12240
Electrokinetic potential and stability of SiC suspensions in electrolyte solutions
[NASA-TM-77492] 04 p0469 N85-12984
Zeta potential in ceramic industry
[NASA-TM-77478] 04 p0478 N85-13047
Study program for encapsulation materials interface for Flat-plate Solar Array (FSA) project
[NASA-CR-174152] 04 p0530 N85-13385
Flywheel-powered X-ray generator
05 p0605 N85-13661
Westinghouse programs in pulsed homopolar power supplies 05 p0606 N85-13662
Potential of flywheels for spacecraft energy storage
05 p0609 N85-13690
Behaviour of lead-silver anodes in zinc electrodeposition from sulphuric acid baths
[BLL-MINTEK-TR-1180-(5810.5758)]
06 p0764 N85-14887
Device for measuring average power of laser radiation
06 p0786 N85-15026
High-speed power thyristors with excellent switching and load characteristics 06 p0793 N85-15070
Gallium-arsenide power devices
06 p0794 N85-15076
Current-voltage characteristics of semiconductor power devices operating at high current densities
06 p0795 N85-15079
Two programs for the HP9836C computer to acquire frequency or voltage data from a source
[AD-A146832] 06 p0854 N85-15430
Measurement of proton autoneutralization potential
[DE85-001752] 06 p0865 N85-15501
The anode mechanism of a thermal argon arc
[NASA-TM-77754] 07 p0921 N85-15835
Studies on copper alloys containing chromium on the copper side phase diagram
[NASA-TM-77752] 07 p0927 N85-15876
Transmission line biased coherent array of Josephson oscillators
[AD-D011323] 07 p0944 N85-15979
Analog to digital converter
[AD-D011338] 07 p0945 N85-15983
Dependence of breakdown voltage for p-n junction on parameters of ion implantation and semiconductor heat treatment 07 p0954 N85-16046
Battery control and fault detection method
[AD-D011384] 07 p0993 N85-16307
Data and results of a laboratory investigation of microprocessor upset caused by simulated lightning-induced analog transients
07 p0999 N85-16345
The ac power line protection for an IEEE 587 Class B environment 07 p1000 N85-16347
Natural electrical activity of human sympathetic nerve fibers, recorded from body surface
07 p1013 N85-16433
Potential dependence of electrical conductivity and chemical charge storage of poly(pyrrole) films on electrodes
[AD-A148513] 08 p1122 N85-17075
Calculations of high-current characteristics of silicon diodes at microwave frequencies
[AD-A147406] 09 p1314 N85-18281
Development of photoconductive power switch technology
[DE85-001514] 09 p1315 N85-18270
Electrical resistivity technique to assess the integrity of geomembrane liners
[PB85-122414/GAR] 09 p1325 N85-18327
Large electrostatic accelerators
[DE85-001120] 09 p1382 N85-18689
High energy pulsed particle accelerator
[AD-A149247] 10 p1554 N85-19797

Thermal investigation of an electrical high-current arc with porous gas-cooled anode
[NASA-TM-77789] 11 p1627 N85-20245
Angular measurement system
[NASA-CASE-MFS-25825-1] 11 p1635 N85-20298
Electrical and thermal performance during charging and discharging a Phase 1 gel cell battery
[PB85-114312] 11 p1677 N85-20565
Topography of human brain electric potentials and dominance 11 p1691 N85-20633
Review of anode phenomena in vacuum arcs
[DE85-002736] 12 p1926 N85-22101
Electrical performance of semiconductor devices at cryogenic temperatures 12 p1948 N85-22239
Discharges on a negatively biased solar cell array in a charged-particle environment 13 p1994 N85-22499
EMI characteristics of a potential control system 13 p1994 N85-22502
Characteristics of EMI generated by negative metal-positive dielectric voltage stresses due to spacecraft charging 13 p1995 N85-22505
Space test program of high-voltage solar array-space plasma interactions 13 p1997 N85-22519
Stability of highly nonlinear oxide-zinc resistors under continuous voltage of industrial frequency 13 p2067 N85-23030
Comparison of flame photometer data with total particle volume calculated from laser spectrometer particle count data
[AD-A151006] 14 p2252 N85-23958
An improved battery state-of-charge indicator
[NASA-CR-175701] 14 p2296 N85-24227
Thermocouple modeling
[DE85-005172] 14 p2306 N85-24273
Electric potential of satellite in electron emitting experiments in initial stage of electron beam injection in steady-state mode 15 p2480 N85-25309
Transient voltage oscillations in coils
[DE85-006715] 15 p2550 N85-25738
High speed electric field and voltage measurements with field coupled sensors
[DE85-006637] 15 p2642 N85-26299
Studies in electron phenomena in MOS structures: The pulsed C-V method 15 p2659 N85-26407
Sources of improvement in quality of contact butt welding of wire
[BLL-M-36085-(5828.4)] 16 p2793 N85-27225
Investigation of pseudo bi-polar nickel cadmium batteries as filter elements for pulsed power loads
[AD-A152112] 16 p2819 N85-27389
Streak tube characterization
[DE85-009674] 17 p2956 N85-28255
Crack tip chemistry modeling of intergranular stress corrosion cracks of nickel containing segregated phosphorus and sulphur
[DE85-010059] 18 p3076 N85-29028
High voltage power supply
[NASA-CASE-GSC-12818-1] 18 p3093 N85-29147
Magnetically switched power supply systems for lasers
[NASA-CASE-NPO-16402-1] 18 p3112 N85-29265
A collective interaction klystron specification
[AD-D011704] 19 p3255 N85-30186
High efficiency large area polysilicon solar cells 20 p3482 N85-31639
Density gradient electrophoresis of cultured human embryonic kidney cells 20 p3501 N85-31763
Plasma erosion opening switch
[DE85-011384] 20 p3535 N85-31998
Module Hipot and ground continuity test results 21 p3612 N85-32447
R, L, C, G measurement 21 p3666 N85-32784
Recent advances in d-c relaxation techniques for the measurement of kinetics of fast electrode reactions
[DE85-005029] 22 p3745 N85-33216
Transparent electrode for optical switch
[DE85-011618] 22 p3761 N85-33310
IEA-SSPS CRS calibration report: Calibration of relevant measuring sensors
[DE85-010174] 22 p3766 N85-33466
Surface voltage gradient role in high voltage solar array-plasma interaction: Center Director's discretionary fund
[NASA-TM-86516] 22 p3805 N85-33567
Experimental evaluation of the thermodynamic properties of concentrated aqueous potassium hydroxide solutions
[DE85-010628] 23 p3912 N85-34238
Reversing-counterpulse repetitive-pulse inductive storage circuit
[DE85-006409] 23 p3928 N85-34344
Modulated voltage metastable ionization detector
[NASA-CASE-ARC-11503-1] 23 p3933 N85-34374
Rapid annealing of temperature-compensated, precision voltage references following fast-neutron irradiation
[DE85-009621] 23 p3970 N85-34609
Statistical distribution of breakdown voltages in rep-rate spark gaps
[DE85-012813] 24 p4090 N85-35354
System expectations for Pioneer 1 foil implosion experiments
[DE85-014129] 24 p4091 N85-35359

ELECTRIC POWER

Survey of remote data monitoring systems
[DE85-001365] 09 p1323 N85-18313

ELECTRIC POWER CONVERSION

U ELECTRIC GENERATORS

ELECTRIC POWER PLANTS

NT FUEL CELL POWER PLANTS
NT NUCLEAR POWER PLANTS
NT SOLAR THERMAL ELECTRIC POWER PLANTS

Manual of phosphoric acid fuel cell power plant optimization model and computer program
[NASA-CR-174721] 01 p0067 N85-10445
Phosphoric acid fuel cell power plant system performance model and computer program
[NASA-CR-174636] 02 p0222 N85-11456
Fabric filter system study
[PB84-229749] 03 p0342 N85-12206
Electrostatic augmentation of fabric filtration: Reverse-air pilot unit experience
[PB84-230002] 03 p0343 N85-12207
Analytical models 05 p0666 N85-14282
A summary description of a computer program concept for the design and simulation of solar pond electric power generation systems 05 p0666 N85-14285
Salton Sea solar pond power plant design study and regional applicability 05 p0667 N85-14290
The upwind power plant Manzanares 05 p0669 N85-14305
Progress in developing tidal electric power plants reported 07 p0994 N85-16314
Geothermal wells drilled in Transcarpathiens 07 p0994 N85-16315
On-line monitoring of the true corrosion rate in problems related to power plants
[CISE-2335] 08 p1131 N85-17126
Advancement of remote technology: Past perspectives and future plans
[DE85-000934] 09 p1327 N85-18342
Conceptual design of a 10 MW shore-based OTEC plant
[DE84-015606] 10 p1511 N85-19532
Work physiology of operating personnel at power plants in arid regions 10 p1523 N85-19606
Leak monitoring in high pressure preheaters by a noninvasive ultrasonic method
[CISE-2373] 11 p1650 N85-20394
Leak detection by acoustic emission monitoring in power plant high pressure preheaters
[CISE-2392] 11 p1650 N85-20395
Underground pumped hydroelectric storage
[DE85-000288] 11 p1676 N85-20560
Program plan for research and development of dielectric materials for electric power systems
[DE85-001327] 12 p1836 N85-21520
Heat Cycle Research Experimental Program report, FY-84
[DE85-003556] 12 p1882 N85-21811
Comprehensive evaluation of cost effectiveness of solar electric power plants 14 p2265 N85-24036
Tribological sinks: Money down the drain
[DE85-010019] 17 p2974 N85-28376
A program for the calculation of paraboloidal-dish solar thermal power plant performance
[NASA-CR-175674] 17 p2985 N85-28449
Silica problem in the design of geothermal power plants
[DE85-008245] 17 p2986 N85-28453
Fuel cell applications literature review
[DE85-011891] 22 p3809 N85-33592
Fusion facility siting considerations
[DE85-012894] 22 p3843 N85-33805

ELECTRIC POWER SUPPLIES

NT AIRCRAFT POWER SUPPLIES
NT SPACECRAFT POWER SUPPLIES

Power subsystem automation study
[NASA-CR-171213] 03 p0358 N85-12299
Comparative energy storage assessment item 05 p0605 N85-13858
Westinghouse programs in pulsed homopolar power supplies 05 p0606 N85-13862
High-efficiency power conversion options for flywheel energy storage systems 05 p0607 N85-13876
A historical overview of the electrical power systems in the US manned and some US unmanned spacecraft
[NASA-CR-174806] 05 p0612 N85-13910
Energy supply problems for emergency telephones 05 p0663 N85-14265
Project Pellworm: Solar electric energy supply for a health center 05 p0664 N85-14268
High-speed power thyristors with excellent switching and load characteristics 06 p0793 N85-15070
Evaluation of miniature vacuum ultraviolet lamps for stability and operating characteristics, Lyman-Alpha task
[NASA-CR-171345] 10 p1477 N85-19323
The 35 kilowatt peak power photovoltaic system
[DE85-000189] 10 p1511 N85-19537
Microprocessor-based monitoring and control project, phase 1
[DE84-901974] 10 p1538 N85-19699
15KW power supply development
[DE85-001057] 11 p1629 N85-20260
Feasibility of producing commodities and electricity for space shuttle operations at Vandenberg Air Force Base
[DCN-84-203-001-80-21] 12 p1789 N85-21230
New types of power supplies for ultrasonic processing equipment 12 p1843 N85-21566
Autonomous uninterruptable power supply apparatus
[AD-D011571] 14 p2298 N85-24232
Basic research on inertial confinement fusion by LIMAY-I 15 p2655 N85-26363
Maintenance of photovoltaic power systems
[AD-A152299] 16 p2819 N85-27390
Large scale electricity production scheduling via nonlinear optimization
[REPT-84-07] 17 p3017 N85-29655
High voltage power supply
[NASA-CASE-GSC-12818-1] 18 p3093 N85-29147
Dynamic simulation of dispersed, grid-connected photovoltaic power systems: System studies
[DE85-011179] 19 p3262 N85-30231
Experimental investigation of a variable speed constant frequency electric generating system from a utility perspective
[NASA-CR-174950] 21 p3579 N85-32251
Applicability of 100kWe-class of space reactor power systems to NASA manned space station missions
[NASA-CR-174696] 24 p4149 N85-35728

ELECTRIC POWER TRANSMISSION

Laboratory evaluation of Electromagnetic Pulse (EMP) hardness testing concepts for electrical conduit systems
[AD-A145466] 02 p0190 N85-11273
Power subsystem automation study
[NASA-CR-171213] 03 p0358 N85-12299
Electromagnetic pulse and the electric power network
[DE84-015403] 04 p0493 N85-13143
Electrical/electronics working group summary 05 p0604 N85-13853
Effects of Formvar coating and copper-nickel outer sheath on the ac losses of multi-strand subsize cables
[DE85-010413] 18 p3096 N85-29166
Protection products for the conductors of high voltage overhead lines
[BLL-OA-TRANS-3219-(6196.300)] 20 p3429 N85-31269

ELECTRIC PROPULSION

NT ELECTROMAGNETIC PROPULSION
NT ELECTROSTATIC PROPULSION
NT ION PROPULSION
NT PLASMA PROPULSION

Development of the Engineering Test Satellite-3 (ETS-3) ion engine system
[NASA-TM-77538] 01 p0017 N85-10101
Research, development, and demonstration of nickel-iron batteries for electric vehicle propulsion
[DE84-017430] 05 p0632 N85-14054
Experimental research on electric propulsion. Note 7: Analysis of the performance of an arc-jet driven by means of hydrogen and nitrogen
[NASA-TM-77473] 06 p0760 N85-14861
Extended performance technology study 30-cm thruster
[NASA-CR-168259] 07 p0917 N85-15606
High frequency plasma generator for ion thrusters
[NASA-CR-174772] 08 p1114 N85-17023
Proceedings of the AFOSR/AFRPL Rocket Propulsion Research Meeting: Abstracts and Agenda
[AD-A148818] 09 p1288 N85-18085
Preliminary assessment of power-generating tethers in space and of propulsion for their orbit maintenance 13 p1997 N85-22520
Station keeping of geostationary satellites by electric propulsion
[NASA-TM-77820] 14 p2320 N85-24337
Analysis of orbit transfer vehicles for GPS Block 3 satellites
[AD-A152021] 16 p2732 N85-26860
Primary propulsion of electrothermal, ion and chemical systems for space-based radar orbit transfer
[NASA-TM-87043] 17 p2916 N85-27972
Experimental research on electrical propulsion. Note 2: Experimental research on a plasma jet with vortex type stabilization for propulsion
[NASA-TM-77674] 18 p3067 N85-28968
Experimental research on electrical propulsion
[NASA-TM-77876] 18 p3067 N85-29969

Experiments in plasma initiation and laser absorption in flowing gases
[AD-A154303] 19 p3276 N85-30313

ELECTRIC PULSES
Influence of radiation wavelength on elastic pulse shape during laser excitation 02 p0257 N85-11681
Pulsed-power system diagnostics: Electromagnetic data interpretation along pulse lines
[AD-A146807] 06 p0810 N85-15148
Basic research on inertial confinement fusion by LIMAY-I 15 p2655 N85-26383

ELECTRIC RELAYS
Isolated load switching with surge suppression
[AD-D011218] 01 p0042 N85-10274
High or low-side solid state relay with current limiting and operational testing
[AD-D011260] 05 p0631 N85-14046

ELECTRIC ROCKET ENGINES
NT ARC JET ENGINES
NT ELECTROSTATIC ENGINES
NT ELECTROTHERMAL ENGINES
NT ION ENGINES
NT MERCURY ION ENGINES
NT PLASMA ENGINES
NT RESISTOJET ENGINES
NT RIT ENGINES

ELECTRIC SPARKS
Bibliography of data on electrical breakdown in gases
[PB84-218049] 01 p0045 N85-10294
Evaluation of minimum ignition energy measurement technique used at P.E.R.M.E.
[SG83/A258] 09 p1301 N85-18160
A new theory aiming to define the mechanisms of material removal in electroerosion
[NASA-TM-77875] 18 p3176 N85-29689
Apparatus and method for the spectrochemical analysis of liquids using the laser spark
[DE85-005749] 23 p3935 N85-34367

ELECTRIC SWITCHES
NT THERMOSTATS
Automation of assembly of electrical products
03 p0346 N85-12228
Semiconductor submicrosecond power commutator switches 06 p0795 N85-15081
Electromechanical switch
[AD-D011400] 07 p0948 N85-16009
Metal vapor arc switch electromagnetic accelerator technology
[NASA-CR-174360] 09 p1314 N85-18259
High voltage disconnect protection
[AD-D011480] 10 p1481 N85-19353
High-voltage, high-power, solid-state remote power controllers for aerospace applications
[NASA-TP-2437] 12 p1795 N85-21263
Basic studies of gases for fast switches
[AD-A149828] 12 p1835 N85-21514
Comparison of shock-induced displacements with displacements produced by a centrifuge acceleration
[DE85-000467] 12 p1852 N85-21618
Current distribution in a plasma erosion opening switch
[AD-A150967] 14 p2424 N85-24949
System of light protection of antenna-mast structures of radio-relay lines 15 p2527 N85-25583
Erosion of electrodes due to switching of capacitor-bank discharge circuits
[AD-A151207] 15 p2547 N85-25718
A study of reflex optoelectronic switching matrices and their derivatives
[CRC-TN-720] 19 p3253 N85-30189
Fast transient behavior of thyristor switches
[AD-A154109] 19 p3259 N85-30206

ELECTRIC WELDING
NT ARC WELDING
NT ELECTRON BEAM WELDING
NT ELECTROSLAG WELDING
NT GAS TUNGSTEN ARC WELDING
NT PLASMA ARC WELDING
International exhibition: Industrial Robots, 1982
03 p0345 N85-12224
Robotization of electric welding processes
03 p0345 N85-12225
Robotization of technological processes in high-frequency heating and welding
03 p0345 N85-12226
Electric Welding Institute's space-technology test results 03 p0352 N85-12267
Cosmonauts report on space welding at conference
15 p2484 N85-25329
Contact point and seam welding of heat-resistant alloys 15 p2501 N85-25429
Sources of improvement in quality of contact butt welding of wire
[BLL-M-96085-(5825.4)] 18 p2793 N85-27225

Removal of longitudinal internal flash from electrically welded tubes
[BLL-BISI-TRANS-22360-(9022.06)]
17 p2936 N85-28136
Production of thin-walled electricity welded tubes with reduced internal flash
[BLL-BISI-TRANS-22361-(9022.06)]
17 p2973 N85-28364
Production of electrically welded tubes with removed internal flash
[BLL-BISI-TRANS-22362-(9022.06)]
17 p2973 N85-28367

ELECTRIC WIRE
NT BEAM LEADS
The HEMP (High-altitude Electromagnetic Pulse) response of a long transmission line buried in the earth
[AD-A146517] 06 p0800 N85-15108
Safety requirements for wiring systems and connectors for photovoltaic systems
[NASA-CR-174211] 08 p0803 N85-15110
Hardwire missile receiver coupler
[AD-D011350] 07 p0937 N85-15936
Flashover failures from wet-wire arcing and tracking
[AD-A149055] 10 p1476 N85-19332
Signal propagation delay, wire length distribution and the efficiency of VLSI circuits
[CWI-CS-R8412] 11 p1830 N85-20266
Liquid thickness gage
[NASA-CASE-LAR-13342-1] 11 p1835 N85-20297
Releasable cable connector assembly for use between a mobile and stationary object
[AD-D011536] 12 p1858 N85-21655
Properties of Ti alloyed multifilamentary Nb3Sn wires by internal tin process
[DE85-003212] 12 p1941 N85-22191
Multiconductor flat cable
[AD-D011695] 17 p2950 N85-28218
Unalloyed and alloyed fine wires of improved properties
[BLL-BISI-TRANS-21930-(9022.06)]
18 p3073 N85-29006
Critical current density and microstructural state of an internal tin multifilamentary superconducting wire
[DE85-009966] 22 p3761 N85-33308

ELECTRIC WIRING
U ELECTRIC WIRE
U WIRING

ELECTRICAL BREAKDOWN
U ELECTRICAL FAULTS

ELECTRICAL CONDUCTIVITY
U ELECTRICAL RESISTIVITY

ELECTRICAL CONDUCTIVITY METERS
Atmospheric research aircraft — conductivity/charge measurements
[ONERA-RS-87/7154/PY] 11 p1682 N85-20596
Method of separately determining electrophysical properties of bulky conductor 13 p2073 N85-22951

ELECTRICAL ENERGY
U ELECTRIC POWER

ELECTRICAL ENGINEERING
Center for Electronics and Electrical Engineering Technical Bulletin covering center programs with 1984 CEEE events calendar
[PB84-222765] 01 p0045 N85-10292
Center for Electronics and Electrical Engineering Technical Bulletin covering center programs with 1984 CEEE events calendar
[PB84-223084] 01 p0045 N85-10293
Center for Electronics and Electrical Engineering Technical Bulletin covering center programs
[PB84-219716] 01 p0045 N85-10295
Center for Electronics and Electrical Engineering Technical Bulletin covering center programs
[PB84-218056] 01 p0045 N85-10296
Singular perturbations, coherency and aggregation of dynamic systems
[DE84-014166] 01 p0114 N85-10772
Activities report of the Department of Engineering
03 p0342 N85-12202
USSR report: Electronics and electrical engineering
[JPRS-UEE-84-014] 03 p0344 N85-12215
International exhibition: Industrial Robots, 1982
03 p0345 N85-12224
Center for Electronic and Electrical Engineering Technical Progress Bulletin, January - March 1983, no. 2
[PB84-231224] 03 p0360 N85-12308
USSR report: Electronics and electrical engineering
[JPRS-UEE-84-010] 04 p0485 N85-13095
NMOS test chip for a course in semiconductor parameter measurements
[PB84-216506] 04 p0497 N85-13174
USSR report: Electronics and electrical engineering
[JPRS-UEE-84-012] 06 p0781 N85-14991
USSR report: Electronics and electrical engineering
[JPRS-UEE-84-011] 06 p0789 N85-15042
A summary of the foundation research program
[AD-A146524] 06 p0891 N85-15856
Target detection using microwave irradiances from natural sources: A passive, local and global surveillance system
[NASA-CR-174260] 07 p0948 N85-15991
Basic research in electronic (JSEP): Joint Services Electronics Program
[AD-A147891] 07 p0948 N85-16007
USSR report: Electronics and electrical engineering
[JPRS-UEE-84-018] 07 p0949 N85-16014
USSR report: Electronics and electrical engineering
[JPRS-UEE-84-017] 07 p0951 N85-16025
Chemical, material electronics studies established
08 p1142 N85-17200
Flexible applications robot used in Moscow training course 10 p1462 N85-19217
China report: Science and technology
[JPRS-CST-84-025] 11 p1620 N85-20197
Electronics Engineering Department: EE technical review
[DE85-004360] 11 p1629 N85-20259
East Europe report: Scientific affairs
[JPRS-ESA-84-006] 11 p1700 N85-20684
USSR report: Electronics and electrical engineering
[JPRS-UEE-85-004] 12 p1837 N85-21531
The DFS-Kopernikus solar generator electrical design
13 p2008 N85-22590
The DFS-Kopernikus solar generator
13 p2008 N85-22591
Electrical design of the Intelsat 6 solar generator
13 p2008 N85-22592
Development and qualification of the electrical part of the Advanced Rigid Array (ARA) — solar array
13 p2008 N85-22594
Design and qualification testing of the Olympus solar array blanket 13 p2009 N85-22600
Electronics Engineering Department EE Technical Review
[UCRL-50025-84-1] 13 p2063 N85-22867
USSR report: Electronics and electrical engineering
[JPRS-UEE-85-002] 13 p2096 N85-22907
USSR report: Electronics and electrical engineering
[JPRS-UEE-85-001] 13 p2078 N85-22976
Microcomputers and the electrical engineer
[AD-A150499] 13 p2147 N85-23325
China report: Science and technology
[JPRS-CST-85-003] 13 p2166 N85-23433
Basic research in electronics (JSEP)
[AD-A151002] 14 p2296 N85-24230
USSR report: Electronics and electrical engineering
[JPRS-UEE-85-005] 15 p2524 N85-25565
China report: Science and technology
[JPRS-CST-85-011] 15 p2551 N85-25748
A concept for the intrinsic dielectric strength of electrical insulation materials
[NASA-CR-176040] 20 p3448 N85-31410
Failure mechanisms in metal-sheathed thermocouples
[DE85-011929] 21 p3590 N85-32317
USSR report: Electronics and electrical engineering
[JPRS-UEE-84-015] 22 p3762 N85-33314
USSR report: Electronics and electrical engineering
[JPRS-UEE-84-009] 22 p3773 N85-33381
Joint services electronics program
[AD-A154748] 23 p3927 N85-34338
Center for Electronics and Electrical Engineering technical progress bulletin covering center programs, July-September with 1985 CEEE events calendar
[PB85-191393] 24 p4091 N85-35383

ELECTRICAL FAULTS
NT SHORT CIRCUITS
Bibliography of data on electrical breakdown in gases
[PB84-218049] 01 p0045 N85-10294
Luminous points and breakdown in structure of GaAs transistors 02 p0257 N85-11684
Glow spots and breakdown in GaAs transistor structure 04 p0487 N85-13107
Determination of threshold and maximum operating electric stresses for selected high voltage insulation. Task 3: Investigation of high voltage capacitor insulation
[DE84-017081] 09 p1316 N85-18274
Flashover failures from wet-wire arcing and tracking
[AD-A149055] 10 p1476 N85-19332
Mass analysis of neutral particles and ions released during electrical breakdowns on spacecraft surfaces
[NASA-CR-175585] 12 p1793 N85-21250
Concurrent simulation techniques exploiting hierarchy
[AD-A149783] 12 p1835 N85-21512
Basic studies of gases for fast switches
[AD-A149828] 12 p1835 N85-21514
Galileo internal electrostatic discharge program
13 p1995 N85-22504
Mass spectra of neutral particles released during electrical breakdown of thin polymer films
13 p1996 N85-22511

Electrical conduction in polymer dielectrics
13 p1998 N85-22514
Breakdown of thin plates by radiation
13 p2028 N85-22709
High field RF superconductivity: To pulse or not to pulse
[DE85-004381] 14 p2429 N85-24977
Experimental investigation of the electric breakdown in SF6
[BLL-CE-TRANS-7987-(9022.09)]
15 p2546 N85-25714
Field-induced phenomena in electrical insulation
[AD-A151234] 15 p2547 N85-25719
Energy considerations in second breakdown
[AD-A152389] 17 p2952 N85-28229
Analysis of time dependent dielectric failures
[AD-A153200] 17 p2954 N85-28243
Performance and electric field limitations in Inflow disk MHD generators 20 p3534 N85-31987
Vacuum interface flashover with bipolar electric fields
[DE85-012027] 22 p3755 N85-33275
Model that predicts pulse charged gas switching breakdown phenomena
[DE85-013119] 22 p3761 N85-33313
Method and apparatus for transfer function simulator for testing complex systems
[NASA-CASE-NPO-15696-1] 23 p3926 N85-34333
Solar system fault detection
[DE85-005987] 23 p3948 N85-34458
Statistical distribution of breakdown voltages in rep-rate spark gaps
[DE85-012813] 24 p4090 N85-35354

ELECTRICAL GROUNDING
Human engineering laboratory grounding analysis: Project Helga
[AD-A145728] 02 p0195 N85-11300
Exact design formulas for field intensity of dipole deployed above flat homogeneous Earth with finite conductivity 13 p2081 N85-22998

ELECTRICAL IMPEDANCE
NT CONTACT RESISTANCE
NT ELECTRICAL RESISTANCE
Impedance of vertical dipoles above a dissipative ground
[REPT-S-152] 02 p0192 N85-11297
An automated immittance measuring system for electroacoustic transducers
[AD-A145701] 02 p0200 N85-11336
Determination of the pressure sensitivity of 1 inch condenser microphones
[PTB-AK-28] 05 p0633 N85-14058
Deer control using 7 strand vertical fence
11 p1581 N85-19958
Effectiveness of an overhead wire barrier system in reducing gull use at the BFI Jedburg sanitary landfill, Berkeley and Dorchester counties, South Carolina
[AD-P004200] 11 p1582 N85-19967
Semiconductor electrochemistry approach to the study of oxide films on nickel electrodes
[DE85-009042] 11 p1630 N85-20264
Change of electrical characteristics of radio-frequency cables under thermal effect 13 p2081 N85-22999
Quality control of radioelectronic apparatus components on basis of external characteristics in frequency domain
15 p2529 N85-25590
A computation of fin-line impedance
[AD-A154080] 19 p3258 N85-30204
Changes in the impedance and bioelectrical activity of the cerebral cortex of rats under the action of anaesthetic drugs
[HSE-TRANS-10371] 19 p3327 N85-30617
Measurement of electrical parameters and current components in the bulk of silicon solar cells
20 p3481 N85-31635
R, L, C, G measurement 21 p3668 N85-32784

ELECTRICAL INSULATION
Development of power system management
[PB84-216530] 04 p0497 N85-13173
USSR report: Electronics and electrical engineering
[JPRS-UEE-84-012] 06 p0781 N85-14991
Choice of criteria for rejection of insulating components in high-voltage surge equipment
06 p0785 N85-15021
Diagnosis of insulation defects in 1000+ V distribution networks with insulated neutral
07 p0954 N85-16044
Determination of threshold and maximum operating electric stresses for selected high voltage insulation. Task 3: Investigation of high voltage capacitor insulation
[DE84-017051] 09 p1316 N85-18274
Transients during the switching of SF6-insulated isolating switches
[BLL-CE-TRANS-7986-(9022.09)]
15 p2546 N85-25713
Statistical analysis of partial discharge inception in high voltage 15 p2548 N85-25715
Field-induced phenomena in electrical insulation
[AD-A151234] 15 p2547 N85-25719
The ESFET: Evaporated Sensing Field Effect Transistor 19 p3256 N85-30188
A concept for the intrinsic dielectric strength of electrical insulation materials
[NASA-CR-176040] 20 p3448 N85-31410
Failure mechanisms in metal-sheathed thermocouples
[DE85-011929] 21 p3590 N85-32317
Partial discharges in and electric strength of high-voltage polymer insulation at cryogenic temperatures
22 p3770 N85-33364

ELECTRICAL LEADS
U ELECTRIC CONDUCTORS

ELECTRICAL MEASUREMENT
NT COULOMETRY
NT POLAROGRAPHY
Electrical parameters in 60-Hz biological exposure systems and their measurement: A primer
[PB84-217793] 03 p0400 N85-12548
Development of power system management
[PB84-216530] 04 p0497 N85-13173
Electrochemistry in near-critical and supercritical fluids. I. Ammonia
[AD-A146429] 06 p0765 N85-14894
Apparatus for measuring dielectric characteristics of polymer materials in millimetric range of wavelengths at 4.2-300 K temperatures 06 p0788 N85-15032
An indirect measure of below-ground electric field, conductivity, and dielectric constant
[AD-A146518] 06 p0804 N85-15115
Electronic and redox properties of stacked-ring silicon phthalocyanines from molecular orbital theory
[AD-A147161] 07 p0922 N85-15844
A narrow band pulsed eddy current instrument for materials testing
[AERE-R-11229] 07 p0968 N85-16149
Monitoring cure of epoxy resins using a microdielectrometer
[AD-A145618] 08 p1119 N85-17054
The use of microdielectrometry in monitoring the cure of resins and composites
[AD-A146619] 08 p1119 N85-17055
Voltammetry and coulometry with immersed thin layer electrodes. Part 1: Model for effects of solution resistivity in linear sweep voltammetry
[AD-A146655] 08 p1159 N85-17313
Voltammetry and coulometry with immersed thin layer electrodes. Part 2: Practical considerations and experimental results
[AD-A146656] 08 p1159 N85-17314
Multimode harmonic power measurement of 40 MW pulsed S-band klystrons
[DE85-001580] 09 p1316 N85-18272
Charge depletion meter
[AD-D011484] 10 p1468 N85-19393
High-current measurement techniques
[PB85-100444] 11 p1637 N85-20311
Development of a low cost electrochemical CO monitor based on anodic scanning voltammetry in nonaqueous electrolyte
[PB85-113486] 11 p1637 N85-20314
Electromagnetic pulse (EMP) injection on cable entries, type ERA; EMP memo no. 10
[FOA-E-30003-A3] 12 p1830 N85-21484
Program for controlling electrical measuring contact instrument on glow-discharge indicator panel
12 p1842 N85-21558
MFTF sensor verification computer program
[DE85-004452] 12 p1916 N85-22029
The high voltage silicon cell: A comparative analysis
13 p2005 N85-22569
Inverse behavior of silicon photovoltaic cells
13 p2010 N85-22604
Comparing different theoretical designs of six-port reflectometer junctions
[AD-A149419] 13 p2054 N85-22861
Portable electrochemical cell interrogator
[DE85-005186] 13 p2065 N85-22901
Measuring intensity of electric field produced by electromagnetic pulse with aid of active probes
13 p2075 N85-22958
Contactless determination of the conductivity of the white paint PCB-Z — Giotto spacecraft thermal control coating 14 p2243 N85-23907
Thermocouple modeling
[DE85-005172] 14 p2306 N85-24273
Instrument for measuring dispersional distortions in optical fibers and cables 15 p2530 N85-25595
A comparison of alternative analytic models for event related potential records
[AD-A151977] 15 p2618 N85-26134
Measurement methods for accurate microwave characterization and modeling of MESFET chips
[AD-A152360] 17 p2952 N85-28227
Voltammetric analysis of ordnance materials. Part 2: A portable digital voltammeter for use with a silver wire working electrode
[AD-A152460] 17 p2967 N85-28325
Electrical and structural characterization of web dendrite crystals 20 p3461 N85-31633
Measurement of electrical parameters and current components in the bulk of silicon solar cells
20 p3481 N85-31635
Modelling and parameter estimation for distributed vibratory systems
[AD-A154518] 21 p3598 N85-32344
East Europe report: Science and technology. Selections on CSSR computer technology
[JPRS-ESA-84-017] 21 p3668 N85-32781
R, L, C, G measurement 21 p3668 N85-32784
The measurement of high value resistances at the NPL — electrical resistance
[NPL-DES-81] 22 p3758 N85-33291

ELECTRICAL PROPERTIES
NT CAPACITANCE
NT CARRIER MOBILITY
NT CHARGE DISTRIBUTION
NT CONTACT RESISTANCE
NT DIELECTRIC PROPERTIES
NT ELECTRIC MOMENTS
NT ELECTRICAL IMPEDANCE
NT ELECTRICAL RESISTANCE
NT ELECTRICAL RESISTIVITY
NT ELECTRON MOBILITY
NT ELECTROSTRICTION
NT FERROELECTRICITY
NT HOLE MOBILITY
NT INDUCTANCE
NT IONOSPHERIC CONDUCTIVITY
NT KONDO EFFECT
NT MAGNETORESISTIVITY
NT PERMITTIVITY
NT PHOTOCONDUCTIVITY
NT PHOTOVOLTAIC EFFECT
NT PIEZOELECTRICITY
NT PLASMA CONDUCTIVITY
NT POLARIZATION CHARACTERISTICS
NT PROXIMITY EFFECT (ELECTRICITY)
NT PYROELECTRICITY
NT SUPERCONDUCTIVITY
Solution of the Boltzmann transport equations for a permeable base transistor
[AD-A144969] 01 p0112 N85-10757
A high-voltage discharger
[AD-A145659] 02 p0194 N85-11299
Use of magnetic compression based on amorphous alloys as a drive for induction linacs
[DE84-014524] 02 p0277 N85-11805
Materials modification by ion beam mixing
[AD-P003948] 02 p0286 N85-11864
Characteristics of ion implanters for fabrication of electronic devices
[AD-P003949] 02 p0286 N85-11865
Review of the University of Manchester Ion Implantation Conference
[AD-P003950] 02 p0286 N85-11866
Relationships between electronic structure and stability of metallic glasses
[AD-A145506] 02 p0287 N85-11874
Electric properties of neovolcanic rocks of central and east Slovakia
[REPT-558] 03 p0376 N85-12401
Electron channeling and EBIC studies of polycrystalline silicon sheets
[DE84-004515] 05 p0670 N85-14309
Electrical properties of 10-50 nm TEOS (Tetraethoxysilane) LPCVD (Low Pressure Chemical Vapor Deposition) films
[AD-A146416] 06 p0803 N85-15111
Investigation of structural and electrical properties of low-angle silicon sheet 06 p0831 N85-15288
Analysis of optical and electrical performance of a TCP-coated solar cell 06 p0832 N85-15293
The growth and properties of semiconductor strained-layer superlattices
[DE84-012979] 06 p0868 N85-15515
Characterization of bicrystal grain boundary properties using device structures
[DE84-004509] 06 p0869 N85-15523
Optical properties of composite materials
[AD-A146768] 07 p0920 N85-15828
Thermally induced quasiparticle branch imbalance in thin film superconductors 09 p1396 N85-18786
Robotic safety
[DE85-002314] 10 p1493 N85-19431
Stress studies in EFG
[NASA-CR-174441] 10 p1508 N85-19515
High energy pulsed particle accelerator
[AD-A149247] 10 p1554 N85-19797

Material growth and characterization for solid state devices
[NASA-CR-174410] 10 p1561 N85-19847
Investigation of electric and magnetic properties of intercalated graphite
[AD-A149601] 12 p1797 N85-21274
Electric and magnetic properties of intercalated graphite
[AD-A149648] 12 p1798 N85-21276
Proceedings of the Symposium on Electromagnetic Windows (17th) held at Georgia Inst. of Technology, Engineering Experiment Station, Atlanta, Georgia on 25-27 July 1984. Part 2
[AD-A149125] 12 p1824 N85-21444
Dual band radome wall design
[AD-P004357] 12 p1825 N85-21451
Broadband thermoplastic radomes
[AD-P004369] 12 p1827 N85-21463
Development of the F-20 nose radome
[AD-P004374] 12 p1827 N85-21468
Studies of electrical properties of surface films and localization during electrochemical dimensional working of titanium 13 p2032 N85-22729
High sheet resistance, arsenic implanted polycrystalline silicon for integrated circuit resistors
[DE85-004355] 13 p2065 N85-22902
Electrical and thermal transport property studies of high-temperature thermoelectric materials
[AD-A150167] 13 p2163 N85-23417
AlN insulator for 3-5 MIS applications
[AD-A150674] 14 p2426 N85-24962
Structure and properties of ion-implanted Al sub 2 O sub 3
[DE85-005374] 14 p2430 N85-24967
The structural and electronic properties of amorphous silicon based alloy materials
[DE85-002909] 15 p2660 N85-26419
A transduction path method of solid state sensor analysis and investigation
[AD-A152123] 16 p2870 N85-27707
Completely consumed carbide: A new process for dielectric isolation
[AD-A152379] 17 p2918 N85-27987
Effects of processing chemistry on electrical properties of high field ZnO varistors
[DE85-007688] 17 p2956 N85-28254
GaAs MESFET with lateral non-uniform doping 17 p3043 N85-28827
Materials-process interactions in ternary alloy semiconductors
[AD-A153133] 17 p3043 N85-28832
Properties of defects in Hg(1-x)Cd(x)Te
[AD-A153243] 17 p3044 N85-28835
Growth mechanism and properties of the thermal and anodic oxides of the 3-5 compound semiconductors
[AD-A153406] 18 p3193 N85-29803
Photoelectronic properties of zinc phosphide crystals and heterojunctions
[DE85-006777] 19 p3307 N85-30501
Special materials: Carbons
[SNIAS-851-551-104] 20 p3421 N85-31235
Electrochemistry of Hexanitroazobenzene (HNAB)
[DE85-010807] 21 p3585 N85-32171
Electrical properties of bulk grown nitrogen doped silicon
[AD-A155471] 21 p3581 N85-32266
Failure analysis of thin-film amorphous-silicon solar-cell modules 21 p3613 N85-32452
Electronic phenomena near semiconductor grain boundaries
[DE85-011543] 21 p3711 N85-33035
Grain boundary and surface diffusion in oxide systems
[DE85-007291] 23 p3985 N85-34715
Electronic structure and lattice dynamics of dimensionally constrained and disordered solids
[AD-A155927] 24 p4161 N85-35797

ELECTRICAL RESISTANCE
NT CONTACT RESISTANCE
Human engineering laboratory grounding analysis: Project Helga
[AD-A145728] 02 p0195 N85-11300
Instrumentation techniques for measuring large, high rate strains with foil resistance strain gages
[AD-A146248] 03 p0364 N85-12337
Zeta potential in ceramic industry
[NASA-TM-77478] 04 p0478 N85-13047
Electrical resistance measurements of metals to 40 GPa in the diamond cell
[DE85-001009] 11 p1629 N85-20262
Liquid thickness gage
[NASA-CASE-LAR-13342-1] 11 p1635 N85-20297
On filter binary processes
[AD-A150328] 13 p2063 N85-22890
Plasma-edge studies using carbon resistance probes
[DE85-005569] 14 p2424 N85-24955
Temperature variation of resistivity of certain alloys based on transition and simple metals in amorphous and crystalline states 15 p2496 N85-25399
A strain gauge manual
[AD-A151802] 16 p2787 N85-27197
Ohmic potential drop and gas bubble radius distribution in alkaline water electrolysis 17 p2924 N85-28025
Thin films properties of sputtered niobium silicide on SiO2, Si3N4 and on n+ poly-Si
[AD-A152378] 17 p2952 N85-28228
Effects of the structural state in thermo-bimetals on their resistance to microscopic plastic deformation
[BLL-BISI-TRANS-22403-(9022.06)] 17 p2979 N85-28412
Leakage effects in n-GaAs MESFET with n-GaAs buffer layer 17 p3043 N85-28826
Studies on surface processes during friction and wear
[AD-A153509] 18 p3117 N85-29296
Quantized Hall effect in two-dimensional electron systems
[AD-A154347] 19 p3259 N85-30211
Cells for measuring thermoelectromotive force and electrical resistance of metals in temperature range of 20-950 degrees Celsius
[BLL-M-36240-(5828.4)] 20 p3457 N85-31473
Resistance of polyaniline films as a function of electrochemical potential and the fabrication of polyaniline-based microelectronic devices
[AD-A154999] 21 p3569 N85-32201
The measurement of high value resistances at the NPL — electrical resistance
[NPL-DES-81] 22 p3758 N85-33291
Tensile testing apparatus
[NASA-CASE-LAR-13243-1] 23 p3933 N85-34375

ELECTRICAL RESISTIVITY
NT IONOSPHERIC CONDUCTIVITY
NT KONDO EFFECT
NT MAGNETORESISTIVITY
NT PHOTOCONDUCTIVITY
NT PLASMA CONDUCTIVITY
NT SUPERCONDUCTIVITY
Dynamics of graphite fiber intercalation: In situ resistivity measurements with a four point probe
[NASA-TM-86858] 01 p0017 N85-10105
Electrically conductive rigid polyurethane foam
[DE84-014490] 01 p0033 N85-10203
Platinum thin film resistors as accurate and stable temperature sensors
[NASA-TM-77728] 01 p0049 N85-10322
Preparation and properties of single crystals of hydrogen bis(phthalocyaninato) neodymium(3)
[AD-A144933] 01 p0123 N85-10846
Trivalent ion exchange in beta alumina
[AD-A145373] 02 p0172 N85-11151
P-doping of (CH)x to the metallic regime with gaseous oxygen. Application to oxygen fuel cell type electrodes
[AD-A145477] 02 p0186 N85-11242
The concept of doping of conducting polymers. The role of reduction potentials
[AD-A145480] 02 p0186 N85-11243
Ceramic materials for MHD electrodes
[DE84-015580] 02 p0187 N85-11250
Resistance and inductance calculations for helical flux compression generators
[DE84-015068] 02 p0195 N85-11306
Mechanisms of electrical conductivity in olivine
[DE84-014333] 04 p0495 N85-13159
Magnetic susceptibility, electrical resistivity, and specific heat of single crystal LaFe-4P-12
[DE84-009979] 04 p0570 N85-13633
Evidence for d-band conduction in metallic glasses containing transition metal elements
[DE84-014822] 04 p0570 N85-13635
Diffusion mechanisms and point defects in transition-metal oxides
[DE84-016238] 04 p0571 N85-13639
On the Apollo subsatellite evidence for a lunar core 04 p0581 N85-13714
Low frequency electrical properties of selected dielectrics
[DE84-016220] 05 p0632 N85-14052
Polymer-carbon black interaction in electrically conducting fiber-forming composites 06 p0762 N85-14875
Semiconductor high-voltage power devices: State of art and outlook 06 p0794 N85-15074
An indirect measure of below-ground electric field, conductivity, and dielectric constant
[AD-A146518] 06 p0804 N85-15115
An investigation of the electrical conductivity in highly oriented graphite intercalation compounds
[AD-A146539] 06 p0804 N85-15116
Studies on copper alloys containing chromium on the copper side phase diagram
[NASA-TM-77752] 07 p0927 N85-15876
Polyphosphazene solid electrolytes
[AD-A147006] 07 p0931 N85-15902
The relationship between radiation sensitivity and redox equilibria — glass processing variables
[AD-A147216] 07 p0932 N85-15906
Electrically conducting complexes of poly(3,6-n-methylcarbazolyl methylene)
[AD-A147884] 07 p0933 N85-15914
The constant current strain gauge bridge
[ARL/STRUC-TM-385] 07 p0962 N85-16097
On reversion phenomena in Cu-Zr-Cr alloys
[NASA-TM-77791] 08 p1125 N85-17092
Reversion phenomena of Cu-Cr alloys
[NASA-TM-77780] 08 p1125 N85-17094
EDP computer tapes described 08 p1142 N85-17203
An experimental and theoretical investigation of optogalvanic effects
[AD-A148089] 08 p1157 N85-17299
Voltammetry and coulometry with immersed thin layer electrodes. Part 1: Model for effects of solution resistivity in linear sweep voltammetry
[AD-A148655] 08 p1159 N85-17313
Electronic structure, chemical bonding, and electron conductivity of thin-film transition-metal silicides
[AD-A147721] 08 p1226 N85-17718
Characterization of III-V compound semiconductor device materials
[AD-A148203] 08 p1228 N85-17719
Resistivity of alloys
[DE85-000906] 09 p1296 N85-18138
Electrical resistivity and structural changes upon relaxation and crystallization of (Mo/sub 0.6/Ru/sub 0.4)sub 100-x/B/sub x/ metallic glasses
[DE84-017281] 09 p1299 N85-18160
Electrical resistivity technique to assess the integrity of geomembrane liners
[PB85-122414/GAR] 09 p1325 N85-18327
Practical application of earth resistivity methods in phase 2 of the installation restoration program
[AD-P004148] 09 p1348 N85-18484
Compositional, structural, and physical studies of some graphite hexafluoroarsenates and their relatives
[DE85-000855] 10 p1432 N85-19030
Initial aging phenomena in copper-chromium alloys
[NASA-TM-77790] 10 p1439 N85-19070
Water absorption and conductivity in poly(ethylene oxide)-lithium tetrafluoroborate films
[AD-A147969] 10 p1450 N85-19138
Polymer electrolytes: An investigation of some poly (N-propylaziridine)/lithium salt compositions
[AD-A149444] 10 p1452 N85-19146
Microwave surface resistivity of several materials at ambient temperature 10 p1463 N85-19226
Generation of Alfven waves due to thermal modulation of the electrical conductivity
[AD-A149389] 10 p1558 N85-19826
Vacuum ultraviolet electronic properties of liquids
[DE85-000305] 10 p1583 N85-19858
Conductivity changes in neutron-irradiated commercial copper alloys at approximately 450(C)C
[DE85-003007] 11 p1606 N85-20100
Liquid thickness gage
[NASA-CASE-LAR-13342-1] 11 p1635 N85-20297
Normal mode analysis for linear resistive magnetohydrodynamics
[IPP-6/235] 11 p1730 N85-20878
Theory of resistivity-gradient-driven turbulence
[DE85-002175] 11 p1733 N85-20896
Solid electrolytes: Mechanisms for achieving optimal conductivity
[AD-A150116] 12 p1801 N85-21296
Characterization of high temperature electrically conducting oxides
[DE85-004296] 12 p1803 N85-21307
Update of thermal conductivity and electrical resistivity of electrolytic iron, tungsten and stainless steel
[PB85-115814] 12 p1803 N85-21311
Control of electronic, magnetic and optical properties of doped polyacetylene conductors
[AD-A150117] 12 p1814 N85-21375
Fine-grained, isotropic graphite for use as NBS (National Bureau of Standards) thermophysical property RM's from 5 to 2500 K
[PB85-112886] 12 p1814 N85-21381
Research on separators for alkaline zinc batteries
[DE85-003082] 12 p1836 N85-21523
Distribution of atmospheric electric current in the global circuit
[CONTRIB-87] 12 p1868 N85-21852
The liner package: An incipient MHD capability for CCUBE
[LA-9969-MS] 12 p1913 N85-22007
Preliminary investigation of the electrodynamics of a conducting tether 13 p1997 N85-22521

HREELS and Auger studies of conducting polymers
[DE85-004541] 13 p2038 N85-22764
Exact design formulas for field intensity of dipole deployed above flat homogeneous Earth with finite conductivity 13 p2081 N85-22998
Induction excitation of deep conducting zones 13 p2111 N85-23154
Variations in resistivity of upper crustal layer 13 p2113 N85-23164
Contactless determination of the conductivity of the white paint PCB-Z — Giotto spacecraft thermal control coating 14 p2243 N85-23907
Applications of eddy currents 14 p2316 N85-24315
Tunneling in magnetic superconducting systems
[AD-A150677] 14 p2426 N85-24963
Electrically conductive polymer concrete overlays
[DE85-006728] 15 p2522 N85-25549
Status of French research in plastic batteries 15 p2530 N85-25603
Graphite fiber intercalation: Dynamics of the bromine intercalation process
[NASA-TM-87015] 16 p2742 N85-26921
Electrical resistivity in amorphous metals: Consequences of phonon ineffectiveness in the diffraction model
[AD-A152130] 16 p2779 N85-27150
Impurity bands associated with MOS inversion layers
[INPE-3483-PRE/726] 16 p2870 N85-27704
Electrochemistry of polymer films not immersed in solution: Electron transfer on an ion budget
[AD-A152980] 17 p2920 N85-27998
Electrical conductivity and phase diagram of binary alloys. 21: The system palladium-chromium
[NASA-TM-77663] 18 p3073 N85-29009
Molten carbonate fuel cell cathode material development
[DE85-010268] 18 p3081 N85-29057
ZnSP2 as an improved semiconductor for photovoltaic solar cells
[DE85-008772] 18 p3097 N85-29171
Processable and stable conductive polymers
[AD-D011684] 19 p3249 N85-30143
Transport properties of Topopah Spring tuff
[DE85-010448] 19 p3270 N85-30278
Fractional statistics and fractional quantized Hall effect
[DE85-007833] 19 p3375 N85-30940
Electrical and mechanical properties of intercalated graphite fibers
[AD-A155560] 21 p3570 N85-32205
Electron-donor dopant, method of improving conductivity of polymers by doping therewith, and a polymer so treated
[DE85-011640] 22 p3752 N85-33257
Radiation-hardened polymeric films
[DE85-011636] 22 p3752 N85-33259
Optimization of design parameters for alternating current stabilizer based on magnetic suspension 22 p3772 N85-33374
Molten carbonate fuel cell separator
[DE85-011615] 22 p3806 N85-33577
Electrical resistivity and hysteresis of the equiatomic nickel-titanium alloy near the martensitic transformation temperature 23 p3904 N85-34181
Instrumentation for sensing moisture content of material using a transient thermal pulse
[NASA-CASE-NPO-15493-2] 23 p3933 N85-34373
Electrically conductive containment vessel for molten aluminum
[DE85-006516] 23 p3939 N85-34415
Electrically conductive doped block copolymer of polyacetylene and polyisoprene
[DE85-009500] 24 p4082 N85-35301
Conduction and aging of piezoelectric PZT ceramics 24 p4099 N85-35346
Two-dimensional inversion of resistivity monitoring data from the Cerro Prieto geothermal field
[DE85-012554] 24 p4113 N85-35494

ELECTRICALLY SUSPENDED GYROSCOPES

U ELECTROSTATIC GYROSCOPES

ELECTRICITY

NT ALTERNATING CURRENT
NT ATMOSPHERIC ELECTRICITY
NT AURORAL ELECTROJETS
NT ELECTROJETS
NT EQUATORIAL ELECTROJET
NT GEOELECTRICITY
NT HYDROELECTRICITY
NT IONOSPHERIC CURRENTS
NT STATIC ELECTRICITY
NT TELLURIC CURRENTS

Designing an expert system for training automotive electrical troubleshooting
[AD-P003926] 02 p0246 N85-11606
US energy for the rest of the century, 1984 edition
[PB84-207406] 04 p0531 N85-13393
Electromagnetic pulse (EMP) interaction with electric power systems. Power Systems Technology Program
[DE85-000166] 09 p1312 N85-18244
Light your runways and taxiways without electricity
[DE85-000269] 11 p1586 N85-19991
Electricity production from coal through molten-carbonate fuel cells
[TI85-005072] 14 p2351 N85-24534
Electricity from sunlight: The emergence of photovoltaics, revised edition
[DE85-002920] 19 p3307 N85-30502
Superconducting magnetic energy storage for asynchronous electrical systems
[DE85-005988] 22 p3847 N85-33832

ELECTRIFICATION

Electronic information management and productivity
[DE85-013362] 24 p4164 N85-35818

ELECTRO-OPTICAL EFFECT

Integrated optical components utilizing acoustooptic and electrooptic diffraction in micro-waveguides 13 p2089 N85-23044
Modular Optoelectronic Multispectral Scanner (MOMS) for Earth observation. First results of STS-7 mission
[MBB-UR-717/83-O] 16 p2874 N85-27732
Transparent electrode for optical switch
[DE85-011618] 22 p3761 N85-33310
OMEGA: Optoelectronic measurement of the incidence angle of a projectile
[ISL-CO-223/84] 23 p3974 N85-34634

ELECTRO-OPTICAL PHOTOGRAPHY

Investigations of the accuracy of the Digital Photogrammetry System (DPS), a rigorous three-dimensional compilation process for pushbroom imagery
[MBB-UA-753/83-O] 16 p2874 N85-27734
Magnetic materials
[AD-A154679] 21 p3580 N85-32256

ELECTRO-OPTICS

The development of an optoelectronic assembly applied to computer systems
[AD-A145026] 01 p0120 N85-10821
Visible wavelength interferometer for high speed electron density diagnostics
[AD-A145686] 02 p0277 N85-11803
Optical waveguide spatial filters
[AD-A145674] 02 p0280 N85-11825
Thermal deformation measurements of heat-resistant structural materials for aircraft by electro optical displacement transducer
[NAL-TR-810] 03 p0325 N85-12092
USSR report: Electronics and electrical engineering
[JPRS-UEE-84-014] 03 p0344 N85-12215
Dielectric and optical properties of sputtered thin films
[AD-A146210] 03 p0420 N85-12881
Research on materials and components for opto-electronic signal processing
[AD-A145608] 03 p0433 N85-12754
A physical interpretation of the structure and electron-optical data for spinel (MgAl2O4)
[AERE-R-11278] 03 p0434 N85-12767
An overview of Multispectral Electro-Optical Stereo Scanner (MEOSS) mission 04 p0458 N85-12908
The Monocular Electro-Optical Stereo Scanner Experiment (MEOSS) 04 p0459 N85-12910
Heavy duty precision pan and tilt head
[AD-A146869] 04 p0509 N85-13246
Imaging of surfaces and defects of crystals
[DE84-016449] 04 p0570 N85-13632
Electrooptical matrix multiplication using the twos complement arithmetic for improved accuracy
[AD-D011252] 05 p0728 N85-14682
Advanced cube processor
[AD-D011262] 05 p0729 N85-14683
Measurement of parameters defining orientation of liquid crystals in electrooptic cells 06 p0777 N85-14971
USSR report: Electronics and electrical engineering
[JPRS-UEE-84-012] 06 p0781 N85-14991
Electrooptical sensor for automatic detection of objects 06 p0789 N85-15040
Improvements in avalanche-transistor sweep circuitry for electrooptic streak cameras
[DE84-016195] 06 p0811 N85-15155
The growth and properties of semiconductor strained-layer superlattices
[DE84-012979] 06 p0868 N85-15515
USSR report: Electronics and electrical engineering
[JPRS-UEE-84-018] 07 p0949 N85-16014
Precision electrooptical deflector based on corrugated light guide 07 p0950 N85-16020
Multichannel electrooptical modulators for digital information storage and processing systems 07 p0950 N85-16021
Stereo Electro-optical Tracking System (SETS)
[NASA-CR-172471] 07 p0962 N85-16098
Measurement of high temperature strain by the laser-speckle strain gauge
[NASA-TM-77751] 07 p0977 N85-16207
Electro-optical target detection
[AD-D011366] 07 p1042 N85-16617
The development and test of ultra-large-format multi-anode microchannel array detector systems
[NASA-CR-174247] 07 p1043 N85-16622
Optics and opto-electronic systems
[AD-A147277] 07 p1044 N85-16630
Crystal growth and characterization of BaMgF4
[AD-A146805] 07 p1047 N85-16650
Evaluation of nose, roof, and mast mounted sensor platforms for piloting and sighting, integrated in future combat helicopters 08 p1074 N85-16808
Recent development in astronomic position determinations
[AD-A148335] 08 p1082 N85-16858
Challenges of developing an electro-optical system for measuring man's operational envelope 08 p1095 N85-16921
Telecommunications equipment at 1984 Leipzig Spring Fair 08 p1140 N85-17179
Chemical, material electronics studies established 08 p1142 N85-17200
General assessment of GDR microelectronics industry, applications 08 p1142 N85-17202
Study in spurious sensitivity of electronics in space
[AD-A148386] 08 p1158 N85-17305
Guidelines for atmospheric measurements in support of electro-optical systems testing
[AD-A148090] 08 p1186 N85-17474
Matrix-matrix multiplication using an electrooptical systolic-engagement array processing architecture
[AD-D011410] 08 p1223 N85-17704
High-speed, eight-frame electro-optic camera with multipulsed ruby laser illuminator
[DE85-001748] 09 p1323 N85-18314
Data acquisition, measurement devices at 1984 Leipzig Spring Fair 09 p1378 N85-18661
A methodology for the determination of rotary wing aircraft vulnerabilities in air-to-air combat simulation
[AD-A148984] 10 p1424 N85-18984
The cockpit of the year 2000: How big a step? 10 p1534 N85-19667
An electro-optic spatial light modulator for thermo-elastic generation of programmably focused ultrasound
[AD-A149078] 10 p1553 N85-19794
Modulation Transfer Function (MTF) measurement techniques for lenses and linear detector arrays
[NASA-TM-86168] 10 p1558 N85-19812
Control technology for integrated circuit fabrication at Honeywell Optoelectronics Division, Richardson, Texas
[PB85-109023] 11 p1616 N85-20162
Status of specific FRG high tech research funded by BMFT 11 p1618 N85-20181
Miniature electrooptical air flow sensor
[NASA-CASE-LAR-13065-1] 11 p1635 N85-20295
Photorefractor ocular screening system
[NASA-CASE-MFS-28011-1SB] 11 p1692 N85-20639
Imaging apparatus for transverse electrode electro-optic tunable filter
[AD-D011524] 12 p1832 N85-21497
USSR report: Electronics and electrical engineering
[JPRS-UEE-85-004] 12 p1837 N85-21531
Topics in optical materials and device research, 3: Volume 1
[AD-A149726] 12 p1933 N85-22145
USSR report: Engineering and equipment
[JPRS-UEQ-85-003] 13 p2042 N85-22782
Optoelectronic safety system for robotized technological complex 13 p2046 N85-22805
Mathematical modeling of two-frequency laser sounding of scattering media 13 p2089 N85-23045
Accuracy of random signal spectral parameter estimation against interference background in acoustooptical spectrum analyzers 13 p2090 N85-23052
OMEGA: An optronic device to measure the incidence angle of a projectile
[ISL-CO-207/83] 14 p2306 N85-24274
Feasibility of optical instruments based on multiaperture optics
[AD-A150868] 14 p2421 N85-24936
Ferroelectric tungsten bronze bulk crystals and epitaxial thin films for electro-optic device applications
[AD-A151044] 14 p2427 N85-24970
InGaAs/GaAs, Strained-Layer Superlattice (SLS), junction photodetectors, LED's, injection LASER's and FET's for optoelectronic IC applications
[DE85-001940] 14 p2430 N85-24986
An electro-optic spatial light modulator for thermoelastic generation of programmably focused ultrasound
[AD-A152066] 15 p2646 N85-26323

Electron-bombarded silicon spatial light modulator
[AD-D011579] 15 p2652 N85-26355
Charge isolation in a spatial light modulator
[AD-D011581] 15 p2652 N85-26356
Studies of electro-optical attenuation in the vicinity of cloud base
[AD-A151745] 15 p2653 N85-26360
Technical evaluation report on Avionics Panel Specialists' Meeting on Digital Optical Circuit Technology
[AGARD-AR-202] 15 p2653 N85-26367
Interaction of liquid crystals with inhomogeneous surfaces
[AD-A151557] 15 p2660 N85-26413
ACT applied to helicopter flight control
16 p2712 N85-26738
INPE's line imaging camera: Preliminary results
[INPE-3476-PRE/719] 16 p2787 N85-27194
Construction and analysis of a PRIZ spatial light modulator exhibiting dynamic image selection
[AD-A152318] 17 p3037 N85-28787
Spatial light modulator having a capacitively coupled photoconductor
[AD-D011646] 17 p3037 N85-28790
InP materials
[AD-A152341] 17 p3043 N85-28828
Mass spectrometry technology at the Jet Propulsion Laboratory (JPL) 18 p3157 N85-29552
Digital Optical Circuit Technology
[AGARD-CP-362] 18 p3185 N85-29757
Optical modulators and bistable devices using molecular gases 18 p3186 N85-29761
Integrated electrooptical components using dielectric substrates 18 p3187 N85-29767
The potential of semiconductors for optical integrated circuits 18 p3187 N85-29768
Picosecond photoconductive devices for 10 Gbit/s optoelectronic switching 18 p3187 N85-29770
Electro-optic techniques for VLSI interconnect
18 p3188 N85-29774
The vector magnetograph of the Sayan Solar Observatory 18 p3206 N85-29887
A study of reflex optoelectronic switching matrices and their derivatives
[CRC-TN-720] 19 p3253 N85-30169
Experimental demonstration of an optoelectronic switch matrix for satellite-switched TDMA signals in the 0.3-4.0 GHz band
[CRC-TN-717] 19 p3253 N85-30170
Strained-layer-superlattice optoelectronic devices
[DE85-009148] 19 p3377 N85-30953
Advanced simulator for pilot training and helmet-mounted visual display configuration comparisons
[AD-A155326] 21 p3667 N85-32776
System for electro-optical ceramic recrystallization
21 p3682 N85-32872
Transformation of charged particle beams by concentrating electro-optical systems
21 p3690 N85-32925
Conceptual design and analysis of high-speed electronic imaging
[LA-10072-MS] 22 p3758 N85-33292
Influence of edge effects on performance of electrooptical lens 22 p3770 N85-33366
Design of electrooptical system with annular cathode and electrostatic compressor 22 p3770 N85-33367
USSR report: Electronics and electrical engineering
[JPRS-UEE-84-003] 22 p3773 N85-33381
Electro-optic harmonic conversion to switch a laser beam out of a cavity
[DE85-011619] 22 p3790 N85-33483
Differentiating spatial light modulator
[AD-D011727] 23 p3973 N85-34632

ELECTROACOUSTIC TRANSDUCERS
NT HYDROPHONES
NT LOUDSPEAKERS
NT MICROPHONES
Electromagnetic-acoustic-transducer e system for thick-weld inspection
[PB84-219492] 01 p0051 N85-10336
An automated immittance measuring system for electroacoustic transducers
[AD-A145701] 02 p0200 N85-11338
Acoustic transducers for fast reactor instrumentation
[BLL-RISLEY-TR-4979-(9091.3F)]
07 p0961 N85-16091
Lightweight, broadband Rayleigh wave transducer
[AD-D011345] 07 p1037 N85-16584
Method and apparatus for detecting acoustic emissions from metal matrix wire
[AD-D011556] 12 p1927 N85-22107
Electroacoustical imaging technique for encoding incoherent radiance fields as Gabor elementary signals
[NASA-TM-86372] 13 p2094 N85-23067
High-frequency acoustic variability in the arctic
[AD-A150550] 13 p2155 N85-23383
Piezoelectric and electrostatic polymeric transducers for acoustic emission detection
[AD-A150883] 14 p2306 N85-24272
System of phase-lock automatic frequency control with acoustoelectronic convolver 15 p2526 N85-25573
Acoustic imaging systems (for robotic object acquisition)
[AD-A154043] 19 p3351 N85-30772
The moving thermoacoustic array: A theoretical feasibility study
[AD-A154510] 21 p3699 N85-32980

ELECTROACOUSTIC WAVES
Bragg reflection of surface electroacoustic shear waves 04 p0485 N85-13096
Electroacoustical imaging technique for encoding incoherent radiance fields as Gabor elementary signals
[NASA-TM-86372] 13 p2094 N85-23067

ELECTROANESTHESIA
Electroanesthesia as a means of controlling cold stress of local hypothermia 22 p3823 N85-33687

ELECTROCARDIOGRAMS
U ELECTROCARDIOGRAPHY

ELECTROCARDIOGRAPHY
Frequency and nature of electrocardiographic disturbances in dogs during single and repeated exposure to +G sub z accelerations 01 p0092 N85-10619
Changes in the impedance and bioelectrical activity of the cerebral cortex of rats under the action of anaesthetic drugs
[HSE-TRANS-10371] 19 p3327 N85-30617
Three-dimensional ballistocardiography in microgravity
20 p3510 N85-31818

ELECTROCATALYSTS
Phosphoric and electric utility fuel cell technology development
[NASA-CR-174215] 06 p0805 N85-15124
Electrocatalysis research
[NASA-CR-174352] 10 p1437 N85-19054
Preparation and evaluation of advanced catalysts for phosphoric acid fuel cells
[NASA-CR-168223] 10 p1508 N85-19511
Oxygen evolution on NiCo2O4 electrodes
17 p2924 N85-29026
Molten carbonate fuel cell cathode material development
[DE85-010268] 18 p3081 N85-29057
Regenerative fuel cell systems for space station
20 p3443 N85-31372
Method of preparing thin porous sheets of ceramic material
[DE85-006399] 24 p4082 N85-35300

ELECTROCHEMICAL CELLS
NT ALKALINE BATTERIES
NT ELECTRIC BATTERIES
NT FUEL CELLS
NT LEAD ACID BATTERIES
NT LITHIUM SULFUR BATTERIES
NT NICKEL CADMIUM BATTERIES
NT NICKEL HYDROGEN BATTERIES
NT NICKEL ZINC BATTERIES
NT PHOSPHORIC ACID FUEL CELLS
NT PRIMARY BATTERIES
NT REDOX CELLS
NT REGENERATIVE FUEL CELLS
NT SILVER HYDROGEN BATTERIES
NT SODIUM SULFUR BATTERIES
NT STORAGE BATTERIES
NT THERMAL BATTERIES
NT ZINC-BROMIDE BATTERIES
NT ZINC-CHLORINE BATTERIES
Advanced nickel-hydrogen cell configuration study
[NASA-CR-174775] 01 p0067 N85-10444
Effects of additives and KOH electrolyte concentration on dissolution of iron electrodes
[DE84-014840] 02 p0173 N85-11102
Method of making a porous carbon cathode: A porous carbon cathode so made, and electrochemical cell including the porous carbon cathode
[AD-D011243] 02 p0195 N85-11301
Research on photoelectrochemical cells based on CdSe, CdSe/sub 1-x/Te/sub x and other photoelectrode materials
[DE84-004527] 02 p0224 N85-11466
Investigation of materials for inert electrodes in aluminum electrodeposition cells
[DE84-015036] 05 p0617 N85-13947
High capacity inorganic oxyhalide electrochemical cell
[AD-D011321] 07 p0923 N85-15845
Voltammetry and coulometry with immersed thin layer electrodes. Part 2: Practical considerations and experimental results
[AD-A148656] 08 p1159 N85-17314
Continuous organic electrochemical synthesis
[DE85-001400] 10 p1437 N85-19057
Development of a low cost electrochemical CO monitor based on anodic scanning voltammetry in nonaqueous electrolyte
[PB85-113488] 11 p1637 N85-20314
Electrochemical cell to measure corrosion rates in noncondensing environments
[DE85-003148] 12 p1807 N85-21338
Portable electrochemical cell interrogator
[DE85-005186] 13 p2065 N85-22901
Influence of uncompensated solution resistance upon the evaluation of rate constants for rapid electrochemical reactions
[AD-A150657] 14 p2250 N85-23942
Cycling performance of the iron-chromium redox energy storage system
[NASA-TM-87034] 16 p2819 N85-27387
Research on electrochemical photovoltaic cells
[DE85-008775] 18 p3131 N85-29392
Consolidated fuel reprocessing program
[DE85-010591] 19 p3358 N85-30818
Method for determining the point of zero zeta potential of semiconductor
[NASA-CASE-LAR-12993-1] 19 p3373 N85-30923
Multikilowatt hydrogen-nickel oxide battery system
20 p3443 N85-31373
Improvements in safety testing of lithium cells
20 p3444 N85-31379
Design evaluation of high reliability lithium batteries
20 p3444 N85-31380
RAY-O-VAC BR2325 lithium carbon monofluoride cell performance 20 p3444 N85-31382
Safety of Li-SOCl2 cells 20 p3444 N85-31383
Polymer blends for use in photoelectrochemical cells for conversion of solar energy to electricity
[DE85-011602] 22 p3752 N85-33256
Electrochemical methane sensor
[DE85-011683] 22 p3787 N85-33464
Stable n-CuInSe/sub 2/iodide-iodine photoelectrochemical cell
[DE85-011597] 22 p3806 N85-33576
Experimental evaluation of the thermodynamic properties of concentrated aqueous potassium hydroxide solutions
[DE85-010628] 23 p3912 N85-34236

ELECTROCHEMICAL CORROSION
The modification of metallic corrosion by ion implantation: Engineering applications and fundamental studies
[AD-P003954] 02 p0286 N85-11870
Corrosion of a zinc rotating disk in one molar hydrochloric acid
[DE84-015974] 04 p0474 N85-13015
Electrochemical pitting evaluation of aluminum alloy 7075 in machining coolant
[DE84-016844] 04 p0475 N85-13026
Research approaches to qualify aluminum for Ocean Thermal Energy Conversion (OTEC) systems
[DE84-013007] 04 p0476 N85-13034
Interactions between corrosion and creep of uncoated and coated superalloys in sulfate melts
04 p0477 N85-13033
Predicting electrochemical breakdown in terrestrial photovoltaic modules 06 p0830 N85-15273
On-line monitoring of the true corrosion rate in problems related to power plants
[CISE-2335] 09 p1131 N85-17126
An electrochemical study of the corrosion behavior of primer coated 2219-T87 aluminum
[NASA-TP-2459] 13 p2021 N85-22662
Localized corrosion currents from graphite/aluminum and welded SiC/Al metal matrix composites
[AD-A150988] 14 p2256 N85-23080
Theoretical and experimental comparisons of nearfield electrogalvanic fields due to nonlinear polarization layers
[AD-A152085] 16 p2779 N85-27149
Electrical research on solar cells and photovoltaic materials
[NASA-CR-175897] 17 p2986 N85-28452
Marine corrosion
[AD-A153843] 18 p3074 N85-29012
Theoretical modelling of the electro-chemistry in a corrosion fatigue crack. Part 2: Mathematical aspects of associated unsteady reaction equations
[NPL-DMA(A)-100-PT-2] 20 p3465 N85-31529
Theoretical aspects of corrosion and practical implications for aircraft and related systems
22 p3749 N85-33240
Corrosion fatigue strength and crack growth in prestrained 0.18% C carbon steel
23 p3905 N85-34192

ELECTROCHEMICAL MACHINING
Simulation of the electrochemical machining process
[DE85-003797] 11 p1616 N85-20159

Role of residual stresses in stress corrosion cracking in alloy 600 tubes. Part 1: Determination of throughwall residual stresses and their modification by transient heat treatment
[DE85-004648] 14 p2257 N85-23988
Electrolytic cell
[DE85-011598] 22 p3807 N85-33578

ELECTROCHEMICAL OXIDATION

Two silicon phthalocyanines and a silicon naphthalocyanine: Synthesis, electrochemistry and electrogenerated chemiluminescence
[AD-A144780] 01 p0023 N85-10145
The concept of doping of conducting polymers. The role of reduction potentials
[AD-A145480] 02 p0186 N85-11243
Electrochemistry at very high potentials: The use of ultramicroelectrodes in the anodic oxidation of short chain alkanes
[AD-A148654] 08 p1123 N85-17078
Homogeneous reaction involving components of different redox couples. 1: Theoretical considerations and digital simulation
[AD-A148666] 08 p1124 N85-17084
Polymeric electrolytes for ambient temperature lithium batteries
[DE85-001032] 12 p1835 N85-21518
Diagrams of chemical and electrochemical equilibria in the presence of oxygen and sulphur
[AD-A150929] 14 p2251 N85-23953
Resistance of polyaniline films as a function of electrochemical potential and the fabrication of polyaniline-based microelectronic devices
[AD-A154999] 21 p3569 N85-32201

ELECTROCHEMISTRY

NT COULOMETRY
NT ELECTROLYSIS
NT PHOTOELECTROCHEMISTRY

An electrochemical approach to the prevention of biofouling phenomena
[PB84-202613] 01 p0025 N85-10155
Preparation and properties of single crystals of hydrogen bis(phthalocyaninato) neodymium(3)
[AD-A144933] 01 p0123 N85-10646
The driving-force dependence of electrochemical rate parameters: Origins of anodic-cathodic asymmetries for metal aquo redox couples
[AD-A145605] 02 p0172 N85-11153
Kinetics of simple inner- and outer-sphere electrochemical reactions at rotating silver electrodes as examined using surface-enhanced Raman spectroscopy
[AD-A145606] 02 p0172 N85-11154
Surface environmental effects in electrochemical kinetics: Outer-sphere chromium(3) reductions at mercury, gallium, lead, and thallium surfaces
[AD-A145607] 02 p0172 N85-11155
Solvent effects upon electrochemical kinetics: Influences of interfacial solvation and solvent relaxation dynamics
[AD-A145624] 02 p0173 N85-11156
An electrochemical study of hydrogen uptake and elimination by bare and gold-plated waspaloy
[NASA-TM-86479] 02 p0182 N85-11222
Method of making a porous carbon cathode: A porous carbon cathode so made, and electrochemical cell including the porous carbon cathode
[AD-D011243] 02 p0195 N85-11301
Electrochemistry of rare-earth diphthalocyanines
[AD-A145813] 03 p0327 N85-12106
Feasibility of the electrochemical method of determining nitrogen content in metallic melts
[BLL-M-35730-(5828.4)] 03 p0330 N85-12124
Related studies to cathodic protection of reinforced concrete structures
[PB84-218114] 03 p0333 N85-12145
Electrochemical and surface science research on fuel cells
[DE84-015982] 03 p0359 N85-12307
NASA Redox Storage System Development Project
[NASA-TM-83677] 03 p0365 N85-12465
Electrochemical investigations of novel electrode materials
[DE84-014352] 04 p0495 N85-13158
Electrochemistry and storage
05 p0609 N85-13689
The electrochemical deoxidation of molten oxide substances
[BLL-M-35982-(5828.4)] 05 p0614 N85-13920
Chemically modified electrodes and related solution chemistry
[DE84-017110] 05 p0614 N85-13924
USSR report: Chemistry
[JPRS-UCH-84-012] 06 p0761 N85-14865
Electrochemical behaviour of TiCl4 solutions in low melting point organic media
[BLL-OA-TRANS-3174-(6196.3)]
06 p0764 N85-14888
Space charge, interfacial kinetics, and electrical response of condensed matter
[AD-A146364] 06 p0765 N85-14893
Electrochemistry in near-critical and supercritical fluids. I. Ammonia
[AD-A146429] 06 p0765 N85-14894
A silicon phthalocyanine and a silicon naphthalocyanine: Synthesis, electrochemistry, and electrogenerated chemiluminescence
[AD-A146441] 06 p0765 N85-14895
Proceedings of the 23rd Project Integration Meeting
[NASA-CR-174186] 06 p0829 N85-15260
Electrochemical production of silicon
06 p0832 N85-15290
High capacity inorganic oxyhalide electrochemical cell
[AD-D011321] 07 p0923 N85-15845
Correlation of electronic charge transfer transitions and electrochemical potentials. The Bipyrazine(Tetracarbonyl)Molybdenum(O) system in various solvents
[AD-A147660] 08 p1120 N85-17062
Estimation of the rate of electron transfers between 2 contacting polymer surfaces
[AD-A148416] 08 p1122 N85-17072
Electrochemistry at very high potentials: The use of ultramicroelectrodes in the anodic oxidation of short chain alkanes
[AD-A148654] 08 p1123 N85-17078
The construction and behaviour of ultramicroelectrodes: investigations of novel electrochemical systems
[AD-A148656] 08 p1123 N85-17079
Subtractively normalized interfacial Fourier transform infrared spectroscopy of difluorobenzene adsorbed at polycrystalline platinum electrodes
[AD-A148660] 08 p1123 N85-17080
Electrochemical features of the ferric sulfate leaching of CuFeS2/C aggregates
[AD-A148661] 08 p1123 N85-17081
The adsorption of acrylonitrile at a gold electrode: An EMIRS measurement of the electrochemical stark effect
[AD-A148664] 08 p1123 N85-17082
Modulated surface vibrational spectroscopies at electrode/electrolyte interfaces
[AD-A148665] 08 p1123 N85-17083
Homogeneous reaction involving components of different redox couples. 2: Polarographic studies of the interactions of alkali metal cations with anthracene and fluoranthene dianions in N,N-dimethylformamide and acetonitrile
[AD-A148667] 08 p1124 N85-17085
Application of electrochemical engineering methods and theory to solving corrosion and adhesion problems with organic coatings
[AD-A147799] 08 p1129 N85-17115
Electrochemistry of polymer films. Applications to chemical analysis and energy conversion
[AD-A147737] 08 p1132 N85-17136
The kinetics of electron transfer reactions in and at films of electroactive polymers
[AD-A148597] 08 p1134 N85-17149
Voltammetry and coulometry with immersed thin layer electrodes. Part 1: Model for effects of solution resistivity in linear sweep voltammetry
[AD-A148655] 08 p1159 N85-17313
Voltammetry and coulometry with immersed thin layer electrodes. Part 2: Practical considerations and experimental results
[AD-A148656] 08 p1159 N85-17314
Electrochemical interfaces and electrode processes
[AD-A147414] 09 p1290 N85-18098
Electrocatalysis research
[NASA-CR-174352] 10 p1437 N85-19054
Continuous organic electrochemical synthesis
[DE85-001400] 10 p1437 N85-19057
Positive electrodes of nickel-cadmium batteries
[NASA-TM-77808] 10 p1478 N85-19330
Bioelectrochemistry 2: Membrane phenomena
[AD-A149132] 10 p1522 N85-19602
Semiconductor electrochemistry approach to the study of oxide films on nickel electrodes
[DE85-003042] 11 p1630 N85-20264
Development of a low cost electrochemical CO monitor based on stripping voltammetry
[PB85-113470] 11 p1637 N85-20312
Electrochemistry and electrochemical methodology in molten salts
[AD-A149613] 12 p1799 N85-21284
Electrochemical processes at the sodium (BETA)'' alumina interface
[DE85-004653] 12 p1802 N85-21305
In situ monitoring of electrochemical reactions by surface enhanced Raman scattering
[PB85-149789] 12 p1803 N85-21312
Hydrogen embrittlement of cadmium-plated ultra-high strength steels in paint strippers
[ARL/MAT-R-117] 12 p1806 N85-21326
Stress corrosion cracking behavior of tungsten heavy alloys
[AD-A149843] 12 p1806 N85-21329
Application of modulated hydrodynamic voltammetry to the study of anodic electrocatalysis
[DE85-004182] 13 p2018 N85-22653
Local electrochemistry of pitting corrosion in stainless steels
[DE85-005207] 13 p2023 N85-22673
Studies of electrical properties of surface films and localization during electrochemical dimensional working of titanium 13 p2032 N85-22729
Raman structural studies of the nickel electrode
[NASA-CR-175619] 13 p2162 N85-23414
Ligand structural influences upon electrochemical reactivity: Organic substituent effects upon Carboxylatopentaamminecobalt(3) reductions at mercury and gold electrodes
[AD-A150685] 14 p2250 N85-23944
Evaluation of unimolecular rate constants for some outer-sphere electrochemical reactions
[AD-A150758] 14 p2250 N85-23946
USSR report: Materials science and metallurgy
[JPRS-UMS-85-004] 15 p2513 N85-25503
Electrochemical behavior of amorphous alloys based on iron, cobalt and nickel in H3PO4 solutions alone and mixed with HF 15 p2513 N85-25505
Status of French research in plastic batteries
15 p2530 N85-25603
Calcium/thionyl chloride battery technology
[AD-A151975] 15 p2586 N85-25945
Sixth DOE Electrochemical Contractor's Review. Extended abstracts
[DE84-013679] 16 p2779 N85-27151
Dual electrochemical system
[AD-D011616] 16 p2817 N85-27376
Electrochemistry of polymer films not immersed in solution: Electron transfer on an ion budget
[AD-A152989] 17 p2920 N85-27998
Localized ionic currents from a corroding iron-copper galvanic couple
[AD-A153627] 18 p3074 N85-29011
Effects of H2S on molten carbonate fuel cells
[DE85-008310] 18 p3130 N85-29386
Improved acid electrolytes for fuel cells
[PB85-178053] 18 p3132 N85-29397
Electrochemical studies in liquid crystals
[AD-A154317] 19 p3234 N85-30050
Effect of multi-functional inhibitors on the electrochemistry within corrosion crack
19 p3238 N85-30075
Lithium cell reactions
[AD-A154429] 19 p3305 N85-30484
Electrochemical reduction of titanium in dimethyl sulphoxide
[BLL-OA-TRANS-3225-(6196.300)]
20 p3429 N85-31267
Regenerative fuel cell systems for space station
20 p3443 N85-31372
System level electrochemical principles
20 p3443 N85-31375
Electrochemistry of Hexanitroazobenzene (HNAB)
[DE85-010807] 21 p3565 N85-32171
Topics in electrochemical degradation of photovoltaic modules 21 p3608 N85-32410
Characteristics of optogalvanic effect in media with inverse populations 21 p3693 N85-32944
Chemistry division report
[DE85-010566] 24 p4071 N85-35228
Electrochemical method for investigation of the susceptibility of corrosion-resistant steels to intercrystalline corrosion
[BLL-CE-TRANS-8082-(9022.09)]
24 p4077 N85-35269

ELECTROCHROMISM

Investigation of absorptive electrochemical systems for display applications
[BMFT-FB-T-84-301] 15 p2507 N85-25467
Electrochromic display device
[AD-D011733] 22 p3759 N85-33299

ELECTROCONDUCTIVITY

U ELECTRICAL RESISTIVITY

ELECTRODE FILM BARRIERS

Studies of electrical properties of surface films and localization during electrochemical dimensional working of titanium 13 p2032 N85-22729

ELECTRODE MATERIALS

Behaviour of lead-silver anodes in zinc electrodeposition from sulphuric acid baths
[BLL-MINTEK-TR-1180-(5810.5759)]
06 p0764 N85-14887
Structural studies on lead dioxides
[DE84-015837] 06 p0805 N85-15127
Preparation and evaluation of advanced catalysts for phosphoric acid fuel cells
[NASA-CR-168223] 10 p1508 N85-19511

Conductor-polymer composite electrode materials
[DE85-005766] 23 p3920 N85-34293
ELECTRODELESS DISCHARGES
Neodymium YAG laser pumped with radiation from high frequency electrodeless discharge
13 p2044 N85-22796
ELECTRODEPOSITION
NT ELECTROPLATING
Methods for producing platinum-group metal coatings from molten alkali cyanides
[PB84-225994] 01 p0029 N85-10181
Electroforming of nickel
[SNIAS-841-501-101] 04 p0484 N85-13065
Investigation of materials for inert electrodes in aluminum electrodeposition cells
[DE84-015036] 05 p0617 N85-13947
Behaviour of lead-silver anodes in zinc electrodeposition from sulphuric acid baths
[BLL-MINTEK-TR-1180-(5810.5759)]
06 p0764 N85-14887
Laser-assisted solar-cell metallization processing
06 p0831 N85-15282
The kinetics of electron transfer reactions in and at films of electroactive polymers
[AD-A148597] 08 p1134 N85-17149
Effect of rhodamine-B on the electrodeposition of lead on copper, revision
[DE85-000674] 11 p1606 N85-20101
Mechanical properties of electrodeposited nickel and copper
[DE85-005321] 13 p2023 N85-22677
Film and interstitial formation of metals in plasma-sprayed ceramics
[NASA-TM-86993] 13 p2036 N85-22756
Demonstration of feasibility of depositing semiconductor layers using microwave enhanced plasma techniques
[NASA-CR-174392] 13 p2163 N85-23421
Pulsed electrodeposition
[DE85-007057] 16 p2747 N85-26950
Electrohydrodynamic process for the production of large area polycrystalline silicon sheet
[DE85-006781] 19 p3261 N85-30225
Development of low-melting fused salts 6: Formation of molybdenum film from molten ammonium formate bath
[BLL-OA-TRANS-3195-(6196.300)]
20 p3429 N85-31264
Electrodeposition of chromium and copper in magnetic fields
[AD-A154648] 21 p3566 N85-32180
ELECTRODERMAL RESPONSE
U GALVANIC SKIN RESPONSE
ELECTRODES
NT ANODES
NT CATHODES
NT CELL ANODES
NT CELL CATHODES
NT COLD CATHODES
NT HOLLOW CATHODES
NT HOT CATHODES
NT IMPLANTED ELECTRODES (BIOLOGY)
NT ION SELECTIVE ELECTRODES
NT PHOTOCATHODES
NT PLASMA ELECTRODES
NT SHELL ANODES
NT THERMIONIC CATHODES
NT TUBE ANODES
NT TUBE CATHODES
P-doping of (CH)x to the metallic regime with gaseous oxygen. Application to oxygen fuel cell type electrodes
[AD-A145477] 02 p0186 N85-11242
The concept of doping of conducting polymers. The role of reduction potentials
[AD-A145480] 02 p0186 N85-11243
Chemical derivatization of an array of three gold microelectrodes with polypyrrole: Fabrication of a molecule-based transistor
[AD-A146221] 03 p0359 N85-12304
Photoelectrochemistry with chemically modified electrodes
[DE84-016798] 04 p0471 N85-12997
Bulletin of the Faculty of Engineering, Hokkaido University, no. 123
[ISSN-0385-602-X] 04 p0482 N85-13075
Determination of Faradaic current through a bipolar electrode in acidic bichromate 04 p0483 N85-13077
Electrochemical investigations of novel electrode materials
[DE84-014352] 04 p0495 N85-13158
Chemically modified electrodes and related solution chemistry
[DE84-017110] 05 p0614 N85-13924
Investigation of materials for inert electrodes in aluminum electrodeposition cells
[DE84-015036] 05 p0617 N85-13947
Optimization of toughness properties of HSCA shielded metal arc welding electrodes
[BMFT-FB-T-84-186] 05 p0646 N85-14148
Photoluminescent and electroluminescent properties of Cd sub 0.95 Mn sub 0.05 Se electrodes
[AD-A146775] 07 p0946 N85-15995
Microwave resonator using lateral excitation
[AD-D011374] 07 p1039 N85-16596
Potential dependence of electrical conductivity and chemical charge storage of poly(pyrrole) films on electrodes
[AD-A148513] 08 p1122 N85-17075
The construction and behaviour of ultramicroelectrodes: Investigations of novel electrochemical systems
[AD-A148658] 08 p1123 N85-17079
Subtractively normalized interfacial Fourier transform infrared spectroscopy of difluorobenzene adsorbed at polycrystalline platinum electrodes
[AD-A148660] 08 p1123 N85-17080
The adsorption of acrylonitrile at a gold electrode: An EMIRS measurement of the electrochemical stark effect
[AD-A148664] 08 p1123 N85-17082
Modulated surface vibrational spectroscopies at electrode/electrolyte interfaces
[AD-A148665] 08 p1123 N85-17083
Voltammetry and coulometry with immersed thin layer electrodes. Part 1: Model for effects of solution resistivity in linear sweep voltammetry
[AD-A148655] 08 p1159 N85-17313
Voltammetry and coulometry with immersed thin layer electrodes. Part 2: Practical considerations and experimental results
[AD-A148656] 08 p1159 N85-17314
Electrodes for repairing power engineering equipment made from creep resisting steel
[BLL-CE-TRANS-8064-(9022.09)]
08 p1167 N85-17360
Electric utility acid fuel cell stack technology advancement
[NASA-CR-174804] 08 p1178 N85-17422
Electrochemical interfaces and electrode processes
[AD-A147414] 09 p1290 N85-18098
A two photoelectrode solid-state photoelectrochemical cell
[AD-A148982] 10 p1434 N85-19038
Production method of nickel electrode
[NASA-TM-76946] 10 p1439 N85-19069
Method of producing nickel electrode
[NASA-TM-76944] 10 p1440 N85-19077
Study of surface damage in cathode composite materials in a high flux CO2 laser 10 p1444 N85-19098
Positive electrodes of nickel-cadmium batteries
[NASA-TM-77806] 10 p1478 N85-19330
Thermionic converter for space reactor described
11 p1621 N85-20208
Semiconductor electrochemistry approach to the study of oxide films on nickel electrodes
[DE85-003042] 11 p1630 N85-20264
High-temperature, solid oxide electrolyte fuel cell power generation system
[DE85-002978] 11 p1675 N85-20552
Carbon monoxide adsorption on a platinum electrode studied by polarization modulated FT-IRRAS (Fourier Transform-IR Reflection Adsorption Spectroscopy). Part 1: CO adsorbed in the double layer potential region and its oxidation in acids
[AD-A149751] 12 p1800 N85-21288
Electrochemical processes at the sodium (BETA)" alumina interface
[DE85-004653] 12 p1802 N85-21305
Solar-assisted hydrogen generation by photoelectrocatalysis
[PB85-149706] 12 p1804 N85-21314
Suspension torques on a gimballed electrostatically supported gyroscope and requirements on the gyroscope and spacecraft for the relativity gyroscope experiment
12 p1851 N85-21608
EXAFS of monolayers on silver electrodes: SSRL proposal number 717M
[AD-A150623] 13 p2018 N85-22652
Applications of the vibration probe to localized current measurements
[DE85-004702] 13 p2023 N85-22675
Electrodynamic stability of composite liquid-metal contacts 13 p2087 N85-23031
Molten carbonate fuel cell performance model update, draft
[DE85-005423] 13 p2129 N85-23252
Raman structural studies of the nickel electrode
[NASA-CR-175619] 13 p2162 N85-23414
Erosion of electrodes due to switching of capacitor-bank discharge circuits
[AD-A151207] 15 p2547 N85-25718
Numerical modeling of gas dynamic phenomena during supersonic flow of viscous gas in channel with electrical flow discharge 15 p2643 N85-26304
Material for electrodes of pulsed and arc sources of light
[DE85-007453] 16 p2780 N85-27156
Method of fabricating material for the electrodes of gas discharge devices
[DE85-007452] 16 p2780 N85-27157
Investigation of pseudo bi-polar nickel cadmium batteries as filter elements for pulsed power loads
[AD-A152112] 16 p2819 N85-27389
Electrochemistry of polymer films not immersed in solution: Electron transfer on an ion budget
[AD-A152969] 17 p2920 N85-27998
The behaviour of nitride inclusions in nickel-base alloys
[BLL-BISI-TRANS-22396-(9022.05)]
17 p2927 N85-28058
Spark gap electrode erosion
[AD-A152802] 17 p2953 N85-28237
Electrodes for flash discharge lamps
[DE85-008897] 17 p2955 N85-28250
Electrode for flash discharge lamps
[DE85-008896] 17 p2955 N85-28252
Electrogenerated chemiluminescence
[AD-A153547] 18 p3070 N85-28990
Localized ionic currents from a corroding iron-copper galvanic couple
[AD-A153827] 18 p3074 N85-29011
Electrical line source and point source interactions with anomalies in the ground
[DE85-009777] 18 p3095 N85-29161
Trace water sensor
[NASA-CASE-NPO-15722-1] 18 p3103 N85-29212
Electrochemical and morphological study of the effect of temperature on the restructuring and loss of capacity of alkaline battery electrodes
[DE85-006669] 18 p3129 N85-29378
Energizing arrangement for charge coupled device control electrodes
[AD-D011712] 19 p3261 N85-30220
Gyrotron traveling-wave device including quarter wavelength anti-reflective dielectric layer to enhance microwave absorption
[AD-D011600] 19 p3271 N85-30285
High discharge rate characteristics of nickel-cadmium batteries for pulse load filtering
20 p3448 N85-31391
Nickel hydrogen bipolar battery electrode design
20 p3447 N85-31402
The failure mechanism of a nickel electrode in a nickel-hydrogen cell 20 p3448 N85-31408
Operation of the Zeiss cytopherometer with Zn/ZnSO4 electrode system of Tenforde et al
20 p3499 N85-31752
Thermal contraction of current flow through electrode turbulent boundary layer 21 p3690 N85-32926
Recent advances in d-c relaxation techniques for the measurement of kinetics of fast electrode reactions
[DE85-005029] 22 p3745 N85-33216
Transparent electrode for optical switch
[DE85-011618] 22 p3761 N85-33310
Integrated current collector and catalyst support
[DE85-011616] 22 p3761 N85-33311
Model that predicts pulse charged gas switching breakdown phenomena
[DE85-013119] 22 p3761 N85-33313
Electrochemical methane sensor
[DE85-011663] 22 p3787 N85-33484
Stable n-CuInSe/sub 2/iodide-iodine photoelectrochemical cell
[DE85-011597] 22 p3806 N85-33576
Accelerator vibration issues
[DE85-010766] 22 p3842 N85-33791
Electrode erosion in arc discharges at atmospheric pressure
[NASA-TM-87067] 23 p3903 N85-34178
Experimental evaluation of the thermodynamic properties of concentrated aqueous potassium hydroxide solutions
[DE85-010628] 23 p3912 N85-34238
Conductor-polymer composite electrode materials
[DE85-005766] 23 p3920 N85-34293
Nonsaturable microdryer
[DE85-005760] 23 p3946 N85-34457
Negative ion sources equipped with continuous annular and spherical geometry surface ionizers
[DE85-011939] 23 p3971 N85-34619
Thermodynamics of the corrosion of chromium in molten carbonates
[DE85-011407] 24 p4079 N85-35282
Method of preparing thin porous sheets of ceramic material
[DE85-006399] 24 p4082 N85-35300
Development of electrodes for the NASA iron/chromium
[NASA-CR-174724] 24 p4109 N85-35471

ELECTRODIALYSIS
An evaluation of the electrodialysis reversal process (Edr) for the desalination of brackish water from the Omaruru delta (SWA/Namibia)
01 p0023 N85-10141
Research and development work on a single cation specific membrane for the recovery of raw materials with electrodialysis
[BMFT-FB-T-84-163] 03 p0329 N85-12120

ELECTRODYNAMICS
NT ELECTROHYDRODYNAMICS
NT ELECTROMECHANICS
NT QUANTUM ELECTRODYNAMICS
Proceedings of a Workshop on the Applications of Tethers in Space, Volume 1
[NASA-CR-171196] 03 p0322 N85-12076
Proceedings of a Workshop on Applications of Tethers in Space, Volume 2
[NASA-CR-171197] 03 p0322 N85-12077
Short-period seismograph SVSN-6
[REPT-554] 03 p0376 N85-12397
Laboratory electron beam simulation of cosmic radio jets
[DE84-016179] 04 p0590 N85-13764
Electrodynamic tethers. 1: Power generator in LEO. 2: Thrust for propulsion and power storage
05 p0611 N85-13901
Analysis of flat finite antenna consisting of waveguide radiators 06 p0790 N85-15048
The investigation of tethered satellite system dynamics
[NASA-CR-171278] 07 p0912 N85-15772
Science Applications, part 1 11 p1643 N85-20346
Electrodynamic interactions 11 p1643 N85-20348
Transportation applications, part 1
11 p1643 N85-20349
Summary presentation of the Science Applications Panel 11 p1644 N85-20355
Summary presentation of the Electrodynamics Interactions Panel 11 p1644 N85-20356
Applications of Tethers in Space, volume 2
[NASA-CP-2365] 11 p1644 N85-20361
Report of the Electrodynamic Interactions Panel
11 p1645 N85-20363
Report of the Transportation Panel
11 p1645 N85-20364
Report of the Technology and Test Panel
11 p1646 N85-20370
MAP activities in Hungary 11 p1657 N85-20440
Spacecraft Environmental Interactions Technology, 1983
[NASA-CP-2359] 13 p1989 N85-22470
Preliminary investigation of the electrodynamics of a conducting tether 13 p1997 N85-22521
Elasticity formulas for thin-walled shells with piezoceramic layers 13 p2047 N85-22816
Electrodynamic stability of composite liquid-metal contacts 13 p2087 N85-23031
Synthesis of optimum smooth transition in microstrip through line on microwave integrated circuit
13 p2089 N85-23041
Particle shape characterization
[AD-A151981] 15 p2544 N85-25707
The gravito-electrodynamics of charged dust in planetary ring systems 15 p2677 N85-26531
Ultrasonic testing of tubes
[BLL-BISI-TRANS-22337-(9022.06)]
16 p3118 N85-29304
Electrodynamic transducers for ultrasonic reception
16 p3119 N85-29306

ELECTRODYNAMOMETERS
U DYNAMOMETERS

ELECTROENCEPHALOGRAM
U ELECTROENCEPHALOGRAPHY

ELECTROENCEPHALOGRAPHY
Kolmogorov-Smirnov goodness-of-fit test: Corrected for use with EEG-like data
[AD-A144711] 01 p0110 N85-10745
Evidence for multiple areas in the human auditory cortex
[AD-A146086] 03 p0401 N85-12555
In search of a visual-cortical describing function: A summary of work in progress 05 p0707 N85-14538
Visual evoked potentials with disrupted functioning of nonspecific cerebral systems 07 p1013 N85-16437
Neurocognitive pattern analysis of an auditory and visual numeric motor control task. Part 1: Development of methods
[AD-A148809] 09 p1364 N85-18578
Effects of partial deprivation of slow-wave sleep on sleep-wakefulness cycles 10 p1524 N85-19613
Psychological aspects of phenomenon of spatial synchronization of EEG potential
11 p1661 N85-20632
Functional significance of some EEG parameters and dominant principle 11 p1691 N85-20634
Thermoregulatory and vestibular systems in the rat
15 p2610 N85-26082
Measurement and modification of sensory system EEG (electroencephalographic) characteristics during visual-motor performance
[AD-A151901] 15 p2618 N85-26133
A communications link for an implantable electrode array
[AD-A152238] 16 p2840 N85-27510
The origin of brain potentials associated with selective visual attention
[AD-A152291] 16 p2840 N85-27511
Changes in the impedance and bioelectrical activity of the cerebral cortex of rats under the action of anaesthetic drugs
[HSE-TRANS-10371] 19 p3327 N85-30617
Resource allocation in cerebral specialization of function: Behavioral and electrophysiological studies
[AD-A155092] 21 p3664 N85-32759

ELECTROEPITAXY
Producing gallium arsenide crystals in space
02 p0151 N85-11023

ELECTROEROSION
U SPARK MACHINING

ELECTROEXPLOSIVE DEVICES
U INITIATORS (EXPLOSIVES)

ELECTROFORMING
Electroforming of nickel
[SNIAS-841-501-101] 04 p0484 N85-13085
Study of high performance alloy electroforming
[NASA-CR-174276] 07 p0927 N85-15875
Study of high performance alloy electroforming
[NASA-CR-175494] 11 p1596 N85-20040
Study of high performance alloy electroforming
[NASA-CR-175741] 15 p2508 N85-25473

ELECTROGENERATORS
U ELECTRIC GENERATORS

ELECTROHYDRAULIC CONTROL
U ELECTRIC CONTROL
U HYDRAULIC CONTROL

ELECTROHYDRAULIC FORMING
Results of an interlaboratory fatigue test program conducted on alloy 800H at room and elevated temperatures
[NASA-CR-174940] 21 p3597 N85-32340

ELECTROHYDRODYNAMICS
IMS advances in studies of field-aligned currents and their related electrodynamics 14 p2359 N85-24578
Electrodynamics of magnetosphere-ionosphere coupling 14 p2359 N85-24579
Characteristics of the electrodynamics of auroral arcs as inferred from rocket and ground-base observations during IMS 14 p2363 N85-24601
Ac field-induced order in dense colloidal systems
[DE85-009107] 17 p2935 N85-28119
A new theory aiming to define the mechanisms of material removal in electroerosion
[NASA-TM-77875] 18 p3176 N85-29689
Electrohydrodynamic process for the production of large area polycrystalline silicon sheet
[DE85-008781] 19 p3261 N85-30225
Electrodynamic tether 23 p3902 N85-34168
Elastohydrodynamic lubrication calculations used as a tool to study scuffing
[NASA-TM-87097] 23 p3938 N85-34408

ELECTROJETS
NT AURORAL ELECTROJETS
NT EQUATORIAL ELECTROJET
Periodic substorm activity in the geomagnetic tail
[NASA-CR-175629] 13 p2161 N85-23409

ELECTROKINETICS
Electrokinetic potential and stability of SiC suspensions in electrolyte solutions
[NASA-TM-77492] 04 p0469 N85-12984
Zeta potential in ceramic industry
[NASA-TM-77478] 04 p0478 N85-13047
Circulation and internal waves in a cold Gulf Stream wave
[AD-A149704] 12 p1898 N85-21918
Pre-flight report on cultured human embryonic kidney cell handling and cell electrophoresis. Prepared prior to continuous-flow electrophoretic separation experiments aboard space shuttle flight STS-8
20 p3503 N85-31775

ELECTROLESS DEPOSITION
Low temperature deposition of nickel films
[AD-D011568] 12 p1805 N85-21319

ELECTROLUMINESCENCE
Brightness comparison of electroluminescent versus incandescent lighting: A photometric validation
[AD-A145395] 02 p0280 N85-11822
Luminescent properties of graded cadmium sulfoselenide electrodes prepared from cadmium sulfide substrates
[AD-A146710] 06 p0766 N85-14898
Photoluminescent and electroluminescent properties of Cd sub 0.95 Mn sub 0.05 Se electrodes
[AD-A146775] 07 p0946 N85-15995
Research on electroluminescence in thin film yttrium oxysulfide
[AD-A146909] 07 p1037 N85-16582

ELECTROLUMINESCENT LAMPS
U ELECTROLUMINESCENCE
U LUMINAIRES

ELECTROLYSIS
NT COULOMETRY
Solid electrolytes for medium temperature steam electrolysis
[DE84-014384] 04 p0463 N85-12938
High-temperature steam electrolysis: Technical and economic evaluation of alternative process designs
[DE84-015702] 04 p0469 N85-12986
Photoelectrochemistry with chemically modified electrodes
[DE84-016798] 04 p0471 N85-12997
Measurement of oxide ion concentration in NaCl-ZnCl2 molten salt and several applications
[BLL-AWRE-TRANS-74-(9091.9F)]
06 p0764 N85-14886
Electrolytic deposition of chromium from aqueous chromium solutions containing foreign anions
[BLL-MINTEK-TR-1170-(5810.5759)]
06 p0764 N85-14889
Study of the liquid vapor equilibrium in the bromine-hydrobromic acid-water system
[NASA-TM-77787] 07 p0921 N85-15836
Engineering model system study for a regenerative fuel cell: Study report
[NASA-CR-174801] 07 p0991 N85-16292
Hydrogen from solar energy
[DE85-001914] 10 p1437 N85-19055
Electrolysis of simulated lunar melts
15 p2681 N85-26561
Ohmic potential drop and gas bubble radius distribution in alkaline water electrolysis 17 p2924 N85-28025
Oxygen evolution on NiCo2O4 electrodes
17 p2924 N85-28026
Corrosion characteristics of some steels produced through a self-cleaning rotating electrode
[BLL-BISI-TRANS-22046-(9022.06)]
17 p2925 N85-28034
Feasibility of electrolytic hydrogen production in the Pacific Northwest
[DE85-009656] 18 p3084 N85-29060
Photoeffects of semiconductor electrolyte interfaces
[AD-A154163] 20 p3449 N85-31411
High temperature solar electrothermal processing 2. Zinc from zinc oxide
[AD-A154747] 21 p3562 N85-32159
Electrolytic cell
[DE85-011598] 22 p3807 N85-33578
Electrolytic synthesis of colored eta alumina film
23 p3906 N85-34201
Deposition of nickel-cobalt alloys by controlled-potential electrolysis
[PB85-198562] 24 p4081 N85-35291

ELECTROLYTE METABOLISM
Voluntary dehydration and electrolyte losses during prolonged exercise in the heat
[AD-A145157] 01 p0095 N85-10639
Analysis of head-down tilt as an analog of weightlessness using a mathematical simulation model
[NASA-CR-171870] 15 p2616 N85-26118
The behavior of renal-regulating hormones during hypogravic stress
[NASA-CR-171877] 15 p2616 N85-26123
Fluid-electrolyte responses during prolonged space flight: A review and interpretation of significant findings
[NASA-CR-171878] 15 p2617 N85-26124
Mathematical modeling of fluid-electrolyte alterations during weightlessness
[NASA-CR-171881] 15 p2617 N85-26125
Evaluation of a field expedient technique for sweat sample collection
[AD-A151916] 16 p2841 N85-27521
Fluid-electrolyte metabolism and renal function in cosmonauts following 185-day spaceflight
23 p3952 N85-34495

ELECTROLYTES
NT ION EXCHANGE MEMBRANE ELECTROLYTES
NT MOLTEN SALT ELECTROLYTES
NT NONAQUEOUS ELECTROLYTES
NT SOLID ELECTROLYTES
Influence of parameters of alumimun alloy anodizing process on oxide coating thickness
01 p0018 N85-10113
Methods for producing platinum-group metal coatings from molten alkali cyanides
[PB84-225994] 01 p0029 N85-10161
Advanced fuel cell development
[DE84-014847] 01 p0044 N85-10289

Voluntary dehydration and electrolyte losses during prolonged exercise in the heat
[AD-A145157] 01 p0095 N85-10639
Effects of additives and KOH electrolyte concentration on dissolution of iron electrodes
[DE84-014840] 02 p0173 N85-11162
Electrochemical and surface science research on fuel cells
[DE84-015982] 03 p0359 N85-12307
Electrokinetic potential and stability of SiC suspensions in electrolyte solutions
[NASA-TM-77492] 04 p0469 N85-12984
Materials for high-temperature fuel cells
[DE84-016316] 04 p0479 N85-13054
Phosphoric and electric utility fuel cell technology development
[NASA-CR-174215] 06 p0805 N85-15124
Modulated surface vibrational spectroscopies at electrode/electrolyte interfaces
[AD-A148665] 08 p1123 N85-17083
Polymeric electrolytes for ambient temperature lithium batteries
[DE85-001032] 12 p1835 N85-21518
Research to explore the feasibility of sulfolanes as electrolytic solvents for rechargeable lithium batteries
[DE85-004345] 12 p1837 N85-21525
Development of molten carbonate fuel cell power plant technology
[DE84-016639] 14 p2352 N85-24536
Calcium/thionyl chloride battery technology
[AD-A151975] 15 p2586 N85-25945
Quantitation of Na+, K+-ATPase enzyme activity in tissues of the mammalian vestibular system
15 p2613 N85-26102
Process for clarification of water
[DE85-007864] 17 p2923 N85-28023
Investigation of the structure and dynamics of electrolytes in solvents used for primary and secondary Li-batteries
[AD-A153099] 17 p2954 N85-28240
Bifunctional oxygen electrodes
[DE85-006871] 17 p2955 N85-28248
GAMPHI: A database of activity and osmotic coefficients for aqueous electrolyte solutions
[PB85-163390] 18 p3072 N85-29002
Corrosion Research Center of the University of Minnesota
[DE85-009418] 18 p3075 N85-29022
Aluminum-air power cell: The M3-3 experiment
[DE85-008678] 18 p3096 N85-29166
Trace water sensor
[NASA-CASE-NPO-15722-1] 18 p3103 N85-29212
Improved acid electrolytes for fuel cells
[PB85-176053] 18 p3132 N85-29397
The ESFET: Evaporated Sensing Field Effect Transistor 19 p3256 N85-30188
Develop and test fuel cell powered on-site integrated total energy systems. Phase 3: Full-scale power plant development
[NASA-CR-168338] 19 p3304 N85-30483
New catalysts and new electrolytes for acid fuel cells
[DE85-000940] 19 p3307 N85-30498
Photoeffects of semiconductor electrolyte interfaces
[AD-A154163] 20 p3449 N85-31411
A gel-halo sample pellet: The best of both worlds? Stubby zones without a constricted sample gate
20 p3502 N85-31770
Electrodeposition of chromium and copper in magnetic fields
[AD-A154648] 21 p3566 N85-32180
Rechargeable lithium-organic electrolyte battery having overcharge protection and method of providing overcharge protection for a lithium-organic electrolyte battery
[AD-D011738] 22 p3806 N85-33575
Stable n-CuInSe/sub 2/iodide-iodine photoelectrochemical cell
[DE85-011597] 22 p3806 N85-33576
Nonsaturable microdryer
[DE85-005760] 23 p3946 N85-34457
Aqueous volatile weak electrolyte equilibria to 300 C
[DE85-013840] 24 p4076 N85-35261

ELECTROLYTIC CELLS
Development and testing of thin film cells for high temperature water vapor electrolysis
[BMFT-FB-T-84-146] 04 p0471 N85-13001
Development and testing of TiB2, used as cathode material in Al-electrolysis cells
[BMFT-FB-T-84-176] 05 p0633 N85-14060
Physico-chemical investigations on the electronic partial conductivity of molten electrolytes, especially of the eutectic mixture LiCl-KCl
[BMFT-FB-T-84-205] 05 p0633 N85-14063
Hydrogen production employing high-temperature solid oxide cells
[DE84-014559] 06 p0766 N85-14901
High capacity inorganic oxyhalide electrochemical cell
[AD-D011321] 07 p0923 N85-15845
Engineering model system study for a regenerative fuel cell: Study report
[NASA-CR-174601] 07 p0991 N85-16292
Method for increasing linearity of load cell
11 p1623 N85-20221
State-of-charge coulometer
[NASA-CASE-NPO-15759-1] 12 p1849 N85-21596
New electronic measurement, control devices
14 p2289 N85-24192
Method of production of metals by cathodic solution of their compounds in electrolytic cells
[BLL-OA-TRANS-3207-(6196.300)]
20 p3429 N85-31266
An update of the JPL program to develop Li-SOCl2 cells 20 p3445 N85-31384
Electrolytic cell
[DE85-011596] 22 p3807 N85-33578

ELECTROLYTIC GRINDING
U ELECTROCHEMICAL MACHINING

ELECTROLYTIC POLARIZATION
Indications of mineral zoning in a fossil hydrothermal system at the Meager Creek geothermal prospect, British Columbia, Canada from induced polarization studies
[DE85-011962] 22 p3815 N85-33636

ELECTROLYTIC POLISHING
U ELECTROPOLISHING

ELECTROMAGNETIC ABSORPTION
NT GAMMA RAY ABSORPTION
NT INFRARED ABSORPTION
NT MULTIPHOTON ABSORPTION
NT PHOTOABSORPTION
NT ULTRAVIOLET ABSORPTION
NT X RAY ABSORPTION
Magnetoabsorption of weak light wave in presence of intense light wave in semiconductor with narrow forbidden band 02 p0267 N85-11743
The winter anomaly in ionospheric absorption (with special reference to the results obtained in Spain)
04 p0522 N85-13338
Possible anomaly prediction system for the middle atmosphere — ionospheric absorption
04 p0522 N85-13339
Direct measurements of nitrous acid, nitrogen dioxide and formaldehyde in auto exhaust by differential optical absorption spectroscopy
[PB84-229269] 06 p0767 N85-14905
Optical properties of composite materials
[AD-A148768] 07 p0920 N85-15828
Study of optical sound generation and amplification
[AD-A147359] 07 p1039 N85-16582
An experimental and theoretical investigation of optogalvanic effects
[AD-A148089] 08 p1157 N85-17299
An experimental and theoretical investigation of optogalvanic effects
[AD-A148456] 08 p1223 N85-17700
Development of photoconductive power switch technology
[DE85-001514] 09 p1315 N85-18270
Synopsis of mid-latitude radio wave absorption in Europe 11 p1659 N85-20454
Ionospheric absorption on 1539 kHz in relation to solar ionizing radiation 11 p1659 N85-20455
Measurements of partial reflections at 3.18 MHz using the CW radar technique 11 p1659 N85-20457
Abnormal circulation changes in the winter stratosphere, detected through variations of D region ionospheric absorption 11 p1659 N85-20458
Autumn and winter anomalies in ionospheric absorption as measured by riometers 11 p1660 N85-20460
Winter anomaly 1982/83 in comparison with earlier winters (1960-82) 11 p1660 N85-20461
Explanation of the normal winter anomaly from the seasonal variation of short wave absorption
11 p1660 N85-20463
Millimeter wave dielectric property measurement of gyrotron window materials
[DE85-004430] 12 p1802 N85-21304
Aerosol multiple-scanning code, ASCAT
[LA-10046-MS] 12 p1823 N85-21440
Inelastic scattering in condensed matter with high intensity Moessbauer radiation
[DE85-003531] 12 p1854 N85-21627
Anisotropy of Alfven wave absorption in ionosphere
14 p2339 N85-24464
Electroreflectance spectroscopy as a probe of the electronic structure at the metal-electronic interface
[DE85-003541] 14 p2428 N85-24976
Study on a prismatic dye vat — laser systems
[CERT-2/6124-04-RO] 16 p2791 N85-27217
Upgrade of the LLNL EM transient range monocone antenna
[DE85-006639] 18 p3097 N85-29172
Optical 3-D signature device for detecting chemical agents
[AD-D011689] 19 p3272 N85-30293
Differential optical absorption techniques for diagnostics of coal gasification
[DE85-010177] 19 p3368 N85-30890
Cyclotron absorption of fast magnetosonic wave in stellarator 21 p3693 N85-32945
Dangling bonds and sub-gap optical absorption in silicon
[DE85-011752] 24 p4082 N85-35302
Muons in gamma showers
[HE-4.5-3] 24 p4195 N85-36027

ELECTROMAGNETIC ACCELERATION
Possibilities and limits of electromagnetic acceleration in space applications
[ILR-MITT-136] 02 p0193 N85-11292
Electromagnetic acceleration of macroparticles to hypervelocities in axisymmetric geometry
[IPPJ-696] 06 p0883 N85-15484
Distributed energy store railguns experiment and analysis 09 p1313 N85-18256
Plasma mass and effective inductance in a small railgun
[MRL-R-947] 12 p1936 N85-22162
High energy particle acceleration by coherent electromagnetic waves propagating across the magnetic field
[IPPJ-717] 16 p2866 N85-27679
Pulsars as cosmic ray accelerators: Energy development of protons
[OG-8.2-22] 23 p4021 N85-34918
Pulsars as cosmic ray particle accelerators: Dynamics of electrons
[OG-8.2-23] 23 p4021 N85-34919

ELECTROMAGNETIC COMPATIBILITY
Planning guide for the review of telecommunications systems for frequency availability and electromagnetic compatibility
[PB84-210238] 01 p0041 N85-10268
Basic EMC (Electromagnetic Compatibility) technology advancement for C3 systems, macromodeling of digital circuits, volume 2B
[AD-A146333] 03 p0359 N85-12306
EMC (Electromagnetic compatibility) spec criteria in Volterra systems
[AD-A147659] 08 p1151 N85-17263
EMC enhanced constant Z modulator
[AD-A147715] 08 p1157 N85-17297
Assessment of satellite power flux-density limits in the 2025-2300 MHz frequency range, part 2
[PB85-101244] 11 p1625 N85-20236
Algorithm for statistical simulation of electromagnetic compatibility characteristics of high-frequency transmission channels in radioelectronic facilities
12 p1842 N85-21580
Design guidelines for assessing and controlling spacecraft charging effects 13 p1994 N85-22500
Basic EMC (Electromagnetic Compatibility) technology advancement for C3 systems. Volume 4E: Modeling of transmission lines. A comparison of lumped-circuit iterative models and the transmission line model
[AD-A150652] 14 p2291 N85-24201
Basic EMC (Electromagnetic Compatibility) technology advancement for C3 systems: Model revision for IEMCAP (Intrasystem Electromagnetic Compatibility Analysis Program)
[AD-A150795] 14 p2292 N85-24206
Basic EMC (Electromagnetic compatibility) technology advancement for C3 systems. Volume 4D: Modeling crosstalk in balanced twisted pairs
[AD-A153678] 18 p3090 N85-29125
Basic EMC (Electromagnetic Compatibility) technology advancement for C3 systems. Volume 1B: Demodulation radio frequency interference effects in operational amplifier circuits
[AD-A154121] 20 p3440 N85-31350
Electromagnetic compatibility conference features biological interactions
[AD-A155813] 24 p4144 N85-35992

ELECTROMAGNETIC CONTROL
U ELECTROMAGNETS
U REMOTE CONTROL

ELECTROMAGNETIC DEDUCTION
U MAGNETIC INDUCTION

ELECTROMAGNETIC FIELDS
NT FAR FIELDS
NT NEAR FIELDS
NT SYSTEM GENERATED ELECTROMAGNETIC PULSES
The case for concern about very low frequency fields from visual display terminals: The need for further research and shielding of VDTs
[CCOHS-P83-2E] 02 p0234 N85-11526
Transformation of heterogeneous surface waves by skewed streams 02 p0259 N85-11697

On generating function of Weber parabolic cylinder functions with a negative integer index and radio pulse deformation by a medium
[PR-213] 03 p0354 N85-12276
Free-space propagation of light pulses
[PB84-217108] 03 p0421 N85-12889
Nonthermal mechanism for laser annealing of semiconductors and formation of super structure 04 p0487 N85-13109
Calibrating and measuring systems for electromagnetic fields 05 p0830 N85-14041
Invariance of mean-square effective area of synthesized apertures 06 p0784 N85-15009
Measurement of electromagnetic field components from arbitrarily oriented gyro platforms 06 p0787 N85-15030
Investigating phase structure of electromagnetic field in local inhomogeneities by modeling method 06 p0822 N85-15220
Khibiny experiment described 07 p0981 N85-16230
A comparison of lightning and nuclear electromagnetic pulse response of a helicopter 07 p1000 N85-16349
A comparison of lightning and nuclear electromagnetic pulse response of tactical shelters 07 p1000 N85-16350
Forces on neutral atoms due to electromagnetic fields
[AD-A146984] 07 p1040 N85-16803
Electromagnetic fields from the generation and absorption of discontinuous linear current fronts
[AD-A148076] 08 p1151 N85-17268
Theoretical issues involving traps for neutral spin-polarized atoms
[AD-A148035] 08 p1220 N85-17682
European Scientific Notes, volume 38, number 12
[AD-A148713] 09 p1418 N85-18946
Propagation of electromagnetic fields along the sea/sea-bed interface
[AD-A149523] 10 p1467 N85-19257
Effects of electromagnetic fields produced by high voltage transmission lines
[DE85-900034] 11 p1625 N85-20230
The ULF/ELF/VLF electromagnetic fields generated in a sea of finite depth by elevated dipole sources
[AD-A149638] 12 p1828 N85-21470
Determining distribution of complex dielectric permittivity over cylindrical body of intricate cross section from electromagnetic field measurement 12 p1842 N85-21559
Characteristics of the boat inductor for keeping liquid metal in the suspended state
[NASA-TM-77816] 12 p1851 N85-21611
Non-contacting electromagnetic de-spin system for Earth orbiting satellites 12 p1946 N85-22225
Models of discontinous random fields 13 p2079 N85-22963
Problem of diffraction by wavy surface: Comparison of numerical methods of solution 13 p2079 N85-22985
Observation of pure resonance and threshold effects in electron impact experiments in high intensity laser fields
[AD-A150725] 14 p2309 N85-24293
Electromagnetic field of currents and its use to estimate total conductivity of sedimentary deposits in Western Black Sea 14 p2334 N85-24434
Electromagnetic fields migration method 14 p2343 N85-24487
Hygienic standardization of electromagnetic fields of radar systems 14 p2367 N85-24703
High field RF superconductivity: To pulse or not to pulse
[DE85-004381] 14 p2429 N85-24977
Solutions of field equations in General Relativity with spinor connection 15 p2663 N85-26436
The Impact of Proposed Radio Frequency Radiation Standards on Military Operations
[AGARD-LS-138] 16 p2775 N85-27128
Hazards of VLF electromagnetic fields 16 p2776 N85-27136
ELF (Extremely Low Frequency) communications system ecological monitoring program: Measurements of ELF electromagnetic fields for site selection and characterization, 1983
[AD-A153120] 17 p2949 N85-28209
Biological and human health effects of extremely low frequency electromagnetic fields. Post-1977 literature review
[AD-A152731] 17 p2999 N85-28539
Plasma engineering models of tandem mirror devices with high-field test-cell inserts
[DE85-010046] 18 p3192 N85-29797
Hybrid two-dimensional Monte-Carlo electron transport in self-consistent electromagnetic fields
[DE85-010757] 19 p3348 N85-30756
Profile of a relativistic electron beam propagated through a linear wiggler and an axial guide field
[AD-A154403] 19 p3353 N85-30783
Guided-mode launching in a slab waveguide by way of diffraction at the edge of a conducting screen residing on one surface of the slab
[AD-A154866] 21 p3575 N85-32232
Calculation of the propagation constant in a rectangular waveguide containing an inhomogeneous longitudinally magnetized plasma
[DE85-012072] 21 p3577 N85-32250
Lower bounds of propagation velocity of steady ionizing waves in field of strong electromagnetic wave 21 p3692 N85-32940
Equations of motion for electromagnetic waves in 4-dimensional Euclidian space 21 p3697 N85-32970
Research in particles and fields
[NASA-CR-176089] 21 p3724 N85-33103
Pulsars as cosmic ray accelerators: Energy development of protons
[OG-9.2-22] 23 p4021 N85-34918
Theory of mutual impedances and multiple reflections in an N-element array environment
[PB85-191419] 24 p4092 N85-35364
Electromagnetic compatibility conference features biological interactions
[AD-A155813] 24 p4144 N85-35692

ELECTROMAGNETIC INTERACTIONS
NT LASER PLASMA INTERACTIONS
NT PLASMA-ELECTROMAGNETIC INTERACTION
Electromagnetic shower development and applications to sampling calorimeters
[DE84-016355] 04 p0493 N85-13142
Metal-support interactions: Their effects upon adsorption, electronics, and activity/selectivity properties of cobalt in hydrogenation
[DE85-003316] 09 p1292 N85-18113
Applications of Tethers in Space, volume 2
[NASA-CP-2365] 11 p1644 N85-20361
Report of the Electrodynamic Interactions Panel 11 p1645 N85-20363
Investigations of the structure and electromagnetic interactions of few-body systems
[DE85-002654] 11 p1721 N85-20824
Theoretical aspects of electroweak and other interactions in medium-energy nuclear physics
[DE85-003621] 13 p2157 N85-23392
Velocity space diffusion of high energy ions induced by a lower hybrid wave in a nonuniform magnetic field
[IPPJ-714] 16 p2666 N85-27681
Modern test of chiral anomalies
[DE85-005692] 17 p3020 N85-28680
Electroweak interactions in nuclei
[DE85-007811] 17 p3033 N85-28782
Energy and Technology Review
[DE85-004358] 17 p3049 N85-28868
Basic EMC (Electromagnetic compatibility) technology advancement for C3 systems. Volume 4D: Modeling crosstalk in balanced twisted pairs
[AD-A153678] 18 p3090 N85-29125
Interactions between electromagnetic fields
[AD-A153796] 18 p3091 N85-29129
Theoretical investigations of the propagation and interactions of surface waves
[AD-A153548] 18 p3185 N85-29753
Effects of CP violation in SU(2) sub L x SU(2) sub R x U(1) electroweak models
[DE85-010801] 20 p3531 N85-31965

ELECTROMAGNETIC INTERFERENCE
NT ATMOSPHERICS
NT CROSSTALK
NT DAWN CHORUS
NT ELECTROMAGNETIC NOISE
NT HISS
NT IONOSPHERIC NOISE
NT JAMMING
NT RADIO FREQUENCY INTERFERENCE
NT SHOT NOISE
NT THERMAL NOISE
NT WHISTLERS
NT WHITE NOISE
Center for Electronics and Electrical Engineering Technical Bulletin covering center programs with 1984 CEEE events calendar
[PB84-223884] 01 p0045 N85-10293
Center for Electronic and Electrical Engineering Technical Progress Bulletin, January - March 1983, no. 2
[PB84-231224] 03 p0360 N85-12308
Interference immunity of digital equipment for coherent processing of wideband signals 04 p0486 N85-13100
Adaptive mutual interference suppression method
[AD-D011266] 05 p0628 N85-14024
Characterization of newly developed conductive composites
[AD-A146652] 06 p0764 N85-14884
Measurement of external antenna characteristics with allowance for distorting factors (review) 06 p0790 N85-15046
The effect of aircraft generated electromagnetic interference (EMI) on future avionics systems: A compendium
[AD-A146380] 06 p0799 N85-15101
Natural interference phenomena affecting spaceborne receivers
[NASA-CR-174256] 07 p0916 N85-15798
EMI (electromagnetic interference) filter capacitor unit
[AD-D011392] 07 p0937 N85-15941
Upset susceptibility study employing circuit analysis and digital simulation — digital systems and electromagnetic interference 07 p0999 N85-16344
Data and results of a laboratory investigation of microprocessor upset caused by simulated lightning-induced analog transients 07 p0999 N85-16345
Adaptive antenna arrays for weak interfering signals
[NASA-CR-174336] 08 p1150 N85-17258
Subjective evaluation of the effect of noise and interference on frequency modulated NTSC television signals
[CRC-1367] 09 p1310 N85-18230
Electromagnetic compatibility of measurement and control equipment in nuclear installations
[BLL-WH-807-(9091.9F)] 11 p1623 N85-20222
Shuttle electrical environment 13 p1990 N85-22475
EMI characteristics of a potential control system 13 p1994 N85-22502
Characteristics of EMI generated by negative metal-positive dielectric voltage stresses due to spacecraft charging 13 p1995 N85-22505
Basic EMC (electromagnetic interference) technology advancement for c3 systems. Volume 3A: Probabilistic analysis of combinational circuits with random delays
[AD-A150349] 13 p2055 N85-22866
Efficiency of digital compensator of strong non-Gaussian interference 13 p2072 N85-22942
Interference immunity of binary systems with second-order phase-difference modulation in various reception modes 13 p2072 N85-22944
Spectra of incidental interference resulting from nonlinear conversion of signals from transmitters 13 p2073 N85-22950
Interference flux during reflection of heterogeneous waves 13 p2078 N85-22977
Models of discontinous random fields 13 p2079 N85-22983
Applicability of log-normal model to probabilistic description of quasi-pulse interference 13 p2084 N85-23014
Frequency selection for dispersion signal in satellite communication lines 15 p2528 N85-25584
Preliminary estimation of mutual interference between fixed satellite service systems 15 p2528 N85-25586
An update on experience on the fly by wire Jaguar equipped with a full-time digital flight control system 16 p2712 N85-26740
Thin layered interference mirrors to reduce radiation damage
[DE85-009763] 18 p3185 N85-29756
Theoretical investigation of single-frequency 8-element localizer signal scattering for critical area determination
[FAA-PM-85-4] 20 p3391 N85-31037
Basic EMC (Electromagnetic Compatibility) technology advancement for C3 systems. Volume 1B: Demodulation radio frequency interference effects in operational amplifier circuits
[AD-A154121] 20 p3440 N85-31350
Study of the interferences of 2 GHz radio beams with a DORIS system — precise low orbit determination system (DORIS)
[CNES-CT/DRT/TIT/RL-84/140-T] 20 p3442 N85-31362
Center for Electronics and Electrical Engineering technical progress bulletin covering center programs, April-June 1984 with 1984 CEEE (Center for Electronics and Electrical Engineering) events calendar, issue 7
[PB85-187540] 20 p3450 N85-31419
Stripe filters on multispectral linear arrays
[NASA-CR-175305] 21 p3579 N85-32252
Effect of interference on the performance of a minimum TCAS 2
[FAA-PM-84-33] 23 p3895 N85-34131
Actuator rigging test set electromagnetic interference test (CE03)
[AD-A155819] 24 p4086 N85-35327
Center for Electronics and Electrical Engineering technical progress bulletin covering center programs, July-September with 1985 CEEE events calendar
[PB85-191393] 24 p4091 N85-35363

ELECTROMAGNETIC MEASUREMENT
NT ELECTROMAGNETIC NOISE MEASUREMENT

Special Developments and Methods in High Frequency Measuring Techniques — conferences
[PTB-E-24] 05 p0629 N85-14030
Present status and development tendencies in the field of high frequency measuring techniques
05 p0629 N85-14031
Improvement of the accuracy of reflection factor measurements by a computer 05 p0629 N85-14033
A computer controlled measuring system for the calibration of HF components 05 p0630 N85-14037
Fundamentals and applications of the six port measuring technique — reflectometer 05 p0630 N85-14039
Calibrating and measuring systems for electromagnetic fields 05 p0630 N85-14041
Evaluation and results of national and international intercomparison measurements — electromagnetic measurement 05 p0631 N85-14043
Measurement of electromagnetic field components from arbitrarily oriented gyro platforms
06 p0787 N85-15030
Measurement of external antenna characteristics with allowance for distorting factors (review)
06 p0790 N85-15046
Structure of temperature field based on observations of refraction from high meteorological mast
06 p0819 N85-15199
Two-dimensional signal processing and storage and theory and applications of electromagnetic measurements. Supplemental appendix
[AD-A146848] 07 p0939 N85-15953
Khibiny experiment described
07 p0981 N85-16230
Determining distribution of complex dielectric permittivity over cylindrical body of intricate cross section from electromagnetic field measurement
12 p1842 N85-21589
Two-dimensional signal processing and storage and theory and applications of electromagnetic measurements
[AD-A150590] 13 p2065 N85-22899
Discrimination of normal and anomalous magnetic and electric fields in geoelectromagnetic variations
13 p2114 N85-23166
Analytical studies and experimental measurements of amplitude and phase of near-field range antenna probes
[AD-A150922] 14 p2293 N85-24212
Lightning strikes on aircraft. The TRIP 82 experiment and 3-dimensional electromagnetic interferometry
[ONERA-RF-88/7154-PY] 16 p2703 N85-28690
Magnetoconductance in aluminum films, wires, and cylinders 19 p3374 N85-30928

ELECTROMAGNETIC NOISE
NT ATMOSPHERICS
NT DAWN CHORUS
NT HISS
NT IONOSPHERIC NOISE
NT SHOT NOISE
NT THERMAL NOISE
NT WHISTLERS
NT WHITE NOISE
A coaxial noise standard for the 1 GHz to 12.4 GHz frequency range
[PB84-217884] 01 p0042 N85-10272
High frequency phase-noise in semiconductor lasers
[FUB-20-1983] 01 p0053 N85-10353
Energy correlation between natural extra-low-frequency noises at various frequencies 06 p0784 N85-15010
Low frequency noise in oscillator with limited space-charge accumulation 06 p0786 N85-15024
Peculiarities of microprocessor implementation of algorithms for processing radio signals and noise in large antenna arrays 06 p0792 N85-15059
Observation of natural noise near upper hybrid resonance in terrestrial magnetosphere by Prognoz-5 satellite 06 p0822 N85-15221
Estimation of requirements for acceptable noise radiation level of communication transmitters
07 p0949 N85-16017
NBS (National Bureau of Standards) switching radiometers
[PB84-235894] 07 p0968 N85-16147
Noise jammer discrimination by noise modulation bandwidth
[AD-D011473] 10 p1468 N85-19264
Fundamental limits to synchronization and tracking
[AD-A149823] 12 p1833 N85-21504
Research on ocean floor electrical surveys
[AD-A149831] 12 p1899 N85-21920
Statistical phenomena in particle beams
[DE85-001050] 12 p1929 N85-22118
Prefiltration in Kalman filter with a priori indeterminacy
13 p2071 N85-22939
Comparative analysis of noise tolerance of quasi-coherent phase shift keying signal demodulators
13 p2072 N85-22946
Magnetic noise in single-machine rotating frequency converters 13 p2077 N85-22969
Playback amplifier with high interference immunity
13 p2077 N85-22970
An examination of signal-to-noise enhancement at the Edzell CDAA (Circular Disposed Antenna Array)
[AD-A150706] 14 p2291 N85-24204
Study of 1/f noise in solids
[AD-A151069] 14 p2428 N85-24972
The effects of seeing on noise
14 p2443 N85-25077
Analysis and interpretation of synthetic time strings of oscillation data 14 p2444 N85-25079
Adaptive detection of noise signal according to Neumann-Pearson criterion 15 p2527 N85-25580
Noise characteristics of an avalanche photodiode
[AD-A154096] 19 p3258 N85-30205
Overview of applications of SQUIDS
[DE85-009942] 20 p3458 N85-31480
The role of long term lamp fluctuations in the random walk of frequency behavior of the rubidium frequency standard: A case study
[AD-A155338] 21 p3590 N85-32314
Design of a freestanding noise measurement and recording system to predict the intensity and location of electromagnetic radiation from earthquakes
[AD-A155070] 21 p3632 N85-32563
A real time index of geomagnetic background noise for the MAD (Magnetic Anomaly Detection) frequency band
[AD-A155717] 22 p3814 N85-33627
Noise in silver beta alumina ceramics
[AD-A156135] 24 p4082 N85-35297

ELECTROMAGNETIC NOISE MEASUREMENT
FCC (Federal Communication Commission) methods of measurement of radio noise emissions from computing devices
[PB84-243591] 08 p0849 N85-15387

ELECTROMAGNETIC PROPAGATION
U ELECTROMAGNETIC WAVE TRANSMISSION

ELECTROMAGNETIC PROPERTIES
NT ABSORPTANCE
NT ABSORPTIVITY
NT BIREFRINGENCE
NT BRIGHTNESS
NT BRIGHTNESS DISTRIBUTION
NT CAPACITANCE
NT CARRIER MOBILITY
NT COLOR
NT DICHROISM
NT DIELECTRIC PROPERTIES
NT ELECTRICAL PROPERTIES
NT ELECTROMAGNETIC ABSORPTION
NT ELECTRON MOBILITY
NT FARADAY EFFECT
NT FERROELECTRICITY
NT HOLE MOBILITY
NT INDUCTANCE
NT INFRARED ABSORPTION
NT LUMINOSITY
NT OPACITY
NT OPTICAL BISTABILITY
NT OPTICAL PROPERTIES
NT OPTICAL REFLECTION
NT PERMITTIVITY
NT PHOSPHORESCENCE
NT PHOTOCONDUCTIVITY
NT PHOTOELASTICITY
NT PHOTOELECTRIC EFFECT
NT PHOTOELECTRIC EMISSION
NT PHOTOIONIZATION
NT PHOTOVISCOELASTICITY
NT PHOTOVOLTAIC EFFECT
NT PROXIMITY EFFECT (ELECTRICITY)
NT RADIANCE
NT REFLECTANCE
NT REFRACTIVITY
NT SKY BRIGHTNESS
NT SOLAR GRANULATION
NT STELLAR LUMINOSITY
NT STIGMATISM
NT TRANSLUCENCE
NT TRANSMISSIVITY
NT TRANSMITTANCE
NT TRANSPARENCE
NT TURBIDITY
NT WATER COLOR
The effect of aircraft generated electromagnetic interference (EMI) on future avionics systems: A compendium
[AD-A148380] 08 p0799 N85-15101
Shielded enclosures for experimental studies of shielding topology
[AD-A149292] 11 p1624 N85-20227
Electromagnetic analysis of radomes by the moment method
[AD-P004351] 12 p1824 N85-21445
A radome for air traffic control SSR radar systems
[AD-P004373] 12 p1827 N85-21467
Simulation of thermal and electromagnetic processes in induction plasmatrons 12 p1841 N85-21552
Research on ocean floor electrical surveys
[AD-A149831] 12 p1899 N85-21920
Determination of electromagnetic properties of mesh material using advanced radiometer techniques
14 p2235 N85-23955
Design and testing of a pulsed current transformer
[AD-A154228] 19 p3259 N85-30208
Comparison of the electromagnetic properties of lightning and EMP (Electromagnetic pulse): Results of recent lightning studies
[AD-A154325] 19 p3317 N85-30560
Possibilities for studying short-lived nuclei produced at LAMPF
[DE85-010740] 19 p3365 N85-30984
SAPIENS Memo 8: Electromagnetic properties of the EMP simulator SAPIENS
[FOA-C-30382-A3] 20 p3442 N85-31365
A review of the physics and response models for burnout of semiconductor devices
[AD-A155031] 21 p3709 N85-33028
Analysis of the nonlinear equations describing the elastic, thermal, and electromagnetic behavior of solids: Existence of solutions of semi-inverse problems
24 p4100 N85-35415

ELECTROMAGNETIC PROPULSION
NT MASS DRIVERS (PAYLOAD DELIVERY)
Preliminary analysis of space mission applications for electromagnetic launchers
[NASA-CR-174067] 03 p0321 N85-12071
Plasma mass and effective inductance in a small railgun
[AD-A154644] 21 p3589 N85-32304

ELECTROMAGNETIC PULSES
NT SYSTEM GENERATED ELECTROMAGNETIC PULSES
Laboratory evaluation of Electromagnetic Pulse (EMP) hardness testing concepts for electrical conduit systems
[AD-A145486] 02 p0190 N85-11273
Microwave susceptibility experiments
[DE84-016188] 02 p0192 N85-11281
EMP injection on conduit entries, type Brattberg — electromagnetic pulse (EMP) injection
[FOA-E-30001-A3] 02 p0193 N85-11290
The case for concern about very low frequency fields from visual display terminals: The need for further research and shielding of VDTs
[CCOHS-P83-2E] 02 p0234 N85-11526
Generation of superpowerful microsecond electromagnetic radiation pulses
03 p0347 N85-12234
Free-space propagation of light pulses
[PB84-217108] 03 p0421 N85-12889
Electromagnetic pulse and the electric power network
[DE84-015403] 04 p0493 N85-13143
Tests for susceptibility to electromagnetic attack
[SNIAS-842-422-101] 04 p0494 N85-13154
Pulse injection on a power cable penetrating a shielding wall by feed-through capacitors
[FOA-C-30372-A3] 04 p0497 N85-13171
The HEMP (High-altitude Electromagnetic Pulse) response of a long transmission line buried in the earth
[AD-A146517] 06 p0800 N85-15108
Dynamic response of electromagnetic current meters
[PB84-229731] 06 p0842 N85-15344
Multiple scattering effects on transmission through the atmosphere
[AD-A147527] 07 p0941 N85-15969
Real-time analysis of space characteristics of microwave electromagnetic pulse fields by means of controllable layer structures 07 p0955 N85-16052
A comparison of lightning and nuclear electromagnetic pulse response of a helicopter 07 p1000 N85-16349
A comparison of lightning and nuclear electromagnetic pulse response of tactical shelters
07 p1000 N85-16350
Nonradial pulsation and mass loss in early B stars
08 p1232 N85-17759
Electromagnetic pulse (EMP) interaction with electric power systems. Power Systems Technology Program
[DE85-000186] 09 p1312 N85-18344
Multiple parallel wires above a finitely conducting plane earth in the presence of a plane wave (EMP)
[DE85-001116] 11 p1625 N85-20231
Distortion of temporal characteristics during parametric up-conversion of ultrashort laser pulses
11 p1717 N85-20803
Numerical investigation of propagation of radiation pulse at xxx 11 p1718 N85-20809
Four-wave hypersonic reversing mirrors in saturated mode 11 p1719 N85-20812

Electromagnetic pulse (EMP) injection on cable entries, type ERA; EMP memo no. 10
[FOA-E-30003-A3] 12 p1830 N85-21484
Intense, broadband, pulsed I-R source at the National Synchrotron Light Source
[DE84-010542] 12 p1935 N85-22154
Design guidelines for assessing and controlling spacecraft charging effects 13 p1994 N85-22500
Processing of signals in experiments with scattering of short radio pulses by conducting sphere 13 p2068 N85-22917
Measuring intensity of electric field produced by electromagnetic pulse with aid of active probes 13 p2075 N85-22958
Use of electronic coding-frequency meters to measure parameters of pulsed radio signals 13 p2076 N85-22964
Pulsations of cosmic ray intensities before increasing flux of relativistic particles from solar flares 15 p2477 N85-25292
Signal processing for the analysis of transient electromagnetic data
[DE85-007244] 16 p2774 N85-27125
Optically triggered transferred-electron device microwave burst and single pulse generators
[AD-D011614] 16 p2778 N85-27141
A synchrotron/inverse Compton interpretation of a solar burst producing fast pulses at lambda 3 mm and hard X-rays 16 p2887 N85-27815
Energy and Technology Review
[DE85-004358] 17 p3049 N85-28868
Comparison of the electromagnetic properties of lightning and EMP (Electromagnetic pulse): Results of recent lightning studies
[AD-A154325] 19 p3317 N85-30560
SAPIENS Memo 8: Electromagnetic properties of the EMP simulator SAPIENS
[FOA-C-30382-A3] 20 p3442 N85-31365
A theory of electromagnetic shielding with applications to MIL-STD-285, IEEE-299, and EMP simulation
[AD-A154905] 21 p3575 N85-32233
Plasmodynamic methods for generating powerful light puses 21 p3693 N85-32943
Methods for measuring and analyzing dispersion properties of multimode fiber optic lightpipes (a review) 21 p3695 N85-32960
Study to assess the effects of magnetohydrodynamic electromagnetic pulse on electric power systems, phase 1, volume 3
[DE85-011301] 24 p4156 N85-35771

ELECTROMAGNETIC RADIATION
NT AIRGLOW
NT BLACK BODY RADIATION
NT BREMSSTRAHLUNG
NT CENTIMETER WAVES
NT CERENKOV RADIATION
NT CN EMISSION
NT COHERENT ELECTROMAGNETIC RADIATION
NT COHERENT LIGHT
NT COMET TAILS
NT COSMIC X RAYS
NT CYCLOTRON RADIATION
NT DECAMETRIC WAVES
NT DECIMETER WAVES
NT ELECTROMAGNETIC PULSES
NT ELECTROMAGNETIC SURFACE WAVES
NT EXTRATERRESTRIAL RADIO WAVES
NT EXTREME ULTRAVIOLET RADIATION
NT FAR INFRARED RADIATION
NT FAR ULTRAVIOLET RADIATION
NT GALACTIC RADIO WAVES
NT GAMMA RAY BEAMS
NT GAMMA RAY BURSTS
NT GAMMA RAYS
NT GEOCORONAL EMISSIONS
NT HYDROXYL EMISSION
NT INFRARED RADIATION
NT KILOMETRIC WAVES
NT LIGHT (VISIBLE RADIATION)
NT LIGHT BEAMS
NT LONG WAVE RADIATION
NT LYMAN ALPHA RADIATION
NT MICROWAVE EMISSION
NT MICROWAVES
NT MILLIMETER WAVES
NT MODULATED CONTINUOUS RADIATION
NT MONOCHROMATIC RADIATION
NT NEAR INFRARED RADIATION
NT NIGHTGLOW
NT NONEQUILIBRIUM RADIATION
NT NORTH POLAR SPUR (ASTRONOMY)
NT PHOTON BEAMS
NT PLANETARY RADIATION
NT PLASMONS
NT POLARIZED ELECTROMAGNETIC RADIATION
NT POLARIZED LIGHT
NT RADIO BURSTS
NT RADIO EMISSION
NT RADIO WAVES
NT SHORT WAVE RADIATION
NT SKY RADIATION
NT SKY WAVES
NT SOLAR RADIO BURSTS
NT SOLAR RADIO EMISSION
NT SOLAR X-RAYS
NT SOMMERFELD WAVES
NT SUBMILLIMETER WAVES
NT SUNLIGHT
NT SYNCHROTRON RADIATION
NT SYSTEM GENERATED ELECTROMAGNETIC PULSES
NT TERRESTRIAL RADIATION
NT THERMAL RADIATION
NT TWILIGHT GLOW
NT TYPE 3 BURSTS
NT TYPE 4 BURSTS
NT ULTRAVIOLET RADIATION
NT X RAYS
NT ZODIACAL LIGHT

Theory of near-field phased arrays for electromagnetic susceptibility testing
[PB84-217636] 01 p0042 N85-10273
Activities report of the Radio Laboratory
[REPT-S-153] 02 p0192 N85-11288
Scattering of electromagnetic waves by plasma half-space after initiation of motion 02 p0264 N85-11729
Diffraction of electromagnetic wave by screen of arbitrary shape 02 p0273 N85-11778
Diffraction of plane electromagnetic waves on semiinfinite grid of parallel conductors arranged at angle to its edge 03 p0344 N85-12217
Scattering of electromagnetic waves in flat waveguide with bilateral diaphragms 03 p0347 N85-12235
Characteristics of absorption and frequency filtration of ULF electromagnetic waves in the ionosphere 03 p0376 N85-12402
Research activities of the Illinois University Coordinated Science Laboratory
[AD-A145589] 03 p0449 N85-12856
Field/cell interaction model
[DE84-011914] 04 p0544 N85-13485
Aharonov-Bohm effect in absorption of electromagnetic wave 06 p0786 N85-15022
Optimization of energy conversion during locking of electron bunches by electromagnetic wave in longitudinal electrostatic field 06 p0786 N85-15025
Diurnal variation harmonics and spatial change in cosmic ray flux 06 p0824 N85-15230
Method for forming electromagnetic-wave-screening composite 07 p0936 N85-15930
Two-dimensional signal processing and storage and theory and applications of electromagnetic measurements. Supplemental appendix
[AD-A146848] 07 p0939 N85-15953
Transformation of electromagnetic waves in plasma with randomly-heterogeneous magnetic field 07 p0953 N85-16039
Tolerance synthesis of multilayer radome walls 07 p0953 N85-16041
Methodical approaches to determination of sanitation protective zone dimensions around TV centers and TV retransmitters 09 p1361 N85-18563
Current measurements by Faraday rotation in single mode optical fibers
[DE85-002025] 09 p1384 N85-18707
Proceedings of the 17th Symposium on Electromagnetic Windows, part 1
[AD-A149185] 10 p1466 N85-19253
Nonlinear saturation of stimulated Raman scattering in collisional homogeneous plasma
[DE85-002814] 10 p1559 N85-19631
Multiple parallel wires above a finitely conducting plane earth in the presence of a plane wave (EMP)
[DE85-001116] 11 p1625 N85-20231
Coronal spectroscopy in laser plasmas
[DE85-002617] 11 p1730 N85-20660
Covariant lie-transformed plasma action principle
[DE85-000285] 11 p1732 N85-20691
Detection of angular modulated electromagnetic signals
[AD-D011563] 12 p1823 N85-21437
Proceedings of the Symposium on Electromagnetic Windows (17th) held at Georgia Inst. of Technology, Engineering Experiment Station, Atlanta, Georgia on 25-27 July 1984. Part 2
[AD-A149125] 12 p1824 N85-21444
Arguments for fundamental emission by the parametric process L yields T + S in interplanetary type III bursts — langmuir, electromagnetic, ion acoustic waves (L, T, S) 12 p1958 N85-22311
Small scale structure and the Spinar model for active galactic nuclei 12 p1959 N85-22316
Numerical/Electromagnetics Code (NEC)
[DE85-004999] 13 p2056 N85-22674
Natural electromagnetic radiation in seismically active regions 13 p2111 N85-23152
Disturbances in structure of lower ionosphere at terminators based on results of winde-band LW sounding 14 p2339 N85-24467
Rain rate determinations from electronic weight measurements: Instrument description and data reduction techniques
[AD-A150765] 14 p2378 N85-24681
Particle shape characterization
[AD-A151981] 15 p2544 N85-25707
A plasma initiation-flow chamber to study CW laser beamed energy absorption in light gases
[AD-A151225] 15 p2562 N85-25806
Amplification of scattered induced radiation flux in high-gain laser rods 15 p2644 N85-26309
Characteristic functionals of stochastic wave processes
[REPT-14/1984] 16 p2768 N85-27084
Multiple scattering of electromagnetic waves in discrete random media
[AD-A151788] 16 p2772 N85-27112
Biological influences of low-frequency sinusoidal electromagnetic signals alone and superimposed on RF carrier waves
[PB85-161248] 16 p2842 N85-27527
DARPA/TTO program IR binary optics
[AD-A152196] 16 p2865 N85-27672
Study of the degradation of short-circuit current and the open-circuit tension of spatial solar cells as a function of the fluency of 1MeV electrons
[INPE-3356-PRE/634] 16 p2887 N85-27814
Solar-Geophysical Data Number 484, December 1984. Part 1 (prompt reports): Data for November 1984, October 1984 and late data
[NASA-CR-175829] 16 p2888 N85-27819
X-ray emission and the winds of cataclysmic variables
[DE85-007663] 17 p3053 N85-28902
Upgrade of the LLNL EM transient range monocone antenna
[DE85-006639] 18 p3097 N85-29172
All-optical logic gates with external switching by laser and incoherent radiation 18 p3167 N85-29766
Electromagnetic solitary waves in magnetized plasmas
[DE85-010064] 18 p3190 N85-29788
Scattering by distributions of small thin particles 19 p3253 N85-30172
Heating of electrons in a high density tokamak by a micro-wave near second harmonic frequency
[DE85-010662] 19 p3359 N85-30822
Electromagnetic lateral waves in layered media 19 p3369 N85-30894
Localization of waves in a disordered medium 19 p3373 N85-30926
Theoretical investigation of single-frequency 8-element localizer signal scattering for critical area determination
[FAA-PM-85-4] 20 p3391 N85-31037
Simulation and analysis of airborne antenna radiation patterns 20 p3439 N85-31342
Numerical modeling of subsurface communication
[DE85-012618] 21 p3577 N85-32249
Some recent developments in the interpretation of MST rader returns from clear air (keynote paper), part 2 21 p3618 N85-32480
Design of a freestanding noise measurement and recording system to predict the intensity and location of electromagnetic radiation from earthquakes
[AD-A155070] 21 p3632 N85-32563
USAFSAM review and analysis of radiofrequency radiation bioeffects literature
[AD-A155113] 21 p3664 N85-32760
Investigation of ion-acoustic plasma turbulence in field of powerful electromagnetic wave by CO2-laser radiation scattering 21 p3691 N85-32935
Lower bounds of propagation velocity of steady ionizing waves in field of strong electromagnetic wave 21 p3692 N85-32940
Amplification of electromagnetic wave by electron stream with negative velocity differences 21 p3692 N85-32941
Electromagnetic wave amplification during cyclotron resonance in a medium 21 p3693 N85-32942
Effective brightness of zero-point fluctuations of the electromagnetic vacuum accompanying parametric scattering of light 21 p3694 N85-32951
Existence of smooth solutions in problems of electromagnetic radiation focusing 21 p3697 N85-32972
Ice fog as an electro-optical obscurant
[AD-A155059] 21 p3705 N85-33015

Method of characterizing critical timing paths and analyzing timing related failure modes in very large scale integrated circuits
[AD-D011731] 22 p3759 N85-33298
Surface wave modes of a multilayered medium backed by a perfectly conducting ground plane: Computation of propagation constants
[DE85-011454] 22 p3829 N85-33715
Recoverable Plasma Diagnostics Package (RPDP) 23 p3902 N85-34167
Simulation studies on stability of hot electron plasma 23 p3978 N85-34664
Pulse effect in a light ion beam propagation through a Z-discharge plasma channel 23 p3981 N85-34684
Source energy spectra from demodulation of solar particle data by interplanetary and coronal transport
[SH-1.3-13] 23 p3994 N85-34758
Solar source regions of 3HE-rich particle events
[SH-2.2-4] 23 p4000 N85-34799
RF stabilization of interchange-ballooning modes
[DE85-012080] 24 p4090 N85-35353
Theory of mutual impedances and multiple reflections in an N-element array environment
[PB85-191419] 24 p4092 N85-35364
High energy radiation from neutron stars
[DE85-014353] 24 p4169 N85-35843
Analytical-numerical methods of calculations of energy and three-dimensional particle distributions in electromagnetic cascades
[HE-3.5-13] 24 p4184 N85-35950
The lateral distributions of charged particles of energy greater than 0.9 E sub crit in electron-photon cascades in lead and air
[HE-3.6-10] 24 p4185 N85-35957
Result of Monte-Carlo simulation of electron-photon cascades in lead and layers of lead-scintillator
[HE-3.6-11] 24 p4185 N85-35958
On mini-cluster observed by Chacaltaya emulsion chamber experiment
[HE-3.6-12] 24 p4185 N85-35959
A comparative analysis of gamma and hadron families at the superhigh energies recorded in experiment Pamir
[HE-3.7-1] 24 p4185 N85-35960
Structured events in Pamir carbon X-ray chambers
[HE-3.7-7] 24 p4186 N85-35965
Peculiarities of gamma-quants distribution at 20 TeV energy
[HE-3.7-10] 24 p4186 N85-35967

ELECTROMAGNETIC SCATTERING
NT HALOS
NT LIGHT SCATTERING
NT MICROWAVE SCATTERING
NT MIE SCATTERING
NT RAMAN SPECTRA
NT RAYLEIGH SCATTERING
NT THOMSON SCATTERING
NT X RAY SCATTERING
Planarity criteria in electromagnetic topology
[AD-A145279] 01 p0038 N85-10241
Gaussian Wide Sense Stationary Uncorrelated Scattering (GWSSUS) channel simulation program to be used for mobile radio systems
[FUB-40-1983] 01 p0041 N85-10265
Theory of near-field phased arrays for electromagnetic susceptibility testing
[PB84-217836] 01 p0042 N85-10273
Scattering of electromagnetic waves by plasma half-space after initiation of motion 02 p0264 N85-11729
Scattering of radio waves on magnitized meteor trail 03 p0344 N85-12221
Scattering of electromagnetic waves in flat waveguide with bilateral diaphragms 03 p0347 N85-12235
Research activities of the Illinois University Coordinated Science Laboratory
[AD-A145589] 03 p0449 N85-12656
Scattering from randomly oriented scatterers of arbitrary shape in the low-frequency limit with application to vegetation 04 p0525 N85-13362
Scattering from randomly oriented circular discs with application to vegetation 04 p0525 N85-13363
A comparison between active and passive sensing of soil moisture from vegetated terrains 04 p0526 N85-13364
Scattering of electromagnetic waves by surface with small asperities 06 p0784 N85-15013
Approach to solution of diffraction problem for waves at rough surface 06 p0784 N85-15014
Scattering from thin dielectric disks
[NASA-TM-86155] 06 p0798 N85-15098
Far-infrared laser diagnostic on EBT and extreme far-forward laser scattering on ISX
[DE85-001788] 07 p1046 N85-16843
Second order Bragg scattering in a SAR
[AD-A148905] 08 p1152 N85-17275
Scattering of electromagnetic waves by human body and its applications 09 p1383 N85-18572
Numerical methods for analyzing electromagnetic scattering
[NASA-CR-175507] 12 p1823 N85-21438
Inelastic scattering in condensed matter with high intensity Mossebauer radiation
[DE85-003531] 12 p1854 N85-21827
Research efforts in support of resonance extraction studies. Volume 1: Improvement and validation of TWFD (Thin-Wire Frequency-Domain): A thin-wire frequency-domain scattering code
[AD-A150296] 13 p2054 N85-22864
Scattering of electromagnetic waves by charged particles 13 p2067 N85-22913
Diffraction of plane TM-wave on continuously irregular elliptical plasma 13 p2067 N85-22914
Extraction of surface-wave energy from plasma waveguide 13 p2077 N85-22974
Scattering of waves by axisymmetrical edge 13 p2080 N85-22987
Analysis of the electromagnetic scattering from an inlet geometry with lossy walls
[NASA-CR-175743] 15 p2541 N85-25686
Electromagnetic scattering by arbitrarily shaped reflectors: Subreflector efficiency
[AD-A149224] 15 p2541 N85-25687
Scattering center analysis for radar cross section modification 16 p2769 N85-27065
Optical non-line-of-sight covert, secure high data communication system
[AD-D011607] 16 p2769 N85-27067
Application of forward scattering renormalization to scattering in turbid media
[AD-A153232] 17 p2959 N85-28271
The stability and dynamics of elastic structures and fluid flows
[AD-A154166] 19 p3266 N85-30252
Active and passive remote sensing of ice
[AD-A154406] 19 p3300 N85-30459
Radar target identification through electromagnetic scattering studies
[AD-A154596] 21 p3573 N85-32220
Scattering from foliage covered terrain
[AD-A154724] 21 p3574 N85-32228
Head-on scattering of a tubular cylinder of finite length for radar target identification purposes
[AD-A155808] 21 p3577 N85-32246
Broadside scattering of a tubular cylinder for evaluation of target identification
[AD-A155739] 21 p3577 N85-32248
Minimizing field scattered by slender dipoles 22 p3774 N85-33388
On the convergence of an iterative formulation of the electromagnetic scattering from an infinite grating of thin wires 24 p4085 N85-35319
Penetrative nature of high energy showers observed in Chacaltaya emulsion chamber
[HE-3.3-5] 24 p4180 N85-35923
Anomalous correlation between hadron and electromagnetic particles in hadron and gamma-ray families
[HE-3.3-6] 24 p4180 N85-35924

ELECTROMAGNETIC SHIELDING
Laboratory evaluation of Electromagnetic Pulse (EMP) hardness testing concepts for electrical conduit systems
[AD-A145466] 02 p0190 N85-11273
Pulse injection on a power cable penetrating a shielding wall by feed-through capacitors
[FOA-C-30372-A3] 04 p0497 N85-13171
A comparison of lightning and nuclear electromagnetic pulse response of tactical shelters 07 p1000 N85-16350
Shielded enclosures for experimental studies of shielding topology
[AD-A149292] 11 p1624 N85-20227
Model calculations for a CO2 mixing laser with screen nozzle
[ESA-TT-859] 11 p1640 N85-20336
Electromagnetic pulse (EMP) injection on cable entries, type ERA; EMP memo no. 10
[FOA-E-30003-A3] 12 p1830 N85-21484
A theory of electromagnetic shielding with applications to MIL-STD-285, IEEE-299, and EMP simulation
[AD-A154905] 21 p3575 N85-32233
Actuator rigging test set electromagnetic interference test (CE03)
[AD-A155819] 24 p4086 N85-35327

ELECTROMAGNETIC SPECTRA
NT BALMER SERIES
NT D LINES
NT ELECTRONIC SPECTRA
NT FRAUNHOFER LINES
NT GAMMA RAY SPECTRA
NT H ALPHA LINE
NT H LINES
NT INFRARED SPECTRA
NT K LINES
NT LINE SPECTRA
NT LYMAN SPECTRA
NT MICROWAVE SPECTRA
NT RADIO SPECTRA
NT RAMAN SPECTRA
NT RYDBERG SERIES
NT SOLAR SPECTRA
NT STELLAR SPECTRA
NT UBV SPECTRA
NT ULTRAVIOLET SPECTRA
NT VIBRATIONAL SPECTRA
NT VISIBLE SPECTRUM
NT X RAY SPECTRA
Summary of the origin of nonradiative heating/momentum in hot stars 08 p1236 N85-17789
Basic principles of industrial radiography 14 p2316 N85-24310
Analytical techniques used to calculate the fields due to refraction and diffraction of electromagnetic waves
[AD-A151705] 15 p2543 N85-25698
A position sensitive phoswich hard X-ray detector system
[OG-9.3-12] 23 p4028 N85-34967
The ISAVF opto-mechanical test bed
[NASA-TM-87505] 24 p4067 N85-35208

ELECTROMAGNETIC SURFACE WAVES
Image theory for a vertical electric dipole above a wire grid with square cells
[REPT-S-150] 02 p0192 N85-11286
Extraction of surface-wave energy from plasma waveguide 13 p2077 N85-22974

ELECTROMAGNETIC WAVE FILTERS
NT BANDPASS FILTERS
NT BIREFRINGENT FILTERS
NT CRYSTAL FILTERS
NT DIGITAL FILTERS
NT ELECTRIC FILTERS
NT FIR FILTERS
NT MATCHED FILTERS
NT MICROWAVE FILTERS
NT OPTICAL FILTERS
NT RADAR FILTERS
NT RADIO FILTERS
NT TRACKING FILTERS
NT WAVEGUIDE FILTERS
Environmentally independent fiber optic rotation sensor
[AD-D011219] 01 p0119 N85-10818
Method for forming electromagnetic-wave-screening composite 07 p0936 N85-15930
Filter and passband problems 08 p1252 N85-17910
Space-time response characteristics of acoustooptic filter for compression of linearly frequency-modulated signal 13 p2071 N85-22937
Some design considerations for a satellite-borne magnetograph 18 p3204 N85-29879
The inference of vector magnetic fields from polarization measurements with limited spectral resolution 18 p3207 N85-29896

ELECTROMAGNETIC WAVE TRANSMISSION
NT HALOS
NT IONOSPHERIC PROPAGATION
NT LIGHT SCATTERING
NT LIGHT TRANSMISSION
NT MANDELSTAM REPRESENTATION
NT MICROWAVE ATTENUATION
NT MICROWAVE TRANSMISSION
NT MULTIPATH TRANSMISSION
NT RADAR TRANSMISSION
NT RADIO TRANSMISSION
NT SCATTER PROPAGATION
NT SHORT WAVE RADIO TRANSMISSION
NT SINGLE SIDEBAND TRANSMISSION
NT SPREAD SPECTRUM TRANSMISSION
NT TELEVISION TRANSMISSION
NT TRANSEQUATORIAL PROPAGATION
Activities report of the Radio Laboratory
[REPT-S-153] 02 p0192 N85-11288
Effects of atmospheric water vapor and clouds on NOAA (National Oceanic and Atmospheric Administration) AVHRR (Advanced Very High Resolution Radiometer) satellite data
[AD-A145425] 02 p0280 N85-11824
Nonlinear electromagnetic waves in ferromagnetic conducting media 03 p0346 N85-12232
The development of new methods for solving the target identification or inverse scattering problem for time-harmonic acoustic and electromagnetic waves
[AD-A145821] 03 p0415 N85-12657
A comparison of evaporation duct models for IREPS (Integrated Refractive Effects Prediction System)
[AD-A146471] 06 p0799 N85-15103

Beam propagation studies at NRL (Naval Research Laboratory) July 1983 to June 1984, volume 2
[AD-A148198] 08 p1152 N85-17270
Methodical approaches to determination of sanitation protective zone dimensions around TV centers and TV retransmitters 09 p1361 N85-18563
Propagation of electromagnetic fields along the sea/sea-bed interface
[AD-A149523] 10 p1467 N85-19257
Generation of Alfven waves due to thermal modulation of the electrical conductivity
[AD-A149369] 10 p1558 N85-19826
Survivable propagation
[AD-A150070] 12 p1829 N85-21478
Analysis and computations of microwave-atmospheric interactions
[AD-A149668] 12 p1869 N85-21654
The use of the spectral matrix in analyzing the propagation characteristics of electromagnetic emissions --- magnetosphere 14 p2371 N85-24658
Statistical/Trend analysis of the marine atmospheric boundary layer model
[AD-A151053] 14 p2374 N85-24673
Meteorological conditions affecting electromagnetic propagation on the Arabian Peninsula
[AD-A152019] 15 p2544 N85-25708
The weighting function for scintillation on a folded path
[AD-A152659] 17 p2949 N85-28206
Electromagnetic transmission through a slot in a perfectly conducting plane
[AD-A153224] 17 p2949 N85-28210
Electromagnetic lateral waves in layered media 19 p3369 N85-30694
Control of large antennas based on electromagnetic performance criteria 20 p3409 N85-31158
Effects of hydrometeors on electromagnetic wave propagation
[AD-A155379] 22 p3759 N85-33297
Injection of energetic particles following the gamma-ray flares on June 7, 1980, as observed on Helios 1
[SH-1.3-9] 23 p3993 N85-34756

ELECTROMAGNETIC WAVES
U ELECTROMAGNETIC RADIATION

ELECTROMAGNETICS
U ELECTROMAGNETISM

ELECTROMAGNETISM
NT MAGNETOSTATICS
Joint services electronics program
[AD-A145085] 01 p0042 N85-10276
ASP: A new PEP experiment to measure single photons
[DE84-015732] 04 p0560 N85-13563
Electromechanical/electromagnetics working group summary 05 p0604 N85-13852
Experimental research on electric propulsion. Note 7: Analysis of the performance of an arc-jet driven by means of hydrogen and nitrogen
[NASA-TM-77473] 06 p0760 N85-14861
Two-dimensional signal processing and storage and theory and applications of electromagnetic measurements. Supplemental appendix
[AD-A146848] 07 p0939 N85-15953
USSR report: Electronics and electrical engineering
[JPRS-UEE-84-017] 07 p0951 N85-16025
Electromagnetic inspection of wire ropes using sensor arrays
[AD-A148317] 08 p1170 N85-17379
Electromagnetic braking of a metallic projectile in flight
[AD-A149424] 10 p1480 N85-19345
Electromagnetic inspection of wire ropes using sensor arrays
[AD-A149016] 10 p1495 N85-19436
Linear magnetic bearings
[NASA-CASE-GSC-12582-2] 11 p1641 N85-20337
Magnetic location of Earth's core-mantle boundary and estimates of the adjacent fluid motion 13 p2131 N85-23260
Magnetic field interactions with material discontinuities
[AD-A150197] 13 p2154 N85-23373
Electro-science requirements for shuttle-attached antenna flight experiments 14 p2237 N85-23866
Basic research in electronics (JSEP)
[AD-A151002] 14 p2298 N85-24230
Small aperture analysis of the dual TEM (transverse electromagnetic) cell and an investigation of test object scattering in a single TEM cell
[PB85-156952] 14 p2306 N85-24277
Annual report on electronics research at the University of Texas at Austin
[AD-A150836] 14 p2415 N85-24901
Los Alamos Science, Number 11, Summer-Fall, 1984
[DE85-004634] 14 p2419 N85-24926
A literature review of EMATs, with stress calculations for simple EMAT geometries
[AERE-R-11415] 15 p2642 N85-26295
Joint services electronics program
[AD-A154348] 19 p3375 N85-30939
Electromagnetic inspection of wire ropes using sensor arrays
[AD-A155412] 22 p3795 N85-33509
Diagnostic of electromagnetic conditions in space using cosmic rays
[SH-4.5-19] 23 p4038 N85-35036
Moment-method formulation of the cavity-probe aperture antenna
[DE85-013264] 24 p4088 N85-35338

ELECTROMAGNETS
NT SUPERCONDUCTING MAGNETS
Magnetic spin reduction system for free spinning objects
[NASA-CASE-MFS-25966-1] 02 p0166 N85-11122
Design of electromagnetic bearing for vibration control of flexible transmission shaft 05 p0645 N85-14136
Code lock with microcircuit 13 p2071 N85-22935
The development of a transducer system for the accurate measurement of ultrasonic phase delay of SH plate waves
[AERE-R-11598] 15 p2559 N85-25790
Major facility overhauls at LAMPF
[DE85-012724] 24 p4156 N85-35765

ELECTROMECHANICAL DEVICES
Shock electromechanical energy converter with permanent magnet
[AD-D011226] 01 p0115 N85-10781
Electromechanical/electromagnetics working group summary 05 p0604 N85-13852
Systems study for an Integrated Digital-Electric Aircraft (IDEA)
[NASA-CR-3840] 07 p0902 N85-15714
Electromechanical switch
[AD-D011400] 07 p0948 N85-16009
Improvement of electromechanical systems by utilization of microelectronic technology 07 p0955 N85-16053
Design and test of a four channel motor for electromechanical flight control actuation
[NASA-CR-171838] 08 p1156 N85-17294
The development of a microprocessor-controlled linearly-actuated valve assembly
[NASA-CR-174437] 10 p1491 N85-19415
Design and fabrication of a unique electromechanical machine for long-term fatigue testing
[DE85-006524] 15 p2590 N85-25912
Optimum dimensions of power solenoids for magnetic suspension
[NASA-TM-77864] 17 p3026 N85-28716
Electro-expulsive separation system
[NASA-CASE-ARC-11613-1] 18 p3094 N85-29150
Reliability derating procedures
[AD-A153744] 18 p3119 N85-29309
Experiments on the influence of active walls on the initial amplitudes and growths of instability waves
[AD-A154630] 21 p3583 N85-32275

ELECTROMECHANICS
Modular electromechanical industrial robots 03 p0345 N85-12223
Characterization of CNRS Fizeau wedge laser tuner
[NASA-CR-174357] 09 p1325 N85-18328
Activities of Istituto Elettrotecnico Nazionale Galileo Ferraris 18 p3199 N85-29845
Supersonic flow with feeding of energy
[NASA-TM-77912] 24 p4061 N85-35163

ELECTROMETERS
An improved rocket-borne electric field meter for the middle atmosphere
[NASA-CR-175510] 12 p1888 N85-21851
Dielectric measurements in infralow-frequency band 13 p2067 N85-23034

ELECTROMOTIVE FORCES
NT PONDEROMOTIVE FORCES
Measurement of oxide ion concentration in NaCl-ZnCl2 molten salt and several applications
[BLL-AWRE-TRANS-74-(9091.9F)] 06 p0764 N85-14886
Studies on copper alloys containing chromium on the copper side phase diagram
[NASA-TM-77752] 07 p0927 N85-15876
Cells for measuring thermoelectromotive force and electrical resistance of metals in temperature range of 20-950 degrees Celsius
[BLL-M-36240-(5826.4)] 20 p3457 N85-31473

ELECTROMYOGRAMS
U ELECTROMYOGRAPHY

ELECTROMYOGRAPHS
U ELECTROMYOGRAPHY

ELECTROMYOGRAPHY
Electromyographic patterns associated with discrete limb movements 05 p0710 N85-14551

ELECTRON ACCELERATION
Electron acceleration by laser fields in a gas
[DE85-000575] 11 p1639 N85-20323
Electron acceleration
[DE85-002337] 11 p1725 N85-20850
Average and worst-case specifications of precipitating auroral electron environment 13 p1991 N85-22482
Polar plasmas as observed by Dynamics Explorers 1 and 2 13 p1991 N85-22483
Two-dimensional beat wave acceleration simulation
[DE85-005961] 16 p2791 N85-27214
The temporal evolution of a small auroral substorm as viewed from high altitudes with Dynamics Explorer 1
[NASA-CR-176064] 20 p3493 N85-31718
Possibility of potential generation by lower hybrid wave 23 p3977 N85-34654

ELECTRON ACCELERATORS
NT BETATRONS
Accelerator development in support of the NRL (Naval research laboratory) beam dynamic program
[AD-A145976] 03 p0417 N85-12660
Self potentials of an electron ring in a torus for large ring displacement from the minor axis
[AD-A146088] 03 p0421 N85-12691
Survey of initial experiments on ATA beam dynamics
[DE85-004410] 10 p1555 N85-19806
China report: Science and technology
[JPRS-CST-84-025] 11 p1620 N85-20197
A 10/sup 11/W high current pulse electron beam accelerator described 11 p1620 N85-20200
Adaptation of an air-dielectric RF cable for use as an oil-filled high voltage pulse transmission line
[DE84-017414] 11 p1630 N85-20265
Calculations pertaining to the design of a prebuncher for a 150-MeV electron linear accelerator 3. Comparisons with experimental data
[DE85-002866] 11 p1724 N85-20844
High-field dipoles for future accelerators
[DE85-002315] 13 p2157 N85-23391
Transverse electron resonance accelerator
[DE85-008299] 17 p3032 N85-29758
Rapid Electron Beam Accelerators (REBA-TRONS)
[AD-A153835] 18 p3179 N85-29707
Plasma wake field accelerator
[DE85-010538] 18 p3191 N85-29791
High-brightness photoemitter development for electron accelerator injectors
[DE85-009548] 19 p3355 N85-30796
Beam dynamics in MABE
[DE85-010670] 19 p3358 N85-30819
Requirements for very high energy accelerators
[DE85-011173] 20 p3529 N85-31952
Space Experiments with Particle Accelerators (SEPAC) 23 p3901 N85-34165
Vehicle Charging And Potential (VCAP) 23 p3902 N85-34173
Four stage HELIA experiment
[DE85-012026] 24 p4156 N85-35768
Power flow evaluations for HERMES 3
[DE85-013116] 24 p4156 N85-35769

ELECTRON ATTACHMENT
Electron production, electron attachment, and charge recombination process in high pressure gas discharges
[AD-A149535] 10 p1554 N85-19799
Density of impurity states associated to inversion layers
[INPE-3406-PRE/675] 16 p2869 N85-27702

ELECTRON AVALANCHE
LPM effect and primary energy estimations
[HE-3.6-4] 24 p4185 N85-35953

ELECTRON BEAM WELDING
Structure and ductility of fracture of joints produced by electron-beam welding of VT6ch titanium alloy parts 03 p0351 N85-12261
Welding of PM-superalloys
[MTU-TB-910/84] 07 p0975 N85-16191
Application of diffusion welding of nickel based metals and application of electron beam welding of hot isostatically pressed nickel based powdered metals 08 p1169 N85-17375
Fatigue resistance of welded joints of high strength steels produced by electron beam welding 10 p1449 N85-19127
Calculation of mode field in electron beam welding of VT6 titanium alloy 10 p1449 N85-19129
Assessment of effectiveness of electron beam welding of titanium alloys up to 40 mm in thickness by vertical or horizontal beam 11 p1603 N85-20078
Mathematical simulation of thermal processes involved in electron-beam treatment 12 p1843 N85-21565
Structure and mechanical characteristics of heterogeneous joints produced by laser welding 13 p2034 N85-22742
Softening of metal near seam during welding of heat-resistant nickel alloys 13 p2035 N85-22747

Paton comments on results of space welding tests
15 p2484 N85-25330
Brittle fracture resistance of electron beam-welded joints in titanium Alpha alloys
15 p2500 N85-25419
Increasing seam formation stability in electron beam welding of very thick titanium alloys
15 p2500 N85-25420
Some aspects of nuclear plant fabrication in Japan and the UK relating to automatic and robotic arc welding
15 p2566 N85-25834
Institute's contribution to Soviet welding technology noted
16 p2767 N85-27072
Paton Institute expert on GDR-USSR welding research
16 p2768 N85-27078
Underwater pipeline: Welding by high frequency induction
[BLL-WI-TRANS-682-(9312.57)]
16 p2792 N85-27221
Welding methods for high melting metals
22 p3794 N85-33508
Laser welding of 6Al-4V titanium alloy
[DE85-012019] 23 p3936 N85-34413

ELECTRON BEAMS

NT RELATIVISTIC ELECTRON BEAMS

Transverse field interaction multibeam amplifier
[AD-D011241] 01 p0043 N85-10282
Time variability of directionality properties of pulsed EB-EDL (Electron Beam-Electric Discharge Laser) N2-CO2 lasers
[AD-A145546] 02 p0202 N85-11344
The propagation and growth of whistler mode waves generated by electron beams in Earth's bow shock
[AD-A145572] 02 p0228 N85-11492
Theory of free-electron lasers with focusing pumping field
02 p0262 N85-11714
Strong Langmuir turbulence 02 p0284 N85-11851
Fast and precise processing of material by means of an intensive electron beam
[BMFT-FB-T-84-123] 03 p0342 N85-12201
Generation of superpowerful microsecond electromagnetic radiation pulses
03 p0347 N85-12234
Accelerator development in support of the NRL (Naval research laboratory) beam dynamic program
[AD-A145976] 03 p0417 N85-12669
ATA gas propagation: 1 foot tank experiment
[DE84-016396] 04 p0561 N85-13575
Ion beam and laser induced surface modifications
[DE84-016569] 04 p0571 N85-13642
Laboratory electron beam simulation of cosmic radio jets
[DE84-016179] 04 p0580 N85-13764
Practical application of electron beam testing in LSI and VLSI circuits
[BMFT-FB-T-84-185] 05 p0633 N85-14061
Status of beam transport with the ETA and ATA accelerators
[DE84-013206] 05 p0726 N85-14670
Minimizing the energy spread within a single bunch by shaping its charge distribution
[DE84-016172] 05 p0727 N85-14676
Transient attenuation in optical fibers
[DE84-016497] 05 p0729 N85-14687
Pulsed electric discharge laser technology. Electron beam window foil material
[AD-A146420] 06 p0813 N85-15162
Processes of smooth increase and dropoff in intensity of glow line lambda' = 5577 A with exposure of ionosphere to electron beam
06 p0822 N85-15219
Mechanism of damping of plasma oscillations in initial stage of injection of electron beams from spacecraft into ionosphere in active experiments
06 p0823 N85-15225
Electron beam propagation along charged foils
[DE85-002137] 06 p0861 N85-15472
ATA probe beam experiment
[DE84-016017] 06 p0862 N85-15477
FORTRAN version of the quantitative energy-dispersive electron beam X-ray analysis program FRAME C
[PB84-240936] 07 p1027 N85-16519
A low perturbation electron injector for cyclic accelerators
[AD-D011312] 07 p1040 N85-16604
Electrostatic wave observation during a space simulation Beam-Plasma-Discharge (BPD)
[NASA-CR-174286] 07 p1045 N85-16639
A coaxial probe for measuring the current density profile of intense electron beams
[AD-D011407] 08 p1164 N85-17347
Exposure modelling of particle beam lithography
[AD-A147849] 08 p1219 N85-17678
Beam propagation study: Stabilization of the resistive hose instability in intense electron beams
[AD-A149071] 08 p1220 N85-17684
Non-linear transverse electron beam dynamics in a modified betatron accelerator
[AD-A148106] 08 p1220 N85-17685
Virtual cathode oscillator study
[AD-A149268] 10 p1480 N85-19342
Two-stage free electron laser research
[AD-A148951] 10 p1489 N85-19402
A free electron laser with a rotating quadrupole wiggler
[AD-A149052] 10 p1489 N85-19404
Facilities for studing radiation damage in nonmetals during irradiation
[DE85-000590] 10 p1554 N85-19801
Experimental investigation of certain beam transport issues in a pulsed transmission line linear accelerator
[DE85-002310] 10 p1555 N85-19805
Brightness limitations in multi-kiloampere electron beam sources
[DE84-017417] 10 p1555 N85-19807
China report: Science and technology
[JPRS-CST-84-025] 11 p1620 N85-20197
A 10/sup 11/W high current pulse electron beam accelerator described
11 p1620 N85-20200
Electron acceleration by laser fields in a gas
[DE85-000575] 11 p1639 N85-20323
Optical guiding in a free electron laser
[DE85-003141] 11 p1639 N85-20327
High power pulsed accelerators with potential industrial applications
[DE85-001710] 11 p1720 N85-20821
Self-Optimized Sector (SOS) model of self-consistent energy loss and scattering for an electron beam propagating in air
[DE85-003161] 11 p1722 N85-20831
Experiments on ETA comparing wire-conditioned and non-wire-conditioned beam propagation
[DE85-004451] 11 p1725 N85-20848
Electron acceleration
[DE85-002337] 11 p1725 N85-20850
Si-on-insulator formation using a line-source electron beam
[DE85-003449] 11 p1737 N85-20925
S3-3 ONR-118 data analysis
[AD-A149725] 12 p1889 N85-21855
Electron beam charging of Space Shuttle thermal protection system tiles
13 p1990 N85-22478
Sheath ionization model of beam emissions from large spacecraft
13 p1992 N85-22489
Electron yields from spacecraft materials
13 p1996 N85-22512
A simple model of electron beam initiated dielectric breakdown
13 p1996 N85-22516
SEM (Scanning Electron Microscope) investigation of silicon diodes using the electron beam induced current method
[AD-A150356] 13 p2084 N85-22894
Design considerations for a 100 kW CW, 140 GHz gyrotron oscillator
[DE85-005282] 13 p2086 N85-22904
Investigation of generation of oscillations using anomalous Doppler effect
13 p2078 N85-22980
Temperature dependence of propagation of high-current electron beam through drift space
13 p2079 N85-22982
Effect of space-charge field on output characteristics of O-type oscillators with distributed interaction
13 p2089 N85-23043
Los Alamos free electron laser: Accelerator performance
[DE85-005722] 13 p2097 N85-23084
Electric potential of satellite in electron emitting experiments in initial stage of electron beam injection in steady-state mode
15 p2480 N85-25309
High current beam hollowing instability study
[AD-A151301] 15 p2648 N85-26329
Two-beam accelerator
[DE85-004662] 15 p2649 N85-26335
Annual Review, April 1983 - March 1984
[ISSN-0547-1567] 15 p2654 N85-26369
High energy beam experiment
15 p2654 N85-26376
Basic studies. 1: Basic experiments in plasma physics
15 p2655 N85-26379
Experimental studies of the electronic structure of 1-2 and 1-3 intermetallic compounds
[DE85-006979] 15 p2662 N85-26432
Measurements in low pressure flow using an electronic beam detector — wind tunnel tests
16 p2701 N85-26576
Investigation of electron attachment and dissociation rates in C2F6/CH4 electric gas discharges
[AD-A151796] 16 p2662 N85-27649
High efficiency transverse dc electron beams
[AD-A152038] 16 p2662 N85-27651
Energy deposition from particle beams
[DE85-007382] 16 p2662 N85-27654
Survey of experimental and theoretical electron-impact ionization cross sections for transition metal ions in low stages of ionization
[DE85-007605] 16 p2663 N85-27658
In situ HVEM studies of electron beam-driven composition changes in thin film alloys: Displacement-rate gradient effects
[DE85-007992] 17 p2931 N85-28092
Uniaxial angular accelerometers
17 p2944 N85-28173
VULTURE manual
[DE85-008573] 17 p3013 N85-28631
Wake fields and wake field acceleration
[DE85-008054] 17 p3031 N85-28750
Measurement and interpretation of electron angle at MABE beam stop
[DE85-008583] 17 p3032 N85-28755
Transverse electron resonance accelerator
[DE85-008289] 17 p3032 N85-28758
Restrike particle beam experiments on a dense plasma focus. Opening switch research on a dense plasma focus
[AD-A152991] 17 p3039 N85-28802
Beam tests of phosphorescent screens
[DE85-009843] 18 p3097 N85-29170
Operation of a quasioptical electron cyclotron maser
[DE85-008450] 18 p3113 N85-29276
The free electron laser variable bridge coupler
[DE85-009630] 18 p3114 N85-29278
Further studies of the NRL collective particle accelerator via numerical modeling with the MAGIC code
[AD-A153583] 18 p3178 N85-29703
Experimental and theoretical investigation of microwave and millimeter wave radiation from hollow, rotating electron beams
[AD-A153827] 18 p3179 N85-29706
Rapid Electron Beam Accelerators (REBA-TRONS)
[AD-A153835] 18 p3179 N85-29707
Phase and amplitude considerations for the 2-beam accelerator
[DE85-008455] 18 p3180 N85-29715
Accelerator technology working group summary
[DE85-009547] 18 p3180 N85-29717
Calculations of beam dynamics in Sandia linear electron accelerators, 1984
[DE85-010417] 18 p3180 N85-29719
Electron multiple, plural and single scattering
[DE85-010325] 18 p3181 N85-29721
Energy deposition and its effects on the E+ capture section at Sector 20
[DE85-010964] 18 p3182 N85-29727
Experience with a high-brightness storage ring: The NSLS 750 MeV VUV ring
[DE85-010647] 18 p3190 N85-29787
Plasma wake field accelerator
[DE85-010538] 18 p3191 N85-29791
A collective interaction klystron specification
[AD-D011704] 19 p3255 N85-30186
Superconducting electronic film structures
[AD-A154196] 19 p3259 N85-30207
Conversion efficiencies of charged particle beam driven free electron lasers
[AD-A154404] 19 p3276 N85-30316
High-brightness photoemitter development for electron accelerator injectors
[DE85-009548] 19 p3355 N85-30796
Interaction of slow electrons with high-pressure gases (quasi-liquids): Synthesis of our knowledge on slow electron-molecule interactions
[DE85-010061] 19 p3355 N85-30800
Beam dynamics in MABE
[DE85-010670] 19 p3358 N85-30819
Quantum effects in linear collider scaling laws
[DE85-009848] 19 p3363 N85-30851
EBIC characterization and hydrogen passivation in silicon sheet
20 p3481 N85-31634
Methods of Monte Carlo electron transport in particle-in-cell codes
[DE85-010702] 20 p3521 N85-31888
Practicality of electronic beam steering for MST/ST radars, part 6.2A
21 p3624 N85-32516
Trapping of ion conics by downward parallel electric fields
[AD-A155306] 21 p3633 N85-32568
Operation of solid state lasers exposed to electron beam
21 p3665 N85-32895
Amplification of electromagnetic wave by electron stream with negative velocity differences
21 p3692 N85-32941
Electron beam enhanced surface modification for making highly resolved structures
[DE85-011609] 22 p3780 N85-33305
Electron trajectories in a combined wiggler and alternating gradient quadrupole field
[DE85-010727] 22 p3842 N85-33794

Theoretical and Experimental Beam Plasma Physics (TEBPP) 23 p3801 N85-34166
RADLAC technolgy review
[DE85-011995] 23 p3982 N85-34691
Measurement and interpretation of electron angle at MABE beam stop
[DE85-011918] 23 p3983 N85-34698
Technology of magnetically driven accelerators
[DE85-011857] 23 p3983 N85-34700
Note on the detection of high energy primary cosmic gamma rays by air shower observation
[OG-9.5-9] 23 p4031 N85-34986
Observations of accelerated high current low emittance beams in the SLC Linac
[DE85-013073] 24 p4068 N85-35211
Four stage HELIA experiment
[DE85-012026] 24 p4156 N85-35768
Power flow evaluations for HERMES 3
[DE85-013116] 24 p4156 N85-35769
Kinetic loss experiments on Mite
[DE85-012826] 24 p4158 N85-35780
Laser and electron beam processing of semiconductors
[AD-A155914] 24 p4161 N85-35796

ELECTRON BOMBARDMENT
Development of the Engineering Test Satellite-3 (ETS-3) ion engine system
[NASA-TM-77538] 01 p0017 N85-10101
Radiation-induced compositional redistribution and local phase transformation in irradiated alloys
[DE85-000060] 10 p1441 N85-19062
Aluminum work function: Effect of oxidation, mechanical scraping and ion bombardment
[NASA-TM-87079] 23 p3915 N85-34265

ELECTRON BUNCHING
Minimizing the energy spread within a single bunch by shaping its charge distribution
[DE84-016172] 05 p0727 N85-14676
Optimization of energy conversion during locking of electron bunches by electromagnetic wave in longitudinal electrostatic field 06 p0786 N85-15025
Calculated parameters for the initial part of an accelerator with high-frequency quadrupole focusing
[RAE-TRANS-2122] 07 p1040 N85-16600
Los Alamos free electron laser: Accelerator performance
[DE85-005722] 13 p2097 N85-23084
Form factor effects on microwave Cerenkov radiation
[AD-A154577] 21 p3701 N85-32993
Cerenkov radiation from periodic electron bunches for finite emission length in air
[AD-A156156] 24 p4090 N85-35352

ELECTRON CAPTURE
Precipitation of protons with E sub p approximately 1 MeV near plasmopause 02 p0161 N85-11093
Theoretical analysis of physical processes of lasing medium degradation in semiconductor lasers 02 p0269 N85-11759
Electron capture by multiply charged ions from hydrogen atoms at low energies
[DE84-016560] 06 p0661 N85-15475
Theoretical studies of Rydberg atom collisions
[AD-A146556] 08 p1220 N85-17687
One-electron capture processes by highly charged ions from helium: Present status of HICE-IPP 09 p1389 N85-18736
Negative lithium emission from a tungsten surface in a plasma
[DE85-003456] 12 p1936 N85-22167
Electron flux with electron energies above 40 MeV at altitudes of about 500 km in region where capture is possible and outside it when L is 3 or greater 15 p2481 N85-25315
Convoy electron production by heavy ions in solids
[DE85-006256] 15 p2680 N85-26418
Excited state populations and charge-exchange of fast ions in solids
[DE85-006362] 18 p3180 N85-29714
Electron capture to the continuum from atomic hydrogen
[DE85-005269] 18 p3181 N85-29722
Atmospheric chlorofluoromethanes as tracers of ocean circulation and mixing: Measurement and calibration techniques and studies in the Greenland and Norwegian Seas 19 p3319 N85-30573
A theoretical study of electron capture in ion-ion and ion-atom collisions
[DE85-011154] 19 p3362 N85-30842
Study of photon emission by electron capture during solar nuclei acceleration, 1: Temperature-dependent cross section for charge changing processes
[SH-1.1-8] 23 p3990 N85-34735
Study of photon emission by electron capture during solar nuclei acceleration. 2: Delimitation of conditions for charge transfert establishment
[SH-1.1-9] 23 p3990 N85-34736
Study of photon emission by electron capture during solar nuclei acceleration. 3: Photon production evaluations
[SH-1.1-10] 23 p3990 N85-34737
Electron capture decay of cosmic rays: A model of the inhomogeneous interstellar medium
[OG-7.1-10] 23 p4014 N85-34871
Search for stellar collapse with the MACRO detector at Gran Sasso
[HE-5.3-11] 24 p4206 N85-36105

ELECTRON CLOUDS
Excess gamma-rays in the direction of the rho Ophiuchi cloud: An exotic object?
[OG-2.5-1] 22 p3868 N85-33958

ELECTRON COLLISIONS
U ELECTRON SCATTERING

ELECTRON COMPOUNDS
U INTERMETALLICS

ELECTRON CYCLOTRON HEATING
Theoretical studies in tandem mirror physics
[DE84-015634] 04 p0566 N85-13604
Fusion plasma theory. Task 3: ECRH and transport modeling in tandem mirrors and divertor physics
[DE84-014939] 04 p0567 N85-13612
EBT electron energy confinement experiments
[DE84-015402] 04 p0567 N85-13613
High frequency plasma generator for ion thrusters
[NASA-CR-174772] 08 p1114 N85-17023
ORNL ECR multicharged ion source
[DE85-001283] 09 p1380 N85-18681
Present status of Heliotron E experiment 09 p1387 N85-18721
Discharge initiation experiments in the Tokapole II Tokamak
[DE84-017345] 09 p1391 N85-18755
Electron cyclotron resonance heating system for the stellarator W 7-AS
[IPF-84-5] 09 p1395 N85-18779
High power millimeter-wave mode converters in overmoded circular waveguides using periodic wall perturbations
[IPF-84-6] 09 p1395 N85-18780
Wave absorption and transport studies on Electron Cyclotron Resonance (ECR) heated stellarator plasmas in W 7-A
[IPF-84-9] 09 p1395 N85-18782
Activities report of the Institute of Plasma Research 11 p1733 N85-20903
The 60 GHz gyrotron development program
[DE85-000599] 12 p1836 N85-21522
A 60 GHz 200 kW CW gyrotron with high output mode purity
[DE85-005283] 13 p2066 N85-22905
Investigation of generation of oscillations using anomalous Doppler effect 13 p2078 N85-22960
System for lower hybrid current startup 15 p2654 N85-26373
Basic experiments in plasma physics (TPL) 15 p2655 N85-26379
140 GHz gyrotron development program
[DE85-010348] 20 p3537 N85-32013
Influence of ECR-heating on MHD activity of plasma in tokamak-10 installation 21 p3694 N85-32949
Electron and ion cyclotron heating calculations in the tandem-mirror
[DE85-011656] 22 p3842 N85-33797
High-field launch electron cyclotron heating experiments in the ELMO Bumpy Torus
[DE85-012068] 22 p3846 N85-33825
Role of ECRH in potential formation for tandem mirrors
[DE85-011859] 22 p3848 N85-33834
Plug and thermal barrier potential formation in Gamma 10 23 p3976 N85-34648
Effect of ECH and ICH on ambipolar potential in NBT-1M 23 p3978 N85-34661
Transports studies of ECH and ICRH-heated bumpy torus plasma in NBT-1M 23 p3978 N85-34662
Multiple-frequency electron cyclotron heating of hot electron rings in EBT-1
[DE85-011302] 23 p3983 N85-34701
ECH tokamak
[DE85-012074] 23 p3984 N85-34707

ELECTRON DENSITY (CONCENTRATION)
NT CARRIER DENSITY (SOLID STATE)
NT ELECTRON DENSITY PROFILES
NT IONOSPHERIC ELECTRON DENSITY
NT MAGNETOSPHERIC ELECTRON DENSITY
Visible wavelength interferometer for high speed electron density diagnostics
[AD-A145686] 02 p0277 N85-11803
Gas pressure and electron density at the level of the active zone of hollow cathode arc discharges
[NASA-TM-77477] 03 p0414 N85-12648
Behavior of the ionospheric F region in low latitudes and in the equatorial region of Brazil during strong magnetic storms in the 1978 to 1983 period
[INPE-3231-PRE/581] 05 p0675 N85-14333
Nocturnal increases of ionization in the ionospheric F region in the low latitude of Brazil during magnetic storms
[INPE-3271-PRE/596] 05 p0675 N85-14334
The parallax of pulsar 0950+08 and the local free electron density 06 p0679 N85-15584
Gas pressure and electron density in the active zone level of hollow cathode arc discharges
[NASA-TM-77468] 07 p0945 N85-15888
Electronic structure, chemical bonding, and superconductivity of silver films on germanium
[AD-A147720] 08 p1128 N85-17112
Photoionization structure of the Orion Nebula 08 p1246 N85-17863
Imploding plasma X-ray laser research
[DE85-000057] 09 p1326 N85-18331
Basic studies of atomic dynamics
[DE84-015661] 09 p1380 N85-18675
Calorimetric investigation into the possibility of a charge density wave ground state in alkali metals
[DE85-002006] 09 p1397 N85-18795
Hartree-Fock interaction between a helium atom and lithium-metal: A test for the effective medium theory
[AD-A150468] 13 p2156 N85-23387
Structural inhomogeneities in amorphous nickel-phosphorus alloy
[BLL-M-36103-(5828.4)] 16 p2748 N85-26960
EISCAT electron density studies
[AD-A152820] 17 p2993 N85-28498
Electron and ion distributions at high latitudes as measured by the Air Force polar orbiting satellites
[AD-A153242] 17 p2993 N85-28500
Memory function for cyclotron resonance of two-dimensional electron systems
[AD-A152632] 17 p3029 N85-28731
Quantized Hall effect in two-dimensional electron systems
[AD-A154347] 19 p3259 N85-30211
Shifts and widths of hydrogenic ion lines
[DE85-011375] 19 p3277 N85-30323
Hard X-ray measurements of the hot electron rings in Nagoya BUMPY TORUS (NBT-1M)
[IPPJ-720] 19 p3370 N85-30899
Effect of inner subshell ionization on emission lines OIV ions
[IPPJ-719] 19 p3370 N85-30903
Characteristics and sources of E-region ionization in the continuous aurora
[AD-A155018] 21 p3632 N85-32562
Soft X-ray polychromator for the Solar Maximum Mission
[NASA-CR-175297] 21 p3723 N85-33096
Lithology and stratigraphy of drill holes completed during 1984 in LANL use areas of Yucca Flat, Nevada Test Site, volume 6
[DE85-010695] 22 p3815 N85-33631
Digital characterization of particle tracks for microdosimetry
[DE85-012898] 22 p3846 N85-33822
Role of ECRH in potential formation for tandem mirrors
[DE85-011859] 22 p3848 N85-33834
Simultaneous Solar Maximum Mission and Very Large Array (VLA) observations of solar active regions
[NASA-CR-176090] 22 p3859 N85-33897
Electron density distribution analysis for nitroguanidine
[DE85-009598] 23 p3969 N85-34603
Helios 1 energetic particle observations of the solar gamma ray flare events of 7, 21 June 1980 and 3 June 1982
[SH-1.3-8] 23 p3993 N85-34755
Akeno 20 km (2) air shower array (Akeno Branch)
[OG-9.4-8] 23 p4029 N85-34975
Cerenkov radiation from periodic electron bunches for finite emission length in air
[AD-A156156] 24 p4090 N85-35352
Los Alamos free-electron laser
[DE85-012666] 24 p4098 N85-35405
Structured events in Pamir carbon X-ray chambers
[HE-3.7-7] 24 p4186 N85-35965
Performance of a local electron density trigger to select extensive air showers at sea level
[HE-4.6-11] 24 p4196 N85-36048

ELECTRON DENSITY PROFILES
Irregularity decay in an isolated plasma bubble
[AD-A145782] 03 p0392 N85-12506
CO2 laser interferometer array for Big Dee
[DE85-001718] 10 p1490 N85-19411
Winter anomaly of the lower ionosphere and its possible causes 11 p1660 N85-20459

Light diffraction with collective, thermal electron density fluctuation in plasmas with several ionic components
[IPF-84-5] 11 p1733 N85-20904
Rocket observations of the ionosphere during the eclipse of 26 February 1979
[NASA-CR-175513] 12 p1888 N85-21850
Calculation of ionospheric profiles by inverting VLF/LF reflection data. 2. Anisotropic propagation
[AD-A150105] 12 p1890 N85-21859
Contribution of relaxation sounding experiments to the understanding of magnetospheric processes 14 p2371 N85-24655
Determination of ionospheric electron density profiles from satellite UV (ultraviolet) emission measurements
[AD-A150734] 14 p2373 N85-24667
Heavy ion beam study of potential formation in bumpy torus plasma
[IPPJ-711] 15 p2656 N85-26386
Electrons and cosmic ray produced protons in Saturn's inner magnetosphere
[NASA-TM-87489] 15 p2679 N85-26546
Electrons and grain boundary energies in metals
[DE85-009530] 17 p2932 N85-28099
Rocket measurements of mesospheric ionization irregularities
[NASA-CR-176056] 20 p3494 N85-31721
Interstellar turbulence, random density variations, and scintillation measurements
[OG-7.2-13] 23 p4015 N85-34880
Relation between gamma-ray family and EAS core: Monte-Carlo simulation of EAS core
[HE-3.6-7] 24 p4185 N85-35955
Hadrons registration in emulsion chamber with carbon block
[HE-3.7-3] 24 p4186 N85-35962

ELECTRON DIFFRACTION

Electron spin polarization effects in low energy electron diffraction, ion neutralization and metastable atom deexcitation at solid surfaces
[DE84-016550] 04 p0572 N85-13649
Structure determination of molecular adsorbates with dynamical LEED and HREELS
[DE85-002007] 06 p0861 N85-15473
Characterization of CO binding sites on Rh(111) and Rh(331) surfaces by XPS and LEED (Low Energy Electron Diffraction): Comparison to EELS (Electron Energy Loss Spectroscopy) results
[AD-A149331] 10 p1435 N85-19044
Conduction in polymerized polyfunctional diacetylenes
[AD-A149104] 10 p1451 N85-19145
Fundamental study of catalysts using laser Raman, infrared, auger electron spectroscopy and low energy electron diffraction
[DE85-001813] 11 p1595 N85-20033
Electron-diffraction structural examination of amorphous iron-tin alloys 11 p1604 N85-20084
AEM with a convergent beam
[DE85-000667] 11 p1714 N85-20784
HREELS and Auger studies of conducting polymers
[DE85-004541] 13 p2038 N85-22764
Structural characterization by intensity measurements of electron diffraction patterns
[DE85-004803] 13 p2164 N85-23427
Test of the electronic structure of Fe(100) by absorbed current spectroscopy
[DE85-004942] 15 p2661 N85-26422
Low-energy electron diffraction experiment and theory
[DE85-009967] 18 p3195 N85-29820
Determination of kinetic parameters of molecular beam epitaxy
[AD-A155222] 21 p3710 N85-33030
Size and shape dependence of CO adsorption sites on sapphire supported Fe microcrystals
[NASA-CR-176171] 24 p4160 N85-35794

ELECTRON DIFFUSION

Two-level model for formation of night ionosphere of Venus from radio occulation experiments 02 p0162 N85-11100
Estimation of the rate of electron transfers between 2 contacting polymer surfaces
[AD-A148416] 08 p1122 N85-17072
Energetic electron anisotropy and ELF waves onboard GEOS. How does quasi-linear diffusion work 14 p2366 N85-24623
Time-implicit Monte-Carlo collision algorithm for particle-in-cell electron transport models
[DE85-010758] 20 p3521 N85-31900
Onion-shell model for cosmic ray electrons and radio synchrotron emission in supernova remnants
[OG-8.1-10] 23 p4018 N85-34900

ELECTRON DISTRIBUTION

NT ELECTRON DENSITY PROFILES
Electrons in a disordered medium
[NOTA-INTERNA-816] 02 p0279 N85-11819
Extended X-ray absorption fine structure (Exafs) studies of the actinides
[DE84-015833] 04 p0559 N85-13561
Electron distribution function and mobility in 3-5 compounds for high and low fields
[AD-A147447] 07 p1048 N85-16858
Data analysis of electron measurements of the plasma experiment aboard the HELIOS probes
[MPE-185] 09 p1416 N85-18935
Potential at atomic boundaries in the TF (or TFD) model and equations of states 12 p1820 N85-21419
Kapton charging characteristics: Effects of material thickness and electron-energy distribution 13 p1996 N85-22513
Observations of energetic electron and ion distributions near the magnetopause at geosynchronous orbit and related ground effects 14 p2356 N85-24580
Electron and ion distributions at high latitudes as measured by the Air Force polar orbiting satellites
[AD-A153242] 17 p2993 N85-28500
The universal spectrum of AGNs and QSOs
[OG-2.7-9] 22 p3872 N85-33982
EAS fluctuation approach to primary mass composition investigation
[OG-5.2-5] 22 p3883 N85-34082
Electron density distribution analysis for nitroguanidine
[DE85-009598] 23 p3969 N85-34603
The lateral distributions of charged particles of energy greater than 0.3 E sub crit in electron-photon cascades in lead and air
[HE-3.6-10] 24 p4185 N85-35957
Structured events in Pamir carbon X-ray chambers
[HE-3.7-7] 24 p4186 N85-35965
A new study of shower age distribution in near vertical showers by EAS air shower array 24 p4190 N85-35996
Lateral distribution of electrons of air showers 24 p4191 N85-35998
Detailed studies of the electron lateral distribution in extensive air showers with energies around 10(16) eV 24 p4191 N85-35999
Study of muons near shower cores at sea level using the E594 neutrino detector 24 p4191 N85-36000
Measurement of shower electrons and muons using a small air shower array
[HE-4.3-11] 24 p4192 N85-36005
Monte Carlo simulation of EAS generated by 10(14) - 10(16) eV protons
[HE-4.3-14] 24 p4192 N85-36008
Properties of 10 (18)-10 (19)eV EAS at far core distance
[HE-4.7-3] 24 p4198 N85-36054

ELECTRON EMISSION

NT FIELD EMISSION
NT PHOTOELECTRIC EMISSION
NT SECONDARY EMISSION
Polarized electron cyclotron emission in the Tokapole 2 Tokamak
[DE84-014953] 01 p0122 N85-10838
Plasma variables and tribological properties of coatings in low pressure (0.1 - 10.0 torr) plasma systems
[NASA-TM-83798] 02 p0189 N85-11261
Forward electron production in heavy ion-atom and ion-solid collisions
[DE85-001256] 09 p1381 N85-18683
Improved electron emission by use of a cloth fiber cathode
[AD-A149250] 10 p1480 N85-19340
Textured carbon surfaces on copper
[NASA-CASE-LEW-14130-1] 11 p1615 N85-20156
Coincidence techniques to study electron emission in ion-atom collisions
[DE85-003635] 11 p1724 N85-20846
Recent advances in forward electron production studies in ion-atom and ion-solid collisions
[DE85-001255] 11 p1726 N85-20853
The influence of the local solar wind structures on the propagation of low energy particles 12 p1959 N85-22314
Electron yields from spacecraft materials 13 p1996 N85-22512
Non-self-maintained high-voltage low-pressure discharge 13 p2068 N85-23037
Mean delta-ray energies in ion molecule collisions
[DE85-005524] 13 p2157 N85-23395
Impact ionization from gold, aluminum and PCB-Z — Giotto spacecraft paint PCB-Z 14 p2244 N85-23910
A model of plasma cloud expansion generated by a dust particle impact — Giotto mission 14 p2245 N85-23914
Electrodes for flash discharge lamps
[DE85-008897] 17 p2955 N85-28250
Electrode for flash discharge lamps
[DE85-008896] 17 p2955 N85-28252
VULTURE manual
[DE85-008873] 17 p3013 N85-28631
Electron spin resonance study of interface states induced by electron injection in metal-oxide-semiconductor devices
[DE85-009502] 18 p3195 N85-29817
Resolvability of defect ensembles with positron annihilation studies
[DE85-010041] 18 p3196 N85-29823
Method for predicting the performance of cathode materials
[AD-D011685] 19 p3257 N85-30198
Quantitative passive technique for assay of near-surface tritium in materials
[DE85-010661] 19 p3360 N85-30833
Predamage threshold electron emission from insulator and semiconductor surfaces
[DE85-008968] 19 p3377 N85-30954
Hollow cathodes in high pressure arc discharges
[NASA-TM-87098] 23 p3903 N85-34179
Electron photoejection in carbanions
[DE85-011748] 23 p3912 N85-34237
Improved negative ion source
[DE85-008445] 23 p3912 N85-34241
Workshop report on Simulation Techniques for Shock Wave Phenomena and Characteristics of Plasmas in Inertial Confinement Fusion
[IPPJ-725] 23 p3979 N85-34670

ELECTRON ENERGY

NT ELECTRON STATES
Electron energy loss rates in N-2, O-2 and air
[AD-A145158] 01 p0072 N85-10476
Monte Carlo simulation of thermalization of subexcitation electrons in molecular hydrogen
[NAL-TR-815T] 01 p0117 N85-10798
Electronic-to-vibrational energy transfer studies of singlet molecular oxygen and hydrogen halides
[AD-A145587] 02 p0277 N85-11802
Boundary condition effects in the energy loss spectrum of layered systems
[NOTA-INTERNA-802] 02 p0289 N85-11887
Electron energy loss investigation of the electronic and structural properties of palladium
[NOTA-INTERNA-803] 02 p0289 N85-11888
Reflection electron energy loss investigation of the H-GaAs(110) surface
[NOTA-INTERNA-811] 02 p0289 N85-11889
Ion thruster performance model
[NASA-CR-174810] 04 p0482 N85-12935
EBT electron energy confinement experiments
[DE84-015402] 04 p0567 N85-13613
Departures from LTE populations versus anomalous abundances: The effects of heating 08 p1234 N85-17776
Monte Carlo simulation of electron thermalization in rare gases
[NAL-TR-834T] 09 p1375 N85-18643
Effect of inner subshell ionization for emission lines of OIV ion 09 p1388 N85-18729
Spectra of highly-ionized atoms for the diagnostics of the new generation of Tokamaks 09 p1388 N85-18730
Discharge initiation experiments in the Tokapole II Tokamak
[DE84-017345] 09 p1391 N85-18755
Some unique aspects of fouling on copper as compared to titanium or nickel
[AD-A150072] 12 p1906 N85-21332
Observations of bulk electron heating due to return current in a tokamak discharge started up by lower hybrid waves
[IPPJ-708] 12 p1937 N85-22172
Kapton charging characteristics: Effects of material thickness and electron-energy distribution 13 p1996 N85-22513
Research on thermionic plasmas
[AD-A150883] 14 p2423 N85-24944
High current beam hollowing instability study
[AD-A151301] 15 p2648 N85-26329
Time dependent and steady-state solutions of the electron energy distribution in a weakly ionized gas subject to an ac or dc electric field
[AD-A151829] 15 p2656 N85-26391
Time-resolving electron temperature diagnostic for ALCATOR C
[DE85-004916] 16 p2868 N85-27690
Digital filters for application to data analysis in electron energy loss spectroscopy
[DE85-007932] 17 p2923 N85-28020
The mean trajectory approximation for charge and energy transfer processes at surfaces
[AD-A152708] 17 p3043 N85-28830
Hard X-ray measurements of the hot electron rings in Nagoya BUMPY TORUS (NBT-1M)
[IPPJ-720] 19 p3370 N85-30899
Thermal ion heating in the vicinity of the plasmapause
[NASA-CR-176030] 20 p3535 N85-31993

Metal-insulator-metal models of tunneling
20 p3536 N85-32006
CCD-based X-ray spectrometry for on-line determination of laser plasma electron temperature
21 p3692 N85-32938
Contributions to the 19th International Cosmic Ray Conference
[NASA-CR-176060] 21 p3714 N85-33044
The energy spectrum of Jovian electrons in interplanetary space
[SH-1.5-18] 21 p3715 N85-33051
Solar modulation and interplanetary gradients of the galactic electron flux, 1977 - 1984
[PAPER-SH-4.7-4] 21 p3716 N85-33059
Simultaneous Solar Maximum Mission and Very Large Array (VLA) observations of solar active regions
[NASA-CR-176090] 22 p3859 N85-33897
Improved negative ion source
[DE85-008445] 23 p3912 N85-34241
Electron impact ionization of multicharged ions at ORNL: 1980-1984
[DE85-013104] 23 p3972 N85-34622
Recent experiments in Gamma-10
23 p3976 N85-34651
Bounce resonance heating and radial transport of electrons
23 p3977 N85-34656
Transports studies of ECH and ICRH-heated bumpy torus plasma in NBT-1M 23 p3978 N85-34662
Stochastic particle acceleration in flaring stars
[OG-8.3-9] 23 p4022 N85-34927
High-resolution spectroscopy and dynamics of multiphoton processes in atoms and molecules
[AD-A155862] 24 p4147 N85-35714
Proposed FRX-D experiment
[DE85-012796] 24 p4158 N85-35778

ELECTRON FLUX
U ELECTRONS
U FLUX (RATE)

ELECTRON FLUX DENSITY
Ion thruster performance model
[NASA-CR-174810] 04 p0462 N85-12935
Average and worst-case specifications of precipitating auroral electron environment 13 p1991 N85-22482
Three-dimensional calculation of shuttle charging in polar orbit 13 p1992 N85-22486
Polar orbit electrostatic charging of objects in shuttle wake 13 p1992 N85-22487
Electron flux with electron energies above 40 MeV at altitudes of about 500 km in region where capture is possible and outside it when L is 3 or greater
15 p2481 N85-25315
Carbon foil secondary electron emission during ion passage through the 40 to 500 keV energy field
[MPE-190] 16 p3184 N85-29747
EAS fluctuation approach to primary mass composition investigation
[OG-5.2-5] 22 p3883 N85-34062
Spectral shape variation of interstellar electrons at high energies
[OG-6.2-7] 22 p3889 N85-34106

ELECTRON GAS
Stopping powers of solids for low-energy protons
[DE85-001123] 09 p1382 N85-18693
Angle averaged Compton cross sections for degenerate electron gases
[AD-A154484] 19 p3371 N85-30906
Fractional statistics and fractional quantized Hall effect
[DE85-007833] 19 p3375 N85-30940
Breakdown of helium nuclei in matter processed near black holes
[OG-8.2-20] 23 p4021 N85-34916

ELECTRON GUNS
Development of the Antares electron gun
[DE84-014043] 01 p0053 N85-10352
Gyrotron beam generation with helical magnetic fields
[AD-A145967] 03 p0417 N85-12670
High efficiency electron beam gun foil support
[AD-D011434] 08 p1159 N85-17312
The use of synthesis method in the design of gyrotron electron guns
[INPE-3305-PRE/616] 10 p1478 N85-19329
Brightness limitations in multi-kiloampere electron beam sources
[DE84-017417] 10 p1555 N85-19607
Proposal for hollow cathode electron gun for electron cooling
[DE85-002721] 11 p1630 N85-20263
Neutron streak camera electron gun design
[DE85-000820] 11 p1637 N85-20315
Enhancing the performance of a high-gain free electron laser operating at millimeter wavelengths
[DE85-000862] 12 p1857 N85-21646
High efficiency transverse dc electron beams
[AD-A152038] 16 p2862 N85-27651
Design and testing of a high power quasi-optical gyrotron
[AD-A153212] 17 p2968 N85-28330
Induction heating gun
[NASA-CASE-LAR-13161-1] 18 p3085 N85-29083
Generation of intense negative ion beams
[NASA-CASE-NPO-16081-1-CU]
18 p3178 N85-29701
Phase and amplitude feedback control system for the Los Alamos free-electron laser
[DE85-010787] 19 p3277 N85-30325
140 GHz gyrotron development program
[DE85-010348] 20 p3537 N85-32013
Multi-channel pulser for the SLC thermionic electron source
[DE85-014222] 24 p4160 N85-35792

ELECTRON IMPACT
Synergism in materials erosion due to multispecies impact 06 p0864 N85-15494
The coordinated research program at IAEA on atomic collision data for plasma diagnostics
09 p1390 N85-18747
Observation of pure resonance and threshold effects in electron impact experiments in high intensity laser fields
[AD-A150725] 14 p2309 N85-24293
Indirect processes in electron-impact ionization of multiply-charged ions
[DE85-005237] 14 p2419 N85-24825
Many-electron effects in electron impact ionization of multiply charged ions
[DE85-005570] 15 p2649 N85-26340
Theory of electron-impact atomic ionization cross sections
[AD-A151763] 16 p2861 N85-27648
Survey of experimental and theoretical electron-impact ionization cross sections for transition metal ions in low stages of ionization
[DE85-007605] 16 p2863 N85-27658
Measurement of combustion species by electron impact fluorescence
[DE85-011163] 19 p3236 N85-30085
Vibrationally enhanced dissociation of diatomic molecules
[AD-A154827] 21 p3701 N85-32986
Electron impact ionization of multicharged ions at ORNL: 1980-1984
[DE85-013104] 23 p3972 N85-34622

ELECTRON INTENSITY
U ELECTRON FLUX DENSITY

ELECTRON INTERACTIONS
U ELECTRON SCATTERING

ELECTRON IONIZATION
U IONIZATION

ELECTRON IRRADIATION
Neutron irradiation of semiconductors — lattice defects, electron irradiation 03 p0428 N85-12732
Time-of-flight spectroscopy of ionic and metastable fragments from dissociating molecules
[AD-A148068] 06 p1220 N85-17683
Evaluation and prediction of long-term environmental effects of nonmetallic materials
[NASA-CR-171353] 10 p1450 N85-19137
The role of void nucleation in the swelling resistance of ferritic steel
[AERE-R-11525] 11 p1610 N85-20122
Discharge pulse phenomenology
13 p1995 N85-22509
Technological process effect on the carrier lifetime degradation of silicon solar cell base layer irradiated by 1 MeV electrons (boron doping case)
13 p2007 N85-22585
The effects of lithium counterdoping on radiation damage and annealing in n(+)p silicon solar cells
13 p2007 N85-22586
Investigation of the degradation of GaAs photovoltaic cells by proton and electron irradiation
13 p2008 N85-22587
Electron-bombarded silicon spatial light modulator
[AD-D011579] 15 p2652 N85-26355
Electron irradiation of light emitting diodes
[AD-A154441] 19 p3260 N85-30213
Infrared absorption of oxygen complexes in electron-irradiated silicon
[FOA-C-30379-E1,E2,E3,E4] 20 p3538 N85-32015
The degradation of pollutants in water and waste water by means of electron or gamma irradiation
[OEFZS-4317] 22 p3812 N85-33615
Electron irradiation of N type cadmium telluride
[AD-A156117] 24 p4161 N85-35801

ELECTRON MASS
Incorporation of Monte Carlo electron interface studies into photon general cavity theory
[DE85-007674] 17 p3034 N85-28772

ELECTRON MICROSCOPES
Scanning electron microscope facility for examination of radioactive materials
[DE85-006127] 17 p2969 N85-28395
Resolution at its current limit: Applications of the Berkeley ARM
[DE85-009959] 19 p3274 N85-30301
An empirical technique to measure X-ray production and detection efficiencies in the analytical electron microscope
[DE85-010270] 19 p3361 N85-30837

ELECTRON MICROSCOPY
EDS round-robin evaluation of type 308 austenitic stainless steel
[DE84-014574] 02 p0183 N85-11226
Architecture of dermatophyte cell Walls: Electron microscopic and biochemical analysis
[NASA-TM-77441] 03 p0399 N85-12546
Application of extraction replicas and analytical electron microscopy to precipitate phase studies
[DE85-001253] 06 p0769 N85-14919
The structure and function of fungal cells
[NASA-TM-77443] 06 p0842 N85-15348
Comments on the image contrast from inelastically scattered electrons
[DE85-000899] 07 p1041 N85-16809
Transmission electron microscopy of inorganic materials
[DE85-000708] 09 p1291 N85-18107
SANS and TEM studies of carbide precipitation and creep damage in type 304 stainless steel
[DE85-000933] 09 p1296 N85-18139
Metals and Ceramics Division Materials Science Program
[DE85-003795] 11 p1592 N85-20012
Analytical electron microscopy: A potential new tool in the study of materials compatibility
[DE85-003271] 11 p1606 N85-20096
Application of Raman, TEM and other ion based techniques to oxidation problems
[AERE-R-11447] 11 p1610 N85-20121
K and L-shell cross-sections for X-ray microanalysis in an AEM
[DE85-002733] 11 p1721 N85-20822
Research in surface sciences, disordered materials, and solidification and growth
[PB85-132140] 11 p1737 N85-20927
Electron image simulation: A complementary processing technique
[DE85-000885] 12 p1941 N85-22190
TEM/FIM study of modulated microstructures in the Fe-Be system
[DE85-005379] 13 p2023 N85-22678
Grain boundaries in NiO
[DE85-006129] 13 p2025 N85-22687
Decomposition of VTAN alloy solid solution upon irradiation and thermal aging 13 p2029 N85-22712
Impurities in Kevlar 49 fibers
[DE85-004996] 13 p2038 N85-22767
A comprehensive review of black powder
[AD-A150455] 13 p2039 N85-22769
SEM (Scanning Electron Microscope) investigation of silicon diodes using the electron beam induced current method
[AD-A150356] 13 p2064 N85-22894
Structural characterization by intensity measurements of electron diffraction patterns
[DE85-004803] 13 p2164 N85-23427
New analysis aspects of the fatigue crack propagation behavior by SEM in situ microscopy
14 p2320 N85-24335
Secondary fluorescence effects on X-ray microanalysis
[DE85-005565] 15 p2506 N85-25457
Grain boundary composition and intergranular fracture of steels. Volume 1: Detection of grain boundary segregation in steels
[DE85-006850] 15 p2662 N85-26428
Low dose irradiation creep of pure nickel
[DE85-006320] 16 p2751 N85-26975
Tilt grain boundaries in NiO
[DE85-006839] 16 p2751 N85-26976
In situ HVEM studies of electron beam-driven composition changes in thin film alloys: Displacement-rate gradient effects
[DE85-007992] 17 p2931 N85-28092
Journal of Research of the National Bureau of Standards, volume 90, number 1, January - February 1985
[PB85-179063] 20 p3522 N85-31906
Modification of the grain size of sputtered copper with additions of oxygen, krypton, silver, or yttrium
[DE85-010975] 21 p3557 N85-32189
Z-contrast imaging and electron channeling analysis of dopants in semiconductors
[DE85-011410] 21 p3582 N85-32269

Aerosol formation by wave action over Ross Sea, Antarica 21 p3651 N85-32688
An electron microscopic study of urban aerosol 21 p3651 N85-32689
Three-dimensional reconstruction and data display of chromosome structure studied by electron microscope tomography
[DE85-011562] 22 p3825 N85-33697
Microstructures in rapidly solidified Ni-Mo alloys
[NASA-TM-87100] 23 p3915 N85-34266
High resolution electron microscopic characterization of interfaces in ceramics
[DE85-011207] 23 p3920 N85-34289
Intermolecular explosives
[DE85-009609] 23 p3921 N85-34296
The preparation of TEM specimens showing oxide scales in transverse cross-section
[AERE-R-11579] 24 p4078 N85-35276
Size and shape dependence of CO adsorption sites on sapphire supported Fe microcrystals
[NASA-CR-176171] 24 p4160 N85-35794

ELECTRON MOBILITY
Motion of electrons in non polar classical liquids
[DE84-013609] 05 p0727 N85-14672
High-efficiency solar-cell design modeling 06 p0829 N85-15262
Theory of silicon superlattices: Band structure and mobility enhancement 09 p1396 N85-18789
Microscopic structure of two-dimensional electron glass
[DE85-010265] 19 p3376 N85-30942
Air chemistry measurements 2
[AD-A156041] 24 p4117 N85-35520

ELECTRON MULTIPLIERS
U PHOTOMULTIPLIER TUBES

ELECTRON OPTICS
Method to render second order beam optics programs symplectic
[DE85-010631] 20 p3515 N85-31855
Practicality of electronic beam steering for MST/ST radars, part 6.2A 21 p3624 N85-32516
Electrostatic astigmatic tubular lens 21 p3695 N85-32955

ELECTRON ORBITALS
The 13C nuclear magnetic resonance in graphite intercalation compounds
[NASA-CR-174261] 07 p1040 N85-16601
Theoretical cross sections for inner-shell vacancy production by high-energy electrons
[DE84-007346] 11 p1721 N85-20827

ELECTRON OSCILLATIONS
Investigation of generation of oscillations using anomalous Doppler effect 13 p2078 N85-22980

ELECTRON PARAMAGNETIC RESONANCE
Studies of hydrogenated amorphous silicon
[DE84-013038] 01 p0067 N85-10443
Phase diagrams of organic superconductors
[DE84-016219] 05 p0731 N85-14699
EPR linewidth studies of unpaired electrons at the Si-SiO2
[DE84-016727] 05 p0733 N85-14712
Comparison of ionizing radiation and hot electron effects in MOS structures
[DE84-016766] 09 p1400 N85-18809
Characterization of acetylene-terminated resin cure states
[AD-A149463] 10 p1452 N85-19148
Charge-to-mass dispersion methods for abrasion-ablation fragmentation models
[NASA-TM-86340] 11 p1726 N85-20857
Control of electronic, magnetic and optical properties of doped polyacetylene conductors
[AD-A150117] 12 p1814 N85-21375
Ion and polymer chain motion in a superionic sodium-poly(ethylene oxide) complex
[AD-A152290] 16 p2755 N85-27001
Electron spin resonance study of interface states induced by electron injection in metal-oxide-semiconductor devices
[DE85-009502] 18 p3195 N85-29817
Defect formation in amorphous hydrated silicon subjected to laser radiation 21 p3682 N85-32873
An EPR (Electron-Paramagnetic-Resonance) and ENDOR (Electron-Nuclear-Double-Resonance) study of ferroelectric ammonium sulfate
[AD-A155580] 21 p3710 N85-33033

ELECTRON PATHS
U ELECTRON TRAJECTORIES

ELECTRON PHONON INTERACTIONS
Heterocontact effects in point contact electron-phonon spectroscopy of the alkali metals
[AD-A149760] 12 p1800 N85-21290

ELECTRON PHOTON CASCADES
Cascaded solar photovoltaic cells based on In-GaInPAs and InP-CdS heterostructures 02 p0268 N85-11749
Advanced high-efficiency concentrator cells
[DE84-013020] 09 p1344 N85-18459
Advanced high-efficiency concentrator cell
[DE85-000525] 14 p2351 N85-24533
SERI photovoltaic advanced research and development project: FY 1984 accomplishments
[DE85-002939] 18 p3128 N85-29368
Development of the Cascade inertial-confinement-fusion reactor
[DE85-010933] 19 p3357 N85-30812
Energy spectrum of extragalactic gamma-ray sources
[OG-2.7-13] 22 p3872 N85-33966
Fluctuations of development maximum depth and nuclear composition of primary cosmic radiation
[OG-5.1-13] 22 p3882 N85-34054
Coupled electron-photon transport calculations using the method of discrete ordinates
[DE85-009444] 23 p3967 N85-34597
High sensitive X-ray films to detect electron showers in 100 GeV region
[HE-3.1-13] 24 p4178 N85-35911
Comparison of big event with calculations of the air shower development
[HE-3.6-8] 24 p4185 N85-35956
Result of Monte-Carlo simulation of electron-photon cascades in lead and layers of lead-scintillator
[HE-3.6-11] 24 p4185 N85-35958
Theoretical study of EAS hadronic structure 24 p4189 N85-35991
Tskhra-Tskaro complex intended for the investigations of EAS spatial characteristics near axis 24 p4190 N85-35995
Topological aspects of age parameter
[HE-4.3-13] 24 p4192 N85-36007
Lateral-angular and temporal characteristics of EAS optical radiation
[HE-4.4-19] 24 p4194 N85-36025
Energy spectrum of cascades generated by muons in Baksan underground scintillation telescope
[HE-5.1-15] 24 p4202 N85-36077

ELECTRON PLASMA
Charging of DMSP/F6 spacecraft in aurora on 10 January 1983 13 p1991 N85-22481
Average and worst-case specifications of precipitating auroral electron environment 13 p1991 N85-22482
The downshift of electron plasma oscillations in the electron foreshock region
[NASA-CR-175633] 14 p2423 N85-24945
Charge uncovering effects on flute instabilities in hot electron plasmas
[DE85-006957] 16 p2667 N85-27666
Plasma wake field accelerator
[DE85-010538] 18 p3191 N85-29791
Influence of ECR-heating on MHD activity of plasma in tokamak-10 installation 21 p3694 N85-32949

ELECTRON PRECIPITATION
Polar rain: Solar coronal electrons in the Earth's magnetosphere
[NASA-TM-86150] 07 p1060 N85-16726
Pitch angle scattering and particle precipitation in a pulsating aurora: An experimental study
[KGI-185] 09 p1355 N85-18523
The high latitude D region during electron precipitation events 11 p1664 N85-20484
High energy particle effects in the D region during and after geomagnetic storms 11 p1664 N85-20485
Electron and proton precipitation in magnetic substorms — auroral substorms 14 p2360 N85-24585
Coordinated balloon-satellite studies of energetic electron precipitation mechanisms 14 p2360 N85-24587
Observations during a magnetosphere substorm triggered by a Storm Sudden Commencement (SSC): A case study 14 p2361 N85-24588
Auroral X-rays and equatorial electrons in the morning sector — substorm 14 p2361 N85-24590
On the location of the source for X-ray microbursts 14 p2361 N85-24591
On-off characteristics of auroral pulsations 14 p2363 N85-24604
Multiple correlation between auroral and magnetic pulsations 14 p2363 N85-24605
X-ray intensification at balloon altitudes of the South Atlantic magnetic anomaly in association with geomagnetic activity
[INPE-3469-PRE/712] 16 p2627 N85-27437

ELECTRON PROBES
Materials characterization using ion, electron, and photon probes
[DE84-004518] 04 p0560 N85-13568

ELECTRON PUMPING
The 248 nm - new short wavelength for pumping lasers employing vapors of complex molecules 02 p0261 N85-11705
Pulsed excimer laser processing for cost-effective solar cells
[NASA-CR-175700] 14 p2351 N85-24530

ELECTRON RADIATION
NT BETA PARTICLES
NT ELECTRON BEAMS
NT RELATIVISTIC ELECTRON BEAMS
Periodic substorm activity in the geomagnetic tail
[NASA-CR-175629] 13 p2161 N85-23409
Radio-frequency radiation of storm clouds 21 p3692 N85-32939

ELECTRON RECOMBINATION
NT RADIATIVE RECOMBINATION
High lifetime solar cell processing and design 20 p3480 N85-31822

ELECTRON RING ACCELERATORS
U STORAGE RINGS (PARTICLE ACCELERATORS)

ELECTRON SCATTERING
Bremsstrahlung radiation from longitudinal plasma waves caused by subthermal electrons in plasma 02 p0264 N85-11730
Dirac single particle wave functions in inelastic electron scattering
[DE84-015129] 02 p0279 N85-11814
Electron collision processes in molecular gases
[AD-A146078] 03 p0418 N85-12671
Electromagnetic shower development and applications to sampling calorimeters
[DE84-016355] 04 p0493 N85-13142
Measurements of the A-dependence of deep-inelastic electron scattering from nuclei
[DE84-013865] 05 p0728 N85-14678
Comments on the image contrast from inelastically scattered electrons
[DE85-000699] 07 p1041 N85-16609
Pitch angle scattering and particle precipitation in a pulsating aurora: An experimental study
[KGI-185] 09 p1355 N85-18523
An extension of the multiconfiguration Hartree-Fock program for continuum functions
[DE85-002090] 09 p1379 N85-18672
Studies of P-shell nuclei by large momentum transfer electron scattering
[DE84-016603] 09 p1381 N85-18686
Microscopic determinations of lattice and electronic structures of solids
[DE84-017323] 09 p1399 N85-18806
Analytical electron microscopy: A potential new tool in the study of materials compatibility
[DE85-003271] 11 p1606 N85-20096
Effect of impurities on absorption in semiconductors and lasing of semiconductor lasers 11 p1716 N85-20797
Theoretical cross sections for inner-shell vacancy production by high-energy electrons
[DE84-007346] 11 p1721 N85-20827
Recent progress in electron scattering at SLAC
[DE85-002718] 11 p1723 N85-20840
Coincidence studies of secondary electron emission in light ion-atom collisions
[DE85-002373] 11 p1725 N85-20852
Recent advances in forward electron production studies in ion-atom and ion-solid collisions
[DE85-001255] 11 p1726 N85-20853
Activities in nuclear physics and high energy physics 11 p1728 N85-20868
Heterocontact effects in point contact electron-phonon spectroscopy of the alkali metals
[AD-A149760] 12 p1800 N85-21290
Theoretical study of near-threshold electron-molecule scattering
[DE85-004530] 12 p1930 N85-22126
Observation of pure resonance and threshold effects in electron impact experiments in high intensity laser fields
[AD-A150725] 14 p2309 N85-24293
Numerical solution of a first kind Fredholm integral equation arising in electron-atom scattering
[CWI-NM-R8414] 14 p2414 N85-24897
Slowing down of charged particles by the bound electrons in a plasma — ion beams, nuclear fusion
[LP-209] 14 p2419 N85-24929
Approximate closed-form expression for the electron-scattering-induced interaction between magnetic flux lines and grain boundaries
[DE85-004699] 15 p2660 N85-26417
Test of the electronic structure of Fe(100) by absorbed current spectroscopy
[DE85-004942] 15 p2661 N85-26422
Density of impurity states associated to inversion layers
[INPE-3406-PRE/675] 16 p2669 N85-27702
Wake fields and wake field acceleration
[DE85-008054] 17 p3031 N85-28750
Possible indication of an A-dependence of R in deep-inelastic electron scattering from nuclei
[DE85-008174] 17 p3033 N85-28763

Electron multiple, plural and single scattering
[DE85-010325] 18 p3161 N85-29721
Magnetic scattering and polarized neutrons
[DE85-009823] 19 p3355 N85-30794
Interaction of slow electrons with high-pressure gases (quasi-liquids): Synthesis of our knowledge on slow electron-molecule interactions
[DE85-010061] 19 p3355 N85-30800
Deep-inelastic lepton scattering by nuclei: The pion-exchange model
[DE85-010498] 19 p3359 N85-30828
Angle averaged Compton cross sections for degenerate electron gases
[AD-A154484] 19 p3371 N85-30908
Magnetoconductance in aluminum films, wires, and cylinders 19 p3374 N85-30928
Time-Implicit Monte-Carlo collision algorithm for particle-in-cell electron transport models
[DE85-010758] 20 p3521 N85-31900
Inelastic Near-Surface Interactions. Proceedings of the Werner Brandt Workshop on Penetration Phenomena
[DE85-010579] 20 p3526 N85-31928
Metal-insulator-metal models of tunneling 20 p3536 N85-32006
Electron loss process and cross section of multiply charged ions by neutral atoms 23 p3981 N85-34685
X-ray spectra of bursting neutron stars 23 p3981 N85-34686
The propagation of solar flare particles in a turbulent coronal loop
[SH-1.1-3] 23 p3989 N85-34730
Analytical-numerical methods of calculations of energy and three-dimensional particle distributions in electromagnetic cascades
[HE-3.5-13] 24 p4184 N85-35950

ELECTRON SOURCES
Development of a continuous broad-energy-spectrum electron source 13 p1995 N85-22507

ELECTRON SPECTROSCOPY
Electron energy loss investigation of the electronic and structural properties of palladium
[NOTA-INTERNA-803] 02 p0289 N85-11866
A high transmission, 20 channel polychromator for the Thomson scattering diagnostic of TORTUR 3 — plasma diagnostics
[REPT-84-156] 03 p0422 N85-12694
The effect of thin-film growth mode on XPS/UPS/AES intensities
[AD-A146284] 03 p0434 N85-12763
Mossbauer spectroscopy and X-ray diffraction of samples from the Santa Catharina iron meteorite 06 p0885 N85-15624
Electron spectrometry experiments with the use of synchrotron radiation
[DE85-001286] 07 p1041 N85-16610
Nondestructive evaluation of titanium alloys. ESCA (Electron Spectroscopy for Chemical Analysis), ISS (Ion Scattering Spectroscopy), and SIMS (Secondary Ion Mass Spectrometry) examination of titanium alloy solid surfaces
[AD-P004135] 08 p1128 N85-17110
Simultaneous observations of electron spectra in the auroral zone and near the equatorial plane by the DMSP-5D-F2 and GEOS-1 Satellites
[KGI-184] 09 p1355 N85-18522
Surface physics instrumentation
[AD-A148304] 11 p1728 N86-20869
Some unique aspects of fouling on copper as compared to titanium or nickel
[AD-A150072] 12 p1906 N85-21332
Characterization of material surfaces exposed to atomic oxygen on space shuttle missions 12 p1946 N85-22220
Bonding information from Auger spectroscopy
[AD-A150864] 14 p2251 N85-23948
Chemical and localization effects in Auger lineshapes of transition metal compounds
[AD-A150865] 14 p2251 N85-23949
Threshold electron studies of gas-surface interactions
[AD-A151271] 15 p2647 N85-26326
Microscopic study of the influence of impurities on interface bonding
[AD-A151725] 16 p2743 N85-26928
Digital filters for application to data analysis in electron energy loss spectroscopy
[DE85-007932] 17 p2923 N85-28020
Self-sustaining coatings for fusion applications: Copper lithium alloys
[DE85-009740] 18 p3190 N85-29783
Method for predicting the performance of cathode materials
[AD-D011685] 19 p3257 N85-30198
Superconducting electronic film structures
[AD-A154196] 19 p3259 N85-30207
Study of solute segregation at interfaces using Auger electron spectroscopy
[DE85-005709] 20 p3423 N85-31247
Compositional analysis of silicon 20 p3480 N85-31626
Activities of the Physics Division
[DE85-000784] 21 p3702 N85-33002
Size and shape dependence of CO adsorption sites on sapphire supported Fe microcrystals
[NASA-CR-176171] 24 p4160 N85-35794

ELECTRON SPIN
Magnetic alignment theory and the interpretation of polarization 06 p0880 N85-15590
Collisional pumping for the production of intense spin-polarized, neutral beams: Target considerations
[DE85-003459] 11 p1723 N85-20841
Polarization of fast particle beams by collisional pumping
[DE85-011621] 22 p3838 N85-33764

ELECTRON SPIN RESONANCE
U ELECTRON PARAMAGNETIC RESONANCE

ELECTRON STATES
Singlet delta oxygen generator
[AD-D011208] 01 p0012 N85-10072
Actinides, the narrowest bands
[DE84-016463] 05 p0733 N85-14710
Modelling the local interstellar medium as a supernova remnant in a multiphase gas 06 p0879 N85-15585
Application of quantum chemistry of atmospheric chemistry
[AD-A147035] 07 p0922 N85-15843
Electronically excited atomic and molecular oxygen
[AD-A147732] 08 p1121 N85-17064
The Si/SiO2 intrinsic states and interface charges. Chapter 1: Origin, properties, models, impact
[HMI-B-413] 09 p1400 N85-18812
Temperature-dependent surface states and transitions of Si(111)-7x7
[AD-A149156] 10 p1562 N85-19850
Bonding information from Auger spectroscopy
[AD-A150864] 14 p2251 N85-23948
Experimental study of dissociative attachment in optically-pumped lithium molecules
[AD-A152800] 17 p3030 N85-28738
Monte Carlo simulation of thermalization of subexcitation electrons in He, Ne, Ar, Kr and Xe
[NAL-TR-843T] 18 p3178 N85-29702
Calculation of Franck-Condon factors for diatomic molecules
[AD-A154463] 19 p3353 N85-30784
A method to estimate the self-consistency effects on electronic structure calculations
[INPE-3536-PRE/752] 19 p3375 N85-30936
Calculation of molecular constants potential energy curves and Franck-Condon factors for lead oxide
[AD-A154521] 21 p3582 N85-32158
Nonradiative damping of molecular electronic excited states by metal surfaces
[AD-A154619] 21 p3701 N85-32994
Optical properties of heterostructures and superlattices
[AD-A156243] 24 p4162 N85-35802

ELECTRON SWEEPING
U SWEEP FREQUENCY

ELECTRON TELESCOPES
U PARTICLE TELESCOPES

ELECTRON TEMPERATURE
U ELECTRON ENERGY

ELECTRON TRAJECTORIES
Confinement of low-energy electrons near metallic surfaces for plasmon generation
[DE85-001110] 09 p1381 N85-18688
Electron acceleration by laser fields in a gas
[DE85-000575] 11 p1639 N85-20323
Laser measurements of distances from the ORELA neutron target to experiment stations along flight paths 1 and 6
[DE85-009457] 17 p2971 N85-28352
Hybrid two-dimensional Monte-Carlo electron transport in self-consistent electromagnetic fields
[DE85-010757] 19 p3348 N85-30758
Electron trajectories in a combined wiggler and alternating gradient quadrupole field
[DE85-010727] 22 p3842 N85-33794
Relativistic electron in curved magnetic fields
[OG-6.2-11] 22 p3890 N85-34110

ELECTRON TRANSFER
Solvent effects upon electrochemical kinetics: Influences of interfacial solvation and solvent relaxation dynamics
[AD-A145624] 02 p0173 N85-11156
The oxidation of transition-metal ions by molecular oxygen
[BLL-M-29583-(5828.4)] 02 p0175 N85-11172
Intramolecular electron transfer at metal surfaces. 4: Dependence of tunneling probability upon donor-acceptor separation distance
[AD-A145611] 02 p0287 N85-11876
Inclusion of electron transfer in the calculation of K(n)L(v) multiple vacancy production by ion impact
[DE84-016596] 05 p0733 N85-14711
Electrochemistry in near-critical and supercritical fluids. I. Ammonia
[AD-A146429] 06 p0765 N85-14894
Estimation of the rate of electron transfers between 2 contacting polymer surfaces
[AD-A146416] 06 p1122 N85-17072
Homogeneous reaction involving components of different redox couples. 1: Theoretical considerations and digital simulation
[AD-A146666] 06 p1124 N85-17084
The kinetics of electron transfer reactions in and at films of electroactive polymers
[AD-A146597] 06 p1134 N85-17149
Electron production, electron attachment, and charge recombination process in high pressure gas discharges
[AD-A149535] 10 p1554 N85-19700
Energy transfer and photochemistry in biomimetic solar conversion
[PB85-129112] 11 p1677 N85-20566
Correlated 2 electron effects in collisions of multiply charged Au ions with He
[DE85-003064] 11 p1723 N85-20837
Electronic transport in hydrogenated amorphous silicon films
[DE85-002901] 13 p2164 N85-23426
Noncontinuum solvent effects upon the intrinsic free-energy barrier for electron-transfer reactions
[AD-A150662] 14 p2250 N85-23943
Intramolecular electron transfer at metal surfaces. Part 5: Pendant substituent effects upon thiocarboxylate-bridged Cobalt (3) reduction kinetics at mercury and gold electrodes
[AD-A150647] 14 p2254 N85-23971
Sensitization and quenching in the conversion of light energy into chemical energy
[DE85-006301] 14 p2351 N85-24535
Thermolysis of 4-methyl-4-(1-propenyl)malonyl peroxide: Mechanistic limits to chemiluminescence efficiency
[AD-A151567] 15 p2505 N85-25452
Nitrolysis of the CN single bond and related chemistry of nitro and nitroso groups
[AD-A151753] 15 p2505 N85-25453
Applications of photoinduced electron transfer and hydrogen abstraction reactions to chemical and electrochemical conversion processes
[DE85-006068] 15 p2506 N85-25459
Optically triggered transferred-electron device microwave burst and single pulse generators
[AD-D011614] 16 p2778 N85-27141
Electrochemistry of polymer films not immersed in solution: Electron transfer on an ion budget
[AD-A152969] 17 p2920 N85-27998
Photochemistry of coordination complexes: The phthalocyanines
[DE85-007693] 17 p2923 N85-28022
Electrogenerated chemiluminescence
[AD-A153547] 18 p3070 N85-28990
Germanium detectors with a built-in transverse drift field
[DE85-000944] 18 p3096 N85-29185
One- and two-electron transfer processes in ion-surface scattering
[AD-A154208] 19 p3353 N85-30782
Sulfate-reducing bacteria: Microbiology and physiology 21 p3659 N85-32732
Electron photoejection in carbanions
[DE85-011747] 23 p3911 N85-34230
Electron photoejection in carbanions
[DE85-011748] 23 p3912 N85-34237
Study of photon emission by electron capture during solar nuclei acceleration, 1: Temperature-dependent cross section for charge changing processes
[SH-1.1-8] 23 p3990 N85-34735
Vectorial electron transfer on designed surfaces
[PB85-204600] 24 p4076 N85-35263

ELECTRON TRANSITIONS
Molecular beam scattering 03 p0417 N85-12666
Oscillator strengths for OII ions
[NASA-CR-174153] 04 p0559 N85-13558
Infrared emission and atomic transitions
[AD-A147840] 07 p1041 N85-16607
Materials physics
[DE84-017103] 09 p1377 N85-18658
Identification of spectra of highly ionized Mo, Nb, Zr and Y atoms 09 p1390 N85-18745
Indirect processes in electron-impact ionization of multiply-charged ions
[DE85-005237] 14 p2419 N85-24925

Spectroscopic studies of lead oxide in a flow tube
[AD-A151849] 15 p2505 N85-25455
Spectroscopic studies of lasing transitions in the diatomic mercury halides
[AD-A151553] 15 p2563 N85-25809
Spectroscopy of quasimolecular X-rays with H-like decelerated ions
[DE85-006565] 15 p2849 N85-26337
The copper vapor laser 16 p2924 N85-27417
Field theory of the metal-insulator transitions in restricted symmetries
[NOTA-INTERNA-829] 16 p3196 N85-29826
Simplified analytical model for calculation of population inversion in channels of CW gasdynamic lasers operating at various transitions among levels pertaining to coupled upsilon 1 and upsilon 2 modes of CO2
[STN-2] 20 p3461 N85-31498
Multiple inner shell vacancies in laser-irradiated Au plasma 23 p3981 N85-34667

ELECTRON TUBES
NT CAMERA TUBES
NT CATHODE RAY TUBES
NT GAS DISCHARGE TUBES
NT HELITRONS
NT IMAGE DISSECTOR TUBES
NT KLYSTRONS
NT MAGNETRONS
NT MICROWAVE OSCILLATORS
NT MICROWAVE TUBES
NT PICTURE TUBES
NT RETURN BEAM VIDICONS
NT THERMICONS
NT THYRATRONS
NT TRAVELING WAVE TUBES
NT VACUUM TUBES
NT VIDICONS
Magnetically insulated diode for generating pulsed neutron and gamma ray emissions
[DE85-011658] 22 p3760 N85-33308
Los Alamos free-electron laser
[DE85-012666] 24 p4098 N85-35405

ELECTRON TUNNELING
Intramolecular electron transfer at metal surfaces. 4: Dependence of tunneling probability upon donor-acceptor separation distance
[AD-A145611] 02 p0267 N85-11876
Calculation of the scattering function of rotating molecules with emphasis on the tunnel spectra of absorbed molecules 03 p0427 N85-12725
GaAlAs Sb APD optimization
[AD-A149406] 10 p1480 N85-19344
Inelastic tunnel diodes
[NASA-CASE-LEW-13833-1] 12 p1832 N85-21492
Thin film technology of high-critical-temperature superconducting electronics
[AD-A150010] 12 p1940 N85-22185
Macroscopic quantum tunnelling in a current biased Josephson junction
[DE85-004603] 13 p2164 N85-23424
Tunneling in magnetic superconducting systems
[AD-A150677] 14 p2426 N85-24963
Research on superconductive signal-processing devices
[AD-A152703] 17 p2953 N85-28235
Variational transition state theory
[DE85-010685] 19 p3235 N85-30059
Metal-insulator-metal models of tunneling 20 p3536 N85-32008
A theory of exciton photoluminescence for two types of neutral acceptors in silicon. A study of the systems Si:(B, IN), Si:(Al), (Si), Si:(Ga, In), Si:(B, Al), Si:(B, Ga), and Si:(Al, GA)
[AD-A155452] 21 p3710 N85-33031
Design considerations for personnel access penetrations for the superconducting super collider
[DE85-013027] 24 p4162 N85-35807

ELECTRON-HOLE DROPS
Investigations of radiation-induced and carrier-enhanced conductivity 13 p1996 N85-22515

ELECTRON-ION RECOMBINATION
NT RADIATIVE RECOMBINATION
Ionic reactions of atmospheric importance
[AD-A147354] 07 p0997 N85-16333

ELECTRONIC AIRCRAFT
Electronic reconnaissance aircraft of the Soviet Union Navy
[AD-A154706] 21 p3551 N85-32091
DOD Value Engineering Conference report. Value Engineering (VE): A tool that benefits line management held at Leesburg, Virginia on 1-2 November 1984. Part 2: Plenary session
[AD-A156088] 24 p4163 N85-35811

ELECTRONIC AMPLIFIERS
U AMPLIFIERS

ELECTRONIC CONTROL
Motor/generator and electronic control considerations for energy storage flywheels 05 p0608 N85-13878
Commercialization of the power factor controller
[NASA-CR-171500] 17 p2951 N85-28221
Development of mass-producible line-focus tracking concentrating solar collectors. Category 2: Control systems
[DE85-007873] 17 p2987 N85-28459
Closed loop electrostatic levitation system
[NASA-CASE-NPO-15553-1] 18 p3092 N85-29142
Performance improvements of a highly integrated digital electronic control system for an F-15 airplane
[NASA-TM-86748] 21 p3556 N85-32120
A microprocessor-controlled, multichannel fluorimeter for analysis of sea water
[AD-A154966] 21 p3590 N85-32310
Qualification needs for advanced integrated aircraft
[NASA-TM-86731] 22 p3729 N85-33119

ELECTRONIC COUNTERMEASURES
NT CHAFF
Rivista Tecnica Selenia, volume 9, number 1 07 p0938 N85-15945
Equipment for preflight test of an Electronic Countermeasures (ECM) avionic system 07 p0939 N85-15949
Optimum jamming effects on frequency-hopping M-ary FSK (Frequency-Shift Keying) systems under certain ECCM (Electronic counter-countermeasures) receiver design strategies
[AD-A147766] 08 p1151 N85-17267
Integrated defense communications system antijamming antenna system
[AD-D011423] 08 p1154 N85-17285
Simulation of the performance of adaptively controlled Navstar antennas in battlefield scenarios 10 p1472 N85-19292
Research on adaptive antenna techniques 6
[AD-A149341] 11 p1624 N85-20228
Combat capable space systems for tactical support 11 p1713 N85-20775
A survey of radar ECM and ECCM 15 p2536 N85-25853
AN investigation into the control limitations of a bank to turn missile in the terminal homing phase
[AD-A152193] 16 p2704 N85-26696
Digital RF delay line for ECM (electronic countermeasure) look-through
[AD-A152120] 16 p2774 N85-27120
Adaptive nulling at HF using a compact array of active parasitic antennas
[AD-A152562] 17 p2948 N85-28203
An analysis of jamming effects on noncoherent digital receivers
[AD-A153791] 18 p3090 N85-29128

ELECTRONIC EQUIPMENT
NT AVALANCHE DIODES
NT BIPOLAR TRANSISTORS
NT CHARGE COUPLED DEVICES
NT CHARGE INJECTION DEVICES
NT CHARGE TRANSFER DEVICES
NT CMOS
NT DIODES
NT ELECTRONIC FILTERS
NT ELECTRONIC MODULES
NT ELECTRONIC PACKAGING
NT ELECTRONIC TRANSDUCERS
NT FIELD EFFECT TRANSISTORS
NT GALLIUM ARSENIDE LASERS
NT GERMANIUM DIODES
NT GUNN DIODES
NT HETEROJUNCTION DEVICES
NT JFET
NT JUNCTION DIODES
NT JUNCTION TRANSISTORS
NT LIGHT EMITTING DIODES
NT METAL OXIDE SEMICONDUCTORS
NT MIM (SEMICONDUCTORS)
NT MIM DIODES
NT MINIATURE ELECTRONIC EQUIPMENT
NT MIS (SEMICONDUCTORS)
NT MULTISPECTRAL LINEAR ARRAYS
NT PHOTODIODES
NT PHOTOTRANSISTORS
NT PHOTOVOLTAIC CELLS
NT PLASMA DIODES
NT RUBY LASERS
NT SCHOTTKY DIODES
NT SEMICONDUCTOR DEVICES
NT SEMICONDUCTOR DIODES
NT SEMICONDUCTOR LASERS
NT SILICON CONTROLLED RECTIFIERS
NT SILICON TRANSISTORS
NT SIS (SEMICONDUCTORS)
NT SOLID STATE DEVICES
NT SOLID STATE LASERS
NT SPACECRAFT ELECTRONIC EQUIPMENT
NT THERMISTORS
NT THYRISTORS
NT TRANSISTOR AMPLIFIERS
NT TRANSISTORS
NT TUNNEL DIODES
NT VARACTOR DIODES
NT VARISTORS
NT YAG LASERS
Polychlorinated biphenyls (PCBs) in transit system electrical equipment
[PB84-222207] 01 p0045 N85-10291
Center for Electronics and Electrical Engineering Technical Bulletin covering center programs with 1984 CEEE events calendar
[PB84-222785] 01 p0045 N85-10292
Center for Electronics and Electrical Engineering Technical Bulletin covering center programs with 1984 CEEE events calendar
[PB84-223664] 01 p0045 N85-10293
The psychology of technical devices and technical discourse
[AD-P003929] 02 p0246 N85-11809
Artificial intelligence approaches to monitoring system integrity
[AD-P003930] 02 p0246 N85-11810
Model-based probabilistic reasoning for electronics troubleshooting
[AD-P003937] 02 p0247 N85-11817
Knowledge based tools for electronic equipment maintenance
[AD-P003940] 02 p0248 N85-11820
LES: (Lockheed Expert System): A model-based expert system for electronic maintenance
[AD-P003944] 02 p0248 N85-11824
Characteristics of ion implanters for fabrication of electronic devices
[AD-P003949] 02 p0286 N85-11865
Electronics/avionics depots in the United States Air Force Warner Robins Air Logistics Center
[AD-P004000] 03 p0307 N85-11981
Training capabilities test of Electronics Equipment Maintenance Trainer (EEMT): Findings and conclusions
[AD-A146075] 03 p0359 N85-12302
Accelerated stress facility 1978-1983
[AD-A146101] 03 p0359 N85-12303
Ballpark reliability estimation techniques
[AD-A145971] 03 p0389 N85-12357
USSR report: Electronics and electrical engineering
[JPRS-UEE-84-010] 04 p0485 N85-13095
Electronic components for space applications
[CNES-NT-109] 04 p0498 N85-13169
Heavy duty precision pan and tilt head
[AD-A146869] 04 p0509 N85-13246
Space power management and distribution status and trends 05 p0610 N85-13896
USSR report: Electronics and electrical engineering
[JPRS-UEE-84-011] 06 p0789 N85-15042
High-power gate turn-off thyristors 06 p0793 N85-15071
Target detection using microwave irradiances from natural sources: A passive, local and global surveillance system
[NASA-CR-174260] 07 p0946 N85-15991
cost and benefits optimization model for fault-tolerant aircraft electronic systems
[NASA-CR-166043] 07 p0946 N85-15993
USSR report: Electronics and electrical engineering
[JPRS-UEE-84-017] 07 p0951 N85-16025
The electronic typesetting program programmer's manual
[AD-A147500] 07 p1025 N85-16506
Experience of one UK electronic equipment supplier with bite on engine/flight control systems over the past ten years 08 p1054 N85-16736
Outlook for expanding the Federal research in progress system
[AD-A145354] 08 p1229 N85-17737
Acceleration responses of typical LRU's subjected to bench handling and installation shock 09 p1334 N85-18385
Data acquisition, measurement devices at 1984 Leipzig Spring Fair 09 p1378 N85-19861
Vibration isolated cold plate assembly
[AD-D011444] 10 p1484 N85-19368
Design and calibration of a 35GHz dielectrometer
[AD-P004363] 12 p1826 N85-21457
Nose and inlet duct radomes for the firebolt aerial target
[AD-P004375] 12 p1827 N85-21469
Maintainability time standards for electronic equipment
[AD-A149884] 12 p1834 N85-21507
Algorithm for statistical simulation of electromagnetic compatibility characteristics of high-frequency transmission channels in radioelectronic facilities 12 p1842 N85-21580

The future of lightwave technology
[PB85-109759] 12 p1935 N85-22155
Control of cascaded induction generator systems
[AD-A150429] 13 p2065 N85-22597
USSR report: Electronics and electrical engineering
[JPRS-UEE-85-002] 13 p2066 N85-22907
Simple detonation meter 13 p2077 N85-22971
USSR report: Electronics and electrical engineering
[JPRS-UEE-85-001] 13 p2078 N85-22976
User's guide to calibration of analog electronic controllers in HVAC systems
[AD-A150603] 14 p2298 N85-24229
Laser spot welding in the electronics industry
14 p2308 N85-24287
Rain rate determinations from electronic weight measurements: Instrument description and data reduction techniques
[AD-A150785] 14 p2378 N85-24681
USSR report: Electronics and electrical engineering
[JPRS-UEE-85-005] 15 p2524 N85-25565
Evaluation of adequacy pf JP54 protection level for large electric machines 15 p2526 N85-25568
Electronic detection and concealment of film dirt
[BBC-RD-1985/4] 15 p2536 N85-25657
Structural analysis of electronic assembly housing
[DE85-005794] 15 p2580 N85-25913
Future directions in computers
15 p2626 N85-26183
Avionics integrity issues presented during NAECON (National Aerospace and Electronics Convention) 1984
[AD-A151923] 16 p2707 N85-26707
The replacement of precious metal thick film inks using conductive polymer technology
[AD-A152002] 16 p2749 N85-26965
Reliability report for communication networks
[AD-A153764] 18 p3090 N85-29127
Moisture content and gas sampling device
[NASA-CASE-MSC-18666-1] 18 p3103 N85-29213
Avionics and civil aircraft systems: The present and the future
[SNIAS-851-111-104] 20 p3392 N85-31038
Proceedings of the Electronic Test Equipment Division's Annual Program Review of Electronic Test Equipment Industry Response to Emerging Defense Requirements
[AD-A154455] 20 p3436 N85-31320
Air Force bid sample testing 20 p3437 N85-31323
France's LETI reports 1983 electronic components research 20 p3438 N85-31336
Electronics Division research and development
[DE85-011887] 20 p3540 N85-32032
Resistance of polyaniline films as a function of electrochemical potential and the fabrication of polyaniline-based microelectronic devices
[AD-A154999] 21 p3569 N85-32201
Prospects for a new kind of synthesis: Assembly of molecular components to achieve functions
[AD-A155023] 21 p3702 N85-32997
Adaptive modeling of electronic circuits
22 p3766 N85-33345
Conferences of quantum-radiooptics section
22 p3773 N85-33380
Electronic imaging system and technique
[DE85-005740] 23 p3935 N85-34393
Electronic information management and productivity
[DE85-013362] 24 p4164 N85-35818

ELECTRONIC EQUIPMENT TESTS
Investigation of the application of the marginal torsion technique to test electronic devices, phase 3
[ESD-11-301] 02 p0206 N85-11360
Tests for susceptibility to electromagnetic attack
[SNIAS-842-422-101] 04 p0494 N85-13154
Practical application of electron beam testing in LSI and VLSI circuits
[BMFT-FB-T-84-185] 05 p0633 N85-14061
Equipment for preflight test of an Electronic Countermeasures (ECM) avionic system
07 p0939 N85-15049
Evaluation of test equipment for the detection of contamination on electronic circuits --- spacecraft electronics
[ESA-STM-234] 06 p1159 N85-17316
Design of a bit-sliced processor array with built-in-self-test
[AD-A149785] 12 p1835 N85-21513
Built-in tests for VLSI (Very Large Scale Integration) finite-state machines
[AD-A149784] 12 p1911 N85-21997
Measurement of internal thermal resistance for quality control of semiconductor devices
13 p2074 N85-22953
The Avionics Flight Evaluation System (AFES) of DFVLR
[DFVLR-MITT-85-01] 17 p2897 N85-27864
Measurement methods for accurate microwave characterization and modeling of MESFET chips
[AD-A152360] 17 p2952 N85-28227
The GfW handbook for data compilation of irradiation tested electronic components, volume 3
[HMI-B-353-VOL-3] 17 p2956 N85-28258
Reliability derating procedures
[AD-A153744] 18 p3119 N85-29309
Ada compiler validation summary report, University of Karlsruhe-GMD/German MOD Siemens - BS 2000 version 7.30
[AD-A153747] 18 p3163 N85-29581
New measurement solutions for low frequency systems 20 p3437 N85-31325
East Europe report: Science and technology
[JPRS-ESA-85-021] 21 p3568 N85-32190
Transceiver test device
[AD-D011728] 22 p3786 N85-33458
Testbed for sensory control of intelligent machines
[DE85-012355] 24 p4099 N85-35412

ELECTRONIC FILTERS
Filtration of higher harmonic components in two-level digital computing synthesizers 22 p3776 N85-33410

ELECTRONIC LEVELS
U ELECTRON ENERGY
U ENERGY LEVELS

ELECTRONIC MAIL
Efficiency analysis of the electronic mail system (INFOMAIL) on the defense data network
[AD-A151894] 15 p2632 N85-26223
Interfacing the VAX 11/780 using berkeley UNIX 4.2BSD and Ethernet based Xerox Network Systems
[AD-A153174] 17 p3016 N85-28647

ELECTRONIC MODULES
The study of microstrip antenna arrays and related problems
[NASA-CR-174054] 02 p0189 N85-11265
Electronic bandwidth compression module
[AD-A145843] 03 p0366 N85-12343
Analyses to develop models to project failure rates and repair costs of electronic modules and subassemblies
[AD-A146509] 06 p0816 N85-15180
Electronic module insertion and retraction mechanism
[AD-D011309] 07 p0947 N85-16002
Diodes in photovoltaic modules and arrays
[NASA-CR-175454] 10 p1506 N85-19513
ESP (External-Stores Program): A pilot computer program for determining flutter-critical external-store configurations. Volume 3, part 1: Program compilation
[AD-A152270] 16 p2711 N85-26727
Maintenance of photovoltaic power systems
[AD-A152299] 16 p2819 N85-27390
Modular Optoelectronic Multispectral Scanner (MOMS) for Earth observation. First results of STS-7 mission
[MBB-UR-717/83-O] 16 p2874 N85-27732

ELECTRONIC PACKAGING
Component reliability and assembling technologies
[CNES-NT-108] 04 p0511 N85-13258
UCB cosmic ray experiment 09 p1417 N85-18941
The effects of water and hydrogen on materials used in integrated circuit packages
[AD-A151693] 15 p2518 N85-25529

ELECTRONIC PHOTOGRAPHY
U ELECTRO-OPTICAL PHOTOGRAPHY

ELECTRONIC SIGNAL MEASUREMENT
U SIGNAL MEASUREMENT

ELECTRONIC SPECTRA
Boundary condition effects in the energy loss spectrum of layered systems
[NOTA-INTERNA-602] 02 p0289 N85-11687
Scattering experiments on interactions of excited atoms: Differential cross sections of the system Na (3P) + K(4S)
[MPIS-8/1984] 05 p0728 N85-14677
Metal complexes of some heterocyclic ligands
15 p2504 N85-25446
Theory of electron-impact atomic ionization cross sections
[AD-A151763] 16 p2861 N85-27648
The electronic spectra of phthalocyanine radical anions and cations
[AD-A152328] 17 p2918 N85-27986
Local electron spectrum above 100 MeV derived from gamma-ray emissivity spectra
[CG-3.1-7] 22 p3874 N85-33995

ELECTRONIC STRUCTURE
U ATOMIC STRUCTURE

ELECTRONIC SWITCHES
U SWITCHING CIRCUITS

ELECTRONIC TRANSDUCERS
Electromagnetic Acoustic Transducers (EMATs) for erosion monitoring
[DE85-004834] 12 p1854 N85-21628
MFTF sensor verification computer program
[DE85-004452] 12 p1916 N85-22029
Robot use in FRG increases but sensor technology lags 15 p2531 N85-25605
Design of inductive shift transducers
22 p3771 N85-33368
Development of position sensors for microcomputer-oriented sensor systems
[BMFT-FB-T-85-021] 24 p4091 N85-35361
Materials and process development for microcomputer-compatible pressure, temperature, and position sensors
[BMFT-FB-T-85-024] 24 p4097 N85-35399

ELECTRONIC WARFARE
Simulation of the performance of adaptively controlled Navstar antennas in battlefield scenarios
10 p1472 N85-19292
A survey of radar ECM and ECCM
15 p2536 N85-25653
Fin line filters technology and electronic warfare
[AD-A154975] 21 p3576 N85-32237

ELECTRONICS
Joint services electronics program
[AD-A145085] 01 p0042 N85-10276
Center for Electronics and Electrical Engineering Technical Bulletin covering center programs
[PB84-218056] 01 p0045 N85-10296
NAVAIR's (Naval air systems command) AI (Artificial Intelligence) program for ATE (Automated Test Equipment)
[AD-P003935] 02 p0247 N85-11615
DRG theory on the basis of a discrete interaction model
[PR-215] 03 p0358 N85-12297
Research activities of the Illinois University Coordinated Science Laboratory
[AD-A145589] 03 p0449 N85-12856
Electrical/electronics working group summary
05 p0604 N85-13653
USSR report: Electronics and electrical engineering
[JPRS-UEE-85-002] 13 p2066 N85-22907
China report: Science and technology
[JPRS-CST-85-007] 15 p2533 N85-25621
Tutorial discussion of electronic sampling systems for recording wide-bandwidth transient signals
[DE85-006577] 15 p2549 N85-25735
Robotic arc welding 15 p2566 N85-25830
On the relationship between electronics and chemistry
[DRIC-T-7480] 22 p3743 N85-33200
Modeling of electronic circuits with high degree of component integration 22 p3766 N85-33343
USSR report: Electronics and electrical engineering
[JPRS-UEE-84-003] 22 p3773 N85-33381

ELECTRONOGRAPHY
Photometric study of the Saturn E ring
15 p2671 N85-26483

ELECTRONS
NT CONDUCTION ELECTRONS
NT FREE ELECTRONS
NT HIGH ENERGY ELECTRONS
NT HOT ELECTRONS
NT NEGATRONS
NT PHOTOELECTRONS
NT POLARONS
NT RELATIVISTIC ELECTRON BEAMS
NT SOLAR ELECTRONS
Monte Carlo simulation of thermalization of subexcitation electrons in molecular hydrogen
[NAL-TR-915T] 01 p0117 N85-10798
Bremsstrahlung radiation from longitudinal plasma waves caused by subthermal electrons in plasma
02 p0264 N85-11730
Exchange and correlation effects and pair potentials of inter-atomic interaction
[BLL-M-35745-(5828.4)] 02 p0277 N85-11800
Electron traps in the GaAs permeable base transistor
[AD-A145399] 02 p0287 N85-11871
Relationships between electronic structure and stability of metallic glasses
[AD-A145506] 02 p0287 N85-11874
Forced oscillations theory for resonant extended interaction electron devices
[PR-206] 03 p0358 N85-12296
Mechanisms of electrical conductivity in olivine
[DE84-014333] 04 p0495 N85-13159
Evidence for d-band conduction in metallic glasses containing transition metal elements
[DE84-014822] 04 p0570 N85-13635
Motion of electrons in non polar classical liquids
[DE84-013609] 05 p0727 N85-14672
The radiative hydrodynamics of flare loops heated by impulsive bursts of energetic electrons
05 p0745 N85-14781
Generation of suprathermal electrons during plasma current startup by lower hybrid waves in a Tokamak
[IPPJ-697] 06 p0863 N85-15483
Arc-evaporated carbon films: Optical properties and electron mean free paths
[DE85-001246] 06 p0867 N85-15510
Application of the diffraction model to amorphous magnesium zinc alloys
[AD-A147369] 07 p0928 N85-15883

Electron-irradiated effects in metals
[DE84-016699] 09 p1297 N85-18147
The role of fast electrons for the performance characteristics of hydrogen ion sources
09 p1303 N85-18189
Monte Carlo simulation of electron thermalization in rare gases
[NAL-TR-834T] 09 p1375 N85-18643
Electron bounce resonance heating in a bumpy cylinder
[DE85-001732] 10 p1561 N85-19845
Electron-plastic effect in metals
11 p1605 N85-20089
Correlated 2 electron effects in collisions of multiply charged Au ions with He
[DE85-003064] 11 p1723 N85-20837
ITS: The Integrated TIGER Series of coupled electron/photon Monte Carlo transport codes
[DE85-003719] 11 p1725 N85-20847
Velocity distributions of solar wind ions and electrons
12 p1954 N85-22273
Electron-positron pair equilibrium in strongly magnetized plasmas
12 p1957 N85-22296
Electron-positron pairs in a mildly relativistic plasma in active galactic nuclei
12 p1957 N85-22297
Galileo internal electrostatic discharge program
13 p1995 N85-22504
Discharge characteristics of dielectric materials examined in mono-, dual-, and spectral energy electron charging environments
13 p1995 N85-22510
On the choice of coordinates for semiconductor simulation
[AD-A152214] 16 p2870 N85-27708
Atom location by electron channeling analysis
[DE85-007549] 16 p2872 N85-27716
Effects of level broadening on the magnetothermal oscillations in two-dimensional electron systems
[AD-A152639] 17 p3029 N85-28732
Hall mobility in fluid argon
[DE85-007268] 17 p3045 N85-28840
A review of ionospheric effects on Earth-space propagation
18 p3106 N85-29233
Ionospheric limitations to time transfer by satellite
18 p3107 N85-29234
The prospects of the digital optical computer
18 p3188 N85-29771
Study of the equilibrium vacancy ensemble in aluminum using 1D- and 2D-angular correlation of annihilation radiation
[DE85-008967] 18 p3194 N85-29813
Experiments with stored heavy ions
[DE85-009976] 19 p3356 N85-30802
Monte Carlo electron/photon transport
[DE85-010799] 19 p3364 N85-30861
Localization of waves in a disordered medium
19 p3373 N85-30926
Microscopic structure of two-dimensional electron glass
[DE85-010265] 19 p3376 N85-30942
The influence of a turbulent region on the flux of auroral electrons
[KGI-PREPRINT-072] 20 p3494 N85-31723
Methods of Monte Carlo electron transport in particle-in-cell codes
[DE85-010702] 20 p3521 N85-31896
Runaway electrons and plasma turbulence in current ramping by lower hybrid waves in tokamak plasmas
[DE85-011390] 20 p3535 N85-31997
Detection of excited states by laser-induced fluorescence
[AD-A155558] 21 p3592 N85-32326
Solar modulation and interplanetary gradients of the galactic electron flux, 1977 - 1984
[PAPER-SH-4.7-4] 21 p3716 N85-33059
Electron-donor dopant, method of improving conductivity of polymers by doping therewith, and a polymer so treated
[DE85-011640] 22 p3752 N85-33257
Reestimation of the production spectra of cosmic ray secondary positrons and electrons in the ISM
[OG-6.2-8] 22 p3869 N85-34107
Electrons and positrons from expanding supernova envelopes in dense clouds
[OG-6.2-9] 22 p3869 N85-34108
The electron spectra in the synchrotron nebula of the supernova remnant G 29.7-0.3
[OG-6.2-10] 22 p3880 N85-34109
Atmospheric Emission Photometric Imaging (AEPI)
23 p3902 N85-34170
Measuring method and confirmation of H- (D-) ion current by sheet plasma 1
[IPPJ-730] 23 p3974 N85-34638
Electron dynamics and transport in a mirror field
23 p3977 N85-34656
Model of azimuthal non-uniformities induced by RF heating in RFC-XXM
23 p3977 N85-34658
The propagation of solar flare particles in a turbulent coronal loop
[SH-1.1-3] 23 p3989 N85-34730
Stochastic particle acceleration in solar flares
[SH-1.1-4] 23 p3989 N85-34731
Study of non-thermal photon production under different scenarios in solar flares. 2: The Compton inverse and Bremsstrahlung models and fittings
[SH-1.2-3] 23 p3991 N85-34739
Temporal evolution of an energetic electron population in an inhomogeneous medium: Application to solar hard X-ray bursts
[SH-1.2-6] 23 p3991 N85-34741
Quantitative analysis of flare accelerated electrons through their hard X-ray and microwave radiation
[SH-1.2-7] 23 p3991 N85-34742
Two types of electron events in solar flares
[SH-1.2-11] 23 p3992 N85-34746
The energy spectra of solar flare electrons
[SH-1.2-14] 23 p3992 N85-34749
The Jovian electron spectrum: 1978-1984
[SH-1.5-19] 23 p3998 N85-34782
Observations of solar energetic particles at a synchronous orbit
[SH-3.1-1] 23 p4001 N85-34806
Coronal propagation of flare associated electrons and protons
[SH-3.1-3] 23 p4001 N85-34808
Geometry of the diffusive propagation region in the August 14, 1982 solar electron event
[SH-3.1-5] 23 p4001 N85-34809
The dependence of solar modulation on the sign of the cosmic ray particle charge
[SH-4.2-23] 23 p4009 N85-34860
Onion-shell model for cosmic ray electrons and radio synchrotron emission in supernova remnants
[OG-8.1-10] 23 p4018 N85-34900
Pulsars as cosmic ray particle accelerators: Dynamics of electrons
[OG-8.2-23] 23 p4021 N85-34919
Solar modulation and interplanetary gradients of the galactic electrons flux, 1977 - 1984
[SH-4.7-4] 23 p4040 N85-35049
Additional flux of particles and albedo-electrons in upper atmosphere
[SH-6.1-6] 23 p4045 N85-35080
Pulsed-neutron-source models for the astrophysical s-process
[DE85-012927] 24 p4151 N85-35740
Studies of relativistic heavy ion collisions
[DE85-014686] 24 p4152 N85-35745
Mini-clusters
[HE-3.5-3] 24 p4183 N85-35942
Structure of super-families
[HE-3.5-7] 24 p4183 N85-35944
Extremely high energy hadron and gamma-ray families(3). Core structure of the halo of superfamily
[HE-3.5-8] 24 p4183 N85-35945
Numerical analysis of electromagnetic cascades in emulsion chambers
[HE-3.5-9] 24 p4184 N85-35946
An experimental study of correlations in the development of the electron-photon cascades
[HE-3.5-10] 24 p4184 N85-35947
Integral functions of electron lateral distribution and their fluctuations in electron-photon cascades
[HE-3.5-12] 24 p4184 N85-35949
Electrons, muons and hadrons in extensive air showers and how do they depend on nuclear interaction model, part 2
24 p4187 N85-35969
Electrons, muons and hadrons in extensive air showers and how do they depend on nuclear interaction model, part 1
24 p4187 N85-35972
Sensitivity of depth of maximum and absorption depth of EAS to hadron production mechanism
24 p4188 N85-35982
A critical analysis of air shower structure functions and size spectrum measurements with the NBU air shower array
24 p4188 N85-35983
Missing energies at pair creation
[HE-4.4-8] 24 p4193 N85-36016
The hump in the Cerenkov lateral distribution of gamma ray showers
[HE-4.5-9] 24 p4195 N85-36032
Simulation of gamma-initiated showers
[HE-4.5-10] 24 p4195 N85-36033
Phenomenological characteristic of the electron component in gamma-quanta initiated showers
[HE-4.5-11] 24 p4196 N85-36034
Nuclear cascades in electromagnetic showers produced by primary gamma-quanta in the atmosphere
[HE-4.5-16] 24 p4196 N85-36038
Longitudinal development of muons in large air showers studies from the arrival time distributions measured at 900m above sea level
[HE-4.7-4] 24 p4199 N85-36055
Arrival time distributions of electrons in air showers with primary energies above 10 (18)eV observed at 900m above sea level
[HE-4.7-5] 24 p4199 N85-36056
Analysis of the electron component of EAS at observational level 700 g x cm(-2) with a scale breaking interaction model and gammaisation hypothesis
[HE-5.4-8] 24 p4208 N85-36119
Study of photonuclear muon interactions at Baksan underground scintillation telescope
[HE-5.4-10] 24 p4208 N85-36122
Collimated groups of particles as possible manifestation of heavy meson production
[HE-5.4-14] 24 p4208 N85-36124

ELECTROPHORESIS

Opportunities for space bioprocessing
02 p0150 N85-11018
Advances in electrophoretic separations
02 p0156 N85-11054
Commentary on Salyut-7 electrophoresis, plugging mortar experiments
02 p0158 N85-11072
Commentary on derivation of biological materials, cosmonaut adaptation
02 p0158 N85-11074
Electronic autofluorography: Principles, problems and prospects
[DE84-016698] 05 p0639 N85-14097
Bioprocessing in space
05 p0690 N85-14438
Kidney cell electrophoresis
[NASA-CR-171889] 20 p3498 N85-31745
Task description for the 1983 catalog of tasks for the materials processing in space program
20 p3498 N85-31746
Kidney cell electrophoresis, continuing task
20 p3498 N85-31747
Effects of coating rectangular microscopic electrophoresis chamber with methylcellulose
20 p3498 N85-31748
Asymmetric electroosmotic flow and mobility measurements at nonstationary positions in the rectangular chamber
20 p3499 N85-31749
Theoretical prediction of stationary positions in the rectangular chamber during asymmetric electroosmotic flow
20 p3499 N85-31750
A computer program for determining the electrophoretic mobility of cells in a rectangular chamber during asymmetric electroosmotic flow
20 p3499 N85-31751
Operation of the Zeiss cytopherometer with Zn/ZnSO4 electrode system of Tenforde et al
20 p3499 N85-31752
Electrophoretic mobility of cells in a vertical Ficoll gradient
20 p3499 N85-31753
Free-zone electrophoresis of animal cells. 1: Experiments on cell-cell interactions
20 p3499 N85-31754
Development annd testing of electrophoresis solutions. Task I.1: Development of optimal buffer system
20 p3500 N85-31755
Electrophoretic mobilities of erythrocytes in various buffers
20 p3500 N85-31756
Effects of method of detachment on electrophoretic mobility of mammalian cells grown in monolayer culture
20 p3500 N85-31757
Preparative electrophoresis of cultured human cells: Effect of cell cycle phase
20 p3500 N85-31758
Size and DNA distributions of electrophoretically separated cultured human kidney cells
20 p3500 N85-31759
The role of cell size in density gradient electrophoretic separation of mouse leukemia cells according to position in the cell cycle
20 p3500 N85-31760
Electrophoretic mobilities of cultured human embryonic kidney cells in various buffers
20 p3501 N85-31761
Effect of passage number on electrophoretic mobility distributions of cultured human embryonic kidney cells
20 p3501 N85-31762
Density gradient electrophoresis of cultured human embryonic kidney cells
20 p3501 N85-31763
Identification and quantitation of morphological cell types in electrophoretically separated human embryonic kidney cell cultures
20 p3501 N85-31764
Urokinase production by electrophoretically separated cultured human embryonic kidney cells
20 p3501 N85-31765
Summary electrophoretic data base on human embryonic kidney cell strain 8514
20 p3501 N85-31766
Recommendations and calculations concerning physical characteristics of the EEVT apparatus
20 p3502 N85-31769
Evaluation of results of cell electrophoresis experiments on space shuttle STS-3 including pre-flight and post-flight laboratory experiments
20 p3502 N85-31772
Free zone electrophoresis simulation of static column electrophoresis in microgravity on shuttle flight STS-3
20 p3502 N85-31773

Microgravity electrophoresis: A study of the factors that affect free-fluid separation 20 p3502 N85-31774
Properties of electrophoretic fractions of human embryonic kidney cells separated on space shuttle flight STS-8 20 p3503 N85-31776
A computerized system for spot detection and analysis of two-dimensional electrophoresis images 23 p3958 N85-34531

ELECTROPHOTOMETERS
The Torun measuring system for astronomical spectra 07 p0966 N85-16130
The scanning heliometer 14 p2451 N85-25134
Program for observations of Halley's comet 22 p3732 N85-33136

ELECTROPHOTOMETRY
Offerings of the Astronomical Institute of Bonn 15 p2667 N85-26459
Photoelectric observations of contact binary stars [REPT-96] 15 p2667 N85-26460
Photoelectric observations of the dwarf nova VW Hydri during the November 1977 supermaximum [REPT-97] 15 p2667 N85-26461
Photoelectric observations of the eclipsing binary V 836 Cygni [REPT-98] 15 p2668 N85-26462

ELECTROPHYSICS
NT ELECTRO-OPTICS
NT MOLECULAR ELECTRONICS
Complex formation and temperature stability of electrophysical properties of GaAs semiinsulating single crystals 02 p0256 N85-11689
Basic research in electronic (JSEP): Joint Services Electronics Program [AD-A147891] 07 p0948 N85-16007

ELECTROPHYSIOLOGY
Review on physiological and medical problems related to climates ranging from altitude to sub-tropics 05 p0687 N85-14417
Electrophysiologic changes in organophosphorus-induced delayed neurotoxicity [AD-P004025] 06 p0844 N85-15359
Natural electrical activity of human sympathetic nerve fibers, recorded from body surface 07 p1013 N85-16433
Electrosleep therapy advanced at medical institute 10 p1526 N85-19623
Functional system theory in practice 11 p1690 N85-20629
Psychological aspects of phenomenon of spatial synchronization of EEG potential 11 p1691 N85-20632
Topography of human brain electric potentials and dominance 11 p1691 N85-20633
Susceptibility of cat and squirrel monkey to motion sickness induced by visual stimulation: Correlation with susceptibility to vestibular stimulation 11 p1694 N85-20650
Brain mechanisms underlying individual differences in reaction to stress: An animal model [AD-A150195] 13 p2143 N85-23301
A model for generalization and specification by single neurons [AD-A150671] 14 p2391 N85-24724
The origin of brain potentials associated with selective visual attention [AD-A152291] 16 p2840 N85-27511
Interaction of opiate and phencyclidine derivatives with the acetylcholine receptor [AD-A155119] 21 p3664 N85-32761

ELECTROPLATING
Inhibition of hydrogen absorption during plating of high strength steels [AD-A144882] 01 p0028 N85-10174
Laser-assisted solar-cell metallization processing 06 p0831 N85-15282
Effect of rhodamine-B on the electrodeposition of lead on copper, revision [DE85-000674] 11 p1606 N85-20101
Laser-assisted solar cell metallization processing [NASA-CR-176124] 22 p3805 N85-33565
Electrolytic cell [DE85-011598] 22 p3807 N85-33578

ELECTROPOLISHING
An electrochemical study of hydrogen uptake and elimination by bare and gold-plated waspaloy [NASA-TM-86479] 02 p0182 N85-11222
Electrolytic lapping technique for vanadium [DE84-014710] 02 p0183 N85-11227

ELECTROSEISMIC EFFECT
U ELECTRIC CURRENT
U SEISMIC WAVES

ELECTROSLAG PROCESS
Steel castings by the electroslag casting technique [DE85-003812] 12 p1819 N85-21409

ELECTROSLAG REFINING
ESR (Electroslag Refining) technology in Australia: Laboratory research and industrial development [AD-A147776] 06 p1129 N85-17114

ELECTROSLAG WELDING
Institute's contribution to Soviet welding technology noted 16 p2767 N85-27072

ELECTROSTATIC CHARGE
Aerosol sampling bias from differential electrostatic charge and particle size 02 p0224 N85-11467
Charging of the DMSP F-2 spacecraft in the aurora on 10 January 1983 [AD-A146303] 03 p0324 N85-12086
Long-term light induced changes in dark conductivity of kapton [AD-A148791] 08 p1224 N85-17706
Measurement and control of electrostatic charges on solids in a gaseous suspension [DE85-001450] 09 p1291 N85-18105
Electrostatic potentials: A new method for interpreting and predicting molecular reactivities and for designing synthetic pathways. Applications to nitroaromatics, nitramines and nitrated [AD-A150120] 12 p1801 N85-21298
Direct measurements of severe spacecraft charging in auroral ionosphere 13 p1991 N85-22480
Average and worst-case specifications of precipitating auroral electron environment 13 p1991 N85-22482
Galileo internal electrostatic discharge program 13 p1995 N85-22504
Automatic charge control system for satellites 13 p1995 N85-22508
Discharge characteristics of dielectric materials examined in mono-, dual-, and spectral energy electron charging environments 13 p1995 N85-22510
Development and testing of a spacecraft surface potential monitor 13 p2007 N85-22582
Electrostatic discharge testing on a carbon fiber solar panel structure 13 p2007 N85-22584
EOS (electrical overstress) protection for VLSI (Very Large Scale Integration) devices [AD-A150333] 13 p2064 N85-22891
Electrostatic charging of the Giotto spacecraft due to neutral gas impact 14 p2244 N85-23913
Saturn electrostatic discharges 15 p2673 N85-26499
Statistical study of Saturnian electrostatic discharges observed by the Voyager Planetary Radio Astronomy experiment 15 p2673 N85-26500
Multivalued electrostatic potentials; chance or necessity for the charge of solid particles near Saturn? 15 p2677 N85-26529
On the electric charge carried by dust grain excitation of violent discharge — planetary rings 15 p2677 N85-26530
Oil tank electrostatic charging report [DRIC-T-6967] 20 p3436 N85-31319

ELECTROSTATIC ENGINES
Ion thruster performance model [NASA-CR-174810] 04 p0462 N85-12935
Ion thruster project [NASA-TM-77726] 07 p0917 N85-15805
Precision tunable resonant microwave cavity [NASA-CASE-LEW-13935-1] 11 p1628 N85-20248

ELECTROSTATIC EROSION
U SPARK MACHINING

ELECTROSTATIC FIELDS
U ELECTRIC FIELDS

ELECTROSTATIC GENERATORS
Closed loop electrostatic levitation system [NASA-CASE-NPO-15553-1] 18 p3092 N85-29142
A small-scale self-excited rotor electrostatic generator [AD-A155264] 21 p3581 N85-32265

ELECTROSTATIC GYROSCOPES
Suspension torques on a gimballed electrostatically supported gyroscope and requirements on the gyroscope and spacecraft for the relativity gyroscope experiment 12 p1651 N85-21606

ELECTROSTATIC PLASMA
U PLASMAS (PHYSICS)

ELECTROSTATIC PRECIPITATORS
Electrostatic augmentation of fabric filtration: Reverse-air pilot unit experience [PB84-230002] 03 p0343 N85-12207
A system for monitoring radon and its decay products in the atmosphere [INPE-3065-PRE/494] 03 p0391 N85-12502
Third US/USSR Symposium on Particulate Control [PB85-190890] 19 p3310 N85-30522
Evaluation of pilot ESP used with a spray dryer FGD system at Pittsburgh Energy Technology Center, Bruceton, Pennsylvania [DE85-011151] 22 p3746 N85-33217
A study of the control of particulate emissions from turbine engine test cells 24 p4067 N85-35205

ELECTROSTATIC PROBES
Ionic reactions of atmospheric importance [AD-A147354] 07 p0997 N85-16333
A new fast response probe for diffusion studies in atmospheric air — pollution modeling [IC-AERO-84-01] 08 p1180 N85-17437
Cookbook for determining essential transmission characteristics of spherical section electrostatic analyzers [DE85-001404] 09 p1391 N85-18751
Ram-wake effects on plasma current collection of the PIX 2 Langmuir probe 13 p1993 N85-22496
Results of the Langmuir-probe experiment on board Intercosmos-18 — ionosphere-magnetosphere interaction 14 p2362 N85-24596
Measuring electrical field fluctuations by Langmuir Double Probe Method 16 p2720 N85-26789
Rocket measurements of mesospheric ionization irregularities [NASA-CR-176056] 20 p3494 N85-31721
Observations of mesospheric turbulence by rocket probe and VHF radar, part 2.4A 21 p3619 N85-32484
Recoverable Plasma Diagnostics Package (RPDP) 23 p3902 N85-34167
Langmuir probe on ISX-B [DE85-012066] 23 p3983 N85-34697

ELECTROSTATIC PROPULSION
NT ION PROPULSION
Ion thruster performance model [NASA-CR-174810] 04 p0462 N85-12935

ELECTROSTATIC SHIELDING
High voltage isolation transformer [NASA-CASE-GSC-12817-1] 18 p3093 N85-29148

ELECTROSTATIC WAVES
Integral of wave kinetic equation of drift waves 02 p0283 N85-11848
Waves and instabilities in collisionless shocks [AD-A146689] 06 p0881 N85-15597
The flow of plasma in the solar terrestrial environment [NASA-CR-174301] 08 p1224 N85-17707
Simulation of the ion-beam-driven drift instability in a magnetic trap, 1 [AD-A149451] 10 p1452 N85-19147
Simulation of the ion-beam-driven drift instability in a magnetic trap, 2 [AD-A149452] 10 p1554 N85-19798
Pressure-gradient-driven Tokamak resistive MHD instability in the banana-plateau collisionality regime [DE85-004568] 12 p1937 N85-22171
Cosmic ray generation by plasma turbulence: Development of a new paradigm in physics 12 p1955 N85-22286
Generation and propagation of electron cyclotron harmonic waves 14 p2367 N85-24630
Theoretical studies of electric cyclotron harmonic (ECH) waves based on experimental data from GEOS 1 14 p2367 N85-24631
Anomalous heating of ionospheric components (thermal e- and He+) via intense Ion Cyclotron Waves (ICW's) 14 p2368 N85-24633
A method of solving the dispersion equation for electrostatic electron waves in magnetized plasma [KGI-PREPRINT-071] 16 p2669 N85-27697
Quenching of the beam-plasma instability by 3-D spectra of large scale density fluctuations [NASA-CR-175969] 19 p3369 N85-30697
Application of field similitude theory to calculation of stripline heating 22 p3780 N85-33419
Recoverable Plasma Diagnostics Package (RPDP) 23 p3902 N85-34167
Observation of mode-converted by ion Bernstein wave by an HCN laser scattering [IPPJ-724] 23 p3979 N85-34668

ELECTROSTATICS
Research on large, highly accurate, inflatable reflectors [AD-A145080] 01 p0016 N85-10099
Effects of core mixing on solar oscillation frequencies [DE84-015540] 03 p0449 N85-12553
Solid state, surface and catalytic properties of oxides [DE85-002096] 06 p0867 N85-15512
Data appendix: F-number = 1.0 EMR with a flexible back electrode [NASA-CR-172477] 07 p0946 N85-15994
Electrostatic wave observation during a space simulation Beam-Plasma-Discharge (BPD) [NASA-CR-174286] 07 p1045 N85-16639
Large electrostatic accelerators [DE85-001120] 09 p1382 N85-18689
High power pulsed accelerators with potential industrial applications [DE85-001710] 11 p1720 N85-20821
Computerized study of several electrostatic, surface-ionization ion-source configurations [DE85-001512] 11 p1721 N85-20823

Electrostatic confinement in a bumpy torus
[DE85-003794] 12 p1936 N85-22164
Electrostatic forming and testing of polymer films on a 16-foot diameter test fixture
[NASA-TM-86328] 13 p2063 N85-22985
Evaluation of unimolecular rate constants for some outer-sphere electrochemical reactions
[AD-A150758] 14 p2250 N85-23946
VULTURE manual
[DE85-006873] 17 p3013 N85-28631
Global effects of double layers — plasma layers
[TRITA-EPP-84-12] 20 p3536 N85-32002
Electrostatic astigmatic tubular lens
21 p3685 N85-32955
Supermite vacuum interface design
[DE85-012661] 22 p3837 N85-33759
Design status of heavy ion injector program
[DE85-010751] 22 p3842 N85-33793
Friction, impact, and electrostatic discharge sensitivities of energetic materials
[DE85-013321] 24 p4083 N85-35309
The effect of power law body forces on a thermally-driven flow between concentric rotating spheres
[NASA-TM-87596] 24 p4093 N85-35374
Two-dimensional quasineutral description of particles and fields above discrete auroral arcs
[NASA-CR-176170] 24 p4116 N85-35517

ELECTROSTRICTION
Piezoelectric and electrostrictive materials for transducer applications
[AD-A145115] 01 p0043 N85-10277

ELECTROTHERMAL ENGINES
NT ARC JET ENGINES
NT PLASMA ENGINES
NT RESISTOJET ENGINES
Investigation of a pulsed electrothermal thruster system
[NASA-CR-174768] 02 p0169 N85-11132
Qualification of an electrothermal hydrazine thruster with a vacuum thrust of 0.5 to 2.0 N
[BMFT-FB-W-84-043] 07 p0917 N85-15808
Compatibility experiments of facilities, materials, and propellants for electrothermal thrusters
[NASA-TM-86956] 12 p1795 N85-21260

ELECTROWINNING
Using fuel cells or anode depolarization to reduce electrowinning energy consumption
[DE85-006187] 13 p2129 N85-23250

ELEMENT ABUNDANCE
U ABUNDANCE

ELEMENTARY EXCITATIONS
NT EXCITONS
NT MAGNONS
NT PHONONS
NT PLASMONS
NT POLARONS
Quasiparticle aggregation in the Fractional Quantum Hall Effect
[DE85-001574] 10 p1565 N85-19668
Elementary processes of electronically excited particles. Part 5: Deactivation of CHF (A1a' (O, V'2, O) after excitation by a pulsed dye laser
[MPIS-13/1984] 14 p2420 N85-24930
Quasiparticle excitations in valence-fluctuation materials: Effects of band structure and crystal fields
[DE85-010783] 19 p3359 N85-30824

ELEMENTARY PARTICLE INTERACTIONS
NT ELECTRON CAPTURE
NT NUCLEAR CAPTURE
NT NUCLEON-NUCLEON INTERACTIONS
Spline-Galerkin solution of integral equations for 3-body scattering above break-up
[TWISK-327] 01 p0109 N85-10738
Results on weak current from CHARM collaboration — neutrino interactions
[NOTA-INTERNA-810] 02 p0279 N85-11817
Computing the Kac determinant using dual mode techniques and more about the No-ghost theorem
[DE85-001329] 09 p1375 N85-18640
Activities in nuclear physics and high energy physics
11 p1728 N85-20866
Experimental studies of elementary particle interactions at high energies
[DE85-004795] 13 p2157 N85-23394
Glueball candidates
[DE85-003627] 14 p2418 N85-24921
Modern test of chiral anomalies
[DE85-005892] 17 p3020 N85-28680
Elementary particle theory
[DE85-006603] 17 p3034 N85-28771
Topics in intermediate vector boson physics
[NOTA-INTERNA-841] 18 p3184 N85-29743
Activities report of the Werner-Heisenberg Institute for Physics
[ISSN-0173-6256] 18 p3184 N85-29746
Introduction to the Standard Model — weak and electromagnetic interactions
[USIP-85-02] 20 p3532 N85-31970
Nucleon-nucleus interactions from JACEE
24 p4173 N85-35869

ELEMENTARY PARTICLES
NT ALPHA PARTICLES
NT ANTINEUTRINOS
NT ANTINUCLEONS
NT ANTIPARTICLES
NT ANTIPROTONS
NT BARYONS
NT BETA PARTICLES
NT BOSONS
NT COLD NEUTRONS
NT CONDUCTION ELECTRONS
NT DEUTERONS
NT ELECTRONS
NT FAST NEUTRONS
NT FERMIONS
NT FREE ELECTRONS
NT GLUONS
NT HADRONS
NT HIGH ENERGY ELECTRONS
NT HOT ELECTRONS
NT HYPERONS
NT KAONS
NT LEPTONS
NT LIGHT BEAMS
NT MAGNETIC MONOPOLES
NT MESONS
NT MUONS
NT NEGATRONS
NT NEUTRINOS
NT NEUTRON BEAMS
NT NEUTRONS
NT NUCLEONS
NT PHOTOELECTRONS
NT PHOTONS
NT PIONS
NT POLARONS
NT POSITRONS
NT PROTONS
NT QUARKS
NT SOLAR ELECTRONS
NT SOLAR NEUTRINOS
NT SOLAR PROTONS
NT TACHYONS
NT THERMAL NEUTRONS
NT VECTOR MESONS
Research program in theoretical high-energy physics
[DE84-013717] 01 p0119 N85-10817
Research in elementary particle physics
[DE84-013520] 02 p0279 N85-11815
Decaying particles do not heat up the Universe
[DE85-002191] 11 p1763 N85-21091
Cosmology, galactic astronomy and elementary particle physics
12 p1956 N85-22289
Los Alamos Science, Number 11, Summer-Fall, 1984
[DE85-004634] 14 p2419 N85-24926
Activities report of the Werner-Heisenberg Institute for Physics
[ISSN-0173-6256] 18 p3184 N85-29748
The SLC program
[DE85-011433] 19 p3357 N85-30813
Spin dependence of the lamda-nucleus interaction determined by observation of hypernuclear gamma rays
[DE85-011878] 19 p3364 N85-30863
Monte Carlo sampling strategies for lattice gauge calculations
[DE85-010756] 19 p3377 N85-30948
Research in the theory of condensed matter and elementary particles
[DE85-010447] 20 p3531 N85-31968
Phenomenology of the standard and nonstandard Higgs particles
[USIP-85-03] 20 p3532 N85-31971
Depth and size effects on cosmogenic nuclide production in meteorites
[SH-7.1-9] 23 p4048 N85-35101
The identification of gamma ray induced EAS
[HE-4.5-1] 24 p4195 N85-36026

ELEVATION
Prediction of deflections of the vertical by gravimetric methods
[PB84-213727] 01 p0072 N85-10478
Digital Terrain Elevation Data (DTED) anomaly removal through the use of an interactive Fourier frequency filtering process
[AD-A145433] 02 p0219 N85-11445
Special difficulties of retrieving surface elevation over continental ice — satellite radar altimetry
03 p0380 N85-12429
Digital elevation models improve processing of Alaskan gravity data 04 p0515 N85-13295
Automatic terrain elevation mapping and registration
08 p1148 N85-17242
A comparative test of photogrammetrically sampled digital elevation models 08 p1175 N85-17406
Digital elevation model computation using fast Poisson solutions 08 p1175 N85-17412
Sequential data processing for photogrammetric acquisition of digital elevation models
08 p1176 N85-17413
Hypsometric features on Venus
13 p1983 N85-22439
Mathematical modeling of results of geometric leveling in variable gravity field 13 p2114 N85-23170
Surface units on Venus derived from Pioneer-Venus altimetry, roughness, and reflectivity measurements
13 p2177 N85-23510
Derivation of model topography
18 p3141 N85-29449
Comparison of survey and photogrammetry methods to position gravity data, Yucca Mountain, Nevada
[DE85-011665] 21 p3590 N85-32316

ELEVATION ANGLE
Experimental test of the three subaperture method for estimating target elevation angle
[AD-A149687] 12 p1851 N85-21614
A star camera aspect system suitable for use in balloon experiments
[OG-9.3-10] 23 p4029 N85-34965

ELEVATIONS (DRAWINGS)
U DRAWINGS

ELEVATORS (CONTROL SURFACES)
Application of linear optimal control theory to the design of the elevator control system of the DHC-2 Beaver experimental aircraft
[VTH-LR-411] 16 p2711 N85-26729
Proposals for the determination of necessary elevator handling characteristics of sailplanes in high speed range
[DFVLR-FB-84-52] 17 p2900 N85-27882

ELEVATORS (LIFTS)
Hoist
[AD-D011458] 10 p1493 N85-19425
Automated, robotized forge-press systems viewed
14 p2284 N85-24153
Application of lightweight composite materials to naval weapons systems
[PB85-173607] 16 p3069 N85-28981

ELEVONS
Space shuttle elevon seal panel mechanism
08 p1101 N85-16961

ELIMINATION
NT DELETION
Comparison of two algebraic methods for curve/curve intersection 17 p3007 N85-28591

ELLIPSES
What is principal components analysis?
02 p0211 N85-11389
Symmetry breaking for a class of semi-linear elliptic problems
[AD-A149093] 10 p1546 N85-19748
A new method for calculating the flow field in a dump combustor
[AD-A149305] 11 p1631 N85-20271
On MGR (Upsilon) multigrid methods
[AD-A153687] 19 p3345 N85-30733
Use of a minimum-ellipse criterion in the study of ion-beam extraction systems
[DE85-012870] 24 p4148 N85-35721

ELLIPSOIDS
Two lunar global asymmetries
04 p0585 N85-13734
Automatic Monoellipsoidal Mirror Furnace Facility (AMMFF), volume 1 — spaceborne crystal growth
[AMF-RP.100-DS-015-VOL-1] 09 p1285 N85-18073
Computation of the inviscid velocity potential for general ellipsoids on a nearly quadratic surface grid
[REPT-25/84] 11 p1633 N85-20287
Dynamics of solid body with ellipsoidal cavity containing magnetic fluid 14 p2279 N85-24116
Singularity solutions for ellipsoids in Low-Reynolds-Number flows: With applications to the calculation of hydrodynamic interactions in suspensions of ellipsoids
[AD-A153503] 18 p3169 N85-29632
Speckle interferometry applied to asteroids and other solar system objects
[NASA-CR-175978] 19 p3384 N85-30995

ELLIPSOMETERS
Photon scattering and interaction analysis of interfacial corrosion and catalysis
[DE85-002534] 11 p1608 N85-20114
Time-resolved ellipsometry and reflectivity measurements of the optical properties of silicon during pulsed excimer laser irradiation
[DE85-005091] 13 p2096 N85-23079
Interfacial bonding stability 21 p3608 N85-32409

ELLIPTIC DIFFERENTIAL EQUATIONS
NT MONGE-AMPERE EQUATION
On the theory of coercitive linear partial differential operators
[ISSN-0355-0087] 03 p0414 N85-12846
Transformation of two and three-dimensional regions by elliptic systems
[NASA-CR-174176] 04 p0554 N85-13529
Swirling turbulent spray group combustion
09 p1289 N85-16095
Vectorization and implementation of an efficient multigrid algorithm for the solution of elliptic partial differential equations
[AD-A149049] 10 p1545 N85-19743
Domain decomposition techniques for solving elliptic partial differential equations on multiprocessors
[DE85-004448] 10 p1549 N85-19760
On the accuracy of least squares methods in the presence of corner singularities
[NASA-CR-172552] 12 p1919 N85-22050
Analysis of spectral operators in one-dimensional domains
[NASA-CR-172573] 15 p2633 N85-26226
A stability analysis of incomplete LU factorizations
[AD-A152058] 15 p2636 N85-26271
Generation of surface coordinates by elliptic partial differential equations 17 p3006 N85-28583
Numerical methods for stiff ordinary and elliptic partial differential equations
[AD-A153247] 17 p3020 N85-28675
Solving elliptic partial differential equations on the hypercube multiprocessor
[AD-A153464] 18 p3168 N85-29829
Optimization of a numerical method to calculate elliptic flows
[ESA-TT-889] 20 p3457 N85-31472
Some ideas for decomposing the domain of elliptic partial differential equations in the Schwarz process
[DE85-011844] 22 p3834 N85-33739
Absorbing boundary conditions for exterior problems
[NASA-CR-177944] 24 p4142 N85-35576
ELLIPTIC FUNCTIONS
Application of summability methods to Jackson theorems for splines
[AD-A148256] 03 p0412 N85-12835
Some scientific subroutines in LISP
[AD-A147899] 07 p1026 N85-16515
Feedback, adaptivity and A-posterior estimates in finite elements: Aims, theory and experience
[AD-A148869] 07 p1029 N85-16531
Computation of elliptical functions in problems of celestial mechanics 13 p1979 N85-22418
Incorporation of an elliptical boundary condition into the program POISSON
[DE85-006820] 16 p2849 N85-27564
ELLIPTIC INTEGRALS
U ELLIPTIC FUNCTIONS
ELLIPTICAL CYLINDERS
The unsteady boundary layer on an elliptic cylinder following the impulsive onset of translational and rotational motion — dynamic stall 14 p2209 N85-23699
ELLIPTICAL GALAXIES
The relationship between radio structures and stellar dynamics of nearby elliptical galaxies
08 p1236 N85-17794
A comparative study of dust and young stars in three small galaxies 09 p1415 N85-18928
X-ray emission from Centaurus A
[DE85-002030] 09 p1417 N85-18943
Dynamics of elliptical galaxies and the r sup 1/4 luminosity law 12 p1955 N85-22282
ELLIPTICAL ORBITS
NT INTERPLANETARY TRANSFER ORBITS
NT PERIGEES
NT PERIHELIONS
NT TRANSFER ORBITS
Periodic oscillation of gyrostat-satellite about its center of mass in an elliptical orbit 02 p0159 N85-11080
Nonlinear oscillations of 2 body system relative to center of mass in elliptical orbit 02 p0159 N85-11082
Some considerations on elliptic heliocentric orbits
[INPE-3217-PRE/570] 02 p0297 N85-11925
Averaging of equations of cometary orbital motion with allowance for nongravitational effects
13 p1978 N85-22411
Satellite oscillations in elliptical orbit
13 p1981 N85-22429
Periodic movements of axisymmetrical satellite about center of mass due to gravitational moment
13 p2042 N85-22783
Inclinations of the Uranian rings
15 p2672 N85-26487
Integrable cases of restricted doubly averaged 3-body problem 16 p2718 N85-26778
The 6 pi-periodic solutions of plane restricted elliptical 3-body problem in neighborhood of libration points
16 p2718 N85-26779
Dynamics and control of tethers in elliptical orbits
20 p3399 N85-31087
ELLIPTICAL PLASMAS
Elliptical X-ray analyzer spectrograph application to a laser-produced plasma
[DE85-013790] 24 p4097 N85-35398
ELLIPTICITY
Limits of possible operation of the R-Tokamak due to ideal MHD instabilities
[IPPJ-894] 06 p0863 N85-15486
Downwash in the plane of symmetry of an elliptically loaded wing
[NASA-TP-2414] 07 p0898 N85-15693
An experimental investigation of unexcited and excited elliptic jets 15 p2554 N85-25755
Neoclassical diffusion including ellipticity in a heliotron-like configuration 23 p3978 N85-34667
ELONGATION
Equibiaxial extension of two polymer melts: Polystyrene and low density polyethylene
[AD-A144893] 01 p0032 N85-10200
Tensile properties and swelling of 20%-cold-worked Type 316 stainless steel irradiated in HFIR
[DE84-014080] 05 p0617 N85-13948
Development and characterization of ductile Long-Range-Ordered (LRO) alloys (Fe,Co, Ni)3V for high-temperature structural use
[DE84-016750] 06 p0769 N85-14921
Rheology of dissemination
[AD-A150006] 12 p1813 N85-21373
Magnetic method of inspecting mechanical properties of general purpose tubes
[BLL-M-39084-(5826.4)] 16 p2796 N85-27235
Effects of annealing treatments on superplasticity in a thermomechanically processed Aluminum-10.2%Mg-0.52%Mn
[AD-A154414] 19 p3239 N85-30060
EMANATION
U EMISSION
EMBEDDED COMPUTER SYSTEMS
NT AIRBORNE/SPACEBORNE COMPUTERS
Embedded-grid generation with complete continuity across interfaces for multi-element airfoils
02 p0133 N85-10911
Liquid payload moment equations
[AD-A145977] 03 p0362 N85-12319
The embedded test (BIT): Impact on the total cost of possession 06 p1063 N85-16734
Ada (trademark) primer
[AD-A148855] 10 p1539 N85-19703
HLLM software support
[AD-A154828] 21 p3671 N85-32805
EMBEDDING
Embedment system for ultrahigh-burning rate propellants of solid propulsion subsystems
[AD-D011257] 06 p0773 N85-14942
Immobilization of toxic waste by embedding it in bitumen
[OEFZS-4277] 07 p0995 N85-16322
Extracting embedded generalized networks from linear programming problems
[AD-A147565] 07 p1033 N85-16558
Monitoring the execution of plans in SIPE (System for Interactive Planning and Execution) monitoring
[AD-A149138] 10 p1544 N85-19731
Functional equation for the embedding of a homomorphism of the interval into a flow
[DE85-000655] 11 p1713 N85-20760
Embedding graphs in lines, trees and grids
19 p3334 N85-30652
EMBOLISMS
Pathogenesis and treatment of cerebral air embolism and associated disorders
[AD-A146723] 07 p1014 N85-16443
EMBRITTLEMENT
Effect of microstructure and trapping on the hydrogen embrittlement susceptibility of a titanium bearing HSLA steel 02 p0174 N85-11166
The influence of rare Earth elements on the temper embrittlement behaviour and mechanical properties of a low alloy steel 02 p0180 N85-11210
The effects of microstructure on the temper embrittlement susceptibility of a Cr-2-1/4 1Mo forging
[AERE-R-11110] 03 p0334 N85-12151
Susceptibility of 2 1/4 Cr-1Mo steel to liquid metal induced embrittlement by lithium-lead solutions
[DE85-000997] 09 p1294 N85-18130
Study of the mechanism for annealing embrittlement of an iron-based metallic glass
[DE84-016856] 09 p1300 N85-18164
Models for shock damage to marine structural materials 09 p1336 N85-18400
Patterns in the occurrence of the brittle topologically close-packed phases: Al
[DE85-000592] 11 p1607 N85-20106
Chemisorption theory: Adsorption on copper-nickel alloys and titanium surface embrittlement
[DE85-001815] 12 p1807 N85-21334
Influence of oxygen traces on the properties of tungsten heavy metals
[BLL-RARDE-TR-1177-(7291.7965)] 15 p2508 N85-25470
Radiation effects on structural materials
[DE85-007032] 15 p2649 N85-26336
Grain boundary composition and intergranular fracture of steels. Volume 1: Detection of grain boundary segregation in steels
[DE85-006850] 15 p2662 N85-26428
Effect of texture in steel on the susceptibility of hydrogen embrittlement
[BLL-BISI-TRANS-22026-(9022.06)] 17 p2926 N85-28048
Interfacial segregation and fracture
[DE85-009779] 18 p3075 N85-29019
Brittle fracture behaviour of cold formed, welded 10mm to 20 mm thick plate manufactured from plain carbon structural steels
[BLL-BISI-TRANS-21676-(9022.06)] 18 p3120 N85-29311
EMBRYOS
Effects on in vivo and in vitro exposure to excess gravity on growth and differentiation of mammalian embryos
15 p2612 N85-26095
EMERALD
U BERYL
EMERGENCIES
Materials for emergency repair of runways
[AD-A146130] 03 p0320 N85-12068
Design of a scientific information collation and dissemination system, volumes 1 thru 3
[AD-A146002] 03 p0438 N85-12791
Improved robotic equipment for radiological emergencies
[DE84-017637] 04 p0509 N85-13249
Energy supply problems for emergency telephones
05 p0663 N85-14265
Liposome-encapsulated hemoglobin for emergency resuscitation
[AD-A146794] 07 p1015 N85-16446
An approach to planning in the inflight emergency domain
[AD-A151869] 15 p2467 N85-25228
Survivable ground base sensor
[AD-D011647] 17 p2950 N85-28213
US Coast Guard High Frequency Emergency Network (HFEN) implementation plan
[PB85-174167] 18 p3092 N85-29141
Graphic display development program. Volume 2, revision 0: Appendices
[DE85-011078] 19 p3333 N85-30648
Hydrazine and the F-16 20 p3511 N85-31826
Emergency modeling of hazardous air pollutants
[AD-A155441] 21 p3614 N85-32461
Fire service emergency management handbook
[AD-A155780] 24 p4084 N85-35313
EMERGENCY LIFE SUSTAINING SYSTEMS
A life-saving device for ships
[NASA-TM-77670] 23 p3865 N85-34129
EMERGENCY LOCATOR TRANSMITTERS
Recommended improvements for second generation 121.5/243 MHz ELT's
[NASA-CR-175274] 08 p1080 N85-16841
Emergency Locator Transmitter (ELT) batteries guidance and recommendations
[NASA-TM-87436] 11 p1624 N85-20225
Improved legislated emergency locating transmitters and emergency position indicating radio beacons
[NASA-CASE-GSC-12692-1] 11 p1624 N85-20226
Emergency Locator Transmitter (ELT) batteries guidance and recommendations
[NASA-TM-87415] 11 p1672 N85-20533
The 121.5 MHz ELT: Past, present and future — Emergency Locator Transmitter (ELT)
20 p3401 N85-31105
Soviet Emergency Locator Transmitter/Emergency Position Indicating Radio Beacon (ELT/EPIRBs) at 121.5 and 406 MHz 20 p3402 N85-31107
A 406 MHz ELT processor for geostationary satellites — Emergency Locator Transmitter (ELT)
20 p3403 N85-31114
Navigation data for Emergency Position Indicating Radio Beacons (EPIRBs) 20 p3403 N85-31115
The 121.5/243 MHz ELT identification — Emergency Locator Transmitter (ELT) 20 p3404 N85-31119
SARSAT 406 MHz system technical evaluation
20 p3404 N85-31124

The COSPAS/SARSAT demonstration and evaluation. Results of the first year in the United States
20 p3405 N85-31128

EMISSION
NT ACOUSTIC EMISSION
NT BIOLUMINESCENCE
NT CATHODOLUMINESCENCE
NT CHEMILUMINESCENCE
NT CN EMISSION
NT ELECTROLUMINESCENCE
NT ELECTRON EMISSION
NT EXHAUST EMISSION
NT FIELD EMISSION
NT FLUORESCENCE
NT HYDROXYL EMISSION
NT INCANDESCENCE
NT ION EMISSION
NT LIGHT EMISSION
NT LUMINESCENCE
NT MICROWAVE EMISSION
NT NEUTRON EMISSION
NT OPTICAL RESONANCE
NT PARTICLE EMISSION
NT PHOSPHORESCENCE
NT PHOTOELECTRIC EFFECT
NT PHOTOELECTRIC EMISSION
NT PHOTOIONIZATION
NT PHOTOLUMINESCENCE
NT RADIO BURSTS
NT RADIO EMISSION
NT RESONANCE FLUORESCENCE
NT SECONDARY EMISSION
NT SHOCK WAVE LUMINESCENCE
NT SOLAR RADIO BURSTS
NT SOLAR RADIO EMISSION
NT SPECTRAL EMISSION
NT SPONTANEOUS EMISSION
NT STIMULATED EMISSION
NT THERMAL EMISSION
NT THERMIONIC EMISSION
NT THERMOLUMINESCENCE
NT TYPE 3 BURSTS
NT TYPE 4 BURSTS
NT WATER MASERS
NT X RAY FLUORESCENCE

Future scenarios and ozone change
[DE84-014781] 01 p0085 N85-10673

Harmonic emission from high power gyrotron oscillators
[AD-A145821] 02 p0200 N85-11335

Optical detection of alkali compounds
[DE84-015505] 03 p0328 N85-12117

Photoconductivity and emission from the impurity excited states in silicon
[DE84-015563] 04 p0479 N85-13052

VOC emissions from volatile organic liquid storage tanks: Background information for proposed standards
[PB84-237320] 04 p0532 N85-13403

Inclined dislocation emission at a shielded crack tip
[DE84-016703] 06 p0818 N85-15192

SWIR and visible atomic emission from laser-produced oxygen and nitrogen plasmas
[AD-A147528] 07 p1045 N85-16841

Bipolar flows and X-ray emission from young stellar object
08 p1234 N85-17779

Three dimensional ray tracing of the Jovian magnetosphere in the low frequency range
[NASA-CR-175462] 10 p1571 N85-19909

The spatial dependence of the Jovian auroral emissions
11 p1759 N85-21068

Increase in hydrogen emission of upper atmosphere following launches of space vehicles
13 p1981 N85-22431

Review of national emission standards for mercury
[PB85-153006] 16 p2822 N85-27406

Circular-beam ray tracing on a microcomputer
[DE85-010754] 19 p3338 N85-30685

Improved Nominal Operating Cell Temperature (NOCT) test procedure
21 p3612 N85-32449

Dynamics of emission from dye lasers employing synchronous pumping by limited picosecond pulse train
21 p3686 N85-32899

Spectral-luminescence characteristics and induced emission of Nd-3(+) ion in Gd(2-x)Nd(x)(WO4)3 crystals
21 p3688 N85-32912

SCRIBE data of October 23, 1983 flight
[AD-A154864] 21 p3705 N85-33012

The effect of anisotropic emission on the log N-log S curve of gamma-ray bursts
[OG-1.2-4] 22 p3862 N85-33914

Atmospheric Emission Photometric Imaging (AEPI)
23 p3902 N85-34170

Wide Angle Michelson Doppler Imaging Interferometer (WAMDII)
23 p3902 N85-34172

Results on nucleon life-time from the Kolar gold field experiment
[HE-6.2-3] 24 p4211 N85-36139

EMISSION SPECTRA
Local photometric standards for CaII emission stars
01 p0128 N85-10883

A spectroscopic survey of 113 nearby red dwarf stars
01 p0129 N85-10886

Photoluminescent properties of epitaxial p-GaSb
02 p0257 N85-11745

Variations of the H and K emission lines of singly ionized calcium in the eclipsing binary star system AR Lacertae
02 p0296 N85-11921

Lyman-Alpha aurora
02 p0302 N85-11953

Molecular hydrogen emission associated with high velocity flows. A tracer for low velocity shocks
03 p0443 N85-12819

The X-ray spectrum and time variability of narrow emission line galaxies
[NASA-TM-83859] 03 p0446 N85-12842

Local fields in strongly coupled plasmas
[DE84-013375] 04 p0567 N85-13611

Far-infrared line emission from the galaxy
[NASA-CR-174166] 04 p0580 N85-13702

Non-LTE considerations in spectral diagnostics of thermal transport and implosion experiments
[DE84-015187] 05 p0730 N85-14689

Physical conditions in low-luminosity active galactic nuclei
05 p0742 N85-14771

Lower atmospheric composition of Jupiter from Voyagar infrared measurements
[NASA-CR-174198] 05 p0745 N85-14779

Supercell band structure calculations of the two peak photo-and inverse photoemission spectra in Ce and Pr compounds
[DE84-017485] 06 p0867 N85-15513

The IRAS galaxy 0421+040P06: An active spiral (?) galaxy with extended radio lobes
[NASA-CR-174206] 06 p0871 N85-15536

The nature of the soft X-ray emitting region in the direction of the North Polar spur
06 p0877 N85-15568

Polarization of radio molecular lines and mapping of magnetic field direction
06 p0878 N85-15581

The compact radio emission regions in active galactic nuclei — QUASAT VLBI mission
07 p1058 N85-16713

Air quality assessment model validation in complex terrain
[AD-A147690] 08 p1180 N85-17434

Photoemission, vibrational and stimulated desorption studies of metal-semiconductor interfaces and of chemisorbed atoms and molecules
[AD-A147709] 08 p1225 N85-17717

Observations of nonthermal radio emission from early-type stars
08 p1232 N85-17758

X-ray emission from PKS 2155-304 — BL Lac object
08 p1239 N85-17812

X-ray emission from Centaurus A — Vela 5B; radio galaxy
08 p1239 N85-17813

The X-ray spectra of NGC 4151 — Seyfert galaxy
08 p1239 N85-17815

The high energy X-ray spectrum of 3C 273 — quasar
08 p1240 N85-17818

A universal spectrum for AGNs and QSOs — Active Galactic Nuclei (AGN)
08 p1241 N85-17826

An Inverse Compton model of the X-ray emission in Seyfert galaxies
08 p1241 N85-17827

Theoretical studies of emission line variability in type 1 Seyfert galaxies
08 p1242 N85-17839

On the stability of broad line clouds in active galactic nuclei
08 p1243 N85-17840

The 1.5 - 3.5 micron spectroscopy of the Orion H2 source
08 p1246 N85-17864

Far infrared spectroscopy of (O III) in M82
08 p1249 N85-17883

Interpretation of the far infrared emission from our external galaxies
08 p1249 N85-17884

Measurement procedures for the radar spectrum engineering criteria
[PB85-119022/GAR] 09 p1313 N85-18254

Effect of inner subshell ionization for emission lines of OIV ion
09 p1388 N85-18729

Applications of pulsed-laser techniques and thermographic phosphors to dynamic thermometry of rotating surfaces
[DE85-000403] 11 p1639 N85-20328

Ion quadrupole effects in spectral line broadening
[DE85-001504] 11 p1730 N85-20879

Subnanosecond time-resolved emission study of Cu2O and GaAs
[DE85-002070] 11 p1735 N85-20912

IUE spectroscopy of extragalactic H II regions
11 p1745 N85-20974

Coordinated multifrequency observations of the BL LAC objects MRK 180, MRK 421, and MRK 501
11 p1746 N85-20983

Fluorescent excitation of Fe 2, Mn 2, Ti 2, N 1 lines by V 4, N 5, O 6: Emission lines in the spectra of symbiotic stars and Seyfert galaxies
11 p1746 N85-20984

IUE observations of planetary nebulae in the Magellanic Clouds
11 p1747 N85-20986

1983 observations of the eclipsing nucleus of the bipolar planetary nebula NGC 2346
11 p1747 N85-20987

The changing ultraviolet spectrum of Herbig-Haro object No. 1
11 p1747 N85-20989

Short-wavelength observations of HH-2H and HH-24A
11 p1747 N85-20990

A search for young stellar chromospheres in NGC 2264
11 p1748 N85-20993

FP Cygni profiles in HL CMa
11 p1752 N85-21022

Variability of ultraviolet emission lines in the carbon star TX Psc
11 p1753 N85-21027

Temporal UV emission from the peculiar star RX Puppis
11 p1753 N85-21028

UV observations of epsilon aurigae during ingress and totality
11 p1755 N85-21038

Circumstellar material in Algols and Serpentids
11 p1757 N85-21051

Chromospheric emission lines in high-resolution LWR spectra (220 - 3000 alpha) of gamma CRU (M3 3) and alpha ORI (M2 Iab)
11 p1758 N85-21058

Precise measurements of radial velocities of emission lines in the far-ultraviolet spectra of late-type stars
11 p1758 N85-21062

Long term variability of the IO torus
11 p1760 N85-21070

Calibrations of wavelengths in SWP echelle spectra
11 p1761 N85-21077

Formation of optical-line emitting regions in the jets of SS433
12 p1959 N85-22318

Impurities in Kevlar 49 fibers
[DE85-004998] 13 p2038 N85-22767

A standard aircraft diffusion flame: Spectral characteristics and a feasibility study for developing an alternate calibration source for aircraft optical fire detection systems
[AD-A150231] 13 p2039 N85-22768

Measurement of the large-scale anisotropy of the cosmic background radiation at 3 MM
13 p2206 N85-23680

The Fe XIII 10747 A and Fe XIV 5303 A coronal emission lines polarization
14 p2448 N85-25111

Sound emission by particle beam passing through hole in rigid shield
15 p2525 N85-25570

High pressure cosmochemistry applied to major planetary interiors: Experimental studies
[NASA-CR-175715] 15 p2579 N85-26544

A new luminosity component in 3C48
[NASA-CR-175840] 17 p3052 N85-28894

Method for predicting the performance of cathode materials
[AD-D011665] 19 p3257 N85-30198

Self-consistent models for the X-ray emission from supernova remnants
20 p3548 N85-32082

Aerosol analysis and emission spectrometry with free jets
[DE85-010576] 21 p3584 N85-32168

Ionospheric electron density profile and related studies
[AD-A155257] 21 p3632 N85-32567

Investigation of reproducibility of emission wavelength of helium-neon laser with external neon absorption cell (0.63 micrometers)
21 p3683 N85-32884

High-resolution spectrum of Cygnus X-1
[OG-2.4-12] 22 p3868 N85-33956

Inverse-Compton gamma rays in the galaxy
[OG-3.1-2] 22 p3873 N85-33990

Multicomponent analysis of total COS-B gamma-ray data at intermediate latitudes
[OG-3.1-3] 22 p3873 N85-33991

The galactic gamma-ray distribution and the radial cosmic ray gradient
[OG-3.1-4] 22 p3873 N85-33992

Local electron spectrum above 100 MeV derived from gamma-ray emissivity spectra
[OG-3.1-7] 22 p3874 N85-33995

The electron spectra in the synchrotron nebula of the supernova remnant G 29.7-0.3
[OG-6.2-10] 22 p3889 N85-34100

Time-resolved spectroscopic studies of detonating heterogeneous explosives
[DE85-009760] 23 p3921 N85-34297

Apparatus and method for the spectrochemical analysis of liquids using the laser spark
[DE85-006749] 23 p3935 N85-34387

The read-out system of spatial distribution of thermoluminescence in meteorites
[SH-9.1-16] 23 p4052 N85-35131

The structure of Herbig-Haro object 43 and Orion dark cloud extinction
[NASA-TM-87503] 24 p4166 N85-35831
The ionization structure of planetary nebulae. Part 4: NGC 7662
[NASA-CR-176151] 24 p4169 N85-35844

EMISSIVITY
Non equilibrium ionization in the local hot bubble
06 p0879 N85-15687
Experimental investigations of thermal radiation from potassium atoms in magnetohydrodynamic system: Preliminary report
[DE85-003715] 12 p1936 N85-22189
Emissivity enhancement of fused silica for space applications — solar cells 13 p2011 N85-22815
Periodic gamma-ray emissions from Geminga at or = 10(12) eV
[OG-2.4-2] 22 p3867 N85-33949
Search for periodicities near 59 s in the COS-B gamma-ray data of 2CG195+04 (Geminga)
[OG-2.4-3] 22 p3867 N85-33950
Search for gamma-rays above 400 GeV from Geminga
[OG-2.4-4] 22 p3867 N85-33951
Observations on TeV gamma rays from Geminga and PSR 0950+08
[OG-2.4-6] 22 p3868 N85-33953
HEAO 3 upper limits to the expected 1634 KeV line from SS 433
[OG-2.4-9] 22 p3868 N85-33954

EMISSOGRAPHS
U ACTINOMETERS
U RECORDING INSTRUMENTS

EMITTANCE
Energy dependence of the emittance of damping ring beams
[DE85-007080] 15 p2649 N85-26341
A calorimetric approach for measuring emittance and normal spectral absorptance at elevated temperatures
[AD-A151292] 15 p2651 N85-26351
Profile of a relativistic electron beam propagated through a linear wiggler and an axial guide field
[AD-A154403] 19 p3353 N85-30783
Emittance growth caused by current variation in a beam-transport channel
[DE85-010743] 19 p3363 N85-30849
Requirements for very high energy accelerators
[DE85-011173] 20 p3529 N85-31952
Observations of accelerated high current low emittance beams in the SLC Linac
[DE85-013073] 24 p4068 N85-35211
Beam potential measurement of an intense H(-) beam by use of the emissive probe technique
[DE85-012871] 24 p4155 N85-35762
High resolution beam profile monitors in the SLC
[DE85-013375] 24 p4157 N85-35774
Relation between field energy and RMS emittance in intense particle beams
[DE85-012655] 24 p4159 N85-35784

EMITTERS
NT THERMIONIC CATHODES
NT THERMIONIC EMITTERS
Strained-layer superlattice emitter and detector structures using modulation-doped active regions
[DE85-000064] 06 p0867 N85-15511
Power transfer from natural emitters to collection apertures at microwave wavelengths
[NASA-CR-174275] 07 p0945 N85-15969
Research on electroluminescence in thin film yttrium oxysulfide
[AD-A146909] 07 p1037 N85-16582
Study of surface damage in cathode composite materials in a high flux CO2 laser 10 p1444 N85-19098
Development of solid state infrared emitters for gas detection applications
[PB85-148450] 15 p2561 N85-25800

EMOTIONAL FACTORS
Influence of activation of ASFS-2 on human emotional status 08 p1194 N85-17522
Decision making in stressful conditions: A model based on the coping perspective
[FOA-C-55064-H3] 08 p1229 N85-17736
USSR report: Life sciences. Biomedical and behavioral sciences
[JPRS-UBB-85-011] 10 p1525 N85-19616

EMOTIONS
The Reports of Aeromedical Laboratory, volume 25, no. 1/2
[ISSN-0023-2858] 01 p0090 N85-10605
Psychological states (mood, affect or emotion) experienced by JASDF pilots through flying duties. 3: Flying conditions causing pilots psychological disturbances 01 p0090 N85-10606
The relationship between emotional tension scale and psychological uneasiness of JASDF pilots in flying situations 01 p0090 N85-10608
Functional role of type of person's temperament in individual and mutual activity 10 p1525 N85-19621
Electrosleep therapy advanced at medical institute
10 p1526 N85-19623
Methods of monitoring mental work efficiency, emotional activity 10 p1526 N85-19627

EMPENNAGE
U TAIL ASSEMBLIES

EMPLOYEE RELATIONS
Data processing professionals and DP application users' perceptions and expectations of operational roles of persons working in a DP/application user interface group 24 p4165 N85-35821

EMPLOYMENT
Exploratory assessment of second generation robotics and sensor-based systems
[PB85-132793] 11 p1648 N85-20388
A comparison of metropolitan and non-metropolitan employment characteristics: Indications of the size of non-metropolitan mobile communication services user classes
[NASA-CR-175648] 13 p2053 N85-22855
Application of the Hardman methodology to the Single Channel Ground-Airborne Radio System (SINCGARS)
[NASA-CR-175694] 14 p2218 N85-23756
Characteristics of recent science/engineering graduates, 1982: Detailed statistical tables
[PB85-149060] 15 p2663 N85-26437

EMULSIONS
NT NUCLEAR EMULSIONS
NT PHOTOGRAPHIC EMULSIONS
Mist flammability studies of candidate fire-resistant hydraulic fluids
[AD-A148572] 08 p1134 N85-17148
A study of organic chemical reactions in microemulsions
[AD-A150063] 12 p1796 N85-21265
A brief review of the technology of microemulsions and other micellar systems
[AD-A149759] 12 p1800 N85-21269
Research on microemulsions for storage and conversion of solar energy
[DE85-000161] 12 p1882 N85-21807
Combustion and micro-explosion of water/oil emulsions in high pressure environments
[AD-A152960] 17 p2919 N85-27997
Multidimensional analysis of data obtained in experiments with X-ray emulsion chambers and extensive air showers
[HE-3.6-2] 24 p4184 N85-35951
A new method of differential structural analysis of gamma-family basic parameters
[HE-3.6-3] 24 p4184 N85-35952
Hadrons registration in emulsion chamber with carbon block
[HE-3.7-3] 24 p4186 N85-35982
Structured events in Pamir carbon X-ray chambers
[HE-3.7-7] 24 p4186 N85-35985
Ultra high energy events in ECHOS series and primary energy spectrum
[HE-3.7-9] 24 p4186 N85-35986
Search for anomalons using plastic nuclear track detectors
[HE-6.2-12] 24 p4212 N85-36148
Observation of genetic relation among new phenomena Geminion, Chiron and mini-Centauro
[HE-6.2-16] 24 p4212 N85-36152
Detection threshold energy of high energy cascade showers using thermoluminescence PTFE-sheet and hot-gas reader
[HE-7.1-5] 24 p4213 N85-36159
Application of thermoluminescence for detection of cascade shower 2: Detection of cosmic ray cascade shower at Mount Fuji
[HE-7.1-12] 24 p4214 N85-36162

ENAMELS
Production process for steel with decarburized surface adapted for single coating enamelling
[BMFT-FB-T-85-022] 20 p3432 N85-31292
Features of behavior of gas bubbles in molten oxide films during enamelling: Communication 2
[BLL-M-35781-(5828.4)] 23 p3919 N85-34263

ENCAPSULATING
Investigation of liquid encapsulation Chochralski growth of InP
[AD-A146096] 03 p0433 N85-12760
Study program for encapsulation materials interface for Flat-plate Solar Array (FSA) project
[NASA-CR-174152] 04 p0530 N85-13385
Encapsulation design analysis
06 p0829 N85-15268
Encapsulation materials and processing
06 p0830 N85-15269
Photothermal degradation of encapsulants
06 p0830 N85-15270
Polymer-polymer interface bond stability
06 p0830 N85-15271
Polymer-metal interface bond stability
06 p0830 N85-15272
Module flammability research
06 p0830 N85-15274
Process research of non-Cz silicon material
06 p0830 N85-15275
Effect of sealants of the sound absorption coefficients of acoustical friable insulating materials
[AD-A148541] 08 p1218 N85-17674
WESF (173)Cs gamma ray sources
[DE85-000676] 11 p1727 N85-20659
Hot Isostatic Pressing (HIP): Techniques, applications and economical use
[JUEL-SPEZ-268] 17 p2939 N85-28141
Encapsulation and packaging of a semiconductor multielectrode array for cortical implantation
[AD-A153180] 17 p2998 N85-28535
Concretization of high level radioactive source in marine sediment
[AD-D011703] 19 p3249 N85-30146
Photothermal degradation studies of encapsulants
21 p3608 N85-32403
Encapsulation processing and manufacturing yield analysis 21 p3611 N85-32434
Investigation of test methods, material properties, and processes for solar cell encapsulants
[NASA-CR-176132] 23 p3945 N85-34446

ENCELADUS
The E-ring of Saturn 15 p2677 N85-26527

ENCKE COMET
Extended atmospheres of outer planet satellites and comets
[NASA-CR-174338] 08 p1258 N85-17916
Extended atmospheres of outer planet satellites and comets
[NASA-CR-174396] 09 p1416 N85-18933

ENCLOSURE
Heat-transfer enhancement in natural convection enclosure flow
[DE84-013048] 09 p1319 N85-18297

ENCLOSURES
Influence of Prandtl number on natural convection heat transfer correlations
[DE84-013006] 05 p0637 N85-14089
Moisture content and gas sampling device
[NASA-CASE-MSC-18868-1] 18 p3103 N85-29213
Plastic heliostat enclosure analysis
[DE85-009112] 18 p3130 N85-29387
Natural convection in square partitioned enclosures
[AD-A153707] 18 p3197 N85-29828
Sound-insulating enclosures — machine noise
[BMFT-FB-HA-85-005] 20 p3525 N85-31925

ENCODERS
U CODERS

ENCODING
U CODING

END MORAINES
U GLACIAL DRIFT

END-TO-END DATA SYSTEMS
The IRAS end-to-end data system
[NLR-MP-83056-U] 17 p3051 N85-28883

ENDANGERED SPECIES
Environmental management needs
[DE85-007859] 18 p3133 N85-29405

ENDOCRINE GLANDS
NT ADRENAL GLAND
NT PANCREAS
NT PARATHYROID GLAND
NT PITUITARY GLAND
NT THYMUS GLAND
NT THYROID GLAND

ENDOCRINE SECRETIONS
NT ADRENOCORTICOTROPIN (ACTH)
NT ALDOSTERONE
NT HORMONES
NT HYDROXYCORTICOSTEROID
NT INSULIN
NT PROSTAGLANDINS

ENDOCRINE SYSTEMS
Mathematical modeling of fluid-electrolyte alterations during weightlessness
[NASA-CR-171881] 15 p2617 N85-26125

ENDOCRINOLOGY
Endocrine responses to nonhypotensive gravitational stress: Vasopressin and aldosterone
05 p0693 N85-14459
Endocrine responses to hypotensive gravitational stress: Catecholamines, pancreatic polypeptide, and vasopressin 05 p0693 N85-14460
Changes in bone structure and metabolism during simulated weightlessness: Endocrine and dietary factors
[NASA-CR-175961] 18 p3153 N85-29521

ENDOLYMPH
Quantitation of Na+, K+-ATPase enzyme activity in tissues of the mammalian vestibular system
15 p2613 N85-26102

ENDURANCE
The effect of propranolol on the training response to endurance exercise in normal human adults
05 p0696 N85-14479

ENERGETIC PARTICLES
NT ARGON PLASMA
NT BETA PARTICLES
NT BOUNDARY LAYER PLASMAS
NT COLD PLASMAS
NT COLLISIONAL PLASMAS
NT COLLISIONLESS PLASMAS
NT CONDUCTION ELECTRONS
NT COSMIC PLASMA
NT CYLINDRICAL PLASMAS
NT DENSE PLASMAS
NT DEUTERIUM PLASMA
NT ELECTRON PLASMA
NT ELECTRONS
NT ELLIPTICAL PLASMAS
NT HELIUM PLASMA
NT HIGH ENERGY ELECTRONS
NT HIGH TEMPERATURE PLASMAS
NT HOT ELECTRONS
NT LASER PLASMAS
NT METALLIC PLASMAS
NT NEGATRONS
NT NITROGEN PLASMA
NT NONEQUILIBRIUM PLASMAS
NT NONUNIFORM PLASMAS
NT NUCLEI (NUCLEAR PHYSICS)
NT OXYGEN PLASMA
NT PLASMA FOCUS
NT PLASMAS (PHYSICS)
NT RELATIVISTIC PLASMAS
NT ROTATING PLASMAS
NT SEMICONDUCTOR PLASMAS
NT SOLAR WIND
NT SPACE PLASMAS
NT SPHERICAL PLASMAS
NT STELLAR WINDS
NT STRONGLY COUPLED PLASMAS
NT THERMAL PLASMAS
NT TOROIDAL PLASMAS
Atlas of polar cap energetic particle observations. Volume 1: TIROS-N, 1 January 1979 - 28 February 1981
[PB84-233402] 04 p0535 N85-13419
Hot plasma particles in the Earth's outer magnetosphere: New understandings during the IMS
[DE84-016826] 05 p0677 N85-14348
The radiative hydrodynamics of flare loops heated by impulsive bursts of energetic electrons
05 p0745 N85-14781
Fine structure of Alfven maser radiation
06 p0824 N85-15232
An atlas of polar cap energetic particle observations. Volume 2: NOAA-6, 8 July 1979 to 10 May 1983
[PB85-109072] 12 p1891 N85-21868
Suppression of tilting instability of a compact torus by energetic particle beams
[IPPJ-705] 12 p1935 N85-22157
Particle transport in planetary magnetospheres
12 p1954 N85-22275
Hot plasma and energetic particles in the Earth's outer magnetosphere: New understandings during the IMS
14 p2355 N85-24552
The access of energetic charged particles to satellite altitudes
[AD-A150799] 14 p2373 N85-24670
Boundary of modulation diffusion and stochastic instability of high energy protons in inner radiation belt
15 p2482 N85-25316
Substorms in energetic radiation belt particles according to data from Meteor artificial Earth satellite
16 p2719 N85-26788
Characteristics and sources of E-region ionization in the continuous aurora
[AD-A155018] 21 p3632 N85-32562
Contributions to the 19th International Cosmic Ray Conference
[NASA-CR-176060] 21 p3714 N85-33044
Solar coronal and photospheric abundances from solar energetic particle measurements
[PAPER-SH-2.1-5] 21 p3715 N85-33053
Search for gamma-rays from M31 and other extragalactic objects
[OG-2.7-3] 22 p3671 N85-33977
Cosmic rays in the 10(16) to 10(19) eV range from pulsars
[OG-5.4-3] 22 p3886 N85-34080
The primary cosmic ray mass composition at energies above 10(14) eV
[OG-5.4-6] 22 p3886 N85-34083
Two classes of solar energetic particle events associated with impulsive and long duration soft X-ray flares
[SH-1.2-12] 23 p3992 N85-34747
Energetic protons from a disappearing solar filament
[SH-1.3-7] 23 p3993 N85-34754
Injection of energetic particles following the gamma-ray flares on June 7, 1980, as observed on Helios 1
[SH-1.3-9] 23 p3993 N85-34756
Shock and statistical acceleration of energetic particles in the interplanetary medium
[SH-1.5-1] 23 p3996 N85-34771
Energetic ion acceleration at collisionless shocks
[SH-1.5-3] 23 p3996 N85-34772
Latitude dependence of co-rotating shock acceleration
[SH-1.5-14] 23 p3997 N85-34777
Elemental abundances in corotating events
[SH-1.5-15] 23 p3997 N85-34778
Solar and interplanetary particles at 2 to 4 MEV during solar cycles 21, solar cycle variations of event sizes, and compositions
[SH-1.5-16] 23 p3997 N85-34779
Energetic particle observations of the solar-gamma ray/neutron flare events of 3 Jun 1982 and 21 June 1980 isotopic and chemical composition
[SH-2.1-3] 23 p3998 N85-34784
Precision measurements of solar energetic particle elemental composition
[SH-2.1-4] 23 p3998 N85-34785
Solar Coronal and photospheric abundances from solar energetic particle measurements
[SH-2.1-5] 23 p3998 N85-34786
Variations in elemental composition of several MEV/nucleon ions observed in interplanetary space
[SH-2.1-7] 23 p3998 N85-34788
Diffusion in the chromosphere and the composition of the solar corona and energetic particles
[SH-2.1-9] 23 p3999 N85-34790
Anomalous abundances of solar energetic particles and coronal gas: Coulomb effects and First Ionization Potential (FIP) ordering
[SH-2.1-10] 23 p3999 N85-34791
The mean ionic charges of N, Ne, MG, SI and S in solar energetic particle events
[SH-2.1-11] 23 p3999 N85-34792
Calculations of heavy ion charge state distributions for nonequilibrium conditions
[SH-2.1-12] 23 p3999 N85-34793
Isotopic overabundances and the energetic particle model of solar flares
[SH-2.2-1] 23 p4000 N85-34796
Solar source regions of 3HE-rich particle events
[SH-2.2-4] 23 p4000 N85-34799
On the connection between the 3HE-enrichment and spectral index of solar energetic particles
[SH-2.2-9] 23 p4001 N85-34804
A cosmic ray driven instability
[OG-8.1-5] 23 p4018 N85-34895
Cosmogenic-nuclide production by primary cosmic-ray protons
[SH-7.1-6] 23 p4047 N85-35098
A silicon surface barrier telescope for solar particles identification
[SH-9.1-3] 23 p4050 N85-35118
Multiple vacancy production by high energy heavy ions
[DE85-004429] 24 p4162 N85-35805
A search for heavy long lived particles in high energy cosmic rays
[HE-6.2-7] 24 p4211 N85-36143

ENERGY
The energy cost of women walking and running in shoes and boots
[AD-A151022] 14 p2389 N85-24716
The 1000 GeV gamma rays from ms pulsars
[OG-2.3-12] 22 p3867 N85-33948

ENERGY ABSORPTION
NT ELECTROMAGNETIC ABSORPTION
NT GAMMA RAY ABSORPTION
NT INFRARED ABSORPTION
NT MOLECULAR ABSORPTION
NT MULTIPHOTON ABSORPTION
NT PHOTOABSORPTION
NT THERMAL ASSORPTION
NT THERMALIZATION (ENERGY ABSORPTION)
NT ULTRAVIOLET ABSORPTION
NT X RAY ABSORPTION
Mechanisms of laser annealing of semiconductors
02 p0267 N85-11744
Distribution of total solar radiation in Spain
04 p0523 N85-13344
Tests of the load-bearing and deformation behaviour of reinforced concrete spherical shells under point loading
[BLL-RISLEY-TR-4550-9091.9F)]
06 p0816 N85-15182
An orthogonal grid technique for studying internal deformation and energy absorption in target penetration
[AD-A149989] 12 p1860 N85-21685
Jet topologies in hadron-hadron collisions
[DE85-001328] 12 p1929 N85-22119
A plasma initiation-flow chamber to study CW laser beamed energy absorption in light gases
[AD-A151225] 15 p2562 N85-25806
Energy deposition from particle beams
[DE85-007382] 16 p2682 N85-27654
Energy deposition and its effects on the E+ capture section at Sector 20
[DE85-010964] 18 p3182 N85-29727
Impact dynamics research on composite transport structures
[NASA-TM-86391] 19 p3284 N85-30367
Cyclotron resonance in a nonneutral plasma
[AD-A155248] 21 p3707 N85-33017
Development of an energy-absorbing passenger seat for a transport aircraft 22 p3796 N85-33515
Design and testing of an energy-absorbing crewseat for the F/FB-111 aircraft, volume 1
[NASA-CR-3916] 23 p3896 N85-34133
Design and testing of an energy-absorbing crewseat for the F/FB-111 aircraft. Volume 2: Data from seat testing
[NASA-CR-3917] 24 p4084 N85-35184

ENERGY ABSORPTION FILMS
International Congress Centrum Berlin report on photovoltaics 12 p1877 N85-21773
Thin-film solar cells from sputtered and vapor-deposited amorphous silicon 12 p1879 N85-21792
Development of a CdSe thin film solar cell
12 p1880 N85-21796
Selective coatings for solar heat converters
17 p2939 N85-28144

ENERGY BANDS
NT BLOCH BAND
NT CONDUCTION BANDS
NT FORBIDDEN BANDS
Local contributions to the 0.6 keV diffuse X-ray background 06 p0877 N85-15569
Ultrasoft X-ray background observations of the local interstellar medium 06 p0877 N85-15571
Optically induced intervalence-band transitions in germanium by the absorption of 1.06 micrometers picosecond pulses
[DE85-000946] 09 p1399 N85-18803
Angle-resolved photoemission study of AuGa2 and AuIn2 intermetallic compounds
[AD-A150000] 12 p1940 N85-22183
Laser beam shaping system with reduced objective diameter 14 p2275 N85-24095
Electronic density of states for the double donor system Si:P, As
[INPE-3447-PRE/700] 16 p2669 N85-27700
Doping superlattices in organometallic VPE InP
[AD-A155151] 21 p3710 N85-33029

ENERGY BUDGETS
NT ATMOSPHERIC HEAT BUDGET
NT HEAT BUDGET
Energy-active zones in north Atlantic as manifestation of interannual variability of radiation balance
02 p0164 N85-11108
Cage regional energy budgets from the GLAS ATH order model 05 p0685 N85-14402
Eddy correlation measurements of energy partition for Amazonian forest
[INPE-3195-PRE/559] 06 p0827 N85-15252
The influence of deep cumulus convection on large-scale flow during AVE/SESAME 1, 10-11 April 1979
09 p1355 N85-18526
Testing an energy balance model for estimating actual evapotranspiration using remotely sensed data — Hannover, West Germany barley and wheat fields
13 p2125 N85-23236
Accurate albedos of the brightest regions on Io
13 p2195 N85-23618
Small component spectral model of annual course of zonal atmospheric circulation 14 p2337 N85-24453
The Martian climate: Energy balance models with CO2/H2O atmospheres
[NASA-CR-175722] 15 p2579 N85-26547

ENERGY CONSERVATION
ACEE program rationale and implementation
[NASA-TM-84549] 02 p0133 N85-10908
On-board near-optimal climb-dash energy management 02 p0137 N85-10931
Hybrid laminar flow control study
[NASA-CR-165930] 02 p0137 N85-10933

Energy efficient engine flight propulsion system preliminary analysis and design report
[NASA-CR-174701] 02 p0140 N85-10947
Energy-saving technological methods of obtaining controlled atmospheres
[BLL-M-35724-(5828.4)] 02 p0171 N85-11145
ECUT energy data reference series: Lightweight materials for ground transportation
[DE84-015269] 05 p0621 N85-13074
Hangar heating and energy conservation manual
[AD-A147893] 07 p0910 N85-15762
Development of design and economic parameters for passive solar systems
[AD-A147181] 07 p0993 N85-16303
Evaluation of the measured energy performance of four solar systems
[AD-A147912] 07 p0993 N85-16306
Oil-shale exploration expansion urged
07 p0994 N85-16317
MHD performance demonstration experiment, FY 1974 to FY 1984
[DE85-000854] 08 p1224 N85-17709
Collegium on aviation fuel conservation efforts
09 p1278 N85-18034
New lighting technologies, their status and impacts on power densities
[DE85-000712] 09 p1315 N85-18266
Effect of hitch positions on the performance of track-grouser systems
[AD-P004277] 09 p1406 N85-18853
Electrocatalysis research
[NASA-CR-174352] 10 p1437 N85-19054
DOE/ORNL electric systems program overview
[DE85-003334] 10 p1459 N85-19197
ElectriFleet Project
[DE85-001598] 10 p1570 N85-19698
Electric-Hybrid Vehicle (E-HV) demonstration-test project
[DE85-002370] 10 p1570 N85-19699
Power from the Sun: Light at night
[PB85-124097] 12 p1883 N85-21814
Using fuel cells or anode depolarization to reduce electrowinning energy consumption
[DE85-006187] 13 p2129 N85-23250
Deputy minister on civil aviation fuel conservation efforts 14 p2208 N85-23891
Aviation workers plenum reviews fuel conservation progress 15 p2461 N85-25197
USSR report: Transportation
[JPRS-UTR-84-014] 15 p2467 N85-25229
Ilyushin bureau designer on fuel conservation research
15 p2467 N85-25231
Aviation turbine fuels from tar sands bitumen and heavy oils. Part 1: Process analysis
[AD-A151319] 15 p2521 N85-25539
Planning fuel-conservative descents in an airline environmental using a small programmable calculator: Algorithm development and flight test results
[NASA-TP-2393] 16 p2707 N85-26705
General continuous formulations of atmospheric energy laws 16 p2830 N85-27448
A numerical solution technique for multitemperature plasma hydrodynamics
[AD-A152701] 17 p3039 N85-28601
On power effecient operation of the 2m x 2m transonic wind tunnel at the National Aerospace Laboratory
[NAL-TR-847] 18 p3064 N85-28953
Natural convection in square partitioned enclosures
[AD-A153707] 18 p3197 N85-29828
Improving the defense energy information system (DEIS)
[AD-A153524] 18 p3200 N85-29849
Energy accounting software
[DE85-010612] 19 p3340 N85-30694
Auto fuel efficiency standards, part 2
[GPO-41-189] 20 p3435 N85-31309
Energy efficient transport technology: Program summary and bibliography
[NASA-RP-1135] 22 p3729 N85-33116
Monitoring building energy performance: An informal review and characterization of research in progress
[BNL-51765] 23 p3923 N85-34308
Advanced heat pump research and development
[DE85-009540] 23 p3932 N85-34372
Energy Efficient Engine Program technology benefit/cost study, volume 2
[NASA-CR-174766-VOL-2] 24 p4066 N85-35198
Comparative analysis of operational forecasts versus actual weather conditions in airline flight planning, volume 1
[NASA-CR-167862] 24 p4119 N85-35534
Comparative analysis of operational forecasts versus actual weather conditions in airline flight planning, volume 2
[NASA-CR-167863] 24 p4119 N85-35535
Comparative analysis of operational forecasts versus actual weather conditions in airline flight planning, volume 3
[NASA-CR-167864] 24 p4120 N85-35536
Comparative analysis of operational forecasts versus actual weather conditions in airline flight planning, volume 4
[NASA-CR-167865] 24 p4120 N85-35537
Comparative analysis of operational forecasts versus actual weather conditions in airline flight planning: Summary report
[NASA-CR-167866] 24 p4120 N85-35538
Turbulent structure of stably stratified nocturnal slope flows
[AD-A155845] 24 p4123 N85-35559
Phase space factors in multiparticle processes
24 p4175 N85-35888

ENERGY CONSUMPTION

US energy for the rest of the century, 1984 edition
[PB84-207406] 04 p0531 N85-13393
Energy information exchange, 1983
[DE84-901446] 04 p0577 N85-13680
Hangar heating and energy conservation manual
[AD-A147893] 07 p0910 N85-15762
Biocatalyzed processes for production of commodity chemicals: Assessment of future research advances for N-butanol production
[NASA-CR-174264] 07 p0919 N85-15819
Development of design and economic parameters for passive solar systems
[AD-A147181] 07 p0993 N85-16303
Oil-shale exploration expansion urged
07 p0994 N85-16317
Study of low energy density photovoltaic applications under varying rate structures
[DE85-000185] 10 p1511 N85-19538
Synthetic fuels policy
[GPO-34-227] 11 p1613 N85-20143
Digital and color energy maps for graphic display of hourly data
[DE85-000526] 11 p1673 N85-20543
Feoktistov discusses need for space colonization
13 p1965 N85-22454
Using fuel cells or anode depolarization to reduce electrowinning energy consumption
[DE85-006187] 13 p2129 N85-23250
Field use of electric vehicles compared to prototype tests
[DE85-006887] 15 p2667 N85-26458
Improving the defense energy information system (DEIS)
[AD-A153524] 18 p3200 N85-29849
Wind tunnel results of advanced high speed propellers in the takeoff, climb and landing operating regimes
[NASA-TM-87054] 19 p3213 N85-29925
Energy accounting software
[DE85-010612] 19 p3340 N85-30694
Model documentation of the gas analysis modeling system. Volume 1: Model overview
[DE85-010952] 20 p3515 N85-31856
Development of a prototype energy meter
[PB85-198430] 22 p3789 N85-33476

ENERGY CONVERSION

NT BIOMASS ENERGY PRODUCTION
NT GEOTHERMAL ENERGY CONVERSION
NT OCEAN THERMAL ENERGY CONVERSION
NT PHOTOTHERMAL CONVERSION
NT SOLAR ENERGY CONVERSION
NT SOLAR TOTAL ENERGY SYSTEMS
NT WATERWAVE ENERGY CONVERSION
Shock electromechanical energy converter with permanent magnet
[AD-D011228] 01 p0115 N85-10781
Non-oxide ceramics: A new class of engineering materials 02 p0179 N85-11199
Material problems for high-temperature, high-power space energy-conversion systems
[AD-A145940] 03 p0385 N85-12466
FSA field test
[NASA-CR-174114] 04 p0528 N85-13373
Thermomagnetic generator
[DE84-017018] 04 p0530 N85-13388
Analysis of wind energy systems for selected electric utilities
[DE84-013025] 04 p0530 N85-13389
Electromechanical/electromagnetics working group summary 05 p0604 N85-13852
High-efficiency power conversion options for flywheel energy storage systems 05 p0607 N85-13876
Dynamic conversion working group summary
05 p0611 N85-13904
Thermoelectric and thermionic conversion technology
05 p0611 N85-13905
Advanced and nontraditional concepts working group report 05 p0612 N85-13909
Nitinol devices, phase 2, integration of slip ring system and tracking mechanism with memory drive
[BMFT-FB-W-84-032] 05 p0619 N85-13959
Optimization of energy conversion during locking of electron bunches by electromagnetic wave in longitudinal electrostatic field 06 p0786 N85-15025
Performance and cost of energy transport and storage systems for dish applications using reversible chemical reactions
[NASA-CR-174263] 07 p0992 N85-16298
Electrochemistry of polymer films. Applications to chemical analysis and energy conversion
[AD-A147737] 08 p1132 N85-17136
Air quality assessment model validation in complex terrain
[AD-A147690] 08 p1180 N85-17434
MHD performance demonstration experiment, FY 1974 to FY 1984
[DE85-000854] 08 p1224 N85-17709
Available energy method for evaluating thermodynamic performance of heat pump systems
[DE84-017223] 09 p1400 N85-18814
An electro-optic spatial light modulator for thermo-elastic generation of programmably focused ultrasound
[AD-A149078] 10 p1553 N85-19794
Advanced concepts in systems analysis and simulation
[DE85-002728] 11 p1702 N85-20701
JPL highlights
[NASA-CR-175517] 11 p1767 N85-21102
Oceanic role in terrestrial climate
[DE85-004422] 12 p1896 N85-21904
Modulation of light energy transduction in photosynthesis
[DE85-004711] 13 p2141 N85-23292
Spaceborne power systems preference analyses. Volume 1: Summary
[NASA-CR-175644] 14 p2349 N85-24517
Spaceborne power systems preference analyses. Volume 2: Decision analysis
[NASA-CR-175645] 14 p2349 N85-24518
Sensitivities of projected 1980 photovoltaic system costs to major system cost drivers
[NASA-CR-175669] 14 p2349 N85-24519
Test results of an organic Rankine-cycle power module for a small community solar thermal power experiment
[NASA-CR-175696] 14 p2350 N85-24524
Intermediate load modules for test and evaluation
[NASA-CR-175697] 14 p2350 N85-24526
Studies of photosynthetic Energy Conversion
[DE85-005973] 15 p2586 N85-25944
Exploratory wind-tunnel investigation of a wingtip-mounted vortex turbine for vortex energy recovery
[NASA-TP-2468] 16 p2699 N85-26667
Water brake convertor: A simple device to convert mechanical energy into heat energy
[DE85-006021] 16 p2716 N85-26766
General continuous formulations of atmospheric energy laws 16 p2830 N85-27448
Documents of the JPL Photovoltaics Program Analysis and Integration Center: An annotated bibliography
[NASA-CR-175873] 17 p2965 N85-28448
Energy data base: Subject categories and scope
[DE84-017376] 17 p3050 N85-28881
Technology for industrial waste heat recovery by organic Rankine cycle systems
[DE85-006719] 18 p3102 N85-29206
Exploratory study of coal conversion chemistry
[DE85-010393] 19 p3229 N85-30018
Metallophthalocyanine dimers incorporating five atom covalent bridges
[AD-A154365] 19 p3234 N85-30051
Uniform cost-estimation method for biomass production and conversion technologies
[DE85-011714] 19 p3380 N85-30970
Biocatalysis project
[NASA-CR-176044] 20 p3498 N85-31744
Energy from low temperature differences
[DE85-008817] 24 p4112 N85-35492

ENERGY CONVERSION EFFICIENCY

Energy efficient engine high pressure turbine test hardware detailed design report
[NASA-CR-167955] 02 p0147 N85-10995
Efficiency of photoelectric conversion of short radiation pulses 03 p0348 N85-12240
NASA Redox Storage System Development Project
[NASA-TM-83677] 03 p0385 N85-12465
Operating experience with potassium systems — thermal power stations
[OEFZS-4275] 03 p0387 N85-12473
Development and verification of MOD-2 and MOD-0A simulation models
[DE84-017389] 04 p0550 N85-13499

The spectrophotometric method of determining the transmission of solar energy in salt gradient solar ponds
05 p0666 N85-14283
The upwind power plant Manzanares
05 p0669 N85-14305
Gamma-ray to Cerenkov-light conversion efficiency for pure-silica-core optical fibers
[DE84-015041] 05 p0729 N85-14685
Proceedings of the 23rd Project Integration Meeting
[NASA-CR-174186] 06 p0829 N85-15260
High-efficiency silicon solar cell research
06 p0829 N85-15261
Efficiency estimation and sensitivity modeling
06 p0829 N85-15263
Barriers to achieving high efficiency
06 p0829 N85-15264
MBE growth for high-efficiency silicon solar cells
06 p0829 N85-15265
Development and analysis of silicon solar cells near 20% efficiency
06 p0829 N85-15267
Liquid-fueled Ramjet engines
07 p0918 N85-15814
Multijunction cells for concentrators: Technology prospects
[NASA-CR-174259] 07 p0991 N85-16295
Progress in developing tidal electric power plants reported
07 p0994 N85-16314
Actual versus design performance of solar systems in the National Solar Data Network
[DE85-001190] 09 p1344 N85-18456
Soft X-ray spectroscopy of laser produced plasmas
09 p1367 N85-18727
Development of high efficiency solar cells on silicon web
[NASA-CR-174435] 10 p1509 N85-19521
Research on the basic understanding of high efficiency in silicon solar cells
[DE85-000507] 11 p1672 N85-20537
Direct contact heat recovery from molten salt
[DE85-002830] 11 p1674 N85-20550
Performance of solar thermal systems with liquid metal MHD conversion
[DE85-002758] 11 p1675 N85-20555
Development of new process technologies for solar cells with high efficiency starting from purified silicon
12 p1878 N85-21785
Development of high-efficiency economic systems for photovoltaics
12 p1880 N85-21795
Nonlinearity and spectral mismatch problems of solar cells
13 p2010 N85-22605
High output photovoltaic conversion: The quadrispectral project — spacecraft power supplies
13 p2012 N85-22626
Reluctance and doubly-excited reluctance motors
[DE85-003585] 13 p2065 N85-22900
A theoretical analysis of solar-driven natural convection energy conversion systems
[DE84-004431] 13 p2128 N85-23245
Ways of optimization of light energy transformation in primary stages of photosynthesis. Necessity of optimization of photosynthetic unit structure and method for calculating efficiency
14 p2386 N85-24700
Modeling and optimization of a multiple-cell photovoltaic converter system
15 p2585 N85-25934
Development of high-efficiency solar cells on silicon web
[NASA-CR-175707] 15 p2585 N85-25939
Large-scale commercial combustion systems for producing energy from municipal solid waste
[DE85-007097] 15 p2587 N85-25946
Superconducting traveling wave accelerators
[DE85-006247] 15 p2661 N85-26424
Solar elements with distributed parameters
16 p2760 N85-27036
Documentation and solar cell modules
[NASA-CR-175769] 16 p2818 N85-27364
Design and development of a linear Fresnel lens air-cooled photovoltaic module and a stand-alone photovoltaic collector array
[DE85-006654] 16 p2819 N85-27391
Selection of promising sites for magma energy experiments
[DE85-006832] 16 p2820 N85-27393
Overview of the 1985 NASA Lewis Research Center SP-100 free-piston Stirling engine activities
[NASA-TM-87028] 16 p2880 N85-27769
A program for the calculation of paraboloidal-dish solar thermal power plant performance
[NASA-CR-175874] 17 p2985 N85-28449
Advanced evacuated tube collectors
[DE85-010271] 19 p3274 N85-30302
A mathematical model of reciprocating combustion engine dynamics for the diagnosis of deficient energy conversion
19 p3280 N85-30339
Develop and test fuel cell powered on-site integrated total energy systems. Phase 3: Full-scale power plant development
[NASA-CR-168336] 19 p3304 N85-30483
Research on the basic understanding of high efficiency in silicon solar cells
[DE85-008774] 19 p3305 N85-30487
Reciprocating Brayton cycle motor
[REPT-84-RR-336] 20 p3462 N85-31507
Silicon solar cell efficiency improvement: Status and outlook
20 p3479 N85-31619
Some practical considerations for economical back contact formation on high efficiency solar cells
20 p3479 N85-31620
High-efficiency cell concepts on low-cost silicon sheets
20 p3479 N85-31621
Processing technology for high efficiency silicon solar cells
20 p3483 N85-31642
Texture etching of (100) silicon for solar cells
20 p3483 N85-31643
User handbook for block 5 silicon solar cell modules
[NASA-CR-176043] 20 p3483 N85-31644
Nomographs for estimating the levelized cost of energy from flat-plate and concentrator photovoltaic systems
[NASA-CR-176048] 20 p3483 N85-31645
Photovoltaic concentrator research status
[DE85-010119] 20 p3483 N85-31647
Power generation efficiency of piezoelectric crystals
20 p3537 N85-32008
Status of boron combustion research
[AD-A154762] 21 p3563 N85-32160
High-efficiency crystalline silicon technology development
21 p3607 N85-32395
Summary of the high-efficiency crystalline solar cell research forum
21 p3607 N85-32396
High-efficiency module and array research
21 p3607 N85-32397
Flat-plate module efficiency versus cost tradeoffs
21 p3607 N85-32398
The future of crystalline silicon technology in the US Department of Energy program
21 p3607 N85-32399
Georgetown University Photovoltaic Higher Education National Exemplar Facility (PHENEF)
21 p3607 N85-32400
Block V module program
21 p3607 N85-32401
Photothermal degradation studies of encapsulants
21 p3608 N85-32403
Advanced module development overview
21 p3612 N85-32445
Stress and efficiency studies in EFG
[NASA-CR-176125] 22 p3751 N85-33251
Block 5 documentation and solar modules
[NASA-CR-176134] 22 p3805 N85-33564
Development of high-efficiency solar cells on silicon web
[NASA-CR-176101] 22 p3805 N85-33568
Advanced heat pump research and development
[DE85-009540] 23 p3932 N85-34372
Energy Efficient Engine Program technology benefit/cost study, volume 1
[NASA-CR-174766-VOL-1] 24 p4066 N85-35197

ENERGY CONVERTERS
U DIRECT POWER GENERATORS

ENERGY DENSITY
U FLUX DENSITY

ENERGY DISSIPATION
Electron energy loss rates in N-2, O-2 and air
[AD-A145158] 01 p0072 N85-10476
Electric conductivities, currents and energy dissipation in the polar ionosphere
02 p0227 N85-11483
Boundary condition effects in the energy loss spectrum of layered systems
[NOTA-INTERNA-802] 02 p0289 N85-11887
Electron energy loss investigation of the electronic and structural properties of palladium
[NOTA-INTERNA-803] 02 p0289 N85-11888
Reflection electron energy loss investigation of the H-GaAs(110) surface
[NOTA-INTERNA-811] 02 p0289 N85-11889
Theoretical studies of Field-Reversed Configurations (FRC) and experimental study of the FRC during translation
[DE84-016467] 04 p0566 N85-13603
Boundary conditions for artificial dissipation operators — convection
[FFA-TN-1984-53] 09 p1375 N85-18642
Confinement of low-energy electrons near metallic surfaces for plasmon generation
[DE85-001119] 09 p1381 N85-18688
Effect of hitch positions on the performance of track-grouser systems
[AD-P004277] 09 p1406 N85-18853
Carbon vaporization/condensation effects
[NASA-TM-87430] 10 p1436 N85-19048
Temperature-dependent surface states and transitions of Si(111)-7x7
[AD-A149156] 10 p1582 N85-19850
Vacuum ultraviolet electronic properties of liquids
[DE85-000305] 10 p1583 N85-19858
Winds and waves (4 min - 11 yrs) in the upper middle atmosphere (60-110 km) at Saskatoon, Canada (52 deg N, 107 deg W): MF radar (2.2 MHz) soundings 1973 - 1983
11 p1682 N85-20476
Excitation of impurities by heavy particles and radiative losses of thermonuclear plasma
11 p1719 N85-20816
Coincidence studies of secondary electron emission in light ion-atom collisions
[DE85-002373] 11 p1725 N85-20852
Reducing electric power losses in discharge chamber of induction plasmatron
12 p1841 N85-21553
Substorms in the Earth's atmosphere
[DE85-000654] 12 p1890 N85-21861
Dissipation of energy in composite material
13 p2027 N85-22703
Energy losses at leading edge of turbine blade during multirow jet cooling
13 p2049 N85-22826
Near Field/Far Field (NF/FF) energy loss in Electric Discharge Lasers (EDL's): A mode-medium interaction
[AD-A150299] 13 p2096 N85-23075
Special features of computations of vertical distribution of concentration of suspended sediments under marine conditions
13 p2106 N85-23125
Seismic waves and dispersion relations
13 p2118 N85-23181
Stability of the Galilean satellites in deep orbital resonance
13 p2172 N85-23477
Capture of planetesimals into a circumterrestrial swarm
13 p2179 N85-23522
Aspects of CSSR CMOS integrated circuits discussed
15 p2533 N85-25627
Elastic-workhardening SDF (Single-Degree-of-Freedom) system subjected to random blast excitations
[AD-A151866] 15 p2579 N85-25909
Energy deposition from particle beams
[DE85-007382] 16 p2862 N85-27654
Digital filters for application to data analysis in electron energy loss spectroscopy
[DE85-007932] 17 p2923 N85-28020
Energy considerations in second breakdown
[AD-A152389] 17 p2952 N85-28229
Tribological sinks: Money down the drain
[DE85-010019] 17 p2974 N85-28378
Magnetic steels with the lowest specific total losses
[BMFT-FB-T-84-263] 18 p3078 N85-29042
Interpretation of radar returns from the mesosphere, part 2.3A
21 p3619 N85-32485
All particle energy spectrum of cosmic rays in 10 to the 15th power - 10 to the 20th power eV region
[OG-5.1-15] 22 p3882 N85-34056
Monitoring building energy performance: An informal review and characterization of research in progress
[BNL-51765] 23 p3923 N85-34308
Twenty-two-year cycle of the upper limiting rigidity of Daly waves
[SH-4.5-5] 23 p4036 N85-35023
Spallogenic origin of nuclei in meteorites
[SH-7.1-10] 23 p4048 N85-35102
Prediction of turbulent internal recirculating flows with K-epsilon models
24 p4092 N85-35366
Turbulent structure of stably stratified nocturnal slope flows
[AD-A155845] 24 p4123 N85-35559
Proposed FRX-D experiment
[DE85-012766] 24 p4158 N85-35778
Experimental evidence of the decrease of kinetic energy of hadrons in passing through atomic nuclei
24 p4174 N85-35880
Analytical calculation of muon intensities under deep sea-water
[HE-5.2-16] 24 p4204 N85-36092
Photo nuclear energy loss term for muon-nucleus interactions based on xi scaling model of QCD
[HE-5.2-17] 24 p4204 N85-36093
Range fluctuations of high energy muons passing through matter
[HE-5.2-19] 24 p4204 N85-36095
Results from the UCSD magnetic monopole search
[HE-8.1-12] 24 p4210 N85-36137

ENERGY DISTRIBUTION
NT SPECTRAL ENERGY DISTRIBUTION
Measuring local ion energy distribution function in Tuman-3 Tokamak plasma
02 p0271 N85-11788
Emission mechanisms in the liquid metal ion source: A review
[AERE-R-11294] 03 p0418 N85-12675
Minimizing the energy spread within a single bunch by shaping its charge distribution
[DE84-016172] 05 p0727 N85-14678

The IRAS galaxy 0421+040P06: An active spiral (?) galaxy with extended radio lobes
[NASA-CR-174206] 06 p0871 N85-15536
Unidentified IRAS sources: Ultrahigh luminosity galaxies
[NASA-CR-174207] 06 p0872 N85-15537
Morphology of keV-electrons in the Earth's magnetosphere as observed by GEOS 1
[DRI-3-84] 09 p1350 N85-18496
Multifrequency observations of BL LAC objects and violently variable quasars 11 p1746 N85-20081
Ultraviolet observations of Population 2 Cepheids 11 p1754 N85-21034
Ultraviolet analysis of the peculiar F supergiant HD 112374 11 p1754 N85-21035
Acoustic energy balance method 13 p2000 N85-22537
Breakdown of thin plates by radiation 13 p2028 N85-22709
Theoretical thermodynamics of mixtures at high pressures 13 p2183 N85-23550
Measurement of charged secondary particle emission under ion and neutral impact — Giotto mission 14 p2243 N85-23906
Energy dependence of the emittance of damping ring beams
[DE85-007060] 15 p2649 N85-26341
Time dependent and steady-state solutions of the electron energy distribution in a weakly ionized gas subject to an ac or dc electric field
[AD-A151629] 15 p2656 N85-26391
Ionization energies of liquids from energy distribution, quantum yield and second derivative curves
[AD-A152210] 16 p2746 N85-26946
Studies of hot B subdwarfs. Part 2: Energy distributions of three bright sdB/sdOB stars in the 950-5500 angstrom range
[NASA-CR-175854] 16 p2861 N85-27775
Influence of edge effects on performance of electrooptical lens 22 p3770 N85-33366
Observations on TeV gamma rays from Geminga and PSR 0950+08
[OG-2.4-8] 22 p3868 N85-33953
Composition of primary cosmic rays near the bend from a study of hadrons in air showers at sea level
[OG-5.2-2] 22 p3883 N85-34059
Composition of primary cosmic rays at energies 10(15) to approximately 10(16) eV
[OG-5.2-4] 22 p3883 N85-34061
Variations in elemental composition of several MEV/nucleon ions observed in interplanetary space
[SH-2.1-7] 23 p3998 N85-34788
On the retention of high-energy protons and nuclei with charges Z or equal to 2 in large solar flares after the process of their acceleration
[SH-2.1-8] 23 p3998 N85-34789
The response of ionization chambers to relativistic heavy nuclei
[OG-9.1-13] 23 p4024 N85-34938
Clusters and cycles in the cosmic ray age distributions of meteorites
[SH-7.1-11] 23 p4048 N85-35103
Status of the zeta(8.3)
[DE85-013070] 24 p4149 N85-35724
Lateral distribution of high energy hadrons and gamma ray in air shower cores observed with emulsion chambers
[HE-3.3-8] 24 p4160 N85-35926
Size distributions of air showers accompanied with high energy gamma ray bundles observed at Mt. Chacaltaya
[HE-3.3-9] 24 p4161 N85-35927
Comparison of absolute intensity between EAS with gamma-families and general EAS at Mount Norikura
[HE-3.3-11] 24 p4161 N85-35929
Analytical-numerical methods of calculations of energy and three-dimensional particle distributions in electromagnetic cascades
[HE-3.5-13] 24 p4184 N85-35950
Comparison of big event with calculations of the air shower development
[HE-3.6-8] 24 p4185 N85-35956
Character of energy flow in air shower core 24 p4189 N85-35985
The development of air shower in the iron absorber 24 p4189 N85-35987
Longitudinal trial functions and the cosmic ray energy scale 24 p4193 N85-36014
Primary chemical composition from simultaneous recording of muons induced cascades and accompanying muon group underground
[HE-5.1-13] 24 p4201 N85-36075
On method of muon spectrum measurements by the scintillation detectors of a large thickness T4t sub o
[HE-5.2-18] 24 p4204 N85-36094
Characteristics of slow particles emitted in the charged current interactions of neutrinos with emulsion nuclei
[HE-5.3-22] 24 p4207 N85-36113
Relationship of sea level muon charge ratio to primary composition including nuclear target effects
[HE-5.4-10] 24 p4208 N85-36121

ENERGY EFFICIENCY TRANSPORT PROGRAM
U ACEE PROGRAM

ENERGY EQUIPARTITION
U EQUIPARTITION THEOREM

ENERGY EXCHANGE
U ENERGY TRANSFER

ENERGY GAPS (SOLID STATE)
Refractive index of ternary and quaternary compound semiconductors below the fundamental absorption edge: Linear and nonlinear effects
[DE84-012325] 05 p0640 N85-14105
Material models and device structures for GaAs solar cells
[DE85-000501] 05 p0665 N85-14275
Repetitively pulsed metal ion beams for ion implantation
[DE84-014065] 05 p0732 N85-14704
Solar fuel synthesis based on colloidal and particulate semiconductors
[PB85-129104] 11 p1614 N85-20152
Method and apparatus for measuring minority carrier lifetime in a direct band-gap semiconductor
[NASA-CASE-NPO-16337-1-] 11 p1628 N85-20251
Substituent effects on the electrical conductivities of the phenazine derivatives
[NASA-TM-77792] 14 p2249 N85-23938
Theory and calculations of the electronic structure of solids having directional bonding
[AD-A151062] 14 p2428 N85-24971
Novel materials properties of strained-layer superlattices
[DE85-003676] 14 p2430 N85-24989
Modeling and optimization of a multiple-cell photovoltaic converter system 15 p2585 N85-25934
Heavy doping effects in high efficiency silicon solar cells
[NASA-CR-175687] 15 p2585 N85-25937
Heavy doping effects in high efficiency silicon solar cells
[NASA-CR-175681] 15 p2586 N85-25940
The structural and electronic properties of amorphous silicon based alloy materials
[DE85-002909] 15 p2860 N85-26419
Shallow impurity cluster states in n-type semiconductors
[INPE-3495-PRE/732] 16 p2869 N85-27699
Optically nonlinear and bistable behaviour of direct gap semiconductors 16 p3186 N85-29759
Optical bistability in Cd(x)Hg(1-x)Te 16 p3186 N85-29760
Quantized Hall conductance as a topological invariant
[DE85-007796] 16 p3193 N85-29606
Lasertron simulation with a two-gap output cavity
[DE85-011213] 22 p3790 N85-33480

ENERGY LEVELS
NT ATOMIC ENERGY LEVELS
NT ELECTRON STATES
NT GROUND STATE
NT INTERMOLECULAR FORCES
NT MOLECULAR ENERGY LEVELS
Influence of translational and hyperfine relaxation on energy characteristics of oxygen-iodine laser 02 p0261 N85-11707
Determination of bound water in biological tissue and energy dissipated in bound water by low level microwaves
[AD-A143101] 03 p0399 N85-12547
Focusing and confinement
[DE84-016181] 05 p0640 N85-14106
Theoretical studies of atomic transition
[DE85-001325] 09 p1381 N85-18687
Spectroscopy of quasimolecular X-rays with H-like decelerated ions
[DE85-006565] 15 p2649 N85-26337
Fluorinated polyesters
[AD-D011611] 16 p2753 N85-26988
Boson degrees of freedom in Fermion many-body systems
[DE85-006997] 16 p2863 N85-27660
Multiple scattering effects in low energy alkali ion scattering: Application to the analysis of adsorbate ordering and bonding geometry
[DE85-007575] 17 p3032 N85-28757
Extension of the consistent Q formalism to odd-A nuclei in the W-Pt region
[DE85-006284] 17 p3034 N85-28770
Electronic structure calculations for low coverage adlayers
[DE85-007733] 18 p3179 N85-29709
Calculation of Franck-Condon factors for diatomic molecules
[AD-A154463] 19 p3353 N85-30784
Strong-coupling approximations
[DE85-007829] 19 p3353 N85-30785
Atomic data for controlled fusion research. Volume 4: Spectroscopic data for iron
[DE85-009658] 19 p3354 N85-30787
Systematic view of transition intensities in the spectra of actinides and lanthanides in condensed phases
[DE85-010272] 19 p3354 N85-30789
Experimental level-structure determination in odd-odd actinide nuclei
[DE85-010476] 19 p3360 N85-30835
Microscopic structure of two-dimensional electron glass
[DE85-010265] 19 p3376 N85-30942
Antiproton-nucleus inelastic scattering and the spin-isospin dependence of the N anti N interaction
[DE85-010546] 20 p3526 N85-31935
New O(6) region near A = 130 and the interplay of triaxiality and gamma-softness in the IBA
[DE85-010957] 20 p3530 N85-31961
Establishment of steady-state power level in pulse-periodic excimer laser 21 p3685 N85-32896
Ionization detection of stimulated Raman spectra
[DE85-010672] 22 p3746 N85-33218
Vacuum ultraviolet laser
[DE85-011632] 22 p3790 N85-33476
Heavy quarks and CP: Moriond 1985
[DE85-010553] 22 p3841 N85-33790
Capture in the 1.15-keV iron resonance
[DE85-011913] 23 p3970 N85-34612
Duality of two-point functions for confined non-relativistic quark-antiquark systems
[DE85-012334] 23 p3971 N85-34618
Exact solutions for sporadic acceleration of cosmic rays
[OG-8.3-7] 23 p4022 N85-34925
Relativistic transport theory for cosmic-rays
[OG-8.3-8] 23 p4022 N85-34926
The design of an experiment to detect low energy antiprotons
[OG-9.1-1] 23 p4022 N85-34928
The response of ionization chambers to relativistic heavy nuclei
[OG-9.1-13] 23 p4024 N85-34938
Gamma-ray production cross sections for alpha-particle induced reactions on F-19 and Na-23
[DE85-012603] 24 p4150 N85-35732
Standard value for the radiation length in air
[HE-4.4-4] 24 p4193 N85-36013

ENERGY LOSSES
U ENERGY DISSIPATION

ENERGY METHODS
NT STRAIN ENERGY METHODS
A study of the recursion yn+1=yn+tau yn sup m
[CWI-NM-R8403] 05 p0723 N85-14648

ENERGY OF FORMATION
Parameters of detonation waves excited in gas during concentrated release of energy 02 p0268 N85-11751
Energy of stacking fault and dislocation structure of titanium alloys 03 p0351 N85-12259
Autenite transformation in powder-compacted chromium-nickel-molybdenum steels during continuous cooling
[BLL-M-35981-(5628.4)] 05 p0615 N85-13033

ENERGY POLICY
The changing pattern of fossil fuel CO2 emissions
[DOE/OR-21400/2] 02 p0224 N85-11469
Methane-fueled vehicle RD and D
[GPO-37-926] 04 p0481 N85-13064
Information package on photovoltaics 05 p0661 N85-14250
Stimulation of technologies towards photovoltaic energy conversion 05 p0661 N85-14251
Photovoltaic power supply units 05 p0662 N85-14252
Development and construction of a prototype photovoltaic energy supply unit 05 p0662 N85-14254
Siemens solar module: Status of the technique, development tendencies 05 p0662 N85-14255
Development and utilization of CdS/Cu2S 05 p0662 N85-14256
Solar generators made of amorphous silicon 05 p0662 N85-14257
Fundamentals of solar energy conversion based on fluorescence collectors 05 p0662 N85-14258
Biaxial tracking solar generator 05 p0663 N85-14259
Energy storage with lead acid batteries in photovoltaic systems 05 p0663 N85-14260

Energy storage for stationary and mobile operation as a buffer of power supply from additive energy sources
05 p0663 N85-14261
Utilization of solar energy for the production of hydrogen
05 p0663 N85-14262
The 15 photovoltaic pilot projects of the European Communities
05 p0663 N85-14263
Mains-connected photovoltaic system for a house
05 p0664 N85-14267
Project Pellworm: Solar electric energy supply for a health center
05 p0664 N85-14268
Photovoltaic pump systems
05 p0664 N85-14269
Realized field tests — solar generators
05 p0664 N85-14271
Utilization possibilities of photovoltaics in the private sector
05 p0664 N85-14272
Considerations on the dimensioning of photovoltaic supply systems in the low power range
05 p0665 N85-14273
Solar power supplies for ships
05 p0665 N85-14274
Measurement-Technical Investigations of Wind Energy Units
[JUEL-SPEZ-244]
05 p0667 N85-14293
Measurement-technical problems in the investigation of wind energy units
05 p0668 N85-14295
Design criteria for small wind turbines
[NLR-MP-83054-U]
07 p0994 N85-16310
Verification of the fatigue properties of (small) wind turbines
[NLR-MP-83055-U]
07 p0994 N85-16311
Energy and climate: Problems in Latin America
07 p1003 N85-16375
Blade technology program for large wind turbines, phase 1
[BMFT-FB-T-84-217]
08 p1179 N85-17426
The infrastructure for a surge in synfuels production: The potential role of the AE and C industry and of owner operators
[RAND/N-2172-SFC]
09 p1301 N85-18170
Assessment of wave power available at key United Kingdom sites
[IOS-186]
09 p1346 N85-18468
US Amorphous Silicon Research Project
[DE85-000536]
10 p1511 N85-19536
International Congress Centrum Berlin report on photovoltaics
12 p1877 N85-21773
Crystallization methods for solar cell silicon
12 p1877 N85-21774
Pin solar cells made of amorphous silicon
12 p1879 N85-21787
Physical-chemical investigations of copper sulfides for use in CdS/Cu2S solar cells
12 p1880 N85-21794
Development of a CdSe thin film solar cell
12 p1880 N85-21796
Solar process heat: Technology program
[BMFT-FB-T-84-234]
12 p1882 N85-21812
Hydrology and climatic conditions in Greenland
14 p2327 N85-24387
Ilyushin bureau designer on fuel conservation research
15 p2467 N85-25231
Solar house, Freiburg
[BMFT-FB-T-84-249]
15 p2588 N85-25953
Testing and further development of a solar absorption cooling plant
[BMFT-FB-T-84-264]
15 p2588 N85-25954
Transient behavior of a single-blade horizontal-axis wind turbine
[MBB-UD-421/84-O]
16 p2875 N85-27737
USSR report: Engineering and equipment
[JPRS-UEQ-85-004]
17 p2939 N85-28142
Navy geothermal plan
[AD-A152478]
17 p2965 N85-28450
Investigation of the transferability of measures of passive solar energy utilization in the USA to the Federal Republic of Germany
[BMFT-FB-T-84-284]
18 p3132 N85-29306
Environmental management needs
[DE85-007859]
18 p3133 N85-29405
Pacific Index, April 1983 - October 1984
[TIB6-901335]
19 p3320 N85-30582
Wind energy in the north Netherlands region
20 p3485 N85-31661
Wind turbines and environment management
[CP-MEMO-1983-11]
20 p3485 N85-31662
Magnetohydrodynamics and the National Coal Science, Technology, and Engineering Development Acts
[S-HRG-98-1179]
20 p3535 N85-31994
Fusion facility siting considerations
[DE85-012894]
22 p3843 N85-33805
Magnetic Fusion Program plan
[DE85-009661]
22 p3846 N85-33823
Monitoring building energy performance: An informal review and characterization of research in progress
[BNL-51765]
23 p3923 N85-34308
Implementing agreement for cooperation in the development of large scale wind energy conversion systems
[JUEL-SPEZ-278]
24 p4110 N85-35473
General environmental aspects of large scale wind energy utilization
24 p4110 N85-35474
Environmental aspects of large-scale wind-power systems in the UK
24 p4110 N85-35475
Visit to test facility Stoetten (West Germany) May 9, 1984, including the Voith Wind Energy Converter (WEC) 520 turbine. The annual production of various wind energy plants in selected locations
24 p4112 N85-35487

ENERGY REQUIREMENTS

Energy and climate: Problems in Latin America
07 p1003 N85-16375
MHD performance demonstration experiment, FY 1974 to FY 1984
[DE85-000854]
08 p1224 N85-17709
Study of low energy density photovoltaic applications under varying rate structures
[DE85-000185]
10 p1511 N85-19538
The use of heat pumps in district heat supply
[BLL-OA-TRANS-2728-(6198.3)]
16 p2781 N85-27163
Studies related to the deep Earth gas: 1983
[PB85-171114]
16 p2816 N85-27373
Relative potentials of concentrating and two-axis tracking flat-plate photovoltaic arrays for central-station applications
[NASA-CR-175889]
17 p2985 N85-28446

ENERGY SOURCES

Simulation of automatic control of MFTF-B neutral beams
[DE85-010640]
20 p3530 N85-31960
Solar source regions of 3HE-rich particle events
[SH-2.2-4]
23 p4000 N85-34799
Atmospheric neutrinos observed in underground detectors
[HE-5.3-8]
24 p4205 N85-36102
Geophysical searches for three-neutrino oscillations
[HE-5.3-9]
24 p4205 N85-36103

ENERGY SPECTRA

NT ELECTRONIC SPECTRA
NT NEUTRON SPECTRA
Vowel phoneme identification in speech
[FUB-28-1983]
01 p0040 N85-10257
Equatorial energetic distributions of ions of terrestrial radiation belt an function of solar corona temperature response
02 p0160 N85-11067
Measuring local ion energy distribution function in Tuman-3 Tokamak plasma
02 p0271 N85-11768
Solar neutrinos: Prospects for detection and implications
[DE84-015522]
02 p0304 N85-11966
Chlorine and bromine solar neutrino experiments
[DE84-015720]
02 p0304 N85-11969
Comparison of forecast and observed energetics
05 p0683 N85-14389
Spectral energetics diagnoses and FGGE spectral observing periods and energetics analyses of forecast experiments with GLAS GCM
05 p0683 N85-14391
Aharonov-Bohm effect in absorption of electromagnetic wave
06 p0786 N85-15022
Annual energy spectrum for tracking arrays
06 p0832 N85-15297
On the broadband energy spectra of quasars and BL Lac objects
06 p1240 N85-17825
A compact time-of-flight energy analyzer of high resolution — for Tokamaks
[REPT-84-154]
09 p1324 N85-18318
An operational test of a time-of-flight analyzer at the ASDEX Tokamak
[REPT-84-155]
09 p1324 N85-18319
One-electron capture processes by highly charged ions from helium: Present status of HICE-IPP
09 p1389 N85-18736
The energy spectra of slowed-down neutrals from the heating beams in ASDEX — tokamak
[REPT-84-157]
09 p1394 N85-18772
Laser-Electron-Gamma-Source (LEGS)
[DE85-003204]
11 p1638 N85-20322
KMSF X-ray laser experiments, task no. 1
[DE85-001002]
11 p1639 N85-20325
Jet topologies in hadron-hadron collisions
[DE85-001328]
12 p1929 N85-22119
On the spectrum of longitudinal waves in the hot degenerate plasma
12 p1955 N85-22280
Measured electron contribution to Shuttle plasma environment: Abbreviated update
13 p1990 N85-22476
Development of a continuous broad-energy-spectrum electron source
13 p1995 N85-22507
Discharge characteristics of dielectric materials examined in mono-, dual-, and spectral energy electron charging environments
13 p1995 N85-22510
Nonlinearity and spectral mismatch problems of solar cells
13 p2010 N85-22605
Energy spectrum of processes of structural relaxation of amorphous alloy FeCo70Si15B10
13 p2035 N85-22750
Numerical investigation of evolution of energy spectrum of slightly nonlinear Rossby waves
13 p2106 N85-23124
Mean delta-ray energies in ion molecule collisions
[DE85-005524]
13 p2157 N85-23395
Kinetic energies of fragment ions produced by dissociative photoionization of NO
[NASA-CR-175721]
15 p2647 N85-26327
Restrike particle beam experiments on a dense plasma focus. Opening switch research on a dense plasma focus
[AD-A152991]
17 p3039 N85-28802
Comparison of forecast and observed energetics
18 p3143 N85-29459
On the group-theoretical approach to the energy spectra problem of charge carriers in cubic solids
[PREPRINT-435]
18 p3196 N85-29627
LINE: A code which simulates spectral line shapes for fusion reaction products generated by various speed distributions
[DE85-010633]
19 p3341 N85-30702
Comparison of simulation with experiment in an RFQ
[DE85-010770]
19 p3349 N85-30757
Time-resolved energy spectrum of the ion beam generated in the plasma focus
19 p3369 N85-30892
Paired ion chamber constants for fission gamma-neutron fields
[AD-A155069]
21 p3702 N85-32999
Changes in the energy spectrum of anomalous oxygen and helium during 1977 - 1985
[PAPER-SH-4.6-1]
21 p3715 N85-33056
Spectral measurements of magnetic energy and magnetic helicity between 0.29 and 0.97 AU
[IFSI-85-2]
22 p3850 N85-33844
Unthermalized plasma in bursts sources
[OG-1.1-5]
22 p3861 N85-33907
Gamma ray burst size-frequency distributions: Spectral selection effects
[OG-1.2-3]
22 p3862 N85-33913
Observation of an excess of cosmic ray muons of energies 2 TeV from the direction of Cygnus X-3
[OG-2.1-3]
22 p3863 N85-33920
Gamma rays of 0.3 to 30 MeV from PSR 0531+21
[OG-2.3-6]
22 p3866 N85-33945
Pulsed emission of TeV gamma rays from Vela pulsar
22 p3867 N85-33947
On the 1983 observations of the gamma-ray source 2CG195+4
[OG-2.4-5]
22 p3868 N85-33952
Low-energy gamma rays from Cygnus X-1
[OG-2.4-13]
22 p3868 N85-33957
Energy spectrum of extragalactic gamma-ray sources
[OG-2.7-13]
22 p3872 N85-33986
Ultrahigh energy gamma rays: Carriers of cosmological information
[OG-2.7-14]
22 p3872 N85-33987
On some problems of gamma-astronomy
[OG-2.7-15]
22 p3873 N85-33988
Spectrum of the gamma-ray diffuse component observed from HEAO-1
[OG-3.1-12]
22 p3874 N85-34000
Nineteenth International Cosmic Ray Conference. OG sessions, volume 2
[NASA-CP-2376-VOL-2]
22 p3875 N85-34006
Source spectral index of heavy cosmic ray nuclei
[OG-4.1-2]
22 p3875 N85-34008
Relative abundances of sub-iron to iron nuclei in low energy (50-250 MeV/N) cosmic rays as observed in the Skylab experiment
[OG-4.1-4]
22 p3876 N85-34010
Cosmic ray charge and energy spectrum measurements using a new large area Cerenkov x dE/dx telescope
[OG-4.1-5]
22 p3876 N85-34011
Energy spectra of elements with 18 or = Z or = 28 between 10 and 300 GeV/amu
[OG-4.1-8]
22 p3876 N85-34014
Primary cosmic ray spectra in the range 20-60 GeV/n
[OG-4.1-9]
22 p3877 N85-34015
Energy spectrum of cosmic-ray iron nucleus observed with emulsion chamber
[OG-4.1-10]
22 p3877 N85-34016
Measurement of the iron spectrum from 60 to 200 GeV per nucleon
[OG-4.1-11]
22 p3877 N85-34017
Composition and energy spectra of cosmic ray nuclei above 500 GeV/nucleon from the JACEE emulsion chambers
[OG-4.1-13]
22 p3877 N85-34019
Charge composition and energy spectral of cosmic ray primary particles for energies higher than 1 TeV
[OG-4.1-14]
22 p3877 N85-34020

Parametrized energy spectrum of cosmic-ray protons with kinetic energies down to 1 GeV
[OG-4.2-11] 22 p3878 N85-34025
Observations of ultraheavy cosmic ray particles at 10 GV cutoff rigidity
[OG-4.4-2] 22 p3879 N85-34035
Energy spectrum and arrival direction of primary cosmic rays of energy above 10 to the 18th power eV
[OG-5.1-1] 22 p3880 N85-34043
Ultra high energy cosmic ray spectrum
[OG-5.1-2] 22 p3881 N85-34044
The primary cosmic ray spectrum above 10 to the 19th power eV
[OG-5.1-3] 22 p3881 N85-34045
New calorimetric all-particle energy spectrum
[OG-5.1-4] 22 p3881 N85-34046
Primary cosmic ray spectrum in the 10 to the 12th power - 10 to the 16th power eV energy range from the NUSEX experiment
[OG-5.1-5] 22 p3881 N85-34047
A new measurement of the cosmic ray energy spectrum between 3 x 10 to the 15th power eV and 3 x 10 to the 16th power eV
[OG-5.1-6] 22 p3881 N85-34048
Study of composition of cosmic rays with energy .7 E 3 Ee
[OG-5.1-7] 22 p3881 N85-34049
The muon content of EAS as a function of primary energy
[OG-5.1-8] 22 p3881 N85-34050
A new method to determine the chemical composition of the cosmic rays beyond 10 to the 15th power eV
[OG-5.1-11] 22 p3882 N85-34052
Cosmic ray composition between 10 to the 15th power - 10 to the 17th power eV obtained by air shower experiments
[OG-5.1-12] 22 p3882 N85-34053
Fluctuations of development maximum depth and nuclear composition of primary cosmic radiation
[OG-5.1-13] 22 p3882 N85-34054
Estimation of composition of cosmic rays with E sub zero approximately equals 10(17) - 10(18) eV
[OG-5.1-14] 22 p3882 N85-34055
All particle energy spectrum of cosmic rays in 10 to the 15th power - 10 to the 20th power eV region
[OG-5.1-15] 22 p3882 N85-34056
EAS spectrum in the primary energy region above 10 to the 15th power eV by the Akeno and Yakutsk array data
[OG-5.1-16] 22 p3882 N85-34057
Cosmic ray spectra measurements at the Yakutsk EAS array
[OG-5.1-17] 22 p3882 N85-34058
The composition of cosmic rays near the Bend (10 to the 15th power eV) from a study of muons in air showers at sea level
[OG-5.2-3] 22 p3883 N85-34060
Composition of primary cosmic rays at energies 10(15) to approximately 10(16) eV
[OG-5.2-4] 22 p3883 N85-34061
The primary composition beyond 10 to the 5th power GeV as deduced from high energy hadrons and muons in air showers
[OG-5.2-6] 22 p3883 N85-34063
Implication of EAS data for the study of primary cosmic rays above 10 to the 5th power GeV
[OG-5.2-7] 22 p3883 N85-34064
High-energy multiple muons and heavy primary cosmic-rays
[OG-5.2-9] 22 p3883 N85-34065
Composition of primary cosmic rays near the knee
[OG-5.2-10] 22 p3884 N85-34066
EAS Cerenkov measurements of the composition of the cosmic ray flux around 10 to the 16th power eV
[OG-5.2-11] 22 p3884 N85-34067
Electron and muon parameters of EAS and the composition of primary cosmic rays in 10(15) to approximately 10(16) eV
[OG-5.2-12] 22 p3884 N85-34068
Arrival directions of large air showers, low-mu showers and old-age low-mu air showers observed at St. Chacaltaya
[OG-5.3-2] 22 p3884 N85-34069
Energy dependence of cosmic ray composition above 10(15) GeV/nucleus
[OG-5.4-4] 22 p3886 N85-34081
Implications of the experimental results on high energy cosmic rays with regard to their origin
[OG-5.4-5] 22 p3886 N85-34082
Virgo cluster as a high energy cosmic rays source
[OG-5.4-8] 22 p3886 N85-34085
Anisotropy and the knee of the energy spectrum
[OG-5.4-10] 22 p3887 N85-34087
Observed antiprotons and energy dependent confinement of cosmic rays: A conflict?
[OG-6.1-7] 22 p3888 N85-34098
Antiparticles in the extragalactic cosmic radiation
[OG-6.1-8] 22 p3888 N85-34099
Galactic cosmic ray antiprotons and supersymmetry
[OG-6.1-9] 22 p3888 N85-34100
Halo of NGC 4631 and models of cosmic-ray transport
[OG-6.2-3] 22 p3889 N85-34103
An observation of cosmic ray positrons from 10-20 GeV
[OG-6.2-6] 22 p3889 N85-34105
Reestimation of the production spectra of cosmic ray secondary positrons and electrons in the ISM
[OG-6.2-8] 22 p3889 N85-34107
The electron spectra in the synchrotron nebula of the supernova remnant G 29.7-0.3
[OG-6.2-10] 22 p3889 N85-34109
Study of non-thermal photon production under different scenarios in solar flares. 2: The Compton inverse and Bremsstrahlung models and fittings
[SH-1.2-3] 23 p3991 N85-34739
Observations of solar flare photon energy spectra from 20 keV to 7 MeV
[SH-1.2-9] 23 p3992 N85-34744
The energy spectra of solar flare electrons
[SH-1.2-14] 23 p3992 N85-34749
Source energy spectra from demodulation of solar particle data by interplanetary and coronal transport
[SH-1.3-13] 23 p3994 N85-34758
High energy neutron and gamma-radiation generated during the solar flares
[SH-1.4-8] 23 p3995 N85-34768
On the angular and energy distribution of solar neutrons generated in P-P reactions
[SH-1.4-9] 23 p3995 N85-34769
Acceleration of ions and electrons to near-cosmic ray energies in a perpendicular shock: The January 6, 1978 event
[SH-1.5-4] 23 p3996 N85-34773
The energy spectrum of Jovian electrons in interplanetary space
[SH-1.5-18] 23 p3997 N85-34781
Observation of the fluxes of nuclei with energies 10-20 MEV per nucleon during the solar flare of April 26, 1984
[SH-2.1-1] 23 p3998 N85-34783
Silicon to iron abundances in solar cosmic rays and in the sun
[SH-2.1-6] 23 p3998 N85-34787
The 1973-1964 solar modulation of cosmic ray nuclei
[SH-4.1-16] 23 p4006 N85-34836
A numerical study of diffusive shock acceleration of cosmic rays in supernova shocks
[OG-8.2-2] 23 p4019 N85-34903
The origins of cosmic rays and quantum effects on gravity
[OG-8.2-15] 23 p4020 N85-34911
Stochastic particle acceleration in flaring stars
[OG-8.3-9] 23 p4022 N85-34927
An experiment to measure the energy spectrum of cosmic ray antiprotons from 100 to 1000 MeV
[OG-9.1-3] 23 p4022 N85-34929
The development of a high energy cosmic ray detector for Spacelab-2
[OG-9.1-8] 23 p4023 N85-34934
An observatory to study 10 (10) to 10 (17) by EV gamma rays
[OG-9.4-6] 23 p4029 N85-34973
Mini and super mini arrays for the study of highest energy cosmic rays
[OG-9.4-9] 23 p4029 N85-34976
Detection of 10 (1) GeV cosmic neutrinos with a space station
[OG-9.4-10] 23 p4030 N85-34977
The difference in the energy spectra of galactic cosmic rays at the minima of the 19th and 20th solar activity cycles
[SH-4.4-18] 23 p4035 N85-35014
Solar tri-diurnal variation of cosmic rays in a wide range of rigidity
[SH-4.5-3] 23 p4036 N85-35021
Upper cut-off rigidity for corotation anisotropy during solar activity cycles 20 and 21
[SH-4.5-4] 23 p4036 N85-35022
Change of cosmic ray anisotropy with solar activity
[SH-4.5-20] 23 p4036 N85-35037
Changes in the energy spectrum of anomalous oxygen and helium during 1977-1985
[SH-4.6-1] 23 p4039 N85-35039
Radial and latitudinal gradients of anomalous oxygen during 1977 - 1985
[SH-4.6-4] 23 p4039 N85-35042
Observation of pick-up ions in the solar wind: Evidence for the source of the anomalous cosmic ray component?
[SH-4.6-5] 23 p4039 N85-35043
On the anomalous component
[SH-4.6-6] 23 p4039 N85-35044
Time and energy dependence of the cosmic ray gradient in the outer heliosphere
[SH-4.7-2] 23 p4040 N85-35047
Galactic cosmic ray radial gradients and the anomalous He component near maximum solar modulation and to radii beyond 34 AU from the Sun
[SH-4.7-5] 23 p4040 N85-35050
Rigidity spectrum of Forbush decrease
[SH-5.1-6] 23 p4042 N85-35060
Observations of cosmic-ray modulations in the fall, 1984
[SH-5.1-16] 23 p4043 N85-35069
Observation of energy spectrum of electron albedo in low latitude region at Hyderabad, India
[SH-6.1-7] 23 p4045 N85-35081
A bi-directional charged particle telescope to observe flux, energy spectrum and angular distribution of relativistic and non-relativistic particles
[SH-9.1-4] 23 p4050 N85-35119
A suggested standardized format for cosmic ray ground-level event data
[SH-9.1-15] 23 p4052 N85-35130
Measurement of low energy cosmic rays aboard Spacelab-1
[SH-10.1-6] 23 p4053 N85-35137
Scale separation closure and Alfven wave turbulence
[DE85-013124] 24 p4095 N85-35385
Los Alamos free-electron laser
[DE85-012666] 24 p4098 N85-35405
(NAT)Fe(n,n'x) spectra at 65.5 MeV
[AD-A155776] 24 p4150 N85-35730
Some rigorous results concerning spectral theory for ideal MHD
[DE85-013427] 24 p4156 N85-35770
Proton-air and proton-proton cross sections from air shower data
[HE-1.1-1] 24 p4170 N85-35849
Proton-air inelastic cross section at S(1/2) = 30 TeV
[HE-1.1-2] 24 p4170 N85-35850
Hadron cross sections at ultra high energies and unitarity bounds on diffraction dissociation
[HE-1.1-3] 24 p4170 N85-35851
On total cross sections and slopes at superhigh energies
[HE-1.1-4] 24 p4170 N85-35852
On a possibility of inelasticity partial coefficient K sub gamma determination in pi C and pi Pb interactions at 10 to the 14th power eV (experiment PAMIR 1)
[HE-1.1-12] 24 p4171 N85-35859
1Single particle momentum and angular distributions in hadron-hadron collisions at ultrahigh energies
[HE-1.2-1] 24 p4171 N85-35860
Empirical description of the hadron-hadron and hadron-nucleus interaction at the accelerator energy range
[HE-1.2-4] 24 p4171 N85-35862
Angular distribution and multiplicity of backward hadrons in hFe interactions at 0.5-5.0 TeV energies (PION Experiment)
[HE-1.2-8] 24 p4172 N85-35866
Scaling violation in the fragmentation region of inclusive nucleon spektrum 24 p4173 N85-35874
Intensities of high-energy cosmic rays at Mount Kanbala
[HE-3.1-2] 24 p4177 N85-35902
High energy gamma-rays and hadrons at Mount Fuji
[HE-3.1-3] 24 p4177 N85-35903
Hadron intensity and energy spectrum at 4360 m above level
[HE-3.1-7] 24 p4178 N85-35905
The nucleon intensity in the atmosphere and the Pt distribution
[HE-3.1-9] 24 p4178 N85-35907
Energy spectra of proton and nuclei of primary cosmic rays in energy region 10 TeV/particle
[HE-3.1-10] 24 p4178 N85-35906
Atmospheric interactions detected in both the upper and the lower chambers at Chacaltaya
[HE-3.3-7] 24 p4180 N85-35925
A cosmic ray super high multicore family event. 1: Experiment and general features
[HE-3.4-1] 24 p4181 N85-35930
Observation of super high energy big family with large scale Fe emulsion chambers
[HE-3.4-3] 24 p4182 N85-35932
Super-family P2 C-96-125 observed by Japan-URSS Joint Emulsion Chamber Experiment
[HE-3.4-8] 24 p4182 N85-35936
Integral functions of electron lateral distribution and their fluctuations in electron-photon cascades
[HE-3.5-12] 24 p4184 N85-35949
Comparison of big event with calculations of the air shower development
[HE-3.6-8] 24 p4185 N85-35956

Hadrons registration in emulsion chamber with carbon block
[HE-3.7-3] 24 p4186 N85-35962
Intensities of high-energy cosmic rays at Mount Kanbala
[HE-3.7-5] 24 p4186 N85-35964
Ultra high energy events in ECHOS series and primary energy spectrum
[HE-3.7-9] 24 p4186 N85-35966
The maximum depth of shower with E sub 0 larger than 10(17) eV on average characteristics of EAS different components 24 p4188 N85-35981
Monte Carlo simulation of EAS generated by 10(14) - 10(16) eV protons
[HE-4.3-14] 24 p4192 N85-36008
Lateral distribution of high energy muons in EAS of sizes Ne approximately equals 10(5) and Ne approximately equals 10(6)
[HE-4.3-16] 24 p4192 N85-36010
Energy calibration of the fly's eye detector
[HE-4.4-1] 24 p4192 N85-36011
The structure of EAS at E 0.1 EeV
[HE-4.4-2] 24 p4193 N85-36012
Longitudinal trial functions and the cosmic ray energy scale 24 p4193 N85-36014
EAS development curve at energy of 10(16) - 10(18) eV measured by optical Cerenkov light
[HE-4.4-7] 24 p4193 N85-36015
Missing energies at pair creation
[HE-4.4-8] 24 p4193 N85-36016
On the determination of the depth of EAS development maximum using the lateral distribution of Cerenkov light at distances 150 m from EAS axis
[HE-4.4-13] 24 p4194 N85-36019
Study of the energy spectrum of primary cosmic rays: EAS size fluctuations at a fixed primary energy
[HE-4.4-14] 24 p4194 N85-36020
Preliminary results of the Cerenkov EAS flashes the Crimean Astrophysical Observatory
[HE-4.4-17] 24 p4194 N85-36023
The experimental cascade curves of EAS at E sub 0 10(17) eV obtained by the method of detection of Cherenkov pulse shape
[HE-4.4-18] 24 p4194 N85-36024
Muons in gamma showers
[HE-4.5-3] 24 p4195 N85-36027
Muon spectrum in air showers initiated by gamma rays
[HE-4.5-4] 24 p4195 N85-36028
Expected rates with mini-arrays for air showers
[HE-4.7-8] 24 p4199 N85-36059
The spectrum of cosmic ray muons obtained with 100-ton scintillation detector underground and the analysis of recent experimental data
[HE-5.1-6] 24 p4201 N85-36071
A new world survey expression for cosmic ray vertical intensity vs. depth in standard rock
[HE-5.1-10] 24 p4201 N85-36073
Muon groups and primary composition at 10 to the 13th power to 10 to the 15th power eV
[HE-5.1-12] 24 p4201 N85-36074
On muon energy spectrum in muon groups underground
[HE-5.1-14] 24 p4201 N85-36076
Underwater measurements of muon intensity
[HE-5.1-16] 24 p4202 N85-36078
Hybrid TLC-pair meter for the Sphinx Project
[HE-5.2-10] 24 p4203 N85-36086
An upper limit of muon flux of energies above 100 TeV determined from horizontal air showers observed at Akeno
[HE-5.2-12] 24 p4203 N85-36088
Energy spectrum of cascade showers induced by cosmic ray muons in the range from 50 GeV to 5 TeV
[HE-5.2-14] 24 p4203 N85-36090
Analytical calculation of muon intensities under deep sea-water
[HE-5.2-16] 24 p4204 N85-36092
On method of muon spectrum measurements by the scintillation detectors of a large thickness T4t sub o
[HE-5.2-18] 24 p4204 N85-36094
Range fluctuations of high energy muons passing through matter
[HE-5.2-19] 24 p4204 N85-36095
The spectrum of neutrons at 60 hg m(-2)
[HE-5.2-20] 24 p4204 N85-36096
A transient digitiser for fast air shower events
[HE-5.2-21] 24 p4204 N85-36097
Results of low energy background measurements with the Liquid Scintillation Detector (LSD) of the Mont Blanc Laboratory
[HE-5.3-5] 24 p4205 N85-36099
Measurement of neutrino oscillations in MACRO experiment
[HE-5.3-10] 24 p4206 N85-36104
The capability of the existing network of installations for detecting the antineutrino burst from collapsing stars
[HE-5.3-13] 24 p4206 N85-36107
Energy spectra of high energy atmospheric neutrinos
[HE-5.3-14] 24 p4206 N85-36108
Relationship of sea level muon charge ratio to primary composition including nuclear target effects
[HE-5.4-10] 24 p4208 N85-36121

ENERGY STORAGE
NT ELECTRIC ENERGY STORAGE
NT HEAT STORAGE
NT MAGNETIC ENERGY STORAGE
NASA Redox Storage System Development Project
[NASA-TM-83677] 03 p0385 N85-12465
The limp flywheel
[AD-A148034] 03 p0386 N85-12467
Dynamic and other secondary benefits of compressed air energy storage
[DE84-015571] 03 p0386 N85-12468
Regenerative fuel cell energy storage system for a low Earth orbit space station
[NASA-CR-174802] 04 p0527 N85-13371
An Assessment of Integrated Flywheel System Technology
[NASA-CP-2346] 05 p0604 N85-13850
Rotating assembly working group summary 05 p0604 N85-13851
Electrical/electronics working group summary 05 p0604 N85-13853
Dynamics and controls working group summary 05 p0604 N85-13854
A summary of the 1983 Integrated Flywheel Technology Workshop 05 p0605 N85-13855
European development experience on energy storage wheels for space 05 p0605 N85-13856
Merits of flywheels for spacecraft energy storage 05 p0605 N85-13857
Comparative energy storage assessment item 05 p0605 N85-13858
Inertial storage for satellites 05 p0605 N85-13859
Perspectives on energy storage wheels for space station application 05 p0605 N85-13860
Flywheel-powered X-ray generator 05 p0605 N85-13861
Description of a laboratory model Annular Momentum Control Device (AMCD) 05 p0606 N85-13863
Generic composite flywheel designs 05 p0606 N85-13864
Flexible matrix composite laminated disk/ring flywheel 05 p0606 N85-13866
Flywheel containment and safety considerations 05 p0606 N85-13869
Magnetically suspended reaction wheel assembly 05 p0607 N85-13870
Magnetically suspended flywheel system study 05 p0607 N85-13873
Reaction wheels for kinetic energy storage 05 p0607 N85-13874
High-efficiency power conversion options for flywheel energy storage systems 05 p0607 N85-13876
Motor/generator and electronic control considerations for energy storage flywheels 05 p0608 N85-13878
Torque command steering law for double-gimbaled control moment gyros applied to rotor energy storage 05 p0608 N85-13879
Potential of flywheels for spacecraft energy storage 05 p0609 N85-13890
Space power management and distribution status and trends 05 p0610 N85-13896
Electrochemistry and storage panel report 05 p0611 N85-13903
Advanced and nontraditional concepts working group report 05 p0612 N85-13909
Engineering model system study for a regenerative fuel cell: Study report
[NASA-CR-174801] 07 p0991 N85-16292
Performance and cost of energy transport and storage systems for dish applications using reversible chemical reactions
[NASA-CR-174263] 07 p0992 N85-16296
Eigenvalues of rotating machinery 08 p1167 N85-17361
Hybrid system for producing and storing ice
[DE84-017474] 09 p1304 N85-18195
Comparison of energy storage systems in the United States chilled water versus two types of ice storage systems
[DE85-001102] 09 p1344 N85-18452
Ultrasonic characterization of advanced composite flywheels
[DE85-000158] 11 p1593 N85-20026
Underground pumped hydroelectric storage
[DE85-000288] 11 p1676 N85-20560
Power circuit utilizing self-excited Hall effect switch means
[AD-D011506] 12 p1832 N85-21496
Research on microemulsions for storage and conversion of solar energy
[DE85-000181] 12 p1882 N85-21807
Evaluation of ettringite and related compounds for use in solar energy storage
[DE85-003249] 12 p1882 N85-21809
Evaluation of ettringite and related compounds for use in solar energy storage
[PB85-146876] 12 p1883 N85-21818
Cyclic industrial robots with mechanical energy storing devices: Multipositional system with one or several degrees of freedom 13 p2045 N85-22803
Cyclic industrial robots with mechanical energy storing devices: Principles of drive design 13 p2046 N85-22807
Sensitization and quenching in the conversion of light energy into chemical energy
[DE85-006301] 14 p2351 N85-24535
The role of differential rotation in magnetic energy storage — coronal loops 14 p2449 N85-25119
Multikilowatt hydrogen-nickel oxide battery system
[DE85-003339] 15 p2550 N85-25737
Advanced energy storage systems
[AD-A152244] 16 p2741 N85-26915
Low pressure storage of methane on interlayered clays for potential vehicular applications
[DE85-006949] 16 p2758 N85-27017
Operating characteristics of a 0.87 kW-hr flywheel energy storage module
[NASA-TM-87038] 17 p2974 N85-28371
Relative potentials of concentrating and two-axis tracking flat-plate photovoltaic arrays for central-station applications
[NASA-CR-175889] 17 p2985 N85-28446
Documents of the JPL Photovoltaics Program Analysis and Integration Center: An annotated bibliography
[NASA-CR-175873] 17 p2985 N85-28448
SERI Solar Energy Storage Program: FY 1984
[DE85-002936] 18 p3130 N85-29385
Electrochemical Energy Storage Branch
[DE85-007592] 18 p3131 N85-29391
Control of energy-storage dc-to-dc converters: The large-signal time-domain approach 19 p3257 N85-30196
Thermal Energy Storage Program annual operating plan FY 1985
[DE85-006745] 19 p3307 N85-30499
Regenerative fuel cell systems for space station 20 p3443 N85-31372
System level electrochemical principles 20 p3443 N85-31375
Advances in rechargeable lithium molybdenum disulfide batteries 20 p3444 N85-31376
Capacitive energy storage at cryogenic temperatures
[AD-A154506] 21 p3579 N85-32253
A fast discharge excimer laser with symmetric geometry
[AD-A155294] 21 p3592 N85-32322
Transient two-dimensional simulation of SEU in a CMOS SRAM cell
[DE85-008419] 22 p3890 N85-34111
Series-counterpulse repetitive-pulse inductive storage circuit
[DE85-006438] 23 p3928 N85-34342
Reversing-counterpulse repetitive-pulse inductive storage circuit
[DE85-006409] 23 p3928 N85-34344
Evaluation of developmental membranes for the mixed reactant iron-chromium redox system
[NASA-TM-87074] 23 p3944 N85-34443
Wind energy battery storage, phase 2
[DE85-009753] 23 p3945 N85-34450
Solar heat pump
[DE85-011323] 23 p3946 N85-34453
Ion energy storage for post-flare loops
[SH-1.2-10] 23 p3992 N85-34745
Solar pond technology for Navy applications
[AD-A155877] 24 p4112 N85-35488
Strategic defense initiative
[DE85-012778] 24 p4150 N85-35735
Analysis of a pulsed power system containing rotating machine
[DE85-014125] 24 p4159 N85-35788

ENERGY STORAGE DEVICES
U ENERGY STORAGE

ENERGY TECHNOLOGY
NT GEOTHERMAL TECHNOLOGY
Solar heating and cooling R and D program coordination support
[DE84-013479] 01 p0068 N85-10449
Fusion and its future in Illinois
[DE84-014868] 01 p0122 N85-10833
Agribusiness and space: No limits to growth 02 p0152 N85-11029
Executive information system
[DE84-015355] 04 p0576 N85-13675

Activities report in technology
[ISBN-951-38-1998-1] 04 p0577 N85-13681
Electrical/electronics working group summary
05 p0804 N85-13853
Merits of flywheels for spacecraft energy storage
05 p0805 N85-13857
Stimulation of technologies towards photovoltaic energy conversion 05 p0861 N85-14251
Photovoltaic power supply units
05 p0862 N85-14252
Development and construction of a prototype photovoltaic energy supply unit
05 p0862 N85-14254
Siemens solar module: Status of the technique, development tendencies 05 p0862 N85-14255
Solar energy supplied mobile water purification unit
05 p0864 N85-14270
Utilization possibilities of photovoltaics in the private sector 05 p0864 N85-14272
Measurement-Technical investigations of Wind Energy Units
[JUEL-SPEZ-244] 05 p0867 N85-14293
Measurement-technical investigations of wind energy units in the short-time range — spectrum analysis
05 p0868 N85-14294
VOITH: Wind energy converter WEC 520
05 p0868 N85-14299
The upwind power plant Manzanares
05 p0869 N85-14305
USSR report: Engineering and equipment
[JPRS-UEQ-84-007] 06 p0775 N85-14954
Viscosity measurements for thick-film pastes
06 p0831 N85-15260
Emerging role of the national laboratory in the development and transfer of materials technology
[DE85-001252] 09 p1286 N85-18086
The influence of modern control techniques on the gas industry
[ERS-E.395] 09 p1325 N85-18326
The 35 kilowatt peak power photovoltaic system
[DE85-000189] 10 p1511 N85-19537
Advanced concepts in systems analysis and simulation
[DE85-002728] 11 p1702 N85-20701
Materials refining for solar cell silicon
12 p1877 N85-21775
Flat-plate silicon for solar cells
12 p1877 N85-21776
Carbothermic production of silicon solar cells using high-purity starting materials 12 p1877 N85-21777
Development of silicon nitride materials for the casting of solar cell silicon 12 p1878 N85-21779
Photovoltaic roofing tile systems
12 p1878 N85-21783
Optimization of silicon-nitride-inversion layer solar cells
12 p1878 N85-21784
Development of new process technologies for solar cells with high efficiency starting from purified silicon
12 p1878 N85-21785
Development of new solar cells
12 p1880 N85-21797
Multi-year plan for Experimental Systems Research: Passive and hybrid solar energy program
[DE85-004696] 12 p1882 N85-21810
Solar process heat: Technology program
[BMFT-FB-T-84-234] 12 p1882 N85-21812
New high-efficiency silicon solar cells
[NASA-CR-175643] 13 p2128 N85-23244
Production technology of an electrolyte for Na/S batteries
[BMFT-FB-T-84-277] 15 p2550 N85-25742
Role of supercomputers in energy research programs
[DE85-006665] 15 p2624 N85-26172
Energy Data Base: Subject thesaurus permutated listing. Revision 6, appendix
[DE84-016963] 15 p2666 N85-26454
USSR report: Engineering and equipment
[JPRS-UEQ-84-006] 16 p2760 N85-27035
Parametric study of potential early commercial power plants Task 3-A MHD cost analysis
[NASA-CR-175839] 16 p2817 N85-27377
Wind energy technology program summary
[DE85-007349] 16 p2820 N85-27392
Current alternative energy research and development in Illinois
[PB85-163137] 16 p2820 N85-27397
Energy data base: Subject thesaurus
[DE84-010566] 16 p2878 N85-27761
Documents of the JPL Photovoltaics Program Analysis and Integration Center: An annotated bibliography
[NASA-CR-175873] 17 p2965 N85-28448
Shenandoah parabolic dish solar collector
[DE85-006326] 17 p2967 N85-28460
Multicriteria decision analysis as an aid to strategic planning of energy research and development
[REPT-84-02] 17 p3049 N85-28870
Energy data base: Subject categories and scope
[DE84-017376] 17 p3050 N85-28881
Absorber coatings degradation
[DE85-008628] 18 p3128 N85-29367
Improved acid electrolytes for fuel cells
[PB85-176053] 18 p3132 N85-29397
Activities report in energy technology
[OEFZS-4302] 18 p3199 N85-29846
Thermochemical energy transport using a hydrogen rich working fluid
[AD-D011696] 19 p3233 N85-30042
Air Force Federal Photovoltaic Utilization Program
[DE85-010812] 20 p3484 N85-31648
Renewable energy research and development outlook, volume 1
[DE85-011577] 20 p3540 N85-32033
Proceedings of the 24th Project Integration Meeting
[NASA-CR-176058] 21 p3607 N85-32394
High-efficiency crystalline silicon technology development 21 p3607 N85-32395
Energy and Technology Review
[DE85-011767] 21 p3716 N85-33061
Arctic and offshore research
[DE85-001995] 22 p3818 N85-33653
Logical and physical modeling and design of scientific and statistical databases for energy research
[DE85-006081] 22 p3833 N85-33737
Federal export assistance programs applicable to the US photovoltaic industry
[NASA-CR-176114] 22 p3849 N85-33841
Monitoring building energy performance: An informal review and characterization of research in progress
[BNL-51765] 23 p3923 N85-34306
New technologies at the forefront of industrial developments 24 p4061 N85-35168
Chemistry division report
[DE85-010586] 24 p4071 N85-35228
Photovoltaics technology program summary
[DE85-013098] 24 p4112 N85-35493

ENERGY TRANSFER
NT LINEAR ENERGY TRANSFER (LET)
Electronic-to-vibrational energy transfer studies of singlet molecular oxygen and hydrogen halides
[AD-A145587] 02 p0277 N85-11802
Study of vibrational energy transfer at a liquid tin surface
[AD-A145741] 02 p0277 N85-11804
High temperature gas energy transfer
[AD-A146134] 03 p0326 N85-12113
Fluid layer between infinite elastic plates II. Distribution of power flow
[AD-A146680] 03 p0361 N85-12312
Vector magnetic field analysis of Lorentz forces acting in the solar atmosphere
[AD-A145941] 03 p0449 N85-12852
Study of combustion and flame processes initiated by laser-induced multiple-photon absorption
[DE84-017095] 04 p0471 N85-12996
Laser-driven particle accelerators
[DE84-015953] 04 p0506 N85-13227
Energy transfer in atom-molecule scattering experiments in the 1eV region with SF6-Ar, CF4-Ne and Xe-CO2 systems as examples
[REPT-11/1983] 04 p0563 N85-13588
Energy information exchange, 1983
[DE84-901446] 04 p0577 N85-13680
The Interaction of Global Biochemical Cycles
[NASA-CR-174184] 05 p0652 N85-14183
Biogeochemical cycles: Interactions in global metabolism 05 p0652 N85-14184
Power transfer from natural emitters to collection apertures at microwave wavelengths
[NASA-CR-174275] 07 p0945 N85-15989
Collisional energy exchange in polyatomic molecules
[AD-A147710] 08 p1219 N85-17679
Evaluation of the Fundamental Research on Explosives (FRE) program
[DE85-001537] 09 p1301 N85-18172
Optical studies of dynamical processes in disordered materials
[DE85-002400] 10 p1453 N85-19158
Thermal investigation of an electrical high-current arc with porous gas-cooled anode
[NASA-TM-77789] 11 p1627 N85-20245
UK participation in the Middle Atmosphere Programme
11 p1655 N85-20426
Application of dimensional analysis to the problem of solar wind-magnetosphere energy coupling
[DE85-002414] 11 p1674 N85-20551
Energy transfer and photochemistry in biomimetic solar conversion
[PB85-129112] 11 p1677 N85-20566
Primary light harvesting system: The relationship of phycobiliscomes to photosystem 1 and 2
[DE86-003075] 11 p1689 N85-20622
Saturation kinetics of active medium of oxygen-iodine laser 11 p1718 N85-20807
Two-dimensional measurements of OH concentration and temperature in reactive flows
[AD-A149849] 12 p1800 N85-21292
Acoustic energy exchange in sheared mean flows — solid rocket motors 13 p1999 N85-22534
Repetitive energy transfers from an inductive energy store 13 p2062 N85-22881
Numerical investigation of evolution of energy spectrum of slightly nonlinear Rossby waves
13 p2106 N85-23124
The effects of internal waves on acoustic normal modes
[AD-A150235] 13 p2155 N85-23379
Molecular dynamics studies of energy transfer processes in crystal systems
[AD-A150161] 13 p2163 N85-23416
A fundamental study of liquid phase particle breakup. Revision
[AD-A150791] 14 p2301 N85-24249
The structure, stability, wave transmission and energy transfer at the Earth's magnetopause
14 p2372 N85-24661
Ways of optimization of light energy transformation in primary stages of photosynthesis. Necessity of optimization of photosynthetic unit structure and method for calculating efficiency 14 p2386 N85-24700
Ways of optimization of light energy transformation in primary stages of photosynthesis. Optimization of lattice structure of uniform photosynthetic unit
14 p2386 N85-24701
Intermolecular energy transfer between the individual zero-field levels of triplet traps in an orientationally disordered solid
[AD-A150751] 14 p2417 N85-24914
Energy trapping, release, and transport in three-dimensional energetic solids and molecular crystals: Theory of defects and impurities
[AD-A151071] 14 p2428 N85-24973
Direct electron and ion fluid computation of high electrostatic fields in dense inhomogeneous plasma with subsequent nonlinear optical and dynamical laser interaction 15 p2656 N85-26368
Molecular dynamics studies of energy transfer processes in crystal systems
[DE85-007247] 15 p2662 N85-26426
Spectroscopic investigation of materials for frequency agile laser systems
[AD-A151731] 16 p2790 N85-27208
Electric field and energy transfer by magnetopause reconnection
[INPE-3448-PRE/701] 16 p2826 N85-27432
Rotational energy transfer in highly vibrationally excited hydrogen fluoride and deuterium fluoride
[AD-A152003] 16 p2862 N85-27650
Energy reflection coefficient for H+ ions at energies between 10 and 80 keV
[DE85-007547] 16 p2863 N85-27662
CALTECH-DOE program on numerical analysis, computing and fundamental studies of motion, energy and mass transfer in fluids
[DE85-008106] 17 p2959 N85-28274
Flow characteristics of a partially submerged liquid pickup
[DE85-006744] 17 p2959 N85-28276
Theory of laser-stimulated surface process. 2: A generalized-master-equation approach to energy transfer between an IR laser, an aspecties and phonons
[AD-A153063] 17 p2970 N85-28344
Average collisional vibrational energy transfer quantities and the inversion temperature
[AD-A152674] 17 p3029 N85-28733
Electronically excited alkaline earth oxides: Chemical production and collisional energy transfer processes
[AD-A153172] 17 p3044 N85-28833
Laser-stimulated vibrational excitation of an adspecies studied by a generalized master equation: Neutral atomic hydrogen on hydrated KCl(001)
[AD-A153665] 18 p3112 N85-29268
Thermochemical energy transport using a hydrogen rich working fluid
[AD-D011696] 19 p3233 N85-30042
Correction of calculated estimate of fatigue properties of materials under biharmonic loading
19 p3244 N85-30113
A numerical solution of a nonisothermal wall using the two-dimensional Navier-Stokes equations
[AD-A154467] 19 p3266 N85-30257
Progress in inertial fusion at LLNL
[DE85-010931] 19 p3277 N85-30321
Production of gallium atoms by excimer laser photolysis of trimethyl gallium
[DE85-010742] 19 p3278 N85-30331

A study of the turbulent layer in the water at an air-water interface
[AD-A154117] 19 p3319 N85-30578
Vibrational energy transfer in benzene-argon collisions
[DE85-009803] 19 p3355 N85-30797
Energy transfer and excimer formation in rare gas solids 19 p3374 N85-30930
Solar-wind magnetosphere energy input functions
[NASA-CR-176021] 19 p3385 N85-31001
Meteorological weapons
[AD-A154735] 21 p3635 N85-32575
Resonant energy transfer during strong excitation 21 p3689 N85-32922
Implicit Monte Carlo methods and non-equilibrium Marshak wave radiative transport
[DE85-010711] 22 p3835 N85-33743
A dominant role for protons at the onset of solar flares
[SH-1.2-13] 23 p3992 N85-34748
Friction, impact, and electrostatic discharge sensitivities of energetic materials
[DE85-013321] 24 p4063 N85-35309
Scaling violation in hadron-nucleus interaction
[HE-3.2-8] 24 p4179 N85-35916
Few-particles generation channels in inelastic hadron-nuclear interactions at energy approximately equals 400 GeV
[HE-3.2-9] 24 p4179 N85-35917
Sub-luminal pulses from cosmic ray air showers
[HE-4.7-13] 24 p4200 N85-36063

ENGINE AIRFRAME INTEGRATION

Predicted performance benefits of an adaptive digital engine control system of an F-15 airplane
[NASA-TM-85916] 07 p0905 N85-15729
Energy efficient engine component development and integration program
[NASA-CR-172846] 19 p3219 N85-29958

ENGINE ANALYZERS

DEAN: A program for dynamic engine analysis
[NASA-TM-87033] 18 p3062 N85-28945

ENGINE CONTROL

NT ROCKET ENGINE CONTROL
NT TURBOJET ENGINE CONTROL
Study on control of ion engine system
[EL-847] 07 p0916 N85-15800
Energy Efficient Engine (E3) controls and accessories detail design report
[NASA-CR-168017] 19 p3218 N85-29957
Performance improvements of a highly integrated digital electronic control system for an F-15 airplane
[NASA-TM-86748] 21 p3556 N85-32120

ENGINE COOLANTS

Columbium chamber fabrication study
[AD-A145230] 01 p0017 N85-10102
Vortex-generating coolant-flow-passage design for increased film-cooling effectiveness and surface coverage
[NASA-TP-2388] 03 p0361 N85-12314
Improvement of gas turbine engine performance by water injection into turbine cooling air 09 p1307 N85-18209
Development of a high-temperature coolant for advanced diesel engines
[AD-A153660] 18 p3117 N85-29297

ENGINE DESIGN

NT ROCKET ENGINE DESIGN
Development trends and requirements of propulsion system technology for civil aircraft 01 p0011 N85-10066
Computational thermo-fluid dynamics contributions to advanced gas turbine engine design
[NASA-TM-86865] 01 p0011 N85-10069
Preliminary mechanical redesign of an existing gas-turbine engine to incorporate a high-efficiency, low-pressure-ratio, highly regenerative cycle for marine applications
[AD-A144808] 01 p0011 N85-10070
Free-piston Stirling engine development
[PB84-237767] 01 p0056 N85-10369
Energy efficient engine flight propulsion system preliminary analysis and design report
[NASA-CR-174701] 02 p0140 N85-10947
Energy efficient engine component development and integration program
[NASA-CR-170934] 02 p0146 N85-10990
Energy efficient engine ICLS Nacelle detail design report
[NASA-CR-167870] 02 p0146 N85-10993
Energy efficient engine. Low pressure turbine test hardware detailed design report
[NASA-CR-167956] 02 p0147 N85-10994
Energy efficient engine ICLS engine bearings, drives and configuration: Detail design report
[NASA-CR-167871] 02 p0147 N85-10997
External fuel vaporization study, phase 2
[NASA-CR-174079] 02 p0187 N85-11252
Liquid-piston Stirling machines
[DE84-014255] 02 p0205 N85-11361
Propulsion — jet aircraft engines
[PNR-90208] 03 p0320 N85-12062
Stirling material technology
[NASA-TM-86888] 04 p0472 N85-13007
Advanced automotive diesel assessment program
[NASA-CR-168285] 04 p0507 N85-13235
Advanced automotive diesel engine system study 04 p0508 N85-13240
A.A.D. engine noise evaluation 04 p0508 N85-13241
Boundary layer simulator improvement
[NASA-CR-174199] 05 p0597 N85-13802
Fabrication and quality assurance processes for superhybrid composite fan blades
[NASA-TM-83354] 06 p0763 N85-14882
USSR report: Engineering and equipment
[JPRS-UEQ-84-007] 06 p0775 N85-14954
Optimum thermogasdynamic design of gas turbine engines by characteristics of element prototypes 06 p0777 N85-14965
Cyclic endurance testing of the RB211-22B cast HP turbine blade 07 p0908 N85-15747
The aircraft engine of the future
[PNR-90226] 08 p1087 N85-16875
SSME lifetime prediction and verification, integrating environments, structures, materials: The challenge 08 p1095 N85-16918
Orbital Maneuvering system design evolution 08 p1098 N85-16943
Vehicle/engine integration — orbit transfer vehicles 08 p1109 N85-17008
Orbital transfer vehicle propulsion issues 08 p1109 N85-17009
USSR report: Engineering and equipment
[JPRS-UEQ-85-001] 09 p1305 N85-18200
On one design principle of surge protector for gas turbine engine compressor 09 p1306 N85-18206
Experimental study of influence of size of upper and lower laps on operational efficiency of centripetal full-inlet air driven microturbines 09 p1307 N85-18211
Advanced Gas Turbine (AGT) powertrain system development for automotive applications
[NASA-CR-174809] 09 p1403 N85-18831
SSME thrust chamber simulation using Navier-Stokes equations
[NASA-CR-171349] 10 p1430 N85-19017
Creep-rupture behavior of iron superalloys in high-pressure hydrogen
[NASA-CR-174411] 10 p1441 N85-19078
Analytical fuel property effects: Small combustors, phase 2
[NASA-CR-174848] 10 p1456 N85-19175
Initial testing of a variable-stroke Stirling engine
[NASA-TM-86875] 10 p1569 N85-19695
Lubrication and performance of high-speed rolling-element bearings
[NASA-TM-86958] 12 p1859 N85-21658
Some solar dish/heat engine design considerations
[DE85-003479] 12 p1881 N85-21802
Experimental determination of optimum ratio of runner blade height at exit to runner blade height at entrance of radial inward-flow microturbines 13 p2049 N85-22827
Hydrodynamic simulation of transient processes in injection system of aircraft engines during pump unswirling 13 p2050 N85-22829
Parameters of symmetric rhombic drive mechanism for single-cylinder Stirling engine 14 p2271 N85-24072
Special course on V/STOL aerodynamics: An assessment of European jet lift aircraft
[AGARD-R-710-ADDENDUM] 15 p2460 N85-25188
Ceramic technology for advanced heat engines project
[DE85-004796] 16 p2755 N85-27002
Ceramic applications in turbine engines
[NASA-CR-174715] 17 p2934 N85-28109
Analysis of physical-chemical processes governing SSME internal fluid flows
[NASA-CR-175893] 17 p2957 N85-28261
Use of ceramics in internal combustion engines 18 p3088 N85-29114
Reciprocating Brayton cycle motor
[REPT-84-RR-336] 20 p3462 N85-31507
Energy efficient engine. Fan and quarter-stage component performance report
[NASA-CR-168070] 23 p3897 N85-34141
Shroud segments for unshrouded blade turbines
[PNR-90260] 23 p3897 N85-34143

ENGINE FAILURE

Stall elimination and restart enhancement device
[AD-D011217] 01 p0010 N85-10062
A theory of post-stall transients in multistage axial compression systems
[NASA-CR-3678] 12 p1771 N85-21117
Effects of inlet distortion on a static pressure probe mounted on the engine hub in an F-15 airplane
[NASA-TP-2411] 13 p1974 N85-22304
Safety recommendation(s), A-84-128 through -133
[REPT-3996C/41] 15 p2466 N85-25221
Nonlinear global stability analysis of compressor stall phenomena
[NASA-CR-174908] 19 p3219 N85-29960
Fault detection and accommodation testing on an F100 engine in an F-15 airplane
[NASA-TM-86735] 19 p3219 N85-29962
Weibull distribution based on maximum likelihood with interval inspection data
[NASA-TM-86515] 21 p3678 N85-32847

ENGINE INLETS

A study of bird ingestions into large high bypass ratio turbine aircraft engines
[DOE/FAA/CT-84/13] 01 p0005 N85-10026
Effect of steady-state temperature distortion on inlet flow to a high-bypass-ration turbofan engine
[NASA-TM-86896] 07 p0904 N85-15725
Ramjet air induction system design for tactical missile application 07 p0918 N85-15811
Air intake efficiency at zero speed and lip suction — jet engines
[BAE-KRS-N-GEN-303] 09 p1272 N85-17998
Research and development for semi-spherical inflow control device
[NAL-TR-833] 09 p1281 N85-18056
Experimental study of aerodynamic shielding of turbojet engine air intake against exhaust gases 09 p1307 N85-18210
Description of a technique to measure spray distribution in an air stream
[AD-A149780] 12 p1771 N85-21122
Selection of air intake parameters for supersonic-flow operation 13 p2051 N85-22837
Shock waves in adjacent engine inlets
[ISL-R-104/84] 20 p3396 N85-31066
Calculation of compressible flow about three-dimensional inlets with auxiliary inlets, slats and vanes by means of a panel method
[NASA-CR-174975] 24 p4060 N85-35162

ENGINE MONITORING INSTRUMENTS

A comparative evaluation of EMADS (Engine Monitoring and Display System) and conventional engine instruments
[AD-A145901] 03 p0319 N85-12060
The applications of fibre optics in gas turbine engine instrumentation
[PNR-90209] 03 p0420 N85-12587
Advanced High Pressure O2/H2 Technology
[NASA-CP-2372] 16 p2733 N85-26662
A device to detect Top Dead Center (TDC) position in motored engines
[REPT-84-RR-347] 20 p3456 N85-31475
Design, development and operation of a high simultaneous capacity digital telemetry system — turbomachine blade flutter
[PNR-90261] 23 p3890 N85-34151

ENGINE NOISE

Energy efficient engine component development and integration program
[NASA-CR-168496] 02 p0146 N85-10989
Jet noise suppression by porous plug nozzles
[NASA-CR-3613] 02 p0275 N85-11790
Turbofan noise generation. Volume 2: Computer programs
[NASA-CR-167952] 02 p0275 N85-11791
A.A.D. engine noise evaluation 04 p0508 N85-13241
Experimental investigation of shock-cell noise reduction for dual-stream nozzles in simulated flight
[NASA-CR-3846] 04 p0557 N85-13549
Static jet noise test results of four 0.35 scale-model QCGAT mixer nozzles
[NASA-TM-86871] 04 p0558 N85-13551
Vibroacoustic control diagnostics of selected machines based on research on the slide bearing of an automobile engine and the alternator
[ISSN-0208-5658] 05 p0641 N85-14112
Research and development for semi-spherical inflow control device
[NAL-TR-833] 09 p1281 N85-18056
Fan noise suppression in turbofan engines
[B8580078] 17 p2868 N85-27872
Development of guidelines for setting physiological and hygienic standards for noise levels in aerospace medicine 19 p3323 N85-30584
Sound-insulating enclosures — machine noise
[BMFT-FB-HA-85-005] 20 p3525 N85-31925
Experimental study of engine knock
[DE85-009651] 22 p3754 N85-33268

ENGINE PARTS
Combustion modeling of a 2 cylinder cycle reciprocating engine
[AD-A144782] 01 p0055 N85-10364
Component-specific modeling
02 p0143 N85-10971
Constitutive model development for isotropic materials
02 p0144 N85-10975
Energy efficient engine ICLS engine bearings, drives and configuration: Detail design report
[NASA-CR-167871] 02 p0147 N85-10997
Jet engine blade repair at the Oklahoma Air Logistics Center, Propulsion Division
[AD-P004003] 03 p0307 N85-11983
Bulletin of the Faculty of Engineering, Hokkaido University, no. 123
[ISSN-0385-602-X] 04 p0482 N85-13075
Experimental study on the glow plug aided alcohol driven diesel engine 04 p0483 N85-13076
Roller crosshead analysis 04 p0507 N85-13238
Screw expander for light duty diesel engines
04 p0508 N85-13242
Thermal and mechanical analysis of major components for the advanced adiabatic diesel engine
04 p0508 N85-13243
Optimum thermogasdynamic design of gas turbine engines by characteristics of element prototypes
06 p0777 N85-14965
Longevity of thin-walled engine parts subjected to transient stresses under creep conditions
06 p0777 N85-14966
Constitutive modeling of engine materials
[AD-A146630] 06 p0817 N85-15189
Overview of the AGARD SMP activities on turbine engine materials technology in the 1972 - 1982 period
07 p0906 N85-15736
Cumulative damage modeling of fatigue crack growth
07 p0907 N85-15741
Problems and possibilities for life extension in gas turbine components 07 p0907 N85-15742
Disc fatigue life predictions for gas turbine engines
07 p0907 N85-15743
Life prediction at high temperature under multiaxial loading 07 p0907 N85-15745
Cyclic endurance testing of the RB211-22B cast HP turbine blade 07 p0908 N85-15747
An investigation of enhanced capability thermal barrier coating systems for diesel engine components
[NASA-CR-174820] 09 p1298 N85-18154
On selecting bypass mixers for turbofan engines
09 p1306 N85-18207
Influence of setting angle of jet cooling nozzles on temperature and stress state of a turbine wheel
09 p1306 N85-18208
Advanced Gas Turbine (AGT) powertrain system development for automotive applications
[NASA-CR-174809] 09 p1403 N85-18831
Tribological systems as applied to aircraft engines
[NASA-TM-86965] 12 p1858 N85-21657
Parameters of symmetric rhombic drive mechanism for single-cylinder Stirling engine 14 p2271 N85-24072
Estimate of fatigue stability of gas-turbine engine compressor vanes in probabilistic aspect
14 p2287 N85-24169
Laser drilling of aeroengine components
14 p2309 N85-24290
Flat conduuis R and D in ceramic parts for diesel engine 15 p2534 N85-25637
Advanced High Pressure O2/H2 Technology
[NASA-CP-2372] 16 p2733 N85-26862
Manufacturing and producibility technology
16 p2733 N85-26866
Ceramics for advanced O2/H2 application
16 p2734 N85-26868
Vacuum plasma coatings for turbine blades
16 p2734 N85-26869
Properties and microstructures for dual alloy combinations of three superalloys with alloy 901
[NASA-TM-86987] 16 p2749 N85-26963
Ceramic technology for advanced heat engines project
[DE85-004798] 16 p2755 N85-27002
Spacer structure
[AD-D011641] 17 p2897 N85-27866
Optical strain measurement system development
17 p2915 N85-27969
Ceramic applications in turbine engines
[NASA-CR-174715] 17 p2934 N85-28109
Determination of wear intensity and resource of crankshafts and cylinder liners of ZIL-130 and ZMZ-53 engines
[BLL-BISI-TRANS-21393-(9022.06)]
17 p2972 N85-28355
Ceramic turbochargers: A case study of a near-term application of high-strength ceramics
[DE85-006495] 17 p2975 N85-28379
Future of ceramic turbochargers: Promises and pitfalls
[DE85-006209] 17 p2975 N85-28380
Ceramic Technology for Advanced Heat Engines Project
[DE85-008755] 18 p3080 N85-29052
Energy efficient engine component development and integration program
[NASA-CR-172646] 19 p3219 N85-29958
Correction of calculated estimate of fatigue properties of materials under biharmonic loading
19 p3244 N85-30113
Creep fatigue life prediction for engine hot section materials (isotropic)
[NASA-CR-168228] 20 p3394 N85-31057
SSME seal test program: Test results for hole-pattern damper seals
[NASA-CR-171595] 20 p3395 N85-31059
Reliability of welds to repair defects in cast components made from CrMoV steel
[BLL-CE-TRANS-8054-(9022.09)]
20 p3461 N85-31501
Component-specific modeling
[NASA-CR-174925] 21 p3556 N85-32119
ENGINE STARTERS
Stall elimination and restart enhancement device
[AD-D011217] 01 p0010 N85-10062
ENGINE TESTS
NT COLD FLOW TESTS
NT STATIC FIRING
Cylinder power fault diagnosis in military diesel engines
[TT-8405] 01 p0053 N85-10354
Measurement and analysis of spark ignition engine pressure data to determine heat release profiles
[AD-A144770] 01 p0055 N85-10363
Dilution jet mixing 02 p0145 N85-10985
Combustion system for radiation investigations
02 p0145 N85-10986
HOST liner cyclic facilities: Facility description
02 p0146 N85-10988
Energy efficient engine component development and integration program
[NASA-CR-170034] 02 p0146 N85-10990
Advanced blade tip seal system, volume 2
[NASA-CR-167851] 02 p0147 N85-10999
The KZD-85 engine test. Engine type: 1 cylinder, 2 stroke motor 2100 Husquarna
[FWE-FO-1717] 02 p0205 N85-11354
Predicting changes in reliability characteristics of gas turbine engines during operation
06 p0776 N85-14964
Temperature distortion generator for turboshaft engine testing
[NASA-TM-83748] 07 p0893 N85-15658
Engine Cyclic Durability by Analysis and Testing
[AGARD-CP-368] 07 p0905 N85-15733
Accelerated Mission Endurance Testing (AMET)
07 p0906 N85-15736
Design and test requirements for development of today's engines 07 p0906 N85-15737
Cyclic endurance testing of the RB211-22B cast HP turbine blade 07 p0908 N85-15747
Qualification of an electrothermal hydrazine thruster with a vacuum thrust of 0.5 to 2.0 N
[BMFT-FB-W-84-043] 07 p0917 N85-15808
Integrated exhaust gas analysis system for aircraft turbine engine component testing
[NASA-TP-2424] 07 p0962 N85-16100
Laboratory simulation of smoke reduction from aircraft engine test cell exhaust using a fluidized bed filter
[AD-A146800] 08 p1089 N85-16986
Study of advanced fuel system concepts for commercial aircraft
[NASA-CR-174751] 11 p1584 N85-19978
China report: Science and technology
[JPRS-CST-84-032] 11 p1621 N85-20202
New air supply-prime mover facility for engine tests detailed 11 p1621 N85-20204
Diesel combustion: Advances in analysis and simulation 14 p2253 N85-23965
Ceramic applications in turbine engines
[NASA-CR-174715] 17 p2934 N85-28109
Determination of wear intensity and resource of crankshafts and cylinder liners of ZIL-130 and ZMZ-53 engines
[BLL-BISI-TRANS-21393-(9022.06)]
17 p2972 N85-28355
Energy efficient engine high-pressure turbine component rig performance test report
[NASA-CR-168189] 19 p3218 N85-29955
Free-piston Stirling engine/linear alternator 1000-hour endurance test
[NASA-CR-174771] 19 p3304 N85-30481
SSME seal test program: Test results for hole-pattern damper seals
[NASA-CR-171595] 20 p3395 N85-31059
Experimental study of engine knock
[DE85-009851] 22 p3754 N85-33268
Energy efficient engine. Fan and quarter-stage component performance report
[NASA-CR-168070] 23 p3897 N85-34141
A study of the control of particulate emissions from turbine engine test cells 24 p4067 N85-35205
ENGINEERING
Experimenting with the Rolm Ada language workshop for specifying and designing 03 p0408 N85-12607
Emergency Mathematics and Science Education Act
[GPO-29-561] 03 p0435 N85-12770
Write while you work: Painless technical writing for Sandia engineers
[DE84-010869] 04 p0577 N85-13679
Computational mechanics: A perspective on problems and opportunities for increasing productivity and quality of engineering
[PB85-128106] 12 p1950 N85-22252
Characteristics of recent science/engineering graduates, 1982: Detailed statistical tables
[PB85-149060] 15 p2683 N85-26437
Academic science and engineering: Graduate enrollment and support, fall 1982 (detailed statistical tables)
[PB85-154730] 15 p2684 N85-26438
Academic science and engineering: R and D funds, fiscal year 1982 (detailed statistical tables)
[PB85-154763] 15 p2684 N85-26443
Engineering education based on computer simulation
[CFD/85/1] 20 p3512 N85-31829
ENGINEERING DEVELOPMENT
U PRODUCT DEVELOPMENT
ENGINEERING DRAWINGS
High reliability mechanical-hydraulic converter
14 p2268 N85-24055
Aircraft skin penetrator and agent applicator. Volume 2: Test and evaluation
[AD-A151609] 15 p2466 N85-25225
An analysis of grid-based line drawing quantization methods
[AD-A151847] 15 p2522 N85-25547
An extension of a microcomputer based system for analysis of line drawing quantization schemes
[AD-A152006] 15 p2624 N85-26171
Water brake convertor: A simple device to convert mechanical energy into heat energy
[DE85-008021] 16 p2716 N85-26766
X-ray satellite
[NASA-TM-77898] 20 p3407 N85-31144
Low-head hydroelectric power demonstration project: City of Gonzales, Texas
[DE85-010403] 22 p3809 N85-33595
A rational approach to cam design
23 p3923 N85-34311
ENGINEERING MANAGEMENT
Computers and the consulting engineer
15 p2626 N85-26184
Thin-film reliability and engineering overview
21 p3612 N85-32450
DoD Value Engineering conference report. Value Engineering (VE): A tool that benefits line management. Part 4, Workshop B: VE on spare parts
[AD-A156070] 24 p4163 N85-35813
DoD Value Engineering conference report. Value Engineering (VE): A tool that benefits line management. Part 7, Workshop E: VE in construction and architect engineer contracts
[AD-A156073] 24 p4164 N85-35816
ENGINES
NT AIR BREATHING ENGINES
NT ARC JET ENGINES
NT BOOSTER ROCKET ENGINES
NT DIESEL ENGINES
NT DUCTED ROCKET ENGINES
NT ELECTROSTATIC ENGINES
NT ELECTROTHERMAL ENGINES
NT EXTERNAL COMBUSTION ENGINES
NT GAS TURBINE ENGINES
NT HYDRAZINE ENGINES
NT HYDROGEN OXYGEN ENGINES
NT INTERNAL COMBUSTION ENGINES
NT ION ENGINES
NT J-52 ENGINE
NT J-85 ENGINE
NT JET ENGINES
NT LIQUID PROPELLANT ROCKET ENGINES
NT MERCURY ION ENGINES
NT MICROROCKET ENGINES
NT ORBIT MANEUVERING ENGINE (SPACE SHUTTLE)
NT PISTON ENGINES
NT PLASMA ENGINES

NT PULSED JET ENGINES
NT RAMJET ENGINES
NT RESISTOJET ENGINES
NT REUSABLE ROCKET ENGINES
NT RIT ENGINES
NT RL-10 ENGINES
NT ROCKET ENGINES
NT ROTARY ENGINES
NT SOLID PROPELLANT ROCKET ENGINES
NT SPACE SHUTTLE MAIN ENGINE
NT SUPERSONIC COMBUSTION RAMJET ENGINES
NT TF-34 ENGINE
NT TURBINE ENGINES
NT TURBOFAN ENGINES
NT TURBOJET ENGINES
NT TURBOPROP ENGINES
NT TURBOROCKET ENGINES
NT UPPER STAGE ROCKET ENGINES
NT VARIABLE CYCLE ENGINES
Development of a Braun linear engine-driven, heat-actuated heat pump
[DE84-016647] 04 p0500 N85-13188
Effect of water on hydrogen permeability --- Stirling engines
[NASA-TM-86904] 06 p0761 N85-14864
A simulation model for Air Launched Cruise Missile engine management
[AD-A147018] 07 p1051 N85-16672
Technological and economic assessment of advanced ceramic materials. Volume 2: A case study of ceramics in heat engine applications
[PB85-113090] 12 p1815 N85-21384
Parameters of symmetric rhombic drive mechanism for single-cylinder Stirling engine 14 p2271 N85-24072
Nonlinear analysis of an axisymmetric structure subjected to non-axisymmetric loading
20 p3468 N85-31549
FAA/GAMA (Federal Aviation Administration/General Aviation Manufacturer's Association) propeller aircraft noise test program, Salina Municipal Airport, Salina, Kansas
[AD-A154818] 21 p3699 N85-32983
High temperature structural insulating material
[DE85-006361] 23 p3920 N85-34291
ENGLAND
Accidents and serious incidents to civil aircraft due to birstrikes
[AD-P004180] 11 p1578 N85-19942
ENGLISH LANGUAGE
Research on knowledge delivery
[AD-A149565] 10 p1538 N85-19698
Character recognition using correlation techniques
[AD-A152006] 16 p2847 N85-27549
ENGRAVING
Fast and precise processing of material by means of an intensive electron beam
[BMFT-FB-T-84-123] 03 p0342 N85-12201
Applications of lasers in manufacturing
14 p2308 N85-24279
Automatic engraving of map frames in the revision of the TK 25, 1:25,000 topographical map
16 p2814 N85-27362
T sub EX font tables
[DE85-011394] 19 p3339 N85-30687
ENHANCEMENT
U AUGMENTATION
ENLARGING
U EXPANSION
ENRICHMENT
NT ISOTOPIC ENRICHMENT
NT JET MEMBRANE PROCESS
Development and demonstration of a spiral-wound thin-film composite membrane system for the economical production of oxygen-enriched air, phase 4
[DE85-012380] 23 p3920 N85-34288
Measurement of uranium enrichment for gaseous uranium at low pressure
[DE85-012697] 24 p4150 N85-35733
ENSKOG-CHAPMAN THEORY
U CHAPMAN-ENSKOG THEORY
ENSTATITE
High temperature deformation of hot-pressed polycrystalline orthoenstatite
[NASA-CR-174026] 02 p0285 N85-11861
The rheology of icy satellites
[NASA-CR-174024] 02 p0302 N85-11969
ENSTROPHY
U VORTICITY
ENTERPRISE (ORBITER)
Space shuttle flight readiness firing dress rehearsal for STS-1 08 p1097 N85-16929
ENTHALPY
Thermodynamic properties and environmental chemistry of chromium
[DE84-015123] 01 p0025 N85-10152
Thermodynamic properties of isobutane-isopentane mixtures from -40 to +600(0)F and up to 1000 psia
[DE84-015137] 01 p0124 N85-10850
Engineering method of calculating a turbulent diffusion flame
[BLL-M-35781-(5828.4)] 02 p0171 N85-11147
External fuel vaporization study, phase 2
[NASA-CR-174079] 02 p0187 N85-11252
Procedural aspects of testing aerodynamic models with combustion in high-enthalpy transient-mode installations
05 p0725 N85-14658
Hydrogen embrittlement of nickel
[AD-A148322] 08 p1129 N85-17119
Development of media for dynamic latent heat storage for the low-temperature range. Part 1: Thermal analyses of selected salt hydrate systems
[NASA-TM-77778] 10 p1507 N85-19510
The physical modelling of transition metal alloying: The roles that different levels of theory play
[DE85-000591] 11 p1607 N85-20105
Evaluation of ettringite and related compounds for use in solar energy storage
[DE85-003249] 12 p1882 N85-21809
Heat of mixing experiments for liquified gases
[PB85-183697] 18 p3084 N85-29081
The moist available energy of a conditionally unstable atmosphere 18 p3145 N85-29473
Determination of the vacancy formation enthalpy in chromium by positron annihilation
[DE85-010266] 19 p3239 N85-30084
PAS determination of the vacancy formation enthalpy in tungsten
[DE85-010263] 19 p3240 N85-30086
Liquid-phase compositions from vapor-phase analyses 2: Adaptation of the Prausnitz program to UF6 and some of its potential impurities
[DE85-011521] 21 p3673 N85-32819
Thermodynamic properties of alloys in the Fe-Ti system
[NPL-DMA(A)-96] 22 p3748 N85-33229
Drying of pulverized material with heated condensible vapor
[DE85-011656] 22 p3783 N85-33438
Enthalpy transients in fractured two-phase geothermal systems
[DE85-011968] 22 p3808 N85-33587
Enthalpies of formation of liquid Fe-Ce-Si and Fe-Ce-Al three-component alloys
[BLL-M-36296-(5828.4)] 23 p3913 N85-34247
Dynamics of the melting of chromium-manganese alloys in molten steel
[BLL-M-35850-(5828.4)] 23 p3914 N85-34252
Results of variable enthalpy tests of CPR-488 TIP panels in MSFC Hot Gas Facility
[NASA-CR-170689] 24 p4072 N85-35237
Thermodynamics of the corrosion of chromium in molten carbonates
[DE85-011407] 24 p4079 N85-35282
ENTIRE FUNCTIONS
Boundary behavior of analytic functions, analytic wave front sets and the intersection problem of Ehrenpreis
[PREPRINT-809] 01 p0114 N85-10778
On generating function of Weber parabolic cylinder functions with a negative integer index and radio pulse deformation by a medium
[PR-213] 03 p0354 N85-12276
Solutions of problems of miller and rubel
10 p1538 N85-19685
Pade tables of a class of entire functions
[CSIR-TWISK-337] 14 p2413 N85-24877
Annals of the Scientific Academy of Finland, series A. 1: Mathematics, volume 9
[ISSN-0066-1953] 15 p2633 N85-26229
Iteration of exponential functions
15 p2633 N85-26233
On the length of asymptotic paths of meromorphic functions of order zero 15 p2633 N85-26234
A note on integral operators
[REPT-83-26] 17 p3021 N85-28688
ENTRAINMENT
Experiments on turbulent mixing and chemical reactions in a liquid mixing layer 02 p0134 N85-10912
Characteristics of a turbulent plane offset jet
02 p0196 N85-11310
Particle entrainment in a compressible vortex
[ISL-CO-230/83] 04 p0500 N85-13192
The properties of a round turbulent buoyant jet
[NAL-TR-826] 05 p0808 N85-15136
A wind-tunnel study of the saltation of heterogeneous (size, density) sands 08 p1182 N85-17449
Simulation of entrainment at the top of the atmospheric boundary layer for use in General Circulation Models (GCM)
[DM-42] 09 p1355 N85-18525
The physics of the marine stratocumulus-capped mixed layer 15 p2593 N85-25979
Buoyant jet entrainment in stratified fluids
19 p3263 N85-30238
Density and confinement effects on mixing characteristics of an axisymmetrical CO(2) jet
[AD-A154468] 19 p3267 N85-30258
Performance characteristics of gravity-assisted potassium heat pipes
[DE85-010717] 19 p3287 N85-30387
ENTRAPMENT
Control of mammals at airports
[AD-P004192] 11 p1580 N85-19957
ENTROPY
Thermodynamic properties and environmental chemistry of chromium
[DE84-015123] 01 p0025 N85-10152
Research into topics in transonic flow theory
[AD-A148526] 08 p1078 N85-16837
Construction of solutions for two-dimensional Riemann problems
[DE85-003136] 10 p1549 N85-19770
Entrop production determination of the ambipolar solution nearest equilibrium
[DE85-003049] 10 p1560 N85-19836
Decaying particles do not heat up the Universe
[DE85-002191] 11 p1783 N85-21091
Entropy production during fatigue as a criterion for failure. A local theory of fracture in engineering materials
[AD-A151289] 15 p2578 N85-25902
Cluster production and entropy
[DE85-007626] 17 p3032 N85-28752
Heat of mixing experiments for liquified gases
[PB85-183697] 18 p3084 N85-29081
Entropy of He 2 and universality near the superfluid in He(4) 19 p3378 N85-30957
Biological modulation of planetary atmospheres: The early Earth scenario 22 p3854 N85-33867
ENTROPY (STATISTICS)
NT MAXIMUM ENTROPY METHOD
NT MINIMUM ENTROPY METHOD
Stochastic runaway of dynamical systems
[IPP-6/244] 11 p1706 N85-20745
The role of duality in optimization problems involving entropy functionals, with applications to information theory
[AD-A152338] 17 p3026 N85-28713
ENUMERATION
Isomer enumeration in polytertiary phosphines and related compounds
[AD-A148058] 09 p1290 N85-18099
ENVIRONMENT EFFECTS
Space Shuttle Environmental Effects: The First 5 Flights
[NASA-CR-171812] 01 p0069 N85-10457
State of knowledge of environmental concerns related to natural gas-fueled vehicles
[DE84-015894] 01 p0070 N85-10461
Land use/land cover 02 p0214 N85-11410
Analysis of potential combustion sorce impacts on acid deposition using an independently derived inventory, volume 1
[DE84-012005] 02 p0225 N85-11471
Design of alternate launch and recovery surfaces for environmental effects
[AD-A145800] 03 p0320 N85-12068
Dynamic and other secondary benefits of compressed air energy storage
[DE84-015571] 03 p0386 N85-12468
Modeling effects of toxicants on aquatic systems
[DE84-016594] 04 p0531 N85-13396
Health and environmental effects document for photovoltaic energy systems, 1983
[DE84-017179] 04 p0532 N85-13399
Ocean services user needs assessment. Volume 1: Survey results, conclusions and recommendations
[NASA-CR-174104] 04 p0541 N85-13445
Space nuclear safety program
[DE84-015983] 04 p0584 N85-13591
Global carbon - nitrogen - phosphorus cycle interactions: A key to solving the atmospheric CO2 balance problem?
05 p0652 N85-14188
Summary of salt gradient solar pond research
05 p0667 N85-14292
Activities report in Earth and planetary environments physics
[CRPE-NT-134] 05 p0734 N85-14720
Tides and tidal currents of the inland waters of Western Washington
[PB84-237379] 06 p0842 N85-15348
Ecological impacts of hydroelectric projects in Amazonia 07 p1003 N85-16374
The Amazon and climate 07 p1003 N85-16376
Simulating responses to expected climate change in eastern North America: Applications to decision-making in the forest industry
[DE85-001272] 07 p1008 N85-16406

Installation restoration program. Phase 2: Stage 1 problem confirmation study, Duluth International Airport Duluth, Minnesota
[AD-A148316] 08 p1089 N85-16885
Shuttle on-orbit contamination and environmental effects 08 p1104 N85-16960
Preliminary survey of wind generation in Washington: Site studies and selected wind speed data
[DE85-000058] 09 p1345 N85-18462
Monitoring environmental and related performance parameters for a Rankine-cycle turbine electric generator utilizing geothermal energy at the Gila Hot Springs, New Mexico
[DE84-901772] 09 p1345 N85-18465
Consideration of future climatic changes in three geologic settings
[DE85-001704] 09 p1357 N85-18537
A preliminary assessment of environmental noise from large Wind Energy Conversion Systems (WECS) based on experiences from Swedish prototypes
[FFA-TN-1984-48] 09 p1379 N85-18668
Airport site selection and design
[AD-P004193] 11 p1581 N85-19959
Effects of electromagnetic fields produced by high voltage transmission lines
[DE85-000034] 11 p1625 N85-20230
Effect of water vapor and water droplets on the RAM-1 (Real-Time Aerosol Monitor): Preliminary results
[PB85-109429] 11 p1637 N85-20313
Proceedings of a Workshop on Environment of West Antarctica: Potential CO2-induced changes
[PB85-110757] 11 p1671 N85-20527
Environmental effects of space activities 11 p1678 N85-20577
Combined effects of atmospheric deposition, internal acid production, and harvesting on nutrient gains and losses from forest ecosystems
[DE85-002325] 12 p1884 N85-21821
Ecological observations at the site of the 10 MWe solar thermal power system (1978-1984)
[DE85-004572] 12 p1885 N85-21827
Assessment of hazardous waste surface impoundment technology case studies and perspectives of experts
[PB85-117059] 12 p1886 N85-21834
Standard analytical procedures of the NOAA National Analytical Facility, 1984-85: Extractable toxic organic compounds
[PB85-126282] 12 p1887 N85-21840
Summary report of the Workshop on Structure Activity Concepts in Environmental Sciences
[PB85-137339] 12 p1887 N85-21841
Impact of aerosols on visibility and climate: A report prepared for Panel 3, Environmental Impact, of the NATO/CCMS Air Pollution Pilot Study on Air Pollution Control Strategies and Impact Modelling
[PB85-106744] 12 p1897 N85-21906
USC (University of Southern California) Sea Grant Program Directory, 1984-1985
[PB85-135051] 12 p1899 N85-21922
Effect of high ammonia content in closed environment on some parameters of human nitrogen and carbohydrate metabolism against background of a controlled diet 12 p1903 N85-21948
Areas with forest soils sensitive to acidic deposition under alternative damage hypotheses
[DE85-005257] 13 p2130 N85-23257
Effects of interactive transport and scavenging of smoke on the calculated temperature change resulting from large amounts of smoke
[DE85-006450] 14 p2378 N85-24684
A comparative evaluation of the effects of acid precipitation, natural acid production and harvesting of cation removal from forests
[DE85-005254] 15 p2589 N85-25961
The role of gravity on the reproduction of arabidopsis plants 15 p2607 N85-26089
Oil resistant silicone elastomers
[AD-131523] 16 p2753 N85-26967
Acid rain: Effects on fish and wildlife
[PB85-154672] 16 p2821 N85-27402
Impact of ozone on vegetation
[PB85-159937] 16 p2821 N85-27403
ELF (Extremely Low Frequency) communications system ecological monitoring program: Measurements of ELF electromagnetic fields for site selection and characterization, 1983
[AD-A153120] 17 p2949 N85-28209
Investigation of air pollution impact in Eastern Bavaria: Measurement results from August and September, 1984
[DFVLR-FB-85-03] 17 p2968 N85-28471
Ozone and temperature trends due to the injection of trace species in the atmosphere
[AERONOMICA-ACTA-A-288-1984] 18 p3132 N85-29399
Applied climatology — regional planning 18 p3147 N85-29486
Ambient air contamination: Characterization and detection techniques 18 p3157 N85-29546
Program planning using the GMAP procedure in SAS/GRAPH software
[DE85-008356] 18 p3199 N85-29842
Activities report in energy technology
[OEFZS-4302] 18 p3199 N85-29846
Environmental Sciences Division report
[DE85-910452] 19 p3308 N85-30506
Applied Science Division's Environmental Research Program
[DE85-010637] 19 p3308 N85-30510
Analysis of leachate production in closed hazardous waste landfills
[DE85-010978] 19 p3310 N85-30520
Aviation noise effects
[AD-A154319] 19 p3352 N85-30776
Annual environmental monitoring report, January-December 1984
[DE85-011689] 20 p3486 N85-31685
Ozone in the 21st century: Increase or decrease
[AERONOMICA-ACTA-A-291-1984] 20 p3489 N85-31687
Thin-film reliability and engineering overview 21 p3612 N85-32450
Effects of environment on spacecraft materials 22 p3733 N85-33144
Procedure for estimating orbital debris risks
[NASA-TP-2507] 22 p3738 N85-33189
Small-hydropower development: The process, pitfalls, and experience. Volume 1: Feasibility studies summary and analysis
[DE85-010839] 22 p3806 N85-33589
Acid rain in Europe
[COMMITTEE-PRINT-99-F] 22 p3810 N85-33601
Environmental monitoring at Lawrence Livermore National Laboratory: 1984 report
[DE85-011593] 22 p3811 N85-33606
A 1984 environmental summary: Sandia National Laboratories Tonopah Test Range, Tonopah, Nevada
[DE85-011145] 22 p3812 N85-33612
Nordic Association for Aerosol Research (NOSA) Aerosol Symposium: Program and abstracts
[FOA-E-40019] 22 p3812 N85-33616
Organic solvent alteration of hydraulic properties of sedimentary rocks of low permeability: A review
[DE85-012537] 22 p3815 N85-33635
Meteorology and Society: Statements presented at the 9th congress under agenda item 12 — World Meteorological Organization
[WMO-643] 22 p3817 N85-33644
Fusion facility siting considerations
[DE85-012894] 22 p3843 N85-33805
Near-threshold fatigue: An overview of the role of microstructure and environment
[DE85-009903] 23 p3941 N85-34431
Effects of acid rain on forest nutrient status
[DE85-012486] 23 p3947 N85-34463
Agents and effects of ozone trends in the atmosphere
[AERONOMICA-ACTA-A-287-1984] 23 p3948 N85-34466
Effect of hypokinesia and +Gz accelerations on transport function of human blood 23 p3952 N85-34497
Contribution to the properties of carbon fiber reinforced composites — structural mechanics
[ESA-TT-849] 24 p4074 N85-35246
Implementing agreement for cooperation in the development of large scale wind energy conversion systems
[JUEL-SPEZ-278] 24 p4110 N85-35473
General environmental aspects of large scale wind energy utilization 24 p4110 N85-35474
GROWIAN: First observations of the environmental impact at the GROWIAN site — wind energy converter 24 p4110 N85-35476
Environmental aspects of large-scale wind-power systems in the UK 24 p4110 N85-35478
Environmental Monitoring Burger Hill, Orkney wind turbine generator site and similar work at other UK WTG sites 24 p4111 N85-35482
Environmental aspects of the Netherlands wind farm project 24 p4111 N85-35485

ENVIRONMENT MANAGEMENT

EPA (Environmental Protection Agency) environmental data base and model directory, volume 1
[PB84-207562] 01 p0126 N85-10868
Proceedings of the Environmental Systems Symposium (13th) held at Bethesda, Md., 20-22 March 1984
[AD-A148194] 09 p1346 N85-18471
The application of emissions trading to DoD installations
[AD-P004136] 09 p1346 N85-18472
Compatible goals: Defense and environmental protection
[AD-P004137] 09 p1347 N85-18473
Environmental and energy audits of Air Force government owned-contractor operated installations
[AD-P004138] 09 p1347 N85-18474
Strategies for preparing and submitting a part B application for a DoD facility
[AD-P004139] 09 p1347 N85-18475
Assessment of environmental costs at ordnance activities
[AD-P004140] 09 p1347 N85-18476
Landscape management on airports for reduction of bird populations
[AD-P004194] 11 p1581 N85-19960
Inexpensive multipurpose landscaping 11 p1581 N85-19961
Reducing gull use of some attractions near airports
[AD-P004195] 11 p1581 N85-19962
Effectiveness of an overhead wire barrier in deterring gulls from feeding at a sanitary landfill
[AD-P004199] 11 p1582 N85-19966
Environmental management needs
[DE85-007859] 18 p3133 N85-29405
Wind turbines and environment management
[CP-MEMO-1983-11] 20 p3485 N85-31662
Marine environmental quality assessment program, five-year plan (FY 1984 - 1988)
[AD-A154715] 21 p3613 N85-32459
A guide for new environmental coordinators
[AD-A156327] 24 p4113 N85-35498
Land Disposal of Hazardous Waste
[PB85-196376] 24 p4113 N85-35500

ENVIRONMENT MODELS

EPA (Environmental Protection Agency) environmental data base and model directory, volume 1
[PB84-207562] 01 p0126 N85-10868
Measurements 12 p1787 N85-21222
The accuracy in calculations of intervisibility with digital terrain models — digital models
[FOA-C-20557-D8(E1)] 12 p1909 N85-21983
Empirical methods for predicting eutrophication in impoundments. Report 3. Phase 2. Model refinements
[AD-A155483] 21 p3614 N85-32462
Global environmental transport models for tritium
[DE85-011437] 22 p3816 N85-33639
Oxidation states of iron in the terrestrial planets: Evidence and implications for accretion models 22 p3852 N85-33854

ENVIRONMENT POLLUTION

NT AIR POLLUTION
NT GLOBAL AIR POLLUTION
NT INDOOR AIR POLLUTION
NT OIL POLLUTION
NT WATER POLLUTION
HS and E environmental sciences
[DE84-016183] 05 p0672 N85-14314
Something in the air at Windscale — radioactive contaminants from the Sellafield nuclear Complex for reprocessing and storing irradiated fuel
[BLL-RISLEY-TR-4996-(9091.9F)] 08 p1179 N85-17429
Penetration of the atmosphere by flammable mixtures as a result of spillage of LNG on the ground 08 p1179 N85-17432
Atmospheric acidification chemistry: A review
[PB84-215490] 09 p1350 N85-18495
Research in environmental biology reviewed 11 p1622 N85-20211
National Acid Precipitation Assessment Program. Report to the President and Congress (1983)
[PB85-116713] 11 p1679 N85-20581
China report: Science and technology
[JPRS-CST-84-036] 11 p1696 N85-20661
Report on the Second Annual Review Meeting of the National Acid Precipitation Assessment Program. Research to assist decisionmaking: Summary
[DE85-003003] 12 p1884 N85-21820
Feoktistov discusses need for space colonization 13 p1985 N85-22454
An ultrasensitive and element specific photoionization detection system for environmental analysis
[AD-A153365] 17 p2968 N85-28332
Technical support for geopressured-geothermal well activities in Louisiana
[DE85-010462] 18 p3102 N85-29203
North American acid deposition data base system (ADS) and its use in spatial analysis
[PB85-173235] 18 p3201 N85-29856
Environmental monitoring report for Pantex Plant covering, 1984
[DE85-010624] 19 p3308 N85-30508
Analysis of leachate production in closed hazardous waste landfills
[DE85-010978] 19 p3310 N85-30520
Radioactivity in gaseous waste discharged from the separations facilities during 1984
[DE85-011373] 19 p3360 N85-30831

Bulk and thermal properties of the functional Tuffaceous Beds in holes USW G-1, UE-25 no. 1, and USW G-2, Yucca Mountain, Nevada
[DE85-011181] 19 p3365 N85-30866
Soil extraction kit
[AD-D011736] 22 p3742 N85-33190

ENVIRONMENT PROTECTION

Estuaries of the Cape. Part 2: Synopses of available information on individual systems. Report no. 17: Lourens (CSW 7)
[CSIR-RR-416-PT-2] 01 p0087 N85-10586
National Photovoltaics Program Annual Review Meeting, abstracts
[DE84-013003] 04 p0530 N85-13390
Proceedings of the Environmental Systems Symposium (13th) held at Bethesda, Md., 20-22 March 1984
[AD-A148194] 09 p1346 N85-18471
Compatible goals: Defense and environmental protection
[AD-P004137] 09 p1347 N85-18473
Environmental and energy audits of Air Force government owned-contractor operated installations
[AD-P004138] 09 p1347 N85-18474
Strategies for preparing and submitting a part B application for a DoD facility
[AD-P004139] 09 p1347 N85-18475
Assessment of environmental costs at ordnance activities
[AD-P004140] 09 p1347 N85-18476
Remedial action of hazardous waste US Army Corps of Engineers, Anniston, Alabama
[AD-P004141] 09 p1347 N85-18477
Practical application of earth resistivity methods in phase 2 of the installation restoration program
[AD-P004148] 09 p1348 N85-18484
The Hazardous Materials Technical Center
[AD-P004149] 09 p1349 N85-18485
Community relations activities at Department of Defense sites
[AD-P004150] 09 p1349 N85-18486
Atmospheric diffusion in hilly region on middle reaches of the Chang Jiang 11 p1620 N85-20196
Urban climate and air hygiene before, during, and after the lifework of Hellmut Berg. Overview of a branch of applied meteorology 18 p3147 N85-29487
Radionuclide mobility in the shallow portion of an active high-temperature geothermal system
[DE85-010293] 18 p3182 N85-29729
Reference data source documentation for performance assessment studies, Basalt Waste Isolation Project, Hanford Site, Washington
[DE85-010543] 19 p3301 N85-30468
Magnetohydrodynamics and the National Coal Science, Technology, and Engineering Development Acts
[S-HRG-99-1179] 20 p3535 N85-31994
Corrosion resistant storage container for radioactive material
[DE85-011666] 22 p3838 N85-33765
A guide for new environmental coordinators
[AD-A156327] 24 p4113 N85-35498

ENVIRONMENT SIMULATION

NT ALTITUDE SIMULATION
NT SPACE ENVIRONMENT SIMULATION
NT THERMAL SIMULATION
NT WEIGHTLESSNESS SIMULATION

Evaluation of thermocouple junction temperature
[DE84-015159] 04 p0502 N85-13206
Growth of soil bacteria in presence of Martian soil analog, carbon dioxide and hydrogen peroxide 09 p1361 N85-18580
Ribbon burner simulation of T-700 turbine shroud for ceramic lined seals research
[NASA-TM-86940] 10 p1483 N85-19364
Potential bedforms on Venus: Wind tunnel simulations 13 p2189 N85-23583
Microdunes and other aeolian bedforms on Venus: Wind tunnel simulations 13 p2189 N85-23584
Simulated microgravity as a probe for understanding the mechanisms of early pattern specification 15 p2611 N85-26092
Testing of materials and coatings for jet engine components under simulated operational conditions
[B8580073] 17 p2890 N85-27873
An environmentally-controlled extended-use small animal hypobaric chamber
[AD-A153735] 19 p3221 N85-29974
The deep diving simulator TITAN: Physiological problems associated with staying in great depths of water 24 p4130 N85-35604

ENVIRONMENT SIMULATORS

NT SOLAR SIMULATORS
NT SPACE SIMULATORS

Impedance measurements on a VLF multi-turn loop antenna in a space plasma simulation chamber
[AD-A145104] 04 p0492 N85-13141
Natural exposure versus chamber simulation
[AD-A149538] 10 p1495 N85-19437

ENVIRONMENTAL CHAMBERS

U TEST CHAMBERS

ENVIRONMENTAL CHEMISTRY

NT AEROTHERMOCHEMISTRY
NT ATMOSPHERIC CHEMISTRY
NT BIOCHEMISTRY
NT BIOGEOCHEMISTRY
NT GEOCHEMISTRY
NT PHYSIOCHEMISTRY

Thermodynamic properties and environmental chemistry of chromium
[DE84-015123] 01 p0025 N85-10152
Estuaries of the Cape. Part 2: Synopses of available information on individual systems. Report no. 17: Lourens (CSW 7)
[CSIR-RR-416-PT-2] 01 p0087 N85-10586
Summary report of the Workshop on Structure Activity Concepts in Environmental Sciences
[PB85-137339] 12 p1887 N85-21841
Design of the National Trends Network for monitoring the chemistry of atmospheric precipitation
[GS-CIRC-864] 20 p3486 N85-31864
The 1984 effluent and environmental monitoring report for the Bettis Atomic Power Laboratory
[DE85-011533] 22 p3810 N85-33602

ENVIRONMENTAL CONTROL

Toxicological evaluation of Columbia spacecraft 01 p0094 N85-10831
Conceptual design and evaluation of selected Space Station concepts, volume 2
[NASA-TM-87384] 02 p0166 N85-11130
Challenges in the development of the orbiter atmosphere revitalization subsystem 08 p1095 N85-16920
Other challenges in the development of the orbiter environmental control hardware 08 p1096 N85-16924
Operating and maintenance guidelines for the kinergetics (trade name) environmental control system. Carbon dioxide scrubber model DH-10 and heat exchanger model CCU-01
[AD-A148107] 08 p1200 N85-17557
Control technology for fiber reinforced plastics industry at AMF Hatteras Yachts, New Bern Division, New Bern, North Carolina
[PB85-109015] 10 p1460 N85-19198
Extended mission life support systems 18 p3157 N85-29547
An environmentally-controlled extended-use small animal hypobaric chamber
[AD-A153735] 19 p3221 N85-29974
Space station ECLSS integration analysis: Simplified General Cluster Systems Model, ECLS System Assessment Program enhancements
[NASA-CR-176069] 21 p3670 N85-32796
Evaluation of source strength and dispersion model predications with data from large nitrogen tetroxide field experiments
[DE85-011655] 23 p3947 N85-34485

ENVIRONMENTAL ENGINEERING

Compilation of annual reports of the Navy ELF (Extremely Low Frequency) communications system ecological monitoring program. Volume 1: Tabs A-E
[AD-A148326] 08 p1152 N85-17272
Compilation of annual reports of the Navy ELF (Extremely Low Frequency) communications system ecological monitoring program (1983). Volume 2: Tabs F-J
[AD-A148327] 08 p1152 N85-17273
Research in environmental biology reviewed 11 p1622 N85-20211
Design of computer-related workstations in relation to job functions and productivity
[AD-A151938] 16 p2844 N85-27534
Recommendations for the design and equipping of engineering metrology laboratories
[NPL-MOM-22] 23 p3898 N85-34145

ENVIRONMENTAL LABORATORIES

Activities report in Earth and planetary environments physics
[CRPE-NT-134] 05 p0734 N85-14720
Environmental research laboratories (of the National Oceanic and Atmospheric Administration) programs and plans: FY 1983 programs and FY 1984 plans
[PB84-226729] 06 p0840 N85-15336
Making sure: A brief outline and history of ESA's test and checkout services
[ESA-BR-22] 09 p1286 N85-18077
Environmental Research Laboratories publication abstracts, FY 1984
[PB85-180594] 19 p3313 N85-30540
Environmental background measurement program
[AD-A153980] 19 p3319 N85-30577
Adaptive aiding for symbiotic human-computer control: Conceptual model and experimental approach
[AD-A153870] 19 p3332 N85-30644
European Space Tribology Laboratory: Facilities, services, capabilities
[ESA-BR-12] 20 p3396 N85-31080

ENVIRONMENTAL MONITORING

EPA (Environmental Protection Agency) environmental data base and model directory, volume 1
[PB84-207562] 01 p0126 N85-10866
Economic evaluation of space survey materials use in land improvement engineering field work 02 p0165 N85-11115
Analysis of radiocobalt in environmental samples
[DRIC-T-7334] 03 p0367 N85-12477
A system for monitoring radon and its decay products in the atmosphere
[INPE-3085-PRE/494] 03 p0391 N85-12502
A comparison of TIROS-N series satellite data and LANDSAT data over Scotland 05 p0656 N85-14210
Monitoring and mapping global vegetation cover using data from meteorological satellites 05 p0656 N85-14211
A geoinformation expert system for synergetic use of map and image data 05 p0659 N85-14233
Inventory and monitoring of national park landscapes — remote sensing 05 p0660 N85-14245
Environmental data inventory for the antarctic area
[PB85-107944] 06 p0819 N85-15195
Early detection of environmental exposure
[AD-P004039] 06 p0845 N85-15369
Compilation of annual reports of the Navy ELF (Extremely Low Frequency) communications system ecological monitoring program. Volume 1: Tabs A-E
[AD-A148326] 08 p1152 N85-17272
Compilation of annual reports of the Navy ELF (Extremely Low Frequency) communications system ecological monitoring program (1983). Volume 2: Tabs F-J
[AD-A148327] 08 p1152 N85-17273
Pilot climate data system
[NASA-CR-174321] 08 p1187 N85-17481
Remote sensing technology now playing practical roles 11 p1619 N85-20190
Environmental Monitoring Improvement Act
[GPO-39-742] 11 p1677 N85-20568
National Acid Precipitation Assessment Program. Report to the President and Congress (1983)
[PB85-116713] 11 p1679 N85-20581
On the P1 data from GMS-SEM 12 p1894 N85-21890
The development of image processing of NOAA AVHRR data and its application to sea surface temperature 12 p1895 N85-21891
Combined analysis of the dynamics of complex ecosystems based on repeated remote measurements 13 p1985 N85-22450
Data Collection and Platform Location by Satellite: ARGOS Users' Conference 14 p2237 N85-23669
The ARGOS system status report after 2 years operation 14 p2237 N85-23670
System performance, data distribution and technical files — ARGOS project 14 p2237 N85-23671
Report on the panel discussion of the Workshop on Data Collection Platform Networks 14 p2239 N85-23680
The ARGOS system status report 14 p2239 N85-23684
Equipment for the ARGOS system from Eidsvoll Electronics A.S. 14 p2239 N85-23685
The ARGOS system main characteristics — satellite based localization 14 p2325 N85-24367
The ARGOS system after 3 years operation 14 p2325 N85-24368
Environmental satellites 14 p2328 N85-24392
Evaluation of carrying capacity and landscape damage in northern Kenya by multistage remote sensing
[DFVLR-FB-84-47] 14 p2347 N85-24514
The ARGOS program — satellite based localization 14 p2397 N85-24775
Thermally modulated electron affinity detector for priority pollutant analysis
[PB85-158145] 15 p2508 N85-25469
NOAA satellite operations: Programs briefing — Environmental satellites, LANDSAT, and space station polar platform 15 p2599 N85-26020
The impact of weather on aviation safety
[GPO-95-520] 16 p2703 N85-26685
Shuttle imaging radar-A (SIR-A) data analysis — geology of the Ozark Plateau of southern Missouri, land use in western Illinois, and vegetation types at Koonamore Station, Australia
[NASA-CR-175785] 16 p2809 N85-27324
Monitoring of marine environment 16 p2812 N85-27341

Contribution of the NOAA-7 and 8 and ARGOS partnership to white tuna fishing in the northeast Atlantic
16 p2813 N85-27365
Location and data collection satellite system ARGOS. User's guide — satellite based localization
16 p2816 N85-27371
Investigation of air pollution impact in Eastern Bavaria: Measurement results from August and September, 1984
[DFVLR-FB-85-03] 17 p2988 N85-28471
DFVLR measuring system for the determination of the spatial distribution of environmental parameters of the atmosphere by means of mobile instrumented platforms
[DFVLR-FB-85-09] 17 p2989 N85-28472
Technical support for geopressured-geothermal well activities in Louisiana
[DE85-010462] 18 p3102 N85-29203
Field measurements with the TAMS-2B and development of methods for measuring HCHO, HCl and HONO in real air
[PB85-172955] 18 p3135 N85-29419
North American acid deposition data base system (ADS) and its use in spatial analysis
[PB85-173235] 18 p3201 N85-29856
Environmental Sciences Division report
[DE85-010452] 19 p3306 N85-30506
Environmental monitoring report for Pantex Plant covering, 1984
[DE85-010624] 19 p3306 N85-30508
Environmental monitoring at Argonne National Laboratory
[DE85-010613] 19 p3309 N85-30516
Radioactive liquid wastes discharged to ground in the 200 areas during 1984
[DE85-010619] 19 p3310 N85-30517
Environmental Research Laboratories publication abstracts, FY 1984
[PB85-180594] 19 p3313 N85-30540
Radioactivity in gaseous waste discharged from the separations facilities during 1984
[DE85-011373] 19 p3360 N85-30631
Design of the National Trends Network for monitoring the chemistry of atmospheric precipitation
[GS-CIRC-964] 20 p3486 N85-31664
Annual environmental monitoring report, January-December 1984
[DE85-011689] 20 p3486 N85-31665
Particulate contamination control in clean rooms by particle fallout (PFO) measurements
[ESA-PSS-01-204-ISSUE-1] 20 p3487 N85-31673
Offshore oceanographic and environmental monitoring services for the Strategic Petroleum Reserve, volume 3
[DE85-009907] 20 p3497 N85-31741
Environmental factors in corrosion and deterioration of materials 22 p3750 N85-33241
The 1984 effluent and environmental monitoring report for the Battle Atomic Power Laboratory
[DE85-011533] 22 p3810 N85-33602
Environmental summary for calendar year 1984
[DE85-012020] 22 p3810 N85-33604
Environmental monitoring at Lawrence Livermore National Laboratory: 1984 report
[DE85-011593] 22 p3811 N85-33606
The 1984 environmental monitoring program report for Idaho National Engineering Laboratory site
[DE85-011209] 22 p3812 N85-33611
Dynamics of Mesoscale Weather Systems: 1984 Summer Colloquium
[PB85-188266] 22 p3817 N85-33649
Multi-solute subsurface transfer modeling for energy solid wastes: Highlights FY 1984
[DE85-012788] 23 p3966 N85-34591
Environmental Monitoring Burger Hill, Orkney wind turbine generator site and similar work at other UK WTG sites 24 p4111 N85-35482
Current inventory of anthropogenic carbon dioxide in the North Pacific Subarctic Gyre
[PB85-187938] 24 p4125 N85-35570

ENVIRONMENTAL QUALITY
NT AIR QUALITY
NT WATER QUALITY
Illinois Climate: Trends, Impacts and Issues
[PB84-211986] 01 p0066 N85-10577
Corporate use of information regarding natural resources and environmental quality
[PB84-222736] 03 p0439 N85-12794
Integrated global background monitoring network
[DE84-016996] 04 p0532 N85-13398
Air quality assessment model validation in complex terrain
[AD-A147690] 08 p1160 N85-17434
Quality assurance for environmental analytical chemistry, 1983
[DE84-016045] 09 p1349 N85-18489
China report: Science and technology
[JPRS-CST-84-040] 11 p1623 N85-20219
China report: Science and technology
[JPRS-CST-85-003] 13 p2166 N85-23433
China report: Science and technology
[JPRS-CST-85-009] 15 p2530 N85-25596
China report: Science and technology
[JPRS-CST-85-013] 15 p2536 N85-25652
China report: Science and technology
[JPRS-CST-85-011] 15 p2551 N85-25748
China report: Science and technology
[JPRS-CST-85-010] 15 p2564 N85-25819
An ultrasensitive and element specific photoionization detection system for environmental analysis
[AD-A153365] 17 p2968 N85-28332
Mathematical model of global processes in the biosphere 19 p3295 N85-30431
Assessment of the role of nitrogen oxides in nonurban ozone formation
[PB85-173680] 19 p3311 N85-30524
Marine environmental quality assessment program, five-year plan (FY 1984 - 1988)
[AD-A154715] 21 p3613 N85-32459
Air force technical objective document, Aerospace Medical Division, Fiscal Year 1986
[AD-A155195] 21 p3664 N85-32762
Practical consequences of the assessment of different energy health risks
[DE85-004538] 22 p3825 N85-33696

ENVIRONMENTAL SURVEYS
A geoinformation expert system for synergetic use of map and image data 05 p0659 N85-14233
Inventory and monitoring of national park landscapes — remote sensing 05 p0660 N85-14245
Helicopter noise survey performed at Las Vegas, Nevada, 19-21 January, 1984
[AD-A147392] 07 p1039 N85-16593
Extremely Low Frequency (ELF) Communications System Ecological Monitoring Program: Summary of 1983 progress
[AD-A147704] 08 p1151 N85-17265
Noise measurement flight test: Data-analyses Aerospatiale AS 350D AStar helicopter
[AD-A148498] 08 p1218 N85-17672
Marine environmental quality assessment program, five-year plan (FY 1984 - 1988)
[AD-A154715] 21 p3613 N85-32459
Environmental surveillance at Los Alamos during 1984
[DE85-011866] 22 p3811 N85-33605
Design analysis for a repository in crystalline rock
[DE85-011802] 22 p3839 N85-33771
Environmental-physical measurements and determination of atmospheric turbulence with the ASK-16 motor glider 24 p4122 N85-35549

ENVIRONMENTAL TEMPERATURE
U AMBIENT TEMPERATURE

ENVIRONMENTAL TESTS
NT CORROSION TESTS
NT HIGH TEMPERATURE TESTS
NT LOW TEMPERATURE TESTS
NT SALT SPRAY TESTS
NT UNDERWATER TESTS
Motion sensor evaluation using simulation
[DE84-014989] 01 p0050 N85-10331
Selection, procurement and description of Salem Limestone samples used to study the effects of acid rain
[PB84-231067] 04 p0484 N85-13088
Effects of restricted water intake on performance in a cold environment
[AD-A146904] 07 p1015 N85-16450
Initial investigation of cryogenic wind tunnel model filler materials
[NASA-TM-86363] 09 p1283 N85-18069
Acceleration responses of typical LRU's subjected to bench handling and installation shock
09 p1334 N85-18385
Impact of 810D on dynamic test laboratories
09 p1334 N85-18386
NBS (National Bureau of Standards) solar collector durability-reliability test program
[PB85-113603/GAR] 09 p1346 N85-18469
Natural exposure versus chamber simulation
[AD-A149538] 10 p1495 N85-19437
Evaluation of corrosion-erosion behavior of various ceramic materials
[AD-A149756] 12 p1812 N85-21367
Performance assessment of Class 1E pressure transmitters subjected to environmental stresses
[DE85-001623] 12 p1854 N85-21626
A study of fatigue crack growth in 2 1/4 Cr1Mo steel. Part 1: The influences of environment and material condition
[AERE-R-11472] 14 p2258 N85-23993
Ten year environmental test of glass fiber/epoxy pressure vessels
[NASA-TM-87058] 19 p3231 N85-30034
Module Hipot and ground continuity test results
21 p3612 N85-32447
Flight service evaluation of composite helicopter components
[NASA-CR-172562] 23 p3909 N85-34222

ENVIRONMENTS
NT AEROSPACE ENVIRONMENTS
NT CHROMOSPHERE
NT DEEP SPACE
NT EARTH ENVIRONMENT
NT EXTRATERRESTRIAL ENVIRONMENTS
NT GEOMAGNETIC TAIL
NT HELIUM HYDROGEN ATMOSPHERES
NT HIGH ALTITUDE ENVIRONMENTS
NT HIGH GRAVITY ENVIRONMENTS
NT HIGH TEMPERATURE ENVIRONMENTS
NT ICE ENVIRONMENTS
NT INNER RADIATION BELT
NT INTERPLANETARY SPACE
NT INTERSTELLAR SPACE
NT IONOSPHERE
NT JUPITER ATMOSPHERE
NT LOW TEMPERATURE ENVIRONMENTS
NT LOWER IONOSPHERE
NT LUNAR ATMOSPHERE
NT MAGNETOPAUSE
NT MAGNETOSPHERE
NT MARINE ENVIRONMENTS
NT MARS ATMOSPHERE
NT MARS ENVIRONMENT
NT MESOPAUSE
NT MESOSPHERE
NT MIDLATITUDE ATMOSPHERE
NT NEPTUNE ATMOSPHERE
NT PLANETARY ATMOSPHERES
NT PLANETARY ENVIRONMENTS
NT ROTATING ENVIRONMENTS
NT SATELLITE ATMOSPHERES
NT SATURN ATMOSPHERE
NT SOLAR ATMOSPHERE
NT SPACECRAFT ENVIRONMENTS
NT STELLAR ATMOSPHERES
NT THERMAL ENVIRONMENTS
NT URANUS ATMOSPHERE
NT VENUS ATMOSPHERE
Natural environment design criteria for the Advanced X-ray Astrophysics Facility (AXAF) definition and preliminary design
[NASA-TM-86481] 01 p0014 N85-10089
Software engineering environments for mission critical applications: STARS alternative programmatic approaches
[AD-A145285] 02 p0241 N85-11571
Human aspects in office automation
[PB84-240738] 06 p0847 N85-15376
Implementation of a Zilog Z-80 base realization library for the computer systems design environment
[AD-A148359] 06 p0853 N85-15423
USSR report: Life sciences. Biomedical and behavioral sciences
[JPRS-UBB-85-002] 09 p1360 N85-18559
Role of environments in managing data analysis
[DE85-000397] 09 p1369 N85-18602
Computing environments for data analysis. Part 1. Introduction
[AD-A148677] 09 p1373 N85-18632
Computing environments for data analysis. Part 2. Hardware
[AD-A148678] 09 p1374 N85-18633
Reliability of adhesive bonds under severe environments. Report of the Committee on Reliability of Adhesive Bonds in Severe Environments
[AD-A149010] 10 p1451 N85-19140
Construction and application of a questionnaire for the social scientific investigation of environmental noise effects
[NASA-TM-75492] 10 p1512 N85-19544
Development of satellite data presentation for environmental forecasting 11 p1712 N85-20770
Environmental cycling of cellulosic thermal insulation and its influence on fire performance
[DE85-004295] 13 p2041 N85-22776
Principles of software engineering environment design
[AD-A150352] 13 p2147 N85-23324
Recognition of objects in their natural environment — parallel processing 15 p2622 N85-26158
Computing environments for data analysis. Part 1: Introduction
[DE85-007919] 17 p3009 N85-28603
Computing environments for data analysis. Part 2: Hardware
[DE85-006320] 17 p3009 N85-28604
Use of environmental health-risk analysis for managing toxic substances
[DE85-006964] 18 p3160 N85-29574
Satellite measurements of atmospheric aerosols
[AD-A153807] 19 p3316 N85-30558

Anaerobic microbial transformations in subsurface environments: Project description
[DE85-012789] 23 p3951 N85-34486
Circuit approaches to increasing SRAM performance in total dose environments
[DE85-009441] 23 p3966 N85-34586
International flight planning handbook
[AD-A156330] 24 p4062 N85-35177

ENZYME ACTIVITY
NT FERMENTATION
Induced changes in the cholinergic system of sciatic nerve and slow and fast twitch muscle of rats
15 p2609 N85-26081
Neural mechanism by which gravitational stimulus and stress affect the secretion of renin and other hormones
15 p2610 N85-26083
Lipid hydrolysis in man during antiorthostatic hypokinesia 23 p3953 N85-34500
Lipogenesis in rat liver after flight aboard Cosmos-1129 biosatellite 23 p3954 N85-34508

ENZYMES
NT CATALASE
NT CHOLINESTERASE
NT OXIDASE
NT PROTEASE
NT TRYPSIN
Construction of a bacterium to convert cellulose to ethanol
[TI84-901639] 04 p0481 N85-13068
Acid phosphatase and protease activities in immobilized rat skeletal muscles
[NASA-CR-174340] 08 p1192 N85-17509
A comparison of rat myosin from fast and slow skeletal muscle and the effect of disuse
[NASA-CR-174339] 08 p1192 N85-17510
Ethanol production by enzymatic hydrolysis: Parametric analysis of a base-case process
[DE84-013105] 11 p1614 N85-20147
Development of a new class of chemical and biological ultrasensors: Ribonuclease contamination and control
[NASA-CR-175466] 11 p1635 N85-20296
USSR report: Space Biology and Aerospace Medicine, volume 18, no. 6, November - December 1984
[JPRS-USB-85-002] 12 p1900 N85-21931
Parameters of carbohydrate metabolism and blood serum enzyme activity after short-term spaceflights
12 p1903 N85-21951
Quantitative alterations in the function of bone forming cells due to reduced weight bearing
15 p2609 N85-26075
Quantitation of Na+, K+-ATPase enzyme activity in tissues of the mammalian vestibular system
15 p2613 N85-26102
Differential effect of denervation on free radical scavenging enzymes in slow and fast muscle of rat
[NASA-CR-175719] 15 p2614 N85-26110
Radiation damage and repair in cells and cell component, part 1
[DE85-008667] 18 p3152 N85-29519
Galactose oxidase in stereospecific oxidation of primary alcohols
[AD-A154059] 19 p3234 N85-30048
Blood serum enzyme activity following long term spaceflights 19 p3326 N85-30604
Biocatalysis project
[NASA-CR-176044] 20 p3498 N85-31744
Urokinase production by electrophoretically separated cultured human embryonic kidney cells
20 p3501 N85-31765
The Fibrin slide assay for detecting urokinase activity in human fetal kidney cells 20 p3502 N85-31768
Structural changes in thyroid due to high-altitude adaptation in Kirghizia 22 p3820 N85-33666

EOS
U LANDSAT SATELLITES

EOSS
In situ orbital debris experiment concepts
12 p1784 N85-21198

EPHEMERIDES
NT PLANET EPHEMERIDES
The solar system: Improving knowledge of the system
14 p2396 N85-24782
The astrometry network of the IHW and the P/Crommelin trial run results 14 p2435 N85-25016
The orbits of Comets Halley and Giacobini-Zinner
14 p2437 N85-25039
The work on Comet Halley's orbit at ESOC
14 p2438 N85-25041
Determination of the observation conditions of celestial bodies with the aid of the DISPO system
[NAS 1.15:77632] 14 p2438 N85-25044
Ephemeral regions versus pseudo ephemeral regions
18 p3208 N85-29901

EPHEMERIS TIME
Altimetry, orbits and tides
[E85-10066] 08 p1174 N85-17404
HEAO 3 upper limits to the expected 1634 KeV line from SS 433
[OG-2.4-9] 22 p3868 N85-33954

EPICYCLOIDS
High powered epicyclic gears: Some recent development 23 p3924 N85-34316

EPIDEMIOLOGY
USSR report: Life sciences. Biomedical and behavioral sciences
[JPRS-UBB-84-025] 04 p0543 N85-13453
Epidemiologic methods applied to the study of the relationship between climate and human health
05 p0687 N85-14418
The epidemiology and toxicology of Agent Orange
[AD-P004038] 06 p0845 N85-15368
USSR report: Life sciences. Biomedical and behavioral sciences
[JPRS-UBB-84-015] 07 p1010 N85-16416
Health examination findings among active civil airmen
[AD-A148325] 08 p1195 N85-17533
USSR report: Life sciences. Biomedical and behavioral sciences
[JPRS-UBB-85-002] 09 p1360 N85-18559
Review of epidemiological studies of human exposures to radiofrequency radiation 16 p2776 N85-27134
Geothermal hydrogen and health in Rotorua, New Zealand
[DE85-901283] 19 p3301 N85-30467
USSR report: Life sciences. Biomedical and behavioral sciences
[JPRS-UBB-85-017] 20 p3504 N85-31785
Using the information of cosmic rays to predict influence epidemic
[SH-10.1-2] 23 p4053 N85-35134

EPINEPHRINE
NT NOREPINEPHRINE
Distinctive morphological manifestations of acute stress reaction in adrenal cortex of hypokinetic rats
12 p1902 N85-21944
Studies of circulatory and metabolic changes during ketamine narcosis
[AD-A154512] 21 p3663 N85-32756

EPITAXY
NT ELECTROEPITAXY
NT LIQUID PHASE EPITAXY
NT MOLECULAR BEAM EPITAXY
NT VAPOR PHASE EPITAXY
Photoluminescent properties of epitaxial p-GaSb
02 p0257 N85-11745
Laser diodes for infrared spectroscopy
[BMFT-FB-T-84-131] 05 p0640 N85-14109
Efficiency estimation and sensitivity modeling
06 p0829 N85-15263
Formation of amorphous layers in Al2O3 by ion implantation
[DE85-001269] 09 p1397 N85-18794
Ion beam processes in Si
[DE85-001254] 09 p1399 N85-18808
Use of alternative solvents for low-temperature LPE growth of CdTe films
[AD-A149418] 10 p1562 N85-19853
Low stress semiconductor-insulator interface for cryogenic device applications
[NASA-CASE-NPO-16394-1] 11 p1734 N85-20906
Method for the fabrication of dielectric isolated junction field effect transistor and PNP transistor
[AD-D011500] 12 p1832 N85-21494
Method for the preparation of epitaxial films of mercury cadmium telluride
[AD-D011532] 12 p1938 N85-22175
Enhanced diffusion from interstitial trapping during solid-phase-epitaxial growth of silicon alloys
[DE85-001285] 12 p1941 N85-22193
Technology of thin silicon foils for the fabrication of monolithic integrated sensors
[BMFT-FB-T-84-209] 12 p1943 N85-22202
Clustering and ordering in 3-5 alloys
[AD-A150604] 13 p2022 N85-22870
Raman scattering of light in epitaxial films of solid phosphide-gallium arsenide solutions
15 p2643 N85-26301
Experimental method for measuring positronium reflection from surfaces
[DE85-010949] 20 p3531 N85-31967
Microwave semiconductor research: Materials, devices and circuits and gallium arsenide ballistic electron transistors
[AD-A154666] 21 p3709 N85-33024
Modulation doped GaAs/Al(x)Ga(1-x)As layered structures with applications to field effect transistors
[AD-A155360] 22 p3759 N85-33296
Process for improving the quality of epitaxial silicon films grown on insulating substrates
[AD-D011730] 22 p3847 N85-33828

EPITHELIUM
Preparative electrophoresis of cultured human cells: Effect of cell cycle phase 20 p3500 N85-31758
A critical synopsis: Continuous growth of proximal tubular kidney epithelial cells in hormone-supplemented serum-free medium 20 p3501 N85-31767
Mammalian tissue sensitivity to long-term exposure to high-intensity stationary magnetic fields
22 p3823 N85-33666

EPNL
U EFFECTIVE PERCEIVED NOISE LEVELS

EPOCHS
U TIME MEASUREMENT

EPOXIDES
U EPOXY COMPOUNDS

EPOXY COMPOUNDS
NT ETHYLENE OXIDE
Laboratory investigation on adhesives for Naval facilities construction
[AD-A147453] 07 p0932 N85-15809
Preliminary evaluation of an improved flammability test method for aircraft materials
[FAA-CT-84-22] 08 p1080 N85-16840
Rubber-modified epoxies. Part 2: Morphology, transitions, and mechanical properties
[AD-A147962] 08 p1132 N85-17137
Study of reaction kinetics and development of elastic properties in network polymerization systems by the impulse technique
[AD-A148187] 08 p1133 N85-17141
Crystallization behavior of poly(3,3-bis(Ethoxymethyl) oxetane) and poly(3,3-bis(Azidomethyl) oxetane)
[AD-A148271] 08 p1226 N85-17720
Evaluation of Epoxo 300-C nonskid coating for use on bridge decks
[PB85-108843] 12 p1819 N85-21412
Ten year environmental test of glass fiber/epoxy pressure vessels
[NASA-TM-87058] 19 p3231 N85-30034
Impact fracture mechanism of polymer plates containing a heavy inner material 23 p3905 N85-34215
Molecular biology of environmental aromatic hydrocarbons
[DE85-015036] 24 p4126 N85-35583

EPOXY MATRIX COMPOSITES
Investigating compression failure mechanisms in composite laminates with a transparent fiberglass-epoxy birefringent materials
[NASA-TM-86306] 02 p0170 N85-11137
Development of failure criterion for Kevlar-epoxy fabric laminates
[NASA-CR-172465] 02 p0170 N85-11138
The silane interphase of composites: Effects of process conditions on gamma-aminopropyltriethoxysilane
[AD-A145578] 02 p0171 N85-11143
Influence of test method and material stiffness on the damage produced by low velocity impacts on carbon-epoxy composites No. 45.387/1
[REPT-45.387/1] 03 p0326 N85-12100
Tough Composite Materials
[NASA-CP-2334] 04 p0463 N85-12941
Effects of constituent properties on compression failure mechanisms 04 p0464 N85-12948
Composite property dependence on the fiber, matrix, and the interphase 04 p0465 N85-12954
Variation of resin properties through the thickness of cured samples 04 p0468 N85-12974
Protective coverings for fiber reinforced epoxy composites
[PB84-231059] 04 p0480 N85-13063
Imide modified epoxy matrix resins
[NASA-CR-174695] 07 p0930 N85-15892
Ultrasonic analysis of spherical composite test specimens
[DE85-001591] 07 p0978 N85-16197
Fracture mechanics analysis and prediction of delamination growth in composite structures
[FFA-TN-1984-45] 09 p1289 N85-18092
Comparison of methods for predicting fiber stresses in a cracked Kevlar/epoxy monolayer
[DE84-016118] 11 p1583 N85-20022
Ultrasonic characterization of advanced composite flywheels
[DE85-000158] 11 p1593 N85-20026
Preliminary review of statistical treatment of S-glass/epoxy stress rupture data
[AD-A140810] 12 p1797 N85-21275
Directional dependent engineering properties of aluminum-aramid-epoxy laminates
[CCMS-85-02] 13 p2015 N85-22838
Development of a field repair technique for mini-sandwich Kevlar/epoxy aircraft skin
[AD-A151399] 15 p2503 N85-25439
Improved materials for composites and adhesive joints
[AD-A154918] 21 p3661 N85-32152

Improved materials for composite and adhesive joints
[AD-A155085] 21 p3562 N85-32153

EPOXY RESINS

Infrared spectroscopy study of the SP-250 epoxy resin system
[AD-A145860] 03 p0337 N85-12167
Investigation of toughened neat resins and their relations to advanced composite mechanical properties
04 p0464 N85-12949
The effect of cross-link density on the toughening mechanism of elastomer-modified epoxies
04 p0465 N85-12951
The chemical nature of the fiber/resin interface in composite materials 04 p0465 N85-12953
Modified epoxy composites 04 p0466 N85-12957
Variation of resin properties through the thickness of cured samples 04 p0468 N85-12974
Toughening mechanism in elastomer-modified epoxy resins, part 2
[NASA-CR-3852] 04 p0478 N85-13046
Investigation of the relations between neat resin and advanced composite mechanical properties. Volume 1: Results
[NASA-CR-172303] 05 p0612 N85-13911
Parametric study of the P9 HT glass fiber finish (Fatigue resistance). Lot no. 1: Report on the microfatigue tests
[CS-794] 05 p0620 N85-13968
Investigation of the relations between resin and advanced composite mechanical properties. Volume 2: Appendices
[NASA-CR-172303-VOL-2] 06 p0763 N85-14880
Imide modified epoxy matrix resins
[NASA-CR-174895] 07 p0930 N85-15892
Rubber-modified epoxies. 1: Cure, transitions, and morphology
[AD-A147377] 07 p0932 N85-15908
All-composite Airbus empennage
07 p0936 N85-15931
Monitoring cure of epoxy resins using a microdielectrometer
[AD-A148618] 08 p1119 N85-17054
Adhesive joint formation under field conditions
[AD-D011478] 10 p1453 N85-19153
Characterization of the network structure of a hardened epoxy resin (TGMDA/DDS system)
[ONERA-RT-3/3346-M] 11 p1613 N85-20140
Rubber modified epoxy adhesive
[AD-D011527] 12 p1810 N85-21354
SRM filament wound case resin characterization studies 12 p1944 N85-22212
Theoretical and experimental investigation of mechanically fastened composites
[AD-A150961] 14 p2248 N85-23935
Chemical interpretation of the relaxed permittivity during epoxy resin cure
[AD-A150855] 14 p2260 N85-24005
Compressive strength of epoxy resin chocks subjected to elevated temperatures
[AD-A152018] 15 p2519 N85-25532
Experimental study of the effect of moist environments on epoxy resin chocks
[AD-A152052] 15 p2568 N85-25649
Characterization-curing-property studies of HBRF 55A resin formulations
[NASA-CR-175838] 16 p2753 N85-26980
Evaluation of experimental epoxy monomers
[NASA-TM-87476] 16 p2754 N85-26996
New polymers for composites: A summary of research on polystyrylpyridines
[NASA-CR-175886] 17 p2933 N85-28106
Flight-service program for advanced composite rudders on transport aircraft
[NASA-CR-174537] 19 p3217 N85-29950
Development of fracture mechanics maps for composite materials, volume 1
[ESA-CR(P)-2017-VOL-1] 20 p3471 N85-31573
Development of fracture mechanics maps for composite materials, volume 2
[ESA-CR(P)-2017-VOL-2] 20 p3471 N85-31574
Development of fracture mechanics maps for composite materials. Volume 3: Appendices A-E
[ESA-CR(P)-2017-VOL-3] 20 p3472 N85-31575
Development of fracture mechanics maps for composite materials. Volume 4: Appendices F-K
[ESA-CR(P)-2017-VOL-4] 20 p3472 N85-31576
Improved materials for composite and adhesive joints
[AD-A155085] 21 p3562 N85-32153
The effect of mould size on the exothermic reaction and compressive strength of epoxy resin chocks
[AD-A155102] 21 p3570 N85-32203
Influence of cyclic thermal loading on internal stress in casted epoxy resin 23 p3908 N85-34211
Time and temperature dependence of fracture surface in soft epoxy resin 23 p3908 N85-34213
Study on fracture behavior of epoxy resin
23 p3909 N85-34216
Metal (2) 4,4',4',4'' phthalocyanine tetraamines as curing agents for epoxy resins
[NASA-CASE-ARC-11424-1] 23 p3919 N85-34281
Process for improving moisture resistance of epoxy resins by addition of chromium ions
[NASA-CASE-LAR-13226-1] 23 p3919 N85-34282

EQUALIZERS (CIRCUITS)

Adaptive signal processing for radio communications
10 p1473 N85-19295
Time and space domain filtering for improved HF communication 10 p1473 N85-19298

EQUATIONS

On the dependence of the convergence of Gummel's algorithm on the regularity of the solution
[AD-A154628] 21 p3675 N85-32832

EQUATIONS OF MOTION

NT EULER EQUATIONS OF MOTION
NT HELMHOLTZ VORTICITY EQUATION
NT HYDRODYNAMIC EQUATIONS
NT KINEMATIC EQUATIONS
NT KINETIC EQUATIONS
NT NAVIER-STOKES EQUATION
NT REYNOLDS EQUATION

Stable and chaotic dynamical systems and their singularities in the complex time plan
[DE84-011780] 01 p0035 N85-10222
K-shell yield scaling law for conventional PRS loads
[AD-A145155] 01 p0121 N85-10831
Control of lateral conjectory motion of spacecraft in atmosphere 02 p0160 N85-11085
Effect of the Basset term on particle relaxation behind normal shock waves
[AD-A145446] 02 p0196 N85-11320
Nonsteady motion of solid sphere in compressible viscous fluid 02 p0269 N85-11753
Propagation of longitudinal elastic waves in multilayered half-space 02 p0273 N85-11779
Numerical simulation of the subsonic wing-rock phenomenon 03 p0320 N85-12064
Damping synthesis for a spacecraft using substructure and component data
[CRC-1385] 03 p0323 N85-12082
A dynamical model for a towed linear sonar antenna
[REPT-6-84] 04 p0512 N85-13263
A numerical investigation of planetesimal collision trajectories with a Moon accumulating in Earth orbit
04 p0586 N85-13740
Laboratory electron beam simulation of cosmic radio jets
[DE84-016179] 04 p0590 N85-13764
Solving equations of movement with variable inertia moment
[BLL-M-35975-(5828.4)] 05 p0641 N85-14111
Saint Venant conditions in theory of piezoelastic shells
06 p0780 N85-14987
Motion of heavy symmetric body with flexible bars about stationary point 06 p0780 N85-14989
Analysis of the impact of a deformable missile model on a deformable obstruction
[BLL-RISLEY-TR-8534-(9091.9F)]
06 p0859 N85-15459
More than you want to know about maximum likelihood estimation
[NASA-TM-85905] 07 p0909 N85-15752
Bulk cavitation caused by a plane shock wave
[AD-A147031] 07 p0958 N85-16072
Optimum performance parameters for ski-jump operations of USAF fighter aircraft
[AD-A148532] 08 p1084 N85-16867
Acceleration of an electron ring in a modified betatron with transverse pressure
[AD-A148626] 08 p1221 N85-17688
On vortex transport in turbine channels
09 p1308 N85-18217
Parallel algorithms for robot dynamics
[DE84-016563] 09 p1369 N85-18605
A numerical approach for the vibration analysis of an axisymmetric shell structure with a nonuniform edge constraint
[AD-A149288] 11 p1651 N85-20402
Note of the dynamic behavior of a magnet system suspended by a thin fiber, with special reference to the Quartz Horizontal Magnetometer (QHM)
[DMI-GEOPHYS-PAPERS-R-70]
11 p1714 N85-20785
A Lagrange-D'Alembert formulation of the equations of motion of a helicopter carrying an externally suspended load
[NASA-TM-85864] 12 p1776 N85-21149
A 3-D treatment of convective flow in the Earth's mantle
[DE85-003734] 12 p1890 N85-21863
An analytic model for hydromagnetospheres --- stellar winds; pulsars; cosmic jets 12 p1959 N85-22313
Dynamics of solid body with ellipsoidal cavity containing magnetic fluid 14 p2279 N85-24116
Stability of permanent rotation modes of asymmetric heavy solid body 14 p2279 N85-24118
Stabilization of steady motion of mechanical systems
14 p2280 N85-24122
Quaternion algorithms of 3-dimensional inertial navigational systems 14 p2287 N85-24173
Motion of satellite with total dynamic symmetry around rotating aspherical Earth 14 p2287 N85-24174
Comets and nongravitational forces
14 p2437 N85-25038
The orbital motion of Comet Halley
14 p2437 N85-25040
A user's manual for AMEER flight path trajectory simulation code
[DE85-006580] 15 p2472 N85-25260
Vortex dynamics
[AD-A151278] 15 p2637 N85-26260
Optimum rotation of solid body with 1 axis of symmetry 16 p2718 N85-26781
Identification and control of structures in space
[NASA-CR-175790] 16 p2731 N85-26850
Effects of bearing deadbands on bearing loads and rotor stability 16 p2737 N85-26889
Use of quaternions in flight mechanics
[AD-A152616] 17 p2899 N85-27875
Incorporating control into the optimal structural design of large flexible space structures
[AD-A152958] 17 p2909 N85-27937
Stability in dynamical systems
[DE85-006698] 17 p3034 N85-28766
The role of thermal motions of air particles for fireballs
[PUBL-59] 17 p3053 N85-28900
Extraction of aerodynamic parameters for aircraft at extreme flight conditions
[NASA-TM-86730] 18 p3175 N85-29686
Application of Floquet theory to helicopter blade flapping stability
[AD-A154460] 19 p3218 N85-29952
Random vibration of nonlinear, parametrically excited systems 19 p3282 N85-30351
The initiation and growth of adiabatic shear bands
[AD-A154459] 19 p3287 N85-30382
Extended semiclassical calculations
[DE85-007824] 19 p3346 N85-30736
Robust adaptive control 20 p3417 N85-31207
Maximum likelihood estimation with emphasis on aircraft flight data 20 p3417 N85-31208
Transition in Turbines
[NASA-CP-2386] 20 p3452 N85-31433
Longitudinal tune control in synchrotrons
[DE85-010745] 20 p3527 N85-31937
Hadley circulation in planetary atmospheres
20 p3546 N85-32067
Optimal low thrust transfer using a first-order perturbation model
[AD-A154761] 21 p3676 N85-32835
Classical emission of relativistic charged particles during axial channeling 21 p3681 N85-32871
Theoretical foundations of turbulent flows
21 p3683 N85-32880
Equations of motion for electromagnetic waves in 4-dimensional Euclidian space 21 p3697 N85-32970
Space station rotational equations of motion
[NASA-TP-2511] 23 p3899 N85-34148
Optimisation in the computer aided design of mechanisms 23 p3924 N85-34321
Conjugated symmetrical coupler curves, produced by 4-bar linkages having the same transmission angles
23 p3924 N85-34322
Intermittent motion 23 p3925 N85-34323
The dynamics of articulated rigid bodies for purposes of animation 23 p3965 N85-34579
The model-independence of cosmic ray source determinations
[OG-7.2-1] 23 p4014 N85-34873
Identification and control of structures in space
[NASA-CR-176175] 24 p4069 N85-35214
The compliance of end effector force sensors for robot manipulator control 24 p4098 N85-35406
Time-dependent response of the climate to increasing atmospheric carbon dioxide 24 p4119 N85-35532

EQUATIONS OF STATE

NT HUGONIOT EQUATION OF STATE

Equation of state study for polar fluids
[PB84-222801] 01 p0025 N85-10157
Universal binding energy relations in metallic adhesion
[NASA-TM-86889] 03 p0331 N85-12132
On experimental equations of state for Bosen gases
[PTB-ME-61] 04 p0574 N85-13659
Research in nuclear astrophysics: Stellar collapse and supernovae
[DE84-015550] 05 p0743 N85-14776
A virial equation of state option for the TIGER computer program
[AD-A147490] 07 p1025 N85-16507

A research proposal for the theoretical study of the thermodynamic and transport properties of dense plasmas
[AD-A148040] 08 p1224 N85-17708
Experimental high pressure equation of state of a very fast burning gun propellant
[DE85-001749] 10 p1458 N85-19184
A Galerkin method for the estimation of parameters in hybrid systems governing the vibration of flexible beams with tip bodies
[NASA-CR-172537] 10 p1544 N85-19734
User's manual for GRIZZLY
[DE85-001405] 11 p1702 N85-20702
Wavecode constitutive models: Nonhomogeneous mixtures
[DE85-000836] 12 p1798 N85-21278
Simple EOS for the silicone rubber Sylgard 184
[DE85-001394] 12 p1814 N85-21376
Potential at atomic boundaries in the TF (or TFD) model and equations of states 12 p1820 N85-21419
Control of nonlinear objects 12 p1842 N85-21561
Synthesis of digital control for object with lag 12 p1843 N85-21562
H-division materials physics progress
[DE85-004990] 13 p2165 N85-23430
Cooling of neutron stars with hyperons
[DE85-004641] 13 p2171 N85-23472
Impact cratering calculation 13 p2180 N85-23531
Reaction of piezoceramic shell to concentrated forces 14 p2279 N85-24115
Steady state solution of the Fokker-Planck equation combined with unidirectional quasilinear diffusion under detailed balance conditions
[DE85-004917] 14 p2425 N85-24959
Ionization equilibrium and equation of state in the solar interior 14 p2445 N85-25088
The sensitivity of solar eigenfrequencies to the treatment of the equation of state 14 p2445 N85-25089
Measurement of material properties to Mbar pressures using time-resolved shock wave techniques
[DE85-007319] 15 p2558 N85-25780
Equations of state of strongly coupled plasma mixtures
[DE85-006163] 15 p2657 N85-26393
Equation of state and two-body correlations for fluids of non-spherical molecules
[AD-A151969] 16 p2783 N85-27174
Cluster production and entropy
[DE85-007628] 17 p3032 N85-28752
Equation of state for detonation products
[DE85-009006] 18 p3084 N85-29079
A state variable approach to transient creep deformation in stress reduction experiments
[DE85-009492] 18 p3122 N85-29331
State variable theories based on Hart's formulation
[DE85-009474] 19 p3239 N85-30082
Shear deflection in a three-point bend beam of a solid circular cross-section
[AD-A154458] 19 p3287 N85-30381
Pion production and the nuclear equation of state
[DE85-009941] 19 p3365 N85-30870
Decentralized control synthesis method for large-scale interconnected systems
[DE85-000748] 20 p3518 N85-31678
BLAF: A blast field reconstruction program from pressure histories
[AD-A155300] 21 p3586 N85-32283
Liquid-phase compositions from vapor-phase analyses 2: Adaptation of the Prausnitz program to UF6 and some of its potential impurities
[DE85-011521] 21 p3673 N85-32819
A system of magnetohydrodynamic-type equations 21 p3693 N85-32946
A new problem in mathematical physics associated with the problem of coherent phase transformation 21 p3698 N85-32976
KRAK: A computer program for two-phase two-component porous flow and fracture
[LA-9703] 22 p3782 N85-33434
Planetary fluids He and NH3 at high shock pressures and temperatures
[DE85-011851] 22 p3859 N85-33836
Comparison of experimental data on detonation velocity and Chapman-Jouget pressure vs initial HE density with predictions from Ree's model equation of state
[DE85-007266] 23 p3922 N85-34304
Detonation of condensed explosives: Evolution of knowledge in the last 40 years
[ISL-CO-228/84] 23 p3923 N85-34307
Shock and release equation of state of calcite
[DE85-013151] 23 p3942 N85-34432
Calculations of heavy ion charge state distributions for nonequilibrium conditions
[SH-2.1-12] 23 p3969 N85-34793
Equation of state study for polar fluids
[PB85-204345] 24 p4076 N85-35262
Experimental technique for measuring the isentrope of hydrogen to several megabars
[DE85-014332] 24 p4095 N85-35386

EQUATORIAL ATMOSPHERE
Equatorial energetic distributions of ions of terrestrial radiation belt as function of solar corona temperature response 02 p0160 N85-11087
Inference of equatorial field-line integrated electron density values using whistlers
[AD-A145822] 03 p0392 N85-12507
Ionospheric scintillation: A brief review 04 p0522 N85-13337
Behavior of the ionospheric F region in low latitudes and in the equatorial region of Brazil during strong magnetic storms in the 1978 to 1983 period
[INPE-3231-PRE/581] 05 p0675 N85-14333
Medium- and large-scale wave disturbances and heterogeneities of electron concentration in outer ionosphere in middle and low latitudes 06 p0825 N85-15241
Equatorial transionospheric propagation conditions affecting digital communications 10 p1470 N85-19275
Ionospheric research at INPE
[INPE-3279-PRE/602] 10 p1514 N85-19556
Middle Atmosphere Program. Handbook for MAP, volume 7
[NASA-CR-175479] 11 p1656 N85-20437
PMP-2 report: Equatorial wave dynamics 11 p1657 N85-20442
Meteor wind results from Atlanta, USA, and Ramey, Puerto Rico 11 p1662 N85-20474
Kinetic Rayleigh-Taylor instability theory in the ionosphere near equator 13 p2067 N85-22911
Ionspheric effects of seasonal and diurnal variations of electric fields in equatorial F-region 14 p2338 N85-24459
Investigating statistical characteristics of atmospheric background brightness and star background density in equatorial region of celestial sphere 15 p2478 N85-25298
Determining effective rate of plasma heating in outer equatorial ionosphere using data from ISIS-1 and ISIS-2 satellites 16 p2721 N85-26797
Dependence of equatorial F-region plasma bubble rise velocity and dynamo electric field on solar cycle
[INPE-3439-PRE/696] 16 p2826 N85-27434

EQUATORIAL ELECTROJET
Role of equatorial Electron Cyclotron Harmonic (ECH) waves in the generation of diffuse auroras. Contribution of the GEOS IMS spacecraft 14 p2367 N85-24832

EQUATORIAL ORBITS
NT STATIONARY ORBITS

EQUATORIAL REGIONS
The marine geochemistry of the rare earth elements
[AD-A145132] 01 p0068 N85-10598
Near infrared modeling of the equatorial regions of Jupiter and Saturn 09 p1415 N85-18930
Investigations of the Mars cratered terrain: Smooth plains boundary in the eastern equatorial region 13 p2191 N85-23598
The French Ocean Climate in Equatorial Atlantic (FOCAL) Drifter Program, 1983-1984 14 p2329 N85-24399
Applications of ARGOS measurements in equatorial Pacific Ocean-atmosphere interaction studies 14 p2331 N85-24414
A study of the generation mechanisms of high latitude and equatorial F-region irregularities using DE-2 data
[NASA-CR-175745] 16 p2825 N85-27423
Equatorial F-region irregularity latitudinal extension and dynamo electric field
[INPE-3494-PRE/731] 16 p2828 N85-27433
Thermal ion heating in the vicinity of the plasmapause
[NASA-CR-176030] 20 p3535 N85-31993
Equitorial scintillations: Advances since ISEA-6
[AD-A154962] 21 p3631 N85-32559

EQUATORS
NT MAGNETIC EQUATOR

EQUILIBRIUM
Thermodynamics of reactions of deoxidation of nickel melts
[BLL-M-35729-(5828.4)] 02 p0175 N85-11168
Exergetical analysis of turbojet engine cycle 13 p2049 N85-22825

EQUILIBRIUM DIAGRAMS
U PHASE DIAGRAMS

EQUILIBRIUM EQUATIONS
Radiation transport in the Earth atmosphere 04 p0522 N85-13341
Structural relaxation and isoconfigurational flow of a metallic glass near equilibrium
[AD-A147888] 07 p0933 N85-15915
Solar inverse theory 14 p2441 N85-25063
Computer-controlled carburizing
[BLL-OA-TRANS-3204-(6196.300)] 20 p3429 N85-31268
A new problem in mathematical physics associated with the problem of coherent phase transformation 21 p3698 N85-32976
Recombination and ionization in a nitrogen plasma
[AD-A155426] 22 p3845 N85-33813
Analysis of the nonlinear equations describing the elastic, thermal, and electromagnetic behavior of solids: Existence of solutions of semi-inverse problems 24 p4100 N85-35415

EQUILIBRIUM FLOW
NT FROZEN EQUILIBRIUM FLOW
Reducing numerical diffusion for incompressible flow calculations
[NASA-TM-83621] 06 p0756 N85-14840
Structural relaxation and isoconfigurational flow of a metallic glass near equilibrium
[AD-A147888] 07 p0933 N85-15915
Computer-Aided Structural Engineering (CASE) project. Seepage analysis of confined flow problems by the method of fragments (CFRAG)
[AD-A150015] 12 p1875 N85-21762
Time-dependent flow of stream swirled in vortex chamber 13 p2043 N85-22786
Interaction of cylindrical shell with concentrated mass moving along its inner surface 13 p2047 N85-22810
Elastohydrodynamic lubrication calculations used as a tool to study scuffing
[NASA-TM-87097] 23 p3938 N85-34408

EQUILIBRIUM METHODS
Modelling equilibrium and fractional crystallization in the system MgO-FeO-CaO-Al2O3-SiO2 13 p2184 N85-23552

EQUIPARTITION THEOREM
Equipartition threshold in nonlinear large Hamiltonian systems: The Fermi-Pasta-Ulam model
[NOTA-INTERNA-819] 02 p0255 N85-11670

EQUIPMENT
USSR report: Engineering and equipment
[JPRS-UEQ-85-001] 09 p1305 N85-18200
Plasma arc welding, equipment, installation and process control
[DE85-008481] 19 p3373 N85-30921
The CCIR satellite EPIRB coordinated trials programme — Emergency Position Indicating Radio Beacon (EPIRB); International Radio Consultative Committee (CCIR) 20 p3402 N85-31111
The International Radio Consultative Committee (CCIR) recommended satellite Emergency Position Indicating Radio Beacon (EPIRB) system operating through geostationary satellites at 1.6 GHz 20 p3402 N85-31112

EQUIPMENT SPECIFICATIONS
UCB cosmic ray experiment 09 p1417 N85-18941
The helicopter transmission design process 14 p2221 N85-23772
Manufacturing considerations related to aircraft gearboxes 14 p2222 N85-23778
Practical considerations when using water quality and structure monitoring sensors as applied to portable ARGOS satellite tranamitter equipment 14 p2330 N85-24405
Ariane launcher system. Pyrotechnics subsystem: Definition of chains and pyrotechnic components
[CNES-84/CT/DRT/SST/SE/242(1)] 20 p3398 N85-31081
Poseidon altimeter: Study of the hyperfrequency section and specifications of the prototype components
[CNES-84/DRT/TIT/HY/T/145] 20 p3419 N85-31219

EQUIPOTENTIALS
Plasma drift towards a plane equipotential surface
[TRITA-EPP-84-01] 02 p0285 N85-11660

EQUIVALENCE
Shear deformation plate continua of large double-layered space structures 01 p0059 N85-10391
A preliminary study of a cryogenic equivalence principle experiment on Shuttle
[NASA-CR-171300] 10 p1426 N85-18994
Fundamental equivalence of generalised state space systems
[MATHEMATICS-RESEARCH-182] 15 p2642 N85-26293
A trivariate version of Levy's equivalence
[AD-A153157] 17 p3025 N85-28705

EQUIVALENT CIRCUITS
Magnetic field calculation for ideal conductors by method of equivalent currents 06 p0788 N85-15035
An indirect measure of below-ground electric field, conductivity, and dielectric constant
[AD-A146518] 06 p0804 N85-15115

Battery response to pulse loads: A mathematical model
[DE86-001149] 09 p1316 N85-18277
Parameterization of a transient electromagnetic facility and test antennae from transient data
[DE85-006231] 15 p2545 N85-25710
Measurement methods for accurate microwave characterization and modeling of MESFET chips
[AD-A152360] 17 p2952 N85-28227
Magnetic field and equivalent circuit of induction motors with shielded poles 22 p3772 N85-33378

ERBE
U EARTH RADIATION BUDGET EXPERIMENT

ERBIUM
Spin dynamics of rare Earth ions in crystal fields probed by muon spin rotation
[DE84-013805] 02 p0278 N85-11810
Electron-oscillatory spectra of yttrium-erbium-aluminum garnet of crystals and their role in laser pumping 11 p1715 N85-20791
Contact properties of rare-earth silicides and germanides on Si and Ge 19 p3374 N85-30931

ERBIUM COMPOUNDS
Magnitude and range of the RKKy interaction in SmRh4B4
[DE85-012284] 23 p3985 N85-34712

ERECTION
U CONSTRUCTION

ERGODIC PROCESS
Omni transforms: Applications to renewal theory
[AD-A146939] 07 p1029 N85-16534
Conditionally heteroscedastic autoregressions
[AD-A147166] 07 p1035 N85-16567
A non-commutative quasi subadditive ergodic theorem
[AD-A146810] 07 p1037 N85-16581
On the ergodicity of bilinear time series models and some applications
[AD-A146032] 08 p1215 N85-17651
On ergodic actions whose self-joinings are graphs
[CWI-PM-R8408] 12 p1925 N85-22093
Ergodicity and Steady-State-Equilibrium conditions for Markov chains
[AD-A151038] 14 p2409 N85-24854
Sensitivity of the stationary distribution vector for an ergodic Markov chain
[DE85-008079] 16 p2857 N85-27621
Spectral transform approach to Backlund transformations
[PREPRINT-420] 18 p3172 N85-29663
Further results on the equipartition threshold in large nonlinear Hamiltonian systems
[PREPRINT-428] 18 p3173 N85-29668

ERGOMETERS
Comparison between cycle ergometers with different mechanical braking systems
[FOA-C-54058-H1] 07 p0975 N85-16193

ERGONOMICS
U HUMAN FACTORS ENGINEERING

EROSION
NT RAIN EROSION
NT SOIL EROSION
NT WATER EROSION
NT WIND EROSION
Simulation of contact surface erosion for impact problems 01 p0060 N85-10398
Erosion of sintered WC-Co alloys 02 p0179 N85-11201
Optical properties of laser erosion flares in plasma 02 p0270 N85-11764
Erosion of multiphase materials
[DE84-015816] 04 p0474 N85-13018
High-temperature erosion of plasma-sprayed, yttria-stabilized zirconia in a simulated turbine environment
[NASA-TP-2408] 04 p0478 N85-13045
Bridge erosion in electrical contacts 04 p0486 N85-13102
Back end valves: History and modifications
[DE84-009272] 05 p0646 N85-14145
Copper-nickel sheathing study, phase 2. Two-year service performance of test panels on the ARCO TEXAS
[PB84-242411] 06 p0775 N85-14952
Turbine blade test cascade modifications and orations, August 1982 - April 1983
[DE84-009266] 06 p0833 N85-15303
Proceedings of Workshop on Synergistic Effects in Surface Phenomena Related to Plasma-Wall Interactions
[IPPJ-AM-35] 06 p0864 N85-15486
Synergistic effects in fusion machines, session summary 06 p0864 N85-15489
Plasma surface interaction processes and possible synergisms 06 p0864 N85-15490
Synergisms in surface erosion, session summary 06 p0864 N85-15493
Synergism in materials erosion due to multispecies impact 06 p0864 N85-15494
Solar wind and cosmic ray irradiation of grains and ices - application to erosion and synthesis of organic compounds in the solar system 08 p0888 N85-15637
Arc erosion of metal in current interval of 1-10 amperes 07 p0953 N85-16042
Cavitation erosion resistant coatings for pumps
[PB85-120210/GAR] 09 p1300 N85-18167
Influence of turbulence on erosion by a particle-laden fluid jet
[DE84-014365] 09 p1320 N85-18301
Characterization of erosion of metallic materials under cavitation attack in a mineral oil
[NASA-TM-86934] 10 p1440 N85-19075
Study of surface damage in cathode composite materials in a high flux CO2 laser 10 p1444 N85-19098
Nautical charting with remotely sensed imagery, volume 1
[AD-A149361] 10 p1506 N85-19503
Nautical charting with remotely sensed imagery. Volume 2: Case studies
[AD-A149362] 10 p1506 N85-19504
California coastal erosion and storm damage during the winter 1982 - 1983, a reconnaissance report
[PB85-121705] 10 p1521 N85-19591
Effect of microstructure on solid particle erosion in multiphase materials
[DE85-000426] 11 p1608 N85-20109
Causes and means of prevention of erosion of exit edges of drive vanes in final stages of K-300-240 turbine 14 p2272 N85-24076
Brittle fracture resistance of electron beam-welded joints in titanium Alpha alloys 15 p2500 N85-25419
The influence of abrasive blast cleaning and corrosion inhibitors on protective paint coatings 15 p2517 N85-25522
Erosion of electrodes due to switching of capacitor-bank discharge circuits
[AD-A151207] 15 p2547 N85-25718
Self-sustaining low-Z coatings for fusion applications 2 - copper-lithium
[DE85-002553] 15 p2658 N85-26403
Erosion of multiphase materials
[DE85-006895] 18 p3068 N85-28978
Elevated temperature erosion corrosion of 9Cr1Mo steel
[DE85-008445] 18 p3074 N85-29016
Surface degradation of ductile metal in elevated temperature gas-particle streams
[DE85-008428] 18 p3074 N85-29017
Elevated temperature erosion of steels
[DE85-008503] 18 p3075 N85-29018
Corrosion-erosion rates/mechanisms of 9Cr1Mo steel
[DE85-008506] 18 p3076 N85-29029
The effect of temperature on the corrosion-erosion of 9Cr1Mo steel
[DE85-008507] 18 p3076 N85-29030
Long-Term Materials Test Program
[DE85-003248] 18 p3077 N85-29034
Cavitation erosion of plasma sprayed alloys
[DE85-000542] 18 p3077 N85-29036
A new theory aiming to define the mechanisms of material removal in electroerosion
[NASA-TM-77875] 18 p3176 N85-29689
Mechanical protection of DLC films on fused silica slides
[NASA-TM-87056] 19 p3248 N85-30138
Coastal erosion along Monterey Bay
[AD-A155810] 21 p3655 N85-32707
Operational window for a plasma erosion opening switch used for voltage multiplication on pulsed power generators
[AD-A155482] 21 p3707 N85-33020
Electrode erosion in arc discharges at atmospheric pressure
[NASA-TM-87087] 23 p3903 N85-34178
Influence of particle erosion on the microstructural changes in metals and alloys
[TI85-901364] 23 p3917 N85-34276

EROSIVE BURNING
Solid rocket motor certification to meet space shuttle requirements from challenge to achievement 08 p1096 N85-16941
Model of normal and erosive burning of composite propellants
[ONERA-NT-1984-3] 14 p2263 N85-24024

ERROR ANALYSIS
Diagnosis and therapy of geodetic satellite networks of Doppler type — error analysis
[SER-C-293] 01 p0015 N85-10090
An error analysis for the use of presently available lunar radio flux data in broadbeam antenna-system measurements
[PB84-218361] 01 p0016 N85-10097
Measurement assurance programs. Part 1: General introduction
[PB84-217868] 01 p0051 N85-10339
Performance of the h, p and h-p versions 01 p0058 N85-10383
The initialization of mesoscale models 01 p0079 N85-10529
A microcomputer aided measurement equipment for monitoring performance in digital radio relay systems
[FUB-4-1984] 01 p0101 N85-10668
Trajectory estimation using combined time-of-arrival and velocity measurements
[DE84-015872] 02 p0242 N85-11582
Boundary conditions in Chebyshev and Legendre methods
[NASA-CR-172469] 02 p0250 N85-11635
An asymptotic theory for logistic regression when some predictors are measured with error
[AD-A145673] 02 p0254 N85-11666
Unified approach to sensitivity and uncertainty analysis
[DE84-014049] 02 p0255 N85-11669
Minimization of anomalous errors in measuring systems employing search and testing devices 03 p0344 N85-12219
Diffusion of gases in porous solids: Simulation and measurements
[DE84-016292] 04 p0500 N85-13191
Time discretization of parabolic problems by the discontinuous Galerkin method
[CTH-MATH-1984-16] 04 p0556 N85-13543
TCAS 2 logic performance during phase one operational evaluation
[DOT/FAA/PM-84/20] 05 p0595 N85-13793
Submilliarcsecond VLBI using compact close pairs of radio sources: Error analysis 05 p0622 N85-13981
VLBI solutions for the time variation of DSN baselines: 1978 - 1983 05 p0623 N85-13983
Contributions to the error analysis in the relativity gyroscope experiment 05 p0638 N85-14095
The role of knowledge structures in fault diagnosis 05 p0703 N85-14509
Some error estimates for the p-version of the finite element method
[CTH-MATH-1984-21] 05 p0719 N85-14614
Use of least-squares method for estimating errors of turbine blade type parts during fabrication 06 p0776 N85-14983
NBS (National Bureau of Standards) and WR62 and WR90 reference noise standards
[PB84-235704] 07 p0942 N85-15977
Errors of analog of inertial coordinate systems modeled in astronavigation system 07 p0951 N85-16028
NBS (National Bureau of Standards) switching radiometers
[PB84-235894] 07 p0968 N85-16147
Modeling of human motion by computer considering measurement errors in initial data 07 p1012 N85-16429
A complete characterization of triply balanced matrices with applications to survey sampling
[AD-A147083] 07 p1031 N85-16542
Bayesian estimation of undetected errors
[AD-A147198] 07 p1031 N85-16545
Data stimulated on-line-checking (IROLD) 08 p1066 N85-16754
Altimetry, orbits and tides
[E85-10066] 08 p1174 N85-17404
Multimodels increase accuracy: Summary of an experiment — photogrammetry 08 p1175 N85-17409
A feedback finite element method with a posteriori error estimation. Part 1. The finite element method and some basic properties of the A posteriori error estimator
[AD-A148345] 08 p1212 N85-17631
Filter and passband problems 08 p1252 N85-17910
Cockpit resources management and the theory of the situation 09 p1276 N85-18022
Extrpolation in finite element analysis 09 p1331 N85-18365
An objective error measure for the comparison of calculated and measured transient response histories 09 p1335 N85-18395
A new method of approximating normal and t-tail areas
[AD-A149457] 10 p1548 N85-19761
Blunder detection using a sequential least squares adjustment
[AD-A149514] 10 p1548 N85-19765
On the application of compatibility checking techniques to dynamic flight test data
[ARL/AERO-R-161] 12 p1776 N85-21151
Estimating algorithmic error of digital recursive filters 12 p1839 N85-21543

Preliminary investigation into using the sun as a source for G/T (Gain to System Noise Temperature) measurements
[PB85-128148] 12 p1952 N85-22265
Expansion of functions describing planetary surface and gravity field 13 p1978 N85-22410
Analysis of systematic errors in systems of selenodetic coordinates 13 p1982 N85-22435
Noise tolerance of digital demodulator for complex signal system employing binary quantization 13 p2070 N85-22929
Influence of axial shaft load on operation of magnetoelastic torque transducer 14 p2270 N85-24065
Error analysis of heliostat alignment methods 14 p2281 N85-24128
Investigation of errors of acoustic goniometer information-measurement systems on rocking base 14 p2283 N85-24139
Geometric error analysis for shuttle imaging spectrometer experiment
[NASA-CR-175665] 14 p2305 N85-24269
Propagation of numerical errors in computers and numerical quality 14 p2396 N85-24760
Reliable computation with cellular automata
[AD-A150656] 14 p2399 N85-24790
Laser gyroscope random walk determination using a fast filtering technique 16 p2696 N85-26647
Simulation of a low orbit restitution. Covariance analysis of the position-velocity by Doppler and accelerometer measurements
[CNES-CT/DTI/MS/AE/166] 16 p2728 N85-26836
An evaluation of the performance of a new storm tracking methodology
[AD-A152234] 16 p2e35 N85-27484
Evaluation of a fault tolerant system for an integrated avionics sensor configuration with TSRV flight data
[NASA-CR-172589] 18 p3062 N85-28941
Accepting error to make less error
[AD-A153949] 18 p3171 N85-29651
Satellite measurements of atmospheric aerosols
[AD-A153607] 19 p3316 N85-30556
Evaluation of curve-smoothing techniques
[HSE-TRANS-11106] 19 p3349 N85-30759
Simulations of strapdown-system errors and error compensation methods — transport aircraft navigation
[DFVLR-MITT-84-22] 20 p3392 N85-31040
Using regression analysis for determining air data sensor errors by means of an inertial navigation system
[ESA-TT-886] 20 p3392 N85-31041
Search and rescue satellite (SARSAT) error analysis of the 406 MHz system 20 p3403 N85-31118
Numerical experimentation with maximum likelihood identification in static distributed systems 20 p3418 N85-31214
Comparative analysis of laboratory and fullscale experimental data for metal flow displacements and speeds
[BLL-M-36266-(5828.4)] 20 p3430 N85-31276
Influence of error of determination of moire isotach orders on the stability of their approximation
[BLL-M-36277-(5828.4)] 20 p3450 N85-31423
Error spectrum of Goddard satellite models for the gravity field 20 p3491 N85-31704
Spaceborne gradiometer error analysis 20 p3492 N85-31707
TOPEX error budget 20 p3493 N85-31717
Performance and evaluation of real-time multicomputer control systems
[NASA-CR-176098] 21 p3673 N85-32821
Introduction to adaptive techniques for voice signal processing
[FUB-52-1983] 22 p3756 N85-33267
Design of inductive shift transducers 22 p3771 N85-33368
Error evaluation in measurements with thermoluminescent dosimeters
[ISS-T-84/6] 22 p3788 N85-33471
Implications of cross section errors for cosmic ray propagation
[OG-7.2-3] 23 p4014 N85-34875
Gravity gradiometer survey data processing
[AD-A156165] 24 p4117 N85-35522
A comparison between Falcon data and motor glider data 24 p4121 N85-35547
Accuracy and error analysis — airborne instruments 24 p4123 N85-35557
Study of fault tolerant software technology for dynamic systems
[NASA-CR-172618] 24 p4137 N85-35642
Specifying and verifying concurrent programs
[AD-A156190] 24 p4138 N85-35652

ERROR BAND
U ACCURACY

ERROR CORRECTING CODES
Throughput increase in frequency hopped multiple access channels by means of discrimination against partially overlapping interference
[AD-A145540] 02 p0191 N85-11275
Linear intersecting codes — error correction
[ENST-C-84002] 03 p0356 N85-12291
Simplified continued fraction calculation of spherical Bessel functions
[AD-A146644] 06 p0858 N85-15455
The algebraic structure of convolutional codes with application to code construction and decoding
[AD-A148770] 08 p1206 N85-17591
On the binary weight distribution of some Reed-Solomon codes
[NASA-CR-174375] 09 p1373 N85-18628
Error correction coding for a self-adaptive modem: Theoretical and experimental results 10 p1474 N85-19303
Processing circuit with asymmetry corrector and convolutional encoder for digital data
[NASA-CASE-MSC-20187-1] 11 p1628 N85-20249
Reed-Solomon decoder — applicable to Galileo Project requirements
[NASA-CASE-NPO-15982-1] 11 p1699 N85-20680
Redundancy of codes for detection and correction of unidirectional errors 12 p1842 N85-21557
A concatenated coding scheme for error control
[NASA-CR-175504] 12 p1912 N85-22001
A concatenated coding scheme for error control
[NASA-CR-176006] 19 p3334 N85-30655
Error-correcting codes for computer memories 24 p4136 N85-35636
Pruned error-trellis decoding of certain non-systematic convolutional codes
[AD-A156122] 24 p4138 N85-35650

ERROR CORRECTING DEVICES
DISCUS multiprocessor enhancements — Distributed Control Microprocessor System (DISCUS)
[RSRE-MEMO-3591] 02 p0239 N85-11554
Methods of digital correction for channels of multichannel radar receivers 13 p2082 N85-23005
Decomposition in problem of correcting inertial navigation systems 14 p2287 N85-24172
SC filters and design centering of integrated circuits. Part 2: Design centering of integrated circuits
[BMFT-FB-T-84-265-PT-2] 17 p2956 N85-28257
Development and evaluation of a Fault-Tolerant Multiprocessor (FTMP) computer. Volume 3: FTMP test and evaluation
[NASA-CR-166073] 19 p3341 N85-30707
Satellite links in the ISO architecture: Models and performance evaluation
[ENST-84E017] 22 p3756 N85-33284
High-speed adaptation algorithm for harmonic corrector 22 p3765 N85-33336

ERROR DETECTION CODES
Analysis of the impact of error detection on computer performance
[NASA-CR-174167] 04 p0547 N85-13477
The undetected error probability for shortened hamming codes
[NASA-CR-174175] 04 p0555 N85-13535
Automatic error detection and recovery techniques in onboard intelligent units for space and avionic application 08 p1066 N85-16756
Meta-level control through fault detection and diagnosis
[AD-A149084] 10 p1540 N85-19709
Ada compiler validation summary report, Dansk Datamatik Center, VAX 11 compiler version 1.1
[AD-A149340] 11 p1699 N85-20681
The 20:16 block code for digital recording and transmission channels
[BBC-RD-1985/1] 12 p1824 N85-21443
Redundancy of codes for detection and correction of unidirectional errors 12 p1842 N85-21557
A concatenated coding scheme for error control
[NASA-CR-175504] 12 p1912 N85-22001
Error probability during optimal noncoherent reception of binary signals in multibeam channel 13 p2069 N85-22922
Experimental development of a failure detection scheme for large space structures 14 p2234 N85-23646
Care 3 model overview and user's guide, first revision
[NASA-TM-86404] 15 p2627 N85-26192
Development and evaluation of a Fault-Tolerant Multiprocessor (FTMP) computer. Volume 3: FTMP test and evaluation
[NASA-CR-166073] 19 p3341 N85-30707
Synthesis of tests for programmable logic arrays 22 p3777 N85-33406
Detection of and search for faults in programmable logic arrays 22 p3778 N85-33409
Study of fault tolerant software technology for dynamic systems
[NASA-CR-172618] 24 p4137 N85-35642
AUTOSIM: An automated repetitive software testing tool
[NASA-CR-177930] 24 p4137 N85-35643
Pruned error-trellis decoding of certain non-systematic convolutional codes
[AD-A156122] 24 p4138 N85-35650
Design of a microprogram control unit with concurrent error detection
[AD-A156447] 24 p4139 N85-35655

ERROR FUNCTIONS
The undetected error probability for shortened hamming codes
[NASA-CR-174175] 04 p0555 N85-13535
The method of residual minimization in compressible steady flows
[AD-A153924] 18 p3100 N85-29193

ERROR SIGNALS
Comparator with noise suppression
[NASA-CASE-LAR-13151-1] 11 p1627 N85-20247
Reception of signal with unknown amplitude and duration submerged in white noise 13 p2084 N85-23016
An error generator to support the trials of the ZODIAC prototype system — raster links
[PHL-1984-71] 14 p2293 N85-24216
Ziv-Zakai bound applied to an amplitude-comparison monopulse radar
[AD-A151937] 16 p2773 N85-27118
LANDSAT-4/5 image data quality analysis
[E85-10105] 24 p4107 N85-35463

ERRORS
NT BORESIGHT ERROR
NT INSTRUMENT ERRORS
NT PHASE ERROR
NT PILOT ERROR
NT POSITION ERRORS
NT RANDOM ERRORS
NT ROOT-MEAN-SQUARE ERRORS
NT TRUNCATION ERRORS
Metrological consequences of the hard optical boundary assumption
[PB84-229577] 01 p0121 N85-10827
EDS round-robin evaluation of type 308 austenitic stainless steel
[DE84-014574] 02 p0183 N85-11226
Eyelid motion sequences predictive of decision errors
[AD-A145702] 02 p0235 N85-11531
An asymptotic theory for logistic regression when some predictors are measured with error
[AD-A145673] 02 p0254 N85-11686
Accounting for error stochasticity in terminal homing of aircraft 04 p0489 N85-13115
Comparability and accuracy of industry codes in different data systems
[PB84-215607] 04 p0548 N85-13482
Treatment and expression of measurement uncertainties 05 p0630 N85-14042
Mean and random errors of visual roll rate perception from central and peripheral visual displays 05 p0704 N85-14519
Types of tracking errors induced by concurrent secondary manual task 05 p0711 N85-14561
Approximating true radioluminance distribution from observations on aperture synthesis systems 06 p0783 N85-15003
Indirect estimation of convective boundary layer structure for use in routine dispersion models
[PB84-236260] 06 p0834 N85-15309
Error analysis of wind determined using a VLF Omega sonde
[WSRL-0361-TM] 06 p0836 N85-15321
Computer science and technology: Overview of computer security certification and accreditation
[PB84-217619] 06 p0848 N85-15384
Array sidelobes, error tolerance, gain, and beamwidth
[AD-A147004] 07 p0940 N85-15956
High accuracy Doppler navigation employing optimum integrated position fix information 08 p1073 N85-16803
Error and uncertainty — metrology
[NPL-DPMA-2] 08 p1137 N85-17181
A moving finite element method for time dependent partial differential equations with error estimation and refinement
[AD-A147719] 08 p1210 N85-17617
A note on the prediction error for small time lags into the future
[AD-A148221] 08 p1215 N85-17654
The atmospheric extinction problem 08 p1251 N85-17901
Gain instabilities in photomultipliers: How accurate are photon counting measurements? 08 p1251 N85-17903

CCDs: Their cause and cure
09 p1252 N85-17905
Automatic land vehicle navigation using road map data
[DE84-017178] 09 p1278 N85-18043
Sampling errors. They may deprive the analytical results of any meaning
[BLL-MINTEK-TR-1169-(5810.5759)] 09 p1373 N85-18625
Fixed vs. variable order Runge-Kutta
[DE85-001320] 09 p1374 N85-18639
Analysis of a visual performance experiment
[DE85-000710] 10 p1530 N85-19845
Rejection of anomalous observations when determining spacecraft trajectories 13 p1979 N85-22421
Analysis of systematic errors in systems of selenodetic coordinates 13 p1982 N85-22435
A Monte Carlo sampling plan for estimating network reliability
[AD-A150511] 13 p2065 N85-22898
Noise tolerance of diversity reception in frequency-adaptive digital transmission systems
13 p2086 N85-23024
Investigation of influence of communications link and synchronization error on noise tolerance of group transmission of binary information based on orthogonal Walsh function 13 p2086 N85-23026
Runge-Kutta formula with cheap error estimate
[DE85-005674] 13 p2152 N85-23363
Scheme for measuring specular reflection coefficient at 10.6 microns wavelength with zigzag-path cell and integrating sphere 14 p2275 N85-24097
Propagation of numerical errors in computers and numerical quality 14 p2306 N85-24760
Reliable computation with cellular automata
[AD-A150656] 14 p2399 N85-24790
Spline techniques for magnetic fields
[DE85-004919] 14 p2415 N85-24902
Astrometric plates obtained at the primary focus of large aperture reflectors 14 p2436 N85-25022
Problems and procedures of cometary astrometry
14 p2436 N85-25024
Implications of observed frequencies of solar P modes
14 p2443 N85-25073
Evaluating identifiability in remote sensing problems
15 p2486 N85-25347
The effect of inaccuracies in structural models on the control of large space structures
[AD-A151794] 16 p2732 N85-26858
Estimates of errors of a gyroscope stabilized platform
16 p2763 N85-27050
Radial orbit error spectrum for Topex
16 p2805 N85-27292
Synthetic aperture side-looking radar image adjustment 16 p2808 N85-27304
Error reduction program --- combustor performance evaluation codes
[NASA-CR-174776] 16 p2852 N85-27584
Inherent magnetic field error measurements in ELMO Bumpy Torus
[DE85-005855] 16 p2867 N85-27685
Spectral decomposition and verification of NOGAPS 500MB medium-range forecasts
[AD-A152550] 17 p2996 N85-28520
A high-accuracy optical linear algebra processor for finite element applications
[NASA-CR-175894] 17 p3017 N85-28658
Effects of inspection errors on curtailed Dorfman-type procedures
[AD-A152376] 17 p3024 N85-28699
Statistical effects of imperfect inspection sampling. Part 2: Double sampling, link sampling and grading
[AD-A152377] 17 p3024 N85-28700
A factored implicit scheme for numerical weather prediction with small factorization error
18 p3141 N85-29447
Error growth in operational 10-day forecasts
18 p3143 N85-29460
A constant altitude flight survey method for mapping atmospheric ambient pressures and systematic radar errors
[NASA-TM-86733] 19 p3217 N85-29951
The effect of sensor and actuator errors on static shape control for large space structures
[NASA-TM-86446] 19 p3225 N85-29998
Inherent angular tracking error in an amplitude comparison monopulse radar
[AD-A154212] 19 p3255 N85-30185
Filter induced errors in laser anemometer measurements using counter processors
[NASA-TM-87047] 19 p3272 N85-30288
Development and evaluation of a fault-tolerant multiprocessor (FTMP) computer. Volume 1: FTMP principles of operation
[NASA-CR-166071] 19 p3341 N85-30705
Wideband disturbance accomodation in precision flexible space structures 20 p3415 N85-31194
A comparison of millimeter wave, direct detect and heterodyne laser intersatellite links
[AD-A151964] 20 p3461 N85-31496
Errors and parameterizations of sub-grid scale processes in regional-scale atmospheric models
20 p3488 N85-31682
Hubble space telescope: Pointing error effects on nonlinear ball joints
[NASA-TM-86511] 20 p3545 N85-32058
In-situ measurement of wall thermal performance: Data interpretation and apparatus design recommendations
[DE85-011979] 21 p3586 N85-32289
Comparison of survey and photogrammetry methods to position gravity data, Yucca Mountain, Nevada
[DE85-011685] 21 p3590 N85-32316
Art of programming programmable microcalculators, part 4: errors of calculations 22 p3778 N85-33411
Search of the VAXintosh customizing VMS V4.0 for DCL windows
[DE85-011306] 22 p3831 N85-33729
Assessment of magnetic field asymmetries in ELMO Bumpy square
[DE85-011905] 22 p3846 N85-33819
Nonsimultaneous coupled laser velocimeter measurement technique: Error prediction for spatially noncoincident measurements
[NASA-TM-86718] 23 p3934 N85-34379
Comparative analysis of operational forecasts versus actual weather conditions in airline flight planning, volume 4
[NASA-CR-167865] 24 p4120 N85-35537
Comparative analysis of operational forecasts versus actual weather conditions in airline flight planning: Summary report
[NASA-CR-167866] 24 p4120 N85-35538
Error message recording and reporting in the SLC control system
[DE85-013057] 24 p4140 N85-35664
Multidimensional analysis of data obtained in experiments with X-ray emulsion chambers and extensive air showers
[HE-3.6-2] 24 p4184 N85-35951

ERS-1 (ESA SATELLITE)
ERS-1 radar altimeter data products --- conferences
[ESA-SP-221] 03 p0379 N85-12419
The ESA remote sensing satellite system (ERS-1)
03 p0379 N85-12420
The ERS-1 radar altimeter: An overview
03 p0379 N85-12421
The ERS-1 radar altimeter instrument
03 p0379 N85-12422
The current formal status of the ERS-1 ground segment 03 p0380 N85-12423
Tracking requirements for precise ERS-1 orbit determination 03 p0380 N85-12431
Determination of geoid undulations and ocean heights from ERS-1 radar altimetry data
03 p0381 N85-12432
Factors affecting the archiving, processing and dissemination of ERS-1 altimeter data
03 p0381 N85-12435
ERS-1 altimeter ground segment relations to other sensors and programs 03 p0381 N85-12436
Impact of ERS-1 observations on wave forecasting in the North Sea 03 p0381 N85-12437
SEASAT altimeter data over the Mediterranean: Implications for ERS-1 03 p0382 N85-12443
The Precise Range and Range Rate Equipment (PRARE) and its possible support to the radar altimeter measurement for ERS-1 03 p0382 N85-12445
Determination of the altimetric geoid and gravity anomalies in the North Sea: Implications for a solution of the general circulation problem using ERS-1 data
03 p0382 N85-12446
Ice sheets as invariant surfaces for radar altimeter calibration and orbit determination
03 p0383 N85-12449
ERS-1 radar altimeter system performance evaluation and calibration 03 p0383 N85-12451
Simulation of information extraction from radar altimeter return echoes --- ERS-1 (ESA satellite)
03 p0383 N85-12452
Lessons from the SEASAT and GEOS-3 altimeters data projects 03 p0384 N85-12457
Technology for the ERS-1 SAR antenna
05 p0626 N85-14008
ERS-1 and its potential for industrial utilization
05 p0659 N85-14235
Dissemination of ERS-1 low bit rate data and the use of L-band receiving stations
[NLR-TR-83049-U] 09 p1358 N85-18542
Quantization study for ERS-1 wave mode
[DFVLR-FB-84-39] 11 p1625 N85-20234
The ESA remote sensing satellite system (ERS-1)
11 p1713 N85-20777
Bonded stripline power splitter for ERS-1
[RML-009-84-124] 15 p2550 N85-25740
Comparison of ERS-1 scatterometer Monte Carlo performance simulations using a weighted nonlinear least squares and a maximum likelihood estimation method
20 p3420 N85-31224
AMI calibration study. Volume 1: SAR calibration. Volume 2: Ground Targets. Volume 3: Scatterometer calibration --- Active Microwave Instrument (AMI) ERS-1
[C2248/4/4-VOL-1] 23 p3936 N85-34394

ERTS
U LANDSAT SATELLITES

ERTS-A
U LANDSAT 1

ERTS-D
U LANDSAT 4

ERYTHROCYTES
Hemopoiesis in rats submitted to weightlessness
01 p0091 N85-10613
Functional and structural changes in human erythrocyte surface after irradiation by UV waves of various wavelengths. Report 1: Expression of ABO and Rhesus system antigen 09 p1361 N85-18564
Functional and structural changes in human erythrocyte surface after irradiation by UV waves of various wavelentghts. Report 2: Adsorption of alcyan blue by external premembranous components
09 p1361 N85-18565
The effect of inert gases on ion transport across the erythrocyte membrane
[AD-A148889] 10 p1527 N85-19635
A detailed analysis of the erythropoietic control system in the human, squirrel, monkey, rat and mouse
[NASA-CR-171879] 15 p2614 N85-26107
Research opportunities in loss of red blood cell mass in space flight
[NASA-CR-175808] 16 p2841 N85-27517
Threshold effects and cellular recognition
[DE85-010816] 19 p3327 N85-30614
Electrophoretic mobilities of erythrocytes in various buffers 20 p3500 N85-31756
Evaluation of results of cell electrophoresis experiments on space shuttle STS-3 including pre-flight and post-flight laboratory experiments 20 p3502 N85-31772
Free zone electrophoresis simulation of static column electrophoresis in microgravity on shuttle flight STS-3
20 p3502 N85-31773
Microgravity electrophoresis: A study of the factors that affect free-fluid separation 20 p3502 N85-31774
Pre-flight report on cultured human embryonic kidney cell handling and cell electrophoresis. Prepared prior to continuous-flow electrophoretic separation experiments aboard space shuttle flight STS-8
20 p3503 N85-31775
A systems analysis of the erythropoietic responses to weightlessness. Volume 1: Mathematical model simulations of the erythropoietic responses to weightlessness
[NASA-CR-171890] 20 p3506 N85-31794
A systems analysis of the erythropoietic responses to weightlessness. Volume 2: Description of the model of erythropoiesis regulation. Part A: Model for regulation of erythropoiesis. Part B: Detailed description of the model for regulation of erythropoiesis
[NASA-CR-171891] 20 p3506 N85-31795
Spacelab 1 hematology experiment (INS103): Influence of space flight on erythrokinetics in man
[NASA-TM-58268] 22 p3824 N85-33693

ESA
U EUROPEAN SPACE AGENCY

ESA SATELLITES
NT COS-B SATELLITE
NT ERS-1 (ESA SATELLITE)
NT EUROPEAN COMMUNICATIONS SATELLITE
NT EXOSAT SATELLITE
NT GEOS SATELLITES (ESA)
NT HEOS B SATELLITE
NT L-SAT
NT METEOSAT SATELLITE
NT OTS (ESA)

ESA SPACECRAFT
NT COS-B SATELLITE
NT GIOTTO MISSION
NT L-SAT
NT METEOSAT SATELLITE
NT OTS (ESA)

ESAKI DIODES
U TUNNEL DIODES

ESCAPE (ABANDONMENT)
Study of several factors affecting crew escape trajectories from the Space Shuttle Orbiter at low-subsonic speeds
[NASA-TM-86303] 10 p1428 N85-19008

ESCAPE SYSTEMS
Aeronautical systems technology needs: Escape, rescue and survival, test facilities and test equipment and training-simulation equipment
[AD-A145059] 01 p0001 N85-10002
MC2969 escapement study
[DE84-014542] 05 p0645 N85-14143
A Generalized Escape System Simulation (GESS) computer program. Volume 2: GESS programmer's manual, version 2
[AD-A148363] 06 p1081 N85-16845
Personnel protection concepts for advance escape system design 10 p1532 N85-19858
Chemical and photographic evaluation of rigid explosive transfer lines
[AD-A149303] 11 p1613 N85-20145
Approach for service life extension of explosive devices for aircraft escape systems
[NASA-TM-86323] 13 p1971 N85-22381
Preliminary design of a limb restraint evaluator
[AD-A151749] 15 p2466 N85-25226
Generalized escape system simulation: Its purpose, recent modifications and potential
[DE85-005571] 16 p2703 N85-26689
Design and testing of an energy-absorbing crewseat for the F/FB-111 aircraft, volume 1
[NASA-CR-3916] 23 p3896 N85-34133
Design and testing of an energy-absorbing crewseat for the F/FB-111 aircraft. Volume 2: Data from seat testing
[NASA-CR-3917] 24 p4064 N85-35184
ESCARPMENTS
Lithologic and structural control on slope morphology in the Valles Marineris 13 p2201 N85-23651
ESCHERICHIA
Toxicity, mutagenesis and aging due to endogenous oxygen radicals
[AD-A150121] 12 p1900 N85-21928
Structural-functional changes in bacterial cells under spaceflight conditions 16 p2724 N85-26812
ESG (GYROSCOPES)
U ELECTROSTATIC GYROSCOPES
ESKERS
U GLACIAL DRIFT
ESRO
U EUROPEAN SPACE AGENCY
ESTERS
NT ACRYLATES
NT ASPARTATES
NT CELLULOSE NITRATE
NT DIISOCYANATES
NT GLUTAMATES
NT ISOCYANATES
NT MALEATES
NT NITRATE ESTERS
NT PETN
NT PHTHALATES
NT POLYCARBONATES
NT POLYESTERS
NT POLYETHYLENE TEREPHTHALATE
NT SULFONATES
NT URETHANES
Chemistry and metabolism of delayed neurotoxic organophosphorus esters
[AD-P004023] 06 p0844 N85-15357
Fluorinated diacrylic esters
[AD-D011328] 07 p0929 N85-15689
Acute oral toxicity (LD50) of 4-nitrophenyl monochloromethyl (Phenyl) phosphinate (TA000) in male rats
[AD-A148337] 08 p1192 N85-17513
Plasticizer system for propellant compositions
[AD-D011514] 12 p1817 N85-21393
Plasticizer system for propellant compositions
[AD-D011516] 12 p1817 N85-21394
Plasticizer system for propellant compositions
[AD-D011517] 12 p1817 N85-21395
Condensation of anhydrides or dicarboxylic acids with compounds containing active methylene groups. Part 19: Condensation of phthalic and substituted phthalic anhydrides with benzoylacetic ester
[NASA-TM-77885] 19 p3227 N85-30009
Condensation of anhydrides or dicarboxylic acids with compounds containing active methylene groups. Part 1: Condensation of phthalic anhydride with acetoacetic and malonic ester
[NASA-TM-77886] 19 p3227 N85-30010
ESTIMATES
NT COST ESTIMATES
Estimation of the potential and probable source regions for acid precipitation
[DE84-015119] 02 p0225 N85-11472
Nonparametric maximum penalized likelihood estimation of a density from arbitrarily right-censored observations
[AD-A145569] 02 p0251 N85-11644
Signal processing algorithms
[AD-A145748] 03 p0406 N85-12590
The ML (Maximum Likelihood) method for frequency estimation of real sinusoids in noise
[AD-A146053] 03 p0411 N85-12628
Measurement of range-resolved water vapor concentration by coherent CO2 differential absorption lidar
[PB84-236892] 04 p0535 N85-13420
Some error estimates for the p-version of the finite element method
[CTH-MATH-1984-21] 05 p0719 N85-14614
Numerical estimation of charge transfer time in charge-coupled device employing latent gallium arsenide channel 06 p0793 N85-15069
Repulsive force of magnetic clouds during solar flares and magnetospheric substorms 06 p0824 N85-15233
Characteristic scale of inner mixing layers in stably stratified atmosphere 06 p0824 N85-15235
Geostatistics for resource and reserve estimation
[PB85-105781/GAR] 07 p0989 N85-16286
Forest area estimates from LANDSAT MSS and forest inventory plot data
[PB85-105617/GAR] 07 p0990 N85-16290
Estimation for a semimartingale regression model using the method of sieves
[AD-A146809] 07 p1028 N85-16527
Determination of crustal and upper mantle structure from analysis of broadband teleseismic P-waveforms 08 p1181 N85-17440
A moving finite element method for time dependent partial differential equations with error estimation and refinement
[AD-A147719] 08 p1210 N85-17617
Research in stochastic processes
[AD-A148822] 08 p1216 N85-17660
On the local behaviour of solutions of degenerate parabolic equations with measurable coefficients
[AD-A147412] 09 p1373 N85-18631
Simple approximate variances for b-letter values. A sampling enquiry: Supplement
[DE85-001410] 09 p1376 N85-18647
Data-driven choice of a spectrum estimate: Extending the applicability of cross-validation methods
[DE85-001411] 10 p1437 N85-19058
On the modified likelihood for density estimation
[AD-A149437] 10 p1547 N85-19758
The inefficiency of least squares: Extensions of Kantorovich inequality
[AD-A149568] 10 p1549 N85-19768
Estimation of variance of the regression estimator
[AD-A149407] 10 p1551 N85-19780
Statistical analysis of autoregressive spectral estimates for noise corrupted autoregressive series
[AD-A149543] 11 p1708 N85-20747
AFOS (Automation of Field Operations and Services)-ERA forecast verification, September 1984
[PB85-137578] 12 p1897 N85-21912
An asymptotically efficient solution to the bandwidth problem of kernel density estimation, revision
[AD-A149600] 12 p1920 N85-22056
Estimation of gas turbine engine boost provided by injecting water behind compressor 13 p2051 N85-22838
Accuracy of approximation of Bayes estimates in presence of noninformative parameters 13 p2084 N85-23015
A note about the strong convergence of the nonparametric estimation of a regression function
[AD-A150325] 13 p2151 N85-23353
Runge-Kutta formula with cheap error estimate
[DE85-005674] 13 p2152 N85-23363
Monthly and Seasonal Weather Outlook for mid-December 1984 mid-January 1985, volume 38, number 24, 14 December 1984 14 p2379 N85-24687
Nonparametric estimation of density and hazard rate functions when samples are censored
[AD-A150946] 14 p2411 N85-24868
Residual oxygen pressure in contact gap upon diffusion welding of titanium 15 p2499 N85-25418
High frequency estimation of 2-dimensional cavity scattering
[AD-A151697] 15 p2542 N85-25696
The measurement of human time estimating ability using a modified jerison device
[AD-A151870] 15 p2620 N85-26141
Some estimates of harmonic majorants 15 p2634 N85-26237
A non-parametric probability density estimator and some applications
[AD-A151853] 15 p2641 N85-26287
Sensitivity of conditions for lumping finite Markov chains
[AD-A152122] 16 p2855 N85-27604
Formulas for updating the generalized inverse of a symmetric matrix perturbed by a symmetric rank 2 matrix composed of 2 nonsymmetric DYADS
[AD-A151736] 16 p2858 N85-27628
Conformational and mechanical properties at high strain rates
[AD-A153401] 17 p2959 N85-28272
Computer-aided thermohydraulic design of TEMA type E shell and tube heat exchangers for use in low pressure, liquid-to-liquid, single phase applications
[AD-A153779] 18 p3100 N85-29191
Extent to which least-squares cross-validation minimizes integrated square error in nonparametric density estimation
[AD-A153789] 18 p3174 N85-29679
Precipitation estimation using collocated GOES satellite and surface data
[AD-A154248] 19 p3317 N85-30559
Estimating ability with the wrong model
[AD-A154071] 19 p3335 N85-30663
The optimality of lower confidence limits for the reliability of series systems obtained by the method of key test results or other related techniques
[AD-A154880] 21 p3597 N85-32338
Parameter estimation in communication system tracking satellite observations
[AD-A155137] 21 p3636 N85-32582
Identification of unsteady aerodynamics and aeroelastic integro-differential systems
[NASA-TM-86749] 21 p3678 N85-32851
A simulation study of Sylvester's problem in three dimensions
[AD-A155266] 21 p3679 N85-32854
Procedure for estimating orbital debris risks
[NASA-TP-2507] 22 p3738 N85-33169
Estimating angular position of optical radiation source when received by array of photodetectors 22 p3778 N85-33413
Estimating the change in asymptotic direction due to secular changes in the geomagnetic field
[SH-6.1-13] 23 p4045 N85-35086
Optimal estimation of a high degree gravity field from a global set of 1 deg x 1 deg anomalies to degree and order 250
[AD-A156008] 24 p4117 N85-35519
Gravity gradiometer survey data processing
[AD-A156165] 24 p4117 N85-35522
Atlantic coast hindcast. Phase 2: Wave information, additional extremal estimates
[AD-A156137] 24 p4125 N85-35575
Error-correcting codes for computer memories 24 p4136 N85-35636
ESTIMATING
NT ORBITAL POSITION ESTIMATION
NT PARAMETER IDENTIFICATION
NT SYSTEM IDENTIFICATION
Recursive algorithms for adaptive arrays based on estimates
[REPT-5-84] 01 p0107 N85-10719
Construction of approximate confidence intervals for probability-of-kill via the bootstrap
[AD-A144761] 01 p0113 N85-10784
Decision tree rating scales for workload estimation: Theme and variations
[NASA-CR-174062] 02 p0237 N85-11544
Auto-regressive moving average spectral estimation using modified and least squares modified Yule-Walker estimates
[AD-A145516] 02 p0254 N85-11883
Programming effort estimation
[AD-A145839] 03 p0406 N85-12595
Maximum likelihood and Bayesian parameter estimation in item response theory
[AD-A145775] 03 p0413 N85-12644
Noise analysis of the Coarse Optical Power Spectrum Estimator (COPSE) data acquisition system
[AD-A145918] 03 p0419 N85-12677
Improved carrier tracking by smoothing estimators 05 p0623 N85-13989
Performance of Bayes-optimal angle-of-arrival estimators
[AD-A146594] 06 p0858 N85-15454
Efficient scores, variance decompositions and Monte Carlo swindles
[AD-A146873] 06 p0858 N85-15458
Electronics research at the University of Texas at Austin
[AD-A146900] 07 p0947 N85-15988
Bayesian estimation of undetected errors
[AD-A147198] 07 p1031 N85-16545
Hybrid state estimation approach to multiobject tracking for airborne surveillance radars
[AD-A148459] 08 p1153 N85-17279
Research on optimal control, stabilization and computational algorithms for aerospace applications
[NASA-CR-174318] 08 p1209 N85-17803

A feedback finite element method with a posteriori error estimation. Part 1. The finite element method and some basic properties of the A posteriori error estimator
[AD-A148345] 08 p1212 N85-17631
Antiesampling for estimation: An overview
[AD-A148545] 08 p1216 N85-17659
Three position estimation procedures
[AD-A148748] 09 p1278 N85-18042
Comparing computing formulas for estimating concentration ratios
[DE84-008644] 09 p1349 N85-18490
Estimating the scale parameter of an exponential distribution from a sample of time-censored r-th order statistics
[AD-A148060] 09 p1375 N85-18644
Rain volume estimation over areas using satellite and radar data
[NASA-CR-174434] 10 p1518 N85-19568
Simulation of estimating periodicity of seasonally stationary time series
[DE85-003517] 11 p1708 N85-20748
Care 3 model overview and user's guide, first revision
[NASA-TM-86404] 15 p2627 N85-26192
Estimation theory applied to improving dynamic structural models
[DE85-004148] 15 p2630 N85-26210
Theory and Applications of State Estimation. NRIMS Summer Seminar Series
[CSIR-SWISK-37] 15 p2635 N85-26244
Nonlinear estimation 15 p2635 N85-26245
Some aspects of decentralized Kalman filtering 15 p2635 N85-26250
State estimation with interrupted observations 15 p2635 N85-26251
Estimation of manouvering targets 15 p2636 N85-26253
Bayesian estimation of one dimensional discrete markov random fields
[AD-A151503] 15 p2640 N85-26284
Construction of efficient algorithms for the estimation of multivariate probability densities
[AD-A151509] 15 p2640 N85-26285
Estimation of launch vehicle performance parameters
[AD-A151927] 16 p2728 N85-26639
A data based algorithm for choosing the window width when estimating the integral of f2(x)
[AD-A152093] 16 p2847 N85-27553
Some new estimation methods for weighted regression when there are possible outliers
[AD-A152104] 16 p2854 N85-27602
Multivariable statistical modeling and its application 16 p2857 N85-27617
Methods for optimal recursive estimation of non-stationary time series, applications to atomic time and frequency metrology 17 p2965 N85-28312
Numerical estimation of the curvature of biological surfaces 17 p3006 N85-28588
Nonsmooth analysis and Frechet differentiability of M-functionals
[AD-A152932] 17 p3019 N85-28668
Nonparametric estimation of the probability of ruin
[AD-A153523] 18 p3174 N85-29674
A robust estimator of location using an adaptive spline model
[AD-A153682] 18 p3174 N85-29676
On the characterization of nonnegatively estimable linear combinations of variance components
[AD-A153786] 18 p3174 N85-29678
Estimating ability with the wrong model
[AD-A154071] 19 p3335 N85-30663
A comparison of four Monte Carlo methods for estimating the probability OF S=T connectedness
[AD-A154264] 19 p3348 N85-30749
Nomographs for estimating the levelized cost of energy from flat-plate and concentrator photovoltaic systems
[NASA-CR-176048] 20 p3483 N85-31645
A modal parameter extraction procedure applicable to linear time-invariant dynamic systems
[NASA-CR-176120] 22 p3835 N85-33747
Monte Carlo techniques for analyzing deep penetration problems
[DE85-011436] 23 p3968 N85-34598
Estimation of flight mechanical variables by means of Kalman filters 24 p4062 N85-35171
LANDSAT-4/5 image data quality analysis
[E85-10105] 24 p4107 N85-35483

ESTIMATORS
Asymptotics for configural estimators
[AD-A150106] 12 p1924 N85-22087

ESTUARIES
The SANCOR estuaries programme, 1982-1986
[ISBN-0-7988-2662-2] 01 p0068 N85-10454
Ecology of estuarine channels of the pacific northwest coast: A community profile
[PB84-209709] 01 p0070 N85-10464
Estuaries of the Cape. Part 2: Synopses of available information on individual systems. Report 12: Buffels (WES) (CSW 1), Elsies (CSW 2), Sir Lowry's Pass (CSW8), Steenbras (CSW 9), and Buffels (OOS) (CSW 11)
[CSIR-RR-411-PT-2] 01 p0066 N85-10581
Estuaries of the Cape. Part 2: Synopses of available information on individual systems. Report 13: Silvermine (CSW 3)
[CSIR-RR-412-PT-2] 01 p0066 N85-10582
Estuaries of the Cape. Part 2: Synopses of available information on individual systems. Report no. 14: Sand (CSW 4)
[CSIR-RR-413-PT-2] 01 p0066 N85-10583
Estuaries of the Cape. Part 2: Synopses of available information on individual systems. Report no. 15: Zeekoe (CSW 5)
[CSIR-RR-414-PT-2] 01 p0067 N85-10584
Estuaries of the Cape. Part 2: Synopses of available information on individual systems. Report no. 16: Eerste (CSW 6)
[CSIR-RR-415-PT-2] 01 p0067 N85-10585
Estuaries of the Cape. Part 2: Synopses of available information on individual systems. Report no. 17: Lourens (CSW 7)
[CSIR-RR-416-PT-2] 01 p0067 N85-10586
Estuaries of the Cape. Part 2: Synopses of available information on individual systems. Report no. 18: Bot/Kleinmond system (CSW 13)
[CSIR-RR-417-PT-2] 01 p0067 N85-10587
Estuaries of the Cape. Part 2: Synopses of available information on individual systems. Report no. 19: Groot (WES) (CMS 23) and Sout (CMS 22)
[CSIR-RR-418] 01 p0067 N85-10588
Radiotracer studies of the dispersion of solid pollutants in marine and estuarial environment: Measurement of diffusion coefficients and the phenomenon of dispersion by currents
[BLL-DRIC-TRANS-7104-(3623.66)] 02 p0224 N85-11468
Verification of a model of the Eastern Scheldt
[RAND/R-3106-NETH] 09 p1354 N85-18518
Field-work report: Medway Estuary, 28 June - 18 July 1983
[RNC/NS/TR8] 13 p2041 N85-22773
Ecology of Pamlico River, North Carolina: An estuarine profile
[PB85-155703] 16 p2822 N85-27404
Review and annotated bibliography of benthic studies in coastal and estuarine areas of Florida with a selected compilation of worldwide benthic methodological references and southeastern United States benthic taxonomic references
[PB85-151041] 16 p2822 N85-27405
Water quantity and quality research for the Rhine Meuse estuary
[PUBL-325] 17 p2968 N85-28470

ETCHING
Fabrication of monocrystalline GaAs solar cells utilizing NaCl sacrificial substrates
[DE84-013016] 11 p1673 N85-20544
Laser-plasma interactions for the deposition and etching of semiconductor materials
[DE85-000458] 11 p1731 N85-20885
The characterisation of oxide films on treated aluminium alloys
[MOAD-R-849] 13 p2022 N85-22667
Apparatus for etching vertical junction solar cell wafers
[AD-D011653] 17 p2964 N85-28443
Morphology of GaAs/sub 1-x/P/sub x/ superlattices grown by MOCVD and chloride VPE
[DE85-002944] 17 p3045 N85-28642
Micro-reactions of metal contacts on various types of GaAs surfaces
[AD-A153650] 18 p3193 N85-29606

ETHANE
Laser schlieren, shock tube studies of high temperature hydrocarbon pyrolysis rates
[DE85-003314] 11 p1636 N85-20303
Mechanisms of heat and mass transfer across a double-diffusive interface
[PB85-148468] 12 p1848 N85-21594
Optical waveguide sensor for methane gas
[AD-D011691] 19 p3273 N85-30294
Shock tube measurements of growth constants in the branched-chain ethane-carbon monoxide-oxygen system
[NASA-TM-87068] 21 p3562 N85-32156

ETHERS
NT POLYPHENYL ETHER
Morphology and dynamic mechanical properties of diglycidyl ether of bisphenol-A toughened with carboxyl-terminated butadiene-acrylonitrile 04 p0488 N85-12958
Thermally stable thermoset resin compositions
[AD-D011274] 05 p0620 N85-13963
Fluorinated aliphatic polyalkylether lubricant with an additive composed of an aromatic phosphine substituted with perfluoroalkylether groups
[AD-D011286] 06 p0770 N85-14927
Plasticizer system for propellant compositions
[AD-D011508] 12 p1816 N85-21391
Azido nitramino ether containing solid propellants
[AD-D011511] 12 p1816 N85-21392
Plasticizer system for propellant compositions
[AD-D011516] 12 p1817 N85-21394
Chemical interpretation of the relaxed permittivity during epoxy resin cure
[AD-A150955] 14 p2260 N85-24005
Polyaromatic ether-sulfone-ketones with fluoro-substituted-p-cyclophane units as cross-linking sites
[AD-D011649] 17 p2933 N85-28105
Processable and stable conductive polymers
[AD-D011684] 19 p3249 N85-30143
Synthesis and properties of arylethersulfone thermoset systems
[AD-A154811] 21 p3569 N85-32198
The use of perfluoroether lubricants in unprotected space environments 22 p3797 N85-33523

ETHYL ALCOHOL
Construction of a bacterium to convert cellulose to ethanol
[TI84-901639] 04 p0481 N85-13068
Bulletin of the Faculty of Engineering, Hokkaido University, no. 123
[ISSN-0385-602-X] 04 p0482 N85-13075
Experimental study on the glow plug aided alcohol driven diesel engine 04 p0483 N85-13078
Alcohol fuel from Ohio farms: An introduction
[TI-84-901290] 05 p0621 N85-13970
Renewable energy: Energy from agricultural products
[TI84-901769] 05 p0669 N85-14307
Biocatalyzed processes for production of commodity chemicals: Assessment of future research advances for N-butanol production
[NASA-CR-174264] 07 p0919 N85-15819
Ethanol production by enzymatic hydrolysis: Parametric analysis of a base-case process
[DE84-013105] 11 p1614 N85-20147
Developments in the production and use of ethanol fuels
[GPO-40-678] 12 p1817 N85-21398
Alcohol Fuels Program technical review, spring 1984
[DE85-002919] 17 p2938 N85-28134
Ignition characterization of LOX/hydrocarbon propellants
[NASA-CR-171884] 18 p3083 N85-29070
Ignition characterization of LOX/hydrocarbon propellants
[NASA-CR-171882] 18 p3083 N85-29071

ETHYL COMPOUNDS
Interactions of ketones and hexacarbons
[AD-P004019] 06 p0843 N85-15353
Dynamics of vapor explosions
[DE85-006845] 18 p3101 N85-29194

ETHYLENE
NT VINYLIDENE
A thermodynamic surface for the critical region of ethylene
[PB84-217850] 01 p0025 N85-10159
Transport and relaxation processes in supercritical fluids
[DE84-006591] 05 p0731 N85-14698
Field test results of experimental EPDM (Ethylene Propylene Diene Monomer) and PUF (Polyurethane Foam) roofing
[AD-A147697] 08 p1132 N85-17133
Cars temperature measurements in sooting, laminar diffusion flames
[AD-A148601] 09 p1319 N85-18294
Laser schlieren, shock tube studies of high temperature hydrocarbon pyrolysis rates
[DE85-003314] 11 p1636 N85-20303
An indirect role for ethylene in shoot-inversion release of apical dominance in Pharbitis nil 15 p2611 N85-26090
Participation of ethylene in two modes of gravistimulation of shoots 15 p2613 N85-26101
Flash pyrolysis of biomass with reactive and non-reactive gases
[DE85-010962] 19 p3306 N85-30496
Preparation of ethylenediamine dinitrate
[DE85-006423] 23 p3922 N85-34305

ETHYLENE COMPOUNDS
NT CHLOROETHYLENE
NT ETHYLENEDIAMINE
Investigation of bromine complexed hydrogen/bromine regenerative fuel cells for portable electric power
[AD-A146401] 06 p0833 N85-15300

Ionization energies of liquids from energy distribution, quantum yield and second derivative curves
[AD-A152210] 16 p2746 N85-26946

ETHYLENE OXIDE
Water absorption and conductivity in poly(ethylene oxide)-lithium tetrafluoroborate films
[AD-A147969] 10 p1450 N85-19138
Hazardous air pollutants: Wet removal rates and mechanisms
[PB85-138626] 12 p1887 N85-21842
Influence of hydrogen bonding in block copolymers and their blends 13 p2036 N85-22752
Characterization of poly(ethylene oxide) drawn by solid state extrusion
[AD-A150967] 14 p2260 N85-24006
Ion and polymer chain motion in a superionic sodium-poly(ethylene oxide) complex
[AD-A152290] 16 p2755 N85-27001

ETHYLENEDIAMINE
The IMX double direct process
[AD-A146250] 03 p0340 N85-12188
Ethylenediamine salt of 5-nitrotetrazole and preperation
[DE85-005738] 23 p3923 N85-34306

EUCLIDEAN GEOMETRY
NT ANALYTIC GEOMETRY
NT ANGLE OF ATTACK
NT ANGLES (GEOMETRY)
NT BRAGG ANGLE
NT CARTESIAN COORDINATES
NT CATENARIES
NT CIRCLES (GEOMETRY)
NT CIRCUMFERENCES
NT CONICS
NT DESCRIPTIVE GEOMETRY
NT ELEVATION ANGLE
NT ELLIPSES
NT EPICYCLOIDS
NT FIXED POINTS (MATHEMATICS)
NT GEODESIC LINES
NT HYPERBOLAS
NT INFLECTION POINTS
NT LINES (GEOMETRY)
NT LOCI
NT MERCATOR PROJECTION
NT OBLATE SPHEROIDS
NT PARABOLAS
NT PARALLELEPIPEDS
NT POINTS (MATHEMATICS)
NT POLYGONS
NT PROJECTIVE GEOMETRY
NT PYRAMIDS
NT RADII
NT RECTANGLES
NT SPHEROIDS
NT TANGENTS
NT TORUSES
Model diagnosis in two-way tables by means of row and column Euclidean maps
[CSIR-TWISK-307] 01 p0108 N85-10730
Schur-Ostrowski theorems for functionals on l1(0,1)
[AD-A150193] 13 p2150 N85-23346
A factorization approach to the linear regulator quadratic cost problem 20 p3413 N85-31178
A new description of combined trellis coding with asymmetric modulation
[NASA-CR-176197] 24 p4086 N85-35323

EUCLIDEAN SPACE
U EUCLIDEAN GEOMETRY

EULER BUCKLING
Interactive buckling of thin-walled structural components under static and dynamic loads
01 p0059 N85-10392
Nonlinear deformation and static linear buckling of structures under pressure
[CETIM-11-E-350] 04 p0514 N85-13281

EULER EQUATIONS OF MOTION
Shock capturing finite difference algorithms for supersonic flow past fighter and missile type configurations
[NASA-CR-174051] 02 p0134 N85-10913
Model equations describing unsteady fluid motion
[ESA-TT-850] 04 p0501 N85-13194
A comparative study of the nonuniqueness problem of the potential equation
[NASA-TP-2385] 07 p0898 N85-15694
A Van Leer shock capturing algorithm for the Euler equations
[AD-A148761] 08 p1163 N85-17335
Flow instabilities in transonic small disturbance theory
[NASA-TM-86251] 09 p1273 N85-18000
An implicit, conservative, zonal-boundary scheme for Euler equation calculations
[NASA-CR-3865] 09 p1318 N85-18290
Researched applied to transonic compressors in numerical fluid mechanics of inviscid flow and viscous flow
[NASA-CR-174353] 09 p1319 N85-18291
Algorithms for the Euler and Navier-Stokes equations for supercomputers
[NASA-CR-172543] 10 p1539 N85-19701
Collision detection for moving polyhedra
[AD-A148961] 10 p1544 N85-19735
Contribution to the study of a numerical implicit method for solving the Euler equations
[ESA-TT-872] 10 p1549 N85-19771
A convergent series expansion for hyperbolic systems of conservation laws
[NASA-CR-172557] 12 p1910 N85-21990
Calculation of harmonic aerodynamic forces of aerofoils and wings from the Euler equations
15 p2458 N85-25177
A new implicit plus minus splitting method for the solution of the Euler equations in the transonic flow regime
15 p2461 N85-25200
A 3-dimensional Navier-Stokes-Euler code for blunt-body flow computations
[NASA-TM-58266] 15 p2483 N85-25211
Vortex dynamics
[AD-A151278] 15 p2637 N85-26260
Redistribution of the inlet temperature profile through the SSME fuel turbine 16 p2739 N85-26901
Evaluation of an algorithm for the solution of the time-dependent Euler equations
[AD-A151993] 16 p2854 N85-27600
Upwind-difference methods for aerodynamic problems governed by the Euler equations
[REPT-84-23] 17 p2893 N85-27834
Unsteady flow in multistage turbines
17 p2911 N85-27946
Relaxation methods for hyperbolic equations
[REPT-84-20] 17 p3021 N85-28687
Chemical transformation modules for Eulerian acid deposition models. Volume 1: The gas-phase chemistry
[PB85-173714] 18 p3072 N85-29001
The dynamics and control of large flexible space structures, 8
[NASA-CR-175986] 19 p3225 N85-29996
An elliptic calculation procedure for 3-D viscous flow
21 p3587 N85-32297
Calculation of 3-D flow without numerical mixing
21 p3588 N85-32301
Three-dimensional hydrodynamic hot-spot model
[DE85-009587] 23 p3922 N85-34301
Compressible two-phase flow instabilities simulated with a hybrid Lagrange-Euler pseudospectral method
[DE85-009904] 23 p3931 N85-34361
A stream function approach to solving the conservative Euler equations for transonic flows
24 p4059 N85-35156
Numerical studies of 2-dimensional flows
[NASA-CR-3930] 24 p4060 N85-35160

EULER-CAUCHY EQUATIONS
A study of the recursion yn+1=yn+tau yn sup m
[CWI-NM-R8403] 05 p0723 N85-14648
Propagation of non-axisymmetric elastic waves through shell with filler under radial load at one end
17 p2943 N85-28169

EULER-LAGRANGE EQUATION
Hamiltonian and Lagranglan theory of gyrokinetic equations 02 p0283 N85-11845
The perfecting of the method of experimental-analytic solution of the problem of stationary plastic flow
[BLL-M-35836-(5828.4)] 05 p0634 N85-14065
Influence of turbulence on erosion by a particle-laden fluid jet
[DE84-014365] 09 p1320 N85-18301
Adaptive meshes in the 2DL code
[LA-9936-MS] 12 p1914 N85-22011
Elements of celestial mechanics
14 p2396 N85-24782
Development of a dynamic finite element model for unrestrained flexible structures
[AD-A151176] 15 p2636 N85-26259
FEMALE: Finite Element Method for Arbitrary Lagrangian and Eulerian elements
23 p3979 N85-34671
Two-dimensional simulation of LIB target implosion
23 p3980 N85-34678

EURECA (ESA)
European retrievable carrier (Eureca) and evolutionary space carrier for microgravity, Earth observation and technology demonstration 02 p0152 N85-11032
Botany facility, phase A study. Part 1: Executive summary --- EURECA
[BF-DOC-10-VOL-1] 08 p1110 N85-17015
The EURECA Automatic Gradient Heating Facility (AGHF), phase A study
[ESA-CR(P)-1939] 11 p1591 N85-20005
Solution growth facility, phase A design study, executive summary --- EURECA
[RPT/SGF/00014/TER] 11 p1591 N85-20006
Botany facility phase A study. Core payload number 8 EURECA carrier, volume 1
[ESA-CR(P)-1978-VOL-1] 17 p2906 N85-27918
Botany facility phase A study. Core payload number 8 for EURECA carrier, volume 2
[BF-TD-DRD-03-VOL-2] 17 p2906 N85-27919
German payloads for EURECA 1
[BMFT-FB-W-85-003] 20 p3419 N85-31223
The EURECA solution growth facility conceptual design study. Executive summary
[ESA-CR(P)-2007] 20 p3536 N85-32018

EUROPA
Multispectral and geomorphic studies of processed Voyager 2 images of Europa
[NASA-CR-174075] 03 p0448 N85-12848
Patterns of fracture and tidal stresses due to nonsynchronous rotation: Implications for fracturing on Europa 13 p2173 N85-23483
Planetary analogs in Antarctica: Icy satellites
13 p2193 N85-23605
Spectral units on Europa and Ganymede
13 p2196 N85-23621
Fault offsets and lateral crustal movement on Europa
13 p2201 N85-23656

EUROPE
Project COST 72 (The European weather radar project) today 01 p0084 N85-10561
Heat flow map of Europe: Brief summary of the geophysical implications
[REPT-562] 03 p0377 N85-12405
Terrestrial heat flow in Europe and general features of its regional distribution
[REPT-563] 03 p0377 N85-12406
Determination of the longitude differences Munich-Lissabon-San Fernando, Munich-Wettzell, and Munich-Karlsruhe-Niederrealterberg
[ASTRON-GEODAET-ARB-44]
04 p0524 N85-13353
Determination of astronomical longitude differences for the European longitude reference system for 1980. Relative right ascension corrections for 125 FK4 and FK4 Sup stars 04 p0524 N85-13354
European scientific notes. Volume 38, number 11
[AD-A148228] 08 p1230 N85-17745
West Europe report: Science and technology
[JPRS-WST-85-009] 09 p1309 N85-18224
Analysis of bird strikes reported by European airlines, 1976 - 1980
[AD-P004181] 11 p1578 N85-19943
West Europe report: Science and technology
[JPRS-WST-85-005] 11 p1592 N85-20013
West Europe report: Science and technology
[JPRS-WST-85-008] 11 p1618 N85-20183
The Middle Atmosphere Program: Winter in Northern Europe (MAP/WINE) 11 p1655 N85-20429
Winter in Northern Europe (WINE) project
11 p1657 N85-20439
Large scale winter time disturbances in meteor winds over central and eastern Europe
11 p1661 N85-20487
Changes in the ozone content over central Europe during reversals of stratospheric circulation in late winter
11 p1661 N85-20489
An air-breathing ballistic space transporter for Europe
[NASA-TM-77845] 12 p1792 N85-21244
Lateral inhomogeneity of mantle surface in western Eurasia 14 p2344 N85-24497
West Europe report: Science and technology
[JPRS-WST-85-014] 15 p2480 N85-25382
West Europe report: Science and technology
[JPRS-WST-84-012] 15 p2523 N85-25552
East European report: Science and technology
[JPRS-ESA-85-010] 15 p2524 N85-25560
West Europe report: Science and technology
[JPRS-WST-84-008] 15 p2531 N85-25606
East Europe report: Science and technology
[JPRS-ESA-84-016] 15 p2533 N85-25624
West Europe report: Science and technology
[JPRS-WST-84-020] 15 p2534 N85-25633
West Europe report: Science and technology
[JPRS-WST-84-003] 15 p2534 N85-25635
West Europe report: Science and technology
[JPRS-WST-84-010] 15 p2535 N85-25644
East Europe report: Science and technology
[JPRS-ESA-85-018] 15 p2537 N85-25658
Frequency dependence of Q in the mantle underlying the shield areas of eurasia
[AD-A151387] 15 p2592 N85-25978
East Europe report: Science and technology
[JPRS-ESA-84-032] 16 p2727 N85-26833
Rotterdam Airport and the Common Market
17 p2894 N85-27840

West Europe report: Science and technology
[JPRS-WST-84-024] 17 p2945 N85-28183
Air Weather Service (AWS) climatic briefs: Europe
[AD-A152528] 17 p2996 N85-28519
Forecast impact simulation studies
18 p3139 N85-29435
Reduced to pole long-wavelength magnetic anomalies of Africa and Europe 20 p3475 N85-31595
Euro-African MAGSAT anomaly-tectonic observations
20 p3475 N85-31596
Long-wavelength magnetic and gravity anomaly correlations on Africa and Europe
20 p3476 N85-31597
A transportable, machine oriented library of european sky and terrain radiance distributions with contemporary radiometric and meteorological profiles
[AD-A155254] 21 p3637 N85-32590
Supersaturation spect A of Ice Nuclei at different locations in Europe and over the North-Atlantic
21 p3640 N85-32615
Space-age Europe, 1957-1980
23 p4057 N85-35148
Introduction to European air traffic control
[AD-A156326] 24 p4062 N85-35176

EUROPEAN AIRBUS
NT A-310 AIRCRAFT
NT A-320 AIRCRAFT
Insight. Background information for multipurpose pilots: Flight phenomena 02 p0136 N85-10940
All-composite Airbus empennage
07 p0936 N85-15931
West Europe report: Science and technology
[JPRS-WST-85-006] 11 p1616 N85-20183
Airbus fatigue tests 11 p1616 N85-20186
A 320 to have combined automatic pilot, flight control system 14 p2289 N85-24186
West Europe report: Science and technology
[JPRS-WST-84-027] 15 p2532 N85-25612
MBB cost-reduction plan for Airbus construction described 15 p2532 N85-25616
FRG journal analyzes state, prospects of airbus programs: General analysis 15 p2535 N85-25638
Financial, economic commentary on Airbus, European aviation 15 p2536 N85-25649
Lightning-safe carbon fiber composite for Airbus tail unit 18 p3087 N85-29100
Avionics and civil aircraft systems: The present and the future
[SNIAS-851-111-104] 20 p3392 N85-31038

EUROPEAN COMMUNICATIONS SATELLITE
Station for in-orbit testing of satellites
[MBB-UR-708/84-O] 16 p2874 N85-27733

EUROPEAN LARGE TELECOMM SATELLITE
U L-SAT

EUROPEAN RETRIEVABLE CARRIER
U EURECA (ESA)

EUROPEAN SPACE AGENCY
Non-US approaches to space commercialization
02 p0150 N85-11012
Space research in Norway
[SAD-110-T] 03 p0321 N85-12072
Space research in Sweden 03 p0321 N85-12073
The ESA product assurance specification system: Explanatory note 04 p0511 N85-13259
International involvement in a civilian space station program 07 p0915 N85-15789
FRG study looks at participation in ESA, US space station 08 p1141 N85-17191
Making sure: A brief outline and history of ESA's test and checkout services
[ESA-BR-22] 09 p1286 N85-18077
Commercial space: Europe should have independent strategy 10 p1460 N85-19205
European views differ on space station concept
15 p2531 N85-25608
West Europe report: Science and technology
[JPRS-WST-84-010] 15 p2535 N85-25644
European space science horizon 2000
[ESA-SP-1070] 16 p2717 N85-26771
Timing of spacecraft data: Time accuracy requirements and timing facilities of the European Space Agency (ESA) 17 p2964 N85-28307
Documentation for the West German Federal Cabinet's space policy decision 17 p3051 N85-28886
Some Europeans voice opposition to space station participation 18 p3066 N85-28961
West Europe report: Science and technology
[JPRS-WST-84-022] 18 p3085 N85-29066
ESA presents plans for European manned space station 18 p3085 N85-29067
West Europe report: Science and technology
[JPRS-WST-84-032] 18 p3086 N85-29095
New ESA director on Ariane, space station, future trends 18 p3088 N85-29096
FRG weighs ESA participation, budget issues
18 p3088 N85-29110
The ESA field emission electric propulsion program
[ESA-STR-213] 20 p3420 N85-31229
Space-age Europe, 1957-1980
23 p4057 N85-35148

EUROPEAN SPACE PROGRAMS
Non-US approaches to space commercialization
02 p0150 N85-11012
European retrievable carrier (Eureca) and evolutionary space carrier for microgravity, Earth observation and technology demonstration 02 p0152 N85-11032
Space research in Norway
[SAD-110-T] 03 p0321 N85-12072
Space research in Sweden 03 p0321 N85-12073
Colloquium about Joint Projects within DFVLR/ISRO Cooperation
[DFVLR-MITT-84-12] 04 p0458 N85-12907
Presentation of Indian Space Research Organization (ISRO)/DFVLR cooperation 04 p0459 N85-12912
The Telecom 1 satellite telecommunication system
04 p0493 N85-13147
Antenna mechanical technologies within ESA
05 p0625 N85-14000
The METEOSAT exploitation project, operational use of a remote sensing system 05 p0658 N85-14223
Overview of German microgravity activities in the field of life science 05 p0695 N85-14476
Space research in Spain 06 p1231 N85-17751
United Kingdom report on space research
06 p1231 N85-17752
Space research in Denmark 06 p1231 N85-17753
Space activities in Finland 06 p1231 N85-17754
Space research in the Federal Republic of Germany
09 p1285 N85-18074
Gravity and biological systems: Emphasis on human physiology
[ESA-BR-21] 09 p1360 N85-18558
Activities report in space research in Austria
11 p1587 N85-19994
Preliminary concepts of candidate elements for a potential European participation in a manned space station
[MBB-UR-E-749-84-O] 11 p1587 N85-19996
Future launching systems, 3rd prospective phase
[SNIAS-S/DT/Y-25-083] 11 p1589 N85-19999
West Europe report: Science and technology
[JPRS-WST-85-013] 14 p2289 N85-24183
Science with the Solar and Heliospheric Observatory (SOHO) 14 p2449 N85-25121
Studies on rocket engines for future European launchers
[SEP-TPRL/K-19572/84] 15 p2495 N85-25393
European space science horizon 2000
[ESA-SP-1070] 16 p2717 N85-26771
European utilization aspects of a US manned space station, volume 1
[ESA-CR(P)-1987-VOL-1] 17 p2907 N85-27926
European utilization aspects of a US manned space station, volume 2
[ESA-CR(P)-1987-VOL-2] 17 p2907 N85-27927
In orbit infrastructure. Volume 1: Executive summary — European space programs
[RX0011-002/84-VOL-1] 17 p2908 N85-27928
Documentation for the West German Federal Cabinet's space policy decision 17 p3051 N85-28886
In orbit infrastructure — european space programs
[SNIAS-S/DT-24-996] 18 p3064 N85-28956
Space station study
[BL-6167] 18 p3066 N85-28959
Maintenance of long life space systems, volume 1
[MATRA-0316/DX80-VOL-1] 18 p3066 N85-28964
Maintenance of long life space systems, volume 2
[MATRA-0350/DX80-VOL-2] 18 p3066 N85-28965
DFVLR official on areas of US-FRG Space Station cooperation 18 p3066 N85-29091
Ariane space general director on satellite launcher market 18 p3067 N85-29103
Study of a medium term flexible fixed satellite service mission
[DM51/CC-IM-0185.83] 18 p3091 N85-29136
Looking down looking forward: Earth observation, sciences and applications, a perspective
[ESA-SP-1073] 18 p3149 N85-29497
ERS economic impace study
[ESA-CR(P)-1979] 18 p3199 N85-29847
A study of the ESA-NAVSAT control segment
[ESA-CR(P)-2000] 20 p3396 N85-31079
Studies toward a manned space station: Participation of European industry in NASA space station (MSS)
[SNIAS-S/DT-Y-25-212] 20 p3418 N85-31217
Study of terrestrial mobile systems for personal communications
[MCS-8436] 20 p3441 N85-31357
Thermal protection systems for reentry vehicles
[CNES-NT-113] 23 p3900 N85-34157

EUROPEAN SPACE RESEARCH ORGANIZATION
U EUROPEAN SPACE AGENCY

EUROPIUM COMPOUNDS
Fluorescence quenching by metal semiconductor and insulator surfaces 19 p3374 N85-30929

EUTECTIC ALLOYS
The influence of the carbide distribution on the abrasive wear of ledeburitic chromium steels
01 p0054 N85-10359
Microstructure and creep behaviour at elevated temperature of unidirectionally solidified eutectic nickel base superalloys 02 p0181 N85-11216
Reciprocal solubility of phases in multi-component systems
[BLL-M-36003-(5828.4)] 07 p0926 N85-15870
Alloys and method of making
[AD-D011337] 07 p0927 N85-15874
Research on rapidly solidified alloys
[AD-A149380] 10 p1441 N85-19080
Dependence of superplastic flow on state of grain boundaries 13 p2025 N85-22689
Study of processes of modification of Al-Si alloys
13 p2026 N85-22695
Aluminum alloy ATs5K5 (5% Zn + 5% Ca) for superplastic forming 13 p2026 N85-22697
Influence of solidification parameters on the formation of the gamma-M7C3 eutectic structure of 2% C-12%Cr steel 15 p2512 N85-25500
Dissolution of solid solutions in absence of internal mass transfer
[BLL-M-36092-(5828.4)] 16 p2748 N85-26959
Ca-Ga, Sr-Ga and Ba-Ga binary systems
[DE85-006454] 16 p2751 N85-26980
Multi-phase crystallization of ferrous alloys
[BLL-BISI-TRANS-22441-(9022.06)]
17 p2925 N85-28037
Properties of heat resistant Ni-Al-Nb alloys with unidirectional eutectic structure
19 p3247 N85-30133
Directional solidification of an eutectic Bi-MnBi alloy
[BLL-M-36270-(5828.4)] 20 p3430 N85-31275

EUTECTIC DIAGRAMS
U PHASE DIAGRAMS

EUTECTICS
NT EUTECTIC ALLOYS
Eutectic explosives containing ammonium nitrate
[DE84-015705] 01 p0034 N85-10213
The effect of heat treatment on wear resistance of gas-plasma eutectic coatings
[BLL-M-35756-(5828.4)] 03 p0329 N85-12122
The IMX double direct process
[AD-A146250] 03 p0340 N85-12188
Effect of a thermal gradient applied to a sinusoidal surface profile
[DE84-015649] 03 p0434 N85-12785
Investigation of the dissolution of CaCrO4 in molten LiCl-KCl eutectic
[DE84-016394] 04 p0469 N85-12985
The growth of metastable peritectic compounds
[NASA-CR-171289] 07 p0920 N85-15824
Studies on copper alloys containing chromium on the copper side phase diagram
[NASA-TM-77752] 07 p0927 N85-15876
SPAR X technical report for experiment 76-22 directional solidification of magnetic composites
[NASA-CR-171271] 07 p0927 N85-15880
Advanced latent heat storage media for high-temperature industrial applications
[DE85-000907] 09 p1345 N85-18461
Development of media for dynamic latent heat storage for the low-temperature range. Part 1: Thermal analyses of selected salt hydrate systems
[NASA-TM-77776] 10 p1507 N85-19510
Influence of eutectic silicate inclusions on micro-processes during deformation and fracture of 12GS steel
[BLL-BISI-TRANS-22296-(9022.06)]
17 p2929 N85-28073
Binary phase diagram determinations
[DE85-010656] 19 p3235 N85-30058
A study of freezing and melting with eutectic interactions 19 p3378 N85-30958
Influence of yttrium on eutectoid transformation in irons
[BLL-M-35787-(5828.4)] 24 p4078 N85-35270

EUTROPHICATION
Geographic variation in the relationships of temperature, salinity or sigma sub t versus plant nutrient concentrations in the world ocean — silicic acid, nitrate, and phosphate concentration
[NASA-CR-176621] 13 p2140 N85-23287
Empirical methods for predicting eutrophication in impoundments. Report 3. Phase 2. Model refinements
[AD-A155483] 21 p3614 N85-32482
Sulfur cycling in freshwater sediments
21 p3658 N85-32726

EUVE
U EXTREME ULTRAVIOLET EXPLORER SATELLITE

EVACUATING (TRANSPORTATION)
The helicopter, instrument of choice for health evacuation
[SNIAS-651-220-101] 20 p3393 N85-31051
EVACUATING (VACUUM)
Evacuate and backfill apparatus and method
[DE85-006018] 23 p3935 N85-34411
EVALUATION
NT TRAINING EVALUATION
Performance evaluation of A-10 aircraft maintenance units and aircraft using constrained facet analysis
[AD-A146955] 07 p0893 N85-15660
An evaluation and comparison of vertical profile data from the VISSR Atmospheric Sounder (VAS)
[NASA-TP-2425] 07 p1000 N85-16351
A survey and evaluation of software quality assurance
[AD-A147552] 07 p1026 N85-16510
Flight service evaluation of advanced composite aileron on the L-1011 transport aircraft
[NASA-CR-172483] 08 p1118 N85-17049
Development and evaluation of techniques for using combined microwave and optical image data for vegetation studies 08 p1148 N85-17240
A study of Air Force Quality Circle program effectiveness as viewed through facilitator's perceptions
[AD-A147633] 08 p1170 N85-17377
Design of an evaluation system to measure performance degradation due to continuous operations
[AD-A148188] 08 p1200 N85-17558
Performance management system enhancement and maintenance
[NASA-CR-175271] 08 p1202 N85-17564
Evaluation of the Fundamental Research on Explosives (FRE) program
[DE85-001537] 09 p1301 N85-18172
Evaluation of the particulate levels occurring under 1.0/1.2 g/mi nitrogen oxide standards for light duty diesel vehicles and light duty diesel trucks
[PB85-115939/GAR] 09 p1350 N85-18494
Partial evaluation as a means of language extensibility
[AD-A148730] 09 p1368 N85-18596
Applicability of laboratory kinetics studies to the evaluation of aqueous phase atmospheric oxidation of sulfur-4
[DE85-000586] 12 p1883 N85-21819
Electrical characterization of analog microprocessors
[AD-A149829] 12 p1911 N85-21995
Operational performance of the photovoltaic-powered grain mill and water pump at Tangaye, Burkina Faso (formerly Upper Volta)
[NASA-TM-86970] 13 p2126 N85-23243
MSFC data analysis of the SAFE/DAE experiment 14 p2233 N85-23843
Robotic deburring. Part 2: Evaluation of cutters and noncompliant tooling
[DE85-006182] 14 p2311 N85-24306
US Army Aviation Engineering Flight Activity (USAAEFA) report bibliography update 1983 - 1984
[AD-A151381] 15 p2457 N85-25166
An evaluation of the performance of a new storm tracking methodology
[AD-A152234] 16 p2835 N85-27484
Evaluation of the PROFS (Program for Regional Observing and Forecasting Services) 1982, real-time forecast experiment
[PB85-159747] 16 p2837 N85-27495
Evaluation of used crankcase oils using computerized infrared spectrometry. Appendices
[AD-A152994] 17 p2920 N85-28000
On-orbit frequency stability analysis of the GPS NAVSTAR's 3 and 4 rubidium clocks and NAVSTAR's 5 and 6 cesium clocks 17 p2963 N85-28296
Test and evaluation plan for the Centralized Storm Information System 17 p2994 N85-28508
CSIS test and evaluation 17 p2994 N85-28509
DC-10 winglet flight evaluation
[NASA-CR-3704] 19 p3217 N85-29949
Fundamental studies related to failure of adhesively bonded structures
[AD-A154072] 19 p3285 N85-30374
Nickel cadmium cell design variable program data analysis 20 p3445 N85-31387
High discharge rate characteristics of nickel-cadmium batteries for pulse load filtering 20 p3446 N85-31391
Improved materials for composite and adhesive joints
[AD-A155065] 21 p3562 N85-32153
Fabrication and test of modified quadrupole mass spectrometer
[AD-A155186] 21 p3580 N85-32312
Photovoltaics technical information guide
[DE85-002924] 22 p3808 N85-33585
Fuel cell applications literature review
[DE85-011891] 22 p3809 N85-33592
Effect of interference on the performance of a minimum TCAS 2
[FAA-PM-84-33] 23 p3895 N85-34131
Evaluation of low-temperature geothermal potential in Utah and Goshen Valleys and adjacent areas, Utah. Part 2: Water temperature and chemistry
[DE85-009344] 23 p3943 N85-34438
Expert systems research in regional resource evaluation: Experiences in the application of microcomputer technologies 24 p4105 N85-35450
EVAPORATION
NT EVAPOTRANSPIRATION
NT PROPELLANT EVAPORATION
NT TRANSPIRATION
A comparison of evaporation duct models for IREPS (Integrated Refractive Effects Prediction System)
[AD-A146471] 06 p0799 N85-15103
Eddy correlation measurements of energy partition for Amazonian forest
[INPE-3195-PRE/559] 06 p0827 N85-15252
Practical application of IREPS (Integrated Refractive Effects Prediction System)
[AD-A146528] 06 p0838 N85-15323
Thermal evaporation in blast waves: A model for aneurism formation in the NRL (Naval Research Laboratory) LASER-HANE simulation experiment
[AD-A147006] 07 p0978 N85-16210
Climate at CRREL (Cold Regions Research and Engineering Laboratory) Hanover, New Hampshire
[AD-A148400] 08 p1189 N85-17495
Exciplex systems for vapor-liquid visualization of fuel sprays
[AD-A149360] 10 p1457 N85-19181
Modeling interception of rainfall by forests and the role of interception in the water balance
[DE85-002822] 12 p1884 N85-21825
Effects of temperature variation among droplets in an evaporating fuel spray 13 p2004 N85-22582
Fabrication and I-V characterization of AlGaAs/GaAs MODFETs with P-type surface layers grown by molecular beam epitaxy
[AD-A151695] 15 p2660 N85-26415
Research test facility for evaporation and combustion of alternative jet fuels at high air temperatures
[AD-A153830] 18 p3083 N85-29073
Analysis and model/data comparisons of large-scale releases of nitrogen tetroxide
[DE85-009989] 18 p3133 N85-29406
Laser-induced fluorescence measurement of vapor concentration surrounding evaporating droplets
[DE85-009409] 19 p3277 N85-30320
Influence of spatial variability of hydraulic characteristics of soils on surface parameters obtained from remote sensing data in infrared and microwave
[NASA-TM-77902] 20 p3477 N85-31604
Vaporization from a heated surface into a saturated stream
[DE85-010484] 20 p3530 N85-31958
Emergency modeling of hazardous air pollutants
[AD-A155441] 21 p3614 N85-32461
Superheated fuel injection for combustion of liquid-solid slurries
[DE85-011624] 22 p3753 N85-33266
Volatile loss following very large impacts 22 p3853 N85-33862
Evaluation of source strength and dispersion model predications with data from large nitrogen tetroxide field experiments
[DE85-011855] 23 p3947 N85-34465
How are particle production, nucleon emission and target fragment evaporation processes interrelated in hadron-nucleus collisions? 24 p4174 N85-35878
EVAPORATION RATE
Vapor pressure and evaporation rate of certain heat-resistant compounds in a vacuum at high temperatures
[NASA-TM-77607] 10 p1434 N85-19036
EVAPORATIVE COOLING
NT FILM COOLING
NT SWEAT COOLING
Performance evaluation of an active solar cooling system utilizing low cost plastic collectors and an evaporatively-cooled absorption chiller
[DE84-010813] 12 p1880 N85-21798
Evaporatively cooled chiller for solar air conditioning systems design and field test
[DE84-014154] 20 p3484 N85-31652
EVAPORATORS
Development of a preprototype times wastewater recovery subsystem
[NASA-CR-171815] 03 p0388 N85-12480
Addendum: Development of a preprototype times wastewater recovery subsystem
[NASA-CR-171816] 03 p0388 N85-12481
Development of a preprototype times wastewater recovery subsystem: Appendices
[NASA-CR-171817] 03 p0388 N85-12482
Open cycle OTEC thermal-hydraulic systems analysis and parametric studies
[DE84-013011] 04 p0530 N85-13391
Open-cycle centrifugal vapor-compression heat pump
[PB85-113405/GAR] 09 p1328 N85-18348
Operation of a low temperature absorption chiller at rating point and at reduced evaporator temperature
[DE85-006306] 16 p2760 N85-27030
Spacecraft, straight-tube evaporator design
[AD-A154462] 19 p3226 N85-30003
An experimental apparatus to study nucleate pool boiling of R-114 and oil mixtures
[AD-A154077] 19 p3265 N85-30249
EVAPOTRANSPIRATION
Multispectral Imaging Science Working Group for Hydrologic Science: Executive summary 02 p0214 N85-11414
Remote Sensing of Snow and Evapotranspiration
[NASA-CP-2363] 13 p2123 N85-23223
General report of the researches of snowpack properties, snowmelt runoff and evapotranspiration in Japan 13 p2124 N85-23225
Estimation of regional evapotranspiration using remotely sensed land surface temperature. Part 1: Measurement of evapotranspiration at the Environmental Research Center and determination of Priestley-Taylor parameter 13 p2125 N85-23233
Estimation of regional evapotranspiration using remotely sensed land surface temperature. Part 2: Application of equilibrium evaporation model to estimate evapotranspiration by remote sensing technique — Japan 13 p2125 N85-23234
Testing an energy balance model for estimating actual evapotranspiration using remotely sensed data — Hannover, West Germany barley and wheat fields 13 p2125 N85-23236
Soil moisture and evapotranspiration estimates based on satellite data 15 p2596 N85-25996
EVASIVE ACTIONS
Simple-motion pursuit-evasion differential games in the plane
[CSIR-TWISK-336] 14 p2412 N85-24874
Stochastic pursuit-evasion differential games in the plane
[CSIR-TWISK-343] 14 p2412 N85-24875
EVECTION
U LUNAR ORBITS
U ORBIT PERTURBATION
U SOLAR GRAVITATION
EVEN-EVEN NUCLEI
Boson-fermion symmetries in the W-Pt region
[DE85-009755] 19 p3362 N85-30845
EVENTS
An investigation of the relationship between stressful life events and psychological, behavioral and physiological outcomes
[AD-A147754] 08 p1197 N85-17541
Software for event oriented processing on multiprocessor systems
[DE84-016720] 09 p1370 N85-18607
A replication and extension of the inducement of the availability heuristic
[AD-A149755] 12 p1923 N85-22083
A comparison of alternative analytic models for event related potential records
[AD-A151977] 15 p2618 N85-26134
EVOKED RESPONSE (PSYCHOPHYSIOLOGY)
An optically isolated amplifier
[CSIR-SR-ELEK-257] 01 p0049 N85-10321
Pattern reversal visual evoked potentials and reaction time
[CSIR-SR-PERS-354] 01 p0097 N85-10644
An investigation of the use of steady-state evoked potentials for human performance and workload assessment and control
[AD-A145727] 02 p0237 N85-11541
Visually evoked responses from non-occipital areas of the human cortex
[AD-A146079] 03 p0400 N85-12553
Evidence for multiple areas in the human auditory cortex
[AD-A146088] 03 p0401 N85-12555
Reflection of lateralization of sound stimuli in evoked potentials of human brain 04 p0544 N85-13483
ERPS to monitor non-conscious mentation 05 p0707 N85-14536
Performance enhancements under dual-task conditions 05 p0707 N85-14537
In search of a visual-cortical describing function: A summary of work in progress 05 p0707 N85-14538
Measurement of workload: Physics, psychophysics, and metaphysics 05 p0708 N85-14539

Central regulation of sensory flow in human visual system 07 p1013 N85-16435
Visual evoked potentials with disrupted functioning of nonspecific cerebral systems 07 p1013 N85-16437
Nicholet MED-80 (trademark) programs in the Naval Biodynamics Laboratory evoked potential series [AD-A147105] 07 p1016 N85-16451
Laboratory note: Effect on sleep latency of pre-sleep AEP (Auditory Evoked Potential) procedures [AD-A147620] 08 p1194 N85-17527
Brain mechanisms underlying individual differences in reaction to stress: An animal model [AD-A150195] 13 p2143 N85-23301
Effect of triphthasine and elenium on changes in evoked bioelectrical activity of the brain exposed to stationary magnetic field 19 p3325 N85-30601
Matched filtering of visual evoked potentials to detect acceleration (+Gz) induced blackout [AD-A155912] 24 p4131 N85-35609

EVOLUTION
Sedimentary and tectonic evolution of the western Taiwan foredeep 03 p0369 N85-12491
Global aspects of stream evolution in the solar wind [DE85-002207] 11 p1766 N85-21101

EVOLUTION (DEVELOPMENT)
NT ABIOGENESIS
NT BIOLOGICAL EVOLUTION
NT CHEMICAL EVOLUTION
NT GALACTIC EVOLUTION
NT LUNAR EVOLUTION
NT PLANETARY EVOLUTION
NT STELLAR EVOLUTION
NT STELLAR MASS ACCRETION
Phylogenic distribution of the large 55 rRNA from Halococcus morrhuae [NASA-CR-174019] 02 p0234 N85-11523
Origin and evolution of the Uranian and Neptunian satellites: Some dynamical considerations 02 p0300 N85-11943
Composition, structure and evolution of Uranian and Neptunian satellites 02 p0300 N85-11944
Structure and evolution of the large scale solar and heliospheric magnetic fields 05 p0746 N85-14782
Evolutionary history of CI and CM chondrites 06 p0864 N85-15615
The development of the vestibular apparatus under conditions of weightlessness [NASA-TM-77517] 07 p1011 N85-16422
The origin and evolution of terrestrial and Martian rock labyrinths [NASA-CR-175511] 12 p1961 N85-22326
Asteroid collisional evolution studies 13 p2176 N85-23501
The legacy of science 14 p2432 N85-24995
Monitoring tropical cyclone growth using GOES VISSR/VAS and Nimbus-7 TOMS data 15 p2595 N85-25869
The evolution of meteor streams 15 p2678 N85-26539
Origin and evolution of ordinary chondrite meteorites 15 p2683 N85-26571
Origin of mesosiderites as a natural consequence of planet formation 15 p2683 N85-26574
Theoretical approach to evolution of solar magnetic field 18 p3204 N85-29874
The origin and evolution of the Earth's atmosphere and hydrosphere 19 p3312 N85-30633
The evolution of complex and higher organisms [NASA-SP-478] 21 p3656 N85-32708
Heat transfer and brine evolution in magma-hydrothermal systems 24 p4104 N85-35441
Origin of sedimentary humic acids, potential carriers of ore-forming elements 24 p4104 N85-35443

EVOLUTION (LIBERATION)
NT GAS EVOLUTION
Evolution of strong inhomogeneities in ionospheric plasma, part 1 14 p2330 N85-24463

EXACTNESS
U PRECISION

EXAMINATION
Method of examining microcircuit patterns [NASA-CASE-NPO-16299-1] 11 p1628 N85-20250

EXCAVATION
Impacts in ice: Commissions of solar system crater population 13 p2161 N85-23538

EXCHANGING
NT CHARGE EXCHANGE
NT GAS EXCHANGE
NT ION EXCHANGING
NT SPIN EXCHANGE
Deep-inelastic lepton scattering by nuclei: The pion-exchange model. [DE85-010486] 19 p3359 N85-30628
Tropospheric-stratospheric exchange, part 1.1A 21 p3615 N85-32466

EXCIMER LASERS
Manual for Raman cells [NASA-TM-77756] 01 p0052 N85-10342
The 248 nm - new short wavelength for pumping lasers employing vapors of complex molecules 02 p0261 N85-11705
RF laser plasma measurements [AD-A145936] 03 p0366 N85-12344
A high-repetition rate, inductively stabilized, long-pulse excimer laser [DE84-016827] 04 p0506 N85-13229
Development of prototypes for versatile fast discharge systems for pulsed gas lasers, especially excimer lasers [BMFT-FB-T-84-174] 06 p0813 N85-15165
Visible and ultraviolet lasers based on excimer transitions in the homonuclear halogens [AD-D011311] 07 p0971 N85-16163
Excimer laser photofragmentation of organophosphonates. 1: Detection of the PO radical from dimethyl methyl phosphonate (DMMP) [AD-A149471] 10 p1490 N85-19407
Pulsed excimer laser processing for cost-effective solar cells [NASA-CR-174429] 10 p1509 N85-19517
Investigation of dye lasers pumped by high-power KrF laser radiation 11 p1718 N85-20806
Non-linear optical techniques for visible and UV lasers and thin film deposition [AD-A150489] 13 p2096 N85-23077
Time-resolved ellipsometry and reflectivity measurements of the optical properties of silicon during pulsed excimer laser irradiation [DE85-005091] 13 p2096 N85-23079
Low jitter trigger for an excimer laser [DE85-005732] 13 p2097 N85-23080
Excimer laser annealing to fabricate low cost solar cells [NASA-CR-175702] 14 p2351 N85-24529
Pulsed excimer laser processing for cost-effective solar cells [NASA-CR-175700] 14 p2351 N85-24530
Kinetic studies following state selective laser excitations [DE85-007173] 15 p2564 N85-25816
Discharge characteristics of high-pressure, fast-discharge XeCl excimer laser 15 p2564 N85-25820
Flat-plate solar array project process development area: Process research of non-CZ silicon material [NASA-CR-175777] 16 p2818 N85-27382
Production of gallium atoms by excimer laser photolysis of trimethyl gallium [DE85-010742] 19 p3278 N85-30331
Theoretical modeling of the discharge-pumped XeCl excimer laser 20 p3460 N85-31495
A fast discharge excimer laser with symmetric geometry [AD-A155294] 21 p3592 N85-32322
Investigation of plasma processes in electronic transition lasers [AD-A155598] 21 p3593 N85-32327
Pulsed excimer laser processing for cost-effective solar cells 21 p3611 N85-32432
Excimer laser annealing for fabrication of low-cost solar cells 21 p3611 N85-32433
Establishment of steady-state power level in pulse-periodic excimer laser 21 p3685 N85-32896
Saturation effect in multilevel lasing media 21 p3686 N85-32901
Excimer-laser generator of powerful UV picosecond pulses synchronized with picosecond pulses in visible and IR bands 21 p3686 N85-32903
Powerful XeCl excimer electric discharge laser with good temporal stability and fast response time 21 p3688 N85-32911
Sliding discharge in CO2 and excimer lasers 22 p3773 N85-33379
Flat-plate solar array project process development area process research of non-CZ silicon material [NASA-CR-176117] 23 p3945 N85-34445
Generation of stimulated emission in the soft X-ray range by nonlinear processes with excimer lasers [DE85-012465] 24 p4096 N85-35403

EXCIMERS
E-beam-induced fluorescence of excimers in cryogenic solutions [DE85-010703] 19 p3278 N85-30328
Energy transfer and excimer formation in rare gas solids 19 p3374 N85-30930
A fast discharge excimer laser with symmetric geometry [AD-A155294] 21 p3592 N85-32322

EXCITATION
NT ACOUSTIC EXCITATION
NT ATOMIC EXCITATIONS
NT MOLECULAR EXCITATION
NT SELF EXCITATION
NT WAVE EXCITATION
Experimental studies of atomic inner shell ionization phenomena [DE84-013448] 01 p0118 N85-10805
Excitation of quasi-static magnetic fields with axial structure 02 p0259 N85-11696
Search for white dwarf companions of cool stars with peculiar element abundances [NASA-CR-174030] 02 p0297 N85-11923
RF laser plasma measurements [AD-A145936] 03 p0366 N85-12344
An inverse source problem for elastic waves 03 p0371 N85-12368
Laser excitation of coupled surface electromagnetic and acoustic waves and of static structures in solids 05 p0723 N85-14652
Raman study of neutron irradiated GaAs [DE84-016056] 05 p0731 N85-14702
The correlation between excitation parameter and nebular luminosity for galactic HII regions with application to regions of star formation in M83 05 p0743 N85-14773
Flight test technique for evaluation of gust load alleviation analysis methodology [NASA-TM-86344] 06 p0754 N85-14833
Experimental determination of propagation rate of ELF signals employed by Omega radio navigation system for phase measurements 06 p0793 N85-15066
Intense excitation source of blue-green laser [AD-A147450] 07 p0971 N85-16168
Theoretical study of laser-induced surface excitations on a grating [AD-A147855] 07 p0972 N85-16172
Microwave resonator using lateral excitation [AD-D011374] 07 p1039 N85-16506
Pion inelastic scattering to the first three excited states of Lithium-6 [AD-A147560] 07 p1041 N85-16606
Phase-dissipative mechanisms for laser-induced surface desorption-dissociation processes [AD-A147961] 08 p1121 N85-17065
Instrumentation for particle-beams research using laser excited merging beams [AD-A147968] 08 p1220 N85-17681
Degenerate four-wave mixing lineshapes in sodium vapor under pulsed excitation [AD-A148211] 08 p1222 N85-17696
Atomic and molecular collision processes [DE85-001604] 09 p1382 N85-18690
The coordinated research program at IAEA on atomic collision data for plasma diagnostics 09 p1390 N85-18747
A picosecond population modulation study of near interband resonances in semiconductors 09 p1396 N85-18787
Excitation modes and parameters of stress waves in metal exposed to single laser pulses 10 p1446 N85-19109
Infrared excitation of clusters and ions of atmospheric interest [DE85-002098] 10 p1516 N85-19564
Plane-wave born collision strengths for electron-ion excitation: Comparison with other theoretical methods [DE85-002348] 10 p1555 N85-19802
Hydrodynamic response of a radiating Al plasma excited by a proton beam [AD-A148904] 10 p1558 N85-19824
KMSF X-ray laser experiments, task no. 2 [DE85-000291] 11 p1640 N85-20335
Mini-modal testing of wind turbines using novel excitation [DE85-000868] 11 p1654 N85-20417
Excitation of impurities by heavy particles and radiative losses of thermonuclear plasma 11 p1719 N85-20816
Hydrogen vibrational population distributions and negative ion generation in tandem high density hydrogen discharges [DE85-001207] 11 p1722 N85-20834
Large amplitude forcing of a high speed 2-dimensional jet [NASA-CR-175646] 13 p1974 N85-22393
Use of markets to elucidate reacting sputtering processes [DE85-005723] 13 p2018 N85-22655
Exitation of low-frequency resonance waves by moving conductor in space plasma 13 p2067 N85-22912
Induction excitation of deep conducting zones 13 p2111 N85-23154
Study of resolution of deep MT soundings by means of physical model 13 p2112 N85-23155

Observation of a novel low-lying excited state in zinc complexes
[AD-A150188] 13 p2156 N85-23385
Sequential excitation preparation of molecular energy levels with special structural and chemical properties
[AD-A150301] 13 p2156 N85-23386
Electron stimulated desorption and the role of secondary electrons
[AD-A150974] 14 p2252 N85-23965
Computer simulations of rare earth sites in glass: Experimental tests and applications to laser materials
[DE85-006156] 14 p2261 N85-24013
Sensitization and quenching in the conversion of light energy into chemical energy
[DE85-006301] 14 p2351 N85-24535
Ion kinetics, small neutral and excited components in D-region with elevated ionization level. Part 2: Variations in small neutral and excited components
15 p2480 N85-25307
Electric discharge excitation and energy source integration
[AD-A151502] 15 p2562 N85-25808
Calculations of collision-induced optical gain in high-density mixtures of D2 or HD with a buffer gas
[AD-A151372] 15 p2648 N85-26330
Neutralization and excitation in low-energy ion-surface collisions
[AD-A151568] 15 p2660 N85-26414
A study of excitations during collisionally-induced electron detachment of negative ions
[AD-A152879] 17 p3030 N85-28739
Extension of the consistent Q formalism to odd-A nuclei in the W-Pt region
[DE85-008264] 17 p3034 N85-28770
Magnetically switched power supply systems for lasers
[NASA-CASE-NPO-16402-1] 18 p3112 N85-29265
Laser-stimulated vibrational excitation of an adspecies studied by a generalized master equation: Neutral atomic hydrogen on hydrated KCl(001)
[AD-A153665] 18 p3112 N85-29268
Review of short wavelength lasers
[DE85-009858] 18 p3114 N85-29277
Monte Carlo simulation of thermalization of subexcitation electrons in He, Ne, Ar, Kr and Xe
[NAL-TR-843T] 18 p3178 N85-29702
Excited state populations and charge-exchange of fast ions in solids
[DE85-009362] 18 p3180 N85-29714
Excited leptons contribution to muon g-2
[PREPRINT-432] 18 p3184 N85-29745
Alkali atom - SbCl(5) reactions: Blue-green chemiluminescence from an inverted population in SbCl
[AD-A154371] 19 p3276 N85-30315
Excitation of turbulence by density waves
[NASA-CR-3905] 19 p3314 N85-30546
Instrumentation for particle-beams research using excited merging beams
[AD-A154155] 19 p3356 N85-30607
Energy transfer and excimer formation in rare gas solids 19 p3374 N85-30930
Predamage threshold electron emission from insulator and semiconductor surfaces
[DE85-008968] 19 p3377 N85-30954
Antiproton-nucleus inelastic scattering and the spin-isospin dependence of the N anti N interaction
[DE85-010546] 20 p3526 N85-31935
Ab initio calculations of materials properties
[DE85-011167] 20 p3531 N85-31964
Detection of excited states by laser-induced fluorescence
[AD-A155558] 21 p3592 N85-32326
Toward a theory of excitation of atoms during nuclear and magnetic neutron scattering
21 p3689 N85-32918
Radiative-collision generation of sound in gases subjected to single-pulse optical excitation
21 p3689 N85-32920
Resonant energy transfer during strong excitation
21 p3689 N85-32922
Exotic events of p bar p-collider: Excited quark or excited color boson?
21 p3691 N85-32930
Vibrationally enhanced dissociation of diatomic molecules
[AD-A154827] 21 p3701 N85-32996
Electron photoejection in carbanions
[DE85-011748] 23 p3912 N85-34237
Pressure cross spectra in turbulent boundary layers in water
[AD-A156153] 24 p4094 N85-35378
Investigations of the molecular beam epitaxial growth and characteristics of external excitation induced non-equilibrium phases of immiscible 3-5 compound semiconductors
[AD-A156325] 24 p4182 N85-35804
Observations of far-infrared transitions between excited states of OH
[NASA-TM-86722] 24 p4167 N85-35833

EXCITED STATES
U EXCITATION

EXCITONS
Photophysical studies of triplet exciton processes in pure polymer films
[DE84-016258] 05 p0620 N85-13965
Spectroscopic investigation of materials for frequency agile laser systems
[AD-A151731] 16 p2790 N85-27208
Photophysical studies of triplet exciton processes in pure polymer films
[DE85-008571] 18 p3080 N85-29056
Stationary properties and switching characteristics of dispersive optical bistability in CuCl
18 p3186 N85-29763
A theory of exciton photoluminescence for two types of neutral acceptors in silicon. A study of the systems Si:(B, IN), Si:(Al), (Si), Si:(Ga, In), Si:(B, Al), Si:(B, Ga), and Si:(Al, GA)
[AD-A155452] 21 p3710 N85-33031
Time-resolved and infrared spectroscopy of excitons
[DE85-011879] 23 p3912 N85-34235
Pairing correction of particle-hole state densities for two kinds of fermions
[DE85-011549] 23 p3971 N85-34620
Optical properties of heterostructures and superlattices
[AD-A156243] 24 p4162 N85-35802

EXCLUSION
Some recent developments in systems reliability
[AD-A150661] 14 p2317 N85-24318

EXCRETION
Circadian dynamics of potassium excretion in urine as related to working on one and two shifts
19 p3325 N85-30598

EXECUTIVE AIRCRAFT
U GENERAL AVIATION AIRCRAFT
U PASSENGER AIRCRAFT

EXERCISE
U PHYSICAL EXERCISE

EXERCISE PHYSIOLOGY
Voluntary dehydration and electrolyte losses during prolonged exercise in the heat
[AD-A145157] 01 p0095 N85-10639
A machine for weight-lift testing
[AD-A146816] 07 p0973 N85-16182
Effects of restricted water intake on performance in a cold environment
[AD-A146904] 07 p1015 N85-16450
Thermoregulatory responses during exercise at graded hypohydration levels
[AD-A147733] 08 p1195 N85-17528
The effect of beta adrenergic blockade on ratings of perceived exertion
[AD-A148053] 08 p1195 N85-17530
Cognitive performance during successive sustained physical work episodes
[AD-A148061] 08 p1200 N85-17556
Blood viscosity responses to acute exercise and aerobic conditioning in women 09 p1363 N85-18573
Sleep deprivation and exercise tolerance
[AD-A150566] 13 p2142 N85-23296
Aerobic and anaerobic exercise tolerance in the heat: Effect and acclimatization 14 p2388 N85-24707
SPARTEN (Scientific Program of Aerobic and Resistance Training Exercise in the Navy): A total body fitness program for health and physical readiness
[AD-A150869] 14 p2388 N85-24711
Preparing Alberto Salazar for the heat of the 1984 Olympic Marathon
[AD-A150942] 14 p2389 N85-24714
Exercise-heat strain during hypohydration: Interaction with heat acclimation and aerobic fitness
[AD-A151023] 14 p2389 N85-24717
Physiological differences between men and women in exercise-heat tolerance and heat acclimation
[AD-A152048] 15 p2618 N85-26135
Comparative anaerobic power of males and females
[AD-A151960] 16 p2842 N85-27523
Relationship between the Army two mile run test and maximal oxygen uptake
[AD-A153914] 18 p3154 N85-29526
Regional circulation during testing on isokinetic dynamometer following 14-day bedrest
19 p3323 N85-30590
Heat injury: Prevention is the key
[AD-A153734] 19 p3328 N85-30622
Effect of short-term antiorthostatic hypokinesia on dynamics of cardiorespiratory parameters during graded physical exercise 22 p3622 N85-33677
Weight loss, rectal temperature and heart rates following the 1984 Boston Marathon
[AD-A155984] 24 p4132 N85-35612
Thirst and fluid intake following graded hypohydration levels in humans
[AD-A156201] 24 p4132 N85-35615

EXERTION
U PHYSICAL WORK

EXHAUST DIFFUSERS
Energy efficient engine combustor test hardware detailed design report
[NASA-CR-167945] 02 p0140 N85-10950
Strutless diffuser for gas turbine engine
[AD-D011662] 18 p3062 N85-28943

EXHAUST EMISSION
Size specific total particulate emission factors for mobile sources
[PB84-226653] 01 p0071 N85-10471
Mobile source exposure estimation
[PB84-224518] 01 p0095 N85-10643
Energy efficient engine component development and integration program
[NASA-CR-168496] 02 p0146 N85-10969
The changing pattern of fossil fuel CO2 emissions
[DOE/OR-21400/2] 02 p0224 N85-11469
Analysis of potential combustion sorce impacts on acid deposition using an independently derived inventory, volume 1
[DE84-012005] 02 p0225 N85-11471
Dissociated methanol vehicle test results
[DE84-004507] 04 p0509 N85-13248
Outline of a new emissions model for military and civilian aircraft facilities
[DE84-016455] 04 p0531 N85-13394
Facility safety study
[NASA-CR-174280] 07 p0910 N85-15759
Impact of aircraft emissions on air quality in the vicinity of airports. Volume 3: Air quality and emission modeling needs
[AD-A147951] 08 p1180 N85-17435
The application of emissions trading to DoD installations
[AD-P004138] 09 p1346 N85-18472
The influence on IR emission of engine parameters for an afterburn case. A sensitivity study on NATO infrared air target model (NIRATAM) version: 0.0
[AD-B089311L] 12 p1779 N85-21171
Stability of organic audit materials and results of source test analysis audits
[PB85-116184] 12 p1885 N85-21632
Composition and photochemical reactivity of turbine engine exhaust
[AD-A150559] 13 p2130 N85-23256
Emission inventory applications to regional acid deposition modeling
[PB85-157386] 16 p2760 N85-27033
Air quality benefit analysis for Los Angeles and San Francisco based on housing values and visibility
[PB85-166049] 16 p2822 N85-27409
Effect of traffic and meteorology on air pollution
16 p2830 N85-27452
Clean-burning diesel engines
[AD-A152606] 17 p2974 N85-28374
Mechanisms of exhaust pollutants and plume formation in continuous combustion
[AD-A154169] 20 p3435 N85-31310
Toxic hazards tests for vehicles and other equipment
[AD-A149164] 20 p3506 N85-31797
A study of the control of particulate emissions from turbine engine test cells 24 p4067 N85-35205

EXHAUST FLOW SIMULATION
NT ATMOSPHERIC ENTRY SIMULATION
Calculation of flow about posts and powerhead model — space shuttle main engine
[NASA-CR-171344] 10 p1483 N85-19382
The influence on IR emission of engine parameters for an afterburn case. A sensitivity study on NATO infrared air target model (NIRATAM) version: 0.0
[AD-B089311L] 12 p1779 N85-21171
Calculation of viscous compressible flows in small gas turbines 17 p2912 N85-27950
Numerical simulations of the effect of floor and ceiling venting on fire and smoke spread in aircraft cabins
[PB85-178333] 19 p3216 N85-29939
The highly underexpanded exhaust plume from nozzles with boundary layers
[DFVLR-FB-85-10] 20 p3421 N85-31230

EXHAUST GASES
NT FLUE GASES
Space Shuttle Environmental Effects: The First 5 Flights
[NASA-CR-171812] 01 p0069 N85-10457
Clean-burning diesel engines
[AD-A145515] 02 p0205 N85-11349
Impact of alcohol fuels on urban air pollution: Methanol photochemistry study
[DE84-012950] 04 p0531 N85-13397
Overview of waste heat utilization systems
[NASA-TM-86901] 04 p0578 N85-13692

Direct measurements of nitrous acid, nitrogen dioxide and formaldehyde in auto exhaust by differential optical absorption spectroscopy
[PB84-229289] 06 p0767 N85-14905
The toxicity of complex mixtures
[AD-P004033] 06 p0844 N85-15363
Integrated exhaust gas analysis system for aircraft turbine engine component testing
[NASA-TP-2424] 07 p0962 N85-16100
NOx emissions near a heat pump with gas motor
[BLL-WH-782-(9091.9F)] 07 p0995 N85-16319
Laboratory simulation of smoke reduction from aircraft engine test cell exhaust using a fluidized bed filter
[AD-A148600] 08 p1089 N85-16886
Impact of aircraft emissions on air quality in the vicinity of airports. Volume 3: Air quality and emission modeling needs
[AD-A147951] 08 p1160 N85-17435
An analytic model of gas turbine engine installations
[AD-A148708] 09 p1261 N85-18059
Natural gas the new locomotive fuel
[DE84-901624] 09 p1302 N85-18179
Experimental study of aerodynamic shielding of turbojet engine air intake against exhaust gases
09 p1307 N85-18210
Shock propagation in the exhaust gas handling system of the proposed large altitude rocket cell: Methods and preliminary analysis
[DE85-003055] 11 p1591 N85-20010
Diesel engine emissions of particulates and associated organic matter
[PB85-154425] 15 p2590 N85-25964
Papers from the Symposium on Emissions: The Value of Incentives and Guidelines for Control
[S-336] 15 p2590 N85-25967
Transformation of nitrogen oxides while sampling combustion products
[AD-A152184] 16 p2746 N85-26945
Measurements of two-phase exhaust flow parameters of a small caliber gun associated with muzzle flash phenomena
[ISL-CO-212/83] 16 p2784 N85-27182
High resolution spectroscopy of C13O16 in gas mixtures
[AD-A152625] 17 p2919 N85-27991
Clean-burning diesel engines
[AD-A152606] 17 p2974 N85-28374
Opacity control technique for jet engine test cells
[AD-D011668] 19 p3220 N85-29966
Analysis of aldehydes and ketones in the gas phase
[PB85-181895] 20 p3426 N85-31261
Comparative evaluation of three alternative power cycles for waste heat recovery from the exhaust of adiabatic diesel engines
[NASA-TM-86963] 20 p3542 N85-32043
Influence on an industrial site on the characteristics of CCN supersaturation with air masses of different origin
21 p3650 N85-32683
Ames Laboratory measurements of alkali levels in the Curtiss-Wright PFBC gas stream
[DE85-011357] 22 p3745 N85-33214
Modeling of auto exhaust smog chamber data for EKMA development
[PB85-186492] 22 p3813 N85-33619

EXHAUST JETS
U EXHAUST GASES

EXHAUST NOZZLES
NT CONVERGENT-DIVERGENT NOZZLES
NT PLUG NOZZLES
Density distribution in supersonic jet discharged into vacuum from nozzle with bevel tip
02 p0269 N85-11757
The preliminary checkout, evaluation and calibration of a 3-component force measurement system for calibrating propulsion simulators for wind tunnel models
[NASA-CR-174113] 04 p0458 N85-12903
Static jet noise test results of four 0.35 scale-model QCGAT mixer nozzles
[NASA-TM-86871] 04 p0558 N85-13551
Carbon/carbon rocket motor exit cone reinforcement
[AD-D011360] 07 p0916 N85-15799

EXHAUST SYSTEMS
Noise reduction of the exhaust from pneumatic tools
[BMFT-FB-HA-83-021] 02 p0276 N85-11799
Calculation of flow about posts and powerhead model — space shuttle main engine
[NASA-CR-171344] 10 p1483 N85-19362
Pneumatic clamping device
[AD-D011544] 12 p1858 N85-21658
Exhaust systems for passenger vehicles: Test procedure for resistance to internal corrosion of silencers
[BLL-BISI-TRANS-22360-(9022.06)]
17 p2973 N85-28361
Numerical simulations of the effect of floor and ceiling venting on fire and smoke spread in aircraft cabins
[PB85-178333] 19 p3216 N85-29939
Measurement of turbofan-turbojet thrust from tailpipe static pressure
[AD-A154036] 19 p3220 N85-29967

EXHAUST VELOCITY
Particle size, number, composition and velocity from solid rocket motors 12 p1785 N85-21201
Estimation of launch vehicle performance parameters
[AD-A151927] 16 p2728 N85-28839

EXISTENCE THEOREMS
The Boltzmann equation: Global existence for a rare gas in an infinite vacuum
[PREPRINT-78] 01 p0124 N85-10851
The Chinese remainder theorem and multi-PRF radars
[AD-A141375] 13 p2054 N85-22858

EXITS (DOORS)
U DOORS

EXOBIOLOGY
Space medicine and biology, continuing bibliography (supplement 263)
[NASA-SP-7011(263)] 01 p0094 N85-10636
Publications of the exobiology program for 1981: A special bibliography
[NASA-TM-86653] 01 p0099 N85-10657
Aerospace Medicine and Biology, a continuing bibliography with indexes
[NASA-SP-7011(264)] 02 p0234 N85-11525
A survey of space biology and space medicine
[ESA-BR-17] 04 p0545 N85-13486
Aerospace Medicine and Biology, a continuing bibliography with indexes
[NASA-SP-7011(265)] 04 p0545 N85-13487
Plant growth in space 05 p0691 N85-14444
Aerospace medicine and biology: A continuing bibliography with indexes
[NASA-SP-7011(266)] 08 p1194 N85-17525
Aerospace medicine and biology: A continuing bibliography with indexes, supplement 268
[NASA-SP-7011(268)] 08 p1194 N85-17526
Aerospace medicine and biology: A continuing bibliography with indexes
[NASA-SP-7011(269)] 10 p1526 N85-19626
Modular plant culture systems for life support functions
[NASA-CR-171853] 12 p1899 N85-21924
Second Soviet-French Symposium on Space Technology 15 p2483 N85-25326
Aerospace Medicine and Biology: A continuing bibliography with indexes
[NASA-SP-7011(270)] 15 p2615 N85-26114
Aerospace medicine and biology: A continuing bibliography with indexes, supplement 271, May 1985
[NASA-SP-7011(271)] 16 p2840 N85-27514
The cosmic history of the biogenic elements and compounds
[NASA-SP-476] 17 p3003 N85-28582
USSR report: Space Biology and Aerospace Medicine, volume 18, no. 5, September - October 1984
[JPRS-USB-84-007] 19 p3322 N85-30583
Changes in nephron and juxtaglomerular system of primate kidneys under the effect of antiorthostatic hypokinesia 19 p3326 N85-30605
Influence of limboreticular complex on some reactions of rabbits 19 p3326 N85-30607
Aerospace Medicine and Biology: A continuing bibliography with indexes (supplement 272)
[NASA-SP-7011(272)] 19 p3328 N85-30620
Sensitivity of human lymphocytes to microgravity in-vitro 20 p3510 N85-31820
Biostack experiments on STS-flights and the impact for man in space 20 p3510 N85-31821
The global sulfur cycle
[NASA-TM-87570] 21 p3656 N85-32710
Aerospace medicine and biology: A continuing bibliography with indexes, supplement 273
[NASA-SP-7011(273)] 21 p3663 N85-32755
Search for the universal ancestors
[NASA-SP-477] 21 p3667 N85-32777
USSR report: Space Biology and Aerospace Medicine, volume 19, no. 2, March - April 1985
[JPRS-USB-85-004] 22 p3820 N85-33667
Aerospace Medicine and Biology: A continuing bibliography with indexes (supplement 274)
[NASA-SP-7011(274)] 23 p3952 N85-34491
NASA Developmental Biology Workshop: A summary
[NASA-TM-86756] 24 p4126 N85-35578
Vertebrate development in space: Gravity is a drag (and has been for eons and eons) 24 p4126 N85-35580
Report of the NASA Mammalian Developmental Biology Working Group 24 p4126 N85-35581
Report of Amphibian Development Group
24 p4127 N85-35583
Report of the Insect Development Group
24 p4127 N85-35584
Aquatic Invertebrate Development Working Group
24 p4127 N85-35585
Report of the Microbial Development Working Group
24 p4127 N85-35586

EXOSAT SATELLITE
EXOSAT observations of active galactic nuclei
08 p1238 N85-17809
Soft X-ray emission from BL Lac objects
08 p1239 N85-17810

EXOSPHERE
Experimental investigation of neutral plasma beam propagation across a magnetic field
[AD-A150944] 14 p2423 N85-24947
Advances in technology development for exoatmospheric research
[AD-A152581] 17 p2992 N85-28495

EXOTHERMIC REACTIONS
Exothermic processes in solids under low temperatures, their physics and their cryogenic implications
[JUEL-1919] 03 p0414 N85-12651
Theoretical studies on N-bonded pyrazole derivatives of boron
[AD-A150036] 12 p1813 N85-21374
Physical chemistry of exothermic gas-aerosol calorimetry
[AD-A150672] 14 p2251 N85-23950
The effect of mould size on the exothermic reaction and compressive strength of epoxy resin chocks
[AD-A155102] 21 p3570 N85-32203
Optical waveguide along front of exothermic reaction
21 p3694 N85-32954
Pulsed hydrojet propulsion
[DE85-010771] 22 p3784 N85-33448

EXPANDABLE STRUCTURES
NT BALLOONS
NT HIGH ALTITUDE BALLOONS
NT INFLATABLE STRUCTURES
NT JIMSPHERE BALLOONS
NT METEOROLOGICAL BALLOONS
NT MICROBALLOONS
NT SUPERPRESSURE BALLOONS
NT TETHERED BALLOONS
LDR system concepts and technology
14 p2231 N85-23823

EXPANSION
NT GAS EXPANSION
NT KARHUNEN-LOEVE EXPANSION
NT PRANDTL-MEYER EXPANSION
NT SERIES EXPANSION
NT THERMAL EXPANSION
In-situ stress relief of expanded alloy 600 steam generator tubing
[DE84-014560] 04 p0513 N85-13273
Device for measuring relative axial expansion of turbine rotor employing space-vector tracking method
06 p0776 N85-14962
Basic studies of multiple free and confined jets
[AD-A149556] 10 p1485 N85-19374
Tenth-order expansion formulas for the orbital eccentricity function K (sub lpq)(e) obtained using a symbolic algebraic manipulation system
[AD-A153754] 18 p3170 N85-29647
Expedient runway surfacing with post tensioning system for expeditionary airfields
[AD-D011677] 19 p3222 N85-29976
An algorithm for the influence numbers in the expansion of the lumped gravitational potential coefficients in the presence of resonant inclination variation
[AD-A154229] 19 p3336 N85-30689
Acoustic radiation from concentric shells containing an inner fluid
[AD-A155476] 21 p3700 N85-32991

EXPANSION WAVES
U ELASTIC WAVES

EXPECTANCY HYPOTHESIS
Testing of inequality hypotheses in linear models using the Bayes method
[SER-C-292] 01 p0112 N85-10761

EXPENDABLE STAGES (SPACECRAFT)
The Expendable Launch Vehicle Commercialization Act
[GPO-30-838] 04 p0460 N85-12919
Commercial space launches
[S-REPT-98-656] 12 p1788 N85-21225

EXPERIMENT DESIGN
NT FACTORIAL DESIGN
Results of the technical exchange agreement between NASA and DuPont on the containerless drop tube solidification of NiAl3
[NASA-TM-86473] 01 p0014 N85-10087
Determination of vowel zones in speech — speech recognition
[FUB-16-1983] 01 p0040 N85-10253
Fast waves near the lower hybrid frequency
[DE84-015217] 01 p0123 N85-10841

Fluids Experiment Apparatus (FEA)
02 p0155 N85-11048
Design and implementation of a low-gravity solidification experiment package for the F-104
02 p0156 N85-11053
Advances in electrophoretic separations
02 p0156 N85-11054
Laser on copper and gold vapors with space diversity media
02 p0270 N85-11762
The Beatrice experiment and the luminance concept in Dante
[NOTA-INTERNA-823] 02 p0281 N85-11831
An underground search for massive slow particles (hunting Grand Unified Theory (GUT) monopoles)
[NOTA-INTERNA-821] 02 p0292 N85-11894
Definition of ground test for verification of large space structure control
[NASA-CR-171206] 05 p0602 N85-13838
Ground test experiment for large space structures, appendix I
05 p0603 N85-13847
Plant cell cultures in biological space experiments
05 p0690 N85-14434
Comparison of simulation of weightlessness by Head Down Tilt (HDT) and Water Immersion (WI)
05 p0692 N85-14454
Medication interference with space research: An example from a mass-discrimination experiment on Spacelab 1
05 p0695 N85-14472
Response surface designs
[AD-A147202] 07 p1035 N85-16589
Experiment description 08 p1143 N85-17210
UCB cosmic ray experiment 09 p1417 N85-18941
A preliminary study of a cryogenic equivalence principle experiment on Shuttle
[NASA-CR-171300] 10 p1426 N85-18994
Fluid slosh dynamics of surface tension tanks in three axis stabilized spacecraft
[MBB-UR-E-739-84-O] 11 p1634 N85-20291
Human assembly time versus levels of visual and tactile sensory input: Experimental results for five devices
[AD-A149982] 12 p1909 N85-21980
Investigation of dynamics of radiation spectrum of injection lasers by infrared impulse Fourier spectroscopy
13 p2090 N85-23047
Control Of Flexible Structures (COFS) flight experiment background and description 14 p2236 N85-23664
Electro-science requirements for shuttle-attached antenna flight experiments 14 p2237 N85-23666
Determining optimum service conditions for concentrator mirrors by methods of mathematically planned experiment 14 p2274 N85-24090
An interactive computer package for use with simulation models which performs multidimensional sensitivity analysis by employing the techniques of response surface methodology
[AD-A151956] 16 p2846 N85-27548
Botany facility phase A study. Core payload number 6 EURECA carrier, volume 1
[ESA-CR(P)-1978-VOL-1] 17 p2906 N85-27918
Botany facility phase A study. Core payload number 6 for EURECA carrier, volume 2
[BF-TD-DRD-03-VOL-2] 17 p2906 N85-27919
Laboratory research: A question of when, not if
[AD-A153296] 17 p3048 N85-28867
Optimization of single and multi-component analytical techniques
[HSE-TRANS-10987] 19 p3347 N85-30744
Experiments with stored heavy ions
[DE85-009978] 19 p3356 N85-30802
Efficiency tests of samplers for microbiological aerosols, a review
[FOA-C-40199-B1] 20 p3504 N85-31783
Design of simulation experiments
[FEW-123] 20 p3519 N85-31885
Apparatus for unilateral generation of a homogeneous magnetic field
[DE85-008001] 23 p3928 N85-34345
Experimental lithium system
[DE85-013252] 24 p4094 N85-35382
Model robust response surface designs: Scaling two-level factorials
[AD-A156218] 24 p4143 N85-35886

EXPERIMENTAL BREEDER REACTOR 2
SASSYS-1 computer code verification with EBR-2 test data
[DE85-012119] 24 p4139 N85-35657

EXPERIMENTATION
On thermomechanical testing in support of constitutive equation development for high temperature alloys
[NASA-CR-174879] 15 p2577 N85-25894
High pressure cosmochemistry applied to major planetary interiors: Experimental studies
[NASA-CR-175715] 15 p2679 N85-26544
Sensitivity and performance characterization of DINGU
[DE85-010750] 22 p3754 N85-33269
Experimental studies of chemical reactivity during shock initiation of hexanitrostilbene
[DE85-011726] 22 p3754 N85-33270
Separation of gas mixtures by supported complexes
[DE85-011996] 23 p3912 N85-34236
Evaluation of low-temperature geothermal potential in Utah and Goshen Valleys and adjacent areas, Utah. Part 2: Water temperature and chemistry
[DE85-009344] 23 p3943 N85-34438
Throughfall rate and chemistry studies: Whiteface Mountain
[DE85-012407] 23 p3947 N85-34464
The 1984 biotic studies of Yucca Mountain, Nevada test site, Nye County, Nevada
[DE85-011715] 23 p3951 N85-34487
The impact of supercomputers on experimentation: A view from a national laboratory
[NASA-TM-86822] 23 p3955 N85-34510
Analysis of transient radiation upset in a 16K SRAM
[DE85-009442] 23 p3965 N85-34586
Experimental technique for measuring the isentrope of hydrogen to several megabars
[DE85-014332] 24 p4095 N85-35386

EXPERT SYSTEMS
A relational approach to the development of expert diagnostic systems
[NASA-TM-86288] 01 p0099 N85-10658
Diagnosis via causal reasoning: Paths of interaction and the locality principle
[AD-P003920] 02 p0245 N85-11600
A representation for the functioning of devices that supports compilation of expert problem solving structures: An extended summary
[AD-P003921] 02 p0245 N85-11601
Application of the CSRL language to the design of expert diagnosis systems: The Auto-Mech experience
[AD-P003922] 02 p0245 N85-11602
An expert system for representing procedural knowledge
[AD-P003923] 02 p0245 N85-11603
Failure detection processes by pattern recognition and expert systems
[AD-P003924] 02 p0246 N85-11604
Designing an expert system for training automotive electrical troubleshooting
[AD-P003926] 02 p0246 N85-11606
Artificial intelligence approaches to monitoring system integrity
[AD-P003930] 02 p0246 N85-11610
Expert systems in maintenance diagnostics for self-repair of digital flight control systems
[AD-P003933] 02 p0247 N85-11613
DELTA: An expert system for diesel electric locomotive repair
[AD-P003941] 02 p0248 N85-11621
The ACE (Automated Cable Expert) experiment: Initial evaluation of an expert system for preventive maintenance
[AD-P003943] 02 p0248 N85-11623
LES: (Lockheed Expert System): A model-based expert system for electronic maintenance
[AD-P003944] 02 p0248 N85-11624
On the requirements of expert systems for fault isolation
[AD-P003947] 02 p0249 N85-11627
Memory-based expert systems
[AD-A145812] 02 p0249 N85-11628
Expert systems: The application of new computer methods to corrosion problems
[AERE-M-3395] 03 p0334 N85-12153
Power subsystem automation study
[NASA-CR-171213] 03 p0358 N85-12299
Psychological issues in the design of expert systems
[AD-A146061] 03 p0436 N85-12792
Expert systems in design and manufacture
[DE84-005522] 04 p0550 N85-13496
Minimal cut-set methodology for artificial intelligence applications
[DE84-016674] 04 p0553 N85-13518
A distributed expert system for Space Shuttle flight control 05 p0602 N85-13836
The role of expert systems in remote sensing
05 p0661 N85-14246
The application of artificial intelligence to contract management
[AD-A146881] 06 p0857 N85-15448
Mental models and cooperative problem solving with expert systems
[AD-A147843] 07 p1021 N85-16479
Automatic map name placement system
09 p1341 N85-18438
Expert systems in contract management: A pilot study
[AD-A149363] 10 p1566 N85-19873
ESOP expert system model described
11 p1619 N85-20167
The application of expert systems to corrosion problems
[AERE-M-3445] 12 p1804 N85-21316
An interactive environment for the development of an expert system in ZOG
[AD-A149954] 12 p1915 N85-22025
Characterizing the parallelism in rule-based expert systems
[DE85-002432] 12 p1919 N85-22047
Research Reports: 1984 NASA/ASEE Summer Faculty Fellowship Program
[NASA-CR-171317] 12 p1944 N85-22210
Evaluation of expert systems
12 p1947 N85-22229
An expert system for choosing the best combination of options in a general-purpose program for automated design synthesis
[NASA-TM-86329] 14 p2402 N85-24807
Gordon Conference on Fundamentals of Cybernetics
[AD-A151074] 14 p2408 N85-24842
Diagnosis: Using automatic test equipment and an artificial intelligence expert system
[AD-A151918] 16 p2851 N85-27576
Artificial intelligence in space platforms
[AD-A152078] 16 p2851 N85-27578
Composite loads spectra for select space propulsion structural components: Probabilistic load model development 17 p2912 N85-27964
Evidential reasoning in expert systems for image analysis
[AD-A153379] 17 p3013 N85-28627
Alternative theories of inference in expert systems for image analysis
[AD-A153649] 18 p3170 N85-29648
Expanding expertise by use of an expert system
[DE85-010759] 19 p3344 N85-30723
Data communications-Oriented Production System Language (CPSL)
[DE85-011457] 20 p3440 N85-31352
RESO: Expert system applied to company computer networks
[ENST-84E016] 20 p3518 N85-31874
Myoelectric control of a computer based expert system for flight control
[AD-A154981] 21 p3557 N85-32126
NASA space station automation: AI-based technology review
[NASA-CR-176094] 21 p3558 N85-32134
NASA space station automation: AI-based technology review. Executive summary
[NASA-CR-176096] 21 p3558 N85-32135
Research on an expert system for database operation of simulation-emulation math models. Volume 1, Phase 1: Results
[NASA-CR-176087] 21 p3669 N85-32792
Research on an expert system for database operation of simulation-emulation math models. Volume 2, Phase 1: Results
[NASA-CR-176088] 21 p3669 N85-32793
Design of an expert-system flight status monitor
[NASA-TM-86739] 21 p3669 N85-32794
A strategy planner for NASA robotics applications
[NASA-CR-175319] 22 p3834 N85-33738
Research issues in generating graphical explanations
23 p3950 N85-34539
Generative design in architecture using an expert system 23 p3965 N85-34582
Knowledge engineering application in image processing 23 p3965 N85-34583
Robot environment expert system
[NASA-CR-3915] 23 p3967 N85-34588
Implications of artificial intelligence on the design of future onboard systems
[SFENA-DPS/C/S3/84252A] 23 p3967 N85-34596
Expert systems research in regional resource evaluation: Experiences in the application of microcomputer technologies 24 p4105 N85-35450
AUTOSIM: An automated repetitive software testing tool
[NASA-CR-177930] 24 p4137 N85-35643

EXPIRED AIR
Gas analysis techniques for human physiological measurements in space — Spacelab
[A/6537] 20 p3507 N85-31803

EXPLODING CONDUCTOR CIRCUITS
U CIRCUITS
U EXPLODING WIRES

EXPLODING CONDUCTORS
U EXPLODING WIRES

EXPLODING WIRES
Modular detonator device
[AD-D011232] 03 p0340 N85-12184
Analysis of a potential hot-wire ignition problem
[DE84-017254] 09 p1301 N85-18174
Nonprimary-explosive, hot-wire detonator
[DE85-005195] 12 p1818 N85-21409

Lightning strikes on aircraft. The TRIP 82 experiment and 3-dimensional electromagnetic interferometry
[ONERA-RF-86/7154-PY] 16 p2703 N85-26690
Detonation velocity measurements of the explosives Datasheet C and Amatol
[AD-A152298] 16 p2757 N85-27015

EXPLOITATION
Orphans of the Valley: Abandoned surface mines in the Tennessee Valley. Volume 2: Maps
[DE85-901249] 19 p3301 N85-30465
Marine Sample Exploitation Project: Estimates regarding the sensitivity and technology for the detection of nuclear explosion debris in the marine environment
[DE85-013176] 23 p3947 N85-34482

EXPLORATION
NT LUNAR EXPLORATION
NT MINERAL EXPLORATION
NT OIL EXPLORATION
NT SPACE EXPLORATION
Geothermal exploration in Trans-Pecos, Texas/New Mexico
[DE84-015553] 01 p0084 N85-10424
Polar research in Earth sciences described
08 p1142 N85-17204
The discovery circumstances of Earth-approaching asteroids
[NASA-CR-174327] 08 p1258 N85-17920
Workshop on Remote Sensing/Lineament Applications for Energy Extraction
[DE84-009291] 12 p1675 N85-21763
Some recent deposit modeling efforts
24 p4106 N85-35453

EXPLORER SATELLITES
NT DYNAMICS EXPLORER 1 SATELLITE
NT EXPLORER 10 SATELLITE
NT EXPLORER 43 SATELLITE
NT EXPLORER 46 SATELLITE
NT EXPLORER 50 SATELLITE
NT EXPLORER 51 SATELLITE
NT EXTREME ULTRAVIOLET EXPLORER SATELLITE
NT FAR UV SPECTROSCOPIC EXPLORER
NT IMP
NT INTERNATIONAL SUN EARTH EXPLORER 1
NT INTERNATIONAL SUN EARTH EXPLORER 2
NT INTERNATIONAL SUN EARTH EXPLORER 3
NT INTERNATIONAL SUN EARTH EXPLORERS
NT SOLAR MESOSPHERE EXPLORER
Solar Corona Explorer: A mission for the physical diagnosis of the solar corona
[NASA-TM-87416] 10 p1572 N85-19912

EXPLORER 10 SATELLITE
Discovery of the solar wind 12 p1954 N85-22272

EXPLORER 43 SATELLITE
Reduction and analysis of data from the plasma wave instruments on the IMP-6 and IMP-8 spacecraft
[NASA-CR-175127] 04 p0480 N85-12918

EXPLORER 46 SATELLITE
Impacts on Explorer 46 from an Earth orbiting population 12 p1785 N85-21204

EXPLORER 50 SATELLITE
Reduction and analysis of data from the plasma wave instruments on the IMP-6 and IMP-8 spacecraft
[NASA-CR-175127] 04 p0480 N85-12918

EXPLORER 51 SATELLITE
Wakes and differential charging of large bodies in low Earth orbit 13 p1992 N85-22488

EXPLOSION SUPPRESSION
Explosion-proof properties and hydraulic resistance of fire-barrier elements based on knitted metallic screens
11 p1601 N85-20067

EXPLOSIONS
NT AERIAL EXPLOSIONS
NT CHEMICAL EXPLOSIONS
NT GAS EXPLOSIONS
NT NUCLEAR EXPLOSIONS
NT THERMONUCLEAR EXPLOSIONS
NT UNDERGROUND EXPLOSIONS
NT UNDERWATER EXPLOSIONS
Bulletin of the Faculty of Engineering, Hokkaido University, no. 123
[ISSN-0385-802-X] 04 p0482 N85-13075
Estimation of dynamic stresses around the shot point by scale model experiment 04 p0482 N85-13076
China report: Science and technology
[JPRS-CST-84-001] 04 p0557 N85-13545
Measurement of infrasonic waves from remotely detonated artificial explosion 04 p0557 N85-13546
Numerical reconstruction of part of an actual blast-wave flow field to agree with available experimental data
[UTIAS-TN-251] 07 p0998 N85-16061
Nonlinear wave propagation study
[AD-A147011] 07 p0998 N85-16329
Penguin warhead safety tests
08 p1115 N85-17031
The vulnerability of cast double base rocket motors to thermomechanical attack 08 p1115 N85-17033
Ballistic/detonic transition of propellants
08 p1117 N85-17041
Hazard assessment of a hypothetical large rocket motor 08 p1117 N85-17042
Penetration of short duration airblast into protective structures 09 p1336 N85-18404
Preventing explosive propagation in racks or containers of tactical missiles
[AD-P004342] 10 p1455 N85-19166
Analysis of the natural initiation of vapor explosions
[DE85-000166] 11 p1632 N85-20279
Piezoelectric stress transducer used for measurements of explosions in hard rock 11 p1638 N85-20316
Explosive instability of strong electromagnetic wave in plasma 11 p1719 N85-20817
An analysis of short-to-medium-range seismic attenuation tests using a multilayered viscoelastic seismic propagation model
[AD-A149771] 12 p1880 N85-21856
Biological effects of blast and impact waves
[FOA-C-52006-H4-D7] 12 p1906 N85-21968
Adaptive meshes in the 2DL code
[LA-9938-MS] 12 p1914 N85-22011
Electric and hybrid vehicle demonstration project
[DE85-003939] 13 p2169 N85-23455
Centrifuge impact cratering experiments
13 p2181 N85-23533
Hydrovolcanism 13 p2188 N85-23574
Empirical development of ground acceleration, velocity and displacement for accidental explosions at J5 or the proposed large altitude rocket cell at Arnold Engineering Development Center
[DE85-008324] 16 p2758 N85-27020
Pyrotechnic shock simulation using the controlled response of a resonating bar fixture
[DE85-009537] 16 p2784 N85-27181
Combustion and micro-explosion of water/oil emulsions in high pressure environments
[AD-A152960] 17 p2919 N85-27997
Constitutive modeling for blast-induced wave propagation
[AD-A153576] 18 p3099 N85-29187
Dynamics of vapor explosions
[DE85-008845] 18 p3101 N85-29194
Action of plasma and explosion products on alumina
19 p3242 N85-30100
Study of the explosive combustion of drops of sulphur at high temperatures
[HSE-TRANS-11182] 19 p3252 N85-30183
Strain-path modeling for geo-materials
[AD-A154378] 19 p3286 N85-30360
Supernova explosion in dense clouds in the galaxy and the COS-B gamma-ray sources
[OG-2.5-3] 22 p3869 N85-33960

EXPLOSIVE DEVICES
NT BOMBS (ORDNANCE)
NT DETONATORS
NT EXPLODING WIRES
NT INITIATORS (EXPLOSIVES)
NT SHAPED CHARGES
Approach for service life extension of explosive devices for aircraft escape systems
[NASA-TM-86323] 13 p1971 N85-22381

EXPLOSIVE FORMING
Dynamic compaction of powders
[DE85-001062] 11 p1612 N85-20137
Influence of behavior laws in the explosive deformation of metal plates
[ISL-R-122/83] 16 p2760 N85-27032
Computational methods for the explosive and impact compaction of powders
[AD-A156219] 24 p4139 N85-35653

EXPLOSIVE GASES
U FLAMMABLE GASES

EXPLOSIVE WELDING
Some features of the fabrication of multilayer fiber composites by explosive welding
[NASA-TM-77844] 14 p2248 N85-23932
Examination of the regions of the joint of sheets bonded by the explosive welding technique
[BLL-BISI-TRANS-22352-(9022.06)]
17 p2973 N85-28170
Determination of local deformation during explosive welding
[BLL-M-36278-(5828.4)] 20 p3462 N85-31503

EXPLOSIVES
NT CELLULOSE NITRATE
NT RDX
NT TATB
NT TRINITROTOLUENE
Computer simulation of the shock initiation of detonation in solid explosives
[PML-1984-23] 01 p0033 N85-10207
Eutectic explosives containing ammonium nitrate
[DE84-015705] 01 p0034 N85-10213
The 7-Amino-4,6-Dinitrobenzofuroxan, an insensitive high explosive
[AD-A145665] 02 p0188 N85-11257
Official journey to USA, November 1983. Symposium on the Compatibility of Explosives; Mound Laboratory; Naval Surface Weapons Center
[FOA-C-20548-D1] 04 p0482 N85-13072
Laser for determining the ignition conditions of a pyrotechnic mixture
[FOA-C-20542-D1] 04 p0506 N85-13230
Aircraft accident report, Western Helicopters, Inc., Bell UH-1B, N87701, Valencia, California, July 23, 1982
[PB84-910414] 05 p0594 N85-13789
Effects of surface interactions and mechanical properties of PBXs (plastic bonded explosives) on explosive sensitivity
[AD-A146368] 06 p0773 N85-14944
Deformation, fracture and explosive properties of reactive materials
[AD-A146396] 06 p0774 N85-14945
Making high explosive bodies for shaped charges by casting or pressing. Shaped charge research at Research Institute of National Defence (FOA) in 1972 - 1983, part 1
[FOA-C-20554-D4-PT-1] 07 p0935 N85-15923
Sensitiveness and explosiveness assessment at Perrie Waltham Abbey 08 p1115 N85-17029
Numerical simulation of the shock detonation transition 08 p1116 N85-17039
Mass spectrometry/mass spectrometry as a screening method for detecting explosive vapors
[DE85-001276] 09 p1292 N85-18110
Evaluation of the Fundamental Research on Explosives (FRE) program
[DE85-001537] 09 p1301 N85-18172
LX-10 and LX-17 moisture content and release
[DE84-016579] 09 p1301 N85-18173
Incineration of explosives contaminated soils
[AD-P004142] 09 p1347 N85-18478
Polymeric liner selection for military waste impoundments
[AD-P004143] 09 p1348 N85-18479
NATO AC/310 activities report on NATO STANAG 4170 and Allied Ordnance Publication 7 (Manual of Tests for Qualification of Explosive Materials for Military Use)
[AD-P004341] 10 p1454 N85-19165
A thermal-mechanical model of deflagration-to-detonation in granular energetic materials
[AD-P004346] 10 p1455 N85-19170
A summary of the mechanism of delayed detonation
[AD-P004347] 10 p1455 N85-19171
Some aspects of the micromechanics of hot spot formation in energetic materials
[AD-P004348] 10 p1456 N85-19172
Thermodynamics of the reactive flow model
[DE85-004405] 10 p1565 N85-19870
Polymer blends as high explosive binders
[DE85-001210] 11 p1611 N85-20131
Design of explosive logic elements
[DE84-009611] 11 p1614 N85-20148
The response of explosive systems to thermal stimuli: A state-of-the-art assessment
[DE85-000919] 11 p1614 N85-20148
DOE hazard classification for Insensitive High Explosives (IHE)
[DE84-017002] 11 p1614 N85-20149
Waveform control and application of detonation wave in explosives 12 p1820 N85-21420
A comprehensive review of black powder
[AD-A150455] 13 p2039 N85-22769
IHE material qualification tests description and criteria
[DE85-004649] 13 p2040 N85-22770
Detonations of solid explosives
[AD-A152012] 15 p2521 N85-25540
Detonation velocity measurements of the explosives Datasheet C and Amatol
[AD-A152298] 16 p2757 N85-27015
Surveillance program for the dissection and analysis of explosive and pyrotechnic components
[DE85-006105] 16 p2757 N85-27016
A review of safety practices and safety training for the explosives field
[AD-A152295] 16 p2759 N85-27028
Inversion of Rayleigh wave group velocities from high-explosive tests
[AD-A152172] 16 p2783 N85-27175
Detonation behavior of LX-14 and PBX-9404: Theoretical aspect
[DE85-010038] 18 p3084 N85-29076
The shock desensitization of PBX-9404 and composition B-3
[DE85-009604] 18 p3084 N85-29077
Equation of state for detonation products
[DE85-009606] 18 p3084 N85-29079

Diagnostic verification of the GLAS (Goddard Laboratory for Atmospheric Sciences) general circulation model as applied to a case of extratropical maritime explosive cyclogenesis
[AD-A153686] 18 p3148 N85-29494
Deformation, fracture and explosive properties of reactive materials
[AD-A154073] 19 p3251 N85-30157
Burn rates of explosives at high pressures
[DE85-010806] 19 p3251 N85-30159
X-ray photoelectron spectroscopy study of the compatibility of the explosive PETN with candidate plastic bonding materials
[DE85-010604] 19 p3251 N85-30161
SAFEORD: Safety of explosive ordnance databank
[AD-A154058] 19 p3380 N85-30972
Electrochemistry of Hexanitroazobenzene (HNAB)
[DE85-010807] 21 p3565 N85-32171
The determination of dinitrotoluene in single base propellants
[AD-A154672] 21 p3571 N85-32209
TNT equivalency of EAK explosive
[AD-A155737] 21 p3571 N85-32211
Explosive containment study
[DE85-011719] 22 p3753 N85-33267
Sensitivity and performance characterization of DINGU
[DE85-010750] 22 p3754 N85-33269
Experimental studies of chemical reactivity during shock initiation of hexanitrostilbene
[DE85-011726] 22 p3754 N85-33270
Modeling granular explosive detonations with shear band concepts
[DE85-011823] 22 p3754 N85-33271
Hydrazine nitrate based explosives
[ISL-CO-229/84] 22 p3754 N85-33272
Intermolecular explosives
[DE85-009698] 23 p3921 N85-34296
Pressure-shear loading of PBX-9404
[DE85-009682] 23 p3921 N85-34298
Modeling heterogeneous high explosive burn with an explicit hot-spot process
[DE85-009593] 23 p3922 N85-34300
Detonation of condensed explosives: Evolution of knowledge in the last 40 years
[ISL-CO-228/84] 23 p3923 N85-34307
Computational methods for the explosive and impact compaction of powders
[AD-A156219] 24 p4139 N85-35653

EXPONENTIAL FUNCTIONS
NT LOGARITHMS
Simulation uses of the exponential distribution
[AD-A144940] 01 p0112 N85-10756
Likelihood estimation for generalized mixed exponential distributions
[AD-A145675] 02 p0252 N85-11651
A power transformation exponential regression model for censored failure time data
[AD-A146377] 08 p1212 N85-17632
Estimating the scale parameter of an exponential distribution from a sample of time-censored r-th order statistics
[AD-A148060] 09 p1375 N85-18644
Modelling and residual analysis of nonlinear auto-regressive time series in exponential variables
[AD-A149047] 10 p1550 N85-19776
Attainable rates of convergence of maxima
[AD-A150838] 14 p2408 N85-24847
Iteration of exponential functions
15 p2633 N85-26233
Asymptotic expansions of the distribution of test statistics associated with several two parameter exponential distributions
[AD-A151906] 15 p2641 N85-26289
Exponential order statistic models of software reliability growth
[NASA-CR-3909] 20 p3515 N85-31852
Survival function of hypo-exponential distributions
[AD-A155516] 21 p3572 N85-32214

EXPORTS
U INTERNATIONAL TRADE

EXPOSURE
The oxidation behaviour of a 20 percent Cr/25 percent Ni/Nb stabilized stainless steel in carbon dioxide at high temperatures and its improvement by cerium and yttrium
[AERE-R-11228] 01 p0029 N85-10182
Instability in semiconductors exposed to ionizing radiation 02 p0267 N85-11747
NAAQS (National Ambient Air Quality Standards) Exposure Model (NEM) applied to carbon monoxide
[PB84-242551] 06 p0834 N85-15310
Early detection of environmental exposure
[AD-P004039] 06 p0845 N85-15389
Using a Gossen light meter to produce enlarged interpositive film copies from glass plates — astronomical photography 07 p0984 N85-16118
Carotid baroreceptor influences on peripheral circulatory and thermal responses during cold exposure
[AD-A146808] 07 p1015 N85-16447
A crew exposure study. Volume 1: Offshore
[AD-A146884] 07 p1015 N85-16449
Exposure modelling of particle beam lithography
[AD-A147849] 08 p1219 N85-17678
Long-term light induced changes in dark conductivity of kapton
[AD-A148791] 08 p1224 N85-17706
Natural exposure versus chamber simulation
[AD-A149538] 10 p1495 N85-19437
Effects of overall vibration and noise on operational personnel 10 p1523 N85-19606
Mercury health effects update: Health issue assessment
[PB85-123925] 10 p1528 N85-19639
Effect of long-term repeated exposure to high-intensity stationary magnetic field on adrenomedullary activity
12 p1904 N85-21955
Characterization of material surfaces exposed to atomic oxygen on space shuttle missions
12 p1946 N85-22220
The effect of occupational exposure and the body weight to height ratio on exhaled methylene chloride breath concentration in females at one, eighteen and sixty-six hours post exposure 14 p2388 N85-24708
Spectroscopic analysis of radiation-generated changes in tensile properties of a polyetherimide film
[NASA-TP-2429] 15 p2502 N85-25435
A study of the methods for evaluating the noise impact of a proposed airport on a community
15 p2588 N85-25957
Damage caused to polyurethane foams by aging, simulated sunlight exposure, heat and fire
[AD-A152040] 16 p2754 N85-26998
Experiments in microwave exposure in the rat: Body temperature, serum chemistry and the use of chemical restraint
[PB85-156834] 16 p2840 N85-27512
Low-profile fastener
[AD-D011667] 19 p3280 N85-30343
Los Alamos optical materials reliability, maintainability, and exposure testing program
[DE85-011894] 21 p3613 N85-32456
A crew exposure study. Phase II. Volume 2. At sea. Part A
[AD-A155233] 21 p3666 N85-32774
Estimating risks of lead-induced hemoglobin decrements under conditions of uncertainty: Methodology, pilot judgments and illustrative calculations
[DE85-012293] 23 p3952 N85-34493

EXPRESSIONS (MATHEMATICS)
U FORMULAS (MATHEMATICS)

EXPULSION
Electro-expulsive separation system
[NASA-CASE-ARC-11613-1] 18 p3094 N85-29150

EXTENDED DURATION SPACE FLIGHT
U LONG DURATION SPACE FLIGHT

EXTENSIONS
On shrinkage and molecular extension
[AD-A149100] 10 p1451 N85-19144
ODIN: An extensible software environment. Report and user's reference manual
[DE85-008459] 18 p3164 N85-29600

EXTENSOMETERS
Recommendations for the use of Ni-Cr-base alloy extensometers for measurement of creep strain
[NPL-DMA(A)-81] 08 p1164 N85-17342
Some advances in experimentation supporting development of viscoplastic constitutive models
[NASA-CR-174855] 16 p2799 N85-27280
A simple optical extensometer achieving high accuracy
[NPL-DMA(A)-95] 20 p3458 N85-31474
Some advances in experimentation supporting development of viscoplastic constitutive models
20 p3468 N85-31545
Results of an interlaboratory fatigue test program conducted on alloy 800H at room and elevated temperatures
[NASA-CR-174940] 21 p3597 N85-32340
Tensile testing apparatus
[NASA-CASE-LAR-13243-1] 23 p3933 N85-34375

EXTERNAL COMBUSTION ENGINES
Stirling material technology
[NASA-TM-86888] 04 p0472 N85-13007

EXTERNAL STORE SEPARATION
Implementation of the supersonic triplet singularity into the USTORE computer code
[CSIR-NIAST-83/47] 01 p0001 N85-10006
Remote pivot decoupler pylon: Wing/store suppression
[NASA-CASE-LAR-13173-1] 11 p1584 N85-19981
Slide release mechanism — for space shuttle orbiter/external tank connection device
[NASA-CASE-MSC-20060-1] 19 p3279 N85-30334

EXTERNAL STORES
NT PODS (EXTERNAL STORES)
External tank aft cargo carrier
02 p0155 N85-11050
UH-60A external stores support system fixed provision fairings drag determination
[AD-A147188] 07 p0902 N85-15719
ESP (External-Stores Program): A pilot computer program for determining flutter-critical external-store configurations. Volume 3, part 2. Program compilation
[AD-A152271] 16 p2706 N85-26703
ESP (External-Stores Program): A pilot computer program for determining flutter-critical external-store configurations. Volume 1: User's manual
[AD-A152268] 16 p2710 N85-26725
ESP (External-Stores Program): A pilot computer program for determining flutter-critical external-store configurations. Volume 2: Final report on program enhancement and delivery
[AD-A152269] 16 p2711 N85-26726
ESP (External-Stores Program): A pilot computer program for determining flutter-critical external-store configurations. Volume 3, part 1: Program compilation
[AD-A152270] 16 p2711 N85-26727
Flight trials of a modified gulfstream commander carrying external stores
[AD-A153376] 17 p2896 N85-27859
Results of variable enthalpy tests of CPR-488 TIP panels in MSFC Hot Gas Facility
[NASA-CR-170889] 24 p4072 N85-35237

EXTERNAL SURFACE CURRENTS
SEPAC (space experiments with particle accelerators)
01 p0014 N85-10085
Rocket body charge neutralization processes in ARAKS experiment (data from two launches)
13 p1980 N85-22426
Electric field effects on ion currents in satellite wakes
13 p1991 N85-22485
Calculation of secondary-electron escape currents from inclined-spacecraft surfaces in a magnetic field
13 p1992 N85-22491
Surface interactions and high-voltage current collection 13 p1993 N85-22493
Development of a continuous broad-energy-spectrum electron source 13 p1995 N85-22507
Development and testing of a spacecraft surface potential monitor 13 p2007 N85-22582

EXTERNAL TANKS
Vibration, acoustic, and shock design and test criteria for components on the Solid Rocket Boosters (SRB), Lightweight External Tank (LWT), and Space Shuttle Main Engines (SSME)
[NASA-RP-1127] 01 p0061 N85-10405
External tank aft cargo carrier
02 p0155 N85-11050
The variable polarity plasma arc welding process: Its application to the Space Shuttle external tank
[NASA-TM-86482] 05 p0641 N85-14115
Preliminary airworthiness evaluation AH-1S (MC) helicopter with external fuel tanks installed
[AD-A148091] 08 p1084 N85-16865
Space shuttle external tank performance improvements: The challenge 08 p1094 N85-16918
External tank processing from barge to pad
08 p1098 N85-16927
Cryogenic propellant management: Integration of design, performance and operational requirements
08 p1098 N85-16939
External tank GH2 vent arm 08 p1102 N85-16969
Thermal design of the space shuttle external tank
08 p1103 N85-16977
BI-PAC F-15 external fuel tank container modification
[AD-A148636] 09 p1280 N85-18053
STS-1 Pogo analysis
[NASA-TM-87433] 11 p1591 N85-20007
Artificial gravity: Tethers and containers
11 p1645 N85-20367
Results of aeroheating DFI and ET design-data test on a 0.0175-scale model 60-OTS conducted in the Von Karman Gas Dynamics Facility (VKF) 40' supersonic and the 50' hypersonic wind tunnels A and C
[NASA-CR-167693] 13 p1988 N85-22468
Results of a M = 5.3 heat transfer test of the integrated vehicle using phase-change paint techniques on the 0.0175-scale model 56-OTS in the NASA/Ames Research Center 3.5-foot hypersonic wind tunnel
[NASA-CR-167695] 13 p1988 N85-22468
Development of acceptance criteria for batches of silane primer for external tank thermal protection system bonding applications
[NASA-CR-171428] 14 p2259 N85-23998

Development of acceptance criteria for batches of silane primer for external tank thermal protection system bonding applications
[NASA-CR-171436] 15 p2518 N85-25523
Development of acceptance criteria for batches of silane primer for external tank thermal protection system bonding applications
[NASA-CR-175850] 16 p2754 N85-26995
Analysis of heat-transfer measurements from 2 AEDC wind tunnels on the Shuttle external tank
[NASA-CR-171470] 17 p2957 N85-28263
Slide release mechanism — for space shuttle orbiter/external tank connection device
[NASA-CASE-MSC-20060-1] 19 p3279 N85-30334
Results of a study to build a gamma-ray telescope in an external tank
[OG-9.3-3] 23 p4027 N85-34958

EXTINCTION
NT INTERSTELLAR EXTINCTION
Atmospheric extinction in critical environments
[AD-A146102] 03 p0396 N85-12527
Extinction by dielectric particles at optical and infrared wavelengths
[AD-A146305] 03 p0413 N85-12640
Dust in the region of Herbig-Haro objects: The case of NGC 1999 11 p1747 N85-20991
The UV extinction laws in two very young clusters, NGC 6530 in the galaxy and NGC 2100 in the LMC 11 p1748 N85-20994
On the inversion of the lidar equation
[AD-A149653] 12 p1858 N85-21641
Phase function, backscatter, extinction, and absorption for standard radiation atmosphere and El Chichon aerosol models at visible and near-infrared wavelengths
[NASA-TM-86379] 12 p1892 N85-21874
Characteristics and behavior of atmospheric aerosols; application to prediction of infrared extinction
[AD-A150691] 14 p2372 N85-24665
SAM II measurements of the polar stratospheric aerosol. Volume 6: April to October 1981
[NASA-RP-1141] 16 p2625 N85-27422
Visibility and vertical structure measurements in southern Germany
[AD-A154714] 21 p3635 N85-32574
Ice fog as an electro-optical obscurant
[AD-A155059] 21 p3705 N85-33015

EXTINGUISHERS
U FIRE EXTINGUISHERS

EXTINQUISHING
Vortex dynamics simulation of conserved scalar dissipation 22 p3745 N85-33210

EXTRACTION
NT GEOTHERMAL ENERGY EXTRACTION
NT ION EXTRACTION
NT SOLVENT EXTRACTION
Extractor for spring-lock pin connectors
[AD-D011235] 01 p0043 N85-10280
Positron flux concentrator: An update
[DE84-016260] 04 p0561 N85-13576
Solar cell coverslide extraction method and apparatus
[AD-D011275] 05 p0669 N85-14306
Application of extraction replicas and analytical electron microscopy to precipitate phase studies
[DE85-001253] 06 p0769 N85-14919
Analyses of energy extraction efficiency of unstable resonators
[AD-A146391] 06 p0813 N85-15161
Extracting embedded generalized networks from linear programming problems
[AD-A147565] 07 p1033 N85-16558
Parachute extraction device for ultralight gliders
[CH-643499-A5] 16 p2699 N85-26663
Slow extraction of LAMPF 2
[DE85-010744] 19 p3356 N85-30805
Soil extraction kit
[AD-D011736] 22 p3742 N85-33190
Geologic, technical, and economic sensitivity analysis in support of the GRI (Gase Research Institute) tight gas reservoirs project area
[PB85-192276] 22 p3802 N85-33559
Use of a minimum-ellipse criterion in the study of ion-beam extraction systems
[DE85-012670] 24 p4148 N85-35721
Measurement of uranium enrichment for gaseous uranium at low pressure
[DE85-012697] 24 p4150 N85-35733
Synchronous timing of multi-energy fast beam extraction during a single AGS cycle
[DE85-011629] 24 p4158 N85-35781

EXTRAGALACTIC LIGHT
U EXTRATERRESTRIAL RADIATION
U LIGHT (VISIBLE RADIATION)

EXTRAGALACTIC MEDIA
U INTERGALACTIC MEDIA

EXTRAGALACTIC RADIO SOURCES
NT RADIO GALAXIES
Documentation for the machine-readable version of A Catalogue of Extragalactic Radio Source Identifications (Veron-Cetty and Veron 1983)
[NASA-TM-87373] 03 p0405 N85-12587
Dynamical models for radio jets 03 p0449 N85-12854
VLBI solutions for the time variation of DSN baselines: 1978 - 1983 05 p0623 N85-13983
Metric-wave and decimetric-wave aperture synthesis systems (review) 06 p0782 N85-14998
Research in geodesy based upon radio interferometric observations of extragalactic radio sources
[AD-A147581] 07 p0988 N85-16280
The extragalactic nature of H0323+022 08 p1237 N85-17802
Morphology and optical polarization of the 3C 273 jet — radio jet 08 p1238 N85-17803
Spatially resolved optical spectroscopy of the radio jet of the X-ray galaxy NGC 2110 08 p1238 N85-17804
Characteristics of X-ray spectra from galactic and extragalactic X-ray sources 08 p1239 N85-17811
Comments on the physics of active galactic nuclei 08 p1240 N85-17823
The origin of the X-ray background 08 p1243 N85-17841
VLBI observations of compact double radio sources 09 p1417 N85-18940
Arcsecond positions for milliarcsecond VLBI nuclei of extragalactic radio sources. Part 3: 74 sources 10 p1463 N85-19225
Jets in galaxies 12 p1958 N85-22309
All-Union conference of radio astronomers 13 p1977 N85-22408
Extragalactic origin or gamma-ray bursts, revision 1
[DE85-005822] 15 p2686 N85-26585
Evolution of the luminosity function of extragalactic objects
[NASA-CR-175977] 18 p3201 N85-29860
Frequent observations of extragalactic compact sources at 24 GHz 19 p3366 N85-31003
New VLBI technology developments 20 p3491 N85-31702
Variations in the small-scale galactic magnetic field and short time-scale intensity variations of extragalactic radio sources 20 p3549 N85-32084
Observation of gamma-rays from LMC X-4 above 10(16) eV
[OG-2.6-10] 22 p3870 N85-33972
Search for TeV gamma rays from extragalactic sources and the Galactic Center
[OG-2.7-1] 22 p3871 N85-33976
Search for gamma-rays from M31 and other extragalactic objects
[OG-2.7-3] 22 p3871 N85-33977
Energy spectrum of extragalactic gamma-ray sources
[OG-2.7-13] 22 p3872 N85-33986
Ultrahigh energy gamma rays: Carriers of cosmological information
[OG-2.7-14] 22 p3872 N85-33987
Propagation of cosmic rays and new evidence for distributed acceleration
[OG-8.3-5] 23 p4022 N85-34924

EXTRAPOLATION
Signal processing algorithms
[AD-A145748] 03 p0406 N85-12590
Searching for impact craters using space shuttle photography 06 p0869 N85-15845
Combustion kinetics of metal oxide and halide radicals
[AD-A148521] 08 p1122 N85-17076
A note on the prediction error for small time lags into the future
[AD-A148221] 08 p1215 N85-17654
Extrpolation in finite element analysis 09 p1331 N85-18365
Fixed vs. variable order Runge-Kutta
[DE85-001320] 09 p1374 N85-18639
Proposed preliminary design criteria model environment for the 1990's 12 p1784 N85-21194
Real-time enhancement of a climatology or forecast of ocean thermal structure using observed ocean temperatures
[AD-A151118] 15 p2604 N85-26049
Extrapolation methods for multi-dimensional quadrature of singular and regular integrand functions
[DE85-009665] 18 p3172 N85-29655
Extrapolation methods in the finite element method
[BONNER-MATHE-SCHR-158] 19 p3345 N85-30729
An objective analysis technique for extrapolating tidal fields 20 p3493 N85-31715
Changes in lattice cell parameter of film intermetallic compounds RT2
[BLL-M-35874-(5828.4)] 23 p3915 N85-34261

EXTRATERRESTRIAL ENVIRONMENTS
NT CHROMOSPHERE
NT DEEP SPACE
NT HELIUM HYDROGEN ATMOSPHERES
NT INTERPLANETARY SPACE
NT INTERSTELLAR SPACE
NT JUPITER ATMOSPHERE
NT LUNAR ATMOSPHERE
NT MARS ATMOSPHERE
NT MARS ENVIRONMENT
NT NEPTUNE ATMOSPHERE
NT PLANETARY ATMOSPHERES
NT PLANETARY ENVIRONMENTS
NT SATELLITE ATMOSPHERES
NT SATURN ATMOSPHERE
NT SOLAR ATMOSPHERE
NT STELLAR ATMOSPHERES
NT URANUS ATMOSPHERE
NT VENUS ATMOSPHERE
The velocity-age relation for B and A stars 06 p0740 N85-14762
Natural environment design criteria for the Space Station definition and preliminary design
[NASA-TM-86498] 12 p1789 N85-21232

EXTRATERRESTRIAL INTELLIGENCE
The search for extraterrestrial intelligence 15 p2689 N85-26609
Where is everybody? An account of Fermi's question
[DE85-011898] 19 p3383 N85-30988

EXTRATERRESTRIAL LIFE
The impact ejection of living organisms into space 15 p2682 N85-26566
Microbial ecology of extreme environments: Antarctic yeasts and growth in substrate-limited habitats
[NASA-CR-176005] 19 p3326 N85-30609
Where is everybody? An account of Fermi's question
[DE85-011898] 19 p3383 N85-30988

EXTRATERRESTRIAL MATTER
NT COSMIC GASES
NT COSMIC PLASMA
NT INTERSTELLAR GAS
NT NEUTRAL GASES
Minor elements in relict olivine grains of deep-sea spheres: Match with Mg-rich olivines from C2 meteorites 06 p0883 N85-15610
Activities report of the Institute for Extraterrestrial Physics
[MPI-PAE/EXTRATERR-187] 17 p3053 N85-28698
Lead and uranium group abundances in cosmic rays
[OG-7.1-3] 23 p4013 N85-34865

EXTRATERRESTRIAL RADIATION
NT CIRCUMSOLAR RADIATION
NT EXTRATERRESTRIAL RADIO WAVES
NT GALACTIC COSMIC RAYS
NT GALACTIC RADIATION
NT GALACTIC RADIO WAVES
NT GAMMA RAY BURSTS
NT INTERSTELLAR RADIATION
NT LUNAR RADIATION
NT NORTH POLAR SPUR (ASTRONOMY)
NT PLANETARY RADIATION
NT PRIMARY COSMIC RAYS
NT RADIO BURSTS
NT SOLAR CORPUSCULAR RADIATION
NT SOLAR COSMIC RAYS
NT SOLAR ELECTRONS
NT SOLAR NEUTRINOS
NT SOLAR PROTONS
NT SOLAR RADIATION
NT SOLAR RADIO BURSTS
NT SOLAR RADIO EMISSION
NT SOLAR WIND
NT SOLAR X-RAYS
NT STELLAR RADIATION
NT STELLAR WINDS
NT SUNLIGHT
NT TYPE 3 BURSTS
NT TYPE 4 BURSTS
NT ZODIACAL LIGHT
Fluctuations during observations of extraterrestrial sources from outer space through Earth's atmosphere 07 p0953 N85-16040
Cosmology 07 p1056 N85-16701
IUE spectroscopy of extragalactic H II regions 11 p1745 N85-20974
Research in particles and fields
[NASA-CR-175472] 12 p1983 N85-22337
Space radiation monitor observations from Salyut-4 orbital station 15 p2482 N85-25317
Spectroscopic analysis of radiation-generated changes in tensile properties of a polyetherimide film
[NASA-TP-2429] 15 p2502 N85-25435
Space radiation studies — Spacelab 2 Payload
[NASA-CR-171410] 15 p2685 N85-26584

Activities report of the Institute for Extraterrestrial Physics
[MPI-PAE/EXTRATERR-167] 17 p3053 N85-28898
Radio counterparts of galactic gamma-ray sources
20 p3549 N85-32085
Results from radiation monitoring equipment experiments on STS-41C, 41D, 41G and 51A
[AD-A154878] 21 p3560 N85-32142
Nineteenth International Cosmic Ray Conference. Conference program and author index
[NASA-CP-2376] 22 p3860 N85-33901
Standard value for the radiation length in air
[HE-4.4-4] 24 p4193 N85-36013
Samarkand complex setup for investigation of cosmic ray variation in the energy range of 7 10 (9) - 10 (15) eV
[HE-4.6-14] 24 p4198 N85-36050
High energy neutrino astronomy with MACRO
[HE-5.3-12] 24 p4206 N85-36106

EXTRATERRESTRIAL RADIO WAVES
NT GALACTIC RADIO WAVES
NT NORTH POLAR SPUR (ASTRONOMY)
NT RADIO BURSTS
NT SOLAR RADIO BURSTS
NT SOLAR RADIO EMISSION
NT TYPE 3 BURSTS
NT TYPE 4 BURSTS
Solar radio bursts, proton events and geomagnetic activity
[AD-A149018] 10 p1571 N85-19906
Forecast verification of the 10.7 centimeter solar flux and the Ap daily geomagnetic activity indices
[AD-A152959] 17 p2993 N85-28499
High energy radiation from neutron stars
[DE85-014353] 24 p4169 N85-35843

EXTRATERRESTRIAL RESOURCES
Studies on the processing methods for extraterrestrial materials
[NASA-CR-175778] 16 p2716 N85-26788
Hydrogen recovery from extraterrestrial materials using microwave energy
[DE85-006717] 16 p2883 N85-27789

EXTRATERRESTRIAL ROVING VEHICLES
U ROVING VEHICLES

EXTRAVEHICULAR ACTIVITY
EVA of cosmonauts Savitskaya and Dzhanibekov
02 p0158 N85-11076
Commentary on hand tool used in cosmonaut EVA
02 p0159 N85-11077
Further details in welding, spray-coating tool
02 p0159 N85-11078
The human role in space. Volume 1: Executive summary
[NASA-CR-171223] 04 p0546 N85-13473
Aerospace Safety Advisory Panel
[NASA-TM-87426] 13 p1970 N85-22373
Astronaut hazard during free-flight polar EVA
13 p1997 N85-22522
A concept for a mobile remote manipulator system
14 p2236 N85-23859
Assembly Concept for Construction of Erectible Space Structure (ACCESS) neutral buoyancy testing results
14 p2236 N85-23862
National Space Transportation Systems Program mission report
[NASA-TM-87454] 14 p2242 N85-23899
The human role in space (THURIS)
18 p3158 N85-29557
Experiences with neutral buoyance testing mockups
18 p3159 N85-29571
Space station automation and robotics study. Operator-systems interface
[NASA-CR-176096] 22 p3736 N85-33172

EXTRAVEHICULAR MOBILITY UNITS
Challenges in the development of the shuttle extravehicular mobility unit 08 p1095 N85-16922
Swing-arm beam erector (SABER) concept for single astronaut assembly of space structure
[NASA-TP-2379] 10 p1429 N85-19015

EXTREMA
U RANGE (EXTREMES)

EXTREME ULTRAVIOLET EXPLORER SATELLITE
The 1986 National Aeronautics and Space Administration authorization
[GPO-47-635] 24 p4166 N85-35829

EXTREME ULTRAVIOLET RADIATION
A normal-incidence monochromator branch line on the FEL-undulator for experimental studies in the 5 to 30 eV region
[DE84-014379] 04 p0505 N85-13225
Voyager EUV and FUV observations
06 p0675 N85-15554
Absorption and emission of EUV radiation by the local ISM 06 p0676 N85-15583
Measuring EUV line emission from the hot interstellar medium 06 p0680 N85-15595
Spectroscopic instrumentation for Tokamak diagnostics 09 p1388 N85-18732
Research in extreme ultraviolet and far ultraviolet astronomy
[NASA-CR-174432] 10 p1570 N85-19902
Solar flare and IMF sector structure effects in the lower ionosphere 11 p1664 N85-20488
Edge diagnostics for tandem mirror machines
[DE85-001209] 11 p1733 N85-20902
Tasks for observations of close binary systems in the extreme ultraviolet 11 p1757 N85-21054
Studies on radiative collisional and ultraviolet lasers
[AD-A151004] 14 p2310 N85-24206
Free electron lasers for the EUV spectral region
[DE85-006804] 15 p2583 N85-25815
Review of short wavelength lasers
[DE85-009856] 18 p3114 N85-29277
Four-photon resonant third harmonic generation
[DE85-010070] 19 p3367 N85-30883

EXTREMELY HIGH FREQUENCIES
The Finnish approach to microwave remote sensing of snow 05 p0656 N85-14212
The development of a 90 GHz solid state noise source
[CD.6500695] 05 p0733 N85-14715
Potential affiliate stations to work with the EVN — European VLBI Network; QUASAT
07 p1057 N85-16708
Design of mode converters from TE circular om modes in circular waveguides to TE rectangular mo modes in rectangular waveguides for high power applications in the frequency range 1 to 30 GHz
[IPF-84-7] 09 p1395 N85-18781
The effects of mode impurity of Ka-band system performance 10 p1483 N85-19227
EHF air-to-air communications
10 p1489 N85-19273
EHF MILSATCOM systems for tactical users
11 p1709 N85-20755
Tactical military communications by satellite relay at high latitudes 11 p1709 N85-20756
Design and calibration of a 35GHz dielectrometer
[AD-P004363] 12 p1826 N85-21457
Digital processing of passive Ka-band microwave images for sea-ice classification
[AD-A150686] 14 p2347 N85-24511
Analysis of space diversity techniques for EHF (Extremely High Frequency) satellite downlinks
[AD-A151900] 15 p2544 N85-25705
Radiometry: A useful prediction tool — atmospheric attenuation
[ESA-SP-1071] 20 p3399 N85-31084
Preliminary investigations concerning a 90 GHz radiometer satellite experiment
[ESA-TT-860] 20 p3420 N85-31225
Thirty GHz low noise GaAs FET amplifiers — satellite-ground communication
[CD.6500686] 20 p3449 N85-31413
An experimental study of dielectric rod antennas for millimeter-wave imaging applications
[AD-A155832] 24 p4086 N85-35328

EXTREMELY LOW FREQUENCIES
Experimental determination of propagation rate of ELF signals employed by Omega radio navigation system for phase measurements 06 p0793 N85-15086
Electrostatic wave observation during a space simulation Beam-Plasma-Discharge (BPD)
[NASA-CR-174286] 07 p1045 N85-16639
Extremely Low Frequency (ELF) Communications System Ecological Monitoring Program: Summary of 1983 progress
[AD-A147704] 08 p1151 N85-17265
Compilation of annual reports of the Navy ELF (Extremely Low Frequency) communications system ecological monitoring program. Volume 1: Tabs A-E
[AD-A148326] 08 p1152 N85-17272
Compilation of annual reports of the Navy ELF (Extremely Low Frequency) communications system ecological monitoring program (1983). Volume 2: Tabs F-J
[AD-A148327] 08 p1152 N85-17273
Energetic electron anisotropy and ELF waves onboard GEOS. How does quasi-linear diffusion work
14 p2366 N85-24623
ELF chorus in the Earth's outer magnetosphere
14 p2366 N85-24624
Conjugacy of ELF-VHF emissions near L=6 — chorus phenomenon, hiss 14 p2367 N85-24625
Biological and human health effects of extremely low frequency electromagnetic fields. Post-1977 literature review
[AD-A152731] 17 p2999 N85-28539
Numerical modeling of subsurface communication
[DE85-012616] 21 p3577 N85-32249

EXTREMELY LOW RADIO FREQUENCIES
The propagation and growth of whistler mode waves generated by electron beams in Earth's bow shock
[AD-A145572] 02 p0228 N85-11492
Energy correlation between natural extra-low-frequency noises at various frequencies 06 p0784 N85-15010
Propagation of electromagnetic fields along the sea/sea-bed interface
[AD-A149523] 10 p1467 N85-19257
The ULF/ELF/VLF electromagnetic fields generated in a sea of finite depth by elevated dipole sources
[AD-A149638] 12 p1828 N85-21470
Dielectric measurements in infralow-frequency band
13 p2087 N85-23034
Spatial characteristics of ULF pulsations and their modification by the ionosphere: IMS results
14 p2364 N85-24612
An evaluation of the contributions of the IMS to experimental and theoretical studies of ULF plasma
14 p2365 N85-24614
Results of ULF-wave investigations in the USSR
14 p2369 N85-24644
Satellite, auroral radar and ground magnometer observations of transient ULF pulsations
14 p2369 N85-24645

EXTREMUM VALUES
NT LIMITS (MATHEMATICS)
NT MAXIMA
Distributions of extreme values of sequences of autocorrelated random variables
[PB84-240746] 06 p0858 N85-15456
Master Fit users' guide, version 1.0
[DE85-014190] 24 p4140 N85-35667

EXTRUDING
NT PULTRUSION
Optimizing conductive polymer compounds
[BMFT-FB-T-84-145] 03 p0338 N85-12177
Optimization of the die entrance shape for polymeric extrusion
[DE85-001588] 06 p0772 N85-14937
Computer-aided design of extrusion dies by metal-flow simulation 06 p0797 N85-15094
Modelling temperature changes during hot working operations 06 p0798 N85-15095
Materials of the fourth scientific-technical Conference on Questions of the Extrusion of Metals (Selected articles)
[AD-A148578] 08 p1130 N85-17121
High temperature properties of equiatomic FeAl with ternary additions
[NASA-TM-86936] 10 p1439 N85-19072
Evaluation of 7010 aluminium alloy extruded tube in the T76 condition
[BR92019] 11 p1596 N85-20039
Characterization of poly(ethylene oxide) drawn by solid state extrusion
[AD-A150987] 14 p2260 N85-24006
Effect of initial structure on texture of pressed titanium alloy bars 15 p2515 N85-25518
Strain fields for aluminum at different tooling temperatures and extrusion ratios
[DE85-006257] 18 p3075 N85-29020
Downdraw extrusion of ULE(TM) glass
[AD-A153783] 18 p3079 N85-29048
Characterization of modified 9 Cr Mo steel extruded pipe
[DE85-012058] 23 p3941 N85-34430
Solid-state co-extrusion of nylon 6 gel
[AD-A156187] 24 p4082 N85-35298
Establishment of a Computer-Aided Design (CAD)-Computer-Aided Manufacturing (CAM) process for the production of cold forged gears
[AD-A155756] 24 p4137 N85-35644

EYE (ANATOMY)
NT NYSTAGMUS
NT OCULOMOTOR NERVES
NT RETINA
A limbus-sensing eye movement recorder
[AD-A144772] 01 p0049 N85-10323
Eyes for computers 07 p1012 N85-16428
The effect of modified spectacles on the field of view of the helmet display unit of the integrated helmet and display sighting system
[AD-A148693] 09 p1261 N85-18055
Photorefractor ocular screening system
[NASA-CASE-MFS-26011-1SB]
11 p1692 N85-20639
Retinal information mapping system
[AD-D011531] 12 p1849 N85-21601
Application of the system identification technique to goal-directed saccades
[AD-A150132] 12 p1906 N85-21967
Technical support for microwave experiments on the eye lens
[AD-A149702] 12 p1933 N85-22144

Applications of compound eye configurations to smart sensor design
[AD-A150731] 14 p2420 N85-24935
Test and evaluation of the 2.4-micron photorefractor ocular screening system
[NASA-TM-86492] 15 p2615 N85-26115
The 10 MWe solar thermal central receiver pilot plant: Beam safety tests and analyses
[SAND-83-8035] 16 p2818 N85-27379
Pursuit tracking performance and flash disruption: The effects of training the non-dominant eye on target reacquisition
[AD-A153404] 17 p2999 N85-28541
Predictive model of electron beam induced flashblindness
[AD-A155260] 21 p3664 N85-32763

EYE DISEASES
NT CATARACTS
Photorefractor ocular screening system
[NASA-CASE-MFS-26011-1SB] 11 p1692 N85-20639

EYE MOVEMENTS
NT NYSTAGMUS
NT SACCADIC EYE MOVEMENTS
A limbus-sensing eye movement recorder
[AD-A144772] 01 p0049 N85-10323
Eyelid motion sequences predictive of decision errors
[AD-A145702] 02 p0235 N85-11531
Development and evaluation of a performance-based test of saccadic and vestibulo-ocular control
[AD-A145367] 02 p0237 N85-11545
Computerized sleep staging by detecting eye and hand movement, delta EEG activity and EMG, using portable solid state technique — spaceborne experiments
05 p0695 N85-14475
Visual attention to radar displays
05 p0704 N85-14514
No fatigue effect on blink rate
05 p0712 N85-14564
Neuro-linguistic programming: Eye movements as indicators of representational systems
[AD-A147541] 07 p1016 N85-18454
Vestibular and oculomotor function during Gz variations 11 p1693 N85-20645
Prediction of seasickness susceptibility
11 p1693 N85-20647
Sensory and motor properties of the cerebellar uvula and modulus 15 p2613 N85-26104
Eye movement in response to single and multiple targets
[AD-A151115] 15 p2617 N85-26126
Electrooculographic measurement, fatigue and variability of performance in simulated aircraft flight
19 p3217 N85-29948
An error-dependent model of instrument-scanning behavior in commercial airline pilots
[NASA-CR-3908] 21 p3665 N85-32765
The human engineering eye movement measurement research facility
[AD-A156009] 24 p4132 N85-35613

F

F CENTERS
U COLOR CENTERS

F DISPLAYS
U F REGION

F LAYER
U F REGION

F REGION
NT F 2 REGION
Global maps of foF2 derived from observations and theoretical values
[AD-A145686] 03 p0392 N85-12509
Behavior of the ionospheric F region in low latitudes and in the equatorial region of Brazil during strong magnetic storms in the 1978 to 1983 period
[INPE-3231-PRE/581] 05 p0675 N85-14333
Nocturnal increases of ionization in the ionospheric F region in the low latitude of Brazil during magnetic storms
[INPE-3271-PRE/596] 05 p0675 N85-14334
Experience with proposed improvements of the International Reference Ionosphere (IRI)
[PB84-235670] 05 p0678 N85-14353
Observations of plasma bubbles and their zonal drift using polarimeters
[INPE-3219-PRE/572] 05 p0729 N85-14688
Dynamics of the low-latitude thermosphere and ionosphere 09 p1351 N85-18501
Ionspheric effects of seasonal and diurnal variations of electric fields in equatorial F-region
14 p2336 N85-24459
Influence of internal gravity waves on F layer
14 p2336 N85-24460
Anisotropy of Alfven wave absorption in ionosphere
14 p2339 N85-24464
Fabry-Perot interferometer and skymapping photometer determinations of midlatitude f-region neutral winds and temperatures and airglow enhancement/depletions
[AD-A150730] 14 p2373 N85-24666
Fast ion polarization jet in subauroral F-layer and its manifestation in structure of high latitude ionosphere
15 p2480 N85-25306
Influence of tropical F region in ionosphere on propagation of short radio waves
16 p2721 N85-26798
A study of the generation mechanisms of high latitude and equatorial F-region irregularities using DE-2 data
[NASA-CR-175745] 16 p2825 N85-27423
Equatorial F-region irregularity latitudinal extension and dynamo electric field
[INPE-3494-PRE/731] 16 p2826 N85-27433
Dependence of equatorial F-region plasma bubble rise velocity and dynamo electric field on solar cycle
[INPE-3439-PRE/696] 16 p2826 N85-27434
EISCAT electron density studies
[AD-A152820] 17 p2993 N85-28498
Small-scale structure of ionospheric F-region
19 p3297 N85-30440
Equitorial scintillations: Advances since ISEA-6
[AD-A154962] 21 p3631 N85-32559

F 2 REGION
Response of the F2 layer to the polarity of the interplanetary magnetic field
[REPT-561] 03 p0377 N85-12404
Foreshortened short-wave scattering on artificial ionospheric inhomogeneities 14 p2340 N85-24468

F-80 AIRCRAFT
U T-33 AIRCRAFT

F-8 AIRCRAFT
Analytical redundancy management mechanization and flight data analysis for the F-8 digital fly-by-wire aircraft flight control sensors
[NASA-CR-170396] 06 p0757 N85-14844
F-8 refueling boom ground vibration test
[NASA-TM-84914] 07 p0802 N85-15713

F-14 AIRCRAFT
A safety evaluation of the relocation of the ACM (Air Combat Maneuver) panel in the F-14 ( )/AIP (Avionics Integration Program)
[AD-A149596] 12 p1777 N85-21158
F-14A aircraft high-speed flow simulations
[NASA-CR-172559] 14 p2209 N85-23702

F-15 AIRCRAFT
The F-15 flight loads tracking program
07 p0894 N85-15666
Predicted performance benefits of an adaptive digital engine control system of an F-15 airplane
[NASA-TM-85916] 07 p0905 N85-15729
BI-PAC F-15 external fuel tank container modification
[AD-A148836] 09 p1280 N85-18053
Impacts of Space Shuttle thermal protection system tile on F-15 aircraft vertical tile
[NASA-TM-85904] 12 p1792 N85-21245
Effects of inlet distortion on a static pressure probe mounted on the engine hub in an F-15 airplane
[NASA-TP-2411] 13 p1974 N85-22394
Diagnosis: Using automatic test equipment and an artificial intelligence expert system
[AD-A151918] 16 p2851 N85-27576
Fault detection and accommodation testing on an F100 engine in an F-15 airplane
[NASA-TM-86735] 19 p3219 N85-29962
Recent developments in rotary-balance testing of fighter aircraft configurations at NASA Ames Research Center
[NASA-TM-86714] 21 p3551 N85-32090
Performance improvements of a highly integrated digital electronic control system for an F-15 airplane
[NASA-TM-86748] 21 p3556 N85-32120
Development of control laws for a flight test maneuver autopilot for an F-15 aircraft
[NASA-TM-86736] 22 p3730 N85-33122

F-16 AIRCRAFT
F-16 force management, yesterday, today and tomorrow 07 p0895 N85-15674
Implications of guidance and control technology on human factors considerations 10 p1532 N85-19656
Automated radome testing
[AD-P004362] 12 p1826 N85-21456
Dynamic wind-tunnel testing of active controls by the NASA Langley Research Center
13 p1966 N85-22353
Multivariable control law design for the AFTI/F-16 with a failed control surface
[AD-A151906] 15 p2474 N85-25271
Flight control system reconfiguration design using quantitative feedback theory
[AD-A151771] 16 p2710 N85-26722
Application of AFTI/F-16 task-tailored control modes in advanced multirole fighters 17 p2901 N85-27888
Selection procedures for F-16 pilots in the Belgian Air Force 20 p3510 N85-31822

F-17 AIRCRAFT
Dynamic wind-tunnel testing of active controls by the NASA Langley Research Center
13 p1966 N85-22353

F-18 AIRCRAFT
The F-18: A new era for human factors
10 p1534 N85-19671

F-20 AIRCRAFT
Development of the F-20 nose radome
[AD-P004374] 12 p1827 N85-21468

F-27 AIRCRAFT
Safety recommendation(s), A-84-128 through -133
[REPT-3996C/41] 15 p2466 N85-25221
Static longitudinal stability and control characteristics of the Fokker F27 Friendship calculated by simple handbook methods
[VTH-LR-394] 16 p2711 N85-26728

F-104 AIRCRAFT
Testing of the digital flight control system of the German CCV fighter experimental aircraft
13 p1968 N85-22361

F-106 AIRCRAFT
Electromagnetic resonances of cylinders and aircraft model with resistive wires
[NASA-CR-174203] 06 p0838 N85-15319
Comparison of wind velocity in thunderstorms determined from measurements by a ground-based Doppler radar and an F-106B airplane
[NASA-TM-86348] 16 p2703 N85-26687

F-111 AIRCRAFT
Interactions between F-111 fuselage fuel tank sealants. Part 2: Variation in performance properties of polysulfides after contact with polyester degradation products
[AD-A149777] 12 p1812 N85-21368
Automatic flight control modes for the AFTI/F-111 mission adaptive wing aircraft 16 p2714 N85-26756
Automatic flight control modes for the AFTI/F-111 mission adaptive wing aircraft 17 p2905 N85-27909
F-111 automatic test equipment replacement program
20 p3437 N85-31322
Design and testing of an energy-absorbing crewseat for the F/FB-111 aircraft. Volume 3: Data from crew module testing
[NASA-CR-3918] 23 p3896 N85-34134

FAB (PROGRAMMING LANGUAGE)
U FORTRAN

FABRICATION
NT SPACE MANUFACTURING
Development of copper sulfide/cadmium sulfide thin-film solar cells
[DE84-004513] 01 p0044 N85-10287
Automated apparatus for producing gradient gels
[DE84-014507] 01 p0107 N85-10716
Acoustic resonator and method of making same
[DE84-014655] 01 p0116 N85-10792
Characteristics of ion implanters for fabrication of electronic devices
[AD-P003949] 02 p0286 N85-11865
Weld metal solidification cracking in a carbon-manganese steel 03 p0330 N85-12126
Novel techniques for the fabricating and characterization of GaAs MIS (Metal Insulator Semiconductor) structures
[AD-A145766] 03 p0358 N85-12301
Chemical derivatization of an array of three gold microelectrodes with polypyrrole: Fabrication of a molecule-based transistor
[AD-A146221] 03 p0359 N85-12304
The design, fabrication and delivery of a spacelab neutral buoyancy instrument Pointing System (IPS) mockup — underwater training simulator
[NASA-CR-171233] 04 p0462 N85-12934
Ceramic/ceramic seals by microwave heating
[DE84-007486] 04 p0479 N85-13050
Materials for high-temperature fuel cells
[DE84-016316] 04 p0479 N85-13054
NMOS test chip for a course in semiconductor parameter measurements
[PB84-216506] 04 p0497 N85-13174
Development and demonstration of a vertical axis wind turbine POWERHOUSE
[DE84-901449] 04 p0527 N85-13369
Advanced amorphous materials for photovoltaic conversion
[DE84-017198] 04 p0529 N85-13384
Health and environmental effects document for photovoltaic energy systems, 1983
[DE84-017179] 04 p0532 N85-13399
Design, ancillary testing, analysis and fabrication data for the advanced composite stabilizer for Boeing 737 aircraft, volume 2
[NASA-CR-166011] 05 p0612 N85-13914
The variable polarity plasma arc welding process: Its application to the Space Shuttle external tank
[NASA-TM-86482] 05 p0641 N85-14115

Forming fluorine-containing threads from vinylidene fluoride-tetrafluoroethylene copolymer by dry method
06 p0762 N85-14873
Preparation of fire-resistant infusible polycaproamide fiber
06 p0763 N85-14877
Fabrication and quality assurance processes for superhybrid composite fan blades
[NASA-TM-83354] 06 p0763 N85-14882
Effect of substituted phenylnadimides on processing and properties of PMR polyimide composites
[NASA-TM-86902] 06 p0770 N85-14929
Use of least-squares method for estimating errors of turbine blade type parts during fabrication
06 p0776 N85-14963
Oxide charge characteristics of low temperature MOS (Metal-Oxide-Silicon) oxide films
[AD-A148447] 06 p0803 N85-15113
Design and development of a sealed 100-Ah nickel-hydrogen battery
[DE84-016935] 06 p0805 N85-15128
Research on submicrometer structures
[AD-A148578] 06 p0867 N85-15508
Development of short gate FET's
[AD-A147033] 07 p0947 N85-15999
Control technology for integrated circuit fabrication at Micro-Circuit Engineering, Incorporated, West Palm Beach, Florida
[PB85-100717/GAR] 07 p0949 N85-16013
Infrared technology for satellite power conversion — antenna arrays and bolometers
[NASA-CR-174266] 07 p0991 N85-16293
Switchable zero order diffraction gratings as light valves
[AD-A147575] 07 p1044 N85-16633
Advances in composites technology
[NASA-TM-86353] 08 p1118 N85-17048
Materials of the fourth scientific-technical Conference on Questions of the Extrusion of Metals (Selected articles)
[AD-A148578] 08 p1130 N85-17121
Ceramic fabrication process before firing-surface treatment of ceramic powder
[NASA-TM-77437] 08 p1131 N85-17129
Investigation on experimental techniques to detect, locate and quantify gear noise in helicopter transmissions
[NASA-CR-3947] 08 p1217 N85-17667
The fabrication, processing and characterization of multidimensionally braided graphite/epoxy composite materials
[AD-A148729] 09 p1288 N85-18090
An inexpensive vector thin film magnetometer
[AD-A148725] 09 p1323 N85-18310
Mask aligner for solar cell fabrication
[AD-D011450] 10 p1510 N85-19529
Conceptual design of a 10 MW shore-based OTEC plant
[DE84-015808] 10 p1511 N85-19532
Develop and demonstrate manufacturing processes for fabricating graphite filament reinforced polyimide (Gr/PI) composite structural elements
[NASA-CR-172497] 11 p1592 N85-20019
Fabrication and properties of tungsten heavy metal alloys containing 30% - 90% tungsten
[DE85-000152] 11 p1607 N85-20103
Fabrication of fiber-reinforced ceramic composites by chemical vapor infiltration
[DE85-003809] 11 p1611 N85-20132
Control technology for integrated circuit fabrication at Honeywell Optoelectronics Division, Richardson, Texas
[PB85-109023] 11 p1616 N85-20162
Pultrusion process for fabrication of tethers (preliminary concepts)
11 p1646 N85-20371
Excimer laser annealing to fabricate low cost solar cells
[NASA-CR-174394] 11 p1673 N85-20638
Research on separators for alkaline zinc batteries
[DE85-003082] 12 p1836 N85-21523
New high resolution scanning ion microprobe and focused ion beam applications
[AD-A149992] 12 p1852 N85-21616
Low capacitance e-beam fabricated beam-lead Schottky barrier diodes
[AD-A150236] 13 p2063 N85-22888
New high-efficiency silicon solar cells
[NASA-CR-175643] 13 p2128 N85-23244
Structural design of the Sandia 34-M Vertical Axis Wind Turbine
[DE85-002631] 13 p2129 N85-23247
A normal incidence, high resolution X-ray telescope for solar coronal observations
[NASA-CR-175822] 13 p2169 N85-23481
Technology for pressure-instrumented thin airfoil models, phase 1
[NASA-CR-3891] 14 p2227 N85-23804
Extreme precision antenna reflector study results
14 p2232 N85-23830
Some features of the fabrication of multilayer fiber composites by explosive welding
[NASA-TM-77844] 14 p2248 N85-23932
Milling of spherical zones in parts
14 p2266 N85-24041
Fabrication of turbine parts with transportable tools
14 p2267 N85-24046
Design, fabrication and testing of a multibeam forming network
[NASA-CR-175895] 14 p2296 N85-24228
High resistance and raised modulus carbon fibers
[NASA-TM-76864] 15 p2502 N85-25436
Glass, carbon fibers made at Fibre et Mica in France
15 p2534 N85-25634
Welding technology: Japan — Conference
[ISBN-0-85300177-4] 15 p2565 N85-25823
Welding technology and organisation in steel construction
15 p2566 N85-25828
Design and fabrication of a unique electromechanical machine for long-term fatigue testing
[DE85-006524] 15 p2580 N85-25912
Development of a new faster process for the fabrication of ceramic fiber-reinforced ceramic composites by chemical vapor infiltration
[DE85-007550] 16 p2756 N85-27007
Method of fabricating acceleration resistant crystal resonators and acceleration resistant crystal resonators so formed
[AD-D011630] 16 p2778 N85-27145
Method of fabricating material for the electrodes of gas discharge devices
[DE85-007452] 16 p2780 N85-27157
Production and compaction of amorphous metal powders
[BLL-BISI-TRANS-22387-(9022.06)]
17 p2929 N85-28080
Process for making electrodes for discharge tubes
[DE85-006896] 17 p2955 N85-28247
Electrode for flash discharge lamps
[DE85-006896] 17 p2955 N85-28252
Effects of processing chemistry on electrical properties of high field ZnO varistors
[DE85-007688] 17 p2956 N85-28254
Laser welder for fabricating neutron tubes
[DE85-009965] 17 p2974 N85-28377
Inspection of welds and the factors improving its effectiveness in welded structure fabrication
[BLL-BISI-TRANS-22194-(9022.06)]
17 p2976 N85-28387
Low density inorganic foams fabricated using microwaves
[DE85-007708] 18 p3060 N85-29051
Molten carbonate fuel cell cathode material development
[DE85-010268] 18 p3061 N85-29057
LFMR definition study
[AD-A153691] 18 p3090 N85-29126
Coal-Fired MHD Combustor Development Project, Phase 3D
[DE85-008822] 18 p3192 N85-29795
Solar rocket component study
[AD-A154186] 19 p3227 N85-30007
Method for production of ceramic oxide and carbide bodies by polymer inclusion and decomposition
[DE85-011668] 19 p3250 N85-30152
Heterojunction Schottky gate MESFET with lower channel ridge barrier
[AD-D011673] 19 p3258 N85-30199
Glow discharge deposition at high rates using diethane
[DE85-010236] 19 p3263 N85-30235
Design and operation of epitaxial reactor
[DE85-011089] 19 p3306 N85-30491
Materials and techniques for model construction
[NASA-CR-172620] 20 p3398 N85-31066
Design and fabrication of durable owner-built wind turbine blades
[DE85-009200] 20 p3484 N85-31650
Resistance of polyaniline films as a function of electrochemical potential and the fabrication of polyaniline-based microelectronic devices
[AD-A154999] 21 p3569 N85-32201
Parallel simulation of digital LSI circuits
[AD-A154745] 21 p3580 N85-32258
Fabrication and test of modified quadrupole mass spectrometer
[AD-A155186] 21 p3590 N85-32312
Three-dimensional photochemical machining with lasers
[AD-A154711] 21 p3591 N85-32320
Tape casting as an approach to an all-ceramic turbine shroud seal
[NASA-TM-87078] 21 p3596 N85-32333
Status of high-efficiency module design and fabrication
21 p3612 N85-32446
Method of bonding silver to glass and mirrors produced according to this method
[DE85-011642] 22 p3792 N85-33495
Automatic rotary valve actuator
[DE85-012797] 22 p3794 N85-33505
Block 5 documentation and solar modules
[NASA-CR-176134] 22 p3805 N85-33564
Poly-functional building material from fiberglass (its fabrication and properties)
23 p3908 N85-34209
Evacuate and backfill apparatus and method
[DE85-006018] 23 p3938 N85-34411
Electrolyte reservoir for carbonate fuel cells
[DE85-005736] 23 p3947 N85-34480
Method of preparing thin porous sheets of ceramic material
[DE85-006399] 24 p4082 N85-35300
Single-point diamond crushing of Zerodur with in-situ polishing and metrology on a diamond turning machine
[DE85-012918] 24 p4083 N85-35305
SLC arc transport system: Magnet design and construction
[DE85-014289] 24 p4159 N85-35789

FABRICS
NT PARACHUTE FABRICS
NT WOOL
Zero adhesion system
[AD-D011237] 01 p0015 N85-10093
The theory of elastic modulus of fabric composites and its examination by experiments
[NAL-TR-808] 01 p0022 N85-10133
Development of failure criterion for Kevlar-epoxy fabric laminates
[NASA-CR-172465] 02 p0170 N85-11138
Testing of three different flight suits in fire environment — fuel fire
[FOA-C-59012-H1] 02 p0238 N85-11552
Thermoplastic-carbon fiber hybrid yarn
[NASA-CR-3849] 03 p0325 N85-12093
Fabric filter system study
[PB84-229749] 03 p0342 N85-12206
Electrostatic augmentation of fabric filtration: Reverse-air pilot unit experience
[PB84-230002] 03 p0343 N85-12207
Flame-resistant materials for use in pyrotechnic safety clothing
[AD-A148857] 07 p0931 N85-15901
Measurement of stress in clothing: A literature review and methods selected
[AD-A147674] 08 p1132 N85-17132
Ceramic fabric material testing
[DE84-012014] 09 p1300 N85-18165
Improved electron emission by use of a cloth fiber cathode
[AD-A149250] 10 p1480 N85-19340
Hot melt adhesive attachment pad
[NASA-CASE-LAR-12894-1] 11 p1610 N85-20125
Finger materials for air cushion vehicles. Volume 2: Base fabrics for finger materials
[AD-A149701] 12 p1819 N85-21408
Removable cleanable antireflection shield
[AD-D011735] 22 p3844 N85-33810

FABRY-PEROT INTERFEROMETERS
Fabry-Perot interferometer and skymapping photometer determinations of midlatitude f-region neutral winds and temperatures and airglow enhancement/depletions
[AD-A150730] 14 p2373 N85-24666
Evaluation of a magneto-optical filter and a Fabry-Perot interferometer for the measurement of solar velocity fields from space
14 p2442 N85-25067
Linewidth and bandwidth measurements of the q-branch of h2 using CW coherent anti-Stokes Raman spectroscopy
[AD-A151868] 15 p2506 N85-25456
Thermospheric winds observed by OI6300A Doppler shifts at 23 deg S in the Brazilian sector
[INPE-3384-RPE/470] 16 p2834 N85-27479
Optically bistable devices using InSb
18 p3188 N85-29758
Optical bistability in Cd(x)Hg(1-x)Te
18 p3188 N85-29760
Optical modulators and bistable devices using molecular gases
18 p3188 N85-29761
A simple optical extensometer achieving high accuracy
[NPL-DMA(A)-95] 20 p3458 N85-31474

FABRY-PEROT LASERS
U LASERS

FABRY-PEROT SPECTROMETERS
High precision measurement of stellar radial velocity variations
08 p1250 N85-17696

FACE CENTERED CUBIC LATTICES
Kohn anomaly in metastable fcc lanthanum at low temperatures
[DE84-015459] 04 p0569 N85-13628

Irradiation creep induced anisotropy in a/2110 dislocation populations
[DE84-016623] 06 p0668 N85-15520
Computer simulation of grain-boundary properties in ionic crystals and metals
[DE85-000577] 11 p1734 N85-20908
Observation of surface vibrational resonances on (110) surfaces of FCC metals
[AD-A150469] 13 p2163 N85-23419
Defect production and recovery in FCC metals irradiated at 4.2 K
[DE85-010477] 20 p3538 N85-32014

FACETS
U FLAT SURFACES

FACILITIES
Corrosion and coatings review of specifications and drawings of facilities for the Oman Military Construction Program at Masirah Island, Oman
[AD-A149739] 12 p1812 N85-21366

FACSIMILE COMMUNICATION
Facsimile transmission of microforms
[AD-A144855] 01 p0038 N85-10236
APOLLO system requirements specification — electronic document delivery
[ESA-SP-1066] 04 p0494 N85-13150

FACSIMILE TRANSMISSION
U FACSIMILE COMMUNICATION

FACTOR ANALYSIS
Factor analysis applied to a silane coupling agent on E-glass fiber system
[AD-A145687] 02 p0187 N85-11249
What is principal components analysis?
02 p0211 N85-11389
Principal components: A review
02 p0211 N85-11390
A factor analysis for time series
[AD-A147495] 07 p1036 N85-16574
Studies in quality improvement. Part 1: Dispersion effects from fractional designs, revised
[AD-A153516] 18 p3119 N85-29308
Chemometric analysis of multisensor arrays
[AD-A153805] 18 p3174 N85-29680
Factor analysis of atmospheric pollution by polycyclic aromatic hydrocarbons
[HSE-TRANS-10988] 19 p3311 N85-30528
Bayesian factor analysis
[AD-A154184] 19 p3347 N85-30747
Development of improved capabilities for computation of gas supercompressibility factors and other properties
[PB85-188316] 20 p3436 N85-31315
Telecommunication market research processing
[ENST-83E018] 23 p3926 N85-34331

FACTORIAL DESIGN
Model robust response surface designs: Scaling 2-level factorials
[AD-A147494] 07 p1033 N85-16556
Analyzing two-level fractional factorial experiments for possible dispersion effects
[AD-A149455] 10 p1548 N85-19760
Studies in quality improvement. Part 1: Dispersion effects from fractional designs, revised
[AD-A153516] 18 p3119 N85-29308
Model robust response surface designs: Scaling two-level factorials
[AD-A156218] 24 p4143 N85-35686

FACTORIALS
Analysis of unreplicated factorials allowing for possibly faulty observations
[AD-A154813] 21 p3678 N85-32848

FACTORIES
U INDUSTRIAL PLANTS

FACTORIZATION
Augmented weak forms and element-by-element preconditioners: Efficient iterative strategies for structural finite elements. A preliminary study
01 p0058 N85-10384
Most wanted factorizations using the quadratic sieve
[DE84-016206] 05 p0718 N85-14609
Supersonic nonlinear potential analysis
[NASA-CR-172456] 07 p0997 N85-15685
Analysis of inviscid transonic flow around an airfoil by diagonal form of IAF scheme
[NAL-TR-831] 10 p1420 N85-18955
Factorized algorithms for combined spatial and temporal processing of radar signals 13 p2061 N85-22997
A stability analysis of incomplete LU factorizations
[AD-A152058] 15 p2638 N85-26271
Symbolic Givens reduction in large sparse least squares problems
[DE85-006885] 17 p3021 N85-28681
A factored implicit scheme for numerical weather prediction with small factorization error
18 p3141 N85-29447
Intermediate boundary conditions for LOD, ADI and approximate factorization methods
[NASA-CR-172591] 18 p3167 N85-29626
Pipelined Givens method for computing the QR factorization of a sparse matrix
[DE85-009772] 18 p3171 N85-29653
Approximate factorization method for computation of nonhydrostatic mesoscale flows
[DE85-007259] 19 p3313 N85-30537
Bayesian factor analysis
[AD-A154184] 19 p3347 N85-30747
A factorization approach to the linear regulator quadratic cost problem 20 p3413 N85-31178

FACULAE
Variability of the quiet photospheric network
14 p2452 N85-25144
Contribution functions for Zeeman-split lines, and line formation in photospheric faculae
18 p3207 N85-29893

FADDEEV EQUATIONS
Spline-Galerkin solution of integral equations for 3-body scattering above break-up
[TWISK-327] 01 p0109 N85-10738
Configuration space Faddeev calculations
[DE85-005813] 16 p2672 N85-27721

FADING
NT SELECTIVE FADING
NT SIGNAL FADING
Propagation influences on the performance of a reduced bandwidth quadrature phase shift keyed digital radio system 10 p1470 N85-19274
Equatorial transionospheric propagation conditions affecting digital communications
10 p1470 N85-19275
The fading of R coronae borealis
11 p1753 N85-21029
DMSK: A practical 2400-bps receiver for the mobile satellite service: An MSAT-X Report
[NASA-CR-176194] 24 p4086 N85-35324

FAHRENHEIT TEMPERATURE SCALE
U TEMPERATURE SCALES

FAIL-SAFE SYSTEMS
Automatic flight control modes for the AFTI/F-111 mission adaptive wing aircraft 17 p2905 N85-27909
Graphic display development program. Volume 2, revision 0: Appendices
[DE85-011078] 19 p3333 N85-30648

FAILURE
NT ENGINE FAILURE
NT STRUCTURAL FAILURE
NT SYSTEM FAILURES
Fracture, failure, and fragmentation
01 p0059 N85-10390
Life distribution properties of devices subject to deterioration
[AD-A145554] 02 p0208 N85-11358
On discrete failure models
[AD-A145579] 02 p0206 N85-11359
Vertical crustal movements in southern California, 1974 to 1978
[GS-CIRC-905] 02 p0228 N85-11491
Failure detection processes by pattern recognition and expert systems
[AD-P003924] 02 p0246 N85-11604
Luminous points and breakdown in structure of GaAs transistors 02 p0257 N85-11684
Contributions to the 7th International Acoustic Emission Symposium
[AD-A145368] 02 p0275 N85-11792
On-line fatigue life prediction under stochastic loading by the time series modeling 03 p0370 N85-12362
Dynamic shear failure of shallow-buried flat-roofed reinforced concrete structures subjected to blast loading
[AD-A145974] 03 p0373 N85-12376
A comparison of methods for predicting ductile crack growth instability
[AERE-R-11199] 03 p0374 N85-12387
Effects of constituent properties on compression failure mechanisms 04 p0464 N85-12946
Allowable surge currents and failure mechanisms in semiconductor power devices in various modes of operation 06 p0795 N85-15080
Analyses to develop models to project failure rates and repair costs of electronic modules and subassemblies
[AD-A146509] 06 p0816 N85-15180
Predicting electrochemical breakdown in terrestrial photovoltaic modules 06 p0830 N85-15273
Challenges in the development of the orbiter active thermal control subsystem 06 p1096 N85-16923
Completely monotone regression estimates of software failure rates
[NASA-CR-174319] 06 p1204 N85-17575
A power transformation exponential regression model for censored failure time data
[AD-A148377] 06 p1212 N85-17632
Evaluation of failure criterion for graphite/epoxy fabric laminates
[NASA-CR-172547] 10 p1431 N85-19025
Flashover failures from wet-wire arcing and tracking
[AD-A149055] 10 p1478 N85-19332
Fractographic features of titanium alloy fatigue failure under repeated static stress and high frequency vibration 11 p1601 N85-20070
Systems vulnerability and lethality in the development phase
[AD-A149737] 12 p1924 N85-22089
Reliability bounds for fault-tolerant systems with competing responses to component failures
[NASA-TP-2409] 13 p2100 N85-23090
Effects of assuming independent component failure times, if they are actually dependent, in a series system
[AD-A150582] 13 p2101 N85-23092
Sizing capability of automated ultrasonic time-of-flight diffraction in thick section steel and aspects of reliable inspection in practice
[AERE-R-11548] 15 p2571 N85-25855
VLSI (Very large scale integrated circuits) device reliability models
[AD-A153268] 17 p2954 N85-28245
Inequalities for distributions with increasing failure rate
[AD-A152812] 17 p2976 N85-28390
Optimally robust redundancy relations for failure in uncertain systems
[NASA-CR-175953] 17 p2976 N85-28391
Critical conditions for failure in materials subjected to high rates of loading
[AD-A153135] 17 p2980 N85-28420
Nonparametric estimation of the probability of ruin
[AD-A153523] 18 p3174 N85-29674
Deformation, fracture and explosive properties of reactive materials
[AD-A154073] 19 p3251 N85-30157
Effect of confinement on failure in 95 TATB/5 KEL-F
[DE85-010790] 19 p3251 N85-30158
The value of DMT in the selection of pilots
[RAE-TRANS-2127] 19 p3330 N85-30626
Fundamental investigations of failure during superplastic forming process
[AD-A154647] 21 p3568 N85-32194
Accelerated stress factors and failure/degradation mechanisms in terrestrial solar cells
21 p3613 N85-32451
Analysis of long bone and vertebral failure patterns
[AD-A154796] 21 p3663 N85-32758
Method of characterizing critical timing paths and analyzing timing related failure modes in very large scale integrated circuits
[AD-D011731] 22 p3759 N85-33296

FAILURE ANALYSIS
Review of aircraft accident data: US General Aviation
[PB84-230960] 01 p0005 N85-10027
Stochastic properties of a sequence of interfailure times under minimal repair and under revival
[AD-A145003] 01 p0113 N85-10769
Airfoil deposition model 02 p0144 N85-10979
Development of failure criterion for Kevlar-epoxy fabric laminates
[NASA-CR-172465] 02 p0170 N85-11138
Effect of stress concentrations in composite structures
[NASA-CR-173976] 02 p0170 N85-11140
Efficient methods for mechanical and structural reliability analysis and design 02 p0205 N85-11355
LES: (Lockheed Expert System): A model-based expert system for electronic maintenance
[AD-P003944] 02 p0248 N85-11624
On the requirements of expert systems for fault isolation
[AD-P003947] 02 p0249 N85-11627
Composite fracture toughness and impact characterization 04 p0466 N85-12963
Evaluation of fuzzy rulemaking for expert systems for failure detection 05 p0703 N85-14506
Analytical redundancy management mechanization and flight data analysis for the F-8 digital fly-by-wire aircraft flight control sensors
[NASA-CR-170396] 06 p0757 N85-14844
On the effects of delamination damage in fibre composite laminates
[ARL/STRUC-R-403] 06 p0763 N85-14881
Investigation of accelerated stress factors and failure/degradation mechanisms
06 p0832 N85-15295
Investigation of the HPFTP first stage impeller crack
[NASA-CR-171261] 07 p0977 N85-16208
Built-in-test for first line testing
08 p1064 N85-16739
Automatic error detection and recovery techniques in onboard intelligent units for space and avionic application 08 p1066 N85-16758
Ballistic/detonic transition of propellants
08 p1117 N85-17041
Advances in composites technology
[NASA-TM-86353] 08 p1118 N85-17048

Prematurely terminated sequential tests for MIL-STD 781C
[AD-A148417] 08 p1216 N85-17657
finite element analysis of bi-material systems with applications in hydraulic fracturing
09 p1332 N85-18369
Comparison of property regeneration techniques and life prediction procedures applied to laboratory tested and service exposed NI-Cr alloys
[NPL-DMA(A)-91] 09 p1333 N85-18374
Material flow in the manufacturing system: Fault-diagnosis systems as support for the maintenance of highly automated manufacturing systems
[PNR-90238] 09 p1371 N85-18618
Reliability studies of ceramic capacitors
[AD-A149126] 10 p1479 N85-19338
Theoretical and experimental study of crack resistance and macrocrack growth rate in organic fiber reinforced plastic under pure shear condition
11 p1586 N85-20053
Method of constructing diagram of bimetal fatigue failure 11 p1599 N85-20058
Electric vehicle demonstration project
[DE85-002167] 11 p1741 N85-20943
Environment definition, large particles
12 p1787 N85-21220
A summary and assessment of historical reliability and maintainability data for solar hot water and space conditioning systems
[DE84-004521] 12 p1876 N85-21770
Results of the AFRSI rewaterproofing systems screening test in the NASA/Ames Research Center (ARC) 2 x 2-foot transonic wind tunnel
[NASA-CR-167694] 13 p1988 N85-22467
Reliability of robotized welding apparatus
13 p2034 N85-22741
Characteristics of surface crack development in ATiaS aluminum alloy during slow-cycle loading
13 p2034 N85-22745
Advanced life analysis methods. Volume 1: Cracking data survey and NDI (nondestructive inspection) assessment for attachment lugs
[AD-A150419] 13 p2103 N85-23108
A theoretical basis for the analysis of redundant software subject to coincident errors
[NASA-TM-86369] 13 p2145 N85-23317
Contribution of instrumentation and control software to system reliability
[DE85-004693] 13 p2149 N85-23340
Load capacity of cages of roller bearings for planet wheels 14 p2221 N85-23775
Condition monitoring of helicopter gearboxes using automatic vibration analysis techniques
14 p2223 N85-23790
The observation and interpretation of gear tooth failures 14 p2224 N85-23792
Experimental development of a failure detection scheme for large space structures 14 p2234 N85-23846
Convolution of the IFRA (Increasing Failure Rate Average) scaled-mins class
[AD-A151070] 14 p2411 N85-24870
On failure modeling, revised
[AD-A151411] 15 p2637 N85-26263
How to handle failures in advanced flight control systems of future transport aircraft 16 p2714 N85-26752
Recent failures of weather satellites
[S-HRG-98-1070] 16 p2731 N85-26855
Reusable rocket engine turbopump condition monitoring 16 p2740 N85-26907
ACT applied to helicopter flight control
17 p2902 N85-27891
Experimental measurements and analysis of heat transfer and gas dynamics in a rotating turbine stage
17 p2911 N85-27949
Strength and failure analysis of composite laminates with holes at room and elevated temperatures
[AD-A153263] 17 p2917 N85-27961
Influence of thermochemical treatment on properties of low-carbon steel
[BLL-BISI-TRANS-22410-(9022.06)]
17 p2927 N85-28055
Inequalities for distributions with increasing failure rate
[AD-A152812] 17 p2976 N85-28390
Optimally robust redundancy relations for failure in uncertain systems
[NASA-CR-175953] 17 p2976 N85-28391
Method of assessment of start of slow crack growth by acoustic emission technique
[BLL-BISI-TRANS-21762-(9022.06)]
17 p3027 N85-28722
Properties of polyethylene gas piping materials
[PB85-167045] 18 p3082 N85-29068
Fault detection and accommodation testing on an F100 engine in an F-15 airplane
[NASA-TM-86736] 19 p3219 N85-29962
Study of failure mechanism of fibrous composition materials taking into account physicochemical reactions of components 19 p3243 N85-30106
Effect of matrix plasticity on durability of fibrous composition materials 19 p3243 N85-30107
Resistance to corrosion fatigue in aluminum alloy 1561 in sea water 19 p3243 N85-30108
Correction of calculated estimate of fatigue properties of materials under biharmonic loading
19 p3244 N85-30113
Deformation, fracture and explosive properties of reactive materials
[AD-A154073] 19 p3251 N85-30157
Effects of high mean stress on the high-cycle fatigue behavior of PWA 1480
[NASA-CR-176020] 19 p3287 N85-30368
Impurity and particle control systems for tokamak reactor experiments
[DE85-006124] 19 p3366 N85-30673
Failure modes experienced on spacecraft NiCd batteries 20 p3445 N85-31366
The failure mechanism of a nickel electrode in a nickel-hydrogen cell 20 p3448 N85-31408
Automated FMEA (Failure Modes and Effects Analysis) techniques
[AD-A154161] 20 p3464 N85-31518
A comparison of two contemporary creep-fatigue life prediction methods 20 p3467 N85-31538
Geothermal COMPAX drill bit development
[DE85-011353] 20 p3469 N85-31556
Failure mechanisms in metal-sheathed thermocouples
[DE85-011929] 21 p3590 N85-32317
Dynamic fracture of concrete and other heterogeneous materials
[AD-A154513] 21 p3598 N85-32343
Development of improved dynamic failure models
[AD-A155586] 21 p3600 N85-32354
Failure analysis of thin-film amorphous-silicon solar-cell modules 21 p3613 N85-32452
Methods of reliability design of semiconductor power devices 22 p3770 N85-33365
Nonlinear response and failure characteristics of internally pressurized composite cylindrical panels
[NASA-CR-176148] 22 p3800 N85-33546
Data Base Workshop: Availability-Reliability Modeling
[DE85-011570] 22 p3829 N85-33713
Detonation in tungsten-loaded HMX
[DE85-009606] 23 p3922 N85-34299
The use of ultrasound to monitor incipient failure of rolling element bearings 23 p3924 N85-34317
Method and apparatus for transfer function simulator for testing complex systems
[NASA-CASE-NPO-15896-1] 23 p3926 N85-34333
Short-time creep of ice
[NRC/CNR-TT-2111] 23 p3941 N85-34428
A preliminary evaluation of a failure detection filter for detecting and identifying control element failures in a transport aircraft
[NASA-TM-87576] 24 p4067 N85-35204
Reliability prediction of the series system with spares subject to Weibull failure 24 p4100 N85-35413
State-of-the-art of solid-state motor controllers
[TI85-008674] 24 p4162 N85-35806

FAILURE MODES

Determination sample sizes for diversified reliability test programs
[DE84-015003] 04 p0511 N85-13255
General Electric composite ring-disk flywheel: Recent and potential developments 05 p0606 N85-13867
Centrifuge tests to provide closure bounds for switches subjected to random vibration
[DE85-002003] 10 p1482 N85-19357
Characterization of mode 1 and mixed-mode failure of adhesive bonds between composite adherends
[NASA-TM-86355] 12 p1797 N85-21270
Supported liquid membrane battery separators
[DE85-001031] 12 p1836 N85-21519
Use of acoustical emission method to study specifics of fracture of boron reinforced plastic structural elements 13 p2026 N85-22996
Layered composite analysis capability
15 p2573 N85-25868
Signal analysis techniques for incipient failure detection in turbomachinery 16 p2736 N85-26884
The effects of pin elasticity, clearance, and friction on the stresses in a pin-loaded orthotropic plate
[NASA-CR-175816] 16 p2743 N85-26927
Creep-fatigue interaction of notched 304 stainless steel bars 16 p2798 N85-27249
Determination of failure characteristics of materials and structures
[AD-A152073] 16 p2800 N85-27266
Photovoltaic cell reliability research: Investigation of accelerated stress factors and failure-degradation mechanisms in terrestrial solar cells
[NASA-CR-175815] 16 p2819 N85-27388
Recent progress in the dynamic plastic behaviour of structures, part 4 17 p2978 N85-28402
On validity of threshold values of fatigue strength of steel structures
[BLL-BISI-TRANS-22192-(9022.06)]
17 p2978 N85-28408
Properties of polyethylene gas piping materials
[PB85-167045] 18 p3082 N85-29068
Automated FMEA (Failure Modes and Effects Analysis) techniques
[AD-A154161] 20 p3464 N85-31518
A continuous damage model based on stepwise-stress creep rupture tests
[NASA-CR-174941] 21 p3597 N85-32341
Thin-film reliability and engineering overview
21 p3612 N85-32450
Circuit approaches to increasing SRAM performance in total dose environments
[DE85-009441] 23 p3966 N85-34588
Mechanical characterization and failure modes of fiber reinforced angle-ply composites
24 p4072 N85-35234
Structure and properties of polyethylene films used in heavy lift balloons
[NASA-CR-176227] 24 p4083 N85-35308

FAIRCHILD MILITARY AIRCRAFT

U MILITARY AIRCRAFT

FAIRINGS

UH-60A external stores support system fixed provision fairings drag determination
[AD-A147188] 07 p0902 N85-15719
Space shuttle elevon seal panel mechanism
08 p1101 N85-16981
Automating the study of error in discrete aerodynamic fairing design 14 p2268 N85-24178
The development of staging mechanisms for the Japanese satellite launcher Mu-3SII
22 p3798 N85-33528
An automated technique for encasing specific payloads with low-drag fairings 24 p4083 N85-35183

FALKNER-SKAN EQUATION

Numerical solutions of turbulent models for flow over a flat plate with angle of attack
[DE85-010380] 21 p3585 N85-32286

FALLING SPHERES

Computing parameters characterizing possibility of planets falling in star camera field of view during space survey 15 p2487 N85-25351
Applied research and development for falling-sphere air density measuring systems
[AD-A155227] 21 p3552 N85-32099

FALLOUT

Particle size distribution on surfaces in clean rooms
[AD-A146057] 03 p0328 N85-12109
Assessment of radiation dosages obtained by intake of radioactive fallout contaminated food
[VTT-292] 07 p1017 N85-16480
Development and validation of a new fallout transport method using variable spectral winds
[AD-A151871] 15 p2599 N85-26022
On the design of a global detection system for airborne radioactivity
[CM-68] 20 p3487 N85-31670

FAN BLADES

Energy efficient engine. Volume 2. Appendix A: Component development and integration program
[NASA-CR-173085] 02 p0146 N85-10991
Basic study of bladed disk structural response
[AD-A148226] 03 p0319 N85-12061
Fabrication and quality assurance processes for superhybrid composite fan blades
[NASA-TM-83354] 06 p0763 N85-14882
Strength analysis of fan-shaped wing considering temperature deformation and creep deformations
06 p0779 N85-14983
A comparison of measured and predicted unsteady pressure on a fan blade in unstalled supersonic flutter
[PNR-90223] 08 p1079 N85-16839
Fluctuating pressures on fan blades of a turbofan engine, flight test investigation
[NASA-TP-2361] 10 p1553 N85-19790
Effects of vane/blade ratio and spacing on fan noise, volume 1
[NASA-CR-174864] 10 p1553 N85-19791
Effects of vane/blade ratio and spacing on fan noise. Volume 2: Data supplement
[NASA-CR-174865] 10 p1553 N85-19792
Numerical analyses in aerodynamic design of aero-engine fan 16 p2692 N85-26818
Energy Efficient Engine Program technology benefit/cost study, volume 1
[NASA-CR-174766-VOL-1] 24 p4066 N85-35197

FAN IN WING AIRCRAFT

Strength analysis of fan-shaped wing considering temperature deformation and creep deformations
06 p0779 N85-14983

FANS
Sources, paths, and concepts for reduction of noise in the test section of the NASA Langley 4x7m wind tunnel
[NASA-CR-172446-VOL-1] 05 p0726 N85-14666
Comparison of options for reduction of noise in the test section of the NASA Langley 4x7m wind tunnel, including reduction of nozzle area
[NASA-CR-172446-VOL-2] 05 p0726 N85-14667
FAR FIELDS
Transonic wing and far field test data on a high aspect ratio transport wing for three dimensional computational method evaluation 01 p0004 N85-10021
Case study of sample spacing in planar near-field measurement of high gain antennas
[NASA-TM-86672] 01 p0037 N85-10234
Characteristic boundary conditions for three-dimensional transonic unsteady aerodynamics
[NASA-TM-86292] 02 p0134 N85-10915
Time variability of directionality properties of pulsed EB-EDL (Electron Beam-Electric Discharge Laser) N2-CO2 lasers
[AD-A145546] 02 p0202 N85-11344
Efficient computation of reflector antenna aperture distributions and far field patterns
[AD-A147367] 07 p0940 N85-15962
Radiation patterns of a pyramidal horn antenna
09 p1311 N85-18236
A conformal mapping suitable for problems involving interaction between given geometries and known far fields
[AD-A148050] 10 p1545 N85-19744
Near Field/Far Field (NF/FF) energy loss in Electric Discharge Lasers (EDL's): A mode-medium interaction
[AD-A150299] 13 p2096 N85-23075
Space processing of acoustic signals in plane-parallel waveguide — antenna arrays 15 p2525 N85-25572
The method of residual minimization in compressible steady flows
[AD-A153924] 18 p3100 N85-29193
Notes on unsteady transonic cascade flows
[AD-A154829] 21 p3552 N85-32098
Reducing grating lobes due to subarray amplitude tapering
[AD-D011723] 23 p3927 N85-34339
FAR INFRARED RADIATION
Effects of atmospheric water vapor and clouds on NOAA (National Oceanic and Atmospheric Administration) AVHRR (Advanced Very High Resolution Radiometer) satellite data
[AD-A145425] 02 p0260 N85-11824
Developments in far-infrared detection techniques
[AD-A146290] 03 p0420 N85-12663
Far-infrared observations of some regions of star formation 03 p0442 N85-12814
Far-infrared photometry of compact extragalactic sources: OJ 187 and BL Lac
[NASA-TM-86022] 04 p0580 N85-13701
Far-infrared line emission from the galaxy
[NASA-CR-174166] 04 p0580 N85-13702
Far-infrared laser diagnostic on EBT and extreme far-forward laser scattering on ISX
[DE85-001788] 07 p1046 N85-16643
The Lear Jet Observatory: Fifteen years of discovery and rebirth 08 p1244 N85-17850
Far infrared and submillimeter observations of the giant planets 08 p1245 N85-17856
Far-infrared spectroscopy of interstellar gas
08 p1245 N85-17858
Multi-spectral observations of the star formation: The role of far infrared photometry 08 p1245 N85-17859
The Orion molecular cloud at far-infrared wavelengths
08 p1245 N85-17860
First results of submillimeter polarimetry
08 p1246 N85-17861
NGC 2024: Multi-wavelength infrared and radio observations 08 p1246 N85-17865
Far-infrared photometry of low-mass pre-main-sequence stars with broad CO wings 08 p1246 N85-17866
High sensitivity, high angular resolution far-infrared photometry from the KAO 08 p1246 N85-17867
Star formation in globules 08 p1247 N85-17868
Far infrared observations of molecular clouds in the outer galaxy 08 p1247 N85-17869
Far infrared emission from galaxies
08 p1248 N85-17875
Far infrared continuum emission from the galactic center 08 p1248 N85-17876
The 157 micron (C II) luminosity of the galaxy
08 p1248 N85-17877
Variation of oxygen and nitrogen abundances in the galaxy 08 p1248 N85-17878
Far IR observations of the Magellanic clouds
08 p1248 N85-17879
Dust reradiation from NGC 6946
08 p1248 N85-17880
Starbursts in galaxies: Implications of molecular and far-infrared observations 08 p1248 N85-17881
Far-infrared spectroscopy of galaxies: The 158 micron C(+) line 08 p1249 N85-17882
Interpretation of the far infrared emission from our external galaxies 08 p1249 N85-17884
A far infrared Echelle spectrometer for the Kuiper Airborne Observatory 08 p1249 N85-17886
Far-infrared interferometry/polarimetry on the ISX-B Tokamak
[DE84-015401] 10 p1558 N85-19827
Far-infrared line observations of planetary nebulae. 1: The O 3 spectrum
[NASA-TM-86670] 10 p1570 N85-19900
FIR interferometer/polarimeter system on ISX-B Tokamak
[DE85-001129] 11 p1731 N85-20887
Balloon-borne, He-cooled Fourier transform spectrometer for far infrared astronomy
[MPE-IR-41] 17 p3053 N85-28899
Far-infrared emission lines of CO and OH in the Orion-KL molecular shock
[NASA-TM-86721] 24 p4167 N85-35832
Observations of far-infrared transitions between excited states of OH
[NASA-TM-86722] 24 p4167 N85-35833
FAR ULTRAVIOLET RADIATION
NT LYMAN ALPHA RADIATION
Voyager EUV and FUV observations
06 p0675 N85-15554
Radiation/catalytic augmented combustion
[AD-A148758] 09 p1290 N85-18101
Evaluation of miniature vacuum ultraviolet lamps for stability and operating characteristics, Lyman-Alpha task
[NASA-CR-171345] 10 p1477 N85-19323
Vacuum ultraviolet electronic properties of liquids
[DE85-000305] 10 p1583 N85-19958
Research in extreme ultraviolet and far ultraviolet astronomy
[NASA-CR-174432] 10 p1570 N85-19902
Ultraviolet observations of circumstellar matter in Algol type binary systems 11 p1756 N85-21043
Strange F + Be binary star systems
11 p1756 N85-21045
The solar stellar connection in the far ultraviolet
11 p1757 N85-21055
Precise measurements of radial velocities of emission lines in the far-ultraviolet spectra of late-type stars
11 p1758 N85-21082
Documentation for the machine-readable version of the Revised S210 Catalog of Far-Ultraviolet Objects (Page, Carruthers and Heckathorn 1982)
[NASA-TM-87439] 14 p2438 N85-25047
Stimulated Brillouin scattering reflectivity in the presence of various aberrators
[AD-A151750] 15 p2563 N85-25812
Studies of collisional and nonlinear radiative process for development of coherent UV and XUV sources
[AD-A152001] 16 p2865 N85-27670
Photoionization mass spectrometry with VUV hydrogen laser source
[AD-A153362] 17 p2921 N85-28009
Lifetime and quenching measurements of C2H emission produced by vacuum ultraviolet photolysis of C2H2
[DE85-010769] 19 p3278 N85-30330
Energy transfer and excimer formation in rare gas solids 19 p3374 N85-30930
Tuning system for capacitively loaded 1/4 accelerating cavity
[DE85-012516] 24 p4091 N85-35358
FAR UV SPECTROSCOPIC EXPLORER
Future ultraviolet experiments, including FUSE/COLUMBUS 11 p1744 N85-20969
FARADAY EFFECT
Shock electromechanical energy converter with permanent magnet
[AD-D011228] 01 p0115 N85-10781
Beam pulse length determination by spectral analysis
[CSIR-NAC-83-05] 01 p0116 N85-10793
Magnetosphere, rings, and moons of Uranus
02 p0301 N85-11951
The response of mid-latitude total electron content to solar activity 04 p0522 N85-13336
A warm magnetoactive plasma in a large volume of space 06 p0678 N85-15579
Influence of Faraday effect in ionosphere on nonmutuality of meteor radio channel
07 p0952 N85-16037
Current measurements by Faraday rotation in single mode optical fibers
[DE85-002025] 09 p1384 N85-18707
The Faraday rotation experiment — solar corona
16 p2866 N85-27805
Sensitive detection of tunable diode laser absorption by polarization rotation
[DE85-009621] 19 p3277 N85-30322
Variations in the small-scale galactic magnetic field and short time-scale intensity variations of extragalactic radio sources 20 p3549 N85-32084
The Faraday effect in ruby and corundum in strong magnetic fields 21 p3697 N85-32987
Injector losses on Mite
[DE85-012356] 24 p4090 N85-35355
FARADAY ROTATION
U FARADAY EFFECT
FARM CROPS
NT ALFALFA
NT BARLEY
NT CORN
NT FRUITS
NT GRAINS (FOOD)
NT LEGUMINOUS PLANTS
NT OATS
NT POTATOES
NT RICE
NT SUGAR BEETS
NT SUGAR CANE
NT WHEAT
Spatial estimation from remotely sensed data via empirical Bayes models 07 p0985 N85-16258
The climate in food production in Latin America
07 p1001 N85-16359
The challenge of food production: The importance of climate 07 p1001 N85-16361
The management of atmospheric resources in food production 07 p1002 N85-16362
Some stability and control problems with trailed farm tankers on slopes
[AD-P004291] 09 p1408 N85-18668
Characterization of LANDSAT-4 TM and MSS image quality for the interpretation of California's agricultural resources — Central Valley 13 p2118 N85-23190
Evaluation of the area and severity of last night's frosts
[REPT-109] 16 p2833 N85-27473
Irradiation of northwest agricultural products
[DE85-012455] 22 p3843 N85-33803
FARMLANDS
Evaluation of SIR-B imagery for geologic and geomorphic mapping, hydrology, and oceanography in Australia 08 p1146 N85-17229
Remote sensing research for agricultural applications — San Joaquin County, California and Snake River Plain and Twin Falls area, Idaho
[E85-10090] 12 p1873 N85-21752
Characterization of LANDSAT-4 TM and MSS image quality for the interpretation of California's agricultural resources — Central Valley 13 p2118 N85-23190
An initial analysis of LANDSAT-4 Thematic Mapper data for the discrimination of agricultural, forested wetlands, and urban land cover — Poinsett County, Arkansas; and Reelfoot Lake and Union City, Tennessee
13 p2118 N85-23193
Preliminary evaluation of TM for soils information
13 p2121 N85-23206
The use of Thematic Mapper data for land cover discrimination: Preliminary results from the UK SATMaP programme 13 p2121 N85-23207
Mathematical model of the nitrogen cycle in a nonsaturated area of cultivated soil
20 p3478 N85-31610
FAST FOURIER TRANSFORMATIONS
On maximum entropy signal analysis
[AD-A144374] 03 p0410 N85-12618
Fast method for calculating radiation patterns of nonequidistant radiator systems
06 p0791 N85-15052
An adaptive Fast Fourier Transform weighting technique to increase small target sensitivity
[AD-D011424] 08 p1154 N85-17286
Computing convolution of multifrequency signal employing truncated fast Fourier transform algorithms
13 p2065 N85-23019
Spectral information from gapped data. A comparison of technique 14 p2444 N85-25080
Hardware schemes for fast Fourier transform, part 7.4A 21 p3626 N85-32526
Interpolation problems in meteor radar analysis, part 7.6A 21 p3626 N85-32528
Generalization of discrete Fourier transform for interpolation in time domain 22 p3775 N85-33396
Generalization of discrete Fourier transformation for interpolation in time domain 22 p3776 N85-33400
Matched filtering of visual evoked potentials to detect acceleration (+Gz) induced blackout
[AD-A155912] 24 p4131 N85-35609
FAST NEUTRONS
Raman study of neutron irradiated GaAs
[DE84-016056] 05 p0731 N85-14702
Measurement of oxygen contamination in titanium alloy ingots by fast neutron activation analysis
[AD-P004133] 08 p1128 N85-17108

Sulfur activation at the Little Boy-Comet Critical Assembly: A replica of the Hiroshima bomb
[DE85-010261] 20 p3527 N85-31938
Fast-neutron interaction with niobium
[DE85-011471] 24 p4150 N85-35731

FAST NUCLEAR REACTORS
NT EXPERIMENTAL BREEDER REACTOR 2
NT FAST TEST REACTORS
NT LIQUID METAL FAST BREEDER REACTORS
Expected behavior of plutonium in the IFR fuel cycle
[DE85-006225] 18 p3181 N85-29725
A review of the SIMMER-2 analyses of liquid-metal-cooled fast breeder reactor core-disruptive accident fuel escape
[DE85-010803] 19 p3366 N85-30876

FAST TEST REACTORS
Application of robotics in remote fuel fabrication operations
[DE84-011481] 05 p0646 N85-14144
Liquid metal reactor programs: Safeguards and program assurance
[DE85-010621] 19 p3331 N85-30635

FASTENERS
NT ANCHORS (FASTENERS)
NT BOLTS
NT LOCKS (FASTENERS)
NT NUTS (FASTENERS)
NT PINS
NT RIVETS
NT SCREWS
The influence of fastener flexibility on load transfer and fatigue life predictions for multirow bolted and riveted joints — aircraft structures
[LBF-FB-172/84] 07 p0979 N85-16219
Eddy current test probe with circumferential segments and method of testing material surrounding fastener holes
[AD-D011554] 12 p1850 N85-21603
Finite element analysis of problems associated with life enhancement techniques
[ARL/STRUC-R-404] 12 p1862 N85-21676
On the stress analysis of bonded inserts
[ARL/STRUC-R-407] 12 p1865 N85-21698
Stresses in a half-plane containing either a pressurized hole or an interference-fit disc
[ARL/STRUC-R-409] 12 p1865 N85-21700
Elastic response of a half-plane to a bonded interference-fit disc of the same material
[ARL/STRUC-R-406] 12 p1865 N85-21701
Theoretical and experimental investigation of mechanically fastened composites
[AD-A150961] 14 p2248 N85-23935
Daze fasteners
[NASA-CASE-LAR-13009-1] 18 p3116 N85-29285
Mechanical fastener
[NASA-CASE-LAR-12738-2] 19 p3279 N85-30335
Low-profile fastener
[AD-D011667] 19 p3280 N85-30343
Load transfer by analytical methods
[SNIAS-851-111-109] 20 p3470 N85-31561
Mechanical connection for a tubular assembly
[DE85-011590] 22 p3792 N85-33497
Automatic capability to store and retrieve component data and to calculate structural integrity of these components
[DE85-012429] 22 p3831 N85-33728

FASTING
Effect of prolonged hunger during experimental hikes
11 p1692 N85-20637

FATIGUE (BIOLOGY)
NT AUDITORY FATIGUE
NT FLIGHT FATIGUE
NT MUSCULAR FATIGUE
The Reports of Aeromedical Laboratory, volume 25, no. 1/2
[ISSN-0023-2858] 01 p0090 N85-10605
A study of fatigue of shiftworkers in air traffic control and weather service groups in JASDF
01 p0090 N85-10610
The effect of sleep loss on the human visual event-related potential
[AD-A145364] 02 p0234 N85-11528
Man's physical tolerance to heat. Heat storage, burn injury
[FOA-C-54055-H1] 02 p0235 N85-11533
No fatigue effect on blink rate
05 p0712 N85-14564
Human factors survey: C-5 pilots
[AD-A147108] 07 p1020 N85-16477
Methods of monitoring mental work efficiency, emotional activity 10 p1526 N85-19827
Electrooculographic measurement, fatigue and variability of performance in simulated aircraft flight
19 p3217 N85-29948
Human performance in continuous/sustained operations and the demands of extended work/rest schedules. An annotated bibliography
[AD-A155619] 21 p3666 N85-32771
Physiological responses to unvarying (steady) and 2-2-1 shifts: Miami International Flight Service Station
[AD-A155751] 24 p4133 N85-35619

FATIGUE (MATERIALS)
NT BENDING FATIGUE
NT METAL FATIGUE
NT STRUCTURAL STRAIN
NT THERMAL FATIGUE
Influence of aluminum metallization coatings on corrosion fatigue properties of steel
01 p0018 N85-10112
Retardation analytical model to extend service life
[NASA-CR-171177] 01 p0057 N85-10376
Estimation of the threshold in fatigue crack initiation models: A Bayesian approach
[AD-A144847] 01 p0062 N85-10410
Turbine Engine Hot Section Technology (HOST)
[NASA-TM-83022] 02 p0140 N85-10951
Benchmark notch test for life prediction
02 p0140 N85-10953
Life prediction and constitutive models for anisotropic materials 02 p0144 N85-10976
The effect of overload on three different kinds of steel
02 p0174 N85-11165
The adhesion of hard and wear resistant coatings
02 p0179 N85-11203
Fatigue-impact studies in laminated composites
[AD-A142841] 03 p0326 N85-12097
High temperature low-cycle fatigue mechanisms in single crystals of nickel-based superalloy Mar-M 200
[NASA-CR-174739] 03 p0331 N85-12130
Kinetics of fatigue factor of AT3 titanium alloys in air, distilled water and 3.5% aqueous NaCl solution
03 p0350 N85-12255
Fatigue limit analysis involving biaxial stress components 03 p0370 N85-12363
The TA6Zr5D (IMI 685) characterization in strain controlled tests. (Specimens obtained from a forged spinning wheel) no. M4-45870
[M4-45870] 03 p0373 N85-12384
Composite structural materials
[NASA-CR-174077] 04 p0467 N85-12966
Fatigue in composite materials
04 p0467 N85-12968
Ultrasound interaction with partially closed fatigue cracks
[DE84-016360] 04 p0514 N85-13276
Development of damage in fatigue loaded carbon fiber reinforced plastics 05 p0650 N85-14172
Fatigue behavior of bolted joints made of carbon fiber reinforced epoxy resins 05 p0650 N85-14173
Fatigue behavior of sintered steels and measurement criteria for sintered prefabricated parts
05 p0650 N85-14174
Fatigue behavior of continuous fiber silicon-carbide-aluminum composites
[NASA-TM-86332] 06 p0763 N85-14879
On the effects of delamination damage in fibre composite laminates
[ARL/STRUC-R-403] 06 p0763 N85-14881
Study of fatigue fracture in hardened and tempered carbon steel. Report 1: Microscopic observation of the fatigue crack formation process
[BLL-PNR-90242-(8019.3153)]
06 p0767 N85-14909
Investigations into the fatigue crack growth behaviour of X6CrNi 18 11 (1.4948) austenitic stainless steel
[BLL-RISLEY-TR-4544-(9091.9F)]
06 p0768 N85-14911
Influence of the shape and distribution of inclusions of the fatigue strength of bearing steels in rotary bending
[BLL-PNR-90243-(8019.3153)]
06 p0768 N85-14912
The effect of potential on the corrosion fatigue behavior of a precipitation hardened aluminum alloy
[AD-A146537] 06 p0768 N85-14916
Three-dimensional crack location by acoustic emission
[AERE-R-11277] 06 p0618 N85-15193
Operational Loads Data
[AGARD-CP-375] 07 p0894 N85-15664
Operational loads measurement: A philosophy and its implementation 07 p0894 N85-15665
The F-15 flight loads tracking program
07 p0894 N85-15666
Structural load measurements on a Northrop NF-5A
07 p0894 N85-15667
Operational loads data evaluation for individual aircraft fatigue monitoring 07 p0895 N85-15669
In-flight evalution of LCF life consumption of critical rotor components subjected to high transient thermal stress
07 p0906 N85-15734
Monitoring engine thermal stresses
07 p0906 N85-15735
Mechanical aspects of high temperature coatings
07 p0908 N85-15749
Study of residual stresses introduced into TA6ZrO (685) cylinders by quenching
[BLL-PNR-90240-(8019.3153)]
07 p0925 N85-15859
Experimental compliance calibration of the NASA Lewis Research Center Mode 2 fatigue specimen
[NASA-TM-86908] 07 p0977 N85-16205
Verification of the fatigue properties of (small) wind turbines
[NLR-MP-83055-U] 07 p0994 N85-16311
Applicability of linear elastic fracture mechanics to fatigue in polymers and short-fiber composites
09 p1298 N85-18152
Determination of blade service life under irregular loading conditions 09 p1309 N85-18222
Assessing expired fatigue life in large turbine shafts
[DE84-016676] 09 p1340 N85-18427
Fracture resistance of surface layer with technological defects under cyclical loading 10 p1448 N85-19126
Mechanism and pattern of fatigue crack growth in aluminum alloys 11 p1597 N85-20047
Method of constructing diagram of bimetal fatigue failure 11 p1599 N85-20058
Finger materials for air cushion vehicles. Volume 2: Base fabrics for finger materials
[AD-A149701] 12 p1819 N85-21406
The residual strength of cracked specimens representing a section of the flange into wing main spar
[ARL/STRUC-R-408] 12 p1865 N85-21699
Proceedings of the 9th Biennial Army Symposium on Solid Mechanics. Advances in Solid Mechanics for Design and Analysis
[AD-A150042] 12 p1867 N85-21710
Characterisation of fatigue crack extension by quantitative acoustic emission
[AERE-R-11289] 12 p1868 N85-21721
Experimental and numerical analysis of electric currents and electromagnetic blunting of cracks in thin plates
[AD-A150418] 13 p2022 N85-22669
Long-term strength and fracture criteria for EI698VD alloy under complex stress conditions
13 p2030 N85-22723
Some specifics of development of fatigue and creep in heat-resistant alloys with asymmetrical multicycle loading
13 p2031 N85-22724
Load capacity of cages of roller bearings for planet wheels 14 p2221 N85-23775
A study of frequency effects and damage accumulation during the fatigue of graphite/epoxy and glass/epoxy composite materials 14 p2247 N85-23930
An investigation of elevated temperature fatigue crack initiation in 2 and 1/4 cR-1 MO low alloy steel
[AD-A150670] 14 p2255 N85-23973
Variability in constant-load-amplitude fatigue crack growth rates in marine environments
[AD-A150786] 14 p2255 N85-23975
Role of passive surface films on corrosion fatigue crack initiation
[DE85-000436] 14 p2257 N85-23985
Fatigue Crack Topography
[AGARD-CP-376] 14 p2318 N85-24321
Essential features in fatigue fractures and remarkable phenomena in fatigue crack growth
14 p2318 N85-24322
Fatigue fracture topography 14 p2318 N85-24323
Generation of marker lines by means of marker loads
14 p2318 N85-24327
Generation of marker lines on fatigue fracture surfaces 14 p2319 N85-24328
Periodic loading sequences for the systematic marking of fatigue crack fracture surfaces
14 p2319 N85-24329
Modifications of flight by flight load sequences to provide for good fracture surface readability
14 p2319 N85-24330
Effect of fatigue and thermal loads on silicon carbide fiber reinforced glass matrix composites
[DE85-008099] 15 p2503 N85-25441
Mechanisms of corrosion fatigue in high strength I/M (Ingot Metallurgy) and P/M (Powder Metallurgy) aluminum alloys
[AD-A151177] 15 p2509 N85-25478
Damage development during low cycle fatigue of carbon-black loaded SBR
[DE85-006234] 15 p2519 N85-25533
Entropy production during fatigue as a criterion for failure. A local theory of fracture in engineering materials
[AD-A151289] 15 p2578 N85-25902
Crack closure characteristics considering center cracked and compact tension specimens
[AD-A151702] 15 p2579 N85-25907

Creep ratcheting simplified methods experience from structural design of elevated temperature components
[DE85-007433] 15 p2580 N85-25015
Fatigue criterion to system design, life and reliability
[NASA-TM-87017] 16 p2793 N85-27226
Fatigue damage and small crack growth during biaxial loading 16 p2797 N85-27247
Creep-fatigue interaction of notched 304 stainless steel bars 16 p2798 N85-27249
Elevated temperature biaxial fatigue
[NASA-CR-175795] 16 p2800 N85-27263
Initiation, growth and coalescence of small fatigue cracks
[AD-A151799] 16 p2800 N85-27265
The practical and theoretical significance of small cracks: An evaluation
[VTH-LR-432] 16 p2803 N85-27283
Structural Integrity and Durability of Reusable Space Propulsion Systems
[NASA-CP-2381] 17 p2910 N85-27941
Interaction of high-cycle and low-cycle fatigue of Haynes 188 alloy at 1400 F deg 17 p2913 N85-27961
Reexamination of cumulative fatigue damage laws 17 p2914 N85-27962
The synergistic actions of stress corrosion cracking and corrosion fatigue
[BLL-BISI-TRANS-22334-(9022.06)] 17 p2926 N85-28045
Characterization of the fatigue and slow crack growth behavior of partially stabilized zirconia ceramics
[DE85-005240] 17 p2934 N85-28113
Relaxation properties and fatigue fracture resistance of austenitic spring steel
[BLL-BISI-TRANS-22300-(9022.06)] 17 p2978 N85-28406
Fatigue crack propagation characteristics and fatigue fracture toughness in 780 MPa grade high strength steel weldments at low temperature
[BLL-BISI-TRANS-22369-(9022.06)] 17 p2979 N85-28411
Fatigue of synthetic fibers for marine rope applications
[MIT-R84-2] 17 p2979 N85-28414
Fatigue behavior of synthetic fibers, yarns and ropes 17 p2979 N85-28415
The effects of sea water and concentrated salt solutions on the fatigue of nylon 6,6 fibers 17 p2979 N85-28416
Interaction among inhomogeneities and inclusions
[AD-A153114] 17 p2979 N85-28419
Evaluation of interpolative modeling concepts for fatigue crack growth at elevated temperature
[AD-A153222] 17 p2980 N85-28422
Fatigue strength of Inconel 625 plate and weldments used in the DIII-D configuration vacuum vessel
[DE85-006276] 17 p2981 N85-28427
Fatigue and chromium-ferritic steels at elevated temperatures
[DE85-007735] 18 p3074 N85-29015
Fatigue behavior of HY-130 steel weldments containing fabrication discontinuities
[AD-A153930] 18 p3122 N85-29326
Study of the influence of metallurgical factors on fatigue and fracture of aerospace structural materials
[AD-A153913] 18 p3122 N85-29328
Study of failure mechanism of fibrous composition materials taking into account physicochemical reactions of components 19 p3243 N85-30106
Correction of calculated estimate of fatigue properties of materials under biharmonic loading 19 p3244 N85-30113
Fatigue resistance of VT3-1 titanium alloy related to surface cold working 19 p3245 N85-30120
Fatigue resistance of homogeneous and heterogeneous welded joints of T55 titanium alloy 19 p3246 N85-30126
Acoustic emission study of fatigue crack extension position in a stress cycle 19 p3263 N85-30355
Residual stress distributions in (plastically) surface deformed two-phase materials 19 p3263 N85-30356
Experimental and theoretical study of fatigue crack initiation in metals 19 p3263 N85-30357
Multiaxial fatigue and fracture: A literature review
[ARL/STRUC-R-410] 19 p3265 N85-30370
Hold-time effects in elevated temperature fatigue crack propagation
[AD-A154146] 19 p3266 N85-30376
Fatigue-crack propagation behavior of alloy A-286
[DE85-007460] 19 p3268 N85-30391
Fatigue-crack growth and ductile fracture toughness behavior of ASTM A387 Grade 91 steel
[DE85-006495] 20 p3431 N85-31266
Two simplified procedures for predicting cyclic material response from a strain history 20 p3467 N85-31543
The effect of abrasive blasting on the fatigue and corrosion of an aluminum-copper alloy
[AD-A154954] 21 p3566 N85-32182
Measurement and analysis of critical crack tip processes during fatigue crack growth
[NASA-CR-172597] 21 p3596 N85-32342
Tensile fatigue of glass fibers and composites with conventional and surface compressed fibers
[RR-84-4] 22 p3742 N85-33196
Fatigue behavior of chromium-containing ferritic steels at elevated temperature
[DE85-012309] 22 p3748 N85-33231
Application of traction drives as servo mechanisms 22 p3797 N85-33520
Near-threshold fatigue: An overview of the role of microstructure and environment
[DE85-009903] 23 p3941 N85-34431
Fatigue damage detection in steels by optical correlation
[AD-A155830] 24 p4079 N85-35277
Effect of microstructure on the fatigue behavior of Fe-C-X alloys
[DE85-011749] 24 p4080 N85-35285
FATIGUE DIAGRAMS
U S-N DIAGRAMS
FATIGUE LIFE
Distributions of fatigue life and fatigue strength in notched specimens of a carbon 8-harness-satin laminate
[NAL-TR-809T] 01 p0061 N85-10407
Life prediction and constitutive behavior: Overview 02 p0143 N85-10973
Investigation of chemical durability mechanisms in fluoride glasses
[AD-A145420] 02 p0186 N85-11241
The influence of subliminate cracks on the tension fatigue behavior of a graphite epoxy laminate
[FFA-TN-1984-32] 02 p0210 N85-11386
The in-flight estimation and indication of cumulative fatigue damage to helicopter gears
[ARL/AERO-R-164] 03 p0317 N85-12050
On-line fatigue life prediction under stochastic loading by the time series modeling 03 p0370 N85-12362
Turbine blade damping study, introduction 04 p0456 N85-12891
Effect of lubricant extreme-pressure additives on surface fatigue life of AISI 9310 spur gears
[NASA-TP-2406] 04 p0507 N85-13234
Mechanical properties of aligned short carbon fiber reinforced PES and PI laminates
[DFVLR-FB-84-24] 05 p0613 N85-13918
The fourth LBF colloquium
[ISSN-0721-5320] 05 p0648 N85-14163
Welcome and introduction — materials strength 05 p0649 N85-14164
Critical evaluation of methods to calculate fatigue life 05 p0649 N85-14165
Possibilities of fatigue life estimation in the higher cycle range 05 p0649 N85-14166
Low cycle fatigue strength for multiaxial loading of ductile materials 05 p0649 N85-14167
Fatigue life improvement due to mechanically induced compressive residual stresses 05 p0650 N85-14175
Processes to increase the fatigue life of constructions with already initiated cracks 05 p0650 N85-14176
Evaluation of the crack initiation life behavior of fatigue loaded automotive components made from high strength aluminium alloys
[ESA-TT-733] 05 p0651 N85-14181
Operational loads measurement: A philosophy and its implementation 07 p0894 N85-15685
The F-15 flight loads tracking program 07 p0894 N85-15686
Navy operational loads data sources and systems 07 p0895 N85-15668
Structural flight load measurement demonstration of structural integrity 07 p0895 N85-15670
Advanced fatigue monitoring on service aircraft 07 p0895 N85-15671
Flight parameters recording for structure fatigue life monitoring 07 p0896 N85-15682
Disc fatigue life predictions for gas turbine engines 07 p0907 N85-15743
Experiences with the material bevaviour and high temperature low cycle fatigue life prediction of the IN 738 blading alloy 07 p0908 N85-15746
Thermal-mechanical fatigue crack growth in Inconel X-750
[NASA-CR-174740] 07 p0927 N85-15877
Fatigue strength of different sintered steels and design criteria for porous material (PM) parts
[LBF-FB-170/84] 07 p0928 N85-15886
Fundamentals of microcrack nucleation mechanics
[NASA-CR-3651] 07 p0975 N85-16195
Possibilities for a more accurate life prediction of components — gas turbine disks 07 p0976 N85-16196
The influence of fastener flexibility on load transfer and fatigue life predictions for multirow bolted and riveted joints — aircraft structures
[LBF-FB-172/84] 07 p0979 N85-16219
A comparison of fatigue lives under a complex and a much simplified flight-by-flight testing sequence — Mirage 3 aircraft
[ARL/STRUC-TM-388] 09 p1280 N85-18052
Fatigue-creep interaction in + or - 45 deg carbon-resin composites — aircraft construction materials
[ONERA-RT/40/7066/M] 11 p1594 N85-20027
Effect of stress concentration fatigue resistance of refractory nickel alloys under asymmetrical multicycle loading, communication 1 11 p1604 N85-20086
Fatigue crack growth in Aramid Reinforced Aluminum Laminates (ARALL): Mechanisms and predictions
[DFVLR-FB-84-37] 11 p1609 N85-20118
Fatigue crack propagation in mirage 1110 wing main spar specimens and the effects of spectrum truncation on life
[ARL/STRUC-R-405] 12 p1776 N85-21152
Finite element analysis of problems associated with life enhancement techniques
[ARL/STRUC-R-404] 12 p1862 N85-21676
On the stress analysis of bonded inserts
[ARL/STRUC-R-407] 12 p1865 N85-21686
Fatigue and corrosion fatigue resistance of aluminum casting alloy VAL10 and forging alloy AK6 13 p2025 N85-22690
Fatigue life, crack initiation, and propagation of 304 stainless steel with non-proportional axial/torsional strain-paths 13 p2101 N85-23094
Resistance of hydrogenated alpha-titanium alloys to corrosion-fatigue fracture 15 p2499 N85-25413
Fatigue life, fatigue crack propagation and fracture toughness study of 7075 aluminum alloy subjected to thermomechanical processing 15 p2573 N85-25882
A review of fracture mechanics life technology 16 p2733 N85-26863
Fatigue life extension 16 p2733 N85-26864
Thrust chamber life prediction 16 p2733 N85-26865
Rolling contact fatigue life of chromium ion plated 440C bearing steel 16 p2736 N85-26882
Fatigue life analysis of a turboprop reduction gearbox
[NASA-TM-87014] 16 p2793 N85-27228
Experimental measurements and analysis of heat transfer and gas dynamics in a rotating turbine stage 17 p2911 N85-27949
Flow-induced vibration of SSME main injector liquid-oxygen posts 17 p2912 N85-27951
Further investigations to improve the fatigue life of the Mirage 1110 wing main span
[ARL/STRUC-TM-397] 18 p3061 N85-28938
Low-rate discharge of various electrochemical batteries for use with oceanographic instruments
[AD-A153965] 18 p3095 N85-29159
Corrosion fatigue cooperative testing program statistical analysis
[AD-A153886] 19 p3238 N85-30077
Load-carrying capabilities of refractory alloys for space reactor power applications
[DE85-010586] 19 p3240 N85-30087
Effect of prolonged high temperature on durability of coated high-temperature nickel alloys 19 p3243 N85-30105
Experimental and theoretical study of fatigue crack initiation in metals 19 p3263 N85-30357
Fatigue characterization of fabricated ship details for design
[SSC-318] 19 p3265 N85-30371
Effects of high mean stress on the high-cycle fatigue behavior of PWA 1480
[NASA-CR-176020] 19 p3267 N85-30388
Creep fatigue life prediction for engine hot section materials (isotropic)
[NASA-CR-168228] 20 p3394 N85-31057
Mechanical properties of aligned short carbon fiber reinforced PES and PI laminates
[ESA-TT-898] 20 p3422 N85-31240
Influence of recrystallization and solution on the tenacity of the 7010 and 7475 alloys. Oligocyclic fatigue of the 7010 alloy
[ONERA-RT-19/5069-M] 20 p3432 N85-31289
Effect of speed and press fit on fatigue life of roller-bearing inner-race contact
[NASA-TP-2496] 20 p3463 N85-31511
A comparison of two contemporary creep-fatigue life prediction methods 20 p3467 N85-31538
Influence of moisture and elevated temperature on the fatigue properties of WTS-3 glass fiber blade material — wind turbine blade (WTS-3)
[FFA-TN-1984-58] 20 p3470 N85-31558
Controlled indentation flaws for the construction of toughness and fatigue master maps
[PB85-179067] 20 p3473 N85-31582

Voyager 0.2-lbf thruster valve assembly short pulse test report
[NASA-CR-176121] 22 p3741 N85-33185
Joint design for improved fatigue life of diffusion-bonded box-stiffened panels
[NASA-TP-2480] 22 p3799 N85-33537
Corrosion fatigue strength and crack growth in prestrained 0.16% C carbon steel
23 p3905 N85-34192
Statistical pooling method of fatigue data for reliability design 23 p3906 N85-34196
The character of observed porosity and its possible effects on rolling contact fatigue life of M-50 steel
[AD-A155930] 24 p4079 N85-35279
Effect of prior warm rolling on the retained austenite content and hardening response of VIM-VAR (vacuum-induction melted-vacuum-arc remelted) AISI M-50 steel
[AD-A156145] 24 p4079 N85-35281
Development of a mathematical model for predicting the percentage fatigue life increase resulting from shot peened components
[AD-A155774] 24 p4101 N85-35425

FATIGUE TESTING MACHINES

Design and fabrication of a unique electromechanical machine for long-term fatigue testing
[DE85-006524] 15 p2580 N85-25912

FATIGUE TESTS

Strength of welded joints in VT23 alloy upon repeated static loading 01 p0020 N85-10120
Effect of penetrant on fatigue of aluminum alloy lap joints
[NLR-TR-82104-U] 01 p0056 N85-10373
Flight simulation fatigue crack propagation in metal/carbon-epoxy laminates
[NLR-TR-83006-U] 01 p0063 N85-10416
The effect of overload on three different kinds of steel
02 p0174 N85-11185
The influence of subliminate cracks on the tension fatigue behavior of a graphite epoxy laminate
[FFA-TN-1984-32] 02 p0210 N85-11386
Cyclic endurance testing of the RB211-22B cast HP turbine blade — high pressure (HP)
[PNR-90210] 03 p0320 N85-12063
The TA6Zr5D (IMI 685) characterization in strain controlled tests. (Specimens obtained from a forged spinning wheel) no. M4-45870
[M4-45870] 03 p0373 N85-12384
Parametric study of the P9 HT glass fiber finish (Fatigue resistance). Lot no. 1: Report on the microfatigue tests
[CS-794] 05 p0620 N85-13968
Critical evaluation of methods to calculate fatigue life
05 p0649 N85-14165
Possibilities of fatigue life estimation in the higher cycle range 05 p0649 N85-14166
Advanced fatigue monitoring on service aircraft
07 p0895 N85-15671
Design and test requirements for development of today's engines 07 p0906 N85-15737
Inconel 718 alloy resistance to crack propagation
07 p0907 N85-15740
Engine cyclic durability by analysis and material testing 07 p0907 N85-15744
Effect of five lubricants on life of AISI 9310 spur gears
[NASA-TP-2419] 07 p0962 N85-16099
Low cycle fatigue of MAR-M 200 single crystals at 760 and 870 deg C
[NASA-TM-86933] 10 p1440 N85-19074
Airbus fatigue tests 11 p1618 N85-20186
Deflection model of a CT4-A undercarriage
[AD-A149778] 12 p1777 N85-21156
Characterization of mode 1 and mixed-mode failure of adhesive bonds between composite adherends
[NASA-TM-86355] 12 p1797 N85-21270
Comparison of the fatigue resistance (initiation, propagation) of cast TA6V with hot rolled TA6V — titanium alloy
[DGT-25369-PT-1] 12 p1808 N85-21341
Fatigue and corrosion fatigue resistance of aluminum casting alloy VAL10 and forging alloy AK6
13 p2025 N85-22690
Use of acoustical emission method to study specifics of fracture of boron reinforced plastic structural elements 13 p2026 N85-22696
Advanced life analysis methods. Volume 1: Cracking data survey and NDI (nondestructive inspection) assessment for attachment lugs
[AD-A150419] 13 p2103 N85-23108
Analysis and design of hydraulic servo systems within the scope of the improvement of a fatigue testing installation of the Royal Dutch Army
[LEOK-TR-1984-09] 14 p2265 N85-24033
Study of fatigue strength of shafts with segmented channels 14 p2282 N85-24138
Durability calculation of wing panel element
14 p2285 N85-24159
Two recent cases of marker load applications on cargo/fighter aircraft fatigue tests
14 p2318 N85-24325
Generation of marker lines by means of marker loads
14 p2318 N85-24327
Fatigue of clad aluminum materials D16T and 2024-T3 with stepped loading 15 p2496 N85-25397
Fatigue strength of alpha-titanium alloys under cophasal action of variable normal and tangential stresses
15 p2498 N85-25407
The effect of frictional forces on fatigue crack growth in lugs
[AD-A151994] 15 p2578 N85-25898
Initial quality of advanced joining concepts
[AD-A152241] 16 p2759 N85-27027
Lubricant and additive effects on spur gear fatigue life
[NASA-TM-87044] 17 p2974 N85-28373
Tests of low-cycle fatigue of elected steels of class 11
[BLL-BISI-TRANS-22039-(9022.06)] 17 p2978 N85-28404
Fatigue and chromium-ferritic steels at elevated temperatures
[DE85-007735] 18 p3074 N85-29015
Fatigue behavior of HY-130 steel weldments containing fabrication discontinuities
[AD-A153630] 18 p3122 N85-29326
Rolling contact fatigue testing of thermomechanically processed M-50 steel
[AD-A153640] 18 p3122 N85-29327
Corrosion fatigue cooperative testing program statistical analysis
[AD-A153666] 19 p3238 N85-30077
Influence of interface ply orientation on fatigue damage of adhesively bonded composite joints
[NASA-TM-86443] 19 p3284 N85-30365
Investigation of fatigue strength of spring steel after high-temperature thermomechanical working (HTMW) by helical drawing
[BLL-M-36274-(5828.4)] 20 p3465 N85-31525
Multiaxial fatigue low cycle fatigue testing
20 p3468 N85-31544
Influence of the molding joint plane on the fatigue resistance of the alloys 7010 and 7050. Test Report No. M1-631600
[PV-M1-631600] 20 p3470 N85-31562
Design and fabrication of durable owner-built wind turbine blades
[DE85-009200] 20 p3484 N85-31650
The effect of abrasive blasting on the fatigue and corrosion of an aluminium-copper alloy
[AD-A154954] 21 p3566 N85-32182
Results of an interlaboratory fatigue test program conducted on alloy 800H at room and elevated temperatures
[NASA-CR-174940] 21 p3597 N85-32340
Rotating bending fatigue strength of silicon carbide and alumina-fiber reinforced aluminum
23 p3907 N85-34208
Fatigue lives of specimens representing critical locations in Mirage 3 spars under Australian and Swiss test spectra
[ARL-STRUC-R-415] 24 p4064 N85-35187

FATS

NT CHOLINE

Prediction of percent body fat for U.S. Navy women from body circumferences and height
[AD-A146456] 08 p0845 N85-15370

FATTY ACIDS

NT BENZOIC ACID
NT CARBOXYLIC ACIDS
NT DICARBOXYLIC ACIDS

The lipid composition and its alteration during the growth stage in pathogenic fungus, epidermophyton floccosum
[NASA-TM-77440] 07 p1011 N85-16421
Fatty and aromatic acid catabolizing bacteria from methanogenic ecosystems
[DE85-006133] 17 p2998 N85-28537

FAULT MECHANICS

U FRACTURE MECHANICS

FAULT TOLERANCE

Assessing the reliability of computer software and computing networks: An opportunity for partnership with computer scientists
[AD-A145131] 01 p0104 N85-10697
Communications protocols for a fault tolerant, integrated local area network for Space Station applications
[NASA-TM-86304] 01 p0108 N85-10711
Fault tolerant computing research
[AD-A145640] 02 p0244 N85-11590
An expert system for representing procedural knowledge
[AD-P003923] 02 p0245 N85-11603
A generalized model of fault-isolation performance
[AD-P003928] 02 p0246 N85-11606
Artificial intelligence approaches to monitoring system integrity
[AD-P003930] 02 p0246 N85-11610
Depot level problems in the testing of printed circuit boards
[AD-P003932] 02 p0247 N85-11612
Technologies for space station autonomy
[NASA-CR-174112] 04 p0458 N85-12908
Analysis of the impact of error detection on computer performance
[NASA-CR-174167] 04 p0547 N85-13477
Test experience on an ultrareliable computer communication network
[NASA-TM-85915] 04 p0552 N85-13514
cost and benefits optimization model for fault-tolerant aircraft electronic systems
[NASA-CR-166043] 07 p0946 N85-15993
Local area network evaluation by MICROSS extensions
[AD-A146773] 07 p1027 N85-16521
Investigating version dependence in fault-tolerant software 08 p1065 N85-16749
Evolution of shuttle avionics redundancy management/fault tolerance 08 p1090 N85-16890
SSME digital control design characteristics
08 p1091 N85-16893
A unified model for performance and reliability of Fault-Tolerant/Multi-Mode systems
[AD-A148789] 08 p1208 N85-17601
Research on optimal control, stabilization and computational algorithms for aerospace applications
[NASA-CR-174318] 08 p1209 N85-17603
Extended Stochastic Petri Nets: Applications and analysis
[AD-A148439] 08 p1213 N85-17633
SPADE: Series-parallel directed acyclic graph evaluator
[AD-A148458] 09 p1368 N85-18592
Beyond fault trees to fault graphs
[DE84-017022] 09 p1370 N85-18608
An ultra reliable computer communication network: The dispersed sensor processing mesh
09 p1372 N85-18620
AIRLAB: A laboratory for flight-crucial-electronics system research 13 p1968 N85-22362
Reliability bounds for fault-tolerant systems with competing responses to component failures
[NASA-TP-2409] 13 p2100 N85-23090
A theoretical basis for the analysis of redundant software subject to coincident errors
[NASA-TM-86369] 13 p2145 N85-23317
Measurement of SIFT operating system overhead
[NASA-TM-86322] 13 p2149 N85-23337
An experiment in software reliability
[NASA-CR-172553] 14 p2403 N85-24813
Care 3 model overview and user's guide, first revision
[NASA-TM-86404] 15 p2627 N85-26192
An abstract specification language for Markov reliability models
[NASA-TM-86423] 16 p2857 N85-27816
Efficient VLSI (Very Large Scale Integration) fault simulation
[AD-A152661] 17 p2953 N85-28233
Optimal design and use of retry in fault tolerant real-time computer systems
[NASA-CR-175920] 17 p3015 N85-28643
Evaluation of a fault tolerant system for an integrated avionics sensor configuration with TSRV flight data
[NASA-CR-172589] 18 p3062 N85-28941
Guidance on planning and implementing computer system reliability
[PB85-177996] 18 p3161 N85-29581
Research on optimal control, stabilization and computational algorithms for aerospace applications
[NASA-CR-172528] 19 p3221 N85-29970
Ultrareliable, fault-tolerant control systems: A conceptual description
[NASA-TM-86017] 19 p3221 N85-29972
Graceful fault tolerance in large networks of microcomputers 19 p3332 N85-30643
Development and evaluation of a Fault-Tolerant Multiprocessor (FTMP) computer. Volume 2: FTMP software
[NASA-CR-166072] 19 p3341 N85-30706
Development and evaluation of a Fault-Tolerant Multiprocessor (FTMP) computer. Volume 3: FTMP test and evaluation
[NASA-CR-166073] 19 p3341 N85-30707
Fault-tolerant computing research
[AD-A154082] 19 p3342 N85-30710
Implementation of a serial communication process for a fault tolerant, real time, multitransputer operating system
[AD-A154237] 19 p3343 N85-30714

Performance and evaluation of real-time multicomputer control systems
[NASA-CR-176098] 21 p3673 N85-32821
A new fault-tolerant algorithm for clock synchronization
[AD-A154771] 21 p3676 N85-32836
A dual, fault-tolerant aerospace actuator 22 p3798 N85-33530
Design of a dual fault tolerant space shuttle payload deployment actuator 22 p3798 N85-33531
Modeling and measurement of fault-tolerant multiprocessors
[NASA-CR-3920] 22 p3833 N85-33732
Study of fault tolerant software technology for dynamic systems
[NASA-CR-172618] 24 p4137 N85-35842

FAULT TREES
Minimal cut-set methodology for artificial intelligence applications
[DE84-016674] 04 p0553 N85-13518
Avionics fault tree analysis and artifical intelligence for future aircraft maintenance 08 p1068 N85-16755
Beyond fault trees to fault graphs
[DE84-017022] 09 p1370 N85-18608
Calculation through Fault Tree Analysis of the probability of a warhead being armed prior to launch
[AD-P004339] 10 p1454 N85-19163
Contribution of instrumentation and control software to system reliability
[DE85-004693] 13 p2149 N85-23340

FAULTS
Models of natural intelligence in fault diagnosis tasks: Implications for training and aiding of maintenance personnel
[AD-P003927] 02 p0246 N85-11607
Battery control and fault detection method
[AD-D011384] 07 p0993 N85-16307

FAUNA
U ANIMALS

FCC LATTICES
U FACE CENTERED CUBIC LATTICES

FDMA
U FREQUENCY DIVISION MULTIPLE ACCESS

FEAR
NT FEAR OF FLYING

FEAR OF FLYING
The Reports of Aeromedical Laboratory, volume 25, no. 1/2
[ISSN-0023-2858] 01 p0090 N85-10605
The relationship between emotional tension scale and psychological uneasiness of JASDF pilots in flying situations 01 p0090 N85-10608

FEASIBILITY
A preliminary study of the feasibility of detecting the floating macrophytes by means of digital processing of MSS/LANDSAT data
[E85-10005] 02 p0215 N85-11418
Initial feasibility ground test of a proposed photogrammetric system for measuring the shapes of ice accretions on helicopter rotor blades during forward flight
[NASA-TM-87391] 04 p0455 N85-12887

FEASIBILITY ANALYSIS
Exploratory investigation of the need for and feasibility of a Lower Atmosphere Research Satellite (LARS) program
[NASA-CR-17[illegible]161] 01 p0015 N85-10091
Prospectus of the utilization of leafy spurge (Euphorbia Esula L.) as a source of liquid fuel and biomass
[DE84-015203] 01 p0034 N85-10208
Theory of near-field phased arrays for electromagnetic susceptibility testing
[PB84-217836] 01 p0042 N85-10273
The development of a diode laser Doppler velocimeter for boundary layer measurements under ice: A feasibility investigation
[AD-A145076] 01 p0053 N85-10348
Robotics investment decision model user's manual
[AD-A145467] 02 p0204 N85-11347
Research on gallium arsenide diffused junction solar cells
[NASA-CR-174057] 02 p0222 N85-11457
SLIM TDMA ANIK B pilot project
[CRC-REPT-1366] 03 p0354 N85-12278
Feasibility study of a satellite-borne 90 GHz radiometer 04 p0459 N85-12914
Methodology for the implementation of a domestic satellite communications network 04 p0493 N85-13148
Measurement of range-resolved water vapor concentration by coherent CO2 differential absorption lidar
[PB84-236862] 04 p0535 N85-13420
Feasibility of long duration ballooning in Antarctica
[PB84-240571] 04 p0541 N85-13443
Report of the reference designs study group on the superconducting super collider
[DE84-015567] 04 p0569 N85-13630
Results of principal NASA studies on space station uses and functional requirements 07 p0914 N85-15787
Feasibility of producing a range of food products from a limited range of undifferentiated major food components
[NASA-CR-177329] 07 p1020 N85-16473
NSW (National Software Works) lessons learned
[AD-A146737] 07 p1023 N85-16494
Feasibility of measuring technical productivity improvements in Air Force Logistics Command depot-level maintenance using the Data Envelopment Analysis (DEA) and Constrained Facet Analysis (CFA) models
[AD-A147329] 07 p1052 N85-16676
Proposal for a small scheme implementation
[AD-A148707] 09 p1366 N85-18585
Magnetic heat pump feasibility assessment
[DE85-002806] 11 p1632 N85-20276
Advanced glazings research
[DE85-000539] 11 p1674 N85-20549
Feasibility of producing commodities and electricity for space shuttle operations at Vandenberg Air Force Base
[DCN-84-203-001-80-21] 12 p1789 N85-21230
Technological and economic assessment of advanced ceramic materials. Volume 6: A case study of ceramic cutting tools
[PB85-113132] 12 p1815 N85-21387
Shallow magma targets in the western US
[DE85-003274] 12 p1881 N85-21803
Using a data base management system for modelling SSME test history data 12 p1944 N85-22211
A standard aircraft diffusion flame: Spectral characteristics and a feasibility study for developing an alternate calibration source for aircraft optical fire detection systems
[AD-A150231] 13 p2039 N85-22768
Multifunctional elements for integrated optics 13 p2068 N85-22918
Technical and cost analyses of manganese nodule processing techniques and their significant variations
[PB85-148815] 14 p2258 N85-23992
Feasibility study of an installation to simulate the flow of propellant gases in a gun barrel, part 2
[ISL-R-128/83-PT-2] 14 p2303 N85-24263
Feasibility of optical instruments based on multiaperture optics
[AD-A150868] 14 p2421 N85-24936
FRG opinion on Spacelab benefits, space station participation 15 p2532 N85-25618
Application of infrared radiometers for airborne detection of clear air turbulence and low level wind shear, airborne infrared low level wind shear detection test
[NASA-CR-175725] 15 p2594 N85-25985
A practical system for collecting reliable data on the space-time behavior of people
[AD-A151174] 15 p2619 N85-26140
A feasibility study for using low boiling point fluids to change aircraft tire deflection
[AD-A152096] 16 p2706 N85-26701
Feasibility study on Laser Doppler Anemometer (LDA) wind velocity measurements using pulsed visible laser light
[ISL-CO-224/83] 16 p2836 N85-27489
Preliminary technology utilization assessment of the robotic fruit harvester
[NASA-CR-175834] 16 p2844 N85-27532
On various Fourier series utilized for solution of structural mechanics problems
[VTH-LR-429] 16 p2856 N85-27615
Transverse electron resonance accelerator
[DE85-006289] 17 p3032 N85-28758
Some Europeans voice opposition to space station participation 18 p3066 N85-28961
Personal mobile communications by satellite
[REPT-15-4572] 18 p3091 N85-29135
Stability and feasibility of model ecosystems
[PREPRINT-431] 18 p3134 N85-29408
Feasibility study of a fission-suppressed Tokamak fusion breeder
[DE85-009099] 18 p3190 N85-29786
Note for a research feasibility project: High reliability design in the aeronautical field
[REPT-84-RR-350] 20 p3387 N85-31005
Future prospects for a combined INMARSAT polar communication and search and rescue satellite system 20 p3406 N85-31137
Large space structure flight experiment 20 p3410 N85-31163
Preliminary investigations concerning a 90 GHz radiometer satellite experiment
[ESA-TT-860] 20 p3420 N85-31225
Improved turbopump dynamics
[NASA-TM-86514] 20 p3462 N85-31509
Rain volume estimation over areas using satellite and radar data
[NASA-CR-176050] 21 p3634 N85-32570
Feasibility of applications of Competition Decision Assist Package (CDAP) to spare parts
[AD-A154716] 21 p3712 N85-33036
Deficit irrigation feasibility study and demonstration project
[DE85-011531] 22 p3802 N85-33555
Diffusion welding of Cassegrainian concentrator cell stack assemblies
[NASA-CR-176104] 22 p3805 N85-33566
Small-hydropower development: The process, pitfalls, and experience. Volume 1: Feasibility studies summary and analysis
[DE85-010839] 22 p3808 N85-33589
Technology transfer report: Feasibility study for the use of geothermal brine in the Ashdod area, Israel
[DE85-013316] 22 p3810 N85-33598
Thermal protection systems for reentry vehicles
[CNES-NT-113] 23 p3900 N85-34157
Calculations on the feasibility of ultrasonic inspection of steam generator tubing in pressurized water reactors
[AERE-R-10960] 23 p3940 N85-34419
SP-100 Thermionic Technology Program
[DE85-012311] 23 p3972 N85-34625
Miniature infra-red data acquisition and telemetry system
[NASA-CR-177953] 24 p4096 N85-35390

FEATHERING
Study to eliminate ground resonance using active controls
[NASA-CR-166609] 07 p0902 N85-15715
Optimally designed propellers constrained by noise 24 p4065 N85-35196

FEATURE EXTRACTION
U PATTERN RECOGNITION

FECES
Improved orbiter waste collection system study
[NASA-CR-171830] 08 p1199 N85-17548
Space Shuttle Orbiter waste collection system conceptual study
[NASA-CR-171844] 08 p1199 N85-17553
Preliminary assessment of climatic change during late Wisconsin time, southwest Great Basin and vicinity, Arizona, California and Nevada
[DE85-006343] 16 p2836 N85-27488

FEDERAL BUDGETS
Department of Housing and Urban Development, and certain independent agencies appropriations for fiscal year 1985, part 2
[S-REPT-98-889-PT-2] 01 p0127 N85-10670
National Aeronautics and Space Administration 01 p0127 N85-10671
The status of synthetic fuels and cost-shared energy R and D facilities
[GPO-36-903] 03 p0339 N85-12182
Financing considerations and Federal budget impacts 07 p0915 N85-15792
Outlook for expanding the Federal research in progress system
[AD-A148354] 08 p1229 N85-17737
1984 science and technology posture hearing with the director of the Office of Science and Technology Policy
[GPO-41-060] 12 p1949 N85-22244
An agenda for a study of government science policy
[GPO-40-860] 12 p1949 N85-22245
President's private sector survey on cost control, report on research and development
[PB84-173269] 12 p1951 N85-22253
Summary of activities of the Committee on Science and Technology
[H-REPT-98-1189] 12 p1964 N85-22341
Department of Housing and Urban Development-independent agencies appropriations for 1986. Part 6: National Aeronautics and Space Administration
[GPO-47-235] 16 p2879 N85-27768
Selected university laboratory needs in support of national security
[AD-A153511] 18 p3197 N85-29833
Department of Housing and Urban Development-Independent Agencies Appropriation Bill, 1986
[H-REPT-99-212] 19 p3382 N85-30979
National Aeronautics and Space Administration 19 p3382 N85-30980
NASA authorization, 1986, volume 1
[GPO-46-365] 20 p3541 N85-32039
Department of Housing and Urban Development-Independent Agencies Appropriation Act, 1986 20 p3542 N85-32041
National Aeronautics and Space Administration research and development 20 p3542 N85-32042

Testimony of Robert A. Froech before the Subcommittee on HUD and Independent Agencies of the Senate Committee on Appropriations
[NASA-TM-87496] 22 p3738 N85-33173
Department of Housing and Urban Development Independent Agencies Appropriation Bill, 1986
[S-REPT-99-129] 23 p3987 N85-34720
National Aeronautics and Space Administration research and development: Program description
23 p3987 N85-34721
Progress report on implementing the recommendations of the White House Science Council's Federal Laboratory Review Panel, volume 1
[PB85-185072] 24 p4164 N85-35819

FEDERAL REPUBLIC OF GERMANY
U WEST GERMANY

FEED SYSTEMS
Feed system design considerations for large space antenna systems. Part 1: Multiple apertures with non-overlapping feeds 14 p2234 N85-23852
Feed system design considerations for large space antenna systems. Part 2: Single aperture with overlapping feeds 14 p2235 N85-23853
Auxiliary units for Robots 14 p2285 N85-24161
Inspection evaluation and repair of the flawed feedwater nozzle of the 50 MWe Dodewaard GKN boiling water reactor
[ISBN-90-353-0017-3] 17 p2977 N85-28394

FEEDBACK
NT BIOFEEDBACK
NT NEGATIVE FEEDBACK
NT NONLINEAR FEEDBACK
NT SENSORY FEEDBACK
Optimizing search with positive information feedback
[CSIR-TWISK-313] 01 p0125 N85-10855
Qualitative results for distributed systems with discrete damping and stiffness with application to control
[AD-A145525] 02 p0209 N85-11382
Self-modulation of injection laser emission intensity due to external optical feedback 02 p0261 N85-11706
An appraisal of an out-of-phase feed-back system for the variation of damping of dynamic wind-tunnel models
[NMI-189] 03 p0320 N85-12065
Investigation of cloud feedback in the GLAS model
05 p0685 N85-14404
Feedback, adaptivity and A-posterior estimates in finite elements: Aims, theory and experience
[AD-A146869] 07 p1029 N85-16531
Unstable optical resonator with cancelling edge waves
[AD-D011379] 07 p1042 N85-16618
A feedback finite element method with a posteriori error estimation. Part 1. The finite element method and some basic properties of the A posteriori error estimator
[AD-A148345] 08 p1212 N85-17631
A note on the disturbance decoupling problem for retarded systems
[AD-A149045] 10 p1543 N85-19730
The eigenstructure assignment of deadbeat control systems
[AD-A149761] 12 p1834 N85-21510
Total energy-rate feedback for automatic glide-slope tracking during wind-shear penetration
[NASA-TP-2412] 14 p2226 N85-23801
Practical methods for the compensation and control of multivariable systems
[AD-A151047] 14 p2407 N85-24841
Stochastic pursuit-evasion differential games in the plane
[CSIR-TWISK-343] 14 p2412 N85-24875
Positioning of a robotic manipulator through the use of visual feedback
[AD-A151933] 16 p2651 N85-27577
Principles of designing digital compensating accelerometers 17 p2944 N85-28172
Short and long-term robot feedback
[PB85-180735] 19 p3281 N85-30347
Interactive computer program for the analysis and design of linear time invariant systems
[AD-A154076] 19 p3335 N85-30664
Self Q-modulation and generation of short pulses in distributed-feedback lasers 21 p3687 N85-32907

FEEDBACK AMPLIFIERS
Efficiency in integral active antennas
06 p0792 N85-15060
Method of improving dynamic characteristics of DC voltage stabilizers with compound regulation
15 p2528 N85-25589
Eye movement in response to single and multiple targets
[AD-A151115] 15 p2617 N85-26126
Synthesis of high-speed devices using integrated operational amplifiers 22 p3781 N85-33428

FEEDBACK CIRCUITS
Experimental performance of a frequency measurement circuit
[AD-A152951] 17 p2953 N85-28239
A study of reflex optoelectronic switching matrices and their derivatives
[CRC-TN-720] 19 p3253 N85-30169

FEEDBACK CONTROL
NT CASCADE CONTROL
Interactive aircraft flight control and aeroelastic stabilization
[NASA-CR-174025] 02 p0148 N85-11003
Optimal nonlinear feedback control of spacecraft attitude maneuvers 02 p0167 N85-11126
Smith predictor and self-tuning control of muscle relaxant drug administration
[RR-257] 02 p0235 N85-11534
On a class of suboptimal controls for infinite-dimensional bilinear systems
[RR-258] 02 p0249 N85-11630
Control and identification of time varying systems
[AD-A145638] 02 p0252 N85-11649
The numerical range: A tool for robust stability studies — multivariable feedback systems
[RR-255] 02 p0253 N85-11660
CONTROL: A suite of interactive transfer-function analysis programs
[OUEL-1527/84] 03 p0408 N85-12609
On the relationship between Lehtomaki's robustness test and an inverse Nyquist based test
[OUEL-1526/84] 03 p0409 N85-12616
Non-linear systems in infinite dimensional state spaces
[AD-A145828] 03 p0410 N85-12623
Return difference feedback design for robust uncertainty tolerance in stochastic multivariable control systems
[AD-A145861] 03 p0411 N85-12624
Control of linear stationary objects subject to external actions by means of various types of feedback
04 p0488 N85-13114
Frequency response design methods for large scale systems
[DE84-014161] 04 p0553 N85-13517
Experiments in control of flexible structures with uncertain parameters 05 p0602 N85-13837
The acquisition, processing, and use of tactile sensor data in robot control 05 p0641 N85-14114
A nonlinear filter for compensating for time delays in manual control systems 05 p0700 N85-14493
Does McKuer's law hold for heart rate control via biofeedback display? 05 p0706 N85-14528
Active sticks: A new dimension in controller design
05 p0706 N85-14531
An H-infinity-minimax approach to the design of robust control systems
[OUEL-1537/84] 05 p0717 N85-14600
Improvement of the transient response in the finite settling time control
[NAL-TR-823] 06 p0757 N85-14843
Flutter control with unsteady aerodynamic models
[AD-A147858] 07 p0909 N85-15753
Precise control of flexible manipulators
[NASA-CR-174210] 07 p0973 N85-16178
Multivariable flight control with time-scale separation
[NASA-CR-174320] 08 p1087 N85-16873
Time series analysis of closed-loop pilot vehicle dynamics 08 p1087 N85-16876
Research on optimal control, stabilization and computational algorithms for aerospace applications
[NASA-CR-174318] 08 p1209 N85-17603
Improved stability and performance bounds using approximate models — control system design
[RR-260] 08 p1209 N85-17606
Utilization of numerical optimization techniques in the design of robust multi-input, multi-output control systems
[AD-A148289] 08 p1212 N85-17630
Servo operated anti-G suit pressurization system
[AD-D011468] 10 p1531 N85-19651
A note on the disturbance decoupling problem for retarded systems
[AD-A149045] 10 p1543 N85-19730
Tethered satellite system project overview
11 p1642 N85-20341
Analytically redundant output feedback scheme for reduction of structural loads of a flexible transport aircraft
[TT-6303] 12 p1777 N85-21154
Modal control of structural systems
[AD-A149734] 12 p1790 N85-21235
Stability analysis of flexible spacecraft with PID controller
[CRC-1372] 12 p1792 N85-21247
NASA/MSFC ground experiment for large space structure control verification
[NASA-TM-86496] 12 p1792 N85-21248
The eigenstructure assignment of deadbeat control systems
[AD-A149761] 12 p1834 N85-21510
Control of nonlinear objects 12 p1842 N85-21561
Dynamic visual servo control of robots: An adaptive image-based approach
[AD-A150057] 12 p1860 N85-21667
Practical considerations for noninteracting control synthesis
[AD-A150130] 12 p1918 N85-22046
Testing of the digital flight control system of the German CCV fighter experimental aircraft
13 p1968 N85-22361
Periodic binary sequence generators: VLSI circuits considerations
[NASA-CR-175649] 13 p2063 N85-22686
Control of cascaded induction generator systems
[AD-A150429] 13 p2065 N85-22897
Design of multivariable feedback control systems via spectral assignment using reduced-order models and reduced-order observers
[NASA-CR-3869] 14 p2226 N85-23800
Dynamic verification of large space structures
14 p2234 N85-23847
A mathematical formulation of the Scole control problem, part 1
[NASA-CR-172581] 14 p2243 N85-23903
Two-stage gyrocompass 14 p2273 N85-24080
Computer program TRAMP: Inclusion of state space facilities and the analysis of non-linear elements
[BAE-BT-12643] 15 p2626 N85-26181
The modeling and simulation of feedback control systems
[NASA-CR-171675] 15 p2632 N85-26225
Flight control system reconfiguration design using quantitative feedback theory
[AD-A151771] 16 p2710 N85-26722
Application of linear optimal control theory to the design of the elevator control system of the DHC-2 Beaver experimental aircraft
[VTH-LR-411] 16 p2711 N85-26729
Flight testing and development of the F/A-18A digital flight control system 16 p2713 N85-26743
OLGA: An open loop gust alleviation
16 p2713 N85-26744
Optimal open loop and nonlinear feedback control for remote orbital capture
[AD-A151967] 16 p2732 N85-26859
Nonintrusive shaft speed sensor
16 p2740 N85-26908
Digital RF delay line for ECM (electronic countermeasure) lock-through
[AD-A152120] 16 p2774 N85-27120
Development of graphical time response using the OPTSYSX program
[AD-A152221] 16 p2848 N85-27557
Stabilizing force feedback in bio-actuated control systems
[AD-D011634] 17 p3002 N85-28560
Closed loop electrostatic levitation system
[NASA-CASE-NPO-15553-1] 18 p3092 N85-29142
An interactive computer aid for the design and analysis of linear, single input/single output digital and continuous control systems
[AD-A153704] 18 p3162 N85-29589
Research on optimal control, stabilization and computational algorithms for aerospace applications
[NASA-CR-172528] 19 p3221 N85-29970
Evaluation of methods used for the determination of acidity in acid rain samples
[PB85-178309] 19 p3237 N85-30070
Phase and amplitude feedback control system for the Los Alamos free-electron laser
[DE85-010787] 19 p3277 N85-30325
High gain adaptive control of decentralized systems
[DE85-001586] 19 p3343 N85-30717
Multivariable control of a soft coupled space station
20 p3408 N85-31151
Automatic assembly of space stations
20 p3409 N85-31153
Antenna pointing of large flexible telecommunications spacecraft 20 p3409 N85-31158
Proceedings of the Workshop on Identification and Control of Flexible Space Structures, volume 2
[NASA-CR-178052] 20 p3411 N85-31170
Approximation techniques for parameter estimation and feedback control for distributed models of large flexible structures 20 p3413 N85-31179
Parametric stiffness control of flexible structures
20 p3414 N85-31187
Wideband disturbance accomodation in precision flexible space structures 20 p3415 N85-31194
Proceedings of the Workshop on Identification and Control of Flexible Space Structures, volume 3
[NASA-CR-178053] 20 p3415 N85-31195
Eigenvalue placement and stabilization by constrained optimization 20 p3416 N85-31198
Self-tuning adaptive-controller using online frequency identification 20 p3417 N85-31205

Feedforward-feedback control logic for robust target-tracking 20 p3436 N85-31317
Decentralized control synthesis method for large-scale interconnected systems
[DE85-000748] 20 p3518 N85-31878
Ultrasonic position reference systems for an autonomous sentry robot and a robot manipulator arm
[AD-A155481] 21 p3596 N85-32336
Flight test experience and controlled impact of a large, four-engine, remotely piloted airplane
[NASA-TM-86738] 22 p3730 N85-33123
Decentralized control of dynamically interconnected systems
[BU-111] 22 p3835 N85-33744
Method and apparatus for transfer function simulator for testing complex systems
[NASA-CASE-NPO-15666-1] 23 p3926 N85-34333
Feedback regulated induction heater for a flowing fluid
[DE85-006506] 23 p3939 N85-34414
A graph theoretic procedure for the design of feedback patterns
[REPT-110] 24 p4142 N85-35673
Design of dynamic compensators of prescribed pattern
[BU-109] 24 p4142 N85-35674
Spreading the control complexity in decentralized control of interconnected systems
[BU-117] 24 p4144 N85-35688
Decentralized stabilization by high gain feedback
[BU-115] 24 p4144 N85-35689

FEEDERS

Stability indicators for front end loaders
[AD-P004293] 09 p1408 N85-18870
Leak monitoring in high pressure preheaters by a noninvasive ultrasonic method
[CISE-2373] 11 p1650 N85-20394
Leak detection by acoustic emission monitoring in power plant high pressure preheaters
[CISE-2392] 11 p1650 N85-20395
New technique for fluid feed in simultaneous multisurface grinding 13 p2045 N85-22600

FEEDFORWARD CONTROL

Decentralized control synthesis method for large-scale interconnected systems
[DE85-000748] 20 p3518 N85-31878

FEELINGS

U SENSORY FEEDBACK

FEET (ANATOMY)

Translating rudder pedal system
[AD-D011510] 12 p1760 N85-21172

FELDSPARS

Concordant bands of augen gneiss within metasedimentary rocks in the Big Delta C-2 quadrangle, east-central Alaska 04 p0516 N85-13294
Solar cosmic ray produced neon in lunar soils and their implication for gas-rich meteorite studies
06 p0687 N85-15636
Interim rock mass properties and conditions for analyses of a repository in crystalline rock
[DE85-010700] 18 p3125 N85-29352
Conditions for formation of paragenesses containing kyanite-orthoclase in region of Mount Provender and Pratt Peak (Shackleton Range, Antarctica)
19 p3296 N85-30447
Primordial magmaspheres and their lasting consequences 22 p3857 N85-33882

FEMALES

Challenges in the development of the shuttle extravehicular mobility unit 08 p1095 N85-16922
Aviation-related cardiorespiratory effects of blood donation in female pilots
[AD-A148045] 08 p1195 N85-17529
An investigation of spinal injury potential from the use of the ACES 2 ejection seat by lower weight female pilots
[AD-A148449] 08 p1196 N85-17537
Blood viscosity responses to acute exercise and aerobic conditioning in women 09 p1363 N85-18573
Assessment of muscle strength and prediction of lifting capacity in US Army personnel
[AD-A148846] 10 p1527 N85-19633
The effect of occupational exposure and the body weight to height ratio on exhaled methylene chloride breath concentration in females at one, eighteen and sixty-six hours post exposure 14 p2368 N85-24706
The energy cost of women walking and running in shoes and boots
[AD-A151022] 14 p2389 N85-24716
Perceived heterogeneity and its effect on various types of tasks
[AD-A151003] 14 p2392 N85-24729
Physiological differences between men and women in exercise-heat tolerance and heat acclimation
[AD-A152048] 15 p2618 N85-26135
Cosmonaut Savitskaya says many women in cosmonaut training 16 p2717 N85-26774
Comparative anaerobic power of males and females
[AD-A151960] 16 p2842 N85-27523

FEMUR

Locomotion research for the analysis of the human gait and for the determination of the maximum loads of the pelvis-leg skeleton. Volume 1: Two-dimensional analysis
[BMFT-FB-T-83-187-VOL-1] 02 p0236 N85-11535

FENCES (BARRIERS)

Deer control using 7 strand vertical fence
11 p1581 N85-19958
Reducing gull use of some attractions near airports
[AD-P004195] 11 p1581 N85-19962
Effectiveness of an overhead wire barrier in deterring gulls from feeding at a sanitary landfill
[AD-P004199] 11 p1582 N85-19966

FERMENTATION

DOE supported research in alcohol fuel technology development
[DE84-007686] 06 p0774 N85-14948
ECUT, Energy Conversion and Utilization Technologies program: Technical and economic assessment of processes for the production of butanol and acetone. Phase 2: Analysis of research advances
[NASA-CR-175471] 10 p1434 N85-19034
Ethanol production by enzymatic hydrolysis: Parametric analysis of a base-case process
[DE84-013105] 11 p1614 N85-20147
Anaerobic microbial transformations in subsurface environments
[DE85-012790] 22 p3819 N85-33659
Production of butanol by fermentation in the presence of cocultures of clostridium
[NASA-CASE-NPO-16203-1] 24 p4071 N85-35227

FERMI LIQUIDS

Quasiparticle excitations in valence-fluctuation materials: Effects of band structure and crystal fields
[DE85-010783] 19 p3359 N85-30824

FERMI SURFACES

Kohn anomaly in metastable fcc lanthanum at low temperatures
[DE84-015459] 04 p0569 N85-13628
Electronic properties of intercalated graphite and amorphous metals
[AD-A147664] 06 p1225 N85-17716
Fermi surface study of CeSb
[DE85-002532] 10 p1564 N85-19662
First principles theory of Fermi-surface driven concentration waves in Cu/sub c/Pd/sub 1-c/ alloys
[DE85-005367] 13 p2024 N85-22681
Further results on the equipartition threshold in large nonlinear Hamiltonian systems
[PREPRINT-428] 18 p3173 N85-29668
Quantized Hall conductance as a topological invariant
[DE85-007796] 18 p3193 N85-29808
Aspects of silicon bulk lifetimes
20 p3479 N85-31617

FERMI-DIRAC STATISTICS

Potential at atomic boundaries in the TF (or TFD) model and equations of states 12 p1820 N85-21419
First-order shock acceleration in solar flares
[SH-1.1-5] 23 p3969 N85-34732

FERMIONS

NT ANTINEUTRINOS
NT BARYONS
NT COLD NEUTRONS
NT CONDUCTION ELECTRONS
NT FAST NEUTRONS
NT HYPERONS
NT LEPTONS
NT MUONS
NT NEUTRINOS
NT NEUTRONS
NT PROTONS
NT SOLAR NEUTRINOS
NT SOLAR PROTONS
NT THERMAL NEUTRONS

Constraints to the radiative lifetime of a light neutral fermion in the galactic halo from IUE
[NOTA-INTERNA-817] 02 p0279 N85-11820
Measurement of the induced moment magnetic form factor of a heavy fermion superconductor
[DE85-004165] 12 p1942 N85-22194
Canonical analysis of the fermion sector in higher-derivative supergravity
[DE85-007828] 16 p2859 N85-27635
Boson degrees of freedom in Fermion many-body systems
[DE85-006997] 16 p2863 N85-27660
Microscopic analysis of angular momentum projected HFB-states in terms of interacting bosons
[DE85-007629] 16 p2863 N85-27661
Comment on quantum effects on 4-dimensional space-time symmetries
[DE85-007760] 16 p2872 N85-27722
On the definition of topological susceptibility via lattice anomalous Ward identities and its perturbative tail
[PREPRINT-416] 18 p3184 N85-29744
Neutron scattering study of the heavy fermion system UBe-13
[DE85-010955] 19 p3356 N85-30804
Boson-fermion symmetries in the W-Pt region
[DE85-009755] 19 p3362 N85-30845
Monte Carlo simulations of fermion systems: The determinant method
[DE85-010708] 19 p3376 N85-30947
Pairing correction of particle-hole state densities for two kinds of fermions
[DE85-011549] 23 p3971 N85-34820

FERRATES

Analysis of ferrates and ferrites of three transition metals using Moessbauer effects
[BLL-CE-TRANS-8019-(9022.09)]
20 p3430 N85-31273

FERRIC IONS

Dynamics of graphite fiber intercalation: In situ resistivity measurements with a four point probe
[NASA-TM-86858] 01 p0017 N85-10105

FERRIMAGNETS

Static and dynamic disordering in amorphous magnets and crystals 03 p0422 N85-12699

FERRITES

Study to optimize Cr-Mo steels to resist hydrogen and temper embrittlement. A study of carbides formed in low alloy Cr-Mo steels
[DE84-015208] 01 p0029 N85-10179
Symmetry of exchange interaction in crystalline magnetic films 02 p0259 N85-11694
Stability of several substituted ferrites in a reducing atmosphere
[AD-A146106] 03 p0328 N85-12112
Effects of prior austenite and ferrite grain size on fracture properties of a plain carbon steel
[AD-A146276] 03 p0332 N85-12138
Anisotropy and relaxation effects of Co2+ ions in LiTi ferrite
[AD-A146550] 06 p0661 N85-15489
Fundamental tribological properties of ceramics
[NASA-TM-86915] 07 p0930 N85-15893
Defective nature of the crystalline lattice of nickel ferrite-based solid solutions
[BLL-WH-595-(9091.9F)] 07 p1046 N85-16645
Replacement of Fe-3+ ions in nickel ferrites by nonmagnetic Al-3+ and Sc-3+ ions
[BLL-WH-594-(9091.9F)] 08 p1125 N85-17090
Defective nature of the crystalline lattice of nickel ferrite-based solid solutions
[BLL-TRANS-WH-595-(9091.9F)]
10 p1439 N85-19068
Permanent magnet motors
[DE85-000660] 10 p1482 N85-19355
Magnetic and structural properties of shock-synthesized zinc ferrite
[DE85-000469] 11 p1736 N85-20915
Humidity effects on adhesion of nickel-zinc ferrite in elastic contact with magnetic tape and itself
[NASA-TP-2449] 12 p1811 N85-21359
Quenching effects on iron site partitioning in the Apollo 17 orange glass composition 13 p2184 N85-23553
Studies of ferritic filler metals for welding 9 percent nickel steel 15 p2565 N85-25825
Effects of wear on structure-sensitive magnetic properties of ceramic ferrite in contact with magnetic tape
[NASA-TM-87007] 16 p2753 N85-26991
Mechanical stabilization of austenite against epsilon martensite and its effect on deformation behavior in high manganese steels
[DE85-007654] 17 p2932 N85-28097
Analysis of ferrates and ferrites of three transition metals using Moessbauer effects
[BLL-CE-TRANS-8019-(9022.09)]
20 p3430 N85-31273

FERRITIC STAINLESS STEELS

Alloying effects of reactive elements in ferritic stainless steels 02 p0178 N85-11196
Sour-gas cracking in ferritic steels
[AERE-R-10908] 03 p0333 N85-12148
The role of void nucleation in the swelling resistance of ferritic steel
[AERE-R-11525] 11 p1610 N85-20122
Thickness effects of fracture toughness
[DE85-002974] 11 p1653 N85-20409
Investigation of the development possibilities of a ferritic creep and oxidation-resistant steel for application under creep conditions above 650 deg C
[BMFT-FB-T-84-244] 12 p1808 N85-21344
The ferrite permanent magnet AC motor: A technical and economical assessment
[DE85-002480] 13 p2066 N85-22903

Rapid solidification of candidate ferritic steels
[DE85-006596] 16 p2750 N85-26971
Properties of corrosion resistant stabilized ferritic steels
[BLL-BISI-TRANS-22519-(9022.06)] 17 p2925 N85-28039
Stainless steels: Application and welding
[BLL-BISI-TRANS-22357-(9022.06)] 17 p2927 N85-28059
Fatigue behavior of chromium-containing ferritic steels at elevated temperature
[DE85-012309] 22 p3748 N85-33231

FERROALLOYS
U IRON ALLOYS

FERROELECTRICITY
Center for dielectric studies
[AD-A146183] 03 p0434 N85-12761
Ferroelectric tungsten bronze bulk crystals and epitaxial thin films for electro-optic device applications
[AD-A151044] 14 p2427 N85-24970
Capacitive energy storage at cryogenic temperatures
[AD-A154508] 21 p3579 N85-32253
Materials used by industry for the production of piezoelectric transducers. The state of the art of research work performed in the field of PZT ceramics and ferroelectric polymers
[ISL-CO-211/84] 24 p4089 N85-35344
Ferroelectric homopolymer PVF2 and P (VDF-TrFe) copolymers 24 p4089 N85-35347

FERROFLUIDS
Use of ferrofluids in machining of metals 13 p2045 N85-22802
Linear motion valve
[NASA-CASE-MSC-20146-1] 18 p3115 N85-29284

FERROMAGNETIC FILMS
Magnetization of very thin Ni films in epitaxial metal film sandwiches of Cu
[DE85-001840] 10 p1563 N85-19660
Study of amorphous strips and microconductors by ferromagnetic resonance method 15 p2497 N85-25402
Dielectric mirror with ferromagnetic substrate 21 p3696 N85-32966

FERROMAGNETIC MATERIALS
NT FERROFLUIDS
NT FERROMAGNETIC FILMS
NT MAGNETITE
Contributions to the 7th International Acoustic Emission Symposium
[AD-A145368] 02 p0275 N85-11792
Use of magnetic compression based on amorphous alloys as a drive for induction linacs
[DE84-014524] 02 p0277 N85-11805
Nonlinear electromagnetic waves in ferromagnetic conducting media 03 p0348 N85-12232
Effect of external magnetic field on characteristics of current-carrying steel tape 08 p0788 N85-15034
Advanced artificial dielectric materials for millimeter wavelength applications
[AD-A148960] 10 p1431 N85-19027
Application of hysteresis modelling to the non-destructive inspection of stress
[DE85-003081] 11 p1650 N85-20393
The UFe4P12 and CeFe4P12: Non-metallic isotopes of superconducting LaFe4P12
[DE85-003724] 12 p1942 N85-22195
Annealing effects in ferromagnetic amorphous alloys
[AD-A150648] 14 p2255 N85-23972
NMR manometer for measuring high pressures at liquid-helium temperatures 17 p2944 N85-28171
An evaluation and preparation of ferromagnetic liquid composites for use at millimeter wavelengths
[AD-A153939] 18 p3069 N85-28980
Magnetically-localizable, polymerized lipid vesicles and method of disrupting same
[AD-D011686] 19 p3249 N85-30144
An experimental study of the magnetoelastic bending of thin plates made of soft ferromagnetic material 19 p3282 N85-30352
Very low temperature studies of hyperfine effects in metals
[DE85-013367] 22 p3749 N85-33236
Magnetic search system
[PB85-185108] 23 p3949 N85-34477

FERROMAGNETIC RESONANCE
Ferromagnetic resonance in a Ni-Mo superlattice
[DE85-003039] 11 p1735 N85-20911
Study of amorphous strips and microconductors by ferromagnetic resonance method 15 p2497 N85-25402

FERROMAGNETISM
Ferromagnetism in metals at finite temperatures
[DE85-000898] 09 p1377 N85-18656
The Fermi surface and momentum space densities of ferromagnetic Gd using the Positron technique 09 p1395 N85-18788
Fermi surface study of CeSb
[DE85-002532] 10 p1564 N85-19662
Investigation of electric and magnetic properties of intercalated graphite
[AD-A149801] 12 p1797 N85-21274
Magnetic X-ray scattering studies of the rare Earth metal holmium
[DE85-003608] 12 p1807 N85-21335
Behavior of small ferromagnetic particles in traveling magnetic field 12 p1843 N85-21564
Paramagnetic scattering from Ni
[DE85-004207] 12 p1942 N85-22198
Magnetovolume effects in some Y-Ni intermetallic compounds
[ISSN-0066-2003] 13 p2021 N85-22663
Anomalous magnetism of CeRh3B2 under pressure
[DE85-003069] 13 p2164 N85-23425
Material research in microgravity
[NASA-TM-77629] 14 p2228 N85-23811
Peltier heat of a small polaron in a magnetic semiconductor
[DE85-000470] 14 p2430 N85-24983
Lattice overview
[DE85-007282] 15 p2662 N85-26427
Central limit theorems in the area of large deviations for some dependent random variables
[AD-A153125] 17 p3043 N85-28831
A theoretical model for the study of nonlinear dynamics of magnetic bearings 20 p3462 N85-31505
Electronics Division research and development
[DE85-011887] 20 p3540 N85-32032

FERROUS METALS
Strain hardening and strain aging in Fe-Al-Mn alloys 02 p0178 N85-11196
The origin of the Moon 04 p0588 N85-13754
Unsinkability of ferromanganese nodules 06 p0819 N85-15202
Mineralogical-geochemical characteristics of ferromanganese formations in Arabian-Indian Ocean Ridge 19 p3293 N85-30416
Pitting corrosion of ferrous alloys
[AERE-R-11490] 24 p4078 N85-35273
Assessment of metal heating technologies for ferrous forging: A pilot study of the form value of natural gas
[PB85-204394] 24 p4084 N85-35314
Cobalt-rich ferromanganese crusts in the oceans 24 p4104 N85-35444

FERTILITY
Microbial ecology of extreme environments: Antarctic yeasts and growth in substrate-limited habitats
[NASA-CR-175810] 16 p2839 N85-27509

FERTILIZATION
An automatic device for amphibian egg fertilization in space: Technical aspects and biological requirements 05 p0689 N85-14427
Combined effects of atmospheric deposition, internal acid production, and harvesting on nutrient gains and losses from forest ecosystems
[DE85-002325] 12 p1884 N85-21821
Effects of simulated weightlessness on mammalian development. Part 2: Meiotic maturation of mouse oocytes during clinostat rotation 15 p2612 N85-26094

FERTILIZERS
Growth and reflectance characteristics of winter wheat canopies
[E85-10080] 10 p1505 N85-19494
Salinity driven oceanographic upwelling
[DE85-011664] 22 p3818 N85-33652

FET (TRANSISTORS)
U FIELD EFFECT TRANSISTORS

FEVER
China report: Science and technology
[JPRS-CST-84-008] 13 p1972 N85-22384

FEYNMAN DIAGRAMS
Introduction to LINE: A Feynman diagram graphic operator
[DE85-009299] 17 p3013 N85-29832
A test of the Feynman scaling in the fragmentation region
[HE-1.2-9] 24 p4172 N85-35887
General consequences of the violated Feynman scaling 24 p4173 N85-35872

FFT
U FAST FOURIER TRANSFORMATIONS

FIBER COMPOSITES
NT CARBON FIBER REINFORCED PLASTICS
NT GLASS FIBER REINFORCED PLASTICS
Fracture toughness of fibrous composite materials
[NASA-TP-2370] 02 p0170 N85-11136
Microstructural basis of strength and toughness in hardmetals 02 p0177 N85-11185
Effective moduli of elasticity of unidirectional fibrous composite 02 p0265 N85-11733
Tough Composite Materials
[NASA-CP-2334] 04 p0463 N85-12941
Characterization of interlaminar crack growth in composites with the double cantilever beam specimen 04 p0483 N85-12942
Characterizing delamination resistance of toughened resin composites 04 p0484 N85-12943
Composite materials characterization and development at AFWAL 04 p0484 N85-12944
Effect of impact damage and open holes on the compression strength of tough resin/high strain fiber laminates 04 p0484 N85-12945
Effects of constituent properties on compression failure mechanisms 04 p0484 N85-12946
The effect of matrix and fiber properties on impact resistance 04 p0484 N85-12947
Fundamental studies of composite toughness 04 p0484 N85-12948
European development experience on energy storage wheels for space 05 p0605 N85-13858
Generic composite flywheel designs 05 p0606 N85-13864
The creep and creep rupture of SMC-R50 under different thermomechanical conditions 05 p0648 N85-14160
Design procedures for fiber composite structural components: Panels subjected to combined in-plane loads
[NASA-TM-86909] 07 p0919 N85-15823
Titanium Matrix/Continuous Fiber/Continuous fiber composite interface interactions and their influence on mechanical properties
[AD-A147504] 07 p0920 N85-15829
Composite batteries 07 p0936 N85-15932
Applicability of linear elastic fracture mechanics to fatigue in polymers and short-fiber composites 09 p1298 N85-18152
Tribological properties of graphite-fiber-reinforced, partially fluorinated polyimide composites
[NASA-TM-86926] 09 p1298 N85-18153
Calculating residual stresses in composite materials 10 p1443 N85-19095
Spreading upon compacting of fiber composite materials with porous metal matrix 10 p1443 N85-19096
Quantitative estimate of compatibility of fiber composite material components 10 p1444 N85-19099
SEP of France manufactures its first silicon carbide fibers 11 p1618 N85-20184
Estimating degree of development of physical-chemical interaction among components in Al-B fiber composite material 13 p2027 N85-22705
Segregation of silicon in silumin-carbon fiber composites 13 p2028 N85-22706
Some features of the fabrication of multilayer fiber composites by explosive welding
[NASA-TM-77844] 14 p2248 N85-23832
Outlook for polymer composite materials 15 p2497 N85-25403
Research, development of composite materials described 15 p2497 N85-25404
The accuracy of approximate solutions in the analysis of fracture of composites
[NASA-CR-175738] 15 p2503 N85-25437
Homogeneity of pristine and bromine intercalated graphite fibers
[NASA-TM-87016] 15 p2517 N85-25521
Mechanical jointing in Aramid fiber composites: An experimental study
[VTH-LR-371] 16 p2802 N85-27260
Designing for fiber composite structural durability in hygrothermomechanical environment
[NASA-TM-87045] 17 p2917 N85-27978
Titanium metal-matrix composites
[AD-D011643] 17 p2930 N85-28066
Light weight fire resistant graphite composites
[NASA-CASE-ARC-11615-1-SB] 18 p3068 N85-28976
Development of carbon based brake lining materials without asbestos content in the form of carbon-carbon composites and carbon-metal or carbon-carbide composites
[BMFT-FB-T-85-014] 18 p3082 N85-29067
Lightning-safe carbon fiber composite for Airbus tail unit 18 p3087 N85-29100
Arc spray fabrication of metal matrix composite monotape
[NASA-CASE-LEW-13828-1] 19 p3230 N85-30027
Polymer matrix and graphite fiber interface study
[NASA-CR-177357] 19 p3232 N85-30036
Structural characteristics of high temperature composites
[NASA-CR-175998] 19 p3232 N85-30037
Basic cryogenics and materials. Phase 1
[NASA-CR-177932] 21 p3572 N85-32215
Measurement of damping of graphite epoxy materials
[NASA-CR-176073] 21 p3596 N85-32334
Substitution of asbestos by aramid fibers and fiber blends in industrial textiles and composites with organic binders
[BMFT-FB-T-85-006] 23 p3920 N85-34294

FIBER OPTICS
Peripheral vision displays: The future
01 p0009 N85-10058
New type of unique frequency laser communications
[AD-A145128] 01 p0036 N85-10239
Center for Electronics and Electrical Engineering Technical Bulletin covering center programs
[PB84-218056] 01 p0045 N85-10296
Environmentally independent fiber optic rotation sensor
[AD-D011219] 01 p0119 N85-10618
The development of an optoelectronic assembly applied to computer systems
[AD-A145028] 01 p0120 N85-10621
Optical pin apparatus for measuring the arrival time and velocity of shock waves and particles
[DE84-014501] 01 p0120 N85-10624
Fine grained hodoscopes based on scintillating optical fibers
[DE84-014849] 01 p0120 N85-10625
Two novel plasma diagnostic tools: Fiber sensors and phase conjugation
[DE84-014093] 01 p0123 N85-10640
Dual (GaAl) As-heterostructure based injection laser traveling wave amplifier 02 p0261 N85-11708
Fiber cable in optical system with brightness amplifier
02 p0263 N85-11724
Nonlinear symmetrization of picosecond pulses in optical fibers 02 p0264 N85-11725
Using fiber-optics light guides in diagnosing intense shock waves 02 p0272 N85-11773
The effect of temperature on the radiation induced losses of large diameter GPS (Germanium phosphosilicate) and GBS core optical fibers
[AD-A145409] 02 p0280 N85-11823
Fore-optics systems designed for electronic streak cameras using fiber optics
[DE84-014525] 02 p0281 N85-11830
Multiple object spectroscopy: The MX spectrometer design 02 p0296 N85-11920
ONR (Office of Naval Research) Far east Scientific Bulletin, Volume 9, Number 2, April - June 1984
[AD-A145681] 02 p0305 N85-11974
East Europe report: Science and technology
[JPRS-ESA-84-038] 03 p0343 N85-12210
Fiber optics development, prospects assessed
03 p0343 N85-12214
Frequency shifting in multimode fiber optic phase modulation devices 03 p0347 N85-12239
Influence of mode noise suppression in multimode fiber optic light guides 03 p0348 N85-12242
Microshell (trademark)-tipped optical fibers as sensors of high-pressure pulses in adverse environments
[DE84-015520] 03 p0365 N85-12338
Holographic displacement analysis with fiber optics
[AD-A146185] 03 p0420 N85-12880
The applications of fibre optics in gas turbine engine instrumentation
[PNR-90209] 03 p0420 N85-12887
High-temperature optically activated GaAs power switching for aircraft digital electronic control
[NASA-CR-174711] 04 p0457 N85-12901
China report: Science and technology
[JPRS-CST-84-003] 04 p0491 N85-13132
New telecommunications optical fiber developed
04 p0492 N85-13135
Fiber optic data bus using Frequency Division Multiplexing (FDM) and an asymmetric coupler
[NASA-TM-86015] 04 p0492 N85-13139
Scintillator-fiber charged particle track-imaging detector
[NASA-CR-174160] 04 p0559 N85-13560
Fiber optic, Fabry-Perot high temperature sensor
[NASA-CR-174712] 04 p0584 N85-13594
High-bandwidth multichannel fiber optic system for measuring gamma rays
[DE84-014528] 04 p0564 N85-13596
Measuring transient radiation effects in optical fibers
[DE84-015044] 04 p0565 N85-13598
Application of commercial star couplers to increase signal dynamic range
[DE84-014709] 04 p0565 N85-13600
Optical characterization of radiation-resistant fibers
[DE84-015248] 05 p0620 N85-13964
Characterization of fiber optic cables under large tensile loads
[DE84-016816] 05 p0651 N85-14180
Clinical measurements using fiber optics and optrodes
[DE84-015043] 05 p0696 N85-14481
Psychophysical research in development of a fiber-optic helmet mounted display 05 p0701 N85-14501
Contribution to the study and realization of the CARTHAGE multiservice local network
[ENST-84E006] 05 p0716 N85-14595
Gamma-ray to Cerenkov-light conversion efficiency for pure-silica-core optical fibers
[DE84-015041] 05 p0729 N85-14685
100 MHz fiber optic single transient gamma ray detection system
[DE84-016818] 05 p0729 N85-14686
Transient attenuation in optical fibers
[DE84-016487] 05 p0729 N85-14687
A single optical fiber telephone system
[AD-D011293] 06 p0799 N85-15107
Lithium battery safety: A fiber-optic application for safe observation of lithium cells under severe tests
[AD-A146646] 06 p0804 N85-15119
Qualitative and quantitative compositional analysis of shale derived by gas chromatography and combined gas Chromatography/Mass spectrometry. Executive summary
[AD-A148369] 07 p0924 N85-15851
The relationship between radiation sensitivity and redox equilibria — glass processing variables
[AD-A147216] 07 p0932 N85-15906
Holographic directional coupler for fiber optic systems
[AD-D011365] 07 p0937 N85-15939
Micro-waveguide transformers of coherent optical signals 07 p0950 N85-16022
Helmet mounted telescope
[AD-D011355] 07 p1019 N85-16467
Multiwavelength bidirectional coupler-decouplers
[AD-A147009] 07 p1043 N85-16625
Optical fibers with reduced pressure sensitivity to high frequency acoustic field
[AD-D011306] 07 p1043 N85-16627
Bragg cell spectrum analyzer specification
[AD-D011320] 07 p1044 N85-16629
Analytic models for radiation induced loss in optical fibers 2: A physical model
[AD-A147442] 07 p1044 N85-16632
Research and technology, 1984 report
[NASA-TM-83096] 07 p1061 N85-16730
Helicopter Guidance and Control Systems for Battlefield Support
[AGARD-CP-359] 08 p1072 N85-16797
Telecommunications equipment at 1984 Leipzig Spring Fair 08 p1140 N85-17179
East Europe report: Science and technology
[JPRS-ESA-84-047] 08 p1140 N85-17183
UK, FRG, France: R and D in sensors, related fields
08 p1142 N85-17197
RF fiber optic link
[AD-A148679] 08 p1155 N85-17290
Optical frequency domain reflectometry
08 p1222 N85-17695
Application of fiber optics and compound collectors
08 p1253 N85-17912
The fiber-optic helmet-mounted display
[AD-P004330] 09 p1270 N85-17984
Binocular overlap in a fiber optic helmet mounted display
[AD-P004331] 09 p1270 N85-17985
Current measurements by Faraday rotation in single mode optical fibers
[DE85-002025] 09 p1384 N85-18707
Radiation response of optical fibers in a nuclear reactor
[DE84-017221] 09 p1385 N85-18710
Self-induced nonlinear effects in optical fibers: A unified approach
[FUB-67-1982] 09 p1385 N85-18713
Low voltage two wire to four wire telephone circuit converter apparatus
[AD-D011449] 10 p1468 N85-19261
Worldwide report: Telecommunications policy, research and development
[JPRS-TTP-85-002] 10 p1475 N85-19309
NTT (Nippon Telegraph and Telephone Public Corporation) develops new optical fiber
10 p1476 N85-19311
West Europe report: Science and technology
[JPRS-WST-85-008] 11 p1617 N85-20174
Siemens-Corning plant to manufacture optical fibers
11 p1617 N85-20175
Photonic methods of high speed analog data recording
[DE84-016723] 11 p1637 N85-20306
Report of the Technology and Test Panel
11 p1646 N85-20370
Polarization transformation by single-mode fibers — optical fibers
[FI-452-TBR-59] 11 p1729 N85-20876
Wide-field-of-view, helmet-mounted infinity display system development
[AD-A149641] 12 p1777 N85-21159
Optical fiber communications link design in compliance with systems performance standards
[PB85-111037] 12 p1830 N85-21489
1.5 to 1.7 micrometers LEDs (Light-Emitting Diode)
[AD-A149685] 12 p1834 N85-21508
Temperature-insensitive optical fibers
[AD-D011551] 12 p1933 N85-22142
Design of an optical proximity sensor using multiple cones of light for measuring surface shape — application to a robot manipulator
[AD-A150050] 12 p1934 N85-22152
The future of lightwave technology
[PB85-109759] 12 p1935 N85-22155
Analysis of fiber-gyroscopes discussed
13 p2052 N85-22845
Interference immunity of fiber-optic communication lines with spectral multiplexing of channels
13 p2069 N85-22924
AL-124 light-emitting diode in 30 Mbit/s fiber-optic communication line 13 p2069 N85-22925
Optical reflectometer for multimode fiber lightpipes
13 p2075 N85-22961
Dispersion characteristics of small-mode gradient optical fibers 13 p2082 N85-23004
Technical Digest: Symposium on Optical Fiber measurements, 1984
[PB85-114700] 13 p2160 N85-23407
Feasibility study for an AFGL fiber optic data link at WSMR sounding rocket launch area
[AD-A150852] 14 p2240 N85-23894
Use of focons in combination with brightness amplifiers 14 p2274 N85-24088
Research study of fiber-optic interferometry at very low frequencies
[AD-A150906] 14 p2421 N85-24937
Experimental report on a fiber optic light guide made by Galileo Electro-Optics Corporation
[DE85-006161] 14 p2421 N85-24941
Fiber optics applications for MIL-STD-1760
[AD-A151113] 15 p2470 N85-25251
Instrument for measuring dispersional distortions in optical fibers and cables 15 p2530 N85-25595
Wideband fiber optic communications link
[AD-A151704] 15 p2542 N85-25697
Wavelength dependent, tunable, optical time delay system for electrical signals
[AD-D011584] 15 p2548 N85-25725
Length dependent, optical time delay/filter device for electrical signals
[AD-D011594] 15 p2549 N85-25732
Mode dependent, optical time delay system for electrical signals
[AD-D011596] 15 p2553 N85-26363
Three new fiber-optic components
[DE85-006289] 15 p2553 N85-26364
Fiber optic Raman thermometer for Space Shuttle main engine preburner profiling 16 p2739 N85-26904
Reusable rocket engine turbopump condition monitoring 16 p2740 N85-26907
Wavelength multiplexer-demultiplexer
[AD-D011608] 16 p2777 N85-27140
Phase-lock fiber optic interferometer
[AD-D011603] 16 p2786 N85-27191
The utilization of optical fibers in holography
[ISL-R-102/83] 16 p2787 N85-27196
Ultrafast holography using optical fibers
[ISL-CO-238/83] 16 p2788 N85-27204
In-situ stratospheric ozone measurements: Recent results and their implications 16 p2824 N85-27419
A study of topologies and protocols for fiber optic local area network
[NASA-CR-175771] 16 p2864 N85-27669
Performance evaluation of fiber-optic converters
17 p2941 N85-28154
Derated application of parts for (Electronic Systems Division) systems development. Revision
[AD-A153299] 17 p2955 N85-28246
Studies of optical-beam phase-conjugation by nonlinear refraction
[AD-A152865] 17 p3037 N85-28788
Preparation of heavy metal fluoride glasses in the bulk form
[AD-A153784] 18 p3079 N85-29049
West Europe report: Science and technology
[JPRS-WST-84-031] 18 p3086 N85-29089
Philips researches gallium arsenide use for lasers
18 p3087 N85-29106
Rifa of Sweden conducts research in 3-5 materials
18 p3088 N85-29107
Optical fiber magnetic field sensor with nanosecond response time
[DE85-008409] 18 p3110 N85-29259
Optical fiber coupling method and apparatus
[NASA-CASE-NPO-15464-1] 18 p3184 N85-29749
Fiber optics in high dose radiation fields
[DE85-008649] 18 p3185 N85-29755
Fiber optic sensors operating at dc
[AD-D011674] 19 p3271 N85-30283

Fiber optic gyroscope with alternating output signal
[AD-D011689] 19 p3271 N85-30284
Optical 3-D signature device for detecting chemical agents
[AD-D011689] 19 p3272 N85-30293
One-frequency laser interferometer using the optic fiber as a polarization-independent interference phase detector
[DE85-010544] 19 p3277 N85-30326
Fiber optic expanded beam connector
[AD-A154057] 19 p3367 N85-30880
Fiber optics in transient radiation fields
[DE85-010721] 19 p3368 N85-30886
Swedish program for sensor research, development 20 p3438 N85-31338
Data communications-Oriented Production System Language (CPSL)
[DE85-011457] 20 p3440 N85-31352
Optical multiplexing on monomode fibers
[ENST-83E016] 20 p3533 N85-31982
R and D activities of the Systems Engineering Division 20 p3540 N85-32027
Methods for measuring and analyzing dispersion properties of multimode fiber optic lightpipes (a review) 21 p3695 N85-32980
USSR report: Electronics and electrical engineering
[JPRS-UEE-84-015] 22 p3782 N85-33314
Comparative characteristics of optical multiposition pulse signals with intersymbol distortion 22 p3764 N85-33329
Refraction of narrow probing light beam in multilayer optical fiber 22 p3764 N85-33330
Temperature sensitivity of fiber-optic transmission line 22 p3764 N85-33331
Fiber optic moisture sensor
[DE85-011651] 22 p3787 N85-33462
Optical-fiber/microprocessor-based remote velocity sensor
[DE85-010071] 22 p3788 N85-33470
The use of optical fibers in pulsed laser holography
[ISL-CO-226/84] 23 p3936 N85-34395
Fiber optics interface for a dye laser oscillator and method
[DE85-005785] 23 p3973 N85-34833
Bevalac calibration of the SOFIE range and hodoscope detectors
[OG-9.1-7] 23 p4023 N85-34933
Akeno 20 km (2) air shower array (Akeno Branch)
[OG-9.4-8] 23 p4029 N85-34975
Center for Electronics and Electrical Engineering technical progress bulletin covering center programs, July-September with 1985 CEEE events calendar
[PB85-191393] 24 p4091 N85-35363
Optical synthetic aperture techniques
[AD-A156151] 24 p4154 N85-35752
On the possibilities of large-scale radio and fiber optics detectors in cosmic rays
[HE-4.6-2] 24 p4196 N85-36039

FIBER ORIENTATION

Fracture toughness of fibrous composite materials
[NASA-TP-2370] 02 p0170 N85-11136
Experimental study on transonic flutter characteristics of sweptback wing with core composite plates having different fiber orientations
[NAL-TR-827] 06 p0756 N85-14842
Studies of structure and mechanical properties of carbon-reinforced plastic based on spirally reinforced fiber 10 p1444 N85-19100
Initial fracture stages of orthogonally reinforced composite material 11 p1599 N85-20055
Strength properties of unidirectionally reinforced hybrid composites 11 p1599 N85-20058
The orientation distribution of nonspherical aerosol particles within a cloud
[AD-A150600] 13 p2092 N85-23061
Technical Digest: Symposium on Optical Fiber measurements, 1984
[PB85-114700] 13 p2160 N85-23407
Literature survey of discontinuous-fiber-reinforced composites with emphasis on pressure vessels
[DE85-010386] 19 p3232 N85-30038
Strength properties of glassfiber reinforced thermoplastics 23 p3908 N85-34212

FIBER REINFORCED COMPOSITES

Inorganic composites for space applications 02 p0155 N85-11047
Contributions to the 7th International Acoustic Emission Symposium
[AD-A145368] 02 p0275 N85-11792
Thermoplastic-carbon fiber hybrid yarn
[NASA-CR-3849] 03 p0325 N85-12093
Matrix resin characterization in cured graphite composites using diffuse reflectance-FTIR 04 p0496 N85-12959
Composite structural materials
[NASA-CR-174077] 04 p0467 N85-12968
Protective coverings for fiber reinforced epoxy composites
[PB84-231059] 04 p0480 N85-13063
Prefabricated panels for rapidly runway repair and expedient airfield surfacing
[AD-D011277] 05 p0597 N85-13804
On the effects of delamination damage in fibre composite laminates
[ARL/STRUC-R-403] 06 p0763 N85-14881
Carbon fibre reinforced aluminum matrix composites: A critical review
[AD-A146367] 06 p0764 N85-14883
Characterization of newly developed conductive composites
[AD-A146652] 06 p0764 N85-14884
System for rapid repair of damaged airfield runways
[AD-D011325] 07 p0909 N85-15754
Unidirectional fibers and polyurethane elastomer matrix based composites synthesis and properties
[NASA-TM-77501] 07 p0920 N85-15826
Titanium Matrix/Continuous Fiber/Continuous fiber composite interface interactions and their influence on mechanical properties
[AD-A147504] 07 p0920 N85-15829
Verification of the fatigue properties of (small) wind turbines
[NLR-MP-83055-U] 07 p0994 N85-16311
Effects of high energy radiation on the mechanical properties of epoxy-graphite fiber reinforced composites
[NASA-CR-174314] 08 p1118 N85-17047
Disclinations in carbon-carbon composites
[AD-A148290] 08 p1119 N85-17052
The response of metallic structures to dynamic loading 08 p1172 N85-17380
The fabrication, processing and characterization of multidimensionally braided graphite/epoxy composite materials
[AD-A148729] 09 p1288 N85-18090
A comprehensive study on sublaminate crack growth stability and its effects on the load-carrying capacity
[AD-A149037] 10 p1432 N85-19028
Proceedings of Colloquium/Workshop on Composite Materials and Structures, Standardization, Qualification, Certification held at washington, D.C. on 8-10 May 1984
[AD-A149039] 10 p1432 N85-19029
The problem of protecting the structure of a packet composite of optimal thinwall elements 10 p1444 N85-19101
Fiber composite materials with titanium matrix 10 p1445 N85-19105
Fracture toughness of fiber reinforced concrete
[AD-A149403] 10 p1496 N85-19441
Thermoviscoelastic analysis of dimensionally stable fiber composite space structures
[AD-A149275] 11 p1593 N85-20021
Fatigue crack growth in Aramid Reinforced Aluminum Laminates (ARALL): Mechanisms and predictions
[DFVLR-FB-84-37] 11 p1609 N85-20118
Fabrication of fiber-reinforced ceramic composites by chemical vapor infiltration
[DE85-003809] 11 p1611 N85-20132
Aerostructure nondestructive evaluation by thermal field detection. Phase 2: Technique refinement and quantitative determination of flaw detection capabilities
[AD-A149622] 12 p1777 N85-21155
Nonlinear analysis for high-temperature multilayered fiber composite structures --- turbine blades
[NASA-TM-83754] 12 p1797 N85-21273
Behavior of fiber-reinforced composites under dynamic tension
[AD-A150619] 13 p2015 N85-22641
Fibre composite laminated plate analysis using a card programmable calculator (HP41C/CV)
[NIAST-83/88] 13 p2103 N85-23106
Monitoring of laminate cure with microdielectrometry
[AD-A150663] 14 p2249 N85-23934
Synthesis of hydrophobic, crosslinkable resins
[AD-A150658] 14 p2260 N85-24002
Research on composite materials for structural design
[AD-A150602] 14 p2260 N85-24004
A model for the compressive buckling of extended chain polymers
[AD-A151025] 14 p2260 N85-24008
Local elastoplastic fracture of fibrous composite materials 15 p2497 N85-25405
A preliminary investigation into transverse fracture of unidirectional fiber composites
[AERE-R-11494] 15 p2503 N85-25438
Effect of fatigue and thermal loads on silicon carbide fiber reinforced glass matrix composites
[DE85-006069] 15 p2503 N85-25441
Mechanics of polymers and composites: Research opportunities
[DE85-007052] 15 p2503 N85-25442
Fabrication of fiber reinforced ceramic composites by chemical vapor infiltration
[DE85-007565] 15 p2520 N85-25536
Design overview of fiber-reinforced superalloy composites for the Space Shuttle main engine 16 p2734 N85-26871
Nonlinear structural analysis for fiber-reinforced superalloy turbine blades 16 p2737 N85-26887
NASA/aircraft industry standard specification for graphite fiber toughened thermoset resin composite material
[NASA-RP-1142] 16 p2742 N85-26923
Effect of low-velocity or ballistic impact damage on the strength of thin composite and aluminum shear panels
[NASA-TP-2441] 16 p2742 N85-26924
Durability of Aramid reinforced aluminum laminate (ARALL)
[VTH-LR-423] 16 p2744 N85-26933
The effect of low sheet thicknesses on the fracture toughness of an Al alloy (7075-T6) --- Aramid Reinforced Aluminum Laminate (ARALL)
[VTH-LR-425] 16 p2752 N85-26984
Development of a new faster process for the fabrication of ceramic fiber-reinforced ceramic composites by chemical vapor infiltration
[DE85-007550] 16 p2756 N85-27007
The application of BRILES rivets for mechanical jointing of Aramid Reinforced Aluminum Laminate (ARALL)
[VTH-LR-387] 16 p2802 N85-27279
Reaction-bonded and fiber-reinforced SiC static and dynamic gas turbine components
[BMFT-FB-T-84-302] 17 p2899 N85-27874
Aluminum-lithium alloys: The answer of the aluminum industry to the threat of advanced fiber-reinforced materials
[VTH-LR-406] 17 p2932 N85-28102
DFVLR research in aluminum-lithium alloys 18 p3087 N85-29105
Fatigue behavior of unidirectional FP-Al composites with circular holes
[AD-A153466] 18 p3121 N85-29322
Ten year environmental test of glass fiber/epoxy pressure vessels
[NASA-TM-87058] 19 p3231 N85-30034
Literature survey of discontinuous-fiber-reinforced composites with emphasis on pressure vessels
[DE85-010386] 19 p3232 N85-30038
Study of failure mechanism of fibrous composition materials taking into account physicochemical reactions of components 19 p3243 N85-30108
Effect of matrix plasticity on durability of fibrous composition materials 19 p3243 N85-30107
BN coating of ceramic fibers for ceramic fiber composites
[AD-D011700] 19 p3249 N85-30145
Tensile fatigue of glass fibers and composites with conventional and surface compressed fibers
[RR-84-4] 22 p3742 N85-33106
Improved process for the preparation of fiber-reinforced ceramic composites by chemical vapor deposition
[DE85-011584] 22 p3752 N85-33255
Stresses and deformations in cross-ply composite tubes subjected to a uniform temperature change: Elasticity and Approximate Solutions
[NASA-CR-178147] 22 p3800 N85-33545
X-ray measurement of thermal stresses in tungsten fiber-copper composites 23 p3907 N85-34205
Evaluation methods of ceramic fiber reinforced metal matrix composite 23 p3907 N85-34206
Fracture behavior of aluminum composites reinforced with fiber 23 p3907 N85-34207
Rotating bending fatigue strength of silicon carbide and alumina-fiber reinforced aluminum 23 p3907 N85-34208
Mechanical properties of SiC fiber-reinforced reaction-bonded Si3N4 composites
[NASA-TM-87065] 23 p3909 N85-34223
Viscoelastic behavior of short-fiber composite materials
[DE85-011233] 23 p3910 N85-34225
Three-dimensional finite element failure model for predicting failure in fibre reinforced bolted joints
[BR94778] 23 p3940 N85-34423
Mechanical characterization and failure modes of fiber reinforced angle-ply composites 24 p4072 N85-35234
Quantitative non-destructive evaluation of composite materials based on ultrasonic wave propagation
[NASA-CR-178176] 24 p4074 N85-35244
Determination of characteristic values for fiber reinforced materials 24 p4074 N85-35247
Computational techniques for fiber reinforced components 24 p4075 N85-35250
A research program to reduce the interior noise in general aviation aircraft, index and summary
[NASA-CR-178178] 24 p4145 N85-35695

FIBER STRENGTH
High performance fibers for structurally reliable metal and ceramic composites — advanced gas turbine engine materials
[NASA-TM-86878] 03 p0325 N85-12005
Qualitative and quantitative compositional analysis of shale derived by gas chromatography and combined gas Chromatography/Mass spectrometry. Executive summary
[AD-A148369] 07 p0924 N85-15851
Damage to boron fibers during thermal cycling and annealing 10 p1445 N85-19107
High resistance and raised modulus carbon fibers
[NASA-TM-76884] 15 p2502 N85-25436
Effect of surface state on durability of aluminized boron fibers 19 p3244 N85-30115

FIBERGLASS
U GLASS FIBERS

FIBERS
NT BORON FIBERS
NT CARBON FIBERS
NT CERAMIC FIBERS
NT GLASS FIBERS
NT METAL FIBERS
NT NYLON (TRADEMARK)
NT REINFORCING FIBERS
NT SYNTHETIC FIBERS
NT WOOL
Dynamics of graphite fiber intercalation: In situ resistivity measurements with a four point probe
[NASA-TM-86959] 01 p0017 N85-10105
Preparation of silicon carbide fibers
[DE84-014661] 01 p0022 N85-10137
Evaluation of hollow fiber ultrafiltration as a pretreatment for reverse osmosis desalination of seawater
[PB84-212406] 01 p0026 N85-10160
Stability of bromine intercalated graphite fibers
[NASA-TM-86859] 01 p0031 N85-10187
Research in quantitative NDE techniques
[AD-A145990] 03 p0369 N85-12358
Gamma-ray to Cerenkov-light conversion efficiency for pure-silica-core optical fibers
[DE84-015041] 05 p0729 N85-14685
Transient attenuation in optical fibers
[DE84-016487] 05 p0729 N85-14687
Fire retardant cellulosehydrate fibers 06 p0761 N85-14870
Improved uniformity of viscous textile fibers obtained by altering drying procedures 06 p0762 N85-14871
Synthesis of antimicrobial chemical fibers and fibrous materials containing quaternary ammonium compounds and their utilization 06 p0762 N85-14872
Forming fluorine-containing threads from vinylidene fluoride-tetrafluoroethylene copolymer by dry method 06 p0762 N85-14873
Study of effectiveness of fire-resistant activity of antipyranse for fibers of aromatic polyamides 06 p0762 N85-14874
Polymer-carbon black interaction in electrically conducting fiber-forming composites 06 p0762 N85-14875
Effect of polymer matrix on properties of fibers obtained by caking polymer dispersions 06 p0762 N85-14876
Preparation of fire-resistant infusible polycaproamide fiber 06 p0763 N85-14877
Creep of chemically vapor deposited SiC fibers
[NASA-TM-86867] 06 p0763 N85-14878
Flame resistant fibrous materials development
[NASA-CR-167817] 07 p0920 N85-15827
Improved solid-state laser sources, volume 2
[DE85-000759] 09 p1325 N85-18330
Gel drawn fibers of poly(vinyl alcohol)
[AD-A149062] 10 p1435 N85-19040
Behavior and specifics of fracture of porous fiber materials in extension 10 p1447 N85-19118
Thermophysical properties of porous fiber materials 11 p1601 N85-20068
West Europe report: Science and technology
[JPRS-WST-85-006] 11 p1618 N85-20183
Impurities in Kevlar 49 fibers
[DE85-004995] 13 p2038 N85-22767
A model for the compressive buckling of extended chain polymers
[AD-A151025] 14 p2260 N85-24008
Changes in the cholinergic system of rat sciatic nerve and skeletal muscle following suspension induced disuse
[NASA-CR-175718] 15 p2615 N85-26111
A micrographic and gravimetric study of intercalation and deintercalation of graphite fibers
[NASA-TM-87026] 17 p2934 N85-28110
Experiments and micromechanical models for creep-rupture in polymer matrix composites
[DE85-009833] 17 p2935 N85-28118
Thermal expansion coefficients of a 30% glass fiber filled PEEK pyrotechnic charge holder
[DE85-010905] 19 p3251 N85-30155
Woven heat exchanger
[DE85-011633] 22 p3783 N85-33439
Development and characterization of carbon-bonded carbon fiber insulation for radioisotope space power systems
[DE85-013365] 24 p4082 N85-35299

FIBERS (MATHEMATICS)
Annals of the Fourier Institute, volume 34, no. 4 11 p1698 N85-20668
Contribution of the cup-product of Milnor's fiber with /f/ sup 2 lambda poles 11 p1698 N85-20672
Riemann foliations on simply connected varieties 11 p1699 N85-20677

FIBRILLATION
Mapping of mammalian arrhythmias with the cardiac laser scanner 03 p0399 N85-12545

FIBRIN
The Fibrin slide assay for detecting urokinase activity in human fetal kidney cells 20 p3502 N85-31768

FIBROBLASTS
Repair of DNA treated with lambda-irradiation and chemical carcinogens
[DE85-010298] 19 p3327 N85-30616

FIBROUS MATERIALS
U FIBERS

FIDELITY
U ACCURACY

FIELD COILS
Superconducting toroidal field coil current densities for the TFCX
[DE85-010285] 20 p3530 N85-31959

FIELD EFFECT TRANSISTORS
NT JFET
Luminous points and breakdown in structure of GaAs transistors 02 p0257 N85-11684
Novel techniques for the fabricating and characterization of GaAs MIS (Metal Insulator Semiconductor) structures
[AD-A145766] 03 p0358 N85-12301
High-temperature optically activated GaAs power switching for aircraft digital electronic control
[NASA-CR-174711] 04 p0457 N85-12901
Glow spots and breakdown in GaAs transistor structure 04 p0487 N85-13107
Gamma-induced leakage in junction field-effect transistors
[DE84-014990] 04 p0570 N85-13634
Radiation hardened ion-implanted GaAs field effect transistor and method for making the same specification
[AD-D011284] 05 p0731 N85-14697
Dual-gate MESFET variable gain constant output power amplifier
[AD-D011334] 07 p0945 N85-15982
Development of short gate FET's
[AD-A147033] 07 p0947 N85-15999
Linear wideband microwave amplifiers for monolithic integrated microcircuits 07 p0955 N85-16051
Fluctuation phenomena studies in chemically sensitive field effect transistor. Part 1: Corrosion of aluminum
[AD-A148240] 08 p1129 N85-17118
Fluctuation phenomena studies in chemically sensitive field effect transistors. Part 2: Corrosion of silicon oxynitride
[AD-A148227] 08 p1157 N85-17302
A transistor oscillator-doubler
[AD-D011408] 08 p1158 N85-17307
Thin film transistors for addressing flat panel displays
[BMFT-FB-T-84-210] 08 p1227 N85-17726
Transient response of a small-signal microwave GaAs FET to X-rays
[DE85-000066] 09 p1315 N85-18265
Tally cell circuit
[AD-D011492] 11 p1629 N85-20254
Determination of the mobility profile in GaAs-MESFETs
[NASA-TM-77818] 11 p1734 N85-20905
High-voltage, high-power, solid-state remote power controllers for aerospace applications
[NASA-TP-2437] 12 p1795 N85-21263
Factors affecting SOS (Silicon-On-Sapphire) yield and reliability
[AD-A150004] 12 p1835 N85-21515
Pulse transformer package for impedance matching a laser diode to a transmission line
[AD-D011499] 12 p1855 N85-21632
Process for making a heterojunction source-drain insulated gate field-effect transistors utilizing diffusion to form the lattice
[AD-D011536] 12 p1939 N85-22176
Electrical performance of semiconductor devices at cryogenic temperatures 12 p1948 N85-22239
Advanced detectors and signal processing for bubble memories
[NASA-CR-172534] 14 p2297 N85-24219
Proceedings of the Cold Electronics Workshop
[NASA-CR-175682] 14 p2297 N85-24220
Physical electronics of cooled operation of very short compound semiconductor transistors 14 p2297 N85-24223
Si MOS devices at low temperatures 14 p2297 N85-24225
Cryogenically-cooled, low-noise microwave receivers: Present status and future needs 14 p2298 N85-24226
InGaAs/GaAs, Strained-Layer Superlattice (SLS), junction photodetectors, LED's, injection LASER's and FET's for optoelectronic IC applications
[DE85-001940] 14 p2430 N85-24986
Cascode and differential amplifier using field-effect transistors 15 p2529 N85-25501
Assessment of present and future large-scale semiconductor detector systems
[DE85-006806] 15 p2682 N85-26430
Impurity bands associated with MOS inversion layers
[INPE-3483-PRE/726] 16 p2870 N85-27704
A study of Ga(.47)In(.53)As and Al(.48)In(.52)As for very high frequency device applications
[AD-A151995] 16 p2870 N85-27706
Effect of dislocations on gallium arsenide FETs
[AD-A152249] 16 p2870 N85-27709
Measurement methods for accurate microwave characterization and modeling of MESFET chips
[AD-A152360] 17 p2952 N85-28227
Communications and logic systems at millimeter wave frequencies
[NASA-CR-175859] 17 p3042 N85-28824
Communications and logic systems at millimeter wave frequencies, summary 17 p3042 N85-28825
Leakage effects in n-GaAs MESFET with n-GaAs buffer layer 17 p3043 N85-28826
GaAs MESFET with lateral non-uniform doping 17 p3043 N85-28827
Further development of high voltage SIPMOS FET's to fulfill market needs
[BMFT-FB-T-84-255] 17 p3045 N85-28843
Rifa of Sweden conducts research in 3-5 materials 18 p3088 N85-29107
The ESFET: Evaporated Sensing Field Effect Transistor 19 p3256 N85-30188
High speed GaAs device and integrated circuit modelling and simulation 19 p3256 N85-30191
High voltage lateral power transistors: Theory and design 19 p3257 N85-30194
Heterojunction Schottky gate MESFET with lower channel ridge barrier
[AD-D011673] 19 p3258 N85-30199
Self-aligned GaAs FET with low 1/F noise
[AD-D011687] 19 p3260 N85-30215
Optical injection locking of solid-state oscillators by frequency-multiplexed injection-locked, laser diodes
[AD-D011695] 19 p3275 N85-30307
Design and fabrication of monolithic broadband microwave GaAs low noise FET amplifiers 20 p3443 N85-31370
Thirty GHz low noise GaAs FET amplifiers — satellite-ground communication
[CD.6500686] 20 p3449 N85-31413
Evaluation of semiconductor devices for Electric and Hybrid Vehicle (EHV) ac-drive applications, volume 2
[NASA-CR-176103] 22 p3759 N85-33294
Modulation doped GaAs/Al(x)Ga(1-x)As layered structures with applications to field effect transistors
[AD-A155360] 22 p3759 N85-33296
Study of nonlinear distortion in microwave amplifiers using Schottky gate field effect transistors 22 p3780 N85-33423
Two-dimensional numerical modeling of ion implanted GaAs MESFET devices 24 p4088 N85-35341

FIELD EMISSION
Virtual cathode oscillator study
[AD-A149268] 10 p1480 N85-19342
On the electric charge carried by dust grain excitation of violent discharge — planetary rings 15 p2677 N85-26530
Apparatus for mounting a field emission cathode
[NASA-CASE-LEW-14108-1] 18 p3094 N85-29149
Resolution at its current limit: Applications of the Berkeley ARM
[DE85-009959] 19 p3274 N85-30301
The ESA field emission electric propulsion program
[ESA-STR-213] 20 p3420 N85-31229

FIELD INTENSITY METERS
Methodical approaches to determination of sanitation protective zone dimensions around TV centers and TV retransmitters 09 p1361 N85-18563
Automated TEM (Transverse electromagnetic) cell calibration system
[PB85-134377] 11 p1636 N85-20319

FIELD OF VIEW
Investigation of several aspects of LANDSAT 4/5 data quality
[E85-10036] 04 p0525 N85-13357
Direction judgement errors in perspective displays
05 p0705 N85-14520
Helmet mounted telescope
[AD-D011355] 07 p1019 N85-16467
Binocular overlap in a fiber optic helmet mounted display
[AD-P004331] 09 p1270 N85-17985
The effect of modified spectacles on the field of view of the helmet display unit of the integrated helmet and display sighting system
[AD-A146883] 09 p1281 N85-18055
On the error of typhoon intensity estimation by means of IR Dvorak technique occurring when the eye is very small 12 p1894 N85-21886
Focal plane array optical proximity sensor
[NASA-CASE-NPO-15155-1] 12 p1932 N85-22139
Computing parameters characterizing possibility of planets falling in star camera field of view during space survey 15 p2487 N85-25351

FIELD STRENGTH
NT ELECTRIC FIELD STRENGTH
NT MAGNETIC FLUX
Automated TEM (Transverse electromagnetic) cell calibration system
[PB85-134377] 11 p1638 N85-20319
User's manual for the University of Houston individual heliostat layout and performance code
[DE85-004643] 12 p1882 N85-21806
Exact design formulas for field intensity of dipole deployed above flat homogeneous Earth with finite conductivity 13 p2061 N85-22998
MHD channel development
[DE85-008305] 18 p3192 N85-29796
Solar monochromatic images in magneto-sensitive spectral lines and maps of vector magnetic fields
18 p3207 N85-29897
Magnetic field-vector measurements in quiescent prominences via the Hanle effect: Analysis of prominences observed at Pic-du-Midi and at Sacramento Peak
18 p3208 N85-29898
Fractal structure of the interplanetary magnetic field
[NASA-TM-86212] 19 p3383 N85-30867
Short perturbations of cosmic ray intensity and electric field in atmosphere
[SH-6.1-18] 23 p4048 N85-35090

FIELD THEORY (ALGEBRA)
NT QUADRATIC EQUATIONS
Annals of the Fourier Institute, volume 34, no. 4
11 p1698 N85-20668
On the distribution of integral and prime divisors with equal norms 11 p1698 N85-20669
The Milnor link of a local field to a perfect residue field 11 p1698 N85-20670
Nonlinear sigma-models and integration methods
[DE85-004447] 12 p1922 N85-22071
Field theory analysis using the finite element method to determine the deliberation curves of three dimensional fracture mechanics specimens with a semicircular surface crack applying the electrical direct current potential method for crack depth measurement
[GKSS-84-E-53] 17 p2982 N85-28434
Special relativity of Kaluza-Klein
[DE85-007838] 17 p3046 N85-28847

FIELD THEORY (PHYSICS)
NT INSTANTONS
NT QUANTUM CHROMODYNAMICS
NT STRONG INTERACTIONS (FIELD THEORY)
NT UNIFIED FIELD THEORY
NT WEAK INTERACTIONS (FIELD THEORY)
Scattering theory by Enss' method for operator valued matrices: Dirac operator in an electric field
[REPT-64] 01 p0045 N85-10290
Research program in theoretical high-energy physics
[DE84-013717] 01 p0119 N85-10817
Linear conformal gravitation 02 p0265 N85-11735
Renormalization theory in four dimensional scalar fields
[NOTA-INTERNA-824] 02 p0292 N85-11895
Toward unification of elementary particle physics and cosmology in 10-dimensions
[DE84-013950] 05 p0727 N85-14674
Analyses of energy extraction efficiency of unstable resonators
[AD-A146391] 08 p0813 N85-15161
Supermanifolds and Berezin's new integral
[DE85-001833] 11 p1706 N85-20732
Ultraviolet divergences and supersymmetric theories
[DE85-001649] 11 p1729 N85-20875
Research in theoretical physics
[DE85-004286] 12 p1944 N85-22207
Standard model and beyond
[DE85-004269] 14 p2418 N85-24919
Research in theoretical nuclear physics
[DE85-006172] 14 p2418 N85-24920
Los Alamos Science, Number 11, Summer-Fall, 1984
[DE85-004634] 14 p2419 N85-24926
Lattice Monte Carlo calculations of finite temperature QCD
[DE85-004035] 14 p2431 N85-24992
Gravitational effects in theories with interacting fields: Two studies 15 p2863 N85-26435
Solutions of field equations in General Relativity with spinor connection 15 p2863 N85-26436
Neutrino measurements on the Moon
[DE85-007700] 16 p2884 N85-27791
Coherent state description of non-topological solitons and momentum projection
[DE85-007814] 17 p3033 N85-28761
Cavityless optical bistability in systems of two-level atoms 18 p3188 N85-29784
Operation of HFTF to test the MIT 12 T coil
[DE85-010409] 18 p3195 N85-29821
Field theory of the metal-insulator transitions in restricted symmetries
[NOTA-INTERNA-829] 18 p3196 N85-29826
Constructing a bit string universe
[DE85-006317] 18 p3197 N85-29829
Theory of high energy collision processes
[DE85-010183] 19 p3362 N85-30846
The standard model and beyond
[DE85-010239] 19 p3362 N85-30847
Wave propagation and methods of solution of the wave equation for moving disturbances sources
[ESA-TT-824] 20 p3522 N85-31906
Research in the theory of condensed matter and elementary particles
[DE85-010447] 20 p3531 N85-31968
Introduction to the Standard Model — weak and electromagnetic interactions
[USIP-85-02] 20 p3532 N85-31970
Some dynamic electronic properties of semiconductor surfaces and interfaces 20 p3537 N85-32007
Bergson and the unification of the sciences
[DE85-009961] 20 p3538 N85-32018
Lattice theory for nonspecialists, lecture notes
[NIKHEF-H/84-11] 20 p3539 N85-32019
Monopole search below the Parker limit with the MACRO detector at Gran Sasso
[HE-6.1-5] 24 p4209 N85-36131
Limits on monopole fluxes from KFG experiment
[HE-6.1-8] 24 p4209 N85-36132
An experiment to detect gut monopoles
[HE-6.1-7] 24 p4210 N85-36133

FIGHTER AIRCRAFT
NT F-8 AIRCRAFT
NT F-14 AIRCRAFT
NT F-15 AIRCRAFT
NT F-16 AIRCRAFT
NT F-17 AIRCRAFT
NT F-18 AIRCRAFT
NT F-27 AIRCRAFT
NT F-104 AIRCRAFT
NT F-106 AIRCRAFT
NT F-111 AIRCRAFT
NT HARRIER AIRCRAFT
NT JAGUAR AIRCRAFT
NT JET PROVOST AIRCRAFT
NT MIG AIRCRAFT
NT MIRAGE AIRCRAFT
NT MIRAGE 3 AIRCRAFT
Prediction of aerodynamic characteristics of fighter wings at high angles of attack
[AD-A145107] 01 p0003 N85-10017
Shock capturing finite difference algorithms for supersonic flow past fighter and missile type configurations
[NASA-CR-174051] 02 p0134 N85-10913
Avionics Integrity Program (AvIp). Volume 2: Hardware case studies
[AD-A145889] 02 p0139 N85-10944
Status and prospects of computational fluid dynamics for unsteady transonic viscous flows
[NASA-TM-86018] 03 p0315 N85-12037
Quantification of cross-coupling and motion feedthrough for multiaxis controllers used in an air combat flying task
05 p0700 N85-14491
China report: Science and technology
[JPRS-CST-84-042] 06 p0747 N85-14789
New fighter aircraft reported — Jian-8 aircraft
06 p0747 N85-14790
F-7 supersonic day fighter viewed — Jian-7 aircraft
06 p0747 N85-14791
Operational Loads Data
[AGARD-CP-375] 07 p0894 N85-15664
Structural load measurements on a Northrop NF-5A
07 p0894 N85-15667
Navy operational loads data sources and systems
07 p0895 N85-15668
Structural flight load measurement demonstration of structural integrity 07 p0895 N85-15670
Display Techniques for Advanced Crew Stations (DTACS). Phase 1: Display techniques study
[AD-A146922] 07 p0904 N85-15722
Can the Aggressors continue to be effective in the F-5E?
[AD-A146861] 07 p1019 N85-16465
Computer sizing of fighter aircraft
[NASA-TM-86351] 08 p1067 N85-18759
International aviation (selected articles)
[AD-A148704] 08 p1067 N85-16762
Full scale experiments into the use of large eddy breakup devices for drag reduction on aircraft
08 p1071 N85-16790
Optimum performance parameters for ski-jump operations of USAF fighter aircraft
[AD-A148532] 08 p1084 N85-16867
Advances in composites technology
[NASA-TM-86353] 08 p1118 N85-17048
Development of an electro-pneumatic anti-G valve for high performance fighter aircraft
[AD-A148468] 08 p1201 N85-17561
Some fighter aircraft trends
[NASA-TM-86352] 10 p1420 N85-18854
Pictorial format display evaluation
[AD-A149252] 10 p1425 N85-18868
A technical solution to fadings in tactical satellite digital transmissions 10 p1473 N85-19297
Human Factors Considerations in High Performance Aircraft
[AGARD-CP-371] 10 p1532 N85-19653
Aircrew and avionics: Friends or Foes?
10 p1532 N85-19654
Military pilot ergonomics 10 p1532 N85-19655
Impact of future aircombat characteristics on pilot performance and cockpit design
10 p1533 N85-19661
Grasp of information by the pilot in future combat aircraft 10 p1533 N85-19662
The cockpit of the year 2000: How big a step?
10 p1534 N85-19667
Flight mechanics analysis of dynamic derivatives of the Dornier variable wind tunnel model
[ESA-TT-854] 11 p1577 N85-19937
Don't fowl out
[AD-P004179] 11 p1578 N85-19941
Robustness of discrete-time dynamical systems: Application to the multivariable digital control of combat aircraft
[ONERA-NT-1984-2] 11 p1585 N85-19986
Potential impact of Navstar GPS on NATO tactical operations 11 p1711 N85-20763
Development of the F-20 nose radome
[AD-P004374] 12 p1827 N85-21468
Laser clock
[AD-D011513] 12 p1855 N85-21634
Low-speed stability and control wind-tunnel investigations of effects of spanwise blowing on fighter flight characteristics at high angles of attack — Langely 12-ft low-speed tunnel and 30- by 60-ft tunnel
[NASA-TP-2431] 14 p2210 N85-23708
Status and prospects of computational fluid dynamics for unsteady transonic flow 15 p2459 N85-25180
West Europe report: Science and technology
[JPRS-WST-84-012] 15 p2523 N85-25552
Low-resolution target classification from a staring infrared sensor
[AD-A151690] 15 p2552 N85-26358
Some aspects of how to design cost-effective flight control systems 16 p2695 N85-26639
Application of AFTI/F-16 task-tailored control modes in advanced multirole fighters 16 p2712 N85-26735
The STOL and maneuver technology program integrated control system 16 p2715 N85-26757
Some aspects of how to design cost-effective flight control systems
[MBB-LKE-32/S/PUB/143] 16 p2873 N85-27729
Operational and developmental experience with the F/A-18A digital flight control system
17 p2902 N85-27895
Flight testing and development of the F/A-18A digital flight control system 17 p2902 N85-27896
The flight control system for the Experimental Aircraft Programme (EAP) demonstration aircraft
17 p2904 N85-27908
Design and implementation of input signals for identification of pilot/aircraft models
[ESA-TT-880] 20 p3394 N85-31055
Modifications of flight-by-flight load sequences to provide for good fracture surface readability
[NLR-MP-84012-U] 20 p3472 N85-31577
Maintenance and the military environment
22 p3750 N85-33243

Fatigue lives of specimens representing critical locations in Mirage 3 spars under Australian and Swiss test spectra
[ARL-STRUC-R-415] 24 p4064 N85-35187
RAFTS: A T-38 replacement for the 21st century
[AD-A156103] 24 p4065 N85-35191

FIGURE OF MERIT
Transversely reinforced piezoelectric composites
[AD-D011676] 19 p3260 N85-30214

FILAMENT WINDING
The fabrication, processing and characterization of multidimensionally braided graphite/epoxy composite materials
[AD-A148729] 09 p1288 N85-18090
Studies of structure and mechanical properties of carbon-reinforced plastic based on spirally reinforced fiber 10 p1444 N85-19100
SRM filament wound case resin characterization studies 12 p1944 N85-22212
Testing of wound materials for strength with loading in the reinforcement plane 13 p2027 N85-22701
Glass, carbon fibers made at Fibre et Mica in France 15 p2534 N85-25834
SRB filament wound case material property study
[NASA-CR-171469] 17 p2910 N85-27940
Filament wound structures in PSP carbon composite
[RV10/84424] 22 p3743 N85-33198

FILAMENT WOUND CONSTRUCTION
U FILAMENT WINDING

FILAMENTS
Dynamics of liquid filament breakup
[DE84-016006] 04 p0500 N85-13187
Ultrasonic girth weld evaluation for aluminum substrate of spherical Kevlar-epoxy test specimens
[DE85-001592] 06 p0816 N85-15181
Magnetization measurements on multifilamentary Nb3Sn and NbTi conductors
[DE85-001237] 11 p1737 N85-20923
Current enhancement in a conducting channel
[AD-A155418] 22 p3845 N85-33812

FILAMENTS (SOLAR PHYSICS)
U SOLAR PROMINENCES

FILE MAINTENANCE (COMPUTERS)
Storage in the LLNL Octopus network: An overview and reflections
[DE84-014711] 01 p0106 N85-10712
Proceedings of the 5th LAN-Transport Workshop
[PB84-232667] 01 p0107 N85-10715
WXR (hydrologic weather wire and PLT product software package)
[PB84-237221] 04 p0541 N85-13442
OSLOG: Designed to create and maintain a 49 hour observation log file
[PB85-109528] 10 p1519 N85-19579
The identification of semantics for the file/database problem domain and their use in a template-based software environment 14 p2401 N85-24803
An adaptive technique and its application in database design 16 p2877 N85-27748
VIDTEX
[PB85-175689] 19 p3318 N85-30567
Recovery of lost files from VAX/VMS disk structures: A case study
[DE85-010652] 19 p3333 N85-30650
CMP: Code Maintenance Package reference manual, version 2.0
[DE85-011396] 19 p3340 N85-30697
Analysis of spacecraft data
[NASA-CR-171597] 21 p3689 N85-32790
CARE 3 user friendly interface user's guide
[NASA-CR-172608] 21 p3689 N85-32791
CARE 3 MENU maintenance manual
[NASA-CR-172609] 22 p3828 N85-33706
User's operating procedures. Volume 1: Scout project information programs
[NASA-CR-177948] 23 p3956 N85-34518
Using LINE as an interactive graphics package. Interfacing line and Topdraw in 43 and 24 VM
[DE85-012007] 23 p3965 N85-34585

FILLERS
Numerical modeling of complex interaction of shell of revolution and its filler with allowance for friction 06 p0779 N85-14980
Initial investigation of cryogenic wind tunnel model filler materials
[NASA-TM-86363] 09 p1283 N85-18069
Studies of structure and mechanical properties of carbon-reinforced plastic based on spirally reinforced fiber 10 p1444 N85-19100
The effect of filler wire and flux compositions on the microstructure and properties of microalloyed steel weld metal
[AD-A149529] 10 p1492 N85-19423
Studies of ferritic filler metals for welding 9 percent nickel steel 15 p2585 N85-25825
Propagation of non-axisymmetric elastic waves through shell with filler under radial load at one end 17 p2943 N85-28169
Comparison of TT-F-1098 solvent-thinned block fillers with water-thinnable block fillers
[AD-A154207] 19 p3249 N85-30142
Results of tests of weathered K5NA closeout material in the MSFC Hot Gas Facility
[NASA-CR-170893] 24 p4073 N85-35239

FILLETS
Fillet weld stress using finite element methods 15 p2576 N85-25884

FILLING
NT REFILLING
Modifications to SOLA-VOF for flow dynamics in spinning cylinders
[AD-A154093] 19 p3265 N85-30250
Robotic order picking
[AD-D011737] 22 p3792 N85-33493
AUTSKED: An addendum
[DE85-010410] 22 p3829 N85-33712
An analysis and algorithm for filling propagation 23 p3961 N85-34551

FILM BOILING
Theoretical description of film boiling in a two phase flow calculation
[IKE-2-66] 05 p0638 N85-14092
Instability of film boiling of moving liquids
[BLL-WH-603-(9091.9F)] 07 p0956 N85-16056

FILM CONDENSATION
Heat transfer due to film condensation on vertical fluted tubes
[AD-A147258] 07 p0959 N85-16079
Filmwise condensation of steam on low integral-finned tubes
[AD-A152220] 16 p2783 N85-27176
Film condensation of steam on externally finned horizontal tubes
[AD-A155642] 21 p3585 N85-32285

FILM COOLING
Vortex-generating coolant-flow-passage design for increased film-cooling effectiveness and surface coverage
[NASA-TP-2388] 03 p0361 N85-12314
Heat transfer results and operational characteristics of the NASA Lewis Research Center Hot Section Cascade Test Facility
[NASA-TM-86890] 06 p0806 N85-15133
Flow visualization study of the effect of injection hole geometry on an inclined jet in crossflow
[NASA-TM-86936] 11 p1631 N85-20269
Advanced liner-cooling techniques for gas turbine combustors
[NASA-TM-86952] 12 p1770 N85-21115
Optimization of combined convective and film cooling of perforated baffle blades in gas turbines 14 p2270 N85-24067
The effect of injection-stream turbulence on film cooling effectiveness and heat transfer coefficients 20 p3451 N85-31424
Vortex generating flow passage design for increased film cooling effectiveness
[NASA-CASE-LEW-14039-1] 22 p3782 N85-33433

FILM THICKNESS
Effect of interconnection of the ends of a sliding bearing on film thickness
[AD-A147736] 08 p1132 N85-17135
Mechanical interactions of rough surfaces
[DE85-000814] 10 p1494 N85-19434
Nonuniform interference coatings with thickness-dependent refractive index 14 p2281 N85-24131
Fast approach for calculating film thicknesses and pressures in elastohydrodynamically lubricated contacts at high loads
[NASA-TM-87032] 19 p3264 N85-30242
Influence of surface films of petroleum products on conditions for absorption of solar radiation by upper water layer 19 p3269 N85-30396

FILMS
Rep rated long life capacitor development: Phase 1 and 2
[DE85-000719] 11 p1629 N85-20256
Modification of the grain size of sputtered copper with additions of oxygen, krypton, silver, or yttrium
[DE85-010975] 21 p3567 N85-32189
A new large-scale, high-resolution multicolor software display concept
[AD-A155404] 22 p3827 N85-33703

FILTERING
U FILTRATION

FILTERS
Calibration and use of filter test facility orifice plates
[DE84-016851] 04 p0500 N85-13190
Intermediate results of a 1-year study of a laser spectrometer in the DOE filter test facilities
[DE84-016478] 04 p0506 N85-13228
Theory of optimum M-filtration of signals against background of correlated interference 13 p2069 N85-22927
Sigma filter 18 p3142 N85-29450

FILTRATION
NT SPATIAL FILTERING
Noise isolation system for high-speed circuits
[DE84-014229] 01 p0043 N85-10283
Ultrafiltration as pretreatment for the preparation of drinking water by reverse osmosis onboard ships
[PML-1984-32] 01 p0098 N85-10854
Fabric filter system study
[PB84-229749] 03 p0342 N85-12206
Electrostatic augmentation of fabric filtration: Reverse-air pilot unit experience
[PB84-230002] 03 p0343 N85-12207
Characteristics of absorption and frequency filtration of ULF electromagnetic waves in the ionosphere 03 p0376 N85-12402
A method of making the gas-electric removal of highly dispersed particles more effective
[BLL-M-36030-(5826.4)] 06 p0765 N85-14890
Laboratory simulation of smoke reduction from aircraft engine test cell exhaust using a fluidized bed filter
[AD-A148600] 08 p1089 N85-16886
Carbon filter plates for aluminum filtration at casting
[BMFT-FB-T-84-242] 12 p1808 N85-21343
Local behavior of solutions of an elliptic-parabolic equation
[AD-A149624] 12 p1920 N85-22057
Acoustic agglomeration methods and apparatus
[NASA-CASE-NPO-15466-1] 12 p1927 N85-22104
Fine filtration: An attractive route towards lower helicopter operating costs 14 p2221 N85-23774
High-latitude filtering in a global grid-point model using model normal modes 18 p3140 N85-29442
The investigation of natural and artificial ice nuclei by the improved membrane filter method 21 p3642 N85-32626
Determination of sensitivity functions for discrete dynamic systems from results of function modeling on digital computer 22 p3769 N85-33359
Nonlinear filtration of clutter 22 p3777 N85-33404

FINANCE
Financial issues for commercial space ventures: Paying for the dreams 02 p0150 N85-11014
Siemens, Philips megaproject to yield superchip in 5 years 11 p1592 N85-20018
A microcomputer tutorial on spreadsheets and databases with a simulated budget preparation
[AD-A155516] 21 p3672 N85-32813

FINANCIAL MANAGEMENT
Space commercialization: Analysis of R and D investments with long time horizons 02 p0155 N85-11052
Satellite servicing: A business opportunity? 02 p0156 N85-11056
Development and testing of a rural credit supervision system at the level of counties and rural properties utilizing remote sensing techniques
[E85-10018] 02 p0217 N85-11431
Evaluation of the effectiveness of the weighted guidelines to induce contractor's investment in cost reducing facilities equipment
[AD-A147586] 07 p1053 N85-16681
Activities report of the aerospace industry in West Germany
[ISSN-0722-3838] 07 p1053 N85-16686
Activities report of the aerospace industry in West Germany
[ISSN-0722-3838] 07 p1054 N85-16687
Digest of the Deutsche Lufthansa report, 1983
[ISSN-0415-503X] 09 p1418 N85-18948
An analysis of a dynamic project cost problem
[CSIR-TWISK-338] 13 p2149 N85-23341
FRG journal analyzes state, prospects of airbus programs: General analysis 15 p2535 N85-25638
Management communication and financial modeling 15 p2627 N85-26190
Information technology applications in voluntary sector transport operations. SP1: Objectives and programme of work
[TT-8501] 15 p2667 N85-26457
A microcomputer tutorial on spreadsheets and databases with a simulated budget preparation
[AD-A155516] 21 p3672 N85-32813
User's operating procedures. Volume 1: Scout project financial analysis program
[NASA-CR-177949] 23 p3956 N85-34519

FINE STRUCTURE
Study of deformation and fracture of AMg6N weldable aluminum alloy by method of acoustic emission 03 p0352 N85-12266

EXAFS studies of sodium silicate glasses containing dissolved actinides
[DE84-015835] 04 p0479 N85-13051
Extended X-ray absorption fine structure (Exafs) studies of the actinides
[DE84-015833] 04 p0559 N85-13561
Surface structure determination with ARPEFS
[DE84-016904] 04 p0571 N85-13644
Asymmetrical harmonic oscillator and fine-structure constant
[FUB-9-1984] 09 p1401 N85-18818
Synchrotron X-ray fluorescence and extended X-ray absorption fine structure analysis
[DE85-003606] 10 p1438 N85-19063
Structural studies of sputtered Ni-As-O films
[DE85-003229] 11 p1605 N85-20095
Documentation for the machine-readable version of A Finding List for the Multiplet Tables of NSRDS-NBS 3, Sections 1-10 (Adelman, Adelman, Fischel and Warren 1984)
[NASA-TM-87440] 14 p2438 N85-25048
Fine structure of solar acoustic oscillations due to rotation 14 p2445 N85-25087
The intern. rotation of the Sun inferred from the rotational splitting of acoustic and gravity mode multiplets 14 p2449 N85-25122
Effect of zirconium on forming ultrafine-grained structure in Al-Mg-Zr alloy 15 p2513 N85-25504
Test of the electronic structure of Fe(100) by absorbed current spectroscopy
[DE85-004942] 15 p2661 N85-26422
Characterization of thin films and layered structures using X-ray absorption and reflection at grazing incidence
[DE85-006560] 15 p2662 N85-26429

FINES
Drying of pulverized material with heated condensible vapor
[DE85-011656] 22 p3783 N85-33438

FINGERS
Finger materials for air cushion vehicles. Volume 1: Flexible coatings for finger materials
[AD-A151438] 15 p2522 N85-25545

FINISHES
NT ENAMELS
NT GLAZES
NT LACQUERS

FINITE DIFFERENCE THEORY
Development and applications of algorithms for calculating the transonic flow about harmonically oscillating wings
[NASA-CR-172376] 01 p0002 N85-10007
ICARUS: A general one-dimensional heat conduction code
[DE84-016125] 01 p0047 N85-10310
Upwind compact finite difference schemes
[CSIR-TWISK-334] 01 p0110 N85-10742
Shock capturing finite difference algorithms for supersonic flow past fighter and missile type configurations
[NASA-CR-174051] 02 p0134 N85-10913
Finite-difference synthetic seismograms for SH waves
[AD-A145834] 03 p0392 N85-12508
Difference schemes for equations of Schrodinger type
[AD-A145812] 03 p0410 N85-12622
Return difference feedback design for robust uncertainty tolerance in stochastic multivariable control systems
[AD-A145861] 03 p0411 N85-12624
Simulation of separated transonic airfoil flow by finite-difference viscous-inviscid interaction 05 p0591 N85-13768
Numerical methods for bluff body aerodynamics 05 p0593 N85-13782
Numerical integrations of the Navier-Stokes equations for flow over surface-mounted obstacles 05 p0593 N85-13784
Numerical investigations into the parabolized Navier-Stokes equations 05 p0635 N85-14075
Implicit numerical methods in meteorology 05 p0586 N85-14408
A compact finite element method for elastic bodies
[NASA-CR-172467] 06 p0617 N85-15185
An exploratory study of finite difference grids for transonic unsteady aerodynamics
[NASA-TM-84583] 07 p0899 N85-15896
High Marangoni number convection in a square cavity
[NASA-CR-174283] 07 p0959 N85-16078
Laminar flow over a backward-facing step
[AD-A147469] 07 p0960 N85-16084
Finite difference calculations of buoyant convection in an enclosure. Part 2: Verification of the nonlinear algorithm
[PB85-104065/GAR] 07 p0961 N85-16089
A finite difference method for inverse mode calculations of a three-dimensional boundary layer
[ESA-TT-863] 09 p1274 N85-18007
Researched applied to transonic compressors in numerical fluid mechanics of inviscid flow and viscous flow
[NASA-CR-174353] 09 p1319 N85-18291
Accuracy of the finite analytic method for scalar transport calculations
[DE85-001474] 09 p1320 N85-18300
The implementation of irregular grid systems for the finite difference solution of partial differential equations
[LU-MATH-RES-181] 09 p1373 N85-18630
Boundary conditions for artificial dissipation operators — convection
[FFA-TN-1984-53] 09 p1375 N85-18642
Vectorization and implementation of an efficient multigrid algorithm for the solution of elliptic partial differential equations
[AD-A149049] 10 p1545 N85-19743
Numerical solution of semilinear elliptic problems on unbounded domains
[AD-A149559] 10 p1549 N85-19767
Developments in the simulation of compressible inviscid and viscous flow on supercomputers
[NASA-TM-86674] 11 p1575 N85-19924
A fast algorithm of the finite difference method for computation of the transonic flow past an arbitrary airfoil with the conservative full-potential equation 11 p1619 N85-20191
A mixed finite difference analysis of the internal and external transonic flow fields of inlets with centerbody 11 p1619 N85-20192
Finite difference method for solving turbulent boundary layer equations 11 p1619 N85-20193
Finite difference computation of the flow around airfoils in two-dimensional transonic slotted wall wind tunnel 11 p1623 N85-20216
Calculation of oscillating turbulent flows in open channels
[KU-SFB-80/T/228] 11 p1633 N85-20289
Spectral methods in time for parabolic problems
[NASA-CR-172539] 11 p1706 N85-20730
The split-coefficient matrix method for supersonic three dimensional flow 12 p1821 N85-21425
Numerical studies of fluid spin-up from rest in a partially-filled cylinder
[AD-A150079] 12 p1847 N85-21586
Robust calculation of three-dimensional transonic potential flow based on the nonlinear gas multigrid method and a mixed incomplete lower upper decomposition/strongly implicit procedure (ILU/SIP) algorithm
[NLR-MP-84003-U] 12 p1848 N85-21593
Structural sensitivity analysis: Methods, applications and needs
[NASA-TM-85827] 12 p1865 N85-21695
Intensification of tropical instabilities
[AD-A149885] 12 p1896 N85-21899
Asymptotics for configural estimators
[AD-A150106] 12 p1924 N85-22087
Workshop on Nuclear Dynamics 3
[INC-40007-24] 12 p1931 N85-22130
Machine analysis of resonance characteristics of plate-type radio electronic equipment constructions 13 p2085 N85-23018
Calculation of level surface in problems of large-scale ocean circulation 13 p2108 N85-23136
Parallel processing for computational continuum dynamics
[AD-A150513] 13 p2147 N85-23327
Application of adaptive grids in solving the partial differential equations governing fluid flow
[AD-A151175] 15 p2555 N85-25766
Vibration and buckling of rotating, pretwisted, precned beams including Coriolis effects
[NASA-TM-87004] 15 p2577 N85-25883
Inviscid upwind finite difference model for two dimensional vertical axis wind turbines 15 p2585 N85-25933
Recent progress in the development and application of the parabolic equation
[AD-A151475] 15 p2637 N85-26265
Some numerical analyses of flows with seperation 16 p2692 N85-26616
Finite-difference computations of rotor loads
[NASA-TM-86682] 16 p2700 N85-26689
A computer analysis program for interfacing thermal and structural codes
[NASA-TM-87021] 16 p2800 N85-27284
Error reduction program — combustor performance evaluation codes
[NASA-CR-174776] 16 p2852 N85-27584
Evaluation of an algorithm for the solution of the time-dependent Euler equations
[AD-A151993] 16 p2864 N85-27600
Analysis and modeling for thermal focal plane arrays
[AD-A153158] 17 p2968 N85-28329
A discussion of adaptive grids and their applicability in numerical hydrodynamic modeling
[AD-A151843] 17 p3017 N85-28859
Spatial differencing for finite difference codes
[DE85-009902] 17 p3021 N85-28884
A numerical solution technique for multitemperature plasma hydrodynamics
[AD-A152701] 17 p3039 N85-28901
A study of aerodynamic control in stalled flight long laminar separation bubble analysis
[AD-A153650] 18 p3059 N85-28930
Numerical simulation of unsteady motion in a turbulent mixing layer
[NAL-TR-849T] 18 p3099 N85-29183
Limiting processes laser CVD
[DE85-008848] 18 p3114 N85-29279
A model for the combustion of polymethyl methacrylate in air in a laminar diffusion flame
[VTH-LR-439] 18 p3165 N85-29606
Intermediate boundary conditions for LOD, ADI and approximate factorization methods
[NASA-CR-172501] 18 p3167 N85-29626
Shock capturing
[NASA-CR-172502] 18 p3168 N85-29627
Study of second order upwind differencing in a recirculating flow
[NASA-CR-174939] 19 p3264 N85-30243
On the convergence of difference approximations to scalar conservation laws
[NASA-CR-172614] 19 p3344 N85-30726
Floating shock-fitting in transonic potential flow calculations 20 p3387 N85-31007
An implicit finite-difference code for a two-equation turbulence model for three-dimensional flows
[NASA-TM-86752] 20 p3454 N85-31448
Nonnewtonian, unsteady flow in a convergent divergent duct 20 p3456 N85-31463
Generation of three-dimensional body-fitted coordinates using hyperbolic partial differential equations
[NASA-TM-86753] 20 p3519 N85-31887
Calculation of transonic steady and oscillatory pressures on a low aspect ratio model and comparison with experiment
[NASA-TM-86449] 21 p3551 N85-32062
A numerical study of Taylor-Vortex flow
[AD-A154787] 21 p3584 N85-32277
Performance evaluation of flow in turbomachinery blade rows 21 p3587 N85-32299
Numerical solution of the Navier-Stokes equations for 3-D internal flows: An emerging capability 21 p3588 N85-32300
An investigation into the comparisons of the underwater shock effects on a stiffened flat plate to the predictive nature of a computer model
[AD-A155612] 21 p3600 N85-32355
Generalized formulation of a class of explicit and implicit TVD schemes
[NASA-TM-86775] 21 p3675 N85-32830
Oscillatory solutions of the Peaceman-Rachford alternating direction implicit method and a comparison of methods for the solution of the two dimensional heat diffusion equation
[AD-A154670] 21 p3675 N85-32833
Gradient scaling for nonuniform meshes
[DE85-009625] 22 p3784 N85-33443
Selecting step sizes in sensitivity analysis by finite differences
[NASA-TM-86382] 22 p3799 N85-33538
KIVA computer program for multidimensional chemically reactive fluid flows with fuel sprays
[DE85-012730] 22 p3830 N85-33722
Use of a hyperbolic grid generation scheme in simulating supersonic viscous flow about three-dimensional winged configuration
[NASA-TM-85344] 23 p3893 N85-34116
A versatile computer package for mechanism analysis 23 p3924 N85-34314
Block-implicit calculations of three-dimensional laminar flow in strongly curved ducts
[DE85-003047] 23 p3931 N85-34363
Numerical and analytic descriptions of cosmic-ray transport
[SH-4.1-4] 23 p4005 N85-34830
Finite analytic solutions of supersonic flows in two-dimensional non-symmetrical channels 24 p4059 N85-35154
Numerical studies of 2-dimensional flows
[NASA-CR-3930] 24 p4060 N85-35160
Two-dimensional numerical modeling of ion implanted GaAs MESFET devices 24 p4088 N85-35341
Stress analysis of axisymmetric sandwich shells of variable thickness 24 p4101 N85-35419
Thermal evolution of coastal California with implications for hydrocarbon maturation 24 p4115 N85-35509

Three-dimensional finite deformation viscoelastic model accounting for damage effects
[DE85-012951] 24 p4139 N85-35660
The finite element-difference method
24 p4141 N85-35672

FINITE ELEMENT METHOD
Finite element computation on nearest neighbor connected machines 01 p0057 N85-10379
Initial experience with distributing structural calculations among computers operating in parallel
01 p0058 N85-10381
Performance of the h, p and h-p versions
01 p0058 N85-10383
Augmented weak forms and element-by-element preconditioners: Efficient iterative strategies for structural finite elements. A preliminary study
01 p0058 N85-10384
Stress-derivative control of kayostoning deformation in finite element codes 01 p0058 N85-10385
A triangular finite element for thin plates and shells
01 p0058 N85-10386
Crashworthiness of light aircraft fuselage structures: A numerical and experimental investigation
01 p0060 N85-10399
Finite element modelling of buried structures
01 p0061 N85-10403
On the computer analysis of structures and mechanical systems 01 p0061 N85-10404
Solution of contaminant transport equations using an orthogonal-upstream finite element scheme
[DE84-014266] 01 p0070 N85-10483
Applications of a finite-element regional model to very-short-range forecasting 01 p0080 N85-10531
Recursive calculation of curved finite element stiffness matrices
[CSIR-TWISK-303] 01 p0108 N85-10726
Constitutive model development for isotropic materials
02 p0144 N85-10975
The CMC/3DPNS computer program for prediction of three-dimensional, subsonic, turbulent aerodynamic juncture region flow. Volume 3: Programmers' manual
[NASA-CR-165998] 02 p0197 N85-11318
Finite element analysis of thermoelasticity problems
02 p0208 N85-11369
STARS: A general-purpose finite element computer program for analysis of engineering structures
[NASA-RP-1129] 02 p0209 N85-11378
Parallel triangularization of substructured finite element problems
[NASA-CR-172468] 02 p0241 N85-11569
A finite element projection method for the solution of particle transport problems with anisotropic scattering
[AD-A145362] 02 p0250 N85-11637
Numerical methods for singularly perturbed differential equations with applications
[AD-A145839] 02 p0252 N85-11650
Pointwise iterations of finite element modeling of advection-diffusion equations
[DE84-015284] 02 p0253 N85-11656
A finite element method for the solution of two-dimensional transonic flows in cascades
[PNR-90216] 03 p0316 N85-12045
A comparative study of the finite element and boundary element methods as applied to a boundary value problem of a harmonic function
[AD-A146018] 03 p0411 N85-12627
Moving finite elements in 2-D
[AD-A146266] 03 p0412 N85-12637
Analysis of piezoelectric disks and cylinders using finite element method
[AD-A146323] 03 p0414 N85-12650
Numerical calculations of stratified Ekman layer flow over ridges with a finite element model
[DE84-014482] 04 p0499 N85-13179
Finite element method for a class of viscoelastic flows in deforming domains applied to jet breakup
[DE84-014571] 04 p0500 N85-13186
NIKE3D: An implicit, finite-deformation, finite element code for analyzing the static and dynamic response of three-dimensional solids, revision 1
[DE84-017161] 04 p0514 N85-13277
Comparison of free component mode synthesis techniques using MSC/NASTRAN
[DE84-014451] 04 p0514 N85-13278
The determination of eddy current losses in electrical equipment
[DE84-016340] 05 p0632 N85-14050
A finite element method for three dimensional cavity circulation 05 p0635 N85-14071
Dynamic testing of NOVA laser switchyard tower
[DE84-014450] 05 p0640 N85-14103
Finite element method calculation of a necking tension specimen including heat transfer influence
[RUB-IFM-MITT-40] 05 p0648 N85-14162
Some error estimates for the p-version of the finite element method
[CTH-MATH-1984-21] 05 p0719 N85-14614
A lumped mass finite element method with quadrature for a nonlinear parabolic problem
[CTH-MATH-1984-22] 05 p0719 N85-14615
Applications of finite and wave envelope element approximations to acoustic radiation from turbofan engine inlets in flight 05 p0726 N85-14664
Element methods for calculation of sound fields
[RUB-IFM-MITT-41] 05 p0726 N85-14665
A study of crashworthiness of light aircraft fuselage structures: A numerical and experimental investigation
[UTIAS-286] 06 p0750 N85-14803
Iterative method of calculating strength of airframe members using finite element method
06 p0775 N85-14955
Process Modeling Applied to Metal Forming and Thermo-mechanical Processing
[AGARD-LS-137] 06 p0796 N85-15086
Finite element simulation of forging processes
06 p0797 N85-15093
Computer-aided design of extrusion dies by metal-flow simulation 06 p0797 N85-15094
A simple extension to multidimensional problems of the artificial viscosity due to Lapidus
06 p0808 N85-15134
A compact finite element method for elastic bodies
[NASA-CR-172487] 06 p0817 N85-15185
Verification of a computer program for vibration analysis of composite wing cores
[NAL-TR-825] 06 p0817 N85-15187
CFM 56-2. Oligocyclic fatigue of the turbofan disk: Dimensionning and tests for verification and improvements 07 p0908 N85-15750
A study of interply layer effects on the free-edge stress field of angleplied laminates
[NASA-TM-86924] 07 p0919 N85-15822
Finite element procedures applicable to nonlinear analysis of reinforced concrete shell structures
[AD-A146796] 07 p0978 N85-16209
Buckling analysis of cracked, floating ice sheets
[AD-A147330] 07 p0988 N85-16277
Feedback, adaptivity and A-posterior estimates in finite elements: Aims, theory and experience
[AD-A146869] 07 p1029 N85-16531
Solution of finite element problems by preconditioned conjugate gradient and Lanczos methods
[AD-A146921] 07 p1029 N85-16532
Performance of the h, p and h-p versions of the finite element method
[AD-A146940] 07 p1029 N85-16535
A counterexample to a result of Strang and Fix concerning controlled approximation
[AD-A147360] 07 p1032 N85-16550
Splitting methods for the numerical solution of the incompressible Navier-Stokes equations
[AD-A147463] 07 p1032 N85-16554
Analysis of a penalty finite element approximation of the Navier Stokes equations 08 p1161 N85-17321
Finite element calculation for a Y-joint and comparison of results with strain measurements
[BLL-RISLEY-TR-4526-(9091.9F)]
08 p1171 N85-17381
Computational methods for nonlinear dynamics problems in solid and structural mechanics
[AD-A148352] 08 p1172 N85-17392
Response of saturated porous nonlinear materials to dynamic loadings
[AD-A148528] 08 p1173 N85-17394
A moving finite element method for time dependent partial differential equations with error estimation and refinement
[AD-A147719] 08 p1210 N85-17617
A local refinement finite element method for time dependent partial differential equations
[AD-A147943] 08 p1211 N85-17620
A feedback finite element method with a posteriori error estimation. Part 1. The finite element method and some basic properties of the A posteriori error estimator
[AD-A148345] 08 p1212 N85-17631
Analytical and experimental investigation of rubbing interaction in labyrinth seals for a liquid hydrogen fuel pump — space shuttle main engine
[NASA-CR-174857] 09 p1287 N85-18084
Nonlinear analysis of composite laminates
09 p1288 N85-18087
Defect tolerance in pipeline girth welds
[ERS-E.353] 09 p1328 N85-18347
Finite element computation of structural design sensitivity analysis 09 p1330 N85-18353
A finite element analysis of viscoelastic materials with varying time scales 09 p1330 N85-18355
Extrpolation in finite element analysis
09 p1331 N85-18365
finite element analysis of bi-material systems with applications in hydraulic fracturing
09 p1332 N85-18369
Existence, uniqueness and stability conditions for general finite element methods in linear elasticity
09 p1332 N85-18372
Nonlinear finite element analysis of elastic and elastic-plastic buckling of cylinders under complex combined loads 09 p1332 N85-18373
Alternative shock characterizations for consistent shock test specifications 09 p1335 N85-18396
Determination of shear coefficient of a general beam cross section by finite element method
09 p1338 N85-18413
System software for the finite element machine
[NASA-CR-3870] 09 p1372 N85-18622
A 3-dimensional mass conserving element for compressible flows
[NASA-CR-172513] 09 p1373 N85-18626
Grouser effect studies
[AD-P004278] 09 p1406 N85-18854
Condensed antenna structural models for dynamics analysis 10 p1463 N85-19230
Finite element analysis of nonlinear oscillations and flutter of shells of revolution
[AD-A149071] 10 p1496 N85-19440
A program design for an adaptive, non-linear finite element solver
[AD-A148880] 10 p1539 N85-19705
SOLIDGEN: A solid finite element data generator. User's manual
[AD-A149490] 10 p1541 N85-19715
Controlled approximation and a characterization of the local approximation order
[AD-A149095] 10 p1546 N85-19750
Calculation of transmission line impedances using the ANSYS finite element program
[DE84-016715] 11 p1629 N85-20261
Local strain redistribution corrections for a simplified inelastic analysis procedure based on an elastic finite-element analysis
[NASA-TP-2421] 11 p1651 N85-20396
Dynamic investigations of a spherical tank structure filled with liquid using ANSYS three-dimensional fluid elements
[MBB-UR-E-737-83-O] 11 p1654 N85-20418
Resolution of 2-dimensional seismologic problems by a finite element approximation. Application to the Love wave propagation through the Atlantic border of the Iberic Peninsula 11 p1681 N85-20594
Resolution of 2-dimensional seismologic problems by a finite element approximation. Application to the Love wave propagation through the Atlantic border of the Iberic Peninsula. Appendix: Graphs of results — Lagrange coordinates 11 p1681 N85-20595
PASLIB programmer's guide for the finite element machine, revision 2.1-A
[NASA-CR-172281] 11 p1705 N85-20727
Finite element method for solving neutron transport problems
[DE85-001075] 11 p1722 N85-20829
Si-on-insulator formation using a line-source electron beam
[DE85-003449] 11 p1737 N85-20925
Advanced stress analysis methods applicable to turbine engine structures
[NASA-CR-175573] 12 p1778 N85-21165
Nonlinear analysis for high-temperature multilayered fiber composite structures — turbine blades
[NASA-TM-83754] 12 p1797 N85-21273
Algorithm for the simulation of transient viscoelastic flows with free surfaces
[DE85-002713] 12 p1848 N85-21590
Finite element analysis of problems associated with life enhancement techniques
[ARL/STRUC-R-404] 12 p1862 N85-21676
3-D inelastic analysis methods for hot section components (base program) — turbine blades, turbine vanes, and combustor liners
[NASA-CR-174700] 12 p1863 N85-21686
Recent advances in hybrid/mixed finite elements
[NASA-CR-175574] 12 p1863 N85-21687
A study of coupling the boundary and finite element methods in two-dimensional elastostatics
[AD-A149619] 12 p1865 N85-21702
A solution method for large deformation contact problems
[AD-A149842] 12 p1866 N85-21707
Nonlinear analysis of layered composite plates and shells
[PB85-127181] 12 p1868 N85-21719
Geometrically nonlinear analysis of laminated elastic structures
[NASA-CR-175609] 12 p1868 N85-21720

A 3-D treatment of convective flow in the Earth's mantle
[DE85-003734] 12 p1890 N85-21883
On the accuracy of least squares methods in the presence of corner singularities
[NASA-CR-172552] 12 p1919 N85-22050
Experimental and numerical analysis of electric currents and electromagnetic blunting of cracks in thin plates
[AD-A150418] 13 p2022 N85-22669
Micromechanical modeling of microstructural damage in creeping alloys
[DE85-003925] 13 p2022 N85-22671
Analysis of interaction of dynamically adjustable gyroscopes on elastic platform by finite-element method 13 p2048 N85-22822
Pre- and post-processing for stream-function eddy current calculations
[AD-A150417] 13 p2065 N85-22896
HPFTP flow diverter analysis
[NASA-CR-171424] 13 p2091 N85-23057
On Hybrid and mixed finite element methods
[NASA-CR-175551] 13 p2101 N85-23096
Advanced life analysis methods. Volume 2: Crack growth analysis methods for attachment lugs
[AD-A150420] 13 p2103 N85-23109
Exploiting parallel computing with limited program changes using a network of microcomputers
[NASA-TM-86387] 13 p2146 N85-23318
User's and programmer's guide to the mechanics of moving finite element code
[DE85-006165] 13 p2152 N85-23365
Magnetic field interactions with material discontinuities
[AD-A150197] 13 p2154 N85-23373
Unified constitutive material models for nonlinear finite-element structural analysis — gas turbine engine blades and vanes
[NASA-TM-86985] 14 p2320 N85-24338
Stress in axially symmetrical heavy metal projectiles during discharge — numerical simulation
[ISL-CO-219/83] 14 p2321 N85-24345
Finite element model for creep in composite masonry
[PB85-150324] 14 p2322 N85-24347
Space Mathematics for the Preparation and Development of satellite Exploitation
[ISBN-2-85428-115-2] 14 p2395 N85-24753
Finite element methods in space mathematics 14 p2396 N85-24757
Runstreams for using ASKA
[NIAST-84/27] 14 p2403 N85-24812
Implementation of a C1 triangular element based on the p-version of the finite element method
[AD-A150904] 14 p2404 N85-24825
Constrained parabolic approximation of curves in the finite element method
[CSIR-TWISK-340] 14 p2408 N85-24843
Finite Element Methods in South Africa 1983 — conference
[S-332] 14 p2410 N85-24863
Design, fabrication and test of composite curved frames for helicopter fuselage structure
[NASA-CR-172438] 15 p2470 N85-25247
Summary of recent investigations of the mechanical properties of polycrystalline solids
[DE85-006776] 15 p2511 N85-25492
A finite element, Navier-Stokes study of the confined, laminar flow over a downstream facing step 15 p2553 N85-25754
Thirteenth NASTRAN Users' Colloquium
[NASA-CP-2373] 15 p2573 N85-25863
New enhancements in April 85 NASTRAN release 15 p2573 N85-25864
Crack elements for COSMIC/NASTRAN 15 p2573 N85-25866
Layered composite analysis capability 15 p2573 N85-25868
NPLOT: An interactive plotting program for NASTRAN finite element models 15 p2573 N85-25869
COSMIC/NASTRAN-PATRAN interface 15 p2574 N85-25870
Isoparametric 3-D finite element mesh generation using interactive computer graphics 15 p2574 N85-25873
A new NASTRAN capability for data reduction 15 p2574 N85-25874
Symmetric composite laminate stress analysis 15 p2575 N85-25878
On the interconnection of incompatible solid finite element meshes using multipoint constraints 15 p2575 N85-25879
NASTRAN's application in agricultural engineering 15 p2575 N85-25880
Use of COSMIC NASTRAN in a design department 15 p2575 N85-25881
An elastic analysis of a plated bone to determine fracture gap motion 15 p2575 N85-25882
Learjet Model 55 wing analysis with landing loads 15 p2575 N85-25883
Fillet weld stress using finite element methods 15 p2576 N85-25884
The structural finite element model of the C-5A 15 p2576 N85-25885
Using NASTRAN to model missile inertia loads 15 p2576 N85-25886
Experience with free bodies 15 p2576 N85-25887
NASTRAN analysis comparison to shock tube tests used to simulate nuclear overpressures 15 p2576 N85-25888
Finite element prediction of loss factors for structures with frequency-dependent damping treatments 15 p2576 N85-25889
Direct transient analysis of a fuze assembly by axisymmetric solid elements 15 p2576 N85-25890
Transient analysis of a magnetic heat pump 15 p2576 N85-25891
Effect of internal pressure on flexibility and stress intensification factors for pipe elbows analyzed by the finite element method
[AD-A151161] 15 p2578 N85-25901
An experimental investigation into the dynamic response of a stiffened flat plate loaded impulsively by an underwater shockwave
[AD-A151321] 15 p2578 N85-25903
Crack closure characteristics considering center cracked and compact tension specimens
[AD-A151702] 15 p2579 N85-25907
GRID: A FORTRAN program for using a digitizing table to enter a finite element GRID
[AD-A151317] 15 p2628 N85-26196
Enhanced thermal-structural analysis by integrated finite elements
[AD-A151103] 15 p2636 N85-26258
Development of a dynamic finite element model for unrestrained flexible structures
[AD-A151178] 15 p2636 N85-26259
SPLOT: A plot program for finite element data, function versus distance
[DE85-007129] 15 p2636 N85-26273
Sliding interfaces with contact-impact in large scale Lagrangian computations
[DE85-006451] 15 p2639 N85-26277
Two computational methods for cascade flows 16 p2692 N85-26617
The effect of inaccuracies in structural models on the control of large space structures
[AD-A151794] 16 p2732 N85-26858
Theoretical and experimental comparisons of nearfield electrogalvanic fields due to nonlinear polarization layers
[AD-A152085] 16 p2779 N85-27149
Solution of Oseager's equation for a rotating compressible fluid in a multiply-connected domain
[DE85-007048] 16 p2784 N85-27178
Computer modeling of vibrational energy levels of potential laser candidates (dielomic molecules)
[AD-A151765] 16 p2790 N85-27209
Automatic tracking of crack growth via finite elements 16 p2797 N85-27246
Finite axisymmetric deformation of a thin shell of revolution 16 p2798 N85-27251
A computer analysis program for interfacing thermal and structural codes
[NASA-TM-87021] 16 p2800 N85-27264
The nonlinear analysis of thick composite plates using a cubic spline function
[AD-A152115] 16 p2801 N85-27268
Numerical resolution calculation for elastic-plastic impact problems
[AD-A152292] 16 p2801 N85-27270
Hopkinson bar simulation using DYNA2D
[DE85-006766] 16 p2802 N85-27275
Stress analysis of the space telescope focal plane structure joint
[NASA-CR-176797] 16 p2803 N85-27284
A general purpose scatter storage subsystem and a comparison of hashing methods
[NASA-CR-175814] 16 p2845 N85-27542
Finite elements and the method of conjugate gradients on a concurrent processor
[NASA-CR-175812] 16 p2853 N85-27588
Analysis of the convergence of mixed finite element methods
[HTKK-MAT-A227] 16 p2856 N85-27613
Probabilistic finite element development 17 p2913 N85-27958
Probabilistic finite element: Variational theory 17 p2913 N85-27957
Designing for fiber composite structural durability in hygrothermomechanical environment
[NASA-TM-87045] 17 p2917 N85-27978
Analytical shear buckling investigation of curved composite panels
[AD-A153136] 17 p2980 N85-28421
Field theory analysis using the finite element method to determine the deliberation curves of three dimensional fracture mechanics specimens with a semicircular surface crack applying the electrical direct current potential method for crack depth measurement
[GKSS-84-E-53] 17 p2982 N85-28434
Implementation of a general finite element code on an IBM PC compatible microcomputer
[AD-A152681] 17 p3011 N85-28615
TRINITY: A pre- and post-processing program for 2-dimensional finite element data
[DE85-008029] 17 p3013 N85-28628
Numerical benchmark study for the finite element computer code NEPTUNE
[DE85-008400] 17 p3013 N85-28630
A high-accuracy optical linear algebra processor for finite element applications
[NASA-CR-175894] 17 p3017 N85-28658
A discussion of adaptive grids and their applicability in numerical hydrodynamic modeling
[AD-A151843] 17 p3017 N85-28659
A fast implementation of explicit time stepping algorithms with the finite element method for a class of nonlinear evolution problems
[REPT-84-03] 17 p3021 N85-28686
Finite element thermal-structural analysis of cable-stiffened space structures
[AD-A153822] 18 p3066 N85-28993
Localized ionic currents from a corroding iron-copper galvanic couple
[AD-A153627] 18 p3074 N85-29011
Structural Analysis
[DFVLR-MITT-84-21] 18 p3120 N85-29313
Field consistency and the finite element analysis of multifield structural problems 18 p3120 N85-29316
Scattering by distributions of small thin particles 19 p3253 N85-30172
Use of a two-dimensional flow model to quantify aquatic habitat
[AD-A154287] 19 p3266 N85-30253
Comparison and evaluation of field and numerical results from the Site A heater test at Avery Island
[DE85-010625] 19 p3268 N85-30269
Forced structural response using component mode synthesis
[DE85-006479] 19 p3287 N85-30383
Three-dimensional finite element impact analysis of a nuclear waste truck cask
[DE85-010653] 19 p3288 N85-30389
Combined finite element meshing technique using SUPERTAB
[DE85-011393] 19 p3340 N85-30696
Nested dissection on a mesh-connected processor array
[AD-A154088] 19 p3342 N85-30711
Extrapolation methods in the finite element method
[BONNER-MATHE-SCHR-158] 19 p3345 N85-30729
Asymptotic expansions for finite element eigenvalues and finite element solution 19 p3345 N85-30730
Asymptotic expansions for the finite element approximation of parabolic functions 19 p3345 N85-30731
Superconvergence of finite element approximation for Navier-Stokes equations 19 p3345 N85-30732
Space station parametric models 20 p3413 N85-31180
A control concept for large flexible spacecraft using order reduction techniques 20 p3415 N85-31193
Delamination micromechanics analysis
[NASA-CR-172598] 20 p3422 N85-31237
SPAR improved structural-fluid dynamic analysis capability
[NASA-CR-171549] 20 p3454 N85-31449
A new finite element approach: Progress in inviscid flow computations
[NASA-TM-86434] 20 p3454 N85-31450
Application of finite element method to the sizing of mechanical parts — helicopter design
[SNIAS-851-210-105] 20 p3463 N85-31515
Constitutive modeling of superalloy single crystals and directionally solidified materials 20 p3466 N85-31535
A numerical algorithm for endochronic plasticity and comparison with experiment 20 p3467 N85-31539
Finite element modeling of cracked bodies using the Bodner-Partom flow law 20 p3468 N85-31547
Nonlinear analysis of an axisymmetric structure subjected to non-axisymmetric loading 20 p3468 N85-31549
Efficient solution methods for nonlinear finite element analysis 20 p3519 N85-31886
A variable node finite element method applied to the gas dynamics equations
[AD-A155211] 21 p3584 N85-32281

Ductile fracture of dynamically loaded naval structures-compact tension specimen tests and analyses
[AD-A155472] 21 p3600 N85-32353
An investigation into the comparisons of the underwater shock effects on a stiffened flat plate to the predictive nature of a computer model
[AD-A155612] 21 p3600 N85-32355
Analysis of inclined growth of silicon sheet
21 p3612 N85-32442
Edge-defined film-fed growth of thin silicon sheets
21 p3612 N85-32443
Concurrent implementation of the Crank-Nicolson method for heat transfer analysis
[NASA-TM-86445] 21 p3674 N85-32822
DYNA3D, INGRID, and TAURUS: An integrated, interactive software system for crashworthiness engineering
[DE85-010928] 21 p3677 N85-32846
Photo-acoustic effect in finite-dimensional semiconductors 21 p3682 N85-32876
Finite element methods for viscoelastic flow
[AD-A154877] 22 p3783 N85-33437
Selecting step sizes in sensitivity analysis by finite differences
[NASA-TM-86362] 22 p3799 N85-33536
Elevated temperature crack growth
[NASA-CR-174057] 22 p3799 N85-33540
A review of path-independent integrals in elastic-plastic fracture mechanics, task 4
[NASA-CR-174956] 22 p3799 N85-33541
Sideline verification for multilayer pressure vessels and piping analysis including strain hardening
[DE85-005616] 22 p3801 N85-33549
SANCHO: A finite element computer program for the quasistatic, large deformation, inelastic response of two-dimensional solids
[DE85-011456] 22 p3829 N85-33714
Numerical simulation of interior and terminal ballistics phenomena. Investigation of the effects of the parameters and application examples
[ISL-R-112/84] 22 p3831 N85-33731
Behaviors of stress waves in a conical bar
23 p3904 N85-34182
Experimental study of collapse of thick-walled tube under external pressure and axial force
23 p3904 N85-34186
Proceedings of the Mechanisms Conference, volume 1 23 p3923 N85-34309
Proceedings of the Mechanisms Conference, volume 2 23 p3924 N85-34318
An introduction to finite elements
23 p3924 N85-34319
Inertial stresses and deformations in mechanisms
23 p3924 N85-34320
Thermal stress analysis of a new turbine shroud seal concept
[NASA-TM-87062] 23 p3938 N85-34406
Three-dimensional finite element failure model for predicting failure in fibre reinforced bolted joints
[BR94778] 23 p3940 N85-34423
Stresses and strains in a plate resulting from two closely-spaced interference-fit fasteners
[ARL/STRUC-TM-409] 23 p3941 N85-34429
FEMALE: Finite Element Method for Arbitrary Lagrangian and Eulerian elements
23 p3979 N85-34671
Analysis of incompressible cascade flows using state-of-the-art computer programs
[AD-A155850] 24 p4062 N85-35173
Design and behavior of coped beams
24 p4100 N85-35417
Stress-intensity factors for circumferential surface cracks in pipes and rods under tension and bending loads
[NASA-TM-87594] 24 p4101 N85-35424
Prediction of plasticity characteristics for three-dimensional fracture specimens comparison with experiment
[AD-A156425] 24 p4102 N85-35430
The finite element-difference method
24 p4141 N85-35672
A new method for boundary value problems
[AD-A155934] 24 p4143 N85-35683

FINITE IMPULSE RESPONSE FILTERS
U FIR FILTERS

FINITE VOLUME METHOD
Theoretical contributions to transonic flow analysis for transport aircraft
[BMFT-FB-W-84-038] 08 p1076 N85-16838
Thermodynamic evaluation of transonic compressor rotors using the finite volume approach
[NASA-CR-175811] 16 p2708 N85-26712
Unsteady flow in multistage turbines
17 p2911 N85-27946
Calculation of flow around the SF 310 airplane using a full potential equation method
[FFA-TN-1984-63] 20 p3389 N85-31022

FINITE-STATE MACHINES
U TURING MACHINES

FINLAND
Space activities in Finland 08 p1231 N85-17754
Finnair, LOT, SAS reps in USSR on present operations, plans 09 p1278 N85-18035
Precipitation and snow cover data, 1977
[ISBN-951-697-215-2] 17 p2995 N85-28514

FINS
NT COOLING FINS
NT NOSE FINS
The effect of channel convergence on heat transfer in a passage with short pin fins
[NASA-TM-83801] 01 p0046 N85-10303
An experimental study on the induced normal force on tail-fins due to wing-tail interference
[NAL-TR-814] 03 p0318 N85-12051
Oil-flow study of a Space Shuttle orbiter tip-fin controller
[NASA-TM-86276] 04 p0460 N85-12920
Finlet injector
[AD-D011245] 06 p0765 N85-14891
Repair of composites 06 p1120 N85-17058
Modeling and simulation of a fin actuation system
[AD-A149443] 10 p1428 N85-19005
Optimization of a ground coupled heat pump
[DE85-000273] 10 p1486 N85-19380
An exploratory investigation of sharp fin-induced shock wave/turbulent boundary layer interactions at high shock strengths
[AD-A151571] 15 p2556 N85-25772
Subsonic and transonic aerodynamics of a wraparound fin configuration
[AD-A153646] 18 p3059 N85-28927
A computation of fin-line impedance
[AD-A154080] 19 p3258 N85-30204
Fin line filters technology and electronic warfare
[AD-A154975] 21 p3576 N85-32237
Film condensation of steam on externally finned horizontal tubes
[AD-A155642] 21 p3585 N85-32285
Computer simulation of a cruise missile using brushless dc motor fin control
[AD-A155935] 24 p4089 N85-35349

FIR FILTERS
Use of Walsh functions for calculating characteristics of digital filters with impulse response of finite duration
13 p2083 N85-23011

FIRE CONTROL
Voice command weapons launching system
[AD-D011378] 07 p0937 N85-15940
Methodology improvement program for the second generation mine distance radar (MIDI 2)
[AD-A148467] 08 p1153 N85-17281
Acta Electronica Sinica (selected articles)
[AD-A148829] 11 p1628 N85-20252
Ground evaluation of helicopter air-to-air warfare
13 p1967 N85-22360
Research Flight Simulator for Helicopters (RFSH): Description and application to fire control system design
[SNIAS-851-210-106] 20 p3393 N85-31050

FIRE DAMAGE
Testing of three different flight suits in fire environment — fuel fire
[FOA-C-59012-H1] 02 p0238 N85-11552
Post fire interview: Development and field validation of the behavioral sequence interview technique
[NBS-GCR-84-477] 04 p0454 N85-12881
Thermal radiation hazards from Liquified Petroleum Gas (LPG) fireballs
[VTT-304] 09 p1293 N85-18122
Pathophysiological study of poisoning due to thermal degradation of materials — aircraft cabins
[CERMA-84-15] 11 p1692 N85-20640
The role of aircraft panel materials in cabin fires and their properties
[FAA-CT-84-30] 21 p3553 N85-32104
Photovoltaic module spread-of-flame testing
21 p3612 N85-32448

FIRE EXTINGUISHERS
Flow of nitrogen-pressurized Halon 1301 in fire extinguishing systems
[NASA-CR-174271] 07 p0900 N85-15701
Aircraft skin penetrator and agent applicator. Volume 1: Working model development and construction
[AD-A150406] 13 p1970 N85-22374

FIRE FIGHTING
The experimental mod 3 firefighters' aluminized crash-rescue, fire-proximity hood
[AD-A144993] 01 p0098 N85-10655
Fire research publications, 1983
[PB84-217066] 03 p0343 N85-12208
Suppression and control of Class C cargo compartment fires
[FAA-CT-84-21] 12 p1773 N85-21133
Firefighters' communication transceiver test plan
[NASA-CR-171419] 13 p2053 N85-22654
Aircraft skin penetrator and agent applicator. Volume 2: Test and evaluation
[AD-A151609] 15 p2466 N85-25225
Fire protection review revisit no. 2, Argonne National Laboratory, Argonne, Illinois
[DE85-013245] 22 p3755 N85-33276
Fire research publications, 1984
[PB85-208502] 24 p4166 N85-35827

FIRE PREVENTION
Fire research publications, 1983
[PB84-217066] 03 p0343 N85-12208
Fire prevention and control
[GPO-30-743] 04 p0482 N85-13074
The development of fire evaluation system for detention and correctional occupancies
[NBSIR-84-2976] 10 p1459 N85-19192
Legislation to improve airline safety
[GPO-38-222] 12 p1773 N85-21132
Fire resistant polymers based on 1-(diorgano oxyphosphonyl)methyl-2,4- and 2,6-diamino benzenes
[NASA-CASE-ARC-11512-2] 12 p1811 N85-21362
Test results from a comparative evaluation of a condensation nuclei fire detector
[NASA-CR-3674] 12 p1862 N85-21675
Fiscal year 1986 technical objective document
[AD-A151039] 14 p2432 N85-25000
Hazards in welding due to oxygen changes in the workplace atmosphere
[BLL-WI-TRANS-664-(9312.57)]
16 p2792 N85-27224
Evaluation of pyrotechnic fire suppression system for six pyrotechnic compositions
[AD-A152995] 17 p2937 N85-28130
Practical real-time quality control of antimisting kerosene
[DE/FAA/CT-85/1] 18 p3083 N85-29072
Fire protection review revisit no. 2, Argonne National Laboratory, Argonne, Illinois
[DE85-013245] 22 p3755 N85-33276
Scaling parameters of flashover
[NBS-GCR-85-497] 23 p3911 N85-34229
Review of zirconium-zircaloy pyrophoricity
[DE85-011169] 23 p3916 N85-34270
Investigation of experimental lightweight firewall materials for A/C engine bay applications
[AD-A155765] 24 p4062 N85-35175
Proceedings of the 7th Joint Panel Meeting of the UJNR Panel on Fire Research and Safety
[PB85-190545] 24 p4085 N85-35317
Fire research publications, 1984
[PB85-208502] 24 p4166 N85-35827

FIRE RESISTANCE
U FLAMMABILITY

FIRE RETARDANTS
U FLAME RETARDANTS

FIREBREAKS
Explosion-proof properties and hydraulic resistance of fire-barrier elements based on knitted metallic screens
11 p1601 N85-20067
Scaling parameters of flashover
[NBS-GCR-85-497] 23 p3911 N85-34229

FIREPROOFING
Module flammability research
06 p0830 N85-15274
Flame-resistant materials for use in pyrotechnic safety clothing
[AD-A148857] 07 p0931 N85-15901
Environmental cycling of cellulosic thermal insulation and its influence on fire performance
[DE85-004295] 13 p2041 N85-22776
Fire performance of interstitial space construction system
[NBSIR-85-3158] 20 p3436 N85-31318
Aviation safety (aircraft passenger survivability and cabin safety)
[GPO-39-847] 23 p3895 N85-34130
Investigation of experimental lightweight firewall materials for A/C engine bay applications
[AD-A155765] 24 p4062 N85-35175
Fire research publications, 1984
[PB85-208502] 24 p4166 N85-35827

FIRES
The pyrolysis toxic gas analysis of aircraft interior materials
[AD-A146285] 03 p0328 N85-12115
Fire research publications, 1983
[PB84-217066] 03 p0343 N85-12208
Post fire interview: Development and field validation of the behavioral sequence interview technique
[NBS-GCR-84-477] 04 p0454 N85-12881

Fire prevention and control
[GPO-30-743] 04 p0482 N85-13074
Modeling of aircraft cabin fires
[PB85-137685/GAR] 09 p1277 N85-18031
Suppression and control of Class C cargo compartment fires
[FAA-CT-84-21] 12 p1773 N85-21133
A study of intumescent reaction mechanisms
[AD-A149605] 12 p1812 N85-21365
Collection and use of lightning strike data in the western US during summer 1983
[PB85-110534] 12 p1897 N85-21907
Determination of toxicity of combustion products of habitability foams concurrently with flammability studies of these materials
[AD-A149647] 12 p1905 N85-21961
Aircraft skin penetrator and agent applicator. Volume 1: Working model development and construction
[AD-A150498] 13 p1970 N85-22374
Environmental cycling of cellulosic thermal insulation and its influence on fire performance
[DE85-004295] 13 p2041 N85-22778
Thermal response of aircraft cabin ceiling materials during a post-crash, external fuel-spill, fire scenario
[PB85-145647] 14 p2220 N85-23764
Safety recommendation(s), A-84-76 through -78
[REPT-3751E] 15 p2466 N85-25224
Hydrocarbon pool and vapor fire data analysis
[DE85-005857] 15 p2523 N85-25550
Fire pit tests of blue flight coverall program
[AD-A151884] 15 p2620 N85-26149
Evaluation of pyrotechnic fire suppression system for six pyrotechnic compositions
[AD-A152995] 17 p2937 N85-28130
Laboratory modeling of aspects of large fires
[AD-A153152] 17 p2938 N85-28138
Numerical simulations of the effect of floor and ceiling venting on fire and smoke spread in aircraft cabins
[PB85-178333] 19 p3216 N85-29939
Fire performance of interstitial space construction system
[NBSIR-85-3158] 20 p3496 N85-31318
Aviation safety (aircraft passenger survivability and cabin safety)
[GPO-39-847] 23 p3895 N85-34130
The application of models to the assessment of fire hazard from consumer products
[NBSIR-85-3219] 23 p3925 N85-34325

FIREWORKS
U PYROTECHNICS

FIRING (IGNITING)
NT STATIC FIRING
NT TEST FIRING
CP DDT detonators. Part 1: Design sensitivity study
[DE84-017255] 09 p1302 N85-18160
A computer code IB-KB for interior ballistics of recoiling and recoilless guns
[FOA-C-20566-D2] 18 p3164 N85-29602

FISCHER-TROPSCH PROCESS
Michelle-derived catalysts for extended Schulz-Flory
[DE85-005856] 17 p2922 N85-28012
Catalyst and reactor development for a liquid phase Fischer-Tropsch process
[DE85-006894] 17 p2922 N85-28014
CO + H2 reaction over nitrogn-modified iron catalysts
[DE85-013791] 24 p4072 N85-35231

FISH
U FISHES

FISHERIES
The Marine Resources Experiment Program (MAREX)
[NASA-TM-87368] 01 p0066 N85-10580
Climate and fisheries: A Peruvian case study
07 p1003 N85-16373
The use of hydrometeorological data in explaining shrimp cycles in Guyana
07 p1004 N85-16381
Automatic buoys to assist the tuna fishery off the Azores
14 p2238 N85-23879
Contribution of the NOAA-7 and 8 and ARGOS partnership to white tuna fishing in the northeast Atlantic
16 p2813 N85-27355
Ecology of Pamlico River, North Carolina: An estuarine profile
[PB85-155703] 16 p2822 N85-27404

FISHES
NT SHARKS
Modeling effects of toxicants on aquatic systems
[DE84-016594] 04 p0531 N85-13396
The development of the vestibular apparatus under conditions of weightlessness
[NASA-TM-77517] 07 p1011 N85-16422
Mercury health effects update: Health issue assessment
[PB85-123925] 10 p1526 N85-19639
Acid rain: Effects on fish and wildlife
[PB85-154672] 16 p2821 N85-27402
Pollutant body burdens and reproduction in Platichthys stellatus from San Francisco Bay
[DE85-010407] 19 p3308 N85-30509
Chemoreception and detection of micropollutants by means of a telemetric bionic detector
[DRIC-T-7460] 22 p3810 N85-33600

FISHTAILING
U YAW

FISSION
Tests of the lunar hypothesis
04 p0584 N85-13730
A reappraisal of Darwin's fission hypothesis and a possible limit to the primordial angular momentum of the Earth
04 p0585 N85-13736
Numerical simulations of fission
04 p0585 N85-13737
The dynamic fission instability and the origin of the Moon
04 p0586 N85-13738
On the origin of the Moon by rotational fission
04 p0587 N85-13748
Geochemical evidence for the formation of the Moon by impact induced fission of the proto-Earth
04 p0587 N85-13747
Workshop on Nuclear Dynamics 3
[INC-40007-24] 12 p1931 N85-22130
Methodology for evaluating P sub nu distributions: Results to date
[DE85-007286] 20 p3530 N85-31956
Paired ion chamber constants for fission gamma-neutron fields
[AD-A155069] 21 p3702 N85-32999
Nuclear data for MCNP
[DE85-010794] 22 p3840 N85-33782

FISSION PRODUCTS
Hydrolysis, formation and ionization constants at 25(0)C, and at high temperature-high ionic strength
[DE85-010645] 19 p3236 N85-30061
MELCOR Accident Consequence Code System (MACCS)
[DE85-009712] 19 p3339 N85-30689
Source Term Experiments Project (STEP): Aerosol characterization system
[DE85-010248] 19 p3361 N85-30839
Consolidated fuel reprocessing program
[DE85-008750] 19 p3366 N85-30871
Paired ion chamber constants for fission gamma-neutron fields
[AD-A155069] 21 p3702 N85-32999
Neutron detector counting capabilities for (10) B-lined and (235) U fission chambers in high gamma-ray fluxes
[DE85-011893] 22 p3840 N85-33780
Marine Sample Exploitation Project: Estimates regarding the sensitivity and technology for the detection of nuclear explosion debris in the marine environment
[DE85-013176] 23 p3947 N85-34462
Downstream behavior of volatile fission product species
[DE85-012124] 23 p3971 N85-34617
Application of evaluated fission-product delayed-neutron precursor data in reactor kinetics calculations
[DE85-012728] 23 p3972 N85-34624

FISSURES (GEOLOGY)
Radar observations of fissure-fed basaltic lava flows, Craters of the Moon, Idaho 13 p2199 N85-23640
Interpretation of space photolineaments
15 p2487 N85-25353
Transport properties of Topopah Spring tuff
[DE85-010448] 19 p3270 N85-30278

FITNESS
NT PHYSICAL FITNESS

FITTING
Use of ranks to fit a linear model to cross-sectional data with an application to biological rhythms
[MATHEMATICS-RESEARCH-169]
12 p1923 N85-22081
Macro for fitting nonlinear models to Poisson distributed data
[DE84-006569] 14 p2412 N85-24871
A prototype test chamber for fit testing of protective masks in the field
[FOA-C-40208-C1(C2)] 20 p3512 N85-31834

FITTINGS
Tube coupling device
[NASA-CASE-MFS-25964-1] 11 p1647 N85-20378
Development and test of advanced composite components. Center Directors discretionary fund program
[NASA-TM-86512] 21 p3561 N85-32147

FIXED POINT ARITHMETIC
Interval interation methods for nonlinear equation systems: Theory and comparison on computer
[INTERVALL-BER-84/6] 05 p0719 N85-14812

FIXED POINTS (MATHEMATICS)
Towards a uniform topological treatment of streams and functions on streams
[CWI-CS-R8422] 17 p3014 N85-28839

FIXED WINGS
Flight testing the fixed-wing configuration of the Rotor Systems Research Aircraft (RSRA)
[NASA-TM-86782] 23 p3896 N85-34135

FIXED-WING AIRCRAFT
U AIRCRAFT CONFIGURATIONS
U FIXED WINGS

FIXTURES
An alignment fixture for a 2-Degree-of-Freedom (TDF) gyroscope
[AD-A146885] 10 p1422 N85-18969
Electrostatic forming and testing of polymer films on a 16-foot diameter test fixture
[NASA-TM-86328] 13 p2053 N85-22585

FLAME FRONTS
U FLAME PROPAGATION

FLAME HOLDERS
Computational analysis of scramjet dual mode operation
[NASA-CR-174250] 07 p0956 N85-16060
Flameholder with integrated air mixer
[AD-D011549] 12 p1778 N85-21161
The mechanisms of flame holding in the wake of a bluff body
[NASA-CR-3966] 12 p1779 N85-21166
On the coupling of an anchored flame with an acoustic field
[COLL-AERON-8434] 12 p1799 N85-21282

FLAME INTERACTION
U CHEMICAL REACTIONS
U FLAME PROPAGATION

FLAME IONIZATION
Ionization and time structure of flames
[LE-484/1-2] 05 p0614 N85-13925
Large eddy structures in transitional and turbulent flames
[AD-A154520] 21 p3562 N85-32157

FLAME PROBES
Ionization and time structure of flames
[LE-484/1-2] 05 p0614 N85-13925

FLAME PROPAGATION
Gravitational effects on premixed particle cloud flames
02 p0171 N85-11144
Diffusive combustion of fluids with free surface
02 p0274 N85-11785
Laminar flame propagation/quench for a parallel-wall duct
[DE84-009773] 04 p0470 N85-12983
Combustion waves in dispersed-2-phase mixtures
[CFD/84/13] 04 p0472 N85-13003
Ionization and time structure of flames
[LE-484/1-2] 05 p0614 N85-13925
Numerical calculation of the cold-flow characteristics of a bluff-body flame stabilizer
[CFD/84/14] 06 p1124 N85-17088
Radiation/catalytic augmented combustion
[AD-A148758] 09 p1290 N85-18101
Flame propagation and stabilization studies using Rayleigh scattering and laser Doppler velocimetry
[AD-A148802] 09 p1290 N85-18102
Burner stabilized flames in fluids
[DE84-017429] 09 p1291 N85-18109
Turbulent premixed flame study
[DE85-003220] 09 p1292 N85-18112
Long range effect of turbulent pressure pulsations in plane-parallel flows at different velocities with various flame fronts
09 p1308 N85-18220
A thermal-mechanical model of deflagration-to-detonation in granular energetic materials
[AD-P004346] 10 p1455 N85-19170
Research in nonlinear problems of energy: Informal technical report
[DE85-001529] 11 p1595 N85-20031
Flame spread on combustible solar collector glazing materials
[DE85-002598] 11 p1595 N85-20032
Behavior of the lean methane-air flame at zero-gravity
[NASA-CR-175586] 12 p1799 N85-21283
Hydrogen flame acceleration and transition to detonation
[DE85-000611] 12 p1802 N85-21299
Limiting factor of flame propagation in mono-sized sprays of low-volatility fuels
[NAL-TR-839T] 15 p2521 N85-25538
Affect of angle of incidence on plasmas generated during laser welding
[DE85-005724] 15 p2569 N85-25852
Modeling the role of radicals in the ignition of and flame propagation in hydrogen-air and methane-air mixtures
16 p2744 N85-26935
LDA study of non-steady flame propagation in a constant volume duct
[DE85-007233] 16 p2746 N85-26948
On the analytic calculation of premixed flames
[VTH-LR-417] 16 p2747 N85-26954

Significant parameters for predicting flame spread
[PB85-178002] 16 p2760 N85-27034
Polynomial approaches for the characteristic velocity and flame temperature as a function of mixing compounding and pressure for the systems PMMA/O2, PMMA/air, PE/O2, PE/air, PS/O2 and PS/air
[VTH-LR-421] 17 p2924 N85-26024
Laboratory modeling of aspects of large fires
[AD-A153152] 17 p2936 N85-29138
Flame acceleration mechanisms under conditions of partial confinement
[PB85-184083] 18 p3073 N85-29004
LDA study of the unburned gas motion induced by nonsteady flame propagation in a constant volume duct
[DE85-009936] 19 p3270 N85-30277
Wall flames and implications for upward flame spread
[FAA-CT-85-2] 21 p3553 N85-32103
Optical waveguide along front of exothermic reaction
21 p3694 N85-32954
Multiparameter conditionally sampled laser velocimetry measurements during flame propagation in a spark ignition engine
[DE85-009850] 22 p3793 N85-33502
Investigation of the flame speeds of propane/methanol gas mixtures
[DE85-012817] 23 p3912 N85-34239
The use of austenitic stainless steel versus monel (Ni-cu) alloy in pressurized Gaseous Oxygen (GOX) life support systems
[AD-A158305] 24 p4134 N85-35625

FLAME QUENCHING
U EXTINGUISHING
U QUENCHING (COOLING)

FLAME RETARDANTS
Fire retardant cellulosehydrate fibers
06 p0761 N85-14870
Study of effectiveness of fire-resistant activity of antipyrenes for fibers of aromatic polyamides
06 p0762 N85-14874
Preparation of fire-resistant infusible polycaproamide fiber 06 p0763 N85-14877
Flame resistant fibrous materials development
[NASA-CR-167817] 07 p0920 N85-15827
A study of intumescent reaction mechanisms
[AD-A149805] 12 p1812 N85-21305
Polyesters: A review of the literature on products of combustion and toxicity
[NBSIR-85-3139] 20 p3433 N85-31296
Photovoltaic module spread-of-flame testing
21 p3612 N85-32448
Investigation of experimental lightweight firewall materials for A/C engine bay applications
[AD-A155765] 24 p4062 N85-35175
Fire research publications, 1984
[PB85-208502] 24 p4166 N85-35827

FLAME SPECTROSCOPY
Laser Raman techniques for studying flows and flames 11 p1576 N85-19929
Advanced diagnostics for reacting flows
[AD-A150675] 14 p2301 N85-24246
Spectroscopic studies of lead oxide in a flow tube
[AD-A151849] 15 p2505 N85-25455
Shock tube measurements of growth constants in the branched-chain ethane-carbon monoxide-oxygen system
[NASA-TM-87066] 21 p3562 N85-32156

FLAME SPRAYING
Detonation flame spraying extends life of automotive parts 15 p2513 N85-25507
Thermal barrier coating system
[NASA-CASE-LEW-14057-1] 24 p4072 N85-35233

FLAME STABILITY
Linear long-wave stability of cylindrical steady laminar flame in rotating medium 02 p0266 N85-11752
Numerical calculation of the cold-flow characteristics of a bluff-body flame stabilizer
[CFD/84/14] 08 p1124 N85-17088
The mechanisms of flame holding in the wake of a bluff body
[NASA-CR-3866] 12 p1779 N85-21166
Radiative augmented combustion
[AD-A154137] 20 p3423 N85-31246
Wall flames and implications for upward flame spread
[FAA-CT-85-2] 21 p3553 N85-32103

FLAME TEMPERATURE
New concepts for measuring flame spread properties
[NBSIR-84-2943] 03 p0327 N85-12104
Core temperature measurements in sooting, laminar diffusion flames
[AD-A148801] 09 p1319 N85-18294
Ionic mechanisms of soot formation in flames
[AD-A150119] 12 p1801 N85-21297
The influence of fuel quality upon flame-tube temperature and flame radiation in a model gas-turbine primary zone
[K233] 13 p1974 N85-22396
The influence of fuel molecular composition upon flame-tube temperature and flame radiation in a model gas-turbine primary zone
[K234] 13 p2017 N85-22648
Laser diagnostic analyses of sooting flames
[AD-A150478] 13 p2017 N85-22649
On the analytic calculation of premixed flames
[VTH-LR-417] 16 p2747 N85-26954
Elementary reactions of importance in oxidation, combustion ignition and flame inhibitions
[AD-A153139] 17 p2921 N85-26004
Polynomial approaches for the characteristic velocity and flame temperature as a function of mixing compounding and pressure for the systems PMMA/O2, PMMA/air, PE/O2, PE/air, PS/O2 and PS/air
[VTH-LR-421] 17 p2924 N85-26024

FLAMEOUT
The mechanisms of flame holding in the wake of a bluff body
[NASA-CR-174056] 02 p0172 N85-11149

FLAMES
NT DIFFUSION FLAMES
NT PREMIXED FLAMES
Limiting effects during turbulent combustion
02 p0274 N85-11784
Raman and fluorescence spectroscopy in a methane-nitrous oxide laminar flame
[AD-A146092] 03 p0328 N85-12111
Study of combustion and flame processes initiated by laser-induced multiple-photon absorption
[DE84-017095] 04 p0471 N85-12996
The structure of dilute combusting sprays
[NASA-CR-174835] 07 p0905 N85-15728
Burner stabilized flames in fluids
[DE84-017429] 09 p1291 N85-18109
Mechanisms and reaction dynamics related to methane combustion
[PB85-129690] 10 p1438 N85-19065
Theory of flammability limits. Flow gradient effects and flame stretch
[PB85-135077] 10 p1439 N85-19067
Behavior of the lean methane-air flame at zero-gravity
[NASA-CR-175586] 12 p1799 N85-21283
Two-dimensional measurements of OH concentration and temperature in reactive flows
[AD-A149849] 12 p1800 N85-21292
Ionic mechanisms of soot formation in flames
[AD-A150119] 12 p1801 N85-21297
Picosecond lidar techniques in laboratory and field diagnostics
[AD-A150755] 14 p2309 N85-24294
An experimental investigation of two-dimensional flame-vortex interactions 16 p2744 N85-26934
Modeling the role of radicals in the ignition of and flame propagation in hydrogen-air and methane-air mixtures
16 p2744 N85-26935
Elementary reactions of importance in oxidation, combustion ignition and flame inhibitions
[AD-A153139] 17 p2921 N85-26004
Investigation of several low-lying levels of X doublet pi state of NCO using argon laser excited fluorescence
[AD-A153693] 18 p3071 N85-29994
Theoretical studies of combustion chemistry
[DE85-010284] 19 p3237 N85-30069
Intermittency, conditional sampling and turbulent combustion 20 p3424 N85-31249
Rayleigh scattering for density measurements in premixed flames: One point, time series data
20 p3424 N85-31253
Recent measurements in turbulent jet flames at Sandia Combustion Research Facility 20 p3424 N85-31254
Large eddy structures in transitional and turbulent flames
[AD-A154520] 21 p3562 N85-32157
Status of boron combustion research
[AD-A154762] 21 p3563 N85-32160
In-cavity laser IR spectrum analyzer for investigating non-steady-state processes 21 p3695 N85-32994
Experimental study of engine knock
[DE85-009851] 22 p3754 N85-33268
Effects of ambient pressure on the instability of a liquid boiling explosively at the superheat limit
[DE85-009476] 23 p3932 N85-34370
Electronic imaging system and technique
[DE85-005740] 23 p3935 N85-34393
Radiation measurements on magnesium flames
[BLL-CE-TRANS-8110-(9022.09)]
24 p4075 N85-35254

FLAMMABILITY
Development of new and improved polymer matrix resin systems, phase 1
[NASA-CR-166595] 01 p0017 N85-10104
Quasi-steady analysis of aircraft panel flammability
[AD-A145461] 02 p0138 N85-10936
New concepts for measuring flame spread properties
[NBSIR-84-2943] 03 p0327 N85-12104
Modeling of aircraft cabin fires
[NBS-GCR-84-473] 04 p0454 N85-12860
Standardization of flammability tests for hydraulic fluids
[AD-A146468] 06 p0771 N85-14932
Module flammability research
06 p0830 N85-15274
Preliminary evaluation of an improved flammability test method for aircraft materials
[FAA-CT-84-22] 08 p1060 N85-16840
Mist flammability studies of candidate fire-resistant hydraulic fluids
[AD-A148572] 08 p1134 N85-17148
Penetration of the atmosphere by flammable mixtures as a result of spillage of LNG on the ground
08 p1179 N85-17432
Theory of flammability limits. Flow gradient effects and flame stretch
[PB85-135077] 10 p1439 N85-19067
Determination of toxicity of combustion products of habitability foams concurrently with flammability studies of these materials
[AD-A149647] 12 p1905 N85-21961
Light weight fire resistant graphite composites
[NASA-CASE-ARC-11615-1-SB]
18 p3068 N85-28976
Practical real-time quality control of antimisting kerosene
[DE/FAA/CT-85/1] 18 p3063 N85-29072
Working with flammable solvents, thinners, paints and adhesives
[HSE-TRANS-11066] 19 p3250 N85-30154
The role of aircraft panel materials in cabin fires and their properties
[FAA-CT-84-30] 21 p3553 N85-32104
Photovoltaic module spread-of-flame testing
21 p3612 N85-32448
Review of zirconium-zircaloy pyrophoricity
[DE85-011169] 23 p3916 N85-34270
The use of a laser Doppler velocimeter in a standard flammability tube
[NASA-CR-174960] 24 p4096 N85-35389

FLAMMABLE GASES
NT GASEOUS FUELS
NT LIQUEFIED NATURAL GAS
Investigation of the flame speeds of propane/methanol gas mixtures
[DE85-012817] 23 p3912 N85-34239

FLANGE WRINKLING
Design, fabrication and test of composite curved frames for helicopter fuselage structure
[NASA-CR-172438] 15 p2470 N85-25247

FLANGES
High temperature ultra-high vacuum infrared window seal
[AD-D011333] 07 p0929 N85-15890
Fuel cell separator plate with bellows-type sealing flanges
[DE85-005991] 23 p3947 N85-34459

FLAP CONTROL
U AIRCRAFT CONTROL
U FLAPS (CONTROL SURFACES)

FLAPERONS
Wing buffeting active control testing on a transport aircraft configuration in a large sonic windtunnel
17 p2904 N85-27903

FLAPPING
Stochastic motor blade dynamics
[AD-A146312] 03 p0318 N85-12054
Computer analysis of wind turbine blade dynamic loads
[DE85-000530] 12 p1867 N85-21714

FLAPS (CONTROL SURFACES)
NT FLAPERONS
NT JET FLAPS
NT LEADING EDGE FLAPS
NT LEADING EDGE SLATS
NT TRAILING EDGE FLAPS
NT VORTEX FLAPS
NT WING FLAPS
Development of the space shuttle body flap actuation subsystem 08 p1102 N85-16965
An experimental investigation of flap turbulent heat transfer and pressure characteristics in hypersonic flow
12 p1821 N85-21426
Flow over a biconic configuration with an afterbody compression flap
[AD-A151882] 15 p2557 N85-25778
Additional flow field studies of the GA(W)-1 airfoil with 30-percent chord Fowler flap including slot-gap variations and cove shape modifications
[NASA-CR-3687] 19 p3212 N85-29919

FLARE STARS
On the most probable number of flare stars in the Pleiades field 05 p0739 N85-14756

Activity and magnetic fields on stars from radio observations
[NASA-CR-175966] 18 p3202 N85-29861
Stochastic particle acceleration in flaring stars
[OG-8.3-9] 23 p4022 N85-34927
FLASH
Production of thin-walled electricity welded tubes with reduced internal flash
[BLL-BISI-TRANS-22381-(9022.06)] 17 p2973 N85-28364
FLASH BLINDNESS
Pursuit tracking performance and flash disruption: The effects of training the non-dominant eye on target reacquisition
[AD-A153404] 17 p2999 N85-28541
Predictive model of electron beam induced flashblindness
[AD-A155260] 21 p3664 N85-32763
FLASH LAMPS
Electronics Engineering Department: EE technical review
[DE84-016124] 01 p0044 N85-10286
Flares and photoflash items
[AD-A145442] 02 p0187 N85-11253
Performance of a large area flash chamber prototype
[NOTA-INTERNA-807] 02 p0201 N85-11338
An evaluation of flashtube signal characteristics
[AD-A149569] 10 p1423 N85-18974
Characteristics of unstable resonators in flashlamp-pumped organic-compound lasers 11 p1717 N85-20800
Electrodes for flash discharge lamps
[DE85-008897] 17 p2955 N85-28250
Electrode for flash discharge lamps
[DE85-008896] 17 p2955 N85-28252
Dye laser traveling wave amplifier
[NASA-CR-175969] 19 p3275 N85-30308
Switching power supply
[DE85-005993] 22 p3761 N85-33312
FLASH POINT
Removal of longitudinal internal flash from electrically welded tubes
[BLL-BISI-TRANS-22380-(9022.06)] 17 p2938 N85-28136
FLASH TUBES
U FLASH LAMPS
FLASHING (VAPORIZING)
Critical flashing flow of subcooled fluids in nozzles with contour discontinuities
[DE84-017229] 09 p1319 N85-18296
FLASHOVER
Development of power system management
[PB84-216530] 04 p0497 N85-13173
Flashover failures from wet-wire arcing and tracking
[AD-A149055] 10 p1478 N85-19332
Flash radiography 14 p2317 N85-24316
Vacuum interface flashover with bipolar electric fields
[DE85-012027] 22 p3755 N85-33275
Scaling parameters of flashover
[NBS-GCR-85-497] 23 p3911 N85-34229
FLASKS
Dynamic pressure test unit-ratio method
[AD-D011468] 10 p1488 N85-19392
Transmissive Dewar cooling chamber for optically pumped semiconductor ring lasers
[AD-D011550] 12 p1855 N85-21636
FLAT COAXIAL TRANSMISSION LINES
U MICROSTRIP TRANSMISSION LINES
FLAT PLATES
Approximate solution of a laminar flow over a flat plate with suction and pressure gradient
[AD-A145482] 02 p0198 N85-11321
Modular photovoltaic array field
[SAND-83-7028] 02 p0222 N85-11454
Total area of diffusion elements in a reverberation chamber and measured degree of sound absorption
[NRC/CNR-TT-2110] 03 p0415 N85-12653
FSA field test
[NASA-CR-174114] 04 p0528 N85-13373
Thin polymer film collectors as a contribution to the solar industry
[DE84-015299] 04 p0529 N85-13383
Proceedings of the 22nd Project Integration Meeting
[DE85-000334] 06 p0633 N85-15302
A second-order accurate parabolized Navier-Stokes algorithm for internal flows
[NASA-CR-174258] 07 p0956 N85-16059
Free surface effects on the wake of a flat plate
[AD-A146988] 07 p0958 N85-16071
A free shear layer prediction of the turbulent wake of a flat plate towed below a free surface
[AD-A146899] 09 p1319 N85-18293
An experimental investigation into the effects of plate eccentricity and elastic deformation on orifice meter accuracy
[ERS-E.391] 09 p1325 N85-18325
The dependence of soil bearing capacity and drawbar pull on the spacing between track
[AD-P004273] 09 p1406 N85-18849
A multistage time-stepping scheme for the Navier-Stokes equations
[NASA-CR-172527] 10 p1483 N85-19365
MOD silver metallization for photovoltaics
[NASA-CR-175480] 10 p1510 N85-19526
LOVEL-84: A LOw-VELocity aerodynamic heating code for flat plates, wedges, and cones
[DE85-002604] 11 p1576 N85-19933
Pre-turbulence: Transitional Laminar-turbulent flows 11 p1716 N85-20793
Numerical study of large-eddy breakup and its effect on the drag characteristics of boundary layers
[NASA-CR-3884] 12 p1797 N85-21272
Interaction of part-through cracks in a flat plate
[NASA-CR-175588] 12 p1864 N85-21692
A new model for thin plates with rapidly varying thickness. Part 3: Comparison of different scalings
[AD-A149748] 12 p1866 N85-21704
Scattered data interpolation using thin plate splines with tension
[AD-A149803] 12 p1866 N85-21705
Nonlinear analysis of layered composite plates and shells
[PB85-127181] 12 p1868 N85-21719
Calculating isothermal flow in wake beyond injection zone 14 p2287 N85-24175
Heat transfer to vertical flat plates in a rectangular gas-fluidized bed
[AD-A150785] 14 p2301 N85-24248
Silicon-sheet and thin-film cell and module technology potential: Issue study
[NASA-CR-175854] 14 p2349 N85-24520
Intermediate load modules for test and evaluation
[NASA-CR-175897] 14 p2350 N85-24526
Periodic vortex shedding in the supersonic wake of a planar plate
[NASA-TM-77854] 15 p2463 N85-25207
Flow past a flat plat with a vortex/sink combination
[AAA-TR-58] 15 p2464 N85-25215
An experimental investigation into the dynamic response of a stiffened flat plate loaded impulsively by an underwater shockwave
[AD-A151321] 15 p2578 N85-25903
Electrical research on solar cells and photovoltaic materials
[NASA-CR-175899] 15 p2585 N85-25935
Turbulent flow of fluid near trailing edge of plate in stream at zero angle of attack 16 p2764 N85-27057
Acceleration sensitivity reduction method
[AD-D011631] 16 p2778 N85-27146
MOD silver metallization for photovoltaics
[NASA-CR-175773] 16 p2818 N85-27381
Turbulent wake of a submerged flat plate
[AD-A153776] 18 p3100 N85-29190
Underwater shock-induced responses of stiffened flat plates: An investigation into the predictive capabilities of the USA-STAGS code
[AD-A154245] 19 p3286 N85-30377
Using PVFORM, a systems performance model, to determine optimum mounting configurations for flat-plate photovoltaic modules
[DE85-011191] 19 p3306 N85-30495
Sub-optimal control of nonlinear flexible space structures 20 p3414 N85-31190
A mathematical analysis of the effect of free stream turbulence on the Blasius boundary layer 20 p3451 N85-31430
Experimental observation of transition behavior on a flat plate 20 p3452 N85-31437
Dynamical study of flat plates by nonlinear elasticity theory
[STN-6] 20 p3471 N85-31572
An analysis of the feasibility of producing silicon for solar cells by a dichlorosilane/fluidized-bed reactor process
[NASA-CR-176036] 20 p3478 N85-31614
Proceedings of the Flat-Plate Solar Array Project Research Forum on High-Efficiency Crystalline Silicon Solar Cells
[NASA-CR-176047] 20 p3478 N85-31615
Nomographs for estimating the levelized cost of energy from flat-plate and concentrator photovoltaic systems
[NASA-CR-176048] 20 p3483 N85-31645
Instability and chaotic behavior in a free-surface flow
[AD-A154879] 21 p3584 N85-32279
Numerical solutions of turbulent models for flow over a flat plate with angle of attack
[DE85-010380] 21 p3585 N85-32286
An investigation into the comparisons of the underwater shock effects on a stiffened flat plate to the predictive nature of a computer model
[AD-A155612] 21 p3600 N85-32355
Proceedings of the 24th Project Integration Meeting
[NASA-CR-176058] 21 p3607 N85-32394
Flat-plate module efficiency versus cost tradeoffs 21 p3607 N85-32398
Block V module program 21 p3607 N85-32401
Reliability physics 21 p3608 N85-32402
MOD silver metallization for photovoltaics 21 p3610 N85-32426
Development of artificially produced perturbations in supersonic boundary layer 21 p3663 N85-32879
Fuel cell separator plate with bellows-type sealing flanges
[DE85-005991] 23 p3947 N85-34459
Vortex boundary-layer interactions
[NASA-CR-176192] 24 p4093 N85-35373
FLAT SURFACES
Local stability analysis for a planar shock wave
[NASA-TP-2367] 04 p0452 N85-12984
An experimental investigation of a turbulent junction vortex
[NASA-CR-175915] 17 p2957 N85-28259
Boundary to constructive solid geometry mappings: A focus on 2-D issues 17 p3004 N85-28570
Numerical estimation of the curvature of biological surfaces 17 p3006 N85-28588
FLATNESS
Development of a measuring procedure for the automatic evaluation of the flatness of reflective surfaces
[BMFT-FB-T-84-168] 03 p0421 N85-12688
FLATS (LANDFORMS)
Surface soil moisture measurements of the White Sands, New Mexico
[NOAA-TM-NESDIS-7] 02 p0219 N85-11441
FLATTENING
Computation of thermal shock-free straightening conditions for aluminum-magnesium alloy welded structures 10 p1449 N85-19131
FLAVOR (PARTICLE PHYSICS)
Heavy quarks and CP: Moriond 1985
[DE85-010553] 22 p3841 N85-33790
FLAW DETECTION
U NONDESTRUCTIVE TESTS
FLAWS
U DEFECTS
FLEXIBILITY
Two- and three-dimensional model and wall data from a flexible-walled transonic test section 03 p0312 N85-12015
Synthesis study of nondestructive testing devices for use in overlay thickness design of flexible pavements
[PB84-216080] 06 p0774 N85-14950
Random vibrations of aircraft engine blades 06 p0777 N85-14957
The influence of fastener flexibility on load transfer and fatigue life predictions for multirow bolted and riveted joints --- aircraft structures
[LBF-FB-172/84] 07 p0979 N85-16219
A Galerkin method for the estimation of parameters in hybrid systems governing the vibration of flexible beams with tip bodies
[NASA-CR-172537] 10 p1544 N85-19734
Simplified theory for the behaviour of buried flexible cylinders under the influence of uniform hoop compression
[PB85-116631] 11 p1654 N85-20419
Finger materials for air cushion vehicles. Volume 2: Base fabrics for finger materials
[AD-A149701] 12 p1819 N85-21408
Effects of triazine components on physicochemical properties of polybutadiene: urethane block copolymers 13 p2014 N85-22635
Optimum design and automated dynamic analysis of flexible mechanisms
[AD-A150152] 13 p2099 N85-23088
A research program in active control/aeroelasticity
[NASA-CR-175874] 14 p2218 N85-23752
Systems design and application of computers with flexible architecture 14 p2401 N85-24900
Effect of internal pressure on flexibility and stress intensification factors for pipe elbows analyzed by the finite element method
[AD-A151161] 15 p2578 N85-25901
Control of a flexible beam
[DE85-007243] 15 p2580 N85-25914
Development of a new faster process for the fabrication of ceramic fiber-reinforced ceramic composites by chemical vapor infiltration
[DE85-007550] 16 p2756 N85-27007
On the accuracy of modelling the dynamics of large space structures 19 p3225 N85-29995
Modeling and analysis of pinhole occulter experiment: Initial study phase
[NASA-CR-175978] 19 p3272 N85-30287
Dynamic response of a flexible space beam
[NASA-TM-86441] 19 p3285 N85-30368
Sub-optimal control of nonlinear flexible space structures 20 p3414 N85-31190

An overview of latest model reduction and control methods of large flexible space structures
20 p3414 N85-31191
A control concept for large flexible spacecraft using order reduction techniques
20 p3415 N85-31193
Wideband disturbance accomodation in precision flexible space structures
20 p3415 N85-31194
STPI/LARC: A 200 deg C polyimide adhesive
[NASA-TM-86447] 20 p3433 N85-31297
An analysis of multi-fingered hands
20 p3482 N85-31504
User's guide for computer program CGFAG, Concrete General Flexure Analysis with Graphics
[AD-A155555] 21 p3570 N85-32204
Thin-film reliability and engineering overview
21 p3612 N85-32450
Removable cleanable antireflection shield
[AD-D011735] 22 p3844 N85-33610
Strength properties of glassfiber reinforced thermoplastics
23 p3908 N85-34212

FLEXIBLE BODIES
NT FLEXIBLE SPACECRAFT
Measurement of the inertial constants of a rigid or flexible structure of arbitrary shape through a vibration test
[NASA-TM-77557] 02 p0209 N85-11361
Experiments in control of flexible structures with uncertain parameters
05 p0602 N85-13837
Low-loss flexible dielectric waveguide for millimeter-wave transmission and its application to devices
[AD-A147846] 07 p0948 N85-16006
Flexible line support assembly
[AD-D011391] 07 p0972 N85-16177
Precise control of flexible manipulators
[NASA-CR-174210] 07 p0973 N85-16178
Identification of vibration parameters of flexible structures
09 p1331 N85-18360
A deformation analysis of flat flexible gear and its equation of original curved surfaces
[NASA-TM-77493] 12 p1859 N85-21660
Planar dynamics of a uniform beam with rigid bodies affixed to the ends
[NASA-CR-175666] 12 p1864 N85-21693
Developments in deployable masts to support flexible solar arrays
13 p2012 N85-22620
Spline-based Rayleigh-Ritz methods for the approximation of the natural modes of vibration for flexible beams with tip bodies
[NASA-CR-172566] 13 p2102 N85-23100
AFWAL space control technology program
14 p2233 N85-23939
Control Of Flexible Structures (COFS) flight experiment background and description
14 p2236 N85-23664
Modeling and control of large flexible structures, phase 1
[AD-A150736] 14 p2403 N85-24817
Model reduction techniques applied to the control of large space structures
[AD-A151784] 16 p2731 N85-26857
Addition of flexible body option to the TOLA computer program, part 1
[NASA-CR-132732-1] 17 p2896 N85-27855
Addition of flexible body option to the TOLA computer program. Part 2: User and programmer documentation
[NASA-CR-132732-2] 17 p2896 N85-27856
LFMR definition study
[AD-A153691] 18 p3090 N85-29126
Spillover minimization: An approach for actuators and sensors placement in distributed parameter study
[INPE-3525-PRE/746] 19 p3272 N85-30289
Application of deformable body mean-axis to dynamics of flexible mechanical systems
19 p3283 N85-30359
AFWAL control technology programs
20 p3408 N85-31150
Attitude control tradeoff study between the use of a flexible beam and a tether configuration for the connection of two bodies in orbit
20 p3412 N85-31174
Approximation techniques for parameter estimation and feedback control for distributed models of large flexible structures
20 p3413 N85-31179
Approximation of optimal infinite dimensional compensators for flexible structures
20 p3413 N85-31181
Control of a flexible space antenna: A finite dimensional perspective based on distributed parameter theory
20 p3413 N85-31182
Optimization of controlled structures
20 p3414 N85-31186
A nonlinear dual-adaptive control strategy for identification and control of flexible structures
20 p3416 N85-31203
Combined state and parameter estimation for a static model of the Maypole (Hoop-Column) antenna suface
20 p3417 N85-31210
Experimental verification of identification algorithms for control of flexible structures
20 p3418 N85-31211
Non-rigid body motion
23 p3964 N85-34576
Analysis of flexible aircraft longitudinal dynamics and handling qualities. Volume 1: Analysis methods
[NASA-CR-177943-VOL-1] 24 p4066 N85-35202
Analysis of flexible aircraft longitudinal dynamics and handling qualities. Volume 2: Data
[NASA-CR-177943-VOL-2] 24 p4067 N85-35203

FLEXIBLE SPACECRAFT
Modular design attitude control system
[NASA-CR-171182] 01 p0016 N85-10098
Qualitative results for distributed systems with discrete damping and stiffness with application to control
[AD-A145525] 02 p0209 N85-11382
A user's guide to the Flexible Spacecraft Dynamics and Control Program
[NASA-TM-87369] 03 p0405 N85-12586
Damping models for flexible communications satellites by substructural damping synthesis
[UTIAS-287] 14 p2237 N85-23868
A mathematical formulation of the Scole control problem, part 1
[NASA-CR-172581] 14 p2243 N85-23903
Numerical experiments on flexible spacecraft with the aid of the Dynamic Control and Analysis Package (DCAP)
[ESA-STM-229] 15 p2493 N85-25382
The effect of sensor and actuator errors on static shape control for large space structures
[NASA-TM-86446] 19 p3225 N85-29998
Dynamic response of a flexible space beam
[NASA-TM-86441] 19 p3265 N85-30368
Proceedings of the Workshop on Identification and Control of Flexible Space Structures, volume 1
[NASA-CR-176051] 20 p3408 N85-31148
Dynamic performance of several large antenna concepts
20 p3409 N85-31155
Antenna pointing of large flexible telecommunications spacecraft
20 p3409 N85-31156
Control of flexible structures
20 p3410 N85-31161
Experiments in structural dynamics and control using a grid
20 p3410 N85-31165
Rationale for an experimental test for flexible space structure attitude control
20 p3411 N85-31167
Numerical and experimental evaluation for single-axis control of an LSS laboratory model
20 p3411 N85-31168
Proceedings of the Workshop on Identification and Control of Flexible Space Structures, volume 2
[NASA-CR-176052] 20 p3411 N85-31170
Vibration/libration interaction dynamics during the orbiter based deployment of flexible members
20 p3411 N85-31171
Design of multivariable controllers using the Integrated Analysis Capability (IAC)
20 p3412 N85-31172
An integrated control and minimum mass structural optimization algorithm for large space structures
20 p3413 N85-31183
ISAAC (Integrated Structural Analysis and Control) via continuum modeling and distributed frequency domain design techniques
20 p3414 N85-31185
Parametric stiffness control of flexible structures
20 p3414 N85-31187
Vibrational stabilization of flexible structures
20 p3414 N85-31188
Stiffness control of large space structures
20 p3414 N85-31189
Proceedings of the Workshop on Identification and Control of Flexible Space Structures, volume 3
[NASA-CR-176053] 20 p3415 N85-31195
Matrix transfer function design for flexible structures: An application
20 p3416 N85-31199
On the stability of collocated controllers in the presence or uncertain nonlinearities and other perils
20 p3416 N85-31201
Maximum likelihood estimation with emphasis on aircraft flight data
20 p3417 N85-31208
Enhancement of the flexible spacecraft dynamics program for open spacecraft
[NASA-CR-175309] 24 p4137 N85-35641

FLEXIBLE WINGS
Transonic pressure distribution computations of a flexible wing
11 p1622 N85-20213
Analytically redundant output feedback scheme for reduction of structural loads of a flexible transport aircraft
[TT-8303] 12 p1777 N85-21154
Transonic calculations for a flexible supercritical wing and comparison with experiment
[NASA-TM-86439] 20 p3388 N85-31012

FLEXING
Long-term thermal aging of 2 graphite-polyimide composite materials
[NASA-TP-2360] 03 p0325 N85-12094
Effect of coupled torsional-flexural vibration of a geared shaft system on the dynamic tooth load
09 p1338 N85-18415
Variable flexing device for targets in internal beams of charged particle accelerators
13 p2044 N85-22797
Machine analysis of resonance characteristics of plate-type radio electronic equipment constructions
13 p2065 N85-23018
Load carrying capacity of double circular arc gears
14 p2221 N85-23776
Reflection and transmission of flexural waves at discontinuities
15 p2572 N85-25661
On geoid heights and flexure of the lithosphere at seamounts
[AD-A151220] 15 p2604 N85-26050
Buckling and bracing of cantilevers
[CE-42] 17 p2879 N85-28413
Study on a flexure hinged pendulum accelerometer
[NAL-TR-844] 18 p3104 N85-29220
Buckling and post-buckling behavior of sparsely connected built-up columns
19 p3283 N85-30358
Graphite/PMR polyimide composites with improved toughness
[NASA-TM-87081] 21 p3561 N85-32148
Reliability of two sintered silicon nitride materials
[NASA-TM-87092] 23 p3919 N85-34284

FLEXURE
U FLEXING

FLICKER
An evaluation of flashtube signal characteristics
[AD-A149569] 10 p1423 N85-18974
Variations in the small-scale galactic magnetic field and short time-scale intensity variations of extragalactic radio sources
20 p3549 N85-32084

FLIGHT ALTITUDE
Global matrix of thermospheric density values for selected solar/geomagnetic conditions and spacecraft orbital attitudes
[NASA-TM-86478] 04 p0533 N85-13409
Safety recommendation(s), A-84-82 through -84
[REPT-3957] 14 p2217 N85-23748

FLIGHT CHARACTERISTICS
Airworthiness and flight characteristics test of the JOH-6A light combat helicopter configured with a wire strike protection system
[AD-A144880] 01 p0006 N85-10038
Airworthiness and Flight Characteristics (A and FC) test of the EH - 1X/EH - 1H helicopter configurations
[AD-A144881] 01 p0007 N85-10039
Active control technology experience with the Space Shuttle in the landing regime
[NASA-TM-85910] 01 p0012 N85-10071
YO-3A acoustics research aircraft systems manual
[NASA-TM-85968] 01 p0012 N85-10074
Simulator study of flight characteristics of several large, dissimilar, cargo transport airplanes during approach and landing
[NASA-TP-2357] 02 p0148 N85-11002
Aircrew-aircraft integration: A summary of US Army research programs and plans
[NASA-TM-85991] 02 p0148 N85-11004
Flying qualities and control system characteristics for superaugmented aircraft
[NASA-CR-170419] 05 p0596 N85-13800
An in-flight investigation of a twin fuselage configuration in approach and landing
[NASA-CR-172366] 05 p0596 N85-13801
STOL simulation requirements for development of integrated flight/propulsion control systems
05 p0701 N85-14499
Maximum normalized rate as a flying qualities parameter
05 p0702 N85-14503
The Sternberg task as a workload metric in flight handling qualities research
05 p0712 N85-14568
Effects of aircraft and flight parameters on energy-efficient profile descents in time-based metered traffic
[NASA-CR-172338-ADD] 07 p0901 N85-15706
Airworthiness and flight characteristics test of the RC-12D Guardrail V
[AD-A148046] 08 p1084 N85-16864
Realization and testing of an experimental color display system for general aviation helicopters and aircraft
[BMFT-FB-W-84-042] 08 p1086 N85-16872
Time series analysis of closed-loop pilot vehicle dynamics
08 p1087 N85-16876
Low-speed longitudinal orbiter qualities
08 p1092 N85-16905
Aerodynamic challenges of ALT
08 p1094 N85-16911
The design of sport and touring aircraft
[NASA TM-77783] 10 p1423 N85-18975
In-flight investigation of the effects of time delay in control system on flying qualities in landing approach
[DFVLR-FB-84-35] 11 p1586 N85-19989
Technical evaluation report on the FDP Symposium on Flight Test Techniques
[AGARD-AR-208] 12 p1777 N85-21157

Low-speed stability and control wind-tunnel investigations of effects of spanwise blowing on fighter flight characteristics at high angles of attack — Langely 12-ft low-speed tunnel and 30- by 60-ft tunnel
[NASA-TP-2431] 14 p2210 N85-23708
The design of high-performance gliders
[NASA-TM-77772] 14 p2217 N85-23750
Simulation of aircraft behaviour on and close to the ground
[NASA-TM-87460] 14 p2218 N85-23754
Preliminary helicopter design decision making based on flight performance factors
[AD-A151488] 15 p2471 N85-25254
Study of longitudinal landing flying qualities evaluation using pilot model theory
[AD-A152194] 16 p2706 N85-26702
Technical evaluation report on the Flight Mechanics Symposium on Active Control Systems: Review, Evaluation and Projections
[AGARD-AR-220] 16 p2711 N85-26730
The state-of-the-art and future of flight control systems 16 p2712 N85-26732
In-flight investigation of the influence of pitch damping and pitch control effectiveness on landing approach flying qualities of statically unstable transport aircraft
[DFVLR-FB-84-12] 17 p2900 N85-27880
Helicopter Aeromechanics
[AGARD-LS-139] 18 p3057 N85-28913
Helicopter aeromechanics: Introduction and historical review 18 p3057 N85-28914
In-flight evaluation of pure time delays in pitch and roll
[NASA-TM-86744] 21 p3556 N85-32123
Ground-based and in-flight simulator studies of flight characteristics of a twin-fuselage passenger transport airplane during approach and landing
[NASA-TP-2451] 23 p3898 N85-34144
Estimation of flight mechanical variables by means of Kalman filters 24 p4062 N85-35171

FLIGHT CLOTHING

The water vapor resistances of some clothing assemblies used by flying personnel of the Swedish Armed Forces: A series of model studies
[FOA-C-59011-H1] 02 p0238 N85-11551
Testing of three different flight suits in fire environment — fuel fire
[FOA-C-59012-H1] 02 p0238 N85-11552
Acceptance-testing procedures for air-line supplied-air suits
[DE84-016960] 05 p0712 N85-14569
The new Navy flier's fire-resistant blue coverall
[AD-A146611] 06 p0846 N85-15375
SPH-4 US Army flight helmet performance, 1972 - 1983
[AD-A148674] 08 p1201 N85-17582
The application of anthropometric survey data to aircrew clothing sizing
[AD-A150545] 13 p2143 N85-23304
Fire pit tests of blue flight coverall program
[AD-A151884] 15 p2620 N85-26149

FLIGHT COMPUTERS

U AIRBORNE/SPACEBORNE COMPUTERS

FLIGHT CONDITIONS

TAF verification (airport weather forecasts)
[GEOPHYSBDBW-FM-205] 05 p0687 N85-14420
Weather satellite products in the Flight Service Automation System (FSAS)
[AD-A146520] 06 p0759 N85-14855
The Altitude Wind Tunnel (AWT): A unique facility for propulsion system and adverse weather testing
[NASA-TM-86921] 09 p1263 N85-18067
Direct-strike lightning photographs, swept-flash attachment patterns, and flight conditions for storm hazards 1982
[NASA-TM-86347] 12 p1892 N85-21877
Safety recommendation(s), A84-111 through -115
[REPT-4011C/27] 14 p2216 N85-23744
Extraction of aerodynamic parameters for aircraft at extreme flight conditions
[NASA-TM-86730] 18 p3175 N85-29686

FLIGHT CONTROL

NT AUTOMATIC FLIGHT CONTROL
NT AUTOMATIC LANDING CONTROL
NT FLY BY WIRE CONTROL
NT POINTING CONTROL SYSTEMS
NT THRUST VECTOR CONTROL
LED multifunction keyboard engineering study
[AD-A145199] 01 p0010 N85-10061
Model simplification of flight control systems
02 p0147 N85-11000
Interactive aircraft flight control and aeroelastic stabilization
[NASA-CR-174025] 02 p0148 N85-11003
Aircrew-aircraft integration: A summary of US Army research programs and plans
[NASA-TM-85991] 02 p0148 N85-11004
Definition of acceptable levels of mismatch for equivalent systems of augmented CTOL (Conventional Take-Off and Landing) aircraft
[AD-A145619] 02 p0149 N85-11007
Expert systems in maintenance diagnostics for self-repair of digital flight control systems
[AD-P003933] 02 p0247 N85-11613
Computer equipment for research in statistics
[AD-A145755] 03 p0406 N85-12591
A unified method for evaluating real-time computer controllers: A case study — aircraft control
[NASA-CR-174166] 04 p0547 N85-13478
Flying qualities and control system characteristics for superaugmented aircraft
[NASA-CR-170419] 05 p0596 N85-13800
A distributed expert system for Space Shuttle flight control 05 p0602 N85-13836
Statistical time series models of pilot control with applications to instrument discrimination
05 p0700 N85-14489
Quantification of cross-coupling and motion feedthrough for multiaxis controllers used in an air combat flying task
05 p0700 N85-14491
A nonlinear filter for compensating for time delays in manual control systems 05 p0700 N85-14493
Predictions of cockpit simulator experimental outcome using system models 05 p0702 N85-14504
Twentieth Annual Conference on Manual Control, volume 2
[NASA-CP-2341-VOL-2] 05 p0707 N85-14535
Performance measures for aircraft landings as a function of aircraft dynamics 05 p0712 N85-14565
Terminal control of gliding in atmosphere
06 p0777 N85-14968
Aircraft thrust control scheme for terrain following system
[AD-D011387] 07 p0901 N85-15711
Effect of aerodynamic and angle-of-attack uncertainties on the May 1979 entry flight control system of the Space Shuttle from Mach 8 to 1.5
[NASA-TP-2365] 07 p0913 N85-15778
Literature review of voice recognition and generation technology for Army helicopter applications
[AD-A146878] 07 p0939 N85-15954
cost and benefits optimization model for fault-tolerant aircraft electronic systems
[NASA-CR-166043] 07 p0946 N85-15993
Experience of one UK electronic equipment supplier with bite on engine/flight control systems over the past ten years 08 p1064 N85-16738
Helicopter Guidance and Control Systems for Battlefield Support
[AGARD-CP-359] 08 p1072 N85-16797
Integrated digital/electric aircraft concepts study
[NASA-CR-3841] 08 p1083 N85-16861
Reference energy-altitude descent guidance: Simulator evaluation — aircraft descent and fuel conservation
[NASA-TP-2383] 08 p1085 N85-16868
Multivariable flight control with time-scale separation
[NASA-CR-174320] 08 p1087 N85-16873
Shuttle avionics software development trials: Tribulations and successes, the backup flight system
08 p1091 N85-16892
SSME digital control design characteristics
08 p1091 N85-16893
Development and implementation of the verification process for the shuttle avionics system
08 p1091 N85-16896
Some effects of digital sampling on orbiter flight control system operation 08 p1092 N85-16903
The development and application of aerodynamic uncertainties: And flight test verification for the space shuttle orbiter 08 p1093 N85-16910
Space Shuttle Technical Conference, part 2
[NASA-CP-2342-PT-2] 08 p1098 N85-16937
Space shuttle rudder/speedbrake actuation subsystem
08 p1102 N85-16965
Design and test of a four channel motor for electromechanical flight control actuation
[NASA-CR-171838] 08 p1156 N85-17294
Implications of guidance and control technology on human factors considerations 10 p1532 N85-19656
Interactive Graphics Simulator: Design, development and effectiveness/cost evaluation
[AD-A149417] 10 p1540 N85-19712
Robustness of discrete-time dynamical systems: Application to the multivariable digital control of combat aircraft
[ONERA-NT-1984-2] 11 p1585 N85-19986
Robustness of continuous multivariable flight controls
[ONERA-RT-12/7224-SY] 11 p1586 N85-19987
Robustness of continuous multivariable flight controls
[ONERA-RT-11/7224-SY] 11 p1586 N85-19988
Translating rudder pedal system
[AD-D011510] 12 p1780 N85-21172
Analytical and flight investigation of the influence of rotor and other high-order dynamics on helicopter flight-control system bandwidth
[NASA-TM-86696] 12 p1780 N85-21174
Optimal symmetric flight studies
[NASA-CR-172508] 12 p1780 N85-21176
Integrated control system engineering support
[AD-A149742] 12 p1780 N85-21177
Activities in flight mechanics and flight control
[ISSN-0720-7808] 14 p2227 N85-23803
On-orbit systems identification of flexible spacecraft
Technol., 1984, Pt. 2 p 485-481
14 p2233 N85-23841
High specific power aircraft turn maneuvers: Tradeoff of time-to-turn versus change in specific energy
[AD-A151701] 15 p2471 N85-25257
Effects of side-stick controllers on rotorcraft handling qualities for terrain flight
[NASA-TM-86668] 15 p2473 N85-25267
Multistep orbital correction algorithms for an Earth satellite using low thrust engine
15 p2479 N85-25303
Harrier 15 p2687 N85-26595
Cost Effective and Affordable Guidance and Control Systems
[AGARD-CP-360] 16 p2695 N85-26636
Some aspects of how to design cost-effective flight control systems 16 p2695 N85-26639
Navigation: Accounting for copy
16 p2695 N85-26641
A cost-efficient control procedure for the benefit of all airspace users 16 p2697 N85-26651
Study of longitudinal landing flying qualities evaluation using pilot model theory
[AD-A152194] 16 p2706 N85-26702
Flight control system reconfiguration design using quantitative feedback theory
[AD-A151771] 16 p2710 N85-26722
A modern control design methodology with application to the CH-47 helicopter
[AD-A151946] 16 p2710 N85-26723
The state-of-the-art and future of flight control systems 16 p2712 N85-26732
A perspective on superaugmented flight control advantages and problems 16 p2712 N85-26733
Aspects of application of ACT systems for pilot workload alleviation 16 p2712 N85-26734
Application of AFTI/F-16 task-tailored control modes in advanced multirole fighters 16 p2712 N85-26735
X-29A digital flight control system design
16 p2712 N85-26736
ACT applied to helicopter flight control
16 p2712 N85-26738
Some flight test results with redundant digital flight control systems 16 p2712 N85-26739
An update on experience on the fly by wire Jaguar equipped with a full-time digital flight control system
16 p2712 N85-26740
ACT flight research experience
16 p2713 N85-26741
Operational and developmental experience with the F/A-18A digital flight control system
16 p2713 N85-26742
Flight testing and development of the F/A-18A digital flight control system 16 p2713 N85-26743
Active control technology experience with the Space Shuttle in the landing regime 16 p2713 N85-26747
How to handle failures in advanced flight control systems of future transport aircraft 16 p2714 N85-26752
Interactive design of specifications for airborne software set (GISELE) 16 p2714 N85-26753
The flight control system for the Experimental Aircraft Programme (EAP) demonstrator aircraft
16 p2714 N85-26755
Automatic flight control modes for the AFTI/F-111 mission adaptive wing aircraft 16 p2714 N85-26756
The STOL and maneuver technology program integrated control system 16 p2715 N85-26757
The evolution of active control technology systems for the 1990's helicopter 16 p2715 N85-26758
Some aspects of how to design cost-effective flight control systems
[MBB-LKE-32/S/PUB/143] 16 p2873 N85-27729
Analysis of control system from a viewpoint of desired pole placement and desired degree of robustness
[AD-A152627] 17 p2899 N85-27876
Design of robust controllers for a multiple input-multiple output control system with uncertain parameters application to the lateral and longitudinal modes of the KC-135 transport aircraft
[AD-A153100] 17 p2900 N85-27877
Controller requirements for uncoupled aircraft motion, volume 1
[AD-A153173] 17 p2900 N85-27878

Active Control Systems: Review, Evaluation and Projections
[AGARD-CP-384] 17 p2901 N85-27883
The state-of-the-art and future of flight control systems 17 p2901 N85-27885
A perspective on supersugmented flight control advantages and problems 17 p2901 N85-27886
ACT applied to helicopter flight control 17 p2902 N85-27891
Some flight test results with redundant digital flight control systems 17 p2902 N85-27892
Active control technology experience with the Space Shuttle in the landing regime 17 p2903 N85-27900
The aerodynamics of control 17 p2903 N85-27901
The STOL and maneuver technology program integrated control system development 17 p2905 N85-27910
The evolution of active control technology systems for the 1990's helicopter 17 p2905 N85-27911
Advanced secondary power system for transport aircraft
[NASA-TP-2463] 18 p3062 N85-28944
Piloted simulation of an algorithm for onboard control of time-optimal intercept
[NASA-TP-2445] 18 p3063 N85-28949
Extraction of aerodynamic parameters for aircraft at extreme flight conditions
[NASA-TM-86730] 18 p3175 N85-29686
Development and evaluation of a Fault-Tolerant Multiprocessor (FTMP) computer. Volume 2: FTMP software
[NASA-CR-166072] 19 p3341 N85-30706
Interactive aircraft flight control and aeroelastic stabilization
[NASA-CR-176035] 20 p3396 N85-31064
Ergonomic problems regarding the interactive touch input via screens in onboard and ground-based flight control
[NASA-TM-77814] 20 p3512 N85-31832
Flight control system for a computer controlled aircraft with limited sensors
[AD-A155107] 21 p3555 N85-32115
Myoelectric control of a computer based expert system for flight control
[AD-A154981] 21 p3557 N85-32126
Flutter clearance of the Schweizer 1-36 deep-stall sailplane
[NASA-TM-85917] 22 p3729 N85-33118
Flight test experience and controlled impact of a large, four-engine, remotely piloted airplane
[NASA-TM-86736] 22 p3730 N85-33123
The interpretation of flying qualities requirements for flight control system design
[NASA-CR-177942] 22 p3730 N85-33125
Intelligent redundant actuation system requirements and preliminary system design
[NASA-CR-177306] 23 p3898 N85-34136

FLIGHT CREWS

NT SPACECREWS

Analysis of on-board CIG (Computer Image Generator) applications for aircrew training
[AD-A145214] 01 p0013 N85-10079
Dark focus: Intersubject variation, intrasubject stability, and relationship to near retinoscopy
[AD-A145489] 02 p0235 N85-11530
System status display information
[NASA-CR-172347] 04 p0455 N85-12869
Decision tree rating scales for workload estimation: Theme and variations 05 p0706 N85-14541
Intelligent interfaces for tactical airborne platforms 06 p0752 N85-14820
Establishment of posture and working movements of pilot in air crash enquiries 07 p1010 N85-16417
Human factors survey: C-5 pilots
[AD-A147106] 07 p1020 N85-16477
An analysis of constraints to coordinated tactical crew interaction in the P-3C aircraft
[AD-A147220] 07 p1021 N85-16478
Video concepts in CRM training 09 p1276 N85-18015
A systems analysis of alternative concepts for aircrew cold weather clothing
[AD-A148605] 09 p1365 N85-18580
Human Factors Considerations in High Performance Aircraft
[AGARD-CP-371] 10 p1532 N85-19653
Aircrew and avionics: Friends or Foes? 10 p1532 N85-19654
Observations of physiological and psychological effects of terrain following flight based on in-flight test experience 10 p1532 N85-19657
Personnel protection concepts for advance escape system design 10 p1532 N85-19658
Results of a longitudinal study of airsickness incidence during Naval flight officer training 11 p1694 N85-20649
Preflight and postflight motion sickness testing of the Spacelab 1 crew 11 p1694 N85-20652
Psychological components in the development and prevention of air sickness 11 p1695 N85-20659
Assessing the behavior and performance of teams in organizations: The case of air transport crews
[AD-A150359] 13 p2143 N85-23302
The application of anthropometric survey data to aircrew clothing sizing
[AD-A150545] 13 p2143 N85-23304
Torso restraint system
[AD-D011609] 16 p2702 N85-26684
Statistical study of the dynamic analysis of the workload in the A310 certification campaign 16 p2844 N85-27531
Guidelines of the Federal Minister of Transportation for the formation and examination of airline personnel, part 4 17 p3002 N85-28558
Human factors in cockpit automation: A field study of flight crew transition
[NASA-CR-177333] 19 p3215 N85-29937
U.S. Civil airmen statistics for calendar year 1984
[AD-A156326] 24 p4059 N85-35153
Introduction to European air traffic control
[AD-A156328] 24 p4062 N85-35176
Models for assessing workload of aircrews on long distance flights 24 p4129 N85-35599

FLIGHT FATIGUE

Tolerance, fatigue, physiological and performance effects of sustained and oscillating lateral accelerations 10 p1533 N85-19659
Mental workload measurement: Event-related potentials and ratings of workload and fatigue
[NASA-CR-177354] 15 p2619 N85-26139

FLIGHT HAZARDS

NT METEOROID HAZARDS

Study of effects of lightning on aircraft systems stressed 03 p0310 N85-12005
Don't fowl out
[AD-P004179] 11 p1578 N85-19941
Analysis of bird strikes reported by European airlines, 1976 - 1980
[AD-P004181] 11 p1578 N85-19943
Birds and aircraft engine strike rates
[AD-P004184] 11 p1579 N85-19946
The use of falconry as mean to persuade the birds to stay out of the airport vicinity 11 p1580 N85-19956
Airport bird hazards associated with solid waste disposal facilities
[AD-P004197] 11 p1581 N85-19964
Evaluation of effectiveness of bird scaring operations at a sanitary landfill site near CFB Trenton, Ontario, Canada
[AD-P004201] 11 p1582 N85-19968
Development of bird hazard reduction for airport operational safety
[AD-P004202] 11 p1582 N85-19969
The bird strike situation and its ecological background in the Copenhagen Airport, Kastrup
[AD-P004203] 11 p1582 N85-19970
Bird control program Orlando International Airport
[AD-P004204] 11 p1583 N85-19971
Staff assistance to bases for bird hazards
[AD-P004205] 11 p1583 N85-19972
Bird strike avoidance system for Dover AFB, Delaware
[AD-P004206] 11 p1583 N85-19973
The potential of the NEXRAD radar system for warning of bird hazards
[AD-P004210] 11 p1583 N85-19977
First stage of equipping a Do 28 as a research aircraft for icing, and first research results
[ESA-TT-855] 11 p1584 N85-19982
An analysis of the impacts of the Airport Radar Service Area (ARSA)
[AD-A150954] 14 p2217 N85-23749
Helicopter user survey: Traffic alert and collision avoidance system (TCAS)
[FAA-PM-85-6] 15 p2468 N85-25236
The impact of weather on aviation safety
[GPO-35-520] 16 p2703 N85-26685
Aircraft accident report: United Airlines Flight 663, Boeing 727-222, N7647U, Denver, Colorado, May 31, 1984
[PB85-910405] 16 p2703 N85-26686
Flying in spite of the weather
[NLR-MP-84021-U] 17 p2895 N85-27847
Contributions on the subject of longitudinal movements of aircraft in wind shears
[NASA-TM-77837] 18 p3139 N85-29432
Space Station crew safety alternatives study. Volume 2: Threat development
[NASA-CR-3855] 21 p3558 N85-32133
System safety study of minimum TCAS 2 for instrument weather conditions
[FAA-PM-85-12] 22 p3728 N85-33113

FLIGHT INSTRUMENTS

NT APPROACH INDICATORS
NT ATTITUDE INDICATORS
NT AUTOMATIC PILOTS
NT FLIGHT TEST INSTRUMENTS
NT GYRO HORIZONS
NT HORIZON SCANNERS
NT RADIO ALTIMETERS

The Malcolm horizon: History and future 01 p0008 N85-10046
A comparative evaluation of EMADS (Engine Monitoring and Display System) and conventional engine instruments
[AD-A145901] 03 p0319 N85-12060
Commerce Laboratory: Mission analysis payload integration study
[NASA-CR-171298] 07 p0911 N85-15764
LPI-radar for helicopter obstacle warning 08 p1074 N85-16810
Crewstation assessment of reach as applied to the OH-58A helicopter
[AD-A149413] 10 p1531 N85-19650
Air Force Academy Aeronautics Digest
[AD-A149614] 12 p1769 N85-21104
A preliminary investigation of handling qualities requirements for helicopter instrument flight during decelerating approach manoeuvers and overshoot
[NRC-24173] 17 p2896 N85-27857
A guide to USAF helicopter instrument flight procedures
[AD-A156102] 24 p4063 N85-35182
Accuracy and error analysis — airborne instruments 24 p4123 N85-35557

FLIGHT LOAD RECORDERS

Operational Loads Data
[AGARD-CP-375] 07 p0894 N85-15664
Operational loads measurement: A philosophy and its implementation 07 p0894 N85-15665
The F-15 flight loads tracking program 07 p0894 N85-15666
Operational loads data evaluation for individual aircraft fatigue monitoring 07 p0895 N85-15669
US Army helicopter operational flight loads 07 p0895 N85-15675
Flight parameters recording for structure fatigue life monitoring 07 p0896 N85-15682
USAF approach to airborne structural data recording: Airborne Data Acquisition Multifunction System (ADAMS) 07 p0897 N85-15683

FLIGHT MANAGEMENT SYSTEMS

Ground and flight testing for aircraft guidance and control
[AGARD-AG-282] 13 p1966 N85-22350
Civil avionics flight testing with the RAE(B) BAC1-11 13 p1967 N85-22354
A flight management algorithm and guidance for fuel-conservative descents in a time-based metered air traffic environment: Development and flight test results 13 p1967 N85-22356
Users guide: The LaRC human-operator-simulator-based pilot model
[NASA-TM-86367] 14 p2390 N85-24721
Planning fuel-conservative descents in an airline environmental using a small programmable calculator: Algorithm development and flight test results
[NASA-TP-2393] 16 p2707 N85-26705

FLIGHT MECHANICS

AGARD bulletin technical programme, 1985
[AGARD-BUL-84-2] 02 p0305 N85-11971
Flight test of the Open Loop Gust Alleviation (OLGA) system
[BMFT-FB-W-84-038] 08 p1068 N85-16681
Flight mechanics analysis of dynamic derivatives of the Dornier variable wind tunnel model
[ESA-TT-854] 11 p1577 N85-19937
Technical evaluation report on the FDP Symposium on Flight Test Techniques
[AGARD-AR-208] 12 p1777 N85-21157
Optimal symmetric flight studies
[NASA-CR-172508] 12 p1780 N85-21176
Dynamic wind tunnel testing for active control research 13 p1966 N85-22352
Activities in flight mechanics and flight control
[ISSN-0720-7808] 14 p2227 N85-23803
Use of quaternions in flight mechanics
[AD-A152616] 17 p2899 N85-27875
Active Control Systems: Review, Evaluation and Projections
[AGARD-CP-384] 17 p2901 N85-27883
Flight-mechanics test with a restricted flying aircraft model in a wind tunnel
[ESA-TT-865] 20 p3394 N85-31053
The Naval Postgraduate School Flight Mechanics Laboratory: A feasibility study
[AD-A154578] 21 p3557 N85-32127

Lectures of a Flight Mechanics Conference — conferences
[ESA-TT-831] 24 p4061 N85-35165
Development of flight mechanics research in Brunswick 24 p4061 N85-35166
The contribution made by flight mechanics to civil aviation 24 p4061 N85-35169
The effect of instrumentation system parameters on the results of a flight mechanical system identification 24 p4061 N85-35170
Estimation of flight mechanical variables by means of Kalman filters 24 p4062 N85-35171
Gust simulation for flight mechanical wind tunnel tests 24 p4062 N85-35172
Control variables in vertical wind determination using simple flight-mechanical equations 24 p4121 N85-35546

FLIGHT OPERATIONS
NT CREW PROCEDURES (INFLIGHT)
New runway enables IL-76 flights to Tenkeli in far north 12 p1769 N85-21106
Ministry officials on improving aircraft technical servicing 14 p2206 N85-23697
Disturbance to the population due to flight operations at landing fields. Questionnaire on community reaction to non-commercial and sporting aviation
[NASA-TM-76531] 14 p2353 N85-24537
Space station systems technology study (add-on task). Volume 2: Trade study and technology selection
[NASA-CR-171416] 15 p2475 N85-25279

FLIGHT OPTIMIZATION
On-board near-optimal climb-dash energy management 02 p0137 N85-10931
Computer assisted flight schedule optimization
[AD-A151689] 16 p2858 N85-27623

FLIGHT PATHS
NT GLIDE PATHS
On-board near-optimal climb-dash energy management 02 p0137 N85-10931
Command flight path display. Phase I and II: Appendix F
[AD-A145858] 03 p0318 N85-12056
Effects of aircraft and flight parameters on energy-efficient profile descents in time-based metered traffic
[NASA-CR-172338-ADD] 07 p0901 N85-15706
Predicted performance benefits of an adaptive digital engine control system of an F-15 airplane
[NASA-TM-85916] 07 p0905 N85-15729
Investigation of semiautomatic aircraft control processes employing time redundancy in on-board digital trajectory control computers 07 p0954 N85-16048
Hot radome boresight error measurements
[AD-P004364] 12 p1626 N85-21458
Minimum time turns using vectored thrust
[AD-A151693] 15 p2471 N85-25256
High specific power aircraft turn maneuvers: Tradeoff of time-to-turn versus change in specific energy
[AD-A151701] 15 p2471 N85-25257
A user's manual for AMEER flight path trajectory simulation code
[DE85-006580] 15 p2472 N85-25260
A method of estimating aircraft attitude from fly by wire flight control system data 16 p2697 N85-26653
Terrain following without use of forward looking sensors 16 p2698 N85-26658
Generation of flight paths using heuristic search
[AD-A151949] 16 p2704 N85-26694
Planning fuel-conservative descents in an airline environmental using a small programmable calculator: Algorithm development and flight test results
[NASA-TP-2393] 16 p2707 N85-26705
Aspects of application of ACT systems for pilot workload alleviation 16 p2712 N85-26734
Probabilistic computer model of optimal runway turnoffs
[NASA-CR-172549] 16 p2715 N85-26760
Status of air traffic control system
[S-HRG-98-1197] 20 p3391 N85-31036
User's manual of the BNDSCO computer program for solving constrained optimal control problems
[DFVLR-MITT-85-05] 20 p3516 N85-31865
Guidelines for the evaluation of visual approach slope indicators
[ARL/SYS-R-32] 23 p3896 N85-34132
Determination of instrument errors by compatibility checking: Results from dynamic flight test data
[ARL/AERO-R-162] 23 p3896 N85-34137
International flight planning handbook
[AD-A156330] 24 p4062 N85-35177
Comparative analysis of operational forecasts versus actual weather conditions in airline flight planning, volume 2
[NASA-CR-167863] 24 p4119 N85-35535
Comparative analysis of operational forecasts versus actual weather conditions in airline flight planning, volume 3
[NASA-CR-167864] 24 p4120 N85-35536
Comparative analysis of operational forecasts versus actual weather conditions in airline flight planning, volume 4
[NASA-CR-167865] 24 p4120 N85-35537
Comparative analysis of operational forecasts versus actual weather conditions in airline flight planning: Summary report
[NASA-CR-167866] 24 p4120 N85-35538

FLIGHT PERFORMANCE
U FLIGHT CHARACTERISTICS

FLIGHT PLANS
Kovtunenko comments on Vega flight plan, instrumentation 15 p2462 N85-25318
International flight planning handbook
[AD-A156330] 24 p4062 N85-35177
Comparative analysis of operational forecasts versus actual weather conditions in airline flight planning, volume 1
[NASA-CR-167862] 24 p4119 N85-35534
Comparative analysis of operational forecasts versus actual weather conditions in airline flight planning, volume 2
[NASA-CR-167863] 24 p4119 N85-35535
Comparative analysis of operational forecasts versus actual weather conditions in airline flight planning: Summary report
[NASA-CR-167866] 24 p4120 N85-35538

FLIGHT RULES
NT INSTRUMENT FLIGHT RULES
NT VISUAL FLIGHT RULES

FLIGHT SAFETY
Flight phase status monitor study. Phase 1: Systems concepts
[DOT/FAA/PM-84/18] 03 p0317 N85-12046
Aircraft navigation and landing technology: Status of implementation
[GPO-38-615] 04 p0454 N85-12883
Flight Training Technology for Regional/Commuter Airline Operations: Regional Airline Association/NASA Workshop Proceedings
[NASA-CP-2348] 09 p1275 N85-18009
Dynamic training devices in CRM training 09 p1276 N85-18018
Safety awareness, pilot education, and incident reporting programs 09 p1276 N85-18020
The aviation safety reporting system 09 p1276 N85-18021
Pilot education and safety awareness programs 09 p1277 N85-18026
Legislation to improve airline safety
[GPO-38-222] 12 p1773 N85-21132
Aerospace Safety Advisory Panel
[NASA-TM-87428] 12 p1774 N85-21135
Improvements in personnel needed for better flight safety 14 p2206 N85-23693
Safety recommendation(s), A84-111 through -115
[REPT-4011C/27] 14 p2216 N85-23744
An analysis of the impacts of the Airport Radar Service Area (ARSA)
[AD-A150954] 14 p2217 N85-23749
Official on Soviet research in deicing techniques 15 p2460 N85-25191
Safety recommendation(s), A-84-96
[REPT-3983A/217] 15 p2466 N85-25223
Safety recommendation(s), A-84-76 through -78
[REPT-3751E] 15 p2466 N85-25224
The impact of weather on aviation safety
[GPO-35-520] 16 p2703 N85-26685
Aircraft accident report: United Airlines Flight 663, Boeing 727-222, N7647U, Denver, Colorado, May 31, 1984
[PB85-910405] 16 p2703 N85-26686
Lightning-safe carbon fiber composite for Airbus tail unit 18 p3087 N85-29100
Hydrazine and the F-16 20 p3511 N85-31826

FLIGHT SIMULATION
Pressure distribution on a swept wing aircraft in flight 01 p0004 N85-10025
A mathematical simulation model of the CH-47B helicopter, volume 1
[NASA-TM-84351-VOL-1] 01 p0006 N85-10033
The Malcolm horizon: History and future 01 p0008 N85-10046
Active control technology experience with the Space Shuttle in the landing regime
[NASA-TM-85910] 01 p0012 N85-10071
Effect of penetrant on fatigue of aluminum alloy lap joints
[NLR-TR-82104-U] 01 p0058 N85-10373
Flight simulation fatigue crack propagation in metal/carbon-epoxy laminates
[NLR-TR-83008-U] 01 p0063 N85-10416
Airborne performance measurement system design: C-5 aircraft
[AD-A145436] 02 p0236 N85-11539
Cyclic endurance testing of the RB211-22B cast HP turbine blade — high pressure (HP)
[PNR-90210] 03 p0320 N85-12063
A spatial model of wind shear and turbulence for flight simulation 03 p0395 N85-12518
An in-flight investigation of a twin fuselage configuration in approach and landing
[NASA-CR-172366] 05 p0596 N85-13801
Investigation of pilot behavior in flight tests with a rate command/attitude hold control system
[DFVLR-FB-84-25] 05 p0699 N85-14486
Quantification of cross-coupling and motion feedthrough for multiaxis controllers used in an air combat flying task 05 p0700 N85-14491
A method for measuring the effective throughput time delay in simulated displays involving manual control 05 p0701 N85-14497
Maximum normalized rate as a flying qualities parameter 05 p0702 N85-14503
Measuring workload differences between short-term memory and long-term memory scenarios in a simulated flight environment 05 p0703 N85-14513
Use of linear perspective scene cues in a simulated height regulation task 05 p0704 N85-14517
Accuracy of system step response roll magnitude estimation from central and peripheral visual displays and simulator cockpit motion 05 p0705 N85-14522
Fractographic observation and estimation of crack growth curve of aluminum alloy under ramdom flight simulation loading
[NAL-TR-824] 06 p0766 N85-14913
NyKINM, a further development of KINM 22 — simulation of a robot attack on an aircraft
[FOA-C-20559-D8(E3)] 07 p0903 N85-15720
Practice makes perfect
[AD-A147124] 07 p1019 N85-16488
Advanced flight simulation for helicopter development 08 p1075 N85-16815
Assessment of simulation fidelity using measurements of piloting technique in flight 08 p1075 N85-16817
The IMAGE 3 Conference Proceedings
[AD-A148636] 09 p1267 N85-17962
Visual perceptual aspects of low level high speed flight and flight simulation
[AD-P004310] 09 p1267 N85-17964
Low altitude high speed flight simulation using video disc technology
[AD-P004312] 09 p1268 N85-17966
SODERN Visualization System (SVS) for flight simulation
[AD-P004320] 09 p1269 N85-17974
CIG (Computer Image Generator) goes to war: The tactical illusion
[AD-P004336] 09 p1271 N85-17990
AVTS (Advanced Visual Technology System): A high fidelity visual simulator
[AD-P004338] 09 p1271 N85-17992
Flight crew training technology: A review 09 p1275 N85-18010
Low-cost training technology 09 p1275 N85-18011
Initiative uses of aircraft for flight training 09 p1277 N85-18027
Innovative approaches to recurrent training 09 p1277 N85-18028
In-flight investigation of the effects of time delay in control system on flying qualities in landing approach
[DFVLR-FB-84-35] 11 p1586 N85-19989
Crack growth geometry in aluminum alloy sheet material under flight simulation loading. 1: A comparison between TWIST and miniTWIST FALSTAFF and short FALSTAFF. 2: Effect of truncating high loads
[VTH-LR-441] 11 p1609 N85-20119
Simulation of aircraft behaviour on and close to the ground
[NASA-TM-87460] 14 p2215 N85-23754
Flight simulation for inertial navigation system 14 p2273 N85-24081
Users guide: The LaRC human-operator-simulator-based pilot model
[NASA-TM-86367] 14 p2390 N85-24721
YAV-8B Harrier 15 p2686 N85-26605
Piloted simulation of one-on-one helicopter air combat at NOE flight levels
[NASA-TM-86686] 16 p2710 N85-26720
The effect of load factor on aircraft handling qualities
[AD-A152118] 16 p2710 N85-26724
Design and specification of a local area network architecture for use in real-time flight simulation
[AD-A152242] 16 p2716 N85-26762
Flight Experiment Demonstration System (FEDS) functional description and interface document
[NASA-CR-175290] 16 p2717 N85-26769

Research and development. Technical and scientific reports 1984 16 p2873 N85-27724
Advanced flight simulation for helicopter development [MBB-UD-416/84-O] 16 p2874 N85-27731
Technical evaluation of the Naval Automated Pilot Aptitude Measurement System (NAPAMS) [AD-A152361] 17 p3000 N85-28547
Adding computationally efficient realism to Monte Carlo turbulence simulation [NASA-TP-2469] 17 p3025 N85-28708
Helicopter Aeromechanics [AGARD-LS-139] 18 p3057 N85-28913
Visual and part-task manipulations for teaching simulated carrier landings [AD-A153622] 18 p3154 N85-29529
Electrooculographic measurement, fatigue and variability of performance in simulated aircraft flight 19 p3217 N85-29948
Crew systems and flight station concepts for a 1995 transport aircraft [NASA-CR-166068] 19 p3221 N85-29973
X-ray satellite [NASA-TM-77606] 20 p3407 N85-31144
Modifications of flight-by-flight load sequences to provide for good fracture surface readability [NLR-MP-84012-U] 20 p3472 N85-31577
Learning and self adaptation applied to the simulation of a human pilot [ONERA-RT-24/5122-SY] 20 p3511 N85-31628
A preliminary investigation of handling qualities requirements for helicopter instrument flight during decelerating approach maneuvers and overshoot [AD-A154650] 21 p3557 N85-32125
The interpretation of flying qualities requirements for flight control system design [NASA-CR-177942] 22 p3730 N85-33125
Energy management of three-dimensional minimum-time intercept [NASA-CR-176174] 24 p4064 N85-35186
Comparative analysis of operational forecasts versus actual weather conditions in airline flight planning, volume 2 [NASA-CR-167863] 24 p4119 N85-35535

FLIGHT SIMULATORS
NT COCKPIT SIMULATORS
Evaluation of the Malcolm horizon in a moving-base flight simulator 01 p0008 N85-10051
Content, variety, and augmentation of simulated visual scenes for teaching air-to-ground attack [AD-A145218] 01 p0013 N85-10060
Simulator study of flight characteristics of several large, dissimilar, cargo transport airplanes during approach and landing [NASA-TP-2357] 02 p0148 N85-11002
Air Force Human Resources Laboratory report: Fiscal year, 1983 [AD-A145647] 02 p0238 N85-11548
Models for the effects of G-seat cuing on roll-axis tracking performance 05 p0707 N85-14532
Determining training device requirements in Army aviation systems 05 p0711 N85-14558
Measuring pilot workload in a moving-base simulator. Part 2: Building levels of workload 05 p0712 N85-14566
Simulation evaluation of two VTOL control/display systems in IMC approach and shipboard landing [NASA-TM-85996] 06 p0756 N85-14841
Situational interactive micro/graphic simulator system for improving maintenance performance [AD-A146677] 06 p0757 N85-14846
Reference energy-altitude descent guidance: Simulator evaluation — aircraft descent and fuel conservation [NASA-TP-2383] 06 p1095 N85-16868
Proceedings of a Workshop on Research Issues in Simulator Sickness [AD-A148543] 06 p1198 N85-17538
Using a limited field of view simulator to instruct high speed, low altitude flying skills [AD-P004309] 09 p1267 N85-17963
Attitude control using action-demanding interactive displays: Toward an active psychophysics [AD-P004311] 09 p1267 N85-17965
Simulating speed and height cues in the C-130 weapon system trainer [AD-P004313] 09 p1268 N85-17967
Automated and interactive data base generation [AD-P004316] 09 p1268 N85-17970
An overview of the research program at the visual technology research simulator [AD-P004321] 09 p1269 N85-17975
Considerations in an optical variable acuity display system [AD-P004323] 09 p1269 N85-17977
Design considerations for an eye tracked ADI (Area of Interest) display system [AD-P004324] 09 p1269 N85-17978
The effects of time delay in man-machine control systems: Implications for design of flight simulator Visual-Display-Delay compensation [AD-P004329] 09 p1270 N85-17983
Binocular overlap in a fiber optic helmet mounted display [AD-P004331] 09 p1270 N85-17985
Global optical metrics for self-motion perception [AD-P004333] 09 p1271 N85-17987
Simulator sickness: Sensorimotor disturbances induced in flight simulators [AD-P004334] 09 p1271 N85-17988
Simulation 09 p1277 N85-18024
Low cost training aids and devices 09 p1277 N85-18025
Pictorial format display evaluation [AD-A149252] 10 p1425 N85-18986
Interactive Graphics Simulator: Design, development and effectiveness/cost evaluation [AD-A149417] 10 p1540 N85-19712
Inflight IFR procedures simulator [NASA-CASE-KSC-11218-1] 11 p1586 N85-19990
Simulator sickness: Reaction to a transformed perceptual world. 6: Preliminary site surveys 11 p1694 N85-20653
Transportation [JPRS-UTR-85-004] 12 p1769 N85-21105
New flight simulators at Vnukovo permit less in-flight training 12 p1769 N85-21107
Visual simulation requirements for aircraft aspect recognition at real world distances [AD-A151040] 14 p2228 N85-23610
Roundtable on effective use of flight simulators 15 p2460 N85-25190
The evaluation of ACS for helicopters: Conceptual simulation studies to preliminary design 16 p2712 N85-26737
Advanced flight simulation for helicopter development [MBB-UD-416/84-O] 16 p2874 N85-27731
The role of simulation 18 p3058 N85-28919
The use of flight simulators in measuring and improving training effectiveness [AD-A153817] 18 p3064 N85-28954
A systematic determination of skill and simulator requirements for airline transport pilot certification [AD-A154135] 19 p3330 N85-30630
Advanced simulator for pilot training and helmet-mounted visual display configuration comparisons [AD-A155326] 21 p3667 N85-32776
Man-vehicle systems research facility advanced aircraft flight simulator throttle mechanism 22 p3798 N85-33527
Langley aeronautics and space test highlights, 1984 [NASA-TM-87565] 23 p4057 N85-35151

FLIGHT STABILITY TESTS
Flight test of the Open Loop Gust Alleviation (OLGA) system [BMFT-FB-W-84-038] 08 p1088 N85-16881
Identification of gust input and gust response characteristics from Do 28 TNT flight test data [DFVLR-FB-84-48] 17 p2900 N85-27881
Proposals for the determination of necessary elevator handling characteristics of sailplanes in high speed range [DFVLR-FB-84-52] 17 p2900 N85-27882
Real scale test of the Petit Canard aircraft in the number 3 section, 47 sqm, of the SIMA wind tunnel, May 1984 [ONERA-PV-1/0772-GY] 20 p3369 N85-31018

FLIGHT STRESS (BIOLOGY)
NT SPACE FLIGHT STRESS
The Reports of Aeromedical Laboratory, volume 25, no. 1/2 [ISSN-0023-2858] 01 p0090 N85-10605
Psychological states (mood, affect or emotion) experienced by JASDF pilots through flying duties. 3: Flying conditions causing pilots psychological disturbances 01 p0090 N85-10606
The relationship between emotional tension scale and psychological uneasiness of JASDF pilots in flying situations 01 p0090 N85-10606
Results of a longitudinal study of airsickness during naval flight officer training: Executive summary [AD-A150687] 14 p2368 N85-24712
Blood serum enzyme activity following long term spaceflights 19 p3326 N85-30604
Microorganisms in space flight 23 p3951 N85-34490

FLIGHT TECHNICAL ERROR
U PILOT ERROR

FLIGHT TEST INSTRUMENTS
Flight test support aircraft Advanced Technologies Testing Aircraft System (ATTAS) for the DFVLR [MBB-FE-732/S/PUB/154] 16 p2874 N85-27730

FLIGHT TEST VEHICLES
Flight test support aircraft Advanced Technologies Testing Aircraft System (ATTAS) for the DFVLR [MBB-FE-732/S/PUB/154] 16 p2874 N85-27730
B-52B/DTV (Drop Test Vehicle) flight test results: Drop test missions [NASA-CR-171830] 19 p3215 N85-29934

FLIGHT TESTS
NT FLIGHT STABILITY TESTS
NT SPACE TRANSPORTATION SYSTEM FLIGHTS
NT SPACE TRANSPORTATION SYSTEM 1 FLIGHT
NT SPACE TRANSPORTATION SYSTEM 3 FLIGHT
NT SPACE TRANSPORTATION SYSTEM 4 FLIGHT
Pressure distribution on a swept wing aircraft in flight 01 p0004 N85-10025
Airworthiness and flight characteristics test of the JOH-6A light combat helicopter configured with a wire strike protection system [AD-A144880] 01 p0006 N85-10038
Airworthiness and Flight Characteristics (A and FC) test of the EH - 1X/EH - 1H helicopter configurations [AD-A144881] 01 p0007 N85-10039
A preliminary flight evaluation of the peripheral vision display using the NT-33A aircraft [AD-A145123] 01 p0010 N85-10060
YO-3A acoustics research aircraft systems manual [NASA-TM-85968] 01 p0012 N85-10074
Nonlinear system identification methodology development based on F-4S flight test data analysis [AD-A146289] 03 p0318 N85-12053
Flight and wind-tunnel comparisons of the inlet-airframe interaction of the F-15 airplane [NASA-TP-2374] 04 p0455 N85-12884
Flight tests of the Digital Integrated Automatic Landing System (DIALS) [NASA-CR-3959] 04 p0457 N85-12900
The DG400 propulsed glider [CEV/IS/SE/AV/84] 05 p0595 N85-13795
Maximum normalized rate as a flying qualities parameter 05 p0702 N85-14503
Maximum likelihood estimation of parameters in linear systems from flight test data: A FORTRAN program [AD-B087198L] 05 p0715 N85-14588
Flight test technique for evaluation of gust load alleviation analysis methodology [NASA-TM-86344] 06 p0754 N85-14833
Flight test results on stall characteristics of a large jet transport [NAL-TR-817] 06 p0754 N85-14835
Structural flight load measurement demonstration of structural integrity 07 p0895 N85-15670
CF-5 vertical stabilizer flight load survey 07 p0895 N85-15673
Ground-effect analysis of a jet transport airplane [NASA-TM-85920] 07 p0897 N85-15687
The UH-1H helicopter icing flight test program: An overview [NASA-TM-86925] 07 p0900 N85-15702
Flight testing of Litton laser gyro strapdown system LTN-90 for general aviation [DFVLR-MITT-84-16] 07 p0901 N85-15709
Noise measurement flight test: Data-analyses aerospatiale AS-355F TwinStar helicopter [AD-A147497] 07 p1039 N85-16595
Built-in-test for first line testing 08 p1084 N85-16739
Flight tests with a new helicopter Force Feel System (FFS) 08 p1075 N85-16818
Development and flight test of a helicopter compact, portable, precision landing system concept 08 p1076 N85-16821
Airworthiness and flight characteristics test of the RC-12D Guardrail V [AD-A148046] 08 p1084 N85-16864
Preliminary airworthiness evaluation AH-1S (MC) helicopter with external fuel tanks installed [AD-A148091] 08 p1084 N85-16865
Noise measurement flight test for Boeing Vertol 234/CH 47-d helicopter: Data/analyses [AD-A148172] 08 p1216 N85-17670
Noise measurement flight test: Data-analyses Aerospatiale AS 350D AStar helicopter [AD-A148496] 08 p1218 N85-17672
Noise measurement flight test: Data-analyses, Sikorsky S-76A helicopter [AD-A148525] 08 p1218 N85-17673
Activities at Mil Experimental Design Bureau 09 p1278 N85-18036
Modeling of aircraft performance from flight test results using quasi steady-state test techniques 09 p1279 N85-18047
A comparison of fatigue lives under a complex and a much simplified flight-by-flight testing sequence — Mirage 3 aircraft [ARL/STRUC-TM-368] 09 p1280 N85-18052

NASA-VCOSS dynamic test facility
[NASA-TM-86491] 10 p1427 N85-18998
Observations of physiological and psychological effects of terrain following flight based on in-flight test experience 10 p1532 N85-19657
Collision avoidance for Naval training aircraft
[FAA-PM-84-4] 12 p1774 N85-21136
On the application of compatibility checking techniques to dynamic flight test data
[ARL/AERO-R-161] 12 p1776 N85-21151
Technical evaluation report on the FDP Symposium on Flight Test Techniques
[AGARD-AR-206] 12 p1777 N85-21157
Civil avionics flight testing with the RAE(B) BAC1-11 13 p1967 N85-22354
Guidance and control research flight testing with HFB 320 test aircraft 13 p1967 N85-22355
A flight management algorithm and guidance for fuel-conservative descents in a time-based metered air traffic environment: Development and flight test results 13 p1967 N85-22356
Avionics Flight Evaluation System (AFES) 13 p1967 N85-22357
Improved Y-11 general-purpose transport designated Y-12 13 p1972 N85-22365
Operational loads measurement: A philosophy and its implementation — aircraft structures
[AD-A149445] 13 p2144 N85-23308
Glider Nimbus 3-24.5. Partial certification test results for importation in the U category
[REPT-CEV/IS/SE/AV/84] 14 p2220 N85-23763
Solar Array Experiment (SAE) flight experience 14 p2236 N85-23861
Location and data collection for long stratospheric balloon flights 14 p2326 N85-24377
US Army Aviation Engineering Flight Activity (USAAEFA) report bibliography update 1983 - 1984
[AD-A151381] 15 p2457 N85-25168
Trajectory measurements for take-off and landing tests and other short-range applications, volume 16
[AGARD-AG-160-VOL-16] 15 p2581 N85-25801
Navigation and flight director guidance for the NASA/FAA helicopter MLS curved approach flight test program
[NASA-CR-177350] 16 p2704 N85-26691
Planning fuel-conservative descents in an airline environmental using a small programmable calculator: Algorithm development and flight test results
[NASA-TP-2393] 16 p2707 N85-26705
Development and flight test of a helicopter, X-band, portable precision landing system concept
[NASA-TM-86710] 16 p2710 N85-26721
A modern control design methodology with application to the CH-47 helicopter
[AD-A151946] 16 p2710 N85-26723
The effect of load factor on aircraft handling qualities
[AD-A152118] 16 p2710 N85-26724
Some flight test results with redundant digital flight control systems 16 p2712 N85-26739
Flight testing and development of the F/A-18A digital flight control system 16 p2713 N85-26743
OLGA: An open loop gust alleviation 16 p2713 N85-26744
Space Shuttle program communication and tracking systems interface analysis
[NASA-CR-171862] 16 p2729 N85-26841
In-situ stratospheric ozone measurements: Recent results and their implications 16 p2824 N85-27419
Station for in-orbit testing of satellites
[MBB-UR-706/84-O] 16 p2874 N85-27733
USSR report: Transportation
[JPRS-UTR-84-025] 17 p2894 N85-27841
Test flight of IL-76TD long-range transport variant 17 p2894 N85-27842
A preliminary investigation of handling qualities requirements for helicopter instrument flight during decelerating approach maneuvers and overshoot
[NRC-24173] 17 p2896 N85-27857
Flight trials of a modified gulfstream commander carrying external stores
[AD-A153376] 17 p2896 N85-27859
Parameter identification results of tests in nonsteady symmetric flight with the Hawker Hunter Mk 7
[NLR-TR-83042-U] 17 p2897 N85-27860
The Avionics Flight Evaluation System (AFES) of DFVLR
[DFVLR-MITT-85-01] 17 p2897 N85-27864
In-flight investigation of the influence of pitch damping and pitch control effectiveness on landing approach flying qualities of statically unstable transport aircraft
[DFVLR-FB-84-12] 17 p2900 N85-27880
Some flight test results with redundant digital flight control systems 17 p2902 N85-27892
ACT flight research experience 17 p2902 N85-27894
Flight testing and development of the F/A-18A digital flight control system 17 p2902 N85-27896
OLGA: An open loop gust alleviation system 17 p2903 N85-27897
Flight testing for performance and flying qualities 18 p3056 N85-28920
DC-10 winglet flight evaluation
[NASA-CR-3704] 19 p3217 N85-29849
Flight testing the Litton LTN 90 laser gyro strapdown system for civil aviation
[ESA-TT-904] 20 p3392 N85-31042
Design and implementation of input signals for identification of pilot/aircraft models
[ESA-TT-880] 20 p3394 N85-31055
Large space structure flight experiment 20 p3410 N85-31163
Design, manufacture and testing of a medium accuracy star tracker
[REPT-TR/84-048] 20 p3459 N85-31488
Artificial and natural icing tests YEH-60A quick fix helicopter
[AD-A155147] 21 p3555 N85-32116
Design of an expert-system flight status monitor
[NASA-TM-86739] 21 p3669 N85-32794
Qualification needs for advanced integrated aircraft
[NASA-TM-86731] 22 p3729 N85-33119
Development of a temperature-compensated hot-film anemometer system for boundary-layer transition detection on high-performance aircraft
[NASA-TM-86732] 22 p3730 N85-33121
Development of control laws for a flight test maneuver autopilot for an F-15 aircraft
[NASA-TM-86736] 22 p3730 N85-33122
Flight test experience and controlled impact of a large, four-engine, remotely piloted airplane
[NASA-TM-86738] 22 p3730 N85-33123
The interpretation of flying qualities requirements for flight control system design
[NASA-CR-177942] 22 p3730 N85-33125
Flight testing the fixed-wing configuration of the Rotor Systems Research Aircraft (RSRA)
[NASA-TM-86762] 23 p3896 N85-34135
Determination of instrument errors by compatibility checking: Results from dynamic flight test data
[ARL/AERO-R-162] 23 p3896 N85-34137
A comparison between Falcon data and motor glider data 24 p4121 N85-35547

FLIGHT TIME
General aviation activity and avionics survey
[AD-A149572] 12 p1769 N85-21103

FLIGHT TRAINING
NT SPACE FLIGHT TRAINING
Analysis of on-board CIG (Computer Image Generator) applications for aircrew training
[AD-A145214] 01 p0013 N85-10079
Workload demand and CNS depressant stressor effects on spatial orientation information processing
[AD-A145211] 01 p0098 N85-10851
Airborne performance measurement system design: C-5 aircraft
[AD-A145436] 02 p0236 N85-11539
Air Force Human Resources Laboratory report: Fiscal year, 1983
[AD-A145647] 02 p0238 N85-11548
Can the Aggressors continue to be effective in the F-5E?
[AD-A146861] 07 p1019 N85-16465
Practice makes perfect
[AD-A147124] 07 p1019 N85-16466
Directions of the West German Ministry of Transport for education and control of airline personnel (section 3, chapters 2 and 12) 08 p1081 N85-16848
Directions of the West German Ministry of Transport for education and control or airline personnel, Report 6; chapters 3/A and 3/B 08 p1081 N85-16849
The value and utility of inflight onboard simulation
[AD-A148033] 08 p1196 N85-17543
Flight Training Technology for Regional/Commuter Airline Operations: Regional Airline Association/NASA Workshop Proceedings
[NASA-CP-2348] 09 p1275 N85-18009
Flight crew training technology: A review 09 p1275 N85-18010
Low-cost training technology 09 p1275 N85-18011
Captain development training at US Air 09 p1275 N85-18012
Management training for cockpit crews at Piedmont flight 09 p1276 N85-18013
Integrated approach to flight crew training 09 p1276 N85-18014
Video concepts in CRM training 09 p1276 N85-18015
Use of simplifier scenarios for CRM training 09 p1276 N85-18016
Use of airplanes for loft training 09 p1276 N85-18019
Low cost training aids and devices 09 p1277 N85-18025
Initiative uses of aircraft for flight training 09 p1277 N85-18027
Innovative approaches to recurrent training 09 p1277 N85-18028
Interactive Graphics Simulator: Design, development and effectiveness/cost evaluation
[AD-A149417] 10 p1540 N85-19712
Inflight IFR procedures simulator
[NASA-CASE-KSC-11218-1] 11 p1586 N85-19990
Results of a longitudinal study of airsickness incidence during Naval flight officer training 11 p1694 N85-20649
New flight simulators at Vnukovo permit less in-flight training 12 p1769 N85-21107
Results of a longitudinal study of airsickness during naval flight officer training: Executive summary
[AD-A150867] 14 p2388 N85-24712
Roundtable on effective use of flight simulators 15 p2460 N85-25190
Trends shaping advanced aircrew training capabilities through the 1990s
[AD-A152277] 16 p2843 N85-27530
Guidelines of the Federal Minister of Transportation for the formation and examination of airline personnel, part 4 17 p3002 N85-28558
The use of flight simulators in measuring and improving training effectiveness
[AD-A153617] 18 p3064 N85-28954
Visual and part-task manipulations for teaching simulated carrier landings
[AD-A153622] 18 p3154 N85-29529

FLIGHT VEHICLES
Approximate analytic method of calculating trajectories of movement of a flight vehicle in the atmosphere 14 p2279 N85-24121

FLIP-FLOPS
Experimental test of the three subaperture method for estimating target elevation angle
[AD-A149687] 12 p1851 N85-21614
A two-cycle shift register with error detection
[AD-A150768] 14 p2400 N85-24791

FLIR DETECTORS
Some thoughts on the implementation of pilot night vision devices for helicopters 06 p0751 N85-14814
Application of infrared radiometers for airborne detection of clear air turbulence and low level wind shear, airborne infrared low level wind shear detection test
[NASA-CR-175725] 15 p2594 N85-25985
An analysis of the economic impact of the AN/APS-134 FLAR (Forward Looking Airborne Radar) retrofit on Coast Guard HC-130 aircraft
[AD-A152619] 17 p2949 N85-28204
Thin film phase transition materials development program
[AD-A154260] 19 p3259 N85-30209

FLOAT ZONES
Research on the basic understanding of high efficiency in silicon solar cells
[DE85-000507] 11 p1672 N85-20537
Microgravity silicon zoning investigation
[NASA-CR-171531] 20 p3397 N85-31073
Advanced module development overview 21 p3612 N85-32445

FLOATING
Development of a floating element wall shear transducer
[AD-A144794] 01 p0049 N85-10324
Buckling analysis of cracked, floating ice sheets
[AD-A147330] 07 p0968 N85-16277

FLOATING POINT ARITHMETIC
Function algorithms for MPP scientific subroutines, volume 1
[NASA-CR-175248] 01 p0102 N85-10678
Floating-point function generation routines for 16-bit microcomputers
[NASA-TM-83783] 01 p0102 N85-10683
ES devices at fair 08 p1141 N85-17187
Programmable realtime interface between a block floating point processor and memory
[AD-D011431] 08 p1203 N85-17571
Hardware math for the 6502 microprocessor
[NASA-TM-86517] 23 p3955 N85-34511

FLOATS
Air carrier overwater emergency equipment and procedures
[PB85-917006] 21 p3553 N85-32105

FLOCCULATING
Mechanism and process of flocculation by polymeric flocculant 09 p1303 N85-18185

FLOOD PLAINS
Deforestation, floodplain dynamics, and carbon biogeochemistry in the Amazon Basin
08 p1144 N85-17218
Application of hierarchical data structures to geographical information systems
[AD-A152169] 16 p2877 N85-27753
FLOOD PREDICTIONS
NESDIS operational precipitation estimation techniques 01 p0076 N85-10505
Short period forecasts in West Africa using Meteosat data 01 p0079 N85-10526
Parameterizing extreme still water levels and waves in design level studies
[IOS-163] 03 p0398 N85-12542
FLOODS
Paleohydrology and geomorphology of selected reaches of the upper Wabash Valley, Indiana 02 p0226 N85-11481
Heat sources in the tropics and large scale flow anomalies associated with precipitation anomalies in northeast Brazil
[INPE-3211-TDL/175] 04 p0538 N85-13421
Probable maximum flood estimation - Eastern United States
[AD-A146536] 06 p0839 N85-15324
Droughts and floods in South America due to the 1982-83 El Nino-southern oscillation episode
[INPE-3408-PRE/677] 09 p1357 N85-18535
Catastrophic-flood features in Swedish Lapland as a terrestrial analog for Martian channel flows 13 p2190 N85-23587
Flood-runoff forecasting with HEC1F
[AD-A154286] 19 p3300 N85-30456
Military hydrology. Report 9: State-of-the-art review and annotated bibliography of dam-breach flood forecasting
[AD-A155383] 22 p3801 N85-33553
FLOORS
Full-scale crash-test evaluation of two load-limiting subfloors for general aviation airframes
[NASA-TP-2360] 04 p0512 N85-13267
The development of a method for the shock-resistant securing of large batteries in submarines 09 p1335 N85-18391
Fire performance of interstitial space construction system
[NBSIR-85-3158] 20 p3436 N85-31318
Airborne sound transmission loss characteristics of wood-frame construction
[AD-A154174] 20 p3524 N85-31919
FLOQUET THEOREM
Application of Floquet theory to helicopter blade flapping stability
[AD-A154460] 19 p3218 N85-29952
FLORA
U PLANTS (BOTANY)
FLORIDA
Water resources data, Florida, water year 1982. Volume 4: Northwest Florida
[PB84-223445] 01 p0066 N85-10437
Revised Uniform Summary of Surface Weather Observations (RUSSWO). Parts A-F: Homestead AFB, Florida
[AD-A147203] 07 p1007 N85-16396
Surface pressure produced by Space Transportation System flight 41B
[AD-A150793] 14 p2242 N85-23901
Review and annotated bibliography of benthic studies in coastal and estuarine areas of Florida with a selected compilation of worldwide benthic methodological references and southeastern United States benthic taxonomic references
[PB85-151041] 16 p2622 N85-27405
FLOTATION
Investigations into the improvement of processing of Bolivian tin ores
[BMFT-FB-T-84-184] 07 p0917 N85-15807
Flotation tires and subsurface compaction
[AD-P004299] 09 p1409 N85-18878
Investigation of foam flotation and phase partitioning techniques 12 p1945 N85-22218
FLOTATION SYSTEMS
U FLOATS
FLOUR (FOOD)
Compilation of elemental concentration data for NBS (National Bureau of Standards) biological, geological and environmental standard reference materials, 1982
[PB84-218338] 01 p0025 N85-10158
FLOW CHAMBERS
Jet pump-drive system for heat removal
[NASA-CASE-NPO-16494-1-CU] 18 p3099 N85-29182
Fluidic angular velocity sensor
[NASA-CASE-NPO-16479-1-CU] 18 p3104 N85-29219
FLOW CHARACTERISTICS
NT BOUNDARY LAYER STABILITY
NT FLAME STABILITY
NT FLOW DISTRIBUTION
NT FLOW STABILITY
NT FLOW VELOCITY
NT MAGNETOHYDRODYNAMIC STABILITY
NT WEIBEL INSTABILITY
Coolant passage heat transfer with rotation 02 p0143 N85-10988
Vortex-generating coolant-flow-passage design for increased film-cooling effectiveness and surface coverage
[NASA-TP-2368] 03 p0361 N85-12314
Modelling the aerodynamics in a system of continuous channels and experimentation procedure
[BLL-M-35923-(5828.4)] 05 p0634 N85-14067
Analytical modeling of circuit aerodynamics in the new NASA Lewis wind tunnel
[NASA-TM-86912] 07 p0897 N85-15688
Flow of nitrogen-pressurized Halon 1301 in fire extinguishing systems
[NASA-CR-174271] 07 p0900 N85-15701
Turbulent bouyant flow and pressure variations around a circular cylinder in a cross uniform flow near the ground 09 p1318 N85-18287
Flow through very porous screens
[NASA-TP-2436] 11 p1631 N85-20270
A probe for direct measurement of flow direction
[ESA-TT-853] 11 p1637 N85-20310
TRACR3D: A model of flow and transport in porous/fractured media
[LA-9667-MS] 12 p1845 N85-21576
Calibration of wind tunnel flow quality 13 p1976 N85-22399
Hydraulic brakes for industrial robots 13 p2046 N85-22806
Design of piping for oil drain from turbine bearings 14 p2271 N85-24073
Analysis of selected problems involving vortical flows
[NASA-CR-177347] 15 p2463 N85-25212
Flow past a flat plat with a vortex/sink combination
[JIAA-TR-58] 15 p2464 N85-25215
The effect of air holes on combustor liner wall temperature profile: Experiments
[NAL-TR-840] 15 p2504 N85-25443
Flow through very porous inclined screens
[NASA-TM-86979] 15 p2555 N85-25761
Inviscid upwind finite difference model for two dimensional vertical axis wind turbines 15 p2585 N85-25933
Fuel and oxidizer turbine loss analysis 16 p2739 N85-26900
Analysis of the NASA/MSFC airborne Doppler lidar results from San Gorgonio Pass, California
[NASA-CR-3901] 16 p2832 N85-27463
New flow physical aspects in aerodynamics
[MBB-FE-122/S/PUB/133] 16 p2873 N85-27725
Dependence of characteristics of centrifugal magnetohydrodynamic conduction pump on electrical conductance of end walls. Part 1: Experiment 17 p2939 N85-28146
Transport characteristics of slurries in pipelines: Flow regimes and pressure drop
[DE85-009453] 18 p3101 N85-29198
Inferred flows of electric currents in solar active regions 18 p3208 N85-29899
Microgravity silicon zoning investigation
[NASA-CR-171531] 20 p3397 N85-31073
Flow characteristics of the Cascade granular blanket
[DE85-010932] 20 p3420 N85-31227
Flow modeling at the base region of missiles
[SNIAS-851-320-101] 20 p3420 N85-31228
Detailed studies of aviation fuel flowability
[NASA-CR-174938] 20 p3435 N85-31308
A comparison of two bench scale tests of fuel low temperature flow properties
[AD-A154477] 20 p3435 N85-31311
Transition in Turbines
[NASA-CP-2366] 20 p3452 N85-31433
Investigation of influence of gas exit modes on characteristics of N2O - N2 - He discharge laser 21 p3684 N85-32988
Compressible two-phase flow instabilities simulated with a hybrid Lagrange-Euler pseudospectral method
[DE85-009904] 23 p3931 N85-34361
FLOW CHARTS
Flowcharting with D-charts
[NASA-CR-175641] 14 p2402 N85-24806
A test methodology for an automated and interactive software development environment
[AD-A152857] 17 p3011 N85-28618
Resource management for the tagged token dataflow architecture
[AD-A154773] 21 p3667 N85-32779
A rational approach to cam design 23 p3923 N85-34311
FLOW COEFFICIENTS
Measurement of the development of the boundary layer in the annulus walls of a fourstage compressor
[CUED/A-TURBO-TR-121] 01 p0046 N85-10299
Analysis of experimental shaft seal data for high-performance turbomachines, as for Space Shuttle main engines
[NASA-TM-86926] 12 p1844 N85-21569
FLOW DEFLECTION
Turbulent flow around circular cylinder uniformly rotating in infinite incompressible fluid 14 p2277 N85-24109
FLOW DIRECTION INDICATORS
NT WIND VANES
Determination of corrections to flow direction measurements obtained with a wing-tip mounted sensor
[NASA-CR-174412] 10 p1421 N85-18982
Miniature electrooptical air flow sensor
[NASA-CASE-LAR-13065-1] 11 p1635 N85-20295
Determination of boundary line between reverse jet and surrounding stream 13 p2043 N85-22789
FLOW DISTORTION
On vortex bursting
[NASA-TM-77587] 01 p0002 N85-10008
Natural environment analysis
[NASA-CR-171333] 10 p1428 N85-19010
Experimental and analytical investigation of fan flow interaction with downstream struts
[NASA-CR-175756] 15 p2462 N85-25201
Development of artificially produced perturbations in supersonic boundary layer 21 p3683 N85-32879
FLOW DISTRIBUTION
Numerical analysis of the 3-dimensional inviscid hypersonic flow around capsule-type bodies by the alternate directional implicit method
[NAL-TR-799] 01 p0002 N85-10012
Computational methods for complex flowfields
[AD-A145219] 01 p0004 N85-10019
Measurement of the development of the boundary layer in the annulus walls of a fourstage compressor
[CUED/A-TURBO-TR-121] 01 p0046 N85-10299
Oil flow patterns of separated flow on a hemispherical cylinder at incidence
[DFVLR-FB-84-20] 01 p0048 N85-10313
Estuaries of the Cape. Part 2: Synposes of available information on individual systems. Report no. 19: Groot (WES) (CMS 23) and Sout (CMS 22)
[CSIR-RR-418] 01 p0087 N85-10588
Experimental trim drag values and flow-field measurements for a wide-body transport model with conventional and supercritical wings
[NASA-TP-2071] 02 p0135 N85-10920
Hot section laser anemometry 02 p0142 N85-10962
Jet array impingement flow distributions and heat transfer characteristics: Effects of initial crossflow and nonuniform array geometry 02 p0142 N85-10967
Energy efficient engine high pressure turbine test hardware detailed design report
[NASA-CR-167955] 02 p0147 N85-10995
An experimental study of jet impingement on a circular cylinder
[AD-A145583] 02 p0198 N85-11326
Problem of reduction to ideal wind tunnel in experimental aerodynamics 02 p0260 N85-11702
Navier-Stokes solution of 3-dimensional hypersonic afterbody flowfields over capsule-type vehicles
[NAL-TR-819] 03 p0311 N85-12010
Wind Tunnel Wall Interference Assessment and Correction, 1983
[NASA-CP-2319] 03 p0311 N85-12011
Wall interference measurements for three-dimensional models in transonic wind tunnels: Experimental difficulties 03 p0311 N85-12012
Survey of ONERA activities on adaptive-wall applications and computation of residual corrections 03 p0312 N85-12013
Investigations of flow field perturbations induced on slotted transonic-tunnel walls 03 p0312 N85-12018
NLR activities in the field of wind tunnel wall interference 03 p0313 N85-12024
Interaction between an airfoil and a streamwise vortex
[AD-A145823] 03 p0316 N85-12041
An inviscid computational method for supersonic inlets
[AD-A145997] 03 p0316 N85-12042
Structure and properties of titanium alloys after isothermal deformation at low speeds 03 p0351 N85-12260
Fluid layer between infinite elastic plates II. Distribution of power flow
[AD-A146690] 03 p0361 N85-12312
Fluid motion in a rotating and nutating container
[AD-A146175] 03 p0362 N85-12322

Laser velocimeter measurements and analysis in turbulent flows with combustion. Part 3: A correction lens for laser Doppler measurements in a cylindrical tube
[AD-A146206] 03 p0386 N85-12348
Terrestrial heat flow in Europe and general features of its regional distribution
[REPT-563] 03 p0377 N85-12406
Dynamic occlusion analysis in optical flow fields
[AD-A145805] 03 p0406 N85-12594
A study of flow past an airfoil with a jet issuing from its lower surface
[NASA-CR-166610] 04 p0451 N85-12860
Viscous-inviscid aerodynamic analysis of two-dimensional thrust augmentors
[NASA-CR-177321] 04 p0451 N85-12861
Development of computational fluid dynamics at NASA Ames Research Center
[NASA-TM-86021] 04 p0452 N85-12866
An experimental investigation of two-dimensional thrust augmenting ejectors, part 2
[NASA-CR-174110] 04 p0456 N85-12895
The preliminary checkout, evaluation and calibration of a 3-component force measurement system for calibrating propulsion simulators for wind tunnel models
[NASA-CR-174113] 04 p0458 N85-12903
Calibration and use of filter test facility orifice plates
[DE84-016851] 04 p0500 N85-13190
Model equations describing unsteady fluid motion
[ESA-TT-850] 04 p0501 N85-13194
Effect of two inner-ring oil-flow distribution schemes on the operating characteristics of a 35 millimeter bore ball bearing to 2.5 million DN
[NASA-TP-2404] 04 p0507 N85-13233
Magnetohydrodynamic and gasdynamic theories for planetary bow waves
[NASA-CR-174135] 04 p0589 N85-13760
Experimental studies of transonic airfoil trailing edge and wake flowfield properties 05 p0592 N85-13773
Flow Around Bluff Bodies: Numerical and Experimental Approaches — conferences
[VKI-LS-1984-06] 05 p0593 N85-13778
Flow around bluff bodies 05 p0593 N85-13779
Acceleration of bluff bodies through fluids 05 p0593 N85-13786
Direct numerical simulation of curved turbulent channel flow 05 p0635 N85-14072
Experiments on the structure of turbulent reattaching flow 05 p0635 N85-14074
Vaneless diffusers — flow in centrigal compressors 05 p0637 N85-14084
Theoretical approach to labyrinth seal forces - cross-coupled stiffness of a straight-through labyrinth seal 05 p0643 N85-14127
Experimental investigation of lateral forces induced by flow through model labyrinth glands 05 p0643 N85-14128
Analysis of dynamic characteristics of fluid force induced by labyrinth seal 05 p0643 N85-14129
Friction and heat exchange in laminar and turbulent boundary layers with axisymmetrical bodies exposed to heterogeneous supersonic flow 05 p0724 N85-14655
A three-dimensional axisymmetric calculation procedure for turbulent flows in a radial vaneless diffuser
[NASA-TM-86903] 06 p0749 N85-14798
Analysis of physical-chemical processes governing SSME internal fluid flows
[NASA-CR-174245] 06 p0760 N85-14862
Special topics reports for the reference tandem mirror fusion breeder: Liquid metal MHD pressure drop effects in the packet bed blanket, volume 1
[DE85-002142] 06 p0865 N85-15500
Supersonic nonlinear potential analysis
[NASA-CR-172456] 07 p0897 N85-15685
An exploratory study of finite difference grids for transonic unsteady aerodynamics
[NASA-TM-84583] 07 p0899 N85-15696
Analysis of the flow field about a T-45 using PANAIR
[AD-A146811] 07 p0899 N85-15699
Columbia: The first 5 flights entry heating data series. Volume 1: An overview
[NASA-CR-171820] 07 p0913 N85-15777
High altitude chemically reacting gas particle mixtures. Volume 1: A theoretical analysis and development of the numerical solution — rocket nozzle and orbital plume flow fields
[NASA-CR-171826] 07 p0916 N85-15801
High altitude chemically reacting gas particle mixtures. Volume 2: Program manual for RAMP2 — rocket nozzle and orbital plume flow fields
[NASA-CR-171827] 07 p0916 N85-15802
High altitude chemically reacting gas particle mixtures. Volume 3: Computer code user's and applications manual — rocket nozzle and orbital plume flow fields
[NASA-CR-171828] 07 p0917 N85-15803
Computational analysis of scramjet dual mode operation
[NASA-CR-174250] 07 p0956 N85-16060
Numerical reconstruction of part of an actual blast-wave flow field to agree with available experimental data
[UTIAS-TN-251] 07 p0956 N85-16061
Numerical studies of interacting vortices
[NASA-TM-86325] 07 p0957 N85-16062
Aero-optics experimental techniques
[AD-A146755] 07 p0957 N85-16067
Bulk cavitation caused by a plane shock wave
[AD-A147031] 07 p0958 N85-16072
Contamination and distortion of steady flow field induced by discrete frequency in aircraft gas turbines
[AD-A147092] 07 p0958 N85-16073
High Marangoni number convection in a square cavity
[NASA-CR-174283] 07 p0959 N85-16078
Calculation of the velocity field generated by a helicopter main and tail rotors in hover
[AD-A147731] 08 p1078 N85-16833
The orbiter air data system 08 p1094 N85-16912
Shuttle system ascent aerodynamic and plume heating 08 p1103 N85-16975
Aerothermal tests of a 12.5 percent cone at Mach 6.7 for various Reynolds numbers, angles of attack and nose shapes — conducted in Langley 8-foot high temperature tunnel
[NASA-TP-2345] 08 p1161 N85-17322
Computation of flow and heat transfer in flow around a 180 deg bend
[AD-A148065] 08 p1162 N85-17330
Steady flow model user's guide
[DE85-002001] 08 p1163 N85-17337
Genesis of unsteady separation
[AD-P004173] 09 p1266 N85-17958
Corrections for attached sidewall boundary-layer effects in 2-dimensional airfoil testing
[NASA-CR-3873] 09 p1272 N85-17997
Effect of jet exit vanes on flow pulsations in an open-jet wind tunnel
[NASA-TM-86299] 09 p1273 N85-17999
Theory of wing rock 09 p1282 N85-18064
Flow quality of NAL 2-dimensional transonic wind tunnel. Part 2: Extensive and systematic pressure fluctuations study in the settling chamber, test section and second throat of the NAL 2-D transonic wind tunnel
[NAL-TR-836-PT2] 09 p1283 N85-18066
On vortex transport in turbine channels 09 p1308 N85-18217
Analysis of sudden expansion flow in a two-dimensional duct with and without side-wall injection using the k-epsilon turbulence model 09 p1317 N85-18262
The boundary layer on compressor cascade blades
[NASA-CR-174389] 09 p1319 N85-18292
Force balance limiting current for charged particle beams
[DE84-016976] 09 p1381 N85-18685
Hydrodynamic flow structures in quantum field theory
[DE84-015513] 09 p1401 N85-18817
Aerodynamic improvements by discrete wing tip jets
[AD-A148981] 10 p1421 N85-18964
Capabilities of laser diagnostics for combustion and flow fields
[DE85-002661] 10 p1438 N85-19064
Theory of flammability limits. Flow gradient effects and flame stretch
[PB85-135077] 10 p1439 N85-19067
A shock wave capability for the improved Two-Dimensional Kinetics (TDK) computer program
[NASA-CR-171302] 10 p1483 N85-19360
A frozen vorticity approach to the axisymmetric strong interaction problem
[AD-A149101] 10 p1484 N85-19369
Averaging effects in models of three-dimensional two-phase flows
[AD-A149313] 10 p1484 N85-19371
Optimization of a ground coupled heat pump
[DE85-000273] 10 p1486 N85-19380
Mixing chemical reaction and flow field development in ducted rockets
[DE85-002710] 11 p1591 N85-20009
A mixed finite difference analysis of the internal and external transonic flow fields of inlets with centerbody 11 p1619 N85-20192
Flow through very porous screens
[NASA-TP-2436] 11 p1631 N85-20270
A new method for calculating the flow field in a dump combustor
[AD-A149305] 11 p1631 N85-20271
A study of degenerate and nondegenerate critical points in three-dimensional flow fields
[DFVLR-FB-84-36] 11 p1633 N85-20286
A study of eddy-mean flow interactions using Eliassen-Palm diagnostics: FGGE SOP-1 data and the NASA GLAS general circulation model compared
[NASA-CR-175509] 11 p1686 N85-20804
Reconstruction of a 3-dimensional transonic rotor flow field from holographic interferogram data
[NASA-TM-86690] 12 p1770 N85-21112
An investigation of turbulence mechanisms in V/STOL upwash flow fields
[AD-A149786] 12 p1772 N85-21123
Unsteady flows around 3-dimensional wings
[AD-A149993] 12 p1772 N85-21124
Investigation of flowfields found in typical combustor geometries
[NASA-CR-3869] 12 p1779 N85-21167
Aerodynamic behavior of ventilated wind tunnel walls 13 p1968 N85-22363
On the solution of the three-dimensional flowfield about a flow-through nacelle
[NASA-TM-87448] 13 p1969 N85-22371
Results of the AFRSI rewaterproofing systems screening test in the NASA/Ames Research Center (ARC) 2 x 2-foot transonic wind tunnel
[NASA-CR-167694] 13 p1968 N85-22467
HPFTP flow diverter analysis
[NASA-CR-171424] 13 p2091 N85-23057
Centrifuge impact cratering experiments 13 p2181 N85-23533
The nature of Martian flow ejecta craters 13 p2183 N85-23545
Interaction of Martian flow ejecta blankets with pre-existing impact craters: Morphological observations 13 p2183 N85-23546
Comparison of measured and computed boundary layers at the tail-end of an axisymmetric body in an air-jet
[AMTE(N)-TM-83053] 14 p2209 N85-23700
Estimating unsteady aerodynamic forces on a cascade in a three-dimensional turbulence field
[NASA-TM-86701] 14 p2209 N85-23704
Transonic merging separated flows
[AD-A150667] 14 p2213 N85-23724
Mixing, chemical reaction and flow field development in ducted rockets
[DE85-004083] 14 p2247 N85-23928
Experimental simulation of the flow inside a gun barrel
[ISL-CO-208/83] 14 p2302 N85-24252
Measurements in the flow field of a cylinder with a laser transit anemometer and a drag rake in the Langley 0.3 m transonic cryogenic tunnel
[NASA-TM-86399] 14 p2305 N85-24270
A study of the turbulent layer in the water at an air-water interface 14 p2378 N85-24679
A new implicit plus minus splitting method for the solution of the Euler equations in the transonic flow regime 15 p2461 N85-25200
A 3-dimensional Navier-Stokes-Euler code for blunt-body flow computations
[NASA-TM-58266] 15 p2463 N85-25211
An experimental study of hairpin-type vortices as a potential flow structure of turbulent boundary layers 15 p2553 N85-25751
The influence of jet-grid turbulence on heat transfer from the stagnation region of a cylinder in crossflow
[NASA-TM-87011] 15 p2554 N85-25760
Flow over a biconic configuration with an afterbody compression flap
[AD-A151882] 15 p2557 N85-25778
Viscous effects on blast wave flowfields
[AD-A152013] 15 p2558 N85-25779
Numerical analysis of supersonic reactive flow in wake of reverse step 15 p2643 N85-26303
An evaluation of proposed acoustic treatments for the NASA LaRC 4 x 7 meter wind tunnel
[NASA-CR-172577] 15 p2646 N85-26319
Navier-Stokes solution of hypersonic blunt-nosed body flowfields 16 p2693 N85-26624
The role of computational fluid dynamics in aeronautical engineering 16 p2694 N85-26629
A method for simulating 3-D aircraft flow fields with jet plume effects
[NASA-CR-175802] 16 p2699 N85-26664
Application of CFD techniques toward the validation of nonlinear aerodynamic models
[NASA-TM-86715] 16 p2700 N85-26671
Measurements in low pressure flow using an electronic beam detector — wind tunnel tests 16 p2701 N85-26678
Turbulence characteristics of swirling flowfields
[NASA-CR-174918] 16 p2709 N85-26717
Numerical analysis of flow non-uniformity in the hot gas manifold of the Space Shuttle main engine 16 p2736 N85-26899
Analysis of combustion oscillations in heterogeneous systems
[AD-A151999] 16 p2745 N85-26942
Simulation of interior ballistics flows in a shock tube
[ISL-CO-222/83] 16 p2784 N85-27183
Structural stability and bifurcation in conical flow fields
[VTH-LR-424] 16 p2803 N85-27282

Static and dynamic pressure measurements on a NACA 0012 airfoil in the Ames High Reynolds Number Facility
[NASA-TP-2485] 17 p2891 N85-27823
User's manual for airfoil flow field computer code SRAIR
[NASA-CR-172585] 17 p2891 N85-27825
Predictions and measurements of isothermal flowfields in axisymmetric combustor geometries
[NASA-CR-174916] 17 p2898 N85-27867
The gust simulation apparatus of the 3m x 3m low speed wind tunnel of the DFVLR in Goettingen, West Germany
[DFVLR-FB-85-04] 17 p2906 N85-27920
Simulation of multistage turbine flows
17 p2911 N85-27945
Unsteady flow in multistage turbines
17 p2911 N85-27946
Feasibility of mapping velocity flow fields in SSME powerhead by laser anemometry techniques
17 p2915 N85-27971
Proceedings of the 9th US Air Force and the Federal Republic of Germany Data Exchange Agreement Meeting, Viscous and Interacting Flow Field Effects
[AD-A153020] 17 p2958 N85-28266
Vortices in non-Newtonian fluids
[AD-A153169] 17 p2958 N85-28269
Numerical computation of space shuttle orbiter flow field
[NASA-CR-175912] 18 p3058 N85-28921
Transverse vorticity measurements using an array of four hot-wire probes
[FSFL-R-85-006] 18 p3099 N85-29184
On the origin of streamwise vortices in a turbulent boundary layer
[AD-A153651] 18 p3100 N85-29188
The method of residual minimization in compressible steady flows
[AD-A153924] 18 p3100 N85-29193
A model for the combustion of polymethyl methacrylate in air in a laminar diffusion flame
[VTH-LR-439] 18 p3165 N85-29606
Wake effects of the aerodynamic performance of horizontal axis wind turbines 19 p3211 N85-29915
Additional flow field studies of the GA(W)-1 airfoil with 30-percent chord Fowler flap including slot-gap variations and cove shape modifications
[NASA-CR-3687] 19 p3212 N85-29919
Vapor-screen technique for flow visualization in the Langley Unitary Plan Wind Tunnel
[NASA-TM-86384] 19 p3214 N85-29929
Turbine blade-tip clearance excitation forces
[NASA-CR-171534] 19 p3220 N85-29963
Flow field effects on nucleation in a reacting mixing layer
[ARL/AERO-R-165] 19 p3263 N85-30237
Highly accurate shock flow calculations with moving grids and mesh refinements, revision 1
[DE85-010929] 19 p3267 N85-30260
SANDRAG: A computer code for predicting drag of bodies of revolution at zero angle of attack in incompressible flow
[DE85-011170] 19 p3338 N85-30684
A theory of quasi-conical solutions of noninteger degree — flow fields on supersonic wings
[UTH-LR-420] 20 p3390 N85-31024
Mechanisms of exhaust pollutants and plume formation in continuous combustion
[AD-A154169] 20 p3435 N85-31310
An experimental investigation of confined, multiple, turbulent jet mixing with recirculation
20 p3451 N85-31426
Numerical and experimental investigation of turbomachinery rotor flow fields
20 p3451 N85-31429
Direct simulation techniques for the Boltzmann equation
[DFVLR-FB-85-13] 20 p3457 N85-31470
Geologic and hydrologic characterization and evaluation of the basin and range province relative to the disposal of high-level radioactive waste. Part 1: Introduction and guidelines
[GS-CIRC-904-A] 20 p3526 N85-31932
Geologic and hydrologic characterization and evaluation of the basin and range province relative to the disposal of high-level radioactive waste. Part 2: Geologic and hydrologic characterization
[GS-CIRC-904-B] 20 p3526 N85-31933
BLAF: A blast field reconstruction program from pressure histories
[AD-A155300] 21 p3585 N85-32263
Techniques for the study of gravity waves and turbulence (keynote paper), part 4 21 p3621 N85-32499
Calculation of steady and unsteady airfoil flow fields via the Navier-Stokes equations
[NASA-CR-3809] 22 p3727 N85-33105
Sandia Cooperative Group on the Aerothermochemistry of Turbulent Combustion. Discussion record of the second meeting
[DE85-007493] 22 p3743 N85-33203
Pressure correlations in turbulent reacting flows
22 p3744 N85-33205
Second order modelling in non-constant density flows
22 p3744 N85-33206
KRAK: A computer program for two-phase two-component porous flow and fracture
[LA-9703] 22 p3782 N85-33434
A three-dimensional viscous flow analysis for the helicopter tip vortex generation problem
[NASA-CR-3906] 23 p3893 N85-34114
A comparison of laser Doppler anemometry and probe measurements within the boundary layer of an airfoil at subsonic flow
[ISL-CO-219/84] 23 p3895 N85-34127
Prediction of the flow-field interference induced by the long-range laser velocimeter in the Ames 40- by 80-foot and the 80- by 120-foot wind tunnels
[NASA-TM-86763] 23 p3896 N85-34146
A three-dimensional turbulent boundary layer undergoing transverse strain and streamwise pressure gradient
[NASA-TM-86768] 23 p3930 N85-34358
Block-implicit calculations of three-dimensional laminar flow in strongly curved ducts
[DE85-003047] 23 p3931 N85-34363
Mathematical modeling of ultimate heat sink cooling ponds
[TI85-009747] 23 p3932 N85-34369
General design method for 3-dimensional, potential flow fields. Part 2: Computer program DIN3D1 for simple, unbranched ducts
[NASA-CR-3926] 24 p4060 N85-35159
Calculation of compressible flow about three-dimensional inlets with auxiliary inlets, slats and vanes by means of a panel method
[NASA-CR-174975] 24 p4060 N85-35162
The effect of power law body forces on a thermally-driven flow between concentric rotating spheres
[NASA-TM-87595] 24 p4093 N85-35374
The kinematic structure of cold frontal rainbands
24 p4119 N85-35531

FLOW EQUATIONS
NT HELMHOLTZ VORTICITY EQUATION
NT VORTICITY EQUATIONS
Second order modeling of scalar turbulent flows
03 p0360 N85-12311
Multigrid iteration solution procedure for solving two-dimensional sets of coupled equations
[DE84-016554] 04 p0555 N85-13533
Vectorizable multigrid algorithms for transonic flow calculations
[NASA-CR-174326] 06 p1077 N85-18827
Front tracking for gas dynamics
[DE85-000571] 06 p1163 N85-17336
Closure problem and numerical studies of turbulence
06 p1209 N85-17606
Numerical approach for the aerodynamic analysis if airfoils with laminar separation
[NASA-CR-172496] 09 p1273 N85-18001
Notes on compressible flow equations for thermodynamics of hot jets
[BAE-KRS-N-GEN-273] 09 p1318 N85-18289
An implicit, conservative, zonal-boundary scheme for Euler equation calculations
[NASA-CR-3895] 09 p1318 N85-18290
Accuracy of the finite analytic method for scalar transport calculations
[DE85-001474] 09 p1320 N85-18300
Nicolai maps and stochastic observables from a coupling constant flow
[BONN-HE-84-26] 09 p1376 N85-18853
Triple layer system for numerical integration of equations of gas dynamics and nonlinear heat conduction equation
[DE85-000297] 11 p1632 N85-20277
Evaluation of time integrators for the shallow water equations
[CWI-NM-R8406] 11 p1634 N85-20292
High order difference schemes with reduced dispersion for hyperbolic differential equations
[CWI-NM-R8408] 11 p1634 N85-20293
Space nuclear-power reactor design based on combined neutronic and thermal-fluid analyses
[DE85-002433] 11 p1727 N85-20864
Calculation of harmonic aerodynamic forces of aerofoils and wings from the Euler equations
15 p2458 N85-25177
Mathematical modeling of the AEDC (Arnold Engineering Development Center) propulsion wind tunnel (16T)
[AD-A151293] 15 p2475 N85-25275
Solution of Onsager's equation for a rotating compressible fluid in a multiply-connected domain
[DE85-007048] 16 p2784 N85-27178
Steady, incompressible, inviscid flow through a finite collapsible tube under longitudinal tension
[REPT-84-01] 17 p2959 N85-28278
A second-order pressure-correction method for viscous incompressible flow
[REPT-84-15] 17 p2960 N85-28280
Flow through finite collapsible tubes: A branching problem
[REPT-84-29] 17 p2960 N85-28281
On Long's solution to hydrostatic flow over mountains
[DFVLR-MITT-84-02] 17 p2994 N85-28503
Relaxation methods for hyperbolic equations
[REPT-84-20] 17 p3021 N85-28687
Fluid modeling of magnetized plasmas
[DE85-007679] 17 p3039 N85-28604
An investigation of hydraulic transients in combination free surface and pressurized flows
19 p3264 N85-30239
Use of a two-dimensional flow model to quantify aquatic habitat
[AD-A154287] 19 p3266 N85-30253
An implicit finite-difference code for a two-equation turbulence model for three-dimensional flows
[NASA-TM-86752] 20 p3454 N85-31448
Some remarks on the constitutive equations of stratified gas-liquid flow
[EME-137] 20 p3456 N85-31466
Optimization of a numerical method to calculate elliptic flows
[ESA-TT-889] 20 p3457 N85-31472
The calculation of fully three dimensional flow through any type of turbomachine blade row
21 p3587 N85-32294
Tabular and graphical solutions of regular and Mach reflections in pseudo-stationary frozen and vibrational-equilibrium flows, part 1
[UTIAS-283-PT-1] 23 p3893 N85-34117
Tabular and graphical solutions of regular and Mach reflections in pseudo-stationary frozen and vibrational-equilibrium flows, part 2
[UTIAS-283-PT-2] 23 p3894 N85-34118

FLOW FIELDS
U FLOW DISTRIBUTION

FLOW GEOMETRY
Geometric characteristics of turbulent boundary layer separation upon action with direct shock wave in conical flows 02 p0269 N85-11755
An improved computer model for prediction of axial gas turbine performance losses
[NASA-CR-174246] 07 p0904 N85-15724
TRACR3D: A model of flow and transport in porous/fractured media
[LA-9667-MS] 12 p1845 N85-21576
Grid generation for a pump collector
[AD-A150217] 13 p2092 N85-23059
Numerical calculation of subsonic jets in crossflow with reduced numerical diffusion
[NASA-TM-87003] 15 p2472 N85-25283
Computational aerodynamics in designing aircraft
16 p2693 N85-28622
Boundary layer and parabolic flows
[DFVLR-FB-84-46] 17 p2960 N85-28285

FLOW MEASUREMENT
Pressure distribution on a swept wing aircraft in flight
01 p0004 N85-10025
Measurement of the development of the boundary layer in the annulus walls of a fourstage compressor
[CUED/A-TURBO-TR-121] 01 p0046 N85-10299
Development in UK of a method for calculating tunnel wall corrections from flow measurements
03 p0314 N85-12026
Comparative review of laser Doppler and laser two-focus anemometry in turbomachinery applications
[VKI-TM-34] 03 p0367 N85-12350
Study of the structure of turbulent shear flows at supersonic speeds and high Reynolds number
[NASA-CR-174144] 04 p0452 N85-12865
Magnetic inductive flowmeter for low conducting liquids
[BMFT-FB-T-84-136] 04 p0504 N85-13216
Flow Around Bluff Bodies: Numerical and Experimental Approaches — conferences
[VKI-LS-1984-06] 05 p0593 N85-13778
Experimental techniques and instrumentation for bluff body aerodynamics 05 p0593 N85-13781
Experimental observation of the flow in impellers and diffusers — centrifugal compressors
05 p0636 N85-14080
Turbulence measurement interferometer apparatus
[AD-D011377] 07 p0970 N85-16156
Investigation of the ice dynamics in the marginal ice zone
[AD-A146729] 07 p1009 N85-16411
Advanced diagnostics for reacting flows
[AD-A148479] 08 p1162 N85-17334

Halogen mass flow rate detection system
[AD-D011398] 08 p1166 N85-17352
Experimental study of aerodynamic shielding of turbojet engine air intake against exhaust gases
09 p1307 N85-18210
Modeling turbulent flow in compressible fluids: Metrological aspects — conferences
11 p1575 N85-19926
Comparison of two-dimensional laser and hot-wire velocimetry for a supersonic turbulent boundary layer
11 p1576 N85-19927
Characterization of jet turbulence using infrared radiometry 11 p1576 N85-19928
Laser Raman techniques for studying flows and flames 11 p1576 N85-19929
Velocity and volumetric measurement in free jets
11 p1576 N85-19931
Laser Doppler Anemometry (LDA) signal triggering and effective particle size range
[KU-SFB-210/E/5] 11 p1634 N85-20290
Miniature electrooptical air flow sensor
[NASA-CASE-LAR-13085-1] 11 p1635 N85-20295
Examples of environment services: Hydrological and pollution measurements in the Po River (Italy)
[CISE-2299] 11 p1679 N85-20578
Liquid mass flow rate computer
13 p2075 N85-22962
Turbulent flows of surfacant solutions
[AD-B069137L] 13 p2092 N85-23058
Mean flow and turbulence in complex terrain NPS (Naval Postgraduate School)/Vandenberg measurement system
[AD-A150184] 13 p2138 N85-23274
Field measurements of the 1983 Royal Gardens lava flows, Kilauea Volcano, and 1984 Mauna Loa lava flows, Hawaii 13 p2166 N85-23565
Calibration of sonic valves for the laminar flow control, leading-edge flight test
[NASA-TP-2423] 14 p2210 N85-23707
Advanced diagnostics for reacting flows
[AD-A150675] 14 p2301 N85-24246
Experimental and analytical investigation of fan flow interaction with downstream struts
[NASA-CR-175756] 15 p2462 N85-25201
Measurements in low pressure flow using an electronic beam detector — wind tunnel tests
16 p2701 N85-26676
Measurements of two-phase exhaust flow parameters of a small caliber gun associated with muzzle flash phenomena
[ISL-CO-212/83] 16 p2784 N85-27182
Vibration-free Raman Doppler velocimeter
[NASA-CASE-LAR-13268-1] 18 p3104 N85-29216
Use of a two-dimensional flow model to quantify aquatic habitat
[AD-A154287] 19 p3266 N85-30253
Accuracy in determining velocity of fluid movement by Doppler method 19 p3293 N85-30419
Measurement and analysis of two-phase flow through low permeability media, task 3
[PB85-188373] 20 p3435 N85-31313
Velocity visualization in gaseous flows
[NASA-CR-174954] 20 p3453 N85-31445
Study of requirements for and method of multidimensional acoustic imaging — spaceborne experiments
[ESA-CR(P)-2020] 20 p3525 N85-31924
Injection of drag reducing additives into turbulent water flows: Two-component velocity measurements and mixing length model predictions
[AD-A154604] 21 p3583 N85-32274
Laser Doppler Anemometer (LDA) measurements in the turbulent near-wake of blunt bodies
[ISL-CO-212/84] 22 p3785 N85-33450
Measurement of velocity and concentration in free jets
[ISL-CO-215/84] 22 p3785 N85-33451
Improved flow cytometer measurement of binding assays
[DE85-006407] 23 p3935 N85-34390

FLOW PATTERNS
U FLOW DISTRIBUTION

FLOW RATE
U FLOW VELOCITY

FLOW REGULATORS
Research and development for semi-spherical inflow control device
[NAL-TR-833] 09 p1281 N85-18056
Flow through very porous inclined screens
[NASA-TM-86979] 15 p2555 N85-25761
Combined riblet and LEBU drag reduction system
[NASA-CASE-LAR-13286-1] 18 p3058 N85-28822
Fluidized bed desulfurization
[NASA-CASE-NPO-15924-1] 24 p4075 N85-35253

FLOW RESISTANCE
NT AERODYNAMIC DRAG
NT FRICTION DRAG
NT VISCOUS DRAG
Turbulent flows of surfacant solutions
[AD-B069137L] 13 p2092 N85-23058

FLOW SEPARATION
U BOUNDARY LAYER SEPARATION
U SEPARATED FLOW

FLOW STABILITY
NT BOUNDARY LAYER STABILITY
NT FLAME STABILITY
NT MAGNETOHYDRODYNAMIC STABILITY
NT WEIBEL INSTABILITY
On vortex bursting
[NASA-TM-77587] 01 p0002 N85-10008
Stability of fluid flow in a cylindrical annulus
[NASA-TM-77720] 01 p0046 N85-10300
Computation of the nonequilibrium flow in a gasdynamic laser
[AD-A141022] 04 p0505 N85-13224
Experiences with nonsynchronous forced vibration in centrifugal compressors 05 p0642 N85-14119
Preliminary investigation of labyrinth packing pressure drops at onset of swirl-induced rotor instability
05 p0644 N85-14132
Stability of lubricant film in gas dynamic bearing
06 p0778 N85-14977
Stability of rigid motions and rollers in bicomponent flows of immiscible liquids
[AD-A147302] 07 p0960 N85-16081
An experimental study on the instability of a mixing-layer with laminar wake as the initial condition
06 p1076 N85-16824
Flow instabilities in transonic small disturbance theory
[NASA-TM-86251] 09 p1273 N85-18000
Acoustic energy balance method
13 p2000 N85-22537
Lyapunov stability of very simple steady solutions of prognostic systems 14 p2333 N85-24429
Stability calculations of the two-dimensional boundary layer along a concave wall: Part 1: A numerical method of solution for the simultaneous ordinary differential equations governing disturbances
[NAL-TR-841] 15 p2554 N85-25758
Instability of solar wind near streamlined bodies
16 p2720 N85-26794
Vortex shedding flowmeters for liquids at high flow velocities 16 p2740 N85-26906
A numerical study of nonspherical black hole accretion 16 p2881 N85-27780
Generation of capillary instabilities by external disturbances in a liquid jet
[NASA-TM-87041] 19 p3265 N85-30246
Development of thermoconvective instabilities in porous media. Influence of boundary conditions
20 p3458 N85-31461
Moist barotropic instability in the tropics
20 p3489 N85-31683
Experiments on the influence of active walls on the initial amplitudes and growths of instability waves
[AD-A154630] 21 p3583 N85-32275
Instability and chaotic behavior in a free-surface flow
[AD-A154879] 21 p3584 N85-32279
Stability of implosion dynamics
23 p3980 N85-34680
Couette flow of two fluids between concentric cylinders
[AD-A155827] 24 p4093 N85-35376

FLOW THEORY
NT MIXING LENGTH FLOW THEORY
Magnetohydrodynamic and gasdynamic theories for planetary bow waves
[NASA-CR-174135] 04 p0589 N85-13760
Acceleration of bluff bodies through fluids
05 p0593 N85-13788
Wave propagation in compliant tubes containing a heat-conducting viscous fluid
[WTHD-163] 05 p0636 N85-14094
Flow-based analyses of metal deformation processes: An overview 06 p0796 N85-15067
Investigation of the local mass transfer of a laminar and turbulent falling liquid film
[BLL-T6368/BG/WH792/84] 06 p0807 N85-15130
The stability of an infinite elastic pipe with uniform mean flow
[AD-A146686] 08 p1161 N85-17326
Large deformations of a nonlinear elastic solid and the diffusion of an ideal fluid treated as interacting continua
09 p1330 N85-18356
Study proposal for the possible use of ISS as an aerodynamic facility for aerospace applications
11 p1648 N85-20374
Computational aerodynamics in designing aircraft
16 p2693 N85-26822
La Recherche Aerospatiale Bimonthly Bulletin Number 1984-2, 219/March-April
[ESA-TT-878] 16 p2694 N85-26835
Conical stagnation points in the flow around an external corner — delta wings
[VTH-LR-396] 16 p2701 N85-26880
New flow physical aspects in aerodynamics
[MBB-FE-122/S/PUB/133] 16 p2873 N85-27725
Calculation of viscous compressible flows in small gas turbines 17 p2912 N85-27950
Boundary layer and parabolic flows
[DFVLR-FB-84-46] 17 p2960 N85-28265
Progress in the development of a two-fluid model of turbulence: A set of 42 lecture panels
[CFD/84/20] 20 p3457 N85-31469
Explosion in flight 21 p3683 N85-32883
A curvilinear coordinate method for the solutions of initial value problems using the third-order upwind differencing scheme
[IPPJ-734] 23 p3975 N85-34642
Bibliography on tidal hydraulics. Report 2. Supplement 9: Supplementary material compiled from June 1980 - June 1983. Tidal flows in rivers and harbors
[AD-A155990] 24 p4125 N85-35574

FLOW VELOCITY
NT SOLAR WIND VELOCITY
Water resources data for Michigan, water year 1983
[PB84-225178] 01 p0066 N85-10442
Chemical vapor deposition of amorphous silicon films produced by using higher order silanes
[DE84-004519] 01 p0123 N85-10847
Laser anemometer optimization
02 p0142 N85-10963
Characteristics of a turbulent plane offset jet
02 p0196 N85-11310
Some of the features of movement of gas through a layer of free-flowing substances
[BLL-M-35732-(5828.4)] 02 p0196 N85-11312
NLR activities in the field of wind tunnel wall interference 03 p0313 N85-12024
Flow around bluff bodies 05 p0593 N85-13779
A finite element method for three dimensional cavity circulation 05 p0635 N85-14071
Flow rates and pressure profiles for one to four axially aligned Borda inlets
[NASA-TP-2390] 05 p0636 N85-14078
Plasma and magnetospheric research
[NASA-CR-171293] 06 p1183 N85-17451
Studies on reactive mufflers. Part 2: Mufflers with air flow 09 p1303 N85-18184
Determination of total pressure losses in stepped annular diffusers with curvilinear outer walls and uniform velocity field at inlet 09 p1306 N85-18203
Influence of secondary flow rate on dynamic stresses in turbine rotor blades 09 p1306 N85-18205
Long range effect of turbulent pressure pulsations in plane-parallel flows at different velocities with various flame fronts 09 p1308 N85-18220
Developing a flowmeter for streams with high solids content
[DE84-016643] 09 p1323 N85-18316
Optical flow and texture variables useful in detecting decelerating and accelerating self-motion
[AD-A148718] 09 p1384 N85-18703
Critical velocities in He II for independently varied superfluid and normal fluid velocities
09 p1396 N85-18784
Velocity measurements in a 3D shock wave laminar boundary layer interaction. Part 1: Low speed 2D LDV measurements
[AD-A149533] 10 p1485 N85-19373
Computation of the inviscid velocity potential for general ellipsoids on a nearly quadratic surface grid
[REPT-25/84] 11 p1633 N85-20287
Preliminary analysis of tone-excited two-stream jet velocity decay
[NASA-TM-86951] 12 p1770 N85-21114
Liquid mass flow rate computer
13 p2075 N85-22962
Turbulence measurements in shock induced flows
13 p2091 N85-23055
Hydraulic characteristics of reduction installation valves 14 p2289 N85-24060
Heat transfer to vertical flat plates in a rectangular gas-fluidized bed
[AD-A150785] 14 p2301 N85-24248
Modeling longitudinal motions of thermal O+ and H+ ions in magnetic field tube convective through daytime polar cusp 15 p2481 N85-25314
An experimental technique for the study of velocity profiles in a laminar jet using a pulsed nitrogen laser
[AD-A151496] 15 p2556 N85-25771
Fuel and oxidizer turbine loss analysis
16 p2739 N85-26900
Vortex shedding flowmeters for liquids at high flow velocities 16 p2740 N85-26906
Aerodynamic forces developing in channels between vanes in turbine drive wheels 16 p2765 N85-27082

Flow rate and pressure profiles for 1 to 4 axially aligned orifice inlets
[NASA-TP-2460] 16 p2782 N85-27165
Supersonic flow around blunt wedge
17 p2942 N85-28158
Flow quality of National Aerospace Laboratory two-dimensional transonic wind tunnel. Part 3: Flow turbulence level and measuring method
[NAL-TR-842-PT-3] 18 p3064 N85-28952
Burner rig corrosion of SiC at 1000 deg C
[NASA-TM-87061] 19 p3227 N85-30011
Transient combustion dynamics
[AD-A154430] 19 p3235 N85-30052
Improved fluid flow meter for measuring the rate of fluid flow in a conduit
[NASA-CASE-MFS-28030-1] 19 p3271 N85-30286
Accuracy in determining velocity of fluid movement by Doppler method 19 p3293 N85-30419
Combustor turbulence 20 p3452 N85-31434
Preliminary results of a study of the relationship between free-stream turbulence and stagnation region heat transfer 20 p3452 N85-31435
Transition in a disturbed environment
20 p3452 N85-31436
Velocity visualization in gaseous flows
[NASA-CR-174954] 20 p3453 N85-31445
A panel method study of vortex sheets with special emphasis on sheets of axisymmetric geometry
[NASA-CR-177365] 21 p3552 N85-32095
A comparison of laser Doppler anemometry and probe measurements within the boundary layer of an airfoil at subsonic flow
[ISL-CO-219/84] 23 p3895 N85-34127
Flow modifying device
[NASA-CASE-LEW-13562-2] 24 p4065 N85-35195
The use of a laser Doppler velocimeter in a standard flammability tube
[NASA-CR-174980] 24 p4096 N85-35369

FLOW VISUALIZATION
NT NUMERICAL FLOW VISUALIZATION
On vortex bursting
[NASA-TM-77587] 01 p0002 N85-10008
Pressure distributions measured on research wing M86 mounted on an axisymmetric body
01 p0004 N85-10024
Oil flow patterns of separated flow on a hemispherical cylinder at incidence
[DFVLR-FB-84-20] 01 p0048 N85-10313
Three dimensional separation and vortex formation
02 p0196 N85-11308
New approaches to hydrodynamic flow visualization on surfaces
[AD-A145528] 02 p0196 N85-11324
Preliminary results using a rapid photographic wake traverse system — in a wind tunnel
[RAE-TM-AERO-1987] 02 p0200 N85-11332
Experiences with a high-blockage model tested in the NASA Ames 12-foot pressure wind tunnel
03 p0315 N85-12032
Flow visualization study of a vortex-wing interaction
[NASA-TM-86656] 03 p0316 N85-12040
The role of freestream turbulence scale in subsonic flow separation
[NASA-CR-174172] 04 p0452 N85-12870
An experimental investigation of the parallel blade-vortex interaction
[NASA-TM-86005] 05 p0592 N85-13777
A collection of flow visualization techniques used in the Aerodynamic Research Branch
[NASA-TM-85996] 06 p0806 N85-15135
Channel constructed to provide well defined boundary layers for vorticity optical probe measurements
[AD-A146679] 06 p0809 N85-15140
Investigation of light source and scattering medium related to vapor-screen flow visualization in a supersonic wind tunnel
[NASA-TM-86290] 06 p0810 N85-15144
Unsteady flow characteristics in the near-wake of a two-dimensional obstacle
[NASA-TM-77762] 07 p0897 N85-15684
Unsteady pressure measurements on a biconvex airfoil in a transonic oscillating cascade
[NASA-TM-86914] 07 p0898 N85-15689
A 3-dimensional turbulent boundary layer upstream and around a junction vortex flow 08 p1160 N85-17319
Advanced diagnostics for reacting flows
[AD-A148479] 08 p1162 N85-17334
Simultaneous flow visualization and unsteady lift measurement on an oscillating lifting surface
[AD-P004157] 09 p1264 N85-17942
A visual study of a delta wing in steady and unsteady motion
[AD-P004158] 09 p1264 N85-17943
Comparative visualization of accelerating flow around various bodies, starting from rest
[AD-P004159] 09 p1264 N85-17944
Unsteady separated flows: Generation and use by insects
[AD-P004168] 09 p1266 N85-17953
Aerodynamic improvements by discrete wing tip jets
[AD-A148981] 10 p1421 N85-18964
Capabilities of laser diagnostics for combustion and flow fields
[DE85-002661] 10 p1438 N85-19084
Mixing characteristics of an underexpanded multiple jet ejector
[AD-A149557] 10 p1485 N85-19375
Momentum and heat transfers in a complex, but well-defined turbulent fluid flow
[DE85-002857] 10 p1486 N85-19381
Flow visualization study of the effect of injection hole geometry on an inclined jet in crossflow
[NASA-TM-86936] 11 p1631 N85-20269
Experimental investigation of a pulse combustor: Flow visualization by Schlieren photography
[DE85-002862] 11 p1636 N85-20304
Use of laser flow visualization techniques in reactor component thermal-hydraulic studies
[DE84-014768] 11 p1639 N85-20330
Unsteady flows around 3-dimensional wings
[AD-A149993] 12 p1772 N85-21124
Continuous laminar smoke generator
[NASA-CASE-LAR-13014-1] 12 p1781 N85-21178
Experimental studies of Quasi-Two-Dimensional and three-dimensional viscous interaction regions induced by skewed-shock and swept-shock boundary layer interactions
[AD-A150060] 12 p1847 N85-21587
Deflected jet experiments in a turbulent combustor flowfield
[NASA-CR-174863] 13 p1973 N85-22390
An experimental investigation of the chopping of helicopter main rotor tip vortices by the tail rotor
[NASA-CR-177338] 13 p2154 N85-23376
Stability of vortex structures during separation flow past array of wings 14 p2278 N85-24110
Advanced diagnostics for reacting flows
[AD-A150675] 14 p2301 N85-24246
Fluid mechanics and heat transfer spirally fluted tubing
[AD-A150774] 14 p2301 N85-24247
Experimental simulation of the flow inside a gun barrel
[ISL-CO-208/83] 14 p2302 N85-24252
Visualization of velocity fields with Doppler images
[ISL-CO-218/83] 14 p2302 N85-24256
Experimental and theoretical investigation of the motion of particles in a compressible vortex
[ISL-R-129/83] 14 p2303 N85-24264
Modifications to the nozzle test chamber to extend nozzle static-test capability
[NASA-TM-86368] 15 p2464 N85-25216
An experimental study of hairpin-type vortices as a potential flow structure of turbulent boundary layers
15 p2553 N85-25751
An experimental investigation of unexcited and excited elliptic jets 15 p2554 N85-25755
An experimental technique for the study of velocity profiles in a laminar jet using a pulsed nitrogen laser
[AD-A151496] 15 p2556 N85-25771
Simulation of interior ballistics flows in a shock tube
[ISL-CO-222/83] 16 p2784 N85-27183
Convective storm downdraft outflows detected by NASA/MSFC's Airborne 10.6 micron pulsed Doppler Lidar System
[NASA-CR-3896] 17 p2995 N85-28511
Multi-ducted inlet combustor research and development
[AD-A153753] 18 p3063 N85-28946
Lee-side flow over delta wings at supersonic speeds
[NASA-TP-2430] 19 p3212 N85-29921
Vapor-screen technique for flow visualization in the Langley Unitary Plan Wind Tunnel
[NASA-TM-86364] 19 p3214 N85-29929
Density and confinement effects on mixing characteristics of an axisymmetrical CO(2) jet
[AD-A154468] 19 p3267 N85-30258
Flow visualization study of inverted annular flow of post dryout heat transfer region
[DE85-010482] 19 p3269 N85-30275
An experimental investigation of confined, multiple, turbulent jet mixing with recirculation
20 p3451 N85-31426
Preliminary results of a study of the relationship between free-stream turbulence and stagnation region heat transfer 20 p3452 N85-31435
Velocity visualization in gaseous flows
[NASA-CR-174954] 20 p3453 N85-31445
Two-phase flow visualization in a transparent, atmospheric pressure, boiling water loop
[DE84-016657] 21 p3586 N85-32288
Computer and water-model simulation of flow through poppet valves
[CFD/85/2] 22 p3785 N85-33449
Experimental simulation of in-bore flows using a high pressure shock tube
[ISL-CO-217/84] 22 p3785 N85-33452
Circulation control lift generation experiment: Hardware development 22 p3799 N85-33535
The influence of helicopter tail shape on drag: An aerodynamic study using a low speed wind tunnel
[AD-A156304] 24 p4062 N85-35174

FLOWMETERS
NT GAS METERS
NT HOT-WIRE FLOWMETERS
NT RHEOMETERS
Magnetic inductive flowmeter for low conducting liquids
[BMFT-FB-T-84-136] 04 p0504 N85-13216
Dynamic response of electromagnetic current meters
[PB84-229731] 06 p0842 N85-15344
Flow measurement device
[AD-D011432] 08 p1168 N85-17369
Developing a flowmeter for streams with high solids content
[DE84-016643] 09 p1323 N85-18316
Miniature electrooptical air flow sensor
[NASA-CASE-LAR-13065-1] 11 p1635 N85-20295
State-of-charge coulometer
[NASA-CASE-NPO-15759-1] 12 p1849 N85-21596
Field-work report: Medway Estuary, 28 June - 18 July 1983
[RNC/NS/TR8] 13 p2041 N85-22773
Vortex shedding flowmeters for liquids at high flow velocities 16 p2740 N85-26906
Improved fluid flow meter for measuring the rate of fluid flow in a conduit
[NASA-CASE-MFS-28030-1] 19 p3271 N85-30286
MHD generator CDIF
[DE85-011389] 20 p3536 N85-32001
IEA-SSPS CRS calibration report: Calibration of relevant measuring sensors
[DE85-010174] 22 p3788 N85-33468
Acoustic cross-correlation flowmeter for solid-gas flow
[DE85-005988] 23 p3935 N85-34391

FLUCTUATION
U VARIATIONS

FLUCTUATION THEORY
Range fluctuations of high energy muons passing through matter
[HE-5.2-19] 24 p4204 N85-36095

FLUE GASES
Comparative usefulness of flue gas oxygen and carbon dioxide analysis
[BLL-TRANS-T6358/BG/WH783/84]
06 p1179 N85-17430
Components of the combustion gases of propellant charge powders after reaction in the high pressure bomb in the pressure range up to 1000 MPa. Part 1: Nitroglycerine powder GB Pa 125
[ISL-CO-217/83-PT-1] 14 p2264 N85-24027
Development of corrosion resistant heat exchangers for flue gas desulfurization
[BMFT-FB-T-84-281] 18 p3103 N85-29211
Evaluation of the Santee limestone for use in flue-gas desulfurization systems
[DE85-901277] 19 p3249 N85-30148
Evaluation of pilot ESP used with a spray dryer FGD system at Pittsburgh Energy Technology Center, Bruceton, Pennsylvania
[DE85-011151] 22 p3746 N85-33217

FLUENCE
Critical assessment of low fluence irradiation creep mechanisms
[DE84-015578] 02 p0184 N85-11232
Beam profiling in gigawatt 1064-nm lasers used in research on optical materials at Livermore
[DE84-007226] 04 p0505 N85-13223
Structure and properties of ion-implanted Al sub 2 O sub 3
[DE85-005374] 14 p2430 N85-24987
Incorporation of Monte Carlo electron interface studies into photon general cavity theory
[DE85-007674] 17 p3034 N85-28772
Solar flare gamma-ray line spectroscopy
[SH-2.1-14] 23 p3999 N85-34795

FLUID AMPLIFICATION
U FLUID AMPLIFIERS

FLUID AMPLIFIERS
Design guide for fluidic laminar proportional amplifiers and laminar jet angular rate sensors
[AD-A147730] 08 p1161 N85-17328

FLUID BOUNDARIES
NT GAS-SOLID INTERFACES
NT JET BOUNDARIES
NT LIQUID-LIQUID INTERFACES
NT LIQUID-SOLID INTERFACES
NT LIQUID-VAPOR INTERFACES
Instability of film boiling of moving liquids
[BLL-WH-603-(9091.9F)] 07 p0956 N85-16056

Perturbation of a multiple eigenvalue in the Benard problem for two fluid layers
[AD-A149068] 10 p1546 N85-19745
Application of the MHD energy principle to magnetostatic atmospheres
[NASA-CR-175967] 18 p3136 N85-29420
An investigation of hydraulic transients in combination free surface and pressurized flows
19 p3264 N85-30239
The Konstantinov effect and absorption of sound in inhomogeneous media 21 p3680 N85-32981

FLUID DYNAMICS
NT AERODYNAMICS
NT AEROTHERMODYNAMICS
NT COMPUTATIONAL FLUID DYNAMICS
NT CYLINDRICAL PLASMAS
NT ELASTOHYDRODYNAMICS
NT ELECTROHYDRODYNAMICS
NT GAS DYNAMICS
NT HYDRODYNAMICS
NT INTERACTIONAL AERODYNAMICS
NT MAGNETOHYDRODYNAMICS
NT RAREFIED GAS DYNAMICS
NT ROTONS
NT ROTOR AERODYNAMICS
NT SUPERSONICS
NT VORTEX SHEDDING
The properties of plane turbulent buoyant jet
[NAL-TR-798] 01 p0046 N85-10304
Highlights of the Institute of Sound and Vibration Research 01 p0131 N85-10905
Further development of a transonic cascade analysis
[AD-A145410] 02 p0198 N85-11319
USSR report: Physics and mathematics
[JPRS-UPM-84-004] 02 p0266 N85-11737
AGARD bulletin technical programme, 1985
[AGARD-BUL-84-2] 02 p0305 N85-11971
Report of the Department of Aerospace Engineering
03 p0307 N85-11977
Fluid motion in a rotating and nutating container
[AD-A146175] 03 p0362 N85-12322
Report of the Division of Atmospheric Physics, 1980-1983 03 p0391 N85-12501
Flow in Centrifugal Compressors — conferences
[VKI-LS-1984-07] 05 p0636 N85-14079
Salt-gradient solar ponds: Summary of US Department of Energy sponsored research
[NASA-CR-174183] 05 p0667 N85-14286
Solar pond fluid dynamics and heat transfer
05 p0667 N85-14288
Intraocular fluid dynamics in microgravity
05 p0693 N85-14455
USSR report: Physics and mathematics
[JPRS-UPM-84-007] 05 p0723 N85-14651
A method for solving the inverse problem of transonic cascade flow
[AD-A146739] 07 p0699 N85-15698
Dynamical characteristics of weak turbulence
[AD-A147186] 07 p0959 N85-16075
Solution of partial differential equations on vector and parallel computers
[NASA-CR-172500] 07 p1028 N85-16525
Advanced diagnostics for reacting flows
[AD-A148479] 08 p1162 N85-17334
Researched applied to transonic compressors in numerical fluid mechanics of inviscid flow and viscous flow
[NASA-CR-174353] 09 p1319 N85-18291
Solution of the h-equation for a single point source excitation of magnitude K
[DE84-017574] 09 p1374 N85-18638
Materials physics
[DE84-017103] 09 p1377 N85-18658
Effect of alpha particles on the stability of Elmo Bumpy Torus (EBT) reactor
[DE84-017266] 09 p1392 N85-18759
Summer study program in geophysical fluid dynamics, the Woods Hole Oceanographic Institution, dynamic differentiation
[AD-A149386] 10 p1521 N85-19595
Fluid temperature and concentration gradient measurement study — for spaceborne experiments
[CISE-R/FL/1/04] 11 p1637 N85-20309
MAP in India 11 p1655 N85-20424
The Middle Atmosphere Program: A special project for the Antarctic Middle Atmosphere (AMA)
11 p1656 N85-20430
Three-dimensional baroclinic instability of a Hadley cell for small Richardson number
[NASA-TP-2450] 11 p1687 N85-20605
Advanced research and technology programs for advanced high-pressure oxygen-hydrogen rocket propulsion
[NASA-TM-86969] 12 p1789 N85-21231
Numerical studies of fluid spin-up from rest in a partially-filled cylinder
[AD-A150079] 12 p1847 N85-21586
Analysis of the NASA/MSFC Airborne Doppler Lidar results from San Gorgonio Pass, California
[NASA-CR-171355] 12 p1892 N85-21873
Research Reports: 1984 NASA/ASEE Summer Faculty Fellowship Program
[NASA-CR-171317] 12 p1944 N85-22210
A study of the compatibility of an existing CFD package with a broader class of material constitutions
12 p1945 N85-22219
Evaluation of PHOENICS as a design analysis tool for SSME 12 p1949 N85-22240
Oversight review of the five-year outlook report on science and technology
[GPO-41-058] 12 p1949 N85-22243
Current problems in turbomachinery fluid dynamics
[AD-A150533] 13 p1974 N85-22397
The low frequency behaviour of an immersed structure at a standstill in a high density fluid with free surface
[TP-1983-31] 13 p2103 N85-23105
Effect of apparent fluid masses on natural vibration frequencies of impellers of multistage centrifugal pumps
14 p2277 N85-24108
Determination of gravity wave envelope solitons on surface of stratified fluid interacting with wind
14 p2334 N85-24433
One physical mechanism of formation of fine structure of ocean waters 14 p2334 N85-24436
Circulation statistics based on FGGE (First GARP Global Experiment) level 3-B analyses produced by GFDL (Geophysics Fluid Dynamics Laboratory)
[PB85-149318] 14 p2379 N85-24688
Magneto-fluid-dynamic issues for fusion first wall and blanket systems
[DE85-004022] 14 p2424 N85-24954
Heat transfer and fluid mechanics measurements in the turbulent reattaching flow behind a backward-facing step
15 p2553 N85-25753
Gasdynamic evaluation of choking cascade turns
[AD-A151854] 15 p2557 N85-25776
Geophysical Fluid Dynamics Laboratory activities, FY84, plans, FY85
[PB85-147601] 15 p2558 N85-25783
USSR report: Physics and mathematics
[JPRS-UPM-85-003] 15 p2642 N85-26300
Mean free paths, viscosity, and the limitations of perfect fluid hydrodynamics in the description of the quark-gluon plasma
[DE85-005501] 15 p2649 N85-26339
Progress of computational fluid dynamics in the world
16 p2691 N85-26612
Flow dynamic environment data base development for the SSME 16 p2736 N85-26885
Experimental evaluation of an advanced Space Shuttle main engine hot-gas manifold design concept
16 p2738 N85-26898
Analytical study of flow phenomena in SSME turnaround duct geometries 16 p2739 N85-26902
Liquid rocket combustor computer code development
16 p2740 N85-26910
Laser Schlieren and ultraviolet diagnostics of rocket combustion 16 p2740 N85-26911
USSR report: Engineering and equipment
[JPRS-UEQ-84-006] 16 p2760 N85-27035
An incremental multigrid strategy for the fluid dynamics equations
[AD-A151953] 16 p2783 N85-27172
A study of the effect of gently varying terrain on atmospheric flow near the surface
16 p2823 N85-27411
Fluid-dynamic model of a downburst
[UTIAS-271] 16 p2829 N85-27441
Air flow of the western coastal boundary of South Africa and its influence on the ocean 16 p2831 N85-27459
Apparatus for measuring velocity of sound in fluids
17 p2944 N85-28175
Vortices in non-Newtonian fluids
[AD-A153169] 17 p2958 N85-28269
FLOWPLOT 2: A fluid dynamics and heat transfer plotting package
[DE85-009802] 17 p2959 N85-28277
Morphological stability and fluid dynamics of vapor crystal growth
[NASA-CR-175879] 17 p3042 N85-28822
Morphological stability and fluid dynamics of vapor crystal growth
[NASA-CR-175880] 17 p3042 N85-28823
Activities of the Department of Aerospace Engineering
18 p3199 N85-29844
Buoyant jet entrainment in stratified fluids
19 p3263 N85-30238
Modifications to SOLA-VOF for flow dynamics in spinning cylinders
[AD-A154093] 19 p3265 N85-30250
Destruction of density jumps in ocean by turbulence
19 p3291 N85-30407
A device for generating motive force through the expansion of a non-elastic dense fluid
[NASA-TM-77664] 20 p3454 N85-31446
Notes on unsteady transonic cascade flows
[AD-A154829] 21 p3552 N85-32096
Experiments on the influence of active walls on the initial amplitudes and growths of instability waves
[AD-A154830] 21 p3583 N85-32275
Characteristics of a numerical fluid dynamics simulator
[DE85-009602] 21 p3586 N85-32290
Simulation of instability of cylindrically converging shock waves 23 p3960 N85-34679

FLUID FILLED SHELLS
NT LIQUID FILLED SHELLS
Acoustic radiation from concentric shells containing an inner fluid
[AD-A155476] 21 p3700 N85-32991

FLUID FILMS
NT SQUEEZE FILMS
Investigation of the local mass transfer of a laminar and turbulent falling liquid film
[BLL-T6368/BG/WH792/84] 06 p0807 N85-15130
Effect of interconnection of the ends of a sliding bearing on film thickness
[AD-A147736] 08 p1132 N85-17135
Tunable microwave transversal filters
[AD-A148370] 08 p1158 N85-17304
Mechanical interactions of rough surfaces
[DE85-000814] 10 p1494 N85-19434

FLUID FILTERS
NT AIR FILTERS
Laboratory simulation of smoke reduction from aircraft engine test cell exhaust using a fluidized bed filter
[AD-A148600] 08 p1089 N85-16866
Carbon filter plates for aluminum filtration at casting
[BMFT-FB-T-84-242] 12 p1806 N85-21343
Molecular and macromolecular sieving by asymmetric ultrafiltration membranes
[PB85-157766] 24 p4077 N85-35286

FLUID FLOW
NT AIR CURRENTS
NT AIR FLOW
NT AIR JETS
NT ANNULAR FLOW
NT AXIAL FLOW
NT AXISYMMETRIC FLOW
NT BAROTROPIC FLOW
NT BASE FLOW
NT BLASIUS FLOW
NT BLOOD FLOW
NT BOUNDARY LAYER FLOW
NT BOUNDARY LAYER SEPARATION
NT CAPILLARY FLOW
NT CASCADE FLOW
NT CAVITATION FLOW
NT CHANNEL FLOW
NT COAXIAL FLOW
NT COMBUSTIBLE FLOW
NT COMPRESSIBLE FLOW
NT CONICAL FLOW
NT CONTINUUM FLOW
NT CONVECTIVE FLOW
NT CORE FLOW
NT CORNER FLOW
NT COUETTE FLOW
NT COUNTERFLOW
NT CRITICAL FLOW
NT CROSS FLOW
NT DUCTED FLOW
NT EQUILIBRIUM FLOW
NT EQUIPOTENTIALS
NT FREE FLOW
NT FREE MOLECULAR FLOW
NT FROZEN EQUILIBRIUM FLOW
NT FUEL FLOW
NT GAS FLOW
NT HELICAL FLOW
NT HYPERSONIC FLOW
NT HYPERVELOCITY FLOW
NT INCOMPRESSIBLE FLOW
NT INLET FLOW
NT INVISCID FLOW
NT ISOTHERMAL FLOW
NT JET FLOW
NT JET MIXING FLOW
NT JET STREAMS (METEOROLOGY)
NT KNUDSEN FLOW
NT LAMINAR FLOW
NT LIQUID FLOW
NT MAGNETOHYDRODYNAMIC FLOW
NT MASS FLOW
NT MERIDIONAL FLOW
NT MOLECULAR FLOW
NT MULTIPHASE FLOW

NT NONEQUILIBRIUM FLOW
NT NONNEWTONIAN FLOW
NT NONUNIFORM FLOW
NT NOZZLE FLOW
NT ONE DIMENSIONAL FLOW
NT OPEN CHANNEL FLOW
NT ORIFICE FLOW
NT OSCILLATING FLOW
NT OUTLET FLOW
NT PARALLEL FLOW
NT PIPE FLOW
NT PLASTIC FLOW
NT POTENTIAL FLOW
NT PRESSURE HEADS
NT PROPELLANT TRANSFER
NT RADIAL FLOW
NT REATTACHED FLOW
NT RECIRCULATIVE FLUID FLOW
NT REVERSED FLOW
NT SECONDARY FLOW
NT SEPARATED FLOW
NT SHEAR FLOW
NT SMALL PERTURBATION FLOW
NT SOLIDS FLOW
NT STAGNATION FLOW
NT STEADY FLOW
NT STOKES FLOW
NT STRATIFIED FLOW
NT SUBCRITICAL FLOW
NT SUBSONIC FLOW
NT SUPERCRITICAL FLOW
NT SUPERSONIC FLOW
NT SUPERSONIC JET FLOW
NT THREE DIMENSIONAL FLOW
NT TRANSITION FLOW
NT TRANSONIC FLOW
NT TRESCA FLOW
NT TURBULENT FLOW
NT TWO DIMENSIONAL FLOW
NT TWO PHASE FLOW
NT UNIFORM FLOW
NT UNSTEADY FLOW
NT VERTICAL AIR CURRENTS
NT VISCOUS FLOW
NT WALL FLOW
NT WATER FLOW
NT WEDGE FLOW

Implementation of the supersonic triplet singularity into the USTORE computer code
[CSIR-NIAST-83/47] 01 p0001 N85-10006

Collapsable seal member
[DE84-014300] 01 p0055 N85-10367

Observations of the vertical structure of the eddy field in the Kuroshio extension
[AD-A145178] 01 p0089 N85-10590

Upwind compact finite difference schemes
[CSIR-TWISK-394] 01 p0110 N85-10742

Experiments on turbulent mixing and chemical reactions in a liquid mixing layer 02 p0134 N85-10912

Spatial relationships in stream flow residuals 02 p0212 N85-11397

A study on dynamic characteristics of liquid oxygen pumps for rocket engines
[NAL-TR-806] 03 p0324 N85-12068

NBS (National Bureau of Standards): Materials measurements
[NASA-CR-174036] 03 p0332 N85-12143

Analysis of physical-chemical processes governing SSME internal fluid flows
[NASA-CR-171247] 04 p0451 N85-12859

A preliminary study of numerical simulation of thermosolutal convection of interest to crystal growth
[NASA-TP-2394] 04 p0498 N85-13175

Analysis of dynamic characteristics of fluid force induced by labyrinth seal 05 p0643 N85-14129

Atmospheric studies in complex terrain
[DE84-006553] 05 p0676 N85-14345

Analysis of physical-chemical processes governing SSME internal fluid flows
[NASA-CR-174245] 06 p0760 N85-14862

Towing tank studies of stratified flow over ridges and valleys
[DE84-011418] 06 p0839 N85-15329

Stability of rigid motions and rollers in bicomponent flows of immiscible liquids
[AD-A147302] 07 p0960 N85-16081

Numerical solutions for steady natural convection in a square cavity
[PB84-245752] 07 p0961 N85-16090

Steady flow model user's guide
[DE85-002001] 08 p1163 N85-17337

New discovery in supersonic flight research 09 p1278 N85-18041

Supercritical fluid chromatography/supersonic jet spectroscopy
[DE85-003310] 09 p1292 N85-18115

Microscopic study of fluid flow 09 p1317 N85-18280

Convective heat transfer coefficients for pipe flow with curvature induced secondary motion 09 p1318 N85-18285

Accuracy of the finite analytic method for scalar transport calculations
[DE85-001474] 09 p1320 N85-18300

Thermal striping downstream of a horizontal elbow under thermally stratified transient flow conditions
[DE84-014887] 09 p1320 N85-18302

Survey of remote data monitoring systems
[DE85-001385] 09 p1323 N85-18313

Analysis of compact heat exchanger performance
[DE84-012624] 10 p1485 N85-19377

Perturbation of a multiple eigenvalue in the Benard problem for two fluid layers
[AD-A149068] 10 p1546 N85-19745

Thermodynamics of the reactive flow model
[DE85-004405] 10 p1565 N85-19870

Leakage-flow-induced vibration of a tube-in-tube slip joint
[DE84-007301] 11 p1652 N85-20406

Flow-induced tube vibration thresholds in heat exchangers from shellside water tests
[DE84-006603] 11 p1652 N85-20407

Algorithm for the simulation of transient viscoelastic flows with free surfaces
[DE85-002713] 12 p1848 N85-21590

Response time correlations for platinum resistance thermometers in flowing fluids
[NASA-CR-172523] 12 p1850 N85-21606

A two-axis, self-nulling skin friction balance
[NASA-CASE-LAR-13294-1] 12 p1851 N85-21610

Computer-Aided Structural Engineering (CASE) project. Seepage analysis of confined flow problems by the method of fragments (CFRAG)
[AD-A150015] 12 p1875 N85-21782

Results of the AFRSI rewaterproofing systems screening test in the NASA/Ames Research Center (ARC) 2 x 2-foot transonic wind tunnel
[NASA-CR-167694] 13 p1988 N85-22467

Workshop report: Swirl Enhanced Combustion 13 p2005 N85-22584

HPFTP flow diverter analysis
[NASA-CR-171424] 13 p2091 N85-23057

Effects of fracture roughness on fluid flow through a single deformable fracture
[DE85-004593] 13 p2092 N85-23062

Emplacement of long lava flows on Mauna Loa (Hawaii) and Alba (Mars) 13 p2186 N85-23563

Thermal infrared observations of lava flows during the 1984 Mauna Loa eruption 13 p2186 N85-23564

Surface structures of Hawaiian lavas 13 p2186 N85-23566

Basaltic pressure ridges: Formation and relationship to flow emplacement 13 p2186 N85-23567

Model of friction bearing hydrodynamics 14 p2288 N85-24178

Application of adaptive grids in solving the partial differential equations governing fluid flow
[AD-A151175] 15 p2555 N85-25766

Thermal traction contact performance evaluation under fully flooded and starved conditions
[NASA-CR-168173] 15 p2568 N85-25848

Variational bounds on Darcy's constant
[DE85-006638] 15 p2580 N85-25916

The effect of the Benthic Boundary Layer on the physics of intense mesoscale eddies
[AD-A153193] 17 p2958 N85-28270

Experimental and theoretical studies on transport processes in laser welding
[DE84-006572] 17 p2975 N85-28378

Numerical benchmark study for the finite element computer code NEPTUNE
[DE85-008400] 17 p3013 N85-28630

Fluid modeling of magnetized plasmas
[DE85-007679] 17 p3039 N85-28804

Multi-ducted inlet combustor research and development
[AD-A153753] 18 p3063 N85-28946

Theoretical and experimental studies of the mechanics of viscoelastic liquids
[AD-A153505] 18 p3070 N85-28987

Variational bounds on Darcy's constant
[DE85-006959] 18 p3101 N85-29195

Transport characteristics of slurries in pipelines: Flow regimes and pressure drop
[DE85-009453] 18 p3101 N85-29196

Laboratory investigation of formation damage of an artificial fracture at simulated geothermal conditions
[DE85-010301] 18 p3102 N85-29201

Applications of Canuto's method to Rayleigh-Taylor-initiated turbulence
[DE85-010635] 18 p3102 N85-29202

Pressure measurement: Short course
[DE85-008644] 18 p3102 N85-29205

Conceptual hydrologic model of flow in the unsaturated zone, Yucca Mountain, Nevada
[DE85-006346] 18 p3125 N85-29350

Interim rock mass properties and conditions for analyses of a repository in crystalline rock
[DE85-010700] 18 p3125 N85-29352

Colloidal particle transport with simultaneous birth, growth and capture
[DE85-010368] 19 p3235 N85-30055

The stability and dynamics of elastic structures and fluid flows
[AD-A154188] 19 p3266 N85-30252

A method for predicting additive drag reduction from small-diameter pipe flows
[AD-A154411] 19 p3266 N85-30254

Mathematics of oil production
[DE85-011235] 19 p3267 N85-30261

Pressure recovery in a cylindrical heat pipe at high radial Reynolds numbers and at high Mach numbers
[DE85-010718] 19 p3269 N85-30274

LDA study of the unburned gas motion induced by nonsteady flame propagation in a constant volume duct
[DE85-009938] 19 p3270 N85-30277

Improved fluid flow meter for measuring the rate of fluid flow in a conduit
[NASA-CASE-MFS-28030-1] 19 p3271 N85-30286

Accuracy in determining velocity of fluid movement by Doppler method 19 p3293 N85-30419

Preliminary evaluation of alterant geophysical tomography in welded tuff
[DE85-010826] 19 p3302 N85-30469

KIVA: A computer program for two- and three-dimensional fluid flows with chemical reactions and fuel sprays
[DE85-010334] 19 p3339 N85-30693

Observations of the use of the setapoint detector
[AD-A154533] 21 p3571 N85-32208

Weak shock waves propagating in fluid-gas mixtures
[AD-A154759] 21 p3584 N85-32276

Finite element methods for viscoelastic flow
[AD-A154877] 22 p3783 N85-33437

Gradient scaling for nonuniform meshes
[DE85-009625] 22 p3784 N85-33443

Linear boundary detection using pressure buildup tests
[DE85-009926] 22 p3784 N85-33444

KIVA computer program for multidimensional chemically reactive fluid flows with fuel sprays
[DE85-012730] 22 p3830 N85-33722

The application of models to the assessment of fire hazard from consumer products
[NBSIR-85-3219] 23 p3925 N85-34325

Refrigerated dynamic seal to 6.9 MPa (1000 psi)
[NASA-TM-87108] 23 p3930 N85-34356

Feedback regulated induction heater for a flowing fluid
[DE85-006506] 23 p3939 N85-34414

Studies in thermo-hydro-chemical transport in porous and fractured media
[DE85-012555] 23 p3949 N85-34473

Flow modifying device
[NASA-CASE-LEW-13562-2] 24 p4065 N85-35195

The effect of power law body forces on a thermally-driven flow between concentric rotating spheres
[NASA-TM-87596] 24 p4093 N85-35374

Noise-sustained structure, intermittency and the Ginzburg-Landau equation
[DE85-009626] 24 p4094 N85-35379

Transient three-phase three-component systems. Part 1: Formulation of the system of differential equations
[DE85-013267] 24 p4095 N85-35384

FLUID INJECTION
NT DEEP WELL INJECTION (WASTES)
NT GAS INJECTION
NT LIQUID INJECTION
NT WATER INJECTION

Geothermal injection treatment: Process chemistry, field experiences, and design options
[DE85-002873] 11 p1675 N85-20554

Calculating isothermal flow in wake beyond injection zone 14 p2287 N85-24175

Micro-scale methods for characterization of supercritical fluid extraction and fractionation processes
[DE85-010966] 20 p3455 N85-31456

FLUID JET AMPLIFIERS
U FLUID AMPLIFIERS

FLUID JETS
NT AIR JETS
NT FREE JETS
NT GAS JETS
NT HYDRAULIC JETS
NT VAPOR JETS

Supercritical fluid chromatography/supersonic jet spectroscopy
[DE84-016199] 04 p0471 N85-12998

Transition and mixing in axisymmetric jets and vortex rings 05 p0591 N85-13769
Influence of turbulence on erosion by a particle-laden fluid jet
[DE84-014365] 09 p1320 N85-18301
Algorithm for the simulation of transient viscoelastic flows with free surfaces
[DE85-002713] 12 p1848 N85-21590
Fluid-dynamic model of a downburst
[UTIAS-271] 16 p2829 N85-27441
Buoyant jet entrainment in stratified fluids 19 p3263 N85-30238
Generation of capillary instabilities by external disturbances in a liquid jet
[NASA-TM-87041] 19 p3265 N85-30246
Supercritical fluid chromatography/supersonic jet spectroscopy
[DE85-007005] 22 p3746 N85-33221

FLUID MANAGEMENT
Space station task force perspective 08 p1106 N85-16992
Technology requirements to be addressed by the NASA Lewis Research Center Cryogenic Fluid Management Facility program
[NASA-TM-87048] 19 p3224 N85-29987

FLUID MECHANICS
NT AERODYNAMICS
NT AEROTHERMODYNAMICS
NT COMPUTATIONAL FLUID DYNAMICS
NT CYLINDRICAL PLASMAS
NT ELASTOHYDRODYNAMICS
NT ELECTROHYDRODYNAMICS
NT FLUID DYNAMICS
NT GAS DYNAMICS
NT HYDRODYNAMICS
NT HYDROMECHANICS
NT HYDROSTATICS
NT INTERACTIONAL AERODYNAMICS
NT MAGNETOHYDRODYNAMICS
NT PNEUMATICS
NT RAREFIED GAS DYNAMICS
NT ROTONS
NT ROTOR AERODYNAMICS
NT SUPERSONICS
NT VORTEX SHEDDING
Equation of state study for polar fluids
[PB84-222601] 01 p0025 N85-10157
Space research and the new approach to the mechanics of fluid media in cosmos
[TRITA-EPP-84-04] 03 p0447 N85-12844
Experimental and theoretical study of a solar thermochemical receiver module
[NASA-CR-174107] 04 p0528 N85-13374
USSR report: Engineering and equipment
[JPRS-UEQ-84-007] 06 p0775 N85-14954
Large-eddy simulation. Guidelines for its application to planetary boundary layer research
[AD-A146381] 06 p0890 N85-15851
An update of the Canada/USA augmentor-wing project 06 p1070 N85-16781
USSR report: Engineering and equipment
[JPRS-UEQ-85-001] 09 p1305 N85-18200
An experimental study of single and multiple turbulent buoyant jets in crossflow 09 p1317 N85-18281
Evaluation of inviscid/boundary layer and parabolized Navier-Stokes solutions for design of reentry vehicles
[DE84-014329] 10 p1428 N85-19006
Overview of leading-edge research at French CNRS lab 11 p1618 N85-20179
Acoustic resonance in heat exchanger tube banks
[DE85-004305] 11 p1632 N85-20281
Advanced research and technology programs for advanced high-pressure oxygen-hydrogen rocket propulsion
[NASA-TM-86969] 12 p1789 N85-21231
Nested subcritical flows within supercritical systems
[NASA-TM-86960] 12 p1845 N85-21574
Arc-driven rail gun research
[NASA-CR-174816] 12 p1859 N85-21682
Space research and the new approach to the mechanics of fluid media in cosmos 12 p1953 N85-22271
USSR report: Engineering and equipment
[JPRS-UEQ-85-003] 13 p2042 N85-22782
Coupling between velocity oscillations and solid propellant combustion
[AD-A151081] 14 p2247 N85-23927
Abatement of noise and vibration in pipelines of hydro systems 14 p2276 N85-24102
USSR report: Engineering and equipment
[JPRS-UEQ-84-006] 14 p2285 N85-24157
Fluid mechanics and heat transfer spirally fluted tubing
[AD-A150774] 14 p2301 N85-24247
Adaptive grid generation for numerical solution of Burger's equation
[AD-A152217] 16 p2855 N85-27606
USSR report: Engineering and equipment
[JPRS-UEQ-85-004] 17 p2939 N85-28142
Buildup of oscillation of bodies in stratified fluid 17 p2941 N85-28157
Fluid surface behavior in low gravity. Center discretionary fund no. 83-21
[NASA-TP-2486] 17 p2957 N85-28260
TRINITY: A pre- and post-processing program for 2-dimensional finite element data
[DE85-008029] 17 p3013 N85-28626
Turbulent wake of a submerged flat plate
[AD-A153776] 18 p3100 N85-29190
Pattern selection and instability in nonlinear wave equation: An aspect of soliton and chaos
[DE85-009578] 18 p3101 N85-29197
Dynamic stability of a spinning tube conveying a flowing fluid
[DE85-007563] 18 p3102 N85-29207
Highly accurate shock flow calculations with moving grids and mesh refinements, revision 1
[DE85-010929] 19 p3267 N85-30260
Analysis of seismic sloshing of reactor tanks considering submerged components and seismic isolation
[DE85-010499] 19 p3269 N85-30273
Transition in Turbines
[NASA-CP-2386] 20 p3452 N85-31433
Heat transfer and fluid mechanics measurements in transitional boundary layer flows 20 p3453 N85-31439
R and D activities of the Aerodynamics Division 20 p3539 N85-32023
Bubble dynamics in polymer solutions undergoing shear
[AD-A154575] 21 p3568 N85-32193
Experiments on the influence of active walls on the initial amplitudes and growths of instability waves
[AD-A154630] 21 p3583 N85-32275
USSR report: Physics and mathematics
[JPRS-UPM-85-004] 21 p3660 N85-32860
Basic research on pulse-combustion phenomena
[PB85-200226] 24 p4077 N85-35265

FLUID POWER
Fluid layer between infinite elastic plates II. Distribution of power flow
[AD-A146690] 03 p0361 N85-12312
Rotordynamic Instability Problems in High-Performance Turbomachinery
[NASA-CP-2338] 05 p0642 N85-14116
Lateral fluid forces acting on a whirling centrifugal impeller in vaneless and vaned diffuser 05 p0643 N85-14123
Two-dimensional unsteady analysis of fluid forces on a whirling centrifugal impeller in a volute 05 p0643 N85-14126

FLUID PRESSURE
NT WATER PRESSURE
Evaluation of subsurface fracture geometry using fluid pressure response to solid earth tidal strain
[DE85-003294] 12 p1890 N85-21884
Investigation, development, and certification of a burst disk for cryogenic fuel tanks
[GCP-3/MT-CM-21-2546] 18 p3067 N85-28972
Damping seal for turbomachinery
[NASA-CASE-MFS-25842-2] 19 p3260 N85-30341
Polymer solution-supercritical fluid behavior
[AD-A154514] 21 p3568 N85-32192

FLUID SWITCHING ELEMENTS
An investigation into the advantages of fluidics in fluid processing. Part 1: An overview of fluidics
[FFA-TN-1984-15-PT-1] 02 p0199 N85-11328

FLUID TRANSMISSION LINES
Dynamic response of fluid transmission lines
[AD-A151926] 16 p2782 N85-27171

FLUID TRANSPIRATION
U TRANSPIRATION

FLUID-SOLID INTERACTIONS
NT GAS-METAL INTERACTIONS
NT GAS-SOLID INTERACTIONS
Normal mode method of solving problem forced oscillations of rib-reinforced shell of revolution in liquid 02 p0273 N85-11781
Leakage-flow induced vibrations of a chimney structure suspended in a liquid flow — nuclear reactors 09 p1339 N85-18420
Effect of air cavity on the vibration analysis of loaded drums 09 p1339 N85-18422

FLUIDIC CIRCUITS
NT FLIP-FLOPS
An investigation into the advantages of fluidics in fluid processing. Part 1: An overview of fluidics
[FFA-TN-1984-15-PT-1] 02 p0199 N85-11328

FLUIDICS
An investigation into the advantages of fluidics in fluid processing. Part 1: An overview of fluidics
[FFA-TN-1984-15-PT-1] 02 p0199 N85-11328
Design guide for fluidic laminar proportional amplifiers and laminar jet angular rate sensors
[AD-A147730] 06 p1161 N85-17328
Dynamic response of fluid transmission lines
[AD-A151926] 16 p2782 N85-27171

FLUIDIZED BED PROCESSORS
Overall heat transfer coefficients for a horizontal cylinder in a fluidized bed
[AD-A144878] 01 p0124 N85-10849
Dynamics of burnout of solid fuel in fluidized bed of finely divided inert particles 02 p0273 N85-11782
Electrochemical production of silicon 06 p0832 N85-15290
JPL in-house fluidized-bed reactor research 06 p0832 N85-15291
Advanced technology cogeneration system conceptual design study: Closed cycle gas turbines
[NASA-CR-168222] 07 p0992 N85-18300
Laboratory simulation of smoke reduction from aircraft engine test cell exhaust using a fluidized bed filter
[AD-A148600] 08 p1089 N85-16686
Liquid phase methanol process development unit: Installation, operation, and support studies
[DE85-001311] 09 p1301 N85-18171
Heat transfer to vertical flat plates in a rectangular gas-fluidized bed
[AD-A150785] 14 p2301 N85-24248
Conversion of methanol to gasoline: Engineering and construction of the demonstration plant
[DE85-003237] 17 p2937 N85-28133
Current status of TVA's atmospheric fluidized bed combustion development efforts
[DE85-901209] 19 p3308 N85-30507
An analysis of the feasibility of producing silicon for solar cells by a dichlorosilane/fluidized-bed reactor process
[NASA-CR-176036] 20 p3478 N85-31614
An investigation into the fluidization and heat transfer of low density particles in a fluidized bed with applications
[AD-A155259] 21 p3584 N85-32282
A fluidized-bed reactor for silane pyrolysis 21 p3609 N85-32413
JPL in-house fluidized-bed reactor research 21 p3609 N85-32414
Modeling of the silane FBR system 21 p3609 N85-32415
Solids mixing in a three phase fluidized bed containing spherically shaped-porous solid particles
[PB85-187961] 22 p3785 N85-33483
Fluidized bed desulfurization
[NASA-CASE-NPO-15924-1] 24 p4075 N85-35253

FLUIDS
On the co-variant formulation of the law of motion of passive particles in a field of turbulence
[REPT-584] 03 p0377 N85-12407
Convection heat transfer in the critical region of fluid mixtures
[DE85-001282] 11 p1633 N85-20285
Self-charging metering and dispensing device for fluids
[NASA-CASE-MSC-20275-1] 12 p1848 N85-21585
Dynamics of solid body with ellipsoidal cavity containing magnetic fluid 14 p2279 N85-24116
Mathematical modeling of fluid-electrolyte alterations during weightlessness
[NASA-CR-171881] 15 p2617 N85-26125
An experimental study of the pressure in a fast bottom beneath the apex of an overlying fluid wedge
[AD-A153618] 18 p3177 N85-29696

FLUORESCENCE
NT PHOSPHORESCENCE
NT RESONANCE FLUORESCENCE
NT X RAY FLUORESCENCE
Raman and fluorescence spectroscopy in a methane-nitrous oxide laminar flame
[AD-A146092] 03 p0326 N85-12111
Microfluorescence studies of zirconium oxide
[DE84-016116] 03 p0329 N85-12118
Time-resolved spectroscopy of evanescent-wave excited fluorescence
[DE84-015213] 04 p0473 N85-13013
Fluorescent dyes for luminescent solar concentrators
[BMFT-FB-T-84-164] 04 p0480 N85-13061
Secondary fluorescence effects on X-ray microanalysis
[DE84-016600] 05 p0618 N85-13951
Determining lamp/ballast system performance with a temperature-controlled integrating chamber
[DE84-014606] 05 p0631 N85-14049
Fundamentals of solar energy conversion based on fluorescence collectors 05 p0662 N85-14258
Fundamental equations of the LIF hydroxyl measurements, appendix A 05 p0676 N85-14338
Saturation phenomena in LIF measurements, appendix B 05 p0676 N85-14339

Detailed performance calculations: Wayne State University and Ford Motor Company, appendix C
05 p0676 N85-14340
Detailed performance calculations: Portland State Group, appendix F
05 p0676 N85-14343
Detailed performance calculations: Harvard Group, appendix G
05 p0676 N85-14344
Clinical measurements using fiber optics and optrodes
[DE84-015043] 05 p0696 N85-14481
Measurements of X-ray spectra from laser produced plasma
06 p0748 N85-14794
Solar energy conversion based on the principle of fluorescent collectors. Installation of a test collector to deliver several Watts power
[BMFT-FB-T-84-192] 07 p0993 N85-16308
Solar energy conversion based on the principle of fluorescent collectors
[BMFT-FB-T-84-193] 07 p0994 N85-16309
Combustion kinetics of metal oxide and halide radicals
[AD-A148521] 08 p1122 N85-17076
New lighting technologies, their status and impacts on power densities
[DE85-000712] 09 p1315 N85-18265
Alignment of high Rydberg states in hydrogen
[DE85-000582] 09 p1380 N85-18677
Developments and applications of laser fluorescence spectroscopy for studies of particle behaviours in fusion plasmas
09 p1389 N85-18735
Measurements of electric fields in plasmas by using beam probe and laser fluorescence techniques
09 p1389 N85-18737
Laser-induced-fluorescence-spectroscopy of atomic processes under a high magnetic field
09 p1389 N85-18740
The fluorescence of cometary OH and CN
09 p1411 N85-18896
Exciplex systems for vapor-liquid visualization of fuel sprays
[AD-A149360] 10 p1457 N85-19181
Excimer laser photofragmentation of organophosphonates. 1: Detection of the PO radical from dimethyl methyl phosphonate (DMMP)
[AD-A149471] 10 p1490 N85-19407
Applications of pulsed-laser techniques and thermographic phosphors to dynamic thermometry of rotating surfaces
[DE85-000400] 11 p1639 N85-20328
Fluorescent excitation of Fe 2, Mn 2, Ti 2, N 1 lines by V 4, N 5, O 6: Emission lines in the spectra of symbiotic stars and Seyfert galaxies
11 p1746 N85-20984
Two-dimensional measurements of OH concentration and temperature in reactive flows
[AD-A149849] 12 p1600 N85-21292
Application of fluorescence to measurement of surface temperature in solid propellants
13 p2002 N85-22548
Luminescence in the ocean
[AD-B069136L] 13 p2140 N85-23268
Ion transport in beam-plasma interactions
[AD-A150145] 13 p2161 N85-23410
Computer simulations of rare earth sites in glass: Experimental tests and applications to laser materials
[DE85-006188] 14 p2261 N85-24013
Application of atomic fluorescence to measurement of combustion temperature in solid propellants
[AD-A150733] 14 p2263 N85-24021
Secondary fluorescence effects on X-ray microanalysis
[DE85-006585] 15 p2506 N85-25457
Water vapor
16 p2824 N85-27420
Measurement of Franck-Condon factors for the v'=0 progression in the B-X system of PO
[AD-A152734] 17 p2919 N85-27993
Investigation of several low-lying levels of X doublet pi state of NCO using argon laser excited fluorescence
[AD-A153993] 18 p3071 N85-28994
Measurement of radical species concentrations and polycyclic aromatic hydrocarbons in flames by fluorescence and absorption using a tunable dye laser
[DE85-009624] 18 p3113 N85-29274
Quantitative studies for photoabsorption and fluorescence of HCl
[NASA-CR-175985] 19 p3233 N85-30043
Measurement of combustion species by electron impact fluorescence
[DE85-011163] 19 p3236 N85-30065
Improvements in the energy resolution and high-count-rate performance of bismuth germanate
[DE85-010763] 19 p3240 N85-30092
Laser-induced fluorescence measurement of vapor concentration surrounding evaporating droplets
[DE85-009409] 19 p3277 N85-30320
E-beam-induced fluorescence of excimers in cryogenic solutions
[DE85-010703] 19 p3278 N85-30328
Development of a technique for in situ detection of stratospheric nitrogen dioxide
19 p3312 N85-30534
Fluorescence quenching by metal semiconductor and insulator surfaces
19 p3374 N85-30920
Chromophores with auxochrome-like function
[NASA-TM-77849] 20 p3421 N85-31233
Recent measurements in turbulent jet flames at Sandia Combustion Research Facility
20 p3424 N85-31254
Velocity visualization in gaseous flows
[NASA-CR-174954] 20 p3453 N85-31445
Multidimensional luminescence measurements
[AD-A154950] 21 p3563 N85-32162
A microprocessor-controlled, multichannel fluorimeter for analysis of sea water
[AD-A154986] 21 p3590 N85-32310
Detection of excited states by laser-induced fluorescence
[AD-A155558] 21 p3592 N85-32326
Photofragment fluorescence as a sensitive probe for gas-phase alkali compounds and their photochemistry
[DE85-010707] 22 p3746 N85-33219
Laser probes of natural gas ignition chemistry
[PB85-200210] 24 p4077 N85-35264
Atmospheric nitrogen oxides: Their detection and chemistry
[PB85-193910] 24 p4114 N85-35502
Lateral-angular and temporal characteristics of EAS optical radiation
[HE-4.4-19] 24 p4194 N85-36025
Air fluorescence detection of large air showers below the horizon
[HE-4.6-6] 24 p4197 N85-36043

FLUORESCENT EMISSION
U FLUORESCENCE

FLUORIDES
NT BERYLLIUM FLUORIDES
NT BORON FLUORIDES
NT CADMIUM FLUORIDES
NT CALCIUM FLUORIDES
NT DEUTERIUM FLUORIDES
NT DIFLUORIDES
NT HYDROFLUORIC ACID
NT LITHIUM FLUORIDES
NT MAGNESIUM FLUORIDES
NT METAL FLUORIDES
NT OXYFLUORIDES
NT POLYVINYL FLUORIDE
NT STRONTIUM FLUORIDES
NT SULFUR FLUORIDES
NT URANIUM FLUORIDES

Method for the preparation of poly(carbonyl fluoride) oligomers
[AD-D011207] 01 p0030 N85-10184
Comparison study of analytical methods for the determination of fluoride, chloride, and bromide in plastics
[DE84-015008] 04 p0470 N85-12989
Effects of silver and group 2 fluorides addition to plasma sprayed chromium carbide high temperature solid lubricant for foil gas bearing to 650 deg C
[NASA-TM-88895] 06 p0770 N85-14928
Compositional, structural, and physical studies of some graphite hexafluoroarsenates and their relatives
[DE85-000855] 10 p1432 N85-19030
Optically pumped iodine monofluoride laser
[AD-D011555] 12 p1855 N85-21637
Synthesis and characterization of poly(vinylidene fluoride)
[AD-A150291] 13 p2037 N85-22759
Mixed valence materials
[AD-A151009] 14 p2252 N85-23959
Preparation of heavy metal fluoride glasses in the bulk form
[AD-A153784] 18 p3079 N85-29049
RAY-O-VAC BR2325 lithium carbon monofluoride cell performance
20 p3444 N85-31382
Method for fluorination of actinide fluorides and oxyfluorides using O2F2
[DE85-011646] 22 p3743 N85-33202
Environmental surveillance at Los Alamos during 1984
[DE85-011886] 22 p3811 N85-33605
A new large-scale, high-resolution multicolor software display concept
[AD-A155404] 22 p3827 N85-33703

FLUORINATION

Fluorinated diamond particles bonded in a filled fluorocarbon resin matrix
[DE84-014444] 01 p0022 N85-10136
Method for introducing fluorine into an aromatic ring
[AD-D011397] 08 p1120 N85-17061
Effective antireflection coatings of transparent polymeric materials by gas-phase surface fluorination
[DE84-013027] 09 p1385 N85-18711
Fluorinated polyesters
[AD-D011611] 16 p2753 N85-26988
Method for fluorination of actinide fluorides and oxyfluorides using O2F2
[DE85-011646] 22 p3743 N85-33202

FLUORINE

Nuclear moments and nuclear structure
[DE84-015847] 04 p0561 N85-13573
Forming fluorine-containing threads from vinylidene fluoride-tetrafluoroethylene copolymer by dry method
06 p0762 N85-14673
Alabama Tin Belt: Metallogenesis and mineral resource evaluation. Year-end report
[DE84-901335] 07 p0989 N85-16283
Method for introducing fluorine into an aromatic ring
[AD-D011397] 08 p1120 N85-17061
Time dependent Hartree-Fock theory of ion-atom collisions: Application to F(9+) + Ne
[DE85-003083] 11 p1723 N85-20638
Preparation of nitrocompounds
[AD-A153687] 18 p3071 N85-28993
Slow chemistry effects in a turbulent mixing layer
20 p3424 N85-31252
Synthesis of energetic materials
[AD-A154687] 21 p3571 N85-32210
Vacuum ultraviolet laser
[DE85-011632] 22 p3790 N85-33478

FLUORINE COMPOUNDS
NT BERYLLIUM FLUORIDES
NT BORON FLUORIDES
NT CADMIUM FLUORIDES
NT CALCIUM FLUORIDES
NT CARBON TETRAFLUORIDE
NT DEUTERIUM FLUORIDES
NT DIFLUORIDES
NT DIFLUORO COMPOUNDS
NT FLUORIDES
NT FLUORINE ORGANIC COMPOUNDS
NT FLUORITE
NT FLUORO COMPOUNDS
NT FLUOROCARBONS
NT FLUOROHYDROCARBONS
NT FLUOROPOLYMERS
NT HYDROFLUORIC ACID
NT LITHIUM FLUORIDES
NT MAGNESIUM FLUORIDES
NT METAL FLUORIDES
NT OXYFLUORIDES
NT PERFLUOROALKANE
NT POLYTETRAFLUOROETHYLENE
NT POLYVINYL FLUORIDE
NT STRONTIUM FLUORIDES
NT SULFUR FLUORIDES
NT URANIUM FLUORIDES

Synthesis of pentafluorotellurium hypofluorite
[AD-D011212] 01 p0023 N85-10139
Electron oxidation of graphite by fluorospecies
[DE85-001196] 11 p1595 N85-20034
New catalysts and new electrolytes for acid fuel cells
[DE85-009940] 19 p3307 N85-30498

FLUORINE ORGANIC COMPOUNDS
NT CARBON TETRAFLUORIDE
NT FLUOROCARBONS
NT FLUOROHYDROCARBONS
NT FLUOROPOLYMERS
NT PERFLUOROALKANE
NT POLYVINYL FLUORIDE

Development and application of fluorine-containing reagents in the gas chromatography of carbonyl compounds
[BLL-DRIC-TRANS-7205-(3623.66)]
01 p0023 N85-10140

FLUORITE

A mixed-basis band structure interpolation scheme applied to the fluorite structure compounds NiSi2, AuAl2, AuGa2 and AuIn2
[AD-A150131] 12 p1940 N85-22187

FLUORO COMPOUNDS
NT CARBON TETRAFLUORIDE
NT DIFLUORO COMPOUNDS
NT FLUORINE ORGANIC COMPOUNDS
NT FLUOROCARBONS
NT FLUOROHYDROCARBONS
NT FLUOROPOLYMERS
NT PERFLUOROALKANE
NT POLYTETRAFLUOROETHYLENE

Measurement of state and dynamic solid state properties in nonmetals using excited probe nuclei on the Erlangen 12 MeV tandem accelerator
03 p0428 N85-12730
Pseudo-p-1,2,2,9,9,10,10-octofluoro (2,2)-p-cyclophane bis-acid chloride
[AD-D011393] 07 p0919 N85-15818
Water-resistance and some other properties of polyalkali fluorophosphate glasses
14 p2281 N85-24133
Improved acid electrolytes for fuel cells
[PB85-176053] 18 p3132 N85-29397

FLUOROCARBONS
Fluorinated diamond particles bonded in a filled fluorocarbon resin matrix
[DE84-014444] 01 p0022 N85-10136
Apparatus for measuring dielectric characteristics of polymer materials in millimetric range of wavelengths at 4.2-300 K temperatures 06 p0788 N85-15032
Cross-Appalachian Tracer Experiment (CAPTEX '83)
[PB84-238641] 06 p0834 N85-15307
New approaches to functionalized fluorocarbons
[AD-A154205] 19 p3248 N85-30141
Basic research in novel inorganic reagents and fluorocarbon chemistry
[AD-A155340] 21 p3584 N85-32165
Reaction of uranium and the fluorocarbon FC-75
[DE85-012322] 22 p3843 N85-33802

FLUOROHYDROCARBONS
NT CARBON TETRAFLUORIDE
Working medium for sorption heat pumps
[BLL-T6360/BG/WH785/84] 06 p0807 N85-15131
Fluorinated diacrylic esters
[AD-D011328] 07 p0929 N85-15889
Elementary processes of electronically excited particles. Part 5: Deactivation of CHF (A1a' (O, V'2, O) after excitation by a pulsed dye laser
[MPIS-13/1984] 14 p2420 N85-24930
New approaches to functionalized fluorocarbons
[AD-A154205] 19 p3248 N85-30141
Atmospheric chlorofluromethanes as tracers of ocean circulation and mixing: Measurement and calibration techniques and studies in the Greenland and Norwegian Seas 19 p3319 N85-30573

FLUOROMICA
U MICA

FLUOROPLASTICS
U FLUOROPOLYMERS

FLUOROPOLYMERS
NT POLYTETRAFLUOROETHYLENE
NT POLYVINYL FLUORIDE
NT TEFLON (TRADEMARK)
Fluorinated aliphatic polyalkylether lubricant with an additive composed of an aromatic phosphine substituted with perfluoroalkylether groups
[AD-D011286] 06 p0770 N85-14927
Fluorinated diacrylic esters
[AD-D011328] 07 p0929 N85-15889
Dynamic polymer pressure transducer with temperature compensation
[AD-D011373] 07 p0967 N85-16142
Polymer blends as high explosive binders
[DE85-001210] 11 p1611 N85-20131
Fluorinated polyurethanes
[AD-D011526] 12 p1810 N85-21353
Ion transporting composite membranes. 1: Nafion impregnated gore-tex
[AD-A151020] 14 p2252 N85-23960

FLUSHING
Nitrogen flushing during exposure of large Schmidt telescope plates 07 p0963 N85-16109

FLUTING
U GROOVING

FLUTTER
NT AEROELASTIC RESEARCH WINGS
NT SUBSONIC FLUTTER
NT SUPERSONIC FLUTTER
NT TRANSONIC FLUTTER
Results of winglet development studies for DC-10 derivatives
[NASA-CR-3677] 02 p0138 N85-10936
Interactive aircraft flight control and aeroelastic stabilization
[NASA-CR-174025] 02 p0148 N85-11003
Status and prospects of computational fluid dynamics for unsteady transonic viscous flows
[NASA-TM-86018] 03 p0315 N85-12037
Flutter parametric studies of cantilevered twin-engine-transport type wing with and without winglet. Volume 1: Low-speed investigations
[NASA-CR-172410-VOL-1] 04 p0513 N85-13269
Flutter parametric studies of cantilevered twin-engine transport type wing with and without winglet. Volume 2: Transonic and density effect investigations
[NASA-CR-172410-VOL-2] 04 p0513 N85-13270
Flutter control with unsteady aerodynamic models
[AD-A147858] 07 p0909 N85-15753
Finite element analysis of nonlinear oscillations and flutter of shells of revolution
[AD-A149071] 10 p1496 N85-19440
Remote pivot decoupler pylon: Wing/store suppression
[NASA-CASE-LAR-13173-1] *1 p1584 N85-19981
Flutter taming: A new tool for the aeroelastic designer
[AD-A150834] 14 p2226 N85-23802
Transonic Unsteady Aerodynamics and its Aeroelastic Applications
[AGARD-CP-374] 15 p2457 N85-25171
Status and prospects of computational fluid dynamics for unsteady transonic flow 15 p2459 N85-25180
Application of time-linearized methods to oscillating wings in transonic flow and flutter 15 p2459 N85-25182
The application of transonic unsteady methods for calculation of flutter airloads 15 p2460 N85-25186
The design and operation of a simple low-speed flutter-suppression model
[AD-A151610] 15 p2474 N85-25269
Active control of forward swept wings with divergence and flutter aeroelastic instabilities
[AD-A151837] 15 p2474 N85-25270
Aerodynamic detuning analysis of an unstalled supersonic turbofan cascade
[NASA-TM-87001] 16 p2700 N85-26670
ESP (External-Stores Program): A pilot computer program for determining flutter-critical external-store configurations. Volume 3, part 2. Program compilation
[AD-A152271] 16 p2706 N85-26703
ESP (External-Stores Program): A pilot computer program for determining flutter-critical external-store configurations. Volume 1: User's manual
[AD-A152268] 16 p2710 N85-26725
ESP (External-Stores Program): A pilot computer program for determining flutter-critical external-store configurations. Volume 2: Final report on program enhancement and delivery
[AD-A152269] 16 p2711 N85-26726
ESP (External-Stores Program): A pilot computer program for determining flutter-critical external-store configurations. Volume 3, part 1: Program compilation
[AD-A152270] 16 p2711 N85-26727
Flight trials of a modified gulfstream commander carrying external stores
[AD-A153376] 17 p2896 N85-27859
The application of bispectral analyses to aeroelastic phenomena 24 p4060 N85-35157
Unsteady flow in a supersonic cascade with two in-passage shocks
[NASA-CR-3925] 24 p4060 N85-35158

FLUTTER ANALYSIS
NT AEROELASTIC RESEARCH WINGS
Flutter parametric studies of cantilevered twin-engine-transport type wing with and without winglet. Volume 1: Low-speed investigations
[NASA-CR-172410-VOL-1] 04 p0513 N85-13269
Viscous effects on transonic airfoil stability and response
[NASA-TM-86374] 10 p1421 N85-18961
Exploratory flutter test in a cryogenic wind tunnel
[NASA-TM-86380] 12 p1863 N85-21689
Dynamic wind-tunnel testing of active controls by the NASA Langley Research Center 13 p1966 N85-22353
Two degree-of-freedom flutter solution for a personal computer
[NASA-TM-86381] 13 p1971 N85-22379
Experience with transonic unsteady aerodynamic calculations 15 p2458 N85-25176
A semi-empirical unsteady transonic method with supersonic free stream 15 p2458 N85-25179
A study of transonic flutter of a two-dimensional airfoil using the U-g and p-k methods
[AD-A151463] 15 p2473 N85-25268
Verification of calculation methods for unsteady airloads in the precipitation of transonic flutter
[NLR-MP-84016-U] 20 p3390 N85-31027
Flutter clearance of the Schweizer 1-36 deep-stall sailplane
[NASA-TM-85917] 22 p3729 N85-33118
Design, development and operation of a high simultaneous capacity digital telemetry system — turbomachine blade flutter
[PNR-90261] 23 p3899 N85-34151

FLUX
Stellar ultraviolet flux distributions in the 912-1200 A wavelength range 11 p1782 N85-21061
Limits on deeply penetrating particles in the 10(17) eV cosmic ray flux
[HE-5.3-1] 24 p4205 N85-36098
Atmospheric neutrinos observed in underground detectors
[HE-5.3-8] 24 p4205 N85-36102

FLUX (RATE PER UNIT AREA)
U FLUX DENSITY

FLUX (RATE)
NT HEAT FLUX
NT MAGNETIC FLUX
NT SOLAR FLUX
Method and apparatus for determining the content and distribution of a thermal neutron absorbing material in an object
[DE84-014319] 01 p0117 N85-10801
Mid-Infrared spectroscopy of planetary nebulae 08 p1247 N85-17872
The high latitude D region during electron precipitation events 11 p1664 N85-20484
Absolute measurements of radiation intensity from Cassiopeia-A, Cygnus-A and crab nebula in 60-100 cm band 13 p2078 N85-22978
Study of integral and spectral direct solar radiation over Atlantic 14 p2341 N85-24475
The behavior of the atmosphere in the desert planetary boundary layer
[AD-A151286] 15 p2592 N85-25977
Proposed solar neutrino experiment using (81)Br(nu,e(-e)) (81)Kr
[DE85-004802] 15 p2684 N85-26579
Periodicity of variations in galactic cosmic ray fluxes and solar activity parameters near 20th cycle minimum 16 p2720 N85-26791
Variations in intensity of secondary cosmic radiation observed on 10-11 August 1981 16 p2721 N85-26796
Measurements of fluxes of high-energy protons and electrons by 2 oppositely oriented spectrometers aboard Cosmos-988 artificial Earth satellite 16 p2722 N85-26800
On the choice of coordinates for semiconductor simulation
[AD-A152214] 16 p2870 N85-27708
Parameterization of surface fluxes in the VVR Fourth Order GCM 18 p3142 N85-29454
On the global distribution of three-dimensional Eliassen-Palm fluxes by stationary waves 18 p3145 N85-29469
Dynamic models of flux tubes in the interpretation of polarization measurements 18 p3206 N85-29891
The influence of a turbulent region on the flux of auroral electrons
[KGI-PREPRINT-072] 20 p3494 N85-31723
Use of the VAD technique and measurements of momentum flux in the stratosphere at Aercibo, part 4.3A 21 p3622 N85-32505
Momentum flux measurements: Techniques and needs, part 4.5A 21 p3623 N85-32508
Characteristics and sources of E-region ionization in the continuous aurora
[AD-A155018] 21 p3632 N85-32562
Horizontal and vertical structure of velocity, potential vorticity and energy in the gulf stream
[AD-A154753] 21 p3655 N85-32702
Sulfur Cycle 21 p3662 N85-32748
Solar cycle variation of ephemeral regions
[AD-A154967] 21 p3723 N85-33097
Scientific Opportunities with Advanced Facilities for Neutron Scattering
[DE85-012113] 22 p3839 N85-33770
Neutron flux, spectrum and dose equivalent measurements for a 4500-W(th) 238 PuO2 general purpose heat source
[DE85-011361] 22 p3841 N85-33786
Observations of the Crab Nebula at energies 4.10(11)
[OG-2.3-1] 22 p3865 N85-33938
Search for gamma-rays above 400 GeV from Geminga
[OG-2.4-4] 22 p3867 N85-33951
Balloon observations of hard X-rays from some galactic X-ray sources
[OG-2.5-11] 22 p3870 N85-33966
All sky Northern Hemisphere 10(15) EV gamma-ray survey
[OG-2.6-3] 22 p3870 N85-33968
Search for the gamma-ray fluxes with energies above 10915) eV from various objects
[OG-2.6-14] 22 p3871 N85-33975
Cosmic rays in the 10(16) to 10(19) eV range from pulsars
[OG-5.4-3] 22 p3886 N85-34080
The primary cosmic ray mass composition at energies above 10(14) eV
[OG-5.4-6] 22 p3886 N85-34083
UHE particle production in close binary systems
[OG-5.4-7] 22 p3886 N85-34084
Modeling cosmic ray anisotropies near 10(18) eV
[OG-5.4-9] 22 p3886 N85-34086
A search for solar neutrons on a long duration balloon flight
[SH-1.4-6] 23 p3905 N85-34706
Observation of the fluxes of nuclei with energies 10-20 MEV per nucleon during the solar flare of April 26, 1984
[SH-2.1-1] 23 p3998 N85-34783
The 3HE in solar non-relativistic electron events
[SH-2.2-5] 23 p4000 N85-34800
The dependence of solar modulation on the sign of the cosmic ray particle charge
[SH-4.2-23] 23 p4009 N85-34860
Scaling from Jupiter to pulsars and the acceleration of cosmic ray particles by pulsars, 3
[OG-6.2-3] 23 p4019 N85-34904

The design of an experiment to detect low energy antiprotons
[OG-9.1-1] 23 p4022 N85-34928
Cosmic ray modulation by high-speed solar wind fluxes
[SH-5.1-22] 23 p4044 N85-35074
Additional flux of particles and albedo-electrons in upper atmosphere
[SH-6.1-6] 23 p4045 N85-35080
Empirical model for the Earth's cosmic ray shadow at 400 KM: Prohibited cosmic ray access
[SH-6.1-14] 23 p4046 N85-35087
Limiter
[DE85-011620] 24 p4150 N85-35736
Hadron intensity and energy spectrum at 4360 m above level
[HE-3.1-7] 24 p4178 N85-35905
Scaling violation in fragmentation region at energies above 10-15 eV based on the data on cosmic ray hadron component
[HE-3.1-11] 24 p4178 N85-35909
Monte Carlo simulations of electron lateral distributions in the core region of 10(13) - 10(16) eV air showers 24 p4190 N85-35992
The Nagoya cosmic-ray muon spectrometer 3, part 1: Preliminary observations
[HE-5.2-2] 24 p4202 N85-36080
Angular distribution of muons produced by cosmic ray neutrinos in rock
[HE-5.3-24] 24 p4207 N85-36115
Muon and neutrino fluxes
[HE-6.2-18] 24 p4213 N85-36154

FLUX DENSITY
NT CURRENT DENSITY
NT ELECTRON FLUX DENSITY
NT ILLUMINANCE
NT IRRADIANCE
NT LUMINANCE
NT LUMINOUS INTENSITY
NT NEUTRON FLUX DENSITY
NT PARTICLE FLUX DENSITY
NT PHOTON DENSITY
NT PROTON FLUX DENSITY
NT RADIANCE
NT RADIANT FLUX DENSITY
NT SOLAR CONSTANT
NT SOLAR FLUX DENSITY
NT SOUND INTENSITY

An error analysis for the use of presently available lunar radio flux data in broadbeam antenna-system measurements
[PB84-218361] 01 p0016 N85-10097
Bremsstrahlung radiation from longitudinal plasma waves caused by subthermal electrons in plasma 02 p0264 N85-11730
X-ray observations of the Seyfert 1 galaxies AKN120 and MCG8-11-11
[NASA-TM-86663] 03 p0446 N85-12839
Positron flux concentrator: An update
[DE84-016260] 04 p0561 N85-13576
Potential of flywheels for spacecraft energy storage 05 p0809 N85-13890
Diurnal variation harmonics and spatial change in cosmic ray flux 06 p0824 N85-15230
Grain boundary structure in NiO
[DE84-016242] 06 p0868 N85-15519
The nature of the soft X-ray emitting region in the direction of the North Polar spur 06 p0877 N85-15568
Inverse relations between 0.25 keV counts and local interstellar dust 06 p0877 N85-15572
The Orion molecular cloud at far-infrared wavelengths 06 p1245 N85-17860
Techniques for measuring intercepted and absorbed PAR in corn canopies
[E85-10081] 10 p1505 N85-19495
Study of low energy density photovoltaic applications under varying rate structures
[DE85-000185] 10 p1511 N85-19538
Quasi-thermodynamic prediction of hydrogen reemission behavior from titanium films
[DE85-003667] 10 p1564 N85-19864
Assessment of satellite power flux-density limits in the 2025-2300 MHz frequency range, part 2
[PB85-101244] 11 p1625 N85-20238
Absorption of ozone molecules in strong field of tea CO2 injection laser 11 p1718 N85-20808
Coordinated multifrequency observations of the BL LAC objects MRK 180, MRK 421, and MRK 501 11 p1746 N85-20983
The physical implications of an isothermal model for the hot intracluster medium
[NASA-TM-86174] 11 p1763 N85-21089
Mass analysis of neutral particles and ions released during electrical breakdowns on spacecraft surfaces
[NASA-CR-175585] 12 p1793 N85-21250
Magnetic field in main gap of separator 12 p1843 N85-21563
Dual electrochemical system
[AD-D011616] 16 p2817 N85-27376
Investigation of pseudo bi-polar nickel cadmium batteries as filler elements for pulsed power loads
[AD-A152112] 16 p2819 N85-27389
High efficiency ionizer using a hollow cathode discharge plasma
[DE85-006690] 16 p2868 N85-27693
Nickel-cadmium cell design variable program data analysis
[NASA-TM-86196] 19 p3258 N85-30203
Frequent observations of extragalactic compact sources at 24 GHz 19 p3386 N85-31003
Results of analysis on the design variable cells 20 p3445 N85-31388
Improved specific energy Ni-H2 cell 20 p3447 N85-31399
Density gradient electrophoresis of cultured human embryonic kidney cells 20 p3501 N85-31763
Spectral methods for the estimation of acoustic intensity, energy density, and surface velocity using a multimicrophone probe 20 p3524 N85-31916
Hit-size effectiveness theory applied to high doses of low LET radiation for pink mutations in Tradescantia
[DE85-011835] 22 p3819 N85-33657
Very high energy gamma rays from the Crab Nebula
[OG-2.3-3] 22 p3866 N85-33940
Periodic gamma-ray emissions from Geminga at or = 10(12) eV
[OG-2.4-2] 22 p3867 N85-33949
On the 1983 observations of the gamma-ray source 2CG195+4
[OG-2.4-5] 22 p3868 N85-33952
SMM detection of interstellar Al-26 gamma radiation
[OG-3.2-1] 22 p3874 N85-34001
The muon content of EAS as a function of primary energy
[OG-5.1-8] 22 p3881 N85-34050
EAS spectrum in the primary energy region above 10 to the 15th power eV by the Akeno and Yakutsk array data
[OG-5.1-16] 22 p3882 N85-34057
Composition of primary cosmic rays at energies 10(15) to approximately 10(16) eV
[OG-5.2-4] 22 p3883 N85-34061
Implication of EAS data for the study of primary cosmic rays above 10 to the 5th power GeV
[OG-5.2-7] 22 p3883 N85-34064
EAS Cerenkov measurements of the composition of the cosmic ray flux around 10 to the 16th power eV
[OG-5.2-11] 22 p3884 N85-34067
Analytic and numerical calculations of the ambipolar electric field in a stellarator 23 p3978 N85-34665
Spectral analysis of the Forbush decrease of 13 July 1982
[SH-5.1-7] 23 p4042 N85-35061
Transient cosmic ray increase associated with a geomagnetic storm
[SH-5.1-8] 23 p4042 N85-35062
Short perturbations of cosmic ray intensity and electric field in atmosphere
[SH-6.1-18] 23 p4046 N85-35090
Diurnal variations of cosmic ray geomagnetic cut-off threshold rigidities
[SH-6.1-21] 23 p4046 N85-35092
The influence of the Earth's magnetosphere on the high-energy solar protons
[SH-6.1-22] 23 p4046 N85-35093
Observation of nuclei with energies 8-30 MeV per nucleon in the Earth's magnetosphere at the altitudes 350 KM
[SH-10.1-5] 23 p4053 N85-35136
Proton-air and proton-proton cross sections from air shower data
[HE-1.1-1] 24 p4170 N85-35849
Multiplicity distributions in interaction models used for cascade simulations
[HE-1.2-5] 24 p4172 N85-35863
Connection between variations of the atmosphere temperature profile and variations of the meson component intensity
[HE-3.1-12] 24 p4178 N85-35910
The model of independent particles emission in the multiparticle production theory
[HE-3.2-10] 24 p4179 N85-35918
A critical analysis of air shower structure functions and size spectrum measurements with the NBU air shower array 24 p4188 N85-35983
Measurement of the local density spectrum 24 p4189 N85-35984
Transition effect of air shower particles in plastic scintillators
[HE-4.4-9] 24 p4193 N85-36017
On the determination of the depth of EAS development maximum using the lateral distribution of Cerenkov light at distances 150 m from EAS axis
[HE-4.4-13] 24 p4194 N85-36019
An upper limit of muon flux of energies above 100 TeV determined from horizontal air showers observed at Akeno
[HE-5.2-12] 24 p4203 N85-36088
Energy spectrum of cascade showers induced by cosmic ray muons in the range from 50 GeV to 5 TeV
[HE-5.2-14] 24 p4203 N85-36090
Measurement of muon intensity by Cerenkov method
[HE-5.2-15] 24 p4204 N85-36091
Analytical calculation of muon intensities under deep sea-water
[HE-5.2-16] 24 p4204 N85-36092
The spectrum of neutrons at 60 hg m(-2)
[HE-5.2-20] 24 p4204 N85-36096
Geophysical searches for three-neutrino oscillations
[HE-5.3-9] 24 p4205 N85-36103
Angular distribution of muons produced by cosmic ray neutrinos in rock
[HE-5.3-24] 24 p4207 N85-36115
Atmospheric muons and neutrinos, and the neutrino-induced muon flux underground
[HE-5.4-7] 24 p4207 N85-36118
Results of investigation of muon fluxes of superhigh energy cosmic rays with X-ray emulsion chambers
[HE-5.4-16] 24 p4208 N85-36126

FLUX MAPPING
U FLUX DENSITY
U MAPPING

FLUX PINNING
Flux-line pinning by the grain boundary in niobium bicrystals
[DE84-016668] 04 p0570 N85-13638
Ballooning instabilities on a magnetic separatrix
[DE85-010855] 19 p3372 N85-30915
Flux pinning and flux flow studies in superconductors using flux flow noise techniques
[DE85-010814] 19 p3376 N85-30945

FLUXES
Suppressing porosity in weld joints of 1420 aluminum alloy 01 p0020 N85-10123
Densification of submicron YSZ (Yttria-Stabilized Zirconia) powders with alumina and borate additives
[AD-A149520] 10 p1452 N85-19150
The effect of filler wire and flux compositions on the microstructure and properties of microalloyed steel weld metal
[AD-A149529] 10 p1492 N85-19423
Automatic multi-layer welding of thick cylindrical structures under flux 13 p2035 N85-22746
Microcomputer-controlled system for measuring atmospheric particle fluxes
[DE85-007910] 17 p2988 N85-28469

FLUXMETERS
U MAGNETIC MEASUREMENT
U MEASURING INSTRUMENTS

FLY ASH
Compressive strength-maturity relationships of mortar containing fly ash
[AD-A148705] 09 p1339 N85-18423
Adherence of ash particles from the combustion of micronized coal
[DE85-008600] 19 p3229 N85-30023
Third US/USSR Symposium on Particulate Control
[PB85-190890] 19 p3310 N85-30522
Evaluation of pilot ESP used with a spray dryer FGD system at Pittsburgh Energy Technology Center, Bruceton, Pennsylvania
[DE85-011151] 22 p3746 N85-33217

FLY BY WIRE CONTROL
Role of research aircraft in technology development
[NASA-TM-85913] 02 p0137 N85-10932
Integrated digital/electric aircraft concepts study
[NASA-CR-3841] 08 p1083 N85-16861
Some aspects of the design of a fly-by-wire flying control system for a supersonic V/STOL fighter aircraft
[COLL-AERON-8413] 12 p1780 N85-21175
Guidance and conirol research flight testing with HFB 320 test aircraft 13 p1967 N85-22355
Multivariable control law design for the X-29 aircraft
[AD-A151828] 15 p2472 N85-25259
A method of estimating aircraft attitude from fly by wire flight control system data 16 p2697 N85-26853
An update on experience on the fly by wire Jaguar equipped with a full-time digital flight control system 16 p2712 N85-26740
Application of AFTI/F-16 task-tailored control modes in advanced multirole fighters 17 p2901 N85-27886
X-29 digital flight control system design 17 p2901 N85-27889
An update of experience on the fly by wire Jaguar equipped with a full-time digital flight control system 17 p2902 N85-27893

Operational and developmental experience with the F/A-18A digital flight control system
17 p2902 N85-27895
How to handle failures in advanced flight control systems of future transport aircraft 17 p2904 N85-27905
The flight control system for the Experimental Aircraft Programme (EAP) demonstration aircraft
17 p2904 N85-27908
Crew systems and flight station concepts for a 1995 transport aircraft
[NASA-CR-166068] 19 p3221 N85-29973

FLYBY MISSIONS
NT ASTEROID MISSIONS
NT GIOTTO MISSION
Sample return from a comet flyby
06 p0889 N85-15646
The violet absorber on Io: Disulfur monoxide derivatives 13 p2173 N85-23482
Dark halo craters and the thickness of grooved terrain on Ganymede 13 p2173 N85-23484
Formation of bright terrain bands on Ganymede by unstable lithosphere extension 13 p2173 N85-23485
Dynamical studies of Saturn's rings
13 p2174 N85-23489
The astrometry network of the IHW and the P/Crommelin trial run results 14 p2435 N85-25016
Comments on Vega mission 15 p2482 N85-25319
Press conference on flight of Vega spacecraft
15 p2482 N85-25320
Interpretation of Venus gravitational anomalies
15 p2483 N85-25322
TASS update on flights of Vega-1 and Vega-2
16 p2722 N85-26803
Kovtunenko discusses Vega Project
16 p2722 N85-26804

FLYING BEDSTEAD AIRCRAFT
U FLYING PLATFORMS

FLYING PERSONNEL
NT AIRCRAFT PILOTS
NT ASTRONAUTS
NT COSMONAUTS
NT FLIGHT CREWS
NT PILOTS (PERSONNEL)
NT SPACECREWS
Review of US manual of clinical aviation medicine
12 p1904 N85-21957
Review of US guide on medication and flying
12 p1904 N85-21958

FLYING PLATFORM STABILITY
U AERODYNAMIC STABILITY
U FLYING PLATFORMS

FLYING PLATFORMS
Intelligent interfaces for tactical airborne platforms
06 p0752 N85-14820

FLYING QUALITIES
U FLIGHT CHARACTERISTICS

FLYWHEELS
The limp flywheel
[AD-A146034] 03 p0386 N85-12467
An Assessment of Integrated Flywheel System Technology
[NASA-CP-2346] 05 p0604 N85-13850
Rotating assembly working group summary
05 p0604 N85-13851
Electromechanical/electromagnetics working group summary 05 p0604 N85-13852
Electrical/electronics working group summary
05 p0604 N85-13853
Dynamics and controls working group summary
05 p0604 N85-13854
A summary of the 1983 Integrated Flywheel Technology Workshop 05 p0605 N85-13855
European development experience on energy storage wheels for space 05 p0605 N85-13856
Merits of flywheels for spacecraft energy storage
05 p0605 N85-13857
Comparative energy storage assessment item
05 p0605 N85-13858
Inertial storage for satellites 05 p0605 N85-13859
Flywheel-powered X-ray generator
05 p0605 N85-13861
Generic composite flywheel designs
05 p0606 N85-13864
Summary results of the DOE flywheel development effort 05 p0606 N85-13865
Flexible matrix composite laminated disk/ring flywheel
05 p0606 N85-13866
General Electric composite ring-disk flywheel: Recent and potential developments 05 p0606 N85-13867
The multipurpose composite flywheel
05 p0606 N85-13868
Flywheel containment and safety considerations
05 p0606 N85-13869
Magnetically suspended flywheel system study
05 p0607 N85-13873
Reaction wheels for kinetic energy storage
05 p0607 N85-13874
High-efficiency power conversion options for flywheel energy storage systems 05 p0607 N85-13876
Motor/generator and electronic control considerations for energy storage flywheels 05 p0608 N85-13878
Torque command steering law for double-gimbaled control moment gyros applied to rotor energy storage
05 p0608 N85-13879
Potential of flywheels for spacecraft energy storage
05 p0609 N85-13890
Ultrasonic characterization of advanced composite flywheels
[DE85-000158] 11 p1593 N85-20026
Operating characteristics of a 0.87 kW-hr flywheel energy storage module
[NASA-TM-87036] 17 p2974 N85-28371
Strategic defense initiative
[DE85-012778] 24 p4150 N85-35735

FOAMS
Design, manufacture, and testing of compliant coatings for reduction of turbulent drag
[AD-A145510] 02 p0198 N85-11323
Insulation bonding test system
[NASA-CASE-MFS-25662-1] 11 p1610 N85-20126
X-ray gauge measures areal density variations as small as 0.1%
[DE85-003774] 12 p1854 N85-21629
Hydrolysis of plastic wastes with the aim of recovering and reprocessing the starting components (recycling)
[BMFT-FB-T-84-250] 12 p1865 N85-21828
Determination of toxicity of combustion products of habitability foams concurrently with flammability studies of these materials
[AD-A149647] 12 p1905 N85-21961
Exploratory development of foams from liquid crystal polymers
[NASA-CR-172510] 13 p2036 N85-22754
Development of nitrile rubbers and foams having a high static modulus and low creep
[BR91465] 14 p2259 N85-24001
Atmospheric frontal zone studies
[NASA-CR-175293] 16 p2833 N85-27480
Low density inorganic foams fabricated using microwaves
[DE85-007708] 18 p3060 N85-29051
Dynamics of thin-film breakup in a constricted pore
[DE85-008442] 18 p3101 N85-29199
Foamglass solar window collector
[DE85-009197] 18 p3129 N85-29374
Results of variable enthalpy tests of CPR-488 TIP panels in MSFC Hot Gas Facility
[NASA-CR-170889] 24 p4072 N85-35237
Results of tests of Insta-Foam Thermal Protection System (TPS) material for protection of equipment inside the SRB aft skirt
[NASA-CR-170892] 24 p4081 N85-35295

FOCI
NT PLASMA FOCUS
New focal plane detector system for the broad range spectrometer
[DE85-005370] 16 p2768 N85-27201

FOCUSING
NT DEFOCUSING
NT SELF FOCUSING
Ultrasonic synthetic aperture focusing using unfocused pulse-echo transducers
[AERE-R-11230] 01 p0057 N85-10374
Dark focus: Intersubject variation, intrasubject stability, and relationship to near retinoscopy
[AD-A145489] 02 p0235 N85-11530
Focusing beam of 1-GeV protons with volumetric capture to the mode of channeling by bent single crystal
02 p0268 N85-11750
Focusing effects of a laser beam in the nonresonant multiphoton ionization (MPI) of gases
[LP-207] 04 p0506 N85-13231
Focussing and confinement
[DE84-016161] 05 p0640 N85-14106
Calculated parameters for the initial part of an accelerator with high-frequency quadrupole focusing
[RAE-TRANS-2122] 07 p1040 N85-16600
Emerging technology of synthetic aperture focusing for ultrasonic testing
[DE85-000373] 09 p1378 N85-18664
Subreflector focusing techniques applied to new DSS-15 and DSS-45 34-meter antennas
10 p1484 N85-19233
Axial focusing of signal from distant point radiator reflected twice in deep paraboloid
13 p2078 N85-22979
Effects of focusing on HRS focal-plane polarimeter measurements
[DE85-004627] 13 p2160 N85-23406
Design of a variable-focal-length optical system
[NASA-CR-175710] 15 p2951 N85-26349
Streak tube characterization
[DE85-009874] 17 p2958 N85-28255
DOE/Sandia point-focus concentrator program, draft
[DE85-008200] 17 p3038 N85-28793
Mass spectrometry technology at the Jet Propulsion Laboratory (JPL) 18 p3157 N85-29552
Applications and investigations of second harmonic generation 19 p3367 N85-30878
Advanced ultrasonic imaging of piping in Dresden and Vermont Yankee reactors
[TI85-010049] 20 p3464 N85-31520
Particle sizing from forward scattered light at two angles using a Variable-Focal-Length optical system
[AD-A154164] 20 p3533 N85-31960
Background equatorial astronomical measurements focal plane assembly (refurbished HI STAR SOUTH)
[AD-A155215] 21 p3590 N85-32313
Existence of smooth solutions in problems of electromagnetic radiation focusing
21 p3697 N85-32972
Theoretical and computational research on the focused transport of intense charged particle beams
[DE85-012960] 23 p3972 N85-34821
Parametric stability of analytical close-range photogrammetry 24 p4107 N85-35461

FOG
An operational numerical model for prediction of fog and stratus 01 p0080 N85-10537
A 1-dimensional model with a sub-grid scale condensation scheme for stratiform clouds and fog
01 p0080 N85-10538
An operational forecasting system for stratus and fog with sodar 01 p0081 N85-10539
Preparation steps for the use of one-dimensional interpretation models for nowcasting purposes in the German weather net 01 p0081 N85-10540
Studies of the ocean surface and the coupling between the sea and the atmosphere
[AD-A146546] 06 p0841 N85-15339
An evaluation of an advection fog prediction model
[AD-A147436] 07 p1008 N85-16403
Fog advection in the Namib 16 p2831 N85-27454
Fog activation and supersaturation
21 p3650 N85-32678
The interaction of polynuclear aromatic hydrocarbons PAH's with water vapor and their role as condensation nuclei in the formation of haze and fog
21 p3652 N85-32695
Ice fog as an electro-optical obscurant
[AD-A155059] 21 p3705 N85-33015

FOIL BEARINGS
Effects of silver and group 2 fluorides addition to plasma sprayed chromium carbide high temperature solid lubricant for foil gas bearing to 650 deg C
[NASA-TM-86695] 06 p0770 N85-14928

FOILS (MATERIALS)
NT METAL FOILS
Progress on solar absorber selective paint research
[DE84-015536] 04 p0480 N85-13059
Strong-coupling superconductivity of Mg in proximity to Ta
[DE84-015482] 04 p0569 N85-13827
Pulsed electric discharge laser technology. Electron beam window foil material
[AD-A146420] 06 p0813 N85-15162
Electron beam propagation along charged foils
[DE85-002137] 06 p0861 N85-15472
High efficiency electron beam gun foil support
[AD-D011434] 08 p1159 N85-17312
Beam-foil spectroscopy of highly ionized aluminum atoms 09 p1390 N85-18746
AEM with a convergent beam
[DE85-000867] 11 p1714 N85-20784
Time-integrated yield for the Joint European Torus (JET), April - September 1984
[AERE-M-3449] 17 p3038 N85-28797
Flux pinning and flux flow studies in superconductors using flux flow noise techniques
[DE85-010814] 19 p3376 N85-30945
Plasma mass and effective inductance in a small railgun
[AD-A154644] 21 p3589 N85-32304
Plating density standards
[DE85-010014] 21 p3591 N85-32318
Rhodium-103 and Indium-115 inelastic scattering reactions for fission neutron dosimetry
21 p3703 N85-33004
Buildup of electric charge in foil dielectrics during gamma irradiation 22 p3770 N85-33383
Fast shutter apparatus
[DE85-006501] 23 p3928 N85-34343
System expectations for Pioneer 1 foil implosion experiments
[DE85-014129] 24 p4091 N85-35359

Diagnostics for Pioneer 1 imploding plasma experiments
[DE85-014120] 24 p4159 N85-35787
FOKKER AIRCRAFT
NT F-27 AIRCRAFT
FOKKER BOND TESTERS
U ADHESION TESTS
FOKKER F 27 AIRCRAFT
U F-27 AIRCRAFT
FOKKER FRIENDSHIP AIRCRAFT
U F-27 AIRCRAFT
FOKKER-PLANCK EQUATION
Stochastic methods for the description of multiparticle production
[DE84-009861] 10 p1556 N85-19810
Beam loss due to the aperture limitation resulting from intrabeam scattering
[DE85-006138] 12 p1930 N85-22124
On filter binary processes
[AD-A150328] 13 p2063 N85-22800
Steady state solution of the Fokker-Planck equation combined with unidirectional quasilinear diffusion under detailed balance conditions
[DE85-004917] 14 p2425 N85-24959
Kinetic theory and simulation of multi-species plasmas in Tokamaks excited with ICRF microwaves
[DE85-006119] 16 p2668 N85-27691
Random vibration of nonlinear, parametrically excited systems 19 p3282 N85-30351
Fokker-Planck calculation of hot electron formation in the thermal barrier region of tandem mirror Gamma-10
[IPPJ-726] 23 p3979 N85-34669
Pitch angle distributions of solar energetic particles and the local scattering properties of the interplanetary magnetic field
[SH-3.1-13] 23 p4002 N85-34816
Numerical descriptions of cosmic-ray transport
[SH-4.1-3] 23 p4004 N85-34829
FOLDING STRUCTURES
Large-diameter astromast development
[NASA-CR-171201] 03 p0342 N85-12200
High performance deployable antenna structures 05 p0625 N85-14001
Development of a foldline concept for automatic refolding of a flexible blanket (folding analysis) — spaceborne solar generators
[ESA-CR(P)-1933] 06 p1179 N85-17428
Deployable folded antenna apparatus
[AD-D011503] 12 p1832 N85-21495
Variable geometry truss concept
[REPT-614] 12 p1865 N85-21697
SPOT solar array 13 p2009 N85-22595
Retractable Rigid Solar Generator (GSR) 13 p2009 N85-22597
Blanket integrated cushioning of foldable and retractable solar arrays 13 p2011 N85-22612
Synchronously deployable tetrahedral truss reflector 14 p2231 N85-23827
Retractable Rigid Solar Generator (GSR)
[SNIAS-851-440-101] 20 p3484 N85-31654
The SPOT solar array
[SNIAS-851-440-103] 20 p3485 N85-31656
FOLDS (GEOLOGY)
Structural observations in the Circle quadrangle, Yukon-Tanana Upland, Alaska 04 p0517 N85-13298
Structural investigation of the Grenville Province by radar and other imaging and nonimaging sensors 08 p1147 N85-17237
Structural morphology and associated strain within parts of the US section of the Kootenay Arc, NE, Washington 09 p1352 N85-18505
Normal-fault and fold development in sedimentary rocks above a pre-existing basement normal fault 13 p2131 N85-23259
Mechanisms of basalt-plains ridge formation 13 p2199 N85-23643
Terrestrial analogs for planetary wrinkle ridges 13 p2199 N85-23644
Using remote photographs in prospecting for hydrocarbons on the Kerch Peninsula 22 p3735 N85-33154
FOLIAGE
Scattering from foliage covered terrain
[AD-A154724] 21 p3574 N85-32228
Throughfall rate and chemistry studies: Whiteface Mountain
[DE85-012407] 23 p3947 N85-34464
FOOD
Assessment of radiation dosages obtained by intake of radioactive fallout contaminated food
[VTT-292] 07 p1017 N85-16460
Characterization of heat transfer in nutrient materials — space flight feeding
[NASA-CR-171841] 08 p1199 N85-17551
Controlled Ecological Life Support Systems (CELSS) 15 p2668 N85-26604
FOOD CHAIN
Hollings hungry mantid model for the invertebrate functional response considered as a Markov process. Part 3: Mathematical elaborations
[CWI-AM-R8407-PT-3] 05 p0722 N85-14639
Models and parameters for environmental radiological assessments
[DE81-027154] 11 p1678 N85-20573
From microbial communities to cells 21 p3659 N85-32728
The 1984 environmental monitoring report, Sandia National Laboratories, Albuquerque, New Mexico
[DE85-011175] 22 p3811 N85-33607
The 1984 environmental monitoring program report for Idaho National Engineering Laboratory site
[DE85-011209] 22 p3812 N85-33611
Chemical composition of Musca domestica L. larval and pupal biomass when developing in organic waste of biological life-support system for man 22 p3824 N85-33691
FOOD PROCESSING
NT CANNING
NT PRESERVING
USSR report: Life sciences. Biomedical and behavioral sciences
[JPRS-UBB-84-015] 07 p1010 N85-16416
Feasibility of producing a range of food products from a limited range of undifferentiated major food components
[NASA-CR-177329] 07 p1020 N85-16473
Food Service and Nutrition for the Space Station
[NASA-CP-2370] 14 p2393 N85-24733
The context for food service and nutrition in the space station 14 p2393 N85-24734
Food service management 14 p2393 N85-24736
Preparation methods: Past and potential methods of food preparation for space 14 p2393 N85-24738
Use of irradiated foods 14 p2393 N85-24740
Equipment for hot-to-serve foods 14 p2393 N85-24741
Packaging's contribution for the effectiveness of the space station's food service operation 14 p2394 N85-24746
Packaging for food service 14 p2394 N85-24747
FORBIDDEN BANDS
Forbidden lines of oxygen in comet spectra 02 p0163 N85-11105
Formation of lattice defects by nitrogen laser exposure in A2B6 semiconductors with wide forbidden band 02 p0258 N85-11692
Nonlinear absorption of laser radiation in InP and in GaAs 02 p0266 N85-11740
Magnetoabsorption of weak light wave in presence of intense light wave in semiconductor with narrow forbidden band 02 p0267 N85-11743
Cascaded solar photovoltaic cells based on InP-GaInPAs and InP-CdS heterostructures 02 p0268 N85-11749
FORBIDDEN TRANSITIONS
Collision-induced dipole moments
[AD-A147682] 08 p1121 N85-17063
Theoretical studies of atomic transition
[DE85-001325] 09 p1381 N85-18687
Excitation of some alkaline Earth-like ions
[DE85-010737] 20 p3529 N85-31951
Ionization detection of stimulated Raman spectra
[DE85-010672] 22 p3746 N85-33218
FORBUSH DECREASES
Some features of the interplanetary medium during Forbush decreases
[NOTA-INTERNA-836] 18 p3202 N85-29866
The longitudinal asymmetry of the interplanetary perturbation producing Forbush decreases
[IFSI-84-18] 20 p3546 N85-32065
Interplanetary disturbances during Forbush decreases
[IFSI-84-10] 20 p3547 N85-32075
Some properties of flare-not-associated Forbush decreases
[IFSI-84-13] 20 p3548 N85-32077
the role of shock waves in modulation of galactic cosmic rays
[SH-4.1-7] 23 p4005 N85-34831
The intensity recovery of Forbush-type decreases as a function of heliocentric distance and its relationship to the 11-year variation
[SH-4.1-9] 23 p4005 N85-34832
Cumulative effect of Forbush decreases in the heliospheric modulation during the present solar cycle
[SH-4.1-10] 23 p4005 N85-34833
Drift and Forbush decreases
[SH-5.1-2] 23 p4041 N85-35056
Anomalous short-term increases in the galactic cosmic ray intensity: Are they related to the interplanetary magnetic cloud-like structures?
[SH-5.1-3] 23 p4041 N85-35057
The flare origin of Forbush decreases not associated with solar flares on the visible hemisphere of the Sun
[SH-5.1-4] 23 p4041 N85-35058
Longitudinal dependence of the interplanetary perturbation produced by energetic type 4 solar flares and of the associated cosmic ray modulation
[SH-5.1-5] 23 p4042 N85-35059
Rigidity spectrum of Forbush decrease
[SH-5.1-6] 23 p4042 N85-35060
Spectral analysis of the Forbush decrease of 13 July 1982
[SH-5.1-7] 23 p4042 N85-35061
The theoretical and experimental investigation of cosmic ray Forbush-effects
[SH-5.1-20] 23 p4044 N85-35072
Peculiarities of Galactic Cosmic Ray (GCR) anisotropy variation in connection with the recurrent and sporadic Forbush effects
[SH-5.1-21] 23 p4044 N85-35073
Cosmic ray modulation by high-speed solar wind fluxes
[SH-5.1-22] 23 p4044 N85-35074
The neutron moderated detector and groundbased cosmic ray modulation studies
[SH-9.1-13] 23 p4052 N85-35128
The influences of the galactic cosmic ray on the atmospheric ozone
[SH-10.1-1] 23 p4053 N85-35133
FORBUSH EFFECT
U FORBUSH DECREASES
FORCE
Primer for mass metrology
[PB85-121424/GAR] 09 p1305 N85-18199
FORCE DISTRIBUTION
Control of the dynamic response of a damped membrane by distributed forces
[CSIR-TWISK-312] 01 p0061 N85-10406
Flight and wind-tunnel comparisons of the inlet-airframe interaction of the F-15 airplane
[NASA-TP-2374] 04 p0455 N85-12884
Mathematical modeling of assembly processes involving use of sensitized robots 04 p0488 N85-13111
On the use of marker loads and replicas for measuring growth rates for small cracks 14 p2319 N85-24331
Experimental and theoretical determination of the wing-induced lateral wind on the tail surfaces in oscillating rolling motion. Part 1: Application of the Mobile Oscillating Derivatives (MOD) on an experimental part
[IFD-1/84-PT-1] 18 p3061 N85-28939
Application of two-dimensional unsteady aerodynamic to a free-tip rotor response analysis
[NASA-CR-177348] 19 p3215 N85-29933
Turbine blade-tip clearance excitation forces
[NASA-CR-171534] 19 p3220 N85-29963
On high strain rate fragmentation of a closed vessel 23 p3904 N85-34187
FORCE FIELDS
U FIELD THEORY (PHYSICS)
FORCE-FREE MAGNETIC FIELDS
Measurements of Solar Vector Magnetic Fields
[NASA-CP-2374] 18 p3203 N85-29869
On the numerical computation of nonlinear force-free magnetic fields 18 p3203 N85-29871
Modeling solar magnetic structures 18 p3203 N85-29872
FORCED CONVECTION
Internal forced convection to low Prandtl number gas mixtures
[AD-A148932] 10 p1484 N85-19366
Heat transfer in aeropropulsion systems
[NASA-TM-87066] 20 p3453 N85-31444
Forced convection on solar collector arrays
[DE85-010381] 21 p3585 N85-32287
FORCED OSCILLATION
U FORCED VIBRATION
FORCED VIBRATION
Normal mode method of solving problem forced oscillations of rib-reinforced shell of revolution in liquid 02 p0273 N85-11781
The Shock and Vibration Digest, volume 16, no. 9
[AD-A146779] 07 p0976 N85-16200
A review of approximate methods for determining the vibrational modes of membranes 09 p1331 N85-18363
Journal of Research of the National Bureau of Standards, volume 89, number 2, March - April 1984
[PB85-115426] 12 p1926 N85-22103
A preliminary investigation of the dynamic force-calibration of a magnetic suspension and balance system
[NASA-CR-172580] 14 p2228 N85-23808
Study of dynamic characteristics of prefabricated gas turbine compressor rotor 14 p2272 N85-24078
A study of internal and distributed damping for vibrating turbomachiner blades
[NASA-CR-175901] 17 p2898 N85-27868

FORCED VIBRATORY MOTION EQUATIONS
U EQUATIONS
U FORCED VIBRATION
FOREBODIES
NT NOSE CONES
NT NOSES (FOREBODIES)
Effects of body shape on the aerodynamics of a body of revolution at Mach numbers from 1.6 to 4.6
[NASA-TM-86345] 07 p0893 N85-15657
Free-surface boundary layer and the origin of bow vortices
[AD-A147427] 07 p0960 N85-16083
FORECASTING
NT DELPHI METHOD (FORECASTING)
NT LONG RANGE WEATHER FORECASTING
NT NOWCASTING
NT NUMERICAL WEATHER FORECASTING
NT PATTERN METHOD (FORECASTING)
NT PERFORMANCE PREDICTION
NT PREDICTION ANALYSIS TECHNIQUES
NT PROFILE METHOD (FORECASTING)
NT STATISTICAL WEATHER FORECASTING
NT TECHNOLOGICAL FORECASTING
NT WEATHER FORECASTING
Future scenarios and ozone change
[DE84-014781] 01 p0085 N85-10573
Outline of a new emissions model for military and civilian aircraft facilities
[DE84-016455] 04 p0531 N85-13394
Subhourly wind forecasting techniques for wind turbine operations
[DE84-016205] 04 p0539 N85-13427
General model of earthquakes and the place of warnings in it 07 p0981 N85-16232
Earthquake forecasting research in the Ukraine 07 p0981 N85-16233
Crop yield forecasting 07 p1001 N85-16360
A note on using the integrated form of ARIMA forecasts
[AD-A146965] 07 p1030 N85-16536
Life cycle cost management master plan for the Defense Communications Agency
[AD-A146876] 07 p1050 N85-16668
The Air Force can improve its forecasts of aircraft spare parts requirements
[AD-A147911] 07 p1053 N85-16682
On seismic waves 08 p1171 N85-17383
An HF communications frequency-management procedure for forecasting the frequency of optimum transmission
[AD-A149191] 10 p1467 N85-19254
A model for forecasting runway surface temperature and verification with subjective forecasts
[TR-28] 10 p1518 N85-19569
Bootstrapping the Kalman filter
[AD-A150509] 13 p2153 N85-23370
Real-time enhancement of a climatology or forecast of ocean thermal structure using observed ocean temperatures
[AD-A151118] 15 p2604 N85-26049
Role of supercomputers in energy research programs
[DE85-006865] 15 p2624 N85-26172
Kalman filtering and exponential smoothing in economics 15 p2635 N85-26248
Intermediate term forecasting techniques for management
[AD-A151370] 15 p2637 N85-26262
Satellite provided customer promises services, a forecast of potential domestic demand through the year 2000. Volume 4: Sensitivity analysis
[NASA-CR-174662] 16 p2769 N85-27092
Use of forest modeling to project acid rain effects
[DE85-005251] 16 p2821 N85-27400
An evaluation of discretized conditional probability and linear regression threshold techniques in model output statistics forecasting of visibility over the north Atlantic Ocean
[AD-A151955] 16 p2857 N85-27619
Historical perspective on the Moon base: The British perspective
[DE85-005905] 17 p2907 N85-27925
Forecast verification of the 10.7 centimeter solar flux and the Ap daily geomagnetic activity indices
[AD-A152950] 17 p2993 N85-28489
Discovery in earthquake forecasting and seismic zoning recorded 19 p3295 N85-30426
Flood-runoff forecasting with HEC1F
[AD-A154286] 19 p3300 N85-30456
Optimization of single and multi-component analytical techniques
[HSE-TRANS-10987] 19 p3347 N85-30744
New estimating procedures for surface runoff, sediment yield, and contaminant transport in Los Alamos County, New Mexico
[DE85-011890] 21 p3606 N85-32393
Forecasting atmospheric visibility over the summer north Atlantic using the principal discriminant method
[AD-A155537] 21 p3637 N85-32593
Study to encourage and facilitate industrial investment and involvement in space
[NASA-CR-176152] 23 p3898 N85-34147
The NORDA/FNOC (Naval Ocean Research and Development Activity's/Fleet Numerical Oceanography Center) Polar Ice Prediction System (PIPS)-Arctic: A technical description
[AD-A156332] 24 p4126 N85-35577
FORECASTS
U FORECASTING
FOREIGN POLICY
NT INTERNATIONAL COOPERATION
NT INTERNATIONAL RELATIONS
NT OUTER SPACE TREATY
FORENSIC SCIENCES
U LAW (JURISPRUDENCE)
FOREST FIRE DETECTION
Aerospace technology determines forest-fire danger 19 p3295 N85-30427
FOREST MANAGEMENT
The 1984 NASA/ASEE summer faculty fellowship program
[NASA-CR-174138] 04 p0574 N85-13863
Modeling long-term changes in forested landscapes and their relation to the Earth's energy balance 05 p0653 N85-14194
Forest cover monitoring by remote sensing in Great Britain 05 p0656 N85-14214
Integrative investigation on forest damage detection based on airborne Multispectral Scanner data 05 p0656 N85-14215
Response of unmanaged forests to CO2-induced climate change: Available information, initial tests and data requirements
[DOE/NSB-0053] 12 p1883 N85-21817
Remote sensing used for study of forest resources 13 p1983 N85-22440
Technologies to sustain tropical forest resources
[TI85-901085] 13 p2126 N85-23241
FORESTS
NT RAIN FORESTS
Fungi of Mt. Babia Gora. 2: Indicative value of macromycetes in forest associations. A: Initial considerations
[NASA-TM-77485] 01 p0094 N85-10632
Fungi of Mount Babia Gora. 3: The indicating value of macromycetes in the forest associations
[NASA-TM-77486] 01 p0094 N85-10633
Remote sensing applied to forest resources
[E85-10012] 02 p0216 N85-11425
Shuttle Experimental Radar for Geological Exploration (SERGE) project: Field work relating to the Shuttle Experimental Radar A (SIR-A) in Brazil (phase 2)
[NASA-CR-174033] 02 p0219 N85-11444
Some principles of plant resources evaluation using remotely sensed data 04 p0543 N85-13459
Integrative investigation on forest damage detection based on airborne Multispectral Scanner data 05 p0656 N85-14215
Acid rain and tree physiology: Some hypotheses for observed changes in forest productivity
[DE84-016568] 05 p0672 N85-14318
Image variance and spatial structure in remotely sensed scenes — South Dakota, California, Missouri, Kentucky, Louisiana, Tennessee, District of Columbia, and Oregon 07 p0998 N85-16265
Forest area estimates from LANDSAT MSS and forest inventory plot data
[PB85-105617/GAR] 07 p0990 N85-16290
Deciduous forest radiation regimes: Effects of forest structure, phenology and Earth-Sun geometry upon their spatial, temporal and spectral variability
[AD-A146804] 07 p0998 N85-16327
Simulating responses to expected climate change in eastern North America: Applications to decision-making in the forest industry
[DE85-001272] 07 p1008 N85-16406
New Zealand SIR-B science investigations 08 p1144 N85-17218
Microwave and optical remote sensing of forest vegetation 08 p1146 N85-17228
The extension of an invertible coniferous forest canopy reflectance model using SIR-B and LANDSAT data 08 p1149 N85-17246
Test plan for the forest-echo experiment
[DE84-017175] 09 p1343 N85-18447
Smoother terrain-machine
[AD-P004296] 09 p1409 N85-18873
UHF radiowave propagation through forests
[AD-A149518] 10 p1467 N85-19256
UHF communications through forested propagation channels 10 p1470 N85-19290
Analysis of data acquired by synthetic aperture radar and LANDSAT Multispectral Scanner over Kershaw County, South Carolina, during the summer season
[E85-10071] 10 p1503 N85-19485
Anayis of the quality of image data required by the LANDSAT-4 Thematic Mapper and Multispectral Scanner — agricultural and forest cover types in California
[E85-10074] 10 p1504 N85-19488
Effects of air pollution and acid rain on forest decline
[GPO-37-459] 12 p1883 N85-21818
Modeling interception of rainfall by forests and the role of interception in the water balance
[DE85-002822] 12 p1884 N85-21825
The use of Thematic Mapper data for land cover discrimination: Preliminary results from the UK SATMaP programme 13 p2121 N85-23207
Areas with forest soils sensitive to acidic deposition under alternative damage hypotheses
[DE85-005257] 13 p2130 N85-23257
A comparative evaluation of the effects of acid precipitation, natural acid production and harvesting of cation removal from forests
[DE85-005254] 15 p2589 N85-25961
Use of forest modeling to project acid rain effects
[DE85-005251] 16 p2821 N85-27400
A transport theory of millimeter wave propagation in woods and forests
[AD-A151883] 17 p2947 N85-28196
A comparative evaluation of the effects of acid precipitation, natural acid production and harvesting on cation removal from forests
[DE85-010821] 19 p3309 N85-30511
Study of the formation of particles from natural hydrocarbons released by vegetation 21 p3644 N85-32840
Snow cover in the Siberian forest-steppe
[NASA-TM-77914] 23 p3943 N85-34435
Effects of acid rain on forest nutrient status
[DE85-012486] 23 p3947 N85-34463
FORGING
Calculation of the optimum conditions for the forging of plates
[BLL-M-35757-(5828.4)] 02 p0189 N85-11280
Tensile and crack propagation tests on aluminum alloys of the 2000 and 7000 series in laminated plate and forged products
[M2-578300] 03 p0373 N85-12383
The role of microstructure in the modelling of plastic flow in P/M superalloys at forging temperatures and strain rate 06 p0796 N85-15090
Control of microstructure during hot working of Ti-6242 06 p0797 N85-15091
Static and dynamic fracture toughness characterization of SA508 forging and SA533B welded plate — pressure vessel steels
[CISE-2258] 08 p1131 N85-17127
Application of electricity to the reheating of metals prior to forming. Forging, lamination, induction
[BLL-TR-T6399/BG/MRS14903/84] 08 p1137 N85-17160
Engineering property comparisons of PM and IM aluminum alloy forgings
[AD-B088146L] 08 p1173 N85-17398
Correction of engraving stamp for forming blanks of gas turbine engine blades 09 p1307 N85-18213
Robotized blanks loader for new forge press 10 p1481 N85-19218
Dependence of mechanical properties of large VT3-1 alloy forgings on microstructure parameters 11 p1602 N85-20072
Weldability and mechanical property characterization of weld clad alloy 800H tubesheet forging
[DE85-001737] 11 p1609 N85-20116
USSR report: Machine tools and metalworking equipment
[JPRS-UMM-85-005] 13 p2051 N85-22839
Experience in use of optical theodolite for machine construction 14 p2267 N85-24049
Clutchless mechanism for engagement of forging press 14 p2268 N85-24051
USSR report: Machine tools and metalworking equipment
[JPRS-UMM-85-004] 14 p2284 N85-24152
Automated, robotized forge-press systems viewed 14 p2284 N85-24153
Robots for application in forge-press operation 14 p2284 N85-24154
Titanium alloys, products, standards listed 15 p2533 N85-25626
Automatic manipulators for forging rollers 16 p2762 N85-27042
Industrial robots and automatic manipulators for forging and pressing operations at Second International Exhibition 16 p2762 N85-27044

Precision die forging of blades or gas turbines
17 p2940 N85-28148
Mechanizing of handling operations in drop forging with hammers and presses (conducted ergonomical examinations)
[BMFT-FB-HA-84-051] 17 p3002 N85-28581
Powder metallurgy forged gear development
[NASA-TM-87483] 18 p3117 N85-29295
Distribution of density in closed-impression die forging of axisymmetrical products from metal powders
19 p3245 N85-30118
Influence of the molding joint plane on the fatigue resistance of the alloys 7010 and 7050. Test Report No. M1-631600
[PV-M1-631600] 20 p3470 N85-31582
Assessment of metal heating technologies for ferrous forging: A pilot study of the form value of natural gas
[PB85-204394] 24 p4084 N85-35314
Establishment of a Computer-Aided Design (CAD)-Computer-Aided Manufacturing (CAM) process for the production of cold forged gears
[AD-A155756] 24 p4137 N85-35844

FORM
U SHAPES

FORM FACTORS
Dirac single particle wave functions in inelastic electron scattering
[DE84-015129] 02 p0279 N85-11814
Measurement of the induced moment magnetic form factor of a heavy fermion superconductor
[DE85-004165] 12 p1942 N85-22194
Paramagnetic form factors from itinerant electron theory
[DE85-005272] 16 p2750 N85-26973

FORM PERCEPTION
U SPACE PERCEPTION

FORMALDEHYDE
Direct measurements of nitrous acid, nitrogen dioxide and formaldehyde in auto exhaust by differential optical absorption spectroscopy
[PB84-229269] 06 p0767 N85-14905
Long term durability of urea formaldehyde glued joints removed from Vampire aircraft
[AD-A149053] 10 p1424 N85-18985
The decomposition of gas phase formaldehyde by plasma discharge
[AD-A153202] 17 p2921 N85-28007
Synthesis of 2,4,8,10-tetraoxaspiro5,5undecane
[NASA-CASE-ARC-11243-2] 22 p3741 N85-33187
Oxidation of formaldehyde solutions used for the preservation of reverse osmosis membranes
[PB85-185585] 22 p3742 N85-33194
Modeling of auto exhaust smog chamber data for EKMA development
[PB85-186492] 22 p3813 N85-33619

FORMALISM
Model theory for infinitely deep languages
[ISSN-0355-0087] 01 p0101 N85-10674
On the formal description and derivation of temporal proof rules for program properties
[TUM-I8405] 01 p0101 N85-10675
Experimental techniques of formal specifications for the design of tested and reliable computer programs
[ENST-84E007] 05 p0716 N85-14591
The period of orbit as a test of the general theory of relativity
05 p0742 N85-14772
Analysis of the impact of a deformable missile model on a deformable obstruction
[BLL-RISLEY-TR-8534-(9091.9F)]
06 p0859 N85-15459
Self-induced nonlinear effects in optical fibers: A unified approach
[FUB-67-1982] 09 p1385 N85-18713
An algorithm to test for confluence in a system of left to right rewrite rules
[AD-A154066] 19 p3335 N85-30662

FORMAT
Standardization of data formats for radar altimeter data
03 p0384 N85-12455
WXR (hydrologic weather wire and PLT product software package)
[PB84-237221] 04 p0541 N85-13442
Formats for numerical and textual data in data processing
[DFVLR-MITT-84-07] 04 p0551 N85-13504
Distribution of the K-corona over the polar regions of the solar disk: 1965-1983
[PB84-230077] 06 p0835 N85-15317
Standard SHEF (Standard Hydrometeorologic Exchange Format) decoder Version 1.1
[PB85-106506/GAR] 06 p0840 N85-15332
RATFOR user's guide version 2.0
[NASA-CR-166601] 07 p1023 N85-16490
Document interchange format
[PB84-217033] 07 p1027 N85-16517
Technical order managers handbook: Utilization assessment
[AD-A147579] 07 p1055 N85-16694
Introduction to LBL graphics
[DE85-000389] 09 p1369 N85-18600
Pictorial format display evaluation
[AD-A149252] 10 p1425 N85-18986
Standardized format for computer series
[PB85-109668] 11 p1705 N85-20724
Atmospheric handbook: Atmospheric data tables available on computer tape
[PB85-108512] 12 p1891 N85-21867
The four forms of omega
[AD-A149694] 12 p1915 N85-22020
M68000 RNF text formatter user's manual
[NASA-TM-86327] 13 p2146 N85-23320
Multiple resources and display formatting: The implications of task integration in a simulated air traffic control task
[AD-A150713] 14 p2292 N85-24205
Factors affecting dwell times on digital displaying
[NASA-TM-86406] 14 p2390 N85-24722
Use of COSMIC NASTRAN in a design department
15 p2575 N85-25881
User manual for IMAGER: The DREO (Defence Research Establishment Ottawa) image processing system
[AD-A151754] 15 p2653 N85-26362
Design of an interface to an information retrieval network
16 p2877 N85-27750
A method to calculate the parameters of wings of arbitrary planform
[AD-A152689] 17 p2892 N85-27831
Airport and airway system cost allocation model. Volume 7: User's manual
[AD-A152877] 17 p2906 N85-27917
VIDTEX
[PB85-175869] 19 p3316 N85-30567
Cultural data base implementation study and computer-aided scene modeling system users manual
[AD-A154232] 19 p3333 N85-30646
T sub EX font tables
[DE85-011394] 19 p3339 N85-30687
A model for a document maintenance system
23 p3960 N85-34542

FORMATION
Ionic mechanisms of soot formation in flames
[AD-A150119] 12 p1801 N85-21297

FORMATION HEAT
U HEAT OF FORMATION

FORMATIONS
A paleomagnetic study of the Prince William terrane and Nixon Fork terrane, Alaska 02 p0226 N85-11478
Paleozoic limestones of the Crazy Mountains and vicinity, Circle quadrangle, east-central Alaska
04 p0517 N85-13296
Late Paleozoic and early Mesozoic radiolarians in the Circle quadrangle, east-central Alaska
04 p0517 N85-13297
Morphology and mechanics of terraces in lunar craters
13 p2182 N85-23543
Application of far-field models to the disposal of nuclear waste in geologic formations
[DE85-005489] 14 p2420 N85-24932
Thermal-cycle testing of the G-tunnel heated block
[DE85-008408] 18 p3126 N85-29359
Implications for the Earth of the early dynamical environment 21 p3719 N85-33079

FORMING TECHNIQUES
NT CASTING
NT CENTRIFUGAL CASTING
NT COLD ROLLING
NT COLD WORKING
NT ELECTROFORMING
NT ELECTROHYDRAULIC FORMING
NT EXPLOSIVE FORMING
NT EXTRUDING
NT FORGING
NT HOT WORKING
NT INJECTION MOLDING
NT MAGNETIC FORMING
NT METAL DRAWING
NT METAL SPINNING
NT PRESSING (FORMING)
NT PULTRUSION
NT ROLL FORMING
NT SLIP CASTING
NT STAMPING
International Conference on Recent Developments in Specialty Steels and Hard Materials. Conference abstracts
[CSIR-S-256] 02 p0176 N85-11177
Process Modeling Applied to Metal Forming and Thermomechanical Processing
[AGARD-LS-137] 06 p0796 N85-15086
Microstructure, texture and formability of thin aluminium sheets 06 p0796 N85-15088
Numerical methods in metalforming
06 p0797 N85-15092
Finite element simulation of forging processes
06 p0797 N85-15093
Heliostat tested 07 p0994 N85-16318
USSR report: Machine tools and metalworking equipment
[JPRS-UMM-85-001] 08 p1139 N85-17172
Electromagnetic processing of materials
[AD-A148804] 09 p1311 N85-18241
Factors influencing the ball milling of SI3N4 in water
[NASA-TM-86932] 10 p1450 N85-19136
Developments in GDR metal forming technology assessed 11 p1617 N85-20168
Aluminum alloy ATs5K5 (5% Zn + 5% Ca) for superplastic forming 13 p2026 N85-22897
Electrostatic forming and testing of polymer films on a 16-foot diameter test fixture
[NASA-TM-86328] 13 p2063 N85-22885
Equipment for performing surfaces of optical parts
14 p2266 N85-24043
Powder metallurgy production problems
15 p2497 N85-25406
New material, process spins off from Volvo LCP 2000 program 15 p2536 N85-25648
Preparation of metal for cold upsetting
[BLL-BISI-TRANS-22383-(9022.06)]
17 p2926 N85-28043
Application of 4-wire submerged arc method to welding UOE pipe
[BLL-BISI-TRANS-22417-(9022.06)]
17 p2972 N85-28358
State of stress and penetration of plastic deformation in forming
[BLL-BISI-22199-(9022.06)] 17 p2977 N85-28396
French, UK, Swedish research in powder metallurgy, HIP 18 p3088 N85-29109

FORMULAS (MATHEMATICS)
Model theory for infinitely deep languages
[ISSN-0355-0087] 01 p0101 N85-10674
What formulas are good for representing dipole and generalized oscillator-strength spectra
[DE84-014641] 02 p0278 N85-11809
Spatial mechanics formulas and exercises
05 p0601 N85-13832
Consolidation theory with consideration of frame plasticity
[REPT-9/1984] 16 p2796 N85-27240
Formulas for updating the generalized inverse of a symmetric matrix perturbed by a symmetric rank 2 matrix composed of 2 nonsymmetric DYADS
[AD-A151736] 16 p2858 N85-27629
The method of residual minimization in compressible steady flows
[AD-A153924] 18 p3100 N85-29193
About product formulas with variable step-size
[AD-A153527] 18 p3169 N85-29636
Tenth-order expansion formulas for the orbital eccentricity function K (sub lpq)(e) obtained using a symbolic algebraic manipulation system
[AD-A153754] 18 p3170 N85-29647
Aspects of SAR image segmentation
[AD-A154965] 21 p3575 N85-32236

FORMULATIONS
Finding the largest l(p)-ball in a polyhedral set
[AD-A153542] 18 p3170 N85-29643

FORTRAN
Three degree of freedom steady state point performance program: Updated version 1
[CSIR-NIAST-83/48] 01 p0001 N85-10005
Application guide for Hydrological Simulation Program FORTRAN (HSPF)
[PB84-215763] 01 p0064 N85-10427
Manual of phosphoric acid fuel cell stack three-dimensional model and computer program
[NASA-CR-174722] 01 p0067 N85-10447
ADS: A FORTRAN program for automated design synthesis, version 1.00
[NASA-CR-172460] 01 p0102 N85-10684
The CMC/3DPNS computer program for prediction of three-dimensional, subsonic, turbulent aerodynamic juncture region flow. Volume 3: Programmers' manual
[NASA-CR-165998] 02 p0197 N85-11318
Phosphoric acid fuel cell power plant system performance model and computer program
[NASA-CR-174638] 02 p0222 N85-11456
Proposal for a semiautomatic program testing system
[INPE-3262-TDL/178] 02 p0240 N85-11561
SMILE user's guide: A macro preprocessor for extending FORTRAN
[DE84-015984] 02 p0243 N85-11584
Programmer's guide for ASKF 77: A tool for programming of dialogs in FORTRAN and PASCAL
[FOA-C-30366-E1] 02 p0243 N85-11585

Convergent Technologies, mega frame, CTIX FORTRAN 77 version 2.1
[PB84-227768] 03 p0404 N85-12580
Digital Equipment Corp., VAX-11/782, VAX FORTRAN version 4.0
[PB84-227701] 03 p0405 N85-12582
Conversion of FEB (Fast and Easy Binary) utilities to ASCII FORTRAN
[AD-A145840] 03 p0406 N85-12596
Vertical coherence along a macroray path in an inhomogeneous anisotropic ocean
[AD-A145992] 03 p0416 N85-12660
Prime Computer, Inc., PRIME 750, FORTRAN-77 revision 19.4
[PB84-227628] 04 p0548 N85-13487
Control Data Corporation CYBER 205 model 442, FORTRAN 200 (G201-25)
[PB84-216290] 04 p0551 N85-13510
United Information Services, Inc., CRAY 1-S/2000, FORTRAN CFT 1.10
[PB84-227685] 04 p0552 N85-13512
Multigrid iteration solution procedure for solving three-dimensional sets of coupled equations
[DE84-016515] 04 p0555 N85-13532
Use of monitors in FORTRAN: A tutorial on the barrier, self-scheduling DO-loop and Askfor monitors
[DE84-016506] 05 p0715 N85-14587
Efficient sorting routines in FORTRAN 77
[OUEL-1529/84] 05 p0716 N85-14590
Some implementations of multigrid linear system solvers
[CWI-NM-R8401] 05 p0720 N85-14626
Digital Research Incorporated, IBM PC XT, FORTRAN-77 V4.0
[PB84-243633] 06 p0849 N85-15388
Perkin-Elmer, Perkin-Elmer 3230, FORTRAN 7 D R00-00
[PB84-243682] 06 p0849 N85-15389
Gould Incorporated, Gould PS-3000, Gould PS-3000 FORTRAN 77 V2.1
[PB84-229178] 06 p0849 N85-15390
Digital Equipment Corporation, PDP-11/23-PLUS PDP-11 FORTRAN-77 V5.0
[PB84-227610] 06 p0851 N85-15405
Plexus Computers, Inc., Plexus P/60, Plexus FORTRAN 77 Version 1.1
[PB84-227859] 06 p0851 N85-15407
Modular Computer Systems, Incorporated, MODCOMP CLASSIC 7860, MODCOMP FORTRAN 77/16 Version A.0
[PB84-230558] 06 p0852 N85-15411
Modular Computer Systems, Incorporated, MODCOMP CLASSIC 7860, MODCOMP NASA EXTENDED FORTRAN 78 Version A.40
[PB84-230549] 06 p0852 N85-15412
Sperry Corporation, 1100/80 ASC2 FORTRAN Level 11R1
[PB84-229194] 06 p0852 N85-15416
Wang Laboratories, Incorporated, Wang VS100, FORTRAN 77 Version 01.00.02
[PB84-228014] 06 p0852 N85-15419
Digital Equipment Corporation, DECSYSTEM-20 2060 Model B, FORTRAN-20 Version 10
[PB84-227974] 06 p0853 N85-15422
Convergent Technologies, NGEN CP001, CT FORTRAN Version 9.0
[PB84-229210] 06 p0856 N85-15442
Simplified continued fraction calculation of spherical Bessel functions
[AD-A146844] 06 p0858 N85-15455
RATFOR user's guide version 2.0
[NASA-CR-166601] 07 p1023 N85-16490
NOISEMAP 4.4 computer program update, operator's manual, addendum 1
[AD-A147091] 07 p1025 N85-16503
FORTRAN version of the quantitative energy-dispersive electron beam X-ray analysis program FRAME C
[PB84-240936] 07 p1027 N85-16519
Using the control system design environment in the design of a data link receiver unit for the Coast Guard HH-65A helicopter
[AD-A146824] 08 p1088 N85-16880
Validation of the communications link analysis and simulation system (CLASS) 08 p1100 N85-16954
Developing double sampling plans for attributes to meet sample size criteria
[AD-A148144] 08 p1205 N85-17587
COPES/ADS (Control Program for Engineering Synthesis) (Automated Design Synthesis) using the ADS optimization program
[AD-A148576] 08 p1206 N85-17588
Multitasking kernel for the C and FORTRAN programming languages
[DE85-001799] 09 p1370 N85-18609
Documentation for an instrument database system
[DE84-017392] 09 p1402 N85-18826
FORTRAN 66 analyser: User's manual
[PB85-111748] 10 p1542 N85-19724
DOS 21: PCDOS 2.0 support subroutine package for the IBM personal computer
[LA-10142-MS] 12 p1914 N85-22012
HGRAPH: A subroutine package for the IBM personal computer to support the Hercules Graphic Card
[LA-10144-MS] 12 p1914 N85-22013
ZTLCK: A subroutine package for the IBM personal computer to support the Zistech ZT1488 real time clock
[LA-10146-MS] 12 p1914 N85-22014
Ryan-McFarland Corporation, IBM PC model XT, RM/FORTRAN, version 2.0.0
[PB85-107993] 12 p1917 N85-22037
Ryan-McFarland Corporation, sun microsystem with sky fast floating point processor, RM/FORTRAN version 1.5.0
[PB85-108009] 12 p1917 N85-22038
Selection and use of general-purpose programming-language: Program examples, volume 2
[PB85-122000] 12 p1917 N85-22039
Selection and use of general-purpose programming language: Overview, volume 1
[PB85-122018] 12 p1917 N85-22040
Validation summary report, Burroughs Corporation, B20 FORTRAN release 4.0
[PB84-227792] 13 p2145 N85-23316
FORTRAN in the 90's
[DE85-006154] 13 p2148 N85-23332
Guidelines for development structured FORTRAN programs
[NASA-TM-86407] 14 p2402 N85-24808
Easyplot: An interactive, user-friendly graphics program
[AD-A150779] 14 p2404 N85-24824
A fast ray tracing routine for laterally inhomogeneous media
[AD-A150984] 14 p2421 N85-24936
A FORTRAN program for deep space sensor analysis
[AD-A151700] 15 p2489 N85-25366
The interactive plotting program: GRAPH
[AD-A151371] 15 p2523 N85-26165
GRID: A FORTRAN program for using a digitizing table to enter a finite element GRID
[AD-A151317] 15 p2626 N85-26196
Recent trends in software technology for vector processors 16 p2691 N85-26815
Pulsewidth modulated speed control of brushless dc motors
[AD-A151966] 16 p2778 N85-27148
An interactive computer package for use with simulation models which performs multidimensional sensitivity analysis by employing the techniques of response surface methodology
[AD-A151956] 16 p2846 N85-27548
Development of graphical time response using the OPTSYSX program
[AD-A152221] 16 p2848 N85-27557
Graphics package, version 4: User reference manual
[DE85-007694] 16 p3163 N85-29596
Introduction to programming multiple-processor computers
[DE85-010274] 18 p3164 N85-29599
Using MATHLIB on the IBM computer and sundry plotting examples with a taste of IMSL
[DE85-011395] 19 p3340 N85-30695
HANDTC: A FORTRAN program to calculate inner-zone terrain corrections
[DE85-011196] 19 p3340 N85-30699
Reliability of void detection in structural ceramics using scanning laser acoustic microscopy
[NASA-TM-87035] 21 p3597 N85-32337
SIGMA - A stochastic-integration global minimization algorithm
[AD-A154878] 21 p3671 N85-32806
A device-independent 2D plotting package written in FORTRAN
[RSRE-MEMO-3776] 23 p3956 N85-34514
CRAYCDC
[NASA-CR-177374] 24 p4137 N85-35639
CDCCRAY
[NASA-CR-177375] 24 p4137 N85-35640

FORWARD LOOKING INFRARED DETECTORS
U FLIR DETECTORS

FORWARD SCATTERING
Characterization of atmospheric conditions along transmission paths from a remotely piloted vehicle
[AD-A145527] 02 p0232 N85-11511
Description of amplitude scintillations on a 11 GHz slant path in terms of forward scattering from turbulent layers
[FI-455-TBR-76] 11 p1825 N85-20232
Surface forward scattering and reflection
[AD-A150115] 12 p1928 N85-22112
Application of forward scattering renormalization to scattering in turbid media
[AD-A153232] 17 p2959 N85-28271
Particle sizing from forward scattered light at two angles using a Variable-Focal-Length optical system
[AD-A154164] 20 p3533 N85-31980

FOSSIL FUELS
NT COAL
NT CRUDE OIL
NT LIGNITE
NT NATURAL GAS
NT PEAT
Analysis of potential combustion sorce impacts on acid deposition using an independently derived inventory, volume 1
[DE84-012005] 02 p0225 N85-11471
Humidity/cloud-radiation feedback on possible climate perturbation due to fossil fuel utilization
[DE85-006886] 18 p3133 N85-29402
Coal-Fired MHD Combustor Development Project, Phase 3D
[DE85-008822] 18 p3192 N85-29795
Control of acid deposition precursors through dry scrubbing
[DE85-010281] 19 p3235 N85-30056
Fracture detection and mapping for geothermal reservoir definition: An assessment of current technology, research, and research needs
[DE85-010627] 19 p3301 N85-30464
Current status of TVA's atmospheric fluidized bed combustion development efforts
[DE85-901209] 19 p3308 N85-30507
Technical guide for estimating fugitive dust impacts from coal handling operations. Volume 1: Project summary
[DE85-010948] 19 p3309 N85-30515

FOSSIL METEORITE CRATERS
U FOSSILS
U METEORITE CRATERS

FOSSILS
Post-Sonoman conodont biofacies of the Triassic of northwestern Nevada 03 p0390 N85-12497
Geographic and stratigraphic distribution of Miocene palynomorphs in north Idaho 03 p0390 N85-12498
Constraints on lunar origin: Evidence preserved in Precambrian stromatolites 04 p0584 N85-13731
Preliminary assessment of climatic change during late Wisconsin time, southwest Great Basin and vicinity, Arizona, California and Nevada
[DE85-008343] 16 p2836 N85-27488
Cyanobacterial mats: Microanalysis of community metabolism 21 p3661 N85-32743
Indications of mineral zoning in a fossil hydrothermal system at the Meager Creek geothermal prospect, British Columbia, Canada from induced polarization studies
[DE85-011982] 22 p3815 N85-33636

FOULING
NT ANTIFOULING
Operating experiences of reverse osmosis plants treating Rand Water Board (RWB) water: Pitfalls and problems 01 p0023 N85-10142
An electrochemical approach to the prevention of biofouling phenomena
[PB84-202813] 01 p0025 N85-10155
Biofouling and corrosion studies at the Seacoast Test Facility in Hawaii
[DE84-014643] 01 p0029 N85-10180
Hot-gas cleanup for molten carbonate fuel cells-dechlorination and soot formation
[DE84-003072] 01 p0068 N85-10450
Copper-nickel sheathing study, phase 2. Two-year service performance of test panels on the ARCO TEXAS
[PB84-242411] 06 p0775 N85-14952
Study of deposition control using transpiration
[DE85-002339] 10 p1485 N85-19378
Ocean energy systems
[PB85-110856] 11 p1678 N85-20584
Investigation of the initial events in biofouling
[AD-A149965] 12 p1900 N85-21927
Heat transfer monitor for measurements of fouling of industrial heat exchangers
[DE85-010257] 20 p3455 N85-31455
Ocean thermal energy conversion
[DE85-012291] 23 p3948 N85-34456

FOUNDATIONS
NT PILE FOUNDATIONS
Response and characteristics of structures subjected to S-H waves 01 p0060 N85-10396
The effect of an elastic foundation and of dissipative forces on the stability of fluid conveying pipes
[TAE-563] 12 p1863 N85-21868
Analysis of slabs-on-grade for a variety of loading and support conditions
[AD-A150965] 14 p2264 N85-24030
Repair of the DSS-14 pedestal concrete 16 p2772 N85-27106

FOUNDRIES
Theoretical and experimental investigations of dust loaded flow fields in industrial halls
[BMFT-FB-HA-84-044] 12 p1819 N85-21411

FOUR BODY PROBLEM
Investigations of the structure and electromagnetic interactions of few-body systems
[DE85-002854] 11 p1721 N85-20824

FOURIER ANALYSIS
NT FOURIER SERIES
Analysis of the Frascati and Geneva gravitational wave antenna background exhibiting the one half sideral day period
[NOTA-INTERNA-601] 02 p0192 N85-11283
Hardware and software selection for experimental modal analysis 02 p0208 N85-11373
Digital Terrain Elevation Data (DTED) anomaly removal through the use of an interactive Fourier frequency filtering process
[AD-A145433] 02 p0219 N85-11445
Local geomagnetic characteristics of solar activity (Dourbes 1960-1978) 04 p0521 N85-13326
Development of holographic particle field data reduction by Fourier analysis
[AD-A148684] 06 p1165 N85-17348
Precision measurement of torsional oscillations induced by gear errors 09 p1336 N85-18416
The eigenvalues of the pseudospectral Fourier approximation to the operator sin (2x) d/dx
[NASA-CR-172536] 11 p1706 N85-20729
Research in image understanding as applied to 3-D tomographic imaging with near optical resolution
[AD-A150098] 12 p1829 N85-21483
Mathematical simulation of thermal processes involved in electron-beam treatment 12 p1843 N85-21585
A two-dimensional smoothing spline and a regression problem
[AD-A149624] 12 p1921 N85-22067
Nonlinear behavior and stability of thin spherical shells subjected to non-axisymmetrical loading 13 p2048 N85-22821
Analysis of short-period changes in intensity of hard X-radiation of solar flares registered aboard Venera-13 and Venera-14 spacecraft 16 p2723 N85-26806
The development and implementation of an optical communications laboratory
[AD-A151682] 16 p2772 N85-27111
Head-on scattering of a tubular cylinder of finite length for radar target identification purposes
[AD-A155608] 21 p3577 N85-32246
Analysis of spacecraft data
[NASA-CR-171587] 21 p3669 N85-32789
SCRIBE data of October 23, 1983 flight
[AD-A154864] 21 p3705 N85-33012
Clusters and cycles in the cosmic ray age distributions of meteorites
[SH-7.1-11] 23 p4048 N85-35103

FOURIER SERIES
Controlled approximation and a characterization of the local approximation order
[AD-A149095] 10 p1546 N85-19750
A numerical approach for the vibration analysis of an axisymmetric shell structure with a nonuniform edge constraint
[AD-A149286] 11 p1651 N85-20402
Nonparametric estimation of density and hazard rate functions when samples are censored
[AD-A150946] 14 p2411 N85-24888
Natural convection in cylindrical containers 15 p2555 N85-25763
On various Fourier series utilized for solution of structural mechanics problems
[VTH-LR-429] 16 p2656 N85-27615
Extension of three theorems of Fourier series on the disc to the torus
[AD-A153017] 17 p3019 N85-28689
Fourier coding and reconstruction of complicated contours
[REPT-84-39] 17 p3022 N85-28691
Sigma filter 18 p3142 N85-29450
An extension to complex-valued functions of an algorithm for numerically inverting the Laplace transform
[DE85-010701] 19 p3347 N85-30743
Stress analysis of axisymmetric sandwich shells of variable thickness 24 p4101 N85-35419

FOURIER TRANSFORMATION
NT FAST FOURIER TRANSFORMATIONS
Shift-variant multidimensional systems
[AD-A144756] 01 p0111 N85-10752
Beam pulse length determination by spectral analysis
[CSIR-NAC-83-05] 01 p0116 N85-10793
Fast Fourier transform for unequally spaced data 01 p0128 N85-10876
Holographic subtraction of images by Fourier plane recording and spatial filtration with a narrow beam 02 p0203 N85-11721
Optical constant determination of thin polymer films in the infrared
[AD-A145669] 02 p0287 N85-11877
Thermomechanical cracking in layered media from moving friction load
[AD-A146022] 03 p0373 N85-12379
Meteorological analysis for clusters of wind turbines
[DE84-013164] 04 p0539 N85-13425
Surface structure determination with ARPEFS
[DE84-016904] 04 p0571 N85-13644
Phase problem in aperture synthesis systems 06 p0782 N85-15002
Micro-waveguide transformers of coherent optical signals 07 p0950 N85-16022
GC-FTIR (Fourier Transform Infrared Spectrometry) of jet fuels
[AD-A148272] 08 p1135 N85-17155
Signal reconstruction from Fourier transform sign information
[AD-A148039] 08 p1211 N85-17624
Molecular dynamics in nitramines and modified nitramines
[AD-A148515] 08 p1220 N85-17686
Effect of ultraviolet radiation on transparent polymer films as determined using in situ FTIR-RA spectroscopy. Volume 2: Photophysics of poly(vinylidene fluoride) films
[DE84-013040] 09 p1299 N85-18159
Shock response analysis by personal computer using the extended IFT algorithm 09 p1335 N85-18397
PCB analysis by capillary gas chromatography coupled with matrix isolation-Fourier transform infrared spectroscopy
[DE84-009201] 10 p1437 N85-19059
An object-oriented signal processing environment: The knowledge-based signal processing package
[AD-A148963] 10 p1466 N85-19251
Some qualitative properties of bivariate Euler-Frobenius polynomials
[AD-A149406] 10 p1547 N85-19755
Characteristic functional of a probability measure absolutely continuous with respect to a Gaussian radon measure
[AD-A149462] 10 p1548 N85-19763
Fourier densitometry: A new optical method for measuring density fluctuations by Rayleigh scattering — turbulent jets 11 p1576 N85-19932
Interim protocol for the automated analysis of semivolatile organic compounds by Gas Chromatography/Fourier Transfer Infrared (GC/FT-IR) spectrometry
[PB85-115186] 11 p1595 N85-20035
Signal processing and range spreading in the FM-CW radar
[PB85-108256] 11 p1626 N85-20239
Classic Fourier microdistributions in the real analytic case 11 p1698 N85-20873
Carbon monoxide adsorption on a platinum electrode studied by polarization modulated FT-IRRAS (Fourier Transform-IR Reflections Adsorption Spectroscopy). Part 1: CO adsorbed in the double layer potential region and its oxidation in acids
[AD-A149751] 12 p1800 N85-21288
Effect of ultraviolet radiation on transparent polymer films as determined using in situ FTIR-RA spectroscopy. Volume 1: Photodegradation of transparent polymer films
[DE84-013039] 12 p1814 N85-21377
Application of the system identification technique to goal-directed saccades
[AD-A150132] 12 p1906 N85-21967
Acousto-optically addressed Fourier transform matched filters
[AD-A150298] 13 p2063 N85-22889
Processing of signals in experiments with scattering of short radio pulses by conducting sphere 13 p2068 N85-22917
Synthesis of quasi-optimum algorithms for signal recognition against background of correlated noise employing discrete spectral transformations 13 p2085 N85-23020
New convolution and discrete Fourier transformation algorithms based on rectangular transformations over field of roots of unity 13 p2085 N85-23022
Algorithms for reconstruction of partially known, band limited Fourier transform pairs from noisy data
[AD-A150194] 13 p2150 N85-23347
Optical processing in radon space
[AD-A150289] 13 p2159 N85-23402
Wave propagation in heterogeneous media
[AD-A150600] 14 p2321 N85-24341
Fourier transform of wave data on ARGOS buoys 14 p2323 N85-24351
Detection of solar gravity mode oscillations 14 p2442 N85-25070
Processing speech for analysis using optical Fourier techniques
[AD-A151898] 15 p2544 N85-25704
Rayleigh criteria resolution of optical correlations
[AD-A151711] 15 p2652 N85-26359
An experimental investigation of two-dimensional flame-vortex interactions 16 p2744 N85-26934
Fourier transform infrared spectrophotometric analysis of resin mix stoichiometry, revision 1
[DE85-007272] 16 p2747 N85-26951
Techniques for computing the DFT using the residue Fermat number systems and VLSI 16 p2770 N85-27097
Balloon-borne, He-cooled Fourier transform spectrometer for far infrared astronomy
[MPE-IR-41] 17 p3053 N85-28699
Transform domain adaptive filtering using a recursive DFT
[DE85-008965] 18 p3172 N85-29656
Novel analytical approaches to coal beneficiation
[DE85-010437] 19 p3229 N85-30021
An extension to complex-valued functions of an algorithm for numerically inverting the Laplace transform
[DE85-010701] 19 p3347 N85-30743
Highly dispersed metal atoms in zeolites
[DE85-010515] 19 p3354 N85-30792
Speciation of hazardous inorganic compounds by Fourier transform infrared (FTIR) spectroscopy
[PB85-188969] 20 p3426 N85-31262
On the solution for the sound field in a semi-infinite uniform duct with sheared mean flow 20 p3523 N85-31912
In-situ measurement of wall thermal performance: Data interpretation and apparatus design recommendations
[DE85-011979] 21 p3586 N85-32269
Qualitative analysis of sign-bit processing
[AD-A154776] 21 p3671 N85-32804
Adaptive corrector operating in frequency domain 22 p3765 N85-33397
Substructure coupling in the frequency domain
[NASA-CR-176140] 22 p3800 N85-33543
Pulse effect in a light ion beam propagation through a Z-discharge plasma channel 23 p3961 N85-34684
The conjecture concerning time variations in the solar neutrino flux
[SH-8.1-6] 23 p4049 N85-35111
Methods and software for cosmic ray scintillation studies
[SH-9.1-17] 23 p4052 N85-35132

FRACTALS
Stable distribution and Levy process in fractal turbulence 02 p0283 N85-11846
A case of a not-so-strange strange attractor
[CWI-AM-R8406] 06 p1214 N85-17643
Fractal structure of the interplanetary magnetic field
[NASA-TM-86212] 19 p3383 N85-30967
On the multifractal nature of fully developed turbulence and chaotic systems
[PREPRINT-413] 20 p3455 N85-31458
Attractors for the Kuramoto-Sivashinsky equations
[DE85-009631] 20 p3520 N85-31892

FRACTIONATION
NT CHEMICAL FRACTIONATION
Geophysical and geochemical constraints favoring the capture hypothesis 04 p0581 N85-13710
Synthesis and characterization of a 1,4 Polybutadiene/Isotactic polypropylene block copolymer
[AD-A148199] 06 p1133 N85-17142
Molecular toxicology of chromatin: The role of Poly(ADP-Ribose) in gene control
[AD-A154415] 19 p3327 N85-30611
Micro-scale methods for characterization of supercritical fluid extraction and fractionation processes
[DE85-010966] 20 p3455 N85-31456
Supercritical fluid chromatography/supersonic jet spectroscopy
[DE85-007005] 22 p3746 N85-33221
Nebular volatile fractionations associated with chondrule formation 22 p3852 N85-33855

FRACTOGRAPHY
Applications of synchrotron X-ray diffraction topography to fractography
[DE84-016257] 04 p0513 N85-13274
Fractographic study of stress corrosion cracking of SUS 304 stainless steel in various environments
[BLL-RISLEY-TR-4598-(9091.9F)] 05 p0615 N85-13926
Fractographic observation and estimation of crack growth curve of aluminum alloy under ramdom flight simulation loading
[NAL-TR-824] 06 p0768 N85-14913
Damage to boron fibers during thermal cycling and annealing 10 p1445 N85-19107
Fractographic features of titanium alloy fatigue failure under repeated static stress and high frequency vibration 11 p1601 N85-20070
Micrographic and fractographic examination of alloys 2214 and 2024 for conditions which would cause burning of the metal on being put into solution, trial 17/175
[DGT-23.419] 11 p1609 N85-20117

Fatigue Crack Topography
[AGARD-CP-376] 14 p2318 N85-24321
Fatigue fracture topography 14 p2318 N85-24323
Fatigue crack propagation and fracture in 7050 and 7091 aluminum alloy forgings 14 p2318 N85-24324
Two recent cases of marker load applications on cargo/fighter aircraft fatigue tests 14 p2318 N85-24325
Effect of flight sequences in complex load histories on crack front marking 14 p2318 N85-24326
Generation of marker lines by means of marker loads 14 p2318 N85-24327
Generation of marker lines on fatigue fracture surfaces 14 p2319 N85-24328
Fatigue crack topography and crack growth analysis — wrought and cast aluminum 14 p2319 N85-24333
Application of optical and electron microscopic techniques in the fractographic determination of fatigue crack growth rates 14 p2320 N85-24334
New analysis aspects of the fatigue crack propagation behavior by SEM in situ microscopy 14 p2320 N85-24335
Crack propagation under constant and variable stress amplitudes: A comparison of calculations based on the Striation spacing and tests 14 p2320 N85-24336
Journal of Research of the National Bureau of Standards, volume 89, no. 6, November - December 1984
[PB85-179042] 20 p3472 N85-31580
Indentation fractography: A measure of brittleness
[PB85-179059] 20 p3473 N85-31581
A fractographic study on mode 2 and mode 3 SCC crack growth in an Al-Zn-Mg alloy 23 p3905 N85-34191
Fractographic analysis for nonpropagating conditions of fatigue crack at high stress ratios in mild steel 23 p3905 N85-34194

FRACTURE MECHANICS

USSR report: Materials science and metallurgy, no. 93
[JPRS-84810] 01 p0016 N85-10110
Influence of annealing on properties of AT3 alloy welded joints 01 p0019 N85-10118
The effects of radial yarns, 3-dimensionally reinforced carbon-carbon composite
[AD-A144751] 01 p0022 N85-10134
On the treatment of material laws for approximate J-estimation methods
[GKSS-84-E-15] 01 p0062 N85-10414
HOST high temperature crack propagation 02 p0144 N85-10977
Tensile strength of composite sheets with unidirectional stringers and crack-like damage: A brief report
[NASA-TM-86310] 02 p0170 N85-11139
Toughness in high speed steels and hard metals 02 p0176 N85-11181
The role of molybdenum as an alloy element in adhesive wear resistance 02 p0181 N85-11212
A study of environmental characterization of conventional and advanced aluminum alloys for selection and design. Phase 2: The breaking load test method
[NASA-CR-172387-PHASE-2] 02 p0182 N85-11219
Short cracks and crack closure in AL 2024-T3
[FFA-TN-1984-40] 02 p0210 N85-11387
Effective moduli of elasticity of unidirectional fibrous composite 02 p0265 N85-11733
European Scientific Notes, Number 38-9
[AD-A145683] 02 p0306 N85-11975
Study of delamination cracking under static and cyclic loads of carbon-epoxy composite materials
[REPT-42-727/F] 03 p0327 N85-12102
The influence of aluminum on the qualities of low and medium carbon steel
[BLL-M-35754-(5826.4)] 03 p0330 N85-12123
Sour-gas cracking in ferritic steels
[AERE-R-10908] 03 p0333 N85-12148
Thermal ageing studies of 9%Cr 1%Mo steel
[AERE-R-11109] 03 p0333 N85-12149
Stress-driven solute enrichment of crack-tips during low ductility intergranular fracture of low-alloy steel
[AERE-R-11120] 03 p0333 N85-12150
Microstructure of ceramics fabricated by unidirectional solidification
[NASA-TM-77423] 03 p0336 N85-12157
HIP glassmaking for high nitrogen compositions in the Y-Si-Al-O-N system
[DE84-015548] 03 p0338 N85-12175
Features of plastic deformation and fracture of EP 741 nickel alloy under thermal strain 03 p0349 N85-12250
Kinetics of fatigue factor of AT3 titanium alloys in air, distilled water and 3.5% aqueous NaCl solution 03 p0350 N85-12255
Structure of two-phase titanium alloys with different microstructures 03 p0351 N85-12257
Penetrator/armour interactions: Background to Australian work
[MRL-R-936] 03 p0367 N85-12353
Viscoplastic finite element analysis of rapid fracture 03 p0370 N85-12365
Applications of integral equations with strong singularities in fracture mechanics 03 p0371 N85-12367
Bending strength studies on hot-pressed silicon carbide
[NASA-TM-77512] 03 p0371 N85-12369
Stress intensity factors for a circular ring with uniform array of radial cracks of unequal depth
[AD-A145893] 03 p0372 N85-12377
Thermomechanical cracking due to moving frictional loads
[AD-A146271] 03 p0373 N85-12381
Eta values for compact geometry specimens to calculate the J integral
[AERE-R-11126] 03 p0374 N85-12385
Removal of singularities in Tresca and Mohr-Coulomb yield functions
[OUEL-1528/84] 03 p0413 N85-12642
Morphology and dynamic mechanical properties of diglycidyl ether of bisphenol-A toughened with carboxyl-terminated butadiene-acrylonitrile 04 p0466 N85-12958
Composite fracture toughness and impact characterization 04 p0466 N85-12963
Constituent properties and interrelationships 04 p0467 N85-12964
Impact of NDE unreliability on pressure vessel fracture predictions
[DE84-015586] 05 p0647 N85-14151
Welcome and introduction — materials strength 05 p0649 N85-14164
Fatigue behavior of continuous fiber silicon-carbide-aluminum composites
[NASA-TM-86332] 06 p0763 N85-14879
Study of fatigue fracture in hardened and tempered carbon steel. Report 1: Microscopic observation of the fatigue crack formation proces
[BLL-PNR-90242-(8019.3153)] 06 p0767 N85-14909
Deformation, fracture and explosive properties of reactive materials
[AD-A146396] 06 p0774 N85-14945
Constitutive modeling of engine materials
[AD-A146630] 06 p0817 N85-15189
Three-dimensional crack location by acoustic emission
[AERE-R-11277] 06 p0818 N85-15193
Engine Cyclic Durability by Analysis and Testing
[AGARD-CP-368] 07 p0905 N85-15733
Investigation of the creep behaviour of soft soldered joints with solder L-SnAg5 at ambient temperature
[BLL-T6383/BG/WH798/84] 07 p0926 N85-15865
Influence of pressure on compaction during compression of powders of iron and 40Kh and 10R6MS steels
[BLL-M-35995-(5828.4)] 07 p0926 N85-15866
Nondestructive tests and fracture mechanics investigations in the Component Integrity Research Programme
[BLL-RISLEY-TR-4541-(9091.9F)] 07 p0976 N85-16199
A general theory of circuit analogy in fracture diagnosis
[AD-A147177] 07 p0978 N85-16212
A hydrogen partitioning model for hydrogen assisted crack growth
[AD-A147385] 07 p0978 N85-16214
New aspects of thermoelastic contact
[AD-A147554] 07 p0979 N85-16217
Buckling analysis of cracked, floating ice sheets
[AD-A147330] 07 p0988 N85-16277
Crack growth in propellants 08 p1116 N85-17034
Shock and impact response of solid rocket propellants: Experimental and theoretical 08 p1116 N85-17040
The influence of strain rate and porosity on the deformation and fracture of titanium and nickel
[AD-A148670] 08 p1130 N85-17123
The influence of porosity on the deformation and fracture of alloys
[AD-A148766] 08 p1130 N85-17124
High pressure physics research focusing on composite materials 08 p1140 N85-17185
Electrodes for repairing power engineering equipment made from creep resisting steel
[BLL-CE-TRANS-8064-(9022.09)] 08 p1167 N85-17360
Numerical solution of elastodynamic problems in fracture mechanics 08 p1171 N85-17365
Tensile test of pressureless-sintered silicon nitride at elevated temperature
[NASA-TM-77777] 08 p1172 N85-17390
A simple engineering treatment of center cracked tension panels in the regime of nonlinear fracture mechanics under plane stress conditions
[GKSS-84-E-38] 08 p1173 N85-17396
Modeling of large-scale accretionary wedge and thin-skinned trust-and-fold belt mechanics 08 p1181 N85-17442
Fracture mechanics analysis and prediction of delamination growth in composite structures
[FFA-TN-1984-45] 09 p1289 N85-18092
Deformation and fracture of P/M (Powder/Metallurgy) titanium alloys
[AD-A148672] 09 p1294 N85-18128
Applicability of linear elastic fracture mechanics to fatigue in polymers and short-fiber composites 09 p1298 N85-18152
Analysis of a potential hot-wire ignition problem
[DE84-017254] 09 p1301 N85-18174
Method of testing carbide inserts for premature fracture by face milling of cylindrical workpieces 09 p1303 N85-18183
Determination of blade service life under irregular loading conditions 09 p1309 N85-18222
finite element analysis of bi-material systems with applications in hydraulic fracturing 09 p1332 N85-18369
The influence of mechanical damage on transmission pipeline integrity
[ERS-E.351] 09 p1340 N85-18431
Recent studies of the significance of mechanical damage in pipelines
[ERS-E.367] 09 p1341 N85-18433
Fracture resistance of surface layer with technological defects under cyclical loading 10 p1448 N85-19128
Crack problems for bonded nonhomogeneous materials under antiplane shear loading
[NASA-CR-172532] 10 p1495 N85-19438
Interaction between a crack and a soft inclusion
[NASA-CR-172533] 10 p1495 N85-19439
Fracture toughness of fiber reinforced concrete
[AD-A149403] 10 p1496 N85-19441
Mechanisms of damage accumulation in time-dependent cyclic deformation
[DE85-001004] 10 p1496 N85-19443
European Scientific Notes. Volume 39, number 2
[AD-A148994] 10 p1573 N85-19919
Fracture analysis of notched composites
[NASA-CR-172563] 11 p1593 N85-20020
Rapidly solidified NiAl and FeAl
[NASA-TM-86941] 11 p1597 N85-20042
Initial fracture stages of orthogonally reinforced composite material 11 p1599 N85-20055
Direct comparison of unloading compliance and potential drop techniques in J-integral testing
[DE85-001550] 11 p1650 N85-20392
Effect of input distributions on the probabilistic fracture mechanics analysis of reactor pressure vessels
[DE85-000832] 11 p1652 N85-20403
Thickness effects of fracture toughness
[DE85-002974] 11 p1653 N85-20409
Simulation of brittle fracture via molecular dynamics
[DE85-001081] 11 p1653 N85-20410
Requirements of quantitative NDE in developing fracture control plans
[DE85-003147] 11 p1654 N85-20415
Translational and extensional energy release rates (the J- and M-integrals) for a crack layer in thermoelasticity
[NASA-CR-174872] 12 p1863 N85-21685
Fracture analysis of cracks in complete cylindrical shells
[AD-A150091] 12 p1887 N85-21711
Evaluation of subsurface fracture geometry using fluid pressure response to solid earth tidal strain
[DE85-003294] 12 p1890 N85-21864
Reliability of structural brittle materials 12 p1948 N85-22222
Longitudinal splitting in unidirectional composites, analysis and experiments
[NASA-CR-3881] 13 p2015 N85-22639
Behavior of fiber-reinforced composites under dynamic tension
[AD-A150619] 13 p2015 N85-22641
Creep crack growth in ductile alloys
[DE85-003937] 13 p2023 N85-22676
Long-term strength and fracture criteria for EI698VD alloy under complex stress conditions 13 p2030 N85-22723
Advanced life analysis methods. Volume 2: Crack growth analysis methods for attachment lugs
[AD-A150420] 13 p2103 N85-23109
Scattering of elastic waves on fractures randomly distributed in a three-dimensional medium 13 p2111 N85-23151
Patterns of fracture and tidal stresses due to nonsynchronous rotation: Implications for fracturing on Europa 13 p2173 N85-23483
Research on composite materials for structural design
[AD-A150902] 14 p2260 N85-24004
On the corner singularity of a 3-D Griffith crack
[AD-A150989] 14 p2321 N85-24342

A preliminary investigation into transverse fracture of unidirectional fiber composites
[AERE-R-11494] 15 p2503 N85-25438
Influence of oxygen traces on the properties of tungsten heavy metals
[BLL-RARDE-TR-1177-(7291.7965)] 15 p2506 N85-25470
Transformation toughened ceramics: A potential material for light diesel engine application
[AD-A151421] 15 p2516 N85-25526
The effect of overload cycles on fatigue crack propagation in structural steels 15 p2577 N85-25897
Fracture problems in power law viscoelastic materials
[AD-A149221] 15 p2578 N85-25900
Crack closure characteristics considering center cracked and compact tension specimens
[AD-A151702] 15 p2579 N85-25907
A study of the time dependence in fracture processes relating to service prediction of adhesive joints and advanced composites
[AD-A152064] 15 p2579 N85-25910
A review of fracture mechanics life technology 16 p2733 N85-26863
Microscopic study of the influence of impurities on interface bonding
[AD-A151725] 16 p2743 N85-26928
Multiaxial and thermomechanical fatigue considerations in damage tolerant design
[NASA-TM-87022] 16 p2749 N85-26964
Automatic tracking of crack growth via finite elements 16 p2797 N85-27246
Full statistical characteristics of microdeformation
[BLL-M-36076-(5826.4)] 16 p2798 N85-27254
Predicting fully plastic mode 2 crack growth from an asymmetric defect
[AD-A152227] 16 p2801 N85-27269
Interaction of high-cycle and low-cycle fatigue of Haynes 188 alloy at 1400 F deg 17 p2913 N85-27961
Experiments and micromechanical models for creep-rupture in polymer matrix composites
[DE85-009533] 17 p2935 N85-28118
Conformational and mechanical properties at high strain rates
[AD-A153401] 17 p2959 N85-28272
Inspection evaluation and repair of the flawed feedwater nozzle of the 50 MWe Dodewaard GKN boiling water reactor
[ISBN-90-353-0017-3] 17 p2977 N85-28394
Measurement of fracture macro-geometry in evaluating fracture toughness
[BLL-BISI-TRANS-22241-(9022.06)] 17 p2978 N85-28403
Fracture mechanics analysis of cold drawn Si-Cr valve steel
[BLL-BISI-TRANS-22216-(9022.06)] 17 p2978 N85-28405
Relaxation properties and fatigue fracture resistance of austenitic spring steel
[BLL-BISI-TRANS-22300-(9022.06)] 17 p2978 N85-28406
Critical conditions for failure in materials subjected to high rates of loading
[AD-A153135] 17 p2980 N85-28420
High temperature fracture mechanics of silicon nitride
[BMFT-FB-T-84-285] 17 p2981 N85-28433
Field theory analysis using the finite element method to determine the deliberation curves of three dimensional fracture mechanics specimens with a semicircular surface crack applying the electrical direct current potential method for crack depth measurement
[GKSS-84-E-53] 17 p2982 N85-28434
Laboratory investigation of formation damage of an artificial fracture at simulated geothermal conditions
[DE85-010301] 18 p3102 N85-29201
Brittle fracture behaviour of cold formed, welded 10mm to 20 mm thick plate manufactured from plain carbon structural steels
[BLL-BISI-TRANS-21676-(9022.06)] 18 p3120 N85-29311
An effective substructure technique applied to crack problems 18 p3121 N85-29319
Study of the influence of metallurgical factors on fatigue and fracture of aerospace structural materials
[AD-A153913] 18 p3122 N85-29328
Fracture of laminated composite materials 19 p3230 N85-30030
The mechanics of internal stress and microcrack toughening mechanisms in ceramics
[AD-A154049] 19 p3248 N85-30139
Fracture mechanics formulas on microcomputers
[NASA-TM-77850] 19 p3284 N85-30362
Computational methods in advanced stress and durability analyses
[AD-A154119] 19 p3286 N85-30375
Micromechanism of fracture for stage 1 hydrogen-induced crack growth
[DE85-010027] 19 p3288 N85-30390
Delamination micromechanics analysis
[NASA-CR-172598] 20 p3422 N85-31237
Prediction of lifetime for ceramic materials in the elastic and viscoelastic region by fracture mechanical methods
[ESA-TT-825] 20 p3434 N85-31305
On elastic-plastic fracture criterion 20 p3465 N85-31528
Numerical study of ductile rupture in plane deformations
[ONERA-RT-23/7169-RY-072-R] 20 p3469 N85-31557
Numerical study of tensile fracture in plane stress
[ONERA-RT-22/7169-RY-070-R] 20 p3470 N85-31563
On the variation of the stress intensity factor along the front of a surface flaw
[OUEL-1565/85] 20 p3471 N85-31568
Development of fracture mechanics maps for composite materials, volume 1
[ESA-CR(P)-2017-VOL-1] 20 p3471 N85-31573
Development of fracture mechanics maps for composite materials, volume 2
[ESA-CR(P)-2017-VOL-2] 20 p3471 N85-31574
Development of fracture mechanics maps for composite materials. Volume 3: Appendices A-E
[ESA-CR(P)-2017-VOL-3] 20 p3472 N85-31575
Development of fracture mechanics maps for composite materials. Volume 4: Appendices F-K
[ESA-CR(P)-2017-VOL-4] 20 p3472 N85-31576
The three-dimensional J-integral. An investigation into its use for post-yield fracture safety assessment
[WTHD-167] 20 p3472 N85-31578
Indentation fractography: A measure of brittleness
[PB85-179059] 20 p3473 N85-31581
Simulation model of acoustic emission due to microscopic fracture in metals
[BLL-BISI-TRANS-22367-(9022.06)] 20 p3523 N85-31909
Influence of the resin on interlaminar mixed-mode fracture
[NASA-TM-87571] 21 p3561 N85-32150
Comparisons of various configurations of the edge delamination test for interlaminar fracture toughness
[NASA-TM-86433] 21 p3561 N85-32151
Effects of weak interfaces on thermostructural behavior of carbon-carbon composites
[AD-A155330] 21 p3562 N85-32154
The shearing contribution in transformation toughening of brittle materials
[AD-A154656] 21 p3568 N85-32195
Stress corrosion of ceramic materials
[AD-A155020] 21 p3570 N85-32202
Dynamic fracture behavior of structural materials
[AD-A154568] 21 p3598 N85-32345
Ductile fracture of dynamically loaded naval structures-compact tension specimen tests and analyses
[AD-A155472] 21 p3600 N85-32353
Development of improved dynamic failure models
[AD-A155586] 21 p3600 N85-32354
Relating corrosion maintenance to environmental factors 22 p3750 N85-33247
Elevated temperature crack growth
[NASA-CR-174957] 22 p3799 N85-33540
A review of path-independent integrals in elastic-plastic fracture mechanics, task 4
[NASA-CR-174956] 22 p3799 N85-33541
Proceedings of the Twentyseventh Japan Congress on Materials Research
[ISSN-0368-3141] 23 p3903 N85-34180
On the methods to determine the stress intensity factors in boundary element method 23 p3905 N85-34189
Experimental study on time and temperature dependent behavior of crack growth in viscoelastic strip 23 p3905 N85-34193
Fatigue crack retardation phenomenon caused by single-multiple overloads in 2017-T3 aluminum allow 23 p3906 N85-34196
Fracture behavior of aluminum composites reinforced with fiber 23 p3907 N85-34207
Time and temperature dependence of fracture surface in soft epoxy resin 23 p3908 N85-34213
Impact fracture mechanism of polymer plates containing a heavy inner material 23 p3908 N85-34215
Study on fracture behavior of epoxy resin 23 p3909 N85-34216
1983 review of experimental stress and strain analysis
[DRIC-T-7489] 24 p4101 N85-35422
Subcritical fracture propagation in rocks: An examination using the methods of fracture mechanics and non-destructive testing 24 p4116 N85-35516

FRACTURE RESISTANCE
U FRACTURE STRENGTH

FRACTURE STRENGTH
Fracture toughness characteristics of welded joints in VT65 and AT6 titanium alloys 01 p0020 N85-10121
Delayed fracture of high-strength steels in spherical tanks for LP gas
[BLL-RISLEY-TR-4926-(9091.9F)] 01 p0026 N85-10162
Fracture toughness of fibrous composite materials
[NASA-TP-2370] 02 p0170 N85-11136
Development of powder metallurgy 2XXX series Al alloys for high temperature aircraft structural applications
[NASA-CR-172408] 02 p0182 N85-11220
Effects of prior austenite and ferrite grain size on fracture properties of a plain carbon steel
[AD-A146276] 03 p0332 N85-12138
Structure and ductility of fracture of joints produced by electron-beam welding of VT6ch titanium alloy parts 03 p0351 N85-12261
An experimental evaluation of the J integral in 50% sidegrooved compact geometry specimens
[AERE-R-11202] 03 p0374 N85-12386
Tough Composite Materials
[NASA-CP-2334] 04 p0463 N85-12941
Characterization of interlaminar crack growth in composites with the double cantilever beam specimen 04 p0463 N85-12942
Characterizing delamination resistance of toughened resin composites 04 p0464 N85-12943
Composite materials characterization and development at AFWAL 04 p0464 N85-12944
Fundamental studies of composite toughness 04 p0464 N85-12948
The effect of cross-link density on the toughening mechanism of elastomer-modified epoxies 04 p0465 N85-12951
Toughening mechanism in elastomer-modified epoxy resins, part 2
[NASA-CR-3852] 04 p0478 N85-13046
Effects of irradiation fluence and creep on fracture toughness of 347/348 stainless steel
[DE84-016091] 05 p0618 N85-13953
Welcome and introduction — materials strength 05 p0649 N85-14164
Influence of residual stresses resulting from manufacturing on the fatigue strength of welded joints 05 p0650 N85-14177
Applicability of fatigue strength data obtained from small separately cast specimens on large cast components 05 p0651 N85-14178
Effect of crack-tip region constraint on fracture in the ductile-to-brittle transition
[PB84-237395] 06 p0770 N85-14926
Strength analysis of fan-shaped wing considering temperature deformation and creep deformations 06 p0779 N85-14983
Inconel 718 alloy resistance to crack propagation 07 p0907 N85-15740
Dispersed metal-toughened ceramics and ceramic brazing
[NASA-CR-174284] 07 p0933 N85-15916
Static and dynamic fracture toughness characterization of SA508 forging and SA533B welded plate — pressure vessel steels
[CISE-2258] 08 p1131 N85-17127
A discussion of problems encountered in the dynamic fracture toughness testing of materials
[OUEL-1524/84] 08 p1173 N85-17397
Engineering property comparisons of PM and IM aluminum alloy forgings
[AD-B088146L] 08 p1173 N85-17398
Surface mechanical properties and wear behavior of ion implanted TiB2
[DE85-001130] 09 p1295 N85-18133
Fabrication of ceramic-ceramic composites by chemical vapor deposition
[DE85-000981] 09 p1298 N85-18155
Fracture toughness of austenitic stainless steel weld metal at 4 K
[DE84-016638] 09 p1340 N85-18425
Preliminary report on tests of tensile specimens with a part-through surface notch for a filament wound graphite/epoxy material
[NASA-CR-172545] 10 p1431 N85-19026
K sub 1° -n diagram of cyclical crack resistance of aluminum alloys 10 p1442 N85-19090
Influence of excess phases on fracture toughness of cast alumiun-magnesium-zinc alloy 10 p1442 N85-19091
Strength and failure of ceramic-metallic material 10 p1446 N85-19112
Behavior and specifics of fracture of porous fiber materials in extension 10 p1447 N85-19118
Influence of gaseous hydrogen on strength and ductility of nickel heat-resistant alloys 10 p1447 N85-19119
Fracture toughness of fiber reinforced concrete
[AD-A149403] 10 p1496 N85-19441

Effect of ingot structure of failure ductility of pressed semifinished products of high-durability aluminum alloys
11 p1597 N85-20045
Thickness effects of fracture toughness
[DE85-002974] 11 p1653 N85-20409
Slit-ring test for evaluating fracture in tubular cross sections
[DE85-003550] 11 p1654 N85-20416
Fatigue crack propagation in mirage 1110 wing main spar specimens and the effects of spectrum truncation on life
[ARL/STRUC-R-405] 12 p1776 N85-21152
Stress corrosion cracking and oxidation characteristics of boride-strengthened microcrystalline iron and nickel based alloys
[AD-A149605] 12 p1806 N85-21326
Effects of neutron irradiation on the fracture properties of HT-9 weld
[DE85-001068] 12 p1807 N85-21339
Fracture toughness of materials
[DE85-004306] 12 p1857 N85-21713
Interlaminar fracture toughness in resin matrix composites
[AD-A150565] 13 p2015 N85-22640
Particulate toughened silicon carbide
[DE85-004797] 13 p2016 N85-22643
Prediction of the resistance of structural materials to cavitation erosion
[BLL-DRIC-TRANS-7435-(3623.66)]
13 p2020 N85-22659
Fatigue and corrosion fatigue resistance of aluminum casting alloy VAL10 and forging alloy AK6
13 p2025 N85-22690
Structural strenght of strip D16T aluminum alloy with low copper and magnesium content
13 p2025 N85-22691
Use of acoustical emission method to study specifics of fracture of boron reinforced plastic structural elements 13 p2026 N85-22696
Mechanical properties and brittle fracture resistance of welded multilayer elements for high pressure vessels
13 p2033 N85-22736
Analysis of strength and ductility of welded joints in AMtsS and AMg5 aluminum alloys
13 p2033 N85-22737
Effect of protective medium on durability and fracture structure on seam zones of thin-walled titanium articles produced by diffusion welding 13 p2033 N85-22738
Dispersed-metal-toughened alumina
[NASA-CR-174667] 13 p2037 N85-22758
Fracture mechanics evaluation of GaAs
[NASA-CR-175657] 13 p2102 N85-23101
The effect of notch acuity on the fracture toughness of silicon carbide/aluminum metal matrix composites
[AD-A150970] 14 p2248 N85-23936
Fracture toughness of HY-130 steel weld metals
[AD-A150841] 14 p2255 N85-23976
Cast-iron technology: Metallographic and mechanical testing results
[DE85-002684] 14 p2257 N85-23984
Effect of elevated-temperature neutron irradiation on fracture toughness of ceramics
[DE85-000652] 14 p2261 N85-24010
Correlation of uniaxial and biaxial fracture strengths of ceramics
[DE85-003779] 14 p2261 N85-24011
Effect of deep cooling on crack resistance and low-temperature hardening of aluminum alloys
15 p2496 N85-25396
Fatigue strength of alpha-titanium alloys under cophasal action of variable normal and tangential stresses
15 p2496 N85-25407
The accuracy of approximate solutions in the analysis of fracture of composites
[NASA-CR-175738] 15 p2503 N85-25437
Fatigue life, fatigue crack propagation and fracture toughness study of 7075 aluminum alloy subjected to thermomechanical processing 15 p2573 N85-25862
Tensile and fracture toughness properties of Mirage III spars
[AR-003-019] 15 p2576 N85-25899
Particulate and whisker toughened alumina composites
[DE85-005239] 16 p2743 N85-26930
Simultaneous chemical vapor deposition of SiC-dispersed phase composites
[DE85-007751] 16 p2744 N85-26931
The effect of low sheet thicknesses on the fracture toughness of an Al alloy (7075-T6) — Aramid Reinforced Aluminum Laminate (ARALL)
[VTH-LR-425] 16 p2752 N85-26984
An improved torsional method for determining the fracture toughness of stiff materials and of adhesive joints
[AD-A152091] 16 p2900 N85-27267
Reaction-bonded and fiber-reinforced SiC static and dynamic gas turbine components
[BMFT-FB-T-84-302] 17 p2899 N85-27674
Fracture toughness of MgCr(sub)2O(sub)4-ZrO(sub)2
[DE85-007945] 17 p2917 N85-27982
Preparation of metal for cold upsetting
[BLL-BISI-TRANS-22363-(9022.06)]
17 p2926 N85-28043
Measurement of fracture macro-geometry in evaluating fracture toughness
[BLL-BISI-TRANS-22241-(9022.06)]
17 p2978 N85-28403
On validity of threshold values of fatigue strength of steel structures
[BLL-BISI-TRANS-22192-(9022.06)]
17 p2978 N85-28408
Specimen thickness effects for elastic-plastic CTOD toughness of A36 steel
[DE85-006992] 18 p3077 N85-29038
Load-carrying capabilities of refractory alloys for space reactor power applications
[DE85-010568] 19 p3240 N85-30087
Mechanism of strength degradation for hot corrosion of alpha-SiC
[NASA-TM-87052] 19 p3248 N85-30135
The mechanics of internal stress and microcrack toughening mechanisms in ceramics
[AD-A154049] 19 p3248 N85-30139
Fatigue-crack growth and ductile fracture toughness behavior of ASTM A387 Grade 91 steel
[DE85-006495] 20 p3431 N85-31286
Application of the unloading compliance methods in fracture toughness measurements of a quenched and tempered steel
[BLL-CE-TRANS-7953-(9022.09)]
20 p3465 N85-31523
Assessment of dynamic test methods for the measurement of fracture toughness — steels
[OUEL-1561/85] 20 p3470 N85-31565
The Hopkinson pressure bar: An alternative to the instrumented pendulum for Charpy tests
[OUEL-1566/85] 20 p3471 N85-31569
Journal of Research of the National Bureau of Standards, volume 89, no. 6, November - December 1984
[PB85-179042] 20 p3472 N85-31580
Indentation fractography: A measure of brittleness
[PB85-179059] 20 p3473 N85-31581
Controlled indentation flaws for the construction of toughness and fatigue master maps
[PB85-179067] 20 p3473 N85-31582
Influence of the resin on interlaminar mixed-mode fracture
[NASA-TM-87571] 21 p3561 N85-32150
Comparisons of various configurations of the edge delamination test for interlaminar fracture toughness
[NASA-TM-86433] 21 p3561 N85-32151
Metallurgical origins of fracture toughness and microstructure and fracture toughness of an HSLA (High-Strength/Low-Alloy) steel
[AD-A155530] 21 p3567 N85-32167
Thin-film reliability and engineering overview
21 p3612 N85-32450
Dispersion toughened ceramic composites and method for making same
[DE85-011601] 22 p3751 N85-33252
KRAK: A computer program for two-phase two-component porous flow and fracture
[LA-9703] 22 p3782 N85-33434
On high strain rate fragmentation of a closed vessel
23 p3904 N85-34187
Study on fracture behavior of epoxy resin
23 p3909 N85-34216

FRACTURE TOUGHNESS
U FRACTURE STRENGTH

FRACTURES (MATERIALS)
Delayed fracture of high-strength steels in spherical tanks for LP gas
[BLL-RISLEY-TR-4926-(9091.9F)]
01 p0028 N85-10162
Turbine Engine Hot Section Technology (HOST)
[NASA-TM-83022] 02 p0140 N85-10951
Contributions to the 7th International Acoustic Emission Symposium
[AD-A145368] 02 p0275 N85-11792
Study of deformation and fracture of AMg6N weldable aluminum alloy by method of acoustic emission
03 p0352 N85-12266
Influence of cyclic tangential loading on indentation fracture
[DE84-015869] 03 p0373 N85-12362
Investigation of toughened neat resins and their relations to advanced composite mechanical properties
04 p0484 N85-12949
Numerical investigation of the micromechanics of composite fracture 04 p0467 N85-12970
Fundamental tribological properties of ceramics
[NASA-TM-86915] 07 p0930 N85-15893
Effects of fracture roughness on fluid flow through a single deformable fracture
[DE85-004593] 13 p2092 N85-23082
Scattering of elastic waves on fractures randomly distributed in a three-dimensional medium
13 p2111 N85-23151
Study of resolution of deep MT soundings by means of physical model 13 p2112 N85-23155
Durability calculation of wing panel element
14 p2285 N85-24159
Essential features in fatigue fractures and remarkable phenomena in fatigue crack growth
14 p2318 N85-24322
Generation of marker lines on fatigue fracture surfaces 14 p2319 N85-24328
Periodic loading sequences for the systematic marking of fatigue crack fracture surfaces
14 p2319 N85-24329
Modifications of flight by flight load sequences to provide for good fracture surface readability
14 p2319 N85-24330
The effect of overload cycles on fatigue crack propagation in structural steels
15 p2577 N85-25897
Creep-fatigue interaction of notched 304 stainless steel bars 16 p2796 N85-27249
Laboratory investigation of formation damage of an artificial fracture at simulated geothermal conditions
[DE85-010301] 18 p3102 N85-29201
Multiaxial fatigue and fracture: A literature review
[ARL/STRUC-R-410] 19 p3265 N85-30370
Dynamic fracture behavior of structural materials
[AD-A154568] 21 p3598 N85-32345
Automatic capability to store and retrieve component data and to calculate structural integrity of these components
[DE85-012429] 22 p3831 N85-33728
Special features of the fracture of ball-bearing steel close to non-metallic inclusion eutectics
[BLL-M-35809-(5828.4)] 23 p3914 N85-34258
On size effects in plane stress crack-growth resistance
[AD-A155826] 24 p4102 N85-35425

FRACTURING
NT CRUSTAL FRACTURES
Fracture, failure, and fragmentation
01 p0059 N85-10390
Quantum characteristics of kinetic fracturing of solids
02 p0265 N85-11732
Composite materials characterization and development at AFWAL 04 p0464 N85-12944
Effects of irradiation fluence and creep on fracture toughness of 347/348 stainless steel
[DE84-016091] 05 p0618 N85-13963
Tests of the load-bearing and deformation behaviour of reinforced concrete spherical shells under point loading
[BLL-RISLEY-TR-4560-9091.9F)]
06 p0616 N85-15182
Modelling of deformation and fracture in high-temperature structural materials
[DE84-016906] 06 p0618 N85-15191
Role of hydrogen in processes of deformation and fracture of metals 10 p1449 N85-19132
Rock mechanics: Issues and research needs in the disposal of wastes in hydraulic fractures
[DE85-001399] 10 p1556 N85-19809
Micro-deformation of quartz under dynamic action and its applications 11 p1620 N85-20201
Simulation of brittle fracture via molecular dynamics
[DE85-001061] 11 p1653 N85-20410
Requirements of quantitative NDE in developing fracture control plans
[DE85-003147] 11 p1654 N85-20415
Reliability of structural brittle materials
12 p1946 N85-22222
Physiography of the Martian west equatorial uplift
12 p1961 N85-22325
Hydrogen effects in austenitic stainless steels based on the Fe-Cr-Mn-N system
[DE85-003617] 13 p2023 N85-22672
Hydrovolcanism 13 p2188 N85-23574
Structural Integrity and Durability of Reusable Space Propulsion Systems
[NASA-CP-2381] 17 p2910 N85-27941
Designing for fiber composite structural durability in hygrothermomechanical environment
[NASA-TM-87045] 17 p2917 N85-27978
Part played by non-metallic inclusions during deformation and fracture of steel with different grain sizes
[BLL-BISI-TRANS-22321-(9022.06)]
17 p2928 N85-28072

Laboratory investigation of formation damage of an artificial fracture at simulated geothermal conditions
[DE85-010301] 18 p3102 N85-29201
Hot Dry Rock Geothermal Energy Developement Program
[DE85-010570] 19 p3268 N85-30264
Failure analysis of fractured capscrews in centrifugal coolant compressor
[DE85-010029] 19 p3287 N85-30384
Comprehensive fracture diagnostics experiement. Part 2: Comparison of seven fracture azimuth measurements
[DE85-011707] 23 p3948 N85-34470

FRAGMENTATION
Fracture, failure, and fragmentation
01 p0059 N85-10390
Theoretical studies in molecular fragmentation: Processes, energetics and diagnostics
[AD-A146310] 03 p0418 N85-12673
The fragmentation of molecular clouds and the IMF
05 p0740 N85-14759
Study of the transition from deflagration to detonation of previously fragmented propellants
08 p1115 N85-17032
Experiment on triggered fragmentation on a molten copper droplet in water
[BLL-WH-602-(9091.9F)] 08 p1125 N85-17091
A T-matrix theory of galactic heavy-ion fragmentation
[NASA-TP-2363] 08 p1221 N85-17690
Fragmentation and turbulence in collapsing gas clouds
[DE85-003745] 11 p1633 N85-20282
Statistical theory of fragmentation processes
[DE85-002206] 11 p1653 N85-20414
Charge-to-mass dispersion methods for abrasion-ablation fragmentation models
[NASA-TM-86340] 11 p1726 N85-20857
Workshop on Nuclear Dynamics 3
[INC-40007-24] 12 p1931 N85-22130
Hydrovolcanism
13 p2188 N85-23574
Collisional outcomes in the asteroid belt
15 p2678 N85-26538
Frangibility of obstacles at airports
[NLR-MP-84002-U] 17 p2981 N85-28431
On high strain rate fragmentation of a closed vessel
23 p3904 N85-34187
On the importance of interstellar helium for the propagation of heavy cosmic rays
[OG-7.2-11] 23 p4015 N85-34879
Measurements of the fragmentation of (40)Ar, (28)Si and (12)C in CH2C and H targets between 300 and 1500 MeV/nuc at the Bevalac
[OG-7.2-19] 23 p4016 N85-34886
Measurements of Fe and Ar fragmentation cross sections
[OG-7.2-20] 23 p4016 N85-34887
Cross sections for the production of fragments with Z greater than or equal to 8 by fragmentation of Z greater than or equal to 9 and less than or equal to 26 nuclei
[OG-7.2-22] 23 p4016 N85-34889
Experimental data for characterizing perforating impacts: Fragmentation processes
[AD-A156370] 24 p4102 N85-35427
A test of the Feynman scaling in the fragmentation region
[HE-1.2-9] 24 p4172 N85-35867
Scaling violation in fragmentation region at energies above 10-15 eV based on the data on cosmic ray hadron component
[HE-3.1-11] 24 p4178 N85-35909
Peculiarities of gamma-quanta distribution at 20 TeV energy
[HE-3.7-10] 24 p4186 N85-35967

FRAGMENTS
Holographic assembly for measuring velocity fields of supersonic ballistic splinters at a large distance
[ISL-CO-203/84] 20 p3458 N85-31487
How are particle production, nucleon emission and target fragment evaporation processes interrelated in hadron-nucleus collisions?
24 p4174 N85-35878

FRAMES
NT AIRFRAMES
NT CHASSIS
NT UNDERCARRIAGES
Studies on reliability of structural systems
02 p0206 N85-11362
Iterative method for determining the distortion of elastic-plastic frames
[ISSN-0208-5658] 05 p0647 N85-14158
A general theory of circuit analogy in fracture diagnosis
[AD-A147177] 07 p0978 N85-16212
A study on a medium-sized rocket with Burnout frame
[NAL-TR-821] 09 p1287 N85-18082
Alternative approximation concepts for space frame synthesis
[NASA-CR-172526] 12 p1776 N85-21150
Spline curves, wire frames and B-value
17 p3006 N85-28587
Airborne sound transmission loss characteristics of wood-frame construction
[AD-A154174] 20 p3524 N85-31919

FRAMES (DATA PROCESSING)
Low-resolution target classification from a staring infrared sensor
[AD-A151690] 15 p2652 N85-26358
ZOG-Vinson technology demonstration project. Volume 2: System description
[AD-A153871] 19 p3333 N85-30645
ZOG/VINSON technology demonstration project system description. Volume 1
[AD-A154211] 19 p3342 N85-30713

FRAMING CAMERAS
Design and fabrication of a CCD camera for use with relay optics in solar X-ray astronomy
[NASA-CR-174334] 08 p1164 N85-17344

FRANCE
The French weather radar network: A status report
01 p0062 N85-10550
Deformation mechanisms associated with mesoscopic kinkbands, Jura Mountains (Switzerland) and Chaines Subalpines (France)
03 p0369 N85-12492
French commentary on Soviet industrial espionage
10 p1461 N85-19210
French panel makes specific proposals for robotics research. Current state of French robotics
11 p1618 N85-20180
French research minister on policy, technology transfer
11 p1618 N85-20182
SEP of France manufactures its first silicon carbide fibers
11 p1618 N85-20184
French activities relevant to middle atmosphere research
11 p1655 N85-20423
Statistics of french Armee de l'air ejections 1970 - 1980
12 p1906 N85-21971
Evaluation of wave energy resources on the French Atlantic seaboard
14 p2325 N85-24389
The ARGOS system and hydrology: The use of Platform Terminal Transmitter (PTT) with built-in memory and direct reception by the Seine basin hydrology service
14 p2326 N85-24389
Second Soviet-French Symposium on Space Cytology
14 p2366 N85-24699
West Europe report: Science and technology
[JPRS-WST-84-007] 15 p2530 N85-25600
Search and rescue of aircraft in distress in France. Organization, means
20 p3401 N85-31096
Specific aspects of maritime search and rescue in French metropolitan and overseas territories: Expected benefits from a detection and location of distress system by satellites
20 p3401 N85-31097
The SARSAT-COSPAS demonstration in France
20 p3405 N85-31131

FRANCK-CONDON PRINCIPLE
Measurement of Franck-Condon factors for the v'=0 progression in the B-X system of PO
[AD-A152734] 17 p2919 N85-27993
Calculation of Franck-Condon factors for diatomic molecules
[AD-A154463] 19 p3353 N85-30784

FRAUNHOFER LINES
Ten years observations of long-period oscillations of the Sun
14 p2450 N85-25123

FRAUNHOFER REGION
U FAR FIELDS

FREDHOLM EQUATIONS
Numerical solution of a first kind Fredholm integral equation arising in electron-atom scattering
[CWI-NM-R8414] 14 p2414 N85-24897
A program for solving first kind Fredholm integral equations by means of regularization
[CWI-NM-R8416] 17 p3022 N85-28697

FREDHOLM OPERATORS
U FREDHOLM EQUATIONS
U OPERATORS (MATHEMATICS)

FREE ATMOSPHERE
C2 sub n (optical) studies in the free atmosphere based on rawinsonde data
[AD-A147307] 07 p0997 N85-16332
A turbulent closure model for the free atmosphere
09 p1351 N85-18502

FREE BOUNDARIES
Diffusive combustion of fluids with free surface
02 p0274 N85-11785
Regularity of the free boundary for the porous medium equation
[AD-A147299] 08 p1210 N85-17611
Initial velocity of the emerging free boundary in a two-phase Stefan problem with imposed flux
[DE85-003813] 11 p1631 N85-20272
A new approach to queer differential equations
[AD-A149321] 15 p2638 N85-26272
A Navier-Stokes capillary free boundary in open boat crystal growth
[REPT-84-34] 17 p2960 N85-28283

FREE CONVECTION
Vertical channel free convection for a power law fluid with a constant heat flux
[DE84-014551] 01 p0047 N85-10311
Influence of Prandtl number on natural convection heat transfer correlations
[DE84-013006] 05 p0637 N85-14089
Theoretical description of film boiling in a two phase flow calculation
[IKE-2-66] 05 p0638 N85-14092
Unsteady free-convection heat transfer inside an annular cavity
[CFD/84/16] 08 p1163 N85-17339
Natural convection during heat accumulation by substances with change of aggregate state
13 p2043 N85-22787
Numerical benchmark study for the finite element computer code NEPTUNE
[DE85-006400] 17 p3013 N85-29630
Surface temperature distribution along a thin liquid layer due to thermocapillary convection
[NASA-TM-87115] 23 p3930 N85-34357

FREE ELECTRON LASERS
NRL (Naval Research Laboratory) FEL (Free Electron Laser) program
[AD-A145057] 01 p0052 N85-10347
Free electron lasers
[AD-A145109] 01 p0053 N85-10349
A covariant derivation of the ponderomotive force
[AD-A145054] 01 p0121 N85-10830
Summary discussion: Theoretical aspects of XUV free electron lasers
[AD-A145475] 02 p0202 N85-11343
Theory of free-electron lasers with focusing pumping field
02 p0262 N85-11714
Linear theory of free-electron lasers with cylindrical interaction space
02 p0262 N85-11716
A normal-incidence monochromator branch line on the FEL-undulator for experimental studies in the 5 to 30 eV region
[DE84-014379] 04 p0505 N85-13225
Laser-driven particle accelerators
[DE84-015953] 04 p0506 N85-13227
Accelerator Technology Program
[DE84-017083] 04 p0563 N85-13586
A proton laser accelerator by means of the inverse free electron laser mechanism
[DE85-000231] 06 p0813 N85-15163
Rippled-field magnetron apparatus
[AD-D011354] 07 p0969 N85-16154
A new free electron laser using a relativistic beam with spiralling electron
[AD-D011318] 07 p0971 N85-16165
Technology for satellite power conversion
[NASA-CR-174335] 09 p1343 N85-18451
Two-stage free electron laser research
[AD-A148951] 10 p1489 N85-19402
The axial velocity spread acceptance of free electron lasers
[AD-A149024] 10 p1489 N85-19403
A free electron laser with a rotating quadrupole wiggler
[AD-A149052] 10 p1489 N85-19404
Construction tolerances for low loss, dielectric coated, metallic waveguide for transmission optical radiation
[DE85-004056] 10 p1558 N85-19822
A free electron laser with two-component wiggler
11 p1623 N85-20217
Progress toward free electron lasers for applications
[DE85-002208] 11 p1639 N85-20326
Optical guiding in a free electron laser
[DE85-003141] 11 p1639 N85-20327
Novel probe for determining the size and position of a relativistic electron beam
[DE85-001044] 11 p1723 N85-20836
Betatron-synchrotron detrapping in a tapered wiggler free electron laser
[AD-A149686] 12 p1856 N85-21642
Resonance between betatron and synchrotron oscillations in a free electron laser: A 3-D numerical study
[AD-A150059] 12 p1857 N85-21645
Enhancing the performance of a high-gain free electron laser operating at millimeter wavelengths
[DE85-000862] 12 p1857 N85-21646
Los Alamos free electron laser: Accelerator performance
[DE85-005722] 13 p2097 N85-23084
Principle and design of a medium-enhanced free-electron laser
15 p2561 N85-25802
Stimulated Brillouin scattering reflectivity in the presence of various aberrators
[AD-A151750] 15 p2563 N85-25812

Free electron lasers for the EUV spectral region
[DE85-006804] 15 p2563 N85-25815
Microwave emission from relativistic electron beams
[AD-A151472] 15 p2648 N85-26333
Two-beam accelerator
[DE85-004662] 15 p2649 N85-26335
Low voltage free electron laser development
[AD-A152917] 17 p2970 N85-26342
Resonator optical designs for free electron lasers
[DE85-007678] 17 p2971 N85-26347
Report of the Working Group on Other Acceleration Schemes
[DE85-008447] 17 p3033 N85-28764
Review of short wavelength lasers
[DE85-009658] 18 p3114 N85-29277
The free electron laser variable bridge coupler
[DE85-009630] 18 p3114 N85-29278
Hamiltonian picture of the free electron laser and unitary symmetries
[PREPRINT-436] 18 p3114 N85-29281
Phase and amplitude considerations for the 2-beam accelerator
[DE85-008455] 18 p3180 N85-29715
Coherent X-rays and vacuum-ultraviolet radiation from storage-ring-based undulators and free electron lasers
[DE85-009968] 18 p3183 N85-29738
Conversion efficiencies of charged particle beam driven free electron lasers
[AD-A154404] 19 p3276 N85-30316
Recent results of the Los Alamos free-electron laser oscillator experiment
[DE85-010736] 19 p3277 N85-30324
Phase and amplitude feedback control system for the Los Alamos free-electron laser
[DE85-010787] 19 p3277 N85-30325
Los Alamos Free-Electron Laser (FEL) RF system
[DE85-010719] 19 p3278 N85-30329
High-brightness photoemitter development for electron accelerator injectors
[DE85-009548] 19 p3355 N85-30796
Grazing incidence beam expander
[DE85-010784] 19 p3368 N85-30889
New concepts in free electron lasers
20 p3480 N85-31493
Cerenkov maser and Cerenkov laser devices
[AD-A155443] 21 p3592 N85-32324
ATA upgrade to 150 MeV
[DE85-013174] 24 p4098 N85-35404
Los Alamos free-electron laser
[DE85-012866] 24 p4098 N85-35405

FREE ELECTRONS
A free electron laser with two-component wiggler
11 p1623 N85-20217
RF-Primed high power halogen vial apparatus
[AD-D011545] 12 p1935 N85-22158

FREE ENERGY
Thermodynamic properties and environmental chemistry of chromium
[DE84-015123] 01 p0025 N85-10152
Equation of state study for polar fluids
[PB84-222801] 01 p0025 N85-10157
Free energy and effective mass of the polaron at finite temperatures
[TUM-M8401] 03 p0417 N85-12667
Correlation of electronic charge transfer transitions and electrochemical potentials. The Bipyrazine(Tetracarbonyl)Molybdenum(O) system in various solvents
[AD-A147660] 08 p1120 N85-17062
Simple EOS for the silicone rubber Sylgard 184
[DE85-001394] 12 p1814 N85-21376
Low-dimensional behavior of the pattern formation Cahn-Hilliard equation
[DE85-003727] 12 p1922 N85-22072
Green's function solution of the Kondo problems and universality of the thermodynamic properties
[DE85-002739] 12 p1943 N85-22206
Noncontinuum solvent effects upon the intrinsic free-energy barrier for electron-transfer reactions
[AD-A150662] 14 p2250 N85-23943
Detonation behavior of LX-14 and PBX-9404: Theoretical aspect
[DE85-010038] 18 p3084 N85-29076
Influence of particle arrangement on sintering
[AD-A155337] 21 p3599 N85-32352

FREE FALL
Research relative to the development of a cryogenic microwave cavity gradiometer for orbital use
[NASA-CR-174249] 07 p0982 N85-16095
Reinterpretation of otolith input as a primary factor in space motion sickness 20 p3509 N85-31612

FREE FLIGHT
Thermal and cryogenic design study for space infrared telescope facility (SIRTF)
[NASA-CR-166613] 07 p0915 N85-15793

FREE FLIGHT TEST APPARATUS
The effect of instrumentation system parameters on the results of a flight mechanical system identification
24 p4061 N85-35170

FREE FLOW
Numerical analysis of the 3-dimensional inviscid hypersonic flow around capsule-type bodies by the alternate directional implicit method
[NAL-TR-799] 01 p0002 N85-10012
Preliminary results of a study of the relationship between free stream turbulence and stagnation region heat transfer
[NASA-TM-86684] 02 p0197 N85-11317
Solid sorbent air sampler
[NASA-CASE-MSC-20653-1] 11 p1636 N85-20301
Investigation of internal friction of free-flowing material during discharge
[BLL-M-36141-(5828.4)] 15 p2553 N85-25752
Study of the coupling between average, coherent and turbulent fields in a circular excited free jet
[ISL-R-115/83] 16 p2785 N85-27184
Computation model of turbulent free flow: Application to axisymmetric jets
[ISL-R-126/83] 16 p2785 N85-27185
Analyses of orderly structures in jets and the relationship with emitted noise
[ISL-R-117/83] 16 p2861 N85-27646
Transverse vorticity measurements using an array of four hot-wire probes
[FSFL-R-85-006] 18 p3099 N85-29184
On Fotonoff's mode 18 p3145 N85-29471
Transient combustion dynamics
[AD-A154430] 19 p3235 N85-30052
An investigation of hydraulic transients in combination free surface and pressurized flows
19 p3264 N85-30239
An experimental investigation of curvature and freestream turbulence effects on heat transfer and fluid mechanics in transitional boundary layer flows
19 p3264 N85-30240
Vortex simulation of v-shaped flame
20 p3425 N85-31259
A mathematical analysis of the effect of free stream turbulence on the Blasius boundary layer
20 p3451 N85-31430
Preliminary results of a study of the relationship between free-stream turbulence and stagnation region heat transfer
20 p3452 N85-31435
Vaporization from a heated surface into a saturated stream
[DE85-010484] 20 p3530 N85-31958
Experiments on the influence of active walls on the initial amplitudes and growths of instability waves
[AD-A154630] 21 p3583 N85-32275
Numerical solutions of turbulent models for flow over a flat plate with angle of attack
[DE85-010380] 21 p3585 N85-32286
Nozzle wall roughness effects on free-stream noise and transition in the pilot low-disturbance tunnel
[NASA-TM-86389] 23 p3930 N85-34355
Experimental study of free and mixed convective flow of air in a heated cavity
[DE85-012536] 24 p4094 N85-35380

FREE JETS
Computation of noise radiation from a free jet perpendicular to its axis via laser anemometry measurements
[ESA-TT-870] 09 p1379 N85-18669
Basic studies of multiple free and confined jets
[AD-A149556] 10 p1485 N85-19374
Velocity and volumetric measurement in free jets
11 p1576 N85-19931
Fourier densitometry: A new optical method for measuring density fluctuations by Rayleigh scattering — turbulent jets 11 p1576 N85-19932
Time-dependent flow of stream swirled in vortex chamber 13 p2043 N85-22786
Application of laser anemometry to jets in combustion chambers
[ISL-CO-210/83] 14 p2302 N85-24253
Laser anemometry two dimensional measurement of velocity fluctuations in an excited jet
[ISL-CO-213/83] 14 p2302 N85-24254
An automatic traversing system for Laser Doppler Anemometer (LDA) applications to wind tunnels and to free jets
[ISL-CO-225/83] 16 p2838 N85-27400
Aerosol analysis and emission spectrometry with free jets
[DE85-010576] 21 p3564 N85-32168
Measurement of velocity and concentration in free jets
[ISL-CO-215/84] 22 p3785 N85-33451

FREE MOLECULAR FLOW
Relation of core structure to high velocity outflow in G35.2-0.74 and other molecular clouds
03 p0443 N85-12818

FREE OSCILLATIONS
U FREE VIBRATION

FREE RADICALS
NT HYDROXYL RADICALS
Analysis of glow discharges for understanding the process of film formation
[NASA-TM-83750] 01 p0022 N85-10138
USSR report: Chemistry
[JPRS-UCH-84-012] 06 p0761 N85-14885
Time-resolved studies of free radicals and laser-initiated chain reactions
[DE85-002100] 09 p1326 N85-18332
Characterization of acetylene-terminated resin cure states
[AD-A149463] 10 p1452 N85-19148
Synthesis of hydrophobic, crosslinkable resins
[AD-A150858] 14 p2280 N85-24002
Free radicals in the stratosphere: A new observational technique 16 p2824 N85-27415
Role and fate of ozone in the atmosphere
16 p2824 N85-27421
Chemical transformation modules for Eulerian acid deposition models. Volume 1: The gas-phase chemistry
[PB85-173714] 18 p3072 N85-29001
Shock tube measurements of growth constants in the branched-chain ethane-carbon monoxide-oxygen system
[NASA-TM-87068] 21 p3562 N85-32158

FREE STREAM EFFECTS
U FREE FLOW

FREE STREAMS
U FREE FLOW

FREE VIBRATION
A rigid body mechanism in structural dynamics
02 p0206 N85-11361
The Shock and Vibration Digest, volume 16, no. 9
[AD-A146779] 07 p0976 N85-16200
A review of approximate methods for determining the vibrational modes of membranes
09 p1331 N85-18363
Effect of coupled torsional-flexural vibration of a geared shaft system on the dynamic tooth load
09 p1336 N85-18415
Effect of air cavity on the vibration analysis of loaded drums 09 p1339 N85-18422
A study of internal and distributed damping for vibrating turbomachiner blades
[NASA-CR-175901] 17 p2866 N85-27868
Applications of the Galerkin formalism in the coupling of the earth's free oscillations 24 p4116 N85-35514

FREEZE DRYING
Polyactic-polyglycolic acid copolymer combined with decalcified freeze-dried bone for use as a bone repair material
[AD-D011438] 10 p1451 N85-19142

FREEZING
NT ZONE MELTING
Forecasting water temperature decline and freeze-up in rivers
[AD-A147088] 07 p0987 N85-16274
Diurnal freeze-thaw frequencies in selected regions of the high latitudes
[AD-A147276] 07 p1007 N85-16400
Lake ice occurrence as a possible detector of atmospheric CO2 effects on climate
[DE85-002951] 11 p1687 N85-20806
Jet fuel property changes and their effect on producibility and cost in the U.S., Canada, and Europe
[NASA-CR-174840] 16 p2757 N85-27012
Fuel freeze point investigations
[AD-A152801] 17 p2937 N85-28129
The distribution of higher n-alkanes in partially frozen middle distillate fuels
[AD-A153940] 18 p3083 N85-29074
Onset of freezing in residential air-to-air heat exchangers
[DE85-009990] 19 p3267 N85-30259
A study of freezing and melting with eutectic interactions 19 p3378 N85-30858
On the problem of possible mechanism of ice nuclei formation in convective clouds 21 p3640 N85-32610
Supersaturation spect A of Ice Nuclei at different locations in Europe and over the North-Atlantic
21 p3640 N85-32615
Concentrations of ice nuclei of different modes of activities 21 p3641 N85-32616
Ice nucleating characteristics of Capparis Aphylla, an Indian herb 21 p3641 N85-32619
Ice-forming efficiency of the soluble and insoluble portions of dust contained in snow
21 p3643 N85-32631
Critical supersaturations with respect to water for fast condensation-freezing ice nucleation
21 p3643 N85-32632

Aircraft accident report: World Airways Inc., Flight 30H, McDonnell Douglas DC-10-30CF, N113WA, Boston-Logan International Airport, Boston, Massachusetts, January 23, 1982
[PB85-910406] 22 p3728 N85-33114
Land vehicle corrosion management 22 p3750 N85-33248
Refrigerated dynamic seal to 6.9 MPa (1000 psi)
[NASA-TM-87108] 23 p3930 N85-34356
Lake ice occurence as a possible detector of atmospheric CO2 effects on climate
[DE85-012987] 23 p3950 N85-34480

FREEZING POINTS
U MELTING POINTS

FREIGHT
U CARGO

FRENCH SATELLITES
NT SPOT (FRENCH SATELLITE)

FRENCH SPACE PROGRAMS
Non-US approaches to space commercialization 02 p0150 N85-11012
The 2 GHz network and the network operations center — satellite tracking 05 p0599 N85-13817
MATRA has Europe's largest white room for satellites 10 p1477 N85-19320
CNES, INRA do joint remote-sensing research 10 p1477 N85-19321
Activities in French aerospace 11 p1587 N85-19995
France officially proposes development of Ariane 5 to ESA 15 p2532 N85-25813
SEP of France to make Ariane HM-60 cryogenic engine 15 p2532 N85-25814
The French space program 22 p3731 N85-33127

FREON
Characteristics of controlled-oscillating annular cascade test facility with Freon gas
[NAL-TR-812] 01 p0003 N85-10014
Challenges in the development of the orbiter active thermal control subsystem 08 p1096 N85-16923
A feasibility study for using low boiling point fluids to change aircraft tire deflection
[AD-A152096] 16 p2706 N85-26701
Special features of the temperature dependence of the capillary constant in the vicinity of the critical point
[BLL-T6436/BG/LRS/LRST750/85] 16 p2659 N85-27632
Thermodynamic study of CO2-organic compound interaction at high pressures and temperatures
[DE85-010999] 19 p3268 N85-30266

FREQUENCIES
NT AUDIO FREQUENCIES
NT BEAT FREQUENCIES
NT BROADBAND
NT C BAND
NT CARRIER FREQUENCIES
NT CRITICAL FREQUENCIES
NT CYCLOTRON FREQUENCY
NT EXTREMELY HIGH FREQUENCIES
NT EXTREMELY LOW FREQUENCIES
NT EXTREMELY LOW RADIO FREQUENCIES
NT HIGH FREQUENCIES
NT INFRASONIC FREQUENCIES
NT INTERMEDIATE FREQUENCIES
NT LOW FREQUENCIES
NT MICROWAVE FREQUENCIES
NT PLASMA FREQUENCIES
NT RADIO FREQUENCIES
NT RESONANT FREQUENCIES
NT SUPERHIGH FREQUENCIES
NT SWEEP FREQUENCY
NT ULTRAHIGH FREQUENCIES
NT VERY HIGH FREQUENCIES
NT VERY LOW FREQUENCIES
Anomalies in frequency characteristics of solid-state ring laser 02 p0271 N85-11765
Characteristics of light diffraction by two acoustic waves, one with complex frequency composition 03 p0348 N85-12243
The investigation of short wave signal structure in the vicinity of the caustic by means of a high-directed antenna
[PR-194] 03 p0354 N85-12277
The ML (Maximum Likelihood) method for frequency estimation of real sinusoids in noise
[AD-A146053] 03 p0411 N85-12828
Analysis of frequency-selective integrated circuits in system of normal coordinates 04 p0489 N85-13119
Two programs for the HP9836C computer to acquire frequency or voltage data from a source
[AD-A146832] 06 p0854 N85-15430
An evaluation of flashtube signal characteristics
[AD-A146569] 10 p1423 N85-18974
Condensed antenna structural models for dynamics analysis 10 p1483 N85-19230
Spectrum resource assessment of the Aeronautical Mobile Service between 400 MHz and 17.7 GHz
[PB85-125995] 11 p1626 N85-20241
Frequency spectra of turbulent pulsations in stability of laminar boundary layer 11 p1716 N85-20795
Study of light shifts in laser pumped quantum discriminator frequency 11 p1716 N85-20798
Externally compensated crystal oscillator (ECXO) study
[AD-A150335] 13 p2084 N85-22893
Programmable filter with fanned interdigital surface acoustic wave transducer 13 p2083 N85-23008
Adsorption site, adsorption energy and normal vibration frequency of H/Ni(100) via total energy calculations
[AD-A150555] 13 p2156 N85-23388
A study of frequency effects and damage accumulation during the fatigue of graphite/epoxy and glass/epoxy composite materials 14 p2247 N85-23930
Design and measured performance of a broadband Archimedes spiral antenna
[R-NIAS-22] 14 p2290 N85-24194
The sensitivity of solar eigenfrequencies to the treatment of the equation of state 14 p2445 N85-25089
Frequency selective signals-to-noise enhancer/limiter apparatus
[AD-D011583] 15 p2548 N85-25724
Adjustment of the frequency-temperature characteristics of crystal oscillators
[AD-D011588] 15 p2548 N85-25726
An atlas of pure water vapor spectra from 500 to 5000/cm, Volume 2
[AD-A151757] 16 p2745 N85-26940
Relationship between Allan variances and Kalman Filter parameters 16 p3107 N85-29238
Temperature sensitive oscillator
[NASA-CASE-GSC-12956-1] 19 p3258 N85-30201
Experimental determination of the mixing frequency parameter for coalescence/dispersion modeling of turbulent combustion
[DE85-011468] 19 p3270 N85-30260
Some studies in filtering of atmospheric turbulence
[AD-A154042] 19 p3316 N85-30557
The problem of brightness enhancement during laser frequency doubling 21 p3686 N85-32897
International prototype network in Dubna experimental satellite communications system 22 p3773 N85-33383
Gradiental adaptive corrector with optimum tuning step 22 p3776 N85-33403
Calculating dominant (quasi-t) mode group velocity in shielded microstrip line 22 p3780 N85-33422

FREQUENCY ANALYZERS
Magnetostatic wave frequency analyzer apparatus
[AD-D011249] 05 p0631 N85-14044
Use of electronic coding-frequency meters to measure parameters of pulsed radio signals 13 p2076 N85-22964
Rotor blade test apparatus
[AD-D011725] 23 p3934 N85-34381

FREQUENCY ASSIGNMENT
Planning guide for the review of telecommunications systems for frequency availability and electromagnetic compatibility
[PB84-210238] 01 p0041 N85-10268
Radar frequency selection strategies
[AD-A147493] 07 p0941 N85-15867
A commentray on the utilization of real-time channel evaluation systems in HF spectrum management
[AD-A148616] 08 p1154 N85-17289
A description of the NRL oblique-incidence-ionogram data base
[AD-A148625] 08 p1230 N85-17748
Spectrum resource assessment of the 1530-1660.5 MHz band
[NTIA/REPT-84/160] 10 p1469 N85-19268
Spectrum resource assessment of the 7125-8500 MHz band
[PB85-127413] 11 p1626 N85-20242
Spectrum resource assessment of the fixed and mobile services in the 947-17,700 MHz band, phase 1
[PB85-128286] 11 p1626 N85-20243
Engineering calculations for communications satellite systems planning
[NASA-CR-175552] 12 p1789 N85-21233
Frequency selection for dispersion signal in satellite communication lines 15 p2528 N85-25584
Propagation considerations in land mobile satellite transmission
[NASA-CR-175733] 15 p2540 N85-25684
Optimal frequencies for broadcast transmitters in the UHF domain: Report
[TUM-M8404] 16 p2769 N85-27068
Generalized graph coloring: A frequency assignment method for VHF broadcasting
[TUM-M8405] 16 p2844 N85-27535
Criteria for site selection and frequency allocation (keynote paper), part 5 21 p3623 N85-32511
Frequency and site selection criteria for MST radars, part 5.1A 21 p3624 N85-32512

FREQUENCY BANDS
U FREQUENCIES

FREQUENCY CONTROL
NT AUTOMATIC FREQUENCY CONTROL
Diagnostic apparatus for radar pulse repetition frequency control circuit card
[AD-D011364] 07 p0937 N85-15938
Low noise multiple crystal-controlled oscillator
[AD-D011401] 07 p0948 N85-16010
Improved magnetic bias and delay linearity in a magnetostatic wave delay line
[AD-D011441] 10 p1479 N85-19337
Stereo decoder without subcarrier restoration 13 p2068 N85-22921
Gyrator frequency selectors with bandwidth independent of input signal level 13 p2083 N85-23009
System of phase-lock automatic frequency control with acoustoelectronic convolver 15 p2526 N85-25573
Simultaneous phase and frequency control of a three-phase inductor-convertor bridge
[DE85-006197] 18 p3086 N85-29164
Rubidium and cesium frequency standards status and performance on the GPS program 18 p3106 N85-29226
A miniature tactical Rb frequency standard 18 p3106 N85-29229
The Rubidium-Crystal Oscillator Hybrid Development Program 18 p3106 N85-29230
New features of different frequency generating systems due to the use of electrodeless rigidly mounted VBA quartz crystal resonator 18 p3106 N85-29231
The system design of a rubidium maser frequency standard 18 p3106 N85-29232
Maintenance of time and frequency in the Jet Propulsion Laboratory's Deep Space Network using the Global Positioning System 18 p3109 N85-29249
A variable frequency control for three-phase induction motors 19 p3256 N85-30190

FREQUENCY CONVERSION
U FREQUENCY CONVERTERS

FREQUENCY CONVERTERS
NT DOWN-CONVERTERS
NT FREQUENCY DIVIDERS
NT FREQUENCY MULTIPLIERS
NT FREQUENCY SYNTHESIZERS
NT PARAMETRIC FREQUENCY CONVERTERS
NT UP-CONVERTERS
15 kW general purpose frequency changer performance improvement
[AD-A145503] 02 p0194 N85-11297
A means of extending streak camera recording into the important 1300-1600 nm wavelength regime: Parametric frequency upconversion
[DE84-015666] 04 p0503 N85-13208
VLBI system (BLK I) IF-video down conversion design 05 p0625 N85-13998
Charge depletion meter
[AD-D011484] 10 p1488 N85-19393
Development of a 20 GHz modulator for the payload of a satellite for propagation and transmission experiments, including the required converters of the test equipment
[BMFT-FB-W-84-044] 11 p1590 N85-20004
Wideband phase keyers 12 p1839 N85-21544
Magnetic noise in single-machine rotating frequency converters 13 p2077 N85-22969
Converters of sum/difference of codes to frequency 15 p2526 N85-25578
Lidar ER2 (ozone). Crystal characterization for harmonic conversion — laser systems
[CERT-2/6129-00] 16 p2872 N85-27717

FREQUENCY DISCRIMINATORS
Multiple passband transducers for tone selection from a frequency comb generator
[RSRE-MEMO-3647] 02 p0194 N85-11295
Analysis of characteristics of digital discriminators for phase-shift keyed signals 13 p2070 N85-22930

FREQUENCY DISTRIBUTION
Three algorithms for parametric frequency domain system identification
[DE85-002801] 11 p1706 N85-20735
Problem of frequency space variation of sonic field in stratified media 11 p1715 N85-20787
Noise immunity of information transmission system with pseudorandom frequency switching under worst-case interference conditions 13 p2066 N85-23029
A statistical treatment of the regional slope characteristics of Venus and Earth 13 p2178 N85-23517
Transient combustion dynamics
[AD-A154430] 19 p3235 N85-30052

The determination of daily usage or occupancy in the land-mobile band 138-174 MHz at Montreal
[CRC-1383] 19 p3253 N85-30167
Scattering by distributions of small thin particles
19 p3253 N85-30172
Coding schemes for improving MST radar performance, part 7.1A 21 p3625 N85-32520
Gamma ray burst size-frequency distributions: Spectral selection effects
[OG-1.2-3] 22 p3862 N85-33913
Burst size distributions in the digitized data of the ion chambers t Mt. Norikura and sea level stations
[SH-9.1-9] 23 p4051 N85-35124
Performance of a local electron density trigger to select extensive air showers at sea level
[HE-4.6-11] 24 p4186 N85-36048

FREQUENCY DIVIDERS
Investigation of characteristics of phased antenna array considering interaction between radiators and properties of power divider 06 p0790 N85-15051
A noise-suppressing digital frequency meter
06 p0796 N85-15084

FREQUENCY DIVISION MULTIPLE ACCESS
Throughput increase in frequency hopped multiple access channels by means of discrimination against partially overlapping interference
[AD-A145540] 02 p0191 N85-11275

FREQUENCY DIVISION MULTIPLEXING
Fiber optic data bus using Frequency Division Multiplexing (FDM) and an asymmetric coupler
[NASA-TM-86015] 04 p0492 N85-13139
Preliminary estimation of mutual interference between fixed satellite service systems 15 p2526 N85-25586

FREQUENCY HOPPING
Throughput increase in frequency hopped multiple access channels by means of discrimination against partially overlapping interference
[AD-A145540] 02 p0191 N85-11275
Spread-spectrum communications
[AD-A146135] 03 p0355 N85-12285
Optimum jamming effects on frequency-hopping M-ary FSK (Frequency-Shift Keying) systems under certain ECCM (Electronic counter-countermeasures) receiver design strategies
[AD-A147786] 06 p1151 N85-17267
Research on adaptive antenna techniques 6
[AD-A149341] 11 p1624 N85-20228
Tactical satellite terminals for land and airborne C3 applications 11 p1710 N85-20760
Spread spectrum mobile radio communications
[AD-A149936] 12 p1829 N85-21477
FH/MFSK performance in multitone jamming
[NASA-CR-175667] 14 p2290 N85-24197
Spectroscopic investigation of materials for frequency agile laser systems
[AD-A151731] 16 p2790 N85-27206
Measured noise performance of a new method of frequency hopping
[AD-A152679] 17 p2953 N85-28234

FREQUENCY MEASUREMENT
Spectral noise density and random errors of pulse frequency characteristic meters
03 p0346 N85-12231
A group delay standard for the MHz frequency range
05 p0630 N85-14040
Infralow-frequency digital phase meter
06 p0787 N85-15031
A noise-suppressing digital frequency meter
06 p0796 N85-15084
NBS frequency measurement system from a user's viewpoint
[DE84-016782] 09 p1315 N85-18268
Historical cost curves for hydrogen masers and cesium beam frequency and timing standards
10 p1465 N85-19245
Use of electronic coding-frequency meters to measure parameters of pulsed radio signals
13 p2076 N85-22964
Space-based antenna measurement system concepts for space station operation 14 p2236 N85-23660
Experimental performance of a frequency measurement circuit
[AD-A152951] 17 p2953 N85-28239
New time and frequency services at the National Bureau of Standards 17 p2961 N85-28289
Methods for optimal recursive estimation of non-stationary time series, applications to atomic time and frequency metrology 17 p2965 N85-28312
Ionospheric limitations to time transfer by satellite
18 p3107 N85-29234
Maintenance of time and frequency in the Jet Propulsion Laboratory's Deep Space Network using the Global Positioning System 18 p3109 N85-29249
Using GPS and VLBI technology to maintain 14 digit synchronization 18 p3109 N85-29250
Performance test results of a low cost GPS time and frequency monitor 18 p3109 N85-29252
Fiber optic sensors operating at dc
[AD-D011674] 19 p3271 N85-30283
New measurement solutions for low frequency systems 20 p3437 N85-31325
Characterization of microstrip discontinuities in the time and frequency domains
[NASA-CR-176190] 24 p4066 N85-35342

FREQUENCY MODULATION
NT FREQUENCY SHIFT KEYING
NT PULSE FREQUENCY MODULATION
Self-modulation of injection laser emission intensity due to external optical feedback 02 p0261 N85-11706
Analog voice processing for FM transmission in a telephone channel
[INPE-2798-PRE/359] 03 p0354 N85-12279
Radio telemetry formula applications. A practical users guide
[AD-A146247] 03 p0356 N85-12286
Television transmission in frequency modulation
04 p0493 N85-13146
Structure of frequency modulated and phase-shift keyed signals reflected from ionosphere at near-critical frequencies 07 p0952 N85-16035
BBC receiving terminal for the European orbital test satellite
[BBC-RD-1984/15] 08 p1142 N85-17205
EMC enhanced constant Z modulator
[AD-A147715] 08 p1157 N85-17297
Subjective evaluation of the effect of noise and interference on frequency modulated NTSC television signals
[CRC-1367] 09 p1310 N85-18230
Generation of Alfven waves due to thermal modulation of the electrical conductivity
[AD-A149389] 10 p1558 N85-19826
Signal processing and range spreading in the FM-CW radar
[PB85-108256] 11 p1626 N85-20239
Space-time response characteristics of acoustooptic filter for compression of linearly frequency-modulated signal 13 p2071 N85-22937
Simple detonation meter 13 p2077 N85-22971
Synthesis of optimum single-channel discrete signals and filters 13 p2080 N85-22990
Analysis of interference caused by interfering radio signals in communications systems with frequency separation of telephone channels and frequency modulation 13 p2088 N85-23025
Preliminary estimation of mutual interference between fixed satellite service systems 15 p2526 N85-25586
An analysis of jamming effects on noncoherent digital receivers
[AD-A153791] 18 p3090 N85-29128
Analog frequency modulated laser using magnetostriction
[AD-D011701] 19 p3276 N85-30318
Use of radar with frequency modulation for studying atmospheric boundary layer 19 p3296 N85-30437
Controllable companding in low-frequency FM radio communication systems 22 p3776 N85-33402
Device for frequency modulation of a laser output spectrum
[DE85-011634] 22 p3790 N85-33479

FREQUENCY MULTIPLIERS
Infralow-frequency digital phase meter
06 p0787 N85-15031
A phase-locked frequency multiplier for the signal averaging of the vibration of the Wessex helicopter input spiral bevel pinion
[AD-A154914] 21 p3555 N85-32113

FREQUENCY RANGES
Statistical properties of geomagnetic pulsations at the Observatory of Fuerstenfeldbruck determined with the aid of pulsation indices. Part 2: Periodicity in the occurrence of pulsations
[REPT-566] 03 p0376 N85-12369
Propagation and scattering considerations for the 0.2-3.0 GHz frequency range for a space-based radar
[AD-A148504] 08 p1153 N85-17282
Solid Rocket Motor Case (SRMC) dynamic sensitivity to changes in composite properties
12 p1948 N85-22238
Observations of intermediate-degree solar oscillations
14 p2442 N85-25069
The medical results of human exposures to radio frequency radiation 16 p2776 N85-27133
Frequent observations of extragalactic compact sources at 24 GHz 19 p3386 N85-31003
VLF (Very low frequency) workshop held at San Diego California, 24-25 January 1985
[AD-A154652] 21 p3573 N85-32224

FREQUENCY REGULATION
U FREQUENCY CONTROL

FREQUENCY RESPONSE
Complex frequency analysis of damped thin-walled beams with open cross sections
03 p0371 N85-12366
Frequency response design methods for large scale systems
[DE84-014161] 04 p0553 N85-13517
Application of the hydraulic system frequency response program to propellant feed systems
[AD-A151624] 16 p2741 N85-26914
An interactive computer aid for the design and analysis of linear, single input/single output digital and continuous control systems
[AD-A153704] 18 p3162 N85-29589

FREQUENCY REUSE
Mechanical/thermal design of a polarization sensitive reflector — communication satellites
05 p0626 N85-14009

FREQUENCY SCANNING
Optical 3-D signature device for detecting chemical agents
[AD-D011669] 19 p3272 N85-30293

FREQUENCY SHIFT
Frequency shifting in multimode fiber optic phase modulation devices 03 p0347 N85-12239
Tropospheric and ionospheric phase perturbations and Doppler frequency shift effects
[AD-A148579] 08 p1154 N85-17283
Atmospheric limitations in stellar seismology: Should one measure radial velocity or brightness fluctuations?
08 p1251 N85-17899
Propagation effects on the Doppler frequency shift of satellite transmissions 10 p1470 N85-19276
Nonlinear saturation of stimulated Raman scattering in homogeneous plasma
[DE85-003120] 10 p1560 N85-19837
Study of light shifts in laser pumped quantum discriminator frequency 11 p1716 N85-20796
Experimental studies of low temperature surface interactions of atomic hydrogen using maser technique
[AD-A150216] 13 p2017 N85-22647
Acceleration-resistant crystal resonator
[AD-D011627] 16 p2778 N85-27144
On the accuracy of Cs beam primary frequency standards 18 p3105 N85-29224
Performance data of US Naval Observatory VLG-11 hydrogen masers since September, 1983
18 p3108 N85-29244
Accuracy in determining velocity of fluid movement by Doppler method 19 p3293 N85-30419
Design of a jamming simulator for a binary communication system
[AD-A154617] 21 p3573 N85-32221
Mesospheric measurements of irregularity patches using a 3-antenna interferometer, part 3.6B
21 p3621 N85-32496
Doppler spectrometer for measuring narrow photochemical gaps in inhomogeneously broadened spectra 21 p3689 N85-32921
HEAO 3 upper limits to the expected 1634 KeV line from SS 433
[OG-2.4-9] 22 p3868 N85-33954
Search for gamma ray lines from SS433
[OG-2.4-11] 22 p3868 N85-33955
DMSK: A practical 2400-bps receiver for the mobile satellite service: An MSAT-X Report
[NASA-CR-176194] 24 p4086 N85-35324
Scale separation closure and Alfven wave turbulence
[DE85-013124] 24 p4095 N85-35385

FREQUENCY SHIFT KEYING
Optimum jamming effects on frequency-hopping M-ary FSK (Frequency-Shift Keying) systems under certain ECCM (Electronic counter-countermeasures) receiver design strategies
[AD-A147786] 06 p1151 N85-17267
Ionospheric distortions of digital signals with wideband modulation 13 p2072 N85-22945
FH/MFSK performance in multitone jamming
[NASA-CR-175667] 14 p2290 N85-24197
Rational pulse-shaping filters for almost MSK-like modulation
[AD-A153065] 17 p2949 N85-28206

FREQUENCY STABILITY
Frequency stabilized laser
[AD-D011223] 01 p0053 N85-10351
Device for frequency stabilization of microwave oscillators 06 p0789 N85-15033
Reference oscillator stability effect on clutter cancellation in a radar system 07 p0938 N85-15946
Low noise multiple crystal-controlled oscillator
[AD-D011401] 07 p0948 N85-16010
The Statistical Loop Analyzer (SLA)
06 p1100 N85-16955
Measurement procedures for the radar spectrum engineering criteria
[PB85-119022/GAR] 09 p1313 N85-18254

Synthesis of digital nonrecursive band-elimination filters for moving-target selectors 12 p1840 N85-21545
Coupled acoustic and hydrodynamic wave instabilities 13 p2000 N85-22536
Spectral frequency of eigenvalues in optimal problems of stability of cylindrical shells of variable thickness 13 p2047 N85-22815
Effect of variance of photoreceiver frequency characteristics on characteristics of measuring instruments 13 p2076 N85-22965
Experimental study of high-stability oscillator with surface-acoustic-wave resonator in feedback loop 13 p2090 N85-23053
Separating the variances of noise components in the Global Positioning System [AD-P004576] 17 p2963 N85-28295
A new precision time and frequency source for stationary PTTI applications 17 p2963 N85-28297
On-orbit frequency stability analysis of the GPS NAVSTAR's 3 and 4 rubidium clocks and NAVSTAR's 5 and 6 cesium clocks 17 p2963 N85-28296
Improved master clock reference system at USNO 17 p2963 N85-28300
Test results for prototype GPS rubidium clocks 17 p2964 N85-28302
Clock characterization tutorial 17 p2965 N85-28311
The measurement of linear frequency drift in oscillators 17 p2966 N85-28316
High performances from a new design of crystal oscillator 17 p2966 N85-28318
Recent results on the peformance of EFOS, NP and NX hydrogen masers 17 p2966 N85-28320
Physics element design aspects for a tactical rubidium frequency standard 17 p2967 N85-28321
Proceedings of the Sixteenth Annual Precise Time and Time Interval (PTTI) Applications and Planning Meeting [NASA-TM-87561] 18 p3105 N85-29221
On-orbit frequency stability analysis of the GPS NAVSTAR-1 quartz clock and the NAVSTARs-6 and -8 rubidium clocks 18 p3105 N85-29227
Investigation of fast reaction SAW (Surface Acoustic Wave) accelerometer [AD-A153676] 19 p3216 N85-29943
Self-tuning adaptive-controller using online frequency identification 20 p3417 N85-31205
RF stabilization of interchange-ballooning modes [DE85-012090] 24 p4090 N85-35953

FREQUENCY STANDARDS
Portable real-time clock [AD-A146218] 03 p0364 N85-12336
NBS frequency measurement system from a user's viewpoint [DE84-016782] 09 p1315 N85-18268
Experimental studies of low temperature surface interactions of atomic hydrogen using maser technique [AD-A150216] 13 p2017 N85-22647
Lifetime and reliability of rubidium discharge lamps for use in atomic frequency standards [AD-A150787] 14 p2417 N85-24915
Maintenance of time and frequency in the DSN using the global positioning system 16 p2771 N85-27105
New time and frequency services at the National Bureau of Standards 17 p2961 N85-28289
Recent improvements in the atomic time scales of the National Bureau of Standards 17 p2962 N85-28290
Enhacements to the TTS-502 time transfer system 17 p2963 N85-28296
A new precision time and frequency source for stationary PTTI applications 17 p2963 N85-28297
Improved master clock reference system at USNO 17 p2963 N85-28300
Test results for prototype GPS rubidium clocks 17 p2964 N85-28302
Timing-system design considerations for a mobile astrolabe 17 p2965 N85-28309
A plan for the development of inertial reconstruction of initial state clock (IRIS) 17 p2966 N85-28317
Physics element design aspects for a tactical rubidium frequency standard 17 p2967 N85-28321
The superconducting cavity stability ruby maser oscillator 17 p2967 N85-28324
Proceedings of the Sixteenth Annual Precise Time and Time Interval (PTTI) Applications and Planning Meeting [NASA-TM-87561] 18 p3105 N85-29221
Prospects for atomic frequency standards 18 p3105 N85-29222
Frequency and time standards based on stored ions 18 p3105 N85-29223
On the accuracy of Cs beam primary frequency standards 18 p3105 N85-29224
Methods to recover the narrow Dicke sub-Doppler feature in evacuated wall-coated cells without restrictions on cell size 18 p3105 N85-29225
Diode laser 87Rb optical pumping in an evacuated wall-coated cell 18 p3105 N85-29226
Rubidium and cesium frequency standards status and performance on the GPS program 18 p3106 N85-29228
A miniature tactical Rb frequency standard 18 p3106 N85-29229
The Rubidium-Crystal Oscillator Hybrid Development Program 18 p3106 N85-29230
New features of different frequency generating systems due to the use of electrodeless rigidly mounted VBA quartz crystal resonator 18 p3106 N85-29231
The system design of a rubidium maser frequency standard 18 p3106 N85-29232
Maser and secondary clock in telecommunications networks 18 p3108 N85-29248
The time and frequency comparisons via Loran-C and National TV Network in Yugoslavia 18 p3109 N85-29248
The role of long term lamp fluctuations in the random walk of frequency behavior of the rubidium frequency standard: A case study [AD-A155338] 21 p3500 N85-32314

FREQUENCY SYNCHRONIZATION
Fundamental limits to synchronization and tracking [AD-A149623] 12 p1833 N85-21504
Foreshortened short-wave scattering on artificial ionospheric inhomogeneities 14 p2340 N85-24468
Clock synchronization by the Symphonie and Laser Synchronization from Stationary Orbit (LASSO) geostationary satellites 14 p2398 N85-24778
Timing accuracy of LF and TV synchronization techniques 17 p2961 N85-28288
The role of a low Earth orbiter in intercontinental time synchronization via GPS satellites 17 p2964 N85-28306
Using GPS and VLBI technology to maintain 14 digit synchronization 18 p3109 N85-29250
Global positioning system carrier phase: Description and use [PB85-174126] 19 p3216 N85-29946
General design principles of high speed frequency synthesizers based on phase synchronization systems 22 p3779 N85-33417

FREQUENCY SYNTHESIZERS
EMC enhanced constant Z modulator [AD-A147715] 08 p1157 N85-17297
Tranedigitizer for relaying signals from Global Positioning System (GPS) satellites [AD-D011442] 10 p1422 N85-18970
Regular synthesis of pairs of phase-keyed binary minimax signals 13 p2069 N85-22923
Theory of optimum M-filtration of signals against background of correlated interference 13 p2069 N85-22927
Optimal synthesis of surface acoustic wave filters 13 p2070 N85-22933
Simple sweep frequency generator 13 p2075 N85-22960
Reactanceless synthesized impedance bandpass amplifier [NASA-CASE-GSC-12768-1] 18 p3093 N85-29145
A low noise synthesizer for autotuning and performance testing of hydrogen masers 18 p3108 N85-29242
Design of high-order analog and digital filters with identical sections 22 p3766 N85-33341
General design principles of high speed frequency synthesizers based on phase synchronization systems 22 p3779 N85-33417

FREQUENCY TRANSLATION
U FREQUENCY CONVERTERS

FRESH WATER
Identification and parameter estimation of phosphate balance models in drinking water reservoirs [PUBL-313] 06 p1181 N85-17439
Operational performance of the photovoltaic-powered grain mill and water pump at Tangaye, Burkina Faso (formerly Upper Volta) [NASA-TM-86970] 13 p2128 N85-23243
Sulfur cycling in freshwater sediments 21 p3658 N85-32726

FRESNEL DIFFRACTION
Optimization piezoelectric transducer width of acousto-optical devices 07 p0950 N85-16024
The evaluation of a deformable diffraction grating for a stigmatic EUV spectrohelliometer [NASA-CR-174248] 07 p1042 N85-16821
Morphology of the scattering targets: Fresnel and turbulent mechanisms, part 2.1A 21 p3618 N85-32481

FRESNEL LENSES
Research on materials and components for opto-electronic signal processing [AD-A145808] 03 p0433 N85-12754
A second generation WAVIDS (Wide Angle Virtual Image Display System) [AD-P004328] 09 p1270 N85-17982
Phase 2 fabrication and construction of the Sky Harbor Airport, solar photovoltaic concentrator project [DE85-000019] 11 p1676 N85-20561
Design and development of a linear Fresnel lens air-cooled photovoltaic module and a stand-alone photovoltaic collector array [DE85-006854] 16 p2819 N85-27391
Development of a second-generation linear Fresnel Photovoltaic and Thermal (PVT) concentrator array, including fabrication and installation of a 200 square meter collector field [DE85-008473] 17 p2988 N85-28485
DOE/Sandia point-focus concentrator program, draft [DE85-008209] 17 p3038 N85-28793
Visual and part-task manipulations for teaching simulated carrier landings [AD-A153822] 18 p3154 N85-29529

FRESNEL REFLECTORS
Magnetism at interfaces and surfaces, as probed by neutron scattering [DE85-007987] 18 p3176 N85-29690

FRESNEL REGION
A modified Fresnel scattering model for the parameterization of Fresnel returns, part 2.3A 21 p3618 N85-32483

FRETTING
Fretting corrosion and fretting fatigue of medium carbon steels 01 p0054 N85-10358
Effect of humidity on fretting wear of several pure metals [NASA-TP-2403] 04 p0472 N85-13006
Comparison of the fatigue resistance (initiation, propagation) of cast TA6V with hot rolled TA6V — titanium alloy [DGT-25369-PT-1] 12 p1808 N85-21341

FRETTING CORROSION
Fretting corrosion and fretting fatigue of medium carbon steels 01 p0054 N85-10358

FRICTION
NT AERODYNAMIC DRAG
NT DRY FRICTION
NT FLOW RESISTANCE
NT FRICTION DRAG
NT INTERNAL FRICTION
NT KINETIC FRICTION
NT SKIN FRICTION
NT SLIDING FRICTION
NT VISCOUS DRAG
Pavement friction measurements on nontangent sections of roadways, vol. 1 [PB84-219732] 01 p0036 N85-10227
Laminar flow heat exchangers. Viscosity induced non-uniform flow [AD-A144777] 01 p0047 N85-10307
Structure and wear workshop colloquium 01 p0054 N85-10356
The influence of surface layers on the friction and wear behavior of materials 01 p0054 N85-10357
Friction and wear of polymers and polymer composite materials 01 p0054 N85-10361
Friction, wear and structure of heterogeneous materials 01 p0055 N85-10362
Surface segregation of sulfur during oscillatory pin-on-plate wear studies of precious metal electrical contact alloys. 1: Friction and electrical contact resistance [DE84-006962] 02 p0195 N85-11303
Comparison of predicted and measured friction for a tilt-pad thrust bearing with crown and roughness under hydrodynamic and mixed lubrication [AD-A145752] 03 p0371 N85-12371
Thermomechanical cracking in layered media from moving friction load [AD-A146022] 03 p0373 N85-12379
Roller crosshead analysis 04 p0507 N85-13238
Alternatives for runway rubber removal from porous friction surfaces [DOT/FAA/PM-84/28] 05 p0597 N85-13803
An Iwatsubo-based solution for labyrinth seals - comparison with experimental results 05 p0644 N85-14131
Analysis for leakage and rotordynamic coefficients of surface roughened tapered annular gas seals 05 p0644 N85-14135
Conditions for assembling dies for drawing under hydrodynamic friction conditions [BLL-M-35954-(5826.4)] 05 p0647 N85-14153
Friction and heat exchange in laminar and turbulent boundary layers with axisymmetrical bodies exposed to heterogeneous supersonic flow 05 p0724 N85-14655
The fate of globular clusters 05 p0739 N85-14751
Effects of silver and group 2 fluorides addition to plasma sprayed chromium carbide high temperature solid lubricant for foil gas bearing to 650 deg C [NASA-TM-86895] 06 p0770 N85-14928

Fundamental tribological properties of ceramics
[NASA-TM-88915] 07 p0930 N85-15893
Experimental test program for evaluation of solid lubricant coating as applied to compliant foil gas bearings to 315 deg C
[NASA-CR-174837] 07 p0930 N85-15895
Surface effects of corrosive media on hardness, friction, and wear of materials
[NASA-TM-83711] 07 p0930 N85-15896
Antifriction nickel-phosphorous coatings on aluminum alloy products 09 p1309 N85-18221
Temperature prediction in mechanical components, an analytical approach 09 p1327 N85-18339
Stochastic dynamic analysis of a structure with frictional joints 09 p1337 N85-18406
Antifriction properties of gas thermal coatings of clad carbine powders 10 p1447 N85-19115
Effect of implantation species on the tribological response of stainless steel surfaces
[DE85-003530] 10 p1493 N85-19432
Techniques to analyze vehicle coastdown data
[DE85-005159] 12 p1772 N85-21127
Tribological properties of boron nitride synthesized by ion beam deposition
[NASA-TM-86962] 12 p1810 N85-21355
Tribological systems as applied to aircraft engines
[NASA-TM-86965] 12 p1858 N85-21657
Skid steering of wheeled and tracked vehicles: Analysis with Coulomb friction assumptions
[AD-A149826] 12 p1860 N85-21664
Dissipation of energy in composite material 13 p2027 N85-22703
High temperature antifriction properties of Ti sub 1-sub xNb sub x C sub 0.5N sub 0.5 alloys 13 p2029 N85-22715
Effect of zero-wear in friction pairs operating in abrasive media 13 p2045 N85-22801
Model of friction bearing hydrodynamics 14 p2288 N85-24178
Hermetic sealing of nonlubricated gas seal and friction characteristics, chapter 7
[DE85-006375] 15 p2569 N85-25851
Metal armatures for railguns
[AD-A152129] 16 p2728 N85-26838
Breakway friction and dynamic friction/wear measurements of various ceramic materials from 25 C (75 F) to 650 C (1200 F)
[NASA-CR-174803] 16 p2754 N85-26994
Friction and wear behavior of aluminum and composite I-beam stiffened airplane skins
[NASA-TM-86418] 17 p2895 N85-27852
Studies on surface processes during friction and wear
[AD-A153509] 18 p3117 N85-29296
Study of the chemical mechanism in lubrication
[DE85-010768] 19 p3228 N85-30013
Mechanical modification of friction surfaces of aluminum alloys by friction transfer 19 p3241 N85-30097
Numerical solutions of turbulent models for flow over a flat plate with angle of attack
[DE85-010360] 21 p3585 N85-32286
Surface roughness effects in elastohydrodynamic contacts
[NASA-TP-2468] 21 p3595 N85-32329
The stress distribution in pin-loaded orthotropic plates
[NASA-CR-176146] 22 p3800 N85-33547
Three body abrasive wear in various metal combinations 23 p3906 N85-34200
Lubrication and cooling for high speed gears
[NASA-TM-87096] 23 p3938 N85-34407
Friction, impact, and electrostatic discharge sensitivities of energetic materials
[DE85-013321] 24 p4083 N85-35309
The use of austenitic stainless steel versus monel (Ni-cu) alloy in pressurized Gaseous Oxygen (GOX) life support systems
[AD-A156305] 24 p4134 N85-35625

FRICTION COEFFICIENT
U COEFFICIENT OF FRICTION

FRICTION DRAG
NT AERODYNAMIC DRAG
NT VISCOUS DRAG
Distributed energy store railguns experiment and analysis 09 p1313 N85-18256
A survey of the turbulent drag reduction using passive devices
[NMI-R-193] 11 p1630 N85-20268
Design of apparatus for the determination of aerodynamic drag coefficients of automobiles
[AD-A151642] 15 p2464 N85-25219
Calculation of friction at spherical bearing journals in turbomachines 17 p2940 N85-28150
Combined riblet and LEBU drag reduction system
[NASA-CASE-LAR-13268-1] 18 p3058 N85-28922
Drag-compensated, precision-powered hinge system 22 p3796 N85-33517

FRICTION FACTOR
Numerical modeling of complex interaction of shell of revolution and its filler with allowance for friction 06 p0779 N85-14960
Experimental study of heat transfer from shaft in cooled radial bearing of GNT-25 gas turbine 14 p2270 N85-24068
Study of axial bearings without oil bath with radial cooling of blocks 14 p2286 N85-24164
Turbine blade friction damping study 16 p2736 N85-26886

FRICTION LOSS COEFFICIENT
U FRICTION FACTOR

FRICTION MEASUREMENT
Skin friction measurements for 2 relatively thick airfoil sections at high Reynolds number
[AD-A150021] 12 p1772 N85-21125
A two-axis, self-nulling skin friction balance
[NASA-CASE-LAR-13294-1] 12 p1851 N85-21610

FRICTION PRESSURE DROP
U SKIN FRICTION

FRICTION REDUCTION
Microscopic aspects of the effect of friction reducers at the lubrication limit
[NASA-TM-77413] 03 p0367 N85-12354
Implantation of Ti + C for reduced friction and wear of steels
[DE85-001606] 09 p1295 N85-18135
The analysis by the lumped parameter method of slade platform friction dampers used in the high pressure fuel turbopump on the space shuttle main engine 09 p1338 N85-18417
Selection of bearing type for large steam turbines 14 p2271 N85-24069
Study of axial bearings without oil bath with radial cooling of blocks 14 p2286 N85-24164
Lubricant and additive effects on spur gear fatigue life
[NASA-TM-87044] 17 p2974 N85-28373
Tribological sinks: Money down the drain
[DE85-010019] 17 p2974 N85-28376
Mechanical modification of friction surfaces of aluminum alloys by friction transfer 19 p3241 N85-30097

FRICTION WELDING
Welding of PM-superalloys
[MTU-TB-910/84] 07 p0975 N85-16191

FRINGE MULTIPLICATION
Measurement of ultrasonic fields in transparent media using a scanning differential interferometer
[NASA-CR-175921] 17 p3026 N85-28726

FRINGE PATTERNS
U DIFFRACTION PATTERNS

FROGS
Spacelab mission D1 Frog statolith experiment STATEX: Hardware family and experiment operational sequence 05 p0689 N85-14426

FRONTAL AREAS (METEOROLOGY)
U FRONTS (METEOROLOGY)

FRONTAL WAVES
Frontal nature of Cromwell Current 14 p2336 N85-24445

FRONTS (METEOROLOGY)
NT COLD FRONTS
Layered sloping mesoscale structures and rainbands in atmospheric frontal regions and their relation to symmetric instability 01 p0075 N85-10497
About the influence of nonadiabatic processes on frontogenesis near the ground 01 p0075 N85-10498
Black Sea coastal frontogenesis 01 p0075 N85-10500
Doppler radar analysis of a frontal zone prior to convective development 01 p0077 N85-10515
Plans for the NRL/NORDA (Naval Research Laboratory-Naval Ocean Research and Development Activity) fine-scale variability experiment - 1984 (FVX-84)
[AD-A146041] 03 p0398 N85-12540
A study of the adequacy of quasi-geostrophic dynamics for modeling the effect of frontal cyclones on the larger scale flow 05 p0684 N85-14396
Meridional penetration of frontal systems in South America and its relation to organized convection in the Amazon
[INPE-3407-PRE/676] 10 p1518 N85-19572
Numerical studies of frontal dynamics 15 p2598 N85-26014
The sensitivity of mesoscale cyclogenesis forecasts to detailed three-dimensional isentropic initial analyses and varied vertical model resolution 15 p2598 N85-26015
A survey of major east coast snowstorms, 1960-1983. Part 2. Summary of surface and upperlevel characteristics
[NASA-TM-86195] 16 p2833 N85-27471
A survey of major east coast snowstorms, 1960-1983. Part 2: Case studies of eighteen storms
[NASA-TM-86196] 16 p2833 N85-27472
Statistical interpretation of the ECMWF model using MOS to predict surface wind and temperature
[WSR-2] 17 p2995 N85-28515
Automatic detection of gust fronts
[FAA-PM-85-11] 17 p2995 N85-28516
A study of the adequacy of quasi-geostrophic dynamics for modeling the effect of frontal cyclones on the larger scale flow
[NASA-CR-176065] 20 p3495 N85-31731
Observations of frontal zone structures with a VHF Doppler radar and radiosondes, part 1.2A 21 p3616 N85-32469
Thunderstorm phenomena and weather radar scanning strategies
[DOT/FAA/PM-85/14] 21 p3634 N85-32573

FROST
Frost nowcasting in the agricultural area of Valencia (Spain) --- meteorological satellites 05 p0658 N85-14225
Salt action on concrete
[AD-A147812] 07 p0933 N85-15912
Ice segregation and frost heaving
[PB85-122430] 10 p1460 N85-19199
The violet absorber on Io: Disulfur monoxide derivatives 13 p2173 N85-23482

FROST DAMAGE
Evaluation of the area and severity of last night's frosts
[REPT-109] 16 p2833 N85-27473

FROZEN EQUILIBRIUM FLOW
Tabular and graphical solutions of regular and Mach reflections in pseudo-stationary frozen and vibrational-equilibrium flows, part 1
[UTIAS-283-PT-1] 23 p3863 N85-34117
Tabular and graphical solutions of regular and Mach reflections in pseudo-stationary frozen and vibrational-equilibrium flows, part 2
[UTIAS-283-PT-2] 23 p3894 N85-34118

FROZEN SOILS
U PERMAFROST

FRUITS
Packaging for food service 14 p2394 N85-24747
Preliminary technology utilization assessment of the robotic fruit harvester
[NASA-CR-175834] 16 p2844 N85-27532

FUEL CAPSULES
General-purpose heat source development: Safety test program. Postimpact evaluation, design iteration test 4
[LA-10217-SR] 12 p1930 N85-22128
General-purpose heat source development: Safety test program. Postimpact evaluation, design iteration test 5
[LA-10232-SR] 12 p1931 N85-22129
Evacuate and backfill apparatus and method
[DE85-008018] 23 p3938 N85-34411

FUEL CELL CATALYSTS
U ELECTROCATALYSTS

FUEL CELL POWER PLANTS
Phosphoric and electric utility fuel cell technology development
[NASA-CR-174215] 06 p0605 N85-15124
Electric utility acid fuel cell stack technology advancement
[NASA-CR-174804] 08 p1178 N85-17422
Development of molten carbonate fuel cell power plant technology
[DE84-016839] 14 p2352 N85-24536
Effects of H2S on molten carbonate fuel cells
[DE85-008310] 18 p3130 N85-29396
Development of molten carbonate fuel cell power plant, volume 1
[DE85-008743] 18 p3131 N85-29394
F-CAP documentation
[DE85-003369] 19 p3307 N85-30503
Reactant pressure differential control for fuel cell gases
[NASA-CASE-MSC-20127-2] 23 p3937 N85-34403

FUEL CELLS
NT PHOSPHORIC ACID FUEL CELLS
NT REGENERATIVE FUEL CELLS
Advanced fuel cell development
[DE84-014847] 01 p0044 N85-10289
Hot-gas cleanup for molten carbonate fuel cells-dechlorination and soot formation
[DE84-003072] 01 p0068 N85-10450
P-doping of (CH)x to the metallic regime with gaseous oxygen. Application to oxygen fuel cell type electrodes
[AD-A145477] 02 p0186 N85-11242
Effects of H2S on molten carbonate fuel cells
[DE84-015166] 02 p0195 N85-11307
Electrochemical and surface science research on fuel cells
[DE84-015982] 03 p0359 N85-12307
Materials for high-temperature fuel cells
[DE84-016316] 04 p0479 N85-13054

Phosphoric and electric utility fuel cell technology development
[NASA-CR-174215] 06 p0805 N85-15124
Space shuttle electrical power generation and reactant supply system 08 p1099 N85-16947
5 kW sleeps inverter. Revision
[AD-A149526] 10 p1510 N85-19528
High-temperature, solid oxide electrolyte fuel cell power generation system
[DE85-002978] 11 p1675 N85-20552
Using fuel cells or anode depolarization to reduce electrowinning energy consumption
[DE85-006187] 13 p2129 N85-23250
Molten carbonate fuel cell performance model update, draft
[DE85-005423] 13 p2129 N85-23252
Cathode materials for molten carbonate fuel cells
[DE85-004078] 13 p2130 N85-23254
Electricity production from coal through molten-carbonate fuel cells
[TI86-005072] 14 p2351 N85-24534
Long-life high performance fuel cell program
[NASA-CR-174874] 15 p2494 N85-25384
Molten carbonate fuel cell performance model update
[DE85-003356] 17 p2986 N85-28454
Fuel cells: A bibliography
[DE85-004565] 18 p3128 N85-29371
Effects of H2S on molten carbonate fuel cells
[DE85-006310] 18 p3130 N85-29386
Improved acid electrolytes for fuel cells
[PB85-176053] 18 p3132 N85-29397
Plasma spray screen repair method
[AD-D011713] 19 p3281 N85-30346
Advanced fuel cell development
[DE85-009662] 19 p3306 N85-30497
F-CAP documentation
[DE85-003369] 19 p3307 N85-30503
Integrated current collector and catalyst support
[DE85-011616] 22 p3761 N85-33311
Molten carbonate fuel cell separator
[DE85-011615] 22 p3806 N85-33577
Effects of H2S on molten carbonate fuel cells. Literature review on the impact of SO2 in the oxidant supplied to molten carbonate fuel cells
[DE85-011668] 22 p3806 N85-33586
Transfer of battery technology developed by the US Department of Energy
[DE85-009668] 22 p3808 N85-33588
Fuel cell applications literature review
[DE85-011891] 22 p3809 N85-33592
Reactant pressure differential control for fuel cell gases
[NASA-CASE-MSC-20127-2] 23 p3937 N85-34403
Evaluation of developmental membranes for the mixed reactant iron-chromium redox system
[NASA-TM-87074] 23 p3944 N85-34443
Fuel cell separator plate with bellows-type sealing flanges
[DE85-005991] 23 p3947 N85-34459
Electrolyte reservoir for carbonate fuel cells
[DE85-005736] 23 p3947 N85-34460
Thermodynamics of the corrosion of chromium in molten carbonates
[DE85-011407] 24 p4079 N85-35282

FUEL COMBUSTION
Combustion gas properties I-ASTM jet A fuel and dry air
[NASA-TP-2359] 01 p0010 N85-10084
The mechanisms of flame holding in the wake of a bluff body
[NASA-CR-174058] 02 p0172 N85-11149
Alternate fuels combustion research
[AD-A145891] 02 p0188 N85-11258
Analysis of potential combustion sorce impacts on acid deposition using an independently derived inventory, volume 1
[DE84-012005] 02 p0225 N85-11471
Dynamics of burnout of solid fuel in fluidized bed of finely divided inert particles 02 p0273 N85-11782
Combustion waves in dispersed-2-phase mixtures
[CFD/84/13] 04 p0472 N85-13003
Liquid-fueled Ramjet engines 07 p0918 N85-15814
Ramjets with supersonic combustion 07 p0918 N85-15817
Catalytic ignition and combustion of lean mixtures
[AD-A148101] 08 p1121 N85-17067
Radiation/catalytic augmented combustion
[AD-A148758] 09 p1290 N85-18101
Mechanisms and reaction dynamics related to methane combustion
[PB85-129880] 10 p1436 N85-19065
Fuels combustion research
[AD-A149106] 10 p1457 N85-19178
The mechanisms of flame holding in the wake of a bluff body
[NASA-CR-3866] 12 p1779 N85-21186
Ignition of mixtures of SiH sub 4, CH sub 4, O sub 2, and Ar or N sub 2 behind reflected shock waves
[NASA-TP-2415] 13 p1974 N85-22395
The influence of fuel quality upon flame-tube temperature and flame radiation in a model gas-turbine primary zone
[K233] 13 p1974 N85-22396
Workshop report: Swirl Enhanced Combustion 13 p2005 N85-22564
The influence of fuel molecular composition upon flame-tube temperature and flame radiation in a model gas-turbine primary zone
[K234] 13 p2017 N85-22646
Laser diagnostic analyses of sooting flames
[AD-A150478] 13 p2017 N85-22649
Dependence of combustion of homogeneous kerosene-air mixtures on humidity of air 13 p2051 N85-22835
Diesel combustion: Advances in analysis and simulation 14 p2253 N85-23965
Shock tube study of the fuel structure effects on the chemical kinetic mechanisms responsible for soot formation, part 2
[NASA-CR-174880] 15 p2504 N85-25444
Influence of fuel properties on gas turbine combustion performance
[AD-A151464] 15 p2504 N85-25448
Studies of the combustion of model fuels with low hydrogen content (pyrolysis of polycyclic aromatics-detection of soot precursors)
[DE85-005422] 15 p2521 N85-25541
Numerical analysis of supersonic reactive flow in wake of reverse step 15 p2643 N85-26303
Analytical fuel property effects--small combustors
[NASA-CR-174738] 16 p2708 N85-26709
Research test facility for evaporation and combustion of alternative jet fuels at high air temperatures
[AD-A153830] 18 p3063 N85-29073
An experimental investigation of fuel regression rate control in solid fuel ramjets
[AD-A154251] 19 p3227 N85-30008
The effect of surface reactions in catalytic combustion
[AD-A154217] 19 p3234 N85-30049
Injection, atomization, ignition and combustion of liquid fuels in high-speed air streams
[AD-A154056] 19 p3251 N85-30156
Investigation of the behavior of fuel in the intake manifold and its relation to SI engines, 1980 - 1983 19 p3279 N85-30337
Fuel-rich catalytic combustion: A soot-free technique for in situ hydrogen-like enrichment
[NASA-TP-2496] 20 p3423 N85-31244
Toxic hazards tests for vehicles and other equipment
[AD-A149164] 20 p3506 N85-31797
Jet flows: Modelling and experiments 22 p3744 N85-33208
Ames Laboratory measurements of alkali levels in the Curtiss-Wright PFBC gas stream
[DE85-011357] 22 p3745 N85-33214
Current inventory of anthropogenic carbon dioxide in the North Pacific Subarctic Gyre
[PB85-187936] 24 p4125 N85-35570

FUEL CONSUMPTION
ACEE program rationale and implementation
[NASA-TM-84549] 02 p0133 N85-10908
Fuel efficiency through new airframe technology
[NASA-TM-84548] 02 p0133 N85-10909
Hybrid laminar flow control study
[NASA-CR-165930] 02 p0137 N85-10933
Energy efficient engine flight propulsion system preliminary analysis and design report
[NASA-CR-174701] 02 p0140 N85-10947
Energy efficient engine. Volume 1: Component development and integration program
[NASA-CR-173084] 02 p0146 N85-10992
Analysis and simulation of the I C engine Otto cycle using the second law of thermodynamics 02 p0291 N85-11891
Advanced Automotive Diesel Assessment Program, executive summary 04 p0507 N85-13236
Dissociated methanol vehicle test results
[DE84-004507] 04 p0509 N85-13248
Combined cycle ramjet engine
[AD-D011247] 06 p0760 N85-14859
Copper-nickel sheathing study, phase 2. Two-year service performance of test panels on the ARCO TEXAS
[PB84-242411] 06 p0775 N85-14862
Reference energy-altitude descent guidance: Simulator evaluation — aircraft descent and fuel conservation
[NASA-TP-2383] 08 p1085 N85-16868
Collegium on aviation fuel conservation efforts 09 p1278 N85-18034
Dissociated methanol citation
[DE85-000605] 10 p1458 N85-19188
Fiat introduces 1000-CC engine 11 p1618 N85-20185
Effect of water injection into air for turbine cooling on economy of operation of gas turbine engine with afterburning 13 p2050 N85-22630
Deputy minister on civil aviation fuel conservation efforts 14 p2208 N85-23691
Safety recommendation(s), A-84-103
[REPT-3909B/101B] 14 p2216 N85-23745
Aviation workers plenum reviews fuel conservation progress 15 p2461 N85-25197
Ilyushin bureau designer on fuel conservation research 15 p2467 N85-25231
Planning fuel-conservative descents in an airline environmental using a small programmable calculator: Algorithm development and flight test results
[NASA-TP-2393] 16 p2707 N85-26705
Energy efficient engine high-pressure turbine component rig performance test report
[NASA-CR-168189] 19 p3218 N85-29955
Energy efficient engine integrated core/low spool test hardware design report
[NASA-CR-168137] 19 p3218 N85-29956
Energy Efficient Engine (E3) controls and accessories detail design report
[NASA-CR-168017] 19 p3218 N85-29957
Auto fuel efficiency standards, part 2
[GPO-41-169] 20 p3435 N85-31309
FAA requirements for model to support capacity, delay, noise and energy programs
[AD-A155815] 24 p4063 N85-35179
Comparative analysis of operational forecasts versus actual weather conditions in airline flight planning, volume 1
[NASA-CR-167862] 24 p4119 N85-35534
Comparative analysis of operational forecasts versus actual weather conditions in airline flight planning, volume 2
[NASA-CR-167863] 24 p4119 N85-35535
Comparative analysis of operational forecasts versus actual weather conditions in airline flight planning, volume 3
[NASA-CR-167864] 24 p4120 N85-35536
Comparative analysis of operational forecasts versus actual weather conditions in airline flight planning, volume 4
[NASA-CR-167865] 24 p4120 N85-35537

FUEL CONTAMINATION
Sound speed measurements in liquid oxygen-liquid nitrogen mixtures
[NASA-TP-2464] 24 p4063 N85-35307

FUEL CONTROL
Engine wear and cold startability of methanol fueled engines.
[DE85-001206] 11 p1647 N85-20381
Energy Efficient Engine (E3) controls and accessories detail design report
[NASA-CR-168017] 19 p3218 N85-29957
An experimental investigation of fuel regression rate control in solid fuel ramjets
[AD-A154251] 19 p3227 N85-30008

FUEL ELEMENTS (NUCLEAR REACTORS)
U NUCLEAR FUEL ELEMENTS

FUEL FLOW
NT PROPELLANT TRANSFER
Energy efficient engine high-pressure turbine component rig performance test report
[NASA-CR-168189] 19 p3218 N85-29955
Detailed studies of aviation fuel flowability
[NASA-CR-174938] 20 p3435 N85-31308
A comparison of two bench scale tests of fuel low temperature flow properties
[AD-A154477] 20 p3435 N85-31311

FUEL GAGES
Assessment study of liquid content measurement methods applicable to space missions — Infrared Space Observatory
[TU-HH-TRI-ESA-84-2] 17 p2938 N85-28135

FUEL INJECTION
Combustion modeling of a 2 cylinder cycle reciprocating engine
[AD-A144782] 01 p0055 N85-10364
Finiet injector
[AD-D011245] 06 p0765 N85-14891
Experimental study of the spray characteristics of a research airblast atomizer
[NASA-TM-86911] 07 p0904 N85-15727
Catalytic ignition and combustion of lean mixtures
[AD-A148101] 08 p1121 N85-17067
A study of air breathing rockets. Part 4: Direct fuel injection into a secondary combustor
[NAL-TR-832] 09 p1287 N85-18083

Hypergolic combustion demonstration in a reciprocating internal combustion engine
[AD-A150846] 14 p2311 N85-24303
Small gas turbine combustor study: Fuel injector performance in a transpiration-cooled liner
[NASA-TM-86989] 15 p2473 N85-25264
Installation, maintenance and operating manual for the Lucas-type fuel injection system of the 3 B rotary engine
[NASA-TM-77872] 15 p2568 N85-25846
Numerical analysis of supersonic reactive flow in wake of reverse step 15 p2643 N85-26303
Segmented zoned fuel injection system for use with a combustor
[AD-D011640] 17 p2897 N85-27865
Research test facility for evaporation and combustion of alternative jet fuels at high air temperatures
[AD-A153830] 18 p3083 N85-29073
Injection, atomization, ignition and combustion of liquid fuels in high-speed air streams
[AD-A154056] 19 p3251 N85-30156
The design of Direct Injection (DI) diesel engines. Injection system by a numerical optimization technique
[REPT-84-RR-346] 20 p3462 N85-31508
Superheated fuel injection for combustion of liquid-solid slurries
[DE85-011624] 22 p3753 N85-33266

FUEL OILS
US energy for the rest of the century, 1984 edition
[PB84-207406] 04 p0531 N85-13393
USSR report: Energy
[JPRS-UEN-84-038] 07 p0994 N85-16312
Oil tank electrostatic charging report
[DRIC-T-6967] 20 p3436 N85-31319

FUEL PRODUCTION
Alcohol fuel from Ohio farms: An introduction
[TI-84-901290] 05 p0621 N85-13970
Application of robotics in remote fuel fabrication operations
[DE84-011481] 05 p0648 N85-14144
Advancement of remote technology: Past perspectives and future plans
[DE85-000934] 09 p1327 N85-18342
Catalytic conversion of C3-C4 paraffins to gasoline
[DE85-004181] 10 p1458 N85-19187
Test report for Getty Synthetic Fuels, Inc., Calumet City, Illinois
[PB85-119493] 10 p1459 N85-19191
Research and development of shallow algal mass culture systems for the production of oils
[DE85-000518] 11 p1680 N85-20624
Microalgae culture collection, 1984-1985
[DE84-013035] 11 p1690 N85-20626
Developments in the production and use of ethanol fuels
[GPO-40-678] 12 p1817 N85-21398
Trifunctional catalysts for conversion of syngas to alcohols
[DE85-004577] 13 p2040 N85-22771
Anaerobic digestion of biomass: status summary and research development needs, 1983
[PB85-161925] 13 p2040 N85-22772
PSA, Renault work on all fuel automobile engine 15 p2531 N85-25604
Jet fuel property changes and their effect on producibility and cost in the U.S., Canada, and Europe
[NASA-CR-174840] 16 p2757 N85-27012
Technical and economic analysis of liquid fuel production from microalgae
[DE85-002926] 16 p2758 N85-27018
Conversion of methanol to gasoline: Engineering and construction of the demonstration plant
[DE85-003237] 17 p2937 N85-28133
Alcohol: An alternate energy resource for community use
[DE85-007731] 18 p3084 N85-29075
Feasibility study of a fission-suppressed Tokamak fusion breeder
[DE85-009099] 18 p3190 N85-29786
Consolidated fuel reprocessing program
[DE85-010591] 19 p3358 N85-30818
Linking R and D to problems experienced in solids processing
[AD-A154238] 19 p3380 N85-30988

FUEL PUMPS
Analytical and experimental investigation of rubbing interaction in labyrinth seals for a liquid hydrogen fuel pump — space shuttle main engine
[NASA-CR-174857] 09 p1287 N85-18084
Hydrodynamic simulation of transient processes in injection system of aircraft engines during pump unswirling 13 p2050 N85-22829
HPFTP flow diverter analysis
[NASA-CR-171424] 13 p2091 N85-23057
Ceramics for advanced O2/H2 application 16 p2734 N85-26868

FUEL SPRAYS
Exciplex systems for vapor-liquid visualization of fuel sprays
[AD-A149360] 10 p1457 N85-19181
Liquid fuel spray processes in high-pressure gas flow
[NASA-TM-86944] 12 p1844 N85-21570
Research test facility for evaporation and combustion of alternative jet fuels at high air temperatures
[AD-A153830] 18 p3083 N85-29073
KIVA: A computer program for two- and three-dimensional fluid flows with chemical reactions and fuel sprays
[DE85-010334] 19 p3339 N85-30693
Particle sizing from forward scattered light at two angles using a Variable-Focal-Length optical system
[AD-A154164] 20 p3533 N85-31980
KIVA computer program for multidimensional chemically reactive fluid flows with fuel sprays
[DE85-012730] 22 p3830 N85-33722

FUEL SYSTEMS
NT AIRCRAFT FUEL SYSTEMS
Application of the CSRL language to the design of expert diagnosis systems: The Auto-Mech experience
[AD-P003922] 02 p0245 N85-11602
Heat management system for aircraft
[AD-D011658] 18 p3061 N85-28936
Energy Efficient Engine (E3) controls and accessories detail design report
[NASA-CR-168017] 19 p3218 N85-29957
Special tools used by cosmonauts in EVA 22 p3731 N85-33129

FUEL TANKS
NT WING TANKS
Aircraft wing fuel tank environmental simulator tests for evaluation of antimisting fuels
[FAA-CT-84-15] 07 p0934 N85-15920
Distribution and storage of aviation turbine fuel for military operations in northern Australia
[AD-A147180] 07 p0935 N85-15921
Preliminary airworthiness evaluation AH-1S (MC) helicopter with external fuel tanks installed
[AD-A148091] 08 p1084 N85-16865
BI-PAC F-15 external fuel tank container modification
[AD-A148836] 09 p1290 N85-18053
Interactions between F-111 fuselage fuel tank sealants. Part 2: Variation in performance properties of polysulfides after contact with polyester degradation products
[AD-A149777] 12 p1812 N85-21368
Fuel freeze point investigations
[AD-A152801] 17 p2937 N85-28129
Investigation, development, and certification of a burst disk for cryogenic fuel tanks
[GCP-3/MT-CM-21-2546] 18 p3067 N85-28972
Fuel containment and damage tolerance in large composite primary aircraft structures
[NASA-CR-166083] 19 p3231 N85-30032
Fuel containment and damage tolerance for large composite primary aircraft structures. Phase 1: Testing
[NASA-CR-166091] 24 p4073 N85-35241

FUEL TESTS
NT REACTOR STARTUP TESTS
Rapid estimation of concentration of aromatic classes in middistillate fuels by high-performance liquid chromatography
[NASA-TP-2495] 20 p3434 N85-31307
Observations of the use of the setapoint detector
[AD-A154533] 21 p3571 N85-32208

FUEL VALVES
Man-vehicle systems research facility advanced aircraft flight simulator throttle mechanism 22 p3796 N85-33527

FUEL-AIR RATIO
Gas dynamics of combustion of gas-air mixture in semi-closed space with relief of pressure into gasless adjacent space 02 p0260 N85-11699
Finlet injector
[AD-D011245] 06 p0765 N85-14891
Catalytic ignition and combustion of lean mixtures
[AD-A148101] 08 p1121 N85-17067
Combustion gas properties. 2: Natural gas fuel and dry air
[NASA-TP-2435] 12 p1779 N85-21168
Behavior of the lean methane-air flame at zero-gravity
[NASA-CR-175586] 12 p1799 N85-21283
The behaviour of detonation waves in single phase heterogeneous systems
[AD-A149825] 12 p1846 N85-21581
Dependence of combustion of homogeneous kerosene-air mixtures on humidity of air 13 p2051 N85-22835
Limiting factor of flame propagation in mono-sized sprays of low-volatility fuels
[NAL-TR-839T] 15 p2521 N85-25536
Detailed chemical kinetic study of the effect of molecular structure on autoignition of fuel-air mixtures
[DE85-004424] 17 p2921 N85-28010
The effect of surface reactions in catalytic combustion
[AD-A154217] 19 p3234 N85-30049
Experimental determination of the mixing frequency parameter for coalescence/dispersion modeling of turbulent combustion
[DE85-011468] 19 p3270 N85-30280
Flow modifying device
[NASA-CASE-LEW-13582-2] 24 p4085 N85-35195

FUELING
U REFUELING

FUELS
NT ACTIVATED CARBON
NT AIRCRAFT FUELS
NT AUTOMOBILE FUELS
NT CERAMIC NUCLEAR FUELS
NT CHARCOAL
NT CHEMICAL FUELS
NT COAL
NT CRYOGENIC ROCKET PROPELLANTS
NT DIESEL FUELS
NT DOUBLE BASE ROCKET PROPELLANTS
NT FOSSIL FUELS
NT FUEL OILS
NT GASEOUS FUELS
NT GASOHOL (FUEL)
NT GASOLINE
NT HYDROCARBON FUELS
NT HYDROGEN FUELS
NT HYPERGOLIC ROCKET PROPELLANTS
NT JET ENGINE FUELS
NT JP-4 JET FUEL
NT JP-5 JET FUEL
NT JP-8 JET FUEL
NT KEROSENE
NT LIQUEFIED NATURAL GAS
NT LIQUID FUELS
NT LIQUID ROCKET PROPELLANTS
NT MONOPROPELLANTS
NT NUCLEAR FUELS
NT PEAT
NT SLURRY PROPELLANTS
NT SOLID ROCKET PROPELLANTS
NT SPENT FUELS
NT SYNTHETIC FUELS
External fuel vaporization study, phase 2
[NASA-CR-174079] 02 p0187 N85-11252
DOE supported research in alcohol fuel technology development
[DE84-007686] 06 p0774 N85-14948
Phase 1-A development kinematic Sterling/Rankine commercial gas-fired heat pump research program
[PB85-100931/GAR] 07 p0936 N85-15928
Research and development of alcohol fuel usage in spark ignited engines 09 p1301 N85-18175
Morbidity and mortality associated with exposure to Otto Fuel II in the U.S. Navy 1966-1979
[AD-A148726] 09 p1363 N85-18574
Investigation of fuel additive effects on sooting flames
[AD-A149154] 10 p1457 N85-19179
Alternative fuels for buses: Current assessment and future perspectives
[PB85-116325] 10 p1459 N85-19190
Peat resources of Maine. Volume 2: Penobscot County
[DE85-004196] 11 p1670 N85-20522
Peat resources of Maine. Volume 5: Washington County
[DE85-004197] 11 p1670 N85-20523
Limiting factor of flame propagation in mono-sized sprays of low-volatility fuels
[NAL-TR-839T] 15 p2521 N85-25536
Evaluation of used crankcase oils using computerized infrared spectrometry
[AD-A152993] 17 p2920 N85-27999
Alcohol Fuels Program technical review, spring 1984
[DE85-002919] 17 p2936 N85-28134
Urban vehicle research project
[DE85-005444] 17 p3052 N85-28889
Effects of H2S on molten carbonate fuel cells
[DE85-008310] 18 p3130 N85-29366
Impact of alcohol fuels on urban air pollution: Methanol photochemistry study
[DE85-009539] 18 p3133 N85-29403
Investigation of the behavior of fuel in the intake manifold and its relation to SI engines, 1980 - 1983 19 p3279 N85-30337
Coal slurry ignition in a diesel engine simulator
[DE85-010987] 20 p3463 N85-31513

FULL SCALE TESTS
Full-scale testing, production and cost analysis data for the advanced composite stabilizer for Boeing 737 aircraft. Volume 1: Technical summary
[NASA-CR-3649] 05 p0612 N85-13912

Full-scale testing, production and cost analysis data for the advanced composite stabilizer for Boeing 737 aircraft, volume 2
[NASA-CR-166012] 05 p0613 N85-13915

FUMES

Pathophysiological study of poisoning due to thermal degradation of materials — aircraft cabins
[CERMA-84-15] 11 p1692 N85-20640

Material thermolysis product toxicity: Definition of a hazard evaluation methodology
[CERMA-84-08] 11 p1692 N85-20641

FUMIGATION

Methanol vaporization: Effects on volumetric efficiency and on determination of optimum fuel delivery system
[PB84-243914] 09 p1302 N85-18181

FUNCTION GENERATORS

Technical data on new engineering products
10 p1460 N85-19201

Precision linear ramp function generator
[DE85-011647] 22 p3760 N85-33304

FUNCTION SPACE

NT BANACH SPACE
NT HILBERT SPACE
NT SOBOLEV SPACE

Partitions of unity and approximation
[AD-A144717] 01 p0110 N85-10746

A simple transport model 02 p0264 N85-11853

Condenser capacities and removable sets in W1p1
10 p1536 N85-19682

Asymptotic behavior of matrix coefficients related to reductive symmetric spaces
[CWI-PM-R8410] 12 p1925 N85-22095

A problem of Burkholder and the existence of harmonic majorants of the absolute value of x sup p in certain domains in R sup d 15 p2634 N85-26236

Quadratic spaces over discrete Hodge algebras
16 p2653 N85-27593

A study of the effect of a mismatch in gamma and gamma prime phase lattice spacings on the high temperature strength characteristics of dispersion-hardened nickel alloys
[BLL-CE-TRANS-6048-(9022.00)]
20 p3430 N85-31279

FUNCTIONAL ANALYSIS

NT BANACH SPACE
NT CONVOLUTION INTEGRALS
NT FOURIER TRANSFORMATION
NT FREDHOLM EQUATIONS
NT HARMONIC ANALYSIS
NT HILBERT SPACE
NT HILBERT TRANSFORMATION
NT INTEGRAL EQUATIONS
NT INTEGRAL TRANSFORMATIONS
NT J INTEGRAL
NT LAPLACE TRANSFORMATION
NT SINGULAR INTEGRAL EQUATIONS
NT SOBOLEV SPACE
NT TESSERAL HARMONICS
NT VOLTERRA EQUATIONS
NT WIENER HOPF EQUATIONS
NT ZONAL HARMONICS

Markovian control problems: Functional equations and algorithms
[MCTH-97] 01 p0107 N85-10717

Applications of functional analytic and Martingale methods
[AD-A145555] 02 p0255 N85-11672

Nonlinear regression with emphasis on spline methods
[AD-A146192] 03 p0412 N85-12633

Interpolating sequences for H to infinity in the ball
[CTH-MATH-1984-15] 04 p0556 N85-13542

Simplified proofs of some basic theorems for quasiregular mappings 10 p1535 N85-19677

Functional equation for the embedding of a homomorphism of the interval into a flow
[DE85-000655] 11 p1713 N85-20780

Schur-Ostrowski theorems for functionals on l1(0,1)
[AD-A150193] 13 p2150 N85-23346

A database design for the Brazilian Air Force Flying Unit Operational Control System
[AD-A151846] 15 p2666 N85-26452

Infinite dimensional linear systems with unbounded control and observation: A functional analytic approach
[AD-A153535] 18 p3169 N85-29639

Conceptualizing in assembly tasks
[AD-A155564] 21 p3665 N85-32770

FUNCTIONAL DESIGN SPECIFICATIONS

Vibration, acoustic, and shock design and test criteria for components on the Solid Rocket Boosters (SRB), Lightweight External Tank (LWT), and Space Shuttle Main Engines (SSME)
[NASA-RP-1127] 01 p0061 N85-10405

The multipurpose composite flywheel
05 p0606 N85-13868

Operational problems with radiation survey meters: The university and accelerator
[DE84-015703] 06 p0811 N85-15151

Design study of technology requirements for high performance single-propeller-driven business airplanes
[NASA-CR-3863] 07 p0898 N85-15892

A digital piloting system for the combat helicopter
08 p1074 N85-16806

The orbiter mate/demate device
08 p1103 N85-16972

High level languages in protocol specification and verification
[FUB-51-1983] 09 p1370 N85-18611

Parallel input and feedback in dialogue cells
[CWI-CS-R8413] 11 p1703 N85-20708

Possible technological answers to new design requirements for power transmission systems
14 p2222 N85-23779

SC filters and design centering of integrated circuits. Part 2: Design centering of integrated circuits
[BMFT-FB-T-84-265-PT-2] 17 p2956 N85-28257

Search of the VAXintosh customizing VMS V4.0 for DCL windows
[DE85-011306] 22 p3831 N85-33729

Product definition: Technical specification of needs
[SNIAS-851-430-104] 23 p3910 N85-34226

FUNCTIONALS

Analytical construction of flight vehicle surfaces
06 p0775 N85-14957

On the probability generating functional for point processes
[AD-A147692] 09 p1210 N85-17615

A data based algorithm for choosing the window width when estimating the integral of f2(x)
[AD-A152093] 16 p2647 N85-27553

Stability of functionals determined by moment conditions
[TRITA-NA-8310] 16 p2652 N85-27585

The role of duality in optimization problems involving entropy functionals, with applications to information theory
[AD-A152336] 17 p3026 N85-28713

Comments on estimating quantiles for Gaussian functionals by simulation
[AD-A154302] 19 p3348 N85-30750

FUNCTIONS

Statistical comparison of pooled nitrogen washout data of various altitude decompression response groups
[NASA-TM-58265] 15 p2639 N85-26278

DLA: Data/data base administration analysis
[AD-A153031] 17 p3050 N85-28879

FUNCTIONS (MATHEMATICS)

NT ABEL FUNCTION
NT AIRY FUNCTION
NT ANALYTIC FUNCTIONS
NT ASYMPTOTES
NT BOOLEAN FUNCTIONS
NT COMPOSITE FUNCTIONS
NT CONFORMAL MAPPING
NT COORDINATE TRANSFORMATIONS
NT DELTA FUNCTION
NT DISCRETE FUNCTIONS
NT DISCRIMINANT ANALYSIS (STATISTICS)
NT DISTRIBUTION FUNCTIONS
NT ELLIPTIC FUNCTIONS
NT ENTIRE FUNCTIONS
NT ERROR FUNCTIONS
NT EXPONENTIAL FUNCTIONS
NT FOURIER TRANSFORMATION
NT GAMMA FUNCTION
NT GREEN'S FUNCTIONS
NT HAMILTONIAN FUNCTIONS
NT HARMONIC FUNCTIONS
NT HYPERBOLIC FUNCTIONS
NT HYPERGEOMETRIC FUNCTIONS
NT KERNEL FUNCTIONS
NT LAGUERRE FUNCTIONS
NT LAPLACE TRANSFORMATION
NT LEGENDRE FUNCTIONS
NT LIAPUNOV FUNCTIONS
NT LINEAR TRANSFORMATIONS
NT LOGARITHMS
NT LORENTZ TRANSFORMATIONS
NT MAXWELL-BOLTZMANN DENSITY FUNCTION
NT MEROMORPHIC FUNCTIONS
NT MODULATION TRANSFER FUNCTION
NT MONOTONE FUNCTIONS
NT NORMAL DENSITY FUNCTIONS
NT OPTICAL TRANSFER FUNCTION
NT ORTHOGONAL FUNCTIONS
NT ORTHONORMAL FUNCTIONS
NT PEARSON DISTRIBUTIONS
NT PENALTY FUNCTION
NT PERIODIC FUNCTIONS
NT POINT SPREAD FUNCTIONS
NT POISSON DENSITY FUNCTIONS
NT PROBABILITY DENSITY FUNCTIONS
NT PROBABILITY DISTRIBUTION FUNCTIONS
NT RAMP FUNCTIONS
NT RAYLEIGH DISTRIBUTION
NT RECURSIVE FUNCTIONS
NT SPACE-TIME FUNCTIONS
NT SPHERICAL HARMONICS
NT SPLINE FUNCTIONS
NT STRESS FUNCTIONS
NT TANGENTS
NT TIME FUNCTIONS
NT TRANSCENDENTAL FUNCTIONS
NT TRANSFER FUNCTIONS
NT WALSH FUNCTION
NT WEIBULL DENSITY FUNCTIONS
NT WEIGHTING FUNCTIONS

Implementation of the supersonic triplet singularity into the USTORE computer code
[CSIR-NIAST-83/47] 01 p0001 N85-10008

Simultaneous rational approximation of a function and its derivatives in the complex plane
[CSIR-TWISK-311] 01 p0109 N85-10733

On two concepts of fundamental matching
[CSIR-TWISK-335] 01 p0110 N85-10743

Computing the reliability of k out of n systems
[AD-A145505] 02 p0206 N85-11357

About ambiguity and Q-functions
[AD-A145293] 02 p0250 N85-11636

Algebraic functions of H-functions with specific dependency structure
[AD-A145598] 02 p0252 N85-11647

Maximum likelihood estimation of the survival functions of N stochastically ordered random variables
[AD-A145429] 02 p0254 N85-11662

A proposal for standard basic functions in Ada
[NPL-DITC-45/84] 05 p0715 N85-14584

The resistance and mobility functions of two equal spheres in low Reynolds number flow
[AD-A147301] 07 p0959 N85-16080

Estimation for a semimartingale regression model using the method of sieves
[AD-A146809] 07 p1028 N85-16527

Conjunctive and disjunctive item response functions
[AD-A147815] 07 p1033 N85-16561

Modules of continuum structures, revised
[AD-A148620] 08 p1213 N85-17639

Bounding the stochastic performance of continuum structure functions 1
[AD-A148621] 08 p1213 N85-17640

Generating positively correlated random variables from a sequence of independent random variables with symmetric logarithmically concave densities
[AD-A148438] 08 p1216 N85-17658

Generalized convex functions: Properties, optimality and duality
[DE85-001553] 09 p1376 N85-18652

On rotation automorphic functions with descrete rotation groups 10 p1536 N85-19686

Computable real analysis
[AD-A149079] 10 p1546 N85-19747

Bounding the stochastic performance of continuum structure functions 2
[AD-A149458] 10 p1548 N85-19762

Sequential minimization for sum of squares of unknown functions
[DE85-004182] 11 p1707 N85-20736

Axiomatic characterizations of continuum structure functions
[AD-A149617] 12 p1866 N85-21706

Software for special functions
[DE85-004684] 12 p1917 N85-22033

A note about the strong convergence of the nonparametric estimation of a regression function
[AD-A150325] 13 p2151 N85-23353

The complexity of reliability computations in planar and acyclic graphs
[AD-A150759] 14 p2408 N85-24845

Disproof of the Mertens conjecture
[CWI-NM-R8412] 14 p2414 N85-24896

A remark on the conformal capacity of Groetzsch's condenser in space 15 p2634 N85-26240

Schubert varieties are arithmetically Cohen-Macaulay
16 p2653 N85-27592

Convergence of Newton's method for a single real equation
[NASA-TP-2489] 17 p3017 N85-28656

The origin of the binary-search paradigm
[AD-A154367] 19 p3337 N85-30677

On the solution for the sound field in a semi-infinite uniform duct with sheared mean flow
20 p3523 N85-31912

On the dependence of the convergence of Gummel's algorithm on the regularity of the solution
[AD-A154628] 21 p3675 N85-32832

New developments on the core function for efficient implementation of the difficult residue number system operations
[AD-A154678] 21 p3676 N85-32834
USSR report: Physics and mathematics
[JPRS-UPM-85-004] 21 p3680 N85-32860
Two methods of global data assimilation
[AD-A155981] 24 p4143 N85-35684
FUNGI
NT YEAST
Aquatic plant control research program. Evaluation of Fusarium roseum Culmorum as a biological control agent for Hydrilla verticillata
[AD-A145228] 01 p0069 N85-10459
Fungi of Mt. Babia Gora. 2: Indicative value of macromycetes in forest associations. A: Initial considerations
[NASA-TM-77485] 01 p0094 N85-10632
Fungi of Mount Babia Gora. 3: The indicating value of macromycetes in the forest associations
[NASA-TM-77486] 01 p0094 N85-10633
Fungi of Mt. Babia Gora. 1: Mycoflora of forests
[NASA-TM-77484] 02 p0234 N85-11522
Architecture of dermatophyte cell Walls: Electron microscopic and biochemical analysis
[NASA-TM-77441] 03 p0399 N85-12546
Structure and functions of fungal cell surfaces
[NASA-TM-77439] 06 p0842 N85-15347
The structure and function of fungal cells
[NASA-TM-77443] 06 p0842 N85-15348
The lipid composition and its alteration during the growth stage in pathogenic fungus, epidermophyton floccosum
[NASA-TM-77440] 07 p1011 N85-16421
Nitrogen control of photosynthetic protein synthesis
[DE85-009513] 11 p1690 N85-20623
FUNNELS
Proposed use of the radio-frequency quadrupole structure to funnel high-current ion beams
[DE85-010746] 19 p3364 N85-30857
FURAN RESINS
NT KEVLAR (TRADEMARK)
NT POLYAMIDE RESINS
FURANS
NT TETRAHYDROFURAN
FURLABLE ANTENNAS
Offset unfurlable antenna concepts
05 p0625 N85-14002
Antenna Technology for QUASAT application --- radio antenna for very long base interferometry missions
14 p2231 N85-23628
FURNACES
NT ELECTRIC FURNACES
NT IMAGE FURNACES
NT SOLAR FURNACES
NT VACUUM FURNACES
Results of the technical exchange agreement between NASA and DuPont on the containerless drop tube solidification of NiAl3
[NASA-TM-86473] 01 p0014 N85-10087
Some of the features of movement of gas through a layer of free-flowing substances
[BLL-M-35732-(5628.4)] 02 p0196 N85-11312
Development of a capacitive sensor system for high temperature application
[BMFT-FB-HA-84-027] 05 p0648 N85-14147
Procedure for investigating high-temperature properties of iron-ore materials
[BLL-M-36020-(5628.4)] 07 p0926 N85-15868
Heliostat tested 07 p0994 N85-16318
Application of electricity to the reheating of metals prior to forming. Forging, lamination, induction
[BLL-TR-T6399/BG/MRS14903/84]
08 p1137 N85-17160
Comparative usefulness of flue gas oxygen and carbon dioxide analysis
[BLL-TRANS-T6356/BG/WH783/84]
08 p1179 N85-17430
The EURECA Automatic Gradient Heating Facility (AGHF), phase A study
[ESA-CR(P)-1939] 11 p1591 N85-20005
Development of AK18 alloy production technology based on electrothermic silumin
11 p1598 N85-20048
Three-dimensional analysis of heat transfer and gas flow in a radiant furnace
[DE84-011732] 11 p1633 N85-20284
Study of a constricted electric arc cooled by transpiration
[NASA-TM-77846] 17 p3038 N85-28798
Concept development evaluation for John Deere/UA STS middeck experiment location
[NASA-CR-171541] 20 p3397 N85-31071
High-frequency furnace
[DE85-011210] 21 p3588 N85-32291
The design, construction and operation of a large-area, high-temperature, thermal conductance apparatus --- furnace insulation
[NPL-DMA(A)-84] 22 p3786 N85-33455
FUSELAGE MOUNTING
U AIRCRAFT PRODUCTION
FUSELAGES
Crashworthiness of light aircraft fuselage structures: A numerical and experimental investigation
01 p0060 N85-10399
Analysis of a transport fuselage section drop test
01 p0060 N85-10400
Modeling of aircraft cabin fires
[NBS-GCR-84-473] 04 p0454 N85-12660
Second sailplane project: The RP-2
04 p0468 N85-12977
An in-flight investigation of a twin fuselage configuration in approach and landing
[NASA-CR-172366] 05 p0596 N85-13601
A study of crashworthiness of light aircraft fuselage structures: A numerical and experimental investigation
[UTIAS-266] 08 p0750 N85-14803
Turbulent drag reduction research
08 p1071 N85-16788
Forced corrosion tests of construction components of passenger aircraft fuselages 11 p1600 N85-20062
Study for prediction of rotor/wake/fuselage interference, part 1
[NASA-CR-177340-VOL-1] 13 p1965 N85-22346
Study for prediction of rotor/wake/fuselage interference. Part 2: Program users guide
[NASA-CR-177340-VOL-2] 13 p1966 N85-22347
Redesign of fuselage compartments by method of special contours 13 p2042 N85-22784
Normal mode calculations for fuselage type intricate structures by regarding them as systems with superposed constraints 13 p2048 N85-22817
Development of a fuselage forward section in Carbon Fiber Reinforced Plastic (CFRP) type of construction
[MBB/LFA34/CFK/PUB/006] 17 p2695 N85-27851
A survey of recent development in helicopter aerodynamics 18 p3057 N85-28915
Impact dynamics research on composite transport structures
[NASA-TM-86391] 19 p3284 N85-30367
Fuselage upwash effects on RSRA rotor systems
[NASA-CR-177349] 20 p3388 N85-31015
Estimation of dynamic rotor loads for the rotor systems research aircraft: Methodology development and validation
[NASA-CR-177362] 20 p3393 N85-31045
Simulation and analysis of airborne antenna radiation patterns 20 p3439 N85-31342
Wind tunnel drag evaluations of helicopter nose sections
[AD-A155489] 21 p3553 N85-32100
Aerodynamic characteristics of a distinct wing-body configuration at Mach 6: Experiment, theory, and the hypersonic isolation principle
[NASA-TP-2467] 22 p3727 N85-33107
Ground-based and in-flight simulator studies of flight characteristics of a twin-fuselage passenger transport airplane during approach and landing
[NASA-TP-2451] 23 p3898 N85-34144
FUSES (ORDNANCE)
Safing and arming mechanism
[AD-D011261] 05 p0621 N85-13969
Calculation through Fault Tree Analysis of the probability of a warhead being armed prior to launch
[AD-P004339] 10 p1454 N85-19163
Direct transient analysis of a fuze assembly by axisymmetric solid elements 15 p2576 N85-25890
Properties of Ti-6Al-4V spun formed fuze supports
[DE85-011968] 22 p3792 N85-33498
FUSIFORM SHAPES
U CONES
FUSION
The 1984 review of the Applied Plasma Physics Program
[DE85-002136] 10 p1560 N85-19840
FUSION (MELTING)
Biform resolidification and amorphous phases in a laser and electron beam processed tantalum-iridium alloy
[DE84-013334] 02 p0184 N85-11234
Induction heating gun
[NASA-CASE-LAR-13181-1] 18 p3085 N85-29083
Development of low-melting fused salts 8: Formation of molybdenum film from molten ammonium formate bath
[BLL-OA-TRANS-3195-(5196.500)]
20 p3429 N85-31264
Preparation and use of very pure o-D2
[DE85-009415] 22 p3843 N85-33800
Summary of activities, 1983
[LBL-18500] 23 p3969 N85-34805
FUSION REACTORS
NT SPHEROMAKS
Engineering Physics Division
[DE84-007778] 02 p0274 N85-11787
Review: Role of refractory metal alloys in fusion reactor applications
[AERE-R-11317] 03 p0422 N85-12695
Volatility of vanadium from a candidate fusion tractor alloy
[DE84-015277] 05 p0618 N85-13655
Passive stabilization of vertical instability in Tokamak reactor 06 p0775 N85-14958
Proceedings of Workshop on Synergistic Effects in Surface Phenomena Related to Plasma-Wall Interactions
[IPPJ-AM-35] 06 p0864 N85-15488
Synergistic effects in fusion machines, session summary 06 p0864 N85-15489
Plasma surface interaction processes and possible synergisms 06 p0864 N85-15490
Steady state hydrogen transport in solids
06 p0864 N85-15492
Special topics reports for the reference tandem mirror fusion breeder: Liquid metal MHD pressure drop effects in the packet bed blanket, volume 1
[DE85-002142] 06 p0865 N85-15500
Identification of spectra of highly ionized Mo, Nb, Zr and Y atoms 09 p1390 N85-18745
CTR plasma engineering studies
[DE84-017447] 09 p1392 N85-18762
Magnetic fusion energy plasma interactive and high heat flux components. Volume 2: Technical assessment of the critical issues and problem areas in high heat flux materials and component development
[DE85-001155] 09 p1393 N85-18764
Magnetic fusion energy plasma interactive and high heat flux components. Volume 3: Strategy for international collaborations in the areas of plasma materials interactions and high heat flux materials and components development
[DE85-001145] 10 p1559 N85-19829
Small, octopole-stabilized tandem mirror reactor
[DE85-002144] 10 p1559 N85-19832
Fusion Energy Division
[DE85-001701] 11 p1731 N85-20884
Magneto-fluid-dynamic issues for fusion first wall and blanket systems
[DE85-004022] 14 p2424 N85-24954
Nagoya bumpy torus 15 p2655 N85-26377
Basic research on inertial confinement fusion by LIMAY-I 15 p2655 N85-26383
Plasma theory and computations
15 p2655 N85-26384
Ballooning beta limits of dee and bean shaped Tokamaks
[IPPJ-713] 16 p2866 N85-27676
TOKASTAR: A Tokamak stellarator hybrid with possible bean-shaped operation
[IPPJ-718] 16 p2866 N85-27680
Prospects for developing attractive magnetic fusion concepts
[DE85-006825] 16 p2867 N85-27684
Fusion-power-core design of a Compact Reversed-Field Pinch Reactor (CRFPR)
[DE85-007710] 16 p2868 N85-27692
Heavy ion fusion accelerator research in the US
[DE85-008485] 17 p3034 N85-28767
An Impurity Control Test Facility (ICTF) for the study of fusion reactor/plasma edge materials
[DE85-007948] 17 p3040 N85-28810
Radiation damage experiments and lifetime estimates for beryllium components in fusion systems
[DE85-008038] 17 p3040 N85-28811
Two-dimensional TBR calculations for conceptual compact reversed-field pinch reactor blanket
[DE85-007836] 17 p3040 N85-28812
Pulse star inertial confinement fusion reactor
[DE85-010040] 18 p3181 N85-29726
Inertial fusion reactors and magnetic fields
[DE85-009571] 18 p3191 N85-29789
SHAPS-2: A three-dimensional computer program for linear/non-linear, static/dynamic analyses of piping systems
[DE85-010500] 19 p3335 N85-30658
Test cell modeling and optimization for FPD-2
[DE85-010636] 19 p3358 N85-30821
TFCX shielding optimization
[DE85-010503] 19 p3359 N85-30826
Qualitative comparison of fusion reactor materials for waste handling and disposal
[DE85-010473] 19 p3360 N85-30830
Poloidal variations in toroidal fusion reactor wall power loadings
[DE85-009505] 19 p3362 N85-30848
Tritium system design for the mirror reactors FPD-1, FPD-2 and FPD-3
[DE85-010490] 19 p3363 N85-30852

Molten salt cooling/17Li-83Pb breeding blanket concept
[DE85-010522] 19 p0363 N85-30854
Magnetic fusion 1995: What next?
[DE85-009953] 19 p0365 N85-30868
Steady-state spheromak reactor studies
[DE85-009585] 19 p0372 N85-30916
Current state of development and expected performance of copper-lithium alloys as an impurity control system in fusion applications
[DE85-009573] 19 p0372 N85-30917
Fusion reactions at low energy
[DE85-010561] 20 p0526 N85-31944
MFTF-(alpha) + T shield design
[DE85-010496] 20 p0529 N85-31948
Superconducting toroidal field coil current densities for the TFCX
[DE85-010285] 20 p0530 N85-31950
Fusion facility siting considerations
[DE85-012804] 22 p0843 N85-33805
Key issues of fusion nuclear technology development (FINESSE)
[DE85-012599] 22 p0845 N85-33817
Fusion Power Demonstration (FPD) maintenance and disassembly considerations
[DE85-011413] 22 p0846 N85-33820
Magnetic Fusion Program plan
[DE85-009681] 22 p0848 N85-33823
Blanket optimization studies for Cascade
[DE85-010002] 22 p0846 N85-33824
Data on the backscattering coefficients on light ions from solids: A revision
[IPPJ-AM-41-REV] 23 p0982 N85-34689
Advanced Toroidal Facility (ATF)
[DE85-011567] 23 p0983 N85-34699
Perspective on the next ten years in plasma physics
[DE85-011849] 23 p0984 N85-34706
ECH tokamak
[DE85-012074] 23 p0984 N85-34707

FUSION WELDING
NT ARC WELDING
NT BRAZING
NT ELECTRON BEAM WELDING
NT ELECTROSLAG WELDING
NT GAS TUNGSTEN ARC WELDING
NT LOW TEMPERATURE BRAZING
NT PLASMA ARC WELDING
New application possibilities for clad steel by reducing surface treatment expenditure and by using improved welding technology
[BMFT-FB-T-84-236] 12 p1861 N85-21672

FUZZY SETS
An investigation into fuzzy clustering and classification
[AD-A145571] 02 p0251 N85-11645
Induction of fuzzy decision rules
[INPE-3053-PRE/474] 04 p0554 N85-13525
R and D project selection with nonnumerical returns
[INPE-2760-PRE/335] 04 p0575 N85-13665
Evaluation of fuzzy rulemaking for expert systems for failure detection 05 p0703 N85-14508
Looking at multivariate data through fuzzy sets
[DE85-000884] 11 p1702 N85-20706
Some applications of fuzzy sets and the analytical hierarchy process to decision making
[AD-A150720] 14 p2412 N85-24876
Fuzzy hierarchical analysis
[DE85-006149] 17 p3021 N85-28685
Applications of fuzzy set theory to satellite soundings 18 p3141 N85-29445
Applications of some artificial intelligence methods to satellite soundings 18 p3141 N85-29446

FUZZY SYSTEMS
The R and D project selection problem with fuzzy coefficients
[INPE-3329-PRE/626] 10 p1565 N85-19671
Looking at multivariate data through fuzzy sets
[DE85-000884] 11 p1702 N85-20706
Applications of fuzzy clustering techniques to stratified by tropopause MSU temperature retrievals 18 p3141 N85-29444

F9U AIRCRAFT
U F-8 AIRCRAFT

G

G FORCE
U ACCELERATION (PHYSICS)

GADOLINIUM
Thermomagnetic generator
[DE84-017018] 04 p0530 N85-13368
The Fermi surface and momentum space densities of ferromagnetic Gd using the Positron technique 09 p1396 N85-18786
Structural, morphological and optical characteristics of KGd(WO4)2 crystals 14 p2280 N85-24126
Spectral-luminescence characteristics and induced emission of Nd-3(+) ion in Gd(2-x)Nd(x)(WO4)3 crystals 21 p3688 N85-32912

GAGES
U MEASURING INSTRUMENTS

GAIN (AMPLIFICATION)
U AMPLIFICATION

GALACTIC CLUSTERS
NT ANDROMEDA GALAXIES
NT VIRGO GALACTIC CLUSTER
Fractals: From snow flakes to galactic clusters
[NOTA-INTERNA-796] 02 p0295 N85-11918
Multiple object spectroscopy: The MX spectrometer design 02 p0296 N85-11920
On syntheses of the X-ray background with power-law sources
[NASA-TM-82173] 03 p0446 N85-12840
Galaxy and cluster formation in a universe dominated by cold dark matter
[DE84-015879] 04 p0580 N85-13706
On the scale of distances of the galaxy 05 p0737 N85-14735
Cosmology 07 p1056 N85-16701
A search for young stellar chromospheres in NGC 2264 11 p1748 N85-20993
The UV extinction laws in two very young clusters, NGC 6530 in the galaxy and NGC 2100 in the LMC 11 p1748 N85-20994
The physical implications of an isothermal model for the hot intracluster medium
[NASA-TM-86174] 11 p1763 N85-21089
Recent heavy particle decay in a matter dominated universe
[NASA-CR-175501] 11 p1764 N85-21095
Plasma in the clusters of galaxies 12 p1957 N85-22299
Morphology and energetics of narrow angle tail radio sources 14 p2455 N85-25164
A program of ground-based astronomy to complement einstein observations
[AD-A151111] 15 p2668 N85-26466
Spectral constraints on models of gas in clusters of galaxies
[NASA-TM-86188] 15 p2669 N85-26468
Formation of galaxies
[DE85-009537] 18 p3202 N85-29863
Further studies of X-ray structure of the Perseus cluster
[OG-2.5-12] 22 p3870 N85-33967
Cosmic gamma rays from quasars
[OG-2.7-10] 22 p3872 N85-33983

GALACTIC COSMIC RAYS
Characteristics of latitude effect on cosmic ray charged component in atmosphere at altitudes 3-5 KM 13 p1978 N85-22413
Periodicity of variations in galactic cosmic ray fluxes and solar activity parameters near 20th cycle minimum 16 p2720 N85-26791
Tables of nuclear cross sections for galactic cosmic rays: Absorption cross sections
[NASA-RP-1134] 16 p2884 N85-27685
Diffuse galactic annihilation radiation from supernova nucleosynthesis
[OG-3.2-8] 22 p3875 N85-34004
Cosmic ray intensity and the tilt of the neutral sheet
[SH-4.2-8] 23 p4007 N85-34846
Differential measurement of cosmic-ray gradient with respect to interplanetary current sheet
[SH-4.2-9] 23 p4007 N85-34847
Spatial variation of cosmic rays near the heliospheric current sheet
[SH-4.2-10] 23 p4007 N85-34848
Effects of a wavy neutral sheet on cosmic ray anisotropies
[SH-4.2-11] 23 p4008 N85-34849
Effects of solar magnetic field on cosmic rays
[SH-4.2-12] 23 p4008 N85-34850
Determination of galactic cosmic ray latitudinal gradient using Earth based detectors
[SH-4.2-13] 23 p4008 N85-34851
The expected cosmic ray density and stream distributions at the heliolatitudinal asymmetry of solar wind
[SH-4.2-14] 23 p4008 N85-34852
Latitudinal gradients of cosmic rays and the polarity reversal of the heliospheric magnetic field: A preliminary evaluation
[SH-4.2-16] 23 p4008 N85-34853
The influence of nonstationarity of the solar activity and general solar field on modulation of cosmic rays
[SH-4.2-17] 23 p4008 N85-34854
The effect of the neutral sheet structure of the interplanetary magnetic field on cosmic ray distribution in space
[SH-4.2-18] 23 p4008 N85-34855
On the influence of the heliomagnetospheric periphery on the galactic cosmic rays
[SH-4.2-19] 23 p4009 N85-34856
Spatial distribution of cosmic rays in magnetic cycles of the Sun
[SH-4.2-20] 23 p4009 N85-34857
11- and 22-year variations of the cosmic ray density and of the solar wind speed
[SH-4.2-21] 23 p4009 N85-34858
Difference between even and odd 11-year cycles in cosmic ray intensity
[SH-4.2-22] 23 p4009 N85-34859
The dependence of solar modulation on the sign of the cosmic ray particle charge
[SH-4.2-23] 23 p4009 N85-34860
An update on the correlation between the cosmic radiation intensity and the geomagnetic AA index
[SH-4.2-24] 23 p4009 N85-34861
Cosmic ray secondary nuclei and the structure of the galaxy
[OG-7.2-4] 23 p4014 N85-34876
Why do leaky-box models work so fine?
[OG-7.2-8] 23 p4014 N85-34877
On the importance of interstellar helium for the propagation of heavy cosmic rays
[OG-7.2-11] 23 p4015 N85-34879
A model for the origin of high-energy cosmic rays
[OG-8.1-8] 23 p4018 N85-34898
Astrophysical applications of high angular resolution array-telescopes
[OG-9.5-7] 23 p4031 N85-34984
Recording system for the solar neutron monitoring at Mt. Norikura
[SH-9.1-8] 23 p4051 N85-35123
Burst size distributions in the digitized data of the ion chambers t Mt. Norikura and sea level stations
[SH-9.1-9] 23 p4051 N85-35124
Sensitivity of single and multiple cosmic ray neutrons to the surrounding medium in a lead-free monitor
[SH-9.1-10] 23 p4051 N85-35125
Plastic scintillators in coincidence for the study of multi-particle production of sea level cosmic rays in dense medium
[SH-9.1-11] 23 p4052 N85-35126
The neutron moderated detector and groundbased cosmic ray modulation studies
[SH-9.1-13] 23 p4052 N85-35128
New Matsushiro underground cosmic ray station (220 M.W.E. in depth)
[SH-9.1-14] 23 p4052 N85-35129
Methods and software for cosmic ray scintillation studies
[SH-9.1-17] 23 p4052 N85-35132
The influences of the galactic cosmic ray on the atmospheric ozone
[SH-10.1-1] 23 p4053 N85-35133
Observation of nuclei with energies 8-30 MeV per nucleon in the Earth's magnetosphere at the altitudes 350 KM
[SH-10.1-5] 23 p4053 N85-35136
Measurement of low energy cosmic rays aboard Spacelab-1
[SH-10.1-6] 23 p4053 N85-35137
Heavy cosmic ray measurement aboard Spacelab-1
[SH-10.1-7] 23 p4053 N85-35138

GALACTIC EVOLUTION
The Belikt experiment 02 p0159 N85-11079
Galaxy and cluster formation in a universe dominated by cold dark matter
[DE84-015879] 04 p0580 N85-13706
Fifth Conference on Star Clusters and Associations and Their Relation to the Evolution of the Galaxy
[PUBL-56] 05 p0736 N85-14732
Structural properties of open star clusters and their relation to the galaxy 05 p0736 N85-14733
Open star clusters and the evolution of the galactic disk 05 p0736 N85-14734
Local galactic kinematics 05 p0741 N85-14765
The structure and dynamics of ringed galaxies 09 p1415 N85-18926
Comments on the origins and variations of carbon and nitrogen in the ISM of galaxies as evident from IUE spectroscopy of H 2 regions 11 p1745 N85-20973
Axions in astrophysics and cosmology
[DE85-002720] 11 p1763 N85-21094
Recent heavy particle decay in a matter dominated universe
[NASA-CR-175501] 11 p1764 N85-21095
Cosmology, galactic astronomy and elementary particle physics 12 p1956 N85-22289
Jets in galaxies 12 p1958 N85-22309
Galaxy formation 12 p1960 N85-22321
Research on the early history of the solar system 13 p2180 N85-23527

Dark matter, galaxies, and large scale structure in the universe
[DE85-008053] 16 p2882 N85-27786
Formation of galaxies
[DE85-009537] 16 p3202 N85-29863
Integral constraints on stress energy perturbations in general relativity and applications to cosmology
19 p3383 N85-30985
Activities report of the Institute of Astronomy
20 p3545 N85-32059
Primary gamma-rays with E gamma or = to 10(15) eV: Evidence for ultrahigh energy particle acceleration in galactic sources
[OG-2.6-13] 22 p3871 N85-33974
Implications of the experimental results on high energy cosmic rays with regard to their origin
[OG-5.4-5] 22 p3886 N85-34082
Anisotropy of cosmic rays above 10(14) eV
[OG-5.4-11] 22 p3887 N85-34088
A model for the proton spectrum and cosmic ray anisotropy
[OG-5.4-12] 22 p3887 N85-34089
Why do leaky-box models work so fine?
[OG-7.2-8] 23 p4014 N85-34877
Cosmic-ray exposure records and origins of meteorites
[SH-7.1-7] 23 p4047 N85-35099

GALACTIC MAGNETIC FIELDS
U INTERSTELLAR MAGNETIC FIELDS

GALACTIC NUCLEI
Star formation in interacting galaxies
03 p0444 N85-12826
Infrared mapping of galaxian centers: Star forming regions with kiloparsec scale sizes
03 p0444 N85-12827
Spectral components at visual and infrared wavelengths in active galactic nuclei
[NASA-CR-174133] 03 p0445 N85-12832
Continuum distributions of active galactic nuclei
05 p0742 N85-14770
Physical conditions in low-luminosity active galactic nuclei 05 p0742 N85-14771
The IRAS galaxy 0421+040P06: An active spiral (?) galaxy with extended radio lobes
[NASA-CR-174206] 06 p0871 N85-15536
Some aspects of active galactic nuclei
07 p1056 N85-16702
The environment of active galactic nuclei
07 p1057 N85-16712
The compact radio emission regions in active galactic nuclei — QUASAT VLBI mission
07 p1058 N85-16713
Very Long Base Interferometry (VLBI) in space and X-ray observations of compact sources in active galactic nuclei 07 p1058 N85-16716
X-ray and UV Emission from Active Galactic Nuclei — conference
[MPE-184] 08 p1236 N85-17790
Optical and UV emission of active galactic nuclei
08 p1236 N85-17791
BL Lacertae objects: Multifrequency observations and model applications 08 p1236 N85-17792
Radio Seyferts and the forbidden line region
08 p1236 N85-17793
Active inner regions of isolated galaxies
08 p1237 N85-17795
A new estimate of the local luminosity function of Seyfert 1 nuclei 08 p1237 N85-17796
Optical studies of X-ray selected Active Galactic Nuclei (AGN) in the direction of the Large Magellanic Cloud (LMC) 08 p1237 N85-17797
Continuous transition from star burst galaxies to Seyfert galaxies 08 p1237 N85-17798
Preliminary results on the ultraviolet observations of a complete X-ray selected sample of Active Galactic Nuclei (AGN) — HEAO 2 08 p1237 N85-17800
Spatially resolved optical spectroscopy of the radio jet of the X-ray galaxy NGC 2110 08 p1238 N85-17804
Extragalactic cosmic rays from active galaxies
08 p1238 N85-17805
A comparison of some photometric parameters of active and normal spiral galaxies 08 p1238 N85-17806
X-ray emission from active galactic nuclei
08 p1238 N85-17808
EXOSAT observations of active galactic nuclei
08 p1238 N85-17809
Characteristics of X-ray spectra from galactic and extragalactic X-ray sources 08 p1239 N85-17811
X-ray emission from PKS 2155-304 — BL Lac object
08 p1239 N85-17812
X-ray spectra of accretion disks — active galactic nuclei 08 p1239 N85-17814
EXO 1102.8+2539, an X-ray variable Active Galactic Nucleus (AGN) 08 p1239 N85-17816
UV and X-ray observations of AGN: Two comparisons with other wave lengths — Active Galactic Nuclei (AGN)
08 p1240 N85-17819
Comments on the physics of active galactic nuclei
08 p1240 N85-17823
Physical processes in relativistic plasmas — active galactic nuclei 08 p1240 N85-17824
A universal spectrum for AGNs and QSOs — Active Galactic Nuclei (AGN) 08 p1241 N85-17826
Shock acceleration in active galactic nuclei and quasars 08 p1241 N85-17828
Power law X- and gamma-ray emission from relativistic thermal plasmas 08 p1241 N85-17829
Pair production at moderate optical depths — galactic nuclei X ray spectra 08 p1241 N85-17830
On the hydrodynamical equations of astrophysical jets — active galactic nuclei 08 p1241 N85-17831
Collimated winds from active galactic nuclei
08 p1241 N85-17832
An alternative to relativistic beaming in AGN — Active Galactic Nuclei (AGN) 08 p1242 N85-17833
Centrifugally driven magnetohydrodynamic (MHD) winds and the nonthermal emission regions in Active Galactic Nuclei (AGN) 08 p1242 N85-17835
Macroscopic currents and wind perturbations in the frame of the wind and shock model — galactic nuclei
08 p1242 N85-17836
Dueling winds: A model for broad-line regions — galactic nuclei 08 p1242 N85-17837
X-ray spectra of accretion disks — active galactic nuclei 08 p1242 N85-17838
On the stability of broad line clouds in active galactic nuclei 08 p1243 N85-17840
Active galactic nuclei and their cosmological evolution
08 p1243 N85-17842
Very long base interferometry (VLBI) and X-ray observations of complete samples of radio selected active galactic nuclei 08 p1243 N85-17847
Ultraviolet and X-ray observations of active galactic nuclei: Constraints on models of the broad emission line region 11 p1744 N85-20966
Structure of the Seyfert broad line region and absorption region of NGC 4151 11 p1746 N85-20978
Broad emission features in active galactic nuclei
11 p1746 N85-20979
Coordinated multifrequency observations of the BL LAC objects MRK 180, MRK 421, and MRK 501
11 p1746 N85-20983
Interstellar extinction in the nucleus of H PER
11 p1749 N85-21001
X-ray emission from active galactic nuclei
[NASA-TM-86175] 11 p1763 N85-21088
Consequences of hot gas in the broad line region of active galactic nuclei
[NASA-TM-86176] 11 p1763 N85-21090
Electron-positron pairs in a mildly relativistic plasma in active galactic nuclei 12 p1957 N85-22297
Hydrodynamics of astrophysical jets — active galactic nuclei 12 p1958 N85-22307
Viscous jets — extragalactic jets
12 p1958 N85-22308
Small scale structure and the Spinar model for active galactic nuclei 12 p1959 N85-22316
All-Union conference of radio astronomers
13 p1977 N85-22408
IRAS observations of active galaxies
[NASA-CR-175720] 15 p2666 N85-26483
Interactions of galaxies and their nuclear activity
20 p3545 N85-32060
The hydrodynamic effects of nuclear active galaxy winds on host galaxies 20 p3545 N85-32062
Spectra and positions of galactic gamma-ray sources
[OG-2.5-7] 22 p3869 N85-33963
Search for TeV gamma rays from extragalactic sources and the Galactic Center
[OG-2.7-1] 22 p3871 N85-33976
Gamma-radiation with E gamma 5 MeV detected from Seyfert galaxy 3C120 and region with 1° = 190 deg and b° = 20 deg
[OG-2.8-6] 22 p3871 N85-33981
Galactic distribution of interstellar Al-26
[OG-3.2-3] 22 p3874 N85-34002
Cosmic rays in the 10(16) to 10(19) eV range from pulsars
[OG-5.4-3] 22 p3886 N85-34080
Energy dependence of cosmic ray composition above 10(15) GeV/nucleus
[OG-5.4-4] 22 p3886 N85-34081
The 1973-1984 solar modulation of cosmic ray nuclei
[SH-4.1-16] 23 p4006 N85-34836
The effects of newly measured cross sections in hydrogen on the production of secondary nuclei during the propagation of cosmic rays through interstellar H
[OG-7.2-2] 23 p4014 N85-34874
The central engine of quasars and AGNs: A relativistic proton radiative shock
[OG-8.1-7] 23 p4018 N85-34897
Cerenkov light images of EAS produced by primary gamma
[OG-9.5-3] 23 p4030 N85-34979

GALACTIC RADIATION
NT GALACTIC COSMIC RAYS
NT GALACTIC RADIO WAVES
NT NORTH POLAR SPUR (ASTRONOMY)
Constraints to the radiative lifetime of a light neutral fermion in the galactic halo from IUE
[NOTA-INTERNA-817] 02 p0279 N85-11820
Star formation in interacting galaxies
03 p0444 N85-12826
Infrared mapping of galaxian centers: Star forming regions with kiloparsec scale sizes
03 p0444 N85-12827
Spectral components at visual and infrared wavelengths in active galactic nuclei
[NASA-CR-174133] 03 p0445 N85-12832
Far-infrared line emission from the galaxy
[NASA-CR-174166] 04 p0580 N85-13702
The IRAS galaxy 0421+040P06: An active spiral (?) galaxy with extended radio lobes
[NASA-CR-174206] 06 p0871 N85-15536
Optical emission line studies and the warm, ionized component of the local interstellar medium
06 p0875 N85-15555
On the record of galactic cosmic ray flux and traffic break-ups in iron meteorites 06 p0887 N85-15634
The ultraviolet spectra of the narrow line active galaxies NGC 3081 and NGC 4507 06 p1237 N85-17799
Low excitation absorptions in the spectrum of the quasar PKS 1327-206 due to the galaxy MCG 03-34-085
06 p1237 N85-17801
The origin of the X-ray background
06 p1243 N85-17841
Far infrared emission from galaxies
06 p1248 N85-17875
Far infrared continuum emission from the galactic center 06 p1248 N85-17876
Dust reradiation from NGC 6946
06 p1248 N85-17880
Far-infrared spectroscopy of galaxies: The 158 micron C(+) line 06 p1249 N85-17882
Interpretation of the far infrared emission from our external galaxies 06 p1249 N85-17884
X-ray emission from Centaurus A
[DE85-002030] 09 p1417 N85-18943
Coordinated multifrequency observations of the BL LAC objects MRK 180, MRK 421, and MRK 501
11 p1746 N85-20983
IRAS observations of Seyfert galaxies
[NASA-CR-175557] 12 p1953 N85-22287
Morphology and energetics of narrow angle tail radio sources 14 p2455 N85-25164
Results from the Helios galactic and solar cosmic ray experiment (E7) 16 p2666 N85-27607
Differential measurement of cosmic-ray gradient with respect to interplanetary current sheet
[PAPER-SH-4.2-9] 21 p3715 N85-33055
Galactic gamma-ray sources, SNOBs, and giant H2 regions
[OG-2.5-4] 22 p3869 N85-33961
Inverse-Compton gamma rays in the galaxy
[OG-3.1-2] 22 p3873 N85-33990
Radial distribution of cosmic ray intensity in the galaxy from gamma-ray data
[OG-3.1-5] 22 p3873 N85-33993
Local electron spectrum above 100 MeV derived from gamma-ray emissivity spectra
[OG-3.1-7] 22 p3874 N85-33995
Relevance of cosmic gamma rays to the mass of gas in the galaxy
[OG-3.1-8] 22 p3874 N85-33996
A measurement of the cosmic ray elements C to Fe in the two energy intervals 0.5-2.0 GeV/n and 20-60 GeV/n
[OG-4.1-6] 22 p3876 N85-34012
Cosmic ray nuclei of energy 50 GeV/NUC
[OG-4.1-12] 22 p3877 N85-34018
Interstellar propagation and the isotopic composition of hydrogen in the galactic cosmic rays
[OG-4.2-1] 22 p3877 N85-34021
Measurements of galactic hydrogen and helium isotopes from 1978 through 1983
[OG-4.2-2] 22 p3877 N85-34022
Galactic propagation models consistent with the cosmic ray lifetime derived from Be-10 measurements
[OG-4.3-1] 22 p3878 N85-34026
Implications of new measurements of O-16 + p + C-12,13, N-14,15 for the abundances of C, N isotopes at the cosmic ray source
[OG-4.3-2] 22 p3878 N85-34027

The isotopic composition of cosmic ray chlorine
[OG-4.3-3] 22 p3878 N85-34028
Cosmic ray isotope measurements with a new Cerenkov X total energy telescope
[OG-4.3-4] 22 p3878 N85-34029
The isotopic composition of cosmic ray calcium
[OG-4.3-5] 22 p3879 N85-34030
A new analysis of cosmic ray isotopes at 3 GeV/n from HEA03-C2 data
[OG-4.3-6] 22 p3879 N85-34031
The energy dependence of the neon-22 excess in the cosmic radiation
[OG-4.3-7] 22 p3879 N85-34032
Ariel 6 measurements of ultra-heavy cosmic ray fluxes in the region 34 or = Z or = 48
[OG-4.4-3] 22 p3879 N85-34036
Ariel 6 measurements of ultra-heavy cosmic ray fluxes in the region Z or = 46
[OG-4.4-4] 22 p3880 N85-34037
Elemental abundances of cosmic rays with Z 33 as measured on HEAO-3
[OG-4.4-5] 22 p3880 N85-34038
Capabilities of the LDEF-2 heavy nuclei collection
[OG-4.4-6] 22 p3880 N85-34040
Energy spectrum and arrival direction of primary cosmic rays of energy above 10 to the 18th power eV
[OG-5.1-1] 22 p3880 N85-34043
Ultra high energy cosmic ray spectrum
[OG-5.1-2] 22 p3881 N85-34044
The primary cosmic ray spectrum above 10 to the 19th power eV
[OG-5.1-3] 22 p3881 N85-34045
Estimation of composition of cosmic rays with E sub zero approximately equals 10(17) - 10(18) eV
[OG-5.1-14] 22 p3882 N85-34055
On galactic origin of cosmic rays with energy up to 10(19) eV
[OG-5.4-15] 22 p3887 N85-34091
Galactic cosmic ray antiprotons and supersymmetry
[OG-6.1-9] 22 p3888 N85-34100
Effect of seeds of heavy charged particles of galactic cosmic radiation 23 p3954 N85-34505
Abundances from solar-flare gamma-ray line spectroscopy
[SH-2.1-13] 23 p3999 N85-34794
Type 3 solar radio bursts and 3HE-rich events
[SH-2.2-3] 23 p4000 N85-34798
the role of shock waves in modulation of galactic cosmic rays
[SH-4.1-7] 23 p4005 N85-34831
Propagation of the phase of solar modulation
[SH-4.1-12] 23 p4005 N85-34835
Germanium and lead: Significant differences between meteoritic and photospheric abundances?
[OG-7.1-2] 23 p4012 N85-34864
Implications of source abundances of ultraheavy cosmic rays
[OG-7.1-4] 23 p4013 N85-34866
Propagation and nucleosynthesis of ultraheavy cosmic rays
[OG-7.1-5] 23 p4013 N85-34867
On the importance of interstellar helium for the propagation of heavy cosmic rays
[OG-7.2-11] 23 p4015 N85-34879
Cosmic-ray transport in the galactic magnetosphere
[OG-7.2-17] 23 p4016 N85-34884
The role of cosmic rays and Alfven waves in the structure of the galactic halo
[OG-7.2-18] 23 p4016 N85-34885
Do supernovae of type 1 paly a role in cosmic-ray production?
[OG-8.2-5] 23 p4019 N85-34905
Neutron-rich nuclei in cosmic rays and Wolf-Rayet stars
[OG-8.2-6] 23 p4019 N85-34906
Bursting star formation and the overabundance of Wolf-Rayet stars
[OG-8.2-8] 23 p4019 N85-34907
Interstellar (Na-22) as a possible source of the excess (Na-22) in the galactic cosmic ray
[OG-8.2-12] 23 p4020 N85-34908
The electromagnetic ram action of the plasma focus as a paradigm for the generation of cosmic rays and the gigantic jets in active galaxies
[OG-8.2-14] 23 p4020 N85-34910
The origins of cosmic rays and quantum effects on gravity
[OG-8.2-15] 23 p4020 N85-34911
Influence of the source distribution on the age distribution of galactic cosmic rays
[OG-8.3-1] 23 p4021 N85-34920
Explanation of the secondary to primary ratio within the continuous Fermi accelerator model
[OG-8.3-2] 23 p4021 N85-34921
Propagation of cosmic rays and new evidence for distributed acceleration
[OG-8.3-5] 23 p4022 N85-34924
High resolution Cherenkov detectors for cosmic ray isotope experiment
[OG-9.1-4] 23 p4023 N85-34930
A high resolution gas Cerenkov detector for the superconducting magnet facility
[OG-9.1-6] 23 p4023 N85-34932
Mass resolution optimization in a large isotopic composition experiment
[OG-9.1-9] 23 p4023 N85-34935
The difference in the energy spectra of galactic cosmic rays at the minima of the 19th and 20th solar activity cycles
[SH-4.4-18] 23 p4035 N85-35014
Azimuthal and meridional asymmetries of the solar wind and quasiperiodic variations of intensity of Galactic Cosmic Rays (GCR)
[SH-4.4-20] 23 p4035 N85-35016
Long-term modulation of galactic cosmic rays in high-energy region
[SH-4.4-22] 23 p4035 N85-35018
The first three harmonics of solar daily variation caused by the diffusive propagation of galactic cosmic rays through the heliosphere
[SH-4.5-1] 23 p4035 N85-35019
Diurnal variation of galactic cosmic ray intensity on quiet days
[SH-4.5-11] 23 p4037 N85-35029
Solar modulation and interplanetary gradients of the galactic electrons flux, 1977 - 1984
[SH-4.7-4] 23 p4040 N85-35049
Galactic cosmic ray radial gradients and the anomalous He component near maximum solar modulation and to radii beyond 34 AU from the Sun
[SH-4.7-5] 23 p4040 N85-35050
Voyager 1 and 2 measurements of radial and latitudinal cosmic ray gradients during 1981 - 1984
[SH-4.7-6] 23 p4041 N85-35051
The large-scale modulation of cosmic rays in mid-1982: Its dependence on heliospheric longitude and radius
[SH-4.7-9] 23 p4041 N85-35053
Nonstationary modulation of galactic cosmic rays in a nonlinear model
[SH-4.7-10] 23 p4041 N85-35054
Dimensions of the solar wind cavity and of the region of interplanetary cosmic ray modulation
[SH-4.7-11] 23 p4041 N85-35055
Drift and Forbush decreases
[SH-5.1-2] 23 p4041 N85-35056
Anomalous short-term increases in the galactic cosmic ray intensity: Are they related to the interplanetary magnetic cloud-like structures?
[SH-5.1-3] 23 p4041 N85-35057
Longitudinal dependence of the interplanetary perturbation produced by energetic type 4 solar flares and of the associated cosmic ray modulation
[SH-5.1-5] 23 p4042 N85-35059
Galactic cosmic ray currents and magnetic field irregularity degree in high-speed solar wind streams
[SH-5.1-9] 23 p4042 N85-35063
Influence of magnetic clouds on cosmic ray intensity variations
[SH-5.1-12] 23 p4042 N85-35065
Cosmic rays 10Be biennal data and their relationship to auroras and sunspots
[SH-7.1-1] 23 p4047 N85-35094
Cosmogenic-nuclide production by primary cosmic-ray protons
[SH-7.1-6] 23 p4047 N85-35098
Accelerator experiments on the contribution of secondary particles to the production of cosmogenic nuclides in meteorites
[SH-7.1-8] 23 p4048 N85-35100
Depth and size effects on cosmogenic nuclide production in meteorites
[SH-7.1-9] 23 p4048 N85-35101
A search for cosmic sources of high energy neutrinos with small underground detectors
[HE-5.3-16] 24 p4206 N85-36110

GALACTIC RADIO WAVES
NT NORTH POLAR SPUR (ASTRONOMY)
Radio Seyferts and the forbidden line region
08 p1236 N85-17793
The relationship between radio structures and stellar dynamics of nearby elliptical galaxies
08 p1236 N85-17794
All-Union conference of radio astronomers
13 p1977 N85-22408
Radio counterparts of galactic gamma-ray sources
20 p3549 N85-32085

GALACTIC ROTATION
On a spectral theory of the excitation mechanism of galactic spirals
12 p1955 N85-22284
The study of the physics of cometary nuclei
[NASA-CR-175917] 17 p3054 N85-29905
A simulation of high energy cosmic ray propagation 2
[OG-5.4-2] 22 p3885 N85-34079

GALACTIC STRUCTURE
The galactic distribution of open clusters of different ages and the angular velocity of the spiral structure
05 p0737 N85-14737
On collective effects in the rotation of stars in clusters and associations 05 p0737 N85-14739
Excitation of spiral patterns in responsible density wave theory 05 p0740 N85-14764
Local galactic kinematics 05 p0741 N85-14765
Some aspects of active galactic nuclei
07 p1056 N85-16702
The galactic gamma-ray distribution: Implications for galactic structure and the radial cosmic ray gradient
[NASA-TM-86173] 07 p1061 N85-16729
The relationship between radio structures and stellar dynamics of nearby elliptical galaxies
08 p1236 N85-17794
Continuous transition from star burst galaxies to Seyfert galaxies 08 p1237 N85-17796
The structure and dynamics of ringed galaxies
09 p1415 N85-18926
On the morphology of spiral modes — disk galaxies
12 p1955 N85-22283
Drift-accretion theory of the spiral structure of galaxies
12 p1957 N85-22298
Some constraints on magnetic fields in galactic spiral arms 12 p1957 N85-22300
Small scale structure and the Spinar model for active galactic nuclei 12 p1959 N85-22316
The color excesses of classical cepheids and the structure of our galaxy 13 p2169 N85-23459
Gas dynamics of the barred spiral galaxy NGC 3359
13 p2170 N85-23465
Dynamics of gas disks in triaxial galaxies
13 p2171 N85-23469
A rocket-borne X-ray observation of SN1006 with the imaging gas scintillation proportional counter
14 p2435 N85-25014
Formation of galaxies
[DE85-009537] 18 p3202 N85-29883
Cosmic ray secondary nuclei and the structure of the galaxy
[OG-7.2-4] 23 p4014 N85-34876
High energy cosmic ray signature of quark nuggets
[HE-6.2-11] 24 p4212 N85-36147

GALACTOSE
Galactose oxidase in stereospecific oxidation of primary alcohols
[AD-A154059] 19 p3234 N85-30048

GALAXIES
NT ANDROMEDA GALAXIES
NT BARRED GALAXIES
NT DISK GALAXIES
NT ELLIPTICAL GALAXIES
NT GALACTIC CLUSTERS
NT MAGELLANIC CLOUDS
NT MILKY WAY GALAXY
NT RADIO GALAXIES
NT SEYFERT GALAXIES
NT SPIRAL GALAXIES
NT VIRGO GALACTIC CLUSTER
IRAS observations of external galaxies
03 p0443 N85-12825
Galaxy and cluster formation in a universe dominated by cold dark matter
[DE84-015879] 04 p0580 N85-13706
Unidentified IRAS sources: Ultrahigh luminosity galaxies
[NASA-CR-174207] 06 p0672 N85-15537
Supersymmetric inflationary cosmology
[DE85-001331] 06 p0681 N85-15598
Far infrared emission from galaxies
08 p1248 N85-17875
Starbursts in galaxies: Implications of molecular and far-infrared observations 06 p1248 N85-17881
Far-infrared spectroscopy of galaxies: The 158 micron C(+) line 08 p1249 N85-17882
Far infrared spectroscopy of (O III) in M82
08 p1249 N85-17883
Data reduction 09 p1412 N85-18903
Combined ultraviolet studies of astronomical sources
[NASA-CR-174361] 09 p1413 N85-18910
Research in extreme ultraviolet and far ultraviolet astronomy
[NASA-CR-174432] 10 p1570 N85-19902
International Ultraviolet Explorer observations of amorphous hot galaxies
[NASA-CR-174354] 10 p1571 N85-19904
Future of Ultraviolet Astronomy Based on Six Years of IUE Research
[NASA-CP-2349] 11 p1743 N85-20961

Galactic absorption lines measured from the IUE low dispersion spectra of active galaxies
11 p1745 N85-20977
University of Cambridge Institute of Astronomy report of activities
13 p2170 N85-23464
Studies of galactic HI in 21-centimeter absorption
13 p2170 N85-23466
Color evolution in high redshift galaxies
20 p3544 N85-32055
Activities report of the Institute of Astronomy
20 p3545 N85-32059
The kinematic and radial properties of normal luminous SC galaxies
20 p3545 N85-32061
Activities report of the Department of Astrophysics
20 p3546 N85-32064
Search for positron annihilation line and continuum radiation from the Galactic Center
[OG-2.5-5] 22 p3869 N85-33962
Charge 4/3 leptons in cosmic rays
[HE-6.2-14] 24 p4212 N85-36150

GALAXY AIRCRAFT
U C-5 AIRCRAFT

GALERKIN METHOD
The convergence of Garlerkin approximation schemes for second-order hyperbolic equations with dissipation
[CSIR-TWISK-325] 01 p0109 N85-10736
Spline-Galerkin solution of integral equations for 3-body scattering above break-up
[TWISK-327] 01 p0109 N85-10738
Approximation of discontinuous solutions of hyperbolic partial differential equations
[NRIMS-TWISK-302] 02 p0250 N85-11631
Time discretization of parabolic problems by the discontinuous Galerkin method
[CTH-MATH-1984-16] 04 p0556 N85-13543
A lumped mass finite element method with quadrature for a nonlinear parabolic problem
[CTH-MATH-1984-22] 05 p0719 N85-14615
Algorithm for the simulation of transient viscoelastic flows with free surfaces
[DE85-002713] 12 p1848 N85-21590
Low-dimensional behavior of the pattern formation Cahn-Hilliard equation
[DE85-003727] 12 p1922 N85-22072
Spline-based Rayleigh-Ritz methods for the approximation of the natural modes of vibration for flexible beams with tip bodies
[NASA-CR-172566] 13 p2102 N85-23100
Solution of Onsager's equation for a rotating compressible fluid in a multiply-connected domain
[DE85-007048] 16 p2784 N85-27178
A study of internal and distributed damping for vibrating turbomachiner blades
[NASA-CR-175901] 17 p2898 N85-27868
A fast implementation of explicit time stepping algorithms with the finite element method for a class of nonlinear evolution problems
[REPT-84-03] 17 p3021 N85-28686
Applications of the Galerkin formalism in the coupling of the earth's free oscillations 24 p4116 N85-35514

GALILEAN SATELLITES
NT CALLISTO
NT EUROPA
NT GANYMEDE
NT IO
Stability of the Galilean satellites in deep orbital resonance
13 p2172 N85-23477
Creep of ice: Further studies
13 p2201 N85-23655
The Galilean Satellite Geological Mapping Program, 1984
13 p2203 N85-23664
Voyagar cartography
13 p2203 N85-23668
The control networks of the satellites of Jupiter and Saturn
13 p2204 N85-23671
Interpretation of photometric measurements of airless bodies
22 p3855 N85-33871

GALILEO MISSION
U GALILEO PROJECT

GALILEO PROBE
Galileo
15 p2668 N85-26601

GALILEO PROJECT
Mission science value-cost savings from the Advanced Imaging Communication System (AICS)
[NASA-CR-174170] 04 p0458 N85-12905
Reed-Solomon decoder — applicable to Galileo Project requirements
[NASA-CASE-NPO-15982-1] 11 p1699 N85-20660
The 1986 National Aeronautics and Space Administration authorization
[GPO-47-635] 24 p4166 N85-35829

GALILEO SPACECRAFT
Transient vibration test criteria for spacecraft hardware — galileo spacecraft 09 p1338 N85-18418
Solid particle environment and protection for the Galileo Orbiter
12 p1786 N85-21207
Galileo internal electrostatic discharge program
13 p1995 N85-22504
Galileo battery testing and the impact of test automation
20 p3444 N85-31381
The Galeleo spacecraft magnetometer boom
22 p3796 N85-33513

GALL
Biligenic function of white rat liver
01 p0093 N85-10624

GALLIUM
Development of high responsitivity Ge:Ga photoconductors
[DE84-016902] 04 p0571 N85-13643
IUE observations of the gaseous component of the local interstellar medium
06 p0674 N85-15553
Research on the basic understanding of high efficiency in silicon solar cells
[DE85-000507] 11 p1672 N85-20537
Angle-resolved photoemission study of AuGa2 and AuIn2 intermetallic compounds
[AD-A150000] 12 p1940 N85-22183
Annealing of radiation damage in boron and gallium doped silicon solar cells
13 p2012 N85-22624
Improvement in magnetic field properties of vanadium-gallium superconductors by enhancement of spin-orbit scattering
[DE85-002693] 13 p2164 N85-23422
Specificity of (71)Ga(p,n) (71)Ge at 35 MeV for Gamow-Teller strength
[DE85-011837] 23 p3971 N85-34615

GALLIUM ANTIMONIDES
Photoluminescent properties of epitaxial p-GaSb
02 p0267 N85-11745
Cascaded solar photovoltaic cells based on InP-GaInPAs and InP-CdS heterostructures
02 p0268 N85-11749
Raman scattering from metastable GaSb(1-x) Ge(2x) alloys
[AD-A145897] 03 p0327 N85-12108
Inter-zone auger recombination in GaSb laser structures
21 p3682 N85-32875

GALLIUM ARSENIDE LASERS
Space-time characteristics of radiation of single-mode injection lasers
02 p0269 N85-11758
Heatsink requirements for coherent operation of high-power semiconductor laser arrays
[AD-A146184] 03 p0368 N85-12346
Design and chemical synthesis of iodine-containing molecules for application to solar-pumped I* lasers
[NASA-CR-176010] 19 p3275 N85-30310
Phase locked loops for optical homodyne detection, volume 2 — spaceborne receivers
[ESA-CR(P)-2029-VOL-2] 20 p3442 N85-31368
Low-threshold injection InGaAsP/GaAs double heterostructure lasers with separate limiting obtained by liquid-phase epitaxy (lambda = 0.78 divided by 0.87 microns, I sub thr = 460 A/cm 2, T = 300 K)
21 p3687 N85-32908
Influence of technological factors on luminescence characteristics of InGaAsP/InP heterolasers (lambda = 1.55 microns)
21 p3688 N85-32910

GALLIUM ARSENIDES
NT ALUMINUM GALLIUM ARSENIDES
NT SUPERLATTICES
An investigation of the solubility and diffusivity of chromium in gallium arsenide
[AD-A144949] 01 p0024 N85-10148
Solution of the Boltzmann transport equations for a permeable base transistor
[AD-A144969] 01 p0112 N85-10757
Acoustic resonator and method of making same
[DE84-014655] 01 p0116 N85-10792
Plasma deposited diamondlike carbon on GaAs and InP
[NASA-TM-86870] 01 p0123 N85-10844
Producing gallium arsenide crystals in space
02 p0151 N85-11023
Research directions and progress in the SERI advanced high efficiency concept program
[DE84-004582] 02 p0223 N85-11482
Luminous points and breakdown in structure of GaAs transistors
02 p0257 N85-11684
Composition of metal films on gallium arsenide surface
02 p0257 N85-11685
Impurity trapping during gas phase epitaxy of gallium arsenide
02 p0257 N85-11686
Spectral distribution of radiation in n junctions of GaAs during avalanche breakdown
02 p0258 N85-11688
Complex formation and temperature stability of electrophysical properties of GaAs semiinsulating single crystals
02 p0258 N85-11689
Reversible change in parameters of GaAs-based surface-barrier metal-semiconductor diodes induced by hydrogen absorption-desorption
02 p0258 N85-11690
Nonlinear absorption of laser radiation in InP and in GaAs
02 p0266 N85-11740
Injection lasers based on AlGaAsSb/GaSb and InGaAsSb/GaSb heterostructures
02 p0270 N85-11761
Splitting of surface polariton spectrum by holographic grating
02 p0272 N85-11771
Electron traps in the GaAs permeable base transistor
[AD-A145399] 02 p0287 N85-11871
Reflection electron energy loss investigation of the H-GaAs(110) surface
[NOTA-INTERNA-811] 02 p0289 N85-11888
Raman scattering from metastable GaSb(1-x) Ge(2x) alloys
[AD-A145897] 03 p0327 N85-12108
Studies of grown-in defects versus growth parameters in 3-4 compound semiconductors
[AD-A145864] 03 p0433 N85-12755
Folded acoustic and quantized optic phonons in semiconductor superlattices
[AD-A145935] 03 p0433 N85-12756
High-temperature optically activated GaAs power switching for aircraft digital electronic control
[NASA-CR-174711] 04 p0457 N85-12901
Effect of barrier height on friction behavior of the semiconductors silicon and gallium arsenide in contact with pure metals
[NASA-TP-2405] 04 p0478 N85-13044
Glow spots and breakdown in GaAs transistor structure
04 p0487 N85-13107
Lifetime of excess charge carriers in weakly doped epitaxial GaAs layers
04 p0487 N85-13108
Trends in space photovoltaic technology
05 p0609 N85-13666
Material models and device structures for GaAs solar cells
[DE85-000501] 05 p0665 N85-14275
Material models and device structures for GaAs solar cells, introduction
05 p0665 N85-14276
GaAs material properties and models
05 p0665 N85-14277
Comparison of SCAPID/GaAs to experiment
05 p0665 N85-14279
Radiation hardened ion-implanted GaAs field effect transistor and method for making the same specification
[AD-D011264] 05 p0731 N85-14697
Photoluminescence studies of Ga(As,P) strained-layer superlattices
[DE84-015709] 05 p0731 N85-14701
Raman study of neutron irradiated GaAs
[DE84-016056] 05 p0731 N85-14702
Numerical estimation of charge transfer time in charge-coupled device employing latent gallium arsenide channel
06 p0793 N85-15069
Gallium-arsenide power devices
06 p0794 N85-15076
Gallium arsenide compounds tested nondestructively with X-rays
07 p0936 N85-15934
Development of short gate FET's
[AD-A147033] 07 p0947 N85-15999
X-ray and backscattering analysis of ion implantation phenomena in GaAs and related compounds
[AD-A147449] 07 p1048 N85-16659
Aluminum nitride insulator for 3-5 MIS (Metal-Insulator-Semiconductor) applications
[AD-A147842] 07 p1049 N85-16662
French research on gallium arsenide devices
08 p1141 N85-17196
Automated assembly of Gallium Arsenide and 50-micron thick silicon solar cell modules
[NASA-CR-174331] 08 p1168 N85-17364
Characterization of thermally treated gallium arsenide by laser-Raman and Auger spectroscopy
[AD-A148414] 08 p1226 N85-17721
Ion implantation in 3-5 compound semiconductors
[AD-A148462] 08 p1226 N85-17723
ONR (Office of Naval Research) Far East Scientific Bulletin, volume 9, number 3, July to September 1984
[AD-A147282] 08 p1262 N85-17930
Transient response of a small-signal microwave GaAs FET to X-rays
[DE85-000066] 09 p1315 N85-18265
A picosecond population modulation study of near interband resonances in semiconductors
09 p1396 N85-18787
Effect of hydrostatic pressure on trapping centers in strained-layer superlattice structures
[DE85-001382] 09 p1399 N85-18807
Material growth and characterization for solid state devices
[NASA-CR-174410] 10 p1561 N85-19847
Surface and interfacial properties of Ga(0.47) In(0.53)As alloys
[AD-A146891] 10 p1562 N85-19849

Fabrication of monocrystalline GaAs solar cells utilizing NaCl sacrificial substrates
[DE84-013016] 11 p1673 N85-20544
Determination of the mobility profile in GaAs-MESFETs
[NASA-TM-77618] 11 p1734 N85-20905
Low stress semiconductor-insulator interface for cryogenic device applications
[NASA-CASE-NPO-16394-1] 11 p1734 N85-20906
AlAs/GaAs superlattice barrier unipolar diode structure
[DE85-001904] 11 p1736 N85-20921
GaAs and 3-5 compound solar cells status and prospects for use in space
[NASA-TM-86960] 12 p1795 N85-21261
Distributed Gunn effect devices; a numerical analysis of microstrip circuits on thin active GaAs substrates
[FOA-C-30383-E] 12 p1837 N85-21527
New high resolution scanning ion microprobe and focused ion beam applications
[AD-A149992] 12 p1852 N85-21616
Characterization of high purity Si-doped molecular beam epitaxial GaAs
[AD-A149651] 12 p1939 N85-22181
Semiconductor materials for high frequency solid state sources
[AD-A150020] 12 p1940 N85-22186
Evaluation of implantation-disordering of (InGa)As/GaAs strained-layer superlattices
[DE85-003533] 12 p1942 N85-22200
Gallium arsenide arrays versus silicon arrays for space application 13 p2006 N85-22574
Space qualified AlGaAs/GaAs solar cells
13 p2006 N85-22575
Availability of AlGaAs/GaAs solar cells in space
13 p2006 N85-22576
Comparative study of GaAs solar cell potentialities for space applications 13 p2006 N85-22577
Investigation of high output gallium arsenide solar cells 13 p2006 N85-22578
Development of very thin large area GaAs solar cells for space application 13 p2006 N85-22579
GaAs and 3-5 compound solar cells status and prospects for use in space 13 p2007 N85-22580
GaAlAs-GaAs solar cell development: Prospective for space applications under concentration
13 p2007 N85-22581
Investigation of the degradation of GaAs photovoltaic cells by proton and electron irradiation
13 p2008 N85-22587
Isotropic proton irradiation of GaAs solar cells
13 p2012 N85-22622
High output photovoltaic conversion: The quadrispectral project — spacecraft power supplies
13 p2012 N85-22626
Thermally stimulated conductivity in semi-insulating gallium arsenide 13 p2068 N85-23036
Fracture mechanics evaluation of GaAs
[NASA-CR-175857] 13 p2102 N85-23101
Some observations of heated gallium arsenide heteroface solar cells
[NASA-TM-86388] 14 p2246 N85-23925
Physical electronics of cooled operation of very short compound semiconductor transistors
14 p2297 N85-24223
Cryogenically-cooled, low-noise microwave receivers: Present status and future needs
14 p2298 N85-24226
Advanced high-efficiency concentrator cell
[DE85-000525] 14 p2351 N85-24533
Infrared nonlinear processes in semiconductors
[AD-A150966] 14 p2427 N85-24968
Ion implantation disorder in strained-layer superlattices
[DE85-004466] 14 p2430 N85-24984
Dual species ion implantation of ternary compounds based on In-Ga-As
[AD-D011617] 16 p2869 N85-27698
A study of Ga(.47)In(.53)As and Al(.48)In(.52)As for very high frequency device applications
[AD-A151995] 16 p2870 N85-27706
Effect of dislocations on gallium arsenide FETs
[AD-A152249] 16 p2870 N85-27709
TEM investigation of polar-on-nonpolar epitaxy: GaAs-AlGaAs on (100) Ge
[DE85-007613] 16 p2871 N85-27714
Random access memory technologies
[AD-A153089] 17 p3008 N85-28597
Optical waveguide characterization using grating couplers
[AD-A153063] 17 p3037 N85-28789
Activities of the Solid State Physics Research Institute
[NASA-CR-175899] 17 p3042 N85-28818
Leakage effects in n-GaAs MESFET with n-GaAs buffer layer 17 p3043 N85-28826
GaAs MESFET with lateral non-uniform doping
17 p3043 N85-28827
Materials-process interactions in ternary alloy semiconductors
[AD-A153133] 17 p3043 N85-28832
Development of photodetectors
[AD-A153773] 18 p3095 N85-29158
Evaluation of VLSI technology — space applications
[CD.6501702] 18 p3098 N85-29177
Mechanically-stacked multijunction solar cells
[DE85-010389] 18 p3129 N85-29377
Prospects for parallel nonlinear optical signal processing using GaAs etalons and ZnS interference filters
18 p3187 N85-29765
Micro-reactions of metal contacts on various types of GaAs surfaces
[AD-A153650] 18 p3193 N85-29806
TEM combined with Al/sub x/Ga/sub 1-x/ as marker layers as a technique for the study of GaAs MBE growth
[DE85-008451] 18 p3194 N85-29809
Summary of recent studies on AlGaAs/GaAs radiation hardened photodiodes
[DE85-009501] 18 p3194 N85-29812
The photochemical oxidation of GaAs
[AD-A153680] 19 p3233 N85-30045
High speed GaAs device and integrated circuit modelling and simulation 19 p3256 N85-30191
Heterojunction Schottky gate MESFET with lower channel ridge barrier
[AD-D011673] 19 p3258 N85-30199
Self-aligned GaAs FET with low 1/F noise
[AD-D011687] 19 p3260 N85-30215
High-efficiency, low-cost, passively-cooled PV concentrator module
[DE85-010013] 19 p3305 N85-30490
Design and operation of epitaxial reactor
[DE85-011069] 19 p3306 N85-30491
Crystal growth of device quality GaAs in space
[NASA-CR-176024] 19 p3375 N85-30935
A method to estimate the self-consistency effects on electronic structure calculations
[INPE-3536-PRE/752] 19 p3375 N85-30936
Leading-edge microelectronics research at Sweden's Chalmers 20 p3438 N85-31337
Design and fabrication of monolithic broadband microwave GaAs low noise FET amplifiers
20 p3443 N85-31370
Thirty GHz low noise GaAs FET amplifiers — satellite-ground communication
[CD.6500686] 20 p3449 N85-31413
Millimetre wave pulse technology — satellite mapping
[ESA-CR(P)-2004] 20 p3478 N85-31611
Recent improvements in materials for thin GaAs and multibandgap solar cells
[DE85-008800] 20 p3484 N85-31651
Gallium arsenide arrays versus silicon arrays for space application
[SNIAS-851-440-104] 20 p3485 N85-31657
Some dynamic electronic properties of semiconductor surfaces and interfaces 20 p3537 N85-32007
NASA space station automation: AI-based technology review
[NASA-CR-176094] 21 p3558 N85-32134
LSI/VLSI ion implanted planar GaAs IC processing
[AD-A155110] 21 p3581 N85-32262
Effect of powerful pulsed low-energy ion streams on GaAs 21 p3682 N85-32877
Microwave semiconductor research: Materials, devices and circuits and gallium arsenide ballistic electron transistors
[AD-A154698] 21 p3709 N85-33024
Microscopic control of semiconductor surface oxidation
[AD-A154799] 21 p3709 N85-33026
Determination of kinetic parameters of molecular beam epitaxy
[AD-A155222] 21 p3710 N85-33030
Raman scattering studies in solids
[AD-A155528] 21 p3710 N85-33032
Sixty GHz IMPATT diode development
[NASA-CR-174969] 22 p3758 N85-33293
In-situ observations of the development of heavy-ion damage in semiconductors
[DE85-010289] 22 p3761 N85-33307
Numerical simulation of nonisothermal transient processes in GaAs diode structures
22 p3767 N85-33350
Diffusion welding of Cassegrainian concentrator cell stack assemblies
[NASA-CR-176104] 22 p3805 N85-33566
Two-dimensional numerical modeling of ion implanted GaAs MESFET devices 24 p4066 N85-35341
Center for Electronics and Electrical Engineering technical progress bulletin covering center programs, July-September with 1985 CEEE events calendar
[PB85-191393] 24 p4091 N85-35383

GALLIUM COMPOUNDS
NT ALUMINUM GALLIUM ARSENIDES
NT GALLIUM ANTIMONIDES
NT GALLIUM ARSENIDES
NT GALLIUM PHOSPHIDES
Ca-Ga, Sr-Ga and Ba-Ga binary systems
[DE85-006454] 16 p2751 N85-26960
Production of gallium atoms by excimer laser photolysis of trimethyl gallium
[DE85-010742] 19 p3278 N85-30331
GALLIUM PHOSPHIDES
Photoluminescence studies of Ga(As,P) strained-layer superlattices
[DE84-015709] 05 p0731 N85-14701
A picosecond population modulation study of near interband resonances in semiconductors
09 p1396 N85-18787
Effect of hydrostatic pressure on trapping centers in strained-layer superlattice structures
[DE85-001362] 09 p1399 N85-18807
In-situ observations of the development of heavy-ion damage in semiconductors
[DE85-010289] 22 p3761 N85-33307
Time-resolved and infrared spectroscopy of excitons
[DE85-011879] 23 p3912 N85-34235
GALVANIC CELLS
U ELECTROLYTIC CELLS
GALVANIC SKIN RESPONSE
Effects of tasks on responses of human skin mechanoreceptors 11 p1691 N85-20635
GALVANIZING
U ZINC COATINGS
GALVANOMAGNETIC EFFECTS
NT NERNST-ETTINGSHAUSEN EFFECT
Standardization of amplitude characteristics of galvanometric seismographs in the KAPG network
[REPT-552] 03 p0375 N85-12395
Study of resolution of deep MT soundings by means of physical model 13 p2112 N85-23155
GALVANOMAGNETISM
U GALVANOMAGNETIC EFFECTS
GALVANOMETERS
Standardization of amplitude characteristics of galvanometric seismographs in the KAPG network
[REPT-552] 03 p0375 N85-12395
SVKD and SVKM-3 seismographs with a low-sensitivity channel
[REPT-553] 03 p0376 N85-12396
Short-period seismograph SVSN-6
[REPT-554] 03 p0376 N85-12397
GAME THEORY
NT SADDLE POINTS (GAME THEORY)
Model theory for infinitely deep languages
[ISSN-0355-0087] 01 p0101 N85-10674
Effects of alternative chromatic mixed graphics displays in decision support systems
[AD-A145561] 02 p0242 N85-11578
Homomonotone games and monocore solutions, revised
[AD-A146216] 03 p0413 N85-12645
The design and use of subtasks in part training and their relationship to the whole task
05 p0711 N85-14559
A computer-based gaming system for assessing recognition performance (RECOG)
[AD-A149752] 12 p1915 N85-22022
Simple-motion pursuit-evasion differential games in the plane
[CSIR-TWISK-336] 14 p2412 N85-24874
Stochastic pursuit-evasion differential games in the plane
[CSIR-TWISK-343] 14 p2412 N85-24875
A formal analysis of the evolution of cooperation
[AD-A152539] 17 p3018 N85-28662
An extended two-target differential game model for medium-range air combat game analysis
[NASA-CR-175968] 18 p3175 N85-29687
A formulation and analysis of combat games
[NASA-TP-2487] 22 p3835 N85-33745
GAMETOCYTES
Effects of simulated weightlessness on mammalian development. Part 2: Meiotic maturation of mouse oocytes during clinostat rotation 15 p2612 N85-26094
GAMMA FUNCTION
On a random difference equation for matrices and a characterization of the gamma distribution
[AD-A146858] 07 p1029 N85-16529
GAMMA RADIATION
U GAMMA RAYS
GAMMA RAY ABSORPTIOMETRY
Local interstellar medium and gamma-ray astronomy
[OG-3.1-1] 22 p3873 N85-33989

GAMMA RAY ABSORPTION
Electronic structure and lattice dynamics of solid state substances from gamma nuclear resonance absorption and angular correlation measurements
03 p0427 N85-12728
Facilities for studing radiation damage in nonmetals during irradiation
[DE85-000590] 10 p1554 N85-19801
Observations of ultraheavy cosmic ray particles at 10 GV cutoff rigidity
[OG-4.4-2] 22 p3879 N85-34035
GAMMA RAY ASTRONOMY
Choice of orbit for scientific satellites: SIGMA, the submillimeter telescope — Ariane-borne gamma imagery satellite (SIGMA) 05 p0600 N85-13826
Instrumental background in balloon-borne gamma-ray spectrometers and techniques for its reduction
[NASA-TM-86162] 09 p1413 N85-18911
Shuttle flight test of an advanced gamma-ray detection system
[AD-A150316] 13 p1988 N85-22469
Nineteenth International Cosmic Ray Conference. OG sessions, volume 1
[NASA-CP-2376-VOL-1] 22 p3860 N85-33902
Observations of Cygnus X-3 above 10(15) eV from 1979 - 1984
[OG-2.1-6] 22 p3863 N85-33923
Experimental results on gamma-ray sources at E sub 0 = 10(13) - 10(14) eV
[OG-2.2-12] 22 p3865 N85-33937
A coded aperture imaging system optimized for hard X-ray and gamma ray astronomy
[OG-9.2-3] 23 p4024 N85-34942
The Gamma-Ray Imaging Spectrometer (GRIS): A new balloon-borne experiment for gamma-ray line astronomy
[OG-9.2-4] 23 p4025 N85-34943
Operating characteristics of a prototype high energy gamma-ray telescope
[OG-9.2-7] 23 p4025 N85-34946
The gamma-ray telescope Gamma-1
[OG-9.2-10] 23 p4026 N85-34949
The Figaro experiment for the observation of time marked sources in the low energy gamma-ray range
[OG-9.2-11] 23 p4026 N85-34950
GeV gamma-ray astronomy telescopes with high angular resolution
[OG-9.3-4] 23 p4027 N85-34959
The final COS-B database now publicly available
[OG-9.3-8] 23 p4028 N85-34963
The University of Durham Mark 3 very high energy gamma ray telescope
[OG-9.4-2] 23 p4028 N85-34969
Application of imaging to the atmospheric Cherenkov technique
[OG-9.5-4] 23 p4030 N85-34981
A new statistic for the analysis of circular data in gamma-ray astronomy
[OG-9.5-13] 23 p4031 N85-34989
GAMMA RAY BEAMS
Observations of Cygnus X-3 above 10(15) eV from 1979 - 1984
[OG-2.1-6] 22 p3863 N85-33923
1000 GeV gamma rays from Cygnus X-3: An update
[OG-2.1-8] 22 p3863 N85-33925
Evidence for long-term variability in the ultra high energy photon flux from Cygnus X-3
[OG-2.1-10] 22 p3863 N85-33926
A search for gamma-ray point sources with the Carpet shower array
[OG-2.1-12] 22 p3864 N85-33928
GAMMA RAY BURSTS
Pair production at moderate optical depths — galactic nuclei X ray spectra 08 p1241 N85-17830
Gamma-ray burster recurrence timescales
[NASA-TM-86157] 09 p1417 N85-18942
Old and new neutron stars
[DE85-002716] 11 p1762 N85-21085
Extragalactic origin or gamma-ray bursts, revision 1
[DE85-005622] 15 p2686 N85-26588
HEAO-1 observations of gamma ray bursts
[OG-1.1-1] 22 p3860 N85-33903
Soft-spectrum gamma-ray bursts
[OG-1.1-2] 22 p3860 N85-33904
Annihilation radiation in cosmic gamma-ray bursts
[OG-1.1-3] 22 p3861 N85-33905
On the emission region of gamma ray bursts
[OG-1.1-4] 22 p3861 N85-33906
Unthermalized plasma in bursts sources
[OG-1.1-5] 22 p3861 N85-33907
Optical monitoring of gamma-ray source fields
[OG-1.1-7] 22 p3861 N85-33908
Search for optical bursts from the gamma ray burst source GBS 0526-66
[OG-1.1-8] 22 p3861 N85-33909
Search for infrared counterparts of gamma-ray bursters
[OG-1.1-9] 22 p3861 N85-33910
A second catalog of gamma ray bursts: 1978 - 1980 localizations from the interplanetary network
[OG-1.2-1] 22 p3861 N85-33912
Gamma ray burst size-frequency distributions: Spectral selection effects
[OG-1.2-3] 22 p3862 N85-33913
The effect of anisotropic emission on the log N-log S curve of gamma-ray bursts
[OG-1.2-4] 22 p3862 N85-33914
Limits to the burster repetition rate as deduced from the 2nd catalog of the interplanetary network
[OG-1.2-5] 22 p3862 N85-33915
An internally consistent gamma ray burst time history phenomenology
[OG-1.2-6] 22 p3862 N85-33916
Gamma-ray burst variability above 4 MeV
[OG-1.2-7] 22 p3862 N85-33917
Relationships between log N-log S and celestial distribution of gamma-ray bursts
[OG-1.2-10] 22 p3862 N85-33918
Observations of Cygnus X-3 above 10(15) eV from 1979 - 1984
[OG-2.1-6] 22 p3863 N85-33923
On gamma and neutrino radiation from Cyg X-3
[OG-2.1-7] 22 p3863 N85-33924
Variability in the high energy gamma ray emission from Cyg X-3 over a two-year period (1983 - 1984) at E 4 x 10(11) eV
[OG-2.1-11] 22 p3864 N85-33927
Cyg X-3: Not seen in high-energy gamma rays by COS-B
[OG-2.2-2] 22 p3864 N85-33929
Relevance of the observation of UHE gammas to hard X-ray astronomy
[OG-2.2-6] 22 p3865 N85-33932
500 TeV gamma rays from Hercules X-1
[OG-2.2-7] 22 p3865 N85-33933
A model for the UHE gamma-rays from Hercules X-1
[OG-2.2-8] 22 p3865 N85-33934
Hercules X-1: Pulsed gamma-rays detected above 150 GeV
[OG-2.2-9] 22 p3865 N85-33935
Microburst of TeV gamma rays from the Crab pulsar
[OG-2.3-4] 22 p3866 N85-33941
Secondary periodicities of microbursts of TeV gamma rays from the Crab pulsar
[OG-2.3-5] 22 p3866 N85-33942
Search for bursts in air shower data
[OG-5.3-10] 22 p3865 N85-34076
The 1983 international intercomparison of nuclear accident dosimetry systems at Oak Ridge National Laboratory
[DE85-011309] 23 p3934 N85-34382
Helios 1 energetic particle observations of the solar gamma ray flare events of 7, 21 June 1980 and 3 June 1982
[SH-1.3-8] 23 p3993 N85-34755
Injection of energetic particles following the gamma-ray flares on June 7, 1980, as observed on Helios 1
[SH-1.3-9] 23 p3993 N85-34756
Ultrarelativistic electrons and solar flare gamma-radiation
[SH-1.3-11] 23 p3993 N85-34757
North-south asymmetry in activity on the Sun and cosmic ray density gradients
[SH-4.2-7] 23 p4007 N85-34845
Burst and Transient Source Experiment (BATSE) for the Gamma Ray Observatory (GRO)
[OG-9.2-14] 23 p4026 N85-34953
Gamma-ray burst spectroscopy capabilities of the BATSE/GRO experiment
[OG-9.2-15] 23 p4026 N85-34954
Capabilities of the GRO/BATSE for monitoring of discrete sources
[OG-9.2-16] 23 p4026 N85-34955
Astrophysical applications of high angular resolution array-telescopes
[OG-9.5-7] 23 p4031 N85-34984
Angular resolution of an EAS array for gamma ray astronomy energies 5 x 10 (13) eV
[OG-9.5-8] 23 p4031 N85-34985
Note on the detection of high energy primary cosmic gamma rays by air shower observation
[OG-9.5-9] 23 p4031 N85-34986
A new approach to evaluate gamma-ray measurements
[OG-9.5-11] 23 p4031 N85-34988
A new statistic for the analysis of circular data in gamma-ray astronomy
[OG-9.5-13] 23 p4031 N85-34989
Multidimensional analysis of data obtained in experiments with X-ray emulsion chambers and extensive air showers
[HE-3.6-2] 24 p4184 N85-35951
A new method of differential structural analysis of gamma-family basic parameters
[HE-3.6-3] 24 p4184 N85-35952
Relation between gamma-ray family and EAS core: Monte-Carlo simulation of EAS core
[HE-3.6-7] 24 p4185 N85-35955
Comparison of big event with calculations of the air shower development
[HE-3.6-6] 24 p4185 N85-35956
Result of Monte-Carlo simulation of electron-photon cascades in lead and layers of lead-scintillator
[HE-3.6-11] 24 p4185 N85-35958
A study of gamma-families generated in nucleon-nucleus (NA) and pion-nucleus (pi A) interactions
[HE-3.7-2] 24 p4186 N85-35961
New analysis of nuclear interaction observed by Mt. Kanbara emulsion chamber experiment
[HE-3.7-4] 24 p4186 N85-35963
Intensities of high-energy cosmic rays at Mount Kanbala
[HE-3.7-5] 24 p4186 N85-35964
Ultra high energy events in ECHOS series and primary energy spectrum
[HE-3.7-9] 24 p4186 N85-35966
Peculiarities of gamma-quanta distribution at 20 TeV energy
[HE-3.7-10] 24 p4186 N85-35967
Results of low energy background measurements with the Liquid Scintillation Detector (LSD) of the Mont Blanc Laboratory
[HE-5.3-5] 24 p4205 N85-36099
The research program of the Liquid Scintillation Detector (LSD) in the Mont Blanc Laboratory
[HE-5.3-6] 24 p4205 N85-36100
Muon and neutrino fluxes
[HE-6.2-18] 24 p4213 N85-36154
Search for acoustic signals from high energy cascades
[HE-7.1-1] 24 p4213 N85-36155
Exploring results of the possibility on detecting cosmic ray particles by acoustic way
[HE-7.1-3] 24 p4213 N85-36157
GAMMA RAY OBSERVATORY
The Figaro experiment for the observation of time marked sources in the low energy gamma-ray range
[OG-9.2-11] 23 p4026 N85-34950
High energy gamma ray balloon instrument
[OG-9.2-12] 23 p4026 N85-34951
Burst and Transient Source Experiment (BATSE) for the Gamma Ray Observatory (GRO)
[OG-9.2-14] 23 p4026 N85-34953
Gamma-ray burst spectroscopy capabilities of the BATSE/GRO experiment
[OG-9.2-15] 23 p4026 N85-34954
An observatory to study 10 (10) to 10 (17) by EV gamma rays
[OG-9.4-6] 23 p4029 N85-34973
GAMMA RAY SPECTRA
Advances in room-temperature solid-state gamma-ray spectrometry
[DE84-015944] 04 p0469 N85-12987
Fast neutron capture with a white neutron source
[DE84-016799] 04 p0582 N85-13580
Power law X- and gamma-ray emission from relativistic thermal plasmas 08 p1241 N85-17829
A 200-MeV pi(+) induced nucleon removal from 24Mg 17 p3042 N85-28821
Paired ion chamber constants for fission gamma-neutron fields
[AD-A155069] 21 p3702 N85-32999
Kalman filter time series analysis of gamma-ray data from NaI(T1) detectors for the ND6620 computer
[AD-A154995] 21 p3705 N85-33014
Measurement of radionuclides in waste packages
[DE85-011674] 22 p3838 N85-33766
Gamma-ray line intensities for depleted uranium
[DE85-012674] 22 p3843 N85-33804
Soft-spectrum gamma-ray bursts
[OG-1.1-2] 22 p3860 N85-33904
The effect of anisotropic emission on the log N-log S curve of gamma-ray bursts
[OG-1.2-4] 22 p3862 N85-33914
Search for gamma ray lines from SS433
[OG-2.4-11] 22 p3868 N85-33955
Low-energy gamma rays from Cygnus X-1
[OG-2.4-13] 22 p3868 N85-33957
Spectral evolution of gamma-rays from adiabatically expanding sources in dense clouds
[OG-2.5-2] 22 p3869 N85-33959
Capture in the 1.15-keV iron resonance
[DE85-011913] 23 p3970 N85-34812

Abundances from solar-flare gamma-ray line spectroscopy
[SH-2.1-13] 23 p3999 N85-34794
Solar flare gamma-ray line spectroscopy
[SH-2.1-14] 23 p3999 N85-34795
The Gamma-Ray Imaging Spectrometer (GRIS): A new balloon-borne experiment for gamma-ray line astronomy
[OG-9.2-4] 23 p4025 N85-34943
Modeling a high energy gamma-ray telescope
[OG-9.2-5] 23 p4025 N85-34944
Secondary gamma-ray production in a coded aperture mask
[OG-9.2-6] 23 p4025 N85-34945
An experimental assessment of the imaging quality of the low energy gamma-ray telescope ZEBRA
[OG-9.2-8] 23 p4025 N85-34947
Advanced techniques for high resolution spectroscopic observations of cosmic gamma-ray sources
[OG-9.2-9] 23 p4025 N85-34948
The gamma-ray telescope Gamma-1
[OG-9.2-10] 23 p4026 N85-34949
The Figaro experiment for the observation of time marked sources in the low energy gamma-ray range
[OG-9.2-11] 23 p4026 N85-34950
Measured performance of the new University of California gamma ray telescope
[OG-9.2-13] 23 p4026 N85-34952
Burst and Transient Source Experiment (BATSE) for the Gamma Ray Observatory (GRO)
[OG-9.2-14] 23 p4026 N85-34953
Gamma-ray burst spectroscopy capabilities of the BATSE/GRO experiment
[OG-9.2-15] 23 p4026 N85-34954
An improved time of flight gamma-ray telescope to monitor diffuse gamma-ray in the energy range 5 MeV - 50 MeV
[OG-9.3-2] 23 p4027 N85-34957
Neutron-induced 2.2 MeV background in gamma ray telescopes
[OG-9.3-6] 23 p4027 N85-34961
Measurement control for plutonium isotopic measurements using gamma-ray spectrometry
[DE85-013394] 24 p4097 N85-35397
Gamma-ray production cross sections for alpha-particle induced reactions on F-19 and Na-23
[DE85-012603] 24 p4150 N85-35732

GAMMA RAY SPECTROMETERS

Description of the SSB/A (Special Sensor B/Aerospace X-ray spectrometer
[AD-A150040] 12 p1790 N85-21236
Method and apparatus for mapping the distribution of chemical elements in an extended medium
[NASA-CASE-GSC-12808-1] 12 p1798 N85-21279
Proceedings of the Fifth International Conference on Nuclear Methods in Environmental and Energy Research
[DE84-017348] 19 p3310 N85-30521
A miroprocessor based multiscaling data acquisition system for Mossbauer spectroscopy
[USIP-85-01] 20 p3518 N85-31875
Neutral pion production in solar flares
[SH-1.4-7] 23 p3995 N85-34767
A coded aperture imaging system optimized for hard X-ray and gamma ray astronomy
[OG-9.2-3] 23 p4024 N85-34942
The Gamma-Ray Imaging Spectrometer (GRIS): A new balloon-borne experiment for gamma-ray line astronomy
[OG-9.2-4] 23 p4025 N85-34943
Advanced techniques for high resolution spectroscopic observations of cosmic gamma-ray sources
[OG-9.2-9] 23 p4025 N85-34948
Gamma-ray burst spectroscopy capabilities of the BATSE/GRO experiment
[OG-9.2-15] 23 p4026 N85-34954
Monte Carlo calibration of the SMM gamma ray spectrometer for high energy gamma rays and neutrons
[SH-9.1-6] 23 p4051 N85-35121
Noiseless coding for the Gamma Ray spectrometer
[NASA-CR-176201] 24 p4069 N85-35219
Measurement control for plutonium isotopic measurements using gamma-ray spectrometry
[DE85-013394] 24 p4097 N85-35397

GAMMA RAY TELESCOPES

Measurement of nuclear lines with a dual Ge(Li) telescope aboard a stratospheric balloon
[INPE-3360-TDL/185] 11 p1762 N85-21083
Determination of angular resolution of coded aperture gamma-ray telescope 13 p1961 N85-22432
Search for positron annihilation line and continuum radiation from the Galactic Center
[OG-2.5-5] 22 p3669 N85-33962
North-south asymmetry in activity on the Sun and cosmic ray density gradients
[SH-4.2-7] 23 p4007 N85-34845
A balloon-borne imaging gamma-ray telescope
[OG-9.2-2] 23 p4024 N85-34941
Modeling a high energy gamma-ray telescope
[OG-9.2-5] 23 p4025 N85-34944
Operating characteristics of a prototype high energy gamma-ray telescope
[OG-9.2-7] 23 p4025 N85-34946
An experimental assessment of the imaging quality of the low energy gamma-ray telescope ZEBRA
[OG-9.2-8] 23 p4025 N85-34947
The gamma-ray telescope Gamma-1
[OG-9.2-10] 23 p4026 N85-34949
High energy gamma ray balloon instrument
[OG-9.2-12] 23 p4026 N85-34951
Measured performance of the new University of California gamma ray telescope
[OG-9.2-13] 23 p4026 N85-34952
An improved time of flight gamma-ray telescope to monitor diffuse gamma-ray in the energy range 5 MeV - 50 MeV
[OG-9.3-2] 23 p4027 N85-34957
Results of a study to build a gamma-ray telescope in an external tank
[OG-9.3-3] 23 p4027 N85-34958
GeV gamma-ray astronomy telescopes with high angular resolution
[OG-9.3-4] 23 p4027 N85-34959
An approach of reducing the background induced by neutrons
[OG-9.3-5] 23 p4027 N85-34960
A Cerenkov imaging telescope for high energy gamma rays
[OG-9.3-13] 23 p4028 N85-34968
The University of Durham Mark 3 very high energy gamma ray telescope
[OG-9.4-2] 23 p4028 N85-34969
A new ultra high energy gamma ray telescope at Ohya mine
[OG-9.4-3] 23 p4029 N85-34970
An observatory to study 10 (10) to 10 (17) by EV gamma rays
[OG-9.4-6] 23 p4029 N85-34973
A method to improve observations of gamma-ray sources near 10 (15) eV
[OG-9.5-5] 23 p4030 N85-34982
Angular resolution of an EAS array for gamma ray astronomy energies 5 x 10 (13) eV
[OG-9.5-8] 23 p4031 N85-34985
The angular resolution of air shower gamma ray telescopes
[OG-9.5-14] 23 p4031 N85-34990
Construction of a cosmic ray air shower telescope
[HE-4.5-14] 24 p4196 N85-36036
Thickness of the particle swarm in cosmic ray air showers
[HE-4.7-14] 24 p4200 N85-36064
Charge 4/3 leptons in cosmic rays
[HE-6.2-14] 24 p4212 N85-36150

GAMMA RAYS

NT GAMMA RAY BURSTS
Observation of gamma radiation from crab nebula in 5-100 MeV range 02 p0162 N85-11098
Investigation of internal fields and motions, radiation damages and recovery processes using beta and gamma active probe nuclei 03 p0427 N85-12726
High-bandwidth multichannel fiber optic system for measuring gamma rays
[DE84-014526] 04 p0564 N85-13596
Gamma-ray to Cerenkov-light conversion efficiency for pure-silica-core optical fibers
[DE84-015041] 05 p0729 N85-14685
100 MHz fiber optic single transient gamma ray detection system
[DE84-016818] 05 p0729 N85-14686
A microchannel plate streak camera
[DE84-016536] 06 p0811 N85-15153
The galactic gamma-ray distribution: Implications for galactic structure and the radial cosmic ray gradient
[NASA-TM-86173] 07 p1061 N85-16729
The HEAO-1 diffuse component spectrum from 15 to above 500 keV — X and gamma rays 08 p1240 N85-17820
P-I-N CdTe gamma-ray detectors by Liquid Phase Epitaxy (LPE)
[DE84-012276] 09 p1323 N85-18315
Comparison of ionizing radiation and hot electron effects in MOS structures
[DE84-016766] 09 p1400 N85-18809
Directivity of Bremsstrahlung radiation from relativistic beams and the Gamma-Rays from solar flares
[NASA-CR-174433] 10 p1572 N85-19913
Physical aspects of the prediction of solar flares
[NASA-CR-175487] 10 p1572 N85-19915
Laser-Electron-Gamma-Source (LEGS)
[DE85-003204] 11 p1638 N85-20322
Behavior degradation due to 1100-RAD pulsed radiation exposure (5.8:1 neutron/gamma ratio)
[AD-A149284] 11 p1669 N85-20621
MCNP code
[DE85-002585] 11 p1702 N85-20705
WESF (173)Cs gamma ray sources
[DE85-000676] 11 p1727 N85-20859
A remote source system for measuring relative positron annihilation line widths in individual slab cylindrical samples
[AERE-R-10549] 12 p1938 N85-22173
Neutron and gamma-ray signatures for particle acceleration in solar flares 12 p1954 N85-22278
Research in particles and fields
[NASA-CR-175472] 12 p1983 N85-22337
Basic principles of industrial radiography 14 p2316 N85-24310
Radiological safety aspects of industrial radiography 14 p2316 N85-24312
The gamma thermometer: A new type of fixed internal instrumentation developed by EDF
[BLL-CE-TRANS-8080-(9022.09)] 15 p2560 N85-25791
Interstellar Al-26 and excess Mg-26 15 p2680 N85-26551
Results from radiation monitoring equipment experiment on STS-11
[AD-A152531] 17 p2908 N85-27932
Measurement and interpretation of electron angle at MABE beam stop
[DE85-006583] 17 p3032 N85-28755
Incorporation of Monte Carlo electron interface studies into photon general cavity theory
[DE85-007674] 17 p3034 N85-28772
High energy gamma rays from complex particle collisions
[DE85-007871] 17 p3036 N85-28783
Results from radiation monitoring equipment experiment on STS-8
[AD-A153241] 17 p3055 N85-28911
Radiation-induced degradation of trichloroethylene and tetrachloroethylene in drinking water
[OEFZS-4298] 18 p3134 N85-29409
Comparison of calculations and measurements of the off-axis radiation dose (SI) in liquid nitrogen as a function of radiation length
[AD-A153676] 18 p3178 N85-29704
Three-dimensional and tomographic imaging device for X-ray and gamma-ray emitting objects
[NASA-CASE-GSC-12851-1] 19 p3271 N85-30281
Chromosome aberrations in Crepis capillaris exposed to gamma radiation and clinostat 19 p3325 N85-30600
Study of a novel shielding principle for protection against intense gamma-ray beams
[AD-A154374] 19 p3357 N85-30808
Correlation analysis of 1 to 30 MeV celestial gamma rays 20 p3549 N85-32083
Radio counterparts of galactic gamma-ray sources 20 p3549 N85-32085
Study of proton and neutron activation of metal samples in low Earth orbit
[NASA-CR-171596] 21 p3558 N85-32130
Results from radiation monitoring equipment experiments on STS-41C, 41D, 41G and 51A
[AD-A154676] 21 p3560 N85-32142
A practical guide to ionization chamber dosimetry at the AFRRI reactor
[AD-A155185] 21 p3703 N85-33003
Empirical correlation of residual gamma radiation resulting from operation of the Health Physics Research Reactor
[DE85-012075] 21 p3704 N85-33006
Kalman filter time series analysis of gamma-ray data from NaI(T1) detectors for the ND6620 computer
[AD-A154995] 21 p3705 N85-33014
A balloon-borne imaging gamma-ray telescope
[OG-9.2-2] 21 p3714 N85-33049
Balloon-borne video cassette recorders for digital data storage
[OG-9.3-11] 21 p3715 N85-33050
Research in particles and fields
[NASA-CR-176069] 21 p3724 N85-33103
Magnetically insulated diode for generating pulsed neutron and gamma ray emissions
[DE85-011658] 22 p3760 N85-33306
Apparatus and method for identification of matrix materials in which transuranic elements are embedded using thermal neutron capture gamma-ray emission
[DE85-011659] 22 p3786 N85-33454
Control technology for radioactive emissions to the atmosphere at US Department of Energy facilities: The Los Alamos Meson Physics Facility
[DE85-011402] 22 p3811 N85-33609
The degradation of pollutants in water and waste water by means of electron or gamma irradiation
[OEFZS-4317] 22 p3812 N85-33615

Neutron detector counting capabilities for (10) B-lined and (235) U fission chambers in high gamma-ray fluxes
[DE85-011893] 22 p3840 N85-33780
Use of gamma radiation as a form of preservation of sweet potatoes
[DE85-011998] 22 p3841 N85-33787
Gamma-ray line intensities for depleted uranium
[DE85-012674] 22 p3843 N85-33804
Nineteenth International Cosmic Ray Conference. OG sessions, volume 1
[NASA-CP-2376-VOL-1] 22 p3860 N85-33902
Search for gamma rays of energy 10(15) eV from Cygnus X-3
[OG-2.1-1] 22 p3862 N85-33919
Gamma rays of energy or = 10(15) eV from Cyg X-3
[OG-2.1-5] 22 p3863 N85-33922
Experimental results on gamma-ray sources at E sub 0 = 10(13) - 10(14) eV
[OG-2.2-12] 22 p3865 N85-33937
Observations of the Crab Nebula at energies 4.10(11)
[OG-2.3-1] 22 p3865 N85-33938
Search for excess showers from Crab Nebula
[OG-2.3-2] 22 p3866 N85-33939
Very high energy gamma rays from the Crab Nebula
[OG-2.3-3] 22 p3866 N85-33940
Detection of gamma-ray lines from the direction of the Crab Nebula 22 p3866 N85-33943
Gamma rays of 0.3 to 30 MeV from PSR 0531+21
[OG-2.3-8] 22 p3866 N85-33945
The 1000 GeV gamma ray emission from radio pulsars 22 p3867 N85-33946
Pulsed emission of TeV gamma rays from Vela pulsar 22 p3867 N85-33947
The 1000 GeV gamma rays from ms pulsars
[OG-2.3-12] 22 p3867 N85-33948
Periodic gamma-ray emissions from Geminga at or = 10(12) eV
[OG-2.4-2] 22 p3867 N85-33949
Search for periodicities near 59 s in the COS-B gamma-ray data of 2CG195+04 (Geminga)
[OG-2.4-3] 22 p3867 N85-33950
Search for gamma-rays above 400 GeV from Geminga
[OG-2.4-4] 22 p3867 N85-33951
On the 1983 observations of the gamma-ray source 2CG195+4
[OG-2.4-5] 22 p3868 N85-33952
Observations on TeV gamma rays from Geminga and PSR 0950+08
[OG-2.4-6] 22 p3868 N85-33953
HEAO 3 upper limits to the expected 1634 KeV line from SS 433
[OG-2.4-9] 22 p3868 N85-33954
Search for gamma ray lines from SS433
[OG-2.4-11] 22 p3868 N85-33955
High-resolution spectrum of Cygnus X-1
[OG-2.4-12] 22 p3868 N85-33956
Excess gamma-rays in the direction of the rho Ophiuchi cloud: An exotic object?
[OG-2.5-1] 22 p3868 N85-33958
Supernova explosion in dense clouds in the galaxy and the COS-B gamma-ray sources
[OG-2.5-3] 22 p3869 N85-33960
Spectra and positions of galactic gamma-ray sources
[OG-2.5-7] 22 p3869 N85-33963
A search in the COS-B data base for correlated time variability in regions containing objects of interest
[OG-2.5-9] 22 p3869 N85-33964
Radio observations of four anticenter 2CG gamma-ray sources
[OG-2.5-10] 22 p3869 N85-33965
Further studies of X-ray structure of the Perseus cluster
[OG-2.5-12] 22 p3870 N85-33967
All sky Northern Hemisphere 10(15) EV gamma-ray survey
[OG-2.6-3] 22 p3870 N85-33968
A search for sources of ultra high energy gamma rays at air shower energies with Ooty EAS array
[OG-2.6-6] 22 p3870 N85-33970
Observations of potential ultra high energy gamma-ray sources above 10(15) eV
[OG-2.6-9] 22 p3870 N85-33971
Observation of gamma-rays from LMC X-4 above 10(16) eV
[OG-2.6-10] 22 p3870 N85-33972
Primary gamma-rays with E gamma or = to 10(15) eV: Evidence for ultrahigh energy particle acceleration in galactic sources
[OG-2.6-13] 22 p3871 N85-33974
Search for TeV gamma rays from extragalactic sources and the Galactic Center
[OG-2.7-1] 22 p3871 N85-33976
Search for gamma-rays from M31 and other extragalactic objects
[OG-2.7-3] 22 p3871 N85-33977
Some evidence for high energy gamma-ray sources at large galactic latitudes
[OG-2.7-5] 22 p3871 N85-33978
CEN A observation at MeV-energies
[OG-2.7-7] 22 p3871 N85-33980
Gamma-radiation with E gamma 5 MeV detected from Seyfert galaxy 3C120 and region with 1° = 190 deg and b° = 20 deg
[OG-2.8-8] 22 p3871 N85-33981
The universal spectrum of AGNs and QSOs
[OG-2.7-9] 22 p3872 N85-33982
Cosmic gamma rays from quasars
[OG-2.7-10] 22 p3872 N85-33983
Some evidence for large gravitational redshift in Seyfert galaxy NGC 4151
[OG-2.7-11] 22 p3872 N85-33984
Limits on the Doppler factor in relativistic jets by means of gamma-ray observations
[OG-2.7-12] 22 p3872 N85-33985
Energy spectrum of extragalactic gamma-ray sources
[OG-2.7-13] 22 p3872 N85-33986
Ultrahigh energy gamma rays: Carriers of cosmological information
[OG-2.7-14] 22 p3872 N85-33987
On some problems of gamma-astronomy
[OG-2.7-15] 22 p3873 N85-33988
Local interstellar medium and gamma-ray astronomy
[OG-3.1-1] 22 p3873 N85-33989
Inverse-Compton gamma rays in the galaxy
[OG-3.1-2] 22 p3873 N85-33990
Multicomponent analysis of total COS-B gamma-ray data at intermediate latitudes
[OG-3.1-3] 22 p3873 N85-33991
The galactic gamma-ray distribution and the radial cosmic ray gradient
[OG-3.1-4] 22 p3873 N85-33992
Radial distribution of cosmic ray intensity in the galaxy from gamma-ray data
[OG-3.1-5] 22 p3873 N85-33993
Constraints on the galactic distribution of cosmic rays from the COS-B gamma-ray data
[OG-3.1-6] 22 p3873 N85-33994
Local electron spectrum above 100 MeV derived from gamma-ray emissivity spectra
[OG-3.1-7] 22 p3874 N85-33995
Relevance of cosmic gamma rays to the mass of gas in the galaxy
[OG-3.1-8] 22 p3874 N85-33996
COS-B gamma-ray sources and interstellar gas
[OG-3.1-9] 22 p3874 N85-33997
Excess gamma rays from the Loop I supernova remnant
[OG-3.1-10] 22 p3874 N85-33998
Spectrum of the gamma-ray diffuse component observed from HEAO-1
[OG-3.1-12] 22 p3874 N85-34000
SMM detection of interstellar Al-26 gamma radiation
[OG-3.2-1] 22 p3874 N85-34001
Galactic distribution of interstellar Al-26
[OG-3.2-3] 22 p3874 N85-34002
Gamma-ray line emission from Al-26 produced by Wolf-Rayet stars
[OG-3.2-5] 22 p3875 N85-34003
Gamma ray line production from cosmic ray spallation reactions 22 p3875 N85-34005
On the possibility of the determining the average mass composition near 10 to the 14th power eV through the solar magnetic field
[OG-5.1-9] 22 p3882 N85-34061
Arrival directions of large air showers, low-mu showers and old-age low-mu air showers observed at St. Chacaltaya
[OG-5.3-2] 22 p3884 N85-34069
Arrival directions of cosmic rays of E .4 EeV
[OG-5.3-4] 22 p3884 N85-34071
Air shower arrival directions measured at Buckland Park
[OG-5.3-11] 22 p3885 N85-34077
UHE particle production in close binary systems
[OG-5.4-7] 22 p3886 N85-34084
Anisotropy of cosmic rays above 10(14) eV
[OG-5.4-11] 22 p3887 N85-34088
Improved method for the stabilization of NaI-photomultiplier gamma detectors against thermal and other drift
[DE85-011830] 23 p3970 N85-34613
Study of non-thermal photon production under different scenarios in solar flares. 1: Scenarios and formulations
[SH-1.2-2] 23 p3991 N85-34736
Study of non-thermal photon production under different scenarios in solar flares. 2: The Compton inverse and Bremsstrahlung models and fittings
[SH-1.2-3] 23 p3991 N85-34739
The starting conditions for an optically small solar gamma ray flare
[SH-1.3-2] 23 p3993 N85-34751
Observations of solar flare gamma-rays and protons
[SH-1.3-6] 23 p3993 N85-34753
Time extended production of neutrons during a solar flare
[SH-1.4-1] 23 p3994 N85-34782
Further observations of protons resulting from the decay of neutrons ejected by solar flares
[SH-1.4-2] 23 p3994 N85-34783
Suggestions for improving the efficiency of ground-based neutron monitors for detecting solar neutrons
[SH-1.4-3] 23 p3995 N85-34784
Search for solar neutrons using NM-64 equipment
[SH-1.4-5] 23 p3995 N85-34785
Neutral pion production in solar flares
[SH-1.4-7] 23 p3995 N85-34787
High energy neutron and gamma-radiation generated during the solar flares
[SH-1.4-8] 23 p3995 N85-34788
Possible detection of flare-generated positrons by Helios 1 on 3 Jun 1982
[SH-1.4-10] 23 p3996 N85-34770
Energetic particle observations of the solar-gamma ray/neutron flare events of 3 Jun 1982 and 21 June 1990 isotopic and chemical composition
[SH-2.1-3] 23 p3998 N85-34784
Geometry of the diffusive propagation region in the August 14, 1982 solar electron event
[SH-3.1-5] 23 p4001 N85-34809
A very important process of nucleosynthesis in stars
[OG-7.1-11] 23 p4014 N85-34872
Bursting star formation and the overabundance of Wolf-Rayet stars
[OG-8.2-8] 23 p4019 N85-34907
Giant molecular clouds as regions of particle acceleration 23 p4020 N85-34913
A balloon-borne imaging gamma-ray telescope
[OG-9.2-2] 23 p4024 N85-34941
Secondary gamma-ray production in a coded aperture mask
[OG-9.2-6] 23 p4025 N85-34945
The final COS-B database now publicly available
[OG-9.3-8] 23 p4028 N85-34963
The Buckland Park air shower array
[OG-9.4-4] 23 p4029 N85-34971
An EAS experiment at mountain altitude for the detection of gamma-ray sources
[OG-9.4-5] 23 p4029 N85-34972
A new array for the study of ultra high energy gamma-ray sources
[OG-9.4-7] 23 p4029 N85-34974
Cerenkov light images of EAS produced by primary gamma
[OG-9.5-3] 23 p4030 N85-34979
Shower disc sampling and the angular resolution of gamma-ray shower detectors
[OG-9.5-2] 23 p4030 N85-34980
Photometric and spectroscopic gamma-ray observations of solar transient phenomena using long duration balloons
[SH-9.1-5] 23 p4051 N85-35120
Total integrated dose testing of solid-state scientific CD4011, CD4013, and CD4060 devices by irradiation with CO-60 gamma rays
[NASA-CR-176196] 24 p4161 N85-35795
Experiment Pamir-3. Coplanar emission of high energy gamma-quanta at interaction of hadrons with nuclei of air atoms at energies above 10 to the 7th power GeV
[HE-1.4-12] 24 p4177 N85-35899
High energy gamma-rays and hadrons at Mount Fuji
[HE-3.1-3] 24 p4177 N85-35903
The multiplicity and the spectra of secondaries correlated with the leading particle energy
[HE-3.2-11] 24 p4179 N85-35919
Study of hadron bundles observed in Chacaltaya two-story emulsion chamber
[HE-3.3-4] 24 p4180 N85-35922
Lateral distribution of high energy hadrons and gamma ray in air shower cores observed with emulsion chambers
[HE-3.3-8] 24 p4180 N85-35926
Size distributions of air showers accompanied with high energy gamma ray bundles observed at Mt. Chacaltaya
[HE-3.3-9] 24 p4181 N85-35927
EAS accompanied by gamma-families at Mt. Norikura and comparison with Monte Carlo simulation
[HE-3.3-10] 24 p4181 N85-35928
Comparison of absolute intensity between EAS with gamma-families and general EAS at Mount Norikura
[HE-3.3-11] 24 p4181 N85-35929
A cosmic ray super high multicore family event. 1: Experiment and general features
[HE-3.4-1] 24 p4181 N85-35930
A halo event created at 200 m above the Chacaltaya emulsion chamber
[HE-3.4-5] 24 p4182 N85-35933

A binocular-type atmospheric interaction generating sequential exotic features
[HE-3.4-6] 24 p4182 N85-35934
Gamma-hadron families and scaling violation
[HE-3.4-7] 24 p4182 N85-35935
Super-family P2 C-66-125 observed by Japan-URSS Joint Emulsion Chamber Experiment
[HE-3.4-8] 24 p4182 N85-35936
On the halo events observed by Mount Fuji and Mount Kanbala Emulsion Chamber Experiments
[HE-3.4-9] 24 p4182 N85-35937
Experiment Pamir-2. Fianit: A giant super-family with halo (Epsilon sub 0 at approximately 10(17) eV)
[HE-3.4-10] 24 p4182 N85-35938
Experiment Pamir-4: Analysis of superfamily with halo of electromagnetic nature detected in deep XEC
[HE-3.4-11] 24 p4183 N85-35939
Particle interactions at energies over 1000 TeV inferred from gamma-families observed at Mount Fuji
[HE-3.5-1] 24 p4183 N85-35940
A search for mini-clusters in Japan-USSR Joint Experiment at Pamir
[HE-3.5-2] 24 p4183 N85-35941
Mini-clusters
[HE-3.5-3] 24 p4183 N85-35942
Giant mini-clusters as possible origin of halo phenomena observed in super-families
[HE-3.5-4] 24 p4183 N85-35943
The electromagnetic component of albedo from superhigh energy cascades in dense media
[HE-3.5-11] 24 p4184 N85-35948
Integral functions of electron lateral distribution and their fluctuations in electron-photon cascades
[HE-3.5-12] 24 p4184 N85-35949
A comparative analysis of gamma and hadron families at the superhigh energies recorded in experiment Pamir
[HE-3.7-1] 24 p4185 N85-35960
Nineteenth International Cosmic Ray Conference. HE Sessions, volume 7
[NASA-CP-2376-VOL-7] 24 p4186 N85-35968
New aspects in nucleon-nucleus collisions and EAS properties around 10(6) GeV 24 p4187 N85-35974
Application of photodiodes to the detection of electromagnetic bursts 24 p4189 N85-35986
Lateral distribution on charged particles in EAS
[HE-4.3-15] 24 p4192 N85-36009
Longitudinal trial functions and the cosmic ray energy scale 24 p4193 N85-36014
Missing energies at pair creation
[HE-4.4-8] 24 p4193 N85-36016
The identification of gamma ray induced EAS
[HE-4.5-1] 24 p4195 N85-36026
Muons in gamma showers
[HE-4.5-3] 24 p4195 N85-36027
Muon spectrum in air showers initiated by gamma rays
[HE-4.5-4] 24 p4195 N85-36028
Development of electromagnetic cascades in the atmosphere including the Landau-Pomeranchuk-Migdal effect
[HE-4.5-5] 24 p4195 N85-36029
Electromagnetic and muonic structure of showers initiated by gamma-rays and by hadrons
[HE-4.5-6] 24 p4195 N85-36030
The muon content of gamma-ray showers
[HE-4.5-7] 24 p4195 N85-36031
The hump in the Cerenkov lateral distribution of gamma ray showers
[HE-4.5-9] 24 p4195 N85-36032
Simulation of gamma-initiated showers
[HE-4.5-10] 24 p4195 N85-36033
Phenomenological characteristic of the electron component in gamma-quanta initiated showers
[HE-4.5-11] 24 p4196 N85-36034
Construction of a cosmic ray air shower telescope
[HE-4.5-14] 24 p4196 N85-36036
Nuclear cascades in electromagnetic showers produced by primary gamma-quanta in the atmosphere
[HE-4.5-16] 24 p4196 N85-36038
Comments on the measurements of multiple muon phenomena
[HE-5.2-13] 24 p4203 N85-36069
High energy neutrino astronomy with MACRO
[HE-5.3-12] 24 p4206 N85-36106
Analysis of the electron component of EAS at observational level 700 g x cm(-2) with a scale breaking interaction model and gammaisation hypothesis
[HE-5.4-8] 24 p4208 N85-36119
Collimated groups of particles as possible manifestation of heavy meson production
[HE-5.4-14] 24 p4208 N85-36124

GANGLIA
NT NERVES
NT NEURONS

GANTRIES
U GANTRY CRANES

GANTRY CRANES
Specifications, applications of gantry robots viewed
10 p1461 N85-19215

GANYMEDE
Dark halo craters and the thickness of grooved terrain on Ganymede 13 p2173 N85-23484
Formation of bright terrain bands on Ganymede by unstable lithosphere extension 13 p2173 N85-23485
Polar cap formation on Ganymede
13 p2174 N85-23486
Giant planets and their satellites: Cosmochemistry, evolution and structure 13 p2175 N85-23494
Ripple ring basins on Ganymede and Callisto
13 p2183 N85-23547
Planetary analogs in Antarctica: Icy satellites
13 p2193 N85-23605
Spectral units on Europa and Ganymede
13 p2196 N85-23621
Three-layer generic Ganymedes: Structure and evolution 13 p2202 N85-23657
Lineaments on Ganymede: New evidence for late tectonic activity 13 p2202 N85-23658
Global tectonics on Ganymede
13 p2202 N85-23659
Tectonics of the Galileo Regio on Ganymede
13 p2202 N85-23660
Importance of the tectonic motions on Ganymede
13 p2202 N85-23661
Geology of the Ganymede quadrangle Jg7
13 p2203 N85-23665
Ganymede and Callisto: Beauty is only skin deep
15 p2680 N85-26552

GAPS
NT ENERGY GAPS (SOLID STATE)
NT SPARK GAPS
Investigation of current setting procedures for sector magnets
[CSIR-NAC-83-03] 01 p0117 N85-10795
Benthic boundary layer, IOS observational programme: Discovery Gap measurements, March 1984 --- Institute of Oceanographic Sciences (IOS)
[ISO-160] 09 p1359 N85-16552
Magnetic field in main gap of separator
12 p1843 N85-21563
Correlation of ring current and ionospheric gap in morning and evening hours 14 p2339 N85-24466
Residual oxygen pressure in contact gap upon diffusion welding of titanium 15 p2499 N85-25418
The radiation of the Vela pulsar
20 p3548 N85-32080
SRB attach ring phenolic TPS flehtail seal evaluation tests
[NASA-CR-170887] 24 p4098 N85-35407

GAPS (GEOLOGY)
Ridged plains of Lunae Planum: Thickness distribution revised 13 p2185 N85-23559
Mechanisms of basalt-plains ridge formation
13 p2199 N85-23643
Terrestrial analogs for planetary wrinkle ridges
13 p2199 N85-23644

GARBAGE
Effectiveness of an overhead wire barrier in deterring gulls from feeding at a sanitary landfill
[AD-P004199] 11 p1582 N85-19966

GARNETS
NT YTTRIUM-ALUMINUM GARNET
NT YTTRIUM-IRON GARNET
Metamorphic petrology of the Table Mountain area, Circle quadrangle, Alaska 04 p0516 N85-13295
Spectroscopic investigation of materials for frequency agile laser systems
[AD-A151731] 16 p2790 N85-27208
Anorthositic oceanic crust in the Archean Earth
21 p3719 N85-33077
Advanced detectors and signal processing
[NASA-CR-176193] 24 p4068 N85-35343

GARP
U GLOBAL ATMOSPHERIC RESEARCH PROGRAM

GAS ANALYSIS
NT OZONOMETRY
The pyrolysis toxic gas analysis of aircraft interior materials
[AD-A146285] 03 p0328 N85-12115
Portable microprocessor-controlled instrument for sensing, identifying and monitoring gaseous chemicals
[DE84-013431] 04 p0504 N85-13214
Portable instrument for the detection and identification of air pollutants
[DE84-014767] 05 p0672 N85-14316
Formation of reference signals in laser-type gas analyzers with mechanical switching of optical channels
06 p0787 N85-15027
Integrated exhaust gas analysis system for aircraft turbine engine component testing
[NASA-TP-2424] 07 p0962 N85-16100
Analysis of gases in the Earth's crust
[PB85-113397/GAR] 07 p0990 N85-16287
Evaluation of interstitial gas contamination in titanium alloys using induced magnetic field analysis
[AD-P004130] 08 p1127 N85-17105
Evaluation of the thermoelectric method for determination of interstitial gases in titanium
[AD-P004132] 08 p1127 N85-17107
Comparative evaluation of GC/MS (Gas Chromatography/Mass Spectrometry) data analysis processing
[PB85-125864] 11 p1598 N85-20037
Edge diagnostics for tandem mirror machines
[DE85-001209] 11 p1733 N85-20902
Diagnostic verification of the GLAS (Goddard Laboratory for Atmospheric Sciences) general circulation model as applied to a case of extratropical maritime explosive cyclogenesis
[AD-A153686] 18 p3148 N85-29494
Analysis of aldehydes and ketones in the gas phase
[PB85-181865] 20 p3426 N85-31261
Gas analysis techniques for human physiological measurements in space --- Spacelab
[A/6537] 20 p3507 N85-31803
Model documentation of the gas analysis modeling system. Volume 1: Model overview
[DE85-010952] 20 p3515 N85-31856
Gas sensing with surface acoustic wave devices
[DE85-009125] 20 p3524 N85-31921
Participation of singlet oxygen in photodestruction of air-saturated solutions of coumarin dyes
21 p3685 N85-32891
The possibilities of remote analysis of atmospheric gases based on Raman scattering spectroscopy
21 p3685 N85-32892
Experimental studies of glass refining
[NASA-CR-176130] 22 p3751 N85-33248
Method for controlling the viscosity of siloxane oils
[DE85-011586] 23 p3909 N85-34221
Oxygen analyzer
[DE85-006002] 23 p3935 N85-34392
Gas analysis of ore-forming fluids
24 p4105 N85-35447

GAS ATOMIZATION
Rapid solidification of candidate ferritic steels
[DE85-006506] 16 p2750 N85-26971
Atomized magnetism-aluminum protective coatings
19 p3244 N85-30116

GAS BEARINGS
Development of gas-lubricated pistons for heavy duty diesel engine technology program
[NASA-CR-174746] 03 p0441 N85-12808
Stability of lubricant film in gas dynamic bearing
06 p0778 N85-14977
Experimental test program for evaluation of solid lubricant coating as applied to compliant foil gas bearings to 315 deg C
[NASA-CR-174837] 07 p0930 N85-15895
The series 2000: A miniature gas bearing DTG for low cost strapdown guidance and control
16 p2696 N85-26848

GAS CHROMATOGRAPHY
Development and application of fluorine-containing reagents in the gas chromatography of carbonyl compounds
[BLL-DRIC-TRANS-7205-(3623.66)]
01 p0023 N85-10140
The pyrolysis toxic gas analysis of aircraft interior materials
[AD-A146285] 03 p0328 N85-12115
Helium ionization detection apparatus
[NASA-TM-77505] 03 p0364 N85-12332
Measurements of atmospheric carbon disulfide using aircraft platforms and a GC/MS isotopic dilution analysis technique 03 p0391 N85-12500
Gas chromatographic separation of hydrogen isotopes using metal hydrides
[DE84-014455] 04 p0469 N85-12983
Photoelectrochemistry with chemically modified electrodes
[DE84-016798] 04 p0471 N85-12997
Development of acceptance criteria for batches of silane primer for external tank thermal protection system bonding applications
[NASA-CR-171266] 04 p0478 N85-13043
Volatile organic emissions from adhesives with indoor applications
[DE84-015965] 05 p0620 N85-13966
USSR report: Chemistry
[JPRS-UCH-84-012] 06 p0761 N85-14865
Gas chromatographic determination of content of harmful substances in air of industrial locations
06 p0761 N85-14866
Description and operation of a thermal decomposition unit-gas chromatographic system
[PB84-246362] 07 p0968 N85-16146

GC-FTIR (Fourier Transform Infrared Spectrometry) of jet fuels
[AD-A148272] 08 p1135 N85-17155
Multiplex gas chromatography for use in space craft
[NASA-TM-86668] 09 p1290 N85-18097
Prediction of retention indices of polynuclear aromatic hydrocarbons. Part 2: Capillary gas chromatography
[DE85-001301] 10 p1437 N85-19053
PCB analysis by capillary gas chromatography coupled with matrix isolation-Fourier transform infrared spectroscopy
[DE84-009201] 10 p1437 N85-19059
Interim protocol for the automated analysis of semivolatile organic compounds by Gas Chromatography/Fourier Transfer Infrared (GC/FT-IR) spectrometry
[PB85-115186] 11 p1595 N85-20035
Comparative evaluation of GC/MS (Gas Chromatography/Mass Spectrometry) data analysis processing
[PB85-125664] 11 p1596 N85-20037
User's guide for the computer program response factor (REFAC)
[PB85-138600] 11 p1705 N85-20726
Study of the kinetics of hydrogenation using aged catalysts
[DE85-004373] 12 p1802 N85-21302
Isolation, concentration and subsequent analysis by capillary gas chromatography of trace amounts of organophosphorus compounds from aqueous samples
[AD-B089301L] 12 p1803 N85-21308
A GC/MS (Gas Chromatograph/Mass Spectrometer) data management process. Part 1: User's guide, version 1.0
[PB85-116051] 12 p1803 N85-21309
A GC/MS (Gas Chromatograph/Mass Spectrometer) data management process. Part 2: Program documentation, version 1.0
[PB85-116069] 12 p1803 N85-21310
Thermally modulated electron affinity detector for priority pollutant analysis
[PB85-156145] 15 p2508 N85-25469
An ultrasensitive and element specific photoionization detection system for environmental analysis
[AD-A153365] 17 p2968 N85-28332
Gas chromatography: Possible application of advanced instrumentation developed for solar system exploration to space station cabin atmospheres
18 p3157 N85-29551
Technical and administrative activities of the Analytical Chemistry Laboratory (ACL)
[DE85-010150] 19 p3236 N85-30063
Identification and quantification of nitropolynuclear aromatic hydrocarbons in ambient and indoor air particulate samples
[PB85-176790] 19 p3311 N85-30525
Atmospheric chlorofluoromethanes as tracers of ocean circulation and mixing: Measurement and calibration techniques and studies in the Greenland and Norwegian Seas 19 p3319 N85-30573
Micro-scale methods for characterization of supercritical fluid extraction and fractionation processes
[DE85-010968] 20 p3455 N85-31456
The determination of dinitrotoluene in single base propellants
[AD-A154672] 21 p3571 N85-32209
Determination of organobromide compounds in water by gas chromatography-negative ion chemical ionization mass spectrometry
[DRIC-T-7411] 22 p3743 N85-33199
Method for measuring surface activity of silicon nitride powder
[NASA-TM-77906] 24 p4073 N85-35242
Aspects of high-resolution gas chromatography as applied to the analysis of hydrocarbon fuels and other complex organic mixtures. Volume 1
[AD-A156154] 24 p4076 N85-35257

GAS COMPOSITION
NT CARBON DIOXIDE CONCENTRATION
Combustion gas properties I-ASTM jet A fuel and dry air
[NASA-TP-2359] 01 p0010 N85-10084
Analysis of gases in the Earth's crust
[PB85-113397/GAR] 07 p0990 N85-16287
Instrumentation for Application Number 1: Mass spectrometric analysis of the boundary layer associated with the tethered satellite 11 p1646 N85-20372
Possible uses of tunable diode lasers in infrared spectroscopy
[ESA-TT-869] 15 p2564 N85-25818
Equipment for monitoring low concentrations of volatile substances in gases or liquid metals
[BLL-DOUNREAY-TR-949-(9091.9F)]
16 p2786 N85-27190
Comparison of observed and predicted short-term tracer-gas concentrations in the atmosphere
[DE85-007566] 16 p2821 N85-27399
Moisture content and gas sampling device
[NASA-CASE-MSC-18866-1] 18 p3103 N85-29213
Combustion gas properties. Part 3: Hydrogen gas fuel and dry air
[NASA-TP-2477] 20 p3395 N85-31058
Gas composition and molecule velocity in the detonation products of pentaerythritol tetranitrate (PETN) in expansion in a high vacuum container. Analysis by mass spectroscopy and time of flight spectrometry
[ISL-R-109/84] 22 p3747 N85-33226

GAS COOLED REACTORS
NT HIGH TEMPERATURE GAS COOLED REACTORS
NT HIGH TEMPERATURE NUCLEAR REACTORS
Technical assessment of thermal-hydraulics for high heat flux fusion components
[DE85-013178] 23 p3930 N85-34359
Liquid uranium alloy-helium fission reactor
[DE85-006511] 23 p3970 N85-34607

GAS COOLING
Gas cooled fuel cell systems technology development
[NASA-CR-174732] 07 p0991 N85-16291
Exploration of new methods to produce efficient sources of coherent near millimeter wave radiation
[AD-A150094] 12 p1829 N85-21481
Method of calculating cooldown process in cryostat of cryogenic electric machine 12 p1843 N85-21567

GAS DENSITY
Emergency modeling of hazardous air pollutants
[AD-A155441] 21 p3614 N85-32461
Local interstellar medium and gamma-ray astronomy
[OG-3.1-1] 22 p3873 N85-33989
Inverse-Compton gamma rays in the galaxy
[OG-3.1-2] 22 p3873 N85-33990
Radial distribution of cosmic ray intensity in the galaxy from gamma-ray data
[OG-3.1-5] 22 p3873 N85-33993
Excess gamma rays from the Loop I supernova remnant
[OG-3.1-10] 22 p3874 N85-33998

GAS DETECTORS
Investigation of the gas-content of gas-liquid systems
[BLL-M-35748-(5828.4)] 02 p0171 N85-11146
Portable instrument for the detection and identification of air pollutants
[DE84-014767] 05 p0672 N85-14316
Gas contamination detection device
[AD-D011388] 07 p0921 N85-15833
History, design and performance of the space shuttle hazardous gas detection system
06 p1096 N85-16936
General theory and design considerations for optical waveguide chemical vapor sensors
[AD-A148505] 08 p1223 N85-17702
Monte Carlo simulation of gas Cerenkov detectors
[DE85-002422] 10 p1488 N85-19394
Technological and economic assessment of advanced ceramic materials. Volume 5: A case study of ceramic toxic and combustible gas sensors
[PB85-113124] 12 p1815 N85-21386
Portable remote laser sensor for methane leak detection
[NASA-CASE-NPO-15790-1] 12 p1855 N85-21631
Development of solid state infrared emitters for gas detection applications
[PB85-148450] 15 p2561 N85-25800
Development of a stationary carbon monoxide detector
[BMFT-FB-T-84-253] 18 p3134 N85-29413
Field measurements with the TAMS-2B and development of methods for measuring HCHO, HC3 and HONO in real air
[PB85-172955] 18 p3135 N85-29419
Surface acoustic wave devices as chemical vapor microsensors
[AD-A153752] 18 p3177 N85-29606
Gas sensing with surface acoustic wave devices
[DE85-009125] 20 p3524 N85-31921

GAS DIFFUSION
U GASEOUS DIFFUSION

GAS DISCHARGE COUNTERS
U COUNTERS
U GAS DISCHARGE TUBES

GAS DISCHARGE TUBES
NT THYRATRONS
Theoretical elements of photometry
[BLL-RISLEY-TR-5022-(9091.9F)]
02 p0279 N85-11821
Development of novel lamps for study of enhanced production of resonance by low-density mercury discharges
[DE84-016889] 05 p0632 N85-14053
Lifetime and reliability of rubidium discharge lamps for use in atomic frequency standards
[AD-A150787] 14 p2417 N85-24915
Method of fabricating material for the electrodes of gas discharge devices
[DE85-007452] 16 p2780 N85-27157
Process for making electrodes for discharge tubes
[DE85-008696] 17 p2955 N85-28247
Schottky theory of three component plasmas
[AD-A154461] 19 p3371 N85-30907
Space-time characteristics of field in longitudinal pulse-period discharge typical in pumping of self-terminating lasers 21 p3687 N85-32909

GAS DISCHARGES
Bibliography of data on electrical breakdown in gases
[PB84-218049] 01 p0045 N85-10294
Development of prototypes for versatile fast discharge systems for pulsed gas lasers, especially excimer lasers
[BMFT-FB-T-84-174] 06 p0813 N85-15185
An experimental and theoretical investigation of optogalvanic effects
[AD-A148089] 08 p1157 N85-17299
An experimental and theoretical investigation of optogalvanic effects
[AD-A148456] 08 p1223 N85-17700
Evaluation of miniature vacuum ultraviolet lamps for stability and operating characteristics, Lyman-Alpha task
[NASA-CR-171345] 10 p1477 N85-19323
Electron production, electron attachment, and charge recombination process in high pressure gas discharges
[AD-A149535] 10 p1554 N85-19799
RF-Primed high power halogen vial apparatus
[AD-D011545] 12 p1935 N85-22156
Turbulence effects on a glow discharge as derived from continuity and energy considerations
[AD-A151836] 15 p2557 N85-25775
Electric discharge excitation and energy source integration
[AD-A151502] 15 p2562 N85-25808
Predischarge parameters of SF6-CO2 determined by laser 15 p2564 N85-25821
Investigation of electron attachment and dissociation rates in C2F6/CH4 electric gas discharges
[AD-A151798] 16 p2862 N85-27649
The decomposition of gas phase formaldehyde by plasma discharge
[AD-A153202] 17 p2921 N85-28007

GAS DISSOCIATION
Electron collision processes in molecular gases
[AD-A146078] 03 p0418 N85-12671
Dissociated methanol citation
[DE85-000505] 10 p1458 N85-19188

GAS DYNAMICS
NT AERODYNAMICS
NT AEROTHERMODYNAMICS
NT INTERACTIONAL AERODYNAMICS
NT RAREFIED GAS DYNAMICS
NT ROTOR AERODYNAMICS
NT SUPERSONICS
Compressibility and fugacity of gaseous hydrogen
[NLR-TR-83079-U] 01 p0025 N85-10154
DYNKIN: A computer program for the description of detailed gas reactions in interaction with gas dynamics
[AD-B085364] 01 p0046 N85-10298
Gas dynamics of combustion of gas-air mixture in semi-closed space with relief of pressure into gasless adjacent space 02 p0260 N85-11699
Ultraviolet observations of Uranus and Neptune below 3000 Angstrom 02 p0298 N85-11932
Magnetohydrodynamic and gasdynamic theories for planetary bow waves
[NASA-CR-174132] 03 p0448 N85-12850
On experimental equations of state for Boson gases
[PTB-ME-61] 04 p0574 N85-13659
Magnetohydrodynamic and gasdynamic theories for planetary bow waves
[NASA-CR-174135] 04 p0589 N85-13760
Multiple steady states for characteristic initial value problems
[NASA-CR-172486] 06 p0749 N85-14800
Optimum thermogasdynamic design of gas turbine engines by characteristics of element prototypes
06 p0777 N85-14965
Kinematics of nearby gas and stars
06 p0860 N85-15591
A Van Leer shock capturing algorithm for the Euler equations
[AD-A148761] 08 p1163 N85-17335
Front tracking for gas dynamics
[DE85-000571] 08 p1163 N85-17336
On limits of applicability of linear models to dynamics of gas channels in aircraft engines
09 p1308 N85-18219
Microscopic study of fluid flow
09 p1317 N85-18280

Preliminary analysis of selected gas dynamic problems — space shuttle main engine main combustion transients and IUS nozzle flow
[NASA-CR-171343] 10 p1483 N85-19361
TVENT1P user's manual, a computer code for analyzing tornado induced gas dynamic transients in flow networks
[DE85-002346] 10 p1486 N85-19379
Triple layer system for numerical integration of equations of gas dynamics and nonlinear heat conduction equation
[DE85-000297] 11 p1632 N85-20277
Model calculations for a CO2 mixing laser with screen nozzle
[ESA-TT-859] 11 p1640 N85-20336
Study proposal for the possible use of ISS as an aerodynamic facility for aerospace applications
11 p1646 N85-20374
Characteristics of flow of oscillatory-relaxing gas in nozzles with constant cross-sections in throat region
11 p1716 N85-20794
Advanced research and technology programs for advanced high-pressure oxygen-hydrogen rocket propulsion
[NASA-TM-86869] 12 p1769 N85-21231
Front tracking and two dimensional Riemann problems: A conference report
[DE85-002209] 12 p1847 N85-21589
Ideal gas thermodynamic properties for the phenyl, phenoxy, and o-biphenyl radicals
[NASA-TM-83600] 12 p1943 N85-22204
Viscous jets — extragalactic jets
12 p1958 N85-22308
Development of a Global 3-D magnetohydrodynamic computational model for solar wind-cometary and planetary studies
[NASA-CR-175490] 12 p1962 N85-22331
Internal fluid mechanism of solid propellant rocket motors 13 p2001 N85-22544
Hypersonic flow about triangular airfoil at large angles of attack 13 p2044 N85-22782
Gas dynamics of the barred spiral galaxy NGC 3359
13 p2170 N85-23465
Dynamics of gas disks in triaxial galaxies
13 p2171 N85-23469
Automating the study of error in discrete aerodynamic tailing design 14 p2286 N85-24176
Discrete models for the numerical analysis of time-dependent multidimensional gas dynamics
[NASA-CR-172574] 14 p2300 N85-24239
Thirty-three years of research with shock tubes in the Franco-German Research Institute, Saint Louis (France)
[ISL-CO-226/83] 14 p2302 N85-24257
Gasdynamic evaluation of choking cascade turns
[AD-A151654] 15 p2557 N85-25776
Results of recent large-scale NH3 and N2O4 dispersion experiments
[DE85-004988] 15 p2589 N85-25960
Numerical analysis of supersonic reactive flow in wake of reverse step 15 p2643 N85-26303
Numerical modeling of gas dynamic phenomena during supersonic flow of viscous gas in channel with electrical flow discharge 15 p2643 N85-26304
Fluid and gas dynamics 16 p2738 N85-26897
Coadsorption studies on transition metals
[PB85-163713] 18 p3072 N85-29003
Velocity visualization in gaseous flows
[NASA-CR-174954] 20 p3453 N85-31445
R and D activities of the Propulsion Division
20 p3539 N85-32025
A variable node finite element method applied to the gas dynamics equations
[AD-A155211] 21 p3584 N85-32281
The 2-D simulations of the NRL (Naval Research Laboratory) laser experiment
[AD-A154915] 21 p3592 N85-32321
Mechanics of a gaseous film barrier to lubricant wetting of elastohydrodynamically lubricated conjunctions
[NASA-TP-2500] 21 p3595 N85-32330
A comparison of experimental and theoretical results for rotordynamic coefficients of four annular gas seals
[NASA-CR-176086] 21 p3596 N85-32332
Preliminary considerations for the gasdynamic precompression of solid molecular hydrogen
[DE85-013256] 22 p3784 N85-33445
Separation of gas mixtures by supported complexes
[DE85-011996] 23 p3912 N85-34236
Numerical model of a pulse combustor
[DE85-011717] 23 p3912 N85-34240

GAS EVACUATING
U EVACUATING (VACUUM)

GAS EVOLUTION
Change in the nitrogen content when nitrided alloys are heated
[BLL-M-36945-(5828.4)] 05 p0615 N85-13929
Chemical composition and kinetics of libration of gases upon welding of aluminum alloys
19 p3247 N85-30131
Means for reducing hydrogen concentration upon surfacing of antifriction aluminum alloys with powder electrode 19 p3247 N85-30132

GAS EXCHANGE
Interaction between lung mechanics and gas exchange by low volume high frequency pulmonary ventilation in patients with respiratory failure
[AD-A146604] 06 p0646 N85-15372
External respiration, gas exchange and energy expenditures of man in weightlessness
12 p1900 N85-21932
Contribution to theory of ocean-atmosphere gas exchange 13 p2108 N85-23134
Influence of bubbles formed upon breaking of waves on gas exchange between ocean and atmosphere
14 p2335 N85-24439
Controlled Ecological Life Support Systems (CELSS)
15 p2686 N85-26804
Photosynthetic acclimation of Acer saccharum
[DE85-008247] 17 p2996 N85-28536
Atmosphere behavior in gas-closed mouse-algal systems: An experimental and modelling study
18 p3155 N85-29536
Effect of 120-day antiorthostatic bedrest on gas exchange and pulmonary circulation in man
19 p3323 N85-30589

GAS EXPANSION
Regularity of the free boundary for the porous medium equation
[AD-A147299] 08 p1210 N85-17611
Partial bleed expander cycle for low thrust LOX/LH2 rocket engine
[NAL-TR-837T] 10 p1430 N85-19018
Study of stresses on surface of flat barrier immersed in under expanded jet of rarefied gas
16 p2765 N85-27061
The highly underexpanded exhaust plume from nozzles with boundary layers
[DFVLR-FB-85-10] 20 p3421 N85-31230
Expansion ratio influence on population inversion in CO2/Ar CW gasdynamic lasers operating at various transitions within coupled upsilon 1 and upsilon 2 modes of CO2
[STN-4] 22 p3790 N85-33485
Spectral evolution of gamma-rays from adiabatically expanding sources in dense clouds
[OG-2.5-2] 22 p3869 N85-33959
Real time analysis of PETN detonation products
[DE85-009581] 23 p3922 N85-34303

GAS EXPLOSIONS
Experiment on triggered fragmentation on a molten copper droplet in water
[BLL-WH-602-(9091.9F)] 08 p1125 N85-17091
Thermal radiation hazards from Liquified Petroleum Gas (LPG) fireballs
[VTT-304] 09 p1293 N85-18122
Explosion in flight 21 p3663 N85-32683

GAS FLOW
NT AIR CURRENTS
NT AIR FLOW
NT CONTINUUM FLOW
NT EQUILIBRIUM FLOW
NT FREE MOLECULAR FLOW
NT FROZEN EQUILIBRIUM FLOW
NT JET STREAMS (METEOROLOGY)
NT KNUDSEN FLOW
NT MERIDIONAL FLOW
NT MOLECULAR FLOW
NT NONEQUILIBRIUM FLOW
NT PIPE FLOW
NT TRANSITION FLOW
NT VERTICAL AIR CURRENTS
Preliminary mechanical redesign of an existing gas-turbine engine to incorporate a high-efficiency, low-pressure-ratio, highly regenerative cycle for marine applications
[AD-A144808] 01 p0011 N85-10070
Chemical vapor deposition of amorphous silicon films produced by using higher order silanes
[DE84-004519] 01 p0123 N85-10847
Some of the features of movement of gas through a layer of free-flowing substances
[BLL-M-35732-(5828.4)] 02 p0196 N85-11312
Multigrid iteration solution procedure for solving two-dimensional sets of coupled equations
[DE84-016554] 04 p0555 N85-13533
Influence of inter-layer effect on charge gas-permeability
[BLL-M-35919-(5828.4)] 05 p0616 N85-13940
Front tracking for gas dynamics
[DE85-000571] 08 p1163 N85-17336
Replaceable blade turbine and stationary specimen corrosion testing facility
[NASA-TM-86931] 09 p1294 N85-18126
Designing the profile of turbine blades using an iteration technique 09 p1305 N85-18201
Calculating secondary nonviscous gas flows in spatial cascades of turbines 09 p1305 N85-18202
Developments in gas metering technology
[ERS-E.348] 09 p1321 N85-18307
Internal forced convection to low Prandtl number gas mixtures
[AD-A148932] 10 p1484 N85-19366
Averaging effects in models of three-dimensional two-phase flows
[AD-A149313] 10 p1484 N85-19371
Characteristics of flow of oscillatory-relaxing gas in nozzles with constant cross-sections in throat region
11 p1716 N85-20794
Explorations into thermodynamics analogies and critical points in reference to gas-solid transport
[DE85-000816] 11 p1738 N85-20929
Front tracking and two dimensional Riemann problems: A conference report
[DE85-002209] 12 p1847 N85-21589
An investigation of aerowindows for solar receivers
[DE84-010931] 12 p1877 N85-21772
Some unique features of isentropic flow of gas under high pressures 13 p2043 N85-22788
Efficiency of algorithms for gas-air channel diagnostics in gas turbine engines based on gas thermodynamic parameters 13 p2048 N85-22823
Mathematical modeling of transient performance of gas turbine engine 13 p2050 N85-22834
Model for high rate gas flows in deformable and reactive porous beds
[DE85-006140] 14 p2253 N85-23964
Effect of diaphragm leakage on turbine stage characteristics 14 p2286 N85-24168
Heat transfer to vertical flat plates in a rectangular gas-fluidized bed
[AD-A150785] 14 p2301 N85-24248
The significance for laser anemometry of particles carried along in a gas flow
[ISL-CO-205/83] 14 p2301 N85-24251
Experimental simulation of the flow inside a gun barrel
[ISL-CO-208/83] 14 p2302 N85-24252
Solid state compressor
[AD-A150790] 14 p2311 N85-24302
Turbulence effects on a glow discharge as derived from continuity and energy considerations
[AD-A151636] 15 p2557 N85-25775
Numerical modeling of gas dynamic phenomena during supersonic flow of viscous gas in channel with electrical flow discharge 15 p2643 N85-26304
Waveguide phenomena in dense relaxing gases and their use in chemical and gas-dynamic lasers
15 p2644 N85-26308
Aerodynamic forces developing in channels between vanes in turbine drive wheels 16 p2765 N85-27062
Hypersonic nonequilibrium gas flow past zero-aspect wing 16 p2765 N85-27063
Calculation of viscous compressible flows in small gas turbines 17 p2912 N85-27950
Flow characteristics of a partially submerged liquid pickup
[DE85-008744] 17 p2959 N85-28276
Numerical computation of space shuttle orbiter flow field
[NASA-CR-175912] 18 p3058 N85-28921
Unsymmetrical flow in a centrifuge
[DE85-009021] 18 p3103 N85-29208
Computer program for the control/operating system of the gas flow installation for the solid fuel combustion chamber
[VTH-LR-430] 18 p3165 N85-29605
Adherence of ash particles from the combustion of micronized coal
[DE85-008600] 19 p3229 N85-30023
Mathematics of oil production
[DE85-011235] 19 p3267 N85-30261
Development and application of a high power ND-glass laser instrument
[AD-A154366] 19 p3276 N85-30314
Development of improved capabilities for computation of gas supercompressibility factors and other properties
[PB85-186316] 20 p3436 N85-31315
Vaporization from a heated surface into a saturated stream
[DE85-010484] 20 p3530 N85-31958
BLAF: A blast field reconstruction program from pressure histories
[AD-A155300] 21 p3585 N85-32283
Investigation of influence of gas exit modes on characteristics of N2O - N2 - He discharge laser
21 p3664 N85-32886
Integrated current collector and catalyst support
[DE85-011616] 22 p3761 N85-33311
Vortex generating flow passage design for increased film cooling effectiveness
[NASA-CASE-LEW-14039-1] 22 p3782 N85-33433

Unsteady transonic heat transfer in a transient facility
[NASA-CR-176145] 23 p3930 N85-34354
GAS GENERATOR ENGINES
U ENGINES
U GAS GENERATORS
GAS GENERATORS
Singlet delta oxygen generator
[AD-D011208] 01 p0012 N85-10072
Qualification of a hydrazine gas generator system with electrothermal/catalytic gas generator
[BMFT-FB-W-84-040] 08 p1110 N85-17016
Curvilinear solid propellant grain
[AD-D011457] 10 p1458 N85-19183
GAS GIANT PLANETS
NT JUPITER (PLANET)
NT NEPTUNE (PLANET)
NT SATURN (PLANET)
NT URANUS (PLANET)
NT URANUS RINGS
Far infrared and submillimeter observations of the giant planets 08 p1245 N85-17856
Shock compression of liquid helium to 56 GPa (560) kbar 13 p2184 N85-23551
GAS GUNS
NT LIGHT GAS GUNS
Performance of the 10 KSI Wilson valve breech
[DE85-000258] 10 p1493 N85-19430
Behavior of fiber-reinforced composites under dynamic tension
[AD-A150619] 13 p2015 N85-22641
Design and fabrication of projectiles for round bore railguns
[DE85-011871] 20 p3396 N85-31078
Low temperature experimental capability for use with gas guns
[DE85-010418] 22 p3801 N85-33548
Shock and release equation of state of calcite
[DE85-013151] 23 p3942 N85-34432
GAS HEATING
Experimentally determined characteristics of vortex heaters 13 p2050 N85-22833
High Temperature Heating System (HTHS)
[PB85-188340] 24 p4084 N85-35316
GAS INJECTION
Alloying specially low carbon silicon-bearing steel with nitrogen
[BLL-M-35707-(5828.4)] 02 p0175 N85-11170
A 50-kW electric-discharge CO2 laser
[AD-A149779] 12 p1857 N85-21644
Characteristics of heat exchange in the region of injection into a supersonic high-temperature flow
[NASA-TM-77833] 15 p2555 N85-25782
An experimental investigation of fuel regression rate control in solid fuel ramjets
[AD-A154251] 19 p3227 N85-30008
GAS IONIZATION
NT ATMOSPHERIC IONIZATION
NT AURORAL IONIZATION
NT FLAME IONIZATION
Helium ionization detection apparatus
[NASA-TM-77505] 03 p0364 N85-12332
Focusing effects of a laser beam in the nonresonant multiphoton ionization (MPI) of gases
[LP-207] 04 p0506 N85-13231
Highly ionized gas associated with the small Magellanic cloud 11 p1745 N85-20976
Frictional and structural characterization of ion-nitrided low and high chromium steels
[NASA-TM-86991] 13 p2098 N85-23085
Giotto residual ionization 14 p2244 N85-23909
Relative abundances of elements (20 or = Z or = 28) at energies up to 70 GeV/amu using relativistic rise in ion chambers
[OG-4.1-7] 22 p3876 N85-34013
Breakdown of intrinsic ambipolarity for the radial diffusion due to a rotating RF field 23 p3977 N85-34860
GAS JETS
Mechanism of brittle heat fracture of inhomogeneous solids by high temperature gas jets
02 p0265 N85-11731
Study of the velocity-acoustic pressure correlation in a cold jet, centered on the sign and the amplitude of the velocity fluctuations
[ISL-R-124/83] 04 p0501 N85-13193
A neutral gas jet in a low velocity shock front at the boundary of the Draco Nebula 06 p0878 N85-15576
Development of the sonic pump levitator
[NASA-CR-171382] 12 p1782 N85-21186
Apparatus and method to keep the walls of a free-space reactor free from deposits of solid materials
[NASA-CASE-NPO-15851-1] 12 p1858 N85-21652
Ion sensor signal fluctuations during operation of spacecraft reaction engines 16 p2724 N85-26815
Uniaxial angular accelerometers
17 p2944 N85-28173
GAS LASERS
NT CARBON DIOXIDE LASERS
NT CARBON MONOXIDE LASERS
NT DF LASERS
NT EXCIMER LASERS
NT HCN LASERS
NT HELIUM-NEON LASERS
NT HF LASERS
NT KRYPTON FLUORIDE LASERS
NT NITROGEN LASERS
NT TEA LASERS
NT ULTRAVIOLET LASERS
NT XENON CHLORIDE LASERS
NT XENON FLUORIDE LASERS
Peripheral vision displays: The future
01 p0009 N85-10058
Development of prototypes for versatile fast discharge systems for pulsed gas lasers, especially excimer lasers
[BMFT-FB-T-84-174] 06 p0813 N85-15165
High efficiency electron beam gun foil support
[AD-D011434] 08 p1159 N85-17312
Axial flow laser cavity
[AD-D011506] 12 p1855 N85-21633
Optically pumped iodine monofluoride laser
[AD-D011555] 12 p1855 N85-21637
Laser with a hollow copper cathode
[ISL-R-119/83] 14 p2310 N85-24300
DARPA/TTO program IR binary optics
[AD-A152196] 16 p2865 N85-27672
Photochemical ignition studies. 1: Laser ignition of flowing premixed gases
[AD-A153048] 17 p2920 N85-28002
Magnetically switched power supply systems for lasers
[NASA-CASE-NPO-16402-1] 18 p3112 N85-29265
Development of a resistive load for PBFA 2 rimfire gas switch simultaneity and laser triggering tests
[DE85-011080] 19 p3365 N85-30669
Theoretical modeling of the discharge-pumped XeCl excimer laser 20 p3460 N85-31495
Vacuum ultraviolet laser
[DE85-011632] 22 p3790 N85-33478
GAS LIQUEFACTION
U CONDENSING
GAS LUBRICANTS
Dual clearance squeeze film damper
[NASA-CASE-LEW-13506-1] 22 p3791 N85-33490
GAS LUBRICATED BEARINGS
U GAS BEARINGS
GAS MASERS
NT HYDROGEN MASERS
GAS METERS
A simple electronic apparatus for determining the oxidation stability of lubricants and other organic compounds
[AD-A146080] 03 p0338 N85-12172
Developments in gas metering technology
[ERS-E.348] 09 p1321 N85-18307
Buckling and eccentricity effects on orifice metering accuracy — gas meters
[ERS-E.350] 09 p1324 N85-18321
An experimental investigation into the effects of plate eccentricity and elastic deformation on orifice meter accuracy
[ERS-E.391] 09 p1325 N85-18325
GAS MIXTURES
NT AIR
NT COMPRESSED AIR
NT EXPIRED AIR
NT LIQUID AIR
Experimental properties of an inhomogeneously broadened He-Xe unstable ring laser
[AD-A144824] 01 p0052 N85-10344
Experimental and theoretical study of condensation in multicomponent vapors
[DE84-015610] 02 p0174 N85-11164
Recent advances in gaseous dielectrics
[DE84-014279] 02 p0195 N85-11304
Gas dynamics of combustion of gas-air mixture in semi-closed space with relief of pressure into gasless adjacent space 02 p0260 N85-11699
Combustion and detonation of hydrogen-air mixture in free spaces 02 p0274 N85-11783
NaK chemiluminescence
[AD-A146077] 03 p0328 N85-12110
PRIAMUS, a computer program for the calculation of thermophysical properties of gas mixtures containing O2, N2, CO, CO2, He, H2O, H2, CH4
[JUEL-1916] 04 p0472 N85-13002
Experiments with hydrox at 1.3 MPa (13 atm) — for divers
[FOA-C-58014-H1] 04 p0545 N85-13471
Cardiac output measured by mass spectroscopy
05 p0692 N85-14449
Cardiac output measurement with soluble gases
05 p0692 N85-14450
Hypersonic flow of mixture around blunt body
06 p0779 N85-14979
Hydrogen-oxygen (hydrox) breathing at 1.3MPa
[FOA-C-58015-H1] 09 p1364 N85-18577
Separation of gas mixtures with coordination complexes
[DE85-000363] 10 p1438 N85-19062
Influence of temperature on wear resistance of detonation coatings of alloy powders
10 p1447 N85-19116
Internal forced convection to low Prandtl number gas mixtures
[AD-A148932] 10 p1484 N85-19366
Diffusion separation of reacting gas mixtures
11 p1718 N85-20810
Basic studies of gases for fast switches
[AD-A149828] 12 p1835 N85-21514
Resonant coherent anti-Stokes Raman scattering
[ESA-TT-876] 15 p2507 N85-25466
Predischarge parameters of SF6-CO2 determined by laser 15 p2564 N85-25821
Calculations of collision-induced optical gain in high-density mixtures of D2 or HD with a buffer gas
[AD-A151372] 15 p2648 N85-26330
Optical waveguide sensor for methane gas
[AD-D011691] 19 p3273 N85-30294
Combustion gas properties. Part 3: Hydrogen gas fuel and dry air
[NASA-TP-2477] 20 p3396 N85-31058
Weak shock waves propagating in fluid-gas mixtures
[AD-A154759] 21 p3584 N85-32276
Asymptotically stable solutions of some nonlinear equations 21 p3698 N85-32974
Separation of gas mixtures by supported complexes
[DE85-011996] 23 p3912 N85-34236
Investigation of the flame speeds of propane/methanol gas mixtures
[DE85-012817] 23 p3912 N85-34239
GAS PHASES
U VAPOR PHASES
GAS PIPES
The influence of mechanical damage on transmission pipeline integrity
[ERS-E.351] 00 p1340 N85-18431
Results of an EPRG round robin test programme with DWTT specimens — drop weight test (DWTT);pipe steels
[ERS-E.365] 09 p1341 N85-18432
GAS POCKETS
Western gas sands
[DE85-001985] 18 p3126 N85-29360
GAS PRESSURE
Gas pressure and electron density at the level of the active zone of hollow cathode arc discharges
[NASA-TM-77477] 03 p0414 N85-12648
Gas pressure and electron density in the active zone level of hollow cathode arc discharges
[NASA-TM-77488] 07 p0945 N85-15988
Improvement of gas-tightness of OTTG and TBO-5 threaded pipe couplings
[BLL-M-35993-(5828.4)] 07 p0972 N85-16175
Simulation in the design of gas pressure control equipment
[ERS-E.352] 09 p1324 N85-18322
Ignition phenomena of bulk aluminum alloy as a function of oxygen pressure 13 p1999 N85-22531
Molecular dynamics of propellant gases, part 2
13 p2002 N85-22552
Residual oxygen pressure in contact gap upon diffusion welding of titanium 15 p2499 N85-25418
A feasibility study for using low boiling point fluids to change aircraft tire deflection
[AD-A152096] 16 p2706 N85-26701
The loss of material from the cathode of metal arcs
[NASA-TM-77845] 17 p2918 N85-27985
Determination of individual tolerance in hyperbaric oxygen 23 p3854 N85-34507
GAS RECOVERY
Separation of gaz mixtures with coordination complexes
[DE85-000363] 10 p1438 N85-19062
Diffusion separation of reacting gas mixtures
11 p1718 N85-20810
Improved model for fluid-driven cracks in jointed rock
[DE85-008983] 18 p3125 N85-29349
GAS SPECTROSCOPY
NT FLAME SPECTROSCOPY
GAS STREAMS
Stability of lubricant film in gas dynamic bearing
06 p0778 N85-14977
Linear problem of harmonic vibrator acting at supercritical frequencies in subsonic boundary layer
06 p0779 N85-14978
Discharge pulse phenomenology
13 p1995 N85-22509

Method of calculating separation flow of subsonic gas stream around wings 17 p2942 N85-26161
Surface degradation of ductile metal in elevated temperature gas-particle streams [DE85-008428] 18 p3074 N85-29017

GAS TEMPERATURE
HOST instrumentation R and D program overview 02 p0141 N85-10957
Dynamic gas temperature measurement system 02 p0141 N85-10958

GAS TRANSPORT
Aircraft measurements of tracer gas during the 1983 cross Appalachian tracer experiment (CAPTEX) [DE84-015292] 04 p0531 N85-13395
Mechanisms of gas permeation through polymer membranes [DE84-017423] 09 p1293 N85-18117
Formaldehyde and tracer gas transfer between airstreams in enthalpy-type air-to-air heat exchangers [DE84-016951] 11 p1631 N85-20274
Principal patterns of functional changes of human respiratory system in adaptation to high pressure 14 p2387 N85-24704

GAS TUNGSTEN ARC WELDING
Minor element effects on gas tungsten arc weld penetration [PB84-222579] 01 p0056 N85-10370
Recommended aluminum pipe welding procedures for corps of engineers construction [AD-A146712] 06 p0815 N85-15172
Characterization of the heat source distribution of a typical GTAW welding arc [DE85-004322] 12 p1861 N85-21670
Sensor control of robot arc welding 12 p1948 N85-22233
Fracture toughness of HY-130 steel weld metals [AD-A150841] 14 p2255 N85-23976
Laser welding of 6Al-4V titanium alloy [DE85-012019] 23 p3938 N85-34413
Interaction of trace elements and welding parameters on GTA weld shape [DE85-004046] 24 p4060 N85-35284

GAS TURBINE ENGINES
NT J-52 ENGINE
NT J-85 ENGINE
NT JET ENGINES
NT RAMJET ENGINES
NT SUPERSONIC COMBUSTION RAMJET ENGINES
NT TURBOFAN ENGINES
NT TURBOJET ENGINES
NT TURBOPROP ENGINES
Computational thermo-fluid dynamics contributions to advanced gas turbine engine design [NASA-TM-86865] 01 p0011 N85-10069
Thermal fatigue of gas turbine engine blades made of material based on silicon nitride and silicon carbide 01 p0019 N85-10115
A review and analysis of boundary layer transition data for turbine application [NASA-TM-86880] 01 p0047 N85-10306
Energy efficient engine flight propulsion system preliminary analysis and design report [NASA-CR-174701] 02 p0140 N85-10947
Turbine Engine Hot Section Technology (HOST) [NASA-TM-83022] 02 p0140 N85-10951
Equivalent damage: A critical assessment 02 p0140 N85-10952
Benchmark notch test for life prediction 02 p0140 N85-10953
Nonlinear structural and life analyses of a turbine blade 02 p0141 N85-10954
Nonlinear structural and life analyses of a combustor liner 02 p0141 N85-10955
Pre-HOST high temperature crack propagation 02 p0141 N85-10956
High temperature static strain sensor development program 02 p0141 N85-10959
Burner liner thermal/structural load modeling 02 p0143 N85-10970
Component-specific modeling 02 p0143 N85-10971
The 3-D inelastic analysis methods for hot section components: Brief description 02 p0143 N85-10972
Creep-fatigue life prediction for engine hot section materials (isotropic) 02 p0144 N85-10974
Constitutive model development for isotropic materials 02 p0144 N85-10975
Life prediction and constitutive models for anisotropic materials 02 p0144 N85-10976
Surface protection overview 02 p0144 N85-10978
Airfoil deposition model 02 p0144 N85-10979
Effects of surface chemistry on hot corrosion life: Overview 02 p0145 N85-10980
Combustion hot section technology 02 p0145 N85-10981
Aerothermal modeling 02 p0145 N85-10982
Aerothermal modeling program 02 p0145 N85-10983
Dilution zone mixing studies 02 p0145 N85-10984
Studies on the hot corrosion of a nickel-base superalloy, Udimet 700 [NASA-TM-86882] 02 p0183 N85-11224
Hot isostatically pressed manufacture of high strength MERL 76 disk and seal shapes [NASA-CR-165550] 02 p0183 N85-11225
External fuel vaporization study, phase 2 [NASA-CR-174079] 02 p0187 N85-11252
Biaxial constitutive equation development for single crystals [NASA-CR-174056] 02 p0286 N85-11862
High performance fibers for structurally reliable metal and ceramic composites -- advanced gas turbine engine materials [NASA-TM-86878] 03 p0325 N85-12095
Development and fabrication of refractory bodies for gas turbine engines [BMFT-FB-T-84-180] 04 p0457 N85-12899
High-temperature erosion of plasma-sprayed, yttria-stabilized zirconia in a simulated turbine environment [NASA-TP-2406] 04 p0478 N85-13045
Ceramic technology for advanced heat engines program plan [DE84-013567] 04 p0479 N85-13055
Fabrication and quality assurance processes for superhybrid composite fan blades [NASA-TM-83354] 06 p0763 N85-14882
Predicting changes in reliability characteristics of gas turbine engines during operation 06 p0776 N85-14964
Optimum thermogasdynamic design of gas turbine engines by characteristics of element prototypes 06 p0777 N85-14965
Mounting construction for turbine vane assembly [AD-D011395] 07 p0904 N85-15723
Control system design language implementation of a gas turbine starting controller [AD-A147896] 07 p0905 N85-15732
Overview of the AGARD SMP activities on turbine engine materials technology in the 1972 - 1982 period 07 p0906 N85-15736
Comparison between the properties of conventional wrought and powder metallurgical alloys for turbine disc applications 07 p0906 N85-15739
Cumulative damage modeling of fatigue crack growth 07 p0907 N85-15741
Disc fatigue life predictions for gas turbine engines 07 p0907 N85-15743
Engine cyclic durability by analysis and material testing 07 p0907 N85-15744
Life prediction at high temperature under multiaxial loading 07 p0907 N85-15745
Experiences with the material bevaviour and high temperature low cycle fatigue life prediction of the IN 738 blading alloy 07 p0908 N85-15746
Verification of life prediction through component testing 07 p0908 N85-15748
View of future requirements for engine cyclic durability by analysis and testing 07 p0908 N85-15751
Current problems in turbomachinery fluid dynamics [AD-A147127] 07 p0958 N85-16074
Integrated exhaust gas analysis system for aircraft turbine engine component testing [NASA-TP-2424] 07 p0962 N85-16100
The solid rocket booster auxiliary power unit: Meeting the challenge 08 p1099 N85-16946
The effects of manufacturing automation on the surge and mobilization capabilities of the gas turbine engine industry [AD-A147295] 08 p1137 N85-17162
Development of high temperature ceramic parts for vehicular gas turbines [PNR-90245] 09 p1282 N85-18062
On one design principle of surge protector for gas turbine engine compressor 09 p1306 N85-18206
Influence of setting angle of jet cooling nozzles on temperature and stress state of a turbine wheel 09 p1306 N85-18208
Improvement of gas turbine engine performance by water injection into turbine cooling air 09 p1307 N85-18209
Correction of engraving stamp for forming blanks of gas turbine engine blades 09 p1307 N85-18213
Advanced Gas Turbine (AGT) powertrain system development for automotive applications [NASA-CR-174809] 09 p1403 N85-18831
Structural ceramics in transportation: Fuel implications and economic impacts [DE85-003024] 11 p1611 N85-20130
Introducing engine innovations: An examination of future markets for Brayton and Stirling automotive engines [DE84-016319] 11 p1647 N85-20382
Assuring structural integrity in Army systems [NASA-CR-175492] 11 p1651 N85-20396
Advanced liner-cooling techniques for gas turbine combustors [NASA-TM-86952] 12 p1770 N85-21115
Combustion research for gas turbine engines [NASA-TM-86963] 12 p1776 N85-21164
Evaluation results of the 700 deg C Chinese strain gauges -- for gas turbine engine [NASA-TM-86973] 12 p1850 N85-21605
Advanced thin film thermocouples [NASA-CR-175541] 12 p1850 N85-21607
Current problems in turbomachinery fluid dynamics [AD-A150533] 13 p1974 N85-22397
Development of a multiplane multispeed balancing system for turbine systems [NASA-CR-174750] 13 p1976 N85-22400
The influence of fuel molecular composition upon flame-tube temperature and flame radiation in a model gas-turbine primary zone [K234] 13 p2017 N85-22646
Efficiency of algorithms for gas-air channel diagnostics in gas turbine engines based on gas thermodynamic parameters 13 p2048 N85-22823
Effect of water injection into air for turbine cooling on economy of operation of gas turbine engine with afterburning 13 p2050 N85-22830
effect of gas stream sweeping past the effluent of a perforated plate on heat transfer inside the perforations 13 p2051 N85-22836
Estimation of gas turbine engine boost provided by injecting water behind compressor 13 p2051 N85-22838
Thermal state of cooled thin-walled nozzle blade 14 p2270 N85-24066
Optimization of combined convective and film cooling of perforated baffle blades in gas turbines 14 p2270 N85-24067
Experimental study of heat transfer from shaft in cooled radial bearing of GNT-25 gas turbine 14 p2270 N85-24068
Estimate of fatigue stability of gas-turbine engine compressor vanes in probabilistic aspect 14 p2287 N85-24169
Investigation of gas-turbine engine blower impeller vibrations with change in engine intake conditions 14 p2287 N85-24170
Laser drilling of aeroengine components 14 p2309 N85-24290
Experiments in dilution jet mixing effects of multiple rows and non-circular orifices [NASA-TM-86996] 15 p2473 N85-25266
Crack closure characteristics considering center cracked and compact tension specimens [AD-A151702] 15 p2579 N85-25907
Analytical fuel property effects--small combustors [NASA-CR-174738] 16 p2708 N85-26709
Multiaxial and thermomechanical fatigue considerations in damage tolerant design [NASA-TM-87022] 16 p2749 N85-26964
Structural tailoring of SSME blades (vanes) 17 p2913 N85-27960
An investigation into the soot production processes in a gas turbine engine [AD-A152710] 17 p2919 N85-27962
Ceramic applications in turbine engines [NASA-CR-174715] 17 p2934 N85-28109
Report to Congress on the Automotive Technology Development Program [DE85-005640] 17 p3052 N85-28890
Strutless diffuser for gas turbine engine [AD-D011662] 18 p3062 N85-28943
Energy efficient engine high-pressure turbine component rig performance test report [NASA-CR-168189] 19 p3218 N85-29955
Energy efficient engine integrated core/low spool test hardware design report [NASA-CR-168137] 19 p3218 N85-29956
Advanced Gas Turbine (AGT) technology project [NASA-CR-174796] 19 p3219 N85-29961
Hold-time effects in elevated temperature fatigue crack propagation [AD-A154146] 19 p3286 N85-30376
Creep fatigue life prediction for engine hot section materials (isotropic) [NASA-CR-168228] 20 p3394 N85-31057
Gas turbines: Operating conditions, material selection and development [NLR-MP-83046-U] 20 p3395 N85-31062
Flat-plate transition 20 p3452 N85-31436
A review and analysis of boundary layer transition data for turbine application 20 p3453 N85-31440
R and D activities of the Propulsion Division 20 p3539 N85-32025

Tape casting as an approach to an all-ceramic turbine shroud seal
[NASA-TM-87078] 21 p3596 N85-32333
Dual clearance squeeze film damper
[NASA-CASE-LEW-13506-1] 22 p3791 N85-33490
Elevated temperature crack growth
[NASA-CR-174957] 22 p3799 N85-33540
Shroud segments for unshrouded blade turbines
[PNR-90260] 23 p3897 N85-34143
The development and evaluation of the creep and corrosion resistant alloy IN6201
[PNR-90253] 23 p3917 N85-34278
Directionally solidified gas turbine alloys
[PNR-90264] 23 p3917 N85-34279
Oxidizing seal for a turbine tip gas path
[NASA-CASE-LEW-14053-1] 23 p3937 N85-34402
Cost effective single crystals: The Rolls Royce approach — gas turbine components
[PNR-90262] 23 p3985 N85-34717
Energy Efficient Engine Program technology benefit/cost study, volume 2
[NASA-CR-174766-VOL-2] 24 p4066 N85-35198
Energy efficient engine, high pressure turbine thermal barrier coating. Support technology report
[NASA-CR-168037] 24 p4066 N85-35199
Development of advanced high-temperature heat flux sensors. Phase 2: Verification testing
[NASA-CR-174973] 24 p4096 N85-35391

GAS TURBINES

Variable inlet vane assembly for a gas turbine combustion
[AD-D011220] 01 p0010 N85-10063
Preliminary mechanical redesign of an existing gas-turbine engine to incorporate a high-efficiency, low-pressure-ratio, highly regenerative cycle for marine applications
[AD-A144808] 01 p0011 N85-10070
Selecting the proper ceramic material for a regenerator experiencing large temperature gradients
[AD-A144796] 01 p0032 N85-10199
The effect of channel convergence on heat transfer in a passage with short pin fins
[NASA-TM-83801] 01 p0046 N85-10303
Gas side heat transfer: 2-D flow
02 p0142 N85-10965
Jet array impingement flow distributions and heat transfer characteristics: Effects of initial crossflow and nonuniform array geometry 02 p0142 N85-10967
Coolant passage heat transfer with rotation
02 p0143 N85-10968
Structural analysis 02 p0143 N85-10969
Alternate fuels combustion research
[AD-A145891] 02 p0188 N85-11258
Air force plasma spray at SA-ALC (San Antonio Air Logistics Center)
[AD-P004004] 03 p0308 N85-11984
Features of plastic deformation and fracture of EP 741 nickel alloy under thermal strain
03 p0349 N85-12250
Additives for heat engine coal slurry fuels
[DE84-016434] 05 p0821 N85-13971
Control of rotordynamic instability in a typical gas turbine's power system 05 p0842 N85-14120
High pressure combustion test facility for gas turbine research
[NAL-TR-801] 06 p0757 N85-14845
Heat transfer results and operational characteristics of the NASA Lewis Research Center Hot Section Cascade Test Facility
[NASA-TM-86890] 06 p0808 N85-15133
An improved computer model for prediction of axial gas turbine performance losses
[NASA-CR-174246] 07 p0904 N85-15724
In-flight evalution of LCF life consumption of critical rotor components subjected to high transient thermal stress
07 p0906 N85-15734
Accelerated Mission Endurance Testing (AMET)
07 p0906 N85-15736
Mechanical aspects of high temperature coatings
07 p0908 N85-15749
Contamination and distortion of steady flow field induced by discrete frequency in aircraft gas turbines
[AD-A147092] 07 p0958 N85-16073
Possibilities for a more accurate life prediction of components — gas turbine disks
07 p0976 N85-16196
Advanced technology cogeneration system conceptual design study: Closed cycle gas turbines
[NASA-CR-168222] 07 p0992 N85-16300
Combustion chamber floatwall panel attachment arrangement
[AD-D011358] 07 p1047 N85-16647
Experience of one UK electronic equipment supplier with bite on engine/flight control systems over the past ten years 08 p1064 N85-16738
An analytic model of gas turbine engine installations
[AD-A148706] 09 p1261 N85-18059
High pressure combustion test facility for gas turbine research
[NAL-TR-801] 09 p1283 N85-18065
Comparison of property regeneration techniques and life prediction procedures applied to laboratory tested and service exposed Ni-Cr alloys
[NPL-DMA(A)-91] 09 p1333 N85-18374
NASA Lewis Research Center/University Graduate Research Program on Engine Structures
[NASA-TM-86916] 09 p1333 N85-18375
Exciplex systems for vapor-liquid visualization of fuel sprays
[AD-A149360] 10 p1457 N85-19161
Internal forced convection to low Prandtl number gas mixtures
[AD-A148932] 10 p1484 N85-19366
Evaluation of corrosion-erosion behavior of various ceramic materials
[AD-A149756] 12 p1812 N85-21367
Cost comparison of small gas turbines versus electric motors in a variable load industrial application
[PB85-149763] 12 p1837 N85-21530
High pressure turbine rotor two-piece blade retainer
[AD-D011498] 12 p1858 N85-21653
Closed cycle versus open cycle gas turbines. A review of A.D. Little's ICOP report, vol. 3
[DE85-000564] 12 p1861 N85-21671
Optimal design efforts in Shanghai described
13 p1972 N85-22386
Oxidation resistant materials for hot gas turbines and jet engines
[AD-B087399L] 13 p1973 N85-22389
Composition and photochemical reactivity of turbine engine exhaust
[AD-A150550] 13 p2130 N85-23256
Construction of profiles of intermediate blade sections from master profiles given on conical surfaces
14 p2272 N85-24075
Causes and means of prevention of erosion of exit edges of drive vanes in final stages of K-300-240 turbine
14 p2272 N85-24076
Oscillations of gas turbine installation rotors under operating conditions 14 p2272 N85-24077
Study of dynamic characteristics of prefabricated gas turbine compressor rotor 14 p2272 N85-24078
Effect of diaphragm leakage on turbine stage characteristics 14 p2286 N85-24168
Fiscal year 1986 technical objective document
[AD-A151039] 14 p2432 N85-25000
Small gas turbine combustor study: Fuel injector performance in a transpiration-cooled liner
[NASA-TM-86969] 15 p2473 N85-25264
Study of the primary zone of gas turbine hearths
[ONERA-RTS-22/3256-EY] 16 p2709 N85-26719
Transformation of nitrogen oxides while sampling combustion products
[AD-A152184] 16 p2746 N85-26945
Future fundamental combustion research for aeropropulsion systems
[NASA-TM-87049] 17 p2868 N85-27870
Reaction-bonded and fiber-reinforced SiC static and dynamic gas turbine components
[BMFT-FB-T-84-302] 17 p2899 N85-27874
Detailed chemical kinetic study of the effect of molecular structure on autoignition of fuel-air mixtures
[DE85-004424] 17 p2921 N85-28010
Development of high temperature resistant, noncorrosible, non-metallic ceramic materials, especially silicon nitride in gas turbine application
[BMFT-FB-T-85-015] 17 p2936 N85-28125
Development of high temperature resistant noncorrodible silicon carbide components for gas turbine applications, follow-up report
[BMFT-FB-T-85-016] 17 p2936 N85-28126
Precision die forging of blades or gas turbines
17 p2940 N85-28148
Stressed-strained state of tightening buckles in sectional runners of gas turbines 17 p2940 N85-28149
Long-Term Materials Test Program
[DE85-003248] 18 p3077 N85-29034
Research test facility for evaporation and combustion of alternative jet fuels at high air temperatures
[AD-A153830] 18 p3083 N85-29073
Adherence of ash particles from the combustion of micronized coal
[DE85-009800] 19 p3229 N85-30023
Optimisation of MCr Al coating compositions for marine gas turbines
[BR91159] 20 p3394 N85-31056
Mechanisms of exhaust pollutants and plume formation in continuous combustion
[AD-A154169] 20 p3435 N85-31310
A comparison of two bench scale tests of fuel low temperature flow properties
[AD-A154477] 20 p3435 N85-31311
Nonlinear analysis of an axisymmetric structure subjected to non-axisymmetric loading
20 p3468 N85-31549
The effect of stress and hot corrosion on nickel-base superalloys
[AD-A154722] 21 p3566 N85-32181
High powered epicyclic gears: Some recent development 23 p3924 N85-34316
Heat transfer characteristics for two-dimensional arrays of impinging jets with initial crossflow
24 p4092 N85-35365

GAS VALVES

Slow opening valve — valve design for shuttle portable oxygen system
[NASA-CASE-MSC-20112-1] 11 p1642 N85-20338

GAS VISCOSITY

Viscous jets — extragalactic jets
12 p1958 N85-22308

GAS WELDING

NT BRAZING
NT LOW TEMPERATURE BRAZING

GAS-GAS INTERACTIONS

KRAK: A computer program for two-phase two-component porous flow and fracture
[LA-9703] 22 p3782 N85-33434

GAS-LIQUID INTERACTIONS

NT AIR SEA ICE INTERACTIONS
NT AIR WATER INTERACTIONS
Investigation of the gas-content of gas-liquid systems
[BLL-M-35748-(5828.4)] 02 p0171 N85-11148
Development of a mass transfer machine for gas/liquid operations in the absence of gravity
[BMFT-FB-W-84-027] 05 p0837 N85-14091
Intermittent gas-liquid flow modeling in horizontal or weakly inclined pipes
[EME-132] 20 p3456 N85-31465
Mechanics of a gaseous film barrier to lubricant wetting of elastohydrodynamically lubricated conjunctions
[NASA-TP-2500] 21 p3595 N85-32330

GAS-METAL INTERACTIONS

Compressibility and fugacity of gaseous hydrogen
[NLR-TR-83079-U] 01 p0025 N85-10154
Determining the optimum heating parameters for precision alloys — iron-nickel alloys
[BLL-M-35718-(5824.4)] 02 p0174 N85-11167
Hydrogen trapping, diffusion, and recombination in austenitic stainless steels
[DE85-001871] 09 p1294 N85-18129
Hydrogen induced cracking in pipeline steels
[ERS-E.327] 09 p1340 N85-18429
Mechanism of hydrogen induced cracking in pipeline steels
[ERS-E.349] 09 p1340 N85-18430
Effects of MAR-M247 substrate (modified) composition on coating oxidation coating/substrate interdiffusion — protective coatings for hot section components of gas turbine engines
[NASA-CR-174851] 10 p1440 N85-19073
Influence of gaseous hydrogen on strength and ductility of nickel heat-resistant alloys 10 p1447 N85-19119
Role of hydrogen in processes of deformation and fracture of metals 10 p1449 N85-19132
Quasi-thermodynamic prediction of hydrogen reemission behavior from titanium films
[DE85-003667] 10 p1584 N85-19864
Oxidation of PT-7M and OT4-1 titanium alloys in air
11 p1600 N85-20063
Hydrogen attack of steel
[DE85-002845] 11 p1608 N85-20113
Electrochemical cell to measure corrosion rates in noncondensing environments
[DE85-003148] 12 p1807 N85-21338
Oxidation and hot corrosion of hot-pressed Si3N4 at 1000 deg C
[NASA-TM-86977] 12 p1811 N85-21358
Change in microstructure of heat-resistant nickel alloys upon thermal cycling in a current of gas
13 p2031 N85-22725
Hartree-Fock interaction between a helium atom and lithium-metal: A test for the effective medium theory
[AD-A150466] 13 p2156 N85-23387
Effect of protective atmosphere composition on durability of welded joints of niobium alloys
15 p2502 N85-25432
Hot Isostatic Pressing (HIP): Technique, applications and economical use
[JUEL-SPEZ-268] 17 p2939 N85-28141
Changes of structure of EP648-VI alloy as a result of high-temperature gas corrosion
19 p3243 N85-30110
Means for reducing hydrogen concentration upon surfacing of antifriction aluminum alloys with powder electrode 19 p3247 N85-30132

Hydrogen embrittlement testing
[DE85-007352] 23 p3916 N85-34273
GAS-SOLID INTERACTIONS
NT GAS-METAL INTERACTIONS
An investigation of the role of sintering in gas-solid interactions
[DE84-015481] 02 p0288 N85-11884
High temperature gas energy transfer
[AD-A146134] 03 p0328 N85-12113
High altitude chemically reacting gas particle mixtures. Volume 1: A theoretical analysis and development of the numerical solution --- rocket nozzle and orbital plume flow fields
[NASA-CR-171826] 07 p0916 N85-15801
Influence of size grading of sintering ore on the sintering process
[BLL-M-36004-(5826.4)] 07 p0924 N85-15854
Separation of gas mixtures with coordination complexes
[DE85-000363] 10 p1436 N85-19062
High pressure cosmochemistry of major planetary interiors: Laboratory studies of the water-rich region of the system ammonia-water 13 p2183 N85-23549
Threshold electron studies of gas-surface interactions
[AD-A151271] 15 p2647 N85-26328
GAS-SOLID INTERFACES
Space charge, interfacial kinetics, and electrical response of condensed matter
[AD-A146364] 06 p0765 N85-14893
Laser studies of chemical dynamics at the gas-solid interface
[DE84-017580] 11 p1736 N85-20920
GASDYNAMIC LASERS
Microwave discharge in a supersonic flow for the excitation of a gas dynamic CO laser
[ESA-TT-833] 09 p1326 N85-18337
Model calculations for a CO2 mixing laser with screen nozzle
[ESA-TT-859] 11 p1640 N85-20336
Waveguide phenomena in dense relaxing gases and their use in chemical and gas-dynamic lasers
15 p2644 N85-26308
Simplified analytical model for calculation of population inversion in channels of CW gasdynamic lasers operating at various transitions among levels pertaining to coupled upsilon 1 and upsilon 2 modes of CO2
[STN-2] 20 p3461 N85-31498
Requirements for attaining Treanor's distribution of vibrational energy among CO2 levels in CW gasdynamic laser flows
[STN-3] 20 p3461 N85-31499
Expansion ratio influence on population inversion in CO2/Ar CW gasdynamic lasers operating at various transitions within coupled upsilon 1 and upsilon 2 modes of CO2
[STN-4] 22 p3790 N85-33485
GASEOUS CAVITATION
U CAVITATION FLOW
U GAS FLOW
GASEOUS DIFFUSION
NT GASEOUS SELF-DIFFUSION
Mechanisms of gas permeation through polymer membranes
[DE84-017423] 09 p1293 N85-18117
Diffusion separation of reacting gas mixtures
11 p1718 N85-20810
Diffusion of water vapor in Carbon Fiber Reinforced Plastics (CFRP). Measurement of the diffusion coefficient under influence of concentration
[DFVLR-FB-84-41] 14 p2262 N85-24018
Diffusion of gases in porous solids: Simulation and measurements
[DE85-006870] 18 p3101 N85-29198
Diffusion of trace gases in the ground level boundary layer 18 p3148 N85-29489
Technology for increasing the uranium-235 isotopic abundance in natural uranium feed on a productive scale
[DE85-011252] 19 p3357 N85-30810
Preliminary wind tunnel experiments to investigate the effect of heat transfer on the dispersion of cold dense gases
[OUEL-1546/84] 20 p3456 N85-31467
Study of molecular diffusivity influence on mass transfer rate at a water-atmosphere interface
22 p3747 N85-33222
WIPP horizon in situ permeability measurements
[DE85-012687] 22 p3802 N85-33557
GASEOUS FUELS
Status of gaseous fuels for use in highway transportation: A 1983 perspective
[DE84-015205] 01 p0034 N85-10211
GASEOUS ROCKET PROPELLANTS
Ignition characterization of LOX/hydrocarbon propellants
[NASA-CR-171884] 18 p3083 N85-29070
Ignition characterization of LOX/hydrocarbon propellants
[NASA-CR-171882] 18 p3083 N85-29071
GASEOUS SELF-DIFFUSION
Two phase discharge of liquefied gases through pipes. Field experiments with ammonia and theoretical model
[FOA-B-40130-C1] 18 p3103 N85-29209
GASES
NT AIR
NT ARGON
NT ARGON ISOTOPES
NT ARGON PLASMA
NT BOUNDARY LAYER PLASMAS
NT CARBON DIOXIDE
NT CARBON MONOXIDE
NT CHARGED PARTICLES
NT COLD GAS
NT COLD PLASMAS
NT COLLISIONAL PLASMAS
NT COLLISIONLESS PLASMAS
NT COMPRESSED AIR
NT COMPRESSED GAS
NT CONDUCTION ELECTRONS
NT COSMIC GASES
NT DENSE PLASMAS
NT DEUTERIUM
NT DEUTERIUM PLASMA
NT DIATOMIC GASES
NT DISSOLVED GASES
NT ELECTRON PLASMA
NT ELLIPTICAL PLASMAS
NT EVEN-EVEN NUCLEI
NT EXHAUST GASES
NT EXPIRED AIR
NT FLAMMABLE GASES
NT FLUE GASES
NT GAS MIXTURES
NT GAS STREAMS
NT HEAVY NUCLEI
NT HELIUM
NT HELIUM ATOMS
NT HELIUM ISOTOPES
NT HELIUM PLASMA
NT HIGH TEMPERATURE GASES
NT HIGH TEMPERATURE PLASMAS
NT HYDROGEN
NT HYDROGEN ATOMS
NT HYDROGEN IONS
NT HYDROGEN ISOTOPES
NT HYDROGEN PLASMA
NT HYPERNUCLEI
NT IDEAL GAS
NT INTERSTELLAR GAS
NT IONIZED GASES
NT KRYPTON
NT LASER PLASMAS
NT LIQUEFIED GASES
NT LIQUEFIED NATURAL GAS
NT LIQUID AIR
NT LIQUID AMMONIA
NT LIQUID HELIUM
NT LIQUID HELIUM 2
NT LIQUID HYDROGEN
NT LIQUID NITROGEN
NT LIQUID OXYGEN
NT LORENTZ GAS
NT METALLIC PLASMAS
NT MOLECULAR GASES
NT NATURAL GAS
NT NEON
NT NEON ISOTOPES
NT NEUTRAL GASES
NT NITROGEN
NT NITROGEN IONS
NT NITROGEN PLASMA
NT NONCONDENSABLE GASES
NT NUCLEI (NUCLEAR PHYSICS)
NT ODD-EVEN NUCLEI
NT ODD-ODD NUCLEI
NT OXYGEN
NT OXYGEN ATOMS
NT OXYGEN IONS
NT OXYGEN ISOTOPES
NT OXYGEN PLASMA
NT OZONE
NT POLAR GASES
NT RADON
NT RADON ISOTOPES
NT RARE GASES
NT RAREFIED GASES
NT RELATIVISTIC PLASMAS
NT ROTATING PLASMAS
NT SOLAR WIND
NT SOLIDIFIED GASES
NT STELLAR WINDS
NT STRONGLY COUPLED PLASMAS
NT THERMAL PLASMAS
NT TRITIUM
NT XENON
NT XENON ISOTOPES
NT XENON 129
Combustion gas properties I-ASTM jet A fuel and dry air
[NASA-TP-2359] 01 p0010 N85-10064
Bibliography of data on electrical breakdown in gases
[PB84-218049] 01 p0045 N85-10294
Recent advances in gaseous dielectrics
[DE84-014279] 02 p0195 N85-11304
Effects of H2S on molten carbonate fuel cells
[DE84-015166] 02 p0195 N85-11307
Laboratory investigation of coefficients of absorption of air at Lambda = 10.6 microns 02 p0263 N85-11723
Characterization of ion implanted deuterium traps in nickel by equilibration with deuterium gas
[DE84-014958] 02 p0288 N85-11879
The pyrolysis toxic gas analysis of aircraft interior materials
[AD-A146285] 03 p0326 N85-12115
The effect of heat treatment on wear resistance of gas-plasma eutectic coatings
[BLL-M-35756-(5826.4)] 03 p0329 N85-12122
Pulsed neodymium glass laser system for investigating nonlinear optical phenomena in gases
03 p0348 N85-12241
China report: Science and technology
[JPRS-CST-84-003] 04 p0491 N85-13132
Magnetohydrodynamic flow of two-component gas analyzed 04 p0491 N85-13133
Velocity-changing collisional effects in nonlinear atomic spectroscopy and photon echo decay in gases
[NASA-CR-174159] 04 p0559 N85-13559
A method of making the gas-electric removal of highly dispersed particles more effective
[BLL-M-36030-(5826.4)] 06 p0765 N85-14890
Homogeneous condensation of gaseous mixtures of Si, Fe, O, N, and C in relative cosmic abundance and implications for astronomical condensation
06 p0887 N85-15632
Apparatus for determining the liquid water content of a gas
[AD-D011297] 07 p0922 N85-15839
A study of the chemical interaction of gases with activated carbon
[AD-A147342] 07 p0923 N85-15846
Identification of leaks: Internal acoustic method, phase 2
[PB85-101947/GAR] 07 p0936 N85-15927
Phase 1-A development kinematic Sterling/Rankine commercial gas-fired heat pump research program
[PB85-100931/GAR] 07 p0936 N85-15928
Convection heat transfer in the critical region of fluid mixtures
[DE85-002118] 07 p0961 N85-16068
A virial equation of state option for the TIGER computer program
[AD-A147490] 07 p1025 N85-16507
Measurement and control of electrostatic charges on solids in a gaseous suspension
[DE85-001450] 09 p1291 N85-18105
Measurement of gas compressibility factor data for natural gas and synthetic gas components and their mixtures
[PB85-129047] 11 p1614 N85-20151
Electron acceleration by laser fields in a gas
[DE85-000575] 11 p1639 N85-20323
Interaction of large meteoroids with the atmosphere
11 p1656 N85-20431
Photoacoustic effect and its applications
12 p1820 N85-21421
Stability of organic audit materials and results of source test analysis audits
[PB85-116184] 12 p1865 N85-21832
A computer controlled mass spectrometer system for investigating the decomposition of non-metallic materials under atmospheric conditions 12 p1948 N85-22237
Physical chemistry of exothermic gas-aerosol calorimetry
[AD-A150872] 14 p2251 N85-23950
Recording of acoustic wave in gaseous medium with thin-film pyroelectric transducers
15 p2525 N85-25571
Mixing across a gas-gas interface
[AD-A151471] 15 p2556 N85-25770
Action of plasma and explosion products on alumina
19 p3242 N85-30100
Crosswell acoustic surveying in gas sands: Travel-time pattern recognition, seismic Q and channel waves
[DE85-010777] 19 p3352 N85-30778
Interaction of slow electrons with high-pressure gases (quasi-liquids): Synthesis of our knowledge on slow electron-molecule interactions
[DE85-010081] 19 p3355 N85-30800

Radioactivity in gaseous waste discharged from the separations facilities during 1984
[DE85-011373] 19 p3380 N85-30831
Gas hydrates
[DE85-001988] 20 p3477 N85-31607
Toxic hazards tests for vehicles and other equipment
[AD-A149164] 20 p3506 N85-31797
Emergency modeling of hazardous air pollutants
[AD-A155441] 21 p3614 N85-32461
Model that predicts pulse charged gas switching breakdown phenomena
[DE85-013119] 22 p3761 N85-33313
Control technology for radioactive emissions to the atmosphere at US Department of Energy facilities: The Los Alamos Meson Physics Facility
[DE85-011402] 22 p3811 N85-33809
Excess gamma-rays in the direction of the rho Ophiuchi cloud: An exotic object?
[OG-2.5-1] 22 p3868 N85-33956
Description of a test site for large-scale heavy gas dispersion and combustion experiments
[DE85-004987] 23 p3911 N85-34231
Features of behavior of gas bubbles in molten oxide films during enamelling: Communication 2
[BLL-M-35781-(5828.4)] 23 p3919 N85-34283
The cosmic-ray shock structure problem for relativistic shocks
[OG-8.1-1] 23 p4017 N85-34891
Measurement of uranium enrichment for gaseous uranium at low pressure
[DE85-012697] 24 p4150 N85-35733

GASIFICATION
NT COAL GASIFICATION
Biomass thermochemical conversion program
[DE84-017177] 05 p0621 N85-13972
Gasification of boron oxide drops and boron slurry agglomerates in combustion gases
13 p1999 N85-22529
Alcohol Fuels Program technical review, spring 1984
[DE85-002919] 17 p2938 N85-28134
Mechanism of the catalytic gasification and reactivity of graphite
[DE85-009932] 19 p3229 N85-30020
Laminar diffusion flames, carbon gasification, and laser diagnostics applied to combustion systems. 1: Laminar diffusion flames with cylindrical symmetry. 2: Diffusion-controlled gasification of carbon particles. 3: Laser diagnostics applied to combustion systems
20 p3423 N85-31243
Biomass thermochemical conversion program
[DE85-011867] 21 p3572 N85-32213

GASKETS
Response of a BWR Mark 2 containment vessel head to loads beyond the design basis
[DE85-010524] 24 p4103 N85-35432

GASOHOL (FUEL)
Dissociated methanol citation
[DE85-000505] 10 p1458 N85-19188
Developments in the production and use of ethanol fuels
[GPO-40-676] 12 p1817 N85-21396

GASOLINE
Converting gasoline farm tractors to run efficiently on farm-produced alcohol
[DE84-015796] 02 p0205 N85-11350
Some characteristics of automotive gasolines and their performance in a light aircraft engine
[FAA-CT-84-12] 07 p0934 N85-15919
Cooling system investigation of the 3-kW MEP models 016A, 021A, and 026A (60Hz, 400-Hz and 28-V dc) gasoline-engine-driven generator sets
[AD-A147571] 07 p0974 N85-16185
Catalytic conversion of C3-C4 paraffins to gasoline
[DE85-004181] 10 p1458 N85-19187
Volatility of in-use gasoline and gasoline-methanol blends
[PB85-117976] 10 p1459 N85-19189
Trends of petroleum fuels
[DE85-000116] 14 p2263 N85-24023
Conversion of methanol to gasoline: Engineering and construction of the demonstration plant
[DE85-003237] 17 p2937 N85-28133
Durability of oxygen sensors
[PB85-183093] 22 p3789 N85-33477

GASP
U GLOBAL AIR SAMPLING PROGRAM

GASTROINTESTINAL SYSTEM
NT INTESTINES
NT RECTUM
Influence of chemical form, feeding regimen, and animal species on the gastrointestinal absorption of plutonium
[DE85-010291] 21 p3662 N85-32751
Investigation of spectrum of human bile acids during 120-day antiorthostatic hypokinesia
22 p3821 N85-33674
Lipid hydrolysis in man during antiorthostatic hypokinesia
23 p3953 N85-34500

GATES (CIRCUITS)
NT THRESHOLD GATES
Glow spots and breakdown in GaAs transistor structure
04 p0487 N85-13107
High-power gate turn-off thyristors
06 p0793 N85-15071
High-speed power devices with field control
06 p0794 N85-15073
Development of short gate FET's
[AD-A147033] 07 p0947 N85-15999
Development of a 2 micrometer silicon-gate-CMOS-technology for microcomputer oriented VLSI circuits with a supply voltage range between 1.5 and 5 V
[BMFT-FB-T-84-203] 07 p0949 N85-16012
Two carrier dual injector apparatus
[AD-D011357] 07 p1047 N85-16646
A new very high voltage semiconductor switch
[NASA-TM-86957] 11 p1627 N85-20246
Automatic pickup of trajectory by method of sequential analysis taking into account deviation of radar markers from center of strobe
12 p1836 N85-21535
Basic EMC (electromagnetic interference) technology advancement for c3 systems. Volume 3A: Probabilistic analysis of combinational circuits with random delays
[AD-A150349] 13 p2055 N85-22666
All-optical logic gates with external switching by laser and incoherent radiation
18 p3187 N85-29766
Electro-optic techniques for VLSI interconnect
18 p3188 N85-29774
Energizing arrangement for charge coupled device control electrodes
[AD-D011712] 19 p3261 N85-30220
Digital integrated circuits
21 p3669 N85-32787

GAUGE INVARIANCE
Magnetic helicity in the solar corona
05 p0745 N85-14760
Cocycles and magnetic monopole
[DE85-007797] 16 p2856 N85-27612
Canonical analysis of the fermion sector in higher-derivative supergravity
[DE85-007828] 16 p2859 N85-27635
Summary of the discussion of the theory of radiative processes
[DE85-007812] 19 p3371 N85-30914
The dimensional reduction transition
[DE85-003948] 19 p3383 N85-30990
Gauge invariance and fractional quantized Hall effect
[DE85-007832] 23 p3985 N85-34716

GAUGE THEORY
Linear conformal gravitation
02 p0265 N85-11735
Gauge Theory on a Lattice, 1984: Proceedings
[DE84-014856] 02 p0291 N85-11892
Particle physics
[DE84-013834] 05 p0727 N85-14673
SU(2) x U(1) vacuum and the Centauro events
[NASA-TM-86062] 08 p1260 N85-17926
Nicolai maps and stochastic observables from a coupling constant flow
[BONN-HE-84-26] 09 p1376 N85-18653
Standard model and beyond
[DE85-004269] 14 p2418 N85-24919
Lattice overview
[DE85-007282] 15 p2662 N85-26427
Overview of the physics issues at the SSC
[DE85-007074] 16 p2859 N85-27634
Topics in intermediate vector boson physics
[NOTA-INTERNA-841] 18 p3184 N85-29743
Search for neutrino oscillations at the Brookhaven AGS
[DE85-009766] 20 p3530 N85-31957
Effects of CP violation in SU(2) sub L x SU(2) sub R x U(1) electroweak models
[DE85-010801] 20 p3531 N85-31965
Introduction to the Standard Model — weak and electromagnetic interactions
[USIP-85-02] 20 p3532 N85-31970
Does low-energy physics depend on the potential of a heavy Higgs-particle
[NIKHEF-H/85-1] 22 p3838 N85-33763

GAUSS EQUATION
A research program in active control/aeroelasticity in the JIAFS at NASA Langley Research Center
[NASA-CR-174052] 02 p0148 N85-11001
Equivocation limits in Gaussian additive channels
[INPE-2628-PRE/300] 04 p0492 N85-13137
Stochastic dynamic analysis of a structure with frictional joints
09 p1337 N85-18406
Checking the shape of discrete distributions
[DE85-000177] 11 p1706 N85-20733
Mathematical simulation of thermal processes involved in electron-beam treatment
12 p1843 N85-21565
MATRIX: A program that shows how row and column orderings affect matrix fill-in
[DE85-007522] 15 p2630 N85-26213
Special relativity of Kaluza-Klein
[DE85-007838] 17 p3046 N85-28847
Analysis and model/data comparisons of large-scale releases of nitrogen tetroxide
[DE85-009989] 18 p3133 N85-29406
Nested dissection on a mesh-connected processor array
[AD-A154088] 19 p3342 N85-30711
Extended semiclassical calculations
[DE85-007824] 19 p3346 N85-30736
Comments on estimating quantiles for Gaussian functionals by simulation
[AD-A154302] 19 p3348 N85-30750
MANHIST user's guide
[DE85-010684] 19 p3348 N85-30754
Modulation transfer function for two-point and periodic objects using Gaussian and Lorentzian resolution functions
[PB85-187557] 19 p3368 N85-30991
An overview of latest model reduction and control methods of large flexible space structures
20 p3414 N85-31191
Frequency domain control design of large space structures: A practical approach
20 p3415 N85-31192
Diakoptic calculation of characteristics for optimization of linear circuits with respect to parameters of individual branches
22 p3767 N85-33346
Observations of Cygnus X-3 above 10(15) eV from 1979 - 1984
[OG-2.1-6] 22 p3863 N85-33923
Evaluation of source strength and dispersion model predications with data from large nitrogen tetroxide field experiments
[DE85-011655] 23 p3947 N85-34485
Master Fit users' guide, version 1.0
[DE85-014199] 24 p4140 N85-35667

GAUSS FUNCTION
U GAUSS EQUATION

GAUSS-MARKOV THEOREM
Nonlinear digital phase-locked loops with application to Loran-C receivers
24 p4063 N85-35178

GAUSSIAN DISTRIBUTIONS
U NORMAL DENSITY FUNCTIONS

GAUSSIAN NOISE
U RANDOM NOISE

GAUSSMETERS
U MAGNETOMETERS

GCR (REACTORS)
U GAS COOLED REACTORS

GEAR TEETH
Effect of coupled torsional-flexural vibration of a geared shaft system on the dynamic tooth load
09 p1338 N85-18415
Precision measurement of torsional oscillations induced by gear errors
09 p1338 N85-18416
Advanced gearbox technology in small turbo propeller engines
14 p2221 N85-23771
Software for designing teeth for reduction gears and transmissions
14 p2221 N85-23773
Load carrying capacity of double circular arc gears
14 p2221 N85-23776
Manufacturing perspective in the design of bevel gearing
14 p2221 N85-23777
Root stresses in conformal gears-strain gauge and photoelastic investigations
14 p2223 N85-23787
Gear noise origins
14 p2224 N85-23791
The observation and interpretation of gear tooth failures
14 p2224 N85-23792
New technology of finish cutting teeth in large gear blanks
14 p2257 N85-24047
Milling machine with numerical programmed control for cutting teeth
14 p2268 N85-24052
Tooth wear in worm gears in vacuum
16 p2766 N85-27070
Study of meshing of beveled gears with normally decreasing arc teeth
[NASA-TM-77868] 18 p3117 N85-29293
Improvement of conditions for meshing spiral bevel gears
[NASA-TM-77867] 18 p3117 N85-29294
Planetary-gear-support bearing test rig design
[NASA-CR-174927] 24 p4064 N85-35185

GEARS
Energy efficient engine ICLS engine bearings, drives and configuration: Detail design report
[NASA-CR-167871] 02 p0147 N85-10997
Vibrational power transmission of an idealised gearbox
[ISVR-TR-124] 02 p0204 N85-11346
The in-flight estimation and indication of cumulative fatigue damage to helicopter gears
[ARL/AERO-R-164] 03 p0317 N85-12050

Effect of lubricant extreme-pressure additives on surface fatigue life of AISI 9310 spur gears
[NASA-TP-2408] 04 p0507 N85-13234
MC2969 escapement study
[DE84-014542] 05 p0645 N85-14143
Effect of five lubricants on life of AISI 9310 spur gears
[NASA-TP-2419] 07 p0962 N85-16099
Gear case vibration isolation in a geared turbine generator 09 p1338 N85-18414
Precision measurement of torsional oscillations induced by gear errors 09 p1338 N85-18416
The guidelines to design the lever turning gears in articulated vehicles
[AD-P004301] 09 p1409 N85-18678
Characteristics of the elevation drive suspension of the 64-meter antennas 10 p1464 N85-19240
Missile launcher integral shock isolation and running gear system
[AD-D011490] 11 p1589 N85-19998
A deformation analysis of flat flexible gear and its equation of original curved surfaces
[NASA-TM-77493] 12 p1859 N85-21660
Gears and Power Transmission Systems for Helicopters and Turboprops
[AGARD-CP-369] 14 p2220 N85-23765
Summary of drive-train component technology in helicopters 14 p2220 N85-23766
Current transmission systems 14 p2220 N85-23767
Helicopter transmission lubricants 14 p2220 N85-23768
Advanced gearbox technology in small turbo propeller engines 14 p2221 N85-23771
Software for designing teeth for reduction gears and transmissions 14 p2221 N85-23773
Load capacity of cages of roller bearings for planet wheels 14 p2221 N85-23775
Load carrying capacity of double circular arc gears 14 p2221 N85-23776
Manufacturing perspective in the design of bevel gearing 14 p2221 N85-23777
Case depth on flanks of gears for helicopter gearboxes 14 p2222 N85-23780
The characteristics of surface roughness important to gear and rolling bearing problems 14 p2222 N85-23782
Significant parameters of the behavior and of the surface damage of the lubricated Hertzian contact: An application to gears 14 p2222 N85-23783
Problems of elastic hydrodynamic lubrication of helicopter transmission gears 14 p2222 N85-23784
Chemical-mechanical interaction in gears 14 p2223 N85-23785
Root stresses in conformal gears-strain gauge and photoelastic investigations 14 p2223 N85-23787
Transmission of gear noise to aircraft interiors prediction methods 14 p2223 N85-23788
Evolution of the design techniques for helicopter main transmission gearboxes 14 p2223 N85-23789
Condition monitoring of helicopter gearboxes using automatic vibration analysis techniques 14 p2223 N85-23790
Gear noise origins 14 p2224 N85-23791
Problems regarding the practical evaluation of efficiency of worm gears 14 p2224 N85-23793
Transmission error measurements in gearbox development 14 p2224 N85-23794
Modernization of running gear of crane 14 p2286 N85-24163
Tooth wear in worm gears in vacuum 16 p2766 N85-27070
A description of the 64-meter antenna elevation drive gears and their strange wear 16 p2771 N85-27107
An analytical investigation of dynamic coupling in nonlinear, geared rotor systems 16 p2792 N85-27218
Life and reliability modeling of bevel gear reductions
[NASA-TM-87006] 16 p2793 N85-27227
Fatigue life analysis of a turboprop reduction gearbox
[NASA-TM-87014] 16 p2793 N85-27228
Study of a test method for assessing machinability in gear cutting operations
[BLL-BISI-TRANS-22345-(9022.06)] 17 p2972 N85-28359
Assessing the machinability of gearwheel steels during manufacture
[BLL-BISI-TRANS-22343-(9902.06)] 17 p2973 N85-28365
Multi-mesh gear dynamics program evaluation and enhancements
[NASA-CR-174747] 17 p2974 N85-28372
Lubricant and additive effects on spur gear fatigue life
[NASA-TM-87044] 17 p2974 N85-28373
Study of meshing of beveled gears with normally decreasing arc teeth
[NASA-TM-77868] 18 p3117 N85-29293
Improvement of conditions for meshing spiral bevel gears
[NASA-TM-77867] 18 p3117 N85-29294
Powder metallurgy forged gear development
[NASA-TM-87483] 18 p3117 N85-29295
Spiral bevel and circular arc helical gears: Tooth contact analysis and the effect of misalignment on circular arc helical gears
[NASA-TM-87013] 20 p3395 N85-31060
A device for generating motive force through the expansion of a non-elastic dense fluid
[NASA-TM-77664] 20 p3454 N85-31446
A computer-controlled traverse gear for the Oxford wind engineering research group's 4 metre x 2 metre wind tunnel
[OUEL-1525/84] 20 p3463 N85-31514
A phase-locked frequency multiplier for the signal averaging of the vibration of the Wessex helicopter input spiral bevel pinion
[AD-A154914] 21 p3555 N85-32113
Proposal for modifications to the Wessex helicopter main rotor gearbox vibration monitoring program
[AD-A155196] 21 p3555 N85-32117
Department of Energy gear drive unit final prototype testing and design evaluation
[DE85-009296] 22 p3793 N85-33499
The design and development of a spacecraft appendage tie down mechanism 22 p3797 N85-33522
Some problems in high speed gears and gearing 23 p3923 N85-34312
High powered epicyclic gears: Some recent development 23 p3924 N85-34316
The design and analysis of single flank transmission error tester for loaded gears
[NASA-CR-176163] 23 p3937 N85-34404
Generated spiral bevel gears: Optimal machine-tool settings and tooth contact analysis
[NASA-TM-87075] 23 p3937 N85-34405
Lubrication and cooling for high speed gears
[NASA-TM-87096] 23 p3938 N85-34407
Elastohydrodynamic lubrication calculations used as a tool to study scuffing
[NASA-TM-87097] 23 p3938 N85-34408
Planetary-gear-support bearing test rig design
[NASA-CR-174927] 24 p4084 N85-35185
Establishment of a Computer-Aided Design (CAD)-Computer-Aided Manufacturing (CAM) process for the production of cold forged gears
[AD-A155756] 24 p4137 N85-35644

GEL PERMEATION CHROMATOGRAPHY
U LIQUID CHROMATOGRAPHY

GELATION
Study of reaction kinetics and development of elastic properties in network polymerization systems by the impulse technique
[AD-A148187] 08 p1133 N85-17141
Polymers and macromolecules
[DE85-003176] 10 p1454 N85-19160

GELS
NT DOUBLE BASE ROCKET PROPELLANTS
NT SILICA GEL
Automated apparatus for producing gradient gels
[DE84-014507] 01 p0107 N85-10716
Structural evolution during the gel to glass conversion
[DE84-014954] 06 p0772 N85-14939
Turbulent shear fields for dispersion of aqueous drops in organic liquids and application to gel-sphere processes
[DE84-016562] 06 p0809 N85-15141
Gel drawn fibers of poly(vinyl alcohol)
[AD-A149062] 10 p1435 N85-19040
Electrical and thermal performance during charging and discharging a Phase 1 gel cell battery
[PB85-114312] 11 p1677 N85-20565
Sol-gel processing of lead zirconate titanate films
[ATR-85(8343)-2] 18 p3073 N85-29010
A gel-halo sample pellet: The best of both worlds? Stubby zones without a constricted sample gate 20 p3502 N85-31770
Solid-state co-extrusion of nylon 6 gel
[AD-A156187] 24 p4082 N85-35296

GENERAL AVIATION AIRCRAFT
NT AGRICULTURAL AIRCRAFT
NT CESSNA 402B AIRCRAFT
NT DHC 2 AIRCRAFT
NT DO-28 AIRCRAFT
Review of aircraft accident data: US General Aviation
[PB84-230960] 01 p0005 N85-10027
Full-scale crash-test evaluation of two load-limiting subfloors for general aviation airframes
[NASA-TP-2360] 04 p0512 N85-13267
Annual review of aircraft accident data: US general aviation, calendar year, 1981
[PB84-230960] 06 p0750 N85-14805
Design study of technology requirements for high performance single-propeller-driven business airplanes
[NASA-CR-3863] 07 p0898 N85-15892
Some characteristics of automotive gasolines and their performance in a light aircraft engine
[FAA-CT-84-12] 07 p0934 N85-15919
Aerodynamic-structural study of canard wing, dual wing, and conventional wing systems for general aviation applications
[NASA-CR-172529] 08 p1077 N85-16829
The design of sport and touring aircraft
[NASA-TM-77783] 10 p1423 N85-18975
Wind-tunnel investigation of a full-scale canard-configured general aviation airplane
[NASA-TP-2382] 11 p1575 N85-19925
Circulation control propellers for general aviation, including a BASIC computer program
[NASA-CR-165968] 19 p3219 N85-29959
FAA regulation of 9-seat and under passenger aircraft
[GPO-42-703] 20 p3391 N85-31032
Quest for performance: The evolution of modern aircraft
[NASA-SP-468] 21 p3551 N85-32089

GENERAL DYNAMICS AIRCRAFT
NT CL-41 AIRCRAFT
NT CV-990 AIRCRAFT
NT F-106 AIRCRAFT
NT F-111 AIRCRAFT

GENERAL DYNAMICS MILITARY AIRCRAFT
U MILITARY AIRCRAFT

GENERATION
Fuel cell applications literature review
[DE85-011891] 22 p3809 N85-33592

GENERATORS
Continuous laminar smoke generator
[NASA-CASE-LAR-13014-1] 12 p1781 N85-21178
Coal-Fired MHD Combustor Development Project, Phase 3D
[DE85-006822] 18 p3192 N85-29795
Design of a generator for near-tangential transonic swirling outflow
[AD-A155163] 21 p3584 N85-32280
Control system for fluid heated steam generator
[DE85-005734] 23 p3939 N85-34417
Development of the osmium-191 yields iridium-191m radionuclide generator
[DE85-011185] 23 p3970 N85-34611
Current status of the Os-191 yields Ir-191m generator
[DE85-006306] 23 p3971 N85-34614

GENETIC CODE
Genetics in methylotrophic bacteria
[DE85-011460] 19 p3327 N85-30615

GENETIC ENGINEERING
Genetic engineering of plants: Agricultural research opportunities and policy concerns
[DE85-006771] 16 p2840 N85-27513
East Europe report: Science and technology
[JPRS-ESA-85-023] 21 p3572 N85-32217

GENETICS
NT GENETIC CODE
NT MUTATIONS
USSR report: Life sciences. Biomedical and behavioral sciences
[JPRS-UBB-84-025] 04 p0543 N85-13453
Study of mathematical models of mutation and selection in multi-locus systems
[DE85-000973] 09 p1376 N85-18648
Genetic effects of microwave exposure on mammalian cells in vitro. Volume 2, Appendix A: Cytogenetics and growth kinetics data, 850 MHz
[AD-A148866] 10 p1522 N85-19599
Oversight review of the five-year outlook report on science and technology
[GPO-41-058] 12 p1949 N85-22243
USSR report: Life sciences. Biomedical and behavioral sciences
[JPRS-UBB-85-012] 14 p2386 N85-24697
Towards a statistical analysis of genetic sequences data with particular reference to protein sequences
[AD-A153605] 18 p3152 N85-29515
Chromosome aberrations in Crepis capillaris exposed to gamma radiation and clinostat 19 p3325 N85-30600
Genetics in methylotrophic bacteria
[DE85-011460] 19 p3327 N85-30615
Biocatalysis project
[NASA-CR-176044] 20 p3498 N85-31744
Organization of the R region in maize
[DE85-011273] 20 p3504 N85-31780
Search for the universal ancestors
[NASA-SP-477] 21 p3667 N85-32777
USSR report: Life sciences. Biomedical and behavioral sciences
[JPRS-UBB-85-018] 22 p3819 N85-33660

Three-dimensional reconstruction and data display of chromosome structure studied by electron microscope tomography
[DE85-011562] 22 p3625 N85-33697
Genetic and physiological control of protective antigen synthesis by bacillus anthracis
[AD-A156324] 24 p4133 N85-35617
GENITOURINARY SYSTEM
NT BLADDER
GEOASTROPHYSICS
U ASTROPHYSICS
U GEOPHYSICS
GEOBOTANY
Remote sensing as a mineral prospecting technique
[E85-10010] 02 p0216 N85-11429
NASA's land remote sensing plans for the 1980's
13 p2124 N85-23224
Carbon isotope geochemistry and geobiology
21 p3657 N85-32716
GEOCENTRIC COORDINATES
Increasing the accuracy of processing radar pictures by excluding systematic point coordinate error component
15 p2488 N85-25356
Global coordinate system
[AD-A153878] 19 p3299 N85-30454
GEOCHEMISTRY
NT BIOGEOCHEMISTRY
Thermodynamic properties and environmental chemistry of chromium
[DE84-015123] 01 p0025 N85-10152
Hydrogeochemical investigation of thermal springs in the Black Canyon-Hoover Dam area, Nevada and Arizona
[PB84-202472] 01 p0064 N85-10428
The marine geochemistry of the rare earth elements
[AD-A145132] 01 p0068 N85-10598
The Alaskan mineral resources assessment program: Guide to information contained in the folio of geologic and mineral-resource maps of the Medfra Quadrangle, Alaska
[GS-CIRC-928] 02 p0219 N85-11443
The petrology and geochemistry of high cascade volcanics in southern Washington: Mount Saint Helens volcano and the Indian Heaven basalt field
02 p0227 N85-11487
Geology and geochemistry of early Tertiary submarine volcanic rocks of the Aleutian Islands, and their bearing on the development of the Aleutian Island Arc
03 p0369 N85-12493
The United States Geological Survey in Alaska: Accomplishments during 1981
[USGS-CIRC-868] 04 p0515 N85-13283
Geology and geochemical evolution of the Lost River, Alaska, tin deposit 04 p0533 N85-13405
Geophysical and geochemical constraints favoring the capture hypothesis 04 p0581 N85-13710
Tests of the lunar hypothesis
04 p0584 N85-13730
Geochemical evidence for the formation of the Moon by impact induced fission of the proto-Earth
04 p0587 N85-13747
An integrated dynamical and geochemical approach to lunar origin modeling 04 p0587 N85-13748
A circumterrestrial compositional filter
04 p0588 N85-13753
Summaries of physical research in the geosciences
[DE85-001882] 06 p0618 N85-15194
Manganese in recent sediments of Ukrainian SSR Black Sea shelf 06 p0619 N85-15200
Geochemical data for rock samples from the Petersburg and parts of the Port Alexander and Sumdum quadrangles, southeastern Alaska (documentation)
[PB84-234434] 06 p0636 N85-15318
Alabama Tin Belt: Metallogenesis and mineral resource evaluation. Year-end report
[DE84-901335] 07 p0989 N85-16283
Analysis of gases in the Earth's crust
[PB85-113397/GAR] 07 p0990 N85-16287
Earth Sciences Division report, 1983
[DE85-001036] 09 p1341 N85-18436
Correlation and petrological interpretation of abyssal and terrestrial taphra layers 09 p1353 N85-18512
Relationship of gold content to gravity fields in Far East 10 p1501 N85-19475
Radioactive waste isolation in salt: Peer review of the Office of Nuclear Waste Isolation's report on the organic geochemistry of deep groundwaters from the Palo Duro Basin, Texas
[DE85-001439] 10 p1556 N85-19811
Research and development related to the Nevada nuclear waste storage investigations
[DE85-002303] 12 p1932 N85-22138
Reports of the Planetary Geology and Geophysics Program, 1984
[NASA-TM-87563] 13 p2172 N85-23474
Hibonite: Crystal chemistry and origin of blue coloration in meteoritic assemblages 13 p2184 N85-23555
Basalts of Mars: Constraints on volatile evolution
13 p2194 N85-23610
USSR report: Earth sciences
[JPRS-UES-85-004] 14 p2332 N85-24424
Most important geochemical barrier zones in ocean (with example of Atlantic Ocean basin)
14 p2343 N85-24491
Geological information content of reflected wave record form 14 p2345 N85-24502
Deep source gas
[DE85-001984] 18 p3126 N85-29358
Radionuclide mobility in the shallow portion of an active high-temperature geothermal system
[DE85-010293] 18 p3182 N85-29729
Geochemistry of manganese in ocean
19 p3291 N85-30406
Mineralogical-geochemical characteristics of ferromanganese formations in Arabian-Indian Ocean Ridge 19 p3293 N85-30416
Petrologic and geochemical characterization of the Topopah Spring Member of the Paintbrush Tuff: Outcrop samples used in waste package experiments
[DE85-010449] 19 p3302 N85-30470
Proceedings of the Fifth International Conference on Nuclear Methods in Environmental and Energy Research
[DE84-017348] 19 p3310 N85-30521
Subsurface petroleum geology of Santa Rosa sandstone (Triassic), northeast New Mexico
[TI85-901364] 19 p3313 N85-30538
Clay identification and amount measured by laboratory techniques compared to well log responses: Application to tight gas sands and shales
[DE85-010411] 19 p3362 N85-30843
The U.S. Geological Survey in Alaska: Accomplishments during 1982
[US-GEOL-SURV-CIRC-939] 20 p3403 N85-31719
Global Mega-Geomorphology
[NASA-CP-2312] 21 p3600 N85-32357
Carbon isotope geochemistry and geobiology
21 p3657 N85-32716
Geology and geochemistry of sulfide and sulfate deposition 21 p3658 N85-32723
Microbiology of solar salt ponds
21 p3658 N85-32724
Workshop on the Early Earth: The Interval from Accretion to the Older Archean
[NASA-CR-176037] 21 p3717 N85-33062
The relation between the age of the subconducting slab and the recycling of sediments into the mantle
21 p3717 N85-33063
The 3.5 b.y. old Onverwacht Group: A remnant of ancient oceanic crust 21 p3718 N85-33073
A review of noble gas geochemistry in relation to early Earth history 21 p3720 N85-33081
The Aravalli sequence of Rajasthan, India: A Precambrian continental margin?
21 p3720 N85-33084
Carbon and nitrogen in the deep Earth
21 p3721 N85-33085
Chemical evolution of the Earth: Equilibrium or disequilibrium process? 21 p3721 N85-33088
Thermal, dynamic and compositional aspects of the core-forming Earth 21 p3722 N85-33091
Geologic processes on Venus: An update
22 p3857 N85-33883
Geochemical confirmation of the lunar magmasphere hypothesis 22 p3859 N85-33895
Thermally induced chemical migration: A natural analog approach
[DE85-012308] 23 p3949 N85-34474
Chemistry division report
[DE85-010586] 24 p4071 N85-35228
The role of regional subsurface geochemistry in resource assessment in the central United States
24 p4104 N85-35440
The development of assessment techniques program
24 p4106 N85-35457
The Alaska Mineral Resources Assessment Program
24 p4107 N85-35460
GEOCHRONOLOGY
Erosion and sedimentation chronology of three watersheds in Maryland
[PB84-207356] 01 p0071 N85-10467
On gravity from SST, geoid from Seasat, and plate age and fracture zones in the Pacific
[E85-10020] 02 p0217 N85-11433
The United States Geological Survey in Alaska: Accomplishments during 1981
[USGS-CIRC-868] 04 p0515 N85-13283
Reconnaissance geology of the northern part of the Unalakleet quadrangle 04 p0516 N85-13291
Newly recognized sedimentary environments in the Shellkof Formation, Alaska 04 p0516 N85-13292
New ages of radiolarian chert from the Rampart district, east-central Alaska 04 p0516 N85-13293
Paleozoic limestones of the Crazy Mountains and vicinity, Circle quadrangle, east-central Alaska
04 p0517 N85-13298
Late Paleozoic and early Mesozoic radiolarians in the Circle quadrangle, east-central Alaska
04 p0517 N85-13297
Structural observations in the Circle quadrangle, Yukon-Tanana Upland, Alaska 04 p0517 N85-13298
Lacustrine and eolian deposits of Wisconsin age at Riverside Bluff in the upper Tanana River valley, Alaska
04 p0517 N85-13299
Glacial-lake deposits in the Mount Harper area, Yukon-Tanana Upland 04 p0517 N85-13300
Paleogene volcanic rocks of the Matanuska Valley area and the displacement history of the Castle Mountain fault 04 p0518 N85-13303
Progress in lead/uranium zircon studies of lower paleozoic rocks of the southern Alexander terrane
04 p0518 N85-13304
Geology and geochemical evolution of the Lost River, Alaska, tin deposit 04 p0533 N85-13405
The I-Pu-Xe age of the Moon
04 p0584 N85-13729
Constraints on lunar origin: Evidence preserved in Precambrian stromatolites 04 p0584 N85-13731
A tectonic and metamorphic history of the north-central Klamath Mountains, California 05 p0673 N85-14323
Tectonic history of a continent: Island arc boundary, west-central Idaho 05 p0673 N85-14324
Geophysical investigation of precambrian crustal structure and Laramide effects across a precambrian suture in southeastern Wyoming
05 p0674 N85-14328
Quaternary stratigraphy, geochronology and carbon isotope geology of alluvial deposits in the Texas panhandle 09 p1353 N85-18514
Major glaciation events of the past and their geological significance 10 p1497 N85-19450
Post-carboniferous tectonics in the Anadarko Basin, Oklahoma: Evidence from side-looking radar imagery
[NASA-CR-175458] 10 p1505 N85-19498
Crustal dynamics studies in China
[NASA-CR-175617] 13 p2132 N85-23265
Why not a constant early lunar impact rate?
13 p2181 N85-23536
Martian terrain ages 13 p2181 N85-23537
The geology of Mt. Hope, a silicic volcanic center in West Central Arizona 13 p2187 N85-23571
Geomorphology and geology of the Southwestern Margaritifer Sinus and Argyre regions of Mars. Part 2: Crater size-frequency distribution curves and geomorphic unit ages 13 p2192 N85-23601
Chondrule-like particles provide evidence of early Archean meteorite impacts, South Africa and western Australia 15 p2662 N85-26562
Structural and tectonic history of the Golconda allochton, southern Tolyabe Range, Nevada
19 p3312 N85-30529
Global Mega-Geomorphology
[NASA-CP-2312] 21 p3600 N85-32357
Some observations on paleogeomorphology
21 p3601 N85-32363
Landscape inheritance: Report of Working Group Number 2 21 p3604 N85-32383
Precambrian evolution and the rock record
21 p3656 N85-32711
Origin of life 21 p3657 N85-32713
The 3.5 b.y. old Onverwacht Group: A remnant of ancient oceanic crust 21 p3718 N85-33073
Archean sedimentary systems and crustal evolution
21 p3720 N85-33082
The Aravalli sequence of Rajasthan, India: A Precambrian continental margin?
21 p3720 N85-33084
Chemical constraints on the evolution of Archean continental crust 21 p3722 N85-33093
Dating Archean zircon by ion microprobe: New light on an old problem 21 p3722 N85-33094
Geology and petroleum resources of basins in western China
[DE85-013038] 23 p3948 N85-34469
Early and middle Cenozoic volcanic synthesis
24 p4105 N85-35449
Hydrogeology of the lower Glen Rose Aquifer, south-central Texas 24 p4108 N85-35468
GEOCORONAL EMISSIONS
High resolution geocoronal Balmer alpha observations
20 p3489 N85-31686
GEODESIC LINES
Harmonic analysis and Radon transforms on pencils of geodesics
[CWI-PM-R8413] 12 p1922 N85-22074
Reflected wave travel-time curves in stratified media with vertically heterogeneous layers and slightly sloping curved boundaries 13 p2114 N85-23167

Informative geometry of probability spaces
[AD-A150510] 13 p2153 N85-23371
GEODESY
NT CELESTIAL GEODESY
Global positioning system: Geodetic applications
[AD-A144904] 01 p0005 N85-10030
Prediction of deflections of the vertical by gravimetric methods
[PB84-213727] 01 p0072 N85-10478
Use and value of a geodetic reference system
[PB84-216167] 03 p0379 N85-12418
Investigation of several aspects of LANDSAT 4/5 data quality
[E85-10038] 04 p0525 N85-13357
An interactive FORTRAN program for determining reliability of pseudo-range geodetic point positioning using the global positioning system
[AD-A147133] 07 p0988 N85-16275
Altimetry, orbits and tides
[E85-10088] 08 p1174 N85-17404
Mathematical aspects of digital terrain information; Report from International Society for Photogrammetry and Remote Sensing (ISPRS) working group 3:3, 1980 - 1984 — photogrammetry 08 p1175 N85-17407
Using the global positioning system (GPS) phase observable for relative geodesy: Modeling, processing, and results 09 p1341 N85-18437
Activities report of the Department of Applied Research 78 for satellite geodesy of the Technical University, Munich
[ASTRON-GEODAET-ARB-45] 09 p1342 N85-18440
Continental networks: Report on the activities of the International Association of Geodesy (IAG) Commission 10, 1979 - 1983 — geodesy
[SER-B-266] 09 p1342 N85-18441
World Geodetic System, 1984
[AD-A147400] 09 p1342 N85-18445
Computer programs for the adjustment of indirect observation with condition equations between the unknowns
[SER-B-268-MITT-170] 09 p1370 N85-18612
Utilization of mobile VLBI for geodetic measurements 10 p1466 N85-19248
Study of tectonic earthquake precursors by geodetic methods 10 p1502 N85-19479
Geodetic accuracy of LANDSAT 4 Multispectral Scanner and Thematic Mapper data — Washington, DC, California, Alabama, South Dakota, and Illinois 11 p1667 N85-20504
Geometric accuracy assessment of LANDSAT-4 Multispectral Scanner (MSS) data 11 p1667 N85-20505
Program INNAVSAT: Global Positioning System (GPS): Test and demonstration program
[BMFT-FB-W-84-047] 12 p1775 N85-21145
Hybrid method of mapping and photogeodetic control network densification
[PB85-133775] 12 p1876 N85-21766
Use of three omega radionavigation system position lines for solving problems in marine geodesy 13 p2107 N85-23131
Determining vector of radiointerferometer base from observations of natural radio emission with narrow spectrum 13 p2112 N85-23158
Development, achievements in China's cartography work 13 p2166 N85-23434
A unified lunar control network 13 p2203 N85-23669
The control network of Mars: October 1984 13 p2203 N85-23670
The control networks of the satellites of Jupiter and Saturn 13 p2204 N85-23671
Shape of Io 13 p2204 N85-23672
Application of space methods in geodesy 16 p2724 N85-26817
Radial orbit error spectrum for Topex 16 p2805 N85-27292
Astrometric method advances Astronomy, geodesy 16 p2806 N85-27306
Reports on cartography and geodesy. Series 1: Original reports, no. 94
[ISSN-0469-4236] 16 p2814 N85-27357
Use of vector processors in cartographic raster data processing, with special regard to the AP-120B vector processor 16 p2814 N85-27358
Standards and specifications for geodetic control networks
[PB85-166478] 16 p2816 N85-27374
Water vapor radiometry research and development phase
[NASA-CR-175887] 17 p2995 N85-28512
Information relative to cartography and geodesy. Series 2: Translations, number 42, volume 1
[ISSN-0469-4244] 18 p3123 N85-29338
Reports on cartography and geodesy. Series 1: Original reports, number 93
[ISSN-0469-4236] 18 p3124 N85-29343
Use of stereographic projection in marine geodesy 19 p3294 N85-30421
HANDTC: A FORTRAN program to calculate inner-zone terrain corrections
[DE85-011196] 19 p3340 N85-30699
Geodyn systems development 20 p3492 N85-31708
Crustal dynamics project data analysis fixed station VLBI geodetic results
[NASA-TM-86229] 21 p3615 N85-32465
SPLINES. Their equivalence to collocation
[AD-A155250] 21 p3632 N85-32566
Crustal Dynamics Project: Catalogue of site information
[NASA-TM-86218] 22 p3801 N85-33552
GEODETIC ACCURACY
Global positioning system: Geodetic applications
[AD-A144904] 01 p0005 N85-10030
An investigation of several aspects of LANDSAT-5 data quality — Palmer County, Shelby, mt; White sands, NM; Great Salt Lake, UT; San Mattied Bridge and Sacramento, California
[E85-10096] 13 p2122 N85-23214
Minimizing influence of Earth's curvature in projective rectification of space photographs into photoplans and photomaps 16 p2727 N85-26829
New VLBI technology developments 20 p3491 N85-31702
Error spectrum of Goddard satellite models for the gravity field 20 p3491 N85-31704
GEODETIC COORDINATES
Diagnosis and therapy of geodetic satellite networks of Doppler type — error analysis
[SER-C-293] 01 p0015 N85-10090
A strategy for the adjustment and analysis of densification networks — geodetic networks
[SER-C-295] 01 p0063 N85-10420
Testing of a field portable GPS (Global Positioning System) geodetic receiver
[AD-A148336] 08 p1082 N85-16859
Continental networks: Report on the activities of the International Association of Geodesy (IAG) Commission 10, 1979 - 1983 — geodesy
[SER-B-266] 09 p1342 N85-18441
A three-dimensional geometric-physical model for conventional geodetic observations-observables, parameter estimation, and deformation analysis
[SER-C-298] 11 p1665 N85-20493
The 1980 diagnostic adjustment of the German main triangulation network. 4: Network adjustment (part 3)
[SER-B-267-PT-3-MITT-168] 11 p1665 N85-20494
The 1980 diagnostic adjustment of the German main triangulation network. 4: Network adjustment (part 1)
[SER-B-267-PT-1-MITT-168] 11 p1670 N85-20525
The 1980 diagnostic adjustment of the German main triangulation network. 4: Network adjustment (part 2)
[SER-B-267-PT-2-MITT-168] 11 p1670 N85-20526
Evaluating accuracy in determining position of Earth's center of mass and elements of orientation of geodetic coordinate system 13 p1983 N85-22441
Determining vector of radiointerferometer base from observations of natural radio emission with narrow spectrum 13 p2112 N85-23158
Study of phase radiogeodetic systems with phase-locked loops 13 p2115 N85-23172
Location and synchronization — space-time coordinates 14 p2397 N85-24768
UTM (Universal Transverse Mercator) determinations from geographical data
[AD-A152293] 16 p2858 N85-27610
Allowance for differences in ellipsoids and geodetic control coordinate systems in determining ship's position using radio navigation systems 19 p3292 N85-30413
Global coordinate system
[AD-A153878] 19 p3299 N85-30454
Comparing SLR and VLBI geodetic parameters 20 p3491 N85-31703
Basic formulae for the computation of the deflection of the vertical from astronomical star observations
[AD-A154912] 21 p3605 N85-32390
GEODETIC SATELLITES
NT GEOS 1 SATELLITE
NT GEOS 2 SATELLITE
NT GEOS 3 SATELLITE
The motion of the Earth by Doppler observing campaign (MEDOC) 05 p0601 N85-13831
Establishment of hydrographic shore control by Doppler satellite techniques
[AD-A150709] 14 p2347 N85-24512
GEODETIC SURVEYS
NASA Geodynamics Program
[NASA-TM-87359] 01 p0063 N85-10418
Basic research for the geodynamics program
[NASA-CR-174055] 02 p0228 N85-11490
Tides and tidal currents of the inland waters of Western Washington
[PB84-237379] 06 p0842 N85-15346
Continental networks: Report on the activities of the International Association of Geodesy (IAG) Commission 10, 1979 - 1983 — geodesy
[SER-B-266] 09 p1342 N85-18441
Utilization of mobile VLBI for geodetic measurements 10 p1466 N85-19248
A three-dimensional geometric-physical model for conventional geodetic observations-observables, parameter estimation, and deformation analysis
[SER-C-298] 11 p1665 N85-20493
The 1980 diagnostic adjustment of the German main triangulation network. 4: Network adjustment (part 1)
[SER-B-267-PT-1-MITT-168] 11 p1670 N85-20525
The 1980 diagnostic adjustment of the German main triangulation network. 4: Network adjustment (part 2)
[SER-B-267-PT-2-MITT-168] 11 p1670 N85-20526
Hybrid method of mapping and photogeodetic control network densification
[PB85-133775] 12 p1876 N85-21766
Planetary cartography in the next decade (1984 - 1994)
[NASA-SP-475] 12 p1960 N85-22323
Consideration of heterogeneity of gravity fields in local high precision geodetic constructions 13 p2114 N85-23169
Mathematical modeling of results of geometric leveling in variable gravity field 13 p2114 N85-23170
Crustal dynamics project: Catalogue of site information
[NASA-TM-87452] 13 p2131 N85-23258
Estzblishment of hydrographic shore control by Doppler satellite techniques
[AD-A150709] 14 p2347 N85-24512
Preliminary processing of laser ranging data from LAGEOS artificial Earth satellite during short merit program observation period 15 p2488 N85-25355
Increasing the accuracy of processing radar pictures by excluding systematic point coordinate error component 15 p2488 N85-25356
Application of the Siemans Computer Aided Computer (Sicad) system to the surveying management in Baden-Wuerttemberg 16 p2814 N85-27361
Derivation of model topography 18 p3141 N85-29449
A comparison of methods of least squares adjustment of traverses
[AD-A153612] 18 p3170 N85-29645
Application of GPS in a high precision engineering survey network
[DE85-010556] 19 p3313 N85-30539
Carbon fiber strainmeter studies in southern California
[PB85-196889] 24 p4118 N85-35528
GEODYNAMICS
NASA Geodynamics Program
[NASA-TM-87359] 01 p0063 N85-10418
The SANCOR programme on coastal processes, April 1982 - March 1986
[REPT-68] 01 p0069 N85-10455
Basic research for the geodynamics program
[NASA-CR-174055] 02 p0228 N85-11490
General model of earthquakes and the place of warnings in it 07 p0981 N85-16232
Earthquake forecasting research in the Ukraine 07 p0981 N85-16233
Activities report of the Department of Applied Research 78 for satellite geodesy of the Technical University, Munich
[ASTRON-GEODAET-ARB-45] 09 p1342 N85-18440
Structural morphology and associated strain within parts of the US section of the Kootenay Arc, NE, Washington 09 p1352 N85-18505
Mesozoic magmatism of Mongolian-Okhotsk Belt and its possible geodynamic interpretation 10 p1502 N85-19481
Science Applications, part 2 11 p1643 N85-20347
Summary presentation of the Science Applications Panel 11 p1644 N85-20355
Absolute movement of Pacific Ocean plate during last 120 million years 13 p2107 N85-23126
Crustal dynamics project: Catalogue of site information
[NASA-TM-87452] 13 p2131 N85-23258
Crustal dynamics studies in China
[NASA-CR-175617] 13 p2132 N85-23265
Reference systems — in space mechanics 14 p2399 N85-24784
Example of joint use of data from surface studies and space photographs in investigating dynamics of zone of North Zeravshan seismogenic faults 15 p2485 N85-25342

Basic research for the geodynamics program
[NASA-CR-175751] 16 p2825 N85-27424
Kuril-Aleutian subduction 19 p3290 N85-30402
Investigation of dynamic noise affecting geodynamics information in a tethered subsatellite
[NASA-CR-176031] 20 p3476 N85-31602
Geodynamics Branch research program
[NASA-TM-86223] 20 p3489 N85-31688
The Earth's wobble and associated ocean motions 20 p3490 N85-31696
NASA/GSFC TOPEX gravity model operations group 20 p3492 N85-31709
Precambrian evolution and the rock record 21 p3656 N85-32711
Thermal, dynamic and compositional aspects of the core-forming Earth 21 p3722 N85-33091
Mapping of dynamics of deltas by space photography 22 p3737 N85-33163

GEOELECTRICITY
NT TELLURIC CURRENTS
Possible effects of interaction of electric seismic fields with the ionosphere 06 p0823 N85-15226
Brazil future plans in upper atmosphere research in Antarctica
[INPE-3400-PRE/669] 10 p1515 N85-19559
Discrimination of normal and anomalous magnetic and electric fields in geoelectromagnetic variations 13 p2114 N85-23166
Electromagnetic fields migration method 14 p2343 N85-24487
Report of the geomagnetic and geoelectric observations, 1983 (rapid variations)
[REPT-24] 15 p2591 N85-25975

GEOFRACTURES
U GEOLOGICAL FAULTS

GEOGRAPHIC INFORMATION SYSTEMS
Use and value of a geodetic reference system
[PB84-216167] 03 p0379 N85-12418
Building a functional, integrated GIS/remote sensing resource analysis and planning system — Utah
[E85-10092] 12 p1874 N85-21754

GEOGRAPHY
NT HYPSOGRAPHY
NT OROGRAPHY
Environmental geologic atlas of the North Carolina coastal zone: Dare, Hyde, Tyrrell and Washington Counties
[PB84-222975] 01 p0066 N85-10439
The Multispectral Imaging Science Working Group. Volume 1: Executive summary
[E85-10001] 02 p0213 N85-11404
The Multispectral Imaging Science Working Group. Volume 2: Working group reports
[E85-10002] 02 p0213 N85-11405
Geographic and stratigraphic distribution of Miocene palynomorphs in north Idaho 03 p0390 N85-12498
Calculation of the area covered by mobile radio systems using geographic data stored in a computer
[FUB-43-1983] 09 p1312 N85-18247
The sharing of remote sensing techniques in Brazilian geographic research
[INPE-3307-PRE/617] 10 p1506 N85-19502
Review of computer mapping and display techniques applicable to regional analysis
[DE85-003545] 12 p1875 N85-21764
Hexagonal data base study
[AD-A150176] 13 p2167 N85-23448
MAP3S precipitation chemistry network
[DE85-005324] 14 p2353 N85-24539
Activities report of the Laboratory for Computer Science (FOA 32)
[FOA-C-30384-E1] 20 p3516 N85-31661
Applied computer graphics in a geographic information system: Problems and successes 23 p3962 N85-34563

GEOIDS
On gravity from SST, geoid from Seasat, and plate age and fracture zones in the Pacific
[E85-10020] 02 p0217 N85-11433
Determination of geoid undulations and ocean heights from ERS-1 radar altimetry data 03 p0381 N85-12432
Satellite altimetry for sea-surfacing topography determination and geoid improvement 03 p0382 N85-12444
Determination of the altimetric geoid and gravity anomalies in the North Sea: Implications for a solution of the general circulation problem using ERS-1 data 03 p0382 N85-12446
Local geoid determination in mountain regions
[AD-A145799] 03 p0384 N85-12458
Lithospheric structure in the Pacific geoid
[NASA-CR-174155] 04 p0526 N85-13365
Altimetry, orbits and tides
[E85-10066] 08 p1174 N85-17404
Simultaneous determination of the xi and eta components of vertical deflection with a prism astrolabe
[SER-B-270-MITT-171] 09 p1343 N85-18450
The Gauss-Krueger projection of the Earth ellipsoid with direct calculation of elliptic integrals through Landen transformations
[SER-C-296] 11 p1666 N85-20495
Physiography of the Martian west equatorial uplift 12 p1961 N85-22325
On geoid heights and flexure of the lithosphere at seamounts
[AD-A151220] 15 p2604 N85-26050
Altimetry data and the elastic stress tensor of subduction zones
[NASA-CR-175798] 18 p2825 N85-27425
Application of GPS in a high precision engineering survey network
[DE85-010556] 19 p3313 N85-30539
Evolution of the oceanic upper mantle and effects on sea floor subsidence geoid height and heat flow 19 p3319 N85-30575
Spaceborne gradiometer error analysis 20 p3492 N85-31707
Global mean sea surface based upon a combination of the GEOS-3 and SEASAT altimeter data 20 p3492 N85-31710
The time averaged circulation of the oceans from satellite altimetry 20 p3493 N85-31713
Dynamic compensation of Venus's geoid: A comparison with Earth 22 p3858 N85-33888
A dynamic model of Venus's gravity field
[NASA-CR-176173] 24 p4169 N85-35845

GEOLOGICAL FAULTS
NT SAN ANDREAS FAULT
Seismic studies in southern Alaska 04 p0515 N85-13286
Paleogene volcanic rocks of the Matanuska Valley area and the displacement history of the Castle Mountain fault 04 p0518 N85-13303
Petrologic model of the northern Mississippi embayment based on satellite magnetic and ground based geophysical data
[NASA-TM-85075] 04 p0533 N85-13406
Blind zones and aspect ratio bias in acquisition of discontinuity orientation data
[DE84-002718] 04 p0533 N85-13410
Rio Grande rift: Problems and perspectives
[DE84-015492] 04 p0534 N85-13417
Synthesis of proterozoic data as a prerequisite for tectonic and thermal modeling
[NASA-CR-174252] 07 p0995 N85-16323
New Zealand SIR-B science investigations 08 p1144 N85-17218
Analysis of SIR-B radar illumination of geometry for depth of penetration and surface feature and vegetation detection, Nevada and California 08 p1149 N85-17248
Modeling of large-scale accretionary wedge and thin-skinned trust-and-fold belt mechanics 08 p1181 N85-17442
Mesozoic ophiolitic olistostromes and Cenozoic imbricate thrust faulting in the northern California coast ranges: Geology of the Mysterious Valley area, Napa County 08 p1182 N85-17445
Thermal conditions and thinning of lithosphere in late cenozoic in southwestern US 10 p1501 N85-19473
Tectonic position and formation of young alkaline provinces of continents and oceans 10 p1502 N85-19480
Nonlinear seismology 10 p1503 N85-19482
Statistical study of anthropogenic seismic noise with IVK-7 computer system 10 p1503 N85-19483
SIR-A imagery in geologic studies of the Sierra Madre Oriental, northeastern Mexico. Part 1 (Regional stratigraphy): The use of morphostratigraphic units in remote sensing mapping
[NASA-CR-175457] 10 p1505 N85-19497
Post-carboniferous tectonics in the Anadarko Basin, Oklahoma: Evidence from side-looking radar imagery
[NASA-CR-175458] 10 p1505 N85-19498
Tectonic lineaments in the cenozoic volcanics of southern Guatemala: Evidence for a broad continental plate boundary zone
[NASA-CR-175456] 10 p1505 N85-19499
Arctic-North Atlantic rift megasystem 13 p2105 N85-23117
Crustal and upper mantle density model of Owen fault zone 13 p2110 N85-23144
Numerical modeling of plane stick-slip fault 13 p2111 N85-23150
Study of geological media based on scattered earthquake waves 13 p2114 N85-23168
Crustal dynamics project: Catalogue of site information
[NASA-TM-87452] 13 p2131 N85-23258
Normal-fault and fold development in sedimentary rocks above a pre-existing basement normal fault 13 p2131 N85-23259
Crustal dynamics studies in China
[NASA-CR-175617] 13 p2132 N85-23265
Volcanism and rift formation in Beta Regio, Venus: New radar results 13 p2176 N85-23507
Volcanic debris flows in the Elysium region of Mars 13 p2185 N85-23560
Geomorphology and geology of the Southwestern Margaritifer Sinus and Argyre regions of Mars. Part 1: Geological and geomorphological overview 13 p2192 N85-23600
On the absence of strike-slip faults from the planets and satellites 13 p2200 N85-23645
Lunar mascon loading: An example of the importance of fault initiation depth on fault type predictions from stresses on planetary surfaces 13 p2200 N85-23646
Elysium region, Mars: Tests of lithospheric loading models for the formation of tectonic features 13 p2200 N85-23650
Creep of ice: Further studies 13 p2201 N85-23655
Fault offsets and lateral crustal movement on Europa 13 p2201 N85-23656
Laboratory investigation of formation damage of an artificial fracture at simulated geothermal conditions
[DE86-010301] 18 p3102 N85-29201
Structure of Reykjanes Ridge rift zone and Icelandic thermal anomaly 19 p3289 N85-30395
Discovery in earthquake forecasting and seismic zoning recorded 19 p3295 N85-30426
Tectonic structure features of some deep faults in Atlantic and Pacific Oceans (according to deep seismic sounding-reflected waves method data) 19 p3295 N85-30428
Fracture detection and mapping for geothermal reservoir definition: An assessment of current technology, research, and research needs
[DE85-010627] 19 p3301 N85-30464
Comparative study of fracture planes computed from topography and lineaments from imagery with structures and mineralization in the magnetic belt of Washington State
[DE85-010972] 20 p3477 N85-31608
Design of a freestanding noise measurement and recording system to predict the intensity and location of electromagnetic radiation from earthquakes
[AD-A155070] 21 p3632 N85-32563
Spacecraft-aided research discussed at geology Congress 22 p3734 N85-33147
Landscape interpretation capabilities using space photographs of regions of a multistage platform mantle structure 22 p3734 N85-33151
Fracture detection and characterization for geothermal reservoir definition
[DE85-008677] 22 p3815 N85-33630
Indications of mineral zoning in a fossil hydrothermal system at the Meager Creek geothermal prospect, British Columbia, Canada from induced polarization studies
[DE85-011962] 22 p3815 N85-33636
Compressional environment in the location and orientation of planetary dorsa and terrestrial earthquake fault structures 22 p3857 N85-33885
Comprehensive fracture diagnostics experiement. Part 2: Comparison of seven fracture azimuth measurements
[DE85-011707] 23 p3948 N85-34470
Studies in thermo-hydro-chemical transport in porous and fractured media
[DE85-012555] 23 p3949 N85-34473
Geophysical-geological studies of possible extensions of the New Madrid fault zone
[TI85-901341] 23 p3949 N85-34475
Geology: Structural history and fluvial geomorphology of the southern Death Valley Fault Zone, Inyo and San Bernardino Counties, California 24 p4114 N85-35506
Structural development of the west-central Grant Range, Nye County, Nevada 24 p4115 N85-35508

GEOLOGICAL SURVEYS
Evaluating effectiveness of using space information in specialized hydrogeological research 02 p0164 N85-11114
The United States Geological Survey in Alaska: Accomplishments during 1981
[USGS-CIRC-868] 04 p0515 N85-13283
Summary of LANDSAT quadrangle studies in Alaska 04 p0515 N85-13284
Digital elevation models improve processing of Alaskan gravity data 04 p0515 N85-13285
The Kanayut Conglomerate in the westernmost Brooks Range, Alaska 04 p0516 N85-13289
Progress in lead/uranium zircon studies of lower paleozoic rocks of the southern Alexander terrane 04 p0518 N85-13304

Report of the field work performed in the Basins of the Quebra Osso and Tanque Petro Rivers in the Catas Altas quadrangle, Minas Gerais
[INPE-3268-NTE/225] 04 p0525 N85-13359
Methods for correlating geological, geochemical and geophysical data with satellite imagery in central Ireland
05 p0655 N85-14208
Maritime prospecting, mining discussed
07 p0980 N85-16226
Integrated analysis of remote sensing products from basic geological surveys — Brazil
[E85-10052] 07 p0984 N85-16248
Organogenic structures (submerged reefs) in Silhetian limestone of west Bengal basin
10 p1500 N85-19484
LANDSAT 4 investigations of Thematic Mapper and Multispectral Scanner applications — Drum Mountains, Utah and Tonopath, Nevada
[E85-10095] 12 p1874 N85-21757
GADB: A database facility for modelling naturally occurring geophysical fields 13 p2122 N85-23217
NASA's land remote sensing plans for the 1980's
13 p2124 N85-23224
Remote sensing: New tool for China's geologists
14 p2283 N85-24141
Investigative report on using geological research to promote prospecting 14 p2283 N85-24142
Temperature anomalies above ore bodies
14 p2345 N85-24500
Results of studies of wave field internal structure in prediction of geological cross section
14 p2346 N85-24504
Experience in automation of data processing in interpretation and defining of linear elements from space photographs 15 p2486 N85-25349
Interpretation of the data of USGS seismic refraction profile across the Arabian Shield in western Saudi Arabia 17 p2991 N85-28488
Technical support for geopressured-geothermal well activities in Louisiana
[DE85-010462] 18 p3102 N85-29203
Revised draft: Southeastern regional geologic characterization report
[DE85-006265] 18 p3125 N85-29351
Space methods for geological research
19 p3295 N85-30429
Highly important features of regional tectonics of Earth's Arctic sector 19 p3298 N85-30449
Engineering geology of selected areas, US army engineer division, lower Mississippi valley. The American bottom area, MO-IL. Volume 1
[AD-A154256] 19 p3299 N85-30455
Fracture detection and mapping for geothermal reservoir definition: An assessment of current technology, research, and research needs
[DE85-010627] 19 p3301 N85-30464
Evaluation of geothermal potential of Rio Grande rift and Basin and Range province, New Mexico
[DE85-901380] 19 p3301 N85-30466
Melt zones beneath five volcanic complexes in California: An assessment of shallow magma occurrence
[DE85-010644] 19 p3305 N85-30489
Crosswell acoustic surveying in gas sands: Travel-time pattern recognition, seismic Q and channel waves
[DE85-010777] 19 p3352 N85-30778
Petroleum and mineral resources of Antarctica
[US-GEOL-SURV-CIRC-909] 20 p3477 N85-31605
The U.S. Geological Survey in Alaska: Accomplishments during 1982
[US-GEOL-SURV-CIRC-939] 20 p3493 N85-31719
Worldwide directory of national Earth-science agencies and related international organizations
[GS-CIRC-934] 21 p3605 N85-32386
Fracture detection and characterization for geothermal reservoir definition
[DE85-008677] 22 p3815 N85-33630
Indications of mineral zoning in a fossil hydrothermal system at the Meager Creek geothermal prospect, British Columbia, Canada from induced polarization studies
[DE85-011982] 22 p3815 N85-33636
The United States Geological Survey in Alaska: Accomplishments during 1983
[USGS-CIRC-945] 23 p3948 N85-34468
The transient electromagnetic depth sounding technique applied to hydrocarbons and geothermal exploration
[MITT-42] 23 p3949 N85-34476
The development of assessment techniques program
24 p4106 N85-35457
The Conterminous United States Mineral Assessment Program 24 p4106 N85-35458
Federal Mineral Land Information System
24 p4106 N85-35459
The Alaska Mineral Resources Assessment Program
24 p4107 N85-35460
USGS coastal research, studies and maps: A source of information for coastal decision making
[USGS-CIRC-883] 24 p4106 N85-35465
Evaluation: Close-range photogrammetry for slope inventory and monitoring
[PB85-192755] 24 p4108 N85-35470

GEOLOGY

NT CONES (VOLCANOES)
NT CROSSBEDDING (GEOLOGY)
NT GEOCHRONOLOGY
NT GEOMORPHOLOGY
NT GLACIOLOGY
NT HYDROGEOLOGY
NT LITHOLOGY
NT LUNAR GEOLOGY
NT MARS VOLCANOES
NT OROGRAPHY
NT PETROGRAPHY
NT PETROLOGY
NT PHOTOGEOLOGY
NT RADAR GEOLOGY
NT STRUCTURAL PROPERTIES (GEOLOGY)
NT SUBDUCTION (GEOLOGY)
NT TECTONICS
NT VOLCANOES
NT VOLCANOLOGY
A summary of geothermal studies in Montana, through 1983
[DE84-014325] 01 p0064 N85-10422
Geology and geomorphology of the southern central Blue Ridge: An indexed bibliography
[PB84-225119] 01 p0072 N85-10480
Commentary on cosmonauts geological mapping, photography 02 p0156 N85-11069
The Multispectral Imaging Science Working Group. Volume 1: Executive summary
[E85-10001] 02 p0213 N85-11404
The Multispectral Imaging Science Working Group. Volume 2: Working group reports
[E85-10002] 02 p0213 N85-11405
Workshop on the Use of Future Multispectral Imaging Capabilities for Lithologic Mapping: Workshop summary
02 p0214 N85-11413
Remote sensing as a mineral prospecting technique
[E85-10010] 02 p0216 N85-11423
The Alaskan mineral resources assessment program: Guide to information contained in the folio of geologic and mineral-resource maps of the Medfra Quadrangle, Alaska
[GS-CIRC-928] 02 p0219 N85-11443
Sedimentary and tectonic evolution of the western Taiwan foredeep 03 p0389 N85-12491
Abstracts of papers submitted in 1983 for publication
[PB84-217579] 03 p0398 N85-12543
Reconnaissance geology of the northern part of the Unalakleet quadrangle 04 p0516 N85-13291
Archean sedimentation and tectonics in southern Africa
[NASA-CR-174156] 04 p0533 N85-13408
Mars polar volatiles: Topographic and geologic setting
[NASA-CR-174089] 04 p0561 N85-13706
Crystalline rocks of the northeastern United States
[DE84-013674] 05 p0677 N85-14347
Report on United States Antarctic research activities, February 1983 - October 1984 and United States Antarctic research activities planned for October 1984 - September 1985
[PB84-231265] 05 p0677 N85-14352
Potential geological natural landmarks of the East Gulf Coastal Plain
[PB84-230317] 06 p0835 N85-15316
Exploring ocean's mineral wealth
07 p0980 N85-16227
Evaluation of SIR-B imagery for geologic and geomorphic mapping, hydrology, and oceanography in Australia 08 p1148 N85-17229
Boring information and subsurface data base package user's guide
[AD-A148623] 08 p1230 N85-17747
Earth Sciences Division report, 1983
[DE85-001036] 09 p1341 N85-18436
Glacial geology of Barron County, Wisconsin
09 p1351 N85-18500
Late precambrian to ordovician metamorphism and orogenesis in the Blue Ridge and western Piedmont, Virginia Appalachians 09 p1352 N85-18503
Quaternary stratigraphy, geochronology and carbon isotope geology of alluvial deposits in the Texas panhandle 09 p1353 N85-18514
Consideration of future climatic changes in three geologic settings
[DE85-001704] 09 p1357 N85-18537
Spatial distribution of auroras and its relationship to geological structure of Norilsk region
10 p1497 N85-19447
China report: Science and technology
[JPRS-CST-84-040] 11 p1623 N85-20219
Low-temperature geothermal assessment of the Jordan Valley Salt Lake County, Utah
[DE85-000616] 11 p1670 N85-20524
Proceedings of the 1st Glacier Bay Science Symposium
[PB85-115913] 11 p1682 N85-20599
Geological remote sensing develops rapidly, finds broad applications 13 p2052 N85-22848
Application of field X-ray: Radiometric analysis in exploratory geology and means for its improvement
13 p2115 N85-23176
Possibilities of aerial electric prospecting by long cable method for detecting poorly conducting strata
13 p2115 N85-23177
Proceedings of the Geoscience Instrumentation Workshop
[DE85-004359] 13 p2132 N85-23268
China report: Science and technology
[JPRS-CST-85-003] 13 p2186 N85-23433
Rapid advances in geological work
13 p2186 N85-23437
Dark halo craters and the thickness of grooved terrain on Ganymede 13 p2173 N85-23484
Polar cap formation on Ganymede
13 p2174 N85-23486
Studies of planetary rings 13 p2174 N85-23488
Mapping and geological analysis of Mercury and Venus radar ranging data 13 p2198 N85-23633
Bouguer images of the North American craton
13 p2200 N85-23648
China report: Science and technology
[JPRS-CST-84-012] 14 p2283 N85-24140
Evaluating structure-forming role of late Paleozoic and Mesozoic-Cenozoic tectonic movements in Baltic Sea region 14 p2337 N85-24450
Geological information content of reflected wave record form 14 p2345 N85-24502
Use of space information in petroleum- and gas-prospecting work (example of Southern Mangyshlak)
15 p2485 N85-25341
Spectral reflectance of carbonate minerals and rocks in the visible and near infrared (0.35 - 2.55 microns) and its applications in carbonate petrology
[NASA-CR-175763] 15 p2591 N85-25973
Organizing geological work tasks for 1985 outlined
16 p2806 N85-27303
Shales and other argillaceous strata in the United States
[DE85-010453] 18 p3125 N85-29353
Implications about in situ stress at Yucca Mountain
[DE85-008068] 18 p3126 N85-29356
Western gas sands
[DE85-001985] 18 p3126 N85-29360
Sixth All-Union Marine Geology School
19 p3294 N85-30420
Stratigraphic analysis of Pennsylvania rocks using hierarchy of transgressive-regressive units
19 p3312 N85-30531
Inhomogeneous deformation: The theory and geological application of finite strain compatibility
19 p3312 N85-30532
Subsurface petroleum geology of Santa Rosa sandstone (Triassic), northeast New Mexico
[TI85-901364] 19 p3313 N85-30538
Improving the geological interpretation of magnetic and gravity satellite anomalies
[E85-10103] 20 p3473 N85-31585
Geologic analysis of averaged magnetic satellite anomalies 20 p3474 N85-31586
Statistical magnetic anomalies from satellite measurements for geologic analysis
20 p3474 N85-31589
Binning of satellite magnetic anomalies
20 p3474 N85-31590
The south-central United States magnetic anomaly
20 p3474 N85-31591
The south-central United States magnetic anomaly
20 p3475 N85-31592
Gas hydrates
[DE85-001986] 20 p3477 N85-31607
Global Mega-Geomorphology
[NASA-CP-2312] 21 p3600 N85-32357
Space imagery and some geomorphological problems of the Guiana Shield, South America
21 p3602 N85-32368
One application of mega-geomorphology in education
21 p3602 N85-32370
Worldwide directory of national Earth-science agencies and related international organizations
[GS-CIRC-934] 21 p3605 N85-32386
Carbon and sulfur cycling through geologic time
21 p3658 N85-32720
Geology and geochemistry of sulfide and sulfate deposition 21 p3658 N85-32723

Spacecraft-aided research discussed at geology Congress 22 p3734 N85-33147
Tectonic stability and expected ground motion at Yucca Mountain
[DE85-012004] 22 p3814 N85-33629
Bedrock geology of the Brattleboro Quadrangle, Vermont-New Hampshire
[DE85-011027] 22 p3815 N85-33634
Geology and petroleum resources of basins in western China
[DE85-013038] 23 p3948 N85-34469

GEOMAGNETIC ANOMALIES
U MAGNETIC ANOMALIES

GEOMAGNETIC CROTCHETS
U SUDDEN IONOSPHERIC DISTURBANCES

GEOMAGNETIC EFFECTS
U MAGNETIC EFFECTS

GEOMAGNETIC EQUATOR
U MAGNETIC EQUATOR

GEOMAGNETIC FIELD
U GEOMAGNETISM

GEOMAGNETIC HOLLOW
The IMS advances in understanding terrestrial myriametric radiation 14 p2365 N85-24618
Altimetry data and the elastic stress tensor of subduction zones
[NASA-CR-175796] 16 p2625 N85-27425

GEOMAGNETIC LATITUDE
Paleomagnetic latitude of paleocene volcanic rocks of the Cantwell Formation, central Alaska 04 p0517 N85-13302
An atlas of polar cap energetic particle observations. Volume 2: NOAA-6, 8 July 1979 to 10 May 1983
[PB85-109072] 12 p1891 N85-21868
Characteristics of latitude effect on cosmic ray charged component in atmosphere at altitudes 3-5 KM 13 p1978 N85-22413
Deuteron whistlers at low latitudes in the low altitude topside ionosphere 14 p2366 N85-24625
Low-latitude ducted whistlers observed at Sanya, Hainan, China 14 p2367 N85-24626
Whistler observation at Okinawa, Japan during the IMS 14 p2367 N85-24627
The latitudinal variation of geomagnetic pulsation amplitude and phase 14 p2370 N85-24646

GEOMAGNETIC PULSATIONS
Statistical properties of geomagnetic pulsations at the Observatory of Fuerstenfeldbruck determined with the aid of pulsation indices. Part 2: Periodicity in the occurrence of pulsations
[REPT-556] 03 p0376 N85-12399
Seasonal variations of reflexibility and transmissibility of ULF waves propagating through the ionosphere of geomagnetic mid-latitudes
[REPT-560] 03 p0376 N85-12403
Fine structure of Alfven maser radiation 06 p0624 N85-15232
Interpretation of directional magnetotelluric soundings by analytical continuation method 14 p2343 N85-24488
Excitation of geomagnetic Pcl-2 and pulsations with decreasing period during microsubstorms 14 p2344 N85-24494
Directional analysis of wave packets of magnetotelluric field 14 p2344 N85-24495
On-off characteristics of auroral pulsations 14 p2363 N85-24604
Multiple correlation between auroral and magnetic pulsations 14 p2363 N85-24605
Multiple correlation between auroral and magnetic pulsations. Part 2: Determination of electric currents and electric fields around a pulsating auroral patch 14 p2363 N85-24606
Pc 1-2 pulsations and related phenomena: A review — geomagnetic pulsations 14 p2364 N85-24611
Spatial characteristics of ULF pulsations and their modification by the ionosphere: IMS results 14 p2364 N85-24612
Contribution of the Scandinavian Twin Auroral Radar Experiment (STARE) radar to the understanding of the physical mechanisms associated with Pc5 pulsations 14 p2364 N85-24613
Short-period magnetic pulsations during substorms 14 p2368 N85-24636
Substorm associated Pc 1 emission in the morning sub-cleft latitudes 14 p2368 N85-24637
Pc 1 pulsation source regions and their relationship to the plasma pause 14 p2368 N85-24638
Long-period magnetospheric pulsations observed with an electric field experiment in the magnetosphere 14 p2369 N85-24639
Magnetospheric pulsations observed by ISEE 1 and 2 satellites 14 p2369 N85-24640
The SAMBO-GEOS experiment: A Ps-6 event from ground-satellite observations 14 p2369 N85-24641
Sudden Storm Commencement (SSC) associated hydromagnetic variations at geosynchronous altitude and on the ground 14 p2369 N85-24642
Observations of a pulsation event from the ground with balloons and with a geostationary satellite 14 p2369 N85-24643
Results of ULF-wave investigations in the USSR 14 p2369 N85-24644
Satellite, auroral radar and ground magnometer observations of transient ULF pulsations 14 p2369 N85-24645
The latitudinal variation of geomagnetic pulsation amplitude and phase 14 p2370 N85-24646
Magnetic pulsations recorded in northern Scandinavia during the IMS; a study of Pc 4-5 events 14 p2370 N85-24647
Characteristics of Pc 4,5 pulsations and their source mechanisms 14 p2370 N85-24648
Ground magnetic observations of high-latitude Pi2 pulsations: Scandinavian magnetometer array results 14 p2370 N85-24649
Pi2 pulsations and the substorm current wedge - ground observations 14 p2370 N85-24650
Ground-satellite observations of substorm related Pi 2 pulsations and current systems 14 p2370 N85-24651
Implications of the global appearance of Pi2 and Pc 3 bursts 14 p2371 N85-24652
A structural classification of geomagnetic pulsations 14 p2371 N85-24657
Correlated fluctuations of charged particle fluxes and magnetic field according to data from Intercosmos-10 satellite 16 p2722 N85-26802

GEOMAGNETIC STORMS
U MAGNETIC STORMS

GEOMAGNETIC TAIL
Plasma flow in the near and distant geomagnetic tail
[DE84-014029] 04 p0534 N85-13415
Polar rain: Solar coronal electrons in the Earth's magnetosphere
[NASA-TM-86150] 07 p1060 N85-16726
Periodic substorm activity in the geomagnetic tail
[NASA-CR-175629] 13 p2161 N85-23409
Response of magnetospheric substorm activity to changes in the interplanetary magnetized plasma 14 p2357 N85-24583
Magnetotail current sheet and energetic particles observed on ISEE-1 14 p2357 N85-24586
Estimate of the amplitude of transient electric fields in the magnetotail 14 p2358 N85-24588
Timing between particle injections at the geostationary orbit and particle flux decreases in the distant geomagnetic tail during substorms 14 p2358 N85-24589
Streaming reversal of energetic particles in the magnetotail during a substorm 14 p2358 N85-24571
The near Earth current sheet: ISEE-1 and -2 case studies 14 p2358 N85-24573
The dawn-dusk asymmetry of particles near the neutral sheet of geomagnetotail 14 p2358 N85-24574
The ionospheric O+ streams in the magnetotail between 22 RE and 6 RE 14 p2360 N85-24582
Pi2 pulsations and the substorm current wedge - ground observations 14 p2370 N85-24650
Hydromagnetic vortices: An interpretation for dawnside events as on December 11, 1977 — magnetotail 14 p2371 N85-24653
Structure of the distant geotail: ISEE-3 observations 20 p3488 N85-31678
Magnetotails of the terrestrial planets: A comparative study 22 p3656 N85-33675

GEOMAGNETICALLY TRAPPED PARTICLES
U RADIATION BELTS

GEOMAGNETISM
Precipitation of protons with E sub p approximately 1 MeV near plasmopause 02 p0161 N85-11093
The south-central United States magnetic anomaly
[E85-10025] 02 p0218 N85-11438
Basic research for the geodynamics program
[NASA-CR-174055] 02 p0228 N85-11490
Geophysical Works during 1981, volume 29, no. 547-566 03 p0375 N85-12389
Characteristics of absorption and frequency filtration of ULF electromagnetic waves in the ionosphere 03 p0376 N85-12402
Continental and oceanic crustal magnetization modelling
[E85-10034] 03 p0376 N85-12413
Asymptotic orbit theory for trapped electrons in inhomogeneous Whistler field
[AD-A146178] 03 p0392 N85-12510
Scientific contributions in commemoration of Ebro Observatory's 75th anniversary — conference
[ISBN-84-00-05380-X] 04 p0518 N85-13306
Present practice for the recording of the Earth magnetic field — geophysical observatories 04 p0519 N85-13317
Advantages and limitations of spherical harmonic analyses of geomagnetic data 04 p0519 N85-13318
Analysis of the daily geomagnetic variation with the use of MAGSAT data — MAGSAT satellites 04 p0520 N85-13319
Research directions in recent studies of the lunar geomagnetic effects 04 p0520 N85-13320
On derivation and significance of geomagnetic equivalent amplitude indices 04 p0520 N85-13321
A directly obtained geomagnetic activity measure, J3 04 p0520 N85-13322
Resonance model of Pc3 in subtropical regions — geomagnetism 04 p0520 N85-13323
Daily magnetic variations at Ebro, Spain 04 p0520 N85-13325
On the annual and semiannual variation of S sub R at l'Aquila — geomagnetism 04 p0520 N85-13326
On some new features of semiannual variation of the geomagnetic field 04 p0520 N85-13327
Local geomagnetic characteristics of solar activity (Dourbes 1960-1978) 04 p0521 N85-13328
Geomagnetic secular variation: A jerk in 1970 04 p0521 N85-13329
Comparisons of secular variation in two-dipole and spherical harmonic models with observatory data in Eurasia, 1965-1975 04 p0521 N85-13330
Geomagnetic secular variation at Ebro Observatory during the past 70 years 04 p0521 N85-13331
Reversals of the Earth's magnetic field 04 p0521 N85-13332
Petrologic model of the northern Mississippi embayment based on satellite magnetic and ground based geophysical data
[NASA-TM-85075] 04 p0533 N85-13406
Global matrix of thermospheric density values for selected solar/geomagnetic conditions and spacecraft orbital attitudes
[NASA-TM-86478] 04 p0533 N85-13409
Statistical relationship of strong earthquakes with planetary geomagnetic field activity 06 p0820 N85-15209
Anomalous magnetic field in northwestern Pacific Ocean and Pacific Ocean plate kinematics 06 p0820 N85-15210
Correlation radius of gravitational and magnetic anomalies and methods of its determination 06 p0821 N85-15213
Spectrum of geomagnetic field variations in the range of periods between 1 and 10 years 06 p0821 N85-15215
Processes of smooth increase and dropoff in intensity of glow line lambda' = 5577 A with exposure of ionosphere to electron beam 06 p0822 N85-15219
Earth's radiation belts
[AD-A147927] 07 p0996 N85-16339
Artificial ionospheric disturbances caused by powerful radio waves
[AD-A148077] 08 p1186 N85-17473
Algorithm for space-time analysis of data on geomagnetic field
[NASA-TM-77804] 08 p1209 N85-17609
Recent investigations at INPE in magnetospheric physics and geomagnetism
[INPE-3260-PRE/603] 10 p1514 N85-19555
Brazil future plans in upper atmosphere research in Antarctica
[INPE-3400-PRE/669] 10 p1515 N85-19559
Solar radio bursts, proton events and geomagnetic activity
[AD-A149018] 10 p1571 N85-19908
Precursors for Brazilian magnetic anomalies from 1922 to 1969
[INPE-3283-PRE/605] 11 p1681 N85-20590
Solar-Geophysical Data. Part 1: (Prompt reports)
[PB85-112066] 11 p1766 N85-21100
Calculation of ionospheric profiles by inverting VLF/LF reflection data. 2. Anisotropic propagation
[AD-A150105] 12 p1890 N85-21859
Circulation and internal waves in a cold Gulf Stream wave
[AD-A149704] 12 p1898 N85-21918
Research on ocean floor electrical surveys
[AD-A149831] 12 p1899 N85-21920
Models of the upper atmosphere 12 p1945 N85-22217
Particle transport in planetary magnetospheres 12 p1954 N85-22275
One-dimensional model of auroral magnetic force with longitudinal current and cyclotron heating of ions 13 p1980 N85-22424
Auroral-polar cap environment and its impact on spacecraft plasma interactions 13 p1991 N85-22484
Calculation of secondary-electron escape currents from inclined-spacecraft surfaces in a magnetic field 13 p1992 N85-22491

Geomagnetic precursors of intensive earthquakes in the 1-0.-2 Hz frequency range of geomagnetic pulsations
13 p2116 N85-23176
Solution of direct magnetometric problem on spherical Earth
13 p2116 N85-23179
Geomagnetic field dynamics
13 p2116 N85-23182
MAGSAT anomaly field data of the crustal properties of Australia
[E85-10100] 13 p2122 N85-23215
GADB: A database facility for modelling naturally occurring geophysical fields
13 p2122 N85-23217
Data selection techniques in the interpretation of MAGSAT data over Australia
13 p2123 N85-23218
USSR report: Earth sciences
[JPRS-UES-85-004] 14 p2332 N85-24424
Diurnal variations in terrestrial magnetic field and structure of magnetosphere
14 p2344 N85-24493
Dynamic spectra of mean monthly values of geomagnetic field elements based on spectral-time analysis data
14 p2344 N85-24496
Achievements of the International Magnetospheric Study (IMS) — conference
[ESA-SP-217] 14 p2354 N85-24544
The measurements of Prognoz-4, -5, -6, -7 during IMS
14 p2355 N85-24548
The structure and dynamics of the magnetosphere: Progress in the IMS
14 p2355 N85-24550
Magnetic field observations at the dayside magnetopause: ISEE-1 and -2 contributions during the IMS
14 p2356 N85-24555
Magnetic field in the Earth's outer magnetosphere: Prognoz-6, -7 data
14 p2356 N85-24556
Sudden Storm Commencement (SSC) associated hydromagnetic variations at geosynchronous altitude and on the ground
14 p2369 N85-24642
Advances in magnetospheric plasma-wave research during the IMS
14 p2372 N85-24662
The access of energetic charged particles to satellite altitudes
[AD-A150799] 14 p2373 N85-24670
The first effect of the amplitude of a solar cycle
14 p2452 N85-25143
Report of the geomagnetic and geoelectric observations, 1983 (rapid variations)
[REPT-24] 15 p2591 N85-25975
Geophysical responses of dynamics of solar wind transition region
16 p2721 N85-26795
Solar-Geophysical Data Number 484, December 1984. Part 1 (prompt reports): Data for November 1984, October 1984 and late data
[NASA-CR-175829] 16 p2886 N85-27819
The influence of the heliospheric current sheet and angular separation on flare accelerated solar wind
[NASA-CR-175982] 18 p3209 N85-29907
MAGSAT scalar anomaly map of South America
20 p3473 N85-31586
MAGSAT satellite magnetic anomaly map over South America
20 p3474 N85-31587
Geologic analysis of averaged magnetic satellite anomalies
20 p3474 N85-31588
Statistical magnetic anomalies from satellite measurements for geologic analysis
20 p3474 N85-31589
Binning of satellite magnetic anomalies
20 p3474 N85-31590
The south-central United States magnetic anomaly
20 p3474 N85-31591
The south-central United States magnetic anomaly
20 p3475 N85-31592
Reduced to pole long-wavelength magnetic anomalies of Africa and Europe
20 p3475 N85-31595
Euro-African MAGSAT anomaly-tectonic observations
20 p3475 N85-31596
Continental and oceanic magnetic anomalies: Enhancement through GRIM
20 p3476 N85-31598
Continental magnetic anomaly constraints on continental reconstruction
20 p3476 N85-31599
Regional magnetic anomaly constraints on continental rifting
20 p3476 N85-31600
Thermal ion heating in the vicinity of the plasmapause
[NASA-CR-176030] 20 p3535 N85-31993
Fluxgate magnetometer (SSM) for the defense meteorological satellite program (DMSP) block 5D-2, flight 7
[AD-A155229] 21 p3560 N85-32143
Planetary Dynamos
[NASA-CR-176001] 21 p3679 N85-32857
A real time index of geomagnetic background noise for the MAD (Magnetic Anomaly Detection) frequency band
[AD-A155717] 22 p3814 N85-33627
Absolute measurement of Declination (D) by means of a proton magnetometer
[DMI-GEOPHYS-PAPERS-R-86] 22 p3836 N85-33751
Current enhancement in a conducting channel
[AD-A155418] 22 p3845 N85-33812
Planetary surface processes: A review
22 p3855 N85-33869
The magnetic field of planets
22 p3858 N85-33891
Magnetic field generation in the cores of terrestrial bodies
22 p3859 N85-33894
Linear filters as a method of real-time prediction of geomagnetic activity
[DE85-010760] 22 p3860 N85-33899
An update on the correlation between the cosmic radiation intensity and the geomagnetic AA index
[SH-4.2-24] 23 p4009 N85-34861
Dynamics of two-year cosmic ray variations inferred from the data of spacecraft and stratospheric measurements and from the neutron monitor data in 1959-1981
[SH-4.4-21] 23 p4035 N85-35017
Formulation of cosmic-ray solar daily variation and its seasonal variation, produced from generalized stationary anisotropy of solar origin
[SH-4.5-2] 23 p4036 N85-35020
Diurnal variation of galactic cosmic ray intensity on quiet days
[SH-4.5-11] 23 p4037 N85-35029
A relation between the short time variations of cosmic rays and geomagnetic field change
[SH-5.1-14] 23 p4043 N85-35067
Anomalous low level of cosmic ray intensity decreases observed during 1960
[SH-5.1-15] 23 p4043 N85-35068
Frequency spectra of short-period variations of cosmic ray
[SH-5.1-17] 23 p4043 N85-35070
Re-evaluation of cosmic ray cutoff terminology
[SH-6.1-11] 23 p4045 N85-35084
The use of the McIlwain L-parameter to estimate cosmic ray vertical cutoff rigidities for different epochs of the geomagnetic field
[SH-6.1-12] 23 p4045 N85-35085
Estimating the change in asymptotic direction due to secular changes in the geomagnetic field
[SH-6.1-13] 23 p4045 N85-35086
Empirical model for the Earth's cosmic ray shadow at 400 KM: Prohibited cosmic ray access
[SH-6.1-14] 23 p4046 N85-35087
Diurnal variations of cosmic ray geomagnetic cut-off threshold rigidities
[SH-6.1-21] 23 p4046 N85-35092
The influence of the Earth's magnetosphere on the high-energy solar protons
[SH-6.1-22] 23 p4046 N85-35093
Correlation between solar neutrino flux and other solar phenomena
23 p4049 N85-35109
Heavy cosmic ray measurement aboard Spacelab-1
[SH-10.1-7] 23 p4053 N85-35138
Radio wave emitted by an extensive air showers in 10KHz to 1MHz region
[HE-4.6-15] 24 p4198 N85-36051
Measurement of neutrino oscillations in MACRO experiment
[HE-5.3-10] 24 p4206 N85-36104

GEOMETRIC ACCURACY
Canadian plans for Thematic Mapper data
11 p1668 N85-20513
LANDSAT-4 Science Characterization Early Results. Volume 3, part 2: Thematic Mapper (TM)
[E85-10069] 12 p1869 N85-21724
A preliminary assessment of LANDSAT-4 Thematic Mapper data — Windsor, Ontario and Medicine Hat areas, Canada
12 p1869 N85-21728
TM geometric performance: Line to Line Displacement Analysis (LLDA) — New Mexico
12 p1870 N85-21732
A preliminary evaluation of LANDSAT-4 Thematic Mapper data for their geometric and radiometric accuracies
12 p1871 N85-21739

GEOMETRIC RECTIFICATION (IMAGERY)
Specification and preliminary design of the CARTA system for satellite cartography
[E85-10035] 03 p0378 N85-12414
Rectification of single and multiple frames of satellite scanner imagery using points and edges as control
07 p0966 N85-16263
The influence of the number of ground control points on the scene-to-map registration accuracy — Kansas, Louisiana, Mississipp, and Missouri
07 p0966 N85-16264
Anaysis of the quality of image data required by the LANDSAT-4 Thematic Mapper and Multispectral Scanner — agricultural and forest cover types in California
[E85-10074] 10 p1504 N85-19488
Summary of MSS characterization investigations
11 p1666 N85-20497
Radiometric calibration and geocoded precision processing of LANDSAT-4 Multispectral Scanner products by the Canada Centre for Remote Sensing
11 p1667 N85-20501
Geometric accuracy of LANDSAT-4 MSS image data
11 p1667 N85-20503
Geometric accuracy assessment of LANDSAT-4 Multispectral Scanner (MSS) data
11 p1667 N85-20505
LS-4 MSS geometric correction: Methods and results
11 p1668 N85-20507
An overview of the Thematic Mapper geometric correction system
11 p1668 N85-20511
Analysis and evaluation of the LANDSAT-4 MSS and TM sensors and ground data processing systems: Early results
13 p2117 N85-23189
Correction and geological analysis of lunar 3.8 cm radar data
13 p2198 N85-23634
Minimizing influence of Earth's curvature in projective rectification of space photographs into photoplans and photomaps
16 p2727 N85-26829
Looking at more than three dimensions
[DE85-007764] 17 p3009 N85-28600
Reports on cartography and geodesy. Series 1: Original reports, number 93
[ISSN-0469-4236] 18 p3124 N85-29343
Dynamic rectification of airborne scanner digital image recordings
18 p3124 N85-29344
LANDSAT-4/5 image data quality analysis
[E85-10105] 24 p4107 N85-35463

GEOMETRICAL ACOUSTICS
High-frequency asymptotic behavior of reflected and transmitted waves during scattering of sound by hollow elastic sphere filled with fluid
02 p0266 N85-11738
Wave description of sound propagation through stratified moving atmosphere
15 p2525 N85-25567

GEOMETRICAL HYDROMAGNETICS
U MAGNETOHYDRODYNAMICS

GEOMETRICAL OPTICS
Theoretical elements of photometry
[BLL-RISLEY-TR-5022-(9091.9F)]
02 p0279 N85-11821
Influence of geometric conditions on the indicatrix of reflection of the perfect reflecting diffuser
[PTB-OPT-16] 03 p0420 N85-12686
An iteration method for complex scattering problems
[AD-A150038] 12 p1934 N85-22151
Dependence of properties of optical cavity on misalignment
14 p2276 N85-24099
Analytical techniques used to calculate the fields due to refraction and diffraction of electromagnetic waves
[AD-A151705] 15 p2543 N85-25696
Performance evaluation of fiber-optic converters
17 p2941 N85-28154
Optical phenomena in computer vision
[AD-A152970] 17 p3008 N85-28595
Solvability of some inverse problems in laser radiation focusing
21 p3696 N85-32963
Existence of smooth solutions in problems of electromagnetic radiation focusing
21 p3697 N85-32972
Edge detection and geometric methods in computer vision
[AD-A155873] 24 p4135 N85-35630

GEOMETRICAL THEORY OF DIFFRACTION
On aircraft antennas and basic scattering studies
[AD-A146017] 03 p0355 N85-12282
Interpolation methods for GTD analysis of shaped reflectors
10 p1483 N85-19231
Scattering of waves by axisymmetrical edge
13 p2080 N85-22987
Analytical techniques used to calculate the fields due to refraction and diffraction of electromagnetic waves
[AD-A151705] 15 p2543 N85-25696
Guided-mode launching in a slab waveguide by way of diffraction at the edge of a conducting screen residing on one surface of the slab
[AD-A154886] 21 p3575 N85-32232

GEOMETRODYNAMICS
U RELATIVITY

GEOMETRY
NT ANALYTIC GEOMETRY
NT ANGLE OF ATTACK
NT ANGLES (GEOMETRY)
NT BRAGG ANGLE
NT CARTESIAN COORDINATES
NT CATENARIES
NT CIRCLES (GEOMETRY)
NT CIRCUMFERENCES
NT COLLINEARITY
NT CONICS
NT COPLANARITY
NT CRACK GEOMETRY
NT CURVATURE
NT CURVES (GEOMETRY)
NT DESCRIPTIVE GEOMETRY

NT DIFFERENTIAL GEOMETRY
NT DUCT GEOMETRY
NT ELEVATION ANGLE
NT ELLIPSES
NT EPICYCLOIDS
NT EUCLIDEAN GEOMETRY
NT FIXED POINTS (MATHEMATICS)
NT FLOW GEOMETRY
NT FRACTALS
NT GEODESIC LINES
NT HOMOTOPY THEORY
NT HYPERBOLAS
NT INFLECTION POINTS
NT LIE GROUPS
NT LINES (GEOMETRY)
NT LINKS (MATHEMATICS)
NT LOCI
NT MERCATOR PROJECTION
NT METRIC SPACE
NT NOZZLE GEOMETRY
NT OBLATE SPHEROIDS
NT PARABOLAS
NT PARALLELEPIPEDS
NT POINTS (MATHEMATICS)
NT POLYGONS
NT PROJECTIVE GEOMETRY
NT PYRAMIDS
NT RADII
NT RECTANGLES
NT RIEMANN MANIFOLD
NT SPECIMEN GEOMETRY
NT SPHEROIDS
NT SPINOR GROUPS
NT TANGENTS
NT TENSOR ANALYSIS
NT TOPOLOGY
NT TORUSES
NT VECTOR ANALYSIS
NT VORTICITY

Halfspace representations of extrusions, solids of revolution and pyramids
[DE84-015005] 01 p0104 N85-10700

Response of propellants to high dynamic stresses: The uses of gun launch techniques
[DE84-013223] 02 p0188 N85-11259

SMP: A solid modeling program
[NASA-CR-172473] 02 p0241 N85-11570

Formation of radio images by scanning around circle
02 p0264 N85-11727

Analysis of in-plane and out-of-plane ground motions using the boundary element method
[AD-A146229] 03 p0355 N85-12287

An experimental evaluation of the J integral in 50% sidegrooved compact geometry specimens
[AERE-R-11202] 03 p0374 N85-12386

Investigation of an ejector heat pump by analytical methods
[DE84-016675] 04 p0500 N85-13189

Computer-aided design of extrusion dies by metal-flow simulation 06 p0797 N85-15094

Investigation of the creep behaviour of soft soldered joints with solder L-SnAg5 at ambient temperature
[BLL-T6383/BG/WH798/84] 07 p0926 N85-15865

A simple prediction model for soil compaction under various wheel loads and geometries as an aid to vehicle design
[AD-P004296] 09 p1409 N85-18875

A conformal mapping suitable for problems involving interaction between given geometries and known far fields
[AD-A149050] 10 p1545 N85-19744

Geometric Hamiltonian structures and perturbation theory
[DE85-002005] 11 p1707 N85-20737

Experimental study of main rotor tip geometry and tail rotor interactions in hover. Volume 1. Text and figures
[NASA-CR-177336-VOL-1] 13 p1965 N85-22344

Experimental study of main rotor tip geometry and tail rotor interactions in hover. Volume 2: Run log and tabulated data
[NASA-CR-177336-VOL-2] 13 p1965 N85-22345

Magnetostatic-wave propagation in a finite YIG-Loaded rectangular waveguide
[AD-A150332] 13 p2055 N85-22865

Mathematical modeling of results of geometric leveling in variable gravity field 13 p2114 N85-23170

Introduction to combinatorial geometry
[DE85-003268] 13 p2152 N85-23364

Informative geometry of probability spaces
[AD-A150510] 13 p2153 N85-23371

Quantitative analyses of planetary reflectance spectra
13 p2197 N85-23625

Problems regarding the practical evaluation of efficiency of worm gears 14 p2224 N85-23793

Global positioning system: A modification to the baseline satellite constellation for improved geometric performance
[AD-A151692] 15 p2469 N85-25239

Optimum geometry of interblade passages in impellers of thermomolecular vacuum pump
16 p2784 N85-27056

Scattering center analysis for radar cross section modification 16 p2789 N85-27065

Probabilistic structural analysis of SSME turbopump blades: Probabilistic geometry effects
17 p2913 N85-27958

Computational Geometry and Computer-Aided Design
[NASA-CP-2379] 17 p3003 N85-28563

Multivariate spline algorithms for CAGD
17 p3003 N85-28566

Improving the effectiveness of integral property calculation in a CSG solid modeling system by exploiting predictability 17 p3006 N85-28586

A study of aerodynamic control in stalled flight leading-edge vortex formation analysis
[AD-A153758] 18 p3059 N85-28928

Study of meshing of beveled gears with normally decreasing arc teeth
[NASA-TM-77868] 18 p3117 N85-29293

Geometry, velocity structure and penetration depths of descending slabs in the western Pacific
19 p3319 N85-30574

Fast and optimal solution to the Rankine-Hugoniot problem
[NASA-TM-86214] 19 p3344 N85-30724

Mathematics of surfaces
[DE85-010439] 19 p3346 N85-30742

A fast discharge excimer laser with symmetric geometry
[AD-A155294] 21 p0592 N85-32322

Photo-acoustic effect in finite-dimensional semiconductors 21 p3862 N85-32876

MORSE-CGA: A Monte Carlo radiation transport code with array geometry capability
[DE85-012063] 22 p3830 N85-33718

Report of Workshop on Computational Geometry and summary of related research
[AD-A155399] 22 p3833 N85-33734

Thermal transport measurements of UV laser irradiated spherical targets
[DE85-011036] 23 p3931 N85-34365

System maintenance manual for master modeling of aerodynamic surfaces by three-dimensional explicit representation
[NASA-CR-178224] 23 p3956 N85-34517

A simple but systematic CSG system
23 p3963 N85-34569

Low cost geometric modelling system for CAM
23 p3964 N85-34578

GEOMORPHOLOGY

Geology and geomorphology of the southern central Blue Ridge: An indexed bibliography
[PB84-225119] 01 p0072 N85-10480

Estuaries of the Cape. Part 2: Synopses of available information on individual systems. Report no. 18: Bot/Kleinmond system (CSW 13)
[CSIR-RR-417-PT-2] 01 p0087 N85-10587

Geographic science: Executive summary
02 p0214 N85-11408

Geographic science 02 p0214 N85-11409

Geomorphology 02 p0214 N85-11411

Paleohydrology and geomorphology of selected reaches of the upper Wabash Valley, Indiana
02 p0226 N85-11481

Mars-Earth geographical comparisons: A pictorial view
[NASA-TM-86166] 02 p0302 N85-11957

Geology and geochemistry of early Tertiary submarine volcanic rocks of the Aleutian Islands, and their bearing on the development of the Aleutian Island Arc
03 p0389 N85-12493

Metamorphic petrology of the Table Mountain area, Circle quadrangle, Alaska 04 p0516 N85-13295

Paleozoic limestones of the Crazy Mountains and vicinity, Circle quadrangle, east-central Alaska
04 p0517 N85-13296

Late Paleozoic and early Mesozoic radiolarians in the Circle quadrangle, east-central Alaska
04 p0517 N85-13297

Lacustrine and eolian deposits of Wisconsin age at Riverside Bluff in the upper Tanana River valley, Alaska
04 p0517 N85-13299

Landform evaluation through integrated remote sensing methods. A case study in parts of Haryana, India
05 p0657 N85-14221

Some methodological aspects of study of layer associations in continents and oceans
05 p0820 N85-15205

Tectonic, volcanic, and climatic geomorphology study of the Sierras Pampeanas Andes, northwestern Argentina 08 p1144 N85-17215

Geological, structural, and geomorphological analyses from SIR-B 08 p1145 N85-17226

Interlobate comparison of glacial-depositional style as evidenced by small-relief glacial landscape features in Illinois, Indiana, and Ohio, utilizing SIR-B
08 p1146 N85-17231

Evaluation of the L-band scattering characteristics of volcanic terrain in aid of lithologic identification, assessment of SIR-B calibration, and development of planetary geomorphic analogs 08 p1146 N85-17232

Soil formation on tertiary landsurfaces of the New Jersey coastal plain 08 p1181 N85-17441

Post-Laramide history of North Central Wyoming
08 p1181 N85-17444

Structural morphology and associated strain within parts of the US section of the Kootenay Arc, NE, Washington
09 p1352 N85-18505

Basic structural features and probable mechanism of formation of the Kuril Island system
10 p1501 N85-19472

Assessment of LANDSAT for rangeland mapping, Rush Valley, Utah
[E85-10072] 10 p1503 N85-19486

An integrated GIS/remote sensing data base in North Cache soil conservation district, Utah: A pilot project for the Utah Department of Agriculture's RIMS (Resource Inventory and Monitoring System)
[E85-10073] 10 p1504 N85-19487

Nautical charting with remotely sensed imagery, volume 1
[AD-A149361] 10 p1506 N85-19503

Nautical charting with remotely sensed imagery. Volume 2: Case studies
[AD-A149362] 10 p1506 N85-19504

Study of the physical properties of crystalline rocks in the southeast Voronezh anteclise
[NASA-TM-77823] 10 p1514 N85-19551

Physiography of the Martian west equatorial uplift
12 p1961 N85-22325

Planetary geology in the 1960s
[NASA-SP-467] 13 p2169 N85-23457

Geomorphic classification of lava flows on Io
13 p2173 N85-23480

Martian terrain ages 13 p2181 N85-23537

Average spacing for rings of individual multi-ring basins is 2.0(0.5)D 13 p2182 N85-23541

Ring-diameter ratios for multi-ring basins average 2.0(0.5)D 13 p2182 N85-23542

Morphology and mechanics of terraces in lunar craters
13 p2182 N85-23543

Interaction of Martian flow ejecta blankets with pre-existing impact craters: Morphological observations
13 p2183 N85-23546

Ripple ring basins on Ganymede and Callisto
13 p2183 N85-23547

Morphologic evolution of the Mount St. Helens crater area, Washington 13 p2187 N85-23568

The geology of Mt. Hope, a silicic volcanic center in West Central Arizona 13 p2187 N85-23571

A silicic shield volcano in Bolivia
13 p2187 N85-23572

Martian fretted terrain morphometry interpreted using principal components analysis 13 p2192 N85-23597

Distribution and properties of large symmetric knobs on Mars 13 p2192 N85-23598

Enigmatic hills of the mottled plains, Mare Acidalium quadrangle (MC-4), Mars 13 p2192 N85-23599

Geomorphology and geology of the Southwestern Margaritifer Sinus and Argyre regions of Mars. Part 1: Geological and geomorphological overview
13 p2192 N85-23600

Geomorphology and geology of the Southwestern Margaritifer Sinus and Argyre regions of Mars. Part 2: Crater size-frequency distribution curves and geomorphic unit ages 13 p2192 N85-23601

Geomorphology and geology of the Southwestern Margaritifer Sinus and Argyre regions of Mars. Part 3: Valley types and distribution 13 p2193 N85-23602

Geomorphology and geology of the Southwestern Margaritifer Sinus and Argyre regions of Mars. Part 4: Flow ejecta crater distribution 13 p2193 N85-23603

The geomorphology of Rhea
13 p2193 N85-23606

Kasei Valle of Mars: Dating the interplay of tectonics and geomorphology 13 p2201 N85-23654

Chondrule-like particles provide evidence of early Archean meteorite impacts, South Africa and western Australia 15 p2582 N85-26562

The Mars ancient cratered terrain, smooth plains boundary: Implications of Viking color data for evolution of the Amenthes Region 15 p2582 N85-26564

Closer look at lunar volcanism
[DE85-008863] 15 p2583 N85-26576

Space methods for geological research
19 p3295 N85-30429
Engineering geology of selected areas, US army engineer division, lower Mississippi valley. The American bottom area, MO-IL. Volume 1
[AD-A164258] 19 p3299 N85-30455
Geologic and hydrologic characterization and evaluation of the basin and range province relative to the disposal of high-level radioactive waste. Part 1: Introduction and guidelines
[GS-CIRC-904-A] 20 p3526 N85-31932
Global Mega-Geomorphology
[NASA-CP-2312] 21 p3600 N85-32357
A new global geomorphology?
21 p3601 N85-32358
Global geomorphology 21 p3601 N85-32359
Mega-geomorphology: Mars vis a vis Earth
21 p3601 N85-32360
Geomorphological similarity and uniqueness
21 p3601 N85-32361
Regional landform thresholds
21 p3601 N85-32362
Some observations on paleogeomorphology
21 p3601 N85-32363
Ancient landscapes: Their nature and significance for the question of inheritance 21 p3601 N85-32364
Geomorphology, tectonics, and exploration
21 p3601 N85-32365
Mega-geomorphology and neotectonics
21 p3602 N85-32366
Andrean examples of mega-geomorphology themes
21 p3602 N85-32367
Space imagery and some geomorphological problems of the Guiana Shield, South America
21 p3602 N85-32368
Deep sea mega-geomorphology: Progress and problems 21 p3602 N85-32369
One application of mega-geomorphology in education
21 p3602 N85-32370
Use of the synoptic view: Examples from Earth and other planets 21 p3602 N85-32371
Geomorphic classification of Icelandic and Martian volcanoes: Limitations of comparative planetology research from LANDSAT and Viking orbiter images
21 p3603 N85-32372
Aeolian geomorphology from the global perspective
21 p3603 N85-32373
Geomorphic analyses from space imagery
21 p3603 N85-32374
The problem of scale in planetary geomorphology
21 p3603 N85-32375
Quantitative analysis in megageomorphology
21 p3603 N85-32376
Use of spaceborne imaging radar in regional geomorphic studies 21 p3603 N85-32377
Techniques, problems and uses of mega-geomorphological mapping
21 p3604 N85-32378
Quantitative analysis of geomorphic processes using satellite image data at different scales
21 p3604 N85-32380
Quantitative geomorphologic studies from spaceborne platforms 21 p3604 N85-32381
Global geomorphology: Report of Working Group Number 1 21 p3604 N85-32382
Process thresholds: Report of Working Group Number 3 21 p3604 N85-32384
Planetary perspective. Report of Working Group Number 4 21 p3605 N85-32385
Precambrian evolution and the rock record
21 p3656 N85-32711
Considerations of large scale impact and the early Earth 21 p3718 N85-33070
Geologic processes on Venus: An update
22 p3857 N85-33883
The United States Geological Survey in Alaska: Accomplishments during 1983
[USGS-CIRC-945] 23 p3948 N85-34468
Geology and geomorphology of the Roraima group, southeastern Venezuela 24 p4115 N85-35511

GEON (TRADEMARK)
U POLYVINYL CHLORIDE

GEOPHYSICAL FLUIDS
Magnetic location of Earth's core-mantle boundary and estimates of the adjacent fluid motion
13 p2131 N85-23260

GEOPHYSICAL OBSERVATORIES
NT OGO
Scientific contributions in commemoration of Ebro Observatory's 75th anniversary — conference
[ISBN-84-00-05380-X] 04 p0518 N85-13308
The Ebro Observatory and international scientific organizations 04 p0518 N85-13309
Use of Ebro Observatory data at Word Data Center A for Solar-Terrestrial Physics 04 p0518 N85-13310
Present practice for the recording of the Earth magnetic field — geophysical observatories
04 p0519 N85-13317
Daily magnetic variations at Ebro, Spain
04 p0520 N85-13325
On the annual and semiannual variation of S sub R at l'Aquila — geomagnetism 04 p0520 N85-13326

GEOPHYSICAL SATELLITES
NT COSMOS SATELLITES
NT EXPLORER 10 SATELLITE
NT INTERCOSMOS SATELLITES
NT OGO
Application of satellite accelerometer data to improve density models
[AD-A154904] 21 p3631 N85-32558

GEOPHYSICS
Seafloor geosciences division: Missions, technical specialties, accomplishments, and activities, calendar year 1983
[AD-A144849] 01 p0067 N85-10592
A bibliography of planetary geology and geophysics principal investigators and their associates, 1983 - 1984
[NASA-TM-87361] 01 p0127 N85-10874
Cosmonauts complete 4th month aboard Salyut-7
02 p0157 N85-11065
Geophysical experiments, photography aboard Salyut-7 02 p0157 N85-11066
Orbit of Salyut-7 station boosted
02 p0157 N85-11067
Salyut-7 crew in orbit 150 days
02 p0157 N85-11068
Use of gravitational stabilization in performance of experiments 02 p0160 N85-11084
Development of a method for exploring low-reflectance areas through the combined use of different geophysical methods taking the north-west German basin as an example
[BMFT-FB-T-83-180] 02 p0220 N85-11450
Project review on geophysical and ocean sound speed profile inversion
[AD-A145717] 02 p0276 N85-11797
Geophysical Works during 1981, volume 29, no. 547-566 03 p0375 N85-12389
SVKD and SVKM-3 seismographs with a low-sensitivity channel
[REPT-553] 03 p0376 N85-12396
Abstracts of papers submitted in 1983 for publication
[PB84-217579] 03 p0398 N85-12543
International Geosphere/Biosphere Program: 1984
[GPO-39-222] 04 p0578 N85-13691
Activities at the Lunar and Planetary Institute
[NASA-CR-174069] 04 p0579 N85-13694
Activities at the Lunar and Planetary Institute, introduction 04 p0579 N85-13695
NASA's SESAC report on research and analysis in space and Earth sciences 04 p0579 N85-13697
Geophysical and geochemical constraints favoring the capture hypothesis 04 p0581 N85-13710
Geophysical investigation of precambrian crustal structure and Laramide effects across a precambrian suture in southeastern Wyoming
05 p0674 N85-14328
Geology and resources of the Tar Sand Triangle, southeastern Utah
[DE84-012017] 05 p0677 N85-14346
USSR report: Earth sciences
[JPRS-UES-84-007] 06 p0819 N85-15196
Selection of spacing of modular and gradient measurement surveys based on statistical characteristics of measured geomagnetic field
06 p0821 N85-15214
Solar-geophysical data number 478, June 1984. Part 1 (prompt reports): Data for May 1984, Apr. 1984, and late data
[PB84-243153] 06 p0890 N85-15653
Solar-geophysical data number 478, June 1984. Part 2 (comprehensive reports): Data for December 1983 and miscellanea
[PB84-243161] 06 p0890 N85-15654
Deployment of a regional array in Norway
[AD-A147032] 07 p0997 N85-16330
Microprocessors in geophysical instruments discussed
08 p1142 N85-17199
Ground-based measurements of mesosphere temperatures by optical means
08 p1183 N85-17453
A research in support of NASA's space science
[NASA-CR-174267] 08 p1227 N85-17728
European scientific notes. Volume 38, number 11
[AD-A146228] 08 p1230 N85-17745
Air Force space technology center space technology: Emphasis 84 09 p1333 N85-18361
Earth Sciences Division report, 1983
[DE85-001036] 09 p1341 N85-18436
Solar-geophysical data number 476, April 1984. Part 1: (Prompt reports). Data for March 1984, February 1984 and late data
[PB84-215060] 09 p1416 N85-18936
Solar-geophysical data number 476, April 1984. Part 2: (Comprehensive reports). Data for October 1983, June 1981 and miscellanea
[PB84-215078] 09 p1417 N85-18937
USSR report: Earth sciences
[JPRS-UES-85-003] 10 p1497 N85-19446
Organogenic structures (submerged reefs) in Silurian limestone of west Bengal basin
10 p1500 N85-19484
MIZEX (Marginal Ice Zone Program): A program for mesoscale air-ice-ocean interaction experiments in Arctic marginal ice zones. 5. MIZEX 84. Summer experiment PI (Principal Investigator) preliminary reports
[AD-A148986] 10 p1521 N85-19594
Summer study program in geophysical fluid dynamics, the Woods Hole Oceanographic Institution, dynamic differentiation
[AD-A149386] 10 p1521 N85-19595
Structure and application of extremely large geophysical data bases
[DE85-003527] 10 p1568 N85-19688
The global meteor observation system (GLOBMET)
11 p1656 N85-20432
Global meteor observation system (GLOBMET)
11 p1656 N85-20438
Large natural geophysical events: Planetary planning
[DE85-000859] 11 p1763 N85-21092
Solar-geophysical data number 479, July 1984. Part 1: (Prompt reports). Data for June 1984, May 1984 and later data
[NASA-CR-175542] 12 p1962 N85-22333
Aeronautical Engineering: A continuing bibliography with indexes, supplement 185
[NASA-SP-7037(185)] 13 p1965 N85-22342
USSR report: Earth sciences
[JPRS-UES-85-002] 13 p2105 N85-23116
Application of field X-ray: Radiometric analysis in exploratory geology and means for its improvement
13 p2115 N85-23176
Reports of the Planetary Geology and Geophysics Program, 1984
[NASA-TM-87563] 13 p2172 N85-23474
Planetary interior modeling and tectonic implications
13 p2200 N85-23649
USSR report: Earth sciences
[JPRS-UES-85-004] 14 p2332 N85-24424
Electromagnetic field of currents and its use to estimate total conductivity of sedimentary deposits in Western Black Sea 14 p2334 N85-24434
New methods for interpreting seismic time fields in media with variable velocities 14 p2343 N85-24490
Possibility of retrieving dynamics of reflected wave method records beneath low-velocity zone
14 p2346 N85-24503
Observation model and parameter partials for the JPL VLBI parameter estimation software MASTERFIT-F 2.0
[NASA-CR-175640] 14 p2347 N85-24509
Spectral analysis of diurnal nonuniformity of Earth's rotation 15 p2477 N85-25269
High-capacity real-time computer system for processing hydrophysical data 15 p2625 N85-26178
Telescope in lunar orbit 15 p2682 N85-26568
Tenth Conference of Working Group of Socialist Countries on Remote Sensing of Earth under Intercosmos Program 16 p2725 N85-26820
USSR report: Earth sciences
[JPRS-UES-85-005] 16 p2807 N85-27307
Surface exploration geophysics applied to the Moon
[DE85-006714] 16 p2884 N85-27793
Solar-Geophysical Data Number 484, December 1984. Part 1 (prompt reports): Data for November 1984, October 1984 and late data
[NASA-CR-175829] 16 p2888 N85-27819
Solar-Geophysical Data Number 484, December 1984. Part 2 (comprehensive reports): Data for June 1984, January 1982 and Miscellanea
[NASA-CR-175826] 16 p2888 N85-27820
Yearbook of the Bureau of Mineral Resources, Geology and Physics: Geoscientific research, resource assessment, and database development, 1 Jul. 1983 to 30 Jun. 1984
[BMR-84] 17 p2989 N85-28474
Geophysical plasmas and atmospheric modeling
[AD-A152605] 17 p2993 N85-28497
Earth Resources: A continuing bibliography with indexes, issue 45
[NASA-SP-7041(45)] 18 p3123 N85-29336
Deep source gas
[DE85-001984] 18 p3126 N85-29358
Geological-geophysical and gas-biochemical studies in Bering Sea 19 p3291 N85-30404

Projects of the Computer Center of the academy's Siberian branch 19 p3295 N85-30425
Preliminary evaluation of alterant geophysical tomography in welded tuff
[DE85-010826] 19 p3302 N85-30469
Melt zones beneath five volcanic complexes in California: An assessment of shallow magma occurrences
[DE85-010644] 19 p3305 N85-30489
Environmental background measurement program
[AD-A153860] 19 p3319 N85-30577
Contemporary plate motions from LAGEOS
20 p3489 N85-31689
The Earth's wobble and associated ocean motions
20 p3490 N85-31696
Geodyn systems development
20 p3492 N85-31706
Global Mega-Geomorphology
[NASA-CP-2312] 21 p3600 N85-32357
Deep sea mega-geomorphology: Progress and problems 21 p3602 N85-32369
The origin of continental crust: Outlines of a general theory 21 p3720 N85-33083
Landscape interpretation capabilities using space photographs of regions of a multistage platform mantle structure 22 p3734 N85-33151
Questions about Mercury's role in comparative planetary geophysics 22 p3853 N85-33861
Geophysical-geological studies of possible extensions of the New Madrid fault zone
[TI85-901341] 23 p3949 N85-34475
Some geophysical guides to ore in southern and southwestern Alaska 24 p4103 N85-35436
The development of assessment techniques program
24 p4106 N85-35457
The Alaska Mineral Resources Assessment Program
24 p4107 N85-35460
Procedure for editing the fluxgate magnetometer data of the AFGL (Air Force Geophysics Laboratory) magnetometer network
[AD-A156331] 24 p4117 N85-35523

GEOPOTENTIAL
NT GEOPOTENTIAL HEIGHT
Geopotential harmonics of order 15 and 30, from analysis of the orbit of satellite 1971-10B
[RAE-TR-84008] 02 p0165 N85-11121
Individual geopotential coefficients of order 15 and 30, from resonant satellite orbits
[AD-A146887] 06 p0828 N85-15256
Individual geopotential coefficients of order 15 and 30, from resonant satellite orbits
[RAE-TR-84021] 08 p1105 N85-16985
Science Applications, part 2 11 p1643 N85-20347
Approximate perturbing part of geopotential by polynomials of stipulated form 13 p1984 N85-22448
Potential models — Earth gravity
14 p2396 N85-24764
Optimization of system for observing Northern Hemisphere atmospheric pressure field
15 p2485 N85-25338
Satellite physical and orbital characteristics
16 p2604 N85-27287
Radial orbit error spectrum for Topex
16 p2605 N85-27292
The selection of the starting field: General versus tailored model 16 p2605 N85-27294
Improving the geological interpretation of magnetic and gravity satellite anomalies
[E85-10103] 20 p3473 N85-31585
A comparative study of spherical and flat-Earth geopotential modeling at satellite elevations
20 p3475 N85-31593
A comparative study of spherical and flat-Earth geopotential modeling at satellite elevations
20 p3475 N85-31594
Continental and oceanic magnetic anomalies: Enhancement through GRM 20 p3476 N85-31596
Spaceborne gradiometer error analysis
20 p3492 N85-31707
Troposphere-stratosphere (surface-55 km) monthly general circulation statistics for the Northern Hemisphere-four year averages
[NASA-TM-86182] 20 p3495 N85-31730

GEOPOTENTIAL HEIGHT
Middle Atmosphere Program. Handbook for MAP, volume 7
[NASA-CR-175479] 11 p1656 N85-20437
Workshop on Comparison of Data and Derived Dynamical Quantities During Northern Hemisphere (PMP-1) Winters 11 p1657 N85-20444
Changes in the ozone content over central Europe during reversals of stratospheric circulation in late winter
11 p1661 N85-20469
On geoid heights and flexure of the lithosphere at seamounts
[AD-A151220] 15 p2604 N85-26050
The seasonal cycle of storminess as measured by band-pass fluctuations 18 p3144 N85-29467

GEORGIA
Revised Uniform Summary of Surface Weather Observations (RUSSWO). Dobbins AFB, Georgia, parts A-F
[AD-A146916] 07 p1005 N85-16387
Meteor wind results from Atlanta, USA, and Ramey, Puerto Rico 11 p1662 N85-20474
Geometric accuracy of LANDSAT-4 MSS image data
11 p1667 N85-20503

GEOS SATELLITES (ESA)
The structure and dynamics of the magnetosphere: Progress in the IMS 14 p2355 N85-24650
Terrestrial continuum radiation study during the IMS
14 p2365 N85-24619
Contribution of relaxation sounding experiments to the understanding of magnetospheric processes
14 p2371 N85-24655
Contribution of mutual impedance experiments to the understanding of magnetospheric processes — GEOS satellites 14 p2371 N85-24656

GEOS SATELLITES (ESRO)
U GEOS SATELLITES (ESA)

GEOS 1 SATELLITE
Simultaneous observations of electron spectra in the auroral zone and near the equatorial plane by the DMSP-5D-F2 and GEOS-1 Satellites
[KGI-184] 09 p1355 N85-18522
Results from the GEOS-1 and GEOS-2 spacecraft and their contributions to the IMS 14 p2354 N85-24545
Morphology of 2keV-electrons observed by GEOS 1
14 p2360 N85-24581
Energetic electron anisotropy and ELF waves onboard GEOS. How does quasi-linear diffusion work
14 p2366 N85-24623
Theoretical studies of electric cyclotron harmonic (ECH) waves based on experimental data from GEOS 1
14 p2367 N85-24631
Advances in magnetospheric plasma diagnosis by active experiments — IMS satellites 14 p2371 N85-24654
Contribution of relaxation sounding experiments to the understanding of magnetospheric processes
14 p2371 N85-24655

GEOS 2 SATELLITE
Results from the GEOS-1 and GEOS-2 spacecraft and their contributions to the IMS 14 p2354 N85-24545
The GEOS-2 electric field observations at times of solar wind discontinuities 14 p2360 N85-24584
Coordinated balloon-satellite studies of energetic electron precipitation mechanisms
14 p2360 N85-24587
The GEOS-2 E-field behavior during dynamic auroral development near the satellite footpoint
14 p2362 N85-24598
Role of equatorial Electron Cyclotron Harmonic (ECH) waves in the generation of diffuse auroras. Contribution of the GEOS IMS spacecraft 14 p2367 N85-24632
Long-period magnetospheric pulsations observed with an electric field experiment in the magnetosphere
14 p2369 N85-24639
The SAMBO-GEOS experiment: A Pe-6 event from ground-satellite observations 14 p2369 N85-24641
Observations of a pulsation event from the ground with balloons and with a geostationary satellite
14 p2369 N85-24643
Satellite, auroral radar and ground magnometer observations of transient ULF pulsations
14 p2369 N85-24645
Advances in magnetospheric plasma diagnosis by active experiments — IMS satellites 14 p2371 N85-24654

GEOS 3 SATELLITE
Intercomparison of GEOS 3/SEASAT wave data and wave model data 03 p0381 N85-12438
Lessons from the SEASAT and GEOS-3 altimeters data projects 03 p0384 N85-12457
Global mean sea surface based upon a combination of the GEOS-3 and SEASAT altimeter data
20 p3492 N85-31710

GEOS-B SATELLITE
U GEOS 2 SATELLITE

GEOS-C SATELLITE
U GEOS 3 SATELLITE

GEOSTATIONARY OPERATIONAL ENVIRON SATS
U GOES SATELLITES

GEOSTATIONARY PLATFORMS
U SYNCHRONOUS PLATFORMS

GEOSTATIONARY SATELLITES
U SYNCHRONOUS SATELLITES

GEOSTROPHIC WIND
The inducement of planetary boundary layer mass convergence associated with varying vorticity beneath tropospheric wind maximum 01 p0074 N85-10494
An alternative to reduction of surface pressure to sea level
[NASA-CR-174174] 04 p0536 N85-13422
A study of the adequacy of quasi-geostrophic dynamics for modeling the effect of frontal cyclones on the larger scale flow 05 p0684 N85-14398
Spectral modeling of a potential vorticity equation for a barotropic flow on a beta-plane
[CWI-AM-R8408] 08 p1186 N85-17478
Sea-ice motion in response to geostrophic winds
14 p2323 N85-24357
Numerical experiments of jet streak ageostrophic circulations using pseudo-geostrophic initialization and perspectives 15 p2590 N85-25969
Numerical studies of frontal dynamics
15 p2596 N85-26014
A study of the adequacy of quasi-geostrophic dynamics for modeling the effect of frontal cyclones on the larger scale flow
[NASA-CR-176065] 20 p3495 N85-31731

GEOSYNCHRONOUS ORBITS
Relationships between Ariane trajectories and satellite orbits 05 p0599 N85-13815
Satellite positioning — in geosynchronous orbit
05 p0600 N85-13823
Perturbations in geostationary orbit
05 p0600 N85-13824
Stationkeeping strategies for geostationary satellites
05 p0600 N85-13825
Moderate lift-to-drag aeroassist
08 p1107 N85-16995
OTV propulsion tecnology programmatic overview
08 p1107 N85-16997
The rationale and suggested approaches for research geosynchronous satellite measurements for severe storm and mesoscale investigations
[NASA-TM-86185] 09 p1356 N85-18532
Efficient structures for geosynchronous spacecraft solar arrays
[NASA-CR-174448] 10 p1428 N85-19004
Assessment of satellite collision hazards by simulated sampling in space 12 p1784 N85-21195
Geosynchronous satellite collision avoidance
12 p1784 N85-21197
The long term behaviour of Earth orbits and the implications for debris control 12 p1786 N85-21213
Debris in the geostationary orbit ring, the endless shooting gallery: The necessity for a disposal policy
12 p1786 N85-21214
The international environment UNISPACE '82 and the ITU: A relationship between orbit-spectrum resource allocation and orbital debris 12 p1787 N85-21215
Radiation exposure and performance of multiple burn LEO-GEO orbit transfer trajectories
[NASA-TM-86946] 12 p1788 N85-21228
SCATHA (spacecraft charging at high altitudes) plasma interaction experiment: SC-3 high energy particle spectrometer; SC-5 energetic ion composition experiment
[AD-A149729] 12 p1793 N85-21252
Design guidelines for assessing and controlling spacecraft charging effects 13 p1994 N85-22500
Development of a continuous broad-energy-spectrum electron source 13 p1995 N85-22507
Automatic charge control system for satellites
13 p1995 N85-22508
Observations of energetic electron and ion distributions near the magnetopause at geosynchronous orbit and related ground effects 14 p2356 N85-24560
Timing between particle injections at the geostationary orbit and particle flux decreases in the distant geomagnetic tail during substorms 14 p2358 N85-24569
Results of the SCATHA ion composition experiment during the IMS 14 p2359 N85-24580
Sudden Storm Commencement (SSC) associated hydromagnetic variations at geosynchronous altitude and on the ground 14 p2369 N85-24642
Costs, payload of Ariane, US Space Shuttle compared
15 p2530 N85-25601
Station for in-orbit testing of satellites
[MBB-UR-708/84-O] 16 p2674 N85-27733
Geostationary orbit capacity study
[REPT-44-3558] 18 p3091 N85-29134
A 406 MHz geostationary satellite SARSAT experiment 20 p3403 N85-31113
Civilian Space Stations and the US future in Space
[OTA-STI-242] 20 p3418 N85-31215
Geosynchronous performance of a lithium-titanium disulfide battery 20 p3444 N85-31377

GEOSYNCLINES
Deformation mechanisms associated with mesoscopic kinkbands, Jura Mountains (Switzerland) and Chaines Subalpines (France) 03 p0369 N85-12492
Conditions for formation of paragenesses containing kyanite-orthoclase in region of Mount Provender and Pratt Peak (Shackleton Range, Antarctica)
19 p3298 N85-30447

Stratigraphic analysis of Pennsylvania rocks using hierarchy of transgressive-regressive units
19 p3312 N85-30531
GEOTECHNICAL ENGINEERING
Engineering geology of selected areas, US army engineer division, lower Mississippi valley. The American bottom area, MO-IL. Volume 1
[AD-A154258] 19 p3299 N85-30455
GEOTEMPERATURE
Geophysical Works during 1981, volume 29, no. 547-566 03 p0375 N85-12380
Heat flow map of Europe: Brief summary of the geophysical implications
[REPT-562] 03 p0377 N85-12405
Terrestrial heat flow in Europe and general features of its regional distribution
[REPT-563] 03 p0377 N85-12406
Diagenesis of niagaran (middle silurian) pinnacle reefs, northwest Michigan 09 p1352 N85-18506
Thermal conditions and thinning of lithosphere in late cenozoic in southwestern US 10 p1501 N85-19473
Low-temperature geothermal assessment of the Jordan Valley Salt Lake County, Utah
[DE85-000616] 11 p1670 N85-20524
Determining deep heat flow and rate of horizontal percolation from temperature measurements in aquifer
13 p2116 N85-23180
Temperature anomalies above ore bodies
14 p2345 N85-24500
Crustal radiogenic heat production and the selective survival of ancient continental crust
21 p3721 N85-33066
GEOTHERMAL ANOMALIES
Seismic discrimination of a geothermal field: Cerro Prieto
[DE84-014581] 01 p0064 N85-10425
Interpreting geothermal anomalies by special points method 07 p0982 N85-16236
GEOTHERMAL ENERGY CONVERSION
International test and demonstration of a 1-MW wellhead generator: Helical screw expander power plant
[NASA-CR-174161] 04 p0527 N85-13372
USSR report: Energy
[JPRS-UEN-84-038] 07 p0994 N85-16312
Deputy Minister discusses plans for geothermal power
07 p0994 N85-16313
Geothermal injection treatment: Process chemistry, field experiences, and design options
[DE85-002873] 11 p1675 N85-20554
Silica problem in the design of geothermal power plants
[DE85-006245] 17 p2966 N85-28453
Solar energy education. Renewable energy: A background text
[DE85-010365] 23 p3946 N85-34452
GEOTHERMAL ENERGY EXTRACTION
Geothermal wells drilled in Transcarpathians
07 p0994 N85-16315
Thermohydrodynamic model: Hydrothermal system, shallowly seated magma chamber
13 p2115 N85-23173
Western gas sands
[DE85-001985] 18 p3126 N85-29360
Technology transfer report: Feasibility study for the use of geothermal brine in the Ashdod area, Israel
[DE85-013316] 22 p3810 N85-33598
GEOTHERMAL ENERGY UTILIZATION
Deputy Minister discusses plans for geothermal power
07 p0994 N85-16313
Optimization of design and control strategies for geothermal space heating systems
[DE85-000496] 09 p1344 N85-18458
Monitoring environmental and related performance parameters for a Rankine-cycle turbine electric generator utilizing geothermal energy at the Gila Hot Springs, New Mexico
[DE84-001772] 09 p1345 N85-18465
Two-phase flow in geothermal systems
[DE85-004692] 12 p1848 N85-21591
Leak detectors for organic Rankine cycle power plants: On-line and manual methods
[DE85-002792] 12 p1852 N85-21617
Selection of promising sites for magma energy experiments
[DE85-006832] 16 p2620 N85-27369
Pagosa Springs geothermal project
[DE85-011308] 22 p3807 N85-33583
Enthalpy transients in fractured two-phase geothermal systems
[DE85-011998] 22 p3808 N85-33587
GEOTHERMAL RESOURCES
NT GEYSERS
NT VOLCANOES
A summary of geothermal studies in Montana, through 1983
[DE84-014325] 01 p0064 N85-10422
Geothermal resources of the Laramie, Hanna, and Shirley Basins, Wyoming
[DE84-016104] 01 p0064 N85-10423
Geothermal exploration in Trans-Pecos, Texas/New Mexico
[DE84-015553] 01 p0064 N85-10424
Seismic discrimination of a geothermal field: Cerro Prieto
[DE84-014581] 01 p0064 N85-10425
Hydrogeochemical investigation of thermal springs in the Black Canyon-Hoover Dam area, Nevada and Arizona
[PB84-202472] 01 p0064 N85-10426
Investigation of mineral and thermomineral springs in the Eifel Mountains regarding thermal indications
[BMFT-FB-T-84-019] 02 p0220 N85-11451
Similarity considerations in 1-component 2-phase flow
[DE84-016370] 04 p0499 N85-13184
Geothermal studies in Alaska: Conditions at Prudhoe Bay 04 p0516 N85-13290
Geothermal resource assessment for North Dakota
[DE84-016128] 04 p0526 N85-13367
Geothermal assessment of the lower Bear River drainage and northern East Shore ground-water areas, Box Elder County, Utah
[DE84-017358] 04 p0526 N85-13368
International test and demonstration of a 1-MW wellhead generator: Helical screw expander power plant
[NASA-CR-174161] 04 p0527 N85-13372
CO-2-silica geothermometer for low temperature geothermal resource assessment, with application to resources in the Safford Basin, Arizona
[DE84-013958] 04 p0534 N85-13411
Subsurface temperatures in northeastern Wyoming measured by bottom hole temperature records
[TI84-901610] 04 p0534 N85-13413
Thermal energy resources of thermal waters in Kazakhstan 06 p0820 N85-15206
Geothermal assessment of a portion of the Escalante Valley, Utah
[DE84-015964] 06 p0826 N85-15257
Analysis of gases in the Earth's crust
[PB85-113397/GAR] 07 p0990 N85-16287
Coso Monitoring Program, January 1981 through December 1983
[AD-A147894] 07 p0998 N85-16338
Earth Sciences Division report, 1983
[DE85-001036] 09 p1341 N85-18436
Geothermal assessment of part of the east shore area, Davis and Weber Counties, Utah
[DE84-016817] 09 p1342 N85-18446
Heat cycle research program
[DE84-017015] 09 p1344 N85-18455
Field testing of aquifer thermal energy storage
[DE85-000399] 09 p1344 N85-18457
Results from geopressured-geothermal subsidence studies
[DE84-016279] 09 p1354 N85-18520
Low-temperature geothermal assessment of the Jordan Valley Salt Lake County, Utah
[DE85-000616] 11 p1670 N85-20524
Geothermal injection treatment: Process chemistry, field experiences, and design options
[DE85-002873] 11 p1675 N85-20554
Heat Cycle Research Experimental Program report, FY-84
[DE85-003558] 12 p1862 N85-21811
Evaluation of subsurface fracture geometry using fluid pressure response to solid earth tidal strain
[DE85-003294] 12 p1890 N85-21864
Normal and anomalous geothermal fields and their relationship to hierarchy of geological bodies
13 p2113 N85-23163
Thermohydrodynamic model: Hydrothermal system, shallowly seated magma chamber
13 p2115 N85-23173
Navy geothermal plan
[AD-A152478] 17 p2965 N85-28450
Laboratory investigation of formation damage of an artificial fracture at simulated geothermal conditions
[DE85-010301] 18 p3102 N85-29201
Hot Dry Rock Geothermal Energy Developement Program
[DE85-010570] 19 p3268 N85-30264
Lost circulation in geothermal wells: Research and development status
[DE85-009636] 19 p3268 N85-30267
Evaluation of geothermal potential of Rio Grande rift and Basin and Range province, New Mexico
[DE85-001360] 19 p3301 N85-30466
Geothermal hydrogen and health in Rotorua, New Zealand
[DE85-001283] 19 p3301 N85-30467
Linear boundary detection using pressure buildup tests
[DE85-009926] 22 p3784 N85-33444
Pagosa Springs geothermal project
[DE85-011308] 22 p3807 N85-33583
Enthalpy transients in fractured two-phase geothermal systems
[DE85-011998] 22 p3808 N85-33587
Technology transfer report: Feasibility study for the use of geothermal brine in the Ashdod area, Israel
[DE85-013316] 22 p3810 N85-33598
Fracture detection and characterization for geothermal reservoir definition
[DE85-009677] 22 p3815 N85-33630
Proposed resource evaluation plan, Salton Sea scientific drilling program
[DE85-011294] 22 p3815 N85-33633
Geothermal resources of the Laramie, Hanna and Shirley Basins, Wyoming
[DE85-005005] 23 p3943 N85-34436
Depletion modeling of liquid dominated geothermal reservoirs
[DE85-009923] 23 p3943 N85-34437
Evaluation of low-temperature geothermal potential in Utah and Goshen Valleys and adjacent areas, Utah. Part 2: Water temperature and chemistry
[DE85-009344] 23 p3943 N85-34438
Modeling of geothermal systems
[DE85-012553] 23 p3943 N85-34439
Workshop on Recent Research in the Valles Caldera
[DE85-010569] 23 p3949 N85-34472
Early and middle Cenozoic volcanic synthesis
24 p4105 N85-35449
Evaluation of low-temperature geothermal potential in north-central Box Elder County, Utah
[DE85-009541] 24 p4112 N85-35490
Geothermal resources of the Washakie and Great Divide basins, Wyoming
[DE85-013004] 24 p4112 N85-35491
GEOTHERMAL TECHNOLOGY
NT GEOTHERMAL ENERGY CONVERSION
NT GEOTHERMAL ENERGY EXTRACTION
NT GEOTHERMAL ENERGY UTILIZATION
Optimization of design and control strategies for geothermal space heating systems
[DE85-000496] 09 p1344 N85-18458
Geothermal injection treatment: Process chemistry, field experiences, and design options
[DE85-002873] 11 p1675 N85-20554
Two-phase flow in geothermal systems
[DE85-004692] 12 p1848 N85-21591
Thermophysical properties of working fluids for binary geothermal cycles
[DE85-000385] 12 p1881 N85-21804
Alternative heat sources for heat pumps
[DE85-007610] 17 p2959 N85-28275
Hot Dry Rock Geothermal Energy Developement Program
[DE85-010570] 19 p3268 N85-30264
The transient electromagnetic depth sounding technique applied to hydrocarbons and geothermal exploration
[MITT-42] 23 p3949 N85-34476
GEOTHERMOMETRY
U GEOTEMPERATURE
GEOTROPISM
Gravity and cell differentiation in lentil roots
05 p0690 N85-14433
GEP TELESCOPES
U PARTICLE TELESCOPES
GERDIEN ARC HEATERS
U HEATING EQUIPMENT
GERMAN DEMOCRATIC REPUBLIC
U EAST GERMANY
GERMANATES
Recent progress in BGO development for high resolution calorimetry
[MPI-PAE/EXP-E1-129] 01 p0124 N85-10848
Improvements in the energy resolution and high-count-rate performance of bismuth germanate
[DE85-010763] 19 p3240 N85-30092
GERMANIDES
Contact properties of rare-earth silicides and germanides on Si and Ge 19 p3374 N85-30931
GERMANIUM
NT GERMANIUM ISOTOPES
Relationships between electronic structure and stability of metallic glasses
[AD-A145141] 01 p0028 N85-10176
Development of high responsitivity Ge:Ga photoconductors
[DE84-016902] 04 p0571 N85-13643
On the origins of structural defects in BF2(+)-implanted and rapid thermally annealed silicon: Conditions for defect free regrowth
[DE84-016060] 04 p0572 N85-13650
Ge abundances in the lunar mantle and implications for the origin of the Moon 04 p0582 N85-13721
IUE observations of the gaseous component of the local interstellar medium 06 p0874 N85-15553

Electronic structure, chemical bonding, and superconductivity of silver films on germanium
[AD-A147720] 08 p1128 N85-17112
Optically induced intervalence-band transitions in germanium by the absorption of 1.06 micrometers picosecond pulses
[DE85-000946] 09 p1399 N85-18803
Metal-nonmetal transitions in N-doped many-valley Si and Ge
[INPE-3358-PRE/636] 10 p1562 N85-19848
Impurity complexes in pure elemental semiconductors
11 p1736 N85-20919
Germanium resistance thermometer calibration at superfluid helium temperatures
12 p1947 N85-22228
Shuttle flight test of an advanced gamma-ray detection system
[AD-A150316] 13 p1988 N85-22469
Time resolved X-ray studies during pulsed laser irradiation of Ge
[DE85-005263] 13 p2097 N85-23083
Infrared nonlinear processes in semiconductors
[AD-A150986] 14 p2427 N85-24968
TEM investigation of polar-on-nonpolar epitaxy: GaAs-AlGaAs on (100) Ge
[DE85-007613] 16 p2871 N85-27714
Germanium detectors with a built-in transverse drift field
[DE85-009944] 18 p3098 N85-29165
Method for producing high quality germanium-germanium nitride interfaces for germanium semiconductors and device produced thereby
[AD-D011702] 19 p3260 N85-30218
Bismuth germanate scintillators: Applications in nuclear safeguards and health physics
[DE85-010730] 19 p3365 N85-30865
New adatom model for Si(11) 7X7 and Si(111)Ge 5X5 reconstructed surfaces 20 p3480 N85-31625
Thermoelectric properties of beta-boron and some boron compounds
[DE85-011976] 21 p3582 N85-32270
Absorption of 10.6 micrometer laser radiation in electron-hole condensate in germanium
21 p3681 N85-32870
Raman scattering studies in solids
[AD-A155528] 21 p3710 N85-33032
Specificity of (71)Ga(p,n) (71)Ge at 35 MeV for Gamow-Teller strength
[DE85-011837] 23 p3971 N85-34615
Germanium and lead: Significant differences between meteoritic and photospheric abundances?
[OG-7.1-2] 23 p4012 N85-34864

GERMANIUM ALLOYS
Raman scattering from metastable GaSb(1-x) Ge(2x) alloys
[AD-A145897] 03 p0327 N85-12108
Optical properties of composite materials
[AD-A146766] 07 p0920 N85-15828
Alloy supercooling on Salyut-7
11 p1604 N85-20083
Structure and aging of amorphous chromium-germanium alloys 15 p2497 N85-25401
Compensation of dangling bonds in A-Si, Ge:H alloys
[DE85-002905] 15 p2662 N85-26433
LPCVD tungsten deposition on Si-Ge alloy
[DE85-005588] 16 p2750 N85-26970
Theoretical studies on the structures of insulating and metallic glasses
[DE85-010022] 18 p3194 N85-29814
Development of improved thermoelectric materials for space nuclear power systems
[DE85-013079] 22 p3844 N85-33807

GERMANIUM COMPOUNDS
NT GERMANATES
NT GERMANIDES
NT GERMANIUM OXIDES
The effect of temperature on the radiation induced losses of large diameter GPS (Germanium phosphosilicate) and GBS core optical fibers
[AD-A145409] 02 p0280 N85-11823
1985 Amorphous Silicon Review Meeting
[DE85-008794] 22 p3807 N85-33582

GERMANIUM DIODES
Measurement of nuclear lines with a dual Ge(Li) telescope aboard a stratospheric balloon
[INPE-3360-TDL/185] 11 p1762 N85-21083
Intercomparison of the calculated absolute efficiency values between true coaxial and true closed-end coaxial Ge (Li) and NaI detectors
[REPT-5-1984] 20 p3532 N85-31976

GERMANIUM ISOTOPES
Results of ultra-low level 71ge counting for application in the Gallex-solar neutrino experiment at the Gran Sasso Underground Physics Laboratory
[SH-8.1-2] 23 p4049 N85-35108

GERMANIUM OXIDES
The relationship between radiation sensitivity and redox equilibria — glass processing variables
[AD-A147216] 07 p0932 N85-15906

GERMANIUM RECTIFIERS
U GERMANIUM DIODES

GERMANY
Determination of the longitude differences Munich-Lissabon-San Fernando, Munich-Wettzell, and Munich-Karlsruhe-Niederreifenberg
[ASTRON-GEODAET-ARB-44]
04 p0524 N85-13353
Determination of astronomical longitude differences for the European longitude reference system for 1980. Relative right ascension corrections for 125 FK4 and FK4 Sup stars 04 p0524 N85-13354
Determination of astronomical longitude differences: Munich, Karlsruhe, Niederreifenberg in 1974
04 p0524 N85-13355
Limited surface observatins climatic summary (LISOCS). Ansback AHP, Germany
[AD-A147205] 07 p1007 N85-16398

GERMINATORS
U PHYTOTRONS

GERT
A Q-GERT network simulation model for examining pipeline time in the Navy's J-52 intermediate level jet engine repair cycle
[AD-A147269] 07 p0894 N85-15663
Simulation of estimating periodicity of seasonally stationary time series
[DE85-003517] 11 p1708 N85-20748
SINOGRAFO: A system for influencing and forecasting weather
[INPE-3349-PRE/628] 16 p2834 N85-27475

GETTERS
Studies on impurity control and hydrogen pumping with chromium gettering in ISX-B
[DE85-001896] 09 p1394 N85-18771
Neutral beam injector oxygen impurity measurements and concentration reduction via gettering processes
[DE85-000861] 12 p1836 N85-21521
Development of new process technologies for solar cells with high efficiency starting from purified silicon
12 p1878 N85-21785
Vacuum system for the Argonne 6 GeV synchrotron light source
[DE85-012286] 24 p4157 N85-35773

GEYSERS
Categorization of nocturnal drainage flows within the Brush Creek valley in western Colorado and the variability of sigma theta in complex terrain
[DE85-011291] 19 p3300 N85-30461

GIACOBINI-ZINNER COMET
The astrometry network of the IHW and the P/Crommelin trial run results 14 p2435 N85-25016
The IHW reference star catalogs for Comets Halley and Giacobini-Zinner 14 p2436 N85-25031
The orbits of Comets Halley and Giacobini-Zinner
14 p2437 N85-25039
Astrometric needs for the ISEE-3/ICE mission to Comet Giacobini-Zinner 14 p2438 N85-25043
The International Cometary Explorer (ICE)wallsheet teacher's guide
[NASA-TM-87498] 23 p3988 N85-34727

GIANT STARS
NT CARBON STARS
NT RED GIANT STARS
Photoelectric photometry of globular cluster giants
01 p0128 N85-10684
Outer atmospheres of giant and supergiant stars
[NASA-CR-174165] 04 p0580 N85-13703
The behaviour of brighter binaries and yellow giants in open clusters 05 p0737 N85-14738
On the content of nitrogen in atmospheres of late giants derived from molecular bands on NH in the UV spectral range 05 p0740 N85-14761
Theoretical studies of chromospheres and winds in cool stars
[NASA-CR-174204] 06 p0880 N85-15596
The essence of binary star coalescence: A coordinated ground-based photometric and IUE ultraviolet study of FK Comae 11 p1758 N85-21044
Chromospheric activity in M giants
11 p1757 N85-21056
Rotational modulation of chromospheric emission in cool giants and hybrid stars 11 p1759 N85-21064
Stellar granulation 14 p2451 N85-25132

GIMBALS
Orbital transfer vehicle propulsion issues
08 p1109 N85-17009
Determination of directional gyro parameters
14 p2287 N85-24171
Impact of magnetic isolation on pointing system performance in the presence of structural flexibility
[NASA-CR-172481] 16 p2732 N85-26861
A Gimbal sizing analysis for an IPACS rotating assembly
[NASA-CR-172524] 16 p2741 N85-26913

GIOTTO MISSION
A cometary ion mass spectrometer
[NASA-CR-174328] 08 p1164 N85-17343
Giotto solar array: Design, manufacture and test
13 p2008 N85-22589
The Giotto spacecraft impact-induced plasma environment
[ESA-SP-224] 14 p2243 N85-23905
Measurement of charged secondary particle emission under ion and neutral impact — Giotto mission
14 p2243 N85-23906
Contactless determination of the conductivity of the white paint PCB-Z — Giotto spacecraft thermal control coating 14 p2243 N85-23907
Measurements of integral yields of charged secondary particles using neutral beams simulating a cometary fly-by — Giotto mission 14 p2244 N85-23908
Giotto residual ionization 14 p2244 N85-23909
Impact ionization from gold, aluminum and PCB-Z — Giotto spacecraft paint PCB-Z 14 p2244 N85-23910
Experimental investigations on ion emission with dust impact on solid surfaces — Giotto spacecraft
14 p2244 N85-23911
Ion emission from solid surfaces: Comparison of dust impact with other excitations — Giotto mission
14 p2244 N85-23912
Electrostatic charging of the Giotto spacecraft due to neutral gas impact 14 p2244 N85-23913
A model of plasma cloud expansion generated by a dust particle impact — Giotto mission
14 p2245 N85-23914
Giotto plasmasheath and wake charging near Halley's Comet: Revised parameters 14 p2245 N85-23915
Simulations of satellite-plasma interaction, including electron space charges — Giotto mission
14 p2245 N85-23916
Anticipated impact plasma problems for the COPERNIC-RPA experiment in the cometary environment — Giotto mission 14 p2245 N85-23917
An impact plasma monitor for cometary missions — Giotto , VEGA 14 p2245 N85-23918
Plasma environment effects on the Giotto Ion Mass Spectrometer 14 p2245 N85-23919
Thermal design of the Giotto spacecraft
14 p2245 N85-23920
Spacecraft environment during the Giotto-Halley encounter: A summary 14 p2246 N85-23921
Towards the Halley Comet 14 p2399 N85-24783

GLACIAL DRIFT
Glacier dynamics and the development of glacial landforms in the eastern Puget lowland, Washington
03 p0389 N85-12490
The pleistocene geology of Vilas County, Wisconsin
09 p1353 N85-18509

GLACIERS
Late quarterly glaciolacustrine and vegetational history of the Copper River Basin, south-central Alaska
03 p0391 N85-12499
Glacial-lake deposits in the Mount Harper area, Yukon-Tanana Upland 04 p0517 N85-13300
Paleoclimatologists use past to predict weather patterns 06 p0819 N85-15197
Surging as a potential response of ice sheets to CO2-induced changes in the polar environment (SPICAE)
[DE84-016472] 06 p0841 N85-15341
Consideration of future climatic changes in three geologic settings
[DE85-001704] 09 p1357 N85-18537
Decade of the Varilov Kupola
10 p1497 N85-19448
Major glaciation events of the past and their geological significance 10 p1497 N85-19450
Proceedings of the 1st Glacier Bay Science Symposium
[PB85-115913] 11 p1682 N85-20599
Catastrophic-flood features in Swedish Lapland as a terrestrial analog for Martian channel flows
13 p2190 N85-23587
Greenland ice sheet mass balance
15 p2603 N85-26043
Potential climatic effects on the Greenland ice sheet
15 p2603 N85-26044
Modern sedimentation in the northern Barents Sea: Input, dispersal and deposition of suspended sediments from glacial meltwater
[AD-A152520] 17 p2997 N85-29530

GLACIOFLUVIAL DEPOSITS
U GLACIAL DRIFT

GLACIOLOGY
Late quaternary glacial cycles in the Bahamian deep basins and in the adjacent Atlantic Ocean
02 p0226 N85-11476

Interlobate comparison of glacial-depositional style as evidenced by small-relief glacial landscape features in Illinois, Indiana, and Ohio, utilizing SIR-B
08 p1146 N85-17231
Glacial geology of Barron County, Wisconsin
09 p1351 N85-18500
The pleistocene geology of Vilas County, Wisconsin
09 p1353 N85-18509
Decade of the Vavilov Kupola
10 p1497 N85-19448
Major glaciation events of the past and their geological significance
10 p1497 N85-19450
Antarctic glaciation, or what are catastrophes in Earth's history
13 p2105 N85-23118
Numerical experiments with simple model of ocean climate
13 p2106 N85-23123
Reports of the Planetary Geology and Geophysics Program, 1984
[NASA-TM-87563] 13 p2172 N85-23474

GLANDS (ANATOMY)
NT ADRENAL GLAND
NT PANCREAS
NT PARATHYROID GLAND
NT PITUITARY GLAND
NT THYMUS GLAND
NT THYROID GLAND

GLANDS (SEALS)
Life testing of rubber seals — aircraft hydraulic systems
[AD-A143193] 13 p2098 N85-23086

GLARE
Removable cleanable antireflection shield
[AD-D011735] 22 p3844 N85-33810

GLASS
NT BOROSILICATE GLASS
NT GLASS FIBERS
NT METALLIC GLASSES
NT S GLASS
NT SILICA GLASS
NT SPIN GLASS
Potential utilization of glass experiments in space
02 p0151 N85-11020
Inorganic composites for space applications
02 p0155 N85-11047
Investigation of chemical durability mechanisms in fluoride glasses
[AD-A145420] 02 p0186 N85-11241
Silicon nitride joining
[AD-A145668] 02 p0187 N85-11248
Structure of vibrational spectrum and selection rules in Raman and hyper-Raman light scattering spectra of inorganic glasses
02 p0271 N85-11769
Thermal deformation measurements of heat-resistant structural materials for aircraft by electro optical displacement transducer
[NAL-TR-810] 03 p0325 N85-12092
HIP glassmaking for high nitrogen compositions in the Y-Si-Al-O-N system
[DE84-015546] 03 p0338 N85-12175
Evaluation of laterally loaded laminated glass units by theory and experiment
[PB84-216423] 03 p0339 N85-12179
EXAFS studies of sodium silicate glasses containing dissolved actinides
[DE84-015835] 04 p0479 N85-13051
Abundancies of Ni, Cr, CO and major elements in the silicate portion of the Moon: Constraints from primary lunar magmas
04 p0582 N85-13720
Volatile elements in and on lunar volcanic glasses: What do they tell us about lunar genesis?
04 p0584 N85-13728
High temperature corrosion of ceramics
[DE84-017084] 05 p0820 N85-13967
Polyimide-glass multilayer printed wiring boards
[DE84-015092] 05 p0831 N85-14048
Polarization in chemically doped hydrogen-rich glasses
[DE84-017486] 06 p0771 N85-14936
The influence of gravitational body force in meteoritic chondrule and lunar glass formation
06 p0864 N85-15614
Method for bonding insulator to insulator
[AD-D011340] 07 p0829 N85-15891
The relationship between radiation sensitivity and redox equilibria — glass processing variables
[AD-A147216] 07 p0932 N85-15906
Cryogenic glass-to-metal seal
[AD-D011370] 07 p0933 N85-15911
Glass corrosion in liquid lithium
[DE85-002066] 09 p1299 N85-18162
Study of charge transport in the thermoelectret state of some ceramics and glasses
[DE85-001763] 09 p1300 N85-18163
Evaluation of laterally loaded laminated glass units by theory and experiment
[PB85-111532/GAR] 09 p1300 N85-18166
Stabilization of contaminated soils by in situ vitrification
[AD-P004144] 09 p1348 N85-18480
Optical studies of dynamical processes in disordered materials
[DE85-002400] 10 p1453 N85-19158
Ultrasonic characterization of advanced composite flywheels
[DE85-000156] 11 p1593 N85-20026
Kinetics of reaction of metals and non-metals during diffusion welding
11 p1602 N85-20076
Ab initio calculations of the optical properties of ions in glass
[DE85-001008] 11 p1612 N85-20133
Magnetically-induced luminescence of (Ir(2-phoe)(2)C10(4)
[AD-A149659] 12 p1799 N85-21286
Ring-on-ring tests and load capacity of cladding glass
[PB85-108391] 12 p1868 N85-21717
Densification and deformation in the presence of a liquid phase
[DE85-005101] 13 p2036 N85-22763
Experimental methods for quenching structures in lunar-analog silicate melts: Variations as a function of quench media and composition
13 p2184 N85-23554
A study of frequency effects and damage accumulation during the fatigue of graphite/epoxy and glass/epoxy composite materials
14 p2247 N85-23930
Computer simulations of rare earth sites in glass: Experimental tests and applications to laser materials
[DE85-006156] 14 p2261 N85-24013
Density and thermal expansion measurements of several mixed oxide glasses in the solid and liquid regions
[DE85-006134] 14 p2261 N85-24014
Power control of induction equipment for founding optical glass in array of platinum crucibles
14 p2267 N85-24044
Water-resistance and some other properties of polyalkali fluorophosphate glasses
14 p2281 N85-24133
USSR report: Materials science and metallurgy
[JPRS-UMS-85-001] 15 p2496 N85-25395
A statistical approach to relaxation in glassy materials
[AD-A151285] 15 p2518 N85-25524
Low-temperature thermal expansion of glass
15 p2645 N85-26315
Impurity studies
[DE85-006235] 15 p2661 N85-26423
Impact of optical inhomogeneity in sintered interface between glasses on laser emission characteristics
16 p2763 N85-27053
Spectroscopic investigation of materials for frequency agile laser systems
[AD-A151731] 16 p2790 N85-27208
Mechanical properties of lunar materials under anhydrous, hard vacuum conditions: Applications of lunar glass structural components
[DE85-006682] 16 p2801 N85-27271
Accuracy of the calculated stress field around a craze
[DE85-005820] 16 p2801 N85-27272
Dendritic growth from amorphous matrix
[DE85-007630] 16 p2871 N85-27712
Investigation of charge transport in the thermoelectret state of some ceramics and glasses
[DE85-009318] 17 p2936 N85-28122
Investigation of semiconductor clad optical waveguides
[NASA-CR-175870] 17 p3036 N85-28785
Preparation of heavy metal fluoride glasses in the bulk form
[AD-A153784] 18 p3079 N85-29049
Foamglass solar window collector
[DE85-009187] 18 p3129 N85-29374
Structural characteristics of high temperature composites
[NASA-CR-175898] 19 p3232 N85-30037
Weldability/microstructure relationships of high nickel alloys for header applications
[DE85-009337] 19 p3241 N85-30094
Thermal expansion coefficients of a 30% glass fiber filled PEEK pyrotechnic charge holder
[DE85-010805] 19 p3251 N85-30155
Microscopic structure of two-dimensional electron glass
[DE85-010265] 19 p3376 N85-30942
Silicon nitride protective coatings for silvered glass mirrors
[DE85-011637] 20 p3433 N85-31300
Development of processes for the inclusion of radioactive waste in glass-metal compounds and ceramic materials
[BLL-CE-TRANS-8014-(0022.09)]
20 p3526 N85-31931
EVA-glass interface bond stability
21 p3608 N85-32406
Thin-film reliability and engineering overview
21 p3612 N85-32450
Luminescence and absorption of indium-activated potassium-borate glasses subjected to high-power excitation
21 p3661 N85-32868
Tensile fatigue of glass fibers and composites with conventional and surface compressed fibers
[RR-84-4] 22 p3742 N85-33196
Experimental studies of glass refining
[NASA-CR-176130] 22 p3751 N85-33248
Research study for gel precursors as glass and ceramic starting materials for space processing applications research
[NASA-CR-176113] 22 p3751 N85-33250
Sodium nitrate containing mixture for producing ceramic-glass-ceramic seal by microwave heating
[DE85-011610] 22 p3751 N85-33254
Method of bonding silver to glass and mirrors produced according to this method
[DE85-011642] 22 p3792 N85-33495
Technology of off-gas treatment for liquid-fed ceramic melters
[DE85-012467] 22 p3812 N85-33610
Iron and manganese in oxide minerals and in glasses: Preliminary consideration of Eh buffering potential at Yucca Mountain, Nevada
[DE85-011692] 23 p3916 N85-34271
The effect of liquid-liquid phase separation of glass on the properties and crystallization behavior
[NASA-TM-77880] 23 p3919 N85-34285
Single-point diamond crushing of Zerodur with in-situ polishing and metrology on a diamond turning machine
[DE85-012918] 24 p4083 N85-35305

GLASS COATINGS
Advanced glazings research
[DE85-000539] 11 p1674 N85-20549
Development of corrosion resistant heat exchangers for flue gas desulfurization
[BMFT-FB-T-84-281] 18 p3103 N85-29211
Tensile fatigue of glass fibers and composites with conventional and surface compressed fibers
[RR-84-4] 22 p3742 N85-33196
Laser sealed evacuated window glazings
[DE85-000512] 22 p3754 N85-33273

GLASS FIBER REINFORCED PLASTICS
Prediction of long term strength of glass reinforced plastics in wet environments
[NPL-DMA(A)-80] 04 p0477 N85-13041
Non-linear data fitting for the analysis of creep rupture data on GRP materials in aggressive environments — glass reinforced plastics (GRP)
[NPL-DMA(A)-79] 04 p0512 N85-13261
Prefabricated panels for rapidly runway repair and expedient airfield surfacing
[AD-D011277] 05 p0597 N85-13804
System for rapid repair of damaged airfield runways
[AD-D011325] 07 p0909 N85-15754
Stresses in pin-loaded orthotropic plates using photoelasticity
[NASA-CR-172496] 07 p0977 N85-16204
Review of the mechanical properties of SMC and GRP materials
[NPL-DMA(A)-68] 08 p1131 N85-17128
Initial fracture stages of orthogonally reinforced composite material
11 p1599 N85-20055
Strength properties of unidirectionally reinforced hybrid composites
11 p1599 N85-20056
Preliminary review of statistical treatment of S-glass/epoxy stress rupture data
[AD-A149810] 12 p1797 N85-21275
Scale-up of vanadium trineodecanoate
[AD-A149935] 12 p1813 N85-21370
Stability of three-layer glass-reinforced plastic shells of rotation
13 p2047 N85-22813
Finland, Sweden cooperate in composites research
17 p2946 N85-28184
Expedient runway surfacing with post tensioning system for expeditionary airfields
[AD-D011677] 19 p3222 N85-29976
Influence of moisture and elevated temperature on the fatigue properties of WTS-3 glass fiber blade material — wind turbine blade (WTS-3)
[FFA-TN-1984-58] 20 p3470 N85-31558
Long-term strength of glass fibre/phenolic resin composites
[NPL-DMA(A)-88] 22 p3742 N85-33195
Poly-functional building material from fiberglass (its fabrication and properties)
23 p3908 N85-34209
Stress distribution of fiberglass reinforced plastic beam with a delamination under three-point bending
23 p3908 N85-34210
Strength properties of glassfiber reinforced thermoplastics
23 p3908 N85-34212
Effect of strain rate on the initial failure of notched GRP laminates
23 p3908 N85-34214

Design of transversely stiffenend FRP panels under compressive load — fiber reinforced plastic (FRP) ships
[AMTE(S)-R-84104] 23 p3940 N85-34424
GLASS FIBERS
Lightweight composite launcher pod
[AD-D011236] 01 p0016 N85-10092
Investigating compression failure mechanisms in composite laminates with a transparent fiberglass-epoxy birefringent materials
[NASA-TM-86306] 02 p0170 N85-11137
Parametric study of the P9 HT glass fiber finish (Fatigue resistance). Lot no. 1: Report on the microfatigue tests
[CS-794] 05 p0620 N85-13968
Telephoning with light and sun — glass fibers, solar cells 05 p0663 N85-14264
Qualitative and quantitative compositional analysis of shale derived by gas chromatography and combined gas Chromatography/Mass spectrometry. Executive summary
[AD-A148369] 07 p0924 N85-15851
Composite batteries 07 p0936 N85-15932
Preliminary evaluation of an improved flammability test method for aircraft materials
[FAA-CT-84-22] 08 p1080 N85-16840
Studies of structure and mechanical properties of carbon-reinforced plastic based on spirally reinforced fiber 10 p1444 N85-19100
Stress-relieving interlayers for bituminous resurfacings
[PB85-136885] 12 p1820 N85-21415
Development and study of two-matrix glass fiber composite with increased transverse deformation 13 p2027 N85-22700
Theoretical and experimental investigation of mechanically fastened composites
[AD-A150961] 14 p2248 N85-23935
Glass, carbon fibers made at Fibre et Mica in France 15 p2534 N85-25634
Ten year environmental test of glass fiber/epoxy pressure vessels
[NASA-TM-87056] 19 p3231 N85-30034
Transversely reinforced piezoelectric composites
[AD-D011676] 19 p3260 N85-30214
Tensile fatigue of glass fibers and composites with conventional and surface compressed fibers
[RR-84-4] 22 p3742 N85-33196
GLASS LASERS
Pulsed neodymium glass laser system for investigating nonlinear optical phenomena in gases 03 p0348 N85-12241
The development of a high average power glass laser source
[AD-A147471] 07 p0971 N85-16169
Improved solid-state laser sources, volume 2
[DE85-000758] 09 p1325 N85-18330
Research, development of laser glasses in China 13 p2166 N85-23439
Operation of solid state lasers exposed to electron beam 21 p3865 N85-32895
GLASSY CARBON
Experimental study of enthalpy of quasimonocrystal of graphite and carbon glass in temperature range of 2800-3818 deg K 13 p2036 N85-22751
Glassy metals: Now highly resistant material
[BLL-BISI-TRANS-21764-(9022.06)] 17 p2926 N85-26049
GLAUERT COEFFICIENT
U AERODYNAMIC FORCES
U MACH NUMBER
GLAZES
Evaluation of laterally loaded laminated glass units by theory and experiment
[PB85-111532/GAR] 09 p1300 N85-18188
Flame spread on combustible solar collector glazing materials
[DE85-002598] 11 p1595 N85-20032
Advanced glazings research
[DE85-000539] 11 p1674 N85-20549
Vertical solar louver project
[DE84-017335] 11 p1676 N85-20558
Improvements in glazings: SERI materials research in progress
[DE84-013049] 12 p1814 N85-21378
Laser sealed evacuated window glazings
[DE85-000512] 22 p3754 N85-33273
GLIDE ANGLES
U GLIDE PATHS
GLIDE LANDINGS
NT HORIZONTAL SPACECRAFT LANDING
Terminal control of gliding in atmosphere 06 p0777 N85-14968
GLIDE PATHS
Realistic localizer courses for aircraft instrument landing simulators
[NASA-CR-172333] 04 p0455 N85-12885
A cockpit-display concept for executing a multiple glide-slope approach for wake-vortex avoidance
[NASA-TP-2386] 08 p1085 N85-16869
Total energy-rate feedback for automatic glide-slope tracking during wind-shear penetration
[NASA-TP-2412] 14 p2226 N85-23801
Theoretical investigation of single-frequency 8-element localizer signal scattering for critical area determination
[FAA-PM-85-4] 20 p3391 N85-31097
GLIDE SLOPES
U GLIDE PATHS
GLIDERS
NT HANG GLIDERS
NT HYPERSONIC GLIDERS
Minimax optimal control in the reentry of a space glider 02 p0167 N85-11124
A comparison of Wortmann airfoil computer-generated lift and drag polars with flight and wind tunnel results
[NASA-TM-86035] 04 p0452 N85-12868
Initial sailplane project: The RP-1 04 p0468 N85-12976
Second sailplane project: The RP-2 04 p0468 N85-12977
The DG400 propulsed glider
[CEV/IS/SE/AV/84] 05 p0595 N85-13795
The design of high-performance gliders
[NASA-TM-77772] 14 p2217 N85-23750
Glider Nimbus 3-24.5. Partial certification test results for importation in the U category
[REPT-CEV/IS/SE/AV/84] 14 p2220 N85-23763
Parachute extraction device for ultralight gliders
[CH-643499-A5] 16 p2699 N85-26663
Three powered sailplanes as meteorological instrumentation for atmospheric boundary layer studies at DFVLR
[DFVLR-FB-84-50] 17 p2897 N85-27862
Proposals for the determination of necessary elevator handling characteristics of sailplanes in high speed range
[DFVLR-FB-84-52] 17 p2900 N85-27882
Flutter clearance of the Schweizer 1-36 deep-stall sailplane
[NASA-TM-85917] 22 p3729 N85-33118
Proceedings of Meteorological Motor Glider (MEMO) Workshop '84
[DFVLR-MITT-85-04] 24 p4121 N85-35542
Motor glider meteorology 24 p4121 N85-35543
Typical and historical aspects of motor gliders as meteorological measuring aircraft 24 p4121 N85-35544
A comparison between Falcon data and motor glider data 24 p4121 N85-35547
Environmental-physical measurements and determination of atmospheric turbulence with the ASK-16 motor glider 24 p4122 N85-35549
Partitioning of the vertical turbulent energy transport into positive and negative contributions — meteorology 24 p4122 N85-35551
Aircraft measurements during the Bonn Experiment (BONEX 1) — meteorology 24 p4122 N85-35552
Motor glider measurements during the Urban Atmosphere Energy Budget Experiment (EESA 1) 24 p4122 N85-35553
Meteorological measurements with motor gliders in Poland 24 p4122 N85-35555
GLIDING
Terminal control of gliding in atmosphere 06 p0777 N85-14968
The study of thermal forecasting for gliding 16 p2830 N85-27453
GLOBAL AIR POLLUTION
Integrated global background monitoring network
[DE84-016996] 04 p0532 N85-13396
Global model of transport of pollutants in atmosphere 19 p3297 N85-30439
The global sulfur cycle
[NASA-TM-87570] 21 p3858 N85-32710
GLOBAL AIR SAMPLING PROGRAM
GASP cloud- and particle-encounter statistics and their application to LFC aircraft studies. Volume 2: Appendixes
[NASA-TM-85835-VOL-2] 03 p0395 N85-12522
GLOBAL ATMOSPHERIC RESEARCH PROGRAM
Global Scale Atmospheric Processes Research Program Review
[NASA-CP-2344] 05 p0679 N85-14360
Observational-numerical study of maritime extratropical cyclones using FGGE data 05 p0685 N85-14400
Polar regions and climatic change
[PB84-237023] 05 p0688 N85-14421
Global scale diagnoses of FGGE data
[NASA-CR-174356] 09 p1356 N85-18533
A study of eddy-mean flow interactions using Eliassen-Palm diagnostics: FGGE SOP-1 data and the NASA GLAS general circulation model compared
[NASA-CR-175508] 11 p1686 N85-20604
The ARGOS contribution to the First GARP Global Experiment (FGGE) study of drifting buoys 14 p2325 N85-24371
Circulation statistics based on FGGE (First GARP Global Experiment) level 3-B analyses produced by GFDL (Geophysics Fluid Dynamics Laboratory)
[PB85-149316] 14 p2379 N85-24688
Characteristics of precipitation regimes during first global atmospheric research project global experiments
[AD-A151572] 15 p2599 N85-26021
Comparison of circulation statistics based on FGGE (First GARP Global Experiment) level 3-B analyses produced by GFDL (Geophysics Fluid Dynamics Laboratory) and ECMWF (European Centre for Medium Range Weather Forecasts) for special observing periods
[PB85-153948] 16 p2836 N85-27492
Experiments using atmospheric forcing from a FGGE analysis to drive an upper ocean model
[INPE-3503-PRE/738] 19 p3319 N85-30576
Generation of available potential energy and the energy cycle during the global weather experiment
[NASA-CR-175301] 21 p3634 N85-32572
GLOBAL POSITIONING SYSTEM
Global positioning system: Geodetic applications
[AD-A144904] 01 p0005 N85-10030
Autonomous navigation of USAF spacecraft 03 p0321 N85-12074
Time comparison with GPS technique and first results with the DFVLR C/A code receiver
[DFVLR-MITT-84-05] 05 p0595 N85-13794
NAVSTAR GPS (Global Positioning System) marine receiver performance analysis
[AD-A146414] 06 p0753 N85-14831
An interactive FORTRAN program for determining reliability of pseudo-range geodetic point positioning using the global positioning system
[AD-A147133] 07 p0988 N85-16275
Satellite navigation
[S-I-RG-99-856] 08 p1082 N85-16851
Installation options for the NAVSTAR global positioning system in surface ships
[AD-A148190] 08 p1082 N85-16856
Testing of a field portable GPS (Global Positioning System) geodetic receiver
[AD-A148396] 08 p1082 N85-16859
Using the global positioning system (GPS) phase observable for relative geodesy: Modeling, processing, and results 09 p1341 N85-18437
Transdigitizer for relaying signals from Global Positioning System (GPS) satellites
[AD-D011442] 10 p1422 N85-18970
Technical evaluation report on the 46th Symposium of the Avionics Panel on Space System Applications to Tactical Operations
[AGARD-AR-203] 10 p1425 N85-18986
Simulation of the performance of adaptively controlled Navstar antennas in battlefield scenarios 10 p1472 N85-19292
The Global Positioning System (GPS): Program status update 11 p1710 N85-20761
GPS system field testing 11 p1711 N85-20762
Potential impact of Navstar GPS on NATO tactical operations 11 p1711 N85-20763
Coverage and buildup of the Navstar constellation 11 p1711 N85-20764
Tactical applications of GPS user equipment 11 p1711 N85-20765
Program INNAVSAT: Global Positioning System (GPS): Test and demonstration program
[BMFT-FB-W-84-047] 12 p1775 N85-21145
Hybrid method of mapping and photogeodetic control network densification
[PB85-133775] 12 p1876 N85-21766
Accurate baseline determination by radio interferometry on NAVSTAR GPS satellite transmissions
[AD-A150681] 14 p2291 N85-24202
The TRANSIT and Global Positioning System (GPS) systems. Precision navigation and localization 14 p2398 N85-24777
Global positioning system: A modification to the baseline satellite constellation for improved geometric performance
[AD-A151692] 15 p2469 N85-25239
A replenishment phase study for the NAVSTAR global positioning system
[AD-A152030] 16 p2704 N85-26695
Analysis of orbit transfer vehicles for GPS Block 3 satellites
[AD-A152021] 16 p2732 N85-26860
Maintenance of time and frequency in the DSN using the global positioning system 16 p2771 N85-27105
Real-time position determinations using the GPS TI4100/GEOSTAR receiver
[AD-A152551] 17 p2894 N85-27845

Proceedings of the Fifteenth Annual Precise Time and Time Interval (PTTI) Applications and Planning Meeting
[AD-A149163] 17 p2961 N85-26287
International time comparison by a GPS timing receiver 17 p2962 N85-26293
First results of GPS time transfer to Australia 17 p2962 N85-26294
Separating the variances of noise components in the Global Positioning System
[AD-P004578] 17 p2963 N85-26295
Enhancements to the TTS-502 time transfer system 17 p2963 N85-26296
On-orbit frequency stability analysis of the GPS NAVSTAR's 3 and 4 rubidium clocks and NAVSTAR's 5 and 6 cesium clocks 17 p2963 N85-26298
CPS navigation experiment using high precision GPS timing receivers 17 p2963 N85-26299
The steering of GPS time 17 p2964 N85-26301
Test results for prototype GPS rubidium clocks 17 p2964 N85-26302
International time transfer and portable clock evaluation using GPS timing receivers: Preliminary results 17 p2964 N85-26303
Unattended TV time transfer results 17 p2964 N85-26305
The role of a low Earth orbiter in intercontinental time synchronization via GPS satellites 17 p2964 N85-26306
Review and evaluation of plans to incorporate NAVSTAR global positioning system user equipment on military sealift command ships
[AD-A153799] 18 p3060 N85-26934
On-orbit frequency stability analysis of the GPS NAVSTAR-1 quartz clock and the NAVSTARs-6 and -8 rubidium clocks 18 p3105 N85-29227
Rubidium and cesium frequency standards status and performance on the GPS program 18 p3106 N85-29228
Maintenance of time and frequency in the Jet Propulsion Laboratory's Deep Space Network using the Global Positioning System 18 p3109 N85-29249
Using GPS and VLSI technology to maintain 14 digit synchronization 18 p3109 N85-29250
A simplified GPS C/A reciever front end with low noise performance 18 p3109 N85-29251
Performance test results of a low cost GPS time and frequency monitor 18 p3109 N85-29252
Global positioning system carrier phase: Description and use
[PB85-174128] 19 p3216 N85-29946
Application of GPS in a high precision engineering survey network
[DE85-010556] 19 p3313 N85-30539
A study of the application of differential techniques to the global positioning system for a helicopter precision approach
[NASA-CR-177326] 20 p3391 N85-31035
The NAVSTAR Global Positioning System (GPS) receiver development program, phase 1
[BMFT-FB-W-85-002] 20 p3399 N85-31085
Time comparisons using the Global Positioning System (GPS). Method and first results obtained using the DFVLR C/A receiver
[ESA-TT-894] 20 p3460 N85-31490
The potential of the NAVSTAR global positioning system for the Corps of Engineers, civil works
[AD-A154913] 21 p3554 N85-32109
A derivation of relativistic effects in satellite tracking
[AD-A154620] 21 p3558 N85-32132

GLOBAL TRACKING NETWORK
The MEDOC 2: Experimental Doppler measurement of Earth kinematics 14 p2399 N85-24786
CPS navigation experiment using high precision GPS timing receivers 17 p2963 N85-26299

GLOBULAR CLUSTERS
Photoelectric photometry of globular cluster giants 01 p0128 N85-10884
Spectroscopic data for globular cluster giants. 1: Stars of the red giant tip 01 p0128 N85-10885
Fifth Conference on Star Clusters and Associations and Their Relation to the Evolution of the Galaxy
[PUBL-56] 05 p0736 N85-14732
The galactic distribution of open clusters of different ages and the angular velocity of the spiral structure 05 p0737 N85-14737
Binaries and evolution of globular clusters 05 p0738 N85-14744
Evolution of globular clusters 05 p0738 N85-14745
Evolution of globular clusters 05 p0738 N85-14746
Investigation of central parts of globular clusters, performed in Pulkovo 05 p0738 N85-14747
Brightness distribution in globular clusters derived by the narrow-slit scanning method 05 p0738 N85-14748
Lessons from the globular cluster NGC 5466 05 p0739 N85-14749
Galactic orbits of globular clusters 05 p0739 N85-14750
The fate of globular clusters 05 p0739 N85-14751

GLOBULES
Dark cloud and globule distribution for galactic longitudes 230 to 360 degrees 08 p0878 N85-15575
Star formation in globules 08 p1247 N85-17868

GLOBULINS
The influence of angiotensin on the maintenance of venous tone. The effect of Lower Body Negative Pressure (LBNP) and angiotensin blockade 05 p0693 N85-14457

GLOSSARIES
U DICTIONARIES

GLOTRAC (TRACKING NETWORK)
U GLOBAL TRACKING NETWORK

GLOW
U LUMINESCENCE

GLOW DISCHARGES
Analysis of glow discharges for understanding the process of film formation
[NASA-TM-83750] 01 p0022 N85-10136
Numerical investigation of characteristics of current flow for different methods of obtaining discharge in high speed lasers. Mechanism underlying current flow in positive glow discharge column 02 p0264 N85-11728
Glow discharge amorphous silicon tin alloys
[DE84-013001] 05 p0618 N85-13952
Nitriding of titanium and its alloys by N2, NH3 or mixtures of N2 + H2 in a dc arc plasma at low pressures (or = to torr)
[NASA-TM-83803] 06 p0814 N85-15168
Silent discharge carbon dioxide gas laser machining facility
[BLL-CTO-2267-(9091.9F)] 07 p0969 N85-16150
Evaluation of miniature vacuum ultraviolet lamps for stability and operating characteristics, Lyman-Alpha task
[NASA-CR-171345] 10 p1477 N85-19323
Program for controlling electrical measuring contact instrument on glow-discharge indicator panel 12 p1842 N85-21558
Frictional and structural characterization of ion-nitrided low and high chromium steels
[NASA-TM-86991] 13 p2098 N85-23085
Explosive emission cathode plasmas in intense relativistic electron beam diodes
[AD-A150689] 14 p2417 N85-24912
Spatial resolution of small particles in silane discharge
[AD-A150953] 14 p2423 N85-24948
Diagnostics of a glow discharge used to produce hydrogenated amorphous silicon films
[DE85-002914] 15 p2661 N85-26420
The structure of ion plated films in relation to coating properties
[NASA-TM-87055] 18 p3085 N85-29085
Influence of type of processing of AK4 alloy on its surface state and strength of bonding of plasma coatings 19 p3242 N85-30103
Characteristics of optogalvanic effect in media with inverse populations 21 p3693 N85-32944
Investigation of space-time structure of glow of laser plasma colliding with flat screen 21 p3693 N85-32947

GLUCOSE
Glucose tolerance in trained and untrained subjects during head-down tilt (6 deg) 05 p0693 N85-14461
Investigation of adaptive distinctions of mechanism of controlled glycemia in Macaca rhesus monkeys 12 p1902 N85-21946

GLUES
Long term durability of urea formaldehyde glued joints removed from Vampire aircraft
[AD-A149053] 10 p1424 N85-18985

GLUONS
Quark models of hadronic interactions
[DE84-013787] 04 p0561 N85-13570
Very high energy probes of the quark-gluon plasma
[DE84-016992] 09 p1392 N85-18763
Glueball candidates
[DE85-009627] 14 p2418 N85-24921
Resonances in photon-photon scattering
[DE85-004607] 14 p2419 N85-24928
Eleven lectures on the physics of the quark-gluon plasma
[DE85-004321] 15 p2662 N85-26431
Some comments on SSC physics
[DE85-008444] 18 p3179 N85-29712
A comprehensive study of pai meson production
[DE85-006094] 18 p3180 N85-29718
Quark structure of nuclei
[DE85-010781] 22 p3842 N85-33795
Detectors for relativistic nuclear collisions (report from the Fixed-Target Hadron Group) 24 p4148 N85-35701
Very high energy probes of the quark-gluon plasma 24 p4147 N85-35708
Propagation of cosmic rays through the atmosphere in the quark-gluon strings model 24 p4173 N85-35873
The phi-meson and Chiral-mass-meson production in heavy-ion collisions as potential probes of quark-gluon-plasma and Chiral symmetry transitions 24 p4175 N85-35884
Heavy flavours production in quark-gluon plasma formed in high energy nuclear reactions 24 p4175 N85-35886
A cosmic ray super high energy multicore family event. 2: Structure and fragmentation characteristics of the jets
[HE-3.4-2] 24 p4181 N85-35931
Peculiarities of gamma-quanta distribution at 20 TeV energy
[HE-3.7-10] 24 p4186 N85-35967
The maximum depth of shower with E sub 0 larger than 10(17) eV on average characteristics of EAS different components 24 p4188 N85-35981
Calculation of intensity of high energy muon groups observed deep underground
[HE-5.4-13] 24 p4208 N85-36123

GLUTAMATES
Response of amino acids in hindlimb muscles to recovery from hypogravity and unloading by tail-cast suspension
[NASA-CR-176183] 24 p4128 N85-35589
Response of rat hindlimb muscles to 12 hours recovery from tail-cast suspension
[NASA-CR-176182] 24 p4128 N85-35590

GLUTAMINE
Response of amino acids in hindlimb muscles to recovery from hypogravity and unloading by tail-cast suspension
[NASA-CR-176183] 24 p4128 N85-35589
Response of rat hindlimb muscles to 12 hours recovery from tail-cast suspension
[NASA-CR-176182] 24 p4128 N85-35590

GLUTATHIONE
Distribution and abundance of organic thiols 21 p3657 N85-32717
Glutathione in cyanobacteria 21 p3661 N85-32745

GLYCINE
Investigation of spectrum of human bile acids during 120-day antiorthostatic hypokinesia 22 p3821 N85-33674

GLYCOGENS
Possible mechanism for changes in glycogen metabolism in unloaded soleus muscle
[NASA-CR-176184] 24 p4127 N85-35588
Muscle protein and glycogen responses to recovery from hypogravity and unloading by tail-cast suspension
[NASA-CR-176181] 24 p4128 N85-35591

GLYCOLS
Investigation of bromine complexed hydrogen/bromine regenerative fuel cells for portable electric power
[AD-A146401] 06 p0833 N85-15300
Ionization energies of liquids from energy distribution, quantum yield and second derivative curves
[AD-A152210] 16 p2746 N85-26946
Stabilized unsaturated polyesters
[NASA-CASE-NPO-16103-1] 18 p3078 N85-29043
Threshold effects and cellular recognition
[DE85-010816] 19 p3327 N85-30614
Electron-donor dopant, method of improving conductivity of polymers by doping therewith, and a polymer so treated
[DE85-011640] 22 p3752 N85-33257

GNEISS
Concordant bands of augen gneiss within metasedimentary rocks in the Big Delta C-2 quadrangle, east-central Alaska 04 p0516 N85-13294
Conditions for formation of paragneisses containing kyanite-orthoclase in region of Mount Provender and Pratt Peak (Shackleton Range, Antarctica) 19 p3298 N85-30447
Dating Archean zircon by ion microprobe: New light on an old problem 21 p3722 N85-33094

GNOMONIC PROJECTION
Use of stereographic projection in marine geodesy 19 p3294 N85-30421

GOALS
Review of Space Shuttle requirements, operations, and future plans
[GPO-39-101] 04 p0461 N85-12927
Constituent properties and interrelationships 04 p0467 N85-12984
Broadening the debate 07 p0914 N85-15785
Toward a goal-oriented civilian space program 07 p0914 N85-15786
Summary of activities of Aeronautics and Space Engineering Board
[NASA-CR-174294] 08 p1228 N85-17729

High-technology ceramics in Japan
[PB85-125029] 12 p1815 N85-21389
National aeronautical R and D goals: Technology for America's future 19 p3379 N85-30964
Long-term goals for solar thermal technology
[DE85-013032] 22 p3809 N85-33597

GOBI DESERT
Measurements of the surface energy budget in the southern Gobi Desert of China, and in the Rocky Mountains of Colorado
[NASA-CR-175506] 12 p1888 N85-21847

GODDARD EXPERIMENT PACKAGE TELESCOPE
U PARTICLE TELESCOPES

GOERTLER INSTABILITY
Stability calculations of the two-dimensional boundary layer along a concave wall: Part 1: A numerical method of solution for the simultaneous ordinary differential equations governing disturbances
[NAL-TR-841] 15 p2554 N85-25758

GOES SATELLITES
NT GOES 5
Report of the First Session of the International Working Group on Data Management for the International Satellite Cloud Climatology Project (ISCCP)
[WCP-42] 01 p0073 N85-10483
Cloud cover sampling capability of various satellite combinations for ISCCP 01 p0073 N85-10484
ISCCP Cloud Algorithm Intercomparison Workshop 01 p0073 N85-10485
ISSCP Cloud Algorithm Intercomparison Workshop 01 p0073 N85-10486
Use of satellite soundings and imagery for nowcasting and very-short-range forecasting 01 p0076 N85-10504
NESDIS operational precipitation estimation techniques 01 p0076 N85-10505
Geostationary satellite cloud and precipitation analysis using an interactive computer system 01 p0076 N85-10506
A scheme for the delineation and extrapolation of thunderstorms from GOES satellite data 01 p0076 N85-10507
Convective scale weather analysis and forecasting
[NASA-CR-174185] 06 p0836 N85-15320
Solar-geophysical data number 476, June 1984. Part 2 (comprehensive reports): Data for December 1983 and miscellanea
[PB84-243161] 06 p0890 N85-15654
Geostationary Operational Environmental Satellite Data Collection System 14 p2328 N85-24393
Soil moisture and evapotranspiration estimates based on satellite data 15 p2596 N85-25998
New GOES satellite synchronized time code generation 18 p3109 N85-29247
A 406 MHz geostationary satellite SARSAT experiment 20 p3403 N85-31113
Rain volume estimation over areas using satellite and radar data
[NASA-CR-176050] 21 p3634 N85-32570

GOES 5
Test results from RAINSAT 01 p0076 N85-10508

GOGGLES
Some thoughts on the implementation of pilot night vision devices for helicopters 06 p0751 N85-14814
The effect of modified spectacles on the field of view of the helmet display unit of the integrated helmet and display sighting system
[AD-A148693] 09 p1261 N85-18055

GOLD
Ion chromatographic determination of gold in plating baths
[DE84-016187] 02 p0184 N85-11230
Influence of aluminum oxide film on thermocompression bonding of gold wire to evaporated aluminum film
[NASA-TM-77503] 03 p0330 N85-12127
Chemical derivatization of an array of three gold microelectrodes with polypyrrole: Fabrication of a molecule-based transistor
[AD-A146221] 03 p0359 N85-12304
Sputtering of gold irradiated with thermal neutrons 03 p0429 N85-12738
The adsorption of acrylonitrile at a gold electrode: An EMIRS measurement of the electrochemical stark effect
[AD-A148664] 08 p1123 N85-17082
Stability of amorphous metals on semiconductor substrates
[DE84-017256] 09 p1295 N85-18134
Lithography radiation effects study
[AD-A149552] 10 p1468 N85-19280
Relationship of gold content to gravity fields in Far East 10 p1501 N85-19475
Angle-resolved photoemission study of AuGa2 and AuIn2 intermetallic compounds
[AD-A150000] 12 p1940 N85-22183
A mixed-basis band structure interpolation scheme applied to the fluorite structure compounds NiSi2, AuAl2, AuGa2 and AuIn2
[AD-A150131] 12 p1940 N85-22187
High energy facilities advanced projects: Intrabeam scattering for a beam of gold ions
[DE85-000887] 12 p1941 N85-22192
Study of energy versus misorientation for grain boundaries in gold by crystallite rotation method. 1: 001 twist boundaries
[DE85-004586] 12 p1943 N85-22201
WRAP-RIB antenna technology development 14 p2231 N85-23824
Ligand structural influences upon electrochemical reactivity: Organic substituent effects upon Carboxylatopentaamminecobalt(3) reductions at mercury and gold electrodes
[AD-A150665] 14 p2250 N85-23944
Characterization of supported metal catalysts by imaging, microdiffraction and microanalysis techniques
[DE85-005567] 14 p2253 N85-23961
The effects of water and hydrogen on materials used in integrated circuit packages
[AD-A151893] 15 p2518 N85-25529
Current understanding of point defects and diffusion processes in silicon 20 p3481 N85-31632
Resistance of polyaniline films as a function of electrochemical potential and the fabrication of polyaniline-based microelectronic devices
[AD-A154999] 21 p3589 N85-32201
Multiple inner shell vacancies in laser-irradiated Au plasma 23 p3981 N85-34667
Elliptical X-ray analyzer spectrograph application to a laser-produced plasma
[DE85-013790] 24 p4097 N85-35396
Mineral deposit models: Theory and practice 24 p4105 N85-35448
Some recent deposit modeling efforts 24 p4106 N85-35453
The Conterminous United States Mineral Assessment Program 24 p4106 N85-35458
Stopping relativistic Xe, Ho, Au and U nuclei in nuclear emulsions 24 p4173 N85-35876

GOLD ALLOYS
Surface segregation of sulfur during oscillatory pin-on-plate wear studies of precious metal electrical contact alloys. 1: Friction and electrical contact resistance
[DE84-006962] 02 p0195 N85-11303
Critical evaluation of binary rare earth phase diagrams
[DE84-015057] 05 p0614 N85-13922
Surface physics and crystallography
[DE85-003128] 11 p1735 N85-20910
Atomistic studies of grain boundaries with segregated impurities
[DE85-000063] 11 p1737 N85-20924
Sputter-induced compositional modifications in a Ni-Au alloy
[DE85-002771] 12 p1807 N85-21333
Pulsed electrodeposition
[DE85-007057] 16 p2747 N85-26950
Studies of the crystallization process of aluminum-silicon alloys using a high temperature microscope
[NASA-TM-77869] 24 p4078 N85-35272

GOLD COATINGS
Impact ionization from gold, aluminum and PCB-Z — Giotto spacecraft paint PCB-Z 14 p2244 N85-23910

GOLD PLATE
U GOLD COATINGS

GONIOMETERS
NT PHOTOGONIOMETERS
Structural, morphological and optical characteristics of KGd(WO4)2 crystals 14 p2280 N85-24126
Investigation of errors of acoustic goniometer information-measurement systems on rocking base 14 p2283 N85-24139

GOODNESS OF FIT
Kolmogorov-Smirnov goodness-of-fit test: Corrected for use with EEG-like data
[AD-A144711] 01 p0110 N85-10745
Sequential minimization for sum of squares of unknown functions
[DE85-004162] 11 p1707 N85-20738
Tests of fit based on normalized spacings
[AD-A149749] 12 p1821 N85-22062
Identification of a mathematical model 1: Goodness of fit criterion
[HSE-TRANS-11109] 19 p3341 N85-30703
A guide to the statistical analysis of the results of linear and nonlinear least-squares data fitting
[NPL-DITC-63/84] 20 p3521 N85-31895

GORGES
U CANYONS

GOVERNMENT PROCUREMENT
Benefit value to the Air Force of the GIDEP (Government Industry Data Exchange Program) alert
[AD-A145470] 02 p0292 N85-11897
System engineering and integration contract for implementation of the National Airspace System plan, volume 1, sections 1.0-4.0, 6.0
[AD-A145793] 03 p0317 N85-12048
Introduction to software packages
[PB84-217843] 06 p0856 N85-15441
Survey relating to the implementation of cost/schedule control systems criteria within the Department of Defense and industry
[AD-A146664] 06 p0870 N85-15526
A buyer's guide to space infrastructure 07 p0914 N85-15784
Synopsis of the OTA Workshop on Cost Containment of Civilian Infrastructure (Civilian Space Station) Elements 07 p0915 N85-15790
An evaluation of the effect of establishing a minimum Economic Order Quantity (EOQ) on the Air Force EOQ item management system
[AD-A147121] 07 p1051 N85-16673
Evaluation of the effectiveness of the weighted guidelines to induce contractor's investment in cost reducing facilities equipment
[AD-A147586] 07 p1053 N85-16681
An analysis of production competition and award methodology
[AD-A147775] 08 p1226 N85-17733
Excessive Air Force inventories result from duplicative spare parts requirements
[AD-A147777] 08 p1226 N85-17734
Cost-plus-percentage-of-costs in government contracts
[AD-A147779] 08 p1226 N85-17735
Prototype concept design for US Army type 3A Air Traffic Control Tower (ATCT)
[AD-A148840] 09 p1284 N85-18070
Program manager: The Journal of the Defense Systems Management College. Volume 13, Number 6, November-December 1984
[AD-A149548] 11 p1739 N85-20933
Copyright law, computer software, and government acquisition
[AD-A150347] 13 p2168 N85-23453
Life cycle costing in government procurement
[AD-A151878] 15 p2666 N85-26456
Navy program manager's guide, 1985 edition
[AD-A151925] 16 p2676 N85-27744
Automation of the reporting and tracking requirements of architect-engineering type contracts
[AD-A152218] 16 p2676 N85-27745
Cost savings from multiyear contracting
[AD-A153564] 18 p3197 N85-29634
Overhead management guide for aerospace procurements
[AD-A153626] 18 p3198 N85-29635
Capital investment motivational techniques used by prime contractors on subcontractors
[AD-A153660] 18 p3198 N85-29637
Using incentives to improve maintainability
[AD-A153792] 18 p3199 N85-29641
The evolution of the U.S. helicopter industry
[AD-A154290] 19 p3211 N85-29913
Civilian Space Stations and the US future in Space
[OTA-STI-242] 20 p3418 N85-31215
Feasibility of applications of Competition Decision Assist Package (CDAP) to spare parts
[AD-A154716] 21 p3712 N85-33038

GOVERNMENT/INDUSTRY RELATIONS
Second Symposium on Space Industrialization — space commercialization
[NASA-CP-2313] 02 p0149 N85-11011
Non-US approaches to space commercialization 02 p0150 N85-11012
Legal considerations and cooperative opportunities for space commercial activities 02 p0150 N85-11013
Land remote sensing commercialization: A status report 02 p0151 N85-11024
Comments on the commercialization of expendable launch vehicles 02 p0153 N85-11034
Concept for a commercial space station laboratory 02 p0153 N85-11035
Commercial space services 02 p0153 N85-11039
Space commercialization: Analysis of R and D investments with long time horizons 02 p0155 N85-11052
Doing business in space: How to get there from here 02 p0156 N85-11057
Contracting for computer software development: Serious problems require management attention to avoid wasting additional millions
[FGMSD-80-4] 02 p0241 N85-11567
Land Remote-Sensing Commercialization Act
[S-REPT-98-458] 06 p0854 N85-14201

Financing considerations and Federal budget impacts
07 p0915 N85-15792
A weapon system design approach to diagnostics
08 p1066 N85-16752
GIDEP representative interaction
[DE84-016792] 09 p1401 N85-18820
Activities report in aerospace in West Germany
[ISSN-0070-3966] 09 p1418 N85-18947
Electric-Hybrid Vehicle (E-HV) demonstration-test project
[DE85-002370] 10 p1570 N85-19899
1984 science and technology posture hearing with the director of the Office of Science and Technology Policy
[GPO-41-060] 12 p1949 N85-22244
Transfer of technology
[S-REPT-98-664] 12 p1949 N85-22246
Status of the U.K. N.D.T. industry today
14 p2316 N85-24309
Financial, economic commentary on Airbus, European aviation
15 p2536 N85-25649
Criteria for qualifying for FRG federal CAD/CAM subsidies
15 p2536 N85-25651
Biotechnology in Japan
[PB85-169484] 15 p2615 N85-26113
The evolution of the U.S. helicopter industry
[AD-A154290] 19 p3211 N85-29913

GOVERNMENTS
Major institutional arrangements affecting ground water in New York state
[PB84-202508] 01 p0065 N85-10429
Lagging development of biotechnology described
01 p0115 N85-10787
International cooperation and competition in space
[GPO-38-001] 02 p0295 N85-11911
Statement of Otho E. Eskin, Director, Office of Advanced Technology, Department of State
02 p0295 N85-11914
Statement of John H. McElroy, Assistant Administrator for Environmental Satellite, Data and Information Services, National Oceanic and Atmospheric Administration
02 p0295 N85-11915
NESDIS international activities, appendix 2
02 p0295 N85-11917
Ways to improve management of Federal funded computerized models
[LCD-75-111] 03 p0435 N85-12771
Federal Telecommunications Privacy Act of 1984
[H-REPT-98-815] 03 p0441 N85-12807
International comparative study of systems for the government advancement of research and development
[NASA-TM-77589] 04 p0578 N85-13699
Area handbook series. Honduras: A country study
[AD-A146510] 06 p0827 N85-15253
Toward an improved FIPS cost-benefit methodology. Phase 2: Descriptive models, general purpose application software development and maintenance
[PB84-226943] 06 p0870 N85-15527
Publications of the Executive Office of the President: January 20, 1981 - June 30, 1984
[PB84-230671] 06 p0871 N85-15533
Government contract contingent liabilities. The anti-deficiency act, and the hobgoblin of little minds
[AD-A147910] 07 p1053 N85-16684
Provision of Federal government publication in electronic format to depository libraries
[S-PRT-98-260] 10 p1567 N85-19880
Organizations as information processing systems. Toward a strategic contingencies model of budget related influence in municipal government organizations
[AD-A149364] 10 p1567 N85-19883
Airport bird hazards associated with solid waste disposal facilities
[AD-P004107] 11 p1581 N85-19964
The FAA grant-in-aid assurances: FAR part 139, and airport hazards
[AD-P004209] 11 p1583 N85-19976
Oversight review of the five-year outlook report on science and technology
[GPO-41-058] 12 p1949 N85-22243
1984 science and technology posture hearing with the director of the Office of Science and Technology Policy
[GPO-41-060] 12 p1949 N85-22244
A 5-year research plan, 1985-1990. Wind energy technology: Generating power from the wind
[DE85-008427] 17 p2987 N85-28463
U.S.-China conference on science policy
[PB86-176345] 19 p3360 N85-30971
Methodology for assessing benefits and costs of government information collection
[DE85-010584] 19 p3361 N85-30975

GOVERNORS
U SPEED REGULATORS

GRABENS
U GEOLOGICAL FAULTS

GRADIENT INDEX OPTICS
Supersonic missile seeker lens system using gradient index material for first element lens
[AD-A151476] 15 p2490 N85-25367

GRADIENTS
NT ELECTRON DENSITY PROFILES
NT POTENTIAL GRADIENTS
NT PRESSURE GRADIENTS
NT TEMPERATURE GRADIENTS
NT THERMOCLINES
A trivariate Clough-Tocher scheme for tetrahedral data
[AD-A144740] 01 p0111 N85-10751
Solar pond overview
05 p0667 N85-14287
Summary of salt gradient solar pond research
05 p0667 N85-14292
Doubly diffusive linear stability with nonconstant gradients
[DE84-013008] 05 p0670 N85-14310
Modeling localized stress fields in composite laminates
[AD-A148630] 08 p1120 N85-17056
Measurement of the vertical gradient of the semidiurnal tidal wind phase in winter at the 95 km level
11 p1682 N85-20478
Rotating squid magnetometers and gradiometers
[AD-D011529] 12 p1849 N85-21600
Determining object orientation from a single image using multiple information sources
[AD-A149960] 12 p1933 N85-22146
Edge detection in SAR imagery using gradient operators --- synthetic aperture radar (SAR)
[AD-A149411] 13 p2054 N85-22862
Method for processing broad-profile data
13 p2117 N85-23185
Alternating gradient synchrotron
[DE85-005950] 17 p3033 N85-28759
3d calculations of a fixed field alternating gradient synchrotron magnet
[DE85-002742] 18 p3183 N85-29739
Electron trajectories in a combined wiggler and alternating gradient quadrupole field
[DE85-010727] 22 p3842 N85-33794
Differential measurement of cosmic-ray gradient with respect to interplanetary current sheet
[SH-4.2-9] 23 p4007 N85-34847
Determination of galactic cosmic ray latitudinal gradient using Earth based detectors
[SH-4.2-13] 23 p4008 N85-34851
The expected cosmic ray density and stream distributions at the heliolatitudinal asymmetry of solar wind
[SH-4.2-14] 23 p4008 N85-34852
Latitudinal gradients of cosmic rays and the polarity reversal of the heliospheric magnetic field: A preliminary evaluation
[SH-4.2-16] 23 p4008 N85-34853
The dependence of solar modulation on the sign of the cosmic ray particle charge
[SH-4.2-23] 23 p4009 N85-34860
Voyager 1 and 2 measurements of radial and latitudinal cosmic ray gradients during 1981 - 1984
[SH-4.7-6] 23 p4041 N85-35051

GRADIOMETERS
U MAGNETOMETERS

GRADUATION
U CALIBRATING

GRAFTING
Low temperature synthesis of polycaproamide copolymers grafted with polydimethylaminothylmethacrylate
06 p0761 N85-14868

GRAIN BOUNDARIES
Granular boundary segregation in low-alloyed titanium-vanadium alloys
01 p0019 N85-10117
Process Research of Polycrystalline Silicon Material (PROPSM)
[NASA-CR-173838] 01 p0067 N85-10446
Swaged Mo-5 percent W alloy and recrystallized commercially pure molybdenum
02 p0180 N85-11208
Diffusion of Cr-51 tracer in Cr-2O-3 and the growth of Cr-2O-3 films
[AERE-R-11314] 03 p0333 N85-12146
Thermal ageing studies of 9%Cr 1%Mo steel
[AERE-R-11109] 03 p0333 N85-12149
Analysis techniques for tracer studies of oxidation
[NASA-CR-174796] 03 p0336 N85-12162
Structure of two-phase titanium alloys with different microstructures
03 p0351 N85-12257
Transport processes during the growth of oxide films at elevated temperature
[AERE-R-11293] 03 p0434 N85-12766
Ion contrasting chamber for discrimination of grains and textures
[BMFT-FB-T-84-151] 04 p0477 N85-13036
Structure and properties of grain boundaries
[DE84-014968] 04 p0570 N85-13636
Flux-line pinning by the grain boundary in niobium bicrystals
[DE84-016668] 04 p0570 N85-13638
The influence of manganese on intercrystaline internal adsorption of arsenic in low carbon steel
[BLL-M-35965-(5828.4)] 05 p0615 N85-13931
Process Research On Polycrystalline Silicon Material (PROPSM)
[DE84-015276] 08 p0830 N85-15276
Grain boundary structure in NIO
[DE84-016242] 08 p0868 N85-15519
Characterization of bicrystal grain boundary properties using device structures
[DE84-004509] 08 p0869 N85-15523
Design of ordered intermetallic alloys for high-temperature structural use
[DE85-000897] 07 p0928 N85-15865
Grain refining and microstructural modification during solidification
[AD-A147705] 08 p1128 N85-17111
Hydrogen embrittlement of nickel
[AD-A148322] 08 p1129 N85-17119
In-situ formation of a grain boundary in field ion microscopy using a laser
[AD-A148225] 08 p1166 N85-17355
Sub-eutectic densification and second phase formation in Al2O3 - CaO
[DE85-002065] 09 p1398 N85-18796
High temperature properties of equiatomic FeAl with ternary additions
[NASA-TM-86938] 10 p1439 N85-19072
Comparisons between computed and observed grain boundary structures and properties in metals
[DE85-002596] 10 p1442 N85-19085
Investigation of vanadium solid solution and zeta phase regions of vanadium-carbon system
[DE85-002678] 11 p1605 N85-20092
Contributions of segregated phosphorus to the intergranular stress corrosion cracking of nickel
[DE85-003112] 11 p1606 N85-20099
Computer simulation of grain-boundary properties in ionic crystals and metals
[DE85-000577] 11 p1734 N85-20908
Atomistic studies of grain boundaries with segregated impurities
[DE85-000063] 11 p1737 N85-20924
Effects of scatterer spacing statistics on ultrasonic backscatter signal spectra
[DE85-003259] 12 p1928 N85-22114
Study of energy versus misorientation for grain boundaries in gold by crystallite rotation method. 1: 001 twist boundaries
[DE85-004596] 12 p1943 N85-22201
Micromechanical modeling of microstructural damage in creeping alloys
[DE85-003925] 13 p2022 N85-22671
Grain boundaries in NIO
[DE85-006129] 13 p2025 N85-22687
Dependence of superplastic flow on state of grain boundaries
13 p2025 N85-22689
Drift fields and boundary conditions at grain boundaries in bipolar P/N junction silicon devices
13 p2062 N85-22879
Investigation of the effect of annealing on the dislocation and sub-grain boundary content of solvent-evaporation-grown CdTe
[AD-A144067] 13 p2162 N85-23415
Relationship between symmetrical tilt, twist, epecial, and favored grain boundaries
[DE85-004024] 14 p2429 N85-24982
Structural unit/grain boundary dislocation model for twist boundaries in cubic crystals
[DE85-000425] 14 p2430 N85-24985
Superplasticity in a thermo-mechanically processed Aluminum-10.2%Mg-0.52%Mn alloy
[AD-A152016] 15 p2510 N85-25485
Variation in the spacing of dislocations in subgrain boundaries with creep strain in Type 304 stainless steel
[DE85-006184] 15 p2511 N85-25493
Structure of condensed aluminum thin film metallizations
15 p2512 N85-25501
Approximate closed-form expression for the electron-scattering-induced interaction between magnetic flux lines and grain boundaries
[DE85-004699] 15 p2660 N85-26417
Grain boundary composition and intergranular fracture of steels. Volume 1: Detection of grain boundary segregation in steels
[DE85-006850] 15 p2662 N85-26426
Tilt grain boundaries in NIO
[DE85-006839] 16 p2751 N85-26978
Electrons and grain boundary energies in metals
[DE85-009530] 17 p2932 N85-28099
Interfacial segregation and fracture
[DE85-009779] 18 p3075 N85-29019

Quantitative analysis of defects in silicon-characterization of UCP, HAMCO, and microcrystalline material
[NASA-CR-175988] 16 p3079 N85-29046
Effects of annealing treatments on superplasticity in a thermomechanically processed Aluminum-10.2%Mg-0.52%Mn
[AD-A154414] 19 p3239 N85-30060
State variable theories based on Hart's formulation
[DE85-009474] 19 p3239 N85-30082
Structural defects in crystalline silicon
20 p3481 N85-31630
The effect of stress and hot corrosion on nickel-base superalloys
[AD-A154722] 21 p3566 N85-32181
The effect of diffusive hydrogen segregation on fracture of polycrystalline nickel
[AD-A155238] 21 p3567 N85-32186
Influence of particle arrangement on sintering
[AD-A155337] 21 p3599 N85-32352
Electrotransport in thin films
[AD-A155584] 21 p3710 N85-33034
Electronic phenomena near semiconductor grain boundaries
[DE85-011543] 21 p3711 N85-33035
An enhanced photoresponse at dislocation subgrain boundaries revealed by X-ray topography of polysilicon solar cells 22 p3806 N85-33572
Investigation of the microstructure and photovoltaic properties of semicrystalline silicon
22 p3806 N85-33573
High resolution electron microscopic characterization of interfaces in ceramics
[DE85-011207] 23 p3920 N85-34289
Grain boundary and surface diffusion in oxide systems
[DE85-007291] 23 p3985 N85-34715

GRAIN SIZE
Structural recrystallization in titanium
03 p0351 N85-12258
Dependance of microplasticity of beryllium on grain size and heat treatment 03 p0353 N85-12273
Center for dielectric studies
[AD-A146183] 03 p0434 N85-12761
Microstructure, texture and formability of thin aluminium sheets 06 p0796 N85-15088
The role of microstructure in the modelling of plastic flow in P/M superalloys at forging temperatures and strain rate 06 p0796 N85-15090
Grainsize evolution and differential comminution in an experimental regolith 06 p0888 N85-15638
Influence of grain size distribution on the undrained dynamic properties of saturated sand
[PB85-102382/GAR] 09 p1305 N85-18197
Mechanical stabilization of austenite against epsilon martensite and its effect on deformation behavior in high manganese steels
[DE85-007654] 17 p2932 N85-28097
Electrohydrodynamic process for the production of large area polycrystalline silicon sheet
[DE85-008781] 19 p3261 N85-30225
Modification of the grain size of sputtered copper with additions of oxygen, krypton, silver, or yttrium
[DE85-010975] 21 p3567 N85-32189
Nonequilibrium kinetics of growth of oxide layer grains during laser heating of metals in air
21 p3689 N85-32919
Influence of technology of atomization of naturally alloyed iron on grain-size characteristics of powder material
[BLL-M-35810-(5828.4)] 23 p3914 N85-34257

GRAINS
Electron channeling and EBIC studies of polycrystalline silicon sheets
[DE84-004515] 05 p0670 N85-14309
Solar wind and cosmic ray irradiation of grains and ices - application to erosion and synthesis of organic compounds in the solar system
06 p0888 N85-15637

GRAINS (FOOD)
NT BARLEY
NT CORN
NT OATS
NT RICE
NT WHEAT
Determination of the conservation state of long conservation agricultural products by means of capacitive sensors
[NOTA-INTERNA-799] 02 p0220 N85-11447
Alcohol fuel from Ohio farms: An introduction
[TI-84-901290] 05 p0821 N85-13970
Crop yield forecasting 07 p1001 N85-16360
Operational performance of the photovoltaic-powered grain mill and water pump at Tangaye, Burkina Faso (formerly Upper Volta)
[NASA-TM-86970] 13 p2128 N85-23243
Gravity perception and response in shoot of cereal grasses 15 p2611 N85-26091

GRAMMARS
Information-theoretic properties of languages and their grammars
[AD-A146688] 06 p0799 N85-15106
Speech analysis by parametric methods: A survey
[ENST-84C004] 09 p1313 N85-18251
Research on knowledge delivery
[AD-A149565] 10 p1536 N85-19698
An algorithm for generating abstract syntax trees
[NASA-CR-172541] 12 p1912 N85-22003
Construction of a menu-based system
[NASA-CR-172560] 13 p2148 N85-23321
Language design, computers and brains
[AD-A152819] 17 p3008 N85-28594
Polyith: The early goals
[DE85-012534] 24 p4139 N85-35658

GRANITE
Contribution to the radiogeology of Sao Roque, SP, granites
[INPE-3079-PRE/492] 03 p0391 N85-12503
Geology and geochemical evolution of the Lost River, Alaska, tin deposit 04 p0533 N85-13406
Geology, petrology, and tectonic setting of the Mafic rocks of the 1480 Ma old granite-rhyolite terrane of Missouri, USA 05 p0674 N85-14327
Alabama Tin Belt: Metallogenesis and mineral resource evaluation. Year-end report
[DE84-901335] 07 p0989 N85-16283
Creep deformation of compacted decomposed granite soils 09 p1303 N85-18187

GRANTS
National Science Foundation grants and awards for fiscal year 1983, volume 2
[PB84-212323] 01 p0125 N85-10854
A research in support of NASA's space science
[NASA-CR-174267] 08 p1227 N85-17726
Small business innovation research: Abstracts of 1984. Phase 1 awards
[NASA-TM-87427] 13 p2165 N85-23431

GRANULAR MATERIALS
Weak shocks and steady waves in a nonlinear elastic rod or granular material
[AD-A145715] 02 p0209 N85-11383
Influence of inter-layer effect on charge gas-permeability
[BLL-M-35919-(5828.4)] 05 p0816 N85-13940
Atmospheric heating of meteorites: Results from nuclear track studies 06 p0882 N85-15607
Carbon granule probe microphone for leak detection — recovery boilers
[NASA-CASE-NPO-16027-1] 12 p1849 N85-21597
Large-size fine-granular graphite for solar techniques
12 p1878 N85-21780
Effect of annealing procedures on structure and properties of VT6 alloy with initial large-grained structure
15 p2498 N85-25410
The Jovian ring 15 p2672 N85-26492
Voyager planetary radio astronomy: Grain and particle impacts shot noise in Saturn's ring plane
15 p2673 N85-26498
Single-pulse Raman and photoacoustic spectroscopy studies of Triaminotrinitrobenzene (TATB) and related compounds
[DE85-010072] 18 p3084 N85-29078
Granular Flow Project
[DE85-010015] 19 p3270 N85-30279
Effect of nonuniform size on internal stresses in a rapid, simple shear flow of granular materials. Part 1: Two grain sizes
[AD-A154045] 19 p3285 N85-30372
Effect of nonuniform size on internal stresses in a rapid, simple shear flow of granular materials. Part 2: Multiple grain sizes
[AD-A154046] 19 p3285 N85-30373
Flow characteristics of the Cascade granular blanket
[DE85-010932] 20 p3420 N85-31227
Modeling granular explosive detonations with shear band concepts
[DE85-011823] 22 p3754 N85-33271

GRAPH THEORY
A comparative evaluation of algorithms for generalized network problems
[TWISK-289] 01 p0107 N85-10721
New labeling procedures for the basis graph in generalized networks
[AD-A146217] 03 p0407 N85-12601
On the formal development of graph theoretical algorithms by transformation
[TUM-I8403] 04 p0553 N85-13522
The traveling salesman problem on a graph and some related integer polyhedra
[AD-A147953] 08 p1211 N85-17621
Some facets of the tri-index assignment polytope
[AD-A149195] 10 p1547 N85-19753
On large matchings and cycles in sparse random graphs
[AD-A149194] 10 p1550 N85-19778
On matchings and Hamiltonian cycles in random graphs
[AD-A151015] 14 p2409 N85-24851
Generalized graph coloring: A frequency assignment method for VHF broadcasting
[TUM-M8405] 16 p2844 N85-27535
Embedding graphs in lines, trees and grids
19 p3334 N85-30652
Graph-theoretical exorcism
[DE85-011918] 23 p3955 N85-34512
A graph theoretic procedure for the design of feedback patterns
[REPT-110] 24 p4142 N85-35673
Design of dynamic compensators of prescribed pattern
[BU-109] 24 p4142 N85-35674

GRAPHIC ARTS
Description of a data matrix structure and model diagnosis by means of row and column Euclidean maps
02 p0211 N85-11392
Application of correspondence analysis to meteorological data 02 p0211 N85-11393
Representing multidimensional systems using visual displays 05 p0711 N85-14560
Television animation store: Recording pictures on a parallel transfer magnetic disc
[BBC-RD-1984/17] 10 p1462 N85-19220
Draftsman displays: A graphical technique for exploratory data analysis
[AD-A150515] 13 p2041 N85-22775
Digital laser platemaker modifications
[AD-A150190] 13 p2096 N85-23074
Image synthesis: Optical identity or pictorial communication? 23 p3963 N85-34565

GRAPHIC EVALUATION AND REVIEW TECHNIQUES
U GERT

GRAPHITE
NT PYROLYTIC GRAPHITE
Dynamics of graphite fiber intercalation: In situ resistivity measurements with a four point probe
[NASA-TM-86858] 01 p0017 N85-10105
Stability of bromine intercalated graphite fibers
[NASA-TM-86859] 01 p0031 N85-10187
Preparation and properties of evaporated CdTe films compared with single crystal CdTe
[DE85-000502] 02 p0222 N85-11452
Fundamental electronic properties of donor-type graphite intercalated compounds
[AD-A146148] 03 p0326 N85-12099
Influence of test method and material stiffness on the damage produced by low velocity impacts on carbon-epoxy composites No. 45.387/1
[REPT-45.387/1] 03 p0326 N85-12100
Matrix resin characterization in cured graphite composites using diffuse reflectance-FTIR
04 p0466 N85-12959
Thermal contact conductance measurements on Doublet 3 armor tile graphite
[DE84-013554] 05 p0613 N85-13916
Metallographic evaluation of the reactions between boronated graphite and Fe-Ni-Cr alloys
[DE84-015374] 06 p0789 N85-14922
Development of intercalated wire and cable
[AD-A146502] 06 p0774 N85-14949
An investigation of the electrical conductivity in highly oriented graphite intercalation compounds
[AD-A146539] 06 p0804 N85-15116
Experimental test program for evaluation of solid lubricant coating as applied to compliant foil gas bearings to 315 deg C
[NASA-CR-174837] 07 p0930 N85-15895
The 13C nuclear magnetic resonance in graphite intercalation compounds
[NASA-CR-174261] 07 p1040 N85-16801
Structure-property relationships in intercalated graphite
[AD-A147949] 08 p1219 N85-17680
Electronic properties of intercalated graphite and amorphous metals
[AD-A147664] 08 p1225 N85-17716
The fabrication, processing and characterization of multidimensionally braided graphite/epoxy composite materials
[AD-A148720] 09 p1288 N85-18090
Tribological properties of graphite-fiber-reinforced, partially fluorinated polyimide composites
[NASA-TM-86926] 09 p1298 N85-18153
Compositional, structural, and physical studies of some graphite hexafluoroarsenates and their relatives
[DE85-000855] 10 p1432 N85-19030
Method of determining thermal stability of heat-resistant coatings on graphite 10 p1447 N85-19117

Electron oxidation of graphite by fluorospecies
[DE85-001196] 11 p1595 N85-20034
Effect of macrostructure on durability of polycrystalline graphite 11 p1605 N85-20091
Investigation of electric and magnetic properties of intercalated graphite
[AD-A149601] 12 p1797 N85-21274
Electric and magnetic properties of intercalated graphite
[AD-A149848] 12 p1798 N85-21276
Fine-grained, isotropic graphite for use as NBS (National Bureau of Standards) thermophysical property RM's from 5 to 2500 K
[PB85-112886] 12 p1814 N85-21361
Large-size fine-granular graphite for solar techniques 12 p1878 N85-21780
Sound velocity of carbon at high pressures
[DE85-002016] 12 p1926 N85-22113
Neutron scattering studies of graphite intercalation compounds
[DE85-003079] 12 p1942 N85-22196
Silicon carbide-silicon nitride fibers: Preparation and characterization of polycarbosilazane precursors 12 p1945 N85-22214
Experimental study of enthalpy of quasimonocrystal of graphite and carbon glass in temperature range of 2890-3618 deg K 13 p2036 N85-22751
High-temperature X-ray diffraction study of coating-substrate compatibility in yttria-coated graphite
[DE85-005916] 14 p2262 N85-24016
Homogeneity of pristine and bromine intercalated graphite fibers
[NASA-TM-87016] 15 p2517 N85-25521
Carbon isotopes in bulk carbonaceous chondrites 15 p2551 N85-25557
Graphite fiber intercalation: Dynamics of the bromine intercalation process
[NASA-TM-87015] 16 p2742 N85-26921
NASA/aircraft industry standard specification for graphite fiber toughened thermoset resin composite material
[NASA-RP-1142] 16 p2742 N85-26923
Microscopic study of the influence of impurities on interface bonding
[AD-A151725] 16 p2743 N85-26928
Environmental stability of intercalated graphite fibers
[NASA-TM-87025] 16 p2753 N85-26992
Effects of the cooling rate on the structure of the graphite in inoculated irons
[BLL-BISI-TRANS-22305-(9022.06)] 17 p2930 N85-28083
A micrographic and gravimetric study of intercalation and deintercalation of graphite fibers
[NASA-TM-87026] 17 p2934 N85-28110
Bifunctional oxygen electrodes
[DE85-008671] 17 p2955 N85-28248
Light weight fire resistant graphite composites
[NASA-CASE-ARC-11615-1-SB] 18 p3068 N85-29976
Mechanism of the catalytic gasification and reactivity of graphite
[DE85-009932] 19 p3229 N85-30020
Polymer matrix and graphite fiber interface study
[NASA-CR-177357] 19 p3232 N85-30036
USSR report: Materials Science and Metallurgy
[JPRS-UMS-85-005] 19 p3241 N85-30095
New form of graphite 19 p3243 N85-30111
Thermodynamics of high temperature materials
[AD-A154299] 19 p3378 N85-30958
Long-term thermal aging of Celion/V378A composite materials
[NASA-TM-86362] 20 p3421 N85-31236
Electrical and mechanical properties of intercalated graphite fibers
[AD-A155560] 21 p3570 N85-32205
Paired ion chamber constants for fission gamma-neutron fields
[AD-A155089] 21 p3702 N85-32999
Multistage spent particle collector and a method for making same
[NASA-CASE-LEW-13914-1] 22 p3791 N85-33489
Oxidation resistant slurry coating for carbon-based materials
[NASA-CASE-LEW-13923-1] 24 p4077 N85-35267
Applications of the mineral resources data system and the international strategic minerals inventory in mineral-resource assessments by region and commodity 24 p4105 N85-35451

GRAPHITE-EPOXY COMPOSITES
Distributions of fatigue life and fatigue strength in notched specimens of a carbon 8-harness-satin laminate
[NAL-TR-909T] 01 p0061 N85-10407
Advanced composite stabilizer for Boeing 737 aircraft
[NASA-CR-168451] 02 p0137 N85-10934
Deformation measurements of composite multi-span beam shear specimens by Moire interferometry
[NASA-CR-3844] 02 p0169 N85-11135
Fracture toughness of fibrous composite materials
[NASA-TP-2370] 02 p0170 N85-11136
The influence of sublaminate cracks on the tension fatigue behavior of a graphite epoxy laminate
[FFA-TN-1984-32] 02 p0210 N85-11386
Accelerated viscoelastic characterization of T300/5208 graphite-epoxy laminates 03 p0325 N85-12091
Study of delamination cracking under static and cyclic loads of carbon-epoxy composite materials
[REPT-42-727/F] 03 p0327 N85-12102
Effect of impact damage and open holes on the compression strength of tough resin/high strain fiber laminates 04 p0464 N85-12945
Investigation of toughened neat resins and their relations to advanced composite mechanical properties 04 p0464 N85-12949
Composite structural materials
[NASA-CR-174077] 04 p0467 N85-12966
Fatigue in composite materials 04 p0467 N85-12968
Experimental and theoretical studies of moisture and temperature effects on the mechanical properties of graphite/epoxy laminates and neat resins 04 p0467 N85-12969
Free-edge failures of composite laminates 04 p0467 N85-12971
Quantification of Saint-Venant's principle for a general prismatic member 04 p0467 N85-12972
Test report no. 17.206: Statistics of the basic characteristics of carbon-epoxy composites
[DGT-23.426/A] 04 p0466 N85-12979
Influence of relaxation on the mechanical characteristics of a carbon-epoxy composite. Report no. 45.427/1 04 p0466 N85-12980
Polyimide resin characteristics, test
[DGT-24.322] 04 p0479 N85-13049
The dimensional stability of advanced composite antenna reflectors: Analytical and test evaluation — satellite antennas 05 p0626 N85-14014
Passive Orbital Disconnect Strut (PODS 3) structural test program
[NASA-CR-177325] 08 p1113 N85-17020
Effects of high energy radiation on the mechanical properties of epoxy-graphite fiber reinforced composites
[NASA-CR-174314] 08 p1118 N85-17047
Flight service evaluation of advanced composite ailerons on the L-1011 transport aircraft
[NASA-CR-172483] 08 p1118 N85-17049
Contact behavior, impact response and damage in graphite-epoxy laminates subjected to initial stresses 08 p1171 N85-17366
Delamination growth in graphite epoxy laminates under compressive loads 09 p1288 N85-18088
The fabrication, processing and characterization of multidimensionally braided graphite/epoxy composite materials
[AD-A148729] 09 p1288 N85-18090
Simulation of repetitively-pulsed laser irradiation of graphite-epoxy composite
[AD-A148698] 09 p1325 N85-18329
Verification and application of the Iosipescu shear test method
[NASA-CR-174346] 09 p1333 N85-18376
Evaluation of failure criterion for graphite/epoxy fabric laminates
[NASA-CR-172547] 10 p1431 N85-19025
Preliminary report on tests of tensile specimens with a part-through surface notch for a filament wound graphite/epoxy material
[NASA-CR-172545] 10 p1431 N85-19026
Evaluation and prediction of long-term environmental effects of nonmetallic materials
[NASA-CR-171353] 10 p1450 N85-19137
Interleaved array antenna technology development
[NASA-CR-171845] 10 p1477 N85-19326
Characterization of mode 1 and mixed-mode failure of adhesive bonds between composite adherends
[NASA-TM-86355] 12 p1797 N85-21270
Accelerated viscoelastic characterization of T300-5208 graphite-epoxy laminates
[NASA-CR-3871] 12 p1797 N85-21271
Rubber modified epoxy adhesive
[AD-D011527] 12 p1810 N85-21354
SRM filament wound case resin characterization studies 12 p1944 N85-22212
Longitudinal splitting in unidirectional composites, analysis and experiments
[NASA-CR-3881] 13 p2015 N85-22639
Development of epoxy matrices for filament-wound graphite structures
[DE85-003874] 13 p2015 N85-22642
WRAP-RIB antenna technology development 14 p2231 N85-23824
A study of frequency effects and damage accumulation during the fatigue of graphite/epoxy and glass/epoxy composite materials 14 p2247 N85-23930
Measurement of damping of graphite epoxy materials
[NASA-CR-175663] 14 p2248 N85-23931
Design, fabrication and test of composite curved frames for helicopter fuselage structure
[NASA-CR-172438] 15 p2470 N85-25247
Crack growth direction in unidirectional off-axis graphite epoxy
[NASA-CR-175752] 15 p2502 N85-25433
In-plane shear properties of graphite Fibre/Epoxy composites for aerospace applications: Evaluation of test methods by the decision analysis technique
[AD-A151599] 15 p2503 N85-25440
The physical effects of different stress situations on graphite/epoxy compounds 15 p2687 N85-26594
Effect of low-velocity or ballistic impact damage on the strength of thin composite and aluminum shear panels
[NASA-TP-2441] 16 p2742 N85-26924
Measurement of damping of graphite epoxy materials
[NASA-CR-175793] 16 p2743 N85-26925
Temperature: Curvature relationships for unsymmetric graphite-epoxy laminates
[VPI-E-85-08] 16 p2743 N85-26926
Directional thermal conductivities of graphite-epoxy composites: 0/90 and 0/+ or - 45/90
[AD-A152209] 16 p2743 N85-26929
The effect of center delamination on the instability of composite cylindrical panels
[AD-A153494] 16 p3069 N85-28979
DFVLR research in aluminum-lithium alloys 16 p3087 N85-29105
Flight-service program for advanced composite rudders on transport aircraft
[NASA-CR-174537] 19 p3217 N85-29950
Fuel containment and damage tolerance in large composite primary aircraft structures
[NASA-CR-166063] 19 p3231 N85-30032
Influence of interface ply orientation on fatigue damage of adhesively bonded composite joints
[NASA-TM-86443] 19 p3264 N85-30365
Residual thermal and moisture influences on the strain energy release rate analysis of edge delamination
[NASA-TM-86437] 20 p3422 N85-31238
Development and test of advanced composite components. Center Directors discretionary fund program
[NASA-TM-86512] 21 p3561 N85-32147
Comparisons of various configurations of the edge delamination test for interlaminar fracture toughness
[NASA-TM-86433] 21 p3561 N85-32151
Measurement of damping of graphite epoxy materials
[NASA-CR-176073] 21 p3596 N85-32334
Nonlinear response and failure characteristics of internally pressurized composite cylindrical panels
[NASA-CR-176148] 22 p3800 N85-33546
Flight service evaluation of composite helicopter components
[NASA-CR-172562] 23 p3909 N85-34222
Damage induced stress redistribution in composite laminates 24 p4072 N85-35235
Fuel containment and damage tolerance for large composite primary aircraft structures. Phase 1: Testing
[NASA-CR-166091] 24 p4073 N85-35241
Quantitative non-destructive evaluation of composite materials based on ultrasonic wave propagation
[NASA-CR-176176] 24 p4074 N85-35244
Effects of temperature on the tensile strength and elastic modulus of composite material
[AD-A156112] 24 p4075 N85-35251
A normal incidence X-ray telescope sounding rocket payload
[NASA-CR-176169] 24 p4153 N85-35749

GRAPHITE-POLYIMIDE COMPOSITES
Long-term thermal aging of 2 graphite-polyimide composite materials
[NASA-TP-2369] 03 p0325 N85-12094
Develop and demonstrate manufacturing processes for fabricating graphite filament reinforced polyimide (Gr/PI) composite structural elements
[NASA-CR-172497] 11 p1592 N85-20019
Effect of counterface material type and its topography on the tribological properties of polyimide composites
[NASA-TM-87036] 16 p2754 N85-26993
DFVLR research in aluminum-lithium alloys 18 p3087 N85-29105
Graphite/PMR polyimide composites with improved toughness
[NASA-TM-87061] 21 p3561 N85-32148
Thermal expansion of selected graphite reinforced polyimide-, epoxy-, and glass-matrix composite
[NASA-TM-87572] 21 p3561 N85-32149

GRAPHITIZATION
Influence of hydrogen saturation and prior heat treatment on graphitization of white cast iron
[BLL-M-35964-(5828.4)] 05 p0615 N85-13932
Rubber modified epoxy adhesive
[AD-D011527] 12 p1810 N85-21354
Directional thermal conductivities of graphite-epoxy composites: 0/90 and 0/+ or - 45/90
[AD-A152209] 16 p2743 N85-26929
GRAPHOEPITAXY
Research on submicrometer structures
[AD-A146578] 06 p0867 N85-15508
GRAPHS (CHARTS)
Planarity criteria in electromagnetic topology
[AD-A145279] 01 p0038 N85-10241
A method for evaluating the contamination of steel in relation to the solidification curve
[BLL-M-35735-(5828.4)] 02 p0175 N85-11171
On the formal development of graph theoretical algorithms by transformation
[TUM-I8403] 04 p0553 N85-13522
Drifting buoy data from equatorial Pacific Ocean, 31 Aug. 1980 - 30 Apr. 1982
[PB85-120046] 10 p1522 N85-19508
Atlas of the Beaufort Sea
[AD-A149545] 11 p1689 N85-20619
Maximum matchings in a class of random graphs
[AD-A149663] 12 p1920 N85-22060
Introduction to CHART: A graphic analysis and display system, revision
[DE85-004612] 13 p2148 N85-23335
The complexity of reliability computations in planar and acyclic graphs
[AD-A150759] 14 p2406 N85-24845
On matchings and Hamiltonian cycles in random graphs
[AD-A151015] 14 p2409 N85-24851
Graphic simulation of a machine-repairman model
[AD-A151761] 16 p2694 N85-26633
Reliability models for dataflow computer systems
[NASA-CR-175813] 16 p2846 N85-27543
Algorithm for determination of isomorphic graphs
22 p3769 N85-33357
GRASHOF NUMBER
Experimental study of free and mixed convective flow of air in a heated cavity
[DE85-012538] 24 p4094 N85-35380
GRASSES
Relationships between grass canopy characteristics and LANDSAT Thematic Mapper bands
02 p0213 N85-11402
Study of the motion of agricultural vehicles on steep grass-covered slopes
[AD-P004290] 09 p1408 N85-18667
Gravity perception and response in shoot of cereal grasses 15 p2611 N85-26091
GRASSLANDS
Direct regression analysis of remote sensing data (using example of grass cover) 22 p3736 N85-33157
GRASSMANN ALGEBRA
U VECTOR SPACES
GRATINGS (SPECTRA)
NT ECHELETTE GRATINGS
Splitting of surface polariton spectrum by holographic grating 02 p0272 N85-11771
Research on materials and components for opto-electronic signal processing
[AD-A145808] 03 p0433 N85-12754
Method of producing a buried long period grating
[AD-D011351] 07 p0969 N85-16153
Theoretical study of laser-induced surface excitations on a grating
[AD-A147855] 07 p0972 N85-16172
Switchable zero order diffraction gratings as light valves
[AD-A147575] 07 p1044 N85-16833
The evaluation of a deformable diffraction grating for a stigmatic EUV spectrohelioneter
[NASA-CR-174350] 09 p1322 N85-18309
STS atmospheric luminosities
[NASA-CR-175514] 12 p1791 N85-21240
Solar energy converter using surface plasma waves
[NASA-CASE-LEW-13827-1] 12 p1876 N85-21768
High resolution diffraction grating
[AD-D011541] 12 p1933 N85-22141
Properties of chirped grating lenses in optical waveguides
[AD-A150023] 12 p1934 N85-22149
Switchable zero order diffraction gratings as light valves
[AD-A150129] 12 p1934 N85-22153
Study of the potential usefulness of superfine holographic x-ray gratings in AXAF and astrophysics in general 12 p1945 N85-22215
Reflex attachment for line alignment in spectral diffraction devices 13 p2044 N85-22794
Millimeter-wave diffraction devices and materials
[AD-A150876] 14 p2418 N85-24917
Mirror accessory for line straightening in diffraction spectrometers 16 p2764 N85-27054
New image deblurring method described
16 p2806 N85-27305
Optical waveguide characterization using grating couplers
[AD-A153063] 17 p3037 N85-28789
Bandpass filter formed by serial gratings operating in a wood's anomaly region
[AD-D011660] 18 p3093 N85-29148
Switchable zero order diffraction gratings as light valves
[AD-A154471] 20 p3533 N85-31981
Picosecond-pulse damage studies of diffraction gratings
[DE85-010785] 22 p3790 N85-33481
On the convergence of an iterative formulation of the electromagnetic scattering from an infinite grating of thin wires 24 p4085 N85-35319
Redefining the scratch standards
[PB85-194736] 24 p4154 N85-35755
GRAVIMETRY
Analysis of highly precise gravity measurements
[SER-C-294] 01 p0071 N85-10472
Prediction of deflections of the vertical by gravimetric methods
[PB84-213727] 01 p0072 N85-10478
Development of a method for exploring low-reflectance areas through the combined use of different geophysical methods taking the north-west German basin as an example
[BMFT-FB-T-83-180] 02 p0220 N85-11450
Morphological study of monkeys submitted to antiorthostatic hypokinesia 12 p1902 N85-21942
Determination of density of the crust and upper mantle from deep seismic sounding and gravimetry, 2
13 p2111 N85-23153
Polynomial parameterization in inverse gravimetric problem 13 p2115 N85-23174
Determination of crust and upper mantle density based on deep seismic sounding and gravimetry data, part 1
14 p2345 N85-24498
Attempts to localize and identify the gravity sensing device of plant seedlings 15 p2607 N85-26064
Standards and specifications for geodetic control networks
[PB85-166478] 16 p2816 N85-27374
A micrographic and gravimetric study of intercalation and deintercalation of graphite fibers
[NASA-TM-87026] 17 p2934 N85-28110
GRAVIRECEPTORS
NT OTOLITH ORGANS
Mammalian gravity receptors: Structure and metabolism 15 p2605 N85-26055
Effects of weightlessness of Aurelia Ephyra differentiation and statolith synthesis
15 p2605 N85-26056
Gravity perception and cardiac function in the spider
15 p2606 N85-26058
Amyloplast sedimentation kinetics in corn roots
15 p2606 N85-26059
Polyamines as possible modulators of gravity induced calcium transport in plants 15 p2606 N85-26060
Calcium and calmodulin localization in gravitropically-responding plant organs
15 p2606 N85-26061
Role of Ca++ in shoot gravitropism — avena
15 p2607 N85-26065
A possible explanation of why gravitropic growth is detected earlier than straight growth
15 p2607 N85-26067
Gravitropism in leafy dicot stems
15 p2610 N85-26086
Mutant peas as probes in the understanding of growth and gravitropism 15 p2611 N85-26088
Gravity perception and response in shoot of cereal grasses 15 p2611 N85-26091
Are living cells generally sensitive to gravity?
24 p4130 N85-35602
GRAVITATION
NT ARTIFICIAL GRAVITY
NT GRAVITY ANOMALIES
NT PLANETARY GRAVITATION
NT REDUCED GRAVITY
NT SOLAR GRAVITATION
Use of gravitational stabilization in performance of experiments 02 p0160 N85-11084
Gravitational vacuum 02 p0265 N85-11734
Linear conformal gravitation 02 p0265 N85-11735
A geometrical theory of spin motion
[DE84-016537] 04 p0574 N85-13658
Observation of the contractile vacuolar system of Paramecium caudatum on the fast running clinostat
05 p0689 N85-14431
Gravity and cell differentiation in lentil roots
05 p0690 N85-14433
The use of horizontal clinostats in studies of plant statocyte development 05 p0690 N85-14435
Stability of stellar disk and ratio of halo to disk masses in the galaxy 05 p0740 N85-14763
World Geodetic System, 1984
[AD-A147409] 09 p1342 N85-18445
A preliminary study of a cryogenic equivalence principle experiment on Shuttle
[NASA-CR-171300] 10 p1426 N85-18994
Venus gravity: Global field results
13 p2177 N85-23512
The interaction of calcium and auxin in the gravitropic response of roots 15 p2606 N85-26062
Attempts to localize and identify the gravity sensing device of plant seedlings 15 p2607 N85-26064
The role of gravity on the reproduction of arabidopsis plants 15 p2607 N85-26069
Importance of gravity for plant growth and behavior
15 p2608 N85-26070
Structural development and gravity
15 p2608 N85-26071
SU(N,1) inflation
[DE85-003952] 15 p2869 N85-26469
Fluid surface behavior in low gravity. Center discretionary fund no. 83-21
[NASA-TP-2486] 17 p2957 N85-28260
Gravitational properties of antimatter
[DE85-000601] 18 p3197 N85-29832
Research relative to the development of a cryogenic microwave cavity gradiometer for orbital use
[NASA-CR-176002] 19 p3222 N85-29980
Primordial inflation and supergravity
[DE85-009538] 19 p3383 N85-30969
The effect of power law body forces on a thermally-driven flow between concentric rotating spheres
[NASA-TM-87596] 24 p4093 N85-35374
Aeromagnetic and gravity models of the pluton below the Lake City caldera, Colorado
24 p4104 N85-35442
Three-dimensional gravity ideal body studies in rough terrain
[DE85-014097] 24 p4118 N85-35525
GRAVITATION THEORY
Stability questions for gravity in 4 and higher dimensions 05 p0734 N85-14716
The determination of the post-Newtonian parameters in gravitational theory using laser ranging to the Lageos satellite 09 p1414 N85-18924
Supermanifolds and Berezin's new integral
[DE85-001833] 11 p1706 N85-20732
Cosmology in theories with extra dimensions
18 p3202 N85-29664
GRAVITATIONAL COLLAPSE
NT BLACK HOLES (ASTRONOMY)
Iron core collapse models of Type 2 supernovae
[DE84-013909] 05 p0743 N85-14775
Research in nuclear astrophysics: Stellar collapse and supernovae
[DE84-015559] 05 p0743 N85-14776
Fragmentation and turbulence in collapsing gas clouds
[DE85-003745] 11 p1633 N85-20282
Inflation from extra dimensions
[DE85-007834] 16 p2883 N85-27787
GRAVITATIONAL EFFECTS
NT GRAVITATIONAL LENSES
NT LAGRANGIAN EQUILIBRIUM POINTS
NT STELLAR GRAVITATION
Some notes on a tangent plane oriented heading reference — stabilized platforms
[RAE-TM-IEE-144] 02 p0136 N85-10828
Rapid nonresonant rotation of a spacecraft in nominally periodic orbits in limited 3 body problem
02 p0160 N85-11083
Gravitational effects on premixed particle cloud flames
02 p0171 N85-11144
Transport phenomena in the boundary layer during solution solidification under microgravity. Ice growth from a water-salt solution
[BMFT-FB-W-84-031] 03 p0329 N85-12121
Tidal disruption and the origin of the Moon
04 p0586 N85-13739
A testable gravitational capture model for the origin of the Earth's Moon 04 p0586 N85-13742
Orbit perturbation — satellites
05 p0598 N85-13810
Investigation of the Ostwald ripening of separated particles in liquid-liquid systems under microgravity conditions
[BMFT-FB-W-84-037] 05 p0615 N85-13927
Biogeochemical cycles: Interactions in global metabolism 05 p0652 N85-14184
Life Sciences Research in Space — conference
[ESA-SP-212] 05 p0689 N85-14425

Influence of simulated weightlessness on the motility of the acellular slime mold Physarum polycephalum
05 p0689 N85-14430
Observation of the contractile vacuolar system of Paramecium caudatum on the fast running clinostat
05 p0689 N85-14431
Gravity and cell differentiation in lentil roots
05 p0690 N85-14433
The influence of gravitational body force in meteoritic chondrule and lunar glass formation
06 p0884 N85-15614
The growth of metastable peritectic compounds
[NASA-CR-171290] 07 p0920 N85-15825
SPAR X technical report for experiment 76-22 directional solidification of magnetic composites
[NASA-CR-171271] 07 p0927 N85-15880
Comparative effects of auxin and abscisic acid on growth, hydrogen ion efflux and gravitropism in primary roots of maize
[NASA-CR-174365] 09 p1342 N85-18444
Gravity and biological systems: Emphasis on human physiology
[ESA-BR-21] 09 p1360 N85-18558
The restricted problem of 2 + N bodies
09 p1414 N85-18925
Approximation of difference in water table positions by horizontal stratum in studies of their influence on gravity
10 p1502 N85-19478
Influence of gravitoinertial force level on apparent magnitude of coriolis cross-coupled angular accelerations and motion sickness 11 p1693 N85-20644
Vestibular and oculomotor function during Gz variations 11 p1693 N85-20645
Averaging of equations of cometary orbital motion with allowance for nongravitational effects
13 p1978 N85-22411
Lagrangian solutions in photogravitational restricted circular three-body problem 13 p1979 N85-22416
Periodic movements of axisymmetrical satellite about center of mass due to gravitational moment
13 p2042 N85-22783
Problems of space biology. Volume 50: Nystagmometry for evaluation of the status of the vestibular function
[NASA-TM-77616] 14 p2385 N85-24694
Systematic and random deformations of orbits of long-period comets 15 p2479 N85-25299
Resonant rotations of satellite in polar orbit in magnetic and gravitational fields 15 p2479 N85-25302
Investigation of internal friction of free-flowing material during discharge
[BLL-M-36141-(5828.4)] 15 p2553 N85-25752
NASA Space Biology Program: 9th Annual Symposium
[NASA-CP-2336] 15 p2605 N85-26054
Mammalian gravity receptors: Structure and metabolism 15 p2605 N85-26055
Effects of weightlessness of Aurelia Ephyra differentiation and statolith synthesis
15 p2605 N85-26056
Gravity perception in a Cladoceran-Zooplankter: Anatomy of antennal socket setae of Daphnia magna
15 p2605 N85-26057
Gravity perception and cardiac function in the spider
15 p2606 N85-26058
Gravistimulus production in roots of corn
15 p2607 N85-26066
Neural mechanism by which gravitational stimulus and stress affect the secretion of renin and other hormones
15 p2610 N85-26083
Gravity, body mass and composition, and metabolic rate 15 p2610 N85-26084
Homeostasis in primates in the hyperdynamic environment — circadian timekeeping and effects of lower body positive pressure on sleep
15 p2610 N85-26085
Plant growth biophysics: The basis for growth asymmetry induced by gravity 15 p2611 N85-26089
An indirect role for ethylene in shoot-inversion release of apical dominance in Pharbitis nil
15 p2611 N85-26090
Gravity perception and response in shoot of cereal grasses 15 p2611 N85-26091
Simulated microgravity as a probe for understanding the mechanisms of early pattern specification
15 p2611 N85-26092
Development and maturation of the neuromuscular junction in cell culture under conditions of simulated zero-gravity 15 p2611 N85-26093
Effects of simulated weightlessness on mammalian development. Part 2: Meiotic maturation of mouse oocytes during clinostat rotation 15 p2612 N85-26094
Effects on in vivo and in vitro exposure to excess gravity on growth and differentiation of mammalian embryos
15 p2612 N85-26095
Gravitational effects on reproduction, growth and development of mammals 15 p2612 N85-26097
Participation of ethylene in two modes of gravistimulation of shoots 15 p2613 N85-26101
Isolation of hybridomas for golgi-associated proteins and a plant calmodulin 15 p2613 N85-26103
Differential wall growth in gravistimulated corn roots: Its timing and regulation 15 p2614 N85-26105
Gravitational effects in theories with interacting fields: Two studies 15 p2663 N85-26435
The gravitational interaction between inclined, elliptical rings — Uranus rings 15 p2675 N85-26514
Dense but collisionless orbiting rings — Saturn rings
15 p2675 N85-26517
The gravito-electrodynamics of charged dust in planetary ring systems 15 p2677 N85-26531
Effects of posture and water immersion on diaphragmatic function 16 p2840 N85-27515
Optical best arc RMS test results
20 p3492 N85-31706
Sensitivity of human lymphocytes to microgravity in-vitro 20 p3510 N85-31820
G-induced Loss of Consciousness (GLC)
20 p3510 N85-31823
Study of requirements for and method of multidimensional acoustic imaging — spaceborne experiments
[ESA-CR(P)-2020] 20 p3525 N85-31924
Tolerance to +Gz and +Gx accelerations of individuals in older age groups in good health and with early signs of arteriosclerosis 23 p3952 N85-34496
NASA Developmental Biology Workshop: A summary
[NASA-TM-86756] 24 p4126 N85-35578
Effects of microgravity and hypergravity on invertebrate development 24 p4126 N85-35579
Vertebrate development in space: Gravity is a drag (and has been for eons and eons) 24 p4126 N85-35580
Report of the NASA Mammalian Developmental Biology Working Group 24 p4126 N85-35581
Report of the Avian Development Working Group
24 p4127 N85-35582
Report of Amphibian Development Group
24 p4127 N85-35583
Report of the Insect Development Group
24 p4127 N85-35584
Aquatic Invertebrate Development Working Group
24 p4127 N85-35585
Report of the Microbial Development Working Group
24 p4127 N85-35586
Cardiovascular responses to orthostatism and weightlessness 24 p4130 N85-35601
Are living cells generally sensitive to gravity?
24 p4130 N85-35602
Simulation of high +Gz onset in the dynamic environment simulator
[AD-A155963] 24 p4131 N85-35610

GRAVITATIONAL FIELDS
NT STELLAR GRAVITATION
Solution generating technique for the Einstein equations 03 p0435 N85-12768
Digital elevation models improve processing of Alaskan gravity data 04 p0515 N85-13285
Relationship of gold content to gravity fields in Far East 10 p1501 N85-19475
Consideration of heterogeneity of gravity fields in local high precision geodetic constructions
13 p2114 N85-23169
Mathematical modeling of results of geometric leveling in variable gravity field 13 p2114 N85-23170
Polynomial parameterization in inverse gravimetric problem 13 p2115 N85-23174
Gravity field of Venus and comparison with Earth
13 p2178 N85-23514
The support of long wavelength loads on Venus
13 p2178 N85-23515
Gravity field of the Jovian system from Pioneer and Voyager tracking data 13 p2180 N85-23529
A study of terrain reductions, density anomalies and geophysical inversion methods in gravity field modelling
[AD-A150788] 14 p2373 N85-24668
Local covariance functions and density distributions
[AD-A150792] 14 p2373 N85-24669
Potential models — Earth gravity
14 p2396 N85-24764
Elementary sunspot energy model
15 p2476 N85-25287
One method for constructing model of point masses of planetary gravity field 15 p2479 N85-25300
Resonant rotations of satellite in polar orbit in magnetic and gravitational fields 15 p2479 N85-25302
Interpretation of Venus gravitational anomalies
15 p2483 N85-25322
Distribution of gravity and plumb line deflection at Martian surface 15 p2483 N85-25324
Optimization of system for observing Northern Hemisphere atmospheric pressure field
15 p2485 N85-25338
The gravitational interaction between inclined, elliptical rings — Uranus rings 15 p2675 N85-26514
Heliocentric sail problem with variable gravity field reduction 16 p2724 N85-26816
On gravitational waves 16 p2759 N85-27026
Topex Gravity Model Development Team activities during fiscal year 1984
[NASA-TM-86208] 16 p2804 N85-27285
Status of the observational data sets — TOPEX
16 p2804 N85-27286
Satellite selection criteria 16 p2804 N85-27288
Optical best arc RMS test results
16 p2804 N85-27290
The size of a gravitational field model for Topex
16 p2805 N85-27293
The selection of the starting field: General versus tailored model 16 p2805 N85-27294
Comparison of gravity field solution techniques
16 p2805 N85-27295
Gravitational properties of antimatter
[DE85-009601] 18 p3197 N85-29832
An algorithm for the influence numbers in the expansion of the lumped gravitational potential coefficients in the presence of resonant inclination variation
[AD-A154229] 19 p3336 N85-30669
Geodynamics Branch research program
[NASA-TM-86223] 20 p3489 N85-31688
New optical satellite data 20 p3492 N85-31705
Spaceborne gradiometer error analysis
20 p3492 N85-31707
NASA/GSFC TOPEX gravity model operations group
20 p3492 N85-31709
The time averaged circulation of the oceans from satellite altimetry 20 p3493 N85-31713
Global geoid and gravity anomaly predictions using the collocation and point mass techniques
[AD-A154517] 21 p3605 N85-32387
The evolution of complex and higher organisms
[NASA-SP-478] 21 p3656 N85-32708
The effect of power law body forces on a thermally-driven flow between concentric rotating spheres
[NASA-TM-87596] 24 p4093 N85-35374
A dynamic model of Venus's gravity field
[NASA-CR-176173] 24 p4169 N85-35845

GRAVITATIONAL LENSES
QUASAT, gravitational lenses, and studies of the interstellar, intracluster and intergalactic medium
07 p1058 N85-16715
University of Cambridge Institute of Astronomy report of activities 13 p2170 N85-23464
Milliarcsecond morphology of the twin quasar 0957 + 56A,B: The view through a gravitational lens
20 p3544 N85-32054

GRAVITATIONAL PHYSIOLOGY
A survey of space biology and space medicine
[ESA-BR-17] 04 p0545 N85-13486
Spacelab mission D1 Frog statolith experiment STATEX: Hardware family and experiment operational sequence
05 p0689 N85-14428
Experiment 1ES031 on Spacelab 1: Are cells sensitive to gravity? — lymphocyte proliferation
05 p0689 N85-14428
Ultrasonic study of early cardiovascular adaptation to zero gravity 05 p0691 N85-14445
Three-dimensional ballistocardiography in weightlessness (experiment 1ES 026) — Spacelab
05 p0691 N85-14447
Miniature personal physiological tape recorder (experiment 1ES 30) — Spacelab
05 p0692 N85-14448
Physical performance capacity after a 7 day head-down tilt (-6 deg) 05 p0692 N85-14451
Intraocular fluid dynamics in microgravity
05 p0693 N85-14455
Endocrine responses to nonhypotensive gravitational stress: Vasopressin and aldosterone
05 p0693 N85-14459
Endocrine responses to hypotensive gravitational stress: Catecholamines, pancreatic polypeptide, and vasopressin 05 p0693 N85-14460
Sleep physiology in weightlessness (experiment 1ES 030) — Spacelab 05 p0695 N85-14474
Gravity and biological systems: Emphasis on human physiology
[ESA-BR-21] 09 p1360 N85-18558
Modular plant culture systems for life support functions
[NASA-CR-171853] 12 p1899 N85-21924
Evaluation of Results of Space Experiments in Physiology and Medicine and Informal Briefings by the F-16 Medical Working Group 20 p3508 N85-31806

GRAVITATIONAL POTENTIAL
U GRAVITATIONAL FIELDS

GRAVITATIONAL RADIATION
U GRAVITATIONAL WAVES

GRAVITATIONAL WAVE ANTENNAS
Analysis of the Frascati and Geneva gravitational wave antenna background exhibiting the one half sideral day period
[NOTA-INTERNA-801] 02 p0192 N85-11283
Some considerations on the capacitive calibration used for the 2.3 ton cryogenic antenna at CERN — gravitational antennas
[NOTA-INTERNA-809] 02 p0192 N85-11284
Sensitivity improvement of a two-mode gravitational radiation detector through the use of a transducer not perfectly tuned to the antenna
[NOTA-INTERNA-812] 02 p0192 N85-11285
GRAVITATIONAL WAVES
Analysis of the Frascati and Geneva gravitational wave antenna background exhibiting the one half sideral day period
[NOTA-INTERNA-801] 02 p0192 N85-11283
Sensitivity improvement of a two-mode gravitational radiation detector through the use of a transducer not perfectly tuned to the antenna
[NOTA-INTERNA-812] 02 p0192 N85-11285
Improved sensitivities in laser interferometers for the detection of gravitational waves
[MPQ-88] 04 p0506 N85-13232
Internal gravity waves in real atmosphere
06 p0825 N85-15236
Determination of gravity wave envelope solitons on surface of stratified fluid interacting with wind
14 p2334 N85-24433
Two-cycle mechanism of dissipation of tidal energy in ocean
14 p2335 N85-24438
The Record of Electrical and Communication Engineering Conversazione, volume 53, no. 2, November 1984
[ISSN-0385-7719] 16 p2758 N85-27022
On gravitational waves 16 p2759 N85-27026
Interplanetary plasma turbulence and the Doppler detection of a gravitational background radiation
[IFSI-85-1] 20 p3546 N85-32066
Some aspects of internal gravity waves in a multi-layered moving stratified flow 24 p4092 N85-35369
GRAVITROPISM
Comparative effects of auxin and abscisic acid on growth, hydrogen ion efflux and gravitropism in primary roots of maize
[NASA-CR-174355] 09 p1342 N85-18444
Role of Ca++ in shoot gravitropism — avena
15 p2607 N85-26085
Gravitropism in leafy dicot stems
15 p2610 N85-26086
Mutant peas as probes in the understanding of growth and gravitropism 15 p2611 N85-26088
GRAVITY
U GRAVITATION
GRAVITY ANOMALIES
On gravity from SST, geoid from Seasat, and plate age and fracture zones in the Pacific
[E85-10020] 02 p0217 N85-11433
Generalized linear inversion of 2.5 - dimensional gravity and magnetic anomalies 02 p0226 N85-11480
Determination of the altimetric geoid and gravity anomalies in the North Sea: Implications for a solution of the general circulation problem using ERS-1 data
03 p0362 N85-12446
Local geoid determination in mountain regions
[AD-A145799] 03 p0384 N85-12458
Lithospheric structure in the Pacific geoid
[NASA-CR-174155] 04 p0526 N85-13365
Models for volcanic processes in Long Valley, California: Testing by continental drilling
[DE84-014943] 04 p0534 N85-13414
Correlation radius of gravitational and magnetic anomalies and methods of its determination
06 p0821 N85-15213
Selection of spacing of modular and gradient measurement surveys based on statistical characteristics of measured geomagnetic field
06 p0821 N85-15214
Gravity anomaly map of Mars and Moon and analysis of Venus gravity field: New analysis procedures
[NASA-CR-174295] 08 p1258 N85-17819
Prospects and means for development of theory and practice of interpretation of gravitational and magnetic anomalies 10 p1501 N85-19474
Polynomial parameterization in inverse gravimetric problem 13 p2115 N85-23174
Gravity field of Venus and comparison with Earth
13 p2178 N85-23514
The support of long wavelength loads on Venus
13 p2178 N85-23515
Impacts in ice: Comissions of solar system crater population 13 p2181 N85-23538
Interpretation of Venus gravitational anomalies
15 p2483 N85-25322
Improving the geological interpretation of magnetic and gravity satellite anomalies
[E85-10103] 20 p3473 N85-31585
A comparative study of spherical and flat-Earth geopotential modeling at satellite elevations
20 p3475 N85-31593
A comparative study of spherical and flat-Earth geopotential modeling at satellite elevations
20 p3475 N85-31594
Long-wavelength magnetic and gravity anomaly correlations on Africa and Europe
20 p3476 N85-31597
Comparison of survey and photogrammetry methods to position gravity data, Yucca Mountain, Nevada
[DE85-011685] 21 p3590 N85-32316
Global geoid and gravity anomaly predictions using the collocation and point mass techniques
[AD-A154517] 21 p3605 N85-32387
Upward continuation of surface gravity anomalies
[AD-A154973] 21 p3631 N85-32560
Geologic processes on Venus: An update
22 p3857 N85-33883
The non-hydrostatic figures of the terrestrial planets
22 p3858 N85-33887
Optimal estimation of a high degree gravity field from a global set of 1 deg x 1 deg anomalies to degree and order 250
[AD-A156008] 24 p4117 N85-35519
Gravity gradiometer survey data processing
[AD-A156165] 24 p4117 N85-35522
A dynamic model of Venus's gravity field
[NASA-CR-176173] 24 p4189 N85-35845
GRAVITY GRADIENT SATELLITES
NT ATS
Application Number 3: Using tethers for attitude control 11 p1646 N85-20373
GRAVITY GRADIOMETERS
Research relative to the development of a cryogenic microwave cavity gradiometer for orbital use
[NASA-CR-174249] 07 p0962 N85-16095
A preliminary study of a cryogenic equivalence principle experiment on Shuttle
[NASA-CR-171300] 10 p1426 N85-18994
Gravity gradiometer survey data processing
[AD-A156165] 24 p4117 N85-35522
GRAVITY PROBE B
Optical contacting for gravity probe star tracker
[NASA-TM-86475] 01 p0120 N85-10819
Optical analysis of the star-tracker telescope for Gravity Probe
[NASA-TM-86474] 01 p0129 N85-10888
GRAVITY WAVES
NT BAROCLINIC WAVES
Wave phase velocity in a wind gradient — gravity waves 04 p0523 N85-13343
Effect of mountain wave dynamics on orographic storms
[DE84-014713] 04 p0540 N85-13433
Theoretical and observed dispersion of acoustic-gravity waves in atmosphere 04 p0557 N85-13547
Dispersion properties of moving ionospheric perturbations 07 p0952 N85-16036
The interpretation of SIR-B imagery of surface waves and other oceanographic features using in-situ, meteorological satellite, and infrared satellite data
08 p1143 N85-17212
On the classification and nonlinear solution of one type of stratified shear flow
[AD-A146832] 09 p1319 N85-18295
Internal Gravity Waves and Small-Scale Turbulence: Proceedings of the 2nd 'Aha Huliko'a Hawaiian Winter Workshop
[AD-A149510] 10 p1522 N85-19597
PMP-2 report: Equatorial wave dynamics
11 p1657 N85-20442
Winds and waves (4 min - 11 yrs) in the upper middle atmosphere (60-110 km) at Saskatoon, Canada (52 deg N, 107 deg W): MF radar (2.2 MHz) soundings 1973 - 1983 11 p1662 N85-20476
Mesh effects on the computation of non-linear gravity waves of arbitrary discharge
[COLL-AERON-8501] 12 p1888 N85-21848
Radio scintillations observed during atmospheric occultations of Voyager: Internal gravity waves at Titan and magnetic field orientations at Jupiter and Saturn
[NASA-CR-175554] 12 p1961 N85-22327
Analysis and interpretation of observations of airglow at 297 nm in the Venus thermosphere
13 p2172 N85-23473
Influence of internal gravity waves on F layer
14 p2338 N85-24460
Long nonlinear waves in layers of sudden changes in wind velocity 14 p2340 N85-24470
Numerical simulations of convectively excited gravity waves 14 p2444 N85-25062
Resonance generation of inertial waves (in the atmosphere) by Doppler-shift of inertio-gravity modes
15 p2590 N85-25968
Role of frontal circulations and gravity waves in initiating convective storm systems 15 p2598 N85-26010
Wave propagation in density stratified fluids
16 p2781 N85-27162
Turbopause as source of internal gravity waves
16 p2808 N85-27314
Wave dynamics and transport in the stratosphere
[NASA-CR-175789] 16 p2823 N85-27413
Symposium on Atmospheric Sciences in South Africa
[CSIR-S-331] 16 p2829 N85-27442
Atmospherically forced, coastally trapped, long period gravity waves off the south coast of southern Africa
16 p2832 N85-27461
Propagation of gravity waves in the atmosphere and around critical levels
[KNMI-WR-85-1] 18 p3137 N85-29428
High-latitude filtering in a global grid-point model using model normal modes 18 p3140 N85-29442
A laser slope gauge and a spar buoy wave gauge: Tools for the validation of microwave remote sensors
[AD-A154038] 19 p3272 N85-30290
Middle Atmosphere Program. Handbook for MAP. Volume 14: URSI/SCOSTEP Workshop on Technical Aspects of MST Radar
[NASA-CR-176085] 21 p3615 N85-32468
Excerpts from the paper: Research Status and Recommendation from the Alaska Workshop on Gravity Waves and Turbulence in the Middle Atmosphere, part 1.3A 21 p3616 N85-32470
Gravity waves from the stratosphere to the mesosphere, part 1.3B 21 p3616 N85-32471
The suppression of convective wavebreaking by radiative transfer processes, part 1.3C
21 p3616 N85-32472
A simple model for testing the effects of gravity-wave-produced vertical oscillations of scattering irregularities on spaced-antenna, horizontal drift measurements 21 p3619 N85-32489
Interferometer applications of VHF radars, part 3.5A
21 p3621 N85-32497
Techniques for the study of gravity waves and turbulence (keynote paper), part 4 21 p3621 N85-32499
Spectral measurements of turbulence and gravity waves, part 4.2A 21 p3622 N85-32501
Gravity-wave spectra in the atmosphere observed by MST radar, part 4.2B 21 p3622 N85-32502
High resolution evidence for the Garrett-Munk spectrum of stratospheric gravity waves 21 p3622 N85-32503
On the spectrum of atmospheric velocity fluctuations seen by MST/ST radar and their interpretation
21 p3622 N85-32504
Use of the VAD technique and measurements of momentum flux in the stratosphere at Aerobo, part 4.3A
21 p3622 N85-32505
Momentum flux measurements: Techniques and needs, part 4.5A 21 p3623 N85-32508
Tropospheric gravity waves observed by three closely spaced ST radars 21 p3623 N85-32509
Determination of horizontal and vertical wavelengths of gravity waves in the mesosphere by spaced wind measurements 21 p3623 N85-32510
On the limiting configuration of interfacial gravity waves
[AD-A154821] 21 p3631 N85-32557
A new hypothesis for the observed vertical distribution of atmospheric aerosols 21 p3645 N85-32646
GRAZING FLOW
The effect of grazing flow on the impedance of the Helmholtz resonator 05 p0635 N85-14076
GRAZING INCIDENCE
Study of magnetism at surfaces by scattering of neutrons at grazing incidence
[DE84-015850] 10 p1564 N85-19985
A new generation of spectrometer designs for ultraviolet astronomy 11 p1761 N85-21079
Grazing incidence beam expander
[DE85-010784] 19 p3368 N85-30889
GRAZING LANDS
U GRASSLANDS
GREASES
An evaluation of grease type ball bearing lubricants operating in various environments
[NASA-TM-86480] 02 p0185 N85-11239
Performance evaluation of automotive wheel bearing greases
[AD-A145948] 03 p0337 N85-12168
Grease versus oil lubrication of wheel bearings in Army equipment
[AD-A147546] 07 p0973 N85-16184
Corrosion properties of second-generation conductive materials 07 p1000 N85-16348

Protection products for the conductors of high voltage overhead lines
[BLL-OA-TRANS-3219-(6196.300)] 20 p3429 N85-31269

GREAT BRITAIN
U UNITED KINGDOM

GREAT LAKES (NORTH AMERICA)
Homogeneous macroclimatic zones of the lake states
[PB84-215821] 04 p0540 N85-13436
Two-dimensional lake wave prediction system
[PB84-231034] 06 p0841 N85-15342
PATHFINDER: A trajectory prediction system for the Great Lakes
[PB85-115335] 10 p1506 N85-19506
Great Lakes winter weather and ice conditions for 1982-83
[PB85-165009] 16 p2837 N85-27486
EPA (Environmental Protection Agency) research program guide, FY-1985, October 1, 1984 - September 30, 1985
[PB85-181881] 20 p3487 N85-31676
Great Lakes hydrometeorologic and hydraulic data needs 20 p3496 N85-31739

GREAT PLAINS CORRIDOR (NORTH AMERICA)
The influence of soil moisture distribution on the severe-storm environment of the southern Great Plains: A numerical study of the SESAME 4 case 09 p1357 N85-16534

GREEN THEOREM
U GREEN'S FUNCTIONS

GREEN'S FUNCTIONS
An inverse source problem for elastic waves 03 p0371 N85-12368
Applications of Green's boundary formula 05 p0718 N85-14607
Green function in theory of microstrip antennas 06 p0790 N85-15050
A first-order Green's function approach to supersonic oscillatory flow: A mixed analytic and numeric treatment
[NASA-CR-172207] 09 p1273 N85-18002
Noise transmission loss of a rectangular plate in an infinite baffle
[NASA-TP-2398] 12 p1927 N85-22109
Green's function solution of the Kondo problems and universality of the thermodynamic properties
[DE85-002739] 12 p1943 N85-22206
Elastic wave scattering from an interface crack in a layered half space 13 p2101 N85-23095
Surface scattering
[AD-A150252] 13 p2153 N85-23366
Reaction of piezoceramic shell to concentrated forces 14 p2279 N85-24115
First- and second-order charged particle optics
[DE85-006310] 14 p2421 N85-24940
Investigation of the numerical method of moments for digital computer determination of differential equations
[AD-A151698] 15 p2636 N85-26268
Local density theory of heats of formation and short-range order parameters in substitutionally disordered alloys
[DE85-009611] 18 p3075 N85-29021
A first-order time-domain Green's function approach to supersonic unsteady flow
[NASA-CR-172208] 19 p3214 N85-29930
Mutual coupling analysis for conformal microstrip antennas
[AD-A154292] 19 p3259 N85-30210
Integral constraints on stress energy perturbations in general relativity and applications to cosmology 19 p3383 N85-30985
Wave propagation and methods of solution of the wave equation for moving disturbances sources
[ESA-TT-824] 20 p3522 N85-31906
A cracked orthotropic sheet stiffened by a semi-infinite orthotropic sheet
[NASA-TP-2455] 21 p3597 N85-32339
Exact solutions of singular equations for viscous transonic flows 21 p3663 N85-32882

GREENHOUSE EFFECT
A study of greenhouse effects using zero, 1 and 2 dimensional climate models 02 p0230 N85-11498
Carbon dioxide, the greenhouse effect and climate: A primer
[GPO-33-444] 03 p0395 N85-12519
Paleoclimatologists use past to predict weather patterns 06 p0619 N85-15197
Surging as a potential response of ice sheets to CO2-induced changes in the polar environment (SPICAE)
[DE84-016472] 06 p0841 N85-15341
Carbon dioxide and the greenhouse effect
[GPO-39-043] 11 p1677 N85-20569
Modeling of mechanism of positive feedback between mean Earth surface temperature and atmospheric carbon dioxide in geologic time scale 13 p2106 N85-23122
Greenhouse effect in Earth's primordial atmosphere 16 p2807 N85-27310
Humidity/cloud-radiation feedback on possible climate perturbation due to fossil fuel utilization
[DE85-006886] 18 p3133 N85-29402
Climatic consequences of very high CO2 levels in Earth's early atmosphere 22 p3854 N85-33865
Volatiles on satellites of the outer solar system 22 p3854 N85-33868
Carbon dioxide and climate: A working glossary
[DE85-013535] 24 p4124 N85-35582

GREENLAND
Investigation of ice dynamics in the marginal ice zone
[AD-A145110] 01 p0088 N85-10597
Revised Uniform Summary of Surface Weather Observations (RUSSWO). Sondestrom AB, Greenland, parts A-F
[AD-A146919] 07 p1005 N85-16390
Structure and stratigraphy of Midterhuken Peninsula, Belsund, West Spitsbergen 09 p1353 N85-16513
Hydrology and climatic conditions in Greenland 14 p2327 N85-24387
North Atlantic Deep Water Formation
[NASA-CP-2367] 15 p2601 N85-26026
Oceanographic variations in recent decades and their impact on the fertility of the Iceland Sea 15 p2602 N85-26034
North Atlantic Deep Water formation: Information from ice cores 15 p2602 N85-26035
Greenland ice sheet mass balance 15 p2603 N85-26043
Potential climatic effects on the Greenland ice sheet 15 p2603 N85-26044
Origin of the Greenland ice sheet 15 p2604 N85-26046
Mining cosmic dust from the blue ice lakes of Greenland 15 p2682 N85-26563
Operational experiences with the ARGOS system in Greenland 16 p2813 N85-27353
AWS (Air Weather Service) climatic briefs: North America
[AD-A152161] 16 p2835 N85-27483

GRIDS
Comparison of the multigrid and ICCG methods in solving the diffusion equation
[DE84-014409] 02 p0253 N85-11657
Transformation of two and three-dimensional regions by elliptic systems
[NASA-CR-174176] 04 p0554 N85-13529
Multigrid iteration solution procedure for solving three-dimensional sets of coupled equations
[DE84-016515] 04 p0555 N85-13532
Characteristics of polarization grids made of parallel metal strips during hemispherical scanning 06 p0792 N85-15062
An exploratory study of finite difference grids for transonic unsteady aerodynamics
[NASA-TM-84583] 07 p0999 N85-15696
Semianalytic modeling of aerodynamic shapes
[NASA-TP-2413] 12 p1771 N85-21120
An orthogonal grid technique for studying internal deformation and energy absorption in target penetration
[AD-A149989] 12 p1860 N85-21665
Grid generation for a pump collector
[AD-A150217] 13 p2092 N85-23059
GRID: A FORTRAN program for using a digitizing table to enter a finite element GRID
[AD-A151317] 15 p2628 N85-26196
An incremental multigrid strategy for the fluid dynamics equations
[AD-A151953] 16 p2783 N85-27172

GRIDS (MATHEMATICS)
U COMPUTATIONAL GRIDS

GRIFFITH CRACK
On the corner singularity of a 3-D Griffith crack
[AD-A150989] 14 p2321 N85-24342

GRINDING (COMMINUTION)
Milling of Si3N4 with Si3N4 hardware
[NASA-TM-86864] 01 p0031 N85-10191
Metallographic grinding efficiency
[DE85-001520] 09 p1304 N85-18194
Ammonia formation caused by the presence of water in the wet grinding of silicon nitride powder
[NASA-TM-77746] 14 p2249 N85-23937
Drying of pulverized material with heated condensable vapor
[DE85-011656] 22 p3783 N85-33436
Spectral characteristics of grinding sparks used for identification of scrap metals
[PB85-198570] 24 p4080 N85-35290

GRINDING (MATERIAL REMOVAL)
NT METAL GRINDING
In-situ annular face grinder
[AD-D011422] 08 p1168 N85-17367
Factors influencing the ball milling of Si3N4 in water
[NASA-TM-86932] 10 p1450 N85-19136
Parametric evaluation of ball milling of SiC in water
[NASA-TM-86974] 12 p1811 N85-21356
New technique for fluid feed in simultaneous multisurface grinding 13 p2045 N85-22800
Robotic deburring. Part 2: Evaluation of cutters and noncompliant tooling
[DE85-006182] 14 p2311 N85-24306
Study of a test method for assessing machinability in gear cutting operations
[BLL-BISI-TRANS-22345-(9022.06)] 17 p2972 N85-28359

GRINDING MACHINES
In-situ annular face grinder
[AD-D011422] 08 p1168 N85-17367
Diamond cutters' grinders 13 p2051 N85-22841
Role of fluid lubricant-coolant in fine grinding of optical glass by diamond tool 14 p2280 N85-24125
Non-contact hydrostatic bearings 16 p2762 N85-27046
Very high speed lap with positive lift effect
[AD-D011710] 19 p3280 N85-30344
Very high speed lap with negative lift effect
[AD-D011711] 19 p3281 N85-30345

GRINDING MILLS
Milling of Si3N4 with Si3N4 hardware
[NASA-TM-86864] 01 p0031 N85-10191
Improved silicon grinding method and apparatus
[NASA-CASE-NPO-16336-1-CU] 12 p1819 N85-21407
Operational performance of the photovoltaic-powered grain mill and water pump at Tangaye, Burkina Faso (formerly Upper Volta)
[NASA-TM-86970] 13 p2128 N85-23243

GRIT
Process development for the production of technically high quality monocrystalline diamond grits
[BMFT-FB-T-84-204] 08 p1138 N85-17166

GROOVES
Annular groove in compressor casing as device for control of air stream 13 p2050 N85-22832
An X-ray study of residual stresses in narrow groove TIG weldments
[DE85-006485] 16 p2802 N85-27274
Monogroove heat pipe design: Insulated liquid channel with bridging wick
[NASA-CASE-MSC-20497-1] 18 p3098 N85-29180

GROOVING
Stress concentration due to axial tension of loaded nonsymmetric-shaped grooves
[AD-A149425] 10 p1496 N85-19442

GROUND BASED CONTROL
NT AIR TRAFFIC CONTROL
NT AUTOMATED EN ROUTE ATC
NT RADAR APPROACH CONTROL
Planned office and facility consolidations: To improve system effectiveness and efficiency, FY 1985-87
[AD-A150441] 13 p1970 N85-22376
Helios ground operations 16 p2887 N85-27611
Simulation studies of time-control procedures for the advanced air traffic control system
[NASA-TP-2493] 21 p3553 N85-32101
The development of assessment techniques program 24 p4106 N85-35457

GROUND EFFECT (AERODYNAMICS)
Ground-effect analysis of a jet transport airplane
[NASA-TM-85920] 07 p0897 N85-15687
Hover test results of a small-scale twin-tilt nacelle model
[NASA-TM-86665] 14 p2210 N85-23706
Structures and Dynamics Division research and technology plans for FY 1985 and accomplishments for FY 1984
[NASA-TM-86417] 15 p2577 N85-25895
Effect of ground and/or ceiling planes on thrust of rotors in hover
[NASA-TM-86754] 20 p3388 N85-31014
Aerodynamic measurement of the wind flow in the number two section of the SIMA wind tunnel
[ONERA-PV-1/8138-GY] 20 p3389 N85-31019
Ground effect on helicopter aerodynamics and stability 20 p3395 N85-31063

GROUND EFFECT (COMMUNICATIONS)
Development of the microwave antenna range of the national antenna test facility at Paardefontein
[R-NIAS-21] 15 p2539 N85-25669
A short range, high accuracy radar ranging system
[AD-A152195] 16 p2774 N85-27122
Most desirable terrain, e.g., flat vs valley location, part 5.1B 21 p3624 N85-32513

GROUND EFFECT MACHINES
NT CUSHIONCRAFT GROUND EFFECT MACHINE
Finger materials for air cushion vehicles. Volume 2: Base fabrics for finger materials
[AD-A149701] 12 p1819 N85-21408

Impact studies of a 1/3-scale model of an air cushion vehicle
[NASA-TM-86360] 14 p2218 N85-23757
Finger materials for air cushion vehicles. Volume 1: Flexible coatings for finger materials
[AD-A151438] 15 p2522 N85-25545
Operational noise data for the LACV-30 air cushion vehicle
[AD-A154063] 19 p3351 N85-30773

GROUND HANDLING
Mechanical features of the shuttle rotating service structure 08 p1102 N85-16967
Payload transportation at KSC 08 p1103 N85-16970
STS payload ground handling mechanism at John F. Kennedy Space Center 08 p1103 N85-16971
Computer aided processing using laser measurements 08 p1103 N85-16973

GROUND RESONANCE
Study to eliminate ground resonance using active controls
[NASA-CR-166609] 07 p0902 N85-15715
Aerodynamic performance of a wing in ground effect using the PANAIR program
[AD-A153303] 17 p2692 N85-27832

GROUND SPEED
Geomagnetic velocimeter
[AD-D011672] 19 p3218 N85-29653

GROUND STATE
Spurious center of mass effects in a dynamically determined basis
[CSIR-TWISK-310] 01 p0109 N85-10732
Stark broadening of H(-) resonances in large electric fields
[DE84-016974] 04 p0496 N85-13164
Variational calculation of the 2D H2 molecule
[INPE-3304-PRE/615] 10 p1554 N85-19796
Quasiparticle aggregation in the Fractional Quantum Hall Effect
[DE85-001574] 10 p1565 N85-19868
Control of electronic, magnetic and optical properties of doped polyacetylene conductors
[AD-A150117] 12 p1814 N85-21375
Ab initio calculations of materials properties
[DE85-011167] 20 p3531 N85-31984

GROUND STATIONS
NT EARTH TERMINALS
NT POLYSTATION DOPPLER TRACKING SYSTEM
The application of microprocessors in the command and control of satellites by the MECB stations
[INPE-3282-RPE/466] 02 p0239 N85-11553
Determination of astronomical longitude differences: Munich, Karlsruhe, Niederreilenberg in 1974 04 p0524 N85-13355
Mark IVA DSN 26-meter subnet 05 p0624 N85-13995
Antenna microwave subsystem 05 p0625 N85-13997
Potential affiliate stations to work with the EVN — European VLBI Network; QUASAT 07 p1057 N85-16708
Dissemination of ERS-1 low bit rate data and the use of L-band receiving stations
[NLR-TR-83049-U] 09 p1358 N85-18542
The Telecommunications and Data Acquisition Report
[NASA-CR-174366] 10 p1462 N85-19224
Brazilian remote sensing receiving, recording and processing ground systems in the 1980's
[E85-10079] 10 p1504 N85-19493
Computer-assisted data processing and analysis system for ground-based meteorological data collection, report on the Sierra Cooperative Pilot Project
[PB85-115350] 10 p1520 N85-19587
The spot operational remote sensing satellite system: Current status and perspectives 11 p1713 N85-20776
The ARGOS VHF direct readout mini-station and CML-80-MP data collection Platform Transmitter Terminals (PTTs) 14 p2238 N85-23873
ARGOS VHF direct readout mini-station 14 p2239 N85-23886
Consultative Committee for Space Data Systems. Panel 1: Support
[NASA-CR-175786] 16 p2769 N85-27090
The Telecommunications and Data Acquisition Report
[NASA-CR-175842] 16 p2770 N85-27094
A description of the 64-meter antenna elevation drive gears and their strange wear 16 p2771 N85-27107
Repair of the DSS-14 pedestal concrete 16 p2772 N85-27108
Canadian Astronautics Limited's SARSAT ground stations 20 p3401 N85-31104
Ground segment of COSPAS system 20 p3402 N85-31106
The COSPAS/SARSAT local user terminal in Tromso, Norway. Special considerations and experience with high latitude location (69 deg, 43 min N) 20 p3402 N85-31109
Fault tolerant multiprocessor SARSAT-COSPAS 406 MHz local user terminal 20 p3404 N85-31123
The COSPAS-SARSAT system evaluation in Norway 20 p3406 N85-31133

GROUND SUPPORT EQUIPMENT
New airport ground traffic control system planned 03 p0310 N85-12006
National airspace system configuration management interface control document. Maintenance processor subsystem to remote monitoring subsystems and remote monitoring subsystem concentrators
[NAS-MD-790] 07 p0900 N85-15705
Equipment for preflight test of an Electronic Countermeasures (ECM) avionic system 07 p0939 N85-15949
External tank processing from barge to pad 08 p1096 N85-16927
Mechanical features of the shuttle rotating service structure 08 p1102 N85-16967
Payload transportation at KSC 08 p1103 N85-16970
STS payload ground handling mechanism at John F. Kennedy Space Center 08 p1103 N85-16971
Airport ground equipment under development at Riga 09 p1278 N85-18036
Improvements in Kazan airport equipment, facilities 09 p1278 N85-18039
Ministry officials on improving aircraft technical servicing 14 p2206 N85-23697

GROUND SUPPORT SYSTEMS
Integration of ground and on-board system for terminal count 08 p1092 N85-16896
Space shuttle flight readiness firing dress rehearsal for STS-1 08 p1097 N85-16929
Mathematical models for space shuttle ground systems 08 p1097 N85-16933
Support systems design and analysis 08 p1097 N85-16935
Impact of activation optimization on the Vandenberg Ground Support System using Q-GERT analysis
[AD-A148448] 08 p1105 N85-16986
Study of application of space telescope science operations software for SIRTF use
[NASA-CR-177337] 09 p1297 N85-18060
NASA-VCOSS dynamic test facility
[NASA-TM-86491] 10 p1427 N85-18998
MAP-related activities in the United States 11 p1655 N85-20427
A mathematical formulation of the problem of optimal use of ground resources for future space missions 12 p1947 N85-22232

GROUND TESTS
NT COLD FLOW TESTS
NT STATIC FIRING
Definition of ground test for verification of large space structure control
[NASA-CR-171208] 05 p0602 N85-13838
Level of effort 05 p0602 N85-13839
Oral presentation of first year final report, appendix A 05 p0602 N85-13840
Simplified planar model of ground test verification structure, appendix B 05 p0603 N85-13841
Definition of ground test for Large Space Structure (LSS) control verification, appendix G 05 p0603 N85-13845
Ground test experiment for large space structures, appendix I 05 p0603 N85-13847
Test signal generator for coherent air-to-ground radars
[AD-D011278] 05 p0628 N85-14025
A rig for testing the soft soil performance of track systems
[AD-P004272] 09 p1405 N85-18848
NASA-VCOSS dynamic test facility
[NASA-TM-86491] 10 p1427 N85-18998
Ground test experiment for large space structures
[NASA-TM-86489] 10 p1429 N85-19013
NASA/MSFC ground experiment for large space structure control verification
[NASA-TM-86496] 12 p1792 N85-21248
Definition of ground test for Large Space Structure (LSS) control verification
[NASA-TM-86495] 12 p1792 N85-21249
Spacecraft environmental interactions: A joint Air Force and NASA research and technology program 13 p1997 N85-22517
Scientific requirements for ozone measurements 13 p2105 N85-23113
Damping models for flexible communications satellites by substructural damping synthesis
[UTIAS-287] 14 p2237 N85-23868
A suggested standardized format for cosmic ray ground-level event data
[SH-9.1-15] 23 p4052 N85-35130

GROUND TRACKS
NT SATELLITE GROUND TRACKS
Mobility of the small combine (track type) on soft ground-relationship between the position of the center of gravity and the mobility
[AD-P004285] 09 p1407 N85-18862
Distributed control of circuits in multiuser communication networks with circuit precedence and path suitability criteria using failsafe routing concepts
[AD-A151625] 16 p2772 N85-27113

GROUND TRUTH
Evaluating effectiveness of using space information in specialized hydrogeological research 02 p0164 N85-11114
Active microwave measurements of sea ice under fall conditions: The RADARSAT/FIREX fall experiment — in the Canadian Arctic
[E85-10019] 02 p0217 N85-11432
Study of the improvement in analyzing passive microwave remote sensing data by integrated use of ground data 05 p0656 N85-14226
Classification of vegetation communities in the Battle Mountain SE quadrangle, Nevada with MSS digital data
[E85-10043] 06 p0826 N85-15246
Effective use of remote sensing products in litigation
[E85-10048] 06 p0827 N85-15250
Exploring the use of structural models to improve remote sensing agricultural estimates 07 p0965 N85-16259
The influence of the number of ground control points on the scene-to-map registration accuracy — Kansas, Louisiana, Mississipp, and Missouri 07 p0966 N85-16264
Amplitude calibration experiment for SIR-B 08 p1146 N85-17227
Ground truth for SIR-B images obtained by SIR system 8 impulse radar 08 p1149 N85-17251
Spectroradiometric calibration of the Thematic Mapper and Multispectral Scanner system
[E85-10077] 10 p1504 N85-19491
Preliminary evaluation of the airborne imaging spectrometer for vegetation analysis
[NASA-CR-174440] 10 p1505 N85-19496
Intra-eruption geologic map from an x-band radar image during the May 18, 1980 eruption of Mount St. Helens, Washington 13 p2199 N85-23639
Recent VAS imaging/sounding research 15 p2597 N85-26004
Simultaneous Earth observations from 2 satellites
[NASA-TM-86204] 16 p2810 N85-27325
Handbook for obtaining and using aerial photography to map aquatic plant distribution
[AD-A154684] 21 p3905 N85-32388
Interpretation of multiband photographs made during Telefoto-80 experiment for the purpose of discriminating agricultural crops 22 p3735 N85-33152
Direct regression analysis of remote sensing data (using example of grass cover) 22 p3736 N85-33157
LANDSAT-4/5 image data quality analysis
[E85-10105] 24 p4107 N85-35463

GROUND WATER
An evaluation of the electrodialysis reversal process (Edr) for the desalination of brackish water from the Omaruru delta (SWA/Namibia) 01 p0023 N85-10141
Major institutional arrangements affecting ground water in New York state
[PB84-202506] 01 p0065 N85-10429
Water resources data, Mississippi, water year 1982
[PB84-224559] 01 p0065 N85-10434
Water resources data, Florida, water year 1982. Volume 4: Northwest Florida
[PB84-223445] 01 p0066 N85-10437
The use of fixed-bed adsorber models to predict the fluxes of toxic substances in groundwaters and soil environments
[PB84-202563] 01 p0071 N85-10488
The application of remote sensing to resource management and environmental quality programs in Kansas
[E85-10023] 02 p0218 N85-11436
Water resources data for Florida, water year 1983. Volume 3B: Southwest Florida ground water
[PB84-220862] 03 p0364 N85-12459
Water resources data for California, water year 1982. Volume 1: Southern Great Basin from Mexican border to Mono Lake Basin and Pacific Slope Basins from Tijuana River to Santa Maria River
[PB84-220870] 03 p0364 N85-12461
Water resources data for Florida, water year 1982. Volume 3A: Southwest Florida surface water
[PB84-223060] 03 p0364 N85-12462
Water resources data for Nebraska, water year 1982
[PB84-223668] 03 p0365 N85-12463

Water resources data for California, water year 1982. Volume 3: Southern Central Valley Basins and Great Basins from Walker River to Truckee River
[PB84-223728] 03 p0385 N85-12464

Geothermal assessment of the lower Bear River drainage and northern East Shore ground-water areas, Box Elder County, Utah
[DE84-017958] 04 p0526 N85-13368

Subsurface temperatures in northeastern Wyoming measured by bottom hole temperature records
[TI84-901610] 04 p0534 N85-13413

Fate and disposition of trichloroethylene in surface soils
[AD-A147918] 07 p0995 N85-16321

Installation restoration program. Phase 2: Stage 1 problem confirmation study, Duluth International Airport Duluth, Minnesota
[AD-A148318] 08 p1089 N85-16885

Application of SIR-B data for groundwater exploration in the Arabian shield and sand-drift monitoring in the AN Nafud and Al Jafurah fringe areas, Kingdom of Saudi Arabia 08 p1144 N85-17214

German Radar Observation Shuttle Experiment (ROSE) 08 p1148 N85-17245

Electrical resistivity technique to assess the integrity of geomembrane liners
[PB85-122414/GAR] 09 p1325 N85-18327

Geothermal assessment of part of the east shore area, Davis and Weber Counties, Utah
[DE84-016817] 09 p1342 N85-18446

Ground-water level data and preliminary potentiometric-surface maps, Yucca Mountain and vicinity, Nye County, Nevada
[DE85-001771] 09 p1343 N85-18448

Applying an innovative approach to field investigations at a remedial action site
[AD-P004145] 09 p1348 N85-18481

Analysis of geohydrologic data by kriging
[AD-P004152] 09 p1349 N85-18488

Approximation of difference in water table positions by horizontal stratum in studies of their influence on gravity 10 p1502 N85-19478

Nationwide urban runoff program. Relationship of urban runoff to land use and groundwater resources
[PB85-114892] 10 p1506 N85-19505

Water resources data for Illinois, water year 1983. Volume 1: Illinois except Illinois River Basin
[PB85-125755] 10 p1507 N85-19506

Radioactive waste isolation in salt: Peer review of the Office of Nuclear Waste Isolation's report on the organic geochemistry of deep groundwaters from the Palo Duro Basin, Texas
[DE85-001439] 10 p1556 N85-19811

ELECT groundwater transport research code
[DE85-003284] 12 p1884 N85-21824

Shallow land burial technology: Humid
[DE85-004432] 12 p1932 N85-22136

Research and development related to the Nevada nuclear waste storage investigations
[DE85-002303] 12 p1932 N85-22138

Protecting the nation's groundwater from contamination, volume 1
[PB85-154201] 15 p2590 N85-25965

Protecting the nation's groundwater from contamination, volume 2
[PB85-154219] 15 p2590 N85-25966

Report on regional groundwater flow modeling for the Palo Duro Basin, Texas
[DE85-007490] 16 p2815 N85-27370

Groundwater model for an island aquifer: Bribie Island groundwater study
[CE-44] 16 p2821 N85-27398

In situ Tuff water migration/heater experiment
[DE85-010415] 18 p3101 N85-29200

Interim rock mass properties and conditions for analyses of a repository in crystalline rock
[DE85-010700] 18 p3125 N85-29352

Chlorine isotopes as environmental tracers in Columbia River basalt groundwaters
[DE85-011392] 19 p3302 N85-30473

Microwave hydrology: A trilogy
[NASA-CR-176042] 20 p3477 N85-31603

State-of-the-art of aquifer restoration. Volume 1: Sections 1 through 6
[PB85-181071] 20 p3478 N85-31612

State-of-the-art of aquifer restoration. Volume 2: Appendices A through G
[PB85-181089] 20 p3478 N85-31613

EPA (Environmental Protection Agency) research program guide, FY-1985, October 1, 1984 - September 30, 1985
[PB85-181881] 20 p3487 N85-31676

Geologic and hydrologic characterization and evaluation of the basin and range province relative to the disposal of high-level radioactive waste. Part 1: Introduction and guidelines
[GS-CIRC-904-A] 20 p3526 N85-31932

Geologic and hydrologic characterization and evaluation of the basin and range province relative to the disposal of high-level radioactive waste. Part 2: Geologic and hydrologic characterization
[GS-CIRC-904-B] 20 p3526 N85-31933

Geologic and hydrologic characterization and evaluation of the basin and range province relative to the disposal of high-level radioactive waste. Part 3: Geologic and hydrologic evaluation
[GS-CIRC-904-A] 20 p3526 N85-31934

Source-term considerations for a potential radioactive-waste repository located in unsaturated tuff
[DE85-010090] 20 p3529 N85-31953

Stochastic groundwater flow modeling using the second-order method
[DE85-011250] 22 p3802 N85-33556

Environmental surveillance at Los Alamos during 1984
[DE85-011886] 22 p3811 N85-33605

The 1984 environmental monitoring program report for Idaho National Engineering Laboratory site
[DE85-011209] 22 p3812 N85-33611

Anaerobic microbial transformations in subsurface environments: Project description
[DE85-012789] 23 p3951 N85-34486

State-of-the-art construction technology for deep tunnels and shafts in rock
[AD-A156362] 24 p4099 N85-35411

The geostatistical approach to the inverse problem in two-dimensional steady state groundwater modeling 24 p4107 N85-35462

Simulated effects of increased recharge on the ground-water flow system of Yucca Mountain and vicinity, Nevada-California
[DE85-012985] 24 p4108 N85-35469

Evaluation of low-temperature geothermal potential in north-central Box Elder County, Utah
[DE85-009541] 24 p4112 N85-35490

Geothermal resources of the Washakie and Great Divide basins, Wyoming
[DE85-013004] 24 p4112 N85-35491

Groundwater radon studies for earthquake precursors in southern California
[PB85-196871] 24 p4118 N85-35529

GROUND WAVE PROPAGATION

Synoptic observations of the radio noise background in the frequency range 150-180 kHz to provide design data for the low frequency communications designer
[AD-A147438] 07 p0941 N85-15965

Measurements and predictions of HF ground wave radio propagation over irregular, inhomogeneous terrain
[PB85-110666] 12 p1830 N85-21487

GROUND WIND

Atmospheric environment for Space Shuttle (STS-41G) launch
[NASA-TM-86486] 07 p0995 N85-16320

Revised Uniform Summary of Surface Weather Observations (RUSSWO). Alconbury RAF United Kingdom, parts A-F
[AD-A146913] 07 p1004 N85-16384

Revised Uniform Summary of Surface Weather Observations (RUSSWO). McChord AFB, Washington, parts A-F
[AD-A146914] 07 p1005 N85-16385

Revised Uniform Summary of Surface Weather Observations (RUSSWO). Mildenhall RAF, United Kingdom, parts A-F
[AD-A146915] 07 p1005 N85-16386

Revised Uniform Summary of Surface Weather Observations (RUSSWO). Dobbins AFB, Georgia, parts A-F
[AD-A146916] 07 p1005 N85-16387

Revised Uniform Summary of Surface Weather Observations (RUSSWO). Shemya AFB, Alaska, parts A-F
[AD-A146917] 07 p1005 N85-16388

Revised Uniform Summary of Surface Weather Observations (RUSSWO). Pope AFB, Fayetteville, North Carolina, parts A-F
[AD-A146918] 07 p1005 N85-16389

Revised Uniform Summary of Surface Weather Observations (RUSSWO). Sondestrom AB, Greenland, parts A-F
[AD-A146919] 07 p1005 N85-16390

Revised Uniform Summary of Surface Weather Observations (RUSSWO). England AFB, Alexandria, Louisiana, parts A-F
[AD-A146920] 07 p1006 N85-16391

Revised Uniform Summary of Surface Weather Observations (RUSSWO). Parts A-F: Homestead AFB, Florida
[AD-A147203] 07 p1007 N85-16396

On the formation of the nocturnal coastal surface wind speed maximum 09 p1356 N85-18528

Data catalog for the 1982 DFVLR observational Foehn experiment --- alpine wind
[DFVLR-FB-84-33] 09 p1358 N85-18543

Natural environment analysis
[NASA-CR-171333] 10 p1426 N85-19010

Wind shear detection technology
[GPO-38-920] 12 p1893 N85-21879

Preliminary study of inphase gusts and moment force wind loads over the first 150 meters at KSC, Florida
[NASA-TM-86501] 13 p2137 N85-23273

Summary of Meteorological Observations, Surface (SMOS), Bermuda
[AD-A150537] 13 p2138 N85-23278

Summary of Meteorological Observations, Surface (SMOS), Beaufort, South Carolina
[AD-A150539] 13 p2138 N85-23279

Mountain barrier baroclinity effects on surface winds along the Alaskan Arctic coast 14 p2238 N85-23877

Application of infrared radiometers for airborne detection of clear air turbulence and low level wind shear, airborne infrared low level wind shear detection test
[NASA-CR-175725] 15 p2594 N85-25985

Air flow of the western coastal boundary of South Africa and its influence on the ocean 16 p2831 N85-27459

The determination of lee circulation during the foehn wind 24 p4122 N85-35554

Turbulent structure of stably stratified nocturnal slope flows
[AD-A155845] 24 p4123 N85-35559

GROUND-AIR-GROUND COMMUNICATION

Combat capable space systems for tactical support 11 p1713 N85-20775

GROUP BEHAVIOR

U GROUP DYNAMICS

GROUP DYNAMICS

Command control group behaviors. Objective 1: A methodology for and identification of command control group behaviors
[AD-A145690] 02 p0191 N85-11279

An analysis of constraints to coordinated tactical crew interaction in the P-3C aircraft
[AD-A147220] 07 p1021 N85-16478

Integrated approach to flight crew training 09 p1276 N85-18014

Video concepts in CRM training 09 p1276 N85-18015

Research opportunities in human behavior and performance
[NASA-CR-175473] 10 p1529 N85-19640

Effect of prolonged hunger during experimental hikes 11 p1692 N85-20637

Team dimensions: Their identity, their measurement and their relationships
[AD-A149662] 12 p1908 N85-21978

Perceived heterogeneity and its effect on various types of tasks
[AD-A151003] 14 p2392 N85-24729

Individual characteristics and unit performance: A review of research and methods
[AD-A153145] 17 p3001 N85-28550

The impact of group processing on achievement in cooperative learning groups
[AD-A153168] 17 p3001 N85-28551

Oral discussion, group-to-individual transfer and achievement in cooperative learning groups
[AD-A153209] 17 p3001 N85-28552

The effects of controversy and concurrence seeking on effective decision making
[AD-A153370] 17 p3002 N85-28555

Symbolic and interactional perspectives on leadership: An integrative framework
[AD-A155247] 21 p3665 N85-32769

USSR report: Space Biology and Aerospace Medicine, vol. 19, no. 3, May - June 1985
[JPRS-USB-85-005] 23 p3952 N85-34494

GROUP THEORY

NT AUTOMORPHISMS
NT HOMOMORPHISMS

Trilinear alternating forms on a vector space of dimension 7
[CWI-PM-R8402] 05 p0722 N85-14644

Nonlinear semigroups and evolution governed by accretive operators
[AD-A147558] 07 p1033 N85-16557

A note on the G-space version of Glicksberg's theorem
[CWI-PM-R8405] 08 p1217 N85-17665

Chemical applications of topology and group theory. 18: Polyhedral isomerizations of seven-coordinate complexes
[AD-A149461] 10 p1436 N85-19047

Annals of the Fourier Institute, volume 34, no. 4 11 p1698 N85-20668

The Milnor link of a local field to a perfect residue field 11 p1698 N85-20670
A continuous Helson surface in R3 11 p1698 N85-20674
Finite products of commutators in C* algebras 11 p1698 N85-20676
Multi-sample cluster analysis as an alternative to multiple comparison procedures [AD-A149960] 12 p1923 N85-22084
On ergodic actions whose self-joinings are graphs [CWI-PM-R8408] 12 p1925 N85-22093
On localization of injective modules [CSIR-TWISK-342] 14 p2413 N85-24878
On positive vectors, positive matrices and the specialization ordering [CWI-PM-R8407] 14 p2414 N85-24890
Old and new in Moebius groups 15 p2634 N85-26235
Cocycles and magnetic monopole [DE85-007797] 16 p2856 N85-27612
Probabilistic algorithms in group theory [AD-A152253] 16 p2859 N85-27630
On the transformation of derivatives of distributions on surfaces [PREPRINT-434] 18 p3173 N85-29670
On the group-theoretical approach to the energy spectra problem of charge carriers in cubic solids [PREPRINT-495] 18 p3196 N85-29827

GROUP VELOCITY
Dispersion characteristics of small-mode gradient optical fibers 13 p2082 N85-23004
Calculating dominant (quasi-t) mode group velocity in shielded microstrip line 22 p3780 N85-33422

GROUP 7A COMPOUNDS
U HALOGEN COMPOUNDS

GROUT
Mixtures experiment where the amount of the mixture is a factor under study [DE85-010974] 19 p3250 N85-30153
Experimental characterization and stability of salt- and nonsalt-containing grouts and mortars (BCT-1F- and BCT-1FF-related) [DE85-012339] 22 p3753 N85-33263

GROWTH
NT CROP GROWTH
NT CRYSTAL GROWTH
NT CZOCHRALSKI METHOD
NT DIRECTIONAL SOLIDIFICATION (CRYSTALS)
NT ELECTROEPITAXY
NT EPITAXY
NT HYDROTHERMAL CRYSTAL GROWTH
NT LIQUID PHASE EPITAXY
NT MOLECULAR BEAM EPITAXY
NT TRAVELING SOLVENT METHOD
NT VAPOR PHASE EPITAXY
NT VEGETATION GROWTH
Effect of 1,25-dihydroxycholecalciferol and 24,25 dihydroxycholecalciferol on growth and alteration of rat bones during hypokinesia (histomorphometric study) 01 p0092 N85-10622
Acid rain and tree physiology: Some hypotheses for observed changes in forest productivity [DE84-016568] 05 p0672 N85-14318
Comparative effects of auxin and abscisic acid on growth, hydrogen ion efflux and gravitropism in primary roots of maize [NASA-CR-174355] 09 p1342 N85-18444
The use of image registration technique in Brasilia's urban growth monitoring [INPE-3302-PRE/614] 10 p1569 N85-19896
Mechanism and pattern of fatigue crack growth in aluminum alloys 11 p1597 N85-20047
User's guide to the TAMW wheat model as implemented on the IBM 360/195 computer [E85-10084] 12 p1873 N85-21749
Purification and cultivation of human pituitary growth hormone secreting cells [NASA-CR-171646] 12 p1899 N85-21923
Investigation of the MBE growth of InSb and novel quantum well structures [AD-A151014] 14 p2427 N85-24969
Role of Ca++ in shoot gravitropism — avena 15 p2607 N85-26065
A possible explanation of why gravitropic growth is detected earlier than straight growth 15 p2607 N85-26067
Constant fiber number during skeletal muscle atrophy and modified arachidonate metabolism during hypertrophy 15 p2609 N85-26078
Development and maturation of the neuromuscular junction in cell culture under conditions of simulated zero-gravity 15 p2611 N85-26093
Effects on in vivo and in vitro exposure to excess gravity on growth and differentiation of mammalian embryos 15 p2612 N85-26095
Gravitational effects on reproduction, growth and development of mammals 15 p2612 N85-26097
Numerical estimation of the curvature of biological surfaces 17 p3006 N85-28588
Cloud droplet nucleation and initial growth derived from lidar depolarization studies 21 p3644 N85-32635
Chemolithotrophy and physiology of bacterial nutrient limitation 21 p3650 N85-32730
Sulfate-reducing bacteria: Microbiology and physiology 21 p3650 N85-32732
Microbial colonization and growth on metal sulfides and other mineral surfaces 21 p3662 N85-32747
Screening and characterizing oleaginous microalgal species from the southeastern United States [DE85-008787] 23 p3951 N85-34488

GROWTH CHAMBERS
U PHYTOTRONS

GRUMMAN AIRCRAFT
NT F-14 AIRCRAFT
NT F-111 AIRCRAFT
NT OV-1 AIRCRAFT

GRUMMAN OV-1C AIRCRAFT
U OV-1 AIRCRAFT

GRUNEISEN CONSTANT
Low-temperature thermal expansion of glass 15 p2645 N85-26315

GUANIDINES
NT TRIAMINOGUANIDINIUM AZIDE

GUATEMALA
Tectonic lineaments in the cenozoic volcanics of southern Guatemala: Evidence for a broad continental plate boundary zone [NASA-CR-175456] 10 p1505 N85-19499

GUAYULE
Guayule research [GPO-29-562] 04 p0477 N85-13042
Process development for commercial production of natural rubber from Guayule [PB85-124956] 12 p1815 N85-21388

GUIDANCE (MOTION)
NT AIRCRAFT GUIDANCE
NT COMMAND GUIDANCE
NT INERTIAL GUIDANCE
NT LASER GUIDANCE
NT MAP MATCHING GUIDANCE
NT REENTRY GUIDANCE
NT RENDEZVOUS GUIDANCE
NT SATELLITE GUIDANCE
NT SPACECRAFT GUIDANCE
NT STRAPDOWN INERTIAL GUIDANCE
NT TERMINAL GUIDANCE
On-board near-optimal climb-dash energy management 02 p0137 N85-10931
Certification of advanced systems 06 p0753 N85-14829
USSR report: Engineering and equipment [JPRS-UEQ-85-001] 09 p1305 N85-18200
Optimization of guidance and control using function minimization and NAVSTAR/GPS [AD-A149956] 12 p1775 N85-21141
Determination of directional gyro parameters 14 p2287 N85-24171
Multi-rate digital autopilot modeling methodology [AD-A152044] 15 p2474 N85-25272
A cost-efficient control procedure for the benefit of all airspace users 16 p2697 N85-26651

GUIDANCE SENSORS
Study of alternate optical and fine guidance sensor designs for the space infrared telescope facility (SIRTF) [NASA-CR-166614] 07 p0915 N85-15794
Evaluation of nose, roof, and mast mounted sensor platforms for piloting and sighting, integrated in future combat helicopters 08 p1074 N85-16608
Fourth International Conference on Robot Vision and Sensory Controls [AD-A149524] 10 p1492 N85-19422
Gyrolaser guidance system for medium range missiles 16 p2596 N85-26649
The impact of VLSI on guidance and control system design 16 p2697 N85-26654

GUIDE VANES
NT JET VANES
Variable inlet vane assembly for a gas turbine combustion [AD-D011220] 01 p0010 N85-10063
Development and certification of a new stall warning and avoidance system 05 p0702 N85-14507
Mounting construction for turbine vane assembly [AD-D011395] 07 p0904 N85-15723
Influence of normalized frequency on time-dependent aerodynamic characteristics of vane blading profiles 09 p1306 N85-18204
Gasdynamic evaluation of choking cascade turns [AD-A151854] 15 p2557 N85-25778
Spacer structure [AD-D011641] 17 p2897 N85-27866

GUINEA PIGS
Measurement of cochlear acoustic pressure in guinea pigs [ISL-CO-234/83] 16 p2661 N85-27644
Spontaneous transitional cell carcinoma in the urinary bladder of a strain 13 guinea pig [AD-A155845] 21 p3685 N85-32764

GULF OF MEXICO
Hurricane experience levels of coastal county populations: Texas to Maine [PB85-111383] 10 p1520 N85-19581

GULF STREAM
The gulf stream deflection and meander energetics experiment. Current meter and bottom pressure gauge data report for the September, 1981 to April, 1982 mooring period [AD-A144977] 01 p0088 N85-10595
Circulation and internal waves in a cold Gulf Stream wave [AD-A149704] 12 p1896 N85-21918
Biological processes in the water column of the South Atlantic Bight. Volume 1: Published manuscripts [DE85-004610] 12 p1900 N85-21929
Circulation pattern of the North Atlantic, part of the warmwater sphere research effort at Kiel University 14 p2239 N85-23868
Horizontal and vertical structure of velocity, potential vorticity and energy in the gulf stream [AD-A154753] 21 p3655 N85-32702
Numerical simulations of the response of intense ocean currents to atmospheric forcing [AD-A155161] 21 p3655 N85-32704

GULFS
NT GULF OF MEXICO

GUM VULCANIZATES
U VULCANIZED ELASTOMERS

GUMBEL THEORY
U RANGE (EXTREMES)

GUN LAUNCHERS
Response of propellants to high dynamic stresses: The uses of gun launch techniques [DE84-013223] 02 p0188 N85-11259
Response of propellants to high dynamic stresses: The uses of gun launch techniques 08 p1116 N85-17035
Experimental simulation of the flow inside a gun barrel [ISL-CO-208/83] 14 p2302 N85-24252
A method of calculating the aim point for an unguided projectile fired at a moving target [BAE-BT-12717] 15 p2489 N85-25365
Telemetry system for the transmission of data from projectiles during the acceleration phase in the gun barrel [ISL-CO-207/84] 22 p3739 N85-33176
Experimental simulation of in-bore flows using a high pressure shock tube [ISL-CO-217/84] 22 p3785 N85-33452

GUN PROPELLANTS
Response of propellants to high dynamic stresses: The uses of gun launch techniques [DE84-013223] 02 p0188 N85-11259
Thrust characterization of very high burning rate propellants [AD-A145891] 03 p0340 N85-12186
Response of propellants to high dynamic stresses: The uses of gun launch techniques 08 p1116 N85-17035
Effects of perforation L/D ratio and slotting on stick propellant combustion [AD-A149854] 10 p1458 N85-19177
A review of hazard assessment procedures for liquid gun propellants [AD-A149470] 10 p1457 N85-19182
Experimental high pressure equation of state of a very fast burning gun propellant [DE85-001749] 10 p1458 N85-19184
Twenty-first JANNAF Combustion Meeting, volume 1 [AD-A150981] 13 p1998 N85-22526
Study on the combustion of nitramine propulsion powder up to 1500 MPa and comparison of the performance with that of classical propulsion powders [ISL-CO-203/83] 14 p2264 N85-24025
Fiber reinforcement of gun propellant [AD-A152296] 16 p2757 N85-27014
Liquid propellants for use in guns: A review [AD-A153051] 17 p2937 N85-28131
The determination of dinitrotoluene in single base propellants [AD-A154672] 21 p3571 N85-32209

GUNFIRE
Measurements of two-phase exhaust flow parameters of a small caliber gun associated with muzzle flash phenomena [ISL-CO-212/83] 16 p2784 N85-27182

GUNN DIODES
Low frequency noise in oscillator with limited space-charge accumulation 06 p0786 N85-15024
Development of a 20/30 GHz receiving station for propagation experiments with L-SAT
[AD-A148281] 08 p1152 N85-17271
A coaxial cavity gunn oscillator using probe coupled microstrip
[AD-D011437] 10 p1479 N85-19334
An integrated varactor tuned coaxial gunn oscillator for 60 GHz operation
[AD-D011439] 10 p1479 N85-19335
Filter reflection image guide oscillator and solid state line scanning device
[AD-D011440] 10 p1479 N85-19336
Millimetre wave pulse technology — satellite mapping
[ESA-CR(P)-2004] 20 p3478 N85-31611
GUNN EFFECT
Distributed Gunn effect devices: a numerical analysis of microstrip circuits on thin active GaAs substrates
[FOA-C-30363-E] 12 p1837 N85-21527
GUNPOWDER
U GUN PROPELLANTS
GUNS (ORDNANCE)
NT ARTILLERY
Response of propellants to high dynamic stresses: The uses of gun launch techniques 08 p1116 N85-17035
Sealing assembly
[AD-D011463] 10 p1452 N85-19151
An orthogonal grid technique for studying internal deformation and energy absorption in target penetration
[AD-A149989] 12 p1860 N85-21665
Modified Landolt C-ring test to measure the effects of laser filters on visual acuity
[AD-A151164] 15 p2617 N85-26127
Liquid propellants for use in guns: A review
[AD-A153051] 17 p2937 N85-28131
A computer code IB-KB for interior ballistics of recoiling and recoilless guns
[FOA-C-20566-D2] 18 p3164 N85-29602
Inertial navigation system - LAS II for SGT YORK testing
[AD-A154204] 19 p3216 N85-29944
Using synchro-ballistic cameras to determine the velocity and spin rate of high-velocity projectiles
[DE85-010629] 19 p3367 N85-30884
Next generation gunship
[AD-A156381] 24 p4065 N85-35193
GUST ALLEVIATORS
Flight test technique for evaluation of gust load alleviation analysis methodology
[NASA-TM-86344] 06 p0754 N85-14833
Helicopter active control with rotor blades relaxation 08 p1075 N85-16819
Flight test of the Open Loop Gust Alleviation (OLGA) system
[BMFT-FB-W-84-038] 08 p1086 N85-16861
OLGA: An open loop gust alleviation 16 p2713 N85-26744
OLGA: An open loop gust alleviation system 17 p2903 N85-27897
Gust load alleviation of a cantilevered rectangular elastic wing. Wind tunnel experiment and analysis
[NAK-TR-86] 18 p3063 N85-28950
GUST LOADS
Flight test technique for evaluation of gust load alleviation analysis methodology
[NASA-TM-86344] 06 p0754 N85-14833
Evaluating wind flow around buildings on heliport placement
[FAA-PM-84-25] 12 p1893 N85-21881
Dynamic wind tunnel testing for active control research 13 p1966 N85-22352
Qualification of the T2 wind tunnel in cryogenic operation. A: Thermal field, preliminary study of a schematic model
[NASA-TM-77781] 14 p2227 N85-23805
Identification of gust input and gust response characteristics from Do 28 TNT flight test data
[DFVLR-FB-84-48] 17 p2900 N85-27881
OLGA: An open loop gust alleviation system 17 p2903 N85-27897
Gust load alleviation of a cantilevered rectangular elastic wing. Wind tunnel experiment and analysis
[NAK-TR-86] 18 p3063 N85-28950
GUSTS
Aerodynamics of airfoils subject to 3-dimensional periodic gusts
[AD-A145149] 01 p0003 N85-10018
Attitude control using action-demanding interactive displays: Toward an active psychophysics
[AD-P004311] 09 p1267 N85-17965
Unsteady aerodynamic characterization of a military aircraft in vertical gusts
[NASA-TM-77810] 12 p1770 N85-21110
Transonic interactions of unsteady vortical flows
[NASA-TM-86658] 12 p1770 N85-21113
Qualification of the T2 wind tunnel in cryogenic operation. B: Flow fluctuations, particle detection and qualification
[NASA-TM-77782] 14 p2227 N85-23806
Synthesis study: Validation of a gust generator in the presence of a model in a wind tunnel
[ONERA-RT-16/5108-RY-051] 16 p2701 N85-26578
The gust simulation apparatus of the 3m x 3m low speed wind tunnel of the DFVLR in Goettingen, West Germany
[DFVLR-FB-85-04] 17 p2908 N85-27920
Automatic detection of gust fronts
[FAA-PM-85-11] 17 p2995 N85-28516
Lectures of a Flight Mechanics Conference — conferences
[ESA-TT-831] 24 p4061 N85-35165
Gust simulation for flight mechanical wind tunnel tests 24 p4062 N85-35172
GUY WIRES
A novel type of stayed tower for wind turbines
[ISD-295] 15 p2587 N85-25952
Dynamic and aeroelastic action of guy cables
[VTT-18] 16 p2802 N85-27276
GUYANA
The use of hydrometeorological data in explaining shrimp cycles in Guyana 07 p1004 N85-16381
GYMNASTICS
U PHYSICAL EXERCISE
GYRATION
NT EARTH ROTATION
NT MOLECULAR ROTATION
NT MUON SPIN ROTATION
NT PLANETARY ROTATION
NT PRECESSION
NT QUENCHING (ATOMIC PHYSICS)
NT REVOLVING
NT ROTATION
NT SATELLITE ROTATION
NT SOLAR ROTATION
NT STELLAR ROTATION
GYRATORS
NT MICROWAVE FILTERS
Gyrator frequency selectors with bandwidth independent of input signal level 13 p2083 N85-23009
Quasioptical gyroklystron
[AD-D011666] 19 p3356 N85-30601
GYRES
Current inventory of anthropogenic carbon dioxide in the North Pacific Subarctic Gyre
[PB85-187938] 24 p4125 N85-35570
GYRO HORIZONS
Attitude data consistence check of rocket payloads
[BMFT-FB-W-84-049] 12 p1790 N85-21239
Perception of roll rate from an artificial horizon and peripheral displays
[VTH-LR-403] 17 p3002 N85-28557
GYROCOMPASSES
Low cost gyrocompass
[AD-A148295] 08 p1082 N85-16857
Design of single-wheel gyrocompass with correction 14 p2272 N85-24079
Two-stage gyrocompass 14 p2273 N85-24080
Simulation of gyrocompassing alignment and calibration of strapdown inertial navigation system in a swaying vehicle
[DFVLR-MITT-84-20] 17 p2895 N85-27850
Elastic wave gyrometer
[REPT-26/4924/HF] 20 p3459 N85-31484
GYROINTERACTION
U MAGNETIC RIGIDITY
GYROMAGNETISM
Nonlocal and nonadiabatic expression for the ponderomotive force near cyclotron resonance
[IPPJ-736] 23 p3974 N85-34636
GYROPLANES
U HELICOPTERS
GYROS
U GYROSCOPES
GYROSCOPES
NT ATTITUDE GYROS
NT CONTROL MOMENT GYROSCOPES
NT ELECTROSTATIC GYROSCOPES
NT GYRO HORIZONS
NT GYROCOMPASSES
NT GYROSTABILIZERS
NT LASER GYROSCOPES
NT OPTICAL GYROSCOPES
NT ROTARY GYROSCOPES
Periodic oscillation of gyrostat-satellite about its center of mass in an elliptical orbit 02 p0159 N85-11080
Gyrotron beam generation with helical magnetic fields
[AD-A145987] 03 p0417 N85-12870
Development program: Nuclear magnetic resonance gyroscope (NMR-gyro). Phase 1: Development of an experimental model
[BMFT-FB-W-84-041] 05 p0639 N85-14101
Measurement of electromagnetic field components from arbitrarily oriented gyro platforms 06 p0787 N85-15030
A gyro sensor block suspension
[AD-D011411] 08 p1154 N85-17284
Loop radiating elements
[AD-D011409] 08 p1158 N85-17308
Data analysis techniques for vehicle attitudinal, positional and experimental measurements
[AD-A147752] 08 p1188 N85-17484
An alignment fixture for a 2-Degree-of-Freedom (TDF) gyroscope
[AD-A148885] 10 p1422 N85-19969
Analysis of interaction of dynamically adjustable gyroscopes on elastic platform by finite-element method 13 p2046 N85-22822
Determination of directional gyro parameters 14 p2287 N85-24171
Superconducting gyroscope research
[NASA-CR-171406] 15 p2560 N85-25795
Preguidance and piloting with the aid of composite inertial sensors 16 p2696 N85-26646
The series 2000: A miniature gas bearing DTG for low cost strapdown guidance and control 16 p2696 N85-26648
Low cost two gimbal inertial platform and its system integration 16 p2698 N85-26661
Positions of relative equilibrium of satellite-gyrostat 16 p2718 N85-26777
USSR report: Engineering and equipment
[JPRS-UEQ-84-006] 16 p2780 N85-27035
Estimates of errors of a gyroscope stabilized platform 16 p2783 N85-27050
Errors in compensating for image oscillation by means of a gyroscopic head 16 p2783 N85-27051
The DREO (Defence Research Establishment Ottawa) Inertial Navigation Laboratory: Development and test capabilities
[AD-A154425] 19 p3216 N85-29945
Test evaluation of the Honeywell GG1111 Single-Degree-of-Freedom (SDF) strapdown gyroscope
[AD-A154768] 21 p3589 N85-32307
Determining an azimuth with a north seeking gyro
[AD-A155880] 24 p4063 N85-35180
GYROSCOPIC DRIFT
U GYROSCOPES
U GYROSCOPIC STABILITY
GYROSCOPIC STABILITY
Contributions to the error analysis in the relativity gyroscope experiment 05 p0638 N85-14095
Flight dynamics of axisymmetrical rotating bodies in air medium 13 p2043 N85-22791
Test evaluation of the Honeywell GG1111 Single-Degree-of-Freedom (SDF) strapdown gyroscope
[AD-A154768] 21 p3589 N85-32307
GYROSTABILIZERS
Optimum parameters of aerogyroscopic satellite orientation system 16 p2718 N85-26782
GYROSTATS
U GYROSCOPES
GYROTRONS
U CYCLOTRON RESONANCE DEVICES

H

H ALPHA LINE
A warm magnetoactive plasma in a large volume of space 08 p0878 N85-15579
Theoretical studies of chromospheres and winds in cool stars
[NASA-CR-174204] 08 p0880 N85-15596
Increase in hydrogen emission of upper atmosphere following launches of space vehicles 13 p1961 N85-22431
H LINES
NT H ALPHA LINE
Variations of the H and K emission lines of singly ionized calcium in the eclipsing binary star system AR Lacertae 02 p0296 N85-11021
Photoionization structure of the Orion Nebula 08 p1246 N85-17883
The kinematic and radial properties of normal luminous SC galaxies 20 p3545 N85-32061
HABITABILITY
Human response to vibroacoustic environments of space vehicles
[NASA-TM-86316] 01 p0116 N85-10789
NASA's land remote sensing plans for the 1980's 13 p2124 N85-23224

Proceedings of the Seminar on Space Station Human Productivity
[NASA-TM-86673] 18 p3156 N85-29539
Space station crew safety: Human factors interaction model 18 p3156 N85-29540
Space station crew safety alternatives study, third quarter briefing 18 p3156 N85-29541
Habitability sleep accommodations 18 p3159 N85-29566
Rockwell experience applications to Ames space station mockup habitability/productivity studies 18 p3159 N85-29572

HABITATS
Ecology of estuarine channels of the pacific northwest coast: A community profile
[PB84-209709] 01 p0070 N85-10464
The use of digital spaceborne SAR data for the delineation of surface features indicative of malaria vector breeding habitats 08 p1146 N85-17230
Birds on airports: The reason for their presence 11 p1580 N85-19955
Use of a two-dimensional flow model to quantify aquatic habitat
[AD-A154287] 19 p3266 N85-30253
Microbial ecology of extreme environments: Antarctic yeasts and growth in substrate-limited habitats
[NASA-CR-176005] 19 p3326 N85-30609

HADRONS
NT BARYONS
NT KAONS
NT MESONS
NT MUONS
NT VECTOR MESONS
A concept for a hadron calorimeter with photodiode readout
[MPI-PAE/EXP-E1-130] 01 p0050 N85-10332
High intensity hadron accelerators
[DE84-014063] 01 p0119 N85-10812
Stochastic cell model for hadronic multiparticle distributions
[DE84-016480] 04 p0562 N85-13578
Stochastic methods for the description of multiparticle production
[DE84-009961] 10 p1556 N85-19610
Jet topologies in hadron-hadron collisions
[DE85-001328] 12 p1929 N85-22119
Glueball candidates
[DE85-003627] 14 p2418 N85-24921
Parton dynamics in hadronic processes
[DE85-006072] 14 p2418 N85-24922
Space station as quark matter factory
[DE85-004606] 15 p2665 N85-26585
Measurements of heavy quark and lepton lifetimes
[DE85-006321] 18 p3181 N85-29724
Electron-proton collider option for the superconducting super collider
[DE85-010146] 18 p3196 N85-29822
Detector problems at the SSC
[DE85-010217] 21 p3703 N85-33007
Generalized string amplitude and wave equation for hadrons
[DE85-011492] 22 p3842 N85-33798
Composition of primary cosmic rays near the bend from a study of hadrons in air showers at sea level
[OG-5.2-2] 22 p3863 N85-34059
The composition of cosmic rays near the Bend (10 to the 15th power eV) from a study of muons in air showers at sea level
[OG-5.2-3] 22 p3863 N85-34060
The primary composition beyond 10 to the 5th power GeV as deduced from high energy hadrons and muons in air showers
[OG-5.2-6] 22 p3863 N85-34063
Observations of cosmic-ray modulations in the fall, 1984
[SH-5.1-16] 23 p4043 N85-35060
Detector requirements for intensity interferometry measurements 24 p4147 N85-35709
Status of the zeta(8.3)
[DE85-013070] 24 p4149 N85-35724
Hadron cross sections at ultra high energies and unitarity bounds on diffraction dissociation
[HE-1.1-3] 24 p4170 N85-35851
On total cross sections and slopes at superhigh energies
[HE-1.1-4] 24 p4170 N85-35852
Hadron thermodynamics in relativistic nuclear collisions
[HE-1.1-8] 24 p4171 N85-35856
Estimation of the total inelasticity coefficient in interaction of greater than or equal to 20 TeV hadrons with lead
[HE-1.1-9] 24 p4171 N85-35857
1Single particle momentum and angular distributions in hadron-hadron collisions at ultrahigh energies
[HE-1.2-1] 24 p4171 N85-35860
Empirical description of the hadron-hadron and hadron-nucleus interaction at the accelerator energy range
[HE-1.2-4] 24 p4171 N85-35862
Low P sub T hadron-nucleus interactions
[HE-1.2-7] 24 p4172 N85-35865
Angular distribution and multiplicity of backward hadrons in hFe interactions at 0.5-5.0 TeV energies (PION Experiment)
[HE-1.2-8] 24 p4172 N85-35866
Nucleon-nucleus interactions from JACEE
24 p4173 N85-35869
A unification of the interactions and the diffractive processes 24 p4173 N85-35870
Is the inelastic charge-exchange contribution constant at the large X and superhigh energies? Qaut 01Kuchin, I. A. 24 p4173 N85-35871
General consequences of the violated Feynman scaling 24 p4173 N85-35872
Propagation of cosmic rays through the atmosphere in the quark-gluon strings model 24 p4173 N85-35873
Scaling violation in the fragmentation region of inclusive nucleon spektrum 24 p4173 N85-35874
Physical meaning of the multiplicities of emitted nucleons in hadron-nucleus collisions 24 p4174 N85-35877
How are particle production, nucleon emission and target fragment evaporation processes interrelated in hadron-nucleus collisions? 24 p4174 N85-35878
Experimental study of the space-time development of the particle production process in hadron-nucleon collisions, using massive target nucleus as a detector 24 p4174 N85-35879
Experimental evidence of the decrease of kinetic energy of hadrons in passing through atomic nuclei 24 p4174 N85-35880
Energy-range relations for hadrons in nuclear matter 24 p4174 N85-35881
Scattering and stopping of hadrons in nuclear matter 24 p4174 N85-35882
Measurements of hadron mean free path for the particle-producing collisions in nuclear matter 24 p4174 N85-35883
The phi-meson and Chiral-mass-meson production in heavy-ion collisions as potential probes of quark-gluon-plasma and Chiral symmetry transitions 24 p4175 N85-35884
Heavy flavours production in quark-gluon plasma formed in high energy nuclear reactions 24 p4175 N85-35886
Observation of direct hadronic pairs in nucleus-nucleus collisions in JACEE emulsion chambers
[HE-1.4-5] 24 p4176 N85-35893
Inclusive angular distribution of alpha and Li fragments produced in the Fe-C and Fe-Pb collisions at 1.88 GeV/u
[HE-1.4-11] 24 p4177 N85-35898
Experiment Pamir-3. Coplanar emission of high energy gamma-quanta at interaction of hadrons with nuclei of air atoms at energies above 10 to the 7th power GeV
[HE-1.4-12] 24 p4177 N85-35899
Japan - USSR joint emulsion chamber experiment at Pamir
[HE-3.1-1] 24 p4177 N85-35901
Intensities of high-energy cosmic rays at Mount Kanbala
[HE-3.1-2] 24 p4177 N85-35902
High energy gamma-rays and hadrons at Mount Fuji
[HE-3.1-3] 24 p4177 N85-35903
Hadron intensity and energy spectrum at 4380 m above level
[HE-3.1-7] 24 p4178 N85-35905
Some characteristic cosmic ray events and an attempt at their explanation
[HE-3.1-8] 24 p4178 N85-35906
Scaling violation in fragmentation region at energies above 10-15 eV based on the data on cosmic ray hadron component
[HE-3.1-11] 24 p4178 N85-35909
Jets in air-jet family
[HE-3.2-1] 24 p4179 N85-35912
Scaling violation in hadron-nucleus interaction
[HE-3.2-8] 24 p4179 N85-35916
Few-particles generation channels in inelastic hadron-nuclear interactions at energy approximately equals 400 GeV
[HE-3.2-9] 24 p4179 N85-35917
Study of hadron bundles observed in Chacaltaya two-story emulsion chamber
[HE-3.3-4] 24 p4180 N85-35922
Penetrative nature of high energy showers observed in Chacaltaya emulsion chamber
[HE-3.3-5] 24 p4180 N85-35923
Anomalous correlation between hadron and electromagnetic particles in hadron and gamma-ray families
[HE-3.3-6] 24 p4180 N85-35924
Atmospheric interactions detected in both the upper and the lower chambers at Chacaltaya
[HE-3.3-7] 24 p4180 N85-35925
Lateral distribution of high energy hadrons and gamma ray in air shower cores observed with emulsion chambers
[HE-3.3-8] 24 p4180 N85-35926
A cosmic ray super high energy multicore family event. 2: Structure and fragmentation characteristics of the jets
[HE-3.4-2] 24 p4181 N85-35931
Observation of super high energy big family with large scale Fe emulsion chambers
[HE-3.4-3] 24 p4182 N85-35932
A halo event created at 200 m above the Chacaltaya emulsion chamber
[HE-3.4-5] 24 p4182 N85-35933
A binocular-type atmospheric interaction generating sequential exotic features
[HE-3.4-6] 24 p4182 N85-35934
Gamma-hadron families and scaling violation
[HE-3.4-7] 24 p4182 N85-35935
Super-family P2 C-86-125 observed by Japan-URSS Joint Emulsion Chamber Experiment
[HE-3.4-8] 24 p4182 N85-35936
Experiment Pamir-2. Fianit: A giant super-family with halo (Epsilon sub 0 at approximately 10(17) eV)
[HE-3.4-10] 24 p4182 N85-35938
Experiment Pamir-4: Analysis of superfamily with halo of electromagnetic nature detected in deep XEC
[HE-3.4-11] 24 p4183 N85-35939
A search for mini-clusters in Japan-USSR Joint Experiment at Pamir
[HE-3.5-2] 24 p4183 N85-35941
Mini-clusters
[HE-3.5-3] 24 p4183 N85-35942
Giant mini-clusters as possible origin of halo phenomena observed in super-families
[HE-3.5-4] 24 p4183 N85-35943
LPM effect and primary energy estimations
[HE-3.6-4] 24 p4185 N85-35953
Experimental basis for the models of cascade propagation in atmosphere
[HE-3.6-6] 24 p4185 N85-35954
Relation between gamma-ray family and EAS core: Monte-Carlo simulation of EAS core
[HE-3.6-7] 24 p4185 N85-35955
Comparison of big event with calculations of the air shower development
[HE-3.6-8] 24 p4185 N85-35956
On mini-cluster observed by Chacaltaya emulsion chamber experiment
[HE-3.6-12] 24 p4185 N85-35959
A comparative analysis of gamma and hadron families at the superhigh energies recorded in experiment Pamir
[HE-3.7-1] 24 p4185 N85-35960
Hadrons registration in emulsion chamber with carbon block
[HE-3.7-3] 24 p4186 N85-35962
Intensities of high-energy cosmic rays at Mount Kanbala
[HE-3.7-5] 24 p4186 N85-35964
Structured events in Pamir carbon X-ray chambers
[HE-3.7-7] 24 p4186 N85-35965
Analysis of the hadron component in E.A.S.
24 p4187 N85-35971
Electrons, muons and hadrons in extensive air showers and how do they depend on nuclear interaction model, part 1 24 p4187 N85-35972
High energy hadrons in extensive air showers
24 p4187 N85-35976
Dependence of the average spatial and energy characteristics of the hadron-lepton cascade on the strong interaction parameters at superhigh energies
24 p4188 N85-35977
Hadronic components of EAS by rigorous saddle point method in the energy range between 10(5) and 10(8) GeV 24 p4188 N85-35978
About increase of the large transvere momentum processes fraction in hA interactions at energies 5.10(14) - 10(16) eV according to the data on E.A.S. hadrons
24 p4188 N85-35979
Phenomenology of soft hadron interactions and the relevant EAS data 24 p4188 N85-35980
The maximum depth of shower with E sub 0 larger than 10(17) eV on average characteristics of EAS different components 24 p4188 N85-35981
Sensitivity of depth of maximum and absorption depth of EAS to hadron production mechanism
24 p4188 N85-35982
Theoretical study of EAS hadronic structure
24 p4189 N85-35991
Muon spectrum in air showers initiated by gamma rays
[HE-4.5-4] 24 p4195 N85-36028

Electromagnetic and muonic structure of showers initiated by gamma-rays and by hadrons
[HE-4.5-6] 24 p4195 N85-36030
The muon content of gamma-ray showers
[HE-4.5-7] 24 p4195 N85-36031
Simulation of gamma-initiated showers
[HE-4.5-10] 24 p4195 N85-36033
Nuclear cascades in electromagnetic showers produced by primary gamma-quanta in the atmosphere
[HE-4.5-16] 24 p4196 N85-36038
Investigation of cosmic rays in very short time scales
[HE-4.6-7] 24 p4197 N85-36044
A facility for investigation of multiple hadrons at cosmic-ray energies
[HE-4.6-8] 24 p4197 N85-36045
Sub-luminal pulses from cosmic ray air showers
[HE-4.7-13] 24 p4200 N85-36063
Anomalies in cosmic rays: New particles versus charm?
[HE-5.4-9] 24 p4208 N85-36120
Collimated groups of particles as possible manifestation of heavy meson production
[HE-5.4-14] 24 p4208 N85-36124
Energetic delayed hadrons in large air showers observed at 5200m above sea level
[HE-6.2-9] 24 p4211 N85-36145
Observation of genetic relation among new phenomena Geminion, Chiron and mini-Centauro
[HE-6.2-16] 24 p4212 N85-36152
Tien-Shan effect and charmed particles
[HE-6.2-17] 24 p4212 N85-36153

HAFNIUM
Long range ordered alloys modified by addition of niobium and cerium
[DE85-011661] 20 p3431 N85-31285

HAFNIUM ALLOYS
Temperature variation of resistivity of certain alloys based on transition and simple metals in amorphous and crystalline states 15 p2496 N85-25399

HALF LIFE
The I-Pu-Xe age of the Moon
04 p0584 N85-13729
Study of proton and neutron activation of metal samples in low Earth orbit
[NASA-CR-171506] 21 p3558 N85-32130

HALF PLANES
Stresses in a half-plane containing either a pressurized hole or an interference-fit disc
[ARL/STRUC-R-409] 12 p1865 N85-21700
Elastic response of a half-plane to a bonded interference-fit disc of the same material
[ARL/STRUC-R-406] 12 p1865 N85-21701

HALF SPACES
Halfspace representations of extrusions, solids of revolution and pyramids
[DE84-015005] 01 p0104 N85-10700
Propagation of longitudinal elastic waves in multilayered half-space 02 p0273 N85-11779
Acoustic emission waveforms in a half space
[AD-A146322] 03 p0417 N85-12664
Elastic wave scattering from an interface crack in a layered half space 13 p2101 N85-23095
Interaction among inhomogeneities and inclusions
[AD-A153114] 17 p2979 N85-28419
Transient dynamic solutions of some half space problems by the boundary element method
19 p3283 N85-30360
Numerical experiment of elastic wave propagation by framework model
[DRIC-T-7462] 22 p3795 N85-33511

HALIDES
NT ALKALI HALIDES
NT ALUMINUM CHLORIDES
NT BERYLLIUM FLUORIDES
NT BORON FLUORIDES
NT BROMIDES
NT CADMIUM FLUORIDES
NT CALCIUM CHLORIDES
NT CALCIUM FLUORIDES
NT CARBON TETRACHLORIDE
NT CESIUM IODIDES
NT CHLORIDES
NT COPPER CHLORIDES
NT DICHLORIDES
NT DIFLUORIDES
NT FLUORIDES
NT HYDROBROMIC ACID
NT HYDROCHLORIC ACID
NT HYDROFLUORIC ACID
NT HYDROGEN CHLORIDES
NT IRON CHLORIDES
NT LITHIUM CHLORIDES
NT LITHIUM FLUORIDES
NT MAGNESIUM CHLORIDES
NT MAGNESIUM FLUORIDES
NT METAL HALIDES
NT OXYFLUORIDES
NT OXYHALIDES
NT POTASSIUM CHLORIDES
NT SILVER CHLORIDES
NT SILVER HALIDES
NT SILVER IODIDES
NT SODIUM CHLORIDES
NT SODIUM IODIDES
NT STRONTIUM FLUORIDES
NT SULFUR FLUORIDES
NT TITANIUM CHLORIDES
NT URANIUM FLUORIDES
NT ZINC CHLORIDES
Electronic-to-vibrational energy transfer studies of singlet molecular oxygen and hydrogen halides
[AD-A145587] 02 p0277 N85-11802
Combustion kinetics of metal oxide and halide radicals
[AD-A148521] 08 p1122 N85-17076
Spectroscopic studies of lasing transitions in the diatomic mercury halides
[AD-A151553] 15 p2563 N85-25809
Metal vapor lasers and their applications
[ISL-CO-218/84] 22 p3791 N85-33486
Thermodynamic data for mineral technology
[PB85-184331] 22 p3803 N85-33560

HALL COEFFICIENT
U HALL EFFECT

HALL CURRENTS
U ELECTRIC CURRENT
U HALL EFFECT

HALL EFFECT
Calibration of hall probes
[CSIR-NAC-83-04] 01 p0116 N85-10794
A study of defects in neutron transmutation doped silicon: Gallium by hall effect analysis
[AD-A146047] 03 p0433 N85-12758
Implications of the chiral anomaly for quantum Hall effect devices
[NUB-2662] 05 p0629 N85-14029
Motion of electrons in non polar classical liquids
[DE84-013609] 05 p0727 N85-14672
Anomalous electronic transport in boron carbides
[DE84-015820] 06 p0868 N85-15518
Quasiparticle aggregation in the Fractional Quantum Hall Effect
[DE85-001574] 10 p1565 N85-19868
Power circuit utilizing self-excited Hall effect switch means
[AD-D011505] 12 p1832 N85-21496
High temperature position sensors based on monolithic GaAs Hall IC
[BMFT-FB-T-84-266] 17 p2969 N85-28337
Activities of the Solid State Physics Research Institute
[NASA-CR-175899] 17 p3042 N85-28818
Hall mobility in fluid argon
[DE85-007288] 17 p3045 N85-28840
Quantized Hall conductance as a topological invariant
[DE85-007798] 18 p3193 N85-29808
Quantized Hall effect in two-dimensional electron systems
[AD-A154347] 19 p3259 N85-30211
Fractional statistics and fractional quantized Hall effect
[DE85-007833] 19 p3375 N85-30940
Electrical properties of bulk grown nitrogen doped silicon
[AD-A155471] 21 p3581 N85-32266
Gauge invariance and fractional quantized Hall effect
[DE85-007832] 23 p3965 N85-34716

HALLEY'S COMET
A cometary ion mass spectrometer
[NASA-CR-174328] 08 p1184 N85-17343
Airborne observations of comets
08 p1244 N85-17853
Extended atmospheres of outer planet satellites and comets
[NASA-CR-174398] 09 p1416 N85-18933
The international VEGA 'Venus-Halley' (1984-1986 experiment: Description and scientific objectives
[NASA-TM-77536] 12 p1960 N85-22324
Averaging of equations of cometary orbital motion with allowance for nongravitational effects
13 p1978 N85-22411
History and future views on solar cells of Japanese scientific satellites 13 p2005 N85-22566
Giotto solar array: Design, manufacture and test
13 p2008 N85-22589
Development of Halley's Comet explorer PLANET-A solar array 13 p2010 N85-22608
Research in planetary studies and operation of Mauna Kea Observatory
[NASA-CR-175618] 13 p2169 N85-23460
Halley's Comet, a bibliography
[LC-84-600109] 13 p2204 N85-23674
Giotto plasmasheath and wake charging near Halley's Comet: Revised parameters 14 p2245 N85-23915
Anticipated impact plasma problems for the COPERNIC-RPA experiment in the cometary environment — Giotto mission 14 p2245 N85-23917
An impact plasma monitor for cometary missions — Giotto , VEGA 14 p2245 N85-23918
Spacecraft environment during the Giotto-Halley encounter: A summary 14 p2246 N85-23921
Towards the Halley Comet 14 p2399 N85-24783
The astrometry network of the IHW and the P/Crommelin trial run results 14 p2435 N85-25016
Near-nucleus studies of Comet Halley
14 p2435 N85-25018
Kitt Peak measurements of P/Halley positions
14 p2436 N85-25023
The astrometry network of observers in China
14 p2436 N85-25027
The astrometry network of observers in Japan
14 p2436 N85-25026
The astrometry network of observers in USSR
14 p2436 N85-25029
The IHW reference star catalogs for Comets Halley and Giocobini-Zinner 14 p2436 N85-25031
The orbits of Comets Halley and Giocobini-Zinner
14 p2437 N85-25039
The orbital motion of Comet Halley
14 p2437 N85-25040
The work on Comet Halley's orbit at ESOC
14 p2438 N85-25041
Astrometric needs for the ISEE-3/ICE mission to Comet Giocobini-Zinner 14 p2438 N85-25043
Determination of the observation conditions of celestial bodies with the aid of the DISPO system
[NAS 1.15:77632] 14 p2438 N85-25044
Kovtunenko comments on Vega flight plan, instrumentation 15 p2482 N85-25318
Comments on Vega mission 15 p2482 N85-25319
Press conference on flight of Vega spacecraft
15 p2482 N85-25320
Sixteenth Lunar and Planetary Science Conference. Press abstracts
[NASA-CR-175892] 15 p2660 N85-26548
Dust emission of Comet Halley at large heliocentric distances 15 p2661 N85-26556
TASS update on flights of Vega-1 and Vega-2
16 p2722 N85-26803
Kovtunenko discuses Vega Project
16 p2722 N85-26804
French and West German equipment for Vega Project
16 p2722 N85-26805
Swedish space program includes research satellites
18 p3088 N85-29113
Program for observations of Halley's comet
22 p3732 N85-33138
The 1986 National Aeronautics and Space Administration authorization
[GPO-47-835] 24 p4166 N85-35829
Comet Halley returns: A teachers' guide 1985-1986
[NASA-EP-197] 24 p4168 N85-35839

HALOCARBONS
NT FLUOROCARBONS
Flow of nitrogen-pressurized Halon 1301 in fire extinguishing systems
[NASA-CR-174271] 07 p0900 N85-15701
New liquid cathodes for lithium batteries. Part A: Halocarbons
[AD-A148433] 08 p1178 N85-17423

HALOGEN COMPOUNDS
NT ALKALI HALIDES
NT ALUMINUM CHLORIDES
NT AMMONIUM PERCHLORATES
NT BERYLLIUM FLUORIDES
NT BORON FLUORIDES
NT BROMIDES
NT BROMINE COMPOUNDS
NT CADMIUM FLUORIDES
NT CALCIUM CHLORIDES
NT CALCIUM FLUORIDES
NT CARBON TETRACHLORIDE
NT CARBON TETRAFLUORIDE
NT CESIUM IODIDES
NT CHLORIDES
NT CHLORINE COMPOUNDS
NT CHLORINE OXIDES
NT CHLOROSILANES
NT COPPER CHLORIDES
NT DDT
NT DICHLORIDES
NT DIFLUORIDES
NT DIFLUORO COMPOUNDS
NT FLUORIDES
NT FLUORINE COMPOUNDS
NT FLUORINE ORGANIC COMPOUNDS
NT FLUORITE
NT FLUORO COMPOUNDS
NT FLUOROCARBONS
NT FLUOROHYDROCARBONS

NT FLUOROPOLYMERS
NT HALIDES
NT HALOCARBONS
NT HYDROBROMIC ACID
NT HYDROCHLORIC ACID
NT HYDROFLUORIC ACID
NT HYDROGEN CHLORIDES
NT IODIDES
NT IODINE COMPOUNDS
NT IRON CHLORIDES
NT LITHIUM CHLORIDES
NT LITHIUM FLUORIDES
NT LITHIUM IODATES
NT MAGNESIUM CHLORIDES
NT MAGNESIUM FLUORIDES
NT METAL FLUORIDES
NT METAL HALIDES
NT OXYFLUORIDES
NT OXYHALIDES
NT PERCHLORATES
NT PERFLUOROALKANE
NT POLYTETRAFLUOROETHYLENE
NT POTASSIUM CHLORIDES
NT POTASSIUM PERCHLORATES
NT SILVER CHLORIDES
NT SILVER HALIDES
NT SILVER IODIDES
NT SODIUM CHLORIDES
NT SODIUM IODIDES
NT STRONTIUM FLUORIDES
NT SULFUR FLUORIDES
NT TITANIUM CHLORIDES
NT URANIUM FLUORIDES
NT ZINC CHLORIDES
Catalyzed low burning rate propellants for upper-stage solid rocket motor
[NAL-TR-805] 03 p0339 N85-12181
Structural phase transitions in doped hexahalogen metallates 03 p0426 N85-12721

HALOGENATION
NT CHLORINATION
NT FLUORINATION
Process for functionalizing alkanes
[DE85-006420] 23 p3909 N85-34219

HALOGENS
NT BROMINE
NT BROMINE ISOTOPES
NT CHLORINE
NT FLUORINE
NT IODINE
NT IODINE ISOTOPES
Determination of halogens and sulfur in organic compounds and polymers by combustion-ion chromatography
[DE84-016186] 05 p0614 N85-13921
Polymerization and halogen scrambling behavior of phenyl-substituted cyclotriphosphazenes
[AD-A146366] 06 p0771 N85-14930
Halogen mass flow rate detection system
[AD-D011398] 08 p1166 N85-17352
Adsorption thermodynamics and surface transport of metal catalyst poisons
[DE85-003750] 12 p1802 N85-21301
RF-Primed high power halogen vial apparatus
[AD-D011545] 12 p1935 N85-22156

HALOS
Highly ionized gas associated with the small Magellanic cloud 11 p1745 N85-20976
Galactic absorption lines measured from the IUE low dispersion spectra of active galaxies 11 p1745 N85-20977
Dark halo craters and the thickness of grooved terrain on Ganymede 13 p2173 N85-23484
Jupiter's ring system resolved: Physical properties inferred from the Voyager images 20 p3546 N85-32069
Evidence for a dynamical halo around the edge-on galaxy NGC 4631
[OG-6.2-1] 22 p3889 N85-34102
Halo of NGC 4631 and models of cosmic-ray transport
[OG-6.2-3] 22 p3889 N85-34103
The extent of the local hi halo
[NASA-CR-176115] 23 p3987 N85-34724
A cosmic ray super high multicore family event. 1: Experiment and general features
[HE-3.4-1] 24 p4181 N85-35930
A halo event created at 200 m above the Chacaltaya emulsion chamber
[HE-3.4-5] 24 p4182 N85-35933
On the halo events observed by Mount Fuji and Mount Kanbala Emulsion Chamber Experiments
[HE-3.4-9] 24 p4182 N85-35937
Experiment Pamir-2. Flarit: A giant super-family with halo (Epsilon sub 0 at approximately 10(17) eV)
[HE-3.4-10] 24 p4182 N85-35938
Experiment Pamir-4: Analysis of superfamily with halo of electromagnetic nature detected in deep XEC
[HE-3.4-11] 24 p4183 N85-35939
Giant mini-clusters as possible origin of halo phenomena observed in super-families
[HE-3.5-4] 24 p4183 N85-35943
Structure of super-families
[HE-3.5-7] 24 p4183 N85-35944
Extremely high energy hadron and gamma-ray families(3). Core structure of the halo of superfamily
[HE-3.5-8] 24 p4183 N85-35945
Numerical analysis of electromagnetic cascades in emulsion chambers
[HE-3.5-9] 24 p4184 N85-35946

HAMILTON-JACOBI EQUATION
The period of orbit as a test of the general theory of relativity 05 p0742 N85-14772
Viscosity solutions of Hamilton-Jacobi equations at the boundary
[AD-A147444] 07 p1032 N85-16553
Neumann type boundary conditions for Hamilton-Jacobi equations
[AD-A149089] 10 p1546 N85-19746
Hamilton-Jacobi equations in infinite dimensions. Part 1. Uniqueness of viscosity solutions
[AD-A149094] 10 p1546 N85-19749
A remark on regularization in Hilbert spaces
[AD-A149046] 10 p1552 N85-19787

HAMILTONIAN FUNCTIONS
Stable and chaotic dynamical systems and their singularities in the complex time plan
[DE84-011780] 01 p0035 N85-10222
Spurious center of mass effects in a dynamically determined basis
[CSIR-TWISK-310] 01 p0109 N85-10732
Equipartition threshold in nonlinear large Hamiltonian systems: The Fermi-Pasta-Ulam model
[NOTA-INTERNA-819] 02 p0255 N85-11670
Stochasticity and transport in Hamiltonian systems 02 p0282 N85-11836
Long-time tail in the two-wave model 02 p0282 N85-11837
On existence and uniqueness of solutions of Hamilton-Jacobi equations
[AD-A147597] 07 p1033 N85-16560
An invariant measure for the equation u sub tt - u sub xx + u3 = O
[AD-A147300] 08 p1210 N85-17612
Periodic solutions of prescribed energy for a class of Hamiltonian systems
[AD-A149487] 10 p1548 N85-19764
Geometric Hamiltonian structures and perturbation theory
[DE85-002005] 11 p1707 N85-20737
Covariant lie-transformed plasma action principle
[DE85-000285] 11 p1732 N85-20891
Accidental degeneracies, hidden supersymmetries, and spectrum-generating superalgebras
[DE85-003547] 11 p1738 N85-20930
A method of calculating periodic solutions of second order dynamical systems
[AD-A149634] 12 p1920 N85-22058
Stability of permanent rotation modes of asymmetric heavy solid body 14 p2279 N85-24118
Elements of celestial mechanics 14 p2398 N85-24762
On matchings and Hamiltonian cycles in random graphs
[AD-A151015] 14 p2409 N85-24851
Application of quaternions to problems of solid body dynamics in the atmosphere 15 p2481 N85-25313
Eigenvalue approximation methods for quantum lattice Hamiltonians 16 p2858 N85-27627
Hamiltonian picture of the free electron laser and unitary symmetries
[PREPRINT-436] 18 p3114 N85-29281
A numerical investigation of the overlap distribution among pure states in the spin glass phase
[PREPRINT-414] 18 p3172 N85-29650
The Hamiltonian structure of a complex version of the Burgers hierarchy
[PREPRINT-423] 18 p3173 N85-29665
Reduction techniques for infinite-dimensional Hamiltonian systems: Some ideas and applications
[PREPRINT-424] 18 p3173 N85-29666
Further results on the equipartition threshold in large nonlinear Hamiltonian systems
[PREPRINT-428] 18 p3173 N85-29668
Exact invariants in resonance form for time-dependent potentials
[DE85-010733] 19 p3346 N85-30739
One- and two-electron transfer processes in ion-surface scattering
[AD-A154208] 19 p3353 N85-30782
Interacting Boson approximation
[DE85-003016] 22 p3837 N85-33756
Width of nonlinear difference resonances
[DE85-013026] 24 p4148 N85-35719

HAND (ANATOMY)
NT FINGERS
Computerized sleep staging by detecting eye and hand movement, delta EEG activity and EMG, using portable solid state technique — spaceborne experiments 05 p0695 N85-14475
A control model: Interpretation of Fitts' law 05 p0706 N85-14526
Mechanical properties for the grasp of a robotic hand
[AD-A150062] 12 p1860 N85-21669
Instrument for determining spatial coordination of hand movements 14 p2387 N85-24702
Investigation of the requirement for auxiliary heating of Canadian forces personnel
[AD-A151950] 16 p2841 N85-27522
Hand controllers for teleoperation. A state-of-the-art technology survey and evaluation
[NASA-CR-175890] 17 p3002 N85-28559
An analysis of multi-fingered hands 20 p3462 N85-31504

HANDBOOKS
NT USER MANUALS (COMPUTER PROGRAMS)
Information Center handbook
[PB84-211341] 03 p0439 N85-12795
Economic analysis handbook
[AD-A146263] 03 p0441 N85-12805
Vibration data analysis system for SNLA area 3 reference manual
[DE84-016207] 04 p0514 N85-13275
National Bureau of Standards passive solar test facility: Instrumentation and site handbook
[PB85-100451/GAR] 07 p0968 N85-16148
Project manager's handbook for special projects
[AD-A147913] 07 p1053 N85-16683
Technical order managers handbook: Utilization assessment
[AD-A147579] 07 p1055 N85-16684
User's guide for the Photochemical Box Model (PBM)
[PB85-137164] 11 p1682 N85-20602
Instructor's handbook on meteorological instrumentation
[PB85-105930] 11 p1688 N85-20615
Atmospheric handbook: Atmospheric data tables available on computer tape
[PB85-108512] 12 p1891 N85-21867
Review of US guide on medication and flying 12 p1904 N85-21958
An overview of the MIL-HDBK-5 program
[AD-A147788] 14 p2254 N85-23970
Installation, maintenance and operating manual for the Lucas-type fuel injection system of the 3 B rotary engine
[NASA-TM-77872] 15 p2568 N85-25846
AWS (Air Weather Service) climatic briefs: Asia
[AD-A151944] 16 p2835 N85-27481
The GIW handbook for data compilation of irradiation tested electronic components, volume 3
[HMI-B-353-VOL-3] 17 p2956 N85-28258
Handbook on superconductivity: The large-scale applications. Chapter 4
[DE85-008170] 17 p3044 N85-28838
State Weights and Measures Laboratories: Program handbook
[PB85-183358] 18 p3111 N85-29283
Technical guide for estimating fugitive dust impacts from coal handling operations. Volume 1: Project summary
[DE85-010948] 19 p3309 N85-30515
Human Engineering Guide to Equipment Design (HEGED)
[AD-A154087] 19 p3331 N85-30631
User handbook for block 5 silicon solar cell modules
[NASA-CR-178043] 20 p3483 N85-31644
Middle Atmosphere Program. Handbook for MAP, volume 11
[NASA-CR-176107] 22 p3814 N85-33825
International flight planning handbook
[AD-A156330] 24 p4062 N85-35177
Fire service emergency management handbook
[AD-A155780] 24 p4084 N85-35313
A guide for new environmental coordinators
[AD-A156327] 24 p4113 N85-35498
Air university commander's and supervisor's guide on substance abuse
[AD-A156336] 24 p4133 N85-35622
Recommendations for content revision and alternate delivery modes for the Human Engineering Guide to Equipment Design (HEGED)
[AD-A155781] 24 p4134 N85-35624
Time domain reflectometry for SLC BPM system
[DE85-012389] 24 p4155 N85-35758

HANDLING EQUIPMENT
NT CRANES
NT GANTRY CRANES
Depot modernization at the Defense Logistics Agency
[AD-P004008] 03 p0308 N85-11988

Dental multi-purpose slowspeed handpiece test and evaluation
[AD-A155764] 24 p4130 N85-35606
HANDLING QUALITIES
U CONTROLLABILITY
HANG GLIDERS
An assessment of the suitability of the BHGA structural test rig for aerodynamic testing of hang gliders
[CA-9505] 17 p2896 N85-27853
HANGARS
Hangar destratification investigation
[AD-A145049] 01 p0012 N85-10076
Hangar heating and energy conservation manual
[AD-A147893] 07 p0910 N85-15762
HARBORS
USSR report: Transportation
[JPRS-UTR-84-008] 14 p2208 N85-23694
LORAN-C harbor and harbor entrance survey: Charleston, South Carolina
[AD-A154875] 21 p3554 N85-32108
Bibliography on tidal hydraulics. Report 2. Supplement 9: Supplementary material compiled from June 1980 - June 1983. Tidal flows in rivers and harbors
[AD-A155990] 24 p4125 N85-35574
HARDENERS
Structure and abrasive resistance of iron based alloys rich in hardening components 01 p0054 N85-10360
HARDENING
Influence of heat treatment parameters on the properties of induction hardened Ni-Cr-Mo steels
[BLL-BISI-TRANS-2499-(9022.06)] 17 p2926 N85-28053
HARDENING (MATERIALS)
NT CARBURIZING
NT HOT PRESSING
NT NITRIDING
NT PRECIPITATION HARDENING
NT PULSE HEATING
NT SHOT PEENING
NT SILICONIZING
NT STRAIN HARDENING
NT WORK HARDENING
USSR report: Machine tools and metalworking equipment
[JPRS-UMM-84-019] 01 p0035 N85-10214
Electro-spark case-hardening of contoured surfaces 01 p0035 N85-10216
Directional nature of strengthening during thermomechanical treatment
[BLL-M-35746-(5828.4)] 02 p0175 N85-11174
An investigation into the superhardening effect in molybdenum-free steel with specific reference to alloy substitution 02 p0180 N85-11209
The determination of soluble and insoluble boron in steel by emission spectrometry using an inductively coupled plasma and a scanning monochromator 02 p0180 N85-11211
Defining effect of hardening on mean yield strength in deformation zone
[BLL-M-35934-(5828.4)] 05 p0647 N85-14154
Study of superplastic alloys based on Al-Zn-Ca 10 p1442 N85-19092
Influence of laser hardening on mechanical properties of type 45 steel with various preliminary heat treatments 10 p1446 N85-19111
Diffusion welding with forced deformation of heat-resistant nickel-based dispersion hardened alloy 10 p1449 N85-19130
Thermal hardening of welded joints in titanium alloys with various structures 13 p2032 N85-22734
Influence of short-range order on deformation mechanisms in solid solutions
[DE85-006374] 14 p2258 N85-23989
Trapping model analysis of annihilation line narrowing in some plastically deformed metals and alloys
[AERE-R-10593] 14 p2258 N85-23995
Laser surface treatments 14 p2308 N85-24284
Effect of deep cooling on crack resistance and low-temperature hardening of aluminum alloys 15 p2496 N85-25396
Hardening of titanium alloy electric-arc welded joints 15 p2514 N85-25513
Determination of failure characteristics of materials and structures
[AD-A152073] 16 p2800 N85-27266
On the accurate representation of large strain non-proportional plastic flow in ductile materials
[DE85-007106] 16 p2801 N85-27273
Heat resistant Carbon Fiber Reinforced Plastics (CFRP) hardening equipment
[MBB/LFA33/CFK/PUB/007] 17 p2916 N85-27976
X-ray crystallography of steel U8 after pulsed laser hardening
[BLL-BISI-22444-(9022.06)] 17 p2925 N85-28038
Internal structure of GP zones in dilute Al-Cu alloys 19 p3238 N85-30073
Effect of ScAl3 phase dispersion on hardening of alloy Al-6.3 percent Mg-0.21 percent Sc 19 p3241 N85-30096
Durability of reinforced hard-alloy draw plates
[BLL-M-36278-(5828.4)] 20 p3485 N85-31526
Effect of prior warm rolling on the retained austenite content and hardening response of VIM-VAR (vacuum-induction melted-vacuum-arc remelted) AISI M-50 steel
[AD-A156145] 24 p4079 N85-35281
HARDENING (SYSTEMS)
Invited papers: DNA ICBM technical R and D program 09 p1333 N85-16379
Ground shock effect on soil field inclusions 09 p1336 N85-16403
HARDNESS
NT KNOOP HARDNESS
NT MICROHARDNESS
Sintered silicon nitride workpiece
[NASA-TM-77600] 01 p0021 N85-10129
Some reflections on the competition among different hard materials in industrial applications 02 p0177 N85-11192
The chemical nature of the fiber/resin interface in composite materials 04 p0465 N85-12953
Creep-rupture behavior of iron superalloys in high-pressure hydrogen
[NASA-CR-174411] 10 p1441 N85-19078
Effect of temperature and deformation rate on hardness of copper 11 p1605 N85-20090
Investigation of vanadium solid solution and zeta phase regions of vanadium-carbon system
[DE85-002678] 11 p1605 N85-20092
Deposition of diamondlike carbon films
[NASA-CASE-LEW-14080-1] 11 p1615 N85-20153
Case depth on flanks of gears for helicopter gearboxes 14 p2222 N85-23780
Sintering reactions, structure and properties of a cobalt free nonconventional hard material
[DE85-007704] 18 p3076 N85-29025
Age hardening and atomic structure of an aluminum-6 at. % silver alloy
[DE85-009977] 18 p3077 N85-29031
Tests on zirconium nitride coatings applied to SW 18 steel using the chemical vapor deposition method 24 p4076 N85-35271
Effect of thermal ageing on the mechanical properties of PWR pressure vessel steels and weldments
[AERE-R-11460] 24 p4078 N85-35275
HARDNESS TESTS
Laboratory evaluation of Electromagnetic Pulse (EMP) hardness testing concepts for electrical conduit systems
[AD-A145466] 02 p0190 N85-11273
HARDWARE
Microcomputers in Hungary 01 p0115 N85-10786
ATE user's view on design for maintainability 08 p1064 N85-16737
Hardware/software codesign for maintainable systems 08 p1066 N85-16753
Fast arithmetic for microcomputers 08 p1140 N85-17160
VICOM technical description
[REPT-611-0012-REV-A] 08 p1202 N85-17563
Development and operation of a real-time data acquisition system for the NASA-LaRC differential absorption lidar
[NASA-CR-174384] 09 p1366 N85-18583
DDL system: Design systhesis of digital systems
[NASA-CR-170759] 09 p1366 N85-18584
National Machine Tools Conference slated for 1985: Conference agenda, papers 10 p1460 N85-19202
A low-cost, general purpose image processing system
[INPE-3292-PRE/607] 10 p1537 N85-19690
ZTLCK: A subroutine package for the IBM personal computer to support the Zlatech ZT1488 real time clock
[LA-10146-MS] 12 p1914 N85-22014
USSR report: Cybernetics, computers and automation technology
[JPRS-UCC-85-003] 15 p2625 N85-26174
Active control technology: Past, present, future 16 p2711 N85-26731
Flight Experiment Demonstration System (FEDS) functional description and interface document
[NASA-CR-175290] 16 p2717 N85-26769
Multiple array processors for ocean acoustic problems
[AD-A152174] 16 p2860 N85-27641
Shuttle-tethered satellite system definition study extension
[NASA-CR-171473] 17 p2907 N85-27923
Hardware test program for evaluation of baseline range/range rate sensor concept
[NASA-CR-175910] 17 p2947 N85-28194
Synchronization and fault-masking in redundant real-time systems
[NASA-TM-87478] 17 p3015 N85-28644
Energy efficient engine integrated core/low spool test hardware design report
[NASA-CR-168137] 19 p3218 N85-29956
Methods for design and evaluation of integrated hardware-software systems for concurrent computation
[NASA-CR-176066] 20 p3515 N85-31851
HARMONIC ANALYSIS
NT TESSERAL HARMONICS
NT ZONAL HARMONICS
Harmonizable, Cramer, and Karhunen classes of processes
[AD-A144984] 01 p0113 N85-10767
Stochastic motor blade dynamics
[AD-A146312] 03 p0318 N85-12054
NATFREQ users manual: A FORTRAN 4 program for computing natural frequencies, mode shapes and drag coefficients for taut strumming cables with attached masses and spring-mass combinations
[AD-A146058] 03 p0407 N85-12600
Linear harmonic analysis for Stirling machines and second law analysis of four important losses
[DE84-016595] 04 p0573 N85-13655
Linear harmonic analysis of Stirling engine thermodynamics
[DE84-016646] 04 p0574 N85-13657
Effects of vane/blade ratio and spacing on fan noise, volume 1
[NASA-CR-174664] 10 p1553 N85-19791
A study for calculating rotor loads using free vortex concept 11 p1620 N85-20194
Three algorithms for parametric frequency domain system identification
[DE85-002801] 11 p1706 N85-20735
A deformation analysis of flat flexible gear and its equation of original curved surfaces
[NASA-TM-77493] 12 p1859 N85-21660
Harmonic analysis and Radon transforms on pencils of geodesics
[CWI-PM-R8413] 12 p1922 N85-22074
Harmonic analysis of the solar magnetic field 14 p2454 N85-25154
Acoustic radiation from concentric shells containing an inner fluid
[AD-A155476] 21 p3700 N85-32991
Hardy spaces and the L sup P-Neumann problem for Laplace's equation in a Lipschitz domain
[CTH-MATH-1985-02] 22 p3836 N85-33749
Arrival directions of large air showers, low-mu showers and old-age low-mu air showers observed at St. Chacaltaya
[OG-5.3-2] 22 p3884 N85-34069
Aniestropy of cosmic rays of energy 10 (15) eV to 10 (17) eV observed at Akeno
[OG-5.3-3] 22 p3884 N85-34070
Aniestropy and the knee of the energy spectrum
[OG-5.4-10] 22 p3887 N85-34087
Characteristics of cosmic ray pole-equator aniestropy derived from spherical harmonic analysis of neutron monitor data
[SH-4.3-12] 23 p4032 N85-34996
Magnetic fluctuation and cosmic ray diurnal variations
[SH-4.5-21] 23 p4036 N85-35036
On the solar cycle variation in the barometer coefficients of high latitude neutron monitors
[SH-6.1-2] 23 p4044 N85-35077
The conjecture concerning time variations in the solar neutrino flux
[SH-8.1-6] 23 p4049 N85-35111
Optimal estimation of a high degree gravity field from a global set of 1 deg x 1 deg anomalies to degree and order 250
[AD-A156008] 24 p4117 N85-35519
HARMONIC CONTROL
Data processing on the rotor test stand at DFVLR in Brunswick: Microprogrammable interfaces and array processor as key components in a PDP 11 real time data acquisition and processing system
[DFVLR-MITT-85-03] 17 p2906 N85-27921
Fixed gain and adaptive techniques for rotorcraft vibration control
[NASA-CR-177344] 22 p3726 N85-33111
High-speed adaptation algorithm for harmonic corrector 22 p3765 N85-33336
HARMONIC FUNCTIONS
Some families of near-orthonormal analytic and harmonic functions
[AD-A144722] 01 p0110 N85-10748
On some exact solutions in elastostatics in terms of harmonic functions 09 p1332 N85-18367
Annuals of the Finnish Academy of Sciences, series A. 1: Mathematics, volume 8, part 2
[ISSN-0066-1953] 10 p1535 N85-19673
On harmonic functions with integrable maximum modulus 10 p1536 N85-19681
On the integral representation of bisubharmonic functions in Rn 10 p1536 N85-19684

Interwining functions on compact Lie groups
[CWI-TRACT-5] 14 p2414 N85-24895
Annals of the Scientific Academy of Finland, series A. 1: Mathematica, volume 9
[ISSN-0066-1953] 15 p2633 N85-26229
Harmonic univalent functions
15 p2633 N85-26230
A problem of Burkholder and the existence of harmonic majorants of the absolute value of x sup p in certain domains in R sup d
15 p2634 N85-26236
Some estimates of harmonic majorants
15 p2634 N85-26237
The first three harmonics of solar daily variation caused by the diffusive propagation of galactic cosmic rays through the heliosphere
[SH-4.5-1] 23 p4035 N85-35019

HARMONIC GENERATIONS
Multimode harmonic power measurement of 40 MW pulsed S-band klystrons
[DE85-001560] 09 p1316 N85-18272
Optical second harmonic generation for surface studies
[DE85-000670] 11 p1640 N85-20333
Digital detector of harmonic signals
12 p1840 N85-21549
Four-photon resonant third harmonic generation
[DE85-010070] 19 p3367 N85-30883

HARMONIC GENERATORS
Theory of harmonic generation of finite amplitude ultrasonic waves in solids of hexagonal symmetry
[AD-A146936] 06 p0860 N85-15465
Quasi-optical harmonic gyrotron and gyroklystron
[AD-D011308] 07 p0947 N85-16001

HARMONIC OSCILLATION
Flow instabilities in transonic small disturbance theory
[NASA-TM-86251] 09 p1273 N85-18000
Precision measurement of torsional oscillations induced by gear errors
09 p1338 N85-18416
Finite element analysis of nonlinear oscillations and flutter of shells of revolution
[AD-A149071] 10 p1496 N85-19440
Errors in compensating for image oscillation by means of a gyroscopic head
16 p2763 N85-27051
Approximate solution of the problem of fluid oscillations in cavities of revolution
16 p2764 N85-27056
Study of oscillations of composite cylindrical shells using a dynamic stiffness technique
16 p2766 N85-27066
Analysis of unsteady pressure measurements on a supercritical airfoil with a harmonically oscillating trailing edge flap at subsonic and transonic speeds
[DFVLR-FB-84-49] 17 p2893 N85-27837
Filtration of higher harmonic components in two-level digital computing synthesizers
22 p3778 N85-33410
Role of ECRH in potential formation for tandem mirrors
[DE85-011859] 22 p3848 N85-33834

HARMONIC OSCILLATORS
Harmonic emission from high power gyrotron oscillators
[AD-A145621] 02 p0200 N85-11335
Reference oscillator stability effect on clutter cancellation in a radar system
07 p0936 N85-15948
Applications of molecular dynamics to the study of shock-induced chemistry
[AD-A148017] 08 p1121 N85-17066
A transistor oscillator-doubler
[AD-D011408] 08 p1158 N85-17307
Asymmetrical harmonic oscillator and fine-structure constant
[FUB-9-1984] 09 p1401 N85-18818
Coupled-cavity gyrotrons with mode conversion
13 p2076 N85-22967
Optical injection locking of solid-state oscillators by frequency-multiplexed injection-locked, laser diodes
[AD-D011695] 19 p3275 N85-30307
A multiplying slot array
[AD-A155570] 21 p3576 N85-32245

HARMONIC RADIATION
Generation and propagation of electron cyclotron harmonic waves
14 p2367 N85-24630
Theoretical studies of electric cyclotron harmonic (ECH) waves based on experimental data from GEOS 1
14 p2367 N85-24631
Role of equatorial Electron Cyclotron Harmonic (ECH) waves in the generation of diffuse aurorae. Contribution of the GEOS IMS spacecraft
14 p2367 N85-24632
Measurement of RF fields associated with ISM equipment as it relates to aeronautical services
[FAA-ES-84-2] 19 p3254 N85-30180
The problem of brightness enhancement during laser frequency doubling
21 p3686 N85-32897
Cerenkov radiation from periodic electron bunches for finite emission length in air
[AD-A156156] 24 p4090 N85-35352

HARMONICS
NT HARMONIC GENERATIONS
NT HARMONIC OSCILLATION
NT SPHERICAL HARMONICS
NT TESSERAL HARMONICS
NT ZONAL HARMONICS
Use of a first-harmonic RF system in the NSLS booster
[DE84-016432] 02 p0277 N85-11806
Recent observations of tides and tidal currents from the northeastern Bering Sea shelf
[PB84-241785] 04 p0543 N85-13452
Linear problem of harmonic vibrator acting at supercritical frequencies in subsonic boundary layer
06 p0779 N85-14978
Perceptibility of nonlinear distortions in power amplifier
06 p0789 N85-15041
Individual geopotential coefficients of order 15 and 30, from resonant satellite orbits
[AD-A146687] 06 p0828 N85-15256
Nonlinear ultrasonic characterization of oxygen impurities in titanium
[AD-P004123] 08 p1126 N85-17098
Analysis of inverter models and harmonic propagation. Part 1: A physical simulator for large solar cell arrays
[DE85-002312] 09 p1315 N85-18271
Analysis of inverter models and harmonic propagation. Part 2: Harmonic propagation
[DE85-000196] 10 p1482 N85-19356
Some individual differences in human response to infrasound
[UTIAS-282] 12 p1905 N85-21960
The effects of internal waves on acoustic normal modes
[AD-A150235] 13 p2155 N85-23379
Propagation of sound in matter
[AD-A151052] 14 p2416 N85-24906
Internal resonance in nonlinear vibrating systems
[REPT-15/1984] 16 p2797 N85-27245
Guided and radiation wave interactions in periodic dielectric waveguides
19 p3253 N85-30173
An algorithm for the influence numbers in the expansion of the lumped gravitational potential coefficients in the presence of resonant inclination variation
[AD-A154229] 19 p3336 N85-30669
Four-photon resonant third harmonic generation
[DE85-010070] 19 p3367 N85-30883
Upward continuation of surface gravity anomalies
[AD-A154973] 21 p3631 N85-32560
Electro-optic harmonic conversion to switch a laser beam out of a cavity
[DE85-011619] 22 p3790 N85-33483
Sidereal variations deep underground in Tasmania
[SH-4.4-4] 23 p4033 N85-35002
The effect of the interplanetary magnetic field on sidereal variations observed at medium depth underground detectors
[SH-4.4-5] 23 p4033 N85-35003
Cosmic ray intensity variations observed at Matsushiro (220 M.W.E. in depth)
[SH-4.4-9] 23 p4034 N85-35007

HARNESSES
Impact tests of adjusters for the HBU-12 lap belt
[AD-A148021] 08 p1080 N85-16843
Impact tests of automatic lap belt configurations
[AD-A148034] 08 p1081 N85-16844
Double pinch-push contact insertion end-effector
[AD-D011485] 10 p1459 N85-19196
Tight Ribbon Arm Protection (TRAP) for aircrewman ejection
[AD-A150484] 13 p2143 N85-23303
Torso restraint system
[AD-D011609] 16 p2702 N85-26684
Improving inflight negative Gz restraint for aircrewmen
[AD-A151909] 16 p2703 N85-26688
Features of the solar array drive mechanism for the space telescope
22 p3798 N85-33532

HARRIER AIRCRAFT
Multivariable flight control with time-scale separation
[NASA-CR-174320] 08 p1067 N85-16873
Harrier 15 p2687 N85-26595
YAV-8B Harrier 15 p2688 N85-26605

HARTREE APPROXIMATION
Spurious center of mass effects in a dynamically determined basis
[CSIR-TWISK-310] 01 p0109 N85-10732
An extension of the multiconfiguration Hartree-Fock program for continuum functions
[DE85-002080] 09 p1379 N85-18672
Time dependent Hartree-Fock theory of ion-atom collisions: Application to F(9+) + Ne
[DE85-003083] 11 p1723 N85-20838
Hartree-Fock interaction between a helium atom and lithium-metal: A test for the effective medium theory
[AD-A150488] 13 p2156 N85-23387
Microscopic analysis of angular momentum projected HFB-states in terms of interacting bosons
[DE85-007629] 16 p2863 N85-27661
Multiple inner shell vacancies in laser-irradiated Au plasma
23 p3981 N85-34687

HARTREE-APPLETON APPROXIMATION
U HARTREE APPROXIMATION

HARTREE-FOCK APPROXIMATION
U HARTREE APPROXIMATION

HASTELLOY (TRADEMARK)
Elevated temperature biaxial fatigue
[NASA-CR-175795] 16 p2800 N85-27263
A comparison of smooth specimen and analytical simulation techniques for notched members at elevated temperatures
20 p3466 N85-31546

HAULING
A Lagrange-D'Alembert formulation of the equations of motion of a helicopter carrying an externally suspended load
[NASA-TM-85864] 12 p1776 N85-21149

HAWAII
An improved analytical theory of Rossby wave driven Eulerian and Lagrangian mean flows along non-zonal barriers with application to the Hawaiian Ridge
[AD-A144951] 01 p0088 N85-10589
Thermosonde C2N measurements in Hawaii--August 1982
[AD-A148016] 08 p1189 N85-17489
Lidar observations of stratospheric aerosol over Mauna Loa Observatory, 1974 - 1981
[PB85-115061] 11 p1682 N85-20597
Emplacement of long lava flows on Mauna Loa (Hawaii) and Alba (Mars)
13 p2186 N85-23563
Thermal infrared observations of lava flows during the 1984 Mauna Loa eruption
13 p2186 N85-23564
Field measurements of the 1983 Royal Gardens lava flows, Kilauea Volcano, and 1984 Mauna Loa lava flows, Hawaii
13 p2186 N85-23565
Surface structures of Hawaiian lavas
13 p2186 N85-23566

HAWKER SIDDELEY AIRCRAFT
NT DH 115 AIRCRAFT
NT HARRIER AIRCRAFT

HAYNES STELLITE
U STELLITE (TRADEMARK)

HAZARDOUS MATERIAL DISPOSAL (IN SPACE)
A model for the evolution of on-orbit manmade debris environment
12 p1784 N85-21196

HAZARDS
NT AIRCRAFT HAZARDS
NT FLIGHT HAZARDS
NT METEOROID HAZARDS
NT OPERATIONAL HAZARDS
NT RADIATION HAZARDS
NT TOXIC HAZARDS
Review of USAF treatment of solid propellant rocket motor hazards
08 p1114 N85-17027
Sensitiveness and explosiveness assessment at Perme Waltham Abbey
08 p1115 N85-17029
Analysis of Deflagration to Shock to Detonation Transition (DSDT) in porous energetic solid propellants
08 p1115 N85-17030
The vulnerability of cast double base rocket motors to thermomechanical attack
08 p1115 N85-17033
Hazard assessment of a hypothetical large rocket motor
08 p1117 N85-17042
The use of synthetic aperture radar imagery to detect hazards to navigation
[AD-A149324] 10 p1422 N85-18971
The 1984 JANNAF Propulsion Systems Hazards Subcommittee Meeting, volume 1
[AD-A148985] 10 p1454 N85-19162
Report on AGARD Meeting: Hazards Studies for Solid Propellant Rocket Motors
[AD-P004340] 10 p1454 N85-19164
Antiplane cracks in solid propellants
[AD-P004344] 10 p1455 N85-19168
Laser Hazards Bibliography, October 1984
[AD-A149534] 10 p1490 N85-19408
Successful control of gulls and other birds at a sanitary landfill
[AD-P004198] 11 p1582 N85-19965
DOE hazard classification for Insensitive High Explosives (IHE)
[DE84-017002] 11 p1614 N85-20149
A model for the evolution of on-orbit manmade debris environment
12 p1784 N85-21196
Preliminary design of an Earth-based debris detection system using current technology and existing installations
12 p1784 N85-21199
Orbital debris policy issues: Battelle involvement and some personal observations
12 p1787 N85-21218
Spacecraft hazard and shielding requirements
12 p1788 N85-21224
Hazardous air pollutants: Dry-deposition phenomena
[PB85-138279] 12 p1887 N85-21843

Astronaut hazard during free-flight polar EVA
13 p1997 N85-22522
Electric and hybrid vehicle demonstration project
[DE85-003939] 13 p2169 N85-23455
Innovation in earthquake and natural hazards research: Determining soil liquefaction potential
[PB85-149573] 14 p2374 N85-24678
Criteria for the classification of hydrographic positioning data
[AD-A152283] 16 p2705 N85-26607
A review of safety practices and safety training for the explosives field
[AD-A152295] 16 p2759 N85-27026
Hazards in welding due to oxygen changes in the workplace atmosphere
[BLL-WI-TRANS-684-(9312.57)]
16 p2792 N85-27224
Space station crew safety alternatives study, third quarter briefing 18 p3156 N85-29541
Facility for large-scale hazardous gas testing
[DE85-011862] 21 p3564 N85-32169
Fire protection review revisit no. 2, Argonne National Laboratory, Argonne, Illinois
[DE85-013245] 22 p3755 N85-33276
Description of a test site for large-scale heavy gas dispersion and combustion experiments
[DE85-004987] 23 p3911 N85-34231
The application of models to the assessment of fire hazard from consumer products
[NBSIR-85-3219] 23 p3925 N85-34325
Estimating risks of lead-induced hemoglobin decrements under conditions of uncertainty: Methodology, pilot judgments and illustrative calculations
[DE85-012293] 23 p3952 N85-34493
The investigation of tethered satellite system dynamics
[NASA-CR-176180] 24 p4069 N85-35215
Fire service emergency management handbook
[AD-A155780] 24 p4084 N85-35313
Investigation of the lightning vulnerability of nuclear explosive test systems at the Nevada Test Site
[DE85-011761] 24 p4124 N85-35563
National program for inspection of non-federal dams. Woodward reservoir dam (VT 00209), Connecticut River Basin, Plymouth, Vermont. Phase 1 inspection report
[AD-A156256] 24 p4144 N85-35693

HAZE
Method for measuring haze in transparencies
[AD-D011233] 01 p0120 N85-10823
Arctic haze: Meteorological aspects of long-range transport 02 p0230 N85-11499
Water-ice clouds on Mars: Location and seasonal variation 13 p2194 N85-23611
Chemical composition of coastal haze aerosol
14 p2338 N85-24458
Haze over eastern North America. Part 1: Haze properties
[PB85-181857] 19 p3311 N85-30526
Atmospheric cross sections for the Arctic gas and aerosol sampling program, March - April 1983
[NASA-CR-176027] 19 p3314 N85-30541
The measurement of aircraft windscreen haze and its effect on visual performance
[AD-A154949] 21 p3555 N85-32114
Airborne measurements of the vertical distribution of Arctic haze 21 p3647 N85-32657
Condensation nuclei and aerosol size distribution measurements in Arctic haze 21 p3647 N85-32658
The interaction of polynuclear aromatic hydrocarbons PAH's with water vapor and their role as condensation nuclei in the formation of haze and fog
21 p3652 N85-32695

HAZE DETECTION
Haze over eastern North America. Part 1: Haze properties
[PB85-181857] 19 p3311 N85-30526

HBNQ
U NITROGUANIDINE

HC-1 HELICOPTER
U CH-47 HELICOPTER

HCMM
U HEAT CAPACITY MAPPING MISSION

HCN LASERS
Observation of mode-converted by ion Bernstein wave by an HCN laser scattering
[IPPJ-724] 23 p3979 N85-34668

HEAD (ANATOMY)
NT SKULL
Powered articulated headrest system
[AD-D011353] 07 p0901 N85-15710
SPH-4 US Army flight helmet performance, 1972 - 1983
[AD-A148674] 08 p1201 N85-17562
Psychometric evaluation of head injury among fliers referred to the AF School of Aerospace Medicine
[AD-A151479] 15 p2617 N85-26129
Investigation of spectrum of human bile acids during 120-day antiorthostatic hypokinesia
22 p3821 N85-33674
Vascular mechanisms of adaptation to antiorthostatic position 22 p3822 N85-33675
Cerebral hemodynamics and ventricular function in -15 deg antiorthostatic position 22 p3822 N85-33676
Effect of short-term antiorthostatic hypokinesia on dynamics of cardiorespiratory parameters during graded physical exercise 22 p3822 N85-33677
Investigation of some aspects of amino acid metabolism in man during brief exposure to antiorthostatic hypokinesia combined with ultraviolet radiation
22 p3822 N85-33678

HEAD (FLUID MECHANICS)
NT PRESSURE HEADS

HEAD (PRESSURE)
U PRESSURE HEADS

HEAD MOVEMENT
Development and evaluation of a performance-based test of saccadic and vestibulo-ocular control
[AD-A145367] 02 p0237 N85-11545
Inverse modelling to obtain head movement controller signal 05 p0705 N85-14525
Effects of external loads on human head movement control systems 05 p0707 N85-14534
Vestibular and oculomotor function during Gz variations 11 p1693 N85-20645
Analysis of head motion during simulated, rough water operation of a 2200 ton surface effect ship
11 p1695 N85-20656
Sensory and motor properties of the cerebellar uvula and nodulus 15 p2613 N85-26104

HEAD-UP DISPLAYS
The value and utility of inflight onboard simulation
[AD-A148033] 08 p1196 N85-17543
Some effects of display format variables on the perception of aircraft spatial orientation
10 p1534 N85-19666
A safety evaluation of the relocation of the ACM (Air Combat Maneuver) panel in the F-14 ( )/AIP (Avionics Integration Program)
[AD-A149598] 12 p1777 N85-21158
Crew systems and flight station concepts for a 1995 transport aircraft
[NASA-CR-166068] 19 p3221 N85-29973

HEADSETS
U EARPHONES

HEALING
Polyactic-polyglycolic acid copolymer combined with decalcified freeze-dried bone for use as a bone repair material
[AD-D011438] 10 p1451 N85-19142

HEALTH
NT HEALTH PHYSICS
NT MENTAL HEALTH
NT PUBLIC HEALTH
Differences in health risks by aircraft model among US Navy pilots
[AD-A148147] 03 p0401 N85-12558
Report of the Meeting of Experts on Climate and Human Health
[WCP-78] 05 p0687 N85-14413
Organization of the session 05 p0687 N85-14414
Difficulties encountered in determining the potential involvement of consultants on health problems in various climatic zones 05 p0687 N85-14416
Epidemiologic methods applied to the study of the relationship between climate and human health
05 p0687 N85-14418
An update on the capabilities of the Air Force Computerized Occupational Health Program (COHP)
[AD-P004037] 06 p0845 N85-15367
Health examination findings among active civil airmen
[AD-A148325] 08 p1195 N85-17533
Robotic safety
[DE85-002314] 10 p1493 N85-19431
Health standards for general vibration
10 p1523 N85-19607
Assessing the short- and long-term health effects of decompression sickness among US Navy divers
[AD-A151687] 15 p2618 N85-26132
Development of guidelines for setting physiological and hygienic standards for noise levels in aerospace medicine 19 p3323 N85-30584
Flow cytometry for health monitoring in space
[DE85-009572] 19 p3329 N85-30625

HEALTH PHYSICS
NT PUBLIC HEALTH
Symposium on Military Aviation Medicine summarized
11 p1696 N85-20663
The biological effects of radiofrequency radiation
16 p2775 N85-27131
Review of epidemiological studies of human exposures to radiofrequency radiation 16 p2776 N85-27134
Practical consequences of the assessment of different energy health risks
[DE85-004538] 22 p3825 N85-33696
Wholebody radiation counting system
[AD-A155842] 24 p4131 N85-35607

HEALTH PHYSICS RESEARCH REACTOR
Empirical correlation of residual gamma radiation resulting from operation of the Health Physics Research Reactor
[DE85-012075] 21 p3704 N85-33008

HEAO
NT HEAO 1
NT HEAO 2
NT HEAO 3
Optical observations of HEAO-B objects
17 p3052 N85-28895

HEAO A
U HEAO 1

HEAO B
U HEAO 2

HEAO C
U HEAO 3

HEAO 1
Local contributions to the 0.6 keV diffuse X-ray background 06 p0877 N85-15569
HEAO-1 diffuse soft X-ray sky maps
06 p0877 N85-15570
Inverse relations between 0.25 keV counts and local interstellar dust 06 p0877 N85-15572
The HEAO-1 diffuse component spectrum from 15 to above 500 keV — X and gamma rays
08 p1240 N85-17820
HEAO-1 observations of gamma ray bursts
[OG-1.1-1] 22 p3860 N85-33903
Spectra and positions of galactic gamma-ray sources
[OG-2.5-7] 22 p3869 N85-33963

HEAO 2
Is the ratio of observed X-ray luminosity to bolometric luminosity in early-type stars really a constant?
06 p1234 N85-17777
Preliminary results on the ultraviolet observations of a complete X-ray selected sample of Active Galactic Nuclei (AGN) — HEAO 2 06 p1237 N85-17800
X-ray surveys of quasars with the Einstein observatory
06 p1238 N85-17807
Interacting binary systems 11 p1744 N85-20957
A soft X-ray survey of galactic supernova remnants with the Einstein Observatory 14 p2434 N85-25013
Optical pulsar in the Large Magellanic Cloud remnant 0540-69.3
[DE85-006707] 16 p2883 N85-27788

HEAO 3
HEAO 3 upper limits to the expected 1634 KeV line from SS 433
[OG-2.4-9] 22 p3868 N85-33954
High-resolution spectrum of Cygnus X-1
[OG-2.4-12] 22 p3868 N85-33956
Energy spectra of elements with 18 or = Z or = 28 between 10 and 300 GeV/amu
[OG-4.1-8] 22 p3876 N85-34014

HEARING
NT BINAURAL HEARING
Auditory impairment and the onset of disability and handicap in noise-induced hearing loss
[ISVR-TR-126] 20 p3507 N85-31801

HEARING LOSS
U AUDITORY DEFECTS

HEART
NT CARDIAC VENTRICLES
NT MYOCARDIUM
Effect of hyperoxia and increased gas atmosphere density on contractile function of the right ventricle
01 p0093 N85-10628
Influence of geomagnetic disturbances on cardiovascular function of athletes
08 p1193 N85-17516
The EM algorithm for censored data
[AD-A148136] 08 p1212 N85-17626
Development of the cerium-191 yields iridium-191m radionuclide generator
[DE85-011185] 23 p3970 N85-34611
Current status of the Os-191 yields Ir-191m generator
[DE85-008306] 23 p3971 N85-34614

HEART DISEASES
NT CORONARY ARTERY DISEASE
Cardiovascular disease among U.S. Navy pilots
[AD-A145871] 03 p0400 N85-12552
An investigation of the relationship between stressful life events and psychological, behavioral and physiological outcomes
[AD-A147754] 08 p1197 N85-17541
Medically disqualified airline pilots
[AD-A149454] 10 p1526 N85-19637
Longitudinal study of cardiovascular disease in US Navy pilots
[AD-A154331] 19 p3328 N85-30623

HEART FUNCTION
Frequency and nature of electrocardiographic disturbances in dogs during single and repeated exposure to +G sub z accelerations 01 p0092 N85-10619
Mapping of mammalian arrhythmias with the cardiac laser scanner 03 p0399 N85-12545
Left heart ventricular function during a 7 day zero-g simulation (6 deg head down tilt) 05 p0691 N85-14446
Cardiac output measured by mass spectroscopy 05 p0692 N85-14449
Cardiac output measurement with soluble gases 05 p0692 N85-14450
Hemodynamics responses to upright tilt at sea level and high altitude [AD-A148848] 10 p1527 N85-19634
Morphological study of monkeys submitted to antiorthostatic hypokinesia 12 p1902 N85-21942
Changes in cardiovascular function: Weightlessness and ground-based studies 20 p3509 N85-31815
Oxygenation and regional circulation in gingival mucosa during exposure to lower body negative pressure 23 p3953 N85-34496

HEART RATE
NT ARRHYTHMIA
Heart rate variability during 7 day head-down tilt (6 deg) 05 p0692 N85-14453
Does McKuer's law hold for heart rate control via biofeedback display? 05 p0706 N85-14528
Scattering of electromagnetic waves by human body and its applications 09 p1363 N85-18572
Variability of cardiac rhythm during information loading 10 p1525 N85-19619
Exercise-heat strain during hypohydration: Interaction with heat acclimation and aerobic fitness [AD-A151023] 14 p2380 N85-24717
Development of an EM-Based lifeform detector [AD-A153504] 18 p3151 N85-29512
Studies of circulatory and metabolic changes during ketamine narcosis [AD-A154512] 21 p3663 N85-32756
Mathematical analysis of heart rhythm assessment of distinctive features in adaptation to spaceflight conditions 22 p3733 N85-33142
Effect of water immersion of parameters of central hemodynamics in individuals over 45 years old 23 p3953 N85-34499
Effect of acute hypoxia on coronary and systemic hemodynamics 23 p3953 N85-34503
Weight loss, rectal temperature and heart rates following the 1984 Boston Marathon [AD-A155984] 24 p4132 N85-35612

HEAT
NT PROCESS HEAT
Change in energetics of muscular contraction as a result of hyperoxia 01 p0093 N85-10629
Thermite and Fe/KClO4: Some thermodynamic calculations [DE84-016945] 04 p0573 N85-13653
An atropinized heat-stressed rat model: Dose response effects and pharmacokinetics [AD-A148851] 07 p1011 N85-16423
Thermal radiation hazards from Liquified Petroleum Gas (LPG) fireballs [VTT-304] 09 p1293 N85-18122
Heat cycle research program [DE84-017015] 09 p1344 N85-18455
A one dimensional dynamical model of ocean/atmosphere interactions 09 p1358 N85-18545
Correlation of zeolite ZSM-5 acid strength with catalytic activity and selectivity [DE85-005415] 17 p2922 N85-28013
Heat injury: Prevention is the key [AD-A153734] 19 p3328 N85-30622
Advanced regenerative heat recovery system [PB85-199802] 24 p4084 N85-35315

HEAT ACCLIMATIZATION
Skeletal muscle metabolism during exercise is influenced by heat acclimation [AD-A148845] 10 p1527 N85-19632
Preventive effect of acute heat factors during hypokinesia 12 p1902 N85-21945
Preparing Alberto Salazar for the heat of the 1984 Olympic Marathon [AD-A150942] 14 p2389 N85-24714
Physiological differences between men and women in exercise-heat tolerance and heat acclimation [AD-A152048] 15 p2618 N85-26135

HEAT BALANCE
Breakdown of thin plates by radiation 13 p2028 N85-22709
Accurate s'bedos of the brightest regions on Io 13 p2195 N85-23618
Mathematical models relating to human thermoregulation: Basic assumptions, validation, and application. Parts A and B [AD-A151556] 15 p2618 N85-26130
Heating parameter estimation using coaxial thermocouple gages in wind tunnel test articles [AD-A153039] 17 p2958 N85-28328
Maintenance of blocking anticyclones in a general circulation model [PB85-190866] 24 p4124 N85-35567

HEAT BUDGET
NT ATMOSPHERIC HEAT BUDGET
Razrezy program research in the tropical Atlantic 07 p0981 N85-16229
Tropical Ocean and Global Atmosphere (TOGA) heat exchange project: A summary report [NASA-CR-176038] 20 p3496 N85-31738

HEAT CAPACITY
U SPECIFIC HEAT

HEAT CAPACITY MAPPING MISSION
Combining Heat Capacity Mapping Mission (HCMM) LANDSAT and thematic map information into a unique high precision merged multichannel system — climatology 05 p0660 N85-14239
A multiple approach in remote sensing for structural and lithological mapping by use Modular Optoelectronic Multispectral Scanner (MOMS)/LANDSAT/Heat Capacity Mapping Mission (HCMM) data 05 p0660 N85-14244
Comparison of measurement and simulation results of radiation temperatures applied to the thermal mapping of Munich [DFVLR-FB-85-06] 17 p2964 N85-28442

HEAT CONDUCTION
U CONDUCTIVE HEAT TRANSFER

HEAT CONTENT
U ENTHALPY

HEAT DISSIPATION
U COOLING

HEAT DISSIPATION CHILLING
U COOLING

HEAT EFFECTS
U TEMPERATURE EFFECTS

HEAT EQUATIONS
U THERMODYNAMICS

HEAT EXCHANGERS
NT TUBE HEAT EXCHANGERS
Biofouling and corrosion studies at the Seacoast Test Facility in Hawaii [DE84-014643] 01 p0029 N85-10180
Laminar flow heat exchangers. Viscosity induced non-uniform flow [AD-A144777] 01 p0047 N85-10307
Heat exchanger [DE84-014299] 01 p0047 N85-10309
Research approaches to qualify aluminum for Ocean Thermal Energy Conversion (OTEC) systems [DE84-013007] 04 p0476 N85-13034
Evaluation of selected advanced heat exchangers for waste heat recuperation of high temperature streams [DE84-016299] 04 p0499 N85-13180
Review of SERI solar pond work 05 p0687 N85-14289
Allowing for the temperature field in the wall thickness of checkerwork in thermal calculation [BLL-M-36015-(5828.4)] 07 p0956 N85-16058
Challenges in the development of the orbiter active thermal control subsystem 08 p1096 N85-16923
Operating and maintenance guidelines for the kinergetics (trade name) environmental control system. Carbon dioxide scrubber model DH-10 and heat exchanger model CCU-01 [AD-A148107] 08 p1200 N85-17557
Corrosion of ceramics in heat exchanger applications [DE84-017459] 09 p1299 N85-18161
Hybrid system for producing and storing ice [DE84-017474] 09 p1304 N85-18195
Monitoring environmental and related performance parameters for a Rankine-cycle turbine electric generator utilizing geothermal energy at the Gila Hot Springs, New Mexico [DE84-901772] 09 p1345 N85-18485
Acoustic imaging in a water filled metallic pipe — monitoring heat exchangers in nuclear power reactors [DE84-016051] 09 p1378 N85-18665
Effect of inclination, transverse intertip spacing, and logitudinal pitch on crossflow heat transfer from an array of finned tubes 10 p1482 N85-19359
Analysis of compact heat exchanger performance [DE84-012824] 10 p1485 N85-19377
Heat and mass exchange in a partially stratified fluid [DE85-000528] 10 p1486 N85-19384
Conceptual design of a 10 MW shore-based OTEC plant [DE84-015808] 10 p1511 N85-19532
Research on heat-exchanger corrosion [PB85-126316] 11 p1616 N85-20184
Formaldehyde and tracer gas transfer between airstreams in enthalpy-type air-to-air heat exchangers [DE84-016951] 11 p1631 N85-20274
Acoustic resonance in heat exchanger tube banks [DE85-004395] 11 p1632 N85-20281
Theoretical and experimental analysis of vertical, concentric-tube ground-coupled heat exchangers [DE85-000474] 11 p1633 N85-20298
Slit-ring test for evaluating fracture in tubular cross sections [DE85-003550] 11 p1654 N85-20416
Direct contact heat recovery from molten salt [DE85-002830] 11 p1674 N85-20550
Theoretical analysis of condensation in the presence of noncondensable gases as applied to open cycle OTEC condensers [DE84-015809] 11 p1675 N85-20556
Steam generator tube vibration tests [DE85-003599] 12 p1867 N85-21712
Direct-contact condensers for solar pond power production [DE84-004510] 12 p1876 N85-21771
Development of a single-family absorption chiller for use in a solar heating and cooling system, phase 3, volume 2 [DE85-003218] 13 p2130 N85-23253
Advanced radiator concepts [NASA-TM-87008] 14 p2300 N85-24245
Equipment for monitoring low concentrations of volatile substances in gases or liquid metals [BLL-DOUNREAY-TR-949-(9091.9F)] 16 p2786 N85-27190
DOE/ANL/HTRI heat exchanger tube vibration data bank: Addendum 5 [DE85-007730] 17 p2960 N85-28425
Heat management system for aircraft [AD-D011656] 18 p3061 N85-28936
Research test facility for evaporation and combustion of alternative jet fuels at high air temperatures [AD-A153830] 18 p3083 N85-29073
Reciprocating magnetic refrigerator employing tandem porous matrices within a reciprocating displacer [NASA-CASE-NPO-16257-1] 18 p3085 N85-29082
Development of corrosion resistant heat exchangers for flue gas desulfurization [BMFT-FB-T-84-281] 18 p3103 N85-29211
Experimental investigation of turbulent heat transfer in straight and curved rectangular ducts [AD-A154413] 19 p3266 N85-30255
Onset of freezing in residential air-to-air heat exchangers [DE85-000960] 19 p3267 N85-30259
Intrinsically irreversible acoustic heat engines [DE85-007672] 19 p3270 N85-30276
Stability analysis of direct contact heat exchangers subject to system perturbations [DE85-011780] 20 p3455 N85-31452
An investigation into the fluidization and heat transfer of low density particles in a fluidized bed with applications [AD-A155259] 21 p3584 N85-32262
One method of solving the problem of unsteady heat exchange of a body and its ablation 22 p3733 N85-33146
Woven heat exchanger [DE85-011833] 22 p3783 N85-33439
Heat-mass flow enhancement system for a metal hydride assembly [DE85-010698] 22 p3783 N85-33441
Ocean thermal energy conversion [DE85-012291] 23 p3946 N85-34456
High Temperature Heating System (HTHS) [PB85-186340] 24 p4084 N85-35316
Experimental lithium system [DE85-013252] 24 p4094 N85-35382

HEAT FLOW
U HEAT TRANSMISSION

HEAT FLUX
Evaluation of surface sensible heat flux effects on the generation and modification of mesoscale circulations 01 p0079 N85-10527
Heat flux sensors for burner liners and turbine blades and vanes 02 p0142 N85-10961
Numerical analysis of flow and heat transfer in the VAFB LOX storage Dewar tank [NASA-CR-171203] 02 p0197 N85-11315
Resistance of Navy shipboard outerwear garments and fire-resistant fabrics to extreme heat [AD-A145414] 02 p0238 N85-11546
The areal pattern of latent and sensible heat fluxes: The combination of soil physics and remotely sensed data 05 p0656 N85-14213
Modeling influence of three layer cloud cover on outgoing thermal radiation 06 p0825 N85-15242

High temperature thermocouple and heat flux gauge using a unique thin film-hardware hot juncture
[NASA-TM-86986] 07 p0962 N85-16096
Self-generated magnetic fields and thermal flux inhibition
[AD-A147405] 07 p0971 N85-16166
New aspects of thermoelastic contact
[AD-A147554] 07 p0979 N85-16217
Subcooled flow boiling at high heat flux
[OUEL-1540/84] 08 p1163 N85-17338
Magnetic fusion energy plasma interactive and high heat flux components. Volume 2: Technical assessment of the critical issues and problem areas in high heat flux materials and component development
[DE85-001155] 09 p1393 N85-18764
Analysis of the dissipation mechanism within an instationary cathode spot of metal vapor arcs
[AD-A149256] 10 p1558 N85-19825
Thermal investigation of an electrical high-current arc with porous gas-cooled anode
[NASA-TM-77769] 11 p1627 N85-20245
Aspects of planetary wave transports in the middle atmosphere 11 p1661 N85-20471
Envelope thermal test unit: Technical description
[DE84-012254] 11 p1674 N85-20548
Heat flux in Lorentzian plasma
[IPPJ-704] 12 p1935 N85-22158
Experimental investigations of thermal radiation from potassium atoms in magnetohydrodynamic system: Preliminary report
[DE85-003715] 12 p1936 N85-22160
Coupling between velocity oscillations and solid propellant combustion
[AD-A151081] 14 p2247 N85-23927
Parameterization of apparent and latent heat fluxes above water surface in calm weather under natural conditions 14 p2337 N85-24454
Thermal and magnetic properties of neutron stars
16 p2880 N85-27774
Experimental measurements and analysis of heat transfer and gas dynamics in a rotating turbine stage
17 p2911 N85-27949
Heat flux sensor calibrator 17 p2915 N85-27970
Conformational and mechanical properties at high strain rates
[AD-A153401] 17 p2959 N85-28272
Analysis of ocean surface wind fields using SEASAT-A scatterometer data 18 p3139 N85-29434
Objective determination of heat wave patterns
18 p3140 N85-29437
Preliminary results from numerical experiments on the summer 1980 heat wave and drought
18 p3140 N85-29438
Enhanced thermal coupling by a repetitively pulsed laser
[AD-A154435] 19 p3276 N85-30317
Experiments using atmospheric forcing from a FGGE analysis to drive an upper ocean model
[INPE-3503-PRE/736] 19 p3319 N85-30576
One-dimensional model hindcasts of warm anomalies in the North Pacific Ocean
[AD-A154128] 19 p3320 N85-30579
Experimental observation of transition behavior on a flat plate 20 p3452 N85-31437
Stability analysis of direct contact heat exchangers subject to system perturbations
[DE85-011780] 20 p3455 N85-31452
Wall flames and implications for upward flame spread
[FAA-CT-85-2] 21 p3553 N85-32103
Facility for large-scale hazardous gas testing
[DE85-011652] 21 p3564 N85-32169
Technical assessment of thermal-hydraulics for high heat flux fusion components
[DE85-013178] 23 p3930 N85-34359
Sequential regularization solution of the inverse heat conduction problem
[DE85-010657] 23 p3931 N85-34362
Forced convective, nonequilibrium, post-CHF heat transfer experiment data and correlation comparison report
[TIB5-009331] 23 p3932 N85-34371
On the heat flux derived by the moment method in Lorentzian plasma between hot and cold walls
23 p3980 N85-34682
Integral representation for nonlinear heat transport
23 p3981 N85-34683
High Temperature Heating System (HTHS)
[PB85-186340] 24 p4084 N85-35316
Development of advanced high-temperature heat flux sensors. Phase 2: Verification testing
[NASA-CR-174973] 24 p4096 N85-35391
Case studies for flux measurements along a low-flying route to the south of Munich 24 p4121 N85-35548
Two-point closure study of covariance budgets for turbulent Rayleigh-Benard convection
[PB85-189108] 24 p4124 N85-35568

HEAT GAIN
U HEATING

HEAT GENERATION
Temperature prediction in mechanical components, an analytical approach 09 p1327 N85-18339
Thermal profiles of thermite reactions
[DE85-003308] 10 p1438 N85-19081
U, Th, K content, heat production and thermal conductivity of Sao Paulo, Brazil continental shelf sediments: A reconnaissance work
[INPE-3401-PRE/670] 10 p1515 N85-19558
Two-d heat transfer through porous media with heat generation
[AD-A151965] 16 p2783 N85-27173
Generated spiral bevel gears: Optimal machine-tool settings and tooth contact analysis
[NASA-TM-87075] 23 p3937 N85-34405

HEAT MEASUREMENT
.A concept for a hadron calorimeter with photodiode readout
[MPI-PAE/EXP-E1-130] 01 p0050 N85-10332
Time resolved calorimetry of 30 nm Te-films during laser annealing
[AD-A145047] 01 p0052 N85-10346
Recent progress in BGO development for high resolution calorimetry
[MPI-PAE/EXP-E1-129] 01 p0124 N85-10848
Accurate measurement of heat capacity by differential scanning calorimetry 04 p0468 N85-12975
Thermal performance testing of passive solar components in NBS (National Bureau of Standards) calorimeter
[PB85-119345/GAR] 09 p1346 N85-18470
Calorimetric investigation into the possibility of a charge density wave ground state in alkali metals
[DE85-002006] 09 p1397 N85-18795
Synthesis and thermomechanical properties of new AT-Phenylene R systems
[AD-A149961] 12 p1813 N85-21372
Transient technique for measuring heat transfer coefficients on stator airfoils in a jet engine environment
[NASA-TM-87005] 15 p2560 N85-25794
Heat flux sensor calibrator 17 p2915 N85-27970
Objective determination of heat wave patterns
18 p3140 N85-29437
Guest molecules in coal
[DE85-010435] 19 p3228 N85-30016
The effect of prior parent phase cold work on martensite transformation in Cu-Zn-Al shape memory alloys
[AD-A155140] 21 p3566 N85-32183
Cryogenic laser calorimetry for impurity analysis
[NASA-CR-176179] 24 p4097 N85-35395
X-ray film chamber with carbon target of Tien-Shan complex array 24 p4179 N85-35915

HEAT OF FORMATION
Local density theory of heats of formation and short-range order parameters in substitutionally disordered alloys
[DE85-009811] 18 p3075 N85-29021
Heats of formation of gas phase organosulfur molecules, radicals and ions measured by PEPICO and application of (17)O and (33)S NMR spectroscopy to structure determination of organosulfur compounds
[DE85-010658] 24 p4071 N85-35229

HEAT OF FUSION
Natural convection during heat accumulation by substances with change of aggregate state
13 p2043 N85-22787

HEAT OF VAPORIZATION
Analysis of the natural initiation of vapor explosions
[DE85-000188] 11 p1632 N85-20279

HEAT PIPES
Corrosion in alkali metal/molybdenum heat pipes
[DE84-014039] 02 p0184 N85-11233
Titanium-potassium heat pipe corrosion studies
[DE84-015526] 05 p0637 N85-14090
Procedures for testing and evaluating spacecraft-type heat pipes
[AD-A146671] 06 p0809 N85-15139
Power flattening techniques for radioisotopic thermoelectric generators
[AD-A146985] 06 p0833 N85-15299
Thermally isolated structural support link
[AD-D011349] 07 p0972 N85-16176
Capillary Pump Loop (CPL) heat pipe development status report
[NASA-CR-175273] 08 p1161 N85-17323
An evaluation of liquid and two-phase cooling techniques for use in electrical machinery
[AD-A146526] 10 p1464 N85-19372
Space heat rejection radiators: Meteoroid/debris consideration 12 p1788 N85-21210
Heat pipe cooled probe
[NASA-CASE-LAR-12588-1] 12 p1844 N85-21566
Modeling of transient heat pipe operation
[NASA-CR-175496] 12 p1844 N85-21571
Use of heat pipes for heat collection and transmission in solar plants 14 p2265 N85-24037
Sodium and lithium corrosion in molybedenum heat pipes
[DE85-005561] 16 p2784 N85-27179
Heat pipe and method of making same
[AD-D011654] 17 p2959 N85-28273
High thermal power density heat transfer apparatus providing electrical isolation at high temperature using heat pipes
[NASA-CASE-LEW-12950-2] 18 p3066 N85-29179
Pressure recovery in a cylindrical heat pipe at high radial Reynolds numbers and at high Mach numbers
[DE85-010718] 19 p3269 N85-30274
Performance characteristics of gravity-assisted potassium heat pipes
[DE85-010717] 19 p3287 N85-30367
Infrared generation and wave-mixing studies in cesium
[DE85-012883] 24 p4083 N85-35304
Development of a high-efficiency, gas-fired, heat pipe, warm-air heating system
[PB85-199636] 24 p4085 N85-35318

HEAT PUMPS
Chemical heat pump state-of-the-art survey
[DE84-013552] 01 p0048 N85-10312
Determination of optimum Curie point as a function of source and sink temperatures for magnetic heat pumps
[DE84-016995] 04 p0499 N85-13182
Magnetic heat pump cycles for industrial waste heat recovery
[DE84-017016] 04 p0499 N85-13183
Development of a Braun linear engine-driven, heat-actuated heat pump
[DE84-016647] 04 p0500 N85-13188
Investigation of an ejector heat pump by analytical methods
[DE84-016675] 04 p0500 N85-13189
A refined computer program for the transient simulation of ground coupled heat pump systems
[DE84-014098] 05 p0637 N85-14088
Open-cycle vapor compression heat pump
[PB85-101475/GAR] 06 p0775 N85-14951
Working medium for sorption heat pumps
[BLL-T6360/BG/WH785/84] 06 p0807 N85-15131
Phase 1-A development kinematic Sterling/Rankine commercial gas-fired heat pump research program
[PB85-100931/GAR] 07 p0936 N85-15928
NOx emissions near a heat pump with gas motor
[BLL-WH-782-(9091.9F)] 07 p0985 N85-16319
Rotary magnetic heat pump
[DE84-017017] 09 p1320 N85-18303
Sulfuric acid chemical heat pump program, March - November 1982
[DE84-017436] 09 p1320 N85-18304
Open-cycle centrifugal vapor-compression heat pump
[PB85-113405/GAR] 09 p1328 N85-18348
Comparison of energy storage systems in the United States chilled water versus two types of ice storage systems
[DE85-001102] 09 p1344 N85-18452
Available energy method for evaluating thermodynamic performance of heat pump systems
[DE84-017223] 09 p1400 N85-18814
DOE/ORNL electric systems program overview
[DE85-003334] 10 p1459 N85-19197
Optimization of a ground coupled heat pump
[DE85-000273] 10 p1486 N85-19380
An assessment of ground-coil heat-pump technology
[DE85-002567] 10 p1486 N85-19382
Development and demonstration of a Stirling/Rankine heat activated heat pump. Phase 3B: Engine technology development testing
[DE85-004388] 10 p1486 N85-19383
Development and test of a high COP Rankine heat pump for generation of process steam. Phase 2: Fabrication and test
[DE85-002600] 11 p1632 N85-20275
Magnetic heat pump feasibility assessment
[DE85-002606] 11 p1632 N85-20276
Theoretical and experimental analysis of vertical, concentric-tube ground-coupled heat exchangers
[DE85-000474] 11 p1633 N85-20286
Performance evaluation of an active solar cooling system utilizing low cost plastic collectors and an evaporatively-cooled absorption chiller
[DE84-010613] 12 p1880 N85-21798
Magnetic refrigeration and heat pumping design options
[DE85-003405] 13 p2092 N85-23064
Cooling performance improvement of a horizontal ground coupled heat pump
[DE85-002470] 13 p2093 N85-23065
A review of development and application of heat pump technology
[CSIR-RR-585] 14 p2300 N85-24241

Mass and heat transfer in reflux condensers of absorption heat pumps
[DFVLR-FB-83-43] 14 p2304 N85-24266
Transient analysis of a magnetic heat pump 15 p2576 N85-25891
The use of heat pumps in district heat supply
[BLL-OA-TRANS-2728-(6196.3)] 16 p2781 N85-27163
Alternative heat sources for heat pumps
[DE85-007610] 17 p2959 N85-28275
Simplified analysis of Stirling engines and heat pumps
[DE85-008753] 17 p2986 N85-28457
Comparative evaluation of ground-coupled heat pumps that use solar energy
[DE85-010950] 20 p3484 N85-31649
Solid state radiative heat pump
[DE85-011605] 22 p3760 N85-33303
Heat-mass flow enhancement system for a metal hydride assembly
[DE85-010698] 22 p3783 N85-33441
Advanced heat pump research and development
[DE85-009540] 23 p3932 N85-34372
Solar heat pump
[DE85-011323] 23 p3946 N85-34453

HEAT RADIATORS
NT SPACECRAFT RADIATORS
Methods for heat transfer and temperature field analysis of the insulated diesel
[NASA-CR-174783] 07 p1056 N85-16699
Challenges in the development of the orbiter radiator system 08 p1096 N85-16925

HEAT REGULATION
U TEMPERATURE CONTROL

HEAT REJECTION DEVICES
U HEAT RADIATORS

HEAT RESISTANCE
U THERMAL RESISTANCE

HEAT RESISTANT ALLOYS
NT MOLYBDENUM ALLOYS
NT NIOBIUM ALLOYS
NT REFRACTORY METAL ALLOYS
NT RENE 95
NT RHENIUM ALLOYS
NT TANTALUM ALLOYS
NT TUNGSTEN ALLOYS
NT UDIMET ALLOYS
NT WASPALOY
Weldability of aged heat resistant nickel alloys 01 p0021 N85-10125
Morphological changes of gamma prime precipitates in nickel-base superalloy single crystals
[NASA-TM-83698] 01 p0026 N85-10165
The effects of seven alloying elements on the microstructure and stress-rupture behavior of nickle-base superalloys
[NASA-TM-83791] 01 p0027 N85-10168
High temperature static strain sensor development program 02 p0141 N85-10959
The structure of rapidly solidified nickel-base alloys 02 p0181 N85-11215
Microstructure and creep behaviour at elevated temperature of unidirectionally solidified eutectic nickel base superalloys 02 p0181 N85-11216
The transient oxidation of single crystal NiAl+Zr
[NASA-CR-174756] 02 p0182 N85-11221
The effect of tantalum and carbon on the structure/properties of a single crystal nickel-base superalloy
[NASA-CR-174779] 02 p0182 N85-11223
Studies on the hot corrosion of a nickel-base superalloy, Udimet 700
[NASA-TM-86882] 02 p0183 N85-11224
Plastic strain localization in superalloy single crystals
[AD-A145705] 02 p0288 N85-11878
Materials for advanced turbine engines. Project 2: Rene 150 directionally solidified superalloy turbine blades, volume 2
[NASA-CR-167993] 03 p0319 N85-12059
Verification tests of durable TPS concepts
[NASA-TM-86313] 03 p0323 N85-12085
Effects of tin on microstructure and mechanical behavior of Inconel 718
[NASA-TM-86866] 03 p0330 N85-12129
High temperature low-cycle fatigue mechanisms in single crystals of nickel-based superalloy Mar-M 200
[NASA-CR-174739] 03 p0331 N85-12130
The effects of Cr, Co, Al, Mo and Ta on the cyclic oxidation behavior of a prototype cast Ni-base superalloy based on a 2(5) composite statistically designed experiment
[NASA-TM-83784] 03 p0331 N85-12131
The effect of orientation on fatigue growth in a nickel-based single crystal superalloy
[PNR-90207] 03 p0332 N85-12141
Analysis techniques for tracer studies of oxidation
[NASA-CR-174796] 03 p0336 N85-12162
Time-temperature dependence of the strength of commercial zirconia ceramics
[AD-A145233] 03 p0338 N85-12173
Features of plastic deformation and fracture of EP 741 nickel alloy under thermal strain 03 p0349 N85-12250
Structural stability of nickel heat resistant alloys at high temperatures 03 p0350 N85-12251
Interactions between corrosion and creep of uncoated and coated superalloys in sulfate melts 04 p0477 N85-13038
COST 50 - materials for gas turbines, part 1 and 2 3UK9
[NPL-DMA(A)-74] 05 p0617 N85-13943
The microstructural characteristics of revert superalloys — for turbine blades 05 p0617 N85-13945
Controlled directionally solidified precision casting for superalloys and steels
[BMFT-FB-T-84-198] 05 p0619 N85-13960
Method for predicting the creep rupture life of nickel-base precipitation-hardened superalloys from their chemical composition
[BLL-PNR-90241-(8019.3153)] 06 p0768 N85-14910
The role of microstructure in the modelling of plastic flow in P/M superalloys at forging temperatures and strain rate 06 p0796 N85-15090
Method for making alloy additions to base metals having higher melting points
[AD-D011403] 07 p0928 N85-15884
Welding of PM-superalloys
[MTU-TB-910/84] 07 p0975 N85-16191
The effect of the test atmosphere on the formation and propagation of creep cracks in commercial high temperature alloys
[JUEL-1939] 07 p0960 N85-16221
Grain refining and microstructural modification during solidification
[AD-A147705] 08 p1128 N85-17111
Materials of the fourth scientific-technical Conference on Questions of the Extrusion of Metals (Selected articles)
[AD-A148578] 08 p1130 N85-17121
The effect of tantalum on the structure/properties of two polycrystalline nickel-base superalloys: B-1900 + Hf MAR-M247
[NASA-CR-174847] 09 p1294 N85-18127
Resistivity of alloys
[DE85-000906] 09 p1296 N85-18138
Adaptation of remelting procedures for the use of recycled metal in nickel-base superalloy castings
[PNR-90232] 09 p1297 N85-18149
Effects of MAR-M247 substrate (modified) composition on coating oxidation coating/substrate interdiffusion — protective coatings for hot section components of gas turbine engines
[NASA-CR-174851] 10 p1440 N85-19073
Low cycle fatigue of MAR-M 200 single crystals at 760 and 870 deg C
[NASA-TM-86933] 10 p1440 N85-19074
Creep-rupture behavior of iron superalloys in high-pressure hydrogen
[NASA-CR-174411] 10 p1441 N85-19078
Influence of gaseous hydrogen on strength and ductility of nickel heat-resistant alloys 10 p1447 N85-19119
Estimation of endurance characteristics of heat resistant materials. Report 2: Determination of endurance limit of heat resistant alloys over a broad temperature range 10 p1447 N85-19120
Metals and Ceramics Division Materials Science Program
[DE85-003795] 11 p1592 N85-20012
The physical modelling of transition metal alloying: The roles that different levels of theory play
[DE85-000591] 11 p1607 N85-20105
Patterns in the occurrence of the brittle topologically close-packed phases: Al
[DE85-000592] 11 p1607 N85-20106
Weldability and mechanical property characterization of weld clad alloy 800H tubesheet forging
[DE85-001737] 11 p1609 N85-20116
Effect of reduction of strategic Columbium addition in 718 Alloy on the structure and properties
[NASA-CR-174841] 12 p1805 N85-21320
Investigation of the development possibilities of a ferritic creep and oxidation-resistant steel for application under creep conditions above 650 deg C
[BMFT-FB-T-84-244] 12 p1808 N85-21344
Orientation and temperature dependence of some mechanical properties of the single-crystal nickel-base superalloy Rene N4. 3: Tension-compression anisotropy
[NASA-TM-86862] 13 p2021 N85-22660
USSR report: Materials science and metallurgy
[JPRS-UMS-85-002] 13 p2025 N85-22688
Comparison of dynamic-tension and constant-load strength characteristics of heat-resistant materials 13 p2030 N85-22722
Some specifics of development of fatigue and creep in heat-resistant alloys with asymmetrical multicycle loading 13 p2031 N85-22724
Change in microstructure of heat-resistant nickel alloys upon thermal cycling in a current of gas 13 p2031 N85-22725
Softening of metal near seam during welding of heat-resistant nickel alloys 13 p2035 N85-22747
Effect of zero-wear in friction pairs operating in abrasive media 13 p2045 N85-22801
The cyclic stress-strain behavior of nickel-base superalloy poly- and single crystals 14 p2254 N85-23969
Research directed advanced high temperature coating system beyond current state-of-the art systems
[AD-A150698] 14 p2255 N85-23974
Role of passive surface films on corrosion fatigue crack initiation
[DE85-000438] 14 p2257 N85-23985
Contact point and seam welding of heat-resistant alloys 15 p2501 N85-25429
An investigation of the structure and high temperature mechanical properties of oxide dispersion strengthened alloys
[AD-A151107] 15 p2509 N85-25477
Optimizing hot workability and controlling microstructures in difficult to process high strength and high temperature materials
[AD-D011586] 15 p2510 N85-25482
Design of ductile polycrystaline Ni3Al alloys
[DE85-005572] 15 p2511 N85-25491
Reduced-chromium stainless steel substitutes containing silicon and aluminum
[PB85-160786] 15 p2513 N85-25502
Mechanisms of buildup and properties of aluminum coatings on heat-resistant nickel alloys 15 p2513 N85-25506
Modified aluminosilicide coating for heat-resistant nickel alloys 15 p2514 N85-25509
On thermomechanical testing in support of constitutive equation development for high temperature alloys
[NASA-CR-174879] 15 p2577 N85-25894
Crack closure characteristics considering center cracked and compact tension specimens
[AD-A151702] 15 p2579 N85-25907
Fatigue life extension 16 p2733 N85-26864
Design overview of fiber-reinforced superalloy composites for the Space Shuttle main engine 16 p2734 N85-26871
Materials for advanced rocket engine turbopump turbine blades 16 p2734 N85-26872
Development of hydrogen resistant alloys 16 p2735 N85-26873
Relationships between microstructure and microflesuring in alloy 718 16 p2735 N85-26876
Nonlinear structural analysis for fiber-reinforced superalloy turbine blades 16 p2737 N85-26887
Iron rich low cost superalloys
[NASA-CR-174900] 16 p2748 N85-26962
Effects of high mean stress on high-cycle fatigue behavior of PWA 1480 17 p2914 N85-27964
Constitutive cyclic deformation behavior in single-crystal and directionally solidified SSME high-pressure fuel turbopump airfoil materials 17 p2914 N85-27965
High-thermal-gradient superalloy crystal growth 17 p2914 N85-27966
Role of hydrogen and structure on CMSX-2 17 p2915 N85-27967
The characteristic structure of weld metal of high temperature alloy X20CrMoV 121
[BLL-BISI-TRANS-21623-(9022.06)] 17 p2926 N85-28069
Precision die forging of blades or gas turbines 17 p2940 N85-28148
High-temperature oxidation of alloys in mixed oxidants
[DE85-009706] 18 p3077 N85-29035
Study of the influence of metallurgical factors on fatigue and fracture of aerospace structural materials
[AD-A153913] 18 p3122 N85-29329
Effect of prolonged high temperature on durability of coated high-temperature nickel alloys 19 p3243 N85-30105
Properties of heat resistant Ni-Al-Nb alloys with unidirectional eutectic structure 19 p3247 N85-30133
Effects of high mean stress on the high-cycle fatigue behavior of PWA 1480
[NASA-CR-176020] 19 p3287 N85-30388
Mechanical behavior of Ni-Cr-base superalloys in forms and conditions representative of service
[NPL-DMA(A)-94] 20 p3431 N85-31282

Long range ordered alloys modified by addition of niobium and cerium
[DE86-011661] 20 p3431 N86-31285
Micromechanics of high temperature deformation and failure 20 p3466 N86-31534
Constitutive modeling of superalloy single crystals and directionally solidified materials 20 p3466 N86-31535
On the use of internal state variables in thermoviscoplastic constitutive equations 20 p3466 N86-31536
Finite element modeling of cracked bodies using the Bodner-Partom flow law 20 p3466 N86-31547
The effect of stress and hot corrosion on nickel-base superalloys
[AD-A154722] 21 p3586 N86-32181
Strain rate sensitivity estimation from high velocity impact data
[AD-A154703] 21 p3599 N86-32347
Nitriding of super alloys for enhancing physical properties
[DE86-005782] 23 p3917 N86-34275
The development and evaluation of the creep and corrosion resistant alloy IN6201
[PNR-90253] 23 p3917 N86-34278
Directionally solidified gas turbine alloys
[PNR-90264] 23 p3917 N86-34279
Microshrink, tensile properties, and the detection of microshrink
[AD-A155875] 24 p4079 N86-35278

HEAT SHIELDING
NT REENTRY SHIELDING
NT REUSABLE HEAT SHIELDING
Passive storage technologies 08 p1108 N85-17003
Erosion of corrosion-resistant surface treatments on alloy steels
[DE85-006448] 17 p2932 N85-28100
Mechanical fastener
[NASA-CASE-LAR-12736-2] 19 p3279 N85-30335
Experimental aerodynamic heating to simulated space shuttle tiles in laminar and turbulent boundary layers with variable flow angles at a nominal Mach number of 7
[NASA-TP-2307] 23 p3929 N85-34351
Results of tests on a specimen of the SRB aft skirt heat shield curtain in the MSFC LRLF
[NASA-CR-170683] 24 p4070 N85-35221
Results of tests of the SRB aft skirt heat shield curtain in the MSFC Hot Gas Facility
[NASA-CR-170668] 24 p4070 N85-35223

HEAT SINKS
Hot hollow cathode gun assembly
[DE84-014312] 01 p0121 N85-10832
Heatsink requirements for coherent operation of high-power semiconductor laser arrays
[AD-A146184] 03 p0366 N85-12346
Determination of optimum Curie point as a function of source and sink temperatures for magnetic heat pumps
[DE84-016995] 04 p0499 N85-13182
Evaluation of some photovoltaic concentrator solar cell-heat sink coupling materials
[DE84-016027] 04 p0529 N85-13378
High-efficiency, low-cost, passively-cooled PV concentrator module
[DE85-010013] 10 p3305 N85-30490
Heat sinking for printed circuitry
[DE85-011585] 22 p3783 N85-33440
Mathematical modeling of ultimate heat sink cooling ponds
[TI85-009747] 23 p3932 N85-34369

HEAT SOURCES
NT GEOTHERMAL RESOURCES
NT GEYSERS
NT THERMAL RESOURCES
Metallography of Kovar/glass/thermite interfaces
[DE84-015247] 02 p0195 N85-11302
General-purpose heat source development: Safety test program. Postimpact evaluation, design iteration test 2
[DE84-015978] 04 p0564 N85-13592
Infrared thermography of burn front propagation in heat powders
[DE85-003307] 10 p1438 N85-19060
Thermal profiles of thermite reactions
[DE85-003306] 10 p1436 N85-19061
Consolidation around a point heat source
[PB85-116549] 11 p1682 N85-20601
General-purpose heat source development: Safety test program. Postimpact evaluation, design iteration test 4
[LA-10217-SR] 12 p1930 N85-22128
General-purpose heat source development: Safety test program. Postimpact evaluation, design iteration test 5
[LA-10232-SR] 12 p1931 N85-22129
General-purpose heat source development: Safety test program. Postimpact evaluation, design iteration test 1
[LA-9980-SR] 12 p1931 N85-22131
Long-term exposure of pressed plutonium oxide heat sources to aquatic environments
[DE85-007385] 15 p2495 N85-25392
Low gravity exothermic heating/cooling apparatus
[NASA-CASE-MSC-25707-1] 18 p3104 N85-29214
Burn front velocity as a function of pellet density in iron-potassium perchlorate heat powders
[DE85-011448] 21 p3572 N85-32214
Crustal radiogenic heat production and the selective survival of ancient continental crust 21 p3721 N85-33066
Neutron flux, spectrum and dose equivalent measurements for a 4500-W(th) 236 PuO2 general purpose heat source
[DE85-011361] 22 p3841 N85-33786
Contrasts in evolution of Venus and Earth 22 p3857 N85-33860
General-purpose heat source development: Safety test program. Postimpact evaluation, design iteration test
[LA-10034-SR] 23 p3969 N85-34606
Development and characterization of carbon-bonded carbon fiber insulation for radioisotope space power systems
[DE85-013365] 24 p4082 N85-35299

HEAT STORAGE
Man's physical tolerance to heat. Heat storage, burn injury
[FOA-C-54055-H1] 02 p0235 N85-11533
Thermal energy storage at 900 deg C
[DE84-004589] 04 p0530 N85-13387
Possibilities of conjugating binary solutions for thermal energy storage
[DE84-016704] 04 p0531 N85-13392
Trends in concentrator, receiver, and storage development for terrestrial applications 05 p0609 N85-13891
A refined computer program for the transient simulation of ground coupled heat pump systems
[DE84-014098] 05 p0637 N85-14088
Thermodynamical characteristics of heat storage reactors using metal hydrides
[NAL-TR-822] 06 p0869 N85-15524
Thermal energy storage
[DE85-001492] 09 p1344 N85-18454
Field testing of aquifer thermal energy storage
[DE85-000399] 09 p1344 N85-18457
Advanced latent heat storage media for high-temperature industrial applications
[DE85-000907] 09 p1345 N85-18461
Development of media for dynamic latent heat storage for the low-temperature range. Part 1: Thermal analyses of selected salt hydrate systems
[NASA-TM-77778] 10 p1507 N85-19510
Direct contact heat recovery from molten salt
[DE85-002830] 11 p1674 N85-20550
Latent heat storage technology and application workshop. Summary report: Session 6
[DE85-001097] 12 p1882 N85-21806
Phase change thermal energy storage and the model building codes
[PB85-111201] 12 p1883 N85-21813
Natural convection during heat accumulation by substances with change of aggregate state 13 p2043 N85-22787
Latent heat storage in cooling systems
[DE85-005355] 13 p2129 N85-23248
Overview of latent storage for passive solar applications
[DE85-005354] 13 p2129 N85-23249
Central solar heating plants with seasonal storage. Evaluation of systems concepts based on heat storage in aquifers
[DE85-006788] 16 p2820 N85-27396
High temperature composite thermal storage systems
[DE85-005073] 17 p2966 N85-28455
Performance of an active/passive hybrid solar system utilizing vapor transport
[DE85-006627] 17 p2966 N85-28466
Solar pond research at the Los Alamos National Laboratory
[DE85-008631] 18 p3128 N85-29366
High temperature sensible heat storage options
[DE85-000534] 18 p3129 N85-29375
Salt-gradient solar ponds
[DE85-008626] 18 p3129 N85-29380
SERI Solar Energy Storage Program: FY 1984
[DE85-002936] 18 p3130 N85-29385
Stable density stratification solar pond
[NASA-CASE-NPO-15419-2] 19 p3303 N85-30474
Calibration of relevant measuring sensors
[DE85-009820] 19 p3306 N85-30492
DHC: A diurnal heat capacity program for microcomputers
[DE85-009545] 20 p3516 N85-31659
Solar energy education: Renewable energy activities for chemistry and physics
[DE85-010371] 23 p3948 N85-34455

HEAT STROKE
An atropinized heat-stressed rat model: Dose response effects and pharmacokinetics
[AD-A146851] 07 p1011 N85-16423

HEAT TESTS
U HIGH TEMPERATURE TESTS

HEAT TOLERANCE
Man's physical tolerance to heat. Heat storage, burn injury
[FOA-C-54055-H1] 02 p0235 N85-11533
Tolerance endpoint for evaluating the effects of heat stress in dogs
[AD-A148104] 08 p1192 N85-17511
Heat stress and personal protective equipment
[DE85-003552] 10 p1532 N85-19652
Preventive effect of acute heat factors during hypokinesia 12 p1902 N85-21945
Physiological differences between men and women in exercise-heat tolerance and heat acclimation
[AD-A152048] 15 p2618 N85-26135

HEAT TRANSFER
NT AERODYNAMIC HEAT TRANSFER
NT CONDUCTIVE HEAT TRANSFER
NT CONVECTIVE HEAT TRANSFER
NT HYPERSONIC HEAT TRANSFER
NT LAMINAR HEAT TRANSFER
NT RADIATIVE HEAT TRANSFER
NT TURBULENT HEAT TRANSFER
Turbulent boundary layers over rough surfaces hypersonic flow
[AD-A145040] 01 p0003 N85-10018
Real time sensing and control of out-of-plane distortion due to line heating by laser
[AD-A144773] 01 p0027 N85-10169
The effect of channel convergence on heat transfer in a passage with short pin fins
[NASA-TM-83801] 01 p0046 N85-10303
Second All-Union Seminar on Hydromechanics and Heat and Mass Exchange in Weightlessness, summaries of reports
[NASA-TM-77590] 01 p0047 N85-10305
A review and analysis of boundary layer transition data for turbine application
[NASA-TM-86880] 01 p0047 N85-10306
Measurement and analysis of spark ignition engine pressure data to determine heat release profiles
[AD-A144770] 01 p0055 N85-10363
Turbine Engine Hot Section Technology (HOST)
[NASA-TM-83022] 02 p0140 N85-10951
Turbine heat transfer 02 p0142 N85-10964
Gas side heat transfer: 2-D flow 02 p0142 N85-10965
Gas flow environment and heat transfer nonrotating 3D program 02 p0142 N85-10966
Jet array impingement flow distributions and heat transfer characteristics: Effects of initial crossflow and nonuniform array geometry 02 p0142 N85-10967
Coolant passage heat transfer with rotation 02 p0143 N85-10968
Burner liner thermal/structural load modelling 02 p0143 N85-10970
Some of the features of movement of gas through a layer of free-flowing substances
[BLL-M-35732-(5828.4)] 02 p0196 N85-11312
Numerical analysis of flow and heat transfer in the VAFB LOX storage Dewar tank
[NASA-CR-171203] 02 p0197 N85-11315
Preliminary results of a study of the relationship between free stream turbulence and stagnation region heat transfer
[NASA-TM-86884] 02 p0197 N85-11317
Experimental and predicted heating distributions for biconics at incidence in air at Mach 10
[NASA-TP-2334] 03 p0361 N85-12313
Heat transfer and pressure drop in blade cooling channels with turbulence promoters
[NASA-CR-3837] 03 p0361 N85-12315
Off-flow study of a Space Shuttle orbiter tip-fin controller
[NASA-TM-86276] 04 p0480 N85-12920
Proposal for wall function for friction and heat transfer in the presence of roughness and mass transfer
[CFD/84/12] 04 p0501 N85-13198
Multigrid iteration solution procedure for solving three-dimensional sets of coupled equations
[DE84-016515] 04 p0555 N85-13532
Multigrid iteration solution procedure for solving two-dimensional sets of coupled equations
[DE84-016554] 04 p0555 N85-13533
The interaction of Global Biochemical Cycles
[NASA-CR-174184] 06 p0852 N85-14183
Air-sea heat exchange, an element of the water cycle 06 p0853 N85-14195

Salt-gradient solar ponds: Summary of US Department of Energy sponsored research
[NASA-CR-174183] 05 p0667 N85-14286
Solar pond fluid dynamics and heat transfer
05 p0667 N85-14288
Cage regional energy budgets from the GLAS ATH order model
05 p0685 N85-14402
Analysis of physical-chemical processes governing SSME internal fluid flows
[NASA-CR-174245] 06 p0760 N85-14862
Heat transfer results and operational characteristics of the NASA Lewis Research Center Hot Section Cascade Test Facility
[NASA-TM-86890] 06 p0808 N85-15133
Energy active areas of ocean
06 p0820 N85-15204
Indirect estimation of convective boundary layer structure for use in routine dispersion models
[PB84-236260] 06 p0834 N85-15306
Thermodynamical characteristics of heat storage reactors using metal hydrides
[NAL-TR-822] 06 p0869 N85-15524
Engine Cyclic Durability by Analysis and Testing
[AGARD-CP-368] 07 p0905 N85-15733
Monitoring engine thermal stresses
07 p0906 N85-15735
Heat transfer due to film condensation on vertical fluted tubes
[AD-A147258] 07 p0959 N85-16079
High temperature thermocouple and heat flux gauge using a unique thin film-hardware hot juncture
[NASA-TM-86898] 07 p0962 N85-16096
Razrezy program research in the tropical Atlantic
07 p0981 N85-16229
Frazil ice formation
[AD-A147425] 07 p0988 N85-16279
Experiment on triggered fragmentation on a molten copper droplet in water
[BLL-WH-602-(9091.9F)] 08 p1125 N85-17091
Capillary Pump Loop (CPL) heat pipe development status report
[NASA-CR-175273] 08 p1161 N85-17323
Computation of flow and heat transfer in flow around a 180 deg bend
[AD-A148065] 08 p1162 N85-17330
Subcooled flow boiling at high heat flux
[OUEL-1540/84] 08 p1163 N85-17338
Characterization of heat transfer in nutrient materials — space flight feeding
[NASA-CR-171841] 08 p1199 N85-17551
Numerical investigation of phase change heat transfer in a horizontal cylinder including effects of natural convection 09 p1318 N85-18286
Heat-transfer enhancement in natural convection enclosure flow
[DE84-013048] 09 p1319 N85-18297
Optimization of design and control strategies for geothermal space heating systems
[DE85-000498] 09 p1344 N85-18458
Heat transfer and mechanical interactions in fusion nuclear systems
[DE84-016233] 09 p1392 N85-18761
A diffuser heat transfer code
[AD-A149270] 10 p1430 N85-19022
Investigation on the burning of unpulverized coal in a self excited acoustic field
[INPE-3295-PRE/610] 10 p1434 N85-19035
Design of low loss helix circuits for interference fitted and brazed circuits
[NASA-CR-168313] 10 p1478 N85-19328
Effect of inclination, transverse intertip spacing, and logitudinal pitch on crossflow heat transfer from an array of finned tubes 10 p1482 N85-19359
Experimental study of ceramic coated tip seals for turbojet engines
[NASA-TM-86939] 10 p1483 N85-19363
Ribbon burner simulation of T-700 turbine shroud for ceramic lined seals research
[NASA-TM-86940] 10 p1483 N85-19364
Internal forced convection to low Prandtl number gas mixtures
[AD-A148932] 10 p1484 N85-19366
Analysis of compact heat exchanger performance
[DE84-012624] 10 p1485 N85-19377
Momentum and heat transfers in a complex, but well-defined turbulent fluid flow
[DE85-002857] 10 p1486 N85-19381
Heat and mass exchange in a partially stratified fluid
[DE85-000526] 10 p1486 N85-19384
SSPS-CRS advanced sodium receiver: Construction experience report
[DE85-000825] 10 p1511 N85-19533
LOVEL-84: A LOw-VELocity aerodynamic heating code for flat plates, wedges, and cones
[DE85-002804] 11 p1576 N85-19933
Thickness effect in low-density insulation
[DE85-003065] 11 p1631 N85-20273
Envelope thermal test unit: Technical description
[DE84-012254] 11 p1674 N85-20548
Magnetic fluctuations, field reversal maintenance, and anomalous thermal transport in the reversed field pinch
[DE85-003604] 11 p1732 N85-20692
Numerical model for swirl cooling in high-heat-flux particle beam targets and the design of a swirl-flow-based plasma limiter
[DE85-003624] 11 p1732 N85-20694
Advanced liner-cooling techniques for gas turbine combustors
[NASA-TM-86952] 12 p1770 N85-21115
Aerostructure nondestructive evaluation by thermal field detection. Phase 2: Technique refinement and quantitative determination of flaw detection capabilities
[AD-A149622] 12 p1777 N85-21155
Improvements in glazings: SERI materials research in progress
[DE84-013049] 12 p1814 N85-21378
Method of calculating cooldown process in cryostat of cryogenic electric machine 12 p1843 N85-21567
Nested subcritical flows within supercritical systems
[NASA-TM-86960] 12 p1845 N85-21574
Mechanisms of heat and mass transfer across a double-diffusive interface
[PB85-148468] 12 p1848 N85-21594
Response time correlations for platinum resistance thermometers in flowing fluids
[NASA-CR-172523] 12 p1850 N85-21606
Experimental study of steam condensation on water in countercurrent flow in presence of inert gases
[DE84-013028] 12 p1861 N85-21800
Multi-year plan for Experimental Systems Research: Passive and hybrid solar energy program
[DE85-004686] 12 p1862 N85-21810
Heat Cycle Research Experimental Program report, FY-84
[DE85-003558] 12 p1862 N85-21811
Multiyear plan for experimental systems research passive and hybrid solar energy program
[PB85-148666] 12 p1863 N85-21815
General-purpose heat source development: Safety test program. Postimpact evaluation, design iteration test 1
[LA-9660-SR] 12 p1931 N85-22131
Coupling between velocity oscillations and solid propellant combustion 13 p2000 N85-22536
Pressure drop and coefficients of internal heat transfer necessary for transpiration cooling
13 p2050 N85-22831
effect of gas stream sweeping past the effluent of a perforated plate on heat transfer inside the perforations
13 p2051 N85-22836
Two-dimensional numerical model of sensible and latent heat transport in an irrigated field under advective conditions 13 p2131 N85-23261
H-division materials physics progress
[DE85-004990] 13 p2165 N85-23430
Classification of circular features on Venus
13 p2177 N85-23511
Hydrovolcanism 13 p2186 N85-23574
Physics of the inner heliosphere: Mechanisms, models and observational signatures
[NASA-CR-175632] 13 p2205 N85-23677
Experimental study of heat transfer from shaft in cooled radial bearing of GNT-25 gas turbine
14 p2270 N85-24068
Fluid mechanics and heat transfer spirally fluted tubing
[AD-A150774] 14 p2301 N85-24247
Heat transfer to vertical flat plates in a rectangular gas-fluidized bed
[AD-A150785] 14 p2301 N85-24248
Effect of form and clearance of a piston launched in a tube on the boundary layer and the heat transfer
[ISL-CO-216/83] 14 p2302 N85-24255
Mass and heat transfer in reflux condensers of absorption heat pumps
[DFVLR-FB-83-43] 14 p2304 N85-24268
Parameterization of apparent and latent heat fluxes above water surface in calm weather under natural conditions 14 p2337 N85-24454
Equipment for hot-to-serve foods
14 p2393 N85-24741
Two-phase fluid thermal transport for spacecraft
[AD-A151316] 15 p2493 N85-25378
Manveling orbital transfer vehicle propulsion
[NASA-TM-87019] 15 p2494 N85-25386
Heat transfer and fluid mechanics measurements in the turbulent reattaching flow behind a backward-facing step
15 p2553 N85-25753
The influence of jet-grid turbulence on heat transfer from the stagnation region of a cylinder in crossflow
[NASA-TM-87011] 15 p2554 N85-25760
Flow over a biconic configuration with an afterbody compression flap
[AD-A151882] 15 p2557 N85-25778
Transient technique for measuring heat transfer coefficients on stator airfoils in a jet engine environment
[NASA-TM-87005] 15 p2580 N85-25794
NASTRAN's application in agricultural engineering
15 p2575 N85-25880
Summaries of FY 1984 engineering research
[DE85-006273] 15 p2684 N85-26442
Advanced rocket engine cryogenic turbopump bearing thermal model 16 p2735 N85-26879
Analysis of combustion oscillations in heterogeneous systems
[AD-A151999] 16 p2745 N85-26942
The use of heat pumps in district heat supply
[BLL-OA-TRANS-2728-(6196.3)]
16 p2781 N85-27163
Two-d heat transfer through porous media with heat generation
[AD-A151965] 16 p2783 N85-27173
Component-specific modeling
[NASA-CR-174765] 16 p2799 N85-27261
A computer analysis program for interfacing thermal and structural codes
[NASA-TM-87021] 16 p2800 N85-27264
Fog advection in the Namib 16 p2831 N85-27454
Adaptive grid generation for numerical solution of Burger's equation
[AD-A152217] 16 p2855 N85-27606
Future fundamental combustion research for aeropropulsion systems
[NASA-TM-87049] 17 p2898 N85-27870
Investigation of heat transfer to a turbine blade cascade using a shock tube
[AD-A153090] 17 p2898 N85-27871
Overview of aerothermodynamic loads definition study
17 p2910 N85-27942
Fuel freeze point investigations
[AD-A152801] 17 p2937 N85-28129
Stefan-Maxwell relations for plasma diffusion currents in magnetic field 17 p2942 N85-28160
FLOWPLOT 2: A fluid dynamics and heat transfer plotting package
[DE85-008602] 17 p2959 N85-28277
Heating parameter estimation using coaxial thermocouple gages in wind tunnel test articles
[AD-A153039] 17 p2968 N85-28328
Experimental and theoretical studies on transport processes in laser welding
[DE84-008572] 17 p2975 N85-28378
Simplified analysis of Stirling engines and heat pumps
[DE85-008753] 17 p2986 N85-28457
Performance of an active/passive hybrid solar system utilizing vapor transport
[DE85-008827] 17 p2988 N85-28466
TRINITY: A pre- and post-processing program for 2-dimensional finite element data
[DE85-008029] 17 p3013 N85-28626
Large, energetic cluster impacts on surfaces
[DE85-008559] 17 p3034 N85-28789
Handbook on superconductivity: The large-scale applications. Chapter 4
[DE85-006170] 17 p3044 N85-28836
Heat management system for aircraft
[AD-D011658] 18 p3061 N85-28936
High thermal power density heat transfer apparatus providing electrical isolation at high temperature using heat pipes
[NASA-CASE-LEW-12950-2] 18 p3098 N85-29179
Monogroove heat pipe design: Insulated liquid channel with bridging wick
[NASA-CASE-MSC-20497-1] 18 p3098 N85-29180
Circulation and transport in the middle atmosphere: Troposphere and lower atmosphere
18 p3148 N85-29491
Circulation and transport in the middle atmosphere: Mesosphere and lower thermosphere
18 p3148 N85-29492
Energy deposition and its effects on the E+ capture section at Sector 20
[DE85-010984] 18 p3182 N85-29727
Thermochemical energy transport using a hydrogen rich working fluid
[AD-D011696] 19 p3233 N85-30042
An experimental investigation of curvature and freestream turbulence effects on heat transfer and fluid mechanics in transitional boundary layer flows
19 p3264 N85-30240
Turbulent transport and length scale measurement experiments with confined coaxial jets
[NASA-CR-174831] 19 p3266 N85-30245
Mathematics of oil production
[DE85-011236] 19 p3287 N85-30291

Design and operation of solar thermal heat transfer systems
[DE85-009837] 19 p3267 N85-30263
Comparison and evaluation of field and numerical results from the Site A heater test at Avery Island
[DE85-010625] 19 p3268 N85-30269
Loss-of-flow transient characterization in carbide-fueled LMFBRs
[DE85-009552] 19 p3269 N85-30270
Flow visualization study of inverted annular flow of post dryout heat transfer region
[DE85-010482] 19 p3269 N85-30275
Intrinsically irreversible acoustic heat engines
[DE85-007672] 19 p3270 N85-30276
Heat flow through ocean floor and its relationship to lithosphere structure and thickness
19 p3294 N85-30422
Transition in Turbines
[NASA-CP-2366] 20 p3452 N85-31433
Preliminary results of a study of the relationship between free-stream turbulence and stagnation region heat transfer 20 p3452 N85-31435
Transition in a disturbed environment
20 p3452 N85-31436
Flat-plate transition 20 p3452 N85-31438
Heat transfer and fluid mechanics measurements in transitional boundary layer flows
20 p3453 N85-31439
A review and analysis of boundary layer transition data for turbine application 20 p3453 N85-31440
Heat transfer in aeropropulsion systems
[NASA-TM-87065] 20 p3453 N85-31444
Stability analysis of direct contact heat exchangers subject to system perturbations
[DE85-011780] 20 p3455 N85-31452
Heat transfer monitor for measurements of fouling of industrial heat exchangers
[DE85-010257] 20 p3455 N85-31455
Preliminary wind tunnel experiments to investigate the effect of heat transfer on the dispersion of cold dense gases
[OUEL-1546/84] 20 p3456 N85-31457
PHOENICS 84: A multi-dimensional multi-phase general-purpose computer simulator for fluid flow, heat transfer and combustion: 36 lecture panels
[CFD/84/18] 20 p3457 N85-31468
Influence of spatial variability of hydraulic characteristics of soils on surface parameters obtained from remote sensing data in infrared and microwaves
[NASA-TM-77902] 20 p3477 N85-31604
R and D activities of the Propulsion Division
20 p3539 N85-32025
Wall flames and implications for upward flame spread
[FAA-CT-85-2] 21 p3553 N85-32109
Imbedded thermocouples as a solid propellant combustion probe
[AD-A155630] 21 p3564 N85-32167
An investigation into the fluidization and heat transfer of low density particles in a fluidized bed with applications
[AD-A155259] 21 p3584 N85-32282
Numerical solutions of turbulent models for flow over a flat plate with angle of attack
[DE85-010380] 21 p3585 N85-32286
Forced convection on solar collector arrays
[DE85-010381] 21 p3585 N85-32287
Resolution of thermal striping issue downstream of a horizontal pipe elbow in stratified pipe flow
[DE85-006195] 21 p3586 N85-32292
Concurrent implementation of the Crank-Nicolson method for heat transfer analysis
[NASA-TM-86448] 21 p3674 N85-32822
Oscillatory solutions of the Peaceman-Rachford alternating direction implicit method and a comparison of methods for the solution of the two dimensional heat diffusion equation
[AD-A154870] 21 p3675 N85-32833
SHELTER: Description of a program code — indoor climate
[FOA-C-58002-H1] 22 p3755 N85-33278
TEMO and TEB thermoelectronic devices
22 p3779 N85-33415
Local heat-transfer measurements on a large, scale-model turbine blade airfoil using a composite of a heater element and liquid crystals
[NASA-TM-86900] 22 p3782 N85-33435
Heat-mass flow enhancement system for a metal hydride assembly
[DE85-010698] 22 p3783 N85-33441
Advances in open-cycle solid desiccant cooling
[DE85-008797] 22 p3808 N85-33580
Microwave radiation and thermoregulation
[AD-A155719] 22 p3818 N85-33654
Component-specific modeling
[NASA-CR-174765] 23 p3897 N85-34140
Numerical model of a pulse combustor
[DE85-011717] 23 p3912 N85-34240
The application of models to the assessment of fire hazard from consumer products
[NBSIR-85-3219] 23 p3925 N85-34325
Technical assessment of thermal-hydraulics for high heat flux fusion components
[DE85-013178] 23 p3930 N85-34359
Preliminary SPR thermal model description and results for WH-11 and BM-4
[DE85-013171] 23 p3931 N85-34360
Thermal transport measurements of UV laser irradiated spherical targets
[DE85-011036] 23 p3931 N85-34365
Vapor phase heat transport concepts
[DE85-009550] 23 p3931 N85-34366
Forced convective, nonequilibrium, post-CHF heat transfer experiment data and correlation comparison report
[TI85-009331] 23 p3932 N85-34371
Determination of properties of zeolite/refrigerant combinations for solar refrigeration systems
[DE85-012009] 23 p3945 N85-34448
Ocean thermal energy conversion
[DE85-012291] 23 p3946 N85-34456
Studies in thermo-hydro-chemical transport in porous and fractured media
[DE85-012555] 23 p3949 N85-34473
Advanced regenerative heat recovery system
[PB85-199602] 24 p4084 N85-35315
High Temperature Heating System (HTHS)
[PB85-188340] 24 p4084 N85-35316
Heat transfer characteristics for two-dimensional arrays of impinging jets with initial crossflow
24 p4092 N85-35365
A two-phase flow and heat transfer model for zero gravity
[AD-A156097] 24 p4094 N85-35377
Experimental study of free and mixed convective flow of air in a heated cavity
[DE85-012538] 24 p4094 N85-35380
Enhanced heat transfer computations for internally cooled cable superconductor
[DE85-011897] 24 p4095 N85-35383
Transient three-phase three-component systems. Part 1: Formulation of the system of differential equations
[DE85-013267] 24 p4095 N85-35384
Heat transfer and brine evolution in magma-hydrothermal systems 24 p4104 N85-35441
Computer code calculations of the TMI-2 accident: Initial and boundary conditions
[DE85-012613] 24 p4140 N85-35866
Analysis of reactor material experiments investigating oxide fuel crust stability and heat transfer in jet impingement flow
[DE85-012097] 24 p4151 N85-35739

HEAT TRANSFER COEFFICIENTS
Laminar flow heat exchangers. Viscosity induced non-uniform flow
[AD-A144777] 01 p0047 N85-10307
Overall heat transfer coefficients for a horizontal cylinder in a fluidized bed
[AD-A144878] 01 p0124 N85-10849
Internal heat transfer and pressure drop measurements in a variously baffled shell and tube heat exchanger
03 p0360 N85-12310
Calculating heat transfer coefficients for turbine profiles taking surface curvature and elevated flow turbulence into account 09 p1307 N85-18212
Convection heat transfer in the critical region of fluid mixtures
[DE85-001282] 11 p1633 N85-20285
Transport processes in the upper atmosphere
11 p1646 N85-20375
Turbulent convecting flow in a square duct with a 180 deg bend: An experimental and numerical study
[AD-A149969] 12 p1846 N85-21583
Two-phase fluid thermal transport for spacecraft
[AD-A151316] 15 p2493 N85-25378
Characteristics of heat exchange in the region of injection into a supersonic high-temperature flow
[NASA-TM-77833] 15 p2555 N85-25782
Filmwise condensation of steam on low integral-finned tubes
[AD-A152220] 16 p2783 N85-27176
An experimental apparatus to study nucleate pool boiling of R-114 and oil mixtures
[AD-A154077] 19 p3265 N85-30249
The effect of injection-stream turbulence on film cooling effectiveness and heat transfer coefficients
20 p3451 N85-31424
The influence of oil contamination on the nucleate pool-boiling behavior of R-114 from a structured surface
[AD-A155609] 21 p3585 N85-32284
Local heat-transfer measurements on a large, scale-model turbine blade airfoil using a composite of a heater element and liquid crystals
[NASA-TM-86900] 22 p3782 N85-33435
Heat transfer coefficients for particles in liquid in axially rotating cans 24 p4093 N85-35370
A two-phase flow and heat transfer model for zero gravity
[AD-A156097] 24 p4094 N85-35377

HEAT TRANSMISSION
NT AERODYNAMIC HEAT TRANSFER
NT CONDUCTIVE HEAT TRANSFER
NT CONVECTIVE HEAT TRANSFER
NT HEAT TRANSFER
NT HYPERSONIC HEAT TRANSFER
NT LAMINAR HEAT TRANSFER
NT RADIATIVE HEAT TRANSFER
NT TURBULENT HEAT TRANSFER
Investigation of heat exchange on models in subsonic jets of induction plasmatron 02 p0269 N85-11756
Heat flow map of Europe: Brief summary of the geophysical implications
[REPT-562] 03 p0377 N85-12405
Terrestrial heat flow in Europe and general features of its regional distribution
[REPT-563] 03 p0377 N85-12406
Megaregolith thickness, heat flow, and the bulk composition of the Moon 04 p0583 N85-13723
Procedural aspects of testing aerodynamic models with combustion in high-enthalpy transient-mode installations
05 p0725 N85-14658
Interpreting geothermal anomalies by special points method 07 p0962 N85-16238
Thermal conditions and thinning of lithosphere in late cenozoic in southwestern US 10 p1501 N85-19473
Characterization of the heat source distribution of a typical GTAW welding arc
[DE85-004322] 12 p1861 N85-21670
Normal and anomalous geothermal fields and their relationship to hierarchy of geological bodies
13 p2113 N85-23163
Determining deep heat flow and rate of horizontal percolation from temperature measurements in aquifer
13 p2116 N85-23180
Use of heat pipes for heat collection and transmission in solar plants 14 p2265 N85-24037
Structure of cold film in water-air boundary layer
14 p2335 N85-24443
Determination of permissible heating rate of metal
[BLL-M-36107-(5828.4)] 16 p2748 N85-26957
Evolution of the oceanic upper mantle and effects on sea floor subsidence geoid height and heat flow
19 p3319 N85-30575
Stability analysis of direct contact heat exchangers subject to system perturbations
[DE85-011780] 20 p3455 N85-31452
MPS solidification model. Analysis and calculation of macrosegregation in a casting ingot
[NASA-CR-171589] 21 p3568 N85-32178
In-situ measurement of wall thermal performance: Data interpretation and apparatus design recommendations
[DE85-011979] 21 p3586 N85-32289
On the importance of viscous dissipation in Io
22 p3855 N85-33873
Adiabatic thermal models for planetary bodies
22 p3857 N85-33881
Spectral evolution of gamma-rays from adiabatically expanding sources in dense clouds
[OG-2.5-2] 22 p3869 N85-33959
Detailed validation of a liquid and heat flow code against field performance
[DE85-009901] 23 p3932 N85-34368
Advanced regenerative heat recovery system
[PB85-199602] 24 p4084 N85-35315
Geothermal resources of the Washakie and Great Divide basins, Wyoming
[DE85-013004] 24 p4112 N85-35491

HEAT TREATMENT
NT ANNEALING
NT LASER ANNEALING
NT NITRIDING
NT PULSE HEATING
NT STRESS RELIEVING
NT TEMPERING
Heat treatment of welded joints in OT4 and VT20 titanium alloys 01 p0020 N85-10119
Injection molding of silicon carbide capable of being sintered without pressure
[NASA-TM-77736] 01 p0035 N85-10221
Energy-saving technological methods of obtaining controlled atmospheres
[BLL-M-35724-(5828.4)] 02 p0171 N85-11145
Metallurgy of a 12 percent chromium stainless steel
02 p0178 N85-11195

Mechanism of brittle heat fracture of inhomogeneous solids by high temperature gas jets
02 p0285 N85-11731
The effect of heat treatment on wear resistance of gas-plasma eutectic coatings
[BLL-M-35756-(5828.4)] 03 p0329 N85-12122
A study of precipitation and boron distribution in 20 Cr 25Ni base stainless steels
[AERE-M-3353] 03 p0334 N85-12154
Effect of heat treatment on phase composition and crystal structure of thin WSi2 films on silicon substrates
03 p0350 N85-12253
Effect of oxidizing medium and heat treatment on stoichiometry of ZnSe crystal surface
03 p0353 N85-12272
Dependence of microplasticity of beryllium on grain size and heat treatment 03 p0353 N85-12273
The disordering process in an L1sub2 ordered alloy
[DE84-016599] 04 p0475 N85-13028
Change in the nitrogen content when nitrided alloys are heated
[BLL-M-35946-(5828.4)] 05 p0615 N85-13929
Impact toughness of wire after cold deformation and annealing
[BLL-M-35941-(5828.4)] 05 p0615 N85-13930
Influence of hydrogen saturation and prior heat treatment on graphitization of white cast iron
[BLL-M-35964-(5828.4)] 05 p0615 N85-13932
Creep of chemically vapor deposited SiC fibers
[NASA-TM-86897] 06 p0763 N85-14878
The effect of potential on the corrosion fatigue behavior of a precipitation hardened aluminum alloy
[AD-A146537] 06 p0768 N85-14916
Development of high-efficiency solar cells on silicon web
[NASA-CR-174212] 06 p0828 N85-15259
Problems and possibilities for life extension in gas turbine components 07 p0907 N85-15742
The formation of isolated phase precipitates during the decomposition of high-coercive force Fe-Cr-Co alloys
[BLL-M-36028-(5828.4)] 07 p0924 N85-15855
Procedure for investigating high-temperature properties of iron-ore materials
[BLL-M-36020-(5828.4)] 07 p0926 N85-15866
On heat-treatable copper-chromium alloy, 1
[NASA-TM-77753] 07 p0927 N85-15879
Method for bonding insulator to insulator
[AD-D011340] 07 p0929 N85-15891
Dependence of breakdown voltage for p-n junction on parameters of ion implantation and semiconductor heat treatment 07 p0954 N85-16046
Effects of oxygen on the microstructure and properties of titanium 6211 alloys
[AD-P004122] 08 p1126 N85-17097
Electromagnetic processing of materials
[AD-A148804] 09 p1311 N85-18241
New method for heat treatment of metals
10 p1446 N85-19110
Influence of laser hardening on mechanical properties of type 45 steel with various preliminary heat treatments
10 p1446 N85-19111
The response of cobalt-free Udimet 700 type alloy to modified heat treatments
[NASA-TM-86942] 11 p1597 N85-20043
USSR report: Materials science and metallurgy
[JPRS-UMS-84-005] 11 p1597 N85-20044
Micrographic and fractographic examination of alloys 2214 and 2024 for conditions which would cause burning of the metal on being put into solution, trial 17/175
[DGT-23.419] 11 p1609 N85-20117
Chemical and photographic evaluation of rigid explosive transfer lines
[AD-A149303] 11 p1613 N85-20145
Method for refining microstructures of cast titanium articles
[AD-D011518] 12 p1804 N85-21318
Microstructural and electronic characteristics of metallic spin glasses
[AD-A149959] 12 p1813 N85-21371
Influence of laser treatment of structure and mechanical properties if MA21 alloy 13 p2029 N85-22713
Specifics of laser heat treatment of high steel tools
13 p2029 N85-22714
Specifics of kinetics of polymorphous conversion upon heating of low carbon steels 13 p2030 N85-22721
Effect of zero-wear in friction pairs operating in abrasive media 13 p2045 N85-22801
Stability of three-layer glass-reinforced plastic shells of rotation 13 p2047 N85-22813
Microstructural study on the processing and properties of high-field A15 superconducting materials
[DE85-004652] 13 p2164 N85-23423
Case depth on flanks of gears for helicopter gearboxes 14 p2222 N85-23780
Synthesis and properties of elevated temperature P/M aluminum alloys
[AD-A151031] 14 p2256 N85-23981
Role of residual stresses in stress corrosion cracking in alloy 600 tubes. Part 1: Determination of throughwall residual stresses and their modification by transient heat treatment
[DE85-004648] 14 p2257 N85-23988
Robotized system for treating gear wheels
14 p2285 N85-24162
Influence of phosphorus content and heat treatment on the machinability of electroless nickel deposits
[DE85-007250] 15 p2522 N85-25548
Properties and microstructures for dual alloy combinations of three superalloys with alloy 901
[NASA-TM-86987] 16 p2749 N85-26963
Thermodynamic analysis of the plasma nitriding of ferrovanadium
[BLL-BISI-TRANS-22237-(9022.06)]
17 p2924 N85-28032
Thermomechanical softening treatment for bearing and tool steels
[BLL-BISI-TRANS-22432-(9022.06)]
17 p2925 N85-28035
Improving the properties of copper and copper alloys through heat treatment and alloying
[BLL-BISI-TRANS-21939-(9022.06)]
17 p2926 N85-28047
The state of martensite after quenching in a magnetic field
[BLL-BISI-TRANS-22297-(9022.06)]
17 p2926 N85-28051
Influence of heat treatment parameters on the properties of induction hardened Ni-Cr-Mo steels
[BLL-BISI-TRANS-2499-(9022.06)]
17 p2926 N85-28053
Textural transformations taking place during heat and mechanical treatment in triplex steels
[BLL-BISI-TRANS-22404-(9022.06)]
17 p2927 N85-28063
Effects of the phase compositions of cast low-pearlite steels micro-alloyed with vanadium and titanium of their structure and properties
[BLL-BISI-TRANS-22301-(9022.06)]
17 p2928 N85-28067
Technological apparatus for laser treatment of materials 17 p2944 N85-28174
Local heat treatment of welded joints of pipes and rotary vessels
[BLL-BISI-TRANS-22197-(9022.06)]
17 p2972 N85-28354
Technical information: Weldability of stainless steel. Part 1: Austenitic stainless steel
[BLL-BISI-TRANS-22456-(9022.06)]
17 p2973 N85-28362
Effects of the structural state in thermo-bimetals on their resistance to microscopic plastic deformation
[BLL-BISI-TRANS-22403-(9022.06)]
17 p2979 N85-28412
Plasma processing of materials
[AD-A152398] 17 p3039 N85-28800
Evaluation of 7XXX-series aluminum alloys for the W87 aft support ring
[DE85-009987] 18 p3076 N85-29027
Rolling contact fatigue testing of thermomechanically processed M-50 steel
[AD-A153640] 18 p3122 N85-29327
Internal structure of GP zones in dilute Al-Cu alloys
19 p3236 N85-30073
Effects of heat treatment and tracer element impurities on the impact properties of the 12Cr steels
[DE85-010676] 19 p3240 N85-30088
Possible causes of modification and strengthening of aluminum by scandium 19 p3241 N85-30099
Effect of thermochemical processing on fatigue resistance of titanium alloys 19 p3244 N85-30112
Structure and properties of VT23 alloy welded joints after thermocyclic processing 19 p3246 N85-30125
Method for the preparation of photochromic insulating crystals
[DE85-011606] 19 p3262 N85-30229
Plasma spray screen repair method
[AD-D011713] 19 p3281 N85-30346
Long-term thermal aging of Celion/V378A composite materials
[NASA-TM-86362] 20 p3421 N85-31236
Structural transformation of a 9% Cr - 2%Mo steel (type Z10CDNbV 09-02) for use in steam generators for fast neutron reactors
[BLL-CE-TRANS-7943-(9022.09)]
20 p3430 N85-31271
Influence of gamma-phase on magnetic properties and structure of KhK15YuB alloy during strain-aging
[BLL-M-36261-(5828.4)] 20 p3431 N85-31280
Influence of recrystallization and solution on the tenacity of the 7010 and 7475 alloys. Oligocyclic fatigue of the 7010 alloy
[ONERA-RT-19/5069-M] 20 p3432 N85-31289
Electrical and structural characterization of web dendrite crystals 20 p3481 N85-31633
Metallurgical origins of fracture toughness and microstructure and fracture toughness of an HSLA (High-Strength/Low-Alloy) steel
[AD-A155530] 21 p3567 N85-32187
Electrical and mechanical properties of intercalated graphite fibers
[AD-A155560] 21 p3570 N85-32205
Strain rate sensitivity estimation from high velocity impact data
[AD-A154703] 21 p3599 N85-32347
Maintenance and the military environment
22 p3750 N85-33243
The study of the effect of residual microimpurities on the fatigue strength of 5552 steel
[BLL-M-36317-(5828.4)] 23 p3913 N85-34248
The effect of pre-heating on the structure and properties of chromium-molybdenum steels
[BLL-M-35897-(5828.4)] 23 p3914 N85-34255
Properties of tungsten-free steel for cutting tools
[BLL-M-35808-(5828.4)] 23 p3915 N85-34259
Stress corrosion cracking susceptibility of types 316NG and 316 stainless steel in an impurity environment
[TIB5-006884] 23 p3917 N85-34277
The read-out system of spatial distribution of thermoluminescence in meteorites
[SH-9.1-16] 23 p4052 N85-35131
Studies of the crystallization process of aluminum-silicon alloys using a high temperature microscope
[NASA-TM-77669] 24 p4078 N85-35272
The dynamic strain ageing of A533B class 1 nuclear pressure vessel steel
[AERE-R-11485] 24 p4078 N85-35274
Effect of thermal ageing on the mechanical properties of PWR pressure vessel steels and weldments
[AERE-R-11480] 24 p4078 N85-35275
The character of observed porosity and its possible effects on rolling contact fatigue life of M-50 steel
[AD-A155930] 24 p4079 N85-35279
Development of a high strength isothermally heat-treated nodular iron road wheel arm
[AD-A155755] 24 p4099 N85-35406

HEATERS

Experimental study on the glow plug aided alcohol driven diesel engine 04 p0483 N85-13078
Heater block assembly for use in thermal oxidation testing of jet fuel
[AD-D011430] 06 p1123 N85-17077
Experimentally determined characteristics of vortex heaters 13 p2050 N85-22833
Heat resistant sheathed insulated electrical conductors
[AD-D011644] 17 p2951 N85-28219
Physiochemically controlled scour jet array system
[AD-D011688] 19 p3308 N85-30505
Toxic hazards tests for vehicles and other equipment
[AD-A149164] 20 p3506 N85-31797
Feedback regulated induction heater for a flowing fluid
[DE85-006508] 23 p3939 N85-34414

HEATING

NT AERODYNAMIC HEATING
NT ATMOSPHERIC HEATING
NT ELECTRON CYCLOTRON HEATING
NT GAS HEATING
NT INDUCTION HEATING
NT IONOSPHERIC HEATING
NT KINETIC HEATING
NT LASER HEATING
NT PLASMA HEATING
NT PULSE HEATING
NT RADIANT HEATING
NT RADIO FREQUENCY HEATING
NT RESISTANCE HEATING
NT SHOCK HEATING
NT SOLAR HEATING
NT SPACE HEATING (BUILDINGS)
NT SUPERHEATING
NT TRANSIENT HEATING
NT WATER HEATING
Treating silicon carbide sinter by heating in nitrogen
[NASA-TM-77601] 01 p0021 N85-10130
Real time sensing and control of out-of-plane distortion due to line heating by laser
[AD-A144773] 01 p0027 N85-10169
Determining the optimum heating parameters for precision alloys — iron-nickel alloys
[BLL-M-35718-(5824.4)] 02 p0174 N85-11167
Robotization of technological processes in high-frequency heating and welding
03 p0345 N85-12226

Dynamic thermal episodes in the protosolar nebula: Development of models from observations on CAI's
08 p0887 N85-15633
Analysis of the heating process of a body in a melt
[BLL-M-38014-(5828.4)] 07 p0956 N85-16057
The Origin of Nonradiative Heating/Momentum in Hot Stars
[NASA-CP-2358] 08 p1231 N85-17755
Evidence for non-radiative activity in stars with T sub eff 10000 K
08 p1231 N85-17757
Non-radiative energy from differential rotation in hot stars
08 p1234 N85-17776
Nonradiative heating and enhanced mass-loss due to shear turbulence in massive hot stars
08 p1235 N85-17780
A leaky waveguide model for MHD wave driven winds from coronal holes
08 p1235 N85-17781
Radiatively driven winds and what they imply: A review of radiative driven instabilities and their importance in hot stars
08 p1235 N85-17782
Magnetic effects in the heating and modification of flows in the outer stellar atmospheres with application to early type star case
08 p1235 N85-17783
ORNL ECR multicharged ion source
[DE85-001263] 09 p1360 N85-18681
On shrinkage and molecular extension
[AD-A149100] 10 p1451 N85-19144
Method of heating quartz resonators
[AD-D011454] 10 p1481 N85-19347
Picosecond laser pulse interactions with metallic and semiconductor surfaces
[AD-A149112] 10 p1490 N85-19405
VHF radar observations in the stratosphere and mesosphere during a stratospheric warming
11 p1651 N85-20468
Improvements in glazings: SERI materials research in progress
[DE84-013049] 12 p1814 N85-21378
Re-design of ARL/HLF (Heated Laminar Flow) body nose region
[AD-A150063] 12 p1846 N85-21585
Influence of substrate heating and thermal annealing on the surface crystallinity in single Si crystals implanted with high doses of (16)O
[DE85-005264] 13 p2164 N85-23428
Thermal and thermoelastic effects in rolling/sliding contacts
[AD-A150435] 13 p2165 N85-23429
Railgun conductor heating from multiple current pulses
[DE85-005333] 14 p2265 N85-24031
Equipment for hot-to-serve foods
14 p2393 N85-24741
New control design principles based on measured performance and energy analysis of HVAC (Heating, Ventilating, and Air-Conditioning) systems
[AD-A151708] 15 p2522 N85-25546
Numerical simulation of boundary layer excitation by surface heating/cooling
[NASA-CR-172575] 15 p2554 N85-25756
A feasibility study for using low boiling point fluids to change aircraft tire deflection
[AD-A152096] 16 p2706 N85-26701
Metal armatures for railguns
[AD-A152129] 16 p2728 N85-26838
Microwave processing of lunar materials: Potential applications
[DE85-007223] 16 p2755 N85-27003
Investigation of the requirement for auxiliary heating of Canadian forces personnel
[AD-A151950] 16 p2841 N85-27522
Hydrogen recovery from extraterrestrial materials using microwave energy
[DE85-006717] 18 p2883 N85-27789
Thermal donor removal by rapid thermal annealing: Infrared absorption
[DE85-010092] 18 p3081 N85-29059
Low gravity exothermic heating/cooling apparatus
[NASA-CASE-MSC-25707-1] 18 p3104 N85-29214
Tokamak ignition/burn experimental research device
[DE85-009999] 18 p3190 N85-29785
The nature of the anomalies on the polytherms of the properties of molten metallic alloys
[BLL-M-36265-(5826.4)] 20 p3430 N85-31277
Self-heating to ignition measurements and computation of critical size for solar energy collector materials
[PB85-183374] 20 p3485 N85-31663
Development of a prototype energy meter
[PB85-198430] 22 p3789 N85-33476

HEATING EQUIPMENT
NT BOILERS
NT ELECTRIC FURNACES
NT EVAPORATORS
NT FURNACES
NT IMAGE FURNACES
NT SOLAR FURNACES
NT VACUUM FURNACES
NT VAPORIZERS
FORTRAN 77 computer program for test procedure calculations of vented heaters
[PB85-109627/GAR] 09 p1305 N85-18196
Leak monitoring in high pressure preheaters by a noninvasive ultrasonic method
[CISE-2373] 11 p1650 N85-20394
Leak detection by acoustic emission monitoring in power plant high pressure preheaters
[CISE-2382] 11 p1650 N85-20395
Investigation of the requirement for auxiliary heating of Canadian forces personnel
[AD-A151950] 16 p2841 N85-27522
Precision manipulator heating and cooling apparatus for use in UHV systems with sample transfer capability
[NASA-CASE-LAR-13040-1] 18 p3116 N85-29286
Measurement of radiated emissions from industrial heating device equipment as it relates to aeronautical services
[FAA-ES-85-2] 19 p3255 N85-30181
Development of a high-efficiency, gas-fired, heat pipe, warm-air heating system
[PB85-199636] 24 p4085 N85-35318

HEAVING
Ice segregation and frost heaving
[PB85-122430] 10 p1460 N85-19199

HEAVY COSMIC RAY PRIMARIES
U HEAVY NUCLEI
U PRIMARY COSMIC RAYS

HEAVY ELEMENTS
NT AMERICIUM
NT AMERICIUM ISOTOPES
NT AMERICIUM 241
NT CALIFORNIUM ISOTOPES
NT CURIUM
NT CURIUM 244
NT PLUTONIUM
NT PLUTONIUM ISOTOPES
NT PLUTONIUM 238
NT PLUTONIUM 239
NT TRANSURANIUM ELEMENTS
Pulsed-neutron-source models for the astrophysical s-process
[DE85-012927] 24 p4151 N85-35740
Some nuclear data needs in astrophysics
[DE85-012916] 24 p4168 N85-35842

HEAVY IONS
The Berkeley mini-collider
[DE84-014594] 01 p0118 N85-10808
Do the satellites of Uranus control its magnetosphere?
02 p0301 N85-11952
Utilization of a tandem accelerator for the investigation of solid state properties by means of heavy ions
03 p0429 N85-12733
The radiobiological advanced Biostack experiment on Spacelab 1
05 p0691 N85-14442
Research in nuclear astrophysics: Stellar collapse and supernovae
[DE84-015559] 05 p0743 N85-14776
The (20)Ne interaction in extended matter
[NASA-TM-86312] 07 p1061 N85-16728
A T-matrix theory of galactic heavy-ion fragmentation
[NASA-TP-2363] 08 p1221 N85-17690
Forward electron production in heavy ion-atom and ion-solid collisions
[DE85-001256] 09 p1361 N85-18683
Beam-foil spectroscopy of highly ionized aluminum atoms
09 p1390 N85-18746
Applications of the Heavy-Iron Rutherford Backscattering Spectrometry (HIRBS) to the analysis of contact structures on GaAs and Ge
[DE85-000671] 10 p1564 N85-19861
Heavy ion induced crystallization in amorphous phases
[DE85-003114] 11 p1606 N85-20098
Charge-to-mass dispersion methods for abrasion-ablation fragmentation models
[NASA-TM-86340] 11 p1726 N85-20857
Operating experience and construction status of ATLAS — Argonne tandem-linac accelerator
[DE85-002741] 11 p1735 N85-20914
Workshop on Nuclear Dynamics 3
[INC-40007-24] 12 p1931 N85-22130
High energy facilities advanced projects: Intrabeam scattering for a beam of gold ions
[DE85-000887] 12 p1941 N85-22192
Laser-induced fluorescence of metal-atom impurities in a neutral beam
[DE85-004960] 14 p2310 N85-24298
X-ray emission in heavy ion collisions
[DE85-006350] 14 p2419 N85-24927
Future accelerator studies of high energy heavy ion collisions
[DE85-005885] 15 p2650 N85-26346
Nuclear spectroscopic studies
[DE85-006894] 16 p2862 N85-27652
Tables of nuclear cross sections for galactic cosmic rays: Absorption cross sections
[NASA-RP-1134] 16 p2864 N85-27865
Nonrelativistic theory of heavy-ion collisions
[DE85-007538] 17 p3031 N85-28747
Experiments and detectors for high energy heavy ion colliders
[DE85-007927] 17 p3031 N85-28748
Spin distributions in heavy ion fusion at and below the Coulomb barrier
[DE85-007817] 17 p3031 N85-28751
Theoretical studies of heavy ion scattering processes
[DE85-008823] 17 p3032 N85-28753
Heavy ion physics at BNL, the AGS and RHIC
[DE85-005951] 17 p3033 N85-28760
Heavy ion fusion accelerator research in the US
[DE85-008465] 17 p3034 N85-28767
Inertial fusion reactors and magnetic fields
[DE85-009571] 18 p3191 N85-29789
Experiments with stored heavy ions
[DE85-009976] 19 p3356 N85-30602
Research activities of the Physics Division
[DE85-006958] 19 p3357 N85-30611
Ion beam-plasma interactions
[DE85-010202] 19 p3371 N85-30913
Biostack experiments on STS-flights and the impact for man in space
20 p3510 N85-31821
Fusion reactions at low energy
[DE85-010561] 20 p3528 N85-31944
In-situ observations of the development of heavy-ion damage in semiconductors
[DE85-010289] 22 p3761 N85-33307
Ultrahigh vacuum system of the heavy ion transport line at Brookhaven
[DE85-011838] 22 p3840 N85-33778
Heavy ion medical accelerator options
[DE85-011204] 22 p3841 N85-33784
Design status of heavy ion injector program
[DE85-010751] 22 p3842 N85-33793
Physics Division annual review, 1 April 1983 - 31 March 1984
[ANL-84-24] 23 p3969 N85-34602
Summary of activities, 1983
[LBL-18500] 23 p3969 N85-34605
Low-energy sputterings with the Monte Carlo Program ACAT
[IPPJ-AM-40] 23 p3982 N85-34690
Calculations of heavy ion charge state distributions for nonequilibrium conditions
[SH-2.1-12] 23 p3999 N85-34793
The heavy ion composition in 3HE-rich solar flares
[SH-2.2-7] 23 p4000 N85-34802
The plasma mechanism for preferential acceleration of heavy ions
[SH-2.2-10] 23 p4001 N85-34805
A high resolution gas Cerenkov detector for the superconducting magnet facility
[OG-9.1-6] 23 p4023 N85-34932
The heavy ions in space experiment
[OG-9.1-10] 23 p4023 N85-34936
The response of ionization chambers to relativistic heavy nuclei
[OG-9.1-13] 23 p4024 N85-34938
Detector calibration of the Indian cosmic ray experiment (IONS) in Space-Shuttle Spacelab-13
[SH-9.1-2] 23 p4050 N85-35117
Proceedings of the Workshop on Detectors for Relativistic Nuclear Collisions
[LBL-18225] 24 p4146 N85-35700
Summary of the working group on penetrating probes in collider experiments. 1: The collider environment
24 p4146 N85-35704
Fractional charge resolution in music
24 p4147 N85-35712
Calculation of heavy-ion tracks in liquid water
[DE85-012101] 24 p4149 N85-35725
Considerations on collective ion acceleration as an intense ion injector
[DE85-012706] 24 p4155 N85-35757
Ion source development for the Los Alamos heavy ion fusion injector
[DE85-012682] 24 p4156 N85-35766
Applications of decelerated ions
[DE85-011832] 24 p4156 N85-35767
Numerical studies of high current beam compression in heavy ion fusion
[DE85-011874] 24 p4158 N85-35783
Multiple vacancy production by high energy heavy ions
[DE85-004428] 24 p4162 N85-35805
The phi-meson and Chiral-mass-meson production in heavy-ion collisions as potential probes of quark-gluon-plasma and Chiral symmetry transitions
24 p4175 N85-35884

On the mechanism of anomalous nucleus-nucleus interactions at energies above 1 TeV/nucleon
[HE-1.4-8] 24 p4177 N85-35896
Meson multiplicity in nucleus-nucleus collisions above 4 GeV/amu
[HE-1.4-10] 24 p4177 N85-35897
Multidimensional analysis of data obtained in experiments with X-ray emulsion chambers and extensive air showers
[HE-3.6-2] 24 p4184 N85-35951

HEAVY NUCLEI

Anomalon search — heavy cosmic ray interactions
[NOTA-INTERNA-825] 02 p0305 N85-11970
Radiobiological studies on egg systems exposed to heavy nuclei of cosmic galactic radiation — insects
05 p0690 N85-14440
Preliminary results of advanced Biostack experiments with plant seeds and spores — cosmic ray effects
05 p0691 N85-14441
The radiobiological advanced Biostack experiment on Spacelab 1
05 p0691 N85-14442
The propagation of ultraheavy cosmic rays
15 p2685 N85-26582
Heavy ion physics at BNL, the AGS and RHIC
[DE85-005951] 17 p3033 N85-28760
Contributions to the 19th International Cosmic Ray Conference
[NASA-CR-176049] 20 p3543 N85-32044
Energy spectra of elements with 18 less than or equal to Z less than or equal to 28 between 10 and 300 GeV/amu
20 p3543 N85-32045
Elemental abundances of cosmic rays with Z33 as measured on HEAO-3
20 p3543 N85-32046
Abundances of secondary elements among the ultra heavy cosmic rays: Results from HEAO-3
20 p3543 N85-32047
Lead, platinum, and other heavy elements in the primary cosmic radiation: HEAO-3 results ssc wg032961 cb553097
20 p3543 N85-32048
Implications of source abundances of ultraheavy cosmic rays
20 p3543 N85-32049
Interactions of heavy nuclei, Kr, Xe and Ho, in light targets
20 p3544 N85-32050
The response of ionization chambers to relativistic heavy nuclei
20 p3544 N85-32051
Source spectral index of heavy cosmic ray nuclei
[OG-4.1-2] 22 p3875 N85-34008
Energy spectra of elements with 18 or = Z or = 28 between 10 and 300 GeV/amu
[OG-4.1-8] 22 p3876 N85-34014
Elemental abundances of cosmic rays with Z 33 as measured on HEAO-3
[OG-4.4-5] 22 p3880 N85-34038
Abundances of secondary elements among the ultra heavy cosmic rays: Results from HEAO-3
[OG-4.4-6] 22 p3880 N85-34039
Capabilities of the LDEF-2 heavy nuclei collection
[OG-4.4-8] 22 p3880 N85-34040
Ultraheavy cosmic ray tracks in meteorites: A reappraisal, based on calibrations with relativistic ions
[OG-4.4-10] 22 p3880 N85-34041
High-energy multiple muons and heavy primary cosmic-rays
[OG-5.2-9] 22 p3883 N85-34065
Electron and muon parameters of EAS and the composition of primary cosmic rays in 10(15) to approximately 10(16) eV
[OG-5.2-12] 22 p3884 N85-34068
Implications of the experimental results on high energy cosmic rays with regard to their origin
[OG-5.4-5] 22 p3886 N85-34082
The heavy ion composition in 3HE-rich solar flares
[SH-2.2-7] 23 p4000 N85-34802
Variations in the propagation of UH-nuclei
[OG-7.1-1] 23 p4012 N85-34863
Propagation and nucleosynthesis of ultraheavy cosmic rays
[OG-7.1-5] 23 p4013 N85-34867
Sources of the ultraheavy cosmic rays
[OG-7.1-7] 23 p4013 N85-34868
Interactions of heavy nuclei, Kr, Xe and Ho, in light targets
[OG-7.2-21] 23 p4016 N85-34888
The response of ionization chambers to relativistic heavy nuclei
[OG-9.1-13] 23 p4024 N85-34938
The response of ionization chambers to relativistic heavy nuclei
[OG-9.1-13] 23 p4024 N85-34939
Measurement of low energy cosmic rays aboard Spacelab-1
[SH-10.1-6] 23 p4053 N85-35137
Heavy cosmic ray measurement aboard Spacelab-1
[SH-10.1-7] 23 p4053 N85-35138
The response of a scintillation counter below an emulsion chamber to heavy nucleus interactions in the chamber
24 p4175 N85-35889
Heavy nucleus collisions between 20 and 60 GeV/nucleon
[HE-1.4-2] 24 p4175 N85-35890
Characteristics of central collision events in Fe-nucleus interactions for 20 - 60 GeV/nucleon
[HE-1.4-3] 24 p4176 N85-35891
Nucleus-nucleus interaction above several hundred GeV/n
[HE-1.4-4] 24 p4176 N85-35892
Experiment Pamir-3. Coplanar emission of high energy gamma-quanta at interaction of hadrons with nuclei of air atoms at energies above 10 to the 7th power GeV
[HE-1.4-12] 24 p4177 N85-35899
Intensities of high-energy cosmic rays at Mount Kanbala
[HE-3.1-2] 24 p4177 N85-35902
Multidimensional analysis of data obtained in experiments with X-ray emulsion chambers and extensive air showers
[HE-3.6-2] 24 p4184 N85-35951
On mini-cluster observed by Chacaltaya emulsion chamber experiment
[HE-3.6-12] 24 p4185 N85-35959
Monte Carlo simulations of electron lateral distributions in the core region of 10(13) - 10(16) eV air showers
24 p4190 N85-35992
Comparison of simulation results with sea-level experimental data on 10(14) - 10(16) air shower cores
24 p4190 N85-35993
Relevance of multiple muons detected underground to the mass composition of primary cosmic rays
[HE-5.1-4] 24 p4201 N85-36069
Search for stellar collapse with the MACRO detector at Gran Sasso
[HE-5.3-11] 24 p4206 N85-36105
Spatial distribution read-out system for thermoluminescence sheets
[HE-7.1-7] 24 p4213 N85-36161

HEIGHT

The estimation of persistance statistics from cumulative probabilities of wave height
[NMI-R183] 03 p0397 N85-12534
Prediction of wave height of wind-generated seas in finite water depth
[AD-A145996] 03 p0398 N85-12539
Components of the time variation of sea surface height from SEASAT altimeter data
05 p0658 N85-14227
Applications of TOMS ozone data and clustering techniques in satellite soundings
05 p0681 N85-14379
Prediction of percent body fat for U.S. Navy women from body circumferences and height
[AD-A146456] 06 p0845 N85-15370
The 500 millibar sign frequency teleconnection charts: Winter
[PB85-106276/GAR] 07 p1009 N85-16410
Analysis of the inflow layer and air-sea interactions in Hurricane Frederic (1979)
[NASA-CR-175616] 13 p2137 N85-23271
A laser slope gauge and a spar buoy wave gauge: Tools for the validation of microwave remote sensors
[AD-A154038] 19 p3272 N85-30290
Troposphere-stratosphere (surface-55 km) monthly general circulation statistics for the Northern Hemisphere-four year averages
[NASA-TM-86182] 20 p3495 N85-31730
Practical use of a tropopause height determination algorithm on an MST radar data set, part 1.88
21 p3618 N85-32479

HEISENBERG THEORY

Lattice actions improved by block-spin renormalisation group and maximally symmetric lattices
[DE85-007416] 17 p3045 N85-28841

HELICAL ANTENNAS

Measured performance of a broadband matching section for peripherally fed helical antennas
[R-NIAS-25] 15 p2539 N85-25870
Dual sense, circularly polarized helical antenna
[AD-D011680] 19 p3254 N85-30175

HELICAL FLOW

International test and demonstration of a 1-MW wellhead generator: Helical screw expander power plant
[NASA-CR-174161] 04 p0527 N85-13372
Spectral measurements of magnetic energy and magnetic helicity between 0.29 and 0.97 AU
[IFSI-85-2] 22 p3850 N85-33844
Behavior of helically-trapped fast ion orbits in heliotron E
23 p3978 N85-34666
Neoclassical diffusion including ellipticity in a heliotron-like configuration
23 p3978 N85-34667

HELICOPTER ATTITUDE INDICATORS

U ATTITUDE INDICATORS
U HELICOPTERS

HELICOPTER CONTROL

The design and development of an integrated core system for battlefield helicopters
08 p1074 N85-16811
A review of US Army aircrew-aircraft integration research programs
08 p1075 N85-16814
Flight tests with a new helicopter Force Feel System (FFS)
08 p1075 N85-16818
Helicopter active control with rotor blades relaxation
08 p1075 N85-16819
Flight research on visual aids and navigation equipment for helicopter low-level flight at night
08 p1076 N85-16820
A preliminary investigation of handling qualities requirements for helicopter instrument flight during decelerating approach maneuvers and overshoot
[NRC-24173] 17 p2896 N85-27857
The evolution of ACS for helicopters: Conceptual simulation studies to preliminary design
17 p2902 N85-27880
ACT applied to helicopter flight control
17 p2902 N85-27881
The evolution of active control technology systems for the 1990's helicopter
17 p2905 N85-27911
Data processing on the rotor test stand at DFVLR in Brunswick: Microprogrammable interfaces and array processor as key components in a PDP 11 real time data acquisition and processing system
[DFVLR-MITT-85-03] 17 p2906 N85-27921
Helicopter Aeromechanics
[AGARD-LS-139] 18 p3057 N85-28913
The role of simulation
18 p3058 N85-28919

HELICOPTER DESIGN

Helicopter rotor blade design for minimum vibration
[NASA-CR-3825] 01 p0006 N85-10032
DFVLR rotorcraft: Construction and engineering
[NASA-TM-77740] 01 p0006 N85-10035
Applications of numerical optimization methods to helicopter design problems: A survey
[NASA-TM-86010] 01 p0006 N85-10036
YO-3A acoustics research aircraft systems manual
[NASA-TM-85966] 01 p0012 N85-10074
Data input, processing and presentation — helicopter rotor balance measurement
[NASA-TM-77739] 01 p0125 N85-10856
Manufacturing Methods and Technology (MM/T) specifications for miniature cathode ray tube
[AD-A145597] 02 p0194 N85-11298
Avionics system design for requirements for the United States Coast Guard HH-65A Dolphin
06 p0753 N85-14827
Speed benefits of tilt-rotor designs for LHX
[NASA-CR-166437] 07 p0902 N85-15717
Operational requirements versus technological capabilities
08 p1072 N85-16798
Integration of sensor fusion in advanced helicopter cockpit design
08 p1074 N85-16813
Advanced flight simulation for helicopter development
08 p1075 N85-16815
Integrated technology rotor/flight research rotor concept definition study
[NASA-CR-166446] 10 p1424 N85-18980
Transmission efficiency measurements and correlations with physical characteristics of the lubricant
14 p2222 N85-23781
Problems of elastic hydrodynamic lubrication of helicopter transmission gears
14 p2222 N85-23784
Evolution of the design techniques for helicopter main transmission gearboxes
14 p2223 N85-23789
Preliminary helicopter design decision making based on flight performance factors
[AD-A151488] 15 p2471 N85-25254
Determination of quantitative relationships between selected critical helicopter design parameters
[AD-A152034] 16 p2706 N85-26700
The evaluation of ACS for helicopters: Conceptual simulation studies to preliminary design
16 p2712 N85-26737
Advanced flight simulation for helicopter development
[MBB-UD-416/84-O] 16 p2874 N85-27731
Design of helicopter rotor blades for optimum dynamic characteristics
[NASA-CR-176076] 20 p3393 N85-31044
Application of finite element method to the sizing of mechanical parts — helicopter design
[SNIAS-851-210-105] 20 p3463 N85-31515

HELICOPTER PERFORMANCE

DFVLR rotorcraft: Construction and engineering
[NASA-TM-77740] 01 p0006 N85-10035
Applications of numerical optimization methods to helicopter design problems: A survey
[NASA-TM-86010] 01 p0006 N85-10036
Airworthiness and flight characteristics test of the JOH-6A light combat helicopter configured with a wire strike protection system
[AD-A144880] 01 p0006 N85-10038

Airworthiness and Flight Characteristics (A and FC) test of the EH - 1X/EH - 1H helicopter configurations
[AD-A144861] 01 p0007 N85-10039
Estimation of helicopter performance using a program based on blade element analysis
[AD-A146341] 03 p0316 N85-12055
The need for a dedicated public service helicopter design 06 p0753 N85-14828
Preliminary airworthiness evaluation AH-1S (MC) helicopter with external fuel tanks installed
[AD-A148091] 06 p1084 N85-16865
Preliminary helicopter design decision making based on flight performance factors
[AD-A151488] 15 p2471 N85-25254
Wind-tunnel evaluation of a 21-percent-scale powered model of a prototype advanced scout helicopter
[NASA-TP-2420] 18 p3058 N85-28923
Effect of ground and/or ceiling planes on thrust of rotors in hover
[NASA-TM-86754] 20 p3386 N85-31014
Standardization of helicopter certification requirements in the western world
[SNIAS-851-210-103] 20 p3393 N85-31046
The effects of parameter variation on helicopter performance
[AD-A156027] 24 p4064 N85-35189
Development of NATOPS performance software for the SH-3D and SH-3H helicopters
[AD-A156140] 24 p4065 N85-35192

HELICOPTER PROPELLER DRIVE
The in-flight estimation and indication of cumulative fatigue damage to helicopter gears
[ARL/AERO-R-164] 03 p0317 N85-12050
The helicopter transmission design process 14 p2221 N85-23772
Fine filtration: An attractive route towards lower helicopter operating costs 14 p2221 N85-23774
Possible technological answers to new design requirements for power transmission systems 14 p2222 N85-23779

HELICOPTER ROTORS
U ROTARY WINGS

HELICOPTER TAIL ROTORS
Calculation of the velocity field generated by a helicopter main and tail rotors in hover
[AD-A147731] 08 p1078 N85-16833
Numerical analysis of the first static calibration of the RSRA helicopter active-isolator rotor balance system
[NASA-TM-85975] 06 p1083 N85-16863
Repair of composites 06 p1120 N85-17056
Reconstruction of a 3-dimensional transonic rotor flow field from holographic interferogram data
[NASA-TM-86690] 12 p1770 N85-21112
Experimental study of main rotor tip geometry and tail rotor interactions in hover. Volume 1. Text and figures
[NASA-CR-177336-VOL-1] 13 p1965 N85-22344
Experimental study of main rotor tip geometry and tail rotor interactions in hover. Volume 2: Run log and tabulated data
[NASA-CR-177336-VOL-2] 13 p1965 N85-22345
Rotorcraft research testing in the National Full-Scale Aerodynamics Complex at NASA Ames Research Center
[NASA-TM-86687] 17 p2896 N85-27854
Fuselage upwash effects on RSRA rotor systems
[NASA-CR-177349] 20 p3388 N85-31015

HELICOPTER WAKES
Study for prediction of rotor/wake/fuselage interference, part 1
[NASA-CR-177340-VOL-1] 13 p1965 N85-22346
Study for prediction of rotor/wake/fuselage interference. Part 2: Program users guide
[NASA-CR-177340-VOL-2] 13 p1966 N85-22347
Unsteady analysis of rotor blade tip flow
[NASA-CR-3868] 15 p2462 N85-25202
Ground effect on helicopter aerodynamics and stability 20 p3395 N85-31063

HELICOPTERS
NT BO-105 HELICOPTER
NT CH-47 HELICOPTER
NT MILITARY HELICOPTERS
NT P-531 HELICOPTER
NT RIGID ROTOR HELICOPTERS
NT UH-1 HELICOPTER
NT UH-60A HELICOPTER
Rotor systems research aircraft airplane configuration flight-test results
[NASA-TM-85911] 01 p0006 N85-10034
Transonic flow analysis for rotors. Part 1: Three-dimensional quasi-steady, full-potential calculation
[NASA-TP-2375-PT-1] 02 p0134 N85-10914
Aircrew-aircraft integration: A summary of US Army research programs and plans
[NASA-TM-85991] 02 p0148 N85-11004
Structural design guidelines for heliports
[FAA-PM-84-23] 02 p0149 N85-11010
The effects of helicopter vibration on the spinal system
[AD-A146274] 03 p0402 N85-12562
Prediction and modeling of helicopter noise
[AD-A145764] 03 p0415 N85-12856
Initial feasibility ground test of a proposed photogrammetric system for measuring the shapes of ice accretions on helicopter rotor blades during forward flight
[NASA-TM-87391] 04 p0455 N85-12887
Aircraft accident report, Western Helicopters, Inc., Bell UH-1B, N67701, Valencia, California, July 23, 1982
[PB84-910414] 05 p0594 N85-13789
Helicopter pilot performance for discrete-maneuver flight tasks 05 p0702 N85-14502
Technical Workshop: Advanced Helicopter Cockpit Design
[NASA-CP-2351] 06 p0750 N85-14806
Supersugmented rotorcraft program 06 p0750 N85-14807
Helicopter human factors programs and plans 06 p0751 N85-14808
Guidance and navigation programs and plans 06 p0751 N85-14809
Army aviation today and tomorrow 06 p0751 N85-14810
Marine helicopter missions 06 p0751 N85-14811
Civil law enforcement missions 06 p0751 N85-14812
SAR maritime missions 06 p0751 N85-14813
Some thoughts on the implementation of pilot night vision devices for helicopters 06 p0751 N85-14814
HH-65A Dolphin digital integrated avionics 06 p0751 N85-14815
Integrated cockpit design for the Army helicopter improvement program 06 p0751 N85-14816
HH-60D night hawk helicopter 06 p0752 N85-14817
Operational requirements - system concepts 06 p0752 N85-14823
Avionics technology - system concepts 06 p0753 N85-14824
Man-machine interface requirements - advanced technology 06 p0753 N85-14825
Attack helicopter (AH-1T) cockpit systems integration 06 p0753 N85-14826
Avionics system design for requirements for the United States Coast Guard HH-65A Dolphin 06 p0753 N85-14827
The need for a dedicated public service helicopter design 06 p0753 N85-14828
Certification of advanced systems 06 p0753 N85-14829
Operational Loads Data
[AGARD-CP-375] 07 p0694 N85-15964
Helicopter data acquisition in WHL 07 p0696 N85-15676
The UH-1H helicopter icing flight test program: An overview
[NASA-TM-86925] 07 p0900 N85-15702
Study to eliminate ground resonance using active controls
[NASA-CR-166609] 07 p0902 N85-15715
Literature review of voice recognition and generation technology for Army helicopter applications
[AD-A146878] 07 p0939 N85-15954
Helicopter noise survey performed at Las Vegas, Nevada, 19-21 January, 1984
[AD-A147392] 07 p1039 N85-16593
Noise measurement flight test: Data-analyses aerospatiale AS-355F TwinStar helicopter
[AD-A147497] 07 p1039 N85-16595
Helicopter Guidance and Control Systems for Battlefield Support
[AGARD-CP-359] 08 p1072 N85-16797
Automatic briefing and mission management systems for battlefield support 08 p1073 N85-16799
A Computer-generated topographic display system for navigation and mission planning in helicopters 08 p1073 N85-16800
Map display for helicopters 08 p1073 N85-16801
Development of a Helicopter integrated navigation system 08 p1073 N85-16802
Standard Attitude Heading Reference System (SAHRS) full scale development program 08 p1073 N85-16804
Integrated control and display systems for helicopter battlefield mission management 08 p1073 N85-16805
Recent methods for calibrating the anemometry of helicopters at low speeds 08 p1074 N85-16809
LPI-radar for helicopter obstacle warning 08 p1074 N85-16810
Advanced flight simulation for helicopter development 08 p1075 N85-16815
Development and flight test of a helicopter compact, portable, precision landing system concept 08 p1076 N85-16821
Helicopter model rotor-blade vortex interaction impulsive noise: Scalability and parametric variations
[NASA-TM-86007] 08 p1077 N85-16826
Development, production and testing of central control and display unit for helicopters
[BMFT-FB-W-84-039] 08 p1085 N85-16871
Investigation on experimental techniques to detect, locate and quantify gear noise in helicopter transmissions
[NASA-CR-3847] 08 p1217 N85-17667
Noise measurement flight test: Data-analyses Aerospatiale AS 350D AStar helicopter
[AD-A148496] 08 p1218 N85-17672
Noise measurement flight test: Data-analyses, Sikorsky S-76A helicopter
[AD-A148525] 08 p1218 N85-17673
A feasibility study of free-tip rotor application as a passive cyclic control device 09 p1279 N85-18046
Discrete modifications to continuous dynamic structural systems 09 p1337 N85-18410
Inviscid analysis of unsteady blade tip flow correlation studies
[NASA-CR-172506] 10 p1420 N85-18958
Integrated Technology Rotor/Flight Research Rotor (ITR/FRR) concept definition study
[NASA-CR-166444] 10 p1424 N85-18981
Crewstation assessment of reach as applied to the OH-58A helicopter
[AD-A149413] 10 p1531 N85-19650
A Lagrange-D'Alembert formulation of the equations of motion of a helicopter carrying an externally suspended load
[NASA-TM-85864] 12 p1776 N85-21149
Analytical and flight investigation of the influence of rotor and other high-order dynamics on helicopter flight-control system bandwidth
[NASA-TM-86696] 12 p1780 N85-21174
Evaluating wind flow around buildings on heliport placement
[FAA-PM-84-25] 12 p1893 N85-21881
Study for prediction of rotor/wake/fuselage interference, part 1
[NASA-CR-177340-VOL-1] 13 p1965 N85-22346
Study for prediction of rotor/wake/fuselage interference. Part 2: Program users guide
[NASA-CR-177340-VOL-2] 13 p1966 N85-22347
Ground evaluation of helicopter air-to-air warfare 13 p1967 N85-22360
A community survey of helicopter noise annoyance conducted under controlled noise exposure conditions
[NASA-TM-86400] 13 p2154 N85-23374
An experimental investigation of the chopping of helicopter main rotor tip vortices by the tail rotor
[NASA-CR-177338] 13 p2154 N85-23376
Basic consideration of the lifting capability of stoppable rotors
[AD-A150650] 14 p2219 N85-23759
Gears and Power Transmission Systems for Helicopters and Turboprops
[AGARD-CP-369] 14 p2220 N85-23765
Summary of drive-train component technology in helicopters 14 p2220 N85-23766
Current transmission systems 14 p2220 N85-23767
Helicopter transmission lubricants 14 p2220 N85-23768
A state of the art assessment of turboprop transmission technology and projected needs for the next generation 14 p2220 N85-23770
Case depth on flanks of gears for helicopter gearboxes 14 p2222 N85-23780
Condition monitoring of helicopter gearboxes using automatic vibration analysis techniques 14 p2223 N85-23790
Transmission error measurements in gearbox development 14 p2224 N85-23794
Do new aircraft need new technologies and certification rules? 14 p2224 N85-23795
Establishment and maintenance of certification standards for helicopter and turboprop power transmission systems 14 p2224 N85-23798
Recent developments in the dynamics of advanced rotor systems
[NASA-TM-86669] 14 p2317 N85-24320
MI-8 helicopter cargo loading experiment for Arctic shipping 14 p2332 N85-24425
Investigation of technology needs for avoiding helicopter pilot error related accidents
[NASA-CR-3895] 15 p2465 N85-25220
Helicopter user survey: Traffic alert and collision avoidance system (TCAS)
[FAA-PM-85-6] 15 p2466 N85-25236

Calibration loading of a strain-gauged diverless helicopter weapon recovery system
[AD-A151486] 15 p2471 N85-25253
Effects of side-stick controllers on rotorcraft handling qualities for terrain flight
[NASA-TM-86688] 15 p2473 N85-25267
Rotorcraft digital advanced avionics system (Rodaas) 15 p2688 N85-26606
The use of a self-compensated magnetometer in an economical navigation system for the helicopter 16 p2697 N85-26650
Finite-difference computations of rotor loads
[NASA-TM-86682] 16 p2700 N85-26669
Rotor blade flap-lag stability and response in forward flight in turbulent flows 16 p2705 N85-26696
Determination of quantitative relationships between selected critical helicopter design parameters
[AD-A152034] 16 p2706 N85-26700
Development and flight test of a helicopter, X-band, portable precision landing system concept
[NASA-TM-86710] 16 p2710 N85-26721
The evaluation of ACS for helicopters: Conceptual simulation studies to preliminary design 16 p2712 N85-26737
ACT applied to helicopter flight control 16 p2712 N85-26738
The evolution of active control technology systems for the 1990's helicopter 16 p2715 N85-26758
The NAVTAG (Naval Tactical Game) system and its modification to include the SH-60B helicopter
[AD-A152004] 16 p2858 N85-27824
Investigation of imaging and flight guidance concepts for rotorcraft zero visibility approach and landing
[NASA-CR-166571] 17 p2894 N85-27843
Helicopter Aeromechanics
[AGARD-LS-139] 18 p3057 N85-28913
Helicopter aeromechanics: Introduction and historical review 18 p3057 N85-28914
A survey of recent development in helicopter aerodynamics 18 p3057 N85-28915
Rotorcraft noise 18 p3057 N85-28916
Recent developments in the dynamics of advanced rotor systems 18 p3057 N85-28917
Mission requirements and handling qualities 18 p3057 N85-28918
The role of simulation 18 p3058 N85-28919
Flight testing for performance and flying qualities 18 p3058 N85-28920
The evolution of the U.S. helicopter industry
[AD-A154290] 19 p3211 N85-29913
Application of two-dimensional unsteady aerodynamic to a free-tip rotor response analysis
[NASA-CR-177348] 19 p3215 N85-29933
Correlation of rheological characteristics of lubricants with transmission efficiency measurements
[NASA-TM-86686] 19 p3260 N85-30342
A study of the application of differential techniques to the global positioning system for a helicopter precision approach
[NASA-CR-177326] 20 p3391 N85-31035
Standardization of helicopter certification requirements in the western world
[SNIAS-851-210-103] 20 p3393 N85-31048
Automated fabrication of composite structures for helicopters
[SNIAS-851-210-104] 20 p3393 N85-31049
The helicopter, instrument of choice for health evacuation
[SNIAS-851-220-101] 20 p3393 N85-31051
Ground effect on helicopter aerodynamics and stability 20 p3395 N85-31063
Impulsive noise due to transonic blade-vortex interactions 20 p3523 N85-31913
R and D activities of the Structural Sciences Division 20 p3539 N85-32026
Wind tunnel drag evaluations of helicopter nose sections
[AD-A155489] 21 p3553 N85-32100
A phase-locked frequency multiplier for the signal averaging of the vibration of the Wessex helicopter input spiral bevel pinion
[AD-A154914] 21 p3555 N85-32113
Artificial and natural icing tests YEH-60A quick fix helicopter
[AD-A155147] 21 p3555 N85-32116
Proposal for modifications to the Wessex helicopter main rotor gearbox vibration monitoring program
[AD-A155196] 21 p3555 N85-32117
Helicopter noise survey for selected cities in the contiguous US
[AD-A154893] 21 p3609 N85-32985
A three-dimensional viscous flow analysis for the helicopter tip vortex generation problem
[NASA-CR-3906] 23 p3893 N85-34114
An evaluation of three helicopter rotor sections
[NASA-TM-86719] 23 p3893 N85-34115
Flight service evaluation of composite helicopter components
[NASA-CR-172562] 23 p3909 N85-34222
Some problems in high speed gears and gearing 23 p3923 N85-34312
U.S. Civil airmen statistics for calendar year 1984
[AD-A156326] 24 p4059 N85-35153
Laboratory vibration schedules
[AD-A155856] 24 p4064 N85-35188
Development of NATOPS (Naval Air Training and Operating Procedure Standardization) performance software for the H-46D helicopter
[AD-A156089] 24 p4064 N85-35190
Development of NATOPS performance software for the SH-3D and SH-3H helicopters
[AD-A156140] 24 p4065 N85-35192

HELIOCENTRIC ORBITS
U SOLAR ORBITS

HELIOGRAPHS
U SPECTROHELIOGRAPHS

HELIOGRAPHY
U SPECTROHELIOGRAPHS

HELIOMAGNETISM
U SOLAR MAGNETIC FIELD

HELIOMETERS
NT PYROHELIOMETERS
The evaluation of a deformable diffraction grating for a stigmatic EUV spectrohelioneter
[NASA-CR-174350] 09 p1322 N85-18309
The scanning heliometer 14 p2451 N85-25134

HELIOMETRY
U HELIOMETERS
U PYROHELIOMETERS

HELIOS PROJECT
Ten years of Helios
[ISBN-3-88135-156-6] 16 p2884 N85-27794
The Helios missions 16 p2884 N85-27795
Zodiacal light: A replica of the interplanetary dust cloud — Helios space probe 16 p2885 N85-27796
The micrometeorite experiment on Helios — inner solar system 16 p2885 N85-27797
Results from the Helios galactic and solar cosmic ray experiment (E7) 16 p2886 N85-27807
The significance of Helios for Europe 16 p2886 N85-27808
Managerial benefits of Helios for the European industry 16 p2887 N85-27809
The technological gains of Helios for the European industry 16 p2887 N85-27810
Helios project support 16 p2887 N85-27812

HELIOS SATELLITES
NT HELIOS 1
NT HELIOS 2
Data analysis of electron measurements of the plasma experiment aboard the HELIOS probes
[MPE-185] 09 p1416 N85-18935

HELIOS 1
Ten years of Helios
[ISBN-3-88135-156-6] 16 p2884 N85-27794
Ten years solar wind experiments on Helios 1 and Helios 2 16 p2885 N85-27798
Results of the magnetic field experiments E2 and E4 onboard Helios 1 and Helios 2 — magnetometer development 16 p2885 N85-27799
Plasma waves in the solar wind: Ten years of Helios observations 16 p2885 N85-27801
The Helios radio astronomy experiment 16 p2886 N85-27803
Remote sensing of the plasma with time delay measurements (coronal sounding) 16 p2886 N85-27804
The Faraday rotation experiment — solar corona 16 p2886 N85-27805
The fast individualists in the solar system: Cosmic rays 16 p2886 N85-27806
Helios ground operations 16 p2887 N85-27811
Solar wind observations associated with a slow forward shock wave at 0.31 AU
[MPAE-W-79-84-46] 17 p3055 N85-28909
Parallel fast-forward shock within 1 AU: Helios-1 and 2 observations
[MPAE-W-79-84-27] 24 p4169 N85-35847

HELIOS 2
Ten years of Helios
[ISBN-3-88135-156-6] 16 p2884 N85-27794
Ten years solar wind experiments on Helios 1 and Helios 2 16 p2885 N85-27798
Results of the magnetic field experiments E2 and E4 onboard Helios 1 and Helios 2 — magnetometer development 16 p2885 N85-27799
Plasma waves in the solar wind: Ten years of Helios observations 16 p2885 N85-27801
Evidence concerning the generation mechanism of solar type 3 radio bursts 16 p2886 N85-27802
The Helios radio astronomy experiment 16 p2886 N85-27803
Remote sensing of the plasma with time delay measurements (coronal sounding) 16 p2886 N85-27804
The Faraday rotation experiment — solar corona 16 p2886 N85-27805
The fast individualists in the solar system: Cosmic rays 16 p2886 N85-27806
Helios ground operations 16 p2887 N85-27811
Parallel fast-forward shock within 1 AU: Helios-1 and 2 observations
[MPAE-W-79-84-27] 24 p4169 N85-35847

HELIOSEISMOLOGY
Solar Seismology From Space. A conference at Snowmass, Colorado
[NASA-CR-175661] 14 p2441 N85-25060
Overview of solar seismology: Oscillations as probes of internal structure and dynamics in the Sun 14 p2441 N85-25061
What would a dynamo theorist like to know about the dynamics of the solar convection zone? 14 p2441 N85-25062
Solar inverse theory 14 p2441 N85-25063
Rotational inversion from global solar oscillations 14 p2442 N85-25064
Sensitivity of inferred subphotospheric velocity field to mode selection, analysis technique and noise 14 p2442 N85-25065
Evaluation of a magneto-optical filter and a Fabry-Perot interferometer for the measurement of solar velocity fields from space 14 p2442 N85-25067
Optimized response functions for 2-dimensional observations of solar oscillations 14 p2443 N85-25075
The effects of image motion on the l-nu diagram 14 p2443 N85-25076
An excitation mechanism for solar 5-minute oscillation of intermediate and high degree 14 p2444 N85-25085
Solar oscillations 14 p2445 N85-25092
Global solar oscillations in irradiance and velocity: A comparison 14 p2446 N85-25094
The intern. rotation of the Sun inferred from the rotational splitting of acoustic and gravity mode multiplets 14 p2449 N85-25122
Magnetic probing of the solar interior
[NASA-CR-176025] 19 p3385 N85-30968

HELIOSPHERE
Physics of the inner heliosphere 1-10R sub O plasma diagnostics and models
[NASA-CR-174010] 02 p0304 N85-11964
Structure and evolution of the large scale solar and heliospheric magnetic fields 05 p0746 N85-14782
Changes of LISM characteristics in the heliospheric interface 06 p0873 N85-15542
Broadening of the interplanetary helium cone structure due to elastic collisions of LISM helium atoms with solar wind ions 06 p0873 N85-15543
A new radio emission at 3 kHz in the outer heliosphere 12 p1959 N85-22312
Science with the Solar and Heliospheric Observatory (SOHO) 14 p2449 N85-25121
The influence of the heliospheric current sheet and angular separation on flare accelerated solar wind
[NASA-CR-175962] 18 p3209 N85-29907
Nineteenth International Cosmic Ray Conference. SH sessions, volume 4
[NASA-CP-2376-VOL-4] 23 p3969 N85-34729
Latitude dependence of co-rotating shock acceleration
[SH-1.5-14] 23 p3997 N85-34777
The intensity recovery of Forbush-type decreases as a function of heliocentric distance and its relationship to the 11-year variation
[SH-4.1-9] 23 p4005 N85-34832
Cumulative effect of Forbush decreases in the heliospheric modulation during the present solar cycle
[SH-4.1-10] 23 p4005 N85-34833
Latitude variation of recurrent fluxes in the outer solar system
[SH-4.1-13] 23 p4006 N85-34836
Longitudinal distribution of cosmic rays in the heliosphere
[SH-4.1-14] 23 p4006 N85-34837
Evidence for regions of negligible cosmic-ray modulation in the inner heliosphere (10 AU)
[SH-4.1-21] 23 p4006 N85-34840
Drift and observations in cosmic-ray modulation, 1
[SH-4.2-4] 23 p4007 N85-34842
Cosmic ray intensity and the tilt of the neutral sheet
[SH-4.2-8] 23 p4007 N85-34846
Spatial variation of cosmic rays near the heliospheric current sheet
[SH-4.2-10] 23 p4007 N85-34848
Effects of a wavy neutral sheet on cosmic ray anisotropies
[SH-4.2-11] 23 p4008 N85-34849

Determination of galactic cosmic ray latitudinal gradient using Earth based detectors
[SH-4.2-13] 23 p4008 N85-34851
Latitudinal gradients of cosmic rays and the polarity reversal of the heliospheric magnetic field: A preliminary evaluation
[SH-4.2-16] 23 p4008 N85-34853
The effect of the neutral sheet structure of the interplanetary magnetic field on cosmic ray distribution in space
[SH-4.2-18] 23 p4008 N85-34855
On the influence of the heliomagnetospheric periphery on the galactic cosmic rays
[SH-4.2-19] 23 p4009 N85-34856
The dependence of solar modulation on the sign of the cosmic ray particle charge
[SH-4.2-23] 23 p4009 N85-34860
An update on the correlation between the cosmic radiation intensity and the geomagnetic AA index
[SH-4.2-24] 23 p4009 N85-34861
Nineteenth International Cosmic Ray Conference. SH sessions, volume 5
[NASA-CP-2376-VOL-5] 23 p4031 N85-34991
Gradients and anisotropies of high energy cosmic rays in the outer heliosphere
[SH-4.3-7] 23 p4032 N85-34992
IMF-sense-dependent cosmic ray anisotropy produced from diffusion-convection in heliosphere
[SH-4.3-9] 23 p4032 N85-34994
The effect of the interplanetary magnetic field on sidereal variations observed at medium depth underground detectors
[SH-4.4-6] 23 p4033 N85-35003
The first three harmonics of solar daily variation caused by the diffusive propagation of galactic cosmic rays through the heliosphere
[SH-4.5-1] 23 p4035 N85-35019
Time and energy dependence of the cosmic ray gradient in the outer heliosphere
[SH-4.7-2] 23 p4040 N85-35047
The large scale dynamics of the outer heliosphere and the long-term modulation of galactic cosmic rays
[SH-4.7-3] 23 p4040 N85-35048
Voyager 1 and 2 measurements of radial and latitudinal cosmic ray gradients during 1981 - 1984
[SH-4.7-6] 23 p4041 N85-35051
The recovery of the cosmic ray flux from maximum solar modulation at IMP-8 (1 AU) and at Pioneer (R 30 AU)
[SH-4.7-7] 23 p4041 N85-35052
The large-scale modulation of cosmic rays in mid-1982: Its dependence on heliospheric longitude and radius
[SH-4.7-9] 23 p4041 N85-35053
Cosmic rays 10Be biennial data and their relationship to aurorae and sunspots
[SH-7.1-1] 23 p4047 N85-35094

HELIOSTATS
Heliostat tested 07 p0904 N85-16318
User's manual for the University of Houston individual heliostat layout and performance code
[DE85-004843] 12 p1882 N85-21808
Ecological observations at the site of the 10 MWe solar thermal power system (1978-1984)
[DE85-004572] 12 p1885 N85-21827
Error analysis of heliostat alignment methods
14 p2291 N85-24128
The 10 MWe solar thermal central receiver pilot plant: Beam safety tests and analyses
[SAND-83-8035] 16 p2818 N85-27379
Plastic heliostat enclosure analysis
[DE85-009112] 18 p3130 N85-29387
Receiver loss study of optimized solar central receiver systems as a function of receiver thermal loss per unit area
[DE85-010831] 19 p3268 N85-30265
Calibration of relevant measuring sensors
[DE85-009620] 19 p3306 N85-30492
Theory of cellwise optimization for solar central receiver system
[DE85-012586] 22 p3807 N85-33579

HELIPORTS
Heliport snow and ice control methods and guidelines
[DOT/FAA/PM-84/22] 01 p0012 N85-10073
Structural design guidelines for heliports
[FAA-PM-84-23] 02 p0149 N85-11010
Evaluating wind flow around buildings on heliport placement
[FAA-PM-84-25] 12 p1883 N85-21881
Microwave landing systems for heliport operators, owners and users
[FAA-PM-86-7] 19 p3216 N85-29940

HELITRONS
Present status of Heliotron E experiment
09 p1387 N85-16721
Spectroscopic measurement on Heliotron E
09 p1397 N85-16722
Behavior of helically-trapped fast ion orbits in heliotron E 23 p3976 N85-34666
Neoclassical diffusion including ellipticity in a heliotron-like configuration 23 p3978 N85-34667

HELIUM
NT HELIUM ATOMS
NT HELIUM IONS
NT HELIUM ISOTOPES
NT LIQUID HELIUM
NT LIQUID HELIUM 2
Experimental studies of atomic inner shell ionization phenomena
[DE84-013448] 01 p0118 N85-10805
Momentum distributions in superfluid helium: Bose condensate fraction
[DE84-014676] 05 p0731 N85-14700
Pioneer 10 and Voyager observations of the interstellar medium in scattered emission of the He 584 A and H Lya 1216 A lines 06 p0873 N85-15541
Broadening of the interplanetary helium cone structure due to elastic collisions of LISM helium atoms with solar wind ions 06 p0873 N85-15543
Thermal and cryogenic design study for space infrared telescope facility (SIRTF)
[NASA-CR-166613] 07 p0915 N85-15793
Critical velocities in He II for independently varied superfluid and normal fluid velocities
09 p1396 N85-16784
Atomistic studies of grain boundaries with segregated impurities
[DE85-000083] 11 p1737 N85-20924
IUE spectrophotometry of the hot helium-rich PG1159 DO degenerates 11 p1751 N85-21015
A Jamin interferometer to determine the helium abundance in the atmosphere of Jupiter
[BONN-IR-83-17] 12 p1961 N85-22329
NMR imaging and spectroscopy of the mammalian central nervous system after heavy ion radiation
[DE85-004509] 14 p2366 N85-24696
Theoretical and experimental studies of stabilized metastable helium
[AD-A150706] 14 p2417 N85-24913
Infrared telescope
[NASA-CR-171392] 15 p2668 N85-26485
Reciprocating magnetic refrigerator employing tandem porous matrices within a reciprocating displacer
[NASA-CASE-NPO-16257-1] 18 p3085 N85-29082
Intrinsically irreversible acoustic heat engines
[DE85-007672] 19 p3270 N85-30276
Flash pyrolysis of biomass with reactive and non-reactive gases
[DE85-010962] 19 p3306 N85-30496
Possibilities for studying short-lived nuclei produced at LAMPF
[DE85-010740] 19 p3365 N85-30864
Reciprocating Brayton cycle motor
[REPT-84-RR-336] 20 p3462 N85-31507
Design of a helium-cooled molten salt fusion breeder
[DE85-010474] 20 p3528 N85-31943
Investigation of influence of gas exit modes on characteristics of N2O - N2 - He discharge laser
21 p3684 N85-32868
Selective population of N = 3 OVIII level during expansion of laser plasma in helium
21 p3688 N85-32914
Changes in the energy spectrum of anomalous oxygen and helium during 1977 - 1985
[PAPER-SH-4.6-1] 21 p3715 N85-33056
Solar cycle variations of the anomalous cosmic ray component
[PAPER-SH-4.6-2] 21 p3715 N85-33057
Tritium-helium effects in metals
[DE85-011507] 22 p3749 N85-33235
Planetary fluids He and NH3 at high shock pressures and temperatures
[DE85-011551] 22 p3859 N85-33896
Absolute rigidity spectrum of protons and helium nuclei above 10 GV/c
[OG-4.1-1] 22 p3875 N85-34007
The flux of secondary anti-deuterons and antihelium produced in the interstellar medium
[OG-6.1-5] 22 p3886 N85-34096
Combined cold compressor/ejector helium refrigerator
[DE85-006406] 23 p3925 N85-34326
Technical assessment of thermal-hydraulics for high heat flux fusion components
[DE85-013178] 23 p3930 N85-34359
Determination of individual tolerance in hyperbaric oxygen 23 p3954 N85-34507
Observations on (3)He neutron spectrometry
[DE85-010731] 23 p3970 N85-34606
On the importance of interstellar helium for the propagation of heavy cosmic rays
[OG-7.2-11] 23 p4015 N85-34679
Changes in the energy spectrum of anomalous oxygen and helium during 1977-1985
[SH-4.6-1] 23 p4039 N85-35039
Experimental technique for measuring the isentrope of hydrogen to several megabars
[DE85-014332] 24 p4095 N85-35366
Search for magnetic monopoles using proportional counters filled with helium gas
[HE-6.1-1] 24 p4209 N85-36127
Magnetic monopole search by 130 m(2)sr He gas proportional counter
[HE-6.1-2] 24 p4209 N85-36128
Results from the UCSD magnetic monopole search
[HE-6.1-12] 24 p4210 N85-36137

HELIUM ATOMS
Helium atoms in interstellar and interplanetary media, part 3: Temperature and velocity of interstellar wind
02 p0160 N85-11068
Helium atoms in interstellar and interplanetary space. II: Determination of direction of interstellar gas motion relative to Sun 13 p1980 N85-22425
Hartree-Fock interaction between a helium atom and lithium-metal: A test for the effective medium theory
[AD-A150466] 13 p2158 N85-23357

HELIUM HYDROGEN ATMOSPHERES
Shock compression of liquid helium to 56 GPa (560 kbar 13 p2184 N85-23551

HELIUM IONS
Helium ionization detection apparatus
[NASA-TM-77505] 03 p0364 N85-12332
One-electron capture processes by highly charged ions from helium: Present status of HICE-IPP
00 p1389 N85-18736
Anomalous heating of ionospheric components (thermal e- and He+) via intense ion Cyclotron Waves (ICW's)
14 p2368 N85-24633
Data on the backscattering coefficients on light ions from solids: A revision
[IPPJ-AM-41-REV] 23 p3982 N85-34689
Injection of energetic particles following the gamma-ray flares on June 7, 1980, as observed on Helios 1
[SH-1.3-9] 23 p3993 N85-34756
Spectra of solar proton ground level events using neutron monitor and neutron moderated detector recordings
[SH-1.3-14] 23 p3994 N85-34759
Observation of pick-up ions in the solar wind: Evidence for the source of the anomalous cosmic ray component?
[SH-4.6-5] 23 p4039 N85-35043

HELIUM ISOTOPES
Structure and kinetics of physisorption, properties of helium during reduction of the dimension
03 p0432 N85-12749
Development program: Nuclear magnetic resonance gyroscope (NMR-gyro). Phase 1: Development of an experimental model
[BMFT-FB-W-84-041] 05 p0639 N85-14101
Solar He-3-rich events and non-relativistic electron events: A new association
[NASA-TM-86179] 06 p0890 N85-15652
Outlook for realization of proximity effect and Josephson direct current in helium-2 13 p2074 N85-22956
Entropy of He 2 and universality near the superfluid in He(4) 19 p3378 N85-30957
Cosmic ray He3 measurements
[OG-4.2-3] 21 p3714 N85-33045
Constraints on early atmosphere from planetary accretion processes 21 p3717 N85-33064
The degassing history of the Earth: Noble gas studies of Archaean cherts and zero age glassy submarine basalts 21 p3718 N85-33072
Interstellar propagation and the isotopic composition of hydrogen in the galactic cosmic rays
[OG-4.2-1] 22 p3877 N85-34021
Measurements of galactic hydrogen and helium isotopes from 1978 through 1983
[OG-4.2-2] 22 p3877 N85-34022
Cosmic ray He-3 measurements
[OG-4.2-3] 22 p3878 N85-34023
Analysis of experimental data on interstellar antiprotons in the light of measurements of high-energy electrons and He-3 nuclei
[OG-6.1-6] 22 p3886 N85-34097
Type 3 solar radio bursts and 3HE-rich events
[SH-2.2-3] 23 p4000 N85-34798
Solar source regions of 3HE-rich particle events
[SH-2.2-4] 23 p4000 N85-34799
The 3HE in solar non-relativistic electron events
[SH-2.2-5] 23 p4000 N85-34800
The heavy ion composition in 3HE-rich solar flares
[SH-2.2-7] 23 p4000 N85-34802
The mean ionic charge of silicon in 3HE-rich solar flares
[SH-2.2-8] 23 p4000 N85-34803

On the connection between the 3HE-enrichment and spectral index of solar energetic particles
[SH-2.2-9] 23 p4001 N85-34804
Breakdown of helium nuclei in matter processed near black holes
[CG-8.2-20] 23 p4021 N85-34916
The 4He1H ratios in the chemical compositions of solar flare particles and the primordial solar nebula
[SH-7.1-12] 23 p4048 N85-35104
HELIUM PLASMA
Low plasma edge temperatures for the self-pumped limiter
[DE85-010155] 18 p3189 N85-29782
The dependence of solar modulation on the sign of the cosmic ray particle charge
[SH-4.2-23] 23 p4009 N85-34860
HELIUM STARS
U B STARS
HELIUM 2
U HELIUM ISOTOPES
U LIQUID HELIUM
HELIUM 3
U HELIUM ISOTOPES
HELIUM 4
U HELIUM ISOTOPES
HELIUM-NEON LASERS
Scheme for measuring specular reflection coefficient at 10.6 microns wavelength with zigzag-path cell and integrating sphere 14 p2275 N85-24097
Applications of laser technology described 21 p3572 N85-32218
Investigation of reproducibility of emission wavelength of helium-neon laser with external neon absorption cell (0.63 micrometers) 21 p3683 N85-32884
Dielectric mirror with ferromagnetic substrate 21 p3696 N85-32986
HELIX TUBES
U TRAVELING WAVE TUBES
HELIXES
U CURVES (GEOMETRY)
HELMET MOUNTED DISPLAYS
Psychophysical research in development of a fiber-optic helmet mounted display 06 p0701 N85-14501
Helmet mounted telescope
[AD-D011355] 07 p1019 N85-18467
The use of lasers in wide-angle visual systems
[AD-P004322] 09 p1269 N85-17976
Design considerations for an eye tracked AOI (Area of Interest) display system
[AD-P004324] 09 p1269 N85-17978
Air combat visual simulation using a head slaved projector
[AD-P004327] 09 p1270 N85-17981
The fiber-optic helmet-mounted display
[AD-P004330] 09 p1270 N85-17984
Binocular overlap in a fiber optic helmet mounted display
[AD-P004331] 09 p1270 N85-17985
The effect of modified spectacles on the field of view of the helmet display unit of the integrated helmet and display sighting system
[AD-A148693] 09 p1281 N85-18055
Wide-field-of-view, helmet-mounted infinity display system development
[AD-A149841] 12 p1777 N85-21159
Trends shaping advanced aircrew training capabilities through the 1990s
[AD-A152277] 16 p2843 N85-27530
Advanced simulator for pilot training and helmet-mounted visual display configuration comparisons
[AD-A155326] 21 p3667 N85-32776
HELMETS
Direct view helmet mounted telescope
[AD-D011291] 06 p0755 N85-14839
Helmet mounted telescope
[AD-D011355] 07 p1019 N85-18467
SPH-4 US Army flight helmet performance, 1972 - 1983
[AD-A148674] 08 p1201 N85-17562
HELMHOLTZ EQUATIONS
The numerical solution of the Helmholtz equation for wave propagation problems in underwater acoustics
[NASA-CR-172454] 02 p0250 N85-11634
Spheroidal functions: Properties and tabulation. Application to antenna synthesis 14 p2396 N85-24758
HELMHOLTZ RESONATORS
The effect of grazing flow on the impedance of the Helmholtz resonator 05 p0635 N85-14076
A broadband matching network
[AD-D011406] 08 p1219 N85-17675
A research program to reduce the interior noise in general aviation aircraft, index and summary
[NASA-CR-176178] 24 p4145 N85-35695
HELMHOLTZ VORTICITY EQUATION
Diffraction of plane polarized waves by noncircular cylindrical cavity 02 p0269 N85-11754
Three-dimensional, direct and vectorized elliptic solvers for various boundary conditions
[AD-B088266L] 08 p1206 N85-17595
An introduction to vortex breakdown and vortex core bursting
[NAE-AN-28] 17 p2892 N85-27929
On the use of internal state variables in thermoviscoplastic constitutive equations 20 p3466 N85-31536
HELOS (SATELLITE)
U EXOSAT SATELLITE
HEMATOCRIT RATIO
A systems analysis of the erythropoietic responses to weightlessness. Volume 1: Mathematical model simulations of the erythropoietic responses to weightlessness
[NASA-CR-171890] 20 p3506 N85-31794
HEMATOLOGY
Multiple regression method used to assess animal adaptation to hypoxic hypoxia 12 p1902 N85-21947
Chemical characterization and toxicologic evaluation of airborne mixtures. Inhalation toxicology of diesel fuel obscurant aerosol in Sprague-Dawley rats. Phase 3. Subchronic exposures
[AD-A150100] 12 p1905 N85-21966
Research opportunities in loss of red blood cell mass in space flight
[NASA-CR-175808] 16 p2841 N85-27517
HEMATOPOIESIS
Hemopoiesis in rats submitted to weightlessness 01 p0091 N85-10613
Functional and structural changes in human erythrocyte surface after irradiation by UV waves of various wavelengths. Report 1: Expression of ABO and Rhesus system antigen 09 p1361 N85-18564
Functional and structural changes in human erythrocyte surface after irradiation by UV waves of various wavelenghts. Report 2: Adsorption of alcyan blue by external premembranous components 09 p1361 N85-18565
A systems analysis of the erythropoietic responses to weightlessness. Volume 1: Mathematical model simulations of the erythropoietic responses to weightlessness
[NASA-CR-171890] 20 p3506 N85-31794
A systems analysis of the erythropoietic responses to weightlessness. Volume 2: Description of the model of erythropoiesis regulation. Part A: Model for regulation of erythropoiesis. Part B: Detailed description of the model for regulation of erythropoiesis
[NASA-CR-171891] 20 p3506 N85-31795
HEMATOPOIETIC SYSTEM
A detailed analysis of the erythropoietic control system in the human, squirrel, monkey, rat and mouse
[NASA-CR-171879] 15 p2614 N85-26107
HEMODYNAMIC RESPONSES
Distribution of blood flow to brain, kidneys, gut, spleen and posterior extremities in cats in acute hypoxia 07 p1013 N85-16434
Nature of postural changes in human hemodynamics with intake of sydnocarb alone and in combination with obeidan 19 p3325 N85-30597
Analysis of the transient response of temporal artery blood flow data relative to various anti-G suit pressure schedules
[AD-A155242] 21 p3666 N85-32775
Formation of new microvessels in skeletal muscles of rats exposed to hypobaric hypoxia for one week 22 p3820 N85-33662
Effect of hypokinesia and +Gz accelerations on transport function of human blood 23 p3952 N85-34497
Oxygenation and regional circulation in gingival mucosa during exposure to lower body negative pressure 23 p3953 N85-34498
Effect of water immersion of parameters of central hemodynamics in individuals over 45 years old 23 p3953 N85-34499
Effect of acute hypoxia on coronary and systemic hemodynamics 23 p3953 N85-34503
HEMODYNAMICS
NT LOWER BODY NEGATIVE PRESSURE
Compensatory and adaptive regional hemodynamic reactions to weightlessness during long-term spaceflights 01 p0091 N85-10616
Hemodynamics and plasma arginine vasopressin during water immersion in normal man 05 p0693 N85-14458
Hemodynamics responses to upright tilt at sea level and high altitude
[AD-A148648] 10 p1527 N85-19634
Regional circulation during testing on isokinetic dynamometer following 14-day bedrest 19 p3323 N85-30590
Primate adrenal reactions to antiorthostatic hypokinesia 19 p3324 N85-30591
Long term exposure of animals to antiorthostatic (-90 deg) as a model of critical homeostatic disturbances 19 p3324 N85-30592
Nature of postural changes in human hemodynamics with intake of sydnocarb alone and in combination with obeidan 19 p3325 N85-30597
Results and prospects of physiological research during spaceflights 22 p3732 N85-33139
Intracardiac hemodynamics and human heart function in simulated weightlessness 22 p3733 N85-33140
Cosmonauts' cardiovascular system function during long-term orbital flights aboard Salyut-6 station 22 p3733 N85-33141
Effects of blood volume overload on myocardial ultrastructure in relation to adaptation to high altitude hypoxia 22 p3820 N85-33664
USSR report: Space Biology and Aerospace Medicine, volume 19, no. 2, March - April 1985
[JPRS-USB-85-004] 22 p3820 N85-33667
Typological characteristics of hemodynamic states of healthy subjects in orthostatic position 22 p3821 N85-33673
Cerebral hemodynamics and ventricular function in -15 deg antiorthostatic position 22 p3822 N85-33676
Morphological manifestations of hemodynamic changes in lungs of monkeys submitted to antiorthostatic hypokinesia 22 p3824 N85-33688
USSR report: Space Biology and Aerospace Medicine, vol. 19, no. 3, May - June 1985
[JPRS-USB-85-005] 23 p3952 N85-34494
Effect of dibazol on parameters of nonspecific resistance of subjects in pressurized cabins 23 p3954 N85-34504
HEMOGLOBIN
NT OXYHEMOGLOBIN
Effect of maximum physical load on oxygen-transport properties of blood 01 p0093 N85-10627
A systems analysis of the erythropoietic responses to weightlessness. Volume 1: Mathematical model simulations of the erythropoietic responses to weightlessness
[NASA-CR-171890] 20 p3506 N85-31794
A systems analysis of the erythropoietic responses to weightlessness. Volume 2: Description of the model of erythropoiesis regulation. Part A: Model for regulation of erythropoiesis. Part B: Detailed description of the model for regulation of erythropoiesis
[NASA-CR-171891] 20 p3506 N85-31795
Estimating risks of lead-induced hemoglobin decrements under conditions of uncertainty: Methodology, pilot judgments and illustrative calculations
[DE85-012293] 23 p3952 N85-34493
HEMORRHAGES
Fatal hemorrhagic shock and acetate solutions
[AD-A146754] 07 p1014 N85-18444
HEOS B SATELLITE
The Earth magnetosphere: A charged particle accelerator 04 p0519 N85-13315
HEOS SATELLITES
NT HEOS B SATELLITE
HERBICIDES
Proceedings of the 14th Conference on Environmental Toxicology
[AD-A146400] 06 p0643 N85-15350
The epidemiology and toxicology of Agent Orange
[AD-P004036] 06 p0645 N85-15368
Toxicity, mutagenesis and aging due to endogenous oxygen radicals
[AD-A150121] 12 p1900 N85-21928
HERBIG-HARO OBJECTS
Bipolar molecular outflows: T Tauri stars and Herbig-Haro objects 03 p0446 N85-12937
Non-stable motions and instability in stellar associations 05 p0739 N85-14754
UV observations and results on pre-main sequence stars 11 p1744 N85-20970
The changing ultraviolet spectrum of Herbig-Haro object No. 1 11 p1747 N85-20989
Short-wavelength observations of HH-2H and HH-24A 11 p1747 N85-20990
Dust in the region of Herbig-Haro objects: The case of NGC 1999 11 p1747 N85-20991
Plasma processes in Herbig-Haro objects 12 p1957 N85-22301
Low-excitation Herbig-Haro objects and interstellar extinction
[NASA-CR-176142] 23 p3988 N85-34726
The structure of Herbig-Haro object 43 and Orion dark cloud extinction
[NASA-TM-87503] 24 p4188 N85-35831

HERCULES NOVA
EXOSAT observations of the 35d intensity variations of Her X-1 — X ray binary source
11 p1742 N85-20956
Pulse phase spectroscopy of Her X-1 with EXOSAT — X ray binary source
11 p1743 N85-20957
HERMES SATELLITE
U COMMUNICATIONS TECHNOLOGY SATELLITE
HERMETIC SEALS
Qualitative and quantitative compositional analysis of shale derived by gas chromatography and combined gas Chromatography/Mass spectrometry. Executive summary
[AD-A148369] 07 p0924 N85-15851
Method for bonding insulator to insulator
[AD-D011340] 07 p0929 N85-15891
Experimental stiffness of tapered bore seals
[NASA-TM-86978] 15 p2568 N85-25847
Hermetic sealing of nonlubricated gas seal and friction characteristics, chapter 7
[DE85-006375] 15 p2569 N85-25851
Inhibited anticorrosion protection of automotive steel strip in the NLMK
[BLL-M-36250-(5828.4)] 20 p3430 N85-31274
A device for generating motive force through the expansion of a non-elastic dense fluid
[NASA-TM-77664] 20 p3454 N85-31448
X-ray residual stress analysis on the coarse grain of copper and its application to the brazed copper
23 p3907 N85-34202
Hermetic chip carrier compliant soldering pads
[AD-D011722] 23 p3936 N85-34410
HERMITIAN POLYNOMIAL
Monotonicity preserving bicubic interpolation, revision 1
[DE85-007976] 17 p3021 N85-28683
HERTZSPRUNG-RUSSELL DIAGRAM
X-ray spectra of bursting neutron stars
23 p3981 N85-34686
HESSIAN MATRICES
Quasi-Newton algorithms for large scale nonlinear systems
02 p0208 N85-11370
Software for estimating sparse Hessian matrices
[DE85-006121] 17 p3013 N85-28629
HETEROCYCLIC COMPOUNDS
NT ADENOSINE DIPHOSPHATE
NT ADENOSINE TRIPHOSPHATE
NT ADENOSINES
NT ATROPINE
NT AZINES
NT AZOLES
NT CARBAZOLES
NT METHYLENE BLUE
NT OXAZOLE
NT PHTHALOCYANIN
NT PHYLLOQUINONE
NT PYRROLES
NT RDX
NT TETRAHYDROFURAN
NT THIAZINE (TRADEMARK)
NT TRYPTOPHAN
Method of obtaining heterocyclic polymers
[AD-A145127] 01 p0033 N85-10202
Method for making heterocyclic block copolymers
[AD-D011446] 10 p1451 N85-19143
Spray pyrolysis as a synthetic tool
[AD-A153691] 19 p3234 N85-30047
HETERODYNING
NT OPTICAL HETERODYNING
Quantum noise and excess noise in optical homodyne and heterodyne receivers
[AD-A148296] 08 p1157 N85-17303
Pulse heterodyne equipment for measurements of range and velocity of moving targets-pulse radar
[ESA-TT-845] 09 p1312 N85-18248
Injection controlled laser transmitter with twin local oscillators
[AD-D011577] 15 p2563 N85-25810
A comparison of electronic heterodyne moire deflectometry and electronic heterodyne holographic interferometry for flow measurements
[NASA-TM-87071] 21 p3588 N85-32302
Recording small frequency drifts of microwave oscillators
22 p3771 N85-33372
Heterodyne holographic interferometry for visualization of surface acoustic waves
[AD-A155405] 22 p3836 N85-33753
HETEROGENEITY
Friction, wear and structure of heterogeneous materials
01 p0055 N85-10362
Transformation of heterogeneous surface waves by skewed streams
02 p0259 N85-11697
Numerical investigation of characteristics of current flow for different methods of obtaining discharge in high speed lasers. Mechanism underlying current flow in positive glow discharge column
02 p0264 N85-11726
The 6th International Summer Institute in Surface Science 1983)
[AD-A146253] 03 p0434 N85-12762
Heterogeneous data base access
05 p0735 N85-14724
Characteristic scale of inner mixing layers in stably stratified atmosphere
06 p0824 N85-15235
Transformation of electromagnetic waves in plasma with randomly-heterogeneous magnetic field
07 p0953 N85-16039
Fluctuations during observations of extraterrestrial sources from outer space through Earth's atmosphere
07 p0953 N85-16040
In situ monitoring of electrochemical reactions by surface enhanced Raman scattering
[PB85-149789] 12 p1803 N85-21312
The behaviour of detonation waves in single phase heterogeneous systems
[AD-A149625] 12 p1846 N85-21581
Temperature effects of heterogenized annealing on structure and properties of V95 aluminum alloy
13 p2025 N85-22692
Consideration of heterogeneity of gravity fields in local high precision geodetic constructions
13 p2114 N85-23169
Wave propagation in heterogeneous media
[AD-A150800] 14 p2321 N85-24341
Perceived heterogeneity and its effect on various types of tasks
[AD-A151003] 14 p2392 N85-24729
Analysis of combustion oscillations in heterogeneous systems
[AD-A151999] 16 p2745 N85-26942
Quality testing to the specifications of the Stahl-Eisen-Pruefblatt 1570/71 using an automatic image analysis system
[BLL-BISI-TRANS-22253-(9022.06)]
17 p2976 N85-28385
Mechanism of heterogeneous deposition ice nucleation near water-saturation
21 p3638 N85-32597
HETEROJUNCTION DEVICES
Thin film (Al, Ga)As heterojunction solar cells
02 p0258 N85-11691
Preparation and evaluation of ZnSe and ZnS sub X Se sub 1-x epitaxial layers on Ge substrates for applications in surface passivation and heterojunction devices
[AD-A147432] 07 p1048 N85-16657
Heterocontact effects in point contact electron-phonon spectroscopy of the alkali metals
[AD-A149760] 12 p1800 N85-21290
Comparative study of GaAs solar cell potentialities for space applications
13 p2006 N85-22577
GaAs and 3-5 compound solar cells status and prospects for use in space
13 p2007 N85-22580
Photovoltaic cells of InP-CdS heterojunction type and their temperature characteristics under A-M illumination
14 p2275 N85-24092
Physical electronics of cooled operation of very short compound semiconductor transistors
14 p2297 N85-24223
Self-detecting optical sensors
[AD-D011657] 18 p3185 N85-29751
Modulation doped GaAs/Al(x)Ga(1-x)As layered structures with applications to field effect transistors
[AD-A155380] 22 p3759 N85-33296
HETEROJUNCTIONS
Low-threshold injection lasers on grown GaInPAs/InP heterostructures (1.2-1.6 micrometers wavelengths)
02 p0258 N85-11693
Research activities of the Illinois University Coordinated Science Laboratory
[AD-A145589] 03 p0449 N85-12856
The growth and properties of semiconductor strained-layer superlattices
[DE84-012979] 06 p0868 N85-15515
Diffusion barrier for long wavelength laser diodes
[AD-D011390] 07 p0970 N85-16157
Effect of neutron irradiation on the high temperature operation of injection laser diodes
[DE85-000068] 09 p1326 N85-18333
Liquid-phase epitaxial growth of CdTe on HgCdTe
[AD-D011482] 10 p1561 N85-19846
Surface and allied studies in silicon solar cells
[NASA-CR-174447] 11 p1671 N85-20531
Preliminary studies on the low-cost preparation of chalcogenide semiconductors from solution depositions
[DE85-000538] 11 p1736 N85-20918
Multiple double heterojunction buried laser device
[AD-D011519] 12 p1855 N85-21635
Process for making a heterojunction source-drain insulated gate field-effect transistors utilizing diffusion to form the lattice
[AD-D011536] 12 p1939 N85-22176
Development of a planar heterojunction bipolar transistor for very high speed logic
[AD-A150374] 13 p2064 N85-22895
Thin film cadmium telluride and zinc phosphide solar cells
[DE85-002904] 15 p2587 N85-25950
Polycrystalline semiconductor heterojunction modelling (CdS/CuInSe(sub)2)
[DE85-002913] 16 p2871 N85-27713
The construction and study of improved Al(x)Ga(1-x)As-GaAs heterostructure devices
[AD-A153264] 17 p2954 N85-28244
Zn3P2 as an improved semiconductor for photovoltaic solar cells
[DE85-008772] 18 p3097 N85-29171
Heterojunction Schottky gate MESFET with lower channel ridge barrier
[AD-D011673] 19 p3258 N85-30199
Cadmium sulfide/copper ternary heterojunction cell research
[DE85-008778] 19 p3305 N85-30486
Photoelectronic properties of zinc phosphide crystals and heterojunctions
[DE85-008777] 19 p3307 N85-30501
Optical properties of heterostructures and superlattices
[AD-A156243] 24 p4162 N85-35802
HETEROTROPHS
Chemical composition of Musca domestica L. larval and pupal biomass when developing in organic waste of biological life-support system for man
22 p3824 N85-33691
HEURISTIC METHODS
An expert system for representing procedural knowledge
[AD-P003923] 02 p0245 N85-11603
The search for regularity: Four aspects of scientific discovery
[AD-A145939] 03 p0368 N85-12355
New uses for sensitivity analysis: How different movement tasks effect limb model parameter sensitivity
05 p0706 N85-14529
Automatic map name placement system
09 p1341 N85-18438
Spacefilling curves and the planer travelling salesman problem
[AD-A149337] 10 p1551 N85-19786
Heuristics based on spacefilling curves for combinatorial problems in the plane
[AD-A149320] 10 p1552 N85-19788
Learning to search. From weak methods to domain-specific heuristics
[AD-A149949] 12 p1918 N85-22045
A replication and extension of the inducement of the availability heuristic
[AD-A149755] 12 p1923 N85-22083
State dependent priority rules for scheduling
[AD-A149972] 12 p1924 N85-22090
Solving set covering problems using heuristics with branch and bound
[AD-A151905] 15 p2638 N85-26269
Generation of flight paths using heuristic search
[AD-A151949] 16 p2704 N85-26694
A heuristic solution to the spacing problem: Maximizing the minimum Euclidean distance among N points in a convex region
[AD-A152116] 16 p2855 N85-27603
Identifying solution paths in cognitive diagnosis
[AD-A152463] 17 p3000 N85-28549
A practical approach to Karmarkar's algorithm
[AD-A155714] 21 p3673 N85-32818
Heuristic rules for visualization
23 p3965 N85-34584
HEWLETT-PACKARD COMPUTERS
System test: Hewlett-Packard draft
[A-9] 18 p3166 N85-29613
HEXANITROSTILBENE
Experimental studies of chemical reactivity during shock initiation of hexanitrostilbene
[DE85-011726] 22 p3754 N85-33270
HEXENES
Influence of structural parameters of zeolite catalysts on their activity and selectivity
[BMFT-FB-T-83-253] 03 p0329 N85-12119
HF LASERS
Short Wavelength Chemical Laser (SWCL) Workshop
[AD-A151959] 16 p2790 N85-27211
Operating characteristics, absorptivity/reflectivity measurements, and pulse system design of the NPS (Naval Postgraduate School) hydrogen fluoride/deuterium fluoride laser
[AD-A152712] 17 p2970 N85-28341
Chemical lasers
[ISL-R-107/84] 23 p3936 N85-34400
HICAT (RADAR TECHNIQUE)
U HIGH RESOLUTION COVERAGE ANTENNAS
HICAT PROJECT
U HIGH RESOLUTION COVERAGE ANTENNAS

HIERARCHIES
Approximating hierarchical normal priors using a vague component
[CSIR-TWISK-284] 01 p0107 N85-10720
Evidence accumulation for spatial reasoning
07 p0965 N85-16261
Research into self-timed VLSI circuits
[AD-A149140] 10 p1479 N85-19339
A circuit grammar for operational amplifier design
[AD-A149566] 10 p1481 N85-19346
Normal and anomalous geothermal fields and their relationship to hierarchy of geological bodies
13 p2113 N85-23163
The hierarchical database decomposition approach to database concurrency control
[AD-A150612] 13 p2166 N85-23450
Some applications of fuzzy sets and the analytical hierarchy process to decision making
[AD-A150720] 14 p2412 N85-24876
Multigrid algorithms on the hypercube multiprocessor
[AD-A152200] 16 p2647 N85-27556
Application of hierarchical data structures to geographical information systems
[AD-A152169] 16 p2677 N85-27753
Fuzzy hierarchical analysis
[DE85-008149] 17 p3021 N85-28685
The Hamiltonian structure of a complex version of the Burgers hierarchy
[PREPRINT-423] 18 p3173 N85-29665
Inference in hierarchic classification — data bases
[ENST-84E014] 20 p3518 N85-31873
Models for multidimensional tests and hierarchically structured training materials
[AD-A155231] 21 p3665 N85-32768
Hierarchical chamfer matching
[FOA-C-30367-E1] 22 p3802 N85-33558
A hierarchy of knowledge levels implemented in a rule-based production system to calculate bounds on the size of intersections and unions of simple sets
[AD-A155291] 22 p3848 N85-33836
Selection of segment similarity measures for hierarchical picture segmentation
23 p3960 N85-34548
Source hierarchy list. Volume 1: A through H
[AD-A156300] 24 p4165 N85-35825
Source hierarchy list. Volume 2: I through Z
[AD-A156301] 24 p4165 N85-35826

HIGH ACCELERATION
Further cell biology experiments with Physarum polycephalum for a reflight of Biorack
05 p0689 N85-14429

HIGH ALTITUDE
Magnetospheric plasma studies using data from the dynamics high and low altitude plasma instruments
[AD-A145751] 03 p0392 N85-12505
Structure of temperature field based on observations of refraction from high meteorological mast
06 p0819 N85-15199
Hemodynamics responses to upright tilt at sea level and high altitude
[AD-A148848] 10 p1527 N85-19634
Design considerations for high-altitude, long-endurance, microwave-powered aircraft
[NASA-TM-86403] 14 p2218 N85-23751
High altitude sampling program: Radioactivity in the stratosphere
[DE85-005924] 14 p2374 N85-24676
Spectral characteristics of protons at low and high altitudes during geomagnetic storm of 29 July 1977
16 p2719 N85-26786
Technological experiments on high-altitude rockets
16 p2725 N85-26818
Applied research and development for falling-sphere air density measuring systems
[AD-A155227] 21 p3552 N85-32099
Effects of blood volume overload on myocardial ultrastructure in relation to adaptation to high altitude hypoxia
22 p3820 N85-33664
Cardiorespiratory function and work performance during adaptation to industrial labor in midalpine conditions
22 p3820 N85-33665
Structural changes in thyroid due to high-altitude adaptation in Kirghizia
22 p3820 N85-33666
An EAS experiment at mountain altitude for the detection of gamma-ray sources
[OG-9.4-5] 23 p4029 N85-34872
Short perturbations of cosmic ray intensity and electric field in atmosphere
[SH-6.1-19] 23 p4046 N85-35090

HIGH ALTITUDE BALLOONS
NT JIMSPHERE BALLOONS
NT SUPERPRESSURE BALLOONS
Thin film strain transducer — suitable for in-flight measurement of scientific balloon strain
[NASA-CASE-WLP-10055-2] 12 p1849 N85-21598
Observation of cosmic ray flux variations in stratosphere
13 p1981 N85-22430

HIGH ALTITUDE BREATHING
Hemodynamics and neurodynamics of the human brain during exposure to moderate hypoxic hypoxia
01 p0094 N85-10630
Results of study of hypoxia problems
04 p0544 N85-13462

HIGH ALTITUDE ENVIRONMENTS
Fungi of Mt. Babia Gora. 1: Mycoflora of forests
[NASA-TM-77484] 02 p0234 N85-11522
Armed forces special Symposium on Medicine of Altitudes
13 p2166 N85-23441
High-altitude testing of selective optical coatings for solar radiators and collectors
17 p2939 N85-28143

HIGH ALTITUDE FLIGHT
U HIGH ALTITUDE

HIGH ALTITUDE PRESSURE
Cut-off lows and their influence on the weather in Switzerland
[REPT-45] 10 p1519 N85-19574
Formation of new microvessels in skeletal muscles of rats exposed to hypobaric hypoxia for one week
22 p3820 N85-33662
Effects of immobilization and high-altitude adaptation on energy metabolism in rats
22 p3820 N85-33663

HIGH ALTITUDE TESTS
High-altitude testing of selective optical coatings for solar radiators and collectors
17 p2939 N85-28143
The design of an experiment to detect low energy antiprotons
[OG-9.1-1] 23 p4022 N85-34828

HIGH ASPECT RATIO
Flutter parametric studies of cantilevered twin-engine transport type wing with and without winglet. Volume 2: Transonic and density effect investigations
[NASA-CR-172410-VOL-2] 04 p0513 N85-13270
Aileron effectiveness for a subsonic transport model with a high-aspect-ratio supercritical wing
[NASA-TM-85674] 07 p0898 N85-15695
Comparison of analytical and experimental steadyand unsteady-pressure distributions at Mach number 0.78 for a high-aspect-ratio supercritical wing model with oscillating control surfaces
[NASA-TM-84589] 07 p0899 N85-15697
Numerical simulation of transonic flutter of a high-aspect ratio transport wing
16 p2694 N85-26830
Low-speed tests of a high-aspect-ratio, supercritical-wing transport model equipped with a high-lift flap system in the Langley 4- by 7-meter and Ames 12-foot pressure tunnels
[NASA-TP-2097] 20 p3388 N85-31010

HIGH ASPECT RATIO WINGS
U SLENDER WINGS

HIGH CURRENT
A 10/sup 11/W high current pulse electron beam accelerator described
11 p1620 N85-20200
High-current measurement techniques
[PB85-100444] 11 p1637 N85-20311
Surface interactions and high-voltage current collection
13 p1993 N85-22499
Collective acceleration of ions using high current relativistic electron beams
[DE85-004869] 13 p2157 N85-23393
Development of theory of high-current high-pressure pulsed arc
15 p2645 N85-26314
High current beam hollowing instability study
[AD-A151301] 15 p2648 N85-26329
Plasma erosion opening switch
[DE85-011984] 20 p3535 N85-31998
Observations of accelerated high current low emittance beams in the SLC Linac
[DE85-013073] 24 p4068 N85-35211
Numerical studies of high current beam compression in heavy ion fusion
[DE85-011874] 24 p4158 N85-35783

HIGH ECCENTRIC LUNAR OCCULTATION SATELLITE
U EXOSAT SATELLITE

HIGH ENERGY ASTRONOMY OBSERVATORIES
U HEAO

HIGH ENERGY ASTRONOMY OBSERVATORY A
U HEAO 1

HIGH ENERGY ASTRONOMY OBSERVATORY B
U HEAO 2

HIGH ENERGY ASTRONOMY OBSERVATORY C
U HEAO 3

HIGH ENERGY ASTRONOMY OBSERVATORY 1
U HEAO 1

HIGH ENERGY ASTRONOMY OBSERVATORY 2
U HEAO 2

HIGH ENERGY ASTRONOMY OBSERVATORY 3
U HEAO 3

HIGH ENERGY ELECTRONS
NT RELATIVISTIC ELECTRON BEAMS
Energetic electrons in impulsive solar flares
02 p0303 N85-11982
Asymptotic orbit theory for trapped electrons in inhomogeneous Whistler field
[AD-A148178] 03 p0392 N85-12510
Morphology of keV-electrons in the Earth's magnetosphere as observed by GEOS 1
[DRI-3-84] 09 p1360 N85-18496
High energy pulsed particle accelerator
[AD-A149247] 10 p1554 N85-19797
The high latitude D region during electron precipitation events
11 p1684 N85-20484
High energy particle effects in the D region during and after geomagnetic storms
11 p1684 N85-20485
Latitudinal dependence of the energy input into the mesosphere by high energy electrons
11 p1684 N85-20489
Longitude and pitch-angle distributions of streams of high-energy electrons under Earth's radiation belts
13 p1976 N85-22415
The keV electrons and 80 keV protons in the vicinity of the high latitude magnetosphere and at the bow shock
14 p2355 N85-24554
Morphology of 2keV-electrons observed by GEOS 1
14 p2360 N85-24581
Electron flux with electron energies above 40 MeV at altitudes of about 500 km in region where capture is possible and outside it when L is 3 or greater
15 p2481 N85-25315
Measurements of fluxes of high-energy protons and electrons by 2 oppositely oriented spectrometers aboard Cosmos-368 artificial Earth satellite
16 p2722 N85-26800
Fast electromagnetic (EM) shower simulation
[NOTA-INTERNA-831] 18 p3175 N85-29663
Low-energy gamma rays from Cygnus X-1
[OG-2.4-13] 22 p3868 N85-33957
Analysis of experimental data on interstellar antiprotons in the light of measurements of high-energy electrons and He-3 nuclei
[OG-6.1-6] 22 p3868 N85-34097
Spectral shape variation of interstellar electrons at high energies
[OG-6.2-7] 22 p3889 N85-34106
Collisional relaxation of electron tail distribution
[IPPJ-729] 23 p3974 N85-34835
On the retention of high-energy protons and nuclei with charges Z or equal to 2 in large solar flares after the process of their acceleration
[SH-2.1-8] 23 p3998 N85-34789
The influence of the Earth's magnetosphere on the high-energy solar protons
[SH-6.1-22] 23 p4048 N85-35093

HIGH ENERGY INTERACTIONS
NT STRONG INTERACTIONS (FIELD THEORY)
High energy-resolution inelastic X-ray scattering
[DE84-014565] 01 p0118 N85-10604
Research program in theoretical high-energy physics
[DE84-013717] 01 p0119 N85-10617
Response of propellants to high dynamic stresses: The uses of gun launch techniques
08 p1116 N85-17035
Dynamics and mechanisms of catalytic processes and hot chemistry
[DE85-002899] 09 p1292 N85-18114
High energy physics study
[DE84-015803] 09 p1383 N85-18700
Very high energy probes of the quark-gluon plasma
[DE84-016992] 09 p1392 N85-18783
Supersymmetric inflationary cosmology
[DE85-001332] 09 p1415 N85-18929
Experimental and theoretical high energy physics
[DE85-000844] 11 p1726 N85-20858
Activities in nuclear physics and high energy physics
11 p1726 N85-20866
Research and technology: Fiscal year 1984 report
[NASA-TM-85231] 12 p1964 N85-22340
Experimental studies of elementary particle interactions at high energies
[DE85-004795] 13 p2157 N85-23394
Los Alamos Science, Number 11, Summer-Fall, 1984
[DE85-004834] 14 p2419 N85-24926
Summaries of FY 1984 research in high energy physics
[DE85-005841] 14 p2420 N85-24934
Physics, Computer Science and Mathematics Div.
[DE85-006666] 15 p2642 N85-26298
Two-beam accelerator
[DE85-004662] 15 p2649 N85-26335
Mean free paths, viscosity, and the limitations of perfect fluid hydrodynamics in the description of the quark-gluon plasma
[DE85-005501] 15 p2649 N85-26339
Future accelerator studies of high energy heavy ion collisions
[DE85-005865] 15 p2650 N85-26346
Overview of the physics issues at the SSC
[DE85-007074] 16 p2659 N85-27634

USSR report: Engineering and equipment
[JPRS-UEQ-85-004] 17 p2939 N85-28142
Neutron scattering and reactions on 59Co from 1 to 20 MeV
[AERE-R-11439] 17 p3028 N85-28729
Heavy ion physics at BNL, the AGS and RHIC
[DE85-005951] 17 p3033 N85-28760
Particle physics: Recent successes and future prospects
[DE85-008175] 17 p3033 N85-28765
Activities report in nuclear physics and high energy physics
[JF40026] 17 p3035 N85-28777
Physics of (very) high energy e(+)-e(-) colliders
[DE85-008177] 17 p3036 N85-28780
Theoretical studies of high energy phenomenon: Analysis of models of CP and T violation
[DE85-007455] 17 p3036 N85-28782
Physics of High Energy Particle Accelerators. AIP Conference Proceedings no. 127
[DE85-006891] 18 p3182 N85-29733
Slow extraction of LAMPF 2
[DE85-010744] 19 p3356 N85-30805
Theory of high energy collision processes
[DE85-010183] 19 p3362 N85-30846
High-energy particle Monte Carlo at Los Alamos
[DE85-010716] 19 p3363 N85-30856
Work in Amsterdam on local intelligence --- artificial intelligence
[NIKHEF-H/84-9] 20 p3518 N85-31677
Requirements for very high energy accelerators
[DE85-011173] 20 p3529 N85-31952
Research in the theory of condensed matter and elementary particles
[DE85-010447] 20 p3531 N85-31968
High-energy Physics Institute building 3-trillion-ev accelerator 21 p3691 N85-32934
Gamma rays of 0.3 to 30 MeV from PSR 0531+21
[OG-2.3-8] 22 p3866 N85-33945
Search for gamma-rays above 400 GeV from Geminga
[OG-2.4-4] 22 p3867 N85-33951
Primary gamma-rays with E gamma or = to 10(15) eV: Evidence for ultrahigh energy particle acceleration in galactic sources
[OG-2.6-13] 22 p3871 N85-33974
Some evidence for high energy gamma-ray sources at large galactic latitudes
[OG-2.7-5] 22 p3871 N85-33976
High-energy multiple muons and heavy primary cosmic-rays
[OG-5.2-9] 22 p3883 N85-34065
Composition of primary cosmic rays near the knee
[OG-5.2-10] 22 p3884 N85-34066
Electron and muon parameters of EAS and the composition of primary cosmic rays in 10(15) to approximately 10(16) eV
[OG-5.2-12] 22 p3884 N85-34068
The primary cosmic ray mass composition at energies above 10(14) eV
[OG-5.4-6] 22 p3886 N85-34083
Summary of activities, 1983
[LBL-18500] 23 p3969 N85-34605
Calculation of improved spallation cross sections
[OG-7.2-23] 23 p4017 N85-34890
Cerenkov counters for high energy nuclei: Some new developments
[OG-9.1-5] 23 p4023 N85-34931
SONTRAC: A solar neutron track chamber detector
[SH-9.1-12] 23 p4052 N85-35127
A survey of multiplicities and rapidity densities from existing emission data on hadron-nucleus nucleus-nucleus collisions 24 p4146 N85-35706
A simulation of ultra-relativistic nucleus-nucleus collisions 24 p4146 N85-35707
Very high energy probes of the quark-gluon plasma 24 p4147 N85-35708
Detector requirements for intensity interferometry measurements 24 p4147 N85-35709
Forty-five years of e(+)e(-) annihilation physics: 1956 to 2001
[DE85-013052] 24 p4149 N85-35723
Neutrino production of like sign dimuons
[DE85-013594] 24 p4151 N85-35741
SLC Energy Upgrade Program at SLAC
[DE85-014290] 24 p4160 N85-35790
Development of observational and instrumental techniques in hard X-ray and medium energy gamma-ray astronomy
[NASA-CR-176172] 24 p4166 N85-35841
Nineteenth International Cosmic Ray Conference. HE Sessions, volume 6
[NASA-CP-2376-VOL-6] 24 p4170 N85-35848
Estimation of the total inelasticity coefficient in interaction of greater than or equal to 20 TeV hadrons with lead
[HE-1.1-9] 24 p4171 N85-35857
The method for the study of the inelastic cross-section for high energy protons by means of shower arrays with the large calorimetric area
[HE-1.1-11] 24 p4171 N85-35858
On a possibility of inelasticity partial coefficient K sub gamma determination in pi C and pi Pb interactions at 10 to the 14th power eV (experiment PAMIR 1)
[HE-1.1-12] 24 p4171 N85-35859
QCD-motivated description of very high energy particle interactions
[HE-1.2-2] 24 p4171 N85-35861
Empirical description of the hadron-hadron and hadron-nucleus interaction at the accelerator energy range
[HE-1.2-4] 24 p4171 N85-35862
Multiplicity distributions in interaction models used for cascade simulations
[HE-1.2-5] 24 p4172 N85-35863
Transverse momentum distribution of pion deg in the fragmentation region of super high energy interactions 24 p4180 N85-35921
Penetrative nature of high energy showers observed in Chacaltaya emulsion chamber
[HE-3.3-5] 24 p4180 N85-35923
Lateral distribution of high energy hadrons and gamma ray in air shower cores observed with emulsion chambers
[HE-3.3-8] 24 p4180 N85-35926
Size distributions of air showers accompanied with high energy gamma ray bundles observed at Mt. Chacaltaya
[HE-3.3-9] 24 p4181 N85-35927
An experimental study of correlations in the development of the electron-photon cascades
[HE-3.5-10] 24 p4184 N85-35947
A comparative analysis of gamma and hadron families at the superhigh energies recorded in experiment Pamir
[HE-3.7-1] 24 p4185 N85-35960
Nineteenth International Cosmic Ray Conference. HE Sessions, volume 7
[NASA-CP-2376-VOL-7] 24 p4186 N85-35968
Analysis of the hadron component in E.A.S. 24 p4187 N85-35971
Electrons, muons and hadrons in extensive air showers and how do they depend on nuclear interaction model, part 1 24 p4187 N85-35972
Simulation of EAS properties on the basis of high energy interaction model deduced from the accelerator data 24 p4187 N85-35973
High energy hadrons in extensive air showers 24 p4187 N85-35976
Dependence of the average spatial and energy characteristics of the hadron-lepton cascade on the strong interaction parameters at superhigh energies 24 p4188 N85-35977
Hadronic components of EAS by rigorous saddle point method in the energy range between 10(5) and 10(8) GeV 24 p4188 N85-35978
Phenomenology of soft hadron interactions and the relevant EAS data 24 p4188 N85-35980
Development of electromagnetic cascades in the atmosphere including the Landau-Pomeranchuk-Migdal effect
[HE-4.5-5] 24 p4195 N85-36029
Nuclear cascades in electromagnetic showers produced by primary gamma-quanta in the atmosphere
[HE-4.5-16] 24 p4196 N85-36038
Energy spectrum of cascade showers induced by cosmic ray muons in the range from 50 GeV to 5 TeV
[HE-5.2-14] 24 p4203 N85-36090
Range fluctuations of high energy muons passing through matter
[HE-5.2-19] 24 p4204 N85-36095
High energy neutrino astronomy with MACRO
[HE-5.3-12] 24 p4206 N85-36106
The capability of the existing network of installations for detecting the antineutrino burst from collapsing stars
[HE-5.3-13] 24 p4206 N85-36107
Energy spectra of high energy atmospheric neutrinos
[HE-5.3-14] 24 p4206 N85-36108
A standard source for high energy neutrino astronomy
[HE-5.3-15] 24 p4206 N85-36109
A search for cosmic sources of high energy neutrinos with small underground detectors
[HE-5.3-16] 24 p4206 N85-36110
Characteristics of slow particles emitted in the charged current interactions of neutrinos with emulsion nuclei
[HE-5.3-22] 24 p4207 N85-36113
Multiple muons of conventional and exotic origin in DUMAND
[HE-5.4-4] 24 p4207 N85-36117
Study of photonuclear muon interactions at Baksan underground scintillation telescope
[HE-5.4-10] 24 p4208 N85-36122
Calculation of intensity of high energy muon groups observed deep underground
[HE-5.4-13] 24 p4208 N85-36123
Results of investigation of muon fluxes of superhigh energy cosmic rays with X-ray emulsion chambers
[HE-5.4-16] 24 p4208 N85-36126
High energy cosmic ray signature of quark nuggets
[HE-6.2-11] 24 p4212 N85-36147

HIGH ENERGY PROPELLANTS
The DDT process for high energy propellants 08 p1116 N85-17038
Analysis of deflagration to detonation transition in high-energy solid propellants
[AD-A148302] 08 p1135 N85-17156
Analysis of Shock to Detonation Transition (SDT) of porous high energy propellant from ramp-wave compression loading
[AD-A149333] 10 p1457 N85-19180
Analysis of deflagration to detonation transition in high-energy solid propellants 16 p2757 N85-27010

HIGH FREQUENCIES
Resistance to HF jamming interference in mobile radio networks by an adaptive, distributed reconfiguration technique
[AD-A145117] 01 p0038 N85-10238
High frequency radar software reference manual for Product Two
[PB84-210079] 01 p0041 N85-10270
Nonlinear propagation in a depth-dependent ocean
[AD-A145079] 01 p0116 N85-10791
Robotization of technological processes in high-frequency heating and welding 03 p0345 N85-12226
Observations and prognosis of HF wave propagation via the sporadic E layer
[UIO-SR-84-04] 03 p0356 N85-12294
Special Developments and Methods in High Frequency Measuring Techniques --- conferences
[PTB-E-24] 05 p0629 N85-14030
Present status and development tendencies in the field of high frequency measuring techniques 05 p0629 N85-14031
Admittance measurement with twin-T devices in the frequency range between 1 and 300 MHz 05 p0629 N85-14032
A computer controlled measuring system for the calibration of HF components 05 p0630 N85-14037
Voltage dependence of the relative AC-DC transfer difference for HF voltage-transfer standards 05 p0630 N85-14038
A group delay standard for the MHz frequency range 05 p0630 N85-14040
Optical fibers with reduced pressure sensitivity to high frequency acoustic field
[AD-D011306] 07 p1043 N85-16627
Tactical HF communication for military helicopters using the NVIS mode 08 p1074 N85-16807
A commentray on the utilization of real-time channel evaluation systems in HF spectrum management
[AD-A148616] 08 p1154 N85-17269
Standing wave pattern of HF radio waves in the ionospheric reflection region. Part 1: General formulas
[UIO-SR-84-05-PT-1] 09 p1313 N85-18253
An HF communications frequency-management procedure for forecasting the frequency of optimum transmission
[AD-A149191] 10 p1467 N85-19254
Multipath and Doppler observations during transatlantic digital HF propagation experiments 10 p1471 N85-19281
An ionospheric mode detection system for HF communications application 10 p1471 N85-19282
An H.F. simulator for use with real time channel evaluation systems 10 p1473 N85-19293
Time and space domain filtering for improved HF communication 10 p1473 N85-19296
Overview of RADC adaptive antenna developments for communications 10 p1474 N85-19299
Serial data transmission with large output on the HF channel 10 p1475 N85-19305
Effect of interfacial characteristics of metal clad polymeric substrates on electrical high frequency interconnection performance
[NASA-TM-86948] 11 p1624 N85-20223
The Ferranti Tactical SHF SATCOM station (MANSAT) 11 p1710 N85-20759
An electronically-steerable active receiving array for h.f.
[BBC-RD-1985/2] 12 p1822 N85-21430
Surface forward scattering and reflection
[AD-A150115] 12 p1928 N85-22112
Stress compensation crystal device
[AD-D011497] 12 p1941 N85-22189
Computer aided antenna design and frequency selection for HF communications
[AD-A150485] 13 p2055 N85-22869
Coupled-cavity gyrotrons with mode conversion 13 p2076 N85-22967

Alternatives for satellite sound broadcast systems at HF and VHF 14 p2229 N85-23815
Physical electronics of cooled operation of very short compound semiconductor transistors 14 p2297 N85-24223
Observations of the MF-HF plasma wave emissions in active auroras by the sounding rocket experiments at Syowa station 14 p2366 N85-24820
High frequency estimation of 2-dimensional cavity scattering [AD-A151697] 15 p2542 N85-25696
Scattering center analysis for radar cross section modification 16 p2769 N85-27085
Predicting the effects of non-Gaussian interference in HF (High-Frequency) broadcasting. Part 1: A methodology for an analytic approach [PB85-171544] 18 p3092 N85-29140
US Coast Guard High Frequency Emergency Network (HFEN) implementation plan [PB85-174167] 18 p3092 N85-29141
Recovery of pyroshock data from distorted acceleration records [NASA-TP-2494] 20 p3407 N85-31141
Seismic discrimination [AD-A154167] 20 p3494 N85-31722
Field antenna handbook [AD-A155204] 21 p3576 N85-32242
High-frequency furnace [DE85-011210] 21 p3586 N85-32291
Multitrunk high-frequency multiplexing of antenna-waveguide channels 22 p3774 N85-33385
Transmitter spectrum analyzer 22 p3774 N85-33389
Optimality criterion for high-frequency channel in receivers of discrete radio signals 22 p3776 N85-33401
KT3127A, KT3128A transistors 22 p3779 N85-33414

HIGH GAIN
Case study of sample spacing in planar near-field measurement of high gain antennas [NASA-TM-86872] 01 p0037 N85-10234
The axial velocity spread acceptance of free electron lasers [AD-A149024] 10 p1489 N85-19403
Instabilities and chaotic behavior of active and passive laser systems [AD-A153366] 17 p2971 N85-28346
High gain adaptive control of decentralized systems [DE85-010040] 19 p3339 N85-30688

HIGH GRAVITY (ACCELERATION)
U HIGH GRAVITY ENVIRONMENTS

HIGH GRAVITY ENVIRONMENTS
Effects on in vivo and in vitro exposure to excess gravity on growth and differentiation of mammalian embryos 15 p2612 N85-26095
Physical training and G tolerance 20 p3511 N85-31824
Centrifuge operations and training in the Royal Netherlands Air Force 20 p3511 N85-31825
Effects of microgravity and hypergravity on invertebrate development 24 p4126 N85-35579

HIGH INTENSITY LASERS
U HIGH POWER LASERS

HIGH LATITUDES
U POLAR REGIONS

HIGH LEVEL LANGUAGES
NT ADA (PROGRAMMING LANGUAGE)
Floating-point function generation routines for 16-bit microcomputers [NASA-TM-83783] 01 p0102 N85-10883
THLL (TRIDENT Higher Level Language) reference manual [AD-A145116] 01 p0104 N85-10696
DATAPLOT: Introduction and overview [PB84-214055] 01 p0105 N85-10708
Tree Query Language Flat (TQLF) specifications [PB84-217116] 06 p0855 N85-15438
Relational Query Language Flat (RQLF) specifications [PB84-217405] 06 p0855 N85-15439
Network Query Language Flat (NQLF) specifications [PB84-217538] 06 p0855 N85-15440
Software test handbook [AD-A146844] 07 p1024 N85-16498
Representation and refinement of visual specifications in PegaSys [AD-A146733] 09 p1368 N85-18598
High level languages in protocol specification and verification [FUB-51-1983] 09 p1370 N85-18611
A Gypsy-to-Ada program compiler [TR-39] 12 p1913 N85-22005
Very-high level concurrent programming [AD-A150009] 12 p1915 N85-22026
Flowcharting with D-charts [NASA-CR-175841] 14 p2402 N85-24806
Design and analysis of a complete relational interface for a multi-backend database system [AD-A151501] 15 p2628 N85-26198
Harnessing computional power: Distributed combinator reduction [DE85-005967] 15 p2631 N85-26216
An abstract specification language for Markov reliability models [NASA-TM-86423] 16 p2857 N85-27616
Multicomputer operating systems and applications [AD-A153205] 17 p3016 N85-28648
MC TRICOMP user's guide [AD-A154339] 19 p3337 N85-30673
VAX TRICOMP user's guide [AD-A154341] 19 p3337 N85-30675
Implementation assessment of the OSI network service. The test definition language [NPL-DITC-52/84] 20 p3514 N85-31849
Study of the applicability of higher order languages for on-board satellite software production [ESA-CR(P)-2024] 20 p3516 N85-31864
HLLM software support [AD-A154828] 21 p3671 N85-32805
The formal specification of an abstract machine: Design and implementation [AD-A155167] 21 p3672 N85-32808
Evaluation of a software design approach: Develop a threat resolution module in Ada (trademark) [AD-A155599] 21 p3672 N85-32815

HIGH MELTING COMPOUNDS
U REFRACTORY MATERIALS

HIGH PASS FILTERS
Frequency-spreading coupler [AD-D011683] 19 p3258 N85-30200

HIGH POWER LASERS
NT NOVA LASER SYSTEM
Summary discussion: Theoretical aspects of XUV free electron lasers [AD-A145475] 02 p0292 N85-11343
High energy laser mirror [AD-D011255] 06 p0812 N85-15158
High power metal vapor laser [AD-D011271] 06 p0813 N85-15159
The development of a high average power glass laser source [AD-A147471] 07 p0971 N85-16169
High-power radiating plasma [NASA-TM-77784] 07 p1045 N85-16637
Status of specific FRG high tech research funded by BMFT 11 p1618 N85-20181
Potential of high-average-power solid state lasers [DE85-003884] 11 p1639 N85-20329
Research, development of laser glasses in China 13 p2166 N85-23439
Observation of pure resonance and threshold effects in electron impact experiments in high intensity laser fields [AD-A150725] 14 p2309 N85-24293
Ground-up-to-Space (GUTS) laser propagation code description and manual [AD-A150783] 14 p2309 N85-24295
High energy lasers: A primer on directed energy weapons for space use [AD-A151279] 15 p2562 N85-25807
Discharge characteristics of high-pressure, fast-discharge XeCl excimer laser 15 p2564 N85-25820
Predischarge parameters of SF6-CO2 determined by laser 15 p2564 N85-25821
West Europe report: Science and technology [JPRS-WST-84-032] 18 p3086 N85-29095
Results of Italian research in high power lasers 18 p3086 N85-29097
Magnetically switched power supply systems for lasers [NASA-CASE-NPO-16402-1] 18 p3112 N85-29265
Intense excitation source for high power laser [AD-A153424] 18 p3112 N85-29267
A simple power meter for high energy pulsed lasers [AD-D011661] 18 p3113 N85-29271
1.5 micrometer GaInAsP high pulsed power diode lasers [AD-A153568] 18 p3193 N85-29805
Development and application of a high power ND-glass laser instrument [AD-A154366] 19 p3276 N85-30314
Research with high-power short-wavelength lasers [DE85-010329] 19 p3276 N85-30332
High-power two-frequency CW dye laser 21 p3686 N85-32900

HIGH PRESSURE
Energy efficient engine high pressure turbine ceramic shroud support technology report [NASA-CR-168036] 02 p0147 N85-10996
Energy efficient engine. High pressure compressor detail design report [NASA-CR-165558] 02 p0147 N85-10998
High pressure cosmochemistry applied to major planetary interiors: Experimental studies [NASA-CR-174032] 02 p0302 N85-11958
Mechanochemical reactions of polymethyl methacrylate and polystyrene at high pressure [DRIC-T-7307] 03 p0337 N85-12165
Qualification of noninvasive systems for on-line leak detection in high pressure feed water preheaters [CISE-2341] 04 p0658 N85-13555
Design and off-design performance prediction of high pressure ratio centrifugal compressors 05 p0836 N85-14062
High pressure combustion test facility for gas turbine research [NAL-TR-801] 06 p0757 N85-14845
Understanding the high pressure properties of molecular solids and molecular surfaces deposited on hetrogeneous substrates [NASA-CR-174262] 07 p1047 N85-16649
High pressure physics research focusing on composite materials 08 p1140 N85-17185
Thermodynamic properties of aqueous NaCl from 273 to 823 K with estimates for higher temperatures [DE85-000392] 09 p1292 N85-18118
Experimental high pressure equation of state of a very fast burning gun propellant [DE85-001749] 10 p1458 N85-19184
Electron production, electron attachment, and charge recombination process in high pressure gas discharges [AD-A149535] 10 p1554 N85-19799
Leak monitoring in high pressure preheaters by a noninvasive ultrasonic method [CISE-2373] 11 p1650 N85-20394
Leak detection by acoustic emission monitoring in power plant high pressure preheaters [CISE-2392] 11 p1650 N85-20395
Liquid fuel spray processes in high-pressure gas flow [NASA-TM-86944] 12 p1844 N85-21570
A 50-kW electric-discharge CO2 laser [AD-A149779] 12 p1857 N85-21644
High pressure turbine rotor two-piece blade retainer [AD-D011498] 12 p1858 N85-21653
Sound velocity of carbon at high pressures [DE85-002016] 12 p1926 N85-22113
High-pressure rocket engine turnaround duct computational fluid dynamics analysis 13 p2003 N85-22556
Possibility of producing monolithic composite materials based on niobium carbide 13 p2028 N85-22707
Some unique features of isentrophic flow of gas under high pressures 13 p2043 N85-22788
High pressure cosmochemistry of major planetary interiors: Laboratory studies of the water-rich region of the system ammonia-water 13 p2163 N85-23549
Theoretical thermodynamics of mixtures at high pressures 13 p2163 N85-23550
Applications of high pressure differential scanning calorimetry to aviation fuel thermal stability research [NASA-TM-87002] 14 p2249 N85-23941
Stability of turbine runners in sliding bearings under external circulation forces 14 p2272 N85-24074
Hypergolic combustion demonstration in a reciprocating internal combustion engine [AD-A150846] 14 p2311 N85-24303
Principal patterns of functional changes of human respiratory system in adaptation to high pressure 14 p2387 N85-24704
Hydrogen resistance of VT1-0 titanium under 150 MPa pressure at room temperature 15 p2490 N85-25414
Calorimeter for measuring high-energy optical pulses [PB85-160695] 15 p2561 N85-25799
Discharge characteristics of high-pressure, fast-discharge XeCl excimer laser 15 p2564 N85-25820
Development of theory of high-current high-pressure pulsed arc 15 p2945 N85-28314
High pressure cosmochemistry applied to major planetary interiors: Experimental studies [NASA-CR-175715] 15 p2979 N85-29544
Material technology 16 p2734 N85-26870
Ignition of metals in high pressure oxygen 16 p2735 N85-26874
High-pressure hydrogen testing of single crystal superalloys for advanced rocket engine turbopump turbine blades 16 p2735 N85-26875
Graphite fiber intercalation: Dynamics of the bromine intercalation process [NASA-TM-87015] 16 p2742 N85-26921
Fog advection in the Namib 16 p2831 N85-27454
Combustion and micro-explosion of water/oil emulsions in high pressure environments [AD-A152960] 17 p2919 N85-27997
Steel Tubes [BLL-BISI-TRANS-22064-(9022.08)] 17 p2973 N85-28369

Principal quality assurance measures in the manufacture of HF-welded high-pressure linepipe
[BLL-BISI-TRANS-21690-(9022.06)] 17 p2976 N85-28389
Energy efficient engine high-pressure turbine component rig performance test report
[NASA-CR-168189] 19 p3218 N85-29955
Burn rates of explosives at high pressures
[DE85-010806] 19 p3251 N85-30159
Thermodynamic study of CO2-organic compound interaction at high pressures and temperatures
[DE85-010999] 19 p3268 N85-30268
Evaluation of a high pressure proportional counter for the detection of radioactive noble gases
[AD-A154436] 19 p3272 N85-30292
Damping seal for turbomachinery
[NASA-CASE-MFS-25842-2] 19 p3280 N85-30341
The use of superoxide mixtures as air-revitalization chemicals in hyperbaric, self-contained, closed-circuit breathing apparatus
[NASA-TM-86709] 20 p3512 N85-31831
High pressure working mode of hollow cathode arc discharges
[NASA-TM-77880] 20 p3535 N85-31992
Identification of vibrational-rotational transitions of Os-192O4 within frequency tuning limits of high pressure CO2 waveguide laser 21 p3669 N85-32917
Static high pressure study of nitric oxide chemistry: Proposed mechanism for nitric oxide detonation
[DE85-010795] 22 p3746 N85-33220
High pressure compressor component performance report
[NASA-CR-168245] 23 p3897 N85-34136
Hollow cathodes in high pressure arc discharges
[NASA-TM-87069] 23 p3903 N85-34179
Determination of individual tolerance in hyperbaric oxygen 23 p3954 N85-34507
Experimental technique for measuring the isentrope of hydrogen to several megabars
[DE85-014332] 24 p4095 N85-35386

HIGH Q
U Q FACTORS

HIGH RESISTANCE
Properties of nitrogen containing stainless alloy designed for high resistance to pitting
[DE85-008282] 17 p2931 N85-28095

HIGH RESOLUTION
The development of a diode laser Doppler velocimeter for boundary layer measurements under ice: A feasibility investigation
[AD-A145076] 01 p0053 N85-10348
Vibration data analysis system for SNLA area 3 reference manual
[DE84-016207] 04 p0514 N85-13275
GLAS fourth order model 05 p0679 N85-14361
Psychophysical research in development of a fiber-optic helmet mounted display 05 p0701 N85-14501
High resolution photoacoustic and photothermal imaging 05 p0723 N85-14649
A geometric approach to high resolution TVD schemes
[NASA-CR-172484] 06 p0957 N85-15449
Topics in high resolution spectroscopy of stored ions
[DE85-002069] 06 p0661 N85-15470
Future studies of the local interstellar medium with Space Telescope and Columbus 06 p0860 N85-15593
A nonlinear technique for high-resolution data processing
[AD-D011415] 08 p1203 N85-17570
Improved real-time ultra-high resolution image projection display using laser-addressed liquid crystal light valve
[AD-D011414] 08 p1223 N85-17705
Acoustic microscopy at cryogenic temperatures
[AD-A146755] 09 p1364 N85-18704
Improved performance for large area triple layer microchannel plate detector for a neutral spectrometer in Doublet III
[DE85-001719] 10 p1488 N85-19395
A progress report on the analysis of long exposure SWP high resolution spectra of cool stars 11 p1758 N85-21057
Statistical classification of IUE low-dispersion stellar spectra: Progress report 11 p1760 N85-21075
Research in image understanding as applied to 3-D tomographic imaging with near optical resolution
[AD-A150096] 12 p1829 N85-21483
New high resolution scanning ion microprobe and focused ion beam applications
[AD-A149902] 12 p1852 N85-21616
High time resolution thermospheric temperature and wind studies in the Arctic
[AD-A150114] 12 p1890 N85-21960
HREELS and Auger studies of conducting polymers
[DE85-004541] 13 p2038 N85-22764
Hot spots on Io: Correlation of infrared emission and visible reflectance 13 p2172 N85-23475
Surfaces of asteroids and cometary nuclei 13 p2176 N85-23503
Venus surface composition from radio/radar measurements 13 p2177 N85-23509
Automated extraction of absorption bands from reflectance special 13 p2197 N85-23624
Viking Lander mosaics of Mars 13 p2203 N85-23667
High time-resolution studies of the auroral ionosphere
[AD-A150945] 14 p2409 N85-24850
Investigations of high resolution imaging through the Earth's atmosphere using speckle interferometry
[AD-A150680] 14 p2439 N85-25053
High resolution hard X-ray spectra of solar and cosmic sources 14 p2455 N85-25163
Asteroid amphitrite: Surface composition and prospects for the possible Galileo flyby 15 p2680 N85-26549
Scheme for atmospheric thermal sensing from satellites with enhanced vertical resolution 16 p2726 N85-26823
High resolution powder diffraction
[DE85-008287] 17 p2922 N85-28015
The HURRA high resolution experimental radar system sampling unit
[FOA-C-30376-E1] 18 p3091 N85-29133
The determination of dinitrotoluene in single base propellants
[AD-A154672] 21 p3571 N85-32209
Antenna induced range smearing in MST radars 21 p3620 N85-32495
High resolution evidence for the Garrett-Munk spectrum of stratospheric gravity waves 21 p3622 N85-32503
The design, development, testing, fabrication, calibration and integration of a High Resolution Imager (HRI) for the Roentgen Satellite (ROSAT)
[NASA-CR-175302] 22 p3741 N85-33184
Ionization detection of stimulated Raman spectra
[DE85-010672] 22 p3746 N85-33218
Electron beam enhanced surface modification for making highly resolved structures
[DE85-011609] 22 p3760 N85-33305
Determination of band oscillator strengths of atmospheric molecules from high resolution vacuum ultraviolet cross section measurements
[NASA-CR-176150] 22 p3814 N85-33624
Heterodyne holographic interferometry for visualization of surface acoustic waves
[AD-A155405] 22 p3836 N85-33753
High-resolution spectrum of Cygnus X-1
[OG-2.4-12] 22 p3868 N85-33956
High resolution electron microscopic characterization of interfaces in ceramics
[DE85-011207] 23 p3920 N85-34289
Acceleration of ions and electrons to near-cosmic ray energies in a perpendicular shock: The January 6, 1978 event
[SH-1.5-4] 23 p3996 N85-34773
Advanced techniques for high resolution spectroscopic observations of cosmic gamma-ray sources
[OG-9.2-9] 23 p4025 N85-34948
High-resolution spectroscopy and dynamics of multiphoton processes in atoms and molecules
[AD-A155662] 24 p4147 N85-35714
High resolution beam profile monitors in the SLC
[DE85-013375] 24 p4157 N85-35774

HIGH RESOLUTION COVERAGE ANTENNAS
Information for space radar designers: Required dynamic range vs resolution and antenna calibration using the Amazon rain forest 08 p1147 N85-17239

HIGH REYNOLDS NUMBER
Study of the structure of turbulent shear flows at supersonic speeds and high Reynolds number
[NASA-CR-174144] 04 p0452 N85-12865
Aeroacoustic data for high Reynolds number supersonic axisymmetric jets
[NASA-TM-86296] 07 p1038 N85-16587
A survey of the turbulent drag reduction using passive devices
[NMI-R-193] 11 p1630 N85-20268
Transition fixing and simulation of high Reynolds number flow at transonic velocities 14 p2212 N85-23721
Investigation of the aerodynamic forces on bluff bodies at high Reynolds numbers
[DFVLR-MITT-84-19] 14 p2213 N85-23727
Mach-10 high Reynolds number development in the NSWC (Naval Surface Weapons Center) hypervelocity facility
[AD-A151241] 15 p2474 N85-25274
Simultaneous measurement of velocity and density in a turbulent nonpremixed flame 22 p3744 N85-33209

HIGH SPEED
Noise isolation system for high-speed circuits
[DE84-014229] 01 p0043 N85-10283
Results of winglet development studies for DC-10 derivatives
[NASA-CR-3677] 02 p0138 N85-10936
Gyrotron beam generation with helical magnetic fields
[AD-A145987] 03 p0417 N85-12570
Effect of two inner-ring oil-flow distribution schemes on the operating characteristics of a 35 millimeter bore ball bearing to 2.5 million DN
[NASA-TP-2404] 04 p0507 N85-13233
High-speed power thyristors with excellent switching and load characteristics 06 p0793 N85-15070
Visual perceptual aspects of low level high speed flight and flight simulation
[AD-P004310] 09 p1267 N85-17964
Low altitude high speed flight simulation using video disc technology
[AD-P004312] 09 p1268 N85-17966
Study on controllability and stability of high speed tracked vehicles
[AD-P004302] 09 p1409 N85-18879
High-speed intercity rail passenger service
[GPO-35-896] 10 p1570 N85-19897
Diesel fuel alternatives for engines in civil works prime movers
[AD-A149738] 12 p1817 N85-21400
Lubrication and performance of high-speed rolling-element bearings
[NASA-TM-86958] 12 p1959 N85-21658
Development of a multiplane multispeed balancing system for turbine systems
[NASA-CR-174750] 13 p1976 N85-22400
Specifics of laser heat treatment of high steel tools 13 p2029 N85-22714
Transition fixing in the high speed range for the development of civil aircraft wings 14 p2211 N85-23716
Advanced gearbox technology in small turbo propeller engines 14 p2221 N85-23771
Gear-cutting tools made of ultra high speed steel coated with TiN
[BLL-RISLEY-TR-5109-(9091.9F)] 15 p2567 N85-25837
Wind tunnel results of advanced high speed propellers in the takeoff, climb and landing operating regimes
[NASA-TM-87054] 19 p3213 N85-29925

HIGH SPEED CAMERAS
NT FRAMING CAMERAS
High-speed, eight-frame electro-optic camera with multipulsed ruby laser illuminator
[DE85-001748] 09 p1323 N85-18314
Positioning errors of commutating lenses and their influence on characteristics of high speed movie cameras 14 p2273 N85-24085

HIGH SPEED FLIGHT
U HIGH SPEED

HIGH SPEED PHOTOGRAPHY
Measurement of shock and induced reaction in rocket propellants by nanosecond infrared radiometry and photography
[DE84-013209] 04 p0482 N85-13070
Development of a dynamic radiographic capability using high-speed video
[DE84-016477] 04 p0511 N85-13256
Method and apparatus for high speed, sustained recording of infrared laser beam patterns
[AD-D011585] 15 p2583 N85-25811
Solids mixing in a three phase fluidized bed containing spherically shaped-porous solid particles
[PB85-187981] 22 p3785 N85-33453

HIGH STRENGTH
Microstructural basis of strength and toughness in hardmetals 02 p0177 N85-11185
Description of a laboratory model Annular Momentum Control Device (AMCD) 05 p0806 N85-13663
Improvement of gas-tightness of OTTG and TBO-5 threaded pipe couplings
[BLL-M-35993-(5628.4)] 07 p0972 N85-16175
Research, development of composite materials described 15 p2497 N85-25404
High resistance and raised modulus carbon fibers
[NASA-TM-76884] 15 p2502 N85-25436
Chain dynamics and structure property relation in high impact strength polycarbonate plastic
[AD-A152011] 15 p2519 N85-25531
Development of a high strength isothermally heat-treated nodular iron road wheel arm
[AD-A155755] 24 p4099 N85-35406

HIGH STRENGTH ALLOYS
NT HIGH STRENGTH STEELS
NT MARAGING STEELS
Methods for producing platinum-group metal coatings from molten alkali cyanides
[PB84-225994] 01 p0029 N85-10161
Design of strong, ductile, duplex low alloy steels 02 p0177 N85-11189
A study of environmental characterization of conventional and advanced aluminum alloys for selection and design. Phase 1: Literature review
[NASA-CR-172397-PHASE-1] 02 p0181 N85-11218

Hot isostatically pressed manufacture of high strength MERL 76 disk and seal shapes
[NASA-CR-165550] 02 p0183 N85-11225
Improved reinforcement metal
03 p0353 N85-12271
Study of high performance alloy electroforming
[NASA-CR-174276] 07 p0927 N85-15875
Distribution of hydrogen in multi-layer welded joints of alloyed steels 11 p1603 N85-20079
The role of hydrogen in the stress corrosion failure of high strength Al-Zn-Mg alloys
[AD-A150691] 14 p2256 N85-23978
Sweden develops new rapid solidification process
15 p2531 N85-25610
High-pressure hydrogen testing of single crystal superalloys for advanced rocket engine turbopump turbine blades 16 p2735 N85-26875
Corrosion test on high-alloy steels
[BLL-BISI-TRANS-21627-(9022.06)]
17 p2926 N85-28046
The influence of temperature on static and dynamic SCC crack growth behavior in aluminum alloy
23 p3905 N85-34190

HIGH STRENGTH STEELS
NT MARAGING STEELS
Delayed fracture of high-strength steels in spherical tanks for LP gas
[BLL-RISLEY-TR-4926-(9091.9F)]
01 p0026 N85-10162
Research on high-strength steels with an improved resistance against weld cracking
[AD-A144830] 01 p0027 N85-10170
Inhibition of hydrogen absorption during plating of high strength steels
[AD-A144882] 01 p0028 N85-10174
Effect of microstructure and trapping on the hydrogen embrittlement susceptibility of a titanium bearing HSLA steel 02 p0174 N85-11166
International Conference on Recent Developments in Specialty Steels and Hard Materials. Conference abstracts
[CSIR-S-256] 02 p0176 N85-11177
Microstructural design and control of sintered hard materials 02 p0176 N85-11180
Toughness in high speed steels and hard metals
02 p0176 N85-11181
Copper-boron low alloy high strength steels
02 p0176 N85-11183
Stress-driven solute enrichment of crack-tips during low ductility intergranular fracture of low-alloy steel
[AERE-R-11120] 03 p0333 N85-12150
Optimization of toughness properties of HSCA shielded metal arc welding electrodes
[BMFT-FB-T-84-186] 05 p0646 N85-14148
Hydrogen induced cracking in pipeline steels
[ERS-E.327] 09 p1340 N85-18429
Mechanism of hydrogen induced cracking in pipeline steels
[ERS-E.349] 09 p1340 N85-18430
Fatigue resistance of welded joints of high strength steels produced by electron beam welding
10 p1449 N85-19127
Assessment of the need for an advanced high-strength chromium-molybdenum steel for construction of third-generation gasifier pressure vessels
[DE85-002865] 11 p1606 N85-20097
High strength steel sheet with dual phase structure
[BMFT-FB-T-84-219] 12 p1808 N85-21342
An investigation of elevated temperature fatigue crack initiation in 2 and 1/4 cR-1 MO low alloy steel
[AD-A150670] 14 p2255 N85-23973
A study of fatigue crack growth in 2 1/4 Cr1Mo steel. Part 1: The influences of environment and material condition
[AERE-R-11472] 14 p2258 N85-23993
Development of high strength ship hull steel for high heat input welding — controlled rolling and accelerated cooling 15 p2565 N85-25827
High-strength weldable steel 03G4N2MAF Sh with improved ductility
[BLL-BISI-TRANS-22233-(9022.06)]
17 p2924 N85-28031
Corrosion test on high-alloy steels
[BLL-BISI-TRANS-21627-(9022.06)]
17 p2926 N85-28046
Effect of texture in steel on the susceptibility of hydrogen embrittlement
[BLL-BISI-TRANS-22026-(9022.06)]
17 p2926 N85-28048
Influence of preliminary cold deformation on fineness of pearlite
[BLL-BISI-TRANS-22409-(9022.06)]
17 p2927 N85-28054
Hydrogen embrittlement of high-strength steel
[B8580075] 17 p2933 N85-28103
Fatigue crack propagation characteristics and fatigue fracture toughness in 780 MPa grade high strength steel weldments at low temperature
[BLL-BISI-TRANS-22369-(9022.06)]
17 p2979 N85-28411
Tendency of selected low-carbon steels to corrosion cracking in nitrates
[BLL-BISI-TRANS-22262-(9022.06)]
18 p3073 N85-29006
Fatigue behavior of HY-130 steel weldments containing fabrication discontinuities
[AD-A153630] 18 p3122 N85-29326
Metallurgical origins of fracture toughness and microstructure and fracture toughness of an HSLA (High-Strength/Low-Alloy) steel
[AD-A155530] 21 p3567 N85-32187
Mechanical properties of Shielded Metal Arc (SMA) and Submerged Arc (SA) welded joints in a steel Raex 366 P Arctic
[VTT-339] 22 p3801 N85-33551

HIGH TEMPERATURE
Stability of bromine intercalated graphite fibers
[NASA-TM-86859] 01 p0031 N85-10187
Equivalent damage: A critical assessment
02 p0140 N85-10952
Benchmark notch test for life prediction
02 p0140 N85-10953
Pre-HOST high temperature crack propagation
02 p0141 N85-10956
Development of powder metallurgy 2XXX series Al alloys for high temperature aircraft structural applications
[NASA-CR-172408] 02 p0182 N85-11220
Mechanism of brittle heat fracture of inhomogeneous solids by high temperature gas jets
02 p0265 N85-11731
High temperature deformation of hot-pressed polycrystalline orthoenstatite
[NASA-CR-174026] 02 p0285 N85-11861
The rheology of icy satellites
[NASA-CR-174024] 02 p0302 N85-11959
Effects of tin on microstructure and mechanical behavior of Inconel 718
[NASA-TM-86866] 03 p0330 N85-12129
NBS (National Bureau of Standards): Materials measurements
[NASA-CR-174038] 03 p0332 N85-12143
Structural stability of nickel heat resistant alloys at high temperatures 03 p0350 N85-12251
High-temperature optically activated GaAs power switching for aircraft digital electronic control
[NASA-CR-174711] 04 p0457 N85-12901
Solid electrolytes for medium temperature steam electrolysis
[DE84-014384] 04 p0463 N85-12938
Surface diffusion of high temperature vapors in porous alumina
[DE84-015968] 04 p0479 N85-13053
Materials for high-temperature fuel cells
[DE84-016316] 04 p0479 N85-13054
High temperature mechanical properties of ceramics
[DE84-016492] 04 p0480 N85-13058
Diffusion of gases in porous solids: Simulation and measurements
[DE84-016292] 04 p0500 N85-13191
Study of the reactive-element effect in oxidation of Fe-Cr alloys using transverse section analytical electron microscopy
[DE84-016237] 04 p0571 N85-13841
High temperature thermoelectric energy conversion
05 p0610 N85-13894
Tensile properties and swelling of 20%-cold-worked Type 316 stainless steel irradiated in HFIR
[DE84-014080] 05 p0617 N85-13948
Effects of irradiation fluence and creep on fracture toughness of 347/348 stainless steel
[DE84-016091] 05 p0618 N85-13953
High temperature corrosion of ceramics
[DE84-017084] 05 p0620 N85-13967
Hydrogen production employing high-temperature solid oxide cells
[DE84-014559] 06 p0766 N85-14901
Development and characterization of ductile Long-Range-Ordered (LRO) alloys (Fe,Co, Ni)3V for high-temperature structural use
[DE84-016750] 06 p0769 N85-14921
Metallographic evaluation of the reactions between boronated graphite and Fe-Ni-Cr alloys
[DE84-015374] 06 p0769 N85-14922
Effects of silver and group 2 fluorides addition to plasma sprayed chromium carbide high temperature solid lubricant for foil gas bearing to 650 deg C
[NASA-TM-86895] 06 p0770 N85-14928
Evaluation of the ion implantation process for production of solar cells from silicon sheet materials
06 p0831 N85-15281
The soft X-ray diffuse background: Implications for the nature of the local interstellar medium
06 p0876 N85-15566
Life prediction at high temperature under multiaxial loading 07 p0907 N85-15745
Experiences with the material bevaviour and high temperature low cycle fatigue life prediction of the IN 738 blading alloy 07 p0908 N85-15746
Mechanical aspects of high temperature coatings
07 p0908 N85-15749
Design of ordered intermetallic alloys for high-temperature structural use
[DE85-000897] 07 p0928 N85-15885
Dispersed metal-toughened ceramics and ceramic brazing
[NASA-CR-174284] 07 p0933 N85-15916
Transformation toughened ceramics for the heavy duty diesel engine technology program
[NASA-CR-174689] 07 p1055 N85-16698
Thermodynamic properties of aqueous NaCl from 273 to 823 K with estimates for higher temperatures
[DE85-000392] 09 p1292 N85-18116
Hydrolysis of Iodine: Equilibria at high temperatures
[DE84-016713] 09 p1293 N85-18119
Notes on compressible flow equations for thermodynamics of hot jets
[BAE-KRS-N-GEN-273] 09 p1316 N85-18289
High temperature properties of equiatomic FeAl with ternary additions
[NASA-TM-86936] 10 p1439 N85-19072
Problems in high temperature thermocouple thermometry
[DE85-000808] 10 p1488 N85-19397
Sputter-induced compositional modifications in a Ni-Au alloy
[DE85-002771] 12 p1807 N85-21333
Chemical approach for controlling nadimide cure temperature and rate
[NASA-CASE-LEW-13770-5] 12 p1810 N85-21352
High-temperature-stable detonators
[DE85-005188] 12 p1818 N85-21402
A millimeter wave apparatus for free-space measurement of dielectric constants at high temperature
[AD-P004361] 12 p1826 N85-21455
3-D inelastic analysis methods for hot section components (base program) — turbine blades, turbine vanes, and combustor liners
[NASA-CR-174700] 12 p1863 N85-21686
Fast times at high temperatures
[DE85-003306] 12 p1943 N85-22205
High temperature antifriction properties of Ti sub 1-sub xNb sub x C sub 0.5N sub 0.5 alloys
13 p2029 N85-22715
Degassification of silicon nitride powders of various origins 13 p2030 N85-22718
Research directed advanced high temperature cooling system beyond current state-of-the art systems
[AD-A150896] 14 p2255 N85-23974
Stability of turbine runners in sliding bearings under external circulation forces 14 p2272 N85-24074
Biophysical evaluation of the wet globe temperature index (Botsball) at high air movements and constant dew point temperature
[AD-A151065] 14 p2378 N85-24883
Structural changes with one- and two-stage aging of alloys Ti-Al-Mo-Fe and Ti-Zr-V-Al-Sn
15 p2499 N85-25415
Swelling behavior of manganese-bearing AISI 216 steel
[DE85-005712] 15 p2512 N85-25486
A calorimetric approach for measuring emittance and normal spectral absorptance at elevated temperatures
[AD-A151292] 15 p2551 N85-26351
Studies on the processing methods for extraterrestrial materials
[NASA-CR-175778] 16 p2718 N85-26768
Multiaxial and thermomechanical fatigue considerations in damage tolerant design
[NASA-TM-87022] 16 p2749 N85-26964
Low dose irradiation creep of pure nickel
[DE85-006320] 16 p2751 N85-26975
Method of investigating accumulations of damage to weld joints in the case of low-cycle creep
[BLL-CE-TRANS-8088-(9022.09)]
16 p2792 N85-27219
Strength and failure analysis of composite laminates with holes at room and elevated temperatures
[AD-A153263] 17 p2917 N85-27981
Improving the properties of copper and copper alloys through heat treatment and alloying
[BLL-BISI-TRANS-21939-(9022.06)]
17 p2926 N85-28047
Powder-metallurgy alloys and steels
[BLL-BISI-TRANS-22239-(9022.06)]
17 p2926 N85-28050

The characteristic structure of weld metal of high temperature alloy X20CrMoV 121
[BLL-BISI-TRANS-21623-(9022.06)] 17 p2928 N85-28069
Influence of eutectic silicate inclusions on micro-processes during deformation and fracture of 12GS steel
[BLL-BISI-TRANS-22296-(9022.06)] 17 p2929 N85-28073
Overload effects on sustained load crack growth at elevated temperature
[AD-A153223] 17 p2931 N85-28091
Electrodes for flash discharge lamps
[DE85-008697] 17 p2955 N85-28250
Evaluation of interpolative modeling concepts for fatigue crack growth at elevated temperature
[AD-A153222] 17 p2960 N85-28422
Average collisional vibrational energy transfer quantities and the inversion temperature
[AD-A152674] 17 p3029 N85-28733
Elevated temperature erosion corrosion of 9Cr1Mo steel
[DE85-008445] 18 p3074 N85-29016
Surface degradation of ductile metal in elevated temperature gas-particle streams
[DE85-008428] 18 p3074 N85-29017
Elevated temperature erosion of steels
[DE85-008503] 18 p3075 N85-29018
Synthesis chemistry of ceramics by solid-state combustion processes in micro-gravity
[DE85-009595] 18 p3081 N85-29061
Research test facility for evaporation and combustion of alternative jet fuels at high air temperatures
[AD-A153830] 18 p3083 N85-29073
Development of a high-temperature coolant for advanced diesel engines
[AD-A153660] 18 p3117 N85-29297
Behavior of reinforced concrete at elevated temperatures
[DE85-009032] 18 p3123 N85-29332
Structural characteristics of high temperature composites
[NASA-CR-175906] 19 p3232 N85-30037
Catalytic hydrotreatment studies with model compounds
[DE85-010187] 19 p3236 N85-30064
An investigation of the irradiation swelling mechanisms in refractory metals at high temperatures
[AD-A154149] 19 p3238 N85-30079
CP DDT detonators. 4: Thermal aging
[DE85-011172] 19 p3251 N85-30160
Thermodynamic study of CO2-organic compound interaction at high pressures and temperatures
[DE85-010990] 19 p3268 N85-30266
Creep fatigue life prediction for engine hot section materials (isotropic)
[NASA-CR-168228] 20 p3304 N85-31057
STPI/LARC: A 200 deg C polyimide adhesive
[NASA-TM-86447] 20 p3433 N85-31297
Investigation of fatigue strength of spring steel after high-temperature thermomechanical working (HTMW) by helical drawing
[BLL-M-36274-(5828.4)] 20 p3465 N85-31525
Constitutive modeling of superalloy single crystals and directionally solidified materials 20 p3466 N85-31535
On numerical integration and computer implementation of viscoplastic models 20 p3467 N85-31542
A comparison of smooth specimen and analytical simulation techniques for notched members at elevated temperatures 20 p3468 N85-31546
Analytical simulation of weld effects in creep range 20 p3468 N85-31550
Current understanding of point defects and diffusion processes in silicon 20 p3481 N85-31632
Recession of graphitic nozzles in rocket motors 21 p3560 N85-32144
Shock tube measurements of growth constants in the branched-chain ethane-carbon monoxide-oxygen system
[NASA-TM-87068] 21 p3562 N85-32156
The effect of stress and hot corrosion on nickel-base superalloys
[AD-A154722] 21 p3566 N85-32161
High temperature electronics technology: Life test report
[AD-A154681] 21 p3580 N85-32257
Results of an interlaboratory fatigue test program conducted on alloy 800H at room and elevated temperatures
[NASA-CR-174940] 21 p3597 N85-32340
Fatigue behavior of chromium-containing ferritic steels at elevated temperature
[DE85-012309] 22 p3748 N85-33231
Multistage spent particle collector and a method for making same
[NASA-CASE-LEW-13914-1] 22 p3791 N85-33489
Reaction of uranium and the fluorocarbon FC-75
[DE85-012322] 22 p3843 N85-33802
X-ray measurement of thermal stresses in tungsten fiber-copper composites 23 p3907 N85-34205
Dynamics of the melting of chromium-manganese alloys in molten steel
[BLL-M-36850-(5828.4)] 23 p3914 N85-34252
High temperature structural insulating material
[DE85-006361] 23 p3920 N85-34291
Depletion modeling of liquid dominated geothermal reservoirs
[DE85-009923] 23 p3943 N85-34437
Effects of temperature on the tensile strength and elastic modulus of composite material
[AD-A156112] 24 p4075 N85-35251

HIGH TEMPERATURE ALLOYS
U HEAT RESISTANT ALLOYS

HIGH TEMPERATURE ENVIRONMENTS
Component-specific modeling 02 p0143 N85-10971
The 3-D inelastic analysis methods for hot section components: Brief description 02 p0143 N85-10972
Life prediction and constitutive behavior: Overview 02 p0143 N85-10973
HOST high temperature crack propagation 02 p0144 N85-10977
Surface protection overview 02 p0144 N85-10978
Airfoil deposition model 02 p0144 N85-10979
A coaxial probe for measuring the current density profile of intense electron beams
[AD-D011407] 08 p1164 N85-17347
Development of a pressure transducer for usage in high-temperature and vibration environments. Phase 1: Feasibility investigation
[AD-A148605] 08 p1165 N85-17349
High-temperature, solid oxide electrolyte fuel cell power generation system
[DE85-002976] 11 p1675 N85-20552
Heat pipe cooled probe
[NASA-CASE-LAR-12588-1] 12 p1844 N85-21568
Evaluation results of the 700 deg C Chinese strain gauges — for gas turbine engine
[NASA-TM-86973] 12 p1850 N85-21605
Design and fabrication of a unique electromechanical machine for long-term fatigue testing
[DE85-006524] 15 p2580 N85-25912
Gas turbines: Operating conditions, material selection and development
[NLR-MP-83048-U] 20 p3395 N85-31082
Thermal barrier coating system
[NASA-CASE-LEW-14057-1] 24 p4072 N85-35233

HIGH TEMPERATURE FLUIDS
NT HIGH TEMPERATURE GASES
Standardization of flammability tests for hydraulic fluids
[AD-A146468] 06 p0771 N85-14932

HIGH TEMPERATURE GAS COOLED REACTORS
Inquiry into disintegration control of irradiated low enrichment uranium for high temperature gas cooled reactors
[OEFZS-7281] 07 p1042 N85-16615
Consolidated fuel reprocessing program
[DE85-008750] 19 p3366 N85-30871

HIGH TEMPERATURE GASES
Hot-gas cleanup for molten carbonate fuel cells-dechlorination and soot formation
[DE84-009072] 01 p0068 N85-10450
High temperature gas energy transfer
[AD-A146134] 03 p0328 N85-12113
Local Interstellar Medium. International Astronomical Union Colloquium No. 81
[NASA-CP-2345] 06 p0872 N85-15539
Modelling the local interstellar medium as a supernova remnant in a multiphase gas 06 p0879 N85-15585
Noncontact photo-thermal probe-beam deflection measurement of thermal diffusivity in an confined hot gas
[AD-A147481] 07 p0971 N85-16170
The environment of active galactic nuclei 07 p1057 N85-16712
Some aspects of the micromechanics of hot spot formation in energetic materials
[AD-P004348] 10 p1456 N85-19172
Consequences of hot gas in the broad line region of active galactic nuclei
[NASA-TM-86176] 11 p1763 N85-21090
Molecular dynamics of propellant gases, part 2 13 p2002 N85-22552
Characteristics of heat exchange in the region of injection into a supersonic high-temperature flow
[NASA-TM-77833] 15 p2555 N85-25762
Fluid and gas dynamics 16 p2738 N85-26897
Experimental evaluation of an advanced Space Shuttle main engine hot-gas manifold design concept 16 p2738 N85-26898
Influence of thermochemical treatment on properties of low-carbon steel
[BLL-BISI-TRANS-22410-(9022.06)] 17 p2927 N85-28055
Changes of structure of EP648-VI alloy as a result of high-temperature gas corrosion 19 p3243 N85-30110
Results of tests of weathered K5NA closeout material in the MSFC Hot Gas Facility
[NASA-CR-170893] 24 p4073 N85-35230
Study of NSI and related cable performance during tests performed in the NASA Hot Gas Facility
[NASA-CR-170886] 24 p4101 N85-35423

HIGH TEMPERATURE MATERIALS
U REFRACTORY MATERIALS

HIGH TEMPERATURE NUCLEAR REACTORS
NT HIGH TEMPERATURE GAS COOLED REACTORS
Reaction of uranium and the fluorocarbon FC-75
[DE85-012322] 22 p3843 N85-33802

HIGH TEMPERATURE PLASMAS
Ion-density correlations and enhancement of thermonuclear reaction rate in dense, inertially confined fusion plasmas 02 p0284 N85-11849
Hot plasma particles in the Earth's outer magnetosphere: New understandings during the IMS
[DE84-016826] 05 p0677 N85-14348
Atomic and molecular collision processes
[DE85-001604] 09 p1382 N85-18690
X-ray spectroscopy of high-Z and high-density plasmas 09 p1387 N85-18726
Identification of spectra of highly ionized Mo, Nb, Zr and Y atoms 09 p1390 N85-18745
Plasma surface interaction processes and possible synergisms
[DE85-001861] 09 p1391 N85-18752
Application of layered synthetic microstructures to high temperature plasma diagnostics
[DE85-002035] 10 p1559 N85-19828
Effects of the solar-terrestrial environment on satellite operations
[DE85-002413] 11 p1590 N85-20003
Excitation of impurities by heavy particles and radiative losses of thermonuclear plasma 11 p1719 N85-20816
Design, construction and initial evaluation of an absolute, time-integrating/time-resolving spectrometer for the diagnostics of pulsed, high temperature plasma X-ray sources in the 100-10,000 eV region
[DE85-003526] 11 p1732 N85-20896
Light diffraction with collective, thermal electron density fluctuation in plasmas with several ionic components
[IPF-84-5] 11 p1733 N85-20904
On the spectrum of longitudinal waves in the hot degenerate plasma 12 p1955 N85-22280
Electron-positron pair equilibrium in strongly magnetized plasmas 12 p1957 N85-22296
Electron-positron pairs in a mildly relativistic plasma in active galactic nuclei 12 p1957 N85-22297
Spacecraft-environment interaction: The environmental plasma aspect 13 p1990 N85-22479
Ruby wavefront-conjugation laser for obtaining high temperature plasma 13 p2044 N85-22795
Hot plasma and energetic particles in the Earth's outer magnetosphere: New understandings during the IMS 14 p2355 N85-24552
Equations of state of strongly coupled plasma mixtures
[DE85-006163] 15 p2557 N85-26393
Charge uncovering effects on flute instabilities in hot electron plasmas
[DE85-006957] 16 p2667 N85-27088
LINE: A code which simulates spectral line shapes for fusion reaction products generated by various speed distributions
[DE85-010833] 19 p3341 N85-30702
Double layer formation due to contact of different temperature plasmas
[IPPJ-722] 19 p3370 N85-30900
Unthermalized plasma in bursts sources
[OG-1.1-5] 22 p3861 N85-33907
Calculations of heavy ion charge state distributions for nonequilibrium conditions
[SH-2.1-12] 23 p3999 N85-34793
A cosmic ray driven instability
[OG-8.1-5] 23 p4018 N85-34895

HIGH TEMPERATURE TESTS
Silicon nitride joining
[AD-A145669] 02 p0187 N85-11248
Special features of the deformation of molybdenum at high temperatures
[BLL-M-36027-(5828.4)] 07 p0924 N85-15856
Tensile test of pressureless-sintered silicon nitride at elevated temperature
[NASA-TM-77777] 08 p1172 N85-17360
Kinetics of oxidation of titanium alloy upon heating to 1000 deg C 10 p1448 N85-19122

Compatibility experiments of facilities, materials, and propellants for electrothermal thrusters
[NASA-TM-86956] 12 p1795 N85-21280
Development of a high temperature single impact rain erosion test capability
[AD-P004371] 12 p1827 N85-21465
Analysis of experimental shaft seal data for high-performance turbomachines, as for Space Shuttle main engines
[NASA-TM-86928] 12 p1844 N85-21589
Performance of Chromel versus Alumel and Nicrosil versus Nisil thermocouple assemblies in vacuum and argon between 1000 deg C and 1200 deg C
[DE85-000810] 12 p1853 N85-21624
Experimental study of enthalpy of quasimonocrystal of graphite and carbon glass in temperature range of 2600-3818 deg K 13 p2036 N85-22751
Exploratory corrosion tests on materials and fluids for advanced high-temperature molten-salt storage
[DE85-002911] 14 p2258 N85-23991
Influence of thermochemical treatment on properties of low-carbon steel
[BLL-BISI-TRANS-22410-(9022.06)] 17 p2927 N85-28055
Evaluation of 7XXX-series aluminum alloys for the W87 aft support ring
[DE85-009987] 18 p3078 N85-29027
Burner rig corrosion of SiC at 1000 deg C
[NASA-TM-87061] 19 p3227 N85-30011
Effect of prolonged high temperature on durability of coated high-temperature nickel alloys 19 p3243 N85-30105
Nonlinear Constitutive Relations for High Temperature Application, 1984
[NASA-CP-2369] 20 p3465 N85-31530
Influence of moisture and elevated temperature on the fatigue properties of WTS-3 glass fiber blade material — wind turbine blade (WTS-3)
[FFA-TN-1984-58] 20 p3470 N85-31558
Friction and wear of solid-lubricated contact in gas turbine engine bearings
[AD-A155042] 21 p3596 N85-32335
The design, construction and operation of a large-area, high-temperature, thermal conductance apparatus — furnace insulation
[NPL-DMA(A)-84] 22 p3786 N85-33455
Space shuttle SRB TPS protective paint test and evaluation in NASA Hot Gas Facility and AEDC Tunnel C
[NASA-CR-170884] 24 p4081 N85-35294

HIGH VACUUM
Interaction of a stream of dielectric spheres in an electric field in a high vacuum
[DE84-014714] 01 p0115 N85-10782
Field installed brazed thermocouple feedthroughs for high vacuum experiments
[DE84-013558] 04 p0503 N85-13207
Vacuum chamber pressure effects on thrust measurements of low Reynolds number nozzles
[NASA-TM-86955] 12 p1794 N85-21259
Cutting structural materials in vacuum 14 p2286 N85-24165
Diffusion vacuum welding 15 p2499 N85-25418
Prospective uses for diffusion welding in vacuum 22 p3733 N85-33145

HIGH VOLTAGES
Resistance and inductance calculations for helical flux compression generators
[DE84-015068] 02 p0195 N85-11308
Circuit transients due to negative bias arcs on a high-voltage solar array in low Earth orbit
[NASA-TP-2407] 06 p0760 N85-14858
Choice of criteria for rejection of insulating components in high-voltage surge equipment 06 p0785 N85-15021
Semiconductor high-voltage power devices: State of art and outlook 06 p0794 N85-15074
Repetitive pulse generation with inductive energy storage: A new technology for defense
[DE84-017090] 06 p0805 N85-15122
Diagnosis of insulation defects in 1000+ V distribution networks with insulated neutral 07 p0954 N85-16044
High voltage effects measured on dummy mannequin 07 p1012 N85-16432
High voltage disconnect protection
[AD-D011480] 10 p1481 N85-19353
Effects of electromagnetic fields produced by high voltage transmission lines
[DE85-900034] 11 p1625 N85-20230
A new very high voltage semiconductor switch
[NASA-TM-86957] 11 p1627 N85-20246
High voltage RF coaxial cable
[AD-D011493] 11 p1629 N85-20255
Adaptation of an air-dielectric RF cable for use as an oil-filled high voltage pulse transmission line
[DE84-017414] 11 p1630 N85-20265
Study of electric field and ion effects on HVDC lines
[DE85-002975] 12 p1833 N85-21503
Spacecraft Environmental Interactions Technology, 1983
[NASA-CP-2359] 13 p1989 N85-22470
Non-self-maintained high-voltage low-pressure discharge 13 p2068 N85-23037
Further development of high voltage SIPMOS FET's to fulfill market needs
[BMFT-FB-T-84-255] 17 p3045 N85-28843
High voltage isolation transformer
[NASA-CASE-GSC-12817-1] 18 p3093 N85-29146
High voltage power supply
[NASA-CASE-GSC-12818-1] 18 p3093 N85-29147
High voltage lateral power transistors: Theory and design 19 p3257 N85-30194
Protection products for the conductors of high voltage overhead lines
[BLL-OA-TRANS-3219-(6196.300)] 20 p3429 N85-31269
Improvements in safety testing of lithium cells 20 p3444 N85-31379
Outline of CCVT (Coupling Capacitor Voltage Transformer) calibration procedure, EPRI-NBS (Electric Power Research Institute/National Bureau of Standards) prototype system. Supplement to EPRI report EL-890 (Field Calibration System for CCVTs, April 1979)
[PB85-182586] 20 p3450 N85-31418
Plasma erosion opening switch
[DE85-011384] 20 p3535 N85-31998
Module Hipot and ground continuity test results 21 p3612 N85-32447
Partial discharges in and electric strength of high-voltage polymer insulation at cryogenic temperatures 22 p3770 N85-33364
Photoconductive pulse power switches: A review
[DE85-014125] 24 p4091 N85-35360

HIGHLANDS
Mapping structures characteristic of the highland boundary scarp on Mars 13 p2191 N85-23585
Mars: Stratigraphy of western highlands and polar regions 13 p2201 N85-23663

HIGHLY MANEUVERABLE AIRCRAFT
Closing the design loop on HiMAT (highly maneuverable aircraft technology)
[NASA-TM-85923] 06 p0754 N85-14836
Autofocus motion compensation for synthetic aperture radar and its compatibility with strapdown inertial navigation sensors on highly maneuverable aircraft
[AD-A151940] 16 p2704 N85-26693

HIGHWAYS
Predictor model for seasonal variations in skid resistance, volume 1
[PB84-226612] 01 p0036 N85-10229
Skid resistance of bituminous surfaces in Ohio
[PB84-234491] 04 p0484 N85-13086
Optimal design efforts in Shanghai described 13 p1972 N85-22366
USSR report: Transportation
[JPRS-UTR-84-008] 14 p2208 N85-23684

HIJACKING
U AIR PIRACY

HILBERT SPACE
NT BANACH SPACE
NT SOBOLEV SPACE
On the commutant of an irreducible set of operators in real Hilbert space
[TUM-M8316] 01 p0114 N85-10774
Orthogonal polynomials and rigged Hilbert space
[TUM-M8313] 03 p0414 N85-12647
Analytic and sequential feynman integrals on abstract Wiener and Hilbert spaces, and A Cameron-Martin formula. Revision
[AD-A149989] 07 p1030 N85-16537
Chandrasekhar equations for infinite dimensional systems
[NASA-CR-172515] 09 p1378 N85-18651
A non-hypoelliptic Dirichlet problem from stochastics 10 p1537 N85-19857
A remark on regularization in Hilbert space
[AD-A149046] 10 p1552 N85-19787
Fake topological Hilbert spaces and characterizations of dimension in terms of negligibility
[CWI-TRACT-2] 14 p2414 N85-24893
Characteristic functionals of stochastic wave processes
[REPT-14/1984] 16 p2768 N85-27084
Finite control in underdamped distributed parameter systems 20 p3412 N85-31176
A factorization approach to the linear regulator quadratic cost problem 20 p3413 N85-31178

HILBERT TRANSFORMATION
Orthogonal polynomials and a Dirichlet problem related to the Hilbert transform
[CWI-PM-R8406] 05 p0723 N85-14647

HILL CURVES
U HILL METHOD

HILL METHOD
Magnetohydrodynamic equilibrium and stability of spheromak with spheroidal plasma-vacuum interface
[PPPL-732] 23 p3974 N85-34640

HILLER MILITARY AIRCRAFT
U MILITARY AIRCRAFT

HILSCH TUBES
Experimentally determined characteristics of vortex heaters 13 p2050 N85-22933

HIMALAYAS
Dist of first Soviet expedition on Mount Everest 19 p3323 N85-30566

HIMAT
U HIGHLY MANEUVERABLE AIRCRAFT

HINDRANCE
U CONSTRAINTS

HINGE MOMENTS
U TORQUE

HINGED ROTOR BLADES
U HINGES
U ROTARY WINGS

HINGELESS ROTORS
U RIGID ROTORS

HINGES
In-orbit performance of INTELSAT V communications antennae deployment systems 05 p0627 N85-14018
Drag-compensated, precision-powered hinge system 22 p3796 N85-33517

HISS
VLF emissions observed by ISIS Satellites during the IMS 14 p2366 N85-24621
Conjugacy of ELF-VHF emissions near L=6 — chorus phenomenon, hiss 14 p2367 N85-24629

HISTOCHEMICAL ANALYSIS
New techniques for studying calcium gradients 15 p2609 N85-26076
The Fibrin slide assay for detecting uroki nase activity in human fetal kidney cells 20 p3502 N85-31766

HISTOGRAMS
Determining object orientation from a single image using multiple information sources
[AD-A149060] 12 p1933 N85-22146
Normal and anomalous geothermal fields and their relationship to hierarchy of geological bodies 13 p2113 N85-23160
CHIL: A comprehensive histogramming language
[DE85-005356] 14 p2405 N85-24630
Nonparametric estimation of density and hazard rate functions when samples are censored
[AD-A150946] 14 p2411 N85-24668
A cluster analysis method for identification of subpopulations of cells in flow cytometric list-mode arrays 20 p3503 N85-31779
How map designers can represent their ideas in thematic maps: Effective user interfaces for thematic map design 23 p3962 N85-34562
Study of spectral/radiometric characteristics of the Thematic Mapper for land use applications
[E85-10106] 24 p4107 N85-35464
Edge information in color images based on histograms of differences
[AD-A156002] 24 p4154 N85-35751

HISTOLOGY
Effect of 1,25-dihydroxycholecalciferol and 24,25 dihydroxycholecalciferol on growth and alteration of rat bones during hypokinesia (histomorphometric study) 01 p0092 N85-10622
Morphological study of monkeys submitted to antiorthostatic hypokinesia 12 p1902 N85-21942
Actual and simulated weightlessness inhibit osteogenesis in long bone metaphysis by different mechanisms 15 p2608 N85-26074
Histological and compositional responses of bone to immobilization and other experimental conditions
[NASA-CR-175837] 16 p2841 N85-27518
Spontaneous transitional cell carcinoma in the urinary bladder of a strain 13 guinea pig
[AD-A155845] 21 p3585 N85-32764

HISTORIES
The Malcolm horizon: History and future 01 p0008 N85-10046
Estuaries of the Cape. Part 2: Synopses of available information on individual systems. Report no. 18: Bot/Kleinmond system (CSW 13)
[CSIR-RR-417-PT-2] 01 p0067 N85-10587
Synthesis of current measurements in Puget Sound, Washington. Volume 1: Index to current measurements made in Puget Sound from 1908-1980 with daily and record averages for selected measurements
[PB84-214105] 01 p0089 N85-10603

Space research benefits national economy
02 p0163 N85-11107
The identification of the scientific community's choice criteria in the history of scientific research: The case of quantum mechanics
[NOTA-INTERNA-797] 02 p0291 N85-11893
Propulsion — jet aircraft engines
[PNR-90208] 03 p0320 N85-12062
Lunar magnetic history 04 p0582 N85-13715
A historical overview of the electrical power systems in the US manned and some US unmanned spacecraft
[NASA-CR-174806] 05 p0612 N85-13910
Man in Space: National Historic Landmark Theme Study
[PB85-107233/GAR] 07 p0911 N85-15768
Polar research in Earth sciences described
08 p1142 N85-17204
Post-Laramide history of North Central Wyoming
08 p1181 N85-17444
The beginnings of airborne astronomy, 1920 - 1930: An historical narrative 08 p1244 N85-17849
History of photometric precision
08 p1250 N85-17893
Chronology of KSC and KSC related events for 1983
[NASA-TM-87400] 08 p1251 N85-17927
On the frontier: Flight research at Dryden 1946-1981
[NASA-SP-4303] 09 p1263 N85-17934
The Prandtl Hergesell project of a national research establishment for aeronautics
[ESA-TT-835] 09 p1272 N85-17993
Flight crew training technology: A review
09 p1275 N85-18010
Making sure: A brief outline and history of ESA's test and checkout services
[ESA-BR-22] 09 p1286 N85-18077
An objective error measure for the comparison of calculated and measured transient response histories
09 p1335 N85-18395
Some fighter aircraft trends
[NASA-TM-86352] 10 p1420 N85-18954
Major glaciation events of the past and their geological significance 10 p1497 N85-19450
A history of full-scale testing of aircraft structures at the National Aeronautical Establishment
[NAE-AN-24] 12 p1777 N85-21153
Discovery of the solar wind 12 p1954 N85-22272
Chronology of KSC and KSC related events for 1983
[NASA-TM-87435] 12 p1963 N85-22339
Feoktistov recalls period leading to Gagarin spaceflight 13 p1995 N85-22451
Model research: The National Advisory Committee for Aeronautics, 1915-1958, volume 1
[NASA-SP-4103-VOL-1] 14 p2207 N85-23663
Model research, the National Advisory Committee for Aeronautics, 1915-1958, volume 2
[NASA-SP-4103-VOL-2] 14 p2207 N85-23664
Basic principles of industrial radiography
14 p2316 N85-24310
Some historical and other notes about the Mertens conjecture and its recent disproof
[CWI-NM-R8415] 14 p2414 N85-24898
O. F. Mossotti and the physics of molecules
[NOTA-INTERNA-822] 14 p2420 N85-24931
Special course on V/STOL aerodynamics: An assessment of European jet lift aircraft
[AGARD-R-710-ADDENDUM] 15 p2460 N85-25188
A climatic data bank for Northern Hemisphere land areas, 1851-1980
[DE85-007663] 16 p2835 N85-27488
The revolution in military affairs and the Soviet system
[AD-P004589] 17 p3048 N85-28863
Air traffic: Instruments, airports, companies, post, cargo and passengers 18 p3060 N85-28932
Environmental management needs
[DE85-007859] 18 p3133 N85-29405
Numerical meteorology 18 p3147 N85-29484
Early study of muons and muon decay
[NOTA-INTERNA-835] 18 p3184 N85-29742
The evolution of the U.S. helicopter industry
[AD-A154290] 19 p3211 N85-29913
The international scope of data evaluation
[DE85-005953] 19 p3349 N85-30760
Historical perspective of barriers to achieving high-efficiency silicon solar cells
20 p3479 N85-31616
Monte Carlo: In the beginning and some great expectations
[DE85-010789] 20 p3518 N85-31872
Quest for performance: The evolution of modern aircraft
[NASA-SP-468] 21 p3551 N85-32089
Ancient landscapes: Their nature and significance for the question of inheritance 21 p3601 N85-32364
One application of mega-geomorphology in education
21 p3602 N85-32370
Space research in the United Kingdom: An assessment
[AD-A155334] 21 p3712 N85-33038
Noble gases and the early history of the Earth: Inappropriate paradigms and assumptions inhibit research and communication 21 p3719 N85-33075
150 years of meteorology in Belgium
22 p3817 N85-33642
An internally consistent gamma ray burst time history phenomenology
[OG-1.2-6] 22 p3862 N85-33916
A spacefaring people: Perspectives on early spaceflight
[NASA-SP-4405] 23 p4056 N85-35142
The next assignment: The state of the literature on space 23 p4057 N85-35146
Opportunities for policy historians: The evolution of the US civilian space program 23 p4057 N85-35147
Space-age Europe, 1957-1980
23 p4057 N85-35148
Space activities in the Soviet Union, Japan, and the People's Republic of China 23 p4057 N85-35149
The idea of space exploration
23 p4057 N85-35150
Development of flight mechanics research in Brunswick 24 p4061 N85-35166
Typical and historical aspects of motor gliders as meteorological measuring aircraft
24 p4121 N85-35544

HMX
HMX combustion modification
[AD-A145071] 01 p0024 N85-10149
Critical analysis of nitramine decomposition data. Preliminary comments on autoacceleration and autoinhibition in HMX and RDX decomposition
[AD-A146570] 06 p0774 N85-14946
Molecular dynamics in nitramines and modified nitramines
[AD-A148615] 08 p1220 N85-17686
Effects of HMX addition on the combustion of energetic binders 13 p2004 N85-22560
The chemistry of RDX and HMX cluster ions
13 p2004 N85-22561
Detonation in tungsten-loaded HMX
[DE85-009606] 23 p3922 N85-34299

HNST
U HEXANITROSTILBENE

HODOGRAPHS
Classical free-streamline flow over a polygonal obstacle
[NASA-CR-172448] 01 p0046 N85-10301
Transonic jets: A numerical approach in the hodograph plane 05 p0592 N85-13774

HODOSCOPES
Fine grained hodoscopes based on scintillating optical fibers
[DE84-014849] 01 p0120 N85-10825
Bevalac calibration of the SOFIE range and hodoscope detectors
[OG-9.1-7] 23 p4023 N85-34933
The response of a scintillation counter below an emulsion chamber to heavy nucleus interactions in the chamber 24 p4175 N85-35689
Results of a search for monopoles and tachyons in horizontal cosmic ray flux
[HE-6.1-3] 24 p4209 N85-36129
Search for acoustic signals from high energy cascades
[HE-7.1-1] 24 p4213 N85-36155

HOGBACKS
U RIDGES

HOHMANN TRAJECTORIES
U ELLIPTICAL ORBITS
U TRANSFER ORBITS

HOHMANN TRANSFER ORBITS
U ELLIPTICAL ORBITS
U TRANSFER ORBITS

HOLDERS
NT FLAME HOLDERS
Contact insertion and wire lay robotic end effector apparatus
[AD-D011451] 10 p1492 N85-19424
Classification of holding jigs for objects of robotized assembly 14 p2266 N85-24039
Apparatus for mounting a field emission cathode
[NASA-CASE-LEW-14108-1] 18 p3094 N85-29149
Thermal expansion coefficients of a 30% glass fiber filled PEEK pyrotechnic charge holder
[DE85-010805] 19 p3251 N85-30155
Results of tests of MTA-2 TPS on the SRB hold-down bolt blast container
[NASA-CR-170891] 24 p4070 N85-35224

HOLE DISTRIBUTION (ELECTRONICS)
Absorption of 10.6 micrometer laser radiation in electron-hole condensate in germanium
21 p3681 N85-32870

HOLE DISTRIBUTION (MECHANICS)
Final magnetic shimming of vacuum chamber suspension holes on the sector magnets
[CSIR-NAC-83-02] 01 p0117 N85-10796

HOLE GEOMETRY (MECHANICS)
Stress analysis of pin-loaded orthotropic plates using orthotropic photoelasticity 02 p0207 N85-11366
Stress intensity factors for corner cracks at holes located near an edge
[FFA-TN-1984-20] 04 p0514 N85-13279
Flow visualization study of the effect of injection hole geometry on an inclined jet in crossflow
[NASA-TM-86936] 11 p1631 N85-20289
Finite element analysis of problems associated with life enhancement techniques
[ARL/STRUC-R-404] 12 p1862 N85-21676
An approximation to the problem of a pin-loaded hole in an orthotropic plate
[VTH-LR-386] 16 p2902 N85-27278
Effect of edge distance on yield initiation in a remotely loaded half-plane containing interference-fit disc of the same material
[ARL/STRUC-R-413] 19 p3285 N85-30369

HOLE MOBILITY
High-efficiency solar-cell design modeling
06 p0829 N85-15262
Collective modes, effective interaction and superconductivity in the electron-hole liquid
20 p3537 N85-32009

HOLES
Stresses in a half-plane containing either a pressurized hole or an interference-fit disc
[ARL/STRUC-R-409] 12 p1865 N85-21700
Elastic response of a half-plane to a bonded interference-fit disc of the same material
[ARL/STRUC-R-406] 12 p1865 N85-21701

HOLES (ELECTRON DEFICIENCIES)
Theoretical analysis of physical processes of lasing medium degradation in semiconductor lasers
02 p0269 N85-11759
Electron and hole effective masses for two-dimensional transport in strained-layer superlattices
[DE84-016222] 04 p0570 N85-13637
Inclusion of elect on transfer in the calculation of K(n)L(v) multiple vacancy production by ion impact
[DE84-016596] 05 p0733 N85-14711
Photoluminescent and electroluminescent properties of Cd sub 0.95 Mn sub 0.05 Se electrodes
[AD-A146775] 07 p0946 N85-15995
Two carrier dual injector apparatus
[AD-D011357] 07 p1047 N85-16646
Chaotic dynamics of instabilities in solids
[DE85-004909] 14 p2429 N85-24978
On the group-theoretical approach to the energy spectra problem of charge carriers in cubic solids
[PREPRINT-435] 18 p3196 N85-29827
Collective modes, effective interaction and superconductivity in the electron-hole liquid
20 p3537 N85-32009
Dangling bonds and sub-gap optical absorption in silicon
[DE85-011752] 24 p4082 N85-35302
Optical properties of heterostructures and superlattices
[AD-A156243] 24 p4162 N85-35802
Multiple vacancy production by high energy heavy ions
[DE85-004428] 24 p4162 N85-35805

HOLLAND
U NETHERLANDS

HOLLOW CATHODES
Hot hollow cathode gun assembly
[DE84-014312] 01 p0121 N85-10832
Gas pressure and electron density at the level of the active zone of hollow cathode arc discharges
[NASA-TM-77477] 03 p0414 N85-12648
Extended performance technology study 30-cm thruster
[NASA-CR-168259] 07 p0917 N85-15806
Gas pressure and electron density in the active zone level of hollow cathode arc discharges
[NASA-TM-77468] 07 p0945 N85-15986
Measurements of electric fields in plasmas by using beam probe and laser fluorescence techniques
09 p1389 N85-18737
Advanced ion thruster research
[NASA-CR-174862] 10 p1430 N85-19021
Proposal for hollow cathode electron gun for electron cooling
[DE85-002721] 11 p1630 N85-20263
Hollow cathode apparatus
[NASA-CASE-NPO-15560-1] 12 p1832 N85-21491
Journal of Research of the National Bureau of Standards, volume 89, number 2, March - April 1984
[PB85-115426] 12 p1926 N85-22103
Laser with a hollow copper cathode
[ISL-R-119/83] 14 p2310 N85-24300

High efficiency ionizer using a hollow cathode discharge plasma
[DE85-006690] 16 p2668 N85-27693
A liquid nitrogen cooled composite wall hollow cathode — molecular spectroscopy
[USIP-85-07] 20 p3526 N85-31930
High pressure working mode of hollow cathode arc discharges
[NASA-TM-77680] 20 p3535 N85-31992
Heaterless ignition of inert gas ion thruster hollow cathodes
[NASA-TM-87086] 23 p3903 N85-34177
Hollow cathodes in high pressure arc discharges
[NASA-TM-87098] 23 p3903 N85-34179

HOLMIUM
Spin dynamics of rare Earth ions in crystal fields probed by muon spin rotation
[DE84-013805] 02 p0278 N85-11810
Magnetic X-ray scattering studies of the rare Earth metal holmium
[DE85-003608] 12 p1807 N85-21335
Interactions of heavy nuclei, Kr, Xe and Ho, in light targets
[OG-7.2-21] 23 p4016 N85-34868
Stopping relativistic Xe, Ho, Au and U nuclei in nuclear emulsions 24 p4173 N85-35876

HOLOGRAMMETRY
Development of holographic particle field data reduction by Fourier analysis
[AD-A148684] 08 p1165 N85-17348
Optical processor for synthetic aperture radar 11 p1621 N85-20203
Hologram-like transmission of pictures 23 p3961 N85-34552

HOLOGRAPHIC INTERFEROMETRY
Distortional measurement of antennas under space simulation conditions by means of holography 05 p0625 N85-14005
Reconstruction of a 3-dimensional transonic rotor flow field from holographic interferogram data
[NASA-TM-86690] 12 p1770 N85-21112
Interferometric velocity measurements in ballistics
[ISL-CO-239/83] 14 p2306 N85-24276
Description of an holographic interferometry nondestructive test installation: Application to bond tests
[SNIAS-851-430-101] 20 p3464 N85-31521
A comparison of electronic heterodyne moire deflectometry and electronic heterodyne holographic interferometry for flow measurements
[NASA-TM-87071] 21 p3586 N85-32302
New method for compensating and measuring any motion of three-dimensional objects in holographic interferometry
[ISL-CO-216/84] 22 p3789 N85-33474
Heterodyne holographic interferometry for visualization of surface acoustic waves
[AD-A155405] 22 p3836 N85-33753
Practical aspects of laser holographic interferometry in wind tunnels
[NASA-TM-86788] 23 p3933 N85-34378

HOLOGRAPHIC SPECTROSCOPY
Simultaneous measuring absorption spectrometer
[BMFT-FB-T-84-132] 03 p0365 N85-12339
Bibliography of Soviet laser developments, number 65, May - June 1983
[AD-A148189] 03 p0366 N85-12347
Investigations of photochemistry using holography and photoacoustic spectroscopy
[AD-A148637] 06 p0810 N85-15149
Fourier transform infrared spectrophotometric analysis of resin mix stoichiometry, revision 1
[DE85-007272] 16 p2747 N85-28951
Holographic corrector in objective with compound main mirror 17 p2941 N85-28153

HOLOGRAPHIC SUBTRACTION
Effect of hydrogen on formation of energy spectrum of multiply charged and copper ions 02 p0263 N85-11720
Holographic subtraction of images by Fourier plane recording and spatial filtration with a narrow beam 02 p0263 N85-11721

HOLOGRAPHY
NT ACOUSTICAL HOLOGRAPHY
NT MICROWAVE HOLOGRAPHY
NT WHITE LIGHT HOLOGRAPHY
Peripheral vision displays: The future 01 p0009 N85-10058
A determination of the photochemical quantum yields from 2 excited triplet states of biacetyl using holography
[AD-A145091] 01 p0050 N85-10328
Acoustic emission linear pulse holography
[DE84-014519] 01 p0050 N85-10330
Formation of radio images by scanning around circle 02 p0264 N85-11727
Modeling holographic recognition system by using number-theory convolution transformation 02 p0272 N85-11774
Holographic displacement analysis with fiber optics
[AD-A146185] 03 p0420 N85-12680
Hologram bleaching 06 p0789 N85-15038
Recording holograms on thin films of titanium dioxide 06 p0789 N85-15039
A collection of flow visualization techniques used in the Aerodynamic Research Branch
[NASA-TM-85998] 06 p0808 N85-15135
Wavelength coded image transmission and holographic optical elements
[AD-A148490] 06 p0810 N85-15147
Investigations of photochemistry using holography and photoacoustic spectroscopy
[AD-A148637] 06 p0810 N85-15149
Holographic directional coupler for fiber optic systems
[AD-D011365] 07 p0937 N85-15939
Solid state research
[NASA-CR-174285] 07 p1048 N85-16656
Advanced diagnostics for reacting flows
[AD-A148479] 08 p1162 N85-17334
Holographic FLI for detection of defects
[AD-A148339] 08 p1164 N85-17345
Development of holographic particle field data reduction by Fourier analysis
[AD-A148684] 08 p1165 N85-17348
Critical flashing flow of subcooled fluids in nozzles with contour discontinuities
[DE84-017229] 09 p1319 N85-18296
Diffraction diffusion screen with holographically-suppressed zero-order beam
[AD-D011445] 10 p1487 N85-19367
X-ray holography of biological specimens
[DE85-002437] 10 p1489 N85-19398
Optical implementation of the synthetic discriminant function
[AD-A149562] 10 p1557 N85-19617
Electronics Engineering Department: EE technical review
[DE85-004360] 11 p1629 N85-20259
KMSF X-ray laser experiments, task no. 2
[DE85-000291] 11 p1640 N85-20335
Study of the potential usefulness of superfine holographic x-ray gratings in AXAF and astrophysics in general 12 p1945 N85-22215
Solid propellant combustion diagnostics and automated data retrieval from holograms 13 p1998 N85-22527
Laser applications in last 10 years reviewed 13 p2052 N85-22844
Space-variant optical systems
[AD-A151032] 14 p2421 N85-24939
Holography in space 15 p2476 N85-25285
Holographic lens for optical correlator 16 p2763 N85-27052
Holoswitch, phase 1
[AD-A152212] 16 p2787 N85-27196
Digital image analysis of four-frame holographic plasma and neutral gas interferograms
[DE85-008397] 16 p2788 N85-27200
Ultrafast holography using optical fibers
[ISL-CO-238/83] 16 p2788 N85-27204
Holographic intensity correlator with PRIS-type photoelectro-optical controlled transparency 17 p2940 N85-28152
Holographic corrector in objective with compound main mirror 17 p2941 N85-28153
Morphological stability and fluid dynamics of vapor crystal growth
[NASA-CR-175879] 17 p3042 N85-28822
Holographic investigation of solid propellant combustion in a two-dimensional motor
[AD-A153546] 18 p3070 N85-29089
Holographic assembly for measuring velocity fields of supersonic ballistic splinters at a large distance
[ISL-CO-203/84] 20 p3459 N85-31487
Infrared laser holography used in fusion plasma studies 21 p3557 N85-32505
Signal processing in quasi-holographic system as an inverse problem 22 p3782 N85-33315
Digital holographic synthesis of pattern-forming transparencies for ring antenna arrays 22 p3783 N85-33326
Depth dimension compression of 3-D images 22 p3784 N85-33332
Pulsed lasers for filming color holographic film images 22 p3781 N85-33429
Holographic cinematography with the help of a pulse YAG laser
[ISL-CO-213/84] 22 p3788 N85-33472
Cineholography
[ISL-CO-214/84] 22 p3788 N85-33473
Methods for the optical processing of signals
[DRIC-T-7439] 22 p3844 N85-33609
Modular digital holographic fringe data processing system
[NASA-CR-177952] 23 p3933 N85-34376
Applications of holography to X-ray imaging
[DE85-010864] 23 p3934 N85-34384
The use of optical fibers in pulsed laser holography
[ISL-CO-226/84] 23 p3936 N85-34395
Fatigue damage detection in steels by optical correlation
[AD-A155930] 24 p4079 N85-35277
Holoswitch
[AD-A155841] 24 p4096 N85-35392

HOLOMORPHISM
U ANALYTIC FUNCTIONS

HOMEOSTASIS
Effects of hypothermia on brain metabolism 11 p1662 N85-20606
Fluid metabolism of monkeys during two-week antiorthostatic hypokinesia 12 p1902 N85-21943
Alterations in gut transport of minerals and in binding proteins during simulated weightlessness
[NASA-CR-175837] 14 p2398 N85-24709
Homeostasis in primates in the hyperdynamic environment — circadian timekeeping and effects of lower body positive pressure on sleep 15 p2610 N85-26085
Primate experiments on SLS-1 15 p2687 N85-26382
Long term exposure of animals to antiorthostatis (-90 deg) as a model of critical homeostatic disturbances 19 p3324 N85-30562
Effect of dibezol on parameters of nonspecific resistance of subjects in pressurized cabins 23 p3954 N85-34504

HOMING
Accounting for error stochasticity in terminal homing of aircraft 04 p0469 N85-13115
Determining an azimuth with a north seeking gyro
[AD-A155880] 24 p4063 N85-35180

HOMING DEVICES
Dual mode radio frequency-infrared frequency system
[AD-D011402] 08 p1081 N85-16850
Applications of compound eye configurations to smart sensor design
[AD-A150731] 14 p2420 N85-24895
Supersonic missile seeker lens system using gradient index material for first element lens
[AD-A151478] 15 p2490 N85-25357
Preguidance and piloting with the aid of composite inertial sensors 18 p2996 N85-28648

HOMODYNE RECEPTION
Quantum noise and excess noise in optical homodyne and heterodyne receivers
[AD-A148298] 09 p1157 N85-17303
Phase-locked loops for optical homodyne detection, volume 1 — spaceborne receivers
[ESA-CR(P)-2029-VOL-1] 20 p3442 N85-31367
Phase locked loops for optical homodyne detection, volume 2 — spaceborne receivers
[ESA-CR(P)-2029-VOL-2] 20 p3442 N85-31368

HOMOGENEITY
Scanning photoacoustic microscopy of aluminum with aluminum oxide, roughness standards and rubber
[AD-A149460] 10 p1441 N85-19081
Surface scattering
[AD-A150252] 13 p2153 N85-23366
Homogeneity of pristine and bromine intercalated graphite fibers
[NASA-TM-87016] 15 p2517 N85-25521
Numerical modeling of subsurface communication
[DE85-012818] 21 p3577 N85-32249
A cracked orthotropic sheet stiffened by a semi-infinite orthotropic sheet
[NASA-TP-2455] 21 p3587 N85-32339
On the principle of uniformity of satellite communications systems 22 p3773 N85-33362
Apparatus for unilateral generation of a homogeneous magnetic field
[DE85-008001] 23 p3926 N85-34345
Why do leaky-box models work so fine?
[OG-7.2-8] 23 p4014 N85-34877

HOMOGENEOUS TURBULENCE
Vortex dynamics simulation of conserved scalar dissipation 22 p3745 N85-33210

HOMOGENIZATION
U HOMOGENIZING

HOMOGENIZING
Optimum convection conditions for Czochralski growth of semiconductors
[INPE-3385-PRE/865] 16 p2670 N85-27703
Effect of polymer additives on characteristics of direct-current motor with liquid dielectric filler 22 p3772 N85-33376

HOMOJUNCTIONS
Comparison of SCAPID/GaAs to experiment 06 p0668 N85-14279

Comparative study of GaAs solar cell potentialities for space applications 13 p2008 N85-22577
Investigation of high output gallium arsenide solar cells 13 p2006 N85-22578
GaAs and 3-5 compound solar cells status and prospects for use in space 13 p2007 N85-22580

HOMOLOGY
Contribution of the cup-product of Milnor's fiber with /f/ sup 2 lambda poles 11 p1698 N85-20672

HOMOMORPHISMS
NT AUTOMORPHISMS
On Bezout domains, elementary divisor rings, and pole assignability
[CSIR-TWISK-330] 01 p0110 N85-10740

HOMOPOLAR GENERATORS
Westinghouse programs in pulsed homopolar power supplies 05 p0606 N85-13862

HOMOSPHERE
NT MIDDLE ATMOSPHERE
NT STRATOSPHERE

HOMOTOPY THEORY
A fast ray tracing routine for laterally inhomogeneous media
[AD-A150984] 14 p2421 N85-24938

HONDURAS
Area handbook series. Honduras: A country study
[AD-A146510] 06 p0627 N85-15253
Interrelationship of atmospheric parameters in Honduras
[AD-A147371] 07 p1007 N85-16401

HONEYCOMB CORES
Nonlinear dynamic analysis of sandwich panels 01 p0080 N85-10394
Integrated insulation wall assembly — for a solid rocket motor case
[AD-D011553] 12 p1794 N85-21257
Aircraft safety improvement 15 p2688 N85-26602
Stress analysis of axisymmetric sandwich shells of variable thickness 24 p4101 N85-35419

HONEYCOMB STRUCTURES
NT HONEYCOMB CORES
Quasi-steady analysis of aircraft panel flammability
[AD-A145461] 02 p0138 N85-10938
Air Force honeycomb shaping at SM-ALC (Sacramento Air Logistics Center)
[AD-P004005] 03 p0308 N85-11985
Verification tests of durable TPS concepts
[NASA-TM-86313] 03 p0323 N85-12085
Composite repair of aircraft structures 08 p1120 N85-17059
Technological parameters of diffusion welding processes in honeycomb titanium alloy structures 13 p2033 N85-22739
Computational methods for the explosive and impact compaction of powders
[AD-A156219] 24 p4139 N85-35653

HOOP COLUMN ANTENNAS
Vibration control experiment design for the 15-m hoop/column antenna 20 p3409 N85-31159

HOOPS
Direct transient analysis of a fuze assembly by axisymmetric solid elements 15 p2576 N85-25890

HORIZON
Stimulus factors in motion perception and spatial orientation 01 p0008 N85-10049
Early Air Force Flight Test Center (AFFTC) experience with Peripheral Vision Horizon Displays (PVHD) 01 p0009 N85-10057
Cockpit window edge proximity effects on judgements of horizon vertical displacement 05 p0704 N85-14518
Mean and random errors of visual roll rate perception from central and peripheral visual displays 06 p0704 N85-14519

HORIZON SCANNERS
Personal experience with the PVHD and opinion of situations in which a wide Field Of View (FOV) PVHD might be helpful 01 p0008 N85-10045
Evaluation of the Malcolm horizon in a moving-base flight simulator 01 p0008 N85-10051
Peripheral vision horizon display on the single seat night attack A-10 01 p0009 N85-10053
Infrared horizon sensor modeling for attitude determination and control: Analysis and mission experience
[NASA-TM-86181] 10 p1429 N85-19016
Autonomous state determination for an Earth orbiting satellite using horizon and star sensors
[AD-A151827] 15 p2493 N85-25379
Studies of the solar mesosphere explorer: Dynamics and horizon sensor performance. Part A: Spin axis precession and atmospheric drag. Part B: Clouds
[NASA-CR-175306] 24 p4069 N85-35213

HORIZON SENSING
U HORIZON SCANNERS

HORIZONTAL ORIENTATION
The Malcolm horizon: History and future 01 p0008 N85-10046
Comparison of wind derived from the LIMS (Limb Infrared Monitor of the Stratosphere) satellite instrument with rocket observations
[NASA-CR-174083] 04 p0541 N85-13444
Experiments in forecasting atmospheric marine horizontal visibility using model output statistics with conditional probabilities of discretized parameters
[AD-A147574] 07 p1008 N85-16404
Intensification of tropical instabilities
[AD-A149985] 12 p1896 N85-21899
Horizontal deflection TS-257 13 p2069 N85-22926
Experimentally determined distribution of stress around a horizontally loaded model pile in dense sand
[CE-43] 16 p2796 N85-27239
Wake effects on the aerodynamic performance of horizontal axis wind turbines
[NASA-CR-174920] 18 p3127 N85-29364
Resolution of thermal striping issue downstream of a horizontal pipe elbow in stratified pipe flow
[DE85-006195] 21 p3586 N85-32292
On the spectrum of atmospheric velocity fluctuations seen by MST/ST radar and their interpretation 21 p3622 N85-32504
Tropospheric gravity waves observed by three closely spaced ST radars 21 p3623 N85-32509
Determination of horizontal and vertical wavelengths of gravity waves in the mesosphere by spaced wind measurements 21 p3623 N85-32510
Horizontal and vertical structure of velocity, potential vorticity and energy in the gulf stream
[AD-A154753] 21 p3655 N85-32702

HORIZONTAL SPACECRAFT LANDING
Active control technology experience with the Space Shuttle in the landing regime 17 p2903 N85-27900

HORIZONTAL STABILIZERS
U STABILIZERS (FLUID DYNAMICS)

HORIZONTAL TAIL SURFACES
Experimental trim drag values and flow-field measurements for a wide-body transport model with conventional and supercritical wings
[NASA-TP-2071] 02 p0135 N85-10920

HORMONE METABOLISMS
Effect of modulated ultrahigh frequency field on behavior and hormone level in female rats under emotional stress 09 p1361 N85-18562
The behavior of renal-regulating hormones during hypogravic stress
[NASA-CR-171877] 15 p2616 N85-26123
Rat plasma hormone levels following flight aboard Cosmos-1129 biosatellite 22 p3823 N85-33681

HORMONES
NT ADRENOCORTICOTROPIN (ACTH)
NT ALDOSTERONE
NT CORTICOSTEROIDS
NT CORTISONE
NT HYDROXYCORTICOSTEROID
NT PROSTAGLANDINS
Modulation of the cytosolic androgen receptor in striated muscle by sex steroids
[NASA-CR-174173] 04 p0545 N85-13468
Comparative effects of auxin and abscisic acid on growth, hydrogen ion efflux and gravitropism in primary roots of maize
[NASA-CR-174355] 09 p1342 N85-18444
Purification and cultivation of human pituitary growth hormone secreting cells
[NASA-CR-171846] 12 p1899 N85-21923
Transduction of the root gravitropic stimulus: Can apical calcium regulate auxin distribution? 15 p2606 N85-26063
Attempts to localize and identify the gravity sensing device of plant seedlings 15 p2607 N85-26064
The salutary effect of dietary calcium on bone mass in a rat model of simulated weightlessness 15 p2608 N85-26073
Neural mechanism by which gravitational stimulus and stress affect the secretion of renin and other hormones 15 p2610 N85-26083
Morphological study of primate hypothalamus and hypophysis after experiment with antiorthostatic hypokinesia 19 p3325 N85-30603
A critical synopsis: Continuous growth of proximal tubular kidney epithelial cells in hormone-supplemented serum-free medium 20 p3501 N85-31767

HORN ANTENNAS
Radiation patterns of a pyramidal horn antenna 09 p1311 N85-18236
Beamwidth control in pyramidal horns
[R-NIAS-27] 13 p2053 N85-22853
Prime-focus parabolic reflector antenna: Theory and measurement
[R-NIAS-20] 14 p2291 N85-24199
Dual sense, circularly polarized helical antenna
[AD-D011680] 19 p3254 N85-30175
Fin-line horn antennas
[AD-A154597] 21 p3580 N85-32255

HORSEPOWER
Tractor power selection with compaction constraints
[AD-P004300] 09 p1409 N85-18677

HOT ATOMS
Observations of absorption lines from highly ionized atoms 08 p0876 N85-15562

HOT CATHODES
Hot hollow cathode gun assembly
[DE84-014312] 01 p0121 N85-10832
Analysis of the dissipation mechanism within an instationary cathode spot of metal vapor arcs
[AD-A149258] 10 p1558 N85-19825

HOT CORROSION
NT TEMPERATURE DEPENDENCE
Effects of surface chemistry on hot corrosion life: Overview 02 p0145 N85-10960
Studies on the hot corrosion of a nickel-base superalloy, Udimet 700
[NASA-TM-86882] 02 p0183 N85-11224
Kinetics of oxidation of titanium alloy upon heating to 1000 deg C 10 p1448 N85-19122
High temperature corrosion of ceramics
[DE85-002179] 11 p1612 N85-20139
Digital temperature and velocity control of mach 0.3 atmospheric pressure durability testing burner riga in long time, unattended cyclic testing
[NASA-TM-86959] 12 p1805 N85-21321
Oxidation and hot corrosion of hot-pressed SI3N4 at 1000 deg C
[NASA-TM-86977] 12 p1811 N85-21358
Effects of surface chemistry on hot corrosion life
[NASA-CR-174915] 16 p2708 N85-26711
Burner rig corrosion of SiC at 1000 deg C
[NASA-TM-87061] 19 p3227 N85-30011
Changes of structure of EP648-VI alloy as a result of high-temperature gas corrosion 19 p3243 N85-30110
High-temperature oxidation of reaction-roasted silicon nitride with various additives 19 p3244 N85-30114
Mechanism of strength degradation for hot corrosion of alpha-SiC
[NASA-TM-87052] 19 p3248 N85-30135
A multiple linear regression analysis of hot corrosion attack on a series of nickel base turbine alloys
[NASA-TM-87020] 20 p3431 N85-31284
The effect of stress and hot corrosion on nickel-base superalloys
[AD-A154722] 21 p3566 N85-32181
Thin-film reliability and engineering overview 21 p3612 N85-32450
High temperature corrosion of ceramics
[DE85-013481] 24 p4083 N85-35303

HOT CYCLE PROPULSION SYSTEM
U TIP DRIVEN ROTORS

HOT ELECTRONS
Non-LTE considerations in spectral diagnostics of thermal transport and implosion experiments
[DE84-015187] 05 p0730 N85-14689
Stabilization of the hot electron precessional mode in a symmetric tandem mirror by the axial variation of radial electric field
[DE84-016389] 05 p0730 N85-14692
The flow of plasma in the solar terrestrial environment
[NASA-CR-174301] 08 p1224 N85-17707
Comparison of ionizing radiation and hot electron effects in MOS structures
[DE84-016766] 09 p1400 N85-18809
A microchannel plate pinhole camera for 20 to 100 keV X-ray imaging
[DE85-001572] 10 p1488 N85-19396
Measurement of hot-electron production and microwave emission by laser-irradiated CH targets
[DE85-003139] 11 p1640 N85-20331
Anomalous heating of ionospheric components (thermal e- and He+) via intense Ion Cyclotron Waves (ICW's) 14 p2368 N85-24833
Hard X-ray measurements of the hot electron rings in Nagoya BUMPY TORUS (NBT-1M)
[IPPJ-720] 19 p3370 N85-30699
Stability of a hot symmetric tandem mirror with thermal barrier
[DE85-010539] 19 p3377 N85-30952
Plug and thermal barrier potential formation in Gamma 10 23 p3976 N85-34648
Effect of ECH and ICH on ambipolar potential in NBT-1M 23 p3976 N85-34661
Simulation studies on stability of hot electron plasma 23 p3976 N85-34664
Fokker-Planck calculation of hot electron formation in the thermal barrier region of tandem mirror Gamma-10
[IPPJ-726] 23 p3979 N85-34669

HOT EXTRUDING
U EXTRUDING
HOT FORMING
U HOT WORKING
HOT GAS SYSTEMS
U HIGH TEMPERATURE GASES
HOT GASES
U HIGH TEMPERATURE GASES
HOT JET EXHAUST
U HIGH TEMPERATURE GASES
U JET EXHAUST
HOT JETS
U JET FLOW
HOT PLASMAS
U HIGH TEMPERATURE PLASMAS
HOT PRESSING
Processing ceramics
[NASA-TM-77603] 01 p0031 N85-10188
Fabrication and characterization of Si3N4 ceramics without additives by high pressure hot pressing
[NASA-TM-77724] 01 p0031 N85-10189
Hot isostatically pressed manufacture of high strength MERL 76 disk and seal shapes
[NASA-CR-165550] 02 p0183 N85-11225
High temperature deformation of hot-pressed polycrystalline orthoenstatite
[NASA-CR-174026] 02 p0285 N85-11861
HIP glassmaking for high nitrogen compositions in the Y-Si-Al-O-N system
[DE84-015546] 03 p0338 N85-12175
Development and fabrication of refractory bodies for gas turbine engines
[BMFT-FB-T-84-180] 04 p0457 N85-12899
Development and production of improved alpha-phase silicon nitride powders for hot pressing and sintering
[BMFT-FB-T-84-208] 07 p0921 N85-15830
Development and production of improved silicon carbide powder for pressureless sintering and hot pressing
[BMFT-FB-T-84-211] 07 p0934 N85-15917
Ti-6Al-4V alloy castings prepared in zircon sand molds and the effect of hot isostatic pressing
[PB85-109932/GAR] 09 p1298 N85-18150
Oxidation and hot corrosion of hot-pressed Si3N4 at 1000 deg C
[NASA-TM-86977] 12 p1811 N85-21358
Pressureless sintered silicon nitride as a promising candidate for radome materials
[AD-P004367] 12 p1826 N85-21461
Particulate toughened silicon carbide
[DE85-004797] 13 p2016 N85-22643
Dispersed-metal-toughened alumina
[NASA-CR-174687] 13 p2037 N85-22758
Sweden invents new ceramic for more durable cutting tools 15 p2536 N85-25645
Development of high temperature resistant, noncorrosible, non-metallic ceramic materials, especially silicon nitride in gas turbine application
[BMFT-FB-T-85-015] 17 p2936 N85-28125
Development of high temperature resistant noncorrodible silicon carbide components for gas turbine applications, follow-up report
[BMFT-FB-T-85-016] 17 p2936 N85-28126
Hot Isostatic Pressing (HIP): Techniques, applications and economical use
[JUEL-SPEZ-268] 17 p2939 N85-28141
Sintering reactions, structure and properties of a cobalt free nonconventional hard material
[DE85-007704] 18 p3076 N85-29025
Hot isostatically pressed Sm(2)(TM)17 magnets
[AD-A155479] 21 p3582 N85-32267
System for electro-optical ceramic recrystallization 21 p3682 N85-32872
HOT STARS
NT A STARS
NT B STARS
NT BLUE STARS
NT O STARS
NT SYMBIOTIC STARS
NT WHITE DWARF STARS
NT WOLF-RAYET STARS
Observations of absorption lines from highly ionized atoms 06 p0876 N85-15582
Strongren trails of hot white dwarfs 06 p0879 N85-15589
The Origin of Nonradiative Heating/Momentum in Hot Stars
[NASA-CP-2358] 08 p1231 N85-17755
Evidence for non-radiative activity in hot stars 08 p1231 N85-17756
Evidence for non-radiative activity in stars with T sub eff 10000 K 08 p1231 N85-17757
Bipolar ejection of matter from hot stars 08 p1233 N85-17767
Stellar winds: Observational evidence for a hot-cool star connection 08 p1233 N85-17768
Corotating interaction regions in stellar winds: Particle acceleration and non-thermal radio emission in hot stars 08 p1234 N85-17773
Synchrotron emission from chaotic stellar winds 08 p1234 N85-17774
Winds from rotating, magnetic, hot stars 08 p1234 N85-17775
Non-radiative energy from differential rotation in hot stars 08 p1234 N85-17778
Bipolar flows and X-ray emission from young stellar object 08 p1234 N85-17779
Nonradiative heating and enhanced mass-loss due to shear turbulence in massive hot stars 08 p1235 N85-17780
A leaky waveguide model for MHD wave driven winds from coronal holes 08 p1235 N85-17781
Magnetic effects in the heating and modification of flows in the outer stellar atmospheres with application to early type star case 08 p1235 N85-17783
Radiative amplification of acoustic waves in hot stars 08 p1235 N85-17786
On the role played by lines in radiatively driven stellar winds depending on the position of the stars in the HR diagram 08 p1236 N85-17787
Summary of the origin of nonradiative heating/momentum in hot stars 08 p1236 N85-17789
International Ultraviolet Explorer observations of amorphous hot galaxies
[NASA-CR-174354] 10 p1571 N85-19904
Radiative ion beams: Hot stellar reactions in the laboratory
[DE85-001570] 11 p1722 N85-20833
IUE absorption line studies of highly ionized interstellar gas 11 p1743 N85-20962
Hot stars: Six years of progress 11 p1743 N85-20963
The usual hot stars in unusual galaxies 11 p1745 N85-20975
The variation of galactic interstellar extinction in the ultraviolet 11 p1749 N85-21000
Coronal effects of the winds of early-type stars 11 p1749 N85-21002
Coordinated ultraviolet and visual observations of Omega Orionis 1982-1983 11 p1750 N85-21007
An episodic red-wing structure of SiIV, lambda 1394A, in gamma Cas 11 p1750 N85-21009
IUE spectrophotometry of the hot helium-rich PG1159 DO degenerates 11 p1751 N85-21015
Eclipse observations of Epsilon Aurigae 11 p1755 N85-21037
Egress spectra of the new eclipsing supergiant 22 Vulfeculae 11 p1755 N85-21039
HOT SURFACES
Problems with electrical interference between solar generators and shunt type regulators 13 p2010 N85-22607
Component-specific modeling
[NASA-CR-174765] 23 p3897 N85-34140
HOT WEATHER
Heat injury: Prevention is the key
[AD-A153734] 19 p3328 N85-30622
HOT WORKING
Mechanical properties of a leaded, resulfurized, rephosphorized steel in various thermo/mechanical conditions
[PB84-216464] 03 p0333 N85-12144
Process Modeling Applied to Metal Forming and Thermomechanical Processing
[AGARD-LS-137] 06 p0796 N85-15086
Control of microstructure during hot working of Ti-6242 06 p0797 N85-15091
Modelling temperature changes during hot working operations 06 p0798 N85-15095
ESR (Electroslag Refining) technology in Australia: Laboratory research and industrial development
[AD-A147776] 08 p1129 N85-17114
Summaries of press automation conference presented 08 p1139 N85-17173
Hot rolling of ceramics by the use of self propagating synthesis
[AD-D011486] 10 p1453 N85-19154
Comparison of the fatigue resistance (initiation, propagation) of cast TA6V with hot rolled TA6V — titanium alloy
[DGT-25369-PT-1] 12 p1808 N85-21341
Optimizing hot workability and controlling microstructures in difficult to process high strength and high temperature materials
[AD-D011586] 15 p2510 N85-25482
New material, process spins off from Volvo LCP 2000 program 15 p2536 N85-25648
Effect of prior warm rolling on the retained austenite content and hardening response of VIM-VAR (vacuum-induction melted-vacuum-arc remelted) AISI M-50 steel
[AD-A156145] 24 p4079 N85-35281
HOT-FILM ANEMOMETERS
Analysis of the Viking Lander 1 surface wind vector for sols 45 to 375
[NASA-CR-174349] 09 p1416 N85-18932
Development of a temperature-compensated hot-film anemometer system for boundary-layer transition detection on high-performance aircraft
[NASA-TM-86732] 22 p3730 N85-33121
HOT-WIRE ANEMOMETERS
Aero-optics experimental techniques
[AD-A146755] 07 p0957 N85-16087
An experimental investigation of unexcited and excited elliptic jets 15 p2554 N85-25755
Velocity and transient measurements in a shock tube using a hot-wire anemometer
[AD-A154694] 21 p3589 N85-32305
HOT-WIRE FLOWMETERS
Comparison of two-dimensional laser and hot-wire velocimetry for a supersonic turbulent boundary layer 11 p1576 N85-19927
Surface shear stress characteristics in turbulent flows 19 p3211 N85-29914
HOT-WIRE TURBULENCE METERS
U HOT-WIRE FLOWMETERS
U TURBULENCE METERS
HOUSEHOLDER TRANSFORMATIONS
Implementation of some concurrent algorithms
[DE85-004687] 13 p2148 N85-23334
HOUSINGS
NT COWLINGS
NT RADOMES
Flywheel containment and safety considerations 05 p0606 N85-13869
Thermally isolated structural support link
[AD-D011349] 07 p0972 N85-16176
Housing flexibility effects on rotor stability 16 p2738 N85-26806
Refrigerated dynamic seal to 6.9 MPa (1000 psi)
[NASA-TM-87108] 23 p3930 N85-34356
HOVERCRAFT
U GROUND EFFECT MACHINES
HOVERING
Reconstruction of a 3-dimensional transonic rotor flow field from holographic interferogram data
[NASA-TM-86690] 12 p1770 N85-21112
Experimental study of main rotor tip geometry and tail rotor interactions in hover. Volume 1. Text and figures
[NASA-CR-177336-VOL-1] 13 p1965 N85-22344
Experimental study of main rotor tip geometry and tail rotor interactions in hover. Volume 2: Run log and tabulated data
[NASA-CR-177336-VOL-2] 13 p1965 N85-22345
Hover test results of a small-scale twin-tilt nacelle model
[NASA-TM-86665] 14 p2210 N85-23706
Harrier 15 p2687 N85-26595
Effect of ground and/or ceiling planes on thrust of rotors in hover
[NASA-TM-86754] 20 p3388 N85-31014
HPRR
U HEALTH PHYSICS RESEARCH REACTOR
HR DIAGRAM
U HERTZSPRUNG-RUSSELL DIAGRAM
HTGR
U HIGH TEMPERATURE GAS COOLED REACTORS
HTPB PROPELLANTS
Study of HTPB-based SOFRAM fuels
[FOA-C-20563-D3] 11 p1614 N85-20150
Effect of variable solid phase thermal properties on propellant combustion 13 p2002 N85-22547
HU-1 HELICOPTER
U UH-1 HELICOPTER
HUBBLE CONSTANT
Ultrahigh energy gamma rays: Carriers of cosmological information
[OG-2.7-14] 22 p3872 N85-33867
HUBBLE DIAGRAM
Cosmology 07 p1058 N85-16701
On the role played by lines in radiatively driven stellar winds depending on the position of the stars in the HR diagram 08 p1236 N85-17787
HUBBLE SPACE TELESCOPE
Algorithm for astronomical, extended source, signal-to-noise radio calculations
[NASA-TP-2396] 03 p0445 N85-12833
Algorithm for astronomical, point source, signal to noise ratio calculations
[NASA-TP-2397] 03 p0445 N85-12834
Local Interstellar Medium. International Astronomical Union Colloquium No. 81
[NASA-CP-2345] 06 p0872 N85-15539

Future studies of the local interstellar medium with Space Telescope and Columbus 06 p0660 N85-15593
Study of application of space telescope science operations software for SIRTF use
[NASA-CR-177337] 09 p1287 N85-18080
Future ultraviolet experiments, including FUSE/COLUMBUS 11 p1744 N85-20969
IUE observations of faint standard stars for calibration of the space telescope 11 p1761 N85-21076
Innovative research in the design and operation of large telescopes for space: Aspects of giant telescopes in space
[NASA-CR-178626] 13 p2170 N86-23462
Telescope in lunar orbit 15 p2662 N85-26508
Hubble space telescope: Pointing error effects on nonlinear ball joints
[NASA-TM-86511] 20 p3545 N85-32058
Astron telescope stabilization system 22 p3732 N85-33133
Features of the solar array drive mechanism for the space telescope 22 p3796 N85-33532
Appendage deployment mechanism for the Hubble Space Telescope program 22 p3796 N85-33533

HUBS
Extended aeroelastic analysis for helicopter rotors with prescribed hub motion and blade appended pendulum vibration absorbers
[NASA-CR-172455] 03 p0315 N85-12038
Integrated technology rotor/flight research rotor hub concept definition
[NASA-CR-166447] 09 p1280 N85-18051
Integrated Technology Rotor/Flight Research Rotor (ITR/FRR) concept definition
[NASA-CR-166443] 10 p1423 N85-18078
Integrated Technology Rotor/Flight Research Rotor (ITR/FRR) concept definition
[NASA-CR-166445] 10 p1423 N85-18079
Integrated technology rotor/flight research rotor concept definition study
[NASA-CR-166446] 10 p1424 N85-18080
Integrated Technology Rotor/Flight Research Rotor (ITR/FRR) concept definition study
[NASA-CR-166444] 10 p1424 N85-18081
Self-locking mechanical center joint
[NASA-CASE-LAR-12864-1] 19 p3279 N85-30336
A new main rotor hub for the AS 332 Super Puma
[SNIAS-851-210-102] 20 p3363 N85-31047

HUGHES MILITARY AIRCRAFT
U MILITARY AIRCRAFT

HUGONIOT ADIABAT
U HUGONIOT EQUATION OF STATE

HUGONIOT EQUATION OF STATE
Dynamic compaction of a monosized spherical tungsten powder
[DE85-014608] 24 p4060 N85-35289

HULLS (STRUCTURES)
NT SHIP HULLS

HUMAN BEHAVIOR
Mathematical Models of the Circadian Sleep-Wake Cycle
[AD-A145712] 02 p0235 N85-11532
Patterns of behavior in lodgings exposed to traffic noise
[NASA-TM-77750] 03 p0387 N85-12479
Evaluation of the National Library of Medicine's programs in the medical behavior sciences. Coverage of the Medical Behavioral Sciences (MBS) literature in monographic databases, study 5
[PB84-230631] 03 p0439 N85-12797
Evaluation of the National Library of Medicine's programs in the medical behavior sciences. Online searchers' reactions to database and vendor capabilities in the Medical Behavioral Sciences (MBS), study 4
[PB84-230623] 03 p0439 N85-12796
Evaluation of the National Library of Medicine's programs in the medical behavior sciences. Quality of indexing: The development and testing of a methodology comparing databases covering the Medical Behavioral Sciences (MBS) literature, study 3
[PB84-230615] 03 p0439 N85-12795
Evaluation of the National Library of Medicine's programs in the medical behavior sciences. Test retrievals in five major databases covering the Medical Behavioral Sciences (MBS) literature, study 2
[PB84-230607] 03 p0440 N85-12800
Evaluation of the National Library of Medicine's programs in the medical behavior sciences. Coverage, overlaps and gaps in bibliographic databases dealing with the Medical Behavioral Sciences (MBS) literature, study 1
[PB84-230490] 03 p0440 N85-12801
Evaluation of the National Library of Medicine's program in the medical behavior sciences. An analysis of the National Library of Medicine's (NLM) handling of Medical Behavioral Sciences (MBS) literatures: Some research tests of methods for evaluating bibliographic databases, executive summary
[PB84-230481] 03 p0440 N85-12802
USSR report: Life Sciences: Biomedical and behavioral sciences
[JPRS-UBB-84-026] 04 p0543 N85-13457
Reflection of lateralization of sound stimuli in evoked potentials of human brain 04 p0544 N85-13463
The human role in space. Volume 2: Research analysis and technology report
[NASA-CR-171224] 04 p0546 N85-13474
The human role in space. Volume 3: Generalizations on human roles in space
[NASA-CR-171225] 04 p0546 N85-13475
Evaluation of fuzzy rulemaking for expert systems for failure detection 05 p0703 N85-14508
An investigation of the relationship between stressful life events and psychological, behavioral and physiological outcomes
[AD-A147754] 08 p1197 N85-17541
Compatibility effects and preference reversals
[AD-A148309] 08 p1198 N85-17544
European scientific notes. Volume 38, number 11
[AD-A148226] 08 p1230 N85-17745
Communications skills for CRM training 09 p1276 N85-18017
European Scientific Notes, volume 38, number 12
[AD-A148713] 09 p1418 N85-18046
USSR report: Life sciences. Biomedical and behavioral sciences
[JPRS-UBB-85-011] 10 p1525 N85-19616
Functional role of type of person's temperament in individual and mutual activity 10 p1525 N85-19621
Research opportunities in human behavior and performance
[NASA-CR-175473] 10 p1529 N85-19640
Aircrew-aircraft integration issues in future US Army helicopters 10 p1535 N85-19672
USSR report: Life sciences. Biomedical and behavioral sciences
[JPRS-UBB-85-010] 11 p1690 N85-20628
Psychological aspects of phenomenon of spatial synchronization of EEG potential 11 p1691 N85-20632
Effect of prolonged hunger during experimental hikes 11 p1692 N85-20637
Psychological components in the development and prevention of air sickness 11 p1695 N85-20659
Assessing the behavior and performance of teams in organizations: The case of air transport crews
[AD-A150359] 13 p2143 N85-23302
Predictors of cold weather health behaviors
[AD-A151910] 16 p2843 N85-27529
Shape with and without redundant colour as coding mechanism for simulated radar displays in a time-extended simple vigilance task
[AD-A151683] 16 p2844 N85-27533
Identifying solution paths in cognitive diagnosis
[AD-A152463] 17 p3000 N85-28549
Individual characteristics and unit performance: A review of research and methods
[AD-A153145] 17 p3001 N85-28550
A formal analysis of the evolution of cooperation
[AD-A152539] 17 p3018 N85-28662
European Science Notes, Volume 39, Number 3
[AD-A152445] 17 p3027 N85-28717
Verbal information processing paradigms: A review of theory and methods
[AD-A153229] 17 p3050 N85-28880
Psychological issues relevant to astronaut selection for long-duration space flight: A review of the literature
[AD-A154051] 19 p3330 N85-30627
Resource allocation in cerebral specialization of function: Behavioral and electrophysiological studies
[AD-A155092] 21 p3664 N85-32759
Rapid determination of cadet discipline by projective tests 22 p3821 N85-33671
Effects of low level carbon monoxide (CO) on tracking and monitoring. An attempt to replicate the findings of Putz et al. (1976) protocol 2
[AD-A155722] 22 p3825 N85-33694
USSR report: Life sciences. Biomedical and behavioral sciences
[JPRS-UBB-85-021] 23 p3951 N85-34489

HUMAN BEINGS
USSR report: Space Biology and Aerospace Medicine, volume 18, no. 4, July - August 1984
[JPRS-USB-84-006] 01 p0091 N85-10611
Functional capacities of elderly subjects exposed to simulated spaceflight factors 01 p0091 N85-10617
Models of natural intelligence in fault diagnosis tasks: Implications for training and aiding of maintenance personnel
[AD-P003927] 02 p0246 N85-11607
Report of the Meeting of Experts on Climate and Human Health
[WCP-78] 05 p0687 N85-14413
Organization of the session 05 p0687 N85-14414
Difficulties encountered in determining the potential involvement of consultants on health problems in various climatic zones 05 p0687 N85-14416
Modeling of human motion by computer considering measurement errors in initial data 07 p1012 N85-16429
Management of vibration sickness in coal mines by hyperbaric oxygenation 10 p1523 N85-19609
Comparative assessment of different treatment modalities in miners with vibration- and noise-induced disease 10 p1524 N85-19610
Aircraft noise effects: An interdisciplinary study of the effects of aircraft noise on man. Part 1: Basic report
[NASA-TM-75819] 10 p1526 N85-19629
Health assessment document for carbon tetrachloride
[PB85-124198] 10 p1528 N85-19638
The effect of jamming/deception on decision making
[AD-A149740] 12 p1828 N85-21472
Human cognition and intelligence: Towards an integrated theoretical perspective
[CSIR-SR-PERS-350] 13 p2143 N85-23300
Photoreactivation and other ultraviolet/visible light effects on DNA in human skin
[DE85-005135] 14 p2390 N85-24719
Functional impairment and structureal cervical injuries in human surrogates
[PB85-167436] 15 p2619 N85-26137
The origin of brain potentials associated with selective visual attention
[AD-A152291] 16 p2840 N85-27511
Evaluation of a field expedient technique for sweat sample collection
[AD-A151916] 16 p2841 N85-27521
Collected epidemiological studies of the late effects of internal radium in man, and mechanistic investigations of those effects, part 2
[DE85-011174] 19 p3331 N85-30636
Task description for the 1983 catalog of tasks for the materials processing in space program 20 p3496 N85-31746
Review of the psychological issues relating to the effectiveness of structured programming
[AD-A154593] 21 p3665 N85-32766
Spacelab 1 hematology experiment (INS103): Influence of space flight on erythrokinetics in man
[NASA-TM-58258] 22 p3824 N85-33693
Tritium hazard via the ingestion pathway
[DE85-012897] 24 p4133 N85-35618

HUMAN BODY
Non-invasive techniques for determining musculoskeleton body composition
[DE84-015718] 04 p0545 N85-13470
Introduction to human biometeorology 05 p0687 N85-14415
In vivo neutron activation analysis: Body composition studies in health and disease
[DE84-014092] 05 p0696 N85-14480
Comparison of thermal responses between rest and leg exercise in water
[AD-A146818] 07 p1015 N85-16448
Effects of body mass and morphology on thermal responses in water
[AD-A147558] 07 p1016 N85-16455
Technique for measuring body circumferences and skinfold thicknesses
[AD-A148166] 08 p1195 N85-17532
Gravity and biological systems: Emphasis on human physiology
[ESA-BR-21] 09 p1360 N85-18558
Scattering of electromagnetic waves by human body and its applications 09 p1363 N85-18572
Health standards for general vibration 10 p1523 N85-19607
The medical results of human exposures to radio frequency radiation
[AD-A149718] 12 p1905 N85-21962
Study of effective physiological temperature 13 p2042 N85-22760
Distribution of radium and plutonium in human bone
[DE85-005025] 13 p2142 N85-23298
Mathematical models relating to human thermoregulation: Basic assumptions, validation, and application. Parts A and B
[AD-A151556] 15 p2618 N85-26130
Human body dimensions: Body outlines and envelope curves at different normal positions and movements
[HSE-TRANS-10666] 19 p3332 N85-30640

Kidney cell electrophoresis, continuing task
20 p3496 N85-31747
A mechanical model of the human body and its application
24 p4129 N85-35598

HUMAN CENTRIFUGES
Susceptability to kinetoses and the amplitude perceived from sensory illusions
11 p1694 N85-20651
Centrifuge operations and training in the Royal Netherlands Air Force
20 p3511 N85-31825

HUMAN ENGINEERING
U HUMAN FACTORS ENGINEERING

HUMAN FACTORS ENGINEERING
NT MOTION SIMULATION
LED multifunction keyboard engineering study
[AD-A145199]
01 p0010 N85-10061
USSR report: Machine tools and metalworking equipment
[JPRS-UMM-84-019]
01 p0035 N85-10214
A review of selected studies of computerized speech recognition conducted at the Naval Postgraduate School
[AD-A144841]
01 p0037 N85-10235
The Reports of Aeromedical Laboratory, volume 25, no. 1/2
[ISSN-0023-2858]
01 p0090 N85-10605
Assessment of the inflating characteristics of the modified anti-G suit
01 p0090 N85-10609
Human response to vibroacoustic environments of space vehicles
[NASA-TM-86316]
01 p0116 N85-10789
Highlights of the Institute of Sound and Vibration Research
01 p0131 N85-10905
Aircrew-aircraft integration: A summary of US Army research programs and plans
[NASA-TM-85991]
02 p0148 N85-11004
Human engineering laboratory grounding analysis: Project Helga
[AD-A145728]
02 p0195 N85-11300
Decision tree rating scales for workload estimation: Theme and variations
[NASA-CR-174062]
02 p0237 N85-11544
Respiratory protection for children 3 - 6 years of age
[FOA-C-40197-C2]
02 p0238 N85-11550
Auditory information systems in military aircraft: Current configurations versus the state of the art
[AD-A145469]
02 p0275 N85-11794
A management workstation concept
[AD-A145617]
02 p0294 N85-11906
Study of annoyance due to urban automobile traffic. Annex 4: A catalog of the characteristics of noise at different measuring points
[NASA-TM-77516]
03 p0387 N85-12478
Patterns of behavior in lodgings exposed to traffic noise
[NASA-TM-77750]
03 p0387 N85-12479
The human operator and system effectiveness
[AD-A146326]
03 p0402 N85-12563
Climate-chamber experiments to improve pilots' work conditions
04 p0543 N85-13454
Impact of space medicine on Earth-based medicine: Academician Ye. I. Chazov comments on the work in orbit of physician O. Atkov
04 p0543 N85-13458
The human role in space. Volume 2: Research analysis and technology report
[NASA-CR-171224]
04 p0546 N85-13474
The human role in space. Volume 3: Generalizations on human roles in space
[NASA-CR-171225]
04 p0546 N85-13475
Investigation and development of multicolored liquid crystal display systems for automotive dashboard application and large format information boards
[BMFT-FB-T-84-187]
04 p0572 N85-13652
Twentieth Annual Conference on Manual Control, volume 1
[NASA-CP-2341-VOL-1]
05 p0699 N85-14487
Time series modeling of human operator dynamics in manual control tasks
05 p0699 N85-14488
Quantification of cross-coupling and motion feedthrough for multiaxis controllers used in an air combat flying task
05 p0700 N85-14491
Evaluation of fuzzy rulemaking for expert systems for failure detection
05 p0703 N85-14508
The role of knowledge structures in fault diagnosis
05 p0709 N85-14509
Twentieth Annual Conference on Manual Control, volume 2
[NASA-CP-2341-VOL-2]
05 p0707 N85-14535
Measurement of workload: Physics, psychophysics, and metaphysics
05 p0708 N85-14539
A comparative study of alternative controls and displays for by the severely physically handicapped
05 p0709 N85-14549
Performance measures for aircraft landings as a function of aircraft dynamics
05 p0712 N85-14565
Measuring pilot workload in a moving-base simulator. Part 2: Building levels of workload
05 p0712 N85-14566
Technical Workshop: Advanced Helicopter Cockpit Design
[NASA-CP-2351]
06 p0750 N85-14806
Helicopter human factors programs and plans
06 p0751 N85-14808
Human factors in cockpit automation
06 p0752 N85-14819
Intelligent interfaces for tactical airborne platforms
06 p0752 N85-14820
Human factors of visual displays
06 p0752 N85-14821
Crewstation design and validation
06 p0752 N85-14822
Avionics technology - system concepts
06 p0753 N85-14824
Man-machine interface requirements - advanced technology
06 p0753 N85-14825
Attack helicopter (AH-1T) cockpit systems integration
06 p0753 N85-14826
Avionics system design for requirements for the United States Coast Guard HH-65A Dolphin
06 p0753 N85-14827
Human aspects in office automation
[PB84-240738]
06 p0847 N85-15378
Human engineer's guide to auditory displays. Volume 2: Elements of signal reception and resolution affecting auditory displays
[AD-A146513]
06 p0859 N85-15462
Human engineer's guide to auditory displays. Volume 1. Elements of perception and memory affecting auditory displays
[AD-A146601]
06 p0860 N85-15464
Biodynamic resistant control stick
[AD-D011380]
07 p0904 N85-15721
USSR report: Life sciences. Biomedical and behavioral sciences
[JPRS-UBB-84-015]
07 p1010 N85-16416
Human factors and training research in military organizations and systems
[AD-A146832]
07 p1020 N85-16475
Human factors characteristics of the Joint Tactical Fusion Test Bed: Field test 467 results
[AD-A146856]
07 p1020 N85-16476
Mental models and cooperative problem solving with expert systems
[AD-A147843]
07 p1021 N85-16479
Operational requirements versus technological capabilities
08 p1072 N85-16798
A Computer-generated topographic display system for navigation and mission planning in helicopters
08 p1073 N85-16800
A review of US Army aircrew-aircraft integration research programs
08 p1075 N85-16814
Impact tests of adjusters for the HBU-12 lap belt
[AD-A148021]
08 p1080 N85-16843
Automatic speech recognition in severe environments
[AD-A148461]
08 p1153 N85-17260
Waste collection subsystem study
[NASA-CR-171836]
08 p1199 N85-17552
Space Shuttle Orbiter waste collection system conceptual study
[NASA-CR-171844]
08 p1199 N85-17553
A computer aided Multi-Man-Machine Work Area Design and Evaluation System (MAWADES)
[AD-A147950]
08 p1199 N85-17554
Development of an electro-pneumatic anti-G valve for high performance fighter aircraft
[AD-A148468]
08 p1201 N85-17561
Simulating speed and height cues in the C-130 weapon system trainer
[AD-P004313]
09 p1268 N85-17967
The fiber-optic helmet-mounted display
[AD-P004330]
09 p1270 N85-17984
Dual arm master controller concept
[DE85-001901]
09 p1327 N85-18344
USSR report: Life sciences. Biomedical and behavioral sciences
[JPRS-UBB-85-002]
09 p1360 N85-18559
Role of engineering psychology
09 p1361 N85-18561
Further development in ride quality assessment
[AD-P004280]
09 p1406 N85-18856
European Scientific Notes, volume 38, number 12
[AD-A148713]
09 p1418 N85-18946
Pictorial format display evaluation
[AD-A149252]
10 p1425 N85-18966
Production turret lathe retrofitted with robot
10 p1461 N85-19214
Be healthy, pilot
10 p1526 N85-19626
Guide to human factors information sources
[AD-A149102]
10 p1531 N85-19649
Human Factors Considerations in High Performance Aircraft
[AGARD-CP-371]
10 p1532 N85-19653
Aircrew and avionics: Friends or Foes?
10 p1532 N85-19654
Military pilot ergonomics
10 p1532 N85-19655
Implications of guidance and control technology on human factors considerations
10 p1532 N85-19656
Observations of physiological and psychological effects of terrain following flight based on in-flight test experience
10 p1532 N85-19657
Impact of future aircombat characteristics on pilot performance and cockpit design
10 p1533 N85-19661
Electronic displays: Their strengths and weaknesses for advanced high performance aircraft
10 p1533 N85-19664
Changing system and display concepts and their impact on aircrew performance
10 p1533 N85-19665
Some effects of display format variables on the perception of aircraft spatial orientation
10 p1534 N85-19666
Pilot workload, performance and aircraft control automation
10 p1534 N85-19670
The F-18: A new era for human factors
10 p1534 N85-19671
Aircrew-aircraft integration issues in future US Army helicopters
10 p1535 N85-19672
European Scientific Notes. Volume 39, number 2
[AD-A148994]
10 p1573 N85-19919
Proceedings of the 14th Army Science Conference. Volume 1: Principal Authors A through H
[AD-A149200]
10 p1573 N85-19920
Biomechanics finds practical applications in aerospace research
11 p1621 N85-20205
Functional system theory in practice
11 p1660 N85-20629
Aviation medicine's role in modern airforce discussed
11 p1696 N85-20662
Symposium on Military Aviation Medicine summarized
11 p1696 N85-20663
Man/machine interface for a nuclear cask remote handling control station: System design requirements
[DE85-000256]
11 p1697 N85-20667
Computer-generated display system guidelines. Volume 1: Display design
[DE85-000679]
11 p1701 N85-20699
Proceedings of the 6th Advanced Aircrew Display Symposium
[AD-A150044]
12 p1778 N85-21160
Human assembly time versus levels of visual and tactile sensory input: Experimental results for five devices
[AD-A149982]
12 p1909 N85-21980
Proceedings of the 6th Human Factors Workshop on Aviation
[AD-A150043]
12 p1909 N85-21982
NASA: Model development for human factors interfacing
[NASA-CR-175584]
12 p1910 N85-21985
Shoulder and hip joint for hard space suits and the like
[NASA-CASE-ARC-11543-1]
12 p1910 N85-21986
Torso sizing ring construction for hard space suit
[NASA-CASE-ARC-11616-1]
12 p1910 N85-21987
Very-high level concurrent programming
[AD-A150009]
12 p1916 N85-22026
TASS update on unmanned flight of Salyut-7
13 p1977 N85-22404
Construction of a menu-based system
[NASA-CR-172580]
13 p2146 N85-23321
Principles of software engineering environment design
[AD-A150352]
13 p2147 N85-23324
Complex program of ergonomic studies Pilot described
14 p2396 N85-24698
Users guide: The LaRC human-operator-simulator-based pilot model
[NASA-TM-86367]
14 p2390 N85-24721
Programmer/analyst workstation evaluation report
[NASA-CR-175289]
14 p2394 N85-24749
Streamlined Test Reporting And Planning (STRAP): Computerized human factors questionnaire
[AD-A150811]
14 p2395 N85-24751
Current approaches for the biophysical and physiological evaluation of combat clothing for environmental extremes
[AD-A151012]
14 p2395 N85-24752
Investigation of technology needs for avoiding helicopter pilot error related accidents
[NASA-CR-3695]
15 p2465 N85-25220
Preliminary design of a limb restraint evaluator
[AD-A151749]
15 p2466 N85-25226
Rotorcraft digital advanced avionics system (RODAAS) functional description
[NASA-CR-166611]
15 p2468 N85-25237
US Army human Engineering Laboratory Communications Survey: A Pilot Study (HELCOMS-PS)
[AD-A151434]
15 p2521 N85-25544
An introductory study of automatic speech recognition systems
[BAE-BT-12296]
15 p2539 N85-25677

A portable battery for objective, non-obstrusive measure of human performance
[NASA-CR-171868] 15 p2588 N85-25942
Computerized biophysical data acquisition system for motion sickness studies
[AD-A151661] 15 p2618 N85-26131
A practical system for collecting reliable data on the space-time behavior of people
[AD-A151174] 15 p2619 N85-26140
Proceedings of the BAe human factors seminar
[BAE-BT-11873] 15 p2620 N85-26145
Human factors department 1981 publications
[BAE-BT-12885] 15 p2620 N85-26147
The human engineering of laboratory data acquisition and control systems
[AD-A151576] 15 p2620 N85-26148
Activities report for FOA 53: Laboratory for man and information systems
[FOA-C-53019-H] 15 p2621 N85-26150
Development of a user support package for CPESIM 2 • (a computer simulation for CPE (Computer Performance Evaluation) use
[AD-A151899] 15 p2624 N85-26170
A comparison of pictorial and speech warning messages in the modern cockpit
[AD-A151917] 16 p2707 N85-26706
The introduction of new cockpit technology: A human factors study
[NASA-TM-86859] 16 p2843 N85-27526
Shape with and without redundant colour as coding mechanism for simulated radar displays in a time-extended simple vigilance task
[AD-A151883] 16 p2844 N85-27533
Design of computer-related workstations in relation to job functions and productivity
[AD-A151938] 16 p2844 N85-27534
Corrective-predictive systems
[BLL-M-36063-(5828.4)] 16 p2851 N85-27573
Information presentation in power plant control rooms
[VTT-320] 16 p2864 N85-27668
Optimizing computational efficiency and user convenience in plasma simulation codes
[DE85-007661] 16 p2866 N85-27682
Utilization of an automated riveting system in aircraft construction
[MBB-UT-11/84-O] 16 p2875 N85-27736
Space Station crew safety alternatives study. Volume 5: Space Station safety plan
[NASA-CR-3858] 17 p2908 N85-27930
Robotic safety systems and methods: Savannah River site
[DE85-006261] 17 p2974 N85-28375
Hand controllers for teleoperation. A state-of-the-art technology survey and evaluation
[NASA-CR-175890] 17 p3002 N85-28559
Mechanizing of handling operations in drop forging with hammers and presses (conducted ergonomical examinations)
[BMFT-FB-HA-84-051] 17 p3002 N85-28561
Space Station crew safety alternatives study. Volume 4: Appendices
[NASA-CR-3857] 18 p3055 N85-29058
The POK project; studies of information handling problems with a new kind of communication device — precoded signals
[FOA-A-53001-H2] 18 p3091 N85-29131
CELSS transportation analysis
18 p3156 N85-29538
Proceedings of the Seminar on Space Station Human Productivity
[NASA-TM-86673] 18 p3156 N85-29539
Space station crew safety: Human factors interaction model 18 p3156 N85-29540
Internal contamination in the space station
18 p3157 N85-29549
The human role in space (THURIS)
18 p3158 N85-29557
Overview: Human factors issues in space station architecture 18 p3158 N85-29558
Human factors issues in space station architecture
18 p3158 N85-29560
Man-machine tradeoff study 18 p3158 N85-29561
Some ideas and questions regarding space station design for human use 18 p3158 N85-29562
Human productivity experience and undersea habitat design 18 p3159 N85-29563
Considerations for space station interior architecture
18 p3159 N85-29564
Human factors in space station architecture: The ECLSS module concept 18 p3159 N85-29565
Habitability sleep accommodations
18 p3159 N85-29566
Customer and mission influence on space station architecture 18 p3159 N85-29567
Simulation for human factors research. A central question: Fidelity 18 p3159 N85-29568
Mockups and human productivity studies
18 p3159 N85-29570
Rockwell experience applications to Ames space station mockup habitability/productivity studies
18 p3159 N85-29572
Human factors in cockpit automation: A field study of flight crew transition
[NASA-CR-177333] 19 p3215 N85-29937
Space station crew safety alternatives study. Volume 3: Safety impact of human factors
[NASA-CR-3856] 19 p3223 N85-29984
Space station crew safety alternatives study, volume 1
[NASA-CR-3854] 19 p3223 N85-29985
Human Engineering Guide to Equipment Design (HEGED)
[AD-A154087] 19 p3331 N85-30831
Physical dimensions of humans; values; the effect of clothing, working clothes and protective equipment on the design of work places
[HSE-TRANS-10666] 19 p3331 N85-30838
The design of working systems on ergonomic principles. The importance of clothes and protective equipment in the design of the workplace
[HSE-TRANS-10665] 19 p3332 N85-30839
Human body dimensions: Body outlines and envelope curves at different normal positions and movements
[HSE-TRANS-10666] 19 p3332 N85-30840
Space Station man-machine automation trade-off analysis
[NASA-CR-176046] 20 p3408 N85-31147
Study to determine potential flight applications and human factors design guidelines for voice recognition and synthesis systems
[NASA-CR-172590] 20 p3440 N85-31349
Ergonomic problems regarding the interactive touch input via screens in onboard and ground-based flight control
[NASA-TM-77814] 20 p3512 N85-31832
The blind and the paralyzed. The notion of the tool revealed and integrated in a different organization environment
[SNIAS-851-422-104] 20 p3513 N85-31835
Human factors engineering contracts in Sweden: An overview
[FOA-C-56043-H2] 20 p3513 N85-31836
Human factors engineering data sources; an overview
[FOA-C-56044-H2] 20 p3513 N85-31837
Physical dimensions of humans, values, envelope curves in different postures
[HSE-TRANS-10669] 20 p3513 N85-31838
Noise reduction in the automotive test cell of the Motor Institute of Naples
[REPT-85-RR-361] 20 p3524 N85-31917
Sound-insulating enclosures — machine noise
[BMFT-FB-HA-85-005] 20 p3525 N85-31925
Space Station crew safety alternatives study. Volume 2: Threat development
[NASA-CR-3855] 21 p3558 N85-32133
USSR report: Life sciences. Biomedical and behavioral sciences
[JPRS-UBB-85-020] 21 p3663 N85-32752
Living aloft: Human requirements for extended spaceflight
[NASA-SP-483] 21 p3666 N85-32772
Design guidelines for user-system interface software
[AD-A154907] 21 p3671 N85-32807
USSR report: Life sciences. Biomedical and behavioral sciences
[JPRS-UBB-85-018] 22 p3819 N85-33660
Speech analysis system for assessing pilots' working fitness 22 p3819 N85-33661
Using percent-done program indicators to enhance user interfaces 23 p3960 N85-34548
Calculation of trajectories of detached wind turbine blades and prediction of site risk levels associated with failures of HAWT's 24 p4110 N85-35475
The human engineering eye movement measurement research facility
[AD-A156099] 24 p4132 N85-35613
Recommendations for content revision and alternate delivery modes for the Human Engineering Guide to Equipment Design (HEGED)
[AD-A155781] 24 p4134 N85-35624
Attacking software crisis: A macro approach
[AD-A155584P] 24 p4136 N85-35645

HUMAN PATHOLOGY
Material thermolysis product toxicity: Definition of a hazard evaluation methodology
[CERMA-84-08] 11 p1692 N85-20641
Selection procedures for F-16 pilots in the Belgian Air Force 20 p3510 N85-31822
Analogies of control mechanisms in flight guidance and medicine 24 p4129 N85-35597

HUMAN PERFORMANCE
NT ASTRONAUT PERFORMANCE
NT OPERATOR PERFORMANCE
NT PILOT PERFORMANCE
The perceptual quality of smoke screens: An analysis of the Oldebroek 2 trials, May 1981
[IZF-1984-20] 01 p0095 N85-10841
The prediction of observer responses from photometric data on smoke screens; an analysis of the Oldebroek 2 trials, May 1981
[IZF-1984-21] 01 p0095 N85-10842
Self-paced instruction. Factors critical to implementation in Air Force technical training: A preliminary inquiry
[AD-A145096] 01 p0097 N85-10847
Ada (trademark) training curriculum. Software engineering for managers m101 teacher's exercise guide
[AD-A145094] 01 p0104 N85-10895
Airborne performance measurement system design: C-5 aircraft
[AD-A145436] 02 p0236 N85-11539
An investigation of the use of steady-state evoked potentials for human performance and workload assessment and control
[AD-A145727] 02 p0237 N85-11541
The effects of feedback and predictability of human judgment
[AD-A145744] 02 p0237 N85-11542
Using gross outline features in long range target identification
[FOA-C-53018-H2] 02 p0237 N85-11543
Overview of training and aiding
[AD-P003917] 02 p0245 N85-11597
The role of physical and physiological capacities and their modification on the tolerance to various stress experienced by Air Force personnel
[AD-A145779] 03 p0400 N85-12550
Experiments with hydrox at 1.3 MPa (13 atm) — for divers
[FOA-C-58014-H1] 04 p0545 N85-13471
Human reliability data bank: Feasibility study
[DE84-015215] 04 p0546 N85-13476
Physical performance capacity after a 7 day head-down tilt (-6 deg) 05 p0692 N85-14451
Medication interference with space research: An example from a mass-discrimination experiment on Spacelab 1 05 p0695 N85-14472
Estimating number, time and length; a baseline study
05 p0695 N85-14473
The effect of propranolol on the training response to endurance exercise in normal human adults
05 p0696 N85-14479
Catecholamine excretion and subjective ratings of tension during autogenic training and mental stress
[REPT-172] 05 p0697 N85-14483
Time series modeling of human operator dynamics in manual control tasks 05 p0699 N85-14488
Multiloop manual control of dynamic systems
05 p0702 N85-14505
The role of knowledge structures in fault diagnosis
05 p0703 N85-14509
Fitts' law? A test of the relationship between information load and movement precision 05 p0705 N85-14523
A production system model of capturing reactive moving targets 05 p0705 N85-14524
Models for the effects of G-seat cuing on roll-axis tracking performance 05 p0707 N85-14532
Subjective workload assessment and voluntary control of effort in a tracking task 05 p0708 N85-14540
Classification systems for individual differences in multiple-task performance and subjective estimates of workload 05 p0708 N85-14543
The representation of action plans in long term memory 05 p0709 N85-14545
On choosing between two probabilistic choice sub-models in a dynamic multitask environment
05 p0711 N85-14563
No fatigue effect on blink rate
05 p0712 N85-14564
Situational interactive micro/graphic simulator system for improving maintenance performance
[AD-A146577] 06 p0757 N85-14848
Performance evaluation of A-10 aircraft maintenance units and aircraft using constrained facet analysis
[AD-A146955] 07 p0893 N85-15660
Nondestructive inspection: Improved capabilities of technicians
[AD-A147388] 07 p0975 N85-16196
Effects of restricted water intake on performance in a cold environment
[AD-A146804] 07 p1015 N85-16450
On the structure of information in software
[AD-A147580] 07 p1026 N85-16511
Efforts to improve aviation medical examiner performance through continuing medical education and annual performance reports
[AD-A148078] 09 p1195 N85-17531

Training high performance skills: Fallacies and guidelines
[AD-A148574] 08 p1198 N85-17545
Design of an evaluation system to measure performance degradation due to continuous operations
[AD-A148188] 08 p1200 N85-17558
Decision making in stressful conditions: A model based on the coping perspective
[FOA-C-55064-H3] 08 p1229 N85-17738
Work capacity of heat and electric power plant operations working 12 hour day and night shifts
09 p1362 N85-18567
Success in learning occupation of chemical production technician as function of certain personality traits and development of psychophysiological functions
09 p1362 N85-18568
Hydrogen-oxygen (hydrox) breathing at 1.3MPa
[FOA-C-58015-H1] 09 p1364 N85-18577
Neurocognitive pattern analysis of an auditory and visual numeric motor control task. Part 1: Development of methods
[AD-A148809] 09 p1364 N85-18578
Bibliography of unclassified reports, FY 1984
[AD-A148836] 09 p1401 N85-18819
Research opportunities in human behavior and performance
[NASA-CR-175473] 10 p1529 N85-19640
The multiple resources model of human performance: Implications for display design 10 p1534 N85-19669
Laboratory tests of motion sickness susceptibility
11 p1694 N85-20648
Space motion sickness monitoring experiment: Spacelab 1 11 p1695 N85-20654
Psychological components in the development and prevention of air sickness 11 p1695 N85-20658
Team dimensions: Their identity, their measurement and their relationships
[AD-A149662] 12 p1908 N85-21978
Human assembly time versus levels of visual and tactile sensory input: Experimental results for five devices
[AD-A149982] 12 p1909 N85-21980
NASA: Model development for human factors interfacing
[NASA-CR-175584] 12 p1910 N85-21985
The man-machine interface
[AD-A149971] 12 p1910 N85-21986
Task influences in the analytic-intuitive approach to decision making
[AD-A149870] 12 p1950 N85-22250
Assessing the behavior and performance of teams in organizations: The case of air transport crews
[AD-A150359] 13 p2143 N85-23302
Personal decision making: The influence of perceived locus of control and degree of rationality on information seeking strategies 13 p2167 N85-23446
Multiple resources and display formatting: The implications of task integration in a simulated air traffic control task
[AD-A150713] 14 p2292 N85-24205
Plans for adaptation research during Antarctic expedition 14 p2333 N85-24428
Instrument for determining spatial coordination of hand movements 14 p2367 N85-24702
The effect of set size on color matching
[AD-A150699] 14 p2368 N85-24713
The effect of set size on color recognition
[AD-A150958] 14 p2391 N85-24726
The effect of strategy in second order manual control on resource competition with a sternberg memory search task
[AD-A150985] 14 p2391 N85-24727
Analysis of team performance in a programmed environment
[NASA-CR-175634] 14 p2392 N85-24728
Perceived heterogeneity and its effect on various types of tasks
[AD-A151003] 14 p2392 N85-24729
Psychophysiological studies. 1: Performance and physiological response in learning, short-term memory and discrimination tasks
[AD-A151018] 14 p2392 N85-24731
US Army human Engineering Laboratory Communications Survey: A Pilot Study (HELCOMS-PS)
[AD-A151434] 15 p2521 N85-25544
A portable battery for objective, non-obstrusive measure of human performances
[NASA-CR-171868] 15 p2586 N85-25942
Measurement and modification of sensory system EEG (electroencephalographic) characteristics during visual-motor performance
[AD-A151901] 15 p2618 N85-26133
Visual search strategy predictions: The use of aspect ratio as a cue
[BAE-ST-15865] 15 p2919 N85-26156
A practical system for collecting reliable data on the space-time behavior of people
[AD-A151174] 15 p2619 N85-26140
Skilled memory
[AD-A152063] 15 p2620 N85-26143
Sleep deprivation and performance: Older age performance and limited sleep period use
[AD-A153102] 17 p2999 N85-28540
Performance Evaluation Tests for Environmental Research (PETER) evaluation of 112 measures
[AD-A152317] 17 p2999 N85-28543
The levels of processing conceptualization of human memory: Some empirical and theoretical issues
[AD-A152321] 17 p3000 N85-28544
The relationship between performance and satisfaction: A utility analysis
[AD-A152342] 17 p3000 N85-28546
Individual characteristics and unit performance: A review of research and methods
[AD-A153145] 17 p3001 N85-28550
Biofeedback and performance: An update
[AD-A153228] 17 p3001 N85-28553
Relationship between the Army two mile run test and maximal oxygen uptake
[AD-A153914] 18 p3154 N85-29526
A task battery for applied human performance assessment research
[AD-A153677] 18 p3154 N85-29530
Proceedings of the Seminar on Space Station Human Productivity
[NASA-TM-86673] 18 p3156 N85-29539
Space station crew safety: Human factors interaction model 18 p3156 N85-29540
Human factors issues in space station architecture
18 p3158 N85-29560
Human factors in cockpit automation: A field study of flight crew transition
[NASA-CR-177333] 19 p3215 N85-29937
Performance envelopes and optimal appropriateness measurement
[AD-A154129] 19 p3330 N85-30629
The design of working systems on ergonomic principles. The importance of clothes and protective equipment in the design of the workplace
[HSE-TRANS-10665] 19 p3332 N85-30639
Individual observer data for the 1955 Stiles-Burch 2 deg pilot investigation — color vision
[NPL-QU-68] 20 p3512 N85-31830
Resource allocation in cerebral specialization of function: Behavioral and electrophysiological studies
[AD-A155092] 21 p3664 N85-32759
Conceptualizing in assembly tasks
[AD-A155564] 21 p3665 N85-32770
Performance of rolling ball and isometric joystick on a 2-D target alignment task
[RSRE-MEMO-3995] 22 p3826 N85-33699
The relationship between personality and performance
24 p4129 N85-35600
The effect of an unphysiological oxygen supply on the organism 24 p4130 N85-35605
An exploratory study of the effect of screen size and resolution on the legibility of graphics in automated job performance aids
[AD-A155869] 24 p4136 N85-35632

HUMAN REACTIONS

A limbus-sensing eye movement recorder
[AD-A144772] 01 p0049 N85-10323
Psychological states (mood, affect or emotion) experienced by JASDF pilots through flying duties. 3: Flying conditions causing pilots psychological disturbances 01 p0090 N85-10606
Post fire interview: Development and field validation of the behavioral sequence interview technique
[NBS-GCR-84-477] 04 p0454 N85-12881
Human reactions to ELF (Extremely Low Frequency) electric and magnetic fields. An annotated bibliography of current literature, fourth edition
[PB84-230356] 04 p0545 N85-13472
Endocrine responses to nonhypotensive gravitational stress: Vasopressin and aldosterone
05 p0693 N85-14459
Fitts' law? A test of the relationship between information load and movement precision 05 p0705 N85-14523
A production system model of capturing reactive moving targets 05 p0705 N85-14524
Inverse modelling to obtain head movement controller signal 05 p0705 N85-14525
A control model: Interpretation of Fitts' law
05 p0706 N85-14526
Human reactions to transient electric currents, volume 12
[PB84-231463] 06 p0846 N85-15374
Construction and application of a questionnaire for the social scientific investigation of environmental noise effects
[NASA-TM-75492] 10 p1512 N85-19544
Functional role of type of person's temperament in individual and mutual activity 10 p1525 N85-19621
Restructuring of the process of visual recognition as perception conditions alter 10 p1526 N85-19624
Effects of tasks on responses of human skin mechanoreceptors 11 p1691 N85-20635
Role of mental work in human tolerance in total-body vibration 12 p1901 N85-21940
Parameters of carbohydrate metabolism and blood serum enzyme activity after short-term spaceflights
12 p1903 N85-21951
Some individual differences in human response to infrasound
[UTIAS-282] 12 p1905 N85-21960
Predictors of transfer adjustment: A longitudinal study
[AD-A152462] 17 p3000 N85-28548
Aviation noise effects
[AD-A154319] 19 p3352 N85-30776
Zinc: Biological effects. Facts and fiction
[USIP-84-12] 20 p3507 N85-31796
The 1984 environmental monitoring report, Sandia National Laboratories, Albuquerque, New Mexico
[DE85-011175] 22 p3811 N85-33607

HUMAN RELATIONS

An investigation of the relationship between stressful life events and psychological, behavioral and physiological outcomes
[AD-A147754] 08 p1197 N85-17541

HUMAN RESOURCES

Strategic management for organizational effectiveness. The effect of human resource planning on retention and related issues, volume 1
[AD-A149398] 10 p1566 N85-19674
Strategic management for organizational effectiveness. The effect of human resource planning on retention and related issues, volume 2
[AD-A149399] 10 p1566 N85-19675
Strategic management for organizational effectiveness. The effect of human resource planning on retention and related issues, volume 3
[AD-A149400] 10 p1566 N85-19676
Strategic management for organizational effectiveness. The effect of human resource planning on retention and related issues: Methodological appendix
[AD-A149401] 10 p1566 N85-19677
Air Force Human Resources Laboratory research and development summary
[AD-A154310] 19 p3331 N85-30632
The Human Resource Management Information Network (HRMIN): A cost comparison in accordance with Office of Management and Budget (OMB) Circular no. A-76, 5 April 1979
[AD-A154583] 21 p3713 N85-33039

HUMAN TOLERANCES

The Reports of Aeromedical Laboratory, volume 25, no. 1/2
[ISSN-0023-2858] 01 p0090 N85-10605
The effects of isotonic training on +Gz tolerance
01 p0090 N85-10607
Assessment of the inflating characteristics of the modified anti-G suit 01 p0090 N85-10609
Effect of fluid and salt supplements to food allowance on endurance of head-to-pelvis accelerations following 7-day dry immersion and under ordinary motor activity conditions 01 p0092 N85-10618
Hemodynamics and neurodynamics of the human brain during exposure to moderate hypoxic hypoxia
01 p0094 N85-10630
Impact of space medicine on Earth-based medicine: Academician Ye. I. Chazov comments on the work in orbit of physician O. Atkov 04 p0543 N85-13458
Endocrine responses to hypotensive gravitational stress: Catecholamines, pancreatic polypeptide, and vasopressin 05 p0693 N85-14460
Glucose tolerance in trained and untrained subjects during head-down tilt (6 deg) 05 p0693 N85-14461
Vityaz specialists study human adaptability to ocean depths 07 p0990 N85-16225
Aircraft noise effects: An inter-disciplinary study of the effect of aircraft noise on men. Part 3: Supplementary analyses of the social-scientific portion of the study on aircraft noise conducted by the DFG
[NASA-TM-75802] 10 p1527 N85-19631
Tolerance, fatigue, physiological and performance effects of sustained and oscillating lateral accelerations
10 p1533 N85-19659
Air quality criteria for ozone and other photochemical oxidants. External review draft, volume 5
[PB85-126076-VOL-5] 11 p1679 N85-20683
Some individual differences in human response to infrasound
[UTIAS-282] 12 p1905 N85-21960
Research on the effect of noise at different times of day: Models, methods and findings
[NASA-CR-3868] 13 p2154 N85-23375

Nutritional criteria for military rations and effects of prolonged feeding on acceptability
14 p2394 N85-24742
Physiological differences between men and women in exercise-heat tolerance and heat acclimation
[AD-A152048] 15 p2618 N85-28135
Positive Gz accelerations tolerance of individuals 41 to 58 years of age 19 p3323 N85-30588
Effect of 120-day antiorthostatic bedrest on gas exchange and pulmonary circulation in man
19 p3323 N85-30589
Pressure chamber simulation of 450-meter dive
20 p3505 N85-31758
Physical training and G tolerance
20 p3511 N85-31824
Centrifuge operations and training in the Royal Netherlands Air Force 20 p3511 N85-31825
Cosmonauts' cardiovascular system function during long-term orbital flights aboard Salyut-6 station
22 p3733 N85-33141
Environmental surveillance at Los Alamos during 1984
[DE85-011886] 22 p3811 N85-33605
Determination of individual tolerance in hyperbaric oxygen 23 p3954 N85-34507

HUMAN WASTES
NT FECES
NT SWEAT
NT URINE
Design concept definition study for an improved shuttle waste collection subsystem
[NASA-CR-171834] 08 p1198 N85-17546
Improved orbiter waste collection system study
[NASA-CR-171830] 08 p1199 N85-17548
Improved orbiter waste collection system study, appendix D
[NASA-CR-171833] 08 p1199 N85-17549
Gas analysis techniques for human physiological measurements in space — Spacelab
[A/6537] 20 p3507 N85-31803

HUMIDITY
RADC/NBS (Rome Air Development Center/National Bureau of Standards) Workshop. Moisture Measurement and Control for Semiconductor Devices, 3
[PB84-219559] 01 p0051 N85-10337
Spectroradiometric calibration of the Thematic Mapper and Multispectral Scanner system
[E85-10026] 02 p0218 N85-11439
Low-frequency sound absorption measurements in air
[NASA-RP-1128] 02 p0275 N85-11789
Effect of humidity on fretting wear of several pure metals
[NASA-TP-2403] 04 p0472 N85-13006
Climate at CRREL (Cold Regions Research and Engineering Laboratory) Hanover, New Hampshire
[AD-A148400] 08 p1189 N85-17495
Survey of remote data monitoring systems
[DE85-001386] 09 p1323 N85-18313
Effect of water vapor and water droplets on the RAM-1 (Real-Time Aerosol Monitor): Preliminary results
[PB85-109429] 11 p1637 N85-20313
Humidity effects on adhesion of nickel-zinc ferrite in elastic contact with magnetic tape and itself
[NASA-TP-2449] 12 p1811 N85-21359
Study of effective physiological temperature
13 p2042 N85-22780
Two-dimensional numerical model of sensible and latent heat transport in an irrigated field under advective conditions 13 p2131 N85-23261
Portable Automated Mesonet (PAM) data from the 1980 experiment in Anderson Creek Valley
[DE85-004361] 13 p2139 N85-23282
Experimental study of the effect of moist environments on epoxy resin chocks
[AD-A152052] 15 p2568 N85-25849
Proper quality of anticorrosion work no matter how bad the atmospheric conditions
[BLL-BISI-TRANS-22080-(9022.06)] 17 p2975 N85-28383
Humidity/cloud-radiation feedback on possible climate perturbation due to fossil fuel utilization
[DE85-006696] 18 p3133 N85-29402
Urban climate and air hygiene before, during, and after the Ilsework of Helimut Berg. Overview of a branch of applied meteorology 18 p3147 N85-29487
Variability of air humidity profiles over ocean determined by lidar sounding 19 p3296 N85-30436
Ice active bacteria as condensation nuclei
21 p3639 N85-32603
Ice crystal nucleation on hygroscopic aerosols
21 p3639 N85-32605
Variation of the submicron aerosol structure
21 p3647 N85-32661
Condensation properties of atmospheric aerosol
21 p3649 N85-32672
Measurements of the critical supersaturation of 0.029 to 0.035 micron radius particles at Washington, District of Columbia 21 p3649 N85-32676
Protective systems and maintenance policies for marine environments 22 p3750 N85-33245
Air-sea interaction with SSM/I and altimeter
[NASA-CR-176105] 22 p3818 N85-33650
Millimeter-wave propagation in moist air: Model versus path data
[AD-A156040] 24 p4087 N85-35331

HUMIDITY MEASUREMENT
Climate-chamber experiments to improve pilots' work conditions 04 p0543 N85-13454
Technology development for thin-film-trace humidity sensors
[BMFT-FB-T-84-268] 17 p2969 N85-28338
Effects of relative humidity gradients on the evaluation of submicron aerosol flux measurements in the atmospheric surface layer
[DE85-010510] 19 p3316 N85-30555
Tropical Ocean and Global Atmosphere (TOGA) heat exchange project: A summary report
[NASA-CR-176038] 20 p3496 N85-31738

HUNGARY
Microcomputers in Hungary 01 p0115 N85-10786

HUNTING P-84 AIRCRAFT
U JET PROVOST AIRCRAFT

HURRICANES
Nowcasting: Advances with McIDAS 3 — Man-computer Interactive Data System System (McIDAS)
01 p0082 N85-10553
Setting hurricane conditions of readiness with high confidence
[AD-A144785] 01 p0085 N85-10570
Mesoscale and convective-scale characteristics of mature hurricanes 03 p0394 N85-12516
Fastest-mile wind speeds in Hurricane Alicia
[PB84-220771] 03 p0397 N85-12532
Hurricane Alicia, Galveston and Houston, Texas, 17-18 August 1983
[PB84-237056] 04 p0541 N85-13441
Annual data and verification tabulation for Eastern North Pacific tropical storms and hurricanes, 1983
[PB85-106635] 10 p1520 N85-19580
Hurricane experience levels of coastal county populations: Texas to Maine
[PB85-111383] 10 p1520 N85-19581
Hurricane plotting program
[PB85-121432] 10 p1521 N85-19592
Hurricane storm surge research
[GPO-40-048] 12 p1893 N85-21880
Hurricane alicia storm surge and wave data
[AD-A149668] 12 p1895 N85-21896
Analysis of the inflow layer and air-sea interactions in Hurricane Frederic (1979)
[NASA-CR-175616] 13 p2137 N85-23271
Hurricane structure and dynamics from stereoscopic and infrared satellite observations and radar data
15 p2594 N85-25988
Analysis of the inflow and air-sea interactions in hurricane Frederic 15 p2595 N85-25990
Forecast of Atlantic seasonal hurricane activity for 1985 16 p2633 N85-27470
Hurricane Research Division, fiscal year 1984 programs, fiscal year 1985 projections 16 p2636 N85-27491
Airborne research meteorological data collected by the National Hurricane Research Laboratory (Hurricane Research Division/AOML) during the 1982-1983 hurricane seasons: Inventory and availability
[PB85-163681] 17 p2997 N85-28528
Forecast of Atlantic seasonal hurricane activity for 1985 20 p3495 N85-31732
Parameter estimation in communication system tracking satellite observations
[AD-A155137] 21 p3636 N85-32582
Kinematic analysis of Hurricane Frederick (1979) using satellite, aircraft and rawinsonde data
[NASA-CR-176167] 24 p4119 N85-35533

HYBRID CIRCUITS
Planning of hybrid integrated circuits for microwave-band oscillators 04 p0490 N85-13124
Qualification of a thick film hybrid
[BMFT-FB-W-84-024] 04 p0497 N85-13170
New designs from electronics R and D center
15 p2538 N85-25666
Hybrid two-dimensional Monte-Carlo electron transport in self-consistent electromagnetic fields
[DE85-010757] 19 p3348 N85-30756
Modeling of electronic circuits with high degree of component integration 22 p3766 N85-33343

HYBRID COMPUTERS
Experiments on the influence of active walls on the initial amplitudes and growths of instability waves
[AD-A154630] 21 p3583 N85-32275

HYBRID NAVIGATION SYSTEMS
Terrain following without use of forward looking sensors 16 p2698 N85-26659

HYBRID PROPULSION
Oxygen-hydrogen thrusters for Space Station auxiliary propulsion systems
[NASA-CR-175691] 15 p2494 N85-25383
Hybrid propulsion technologies for urban bus transit
[PB85-157469] 16 p2880 N85-27773

HYBRID STRUCTURES
Joint services electronics program
[AD-A145085] 01 p0042 N85-10276
Hybrid vehicle program
[DE85-000326] 09 p1410 N85-18886
INEL electric vehicle laboratory qualification: Transition test results and comparisons with JPL ETV1-2 data
[DE85-008006] 16 p2880 N85-27772
Elastic equilibrium of composite shells with finite shear rigidity 17 p2942 N85-28163

HYBRIDS (BIOLOGY)
U GENETIC ENGINEERING

HYDRATES
Development of media for dynamic latent heat storage for the low-temperature range. Part 1: Thermal analyses of selected salt hydrate systems
[NASA-TM-77778] 10 p1507 N85-19510
Chemical weathering of soils from the dry valleys of Antarctica: A terrestrial analog of Martian weathering processes 13 p2197 N85-23626
Volatiles in the outer solar system. 1: Thermodynamics of clathrate hydrates. 2: Ethane ocean on Titan. 3: Evolution of primordial Titan atmosphere
19 p3362 N85-30984
Gas hydrates
[DE85-001986] 20 p3477 N85-31607
Theoretical studies of structure and stability of hydrates of atmospheric sulfur species 21 p3650 N85-32684
Defect formation in amorphous hydrated silicon subjected to laser radiation 21 p3682 N85-32873

HYDRATION
Effect of fluid and salt supplements to food allowance on endurance of head-to-pelvis accelerations following 7-day dry immersion and under ordinary motor activity conditions 01 p0092 N85-10618
Neutron diffraction studies of the hydrogen bonding and water molecules in zeolites
[DE84-016431] 06 p0766 N85-14900
Mechanical properties of adhesively bonded aluminum structures protected with hydration inhibitors
[AD-A148123] 08 p1133 N85-17139
Mechanical properties of adhesively bonded aluminum structures protected with hydration inhibitors
[AD-A153755] 18 p3079 N85-29047
Hydrothermal alteration in the 3.5 b.y. old Onverwacht Group of South Africa 21 p3718 N85-33071

HYDRAULIC ACTUATORS
U ACTUATORS
U HYDRAULIC EQUIPMENT

HYDRAULIC ANALOGIES
Verification of a model of the Eastern Scheldt
[RAND/R-3108-NETH] 09 p1354 N85-18518
Catastrophic-flood features in Swedish Lapland as a terrestrial analog for Martian channel flows
13 p2190 N85-23587

HYDRAULIC CONTROL
Automation of coastal engineering modelling facilities
[CSIR-T/SEA-8304] 01 p0035 N85-10219
Powered articulated headrest system
[AD-D011353] 07 p0901 N85-15710
Hydraulic brakes for industrial robots
13 p2046 N85-22606

HYDRAULIC EQUIPMENT
NT AIRCRAFT HYDRAULIC SYSTEMS
Vehicle-to-vehicle connection mechanism
[AD-D011267] 05 p0645 N85-14142
A study of wear characteristics due to pressure for hydraulic fixed displacement vane pumps
[AD-A146023] 06 p0814 N85-15169
Vehicle anchoring system
[AD-D011292] 06 p0815 N85-15173
Space shuttle orbiter auxiliary power unit development challenges 08 p1099 N85-16945
Materials of the fourth scientific-technical Conference on Questions of the Extrusion of Metals (Selected articles)
[AD-A148578] 08 p1130 N85-17121
Multiple rate shock isolator damping valve
[AD-D011429] 08 p1168 N85-17368
Turning behaviour of articulated frame steering tractor
[AD-P004304] 09 p1409 N85-18881
Integrated paratroop door
[AD-D011507] 12 p1776 N85-21148
Analysis and design of hydraulic servo systems within the scope of the improvement of a fatigue testing installation of the Royal Dutch Army
[LEOK-TR-1984-09] 14 p2265 N85-24033

Pneumohydraulic drive 14 p2268 N85-24050
High reliability mechanical-hydraulic converter 14 p2268 N85-24055
Manufacture of drive wheel vanes for hydraulic turbines on program controlled machine tools 14 p2269 N85-24058
Hydraulic characteristics of reduction installation valves 14 p2269 N85-24060
Hydraulic drag of rod with artificial microroughness in longitudinal flow 14 p2278 N85-24111
Locking of Automative Products hydraulic selector valves
[BAE-EXPER/NOTE-459] 15 p2567 N85-25839
User's guide for concrete strength investigation and design (CSTR)
[AD-A151617] 15 p2579 N85-25906
Application of the hydraulic system frequency response program to propellant feed systems
[AD-A151824] 16 p2741 N85-26914
Active control landing gear for ground load alleviation 17 p2903 N85-27902
Use of a two-dimensional flow model to quantify aquatic habitat
[AD-A154287] 19 p3266 N85-30253

HYDRAULIC FLUIDS
Standardization of flammability tests for hydraulic fluids
[AD-A146468] 06 p0771 N85-14932
Toxic hazards research
[AD-A147857] 07 p1011 N85-16425
Mist flammability studies of candidate fire-resistant hydraulic fluids
[AD-A148572] 08 p1134 N85-17148
Hydraulic drag of rod with artificial microroughness in longitudinal flow 14 p2278 N85-24111
Organic solvent alteration of hydraulic properties of sedimentary rocks of low permeability: A review
[DE85-012537] 22 p3815 N85-33635

HYDRAULIC HEATING SOURCES
U HEAT SOURCES
U HYDRAULIC EQUIPMENT

HYDRAULIC JETS
Potential application of robotics and state-of-the art end effectors at Letterkenny Army Depot
[AD-P004015] 03 p0309 N85-11994
Characterization of jet-contaminant interaction flow in chemical decontamination
[AD-A147298] 08 p1161 N85-17327
The hydrosynclastic infundibulum
[AD-A153849] 18 p3100 N85-29192
Pulsed hydrojet propulsion
[DE85-010771] 22 p3784 N85-33446

HYDRAULIC PUMPS
U HYDRAULIC EQUIPMENT
U PUMPS

HYDRAULIC SHOCK
Rock mechanics: Issues and research needs in the disposal of wastes in hydraulic fractures
[DE85-001399] 10 p1556 N85-19809
Comprehensive fracture diagnostics experiement. Part 2: Comparison of seven fracture azimuth measurements
[DE85-011707] 23 p3948 N85-34470

HYDRAULIC SYSTEMS
U HYDRAULIC EQUIPMENT

HYDRAULIC TEST TUNNELS
The effects of microbubbles on turbulent boundary layer skin friction 20 p3451 N85-31425

HYDRAULIC VALVES
U HYDRAULIC EQUIPMENT
U VALVES

HYDRAULICS
Multigrid iteration solution procedure for solving three-dimensional sets of coupled equations
[DE84-016515] 04 p0555 N85-13532
Hydraulic locking boltwork system
[AD-D011290] 06 p0815 N85-15174
Great Lakes hydrometeorologic and hydraulic data needs 20 p3496 N85-31739
Computer code calculations of the TMI-2 accident: Initial and boundary conditions
[DE85-012613] 24 p4140 N85-35686

HYDRAZINE ENGINES
Heat resistant sheathed insulated electrical conductors
[AD-D011644] 17 p2951 N85-28219

HYDRAZINE NITRATE
Hydrazine nitrate based explosives
[ISL-CO-229/84] 22 p3754 N85-33272

HYDRAZINES
Qualification of a hydrazine gas generator system with electrothermal/catalytic gas generator
[BMFT-FB-W-84-040] 06 p1110 N85-17016
The use of hydrazine as an alternate source of energy
[NASA-CR-175535] 12 p1617 N85-21397
Atmospheric dispersion of hypergolic liquid rocket fuels, volume 1
[AD-A149597] 12 p1617 N85-21399
Hydrazine and the F-16 20 p3511 N85-31526

HYDRIDES
NT BORANES
NT BORON HYDRIDES
NT CARBORANE
NT CHLOROSILANES
NT METAL HYDRIDES
NT PHOSPHINES
NT SILANES
NT ZIRCONIUM HYDRIDES
Influence of 5f electrons on structures and bonding in the actinide-hydrogen intermetallics
[DE84-013693] 01 p0118 N85-10807
Mossbauer effect and contactless conductivity studies of superconducting actinides intermetallics and hydrides. Mossbauer high pressure studies 03 p0430 N85-12743
Neutron scattering for the investigation of solid state materials, utilization in chemical structures 03 p0432 N85-12752
Formation of a limiting composition in the preparation of ternary 3-5 semiconductors by the VPE (Vapor Phase Epitaxy) Hydride technique
[AD-A147639] 08 p1225 N85-17713
An infrared study of the hydrogenation of carbon dioxide on supported rhodium catalysts
[AD-A149477] 10 p1436 N85-19049
Ten degree Kelvin hydride refrigerator
[NASA-CASE-NPO-16393-1-CU] 18 p3085 N85-29084
Method for preparing hydride configurations and reactive metal surface
[DE85-006443] 23 p3917 N85-34274

HYDROACOUSTICS
U UNDERWATER ACOUSTICS

HYDROAEROMECHANICS
U AERODYNAMICS

HYDROBAROPHONES
U HYDROPHONES

HYDROBROMIC ACID
Study of the liquid vapor equilibrium in the bromine-hydrobromic acid-water system
[NASA-TM-77787] 07 p0921 N85-15836
A study of liquid-vapor equilibria of the bromine-hydrobromic acid-water system
[NASA-TM-77748] 14 p2249 N85-23940

HYDROCARBON COMBUSTION
Combustion in high speed air flows
[AD-A148371] 08 p1122 N85-17070
Comprehensive mechanisms for combustion chemistry: An experimental and numerical study with emphasis on applied sensitivity analysis
[DE85-000173] 13 p2018 N85-22656

HYDROCARBON FUEL PRODUCTION
NT ATMOSPHERIC ENERGY SOURCES
Bioenergy, solar biotech research in France, Europe 15 p2536 N85-25646

HYDROCARBON FUELS
NT DIESEL FUELS
NT FOSSIL FUELS
NT GASOLINE
NT JET ENGINE FUELS
NT JP-4 JET FUEL
NT JP-5 JET FUEL
NT JP-8 JET FUEL
Chemistry of fuel deposits and sediments and their precursors
[NASA-CR-174778] 01 p0034 N85-10209
Liquid hydrocarbon fuels from syngas
[DE84-015942] 04 p0482 N85-13089
Analysis of middle distillate fuels by high resolution field ionization mass spectrometry
[AD-A147724] 08 p1135 N85-17153
Combustion gas properties. 2: Natural gas fuel and dry air
[NASA-TP-2435] 12 p1779 N85-21168
PSA, Renault work on all fuel automobile engine 15 p2531 N85-25604
Improved catalysts for liquid hydrocarbon fuels from syngas
[DE85-006569] 16 p2746 N85-26947
Ignition characterization of LOX/hydrocarbon propellants
[NASA-CR-171884] 16 p3083 N85-29070
Ignition characterization of LOX/hydrocarbon propellants
[NASA-CR-171882] 18 p3083 N85-29071
Liquid hydrocarbon fuels from syngas
[DE85-008613] 19 p3228 N85-30017
Fuel-rich catalytic combustion: A soot-free technique for in situ hydrogen-like enrichment
[NASA-TP-2498] 20 p3423 N85-31244
Rapid estimation of concentration of aromatic classes in middledistiate fuels by high-performance liquid chromatography
[NASA-TP-2495] 20 p3434 N85-31307
Aspects of high-resolution gas chromatography as applied to the analysis of hydrocarbon fuels and other complex organic mixtures. Volume 1
[AD-A156154] 24 p4076 N85-35257

HYDROCARBONS
NT ACETYLENE
NT ALKANES
NT ALKENES
NT ALKYNES
NT ANTHRACENE
NT BENZENE
NT BUTADIENE
NT BUTANES
NT BUTENES
NT CAROTENE
NT CYCLIC HYDROCARBONS
NT CYCLOHEXANE
NT CYCLOPROPANE
NT DIENES
NT DURENE
NT ETHANE
NT ETHYLENE
NT HEXENES
NT KEROGEN
NT LIQUEFIED NATURAL GAS
NT METHANE
NT METHYLENE
NT NAPHTHALENE
NT NATURAL GAS
NT NITROPROPANE
NT PARAFFINS
NT PENTANES
NT PROPANE
NT PROPYLENE
NT PYRENES
NT TOLUENE
NT TRIPHENYLS
NT VINYLIDENE
Plasma deposited diamondlike carbon on GaAs and InP
[NASA-TM-86870] 01 p0123 N85-10844
Systematic data interpretation of remote sensing in the reception of hydrocarbons, volume 1
[E85-10008] 02 p0215 N85-11421
Development of a method for exploring low-reflectance areas through the combined use of different geophysical methods taking the north-west German basin as an example
[BMFT-FB-T-83-180] 02 p0220 N85-11450
Magnetic resonance studies of transient radicals and radical ions
[DE84-011699] 03 p0328 N85-12116
Polycyclic aromatic hydrocarbons on the inner surfaces of copper tubing
[AD-A145979] 03 p0337 N85-12189
Organic aerosol formation: OH(hydroxyl radical) versus ozone oxidation pathways
[PB84-219880] 03 p0388 N85-12484
Structure determination of molecular adsorbates with dynamical LEED and HREELS
[DE85-002007] 06 p0661 N85-15473
Analysis of gases in the Earth's crust
[PB85-113397/GAR] 07 p0960 N85-16297
Homogeneous reaction involving components of different redox couples. 1: Theoretical considerations and digital simulation
[AD-A148668] 08 p1124 N85-17084
Impact of aircraft emissions on air quality in the vicinity of airports. Volume 4. Nitrogen dioxide and hydrocarbons
[AD-A148253] 08 p1180 N85-17436
On the importance of light hydrocarbons in multiphase atmospheric systems
[JUEL-1942] 08 p1190 N85-17498
Aromatics determination in middle distillate petroleum fractions by spectrophotometric titration
[PNR-90239] 09 p1293 N85-18123
Initial results for supercritical cycle experiments using pure and mixed-hydrocarbon working fluids
[DE84-017008] 09 p1345 N85-18480
Prediction of retention indices of polynuclear aromatic hydrocarbons. Part 1: HPLC on nitrogen containing normal phase packing materials
[DE85-001302] 10 p1436 N85-19051
Prediction of retention indices of polynuclear aromatic hydrocarbons. Part 2: Capillary gas chromatography
[DE85-001301] 10 p1437 N85-19053
Vapor pressure studies of the solubilization of hydrocarbons by surfactant micelles
[DE85-004319] 12 p1803 N85-21306
Oxidation and gum formation in jet fuels
[AD-A149934] 12 p1818 N85-21401

The body burden of organic vapors in artificial air trial measurements aboard a moored submarine
[AD-A149698] 12 p1910 N85-21988
Applications of high pressure differential scanning calorimetry to aviation fuel thermal stability research
[NASA-TM-87002] 14 p2249 N85-23941
Modelling of photodegradation in solar cell modules of substrate and superstrate design made with ethylene-vinyl acetate as pottant material
[NASA-CR-175690] 14 p2350 N85-24527
C2H(n) fragments on metal surfaces
[AD-A151474] 15 p2505 N85-25449
Studies of the combustion of model fuels with low hydrogen content (pyrolysis of polycyclic aromatics-detection of soot precursors)
[DE85-005422] 15 p2521 N85-25541
The remote detection of polynuclear aromatic hydrocarbons using laser-induced fluorescence
[AD-A152294] 16 p2757 N85-27013
Systematic nomenclature of the nitrogen, oxygen and sulfur functional polycyclic aromatic hydrocarbons
[DE85-007426] 17 p2916 N85-27974
Fuel rich catalytic comustion: The first stage of a two-stage combustor
[NASA-TM-87042] 18 p3069 N85-28983
Study of synthesis gas conversion over metal oxides
[DE85-010136] 18 p3072 N85-28999
Measurement of radical species concentrations and polycyclic aromatic hydrocarbons in flames by fluorescence and absorption using a tunable dye laser
[DE85-006624] 18 p3113 N85-29274
Mechanism of the catalytic gasification and reactivity of graphite
[DE85-009932] 19 p3229 N85-30020
Thermodynamic study of CO2-organic compound interaction at high pressures and temperatures
[DE85-010999] 19 p3268 N85-30266
Identification and quantification of nitropolynuclear aromatic hydrocarbons in ambient and indoor air particulate samples
[PB85-176790] 19 p3311 N85-30525
Factor analysis of atmospheric pollution by polycyclic aromatic hydrocarbons
[HSE-TRANS-10968] 19 p3311 N85-30528
Study of the formation of particles from natural hydrocarbons released by vegetation
21 p3644 N85-32640
The interaction of polynuclear aromatic hydrocarbons PAH's with water vapor and their role as condensation nuclei in the formation of haze and fog
21 p3652 N85-32695
Using remote photographs in prospecting for hydrocarbons on the Kerch Peninsula
22 p3735 N85-33154
Method for removing chlorine compounds from hydrocarbon mixtures
[DE85-011606] 22 p3742 N85-33191
Effect of polymer additives on characteristics of direct-current motor with liquid dielectric filler
22 p3772 N85-33376
Environmental summary for calendar year 1984
[DE85-012020] 22 p3810 N85-33604
Development of a chemical kinetic mechanism for the US EPA (Environmental Protection Agency) regional oxidant model
[PB85-185858] 22 p3813 N85-33618
Modeling of auto exhaust smog chamber data for EKMA development
[PB85-186492] 22 p3813 N85-33619
Process for functionalizing alkanes
[DE85-006420] 23 p3909 N85-34219
FTIR studies of hydrocarbon synthesis on Pd/ZSM5 catalysts
[DE85-012430] 24 p4071 N85-35230
The Conterminous United States Mineral Assessment Program 24 p4106 N85-35458
Thermal evolution of coastal California with implications for hydrocarbon maturation 24 p4115 N85-35509
Molecular biology of environmental aromatic hydrocarbons
[DE85-015036] 24 p4128 N85-35593
Few-particles generation channels in inelastic hadron-nuclear interactions at energy approximately equals 400 GeV
[HE-3.2-9] 24 p4179 N85-35917

HYDROCHLORIC ACID
Photoelectron studies of autoionizing Rydberg states in HCl
[DE85-011613] 21 p3702 N85-33001
A study of the chemistry of alkali metals in the upper atmosphere
[AD-A156349] 24 p4117 N85-35524

HYDROCLIMATOLOGY
Hydrometric telemetry in Canada
14 p2239 N85-23882

HYDRODYNAMIC COEFFICIENTS
Hydraulic brakes for industrial robots
13 p2046 N85-22806
Influence of spatial variability of hydraulic characteristics of soils on surface parameters obtained from remote sensing data in infrared and microwaves
[NASA-TM-77902] 20 p3477 N85-31604

HYDRODYNAMIC EQUATIONS
NT HELMHOLTZ VORTICITY EQUATION
Self-similar expansion of dense matter due to heat transfer by nonlinear conduction
[MPQ-81] 01 p0046 N85-10297
Reduction of nonlinear problems to Schroedinger or heat equations: Formation of Kepler orbits, singular solutions for hydrodynamical equations
[REPT-72] 01 p0129 N85-10892
Equations of plasma transport in a curved magnetic field
[DE84-015625] 05 p0730 N85-14690
On the hydrodynamical equations of astrophysical jets --- active galactic nuclei 08 p1241 N85-17831
Nonlinear waves in the magnetosphere of pulsars
12 p1955 N85-22281
An analytic model for hydromagnetospheres --- stellar winds; pulsars; cosmic jets 12 p1959 N85-22313
Contribution to the theory of stationary separation areas
[NASA-TM-77825] 14 p2300 N85-24244
Lyapunov stability of very simple steady solutions of prognostic systems 14 p2333 N85-24429
General continuous formulations of atmospheric energy laws 16 p2830 N85-27448
Singularity solutions for ellipsoids in Low-Reynolds-Number flows: With applications to the calculation of hydrodynamic interactions in suspensions of ellipsoids
[AD-A153503] 18 p3168 N85-29632
Method for computing evolution of random hydrodynamic fields on basis of adjoint equations
19 p3292 N85-30412
The cosmic-ray shock structure problem for relativistic shocks
[OG-8.1-1] 23 p4017 N85-34891

HYDRODYNAMIC STABILITY
U FLOW STABILITY

HYDRODYNAMICS
NT CYLINDRICAL PLASMAS
NT ELASTOHYDRODYNAMICS
NT ELECTROHYDRODYNAMICS
NT MAGNETOHYDRODYNAMICS
HULL users' manual
[AD-A145000] 01 p0103 N85-10691
A perturbation solution for rigid dumbbell suspensions in steady shear flow
[AD-A144876] 01 p0111 N85-10755
New approaches to hydrodynamic flow visualization on surfaces
[AD-A145528] 02 p0198 N85-11324
Experiences with a high-blockage model tested in the NASA Ames 12-foot pressure wind tunnel
03 p0315 N85-12032
Comparison of predicted and measured friction for a tilt-pad thrust bearing with crown and roughness under hydrodynamic and mixed lubrication
[AD-A145752] 03 p0371 N85-12371
Algebra of hydrodynamic flows of an ideal fluid and the prediction of the behaviour of a system of particles of a passive admixture on Riemann surfaces with a variable curvature
[REPT-565] 03 p0377 N85-12408
Dynamical models for radio jets
03 p0449 N85-12854
Flash radiography as a quantitative tool
[DE84-016465] 04 p0503 N85-13211
Supernova envelope shock origin of cosmic rays: A review
[DE84-016479] 04 p0590 N85-13763
Rotordynamic Instability Problems in High-Performance Turbomachinery
[NASA-CP-2338] 05 p0642 N85-14116
Hydraulic forces on a centrifugal impeller undergoing synchronous whirl 05 p0643 N85-14124
Hydrodynamic impeller stiffness, damping, and inertia in the rotordynamics of centrifugal flow pumps
05 p0643 N85-14125
Damping capacity of a sealed squeeze film bearing
05 p0645 N85-14139
Conditions for assembling dies for drawing under hydrodynamic friction conditions
[BLL-M-35954-(5828.4)] 05 p0647 N85-14153
The radiative hydrodynamics of flare loops heated by impulsive bursts of energetic electrons
05 p0745 N85-14781
Characterization of jet-contaminant interaction flow in chemical decontamination
[AD-A147296] 08 p1161 N85-17327
Hydrodynamic flow structures in quantum field theory
[DE84-015513] 09 p1401 N85-18817
New methods for numerical solution of one class of strongly nonlinear partial differential equations with applications in hydrodynamics
[AD-A149026] 10 p1545 N85-19739
Hydrodynamic response of a radiating Al plasma excited by a proton beam
[AD-A148904] 10 p1558 N85-19824
Ion velocity distributions from spherical 1054 nm and 351 nm laser plasmas
[DE85-002816] 10 p1559 N85-19833
Parallel processing experiences on the Denelcor HEP computer
[DE85-000653] 11 p1702 N85-20703
Hydrodynamic simulations of recurrent novae
11 p1753 N85-21025
Investigation of the initial events in biofouling
[AD-A149995] 12 p1900 N85-21927
Processes and problems in secondary star formation
[DE85-003623] 12 p1960 N85-22322
Coupled acoustic and hydrodynamic wave instabilities
13 p2000 N85-22536
Application of modulated hydrodynamic voltammetry to the study of anodic electrocatalysis
[DE85-004182] 13 p2018 N85-22653
Turbulent flows of surfacant solutions
[AD-B089137L] 13 p2092 N85-23058
Calculation of level surface in problems of large-scale ocean circulation 13 p2108 N85-23136
Double and inverse Taylor-Hogg vortices in a stratified ocean 13 p2108 N85-23137
Model for high rate gas flows in deformable and reactive porous beds
[DE85-006140] 14 p2253 N85-23964
Model of friction bearing hydrodynamics
14 p2288 N85-24178
USSR report: Earth sciences
[JPRS-UES-85-004] 14 p2332 N85-24424
Numerical study of a two-fluid hydrodynamical model of interstellar medium and population 1 stars
14 p2440 N85-25055
The design and construction of a flow channel and rig for corrosion studies
[AERE-M-3455] 15 p2508 N85-25474
Laboratory for laser energetics report
[DE85-007235] 15 p2563 N85-25814
Gravity perception in a Cladoceran-Zooplankter: Anatomy of antennal socket setae of Daphnia magna
15 p2605 N85-26057
Mean free paths, viscosity, and the limitations of perfect fluid hydrodynamics in the description of the quark-gluon plasma
[DE85-005501] 15 p2649 N85-26339
Instability of solar wind near streamlined bodies
16 p2720 N85-26794
Characteristic functionals of stochastic wave processes
[REPT-14/1984] 16 p2768 N85-27084
Optimum convection conditions for Czochralski growth of semiconductors
[INPE-3395-PRE/665] 16 p2870 N85-27703
Catalyst and reactor development for a liquid phase Fischer-Tropech process
[DE85-005894] 17 p2922 N85-28014
A discussion of adaptive grids and their applicability in numerical hydrodynamic modeling
[AD-A151843] 17 p3017 N85-28659
A numerical solution technique for multitemperature plasma hydrodynamics
[AD-A152701] 17 p3039 N85-28801
Multi-ducted inlet combustor research and development
[AD-A153753] 18 p3063 N85-28946
Dynamics of thin-film breakup in a constricted pore
[DE85-008442] 18 p3101 N85-29199
Numerical techniques for steady two-dimensional transcritical stratified flow problems, with an application to the intermediate field dynamics of ocean thermal energy conversion plants
[DE85-008347] 18 p3151 N85-29509
Study of the chemical mechanism in lubrication
[DE85-010768] 19 p3228 N85-30013
Flow visualization study of inverted annular flow of post dryout heat transfer region
[DE85-010482] 19 p3269 N85-30275
Space photographs confirm 40-year-old hydrodynamics discovery 19 p3289 N85-30393
Use of adjoint equations in problems of evaluating state of random hydrodynamic fields
19 p3289 N85-30398
SHAPS-2: A three-dimensional computer program for linear/non-linear, static/dynamic analyses of piping systems
[DE85-010500] 19 p3335 N85-30658

Hybrid two-dimensional Monte-Carlo electron transport in self-consistent electromagnetic fields
[DE85-010757] 19 p3348 N85-30756
Venus thermospheric circulation
[PB85-180420] 19 p3384 N85-30997
Activities report of the Laboratory of Mechanics and Energetics 20 p3437 N85-31328
Hydrodynamic solutions for the diffusion of components in confined media 20 p3456 N85-31464
Hydrodynamics and sanitation
[CT-579] 20 p3487 N85-31672
Compressible Lagrangian hydrodynamics without Lagrangian cells
[DE85-009597] 20 p3520 N85-31891
Self-consistent models for the X-ray emission from supernova remnants 20 p3548 N85-32082
Discovery of a nonpropagating hydrodynamic soliton
[AD-A155569] 21 p3582 N85-32268
Mechanics of a gaseous film barrier to lubricant wetting of elastohydrodynamically lubricated conjunctions
[NASA-TP-2500] 21 p3595 N85-32330
Effect of polymer additives on characteristics of direct-current motor with liquid dielectric filler 22 p3772 N85-33376
Dual clearance squeeze film damper
[NASA-CASE-LEW-13506-1] 22 p3791 N85-33490
Volatile loss following very large impacts 22 p3853 N85-33862
Three-dimensional hydrodynamic hot-spot model
[DE85-009587] 23 p3922 N85-34301
Numerical simulation in astrophysics: Smoothed particle methods 23 p3979 N85-34674
Numerical calculations on shock loaded materials 23 p3980 N85-34676
Dissipation terms in one-dimensional hydrodynamic code for ICF target 23 p3980 N85-34677
Two-dimensional simulation of LIB target implosion 23 p3980 N85-34678
Stability of implosion dynamics 23 p3980 N85-34680
Pulse effect in a light ion beam propagation through a Z-discharge plasma channel 23 p3981 N85-34684
Adaptive rezoner in a two-dimensional Lagrangian hydrodynamic code
[DE85-010108] 24 p4094 N85-35381

HYDROELASTICITY
Time dependent interaction of internal pressure wave with system of two spherical shells 13 p2046 N85-22809
Thermal and thermoelastic effects in rolling/sliding contacts
[AD-A150435] 13 p2165 N85-23429

HYDROELECTRIC POWER STATIONS
International test and demonstration of a 1-MW wellhead generator: Helical screw expander power plant
[NASA-CR-174161] 04 p0527 N85-13372
Ecological impacts of hydroelectric projects in Amazonia 07 p1003 N85-16374
Underground pumped hydroelectric storage
[DE85-000288] 11 p1676 N85-20560
Small-hydropower development: The process, pitfalls, and experience. Volume 1: Feasibility studies summary and analysis
[DE85-010839] 22 p3808 N85-33589
Low-head hydroelectric power demonstration project: City of Gonzales, Texas
[DE85-010403] 22 p3809 N85-33595
Small Hydroelectric Power Plan Demonstration Project
[DE85-011343] 23 p3946 N85-34454

HYDROELECTRICITY
Monitoring environmental and related performance parameters for a Rankine-cycle turbine electric generator utilizing geothermal energy at the Gila Hot Springs, New Mexico
[DE84-901772] 09 p1345 N85-18465
Small-hydropower development: The process, pitfalls, and experience. Volume 1: Feasibility studies summary and analysis
[DE85-010839] 22 p3808 N85-33589
Solar energy education. Renewable energy: A background text
[DE85-010365] 23 p3946 N85-34452
Small Hydroelectric Power Plan Demonstration Project
[DE85-011343] 23 p3946 N85-34454

HYDROFLUORIC ACID
Rotational energy transfer in highly vibrationally excited hydrogen fluoride and deuterium fluoride
[AD-A152003] 16 p2682 N85-27650
Rotational relaxation studies of hydrogen fluoride
[AD-A152711] 17 p3029 N85-28734

HYDROFOIL BOATS
U HYDROFOIL CRAFT

HYDROFOIL CRAFT
A broadband kevlar radome for shipboard
[AD-P004365] 12 p1826 N85-21459

HYDROGEN
NT DEUTERIUM
NT DEUTERIUM PLASMA
NT HYDROGEN ATOMS
NT HYDROGEN IONS
NT HYDROGEN ISOTOPES
NT HYDROGEN PLASMA
NT LIQUID HYDROGEN
NT METALLIC HYDROGEN
NT TRITIUM
Compressibility and fugacity of gaseous hydrogen
[NLR-TR-83079-U] 01 p0025 N85-10154
Inhibition of hydrogen absorption during plating of high strength steels
[AD-A144882] 01 p0028 N85-10174
Monte Carlo simulation of thermalization of subexcitation electrons in molecular hydrogen
[NAL-TR-815T] 01 p0117 N85-10798
Observations of the pulsating hydrogen: Deficient star BD+13 deg 3224, during 1980 - 1981 01 p0128 N85-10882
An electrochemical study of hydrogen uptake and elimination by bare and gold-plated waspaloy
[NASA-TM-86479] 02 p0182 N85-11222
Effects of H2S on molten carbonate fuel cells
[DE84-015166] 02 p0195 N85-11307
Reversible change in parameters of GaAs-based surface-barrier metal-semiconductor diodes induced by hydrogen absorption-desorption 02 p0258 N85-11690
Combustion and detonation of hydrogen-air mixture in free spaces 02 p0274 N85-11783
Surface production of negative hydrogen ions
[AD-A145437] 02 p0277 N85-11801
Molecular hydrogen emission associated with high velocity flows. A tracer for low velocity shocks 03 p0443 N85-12819
Interaction of hydrogen with defects in metals
[DE84-016781] 04 p0476 N85-13032
Theoretical studies of highly ionized species
[DE84-016797] 04 p0561 N85-13574
Influence of hydrogen saturation and prior heat treatment on graphitization of white cast iron
[BLL-M-35964-(5826.4)] 05 p0615 N85-13932
Effect of water on hydrogen permeability — Stirling engines
[NASA-TM-86904] 06 p0781 N85-14864
Investigation of bromine complexed hydrogen/bromine regenerative fuel cells for portable electric power
[AD-A146401] 06 p0833 N85-15300
Synergisms in hydrogen recycling, session summary 06 p0864 N85-15491
Steady state hydrogen transport in solids 06 p0864 N85-15492
Pioneer 10 and Voyager observations of the interstellar medium in scattered emission of the He 584 A and H Lya 1216 A lines 06 p0873 N85-15541
Absorption line studies and the distribution of neutral gas in the local interstellar medium 06 p0873 N85-15544
Synthesis of data on the local interstellar medium 06 p0874 N85-15545
Non-local origin of a substantial portion of the soft X-ray background 06 p0877 N85-15567
The Draco Nebula, a molecular cloud associated with a high velocity cloud? 06 p0878 N85-15577
Nearby molecular hydrogen 06 p0879 N85-15582
Radio and UV observations of high latitude HI 06 p0879 N85-15583
The results of hydrogen hypersensitization of photoemulsions — astronomical photography 07 p0963 N85-16108
The fundamentals of dislocation transport of hydrogen in bcc iron
[AD-A148143] 08 p1129 N85-17117
Photoionization structure of the Orion Nebula 08 p1246 N85-17863
The 1.5 - 3.5 micron spectroscopy of the Orion H2 source 08 p1246 N85-17864
Interpretation of the far infrared emission from our external galaxies 08 p1249 N85-17884
Simultaneous flow visualization and unsteady lift measurement on an oscillating lifting surface
[AD-P004157] 09 p1264 N85-17942
NMR study on rotational fluctuation in solid hydrogen and deuterium 09 p1289 N85-18093
Hydrogen trapping, diffusion, and recombination in austenitic stainless steels
[DE85-001871] 09 p1294 N85-18129
Hydrogen-oxygen (hydrox) breathing at 1.3MPa
[FOA-C-56015-H1] 09 p1364 N85-18577
Alignment of high Ryberg states in hydrogen
[DE85-000582] 09 p1380 N85-18677
Developments and applications of laser fluorescence spectroscopy for studies of particle behaviours in fusion plasmas 09 p1389 N85-18735
Molecular hydrogen and thermal phases in astrophysics 09 p1414 N85-18922
Theoretical studies of the ignition and combustion of silane-hydrogen-air mixtures
[NASA-CR-3876] 10 p1433 N85-19032
Separation of gas mixtures with coordination complexes
[DE85-000383] 10 p1438 N85-19062
Improved operation of transversely exited N2O lasers
[AD-D011488] 10 p1490 N85-19409
Variational calculation of the 2D H2 molecule
[INPE-3304-PRE/615] 10 p1554 N85-19798
Quasi-thermodynamic prediction of hydrogen reemission behavior from titanium films
[DE85-003667] 10 p1564 N85-19864
Effect of hydrogen on fatigue of VT8 alloy 11 p1601 N85-20071
Distribution of hydrogen in multi-layer welded joints of alloyed steels 11 p1603 N85-20079
Low energy antiproton interaction studies at Brookhaven
[DE85-001228] 11 p1720 N85-20820
Vibrational relaxation in H-2 molecules by wall collisions: Applications to negative ion source processes
[DE85-000852] 11 p1721 N85-20828
Direct measurement of the temperature dependence of the velocity of the reaction of deuterium atoms with vibration-excited hydrogen molecules
[MPIS-12/1984] 11 p1726 N85-20856
Atomistic studies of grain boundaries with segregated impurities
[DE85-000063] 11 p1737 N85-20924
Feasibility of producing commodities and electricity for space shuttle operations at Vandenberg Air Force Base
[DCN-84-203-001-80-21] 12 p1789 N85-21230
Hydrogen flame acceleration and transition to detonation
[DE85-000611] 12 p1802 N85-21299
Increase in hydrogen emission of upper atmosphere following launches of space vehicles 13 p1981 N85-22431
Adsorption site, adsorption energy and normal vibration frequency of H/Ni(100) via total energy calculations
[AD-A150555] 13 p2156 N85-23388
Gas dynamics of the barred spiral galaxy NGC 3359 13 p2170 N85-23465
Hydrogen on impurity-covered iron surfaces 14 p2254 N85-23968
Hydrogen resistance of VT1-0 titanium under 150 MPa pressure at room temperature 15 p2499 N85-25414
Linewidth and bandwidth measurements of the q-branch of h2 using CW coherent anti-Stokes Raman spectroscopy
[AD-A151868] 15 p2506 N85-25456
Applications of photoinduced electron transfer and hydrogen abstraction reactions to chemical and electrochemical conversion processes
[DE85-006068] 15 p2506 N85-25459
The effects of water and hydrogen on materials used in integrated circuit packages
[AD-A151893] 15 p2518 N85-25629
Numerical analysis of supersonic reactive flow in wake of reverse step 15 p2643 N85-26303
Compensation of dangling bonds in A-Si, Ge:H alloys
[DE85-002905] 15 p2662 N85-26433
Development of hydrogen resistant alloys 16 p2735 N85-26873
Modeling the role of radicals in the ignition of and flame propagation in hydrogen-air and methane-air mixtures 16 p2744 N85-26935
Transitional metal activation and functionalization of C-H bonds
[DE85-006816] 16 p2748 N85-26949
Study of the kinetics and thermodynamics of hydrogen in Pd-based alloys
[DE85-007341] 16 p2750 N85-26969
Spin-polarized quantum systems
[DE85-006914] 16 p2864 N85-27667
The structure of galactic HI in directions of low total column density
[NASA-CR-175709] 16 p2882 N85-27785
An analysis of alternate hydrogen sources for lunar manufacture
[DE85-007234] 16 p2894 N85-27792
Role of hydrogen and structure on CMSX-2 17 p2915 N85-27967
Photoionization mass spectrometry with VUV hydrogen laser source
[AD-A153362] 17 p2921 N85-28009
Effect of texture in steel on the susceptibility of hydrogen embrittlement
[BLL-BISI-TRANS-22026-(9022.06)] 17 p2926 N85-28048
Construction techniques of a molecular hydrogen laser
[AD-A152928] 17 p2970 N85-28343

Thermodynamic calculations of equilibrium states in metal-carbon-hydrogen-oxygen system
[BLL-BISI-TRANS-22092-(9022.06)] 17 p3045 N85-28544

Hydrogen absorption in metals: A field ion microscopy study
[DE85-010299] 18 p3078 N85-29026

Feasibility of electrolytic hydrogen production in the Pacific Northwest
[DE85-009856] 18 p3084 N85-29080

Electron capture to the continuum from atomic hydrogen
[DE85-005269] 18 p3181 N85-29722

Effect of polarized radiative transfer on the Hanle magnetic field determination in prominences: Analysis of hydrogen H alpha line observations at Pic-du-Midi 18 p3207 N85-29904

Determining partial molar volume of hydrogen in titanium alloys 19 p3245 N85-30119

Means for reducing hydrogen concentration upon surfacing of antifriction aluminum alloys with powder electrode 19 p3247 N85-30132

Flash pyrolysis of biomass with reactive and non-reactive gases
[DE85-010962] 19 p3306 N85-30496

Tables of generalized hydrogen diffusion profiles and permeating fluxes for fusion applications
[DE85-006876] 19 p3372 N85-30919

Slow chemistry effects in a turbulent mixing layer 20 p3424 N85-31252

Assessment of supertayer contribution to the conserved scalar PDF in a hydrogen turbulent jet diffusion flame 20 p3425 N85-31255

Surface passivation and junction formation using low energy hydrogen implants 20 p3480 N85-31628

EBIC characterization and hydrogen passivation in silicon sheet 20 p3481 N85-31634

Detection of excited states by laser-induced fluorescence
[AD-A155558] 21 p3582 N85-32326

Sulfate-reducing bacteria: Microbiology and physiology 21 p3659 N85-32732

Thermophysical properties of fluids for the gas industry
[PB85-196471] 22 p3747 N85-33227

Use of low energy hydrogen ion implants in high efficiency crystalline silicon solar cells
[NASA-CR-176100] 22 p3806 N85-33571

Separation of gas mixtures by supported complexes
[DE85-011966] 23 p3912 N85-34236

Method for preparing hydride configurations and reactive metal surface
[DE85-006443] 23 p3917 N85-34274

Low noise polycrystalline semiconductor resistors by hydrogen passivation
[AD-D011721] 23 p3927 N85-34338

Dual-chamber plasma deposition of A-Si:H solar cells at high rates using disilane
[DE85-011629] 23 p3946 N85-34451

The extent of the local hi halo
[NASA-CR-176115] 23 p3967 N85-34724

Low-excitation Herbig-Haro objects and interstellar extinction
[NASA-CR-176142] 23 p3968 N85-34726

On the detectability of key-MeV solar protons through their nonthermal Lyman-alpha emission
[SH-1.9-5] 23 p3993 N85-34752

The effects of newly measured cross sections in hydrogen on the production of secondary nuclei during the propagation of cosmic rays through interstellar H
[OG-7.2-2] 23 p4014 N85-34874

On the importance of interstellar helium for the propagation of heavy cosmic rays
[OG-7.2-11] 23 p4015 N85-34879

Interactions of heavy nuclei, Kr, Xe and Ho, in light targets
[OG-7.2-21] 23 p4016 N85-34888

CO + H2 reaction over nitrogn-modified iron catalysts
[DE85-013791] 24 p4072 N85-35231

Fluidized bed desulfurization
[NASA-CASE-NPO-15924-1] 24 p4075 N85-35253

Pressure measurements in a hydrogen combustion environment: Hydrogen-air combustion test series 1 and 2 in the FITS tank, volume 1
[TI85-009899] 24 p4076 N85-35259

Vectorial electron transfer on designed surfaces
[PB85-204600] 24 p4076 N85-35263

Effect of temperature and ionic impurities at very low concentrations on stress corrosion cracking of Type 304 stainless steel
[TI85-009048] 24 p4079 N85-35283

Experimental technique for measuring the isentrope of hydrogen to several megabars
[DE85-014332] 24 p4095 N85-35366

Characterization of catalysts with metal-support effects and of the species adsorbed on their surfaces
[DE85-012254] 24 p4096 N85-35394

Cooling high intensity atomic hydrogen beams to liquid helium temperatures
[DE85-012515] 24 p4148 N85-35718

Limiter
[DE85-011620] 24 p4150 N85-35736

Circumstellar shells of late-type stars: A study at millimeter and infrared wavelengths 24 p4167 N85-35836

Some nuclear data needs in astrophysics
[DE85-012916] 24 p4168 N85-35842

HYDROGEN ATOMS

Electron capture by multiply charged ions from hydrogen atoms at low energies
[DE84-016580] 06 p0861 N85-15475

Reactions of butadiyne. 1: The reaction with hydrogen atoms
[NASA-TM-77805] 07 p0921 N85-15834

Dipole active surface vibrational resonances on clean and hydrogen covered Ni(110)
[AD-A150546] 13 p2163 N85-23420

Super hydrides
[AD-A153499] 16 p3070 N85-28966

HYDROGEN BONDS

Influence of hydrogen bonding in block copolymers and their blends 13 p2036 N85-22752

HYDROGEN CHLORIDES

NT HYDROCHLORIC ACID

Space Shuttle Environmental Effects: The First 5 Flights
[NASA-CR-171812] 01 p0069 N85-10457

Measurements on the diffusion of hydrogen chloride in the waste gas plume of incineration ships in the North Sea. Part 1: Methodology, instrumentation and presentation of data
[GKSS-84-E-23-PT-1] 05 p0672 N85-14319

Process for the epitaxial deposition of III-V compounds utilizing a continuous in-situ hydrogen chloride etch
[AD-D011557] 12 p1939 N85-22177

Quantitative studies for photoabsorption and fluorescence of HCl
[NASA-CR-175965] 19 p3233 N85-30043

HYDROGEN CLOUDS

NT ORION NEBULA

The z-dependence of the spin temperature of HI 06 p0878 N85-15580

Cosmic ray secondary nuclei and the structure of the galaxy
[OG-7.2-4] 23 p4014 N85-34876

HYDROGEN COMPOUNDS

NT BORANES
NT BORON HYDRIDES
NT CARBORANE
NT CHLOROSILANES
NT DEUTERIUM COMPOUNDS
NT DEUTERIUM FLUORIDES
NT HYDRIDES
NT HYDROGEN PEROXIDE
NT HYDROGEN SULFIDE
NT METAL HYDRIDES
NT PHOSPHINES
NT SILANES
NT ZIRCONIUM HYDRIDES

Preparation and properties of single crystals of hydrogen bis(phthalocyaninato) neodymium(3)
[AD-A144933] 01 p0123 N85-10848

Electronic-to-vibrational energy transfer studies of singlet molecular oxygen and hydrogen halides
[AD-A146587] 02 p0277 N85-11802

Reflection electron energy loss investigation of the H-GaAs(110) surface
[NOTA-INTERNA-811] 02 p0289 N85-11869

Calculations of collision-induced optical gain in high-density mixtures of D2 or HD with a buffer gas
[AD-A151372] 15 p2648 N85-26330

Intermolecular explosives
[DE85-009809] 23 p3921 N85-34296

HYDROGEN EMBRITTLEMENT

Compressibility and fugacity of gaseous hydrogen
[NLR-TR-83079-U] 01 p0025 N85-10154

Delayed fracture of high-strength steels in spherical tanks for LP gas
[BLL-RISLEY-TR-4926-(9091.9F)] 01 p0026 N85-10162

Study to optimize Cr-Mo steels to resist hydrogen and temper embrittlement. A study of carbides formed in low alloy Cr-Mo steels
[DE84-015208] 01 p0029 N85-10179

Lattice dilation in metal-hydrogen systems
[BLL-M-35768-(5825.4)] 02 p0176 N85-11176

Detection of hydrogen assisted crack growth
[DE84-015920] 02 p0183 N85-11228

Environment-induced embrittlement: Effect of impurity segregation and state of stress
[DE84-015436] 02 p0184 N85-11235

Detection of hydrogen assisted crack growth by measurement of modulus changes and acoustic emission
[DE84-015752] 02 p0184 N85-11236

A hydrogen partitioning model for hydrogen assisted crack growth
[AD-A147385] 07 p0978 N85-16214

Hydrogen embrittlement of nickel
[AD-A148322] 08 p1129 N85-17119

Effect of microstructure and trapping on the hydrogen embrittlement susceptibility of a Ti-bearing HSLA steel
[AD-A148610] 08 p1130 N85-17122

Hydrogen induced cracking in pipeline steels
[ERS-E.327] 09 p1340 N85-18429

Mechanism of hydrogen induced cracking in pipeline steels
[ERS-E.349] 09 p1340 N85-18430

Statistical aspects of shear fracture propagation
[ERS-E.368] 09 p1341 N85-18434

Influence of gaseous hydrogen on strength and ductility of nickel heat-resistant alloys 10 p1447 N85-19119

Role of hydrogen in processes of deformation and fracture of metals 10 p1449 N85-19132

Mechanism of titanium impact on brittle tendency in delayed deformation of martensite-aging steels 11 p1604 N85-20087

Hydrogen attack of steel
[DE85-002645] 11 p1608 N85-20113

Hydrogen embrittlement of cadmium-plated ultra-high strength steels in paint strippers
[ARL/MAT-R-117] 12 p1808 N85-21326

Delayed cracking strength of experimental grades of 42 CD 4 steel in aqueous H2S surroundings
[BLL-T8419/BG/LRS/LRST738/84] 13 p2020 N85-22658

Hydrogen effects in austenitic stainless steels based on the Fe-Cr-Mn-N system
[DE85-009617] 13 p2023 N85-22672

The role of hydrogen in the stress corrosion failure of high strength Al-Zn-Mg alloys
[AD-A150891] 14 p2256 N85-23976

A study of fatigue crack growth in 2 1/4 Cr1Mo steel. Part 1: The influences of environment and material condition
[AERE-R-11472] 14 p2258 N85-23993

Hydrogen induced crack growth in Grade-12 Titanium
[BNL-NUREG-35598] 16 p2751 N85-26976

Study to optimize Cr-Mo steels to resist hydrogen and temper embrittlement
[DE85-005492] 17 p2932 N85-28098

Hydrogen degradation of pipeline steels
[DE85-006930] 17 p2932 N85-28101

Hydrogen embrittlement of high-strength steel
[B8580075] 17 p2933 N85-28103

Feasibility of electrolytic hydrogen production in the Pacific Northwest
[DE85-009856] 18 p3084 N85-29080

Kinetics of H-induced stress corrosion cracking. Part 1: Important features of cracking in respect of high strength steels
[BLL-BISI-TRANS-(9022.06)] 19 p3282 N85-30350

Failure analysis of fractured capscrews in centrifugal coolant compressor
[DE85-010029] 19 p3287 N85-30384

Micromechanism of fracture for stage 1 hydrogen-induced crack growth
[DE85-010027] 19 p3288 N85-30390

The effect of diffusive hydrogen segregation on fracture of polycrystalline nickel
[AD-A155238] 21 p3567 N85-32186

Hydrogen embrittlement testing
[DE85-007352] 23 p3916 N85-34273

HYDROGEN FLUORIDES

U HYDROFLUORIC ACID

HYDROGEN FUELS

Combustion gas properties. Part 3: Hydrogen gas fuel and dry air
[NASA-TP-2477] 20 p3395 N85-31058

Jet flows: Modelling and experiments 22 p3744 N85-33206

HYDROGEN IONS

Hydrogen passivation of electrically active defects in crystalline silicon solar cells
[DE84-004560] 02 p0223 N85-11461

Stark broadening of H(-) resonances in large electric fields
[DE84-016974] 04 p0496 N85-13164

Focusing effects of a laser beam in the nonresonant multiphoton ionization (MPI) of gases
[LP-207] 04 p0506 N85-13231

The role of fast electrons for the performance characteristics of hydrogen ion sources 09 p1303 N85-18189

Comparative effects of auxin and abscisic acid on growth, hydrogen ion efflux and gravitropism in primary roots of maize
[NASA-CR-174355] 09 p1342 N85-18444
Hydrogen vibrational population distributions and negative ion generation in tandem high density hydrogen discharges
[DE85-001207] 11 p1722 N85-20834
Collisional pumping for the production of intense spin-polarized, neutral beams: Target considerations
[DE85-003459] 11 p1723 N85-20841
Three-dimensional calculation of shuttle charging in polar orbit 13 p1992 N85-22486
Hydrogen vibrational population distributions and negative ion generation in tandem high-density hydrogen discharges
[DE85-006764] 16 p2863 N85-27657
Energy reflection coefficient for H+ ions at energies between 10 and 80 keV
[DE85-007547] 16 p2863 N85-27662
Shifts and widths of hydrogenic ion lines
[DE85-011375] 19 p3277 N85-30323
Heating of the deep chromosphere during solar flares
[AD-A155256] 21 p3723 N85-33100
Some physical differences between sheet plasma and multicusp plasma as volume produced H- or D- ion sources
[IPPJ-728] 23 p3974 N85-34637
Data on the backscattering coefficients on light ions from solids: A revision
[IPPJ-AM-41-REV] 23 p3982 N85-34689

HYDROGEN ISOTOPES
NT DEUTERIUM
NT METALLIC HYDROGEN
NT TRITIUM
Gas chromatographic separation of hydrogen isotopes using metal hydrides
[DE84-014455] 04 p0469 N85-12983
Stable isotope studies
[DE84-016752] 04 p0562 N85-13583
Advanced mass spectrometers for hydrogen isotope analyses
[DE85-000716] 06 p0811 N85-15150
Ion beam studies of hydrogen in metals
[DE84-017422] 09 p1297 N85-18145
Plasma-edge studies using carbon resistance probes
[DE85-005589] 14 p2424 N85-24955
Hydrogen recovery from extraterrestrial materials using microwave energy
[DE85-006717] 16 p2863 N85-27789
Cosmic ray He3 measurements
[OG-4.2-3] 21 p3714 N85-33045
Interstellar propagation and the isotopic composition of hydrogen in the galactic cosmic rays
[OG-4.2-1] 22 p3877 N85-34021
Measurements of galactic hydrogen and helium isotopes from 1978 through 1983
[OG-4.2-2] 22 p3877 N85-34022
The 4He1H ratios in the chemical compositions of solar flare particles and the primordial solar nebula
[SH-7.1-12] 23 p4048 N85-35104

HYDROGEN MASERS
Historical cost curves for hydrogen masers and cesium beam frequency and timing standards
10 p1465 N85-19245
Experimental studies of low temperature surface interactions of atomic hydrogen using maser technique
[AD-A150216] 13 p2017 N85-22647
Proceedings of the Fifteenth Annual Precise Time and Time Interval (PTTI) Applications and Planning Meeting
[AD-A149163] 17 p2961 N85-28267
First results of GPS time transfer to Australia
17 p2962 N85-28294
Improved master clock reference system at USNO
17 p2963 N85-28300
Recent results on the performance of EFOS, NP and NX hydrogen masers 17 p2966 N85-28320
Methods to recover the narrow Dicke sub-Doppler feature in evacuated wall-coated cells without restrictions on cell size 18 p3105 N85-29225
Development of hydrogen masers for K-3 VLBI system
18 p3106 N85-29239
Atomic hydrogen maser active oscillator cavity and bulb design optimization 18 p3106 N85-29240
Hydrogen maser oscillation at 10 K
18 p3106 N85-29241
A low noise synthesizer for autotuning and performance testing of hydrogen masers 18 p3106 N85-29242
Atomic hydrogen maser measurements with wall surfaces of carbon tetrafluoride
18 p3106 N85-29243
Performance data of US Naval Observatory VLG-11 hydrogen masers since September, 1983
18 p3106 N85-29244

HYDROGEN OXYGEN ENGINES
LOX/LH2 propulsion system for launch vehicle upper stage, test results
[NASA-TM-77727] 03 p0324 N85-12089
Nonlinear control model of an H2O steam reactor
[DFVLR-FB-84-30] 07 p0975 N85-16192
Cryogenic propellant management: Integration of design, performance and operational requirements
08 p1098 N85-16939
Advanced research and technology programs for advanced high-pressure oxygen-hydrogen rocket propulsion
[NASA-TM-86969] 12 p1789 N85-21231
Advanced High Pressure O2/H2 Technology
[NASA-CP-2372] 16 p2733 N85-26662
Ceramics for advanced O2/H2 application
16 p2734 N85-26666
An evaluation of oxygen-hydrogen propulsion systems for the Space Station
[NASA-TM-87059] 18 p3067 N85-28971
Status of advanced orbital transfer propulsion
[NASA-TM-87069] 24 p4071 N85-35225

HYDROGEN PEROXIDE
Attempted measurement of gaseous H-2O-2 in the ambient atmosphere
[DE85-001937] 05 p0834 N85-15306
Oxygen isotopic study of the oxidation of SO2 by H2O2 in the atmosphere
[DE85-004017] 17 p2968 N85-28468
Chemical transformation in acid rain. Volume 1: New methodologies for sampling and analysis of gas-phase peroxide
[PB85-173425] 19 p3311 N85-30527

HYDROGEN PLASMA
NT DEUTERIUM PLASMA
Density measurements of atomic hydrogen in NBT-IM by laser-induced fluorescence spectroscopy
09 p1389 N85-18739
Control of surface composition and hydrogen recycling by plasma conditioning
[DE85-001859] 11 p1731 N85-20689
Frictional and structural characterization of ion-nitrided low and high chromium steels
[NASA-TM-86991] 13 p2096 N85-23065
Injection of hydrogen macroparticles into T-10 tokamak 21 p3692 N85-32937

HYDROGEN PRODUCTION
Surface production of negative hydrogen ions
[AD-A145437] 02 p0277 N85-11801
Solid electrolytes for medium temperature steam electrolysis
[DE84-014384] 04 p0463 N85-12938
High-temperature steam electrolysis: Technical and economic evaluation of alternative process designs
[DE84-015702] 04 p0469 N85-12968
Hydrogen technology evaluation center at Brookhaven National Laboratory
[DE84-014099] 04 p0470 N85-12968
Development and testing of thin film cells for high temperature water vapor electrolysis
[BMFT-FB-T-84-146] 04 p0471 N85-13001
Utilization of solar energy for the production of hydrogen 05 p0663 N85-14262
Hydrogen production employing high-temperature solid oxide cells
[DE84-014559] 06 p0768 N85-14901
Production of hydrogen by cyanobacteria
[PB85-113421/GAR] 07 p0935 N85-15925
Hydrogen from solar energy
[DE85-001914] 10 p1437 N85-19055
Artificial photosynthesis with algal and reconstituted systems
[DE85-002557] 10 p1523 N85-19604
Alternative anodic reactions in water splitting
[DE85-004159] 12 p1802 N85-21300
Solar-assisted hydrogen generation by photoelectrocatalysis
[PB85-149706] 12 p1804 N85-21314
The effect of water chemistry on the rates of hydrogen generation for galvanized steel corrosion at post-loca conditions
[NUREG/CR-3961] 14 p2253 N85-23963
Solid state hydrogen pumping and storage material
[AD-D011610] 16 p2757 N85-27011
Hydrogen recovery from extraterrestrial materials using microwave energy
[DE85-006717] 16 p2863 N85-27789

HYDROGEN RECOMBINATIONS
Hydrogen trapping, diffusion, and recombination in austenitic stainless steels
[DE85-001871] 09 p1294 N85-18129
Spin-polarized quantum systems
[DE85-006914] 16 p2864 N85-27667

HYDROGEN SULFIDE
The Jovian atmospheric window at 2.7 microns: A search for H2S
[NASA-TM-86661] 03 p0445 N85-12836
Thio and seleno compounds of the transition metals with the d (o) configuration
[BLL-MINTEX-TR-1177-(5810.5758)]
07 p0925 N85-15863
Effects of H2S on molten carbonate fuel cells
[DE85-008310] 18 p3130 N85-29366
Geothermal hydrogen and health in Rotorua, New Zealand
[DE85-901283] 19 p3301 N85-30457
Sulfur transformations at the hydrogen sulfide/oxygen interface in stratified waters and in cyanobacterial mats
21 p3657 N85-32715
The identification of compounds in mustard hydrolysate
[AD-A156381] 24 p4076 N85-35258

HYDROGEN 2
U DEUTERIUM

HYDROGEN 3
U TRITIUM

HYDROGEN-BASED ENERGY
Solid state hydrogen pumping and storage material
[AD-D011610] 16 p2757 N85-27011
Design principles for nickel hydrogen cells and batteries 20 p3447 N85-31398

HYDROGENATION
Studies of hydrogenated amorphous silicon
[DE84-013036] 01 p0067 N85-10443
Process research of polycrystalline silicon material (PROPSM)
[NASA-CR-174130] 05 p0619 N85-13962
Process Research On Polycrystalline Silicon Material (PROPSM) 08 p0830 N85-15276
Cation promotion effects in zeolite-supported F-T catalysts
[DE85-001706] 09 p1291 N85-18108
Process Research on Polycrystalline Silicon Material (PROPSM)
[NASA-CR-175461] 10 p1509 N85-19523
Study of the kinetics of hydrogenation using aged catalysts
[DE85-004373] 12 p1802 N85-21302
Synthesis, static and reactive characterization of supported organometallics
[DE85-004285] 12 p1808 N85-21340
Fire resistant polymers based on 1-(diorgano oxyphosphonyl)methyl-2,4- and 2,6-diamino benzenes
[NASA-CASE-ARC-11512-2] 12 p1811 N85-21362
Resistance of hydrogenated alpha-titanium alloys to corrosion-fatigue fracture 15 p2499 N85-25413
Process Research on Polycrystalline Silicon Material (PROPSM)
[NASA-CR-175761] 15 p2587 N85-25861
Optical properties of hydrogenated amorphous carbon films grown from methane plasma
[NASA-TM-86965] 15 p2658 N85-26406
Chemical vapor deposition of amorphous semiconductor films
[DE85-002917] 15 p2661 N85-26421
Study of synthesis gas conversion over metal oxides
[DE85-010136] 18 p3072 N85-29099
Study of the kinetics of hydrogenation using aged catalysts
[DE85-010427] 19 p3230 N85-30025
Catalytic hydrotreatment studies with model compounds
[DE85-010187] 19 p3236 N85-30064
Effect of thermochemical processing on fatigue resistance of titanium alloys 19 p3244 N85-30112
Reduction of the trapping of positrons in dislocated single crystals of iron when charged with hydrogen
[DE85-010235] 19 p3377 N85-30950
Mechanistic and kinetic studies of the elementary processes in catalytic combustion of methane
[PB85-198306] 20 p3435 N85-31314

HYDROGENOLYSIS
Properties of supported metal catalysts
[DE85-003927] 12 p1802 N85-21303
Exploratory study of coal conversion chemistry
[DE85-010393] 19 p3229 N85-30018

HYDROGEOLOGY
Hydrogeochemical investigation of thermal springs in the Black Canyon-Hoover Dam area, Nevada and Arizona
[PB84-202472] 01 p0064 N85-10428
Seafloor geosciences division: Missions, technical specialties, accomplishments, and activities, calendar year 1983
[AD-A144849] 01 p0087 N85-10592
Evaluating effectiveness of using space information in specialized hydrogeological research
02 p0184 N85-11114

Paleohydrology and geomorphology of selected reaches of the upper Wabash Valley, Indiana
02 p0226 N85-11481
Submarine sand ridges: Geology and development, New Jersey, USA
02 p0227 N85-11482
Glacier dynamics and the development of glacial landforms in the eastern Puget lowland, Washington
03 p0369 N85-12490
Activities of the Coastal Research Center
[PB84-231323] 05 p0672 N85-14320
Application of SIR-B data for groundwater exploration in the Arabian shield and sand-drift monitoring in the AN Nafud and Al Jafurah fringe areas, Kingdom of Saudi Arabia
08 p1144 N85-17214
Deforestation, floodplain dynamics, and carbon biogeochemistry in the Amazon Basin
08 p1144 N85-17216
Radioactive waste isolation in salt: Peer review of the Office of Nuclear Waste Isolation's report on the organic geochemistry of deep groundwaters from the Palo Duro Basin, Texas
[DE85-001439] 10 p1556 N85-19811
Structure and application of extremely large geophysical data bases
[DE85-003527] 10 p1568 N85-19868
Mars: Long term changes in the state and distribution of H2O
13 p2191 N85-23593
Equipment for the ARGOS system from Eidsvoll Electronics A.S.
14 p2239 N85-23865
Remote sensing: New tool for China's geologists
14 p2263 N85-24141
Investigative report on using geological research to promote prospecting
14 p2263 N85-24142
Protecting the nation's groundwater from contamination, volume 1
[PB85-154201] 15 p2590 N85-25985
Protecting the nation's groundwater from contamination, volume 2
[PB85-154219] 15 p2590 N85-25986
Geologic and hydrologic characterization and evaluation of the basin and range province relative to the disposal of high-level radioactive waste. Part 2: Geologic and hydrologic characterization
[GS-CIRC-904-B] 20 p3526 N85-31933
Geologic and hydrologic characterization and evaluation of the basin and range province relative to the disposal of high-level radioactive waste. Part 3: Geologic and hydrologic evaluation
[GS-CIRC-904-A] 20 p3526 N85-31934
Deep sea mega-geomorphology: Progress and problems
21 p3602 N85-32369
Understanding coherence losses incurred by bottom-retained signals
[AD-A155559] 21 p3701 N85-32992
Indications of mineral zoning in a fossil hydrothermal system at the Meager Creek geothermal prospect, British Columbia, Canada from induced polarization studies
[DE85-011982] 22 p3815 N85-33836
Hydrogeology of the lower Glen Rose Aquifer, south-central Texas
24 p4108 N85-35468

HYDROGRAPHY
The Long Term Upper Ocean Study (LOTUS). Cruise summary
[AD-A145767] 03 p0397 N85-12536
The long term upper ocean study (LOTUS). Cruise summary and hydrographic data report, OCEANUS 154, May 1984
[AD-A147908] 07 p1009 N85-16414
Advanced technology for hydrographic mapping
[FOA-C-30371-E1] 08 p1176 N85-17418
Deep water mass circulation in the Western Alboran Basin: Measurements in July and September 1980 (Alboran I experiment)
[AD-A146566] 08 p1191 N85-17504
Analysis of flow within the coastal boundary layer off Long Island, New York
[DE85-001384] 09 p1359 N85-18550
Nautical charting with remotely sensed imagery, volume 1
[AD-A149361] 10 p1506 N85-19503
Nautical charting with remotely sensed imagery. Volume 2: Case studies
[AD-A149362] 10 p1506 N85-19504
Establishment of hydrographic shore control by Doppler satellite techniques
[AD-A150709] 14 p2347 N85-24512
Study of Volga river delta using space photosurvey materials
15 p2485 N85-25340
Report of the Hydrographic Service Royal Australian Navy for the year ended 30th June 1984, issue number 20
[AD-A151460] 15 p2583 N85-25632
Criteria for the classification of hydrographic positioning data
[AD-A152295] 16 p2706 N85-26897
Status of computer aided mapping in hydrographic services
16 p2815 N85-27366
A comparison of methods of least squares adjustment of traverses
[AD-A153612] 18 p3170 N85-29645
Hydrographic data from the OPTOMA (Ocean Prediction Through Observations, Modeling and Analysis) program: OPTOMA15, 24 January to 23 February 1985
[AD-A155012] 21 p3655 N85-32703
Federal Mineral Land Information System
24 p4106 N85-35459

HYDROKINETICS
U HYDROMECHANICS

HYDROLOGY
NT HYDROGEOLOGY
A summary of geothermal studies in Montana, through 1983
[DE84-014325] 01 p0064 N85-10422
Application guide for Hydrological Simulation Program FORTRAN (HSPF)
[PB84-215763] 01 p0064 N85-10427
Water resources data, Mississippi, water year 1982
[PB84-224559] 01 p0065 N85-10434
Water resources data, Florida, water year 1982. Volume 4: Northwest Florida
[PB84-223445] 01 p0066 N85-10437
Water resources data for Michigan, water year 1983
[PB84-225176] 01 p0066 N85-10442
Ecology of estuarine channels of the pacific northwest coast: A community profile
[PB84-209709] 01 p0070 N85-10464
Estuaries of the Cape. Part 2: Synopses of available information on individual systems. Report no. 18: Bot/Kleinmond system (CSW 13)
[CSIR-RR-417-PT-2] 01 p0087 N85-10587
The Multispectral Imaging Science Working Group. Volume 1: Executive summary
[E85-10001] 02 p0213 N85-11404
The Multispectral Imaging Science Working Group. Volume 2: Working group reports
[E85-10002] 02 p0213 N85-11405
Multispectral Imaging Science Working Group for Hydrologic Science: Executive summary
02 p0214 N85-11414
WXR (hydrologic weather wire and PLT product software package)
[PB84-237221] 04 p0541 N85-13442
Contributions to remote sensing: Applications of thermal infrared
[COMMUN-34/1984] 05 p0854 N85-14196
USSR report: Earth sciences
[JPRS-UES-84-008] 07 p0980 N85-16223
Hydrologic characteristics of the Mediterranean and Black Sea
07 p0981 N85-16228
Razrezy program research in the tropical Atlantic
07 p0981 N85-16229
Evaluation of SIR-B imagery for geologic and geomorphic mapping, hydrology, and oceanography in Australia
08 p1148 N85-17229
Earth Sciences Division report, 1983
[DE85-001036] 09 p1341 N85-18436
Analysis of geohydrologic data by kriging
[AD-P004152] 09 p1349 N85-18488
Retrieval procedures for hydrologic data from ARS (Agricultural Research Service) experimental watersheds in the US (REPHLEX)
[PB85-111326/GAR] 09 p1402 N85-18828
Ice segregation and frost heaving
[PB85-122430] 10 p1460 N85-19199
Water resources data for Alabama, water year 1983
[PB85-123842] 10 p1507 N85-19507
Water resources data for Colorado, water year 1983. Volume 1: Missouri River Basin, Arkansas River Basin and Rio Grande Basin
[PB85-123859] 11 p1671 N85-20528
Water resources data for Colorado, water year 1983. Volume 2: River Basin above Dolores River
[PB85-123867] 11 p1671 N85-20529
Review of computer mapping and display techniques applicable to regional analysis
[DE85-003545] 12 p1675 N85-21764
Hydrographic data collected in 1982 and 1983 for EPOCS (Equatorial Pacific Ocean Climate Studies)
[PB85-110799] 12 p1676 N85-21765
Catalog of submarine volcanoes and hydrological phenomena associated with volcanic events: 1500 BC to 31 Dec. 1899
[PB85-117984] 12 p1691 N85-21869
Effects of fracture roughness on fluid flow through a single deformable fracture
[DE85-004593] 13 p2092 N85-23062
Snow reflectance from Thematic Mapper
13 p2120 N85-23205
Hydrovolcanism
13 p2188 N85-23674
Paleohydrologic implications of valley networks of Mars
13 p2190 N85-23585
Catastrophic-flood features in Swedish Lapland as a terrestrial analog for Martian channel flows
13 p2190 N85-23587
The ARGOS system and hydrology. Results obtained by ORSTROM and benefits of a degree of standardization
14 p2239 N85-23861
Automatic hydrological data collection facility using ARGOS
14 p2324 N85-24363
Hydrology and climatic conditions in Greenland
14 p2327 N85-24367
Hydrological data collection from Swedish mountain areas
14 p2327 N85-24388
The ARGOS system and hydrology: The use of Platform Terminal Transmitter (PTT) with built-in memory and direct reception by the Seine basin hydrology service
14 p2328 N85-24389
Preliminary report on the results of hydrological measurements in the southern Tyrrhenian Sea, in the Messina strait and in the western Ionian sea
[PREPRINT-433] 14 p2362 N85-24693
Organizing geological work tasks for 1985 outlined
16 p2806 N85-27303
Present stage of utilization of the ARGOS system by the ORSTOM hydrological service for hydrometric data collection
16 p2813 N85-27348
The ARGOS system in Brazil — hydrology
16 p2813 N85-27349
Report on regional groundwater flow modeling for the Palo Duro Basin, Texas
[DE85-007490] 16 p2815 N85-27370
Ecology of Pamlico River, North Carolina: An estuarine profile
[PB85-155703] 16 p2822 N85-27404
Potential climatic impacts of increasing atmospheric CO2 with emphasis on water availability and hydrology in the United States
[NASA-TM-87479] 17 p2995 N85-28517
Earth Resources: A continuing bibliography with indexes, issue 45
[NASA-SP-7041(45)] 18 p3123 N85-29336
Conceptual hydrologic model of flow in the unsaturated zone, Yucca Mountain, Nevada
[DE85-006346] 18 p3125 N85-29350
Shales and other argillaceous strata in the United States
[DE85-010453] 18 p3125 N85-29353
Surface hydrologic characteristics of proposed repository locations in the Palo Duro Basin of the Texas Panhandle
[DE85-010530] 18 p3126 N85-29355
CSIN (Chemical Substances Information Network) workbook: US Geological Survey training course for Chemical Substances Information Network
[PB85-170058] 18 p3200 N85-29855
Use of a two-dimensional flow model to quantify aquatic habitat
[AD-A154287] 19 p3266 N85-30253
Chlorine isotopes as environmental tracers in Columbia River basalt groundwaters
[DE85-011392] 19 p3302 N85-30473
Synthetic rainfall and its use in hydrologic modeling
19 p3314 N85-30542
Microwave hydrology: A trilogy
[NASA-CR-176042] 20 p3477 N85-31609
SEASAT altimetry for surface height of inland seas
20 p3493 N85-31714
Geologic and hydrologic characterization and evaluation of the basin and range province relative to the disposal of high-level radioactive waste. Part 3: Geologic and hydrologic evaluation
[GS-CIRC-904-A] 20 p3526 N85-31934
Mega-geomorphology and neotectonics
21 p3602 N85-32366
Space imagery and some geomorphological problems of the Guiana Shield, South America
21 p3602 N85-32368
Changes in the organic material in lakes in the blast zone of Mount St. Helens, Washington: Hydrologic effects of the eruptions
[GS-CIRC-850-1] 21 p3630 N85-32551
Military hydrology. Report 9: State-of-the-art review and annotated bibliography of dam-breach flood forecasting
[AD-A155383] 22 p3801 N85-33553
Meteorology and Society: Statements presented at the 9th congress under agenda item 12 — World Meteorological Organization
[WMO-643] 22 p3817 N85-33844
Hydrology
[PB85-182054] 23 p3944 N85-34440
USGS coastal research, studies and maps: A source of information for coastal decision making
[USGS-CIRC-963] 24 p4108 N85-35465
Two-dimensional inversion of resistivity monitoring data from the Cerro Prieto geothermal field
[DE86-012551] 24 p4113 N85-35494

HYDROLOGY MODELS
Hydrologic and economic models for watershed evaluation and research
[PB84-222371] 01 p0066 N85-10436
The use of fixed-bed adsorber models to predict the fluxes of toxic substances in groundwaters and soil environments
[PB84-202583] 01 p0071 N85-10468
Identification and parameter estimation of phosphate balance models in drinking water reservoirs
[PUBL-313] 08 p1181 N85-17439
Verification of a model of the Eastern Scheldt
[RAND/R-3108-NETH] 09 p1354 N85-18518
World ocean level oscillations and their relationship to change in inflow of continental waters
13 p2108 N85-23133
Remote Sensing of Snow and Evapotranspiration
[NASA-CP-2363] 13 p2123 N85-23223
Snowmelt-runoff model utilizing remotely-sensed data
13 p2124 N85-23226
Snowmelt runoff model in Japan
13 p2124 N85-23227
Application of Martinec-Rango model to river basin in Japan
13 p2124 N85-23228
Applications of Kalman filtering and recursive least-squares in river flow modelling
15 p2636 N85-26254
Identification and characterization of watershed models for evaluation of impacts of climate change on hydrology
[DE85-006575] 18 p3125 N85-29348
Hydrology
[PB85-182954] 23 p3944 N85-34440
The development of assessment techniques program
24 p4106 N85-35457

HYDROLYSIS
Ceramic microstructure development
[AD-A145753] 03 p0337 N85-12166
Research in phase transfer catalysis
[AD-A148286] 08 p1121 N85-17068
Hydrolysis of iodine: Equilibria at high temperatures
[DE84-016713] 09 p1293 N85-18119
ECUT, Energy Conversion and Utilization Technologies program: Technical and economic assessment of processes for the production of butanol and acetone. Phase 2: Analysis of research advances
[NASA-CR-175471] 10 p1434 N85-19034
Ethanol production by enzymatic hydrolysis: Parametric analysis of a base-case process
[DE84-013105] 11 p1614 N85-20147
Hydrolysis of plastic wastes with the aim of recovering and reprocessing the starting components (recycling)
[BMFT-FB-T-84-250] 12 p1885 N85-21828
Kinetics of hydrolysis and products of hydrolysis and photolysis of tetryl
[AD-A153144] 17 p2921 N85-28005
Model for the growth of fractal silica polymers
[DE85-007884] 17 p2935 N85-28115
Lipid hydrolysis in man during antiorthostatic hypokinesia
23 p3953 N85-34500
The identification of compounds in mustard hydrolysate
[AD-A156361] 24 p4076 N85-35258
Aqueous volatile weak electrolyte equilibria to 300 C
[DE85-013640] 24 p4076 N85-35251

HYDROMAGNETIC FLOW
U MAGNETOHYDRODYNAMIC FLOW

HYDROMAGNETIC STABILITY
U MAGNETOHYDRODYNAMIC STABILITY

HYDROMAGNETIC WAVES
U MAGNETOHYDRODYNAMIC WAVES

HYDROMAGNETICS
U MAGNETOHYDRODYNAMICS

HYDROMAGNETISM
U MAGNETOHYDRODYNAMICS

HYDROMECHANICS
NT ELASTOHYDRODYNAMICS
NT ELECTROHYDRODYNAMICS
NT HYDRODYNAMICS
NT HYDROSTATICS
NT MAGNETOHYDRODYNAMICS
Second All-Union Seminar on Hydromechanics and Heat and Mass Exchange in Weightlessness, summaries of reports
[NASA-TM-77590] 01 p0047 N85-10305
Free surface effects on the wake of a flat plate
[AD-A146068] 07 p0958 N85-16071
Experiments on the influence of active walls on the initial amplitudes and growths of instability waves
[AD-A154630] 21 p3583 N85-32275

HYDROMETEOROLOGY
NT MARINE METEOROLOGY
Bibliography of climate textbooks and studies
[WCP-84] 02 p0231 N85-11505
Standard SHEF (Standard Hydrometeorologic Exchange Format) decoder Version 1.1
[PB85-101508/GAR] 06 p0840 N85-15332
Use of minicomputers for the formation of hydrological data banks 07 p1001 N85-16358
Water and climate, study of one case
07 p1002 N85-16360
The use of hydrometeorological data in explaining shrimp cycles in Guyana 07 p1004 N85-16361
A scheme for short-term prediction of hydrometeors using advection and physical forcing
[AD-A148011] 08 p1188 N85-17467
Almospheric research aircraft — conductivity/charge measurements
[ONERA-RS-87/7154/PY] 11 p1662 N85-20596
Analysis of hydrometeorological conditions in Antarctic coastal waters according to data from hydrological and satellite observations 15 p2467 N85-25354
Great Lakes hydrometeorologic and hydraulic data needs 20 p3496 N85-31739
Effects of hydrometeors on electromagnetic wave propagation
[AD-A155379] 22 p3759 N85-33297

HYDROPHONES
Effect of axisymmetric vibration modes on sensitivity and directivity characteristics of piezoceramic sphere — hydrophones 15 p2525 N85-25569
Transversely reinforced piezoelectric composites
[AD-D011676] 19 p3260 N85-30214

HYDROPLANING
Runway rubber removal specification development field evaluation procedures development
[FAA-PM-84-27] 12 p1781 N85-21179
Very high speed lap with positive lift effect
[AD-D011710] 19 p3260 N85-30344

HYDROPONICS
Hydroponics developments for spaceship garden
21 p3663 N85-32754

HYDROPOWER STATIONS
U HYDROELECTRIC POWER STATIONS

HYDROSPHERE (EARTH)
U EARTH HYDROSPHERE

HYDROSTATIC PRESSURE
Processing ceramics
[NASA-TM-77603] 01 p0031 N85-10188
Special topics reports for the reference tandem mirror fusion breeder: Liquid metal MHD pressure drop effects in the packet bed blanket, volume 1
[DE85-002142] 06 p0865 N85-15500
Effect of hydrostatic pressure on trapping centers in strained-layer superlattice structures
[DE85-001362] 09 p1399 N85-18807
Hydrostatic bearing pad maximum load and overturning conditions for the 70-meter antenna
10 p1465 N85-19241
Simplified theory for the behaviour of buried flexible cylinders under the influence of uniform hoop compression
[PB85-116531] 11 p1654 N85-20419
Human lung fluid content during 7-day head-down tilt
12 p1902 N85-21941
High pressure environmental conditioning systems and chamber rehabilitation
[AD-A150039] 12 p1905 N85-21964
Effects of posture and water immersion on diaphragmatic function 16 p2840 N85-27515
Distribution of density in closed-impression die forging of axisymmetrical products from metal powders
19 p3245 N85-30118

HYDROSTATICS
Development of gas-lubricated pistons for heavy duty diesel engine technology program
[NASA-CR-174746] 03 p0441 N85-12606
Behavior and characteristics of storm cold outflows
09 p1356 N85-18529
Hydrostatic compression of Fe1-chi O wustite.
15 p2508 N85-25472
Non-contact hydrostatic bearings
16 p2762 N85-27046
On Long's solution to hydrostatic flow over mountains
[DFVLR-MITT-84-02] 17 p2994 N85-28503
Planetary reorientation by surface loads
22 p3858 N85-33886

HYDROTHERMAL CRYSTAL GROWTH
Hydrothermal alteration of CM carbonaceous chondrites: Implications of the identification of tochilinite as one type of meteoritic PCP 06 p0884 N85-15616

HYDROTHERMAL STRESS ANALYSIS
Designing for fiber composite structural durability in hygrothermomechanical environment
[NASA-TM-87045] 17 p2917 N85-27978
EVA-glass interface bond stability
21 p3608 N85-32408
Hydrothermal alteration in the 3.5 b.y. old Onverwacht Group of South Africa 21 p3718 N85-33071

HYDROTHERMAL SYSTEMS
Field testing of aquifer thermal energy storage
[DE85-000396] 09 p1344 N85-18457
Thermohydrodynamic model: Hydrothermal system, shallowly seated magma chamber
13 p2115 N85-23173
Determining deep heat flow and rate of horizontal percolation from temperature measurements in aquifer
13 p2116 N85-23180
Structure of Reykjanes Ridge rift zone and Icelandic thermal anomaly 19 p3299 N85-30095
Melt zones beneath five volcanic complexes in California: An assessment of shallow magma occurrences
[DE85-010844] 19 p3305 N85-30469
Submarine hydrothermal environments as sites for the origin and evolution of life 21 p3719 N85-33074
Indications of mineral zoning in a fossil hydrothermal system at the Meager Creek geothermal prospect, British Columbia, Canada from induced polarization studies
[DE85-011982] 22 p3815 N85-33636
Workshop on Recent Research in the Valles Caldera
[DE85-010569] 23 p3949 N85-34472
Heat transfer and brine evolution in magma-hydrothermal systems 24 p4104 N85-35441
Massive sulfide deposits from the southern Juan de Fuca Ridge 24 p4105 N85-35446
A comparison of LANDSAT thematic mapper, multispectral scanner and airborne sensors for mapping the distribution of alteration minerals: Examples from the southwestern United States 24 p4106 N85-35452
Preliminary results of an ALVIN dive program on active hydrothermal vents at the southern Juan de Fuca Ridge
24 p4106 N85-35454
Ore genesis at the Monterrosas deposit in the Coastal Batholith, Ica, Peru 24 p4115 N85-35510

HYDROX ENGINES
U HYDROGEN OXYGEN ENGINES

HYDROXIDES
NT POTASSIUM HYDROXIDES
The alpha-form of the hydroxides of bivalent metals
[NASA-TM-77508] 04 p0473 N85-13009
Evaluation of ettringite and related compounds for use in solar energy storage
[DE85-003249] 12 p1882 N85-21809
Exploratory corrosion tests on alloys in molten salts at 900(0)C
[DE85-000511] 14 p2257 N85-23983
High performance size exclusion chromatography (IX) bulk and component analysis of silanol groups in polydimethylsiloxanes: Process development endeavor
[DE85-008653] 15 p2506 N85-25458
Sintering phenomena of non-oxide silicon compounds
[DE85-006678] 15 p2520 N85-25535
Investigation of the reaction system NOX/CIOX/HOX under tropospheric and stratospheric conditions
[BPT-11/84] 18 p3137 N85-29427

HYDROXYCORTICOSTEROID
NT CORTISONE
Biochemical status of adrenocortical dysfunction following spaceflight 12 p1901 N85-21935

HYDROXYL COMPOUNDS
NT ALCOHOLS
NT ETHYL ALCOHOL
NT GLYCOLS
NT METHYL ALCOHOLS
NT PHENOLS
NT POLYVINYL ALCOHOL

HYDROXYL EMISSION
Fundamental equations of the LIF hydroxyl measurements, appendix A 05 p0676 N85-14338
Orographic disturbances of upper atmosphere emissions 11 p1663 N85-20480
Twilight intensity variation of the infrared hydroxyl airglow 11 p1663 N85-20481
Far-infrared emission lines of CO and OH in the Orion-KL molecular shock
[NASA-TM-86721] 24 p4167 N85-35832
Observations of far-infrared transitions between excited states of OH
[NASA-TM-86722] 24 p4167 N85-35833

HYDROXYL RADICALS
Organic aerosol formation: OH(hydroxyl radical) versus ozone oxidation pathways
[PB84-219880] 03 p0368 N85-12484
Detailed performance calculations: Wayne State University and Ford Motor Company, appendix C
05 p0676 N85-14340
Detailed performance calculations: Portland State Group, appendix F 05 p0676 N85-14343
Detailed performance calculations: Harvard Group, appendix G 05 p0676 N85-14344
The fluorescence of cometary OH and CN
09 p1411 N85-18888
Application of Monte Carlo and molecular dynamics methods to the calculation of thermodynamic properties of molten salts
[AD-A148667] 10 p1568 N85-19889

Electron stimulated desorption and the role of secondary electrons
[AD-A150974] 14 p2252 N85-23955
The copper vapor laser 16 p2824 N85-27417
Water vapor 16 p2824 N85-27420
Resonant CARS detection of OH radicals
[AD-A153842] 18 p3071 N85-28995
Measurement of radical species concentrations and polycyclic aromatic hydrocarbons in flames by fluorescence and absorption using a tunable dye laser
[DE85-006824] 18 p3113 N85-29274
Passive Q-modulation of optical cavities by KCl crystals containing OH(-) -ions 21 p3688 N85-32915

HYGRAL PROPERTIES
Remote sensing as a mineral prospecting technique
[E85-10010] 02 p0216 N85-11423
Designing for fiber composite structural durability in hygrothermomechanical environment
[NASA-TM-87045] 17 p2917 N85-27978

HYGROMETERS
Trace water sensor
[NASA-CASE-NPO-15722-1] 18 p3103 N85-29212
Fog activation and supersaturation 21 p3660 N85-32678

HYGROSCOPICITY
Structure and property formation mechanism in magnetite alloy-binder composite 10 p1444 N85-19103
Water-resistance and some other properties of polyalkali fluorophosphate glasses 14 p2281 N85-24133

HYPENBARIC CHAMBERS
Hyperbaric physiology (status and prospects) 08 p1194 N85-17521
Management of vibration sickness in coal mines by hyperbaric oxygenation 10 p1523 N85-19609
Peripheral changes in regional sweating responses to exercise in hypobaric environments
[AD-A150757] 14 p2388 N85-24710
Medical planning criteria for implementation of clinical hyperbaric facilities
[AD-A151001] 14 p2389 N85-24715
Light-weight oxygen delivery hood assembly for hyperbaric chamber
[AD-D011709] 19 p3331 N85-30634
Determination of individual tolerance in hyperbaric oxygen 23 p3954 N85-34507

HYPERBOLAS
Efficient parallel solution of linear systems with hyperbolic rotations
[AD-A152365] 17 p3018 N85-28661
Hyperbolic phenomena in the flow of viscoelastic fluids
[AD-A153633] 18 p3099 N85-29186

HYPERBOLIC COORDINATES
Generation of three-dimensional body-fitted coordinates using hyperbolic partial differential equations
[NASA-TM-86753] 20 p3519 N85-31867

HYPERBOLIC DIFFERENTIAL EQUATIONS
The convergence of Garlerkin approximation schemes for second-order hyperbolic equations with dissipation
[CSIR-TWISK-325] 01 p0109 N85-10736
Approximation of discontinuous solutions of hyperbolic partial differential equations
[NRIMS-TWISK-302] 02 p0250 N85-11631
A pseudospectral Legendre method for hyperbolic equations with an improved stability condition
[NASA-CR-172475] 03 p0410 N85-12617
On explicit difference schemes for hyperbolic systems with variable coefficient 2
[PREPRINT-808] 03 p0413 N85-12641
Lolb Sobolev spaces with applications to variational integrals and differential equations
[CTH-MATH-1984-19] 04 p0556 N85-13544
Generation of 3-dimensional body fitted coordinates using hyperbolic partial differential equations
[AD-A148059] 09 p1274 N85-18006
Contribution to the study of a numerical implicit method for solving the Euler equations
[ESA-TT-872] 10 p1549 N85-19771
High order difference schemes with reduced dispersion for hyperbolic differential equations
[CWI-NM-R8408] 11 p1634 N85-20293
A convergent series expansion for hyperbolic systems of conservation laws
[NASA-CR-172557] 12 p1910 N85-21990
Results for second order hyperbolic systems with viscous dumping
[AD-A151100] 15 p2555 N85-25765
On functions with a finite or locally bounded Dirichlet integral 15 p2635 N85-26243
Relaxation methods for hyperbolic equations
[REPT-84-20] 17 p3021 N85-28687
Use of a hyperbolic grid generation scheme in simulating supersonic viscous flow about three-dimensional winged configuration
[NASA-TM-86344] 23 p3893 N85-34116
Workshop report on Simulation Techniques for Shock Wave Phenomena and Characteristics of Plasmas in Inertial Confinement Fusion
[IPPJ-725] 23 p3979 N85-34670
Cubic interpolated pseudo-particle method (CIP) for solving hyperbolic-type equation 23 p3979 N85-34673
Absorbing boundary conditions for exterior problems
[NASA-CR-177944] 24 p4142 N85-35876

HYPERBOLIC FUNCTIONS
Some scientific subroutines in LISP
[AD-A147889] 07 p1026 N85-16515
Generalized formulation of a class of explicit and implicit TVD schemes
[NASA-TM-86775] 21 p3675 N85-32830

HYPERBOLIC NAVIGATION
NT LORAN
NT LORAN C

HYPERBOLIC SPACE
U HYPERBOLIC COORDINATES

HYPERBOLIC SYSTEMS
The experimental computer control of a two-dimensional hyperbolic system 20 p3411 N85-31166

HYPERCAPNIA
Dynamics of external respiration and gas metabolism under combined effect of hypoxia and hypercapnia 08 p1193 N85-17519
Factors determining effectiveness of voluntary decrease in ventilation during muscular work using instrumented feedback 08 p1193 N85-17520

HYPERFINE STRUCTURE
Investigation of solid state problems using the hyperfine interaction between static and dynamic internal fields with short live excited probe nuclei 03 p0428 N85-12729
EXAFS and Moessbauer study of small metal clusters isolated in rare-gas solids
[DE84-015976] 04 p0470 N85-12994
Investigation on K (4 2P3/2) Hg interaction at collision energies from 0.5 to 5.7 eV
[MPIS-15/1983] 04 p0563 N85-13589
The evaluation of a deformable diffraction grating for a stigmatic EUV spectrohellometer
[NASA-CR-174248] 07 p1042 N85-16821
Hyperfine structure and lifetime measurements on electronically excited long-life molecules in a beam experiment
[MPIS-11/1984] 11 p1726 N85-20855
Very low temperature studies of hyperfine effects in metals
[DE85-013367] 22 p3749 N85-33236

HYPERGEOMETRIC FUNCTIONS
Asymptotic expansion of Jacobi polynomials
[REPT-84-35] 17 p3021 N85-28689

HYPERGOLIC ROCKET PROPELLANTS
Atmospheric dispersion of hypergolic liquid rocket fuels, volume 1
[AD-A149597] 12 p1817 N85-21309
Atmospheric dispersion of hypergolic liquid rocket fuels, volume 2
[AD-A150699] 14 p2263 N85-24020

HYPERKINESIA
Alterations in skeletal muscle with disuse atrophy
[NASA-CR-174195] 06 p0643 N85-15349

HYPERNEA
Factors determining effectiveness of voluntary decrease in ventilation during muscular work using instrumented feedback 08 p1193 N85-17520

HYPERNUCLEI
A 1-2 GeV/c beam line for hypernuclear and kaon research
[DE85-007623] 16 p2863 N85-27659
Spin dependence of the lamda-nucleus interaction determined by observation of hypernuclear gamma rays
[DE85-011878] 19 p3364 N85-30863

HYPERONS
Cooling of neutron stars with hyperons
[DE85-004641] 13 p2171 N85-23472

HYPEROXIA
Effect of hyperoxia and increased gas atmosphere density on contractile function of the right ventricle 01 p0093 N85-10626
Change in energetics of muscular contraction as a result of hyperoxia 01 p0093 N85-10629
Mechanisms of oxygen toxicity and methods of protection
[AD-A145830] 03 p0400 N85-12551
Distribution and abundance of organic thiols 21 p3657 N85-32717

HYPERSONIC AIRCRAFT
NT HYPERSONIC GLIDERS
Aerodynamic heating rate distributions induced by trailing edge controls on hypersonic aircraft configurations at Mach 8
[NASA-TM-87453] 13 p1969 N85-22370
Aerodynamic characteristics of a distinct wing-body configuration at Mach 6: Experiment, theory, and the hypersonic isolation principle
[NASA-TP-2467] 22 p3727 N85-33107

HYPERSONIC BOUNDARY LAYER
Experimental studies of Quasi-Two-Dimensional and three-dimensional viscous interaction regions induced by skewed-shock and swept-shock boundary layer interactions
[AD-A150080] 12 p1847 N85-21587
Proceedings of the 9th US Air Force and the Federal Republic of Germany Data Exchange Agreement Meeting, Viscous and Interacting Flow Field Effects
[AD-A153020] 17 p2958 N85-28266
A numerical solution of a nonisothermal wall using the two-dimensional Navier-Stokes equations
[AD-A154467] 19 p3266 N85-30257

HYPERSONIC FLOW
Numerical analysis of the 3-dimensional inviscid hypersonic flow around capsule-type bodies by the alternate directional implicit method
[NAL-TR-799] 01 p0002 N85-10012
Turbulent boundary layers over rough surfaces hypersonic flow
[AD-A145040] 01 p0003 N85-10016
Experimental and predicted heating distributions for biconics at incidence in air at Mach 10
[NASA-TP-2334] 03 p0361 N85-12313
Aerodynamic and thermal characteristics of stellate bodies in hypersonic flow of rarefied gas at angle of attack 06 p0778 N85-14974
Hypersonic flow of mixture around blunt body 06 p0779 N85-14979
Laminar heat-transfer distributions on biconics at incidence in hypersonic-hypervelocity flows
[NASA-TP-2213] 07 p0957 N85-16065
Instrumentation for Application Number 1: Mass spectrometric analysis of the boundary layer associated with the tethered satellite 11 p1646 N85-20372
Hypersonic flow about triangular airfoil at large angles of attack 13 p2044 N85-22792
A 3-dimensional Navier-Stokes-Euler code for blunt-body flow computations
[NASA-TM-58266] 15 p2463 N85-25211
Flow over a biconic configuration with an afterbody compression flap
[AD-A151882] 15 p2557 N85-25778
Hypersonic nonequilibrium gas flow past zero-aspect wing 16 p2765 N85-27063
Cone drag in the transition from continuum to free molecular flow
[OUEL-1538/84] 20 p3390 N85-31023
One method of solving the problem of unsteady heat exchange of a body and its ablation 22 p3733 N85-33146
Experimental aerodynamic heating to simulated space shuttle tiles in laminar and turbulent boundary layers with variable flow angles at a nominal Mach number of 7
[NASA-TP-2307] 23 p3929 N85-34351
Mach 14 flow restrictor thermal stress analysis
[AD-A156215] 24 p4067 N85-35206

HYPERSONIC GLIDERS
Flight tests of experimental shuttle craft described 15 p2533 N85-25625

HYPERSONIC HEAT TRANSFER
Experimental investigation of heat transfer to bluff cylinders and cones in hypersonic rarefied gas flow 11 p1620 N85-20195
An experimental investigation of flap turbulent heat transfer and pressure characteristics in hypersonic flow 12 p1821 N85-21426

HYPERSONIC REENTRY
NT UNCONTROLLED REENTRY (SPACECRAFT)
Columbia: The first 5 flights entry heating data series. Volume 1: An overview
[NASA-CR-171820] 07 p0913 N85-15777

HYPERSONIC SPEED
Fiber reinforced fused silica for hypersonic radome applications
[AD-P004366] 12 p1826 N85-21460

HYPERSONIC VEHICLES
NT HYPERSONIC AIRCRAFT
NT HYPERSONIC GLIDERS
NT LIFTING REENTRY VEHICLES
A model of hypersonic two-dimensional oblique detonation wave ramjet
[UTIAS-TN-257] 23 p3897 N85-34139

HYPERSONIC WIND TUNNELS
NT CASCADE WIND TUNNELS
Aeronautical facilities catalogue. Volume 1: Wind tunnels
[NASA-RP-1132] 10 p1426 N85-18991
Mach-10 high Reynolds number development in the NSWC (Naval Surface Weapons Center) hypervelocity facility
[AD-A151241] 15 p2474 N85-25274

Mach 14 flow restrictor thermal stress analysis
[AD-A156215] 24 p4067 N85-35208
HYPERTENSIN
NT POLYPEPTIDES
HYPERTHERMIA
Effects of hyperthermia on free amino acids in rat brain and in subcellular fractions 11 p1691 N85-20631
HYPERTONIA
U OSMOSIS
HYPERTROPHY
U GROWTH
HYPERVELOCITY
Electromagnetic acceleration of macroparticles to hypervelocities in axisymmetric geometry
[IPPJ-896] 06 p0863 N85-15484
Mach-10 high Reynolds number development in the NSWC (Naval Surface Weapons Center) hypervelocity facility
[AD-A151241] 15 p2474 N85-25274
HYPERVELOCITY ACCELERATORS
U HYPERVELOCITY GUNS
HYPERVELOCITY CRATERING
U HYPERVELOCITY PROJECTILES
U PROJECTILE CRATERING
HYPERVELOCITY FLOW
Laminar heat-transfer distributions on biconics at incidence in hypersonic-hypervelocity flows
[NASA-TP-2213] 07 p0957 N85-18065
HYPERVELOCITY GUNS
NASA-Ames vertical gun 04 p0579 N85-13696
Electromagnetic rail launcher as a circuit element
[AD-A150067] 12 p1835 N85-21516
An orthogonal grid technique for studying internal deformation and energy absorption in target penetration
[AD-A149969] 12 p1860 N85-21685
Design and fabrication of projectiles for round bore railguns
[DE85-011871] 20 p3398 N85-31078
HYPERVELOCITY IMPACT
Particle velocity experiments in anorthosite and gabbro
[NASA-CR-174158] 04 p0533 N85-13407
Orbital Debris
[NASA-CP-2360] 12 p1783 N85-21188
Manmade orbital debris studies at NASA Langley 12 p1783 N85-21192
Hypervelocity impacts on Skylab 4/Apollo windows 12 p1785 N85-21202
Hypervelocity impact investigations and meteoroid shielding experience related to Apollo and Skylab 12 p1785 N85-21206
Debris impact on Earth-orbiting spacecraft 12 p1948 N85-22234
Plasma production by meteoroid impact 13 p2174 N85-23492
Progress on studies of early intense cratering 13 p2181 N85-23535
Martian terrain ages 13 p2181 N85-23537
Morphology and mechanics of terraces in lunar craters 13 p2182 N85-23543
Newly discovered Martian impact basins 13 p2182 N85-23544
Impact ionization from gold, aluminum and PCB-Z — Giotto spacecraft paint PCB-Z 14 p2244 N85-23910
Experimental investigations on ion emission with dust impact on solid surfaces — Giotto spacecraft 14 p2244 N85-23911
Voyager planetary radio astronomy: Grain and particle impacts shot noise in Saturn's ring plane 15 p2573 N85-26498
Experimental data for characterizing perforating impacts: Fragmentation processes
[AD-A156370] 24 p4102 N85-35427
HYPERVELOCITY LAUNCHERS
Preliminary analysis of space mission applications for electromagnetic launchers
[NASA-CR-174067] 03 p0321 N85-12071
Use of the computer programs PARA 80 to study results from firing the railgun ERGS-1M
[MRL-R-900] 22 p3736 N85-33167
HYPERVELOCITY PROJECTILES
Rail accelerator technology and applications
[NASA-TM-86947] 12 p1794 N85-21258
Arc-driven rail gun research
[NASA-CR-174816] 12 p1859 N85-21662
Ion emission from solid surfaces: Comparison of dust impact with other excitations — Giotto mission 14 p2244 N85-23912
A method of accurizing rail guns
[LA-10028-MS] 22 p3737 N85-33168
Experimental data for characterizing perforating impacts: Fragmentation processes
[AD-A156370] 24 p4102 N85-35427
HYPERVELOCITY WIND TUNNELS
NT CASCADE WIND TUNNELS
HYPOBARIC ATMOSPHERES
Small animal hypobaric chamber
[AD-A146196] 03 p0364 N85-12335
An environmentally-controlled extended-use small animal hypobaric chamber
[AD-A153735] 19 p3221 N85-29974
HYPOKINESIA
Dynamics of morphological changes in articulation nervous system under hypokinetic conditions as a model of a spaceflight factor 01 p0092 N85-10621
Effect of 1,25-dihydroxycholecalciferol and 24,25 dihydroxycholecalciferol on growth and alteration of rat bones during hypokinesa (histomorphometric study) 01 p0092 N85-10622
Dynamics of some parameters of carbohydrate and lipid metabolism in recovery period following long-term hypokinesa 01 p0093 N85-10623
Biligenic function of white rat liver 01 p0093 N85-10624
Effect of short-term hypokinesia on rat opioid system reaction 01 p0093 N85-10625
Skeletal muscle metabolism in hypokinetic rats
[NASA-CR-174059] 02 p0233 N85-11520
General resistance of organism of rats under hypokinesia 05 p0694 N85-14462
Effects of prolonged hypokinesia on nervous system 08 p1194 N85-17524
Study of bodily functional status and quality of controlling action of power unit operators with various intensities of labor 09 p1362 N85-18569
Characteristics of human masseter under conditions of hypokinesia 11 p1691 N85-20630
Morphological study of monkeys submitted to antiorthostatic hypokinesia 12 p1902 N85-21942
Fluid metabolism of monkeys during two-week antiorthostatic hypokinesia 12 p1902 N85-21943
Distinctive morphological manifestations of acute stress reaction in adrenal cortex of hypokinetic rats 12 p1902 N85-21944
Preventive effect of acute heat factors during hypokinesia 12 p1902 N85-21945
Rat tissue opioid peptide content during long-term hypokinesia 12 p1904 N85-21954
Effects of muscle atrophy on motor control: Cage size effects 15 p2609 N85-26080
Induced changes in the cholinergic system of sciatic nerve and slow and fast twitch muscle of rats 15 p2609 N85-26081
Use and disuse and the control of acetylcholinesterase activity in fast and slow twitch muscle of rat
[NASA-CR-175717] 15 p2614 N85-26109
Changes in the cholinergic system of rat sciatic nerve and skeletal muscle following suspension induced disuse
[NASA-CR-175718] 15 p2615 N85-26111
Analysis of head-down tilt as an analog of weightlessness using a mathematical simulation model
[NASA-CR-171870] 15 p2616 N85-26118
Regional circulation during testing on isokinetic dynamometer following 14-day bedrest 19 p3323 N85-30590
Primate adrenal reactions to antiorthostatic hypokinesia 19 p3324 N85-30591
Distinctions of rat lymphatic organ reactions to acute stress factor during hypokinesia 19 p3324 N85-30596
Morphological study of primate hypothalamus and hypophysis after experiment with antiorthostatic hypokinesia 19 p3325 N85-30603
Changes in nephron and juxtaglomerular system of primate kidneys under the effect of antiorthostatic hypokinesia 19 p3326 N85-30605
Rat blood serum and liver carbohydrates and lipids in recovery period after 15-day hypokinesia 19 p3326 N85-30606
Analysis of long bone and vertebral failure patterns
[AD-A154796] 21 p3663 N85-32758
Results and prospects of physiological research during spaceflights 22 p3732 N85-33139
Effects of immobilization and high-altitude adaptation on energy metabolism in rats 22 p3820 N85-33663
Investigation of spectrum of human bile acids during 120-day antiorthostatic hypokinesia 22 p3821 N85-33674
Effect of short-term antiorthostatic hypokinesia on dynamics of cardiorespiratory parameters during graded physical exercise 22 p3822 N85-33677
Investigation of some aspects of amino acid metabolism in man during brief exposure to antiorthostatic hypokinesia combined with ultraviolet radiation 22 p3822 N85-33678
Morphological study of antiorthostatic hypokinesia in monkeys 22 p3822 N85-33680
Morphological manifestations of hemodynamic changes in lungs of monkeys submitted to antiorthostatic hypokinesia 22 p3824 N85-33688
Effect of hypokinesia and +Gz accelerations on transport function of human blood 23 p3952 N85-34497
Lipid hydrolysis in man during antiorthostatic hypokinesia 23 p3953 N85-34500
Rat skeletal muscles with simulation of physiological effects of weightlessness (morphological study) 23 p3953 N85-34502
Possible mechanism for changes in glycogen metabolism in unloaded soleus muscle
[NASA-CR-176184] 24 p4127 N85-35588
HYPOTHALAMUS
Influence of hyperthermia on body temperature and content of catecholamines in white rat hypothalamus 10 p1524 N85-19615
Neural mechanism by which gravitational stimulus and stress affect the secretion of renin and other hormones 15 p2610 N85-26083
Morphological study of primate hypothalamus and hypophysis after experiment with antiorthostatic hypokinesia 19 p3325 N85-30603
HYPOTHERMIA
Influence of hyperthermia on body temperature and content of catecholamines in white rat hypothalamus 10 p1524 N85-19615
Effects of hypothermia on brain metabolism 11 p1692 N85-20636
Changes in pentose and glucuronate pathway dehydrogenases in rat brains following single or multiple hypothermic episodes 20 p3505 N85-31790
Electroanesthesia as a means of controlling cold stress of local hypothermia 22 p3823 N85-33687
HYPOTHESES
NT EXPECTANCY HYPOTHESIS
NT NULL HYPOTHESIS
NT VORTICITY TRANSPORT HYPOTHESIS
Distributed hypothesis testing in distributed sensor networks
[AD-A145434] 02 p0294 N85-11905
The search for regularity: Four aspects of scientific discovery
[AD-A145939] 03 p0368 N85-12355
Development of structured regression hypotheses/interactive descriptive geometry through five dimensions
[INT-324] 04 p0554 N85-13524
Invariant tests and likelihood ratio tests for multivariate elliptically contoured distributions
[AD-A155844] 24 p4142 N85-35679
HYPOXEMIA
Pulmonary blood flow and oxygenation of arterial blood in a healthy subject upon 7 days hypokinesia 07 p1014 N85-16439
The effect of an unphysiological oxygen supply on the organism 24 p4130 N85-35605
HYPOXIA
Hemodynamics and neurodynamics of the human brain during exposure to moderate hypoxic hypoxia 01 p0094 N85-10630
The effect of naproxen on acute mountain sickness and vascular responses to hypoxia
[AD-A145144] 01 p0095 N85-10638
USSR report: Life Sciences: Biomedical and behavioral sciences
[JPRS-UBB-84-026] 04 p0543 N85-13457
Results of study of hypoxia problems 04 p0544 N85-13462
Distribution of blood flow to brain, kidneys, gut, spleen and posterior extremities in cats in acute hypoxia 07 p1013 N85-16434
Biochemical evaluation of bodily influence of high and low temperatures 07 p1014 N85-16441
Dynamics of external respiration and gas metabolism under combined effect of hypoxia and hypercapnia 08 p1193 N85-17519
Aviation-related cardiorespiratory effects of blood donation in female pilots
[AD-A148045] 08 p1195 N85-17529
Multiple regression method used to assess animal adaptation to hypoxic hypoxia 12 p1902 N85-21947
Peripheral changes in regional sweating responses to exercise in hypobaric environments
[AD-A150757] 14 p2388 N85-24710
Oxygen uptake as an indicator of animal adaptation to altitude hypoxia 19 p3324 N85-30595
Formation of new microvessels in skeletal muscles of rats exposed to hypobaric hypoxia for one week 22 p3820 N85-33662
Effects of blood volume overload on myocardial ultrastructure in relation to adaptation to high altitude hypoxia 22 p3820 N85-33664
Structural changes in thyroid due to high-altitude adaptation in Kirghizia 22 p3820 N85-33666
Effect of acute hypoxia on coronary and systemic hemodynamics 23 p3953 N85-34503

Monitoring dosage of volatile compounds in tests at low barometric pressure 23 p3954 N85-34506
HYPSOGRAPHY
Hypsometric features on Venus 13 p1983 N85-22439
HYSTERESIS
Input-output stability analysis with magnetic hysteresis non-linearity: A class of multipliers
[AD-A145729] 02 p0253 N85-11654
Theory of the double critical state in type-2 superconductors
[DE84-015461] 02 p0289 N85-11886
Variation of resin properties through the thickness of cured samples 04 p0468 N85-12974
Internal hysteresis experienced on a high pressure syn gas compressor 05 p0842 N85-14122
Anisotropy and relaxation effects of Co2+ ions in LiTi ferrite
[AD-A146550] 06 p0861 N85-15468
Magnetostatic problems in nonlinear media with hysteresis
[DE85-003701] 10 p1482 N85-19358
Application of hysteresis modelling to the non-destructive inspection of stress
[DE85-003081] 11 p1650 N85-20393
Studies in electron phenomena in MOS structures: The pulsed C-V method 15 p2659 N85-26407
An experimental nonlinear optical waveguide device 18 p3186 N85-29762
Application of traction drives as servo mechanisms 22 p3797 N85-33520
Electrical resistivity and hysteresis of the equiatomic nickel-titanium alloy near the martensitic transformation temperature 23 p3904 N85-34181
Monotonous stress-strain properties of structural steel subjected to nonstationary repetitive pre-loading 23 p3904 N85-34185

I

I BEAMS
Yield joint condition for three-dimensional I-beams
[ILR-MITT-137] 12 p1867 N85-21716
Buckling and bracing of cantilevers
[CE-42] 17 p2979 N85-28413
Impact dynamics research on composite transport structures
[NASA-TM-86391] 19 p3284 N85-30367
IBM COMPUTERS
IBM Corporation, IBM 5381 model 5, system/38 COBOL release 6
[PB84-227677] 03 p0405 N85-12584
Digital Research Incorporated, IBM PC XT, FORTRAN-77 V4.0
[PB84-243633] 06 p0849 N85-15388
Northern Telecom, Incorporated, IBM 3033 (compilation), NTI-585/585 (execution), XCOBOL Release 4.1 Version H(01)
[PB84-227875] 06 p0850 N85-15400
ZTL: A subroutine package for the IBM personal computer to support the Ziatech ZT1488 IEEE-488 controller
[LA-10141-MS] 12 p1913 N85-22010
DOS 21: PCDOS 2.0 support subroutine package for the IBM personal computer
[LA-10142-MS] 12 p1914 N85-22012
TRANIO: A subroutine package for the IBM personal computer to support the transfer 6002 CAMAC crate controller
[LA-10145-MS] 12 p1914 N85-22015
ICBM (MISSILES)
U INTERCONTINENTAL BALLISTIC MISSILES
ICE
NT GLACIERS
NT ICE FLOES
NT ICEBERGS
NT LAKE ICE
NT LAND ICE
NT PRESSURE ICE
NT SEA ICE
The development of a diode laser Doppler velocimeter for boundary layer measurements under ice: A feasibility investigation
[AD-A145076] 01 p0053 N85-10348
Executive report: Results of the IRGA-CNPq/INPE experimental project
[E85-10011] 02 p0216 N85-11424
Transport phenomena in the boundary layer during solution solidification under microgravity. Ice growth from a water-salt solution
[BMFT-FB-W-84-031] 03 p0329 N85-12121
Measurement of snow cover thickness by radar sounding 03 p0344 N85-12216
Ice sheets as invariant surfaces for radar altimeter calibration and orbit determination 03 p0383 N85-12449
Initial feasibility ground test of a proposed photogrammetric system for measuring the shapes of ice accretions on helicopter rotor blades during forward flight
[NASA-TM-87391] 04 p0455 N85-12887
Evaluation of thermocouple junction temperature
[DE84-015159] 04 p0502 N85-13206
Solar wind and cosmic ray irradiation of grains and ices - application to erosion and synthesis of organic compounds in the solar system 06 p0888 N85-15637
Salt action on concrete
[AD-A147812] 07 p0933 N85-15912
Pulse transmission through frozen silt
[AD-A147108] 07 p0940 N85-15958
Buckling analysis of cracked, floating ice sheets
[AD-A147330] 07 p0988 N85-16277
Deuterium diffusion in a soil-water-ice mixture
[AD-A148457] 08 p1176 N85-17415
Hybrid system for producing and storing ice
[DE84-017474] 09 p1304 N85-18195
The pleistocene geology of Vilas County, Wisconsin 09 p1353 N85-18509
A model for the climatic behavior of water on Mars 09 p1415 N85-18931
Atlas of snow and ice resources 10 p1497 N85-19449
Freeze-up, breakup and date of maximum ice thickness for the Saint Lawrence River, 1971 - 1978
[PB85-119451] 10 p1507 N85-19509
Ground-based snow and ice crystal observation system used in Sierra Nevada winter orographic storms
[PB85-115343] 10 p1520 N85-19584
MIZEX (Marginal Ice Zone Program): A program for mesoscale air-ice-ocean interaction experiments in Arctic marginal ice zones. 5. MIZEX 84. Summer experiment PI (Principal Investigator) preliminary reports
[AD-A148966] 10 p1521 N85-19594
Lake ice occurrence as a possible detector of atmospheric CO2 effects on climate
[DE85-002951] 11 p1687 N85-20606
Implications of the presence of S2 in cometary ice 11 p1760 N85-21072
Latent heat storage in cooling systems
[DE85-005355] 13 p2129 N85-23248
Variation of Arctic cloud cover in summer
[DE85-004507] 13 p2139 N85-23285
Patterns of fracture and tidal stresses due to nonsynchronous rotation: Implications for fracturing on Europa 13 p2173 N85-23483
Comet thermal modeling 13 p2176 N85-23505
High pressure cosmochemistry of major planetary interiors: Laboratory studies of the water-rich region of the system ammonia-water 13 p2183 N85-23549
Transformation of polar ice sublimate residue into Martian circumpolar sand 13 p2189 N85-23580
Mars: Long term changes in the state and distribution of H2O 13 p2191 N85-23593
Creep of ice: Further studies 13 p2201 N85-23655
North Atlantic Deep Water Formation
[NASA-CP-2367] 15 p2601 N85-26028
Macrostructure and microphysics of Saturn's E-ring 15 p2677 N85-26528
Permafrost, seasonally frozen ground, snow cover and vegetation in the USSR
[AD-A153628] 16 p3124 N85-29346
Active and passive remote sensing of ice
[AD-A154406] 19 p3300 N85-30459
A study of freezing and melting with eutectic interactions 19 p3378 N85-30956
Mesoscale features and atmospheric refraction conditions of the Arctic marginal ice zone
[AD-A155139] 21 p3636 N85-32584
The nucleation of ice at very low temperatures and pressures 21 p3641 N85-32617
The capture of ice nucleating and non ice-nucleating aerosols by ice phase precipitation 21 p3641 N85-32620
Short-time creep of ice
[NRC/CNR-TT-2111] 23 p3941 N85-34428
Lake ice occurence as a possible detector of atmospheric CO2 effects on climate
[DE85-012987] 23 p3950 N85-34480
Elemental tracers of source regions of contaminants in precipitation
[DE85-012858] 24 p4113 N85-35499
ICE ENVIRONMENTS
Sea ice data buoys in the Weddell Sea
[AD-A144953] 01 p0068 N85-10594
Investigation of ice dynamics in the marginal ice zone
[AD-A145110] 01 p0068 N85-10597
Cryospheric data products available through satellite altimetry 03 p0380 N85-12429
Surging as a potential response of ice sheets to CO2-induced changes in the polar environment (SPICAE)
[DE84-016472] 06 p0841 N85-15341
Proceedings of a Workshop on Environment of West Antarctica: Potential CO2-induced changes
[PB85-110757] 11 p1671 N85-20527
Planetary analogs in Antarctica: Icy satellites 13 p2193 N85-23605
Ganymede and Callisto: Beauty is only skin deep 15 p2690 N85-26552
The NORDA/FNOC (Naval Ocean Research and Development Activity's/Fleet Numerical Oceanography Center) Polar Ice Prediction System (PIPS)-Arctic: A technical description
[AD-A156332] 24 p4126 N85-35577
ICE FLOES
Meteorite concentrations in Antarctica: How complete is the picture? 06 p0889 N85-15644
Parachute expedition to Arctic 07 p0982 N85-16240
Mining cosmic dust from the blue ice lakes of Greenland 15 p2682 N85-26563
ICE FORMATION
Automated aircraft icing forecast technique
[AD-A144853] 01 p0065 N85-10571
The rheology of icy satellites
[NASA-CR-174024] 02 p0302 N85-11959
Icing rate on stationary structures under marine conditions
[AD-A145795] 03 p0395 N85-12524
The UH-1H helicopter icing flight test program: An overview
[NASA-TM-86925] 07 p0900 N85-15702
The NASA Altitude Wind Tunnel (AWT): Its role in advanced icing research and development
[NASA-TM-86920] 07 p0910 N85-15758
Frazil ice formation
[AD-A147425] 07 p0988 N85-16279
Snow characterization measurements from SNOW-TWO/Smoke Week 6
[AD-A147423] 07 p1008 N85-16402
Icing flight research: Aerodynamic effects of ice and ice shape documentation with stereo photography
[NASA-TM-86906] 09 p1279 N85-18049
Ice segregation and frost heaving
[PB85-122430] 10 p1480 N85-19199
Frozen precipitation and concurrent weather: A case study for Munchen-Riem, West Germany
[AD-A149227] 10 p1519 N85-19577
First stage of equipping a Do 28 as a research aircraft for icing, and first research results
[ESA-TT-855] 11 p1584 N85-19982
Analysis of hydrometeorological conditions in Antarctic coastal waters according to data from hydrological and satellite observations 15 p2487 N85-25354
Characteristics of snow cover on sea ice and formation of snow ice II 15 p2582 N85-25924
Ice multiplication in summertime cumulus clouds in the BEWMEX area 16 p2829 N85-27445
Ice shapes and the resulting drag increase for a NACA 0012 airfoil
[NASA-TM-83556] 17 p2884 N85-27839
On the state of knowledge on meteorologically caused icing of aircraft in clouds
[ESA-TT-861] 20 p3496 N85-31736
Artificial and natural icing tests YEH-60A quick fix helicopter
[AD-A155147] 21 p3555 N85-32116
Ice nucleation of single water droplet by silver iodide: A laboratory observation 21 p3643 N85-32630
Ice-forming efficiency of the soluble and insoluble portions of dust contained in snow 21 p3643 N85-32631
Monte Carlo studies of H2O layers adsorbed on a model basal face of AgI 21 p3643 N85-32633
Aircraft accident report: World Airways Inc., Flight 30H, McDonnell Douglas DC-10-30CF, N113WA, Boston-Logan International Airport, Boston, Massachusetts, January 23, 1982
[PB85-910406] 22 p3728 N85-33114
Permafrost features on Earth and Mars: Similarities, differences 22 p3855 N85-33870
ICE MAPPING
Ice-soil mixtures: Visual and near-infrared remote sensing techniques
[NASA-CR-174087] 04 p0525 N85-13358
Technology development for unmanned untethered submersible vehicle systems
[AD-A148794] 09 p1304 N85-18190
Analysis of hydrometeorological conditions in Antarctic coastal waters according to data from hydrological and satellite observations 15 p2487 N85-25354

ICE NUCLEI
Ice multiplication in summertime cumulus clouds in the BEWMEX area 16 p2829 N85-27445
SCPP (Sierra Cooperative Pilot Project) data collection and analysis. Volume 1: Executive summary [PB85-156065] 16 p2837 N85-27494
Eleventh International Conference on Atmospheric Aerosols, Condensation and Ice Nuclei, volume 2 [PB85-182418] 21 p3636 N85-32596
Mechanism of heterogeneous deposition ice nucleation near water-saturation 21 p3636 N85-32597
Experimental studies of the kinetics of deposition nucleation on an ice nucleant used in weather modification 21 p3636 N85-32598
Inactivation of silver iodide by atmospheric nucleation inhibitors 21 p3636 N85-32599
Ice nucleation by silver iodine particles with nearly critical sizes 21 p3636 N85-32600
Photoinduced active sites on ice nucleating aerosol of silver iodide 21 p3639 N85-32601
Experimental investigation of properties of ice-forming reagents 21 p3639 N85-32602
Ice active bacteria as condensation nuclei 21 p3639 N85-32603
The effect of supersaturation, temperature and particle size on ice-nucleating ability of atmospheric aerosol 21 p3639 N85-32604
Ice crystal nucleation on hygroscopic aerosols 21 p3639 N85-32605
On the efficiency of the mechanism of ice particles formation in the vapor supersaturation field around a freezing droplet 21 p3639 N85-32606
Generation of lead, lead iodide and iodide aerosols and their ice nucleation 21 p3639 N85-32607
The nucleation of ice crystals during the freezing of large supercooled drops 21 p3640 N85-32608
Ice nucleus measurements 21 p3640 N85-32609
On the problem of possible mechanism of ice nuclei formation in convective clouds 21 p3640 N85-32610
Bacterial ice nuclei of marine origin: Some recent observations 21 p3640 N85-32611
Airborne measurements of atmospheric ice nuclei 21 p3640 N85-32612
Aircraft observations of condensation and ice nuclei at a tropical station 21 p3640 N85-32613
A statistical analysis of ice nuclei concentrations at urban and rural sites in Valladolid, Spain 21 p3640 N85-32614
Supersaturation spect A of Ice Nuclei at different locations in Europe and over the North-Atlantic 21 p3640 N85-32615
Concentrations of ice nuclei of different modes of activities 21 p3641 N85-32616
Observations of the atmospheric ice nucleus at northwest China 21 p3641 N85-32618
Ice nucleating characteristics of Capparis Aphylla, an Indian herb 21 p3641 N85-32619
The capture of ice nucleating and non ice-nucleating aerosols by ice phase precipitation 21 p3641 N85-32620
The investigation of natural and artificial ice nuclei by the improved membrane filter method 21 p3642 N85-32626
Basic ice nucleation mechanisms on mono and microcrystals and ice forming nuclei. Theoretical analysis and experimental results achieved in the laboratory over the past ten years: Review paper 21 p3642 N85-32629
Ice-forming efficiency of the soluble and insoluble portions of dust contained in snow 21 p3643 N85-32631
Critical supersaturations with respect to water for fast condensation-freezing ice nucleation 21 p3643 N85-32632
Concentration and source areas of ice nuclei in the Alaskan atmosphere 21 p3643 N85-32634
Eleventh International Conference on Atmospheric Aerosols, Condensation and Ice Nuclei, volume 1 [PB85-182400] 21 p3644 N85-32636
Effect of ions on cloud formation and its role in solar terrestrial relationship 21 p3653 N85-32997

ICE OBSERVATION
U ICE REPORTING

ICE PACKS
U SEA ICE

ICE PREVENTION
Heliport snow and ice control methods and guidelines [DOT/FAA/PM-84/22] 01 p0012 N85-10073
To take off and to land safely, Hoechst 1678 for ice and snow free runways 05 p0595 N85-13791
Analytical and physical modeling program for the NASA Lewis Research Center's Altitude Wind Tunnel (AWT) [NASA-TM-88918] 07 p0909 N85-15757

ICE REPORTING
Cryospheric data products available through satellite altimetry 03 p0380 N85-12428
Special difficulties of retrieving surface elevation over continental ice — satellite radar altimetry 03 p0380 N85-12429
Sea ice characteristics derived from airborne altimetry 03 p0382 N85-12440
Radar altimetry over sea ice 03 p0382 N85-12441
Use of SIR-B multiincidence-angle imagery to study iceberg detectability and offshore ocean feature extraction 08 p1145 N85-17225
Data report on variations in the composition of sea ice during MIZEX/East'83 with the Nimbus-7 SMMR [NASA-TM-86170] 09 p1342 N85-18443
Data collection and winter ice dynamics in the Beaufort Sea 14 p2238 N85-23578
Results of the MIZEX preliminary campaign: 29 June to 19 July 1983 — Marginal Ice Zone Experiment (MIZEX), satellite observation [CNES-84/142/T/CT/DRT/TIT/RL] 20 p3478 N85-31609

ICE SHELVES
U LAND ICE

ICEBERGS
Arctic ice island and sea ice movements and mechanical properties [DE84-016323] 04 p0542 N85-13450
Use of SIR-B multiincidence-angle imagery to study iceberg detectability and offshore ocean feature extraction 08 p1145 N85-17225
The use of the ARGOS system for the study of the drift of Antarctic icebergs 14 p2240 N85-23690
Main features of Antarctic Ocean circulation as revealed by satellite tracking of icebergs 14 p2325 N85-24372
Radar measurement of thickness of drifting ocean ice employing cepstral signal processing 15 p2644 N85-26313

ICELAND
The structure of the Iceland-Faeroe ridge, derived from geophysical measurements [DRIC-T-7255] 03 p0397 N85-12535
Structure of Iceland and ocean floor spreading 13 p2112 N85-23159
Oceanographic variations in recent decades and their impact on the fertility of the Iceland Sea 15 p2602 N85-26034
Geomorphic classification of Icelandic and Martian volcanoes: Limitations of comparative planetology research from LANDSAT and Viking orbiter images 21 p3603 N85-32372

ICING
U ICE FORMATION

IDAHO
Geology of selected migmatite zones within the bitterroot lobe of the Idaho batholith, Idaho and Montana 03 p0389 N85-12489
Geographic and stratigraphic distribution of Miocene palynomorphs in north Idaho 03 p0390 N85-12498
Multi crop area estimation in Idaho using EDITOR [E85-10064] 06 p0827 N85-15251
Depositional modeling of tetrahedrite in the Coeur d'Alene district, Idaho 08 p1182 N85-17448
The geology of East Butte, a rhyolitic volcanic dome on the Eastern Snake River Plain, Idaho 13 p2187 N85-23570

IDEAL FLUIDS
Algebra of hydrodynamic flows of an ideal fluid and the prediction of the behaviour of a system of particles of a passive admixture on Riemann surfaces with a variable curvature [REPT-585] 03 p0377 N85-12406
Large deformations of a nonlinear elastic solid and the diffusion of an ideal fluid treated as interacting continua 09 p1330 N85-18356

IDEAL GAS
Calculating secondary nonviscous gas flows in spatial cascades of turbines 09 p1305 N85-18202
Ideal gas thermodynamic properties for the phenyl, phenoxy, and o-biphenyl radicals [NASA-TM-83800] 12 p1943 N85-22204

IDENTIFY FRIEND OR FOE
U IFF SYSTEMS (IDENTIFICATION)

IDENTIFYING
NT CROP IDENTIFICATION
NT IFF SYSTEMS (IDENTIFICATION)
NT PARAMETER IDENTIFICATION
NT RAPID BALLISTICS IDENTIFICATION
NT SYSTEM IDENTIFICATION
NT TIMBER IDENTIFICATION
Identification as a function of familiarity for known voices talking over an unprocessed channel and an LPC (Linear Predictive Coding) voice processor [AD-A145545] 02 p0191 N85-11276
Microscopic identification of feathers in order to improve birdstrike statistics [AD-P004187] 11 p1579 N85-19950
Approximation in optimal control and identification of large space structures [AD-A150323] 13 p2151 N85-23351
Stereotype traits can be processed automatically [AD-A150947] 14 p2391 N85-24725
The 121.5/243 MHz ELT identification — Emergency Locator Transmitter (ELT) 20 p3404 N85-31119
A cluster analysis method for identification of subpopulations of cells in flow cytometric list-mode arrays 20 p3503 N85-31779
Distributed name management [AD-A154785] 21 p3712 N85-33037
Results of a search for deuterium at 25-50 GC/c using a magnetic spectrometer [OG-4.2-4] 22 p3878 N85-34024

IFF SYSTEMS (IDENTIFICATION)
A computer analysis of the RF performance of a ground-mounted, air-supported radome [AD-P004352] 12 p1824 N85-21448

IFR (RULES)
U INSTRUMENT FLIGHT RULES

IGFET
U FIELD EFFECT TRANSISTORS

IGNEOUS ROCKS
NT ANORTHOSITE
NT BASALT
NT ECLOGITE
NT GRANITE
NT PERIDOTITE
Petrology of deep crustal xenoliths from the eastern Snake River Plain, Idaho 02 p0226 N85-11477
Particle velocity experiments in anorthosite and gabbro [NASA-CR-174158] 04 p0533 N85-13407
Two lunar global asymmetries 04 p0585 N85-13734
Crystalline rocks of the northeastern United States [DE84-013674] 05 p0677 N85-14347
The search for igneous materials at the Viking landing sites 13 p2194 N85-23609
Bouguer images of the North American craton 13 p2200 N85-23648
Region-to-area screening methodology for the Crystalline Repository Project [DE85-009892] 18 p3125 N85-29354
Design analysis for a repository in crystalline rock [DE85-011802] 22 p3839 N85-33771
Aeromagnetic and gravity models of the pluton below the Lake City caldera, Colorado 24 p4104 N85-35442

IGNIMBRITE
U IGNEOUS ROCKS

IGNITERS
NT DETONATORS
NT INITIATORS (EXPLOSIVES)
Metallography of Kovar/glass/thermite interfaces [DE84-015247] 02 p0195 N85-11302
Hollow cathode apparatus [NASA-CASE-NPO-15560-1] 12 p1832 N85-21491
Oxygen-hydrogen thrusters for Space Station auxiliary propulsion systems [NASA-CR-175691] 15 p2494 N85-25383
Low gravity exothermic heating/cooling apparatus [NASA-CASE-MSC-25707-1] 18 p3104 N85-29214

IGNITION
NT SOLID PROPELLANT IGNITION
NT SPARK IGNITION
Effect of oxide coated thickness on thermal ignition of titanium-based pyrotechnics [DE84-013061] 04 p0481 N85-13065
Bulletin of the Faculty of Engineering, Hokkaido University, no. 123 [ISSN-0385-802-X] 04 p0482 N85-13075
Experimental study on the glow plug aided alcohol driven diesel engine 04 p0483 N85-13078
Laser for determining the ignition conditions of a pyrotechnic mixture [FOA-C-20542-D1] 04 p0506 N85-13230
Catalytic ignition and combustion of lean mixtures [AD-A148101] 08 p1121 N85-17057
Fuel-rich solid propellant boron combustion [AD-A148522] 08 p1136 N85-17157
Spontaneous ignition of organic solids by radiant heating 09 p1289 N85-18098
Evaluation of minimum ignition energy measurement techniques used at P.E.R.M.E. [SG83/A258] 09 p1301 N85-18169
Analysis of a potential hot-wire ignition problem [DE84-017254] 09 p1301 N85-18174
Parameters affecting hot wire ignition of thermite mixtures [DE84-016841] 09 p1301 N85-18176
Theoretical studies of the ignition and combustion of silane-hydrogen-air mixtures [NASA-CR-3876] 10 p1433 N85-19092

Mechanisms and reaction dynamics related to methane combustion
[PB85-129690] 10 p1438 N85-19065
Laser-initiated combustion studies on metallic alloys in pressurized oxygen
[PB85-126114] 10 p1438 N85-19066
Theory of flammability limits. Flow gradient effects and flame stretch
[PB85-135077] 10 p1439 N85-19067
Fuels combustion research
[AD-A149108] 10 p1457 N85-19178
Hydrogen flame acceleration and transition to detonation
[DE85-000611] 12 p1802 N85-21299
Ignition of mixtures of SiH sub 4, CH sub 4, O sub 2, and Ar or N sub 2 behind reflected shock waves
[NASA-TP-2415] 13 p1974 N85-22395
Ignition phenomena of bulk aluminum alloy as a function of oxygen pressure 13 p1999 N85-22531
Combustion of zirconium carbide 13 p1999 N85-22532
Limiting factor of flame propagation in mono-sized sprays of low-volatility fuels
[NAL-TR-839T] 15 p2521 N85-25538
Ignition of metals in high pressure oxygen 16 p2735 N85-26874
Modeling the role of radicals in the ignition of and flame propagation in hydrogen-air and methane-air mixtures 16 p2744 N85-26935
Design of a Mobile Combustion Diagnostic Fixture (MCDF)
[AD-A151814] 16 p2745 N85-26941
Elementary reactions of importance in oxidation, combustion ignition and flame inhibitions
[AD-A153139] 17 p2921 N85-28004
Whist code calculations of ignition margin in an ignition Tokamak
[DE85-009507] 18 p3190 N85-29784
Measurement of combustion species by electron impact fluorescence
[DE85-011163] 19 p3236 N85-30065
Injection, atomization, ignition and combustion of liquid fuels in high-speed air streams
[AD-A154056] 19 p3251 N85-30156
Deformation, fracture and explosive properties of reactive materials
[AD-A154073] 19 p3251 N85-30157
Burn rates of explosives at high pressures
[DE85-010606] 19 p3251 N85-30159
Coal slurry ignition in a diesel engine simulator
[DE85-010987] 20 p3463 N85-31513
Self-heating to ignition measurements and computation of critical size for solar energy collector materials
[PB85-183374] 20 p3485 N85-31663
Burn front velocity as a function of pellet density in iron-potassium perchlorate heat powders
[DE85-011448] 21 p3572 N85-32214
Scaling parameters of flashover
[NBS-GCR-85-497] 23 p3911 N85-34229
Laser probes of natural gas ignition chemistry
[PB85-200210] 24 p4077 N85-35264
Neutral pumping rates for a next step tokamak ignition device
[DE85-012780] 24 p4157 N85-35776

IGNITION LIMITS
New concepts for measuring flame spread properties
[NBSIR-84-2943] 03 p0327 N85-12104
Evaluation of minimum ignition energy measurement techniques used at P.E.R.M.E.
[SGS3/A258] 09 p1301 N85-18169
Theory of flammability limits. Flow gradient effects and flame stretch
[PB85-135077] 10 p1439 N85-19067
Behavior of the lean methane-air flame at zero-gravity
[NASA-CR-175586] 12 p1799 N85-21283
The use of a laser Doppler velocimeter in a standard flammability tube
[NASA-CR-174960] 24 p4096 N85-35389

IGNITION SYSTEMS
Analysis and simulation of the I C engine Otto cycle using the second law of thermodynamics 02 p0291 N85-11691
Studies of ignition and combustion wave propagation in exothermic systems using high-speed photography
[DE84-016482] 04 p0471 N85-12995
Laser ignition of explosives
[FOA-C-20550-D1] 07 p0972 N85-16173
Study of bridgewire size and pyrotechnic density relationships on all-fire levels
[DE84-016946] 09 p1302 N85-18177
Development of a PETN DDT detonator
[DE84-016944] 09 p1302 N85-18178
Tokamak ignition/burn experimental research device
[DE85-009899] 18 p3190 N85-29785
Experimental study of engine knock
[DE85-009851] 22 p3754 N85-33268

IGNITION TEMPERATURE
NT FLASH POINT
Catalytic ignition and combustion of lean mixtures
[AD-A148101] 08 p1121 N85-17067
A program to develop thermite reactions to produce refractory borides and carbides
[AD-A148972] 10 p1434 N85-19037
The reaction of oxygen-nitrogen mixtures with granular activated carbons below the spontaneous ignition temperature
[AD-A149041] 10 p1434 N85-19039
Review of zirconium-zircaloy pyrophoricity
[DE85-011169] 23 p3916 N85-34270

ILLINOIS
Illinois Climate: Trends, Impacts and Issues
[PB84-211986] 01 p0086 N85-10577
Revised Uniform Summary of Surface Weather Observations (RUSSWO). O'Hare International Airport, Chicago, parts A-F
[AD-A147206] 07 p1007 N85-16399
Interlobate comparison of glacial-depositional style as evidenced by small-relief glacial landscape features in Illinois, Indiana, and Ohio, utilizing SIR-B
08 p1146 N85-17231
Water resources data for Illinois, water year 1983. Volume 1: Illinois except Illinois River Basin
[PB85-125755] 10 p1507 N85-19508
Geodetic accuracy of LANDSAT 4 Multispectral Scanner and Thematic Mapper data — Washington, DC, California, Alabama, South Dakota, and Illinois
11 p1667 N85-20504
Evaluation of the radiometric quality of the TM data using clustering, linear transformations and multispectral distance measures — Illinois 12 p1870 N85-21731
Current alternative energy research and development in Illinois
[PB85-163137] 16 p2820 N85-27397

ILLUMINANCE
Effect of aberration in optical system on illuminance distribution over image of strip in semicoherent light
06 p0777 N85-14970
Correlations of solar irradiance and daylight illuminance for building energy analysis
[DE85-001736] 06 p0839 N85-15326
Quantitative analyses of planetary reflectance spectra
13 p2197 N85-23625
Photovoltaic cells of InP-CdS heterojunction type and their temperature characteristics under A-M illumination
14 p2275 N85-24092
Solar cells with distributed parameters: Current-voltage characteristics under uniform and nonuniform illumination 14 p2275 N85-24093
Issue of sky conditions
[DE85-010590] 19 p3317 N85-30562
Immediate visibility after red and white adaptation
[AD-A156271] 24 p4132 N85-35618

ILLUMINATING
Theoretical elements of photometry
[BLL-RISLEY-TR-5022-(9091.9F)]
02 p0279 N85-11821
Evaluation of arctic test of improved tritium radioluminescent lighting
[DE84-014887] 05 p0597 N85-13605
Human factors of visual displays
06 p0752 N85-14821
Analysis of a visual performance experiment
[DE85-000710] 10 p1530 N85-19645
Lighting for remote viewing systems
[DE85-001886] 11 p1729 N85-20873
Power from the Sun: Light at night
[PB85-124097] 12 p1883 N85-21614
Development of robots and application to industrial processes
[NASA-CR-175754] 15 p2567 N85-25840
Use of Goudrian model in studying laws of reflection in vegetation-soil system in optical range. 2: Influence of illumination conditions on spectral brightness coefficients 18 p2726 N85-26827
Electrodeless HID lamp study
[DE85-010626] 18 p3096 N85-29167
Terrain illumination conditions when taking scanning photographs from space 22 p3736 N85-33159
Electrochromic display device
[AD-D011733] 22 p3759 N85-33299

ILLUMINATION
Laser illuminated nano-second microscope
[DE84-016200] 06 p0811 N85-15152
NBS (National Bureau of Standards) daylight availability database
[PB84-245745] 07 p1054 N85-16688

ILLUMINATORS
High-speed, eight-frame electro-optic camera with multipulsed ruby laser illuminator
[DE85-001748] 09 p1323 N85-18314
Analysis of a visual performance experiment
[DE85-000710] 10 p1530 N85-19645

ILLUSIONS
Bulletin of the Faculty of Engineering, Hokkaido University, no. 123
[ISSN-0385-602-X] 04 p0482 N85-13075
A mathematical model of visual perception regarding peripheral vision and its application to the Hermann's illusion 04 p0483 N85-13080
Susceptability to kinetoses and the amplitude perceived from sensory illusions 11 p1694 N85-20651
Effect of body position and immobilization on intensity of spatial illusions in weightlessness
22 p3821 N85-33672

ILS (LANDING SYSTEMS)
U INSTRUMENT LANDING SYSTEMS

ILYUSHIN AIRCRAFT
Testing solution for IL-76 braking system problem
08 p1067 N85-16766

IMAGE ANALYSIS
The Multispectral Imaging Science Working Group. Volume 1: Executive summary
[E85-10001] 02 p0213 N85-11404
The Multispectral Imaging Science Working Group. Volume 2: Working group reports
[E85-10002] 02 p0213 N85-11405
Information Science Panel joint meeting with Imaging Science Panel 02 p0214 N85-11415
Integrated analysis of remote sensing products from basic geological surveys — Brazil
[E85-10052] 07 p0984 N85-16248
LANDSAT-4 Thematic Mapper Modulation Transfer Function (MFT) evaluation — California and New Mexico
[E85-10055] 07 p0984 N85-16250
Proceedings of the Second Annual Symposium on Mathematical Pattern Recognition and Image Analysis Program
[E85-10056] 07 p0984 N85-16251
Estimating location parameters in a mixture
07 p0984 N85-16252
Nonparametric analysis of Minnesota spruce and aspen tree data and LANDSAT data 07 p0984 N85-16253
Texture classification using autoregressive filtering
07 p0984 N85-16254
Bayesian estimation of normal mixture parameters
07 p0985 N85-16255
Spatial estimation from remotely sensed data via empirical Bayes models 07 p0985 N85-16256
Evidence accumulation for spatial reasoning
07 p0985 N85-16261
Power spectral ensity of markov texture fields
07 p0986 N85-16262
Rectification of single and multiple frames of satellite scanner imagery using points and edges as control
07 p0986 N85-16263
The influence of the number of ground control points on the scene-to-map registration accuracy — Kansas, Louisiana, Mississipp, and Missouri
07 p0986 N85-16264
Image variance and spatial structure in remotely sensed scenes — South Dakota, California, Missouri, Kentucky, Louisiana, Tennessee, District of Columbia, and Oregon
07 p0986 N85-16265
Image-to-image correspondence: Linear structure matching 07 p0986 N85-16266
Metric aspects of digital images and digital image processing
[AD-A147211] 07 p0986 N85-16276
The interpretation of SIR-B imagery of surface waves and other oceanographic features using in-situ, meteorological satellite, and infrared satellite data
08 p1143 N85-17212
Southern ocean sea-ice morphology and kinematics
08 p1144 N85-17217
Automatic analysis of speckle photographs by microcomputer
[NPL-DITC-47/84] 09 p1322 N85-18308
Anayis of the quality of image data required by the LANDSAT-4 Thematic Mapper and Multispectral Scanner — agricultural and forest cover types in California
[E85-10074] 10 p1504 N85-19488
Study of spectral/radiometric characteristics of the Thematic Mapper for land use applications
[E85-10075] 10 p1504 N85-19489
Geodetic accuracy of LANDSAT 4 Multispectral Scanner and Thematic Mapper data — Washington, DC, California, Alabama, South Dakota, and Illinois
11 p1667 N85-20504
Geometric accuracy assessment of LANDSAT-4 Multispectral Scanner (MSS) data
11 p1667 N85-20505
Canadian plans for Thematic Mapper data
11 p1668 N85-20513
Image lobe analysis for large radomes
[AD-P004359] 12 p1825 N85-21453

The use of linear feature detection to investigate Thematic Mapper data performance and processing
12 p1872 N85-21740
Method for approximating autocorrelation functions for describing areal photoimage features
13 p1983 N85-22443
Experience in automated interpretation of aerospace photographs 13 p1983 N85-22444
Geoindication method for interpreting aerial and space photographs: Status and prospects
13 p1984 N85-22445
Edge detection in SAR imagery using gradient operators — synthetic aperture radar (SAR)
[AD-A146411] 13 p2054 N85-22862
An investigation of several aspects of LANDSAT-5 data quality — Palmer County, Shelby, mt; White sands, NM; Great Salt Lake, UT; San Matteo Bridge and Sacramento, California
[E85-10096] 13 p2122 N85-23214
Photometric analysis of Jupiter-illuminated images of Io 13 p2196 N85-23620
Using color to separate reflection components
[AD-A150999] 14 p2405 N85-24828
Optical flow-patterns of image velocity and their potential use in guidance and image interpretation
[BAE-BT-12091] 15 p2651 N85-26947
The impact of VLSI on guidance and control system design 16 p2697 N85-26654
Digital image analysis of four-frame holographic plasma and neutral gas interferograms
[DE85-006397] 16 p2788 N85-27200
Air photo analysis, photo interpretation logic, and feature extraction
[AD-A153926] 18 p3124 N85-29347
Alternative theories of inference in expert systems for image analysis
[AD-A153649] 18 p3170 N85-29646
Resource allocation in cerebral specialization of function: Behavioral and electrophysiological studies
[AD-A155092] 21 p3664 N85-32759
Experiments and discussions on the analysis of interferograms with closed-loop fringes
[NPL-MOM-68] 23 p3956 N85-34515
Non-rigid body motion 23 p3964 N85-34576

IMAGE CONTRAST

Ion contrasting chamber for discrimination of grains and textures
[BMFT-FB-T-84-151] 04 p0477 N85-13036
Human factors of visual displays
06 p0752 N85-14821
Comments on the image contrast from inelastically scattered electrons
[DE85-000899] 07 p1041 N85-16609
Alphabet-constrained data compression
[AD-A152987] 17 p3019 N85-29887
Colour spaces and colour contrast
23 p3963 N85-34567

IMAGE CONVERTERS

NT THERMICONS

Use of fecons in combination with brightness amplifiers 14 p2274 N85-24088
Beam tests of phosphorescent screens
[DE85-009843] 18 p3097 N85-29170

IMAGE CORRELATORS

Holographic lens for optical correlator
16 p2763 N85-27052

IMAGE DISSECTOR TUBES

Dynamic visual servo control of robots: An adaptive image-based approach
[AD-A150057] 12 p1860 N85-21687

IMAGE ENHANCEMENT

Effect of hydrogen on formation of energy spectrum of multiply charged and copper ions
02 p0263 N85-11720
Holographic subtraction of images by Fourier plane recording and spatial filtration with a narrow beam
02 p0263 N85-11721
Noise removal in multichannel images
[NASA-CR-174116] 04 p0554 N85-13526
Investigative findings of image enhancement techniques
[AD-A146392] 06 p0853 N85-15424
Information extraction and transmission techniques for spaceborne synthetic aperture radar images
[NASA-CR-174341] 08 p1150 N85-17256
Resolution enhancement of multichannel microwave imagery from the Nimbus-7 SMMR for maritime rainfall analysis
[NASA-CR-174367] 10 p1462 N85-19221
A concept for the processing and display of Thematic Mapper data 13 p2119 N85-23196
A quantitative image evaluation study of a concurrent photon amplification treated emulsion
[AD-A151831] 15 p2560 N85-25796
Looking at more than three dimensions
[DE85-007764] 17 p3009 N85-29800
First results of oceanography utilization of infrared high resolution picture transmission images
[KNMI-TR-59] 18 p3151 N85-29511
Quantizer of images of heat fields obtained by Rubin-type infra-red imagers 22 p3771 N85-33369

IMAGE FILTERS

Investigative findings of image enhancement techniques
[AD-A146392] 06 p0853 N85-15424
On edge detection
[AD-A148573] 08 p1223 N85-17703
Improved continuum definition in high-background IUE images 11 p1761 N85-21078
Hexagonal uniformly redundant arrays for coded-aperture imaging
[OG-9.2-1] 21 p3714 N85-33048

IMAGE FURNACES

Automatic Monoellipsoidal Mirror Furnace Facility (AMMFF), volume 1 — spaceborne crystal growth
[AMF-RP.100-DS-015-VOL-1] 09 p1285 N85-18073

IMAGE INTENSIFIERS

Programmable optical sensor
[AD-D011244] 02 p0281 N85-11829
Development of a dynamic radiographic capability using high-speed video
[DE84-016477] 04 p0511 N85-13256
Electronic autofluorography: Principles, problems and prospects
[DE84-016696] 05 p0639 N85-14097
STS atmospheric luminosities
[NASA-CR-175514] 12 p1791 N85-21240
Research in the optical sciences
[AD-A150196] 13 p2159 N85-23401
Holographic intensity correlator with PRIS-type photoelectro-optical controlled transparency
17 p2940 N85-28152
Quantizer of images of heat fields obtained by Rubin-type infra-red imagers 22 p3771 N85-33369
Application of thermoluminescence for detection of cascade shower 1: Hardware and software of reader system
[HE-7.1-6] 24 p4213 N85-36160
Spatial distribution read-out system for thermoluminescence sheets
[HE-7.1-7] 24 p4213 N85-36161
Application of thermoluminescence for detection of cascade shower 2: Detection of cosmic ray cascade shower at Mount Fuji
[HE-7.1-12] 24 p4214 N85-36162

IMAGE MOTION COMPENSATION

Predicting optical image displacement velocity in survey of Earth's surface 02 p0165 N85-11116
Study of alternate optical and fine guidance sensor designs for the space infrared telescope facility (SIRTF)
[NASA-CR-166614] 07 p0915 N85-15794
Processing dynamic image sequences from a moving sensor
[AD-A149984] 12 p1934 N85-22148
Autofocus motion compensation for synthetic aperture radar and its compatibility with strapdown inertial navigation sensors on highly manouverable aircraft
[AD-A151940] 16 p2704 N85-26693
Errors in compensating for image oscillation by means of a gyroscopic head 16 p2763 N85-27051
New method for compensating and measuring any motion of three-dimensional objects in holographic interferometry
[ISL-CO-216/84] 22 p3789 N85-33474

IMAGE PROCESSING

NT GEOMETRIC RECTIFICATION (IMAGERY)

Analysis of on-board CIG (Computer Image Generator) applications for aircrew training
[AD-A145214] 01 p0013 N85-10079
Detection and coding techniques of contours in image signals
[FUB-8-1983] 01 p0039 N85-10251
Image signals encoding techniques oriented towards the reduction of perceptive redundance
[FUB-23-1983] 01 p0040 N85-10256
Methods for the design of quantizers for image signals
[FUB-38-1983] 01 p0041 N85-10263
A system for meteorological satellite, radar, conventional data and model analysis 01 p0062 N85-10651
A human visual system investigation applicable to image contour coding
[FUB-36-1983] 01 p0095 N85-10640
Detection and estimation of image contours
[FUB-35-1983] 01 p0112 N85-10760
East Europe report: Science and technology
[JPRS-ESA-84-029] 01 p0115 N85-10783
Methods, applications of image processing
01 p0115 N85-10785
LANDSAT data and interactive computer mapping
02 p0152 N85-11028
Technological approach to automation of specialized processing of survey data 02 p0165 N85-11118
The application of principal components analysis to LANDSAT MSS data 02 p0212 N85-11396
Information Science Panel joint meeting with Imaging Science Panel 02 p0214 N85-11415
Mapping land use changes in the carboniferous region of Santa Catarina, report 2
[E85-10017] 02 p0217 N85-11430
Application of digital analysis of MSS to agro-environmental studies
[E85-10024] 02 p0218 N85-11437
Description of the logical support for an image processing system
[INPE-2783-PRE/349] 02 p0240 N85-11563
SITIM system: Object manager module
[INPE-3284-NTE/226] 02 p0240 N85-11564
SITIM system: Supervisor utilization
[INPE-3267-NTE/224] 02 p0240 N85-11565
Utilization of interpolation and transformation for the compression of digital image data
[INPE-3081-PRE/479] 02 p0240 N85-11566
Design of edge detectors for reduced images
[AD-A145700] 02 p0252 N85-11653
Tomographic reconstruction of neutron radiograph images
[AD-A145682] 02 p0260 N85-11826
Production of optically correlated SEASAT-A (SEA satellite) SAR (Synthetic Aperture Radar) imagery at DREO (Defence Research Establishment Ottawa)
[AD-A145970] 03 p0355 N85-12281
LANDAT-4/5 image data quality analysis
[E85-10039] 03 p0379 N85-12417
Automatic recognition and turbuling objects
[AD-A145908] 03 p0419 N85-12676
Multispectral and geomorphic studies of processed Voyager 2 images of Europa
[NASA-CR-174075] 03 p0448 N85-12848
Research activities of the Illinois University Coordinated Science Laboratory
[AD-A145589] 03 p0449 N85-12856
Mission science value-cost savings from the Advanced Imaging Communication System (AICS)
[NASA-CR-174170] 04 p0458 N85-12905
Digital image processing; report from a conference and study trip to the USA and Canada, summer 1984
[FOA-C-30369-E1] 04 p0494 N85-13153
LANDSAT instruments characterization
[E85-10032] 04 p0524 N85-13356
Coastal Zone Color Scanner (CZCS): Imagery of near-surface phytoplankton pigment concentrations from the first coastal ocean dynamics experiment (CODE-1), March - July 1981
[NASA-CR-174169] 04 p0542 N85-13447
Restoration of multichannel microwave radiometric images
[NASA-CR-174115] 04 p0554 N85-13527
Time-resolved tomographic images of a relativistic electron beam
[DE84-015021] 04 p0565 N85-13567
Tomographic reconstruction of axially symmetric objects from a single radiograph
[DE84-016783] 04 p0565 N85-13599
Imaging of surfaces and defects of crystals
[DE84-016449] 04 p0570 N85-13632
Characterizing the scientific potential of satellite sensors
[E85-10031] 05 p0654 N85-14200
The Interactive Planetary Image Processing System (IPIPS): A major facility for research and teaching in remote sensing 05 p0655 N85-14203
Digital comparison and correlation techniques of remote sensing images with differing spatial resolutions
05 p0655 N85-14204
The integrated use of digital cartographic data and remotely sensed imagery 05 p0655 N85-14206
Methodological research in connection with the handling of LANDSAT satellite data for archaeology
05 p0655 N85-14207
The areal pattern of latent and sensible heat fluxes: The combination of soil physics and remotely sensed data 05 p0656 N85-14213
Integration of multispectral data obtained at different view angles for vegetation analysis
05 p0657 N85-14218
Landform evaluation through integrated remote sensing methods. A case study in parts of Haryana, India
05 p0657 N85-14221
Modular Optoelektronischer Multispektraler Scanner (MOMS), interpretation and evaluation of the MOMS image Arica, West Coast of South America — STS-7 flight
05 p0657 N85-14222
A methodology for an integrated spatial data model and its application to image classification
05 p0659 N85-14234
Application of high frequency 2-D digital filtering to remote sensing image processing
05 p0660 N85-14242

A multiple approach in remote sensing for structural and lithological mapping by use Modular Optoelectronic Multispectral Scanner (MOMS)/LANDSAT/Heat Capacity Mapping Mission (HCMM) data
05 p0660 N85-14244

Image texture study for the operational meteorological satellites NOAA 6 and NOAA 7 and its variation with time. Application to the Beauce region
[ENST-84E009] 05 p0661 N85-14249

Vector quantization of digital images
05 p0714 N85-14580

Automatic determination of motion in an image sequence. The interest for interpretation
[ENST-84E012] 05 p0716 N85-14592

Linear associative mapping
[ESA-TT-858] 05 p0719 N85-14611

Some techniques in image processing
05 p0721 N85-14629

Multi-disciplinary techniques for understanding time-varying space-based imagery
[AD-A144357] 05 p0728 N85-14681

Fly's eye sensor nonlinear signal processing
[AD-D011290] 06 p0729 N85-14684

Selection of parameters for image decomposition by television system for recognition of group of point sources 06 p0785 N85-15018

Hologram bleaching 06 p0789 N85-15038

Wavelength coded image transmission and holographic optical elements
[AD-A146490] 06 p0810 N85-15147

Geological effectiveness of automated processing of highly precise aeromagnetic surveys in Caspian region
06 p0821 N85-15216

Experiences with digital processing of images at INPE
[E85-10045] 06 p0826 N85-15247

An integrated LANDSAT/ancillary data classification of desert rangeland
[E85-10046] 06 p0826 N85-15248

A geographic information system for resource managers based on multi-level remote sensing data
[E85-10047] 06 p0827 N85-15249

Effective use of remote sensing products in litigation
[E85-10048] 06 p0827 N85-15250

Support for the Naval Research Laboratory Passive Microwave Clutter Analysis Program
[AD-A146771] 07 p0939 N85-15951

White-light optical information processing and holography
[AD-A146938] 07 p0957 N85-16138

Characterizing the scientific potential of satellite sensors — San Francisco, California
[E85-10044] 07 p0983 N85-16244

Integrated analysis of remote sensing products from basic geological surveys — Brazil
[E85-10052] 07 p0984 N85-16248

Metric aspects of digital images and digital image processing
[AD-A147211] 07 p0988 N85-16276

Enhancement of multispectral scanner images by digital filtering
[ESA-TT-824] 07 p0989 N85-16284

JPL Robotics Laboratory computer vision software library
[NASA-CR-174272] 07 p1023 N85-16491

Surface reconstruction preserving discontinuities
[AD-A146741] 07 p1028 N85-16526

Ultrasonic measurements, X-ray photographs and image processing
[BLL-RISLEY-TR-4586-(9091.9F)] 07 p1037 N85-16583

Rule-based evidence accrual system for image understanding
[AD-A147835] 07 p1044 N85-16634

Manual and automated line generalization and feature displacement: Appendixes
[AD-A143251] 07 p1054 N85-16689

Functional built-in-test in a pipelined image processor
08 p1064 N85-16740

UK, FRG, France: R and D in sensors, related fields
08 p1142 N85-17197

Development and evaluation of techniques for using combined microwave and optical image data for vegetation studies 08 p1148 N85-17240

Automatic terrain elevation mapping and registration
08 p1148 N85-17242

An investigation of ionospheric irregularity effects on SIR-B image processing and information extraction
08 p1149 N85-17247

Analysis of SIR-B radar illumination of geometry for depth of penetration and surface feature and vegetation detection, Nevada and California
08 p1149 N85-17248

Information extraction and transmission techniques for spaceborne synthetic aperture radar images
[NASA-CR-174341] 08 p1150 N85-17256

Hierarchical data structures and algorithms for digital stereoscopical mensuration 08 p1175 N85-17410

Digital elevation model computation using fast Poisson solutions 08 p1175 N85-17412

Interactive digital image processing for terrain data extraction
[AD-A148580] 08 p1176 N85-17417

An auroral X-ray imaging spectrometer
[AD-A147756] 08 p1185 N85-17469

Atmospheric wind and diffusion from analysis of an SF6 release at 350 km altitude
[AD-A147965] 08 p1185 N85-17471

ViCOM technical description
[REPT-611-0012-REV-A] 08 p1202 N85-17563

Hybrid data processing research facility
[AD-A148092] 08 p1202 N85-17567

Image quality on the KAO 08 p1249 N85-17885

A CCD system for photometry of direct and spectroscopic images 08 p1252 N85-17904

The IMAGE 3 Conference Proceedings
[AD-A148636] 09 p1267 N85-17962

The use of lasers in wide-angle visual systems
[AD-P004322] 09 p1269 N85-17976

A second generation WAVIDS (Wide Angle Virtual Image Display System)
[AD-P004328] 09 p1270 N85-17982

Military applications of the Singer Link-Miles IMAGE visual system
[AD-P004337] 09 p1271 N85-17991

AVTS (Advanced Visual Technology System): A high fidelity visual simulator
[AD-P004338] 09 p1271 N85-17992

The evaluation of a deformable diffraction grating for a stigmatic EUV spectrohelioimeter
[NASA-CR-174350] 09 p1322 N85-18309

Field implementation of geophysical diffraction tomography
[DE84-017594] 09 p1343 N85-18449

Data reduction 09 p1412 N85-18903

Diffraction diffusion screen with holographically-suppressed zero-order beam
[AD-D011445] 10 p1487 N85-19387

LANDSAT 4 investigation of Thematic Mapper and Multispectral Scanner applications
[E85-10076] 10 p1504 N85-19490

Thematic Mapper: Design through flight evaluation
[E85-10078] 10 p1504 N85-19492

Processing of Global Area Coverage (GAC) data of the TIROS-N/NOAA series polar orbiters
[AD-A148992] 10 p1519 N85-19576

A low-cost, general purpose image processing system
[INPE-3292-PRE/607] 10 p1537 N85-19690

One-dimensional processing for adaptive image restoration
[AD-A149314] 10 p1557 N85-19815

Image Understanding: Proceedings of the 15th Workshop
[AD-A149496] 10 p1557 N85-19816

The use of image registration technique in Brasilia's urban growth monitoring
[INPE-3302-PRE/614] 10 p1569 N85-19696

LS-4 MSS geometric correction: Methods and results
11 p1668 N85-20507

An overview of LANDSAT-4 and the Thematic Mapper
11 p1668 N85-20509

TM digital image products for applications
11 p1668 N85-20512

Characterization of radiometric calibration of LANDSAT-4 reflective bands 11 p1669 N85-20516

Contour line generalization using digital image processing methods
[SER-C-291] 11 p1700 N85-20688

Digital imaging processing
[INPE-3325-PRE/624] 11 p1701 N85-20696

A modern approach of a synthetic aperture radar processor and its technological aspects
11 p1713 N85-20778

Improved continuum definition in high-background IUE images 11 p1761 N85-21078

Image processing instrumentation for speckle interferometry and imaging
[AD-A149306] 11 p1762 N85-21084

Conclusion of Viking Lander Imaging Investigation: Picture catalog of experiment data record
[NASA-RP-1137] 11 p1765 N85-21099

Wide-field-of-view, helmet-mounted infinity display system development
[AD-A149641] 12 p1777 N85-21159

Imaging apparatus for transverse electrode electro-optic tunable filter
[AD-D011524] 12 p1832 N85-21497

Integrating non-semantic knowledge into image segmentation processes
[AD-A149571] 12 p1851 N85-21612

Relative radiometric calibration of LANDSAT TM reflective bands 12 p1869 N85-21725

Preliminary evaluation of the radiometric calibration of LANDSAT-4 Thematic Mapper data by the Canada Centre for Remote Sensing 12 p1870 N85-21729

The use of linear feature detection to investigate Thematic Mapper data performance and processing
12 p1872 N85-21740

The development of image processing of NOAA AVHRR data and its application to sea surface temperature
12 p1895 N85-21891

Instrumentation award
[AD-A150061] 12 p1912 N85-21999

Processing dynamic image sequences from a moving sensor
[AD-A149984] 12 p1934 N85-22148

Electron image simulation: A complementary processing technique
[DE85-000685] 12 p1941 N85-22190

Method for approximating autocorrelation functions for describing areal photoimage features
13 p1983 N85-22443

Electronic generation of text for television
[BBC-RD-1984/14] 13 p2053 N85-22856

Nature of seismic images with amplitude and time fluctuations of recorded oscillations
13 p2112 N85-23156

LANDSAT-4 Science Characterization Early Results. Volume 4: Applications — agriculture, soils land use, geology, hydrology, wetlands, water quality, biomass identification, and snow mapping
[E85-10070] 13 p2117 N85-23186

A concept for the processing and display of Thematic Mapper data 13 p2119 N85-23196

Early results of investigations of LANDSAT 4 Thematic Mapper and Multispectral Scanner applications — Washington, D.C. 13 p2119 N85-23200

Comparative techniques used to evaluate Thematic Mapper data for land cover classification in Logan County, West Virginia 13 p2121 N85-23209

Comparison of MSS and TM data for landcover classification in the Chesapeake Bay area: A preliminary report — Taylor's Island, Maryland
13 p2121 N85-23210

Distribution of snow and maximum snow water equivalent obtained by LANDSAT data and degree day method 13 p2124 N85-23229

Feature extraction assessment study
[AD-A150189] 13 p2126 N85-23239

On a mathematical structure for an image algebra
[AD-A150228] 13 p2150 N85-23348

Image data compression using uneven knots selection
[AD-A150602] 13 p2152 N85-23359

Hexagonal data base study
[AD-A150176] 13 p2167 N85-23448

Hot spots on Io: Correlation of infrared emission and visible reflectance 13 p2172 N85-23475

Bouguer images of the North American craton
13 p2200 N85-23648

Participation in the Mars Data Analysis Program: Analysis of cloud forms in Viking and Mariner 9 images
[NASA-CR-175604] 13 p2204 N85-23673

New developments in industrial radiography
14 p2317 N85-24317

Evaluation of carrying capacity and landscape damage in northern Kenya by multistage remote sensing
[DFVLR-FB-84-47] 14 p2347 N85-24514

Visual recognition of simple objects by a connection network
[AD-A151043] 14 p2389 N85-24718

Perceptual organization and visual recognition
[AD-A150626] 14 p2391 N85-24723

Synthetic aperture radar data processing
14 p2398 N85-24760

Studies in parallel image processing
14 p2399 N85-24769

Execution of cellular logic operations in spatially continuous, bit slice processor 14 p2401 N85-24796

The Multimission Image Processing Laboratory's virtual frame buffer interface
[NASA-CR-175655] 14 p2402 N85-24805

Video animation system
[DE85-005494] 14 p2405 N85-24831

Photoacoustic imaging
[AD-A150623] 14 p2416 N85-24905

Feasibility of optical instruments based on multiaperture optics
[AD-A150666] 14 p2421 N85-24936

Space-variant optical systems
[AD-A151032] 14 p2421 N85-24939

High resolution Z-contrast imaging and lattice location analysis of dopants in ion-implanted silicon
[DE85-005261] 14 p2429 N85-24980

Efficient contextual measures for classification of multispectral image data 14 p2433 N85-25005

Near-nucleus studies of Comet Halley
14 p2435 N85-25018

Kitt Peak measurements of P/Halley positions
14 p2436 N85-25023
Problems and procedures of cometary astrometry
14 p2436 N85-25024
Desired characteristics of catalogs for cometary astrometry
14 p2436 N85-25030
Investigations of high resolution imaging through the Earth's atmosphere using speckle interferometry
[AD-A150880] 14 p2439 N85-25053
Research on atmospheric dust formations using satellite observation data
15 p2485 N85-25339
Evaluating radiation distortions of optical image of Earth's surface in horizontally inhomogeneous atmosphere
15 p2486 N85-25345
Evaluating identifiability in remote sensing problems
15 p2486 N85-25347
Identifying land use structures of multizonal aerospace photographs using digital data processing
15 p2486 N85-25348
Using SM-4 Omega system in checking and editing digital terrain information
15 p2487 N85-25350
Increasing the accuracy of processing radar pictures by excluding systematic point coordinate error component
15 p2488 N85-25356
French firm develops new kind of CTD camera for robots
15 p2523 N85-25558
Microcomputer controlled image acquisition system
15 p2537 N85-25654
Statistical techniques for signal processing
[AD-A151231] 15 p2541 N85-25690
Experimental investigation of the electric breakdown in SF6
[BLL-CE-TRANS-7987-(9022.09)]
15 p2546 N85-25714
Superfine laser position control using statistically enhanced resolution in real time
[DE85-005643] 15 p2564 N85-25817
Three-dimensional/perspective display techniques for meteorological data sets
15 p2599 N85-26018
Test and evaluation of the 2.4-micron photorefractor ocular screening system
[NASA-TM-86492] 15 p2615 N85-26115
Workshop on Parallel Computer Architectures in Pattern Recognition and Image Processing
[BMFT-FB-DV-84-006] 15 p2622 N85-26154
Posing of the problem, status, and future of parallel computer architecture for image processing
15 p2622 N85-26155
Industrial applications of pattern recognition and image processing
15 p2622 N85-26157
Recognition of objects in their natural environment — parallel processing
15 p2622 N85-26158
Innovative image processing architectures
15 p2622 N85-26159
Influence and possibilities of Very Large Scale Integration (VLSI) in pattern recognition and image processing
15 p2622 N85-26160
Computer architecture for image processing and pattern recognition in the Federal Republic of Germany. Status 1983, a review
15 p2623 N85-26161
Design specifications for IMAGER: The DREO (Defence Research Establishment Ottawa) image processing system
[AD-A151752] 15 p2624 N85-26168
Feasibility studies of optical processing of image bandwidth compression schemes
[AD-A151254] 15 p2651 N85-26350
User manual for IMAGER: The DREO (Defence Research Establishment Ottawa) image processing system
[AD-A151754] 15 p2653 N85-26362
Image formation in terms of the transport equation
[DE85-004993] 15 p2653 N85-26365
SVIT complex for analysis of space photography
16 p2725 N85-26819
Contribution to space program reviewed
16 p2727 N85-26834
Polarimetric image recorder
[AD-D011605] 16 p2787 N85-27192
New image deblurring method described
16 p2806 N85-27305
CNPq/INPE LANDSAT system: Report of activities from October 1, 1983 to September 30, 1984 — Brazil
[E85-10097] 16 p2808 N85-27318
Noise correction on LANDSAT images using a spline-like algorithm
[E85-10098] 16 p2808 N85-27319
Study of the urban evolution of Brasilia with the use of LANDSAT data
[E85-10101] 16 p2809 N85-27321
System of interpretation of remote sensing data when hydrocarbons are present, volume 2
[INPE-3067-TDL/162-VOL-2] 16 p2810 N85-27326
Symbiosis between postgraduate training and research projects: A successful experience
[INPE-3216-PRE/589] 16 p2810 N85-27330
Reports on cartography and geodesy. Series 1: Original reports, no. 94
[ISSN-0469-4236] 16 p2814 N85-27357
Realization of cartographic tasks on the multiprocessor system EGPA — image processing
16 p2814 N85-27360
A concept for map updating using digital image processing methods
16 p2815 N85-27364
Contour line generalization using digital image processing methods
16 p2815 N85-27367
What does digital image processing perform in the production of orthophotomaps
16 p2815 N85-27368
Free-surface phenomena under low- and zero-gravity conditions
[NASA-CR-175885] 17 p2907 N85-27922
Techniques for operating Charge Coupled Devices (CCD's) in very high speed framing mode
[AD-A152878] 17 p2953 N85-28236
Sub-nanosecond cinematography in laser fusion research: Current techniques and applications at the Lawrence Livermore Laboratory
[DE85-007252] 17 p2968 N85-28334
Evidential reasoning in expert systems for image analysis
[AD-A153379] 17 p3013 N85-28627
Application of artificial intelligence (AI) to radar image understanding
[AD-A152519] 17 p3017 N85-28654
Deconvolution methods for multi-sensors
[AD-A152351] 17 p3018 N85-28660
Further study of digital matching of dissimilar images
[AD-A153112] 17 p3019 N85-28672
Spatial light modulator having a capacitively coupled photoconductor
[AD-D011646] 17 p3037 N85-28790
Axial topography from digitized real time radiography
[DE85-006767] 18 p3091 N85-29130
Reports on cartography and geodesy. Series 1: Original reports, number 93
[ISSN-0469-4236] 18 p3124 N85-29343
An information theoretical method for automatic noise elimination in digital image processing
18 p3124 N85-29345
Air photo analysis, photo interpretation logic, and feature extraction
[AD-A153926] 18 p3124 N85-29347
Image processing: Mathematics, engineering or art
[DE85-007666] 18 p3154 N85-29527
The multiple processor machine for image processing, volume 5
[ESA-CR(P)-1976-VOL-5] 18 p3164 N85-29603
Research on signal detection and block truncation coding for image compression
[AD-A153444] 18 p3168 N85-29628
Alternative theories of inference in expert systems for image analysis
[AD-A153649] 18 p3170 N85-29646
Solar physics applications of computer graphics and image processing
18 p3206 N85-29903
Graphic displays of vector magnetograph data
18 p3209 N85-29904
Approaches to digital image registration and recognition
19 p3257 N85-30197
Projects of the Computer Center of the academy's Siberian branch
19 p3295 N85-30425
Texture perception and shape from texture
[AD-A154276] 19 p3336 N85-30672
Target discrimination using infrared techniques: Theoretical considerations
[AD-A154070] 19 p3350 N85-30762
Methods for design and evaluation of integrated hardware-software systems for concurrent computation
[NASA-CR-176066] 20 p3515 N85-31651
Activities report of the Laboratory for Computer Science (FOA 32)
[FOA-C-30384-E1] 20 p3516 N85-31661
Electronics Division research and development
[DE85-011887] 20 p3540 N85-32032
Aspects of SAR image segmentation
[AD-A154985] 21 p3575 N85-32236
Microcomputer processing of LANDSAT Thematic Mapper data for the acquisition of military tactical terrain data
[AD-A154781] 21 p3605 N85-32369
Object identification and manipulation using silhouette moments
[AD-A154755] 21 p3705 N85-33011
Depth dimension compression of 3-D images
22 p3764 N85-33332
Pulsed lasers for filming color holographic film images
22 p3781 N85-33426
Hierarchical chamfer matching
[FOA-C-30387-E1] 22 p3802 N85-33558
Optimal Bayesian estimators for image segmentation and surface reconstruction
[AD-A155732] 22 p3827 N85-33704
Microcomputer controlled image processor
[AD-D011734] 22 p3833 N85-33735
Electronic imaging system and technique
[DE85-005740] 23 p3935 N85-34393
Production of initial estimates of photogrammetric variables
[NPL-MOM-66] 23 p3943 N85-34434
A model for graphics interface tool development
23 p3960 N85-34545
A general purpose image processing package
23 p3961 N85-34549
A new approach to linear quadtrees
23 p3961 N85-34550
Image synthesis: Optical identity or pictorial communication?
23 p3963 N85-34565
Knowledge engineering application in image processing
23 p3965 N85-34583
The read-out system of spatial distribution of thermoluminescence in meteorites
[SH-9.1-16] 23 p4052 N85-35131
Raster functionality for a VDI
[DE85-006734] 24 p4097 N85-35396
Strain measurement using point recognition picture processing
[DRIC-T-7407] 24 p4101 N85-35421
Selected publications in image understanding and computer vision from 1974 to 1983
[AD-A156196] 24 p4136 N85-35634
Edge information in color images based on histograms of differences
[AD-A156002] 24 p4154 N85-35751
Application of thermoluminescence for detection of cascade shower 1: Hardware and software of reader system
[HE-7.1-6] 24 p4213 N85-36160
Spatial distribution read-out system for thermoluminescence sheets
[HE-7.1-7] 24 p4213 N85-36161
Application of thermoluminescence for detection of cascade shower 2: Detection of cosmic ray cascade shower at Mount Fuji
[HE-7.1-12] 24 p4214 N85-36162

IMAGE RECONSTRUCTION

Shift-variant multidimensional systems
[AD-A144756] 01 p0111 N85-10752
Effect of hydrogen on formation of energy spectrum of multiply charged and copper ions
02 p0263 N85-11720
Wavelength coded image transmission and holographic optical elements
[AD-A146490] 06 p0810 N85-15147
One-dimensional processing for adaptive image restoration
[AD-A149314] 10 p1557 N85-19615
Diffraction-limited imaging of space objects 2
[AD-A149344] 11 p1728 N85-20870
Image data compression using uneven knots selection
[AD-A150602] 13 p2152 N85-23359
Holographic intensity correlator with PRIS-type photoelectro-optical controlled transparency
17 p2940 N85-28152
Deconvolution methods for multi-sensors
[AD-A152351] 17 p3018 N85-28660
Optimal Bayesian estimators for image segmentation and surface reconstruction
[AD-A155732] 22 p3827 N85-33704
Advanced instrumentation for Positron Emission Tomography
[DE85-011147] 22 p3840 N85-33779
Hologram-like transmission of pictures
23 p3961 N85-34552

IMAGE RESOLUTION

Test measurements of the 100 m telescope at lambda = 7 mm
[TR-18] 01 p0129 N85-10990
The Multispectral Imaging Science Working Group. Volume 1: Executive summary
[E85-10001] 02 p0213 N85-11404
The Multispectral Imaging Science Working Group. Volume 2: Working group reports
[E85-10002] 02 p0213 N85-11405
Formation of radio images by scanning around circle
02 p0264 N85-11727
Characterizing the scientific potential of satellite sensors
[E85-10031] 05 p0654 N85-14200
A study on the imaging potential of QUASAT — spaceborne VLBI
07 p1057 N85-16707
Potential affiliate stations to work with the EVN — European VLBI Network; QUASAT
07 p1057 N85-16708
Image quality on the KAO
08 p1249 N85-17985
Resolution enhancement of multichannel microwave imagery from the Nimbus-7 SMMR for maritime rainfall analysis
[NASA-CR-174367] 10 p1462 N85-19221

Research in image understanding as applied to 3-D tomographic imaging with near optical resolution
[AD-A150096] 12 p1829 N85-21483
LANDSAT-4 Science Characterization Early Results. Volume 3, part 2: Thematic Mapper (TM)
[E85-10069] 12 p1869 N85-21724
TM geometric performance: Line to Line Displacement Analysis (LLDA) — New Mexico 12 p1870 N85-21732
A preliminary evaluation of LANDSAT-4 Thematic Mapper data for their geometric and radiometric accuracies 12 p1871 N85-21739
Processing dynamic image sequences from a moving sensor
[AD-A149984] 12 p1934 N85-22148
Overview of TM applications research reports 13 p2117 N85-23187
Analysis and evaluation of the LANDSAT-4 MSS and TM sensors and ground data processing systems: Early results 13 p2117 N85-23189
Characterization of LANDSAT-4 TM and MSS image quality for the interpretation of California's agricultural resources — Central Valley 13 p2118 N85-23190
Preliminary evaluation of Thematic Mapper image data quality 13 p2118 N85-23194
Use of focons in combination with brightness amplifiers 14 p2274 N85-24068
A quantitative image evaluation study of a concurrent photon amplification treated emulsion
[AD-A151831] 15 p2560 N85-25796
Holographic intensity correlator with PRIS-type photoelectro-optical controlled transparency 17 p2940 N85-28152
The design, development, testing, fabrication, calibration and integration of a High Resolution Imager (HRI) for the Roentgen Satellite (ROSAT)
[NASA-CR-175302] 22 p3741 N85-33184
An analysis and algorithm for filling propagation 23 p3961 N85-34551
Hologram-like transmission of pictures 23 p3961 N85-34552
An exploratory study of the effect of screen size and resolution on the legibility of graphics in automated job performance aids
[AD-A155969] 24 p4138 N85-35632

IMAGE ROTATION
Three-dimensional data display on the two-dimensional screen
[AD-A150699] 18 p3160 N85-29577

IMAGE TRANSDUCERS
Fly's eye sensor nonlinear signal processing
[AD-D011290] 05 p0729 N85-14684
Construction and analysis of a PRIZ spatial light modulator exhibiting dynamic image selection
[AD-A152318] 17 p3037 N85-28787
Acoustic imaging systems (for robotic object acquisition)
[AD-A154043] 19 p3351 N85-30772

IMAGE TUBES
NT THERMICONS

IMAGE VELOCITY SENSORS
Predicting optical image displacement velocity in survey of Earth's surface 02 p0165 N85-11116

IMAGERY
NT ACOUSTICAL HOLOGRAPHY
NT AERIAL PHOTOGRAPHY
NT ALL SKY PHOTOGRAPHY
NT ASTRONOMICAL PHOTOGRAPHY
NT AUTORADIOGRAPHY
NT BLACK AND WHITE PHOTOGRAPHY
NT CINEMATOGRAPHY
NT CLOUD PHOTOGRAPHY
NT COLOR INFRARED PHOTOGRAPHY
NT COLOR PHOTOGRAPHY
NT COMPUTER AIDED TOMOGRAPHY
NT ELECTRO-OPTICAL PHOTOGRAPHY
NT HOLOGRAPHY
NT INFRARED IMAGERY
NT INFRARED PHOTOGRAPHY
NT LUNAR PHOTOGRAPHY
NT MICROWAVE HOLOGRAPHY
NT MICROWAVE IMAGERY
NT NEUTRON RADIOGRAPHY
NT PHOTOMICROGRAPHY
NT PHOTORECONNAISSANCE
NT RADAR IMAGERY
NT RADAR PHOTOGRAPHY
NT RADIOGRAPHY
NT REPRODUCTION (COPYING)
NT SATELLITE IMAGERY
NT SATELLITE-BORNE PHOTOGRAPHY
NT SCHLIEREN PHOTOGRAPHY
NT SHADOWGRAPH PHOTOGRAPHY
NT SPACEBORNE PHOTOGRAPHY
NT SPECTROHELIOGRAPHS
NT STEREOPHOTOGRAPHY
NT STEREOSCOPY
NT TOMOGRAPHY
NT ULTRAVIOLET PHOTOMETRY
NT WHITE LIGHT HOLOGRAPHY
NT X RAY IMAGERY
Formation of radio images by scanning around circle 02 p0264 N85-11727
Multi-disciplinary techniques for understanding time-varying space-based imagery
[AD-A144357] 05 p0728 N85-14681
Image variance and spatial structure in remotely sensed scenes — South Dakota, California, Missouri, Kentucky, Louisiana, Tennessee, District of Columbia, and Oregon 07 p0986 N85-16265
Analysis of subpixel registration 07 p0986 N85-16267
Radar calibration using direct measurement equipment and oblique photometry
[AD-D011530] 12 p1822 N85-21433
Relationship between brightness spectrum of photographic image and spectrum of rises on a water surface with waves 13 p2115 N85-23171
An assessment of the potential role of multispectral imagery in bathymetric charting
[AD-A152460] 17 p2964 N85-28438
Improved cloud and surface fields derived from HIRS2/MSU 18 p3140 N85-29439
Jupiter's ring system resolved: Physical properties inferred from the Voyager images 20 p3546 N85-32069
Geomorphic classification of Icelandic and Martian volcanoes: Limitations of comparative planetology research from LANDSAT and Viking orbiter images 21 p3603 N85-32372
Geomorphic analyses from space imagery 21 p3603 N85-32374
Process thresholds: Report of Working Group Number 3 21 p3604 N85-32384
Recognition and clear representation of handwritten electronic diagrams 23 p3960 N85-34541
Selected publications in image understanding and computer vision from 1974 to 1983
[AD-A156196] 24 p4136 N85-35634

IMAGES
NT RETINAL IMAGES
Range-resiaduated mappings
[AD-A145148] 01 p0112 N85-10759
Aircraft flow effects on cloud droplet images and concentrations
[AD-A146176] 03 p0396 N85-12529
Analysis of accretion and deletion at boundaries in dynamic scenes
[AD-A145944] 03 p0419 N85-12678
Weather satellite products in the Flight Service Automation System (FSAS)
[AD-A146520] 06 p0759 N85-14855
Effect of aberration in optical system on illuminance distribution over image of strip in semicoherent light 06 p0777 N85-14970
Matrix display simulation
[AD-D011371] 07 p1055 N85-16695
Development and evaluation of techniques for using combined microwave and optical image data for vegetation studies 08 p1148 N85-17240
Filter reflection image guide oscillator and solid state line scanning device
[AD-D011440] 10 p1479 N85-19336
Wide-angle flat field telescope
[NASA-CASE-GSC-12825-1] 11 p1728 N85-20668
Diffraction-limited imaging of space objects 2
[AD-A148344] 11 p1728 N85-20670
Integrating non-semantic knowledge into image segmentation processes
[AD-A149571] 12 p1851 N85-21612
Determining object orientation from a single image using multiple information sources
[AD-A149980] 12 p1933 N85-22146
A posteriori increase of resolving power of optical system forming averaged monochromatic images 13 p2062 N85-23003
Vision algorithms and psychophysics
[AD-A151868] 15 p2620 N85-26142
Asteroid amphitrite: Surface composition and prospects for the possible Galileo flyby 15 p2680 N85-26549
The development and implementation of an optical communications laboratory
[AD-A151682] 16 p2772 N85-27111
Further study of digital matching of dissimilar images
[AD-A153112] 17 p3019 N85-28672
System of white-light density pseudocolor encoding with three primary colors
[AD-D011651] 17 p3037 N85-28791
Images of the Earth's aurora and geocorona from the Dynamics Explorer Mission
[NASA-CR-175983] 18 p3136 N85-29423
Solar monochromatic images in magneto-sensitive spectral lines and maps of vector magnetic fields 18 p3207 N85-29897
Infrared laser holography used in fusion plasma studies 21 p3697 N85-32905
Optical image of bounded objects 21 p3697 N85-32908
Depth dimension compression of 3-D images 22 p3764 N85-33332
LI481 and LI482 vidicons for two-tube color TV cameras with improved image quality 22 p3764 N85-33333
Optimal Bayesian estimators for image segmentation and surface reconstruction
[AD-A155732] 22 p3827 N85-33704
Image synthesis: Optical identity or pictorial communication? 23 p3963 N85-34565
Shadow volumes for non-planar polygons 23 p3965 N85-34580
Remote sensing of hydrologic transport processes using spot simulation data
[DE85-012412] 24 p4108 N85-35467
Edge information in color images based on histograms of differences
[AD-A156002] 24 p4154 N85-35751

IMAGING RADAR
3D (Three-Dimensional) sensor for adaptive suspension vehicle
[AD-A150921] 14 p2311 N85-24305
The Boot Lake MF imaging radar 21 p3628 N85-32537

IMAGING TECHNIQUES
East Europe report: Science and technology
[JPRS-ESA-84-029] 01 p0115 N85-10783
Methods, applications of image processing 01 p0115 N85-10785
Imaging Science Panel. Multispectral Imaging Science Working Group joint meeting with Information Science Panel: Introduction 02 p0213 N85-11408
Workshop on the Use of Future Multispectral Imaging Capabilities for Lithologic Mapping: Workshop summary 02 p0214 N85-11413
Multispectral Imaging Science Working Group for Hydrologic Science: Executive summary 02 p0214 N85-11414
Information Science Panel joint meeting with Imaging Science Panel 02 p0214 N85-11415
Executive report: Results of the IRGA-CNPq/INPE experimental project
[E85-10011] 02 p0216 N85-11424
Application of digital analysis of MSS to agro-environmental studies
[E85-10024] 02 p0218 N85-11437
Holographic subtraction of images by Fourier plane recording and spatial filtration with a narrow beam 02 p0263 N85-11721
Near infrared imaging of Uranus and Neptune 02 p0299 N85-11934
Lyman-Alpha aurora 02 p0302 N85-11953
Infrared images of the Uranian rings 02 p0302 N85-11955
Restoration of multichannel microwave radiometric images
[NASA-CR-174115] 04 p0554 N85-13527
Scintillator-fiber charged particle track-imaging detector
[NASA-CR-174160] 04 p0559 N85-13560
High-speed videography for optical and X-ray imaging
[DE84-012661] 04 p0564 N85-13595
A method for measuring the effective throughput time delay in simulated displays involving manual control 05 p0701 N85-14497
Representing multidimensional systems using visual displays 05 p0711 N85-14560
Some techniques in image processing 05 p0721 N85-14629
High resolution photoacoustic and photothermal imaging 05 p0723 N85-14649
Synthesis of radio image on RATAN-600 radiotelescope 06 p0783 N85-15004
Investigative findings of image enhancement techniques
[AD-A146392] 06 p0853 N85-15424
Image-to-image correspondence: Linear structure matching 07 p0986 N85-16266
The electronic typesetting program programmer's manual
[AD-A147500] 07 p1025 N85-16508
Use of the analytic signal in ultrasonic imaging
[DE84-016843] 07 p1039 N85-16598
Application and calibration of the subsurface mapping capability of SIR-B in desert regions 08 p1148 N85-17244
A cometary ion mass spectrometer
[NASA-CR-174328] 08 p1164 N85-17343
A CCD system for photometry of direct and spectroscopic images 08 p1252 N85-17904

CCDs: Their cause and cure
08 p1252 N85-17905
Automated and interactive data base generation
[AD-P004316] 09 p1268 N85-17970
Geographic subdivision and top level data structures, Columbus, Magellan, and expanding CIG (Computer Image Generation) horizons
[AD-P004317] 09 p1268 N85-17971
CIG (Computer Image generation) data bases in an instance: Bits and pieces
[AD-P004318] 09 p1269 N85-17972
The generation of three-dimensional data bases using a building block approach
[AD-P004319] 09 p1269 N85-17973
SODERN Visualization System (SVS) for flight simulation
[AD-P004320] 09 p1269 N85-17974
An overview of the research program at the visual technology research simulator
[AD-P004321] 09 p1269 N85-17975
Design considerations for an eye tracked ACI (Area of Interest) display system
[AD-P004324] 09 p1269 N85-17978
Control systems analysis program: A tool for analysis of the GE-VSCDP (General Electric-Visual System Component Display Program) image display system
[AD-P004325] 09 p1270 N85-17979
Progress report on an eye-slaved area-of-interest visual display
[AD-P004326] 09 p1270 N85-17980
Baffled eye and confounded brain or using visual illusions to train blind pilots
[AD-P004332] 09 p1271 N85-17986
On-board Computer Image Generator (CIG) applications
[AD-P004335] 09 p1271 N85-17989
CIG (Computer Image Generator) goes to war: The tactical illusion
[AD-P004336] 09 p1271 N85-17990
Military applications of the Singer Link-Miles IMAGE visual system
[AD-P004337] 09 p1271 N85-17991
Acoustic imaging in a water filled metallic pipe — monitoring heat exchangers in nuclear power reactors
[DE84-016051] 09 p1378 N85-18665
A microchannel plate pinhole camera for 20 to 100 keV X-ray imaging
[DE85-001572] 10 p1486 N85-19396
X-ray holography of biological specimens
[DE85-002437] 10 p1489 N85-19398
Fourth International Conference on Robot Vision and Sensory Controls
[AD-A149524] 10 p1492 N85-19422
Imaging through a multiple scattering medium
[DE85-002051] 10 p1557 N85-19621
Airborne remote sensing CCD imaging system
11 p1623 N85-20220
A modern approach of a synthetic aperture radar processor and its technological aspects
11 p1713 N85-20778
Multiparticle 3D imaging technique to study the structure of molecular ions
[DE85-001843] 12 p1929 N85-22122
Grain boundaries in NiO
[DE85-006129] 13 p2025 N85-22667
A posteriori increase of resolving power of optical system forming averaged monochromatic images
13 p2062 N85-23003
Electroacoustical imaging technique for encoding incoherent radiance fields as Gabor elementary signals
[NASA-TM-86372] 13 p2094 N85-23067
Image data compression using uneven knots selection
[AD-A150602] 13 p2152 N85-23359
Optical system
[NASA-CASE-NPO-15801-1] 13 p2158 N85-23396
Photoacoustic imaging
[AD-A150623] 14 p2416 N85-24905
Connection between time- and frequency-domain three-dimensional inverse problems for the Schroedinger equation
[DE85-006814] 15 p2639 N85-26274
Occultation detection of a Neptune ring segment
15 p2661 N85-26558
Validation of the ERBE scanner scene identification methodology: Analysis with Nimbus-7 ERB data
[NASA-CR-172506] 16 p2832 N85-27466
Holographic intensity correlator with PRIS-type photoelectro-optical controlled transparency
17 p2940 N85-28152
Techniques for operating Charge Coupled Devices (CCD's) in very high speed framing mode
[AD-A152878] 17 p2953 N85-28238
Generation and display apparatus
[AD-D011639] 17 p3006 N85-28599
System of white-light density pseudocolor encoding with three primary colors
[AD-D011651] 17 p3037 N85-28791
Digital image mapping of Antarctica using NOAA-7 AVHRR imagery 18 p3124 N85-29340
Graphic displays of vector magnetograph data
18 p3209 N85-29904
Three-dimensional and tomographic imaging device for X-ray and gamma-ray emitting objects
[NASA-CASE-GSC-12851-1] 19 p3271 N85-30281
Texture perception and shape from texture
[AD-A154276] 19 p3336 N85-30672
Acoustic imaging systems (for robotic object acquisition)
[AD-A154043] 19 p3351 N85-30772
Short-time spectroscopic measurement of the temperature of solids
[ISL-CO-202/84] 20 p3459 N85-31486
EBIC characterization and hydrogen passivation in silicon sheet 20 p3481 N85-31634
The temporal evolution of a small auroral substorm as viewed from high altitudes with Dynamics Explorer 1
[NASA-CR-176084] 20 p3493 N85-31716
Study of requirements for and method of multidimensional acoustic imaging — spaceborne experiments
[ESA-CR(P)-2020] 20 p3525 N85-31924
Z-contrast imaging and electron channeling analysis of dopants in semiconductors
[DE85-011410] 21 p3582 N85-32269
One application of mega-geomorphology in education
21 p3602 N85-32370
Hexagonal uniformly redundant arrays for coded-aperture imaging
[OG-9.2-1] 21 p3714 N85-33048
An image compression survey and algorithm switching based on scene activity
[NASA-TP-2458] 22 p3727 N85-33106
Physico-geographical regionalization of Caspian lowland based on space survey materials
22 p3736 N85-33162
Conceptual design and analysis of high-speed electronic imaging
[LA-10072-MS] 22 p3758 N85-33292
Quantizer of images of heat fields obtained by Rubin-type infra-red imagers 22 p3771 N85-33360
Advanced instrumentation for Positron Emission Tomography
[DE85-011147] 22 p3840 N85-33779
Method and apparatus for Delta Kappa synthetic aperture radar measurement of ocean current
[NASA-CASE-NPO-15704-1] 23 p3925 N85-34327
Applications of holography to X-ray imaging
[DE85-010984] 23 p3934 N85-34384
A theoretical and empirical analysis of coherent ray-tracing 23 p3957 N85-34524
Frame buffer algorithms for stochastic models
23 p3957 N85-34525
Specifying stochastic objects in a hierarchical graphics system 23 p3957 N85-34526
Computer analysis techniques for the temporal evaluation of cardiac wall motion
23 p3958 N85-34530
A computerized system for spot detection and analysis of two-dimensional electrophoresis images
23 p3958 N85-34531
An image management kernel for the design of relational and pictorial data bases 23 p3958 N85-34532
Animangine: An engineering animation system
23 p3959 N85-34535
3D computer animation: More an evolution problem than a motion problem 23 p3959 N85-34536
Towards an integrated view of 3-D computer character animation 23 p3959 N85-34538
Research issues in generating graphical explanations
23 p3959 N85-34539
The scientific and technical issues in integrating remotely sensed imagery with geocoded data bases
23 p3960 N85-34547
Selection of segment similarity measures for hierarchical picture segmentation 23 p3960 N85-34548
Hexagonal uniformly redundant arrays for coded-aperture imaging
[OG-9.2-1] 23 p4024 N85-34940
A coded aperture imaging system optimized for hard X-ray and gamma ray astronomy
[OG-9.2-3] 23 p4024 N85-34942
An experimental assessment of the imaging quality of the low energy gamma-ray telescope ZEBRA
[OG-9.2-8] 23 p4025 N85-34947
Advanced techniques for high resolution spectroscopic observations of cosmic gamma-ray sources
[OG-9.2-9] 23 p4025 N85-34948
A Cerenkov imaging telescope for high energy gamma rays
[OG-9.3-13] 23 p4028 N85-34968
The University of Durham Mark 3 very high energy gamma ray telescope
[OG-9.4-2] 23 p4028 N85-34969
Application of imaging to the atmospheric Cherenkov technique
[OG-9.5-4] 23 p4030 N85-34981
An experimental study of dielectric rod antennas for millimeter-wave imaging applications
[AD-A155832] 24 p4066 N85-35328
Strain measurement using point recognition picture processing
[DRIC-T-7407] 24 p4101 N85-35421
Processing of LANDSAT imagery to map surface mineral alteration on the Alaska Peninsula, Alaska
24 p4106 N85-35455
Selected publications in image understanding and computer vision from 1974 to 1983
[AD-A156196] 24 p4136 N85-35634
Optical synthetic aperture techniques
[AD-A156151] 24 p4154 N85-35752

IMIDES
Development of new and improved polymer matrix resin systems, phase 1
[NASA-CR-166595] 01 p0017 N85-10104
A method for obtaining new cyclical imides of derivative benzimidazoles
[AD-A145042] 01 p0017 N85-10106
A new heat-resistant polymer from dimer diamine bismaleimide. Part 1: Preparation and free radical cure of dimer diamine bismaleimide
[AD-A145864] 02 p0186 N85-11247
Polyimide-glass multilayer printed wiring boards
[DE84-015092] 05 p0631 N85-14048
Imide modified epoxy matrix resins
[NASA-CR-174695] 07 p0930 N85-15892
Phosphorus-containing imide resins
[NASA-CASE-ARC-11368-2] 12 p1809 N85-21347
High performance mixed bismide resins and composites based thereon
[NASA-CASE-ARC-11536-1-SB]
19 p3231 N85-30033

IMINES
A soluble linear Schiff-base coordination polymer containing eight-coordinate zirconium(4)
[AD-A151445] 15 p2518 N85-25527
Polyethylene imine-metal salt solid electrolyte
[AD-D011678] 19 p3305 N85-30485

IMMERSION
U SUBMERGING

IMMISCIBILITY
U SOLUBILITY

IMMITTANCE
U ELECTRICAL IMPEDANCE

IMMOBILIZATION
Effect of disuse on sarcoplasmic reticulum in fast and slow skeletal muscle
[NASA-CR-174337] 08 p1191 N85-17508
Acid phosphatase and protease activities in immobilized rat skeletal muscles
[NASA-CR-174340] 08 p1192 N85-17509
A comparison of rat myosin from fast and slow skeletal muscle and the effect of disuse
[NASA-CR-174339] 08 p1192 N85-17510
Histological and compositional responses of bone to immobilization and other experimental conditions
[NASA-CR-176837] 18 p2841 N85-27518

IMMUNITY
Induction of immunity to toxins with anti-idiotypic antibody
[AD-A146793] 07 p1014 N85-16445
Phenomenon of universal rosette-forming cell stimulation by extreme stress 20 p3505 N85-31789

IMMUNOASSAY
Proceedings of the 14th Army Science Conference. Volume 1: Principal Authors A through H
[AD-A149200] 10 p1573 N85-19920

IMMUNOLOGY
USSR report: Life sciences. Biomedical and behavioral sciences
[JPRS-UBB-84-015] 07 p1010 N85-16418
The effects of simulated weightlessness on susceptibility to viral and bacterial infections using a murine model
15 p2613 N85-26100
Rapid rate-kinetic turbidometric assay for quantitation of antiviral complement-fixing antibodies
[AD-A153844] 18 p3152 N85-29516
USSR report: Life sciences. Biomedical and behavioral sciences
[JPRS-UBB-85-017] 20 p3504 N85-31785
East Europe report: Science and technology
[JPRS-ESA-85-021] 21 p3568 N85-32190
East Europe report: Science and technology
[JPRS-ESA-85-023] 21 p3572 N85-32217

IMP
Pluribus satellite IMP development mobile access terminal network
[AD-A147675] 08 p1151 N85-17264
IMP-I
U EXPLORER 43 SATELLITE
IMP-J
U EXPLORER 50 SATELLITE
IMP-S
U EXPLORER 43 SATELLITE
IMP-S
U EXPLORER 50 SATELLITE
IMPACT
NT ECONOMIC IMPACT
NT ELECTRON IMPACT
NT HYPERVELOCITY IMPACT
NT ION IMPACT
Impact phenomena as factors in the evolution of the Earth
[NASA-CR-174015] 01 p0072 N85-10474
Impact of alcohol fuels on urban air pollution: Methanol photochemistry study
[DE84-012950] 04 p0531 N85-13397
Lunar magma ocean and its implication for origin of the Moon 04 p0581 N85-13711
Lunar origin: role of giant impacts 04 p0587 N85-13749
Lunar origin from impact on the Earth 04 p0588 N85-13757
Evaluation of the birdstrike threat to the F-15 present fleet, rapid deployment force, and dual role fighter transparencies
[AD-A148954] 10 p1421 N85-18666
Impacts on Explorer 46 from an Earth orbiting population 12 p1785 N85-21204
Stagnation zone impaction on a simple terrain feature in stable flow 13 p2130 N85-23255
Lunar origin: Role of giant impacts 13 p2179 N85-23519
Impact cratering calculation 13 p2180 N85-23531
Impact crater scaling laws 13 p2181 N85-23532
Sliding interfaces with contact-impact in large scale Lagrangian computations
[DE85-006451] 15 p2639 N85-26277
Volatile loss following very large impacts 22 p3853 N85-33862
Friction, impact, and electrostatic discharge sensitivities of energetic materials
[DE85-013321] 24 p4083 N85-35309
IMPACT ACCELERATION
Biomechanical studies of impact acceleration research
[AD-A149077] 10 p1522 N85-19601
Telemetry system for the transmission of data from projectiles during the acceleration phase in the gun barrel
[ISL-CO-207/84] 22 p3739 N85-33178
IMPACT DAMAGE
NT METEORITIC DAMAGE
Simulation of contact surface erosion for impact problems 01 p0060 N85-10396
Single-drop impact damage prediction for low density, coated ceramic materials — rain erosion 01 p0061 N85-10402
Influence of test method and material stiffness on the damage produced by low velocity impacts on carbon-epoxy composites No. 45.387/1
[REPT-45.387/1] 03 p0326 N85-12100
Effect of impact damage and open holes on the compression strength of tough resin/high strain fiber laminates 04 p0464 N85-12945
The effect of matrix and fiber properties on impact resistance 04 p0464 N85-12947
Development of a heterogeneous laminating resin 04 p0465 N85-12956
On the effects of delamination damage in fibre composite laminates
[ARL/STRUC-R-403] 08 p0763 N85-14881
Contact behavior, impact response and damage in graphite-epoxy laminates subjected to initial stresses 08 p1171 N85-17386
A study of constitutive relations for polycrystalline aluminum during finite dynamic plastic deformation 08 p1172 N85-17388
Water impact laboratory and flight test results for the space shuttle solid rocket booster aft skirt 09 p1335 N85-18394
The influence of mechanical damage on transmission pipeline integrity
[ERS-E.351] 09 p1340 N85-18431
Recent studies of the significance of mechanical damage in pipelines
[ERS-E.367] 09 p1341 N85-18433
Smoother terrain-machine
[AD-P004296] 09 p1409 N85-18873
Birds and aviation
[AD-P004177] 11 p1578 N85-19939
Avoiding serious bird strike incidents
[AD-P004178] 11 p1578 N85-19940
Accidents and serious incidents to civil aircraft due to birdstrikes
[AD-P004180] 11 p1578 N85-19942
Worldwide birdstrike statistics of Lufthansa German Airlines
[AD-P004183] 11 p1579 N85-19945
Birds and aircraft engine strike rates
[AD-P004184] 11 p1579 N85-19946
Orbital Debris
[NASA-CP-2360] 12 p1783 N85-21188
A model for the evolution of on-orbit manmade debris environment 12 p1784 N85-21196
Geosynchronous satellite collision avoidance 12 p1784 N85-21197
In situ orbital debris experiment concepts 12 p1784 N85-21198
General-purpose heat source development: Safety test program. Postimpact evaluation, design iteration test 5
[LA-10232-SR] 12 p1931 N85-22129
Anticipated impact plasma problems for the COPERNIC-RPA experiment in the cometary environment — Giotto mission 14 p2245 N85-23917
Considerations of large scale impact and the early Earth 21 p3718 N85-33070
Design and testing of an energy-absorbing crewseat for the F/FB-111 aircraft, volume 1
[NASA-CR-3916] 23 p3896 N85-34133
Quantitative non-destructive evaluation of composite materials based on ultrasonic wave propagation
[NASA-CR-176176] 24 p4074 N85-35244
IMPACT DECELERATION
U DECELERATION
U IMPACT ACCELERATION
IMPACT FUSION
Investigation of electromagnetic launcher behavior for impact fusion
[DE84-017401] 04 p0563 N85-13585
IMPACT LOADS
Fatigue-impact studies in laminated composites
[AD-A142841] 03 p0326 N85-12097
Constitutive features of solids at shock-wave loading rates
[DE84-015715] 03 p0362 N85-12325
Tests of the load-bearing and deformation behaviour of reinforced concrete spherical shells under point loading
[BLL-RISLEY-TR-4550-9091.9F)] 06 p0618 N85-15182
Analysis of the impact of a deformable missile model on a deformable obstruction
[BLL-RISLEY-TR-8534-(9091.9F)] 06 p0659 N85-15459
Crack growth in propellants 08 p1116 N85-17034
Alternative shock characterizations for consistent shock test specifications 09 p1335 N85-18396
Subreflector focusing techniques applied to new DSS-15 and DSS-45 34-meter antennas 10 p1464 N85-19233
Biological effects of blast and impact waves
[FOA-C-52006-H4-D7] 12 p1906 N85-21968
A search for evidence of large body Earth impacts associated with biological crisis zones in the fossil record 15 p2682 N85-26567
General Aviation Crashworthiness Project. Phase 2: Impact severity and potential injury prevention in general aviation accidents
[PB85-917002] 19 p3215 N85-29938
Analysis of rotorcraft crash dynamics for development of improved crashworthiness design criteria
[FAA-CT-85-11] 20 p3391 N85-31031
Space station dynamic modeling, disturbance accommodation, and adaptive control 20 p3409 N85-31154
Preliminary considerations for the gasdynamic precompression of solid molecular hydrogen
[DE85-013256] 22 p3784 N85-33445
Safety and reliability of steel structural materials under random service impact loads 23 p3906 N85-34197
IMPACT MELTS
Centrifuge impact cratering experiments 13 p2181 N85-23533
Progress on studies of early intense cratering 13 p2181 N85-23535
Why not a constant early lunar impact rate? 13 p2181 N85-23536
IMPACT PREDICTION
Structural modifications by viscoelastic elements 09 p1337 N85-18407
General-purpose heat source development: Safety test program. Postimpact evaluation, design iteration test 1
[LA-9680-SR] 12 p1931 N85-22131
IMPACT PRESSURES
U IMPACT LOADS
IMPACT RESISTANCE
Sensitivity analysis of limit state functions for probability-based plastic design 01 p0059 N85-10386
The influence of inert particulate material on the properties of RDX/polyethylene wax compositions
[MRL-R-929] 03 p0336 N85-12159
The effect of matrix and fiber properties on impact resistance 04 p0464 N85-12947
Fundamental studies of composite toughness 04 p0464 N85-12948
Development of a heterogeneous laminating resin 04 p0465 N85-12956
Modified epoxy composites 04 p0466 N85-12957
Nonlinear analysis of composite laminates 09 p1288 N85-18067
Development of a heterogeneous laminating resin system
[NASA-CR-172459] 09 p1288 N85-18069
General-purpose heat source development: Safety test program. Postimpact evaluation, design iteration test 4
[LA-10217-SR] 12 p1930 N85-22128
Remote control of an impact demonstration vehicle
[NASA-TM-85925] 14 p2225 N85-23797
Development of an impact- and solvent-resistant thermoplastic composite matrix, phase 3
[NASA-CR-172566] 20 p3422 N85-31239
Strain rate sensitivity estimation from high velocity impact data
[AD-A154703] 21 p3599 N85-32347
IMPACT SENSITIVITY
U IMPACT RESISTANCE
IMPACT STRENGTH
Tough Composite Materials
[NASA-CP-2334] 04 p0463 N85-12941
Impact toughness of wire after cold deformation and annealing
[BLL-M-35941-(5828.4)] 05 p0615 N85-13930
Proceedings of the International Conference and Exposition on Structural Impact and Crashworthiness
[AD-A147845] 07 p0900 N85-15703
Contact behavior, impact response and damage in graphite-epoxy laminates subjected to initial stresses 08 p1171 N85-17386
Impact toughness of composites with layered microstructure of OT4 titanium alloy 10 p1445 N85-19104
Fiber composite materials with titanium matrix 10 p1445 N85-19105
Prediction of the resistance of structural materials to cavitation erosion
[BLL-DRIC-TRANS-7435-(3623.66)] 13 p2020 N85-22659
Chain dynamics and structure property relation in high impact strength polycarbonate plastic
[AD-A152011] 15 p2519 N85-25531
Effect of low-velocity or ballistic impact damage on the strength of thin composite and aluminum shear panels
[NASA-TP-2441] 16 p2742 N85-26924
High-strength weldable steel 03G4N2MAF Sh with improved ductility
[BLL-BISI-TRANS-22233-(9022.06)] 17 p2924 N85-28031
Effects of heat treatment and tracer element impurities on the impact properties of the 12Cr steels
[DE85-010576] 19 p3240 N85-30088
Impact fracture mechanism of polymer plates containing a heavy inner material 23 p3908 N85-34215
IMPACT TESTING MACHINES
Instrumented impact testing machine with reduced specimen oscillation effects
[VTT-290] 04 p0504 N85-13218
IMPACT TESTS
NT CHARPY IMPACT TEST
Eutectic explosives containing ammonium nitrate
[DE84-015705] 01 p0034 N85-10213
Crashworthiness of light aircraft fuselage structures: A numerical and experimental investigation 01 p0060 N85-10399
Analysis of a transport fuselage section drop test 01 p0060 N85-10400
Deformation measurements of composite multi-span beam shear specimens by Moire interferometry
[NASA-CR-3844] 02 p0169 N85-11135
Influence of test method and material stiffness on the damage produced by low velocity impacts on carbon-epoxy composites No. 45.387/1
[REPT-45.387/1] 03 p0326 N85-12100
Full-scale crash-test evaluation of two load-limiting subfloors for general aviation airframes
[NASA-TP-2380] 04 p0512 N85-13267
NASA-Ames vertical gun 04 p0579 N85-13696
Deformation, fracture and explosive properties of reactive materials
[AD-A146398] 06 p0774 N85-14945

Impact tests of adjusters for the HBU-12 lap belt
[AD-A148021] 08 p1080 N85-16843
Impact tests of automatic lap belt configurations
[AD-A148034] 08 p1081 N85-16844
Sensitivity tests for solid propellants in Germany
08 p1115 N85-17028
Development of a high temperature single impact rain erosion test capability
[AD-P004371] 12 p1827 N85-21465
General-purpose heat source development: Safety test program. Postimpact evaluation, design iteration test 4
[LA-10217-SR] 12 p1930 N85-22128
Behavior of fiber-reinforced composites under dynamic tension
[AD-A150619] 13 p2015 N85-22641
IHE material qualification tests description and criteria
[DE85-004849] 13 p2040 N85-22770
Progress on Experimental impact studies
13 p2181 N85-23534
Impact studies of a 1/3-scale model of an air cushion vehicle
[NASA-TM-86360] 14 p2218 N85-23757
Six-inch HYGE vertical impact facility
[AD-A150665] 14 p2228 N85-23809
Impact ionization from gold, aluminum and PCB-Z — Giotto spacecraft paint PCB-Z 14 p2244 N85-23910
Experimental investigations on ion emission with dust impact on solid surfaces — Giotto spacecraft
14 p2244 N85-23911
Ion emission from solid surfaces: Comparison of dust impact with other excitations — Giotto mission
14 p2244 N85-23912
Dynamic shock studies of PZT 95/5 ferroelectric ceramic
[DE85-006137] 14 p2261 N85-24015
Hopkinson bar simulation using DYNA2D
[DE85-006766] 16 p2802 N85-27275
Constitutive modeling for blast-induced wave propagation
[AD-A153676] 18 p3099 N85-29167
Effect of thermochemical processing on fatigue resistance of titanium alloys 19 p3244 N85-30112
Study of intermediate velocity penetration of steel spheres into deep aluminum targets
[DE85-010419] 19 p3287 N85-30385
Flight test experience and controlled impact of a large, four-engine, remotely piloted airplane
[NASA-TM-86738] 22 p3730 N85-33123
Design and testing of an energy-absorbing crewseat for the F/FB-111 aircraft, volume 1
[NASA-CR-3916] 23 p3896 N85-34133
Design and testing of an energy-absorbing crewseat for the F/FB-111 aircraft. Volume 3: Data from crew module testing
[NASA-CR-3918] 23 p3896 N85-34134
Design and testing of an energy-absorbing crewseat for the F/FB-111 aircraft. Volume 2: Data from seat testing
[NASA-CR-3917] 24 p4064 N85-35184

IMPACT TOLERANCES
Impacts of Space Shuttle thermal protection system tile on F-15 aircraft vertical tile
[NASA-TM-85904] 12 p1792 N85-21245
Design and testing of an energy-absorbing crewseat for the F/FB-111 aircraft. Volume 2: Data from seat testing
[NASA-CR-3917] 24 p4064 N85-35184

IMPACTORS
Progress on studies of early intense cratering
13 p2181 N85-23535
Why not a constant early lunar impact rate?
13 p2181 N85-23536
Martian terrain ages 13 p2181 N85-23537
Interaction of Martian flow ejecta blankets with pre-existing impact craters: Morphological observations
13 p2183 N85-23546
Development of a microorifice uniform deposit cascade impactor
[DE85-006765] 22 p3812 N85-33614

IMPATT DIODES
U AVALANCHE DIODES

IMPEDANCE
NT ACOUSTIC IMPEDANCE
NT CONTACT RESISTANCE
NT ELECTRICAL IMPEDANCE
NT ELECTRICAL RESISTANCE
Admittance measurement with twin-T devices in the frequency range between 1 and 300 MHz
05 p0629 N85-14032
Space charge, interfacial kinetics, and electrical response of condensed matter
[AD-A146364] 06 p0765 N85-14893
Scattering of H10-mode wave by narrow conducting plate inside rectangular waveguide
06 p0788 N85-15036
The dc SQUID as a tuned radiofrequency amplifier
[DE85-000701] 06 p0805 N85-15123
Investigation of the pressure-and velocity-coupled responses of solid propellants using impedance tube method 09 p1300 N85-18168
Calculation of transmission line impedances using the ANSYS finite element program
[DE84-016715] 11 p1629 N85-20261
Driven global Alfven eigenmodes
[DE85-001056] 11 p1732 N85-20690
Thermocouple modeling
[DE85-005172] 14 p2306 N85-24273
Discharge characteristics of high-pressure, fast-discharge XeCl excimer laser
15 p2564 N85-25820
Measurement of damping of graphite epoxy materials
[NASA-CR-175793] 16 p2743 N85-26925
Ionospheric effects on antenna impedance
[BMFT-FB-W-84-052] 17 p2950 N85-28217
Nonlinear plasma reactions on the antenna impedance of high transmission power satellites
[BMFT-FB-W-84-053] 18 p3192 N85-29799
Mutual coupling analysis for conformal microstrip antennas
[AD-A154292] 19 p3259 N85-30210
Characterization of microstrip discontinuities in the time and frequency domains
[NASA-CR-176190] 24 p4088 N85-35342

IMPEDANCE MATCHING
A broadband matching network
[AD-D011406] 08 p1219 N85-17675
Pulse transformer package for impedance matching a laser diode to a transmission line
[AD-D011499] 12 p1855 N85-21632
Measured performance of a broadband matching section for peripherally fed helical antennas
[R-NIAS-25] 15 p2539 N85-25670
Switching mixer
[AD-D011602] 16 p2777 N85-27139

IMPEDANCE MEASUREMENT
An automated immittance measuring system for electroacoustic transducers
[AD-A145701] 02 p0200 N85-11336
Impedance measurements on a VLF multi-turn loop antenna in a space plasma simulation chamber
[AD-A145104] 04 p0492 N85-13141
Admittance measurement with twin-T devices in the frequency range between 1 and 300 MHz
05 p0629 N85-14032
Experimental verification of eddy-current flaw theory
[DE85-001288] 09 p1329 N85-18350
Generalized method for the calibration of 4-terminal-pair type digital impedance meters
[PB85-126122] 11 p1638 N85-20318
Thermocouple modeling
[DE85-005172] 14 p2306 N85-24273

IMPEDANCE PROBES
Contribution of mutual impedance experiments to the understanding of magnetospheric processes — GEOS satellites 14 p2371 N85-24656

IMPELLER BLADES
U ROTOR BLADES (TURBOMACHINERY)

IMPELLERS
NT PUMP IMPELLERS
Experimental observation of the flow in impellers and diffusers — centrifugal compressors
05 p0636 N85-14060
Answering thermodynamic questions with three-dimensional viscous flow calculations
05 p0636 N85-14061
Lateral fluid forces acting on a whirling centrifugal impeller in vaneless and vaned diffuser
05 p0643 N85-14123
Hydraulic forces on a centrifugal impeller undergoing synchronous whirl 05 p0643 N85-14124
Hydrodynamic impeller stiffness, damping, and inertia in the rotordynamics of centrifugal flow pumps
05 p0643 N85-14125
Two-dimensional unsteady analysis of fluid forces on a whirling centrifugal impeller in a volute
05 p0643 N85-14126
Group technology for working turbine drive wheel disks 14 p2269 N85-24061
Effect of apparent fluid masses on natural vibration frequencies of impellers of multistage centrifugal pumps
14 p2277 N85-24108
Investigation of gas-turbine engine blower impeller vibrations with change in engine intake conditions
14 p2287 N85-24170
Fluidic angular velocity sensor
[NASA-CASE-NPO-16479-1-CU]
18 p3104 N85-29219
A 3-D Euler method for internal transonic flows computation with a multi-domain approach
21 p3587 N85-32298

IMPERFECTIONS
U DEFECTS

IMPERIAL VALLEY (CA)
Investigation of radiometric properties of LANDSAT-4 MSS — California, North Carolina, South Carolina, and New England 11 p1666 N85-20500

IMPINGEMENT
NT JET IMPINGEMENT
Materials characterization with intense positron beams
[DE85-011850] 22 p3839 N85-33769
Experimental aerodynamic heating to simulated space shuttle tiles in laminar and turbulent boundary layers with variable flow angles at a nominal Mach number of 7
[NASA-TP-2307] 23 p3929 N85-34351
Computation of three-dimensional shock wave and boundary-layer interactions
[NASA-TM-86780] 24 p4093 N85-35372

IMPLANTATION
NT ION IMPLANTATION
Ion-implantation doping of strained-layer superlattices
[DE85-001903] 09 p1400 N85-18811
Percutaneous connectors
[NASA-CR-175827] 16 p2839 N85-27506
A communications link for an implantable electrode array
[AD-A152238] 16 p2840 N85-27510
Design evaluation of high reliability lithium batteries
20 p3444 N85-31380

IMPLANTED ELECTRODES (BIOLOGY)
Encapsulation and packaging of a semiconductor multielectrode array for cortical implantation
[AD-A153180] 17 p2998 N85-28535

IMPLOSIONS
K-shell yield scaling law for conventional PRS loads
[AD-A145155] 01 p0121 N85-10831
Imploding plasma radiation sources: Basic concepts
[AD-A145542] 02 p0284 N85-11856
Non-LTE considerations in spectral diagnostics of thermal transport and implosion experiments
[DE84-015187] 05 p0730 N85-14689
Imploding plasma X-ray laser research
[DE85-000057] 09 p1326 N85-18331
Study of opacity effects on line radiation from pellet implosions
[DE85-000380] 10 p1491 N85-19413
Prediction of the resistance of structural materials to cavitation erosion
[BLL-DRIC-TRANS-7435-(3623.66)]
13 p2020 N85-22659
Research with high-power short-wavelength lasers
[DE85-010329] 19 p3276 N85-30332
Workshop report on Simulation Techniques for Shock Wave Phenomena and Characteristics of Plasmas in Inertial Confinement Fusion
[IPPJ-725] 23 p3979 N85-34670
Moving finite element method for ICF target implosion
23 p3980 N85-34675
Two-dimensional simulation of LIB target implosion
23 p3980 N85-34678
Stability of implosion dynamics
23 p3980 N85-34680
System expectations for Pioneer 1 foil implosion experiments
[DE85-014129] 24 p4091 N85-35359
Diagnostics for Pioneer 1 imploding plasma experiments
[DE85-014120] 24 p4159 N85-35787

IMPREGNATING
Theory of kinetics of impregnation of porous bodies
[BLL-M-35817-(5828.4)] 05 p0616 N85-13942
The fabrication, processing and characterization of multidimensionally braided graphite/epoxy composite materials
[AD-A146729] 09 p1288 N85-18090
Utilization of microwave measuring systems for the automation of composite materials manufacturing
[SNIAS-851-430-102] 22 p3742 N85-33197
Implementation of polymer impregnation as a bridge deck sealant
[PB85-185718] 22 p3753 N85-33285

IMPROVEMENT
Improved coordinate measuring machine calibration and control
[DE85-012053] 21 p3590 N85-32315
Land vehicle corrosion management
22 p3750 N85-33248
The properties of VS13sp inoculated steel
[BLL-M-35894-(5828.4)] 23 p3915 N85-34263

IMPULSE GENERATORS
Fast response impulse generator
[AD-D011283] 06 p0759 N85-14853
Application of pulsed power in the simulation of severe natural lightning
[DE85-012666] 24 p4124 N85-35564

IMPULSES
Axisymmetrical oscillations of shell systems subjected to impulse loads 13 p2047 N85-22814
The Record of Electrical and Communication Engineering Conversazione, volume 83, no. 2, November 1984
[ISSN-0365-7719] 16 p2756 N85-27022
Proposal of a method for evaluating accuracy of estimated impulse response of a system 16 p2759 N85-27024
Development of the relativistic impulse approximation
[DE85-006505] 18 p3179 N85-29711
IMPURITIES
NT PSEUDOPOTENTIALS
Nonlinear ultrasonic characterization of oxygen impurities in titanium, 2
[AD-A144857] 01 p0027 N85-10171
Milling of Si3N4 with Si3N4 hardware
[NASA-TM-86864] 01 p0031 N85-10191
Environment-induced embrittlement: Effect of impurity segregation and state of stress
[DE84-015436] 02 p0184 N85-11295
Impurity trapping during gas phase epitaxy of gallium arsenide 02 p0257 N85-11666
RF laser plasma measurements
[AD-A145936] 03 p0366 N85-12344
Investigation of the interaction of atoms with lattice defects using probe methods 03 p0429 N85-12737
Spectroscopic investigations on neutron induced impurity atoms and radiation defects
03 p0430 N85-12742
Paramagnetic impurity effects in NMR determinations of hydrogen diffusion and electronic structure in metal hydrides. Cerium in YH-2 and LaH-2.25
[DE84-014127] 04 p0472 N85-13005
Preparation of low-silicon vanadium metal
[DE84-014916] 04 p0476 N85-13031
Effects of monolayer coverages on substrate sputtering yields
[DE84-016312] 04 p0476 N85-13033
Silicon for solar cells
[DE84-004503] 04 p0529 N85-13361
Contamination analysis of Ti-O2 thin films deposited using ion assisted deposition
[DE84-014944] 05 p0732 N85-14705
Mechanisms of impurity diffusion in rutile
[DE84-014741] 06 p0766 N85-14902
JPL in-house fluidized-bed reactor research
06 p0832 N85-15291
Determination of moments of initial estimate during linear approximation of distribution of ejected impurity
07 p0954 N85-16045
Dependence of breakdown voltage for p-n junction on parameters of ion implantation and semiconductor heat treatment 07 p0954 N85-16046
Prototype wash water renovation system integration with government-furnished wash fixture
[NASA-CR-171629] 08 p1199 N85-17547
Spectroscopic measurement on Heliotron E
09 p1387 N85-18722
Radial profiles of high resolution X-ray spectra from the Alcator C Tokamak 09 p1387 N85-18723
Impurity control by additional current rise and gas puffing during ICRF heating in JIPP T-IIU Tokamak
09 p1387 N85-18725
Sources, densities, and transport of impurities in neutral-beam injected Tokamaks
09 p1388 N85-18731
Transport experiments in the Texas experimental Tokamak 09 p1389 N85-18741
Impact of atomic data on Tokamak modeling
09 p1390 N85-18743
Extended abstract: Ergodic magnetic limiter experiments on TEXT with a 7/3 resonance
[DE85-001390] 09 p1391 N85-18754
Studies on impurity control and hydrogen pumping with chromium gettering in ISX-B
[DE85-001886] 09 p1394 N85-18771
An infrared study of the hydrogenation of carbon dioxide on supported rhodium catalysts
[AD-A149477] 10 p1436 N85-19049
Variational calculation of the 2D H2 molecule
[INPE-3304-PRE/615] 10 p1554 N85-19796
Investigation of vanadium solid solution and zeta phase regions of vanadium-carbon system
[DE85-002678] 11 p1605 N85-20092
Phonon-impurity relaxation and acoustic wave absorption in yttrium-aluminum garnet crystals with impurities 11 p1715 N85-20790
Excitation of impurities by heavy particles and radiative losses of thermonuclear plasma
11 p1719 N85-20816
Atomic processes involving impurities in the plasma edge
[DE85-001277] 11 p1730 N85-20882
Impurity complexes in pure elemental semiconductors
11 p1736 N85-20919
Atomistic studies of grain boundaries with segregated impurities
[DE85-000063] 11 p1737 N85-20924
Electrochemical processes at the sodium (BETA)" alumina interface
[DE85-004653] 12 p1802 N85-21305
Neutral beam injector oxygen impurity measurements and concentration reduction via gettering processes
[DE85-000661] 12 p1836 N85-21521
Spectroscopic study of sources and control of impurities in TMX-U: Revision 1
[DE85-004423] 12 p1937 N85-22170
Americium metal preparation on the multigram scale
[DE85-003735] 13 p2024 N85-22563
Impurities in Kevlar 49 fibers
[DE85-004996] 13 p2036 N85-22767
Hydrogen on impurity-covered iron surfaces
14 p2254 N85-23966
Recent developments in semiconductor research
14 p2297 N85-24222
Laser-induced fluorescence of metal-atom impurities in a neutral beam
[DE85-004980] 14 p2310 N85-24296
Self-substaining low-Z coatings for impurity control. Part 1: General considerations
[DE85-000427] 14 p2425 N85-24956
Energy trapping, release, and transport in three-dimensional energetic solids and molecular crystals: Theory of defects and impurities
[AD-A151071] 14 p2428 N85-24973
Effect of protective atmosphere composition on durability of welded joints of niobium alloys
15 p2502 N85-25432
Structure and properties of VT20L titanium alloy with 0.1-0.3 percent content 15 p2515 N85-25517
Dynamics of recrystallization and redistribution of impurities in semiconductors subjected to millisecond laser pulses 15 p2643 N85-26302
Performance of a copper-lithium alloy as an impurity control system surface material for a fusion reactor
[DE85-006494] 15 p2657 N85-26398
Impurity studies
[DE85-006235] 15 p2661 N85-26423
Microscopic study of the influence of impurities on interface bonding
[AD-A151725] 16 p2743 N85-26926
Sodium and lithium corrosion in molybedenum heat pipes
[DE85-005561] 16 p2784 N85-27179
Periodic cluster simulation of a disordered impurity system
[INPE-3453-PRE/705] 16 p2858 N85-27626
Shallow impurity cluster states in n-type semiconductors
[INPE-3495-PRE/732] 16 p2869 N85-27699
Electronic density of states for the double donor system SiP, As
[INPE-3447-PRE/700] 16 p2869 N85-27700
On some physical impurity properties of doped-indirect gap semiconductors at low and intermediate concentrations
[INPE-3452-PRE/704] 16 p2869 N85-27701
Density of impurity states associated to inversion layers
[INPE-3406-PRE/675] 16 p2869 N85-27702
Atom location by electron channeling analysis
[DE85-007549] 16 p2872 N85-27716
An Impurity Control Test Facility (ICTF) for the study of fusion reactor/plasma edge materials
[DE85-007946] 17 p3040 N85-28810
Impurity control and vacuum pumping system design and analysis for next-generation Tokamaks
[DE85-006291] 17 p3041 N85-28815
The transport of neutral H, D, T and He and O in the boundary layers of a Tokamak plasma
[REPT-84-153] 17 p3041 N85-28817
Magnetic impurities in superconductors
[DE85-006372] 18 p3196 N85-29825
Anisotropic electron-impurity scattering in dilute AlLi: (Small) corrections to the local density approximation
[DE85-002946] 19 p3238 N85-30076
Effects of heat treatment and tracer element impurities on the impact properties of the 12Cr steels
[DE85-010676] 19 p3240 N85-30088
Method of reducing impurity and antisite defects in semiconductor crystal materials, and device and apparatus respectively produced from and utilizing same
[AD-D011698] 19 p3260 N85-30216
Impurity and particle control systems for tokamak reactor experiments
[DE85-006124] 19 p3366 N85-30673
Current state of development and expected performance of copper-lithium alloys as an impurity control system in fusion applications
[DE85-009673] 19 p3372 N85-30917
Compositional analysis of silicon
20 p3480 N85-31628
Oxygen and carbon impurities and related defects in silicon 20 p3481 N85-31631
Z-contrast imaging and electron channeling analysis of dopants in semiconductors
[DE85-011410] 21 p3582 N85-32269
Raman scattering studies in solids
[AD-A155526] 21 p3710 N85-33032
Cryogenic laser calorimetry for impurity analysis
[NASA-CR-176102] 22 p3743 N85-33201
The study of the effect of residual microimpurities on the fatigue strength of 55S2 steel
[BLL-M-36317-(5628.4)] 23 p3913 N85-34246
Stress corrosion cracking susceptibility of types 316NG and 316 stainless steel in an impurity environment
[TI85-006664] 23 p3917 N85-34277
Effect of temperature and ionic impurities at very low concentrations on stress corrosion cracking of Type 304 stainless steel
[TI85-003048] 24 p4079 N85-35283
Cryogenic laser calorimetry for impurity analysis
[NASA-CR-176179] 24 p4097 N85-35395
X-ray fluorescence analysis of uranium concentrates
[DE85-013189] 24 p4148 N85-35717
IMS
U INTERNATIONAL MAGNETOSPHERIC STUDY
IN-FLIGHT MONITORING
Wind shear measuring on board an airliner
[NASA-TM-77463] 03 p0395 N85-12521
Tornado: Structural Usage Monitoring System (SUMS) 07 p0896 N85-15680
Flight parameters recording for structure fatigue life monitoring 07 p0896 N85-15682
USAF approach to airborne structural data recording: Airborne Data Acquisition Multifunction System (ADAMS)
07 p0897 N85-15683
INACTIVATION
U DEACTIVATION
INCANDESCENCE
Personal experience with the PVHD and opinion of situations in which a wide Field Of View (FOV) PVHD might be helpful 01 p0008 N85-10045
Brightness comparison of electroluminescent versus incandescent lighting: A photometric validation
[AD-A145395] 02 p0260 N85-11822
INCENTIVES
NT CONTRACT INCENTIVES
Papers from the Symposium on Emissions: The Value of Incentives and Guidelines for Control
[S-336] 15 p2590 N85-25967
INCIDENCE
NT GRAZING INCIDENCE
Oil flow patterns of separated flow on a hemispherical cylinder at incidence
[DFVLR-FB-84-20] 01 p0048 N85-10313
A Monte Carlo comparison of the recovery of winds near upwind and downwind from the SASS-1 model function by means of the sum of squares algorithm and a maximum likelihood estimator
[NASA-CR-3839] 01 p0064 N85-10421
Performance of Bayes-optimal angle-of-arrival estimators
[AD-A146594] 06 p0858 N85-15454
The effect of changes in the angle of incidence in the event of a richochet at a float step
[RAE-TRANS-2120] 07 p0902 N85-15712
Quantitative use of multiincidence-angle SAR for geologic mapping 08 p1145 N85-17220
Investigation of SIR-B images for lithologic mapping
08 p1146 N85-17241
Australian Multiexperimental Assessment of SIR-B (AMAS) 08 p1146 N85-17243
German Radar Observation Shuttle Experiment (ROSE) 08 p1146 N85-17245
A probe for direct measurement of flow direction
[ESA-TT-853] 11 p1637 N85-20310
Influence of turbulence of incident stream on three dimensional boundary layer 14 p2278 N85-24113
Diffuse reflection of light from turbid conservative medium of finite thickness with incidence of beam on surface of scattering glancing 14 p2342 N85-24481
Characterization of terrestrial solar cells for space applications: Electrical characteristics of thin Westinghouse dendritic web cells as a function of solar intensity, temperature, and incidence angle
[NASA-CR-175842] 14 p2349 N85-24516
Measurement and interpretation of electron angle at MABE beam stop
[DE85-006583] 17 p3032 N85-28755

OMEGA: Optoelectronic measurement of the incidence angle of a projectile
[ISL-CO-223/84] 23 p3974 N85-34634
A normal incidence X-ray telescope sounding rocket payload
[NASA-CR-176169] 24 p4153 N85-35749
INCIDENT RADIATION
Spontaneous ignition of organic solids by radiant heating 09 p1289 N85-18096
Texture etching of (100) silicon for solar cells 20 p3483 N85-31843
Propagation and reflection of a finite amplitude ultrasonic beam including harmonic content: A numeric model 20 p3523 N85-31914
Formulation of cosmic-ray solar daily variation and its seasonal variation, produced from generalized stationary anisotropy of solar origin
[SH-4.5-2] 23 p4036 N85-35020
INCINERATION
U INCINERATORS
INCINERATORS
Measurements on the diffusion of hydrogen chloride in the waste gas plume of incineration ships in the North Sea. Part 1: Methodology, instrumentation and presentation of data
[GKSS-84-E-23-PT-1] 05 p0672 N85-14319
Description and operation of a thermal decomposition unit-gas chromatographic system
[PB84-246362] 07 p0968 N85-16146
Incineration of explosives contaminated soils
[AD-P004142] 09 p1347 N85-18478
Large-scale commercial combustion systems for producing energy from municipal solid waste
[DE85-007097] 15 p2587 N85-25946
Reduction of pollutant formation in combustion processes
[DE85-010161] 19 p3309 N85-30512
INCLUSIONS
Effect of impact damage and open holes on the compression strength of tough resin/high strain fiber laminates 04 p0464 N85-12945
Inclusion formation during solidification of steels with improved machinability
[BMFT-FB-T-84-160] 05 p0619 N85-13957
Influence of the shape and distribution of inclusions of the fatigue strength of bearing steels in rotary bending
[BLL-PNR-90243-(8019.3153)] 06 p0768 N85-14912
Unexplained Fe, Ni and S anomalies in CV chondrite components 06 p0884 N85-15618
Investigation of granules of molybdenum-base alloys obtained with pulsed discharges
[BLL-M-36012-(5628.4)] 07 p0926 N85-15871
Ground shock effect on soil field inclusions 09 p1336 N85-18403
Interaction between a crack and a soft inclusion
[NASA-CR-172533] 10 p1495 N85-19439
Some recent developments in systems reliability
[AD-A150661] 14 p2317 N85-24318
Fracture toughness of MgCr(sub)2O(sub)4-ZrO(sub)2
[DE85-007945] 17 p2917 N85-27982
Weldability of micro-alloy steels as reaction of structure and inclusions
[BLL-BISI-TRANS-22196-(9022.06)] 17 p2924 N85-28027
Physio-chemical mechanisms of the processes of the formation of globular inclusions in ball-bearing metal
[BLL-BISI-TRANS-22235-(9022.06)] 17 p2924 N85-28030
The behaviour of nitride inclusions in nickel-base alloys
[BLL-BISI-TRANS-22396-(9022.06)] 17 p2927 N85-28058
Quality testing to the specifications of the Stahl-Eisen-Pruefblatt 1570/71 using an automatic image analysis system
[BLL-BISI-TRANS-22253-(9022.06)] 17 p2976 N85-28385
Method for production of ceramic oxide and carbide bodies by polymer inclusion and decomposition
[DE85-011668] 19 p3250 N85-30152
Deep-burial diagenesis in carbonates
[DE85-011224] 22 p3802 N85-33554
Viscoelastic behavior of short-fiber composite materials
[DE85-011233] 23 p3910 N85-34225
Special features of the fracture of ball-bearing steel close to non-metallic inclusion eutectics
[BLL-M-35809-(5628.4)] 23 p3914 N85-34258
INCOHERENCE
Fundamental limits to synchronization and tracking
[AD-A149823] 12 p1833 N85-21504
New image deblurring method described 16 p2806 N85-27305
All-optical logic gates with external switching by laser and incoherent radiation 18 p3157 N85-29766
INCOHERENT SCATTER RADAR
Sources of information concerning the ionosphere 04 p0521 N85-13334
Incoherent scatter radar studies of the mesosphere 08 p1184 N85-17463
The magnetospheric convection electric field at ionospheric altitudes: A case study based on STARE and Saint-Santin data 14 p2362 N85-24594
EISCAT electron density studies
[AD-A152820] 17 p2993 N85-28498
Active and passive remote sensing of ice
[AD-A154406] 19 p3300 N85-30459
The Prouet radar 21 p3629 N85-32547
INCOHERENT SCATTERING
Incoherent scatter radar studies of the mesosphere 08 p1184 N85-17463
Error probability during optimal noncoherent reception of binary signals in multibeam channel 13 p2066 N85-22922
A spatially incoherent and temporally coherent source
[AD-A151291] 13 p2157 N85-23390
The Sondrestrom radar: Progress and proposed upgrades for ST work 21 p3628 N85-32541
INCOMPRESSIBILITY
Numerical methods in metalforming 06 p0797 N85-15092
Nonlinear waves in a rod. Results for incompressible elastic materials
[AD-A147485] 07 p0979 N85-16216
Vortices in non-Newtonian fluids
[AD-A153169] 17 p2958 N85-28269
INCOMPRESSIBLE BOUNDARY LAYER
Experimental investigation of a turbulent incompressible boundary layer on a curved wall 11 p1577 N85-19936
Stability of an oscillating boundary layer
[NASA-TM-77827] 14 p2299 N85-24238
A method of determining the suction velocity for laminar flow control of two-dimensional airfoil in incompressible flow
[NAL-TR-845] 18 p3059 N85-28925
INCOMPRESSIBLE FLOW
NT STOKES FLOW
Classical free-streamline flow over a polygonal obstacle
[NASA-CR-172446] 01 p0046 N85-10301
Review of some vortex relations
[NASA-CR-172452] 01 p0046 N85-10302
Accelerated convergence for incompressible flow calculations
[NASA-TM-86863] 02 p0140 N85-10949
Linear long-wave stability of cylindrical steady laminar flame in rotating medium 02 p0268 N85-11752
Incompressible lifting-surface aerodynamics for a rotor-stator combination
[NASA-TM-83767] 03 p0316 N85-12039
Wall effects on the slow steady motion of a particle in a viscous incompressible fluid
[PREPRINT-828] 03 p0363 N85-12327
Algebra of hydrodynamic flows of an ideal fluid and the prediction of the behaviour of a system of particles of a passive admixture on Riemann surfaces with a variable curvature
[REPT-565] 03 p0377 N85-12408
Reducing numerical diffusion for incompressible flow calculations
[NASA-TM-83621] 06 p0756 N85-14840
Laminar flow over a backward-facing step
[AD-A147469] 07 p0980 N85-16084
Numerical solutions for steady natural convection in a square cavity
[PB84-245752] 07 p0981 N85-16090
Calculation of the velocity field generated by a helicopter main and tail rotors in hover
[AD-A147731] 08 p1078 N85-16833
Analysis of sudden expansion flow in a two-dimensional duct with and without side-wall injection using the k-epsilon turbulence model 09 p1317 N85-18282
Algorithms for the Euler and Navier-Stokes equations for supercomputers
[NASA-CR-172543] 10 p1539 N85-19701
Experimental investigation of a breakdown criterion for a vortex in an incompressible flow — delta wing
[ONERA-RT-27/1147-AY] 11 p1577 N85-19935
A three-dimensional spectral algorithm for simulations of transition and turbulence
[NASA-CR-172561] 12 p1845 N85-21575
Local behavior of solutions of an elliptic-parabolic equation
[AD-A149824] 12 p1920 N85-22057
Turbulent flow around circular cylinder uniformly rotating in infinite incompressible fluid 14 p2277 N85-24109
Turbulent flow of fluid near trailing edge of plate in stream at zero angle of attack 18 p2764 N85-27067
Steady, incompressible, inviscid flow through a finite collapsible tube under longitudinal tension
[REPT-84-01] 17 p2959 N85-28278
A second-order pressure-correction method for viscous incompressible flow
[REPT-84-15] 17 p2960 N85-28280
A method of determining the suction velocity for laminar flow control of two-dimensional airfoil in incompressible flow
[NAL-TR-845] 18 p3059 N85-28925
A computational method for wings of arbitrary planform
[AD-A153788] 18 p3059 N85-28929
The hydrocyclastic infundibulum
[AD-A153849] 18 p3100 N85-29192
Dynamic stability of a spinning tube conveying a flowing fluid
[DE85-007583] 18 p3102 N85-29207
A method for computing the core flow in three-dimensional leading-edge vortices
[NASA-TM-87489] 19 p3214 N85-29932
SANDRAG: A computer code for predicting drag of bodies of revolution at zero angle of attack in incompressible flow
[DE85-011170] 19 p3336 N85-30684
Turbulent reacting flows 20 p3451 N85-31427
Numerical and experimental investigation of turbomachinery rotor flow fields 20 p3451 N85-31429
Turbulence modeling in a two-dimensional wake 20 p3452 N85-31431
Turbulent solutions of equations of fluid motion 20 p3453 N85-31441
An implicit finite-difference code for a two-equation turbulence model for three-dimensional flows
[NASA-TM-86752] 20 p3454 N85-31448
Experiments on the influence of active walls on the initial amplitudes and growths of instability waves
[AD-A154630] 21 p3583 N85-32275
Generation by conformal mappings of aerofoil sections and of certain other simple shapes suitable for both aerodynamic and stress-concentration problems
[AD-A154901] 22 p3728 N85-33112
Modeling of unsteady, incompressible separation on an aerofoil using an inviscid flow algorithm
[GU-AERO-8412] 23 p3894 N85-34122
Calculation of flow kinetics of composite media
[BLL-M-35810-(5628.4)] 23 p3929 N85-34348
Stability of two-dimensional immiscible flow to viscous fingering
[DE85-011403] 23 p3931 N85-34364
New semi-implicit method for solving the time-dependent conservation equations for incompressible flow
[DE85-010926] 23 p3931 N85-34367
A curvilinear coordinate method for the solutions of initial value problems using the third-order upwind differencing scheme
[IPPJ-734] 23 p3975 N85-34642
General design method for 3-dimensional, potential flow fields. Part 2: Computer program DIN3D1 for simple, unbranched ducts
[NASA-CR-3925] 24 p4060 N85-35159
INCOMPRESSIBLE FLUIDS
Splitting methods for the numerical solution of the incompressible Navier-Stokes equations
[AD-A147463] 07 p1032 N85-16554
Local behavior of solutions of an elliptic-parabolic equation
[AD-A149824] 12 p1920 N85-22057
Stability of steady rotation of a cylinder filled with a stratified viscous incompressible fluid 14 p2278 N85-24112
Finite element methods for viscoelastic flow
[AD-A154877] 22 p3783 N85-33437
INCONEL (TRADEMARK)
Benchmark notch test for life prediction 02 p0140 N85-10953
Effects of tin on microstructure and mechanical behavior of Inconel 718
[NASA-TM-86868] 03 p0330 N85-12129
Investigation of the isothermal precipitation behavior of nickel-base alloys using electrochemical phase extraction
[JUEL-1903] 05 p0619 N85-13958
Inconel 718 alloy resistance to crack propagation 07 p0907 N85-15740
Experiences with the material bevaviour and high temperature low cycle fatigue life prediction of the IN 738 blading alloy 07 p0908 N85-15746
Thermal-mechanical fatigue crack growth in Inconel X-750
[NASA-CR-174740] 07 p0927 N85-15877
Possibilities for a more accurate life prediction of components — gas turbine disks 07 p0976 N85-16198

Elevated temperature creep behavior of Inconel alloy 625
[DE84-015936] 09 p1297 N85-16144
Non-isothermal irradiation creep of nickel alloys Inconel 706 and PE-16
[DE85-000842] 11 p1607 N85-20102
Stress relief of transition zones
[DE85-000234] 11 p1653 N85-20411
Effect of reduction of strategic Columbium addition in 718 Alloy on the structure and properties
[NASA-CR-174841] 12 p1805 N85-21320
Fatigue life extension 16 p2733 N85-26864
Fatigue strength of Inconel 625 plate and weldments used in the Dill-D configuration vacuum vessel
[DE85-008276] 17 p2981 N85-28427
Preliminary results of the Inconel 617 optimization program. Advanced gas cooled reactor materials program
[DE85-008236] 18 p3075 N85-29024
Hold-time effects in elevated temperature fatigue crack propagation
[AD-A154146] 19 p3286 N85-30378
Finite element analysis of notch behavior using a state variable constitutive equation 20 p3468 N85-31548
Decomposition of sulfuric acid using solar thermal energy
[DE85-012266] 21 p3584 N85-32170
The effect of stress and hot corrosion on nickel-base superalloys
[AD-A154722] 21 p3586 N85-32161

INDENTATION

Influence of cyclic tangential loading on indentation fracture
[DE84-015869] 03 p0373 N85-12382
Elastic fields under a spherical indenter
[AD-A146519] 06 p0817 N85-15188
Journal of Research of the National Bureau of Standards, volume 89, no. 6, November - December 1984
[PB85-179042] 20 p3472 N85-31560
Indentation fractography: A measure of brittleness
[PB85-179059] 20 p3473 N85-31561
Controlled indentation flaws for the construction of toughness and fatigue master maps
[PB85-179067] 20 p3473 N85-31562

INDEPENDENT VARIABLES

NT LATTICE PARAMETERS

A preliminary study of using a strain-gauged balance and parameter estimation techniques for the determination of aerodynamic forces on a model in a very short duration wind tunnel
[AD-A146473] 06 p0810 N85-15145
Some applications of penalty functions in mathematical programming
[AD-A147443] 07 p1032 N85-16552
Optimum performance parameters for ski-jump operations of USAF fighter aircraft
[AD-A146532] 08 p1084 N85-16667
Estimation of launch vehicle performance parameters
[AD-A151927] 16 p2728 N85-26839
An interactive computer package for use with simulation models which performs multidimensional sensitivity analysis by employing the technique of response surface methodology
[AD-A151956] 16 p2848 N85-27548
Development factors and field dependence-independence
[AD-A152337] 17 p3000 N85-28545
Turbulent wake of a submerged flat plate
[AD-A153776] 18 p3100 N85-29190
Computer program for plotting and fairing wind-tunnel data
[NASA-TM-85848] 20 p3387 N85-31009
On the interpretation of variables — simulation and regression models
[FEW-138] 20 p3522 N85-31903
Dialoptic calculation of characteristics for optimization of linear circuits with respect to parameters of individual branches 22 p3767 N85-33346
The effects of parameter variation on helicopter performance
[AD-A156027] 24 p4064 N85-35169
The NORDA/FNOC (Naval Ocean Research and Development Activity's/Fleet Numerical Oceanography Center) Polar Ice Prediction System (PIPS)-Arctic: A technical description
[AD-A156332] 24 p4129 N85-35577

INDEXES (DOCUMENTATION)

Synthesis of current measurements in Puget Sound, Washington. Volume 1: Index to current measurements made in Puget Sound from 1908-1980 with daily and record averages for selected measurements
[PB84-214106] 01 p0090 N85-10603
Catalogue of earthquakes for the territory of Czechoslovakia for the period 1957 - 1980
[REPT-655] 03 p0376 N85-12398
NASA Thesaurus supplement: A 3-part cumulative supplement to the 1982 edition of the NASA Thesaurus
[NASA-SP-7051(SUPPL-2)] 03 p0437 N85-12785
Criss-cross directory of NASA N numbers and DOD AD numbers, 1982-1978 04 p0575 N85-13669
Index of Air Weather Service technical publications, 1 July 1983-30 June 1984
[AD-A149051] 08 p1189 N85-17401
A research in support of NASA's space science
[NASA-CR-174267] 08 p1227 N85-17728
Abstract and index collection
[PB85-119501] 10 p1569 N85-19892
Index to published geologic maps in the region around the potential Yucca Mountain nuclear waste repository site, southern Nye County, Nevada
[DE85-000260] 11 p1669 N85-20518
Aerospace Medicine and Biology: A continuing bibliography with indexes, supplement 267, January 1985
[NASA-SP-7011(267)] 12 p1904 N85-21959
The intelligent database machine 12 p1949 N85-22242
Medical subject headings, tree structures, 1985
[PB84-216092] 12 p1952 N85-22261
Permuted medical subject headings, 1985
[PB84-216100] 12 p1952 N85-22262
NASA Thesaurus supplement, a three part cumulative supplement to the 1982 edition of the NASA Thesaurus
[NASA-SP-7051(SUPPL-3)] 14 p2432 N85-25002
Schema theory in the representation and analysis of text 14 p2433 N85-25004
Air Force Office of Scientific Research (AFOSR): Technical report summaries. Fourth quarter (CY)
[AD-A150660] 14 p2456 N85-25167
DOD manual for standard data elements, part 1
[AD-A152201] 16 p2878 N85-27754
DoD manual for standard data elements, part 2
[AD-A152202] 16 p2878 N85-27755
DoD manual for standard data elements, part 3
[AD-A152203] 16 p2878 N85-27756
DoD manual for standard data elements, part 4
[AD-A152204] 16 p2878 N85-27757
DoD manual for standard data elements, part 5
[AD-A152205] 16 p2878 N85-27758
Bibliography of Lewis Research Center technical publications announced in 1984
[NASA-TM-87012] 17 p3049 N85-28876
Inference in hierarchic classification — data bases
[ENST-84E014] 20 p3518 N85-31573
Air Force Office of Scientific Research (AFOSR). Technical report summaries: First quarter (CY)
[AD-A154757] 21 p3713 N85-33041
Nineteenth International Cosmic Ray Conference. Conference program and author index
[NASA-CP-2376] 22 p3860 N85-33901
Index of laser program publications and related reports, calendar year 1984
[DE85-011863] 23 p3936 N85-34396
Role of solar flare index in long term modulation of cosmic ray intensity
[SH-4.4-12] 23 p4034 N85-35009
A research program to reduce the interior noise in general aviation aircraft, index and summary
[NASA-CR-176178] 24 p4145 N85-35695
Source hierarchy list. Volume 1: A through H
[AD-A156300] 24 p4165 N85-35825
Source hierarchy list. Volume 2: I through Z
[AD-A156301] 24 p4165 N85-35826

INDEXES (RATIOS)

On derivation and significance of geomagnetic equivalent amplitude indices 04 p0520 N85-13321
A directly obtained geomagnetic activity measure, J3 04 p0520 N85-13322
Index cycles simulated by a low order forced barotropic model 07 p1002 N85-16364
The application of a technology index to aircraft turbine engine cost estimating relationships
[AD-A147701] 08 p1087 N85-16874
Biophysical evaluation of the wet globe temperature index (Botsball) at high air movements and constant dew point temperature
[AD-A151065] 14 p2378 N85-24683
Forecast verification of the 10.7 centimeter solar flux and the Ap daily geomagnetic activity indices
[AD-A152950] 17 p2993 N85-29490
Objective determination of heat wave patterns 18 p3140 N85-29437
Performance envelopes and optimal appropriateness measurement
[AD-A154129] 19 p3330 N85-30829
A real time index of geomagnetic background noise for the MAD (Magnetic Anomaly Detection) frequency band
[AD-A155717] 22 p3814 N85-33627

INDIA

Review on physiological and medical problems related to climates ranging from altitude to sub-tropics 05 p0687 N85-14417
MAP in India 11 p1655 N85-20424
Relationship of Indian monsoon intensity to time of onset 13 p2106 N85-23120
Influence of land surface processes on the Indian monsoon: A numerical study 18 p3146 N85-29478
Observation of energy spectrum of electron albedo in low latitude region at Hyderabad, India
[SH-6.1-7] 23 p4045 N85-35081
Proton albedo spectrum observation in low latitude region at Hyderabad, India
[SH-6.1-8] 23 p4045 N85-35082

INDIAN OCEAN

Sea-level in the world ocean. Part 7: The Indian Ocean, a catalogue of measurements
[CSIR-T/SEA-8303-7] 01 p0087 N85-10591
Tide tables 1985, high and low water predictions, central and western Pacific Ocean and Indian Ocean
[PB84-238393] 04 p0542 N85-13451
Late Quaternary deep-water paleoceanography of the eastern equatorial Indian Ocean: Evidence from Bethnic foraminifera, carbonate dissolution, and stable isotopes 08 p1182 N85-17448
Surface currents of the Indian Ocean (to 25 deg S., 100 deg E.)
[IOS-187] 10 p1521 N85-19593
Remanent magnetization model for the broken ridge satellite magnetic anomaly 13 p2123 N85-23219
The BALSAMINE experiment 14 p2238 N85-23876
The Indian Ocean surface dynamics experiment (SINODE) 14 p2325 N85-24370
Parameters of magnetically active layers of Indian Ocean determined from deep drilling data and magnetic surveys 14 p2337 N85-24451
Characteristics of North Indian Ocean tropical cyclone activity
[AD-A153065] 17 p2997 N85-28524
Mineralogical-geochemical characteristics of ferromanganese formations in Arabian-Indian Ocean Ridge 19 p3293 N85-30418
Variability of air humidity profiles over ocean determined by lidar sounding 19 p3296 N85-30436
Mariners weather log, volume 28, number 4, fall 1984
[PB85-178408] 19 p3318 N85-30571
On the interannual variability of the Indian monsoon and the Southern Oscillation 20 p3495 N85-31726

INDIAN SPACE PROGRAM

Colloquium about Joint Projects within DFVLR/ISRO Cooperation
[DFVLR-MITT-84-12] 04 p0458 N85-12907
The Monocular Electro-Optical Stereo Scanner Experiment (MEOSS) 04 p0459 N85-12910
Overview of Autonomous Payload Control Experiment 04 p0459 N85-12911
The space flight of the Soviet-Indian crew
[NASA-TM-77615] 12 p1788 N85-21226

INDIAN SPACE RESEARCH ORGANIZATION

U ISRO

INDIAN SPACECRAFT

An overview of Multispectral Electro-Optical Stereo Scanner (MEOSS) mission 04 p0458 N85-12908
Status of Stretched Rohini Satellite System (SROSS) and Augmented Satellite Launch Vehicle Project (ASLV) 04 p0459 N85-12909
Time synchronization experiments with APPLE 17 p2967 N85-28323

INDIANA

Interlobate comparison of glacial-depositional style as evidenced by small-relief glacial landscape features in Illinois, Indiana, and Ohio, utilizing SIR-B 08 p1146 N85-17231

INDICATING INSTRUMENTS

NT ANEMOMETERS
NT APPROACH INDICATORS
NT ASTROLABES
NT ATTITUDE INDICATORS
NT CLOUD HEIGHT INDICATORS
NT FLOW DIRECTION INDICATORS
NT GYRO HORIZONS
NT GYROCOMPASSES
NT HOT-FILM ANEMOMETERS
NT HOT-WIRE ANEMOMETERS
NT LASER ANEMOMETERS
NT MICROBALANCES
NT MICROWAVE SENSORS
NT PLAN POSITION INDICATORS
NT POSITION INDICATORS
NT RADIO DIRECTION FINDERS
NT SMOKE DETECTORS
NT SPACECRAFT POSITION INDICATORS
NT SPEED INDICATORS

NT TACHOMETERS
NT WEIGHT INDICATORS
NT WIND VANES
Decision tree rating scales for workload estimation: Theme and variations
[NASA-CR-174062] 02 p0237 N85-11544
Fuse status indicator system
[AD-D011294] 06 p0804 N85-15121
Stability indicators for front end loaders
[AD-P004293] 09 p1408 N85-18670
The multiple resources model of human performance: Implications for display design 10 p1534 N85-19669
Adjustable indicating device for load position
[NASA-CASE-MFS-28008-1] 11 p1635 N85-20300
INDIUM
Use of alternative solvents for low-temperature LPE growth of CdTe films
[AD-A149418] 10 p1562 N85-19853
Low cost, sprayed CuInSe2 solar cell research
[DE85-003467] 12 p1881 N85-21790
Angle-resolved photoemission study of AuGa2 and AuIn2 intermetallic compounds
[AD-A150000] 12 p1940 N85-22183
A mixed-basis band structure interpolation scheme applied to the fluorite structure compounds NiSi2, AuAl2, AuGa2 and AuIn2
[AD-A150131] 12 p1940 N85-22187
Effect of dislocations on gallium arsenide FETs
[AD-A152249] 16 p2870 N85-27709
Post-deposition heat treatments of CdS/CuInSe2 solar cells
[DE85-002943] 18 p3128 N85-29373
Optically bistable devices using InSb
18 p3186 N85-29758
Luminescence and absorption of indium-activated potassium-borate glasses subjected to high-power excitation 21 p3661 N85-32668
INDIUM ANTIMONIDES
InAsSb strained-layer superlattices (SLSs) for long wavelength detector applications
[DE84-016111] 05 p0732 N85-14706
Quaternary narrow-band semiconductors (HgTe)x (InSb)1-x for far-infrared detectors
[AD-A149350] 10 p1562 N85-19852
INDIUM ARSENIDES
InAsSb strained-layer superlattices (SLSs) for long wavelength detector applications
[DE84-016111] 05 p0732 N85-14706
Evaluation of implantation-disordering of (InGa)As/GaAs strained-layer superlattices
[DE85-003533] 12 p1942 N85-22200
Ion implantation disorder in strained-layer superlattices
[DE85-004466] 14 p2430 N85-24984
A study of Ga(.47)In(.53)As and Al(.48)In(.52)As for very high frequency device applications
[AD-A151995] 16 p2870 N85-27706
Mechanically-stacked multijunction solar cells
[DE85-010389] 18 p3129 N85-29377
Low-threshold injection InGaAsP/GaAs double heterostructure lasers with separate limiting obtained by liquid-phase epitaxy (lambda = 0.78 divided by 0.87 microns, I sub thr = 460 A/cm 2, T = 300 K)
21 p3687 N85-32908
Adjustment of radiation wavelength of multimode InP-GaInAsP injection heterolasers
21 p3688 N85-32913
INDIUM COMPOUNDS
NT INDIUM ANTIMONIDES
NT INDIUM ARSENIDES
NT INDIUM PHOSPHATES
NT INDIUM PHOSPHIDES
NT INDIUM TELLURIDES
CuInSe2-based photoelectrochemical cells: Their use in characterization of thin CuInSe2 films, and as photovoltaic cells per se
[DE84-004514] 04 p0529 N85-13379
Surface and interfacial properties of Ga(0.47) In(0.53)As alloys
[AD-A148891] 10 p1562 N85-19849
Transport studies of several novel organic conductors
[DE85-003950] 14 p2429 N85-24979
A study of the stability of cadmium sulfide/copper sulfide and cadmium sulfide copper-indium-diselenide solar cells
[DE85-002902] 15 p2587 N85-25947
Dual species ion implantation of ternary compounds based on In-Ga-As
[AD-D011617] 16 p2869 N85-27696
Materials-process interactions in ternary alloy semiconductors
[AD-A153133] 17 p3043 N85-28832
Development of photodetectors
[AD-A153773] 18 p3095 N85-29158
Liquid crystal light valve structures
[NASA-CASE-MSC-20036-1] 22 p3847 N85-33826
INDIUM PHOSPHATES
Cascaded solar photovoltaic cells based on InP-GaInPAs and InP-CdS heterostructures
02 p0268 N85-11749
INDIUM PHOSPHIDES
Plasma deposited diamondlike carbon on GaAs and InP
[NASA-TM-86870] 01 p0123 N85-10844
Studies of grown-in defects versus growth parameters in 3-4 compound semiconductors
[AD-A145864] 03 p0433 N85-12755
Investigation of liquid encapsulation Chochralski growth of InP
[AD-A146096] 03 p0433 N85-12760
Characterization of surface electronic properties of semi-insulating InP
[AD-A146553] 06 p0868 N85-15507
A picosecond population modulation study of near interband resonances in semiconductors
09 p1396 N85-18787
Material growth and characterization for solid state devices
[NASA-CR-174410] 10 p1561 N85-19847
Method for synthesizing indium phosphide
[AD-D011475] 10 p1563 N85-19855
InP materials
[AD-A152341] 17 p3043 N85-28828
Development of photodetectors
[AD-A153773] 18 p3095 N85-29158
Influence of technological factors on luminescence characteristics of InGaAsP/InP heterolasers (lambda = 1.55 microns)
21 p3686 N85-32910
Adjustment of radiation wavelength of multimode InP-GaInAsP injection heterolasers
21 p3688 N85-32913
INDIUM TELLURIDES
Preliminary studies on the low-cost preparation of chalcogenide semiconductors from solution depositions
[DE85-000638] 11 p1736 N85-20918
INDOLES
NT TRYPTOPHAN
INDONESIA
Geologic mapping of Indonesian rain forest with analysis of multiple SIR-B incidence angles
08 p1145 N85-17221
Microwave propagation studies, measurements and education in Surabaya, Indonesia
[B8464833] 24 p4068 N85-35339
INDOOR AIR POLLUTION
A dispersion model for airborne particulates inside a building
[DE84-014961] 02 p0225 N85-11473
Volatile organic emissions from adhesives with indoor applications
[DE84-015965] 05 p0820 N85-13966
Effect of sealants of the sound absorption coefficients of acoustical friable insulating materials
[AD-A148541] 08 p1218 N85-17674
Formaldehyde and tracer gas transfer between airstreams in enthalpy-type air-to-air heat exchangers
[DE84-016951] 11 p1831 N85-20274
Identification and quantification of nitropolynuclear aromatic hydrocarbons in ambient and indoor air particulate samples
[PB85-176790] 19 p3311 N85-30525
INDUCED FLUID FLOW
U FLUID FLOW
INDUCTANCE
NT PROXIMITY EFFECT (ELECTRICITY)
Magnetic and photoconductive repetitive rail-gun opening switches
[DE84-017060] 04 p0496 N85-13163
Plasma mass and effective inductance in a small railgun
[MRL-R-947] 12 p1936 N85-22162
Piezoelectric filter with low-Q inductances
13 p2070 N85-22932
Plasma mass and effective inductance in a small railgun
[AD-A154844] 21 p3589 N85-32304
Use of the computer programs PARA 80 to study results from firing the railgun ERGS-1M
[MRL-R-900] 22 p3738 N85-33167
Predicting electrical performance parameters of underwater cables 22 p3775 N85-33391
New formulation for linear accelerator design
[DE85-011171] 22 p3842 N85-33792
INDUCTION
DC switching regulated power supply for driving an inductive load
[DE84-014238] 01 p0044 N85-10285
Induction voltmeter
[DE84-014321] 01 p0050 N85-10329
RADLAC technology review
[DE85-011995] 23 p3982 N85-34691
INDUCTION (MATHEMATICS)
Induction of fuzzy decision rules
[INPE-3053-PRE/474] 04 p0554 N85-15525
INDUCTION HEATING
High frequency plasma generator for ion thrusters
[NASA-CR-174772] 08 p1114 N85-17023
The heat sensitivity of solid propellants
08 p1117 N85-17043
Application of electricity to the reheating of metals prior to forming. Forging, lamination, induction
[BLL-TR-T8399/BG/MRS14903/84]
08 p1137 N85-17160
Underwater pipeline: Welding by high frequency induction
[BLL-WI-TRANS-682-(9312.57)]
16 p2792 N85-27221
Influence of heat treatment parameters on the properties of induction hardened Ni-Cr-Mo steels
[BLL-BISI-TRANS-2499-(9022.06)]
17 p2926 N85-29053
Induction heating gun
[NASA-CASE-LAR-13181-1] 18 p3085 N85-29083
Feedback regulated induction heater for a flowing fluid
[DE85-006508] 23 p3939 N85-34414
Effect of ECH and ICH on ambipolar potential in NBT-1M 23 p3976 N85-34861
Transports studies of ECH and ICRH-heated bumpy torus plasma in NBT-1M 23 p3976 N85-34862
INDUCTION MOTORS
Variable speed generator technology options for wind turbine generators
[RR-84-4] 10 p1478 N85-19331
Solar powered actuator with continuously variable auxiliary power control
[NASA-CASE-MFS-25637-1] 12 p1876 N85-21769
Power control for ac motor
[NASA-CASE-MFS-25861-1] 13 p2082 N85-22877
Magnetic noise in single-machine rotating frequency converters 13 p2077 N85-22969
The performance of an alternating-current thyristor-controlled motor 15 p2546 N85-25718
Commercialization of the power factor controller
[NASA-CR-171500] 17 p2951 N85-28221
A variable frequency control for three-phase induction motors 19 p3256 N85-30180
Induction motors with minimum waste of magnetic iron
22 p3772 N85-33377
Magnetic field and equivalent circuit of induction motors with shielded poles 22 p3772 N85-33378
Evaluation of half wave induction motor drive for use in passenger vehicles
[NASA-CR-176119] 23 p3926 N85-34334
State-of-the-art of solid-state motor controllers
[TI85-006674] 24 p4162 N85-35806
INDUCTION SYSTEMS
U INTAKE SYSTEMS
INDUCTORS
Characteristics of the boat inductor for keeping liquid metal in the suspended state
[NASA-TM-77816] 12 p1851 N85-21611
Plasma erosion opening switch
[DE85-011384] 20 p3535 N85-31998
INDUSTRIAL AREAS
Influence on an industrial site on the characteristics of CCN supersaturation with air masses of different origin
21 p3650 N85-32683
INDUSTRIAL ENERGY
Advanced technology cogeneration system conceptual design study: Closed cycle gas turbines
[NASA-CR-168222] 07 p0992 N85-16300
Linking R and D to problems experienced in solids processing
[AD-A154238] 19 p3380 N85-30068
INDUSTRIAL MANAGEMENT
NT ENGINEERING MANAGEMENT
NT INVENTORY CONTROLS
NT INVENTORY MANAGEMENT
NT PERSONNEL MANAGEMENT
Business planning for information services under special consideration of German management information systems
[BMFT-FB-ID-83-007] 02 p0294 N85-11910
Primer on the registration of technical information in industry 03 p0438 N85-12768
Value analysis -- industrial competition
[CNES-NT-110] 04 p0577 N85-13684
Evaluation of the effectiveness of the weighted guidelines to induce contractor's investment in cost reducing facilities equipment
[AD-A147568] 07 p1053 N85-16881
USSR report: Machine tools and metalworking equipment
[JPRS-UMM-85-001] 08 p1139 N85-17172
Summaries of press automation conference presented
08 p1139 N85-17173

Plans, developments in robotics
14 p2289 N85-24191
Mini-Seminar on Non-Destructive Testing
[CSIR-TSD-0009/83] 14 p2316 N85-24308
Status of the U.K. N.D.T. industry today
14 p2316 N85-24309
Robot use in FRG increases but sensor technology lags
15 p2531 N85-25605
The development and implementation of advanced welding technology
15 p2565 N85-25824
Robotic arc welding
15 p2566 N85-25830
Welding techniques in pressure part technology
15 p2566 N85-25835
Industrial applications of pattern recognition and image processing
15 p2622 N85-26157
Quality analysis
21 p3668 N85-32785
DOD Value Engineering Conference report. Value Engineering (VE): A tool that benefits line management held at Leesburg, Virginia on 1-2 November 1984. Part 1. Executive summary
[AD-A156067] 24 p4163 N85-35810
DOD Value Engineering Conference report. Value Engineering (VE): A tool that benefits line management held at Leesburg, Virginia on 1-2 November 1984. Part 2. Plenary session
[AD-A156068] 24 p4163 N85-35811

INDUSTRIAL PLANTS
NT FOUNDRIES
User experience of existing corrosion monitoring techniques and the development of Thin Layer Activation (TLA) for corrosion monitoring
[AERE-R-11248] 01 p0029 N85-10183
Growth, future of Soviet robotics sector analyzed
01 p0035 N85-10217
Advanced technology cogeneration system conceptual design study: Closed cycle gas turbines
[NASA-CR-168222] 07 p0992 N85-16300
Manufacturing methods and technology project summary reports
[AD-A148209] 08 p1138 N85-17163
The infrastructure for a surge in synfuels production: The potential role of the AE and C industry and of owner operators
[RAND/N-2172-SFC] 09 p1301 N85-18170
Scania, ASEA of Sweden use robots for all production phases
09 p1310 N85-18229
Thermal energy storage
[DE85-001492] 09 p1344 N85-18454
Flexible applications robot used in Moscow training course
10 p1482 N85-19217
Institute director surveys industrial automation drive
11 p1617 N85-20167
Increased use of CNC in machine tool construction
11 p1617 N85-20170
Siemens-Corning plant to manufacture optical fibers
11 p1617 N85-20175
French panel makes specific proposals for robotics research. Current state of French robotics
11 p1618 N85-20180
Aviation repair plant directors on quality control measures
12 p1769 N85-21106
Optoelectronic safety system for robotized technological complex
13 p2046 N85-22805
Robotized system for treating gear wheels
14 p2285 N85-24162
Mini-Seminar on Non-Destructive Testing
[CSIR-TSD-0009/83] 14 p2316 N85-24308
West Europe report: Science and technology
[JPRS-WST-84-012] 15 p2523 N85-25552
MBB uses new CFC form tool for titanium alloy air intake
15 p2523 N85-25553
French robotics research at Grenoble labs
15 p2523 N85-25555
West Europe report: Science and technology
[JPRS-WST-84-007] 15 p2530 N85-25600
Robot use in FRG increases but sensor technology lags
15 p2531 N85-25605
Pachiney strategy includes development of new materials
15 p2531 N85-25607
MBB/Erno's views, future plans in aerospace activities
15 p2531 N85-25609
West Europe report: Science and technology
[JPRS-WST-84-027] 15 p2532 N85-25612
West Europe report: Science and technology
[JPRS-WST-84-014] 15 p2536 N85-25647
Updating model RPD-1.25 industrial robot
16 p2762 N85-27043
New stage in robotics development
16 p2762 N85-27045
Review of national emission standards for mercury
[PB85-153906] 16 p2822 N85-27406
Conversion of methanol to gasoline: Engineering and construction of the demonstration plant
[DE85-003237] 17 p2937 N85-28133
Robots, automatic devices inside VW's Wolfsburg plant
17 p2946 N85-28186
USSR report: Machine tools and metalworking equipment
[JPRS-UMM-84-014] 17 p2946 N85-28188
Component problems plague French robotics industry
18 p3085 N85-29088
West Europe report: Science and technology
[JPRS-WST-84-031] 18 p3086 N85-29089
Multinational program to develop intelligent robots
18 p3086 N85-29094
West Europe report: Science and technology
[JPRS-WST-84-037] 18 p3088 N85-29108
Some examples of the application of automatically guided vehicle systems
[HSE-TRANS-11134] 19 p3281 N85-30348
Environmental monitoring report for Pantex Plant covering, 1984
[DE85-010824] 19 p3308 N85-30508
West Europe report: Science and technology
[JPRS-WST-85-020] 20 p3438 N85-31333
Centralized surveillance of flexible workshops for the manufacturing of composite materials
[SNIAS-851-430-103] 23 p3910 N85-34227
Solar thermal technologies program summary
[DE85-012253] 23 p3945 N85-34449

INDUSTRIAL SAFETY
Early detection of environmental exposure
[AD-P004039] 06 p0845 N85-15369
Facility safety study
[NASA-CR-174280] 07 p0910 N85-15759
High voltage effects measured on dummy mannequin
07 p1012 N85-16432
A crew exposure study. Volume 1: Offshore
[AD-A146884] 07 p1015 N85-16449
Study of bodily functional status and quality of controlling action of power unit operators with various intensities of labor
09 p1362 N85-18569
Robotic safety
[DE85-002314] 10 p1493 N85-19431
USSR report: Life sciences. Biomedical and behavioral sciences
[JPRS-UBB-85-008] 10 p1523 N85-19605
Health standards for general vibration
10 p1523 N85-19607
Effects of overall vibration and noise on operational personnel
10 p1523 N85-19608
Comparative assessment of different treatment modalities in miners with vibration- and noise-induced disease
10 p1524 N85-19610
Control technology for integrated circuit fabrication at Honeywell Optoelectronics Division, Richardson, Texas
[PB85-109023] 11 p1616 N85-20162
The audiomat: An automatic audiometer for use in occupational audiometry
[DRIC-T-7138] 13 p2142 N85-23294
Safety with industrial manufacturing lasers
14 p2308 N85-24281
Robotic safety systems and methods: Savannah River site
[DE85-006261] 17 p2974 N85-28375
Sound-insulating enclosures — machine noise
[BMFT-FB-HA-85-005] 20 p3525 N85-31925
A crew exposure study. Phase II. Volume 2. At sea. Part A
[AD-A155233] 21 p3668 N85-32774

INDUSTRIAL WASTES
High-level waste processing and disposal
[DE85-003564] 11 p1728 N85-20865
Technology for industrial waste heat recovery by organic Rankine cycle systems
[DE85-006719] 18 p3102 N85-29206
Pollutant body burdens and reproduction in Platichthys stellatus from San Francisco Bay
[DE85-010407] 19 p3308 N85-30509

INDUSTRIES
NT AEROSPACE INDUSTRY
NT AIRCRAFT INDUSTRY
NT CONSTRUCTION INDUSTRY
NT DEFENSE INDUSTRY
Lagging development of biotechnology described
01 p0115 N85-10787
Space commercialization: Analysis of R and D investments with long time horizons
02 p0155 N85-11052
Development, production, application of robots assessed
03 p0343 N85-12211
Modular electromechanical industrial robots
03 p0345 N85-12223
International exhibition: Industrial Robots, 1982
03 p0345 N85-12224
Robotization of electric welding processes
03 p0345 N85-12225
Robotization of technological processes in high-frequency heating and welding
03 p0345 N85-12226
Improving operational reliability and productivity of robotized technological complexes
03 p0346 N85-12227
USSR report: Chemistry
[JPRS-UCH-84-012] 06 p0761 N85-14885
New concepts for industrial robots outlined
06 p0815 N85-15176
West Europe report: Science and technology
[JPRS-WST-84-039] 07 p0936 N85-15929
Airport ground equipment under development at Riga
09 p1278 N85-18036
The infrastructure for a surge in synfuels production: The potential role of the AE and C industry and of owner operators
[RAND/N-2172-SFC] 09 p1301 N85-18170
Scania, ASEA of Sweden use robots for all production phases
09 p1310 N85-18229
East Europe report: Science and technology
[JPRS-ESA-85-005] 09 p1377 N85-18859
Advanced industrial robot control systems
[PB85-110773] 11 p1648 N85-20385
Advanced industrial robot control systems
[PB85-110781] 11 p1648 N85-20386
Technological and economic assessment of advanced ceramic materials. Volume 5: A case study of ceramic toxic and combustible gas sensors
[PB85-113124] 12 p1815 N85-21386
Cost comparison of small gas turbines versus electric motors in a variable load industrial application
[PB85-149763] 12 p1837 N85-21530
The future of lightwave technology
[PB85-109759] 12 p1935 N85-22155
Current plans for development of chemical industry
13 p2014 N85-22633
USSR report: Machine tools and metalworking equipment
[JPRS-UMM-85-006] 14 p2283 N85-24146
Basic principles of industrial radiography
14 p2316 N85-24310
Standing of industrial radiography in South Africa
14 p2316 N85-24311
Radiological safety aspects of industrial radiography
14 p2316 N85-24312
Ultrasonic non-destructive testing technique
14 p2316 N85-24313
Mercedes-Benz auto 2000 achieves low drag coefficient
15 p2530 N85-25602
West Europe report: Science and technology
[JPRS-WST-84-020] 15 p2534 N85-25633
West Europe report: Science and technology
[JPRS-WST-84-003] 15 p2534 N85-25635
West Europe report: Science and technology
[JPRS-WST-84-009] 15 p2535 N85-25639
USSR report: Engineering and equipment
[JPRS-UEQ-85-004] 17 p2939 N85-28142
West Europe report: Science and technology
[JPRS-WST-84-024] 17 p2945 N85-28183
Space station study
[BL-6167] 18 p3066 N85-28959
CEMA cooperation in development of robotics, FMS viewed
20 p3438 N85-31331
Spin-offs from technical commercial infrastructures, no. 2
20 p3540 N85-32035
Quality analysis
21 p3668 N85-32785
New innovative businesses from industry. Experiences in the Netherlands in the successful transfer of technology from university to industry
22 p3849 N85-33643
Forecasting future industrial SO2 and NC/sub x/ emissions, revised
23 p3947 N85-34481

INELASTIC BODIES
U RIGID STRUCTURES

INELASTIC COLLISIONS
Monte Carlo simulation of thermalization of subexcitation electrons in molecular hydrogen
[NAL-TR-815T] 01 p0117 N85-10798
Energy transfer in atom-molecule scattering experiments in the 1eV region with SF6-Ar, CF4-Ne and Xe-CO2 systems as examples
[REPT-11/1983] 04 p0563 N85-13588
Capture of planetesimals into a circumterrestrial swarm
13 p2179 N85-23522
Accumulation of the terrestrial planets
13 p2179 N85-23524
Kinetic studies following state selective laser excitations
[DE85-007173] 15 p2564 N85-25816
Size distribution in collisional systems — planetary rings
15 p2674 N85-26506
Inelastic Near-Surface Interactions. Proceedings of the Werner Brandt Workshop on Penetration Phenomena
[DE85-010579] 20 p3526 N85-31928
Propagation and secondary production of low energy antiprotons in the atmosphere
[OG-8.1-3] 22 p3867 N85-34094

On a possibility of inelasticity partial coefficient K sub gamma determination in pi C and pi Pb interactions at 10 to the 14th power eV (experiment PAMIR 1)
[HE-1.1-12] 24 p4171 N85-35859
Determination of primary energy in nucleus-nucleus collisions and the high P(sub)T tail of alpha-particles
24 p4173 N85-35875

INELASTIC SCATTERING
Study of structure of nuclei with neutrons and nuclear data measurements for MFE
[DE84-015128] 01 p0117 N85-10802
High energy-resolution inelastic X-ray scattering
[DE84-014585] 01 p0118 N85-10804
Dirac single particle wave functions in inelastic electron scattering
[DE84-015129] 02 p0279 N85-11814
Diffuse elastic and inelastic neutron scattering of disorder transitions and boundaries. Phase determination of structure factors 03 p0424 N85-12708
Inelastic neutron scattering on crystals for the clarification of structure and semiconductor properties
03 p0425 N85-12714
Measurements on the triple axis spectrometer UNIDAS for the investigation of dynamic processes in crystals using inelastic neutron scattering 03 p0426 N85-12716
Structural properties of amorphous metals by Raman scattering
[DE84-016947] 04 p0475 N85-13027
Local fields in strongly coupled plasmas
[DE84-013375] 04 p0567 N85-13611
Particle physics
[DE84-013634] 05 p0727 N85-14673
Measurements of the A-dependence of deep-inelastic electron scattering from nuclei
[DE84-013665] 05 p0728 N85-14678
Pion inelastic scattering to the first three excited states of Lithium-6
[AD-A147560] 07 p1041 N85-16606
Comments on the image contrast from inelastically scattered electrons
[DE85-000899] 07 p1041 N85-16609
Notes for lectures in China: The Bethe theory of inelastic collisions of fast charged particles with atoms and molecules
[DE84-017487] 09 p1380 N85-18676
Neutral-current x-distributions
[DE84-016522] 09 p1382 N85-18691
Microscopic determinations of lattice and electronic structures of solids
[DE84-017323] 09 p1399 N85-18806
Theoretical cross sections for inner-shell vacancy production by high-energy electrons
[DE84-007346] 11 p1721 N85-20827
Recent progress in electron scattering at SLAC
[DE85-002718] 11 p1723 N85-20840
Theoretical nuclear physics
[DE85-003466] 12 p1932 N85-22135
Theoretical aspects of the nucleon-nucleon workshop
[DE85-003740] 14 p2420 N85-24933
Neutron scattering and reactions on 59Co from 1 to 20 MeV
[AERE-R-11439] 17 p3028 N85-28729
Experimental studies of diffractive phenomena
[DE85-006812] 17 p3031 N85-28749
Possible indication of an A-dependence of R in deep-inelastic electron scattering from nuclei
[DE85-006174] 17 p3033 N85-28763
New experimental results in two photon physics
[NIKHEF-H/84-16] 17 p3035 N85-28776
SPECTER: Neutron damage calculations for materials irradiations
[DE85-005791] 18 p3180 N85-29716
Intermediate energy nuclear theory
[DE85-010440] 18 p3182 N85-29731
Deep-inelastic lepton scattering by nuclei: The pion-exchange model
[DE85-010498] 19 p3359 N85-30628
Discussion session: Nucleon- and antinucleon-nucleus inelastic scattering and charge exchange
[DE85-010723] 19 p3364 N85-30660
Energy-advanced nuclear data: Measurements and physical interpretations
[DE85-006196] 19 p3366 N85-30672
Magnetoconductance in aluminum films, wires, and cylinders 19 p3374 N85-30928
Inelastic Near-Surface Interactions. Proceedings of the Werner Brandt Workshop on Penetration Phenomena
[DE85-010579] 20 p3526 N85-31928
Antiproton-nucleus inelastic scattering and the spin-isospin dependence of the N anti N interaction
[DE85-010646] 20 p3526 N85-31935
Toward the question of multi-quark configurations in nuclei 21 p3691 N85-32929
Evaluated nuclear-data file for niobium
[DE85-012095] 21 p3704 N85-33009
Calculation of heavy-ion tracks in liquid water
[DE85-012101] 24 p4149 N85-35725
Fast-neutron interaction with niobium
[DE85-011471] 24 p4150 N85-35731
Proton-air and proton-proton cross sections from air shower data
[HE-1.1-1] 24 p4170 N85-35849
Proton-air inelastic cross section at S(1/2) = 30 TeV
[HE-1.1-2] 24 p4170 N85-35850
Hadron cross sections at ultra high energies and unitarity bounds on diffraction dissociation
[HE-1.1-3] 24 p4170 N85-35851
Determination of the cross section of the proton, pion and neutron inelastic interaction with lead and carbon nuclei at 0.5 - 5.0 TeV energies (PION experiment)
[HE-1.1-5] 24 p4170 N85-35853
Estimation of the total inelasticity coefficient in interaction of greater than or equal to 20 TeV hadrons with lead
[HE-1.1-9] 24 p4171 N85-35857
The method for the study of the inelastic cross-section for high energy protons by means of shower arrays with the large calorimetric area
[HE-1.1-11] 24 p4171 N85-35858
Forward particle production in inelastic Ne-22 inteVractions in emulsion at 4.1 A Ge/c
[HE-1.4-7] 24 p4176 N85-35895
Meson multiplicity in nucleus-nucleus collisions above 4 GeV/amu
[HE-1.4-10] 24 p4177 N85-35897
On the characteristics of emulsion chamber family events produced in low heights
[HE-3.1-6] 24 p4178 N85-35904
A study of gamma-families generated in nucleon-nucleus (NA) and pion-nucleus (pi A) interactions
[HE-3.7-2] 24 p4186 N85-35961
QCD analysis of neutrino charged current structure function F2 in deep inelastic scattering
[HE-5.3-23] 24 p4207 N85-36114

INELASTIC STRESS
The 3-D inelastic analysis methods for hot section components: Brief description 02 p0143 N85-10972
Local strain redistribution corrections for a simplified inelastic analysis procedure based on an elastic finite-element analysis
[NASA-TP-2421] 11 p1651 N85-20396
3-D inelastic analysis methods for hot section components (base program) — turbine blades, turbine vanes, and combustor liners
[NASA-CR-174700] 12 p1883 N85-21686
Unified constitutive material models for nonlinear finite-element structural analysis — gas turbine engine blades and vanes
[NASA-TM-86965] 14 p2320 N85-24338
Elastic-plastic analysis for cyclic loading using a linearized yield condition
[PB85-149607] 14 p2322 N85-24346
A survey of unified constitutive theories
20 p3466 N85-31531
Monotonous stress-strain properties of structural steel subjected to nonstationary repetitive pre-loading
23 p3904 N85-34185
Subcritical fracture propagation in rocks: An examination using the methods of fracture mechanics and non-destructive testing 24 p4116 N85-35516

INEQUALITIES
NT SCHWARTZ INEQUALITY
A weighted polynomial inequality
[CSIR-TWISK-332] 01 p0110 N85-10741
On two concepts of fundamental matching
[CSIR-TWISK-335] 01 p0110 N85-10743
Testing of inequality hypotheses in linear models using the Bayes method
[SER-C-292] 01 p0112 N85-10761
An integral inequality with applications to order statistics
[AD-A145081] 01 p0113 N85-10770
Constrained optimization using iterated partial Kuhn-Tucker vectors
[AD-A145476] 02 p0251 N85-11641
Stable monotone variational inequalities
[AD-A147123] 07 p1031 N85-16544
Generating positively correlated random variables from a sequence of independent random variables with symmetric logarithmically concave densities
[AD-A148439] 08 p1216 N85-17658
On the local behaviour of solutions of degenerate parabolic equations with measurable coefficients
[AD-A147412] 09 p1373 N85-18831
Solutions of problems of miller and rubel
10 p1536 N85-19685
Bounding the stochastic performance of continuum structure functions 2
[AD-A149458] 10 p1548 N85-19762
The inefficiency of least squares: Extensions of Kantorovich inequality
[AD-A149568] 10 p1549 N85-19780
Schur-Ostrowski theorems for functionals on l1(0,1)
[AD-A150193] 13 p2150 N85-23346
Nonlinear 0-1 programming. 1: Linearization techniques, revision
[AD-A150960] 14 p2405 N85-24826
Maintaining solution invariants in the numerical solution of ODEs
[DE85-005918] 14 p2410 N85-24857
Squares of Gegenbauer polynomials and Milin type inequalities
[CWI-PM-R8412] 14 p2410 N85-24862
Entire functions with spiral limits
15 p2634 N85-26241
An inequality and its application to the truncated distributions 17 p3020 N85-28673
On the convergence of difference approximations to scalar conservation laws
[NASA-CR-172814] 19 p3344 N85-30728
On the dependence of the convergence of Gummel's algorithm on the regularity of the solution
[AD-A154628] 21 p3675 N85-32832
Sobolev-Poincare's inequality and the Neumann problem for u sub t = divergence of the absolute value of the gradient u to the p-2 power x the gradient u
[AD-A154766] 21 p3676 N85-32839

INERT ATMOSPHERE
Apparatus and method for the horizontal, crucible-free growth of silicon sheet crystals
[DE85-011586] 22 p3847 N85-33829

INERT GASES
U RARE GASES

INERTIA
Vibrational power transmission of an idealized gearbox
[ISVR-TR-124] 02 p0204 N85-11346
Measurement of the inertial constants of a rigid or flexible structure of arbitrary shape through a vibration test
[NASA-TM-77557] 02 p0209 N85-11381
A geometrical theory of spin motion
[DE84-016537] 04 p0574 N85-13658
Hydrodynamic impeller stiffness, damping, and inertia in the rotordynamics of centrifugal flow pumps
05 p0843 N85-14125
Effects of fluid inertia and turbulence on force coefficients for squeeze film dampers
05 p0845 N85-14137
Effects of external loads on human head movement control systems 05 p0707 N85-14534
A tracked vehicle test plant for the simulation of dynamic operation
[AD-P004306] 09 p1410 N85-18682
Resonance generation of inertial waves (in the atmosphere) by Doppler-shift of inertio-gravity modes
15 p2590 N85-25968
The Shock and Vibration Digest, volume 17, no. 2
[AD-A153129] 17 p2977 N85-28400
Recent progress in the dynamic plastic behaviour of structures, part 4 17 p2978 N85-28402

INERTIA MOMENTS
U MOMENTS OF INERTIA

INERTIA WHEELS
U COUNTER-ROTATING WHEELS
U REACTION WHEELS

INERTIAL CONFINEMENT FUSION
NT IMPACT FUSION
Ion-density correlations and enhancement of thermonuclear reaction rate in dense, inertially confined fusion plasmas 02 p0284 N85-11849
Vacuum inductive pulsed power compression for inertial confinement fusion
[DE84-010935] 03 p0421 N85-12692
Inertial confinement fusion: Present status and future potential
[DE84-016177] 04 p0587 N85-13616
Progress in inertial confinement fusion at Lawrence Livermore National Laboratory
[DE84-016227] 04 p0588 N85-13621
Quality assurance in the Antares Laser Fusion Construction Project
[DE84-015493] 05 p0840 N85-14104
Recent ICF research by GEKKO 12 glass layer at ILE Osaka 09 p1387 N85-18726
Basic research on inertial confinement fusion by LIMAY-I 15 p2655 N85-26383
Pulse star inertial confinement fusion reactor
[DE85-010640] 18 p3181 N85-29726
Inertial fusion reactors and magnetic fields
[DE85-009571] 18 p3191 N85-29789
Progress in inertial fusion at LLNL
[DE85-010931] 19 p3277 N85-30321
Summary of research for the Inertial Confinement Fusion Program at Los Alamos National Laboratory
[DE85-010330] 19 p3361 N85-30836

Advances in ICF power reactor design
[DE85-010930] 19 p3381 N85-30841
Ion beam-plasma interactions
[DE85-010932] 19 p3371 N85-30913
Flow characteristics of the Cascade granular blanket
[DE85-010932] 20 p3420 N85-31227
Thomson scattering on Elmo Bumpy Torus
[DE85-010584] 20 p3527 N85-31941
Transparent electrode for optical switch
[DE85-011618] 22 p3761 N85-33310
Workshop report on Simulation Techniques for Shock Wave Phenomena and Characteristics of Plasmas in Inertial Confinement Fusion
[IPPJ-725] 23 p3979 N85-34670
Stellarator approach to fusion plasma confinement
[DE85-011420] 23 p3984 N85-34704

INERTIAL FORCES
U INERTIA

INERTIAL FUSION (REACTOR)
Accelerator Technology Program
[DE84-017083] 04 p0563 N85-13586
Opacity determinations for Inertial Confinement Fusion (ICF) materials using an average atom model
12 p1957 N85-22295
Heavy ion fusion accelerator research in the US
[DE85-008465] 17 p3034 N85-28767
Megajoule-class single-pulse KrF laser test facility as a logical step toward inertial fusion commercialization
[DE85-009590] 18 p3191 N85-29784
Progress in inertial fusion at LLNL
[DE85-010691] 19 p3277 N85-30321
Ion source development for the Los Alamos heavy ion fusion injector
[DE85-012682] 24 p4156 N85-35766

INERTIAL GUIDANCE
NT STRAPDOWN INERTIAL GUIDANCE
Polaris guidance system
[AD-D011324] 07 p0800 N85-15704
Distance-inertial guidance of launch vehicle described
12 p1820 N85-21417
Gyrolaser guidance system for medium range missiles
16 p2696 N85-26649

INERTIAL MEASURING UNITS
U INERTIAL PLATFORMS

INERTIAL NAVIGATION
Errors of analog of inertial coordinate systems modeled in astronavigation system 07 p0951 N85-16028
A discussion of coning errors exhibited by inertial navigation systems
[RAE-TM-RAD-NAV-243] 08 p1082 N85-16854
Potential impact of Navstar GPS on NATO tactical operations 11 p1711 N85-20763
Avionics Flight Evaluation System (AFES)
13 p1967 N85-22357
Flight simulation for inertial navigation system
14 p2273 N85-24061
Decomposition in problem of correcting inertial navigation systems 14 p2287 N85-24172
Quaternion algorithms of 3-dimensional inertial navigational systems 14 p2287 N85-24173
Non-linear methods for inertial navigation system alignment
[BAE-BT-12683] 15 p2468 N85-25232
Assessment of a nonlinear method of INS alignment — inertial navigation systems (INS)
[BAE-BT-12684] 15 p2468 N85-25233
Implementation of an inertial navigation algorithm using a limited wordlength microprocessor for a strapdown navigation computer
[BAE-BT-12782] 15 p2468 N85-25234
Application of quaternions to problems of solid body dynamics in the atmosphere 15 p2481 N85-25313
Combinatorial performance/cost analysis of an autonomous navigation system for aircraft
16 p2695 N85-26640
Navigation: Accounting for copy
16 p2695 N85-26641
Low cost two gimbal inertial platform and its system integration 16 p2698 N85-26661
Observability in problem of correction of inertial navigation systems using additional information from artificial Earth satellite 16 p2719 N85-26765
A system for take-off and landing measurements (STALINS)
[B8500072] 17 p2895 N85-27849
Simulation of gyrocompassing alignment and calibration of strapdown inertial navigation system in a swaying vehicle
[DFVLR-MITT-84-20] 17 p2896 N85-27850
The AFTI/F16 terrain-aided navigation system
[DE85-006411] 18 p3060 N85-28935
Investigation of fast reaction SAW (Surface Acoustic Wave) accelerometer
[AD-A153576] 19 p3216 N85-29943
Inertial navigation system - LAS II for SGT YORK testing
[AD-A154204] 19 p3216 N85-29944
The DREO (Defence Research Establishment Ottawa) Inertial Navigation Laboratory: Development and test capabilities
[AD-A154425] 19 p3216 N85-29945
Simulations of strapdown-system errors and error compensation methods — transport aircraft navigation
[DFVLR-MITT-84-22] 20 p3392 N85-31040
Using regression analysis for determining air data sensor errors by means of an inertial navigation system
[ESA-TT-886] 20 p3392 N85-31041
Development of an active laser gyro for inertial rotation sensing in attitude/heading reference and inertial navigation systems, phase 1
[BMFT-FB-W-85-001] 20 p3480 N85-31489

INERTIAL PLATFORMS
Low cost two gimbal inertial platform and its system integration 16 p2698 N85-26661
The DREO (Defence Research Establishment Ottawa) Inertial Navigation Laboratory: Development and test capabilities
[AD-A154425] 19 p3216 N85-29945

INERTIAL REFERENCE SYSTEMS
Attitude measurements and determination
14 p2397 N85-24767
Reference systems — in space mechanics
14 p2399 N85-24784
Materialization of a reference system via a star catalog 14 p2399 N85-24787
Non-linear methods for inertial navigation system alignment
[BAE-BT-12683] 15 p2468 N85-25232
Assessment of a nonlinear method of INS alignment — inertial navigation systems (INS)
[BAE-BT-12684] 15 p2468 N85-25233
Relating the planetary ephemerides and the radio reference frame 16 p2770 N85-27095

INERTIAL UPPER STAGE
Preliminary analysis of selected gas dynamic problems — space shuttle main engine main combustion transients and IUS nozzle flow
[NASA-CR-171343] 10 p1483 N85-19361

INFARCTION
NT MYOCARDIAL INFARCTION

INFECTIONS
U INFECTIOUS DISEASES

INFECTIOUS DISEASES
NT INFLUENZA
The use of digital spaceborne SAR data for the delineation of surface features indicative of malaria vector breeding habitats 08 p1146 N85-17230
The effects of simulated weightlessness on susceptibility to viral and bacterial infections using a murine model
15 p2613 N85-26100
Differences in susceptibility of inbred mice to bacillus anthracis
[AD-A155648] 21 p3662 N85-32750
Legionnaires' disease bacteria in power plant cooling systems: Phase 2
[DE85-011546] 22 p3825 N85-33695
Molecular biology of environmental aromatic hydrocarbons
[DE85-015036] 24 p4128 N85-35583

INFERENCE
Lower level inference control in statistical database systems
[DE84-016005] 05 p0735 N85-14729
Ambiguity and uncertainty in probabilistic inference
[AD-A147378] 07 p1035 N85-16572
Research in stochastic processes
[AD-A148622] 08 p1216 N85-17660
Multivariate analysis and its applications
[AD-A150324] 13 p2151 N85-23352
The HORNE reasoning system, revision
[AD-A150983] 14 p2405 N85-24827
Inference and state estimation for stochastic point processes
[AD-A151216] 15 p2640 N85-26281
A complete inference system for regular processes with silent moves
[CWI-CS-R8420] 17 p3014 N85-28638
Alternative theories of inference in expert systems for image analysis
[AD-A153649] 18 p3170 N85-29646
Bayesian inference and diagnostics for the 3 parameter logistic model
[AD-A153640] 18 p3175 N85-29681
Manual and computer-aided sequential diagnostic inference
[AD-A156229] 24 p4133 N85-35620

INFESTATION
Irradiation of northwest agricultural products
[DE85-012455] 22 p3843 N85-33803

INFILTRATION
Fabrication of fiber-reinforced ceramic composites by chemical vapor infiltration
[DE85-003809] 11 p1611 N85-20132
Development of a new faster process for the fabrication of ceramic fiber-reinforced ceramic composites by chemical vapor infiltration
[DE85-007550] 16 p2756 N85-27007
Development of high temperature resistant noncorrodible silicon carbide components for gas turbine applications, follow-up report
[BMFT-FB-T-85-016] 17 p2936 N85-28126
Laboratory investigation of formation damage of an artificial fracture at simulated geothermal conditions
[DE85-010301] 18 p3102 N85-29201

INFINITY
Model theory for infinitely deep languages
[ISSN-0355-0087] 01 p0101 N85-10674
A note on the G-space version of Glicksberg's theorem
[CWI-PM-R8405] 08 p1217 N85-17665
Infinite dimensional linear systems with unbounded control and observation: A functional analytic approach
[AD-A153535] 18 p3169 N85-29639
On the convergence of an iterative formulation of the electromagnetic scattering from an infinite grating of thin wires 24 p4085 N85-35319

INFLATABLE DEVICES
U INFLATABLE STRUCTURES

INFLATABLE STRUCTURES
NT BALLOONS
NT HIGH ALTITUDE BALLOONS
NT JIMSPHERE BALLOONS
NT METEOROLOGICAL BALLOONS
NT MICROBALLOONS
NT SUPERPRESSURE BALLOONS
NT TETHERED BALLOONS
Research on large, highly accurate, inflatable reflectors
[AD-A145080] 01 p0016 N85-10099
Collapsable seal member
[DE84-014300] 01 p0055 N85-10367
Large spaceborne antenna reflectors using inflatable space rigidized structures 05 p0625 N85-14004
Tire inflation/deflation system
[AD-D011459] 10 p1493 N85-19426
Tire deflation mechanism
[AD-D011460] 10 p1493 N85-19427
Air bag restraint system
[AD-D011671] 19 p3215 N85-29936

INFLATING
The Reports of Aeromedical Laboratory, volume 25, no. 1/2
[ISSN-0023-2858] 01 p0090 N85-10605
Assessment of the inflating characteristics of the modified anti-G suit 01 p0090 N85-10609
A theoretical view on the stress analysis of fully inflated parachute canopies
[AD-A148387] 08 p1078 N85-16835
SU(N,1) inflation
[DE85-003952] 15 p2669 N85-26469

INFLECTION POINTS
Construction of solutions for two-dimensional Riemann problems
[DE85-003136] 10 p1549 N85-19770

INFLUENCE COEFFICIENT
Development and application of a unified balancing approach with multiple constraints
16 p2737 N85-26891

INFLUENZA
Advances in study of cold injury in Army
14 p2283 N85-24145
Using the information of cosmic rays to predict influence epidemic
[SH-10.1-2] 23 p4053 N85-35134

INFORMATION
A proposed integration among organizational information requirements, media richness and structural design
[AD-A149317] 10 p1567 N85-19681
Report on the Second Annual Review Meeting of the National Acid Precipitation Assessment Program. Research to assist decisionmaking: Summary
[DE85-003003] 12 p1884 N85-21820
Accomplishments of Institute of Cartography summarized 13 p2166 N85-23435
National Telecommunications and Information Administration authorization
[GPO-38-660] 16 p2879 N85-27766
Verbal information processing paradigms: A review of theory and methods
[AD-A153229] 17 p3050 N85-28880
Summary of archived Atlantic coast wave information study pressure, wind, wave, and water level data
[AD-A153782] 18 p3151 N85-29608

Hybrid uncertainty theory
[DE85-006357] 18 p3167 N85-29622
Fracture detection and characterization for geothermal reservoir definition
[DE85-006677] 22 p3815 N85-33630
Colour coding scales and computer graphics
23 p3963 N85-34568

INFORMATION ADAPTIVE SYSTEM
Alphabet-constrained data compression
[AD-A152887] 17 p3019 N85-28667

INFORMATION DISSEMINATION
NT MESSAGES
NT SELECTIVE DISSEMINATION OF INFORMATION
Nowcasting using lightning location techniques
01 p0084 N85-10568
Estuaries of the Cape. Part 2: Synopses of available information on individual systems. Report no. 16: Eerste (CSW 6)
[CSIR-RR-415-PT-2] 01 p0087 N85-10585
Sea-level in the world ocean. Part 6: The South Atlantic and South Pacific Oceans, a catalogue of measurements
[CSIR-T/SEA-8303-6] 01 p0087 N85-10590
Sea-level in the world ocean. Part 7: The Indian Ocean, a catalogue of measurements
[CSIR-T/SEA-8303-7] 01 p0087 N85-10591
Improving technical documents
[AD-B084855] 01 p0126 N85-10866
Depository librarians' views on GPO's administration of the depository library program. Report to the Chairman, Joint Committee on Printing
[PB84-212265] 01 p0126 N85-10867
Opportunities for commercial organizations
02 p0156 N85-11055
A system for the management of requests at an image data bank
[E85-10014] 02 p0216 N85-11427
Remote sensing applications program
[E85-10022] 02 p0218 N85-11435
Artificial Intelligence in Maintenance: Proceedings of the Joint Services Workshop
[AD-A145349] 02 p0244 N85-11592
Benefit value to the Air Force of the GIDEP (Government Industry Data Exchange Program) alert
[AD-A145470] 02 p0292 N85-11897
Collection overlap and coordinated collection development 02 p0293 N85-11902
AGARD Highlights
[AGARD-HIGHLIGHTS-84/2] 02 p0305 N85-11972
Catalogue of earthquakes for the territory of Czechoslovakia for the period 1957 - 1980
[REPT-555] 03 p0376 N85-12398
Factors affecting the archiving, processing and dissemination of ERS-1 altimeter data
03 p0381 N85-12435
NSSDC and WDC-A-R and S document availability and distribution services
[NASA-TM-87374] 03 p0438 N85-12787
Design of a scientific information collation and dissemination system, volumes 1 thru 3
[AD-A146002] 03 p0438 N85-12791
Scientific communications and national security
[GPO-38-093] 04 p0492 N85-13138
The 1984 ASEE-NASA summer faculty fellowship program (aeronautics and research)
[NASA-TM-87303] 04 p0575 N85-13664
FY 1984 scientific and technical reports, articles, papers and presentations
[NASA-TM-86470] 04 p0575 N85-13670
Economic value of consumer information: A selected, annotated bibliography
[PB84-235795] 04 p0576 N85-13673
Energy information exchange, 1983
[DE84-901446] 04 p0577 N85-13680
An electronic documentation system
[SNIAS-842-111-101] 04 p0577 N85-13683
The availability of Japanese scientific and technical information in the United States
[GPO-35-241] 05 p0735 N85-14726
Oceanographic data for development of the US exclusive economic zone
[PB85-106458/GAR] 07 p1010 N85-16415
Outlook for expanding the Federal research in progress system
[AD-A146354] 08 p1229 N85-17737
Safety awareness, pilot education, and incident reporting programs 09 p1276 N85-18020
The aviation safety reporting system
09 p1276 N85-18021
Community relations activities at Department of Defense sites
[AD-P004150] 09 p1349 N85-18486
GIDEP representative interaction
[DE84-016792] 09 p1401 N85-18620
The establishment and experience of the Carbon Dioxide Information Center (CDIC)
[DE85-001934] 09 p1402 N85-18625
Automation of information services furnished by documentation centers and specialized libraries
[FUB-6-1984] 09 p1402 N85-18627
French commentary on Soviet industrial espionage
10 p1461 N85-19210
Proceedings of the 17th Symposium on Electromagnetic Windows, part 1
[AD-A149185] 10 p1466 N85-19253
Commentary on start of scientific data transmissions with USSR 10 p1476 N85-19319
Computer center CDC libraries
[AD-A149005] 10 p1540 N85-19707
Provision of Federal government publication in electronic format to depository libraries
[S-PRT-98-260] 10 p1567 N85-19880
Keyword thesaurus: A list of terms and codes to identify areas of interest for research and other types of sponsored programs (revised October 1984)
[PB85-136893] 10 p1568 N85-19890
Air Force Office of Scientific Research (AFOSR) technical report summaries. Third quarter (CY)
[AD-A148965] 10 p1573 N85-19918
French research minister on policy, technology transfer 11 p1618 N85-20162
Information systems issues 11 p1701 N85-20693
Computer and communications security and privacy
[GPO-39-741] 12 p1911 N85-21994
Electronics Engineering Department EE Technical Review
[UCRL-50025-84-1] 13 p2063 N85-22887
Evaluating the appropriateness of microcomputers for litigation document management using the analytic hierarchy process 14 p2399 N85-24788
The Effect of Computers on the Generation and Use of Technical Data
[NBSIR-84-2907] 14 p2400 N85-24792
Progress through cooperation and exchange of ideas and experiences 15 p2626 N85-26186
Management communication and financial modeling
15 p2627 N85-26190
Energy Data Base: Subject thesaurus permutated listing. Revision 6, appendix
[DE84-016963] 15 p2666 N85-26454
Span graphics display utilities handbook, first edition
[NASA-TM-86500] 16 p2849 N85-27567
Scientific data bases on a VAX-11/780 running VMS
[DE85-007925] 16 p2878 N85-27760
Australian seismological report, 1980
[REPT-252] 17 p2989 N85-28473
Defense data network support concept analysis
[AD-A153214] 17 p3016 N85-28649
Origin, processing, and dissemination of scientific news, with examples from 20 research institutes
[JUEL-1940] 17 p3050 N85-28882
The POK project; studies of information handling problems with a new kind of communication device --- precoded signals
[FOA-A-53001-H2] 18 p3091 N85-29131
Combined catalog of ionosphere vertical soundings data
[PB85-166494] 18 p3138 N85-29430
INEL User Network Exchange, volume 1-85, Jan./Feb. 1985
[DE85-006108] 18 p3166 N85-29615
Noise for medical catalogers, 1984
[PB85-180206] 18 p3200 N85-29853
System enhancements of Mesoscale Analysis and Space Sensor (MASS) computer system
[NASA-CR-171463] 19 p3342 N85-30706
The application of artificial intelligence techniques to large distributed networks
[NASA-CR-177346] 19 p3344 N85-30721
TMI-2 technical information and examination program
[DE85-010614] 19 p3359 N85-30827
Human factors engineering contracts in Sweden: An overview
[FOA-C-56043-H2] 20 p3513 N85-31836
Data base management: MSTRAC (keynote paper), part 8 21 p3626 N85-32530
USSR Space Life Sciences Digest
[NASA-CR-3922] 21 p3656 N85-32709
Remote medical diagnosis 21 p3663 N85-32753
The Human Resource Management Information Network (HRMIN): A cost comparison in accordance with Office of Management and Budget (OMB) Circular no. A-76, 5 April 1979
[AD-A154583] 21 p3713 N85-33039
The flow of scientific and technical information in the US Army Research Laboratories
[AD-A155050] 21 p3713 N85-33043
USGS coastal research, studies and maps: A source of information for coastal decision making
[USGS-CIRC-883] 24 p4108 N85-35485

INFORMATION FLOW
Standards for commercially emerging technologies: A preliminary cost-benefit assessment for the Optical Digital data disk (ODD) technology for mass data storage applications
[PB84-223593] 01 p0101 N85-10869
Information requirements analysis: An application
[AD-A144896] 01 p0125 N85-10858
Information flow in event-driven large-scale systems
[DE84-014167] 05 p0735 N85-14728
Methodology investigation. Streamlined Test Reporting and Planning (STRAP): Data flow procedures
[AD-A146463] 06 p0871 N85-15831
Model of information-reference dialogue system for working with document abstracts
12 p1903 N85-21949
The availability of Japanese scientific and technical information in the United States
[GPO-39-478] 12 p1951 N85-22254
The application of artificial intelligence techniques to large distributed networks
[NASA-CR-177346] 19 p3344 N85-30721
The flow of scientific and technical information in the US Army Research Laboratories
[AD-A155050] 21 p3713 N85-33043
Assured information flow capping architecture
[AD-A155392] 22 p3756 N85-33293

INFORMATION MANAGEMENT
User requirements for very-short-range weather forecasts: Some key issues 01 p0084 N85-10562
Sea-level in the world ocean. Part 6: The South Atlantic and South Pacific Oceans, a catalogue of measurements
[CSIR-T/SEA-8303-6] 01 p0087 N85-10590
Sea-level in the world ocean. Part 7: The Indian Ocean, a catalogue of measurements
[CSIR-T/SEA-8303-7] 01 p0087 N85-10591
Information requirements analysis: An application
[AD-A144896] 01 p0125 N85-10858
Data dictionary systems and their role in information resource management
[AD-A144905] 01 p0125 N85-10859
Collection overlap and coordinated collection development 02 p0293 N85-11902
A management workstation concept
[AD-A145617] 02 p0294 N85-11906
Inclusion of audiovisual media in information services for the special subjects journalism and communication science (pilot study)
[BMFT-FB-ID-83-004] 02 p0294 N85-11909
Business planning for information services under special consideration of German management information systems
[BMFT-FB-ID-83-007] 02 p0294 N85-11910
A research program in computer technology
[AD-A145776] 03 p0402 N85-12585
Five-year plan for meeting the automatic data processing and telecommunications needs of the Federal Government. Volume 1: Planning strategies
[PB84-214501] 03 p0436 N85-12777
Five-year plan for meeting the automatic data processing and telecommunications needs of the Federal Government. Volume 2: Major information technology systems acquisition plans of Federal executive agencies, 1984-1989
[PB84-214519] 03 p0436 N85-12778
Interdisciplinary structure of information science
03 p0436 N85-12779
Information processing for better utilization: Assessing the CLER model as organizer for innovation diffusion and planned change information reported in selected studies in the ERIC system 03 p0437 N85-12780
An approach to interfacing data bases in WWMCCS ADP
[AD-A146350] 03 p0439 N85-12793
Corporate use of information regarding natural resources and environmental quality
[PB84-222736] 03 p0439 N85-12794
IRM (Information Resources Management) long-range plan: Fiscal year 1984-1988 (update). Volume 2: ADP and telecommunications acquisition plan
[PB84-229244] 03 p0439 N85-12796
The 1984 ASEE-NASA summer faculty fellowship program (aeronautics and research)
[NASA-TM-87303] 04 p0575 N85-13664
Economic value of consumer information: A selected, annotated bibliography
[PB84-235795] 04 p0576 N85-13673
Executive information system
[DE84-015355] 04 p0576 N85-13675
Energy information exchange, 1983
[DE84-901446] 04 p0577 N85-13680
Use of minicomputers for the formation of hydrological data banks 07 p1001 N85-16358
Document interchange format
[PB84-217033] 07 p1027 N85-16517

A study of the relationship between user attitudes and the success of the MAJCOM and AFRCE work information management system
[AD-A146868] 07 p1051 N85-16671
Organizations and information processing: A field study of research and development units within the United States Air Force Systems Command
[AD-A147361] 07 p1054 N85-16691
Data user's manual 08 p1150 N85-17254
The establishment and experience of the Carbon Dioxide Information Center (CDIC)
[DE85-001934] 09 p1402 N85-18825
The evolution from data processing to information resource management
[AD-A149429] 10 p1567 N85-19878
The conservation and utilization of scientific research documents: Practical aspects and organization
[NOTA-INTERNA-834] 14 p2433 N85-25008
White paper on new international satellite systems
[PB85-162501] 16 p2775 N85-27127
Information presentation in power plant control rooms
[VTT-S20] 16 p2864 N85-27668
Distributed systems management in wide area networks
[CMI-CS-R8419] 17 p3016 N85-29851
A hierarchy of knowledge levels implemented in a rule-based production system to calculate bounds on the size of intersections and unions of simple sets
[AD-A155291] 22 p3848 N85-33836
Research report program of the US Army in Europe 24 p4061 N85-35167
Electronic information management and productivity
[DE85-013962] 24 p4164 N85-35618
Records Disposal: A guidebook for laboratory offices
[AD-A156064] 24 p4165 N85-35823

INFORMATION RETRIEVAL

Compilation of data sources for existing chemicals
[GSF-A-2/84] 01 p0017 N85-10103
Intelligent information retrieval from on-line technical documentation
[AD-P003946] 02 p0249 N85-11626
Distributed hypothesis testing in distributed sensor networks
[AD-A145434] 02 p0294 N85-11905
Information processing for better utilization: Assessing the CLER model as organizer for innovation diffusion and planned change information reported in selected studies in the ERIC system 03 p0437 N85-12780
NASA Thesaurus supplement: A 3-part cumulative supplement to the 1982 edition of the NASA Thesaurus
[NASA-SP-7051(SUPPL-2)] 03 p0437 N85-12785
Research activities of the Illinois University Coordinated Science Laboratory
[AD-A145569] 03 p0449 N85-12856
FY 1984 scientific and technical reports, articles, papers and presentations
[NASA-TM-86470] 04 p0575 N85-13670
Automated Library Search System (ALSS) user's manual
[DE84-015952] 04 p0576 N85-13672
Some attributes of online search intermediaries that relate to search outcome 05 p0734 N85-14721
Role of DESIGNMANAGER in information engineering
[DE84-016867] 05 p0736 N85-14730
Setting time standards at NISTARS (Naval Integrated Storage and Retrieval System)
[AD-A146371] 06 p0870 N85-15529
Distributed knowledge base systems for diagnosis and information retrieval
[AD-A146890] 07 p1054 N85-16690
Commerce Lab: Mission analysis. Payload integration study
[NASA-CR-171285] 08 p1104 N85-16982
Benchmarking database systems in multiple backend configurations
[AD-A148191] 08 p1202 N85-17568
Performance evaluation of a database system in multiple backend configurations
[AD-A148192] 08 p1229 N85-17743
Boring information and subsurface data base package user's guide
[AD-A148823] 08 p1230 N85-17747
Analytical modeling of a polling protocol --- airline information network
[ENST-84H001] 09 p1277 N85-18029
GIDEP representative interaction
[DE84-016782] 09 p1401 N85-18820
Methodology for evaluating related databases and a computerized algorithm for merging their output 09 p1401 N85-18821
Online database search strategies and thesaural relationship models 09 p1402 N85-18822
The establishment and experience of the Carbon Dioxide Information Center (CDIC)
[DE85-001934] 09 p1402 N85-18825
Automation of information services furnished by documentation centers and specialized libraries
[FUB-6-1984] 09 p1402 N85-18827
Retrieval procedures for hydrologic data from ARS (Agricultural Research Service) experimental watersheds in the US (REPHLEX)
[PB85-111326/GAR] 09 p1402 N85-18828
Guide to human factors information sources
[AD-A149102] 10 p1531 N85-19649
The integrated library system design concepts for a complete serials control subsystem
[AD-A149379] 10 p1568 N85-19884
Post-processing of bibliographic citations from DOE/Recon, NASA/Recon, and DOD/DROLS
[DE85-000617] 11 p1739 N85-20938
AID: Access to Informal Documentation
[DE85-000418] 11 p1740 N85-20939
Requirements formulation subtask 1.A of the Major Item System Mapping (MISM) project
[DE85-000978] 11 p1740 N85-20940
Model of information-reference dialogue system for working with document abstracts 12 p1903 N85-21949
The EEC's information technology program: An update
[AD-A150022] 12 p1951 N85-22258
Evaluation of the vocabulary switching systems
[PB85-127157] 12 p1951 N85-22260
Precedency control and other semantic integrity issues in a workbench database 13 p2123 N85-23220
General design considerations of an Air Force information system
[AD-A150611] 13 p2168 N85-23449
MMCIAC (Metal Matrix Composites Information Analysis Center)
[AD-A150654] 14 p2248 N85-23933
Invariant system of technological preparation of production 14 p2268 N85-24056
Research needs for artificial intelligence applications in support of C3 (Command, Control, and Communication)
[AD-A150867] 14 p2292 N85-24210
Evaluating the appropriateness of microcomputers for litigation document management using the analytic hierarchy process 14 p2399 N85-24788
NASA Thesaurus supplement, a three part cumulative supplement to the 1982 edition of the NASA Thesaurus
[NASA-SP-7051(SUPPL-3)] 14 p2432 N85-25002
The retrieval expert model of information retrieval 14 p2433 N85-25003
Schema theory in the representation and analysis of text 14 p2433 N85-25004
The conservation and utilization of scientific research documents: Practical aspects and organization
[NOTA-INTERNA-834] 14 p2433 N85-25008
Document retrieval from a relational database management system: An investigation of multiple-line query formulation using SEQUEL 15 p2665 N85-26447
A database design for the Brazilian Air Force Flying Unit Operational Control System
[AD-A151648] 15 p2666 N85-26452
Forward library searching of previously-quantitated peaks, using a scan list created from a quantitation list by a novel FORTRAN program for the INCOS data system
[PB85-165835] 16 p2845 N85-27541
Retrieval performance in a full text journal article database 16 p2877 N85-27747
Access path optimization for network database retrieval 16 p2877 N85-27749
Design of an interface to an information retrieval network 16 p2877 N85-27750
Organization of scientific, technical information services 17 p3049 N85-28873
Energy data base: Subject categories and scope
[DE84-017376] 17 p3050 N85-28881
Avionics Data Base users manual
[AD-A153810] 18 p3062 N85-28942
Information science in toxicology
[DE85-007746] 18 p3200 N85-29851
National Archives and Records Service (NARS) twenty year preservation plan
[PB85-177640] 18 p3200 N85-29854
CSIN (Chemical Substances Information Network) workbook: US Geological Survey training course for Chemical Substances Information Network
[PB85-170058] 18 p3200 N85-29855
Using MATHLIB on the IBM computer and sundry plotting examples with a taste of IMSL
[DE85-011395] 19 p3340 N85-30695
SAFEORD: Safety of explosive ordnance databank
[AD-A154058] 19 p3380 N85-30972
Modified dynamic hashing
[DE85-011166] 19 p3381 N85-30974
Individual differences in online search behavior: The effect of learning styles and cognitive abilities on process and outcome 20 p3541 N85-32037
Technology transfer system automation implementation
[PB85-177335] 22 p3849 N85-33838
User's operating procedures. Volume 3: Projects directorate information programs
[NASA-CR-177950] 23 p3956 N85-34520
NAPGEN: Automatic NAPLPS page generator 23 p3964 N85-34575
LOCAT: A data retrieval program
[AD-A156004] 24 p4165 N85-35822
Source header list, supplement 3
[AD-A156100] 24 p4165 N85-35824
Source hierarchy list. Volume 1: A through H
[AD-A156300] 24 p4165 N85-35825
Source hierarchy list. Volume 2: I through Z
[AD-A156301] 24 p4165 N85-35826

INFORMATION SYSTEMS

NT ATMOSPHERIC & OCEANOGRAPHIC INFORM SYS
NT GEOGRAPHIC INFORMATION SYSTEMS
NT INFORMATION ADAPTIVE SYSTEM
NT MANAGEMENT INFORMATION SYSTEMS

Analysis of computer and communication information processing and system development
[AD-A144986] 01 p0100 N85-10660
A technique to model and design physical database systems
[DE84-015337] 01 p0126 N85-10863
A system for the management of requests at an image data bank
[E85-10014] 02 p0216 N85-11427
Yearly report for programming productivity enhancement by the use of application generators
[AD-A145623] 02 p0242 N85-11579
Implications of artificial intelligence for a user defined technical information system
[AD-P003938] 02 p0248 N85-11618
The application of artificial intelligence to a maintenance and diagnostic information system
[AD-P003945] 02 p0249 N85-11625
Memory-based expert systems
[AD-A145612] 02 p0249 N85-11628
Auditory information systems in military aircraft: Current configurations versus the state of the art
[AD-A145469] 02 p0275 N85-11794
An operational system for subject switching between controlled vocabularies: A computational linguistics approach
[NASA-CR-3838] 02 p0293 N85-11903
Distributed hypothesis testing in distributed sensor networks
[AD-A145434] 02 p0294 N85-11905
Use of prototyping for man-machine interface requirements definition on the AWDS (Automated Weather Distribution System) program
[AD-A146033] 03 p0396 N85-12526
Five-year plan for meeting the automatic data processing and telecommunications needs of the Federal Government. Volume 1: Planning strategies
[PB84-214501] 03 p0436 N85-12777
Five-year plan for meeting the automatic data processing and telecommunications needs of the Federal Government. Volume 2: Major information technology systems acquisition plans of Federal executive agencies, 1984-1989
[PB84-214519] 03 p0436 N85-12778
Information processing for better utilization: Assessing the CLER model as organizer for innovation diffusion and planned change information reported in selected studies in the ERIC system 03 p0437 N85-12780
Preserving the time dimension in information systems 03 p0437 N85-12784
Design of a scientific information collation and dissemination system, volumes 1 thru 3
[AD-A146002] 03 p0436 N85-12791
IRM (Information Resources Management) long-range plan: Fiscal year 1984-1988 (update). Volume 2: ADP and telecommunications acquisition plan
[PB84-229244] 03 p0439 N85-12796
Evaluation of the National Library of Medicine's programs in the medical behavior sciences. Coverage of the Medical Behavioral Sciences (MBS) literature in monographic databases, study 5
[PB84-230531] 03 p0439 N85-12797
Evaluation of the National Library of Medicine's programs in the medical behavior sciences. Online searchers' reactions to database and vendor capabilities in the Medical Behavioral Sciences (MBS), study 4
[PB84-230523] 03 p0439 N85-12798

Evaluation of the National Library of Medicine's programs in the medical behavior sciences. Quality of indexing: The development and testing of a methodology comparing databases covering the Medical Behavioral Sciences (MBS) literature, study 3
[PB84-230515] 03 p0439 N85-12799
Evaluation of the National Library of Medicine's programs in the medical behavior sciences. Test retrievals in five major databases covering the Medical Behavioral Sciences (MBS) literature, study 2
[PB84-230507] 03 p0440 N85-12800
Evaluation of the National Library of Medicine's programs in the medical behavior sciences. Coverage, overlaps and gaps in bibliographic databases dealing with the Medical Behavioral Sciences (MBS) literature, study 1
[PB84-230499] 03 p0440 N85-12801
Evaluation of the National Library of Medicine's program in the medical behavior sciences. An analysis of the National Library of Medicine's (NLM) handling of Medical Behavioral Sciences (MBS) literatures: Some research tests of methods for evaluating bibliographic databases, executive summary
[PB84-230481] 03 p0440 N85-12802
Competitive assessment of the US information services industry
[PB84-174804] 03 p0440 N85-12803
Research activities of the Illinois University Coordinated Science Laboratory
[AD-A145569] 03 p0449 N85-12856
Human reliability data bank: Feasibility study
[DE84-015215] 04 p0546 N85-13476
INFORM system 2-year plan, FY 1984-1985
[DE84-016044] 04 p0576 N85-13674
International information networks for material properties
[DE84-013836] 04 p0576 N85-13676
Archiving and exchange of a computerized marine seismic database: The ROSE data archive system
[DE84-901453] 04 p0576 N85-13677
Nuclear criticality information system: Database examples
[DE84-014462] 04 p0576 N85-13678
Activities report in technology
[ISBN-951-39-1998-1] 04 p0577 N85-13681
Information flow in event-driven large-scale systems
[DE84-014167] 05 p0735 N85-14728
Recommended documentation for computer users at ANL
[DE84-016285] 06 p0855 N85-15434
Toward an improved FIPS cost-benefit methodology. Phase 2: Descriptive models, general purpose application software development and maintenance
[PB84-226943] 06 p0870 N85-15527
UK, FRG, France: R and D in sensors, related fields
08 p1142 N85-17197
EDP computer tapes described
08 p1142 N85-17203
DDN directory
[AD-A148213] 08 p1230 N85-17744
Analytical modeling of a polling protocol — airline information network
[ENST-84H001] 09 p1277 N85-18029
Integrating heterogeneous non-geometric information systems using RIM
[DE84-017600] 09 p1402 N85-18823
Online directory of databases for material properties
[DE84-016511] 09 p1402 N85-18824
Retrieval procedures for hydrologic data from ARS (Agricultural Research Service) experimental watersheds in the US (REPHLEX)
[PB85-111326/GAR] 09 p1402 N85-18826
Concepts and tools for the software life cycle
10 p1464 N85-19236
Guide to human factors information sources
[AD-A149102] 10 p1531 N85-19649
The multiple resources model of human performance: Implications for display design 10 p1534 N85-19669
Management challenges encountered in CAD implementation
10 p1541 N85-19716
Predicting the performance of distributed knowledge-based systems: A modeling approach
[AD-A149021] 10 p1545 N85-19738
Structure and application of extremely large geophysical data bases
[DE85-003527] 10 p1568 N85-19888
Research needs on the interaction between information systems and their users: Report of a workshop
[PB85-121523] 10 p1568 N85-19891
Air Force Office of Scientific Research (AFOSR) technical report summaries. Third quarter (CY)
[AD-A148865] 10 p1573 N85-19918
Information systems issues 11 p1701 N85-20693
Requirements formulation subtask 1.A of the Major Item System Mapping (MISM) project
[DE85-000978] 11 p1740 N85-20940
Sourcebook: Gaining access to US government information on the environment and natural resources
[DE84-017419] 11 p1740 N85-20941
Model of information-reference dialogue system for working with document abstracts
12 p1903 N85-21949
The EEC's information technology program: An update
[AD-A150022] 12 p1951 N85-22258
Performance evaluation of distributed systems with unbalanced flows: An analysis of the INFOPLEX data storage hierarchy
[AD-A150528] 13 p2147 N85-23328
Intel IDIS evaluation
[DE85-003748] 13 p2168 N85-23451
MMCIAC (Metal Matrix Composites Information Analysis Center)
[AD-A150654] 14 p2248 N85-23933
An introduction to USAFETAC (USAF Environmental Technical Applications Center)
[AD-A150971] 14 p2378 N85-24682
Selection criteria and computer aided design (CAD) systems
[NLR-MP-84037-U] 14 p2406 N85-24834
Air Force Office of Scientific Research (AFOSR): Technical report summaries. Fourth quarter (CY)
[AD-A150860] 14 p2456 N85-25167
Computerized biophysical data acquisition system for motion sickness studies
[AD-A151691] 15 p2618 N85-26131
Procedures for use in compiling requirements specifications for computerized library systems
[CSTI-76] 15 p2665 N85-26448
Energy Data Base: Subject thesaurus permutated listing. Revision 6, appendix
[DE84-016963] 15 p2666 N85-26454
Information technology applications in voluntary sector transport operations. SP1: Objectives and programme of work
[TT-8501] 15 p2667 N85-26457
Historical perspectives on information transmission engineering 16 p2759 N85-27023
Diagnostic system
[INPE-3350-PRE/659] 16 p2841 N85-27519
Internation information networks for material properties: Revision 1
[DE85-007412] 16 p2850 N85-27572
Compilation of abstracts of theses submitted by candidates for degrees
[AD-A151722] 16 p2875 N85-27739
DoD manual for standard data elements, part 2
[AD-A152202] 16 p2878 N85-27755
DoD manual for standard data elements, part 3
[AD-A152203] 16 p2878 N85-27756
DoD manual for standard data elements, part 4
[AD-A152204] 16 p2878 N85-27757
DoD manual for standard data elements, part 5
[AD-A152205] 16 p2878 N85-27758
Energy data base: Subject thesaurus
[DE84-010568] 16 p2878 N85-27761
The interactive generation of specifications for an onboard software series (GISELE)
17 p2904 N85-27906
US Naval Observatory collection and utilization of time comparison data 17 p2962 N85-28292
Centralized Storm Information System (CSIS)
[NASA-CR-175898] 17 p2994 N85-28506
A report from the Space Science and Engineering Center, the University of Wisconsin-Madison, Madison, Wisconsin 17 p2994 N85-28507
Test and evaluation plan for the Centralized Storm Information System 17 p2994 N85-28508
Efforts at office automation and information systems utilization at Martin Marietta Energy Systems, Incorporated
[DE85-008154] 17 p3013 N85-28633
USSR report: Science and technology policy
[JPRS-UST-85-008] 17 p3049 N85-28872
Organization of scientific, technical information services 17 p3049 N85-28873
The development of information systems at NLR
[B8580079] 17 p3051 N85-28884
Avionics Data Base users manual
[AD-A153810] 18 p3062 N85-28942
Data base of all known, published data on trace elements in oil shale and its products
[DE85-003399] 18 p3126 N85-29357
Ada (trademark) compiler validation summary report. Honeywell information systems GCOS6 Ada version 1.1
[AD-A153748] 18 p3162 N85-29590
Information science in toxicology
[DE85-007746] 18 p3200 N85-29851
Local automation model software benchmarking: Test plan
[AD-A154349] 19 p3337 N85-30676
The international scope of data evaluation
[DE85-005953] 19 p3349 N85-30760
SAFEORD: Safety of explosive ordnance databank
[AD-A154058] 19 p3360 N85-30872
Evaluative report on the Institute for Computer Sciences and Technology, National Bureau of Standards, fiscal year 1984
[PB85-176097] 20 p3514 N85-31848
Activities report of the Laboratory for Computer Science (FOA 32)
[FOA-C-30384-E1] 20 p3516 N85-31861
Individual differences in online search behavior: The effect of learning styles and cognitive abilities on process and outcome 20 p3541 N85-32037
Navy information systems: Planning, policy, organization, and management
[PB85-176113] 20 p3541 N85-32038
Design guidelines for user-system interface software
[AD-A154907] 21 p3671 N85-32807
The flow of scientific and technical information in the US Army Research Laboratories
[AD-A155060] 21 p3713 N85-33043
Fuel cell applications literature review
[DE85-011891] 22 p3809 N85-33592
User's operating procedures. Volume 1: Scout project information programs
[NASA-CR-177948] 23 p3958 N85-34518
User's operating procedures. Volume 1: Scout project financial analysis program
[NASA-CR-177949] 23 p3958 N85-34519
Applied computer graphics in a geographic information system: Problems and successes
23 p3962 N85-34563
Procedure for editing the fluxgate magnetometer data of the AFGL (Air Force Geophysics Laboratory) magnetometer network
[AD-A156331] 24 p4117 N85-35523
Electronic information management and productivity
[DE85-013362] 24 p4164 N85-35818

INFORMATION THEORY

Approximating hierarchical normal priors using a vague component
[CSIR-TWISK-284] 01 p0107 N85-10720
The inferring of preferences from indifferences in multicriteria decision analysis
[CSIR-TWISK-306] 01 p0108 N85-10729
Optimizing search with positive information feedback
[CSIR-TWISK-313] 01 p0125 N85-10855
A mathematical theory of command and control structures
[AD-A145608] 02 p0256 N85-11875
Distributed hypothesis testing in distributed sensor networks
[AD-A145434] 02 p0294 N85-11905
On update semantics and relational views
[AD-A145622] 02 p0294 N85-11907
Spread-spectrum communications
[AD-A146135] 03 p0355 N85-12285
East Europe report: Science and technology
[JPRS-ESA-84-041] 04 p0484 N85-13090
Theory of information, automation in Czechoslovakia
04 p0485 N85-13091
Equivocation limits in Gaussian additive channels
[INPE-2828-PRE/360] 04 p0492 N85-13137
Process algebra for communication and mutual exclusion
[CWI-CS-R8409] 05 p0720 N85-14622
Lower level inference control in statistical database systems
[DE84-016005] 05 p0735 N85-14729
Information-theoretic properties of languages and their grammars
[AD-A146688] 06 p0799 N85-15106
Study of spectral/radiometric characteristics of the Thematic Mapper for land use applications
[E85-10057] 07 p0967 N85-16288
Rule-based evidence accrual system for image understanding
[AD-A147835] 07 p1044 N85-16834
On the complexity of distributed decision problems
[AD-A147174] 07 p1052 N85-16874
Hardware/software codesign for maintainable systems
08 p1086 N85-18753
Data stimulated on-line-checking (IROLD)
08 p1086 N85-18754
Symbol structure, information content and visual form: A carto-semiotic theory of map signs
09 p1342 N85-18439
Smoothing with split linear fits
[AD-A149032] 10 p1545 N85-19740
Relative-entropy minimization with uncertain constraints--theory and application to spectrum analysis
[AD-A149192] 10 p1546 N85-19752

The use of analytical models to interpret data properly
[ERS-E.341] 11 p1651 N85-20399
Investigation of influence of communications link and synchronization error on noise tolerance of group transmission of binary information based on orthogonal Walsh function 13 p2086 N85-23026
A preliminary comparison of the information content of data from the LANDSAT 4 Thematic Mapper and Multispectral Scanner — Arkansas 13 p2119 N85-23199
A perspective on multiaccess channels
[AD-A150183] 13 p2146 N85-23322
Information information networks for material properties: Revision 1
[DE85-007412] 16 p2850 N85-27572
Future information technology, 1984: Telecommunications
[NBS/SP-500/119] 16 p2878 N85-27762
Chemical applications of topology and group theory. 17: An information theoretical approach to polyhedral symmetry
[AD-A152821] 17 p2919 N85-27995
A software simulation study of a (255,223) Reed-Solomon encoder-decoder
[NASA-CR-175872] 17 p2947 N85-28192
Distributed memory
[AD-A153364] 17 p3001 N85-28554
Language design, computers and brains
[AD-A152819] 17 p3008 N85-28594
Counting is easy — Turing machines
[CWI-CS-R8423] 17 p3009 N85-28608
The role of duality in optimization problems involving entropy functionals, with applications to information theory
[AD-A152336] 17 p3026 N85-28713
An information theoretical method for automatic noise elimination in digital image processing 18 p3124 N85-29345
Evaluation of curve-smoothing techniques
[HSE-TRANS-11106] 19 p3349 N85-30759

INFORMATION TRANSFER
Architecture for a demonstration radar-communication link
[AD-A147635] 08 p1150 N85-17260
The Hazardous Materials Technical Center
[AD-P004149] 09 p1349 N85-18485
Graphics translators for computer-aided drafting and design: Interface alternatives for the A/E community
[AD-A148892] 10 p1540 N85-19706
Oral discussion, group-to-individual transfer and achievement in cooperative learning groups
[AD-A153209] 17 p3001 N85-28552
Study of raster metafile formats
[AD-A153322] 17 p3012 N85-28624
Interfacing the VAX 11/780 using berkeley UNIX 4.2BSD and Ethernet based Xerox Network Systems
[AD-A153174] 17 p3016 N85-28647
Myoelectric control of a computer based expert system for flight control
[AD-A154981] 21 p3557 N85-32126
Tight bounds on the complexity of parallel sorting
[AD-A154726] 21 p3667 N85-32778
The flow of scientific and technical information in the US Army Research Laboratories
[AD-A155050] 21 p3713 N85-33043

INFORMATION TRANSMISSION
U DATA TRANSMISSION

INFRARED ABSORPTION
Study of combustion and flame processes initiated by laser-induced multiple-photon absorption
[DE84-017095] 04 p0471 N85-12996
Development of acceptance criteria for batches of silane primer for external tank thermal protection system bonding applications
[NASA-CR-171266] 04 p0478 N85-13043
An analysis of the data obtained by a simultaneous observation of GMS and GMS-2: A study of the difference between the brightness temperatures by GMS and those by GMS-2 12 p1894 N85-21688
VISSR infrared calibration by means of calculated radiances 12 p1894 N85-21689
Infrared aerosol absorption index 13 p2110 N85-23147
A brief comparison of Egyptian with West German atmospheric transmission data in the 8 to 11.5 micron waveband
[BAE-BT-12829] 15 p2594 N85-25983
Infrared absorption of oxygen complexes in electron-irradiated silicon
[FOA-C-30379-E1,E2,E3,E4] 20 p3538 N85-32015

INFRARED ASTRONOMY
Infrared thermal radiation of Venus 02 p0163 N85-11101
Near Infrared Imaging of Uranus and Neptune 02 p0299 N85-11934
Documentation for the machine-readable version of The Revised AFGL Infrared Sky Survey Catalog (Price and Murdock 1983)
[NASA-TM-87377] 03 p0405 N85-12588
IRAS observations of galactic star formation 03 p0442 N85-12813
IRAS observations of external galaxies 03 p0443 N85-12825
Far-infrared line emission from the galaxy
[NASA-CR-174166] 04 p0580 N85-13702
SIRTF: The next step
[NASA-TM-86663] 07 p1059 N85-16724
Airborne Astronomy Symposium. A symposium commemorating the tenth anniversary of operations of the Kuiper Airborne Observatory
[NASA-CP-2353] 08 p1244 N85-17848
The Lear Jet Observatory: Fifteen years of discovery and rebirth 08 p1244 N85-17850
Exploration of the solar system by airborne astronomy 08 p1244 N85-17851
Extreme limb profiles of the Sun at far infrared and submillimeter wavelengths 08 p1244 N85-17852
Airborne observations of comets 08 p1244 N85-17853
Measurements of H2O in Jupiter's atmosphere from 5 microns airborne observations 08 p1244 N85-17854
The 1.5 - 3.5 micron spectroscopy of the Orion H2 source 08 p1245 N85-17864
Far-infrared photometry of low-mass pre-main-sequence stars with broad CO wings 08 p1245 N85-17866
Star formation in globules 08 p1247 N85-17868
Far infrared continuum emission from the galactic center 08 p1248 N85-17876
The 157 micron (C II) luminosity of the galaxy 08 p1248 N85-17877
Variation of oxygen and nitrogen abundances in the galaxy 08 p1248 N85-17878
Far IR observations of the Magellanic clouds 08 p1248 N85-17879
Dust reradiation from NGC 6946 08 p1248 N85-17880
Far infrared spectroscopy of (O III) in M82 08 p1249 N85-17883
Infrared astronomical satellite (IRAS) catalogs and atlases. Explanatory supplement
[NASA-CR-174311] 09 p1411 N85-18898
Infrared astronomical satellite (IRAS) catalogs and atlases: Introduction 09 p1412 N85-18899
The IRAS mission 09 p1412 N85-18901
Sky coverage, confusion, completeness and reliability 09 p1412 N85-18906
BIG MAC: A bolometer array for mid-infrared astronomy, Center Director's Discretionary Fund
[NASA-TM-86502] 13 p2170 N85-23483
Current ideas on the nature of comets 14 p2435 N85-25017
IRAS observations of active galaxies
[NASA-CR-175720] 15 p2668 N85-26463
The infrared astronomical satellite 15 p2668 N85-26464
A new luminosity component in 3C48
[NASA-CR-175840] 17 p3052 N85-28694
Balloon-borne, He-cooled Fourier transform spectrometer for far infrared astronomy
[MPE-IR-41] 17 p3063 N85-28899
The 8.3 and 12.4 micron imaging of the Galactic Center source complex with the Goddard infrared array camera
[NASA-TM-86225] 19 p3362 N85-30982
Activities report of the Aeronomy Department
[G-774-1984] 21 p3833 N85-32569
Evaluation study of mechanical refrigeration systems for application to space missions — infrared astronomy
[SNIAS-1029ACA/LL/V] 22 p3755 N85-33277
Mosaic Infrared Sensor for Space Astronomy (MIRSSA)
[NASA-CR-176154] 22 p3786 N85-33456

INFRARED ASTRONOMY SATELLITE
In-orbit experiments on IRAS for application to the ISO satellite
[FOK-TR-R-84-057] 03 p0322 N85-12078
IRAS observations of galactic star formation 03 p0442 N85-12813
IRAS observations of external galaxies 03 p0443 N85-12825
High sensitivity, high angular resolution far-infrared photometry from the KAO 08 p1246 N85-17867
Infrared astronomical satellite (IRAS) catalogs and atlases. Explanatory supplement
[NASA-CR-174311] 09 p1411 N85-18898
Infrared astronomical satellite (IRAS) catalogs and atlases: Introduction 09 p1412 N85-18899
Satellite description 09 p1412 N85-18900
The IRAS mission 09 p1412 N85-18901
In-flight tests 09 p1412 N85-18902
Data reduction 09 p1412 N85-18903
Flux reconstruction and calibration 09 p1412 N85-18904
Analysis of processing 09 p1412 N85-18905
The low-resolution spectra 09 p1413 N85-18907
The formats of the IRAS catalogs and atlases 09 p1413 N85-18908
Dynamics of long-period comets 13 p2176 N85-23506
The infrared astronomical satellite 15 p2668 N85-26464
IRAS: Space technology from the Netherlands
[B8561841] 17 p2908 N85-27929
The IRAS end-to-end data system
[NLR-MP-83058-U] 17 p3051 N85-28683
The attitude control model tests for the Infrared Astronomical Satellite (IRAS)
[B8580071] 18 p3067 N85-28967
The 1986 National Aeronautics and Space Administration authorization
[GPO-47-635] 24 p4166 N85-35829

INFRARED DETECTORS
NT FLIR DETECTORS
Moving object detection system using infrared scanning
[AD-D011222] 01 p0120 N85-10822
Developments in far-infrared detection techniques
[AD-A146290] 03 p0420 N85-12683
Preliminary study for an IR-vidicon for the 8 to 14 micron range, phase 1
[BMFT-FB-W-84-025] 05 p0633 N85-14057
InAsSb strained-layer superlattices (SLSs) for long wavelength detector applications
[DE84-016111] 05 p0732 N85-14706
Data handling for the Spectral Radiometer (SPERAD)
[FOA-C-30368-E1,E4] 07 p0968 N85-16145
Electro-optical target detection
[AD-D011386] 07 p1042 N85-16617
Buried junction enhanced Schottky barrier device
[AD-D011399] 07 p1044 N85-16635
Study in spurious sensitivity of electronics in space
[AD-A148386] 08 p1158 N85-17305
In-flight tests 09 p1412 N85-18902
Elimination of sensor artifacts from infrared data
[AD-A149048] 10 p1556 N85-19814
Liquid-phase epitaxial growth of CdTe on HgCdTe
[AD-D011482] 10 p1561 N85-19846
Quaternary narrow-band semiconductors (HgTe)x (InSb)1-x for far-infrared detectors
[AD-A149350] 10 p1562 N85-19852
Aerostructure nondestructive evaluation by thermal field detection. Phase 2: Technique refinement and quantitative determination of flaw detection capabilities
[AD-A149622] 12 p1777 N85-21155
Monolithic short wave infrared (SWIR) detector array
[NASA-CR-175284] 12 p1874 N85-21759
Performance estimate of a reflecting light pipe for infrared detectors
[AD-A141269] 13 p2158 N85-23398
BIG MAC: A bolometer array for mid-infrared astronomy, Center Director's Discretionary Fund
[NASA-TM-86502] 13 p2170 N85-23483
Performance of charge-injection-device infrared detector arrays at low and moderate backgrounds
[NASA-TM-86667] 15 p2580 N85-25793
Low-resolution target classification from a staring infrared sensor
[AD-A151690] 15 p2652 N85-26358
Simulation of solidification in a Bridgman cell
[NASA-CR-175838] 16 p2870 N85-27705
Analysis and modeling for thermal focal plane arrays
[AD-A153156] 17 p2968 N85-28329
The 8.3 and 12.4 micron imaging of the Galactic Center source complex with the Goddard Infrared array camera
[NASA-TM-86225] 19 p3362 N85-30982
Background equatorial astronomical measurements focal plane assembly (refurbished HI STAR SOUTH)
[AD-A155215] 21 p3590 N85-32313
Absorption and scattering properties of aerosols of aggregated particles in the infrared spectral region
[AD-A155475] 21 p3637 N85-32591
Bayesian vs MAP multiple model adaptive estimation for field of view expansion in tracking airborne targets
[AD-A155468] 21 p3679 N85-32855
Enhancing precision of remote temperature sensing data from satellites under cloudy atmospheric conditions 22 p3734 N85-33148
Determination of altitude of cloud cover top from Meteor satellite data 22 p3734 N85-33150
Mosaic Infrared Sensor for Space Astronomy (MIRSSA)
[NASA-CR-176154] 22 p3786 N85-33456

INFRARED HORIZON SCANNERS
U HORIZON SCANNERS
U INFRARED SCANNERS

INFRARED IMAGERY
Near infrared imaging of Uranus and Neptune
02 p0299 N85-11934
Image texture study for the operational meteorological satellites NOAA 6 and NOAA 7 and its variation with time. Application to the Beauce region
[ENST-84E009] 05 p0661 N85-14249
An integrated remote sensing approach for identifying ecological range sites — parker mountain
[E85-10050] 07 p0983 N85-16246
Rule-based evidence accrual system for image understanding
[AD-A147835] 07 p1044 N85-16834
The interpretation of SIR-B imagery of surface waves and other oceanographic features using in-situ, meteorological satellite, and infrared satellite data
08 p1143 N85-17212
Evaluation of the radar response to land surfaces and volumes: Examination of theoretical models, target statistics, and applications 08 p1149 N85-17250
Scanning photoacoustic microscopy of aluminum with aluminum oxide, roughness standards and rubber
[AD-A149460] 10 p1441 N85-19081
Civil weather satellite systems
11 p1711 N85-20768
Meteorological and oceanographic support during the Falklands conflict 11 p1712 N85-20769
LANDSAT 4 band 6 data evaluation
[E85-10093] 12 p1874 N85-21755
On the error of typhoon intensity estimation by means of IR Dvorak technique occurring when the eye is very small 12 p1894 N85-21886
A supplement study on the subsynoptic cloud system off the south coast of Japan 12 p1895 N85-21892
Proposed use of system ARGOS with data buoys for calibration of thermal infrared imagery of North British waters for sea surface temperature maps
14 p2240 N85-23689
Hurricane structure and dynamics from stereoscopic and infrared satellite observations and radar data
15 p2594 N85-25988
INPE's line imaging camera: Preliminary results
[INPE-3476-PRE/719] 16 p2767 N85-27194
Technique that uses satellite, radar, and conventional data for analyzing and short-range forecasting of precipitation from extratropical cyclones
[PB85-164994] 16 p2837 N85-27499
Target discrimination using infrared techniques: Theoretical considerations
[AD-A154070] 19 p3350 N85-30782
The 8.3 and 12.4 micron imaging of the Galactic Center source complex with the Goddard infrared array camera
[NASA-TM-86225] 19 p3362 N85-30982
Influence of spatial variability of hydraulic characteristics of soils on surface parameters obtained from remote sensing data in infrared and microwaves
[NASA-TM-77902] 20 p3477 N85-31604
Object identification and manipulation using silhouette moments
[AD-A154755] 21 p3705 N85-33011
Quantizer of images of heat fields obtained by Rubin-type infra-red imagers 22 p3771 N85-33369
Surface cyclogenesis as indicated by satellite imagery
[PB85-191815] 24 p4124 N85-35566
Far-infrared observations of young clusters embedded in the R Coronae Australnae and RHO Ophiuchi dark clouds
[NASA-TM-86681] 24 p4167 N85-35834
INFRARED INSPECTION
Pulsed photothermal radiometry for remote sensing of spectroscopic and physical properties of thin film
[AD-A149060] 10 p1435 N85-19041
Characterization of the heat source distribution of a typical GTAW welding arc
[DE85-004322] 12 p1861 N85-21670
INFRARED INSTRUMENTS
NT FLIR DETECTORS
NT INFRARED DETECTORS
NT INFRARED INTERFEROMETERS
NT INFRARED SCANNERS
NT INFRARED SPECTROMETERS
NT INFRARED SPECTROPHOTOMETERS
Infrared thermography of burn front propagation in heat powders
[DE85-003307] 10 p1438 N85-19060
An airborne infrared thermal scanning system for easy use on Navy P-3 aircraft
[AD-A149690] 12 p1933 N85-22143
Instrumentation for sensing moisture content of material using a transient thermal pulse
[NASA-CASE-NPO-15493-2] 23 p3933 N85-34579
INFRARED INTERFEROMETERS
A Jamin interferometer to determine the helium abundance in the atmosphere of Jupiter
[BONN-IR-83-17] 12 p1861 N85-22329
Analysis of atmospheric interferometer data
[AD-A150682] 14 p2372 N85-24663
Special topics in infrared interferometry — Michelson interferometer development
[NASA-TM-87472] 17 p3038 N85-28794
SCRIBE data of October 23, 1983 flight
[AD-A154864] 21 p3705 N85-33012
INFRARED LASERS
Thick film radiation detector
[AD-D011211] 01 p0048 N85-10318
Laser diodes for infrared spectroscopy
[BMFT-FB-T-84-131] 05 p0640 N85-14109
Advanced infrared laser modulator development
[NASA-CR-172479] 06 p0862 N85-15479
Upgrading flexible infrared waveguides
[AD-A146763] 07 p0970 N85-16160
Design and testing of a refractive laser beam homogenizer
[AD-A146997] 07 p0970 N85-16162
Far-infrared laser diagnostic on EBT and extreme far-forward laser scattering on ISX
[DE85-001788] 07 p1046 N85-16843
RF fiber optic link
[AD-A148679] 08 p1155 N85-17290
Multilayer reflecting systems based on glassy chalcogenides for infrared lasers
14 p2274 N85-24089
Laser with a hollow copper cathode
[ISL-R-119/83] 14 p2310 N85-24300
Laser induced damage of zinc sulphide
[BAE-BT-13363] 15 p2562 N85-25803
Method and apparatus for high speed, sustained recording of infrared laser beam patterns
[AD-D011585] 15 p2563 N85-25811
Theory of laser-stimulated surface process. 2: A generalized-master-equation approach to energy transfer between an IR laser, an aspecies and phonons
[AD-A153063] 17 p2970 N85-28344
Laser-stimulated vibrational excitation of an adspecies studied by a generalized master equation: Neutral atomic hydrogen on hydrated KCl(001)
[AD-A153665] 18 p3112 N85-29268
Spectroscopic investigation of materials for tunable infrared lasers
[AD-A154124] 19 p3272 N85-30291
Cerenkov maser and Cerenkov laser devices
[AD-A155443] 21 p3592 N85-32324
Infrared laser holography used in fusion plasma studies 21 p3687 N85-32905
INFRARED MASERS
U INFRARED LASERS
INFRARED PHOTOGRAPHY
NT COLOR INFRARED PHOTOGRAPHY
Measurement of shock and induced reaction in rocket propellants by nanosecond infrared radiometry and photography
[DE84-013209] 04 p0482 N85-13070
The need for integrating ground thermal measurements with thermal aircraft imagery 05 p0660 N85-14243
Astronomical applications of new infrared films
07 p0964 N85-16111
Infrared presensitization photography
[AD-A146968] 07 p0967 N85-16139
Measurement of shock induced reaction in rocket propellants by nanosecond infrared radiometry and photography
[AD-P004349] 10 p1456 N85-19173
Infrared presensitization photography
16 p2786 N85-27189
The 8.3 and 12.4 micron imaging of the Galactic Center source complex with the Goddard infrared array camera
[NASA-TM-86225] 19 p3362 N85-30982
Interpretation of multiband photographs made during Telefoto-80 experiment for the purpose of discriminating agricultural crops 22 p3736 N85-33152
INFRARED PHOTOMETRY
Far-infrared photometry of compact extragalactic sources: OJ 187 and BL Lac
[NASA-TM-86022] 04 p0580 N85-13701
Multi-spectral observations of the star formation: The role of far infrared photometry 08 p1245 N85-17859
Far-infrared photometry of low-mass pre-main-sequence stars with broad CO wings 08 p1246 N85-17866
High sensitivity, high angular resolution far-infrared photometry from the KAO 08 p1245 N85-17867
INFRARED RADIATION
NT FAR INFRARED RADIATION
NT NEAR INFRARED RADIATION
A limbus-sensing eye movement recorder
[AD-A144772] 01 p0049 N85-10323
Diagnostics of ionization in air produced by infrared radiation from A pulse CO2 laser
[AD-A145376] 02 p0201 N85-11942
Infrared images of the Uranian rings
02 p0302 N85-11965
Infrared mapping of galaxian centers: Star forming regions with kiloparsec scale sizes
03 p0444 N85-12827
A means of extending streak camera recording into the important 1300-1600 nm wavelength regime: Parametric frequency upconversion
[DE84-015666] 04 p0503 N85-13208
Unidentified IRAS sources: Ultrahigh luminosity galaxies
[NASA-CR-174207] 06 p0872 N85-15537
Upgrading flexible infrared waveguides
[AD-A146763] 07 p0970 N85-16160
Variation in spectral response of soybeans with respect to illumination, view, and canopy geometry
[E85-10040] 07 p0982 N85-16241
SWIR and visible atomic emission from laser-produced oxygen and nitrogen plasmas
[AD-A147528] 07 p1045 N85-16841
Radiation parameterization programs for use in general circulation models
[AD-A148015] 08 p1188 N85-17488
Evidence for non-radiative activity in hot stars
08 p1231 N85-17756
Infrared horizon sensor modeling for attitude determination and control: Analysis and mission experience
[NASA-TM-86181] 10 p1429 N85-19016
Infrared excitation of clusters and ions of atmospheric interest
[DE85-002098] 10 p1516 N85-19584
Elimination of sensor artifacts from infrared data
[AD-A149048] 10 p1556 N85-19814
Liquid-phase epitaxial growth of CdTe on HgCdTe
[AD-D011482] 10 p1561 N85-19846
PMP-1: A coordinated study of the behavior of the middle atmosphere in winter 11 p1654 N85-20421
Distortion of temporal characteristics during parametric up-conversion of ultrashort laser pulses
11 p1717 N85-20803
Absorption of ozone molecules in strong field of tea CO2 injection laser 11 p1718 N85-20808
Evaluation of infrared reflectance as a technique for measuring absorber materials degradation
[DE85-002171] 11 p1729 N85-20874
Infrared modulation of photoluminescence in glow discharge amorphous silicon
[DE85-016993] 11 p1737 N85-20922
New results on PU VUL 11 p1753 N85-21023
The influence on IR emission of engine parameters for an afterburn case. A sensitivity study on NATO infrared air target model (NIRATAM) version: 0.0
[AD-B089311L] 12 p1779 N85-21171
Carbon monoxide adsorption on a platinum electrode studied by polarization modulated FT-IRRAS (Fourier Transform-IR Reflections Adsorption Spectroscopy). Part 1: CO adsorbed in the double layer potential region and its oxidation in acids
[AD-A149751] 12 p1800 N85-21286
Progress on transparent yttria
[AD-P004370] 12 p1827 N85-21464
Infrared material optical damage by rain
[AD-P004372] 12 p1827 N85-21466
Intense, broadband, pulsed I-R source at the National Synchrotron Light Source
[DE84-010542] 12 p1935 N85-22154
Below-room-temperature water-vapor continuum absorption within the 8- to 10 micron atmospheric transmission window
[TR-0084(4945-09)-1] 13 p2132 N85-23266
Measurement of the nighttime infrared luminosity of Spacelab 1 in the H- and K-bands
[NASA-TM-86572] 14 p2434 N85-25011
Low-resolution target classification from a staring infrared sensor
[AD-A151660] 15 p2552 N85-26356
Mechanism of formation of low temperatures in nighttime Venusian thermosphere 16 p2723 N85-28007
Scheme for atmospheric thermal sensing from satellites with enhanced vertical resolution
16 p2726 N85-28023
Analysis and modeling for thermal focal plane arrays
[AD-A153156] 17 p2968 N85-28329
On the definition of topological susceptibility via lattice anomalous Ward identities and its perturbative tail
[PREPRINT-416] 18 p3184 N85-28744
Laser forward and backscattering in particulate media
[AD-A154138] 19 p3275 N85-30312
Comparison of 8 to 12 micrometer and 3 to 5 micrometer CVF transmissometer data with LOWTRAN calculations
[AD-A154218] 19 p3350 N85-30769
Double photon excitation of high-Rydberg atoms as a long-lived submillimeter detector
[NASA-CASE-NPO-16972-1] 19 p3352 N85-30779
Calibration and use of clutter data for simulation
[AD-A154788] 21 p3674 N85-32329

Absorption and scattering properties of aerosols of aggregated particles in the infrared spectral region
[AD-A155475] 21 p3637 N85-32591
Ice fog as an electro-optical obscurant
[AD-A155059] 21 p3705 N85-33015
Solid state radiative heat pump
[DE85-011605] 22 p3760 N85-33303
Search for infrared counterparts of gamma-ray bursters
[OG-1.1-9] 22 p3861 N85-33910
Hercules X-1: Pulsed gamma-rays detected above 150 GeV
[OG-2.2-9] 22 p3865 N85-33935
Further studies of X-ray structure of the Perseus cluster
[OG-2.5-12] 22 p3870 N85-33967
Infrared generation and wave-mixing studies in cesium
[DE85-012683] 24 p4063 N85-35304
Miniature infra-red data acquisition and telemetry system
[NASA-CR-177953] 24 p4096 N85-35390
Electronic structure and lattice dynamics of dimensionally constrained and disordered solids
[AD-A155927] 24 p4161 N85-35797

INFRARED RADIOMETERS

Measurement of shock and induced reaction in rocket propellants by nanosecond infrared radiometry and photography
[DE84-013209] 04 p0482 N85-13070
Comparison of wind derived from the LIMS (Limb Infrared Monitor of the Stratosphere) satellite instrument with rocket observations
[NASA-CR-174083] 04 p0541 N85-13444
Remote sensing of plant stress and diseases
05 p0657 N85-14216
Characterization of jet turbulence using infrared radiometry 11 p1578 N85-19628
Analysis of SMIRR data for volcanic and sedimentary terrains of the trans-Pecos region, Texas
13 p2197 N85-23626

INFRARED REFLECTION

Evaluation of infrared reflectance as a technique for measuring absorber materials degradation
[PB85-108486] 11 p1677 N85-20567
The nature and geometry of infrared reflection nebulae 24 p4167 N85-35835

INFRARED SCANNERS

ISSCP Cloud Algorithm Intercomparison Workshop
01 p0073 N85-10486
Description of the Dutch-Danish (DUDA) scanner --- thermal signatures
[AD-B084693] 01 p0121 N85-10826
Infrared-thermal wave scanner for NDE of naval thermal spray coatings
[DE85-002237] 11 p1650 N85-20391
An airborne infrared thermal scanning system for easy use on Navy P-3 aircraft
[AD-A149690] 12 p1933 N85-22143
Thermal infrared observations of lava flows during the 1984 Mauna Loa eruption 13 p2186 N85-23564
Design specifications for IMAGER: The DREO (Defence Research Establishment Ottawa) image processing system
[AD-A151752] 15 p2624 N85-26168
User manual for IMAGER: The DREO (Defence Research Establishment Ottawa) image processing system
[AD-A151754] 15 p2653 N85-26362
Thermal Infrared Multispectral Scanner (TIMS): An investigator's guide to TIMS data
[NASA-CR-175875] 17 p2961 N85-28266
Developments in remote sensing
[B8580069] 17 p2964 N85-28441
Comparison of measurement and simulation results of radiation temperatures applied to the thermal mapping of Munich
[DFVLR-FB-85-06] 17 p2964 N85-28442

INFRARED SPECTRA

Middle infrared spectral studies of geologic materials in their natural state using photothermal beam deflection spectroscopy
[AD-A144894] 01 p0120 N85-10820
Infrared spectroscopy study of the SP-250 epoxy resin system
[AD-A145860] 03 p0337 N85-12167
Spectral components at visual and infrared wavelengths in active galactic nuclei
[NASA-CR-174133] 03 p0445 N85-12832
The Jovian atmospheric window at 2.7 microns: A search for H2S
[NASA-TM-86661] 03 p0445 N85-12836
Development of acceptance criteria for batches of silane primer for external tank thermal protection system bonding applications
[NASA-CR-171266] 04 p0478 N85-13043
Advanced amorphous materials for photovoltaic conversion
[DE84-017198] 04 p0529 N85-13384
Lower atmospheric composition of Jupiter from Voyager infrared measurements
[NASA-CR-174196] 05 p0745 N85-14779
In situ analysis of corrosive and passive surfaces by laser-excited Raman spectroscopy --- lead, galvanized iron, and asbestos-cement pipes
[PB84-229756] 06 p0767 N85-14904
Nitriding of titanium and its alloys by N2, NH3 or mixtures of N2 + H2 in a dc arc plasma at low pressures (or = to torr)
[NASA-TM-83803] 06 p0814 N85-15168
Spectral reflectance studies on the orientale region of the Moon 06 p0888 N85-15639
Demonstration of transparent solar array module design
[NASA-CR-174257] 07 p0992 N85-16302
Infrared emission and atomic transitions
[AD-A147840] 07 p1041 N85-16607
Far infrared and submillimeter observations of the giant planets 08 p1245 N85-17856
Mid-infrared spectroscopy of planetary nebulae
08 p1247 N85-17872
Aromatics determination in middle distillate petroleum fractions by spectrophotometric titration
[PNR-90239] 09 p1293 N85-18123
The formats of the IRAS catalogs and atlases
09 p1413 N85-18908
Near infrared modeling of the equatorial regions of Jupiter and Saturn 09 p1415 N85-18930
PCB analysis by capillary gas chromatography coupled with matrix isolation-Fourier transform infrared spectroscopy
[DE84-009201] 10 p1437 N85-19059
Satellite support to the Sierra Cooperative Pilot Project: 1979/80 and 1980/81
[PB85-115079] 10 p1520 N85-19583
Far-infrared line observations of planetary nebulae. 1: The O 3 spectrum
[NASA-TM-86670] 10 p1570 N85-19900
Thermal band characterization of the LANDSAT-4 Thematic Mapper 12 p1869 N85-21727
The effects of atmospheric water vapor on infrared propagation
[AD-A150030] 12 p1934 N85-22150
IRAS observations of Seyfert galaxies
[NASA-CR-175557] 12 p1953 N85-22267
A method for estimating soil moisture availability
[NASA-CR-175606] 13 p2126 N85-23238
Water-ice clouds on Mars: Location and seasonal variation 13 p2194 N85-23611
Reassignment of the iron (3) absorption bands in the spectra of Mars 13 p2195 N85-23614
Participation in the Mars Data Analysis Program: Analysis of cloud forms in Viking and Mariner 9 images
[NASA-CR-175604] 13 p2204 N85-23673
Radiation effects induced in pin photodiodes by 40- and 85-MeV protons
[NASA-CR-175678] 14 p2426 N85-24980
Selection of a model of Earth's albedo radiation, practical calculation of its effect on the trajectory of a satellite
[NASA-TM-77870] 15 p2591 N85-25972
Estimation of convective rainfall from visible and infrared satellite data 15 p2596 N85-25999
Infrared observations of the Uranian rings
15 p2672 N85-26488
A measurement of the vibrational band strength for the upsilon sub 3 band of the HO2 radical
[NASA-CR-175858] 16 p2744 N85-26936
Fourier transform infrared spectrophotometric analysis of resin mix stoichiometry, revision 1
[DE85-007272] 16 p2747 N85-26951
Evaluation of used crankcase oils using computerized infrared spectrometry
[AD-A152993] 17 p2920 N85-27999
Evaluation of used crankcase oils using computerized infrared spectrometry. Appendices
[AD-A152994] 17 p2920 N85-28000
The spectroscopy and reaction kinetics of coordinated unsaturated metal carbonyls
[AD-A153079] 17 p2920 N85-28003
Thermal donor removal by rapid thermal annealing: Infrared absorption
[DE85-010092] 18 p3061 N85-29059
Screening phase transitions in two-dimensional Coulomb gas
[NOTA-INTERNA-830] 18 p3192 N85-29798
Technical and administrative activities of the Analytical Chemistry Laboratory (ACL)
[DE85-010150] 19 p3236 N85-30063
Compatibility, contamination and IR microspectrophotometry
[DE85-010909] 19 p3273 N85-30297
Comparison of 8 to 12 micrometer and 3 to 5 micrometer CVF transmissometer data with LOWTRAN calculations
[AD-A154218] 19 p3350 N85-30763
Speciation of hazardous inorganic compounds by Fourier transform infrared (FTIR) spectroscopy
[PB85-188969] 20 p3426 N85-31262
Stress corrosion of ceramic materials
[AD-A155020] 21 p3570 N85-32202
Absorption and scattering properties of aerosols of aggregated particles in the infrared spectral region
[AD-A155475] 21 p3637 N85-32591
In-cavity laser IR spectrum analyzer for investigating non-steady-state processes 21 p3685 N85-32894
Voigt line profile computation of infrared lines in the stratosphere and mesosphere
[AERONOMICA-ACTA-A-294-1985]
22 p3813 N85-33622
Acetonitrile in the Earth's atmosphere: An upper limit deduced from infrared solar spectra
[AERONOMICA-ACTA-A-295-1985]
22 p3813 N85-33623
FTIR studies of hydrocarbon synthesis on Pd/ZSM5 catalysts
[DE85-012430] 24 p4071 N85-35230
Infrared generation and wave-mixing studies in cesium
[DE85-012683] 24 p4063 N85-35304

INFRARED SPECTROMETERS

A high transmission, 20 channel polychromator for the Thomson scattering diagnostic of TORTUR 3 --- plasma diagnostics
[REPT-84-156] 03 p0422 N85-12694
Instruments for characterization of carbon black and polymers
[AD-A146475] 06 p0810 N85-15146
Construction of a superheterodyne receiver for 10 micron waves to be put on a Cassegrain optics telescope for spectroscopic research on the Mars and Venus atmospheres
[MPE-183] 06 p0872 N85-15538
GC-FTIR (Fourier Transform Infrared Spectrometry) of jet fuels
[AD-A148272] 08 p1135 N85-17155
The low-resolution spectra 09 p1413 N85-18907
Preliminary evaluation of the airborne imaging spectrometer for vegetation analysis
[NASA-CR-174440] 10 p1505 N85-19496
Hot spots on Io: Correlation of infrared emission and visible reflectance 13 p2172 N85-23475
Evaluation of used crankcase oils using computerized infrared spectrometry. Appendices
[AD-A152994] 17 p2920 N85-28000
Balloon-borne, He-cooled Fourier transform spectrometer for far infrared astronomy
[MPE-IR-41] 17 p3053 N85-28899

INFRARED SPECTROPHOTOMETERS

Evaluation of used crankcase oils using computerized infrared spectrometry
[AD-A152993] 17 p2920 N85-27999

INFRARED SPECTROSCOPY

Middle infrared spectral studies of geologic materials in their natural state using photothermal beam deflection spectroscopy
[AD-A144894] 01 p0120 N85-10820
Optical constant determination of thin polymer films in the infrared
[AD-A145869] 02 p0287 N85-11877
Properties of the upper tropospheres of Uranus and Neptune derived from observations at visible to near-infrared wavelengths 02 p0298 N85-11933
The 6th International Summer Institute in Surface Science 1983)
[AD-A146253] 03 p0434 N85-12762
Development of acceptance criteria for batches of silane primer for external tank thermal protection system bonding applications
[NASA-CR-171266] 04 p0478 N85-13043
Investigations regarding process analysis of liquids in the 1 to 2 micrometer spectral range
[BMFT-FB-T-84-169] 05 p0614 N85-13926
Carbon monoxide study, Anchorage, Alaska, November 22, 1982 to February 11, 1983
[PB84-236595] 05 p0673 N85-14321
Polymer-polymer interface bond stability
06 p0830 N85-15271
A study of the chemical interaction of gases with activated carbon
[AD-A147342] 07 p0923 N85-15846
Analysis of Nonvolatile Residue (NVR) from spacecraft systems
[NASA-TM-86184] 08 p1113 N85-17019
Modulated surface vibrational spectroscopies at electrode/electrolyte interfaces
[AD-A148665] 08 p1123 N85-17083
Molecular dynamics in nitramines and modified nitramines
[AD-A148515] 08 p1220 N85-17686

The Lear Jet Observatory: Fifteen years of discovery and rebirth
08 p1244 N85-17850
Far-infrared spectroscopy of interstellar gas
08 p1245 N85-17858
Mid-infrared spectroscopy of planetary nebulae
08 p1247 N85-17872
Interstellar grain mantles 08 p1247 N85-17874
Far infrared spectroscopy of (O III) in M82
08 p1249 N85-17883
A far infrared Echelle spectrometer for the Kuiper Airborne Observatory 08 p1249 N85-17886
An infrared study of isotopic exchange during methanation over supported rhodium catalysts: an inverse spillover effect
[AD-A146390] 10 p1435 N85-19046
An infrared study of the oxidation of carbon monoxide over supported rhodium catalysts
[AD-A149478] 10 p1436 N85-19050
Water absorption and conductivity in poly(ethylene oxide)-lithium tetrafluoroborate films
[AD-A147969] 10 p1450 N85-19138
Characterization of acetylene-terminated resin cure states
[AD-A149463] 10 p1452 N85-19148
Fundamental study of catalysts using laser Raman, infrared, auger electron spectroscopy and low energy electron diffraction
[DE85-001813] 11 p1595 N85-20033
Middle atmosphere NO and NO2 observed by means of the Spacelab one grille spectrometer
[AERONOMICA-ACTA-A-293-1984]
11 p1680 N85-20588
An infrared study of the dissociation of carbon dioxide over supported rhodium catalysts
[AD-A149813] 12 p1800 N85-21291
Investigation of dynamics of radiation spectrum of injection lasers by infrared impulse Fourier spectroscopy
13 p2000 N85-23047
Spectral reflectance of carbonate minerals and rocks in the visible and near infrared (0.35 - 2.55 microns) and its applications in carbonate petrology
[NASA-CR-175763] 15 p2591 N85-25973
Molecular spectroscopy from the Kuiper Airborne Observatory
[NASA-CR-175748] 16 p2882 N85-27783
Evaluation of used crankcase oils using computerized infrared spectrometry
[AD-A152993] 17 p2920 N85-27999
Evaluation of used crankcase oils using computerized infrared spectrometry. Appendices
[AD-A152994] 17 p2920 N85-28000
Formation and fate of toxic chemicals in California's atmosphere
[PB85-172609] 18 p3134 N85-29414
Lithium cell reactions
[AD-A154429] 19 p3305 N85-30484
Speciation of hazardous inorganic compounds by Fourier transform infrared (FTIR) spectroscopy
[PB85-186969] 20 p3426 N85-31262
Infrared studies of the influence of alkali metals on the C-O bond in chemisorbed carbon monoxide
[DE85-005306] 23 p3911 N85-34232
Time-resolved and infrared spectroscopy of excitons
[DE85-011670] 23 p3912 N85-34235

INFRARED STARS

Documentation for the machine-readable version of The Revised AFGL Infrared Sky Survey Catalog (Price and Murdock 1983)
[NASA-TM-87377] 03 p0405 N85-12588
Compact infrared sources: Protostars before IRAS
03 p0442 N85-12812

INFRARED SUPPRESSION

Airworthiness and flight characteristics test of the RC-12D Guardrail V
[AD-A148046] 08 p1084 N85-16864

INFRARED TELESCOPES

NT SPACE INFRARED TELESCOPE FACILITY
Thermal and cryogenic design study for space infrared telescope facility (SIRTF)
[NASA-CR-166613] 07 p0915 N85-15793
Study of alternate optical and fine guidance sensor designs for the space infrared telescope facility (SIRTF)
[NASA-CR-166614] 07 p0915 N85-15794
Pointing and control system design study for the space infrared telescope facility (SIRTF)
[NASA-CR-166612] 07 p0915 N85-15795
SIRTF: The next step
[NASA-TM-86663] 07 p1059 N85-16724
SIRTF: The next step 08 p1250 N85-17891
The removal, mechanical handling and installation procedures for declination tachometer and itek encoder — United Kingdom Infrared Telescope
[UKIRT-17] 09 p1414 N85-18915
The mechanical procedures for the 8 channel bolometer — United Kingdom Infrared Telescope
[UKIRT-18] 09 p1414 N85-18916
Procedures for the bonding of the E.M.C. mirror onto its INVAR mirror flange — United Kingdom Infrared Telescope
[UKIRT-19] 09 p1414 N85-18917
In situ washing procedures for the UKIRT 3.8 meter primary mirror — United Kingdom Infrared Telescope (UKIRT)
[UKIRT-20] 09 p1414 N85-18918
The removal, mechanical handling and installation procedures for the RA itek encoder
[UKIRT-21] 09 p1414 N85-18919
The UKIRT centre section structural investigation — United Kingdom Infrared Telescope (UKIRT)
[UKIRT-22] 09 p1414 N85-18920
UKIRT spectro-photometry system — United Kingdom Infrared Telescope (UKIRT)
[UKIRT-23] 09 p1414 N85-18921
LDR system concepts and technology
14 p2231 N85-23823
Precision antenna reflector structures
14 p2232 N85-23834
Infrared telescope
[NASA-CR-171392] 15 p2668 N85-26465
IRAS: Space technology from the Netherlands
[B8561841] 17 p2908 N85-27929
Long life feasibility study for the shuttle infrared telescope facility
[NASA-CR-3722] 17 p3052 N85-28893
The nature and geometry of infrared reflection nebulae 24 p4167 N85-35835

INFRARED TRACKING

Dual mode radio frequency-infrared frequency system
[AD-D011402] 08 p1081 N85-16850
Elimination of sensor artifacts from infrared data
[AD-A149048] 10 p1556 N85-19614
Presentations at the Tri-Service Cloud Modeling Workshop (2nd), held at the Naval Surface Weapons Center, White Oak, Maryland, 26-27 June 1984, volume 1
[AD-A152735] 17 p2996 N85-28522

INFRARED WINDOWS

High temperature ultra-high vacuum infrared window seal
[AD-D011333] 07 p0929 N85-15800
Continuum absorption by H2O in the 700-1200 cm(-1) and 2400-280 cm(-1) windows
[AD-A147391] 07 p0997 N85-16334

INFRASONIC FREQUENCIES

China report: Science and technology
[JPRS-CST-84-001] 04 p0557 N85-13545
Measurement of infrasonic waves from remotely detonated artificial explosion 04 p0557 N85-13546
Theoretical and observed dispersion of acoustic-gravity waves in atmosphere 04 p0557 N85-13547
Long-distance propagation of infrasound in atmosphere near Earth's surface 06 p0825 N85-15238
Seismic observation of infrasonic signals
[AD-A149574] 12 p1889 N85-21853
Some individual differences in human response to infrasound
[UTIAS-282] 12 p1905 N85-21960
Field of point source of low-frequency sound in atmosphere with altitudinally nonuniform wind
15 p2524 N85-25566

INGESTION (BIOLOGY)

NT EATING

INGESTION (ENGINES)

Temperature distortion generator for turboshaft engine testing
[NASA-TM-83748] 07 p0893 N85-15658
Avoiding serious bird strike incidents
[AD-P004178] 11 p1578 N85-19940
Accidents and serious incidents to civil aircraft due to birstrikes
[AD-P004180] 11 p1578 N85-19942
Birds and aircraft engine strike rates
[AD-P004184] 11 p1579 N85-19946
Review of engine ingestions to wide body transport aircraft
[AD-P004185] 11 p1579 N85-19947

INGOTS

Engineering property comparisons of PM and IM aluminum alloy forgings
[AD-B086146L] 06 p1173 N85-17398
USSR report: Materials science and metallurgy
[JPRS-UMS-84-005] 11 p1597 N85-20044
Effect of ingot structure of failure ductility of pressed semifinished products of high-durability aluminum alloys
11 p1597 N85-20045
Nondestructive testing of stainless steel to improve quality and output efficiency of the processing of ingot and continuous casting
[BMFT-FB-T-84-240] 12 p1808 N85-21345
Mechanisms of corrosion fatigue in high strength I/M (Ingot Metallurgy) and P/M (Powder Metallurgy) aluminum alloys
[AD-A151177] 15 p2509 N85-25478
MPS solidification model. Analysis and calculation of macrosegregation in a casting ingot
[NASA-CR-171589] 21 p3566 N85-32178

INHALATION

U RESPIRATION

INHIBITION (PSYCHOLOGY)

Inhibition of return: Neural basis and function
[AD-A145242] 01 p0096 N85-10652

INHIBITORS

NT WEAR INHIBITORS
Mechanical properties of adhesively bonded aluminum structures protected with hydration inhibitors
[AD-A148123] 08 p1133 N85-17139
Effects of pyridostigmine on psychomotor and visual performance
[AD-A148553] 08 p1196 N85-17539
Adsorption thermodynamics and surface transport of metal catalyst poisons
[DE85-002966] 10 p1441 N85-19084
Corrosion inhibitor formulation for molybdenum, tungsten and other metals
[AD-D011593] 15 p2510 N85-25486
Mechanical properties of adhesively bonded aluminum structures protected with hydration inhibitors
[AD-A153755] 18 p3079 N85-29047
Effect of multi-functional inhibitors on the electrochemistry within corrosion crack
19 p3236 N85-30075
Molecular biology of environmental aromatic hydrocarbons
[DE85-015036] 24 p4128 N85-35580

INHOMOGENEITY

Mechanism of brittle heat fracture of inhomogeneous solids by high temperature gas jets
02 p0265 N85-11731
Crack problems for bonded nonhomogeneous materials under antiplane shear loading
[NASA-CR-172532] 10 p1495 N85-19438
Boundary velocities of longitudinal seismic waves and lateral inhomogeneities of upper ocean mantle
13 p2113 N85-23165
Spreading of greatly extended inhomogeneities in upper ionosphere 14 p2339 N85-24462
Evolution of strong inhomogeneities in ionospheric plasma, part 1 14 p2339 N85-24463
Waves in inhomogeneous media — magnetohydrodynamic waves; solar atmosphere
14 p2449 N85-25116
Structural inhomogeneities in amorphous nickel-phosphorus alloy
[BLL-M-38103-(5828.4)] 16 p2748 N85-26960
Impact of optical inhomogeneity in sintered interface between glasses on laser emission characteristics
16 p2763 N85-27053
Optimum convection conditions for Czochralski growth of semiconductors
[INPE-3395-PRE/666] 16 p2870 N85-27703
Reflection of acoustic beam from inhomogeneous boundary 21 p3560 N85-32964
Relaxation lens in inhomogeneous binary mixture
21 p3695 N85-32957
Vortex dynamics simulation of conserved scalar dissipation 22 p3745 N85-33210
Cosmic ray secondary nuclei and the structure of the galaxy
[OG-7.2-4] 23 p4014 N85-34878

INITIAL VALUE PROBLEMS

U BOUNDARY VALUE PROBLEMS

INITIATION

Computer simulation of the shock initiation of detonation in solid explosives
[PML-1984-23] 01 p0033 N85-10207
Analysis of the natural initiation of vapor explosions
[DE85-000168] 11 p1632 N85-20279
Evidence concerning the generation mechanism of solar type 3 radio bursts 16 p2866 N85-27802
Experimental studies of chemical reactivity during shock initiation of hexanitrostilbene
[DE85-011726] 22 p3754 N85-33270

INITIATORS (EXPLOSIVES)

NT DETONATORS
NT EXPLODING WIRES
Fast response impulse generator
[AD-D011283] 06 p0759 N85-14853
Laser ignition of explosives
[FOA-C-20550-D1] 07 p0972 N85-16173
Study of bridgewire size and pyrotechnic density relationships on all-fire levels
[DE84-016948] 09 p1302 N85-18177
Generation of detonation waves of given spatial and temporal characteristics
[ISL-R-103/83] 16 p2758 N85-27021

Deformation, fracture and explosive properties of reactive materials
[AD-A154073] 19 p3251 N85-30157

INJECTION
NT CARRIER INJECTION
NT DEEP WELL INJECTION (WASTES)
NT FLUID INJECTION
NT FUEL INJECTION
NT GAS INJECTION
NT ION INJECTION
NT LIQUID INJECTION
NT WATER INJECTION

Transonic shock interaction with a tangentially-injected turbulent boundary layer 08 p1072 N85-16796
Simulation of the ion-beam-driven drift instability in a magnetic trap, 2
[AD-A149452] 10 p1554 N85-19796
A new very high voltage semiconductor switch
[NASA-TM-86957] 11 p1627 N85-20246
Mechanisms of exhaust pollutants and plume formation in continuous combustion
[AD-A154169] 20 p3435 N85-31310
The effect of injection-stream turbulence on film cooling effectiveness and heat transfer coefficients 20 p3451 N85-31424
Method of characterizing critical timing paths and analyzing timing related failure modes in very large scale integrated circuits
[AD-D011731] 22 p3759 N85-33298
Computer simulation of integrated injection logic 22 p3767 N85-33349
Method for determining depth and shape of a sub-surface conductive object
[DE85-006502] 23 p3935 N85-34389

INJECTION CARBURETORS
U FUEL INJECTION

INJECTION LASERS
Low-threshold injection lasers on grown GaInPAs/InP heterostructures (1.2-1.6 micrometers wavelengths) 02 p0256 N85-11693
Self-modulation of injection laser emission intensity due to external optical feedback 02 p0261 N85-11706
Spectrally matched modulation of radiation of injection laser in traveling-wave amplifier below 2 GHz 02 p0262 N85-11712
Space-time characteristics of radiation of single-mode injection lasers 02 p0269 N85-11758
Quantum noise effects in single-mode injection lasers
[FUB-11-1984] 09 p1327 N85-18338
The noise of laser diodes with modulated injection current
[FI-465-TBR-23] 11 p1625 N85-20233
Investigation of dynamics of radiation spectrum of injection lasers by infrared impulse Fourier spectroscopy 13 p2090 N85-23047
Injection controlled laser transmitter with twin local oscillators
[AD-D011577] 15 p2563 N85-25810
Injection laser structure design
[AD-A153210] 17 p2971 N85-28345
Definition of requirements for injection locking of pulsed UV lasers
[DE85-010126] 18 p3113 N85-29275
Arrangement for damping the resonance in a laser diode
[NASA-CASE-NPO-15980-1] 19 p3274 N85-30305
Dye laser traveling wave amplifier
[NASA-CR-175869] 19 p3275 N85-30308
Low-threshold injection InGaAsP/GaAs double heterostructure lasers with separate limiting obtained by liquid-phase epitaxy (lambda = 0.78 divided by 0.87 microns, I sub thr = 460 A/cm 2, T = 300 K) 21 p3687 N85-32906
Adjustment of radiation wavelength of multimode InP-GaInAsP injection heterolasers 21 p3688 N85-32913

INJECTION LOCKING
Definition of requirements for injection locking of pulsed UV lasers
[DE85-010126] 18 p3113 N85-29275
Optical injection locking of solid-state oscillators by frequency-multiplexed injection-locked, laser diodes
[AD-D011695] 19 p3275 N85-30307
Dye laser traveling wave amplifier
[NASA-CR-175869] 19 p3275 N85-30308

INJECTION MOLDING
Injection molding of silicon carbide capable of being sintered without pressure
[NASA-TM-77736] 01 p0035 N85-10221
Optimization of the injection process for thermostatic polyether-ether-ketone (Peek) thermoplastics reinforced with short carbon fibers
[SNIAS-842-422-102] 04 p0480 N85-13062

INJECTORS
Finlet injector
[AD-D011245] 06 p0785 N85-14891
Low loss injector for liquid propellant rocket engines
[NASA-CASE-MFG-25989-1] 11 p1591 N85-20008
Oxygen-hydrogen thrusters for Space Station auxiliary propulsion systems
[NASA-CR-175891] 15 p2494 N85-25383
Segmented zoned fuel injection system for use with a combustor
[AD-D011640] 17 p2897 N85-27865
Physiochemically controlled scour jet array system
[AD-D011688] 19 p3308 N85-30505
High-brightness photoemitter development for electron accelerator injectors
[DE85-009548] 19 p3355 N85-30798
Design status of heavy ion injector program
[DE85-010751] 22 p3842 N85-33793
Solid state high power amplifier for driving the SLC injector klystron
[DE85-013063] 24 p4090 N85-35356

INJURIES
NT BAROTRAUMA
NT BURNS (INJURIES)
NT CRASH INJURIES
NT EJECTION INJURIES
NT LESIONS
NT NOISE INJURIES
NT PULMONARY LESIONS
NT RADIATION INJURIES
Establishment of posture and working movements of pilot in air crash enquiries 07 p1010 N85-16417
Fatal hemorrhagic shock and acetate solutions
[AD-A146754] 07 p1014 N85-16444
An investigation of spinal injury potential from the use of the ACES 2 ejection seat by lower weight female pilots
[AD-A148449] 08 p1196 N85-17537
SPH-4 US Army flight helmet performance, 1972 - 1983
[AD-A148674] 08 p1201 N85-17562
Interaction of metals and metalloids with biomembranes
[DE85-004902] 13 p2141 N85-23293
Psychometric evaluation of head injury among fliers referred to the AF School of Aerospace Medicine
[AD-A151479] 15 p2617 N85-26129
Heat injury: Prevention is the key
[AD-A153734] 19 p3328 N85-30622
The helicopter, instrument of choice for health evacuation
[SNIAS-851-220-101] 20 p3393 N85-31051
Design and testing of an energy-absorbing crewseat for the F/FB-111 aircraft, volume 1
[NASA-CR-3916] 23 p3896 N85-34133

INKS
Mod silver metallization for photovoltaics
[NASA-CR-174444] 10 p1509 N85-19518
Use of optical techniques in studies of wear rates of anodized aluminum and polymer coatings on aluminum 14 p2259 N85-23907
Procedure for certifying quantity of volatile organic compounds emitted by paint, ink and other coatings
[PB85-159044] 15 p2520 N85-25537
Ink jet printing of silver metallization for photovoltaics
[NASA-CR-175798] 15 p2586 N85-25943
The replacement of precious metal thick film inks using conductive polymer technology
[AD-A152002] 16 p2749 N85-26965
Ink jet printing of silver metallization for photovoltaics
[NASA-CR-176019] 19 p3343 N85-30720
Ink jet printing of silver metallization for photovoltaics
[NASA-CR-176054] 22 p3805 N85-33589

INLAND WATERS
NT GROUND WATER
Investigation of mineral and thermomineral springs in the Eifel Mountains regarding thermal indications
[BMFT-FB-T-84-019] 02 p0220 N85-11451

INLET AIRFRAME CONFIGURATIONS
Flight and wind-tunnel comparisons of the inlet-airframe interaction of the F-15 airplane
[NASA-TP-2374] 04 p0455 N85-12884
Some aspects of engine and airframe integration for Ramjet and Ramrocket powered missiles 07 p0918 N85-15812
Performance and surge limits of a TF30-P-3 turbofan engine/axisymmetric mixed-compression inlet propulsion system at Mach 2.5
[NASA-TP-2461] 15 p2472 N85-25261

INLET FLOW
Flow rates and pressure profiles for one to four axially alined Borda inlets
[NASA-TP-2390] 05 p0636 N85-14078
Experimental observation of the flow in impellers and diffusers — centrifugal compressors 05 p0636 N85-14080
Effect of steady-state temperature distortion on inlet flow to a high-bypass-ration turbofan engine
[NASA-TM-86896] 07 p0904 N85-15725
Some aspects of engine and airframe integration for Ramjet and Ramrocket powered missiles 07 p0918 N85-15812
Current problems in turbomachinery fluid dynamics
[AD-A147127] 07 p0956 N85-16074
Interest of internal bleed for a two-dimensional air intake operating in a wide Mach number range (1.8-3 plus) 08 p1071 N85-16793
Research and development for semi-spherical inflow control device
[NAL-TR-833] 09 p1281 N85-18056
Determination of total pressure losses in stepped annular diffusers with curvilinear outer walls and uniform velocity field at inlet 09 p1306 N85-18203
A mixed finite difference analysis of the internal and external transonic flow fields of inlets with centerbody 11 p1619 N85-20192
Effects of inlet distortion on a static pressure probe mounted on the engine hub in an F-15 airplane
[NASA-TP-2411] 13 p1974 N85-22394
Experimentally determined characteristics of vortex heaters 13 p2050 N85-22933
Dependents of velocity distribution in exit section of converging channel on shape of inlet channel in regulating valve 14 p2277 N85-24106
Aerodynamic detuning analysis of an unstalled supersonic turbofan cascade
[NASA-TM-87001] 16 p2700 N85-26670
A numerical simulation of the NFAC (National Full-scale Aerodynamics Complex) open-return wind tunnel inlet flow
[NASA-TM-86724] 16 p2700 N85-26672
Flow rate and pressure profiles for 1 to 4 axially alined orifice inlets
[NASA-TP-2460] 16 p2782 N85-27165
SSME turbopump turbine computations 17 p2911 N85-27944
Analysis of physical-chemical processes governing SSME internal fluid flows
[NASA-CR-175893] 17 p2957 N85-28261
Application of computational fluid dynamics to complex inlet ducts
[NASA-TM-87060] 19 p3265 N85-30247

INLET NOZZLES
Heat exchanger
[DE84-014299] 01 p0047 N85-10309
Experimental observation of the flow in impellers and diffusers — centrifugal compressors 05 p0636 N85-14080
Vaned diffusers — in centrifugal compressors 05 p0637 N85-14085
Low solidity cascade diffusers for wide flow range centrifugal blowers 05 p0637 N85-14086
Interest of internal bleed for a two-dimensional air intake operating in a wide Mach number range (1.8-3 plus) 08 p1071 N85-16793
Investigation of heat transfer to a turbine blade cascade using a shock tube
[AD-A153090] 17 p2898 N85-27871
Inspection evaluation and repair of the flawed feedwater nozzle of the 50 MWe Dodewaard GKN boiling water reactor
[ISBN-90-353-0017-3] 17 p2977 N85-28394
Quasi non-intrusive sampling and analysis of gases associated with the boundary layer on the tethered satellite and similar supersonic and hypersonic research vehicles
[NASA-CR-176075] 20 p3407 N85-31140

INLET PRESSURE
Inlet and airframe compatibility for a V/STOL fighter/attack aircraft with top-mounted inlets
[NASA-TM-84252] 01 p0003 N85-10015
Flow rates and pressure profiles for one to four axially alined Borda inlets
[NASA-TP-2390] 05 p0636 N85-14078
Investigation of heat transfer to a turbine blade cascade using a shock tube
[AD-A153090] 17 p2898 N85-27871

INLET TEMPERATURE
Methanol vaporization: Effects on volumetric efficiency and on determination of optimum fuel delivery system
[PB84-243914] 09 p1302 N85-18161
Redistribution of the inlet temperature profile through the SSME fuel turbine 16 p2739 N85-26901
SSME fuel preburner two-dimensional analysis 17 p2911 N85-27943
Onset of freezing in residential air-to-air heat exchangers
[DE85-009960] 19 p3267 N85-30259

INLETS (DEVICES)
U INTAKE SYSTEMS

INLETS (TOPOGRAPHY)
NT BAYOUS

INNER RADIATION BELT
Boundary of modulation diffusion and stochastic instability of high energy protons in inner radiation belt 15 p2482 N85-25316

INOCULATION
Induction of immunity to toxins with anti-idiotypic antibody
[AD-A146793] 07 p1014 N85-16445
Inoculation of non-metallic inclusions in steel 17GS
[BLL-BISI-TRANS-22431-(9022.06)] 17 p2925 N85-28042
Effects of the cooling rate on the structure of the graphite in inoculated irons
[BLL-BISI-TRANS-22305-(9022.06)] 17 p2930 N85-28083

INORGANIC CHEMISTRY
The synthesis, structural characterization and reactions of closo-Rhodecarborane Anions containing a formal d8 metal vertex 1,2
[AD-A149640] 12 p1799 N85-21285
Abstracts of the 36th Southeastern Regional Meeting of the American Chemical Society
[AD-A151506] 15 p2498 N85-25394
Basic research in novel inorganic reagents and fluorocarbon chemistry
[AD-A155340] 21 p3564 N85-32185

INORGANIC COATINGS
NT ANODIC COATINGS
NT CERAMIC COATINGS

INORGANIC COMPOUNDS
NT AMMONIA
NT LIQUID AMMONIA
Structure of vibrational spectrum and selection rules in Raman and hyper-Raman light scattering spectra of inorganic glasses 02 p0271 N85-11769
USSR report: Chemistry
[JPRS-UCH-84-012] 06 p0761 N85-14865
High capacity inorganic oxyhalide electrochemical cell
[AD-D011321] 07 p0923 N85-15845
Preliminary report on the results of hydrological measurements in the southern Tyrrhenian Sea, in the Messina strait and in the western Ionian sea
[PREPRINT-433] 14 p2362 N85-24693
Chemicals identified in human biological media, a data base, volume 6, part 1
[DE85-006768] 17 p2999 N85-28542
Aerobic sulfur-oxidizing bacteria: Environmental selection and diversification 21 p3656 N85-32712
Anaerobic microbial transformations in subsurface environments: Project description
[DE85-012769] 23 p3951 N85-34486

INORGANIC NITRATES
NT AMMONIUM NITRATES
NT HYDRAZINE NITRATE
NT SODIUM NITRATES

INORGANIC PEROXIDES
NT HYDROGEN PEROXIDE
The use of superoxide mixtures as air-revitalization chemicals in hyperbaric, self-contained, closed-circuit breathing apparatus
[NASA-TM-86709] 20 p3512 N85-31831
Improved oxygen sources for breathing apparatus
[NASA-TM-86671] 24 p4134 N85-35623

INORGANIC SULFIDES
NT BARIUM SULFIDES
NT CADMIUM SULFIDES
NT CALCIUM SULFIDES
NT COPPER SULFIDES
NT HYDROGEN SULFIDE
NT MOLYBDENUM DISULFIDES
NT POLYSULFIDES
NT ZINC SULFIDES

INPUT
Determination of the input-output characteristics of time-invariant memoryless nonlinear devices
[FUB-41-1983] 01 p0100 N85-10667
Theory of diaphragm light modulators with electrical input signal 13 p2062 N85-23002
Gyrator frequency selectors with bandwidth independent of input signal level 13 p2083 N85-23009
Multivariable statistical modelling and its application 16 p2857 N85-27617
A study of error rates in voice recognition
[AD-A153282] 17 p2949 N85-28211
The touch panel system: Design and development
[AD-A153014] 17 p3008 N85-28596
A comparison of numeric data entry with touch-sensitive and conventional numeric keypads
[AD-A153276] 17 p3008 N85-28598
Frequency-spreading coupler
[AD-D011683] 19 p3258 N85-30200
Bayesian factor analysis
[AD-A154184] 19 p3347 N85-30747
Microwave SAW (Surface Acoustic Wave) monochromator
[AD-D011718] 21 p3590 N85-32311
Visibility and vertical structure measurements in southern Germany
[AD-A154714] 21 p3635 N85-32574
Issues and techniques in touch-sensitive tablet input (executive summary) 23 p3960 N85-34543
Aspects of input signal design for order and parameter estimation in linear dynamical systems
[ER-83/05] 24 p4091 N85-35362
Software maintenance relating to the input translator and z-80 realization volume of the computer systems design environment
[AD-A155849] 24 p4138 N85-35846

INPUT/OUTPUT ROUTINES
THLL (TRIDENT Higher Level Language) reference manual
[AD-A145116] 01 p0104 N85-10696
Input-output stability analysis with magnetic hysteresis non-linearity: A class of multipliers
[AD-A145729] 02 p0253 N85-11654
NATFREQ users manual: A FORTRAN 4 program for computing natural frequencies, mode shapes and drag coefficients for taut strumming cables with attached masses and spring-mass combinations
[AD-A146058] 03 p0407 N85-12600
Investigative findings of image enhancement techniques
[AD-A146392] 06 p0853 N85-15424
High altitude chemically reacting gas particle mixtures. Volume 3: Computer code user's and applications manual — rocket nozzle and orbital plume flow fields
[NASA-CR-171628] 07 p0917 N85-15803
Console I/O routines
[DE85-002644] 11 p1702 N85-20700
New enhancements in April 85 NASTRAN release 15 p2573 N85-25864
Sample problems for STAGSC-1
[AD-A153142] 17 p3012 N85-28621
Complete development and implement AFIT/ENG database management system, volume 1
[AD-A153043] 17 p3048 N85-28886
An interactive computer aid for the design and analysis of linear, single input/single output digital and continuous control systems
[AD-A153704] 18 p3162 N85-29589
MC TRICOMP user's guide
[AD-A154339] 19 p3337 N85-30673
BP (Basic Processor) TRICOMP user's guide
[AD-A154340] 19 p3337 N85-30674
VAX TRICOMP user's guide
[AD-A154341] 19 p3337 N85-30675
Flight control system for a computer controlled aircraft with limited sensors
[AD-A155107] 21 p3555 N85-32115
Flexible satellite communications systems simulator, phase 3
[AD-A155647] 21 p3577 N85-32247

INSAT SATELLITES
U INDIAN SPACECRAFT

INSECT DAMAGE
U INFESTATION

INSECTICIDES
NT DDT
NT URETHANES

INSECTS
NT LARVAE
Radiobiological studies on egg systems exposed to heavy nuclei of cosmic galactic radiation — insects 05 p0690 N85-14440
Unsteady separated flows: Generation and use by insects
[AD-P004166] 09 p1266 N85-17953
Irradiation of northwest agricultural products
[DE85-012455] 22 p3843 N85-33803
Effects of microgravity and hypergravity on invertebrate development 24 p4126 N85-35579
Report of the Insect Development Group 24 p4127 N85-35584

INSENSITIVITY
U SENSITIVITY

INSERTION
Electronic module insertion and retraction mechanism
[AD-D011309] 07 p0947 N85-16002
Developments in gas metering technology
[ERS-E.348] 09 p1321 N85-18307

INSERTION LOSS
Fiber optic expanded beam connector
[AD-A154057] 19 p3367 N85-30880

INSERTS
NT NOZZLE INSERTS
Method of testing carbide inserts for premature fracture by face milling of cylindrical workpieces 09 p1303 N85-18183
Ultrasonic test evaluation of the insert bond on hermetic connectors
[DE85-008394] 18 p3120 N85-29310

INSHORE ZONES
U BEACHES

INSOLATION
Solar energy resource assessment in Eastern New Mexico and solar and wind energy resource assessment in Eastern New Mexico
[DE84-001511] 04 p0527 N85-13370
Global radiation in West Germany — solar generators 05 p0662 N85-14253
Weather data for simplified energy calculation methods. Volume 3: Western United States: TRY data
[DE85-000495] 09 p1358 N85-18540
Weather data for simplified energy calculation methods. Volume 1: Eastern United States: TRY data
[DE85-000493] 09 p1358 N85-18541
Weather data for simplified energy calculation methods. Volume 2: Middle United States: TRY data
[DE85-000494] 11 p1687 N85-20808
Some solar dish/heat engine design considerations
[DE85-003479] 12 p1881 N85-21802
Evaluation of satellite derived estimates of solar radiation
[E85-10087] 14 p2346 N85-24507
Screening ceramic materials for intense radiant heat applications
[DE85-006989] 16 p2756 N85-27006
The influence of global dust storms on the mean seasonal daily insolations at the Martian surface
[AERONOMICA-ACTA-A-289-1984] 18 p3203 N85-29668
View-limiting shrouds for insolation radiometers
[NASA-CR-176041] 20 p3458 N85-31476
Insolation changes on Pluto caused by orbital element variations
[AERONOMICA-ACTA-A-290-1984] 20 p3546 N85-32070
Improved Nominal Operating Cell Temperature (NOCT) test procedure 21 p3612 N85-32449
Resource evaluation and site selection for microalgae production systems
[DE85-006807] 23 p3951 N85-34485

INSPECTION
NT INFRARED INSPECTION
NT X RAY INSPECTION
Advanced blade tip seal system, volume 2
[NASA-CR-167851] 02 p0147 N85-10999
Modernization of IDTs-6 ultrasonic installation
[BLL-M-35716-(5828.4)] 02 p0206 N85-11356
Procedures for precap visual inspection
[NASA-RP-1122] 04 p0495 N85-13156
Nondestructive inspection: Improved capabilities of technicians
[AD-A147388] 07 p0975 N85-16196
Mobile accelerator neutron radiography system
[AD-A148808] 09 p1323 N85-18311
Ultrasonic inspection of alloyed tungsten bars
[AD-A148900] 10 p1495 N85-19435
Electromagnetic inspection of wire ropes using sensor arrays
[AD-A149016] 10 p1495 N85-19436
Application of hysteresis modelling to the non-destructive inspection of stress
[DE85-003081] 11 p1650 N85-20393
Aerostructure nondestructive evaluation by thermal field detection. Phase 2: Technique refinement and quantitative determination of flaw detection capabilities
[AD-A149622] 12 p1777 N85-21155
The state of the art in printed wiring board inspection
[AD-A149871] 12 p1882 N85-21679
Sizing capability of automated ultrasonic time-of-flight diffraction in thick section steel and aspects of reliable inspection in practice
[AERE-R-11548] 15 p2571 N85-25855
Magnetic flux leakage inspection: Principles and applications
[BLL-BISI-TRANS-22248-(9022.06)] 17 p2975 N85-28382
Inspection of welds and the factors improving its effectiveness in welded structure fabrication
[BLL-BISI-TRANS-22194-(9022.06)] 17 p2976 N85-28387
Effects of inspection errors on curtailed Dorfman-type procedures
[AD-A152376] 17 p3024 N85-28689
Statistical effects of imperfect inspection sampling. Part 2: Double sampling, link sampling and grading
[AD-A152377] 17 p3024 N85-28700
Production verification of the acoustic emission weld monitor
[AD-A154168] 20 p3464 N85-31519
In-service supervision of a pressurized concrete pressure vessel
[CEFZS-4308] 20 p3470 N85-31584
Infrared laser holography used in fusion plasma studies 21 p3667 N85-32905
Corrosion management strategies for aircraft and related systems 22 p3749 N85-33239

Relating corrosion maintenance to environmental factors 22 p3750 N85-33247
Towards the year 2000: Developments in inspection and product assurance to be anticipated during the next 15 years — aircraft engines
[PNR-90258] 23 p3940 N85-34421
National program for inspection of non-federal dams. Woodward reservoir dam (VT 00209), Connecticut River Basin, Plymouth, Vermont. Phase 1 inspection report
[AD-A158256] 24 p4144 N85-35693

INSTABILITY
U STABILITY

INSTALLATION
U INSTALLING

INSTALLATION MANUALS
Installation, maintenance and operating manual for the Lucas-type fuel injection system of the 3 B rotary engine
[NASA-TM-77872] 15 p2588 N85-25846

INSTALLING
Automated installation methods for photovoltaic arrays 2
[SAND-84-7036] 02 p0222 N85-11453
Installation options for the NAVSTAR global positioning system in surface ships
[AD-A148190] 06 p1082 N85-16856
The removal, mechanical handling and installation procedures for the RA Itek encoder
[UKIRT-21] 09 p1414 N85-18919
Plasma arc welding, equipment, installation and process control
[DE85-008461] 19 p3373 N85-30921

INSTANTONS
Stability questions for gravity in 4 and higher dimensions 05 p0734 N85-14716
Strong-coupling approximations
[DE85-007829] 19 p3353 N85-30785

INSTITUTIONS
Model research: The National Advisory Committee for Aeronautics, 1915-1958, volume 1
[NASA-SP-4103-VOL-1] 14 p2207 N85-23683
Model research, the National Advisory Committee for Aeronautics, 1915-1958, volume 2
[NASA-SP-4103-VOL-2] 14 p2207 N85-23684

INSTRUCTION SETS (COMPUTERS)
System of microprocessor instructions 22 p3770 N85-33362

INSTRUCTIONS
U EDUCATION

INSTRUCTORS
Ada (trademark) training curriculum. Advanced Ada topics L305 teacher's guide exercises
[AD-A154621] 21 p3670 N85-32796

INSTRUMENT APPROACH
Realistic localizer courses for aircraft instrument landing simulators
[NASA-CR-172333] 04 p0455 N85-12865
Safety recommendation(s), A-84-123 and -124
[REPT-3904B/89] 15 p2468 N85-25222

INSTRUMENT COMPENSATION
NT TEMPERATURE COMPENSATION
Compensation of skew passband of a SAW filter using predistortion 12 p1621 N85-21422
Sphericity gauge for wavefront of laser radiation 14 p2275 N85-24098
The use of a self-compensated magnetometer in an economical navigation system for the helicopter 16 p2697 N85-26850
Development of a prototype energy meter
[PB85-166430] 22 p3789 N85-33476
The final COS-B database: In-flight calibration of instrumental parameters
[OG-9.3-9] 23 p4028 N85-34964

INSTRUMENT DRIFT
U DRIFT (INSTRUMENTATION)

INSTRUMENT ERRORS
Problem of reduction to ideal wind tunnel in experimental aerodynamics 02 p0200 N85-11702
Minimization of anomalous errors in measuring systems employing search and testing devices 03 p0344 N85-12219
Buckling and eccentricity effects on orifice metering accuracy — gas meters
[ERS-E.350] 09 p1324 N85-18321
An experimental investigation into the effects of plate eccentricity and elastic deformation on orifice meter accuracy
[ERS-E.391] 09 p1325 N85-18325
On the application of compatibility checking techniques to dynamic flight test data
[ARL/AERO-R-161] 12 p1776 N85-21151
On the wind error of the Finnish raingauge
[REPT-37] 12 p1893 N85-21883

INSTRUMENT FLIGHT RULES
National airspace review: Airport radar service area operational confirmation report
[DOT/FAA/AT-84/2] 07 p0901 N85-15707
A guide to USAF helicopter instrument flight procedures
[AD-A156102] 24 p4083 N85-35182

INSTRUMENT LANDING SYSTEMS
NT ALL-WEATHER LANDING SYSTEMS
NT AUTOMATIC LANDING CONTROL
Use of microprocessor techniques and new antenna systems to improve the navigation aids very high frequency omnidirectional radar (VOR), Doppler VOR and Instrument Landing System (ILS)
[BMFT-FB-W-84-026] 02 p0137 N85-10930
Realistic localizer courses for aircraft instrument landing simulators
[NASA-CR-172333] 04 p0455 N85-12865
Investigation of pilot behavior in flight tests with a rate command/attitude hold control system
[DFVLR-FB-84-25] 05 p0699 N85-14486
Measurement of signal separation between radio service and air navigation service
[IRT-TB-B-40/82] 08 p1083 N85-16860
A preliminary investigation of handling qualities requirements for helicopter instrument flight during decelerating approach maneuvers and overshoot
[AD-A154650] 21 p3557 N85-32125

INSTRUMENT ORIENTATION
The design, fabrication and delivery of a spacelab neutral buoyancy Instrument Pointing System (IPS) mockup — underwater training simulator
[NASA-CR-171233] 04 p0462 N85-12934
Operational experience with ion concentration sensors in orientation systems 13 p1980 N85-22422
Evaluating accuracy in orientation of topographic photograph and satellite-centered direction from star photograph 13 p1983 N85-22442
Mobile antenna and beam pointing studies for satellite mobile communications
[NASA-CR-175736] 15 p2540 N85-25679
Modeling and analysis of pinhole occulter experiment: Initial study phase
[NASA-CR-175978] 19 p3272 N85-30287

INSTRUMENT PACKAGES
Recommended improvements for second generation 121.5/243 MHz ELT's
[NASA-CR-175274] 08 p1080 N85-16841

INSTRUMENT RECEIVERS
Development of a 20/30 GHz receiving station for propagation experiments with L-SAT
[AD-A148261] 06 p1152 N85-17271

INSTRUMENTAL ANALYSIS
U ANALYZING
U AUTOMATION

INSTRUMENTATION
U INSTRUMENTS

INSTRUMENTS
HOST instrumentation R and D program overview 02 p0141 N85-10957
Magnetospheric plasma studies using data from the dynamics high and low altitude plasma instruments
[AD-A145751] 03 p0392 N85-12505
Instrumentation technology overview 16 p2739 N85-26903

INSULATING MATERIALS
U INSULATION

INSULATION
NT ELECTRICAL INSULATION
NT MULTILAYER INSULATION
NT THERMAL INSULATION
Manifold insulated with knitted impregnated sleeve
[AD-D011270] 06 p0614 N85-15167
Passive storage technologies 09 p1106 N85-17003
Effect of sealants of the sound absorption coefficients of acoustical friable insulating materials
[AD-A148541] 06 p1218 N85-17674
High voltage RF coaxial cable
[AD-D011493] 11 p1629 N85-20255
Advanced glazings research
[DE85-000539] 11 p1674 N85-20549
International Conference on Defects in Insulating Crystals
[AD-A149611] 12 p1939 N85-22160
Optimization of overall dimensions of enclosures for low-voltage devices and equipment 13 p2067 N85-23033
AlN insulator for 3-5 MIS applications
[AD-A150674] 14 p2426 N85-24962
Theory and calculations of the electronic structure of solids having directional bonding
[AD-A151062] 14 p2426 N85-24971
Electrical research on solar cells and photovoltaic materials
[NASA-CR-175699] 15 p2585 N85-25935
Theoretical studies on the structures of insulating and metallic glasses
[DE85-010022] 18 p3194 N85-29814
Processable and stable conductive polymers
[AD-D011684] 19 p3249 N85-30143
Method for the preparation of photochromic insulating crystals
[DE85-011606] 19 p3262 N85-30229
A numerical solution of a nonisothermal wall using the two-dimensional Navier-Stokes equations
[AD-A154467] 19 p3266 N85-30257
Basic cryogenics and materials. Phase 1
[NASA-CR-177932] 21 p3572 N85-32215
Induction motors with minimum waste of magnetic iron 22 p3772 N85-33377
Results of variable enthalpy tests of CPR-488 TIP panels in MSFC Hot Gas Facility
[NASA-CR-170869] 24 p4072 N85-35237
Development and characterization of carbon-bonded carbon fiber insulation for radioisotope space power systems
[DE85-013365] 24 p4082 N85-35299
Injector losses on Mite
[DE85-012356] 24 p4090 N85-35355
Laser and electron beam processing of semiconductors
[AD-A155914] 24 p4161 N85-35796

INSULATORS
Optimized conditions for the formation of buried insulating layers in Si by high dose implantation of oxygen
[DE84-015389] 02 p0288 N85-11882
Effect of doping on the voltage holdoff performance of alumina insulators in vacuum
[DE84-017163] 04 p0480 N85-13060
Development of power system management
[PB84-216530] 04 p0497 N85-13173
Technology status of thermionic fuel elements for space nuclear power 05 p0610 N85-13893
Method for bonding insulator to insulator
[AD-D011340] 07 p0929 N85-15801
Moisture absorbing anti-arcing coating and method for applying same
[AD-D011310] 07 p0932 N85-15904
Dispersed metal-toughened ceramics and ceramic brazing
[NASA-CR-174284] 07 p0933 N85-15916
Two carrier dual injector apparatus
[AD-D011357] 07 p1047 N85-16846
Determination of threshold and maximum operating electric stresses for selected high voltage insulation. Task 3: Investigation of high voltage capacitor insulation
[DE84-017051] 09 p1316 N85-18274
Optical studies of dynamical processes in disordered materials
[DE85-002400] 10 p1453 N85-19158
Self-consistent simulation of plasma interactions with secondary-emitting insulators 13 p1993 N85-22492
Investigation of charge transport in the thermoelectret state of some ceramics and glasses
[DE85-009318] 17 p2936 N85-28122
Field theory of the metal-insulator transitions in restricted symmetries
[NOTA-INTERNA-829] 18 p3196 N85-29826
Fluorescence quenching by metal semiconductor and insulator surfaces 19 p3374 N85-30929
Predamage threshold electron emission from insulator and semiconductor surfaces
[DE85-008988] 19 p3377 N85-30954
Nuclear responses in INTOR plasma stabilization elements
[DE85-010489] 20 p3535 N85-31995
Metal-insulator-metal models of tunneling 20 p3536 N85-32006
Electronic structure and lattice dynamics of dimensionally constrained and disordered solids
[AD-A155927] 24 p4161 N85-35797

INSULIN
Investigation of adaptive distinctions of mechanism of controlled glycemia in Macaca rhesus monkeys 12 p1902 N85-21946

INTAKE SYSTEMS
NT AIR INTAKES
NT ENGINE INLETS
NT INLET AIRFRAME CONFIGURATIONS
NT SUPERSONIC INLETS
Inlet and airframe compatibility for a V/STOL fighter/attack aircraft with top-mounted inlets
[NASA-TM-84252] 01 p0003 N85-10015
A study of bird ingestions into large high bypass ratio turbine aircraft engines
[DOE/FAA/CT-84/13] 01 p0005 N85-10028
Developed turbulent flow under conditions of internal and external problems 02 p0260 N85-11700
Flow rates and pressure profiles for one to four axially aligned Borda inlets
[NASA-TP-2360] 05 p0636 N85-14078

Applications of finite and wave envelope element approximations to acoustic radiation from turbofan engine inlets in flight 05 p0726 N85-14684
Continuous laminar smoke generator [NASA-CASE-LAR-13014-1] 12 p1781 N85-21178
The role of convective perturbations in supercritical inlet oscillations 13 p2004 N85-22563
Performance and surge limits of a TF30-P-3 turbofan engine/axisymmetric mixed-compression inlet propulsion system at Mach 2.5 [NASA-TP-2461] 15 p2472 N85-25261
Multi-ducted inlet combustor research and development [AD-A153763] 18 p3063 N85-28946
An experimental investigation of fuel regression rate control in solid fuel ramjets [AD-A154251] 19 p3227 N85-30008
Investigation of the behavior of fuel in the intake manifold and its relation to SI engines, 1980 - 1983 19 p3279 N85-30337
Calculation of compressible flow about three-dimensional inlets with auxiliary inlets, slats and vanes by means of a panel method [NASA-CR-174975] 24 p4080 N85-35162

INTEGERS
Formats for numerical and textual data in data processing [DFVLR-MITT-84-07] 04 p0551 N85-13504
VLSI architectures for the multiplication of integers modulo a Fermat number 06 p0824 N85-13993
Techniques for computing the DFT using the residue Fermat number systems and VLSI 16 p2770 N85-27097

INTEGRAL CALCULUS
On the integral representation of bisubharmonic functions in Rn 10 p1536 N85-19684

INTEGRAL EQUATIONS
NT FREDHOLM EQUATIONS
NT J INTEGRAL
NT SINGULAR INTEGRAL EQUATIONS
NT VOLTERRA EQUATIONS
NT WIENER HOPF EQUATIONS
Integral equation of lifting surfaces in Laplace domain and analytic continuation of its pressure kernel [NAL-TR-795T] 01 p0002 N85-10009
Spline-Galerkin solution of integral equations for 3-body scattering above break-up [TWISK-327] 01 p0109 N85-10738
An integral method for analyzing incompressible two dimensional turbulent boundary layers with separation 02 p0196 N85-11309
Applications of integral equations with strong singularities in fracture mechanics 03 p0371 N85-12367
Loeb Sobolev spaces with applications to variational integrals and differential equations [CTH-MATH-1984-19] 04 p0556 N85-13544
A theoretical design method for 3-dimensional transonic wings [NAL-TR-830] 06 p0754 N85-14834
Analytic and sequential feynman integrals on abstract Wiener and Hilbert spaces, and A Cameron-Martin formula. Revision [AD-A146969] 07 p1030 N85-16537
Single integral constitutive equations for viscoelastic fluids [AD-A149410] 10 p1547 N85-19756
Algebraic decay in self-similar Markov chains [DE85-003162] 11 p1707 N85-20740
Evaluation of resonant modes in isolated dielectric resonators using a surface integral equation formulation [PB85-110631] 12 p1837 N85-21528
Noise transmission loss of a rectangular plate in an infinite baffle [NASA-TP-2398] 12 p1927 N85-22109
Magnetostatic-wave propagation in a finite YIG-Loaded rectangular waveguide [AD-A150332] 13 p2055 N85-22865
Axisymmetric magnetofluidstatic (MFS) equilibria of solar coronal loops: An integral equation approach 14 p2449 N85-25118
On the relation between upwind-differencing schemes of Godunov, Engquist-Osher and Roe [NASA-CR-175805] 16 p2852 N85-27583
On Long's solution to hydrostatic flow over mountains [DFVLR-MITT-84-02] 17 p2904 N85-28603
Quantized Hall effect in two-dimensional electron systems [AD-A154347] 19 p3259 N85-30211
Solving Volterra integral equations with ODE codes [DE85-011216] 19 p3346 N85-30740
A cracked orthotropic sheet stiffened by a semi-infinite orthotropic sheet [NASA-TP-2455] 21 p3597 N85-32339
Some properties of Loeb-Sobolev spaces [CTH-MATH-1985-01] 22 p3835 N85-33748
Integral equation formulation for three-dimensional unsteady transonic flow [ARL/STRUC-R-416] 23 p3894 N85-34119
Nonlinear adhesive behavior effects in a cracked orthotropic sheet stiffened by a semi-infinite orthotropic sheet [NASA-TM-87584] 23 p3941 N85-34428
A new method of differential structural analysis of gamma-family basic parameters [HE-3.6-3] 24 p4184 N85-35952

INTEGRAL FUNCTIONS
U ENTIRE FUNCTIONS

INTEGRAL TRANSFORMATIONS
NT CONVOLUTION INTEGRALS
NT FAST FOURIER TRANSFORMATIONS
NT FOURIER TRANSFORMATION
NT HILBERT TRANSFORMATION
NT LAPLACE TRANSFORMATION
Simplified proofs of some basic theorems for quasiregular mappings 10 p1535 N85-19677
The Gauss-Krueger projection of the Earth ellipsoid with direct calculation of elliptic integrals through Landen transformations [SER-C-296] 11 p1666 N85-20495
A note on the use of polynomial transformations in evaluating singular integrals [MATHEMATICS-RESEARCH-165] 12 p1920 N85-22053
The implementation of the Tanh transformations in the evaluation of singular integrals [MATHEMATICS-RESEARCH-171] 12 p1920 N85-22054
Uniform asymptotic expansions of integrals [CWI-AM-R8412] 17 p3022 N85-28694
Dynamical systems and numerical integration [CWI-AM-R8413] 17 p3022 N85-28695
Spectral transform approach to Backlund transformations [PREPRINT-420] 18 p3172 N85-29663
On the solution for the sound field in a semi-infinite uniform duct with sheared mean flow 20 p3523 N85-31912

INTEGRALS
Recursive calculation of curved finite element stiffness matrices [CSIR-TWISK-303] 01 p0108 N85-10728
An integral inequality with applications to order statistics [AD-A145081] 01 p0113 N85-10770
Integral of wave kinetic equation of drift waves 02 p0283 N85-11848
Analytic and sequential feynman integrals on abstract Wiener and Hilbert spaces, and A Cameron-Martin formula. Revision [AD-A146969] 07 p1030 N85-16537
On the distribution of integral and prime divisors with equal norms 11 p1698 N85-20669
Supermanifolds and Berezin's new integral [DE85-001833] 11 p1706 N85-20732
Translational and extensional energy release rates (the J- and M-integrals) for a crack layer in thermoelasticity [NASA-CR-174872] 12 p1863 N85-21685
An integral representation of the generalized Euler-Mascheroni constants [NASA-TP-2456] 13 p2144 N85-23305
Study of integral and spectral direct solar radiation over Atlantic 14 p2341 N85-24475
On the boundary behaviour of a rotation automorphic function with finite spherical Dirichlet integral 15 p2634 N85-26238
A remark on the conformal capacity of Groetzsch's condenser in space 15 p2634 N85-26240
Extrapolation methods for multi-dimensional quadrature of singular and regular integrand functions [DE85-009665] 18 p3172 N85-29655
Admissible convergence of Poisson integrals in symmetric spaces [CTH-MATH-1985-04] 22 p3836 N85-33750
Applications of the Kirchoff-Helmholtz integral to problems in body wave seismology 24 p4116 N85-35515

INTEGRATED CIRCUITS
NT LARGE SCALE INTEGRATION
NT TTL INTEGRATED CIRCUITS
NT VERY LARGE SCALE INTEGRATION
NT VHSIC (CIRCUITS)
RADC/NBS (Rome Air Development Center/National Bureau of Standards) Workshop. Moisture Measurement and Control for Semiconductor Devices, 3 [PB84-219559] 01 p0051 N85-10337
Hardware implementation of a support system for the 2501 Western digital LSI, complete controller of the second level, first version of the CCITT 25 (CAP) recommendations [FUB-80-1982] 01 p0100 N85-10668
Cosmic ray effects on microelectronics. Part 3: Propagation of cosmic rays in the atmosphere [AD-A145026] 01 p0131 N85-10902
Microwave susceptibility experiments [DE84-016188] 02 p0192 N85-11281
Investigation of the application of the marginal tension technique to test electronic devices, phase 3 [ESD-11-301] 02 p0206 N85-11360
Guided-wave optic devices for integrated optic information processing [AD-A145695] 02 p0280 N85-11827
Influence of aluminum oxide film on thermocompression bonding of gold wire to evaporated aluminum film [NASA-TM-77503] 03 p0330 N85-12127
West Europe report: Science and technology, no. 168 [JPRS-84845] 03 p0341 N85-12190
Integrated circuits, MBM's, form focus of work at French LETI 03 p0341 N85-12194
Problems in CEMA microelectronic cooperation noted 03 p0341 N85-12196
Numerical investigation of diffraction models of microwave integrated circuits 03 p0347 N85-12233
Functional checking of microprocessors and microprocessor systems 03 p0347 N85-12236
Basic EMC (Electromagnetic Compatibility) technology advancement for C3 systems, macromodeling of digital circuits, volume 2B [AD-A146333] 03 p0359 N85-12306
VLSI (Very Large Scale Integration) design tools reference manual, release 1.0 [AD-A146273] 03 p0408 N85-12604
Research activities of the Illinois University Coordinated Science Laboratory [AD-A145589] 03 p0449 N85-12858
Analysis of frequency-selective integrated circuits in system of normal coordinates 04 p0488 N85-13119
Machine computation of delay and capacitance of transistor structures of subnanosecond large integrated circuits 04 p0490 N85-13120
Comparison analysis of algorithm for construction of functional tests for combined large-scale integrated circuits 04 p0490 N85-13121
Quasi-three dimensional modeling of functionally-integrated elements of large-scale integrated circuits 04 p0490 N85-13122
Analysis of dynamic characteristics and ways of development of bipolar main memory with miniaturization of integrated circuit elements 04 p0490 N85-13123
Planning of hybrid integrated circuits for microwave-band oscillators 04 p0490 N85-13124
Propagation of acoustic shear waves through active periodic structure 04 p0490 N85-13125
Standard cell initial placement strategy [DE84-016921] 05 p0632 N85-14051
User-oriented development and production of integrated circuits in small and medium quantities [BMFT-FB-T-84-171] 05 p0633 N85-14059
Practical application of electron beam testing in LSI and VLSI circuits [BMFT-FB-T-84-185] 05 p0633 N85-14061
Fly's eye sensor nonlinear signal processing [AD-D011290] 05 p0729 N85-14884
Efficiency in integral active antennae 06 p0792 N85-15060
Computer investigation of effects of high injection in transistor large integrated circuit structures 06 p0793 N85-15068
Trends in development of bipolar power transistors 06 p0793 N85-15072
Quality control of integrated circuits by parametric identification methods 06 p0796 N85-15085
Characterization of MMIC devices for active array antennas [NASA-TM-86907] 07 p0913 N85-15779
Investigation of planar waveguides and components for millimeter-wave integrated circuits [AD-A147380] 07 p0948 N85-16005
Control technology for integrated circuit fabrication at Micro-Circuit Engineering, Incorporated, West Palm Beach, Florida [PB85-100717/GAR] 07 p0949 N85-16013
Linear wideband microwave amplifiers for monolithic integrated microcircuits 07 p0955 N85-16051
Trends in development of software for computer-aided analysis of large-scale integrated circuits 07 p0955 N85-16055
Built-in test and self repair mechanisms in a digital correlator integrated circuit 08 p1064 N85-16741
Chemical, material electronics studies established 08 p1142 N85-17200
General assessment of GDR microelectronics industry, applications 08 p1142 N85-17202
Data acquisition channel apparatus [AD-D011429] 08 p1159 N85-17311

Configuration study for a 30 GHz monolithic receive array: Technical assessment
[NASA-CR-174997] 09 p1311 N85-18238
Device modeling for advanced integrated circuits
09 p1314 N85-18258
The planned expansion of microelectronics capability at Sandia National Laboratory
[TI85-004326] 09 p1314 N85-18260
An inexpensive vector thin film magnetometer
[AD-A148725] 09 p1323 N85-18310
DDL system: Design synthesis of digital systems
[NASA-CR-170759] 09 p1366 N85-19584
Semiconductors at Leipzig Spring Fair
09 p1377 N85-19660
Bondability of Al-Si thin film in thermosonic gold wire bonding — integrated circuits
[NASA-TM-77765] 10 p1439 N85-19071
Researchers, projects at French intelligent machine center
10 p1460 N85-19207
Siemens' CAD system designs VLSI circuits
10 p1461 N85-19209
Research into self-timed VLSI circuits
[AD-A149140] 10 p1479 N85-19339
Qualitative of analysis of MOS circuits
[AD-A148937] 10 p1480 N85-19341
Advanced inverter technology
[AD-A149335] 10 p1480 N85-19343
Integrated circuit tunable cavity oscillator
[AD-D011474] 10 p1481 N85-19351
Linear, position-sensitive X-ray detector used for real-time calculations of small-angle scattering parameters with submillisecond resolution
[DE85-002530] 10 p1489 N85-19401
Liquid-phase epitaxial growth of CdTe on HgCdTe
[AD-D011482] 10 p1561 N85-19946
Control technology for integrated circuit fabrication at Honeywell Optoelectronics Division, Richardson, Texas
[PB85-109023] 11 p1616 N85-20162
China report: Science and technology
[JPRS-CST-84-039] 11 p1621 N85-20206
High quality super-large circuits developed
11 p1622 N85-20209
Method of examining microcircuit patterns
[NASA-CASE-NPO-16299-1] 11 p1628 N85-20250
Design of a semi-custom integrated circuit for the SLAC SLC timing control system
[DE85-003091] 11 p1629 N85-20258
Description of 8048 microcomputer operation published
11 p1700 N85-20685
Method for the fabrication of dielectric isolated junction field effect transistor and PNP transistor
[AD-D011500] 12 p1632 N85-21494
Monolithic thin film SAW (Surface Acoustic Wave) structures
[AD-A149782] 12 p1635 N85-21511
Concurrent simulation techniques exploiting hierarchy
[AD-A149783] 12 p1635 N85-21512
Design of a bit-sliced processor array with built-in-self-test
[AD-A149785] 12 p1635 N85-21513
Factors affecting SOS (Silicon-On-Sapphire) yield and reliability
[AD-A150004] 12 p1635 N85-21515
Universal file processing program for field programmable integrated circuits
[DE85-004364] 12 p1637 N85-21526
Built-in tests for VLSI (Very Large Scale Integration) finite-state machines
[AD-A149784] 12 p1911 N85-21997
X-ray lithography and VLSI circuits
13 p2052 N85-22846
Basic EMC (electromagnetic interference) technology advancement for c3 systems. Volume 3A: Probabilistic analysis of combinational circuits with random delays
[AD-A150349] 13 p2055 N85-22866
Advanced mixed-mode simulation techniques
13 p2062 N85-22883
Low capacitance e-beam fabricated beam-lead Schottky barrier diodes
[AD-A150236] 13 p2063 N85-22886
EOS (electrical overstress) protection for VLSI (Very Large Scale Integration) devices
[AD-A150333] 13 p2064 N85-22891
High sheet resistance, arsenic implanted polycrystalline silicon for integrated circuit resistors
[DE85-004355] 13 p2065 N85-22902
Algorithm in Walsh function basis for analysis of integrated microcircuits on MOS-structures
13 p2083 N85-23006
Synthesis of optimum smooth transition in microstrip through line on microwave integrated circuit
13 p2089 N85-23041
Parallel test method for LSI (Large Scale Integration) microprocessors
[AD-A150237] 13 p2144 N85-23310
Design for tactical avionics maintainability, technical evaluation report
[AGARD-AR-204] 14 p2225 N85-23798
Onboard demand scheduling of a multibeam SS/TDMA satellite with integrated circuit and packet switching
14 p2229 N85-23812
Plans, developments in robotics
14 p2289 N85-24191
Proceedings of the Cold Electronics Workshop
[NASA-CR-175862] 14 p2297 N85-24220
Cold electronics: An overview
14 p2297 N85-24221
The effects of cooling on delay-time limits in IC's
14 p2297 N85-24224
Bipolar nonswitching logic arrays: Universal components of function expanders for computation of elementary functions
14 p2400 N85-24797
UW/NW (University of Washington/Northwest) VLSI Consortium
[AD-A150740] 14 p2404 N85-24818
The effects of water and hydrogen on materials used in integrated circuit packages
[AD-A151693] 15 p2518 N85-25529
Computer-aided identification of complete constitution model of transistor structure for design of submicrosecond large-scale-integrated circuits 15 p2529 N85-25594
Developments in microelectronics: Past and future
15 p2530 N85-25597
East Europe report: Science and technology
[JPRS-ESA-84-016] 15 p2533 N85-25624
Aspects of CSSR CMOS integrated circuits discussed
15 p2533 N85-25627
Recent developments 15 p2533 N85-25628
MHB4046 phase-lock circuit 15 p2533 N85-25629
Improved, cheaper SIPMOS circuits no. 10, 1983 p 370
15 p2534 N85-25630
Phase-locked loop design with MHB4046
15 p2534 N85-25631
Additional PLL designs 15 p2534 N85-25632
New designs from electronics R and D center
15 p2536 N85-25666
Conversion of algorithms to custom integrated circuit devices
[AD-A151288] 15 p2547 N85-25720
Analysis of the capability to effectively design complementary metal oxide semiconductor integrated circuits
[AD-A151832] 15 p2548 N85-25726
Designing VLSI (Very Large Scale Integrated) circuits for testability
[AD-A151834] 15 p2549 N85-25729
A microcomputer-based program for printing check plots of integrated circuits specified in Caltech Intermediate form
[AD-A151715] 15 p2629 N85-26205
Technical evaluation report on Avionics Panel Specialists' Meeting on Digital Optical Circuit Technology
[AGARD-AR-202] 15 p2653 N85-26367
The impact of VLSI on guidance and control system design 16 p2697 N85-26654
An integrated UNIX-based CAD system for the design and testing of custom VLSI chips
16 p2771 N85-27102
System design of automated VLSI (Very Large Scale Integrated) test station and implementation of selected system aspects
[AD-A151961] 16 p2776 N85-27147
Radiation hardening for VLSI applications
[DE85-005493] 16 p2780 N85-27155
Bond test data acquisition and analysis system
[DE85-007021] 16 p2780 N85-27158
The systematic integration of very large scale integrated circuit computer-aided design tools into a toolkit optimized for academic applications
[AD-A151813] 16 p2845 N85-27536
East Europe report: Science and technology
[JPRS-ESA-85-017] 17 p2945 N85-28177
Goals, achievements of microelectronics program
17 p2945 N85-28179
Uses of, experiences in production of custom designed IC's 17 p2945 N85-28180
Modern equipment for manufacture of IC's in Hungary
17 p2945 N85-28181
SC filters and design centering of integrated circuits. Part 2: Design centering of integrated circuits
[BMFT-FB-T-84-265-PT-2] 17 p2956 N85-28257
Investigation of semiconductor clad optical waveguides
[NASA-CR-175870] 17 p3096 N85-28785
Development of thin film hybrid IC active filter for video band use
[NHK-LABS-NOTE-312] 18 p3094 N85-29153
System design of multi-layer (3-dimensional) integrated circuits
[AD-A153468] 18 p3094 N85-29154
The use of VLSI technology for the real-time generation of graphics displays: A proposal
[AD-A153786] 18 p3160 N85-29578
The potential of semiconductors for optical integrated circuits 18 p3167 N85-29788
Split-cross-bridge resistor for testing for proper fabrication of integrated circuits
[NASA-CASE-NPO-16021-1] 19 p3256 N85-30187
High speed GaAs device and integrated circuit modelling and simulation 19 p3256 N85-30191
A comparison of the radiation hardness of various VLSI technologies for defense applications
[DE85-006973] 19 p3263 N85-30236
Leading-edge microelectronics research at Sweden's Chalmers 20 p3438 N85-31337
Globally-asynchronous locally-synchronous systems
[AD-A154624] 21 p3573 N85-32222
Parallel simulation of digital LSI circuits
[AD-A154745] 21 p3580 N85-32258
GAO (General Accounting Office) assessment of DOD's Very High Speed Integrated Circuits (VHSIC) technology program
[AD-A155109] 21 p3581 N85-32261
LSI/VLSI ion implanted planar GaAs IC processing
[AD-A155110] 21 p3581 N85-32262
Tight bounds on the complexity of parallel sorting
[AD-A154726] 21 p3667 N85-32778
Digital integrated circuits 21 p3669 N85-32787
Development of a dedicated speech work station
[AD-A155465] 21 p3674 N85-32824
Adaptive modeling of electronic circuits
22 p3766 N85-33345
Software for frequency analysis of microwave circuits
22 p3768 N85-33352
USSR report: Electronics and electrical engineering
[JPRS-UEE-84-003] 22 p3773 N85-33381
Multidiode integrated-circuit protective device
22 p3781 N85-33425
Synthesis of metrico-topological model for layout of topology of large-scale-integration arrays
22 p3781 N85-33427
Synthesis of high-speed devices using integrated operational amplifiers 22 p3781 N85-33428
Joint services electronics program
[AD-A154748] 23 p3927 N85-34336
Multi-robot assembly of IC's 23 p3964 N85-34577
Analog, still without fear
[AD-A155920] 24 p4089 N85-35348
A methodology for the design of testable custom large-scale integrated circuits
[AD-A156098] 24 p4090 N85-35351
Monolithic photovoltaic series array for an energy coupler
[BMFT-FB-T-85-023] 24 p4113 N85-35496
Computer Aided Design (CAD) methods for very large scale integration systems
[BMFT-FB-T-85-029] 24 p4141 N85-35668
Laser and electron beam processing of semiconductors
[AD-A155914] 24 p4161 N85-35796

INTEGRATED ENERGY SYSTEMS

An Assessment of Integrated Flywheel System Technology
[NASA-CP-2346] 05 p0604 N85-13850
Comparative energy storage assessment item
05 p0605 N85-13858
Develop and test fuel cell powered on-site integrated total energy systems. Phase 3: Full-scale power plant development
[NASA-CR-174887] 15 p2586 N85-25941

INTEGRATED OPTICS

Guided-wave optic devices for integrated optic information processing
[AD-A145885] 02 p0280 N85-11827
Advanced infrared laser modulator development
[NASA-CR-172479] 06 p0862 N85-15479
Technological and economic assessment of advanced ceramic materials. Volume 1: Summary and conclusions
[PB85-113082] 12 p1615 N85-21383
Technological and economic assessment of advanced ceramic materials: Volume 4: A case study of integrated optic devices
[PB85-113116] 12 p1615 N85-21385
Technological and economic assessment of advanced ceramic materials. Volume 6: A case study of ceramic cutting tools
[PB85-113132] 12 p1615 N85-21387
Multifunctional elements for integrated optics
13 p2066 N85-22918
Integrated optical components utilizing acoustooptic and electrooptic diffraction in micro-waveguides
13 p2089 N85-23044
Investigation of semiconductor clad optical waveguides
[NASA-CR-175870] 17 p3096 N85-28785

Digital Optical Circuit Technology
[AGARD-CP-362] 16 p3185 N85-29757
Integrated electrooptical components using dielectric substrates 16 p3187 N85-29767
Solar adaptive optics
[AD-A155434] 21 p3724 N85-33101
INTEGRATION (REAL VARIABLES)
U MEASURE AND INTEGRATION
INTEGRATORS
NT DIGITAL INTEGRATORS
Integrated control and display systems for helicopter battlefield mission management 08 p1073 N85-16805
Evaluation of time integrators for the shallow water equations
[CWI-NM-R8408] 11 p1634 N85-20292
Numerical optical computing at the Ohio State University 16 p3188 N85-29775
INTEGRITY
NT COMPUTER PROGRAM INTEGRITY
Avionics integrity program (Awip). Volume 4: Force management. Economic life considerations
[AD-A145592] 02 p0136 N85-10941
Artificial intelligence approaches to monitoring system integrity
[AD-F009930] 02 p0246 N85-11610
INTEGRODIFFERENTIAL EQUATIONS
U DIFFERENTIAL EQUATIONS
U INTEGRAL EQUATIONS
INTELLECT
Manual and computer-aided sequential diagnostic inference
[AD-A156229] 24 p4133 N85-35620
INTELLIGENCE
NT ARTIFICIAL INTELLIGENCE
NT EXPERT SYSTEMS
NT EXTRATERRESTRIAL INTELLIGENCE
NT INTELLECT
Conjunctive and disjunctive item response functions
[AD-A147815] 07 p1033 N85-16561
Transfer of technology
[S-REPT-98-884] 12 p1949 N85-22246
Human cognition and intelligence: Towards an integrated theoretical perspective
[CSIR-SR-PERS-350] 13 p2143 N85-23900
Military journal on US intelligence satellites 16 p2727 N85-26832
Design and implementation of an intelligence database
[AD-A154095] 19 p3381 N85-30973
INTELLIGIBILITY
NT SPEECH RECOGNITION
Hearing protection and speech intelligibility of two nonstandard inflight communication headsets
[AD-A146110] 03 p0355 N85-12284
INTELSAT SATELLITES
Television transmission in frequency modulation 04 p0493 N85-13146
Electrical design of the Intelsat 6 solar generator 13 p2008 N85-22592
INTENSIFICATION
U AMPLIFICATION
INTENSIFIER TUBES
U IMAGE INTENSIFIERS
INTENSIFIERS
NT IMAGE INTENSIFIERS
INTENSITY
Interplanetary cosmic ray intensity: 1972-1984 and out to 32 AU
[AD-A145130] 01 p0131 N85-10008
Beam profiling in gigawatt 1064-nm lasers used in research on optical materials at Livermore
[DE84-007226] 04 p0505 N85-13223
Hurricane Alicia, Galveston and Houston, Texas, 17-18 August 1983
[PB84-237056] 04 p0541 N85-13441
Magnetic constraints on early lunar evolution revisited: Limits on accuracy imposed by methods of paleointensity measurements 04 p0582 N85-13716
Effect of stationary magnetic field on bleeding time 12 p1904 N85-21956
INTERACTIONAL AERODYNAMICS
Calculation of unsteady transonic separated flows by viscous-inviscid interaction 15 p2458 N85-25176
An experimental and analytical study of the aerodynamic interference effects between two Sears-Haack bodies at Mach 2.7
[NASA-TM-85729] 16 p2700 N85-26873
Flow around rotating and nonmoving circular cylinder near flat screen. Report 1: Aerodynamic forces in cylinder 16 p2765 N85-27059
Study of stresses on surface of flat barrier immersed in under expanded jet of rarefied gas 16 p2765 N85-27061
Propulsion efficiency of vibrating bodies in subsonic gas stream 17 p2942 N85-28159
INTERACTIONS
Metal-support interactions: Their effects upon adsorption, electronics, and activity/selectivity properties of cobalt in hydrogenation
[DE85-003316] 09 p1292 N85-18113
Electromagnetic pulse (EMP) interaction with electric power systems. Power Systems Technology Program
[DE85-000166] 09 p1312 N85-18244
A frozen vorticity approach to the subsymmetric strong interaction problem
[AD-A149101] 10 p1484 N85-19369
INTERACTIVE CONTROL
Interactive graphics nonlinear constrained optimization 01 p0058 N85-10367
Interactive color-graphics interface for energy monitoring and control systems
[AD-A147536] 07 p1025 N85-16509
MINDS: A microcomputer interactive data system for 8086-based controllers
[NASA-TP-2378] 08 p1204 N85-17576
Further development of an Interactive Control Engineering Computer Analysis Package (ICECAP) for discrete and continuous systems
[AD-A151783] 16 p2948 N85-27548
A modern control theory enhancement to an Interactive Control Engineering Computer Analysis Package (ICECAP)
[AD-A153249] 17 p3012 N85-29822
Interactive computer program for the analysis and design of linear time invariant systems
[AD-A154076] 19 p3335 N85-30684
Interactive aircraft flight control and aeroelastic stabilization
[NASA-CR-176035] 20 p3396 N85-31064
INTERACTIVE GRAPHICS
U COMPUTER GRAPHICS
INTERATOMIC FORCES
Quantum characteristics of kinetic fracturing of solids 02 p0265 N85-11732
Atomistic studies of grain boundaries with segregated impurities
[DE85-000063] 11 p1737 N85-20924
Planetary fluids He and NH3 at high shock pressure and temperatures
[DE85-011651] 22 p3859 N85-33895
INTERCALATION
Dynamics of graphite fiber intercalation: In situ resistivity measurements with a four point probe
[NASA-TM-86858] 01 p0017 N85-10105
Stability of bromine intercalated graphite fibers
[NASA-TM-86859] 01 p0091 N85-10187
Reaction mechanisms in the formation of intercalation complexes, and properties of intercalated molecules 03 p0431 N85-12745
An investigation of the electrical conductivity in highly oriented graphite intercalation compounds
[AD-A146539] 06 p0804 N85-15116
The 13C nuclear magnetic resonance in graphite intercalation compounds
[NASA-CR-174261] 07 p1040 N85-16601
Structure-property relationships in intercalated graphite
[AD-A147948] 08 p1219 N85-17680
Electronic properties of intercalated graphite and amorphous metals
[AD-A147664] 08 p1225 N85-17716
Compositional, structural, and physical studies of some graphite hexafluoroarsenates and their relatives
[DE85-000855] 10 p1432 N85-19030
Investigation of electric and magnetic properties of intercalated graphite
[AD-A148001] 12 p1797 N85-21274
Electric and magnetic properties of intercalated graphite
[AD-A148648] 12 p1798 N85-21276
Neutron scattering studies of graphite intercalation compounds
[DE85-003079] 12 p1942 N85-22186
Homogeneity of pristine and bromine intercalated graphite fibers
[NASA-TM-87016] 15 p2517 N85-25521
Graphite fiber intercalation: Dynamics of the bromine intercalation process
[NASA-TM-87015] 16 p2742 N85-26921
Environmental stability of intercalated graphite fibers
[NASA-TM-87025] 16 p2763 N85-26992
A micrographic and gravimetric study of intercalation and deintercalation of graphite fibers
[NASA-TM-87026] 17 p2934 N85-28110
Structural and physical studies on a new class of low-dimensional conducting material: FeOCl intercalated with TTF and related molecules
[DE85-009701] 18 p3198 N85-29824
INTERCEPTION
LPI-radar for helicopter obstacle warning 08 p1074 N85-16810
Modeling interception of rainfall by forests and the role of interception in the water balance
[DE85-002822] 12 p1884 N85-21825
Space interception guidance with uncertain factors 13 p2042 N85-22781
INTERCEPTOR AIRCRAFT
U FIGHTER AIRCRAFT
INTERCONNECTION
U JOINING
INTERCONTINENTAL BALLISTIC MISSILES
NT MINUTEMAN ICBM
Invited papers: DNA ICBM technical R and D program 09 p1333 N85-18379
INTERCOSMOS SATELLITES
Space-time features of solar cosmic ray penetration into high latitude regions of Earth's magnetosphere based on Intercosmos-19 satellite data 15 p2481 N85-25310
Interkosmos program of space communication development 15 p2539 N85-25585
INTERDIGITAL TRANSDUCERS
Experimental study of high-stability oscillator with surface-acoustic-wave resonator in feedback loop 13 p2060 N85-23053
Compensation of acoustic wave devices
[AD-D011582] 15 p2648 N85-26322
Microwave SAW (Surface Acoustic Wave) monochromator
[AD-D011718] 21 p3580 N85-32311
INTERFACE STABILITY
Thermal conductivity and interface resistance of particle-filled silicone resin
[DE84-011691] 04 p0479 N85-13056
Polymer-polymer interface bond stability 06 p0830 N85-15271
Polymer-metal interface bond stability 06 p0830 N85-15272
Instability of film boiling of moving liquids
[BLL-WH-603-(8091.9F)] 07 p0958 N85-16056
Instability at the interface between two shearing fluids in a channel
[AD-A153532] 18 p3099 N85-29185
Application of the MHD energy principle to magnetostatic atmospheres
[NASA-CR-175967] 18 p3136 N85-29420
Compressible two-phase flow instabilities simulated with a hybrid Lagrange-Euler pseudospectral method
[DE85-009904] 23 p3931 N85-34361
INTERFACES
NT FLUID BOUNDARIES
NT GAS-SOLID INTERFACES
NT JET BOUNDARIES
NT LIQUID-LIQUID INTERFACES
NT LIQUID-SOLID INTERFACES
NT LIQUID-VAPOR INTERFACES
NT SOLID-SOLID INTERFACES
Automation of coastal engineering modelling facilities
[CSIR-T/SEA-8304] 01 p0035 N85-10219
Electronics Engineering Department: EE technical review
[DE84-016124] 01 p0044 N85-10288
PDSS/IMC CIS user's guide
[NASA-CR-171179] 01 p0102 N85-10882
Surface environmental effects in electrochemical kinetics: Outer-sphere chromium (3) reductions at mercury, gallium, lead, and thallium surfaces
[AD-A145807] 02 p0172 N85-11155
Pluribus satellite IMP (Interface Message Provision) development mobile access terminal network
[AD-A145348] 02 p0190 N85-11269
Multiplexing the ethernet interface among VAX/VMS users
[AD-A145539] 02 p0243 N85-11588
Checking optical-polarization measurements at interfaces 02 p0271 N85-11770
An approach to interfacing data bases in WWMCCS ADP
[AD-A148350] 03 p0439 N85-12793
The chemical nature of the fiber/resin interface in composite materials 04 p0485 N85-12953
Composite property dependence on the fiber, matrix, and the interphase 04 p0485 N85-12954
Study program for encapsulation materials interface for Flat-plate Solar Array (FSA) project
[NASA-CR-174162] 04 p0580 N85-13385
Physical database processor preliminary interface specifications
[PB84-217561] 04 p0548 N85-13483
Elastodynamic stress intensity factors of an interface finite-width crack
[DE84-016608] 06 p0817 N85-15190
High speed magnetic tape interface for a microcomputer
[CSIRO-TP-7] 06 p0847 N85-15377
A standard operating system interface for microcomputer software development
[AD-A148884] 08 p0864 N85-15428

Design and analysis of an SQL (Structured Query Language) interface for a multi-backend database system
[AD-A146534] 06 p0856 N85-15447
Titanium Matrix/Continuous Fiber/Continuous fiber composite interface interactions and their influence on mechanical properties
[AD-A147504] 07 p0920 N85-15629
Interactive color-graphics interface for energy monitoring and control systems
[AD-A147538] 07 p1025 N85-16509
Hardware/software codesign for maintainable systems
08 p1066 N85-16753
Integrated design checkout of shuttle payload avionics interfaces 08 p1092 N85-16899
Kernel Ada Programming Support Environment (KAPSE) interface team public report, volume 4
[AD-A147648] 08 p1205 N85-17581
Electrochemical interfaces and electrode processes
[AD-A147414] 09 p1290 N85-18098
Photoacoustic spectroscopy at electrode-solution interface
[DE85-001872] 09 p1292 N85-18111
Nondestructive characterization of semiconductor surfaces and interfaces 09 p1329 N85-18349
Influence of the amorphous-crystalline interface morphology on dislocation nucleation in pre-amorphized silicon
[DE85-002088] 09 p1398 N85-18800
A comprehensive study on sublaminate crack growth stability and its effects on the load-carrying capacity
[AD-A149037] 10 p1432 N85-19028
Numerical simulations of liquid propellant combustion instability: Onset and growth
[DE85-000743] 10 p1458 N85-19186
Man-machine interaction: Operator
[AD-A149075] 10 p1531 N85-19648
Management challenges encountered in CAD implementation
[DE85-002072] 10 p1541 N85-19716
Effect of interfacial characteristics of metal clad polymeric substrates on electrical high frequency interconnection performance
[NASA-TM-86948] 11 p1624 N85-20223
Elastic compliance of imperfect interfaces: Review and relationship to ultrasonic scattering
[DE85-003068] 11 p1652 N85-20404
Electrochemical processes at the sodium (BETA)" alumina interface
[DE85-004653] 12 p1802 N85-21305
DOS 21: PCDOS 2.0 support subroutine package for the IBM personal computer
[LA-10142-MS] 12 p1914 N85-22012
ZTLCK: A subroutine package for the IBM personal computer to support the Zlatech ZT1488 real time clock
[LA-10148-MS] 12 p1914 N85-22014
Interface specifications for SCR (Software Cost Reduction) (A-7E) extended computer module, revised
[AD-A149948] 12 p1915 N85-22024
A formal method for specifying computer resources in an implementation independent manner
[AD-A149955] 12 p1918 N85-22043
Numerical methods for tracking interfaces
[LA-9917-MS] 12 p1919 N85-22052
Nucleation of phase transitions in the vicinity of phase boundary. Part 1: Comparison of various idolated mechanisms. Part 2: Coupled cluster growth processes
[N-0208-5058] 12 p1938 N85-22174
Problems with electrical interference between solar generators and shunt type regulators
13 p2010 N85-22607
Presentation based user interfaces
[AD-A150311] 13 p2144 N85-23311
A design analysis and implementation of a user-friendly interface for the UNIX operating system
[AD-A150558] 13 p2145 N85-23312
The Multimission Image Processing Laboratory's virtual frame buffer interface
[NASA-CR-175655] 14 p2402 N85-24805
A fast ray tracing routine for laterally inhomogeneous media
[AD-A150984] 14 p2421 N85-24938
Electroreflectance spectroscopy as a probe of the electronic structure at the metal-electronic interface
[DE85-003541] 14 p2428 N85-24976
Mixing across a gas-gas interface
[AD-A151471] 15 p2556 N85-25770
COSMIC/NASTRAN-PATRAN interface
15 p2574 N85-25870
Orbiter middeck/payload standard interfaces control document
[NASA-TM-87473] 16 p2729 N85-26840
Microscopic study of the influence of impurities on interface bonding
[AD-A151725] 16 p2743 N85-26928
Continued development and implementation of the Universal Network Interface Device (UNID) 2 in the Digital Engineering Laboratory Network (DELNET), volume 2
[AD-A151947] 16 p2850 N85-27570
A new technique for system-to-system transfer of surface data 17 p3007 N85-28589
CAMAC 488 module: 68000 based GPIB interface module
[DE85-006367] 17 p3014 N85-28635
Incorporation of Monte Carlo electron interface studies into photon general cavity theory
[DE85-007674] 17 p3034 N85-28772
The effect of ion-bombardment-induced atomic mixing on depth-profiling of interfaces
[AD-A153199] 17 p3044 N85-28834
LDV multiplexer interface
[NASA-CASE-ARC-11536-1] 19 p3258 N85-30202
Method for producing high quality germanium-germanium nitride interfaces for germanium semiconductors and device produced thereby
[AD-D011702] 19 p3260 N85-30218
VUV synchrotron light as a technique for studying the interface quality and properties of thin overlayers
[DE85-009822] 19 p3262 N85-30227
BREED: A CDC-7600 computer program for the automation of breeder reactor design analysis (LWBR Development Program)
[DE85-010327] 19 p3338 N85-30686
Photoeffects of semiconductor electrolyte interfaces
[AD-A154163] 20 p3449 N85-31411
Chemical structure of interfaces
20 p3480 N85-31629
Effects of contact area of an interface on acoustic wave transmission characteristics
[DE85-009935] 20 p3524 N85-31920
Some dynamic electronic properties of semiconductor surfaces and interfaces 20 p3537 N85-32007
Improved materials for composite and adhesive joints
[AD-A155065] 21 p3562 N85-32153
Interface chemistry of Hg(1-x)Cd(x)Te
[AD-A154876] 21 p3563 N85-32161
EVA-glass interface bond stability
21 p3608 N85-32408
Interfacial bonding stability 21 p3608 N85-32409
On the limiting configuration of interfacial gravity waves
[AD-A154821] 21 p3631 N85-32557
Experimental studies of chemical reactivity during shock initiation of hexanitrostilbene
[DE85-011726] 22 p3754 N85-33270
Module for interfacing microprocessors and microcomputer 22 p3774 N85-33390
Supermite vacuum interface design
[DE85-012861] 22 p3837 N85-33759
High resolution electron microscopic characterization of interfaces in ceramics
[DE85-011207] 23 p3920 N85-34289
The interactive planning work station: A graphics-based UNIX (trademark) tool for application users and developers 23 p3957 N85-34527
An image management kernel for the design of relational and pictorial data bases 23 p3958 N85-34532
Graphics interaction in databases
23 p3958 N85-34534
Issues and techniques in touch-sensitive tablet input (executive summary) 23 p3960 N85-34543
Efficient recovery and reversal in graphical user interfaces generated by the Higgens system
23 p3960 N85-34544
A model for graphics interface tool development
23 p3960 N85-34545
Using percent-done program indicators to enhance user interfaces 23 p3960 N85-34546
The CADME approach to the interface of solid modellers 23 p3961 N85-34554
An innovative user interface for microcomputer-based computer-aided design 23 p3961 N85-34555
How map designers can represent their ideas in thematic maps: Effective user interfaces for thematic map design
23 p3962 N85-34562
Pluribus satellite IMP (Interface Message Processors) development mobile access terminal network
[AD-A155754] 24 p4069 N85-35216
Raster functionality for a VDI
[DE85-006734] 24 p4097 N85-35396
DSS/MIS (Decision Support Systems/Management Information Systems) design and implementation for LAMPS Mk 3 utilizing a microcomputer and a maintenance personnel assignment program
[AD-A155852] 24 p4135 N85-35629
Research on GaSb/AlSb multi-quantum well superlattices
[AD-A156080] 24 p4161 N85-35800

INTERFACIAL ENERGY
HgCdTe surface and defect study program
[AD-A156079] 24 p4161 N85-35799

INTERFACIAL STRAIN
U INTERFACIAL TENSION

INTERFACIAL TENSION
Minor element effects on gas tungsten arc weld penetration
[PB84-222579] 01 p0056 N85-10370
Evaluation of interfacial stresses from the amplitude of reflected ultrasonic signal
[DE84-015472] 02 p0276 N85-11798
NBS (National Bureau of Standards): Materials measurements
[NASA-CR-174036] 03 p0332 N85-12143
Dynamics of liquid filament breakup
[DE84-016008] 04 p0500 N85-13187
Contact angle and surface tension measurements of a five-ring polyphenyl ether
[NASA-TM-86927] 07 p0930 N85-15897
Investigation of surface tension phenomena using the KC-135 aircraft
[NASA-TM-82508] 10 p1426 N85-18695
Characterization and adhesive bonding of poly(etheretherketone) resins and composites
[DE85-002526] 11 p1593 N85-20023
Fluid slosh dynamics of surface tension tanks in three axis stabilized spacecraft
[MBB-UR-E-739-84-O] 11 p1634 N85-20291
Dynamic investigations of a spherical tank structure filled with liquid using ANSYS three-dimensional fluid elements
[MBB-UR-E-737-83-O] 11 p1654 N85-20418
Vapor pressure studies of the solubilization of hydrocarbons by surfactant micelles
[DE85-004319] 12 p1803 N85-21306
Tribological properties of boron nitride synthesized by ion beam deposition
[NASA-TM-86962] 12 p1810 N85-21355
Properties of materials using acoustic waves
[AD-A150465] 13 p2155 N85-23382
Mixing across a gas-gas interface
[AD-A151471] 15 p2556 N85-25770
Effects of thermal fluctuations on systems with small surface tension
[PREPRINT-437] 18 p3152 N85-29520
Effects of weak interfaces on thermostructural behavior of carbon-carbon composites
[AD-A155330] 21 p3562 N85-32154
Hertzian contact in two and three dimensions
[NASA-TP-2473] 21 p3596 N85-32331
The Konstantinov effect and absorption of sound in inhomogeneous media 21 p3680 N85-32861
Hydrogen embrittlement testing
[DE85-007352] 23 p3916 N85-34273

INTERFERENCE
Using two-beam interference method for measuring wavelength of tunable pulse lasers
02 p0272 N85-11772
Experiments suitable for wind tunnel wall interference assessment/correction 03 p0313 N85-12021
Asymptotic methods for wind tunnel wall corrections at transonic speed 03 p0313 N85-12022
NLR activities in the field of wind tunnel wall interference 03 p0313 N85-12024
Progress in wind tunnel wall interference assessment/correction procedures at the NAE
03 p0314 N85-12025
The susceptibility of aeronautical navigational aids to interference from adjacent-band broadcast transmissions
[BBC-RD-1984/12] 09 p1311 N85-18234
Pseudospectral calculations of two-dimensional transonic flow (Task 1). Numerical investigation of VTOL aerodynamics (Task 2)
[AD-A150123] 12 p1772 N85-21126

INTERFERENCE DRAG
Installed nacelle drag-improvement tests of an M = 0.8 turboprop transport configuration
[NASA-TM-84302] 07 p0902 N85-15716

INTERFERENCE GRATING
Extraction of signals from background interference with unknown parameters in quantized sample
13 p2084 N85-23013
Probability of detection of pulsed signals employing zero-gating interference suppression
13 p2085 N85-23021
Laser plasma LINAC
[DE85-006294] 17 p2971 N85-28348
Measurement of ultrasonic fields in transparent media using a scanning differential interferometer
[NASA-CR-175921] 17 p3026 N85-28726
Prospects for parallel nonlinear optical signal processing using GaAs etalons and ZnS interference filters
18 p3187 N85-29765
Modular digital holographic fringe data processing system
[NASA-CR-177952] 23 p3933 N85-34376

INTERFERENCE IMMUNITY
Interference immunity of digital equipment for coherent processing of wideband signals
04 p0486 N85-13100
Interference immunity of fiber-optic communication lines with spectral multiplexing of channels
13 p2069 N85-22924
Interference immunity of binary systems with second-order phase-difference modulation in various reception modes
13 p2072 N85-22944
Playback amplifier with high interference immunity
13 p2077 N85-22970
Interference immunity of optical radar system with phased antenna array
15 p2526 N85-25575
INTERFERENCE LIFT
Assessment of lift- and blockage-induced wall interference in a three-dimensional adaptive-wall tunnel
03 p0312 N85-12016
Wind tunnel wall interference correction for aircraft models
03 p0314 N85-12029
INTERFERENCE MONOCHROMATIZATION
U DIFFRACTION
U MONOCHROMATIZATION
INTERFEROGRAMS
U INTERFEROMETRY
INTERFEROMETERS
NT FABRY-PEROT INTERFEROMETERS
NT INFRARED INTERFEROMETERS
NT MICHELSON INTERFEROMETERS
NT MICROWAVE INTERFEROMETERS
NT RADIO INTERFEROMETERS
Neutron interferometry and double diffractometer for condensed matter
03 p0424 N85-12705
Imaging polarimeter-interferometer arrays for Tokamak measurements
[DE84-015916]
05 p0730 N85-14693
Decimetric-wave aperture synthesis system at Scientific Research Institute of Radiophysics
06 p0782 N85-15000
Software for Crimea-Pushchino radiointerferometer
06 p0783 N85-15007
Turbulence measurement interferometer apparatus
[AD-D011377]
07 p0970 N85-16156
Far-infrared interferometry/polarimetry on the ISX-B Tokamak
[DE84-015401]
10 p1558 N85-19627
KMSF X-ray laser experiments, task no. 2
[DE85-000291]
11 p1640 N85-20335
FIR interferometer/polarimeter system on ISX-B Tokamak
[DE85-001129]
11 p1731 N85-20887
Comparison reference etalon of unit laser radiation power
13 p2074 N85-22957
Phase-lock fiber optic interferometer
[AD-D011603]
16 p2766 N85-27191
Fiber optic gyroscope with alternating output signal
[AD-D011689]
19 p3271 N85-30284
Mesospheric measurements of irregularity parameters using a 3-antenna interferometer, part 3.6B
21 p3621 N85-32498
Automatic sphericity interferometer for testing lens radii
[AD-A155736]
22 p3786 N85-33457
Optical synthetic aperture techniques
[AD-A156151]
24 p4154 N85-35752
INTERFEROMETRY
NT DIFFERENTIAL INTERFEROMETRY
NT HOLOGRAPHIC INTERFEROMETRY
NT LASER INTERFEROMETRY
NT MOIRE INTERFEROMETRY
NT VERY LONG BASE INTERFEROMETRY
Two novel plasma diagnostic tools: Fiber sensors and phase conjugation
[DE84-014033]
01 p0123 N85-10840
Modern radioastronomical aperture synthesis systems (review)
06 p0782 N85-14997
SIR-B interferometric topography
08 p1145 N85-17224
Two-photon coherent state light - its generation and potential applications
[AD-A146245]
08 p1166 N85-17356
Diffraction-limited imaging of space objects 2
[AD-A149344]
11 p1728 N85-20870
Research study of fiber-optic interferometry at very low frequencies
[AD-A150906]
14 p2421 N85-24837
Investigations of high resolution imaging through the Earth's atmosphere using speckle interferometry
[AD-A150660]
14 p2439 N85-25053
Optical monitoring of photo-acoustic pulse propagation in silicon wafers
[AD-A151333]
15 p2651 N85-26352
Digital image analysis of four-frame holographic plasma and neutral gas interferograms
[DE85-008397]
16 p2788 N85-27200
Acoustooptic pulse-echo transducer system
[NASA-CR-175919]
17 p2951 N85-28224
Transport in aqueous battery systems
[DE85-007246]
17 p2955 N85-28251
Water vapor radiometry research and development phase
[NASA-CR-175887]
17 p2995 N85-28512
Prospects for parallel nonlinear optical signal processing using GaAs etalons and ZnS interference filters
18 p3167 N85-29765
Dual differential interferometer
[NASA-CASE-LAR-12966-1]
19 p3271 N85-30282
Interferometric creep testing
[AD-A154249]
19 p3286 N85-30378
Speckle interferometry applied to asteroids and other solar system objects
[NASA-CR-175976]
19 p3384 N85-30995
Status of the Jicamarca radar
21 p3627 N85-32535
SCRIBE data of October 23, 1983 flight
[AD-A154864]
21 p3705 N85-33012
Ranging system which compares an object reflected component of a light beam to a reference component of the light beam
[NASA-CASE-NPO-15865-1]
23 p3973 N85-34629
INTERGALACTIC MEDIA
Star formation in interacting galaxies
03 p0444 N85-12826
QUASAT, gravitational lenses, and studies of the interstellar, intracluster and intergalactic medium
07 p1058 N85-16715
Extragalactic cosmic rays from active galaxies
08 p1238 N85-17805
Extragalactic origin or gamma-ray bursts, revision 1
[DE85-005622]
15 p2686 N85-26588
Interactions of heavy nuclei, Kr, Xe and Ho, in light targets
20 p3544 N85-32050
Activities report of the Department of Astrophysics
20 p3548 N85-32064
Galactic antiprotons of 0.2-2 GeV energy
[OG-6.1-11]
22 p3888 N85-34101
Evidence for a dynamical halo around the edge-on galaxy NGC 4631
[OG-6.2-1]
22 p3889 N85-34102
Interstellar turbulence, random density variations, and scintillation measurements
[OG-7.2-13]
23 p4015 N85-34880
INTERGRANULAR CORROSION
Bending strength studies on hot-pressed silicon carbide
[NASA-TM-77512]
03 p0371 N85-12389
In-situ stress relief of expanded alloy 600 steam generator tubing
[DE84-014560]
04 p0513 N85-13273
Testing of non-alloyed and low-alloyed steels for their behaviour with respect to intercrystalline stress corrosion cracking
[BLL-RISLEY-TR-4548-(9091.8F)]
07 p0925 N85-15861
Contributions of segregated phosphorus to the intergranular stress corrosion cracking of nickel
[DE85-003112]
11 p1606 N85-20090
Stress relief of transition zones
[DE85-000234]
11 p1653 N85-20411
Role of segregated P and S in intergranular stress corrosion cracking of nickel
[DE85-004547]
13 p2024 N85-22679
Crack tip chemistry modeling of intergranular stress corrosion cracks of nickel containing segregated phosphorus and sulphur
[DE85-010059]
18 p3076 N85-29028
Electrochemical method for investigation of the susceptibility of corrosion-resistant steels to intercrystalline corrosion
[BLL-CE-TRANS-6062-(9022.09)]
24 p4077 N85-35269
INTERIM STAGES (SPACECRAFT)
NT INERTIAL UPPER STAGE
INTERIM UPPER STAGE (STS)
U INERTIAL UPPER STAGE
INTERIOR BALLISTICS
Intercomparison between West Germany and US thermodynamic codes
[AD-A146622]
06 p0869 N85-15525
Experimental high pressure equation of state of a very fast burning gun propellant
[DE85-001749]
10 p1458 N85-19184
Averaging effects in models of three-dimensional two-phase flows
[AD-A146313]
10 p1484 N85-19371
Molecular dynamics of propellant gases, part 2
13 p2002 N85-22552
Experimental simulation of the flows in front of and behind a projectile with and without gas slippage
[ISL-CO-232/83]
14 p2302 N85-24258
The utilization of a light-gas gun to simulate interior ballistic flow
[ISL-CO-233/83]
14 p2303 N85-24259
Unsteady flows in a tube with combustion reaction
[ISL-R-118/83]
14 p2303 N85-24261
Feasibility study of an installation to simulate the flow of propellant gases in a gun barrel, part 2
[ISL-R-128/83-PT-2]
14 p2303 N85-24263
Simulation of interior ballistics flows in a shock tube
[ISL-CO-222/83]
16 p2784 N85-27183
A computer code IB-KB for interior ballistics of recoiling and recoilless guns
[FOA-C-20566-D2]
18 p3164 N85-29802
Experimental simulation of internal ballistic flows
[ISL-CO-208/84]
20 p3435 N85-31312
Telemetry system for the transmission of data from projectiles during the acceleration phase in the gun barrel
[ISL-CO-207/84]
22 p3739 N85-33178
Experimental simulation of in-bore flows using a high pressure shock tube
[ISL-CO-217/84]
22 p3785 N85-33452
Numerical simulation of interior and terminal ballistics phenomena. Investigation of the effects of the parameters and application examples
[ISL-R-112/84]
22 p3831 N85-33731
INTERLACING DRAINAGE
U DRAINAGE PATTERNS
INTERLAYERS
NT MULTILAYER INSULATION
Influence of inter-layer effect on charge gas-permeability
[BLL-M-35919-(5826.4)]
05 p0616 N85-13940
Stress-relieving interlayers for bituminous resurfacings
[PB85-136865]
12 p1820 N85-21415
Graphite fiber intercalation: Dynamics of the bromine intercalation process
[NASA-TM-87015]
16 p2742 N85-26921
X-ray diffractometric measurements and calculations of limiting values of discrepancy between lattices and layer thicknesses, preventing generation of dislocations during growth of multilayer heterostructures
21 p3681 N85-32866
INTERLOCKING
U LOCKING
INTERMEDIATE FREQUENCIES
VLBI system (BLK I) IF-video down conversion design
05 p0625 N85-13998
Digital coherent detector
[AD-D011560]
12 p1833 N85-21501
Observations of the MF-HF plasma wave emissions in active auroras by the sounding rocket experiments at Syowa station
14 p2366 N85-24620
Coherently pumped two-frequency laser-type devices
[AD-A154065]
19 p3275 N85-30311
INTERMEDIATE RANGE BALLISTIC MISSILES
NT POLARIS MISSILES
INTERMETALLICS
Influence of 5f electrons on structures and bonding in the actinide-hydrogen intermetallics
[DE84-013693]
01 p0118 N85-10807
Photoelectric effect in liquid crystals
02 p0259 N85-11695
Magnetic properties of intermetallic phases and simple systems — neutron diffraction
03 p0422 N85-12697
Magnetism of the rare earth compounds — intermetallic compounds
03 p0424 N85-12707
Moessbauer effect and contactless conductivity studies of superconducting actinides intermetallics and hydrides. Moessbauer high pressure studies
03 p0430 N85-12743
Cerium compounds in the fashion of the light actinides
[DE84-014642]
04 p0475 N85-13024
Storage life of thermal detents
[DE84-016934]
04 p0476 N85-13030
Thermomagnetic generator
[DE84-017018]
04 p0530 N85-13398
Electronic bandstructure of an incommensurate crystal
[DE84-016891]
05 p0733 N85-14714
High temperature properties of equiatomic FeAl with ternary additions
[NASA-TM-86938]
10 p1439 N85-19072
The B2 aluminides as alternative materials
[NASA-TM-86937]
10 p1440 N85-19076
Alloys based on NiAl for high temperature applications
[NASA-TM-86976]
12 p1805 N85-21322
Angle-resolved photoemission study of AuGa2 and AuIn2 intermetallic compounds
[AD-A150000]
12 p1940 N85-22183
A mixed-basis band structure interpolation scheme applied to the fluorite structure compounds NiSi2, AuAl2, AuGa2 and AuIn2
[AD-A150131]
12 p1940 N85-22187
Magnetic studies of Ni3Al(Fe) compounds
[DE85-005262]
13 p2025 N85-22686

Structure and aging of amorphous chromium-germanium alloys 15 p2497 N85-25401
Experimental studies of the electronic structure of 1-2 and 1-3 intermetallic compounds
[DE85-009978] 15 p2662 N85-26432
Changes in lattice cell parameter of film intermetallic compounds RT2
[BLL-M-35874-(5828.4)] 23 p3915 N85-34261
Oxidizing seal for a turbine tip gas path
[NASA-CASE-LEW-14053-1] 23 p3937 N85-34402
Oxidation resistant slurry coating for carbon-based materials
[NASA-CASE-LEW-13923-1] 24 p4077 N85-35267

INTERMITTENCY
Diffusion and intermittency in an extended one-dimensional maps 02 p0262 N85-11834
Characterization of intermittency in chaotic systems
[PREPRINT-429] 18 p3173 N85-29669
Intermittent gas-liquid flow modeling in horizontal or weakly inclined pipes
[EME-132] 20 p3458 N85-31465
Intermittent motion 23 p3925 N85-34323
Noise-sustained structure, intermittency and the Ginzburg-Landau equation
[DE85-009626] 24 p4094 N85-35379

INTERMODULATION
Simulation of a transmission circuit composed of slightly nonlinear elements. Computation of the intermodulation on signals composed of N carriers
[CNES-NT-105] 04 p0496 N85-13167
The susceptibility of aeronautical navigational aids to interference from adjacent-band broadcast transmissions
[BBC-RD-1984/12] 09 p1311 N85-18234

INTERMOLECULAR FORCES
Some unique features of isentrophic flow of gas under high pressures 13 p2043 N85-22768
Molecular dynamics studies of energy transfer processes in crystal systems
[DE85-007247] 15 p2662 N85-26426
Simulation studies for surfaces and materials strength
[NASA-CR-175766] 16 p2900 N85-27262

INTERMONTANE FLOORS
U VALLEYS

INTERNAL COMBUSTION ENGINES
NT DIESEL ENGINES
NT GAS TURBINE ENGINES
NT J-52 ENGINE
NT J-85 ENGINE
NT JET ENGINES
NT RAMJET ENGINES
NT ROTARY ENGINES
NT SUPERSONIC COMBUSTION RAMJET ENGINES
NT TURBOFAN ENGINES
NT TURBOJET ENGINES
NT TURBOPROP ENGINES
Measurement and analysis of spark ignition engine pressure data to determine heat release profiles
[AD-A144770] 01 p0055 N85-10363
The KZD-85 engine test. Engine type: 1 cylinder, 2 stroke motor 2100 Husquarna
[FWE-FO-1717] 02 p0205 N85-11354
Advanced concepts for methanol fuel vehicles
[DE84-013812] 04 p0482 N85-13071
Detailed performance analysis of the A.A.D. - concept B 04 p0507 N85-13237
A.A.D. engine noise evaluation 04 p0508 N85-13241
Phase 1-A development kinematic Sterling/Rankine commercial gas-fired heat pump research program
[PB85-100931/GAR] 07 p0936 N85-15928
Cooling system investigation of the 3-kW MEP models 016A, 021A, and 026A (60Hz, 400-Hz and 28-V dc) gasoline-engine-driven generator sets
[AD-A147571] 07 p0974 N85-16185
Research and development of alcohol fuel usage in spark ignited engines 09 p1301 N85-18175
Knock syndrome: Its cures and its victims
[NASA-CR-174395] 10 p1456 N85-19185
Modeling the internal combustion engine
[NASA-RP-1094] 10 p1544 N85-19733
Structural ceramics in transportation: Fuel implications and economic impacts
[DE85-003024] 11 p1611 N85-20130
NDE for heat engine ceramics
[NASA-TM-86940] 11 p1649 N85-20389
Stratified charge rotary aircraft engine technology enablement program
[NASA-CR-174812] 12 p1778 N85-21163
Laboratory tests of reciprocating internal combustion engines
[AD-A150143] 13 p2096 N85-23087
Hypergolic combustion demonstration in a reciprocating internal combustion engine
[AD-A150646] 14 p2311 N85-24303
Exhaust systems for passenger vehicles: Test procedure for resistance to internal corrosion of silencers
[BLL-BISI-TRANS-22360-(9022.06)] 17 p2973 N85-28361
Urban vehicle research project
[DE85-005444] 17 p3052 N85-28689
Use of ceramics in internal combustion engines 18 p3088 N85-29114
KIVA: A comprehensive model for 2D and 3D engine simulations
[DE85-005562] 18 p3118 N85-29296
Investigation of the behavior of fuel in the intake manifold and its relation to SI engines, 1960 - 1983 19 p3279 N85-30337
KIVA: A computer program for two- and three-dimensional fluid flows with chemical reactions and fuel sprays
[DE85-010334] 19 p3339 N85-30693
Friction and wear of solid-lubricated contact in gas turbine engine bearings
[AD-A155042] 21 p3596 N85-32335

INTERNAL CONVERSION
Inelastic scattering in condensed matter with high intensity Moessbauer radiation
[DE85-003531] 12 p1854 N85-21627

INTERNAL ENERGY
Investigation of internal fields and motions, radiation damages and recovery processes using beta and gamma active probe nuclei 03 p0427 N85-12726
Investigation of solid state problems using the hyperfine interaction between static and dynamic internal fields with short live excited probe nuclei 03 p0428 N85-12729
On the use of internal state variables in thermoviscoplastic constitutive equations 20 p3466 N85-31536

INTERNAL FRICTION
Internal friction, microstructure and radiation effects
[DE84-013905] 02 p0288 N85-11880
Control of rotordynamic instability in a typical gas turbine's power system 05 p0642 N85-14120
Interaction of cylindrical shell with concentrated mass moving along its inner surface 13 p2047 N85-22810
Steady-state reaction of three-layered cylindrical shell to effect of moving load 13 p2047 N85-22811
Investigation of internal friction of free-flowing material during discharge
[BLL-M-36141-(5828.4)] 15 p2553 N85-25752
Acoustic oscillations of rods and plates 17 p2944 N85-28170
Experimental investigations of the unsteady turbulent friction behavior with pressure impulses in a circular pipe
[IWAWI-MITT-102] 18 p3103 N85-29210

INTERNAL PRESSURE
Optimization of pressure vessels with standard intercepting spheres
[INPE-3276-PRE/600] 11 p1651 N85-20397
Effect of internal pressure on flexibility and stress intensification factors for pipe elbows analyzed by the finite element method
[AD-A151161] 15 p2578 N85-25901
Mechanical ratcheting behaviors of a steel pipe under combined cyclic axial load and internal pressure 23 p3904 N85-34184

INTERNAL STRESS
U RESIDUAL STRESS

INTERNAL WAVES
NT PLANETARY WAVES
An improved analytical theory of Rossby wave driven Eulerian and Lagrangian mean flows along non-zonal barriers with application to the Hawaiian Ridge
[AD-A144951] 01 p0088 N85-10593
Internal waves in ocean 06 p0819 N85-15201
Internal gravity waves in real atmosphere 06 p0825 N85-15236
The investigation of selected oceanographic applications of spaceborne synthetic-aperture radar 08 p1146 N85-17233
SAR internal wave signature experiment 08 p1149 N85-17253
Solitons and SEASAT
[AD-A148396] 08 p1176 N85-17414
On the classification and nonlinear solution of one type of stratified shear flow
[AD-A148832] 09 p1319 N85-18295
Internal Gravity Waves and Small-Scale Turbulence: Proceedings of the 2nd 'Aha Huliko'a Hawaiian Winter Workshop
[AD-A149510] 10 p1522 N85-19597
The imaging of internal waves by the SEASAT-A synthetic aperture radar
[AD-A149808] 12 p1875 N85-21761
Circulation and internal waves in a cold Gulf Stream wave
[AD-A149704] 12 p1898 N85-21918
The imaging of internal waves by the SEASAT-A synthetic aperture radar
[ARE(PORTLAND)TN-720/84] 13 p2054 N85-22860
The effects of internal waves on acoustic normal modes
[AD-A150235] 13 p2155 N85-23379
Influence of internal gravity waves on F layer 14 p2338 N85-24460
SEASAT report
[AD-A151283] 15 p2583 N85-25931
Sound propagation through directional internal wave fields
[AD-A151168] 15 p2648 N85-26321
Wave propagation in density stratified fluids 16 p2781 N85-27162
Internal waves in layers of Earth's upper mantle 16 p2807 N85-27312
Turbopause as source of internal gravity waves 16 p2808 N85-27314
Internal waves in marine straits
[PREPRINT-415] 18 p3151 N85-29510
Excerpts from the paper: Research Status and Recommendation from the Alaska Workshop on Gravity Waves and Turbulence in the Middle Atmosphere, part 1.3A 21 p3616 N85-32470
On the limiting configuration of interfacial gravity waves
[AD-A154821] 21 p3631 N85-32557
Theory of soliton waves
[AD-A154784] 21 p3676 N85-32837
Some aspects of internal gravity waves in a multi-layered moving stratified flow 24 p4092 N85-35369

INTERNATIONAL COMETARY EXPLORER
U INTERNATIONAL SUN EARTH EXPLORER 3

INTERNATIONAL COOPERATION
NT OUTER SPACE TREATY
Space Research in Japan. National report 01 p0013 N85-10082
SEPAC (space experiments with particle accelerators) 01 p0014 N85-10085
Balloon observations 01 p0014 N85-10086
Availability of transmission systems in continental and intercontinental connections --- telecommunication
[FUB-33-1983] 01 p0040 N85-10261
Solar heating and cooling R and D program coordination support
[DE84-013479] 01 p0068 N85-10449
Report of the First Session of the International Working Group on Data Management for the International Satellite Cloud Climatology Project (ISCCP)
[WCP-42] 01 p0073 N85-10483
Cloud cover sampling capability of various satellite combinations for ISCCP 01 p0073 N85-10484
ISCCP Cloud Algorithm Intercomparison Workshop 01 p0073 N85-10485
ISSCP Cloud Algorithm Intercomparison Workshop 01 p0073 N85-10486
Project COST 72 (The European weather radar project) today 01 p0084 N85-10561
Development of space instrumentation of Intercosmos member countries 02 p0163 N85-11106
International cooperation and competition in space
[GPO-38-001] 02 p0295 N85-11911
International cooperation and competition in space. Introduction 02 p0295 N85-11912
Statement of Kenneth S. Pedersen, Director, International Affairs Division, National Aeronautics and Space Administration 02 p0295 N85-11913
Statement of Otho E. Eskin, Director, Office of Advanced Technology, Department of State 02 p0295 N85-11914
Statement of John H. McElroy, Assistant Administrator for Environmental Satellite, Data and Information Services, National Oceanic and Atmospheric Administration 02 p0295 N85-11915
International cooperation and competition in civilian space activities, summary, appendix 1 02 p0295 N85-11916
NESDIS international activities, appendix 2 02 p0295 N85-11917
AGARD Highlights
[AGARD-HIGHLIGHTS-84/2] 02 p0305 N85-11972
West Europe report: Science and technology
[JPRS-WST-84-004] 03 p0309 N85-11998
French, Soviets decide to launch Sigma space telescope 03 p0341 N85-12191
International banking of satellite and in-situ wave data by the Marine Information and Advisory Services (MIAS) 03 p0361 N85-12434
Competitive assessment of the US information services industry
[PB84-174804] 03 p0440 N85-12803
The structures and the role of an international agency for the control of satellites
[NASA-TM-76765] 03 p0441 N85-12806

Colloquium about Joint Projects within DFVLR/ISRO Cooperation
[DFVLR-MITT-84-12] 04 p0458 N85-12907
Presentation of Indian Space Research Organization (ISRO)/DFVLR cooperation 04 p0459 N85-12912
Launching systems
[CNES-NT-111] 04 p0460 N85-12917
The Ebro Observatory and international scientific organizations 04 p0518 N85-13309
Use of Ebro Observatory data at Word Data Center A for Solar-Terrestrial Physics 04 p0518 N85-13310
International coordination in scientific research 04 p0519 N85-13311
International cooperation in remote sensing applications 05 p0656 N85-14209
International Conference on Physics of Clouds 05 p0619 N85-15196
Broadening the debate 07 p0914 N85-15785
International involvement in a civilian space station program 07 p0915 N85-15789
West Europe report: Science and technology
[JPRS-WST-84-039] 07 p0936 N85-15929
Maritime prospecting, mining discussed 07 p0960 N85-16226
The challenge of food production: The importance of climate 07 p1001 N85-16361
The potential contributions of the World Climate Program (WCP) to the economies of developing countries 07 p1003 N85-16371
International projects, other work of Aeroproyekt Institute 08 p1068 N85-16767
FRG study looks at participation in ESA, US space station 08 p1141 N85-17191
UK, FRG, France: R and D in sensors, related fields 08 p1142 N85-17197
International cooperation and competition in civilian space activities
[OTA-ISC-240] 08 p1231 N85-17750
High-technology ceramics in Japan
[TI85-900369] 09 p1299 N85-18157
The Venus Balloon Project 10 p1465 N85-19243
Commentary on start of scientific data transmissions with USSR 10 p1476 N85-19319
Magnetic fusion energy plasma interactive and high heat flux components. Volume 3: Strategy for international collaborations in the areas of plasma materials interactions and high heat flux materials and components development
[DE85-001145] 10 p1559 N85-19829
Window on science visit to the USA, 21 March - 22 April, 1984 — ramjets and solid propellant rocketry
[VTH-LR-426] 11 p1592 N85-20011
FRG's DFVLR ready for participation in space station 11 p1618 N85-20176
TSS Satellite overview 11 p1642 N85-20343
The Middle Atmosphere Program: A special project for the Antarctic Middle Atmosphere (AMA) 11 p1656 N85-20430
Large natural geophysical events: Planetary planning
[DE85-000859] 11 p1783 N85-21092
INMARSAT marine satellite organization 13 p1985 N85-22456
The astrometry network of the IHW and the P/Crommelin trial run results 14 p2435 N85-25016
International conference on COSPAS-SARSAT system 15 p2484 N85-25336
Financial, economic commentary on Airbus, European aviation 15 p2536 N85-25849
NOAA satellite operations: Programs briefing — Environmental satellites, LANDSAT, and space station polar platform 15 p2599 N85-26020
Progress through cooperation and exchange of ideas and experiences 15 p2626 N85-26186
AGARD bulletin: Meetings, publications, membership
[AGARD-BUL-85-1] 15 p2686 N85-26589
Tass reports program for Salyut-7 fully completed 16 p2717 N85-26773
East Europe report: Science and technology
[JPRS-ESA-85-019] 16 p2767 N85-27077
International cooperation in space exploration 16 p2769 N85-27079
The relevance of remote sensing to Brazil
[INPE-3421-PRE/686] 16 p2811 N85-27332
Intemation information networks for material properties: Revision 1
[DE85-007412] 16 p2850 N85-27572
East-West cooperation in outer space
[S-HRG-98-1064] 16 p2879 N85-27767
Construction 1976-1980: Design, manufacturing, calibration of the German-Dutch wind tunnel (DNW) 17 p2905 N85-27913
European utilization aspects of a US manned space station, volume 1
[ESA-CR(P)-1967-VOL-1] 17 p2907 N85-27926
European utilization aspects of a US manned space station, volume 2
[ESA-CR(P)-1967-VOL-2] 17 p2907 N85-27927
Finland, Sweden cooperate in composites research 17 p2946 N85-28184
New ESA director on space station, military space 18 p3066 N85-28962
West Europe report: Science and technology
[JPRS-WST-84-031] 18 p3068 N85-29089
DFVLR official on areas of US-FRG Space Station cooperation 18 p3068 N85-29091
New ESA director on Ariane, space station, future trends 18 p3068 N85-29096
FRG weighs ESA participation, budget issues 18 p3068 N85-29110
DFVLR study recommends European independence in space systems 18 p3068 N85-29111
United States participation in International Energy Agency Task IX, Subtask (C): Pyranometry. 1984 participation
[DE85-009615] 18 p3110 N85-29256
Forecast impact simulation studies 18 p3139 N85-29435
Standards Committee activities of the National Bureau of Standards: 1984 highlights
[PB85-183382] 19 p3350 N85-30764
Report to the Working Group on Technology, Growth and Employment
[DE85-010320] 19 p3372 N85-30920
Cost and schedule implications of multinational coproduction
[AD-A154358] 19 p3380 N85-30969
The international organization of maritime search and rescue 20 p3400 N85-31089
Search and rescue services for international civil aviation 20 p3400 N85-31090
Maritime search and rescue cooperation and planning 20 p3400 N85-31093
The development of an institutional structure for the Future Global Satellite System for Search and Rescue 20 p3406 N85-31138
Studies toward a manned space station: Participation of European industry in NASA space station (MSS)
[SNIAS-S/DT-Y-25-212] 20 p3418 N85-31217
CEMA cooperation in development of robotics, FMS viewed 20 p3438 N85-31331
Antarctica
[S-HRG-98-1181] 20 p3473 N85-31584
United States-Soviet satellite accord: SARSAT/Cospas search-and-rescue program
[GPO-41-113] 20 p3541 N85-32040
International prototype network in Dubna experimental satellite communications system 22 p3773 N85-33383
Research report program of the US Army in Europe 24 p4061 N85-35167
Microwave propagation studies, measurements and education in Surabaya, Indonesia
[B8464833] 24 p4088 N85-35339

INTERNATIONAL GEOSPHERE-BIOSPHERE PROGRAM
International Geosphere/Biosphere Program: 1984
[GPO-39-222] 04 p0578 N85-13691

INTERNATIONAL LAW
NT AIR LAW
NT SPACE LAW

INTERNATIONAL MAGNETOSPHERIC STUDY
Achievements of the International Magnetospheric Study (IMS) — conference
[ESA-SP-217] 14 p2354 N85-24544
Results from the GEOS-1 and GEOS-2 spacecraft and their contributions to the IMS 14 p2354 N85-24545
Observations of auroras and related plasma phenomena by the Kyokko and Jikken satellite in IMS — EXOS-A and B satellite 14 p2354 N85-24547
The measurements of Prognoz-4, -5, -6, -7 during IMS 14 p2355 N85-24548
The Earth's magnetopause — International Magnetospheric Study 14 p2355 N85-24549
The structure and dynamics of the magnetosphere: Progress in the IMS 14 p2355 N85-24550
Observations of the magnetospheric boundary layers — International Magnetospheric Study 14 p2355 N85-24551
Hot plasma and energetic particles in the Earth's outer magnetosphere: New understandings during the IMS 14 p2355 N85-24552
Magnetic field observations at the dayside magnetopause: ISEE-1 and -2 contributions during the IMS 14 p2356 N85-24555
Ground-based and near-Earth observations during the IMS 14 p2359 N85-24575
IMS advances in studies of field-aligned currents and their related electrodynamics 14 p2359 N85-24578
Results of the SCATHA ion composition experiment during the IMS 14 p2359 N85-24580
Achievements of the plasma composition experiment on ISEE-1 during the IMS 14 p2360 N85-24583
A brief summary of results derived from Scandinavian Twin Auroral Radar Experiment (STARE) observations during IMS — ionospheric electric fields 14 p2362 N85-24595
Characteristics of the electrodynamics of auroral arcs as inferred from rocket and ground-base observations during IMS 14 p2363 N85-24601
An evaluation of the contributions of the IMS to experimental and theoretical studies of ULF plasma 14 p2365 N85-24614
The IMS advances in understanding terrestrial myriametric radiation 14 p2365 N85-24618
Terrestrial continuum radiation study during the IMS 14 p2365 N85-24619
VLF emissions observed by ISIS Satellites during the IMS 14 p2366 N85-24621
Whistler mode waves near the plasmapause: Results from the IMS VLF experiment at Halley, Antarctica 14 p2367 N85-24628
Role of equatorial Electron Cyclotron Harmonic (ECH) waves in the generation of diffuse auroras. Contribution of the GEOS IMS spacecraft 14 p2367 N85-24632
Results of ULF-wave investigations in the USSR 14 p2369 N85-24644
Magnetic pulsations recorded in northern Scandinavia during the IMS; a study of Pc 4-5 events 14 p2370 N85-24647
Advances in magnetospheric plasma diagnosis by active experiments — IMS satellites 14 p2371 N85-24654
The IMS contributions to the understanding of auroral precipitation, transport and particle sources 14 p2372 N85-24660
Advances in magnetospheric plasma-wave research during the IMS 14 p2372 N85-24662
IMS (International Magnetospheric Study) contributions to the understanding of auroral precipitation, transport, and particle sources
[AD-A152320] 17 p2992 N85-28492

INTERNATIONAL PRACTICAL TEMPERATURE
U TEMPERATURE SCALES

INTERNATIONAL RELATIONS
NT INTERNATIONAL COOPERATION
NT OUTER SPACE TREATY
Technology transfer to the Middle East
[PB85-127744] 12 p1952 N85-22254
East-West cooperation in outer space
[S-HRG-98-1064] 16 p2879 N85-27767
Technology and Soviet political choices
[AD-P004566] 17 p3048 N85-28861
Close encounters with S/T (science and technology) in the Soviet Union
[AD-P004570] 17 p3048 N85-28864
Sub-committee on advanced technology and technology transfer
[AD-A153645] 18 p3198 N85-29636
U.S.-China conference on science policy
[PB85-178345] 19 p3360 N85-30971

INTERNATIONAL SATS FOR IONOSPHERIC STUDY
U ISIS SATELLITES

INTERNATIONAL SUN EARTH EXPLORER 1
Observation of a westward travelling surge from satellites at low, medium and high altitudes
[NASA-TM-87434] 09 p1342 N85-18442
Anomalously high potentials observed on ISEE 13 p1994 N85-22503
Some contributions to knowledge of the magnetospheric plasma by ISEE-1 investigators 14 p2354 N85-24548
Magnetic field observations at the dayside magnetopause: ISEE-1 and -2 contributions during the IMS 14 p2356 N85-24555
Magnetotail current sheet and energetic particles observed on ISEE-1 14 p2357 N85-24566
Plasma sheet dynamics deduced from ISEE-1 and -2 energetic particle flux data 14 p2358 N85-24570
The near Earth current sheet: ISEE-1 and -2 case studies 14 p2358 N85-24573
Achievements of the plasma composition experiment on ISEE-1 during the IMS 14 p2360 N85-24583
Magnetospheric pulsations observed by ISEE 1 and 2 satellites 14 p2369 N85-24640
Advances in magnetospheric plasma diagnosis by active experiments — IMS satellites 14 p2371 N85-24654
The downshift of electron plasma oscillations in the electron foreshock region
[NASA-CR-175833] 14 p2423 N85-24945
On the use of a sunward-libration-point orbiting spacecraft as an IMF monitor for magnetospheric studies
[NASA-CR-175809] 16 p2825 N85-27426
Interaction between an interplanetary shock and the Earth's magnetosphere on 27 August 1978: ISEE-1 electric field and ISEE-2 plasma observations
[IFSI-84-15] 20 p3548 N85-32078

ISEE-1 data reduction and analysis plasma composition experiment
[NASA-CR-175306] 21 p0630 N85-32552
INTERNATIONAL SUN EARTH EXPLORER 2
Magnetic field observations at the dayside magnetopause: ISEE-1 and -2 contributions during the IMS 14 p2356 N85-24555
Plasma sheet dynamics deduced from ISEE-1 and -2 energetic particle flux data 14 p2358 N85-24570
The near Earth current sheet: ISEE-1 and -2 case studies 14 p2358 N85-24573
Magnetospheric pulsations observed by ISEE 1 and 2 satellites 14 p2369 N85-24640
Interaction between an interplanetary shock and the Earth's magnetosphere on 27 August 1978: ISEE-1 electric field and ISEE-2 plasma observations
[IFSI-84-15] 20 p3548 N85-32078
INTERNATIONAL SUN EARTH EXPLORER 3
Isotopic composition of primary cosmic rays H-Fe for ISEE-C
[NASA-CR-175286] 05 p0746 N85-14783
Astrometric needs for the ISEE-3/ICE mission to Comet Giacobini-Zinner 14 p2436 N85-25043
On the use of a sunward-libration-point orbiting spacecraft as an IMF monitor for magnetospheric studies
[NASA-CR-175809] 16 p2825 N85-27426
Measurements of galactic hydrogen and helium isotopes from 1978 through 1983
[OG-4.2-2] 22 p3677 N85-34022
The International Cometary Explorer (ICE)wallsheet teacher's guide
[NASA-TM-87498] 23 p3988 N85-34727
INTERNATIONAL SUN EARTH EXPLORERS
NT INTERNATIONAL SUN EARTH EXPLORER 1
NT INTERNATIONAL SUN EARTH EXPLORER 2
NT INTERNATIONAL SUN EARTH EXPLORER 3
The structure and dynamics of the magnetosphere: Progress in the IMS 14 p2355 N85-24550
Terrestrial continuum radiation study during the IMS 14 p2365 N85-24619
Contribution of relaxation sounding experiments to the understanding of magnetospheric processes 14 p2371 N85-24655
The boundary layers as the primary transport regions of the Earth's magnetotail
[AD-A152714] 17 p2992 N85-28498
INTERNATIONAL TRADE
East Europe report: Science and technology
[JPRS-ESA-84-036] 03 p0343 N85-12210
International airport study: How to improve the effect of airports on trade and on export-related industries
[PB85-124923] 11 p1586 N85-19992
Transfer of technology
[S-REPT-98-864] 12 p1949 N85-22246
Transfer of technology
[S-HRG-98-666] 12 p1949 N85-22247
Sub-committee on advanced technology and technology transfer
[AD-A153645] 18 p3198 N85-29636
Irradiation of northwest agricultural products
[DE85-012455] 22 p3843 N85-33803
Federal export assistance programs applicable to the US photovoltaic industry
[NASA-CR-178114] 22 p3849 N85-33841
INTERNATIONAL ULTRAVIOLET EXPLORER
U IUE
INTERORBITAL TRAJECTORIES
Radiation exposure and performance of multiple burn LEO-GEO orbit transfer trajectories
[NASA-TM-86946] 12 p1788 N85-21228
INTERPERSONAL RELATIONS
U HUMAN RELATIONS
INTERPLANETARY COMMUNICATION
Performance analysis of the DSN baseband assembly (Bba) Real-Time Combiner (RTC)
[NASA-CR-175878] 17 p2946 N85-28190
INTERPLANETARY DUST
NT ZODIACAL DUST
Discovery of nuclear tracks in interplanetary dust 06 p0669 N85-15647
Evolution of grains in a turbulent solar nebula 13 p2179 N85-23525
A model of plasma cloud expansion generated by a dust particle impact — Giotto mission 14 p2245 N85-23914
Dynamics of neutral small particles — in the solar system 15 p2676 N85-26521
Dynamics of charged small particles — Jupiter, Saturn magnetospheres 15 p2676 N85-26522
Diffusion of dust around a central body — Keplerian orbits 15 p2676 N85-26523
On the electric charge carried by dust grain excitation of violent discharge — planetary rings 15 p2677 N85-26530
French and West German equipment for Vega Project 16 p2722 N85-26805
The influence of global dust storms on the mean seasonal daily insolations at the Martian surface
[AERONOMICA-ACTA-A-269-1984] 18 p3203 N85-29668
Elemental abundance differences between nuclei accelerated in CIR shocks and solar flares
[SH-2.2-6] 23 p4000 N85-34801
INTERPLANETARY FLIGHT
NT ASTEROID MISSIONS
NT LONG DURATION SPACE FLIGHT
Towards the Halley Comet 14 p2399 N85-24783
TASS update on flights of Vega-1 and Vega-2 16 p2722 N85-26803
Kovtunenko discuses Vega Project 16 p2722 N85-26804
Far travelers: The exploring machines
[NASA-SP-480] 22 p3731 N85-33126
INTERPLANETARY MAGNETIC FIELDS
Response of the F2 layer to the polarity of the interplanetary magnetic field
[REPT-561] 03 p0377 N85-12404
Relations between the particle precipitation events in mid-latitudes, the ring current intensity and the polarity of the interplanetary magnetic field 04 p0519 N85-13316
Sun-aligned polar cap auroral arcs
[AD-A146052] 08 p1185 N85-17472
Solar-geophysical data number 476, April 1984. Part 1: (Prompt reports). Data for March 1984, February 1984 and late data
[PB84-215060] 09 p1416 N85-18036
Partial penetration of IMF B(sub y) into the magnetosphere
[DRI-5-84] 10 p1514 N85-19554
Plans for Interbol satellite experiment 13 p1977 N85-22407
The measurements of Prognoz-4, -5, -6, -7 during IMS 14 p2355 N85-24548
Response of magnetospheric substorm activity to changes in the interplanetary magnetized plasma 14 p2357 N85-24563
On the use of a sunward-libration-point orbiting spacecraft as an IMF monitor for magnetospheric studies
[NASA-CR-175809] 16 p2825 N85-27426
An interplanetary magnetic field ensemble at 1 AU
[NASA-TM-86209] 16 p2882 N85-27784
Results of the magnetic field experiments E2 and E4 onboard Helios 1 and Helios 2 — magnetometer development 16 p2885 N85-27799
Rome/Goddard Space Flight Center (GSFC) magnetic field experiment: A summary of results — flux gate magnetometer 16 p2885 N85-27800
Images of the Earth's aurora and geocorona from the Dynamics Explorer Mission
[NASA-CR-175983] 18 p3136 N85-29423
Fractal structure of the interplanetary magnetic field
[NASA-TM-86212] 19 p3383 N85-30987
Solar-wind magnetosphere energy input functions
[NASA-CR-176021] 19 p3385 N85-31001
The longitudinal asymmetry of the interplanetary perturbation producing Forbush decreases
[IFSI-84-16] 20 p3546 N85-32065
Interplanetary disturbances during Forbush decreases
[IFSI-84-10] 20 p3547 N85-32075
Spectral measurements of magnetic energy and magnetic helicity between 0.29 and 0.97 AU
[IFSI-85-2] 22 p3850 N85-33844
Interplanetary magnetic field control of high-latitude electric fields and currents determined from Greenland magnetometer data
[DMI-GEOPHYS-PAPERS-R-60] 22 p3850 N85-33845
Linear filters as a method of real-time prediction of geomagnetic activity
[DE85-010760] 22 p3860 N85-33899
Determination of the pitch-angle distribution and transverse anisotropy of interplanetary particles
[SH-3.1-11] 23 p4002 N85-34815
Pitch angle distributions of solar energetic particles and the local scattering properties of the interplanetary magnetic field
[SH-3.1-13] 23 p4002 N85-34816
Channeled propagation of solar particles
[SH-3.2-3] 23 p4003 N85-34819
The propagation of solar energetic particles in magnetic channels
[SH-3.2-4] 23 p4003 N85-34820
The local characteristic function of interplanetary particle propagation
[SH-3.2-8] 23 p4003 N85-34823
On reflecting boundary behind the Earth's orbit at propagation of fast particles from solar flares
[SH-3.2-13] 23 p4004 N85-34827
The intensity recovery of Forbush-type decreases as a function of heliocentric distance and its relationship to the 11-year variation
[SH-4.1-9] 23 p4005 N85-34832
Cosmic ray modulatin and merged interaction regions
[SH-4.1-11] 23 p4005 N85-34834
Cosmic ray modulation in a random anisotropic magnetic field
[SH-4.1-20] 23 p4006 N85-34839
Drift and observations in cosmic-ray modulation, 1
[SH-4.2-4] 23 p4007 N85-34842
Drift and observations in cosmic-ray modulation, 2
[SH-4.2-5] 23 p4007 N85-34843
Cosmic ray north-south anisotropy 1961 - 1983
[SH-4.2-6] 23 p4007 N85-34844
Cosmic ray intensity and the tilt of the neutral sheet
[SH-4.2-8] 23 p4007 N85-34846
Differential measurement of cosmic-ray gradient with respect to interplanetary current sheet
[SH-4.2-9] 23 p4007 N85-34847
Spatial variation of cosmic rays near the heliospheric current sheet
[SH-4.2-10] 23 p4007 N85-34848
The effect of the neutral sheet structure of the interplanetary magnetic field on cosmic ray distribution in space
[SH-4.2-18] 23 p4008 N85-34855
The dependence of solar modulation on the sign of the cosmic ray particle charge
[SH-4.2-23] 23 p4009 N85-34860
An update on the correlation between the cosmic radiation intensity and the geomagnetic AA index
[SH-4.2-24] 23 p4009 N85-34861
Isotropic intensity waves and features of their occurrence
[SH-4.3-8] 23 p4032 N85-34993
IMF-sense-dependent cosmic ray anisotropy produced from diffusion-convection in heliosphere
[SH-4.3-9] 23 p4032 N85-34994
Characteristics of cosmic ray pole-equator anisotropy derived from spherical harmonic analysis of neutron monitor data
[SH-4.3-12] 23 p4032 N85-34996
The corotating variation of the north-south anisotropy of cosmic rays
[SH-4.3-15] 23 p4033 N85-34999
Sidereal variations deep underground in Tasmania
[SH-4.4-4] 23 p4033 N85-35002
The effect of the interplanetary magnetic field on sidereal variations observed at medium depth underground detectors
[SH-4.4-5] 23 p4033 N85-35003
Corrected sidereal anisotropy for underground muons
[SH-4.4-7] 23 p4033 N85-35005
A study of periodicities and recurrences in solar activity and cosmic ray modulation
[SH-4.4-14] 23 p4034 N85-35010
Solar wind velocity and daily variation of cosmic rays
[SH-4.5-6] 23 p4036 N85-35024
Magnetic fluctuation and cosmic ray diurnal variations
[SH-4.5-21] 23 p4038 N85-35038
Observation of pick-up ions in the solar wind: Evidence for the source of the anomalous cosmic ray component?
[SH-4.6-5] 23 p4039 N85-35043
Possible origin of the anomalous component of cosmic rays
[SH-4.6-7] 23 p4039 N85-35045
Anomalous short-term increases in the galactic cosmic ray intensity: Are they related to the interplanetary magnetic cloud-like structures?
[SH-5.1-3] 23 p4041 N85-35057
Galactic cosmic ray currents and magnetic field irregularity degree in high-speed solar wind streams
[SH-5.1-9] 23 p4042 N85-35063
Influence of magnetic clouds on cosmic ray intensity variations
[SH-5.1-12] 23 p4042 N85-35065
Solar activity beyond the disk and variations of the cosmic ray gradient
[SH-5.1-23] 23 p4044 N85-35075
Parallel fast-forward shock within 1 AU: Helios-1 and 2 observations
[MPAE-W-79-84-27] 24 p4169 N85-35847
INTERPLANETARY MEDIUM
NT INTERPLANETARY DUST
NT ZODIACAL DUST
Helium atoms in interstellar and interplanetary media, part 3: Temperature and velocity of interstellar wind 02 p0160 N85-11088
Dust properties determined from backscattering in the interplanetary and interstellar medium 03 p0446 N85-12838
Broadening of the interplanetary helium cone structure due to elastic collisions of LISM helium atoms with solar wind ions 06 p0673 N85-15543

Solar-geophysical data number 476, April 1984. Part 2: (Comprehensive reports). Data for October 1983, June 1981 and miscellanea
[PB84-215078] 09 p1417 N85-18837
Hydromagnetic precursors of interplanetary plasma burst 13 p1978 N85-22414
Interplanetary shock waves during April and May of 1981 13 p1982 N85-22434
Some features of the interplanetary medium during Forbush decreases
[NOTA-INTERNA-836] 18 p3202 N85-29666
Shocks in the solar wind between 1 and 8.5 AU: Voyager 1 observations
[NASA-CR-175911] 18 p3209 N85-29905
Interplanetary plasma turbulence and the Doppler detection of a gravitational background radiation
[IFSI-85-1] 20 p3546 N85-32066
Interplanetary disturbances during Forbush decreases
[IFSI-84-10] 20 p3547 N85-32075
Some properties of flare-not-associated Forbush decreases
[IFSI-84-13] 20 p3548 N85-32077
Interaction between an interplanetary shock and the Earth's magnetosphere on 27 August 1978: ISEE-1 electric field and ISEE-2 plasma observations
[IFSI-84-15] 20 p3548 N85-32078
Nineteenth International Cosmic Ray Conference. SH sessions, volume 4
[NASA-CP-2376-VOL-4] 23 p3969 N85-34729
Source energy spectra from demodulation of solar particle data by interplanetary and coronal transport
[SH-1.3-13] 23 p3994 N85-34758
Shock and statistical acceleration of energetic particles in the interplanetary medium
[SH-1.5-1] 23 p3996 N85-34771
Energetic ion acceleration at collisionless shocks
[SH-1.5-3] 23 p3996 N85-34772
Particle acceleration due to shocks in the interplanetary field: High time resolution data and simulation results
[SH-1.5-5] 23 p3996 N85-34774
Pitch angle distributions of 35-1000 keV protons at quasi-perpendicular interplanetary shocks
[SH-1.5-6] 23 p3996 N85-34775
Spatial dependence of the local diffusion coefficient measured upstream of the November 12, 1978 interplanetary traveling shock
[SH-1.5-12] 23 p3996 N85-34776
Solar and interplanetary particles at 2 to 4 MEV during solar cycles 21, solar cycle variations of event sizes, and compositions
[SH-1.5-16] 23 p3997 N85-34779
Cosmic ray acceleration by stellar wind. Simulation for heliosphere
[SH-1.5-17] 23 p3997 N85-34780
Low energy proton bidirectional anisotropies and their relation to transient interplanetary magnetic structures: ISEE-3 observations
[SH-3.1-9] 23 p4002 N85-34813
Latitudinal gradients of cosmic rays and the polarity reversal of the heliospheric magnetic field: A preliminary evaluation
[SH-4.2-16] 23 p4008 N85-34853
Solar modulation and interplanetary gradients of the galactic electrons flux, 1977 - 1984
[SH-4.7-4] 23 p4040 N85-35049
Anomalous short-term increases in the galactic cosmic ray intensity: Are they related to the interplanetary magnetic cloud-like structures?
[SH-5.1-3] 23 p4041 N85-35057
A suggested standardized format for cosmic ray ground-level event data
[SH-9.1-15] 23 p4052 N85-35130

INTERPLANETARY MONITORING PLATFORM
U IMP

INTERPLANETARY NAVIGATION
Interplanetary navigation 14 p2396 N85-24781

INTERPLANETARY PROPULSION
U INTERPLANETARY SPACECRAFT
U ROCKET ENGINES

INTERPLANETARY SPACE
Interplanetary cosmic ray intensity: 1972-1984 and out to 32 AU
[AD-A145130] 01 p0131 N85-10003
Interplanetary radio storms. 2: Emission levels and solar wind speed in the range 0.05-0.8 AU
[NASA-TM-84946] 04 p0589 N85-13781
Electric fields in Earth orbital space
[AD-A146448] 06 p0835 N85-15313
Dependence of the high latitude middle atmosphere ionization on structures in interplanetary space 11 p1664 N85-20487
The Helios radio astronomy experiment 16 p2696 N85-27803
The energy spectrum of Jovian electrons in interplanetary space
[SH-1.5-18] 21 p3715 N85-33051
Possible detection of flare-generated positrons by Helios 1 on 3 Jun 1982
[SH-1.4-10] 23 p3996 N85-34770
Variations in elemental composition of several MEV/nucleon ions observed in interplanetary space
[SH-2.1-7] 23 p3996 N85-34788
On the retention of high-energy protons and nuclei with charges Z or equal to 2 in large solar flares after the process of their acceleration
[SH-2.1-8] 23 p3996 N85-34789
Isotopic overabundances and the energetic particle model of solar flares
[SH-2.2-1] 23 p4000 N85-34796
Radial transport of approximately 1 MeV/nucleon ions during the 22 November 1977 solar particle event
[SH-3.2-5] 23 p4003 N85-34821
Investigation of cosmic ray propagation in interplanetary space
[SH-3.2-9] 23 p4004 N85-34824
Monte Carlo calculations of relativistic solar proton propagation in interplanetary space
[SH-3.2-11] 23 p4004 N85-34826
The influence of nonstationarity of the solar activity and general solar field on modulation of cosmic rays
[SH-4.2-17] 23 p4006 N85-34854
The cosmic ray interplanetary radial gradient from 1972 - 1985
[SH-4.7-1] 23 p4040 N85-35046
The large scale dynamics of the outer heliosphere and the long-term modulation of galactic cosmic rays
[SH-4.7-3] 23 p4040 N85-35048
Study of cosmic ray scintillations from 5-minute data of the scintillations telescope Izmiran and world-wide network stations
[SH-5.1-18] 23 p4043 N85-35071
The theoretical and experimental investigation of cosmic ray Forbush-effects
[SH-5.1-20] 23 p4044 N85-35072
Observation of nuclei with energies 8-30 MeV per nucleon in the Earth's magnetosphere at the altitudes 350 KM
[SH-10.1-5] 23 p4053 N85-35136

INTERPLANETARY SPACECRAFT
NT GALILEO PROBE
NT GALILEO SPACECRAFT
NT JUPITER PROBES
NT MARINER 5 SPACE PROBE
NT MARINER 9 SPACE PROBE
NT MARS PROBES
NT PIONEER SPACE PROBES
NT PIONEER VENUS SPACECRAFT
NT PIONEER 10 SPACE PROBE
NT VENERA SATELLITES
NT VENERA 11 SATELLITE
NT VENUS PROBES
NT VIKING LANDER SPACECRAFT
NT VIKING LANDER 1
NT VIKING ORBITER SPACECRAFT
NT VIKING SPACECRAFT
NT VOYAGER 1 SPACECRAFT
NT VOYAGER 2 SPACECRAFT
Interplanetary plasma turbulence and the Doppler detection of a gravitational background radiation
[IFSI-85-1] 20 p3546 N85-32066
Far travelers: The exploring machines
[NASA-SP-480] 22 p3731 N85-33126

INTERPLANETARY TRAJECTORIES
Interplanetary trajectories 05 p0600 N85-13827
Towards the Halley Comet 14 p2399 N85-24783

INTERPLANETARY TRANSFER ORBITS
Interplanetary trajectories 05 p0600 N85-13827

INTERPOLATION
Interpolation formulas for viscosity of six gases: Air, nitrogen, carbon dioxide, helium, argon and oxygen
[PB84-217801] 01 p0026 N85-10161
Floating-point function generation routines for 16-bit microcomputers
[NASA-TM-83783] 01 p0102 N85-10683
Oscillatory integrals by Hermite interpolatory rules
[CSIR-TWISK-301] 01 p0108 N85-10725
A trivariate Clough-Tocher scheme for tetrahedral data
[AD-A144740] 01 p0111 N85-10751
Utilization of interpolation and transformation for the compression of digital image data
[INPE-3081-PRE/479] 02 p0240 N85-11566
Application of summability methods to Jackson theorems for splines
[AD-A146258] 03 p0412 N85-12635
Spatial and temporal interpolation of NEROS radiosonde winds
[PB84-232545] 04 p0540 N85-13439
Interpolating sequences for H to infinity in the ball
[CTH-MATH-1984-15] 04 p0556 N85-13542
Comparison of optimum interpolation and Cressman analyses 05 p0600 N85-14371
Analytical construction of flight vehicle surfaces 06 p0775 N85-14957
Robust prediction and interpolation for vector stationary processes, part 3
[AD-A147880] 07 p1036 N85-18579
Analysis of geohydrologic data by kriging
[AD-P004152] 09 p1349 N85-18468
Interpolation methods for GTD analysis of shaped reflectors 10 p1463 N85-19231
Some qualitative properties of bivariate Euler-Frobenius polynomials
[AD-A149408] 10 p1547 N85-19755
Scattered data interpolation using thin plate splines with tension
[AD-A149803] 12 p1866 N85-21705
A mixed-basis band structure interpolation scheme applied to the fluorite structure compounds NiSi2, AuAl2, AuGa2 and AuIn2
[AD-A150131] 12 p1940 N85-22167
Digital standards conversion: Interpolation theory and aperture synthesis
[BBC-RD-1984/20] 13 p2053 N85-22857
Analysis of spectral operators in one-dimensional domains
[NASA-CR-172573] 15 p2633 N85-26228
Scattered data interpolation and approximation
[DE85-007495] 15 p2641 N85-26290
An incremental multigrid strategy for the fluid dynamics equations
[AD-A151953] 16 p2783 N85-27172
An interpolation method with the possibility of first derivative correction
[INPE-3352-PRE/631] 16 p2853 N85-27590
Surface interpolation using weighted splines
[INPE-3367-PRE/658] 16 p2853 N85-27591
Evaluation of interpolative modeling concepts for fatigue crack growth at elevated temperature
[AD-A153222] 17 p2980 N85-28422
Shape preserving spline interpolation 17 p3003 N85-28564
A survey of patch methods 17 p3003 N85-28567
Convex interpolating splines of arbitrary degree 17 p3004 N85-28574
A natural bias approach to cardinal spline curves 17 p3004 N85-28575
Monotonicity preserving bicubic interpolation, revision 1
[DE85-007976] 17 p3021 N85-28883
Confidence intervals based on interpolated order statistics
[AD-A152607] 17 p3025 N85-28701
A study of aerodynamic control in stalled flight leading-edge vortex formation analysis
[AD-A153758] 18 p3059 N85-28928
Comparison of optimum interpolation and Cressman analyses 18 p3141 N85-29448
Development and testing of the variable vertical resolution Fourth Order GCM 18 p3142 N85-29453
Developement of an optimum interpolation analysis method for the CYBER 205 18 p3143 N85-29456
Scattered data interpolation codes
[DE85-007337] 18 p3164 N85-29601
Monotonicity preserving bicubic interpolation
[DE85-004206] 18 p3172 N85-29657
Interpolation and differentiation for periodic functions
[PREPRINT-419] 18 p3172 N85-29662
Mathematics of surfaces
[DE85-010439] 19 p3346 N85-30742
An objective analysis technique for extrapolating tidal fields 20 p3493 N85-31715
Interpolation problems in meteor radar analysis, part 7.8A 21 p3626 N85-32528
Heterodyne holographic interferometry for visualization of surface acoustic waves
[AD-A155405] 22 p3836 N85-33753
The improved display of 625-line television pictures: Adaptive interpolation
[BBC-RD-1985/5] 23 p3925 N85-34328
Reports from the German Meteorological Service. No. 166: The optimal spectral density of climatological station networks
[ISBN-3-88148-214-8] 23 p3950 N85-34478
Geometric continuity with interpolating Bezier curves 23 p3983 N85-34570
Users guide for optimum interpolation method of global data assimilation
[AD-A155929] 24 p4138 N85-35848
Two methods of global data assimilation
[AD-A155981] 24 p4143 N85-35884

INTERPOLATORS
U REPEATERS

INTERPROCESSOR COMMUNICATION
Activities of the MIT Laboratory for Computer Science
[AD-A145134] 01 p0100 N85-10661
REMOTE: Modem Communicator Program for the IBM personal computer
[DE84-015047] 01 p0100 N85-10665

Numerical algorithms and parallel testing
[AD-A145090] 01 p0104 N85-10663
The development of an optoelectronic assembly applied to computer systems
[AD-A145089] 01 p0120 N85-10821
Multiplexing the ethernet interface among VAX/VMS users
[AD-A145539] 02 p0243 N85-11586
The design and performance analysis of an arbiter for a multi-processor shared-memory system
[AD-A146074] 03 p0403 N85-12566
Requirements and overview of the LINCS distributed operating system architecture
[DE84-013721] 05 p0714 N85-14577
Design and analysis of an SQL (Structured Query Language) interface for a multi-backend database system
[AD-A146834] 06 p0856 N85-15447
Decentralized control of scheduling in distributed systems
[AD-A147446] 07 p1022 N85-16487
Local area network evaluation by MICROSS extensions
[AD-A146773] 07 p1027 N85-16521
Decentralized control of scheduling in distributed systems
[AD-A147445] 07 p1028 N85-16523
Architecture for a demonstration radar-communication link
[AD-A147835] 08 p1150 N85-17260
NSWC-NADC interactive communication links for AN/UYS-1 loadtape creation and retrieval
[AD-A148418] 08 p1159 N85-17277
Adapting logistics models to a microcomputer for interface with computer-aided design systems
[AD-A147666] 08 p1202 N85-17566
Benchmarking database systems in multiple backend configurations
[AD-A148191] 08 p1202 N85-17568
Some experiences of testing protocol implementations -- open systems interconnection
[NPL-DITC-48/84] 08 p1204 N85-17574
EGP (Exterior Gateway Protocol) gateway under Berkeley UNIX 4.2
[AD-A148056] 08 p1206 N85-17597
Performance evaluation and control of distributed computer communication networks
[AD-A148103] 08 p1206 N85-17598
Asynchronous distributed flow control algorithms
[AD-A148452] 08 p1208 N85-17600
Performance evaluation of a database system in multiple backend configurations
[AD-A148192] 08 p1229 N85-17743
Gateway testing techniques -- computer system interconnection
[NPL-DITC-49/84] 09 p1372 N85-18621
Distributed data processing design methodology
[AD-A149868] 10 p1537 N85-19692
Pluribus Satellite IMP (Interface Message Provision) development mobile access terminal network
[AD-A151201] 15 p2541 N85-25688
Evaluating computer-communication networks with simulation techniques
[AD-A151862] 15 p2832 N85-26222
Interfacing the VAX 11/780 using Berkeley Unix 4.2 BSD and Ethernet based Xerox network systems, volume 1
[AD-A152953] 17 p3015 N85-28645
A real-time executive for multiple-computer clusters
[AD-A152981] 17 p3015 N85-28646
Interfacing the VAX 11/780 using berkeley UNIX 4.2BSD and Ethernet based Xerox Network Systems
[AD-A153174] 17 p3016 N85-28647
Multicomputer operating systems and applications
[AD-A153205] 17 p3016 N85-28648
Distributed elections in a ring of processors using Archimedean time
[CWI-CS-R8419] 17 p3016 N85-28653
Reliability report for communication networks
[AD-A153764] 18 p3090 N85-29127
Performance evaluation of stochastic timed decision-free Petri Nets
[AD-A153887] 18 p3171 N85-29652
Computer center policy
[AD-A154416] 19 p3336 N85-30681
VLSI structures for numerical and digital signal processing computations 20 p3439 N85-31340
Implementation assessment of the OSI network service. The test definition language
[NPL-DITC-52/84] 20 p3514 N85-31849
Broadcasting topology and routing information in computer networks
[AD-A155698] 21 p3674 N85-32827
Parallel Cholesky factorization in message-passing multiprocessor environments
[DE85-012079] 22 p3830 N85-33717
Interprocess communication
[AD-A156337] 24 p4066 N85-35337

INTERRELATIONSHIPS
U RELATIONSHIPS

INTERROGATION
Design and analysis of an SQL (Structured Query Language) interface for a multi-backend database system
[AD-A146834] 06 p0856 N85-15447
Steps towards parsing of query sequences to a database
[AD-A148769] 08 p1206 N85-17590
Design of a pictorial program reference language
[AD-A149323] 10 p1540 N85-19711

INTERRUPTION
A single server queue with mixed types of interruptions
[AD-A148536] 08 p1213 N85-17637
Current interruption by density depression
[DE85-013120] 24 p4169 N85-35846

INTERSECTIONS
An iterative procedure for obtaining I-projections onto the intersection of convex sets
[AD-A145402] 02 p0251 N85-11639
Comparison of two algebraic methods for curve/curve intersection 17 p3007 N85-28591
A comparison of three curve intersection algorithms 17 p3007 N85-28592
Intersection of three-dimensional geometric surfaces
[NASA-TP-2454] 20 p3513 N85-31839

INTERSTELLAR CHEMISTRY
Distribution and properties of molecular clouds in the galaxy 03 p0442 N85-12810
Relation of core structure to high velocity outflow in G35.2-0.74 and other molecular clouds 03 p0443 N85-12818
Time-dependent chemistry of molecular clouds 03 p0443 N85-12822
IUE observations of interstellar lines 11 p1748 N85-20996
Observations of Mg 1 and Mg 2 in the local ISM 11 p1748 N85-20997
The dependence of interstellar element depletions on mean space density 11 p1749 N85-20998

INTERSTELLAR COMMUNICATION
Interstellar mission 04 p0450 N85-12916
The search for extraterrestrial intelligence 15 p2599 N85-26809
Where is everybody? An account of Fermi's question
[DE85-011898] 19 p3383 N85-30988

INTERSTELLAR EXTINCTION
Local interstellar extinction with an emphasis on uvby beta results 06 p0875 N85-15559
Do the arching HI filaments show in local reddening data? 06 p0876 N85-15561
Inverse relations between 0.25 keV counts and local interstellar dust 06 p0877 N85-15572
Nearby molecular hydrogen 06 p0879 N85-15582
The atmospheric extinction problem 08 p1251 N85-17901
Magellanic cloud objects 11 p1744 N85-20985
The variation of galactic interstellar extinction in the ultraviolet 11 p1749 N85-21000
Interstellar extinction in the nucleus of H PER 11 p1749 N85-21001
The UV extinction of HR 5999 11 p1753 N85-21026
Physical models for the UV continua of symbiotic stars 11 p1756 N85-21048
IUE and optical observations of LMC X-ray binaries 11 p1757 N85-21050
Tasks for observations of close binary systems in the extreme ultraviolet 11 p1757 N35-21054
Dynamics of long-period comets 13 p2176 N85-23506
The structure of Herbig-Haro object 43 and Orion dark cloud extinction
[NASA-TM-87503] 24 p4166 N85-35831

INTERSTELLAR GAS
NT NEUTRAL GASES
Relation of core structure to high velocity outflow in G35.2-0.74 and other molecular clouds 03 p0443 N85-12818
Changes of LISM characteristics in the heliospheric interface 06 p0873 N85-15542
Probe of the nearby interstellar medium by the vacant line of sight to Beta CMa 06 p0874 N85-15551
IUE observations of the gaseous component of the local interstellar medium 06 p0874 N85-15553
Optical emission line studies and the warm, ionized component of the local interstellar medium 06 p0875 N85-15555
A high-resolution study of local interstellar sodium 06 p0875 N85-15556
Optical observations of nearby interstellar gas 06 p0875 N85-15557
Local interstellar extinction with an emphasis on uvby beta results 06 p0875 N85-15559
Do the arching HI filaments show in local reddening data? 06 p0876 N85-15561
Absorption and emission of EUV radiation by the local ISM 06 p0876 N85-15563
Observations of highly-ionized interstellar iron 06 p0876 N85-15565
Local contributions to the 0.6 keV diffuse X-ray background 06 p0877 N85-15569
Inverse relations between 0.25 keV counts and local interstellar dust 06 p0877 N85-15572
Dark cloud and globule distribution for galactic longitudes 230 to 360 degrees 06 p0878 N85-15575
The smallest sizes of diffuse interstellar clouds 06 p0878 N85-15578
Polarization of radio molecular lines and mapping of magnetic field direction 06 p0878 N85-15581
Nearby molecular hydrogen 06 p0879 N85-15582
Modelling the local interstellar medium as a supernova remnant in a multiphase gas 06 p0879 N85-15585
Kinematics of nearby gas and stars 06 p0880 N85-15591
The environment of active galactic nuclei 07 p1057 N85-16712
Radio Seyferts and the forbidden line region 08 p1236 N85-17793
On the stability of broad line clouds in active galactic nuclei 08 p1243 N85-17840
Far-Infrared spectroscopy of interstellar gas 08 p1245 N85-17858
Multi-spectral observations of the star formation: The role of far infrared photometry 08 p1245 N85-17859
First results of submillimeter polarimetry 08 p1246 N85-17861
Far-Infrared spectroscopy of galaxies: The 158 micron C(+) line 08 p1249 N85-17882
Molecular hydrogen and thermal phases in astrophysics 09 p1414 N85-18922
IUE absorption line studies of highly ionized interstellar gas 11 p1743 N85-20982
Supernova remnants and the carbon abundance in M33 11 p1745 N85-20972
The UV extinction laws in two very young clusters, NGC 6530 in the galaxy and NGC 2100 in the LMC 11 p1748 N85-20994
Observations of Mg 1 and Mg 2 in the local ISM 11 p1748 N85-20997
The dependence of interstellar element depletions on mean space density 11 p1749 N85-20998
High-velocity interstellar gas in the line-of-sight to HD 50896 11 p1749 N85-20999
Helium atoms in interstellar and interplanetary space. II: Determination of direction of interstellar gas motion relative to Sun 13 p1900 N85-22425
Numerical study of a two-fluid hydrodynamical model of interstellar medium and population 1 stars 14 p2440 N85-25055
Spectral constraints on models of gas in clusters of galaxies
[NASA-TM-86188] 15 p2669 N85-26468
The structure of galactic HI in directions of low total column density
[NASA-CR-175709] 16 p2882 N85-27765
The extent of the local hi halo
[NASA-CR-176115] 23 p3987 N85-34724
On the influence of the heliomagnetospheric periphery on the galactic cosmic rays
[SH-4.2-19] 23 p4009 N85-34858
On the importance of interstellar helium for the propagation of heavy cosmic rays
[OG-7.2-11] 23 p4015 N85-34879
The role of cosmic rays in magnetic hydrodynamics of interstellar medium
[OG-7.2-15] 23 p4015 N85-34882
The HEAO-2 Guest Investigator Program: Non-linear growth of instabilities in line-driven stellar winds
[NASA-CR-176166] 24 p4168 N85-35840

INTERSTELLAR MAGNETIC FIELDS
Models of nonkeplerian accretion disks based on dynamo magnetic field: Application to Active Galactic Nuclei (AGN) 08 p1242 N85-17834
Some constraints on magnetic fields in galactic spiral arms 12 p1957 N85-22300
Variations in the small-scale galactic magnetic field and short time-scale intensity variations of extragalactic radio sources 20 p3549 N85-32084
A simulation of high energy cosmic ray propagation 1
[OG-5.4-1] 22 p3885 N85-34078
Modeling cosmic ray anisotropies near 10(18) eV
[OG-5.4-9] 22 p3886 N85-34086
On galactic origin of cosmic rays with energy up to 10(19) eV
[OG-5.4-15] 22 p3887 N85-34091
Relativistic electron in curved magnetic fields
[OG-6.2-11] 22 p3890 N85-34110

Angular resolution of an EAS array for gamma ray astronomy energies 5 x 10 (13) eV
[OG-8.5-8] 23 p4031 N85-34065
Change of cosmic ray anisotropy with solar activity
[SH-4.5-20] 23 p4036 N85-35037
INTERSTELLAR MASERS
An infrared study of the bi-polar outflow region GGD 12-15
[NASA-TM-86655] 03 p0445 N85-12835
The relevance of QUASAT to the star formation problem 07 p1058 N85-16718
Galactic OH and H2O masers — QUASAT project 07 p1058 N85-16719
Water maser outburst 07 p1058 N85-16720
Water masers and distance measurements: The impact of QUASAT 07 p1059 N85-16721
INTERSTELLAR MATTER
Helium atoms in interstellar and interplanetary media, part 3: Temperature and velocity of interstellar wind 02 p0160 N85-11088
Molecules in external galaxies 03 p0444 N85-12828
Detection of submillimeter polarization in the Orion Nebula
[NASA-TM-86613] 04 p0579 N85-13700
Structural properties of open star clusters and their relation to the galaxy 05 p0736 N85-14733
The dynamical evolution of the environment of an OB association 05 p0739 N85-14752
Local Interstellar Medium. International Astronomical Union Colloquium No. 81
[NASA-CP-2345] 06 p0872 N85-15539
Absorption line studies and the distribution of neutral gas in the local interstellar medium 06 p0873 N85-15544
Synthesis of data on the local interstellar medium 06 p0874 N85-15545
Observations of interstellar HI toward nearby late-type stars 06 p0874 N85-15546
Observations of local interstellar Mg I and Mg II 06 p0874 N85-15547
Mg II spectra of late type stars used to probe the LISM 06 p0874 N85-15548
FeII and MgII in the nearby interstellar medium 06 p0874 N85-15549
A type stars as probes of the local interstellar medium 06 p0874 N85-15550
Deuterium abundance in the local interstellar medium 06 p0874 N85-15552
Voyager EUV and FUV observations 06 p0875 N85-15554
Distances of local clouds from optical line observations 06 p0875 N85-15558
Optical polarization as a probe of the local interstellar medium 06 p0875 N85-15560
Do the arching HI filaments show in local reddening data? 06 p0876 N85-15561
Observations of absorption lines from highly ionized atoms 06 p0876 N85-15562
Absorption and emission of EUV radiation by the local ISM 06 p0876 N85-15563
Detection of narrow C 4 and Si 4 absorption features in spectra of stars within 200 pc f the Sun 06 p0876 N85-15564
Observations of highly-ionized interstellar iron 06 p0876 N85-15565
The soft X-ray diffuse background: Implications for the nature of the local interstellar medium 06 p0876 N85-15566
Non-local origin of a substantial portion of the soft X-ray background 06 p0877 N85-15567
Local contributions to the 0.6 keV diffuse X-ray background 06 p0877 N85-15569
HEAO-1 diffuse soft X-ray sky maps 06 p0877 N85-15570
Ultrasoft X-ray background observations of the local interstellar medium 06 p0877 N85-15571
Inverse relations between 0.25 keV counts and local interstellar dust 06 p0877 N85-15572
Molecular clouds within 100 pc 06 p0877 N85-15573
A wide latitude CO survey of molecular clouds in the northern Milky Way 06 p0877 N85-15574
Non equilibrium ionization in the local hot bubble 06 p0879 N85-15587
Large-scale bubble structure of the interstellar medium (ISM) and properties of the Local Spiral Arm (LSA) 06 p0879 N85-15588
Stromgren trails of hot white dwarfs 06 p0879 N85-15589
Magnetic alignment theory and the interpretation of polarization 06 p0880 N85-15590
Dark matter near the sun: Simulated star counts and the Oort limit 06 p0880 N85-15592
Future studies of the local interstellar medium with Space Telescope and Columbus 06 p0880 N85-15593
Observations of local ISM emission with the Berkeley EUV/FUV shuttle telescope 06 p0880 N85-15594
Measuring EUV line emission from the hot interstellar medium 06 p0880 N85-15595
Far-infrared spectroscopy of interstellar gas 06 p1245 N85-17853
Multi-spectral observations of the star formation: The role of far infrared photometry 06 p1245 N85-17859
The 1.5 - 3.5 micron spectroscopy of the Orion H2 source 06 p1246 N85-17864
High sensitivity, high angular resolution far-infrared photometry from the KAO 06 p1246 N85-17867
Interstellar grain mantles 06 p1247 N85-17874
Boundary conditions for the paleoenvironment: Chemical and physical processes in the pre-solar nebula — molecular clouds, interstellar matter, and abundance
[NASA-CR-174370] 10 p1570 N85-19901
Future of Ultraviolet Astronomy Based on Six Years of IUE Research
[NASA-CP-2349] 11 p1743 N85-20981
Magellanic cloud objects 11 p1744 N85-20985
Comments on the origins and variations of carbon and nitrogen in the ISM of galaxies as evident from IUE spectroscopy of H 2 regions 11 p1745 N85-20973
IUE observations of interstellar lines 11 p1748 N85-20996
Dynamics of long-period comets 13 p2176 N85-23508
A soft X-ray survey of galactic supernova remnants with the Einstein Observatory 14 p2434 N85-25013
The propagation of ultraheavy cosmic rays 15 p2685 N85-26582
The soft X-ray background as a supernova blast wave viewed from inside: Solar abundance models
[NASA-CR-175767] 16 p2887 N85-27813
Photoabsorption and photodissociation of molecules important in the interstellar medium
[NASA-CR-175918] 19 p3363 N85-30966
The hydrodynamic effects of nuclear active galaxy winds on host galaxies 20 p3545 N85-32082
Local interstellar medium and gamma-ray astronomy
[OG-3.1-1] 22 p3873 N85-33889
Multicomponent analysis of total COS-B gamma-ray data at intermediate latitudes
[OG-3.1-3] 22 p3873 N85-33891
Constraints on the galactic distribution of cosmic rays from the COS-B gamma-ray data
[OG-3.1-6] 22 p3873 N85-33894
Relevance of cosmic gamma rays to the mass of gas in the galaxy
[OG-3.1-9] 22 p3874 N85-33896
COS-B gamma-ray sources and interstellar gas
[OG-3.1-9] 22 p3874 N85-33897
SMM detection of interstellar Al-26 gamma radiation
[OG-3.2-1] 22 p3874 N85-34001
Galactic distribution of interstellar Al-26
[OG-3.2-3] 22 p3874 N85-34002
Interpretation of cosmic-ray anisotropy below 10(14) eV
[OG-5.4-13] 22 p3887 N85-34090
The flux of secondary anti-deuterons and antihelium produced in the interstellar medium
[OG-6.1-5] 22 p3888 N85-34096
Analysis of experimental data on interstellar antiprotons in the light of measurements of high-energy electrons and He-3 nuclei
[OG-6.1-6] 22 p3888 N85-34097
Spectral shape variation of interstellar electrons at high energies
[OG-6.2-7] 22 p3889 N85-34106
Reestimation of the production spectra of cosmic ray secondary positrons and electrons in the ISM
[OG-6.2-8] 22 p3889 N85-34107
Variations in the propagation of UH-nuclei
[OG-7.1-1] 23 p4012 N85-34863
Electron capture decay of cosmic rays: A model of the inhomogeneous interstellar medium
[OG-7.1-10] 23 p4014 N85-34871
The effects of newly measured cross sections in hydrogen on the production of secondary nuclei during the propagation of cosmic rays through interstellar H
[OG-7.2-2] 23 p4014 N85-34874
Interstellar turbulence, random density variations, and scintillation measurements
[OG-7.2-13] 23 p4015 N85-34880
Interstellar (Ne-22) as a possible source of the excess (Ne-22) in the galactic cosmic ray
[OG-8.2-12] 23 p4020 N85-34908
Giant molecular clouds as regions of particle acceleration 23 p4020 N85-34913
Secondary to primary ratio and the continuous acceleration
[OG-8.3-4] 23 p4022 N85-34923
Exact solutions for sporadic acceleration of cosmic rays
[OG-8.3-7] 23 p4022 N85-34925
INTERSTELLAR MICROWAVE SPECTRA
U INTERSTELLAR RADIATION
U MICROWAVE SPECTRA
INTERSTELLAR RADIATION
Polarization of radio molecular lines and mapping of magnetic field direction 06 p0876 N85-15581
Radiation exposure and performance of multiple burn LEO-GEO orbit transfer trajectories
[NASA-TM-86946] 12 p1788 N85-21228
Pulsars and interstellar medium 12 p1980 N85-22320
Contributions to the 19th International Cosmic Ray Conference
[NASA-CR-176060] 21 p3714 N85-33044
Observations of Cygnus X-3 above 10(15) eV from 1979 - 1984
[OG-2.1-6] 22 p3883 N85-33623
Interstellar propagation and the isotopic composition of hydrogen in the galactic cosmic rays
[OG-4.2-1] 22 p3877 N85-34021
Influence of the source distribution on the age distribution of galactic cosmic rays
[OG-8.3-1] 23 p4021 N85-34920
INTERSTELLAR REDDENING
U INTERSTELLAR EXTINCTION
INTERSTELLAR SPACE
Dust properties determined from backscattering in the interplanetary and interstellar medium 03 p0446 N85-12836
Helium and hydrogen of the local interstellar medium observed in the vicinity of the Sun 06 p0873 N85-15540
Pioneer 10 and Voyager observations of the interstellar medium in scattered emission of the He 584 A and H Lya 1216 A lines 06 p0873 N85-15541
Changes of LISM characteristics in the heliospheric interface 06 p0873 N85-15542
Broadening of the interplanetary helium cone structure due to elastic collisions of LISM helium atoms with solar wind ions 06 p0873 N85-15543
Synthesis of data on the local interstellar medium 06 p0874 N85-15545
Magnetic alignment theory and the interpretation of polarization 06 p0880 N85-15590
QUASAT, gravitational lenses, and studies of the interstellar, intracluster and intergalactic medium 07 p1058 N85-16715
Pulsars and interstellar medium 12 p1980 N85-22320
Activities report of the Institute for Astronomy and Astrophysics
[MITT-5] 14 p2434 N85-25012
On the influence of the heliomagnetospheric periphery on the galactic cosmic rays
[SH-4.2-19] 23 p4009 N85-34856
Cosmic ray secondary nuclei and the structure of the galaxy
[OG-7.2-4] 23 p4014 N85-34876
On the cosmic ray diffusion in a violent interstellar medium
[OG-7.2-14] 23 p4015 N85-34881
The role of cosmic rays in magnetic hydrodynamics of interstellar medium
[OG-7.2-15] 23 p4015 N85-34882
INTERSTELLAR SPACECRAFT
Interstellar mission 04 p0459 N85-12916
INTERSTELLAR TRAVEL
Where is everybody? An account of Fermi's question
[DE85-011868] 19 p3383 N85-30868
INTERSTITIALS
Investigation of the interaction of atoms with lattice defects using probe methods 03 p0429 N85-12737
Interaction of hydrogen with defects in metals
[DE84-016781] 04 p0476 N85-13032
Evaluation of interstitial gas contamination in titanium alloys using induced magnetic field analysis
[AD-P004130] 08 p1127 N85-17105
Electromagnetic NDE of interstitial contamination in titanium alloy weldments
[AD-P004131] 08 p1127 N85-17106
Evaluation of the thermoelectric method for determination of interstitial gases in titanium
[AD-P004132] 08 p1127 N85-17107
Enhanced diffusion from interstitial trapping during solid-phase-epitaxial growth of silicon alloys
[DE85-001285] 12 p1941 N85-22193
Current understanding of point defects and diffusion processes in silicon 20 p3481 N85-31632
INTERTROPICAL CONVERGENT ZONES
Plans for the NRL/NORDA (Naval Research Laboratory-Naval Ocean Research and Development Activity) fine-scale variability experiment - 1984 (FVX-84)
[AD-A146041] 03 p0398 N85-12540
Simple prediction of convergence zone propagation in waters around australia
[AD-A146988] 03 p0416 N85-12659

INTERVALS
Construction of approximate confidence intervals for probability-of-kill via the bootstrap
[AD-A144761] 01 p0113 N85-10764
Interval mathematics reports
[REPT-84/1] 04 p0556 N85-13536
Interval-mathematical treatment of initial value problems of ordinary differential equations
04 p0556 N85-13538
Interval interation methods for nonlinear equation systems: Theory and comparison on computer
[INTERVALL-BER-84/6] 05 p0719 N85-14612
Bootstrap confidence intervals
[AD-A147572] 07 p1033 N85-16559
Exact simultaneous confidence intervals for pairwise comparisons of three normal means
[AD-A148751] 09 p1375 N85-18645
Confidence intervals using the regenerative method for simulation output analysis
[AD-A150147] 13 p2149 N85-23343
Better bootstrap confidence intervals
[AD-A150798] 14 p2408 N85-24846
The measurement of human time estimating ability using a modified jerison device
[AD-A151870] 15 p2620 N85-26141
Proceedings of the Sixteenth Annual Precise Time and Time Interval (PTTI) Applications and Planning Meeting
[NASA-TM-87561] 18 p3105 N85-29221
Fixed width interval estimation in linear regression
[AD-A153833] 18 p3174 N85-29675
Weibull distribution based on maximum likelihood with interval inspection data
[NASA-TM-86515] 21 p3678 N85-32847
Precision microwave attenuation measurement by time interval ratio
[RSRE-85005] 22 p3755 N85-33280
Limits to the burster repetition rate as deduced from the 2nd catalog of the interplanetary network
[OG-1.2-5] 22 p3862 N85-33915
INTESTINES
NT RECTUM
Distinctions of SPF rats used in experiments aboard biosatellites 07 p1012 N85-16427
Dynamics of quantitative and qualitative changes in conditionally pathogenic microflora of the human intestine during long-term hypokinesia 12 p1903 N85-21953
INTOXICATION
A manual control test for the detection and deterrence of impaired drivers 05 p0709 N85-14550
INTRAMOLECULAR STRUCTURES
Intramolecular electron transfer at metal surfaces. Part 5: Pendant substituent effects upon thiocarboxylate-bridged Cobalt (3) reduction kinetics at mercury and gold electrodes
[AD-A150647] 14 p2254 N85-23971
Determination of the intramolecular potential flow from a neutron diffraction experiment
[B8583199] 20 p3532 N85-31978
INTRAOCULAR PRESSURE
Intraocular fluid dynamics in microgravity 05 p0693 N85-14455
INTRAVEHICULAR ACTIVITY
The human role in space. Volume 1: Executive summary
[NASA-CR-171223] 04 p0548 N85-13473
INTRUSION
Slope water intrusions within the nearshore waters off Long Island, New York
[DE85-001386] 09 p1359 N85-18549
One physical mechanism of formation of fine structure of ocean waters 14 p2334 N85-24436
Device for preventing intrusion of a blade during vibration cutting of intermittent cutting with a lathe
16 p2794 N85-27232
Explanation of Russian models: Saudi Arabian seismic refraction profile 17 p2991 N85-28487
INVALIDITY
U ERRORS
INVARIANCE
NT GAUGE INVARIANCE
Time invariant memoryless nonlinear systems identification method
[FUB-9-1983] 01 p0114 N85-10773
Trilinear alternating forms on a vector space of dimension 7
[CWI-PM-R8402] 05 p0722 N85-14644
An invariant measure for the equation u sub tt - u sub xx + u3 = 0
[AD-A147300] 08 p1210 N85-17612
Recognition of complex 3-dimensional objects using 3-dimensional moment invariants
[AD-A148119] 08 p1212 N85-17625
Connected simple systems and the Conley index of isolated invariant sets
[AD-A149383] 10 p1552 N85-19789
Invariant differential operators on a semisimple symmetric space and finite multiplicities in a Plancherel formula
[CWI-PM-R8409] 12 p1925 N85-22094
Practical methods for the compensation and control of multivariable systems
[AD-A151047] 14 p2407 N85-24841
Generalised translation invariance and systems theory
[CRM-8501] 17 p3017 N85-28657
Exact invariants in resonance form for time-dependent potentials
[DE85-010733] 19 p3346 N85-30739
Application of adaptive noise cancellation to Coast Guard voice communications
[AD-A154798] 21 p3574 N85-32230
A graph theoretic procedure for the design of feedback patterns
[REPT-110] 24 p4142 N85-35673
INVENTIONS
Parabolic tapers for overmoded waveguides
[DE84-014237] 01 p0039 N85-10247
A high-voltage discharger
[AD-A145659] 02 p0194 N85-11299
Novel drives for machine tools
14 p2268 N85-24053
Equipment for monitoring low concentrations of volatile substances in gases or liquid metals
[BLL-DOUNREAY-TR-949-(9091.9F)]
16 p2786 N85-27190
East Europe report: Science and technology
[JPRS-ESA-85-021] 21 p3568 N85-32190
INVENTORIES
NT CROP INVENTORIES
NT TIMBER INVENTORY
International strategic minerals inventory. Summary report: Manganese
[GS-CIRC-830-A] 02 p0219 N85-11442
On some common interests among reliability, inventory and queuing
[AD-A145595] 02 p0251 N85-11646
Environmental data inventory for the antarctic area
[PB85-107944] 06 p0819 N85-15195
Setting time standards at NISTARS (Naval Integrated Storage and Retrieval System)
[AD-A146371] 06 p0870 N85-15529
Excessive Air Force inventories result from duplicative spare parts requirements
[AD-A147777] 08 p1228 N85-17734
Inventory policy for high backorder items
[AD-A153606] 18 p3198 N85-29840
INVENTORY CONTROLS
Probability distribution of leadtime demand
[AD-A144952] 01 p0113 N85-10766
Setting time standards at NISTARS (Naval Integrated Storage and Retrieval System)
[AD-A146371] 06 p0870 N85-15529
An applicatio of Markov chains to the problem of migration in inventory systems
[AD-A151954] 16 p2857 N85-27618
EOQ (Economic Order Quantity) range model
[AD-A153709] 19 p3379 N85-30965
Discrete simulation models - their role in the design, development and management of inventory control systems
[PNR-90249] 23 p3986 N85-34719
INVENTORY MANAGEMENT
NT INVENTORY CONTROLS
Ministry wants better commo facilities for agroaviation
03 p0310 N85-12003
A methodology for comparing the variable costs of the continuous and periodic review models
[AD-A146351] 03 p0436 N85-12776
An evaluation of the effect of establishing a minimum Economic Order Quantity (EOQ) on the Air Force EOQ item management system
[AD-A147121] 07 p1051 N85-16673
The Air Force stock fund and aircraft availability
[AD-A148653] 08 p1067 N85-16761
Inventory policy for high backorder items
[AD-A153606] 18 p3198 N85-29840
EOQ (Economic Order Quantity) range model
[AD-A153709] 19 p3379 N85-30965
INVERSE SCATTERING
The development of new methods for solving the target identification or inverse scattering problem for time-harmonic acoustic and electromagnetic waves
[AD-A145821] 03 p0415 N85-12657
Multidimensional inverse scattering for first order systems
[AD-A148711] 08 p1214 N85-17642
Lax-pair operators for squared-sum and squared-difference eigenfunctions
[AD-B089083L] 09 p1366 N85-18718
Nonlinear sigma-models and integration methods
[DE85-004447] 12 p1922 N85-22071
Connection between time- and frequency-domain three-dimensional inverse problems for the Schroedinger equation
[DE85-005914] 15 p2639 N85-26274
Solvability of some inverse problems in laser radiation focusing 21 p3696 N85-32963
Inverse-Compton gamma rays in the galaxy
[OG-3.1-2] 22 p3873 N85-33990
Multicomponent analysis of total COS-B gamma-ray data at intermediate lattitudes
[OG-3.1-3] 22 p3873 N85-33991
Calculation of heavy-ion tracks in liquid water
[DE85-012101] 24 p4149 N85-35725
INVERSIONS
NT CENTRIFUGING STRESS
NT MAGNETIC FIELD INVERSIONS
NT POPULATION INVERSION
NT TEMPERATURE INVERSIONS
Project review on geophysical and ocean sound speed profile inversion
[AD-A145717] 02 p0276 N85-11797
An extension of the Born inversion method to a depth dependent reference profile
[AD-A146469] 06 p0859 N85-15461
A method for solving the inverse problem of transonic cascade flow
[AD-A146739] 07 p0899 N85-15698
Ill-posed problems and regularization analysis in early vision
[AD-A147753] 08 p1222 N85-17696
Characteristic functional of a probability measure absolutely continuous with respect to a Gaussian radon measure
[AD-A149482] 10 p1548 N85-19763
On the inversion of the lidar equation
[AD-A149653] 12 p1856 N85-21641
Determining conductivity by boundary measurements. Part 2: Interior results
[AD-A149750] 12 p1921 N85-22063
Inverse behavior of silicon photovoltaic cells
13 p2010 N85-22604
Algorithms for reconstruction of partially known, band limited Fourier transform pairs from noisy data
[AD-A150194] 13 p2150 N85-23347
Born inversion with a stratified reference velocity
[AD-A149222] 16 p2853 N85-27584
Efficient parallel solution of linear systems
[AD-A152683] 17 p3018 N85-28663
INVERTEBRATES
NT INSECTS
NT LARVAE
NT PROTOZOA
NT SPIDERS
Hollings hungry mantid model for the invertebrate functional response considered as a Markov process. Part 3: Mathematical elaborations
[CWI-AM-R8407-PT-3] 05 p0722 N85-14639
Effects of acid rain on forest nutrient status
[DE85-012486] 23 p3947 N85-34463
Aquatic Invertebrate Development Working Group
24 p4127 N85-35585
INVERTED CONVERTERS (DC TO AC)
Analysis of inverter models and harmonic propagation. Part 1: A physical simulator for large solar cell arrays
[DE85-002312] 09 p1315 N85-18271
Analysis of inverter models and harmonic propagation. Part 2: Harmonic propagation
[DE85-000198] 10 p1482 N85-19356
5 kW sleeps inverter. Revision
[AD-A149526] 10 p1510 N85-19528
Analysis of inverter models and harmonic propagation. Part 3. Transient processes in inverter models
[DE85-000191] 10 p1510 N85-19530
Airport solar photovoltaic concentrator phase 3
[DE85-006773] 18 p3128 N85-29370
INVERTERS
Advanced inverter technology
[AD-A149335] 10 p1480 N85-19343
IREB (Intense Relativistic Electron Beam) converter to ac pulses
[AD-D011479] 10 p1554 N85-19800
Numerical simulation of inverters with I2L elements including effects of high doping level
13 p2088 N85-23039
Evaluation of half wave induction motor drive for use in passenger vehicles
[NASA-CR-176119] 23 p3926 N85-34334
INVESTIGATION
NT ACCIDENT INVESTIGATION
NT AIRCRAFT ACCIDENT INVESTIGATION
NT INTERNATIONAL MAGNETOSPHERIC STUDY
Holographic investigation of solid propellant combustion in a two-dimensional motor
[AD-A153546] 18 p3070 N85-29989

Studies in quality improvement 2. An analysis for unreplicated fractional factorials
[AD-A153539] 18 p3169 N85-29640
INVESTMENTS
Capital investment motivational techniques used by prime contractors on subcontractors
[AD-A153660] 18 p3196 N85-29837
INVISCID FLOW
NT STAGNATION FLOW
Numerical analysis of the 3-dimensional inviscid hypersonic flow around capsule-type bodies by the alternate directional implicit method
[NAL-TR-799] 01 p0002 N85-10012
Review of some vortex relations
[NASA-CR-172452] 01 p0046 N85-10302
Gas side heat transfer: 2-D flow
02 p0142 N85-10985
Linear long-wave stability of cylindrical steady laminar flame in rotating medium 02 p0266 N85-11752
An inviscid computational method for supersonic inlets
[AD-A145997] 03 p0316 N85-12042
Incorporation of viscous-inviscid interactions in turbomachinery design
[PNR-90219] 04 p0457 N85-12897
The numerical simulation of steady transonic rotational flow using a dual potential formulation
05 p0591 N85-13770
A comparative study of the nonuniqueness problem of the potential equation
[NASA-TP-2385] 07 p0898 N85-15894
Analysis of the flow field about a T-45 using PANAIR
[AD-A146811] 07 p0899 N85-15899
A second-order accurate parabolized Navier-Stokes algorithm for internal flows
[NASA-CR-174258] 07 p0956 N85-16059
Recent advances in computational methods to solve the high-lift multi-component airfoil problem
08 p1068 N85-16774
Inviscid compressible flow past a multi-element aerofoil 08 p1069 N85-16776
Theoretical study of boundary-layer control
08 p1070 N85-16784
Leading edge separation criterion for an oscillating airfoil
[AD-P004175] 09 p1257 N85-17960
Development of multigrid algorithms for problems from fluid dynamics
[GMD-111] 09 p1321 N85-18305
Analysis of inviscid transonic flow around an airfoil by diagonal form of IAF scheme
[NAL-TR-831] 10 p1420 N85-18955
Inviscid analysis of unsteady blade tip flow correlation studies
[NASA-CR-172506] 10 p1420 N85-18958
Efficient self-consistent viscous-inviscid solutions for unsteady transonic flow
[NASA-TM-86335] 10 p1420 N85-18959
Computation of the inviscid velocity potential for general ellipsoids on a nearly quadratic surface grid
[REPT-25/84] 11 p1633 N85-20267
Wind tunnel wall interference
[AD-A151212] 15 p2474 N85-25273
Flow through very porous inclined screens
[NASA-TM-86979] 15 p2555 N85-25761
Investigation of potential and viscous flow effects contributing to dynamic stall
[AD-A151699] 15 p2557 N85-25773
Inviscid upwind finite difference model for two dimensional vertical axis wind turbines
15 p2595 N85-25903
Numerical simulation of inviscid compressible flow through three-dimensional cascade
16 p2892 N85-26619
The role of computational fluid dynamics in aeronautical engineering 16 p2894 N85-26629
Theoretical investigation of three-dimensional shock wave turbulent boundary layer interactions. Part 3
[AD-A152251] 16 p2783 N85-27177
On the relation between upwind-differencing schemes of Godunov, Engquist-Osher and Roe
[NASA-CR-175805] 16 p2852 N85-27583
Steady, incompressible, inviscid flow through a finite collapsible tube under longitudinal tension
[REPT-84-01] 17 p2959 N85-28278
Numerical computation of space shuttle orbiter flow field
[NASA-CR-175912] 18 p3058 N85-28921
Inviscid analysis of two supercritical laminar-flow-control airfoils at design and off-design conditions
[NASA-TM-84657] 19 p3212 N85-29920
Numerical and experimental investigation of turbomachinery rotor flow fields
20 p3451 N85-31429
A new finite element approach: Progress in inviscid flow computations
[NASA-TM-86434] 20 p3454 N85-31450
An evaluation of four methods of numerical analysis for two-dimensional airfoil flows
[AD-A155202] 21 p3552 N85-32096
An analysis of flow models: From Navier-Stokes to potential flow equations 21 p3587 N85-32295
Numerical solution of the Navier-Stokes equations for 3-D internal flows: An emerging capability
21 p3588 N85-32300
Calculation of 3-D flow without numerical mixing
21 p3588 N85-32301
Generation by conformal mappings of aerofoil sections and of certain other simple shapes suitable for both aerodynamic and stress-concentration problems
[AD-A154901] 22 p3728 N85-33112
Modelling of unsteady, incompressible separation on an aerofoil using an inviscid flow algorithm
[GU-AERO-8412] 23 p3894 N85-34122
INVISIBILITY
U VISIBILITY
IO
Do the satellites of Uranus control its magnetosphere?
02 p0301 N85-11952
Temporal and spatial variations in the intensity of ultraviolet emissions from Jupiter and the Io torus
03 p0448 N85-12846
Outer satellite atmospheres: Their nature and planetary interactions
[NASA-CR-174146] 04 p0589 N85-13759
Analysis of Jovian low frequency radio emissions
[NASA-CR-174449] 10 p1571 N85-19908
A modeling analysis program for the JPL Table Mountain Io sodium cloud data
[NASA-CR-175493] 11 p1681 N85-20589
Coincidence techniques to study electron emission in ion-atom collisions
[DE85-003635] 11 p1724 N85-20846
Long term variability of the IO torus
11 p1760 N85-21070
Research in planetary studies and operation of Mauna Kea Observatory
[NASA-CR-175618] 13 p2169 N85-23460
Hot spots on Io: Correlation of infrared emission and visible reflectance 13 p2172 N85-23475
Io: Generation of silicate magma by shear melting at the base of a basaltic lithosphere
13 p2172 N85-23476
Topographic evidence for shield volcanism on Io
13 p2172 N85-23478
Sulfur volcanoes on Io? 13 p2173 N85-23479
Sulfur oxygen processes on Io
13 p2173 N85-23481
The violet absorber on Io: Disulfur monoxide derivatives 13 p2173 N85-23482
Emplacement of long lava flows on Mauna Loa (Hawaii) and Alba (Mars) 13 p2186 N85-23563
Accurate albedos of the brightest regions on Io
13 p2195 N85-23618
Io: Precise comparison of Voyager spectral curves with laboratory measurements 13 p2196 N85-23619
Photometric analysis of Jupiter-illuminated images of Io 13 p2196 N85-23620
Shape of Io 13 p2204 N85-23672
A modeling analysis program for the JPL table mountain Io sodium cloud
[NASA-CR-175851] 16 p2833 N85-27468
On the importance of viscous dissipation in Io
22 p3855 N85-33573
Models of planetary structure and evolution: The case of Io 22 p3855 N85-33574
IODATES
NT LITHIUM IODATES
IODIDES
NT CESIUM IODIDES
NT SILVER IODIDES
NT SODIUM IODIDES
Structural and synthetic organosilicon chemistry
[AD-A147101] 07 p0919 N85-15820
Mercuric iodide photodetectors for scintillation spectroscopy
[DE85-001437] 10 p1437 N85-19056
Generation of lead, lead iodide and iodide aerosols and their ice nucleation 21 p3639 N85-32607
New and revised methods of purifying mercuric iodide
[DE85-011684] 22 p3749 N85-33237
Stable n-CuInSe/sub 2/iodide-iodine photoelectrochemical cell
[DE85-011597] 22 p3808 N85-33576
IODINE
NT IODINE ISOTOPES
Spectrophotometric studies of iodine complexes in an aluminum chloride - butylpyridinium chloride ionic liquid
[AD-A145074] 01 p0024 N85-10150
Hydrolysis of iodine: Equilibria at high temperatures
[DE84-016713] 09 p1293 N85-18119
Ice nucleating characteristics of Capparis Aphylla, an Indian herb 21 p3641 N85-32619
Ice nucleation of single water droplet by silver iodide: A laboratory observation 21 p3643 N85-32630
Monte Carlo studies of H2O layers adsorbed on a model basal face of AgI 21 p3643 N85-32633
Technology of off-gas treatment for liquid-fed ceramic melters
[DE85-012467] 22 p3812 N85-33610
Aqueous volatile weak electrolyte equilibria to 300 C
[DE85-013840] 24 p4076 N85-35281
A new drawing technique for nylon 6 by reversible plasticization with iodine
[AD-A156272] 24 p4162 N85-35803
IODINE COMPOUNDS
NT CESIUM IODIDES
NT IODIDES
NT LITHIUM IODATES
NT SILVER IODIDES
NT SODIUM IODIDES
Spectrophotometric studies of iodine complexes in an aluminum chloride - butylpyridinium chloride ionic liquid
[AD-A145074] 01 p0024 N85-10150
Environmental stability of intercalated graphite fibers
[NASA-TM-87025] 16 p2753 N85-28992
IODINE ISOTOPES
The I-Pu-Xe age of the Moon
04 p0584 N85-13729
Design and chemical synthesis of iodine-containing molecules for application to solar-pumped I* lasers
[NASA-CR-176010] 19 p3275 N85-30310
IODINE LASERS
Saturation kinetics of active medium of oxygen-iodine laser 11 p1718 N85-20607
Optically pumped iodine monofluoride laser
[AD-D011555] 12 p1955 N85-21637
Laser-induced fluorescence measurement of vapor concentration surrounding evaporating droplets
[DE85-009409] 19 p3277 N85-30320
Optical inhomogeneities in a nanosecond-pulse iodine photodissociation laser with slow UV radiation pumping
21 p3686 N85-32902
ION ACCELERATORS
The Berkeley mini-collider
[DE84-014584] 01 p0118 N85-10808
High intensity hadron accelerators
[DE84-014063] 01 p0119 N85-10812
Laser source of neutral atoms for collective-field particle accelerator 02 p0263 N85-11719
Preliminary grouping in A strong-current linear ion accelerator with a low injection energy
[DE84-017192] 04 p0563 N85-13587
Explosive emission cathode plasmas in intensive relativistic electron beam diodes
[AD-A147917] 07 p1046 N85-16842
Status of RF superconductivity at Argonne National Laboratory
[DE85-002145] 09 p1312 N85-18245
Mobile accelerator neutron radiography system
[AD-A148808] 09 p1323 N85-18311
Large electrostatic accelerators
[DE85-001120] 09 p1382 N85-18869
Operating experience and construction status of ATLAS — Argonne tandem-linac accelerator
[DE85-002741] 11 p1736 N85-20914
Theoretical study of collective ion acceleration in the Luce diode
[AD-A150107] 12 p1929 N85-22116
Workshop on Nuclear Dynamics 3
[INC-40007-24] 12 p1931 N85-22130
Effects of magnetic shear on lower hybrid waves in the suprauroral region
[AD-A151980] 15 p2658 N85-26392
Heavy ion physics at BNL, the AGS and RHIC
[DE85-005651] 17 p3033 N85-28760
Heavy ion fusion accelerator research in the US
[DE85-008465] 17 p3034 N85-28767
Ultrahigh vacuum system of the heavy ion transport line at Brookhaven
[DE85-011838] 22 p3840 N85-33778
Heavy ion medical accelerator options
[DE85-011204] 22 p3841 N85-33784
Energetic ion acceleration at collisionless shocks
[SH-1.5-3] 23 p3998 N85-34772
Considerations on collective ion acceleration as an intense ion injector
[DE85-012706] 24 p4155 N85-35757
Applications of decelerated ions
[DE85-011832] 24 p4156 N85-35767
Heavy nucleus collisions between 20 and 60 GeV/nucleon
[HE-1.4-2] 24 p4175 N85-35890
Meson multiplicity in nucleus-nucleus collisions above 4 GeV/amu
[HE-1.4-10] 24 p4177 N85-35897

ION ACOUSTIC WAVES

Arguments for fundamental emission by the parametric process L yields T + S in interplanetary type III bursts — langmuir, electromagnetic, ion acoustic waves (L, T, S) 12 p1958 N85-22311

Research with high-power short-wavelength lasers [DE85-010329] 19 p3278 N85-30332

Ion-acoustic double layer in a magnetic picket fence configuration [INPE-3552-PRE/764] 19 p3360 N85-30698

Investigation of ion-acoustic plasma turbulence in field of powerful electromagnetic wave by CO2-laser radiation scattering 21 p3691 N85-32935

Current interruption by density depression [DE85-013120] 24 p4169 N85-35846

ION ATOM INTERACTIONS

Experimental studies of atomic inner shell ionization phenomena [DE84-013448] 01 p0118 N85-10805

Progress in numerical calculations of ion-atom collisions [DE84-016598] 06 p0661 N85-15474

Electron capture by multiply charged ions from hydrogen atoms at low energies [DE84-016560] 06 p0661 N85-15475

Forward electron production in heavy ion-atom and ion-solid collisions [DE85-001256] 09 p1361 N85-18683

Time dependent Hartree-Fock theory of ion-atom collisions: Application to F(9+) + Ne [DE85-003083] 11 p1723 N85-20838

Inner shell contribution to multiple ionization in ion-atom collisions [DE85-003107] 11 p1723 N85-20839

Classical rainbow scattering of alkali ions on metal surfaces. Application to the investigation of unknown surface structures [MPIS-10/1984] 11 p1726 N85-20854

Vacancy-rearrangement theory in the first Magnus approximation [DE85-004435] 12 p1930 N85-22123

Convoy electron production by heavy ions in solids [DE85-005256] 15 p2660 N85-26418

Spin distributions in heavy ion fusion at and below the Coulomb barrier [DE85-007617] 17 p3031 N85-28751

Theoretical studies of heavy ion scattering processes [DE85-008623] 17 p3032 N85-28753

The production and destruction of metastable negative ions [DE85-011056] 19 p3364 N85-30658

ION BEAMS

Manufacturing methods for microwave circuits [AD-A145237] 01 p0043 N85-10278

Beam pulse length determination by spectral analysis [CSIR-NAC-83-05] 01 p0116 N85-10793

Metastable phase formation in ion implanted metals [DE84-014945] 02 p0183 N85-11229

Neutral beam interactions with materials [AD-A145836] 02 p0265 N85-11857

Materials modification by ion beam mixing [AD-P003948] 02 p0266 N85-11864

The use of ion implantation for materials processing [AD-A145438] 02 p0267 N85-11873

Emission mechanisms in the liquid metal ion source: A review [AERE-R-11294] 03 p0418 N85-12675

Vacuum inductive pulsed power compression for inertial confinement fusion [DE84-010935] 03 p0421 N85-12693

Fast ions as probes in solid state research 03 p0430 N85-12740

Ion beam lithography [BMFT-FB-T-84-182] 04 p0504 N85-13219

Low energy ion-molecule reaction dynamics and chemionization kinetics [DE84-015681] 04 p0559 N85-13562

Intense non-relativistic cesium ion beam [DE84-012575] 04 p0560 N85-13566

Performing (p vector, jic)n), (d vector, n) and (n vector, n) measurements with a rotating magnet beam swinger [DE84-017003] 04 p0562 N85-13582

Ion beam and laser induced surface modifications [DE84-016569] 04 p0571 N85-13642

Repetitively pulsed metal ion beams for ion implantation [DE84-014065] 05 p0732 N85-14704

Ion cluster beam deposition research 06 p0831 N85-15283

Extended performance technology study 30-cm thruster [NASA-CR-168259] 07 p0917 N85-15806

The (20)Ne interaction in extended matter [NASA-TM-86312] 07 p1061 N85-16726

Exposure modelling of particle beam lithography [AD-A147849] 08 p1219 N85-17678

Effect of resonant microwave power on a PIG ion source [DE85-001396] 09 p1379 N85-18673

The energy spectra of slowed-down neutrals from the heating beams in ASDEX — tokamak [REPT-84-157] 09 p1394 N85-18772

Fundamental aspects on ion-beam surface modification: Defect production and migration processes [DE85-000093] 09 p1399 N85-18804

Ion beam processes in Si [DE85-001254] 09 p1399 N85-18806

Advanced ion thruster research [NASA-CR-174862] 10 p1430 N85-19021

Simulation of the ion-beam-driven drift instability in a magnetic trap, 1 [AD-A149451] 10 p1452 N85-19147

Amorphization of ceramics by ion beams [DE85-000936] 10 p1453 N85-19156

Hydrodynamic response of a radiating Al plasma excited by a proton beam [AD-A148904] 10 p1558 N85-19824

Oxidation protection coatings for polymers [NASA-CASE-LEW-14072-1] 11 p1611 N85-20129

Deposition of diamondlike carbon films [NASA-CASE-LEW-14060-1] 11 p1615 N85-20153

Radiative ion beams: Hot stellar reactions in the laboratory [DE85-001570] 11 p1722 N85-20833

Diamondlike flakes [NASA-CASE-LEW-13837-2] 12 p1796 N85-21267

Ion-beam nitriding of steels [NASA-CASE-LEW-14104-1] 12 p1805 N85-21324

Sputter-induced compositional modifications in a Ni-Au alloy [DE85-002771] 12 p1807 N85-21333

New high resolution scanning ion microprobe and focused ion beam applications [AD-A149992] 12 p1852 N85-21616

Beam loss due to the aperture limitation resulting from intrabeam scattering [DE85-005138] 12 p1930 N85-22124

Sheath ionization model of beam emissions from large spacecraft 13 p1992 N85-22489

System for forming and focusing high current beam of deuterium ions 13 p2045 N85-22796

Collective acceleration of ions using high current relativistic electron beams [DE85-004869] 13 p2157 N85-23393

Ion transport in beam-plasma interactions [AD-A150145] 13 p2161 N85-23410

Influences of thermal spikes in ion beam mixing [DE85-006190] 14 p2419 N85-24924

Slowing down of charged particles by the bound electrons in a plasma — ion beams, nuclear fusion [LP-209] 14 p2419 N85-24929

Ion beam mixing of marker layers in Al and Si [DE85-006227] 15 p2511 N85-25490

Effects of ion bombardment on the morphology of lead films [DE85-007232] 15 p2511 N85-25494

Annual Review, April 1983 - March 1984 [ISSN-0547-1567] 15 p2654 N85-26369

Heavy ion beam study of potential formation in bumpy torus plasma [IPPJ-711] 15 p2656 N85-26386

Survey of experimental and theoretical electron-impact ionization cross sections for transition metal ions in low stages of ionization [DE85-007605] 16 p2863 N85-27658

Surface modification of solids [DE85-007543] 16 p2871 N85-27715

Uniaxial angular accelerometers 17 p2944 N85-28173

Heavy ion fusion accelerator research in the US [DE85-008465] 17 p3034 N85-28767

Rastrike particle beam experiments on a dense plasma focus. Opening switch research on a dense plasma focus [AD-A152991] 17 p3039 N85-28802

Intense ion beam diode diagnostics using a tunable dye laser [DE85-008079] 18 p3113 N85-29272

Generation of intense negative ion beams [NASA-CASE-NPO-16081-1-CU] 18 p3178 N85-29701

Wide-angle optics with strong magnetic fields for efficient generation of secondary-particle beams [DE85-007727] 18 p3179 N85-29713

Ion beam sputter-deposited thin film coatings for protection of spacecraft polymers in low Earth orbit [NASA-TM-87051] 19 p3248 N85-30137

Experiments with stored heavy ions [DE85-009976] 19 p3356 N85-30602

Emittance growth caused by current variation in a beam-transport channel [DE85-010743] 19 p3363 N85-30649

Proposed use of the radio-frequency quadrupole structure to funnel high-current ion beams [DE85-010746] 19 p3364 N85-30657

Time-resolved energy spectrum of the ion beam generated in the plasma focus 19 p3369 N85-30692

Ion beam-plasma interactions [DE85-010202] 19 p3371 N85-30913

Analysis of beam interaction of the electrical thruster RIT 10 (particle emission) with surfaces [ESA-TT-826] 20 p3421 N85-31231

The response of ionization chambers to relativistic heavy nuclei 20 p3544 N85-32051

In-situ observations of the development of heavy-ion damage in semiconductors [DE85-010289] 22 p3761 N85-33307

Ultrahigh vacuum system of the heavy ion transport line at Brookhaven [DE85-011838] 22 p3840 N85-33778

Heavy ion medical accelerator options [DE85-011204] 22 p3841 N85-33784

Design status of heavy ion injector program [DE85-010751] 22 p3842 N85-33793

Calculation of mixed depth for some metal-Si systems [DE85-011907] 23 p3971 N85-34616

Diamondlike carbon protective coatings for IR materials [NASA-TM-87083] 23 p3973 N85-34631

Numerical calculations on shock loaded materials 23 p3980 N85-34676

Dissipation terms in one-dimensional hydrodynamic code for ICF target 23 p3980 N85-34677

Pulse effect in a light ion beam propagation through a Z-discharge plasma channel 23 p3981 N85-34684

Repetitive pulse accelerator technology for light ion inertial confinement fusion [DE85-012030] 23 p3982 N85-34693

Light ion sources for ICF [DE85-011544] 23 p3983 N85-34702

Method of precisely modifying predetermined surface layers of a workpiece by cluster ion impact therewith [DE85-006519] 23 p3984 N85-34710

Survey of mixing in metal/insulator systems [DE85-011936] 23 p3985 N85-34714

Injection of energetic particles following the gamma-ray flares on June 7, 1980, as observed on Helios 1 [SH-1.3-9] 23 p3993 N85-34756

Use of a minimum-ellipse criterion in the study of ion-beam extraction systems [DE85-012670] 24 p4148 N85-35721

Neutron production by Ne and Si ions on a thick Cu target at 670 MeV/A with application to radiation protection [DE85-014526] 24 p4152 N85-35746

Ion source development for the Los Alamos heavy ion fusion injector [DE85-012682] 24 p4156 N85-35766

Applications of decelerated ions [DE85-011832] 24 p4158 N85-35767

ION CHAMBERS

U IONIZATION CHAMBERS

ION CHARGE

Relative abundances of sub-iron to iron nuclei in low energy (50-250 MeV/N) cosmic rays as observed in the Skylab experiment [OG-4.1-4] 22 p3876 N85-34010

The mean ionic charges of N, Ne, MG, Si and S in solar energetic particle events [SH-2.1-11] 23 p3999 N85-34792

The mean ionic charge of silicon in 3HE-rich solar flares [SH-2.2-6] 23 p4000 N85-34803

ION CONCENTRATION

Measuring system with ion selective electrodes [BMFT-FB-T-84-170] 05 p0639 N85-14100

Maximum current densities from tandem high density systems [DE85-006906] 18 p3180 N85-29720

ION CURRENTS

NT ION BEAMS

Rocket and satellite observations of electric fields and ion convection in the dayside auroral ionosphere [TRITA-EPP-84-05] 02 p0229 N85-11497

Quasielastic neutron scattering on single crystals of solid ionic conductor 03 p0426 N85-12719

Solid electrolytes: Mechanisms for achieving optimal conductivity [AD-A150116] 12 p1801 N85-21296

Achievements of the plasma composition experiment on ISEE-1 during the IMS 14 p2360 N85-24583

Ionic conduction and water diffusion in Li (BETA)-alumina [DE85-007548] 16 p2755 N85-27005

Electrochemistry of polymer films not immersed in solution: Electron transfer on an ion budget [AD-A152969] 17 p2920 N85-27998

Localized ionic currents from a corroding iron-copper galvanic couple
[AD-A153627] 18 p3074 N85-29011
Maximum current densities from tandem high density systems
[DE85-008666] 18 p3180 N85-29720
Ion waves generated by ion loss-cone distributions or drifting particles
[KGI-PREPRINT-070] 20 p3549 N85-32087
Some physical differences between sheet plasma and multicusp plasma as volume produced H- or D- ion sources
[IPPJ-728] 23 p3974 N85-34637
Measuring method and confirmation of H- (D-) ion current by sheet plasma 1
[IPPJ-730] 23 p3974 N85-34638
Feasibility study of radar-transmitting materials
[AD-A155839] 24 p4087 N85-35329
Ion composition measurements of the disturbed and quiet D-region in 1980 - 1981
[AD-A156055] 24 p4117 N85-35521

ION CYCLOTRON RADIATION
Slow wave antenna coupling to ion Bernstein waves for plasma heating in ICRF
[AD-B069084L] 09 p1386 N85-18717
Impurity control by additional current rise and gas puffing during ICRF heating in JIPP T-IIU Tokamak
09 p1387 N85-18725
Electron bounce resonance heating in a bumpy cylinder
[DE85-001732] 10 p1561 N85-19845
Analysis of Jovian low frequency radio emissions
[NASA-CR-174449] 10 p1571 N85-19908
Monte Carlo studies of tandem mirror plasmas interacting with waves in the Ion Cyclotron Range of Frequencies (ICRF)
[DE85-002988] 11 p1731 N85-20883
Lower hybrid heating and current drive, and ion cyclotron heating experiments on the Alcator C and the Versator II Tokamaks
[DE85-004916] 13 p2161 N85-23412
Theory and computer simulation of auroral kilometric radiation 14 p2365 N85-24617
Anomalous heating of ionospheric components (thermal e- and He+) via Intense Ion Cyclotron Waves (ICW's)
14 p2368 N85-24633
Propagation and amplification of Ion Cyclotron Waves (ICW's) in a multicomponent plasma. The Earth magnetosphere as a giant maser for Alfven waves
14 p2368 N85-24634
Pc 1 pulsation source regions and their relationship to the plasma pause 14 p2368 N85-24636
Preparatory experiments. 1: JIPP T-IIU
15 p2654 N85-26374
Radio frequency containment
15 p2654 N85-26375
Computational study on excitation, propagation and 3 omega -heating due to the ion Bernstein wave
[IPPJ-733] 23 p3975 N85-34641
Transport issues in Phaedrus-type plasmas
23 p3976 N85-34653
Bounce resonance heating and radial transport of electrons 23 p3977 N85-34655
Effect of ECH and ICH on ambipolar potential in NBT-1M 23 p3976 N85-34661
Simulation studies on stability of hot electron plasma
23 p3976 N85-34664
Observation of mode-converted by ion Bernstein wave by an HCN laser scattering
[IPPJ-724] 23 p3979 N85-34668

ION DENSITY (CONCENTRATION)
NT IONOSPHERIC ION DENSITY
NT MAGNETOSPHERIC ION DENSITY
NT MAGNETOSPHERIC PROTON DENSITY
NT PROTON DENSITY (CONCENTRATION)
Ion-density correlations and enhancement of thermonuclear reaction rate in dense, inertially confined fusion plasmas 02 p0284 N85-11849
Many-body correlations in strongly-coupled plasmas
02 p0284 N85-11850
Analysis of Jovian low frequency radio emissions
[NASA-CR-174449] 10 p1571 N85-19908
Hydrogen vibrational population distributions and negative ion generation in tandem high density hydrogen discharges
[DE85-001207] 11 p1722 N85-20834
Development of Faraday cup onboard MS-T5 for solar wind measurements
[REPT-616] 12 p1794 N85-21255
Ionic mechanisms of soot formation in flames
[AD-A150119] 12 p1801 N85-21297
Study of electric field and ion effects on HVDC lines
[DE85-002975] 12 p1833 N85-21503
Theoretical study of collective ion acceleration in the Luce diode
[AD-A150107] 12 p1929 N85-22116
Evolution of strong inhomogeneities in ionospheric plasma, part 1 14 p2339 N85-24463
Correlation of ring current and ionospheric gap in morning and evening hours 14 p2339 N85-24466
Hydrogen vibrational population distributions and negative ion generation in tandem high-density hydrogen discharges
[DE85-006764] 16 p2863 N85-27657
Electron and ion distributions at high latitudes as measured by the Air Force polar orbiting satellites
[AD-A153242] 17 p2993 N85-28500
Ion thruster performance model
20 p3420 N85-31226
Yakutsk Institute's cosmic ray research facility
22 p3732 N85-33135

ION DISTRIBUTION
Measuring local ion energy distribution function in Tuman-3 Tokamak plasma 02 p0271 N85-11768
Ion velocity distributions from spherical 1054 nm and 351 nm laser plasmas
[DE85-002816] 10 p1559 N85-19833
Observations of energetic electron and ion distributions near the magnetopause at geosynchronous orbit and related ground effects 14 p2356 N85-24560
Results of the SCATHA ion composition experiment during the IMS 14 p2359 N85-24580
Ion sensor signal fluctuations during operation of spacecraft reaction engines 16 p2724 N85-25815
Ion waves generated by ion loss-cone distributions or drifting particles
[KGI-PREPRINT-070] 20 p3549 N85-32087
Stability of ion distribution in strong ion shock structure 23 p3980 N85-34681
Solar Coronal and photospheric abundances from solar energetic particle measurements
[SH-2.1-5] 23 p3998 N85-34786

ION EMISSION
Emission mechanisms in the liquid metal ion source: A review
[AERE-R-11294] 03 p0418 N85-12675
Measurements of integral yields of charged secondary particles using neutral beams simulating a cometary fly-by — Giotto mission 14 p2244 N85-23908
Impact ionization from gold, aluminum and PCB-Z — Giotto spacecraft paint PCB-Z 14 p2244 N85-23910
Experimental investigations on ion emission with dust impact on solid surfaces — Giotto spacecraft
14 p2244 N85-23911
Ion emission from solid surfaces: Comparison of dust impact with other excitations — Giotto mission
14 p2244 N85-23912
The ESA field emission electric propulsion program
[ESA-STR-213] 20 p3420 N85-31229
Workshop report on Simulation Techniques for Shock Wave Phenomena and Characteristics of Plasmas in Inertial Confinement Fusion
[IPPJ-725] 23 p3979 N85-34670

ION ENGINES
NT MERCURY ION ENGINES
NT RIT ENGINES
Investigation of a pulsed electrothermal thruster system
[NASA-CR-174766] 02 p0169 N85-11132
Study on control of ion engine system
[EL-847] 07 p0916 N85-15800
Advanced ion thruster research
[NASA-CR-174862] 10 p1430 N85-19021
Precision tunable resonant microwave cavity
[NASA-CASE-LEW-13935-1] 11 p1628 N85-20248
Multistep orbital correction algorithms for an Earth satellite using low thrust engine
15 p2479 N85-25303
Ion thruster performance model
20 p3420 N85-31226
The ESA field emission electric propulsion program
[ESA-STR-213] 20 p3420 N85-31229
Heaterless ignition of inert gas ion thruster hollow cathodes
[NASA-TM-87066] 23 p3903 N85-34177

ION EXCHANGE MEMBRANE ELECTROLYTES
Research and development work on a single cation specific membrane for the recovery of raw materials with electrodialysis
[BMFT-FB-T-84-163] 03 p0329 N85-12120
Measuring system with ion selective electrodes
[BMFT-FB-T-84-170] 05 p0639 N85-14100
Research and development work concerning liquid membranes
[BMFT-FB-T-84-227] 08 p1124 N85-17087
Development of a lithium secondary battery separator
20 p3444 N85-31378
Evaluation of developmental membranes for the mixed reactant iron-chromium redox system
[NASA-TM-87074] 23 p3944 N85-34443

ION EXCHANGE RESINS
Ion transporting composite membranes. 1: Nafion impregnated gore-tex
[AD-A151020] 14 p2252 N85-23980
Luminescence probe studies of ionomers. I: Steady-state measurements from nafion membrane
[AD-A152475] 17 p3029 N85-28730
Determination of the association constant for pertechnetic acid
[DE85-010224] 19 p3235 N85-30057
Polyethylene solidification of low-level wastes
[DE85-012566] 22 p3843 N85-33799

ION EXCHANGING
Trivalent ion exchange in beta alumina
[AD-A145373] 02 p0172 N85-11151
Ion chromatographic determination of gold in plating baths
[DE84-016187] 02 p0184 N85-11230
Workshop on membrane biophysics
[AD-A148238] 08 p1192 N85-17512
Solid electrolytes: Mechanisms for achieving optimal conductivity
[AD-A150116] 12 p1801 N85-21296
Ion transport in beam-plasma interactions
[AD-A150145] 13 p2161 N85-23410
Feasibility study for small group water desalination equipment
[AD-A155106] 21 p3583 N85-32164
Oxidation of formaldehyde solutions used for the preservation of reverse osmosis membranes
[PB85-185585] 22 p3742 N85-33194
Multi-solute subsurface transfer modeling for energy solid wastes: Highlights FY 1984
[DE85-012788] 23 p3966 N85-34591

ION EXTRACTION
Extended performance technology study 30-cm thruster
[NASA-CR-168259] 07 p0917 N85-15806
Reconsideration of sheath related to negative ion extraction
[IPPJ-706] 12 p1935 N85-22159
Some physical differences between sheet plasma and multicusp plasma as volume produced H- or D- ion sources
[IPPJ-728] 23 p3974 N85-34637

ION GAGES
U IONIZATION GAGES

ION IMPACT
Inclusion of electron transfer in the calculation of K(n)L(v) multiple vacancy production by ion impact
[DE84-016596] 05 p0733 N85-14711
Synergism in materials erosion due to multispecies impact 06 p0884 N85-15494
Measurement of charged secondary particle emission under ion and neutral impact — Giotto mission
14 p2243 N85-23906
Inelastic Near-Surface Interactions. Proceedings of the Warner Brandt Workshop on Penetration Phenomena
[DE85-010579] 20 p3526 N85-31928
Method of precisely modifying predetermined surface layers of a workpiece by cluster ion impact therewith
[DE85-006519] 23 p3984 N85-34710
Air chemistry measurements 2
[AD-A156041] 24 p4117 N85-35520

ION IMPLANTATION
Implantation of ionized monomer into aluminum alloy 6061 for marine corrosion protection
[AD-A144874] 01 p0028 N85-10172
The oxidation behaviour of a 20 percent Cr/25 percent Ni/Nb stabilized stainless steel in carbon dioxide at high temperatures and its improvement by cerium and yttrium
[AERE-R-11228] 01 p0029 N85-10182
Metastable phase formation in ion implanted metals
[DE84-014945] 02 p0193 N85-11229
Studies of laser melting and rapid solidification using amorphous silicon
[DE84-014737] 02 p0202 N85-11345
Proceedings of the Ion Implantation for Army Needs Workshop
[AD-A145474] 02 p0286 N85-11863
Materials modification by ion beam mixing
[AD-P003948] 02 p0286 N85-11864
Characteristics of ion implanters for fabrication of electronic devices
[AD-P003949] 02 p0286 N85-11865
Review of the University of Manchester Ion Implantation Conference
[AD-P003950] 02 p0286 N85-11866
Research and development requirements for ion implantation
[AD-P003951] 02 p0286 N85-11867
Navy programs on ion implantation for materials modification
[AD-P003952] 02 p0286 N85-11868

Use of ion implantation to modify the corrosion behavior of metals
[AD-P003953] 02 p0296 N85-11869
The modification of metallic corrosion by ion implantation: Engineering applications and fundamentals studies
[AD-P003954] 02 p0296 N85-11870
The use of ion implantation for materials processing
[AD-A145436] 02 p0267 N85-11873
Characterization of ion implanted deuterium traps in nickel by equilibration with deuterium gas
[DE84-014958] 02 p0268 N85-11879
Optimized conditions for the formation of buried insulating layers in Si by high dose implantation of oxygen
[DE84-015360] 02 p0286 N85-11882
Characterization of amorphous surface layers in Fe implanted with Ti and C
[DE84-014960] 02 p0269 N85-11885
Annealing of implanted Al-2O-3 in a reducing environment
[DE84-015370] 03 p0332 N85-12140
Formation of subsurface Al2O3 layers in aluminum by oxygen ion implantation
[DE84-015599] 04 p0474 N85-13020
Ion beam and laser induced surface modifications
[DE84-016569] 04 p0571 N85-13642
On the origins of structural defects in BF2(+)-implanted and rapid thermally annealed silicon: Conditions for defect free regrowth
[DE84-016060] 04 p0572 N85-13650
Radiation hardened ion-implanted GaAs field effect transistor and method for making the same specification
[AD-D011264] 05 p0731 N85-14687
Repetitively pulsed metal ion beams for ion implantation
[DE84-014065] 05 p0732 N85-14704
Process for producing carbide coatings
[AD-D011295] 06 p0764 N85-14885
Evaluation of the ion implantation process for production of solar cells from silicon sheet materials
06 p0631 N85-15281
Evidence for pairing of implanted nitrogen in silicon
[DE84-015622] 06 p0668 N85-15517
Dependence of breakdown voltage for p-n junction on parameters of ion implantation and semiconductor heat treatment 07 p0954 N85-16046
Ion implantation and laser processing of III-V compound semiconductors with applications to the fabrication of microwave devices
[AD-A148846] 07 p1047 N85-16651
Laser annealing of ion implanted semiconductors
[AD-A148879] 07 p1047 N85-16652
X-ray and backscattering analysis of ion implantation phenomena in GaAs and related compounds
[AD-A147449] 07 p1048 N85-16659
Ion implantation in 3-5 compound semiconductors
[AD-A148462] 08 p1226 N85-17723
Surface mechanical properties and wear behavior of ion implanted TiB2
[DE85-001130] 09 p1295 N85-18133
Implantation of Ti + C for reduced friction and wear of steels
[DE85-001606] 09 p1295 N85-18135
Ion implantation of surgical Ti-6Al-4V alloy
[DE85-000943] 09 p1296 N85-18142
Ion beam studies of hydrogen in metals
[DE84-017422] 09 p1297 N85-18145
Formation of amorphous layers in Al2O3 by ion implantation
[DE85-001286] 09 p1397 N85-18794
Reactivity of ion implanted silicon carbide
[DE85-001543] 09 p1399 N85-18802
Fundamental aspects on ion-beam surface modification: Defect production and migration processes
[DE85-000093] 09 p1399 N85-18804
Amorphization of ceramics by ion beams
[DE85-000936] 10 p1453 N85-19156
Effect of implantation species on the tribological response of stainless steel surfaces
[DE85-000530] 10 p1493 N85-19432
Pulsed excimer laser processing for cost-effective solar cells
[NASA-CR-175485] 10 p1509 N85-19520
Fundamental studies of growth, doping and transformation in beta silicon carbide
[AD-A149339] 10 p1562 N85-19851
Ion implanted lateral in 2Ga 8As/GaAs strained-layer superlattice photodector
[DE85-001365] 10 p1563 N85-19859
Analysis of diffusion in an ion-implanted alloy using a phenomenological model
[AERE-R-11527] 11 p1609 N85-20120
Excimer laser annealing to fabricate low cost solar cells
[NASA-CR-174394] 11 p1673 N85-20538
Effects of B, Ti and Ta implantation on the wear resistance of Fe and Ni-plated Fe
[AD-A149947] 12 p1806 N85-21330
Enhanced diffusion from interstitial trapping during solid-phase-epitaxial growth of silicon alloys
[DE85-001285] 12 p1941 N85-22193
Evaluation of implantation-disordering of (InGa)As/GaAs strained-layer superlattices
[DE85-003533] 12 p1942 N85-22200
Experiences with implanted Back Surface Field (BSF) solar cells 13 p2005 N85-22571
Use of markets to elucidate reacting sputtering processes
[DE85-005723] 13 p2018 N85-22655
Study of the effects of implantation on the high Fe-Ni-Cr and Ni-Cr-Al alloys
[NASA-CR-175625] 13 p2021 N85-22661
High sheet resistance, arsenic implanted polycrystalline silicon for integrated circuit resistors
[DE85-004355] 13 p2065 N85-22902
Activation of Si-N modes in silicon by pulsed laser annealing
[DE85-003988] 13 p2097 N85-23082
Influence of substrate heating and thermal annealing on the surface crystallinity in single Si crystals implanted with high doses of (16)O
[DE85-005264] 13 p2164 N85-23428
Measurements of radiation-induced segregation and diffusion in ion irradiated alloy using implanted manganese
[AERE-R-11528] 14 p2258 N85-23994
Improvement by cerium and yttrium ion implantation of oxidation behaviour of stabilised stainless steel in carbon dioxide
[AERE-R-11523] 14 p2259 N85-23996
Excimer laser annealing to fabricate low cost solar cells
[NASA-CR-175702] 14 p2351 N85-24529
Laser annealing of ion implanted HgCdTe
[AD-A150875] 14 p2427 N85-24966
High resolution Z-contrast imaging and lattice location analysis of dopants in ion-implanted silicon
[DE85-005261] 14 p2429 N85-24980
Ion implantation disorder in strained-layer superlattices
[DE85-004466] 14 p2430 N85-24984
Structure and properties of ion-implanted Al sub 2 O sub 3
[DE85-005374] 14 p2430 N85-24987
Fundamental studies of growth, doping and transformation in beta silicon carbide
[AD-A152047] 15 p2660 N85-26416
Thin-film polycrystalline silicon research
[DE85-002908] 15 p2663 N85-26434
Dual species ion implantation of ternary compounds based on In-Ga-As
[AD-D011617] 16 p2869 N85-27698
Surface modification of solids
[DE85-007543] 16 p2871 N85-27715
High temperature position sensors based on monolithic GaAs Hall IC
[BMFT-FB-T-84-266] 17 p2969 N85-28337
Electrical research on solar cells and photovoltaic materials
[NASA-CR-175897] 17 p2986 N85-28452
Communications and logic systems at millimeter wave frequencies, summary 17 p3042 N85-28825
Crack tip chemistry modeling of intergranular stress corrosion cracks of nickel containing segregated phosphorus and sulphur
[DE85-010059] 18 p3076 N85-29028
Oxygen-nitrogen interactions in ion-implanted silicon
[DE85-010091] 18 p3195 N85-29819
Wear improvement in titanium alloys by ion implantation
[AD-D011694] 19 p3239 N85-30081
Spectroscopic investigation of materials for tunable infrared lasers
[AD-A154124] 19 p3272 N85-30291
Amorphous alloys of ion-implanted Fe-Ti-C
[DE85-010656] 19 p3360 N85-30834
Leading-edge microelectronics research at Sweden's Chalmers 20 p3438 N85-31337
Surface passivation and junction formation using low energy hydrogen implants 20 p3480 N85-31628
Processing technology for high efficiency silicon solar cells 20 p3483 N85-31842
Use of low energy hydrogen ion implants in high efficiency crystalline silicon solar cells
[NASA-CR-176109] 22 p3806 N85-33571
Calculation of mixed depth for some metal-Si systems
[DE85-011907] 23 p3971 N85-34616
Formation of amorphous silicon by light ion damage
[DE85-012605] 23 p3972 N85-34623
Two-dimensional numerical modeling of ion implanted GaAs MESFET devices 24 p4088 N85-35341

ION INJECTION
Argon ion pollution of the magnetosphere
13 p1998 N85-22523
Timing between particle injections at the geostationary orbit and particle flux decreases in the distant geomagnetic tail during substorms 14 p2356 N85-24569
Experimental study of laser produced ions for collective ion acceleration 20 p3460 N85-31484
ISEE-1 data reduction and analysis plasma composition experiment
[NASA-CR-175306] 21 p3630 N85-32552
Effect of powerful pulsed low-energy ion streams on GaAs 21 p3682 N85-32877
Ultrahigh vacuum system of the heavy ion transport line at Brookhaven
[DE85-011838] 22 p3840 N85-33778
Design status of heavy ion injector program
[DE85-010751] 22 p3842 N85-33793
ION IRRADIATION
NT DEUTERON IRRADIATION
NT PROTON IRRADIATION
Metastable phase formation in ion implanted metals
[DE84-014945] 02 p0183 N85-11229
Hydrogen passivation of electrically active defects in crystalline silicon solar cells
[DE84-004590] 02 p0223 N85-11461
Review: Role of refractory metal alloys in fusion reactor applications
[AERE-R-11317] 03 p0422 N85-12695
Radiation induced defects in superconductors of type 2 03 p0429 N85-12734
Experimental determination of the critical cavity radius in Fe-10% Cr for ion irradiation
[DE84-016570] 04 p0571 N85-13646
Ion beam studies of hydrogen in metals
[DE84-017422] 09 p1297 N85-18145
Plasma surface interaction processes and possible synergisms
[DE85-001661] 09 p1391 N85-18752
Amorphization of ceramics by ion beams
[DE85-000936] 10 p1453 N85-19156
Heavy ion induced crystallization in amorphous phases
[DE85-003114] 11 p1606 N85-20098
Effects of ion bombardment on the morphology of lead films
[DE85-007232] 15 p2511 N85-25494
Neutralization and excitation in low-energy ion-surface collisions
[AD-A151568] 15 p2660 N85-26414
Secondary ion mass spectrometry studies of solids and surfaces
[AD-A151744] 16 p2745 N85-26939
Energy reflection coefficient for H+ ions at energies between 10 and 80 keV
[DE85-007547] 16 p2863 N85-27662
Surface modification of solids
[DE85-007543] 16 p2871 N85-27715
The effect of ion-bombardment-induced atomic mixing on depth-profiling of interfaces
[AD-A153199] 17 p3044 N85-28834
An investigation of the irradiation swelling mechanisms in refractory metals at high temperatures
[AD-A154149] 19 p3238 N85-30079
An investigation of cementation and carbonitriding by means of ionic bombardment
[BLL-OA-TRANS-3203-(6196.300)] 20 p3429 N85-31265
Breakdown of intrinsic ambipolarity for the radial diffusion due to a rotating RF field 23 p3977 N85-34660
Size and shape dependence of CO adsorption sites on sapphire supported Fe microcrystals
[NASA-CR-176171] 24 p4160 N85-35794
ION MICROSCOPES
Ion microscopy of metals and semiconductors
[AD-A147118] 07 p1043 N85-16626
In-situ formation of a grain boundary in field ion microscopy using a laser
[AD-A148225] 08 p1166 N85-17355
New high resolution scanning ion microprobe and focused ion beam applications
[AD-A149992] 12 p1852 N85-21616
Hydrogen absorption in metals: A field ion microscopy study
[DE85-010299] 18 p3076 N85-29026
Chemical constraints on the evolution of Archean continental crust 21 p3722 N85-33093
ION MOTION
Trivalent ion exchange in beta alumina
[AD-A145373] 02 p0172 N85-11151
Simulation of the ion-beam-driven drift instability in a magnetic trap, 1
[AD-A149451] 10 p1452 N85-19147
Fast ion polarization jet in subauroral F-layer and its manifestation in structure of high latitude ionosphere
15 p2480 N85-25306

Ion and polymer chain motion in a superionic sodium-poly(ethylene oxide) complex
[AD-A152290] 16 p2755 N85-27001
Velocity space diffusion of high energy ions induced by a lower hybrid wave in a nonuniform magnetic field
[IPPJ-714] 16 p2666 N85-27681
Behavior of helically-trapped fast ion orbits in heliotron E 23 p3978 N85-34666

ION OSCILLATION
U PLASMA OSCILLATIONS

ION PLATING
Ion chromatographic determination of gold in plating baths
[DE84-016187] 02 p0184 N85-11230
Tribological properties of boron nitride synthesized by ion beam deposition
[NASA-TM-86962] 12 p1810 N85-21355
Corrosion of aircraft Al and Al-Zn ion plated steel fasteners 13 p2021 N85-22666
The structure of ion plated films in relation to coating properties
[NASA-TM-87055] 18 p3085 N85-29085
New metal coating method developed 21 p3568 N85-32191
Advances in sputtered and ion plated solid film lubrication 22 p3797 N85-33524

ION PROBES
Materials characterization using ion, electron, and photon probes
[DE84-004516] 04 p0560 N85-13568
Heavy ion beam study of potential formation in bumpy torus plasma
[IPPJ-711] 15 p2656 N85-26386
Studies in mixed species charged particle beam dynamics
[OUEL-1545/84] 20 p3531 N85-31969

ION PRODUCTION RATES
Modeling longitudinal motions of thermal O+ and H+ ions in magnetic field tube convective through daytime polar cusp 15 p2481 N85-25314

ION PROPULSION
Characterization of 8-cm engineering model thruster
[NASA-CR-174673] 02 p0169 N85-11131
Study on control of ion engine system
[EL-847] 07 p0916 N85-15800
Ion thruster project
[NASA-TM-77725] 07 p0917 N85-15805
Advanced ion thruster research
[NASA-CR-174662] 10 p1430 N85-19021
Ring-cusp ion thruster with shell anode
[NASA-CASE-LEW-13681-1] 12 p1794 N85-21256
The ESA field emission electric propulsion program
[ESA-STR-213] 20 p3420 N85-31229

ION PUMPS
Design study of the vacuum pump of the ESRP — synchrotron radiation
[NIKHEF-MTG-21] 08 p1138 N85-17167
Measurement of NSLS distributed diode sputter ion pump characteristics
[DE85-006550] 16 p2760 N85-27031

ION RECOMBINATION
Surface and allied studies in silicon solar cells
[NASA-CR-175468] 10 p1506 N85-19516
Trends in the electric field enhancement of dielectronic recombination cross sections
[DE85-006920] 16 p2871 N85-27711

ION SCATTERING
Structure of adsorbed monolayers. The surface chemical bond
[DE84-016879] 06 p0861 N85-15471
Chemical information from ion scattering spectrometry
[AD-A148287] 08 p1121 N85-17069
Analysis of Jovian low frequency radio emissions
[NASA-CR-174449] 10 p1571 N85-19908
Classical rainbow scattering of alkali ions on metal surfaces. Application to the investigation of unknown surface structures
[MPIS-10/1984] 11 p1728 N85-20854
Theoretical studies of heavy ion scattering processes
[DE85-008823] 17 p3032 N85-29753
Multiple scattering effects in low energy alkali ion scattering: Application to the analysis of adsorbate ordering and bonding geometry
[DE85-007575] 17 p3032 N85-29757
Solar flare gamma-ray line spectroscopy
[SH-2.1-14] 23 p3999 N85-34795

ION SELECTIVE ELECTRODES
Measuring system with ion selective electrodes
[BMFT-FB-T-84-170] 05 p0639 N85-14100

ION SHEATHS
Advanced ion thruster research
[NASA-CR-174662] 10 p1430 N85-19021
Some physical differences between sheet plasma and multicusp plasma as volume produced H- or D- ion sources
[IPPJ-726] 23 p3974 N85-34637

ION SOURCES
NT PLASMATRONS
Plasma deposited diamondlike carbon on GaAs and InP
[NASA-TM-86870] 01 p0123 N85-10844
Surface production of negative hydrogen ions
[AD-A145437] 02 p0277 N85-11801
Effect of resonant microwave power on a PIG ion source
[DE85-001396] 09 p1379 N85-18673
ORNL ECR multicharged ion source
[DE85-001283] 09 p1380 N85-18681
Vibrational relaxation in H-2 molecules by wall collisions: Applications to negative ion source processes
[DE85-000852] 11 p1721 N85-20826
Hydrogen vibrational population distributions and negative ion generation in tandem high density hydrogen discharges
[DE85-001207] 11 p1722 N85-20834
Collisional pumping for the production of intense spin-polarized, neutral beams: Target considerations
[DE85-003459] 11 p1723 N85-20841
Theoretical study of collective ion acceleration in the Luce diode
[AD-A150107] 12 p1929 N85-22116
Development of an apparatus for obtaining molecular beams in the energy range from 2 to 200 eV
[NASA-TM-77835] 15 p2647 N85-26326
Plasma heating 15 p2654 N85-26372
Maximum current densities from tandem high density systems
[DE85-006966] 18 p3180 N85-29720
An alpha particle diagnostic beam line system to generate an intense Li(O) beam with an ORNL SITEX source
[DE85-010564] 18 p3182 N85-29730
Experimental study of laser produced ions for collective ion acceleration 20 p3460 N85-31484
Aerosol analysis and emission spectrometry with free jets
[DE85-010576] 21 p3564 N85-32168
Acceleration of polarized H(-) in the BNL 200 MeV linac
[DE85-011836] 22 p3840 N85-33777
Improved negative ion source
[DE85-006445] 23 p3912 N85-34241
Negative ion sources equipped with continuous annular and spherical geometry surface ionizers
[DE85-011939] 23 p3971 N85-34619
Light ion sources for ICF
[DE85-011544] 23 p3983 N85-34702
Beam intensity increases at the intense pulsed neutron source accelerator
[DE85-012377] 24 p4155 N85-35764

ION SPECTROMETERS
U MASS SPECTROMETERS

ION STORAGE
Frequency and time standards based on stored ions 18 p3105 N85-29223

ION STRIPPING
Large electrostatic accelerators
[DE85-001120] 09 p1382 N85-18689

ION TEMPERATURE
Equatorial energetic distributions of ions of terrestrial radiation belt as function of solar corona temperature response 02 p0160 N85-11087
Measuring local ion energy distribution function in Tuman-3 Tokamak plasma 02 p0271 N85-11768
A research in support of NASA's space science
[NASA-CR-174267] 08 p1227 N85-17728
Determination of ion temperature and rotation velocity profiles by visible, UV and X-ray spectroscopy on Doublet 3 09 p1388 N85-18734
Beam probe spectroscopic technique for ion temperature and magnetic field measurements 09 p1389 N85-18738
Background calculations for the measurement of the ion temperature in a deuterium plasma
[DE84-016546] 09 p1393 N85-18768
Development of Faraday cup onboard MS-T5 for solar wind measurements
[REPT-616] 12 p1794 N85-21255
Ionic mechanisms of soot formation in flames
[AD-A150119] 12 p1801 N85-21297
Low plasma edge temperatures for the self-pumped limiter
[DE85-010155] 18 p3189 N85-29782
Two-point theory of current-driven ion-cyclotron turbulence
[DE85-010114] 19 p3372 N85-30918
Thermal ion heating in the vicinity of the plasmapause
[NASA-CR-176030] 20 p3535 N85-31993
Low frequency instabilities driven by an ion temperature anisotropy
[AD-A154902] 21 p3707 N85-33018
Soft X-ray polychromator for the Solar Maximum Mission
[NASA-CR-175297] 21 p3723 N85-33096
Transports studies of ECH and ICRH-heated bumpy torus plasma in NBT-1M 23 p3978 N85-34662
Langmuir probe on ISX-B
[DE85-012066] 23 p3983 N85-34697

IONIC COLLISIONS
Theoretical studies of highly ionized species
[DE84-016797] 04 p0561 N85-13574
Monte Carlo studies of transport in stellarators
[DE84-017633] 04 p0568 N85-13625
Particle physics
[DE84-013834] 05 p0727 N85-14673
Inclusion of electron transfer in the calculation of K(n)L(v) multiple vacancy production by ion impact
[DE84-016596] 05 p0733 N85-14711
Progress in numerical calculations of ion-atom collisions
[DE84-016698] 06 p0861 N85-15474
Electron capture by multiply charged ions from hydrogen atoms at low energies
[DE84-016580] 06 p0861 N85-15475
Collision-induced dipole moments
[AD-A147682] 08 p1121 N85-17063
Forward electron production in heavy ion-atom and ion-solid collisions
[DE85-001256] 09 p1381 N85-18683
Plane-wave born collision strengths for electron-ion excitation: Comparison with other theoretical methods
[DE85-002348] 10 p1555 N85-19802
Recent advances in forward electron production studies in ion-atom and ion-solid collisions
[DE85-001255] 11 p1726 N85-20853
Bibliography of atomic and molecular processes, 1983
[DE85-000662] 12 p1929 N85-22121
Multiparticle 3D imaging technique to study the structure of molecular ions
[DE85-001843] 12 p1929 N85-22122
Vacancy-rearrangement theory in the first Magnus approximation
[DE85-004435] 12 p1930 N85-22123
Mean delta-ray energies in ion molecule collisions
[DE85-005524] 13 p2157 N85-23365
Influences of thermal spikes in ion beam mixing
[DE85-006130] 14 p2419 N85-24924
X-ray emission in heavy ion collisions
[DE85-006350] 14 p2419 N85-24927
Many-electron effects in electron impact ionization of multiply charged ions
[DE85-005570] 15 p2649 N85-26340
Convoy electron production by heavy ions in solids
[DE85-006256] 15 p2660 N85-26418
Nuclear spectroscopic studies
[DE85-006894] 16 p2862 N85-27652
Homogeneous processes of atmospheric interest
[NASA-CR-175770] 17 p2969 N85-28475
Experimental approaches to the measurement of dielectronic recombination
[DE85-006927] 17 p3030 N85-28743
Nonrelativistic theory of heavy-ion collisions
[DE85-007536] 17 p3031 N85-28747
Excited state populations and charge-exchange of fast ions in solids
[DE85-006362] 18 p3180 N85-29714
Resonant-transfer-and-excitation for highly charged ions (16 or = Z or = 23) in collisions with helium
[DE85-010550] 19 p3359 N85-30823
A theoretical study of electron capture in ion-ion and ion-atom collisions
[DE85-011154] 19 p3362 N85-30842
Inelastic Near-Surface Interactions. Proceedings of the Werner Brandt Workshop on Penetration Phenomena
[DE85-010579] 20 p3526 N85-31928
Study of photon emission by electron capture during solar nuclei acceleration, 1: Temperature-dependent cross section for charge changing processes
[SH-1.1-9] 23 p3990 N85-34735
Multiple vacancy production by high energy heavy ions
[DE85-004428] 24 p4162 N85-35805
Heavy nucleus collisions between 20 and 60 GeV/nucleon
[HE-1.4-2] 24 p4175 N85-35880
Nucleus-nucleus interaction above several hundred GeV/n
[HE-1.4-4] 24 p4176 N85-35882
Observation of direct hadronic pairs in nucleus-nucleus collisions in JACEE emulsion chambers
[HE-1.4-5] 24 p4176 N85-35883
Excessive production of electron pairs by soft photons in low multiplicity ion interactions
[HE-1.4-6] 24 p4176 N85-35884
On the mechanism of anomalous nucleus-nucleus interactions at energies above 1 TeV/nucleon
[HE-1.4-8] 24 p4177 N85-35886

Inclusive angular distribution of alpha and Li fragments produced in the Fe-C and Fe-Pb collisions at 1.88 GeV/u
[HE-1.4-11] 24 p4177 N85-35899

IONIC CONDUCTIVITY
U ION CURRENTS

IONIC CRYSTALS
Computer simulation of grain-boundary properties in ionic crystals and metals
[DE85-000577] 11 p1734 N85-20908
Ionic crystals
[DE85-009482] 24 p4183 N85-35809

IONIC DIFFUSION
Spreading of greatly extended inhomogeneities in upper ionosphere 14 p2339 N85-24482
Electrogenerated chemiluminescence
[AD-A169547] 18 p3070 N85-29890
Diffusion welding of aluminum with vacuum-tight corundum ceramic 19 p3247 N85-30130
Changes in the impedance and bioelectrical activity of the cerebral cortex of rats under the action of anaesthetic drugs
[HSE-TRANS-10371] 19 p3327 N85-30617
The plasma mechanism for preferential acceleration of heavy ions
[SH-2.2-10] 23 p4001 N85-34805

IONIC MOBILITY
The effect of inert gases on ion transport across the erythrocyte membrane
[AD-A146869] 10 p1527 N85-19635
An investigation of tropospheric ions 16 p2823 N85-27412

IONIC PROPELLANTS
U ION ENGINES

IONIC REACTIONS
Ionic reactions of atmospheric importance
[AD-A147354] 07 p0997 N85-16333
Alternative anodic reactions in water splitting
[DE85-004159] 12 p1802 N85-21300
Use of markers to elucidate reacting sputtering processes
[DE85-005723] 13 p2018 N85-22855
International Conference on Coordination Chemistry (23rd) held at Boulder, Colorado on 29 July - 3 August, 1984
[AD-A150880] 14 p2252 N85-23956
Polymer-water interaction studies 21 p3609 N85-32411
Resonant energy transfer during strong excitation 21 p3699 N85-32922

IONIC WAVES
A new maser effect in plasma turbulence 02 p0264 N85-11852
Caviton collapse of SRS by SBS
[DE85-009605] 20 p3535 N85-31999
Resonant ion acceleration by oblique magnetosonic shock wave in a collisionless plasma
[IPPJ-736] 23 p3975 N85-34843

IONIZATION
NT ATMOSPHERIC IONIZATION
NT AURORAL IONIZATION
NT AUTOIONIZATION
NT FLAME IONIZATION
NT GAS IONIZATION
NT ION PRODUCTION RATES
NT NONEQUILIBRIUM IONIZATION
NT PHOTOIONIZATION
NT SURFACE IONIZATION
Diagnostics of ionization in air produced by infrared radiation from A pulse CO2 laser
[AD-A148376] 02 p0201 N85-11342
Comparison of wide aperture and short residence time ion lenses
[DE84-015274] 03 p0420 N85-12685
Oscillator strengths for OII ions
[NASA-CR-174163] 04 p0559 N85-13558
Non-LTE considerations in spectral diagnostics of thermal transport and implosion experiments
[DE84-015187] 05 p0730 N85-14689
Analysis of middle distillate fuels by high resolution field ionization mass spectrometry
[AD-A147734] 06 p1135 N85-17153
An experimental and theoretical investigation of optogalvanic effects
[AD-A148458] 06 p1223 N85-17700
Effect of scattering on instabilities in line-driven stellar winds 06 p1235 N85-17784
Laser ablation studies using RIS
[DE85-001118] 09 p1326 N85-18336
Effect of inner subshell ionization for emission lines of OIV ion 09 p1368 N85-18729
Identification of spectra of highly ionized Mo, Nb, Zr and Y atoms 09 p1390 N85-18745
The coordinated research program at IAEA on atomic collision data for plasma diagnostics 09 p1390 N85-18747
Ozone measurements in the mesosphere during a solar proton event 11 p1665 N85-20460
Time dependent Hartree-Fock theory of ion-atom collisions: Application to F(9+) + Ne
[DE85-003083] 11 p1723 N85-20838
Inner shell contribution to multiple ionization in ion-atom collisions
[DE85-003107] 11 p1723 N85-20839
Stellar winds in the young galactic cluster NGC 6530 11 p1750 N85-21004
Sheath ionization model of beam emissions from large spacecraft 13 p1992 N85-22489
A simple model of electron beam initiated dielectric breakdown 13 p1996 N85-22516
Mean delta-ray energies in ion molecule collisions
[DE85-005524] 13 p2157 N85-23395
Impact ionization from gold, aluminum and PCB-Z — Giotto spacecraft paint PCB-Z 14 p2244 N85-23910
Correlation of ring current and ionospheric gap in morning and evening hours 14 p2339 N85-24466
Indirect processes in electron-impact ionization of multiply-charged ions
[DE85-005237] 14 p2419 N85-24925
Ionization equilibrium and equation of state in the solar interior 14 p2445 N85-25068
The sensitivity of solar eigenfrequencies to the treatment of the equation of state 14 p2445 N85-25069
Ion kinetics, small neutral and excited components in D-region with elevated ionization level. Part 2: Variations in small neutral and excited components 15 p2480 N85-25307
Survey of experimental and theoretical electron-impact ionization cross sections for transition metal ions in low stages of ionization
[DE85-007605] 16 p2863 N85-27658
Resonance ionization mass spectrometry of carbon
[DE85-009040] 17 p2923 N85-28018
Recent advances in optical measurement methods in physics and chemistry
[DE85-008695] 17 p3037 N85-28792
Numerical studies of ablation and ionization of railgun materials
[DE85-010741] 19 p3223 N85-29983
A study of Co and Mn in ZnO varistors
[DE85-011193] 19 p3263 N85-30233
Atomic data for controlled fusion research. Volume 4: Spectroscopic data for iron
[DE85-009658] 19 p3354 N85-30787
Electron-atom collision studies using optically state selected beams
[DE85-010848] 19 p3368 N85-30886
Predamage threshold electron emission from insulator and semiconductor surfaces
[DE85-009668] 19 p3377 N85-30954
Effects of coronal disturbances on the ionization state of the solar wind
[NASA-CR-175897] 19 p3385 N85-31000
Contributions to the 19th International Cosmic Ray Conference
[NASA-CR-176049] 20 p3543 N85-32044
Energy spectra of elements with 18 less than or equal to Z less than or equal to 28 between 10 and 300 GeV/amu 20 p3543 N85-32045
Elemental abundances of cosmic rays with Z33 as measured on HEAO-3 20 p3543 N85-32046
Abundances of secondary elements among the ultra heavy cosmic rays: Results from HEAO-3 20 p3543 N85-32047
Self-consistent models for the X-ray emission from supernova remnants 20 p3548 N85-32062
Ionization detection of stimulated Raman spectra
[DE85-010672] 22 p3748 N85-33218
Electron impact ionization of multicharged ions at ORNL: 1980-1984
[DE85-013104] 23 p3972 N85-34622
Stability of ion distribution in strong ion shock structure 23 p3980 N85-34681
Solar Coronal and photospheric abundances from solar energetic particle measurements
[SH-2.1-5] 23 p3998 N85-34786
The detection and study of molecular species using time resolved laser spectroscopy
[AD-A155910] 24 p4075 N85-35256
Aqueous volatile weak electrolyte equilibria to 300 C
[DE85-013840] 24 p4076 N85-35281
Infrared generation and wave-mixing studies in cesium
[DE85-012883] 24 p4083 N85-35304
The ionization structure of planetary nebulae. Part 4: NGC 7662
[NASA-CR-176151] 24 p4189 N85-35844
Sub-luminal pulses from cosmic ray air showers
[HE-4.7-13] 24 p4200 N85-36063
Search for acoustic signals from high energy cascades
[HE-7.1-1] 24 p4213 N85-36155

IONIZATION CHAMBERS
NT BUBBLE CHAMBERS
NT CLOUD CHAMBERS
NT PROPORTIONAL COUNTERS
NT SPARK CHAMBERS
Photon and electron dosimetry at the Physikalische-Technische Bundesanstalt in Brunswick
[PTB-DOS-9] 01 p0119 N85-10614
Measurement of soft X-ray absorption spectra with a fluorescent ion chamber detector
[AD-A142213] 07 p0922 N85-15838
Results from a Bragg curve spectrometer
[DE85-007870] 18 p3176 N85-29691
The response of ionization chambers to relativistic heavy nuclei 20 p3544 N85-32051
Paired ion chamber constants for fission gamma-neutron fields
[AD-A155069] 21 p3702 N85-32999
A practical guide to ionization chamber dosimetry at the AFRRI reactor
[AD-A155185] 21 p3703 N85-33003
Digital characterization of particle tracks for microdosimetry
[DE85-012696] 22 p3846 N85-33822
Relative abundances of elements (20 or = Z or = 28) at energies up to 70 GeV/amu using relativistic rise in ion chambers
[OG-4.1-7] 22 p3876 N85-34013
Energy spectra of elements with 18 or = Z or = 28 between 10 and 300 GeV/amu
[OG-4.1-8] 22 p3876 N85-34014
Observations on (3)He neutron spectrometry
[DE85-010731] 23 p3970 N85-34606
The response of ionization chambers to relativistic heavy nuclei
[OG-9.1-13] 23 p4024 N85-34938
Sidereal anisotropy of cosmic rays
[SH-4.4-8] 23 p4034 N85-35006
Long term changes in cosmic ray diurnal variations observed by ion chambers in Hong Kong and Japan
[SH-4.5-14] 23 p4037 N85-35031
Burst size distributions in the digitized data of the ion chambers t Mt. Norikura and sea level stations
[SH-9.1-9] 23 p4061 N85-35124
The influences of the galactic cosmic ray on the atmospheric ozone
[SH-10.1-1] 23 p4053 N85-35133
Fractional charge resolution in music 24 p4147 N85-35712
X-ray film chamber with carbon target of Tien-Shan complex array 24 p4179 N85-35915
Peculiarities of gamma-quanta distribution at 20 TeV energy
[HE-3.7-10] 24 p4186 N85-35967
Observation of genetic relation among new phenomena Geminion, Chiron and mini-Centauro
[HE-6.2-16] 24 p4212 N85-36152

IONIZATION COEFFICIENTS
Ionization coefficient for atomic collisions in meteor trail 16 p2720 N85-26792
Air chemistry measurements 2
[AD-A156041] 24 p4117 N85-35520

IONIZATION COUNTERS
U IONIZATION CHAMBERS
U RADIATION COUNTERS

IONIZATION CROSS SECTIONS
Progress in numerical calculations of ion-atom collisions
[DE84-016598] 06 p0861 N85-15474
Theoretical studies of Rydberg atom collisions
[AD-A148558] 08 p1220 N85-17687
Laser-induced-fluorescence-spectroscopy of atomic processes under a high magnetic field 09 p1389 N85-18740
K and L-shell cross-sections for X-ray microanalysis in an AEM
[DE85-002733] 11 p1721 N85-20822
Correlated 2 electron effects in collisions of multiply charged Au ions with He
[DE85-003084] 11 p1723 N85-20837
Inner shell contribution to multiple ionization in ion-atom collisions
[DE85-003107] 11 p1723 N85-20839
Many-electron effects in electron impact ionization of multiply charged ions
[DE85-005570] 15 p2649 N85-26340
Theory of electron-impact atomic ionization cross sections
[AD-A151763] 16 p2861 N85-27648
Investigation of electron attachment and dissociation rates in C2F6/CH4 electric gas discharges
[AD-A151796] 16 p2862 N85-27649
Survey of experimental and theoretical electron-impact ionization cross sections for transition metal ions in low stages of ionization
[DE85-007605] 16 p2863 N85-27658

Nuclear data needs for fusion energy development
[DE85-010445] 20 p3536 N85-32000
Toward a theory of excitation of atoms during nuclear and magnetic neutron scattering
21 p3689 N85-32918
Contributions to the 19th International Cosmic Ray Conference
[NASA-CR-176080] 21 p3714 N85-33044
Charge and energy dependence of the residence time of cosmic ray nuclei below 15 GeV/nucleon
[OG-4.1-3] 22 p3876 N85-34009
Electron impact ionization of multicharged ions at ORNL: 1980-1984
[DE85-013104] 23 p3972 N85-34622
Electron loss process and cross section of multiply charged ions by neutral atoms 23 p3981 N85-34655
On the importance of interstellar helium for the propagation of heavy cosmic rays
[OG-7.2-11] 23 p4015 N85-34879
EAS accompanied by gamma-families at Mt. Norikura and comparison with Monte Carlo simulation
[HE-3.3-10] 24 p4181 N85-35928

IONIZATION GAGES
Helium ionization detection apparatus
[NASA-TM-77805] 03 p0364 N85-12332
Test results from a comparative evaluation of a condensation nuclei fire detector
[NASA-CR-3874] 12 p1862 N85-21875

IONIZATION POTENTIALS
Photoionization structure of the Orion Nebula
08 p1246 N85-17863
Radiation data and standards for Tokamak diagnostics
09 p1390 N85-18742
Relationship between topological and magnetic order in small metal clusters
[AD-A150547] 13 p2018 N85-22651
Giotto residual ionization 14 p2244 N85-23909
Ionization energies of liquids from energy distribution, quantum yield and second derivative curves
[AD-A152210] 16 p2746 N85-28946
On the role of the magnetic field strength in critical ionization velocity interaction
[TRITA-EPP-85-01] 20 p3536 N85-32003
Contributions to the 19th International Cosmic Ray Conference
[NASA-CR-176080] 21 p3714 N85-33044
Modulated voltage metastable ionization detector
[NASA-CASE-ARC-11503-1] 23 p3933 N85-34374
Anomalous abundances of solar energetic particles and coronal gas: Coulomb effects and First Ionization Potential (FIP) ordering
[SH-2.1-10] 23 p3999 N85-34791
Variations in the propagation of UH-nuclei
[OG-7.1-1] 23 p4012 N85-34863
Germanium and lead: Significant differences between meteoritic and photospheric abundances?
[OG-7.1-2] 23 p4012 N85-34864
Implications of source abundances of ultraheavy cosmic rays
[OG-7.1-4] 23 p4013 N85-34866

IONIZED GASES
NT ARGON PLASMA
NT BOUNDARY LAYER PLASMAS
NT CATIONS
NT CHARGED PARTICLES
NT COLD PLASMAS
NT COLLISIONAL PLASMAS
NT COLLISIONLESS PLASMAS
NT CONDUCTION ELECTRONS
NT COSMIC PLASMA
NT DENSE PLASMAS
NT ELECTRON PLASMA
NT ELLIPTICAL PLASMAS
NT EVEN-EVEN NUCLEI
NT HEAVY NUCLEI
NT HELIUM PLASMA
NT HIGH TEMPERATURE PLASMAS
NT HYPERNUCLEI
NT LASER PLASMAS
NT METALLIC PLASMAS
NT NITROGEN PLASMA
NT NUCLEI (NUCLEAR PHYSICS)
NT ODD-EVEN NUCLEI
NT ODD-ODD NUCLEI
NT PLASMA CLOUDS
NT PLASMA JETS
NT PLASMA LAYERS
NT PLASMA SHEATHS
NT PLASMAS (PHYSICS)
NT RELATIVISTIC PLASMAS
NT ROTATING PLASMAS
NT SEMICONDUCTOR PLASMAS
NT SOLAR WIND
NT SPACE PLASMAS
NT STELLAR WINDS
NT STRONGLY COUPLED PLASMAS
NT THERMAL PLASMAS
NT TOROIDAL PLASMAS
Optical emission line studies and the warm, ionized component of the local interstellar medium
06 p0675 N85-15555
Photoionization structure of the Orion Nebula
08 p1246 N85-17863
Hollow cathode apparatus
[NASA-CASE-NPO-15560-1] 12 p1832 N85-21491
Time dependent and steady-state solutions of the electron energy distribution in a weakly ionized gas subject to an ac or dc electric field
[AD-A151829] 15 p2656 N85-26391
Anomalous abundances of solar energetic particles and coronal gas: Coulomb effects and First Ionization Potential (FIP) ordering
[SH-2.1-10] 23 p3999 N85-34791
The mean ionic charges of N, Ne, MG, SI and S in solar energetic particle events
[SH-2.1-11] 23 p3999 N85-34792

IONIZED PLASMAS
U PLASMAS (PHYSICS)

IONIZERS
High efficiency ionizer using a hollow cathode discharge plasma
[DE85-006690] 16 p2868 N85-27693

IONIZING RADIATION
NT ALPHA PARTICLES
NT BETA PARTICLES
NT COSMIC RAY SHOWERS
NT COSMIC RAYS
NT COSMIC X RAYS
NT EXTREME ULTRAVIOLET RADIATION
NT FAR ULTRAVIOLET RADIATION
NT GALACTIC COSMIC RAYS
NT GAMMA RAY BEAMS
NT GAMMA RAY BURSTS
NT GAMMA RAYS
NT LYMAN ALPHA RADIATION
NT PRIMARY COSMIC RAYS
NT SECONDARY COSMIC RAYS
NT SOLAR COSMIC RAYS
NT SOLAR X-RAYS
NT ULTRAVIOLET RADIATION
NT X RAYS
Radiation measuring system using transistor flux sensors
[AD-D011239] 01 p0050 N85-10328
Energy deposition in microvolumes of silicon from high energy proton reactions
[AD-A144713] 01 p0123 N85-10845
Critical assessment of low fluence irradiation creep mechanisms
[DE84-015578] 02 p0184 N85-11232
Instability in semiconductors exposed to ionizing radiation 02 p0267 N85-11747
A total dose characterization of five commercial analog multiplexers
[AD-A146886] 07 p0948 N85-15997
Chemical protection against ionizing radiation
[AD-A147822] 07 p1016 N85-16457
Beam-foil spectroscopy of highly ionized aluminum atoms 09 p1390 N85-18746
Comparison of ionizing radiation and hot electron effects in MOS structures
[DE84-016766] 09 p1400 N85-18809
Strange F + Be binary star systems
11 p1756 N85-21045
Periodic substorm activity in the geomagnetic tail
[NASA-CR-175829] 13 p2161 N85-23409
Investigation of basic characteristics of laser heating in thermoluminescence and of laser-stimulated luminescence
[AD-A152143] 16 p2790 N85-27212
Study of the degradation of short-circuit current and the open-circuit tension of spatial solar cells as a function of the fluency of 1MeV electrons
[INPE-3358-PRE/634] 16 p2887 N85-27614
Radiation damage and repair in cells and cell component, part 1
[DE85-006667] 18 p3152 N85-29519
Working safely with ionizing radiation sources at the Interuniversity Reactor Institute (IRI) (meant for the introduction of new collaborators)
[IRI-190-84-01] 18 p3160 N85-29576
Fiber optics in transient radiation fields
[DE85-010721] 19 p3368 N85-30888
Development of a recombinant DNA assay system for the detection of genetic change in astronauts cells
[DE85-010103] 20 p3504 N85-31781
The DNA metabolism and poly-(ADP-ribose) synthesis in lymphocytes of persons exposed to low doses of ionizing radiation
[OEFZS-4307] 20 p3507 N85-31800
USAFSAM review and analysis of radiofrequency radiation bioeffects literature
[AD-A155113] 21 p3664 N85-32760
Lower bounds of propagation velocity of steady ionizing waves in field of strong electromagnetic wave
21 p3692 N85-32940
Buildup of electric charge in foil dielectrics during gamma irradiation 22 p3770 N85-33363
The 1984 environmental monitoring program report for Idaho National Engineering Laboratory site
[DE85-011209] 22 p3812 N85-33811
Study of composition of cosmic rays with energy .7 E 3 Ee
[OG-5.1-7] 22 p3881 N85-34049
Composition of primary cosmic rays near the bend from a study of hadrons in air showers at sea level
[OG-5.2-2] 22 p3883 N85-34059

IONOGRAMS
A description of the NRL oblique-incidence-ionogram data base
[AD-A146625] 09 p1230 N85-17748

IONOSONDES
On the study of ionospheric disturbances
04 p0522 N85-13335

IONOSPHERE
NT D REGION
NT E REGION
NT F REGION
NT F 2 REGION
NT LOWER IONOSPHERE
NT SPORADIC E LAYER
NT UPPER IONOSPHERE
USSR report: Space
[JPRS-USP-84-005] 02 p0156 N85-11080
Magnetospheric structures: Uranus and Neptune
02 p0301 N85-11949
Characteristics of absorption and frequency filtration of ULF electromagnetic waves in the ionosphere
03 p0376 N85-12402
Seasonal variations of reliability and transmissibility of ULF waves propagating through the ionosphere of geomagnetic mid-latitudes
[REPT-560] 03 p0376 N85-12403
Scientific contributions in commemoration of Ebro Observatory's 75th anniversary — conference
[ISBN-84-00-06360-X] 04 p0518 N85-13306
Experience with proposed improvements of the International Reference Ionosphere (IRI)
[PB84-235670] 05 p0676 N85-14353
Artificial defocusing lens in ionosphere
05 p0724 N85-14654
Activities report in Earth and planetary environments physics
[CRPE-NT-134] 05 p0734 N85-14720
Processes of smooth increase and dropoff in intensity of glow line lambda' = 5577 A with exposure of ionosphere to electron beam 06 p0822 N85-16219
Mechanism of damping of plasma oscillations in initial stage of injection of electron beams from spacecraft into ionosphere in active experiments
06 p0823 N85-15225
Influence of Faraday effect in ionosphere on nonmutuality of meteor radio channel
07 p0952 N85-16037
Region 1 birkeland currents from a global MHD simulation of the magnetosphere
[AD-A147435] 07 p0967 N85-16335
An investigation of ionospheric irregularity effects on SIR-B image processing and information extraction
08 p1149 N85-17247
X rays from the aurora
[AD-A149628] 08 p1186 N85-17477
A research in support of NASA's space science
[NASA-CR-174267] 08 p1227 N85-17723
Current carriers for the field-aligned current system
[NASA-TM-86161] 08 p1280 N85-17925
Ionospheric research at INPE
[INPE-3279-PRE/602] 10 p1514 N85-19558
Winter anomaly of the lower ionosphere and its possible causes 11 p1660 N85-20459
S3-3 ONR-118 data analysis
[AD-A149725] 12 p1889 N85-21855
Calculation of ionospheric profiles by inverting VLF/LF reflection data. 2. Anisotropic propagation
[AD-A150105] 12 p1890 N85-21859
Direct measurements of severe spacecraft charging in auroral ionosphere 13 p1991 N85-22480
Polar plasmas as observed by Dynamics Explorers 1 and 2 13 p1991 N85-22483
Ionospheric distortions of digital signals with wideband modulation 13 p2072 N85-22945
Evolution of strong inhomogeneities in ionospheric plasma, part 1 14 p2339 N85-24483
Correlation of ring current and ionospheric gap in morning and evening hours 14 p2339 N85-24486

Numberical simulation of the effects of radially injected barium plasma in the ionosphere
[NASA-CR-175636] 14 p2354 N85-24542
Ground-based and near-Earth observations during the IMS 14 p2359 N85-24575
IMS advances in studies of field-aligned currents and their related electrodynamics 14 p2359 N85-24578
Electrodynamics of magnetosphere-ionosphere coupling 14 p2359 N85-24579
Results of the Langmuir-probe experiment on board Intercosmos-18 — Ionosphere-magnetosphere interaction 14 p2362 N85-24596
Comparison of magnetospheric and ionospheric electric fields using different empirical mapping factors 14 p2362 N85-24597
Magnetosphere-ionosphere interaction through hydromagnetic waves 14 p2364 N85-24610
Spatial characteristics of ULF pulsations and their modification by the ionosphere: IMS results 14 p2364 N85-24612
High time-resolution studies of the auroral ionosphere
[AD-A150945] 14 p2409 N85-24850
Magnetic field penetration into cometary ionosphere 15 p2477 N85-25290
Turbopause as source of internal gravity waves 16 p2808 N85-27314
Ionospheric effects on antenna impedance
[BMFT-FB-W-84-052] 17 p2950 N85-28217
The boundary layers as the primary transport regions of the Earth's magnetotail
[AD-A152714] 17 p2992 N85-28496
EISCAT electron density studies
[AD-A152820] 17 p2993 N85-28498
Combined catalog of ionosphere vertical soundings data
[PB85-168494] 18 p3138 N85-29430
Shuttle Molecular Gun: Smog. Potential experiment for the electrodynamic Tethered Satellite System (TSS) mission
[IFSI-84-17] 20 p3419 N85-31221
Fluxgate magnetometer (SSM) for the defense meteorological satellite program (DMSP) block 5D-2, flight 7
[AD-A155229] 21 p3560 N85-32143
Doppler satellite data characteristics
[AD-A154868] 21 p3575 N85-32231
Further developments of EISCAT as an MST radar 21 p3627 N85-32534
Urbana radar systems: Possibilities and limitations 21 p3628 N85-32540
The Sondrestrom radar: Progress and proposed upgrades for ST work 21 p3628 N85-32541
The Adelaide VHF radar: Capabilities and future plans 21 p3629 N85-32546
Ionospheric electron density profile and related studies
[AD-A155257] 21 p3632 N85-32567
Beam diffusion in linear ionospheric layer 21 p3695 N85-32958
Yakutsk Institute's cosmic ray research facility 22 p3732 N85-33135
Magnetotails of the terrestrial planets: A comparative study 22 p3856 N85-33875
Waves in Space Plasmas (WISP) 23 p3901 N85-34164
Electrodynamic tether 23 p3902 N85-34168
Atmospheric Emission Photometric Imaging (AEPI) 23 p3902 N85-34170

IONOSPHERIC ABSORPTION
U ELECTROMAGNETIC ABSORPTION
U IONOSPHERIC PROPAGATION

IONOSPHERIC COMPOSITION
Middle atmospheric ionization. Observations and chemistry 04 p0522 N85-13340

IONOSPHERIC CONDUCTIVITY
Electric conductivities, currents and energy dissipation in the polar ionosphere 02 p0227 N85-11483
Field-aligned currents observed in the vicinity of a moving auroral arc 14 p2363 N85-24603
Multiple correlation between auroral and magnetic pulsations 14 p2363 N85-24605
Multiple correlation between auroral and magnetic pulsations. Part 2: Determination of electric currents and electric fields around a pulsating auroral patch 14 p2363 N85-24606
Effects of Birkeland current limitation on high latitude convection patterns
[TRITA-EPP-84-10] 20 p3494 N85-31725

IONOSPHERIC CURRENTS
NT AURORAL ELECTROJETS
NT ELECTROJETS
NT EQUATORIAL ELECTROJET
Electric conductivities, currents and energy dissipation in the polar ionosphere 02 p0227 N85-11483
Research directions in recent studies of the lunar geomagnetic effects 04 p0520 N85-13320
Dayside cusp aurora 04 p0521 N85-13333
Longitudinal current before westward propagating auroral bend 06 p0823 N85-15223
One-dimensional model of auroral magnetic force with longitudinal current and cyclotron heating of ions 13 p1980 N85-22424
Direct measurements of severe spacecraft charging in auroral ionosphere 13 p1991 N85-22480
Three-dimensional calculation of shuttle charging in polar orbit 13 p1992 N85-22486
Ionspheric effects of seasonal and diurnal variations of electric fields in equatorial F-region 14 p2338 N85-24459
Solar wind control of electric fields and currents in the magnetosphere and ionosphere 14 p2364 N85-24608
Ionosphere-magnetosphere coupling and convection 14 p2364 N85-24609
Effects of Birkeland current limitation on high latitude convection patterns
[TRITA-EPP-84-10] 20 p3494 N85-31725

IONOSPHERIC DISTURBANCES
NT IONOSPHERIC STORMS
NT SUDDEN IONOSPHERIC DISTURBANCES
NT TRAVELING IONOSPHERIC DISTURBANCES
Solar-geophysical data number 477, May 1984. Part 1: (Prompt reports). Data for April 1984, March 1984 and late data. Explanation of data reports issued as number 474 (supplement) February 1984
[PB84-225028] 01 p0131 N85-10901
Global maps of foF2 derived from observations and theoretical values
[AD-A145868] 03 p0392 N85-12509
Occurrences of the polar slant E condition (SEC) at Narssarssuaq, Godhavn, Thule 1982 03 p0393 N85-12514
On the study of ionospheric disturbances 04 p0522 N85-13335
Experimental results of study of artificial perturbation region in upper and lower ionosphere disturbance by the method of vertical probing 06 p0784 N85-15011
Relation between polarization of artificial low frequency radiation and parameters of auroral ionosphere 06 p0785 N85-15016
Possible effects of interaction of electric seismic fields with the ionosphere 06 p0823 N85-15228
Ionospheric turbulence: Interchange instabilities and chaotic fluid behavior
[AD-A147810] 07 p0996 N85-16337
Remote sensing of the high latitude ionosphere
[AD-A147881] 07 p1008 N85-16405
Tropospheric and ionospheric phase perturbations and Doppler frequency shift effects
[AD-A148579] 08 p1154 N85-17283
Artificial ionospheric disturbances caused by powerful radio waves
[AD-A148077] 08 p1186 N85-17473
Ionospheric and magnetospheric modifications caused by VLF waves
[AD-A148210] 08 p1186 N85-17475
X rays from the aurora
[AD-A148628] 08 p1186 N85-17477
Method and apparatus for calibrating the ionosphere and application to surveillance of geophysical events
[NASA-CASE-NPO-15430-1] 12 p1887 N85-21846
Kinetic Rayleigh-Taylor instability theory in the ionosphere near equator 13 p2067 N85-22911
Disturbances in structure of lower ionosphere at terminators based on results of winde-band LW sounding 14 p2339 N85-24467
Foreshortened short-wave scattering on artificial ionospheric inhomogeneities 14 p2340 N85-24468
Disturbance of midlatitude electrodynamic parameters due to the magnetospheric convection 14 p2362 N85-24593
Experimental research on ionospheric disturbance caused by cumulative barium vapor injection 16 p2719 N85-26787
Full shadow phenomenon in Earth's upper atmosphere 16 p2808 N85-27316
Remote sensing of irregularities in the equatorial ionosphere using the radio scintillation technique 16 p2808 N85-27317
Scintillation using NNSS satellites
[AD-A152604] 17 p2949 N85-28207
The Shock and Vibration Digest, volume 17, no. 2
[AD-A153129] 17 p2977 N85-28400
The effects of seismic waves 17 p2978 N85-28401
Ionospheric limitations to time transfer by satellite 18 p3107 N85-29234
Equitorial scintillations: Advances since ISEA-6
[AD-A154962] 21 p3631 N85-32559
Vehicle Charging And Potential (VCAP) 23 p3902 N85-34173
Sporadic radio emission connected with a definite manifestation of solar activity in the near Earth space
[SH-10.1-8] 23 p4053 N85-35139
Near Earth space sporadic radio emission bursts occurring during sunrise
[SH-10.1-9] 23 p4054 N85-35140
Ion composition measurements of the disturbed and quiet D-region in 1980 - 1981
[AD-A156055] 24 p4117 N85-35521

IONOSPHERIC DRIFT
Rocket and satellite observations of electric fields and ion convection in the dayside auroral ionosphere
[TRITA-EPP-84-05] 02 p0229 N85-11497
Fast ion polarization jet in subauroral F-layer and its manifestation in structure of high latitude ionosphere 15 p2480 N85-25306
A study of the generation mechanisms of high latitude and equatorial F-region irregularities using DE-2 data
[NASA-CR-175745] 16 p2825 N85-27423
Geophysical plasmas and atmospheric modeling
[AD-A152805] 17 p2993 N85-28497
A simple model for testing the effects of gravity-wave-produced vertical oscillations of scattering irregularities on spaced-antenna, horizontal drift measurements 21 p3619 N85-32489
Effects of line-of-sight velocity on spaced-antenna measurements, part 3.5A 21 p3621 N85-32496

IONOSPHERIC ELECTRON DENSITY
Two-level model for formation of night ionosphere of Venus from radio occulation experiments 02 p0162 N85-11100
Theoretical study of electron concentration in Venusian atmosphere as function of zenith angle of sun and solar activity in areas of photochemical equilibrium 02 p0163 N85-11104
Inference of equatorial field-line integrated electron density values using whistlers
[AD-A145822] 03 p0392 N85-12507
On the study of ionospheric disturbances 04 p0522 N85-13335
The response of mid-latitude total electron content to solar activity 04 p0522 N85-13336
Middle atmospheric ionization. Observations and chemistry 04 p0522 N85-13340
Observations of plasma bubbles and their zonal drift using polarimeters
[INPE-3219-PRE/572] 05 p0729 N85-14688
Medium- and large-scale wave disturbances and heterogeneities of electron concentration in outer ionosphere in middle and low latitudes 06 p0825 N85-15241
Partial reflection D-region electron densities 08 p1184 N85-17461
Dynamics of the low-latitude thermosphere and ionosphere 09 p1351 N85-18501
Neutral atmosphere properties determining D-region electron densities 11 p1658 N85-20451
Variation of derived mesospheric nitric oxide in relation to wind and temperature in winter 11 p1658 N85-20452
Indirect phase height measurements in central and eastern Europe for monitoring D region plasma 11 p1659 N85-20456
Measurements of partial reflections at 3.18 MHz using the CW radar technique 11 p1659 N85-20457
Method and apparatus for calibrating the ionosphere and application to surveillance of geophysical events
[NASA-CASE-NPO-15430-1] 12 p1887 N85-21846
Rocket observations of the ionosphere during the eclipse of 26 February 1979
[NASA-CR-175513] 12 p1888 N85-21850
Ionspheric effects of seasonal and diurnal variations of electric fields in equatorial F-region 14 p2338 N85-24459
Universal time effects in polar ionosphere 14 p2338 N85-24461
Determination of ionospheric electron density profiles from satellite UV (ultraviolet) emission measurements
[AD-A150734] 14 p2373 N85-24667
Influence of tropical F region in ionosphere on propagation of short radio waves 16 p2721 N85-26798
Full shadow phenomenon in Earth's upper atmosphere 16 p2808 N85-27316
Ionospheric electron density profile and related studies
[AD-A155257] 21 p3632 N85-32567

IONOSPHERIC HEATING
Magnetospheric plasma studies using data from the dynamics high and low altitude plasma instruments
[AD-A145751] 03 p0392 N85-12505

IONOSPHERIC ION DENSITY
Middle atmospheric ionization. Observations and chemistry 04 p0522 N85-13340
Analysis of ionization sources in D region based on theoretical models 06 p0825 N85-15240

One-dimensional model of auroral magnetic force with longitudinal current and cyclotron heating of ions
13 p1980 N85-22424
Results of the SCATHA ion composition experiment during the IMS
14 p2359 N85-24580
The ionospheric O+ streams in the magnetotail between 22 RE and 6 RE
14 p2360 N85-24582
Radar echoes at 2.66 and 40.92 MHz from the mesosphere, part 2.6A
21 p3619 N85-32486

IONOSPHERIC NOISE
NT WHISTLERS
A system for measuring the characteristics of the ionospheric channel by digital transmissions
10 p1472 N85-19287
Sporadic radio emission connected with a definite manifestation of solar activity in the near Earth space [SH-10.1-8]
23 p4053 N85-35139

IONOSPHERIC PROPAGATION
Convection of plasma in polar ionosphere, comparison of measurements from Cosmos-184 with model dependent on interplanetary magnetic field vector
02 p0160 N85-11086
Observations and prognosis of HF wave propagation via the sporadic E layer [UIO-SR-84-04]
03 p0356 N85-12294
Geophysical Works during 1981, volume 29, no. 547-566
03 p0375 N85-12389
Impedance measurements on a VLF multi-turn loop antenna in a space plasma simulation chamber [AD-A145104]
04 p0492 N85-13141
Sources of information concerning the ionosphere
04 p0521 N85-13334
On the study of ionospheric disturbances
04 p0522 N85-13335
Ionospheric scintillation: A brief review
04 p0522 N85-13337
The winter anomaly in ionospheric absorption (with special reference to the results obtained in Spain)
04 p0522 N85-13338
Possible anomaly prediction system for the middle atmosphere — ionospheric absorption
04 p0522 N85-13339
Distortions of radio pulse during reflection from maximum region of ionospheric layer
06 p0792 N85-15061
Medium- and large-scale wave disturbances and heterogeneities of electron concentration in outer ionosphere in middle and low latitudes
06 p0825 N85-15241
Development of a 20/30 GHz receiving station for propagation experiments with L-SAT [AD-A148281]
08 p1152 N85-17271
Propagation and scattering considerations for the 0.2-3.0 GHz frequency range for a space-based radar [AD-A148504]
08 p1153 N85-17282
Standing wave pattern of HF radio waves in the ionospheric reflection region. Part 1: General formulae [UIO-SR-84-05-PT-1]
09 p1313 N85-18253
Equatorial transionospheric propagation conditions affecting digital communications
10 p1470 N85-19275
A system for measuring the characteristics of the ionospheric channel by digital transmissions
10 p1472 N85-19287
A modem with pseudo-orthogonal codes: Experimental results
10 p1474 N85-19302
Error correction coding for a self-adaptive modem: Theoretical and experimental results
10 p1474 N85-19303
Serial data transmission with large output on the HF channel
10 p1475 N85-19305
Ionospheric absorption on 1539 kHz in relation to solar ionizing radiation
11 p1659 N85-20455
Indirect phase height measurements in central and eastern Europe for monitoring D region plasma
11 p1659 N85-20456
Measurements of partial reflections at 3.18 MHz using the CW radar technique
11 p1659 N85-20457
Autumn and winter anomalies in ionospheric absorption as measured by riometers
11 p1660 N85-20460
A model of the influence of neutral air dynamics on the seasonal variation in the low ionosphere
11 p1660 N85-20462
Calculation of ionospheric profiles by inverting VLF/LF reflection data. 2. Anisotropic propagation [AD-A150105]
12 p1890 N85-21859
Anisotropy of Alfven wave absorption in ionosphere
14 p2339 N85-24464
Deuteron whistlers at low latitudes in the low altitude topside ionosphere
14 p2366 N85-24625
Ionosphere effects may replace some communications satellites
15 p2484 N85-25337
Influence of tropical F region in ionosphere on propagation of short radio waves
16 p2721 N85-26798
Results of simultaneous measurements of absorption and polarization of radio waves reflected from ionosphere
16 p2807 N85-27313
Proceedings of the Sixteenth Annual Precise Time and Time Interval (PTTI) Applications and Planning Meeting [NASA-TM-87561]
18 p3105 N85-29221
A review of ionospheric effects on Earth-space propagation
18 p3106 N85-29233
Ionospheric limitations to time transfer by satellite
18 p3107 N85-29234
Waves in Space Plasmas (WISP)
23 p3901 N85-34164

IONOSPHERIC REFLECTION
U IONOSPHERIC PROPAGATION

IONOSPHERIC SOUNDING
Sources of information concerning the ionosphere
04 p0521 N85-13334
Partial reflection D-region electron densities
06 p1184 N85-17461
D1 LF wind measurements in the 90 to 100 km height range
06 p1185 N85-17466
Indirect phase height measurements in central and eastern Europe for monitoring D region plasma
11 p1659 N85-20456
Measurements of partial reflections at 3.18 MHz using the CW radar technique
11 p1659 N85-20457
Method and apparatus for calibrating the ionosphere and application to surveillance of geophysical events [NASA-CASE-NPO-15430-1]
12 p1897 N85-21846
Remote sensing of irregularities in the equatorial ionosphere using the radio scintillation technique
16 p2808 N85-27317
Small-scale structure of ionospheric F-region
19 p3297 N85-30440

IONOSPHERIC STORMS
NT SUDDEN IONOSPHERIC DISTURBANCES
Cold streams of ionospheric oxygen in the plasma sheet during the CDAW-6 event of March 22, 1979 [NASA-CR-174064]
03 p0393 N85-12513

IONOSPHERIC TEMPERATURE
Determining effective rate of plasma heating in outer equatorial ionosphere using data from ISIS-1 and ISIS-2 satellites
16 p2721 N85-26797

IONOSPHERICS
NT DAWN CHORUS
NT HISS

IONS
NT ANIONS
NT ANTIPROTONS
NT CATIONS
NT CESIUM IONS
NT DEUTERONS
NT FERRIC IONS
NT HEAVY IONS
NT HELIUM IONS
NT HYDROGEN IONS
NT LIGHT IONS
NT METAL IONS
NT MOLECULAR IONS
NT NEGATIVE IONS
NT NITROGEN IONS
NT OXYGEN IONS
NT POSITIVE IONS
NT PROTONS
NT RECOIL IONS
NT SOLAR PROTONS
NT TRIVALENT IONS
Spectrophotometric studies of iodine complexes in an aluminum chloride - butylpyridinium chloride ionic liquid [AD-A145074]
01 p0024 N85-10150
Trivalent ion exchange in beta alumina [AD-A145373]
02 p0172 N85-11151
Surface production of negative hydrogen ions [AD-A145437]
02 p0277 N85-11801
Spin dynamics of rare Earth ions in crystal fields probed by muon spin rotation [DE84-013805]
02 p0278 N85-11810
Absolute transition probabilities of lines in the spectra of astrophysical atoms, molecules, and ions [NASA-CR-174141]
04 p0580 N85-13705
Determination of halogens and sulfur in organic compounds and polymers by combustion-ion chromatography [DE84-016186]
05 p0814 N85-13921
Non-LTE considerations in spectral diagnostics of thermal transport and implosion experiments [DE84-015187]
05 p0730 N85-14689
Measurement of oxide ion concentration in NaCl-ZnCl2 molten salt and several applications [BLL-AWRE-TRANS-74-(9091.9F)]
06 p0764 N85-14886
Topics in high resolution spectroscopy of stored ions [DE85-002093]
06 p0861 N85-15470
Observations of local interstellar Mg I and Mg II
06 p0874 N85-15547
FeII and MgII in the nearby interstellar medium
06 p0874 N85-15549
Research relative to plasma transport across the magnetopause [NASA-CR-174300]
07 p1045 N85-16836
A cometary ion mass spectrometer [NASA-CR-174328]
08 p1164 N85-17343
Effect of disuse on sarcoplasmic reticulum in fast and slow skeletal muscle [NASA-CR-174337]
08 p1191 N85-17508
Instrumentation for particle-beams research using laser excited merging beams [AD-A147968]
08 p1220 N85-17681
Time-of-flight spectroscopy of ionic and metastable fragments from dissociating molecules [AD-A148068]
08 p1220 N85-17683
Microstructural analysis of ion containing polymers [DE85-001594]
10 p1453 N85-19157
Ab initio calculations of the optical properties of ions in glass [DE85-001008]
11 p1612 N85-20133
Superionized species and winds in low luminosity B and Be stars
11 p1749 N85-21003
Efficient heating and confinement of ions in an axisymmetric magnetic mirror supplemented with dc electric field [IPPJ-707]
12 p1935 N85-22160
Strong ion accelerating by collisionless magnetosonic shock wave propagating perpendicular to a magnetic field [IPPJ-709]
12 p1935 N85-22161
Velocity distributions of solar wind ions and electrons
12 p1954 N85-22273
Operational experience with ion concentration sensors in orientation systems
13 p1980 N85-22422
The chemistry of RDX and HMX cluster ions
13 p2004 N85-22581
Interaction of the magnetospheric ions with the surfaces of the icy satellites of Saturn
13 p2174 N85-23491
Plasma environment effects on the Giotto Ion Mass Spectrometer
14 p2245 N85-23819
Kinetic energies of fragment ions produced by dissociative photoionization of NO [NASA-CR-175721]
15 p2647 N85-26327
Spectroscopy of quasimolecular X-rays with H-like decelerated ions [DE85-006565]
15 p2649 N85-26337
Comparison of computational results of a few representative three-dimensional transonic potential flow analysis programs
16 p2803 N85-26829
Velocity space diffusion of high energy ions induced by a lower hybrid wave in a nonuniform magnetic field [IPPJ-714]
16 p2866 N85-27661
Selective detection of species in complex matrices by SIMS (Secondary Ion Mass Spectrometry) [AD-D011685]
19 p3235 N85-30063
Systematic view of transition intensities in the spectra of actinides and lanthanides in condensed phases [DE85-010272]
19 p3364 N85-30780
Resonant-transfer-and-excitation for highly charged ions (16 or = Z or = 23) in collisions with helium [DE85-010550]
19 p3369 N85-30823
Effect of inner subshell ionization on emission lines OIV ions [IPPJ-719]
19 p3370 N85-30903
Excitation of some alkaline Earth-like ions [DE85-010737]
20 p3529 N85-31951
Thermal ion heating in the vicinity of the plasmapause [NASA-CR-176030]
20 p3535 N85-31993
Production of stable embryo particles in dense ion tracks of alpha particle emissions in the atmosphere
21 p3644 N85-32938
Formation of particles in the air of the humid tropical forests
21 p3644 N85-32939
Effect of ions on cloud formation and its role in solar terrestrial relationship
21 p3653 N85-32997
Electrostatic ion cyclotron instability due to a nonuniform electric field perpendicular to the external magnetic field [AD-A155474]
21 p3707 N85-33019
Relative abundances of sub-iron to iron nuclei in low energy (50-250 MeV/N) cosmic rays as observed in the Skylab experiment [OG-4.1-4]
22 p3976 N85-34010
Measuring method and confirmation of H- (D-) ion current by sheet plasma 1 [IPPJ-730]
23 p3974 N85-34838
Low frequency instability in a mirror field
23 p3977 N85-34857
Model of azimuthal non-uniformities induced by RF heating in RFC-XXM
23 p3977 N85-34858
Experimental measurements of the ion cyclotron antennas' coupling and RF characteristics [DE85-011569]
23 p3982 N85-34864

Study of photon emission by electron capture during solar nuclei acceleration, 1: Temperature-dependent cross section for charge changing processes
[SH-1.1-8] 23 p3980 N85-34736
Quantitative analysis of flare accelerated electrons through their hard X-ray and microwave radiation
[SH-1.2-7] 23 p3991 N85-34742
Ion energy storage for post-flare loops
[SH-1.2-10] 23 p3992 N85-34745
Energetic protons from a disappearing solar filament
[SH-1.3-7] 23 p3993 N85-34754
Ion composition measurements of the disturbed and quiet D-region in 1980 - 1981
[AD-A156055] 24 p4117 N85-35521
Generalized reduced fluid model with finite ion-gyroradius effects
[DE85-013123] 24 p4157 N85-35777
Noise in sodium beta alumina crystals
[AD-A156025] 24 p4161 N85-35798

IOWA
Shortwave infrared detection of vegetation
[E85-10064] 08 p1174 N85-17402
Quaternary stratigraphy of the lower Iowa and Cedar River Valleys, southeast Iowa 09 p1352 N85-18504
Scan angle and detector effects in Thematic Mapper radiometry — Iowa and Arkansas
12 p1871 N85-21735
Investigation of TM band-to-band registration using the JSC registration processor 12 p1972 N85-21745

IP (IMPACT PREDICTION)
U COMPUTERIZED SIMULATION

IRAN
Microwave hydrology: A trilogy
[NASA-CR-176042] 20 p3477 N85-31603

IRAS
U INFRARED ASTRONOMY SATELLITE

IRAS-ARAKI-ALCOCK COMET
Implications of the presence of S2 in cometary ice
11 p1760 N85-21072
Research in planetary studies and operation of Mauna Kea Observatory
[NASA-CR-175618] 13 p2169 N85-23460

IRASERS
U INFRARED LASERS

IRIDIUM
Magnetically-induced luminescence of (Ir(2=phos)(2)C10(4)
[AD-A149659] 12 p1799 N85-21286
Development of the cerium-191 yields iridium-191m radionuclide generator
[DE85-011165] 23 p3970 N85-34611
Current status of the Os-191 yields Ir-191m generator
[DE85-008306] 23 p3971 N85-34614

IRON
NT FERRIC IONS
NT IRON ISOTOPES
NT IRON 59
Low-gravity solidification of cast iron and space technology applications 02 p0151 N85-11022
Directional solidification of flake and nodular cast iron during KC-135 low-g maneuvers
02 p0154 N85-11040
The reactions of cobalt, iron and nickel in SO-2 atmospheres: Similarities and differences
[NASA-TM-86666] 02 p0161 N85-11217
Detection of hydrogen assisted crack growth
[DE84-015820] 02 p0183 N85-11228
Characterization of amorphous surface layers in Fe implanted with Ti and C
[DE84-014960] 02 p0269 N85-11885
EXAFS and Mossebauer study of small metal clusters isolated in rare-gas solids
[DE84-015076] 04 p0470 N85-12994
The problem of iron partition between Earth and Moon during simultaneous formation as a double planet system 04 p0587 N85-13744
Origin of the Moon 04 p0587 N85-13745
Influence of hydrogen saturation and prior heat treatment on graphitization of white cast iron
[BLL-M-35964-(5828.4)] 05 p0615 N85-13932
Iron core collapse models of Type 2 supernovae
[DE84-013909] 05 p0743 N85-14775
Thermal conductivity of aluminum, copper, iron and tungsten for temperature from 1 K to the melting point
[PB84-235878] 06 p0770 N85-14824
Fell and MgII in the nearby interstellar medium
06 p0874 N85-15549
IUE observations of the gaseous component of the local interstellar medium 06 p0874 N85-15553
Observations of highly-ionized interstellar iron
06 p0876 N85-15585
Procedure for investigating high-temperature properties of iron-ore materials
[BLL-M-36020-(5828.4)] 07 p0926 N85-15666
Surface effects of corrosive media on hardness, friction, and wear of materials
[NASA-TM-83711] 07 p0930 N85-15896
The mineralogy of global magnetic anomalies
[E85-10061] 07 p0987 N85-16272
The fundamentals of dislocation transport of hydrogen in bcc iron
[AD-A148143] 08 p1129 N85-17117
Effect of iron on the performance of IN 625 weld deposits
[BR91456] 08 p1169 N85-17376
Metal-support interactions: Their effects upon adsorption, electronics, and activity/selectivity properties of cobalt in hydrogenation
[DE85-003316] 09 p1292 N85-18113
Alloying effects and microstructure of iron aluminides
[DE85-000903] 09 p1295 N85-18137
Study of the mechanism for annealing embrittlement of an iron-based metallic glass
[DE84-016656] 09 p1300 N85-18164
Liquid phase methanol process development unit: Installation, operation, and support studies
[DE85-001311] 09 p1301 N85-18171
The feasibility of low-G grey solidification of nodular iron in the F-104 experimental furnace package
[NASA-TM-82527] 10 p1426 N85-18996
High temperature properties of equiatomic FeAl with ternary additions
[NASA-TM-86936] 10 p1439 N85-19072
Residual stress after laser processing
11 p1600 N85-20065
Electrical resistance measurements of metals to 40 GPa in the diamond cell
[DE85-001009] 11 p1629 N85-20262
A circum-terrestrial compositional filter
13 p2179 N85-23520
Reassignment of the iron (3) absorption bands in the spectra of Mars 13 p2195 N85-23614
Hydrogen on impurity-covered iron surfaces
14 p2254 N85-23968
The Fe XIII 10747 A and Fe XIV 5303 A coronal emission lines polarization 14 p2448 N85-25111
Weldability of Ni3Al-type aluminide alloys
[DE85-006932] 15 p2512 N85-25496
Test of the electronic structure of Fe(100) by absorbed current spectroscopy
[DE85-004942] 15 p2661 N85-26422
Effect of nickel addition on the thermal, magnetic and magnetomechanical properties of Fe(80)B(15)Si(5)
[AD-A152281] 16 p2749 N85-26967
Effect of superconducting solenoid model coils on spanwise iron magnet roll control
[NASA-TM-86378] 17 p2905 N85-27915
The loss of material from the cathode of metal arcs
[NASA-TM-77845] 17 p2918 N85-27985
Multi-phase crystallization of ferrous alloys
[BLL-BISI-TRANS-22441-(9022.06)]
17 p2925 N85-28037
Effect of the agressive action of soil on metallic pipelines. New possibilities for the passive and active corrosion protection
[BLL-BISI-TRANS-21630-(9022.06)]
17 p2926 N85-28070
Kinetics of the formation of a complex alloyed boride coating on iron and its properties
[BLL-BISI-TRANS-22303-(9022.06)]
17 p2930 N85-28084
Temperature and manganese content dependences of tensile deformation in iron-high manganese binary alloys
[DE85-007656] 17 p2932 N85-28098
Uniaxial stress induced symmetry breaking for muon sites in Fe 17 p3042 N85-28820
Localized ionic currents from a corroding iron-copper galvanic couple
[AD-A153627] 18 p3074 N85-29011
Mineralogical-geochemical characteristics of ferromanganese formations in Arabian-Indian Ocean Ridge 19 p3293 N85-30416
Atomic data for controlled fusion research. Volume 4: Spectroscopic data for iron
[DE85-009658] 19 p3354 N85-30787
Reduction of the trapping of positrons in dislocated single crystals of iron when charged with hydrogen
[DE85-010235] 19 p3377 N85-30950
Concept development evaluation for John Deere/UA STS middeck experiment location
[NASA-CR-171541] 20 p3397 N85-31071
Determination of edge and screw dislocation density in single crystals of high-purity iron
[DE85-010237] 20 p3537 N85-32012
Burn front velocity as a function of pellet density in iron-potassium perchlorate heat powders
[DE85-011448] 21 p3572 N85-32214
Microanalysis of dissolved iron and phosphate in pore waters of hypersaline sediment
21 p3661 N85-32744
Multiphoton production and detection of atoms
[AD-A155561] 21 p3702 N85-33000
Initial results from the Caltech/DSRI balloon-borne isotope experiment
[OG-4.3-8] 21 p3714 N85-33048
Measurements of Fe and Ar fragmentation cross sections
[PAPER-OG-7.2-20] 21 p3714 N85-33047
Was core formation violent enough to homogenize the early mantle? 21 p3718 N85-33068
The problem of the Earth's CO2 content and the iron core 21 p3718 N85-33069
Tritium-helium effects in metals
[DE85-011507] 22 p3749 N85-33235
Induction motors with minimum waste of magnetic iron
22 p3772 N85-33377
Oxidation states of iron in the terrestrial planets: Evidence and implications for accretion models
22 p3852 N85-33854
Relative abundances of sub-iron to iron nuclei in low energy (50-250 MeV/N) cosmic rays as observed in the Skylab experiment
[OG-4.1-4] 22 p3876 N85-34010
A measurement of the cosmic ray elements C to Fe in the two energy intervals 0.5-2.0 GeV/n and 20-60 GeV/n
[OG-4.1-6] 22 p3876 N85-34012
Energy spectrum of cosmic-ray iron nucleus observed with emulsion chamber
[OG-4.1-10] 22 p3877 N85-34016
Measurement of the iron spectrum from 60 to 200 GeV per nucleon
[OG-4.1-11] 22 p3877 N85-34017
A new analysis of cosmic ray isotopes at 3 GeV/n from HEA03-C2 data
[OG-4.3-6] 22 p3879 N85-34031
Calculation of activities of components in liquid alloys of iron with yttrium
[BLL-M-35888-(5826.4)] 23 p3914 N85-34253
Capture in the 1.15-keV iron resonance
[DE85-011913] 23 p3970 N85-34612
Silicon to iron abundances in solar cosmic rays and in the sun
[SH-2.1-6] 23 p3998 N85-34787
Influence of yttrium on eutectoid transformation in irons
[BLL-M-35787-(5828.4)] 24 p4078 N85-35270
Development of a high strength isothermally heat-treated nodular iron road wheel arm
[AD-A155755] 24 p4099 N85-35408
Development of electrodes for the NASA iron/chromium
[NASA-CR-174724] 24 p4109 N85-35471
Ore genesis at the Monterrosas deposit in the Coastal Batholith, Ica, Peru 24 p4115 N85-35510
Size and shape dependence of CO adsorption sites on sapphire supported Fe microcrystals
[NASA-CR-176171] 24 p4160 N85-35794
Characteristics of central collision events in Fe-nucleus interactions for 20 - 60 GeV/nucleon
[HE-1.4-3] 24 p4176 N85-35891
The electromagnetic component of albedo from superhigh energy cascades in dense media
[HE-3.5-11] 24 p4184 N85-35948
The development of air shower in the iron absorber
24 p4189 N85-35967
Monte Carlo simulations of electron lateral distributions in the core region of 10(13) - 10(16) eV air showers
24 p4190 N85-35992
The longitudinal development of muons in cosmic ray air showers at energies 10(15) - 10(17) eV
[HE-4.3-12] 24 p4192 N85-36006
Multiple muons in MACRO
[HE-5.2-1] 24 p4202 N85-36079
The Nagoya cosmic-ray muon spectrometer 3, part 2: Track detector
[HE-5.2-3] 24 p4202 N85-36061

IRON ALLOYS
NT AUSTENITIC STAINLESS STEELS
NT CARBON STEELS
NT CHROMIUM STEELS
NT FERRITIC STAINLESS STEELS
NT HIGH STRENGTH STEELS
NT LOW CARBON STEELS
NT MARAGING STEELS
NT MARTENSITIC STAINLESS STEELS
NT NICKEL STEELS
NT STAINLESS STEELS
NT STEELS
Structure and abrasive resistance of iron based alloys rich in hardening components 01 p0054 N85-10360
Determining the optimum heating parameters for precision alloys — iron-nickel alloys
[BLL-M-35718-(5824.4)] 02 p0174 N85-11167
Rapid solidification of steels: Model and commercial alloys 02 p0176 N85-11184

Effect of annealing in transverse magnetic field on magnetic permeability of amorphous Fe5Co70Si15B10 alloy
03 p0349 N85-12247
Magnetic properties of and superfine interactions in amorphous Fe-Cr-Co-Si-B alloys
03 p0349 N85-12248
Metallurgy Institute's developments for alloy and aircraft producers
03 p0353 N85-12268
Stirling material technology
[NASA-TM-86888] 04 p0472 N85-13007
Radiation effects in amorphous metallic alloys
[DE84-014302] 04 p0475 N85-13025
Thermal conductivity of iron/potassium perchlorate heat powder
[DE84-017071] 04 p0476 N85-13035
Thermomagnetic generator
[DE84-017018] 04 p0530 N85-13388
Study of the reactive-element effect in oxidation of Fe-Cr alloys using transverse section analytical electron microscopy
[DE84-016237] 04 p0571 N85-13641
Experimental determination of the critical cavity radius in Fe-10% Cr for ion irradiation
[DE84-016570] 04 p0571 N85-13646
Metallographic evaluation of the reactions between boronated graphite and Fe-Ni-Cr alloys
[DE84-015374] 06 p0769 N85-14922
A study of tetrataenite
06 p0885 N85-15623
Low temperature diffusion coefficients in the Fe-Ni and FeNiP systems: Application to meteorite cooling rates
06 p0886 N85-15626
Speculations on the formation of metallic meteorite phases
06 p0889 N85-15648
The formation of isolated phase precipitates during the decomposition of high-coercive force Fe-Cr-Co alloys
[BLL-M-36028-(5828.4)] 07 p0924 N85-15855
Laser-initiated combustion studies on metallic alloys in pressurized oxygen
[PB85-126114] 10 p1438 N85-19068
Creep-rupture behavior of iron superalloys in high-pressure hydrogen
[NASA-CR-174411] 10 p1441 N85-19078
Development of AK18 alloy production technology based on electrothermic silumin
11 p1598 N85-20048
Electron-diffraction structural examination of amorphous iron-tin alloys
11 p1604 N85-20084
Heavy ion induced crystallization in amorphous phases
[DE85-003114] 11 p1606 N85-20098
Initial development of nickel and nickel-iron aluminides for structural uses
[DE84-016841] 11 p1608 N85-20108
Development of an automated miniature Charpy test method
[DE85-003011] 11 p1652 N85-20405
Atomistic studies of grain boundaries with segregated impurities
[DE85-000063] 11 p1737 N85-20924
Effects of chromium and aluminum on mechanical and oxidation properties of iron-nickel-base superalloys based on CG-27
[NASA-TP-2443] 12 p1805 N85-21323
Stress corrosion cracking and oxidation characteristics of boride-strengthened microcrystalline iron and nickel based alloys
[AD-A149805] 12 p1806 N85-21328
Formation of alumina layers on iron-base alloys
[BLL-T6418/BG/LRS/LRST737/84] 13 p2020 N85-22657
Study of the effects of implantation on the high Fe-Ni-Cr and Ni-Cr-Al alloys
[NASA-CR-175625] 13 p2021 N85-22661
TEM/FIM study of modulated microstructures in the Fe-Be system
[DE85-005379] 13 p2023 N85-22678
Corrosion-resistant amorphous alloys
13 p2035 N85-22748
Structure of amorphous films of alloys based on Fe, condensed from laser erosion products
13 p2035 N85-22749
Energy spectrum of processes of structural relaxation of amorphous alloy FeCo70Si15B10
13 p2035 N85-22750
Cast-iron technology: Metallographic and mechanical testing results
[DE85-002684] 14 p2257 N85-23984
Contact point and seam welding of heat-resistant alloys
15 p2501 N85-25429
Mossbauer spectrometry: Testing of a new computer based system and its application to a study of an aluminum-iron-cerium alloy
[AD-A151826] 15 p2510 N85-25483
Reduced-chromium stainless steel substitutes containing silicon and aluminum
[PB85-160786] 15 p2513 N85-25502
Iron rich low cost superalloys
[NASA-CR-174900] 16 p2748 N85-28962
The disordering process in an L12 ordered alloy
[DE85-008152] 17 p2931 N85-28093
Hydrogen absorption in metals: A field ion microscopy study
[DE85-010299] 18 p3076 N85-29026
Investigation for low-cost permanent magnets
[AD-A154387] 19 p3260 N85-30212
Experimental and theoretical study of fatigue crack initiation in metals
19 p3283 N85-30357
Long range ordered alloys modified by addition of niobium and cerium
[DE85-011661] 20 p3431 N85-31285
Cells for measuring thermoelectromotive force and electrical resistance of metals in temperature range of 20-950 degrees Celsius
[BLL-M-36240-(5828.4)] 20 p3457 N85-31473
Metallic glass composition
[DE85-011594] 22 p3751 N85-33253
Enthalpies of formation of liquid Fe-Ce-Si and Fe-Ce-Al three-component alloys
[BLL-M-36296-(5828.4)] 23 p3913 N85-34247
Influence of technology of atomization of naturally alloyed iron on grain-size characteristics of powder material
[BLL-M-35810-(5828.4)] 23 p3914 N85-34257
Thermal barrier coating system
[NASA-CASE-LEW-14057-1] 24 p4072 N85-35233

IRON CHLORIDES
Coexistence of antiferromagnetism and spin-glass ordering in the Ising system FeO 55MgO 45Cl2
[DE85-004164] 12 p1942 N85-22197
Environmental stability of intercalated graphite fibers
[NASA-TM-87025] 16 p2753 N85-26992

IRON COMPOUNDS
NT CHROMITES
NT FERRATES
NT FERRITES
NT IRON CHLORIDES
NT IRON CYANIDES
NT IRON OXIDES
NT LIMONITE
NT MAGNETITE
NT PYRITES
NT SIDERITES
NT TROILITE
A circumterrestrial compositional filter
04 p0588 N85-13753
Chemically modified electrodes and related solution chemistry
[DE84-017110] 05 p0614 N85-13924
Electrochemical features of the ferric sulfate leaching of CuFeS2/C aggregates
[AD-A148661] 08 p1123 N85-17081
The UFe4P12 and CeFe4P12: Non-metallic isotopes of superconducting LaFe4P12
[DE85-003724] 12 p1942 N85-22195
Mixed valence materials
[AD-A151009] 14 p2252 N85-23959
Effects of the cooling rate on the structure of the graphite in inoculated irons
[BLL-BISI-TRANS-22305-(9022.06)] 17 p2930 N85-28083
Lithium-alloy/iron sulfide battery design studies
[DE85-007991] 18 p3131 N85-29389

IRON CYANIDES
Development and evaluation of sulfonated polysulfone membranes for the zinc-ferricyanide battery
[DE85-009104] 24 p4090 N85-35357
Cationic exchange membrane for the zinc-ferricyanide battery
[DE85-013152] 24 p4112 N85-35489

IRON ISOTOPES
NT IRON 59
Diffusion of Fe-55 in Fe-2O-3 single crystals
[AERE-R-11286] 03 p0333 N85-12147
Measurements of Fe and Ar fragmentation cross sections
[OG-7.2-20] 23 p4016 N85-34887
The response of ionization chambers to relativistic heavy nuclei
[OG-9.1-13] 23 p4024 N85-34939

IRON METEORITES
Fractionation of siderophiles in cosmic spherules and its implications
06 p0884 N85-15613
Mossbauer spectroscopy and X-ray diffraction of samples from the Santa Catharina iron meteorite
06 p0885 N85-15624
Structural development in the Santa Catharina meteorite
06 p0886 N85-15625
Extreme incompatibility of Pb during the crystallization of magmatic iron meteorites
06 p0886 N85-15627
Experimental and theoretical study of the formation of the 2AB, 3AB, and 8A meteorite chemical groups from the parent liquid
06 p0888 N85-15629
Investigations concerning the magmatic iron meteorites: Static vs. dynamic experiments
06 p0888 N85-15629
On the record of galactic cosmic ray flux and traffic break-ups in iron meteorites
06 p0887 N85-15634
The low-energy secondary cosmic ray flux: Detectors in iron meteorites
06 p0887 N85-15635
Differentiated meteorites and the components of chondrites
[NASA-CR-174201] 06 p0890 N85-15649
Origin of mesosiderites as a natural consequence of planet formation
15 p2683 N85-26574

IRON ORES
Distribution of oxygen between metal and basic slags
[BLL-M-35932-(5828.4)] 05 p0616 N85-13935
World iron ore reserves
[BLL-BISI-TRANS-22280-(9022.06)] 17 p2983 N85-28435

IRON OXIDES
NT CHROMITES
NT MAGNETITE
Effects of additives and KOH electrolyte concentration on dissolution of iron electrodes
[DE84-014840] 02 p0173 N85-11162
An investigation of the role of sintering in gas-solid interactions
[DE84-015481] 02 p0288 N85-11884
Diffusion of Fe-55 in Fe-2O-3 single crystals
[AERE-R-11286] 03 p0333 N85-12147
Thermite and Fe/KClO4: Some thermodynamic calculations
[DE84-016945] 04 p0573 N85-13653
The bulk-Moon MgO/FeO ratio: A highlands perspective
04 p0583 N85-13724
Solid state, surface and catalytic properties of oxides
[DE85-002096] 06 p0867 N85-15512
Kinetics of interaction between carbon and iron oxides of metallized materials in solid phase
[BLL-M-36023-(5828.4)] 07 p0926 N85-15873
Mechanism of burning rate enhancement by ferric oxide
13 p2002 N85-22546
Iron oxides of Mars: Evidence for contemporary weathering
13 p2195 N85-23613
Hydrostatic compression of Fe1-chi O wustite
15 p2508 N85-25472
Influence of eutectic silicate inclusions on micro-processes during deformation and fracture of 12GS steel
[BLL-BISI-TRANS-22296-(9022.06)] 17 p2929 N85-28073
Carbon reduction of mixtures of MnO(2) and Fe(2)O(3)
[BLL-M-36260-(5828.4)] 20 p3422 N85-31241
Iron and manganese in oxide minerals and in glasses: Preliminary consideration of Eh buffering potential at Yucca Mountain, Nevada
[DE85-011892] 23 p3916 N85-34271
Features of behavior of gas bubbles in molten oxide films during enamelling: Communication 2
[BLL-M-35781-(5828.4)] 23 p3919 N85-34283

IRON 59
Mechanisms of impurity diffusion in rutile
[DE84-014741] 06 p0766 N85-14902

IROQUOIS HELICOPTER
U UH-1 HELICOPTER

IRRADIANCE
NT ILLUMINANCE
NT SOLAR CONSTANT
New concepts for measuring flame spread properties
[NBSIR-84-2943] 03 p0327 N85-12104
Annual energy spectrum for tracking arrays
06 p0832 N85-15297
Correlations of solar irradiance and daylight illuminance for building energy analysis
[DE85-001736] 06 p0839 N85-15326
User's guide for the Nimbus 7 ERB Solar Analysis Tape (ESAT)
[NASA-TM-86143] 10 p1572 N85-19914
MSG-7: Atmospheric penetration of solar radiation in the range of Schumann-Runge bands
11 p1657 N85-20443
Report on the Workshop on Intercomparison of Solar UV Irradiance Measurements and Related Instrument Calibration
11 p1658 N85-20448
Optical radiation emissions from selected sources. Part 2: High intensity discharge lamps
[PB85-149136] 15 p2523 N85-25551
Simple solar spectral model for direct and diffuse irradiance on horizontal and tilted planes at the Earth's surface for cloudless atmospheres
[DE85-002933] 18 p3137 N85-29424
Solar Ultraviolet Spectral Irradiance Monitor (SUSIM)
23 p3901 N85-34160
Active Cavity Radiometer (ACR)
23 p3901 N85-34163

IRRADIATION
NT AURORAL IRRADIATION
NT DEUTERON IRRADIATION
NT ELECTRON IRRADIATION
NT ION IRRADIATION
NT NEUTRON IRRADIATION
NT PROTON IRRADIATION
NT X RAY IRRADIATION
Formation of lattice defects by nitrogen laser exposure in A2B6 semiconductors with wide forbidden band
02 p0258 N85-11692
Isotopes in day to day life
[IAEA/PI/A.6S-84-00924] 03 p0417 N85-12668
A study of defects in neutron transmutation doped silicon: Gallium by hall effect analysis
[AD-A146047] 03 p0433 N85-12758
Radiation effects in amorphous metallic alloys
[DE84-014302] 04 p0475 N85-13025
Tensile properties and swelling of 20%-cold-worked Type 316 stainless steel irradiated in HFIR
[DE84-014060] 05 p0617 N85-13948
Raman study of neutron irradiated GaAs
[DE84-016056] 05 p0731 N85-14702
Solar wind and cosmic ray irradiation of grains and ices - application to erosion and synthesis of organic compounds in the solar system
06 p0888 N85-15637
Synergistic sputtering properties of binary alloys
[DE84-017493] 09 p1297 N85-18148
Simulation of repetitively-pulsed laser irradiation of graphite-epoxy composite
[AD-A149698] 09 p1325 N85-18329
Fundamental aspects on ion-beam surface modification: Defect production and migration processes
[DE85-000093] 09 p1399 N85-18804
Radiation-induced compositional redistribution and local phase transformation in irradiated alloys
[DE85-000080] 10 p1441 N85-19082
Facilities for studing radiation damage in nonmetals during irradiation
[DE85-000590] 10 p1554 N85-19801
Study of microstructure of aluminum and copper alloys after processing with continuous CO2 laser beam
11 p1601 N85-20066
Non-isothermal irradiation creep of nickel alloys inconel 706 and PE-16
[DE85-000842] 11 p1607 N85-20102
Measurement of hot-electron production and microwave emission by laser-irradiated CH targets
[DE85-003139] 11 p1640 N85-20331
Development of an automated miniature Charpy test method
[DE85-003011] 11 p1652 N85-20405
Design and use of nonstandard tensile specimens for irradiated materials testing
[DE85-001071] 11 p1652 N85-20406
Plasma states near surface of metal irradiated by CO2 laser 11 p1719 N85-20615
Irradiation effects on fuels for space reactors
[DE84-016460] 12 p1931 N85-22134
Decomposition of VTAN alloy solid solution upon irradiation and thermal aging 13 p2029 N85-22712
Specifics of laser heat treatment of high steel tools
13 p2029 N85-22714
Time-resolved ellipsometry and reflectivity measurements of the optical properties of silicon during pulsed excimer laser irradiation
[DE85-005091] 13 p2096 N85-23079
Time resolved X-ray studies during pulsed laser irradiation of Ge
[DE85-005263] 13 p2097 N85-23083
Time-resolved reflectivity measurement of extrinsic silicon during pulsed laser irradiation
[AD-A150350] 13 p2159 N85-23403
Local phase transformation in alloys during charged-particle irradiation
[DE85-005012] 14 p2258 N85-23990
Sphericity gauge for wavefront of laser radiation
14 p2275 N85-24096
Use of irradiated foods 14 p2393 N85-24740
Experimental report on a fiber optic light guide made by Galileo Electro-Optics Corporation
[DE85-008161] 14 p2421 N85-24941
Solar gravity modes from ACRIM-SWIM irradiance data
14 p2443 N85-25071
Observations of low-degree modes from the solar maximum mission (extended abstract)
14 p2443 N85-25072
Image formation in terms of the transport equation
[DE85-004893] 15 p2653 N85-26365
Low dose irradiation creep of pure nickel
[DE85-006320] 16 p2751 N85-26975
Influence of composition on the microstructural evolution and mechanical properties of irradiated Fe-Ni-Cr ternaries
[DE85-007462] 17 p2931 N85-28004
Effects of gamma-ray irradiation on dislocations in sodium nitrate single crystals
[DE85-008291] 18 p3195 N85-29818
Historical review of californium-252 discovery and development
[DE85-010223] 19 p3362 N85-30844
Defect production and recovery in FCC metals irradiated at 4.2 K
[DE85-010477] 20 p3538 N85-32014
Theoretical modeling of laser induced optical degradation
[AD-A155302] 21 p3592 N85-32323
Effect of powerful pulsed low-energy ion streams on GaAs 21 p3662 N85-32877
Current internal-dosimetry practices at US Department of Energy facilities
[DE85-011718] 22 p3787 N85-33466
Irradiation of northwest agricultural products
[DE85-012455] 22 p3843 N85-33803
Calibration of a high-level photon irradiation
[DE85-013044] 24 p4151 N85-35736
Total integrated dose testing of solid-state scientific CD4011, CD4013, and CD4060 devices by irradiation with CO-60 gamma rays
[NASA-CR-176196] 24 p4161 N85-35795
IRREGULARITIES
Irregularity decay in an isolated plasma bubble
[AD-A145782] 03 p0392 N85-12506
Spectral evaluation of irregularity of superconducting coaxial cables 13 p2062 N85-23000
A study of the generation mechanisms of high latitude and equatorial F-region irregularities using DE-2 data
[NASA-CR-175745] 16 p2825 N85-27423
Mesospheric measurements of irregularity patches using a 3-antenna interferometer, part 3.6B
21 p3621 N85-32498
IRRIGATION
Deficit irrigation feasibility study and demonstration project
[DE85-011531] 22 p3802 N85-33555
IRRITATION
NT TOXICITY AND SAFETY HAZARD
IRROTATIONAL FLOW
U POTENTIAL FLOW
IRS (INDIAN SPACECRAFT)
U INDIAN SPACECRAFT
ISEE
U INTERNATIONAL SUN EARTH EXPLORERS
ISENTROPE
Experimental technique for measuring the isentrope of hydrogen to several megabars
[DE85-014332] 24 p4095 N85-35386
ISENTROPIC PROCESSES
Isentropic objective analysis
[PB85-112167] 11 p1688 N85-20617
Use and interpretation of isentropic analyses
[PB85-132694] 11 p1688 N85-20618
Isotropic plotter
[PB85-175651] 18 p3150 N85-29504
Preliminary considerations for the gasdynamic precompression of solid molecular hydrogen
[DE85-013256] 22 p3784 N85-33445
ISING MODEL
U FERROMAGNETISM
U MATHEMATICAL MODELS
ISIS SATELLITES
NT ALOUETTE 2 SATELLITE
VLF emissions observed by ISIS Satellites during the IMS 14 p2366 N85-24521
ISLAND ARCS
Earthquakes and tectonics of Pacific Ocean margins
06 p0820 N85-15206
Magmatism in continent-ocean transition zone (development of ideas of A. N. Zavaritskiy)
13 p2113 N85-23161
Kuril-Aleutian subduction 19 p3290 N85-30402
ISLANDS
NT ALEUTIAN ISLANDS (US)
NT BERMUDA
NT CUBA
NT GREENLAND
NT HAWAII
NT ICELAND
NT INDONESIA
NT JAPAN
NT KURILE ISLANDS
NT NEW ZEALAND
NT PACIFIC ISLANDS
NT PUERTO RICO
NT TASMANIA
Satellite photographs suggest arctic volcano
07 p0962 N85-16239
Catalog of submarine volcanoes and hydrological phenomena associated with volcanic events: 1500 BC to 31 Dec. 1899
[PB85-117984] 12 p1891 N85-21869
Groundwater model for an island aquifer: Bribie Island groundwater study
[CE-44] 16 p2821 N85-27398
ISOBUTANE
U BUTANES
ISOBUTYLENE
U BUTENES
ISOCHORIC PROCESSES
The isochoric heat capacity of fluid substances in the critical region. Pre-examinations for a Spacelab experiment
[BMFT-FB-W-84-034] 05 p0723 N85-14650
ISOCYANATES
NT DIISOCYANATES
Moisture absorbing anti-arcing coating and method for applying same
[AD-D011310] 07 p0932 N85-15904
Fluorinated polyurethanes
[AD-D011526] 12 p1810 N85-21353
ISOENERGETIC PROCESSES
Application of the isoenergy principle and the A weighting to evaluate lesion risks due to noise in a military environment
[ISL-CO-231/83] 14 p2390 N85-24720
ISOLATION
A generalized model of fault-isolation performance
[AD-P003928] 02 p0248 N85-11606
Battery control and fault detection method
[AD-D011364] 07 p0993 N85-16307
High voltage disconnect protection
[AD-D011480] 10 p1481 N85-19353
High voltage isolation transformer
[NASA-CASE-GSC-12817-1] 18 p3093 N85-29146
Molten carbonate fuel cell seperator
[DE85-011615] 22 p3806 N85-33577
ISOLATORS
NT VIBRATION ISOLATORS
An optically isolated amplifier
[CSIR-SR-ELEK-257] 01 p0049 N85-10321
Numerical analysis of the first static calibration of the RSRA helicopter active-isolator rotor balance system
[NASA-TM-85975] 08 p1063 N85-16863
Multiple rate shock isolator damping valve
[AD-D011429] 08 p1168 N85-17368
Transients during the switching of SF6-insulated isolating switches
[BLL-CE-TRANS-7966-(9022.09)] 15 p2546 N85-25713
ISOMERIZATION
Chemical applications of topology and group theory. 16: Polyhedral isomerizations of seven-coordinate complexes
[AD-A149461] 10 p1436 N85-19047
Chemical applications of topology and group theory. 17: An information theoretical approach to polyhedral symmetry
[AD-A152821] 17 p2919 N85-27995
ISOMERS
EXAFS and Moessbauer study of small metal clusters isolated in rare-gas solids
[DE84-015976] 04 p0470 N85-12994
Isomer enumeration in polytertiary phosphines and related compounds
[AD-A146058] 09 p1290 N85-18099
PCB analysis by capillary gas chromatography coupled with matrix isolation-Fourier transform infrared spectroscopy
[DE84-009201] 10 p1437 N85-19059
Interpretation of 119 Sn isomer shifts and 3d 5/2-core-level shifts based on Dirac-Slater calculations on a number of ionic states
[USIP-85-06] 20 p3532 N85-31973
Noble metals as incipient transition metals
[DE85-013283] 24 p4060 N85-35286
ISOMORPHISM
Moessbauer study of amorphous Fe(67)Co(18)B(14)Si(1)
[AERE-R-11526] 11 p1737 N85-20928
Algorithm for determination of isomorphic graphs
22 p3769 N85-33357
ISOPARAMETRIC FINITE ELEMENTS
Recursive calculation of curved finite element stiffness matrices
[CSIR-TWISK-303] 01 p0106 N85-10726
Nonlinear analysis of composite laminates
09 p1268 N85-19087
Improved accuracy in solid isoparametric elements using selectively reduced integration 15 p2573 N85-25865
A 4-node bilinear isoparametric element in Rockwell NASTRAN 15 p2573 N85-25867
ISOPLETHS
U NOMOGRAPHS
ISOPYCNIC PROCESSES
Local mechanism of equatorial countercurrents
14 p2336 N85-24446

ISOSTATIC PRESSURE
HIP glassmaking for high nitrogen compositions in the Y-Si-Al-O-N system
[DE84-015546] 03 p0338 N85-12175
Mechanical properties and microstructure of centrifugally cast alloy 718
[AD-A147600] 08 p1129 N85-17116
Hot Isostatic Pressing (HIP): Techniques, applications and economical use
[JUEL-SPEZ-268] 17 p2939 N85-28141
Hot isostatically pressed Sm(2)(TM)17 magnets
[AD-A155479] 21 p3562 N85-32267
ISOSTERIC PROCESSES
U ISOPYCNIC PROCESSES
ISOTENSOID STRUCTURES
Mechanics of composite materials, theory and application
[VTH-LR-431] 18 p3123 N85-29334
ISOTHERMAL FLOW
Theoretical and experimental investigations of dust loaded flow fields in industrial halls
[BMFT-FB-HA-84-044] 12 p1819 N85-21411
Calculating isothermal flow in wake beyond injection zone 14 p2267 N85-24175
Predictions and measurements of isothermal flowfields in axisymmetric combustor geometries
[NASA-CR-174916] 17 p2898 N85-27867
Turbulent reacting flows 20 p3451 N85-31427
Nonequilibrium chemistry in an isothermal turbulent flow 22 p3745 N85-33211
ISOTHERMAL LAYERS
The physical implications of an isothermal model for the hot intracluster medium
[NASA-TM-86174] 11 p1763 N85-21089
ISOTHERMAL PROCESSES
Structure and properties of titanium alloys after isothermal deformation at low speeds
03 p0351 N85-12260
ECUT, Energy Conversion and Utilization Technologies program: Isothermal separation processes update
[NASA-CR-175463] 10 p1433 N85-19033
Joining of sintered composite TiC-steel materials by welding
[BLL-M-36253-(5828.4)] 20 p3461 N85-31502
Numerical simulation of nonisothermal transient processes in GaAs diode structures
22 p3767 N85-33350
ISOTHERMS
Accurate measurement of heat capacity by differential scanning calorimetry 04 p0468 N85-12975
Application of computer methods for calculation of multicomponent phase diagrams of high temperature structural ceramics
[AD-A148138] 08 p1133 N85-17140
A survey of major east coast snowstorms, 1960-1983. Part 2. Summary of surface and upperlevel characteristics
[NASA-TM-86195] 16 p2833 N85-27471
ISOTOPE EFFECT
Deuterium isotope effect on the compatibility between polystyrene and polybutadiene
[AD-A148551] 08 p1134 N85-17145
Variational transition state theory
[DE85-010885] 19 p3235 N85-30059
Constraints on the development of the early continental crust from isotopic data 21 p3719 N85-33076
Electron photoejection in carbanions
[DE85-011748] 23 p3912 N85-34237
ISOTOPE SEPARATION
Gas chromatographic separation of hydrogen isotopes using metal hydrides
[DE84-014455] 04 p0469 N85-12983
Methodology for economic evaluation of process technologies in the early research and development stages
[DE84-015883] 05 p0736 N85-14731
An infrared study of isotopic exchange during methanation over supported rhodium catalysts; an inverse spillover effect
[AD-A149390] 10 p1435 N85-19046
Definition of requirements for injection locking of pulsed UV lasers
[DE85-010126] 18 p3113 N85-29275
EDS operator and control software
[DE85-010470] 19 p3340 N85-30698
Possibilities for studying short-lived nuclei produced at LAMPF
[DE85-010740] 19 p3365 N85-30864
ISOTOPE SHIFT
U ISOTOPE EFFECT
ISOTOPES
NT ALUMINUM ISOTOPES
NT ALUMINUM 26
NT AMERICIUM
NT AMERICIUM ISOTOPES
NT AMERICIUM 241
NT ARGON ISOTOPES
NT BERYLLIUM ISOTOPES
NT BERYLLIUM 7
NT BERYLLIUM 9
NT BERYLLIUM 10
NT BORON 10
NT BROMINE ISOTOPES
NT CALCIUM ISOTOPES
NT CALIFORNIUM ISOTOPES
NT CARBON ISOTOPES
NT CARBON 12
NT CARBON 13
NT CARBON 14
NT CERIUM 144
NT CESIUM ISOTOPES
NT CESIUM 134
NT CESIUM 137
NT CHROMIUM ISOTOPES
NT COBALT 60
NT CURIUM
NT CURIUM 244
NT DEUTERIUM
NT GERMANIUM ISOTOPES
NT HELIUM ISOTOPES
NT HYDROGEN ISOTOPES
NT IODINE ISOTOPES
NT IRON ISOTOPES
NT IRON 59
NT KRYPTON ISOTOPES
NT KRYPTON 85
NT LUTETIUM
NT MAGNESIUM ISOTOPES
NT MANGANESE ISOTOPES
NT METALLIC HYDROGEN
NT NEODYMIUM ISOTOPES
NT NEON ISOTOPES
NT NICKEL ISOTOPES
NT NITROGEN ISOTOPES
NT NITROGEN 15
NT OSMIUM ISOTOPES
NT OXYGEN ISOTOPES
NT PLUTONIUM
NT PLUTONIUM ISOTOPES
NT PLUTONIUM 238
NT PLUTONIUM 239
NT POTASSIUM 40
NT RADIOACTIVE ISOTOPES
NT RADON ISOTOPES
NT RUBIDIUM ISOTOPES
NT SCANDIUM ISOTOPES
NT SILICON ISOTOPES
NT SODIUM ISOTOPES
NT STRONTIUM 90
NT TELLURIUM
NT THORIUM ISOTOPES
NT TRANSURANIUM ELEMENTS
NT TRITIUM
NT URANIUM ISOTOPES
NT URANIUM 235
NT XENON ISOTOPES
NT XENON 129
Magnetohydrodynamic flow of two-component gas analyzed 04 p0491 N85-13133
Isotopic composition of primary cosmic rays H-Fe for ISEE-C
[NASA-CR-175266] 05 p0746 N85-14783
Chemical evolution of the solar nebula: A new model
06 p0887 N85-15831
Chlorine isotopes as environmental tracers in Columbia River basalt groundwaters
[DE85-011392] 19 p3302 N85-30473
Technology for increasing the uranium-235 isotopic abundance in natural uranium feed on a productive scale
[DE85-011252] 19 p3357 N85-30810
NBS (National Bureau of Standards) reactor: Summary of activities Jul. 1983 through Jun. 1984
[PB85-184836] 20 p3522 N85-31907
A Cerenkov-delta E-Cerenkov detector for high energy cosmic ray isotopes and an accelerator study of Ar-40 and Fe-56 fragmentation
[NASA-CR-176029] 20 p3549 N85-32066
Contributions to the 19th International Cosmic Ray Conference
[NASA-CR-176060] 21 p3714 N85-33044
Initial results from the Caltech/DSRI balloon-borne isotope experiment
[OG-4.3-8] 21 p3714 N85-33046
Measurements of Fe and Ar fragmentation cross sections
[PAPER-OG-7.2-20] 21 p3714 N85-33047
Nineteenth International Cosmic Ray Conference. OG sessions, volume 2
[NASA-CP-2376-VOL-2] 22 p3875 N85-34006
Results of a search for deuterium at 25-50 GC/c using a magnetic spectrometer
[OG-4.2-4] 22 p3878 N85-34024
Cosmic ray isotope measurements with a new Cerenkov X total energy telescope
[OG-4.3-4] 22 p3878 N85-34029
A new analysis of cosmic ray isotopes at 3 GeV/n from HEAO3-C2 data
[OG-4.3-6] 22 p3879 N85-34031
Initial results from the Caltech/DRSI balloon-borne isotope experiment
[OG-4.3-8] 22 p3879 N85-34033
Abundances of secondary elements among the ultra heavy cosmic rays: Results from HEAO-3
[OG-4.4-6] 22 p3880 N85-34039
High resolution Cherenkov detectors for cosmic ray isotope experiment
[OG-9.1-4] 23 p4023 N85-34930
Mass resolution optimization in a large isotopic composition experiment
[OG-9.1-9] 23 p4023 N85-34935
Measurement of low energy cosmic rays aboard Spacelab-1
[SH-10.1-6] 23 p4063 N85-35137
Stopping relativistic Xe, Ho, Au and U nuclei in nuclear emulsions 24 p4173 N85-35876
ISOTOPIC ENRICHMENT
NT JET MEMBRANE PROCESS
On the connection between the 3HE-enrichment and spectral index of solar energetic particles
[SH-2.2-9] 23 p4001 N85-34804
ISOTOPIC LABELING
Diffusion of Fe-55 in Fe-2O-3 single crystals
[AERE-R-11286] 03 p0333 N85-12147
Isotopes in day to day life
[IAEA/PI/A.6E-84-00624] 03 p0417 N85-12668
Los Alamos MINI-Review: Tracking Antarctic winds
[DE85-004597] 12 p1896 N85-21903
Constraints on the development of the early continental crust from isotopic data 21 p3719 N85-33076
Centrifugal castings of stainless steel spiked with radioactive tracers
[DE85-012003] 22 p3748 N85-33234
Uranium, thorium isotopic analyses and uranium-series ages of calcite and opal and stable isotopic compositions of calcite from drill cores UE25a no. 1, USR G-2 and USW G-3/GU-3, Yucca Mountain, Nevada
[DE85-013039] 23 p3948 N85-34471
ISOTROPIC MEDIA
Compression of a band made of elastic, ideally Coulomb plastic material
[ISSN-0208-5658] 05 p0648 N85-14157
Unified constitutive material models for nonlinear finite-element structural analysis — gas turbine engine blades and vanes
[NASA-TM-86965] 14 p2320 N85-24336
ISOTROPIC TURBULENCE
Decay of a coherent scalar disturbance in a turbulent flow
[NASA-TM-86700] 19 p3264 N85-30244
ISOTROPISM
Trilinear alternating forms on a vector space of dimension 7
[CWI-PM-R8402] 05 p0722 N85-14844
ISOTROPY
NT ISOTROPIC MEDIA
NMR (Nuclear Magnetic Resonance) and macromolecular migration in a melt or in concentrated solutions
[AD-P003908] 01 p0032 N85-10194
Constitutive model development for isotropic materials
02 p0144 N85-10975
Arrival directions of cosmic rays of E .4 EeV
[OG-5.3-4] 22 p3884 N85-34071
ISRAEL
Technology transfer report: Feasibility study for the use of geothermal brine in the Ashdod area, Israel
[DE85-013316] 22 p3810 N85-33568
ISRO
Colloquium about Joint Projects within DFVLR/ISRO Cooperation
[DFVLR-MITT-84-12] 04 p0458 N85-12907
Presentation of Indian Space Research Organization (ISRO)/DFVLR cooperation 04 p0459 N85-12912
ITALY
Examples of environment services: Hydrological and pollution measurements in the Po River (Italy)
[CISE-2290] 11 p1679 N85-20578
ITERATION
NT CONJUGATE GRADIENT METHOD
NT ITERATIVE SOLUTION
A subspace iteration method for determining a dominant span of eigenvectors
[TWISK-329] 01 p0109 N85-10739

The rate of convergence of a class of block Jacobi schemes
[AD-A144738] 01 p0111 N85-10749
Development of a production order release methodology
[AD-A145213] 01 p0124 N85-10852
Generalized linear inversion of 2.5 - dimensional gravity and magnetic anomalies 02 p0226 N85-11480
Parametric analysis for generalized network flow problems
[AD-A145550] 02 p0243 N85-11589
An iterative procedure for obtaining I-projections onto the intersection of convex sets
[AD-A145402] 02 p0251 N85-11639
CHORDS: A new temperature or sound speed profile thinning algorithm
[AD-A145484] 02 p0275 N85-11793
Restoration of multichannel microwave radiometric images
[NASA-CR-174115] 04 p0554 N85-13527
Transformation of two and three-dimensional regions by elliptic systems
[NASA-CR-174176] 04 p0554 N85-13529
Multigrid iteration solution procedure for solving three-dimensional sets of coupled equations
[DE84-016515] 04 p0555 N85-13532
Multigrid iteration solution procedure for solving two-dimensional sets of coupled equations
[DE84-016554] 04 p0555 N85-13533
Iterative method for determining the distortion of elastic-plastic frames
[ISSN-0208-5658] 05 p0647 N85-14156
Very short range statistical forecasting of automated weather observations
[DOT/FAA/PM-84/31] 05 p0679 N85-14359
Interval iteration methods for nonlinear equation systems: Theory and comparison on computer
[INTERVALL-BER-84/6] 05 p0719 N85-14612
Mixed defect correction (iteration) for the solution of a singular perturbation problem
[MC-NW-162/83] 05 p0720 N85-14624
An iterative scheme for linear complementarity problems
[AD-A147464] 07 p1032 N85-16555
Distributed asynchronous relaxation methods for convex network flow problems
[AD-A148027] 08 p1211 N85-17622
Signal reconstruction from Fourier transform sign information
[AD-A148039] 08 p1211 N85-17624
A case of a not-so-strange strange attractor
[CWI-AM-R8406] 08 p1214 N85-17643
Designing the profile of turbine blades using an iteration technique 09 p1305 N85-18201
A turbulent closure model for the free atmosphere
09 p1351 N85-18502
Where are the parallel algorithms?
[NASA-CR-172516] 09 p1373 N85-18627
Transonic pressure distribution computations of a flexible wing 11 p1622 N85-20213
Applied mathematics of transport theory
[DE85-000848] 11 p1633 N85-20283
Complex symmetric matrices with strongly stable iterates
[NASA-CR-172542] 11 p1706 N85-20731
A solution method for large deformation contact problems
[AD-A149842] 12 p1866 N85-21707
State dependent priority rules for scheduling
[AD-A149972] 12 p1924 N85-22090
An iteration method for complex scattering problems
[AD-A150038] 12 p1934 N85-22151
On an iterative scheme for the solution of constrained variational equations
[CSIR-TWISK-341] 13 p2149 N85-23342
Iteration of exponential functions
15 p2633 N85-26233
A decomposition procedure for convex quadratic programs
[AD-A151732] 16 p2854 N85-27595
Nonlinear DSA difference schemes for radiative transfer applications
[DE85-005729] 16 p2856 N85-27611
Polynomial iteration for nonsymmetric indefinite linear systems
[AD-A153094] 17 p3019 N85-28671
A study of aerodynamic control in stalled flight leading-edge vortex formation analysis
[AD-A153758] 18 p3059 N85-28928
Transverse vorticity measurements using an array of four hot-wire probes
[FSFL-R-85-008] 18 p3099 N85-29184
Recent developments in nonlinear normal mode initialization 18 p3142 N85-29451
A robust estimator of location using an adaptive spline model
[AD-A153662] 18 p3174 N85-29676
The origin of the binary-search paradigm
[AD-A154367] 19 p3337 N85-30677
A parallelized point successive over-relaxation method on a multiple instruction multiple data stream computer
[AD-A154377] 19 p3337 N85-30679
Guide on logical database design
[PB85-177970] 19 p3381 N85-30976
Newton's method as a dynamical system: Global convergence and predictability
[AD-A155170] 21 p3632 N85-32564
A practical approach to Karmarkar's algorithm
[AD-A155714] 21 p3673 N85-32818
New developments on the core function for efficient implementation of the difficult residue number system operations
[AD-A154678] 21 p3676 N85-32834
Perturbation-iteration theory for analyzing microwave striplines
[NASA-CR-176180] 24 p4085 N85-35321

ITERATIVE NETWORKS
Analysis and design methodology for VLSI computing networks
[AD-A148030] 03 p0409 N85-12611

ITERATIVE SOLUTION
Augmented weak forms and element-by-element preconditioners: Efficient iterative strategies for structural finite elements. A preliminary study
01 p0058 N85-10384
Parallel, iterative solution of sparse linear systems: Models and architectures
[NASA-CR-172457] 02 p0243 N85-11586
Iterative method of calculating strength of airframe members using finite element method
06 p0775 N85-14955
Use of iterative linear and nonlinear algebraic methods for solving large stiff systems of ODEs
[AD-A148516] 08 p1213 N85-17636
Domain decomposition techniques for solving elliptic partial differential equations on multiprocessors
[DE85-004448] 10 p1549 N85-19769
Some data manipulation requirements for the exploratory analysis of large data sets
[DE85-002541] 10 p1568 N85-19887
On an iterative scheme for the solution of constrained variational equations
[CSIR-TWISK-341] 13 p2149 N85-23342
Solving large linear systems 14 p2396 N85-24759
Synthetic acceleration of coarse-mesh S/sub n/ transport calculations
[DE84-014721] 14 p2409 N85-24855
On the shift parameter in the backward beam method for parabolic problems for preceding times
[CWI-NM-R8411] 14 p2410 N85-24861
Manipulation and simulation of general robots using the zero-position description 15 p2567 N85-25838
Solving the minimal least squares problem subject to bounds on the variables
[TRITA-NA-8215] 16 p2852 N85-27580
Finite elements and the method of conjugate gradients on a concurrent processor
[NASA-CR-175812] 16 p2853 N85-27588
Projected discrete ordinates methods for numerical transport problems
[DE85-005632] 17 p3020 N85-28678
A convolution integral equation solved by Laplace transformation
[CWI-AM-R8409] 17 p3022 N85-28602
Inhomogeneous deformation: The theory and geological application of finite strain compatibility
19 p3312 N85-30532
Multigrid method for multiprocessors
[DE85-007929] 19 p3333 N85-30647
An iterative method for indefinite systems of linear equations
[NASA-CR-172345] 19 p3345 N85-30728
Optimization of a numerical method to calculate elliptic flows
[ESA-TT-889] 20 p3457 N85-31472
On the convergence of an iterative formulation of the electromagnetic scattering from an infinite grating of thin wires 24 p4085 N85-35319

IUE
Constraints to the radiative lifetime of a light neutral fermion in the galactic halo from IUE
[NOTA-INTERNA-617] 02 p0279 N85-11820
Lyman-Alpha aurora 02 p0302 N85-11953
Absorption line studies and the distribution of neutral gas in the local interstellar medium
06 p0673 N85-15544
Synthesis of data on the local interstellar medium
06 p0674 N85-15545
Observations of interstellar HI toward nearby late-type stars 06 p0674 N85-15546
Observations of local interstellar Mg I and Mg II
06 p0674 N85-15547
Mg II spectra of late type stars used to probe the LISM 06 p0674 N85-15548
FeII and MgII in the nearby interstellar medium
06 p0674 N85-15549
Spectroscopic observations of selected stellar systems
[NASA-CR-174288] 06 p1255 N85-17915
Future of Ultraviolet Astronomy Based on Six Years of IUE Research
[NASA-CP-2349] 11 p1743 N85-20961
IUE absorption line studies of highly ionized interstellar gas 11 p1743 N85-20962
Hot stars: Six years of progress
11 p1743 N85-20963
Solar system studies with the IUE: 1982 - 1984
11 p1744 N85-20964
Magellanic cloud objects 11 p1744 N85-20965
Interacting binary systems 11 p1744 N85-20967
Outer atmospheres of cool stars observed with IUE
11 p1744 N85-20968
Future ultraviolet experiments, including FUSE/COLUMBUS 11 p1744 N85-20969
UV observations and results on pre-main sequence stars 11 p1744 N85-20970
White dwarf stars at ultraviolet wavelengths
11 p1744 N85-20971
Supernova remnants and the carbon abundance in M33 11 p1745 N85-20972
Comments on the origins and variations of carbon and nitrogen in the ISM of galaxies as evident from IUE spectroscopy of H 2 regions 11 p1745 N85-20973
IUE spectroscopy of extragalactic H II regions
11 p1745 N85-20974
The usual hot stars in unusual galaxies
11 p1745 N85-20975
Highly ionized gas associated with the small Magellanic cloud 11 p1745 N85-20976
Galactic absorption lines measured from the IUE low dispersion spectra of active galaxies
11 p1745 N85-20977
Self-consistent recalibration of IUE determination of hot DA white dwarf effective temperatures
11 p1751 N85-21016
The fading of R coronae borealis
11 p1753 N85-21029
Observations of RR Lyrae and X Arietis with the IUE satellite 11 p1754 N85-21030
Atmospheric properties of RU Lupi derived from high- and low-resolution IUE spectra
11 p1754 N85-21031
Mg 2 emission of Pop. 2 long-period Cepheids
11 p1754 N85-21032
Blue companions of Cepheids
11 p1754 N85-21033
Ultraviolet observations of Population 2 Cepheids
11 p1754 N85-21034
Ultraviolet analysis of the peculiar F supergiant HD 112374 11 p1754 N85-21035
UV observations of epsilon aurigae during ingress and totality 11 p1755 N85-21038
Egress spectra of the new eclipsing supergiant 22 Vulleculae 11 p1755 N85-21039
The stellar wind in the BO V-type eclipsing binary Y Cygni 11 p1755 N85-21040
Observations of cataclysmic variable star winds
11 p1755 N85-21041
Ultraviolet spectroscopy of the interacting binary U Sagittae 11 p1755 N85-21042
Ultraviolet observations of circumstellar matter in Algol type binary systems 11 p1756 N85-21043
The essence of binary star coalescence: A coordinated ground-based photometric and IUE ultraviolet study of FK Comae 11 p1756 N85-21044
Strange F + Be binary star systems
11 p1756 N85-21045
Multi-year and possibly periodic variations in the UV spectrum of 56 Pegasi 11 p1756 N85-21046
Physical models for the UV continua of symbiotic stars
11 p1756 N85-21048
IUE and optical observations of LMC X-ray binaries
11 p1757 N85-21050
Circumstellar material in Algols and Serpentids
11 p1757 N85-21051
MU Sagittarii and Beta Lyrae: Combined IUE/Voyager observations 11 p1757 N85-21052
A search for the spectroscopic binary companions of Polaris using IUE spectra 11 p1757 N85-21053
The solar stellar connection in the far ultraviolet
11 p1757 N85-21055
Chromospheric activity in M giants
11 p1757 N85-21056
A progress report on the analysis of long exposure SWP high resolution spectra of cool stars
11 p1758 N85-21057

Betagause at maximum luminosity
11 p1758 N85-21061
IUE low-dispersion reference atlas
11 p1760 N85-21073
An IUE High-resolution atlas of O-type spectra
11 p1760 N85-21074
Statistical classification of IUE low-dispersion stellar spectra: Progress report 11 p1760 N85-21075
IUE observations of faint standard stars for calibration of the space telescope 11 p1761 N85-21076
Calibrations of wavelengths in SWP echelle spectra
11 p1761 N85-21077
Improved continuum definition in high-background IUE images 11 p1761 N85-21078

IUS
U INERTIAL UPPER STAGE

IZSAK ELLIPSOID
U ELLIPSOIDS
U GEODESY

J

J INTEGRAL
On the treatment of material laws for approximate J-estimation methods
[GKSS-84-E-15] 01 p0062 N85-10414
Eta values for compact geometry specimens to calculate the J integral
[AERE-R-11126] 03 p0374 N85-12385
An experimental evaluation of the J integral in 50% sidegrooved compact geometry specimens
[AERE-R-11202] 03 p0374 N85-12386
Correlation of stable crack growth with the J-integral and the crack tip opening displacement, effects of geometry, size and material: Report on an investigation of the elastic-plastic R-curve methodology
[GKSS-84-E-37] 08 p1173 N85-17385
Direct comparison of unloading compliance and potential drop techniques in J-integral testing
[DE85-001550] 11 p1650 N85-20392
Translational and extensional energy release rates (the J- and M-integrals) for a crack layer in thermoelasticity
[NASA-CR-174872] 12 p1863 N85-21685
The three-dimensional J-integral. An investigation into its use for post-yield fracture safety assessment
[WTHD-167] 20 p3472 N85-31578
A review of path-independent integrals in elastic-plastic fracture mechanics, task 4
[NASA-CR-174956] 22 p3799 N85-33541

J-52 ENGINE
A Q-GERT network simulation model for examining pipeline time in the Navy's J-52 intermediate level jet engine repair cycle
[AD-A147269] 07 p0884 N85-15663

J-85 ENGINE
Problems and possibilities for life extension in gas turbine components 07 p0907 N85-15742

JACKING EQUIPMENT
U JACKS (LIFTS)

JACKS (ELECTRICAL)
U ELECTRIC CONNECTORS

JACKS (LIFTS)
Improvements in linked-spar motion-compensated lifting system
[AD-D011413] 08 p1138 N85-17165
Cargo handling system
[AD-D011589] 14 p2219 N85-23762

JACOBI MATRIX METHOD
On existence and uniqueness of solutions of Hamilton-Jacobi equations
[AD-A147507] 07 p1033 N85-16560

JACOBI POLYNOMIALS
U HYPERGEOMETRIC FUNCTIONS

JAGUAR AIRCRAFT
Experiences obtained from service fatigue monitoring exercises 07 p0895 N85-15672
An update of experience on the fly by wire Jaguar equipped with a full-time digital flight control system
17 p2902 N85-27593

JAMMERS
Noise jammer discrimir.ation by noise modulation bandwidth
[AD-D011473] 10 p1468 N85-19264
Research on adaptive antenna techniques 6
[AD-A149341] 11 p1624 N85-20228

JAMMING
Resistance to HF jamming interference in mobile radio networks by an adaptive, distributed reconfiguration technique
[AD-A145117] 01 p0038 N85-10238
Noise jammer discrimination by noise spectral bandwidth
[AD-D011234] 01 p0038 N85-10242
Reflector antenna having sidelobe suppression elements
[AD-D011227] 01 p0039 N85-10244
Distributed reservation-based code division multiple access
[AD-A147007] 07 p0940 N85-15957
Parallel processor configuration for adaptive antenna arrays
[AD-D011347] 07 p0942 N85-15970
Optimum jamming effects on frequency-hopping M-ary FSK (Frequency-Shift Keying) systems under certain ECCM (Electronic counter-countermeasure) receiver design strategies
[AD-A147766] 08 p1151 N85-17267
Integrated defense communications system antijamming antenna system
[AD-D011423] 08 p1154 N85-17285
Noise jammer discrimination by noise modulation bandwidth
[AD-D011473] 10 p1468 N85-19264
Narrowband spread spectrum systems
10 p1475 N85-19307
Multiple loop sidelobe canceller
[AD-D011533] 12 p1823 N85-21434
The effect of jamming/deception on decision making
[AD-A149740] 12 p1828 N85-21472
FH/MFSK performance in multitone jamming
[NASA-CR-175667] 14 p2290 N85-24197
A survey of radar ECM and ECCM
15 p2536 N85-25653
Margin leveling algorithm for fully saturated satellite transponder with CDMA (Code Division Multiple Access) signalling
[AD-A151710] 15 p2543 N85-25699
Digital RF delay line for ECM (electronic countermeasure) look-through
[AD-A152120] 16 p2774 N85-27120
An analysis of jamming effects on noncoherent digital receivers
[AD-A153791] 18 p3090 N86-29128
Design of a jamming simulator for a binary communication system
[AD-A154617] 21 p3573 N85-32221

JANUS REACTOR
Microdosimetric spectra measurements of JANUS neutrons
[DE85-012108] 22 p3843 N85-33801

JAPAN
Operational precipitation observation system using digitized radar and rain gages 01 p0082 N85-10549
Analysis of radiocobalt in environmental samples
[DRIC-T-7334] 03 p0387 N85-12477
The availability of Japanese scientific and technical information in the United States
[GPO-35-241] 05 p0735 N85-14728
High-technology ceramics in Japan
[TI85-900380] 09 p1299 N85-18157
MAP in Japan: Organization and projects
11 p1655 N85-20425
High-technology ceramics in Japan
[PB85-125029] 12 p1815 N85-21380
The availability of Japanese scientific and technical information in the United States
[GPO-39-476] 12 p1951 N85-22254
Interrelationship of earthquake magnitude and lithospheric-asthenospheric thermodynamic parameters in seismically active zones 13 p2116 N85-23183
General report of the researches of snowpack properties, snowmelt runoff and evapotranspiration in Japan 13 p2124 N85-23225
Snowmelt runoff model in Japan
13 p2124 N85-23227
Application of Martinec-Rango model to river basin in Japan 13 p2124 N85-23228
Analysis of NIMBUS-7 SMMR data — Hokkaido, Japan snow cover 13 p2125 N85-23232
Estimation of regional evapotranspiration using remotely sensed land surface temperature. Part 2: Application of equilibrium evaporation model to estimate evapotranspiration by remote sensing technique — Japan 13 p2125 N85-23234
Results of comparison of long-wave radiation fluxes measured by Soviet and Japanese actinometric radiosonds 14 p2333 N85-24427
The astrometry network of observers in Japan
14 p2498 N85-25028
Welding technology: Japan — Conference
[ISBN-0-88300177-4] 15 p2565 N85-25823
Observation of precipitating clouds by a vertically pointing radar at Morino in the Iburi District, Hokkaido, Japan 15 p2582 N85-25922
Cosmic ray intensity variations observed at Matsushiro (220 M.W.E. in depth)
[SH-4.4-9] 23 p4084 N86-35007
Space activities in the Soviet Union, Japan, and the People's Republic of China 23 p4087 N85-36149

JAPANESE SPACE PROGRAM
Space Research in Japan. National report
01 p0013 N85-10082
Satellite observations 01 p0013 N85-10083
Non-US approaches to space commercialization
02 p0150 N85-11012
NTT unveils satellite communications equipment
10 p1478 N85-19315
Meteorological Satellite Center Technical Note No. 10, 1984
[MSC-TN-10] 12 p1894 N85-21884
History and future views on solar cells of Japanese scientific satellites 13 p2005 N85-22586

JAPANESE SPACECRAFT
Structural aspects of SAR antenna for Japanese Earth Resources Satellite 1 05 p0526 N85-14007
Development of Halley's Comet explorer PLANET-A solar array 13 p2010 N85-22808
Observations of aurorae and related plasma phenomena by the Kyokko and Jikiken satellite in IMS — EXOS-A and B satellite 14 p2364 N85-24547

JARRING
U MECHANICAL SHOCK

JEEPS
U AUTOMOBILES

JET AIRCRAFT
NT A-7 AIRCRAFT
NT A-310 AIRCRAFT
NT A-320 AIRCRAFT
NT B-70 AIRCRAFT
NT BOEING 727 AIRCRAFT
NT BOEING 737 AIRCRAFT
NT BOEING 747 AIRCRAFT
NT BOEING 767 AIRCRAFT
NT C-5 AIRCRAFT
NT C-135 AIRCRAFT
NT C-141 AIRCRAFT
NT CL-41 AIRCRAFT
NT CONCORDE AIRCRAFT
NT CV-990 AIRCRAFT
NT DC 8 AIRCRAFT
NT DC 9 AIRCRAFT
NT DC 10 AIRCRAFT
NT DH 115 AIRCRAFT
NT DHC 2 AIRCRAFT
NT EUROPEAN AIRBUS
NT F-8 AIRCRAFT
NT F-14 AIRCRAFT
NT F-15 AIRCRAFT
NT F-16 AIRCRAFT
NT F-17 AIRCRAFT
NT F-18 AIRCRAFT
NT F-27 AIRCRAFT
NT F-104 AIRCRAFT
NT F-106 AIRCRAFT
NT F-111 AIRCRAFT
NT JET PROVOST AIRCRAFT
NT L-1011 AIRCRAFT
NT LEAR JET AIRCRAFT
NT MIRAGE AIRCRAFT
NT MIRAGE 3 AIRCRAFT
NT OV-1 AIRCRAFT
NT P-3 AIRCRAFT
NT T-33 AIRCRAFT
NT TURBOFAN AIRCRAFT
NT TURBOPROP AIRCRAFT
NT U-2 AIRCRAFT
Observations from varying the IR and drag inputs to a noise prediction method for supersonic helical tip speed propellers
[NASA-TM-83797] 01 p0115 N85-10788
Development and flight evaluation of an augmented stability active controls concept: Executive summary
[NASA-CR-166009] 02 p0149 N85-11008
Auditory information systems in military aircraft: Current configurations versus the state of the art
[AD-A145469] 02 p0275 N85-11794
Computer programs to predict induced effects of jets exhausting into a crossflow
[NASA-CR-166691] 05 p0692 N85-13776
Advanced fatigue monitoring on service aircraft
07 p0895 N85-15671
Ground-effect analysis of a jet transport airplane
[NASA-TM-85820] 07 p0897 N85-15687
Analysis of the flow field about a T-45 using PANAIR
[AD-A148811] 07 p0899 N85-15699
The influence on IR emission of engine parameters for an afterburn case. A sensitivity study on NATO infrared air target model (NIRATAM) version: 0.0
[AD-B099311L] 12 p1779 N85-21171
Designer O. K. Antonov on new AN-74 arctic transport
15 p2457 N85-25230
A method for simulating 3-D aircraft flow fields with jet plume effects
[NASA-CR-175803] 18 p2999 N85-29664

Flight trials of a modified gulfstream commander carrying external stores
[AD-A153376] 17 p2696 N85-27859
The AFTI/F16 terrain-aided navigation system
[DE85-006411] 18 p3060 N85-28935
JET AIRCRAFT NOISE
Commercial aircraft noise
[PNR-90206] 03 p0417 N85-12665
Experimental investigation of shock-cell noise reduction for dual-stream nozzles in simulated flight
[NASA-CR-3846] 04 p0557 N85-13549
Computation of noise radiation from a free jet perpendicular to its axis via laser anemometry measurements
[ESA-TT-870] 09 p1379 N85-18669
Fan noise suppression in turbofan engines
[B8580076] 17 p2696 N85-27872
JET AIRSTREAMS
U JET STREAMS (METEOROLOGY)
JET AUGMENTED WING FLAPS
U JET FLAPS
U WING FLAPS
JET BLAST EFFECTS
A study of flow past an airfoil with a jet issuing from its lower surface
[NASA-CR-166610] 04 p0451 N85-12660
JET BOUNDARIES
Buoyant jet entrainment in stratified fluids
19 p3263 N85-30238
JET DAMPING
U DAMPING
U SPIN REDUCTION
JET DRIVE
U JET PROPULSION
JET ENGINE FUELS
NT JP-4 JET FUEL
NT JP-5 JET FUEL
NT JP-8 JET FUEL
Combustion gas properties I-ASTM jet A fuel and dry air
[NASA-TP-2359] 01 p0010 N85-10084
Molecular interactions of high energy fuels and jet fuels with oncogenic viruses and endogenous viruses
[AD-A145484] 02 p0186 N85-11255
Lubricity of well-characterized jet and broad-cut fuels by ball-on-cylinder machine
[NASA-TM-83807] 03 p0339 N85-12183
Compound class quantitation of JP-5 jet fuels by high performance liquid chromatography-differential refractive index detection
[AD-A145754] 03 p0340 N85-12185
Liquid phase products and solid deposit formation from thermally stressed model jet fuels
[NASA-TM-86674] 04 p0481 N85-13066
Method for evaluating petrol products corrosivity using piezoelectric crystals. Part 2: Instruction manual — jet engine corrosion tests
[FOA-C-40196-84] 04 p0482 N85-13073
Storage stability of jet fuels
[AD-A146360] 06 p0773 N85-14943
Heater block assembly for use in thermal oxidation testing of jet fuel
[AD-D011430] 09 p1123 N85-17077
GC-FTIR (Fourier Transform Infrared Spectrometry) of jet fuels
[AD-A148272] 09 p1135 N85-17155
Atmospheric photochemical modeling of turbine engine fuels. Phase 1: Experimental studies. Volume 2: Environmental chamber data tabulations
[AD-A147786] 09 p1185 N85-17470
Study of advanced fuel system concepts for commercial aircraft and engines
[NASA-CR-174752] 10 p1456 N85-19176
Quantitative determination of compound classes in jet turbine fuels by high performance liquid Chromatography/Differential refractive index detection: Part 2
[AD-A149299] 11 p1613 N85-20144
Oxidation and gum formation in jet fuels
[AD-A149934] 12 p1816 N85-21401
JP-8 and JP-5 as compression ignition engine fuel
[AD-A150796] 14 p2263 N85-24022
Influence of fuel properties on gas turbine combustion performance
[AD-A151484] 15 p2504 N85-25448
Aviation turbine fuels from tar sands bitumen and heavy oils. Part 1: Process analysis
[AD-A151319] 15 p2521 N85-25539
Jet fuel property changes and their effect on producibility and cost in the U.S., Canada, and Europe
[NASA-CR-174840] 16 p2757 N85-27012
Jet fuel instability mechanisms
[NASA-CR-175856] 17 p2696 N85-26127
Research test facility for evaporation and combustion of alternative jet fuels at high air temperatures
[AD-A153930] 18 p3083 N85-29073
The distribution of higher n-alkanes in partially frozen middle distillate fuels
[AD-A153940] 18 p3083 N85-29074
Measurement and correlation of jet fuel viscosities at low temperatures
[NASA-CR-174911] 23 p3921 N85-34295
Nitrogen analysis by chemiluminescence
[AD-A156197] 24 p4083 N85-35308
Biodegradation of jet fuel by aquatic microbial communities
[PB85-191971] 24 p4084 N85-35311
JET ENGINES
NT J-52 ENGINE
NT J-85 ENGINE
NT RAMJET ENGINES
NT SUPERSONIC COMBUSTION RAMJET ENGINES
NT TURBOFAN ENGINES
NT TURBOJET ENGINES
NT TURBOPROP ENGINES
Air force engine repair - Oklahoma City Air Logistics Center, Propulsion Division
[AD-P003999] 03 p0307 N85-11980
Propulsion — jet aircraft engines
[PNR-90208] 03 p0320 N85-12062
The applications of fibre optics in gas turbine engine instrumentation
[PNR-90209] 03 p0420 N85-12667
Air intake efficiency at zero speed and flp suction — jet engines
[BAE-KRS-N-GEN-303] 09 p1272 N85-17996
Oxidation resistant materials for hot gas turbines and jet engines
[AD-B067369L] 13 p1973 N85-22389
Fabrication of ceramic substrate-reinforced and free forms
[NASA-TM-86694] 14 p2247 N85-23926
Fiscal year 1986 technical objective document
[AD-A151039] 14 p2432 N85-25000
Advanced smoke meter development survey and analysis
[NASA-CR-166267] 15 p2560 N85-25792
Alternatives for jet engine control
[NASA-CR-175831] 16 p2709 N85-26713
Alternatives for jet engine control
[NASA-CR-175832] 16 p2709 N85-26714
Alternatives for jet engine control
[NASA-CR-175833] 16 p2709 N85-26715
Testing of materials and coatings for jet engine components under simulated operational conditions
[B8580073] 17 p2899 N85-27873
Opacity control technique for jet engine test cells
[AD-D011668] 19 p3220 N85-29968
Man-vehicle systems research facility advanced aircraft flight simulator throttle mechanism
22 p3798 N85-33527
Component-specific modeling
[NASA-CR-174765] 23 p3897 N85-34140
JET EXHAUST
A 2-dimensional description of potential perturbations to the ozone layer due to NOx and H-2-O aircraft emissions
[AD-A146292] 03 p0392 N85-12511
Opacity control technique for jet engine test cells
[AD-D011668] 19 p3220 N85-29968
JET FLAMES
U FLAMES
U JET FLOW
JET FLAPS
A study of flow past an airfoil with a jet issuing from its lower surface
[NASA-CR-166610] 04 p0451 N85-12660
JET FLIGHT
U JET AIRCRAFT
JET FLOW
NT AIR JETS
NT SUPERSONIC JET FLOW
Characteristics of a turbulent plane offset jet
02 p0196 N85-11310
Tunnel constraint for a jet in crossflow
03 p0314 N85-12027
Study of the velocity-acoustic pressure correlation in a cold jet, centered on the sign and the amplitude of the velocity fluctuations
[ISL-R-124/83] 04 p0501 N85-13193
Laminar jet issuing into stagnant surroundings — PHOENICS code
[PDR/CFDU-IC/15] 04 p0501 N85-13200
Transition and mixing in axisymmetric jets and vortex rings
05 p0591 N85-13769
Transonic jets: A numerical approach in the hodograph plane
05 p0592 N85-13774
Bicomponent flow problems in rheological fluid mechanics
05 p0635 N85-14073
Characterization of jet-contaminant interaction flow in chemical decontamination
[AD-A147298] 06 p1161 N85-17327
Design guide for fluidic laminar proportional amplifiers and laminar jet angular rate sensors
[AD-A147730] 08 p1161 N85-17326
Bipolar flows and X-ray emission from young stellar object
08 p1234 N85-17779
The sensitivity analysis in k-epsilon turbulence modeling applied to jet flows
09 p1318 N85-18288
Notes on compressible flow equations for thermodynamics of hot jets
[BAE-KRS-N-GEN-273] 09 p1318 N85-18289
Supersonic molecular jet study of the liquid state
[AD-A147416] 09 p1379 N85-18671
Flow visualization study of the effect of injection hole geometry on an inclined jet in crossflow
[NASA-TM-86936] 11 p1631 N85-20269
Preliminary analysis of tone-excited two-stream jet velocity decay
[NASA-TM-86951] 12 p1770 N85-21114
An investigation of turbulence mechanisms in V/STOL upwash flow fields
[AD-A149786] 12 p1772 N85-21123
Pseudospectral calculations of two-dimensional transonic flow (Task 1). Numerical investigation of VTOL aerodynamics (Task 2)
[AD-A150123] 12 p1772 N85-21126
Liquid fuel spray processes in high-pressure gas flow
[NASA-TM-86944] 12 p1844 N85-21570
Large amplitude forcing of a high speed 2-dimensional jet
[NASA-CR-175646] 13 p1974 N85-22393
Flow around axisymmetric bodies with uniform-velocity zones
14 p2276 N85-24103
Localization of sources of equivalent noise in fast cold jets, excited and nonexcited
[ISL-CO-201/83] 14 p2416 N85-24910
Numerical calculation of subsonic jets in crossflow with reduced numerical diffusion
[NASA-TM-87003] 15 p2472 N85-25263
Experiments in dilution jet mixing effects of multiple rows and non-circular orifices
[NASA-TM-86996] 15 p2473 N85-25266
An experimental investigation of unexcited and excited elliptic jets
15 p2554 N85-25755
The influence of jet-grid turbulence on heat transfer from the stagnation region of a cylinder in crossflow
[NASA-TM-87011] 15 p2554 N85-25760
An experimental technique for the study of velocity profiles in a laminar jet using a pulsed nitrogen laser
[AD-A151496] 15 p2556 N85-25771
Numerical experiments of jet streak ageostrophic circulations using pseudo-geostrophic initialization and perspectives
15 p2590 N85-25969
Preliminary wind tunnel study of the influence of a jet on the unsteady aerodynamics of a turbojet engine
[ONERA-RT-12/5115-RY-230-R-231G]
16 p2701 N85-26679
Study of the coupling between average, coherent and turbulent fields in a circular excited free jet
[ISL-R-115/83] 16 p2785 N85-27184
Computation model of turbulent free flow: Application to axisymmetric jets
[ISL-R-126/83] 16 p2785 N85-27185
Contribution to the study of equivalent noise source identification in fast cold jets
[ISL-R-114/83] 16 p2861 N85-27645
Analyses of orderly structures in jets and the relationship with emitted noise
[ISL-R-117/83] 16 p2861 N85-27646
Background noise measurements from jet exit vanes designed to reduced flow pulsations in an open-jet wind tunnel
[NASA-TM-86383] 17 p2906 N85-27918
Turbulent transport and length scale measurement experiments with confined coaxial jets
[NASA-CR-174831] 19 p3265 N85-30245
Density and confinement effects on mixing characteristics of an axisymmetrical CO(2) jet
[AD-A154468] 19 p3267 N85-30258
Hydrodynamic solutions for the diffusion of components in confined media
20 p3456 N85-31484
SCAP: A Shaped Charge Analysis Program. User's manual for SCAP 1.0
[DE85-011182] 20 p3515 N85-31854
Second order modelling in non-constant density flows
22 p3744 N85-33206
Pulsed hydrojet propulsion
[DE85-010771] 22 p3784 N85-33446
The calculation of two-dimensional buoyant surface jets with the k-W model of turbulence — kinetic energy-vorticity fluctuations (k-W)
[CFD/84/21] 22 p3785 N85-33448
Heat transfer characteristics for two-dimensional arrays of impinging jets with initial crossflow
24 p4092 N85-35365

Meteorological data from the OPTOMA (Ocean Prediction Through Observations, Modeling and Analysis) program OPTOMA 2, leg D2. 30 Jun. - 10 Jul. 1984
[AD-A158134] 24 p4123 N85-35560
JET FUELS
U JET ENGINE FUELS
JET IMPINGEMENT
Planar jets impinging on various obstacles and some modes of flow oscillation
[MPIS-MITT-78] 01 p0048 N85-10317
Jet array impingement flow distributions and heat transfer characteristics: Effects of initial crossflow and nonuniform array geometry 02 p0142 N85-10987
An experimental study of jet impingement on a circular cylinder
[AD-A145583] 02 p0198 N85-11326
Analysis of reactor material experiments investigating oxide fuel crust stability and heat transfer in jet impingement flow
[DE85-012097] 24 p4151 N85-35739
JET LAG
Jet lag prevention: Physiological mechanisms and pharmacological therapy
[AD-A145444] 02 p0235 N85-11529
Human performance in continuous/sustained operations and the demands of extended work/rest schedules. An annotated bibliography
[AD-A155619] 21 p3666 N85-32771
JET MEMBRANE PROCESS
Possibilities for studying short-lived nuclei produced at LAMPF
[DE85-010740] 19 p3365 N85-30664
JET MIXING FLOW
Dilution zone mixing studies 02 p0145 N85-10984
Dilution jet mixing 02 p0145 N85-10985
Transition and mixing in axisymmetric jets and vortex rings 05 p0591 N85-13769
Basic studies of multiple free and confined jets
[AD-A149556] 10 p1485 N85-19374
Mixing characteristics of an underexpanded multiple jet ejector
[AD-A149557] 10 p1485 N85-19375
An experimental investigation of an underexpanded rectangular jet ejector
[AD-A149656] 12 p1779 N85-21170
Determination of boundary line between reverse jet and surrounding stream 13 p2043 N85-22789
Development of a temperature measurement system with application to a jet in a cross flow experiment
[NASA-CR-174896] 15 p2472 N85-25282
Experiments in dilution jet mixing effects of multiple rows and non-circular orifices
[NASA-TM-86996] 15 p2473 N85-25288
An experimental investigation of confined, multiple, turbulent jet mixing with recirculation — flow distribution in combustors with injection plates 15 p2555 N85-25764
A theoretical study of two stage thrust augmenting ejectors
[ARL/AERO-R-166] 19 p3218 N85-29954
Buoyant jet entrainment in stratified fluids 19 p3263 N85-30238
Density and confinement effects on mixing characteristics of an axisymmetrical CO(2) jet
[AD-A154488] 19 p3267 N85-30258
An experimental investigation of confined, multiple, turbulent jet mixing with recirculation 20 p3451 N85-31426
Large eddy structures in transitional and turbulent flames
[AD-A154520] 21 p3562 N85-32157
JET NOISE
U JET AIRCRAFT NOISE
JET NOZZLES
Influence of setting angle of jet cooling nozzles on temperature and stress state of a turbine wheel 09 p1308 N85-18208
JET PILOTS
U AIRCRAFT PILOTS
JET PROPULSION
Modeling of propulsive jet plumes-extension of modeling capabilities by utilizing wall curvature effects
[AD-A146282] 03 p0362 N85-12324
Air Force Academy Aeronautics Digest
[AD-A149614] 12 p1769 N85-21104
Fiscal year 1986 technical objective document
[AD-A151039] 14 p2432 N85-25000
A theoretical study of two stage thrust augmenting ejectors
[ARL/AERO-R-166] 19 p3218 N85-29954
JET PROVOST AIRCRAFT
Experiences obtained from service fatigue monitoring exercises 07 p0895 N85-15672
JET PUMPS
Jet pump-drive system for heat removal
[NASA-CASE-NPO-16494-1-CU] 18 p3099 N85-29182
JET STREAMS (METEOROLOGY)
Jet stream errors and tropospheric-stratospheric interactions in the GLAS general circulation model 05 p0683 N85-14392
Small component spectral model of annual course of zonal atmospheric circulation 14 p2337 N85-24453
Role of jet streaks and boundary layer processes in organizing a pre-convective environment 15 p2597 N85-26008
Meso-6 scale numerical simulations of the jet streak adjustments which organized the Carolina tornado outbreak and the subsequent explosive coastal cyclogenesis 15 p2598 N85-26011
Great Lakes winter weather and ice conditions for 1982-83
[PB85-165009] 16 p2837 N85-27496
A preliminary intercomparison between numerical upper wind forecasts and research aircraft measurements of jet streams
[NASA-CR-167884] 24 p4120 N85-35539
JET THRUST
Characteristics of a confined jet thrust vector control nozzle
[AD-A153087] 17 p2958 N85-28268
JET VANES
Effect of jet exit vanes on flow pulsations in an open-jet wind tunnel
[NASA-TM-86299] 09 p1273 N85-17999
Background noise measurements from jet exit vanes designed to reduced flow pulsations in an open-jet wind tunnel
[NASA-TM-86383] 17 p2906 N85-27916
JETAVATORS
U GUIDE VANES
JETS
On the interaction of a sound pulse with the shear layer of an axisymmetric jet. Part 3: Nonlinear effects
[NASA-CR-172512] 09 p1378 N85-18663
Exotic interactions among C-jets and Pb-jets
[HE-3.2-6] 24 p4179 N85-35914
JETTISON SYSTEMS
The development of staging mechanisms for the Japanese satellite launcher Mu-3SII 22 p3796 N85-33528
JFET
Method for the fabrication of dielectric isolated junction field effect transistor and PNP transistor
[AD-D011500] 12 p1832 N85-21494
JIGS
Report on high-precision jig-boring machines 01 p0035 N85-10215
Classification of holding jigs for objects of robotized assembly 14 p2266 N85-24039
JIMSPHERE BALLOONS
Atmospheric environment for Space Shuttle (STS-51A) launch
[NASA-TM-86497] 12 p1692 N85-21675
JITTER
U VIBRATION
JOBS
U TASKS
JOINING
Effect of interconnection of the ends of a sliding bearing on film thickness
[AD-A147736] 08 p1132 N85-17135
Effect of interfacial characteristics of metal clad polymeric substrates on electrical high frequency interconnection performance
[NASA-TM-86948] 11 p1624 N85-20223
NASA welding assessment program
[NASA-CR-175662] 15 p2568 N85-25844
JOINTS (ANATOMY)
NT ELBOW (ANATOMY)
NT KNEE (ANATOMY)
NT WRIST
Dynamics of morphological changes in articulation nervous system under hypokinetic conditions as a model of a spaceflight factor 01 p0092 N85-10621
JOINTS (JUNCTIONS)
NT BEAM LEADS
NT BUTT JOINTS
NT LAP JOINTS
NT METAL JOINTS
NT RIVETED JOINTS
NT SEAMS (JOINTS)
NT SOLDERED JOINTS
NT SPOT WELDS
NT WELDED JOINTS
Silicon nitride joining
[AD-A145868] 02 p0187 N85-11248
Storage life of thermal detents
[DE84-016834] 04 p0476 N85-13030
Detection of cracks in a plastics pipe joint by reflection holography
[NPL-DMA(A)-87/MOM-70] 04 p0502 N85-13202
Exploratory study of shear strength of joints for precast segmental bridges
[PB84-235449] 05 p0651 N85-14182
Translational control of a graphically simulated robot arm by kinematic rate equations that overcome elbow joint singularity
[NASA-TP-2376] 06 p0856 N85-15448
Aeroproyekt develops improved runway surfacing 08 p1068 N85-18770
Space shuttle elevon seal panel mechanism 08 p1101 N85-18961
Finite element calculation for a Y-joint and comparison of results with strain measurements
[BLL-RISLEY-TR-4526-(9091.9F)] 08 p1171 N85-17381
Mechanical properties of Shielded Metal Arc (SMA) and Submerged Arc (SA) welded joints for quenched and tempered steel StE 470.
[VTT-319] 09 p1328 N85-18346
Stochastic dynamic analysis of a structure with frictional joints 09 p1337 N85-18408
Long term durability of urea formaldehyde glued joints removed from Vampire aircraft
[AD-A149063] 10 p1424 N85-19985
Adhesive joint formation under field conditions
[AD-D011478] 10 p1453 N85-19153
Excimer laser annealing to fabricate low cost solar cells
[NASA-CR-174394] 11 p1673 N85-20538
Elbow and knee joint for hard space suits and the like
[NASA-CASE-ARC-11610-1] 11 p1697 N85-20666
Characterization of mode 1 and mixed-mode failure of adhesive bonds between composite adherends
[NASA-TM-86355] 12 p1797 N85-21270
Shoulder and hip joint for hard space suits and the like
[NASA-CASE-ARC-11543-1] 12 p1910 N85-21966
Elasticity solution of an adhesively bonded joint
[NASA-CR-175591] 13 p2101 N85-23097
Scattering of elastic waves on fractures randomly distributed in a three-dimensional medium 13 p2111 N85-23151
Overlays for plain jointed concrete pavements
[PB85-156297] 15 p2523 N85-25557
Reflection and transmission of flexural waves at discontinuities 15 p2572 N85-25861
A study of the time dependence in fracture processes relating to service prediction of adhesive joints and advanced composites
[AD-A152084] 15 p2579 N85-26010
Initial quality of advanced joining concepts
[AD-A152241] 16 p2759 N85-27027
An improved torsional method for determining the fracture toughness of stiff materials and of adhesive joints
[AD-A152091] 16 p2800 N85-27267
Elastic equilibrium of composite shells with finite shear rigidity 17 p2942 N85-28163
Further investigations to improve the fatigue life of the Mirage 1110 wing main span
[ARL/STRUC-TM-397] 18 p3061 N85-29838
Self-locking mechanical center joint
[NASA-CASE-LAR-12864-1] 19 p3279 N85-30336
Fundamental studies related to failure of adhesively bonded structures
[AD-A154072] 19 p3285 N85-30374
Elastomers used in aeronautics industry
[SNIAS-851-551-103] 20 p3434 N85-31304
Joining of sintered composite TiC-steel materials by welding
[BLL-M-36253-(5828.4)] 20 p3461 N85-31502
Hubble space telescope: Pointing error effects on nonlinear ball joints
[NASA-TM-86511] 20 p3545 N85-32058
Improved materials for composites and adhesive joints
[AD-A154918] 21 p3561 N85-32152
Improved materials for composite and adhesive joints
[AD-A155065] 21 p3562 N85-32153
Experimental and theoretical assessment of a new technique for the non-destructive evaluation of laminated panels
[AD-A155822] 21 p3562 N85-32155
Resolution of thermal striping issue downstream of a horizontal pipe elbow in stratified pipe flow
[DE85-006195] 21 p3586 N85-32262
Simultaneous junction formation 21 p3610 N85-32426
Pulsed excimer laser processing for cost-effective solar cells 21 p3611 N85-32432
Mechanical connection for a tubular assembly
[DE85-011590] 22 p3792 N85-33497
The stress distribution in pin-loaded orthotropic plates
[NASA-CR-176146] 22 p3800 N85-33547

Three-dimensional finite element failure model for predicting failure in fibre reinforced bolted joints
[BR94776] 23 p3940 N85-34423
Stresses and strains in a plate resulting from two closely-spaced interference-fit fasteners
[ARL/STRUC-TM-409] 23 p3941 N85-34429
Verification of the SRB motor case pin retainer band tips
[NASA-CR-170882] 24 p4070 N85-35220

JORDAN FORM
Contribution of the cup-product of Milnor's fiber with /1/ sup 2 lambda poles 11 p1698 N85-20672
The eigenstructure assignment of deadbeat control systems
[AD-A149761] 12 p1834 N85-21510

JOSEPHSON JUNCTIONS
Transmission line biased coherent array of Josephson oscillators
[AD-D011323] 07 p0944 N85-15979
Coherent array of Josephson oscillators with external bias leads
[AD-D011367] 08 p1156 N85-17293
Resonant activation of a Josephson junction
[DE85-000702] 10 p1563 N85-19657
Thin film technology of high-critical-temperature superconducting electronics
[AD-A150010] 12 p1940 N85-22185
Macroscopic quantum tunnelling in a current biased Josephson junction
[DE85-004603] 13 p2164 N85-23424
Random access memory technologies
[AD-A153089] 17 p3008 N85-26597

JOULE HEATING
U OHMIC DISSIPATION
U RESISTANCE HEATING

JOURNAL BEARINGS
Damping capacity of a sealed squeeze film bearing
05 p0645 N85-14139
Vibration control of rotor shaft
[NASA-TM-87053] 18 p3117 N85-29292

JOURNALS
NBS (National Bureau of Standards) library serial holdings, 1985
[PB86-191948] 22 p3849 N85-33839

JOURNALS (DOCUMENTS)
U PERIODICALS

JOURNALS (SHAFTS)
U SHAFTS (MACHINE ELEMENTS)

JP-4 JET FUEL
Variability of major organic components in aircraft fuels. Volume 3: Sample data package for the reference JP-4 fuel
[AD-A145483] 02 p0188 N85-11254
Variability of major organic components in aircraft fuels. Volume 1: Technical discussion
[AD-A145574] 02 p0188 N85-11256
Variability of major organic components in aircraft fuels. Volume 2: Illustrations
[AD-A145831] 04 p0481 N85-13067
Effects of temperature variation among droplets in an evaporating fuel spray 13 p2004 N85-22562

JP-5 JET FUEL
Variability of major organic components in aircraft fuels. Volume 3: Sample data package for the reference JP-4 fuel
[AD-A145483] 02 p0188 N85-11254
Variability of major organic components in aircraft fuels. Volume 1: Technical discussion
[AD-A145574] 02 p0188 N85-11256
Variability of major organic components in aircraft fuels. Volume 2: Illustrations
[AD-A145831] 04 p0481 N85-13067
Evaluation of jet fuel deposit kinetics. Lot 4
[AD-A147196] 07 p0935 N85-15822

JP-8 JET FUEL
Effects of temperature variation among droplets in an evaporating fuel spray 13 p2004 N85-22562

JUDGMENTS
The effects of feedback and predictability of human judgment
[AD-A145744] 02 p0237 N85-11542
Direction judgement errors in perspective displays
05 p0705 N85-14520
A theory of preference reversals
[AD-A147952] 08 p1216 N85-17661
Task influences in the analytic-intuitive approach to decision making
[AD-A149870] 12 p1950 N85-22250

JUNCTION DIODES
NT MIM DIODES
Buried junction enhanced Schottky barrier device
[AD-D011399] 07 p1044 N85-16635
Diodes in photovoltaic modules and arrays
[NASA-CR-175454] 10 p1508 N85-19513

JUNCTION FIELD EFFECT TRANSISTORS
U JFET

JUNCTION TRANSISTORS
NT JFET
The study of microstrip antenna arrays and related problems
[NASA-CR-174054] 02 p0189 N85-11265
Gamma-induced leakage in junction field-effect transistors
[DE84-014990] 04 p0570 N85-13634
Simulation of solidification in a Bridgman cell
[NASA-CR-175838] 16 p2870 N85-27705
High voltage lateral power transistors: Theory and design 19 p3257 N85-30194
Method of characterizing critical timing paths and analyzing timing related failure modes in very large scale integrated circuits
[AD-D011731] 22 p3759 N85-33298

JUNGLES
U TROPICAL REGIONS

JUPITER (PLANET)
Charged particle erosion of icy satellites: Coronal atmospheres and surface redistribution
03 p0448 N85-12845
Temporal and spatial variations in the intensity of ultraviolet emissions from Jupiter and the Io torus
03 p0448 N85-12846
Measurements of H2O in Jupiter's atmosphere from 5 microns airborne observations 08 p1244 N85-17854
Analysis of Jovian decametric data: Study of radio emission mechanisms
[NASA-CR-174206] 08 p1258 N85-17917
The spatial dependence of the Jovian auroral emissions 11 p1759 N85-21068
Investigations of planetary ring phenomena
13 p2174 N85-23487
Studies of planetary rings 13 p2174 N85-23488
Orbital resonances and planetary accretion in the solar nebula 13 p2179 N85-23523
Analysis of motions of Jupiter's great red spot and white ovals 15 p2670 N85-26472
The asteroid ring 15 p2678 N85-26536
Direct evidence for solar wind control of Jupiter's hectometer-wavelength radio emission
[NASA-TM-86073] 16 p2883 N85-27790
The coorbital hypothesis 22 p3858 N85-33890
The 1986 National Aeronautics and Space Administration authorization
[GPO-47-635] 24 p4166 N85-35829

JUPITER ATMOSPHERE
The Jovian atmospheric window at 2.7 microns: A search for H2S
[NASA-TM-86661] 03 p0445 N85-12836
Lower atmospheric composition of Jupiter from Voyager infrared measurements
[NASA-CR-174196] 05 p0745 N85-14779
Exploration of the solar system by airborne astronomy
08 p1244 N85-17851
Measurements of H2O in Jupiter's atmosphere from 5 microns airborne observations 08 p1244 N85-17854
Near infrared modeling of the equatorial regions of Jupiter and Saturn 09 p1415 N85-18930
Analysis of Jovian low frequency radio emissions
[NASA-CR-174449] 10 p1571 N85-19908
Three dimensional ray tracing of the Jovian magnetosphere in the low frequency range
[NASA-CR-175462] 10 p1571 N85-19909
The Jovian Stratosphere in the ultraviolet
11 p1760 N85-21069
Particle transport in planetary magnetospheres
12 p1954 N85-22275
A Jamin interferometer to determine the helium abundance in the atmosphere of Jupiter
[BONN-IR-83-17] 12 p1961 N85-22329
Analysis of motions of Jupiter's great red spot and white ovals 15 p2670 N85-26472
Dynamics of charged small particles — Jupiter, Saturn magnetospheres 15 p2676 N85-26522
Galileo 15 p2688 N85-26601
Possible period of Jovian activity and possibility of seasons 16 p2723 N85-26810
Monodeurated methane in the outer solar system. 2. Its detection on Uranus at 1.6 microns
[NASA-CR-175762] 16 p2882 N85-27782
The Jovian electron spectrum: 1978-1984
[SH-1.5-19] 23 p3998 N85-34782

JUPITER PROBES
NT GALILEO PROBE
NT GALILEO SPACECRAFT
Galileo 15 p2688 N85-26601

JUPITER RINGS
The Jovian ring 15 p2672 N85-26492
On planetary rings as sources and sinks of magnetospheric plasmas 15 p2677 N85-26526
Future studies of planetary rings by spaceprobes
15 p2679 N85-26541
Jupiter's ring system resolved: Physical properties inferred from the Voyager images
20 p3546 N85-32089

JUPITER SATELLITES
NT CALLISTO
NT EUROPA
NT GALILEAN SATELLITES
NT GANYMEDE
NT IO
Gravity field of the Jovian system from Pioneer and Voyager tracking data 13 p2180 N85-23529
Jupiter/Voyager data analysis
[NASA-CR-175723] 15 p2679 N85-26545
Sixteenth Lunar and Planetary Science Conference. Press abstracts
[NASA-CR-175692] 15 p2680 N85-26548
The energy spectrum of Jovian electrons in interplanetary space
[SH-1.5-18] 21 p3715 N85-33051
The coorbital hypotheses 22 p3858 N85-33890

K

K BAND
U EXTREMELY HIGH FREQUENCIES

K LINES
Variations of the H and K emission lines of singly ionized calcium in the eclipsing binary star system AR Lacertae
02 p0296 N85-11921

K-MESONS
U KAONS

KA BAND
U EXTREMELY HIGH FREQUENCIES

KALMAN FILTERS
Numerical studies in nonlinear filtering
[TWISK-305] 01 p0108 N85-10728
Robust rate control system designs for a submersible
[AD-A144792] 01 p0111 N85-10753
Detection and estimation of image contours
[FUB-35-1983] 01 p0112 N85-10760
Application of modern guidance control theory to a bank-to-turn missile
[AD-A145646] 02 p0166 N85-11123
Improved carrier tracking by smoothing estimators
05 p0623 N85-13989
Algorithm for tracking manuevering object with ambiguous measurements 06 p0791 N85-15057
A semianalytical, artificial satellite orbit propagation procedure based on optimal parameter estimation
[INPE-3301-PRE/613] 10 p1427 N85-18997
Internal variables in the lattice for cholesky factorization. Kalman filtering and model identification
[AD-A149431] 10 p1547 N85-19757
Robust Kalman filtering and its applications
[AD-A149044] 10 p1550 N85-19775
Acta Electronica Sinica (selected articles)
[AD-A148829] 11 p1628 N85-20252
Reference systems for the evaluation of dead-reckoning navigation equipment 13 p1967 N85-22358
Prefiltration in Kalman filter with a priori indeterminacy
13 p2071 N85-22939
Numerical algorithms and software for matrix Riccati equations
[AD-A150148] 13 p2150 N85-23344
Bootstrapping the Kalman filter
[AD-A150509] 13 p2153 N85-23370
Geophysical interpretation of Venus gravity data
13 p2178 N85-23513
Digital computer applications of Kalman filter in target tracking
[AD-A150770] 14 p2404 N85-24821
Investigation of a failure detection/identification system for a tactical aircraft navigation system
[AD-A151846] 15 p2469 N85-25240
Perturbations of Kalman filtering process
15 p2480 N85-25305
Estimation theory applied to improving dynamic structural models
[DE85-004148] 15 p2630 N85-26210
Theory and Applications of State Estimation. NRIMS Summer Seminar Series
[CSIR-SWISK-37] 15 p2635 N85-26244
The Kalman filter 15 p2635 N85-26246
Linear filtering with non-Gaussian initial conditions
15 p2635 N85-26247
Kalman filtering and exponential smoothing in economics 15 p2635 N85-26248
Some aspects of decentralized Kalman filtering
15 p2635 N85-26250
Tracking filters 15 p2635 N85-26252
Applications of Kalman filtering and recursive least-squares in river flow modelling
15 p2636 N85-26254

Formulation and implementation of nonstationary adaptive estimation algorithm with applications to air-data reconstruction
[NASA-TM-86727] 16 p2706 N85-26689
Applied Kalman filtering: An overview
17 p2965 N85-28313
Kalman filtering with a two-state clock model
17 p2965 N85-28314
Kalman filter estimates of the NAVSTAR satellite clock parameters 17 p2965 N85-28315
A plan for the development of inertial reconstruction of initial state clock (IRIS) 17 p2966 N85-28317
Proceedings of the Sixteenth Annual Precise Time and Time Interval (PTTI) Applications and Planning Meeting
[NASA-TM-87561] 18 p3105 N85-29221
Kalman filter modeling 18 p3107 N85-29237
Relationship between Allan variances and Kalman Filter parameters 18 p3107 N85-29238
Some studies in filtering of atmospheric turbulence
[AD-A154042] 19 p3316 N85-30557
A residuals approach to filtering, smoothing and identification for static distributed systems
20 p3418 N85-31213
Parameter estimation in communication system tracking satellite observations
[AD-A155137] 21 p3636 N85-32582
Bayesian vs MAP multiple model adaptive estimation for field of view expansion in tracking airborne targets
[AD-A155468] 21 p3679 N85-32655
Kalman filter time series analysis of gamma-ray data from NaI(T1) detectors for the ND6620 computer
[AD-A154995] 21 p3705 N85-33014
Lectures of a Flight Mechanics Conference — conferences
[ESA-TT-831] 24 p4061 N85-35165
Estimation of flight mechanical variables by means of Kalman filters 24 p4062 N85-35171
Recursive partitioning estimation
24 p4141 N85-35670

KANSAS
The application of remote sensing to resource management and environmental quality programs in Kansas
[E85-10023] 02 p0218 N85-11436
The influence of the number of ground control points on the scene-to-map registration accuracy — Kansas, Louisiana, Mississipp, and Missouri
07 p0986 N85-16264
Petrography, sedimentology, diagenesis, and reservoir characteristics of some Pennsylvanian phylloid algal limestones: Kansas and Utah, USA
09 p1352 N85-18507
Modeling the backscattering and transmission properties of vegetation canopies
[E85-10099] 16 p2909 N85-27320

KAONS
A 1-2 GeV/c beam line for hypernuclear and kaon research
[DE85-007623] 16 p2863 N85-27659
AGS broad band neutrino beam
[DE85-010954] 19 p3366 N85-30675
K(-) hydrogen bound and continuum states in momentum space
[DE85-010429] 22 p3841 N85-33789

KAPITZA RESISTANCE
High specific heat dielectrics and Kapitza resistance at dielectric boundaries
[AD-A148476] 08 p1217 N85-17666

KAPTON (TRADEMARK)
Long-term light induced changes in dark conductivity of kapton
[AD-A148791] 08 p1224 N85-17706
Laboratory studies of Kapton degradation in an oxygen ion beam 13 p1990 N85-22477
Kapton charging characteristics: Effects of material thickness and electron-energy distribution
13 p1996 N85-22513
Study of Kapton under simulated shuttle environment
[NASA-CR-176009] 19 p3225 N85-29997

KARHUNEN-LOEVE EXPANSION
Harmonizable, Cramer, and Karhunen classes of processes
[AD-A144984] 01 p0113 N85-10767

KARMAN VORTEX STREET
Velocity and transient measurements in a shock tube using a hot-wire anemometer
[AD-A154694] 21 p3589 N85-32305

KC-135 AIRCRAFT
U C-135 AIRCRAFT

KELVIN-HELMHOLTZ INSTABILITY
Magnetohydrodynamic (MHD) turbulence in radio galaxies 12 p1958 N85-22305
Magnetic pulsations recorded in northern Scandinavia during the IMS; a study of Pc 4-5 events
14 p2370 N85-24647
Characteristics of Pc 4,5 pulsations and their source mechanisms 14 p2370 N85-24648
A panel method study of vortex sheets with special emphasis on sheets of axisymmetric geometry
[NASA-CR-177385] 21 p3552 N85-32095

KENTUCKY
Image variance and spatial structure in remotely sensed scenes — South Dakota, California, Missouri, Kentucky, Louisiana, Tennessee, District of Columbia, and Oregon
07 p0986 N85-16265
Lithologic and environmental atlas of Berea Sandstone (Mississippian) in the Appalachian Basin
[PB85-129039] 11 p1682 N85-20600

KENYA
Evaluation of carrying capacity and landscape damage in northern Kenya by multistage remote sensing
[DFVLR-FB-84-47] 14 p2347 N85-24514

KEPLER LAWS
Reduction of nonlinear problems to Schroedinger or heat equations: Formation of Kepler orbits, singular solutions for hydrodynamical equations
[REPT-72] 01 p0129 N85-10692
Keplerian and perturbed motion — satellite motion
05 p0598 N85-13808
Spatial mechanics formulas and exercises
05 p0601 N85-13832
Averaging of equations of cometary orbital motion with allowance for nongravitational effects
13 p1978 N85-22411
Nontraditional method for determining unperturbed orbits of unknown space objects using incomplete optical observational data 13 p1979 N85-22417
Using velocity vector in determining Keplerian orbit of geodectic satellite 15 p2478 N85-25297
Diffusion of dust around a central body — Keplerian orbits 15 p2576 N85-26523

KERNEL FUNCTIONS
Small-sample properties of kernel density estimators from randomly right-censored data
[AD-A148752] 09 p1374 N85-18834
A kernel type estimator of a quantile function from right-censored data
[AD-A148753] 09 p1374 N85-18835
Single integral constitutive equations for viscoelastic fluids
[AD-A149410] 10 p1547 N85-19758
On the modified likelihood for density estimation
[AD-A149437] 10 p1547 N85-19759
Quantum mechanical and semiclassical approaches to molecular dynamics
[DE85-003458] 10 p1555 N85-19603
An asymptotically efficient solution to the bandwidth problem of kernel density estimation, revision
[AD-A149600] 12 p1920 N85-22056
Nonparametric estimation of density and hazard rate functions when samples are censored
[AD-A150946] 14 p2411 N85-24868
Extent to which least-squares cross-validation minimizes integrated square error in nonparametric density estimation
[AD-A153789] 18 p3174 N85-29679
Angle averaged Compton cross sections for degenerate electron gases
[AD-A154464] 19 p3371 N85-30908
Memory effects in dynamical many-body systems: The isomneaic (constant-memory) approximation
[AD-A154160] 20 p3520 N85-31689
The NAS kernel benchmark program
[NASA-TM-86711] 21 p3670 N85-32795

KEROGEN
Comparison of isothermal kerogen decomposition results using reactors with different heat-up rates
[DE85-008563] 19 p3237 N85-30068

KEROSENE
Numerical simulations of fuel droplet flows using a Lagrangian triangular mesh
[AD-A146087] 03 p0362 N85-12320
Aircraft wing fuel tank environmental simulator tests for evaluation of antimisting fuels
[FAA-CT-84-15] 07 p0934 N85-15920
Dependence of combustion of homogeneous kerosene-air mixtures on humidity of air
13 p2051 N85-22835
Practical real-time quality control of antimisting kerosene
[DE/FAA/CT-85/1] 18 p3083 N85-29072
Effect of polymer additives on characteristics of direct-current motor with liquid dielectric filler
22 p3772 N85-33376

KETONES
NT ACETONE
NT ACETYLACETONE
Interactions of ketones and hexacarbons
[AD-P004019] 06 p0843 N85-15353
Pseudo-p-1,2,2,9,9,10,10-octofluoro (2,2)-p-cyclophane bis-acid chloride
[AD-D011393] 07 p0919 N85-15818
Polyaromatic ether-sulfone-ketones with fluoro-substituted-p-cyclophane units as cross-linking sites
[AD-D011649] 17 p2933 N85-26105
Spray pyrolysis as a synthetic tool
[AD-A153891] 19 p3234 N85-30047
Analysis of aldehydes and ketones in the gas phase
[PB85-181865] 20 p3426 N85-31281

KEVLAR (TRADEMARK)
Development of failure criterion for Kevlar-epoxy fabric laminates
[NASA-CR-172485] 02 p0170 N85-11138
Chemical modification of the surface of high modulus carbon fibers 04 p0467 N85-12967
Ultrasonic analysis of spherical composite test specimens
[DE85-001591] 07 p0976 N85-16197
Comparison of methods for predicting fiber stresses in a cracked Kevlar/epoxy monolayer
[DE84-016116] 11 p1593 N85-20022
Ultrasonic analysis of Kevlar-epoxy filament wound spherical test specimens
[DE85-005198] 11 p1593 N85-20024
A broadband kevlar radome for shipboard
[AD-P004365] 12 p1826 N85-21459
Impurities in Kevlar 49 fibers
[DE85-004996] 13 p2038 N85-22767
Development of a field repair technique for mini-sandwich Kevlar/epoxy aircraft skin
[AD-A151369] 15 p2503 N85-25439
Effect of low-velocity or ballistic impact damage on the strength of thin composite and aluminum shear panels
[NASA-TP-2441] 16 p2742 N85-26924
Flight service evaluation of composite helicopter components
[NASA-CR-172562] 23 p3909 N85-34222

KEYING
NT FREQUENCY SHIFT KEYING
NT PHASE SHIFT KEYING
A public key cryptographic algorithm based on a generalization of the knapsack problem
[FUB-7-1984] 09 p1313 N85-18250

KIDNEYS
Bioprocessing in space 05 p0690 N85-14439
Distribution of blood flow to brain, kidneys, gut, spleen and posterior extremities in cats in acute hypoxia
07 p1013 N85-16434
Changes in nephron and juxtaglomerular system of primate kidneys under the effect of antiorthostatic hypokinesia 19 p3326 N85-30605
Kidney cell electrophoresis
[NASA-CR-171869] 20 p3498 N85-31745
Task description for the 1983 catalog of tasks for the materials processing in space program
20 p3498 N85-31746
Kidney cell electrophoresis, continuing task
20 p3498 N85-31747
Effect of passage number on electrophoretic mobility distributions of cultured human embryonic kidney cells
20 p3501 N85-31762
Density gradient electrophoresis of cultured human embryonic kidney cells 20 p3501 N85-31763
Identification and quantitation of morphological cell types in electrophoretically separated human embryonic kidney cell cultures 20 p3501 N85-31764
Urokinase production by electrophoretically separated cultured human embryonic kidney cells
20 p3501 N85-31765
Summary electrophoretic data base on human embryonic kidney cell strain 8514
20 p3501 N85-31766
A critical synopsis: Continuous growth of proximal tubular kidney epithelial cells in hormone-supplemented serum-free medium 20 p3501 N85-31767
The Fibrin slide assay for detecting urokinase activity in human fetal kidney cells 20 p3502 N85-31768
Results of computer calculations for a simulated distribution of kidney cells 20 p3502 N85-31771
Evaluation of results of cell electrophoresis experiments on space shuttle STS-3 including pre-flight and post-flight laboratory experiments 20 p3502 N85-31772
Pre-flight report on cultured human embryonic kidney cell handling and cell electrophoresis. Prepared prior to continuous-flow electrophoretic separation experiments aboard space shuttle flight STS-8
20 p3503 N85-31775
Properties of electrophoretic fractions of human embryonic kidney cells separated on space shuttle flight STS-8 20 p3503 N85-31776
Detection of internal structure by scattered light intensity: Application to kidney cell sorting
20 p3503 N85-31777

Flow cytometry of human embryonic kidney cells: A light scattering approach 20 p3503 N85-31778
KILOMETRIC WAVES
Theory and computer simulation of auroral kilometric radiation 14 p2365 N85-24617
The IMS advances in understanding terrestrial myriametric radiation 14 p2365 N85-24618
Terrestrial continuum radiation study during the IMS 14 p2365 N85-24619
KIMBERLITE
U BIOTITE
U PERIDOTITE
KINEMATIC EQUATIONS
A triangular finite element for thin plates and shells 01 p0058 N85-10386
Local galactic kinematics 05 p0741 N85-14785
Translational control of a graphically simulated robot arm by kinematic rate equations that overcome elbow joint singularity
[NASA-TP-2376] 06 p0856 N85-15448
Equations and algorithms for meteorological applications in air weather service
[AD-A148894] 10 p1519 N85-19575
Kinematic dynamo theory for an arbitrary mean flow 14 p2448 N85-25108
The generation of magnetic fields by a flow with chaotic streamlines 14 p2451 N85-25135
Application of quaternions to problems of solid body dynamics in the atmosphere 15 p2481 N85-25313
Kinematic rate control of simulated robot hand at or near wrist singularity
[NASA-TP-2440] 16 p2851 N85-27575
Computer methods in manipulator kinematics, dynamics and control: A comparative study 20 p3462 N85-31506
Coordinate transformations and programming for small revolute coordinate robots
[RR-273] 20 p3519 N85-31661
KINEMATICS
NT BODY KINEMATICS
Kinematic synthesis of planar cam-link mechanisms for exact path and exact motion generation 03 p0341 N85-12189
Optimization of movements of manipulators with kinematic redundancy 04 p0488 N85-13112
Preliminary grouping in A strong-current linear ion accelerator with a low injection energy
[DE84-017192] 04 p0563 N85-13587
Instantaneous kinematics and joint displacement analysis of fully-parallel robotic devices 05 p0641 N85-14113
Proper motions and kinematical properties of Orion trapezium type stellar systems 05 p0739 N85-14755
Kinematics of B and A stars 05 p0741 N85-14786
Anomalous magnetic field in northwestern Pacific Ocean and Pacific Ocean plate kinematics 06 p0820 N85-15210
Observations of highly-ionized interstellar iron 06 p0876 N85-15565
Kinematics of nearby gas and stars 05 p0880 N85-15591
Phase 1-A development kinematic Sterling/Rankine commercial gas-fired heat pump research program
[PB85-100931/GAR] 07 p0936 N85-15928
Automatic camera tracking for remote manipulators
[DE85-001897] 07 p0974 N85-16187
Modeling of human motion by computer considering measurement errors in initial data 07 p1012 N85-16429
Southern ocean sea-ice morphology and kinematics 06 p1144 N85-17217
The analysis of kinematic restraint and freedom using point contacts
[RR-154/03/75/02] 08 p1169 N85-17372
The synthesis of kinematic restraint and freedom using point contacts
[RR-154/03/75/03] 08 p1169 N85-17373
A free shear layer prediction of the turbulent wake of a flat plate towed below a free surface
[AD-A148699] 09 p1319 N85-18293
Large deformations of a nonlinear elastic solid and the diffusion of an ideal fluid treated as interacting continua 09 p1330 N85-18356
Physics of nonmagnetic relativistic thermal plasmas 09 p1386 N85-18715
The research of driving wheel with movable lugs of the paddy field floating tractor
[AD-P004283] 09 p1407 N85-18880
Advanced stress analysis methods applicable to turbine engine structures
[NASA-CR-175573] 12 p1778 N85-21165
Mechanical properties for the grasp of a robotic hand
[AD-A150062] 12 p1880 N85-21669
Assembly robot control algorithms 13 p2046 N85-22606
On Hybrid and mixed finite element methods
[NASA-CR-175551] 13 p2101 N85-23096
New methods for interpreting seismic time fields in media with variable velocities 14 p2343 N85-24490
Practical methods for the compensation and control of multivariable systems
[AD-A151047] 14 p2407 N85-24841
Mixing in the solar interior 14 p2446 N85-25095
The kinematic control of redundant manipulators 15 p2566 N85-25836
Manipulation and simulation of general robots using the zero-position description 15 p2567 N85-25838
Optimum rotation of solid body with 1 axis of symmetry 16 p2718 N85-26781
Structural design and kinematic configuration of two-armed robots 16 p2761 N85-27037
A general simulation program for robot manipulator arm dynamics
[AD-A152121] 16 p2783 N85-27230
Nonlinear equations for dynamics of preinisted beams undergoing small strains and large rotations
[NASA-TP-2470] 16 p2799 N85-27258
On the accurate representation of large strain non-proportional plastic flow in ductile materials
[DE85-007106] 16 p2801 N85-27273
Dynamic creep buckling: Analysis of shell structures subjected to time-dependent mechanical and thermal loading 17 p2913 N85-27959
The position and mobility of the shoulder, spinal column and pelvis in seated subjects
[AD-A153751] 18 p3153 N85-29524
Application of the ADAMS program to deployable space truss structures
[NASA-CR-177927] 19 p3284 N85-30366
Spiral bevel and circular arc helical gears: Tooth contact analysis and the effect of misalignment on circular arc helical gears
[NASA-TM-87013] 20 p3395 N85-31060
Computer methods in manipulator kinematics, dynamics and control: A comparative study 20 p3462 N85-31506
A versatile computer package for mechanism analysis 23 p3924 N85-34314
Calculation of flow kinetics of composite media
[BLL-M-35819-(5828.4)] 23 p3929 N85-34348
Generated spiral bevel gears: Optimal machine-tool settings and tooth contact analysis
[NASA-TM-87075] 23 p3937 N85-34405
Non-rigid body motion 23 p3964 N85-34576
The kinematic structure of cold frontal rainbands 24 p4119 N85-35531
Kinematic analysis of Hurricane Frederick (1979) using satellite, aircraft and rawinsonde data
[NASA-CR-176167] 24 p4119 N85-35533
KINESCOPES
U PICTURE TUBES
KINESTHESIS
U PROPRIOCEPTION
KINETIC ENERGY
Observations of the vertical structure of the eddy field in the Kuroshio extension
[AD-A145178] 01 p0089 N85-10599
Laser spectroscopy of combustion intermediates
[DE84-016101] 02 p0173 N85-11161
Comparison of wide aperture and short residence time ion lenses
[DE84-015274] 03 p0420 N85-12885
Reaction wheels for kinetic energy storage 05 p0607 N85-13874
Comparison of forecast and observed energetics 05 p0683 N85-14389
Motion of heavy symmetric body with flexible bars about stationary point 06 p0780 N85-14989
Measurement of proton autoneutralization potential
[DE85-001752] 06 p0885 N85-15501
The influence of deep cumulus convection on large-scale flow during AVE/SESAME 1, 10-11 April 1979 09 p1355 N85-18526
IREB (Intense Relativistic Electron Beam) converter to ac pulses
[AD-D011479] 10 p1554 N85-19800
An orthogonal grid technique for studying internal deformation and energy absorption in target penetration
[AD-A149969] 12 p1880 N85-21655
Theoretical study of collective ion acceleration in the Luce diode
[AD-A150107] 12 p1929 N85-22116
A method for the evaluation of the residual energy of a metallic fragment after perforation of a thin target
[ISL-R-113/83] 16 p2794 N85-27233
Applications of Canuto's method to Rayleigh-Taylor-initiated turbulence
[DE85-010835] 18 p3102 N85-29202
Comparison of forecast and observed energetics 18 p3143 N85-29459
An implicit finite-difference code for a two-equation turbulence model for three-dimensional flows
[NASA-TM-86752] 20 p3454 N85-31448
Numerical solutions of turbulent models for flow over a flat plate with angle of attack
[DE85-010380] 21 p3586 N85-32266
The calculation of two-dimensional buoyant surface jets with the k-W model of turbulence — kinetic energy-vorticity fluctuations (k-W)
[CFD/84/21] 22 p3765 N85-33448
Dynamics of Mesoscale Weather Systems: 1984 Summer Colloquium
[PB85-188266] 22 p3817 N85-33849
Parametrized energy spectrum of cosmic-ray protons with kinetic energies down to 1 GeV
[OG-4.2-11] 22 p3878 N85-34025
SONTRAC: A solar neutron track chamber detector
[SH-9.1-12] 23 p4052 N85-35127
Prediction of turbulent internal recirculating flows with K-epsilon models 24 p4092 N85-35366
Kinematic analysis of Hurricane Frederick (1979) using satellite, aircraft and rawinsonde data
[NASA-CR-176167] 24 p4119 N85-35533
Turbulent structure of stably stratified nocturnal slope flows
[AD-A155845] 24 p4123 N85-35559
Two-point closure study of covariance budgets for turbulent Rayleigh-Benard convection
[PB85-189106] 24 p4124 N85-35568
Experimental evidence of the decrease of kinetic energy of hadrons in passing through atomic nuclei 24 p4174 N85-35880
KINETIC EQUATIONS
NT HELMHOLTZ VORTICITY EQUATION
NT HYDRODYNAMIC EQUATIONS
NT KINEMATIC EQUATIONS
Hamiltonian and Lagrangian theory of gyrokinetic equations 02 p0283 N85-11845
Integral of wave kinetic equation of drift waves 02 p0283 N85-11848
Interplanetary trajectories 05 p0600 N85-13627
A propagator expansion method for solving linearized plasma kinetic equations with collisions
[AD-A147524] 07 p1045 N85-16640
Theoretical thermodynamics of mixtures at high pressures 13 p2183 N85-23550
Analysis of nonlinear parabolic equations modeling plasma diffusion across a magnetic field
[DE85-007663] 17 p3040 N85-28607
The effects of weak turubience on parametric processes in an unmagnetized plasma 19 p3369 N85-30866
Collisional transport for a superthermal ion species in a plasma
[DE85-011943] 22 p3845 N85-33818
Guiding center distribution function and longitudinal invariant 23 p3978 N85-34663
KINETIC FRICTION
NT SLIDING FRICTION
Turbine blade damping study
[NASA-CR-171255] 04 p0456 N85-12890
Forced vibrations of friction-damped beam structures in two dimensions
[UDR-TM-82-06] 04 p0456 N85-12892
The effect of frictional forces on fatigue crack growth in lugs
[AD-A151994] 15 p2578 N85-25896
Kinetic friction coefficient of ice
[AD-A155035] 21 p3680 N85-32859
KINETIC HEATING
NT AERODYNAMIC HEATING
NT SHOCK HEATING
An experimental investigation and numerical simulation of the thermomechanical phenomena in compressor rotor tip rubbing 03 p0367 N85-12352
An analysis of the feasibility of producing silicon for solar cells by a dichlorosilane/fluidized-bed reactor process
[NASA-CR-176036] 20 p3478 N85-31614
High pressure working mode of hollow cathode arc discharges
[NASA-TM-77880] 20 p3535 N85-31992
KINETIC THEORY
NT CHAPMAN-ENSKOG THEORY
NT MIXING LENGTH FLOW THEORY
NT TRANSPORT THEORY
A propagator expansion method for solving linearized plasma kinetic equations with collisions
[AD-A147524] 07 p1045 N85-16640
Kinetic Rayleigh-Taylor instability theory in the ionosphere near equator 13 p2067 N85-22911
Kinetic theory and simulation of multi-species plasmas in Tokamaks excited with ICRF microwaves
[DE85-008119] 16 p2868 N85-27691
Megajoule-class single-pulse KrF laser test facility as a logical step toward inertial fusion commercialization
[DE85-009590] 18 p3191 N85-29794

The balancing of complex linkage mechanisms
23 p3924 N85-34313

KINETICS
NT ELECTROKINETICS
NT KINETIC ENERGY
NT NEWTON THEORY
NT REACTION KINETICS
NT VARIABLE MASS SYSTEMS

Experiment on nowcasting of heavy rainfall and severe storms in central China in 1979-1981
01 p0061 N85-10545

Kinetics of simple inner- and outer-sphere electrochemical reactions at rotating silver electrodes as examined using surface-enhanced Raman spectroscopy
[AD-A145608] 02 p0172 N85-11154

Surface environmental effects in electrochemical kinetics: Outer-sphere chromium (3) reductions at mercury, gallium, lead, and thallium surfaces
[AD-A145607] 02 p0172 N85-11155

Solvent effects upon electrochemical kinetics: Influences of interfacial solvation and solvent relaxation dynamics
[AD-A145624] 02 p0173 N85-11156

The observation of a single thermoluminescence glow peak described by kinetics more general than the usual 1st and 2nd order kinetics
[DE84-014697] 02 p0173 N85-11160

Critical assessment of low fluence irradiation creep mechanisms
[DE84-015578] 02 p0184 N85-11232

Kinetics of short-range ordering in metallic glasses: Analysis of the crossover effect
[DE84-015524] 02 p0187 N85-11251

Quantum characteristics of kinetic fracturing of solids
02 p0265 N85-11732

Theory of kinetics of impregnation of porous bodies
[BLL-M-35917-(5828.4)] 05 p0616 N85-13942

An analysis of kinetic response variability
05 p0707 N85-14533

Influence of the mechanical and electrochemical characteristics of austenitic and austenoferritic steels on the propagation rate and morphology of stress corrosion cracking
[BLL-RISLEY-TR-4545-(9091.9F)]
06 p0767 N85-14906

Nitriding of titanium and its alloys by N2, NH3 or mixtures of N2 + H2 in a dc arc plasma at low pressures (or = to torr)
[NASA-TM-83803] 06 p0814 N85-15168

Review of the toxicokinetics of n-hexane
[AD-P004018] 06 p0843 N85-15352

Evaluation of jet fuel deposit kinetics. Lot 4
[AD-A147196] 07 p0935 N85-15922

Variation in photosynthesis with light level for model with two photochemical reactions 07 p1012 N85-16430

Effect of clause on sarcoplasmic reticulum in fast and slow skeletal muscle
[NASA-CR-174337] 08 p1191 N85-17508

Studies of the kinetics and mechanisms of ammonia synthesis and hydrodesulfurization on metal single crystal surfaces
[DE85-001650] 11 p1595 N85-20030

Semiconductor electrochemistry approach to the study of oxide films on nickel electrodes
[DE85-003042] 11 p1630 N85-20264

Saturation kinetics of active medium of oxygen-iodine laser 11 p1718 N85-20807

Shock tube study of the fuel structure effects on the chemical kinetic mechanisms responsible for soot formation, part 2
[NASA-CR-174880] 15 p2504 N85-25444

Kinetics and structure of excited states
[AD-A151902] 15 p2648 N85-26334

Study of the kinetics and thermodynamics of hydrogen in Pd-based alloys
[DE85-007341] 16 p2750 N85-26969

Future fundamental combustion research for aeropropulsion systems
[NASA-TM-87049] 17 p2898 N85-27870

Dynamic creep buckling: Analysis of shell structures subjected to time-dependent mechanical and thermal loading 17 p2913 N85-27959

Research on the kinetics of phase changes in solids
[AD-A152387] 17 p2918 N85-27969

Detailed chemical kinetic study of the effect of molecular structure on autoignition of fuel-air mixtures
[DE85-004424] 17 p2921 N85-28010

Study of the kinetics of hydrogenation using aged catalysts
[DE85-010427] 19 p3230 N85-30025

Kinetics of H-induced stress corrosion cracking. Part 1: Important features of cracking in respect of high strength steels
[BLL-BISI-TRANS-(9022.06)] 19 p3282 N85-30350

Calculation of molecular constants potential energy curves and Franck-Condon factors for lead oxide
[AD-A154521] 21 p3562 N85-32158

The effect of prior parent phase cold work on martensite transformation in Cu-Zn-Al shape memory alloys
[AD-A155140] 21 p3566 N85-32183

Microscopic control of semiconductor surface oxidation
[AD-A154799] 21 p3709 N85-33026

Determination of kinetic parameters of molecular beam epitaxy
[AD-A155222] 21 p3710 N85-33030

KIRCHHOFF LAW OF RADIATION
Toward the theory of acoustic scattering on uneven free surface 21 p3880 N85-32862

Applications of the Kirchoff-Helmholtz integral to problems in body wave seismology
24 p4116 N85-35515

KIRCHHOFF-HELMHOLTZ FLOW
U PIPE FLOW

KIRCHHOFF-HUYGENS PRINCIPLE
U DIFFRACTION
U WAVE PROPAGATION

KITE BALLOONS
U TETHERED BALLOONS

KITS
Robotic order picking
[AD-D011737] 22 p3792 N85-33493

KLYSTRONS
Methods to increase linac efficiency
[DE84-014692] 01 p0116 N85-10609

Quasi-optical harmonic gyrotron and gyroklystron
[AD-D011308] 07 p0947 N85-16001

Multimode harmonic power measurement of 40 MW pulsed S-band klystrons
[DE85-001560] 09 p1316 N85-18272

The effects of mode impurity of Ka-band system performance 10 p1463 N85-19227

Feasibility study for a 34 GHz (Ka band) gyroamplifier
[NASA-CR-174439] 10 p1477 N85-19325

Notes on the RF system for the SLC positron source
[DE85-002628] 11 p1722 N85-20830

Design and testing of gyroklystron amplifiers
[AD-A151026] 14 p2298 N85-24231

VULTURE manual
[DE85-006873] 17 p3013 N85-28631

Coherent X-rays and vacuum-ultraviolet radiation from storage-ring-based undulators and free electron lasers
[DE85-009968] 18 p3183 N85-29736

A collective interaction klystron specification
[AD-D011704] 19 p3255 N85-30186

Los Alamos Free-Electron Laser (FEL) RF system
[DE85-010719] 19 p3278 N85-30329

Quasioptical gyroklystron
[AD-D011666] 19 p3358 N85-30801

Research on gyrotrons
[AD-A154032] 23 p3934 N85-34360

Solid state high power amplifier for driving the SLC injector klystron
[DE85-013063] 24 p4090 N85-35356

SLC Energy Upgrade Program at SLAC
[DE85-014290] 24 p4160 N85-35790

KNEE (ANATOMY)
Elbow and knee joint for hard space suits and the like
[NASA-CASE-ARC-11610-1] 11 p1697 N85-20666

KNIGHT SHIFT
U NUCLEAR MAGNETIC RESONANCE

KNOOP HARDNESS
Surface mechanical properties and wear behavior of ion implanted TiB2
[DE85-001130] 09 p1295 N85-18133

KNOWLEDGE
NT PARADOXES
NT PHILOSOPHY

Knowledge representation and natural-language semantics
[AD-A146025] 03 p0409 N85-12815

Getting mental models and computer models to cooperate 05 p0709 N85-14548

Distributed knowledge base systems for diagnosis and information retrieval
[AD-A146890] 07 p1054 N85-16690

Research on knowledge delivery
[AD-A149565] 10 p1538 N85-19698

Integrating non-semantic knowledge into image segmentation processes
[AD-A149571] 12 p1851 N85-21612

The role of prior knowledge in operating equipment from written instructions
[AD-A151007] 14 p2392 N85-24730

A simple software environment based on objects and relations
[AD-A155704] 21 p3673 N85-32817

Knowledge engineering application in image processing 23 p3965 N85-34583

KNOWLEDGE ENGINEERING
U EXPERT SYSTEMS

KNUDSEN FLOW
Close-spaced high temperature Knudsen flow
[AD-A148477] 08 p1178 N85-17424

KNUDSEN NUMBER
U KNUDSEN FLOW

KOLMOGOROFF THEORY
Closure problem and numerical studies of turbulence
08 p1209 N85-17608

Modeling of shear flow in a stratified fluid
14 p2340 N85-24489

Kolmogorov and scalar spectral regimes in numerical turbulence
[NASA-TM-86699] 17 p2957 N85-28264

KOLMOGOROFF-SMIRNOFF TEST
Kolmogorov-Smirnov goodness-of-fit test: Corrected for use with EEG-like data
[AD-A144711] 01 p0110 N85-10745

A new statistic for the analysis of circular data in gamma-ray astronomy
[OG-9.5-13] 23 p4031 N85-34989

KONDO EFFECT
Green's function solution of the Kondo problems and universality of the thermodynamic properties
[DE85-002739] 12 p1943 N85-22206

Very low temperature studies of hyperfine effects in metals
[DE85-013367] 22 p3749 N85-33236

KOREA
Limited surface observations climatic summary (LISOCS). Camp Casey, Tong Du Chon, Korea
[AD-A147204] 07 p1007 N85-16397

KORTEWEG-DEVRIES EQUATION
Stochastic property of K-dV solitons perturbed by random forces — Korteweg-Devries equation
02 p0283 N85-11843

Lax-pair operators for squared-sum and squared-difference eigenfunctions
[AD-B069083L] 09 p1388 N85-18718

Long nonlinear waves in layers of sudden changes in wind velocity 14 p2340 N85-24470

Internal waves in marine straits
[PREPRINT-415] 18 p3151 N85-29510

Approximate inverse spectral transform for the Korteweg-de Vries equation
[PREPRINT-411] 18 p3172 N85-29658

KOVAR (TRADEMARK)
Sintering and properties of metal-ceramic alloys of the Kovar type
[BLL-BISI-TRANS-21822-(9022.08)]
17 p2927 N85-28080

Slow crack growth in metal reinforced glass composites
[DE85-010094] 18 p3062 N85-29064

KRIGING
Analysis of geohydrologic data by kriging
[AD-P004152] 09 p1349 N85-18488

KRONECKER PRODUCT
U ORTHOGONALITY

KRYPTON
NT KRYPTON ISOTOPES
NT KRYPTON 85

IUE observations of the gaseous component of the local interstellar medium 06 p0874 N85-15553

Optogalvanic measurement of even parity Rydberg levels in krypton gas
[AD-A152113] 16 p2745 N85-26943

Modification of the grain size of sputtered copper with additions of oxygen, krypton, silver, or yttrium
[DE85-010975] 21 p3567 N85-32189

Interactions of heavy nuclei, Kr, Xe and Ho, in light targets
[OG-7.2-21] 23 p4016 N85-34868

KRYPTON FLUORIDE LASERS
An 850 J, 150 ns narrow-band krypton fluoride laser
[DE84-013077] 04 p0508 N85-13228

Investigation of dye lasers pumped by high-power KrF laser radiation 11 p1718 N85-20808

Time-resolved studies of rapid solidification in highly undercooled molten silicon
[DE85-004857] 13 p2038 N85-22765

Design optimization of singlemain-amplifier KrF laser-fusion systems
[DE85-007680] 16 p2791 N85-27215

KrF laser cost/performance model for ICF commercial applications
[DE85-009580] 18 p3182 N85-29728

Megajoule-class single-pulse KrF laser test facility as a logical step toward inertial fusion commercialization
[DE85-009590] 18 p3191 N85-29794

Summary of research for the Inertial Confinement Fusion Program at Los Alamos National Laboratory
[DE85-010930] 19 p3361 N85-30836

Magnetic fields in laser heated plasmas
[DE85-010715] 21 p3707 N85-33022

KRYPTON ISOTOPES
NT KRYPTON 85
Proposed solar neutrino experiment using (81)Br(nu,e(-)) (81)Kr
[DE85-004602] 15 p2684 N85-26579
KRYPTON 85
The 1984 environmental monitoring report, Sandia National Laboratories, Albuquerque, New Mexico
[DE85-011175] 22 p3811 N85-33607
KU BAND
U SUPERHIGH FREQUENCIES
KUIPER AIRBORNE OBSERVATORY
U C-141 AIRCRAFT
KURILE ISLANDS
Basic structural features and probable mechanism of formation of the Kuril Island system
10 p1501 N86-19472

L

L BAND
U ULTRAHIGH FREQUENCIES
L-SAT
Derivation of the Olympus solar array requirements
13 p2009 N85-22598
The Olympus solar array development and test program 13 p2009 N85-22599
Design and qualification testing of the Olympus solar array blanket 13 p2009 N85-22600
The performance of the Olympus power subsystem with its solar array 13 p2009 N85-22601
L-1011 AIRCRAFT
Advanced manufacturing development of a composite empennage component for L-1011 aircraft
[NASA-CR-165885] 02 p0170 N85-11141
Flight service evaluation of advanced composite ailerons on the L-1011 transport aircraft
[NASA-CR-172483] 08 p1116 N85-17049
LABELING (MARKING)
U MARKING
LABOR
New PCB production for robotics application
11 p1617 N85-20169
Cardiorespiratory function and work performance during adaptation to industrial labor in midalpine conditions
22 p3820 N85-33665
LABORATORIES
NT ENVIRONMENTAL LABORATORIES
NT LONG DURATION EXPOSURE FACILITY
NT MANNED ORBITAL LABORATORIES
NT MANNED ORBITAL RESEARCH LABORATORIES
NT SPACE LABORATORIES
NT SPACELAB
NT UNDERWATER RESEARCH LABORATORIES
Spring program summary, 1983
[PB84-222223] 06 p0830 N85-15330
Emerging role of the national laboratory in the development and transfer of materials technology
[DE85-001252] 09 p1288 N85-18086
Robotics in the radiochemical laboratory
[DE85-002824] 10 p1494 N85-19433
The use of small mobile radars to detect, monitor, and quantify bird movements
[AD-P004188] 11 p1580 N85-19951
Personal desktop computing in a research and development laboratory
[DE85-002765] 11 p1705 N85-20728
State measurement laboratories: Program description (part 1). Directory (part 2)
[PB85-137651] 11 p1739 N85-20935
JPL highlights, 1983
[NASA-CR-175558] 12 p1951 N85-22256
Accomplishments of Institute of Cartography summarized 13 p2166 N85-23435
JESS facility modification and environmental/power plans
[NASA-CR-175695] 14 p2227 N85-23607
Fiscal year 1986 technical objective document
[AD-A151039] 14 p2432 N85-25000
AFRPL (Air Force Rocket Propulsion Laboratory) technical objective document FY 85
[AD-A151398] 15 p2495 N85-25389
The human engineering of laboratory data acquisition and control systems
[AD-A151576] 15 p2620 N85-26148
Physics, Computer Science and Mathematics Div.
[DE85-009888] 15 p2642 N85-26298
Design and implementation of the digital engineering laboratory distributed database management system
[AD-A151694] 15 p2665 N85-26460
Guide for the execution of reliability tests in the laboratory — aeronautical equipment
16 p2736 N85-27237
Laboratory research: A question of when, not if
[AD-A153236] 17 p3048 N85-28687
Technical services at NLR
[B6561898] 17 p3049 N85-28871
New technologies to improve laboratory testing
[DE85-006151] 18 p3110 N85-29257
Selected university laboratory needs in support of national security
[AD-A153511] 18 p3197 N85-29633
Current activities and background of technology transfer and exchange program at Lawrence Livermore National Laboratory
[DE85-009526] 18 p3199 N85-29643
Publications of the Jet Propulsion Laboratory 1983
[NASA-CR-175979] 18 p3199 N85-29648
Technical and administrative activities of the Analytical Chemistry Laboratory (ACL)
[DE85-010150] 19 p3236 N85-30063
Clay identification and amount measured by laboratory technique compared to well log responses: Application to tight gas sands and shales
[DE85-010411] 19 p3362 N85-30843
Computerized Laboratory Analytical and Diagnostic Services (CLADS)
[DE85-010854] 20 p3518 N85-31871
The flow of scientific and technical information in the US Army Research Laboratories
[AD-A155050] 21 p3713 N85-33043
The 1984 effluent and environmental monitoring report for the Bettis Atomic Power Laboratory
[DE85-011533] 22 p3810 N85-33602
Environmental monitoring at Lawrence Livermore National Laboratory: 1984 report
[DE85-011593] 22 p3811 N85-33606
Laboratory evaluation and application of microwave absorption properties under simulated conditions for planetary atmospheres
[NASA-CR-176078] 22 p3851 N85-33847
Procedure for editing the fluxgate magnetometer data of the AFGL (Air Force Geophysics Laboratory) magnetometer network
[AD-A156331] 24 p4117 N85-35523
Progress report on implementing the recommendations of the White House Science Council's Federal Laboratory Review Panel, volume 1
[PB85-185072] 24 p4184 N85-35819
Search for proton decay in the Frejus experiment
[HE-6.2-2] 24 p4210 N85-36138
LABORATORY EQUIPMENT
NT IMAGE FURNACES
An inexpensive microcomputer for laboratory data acquisition and test equipment control
[AD-A146095] 03 p0403 N85-12587
Spacelab mission D1 Frog statolith experiment STATEX: Hardware family and experiment operational sequence
05 p0589 N85-14425
Sampling device
[AD-D011256] 06 p0814 N85-15166
A validated methodology for determination of laboratory instrument computer interface efficacy
[AD-A149336] 10 p1487 N85-19391
Robotics at Savannah River site: Activity report
[DE85-003657] 11 p1648 N85-20383
European Space Tribology Laboratory: Facilities, services, capabilities
[ESA-BR-12] 20 p3398 N85-31080
Recommendations and calculations concerning physical characteristics of the EEVT apparatus
20 p3502 N85-31769
A gel-halo sample pellet: The best of both worlds? Stubby zones without a constricted sample gate
20 p3502 N85-31770
Recommendations for the design and equipping of engineering metrology laboratories
[NPL-MOM-22] 23 p3868 N85-34145
LABRADOR
Drifting buoys on the Labrador shelf
14 p2331 N85-24415
LABYRINTH
NT COCHLEA
NT VESTIBULES
Prediction of seasickness susceptibility
11 p1693 N85-20647
Dissociation of autonomic and sensory vestibular reactions 23 p3953 N85-34501
LABYRINTH SEALS
Theoretical approach to labyrinth seal forces - cross-coupled stiffness of a straight-through labyrinth seal 05 p0643 N85-14127
Experimental investigation of lateral forces induced by flow through model labyrinth glands
05 p0643 N85-14128
Analysis of dynamic characteristics of fluid force induced by labyrinth seal 05 p0643 N85-14129
Prediction of force coefficients for labyrinth seals
05 p0644 N85-14130
An Iwatsubo-based solution for labyrinth seals - comparison with experimental results
05 p0644 N85-14131
Preliminary investigation of labyrinth packing pressure drops at onset of swirl-induced rotor instability
05 p0644 N85-14132
Repair welding and brazing procedures for turbine components and investigation of the brazing behavior of thin filler foils
[MTU-TB-906/84] 07 p0974 N85-16180
Analytical and experimental investigation of rubbing interaction in labyrinth seals for a liquid hydrogen fuel pump — space shuttle main engine
[NASA-CR-174657] 09 p1287 N85-18084
LACQUERS
New air-curing lacquer systems with high solids content
[BMFT-FB-T-85-005] 17 p2936 N85-28124
Oxidation resistant slurry coating for carbon-based materials
[NASA-CASE-LEW-13923-1] 24 p4077 N85-35267
LAG (DELAY)
U TIME LAG
LAGEOS (SATELLITE)
Preliminary processing of laser ranging data from LAGEOS artificial Earth satellite during short merit program observation period 15 p2488 N85-25355
Comparison of gravity field solution techniques
16 p2806 N85-27295
Station coordinates and Earth rotation parameters from Lageos laser ranging 16 p2806 N85-27299
Update on the evolution of the LAGEOS orbit
20 p3491 N85-31698
Effect of solar eclipses on the LAGEOS semimajor axis 20 p3491 N85-31699
Effect of diffusely-reflected sunlight on the orbit of LAGEOS 20 p3491 N85-31700
Ocean tidal parameters from LAGEOS
20 p3493 N85-31716
Earth Albedo and the orbit of LAGEOS
[NASA-TM-86210] 21 p3558 N85-32131
LAGRANGE COORDINATES
Model for high rate gas flows in deformable and reactive porous beds
[DE85-006140] 14 p2253 N85-23984
Users manual for coordinate generation code CRDSRA
[NASA-CR-172584] 17 p2891 N85-27824
Compressible Lagrangian hydrodynamics without Lagrangian cells
[DE85-009597] 20 p3520 N85-31891
Two-dimensional simulation of instability growth due to shocks
[DE85-011869] 22 p3784 N85-33442
Compressible two-phase flow instabilities simulated with a hybrid Lagrange-Euler pseudospectral method
[DE85-009904] 23 p3931 N85-34361
Adaptive rezoner in a two-dimensional Lagrangian hydrodynamic code
[DE85-010108] 24 p4094 N85-35381
LAGRANGE EQUATIONS OF MOTION
U EULER-LAGRANGE EQUATION
LAGRANGE MULTIPLIERS
Fracture, failure, and fragmentation
01 p0059 N85-10390
Some concepts in multi-criteria optimization
[CSIR-TWISK-299] 01 p0108 N85-10722
Numerical simulations of fuel droplet flows using a Lagrangian triangular mesh
[AD-A146087] 03 p0362 N85-12320
Skyrmions and vector mesons: A symmetric approach
[DE84-015297] 04 p0563 N85-13584
Existence, uniqueness and stability conditions for general finite element methods in linear elasticity
09 p1332 N85-18372
Recent advances in hybrid/mixed finite elements
[NASA-CR-175574] 12 p1863 N85-21687
On an iterative scheme for the solution of constrained variational equations
[CSIR-TWISK-341] 13 p2149 N85-23342
The nonlinear analysis of thick composite plates using a cubic spline function
[AD-A152115] 16 p2801 N85-27288
Solving the minimal least squares problem subject to bounds on the variables
[TRITA-NA-8215] 16 p2852 N85-27580
Modern test of chiral anomalies
[DE85-006892] 17 p3020 N85-28660
Computable numerical bounds for Lagrange multipliers of stationary points of nonconvex differentiable nonlinear programs
[AD-A153513] 18 p3189 N85-29633
Numerical methods for the solution of stiff delay differential equations 19 p3334 N85-30683

Model building and practical aspects of nonlinear programming
[AD-A155720] 22 p3829 N85-33711

LAGRANGIAN EQUILIBRIUM POINTS
Lagrangian solutions in photogravitational restricted circular three-body problem 13 p1979 N85-22416
The continuous spectrum of an axisymmetric equilibrium with a mixed poloidal and toroidal magnetic field with gravity included 14 p2450 N85-25128

LAGUERRE FUNCTIONS
Modification of the Week's method for numerical inversion of the Laplace transform
[DE85-006576] 14 p2409 N85-24856
A class of polynomials related to those of Laguerre
[CWI-AM-R8411] 17 p3022 N85-29693

LAKE ICE
NT ICE FLOES
Characteristics of snow cover on sea ice and formation of snow ice II 15 p2582 N85-25924
Great Lakes winter weather and ice conditions for 1982-83
[PB85-165009] 16 p2837 N85-27498

LAKES
NT GREAT LAKES (NORTH AMERICA)
Acid Deposition: Processes of Lake Acidification
[PB84-216175] 01 p0070 N85-10466
Investigation of mineral and thermomineral springs in the Eifel Mountains regarding thermal indications
[BMFT-FB-T-84-019] 02 p0220 N85-11451
Satellite altimetric measurements of lake levels 03 p0383 N85-12447
Late quarterly glaciolacustrine and vegetational history of the Copper River Basin, south-central Alaska 03 p0391 N85-12499
Glacial-lake deposits in the Mount Harper area, Yukon-Tanana Upland 04 p0517 N85-13300
Modeling effects of toxicants on aquatic systems
[DE84-016594] 04 p0531 N85-13396
In-lake water quality management for Lake Eureka: Highlights of third year (1983) operation
[PB85-104149/GAR] 07 p0990 N85-16289
Monitoring approaches for assessing quality of high altitude lakes: Colorado Flat Tops Wilderness Area
[PB85-117232] 11 p1679 N85-20579
Lake ice occurrence as a possible detector of atmospheric CO2 effects on climate
[DE85-002951] 11 p1687 N85-20606
Rationale and basic design for experimental acidification of a lake ecosystem in Northern Wisconsin
[PB85-116077] 12 p1865 N85-21829
A first evaluation of LANDSAT TM data to monitor suspended sediments in lakes -- Lake Chicot, Arkansas 13 p2120 N85-23204
Role of natural dissolved organic compounds in determining the concentrations of americium in natural waters
[DE85-010266] 19 p3229 N85-30022
Microwave hydrology: A trilogy
[NASA-CR-176042] 20 p3477 N85-31603
Empirical methods for predicting eutrophication in impoundments. Report 3. Phase 2. Model refinements
[AD-A155483] 21 p3614 N85-32462
Changes in the organic material in lakes in the blast zone of Mount St. Helens, Washington: Hydrologic effects of the eruptions
[GS-CIRC-850-1] 21 p3630 N85-32551
Sulfur cycling in freshwater sediments 21 p3658 N85-32726
Lake ice occurence as a possible detector of atmospheric CO2 effects on climate
[DE85-012987] 23 p3950 N85-34480

LAMB WAVES
Elastic wave gyrometer
[REPT-26/4924/HF] 20 p3459 N85-31484

LAMBERT LAW
U BOUGUER LAW

LAME WAVE EQUATIONS
Spheroidal functions: Properties and tabulation. Application to antenna synthesis 14 p2396 N85-24758

LAMELLA (METALLURGY)
The growth of twins and twin lamellae in synthetic diamond crystals 02 p0181 N85-11213
Determination of local deformation during explosive welding
[BLL-M-36279-(5828.4)] 20 p3462 N85-31503

LAMINA
U LAYERS

LAMINAR BOUNDARY LAYER
Some important problems in unsteady boundary layers including separation. 1: Nature of singularity on oscillating airfoils
[AD-A147897] 07 p0960 N85-16087
Technology developments for laminar boundary layer control on subsonic transport aircraft 08 p1071 N85-16787
Numerical modeling of steady, laminar free-convective boundary layer flow beneath heated or combusting horizonal surfaces 08 p1160 N85-17318
Aerothermal tests of a 12.5 percent cone at Mach 6.7 for various Reynolds numbers, angles of attack and nose shapes --- conducted in Langley 8-foot high temperature tunnel
[NASA-TP-2345] 08 p1161 N85-17322
Leading edge separation criterion for an oscillating airfoil
[AD-P004175] 09 p1267 N85-17960
Numerical approach for the aerodynamic analysis if airfoils with laminar separation
[NASA-CR-172496] 09 p1273 N85-18001
Velocity measurements in a 3D shock wave laminar boundary layer interaction. Part 1: Low speed 2D LDV measurements
[AD-A149533] 10 p1485 N85-19373
Frequency spectra of turbulent pulsations in stability of laminar boundary layer 11 p1716 N85-20795
Re-design of ARL/HLF (Heated Laminar Flow) body nose region
[AD-A150063] 12 p1846 N85-21585
Generation and development of small-amplitude disturbances in a laminar boundary layer in the presence of an acoustic field
[NASA-TM-77826] 14 p2299 N85-24237
Three-dimensional boundary layer research at NLR 15 p2559 N85-25787
Brief review of current work in the UK on three dimensional boundary layers 15 p2559 N85-25788
Proceedings of the 9th US Air Force and the Federal Republic of Germany Data Exchange Agreement Meeting, Viscous and Interacting Flow Field Effects
[AD-A153020] 17 p2958 N85-28266
Experimental observation of transition behavior on a flat plate 20 p3452 N85-31437
Experiments on the influence of active walls on the initial amplitudes and growths of instability waves
[AD-A154630] 21 p3583 N85-32275

LAMINAR BOUNDARY LAYER SEPARATION
U LAMINAR BOUNDARY LAYER

LAMINAR FLAMES
U FLAMES
U LAMINAR FLOW

LAMINAR FLOW
NT BLASIUS FLOW
NT STRATIFIED FLOW
A review and analysis of boundary layer transition data for turbine application
[NASA-TM-86880] 01 p0047 N85-10306
Laminar flow heat exchangers. Viscosity induced non-uniform flow
[AD-A144777] 01 p0047 N85-10307
Analytical modeling of random thermal fluctuations in the NORDA high-frequency sound scattering facility
[AD-A145024] 01 p0116 N85-10790
Hybrid laminar flow control study
[NASA-CR-165930] 02 p0137 N85-10933
Approximate solution of a laminar flow over a flat plate with suction and pressure gradient
[AD-A145482] 02 p0196 N85-11321
Laminar-to-turbulent flow transition under influence of acoustic oscillations 02 p0260 N85-11701
Linear long-wave stability of cylindrical steady laminar flame in rotating medium 02 p0268 N85-11752
Raman and fluorescence spectroscopy in a methane-nitrous oxide laminar flame
[AD-A146092] 03 p0328 N85-12111
Laminar and turbulent boundary layers in a plane of symmetry
[AD-A146261] 03 p0362 N85-12323
Natural laminar flow airfoil design considerations for winglets on low-speed airplanes
[NASA-CR-3853] 04 p0452 N85-12863
Laminar flame propagation/quench for a parallel-wall duct
[DE84-009773] 04 p0470 N85-12993
Laminar jet issuing into stagnant surroundings -- PHOENICS code
[PDR/CFDU-IC/15] 04 p0501 N85-13200
Friction and heat exchange in laminar and turbulent boundary layers with axisymmetrical bodies exposed to heterogeneous supersonic flow 05 p0724 N85-14655
Investigation of the local mass transfer of a laminar and turbulent falling liquid film
[BLL-T6308/BG/WH792/84] 06 p0807 N85-15130
Laminar separation bubble with transition: Prediction test with local interaction
[BLL-PNR-90231-(8019.3153)] 06 p0808 N85-15132
Towing tank studies of stratified flow over ridges and valleys
[DE84-011418] 06 p0839 N85-15329
Laminar flow over a backward-facing step
[AD-A147469] 07 p0960 N85-16084
Aircraft drag reduction technology 08 p1070 N85-16782
Design studies of thick laminar flow airfoils for low speed flight employing turbulent boundary layer suction over the rear part 08 p1070 N85-16786
Pneumatic turbulators: A device for drag reduction at Reynolds numbers below 5 million 08 p1071 N85-16791
Design guide for fluidic laminar proportional amplifiers and laminar jet angular rate sensors
[AD-A147730] 08 p1161 N85-17328
Experiments on controlled, unsteady, separated turbulent boundary layers
[AD-P004172] 09 p1266 N85-17957
Laminar separation bubble with transition: Prediction test with local interaction -- airfoils
[PNR-90231] 09 p1274 N85-18008
Profile design for wings and propellers
[NASA-TM-77765] 10 p1419 N85-18963
A multistage time-stepping scheme for the Navier-Stokes equations
[NASA-CR-172527] 10 p1483 N85-19365
Research in nonlinear problems of energy: Informal technical report
[DE85-001529] 11 p1595 N85-20031
Pre-turbulence: Transitional Laminar-turbulent flows 11 p1716 N85-20793
Flight-measured laminar boundary-layer transition phenomena including stability theory analysis
[NASA-TP-2417] 12 p1771 N85-21118
Continuous laminar smoke generator
[NASA-CASE-LAR-13014-1] 12 p1781 N85-21178
Kinetics of nitric oxide formation in laminar and turbulent methane combustion
[PB85-149698] 12 p1804 N85-21313
Solution of the three-dimensional Navier-Stokes equations for a steady laminar horseshoe vortex flow
[AD-A149651] 12 p1846 N85-21582
Re-design of ARL/HLF (Heated Laminar Flow) body nose region
[AD-A150063] 12 p1846 N85-21585
Computer-Aided Structural Engineering (CASE) project. Seepage analysis of confined flow problems by the method of fragments (CFRAG)
[AD-A150015] 12 p1875 N85-21762
Hydrodynamic stability problem formulated by numerical solutions of the Navier-Stokes equations 12 p1946 N85-22223
Diffusion deposition in fibrous filters for parallel and transverse flow models
[DE85-006149] 13 p2093 N85-23066
Calibration of sonic valves for the laminar flow control, leading-edge flight test
[NASA-TP-2423] 14 p2210 N85-23707
Calculating boundary layer on profile with laminar and turbulent flow zone 14 p2288 N85-24177
A finite element, Navier-Stokes study of the confined, laminar flow over a downstream facing step 15 p2553 N85-25754
An experimental technique for the study of velocity profiles in a laminar jet using a pulsed nitrogen laser
[AD-A151496] 15 p2558 N85-25771
La Recherche Aerospatiale Bimonthly Bulletin Number 1984-3, 220/May-June
[ESA-TT-862] 16 p2695 N85-26636
Low Reynolds number vehicles
[AGARD-AG-286] 16 p2699 N85-26688
Thermodynamic evaluation of transonic compressor rotors using the finite volume approach
[NASA-CR-175811] 16 p2708 N85-26712
Modeling the role of radicals in the ignition of and flame propagation in hydrogen-air and methane-air mixtures 16 p2744 N85-26955
The overall reaction concept in premixed, laminar, steady-state flames. 2: Initial temperatures and pressures
[AD-A152132] 16 p2746 N85-26844
Boundary layer at moving cylinder surface 16 p2785 N85-27084
Dynamic response of fluid transmission lines
[AD-A151926] 16 p2792 N85-27171
Heat transfer in pipes
[NASA-TM-77938] 17 p2957 N85-28262
A method of determining the suction velocity for laminar flow control of two-dimensional airfoil in incompressible flow
[NAL-TR-845] 18 p3089 N85-28925
A study of aerodynamic control in stalled flight long laminar separation bubble analysis
[AD-A153690] 18 p3089 N85-28930
A model for the combustion of polymethyl methacrylate in air in a laminar diffusion flame
[VTH-LR-438] 18 p3165 N85-29606

Inviscid analysis of two supercritical laminar-flow-control airfoils at design and off-design conditions
[NASA-TM-84657] 19 p3212 N85-29920
Nacelle/pylon/wing integration on a transport model with a natural laminar flow nacelle
[NASA-TP-2439] 19 p3213 N85-29924
Sidewall boundary-layer effects in two-dimensional airfoil testing
[NASA-CR-176034] 20 p3398 N85-31065
Laminar diffusion flames, carbon gasification, and laser diagnostics applied to combustion systems. 1: Laminar diffusion flames with cylindrical symmetry. 2: Diffusion-controlled gasification of carbon particles. 3: Laser diagnostics applied to combustion systems
20 p3423 N85-31243
Transition in a disturbed environment
20 p3452 N85-31436
High Re separated flow solutions using the Navier-Stokes and approximate equations
[AD-A152252] 20 p3454 N85-31451
Vaporization from a heated surface into a saturated stream
[DE85-010484] 20 p3530 N85-31958
Numerical solutions of turbulent models for flow over a flat plate with angle of attack
[DE85-010360] 21 p3585 N85-32266
Theoretical foundations of turbulent flows
21 p3683 N85-32880
Block-implicit calculations of three-dimensional laminar flow in strongly curved ducts
[DE85-009047] 23 p3931 N85-34363
Effects of ambient pressure on the instability of a liquid boiling explosively at the superheat limit
[DE85-009476] 23 p3932 N85-34370

LAMINAR FLOW AIRFOILS
Unsteady Navier-Stokes calculations in an accelerated reference frame
[AD-A151751] 15 p2557 N85-25774
A method of determining the suction velocity for laminar flow control of two-dimensional airfoil in incompressible flow
[NAL-TR-845] 18 p3059 N85-28925

LAMINAR FLOW CONTROL
U BOUNDARY LAYER CONTROL
U LAMINAR BOUNDARY LAYER

LAMINAR HEAT TRANSFER
Laminar heat-transfer distributions on biconics at incidence in hypersonic-hypervelocity flows
[NASA-TP-2213] 07 p0957 N85-16065

LAMINAR JETS
U JET FLOW
U LAMINAR FLOW

LAMINAR WAKES
An experimental study on the instability of a mixing-layer with laminar wake as the initial condition
08 p1076 N85-16824
The mechanisms of flame holding in the wake of a bluff body
[NASA-CR-3866] 12 p1779 N85-21166
A panel method study of vortex sheets with special emphasis on sheets of axisymmetric geometry
[NASA-CR-177365] 21 p3552 N85-32095

LAMINATED MATERIALS
U LAMINATES

LAMINATES
NT PLYWOOD
Development of new and improved polymer matrix resin systems, phase 1
[NASA-CR-166595] 01 p0017 N85-10104
Design sensitivity analysis of an antisymmetric angle-ply laminate
[CSIR-TWISK-318] 01 p0021 N85-10128
Cumulative damage model for advanced composite materials
[AD-A144840] 01 p0022 N85-10135
Composite laminate optimization program suitable for microcomputers 01 p0059 N85-10389
Nonlinear dynamic analysis of sandwich panels
01 p0060 N85-10394
Flight simulation fatigue crack propagation in metal/carbon-epoxy laminates
[NLR-TR-83006-U] 01 p0063 N85-10416
Materials studies for magnetic fusion energy applications at low temperatures, 7
[DE84-013487] 01 p0122 N85-10837
Energy efficient engine. Volume 2. Appendix A: Component development and integration program
[NASA-CR-173085] 02 p0146 N85-10991
Fracture toughness of fibrous composite materials
[NASA-TP-2370] 02 p0170 N85-11136
Investigating compression failure mechanisms in composite laminates with a transparent fiberglass-epoxy birefringent materials
[NASA-TM-86306] 02 p0170 N85-11137
Development of failure criterion for Kevlar-epoxy fabric laminates
[NASA-CR-172465] 02 p0170 N85-11138
The influence of sublaminate cracks on the tension fatigue behavior of a graphite epoxy laminate
[FFA-TN-1984-32] 02 p0210 N85-11386
Calculation of critical temperature for Nb-Cu multilayer film superconductor
[AD-A144321] 02 p0274 N85-11786
Accelerated viscoelastic characterization of T300/5208 graphite-epoxy laminates 03 p0325 N85-12091
Fatigue-impact studies in laminated composites
[AD-A142841] 03 p0326 N85-12097
A digital algorithm for composite laminate analysis: FORTRAN, Revised
[AD-A145833] 03 p0326 N85-12098
Modeling the stress field in laminated composite plates near discontinuities
[PB84-219237] 03 p0327 N85-12103
Evaluation of laterally loaded laminated glass units by theory and experiment
[PB84-218423] 03 p0339 N85-12179
Tensile and crack propagation tests on aluminum alloys of the 2000 and 7000 series in laminated plate and forged products
[M2-678300] 03 p0373 N85-12383
Tough Composite Materials
[NASA-CP-2334] 04 p0463 N85-12941
Characterization of interlaminar crack growth in composites with the double cantilever beam specimen
04 p0463 N85-12942
Characterizing delamination resistance of toughened resin composites 04 p0464 N85-12943
Composite materials characterization and development at AFWAL 04 p0464 N85-12944
Effect of impact damage and open holes on the compression strength of tough resin/high strain fiber laminates 04 p0464 N85-12945
Effects of constituent properties on compression failure mechanisms 04 p0464 N85-12946
The effect of matrix and fiber properties on impact resistance 04 p0464 N85-12947
Development of a heterogeneous laminating resin
04 p0465 N85-12956
Free-edge failures of composite laminates
04 p0467 N85-12971
Flexible matrix composite laminated disk/ring flywheel
05 p0606 N85-13866
Mechanical properties of aligned short carbon fiber reinforced PES and PI laminates
[DFVLR-FB-84-24] 05 p0613 N85-13918
Development of damage in fatigue loaded carbon fiber reinforced plastics 05 p0650 N85-14172
A study of interply layer effects on the free-edge stress field of angleplied laminates
[NASA-TM-86924] 07 p0919 N85-15822
Design procedures for fiber composite structural components: Panels subjected to combined in-plane loads
[NASA-TM-86909] 07 p0919 N85-15823
Modeling localized stress fields in composite laminates
[AD-A148630] 08 p1120 N85-17056
Composite repair of aircraft structures
08 p1120 N85-17059
Contact behavior, impact response and damage in graphite-epoxy laminates subjected to initial stresses
08 p1171 N85-17386
Nonlinear analysis of composite laminates
09 p1288 N85-18087
Delamination growth in graphite epoxy laminates under compressive loads 09 p1288 N85-18088
Development of a heterogeneous laminating resin system
[NASA-CR-172459] 09 p1288 N85-18089
Fracture mechanics analysis and prediction of delamination growth in composite structures
[FFA-TN-1984-45] 09 p1289 N85-18092
Mechanical and transient hygrothermal loading of multilayer orthotropic cylinders 09 p1330 N85-18359
Evaluation of failure criterion for graphite/epoxy fabric laminates
[NASA-CR-172547] 10 p1431 N85-19025
A comprehensive study on sublaminate crack growth stability and its effects on the load-carrying capacity
[AD-A149037] 10 p1432 N85-19028
Impact toughness of composites with layered microstructure of OT4 titanium alloy
10 p1445 N85-19104
Simple higher-order theory for laminated composite plates
[NASA-CR-174421] 10 p1496 N85-19445
Develop and demonstrate manufacturing processes for fabricating graphite filament reinforced polymide (Gr/PI) composite structural elements
[NASA-CR-172497] 11 p1592 N85-20019
New method for studying surface crack growth in laminated polymer composite materials
11 p1598 N85-20051
Method of constructing diagram of bimetal fatigue failure 11 p1599 N85-20058
Bending two-layer metal-polymer plates
11 p1604 N85-20085
Aerostructure nondestructive evaluation by thermal field detection. Phase 2: Technique refinement and quantitative determination of flaw detection capabilities
[AD-A149622] 12 p1777 N85-21155
Quantitative non-destructive evaluation of damage in composite materials using transmitted and reflected ultrasound
[NASA-CR-175550] 12 p1796 N85-21289
Accelerated viscoelastic characterization of T300-5208 graphite-epoxy laminates
[NASA-CR-3871] 12 p1797 N85-21271
Fire and heat resistant laminating resins based on maleimido and citraconimido substituted 1-(diorgano oxyphosphonyl)methyl-2,4- and 2,6-diaminobenzenes
[NASA-CASE-ARC-11533-1] 12 p1812 N85-21364
Study of laminated dielectric behavior at microwave and millimeter-wave frequencies
[AD-P004358] 12 p1825 N85-21452
Nonlinear analysis of layered composite plates and shells
[PB85-127181] 12 p1868 N85-21719
Investigation of the effects of NaOH dopant level on the physical and mechanical properties of carbon/phenolic composite material 12 p1945 N85-22213
Solid Rocket Motor Case (SRMC) dynamic sensitivity to changes in composite properties
12 p1948 N85-22238
Directional dependent engineering properties of aluminum-aramid-epoxy laminates
[CCMS-85-02] 13 p2015 N85-22638
Longitudinal splitting in unidirectional composites, analysis and experiments
[NASA-CR-3881] 13 p2015 N85-22639
Interlaminar fracture toughness in resin matrix composites
[AD-A150565] 13 p2015 N85-22640
Mechanical properties and brittle fracture resistance of welded multilayer elements for high pressure vessels
13 p2033 N85-22736
Fibre composite laminated plate analysis using a card programmable calculator (HP41C/CV)
[NIAST-83/88] 13 p2103 N85-23106
Some features of the fabrication of multilayer fiber composites by explosive welding
[NASA-TM-77844] 14 p2248 N85-23932
Monitoring of laminate cure with microdielectrometry
[AD-A150863] 14 p2248 N85-23934
Reduction of free-edge stress concentration
[AD-A150732] 14 p2321 N85-24340
Acoustic radiation from bilaminar plates
14 p2415 N85-24903
Field-induced phenomena in electrical insulation
[AD-A151234] 15 p2547 N85-25719
Layered composite analysis capability
15 p2573 N85-25866
Symmetric composite laminate stress analysis
15 p2575 N85-25878
Design of shear deformable antisymmetric angle-ply laminates to maximize the fundamental frequency and frequency separation
[CSIR-TWISK-333] 15 p2577 N85-25892
Temperature: Curvature relationships for unsymmetric graphite-epoxy laminates
[VPI-E-85-08] 16 p2743 N85-26926
The effects of pin elasticity, clearance, and friction on the stresses in a pin-loaded orthotropic plate
[NASA-CR-175816] 16 p2743 N85-26927
Durability of Aramid reinforced aluminum laminate (ARALL)
[VTH-LR-423] 16 p2744 N85-26933
The effect of low sheet thicknesses on the fracture toughness of an Al alloy (7075-T6) — Aramid Reinforced Aluminum Laminate (ARALL)
[VTH-LR-425] 16 p2752 N85-26984
The nonlinear analysis of thick composite plates using a cubic spline function 16 p2798 N85-27252
The nonlinear analysis of thick composite plates using a cubic spline function
[AD-A152115] 16 p2801 N85-27268
The application of BRILES rivets for mechanical jointing of Aramid Reinforced Aluminum Laminate (ARALL)
[VTH-LR-367] 16 p2802 N85-27279
Mechanical jointing in Aramid fiber composites: An experimental study
[VTH-LR-371] 16 p2802 N85-27280
Solution to eigenvalue problems of antisymmetric cross-ply and antisymmetric angle-ply laminated plates using affine transformations
[AD-A153040] 17 p2917 N85-27980

Strength and failure analysis of composite laminates with holes at room and elevated temperatures
[AD-A153263] 17 p2917 N85-27961
Multiconductor flat cable
[AD-D011635] 17 p2950 N85-28218
Biaxial buckling of specially orthotropic, symmetric composite rectangular plates
[AD-A152956] 17 p2979 N85-28417
Numerical analysis of end effects in symmetric laminated plates
[NAL-TR-850] 18 p3068 N85-28977
The effect of center delamination on the instability of composite cylindrical panels
[AD-A153494] 18 p3069 N85-28979
Crack propation in unidirectional laminates by the stress intensity factors 18 p3121 N85-29320
Fracture of laminated composite materials
19 p3230 N85-30090
Polymer matrix and graphite fiber interface study
[NASA-CR-177357] 19 p3232 N85-30036
Mesophase mechanisms in the formation of graphitic microstructures
[AD-A154100] 19 p3248 N85-30140
Impact dynamics research on composite transport structures
[NASA-TM-86391] 19 p3284 N85-30367
On design of off-axis specimens
[AD-A154328] 19 p3286 N85-30379
Long-term thermal aging of Celion/V378A composite materials
[NASA-TM-86382] 20 p3421 N85-31236
Delamination micromechanics analysis
[NASA-CR-172596] 20 p3422 N85-31237
Residual thermal and moisture influences on the strain energy release rate analysis of edge delamination
[NASA-TM-86437] 20 p3422 N85-31238
Mechanical properties of aligned short carbon fiber reinforced PES and PI laminates
[ESA-TT-898] 20 p3422 N85-31240
Metallographic preparation of materials with various coatings
[BLL-DRIC-TRANS-7522-(3623.66)]
20 p3433 N85-31299
Development of fracture mechanics maps for composite materials, volume 1
[ESA-CR(P)-2017-VOL-1] 20 p3471 N85-31573
Development of fracture mechanics maps for composite materials, volume 2
[ESA-CR(P)-2017-VOL-2] 20 p3471 N85-31574
Development of fracture mechanics maps for composite materials. Volume 3: Appendices A-E
[ESA-CR(P)-2017-VOL-3] 20 p3472 N85-31575
Development of fracture mechanics maps for composite materials. Volume 4: Appendices F-K
[ESA-CR(P)-2017-VOL-4] 20 p3472 N85-31576
Comparisons of various configurations of the edge delamination test for interlaminar fracture toughness
[NASA-TM-86433] 21 p3561 N85-32151
Experimental and theoretical assessment of a new technique for the non-destructive evaluation of laminated panels
[AD-A155622] 21 p3562 N85-32155
Mechanical characterization and failure modes of fiber reinforced angle-ply composites
24 p4072 N85-35234
Damage induced stress redistribution in composite laminates 24 p4072 N85-35235
Methods for nondestructive tests of CFRP laminates
24 p4074 N85-35248
Damage mechanisms in damaged CFRP laminates
24 p4074 N85-35249

LAMINATIONS
U LAMINATES

LAMPS
U LUMINAIRES

LAND
NT ARID LANDS
NT CASCADE RANGE (CA-OR-WA)
NT COASTAL PLAINS
NT DESERTS
NT FARMLANDS
NT FLOOD PLAINS
NT GOBI DESERT
NT GRASSLANDS
NT MARSHLANDS
NT MOJAVE DESERT (CA)
NT NATIONAL PARKS
NT PLAINS
NT RANGELANDS
NT SAHARA DESERT (AFRICA)
NT TUNDRA
NT WETLANDS
Autoregressive modeling and the classification of land clutter — radar signatures
[ENST-C-84003] 03 p0356 N85-12292
Requirements and special problems of land altimetry — satellite altimetry 03 p0380 N85-12430
Earth observations and the polar platform
[NOAA-TR-NESDIS-18] 11 p1669 N85-20517

LAND ICE
Special difficulties of retrieving surface elevation over continental ice — satellite radar altimetry
03 p0380 N85-12429
Diurnal freeze-thaw frequencies in selected regions of the high latitudes
[AD-A147276] 07 p1007 N85-16400
North Atlantic Deep Water formation: Information from ice cores 15 p2602 N85-26035
Greenland ice sheet mass balance
15 p2603 N85-26043
Potential climatic effects on the Greenland ice sheet
15 p2603 N85-26044
Origin of the Greenland ice sheet
15 p2604 N85-26046

LAND MANAGEMENT
Inventory and monitoring of national park landscapes — remote sensing 05 p0660 N85-14245
HS and E environmental sciences
[DE84-016183] 05 p0672 N85-14314
Landscape management on airports for reduction of bird populations
[AD-P004194] 11 p1581 N85-19980
Inexpensive multipurpose landscaping
11 p1581 N85-19981
Combined analysis of the dynamics of complex ecosystems based on repeated remote measurements
13 p1985 N85-22450
Application of interactive graphic systems in land consolidation. Processing of planning maps
16 p2815 N85-27363
Raster or vector processing. Experience with the application of programs for the construction of thematic maps with boundary design in the Lower Saxony (West Germany) Land Administration for ground research
16 p2815 N85-27365

LAND MOBILE SATELLITE SERVICE
RF characteristics of the hoop column antenna for the land mobile satellite system mission
[NASA-CR-3842] 02 p0189 N85-11264
Propagation measurements for land-mobile satellite services in the 800 MHz band
[CRC-TN-724] 09 p1310 N85-18231
Propagation measurements for land-mobile satellite systems at 1541 MHz
[CRC-TN-723] 09 p1310 N85-18232
Measurements of propagation at 900 MHz in an urban zone for establishing a digital radiomobile system
10 p1472 N85-19286
A comparison of metropolitan and non-metropolitan employment characteristics: Indications of the size of non-metropolitan mobile communication services user classes
[NASA-CR-175648] 13 p2053 N85-22855
NASA mobile satellite program
14 p2229 N85-23614
Mobile antenna and beam pointing studies for satellite mobile communications
[NASA-CR-175736] 15 p2540 N85-25679
Trade-off between land vehicle antenna cost and gain for satellite mobile communications
[NASA-CR-175732] 15 p2540 N85-25681
Land vehicle antennas for satellite mobile communications
[NASA-CR-175735] 15 p2540 N85-25682
Propagation considerations in land mobile satellite transmission
[NASA-CR-175733] 15 p2540 N85-25684
Land mobile satellite transmission measurements at 869 MHz: Selected results from the dedicated stratospheric balloon experiment of November 12 and 13, 1984
[NASA-CR-175734] 15 p2541 N85-25685
Spacecraft configuration study for second generation mobile satellite system
[NASA-CR-175774] 16 p2730 N85-26949
Dynamic performance of several large antenna concepts 20 p3409 N85-31155
Control of large antennas based on electromagnetic performance criteria 20 p3409 N85-31158

LAND USE
NT RURAL LAND USE
Satellite reconnaissance
[AD-B085034] 01 p0015 N85-10094
Estuaries of the Cape. Part 2: Synopses of available information on individual systems. Report 13: Silvermine (CSW 3)
[CSIR-RR-412-PT-2] 01 p0086 N85-10582
Estuaries of the Cape. Part 2: Synopses of available information on individual systems. Report no. 16: Eerste (CSW 6)
[CSIR-RR-415-PT-2] 01 p0087 N85-10585
Estuaries of the Cape. Part 2: Synopses of available information on individual systems. Report no. 19: Groot (WES) (CMS 23) and Sout (CMS 22)
[CSIR-RR-418] 01 p0087 N85-10588
Geographic science: Executive summary
02 p0214 N85-11408
Geographic science 02 p0214 N85-11409
Land use/land cover 02 p0214 N85-11410
Utilization of LANDSAT orbital imagery in the soil survey processes at Rio Grande do Norte state
[E85-10009] 02 p0216 N85-11422
Mapping land use changes in the carboniferous region of Santa Catarina, report 2
[E85-10017] 02 p0217 N85-11430
Assessing erosion on US cropland: Land management and physical features
[PB84-219252] 04 p0526 N85-13366
Modeling long-term changes in forested landscapes and their relation to the Earth's energy balance
05 p0653 N85-14194
Integration of multiple thematic data with LANDSAT data: Some results about the feasibility of Mediterranean land cover inventories 05 p0655 N85-14205
Statistics and mapping of land uses by means of LANDSAT MSS imagery 05 p0657 N85-14219
The use of Thematic Mapper data for land cover survey 05 p0657 N85-14220
Detecting agricultural to urban land use change from multi-temporal MSS digital data — Salt Lake County, Utah
[E85-10048] 07 p0983 N85-16245
Calibration or inverse regression: Which is appropriate for crop surveys using LANDSAT data?
07 p0985 N85-16260
Study of spectral/radiometric characteristics of the Thematic Mapper for land use applications
[E85-10057] 07 p0987 N85-16268
Analysis of data acquired by synthetic aperture radar and LANDSAT Multispectral Scanner over Kershaw County, South Carolina, during the summer season
[E85-10071] 10 p1503 N85-19485
Assessment of LANDSAT for rangeland mapping, Rush Valley, Utah
[E85-10072] 10 p1503 N85-19486
An integrated GIS/remote sensing data base in North Cache soil conservation district, Utah: A pilot project for the Utah Department of Agriculture's RIMS (Resource Inventory and Monitoring System)
[E85-10073] 10 p1504 N85-19487
Anaysis of the quality of image data required by the LANDSAT-4 Thematic Mapper and Multispectral Scanner — agricultural and forest cover types in California
[E85-10074] 10 p1504 N85-19488
Study of spectral/radiometric characteristics of the Thematic Mapper for land use applications
[E85-10075] 10 p1504 N85-19489
Nationwide urban runoff program. Relationship of urban runoff to land use and groundwater resources
[PB85-114692] 10 p1506 N85-19505
Control of mammals at airports
[AD-P004192] 11 p1580 N85-19957
Building a functional, integrated GIS/remote sensing resource analysis and planning system — Utah
[E85-10092] 12 p1674 N85-21754
Characterization of LANDSAT-4 TM and MSS image quality for the interpretation of California's agricultural resources — Central Valley 13 p2118 N85-23190
An initial analysis of LANDSAT-4 Thematic Mapper data for the discrimination of agricultural, forested wetlands, and urban land cover — Poinsett County, Arkansas; and Reelfoot Lake and Union City, Tennessee
13 p2118 N85-23193
Quick look analysis of TM data of the Washington, District of Columbia, area 13 p2119 N85-23197
Thematic Mapper data quality and performance assessment in renewable resources/agriculture/remote sensing 13 p2120 N85-23201
Preliminary comparisons of the information content and utility of TM versus MSS data 13 p2120 N85-23202
The use of Thematic Mapper data for land cover discrimination: Preliminary results from the UK SATMaP programme 13 p2121 N85-23207
Preliminary study of information extraction of LANDSAT TM data for a suburban/regional test site
13 p2121 N85-23208
Comparative techniques used to evaluate Thematic Mapper data for land cover classification in Logan County, West Virginia 13 p2121 N85-23209
Comparison of MSS and TM data for landcover classification in the Chesapeake Bay area: A preliminary report — Taylor's Island, Maryland
13 p2121 N85-23210
Atlas of archived vegetation, land-use and seasonal Albedo data sets
[NASA-TM-86199] 14 p2348 N85-24508

Identifying land use structures of multizonal aerospace photographs using digital data processing
15 p2486 N85-25548
A study of the methods for evaluating the noise impact of a proposed airport on a community
15 p2588 N85-25657
Experience of the Institute of Space Research with the use of remote sensing in urban planning studies
[INPE-3159-PRE/533] 16 p2880 N85-27770
Orphans of the Valley: Abandoned surface mines in the Tennessee Valley. Volume 2: Maps
[DE85-901246] 19 p3301 N85-30465
Microcomputer processing of LANDSAT Thematic Mapper data for the acquisition of military tactical terrain data
[AD-A154781] 21 p3605 N85-32389
Cosmonauts participate in multilevel remote sensing experiment 22 p3731 N85-33130
Resource evaluation and site selection for microalgae production systems
[DE85-006807] 23 p3951 N85-34485
Land Disposal of Hazardous Waste
[PB85-196376] 24 p4119 N85-35500

LANDAU DAMPING
Energy spread in SLC linac with Landau damping
[DE84-016259] 05 p0727 N85-14675
I. F. S. (Institute for Fusion Studies) Newsletter, Volume 4, Number 1
[DE85-007917] 17 p3040 N85-26809

LANDAU FACTOR
Some dynamic electronic properties of semiconductor surfaces and interfaces 20 p3537 N85-32007
Analytical-numerical methods of calculations of energy and three-dimensional particle distributions in electromagnetic cascades
[HE-3.5-13] 24 p4184 N85-35950
Development of electromagnetic cascades in the atmosphere including the Landau-Pomeranchuk-Migdal effect
[HE-4.5-5] 24 p4195 N85-36029

LANDFILLS
Electrical resistivity technique to assess the integrity of geomembrane liners
[PB85-122414/GAR] 09 p1325 N85-18327
Test report for Getty Synthetic Fuels, Inc., Calumet City, Illinois
[PB85-119493] 10 p1459 N85-19191
FAA policy regarding solid waste disposal facilities
[AD-P004196] 11 p1581 N85-19963
Successful control of gulls and other birds at a sanitary landfill
[AD-P004198] 11 p1582 N85-19965
Effectiveness of an overhead wire barrier in deterring gulls from feeding at a sanitary landfill
[AD-P004199] 11 p1582 N85-19966
Effectiveness of an overhead wire barrier system in reducing gull use at the BFI Jedburg sanitary landfill, Berkeley and Dorchester counties, South Carolina
[AD-P004200] 11 p1582 N85-19967
Evaluation of effectiveness of bird scaring operations at a sanitary landfill site near CFB Trenton, Ontario, Canada
[AD-P004201] 11 p1582 N85-19968
High-level waste processing and disposal
[DE85-009564] 11 p1728 N85-20665
Assessment of hazardous waste surface impoundment technology case studies and perspectives of experts
[PB85-117059] 12 p1886 N85-21834
Analysis of leachate production in closed hazardous waste landfills
[DE85-010978] 19 p3310 N85-30520

LANDFORMS
NT ALEUTIAN ISLANDS (US)
NT ALPS MOUNTAINS (EUROPE)
NT ANDES MOUNTAINS (SOUTH AMERICA)
NT APPALACHIAN MOUNTAINS (NORTH AMERICA)
NT BARRIERS (LANDFORMS)
NT BAYOUS
NT BERMUDA
NT BIGHORN MOUNTAINS (MT-WY)
NT BRIDGES (LANDFORMS)
NT CALDERAS
NT CANYONS
NT CAPES (LANDFORMS)
NT CARPATHIAN MOUNTAINS (EUROPE)
NT CASCADE RANGE (CA-OR-WA)
NT COASTAL RANGES (CA)
NT CONES (VOLCANOES)
NT CUBA
NT DELTAS
NT DIVIDES (LANDFORMS)
NT DUNES
NT ESCARPMENTS
NT FLATS (LANDFORMS)
NT GAPS (GEOLOGY)
NT GREENLAND
NT HAWAII
NT HIMALAYAS
NT ICELAND
NT INDONESIA
NT ISLAND ARCS
NT ISLANDS
NT JAPAN
NT KURILE ISLANDS
NT MARS VOLCANOES
NT MASSIFS
NT MISSISSIPPI DELTA (LA)
NT MISSOURI RIVER BASIN (US)
NT MOUNTAINS
NT NEW ZEALAND
NT PACIFIC ISLANDS
NT PIEDMONTS
NT PLATEAUS
NT PUERTO RICO
NT PYRENEES MOUNTAINS (EUROPE)
NT REEFS
NT RIVER BASINS
NT ROCKY MOUNTAINS (NORTH AMERICA)
NT SALT BEDS
NT SIERRA NEVADA MOUNTAINS (CA)
NT STEPPES
NT STRUCTURAL BASINS
NT TASMANIA
NT TERRACES (LANDFORMS)
NT TUNDRA
NT VOLCANOES
NT WATERSHEDS
Terrain analysis procedural guide for surface configuration
[AD-A145637] 02 p0219 N85-11446
Submarine sand ridges: Geology and development, New Jersey, USA 02 p0227 N85-11482
Paleoenvironmental interpretation of the upper cretaceous Point Lookout sandstone: Implications for shoreline progradation and basin tectonic history, San Juan basin, New Mexico 02 p0227 N85-11486
Remote sensing for landforms and soils in the arid southwest United States 03 p0378 N85-12410
Glacier dynamics and the development of glacial landforms in the eastern Puget lowland, Washington
03 p0389 N85-12490
Glacial geology of Barron County, Wisconsin
09 p1351 N85-18500
Newly discovered Martian impact basins
13 p2162 N85-23544
Thickness of ridged plains materials in Hesperia Planum, Mars 13 p2165 N85-23561
Submarine volcanic eruptions and potential analogs for Venus 13 p2187 N85-23573
Transformation of polar ice sublimate residue into Martian circumpolar sand 13 p2189 N85-23580
Potential bedforms on Venus: Wind tunnel simulations
13 p2189 N85-23583
Experiments and analyses of the formation of erosional scour marks with implications to the origin of the Martian outflow channels 13 p2190 N85-23588
Distribution and properties of large symmetric knobs on Mars 13 p2192 N85-23598
Enigmatic hills of the mottled plains, Mare Acidalium quadrangle (MC-4), Mars 13 p2192 N85-23599
Geomorphology and geology of the Southwestern Margaritifer Sinus and Argyre regions of Mars. Part 3: Valley types and distribution 13 p2193 N85-23602
The geomorphology of Rhea
13 p2193 N85-23606
Airphoto interpretation of vegetation and landforms for soil mapping 17 p2963 N85-28436
Mineralogical-geochemical characteristics of ferromanganese formations in Arabian-Indian Ocean Ridge 19 p3293 N85-30416
MELSAR: A mesoscale air quality model for complex terrain. Volume 2: Appendices
[DE85-010991] 19 p3310 N85-30519
Global Mega-Geomorphology
[NASA-CP-2312] 21 p3600 N85-32357
The problem of scale in planetary geomorphology
21 p3603 N85-32375
Global geomorphology: Report of Working Group Number 1 21 p3604 N85-32382
Planetary perspective. Report of Working Group Number 4 21 p3605 N85-32385
Massive sulfide deposits from the southern Juan de Fuca Ridge 24 p4105 N85-35448

LANDING
NT AIRCRAFT LANDING
NT CRASH LANDING
NT DITCHING (LANDING)
NT GLIDE LANDINGS
NT HORIZONTAL SPACECRAFT LANDING
NT MARS LANDING
NT PLANETARY LANDING
NT SKID LANDINGS
NT SPACECRAFT LANDING
NT VERTICAL LANDING
NT WATER LANDING
Wind tunnel results of advanced high speed propellers in the takeoff, climb and landing operating regimes
[NASA-TM-87054] 19 p3213 N85-29925
Ground-based and in-flight simulator studies of flight characteristics of a twin-fuselage passenger transport airplane during approach and landing
[NASA-TP-2451] 23 p3898 N85-34144

LANDING AIDS
NT ALL-WEATHER LANDING SYSTEMS
NT APPROACH INDICATORS
NT ARRESTING GEAR
NT AUTOMATIC LANDING CONTROL
NT INSTRUMENT LANDING SYSTEMS
NT LANDING RADAR
NT MICROWAVE LANDING SYSTEMS
NT RUNWAY LIGHTS
Development and flight test of a helicopter, X-band, portable precision landing system concept
[NASA-TM-86710] 16 p2710 N85-26721

LANDING GEAR
Air force landing gear repair - Ogden Air Logistics Center Industrial Products and Landing Gear Division
[AD-P004001] 03 p0307 N85-11982
Determination of parameters of cupped aircraft landing ski 06 p0775 N85-14956
Testing solution for IL-76 braking system problem
06 p1067 N85-16766
Orbiter wheel and tire certification
08 p1101 N85-16959
A literature survey of ground load statistics for landing gear fatigue design purposes
[FFA-TN-1984-39] 09 p1280 N85-18054
Deflection model of a CT4-A undercarriage
[AD-A149778] 12 p1777 N85-21156
Safety recommendation(s), A-84-65
[REPT-3908] 14 p2216 N85-23743
Selection of effective arrangement of heavy undercarriage systems for use with concrete runways
14 p2285 N85-24158
Active control landing gear for ground loads alleviation
16 p2714 N85-26749
Active control landing gear for ground load alleviation
17 p2903 N85-27902

LANDING INSTRUMENTS
NT APPROACH INDICATORS

LANDING LOADS
Development of a preliminary ALRS stabilized material pavement analysis system (SPAS)
[AD-A147116] 07 p0910 N85-15760
Learjet Model 55 wing analysis with landing loads
15 p2575 N85-25883
Active control landing gear for ground load alleviation
17 p2903 N85-27902

LANDING RADAR
Landing control centrals
[AD-A149800] 12 p1775 N85-21140
Investigation of imaging and flight guidance concepts for rotorcraft zero visibility approach and landing
[NASA-CR-166571] 17 p2894 N85-27843

LANDING SIMULATION
Realistic localizer courses for aircraft instrument landing simulators
[NASA-CR-172333] 04 p0455 N85-12685

LANDING SITES
Structural design guidelines for heliports
[FAA-PM-84-23] 02 p0149 N85-11010
STS natural environment analysis
[NASA-CR-171221] 03 p0322 N85-12079
The search for igneous materials at the Viking landing sites 13 p2194 N85-23609
Mars landing sites 22 p3859 N85-33693

LANDING SYSTEMS
U LANDING AIDS

LANDMARKS
Potential geological natural landmarks of the East Gulf Coastal Plain
[PB84-230317] 06 p0835 N85-15316
Man in Space: National Historic Landmark Theme Study
[PB85-107233/GAR] 07 p0911 N85-15768

LANDSAT SATELLITES
NT LANDSAT 1
NT LANDSAT 4
NT LANDSAT 5
Land remote sensing commercialization: A status report 02 p0151 N85-11024
Seminar on Principal Components Analysis in the Atmospheric and Earth Sciences
[CSIR-S-334] 02 p0211 N85-11388
The feasibility of satellite remote sensing as a technique for evaluating coal mine surface features
02 p0213 N85-11401

Relationships between grass canopy characteristics and LANDSAT Thematic Mapper bands
02 p0213 N85-11402
The Alaskan mineral resources assessment program: Guide to information contained in the folio of geologic and mineral-resource maps of the Medfra Quadrangle, Alaska
[GS-CIRC-928] 02 p0219 N85-11443
The United States Geological Survey in Alaska: Accomplishments during 1981
[USGS-CIRC-868] 04 p0515 N85-13283
Summary of LANDSAT quadrangle studies in Alaska
04 p0515 N85-13284
LANDSAT instruments characterization
[E85-10032] 04 p0524 N85-13356
LANDSAT instruments characterization
[E85-10029] 05 p0654 N85-14198
Integration of multiple thematic data with LANDSAT data: Some results about the feasibility of Mediterranean land cover inventories 05 p0655 N85-14205
Methodological research in connection with the handling of LANDSAT satellite data for archaeology
05 p0655 N85-14207
A comparison of TIROS-N series satellite data and LANDSAT data over Scotland 05 p0656 N85-14210
Forest cover monitoring by remote sensing in Great Britain 05 p0656 N85-14214
Statistics and mapping of land uses by means of LANDSAT MSS imagery 05 p0657 N85-14219
Landform evaluation through integrated remote sensing methods. A case study in parts of Haryana, India
05 p0657 N85-14221
Combining Heat Capacity Mapping Mission (HCMM) LANDSAT and thematic map information into a unique high precision merged multichannel system — climatology 05 p0660 N85-14239
A multiple approach in remote sensing for structural and lithological mapping by use Modular Optoelectronic Multispectral Scanner (MOMS)/LANDSAT/Heat Capacity Mapping Mission (HCMM) data
05 p0660 N85-14244
An integrated LANDSAT/ancillary data classification of desert rangeland
[E85-10046] 06 p0826 N85-15248
A geographic information system for resource managers based on multi-level remote sensing data
[E85-10047] 06 p0827 N85-15249
The extension of an invertible coniferous forest canopy reflectance model using SIR-B and LANDSAT data
08 p1149 N85-17246
Assessment of LANDSAT for rangeland mapping, Rush Valley, Utah
[E85-10072] 10 p1503 N85-19486
An integrated GIS/remote sensing data base in North Cache soil conservation district, Utah: A pilot project for the Utah Department of Agriculture's RIMS (Resource Inventory and Monitoring System)
[E85-10073] 10 p1504 N85-19487
Thematic Mapper data quality and performance assessment in renewable resources/agriculture/remote sensing 13 p2120 N85-23201
Study of the urban evolution of Brasilia with the use of LANDSAT data
[E85-10101] 16 p2909 N85-27321
Geomorphic classification of Icelandic and Martian volcanoes: Limitations of comparative planetology research from LANDSAT and Viking orbiter images
21 p3603 N85-32372
Use of spaceborne imaging radar in regional geomorphic studies 21 p3603 N85-32377
Quantitative geomorphologic studies from spaceborne platforms 21 p3604 N85-32381
Microcomputer processing of LANDSAT Thematic Mapper data for the acquisition of military tactical terrain data
[AD-A154781] 21 p3605 N85-32389
Satellites and politics: Weather, communications, and earth resources 23 p4057 N85-35144
A comparison of LANDSAT thematic mapper, multispectral scanner and airborne sensors for mapping the distribution of alteration minerals: Examples from the southwestern United States 24 p4106 N85-35452
Processing of LANDSAT imagery to map surface mineral alteration on the Alaska Peninsula, Alaska
24 p4106 N85-35455

LANDSAT 1
Developments in remote sensing
[B8580069] 17 p2984 N85-28441

LANDSAT 4
LANDAT-4/5 image data quality analysis
[E85-10039] 03 p0379 N85-12417
LANDSAT instruments characterization
[E85-10030] 05 p0654 N85-14199
Characterizing the scientific potential of satellite sensors
[E85-10031] 05 p0654 N85-14200
The use of Thematic Mapper data for land cover survey 05 p0657 N85-14220
Study of spectral/radiometric characteristics of the Thematic Mapper for land use applications
[E85-10057] 07 p0987 N85-16268
LANDSAT 4 investigation of Thematic Mapper and Multispectral Scanner applications
[E85-10076] 10 p1504 N85-19490
Thematic Mapper: Design through flight evaluation
[E85-10078] 10 p1504 N85-19492
LANDSAT-4 Science Characterization Early Results. Volume 1: Multispectral Scanner (MSS)
[E85-10067] 11 p1666 N85-20496
Spectral characterization of the LANDAT-4 MSS sensors 11 p1666 N85-20499
Investigation of radiometric properties of LANDSAT-4 MSS — California, North Carolina, South Carolina, and New England 11 p1666 N85-20500
LANDSAT scene-to-scene registration accuracy assessment 11 p1667 N85-20502
Geometric accuracy of LANDSAT-4 MSS image data
11 p1667 N85-20503
Impact of LANDSAT MSS sensor differences on change detection analysis — New Mexico, San Francisco, CA, New Hampshire, and Connecticut
11 p1667 N85-20506
LANDSAT-4 Science Characterization Early Results. Volume 2, part 1: Thematic Mapper (TM)
[E85-10068] 11 p1668 N85-20508
An overview of LANDSAT-4 and the Thematic Mapper
11 p1668 N85-20509
Radiometric calibration and processing procedure for reflective bands on LANDSAT-4 protoflight Thematic Mapper 11 p1668 N85-20510
An overview of the Thematic Mapper geometric correction system 11 p1668 N85-20511
TM digital image products for applications
11 p1668 N85-20512
Spectral characterization of the LANDSAT Thematic Mapper sensors 11 p1669 N85-20514
Prelaunch absolute radiometric calibration of the reflective bands on the LANDSAT-4 protoflight Thematic Mapper 11 p1669 N85-20515
LANDSAT-4 Science Characterization Early Results. Volume 3, part 2: Thematic Mapper (TM)
[E85-10069] 12 p1669 N85-21724
Relative radiometric calibration of LANDSAT TM reflective bands 12 p1669 N85-21725
Evaluation of the radiometric integrity of LANDSAT 4 Thematic Mapper band 6 data 12 p1669 N85-21726
Thermal band characterization of the LANDSAT-4 Thematic Mapper 12 p1669 N85-21727
A preliminary assessment of LANDSAT-4 Thematic Mapper data — Windsor, Ontario and Medicine Hat areas, Canada 12 p1669 N85-21728
Preliminary evaluation of the radiometric calibration of LANDSAT-4 Thematic Mapper data by the Canada Centre for Remote Sensing 12 p1670 N85-21729
A preliminary analysis of LANDSAT-4 Thematic Mapper radiometric performance 12 p1670 N85-21730
TM geometric performance: Line to Line Displacement Analysis (LLDA) — New Mexico
12 p1670 N85-21732
In-progress absolute radiometric inflight calibration of the LANDSAT-4 sensors — New Mexico
12 p1670 N85-21733
LANDSAT-4 Thematic Mapper calibration and atmospheric correction 12 p1670 N85-21734
MTF analysis of LANDSAT-4 Thematic Mapper
12 p1671 N85-21737
Intraband radiometric performance of the LANDSAT 4 Thematic Mapper — Washington, DC, Arkansas, Massachusetts, Virginia, and Arizona
12 p1671 N85-21738
A preliminary evaluation of LANDSAT-4 Thematic Mapper data for their geometric and radiometric accuracies 12 p1671 N85-21739
The use of linear feature detection to investigate Thematic Mapper data performance and processing
12 p1672 N85-21740
An analysis of the high frequency vibrations in early Thematic Mapper scenes 12 p1672 N85-21742
Assessment of Thematic Mapper band-to-band registration by the block correlation method
12 p1672 N85-21743
Tests of low-frequency geometric distortions in LANDSAT 4 images 12 p1672 N85-21744
Investigation of TM band-to-band registration using the JSC registration processor 12 p1672 N85-21745
Geodetic accuracy of LANDSAT 4 Multispectral Scanner and Thematic Mapper data 12 p1673 N85-21746
LANDSAT 4 band 6 data evaluation
[E85-10093] 12 p1674 N85-21755
LANDSAT-4 Science Characterization Early Results. Volume 4: Applications — agriculture, soils land use, geology, hydrology, wetlands, water quality, biomass identification, and snow mapping
[E85-10070] 13 p2117 N85-23186
Overview of TM applications research reports
13 p2117 N85-23187
Impact of Thematic Mapper sensor characteristics on classification accuracy — suburban Washington, D.C., Maryland, and the Chesapeake Bay
13 p2117 N85-23188
Analysis and evaluation of the LANDSAT-4 MSS and TM sensors and ground data processing systems: Early results 13 p2117 N85-23189
Characterization of LANDSAT-4 TM and MSS image quality for the interpretation of California's agricultural resources — Central Valley 13 p2118 N85-23190
Evaluation of Thematic Mapper performance as applied to hydrocarbon exploration — Ontario, Canada; Cement, Oklahoma; and Death Valley, California
13 p2118 N85-23191
An initial analysis of LANDSAT-4 Thematic Mapper data for the discrimination of agricultural, forested wetlands, and urban land cover — Poinsett County, Arkansas; and Reelfoot Lake and Union City, Tennessee
13 p2118 N85-23193
A preliminary comparison of the information content of data from the LANDSAT 4 Thematic Mapper and Multispectral Scanner — Arkansas
13 p2119 N85-23199
Early results of investigations of LANDSAT 4 Thematic Mapper and Multispectral Scanner applications — Washington, D.C. 13 p2119 N85-23200
Preliminary comparisons of the information content and utility of TM versus MSS data 13 p2120 N85-23202
Snow reflectance from Thematic Mapper
13 p2120 N85-23205
The use of Thematic Mapper data for land cover discrimination: Preliminary results from the UK SATMAP programme 13 p2121 N85-23207
Relative accuracy assessment of LANDSAT-4 MSS and TM data for level 1 land cover inventory — Washington, D.C. 13 p2122 N85-23212
NOAA satellite operations: Programs briefing — Environmental satellites, LANDSAT, and space station polar platform 15 p2599 N85-26020
CNPq/INPE LANDSAT system: Report of activities from October 1, 1983 to September 30, 1984 — Brazil
[E85-10097] 16 p2808 N85-27318
LANDSAT-4/5 image data quality analysis
[E85-10105] 24 p4107 N85-35483
Study of spectral/radiometric characteristics of the Thematic Mapper for land use applications
[E85-10106] 24 p4107 N85-35484

LANDSAT 5
LANDAT-4/5 image data quality analysis
[E85-10039] 03 p0379 N85-12417
LANDSAT instruments characterization
[E85-10030] 05 p0654 N85-14199
Study of spectral/radiometric characteristics of the Thematic Mapper for land use applications
[E85-10057] 07 p0987 N85-16268
Thematic Mapper. Volume 1: Calibration report flight model, LANDSAT 5
[E85-10059] 07 p0987 N85-16270
Thematic Mapper. Volume 2: Flight model preshipment review
[E85-10060] 07 p0987 N85-16271
LANDSAT 4 investigation of Thematic Mapper and Multispectral Scanner applications
[E85-10076] 10 p1504 N85-19490
Spectroradiometric calibration of the Thematic Mapper and Multispectral Scanner system
[E85-10077] 10 p1504 N85-19491
Thematic Mapper: Design through flight evaluation
[E85-10078] 10 p1504 N85-19492
An investigation of several aspects of LANDSAT-5 data quality — Palmer County, Shelby, mt; White sands, NM; Great Salt Lake, UT; San Mattad Bridge and Sacramento, California
[E85-10096] 13 p2122 N85-23214
Spectroradiometric calibration of the Thematic Mapper and Multispectral Scanner system
[E85-10104] 20 p3476 N85-31601
LANDSAT-4/5 image data quality analysis
[E85-10105] 24 p4107 N85-35483
Study of spectral/radiometric characteristics of the Thematic Mapper for land use applications
[E85-10106] 24 p4107 N85-35484

LANDSCAPE
U TERRAIN
U TOPOGRAPHY

LANGMUIR PROBES
U ELECTROSTATIC PROBES

LANGUAGE PROGRAMMING
Evaluation of PHOENICS as a design analysis tool for SSME 12 p1949 N85-22240
Dataflow computation [CWI-TRACT-6] 14 p2406 N85-34833
The design and analysis of a complete hierarchical interface for the multi-backend database system [AD-A151550] 15 p2629 N85-26203
The effect of communication-language designs on software specifications [AD-A155173] 21 p3672 N85-32600

LANGUAGES
NT ADA (PROGRAMMING LANGUAGE)
NT ASSEMBLY LANGUAGE
NT BASIC (PROGRAMMING LANGUAGE)
NT COBOL
NT COMMAND LANGUAGES
NT ENGLISH LANGUAGE
NT FORTRAN
NT HIGH LEVEL LANGUAGES
NT LISP (PROGRAMMING LANGUAGE)
NT NATURAL LANGUAGE (COMPUTERS)
NT PASCAL (PROGRAMMING LANGUAGE)
NT PL/1
NT PROGRAMMING LANGUAGES
NT QUERY LANGUAGES
NT WORDS (LANGUAGE)
Model theory for infinitely deep languages [ISSN-0355-0087] 01 p0101 N85-10674
Information-theoretic properties of languages and their grammars [AD-A146666] 06 p0799 N85-15106
Spanish language equivalents for a glossary of terms used in the field of space exploration [NASA-TM-87403] 08 p1229 N85-17739
Glossary of the soil sciences [PB85-133452] 12 p1952 N85-22263
Expressiveness and language choice [AD-A153280] 17 p3012 N85-28623

LANTHANIDE SERIES METALS
U RARE EARTH ELEMENTS

LANTHANUM
Kohn anomaly in metastable fcc lanthanum at low temperatures [DE84-015459] 04 p0569 N85-13628
Stability of temporal and energy parameters of picosecond lanthanum beryllate laser 11 p1717 N85-20804
Americium metal preparation on the multigram scale [DE85-003735] 13 p2024 N85-22683
Modified aluminosilicide coating for heat-resistant nickel alloys 15 p2514 N85-25509

LANTHANUM COMPOUNDS
Phonon anomalies in superconducting transition metal compounds — lanthanum and niobium compounds 03 p0426 N85-12718
Magnetic susceptibility, electrical resistivity, and specific heat of single crystal LaFe-4P-12 [DE84-009979] 04 p0570 N85-13633
Strength and failure of ceramic-metallic material 10 p1446 N85-19112
The UFe4P12 and CeFe4P12: Non-metallic isotopes of superconducting LaFe4P12 [DE85-003724] 12 p1942 N85-22195
Development of advanced thermoelectric materials [NASA-CR-175684] 14 p2351 N85-24532

LAP JOINTS
Effect of penetrant on fatigue of aluminum alloy lap joints [NLR-TR-82104-U] 01 p0058 N85-10373
Deformations and strains in adhesive joints by moire interferometry [NASA-CR-172474] 02 p0185 N85-11238
The application of BRILES rivets for mechanical joining of Aramid Reinforced Aluminum Laminate (ARALL) [VTH-LR-387] 16 p2802 N85-27279
Influence of interface ply orientation on fatigue damage of adhesively bonded composite joints [NASA-TM-86443] 19 p3284 N85-30365

LAPLACE EQUATION
Boundary element methods in potential theory: Four lectures [NPL-DITC-46/84] 05 p0718 N85-14604
Integral equation formulations in two dimensions 05 p0718 N85-14605
Applications of the simple-layer logarithmic potential 05 p0718 N85-14606
Three-dimensional and axisymmetric problems 05 p0718 N85-14608
Simulation of the electrochemical machining process [DE85-003797] 11 p1616 N85-20150
Computation of elliptical functions in problems of celestial mechanics 13 p1979 N85-22418
Applications of the conformal mapping method to the solution of mechanical vibrations problems 13 p2102 N85-23103
Numerical solutions of the potential distribution within the vacuum region of the FEATRON [AD-A153663] 18 p3178 N85-29705

LAPLACE OPERATORS
U LAPLACE TRANSFORMATION

LAPLACE TRANSFORMATION
Fitting aerodynamic forces in the Laplace domain: An application of a nonlinear nongradient technique to multilevel constrained optimization [NASA-TM-86317] 02 p0134 N85-10917
Omni transforms: Applications to renewal theory [AD-A146939] 07 p1029 N85-16534
Numerical solution of semilinear elliptic problems on unbounded domains [AD-A149559] 10 p1549 N85-19767
Three algorithms for parametric frequency domain system identification [DE85-002901] 11 p1706 N85-20735
Application of the system identification technique to goal-directed saccades [AD-A150132] 12 p1906 N85-21967
Time dependent interaction of internal pressure wave with system of two spherical shells 13 p2046 N85-22609
Modification of the Week's method for numerical inversion of the Laplace transform [DE85-006576] 14 p2409 N85-24856
Implementation of Weeks' method for the inverse Laplace transform problem [DE85-005919] 15 p2639 N85-26275
A convolution integral equation solved by Laplace transformation [CWI-AM-R8409] 17 p3022 N85-28692
Numerical solutions of the potential distribution within the vacuum region of the FEATRON [AD-A153663] 18 p3178 N85-29705
An extension to complex-valued functions of an algorithm for numerically inverting the Laplace transform [DE85-010701] 19 p3347 N85-30743
Art of programming programmable microcalculators: Calculation of response from current values of action 22 p3767 N85-33348
Substructure coupling in the frequency domain [NASA-CR-176140] 22 p3800 N85-33543
Characterizations of generalized hyperexponential distributions [AD-A155855] 24 p4142 N85-35680

LARGE SCALE INTEGRATION
Problems in CEMA microelectronic cooperation noted 03 p0341 N85-12196
Functional checking of microprocessors and microprocessor systems 03 p0347 N85-12236
USSR report: Electronics and electrical engineering [JPRS-UEE-84-010] 04 p0485 N85-13095
Practical application of electron beam testing in LSI and VLSI circuits [BMFT-FB-T-84-185] 05 p0833 N85-14081
Fast algorithms and specialized architectures 05 p0714 N85-14579
Electrooptical sensor for automatic detection of objects 05 p0769 N85-15040
Compository speech output (KOSA) with a very large scale integration speech synthesis chip [FI-13-TBR-18] 07 p0942 N85-15974
Development of a 2 micrometer silicon-gate-CMOS-technology for microcomputer oriented VLSI circuits with a supply voltage range between 1.5 and 5 V [BMFT-FB-T-84-203] 07 p0949 N85-16012
Trends in development of software for computer-aided analysis of large-scale integrated circuits 07 p0955 N85-16055
High quality super-large circuits developed 11 p1622 N85-20209
Method of examining microcircuit patterns [NASA-CASE-NPO-16299-1] 11 p1628 N85-20250
Parallel test method for LSI (Large Scale Integration) microprocessors [AD-A150237] 13 p2144 N85-23310
Computer-aided identification of complete constitution model of transistor structure for design of subnanosecond large-scale-integrated circuits 15 p2529 N85-25594
Recent developments 15 p2533 N85-25628
Research in the design of high-performance reconfigurable systems [NASA-CR-175705] 15 p2621 N85-26153
The impact of VLSI on guidance and control system design 16 p2697 N85-26654
Bond test data acquisition and analysis system [DE85-007021] 16 p2780 N85-27158
Efficient VLSI (Very Large Scale Integration) fault simulation [AD-A152661] 17 p2953 N85-28233
High temperature position sensors based on monolithic GaAs Hall IC [BMFT-FB-T-84-266] 17 p2969 N85-28337
Parallel simulation of digital LSI circuits [AD-A154745] 21 p3580 N85-32258
Modeling of electronic circuits with high degree of component integration 22 p3766 N85-33343
Algorithms and organization of software for computer-aided circuit design 22 p3767 N85-33347
Computer simulation of integrated injection logic 22 p3767 N85-33349
Synthesis of metrico-topological model for layout of topology of large-scale-integration arrays 22 p3781 N85-33427
Laser and electron beam processing of semiconductors [AD-A155914] 24 p4161 N85-35796

LARGE SPACE STRUCTURES
Shear deformation plate continua of large double-layered space structures 01 p0059 N85-10391
IAC user manual [NASA-CR-175300] 01 p0102 N85-10677
Conceptual design and evaluation of selected Space Station concepts: Executive summary [NASA-TM-87382] 02 p0167 N85-11128
Conceptual design and evaluation of selected Space Station concepts, volume 1 [NASA-TM-87383] 02 p0168 N85-11129
Effects of member imperfections on the behavior of space trusses 02 p0207 N85-11363
Qualitative results for distributed systems with discrete damping and stiffness with application to control [AD-A145525] 02 p0209 N85-11382
Definition of technology development missions for early space stations: Large space structures [NASA-CR-171209] 03 p0323 N85-12084
Definition of technology development missions for early Space Station satellite servicing. Volume 1: Executive summary [NASA-CR-171228] 04 p0460 N85-12922
Definition of technology development missions for early Space Station satellite servicing. Volume 2: Technical [NASA-CR-171229] 04 p0461 N85-12923
Conceptual design for scaled truss antenna flight experiment [NASA-TM-85804] 04 p0462 N85-12932
Experiments in control of flexible structures with uncertain parameters 05 p0602 N85-13837
Definition of ground test for verification of large space structure control [NASA-CR-171208] 05 p0602 N85-13838
Level of effort 05 p0602 N85-13839
Oral presentation of first year final report, appendix A 05 p0602 N85-13840
Simplified planar model of ground test verification structure, appendix B 05 p0603 N85-13841
Speed test results and hardware/software study of computational speed problem, appendix D 05 p0603 N85-13843
Section 1. Method of determining mode shapes and natural frequencies of the NASA unmodified test structure. Section 2. Continuous beam closed form solution to the NASA-LSS astromast torsional vibration, appendix E 05 p0603 N85-13844
Definition of ground test for Large Space Structure (LSS) control verification, appendix G 05 p0603 N85-13845
Review of technical papers, appendix H 05 p0603 N85-13846
Ground test experiment for large space structures, appendix I 05 p0603 N85-13847
Environmental interactions working group report 05 p0611 N85-13908
Disturbance propagation in structural networks; control of large space structures 06 p0759 N85-14856
Broadening the debate 07 p0914 N85-15785
Toward a goal-oriented civilian space program 07 p0914 N85-15786
Results of principal NASA studies on space station uses and functional requirements 07 p0914 N85-15787
Space Station truss structures and construction considerations [NASA-TM-86336] 07 p0916 N85-15796
Capillary Pump Loop (CPL) heat pipe development status report [NASA-CR-175273] 08 p1161 N85-17323
The Shock and Vibration Digest, volume 16, no. 11 [AD-A148466] 08 p1171 N85-17382
Research and technology highlights of the Lewis Research Center [NASA-TM-86699] 08 p1261 N85-17928
Modelling and identification of the structural properties of an astromast [CRC-1374] 09 p1329 N85-18352
NASA-VCOSS dynamic test facility [NASA-TM-86491] 10 p1427 N85-18998

Operational fitness of box truss antennas in response to dynamic slewing
[NASA-CR-172470] 10 p1429 N85-19012
Ground test experiment for large space structures
[NASA-TM-86489] 10 p1429 N85-19013
Active control of large space structures: An introduction and overview
[NASA-TM-86490] 10 p1429 N85-19014
Swing-arm beam erector (SABER) concept for single astronaut assembly of space structure
[NASA-TP-2379] 10 p1429 N85-19015
Develop and demonstrate manufacturing processes for fabricating graphite filament reinforced polymide (Gr/PI) composite structural elements
[NASA-CR-172497] 11 p1592 N85-20019
Compensator development and examination of performance and robustness
[NASA-CR-175470] 11 p1627 N85-20244
Modal control of structural systems
[AD-A149734] 12 p1790 N85-21235
NASA/MSFC ground experiment for large space structure control verification
[NASA-TM-86496] 12 p1792 N85-21248
Definition of ground test for Large Space Structure (LSS) control verification
[NASA-TM-86495] 12 p1792 N85-21249
Space Station
[NASA-EP-211] 12 p1793 N85-21251
ACOSS 17 (Active Control of Space Structures)
[AD-A150007] 12 p1793 N85-21253
Structural sensitivity analysis: Methods, applications and needs
[NASA-TM-85827] 12 p1865 N85-21695
Variable geometry truss concept
[REPT-614] 12 p1865 N85-21697
Report on final recommendations for IMPS engineering-science payload
[NASA-CR-175659] 13 p1968 N85-22484
Spacecraft environmental interactions: A joint Air Force and NASA research and technology program
13 p1997 N85-22517
Interactions measurement payload for Shuttle
13 p1997 N85-22518
A quantitative comparison of active and passive damping for large space structures
[UTIAS-TN-249] 13 p1998 N85-22524
Approximation in optimal control and identification of large space structures
[AD-A150323] 13 p2151 N85-23351
Large Space Antenna Systems Technology, 1984
[NASA-CP-2368-PT-1] 14 p2229 N85-23813
NASA mobile satellite program
14 p2229 N85-23814
Alternatives for satellite sound broadcast systems at HF and VHF
14 p2229 N85-23815
Development concerns for satellite-based air traffic control surveillance systems
14 p2230 N85-23816
Application of pushbroom altimetry from space using large space antennas
14 p2230 N85-23817
Orbiting multi-beam microwave radiometer for soil moisture remote sensing
14 p2230 N85-23818
Low-frequency microwave radiometer for N-ROSS
14 p2230 N85-23819
Large space antenna technology applied to radar-imaging, rain-rate measurements, and ocean wind sensing
14 p2230 N85-23820
Advanced 2-frequency ocean sensing radar using high resolution antenna beams
14 p2230 N85-23821
LDR system concepts and technology
14 p2231 N85-23823
WRAP-RIB antenna technology development
14 p2231 N85-23824
Development of the 15-meter hoop-column antenna system
14 p2231 N85-23825
Box truss development and its application
14 p2231 N85-23826
Synchronously deployable tetrahedral truss reflector
14 p2231 N85-23827
Antenna Technology for QUASAT application — radio antenna for very long base interferometry missions
14 p2231 N85-23828
Extreme precision antenna reflector study results
14 p2232 N85-23830
NASA space materials research
14 p2232 N85-23831
New concepts in deployable beam structures
14 p2232 N85-23832
Precision space structures
14 p2232 N85-23833
Precision antenna reflector structures
14 p2232 N85-23834
Space Station structures
14 p2232 N85-23835
Verification for large space structures
14 p2232 N85-23836
An optimization study to minimize surface distortions of a hoop-column antenna
14 p2232 N85-23837
Structural dynamics analysis
14 p2233 N85-23838
AFWAL space control technology program
14 p2233 N85-23839
Large Space Antenna Systems Technology, 1984
[NASA-CP-2368-PT-2] 14 p2233 N85-23840
On-orbit systems identification of flexible spacecraft Technol., 1984, Pt. 2 p 465-481
14 p2233 N85-23841
An eigensystem realization algorithm for application to modal testing
14 p2233 N85-23842
MSFC data analysis of the SAFE/DAE experiment
14 p2233 N85-23843
Langley Research Center photogrammetric measurements of solar array dynamics: Preliminary results
14 p2233 N85-23844
Experimental development of a failure detection scheme for large space structures
14 p2234 N85-23846
Dynamic verification of large space structures
14 p2234 N85-23847
Passive and Active Control of Space Structures (PACOSS)
14 p2234 N85-23848
Application of the maximum entropy/optimal projection control design approach for large space structures
14 p2234 N85-23849
Electromagnetic analysis for surface tolerance effects on large space antennas
14 p2234 N85-23850
Application of modern Aperture Integration (AI) and Geometrical Theory of Diffraction (GTD) techniques for analysis of large reflector antennas
14 p2234 N85-23851
Feed system design considerations for large space antenna systems. Part 1: Multiple apertures with non-overlapping feeds
14 p2234 N85-23852
Feed system design considerations for large space antenna systems. Part 2: Single aperture with overlapping feeds
14 p2235 N85-23853
Diffraction analysis of mesh deployable reflector antennas
14 p2235 N85-23854
The space station as a construction base for large space structures
14 p2235 N85-23856
Large Deployable Reflector (LDR) requirements for space station accommodations
14 p2236 N85-23858
Space-based antenna measurement system concepts for space station operation
14 p2236 N85-23860
Solar Array Experiment (SAE) flight experience
14 p2236 N85-23861
Assembly Concept for Construction of Erectible Space Structure (ACCESS) neutral buoyancy testing results
14 p2236 N85-23862
Space Technology Experiments Platform (STEP) status: An in-space test facility
14 p2236 N85-23863
Control Of Flexible Structures (COFS) flight experiment background and description
14 p2236 N85-23864
Shuttle attached antenna Flight Experiment Definition Study (FEDS)
14 p2237 N85-23865
Electro-science requirements for shuttle-attached antenna flight experiments
14 p2237 N85-23866
Model and controller reduction of uncertain systems using covariance equivalent realizations
14 p2243 N85-23902
ACOSS 11 (Active Control Of Space Structures)
[AD-A150639] 14 p2246 N85-23922
Adaptive techniques for control of large space structures
[AD-A150957] 14 p2246 N85-23923
Technology for large space systems: A bibliography with indexes, supplement 11
[NASA-SP-7046(11)] 15 p2475 N85-25277
Definition of technology development missions for early space stations: Large space structures
[NASA-CR-171446] 15 p2476 N85-25281
Construction in space
15 p2484 N85-25328
Construction in space
[NASA-TM-77630] 15 p2492 N85-25374
Definition of ground test for verification of large space structure control
[NASA-CR-171438] 15 p2492 N85-25377
Structures and Dynamics Division research and technology plans for FY 1985 and accomplishments for FY 1984
[NASA-TM-86417] 15 p2577 N85-25895
Model reduction techniques applied to the control of large space structures
[AD-A151784] 16 p2731 N85-26857
The effect of inaccuracies in structural models on the control of large space structures
[AD-A151794] 16 p2732 N85-26858
Incorporating control into the optimal structural design of large flexible space structures
[AD-A152858] 17 p2909 N85-27937
Mathematical modeling and control of a large space structure as applied to a shuttle-antenna configuration
[AD-A153299] 17 p2910 N85-27939
The Shock and Vibration Digest, volume 17, no. 1
[AD-A151051] 17 p2977 N85-28397
On the accuracy of modelling the dynamics of large space structures
19 p3225 N85-29995
The dynamics and control of large flexible space structures, 8
[NASA-CR-175986] 19 p3225 N85-29996
The effect of sensor and actuator errors on static shape control for large space structures
[NASA-TM-86446] 19 p3225 N85-29998
Submillimeter local oscillators for spaceborne heterodyne applications
[NASA-RP-1147] 19 p3226 N85-30005
Self-locking mechanical center joint
[NASA-CASE-LAR-12864-1] 19 p3279 N85-30336
Control system design for lightly coupled large space structures
20 p3399 N85-31066
AFWAL control technology programs
20 p3406 N85-31150
Dynamic performance of several large antenna concepts
20 p3409 N85-31155
Control of large antennas based on electromagnetic performance criteria
20 p3409 N85-31158
Vibration control experiment design for the 15-m hoop/column antenna
20 p3409 N85-31159
A hardware demonstration of distributed control for a flexible offset-feed antenna
20 p3410 N85-31160
Control of flexible structures
20 p3410 N85-31161
Space station configuration and flight dynamics identification
20 p3410 N85-31162
Large space structure flight experiment
20 p3410 N85-31163
Time-optimal bang-bang slew of rigidized SCOLE configuration
20 p3410 N85-31164
Experiments in structural dynamics and control using a grid
20 p3410 N85-31165
The experimental computer control of a two-dimensional hyperbolic system
20 p3411 N85-31166
Rationale for an experimental test for flexible space structure attitude control
20 p3411 N85-31167
Numerical and experimental evaluation for single-axis control of an LSS laboratory model
20 p3411 N85-31168
On the measurement of material damping in a simulated space environment
20 p3411 N85-31169
Proceedings of the Workshop on Identification and Control of Flexible Space Structures, volume 2
[NASA-CR-176052] 20 p3411 N85-31170
Some asymptotic problems in the optimal control of distributed systems
20 p3412 N85-31175
Approximation techniques for parameter estimation and feedback control for distributed models of large flexible structures
20 p3413 N85-31179
Space station parametric models
20 p3413 N85-31180
An integrated control and minimum mass structural optimization algorithm for large space structures
20 p3413 N85-31183
ISAAC (Integrated Structural Analysis and Control) via continuum modeling and distributed frequency domain design techniques
20 p3414 N85-31185
Vibrational stabilization of flexible structures
20 p3414 N85-31188
Stiffness control of large space structures
20 p3414 N85-31189
Sub-optimal control of nonlinear flexible space structures
20 p3414 N85-31190
An overview of latest model reduction and control methods of large flexible space structures
20 p3414 N85-31191
Frequency domain control design of large space structures: A practical approach
20 p3415 N85-31192
A control concept for large flexible spacecraft using order reduction techniques
20 p3415 N85-31193
Proceedings of the Workshop on Identification and Control of Flexible Space Structures, volume 3
[NASA-CR-176053] 20 p3415 N85-31195
Robust control design for large space structures
20 p3416 N85-31200
On the stability of collocated controllers in the presence or uncertain nonlinearities and other perils
20 p3416 N85-31201
Adaptive filtering for large space structures: A closed-form solution
20 p3417 N85-31206
Experimental verification of identification algorithms for control of flexible structures
20 p3418 N85-31211
NASA space station automation: AI-based technology review
[NASA-CR-176094] 21 p3558 N85-32134
NASA space station automation: AI-based technology review. Executive summary
[NASA-CR-176096] 21 p3558 N85-32135
Space station automation study: Autonomous systems and assembly, volume 2
[NASA-CR-176092] 22 p3739 N85-33175

Research and development activities in unified control-structure modeling and design
[NASA-CR-176129] 22 p3740 N85-33179
Research and development activities in unified control-structure modeling and design
[NASA-CR-176111] 22 p3740 N85-33180
Space station rotational equations of motion
[NASA-TP-2511] 23 p3899 N85-34148
Space Station Engineering and Technology Development: Proceedings of the Panel on In-Space Engineering Research and Technology Development
[NASA-CR-176110] 23 p3899 N85-34153
Box truss analysis and technology development. Task 1: Mesh analysis and control
[NASA-CR-172570] 23 p3900 N85-34156
Technology for large space systems: A bibliography with indexes
[NASA-SP-7046(12)] 24 p4066 N85-35209
Identification and control of structures in space
[NASA-CR-176175] 24 p4066 N85-35214
Structural analysis of imperfect three-legged truss columns for large space structures applications
24 p4100 N85-35416

LARGE SPACE TELESCOPE
U HUBBLE SPACE TELESCOPE

LARMOR RADIUS
Theoretical studies of Field-Reversed Configurations (FRC) and experimental study of the FRC during translation
[DE84-016467] 04 p0566 N85-13603
Finite orbit analysis for long wavelength modes in a plasma with a hot component
[DE85-006696] 15 p2658 N85-26404
Stability of high energy particle plasmas to MHD-like modes
[DE85-007879] 17 p3039 N85-28803

LARVAE
The development of the vestibular apparatus under conditions of weightlessness
[NASA-TM-77517] 07 p1011 N85-16422
Chemical composition of Musca domestica L. larval and pupal biomass when developing in organic waste of biological life-support system for man
22 p3624 N85-33691

LARYNX
Metallic aid and technique in fitting voice prosthesis
[AD-D011356] 07 p1014 N85-16442

LASER ANEMOMETERS
Performance evaluation and estimation of a laser time-of-flight velocimeter 03 p0363 N85-12328
Comparative review of laser Doppler and laser two-focus anemometry in turbomachinery applications
[VKI-TM-34] 03 p0367 N85-12350
Computation of noise radiation from a free jet perpendicular to its axis via laser anemometry measurements
[ESA-TT-870] 09 p1379 N85-18669
Determination of the drag of free flying particles in supersonic flow with a pulsed laser
12 p1773 N85-21129
Development of miniature laser Doppler anemometers
[KU-SFB-210/ET/3] 12 p1857 N85-21648
The significance for laser anemometry of particles carried along in a gas flow
[ISL-CO-205/83] 14 p2301 N85-24251
Application of laser anemometry to jets in combustion chambers
[ISL-CO-210/83] 14 p2302 N85-24253
Laser anemometry two dimensional measurement of velocity fluctuations in an excited jet
[ISL-CO-213/83] 14 p2302 N85-24254
Measurements in the flow field of a cylinder with a laser transit anemometer and a drag rake in the Langley 0.3 m transonic cryogenic tunnel
[NASA-TM-86399] 14 p2305 N85-24270
Feasibility study on Laser Doppler Anemometer (LDA) wind velocity measurements using pulsed visible laser light
[ISL-CO-224/83] 16 p2836 N85-27489
An automatic traversing system for Laser Doppler Anemometer (LDA) applications to wind tunnels and to free jets
[ISL-CO-225/83] 16 p2836 N85-27490
Feasibility of mapping velocity flow fields in SSME powerhead by laser anemometry techniques
17 p2915 N85-27971
LDA study of the unburned gas motion induced by nonsteady flame propagation in a constant volume duct
[DE85-009038] 19 p3270 N85-30277
Filter induced errors in laser anemometer measurements using counter processors
[NASA-TM-87047] 19 p3272 N85-30286
The application of laser anemometry to the study of transonic shock boundary-layer interactions
[ISL-CO-204/84] 20 p3396 N85-31057

LASER ANNEALING
Time resolved calorimetry of 30 nm Te-films during laser annealing
[AD-A145047] 01 p0052 N85-10346
Mechanisms of laser annealing of semiconductors
02 p0267 N85-11744
Nonthermal mechanism for laser annealing of semiconductors and formation of super structure
04 p0487 N85-13109
Laser annealing of ion implanted semiconductors
[AD-A146979] 07 p1047 N85-16652
Residual stress after laser processing
11 p1600 N85-20065
Excimer laser annealing to fabricate low cost solar cells
[NASA-CR-174394] 11 p1673 N85-20538
In-orbit laser regeneration of the radiation damaged solar arrays 13 p2008 N85-22588
Thermodynamic and kinetic studies of pulsed laser annealing from transient conductivity measurements
[DE85-009577] 13 p2096 N85-23078
Activation of Si-N modes in silicon by pulsed laser annealing
[DE85-009988] 13 p2097 N85-23082
Specifications of new industrial lasers reviewed
14 p2284 N85-24150
Laser annealing of ion implanted HgCdTe
[AD-A150875] 14 p2427 N85-24966
Excimer laser annealing for fabrication of low-cost solar cells 21 p3611 N85-32433

LASER APPLICATIONS
NT LASER CUTTING
NT LASER FUSION
Flight demonstration of new NRL real-time data acquisition system and laser video waveform sampler
[AD-A145126] 01 p0053 N85-10350
Optical seam tracking of robotic arc welding
[VTT-272] 01 p0055 N85-10368
Achievements in laser development
01 p0115 N85-10784
Investigation of the application of the marginal tension technique to test electronic devices, phase 3
[ESD-11-301] 02 p0208 N85-11360
Dual (GaAl) As-heterostructure based injection laser traveling wave amplifier 02 p0261 N85-11708
Optical recording of information on paper by CO2 and YAG-lasers 02 p0261 N85-11710
Narrowband tunable dye laser with amplifier pumped by powerful nitrogen laser 02 p0262 N85-11716
Laser source of neutral atoms for collective-field particle accelerator 02 p0263 N85-11719
USSR report: Physics and mathematics
[JPRS-UPM-84-004] 02 p0266 N85-11737
Injection lasers based on AlGaAsSb/GaSb and InGaAsSb/GaSb heterostructures
02 p0270 N85-11761
Laser on copper and gold vapors with space diversity media 02 p0270 N85-11762
ONR (Office of Naval Research) Far east Scientific Bulletin, Volume 9, Number 2, April - June 1984
[AD-A145681] 02 p0305 N85-11974
Laser paint removal
[AD-P004009] 03 p0308 N85-11989
Potential application of robotics and state-of-the art end effectors at Letterkenny Army Depot
[AD-P004015] 03 p0309 N85-11994
Optical detection of alkali compounds
[DE84-015505] 03 p0328 N85-12117
Laser and diffusion welding equipment R and D
03 p0352 N85-12265
Laser balancing system for high material removal rates
[NASA-CR-174731] 03 p0365 N85-12341
Three-dimensional photochemical machining with lasers
[AD-A145792] 03 p0365 N85-12342
Bibliography of Soviet laser developments, number 65, May - June 1983
[AD-A146189] 03 p0366 N85-12347
Mapping of mammalian arrhythmias with the cardiac laser scanner 03 p0399 N85-12545
Deceleration, cooling, and trapping of atoms
[AD-A146234] 03 p0418 N85-12672
Formation of superconductive Al(GeSi) alloys by low temperature laser quenching methods
[DE84-016667] 04 p0474 N85-13021
Laser-driven particle accelerators
[DE84-015953] 04 p0506 N85-13227
Laser for determining the ignition conditions of a pyrotechnic mixture
[FOA-C-20542-D1] 04 p0506 N85-13230
Ion beam and laser induced surface modifications
[DE84-016569] 04 p0571 N85-13642
Fundamental equations of the LIF hydroxyl measurements, appendix A 05 p0676 N85-14338
Saturation phenomena in LIF measurements, appendix B 05 p0676 N85-14339
Detailed performance calculations: Wayne State University and Ford Motor Company, appendix C
05 p0676 N85-14340
Detailed performance calculations: Georgia Institute of Technology Group, appendix E
05 p0676 N85-14342
Detailed performance calculations: Portland State Group, appendix F 05 p0676 N85-14343
Detailed performance calculations: Harvard Group, appendix G 05 p0676 N85-14344
Overview of recent advances in laser applications
05 p0725 N85-14660
Formation of reference signals in laser-type gas analyzers with mechanical switching of optical channels
06 p0787 N85-15027
Development of a van-portable remote-sensing laser system for selective detection of natural gas leaks
[PB85-101939/GAR] 06 p0811 N85-15156
Pulsed electric discharge laser technology. Electron beam window foil material
[AD-A146420] 06 p0813 N85-15162
Laser-assisted solar-cell metallization processing
06 p0831 N85-15282
Sputtering in thin film technology for optics — laser systems 07 p0938 N85-15948
Spacecraft system study: A study to define the impact of laser communication systems on their host spacecraft
[NASA-CR-175272] 07 p0970 N85-16150
Noncontact photo-thermal probe-beam deflection measurement of thermal diffusivity in an confined hot gas
[AD-A147481] 07 p0971 N85-16170
Laser ignition of explosives
[FOA-C-20550-D1] 07 p0972 N85-16173
USSR report: Life sciences. Biomedical and behavioral sciences
[JPRS-UBB-84-015] 07 p1010 N85-16416
Ion implantation and laser processing of III-V compound semiconductors with applications to the fabrication of microwave devices
[AD-A146846] 07 p1047 N85-16651
Laser annealing of ion implanted semiconductors
[AD-A146979] 07 p1047 N85-16652
Research and technology, 1984 report
[NASA-TM-83096] 07 p1061 N85-16730
Phase-dissipative mechanisms for laser-induced surface desorption-dissociation processes
[AD-A147981] 08 p1121 N85-17065
Theoretical and experimental analyses of laser altimeters for barometric measurements over the ocean
08 p1165 N85-17351
NASA three-laser airborne differential absorption lidar system electronics
[NASA-CR-174293] 08 p1166 N85-17353
The use of lasers in wide-angle visual systems
[AD-P004322] 09 p1269 N85-17976
Simulation of repetitively-pulsed laser irradiation of graphite-epoxy composite
[AD-A148698] 09 p1325 N85-18329
Feasibility of alpha particle measurement by CO2 laser Thomson scattering
[DE85-001764] 09 p1326 N85-18334
USSR report: Life sciences. Biomedical and behavioral sciences
[JPRS-UBB-85-002] 09 p1360 N85-18559
Effects of dc electric fields on multipholon ionization spectra in cesium
[DE85-001542] 09 p1381 N85-18684
Recent ICF research by GEKKO 12 glass layer at ILE Osaka 09 p1387 N85-18726
Capabilities of laser diagnostics for combustion and flow fields
[DE85-002661] 10 p1438 N85-19064
Temperature variation of laser mirror stability criteria
10 p1445 N85-19106
Excitation modes and parameters of stress waves in metal exposed to single laser pulses
10 p1446 N85-19109
Study of submicron particle size distributions by laser Doppler measurement of Brownian motion
[AD-A149139] 10 p1487 N85-19368
Bibliography of Soviet laser developments, Number 66, July-August 1983
[AD-A149113] 10 p1490 N85-19406
Laser program annual report 1983
[DE84-017287] 10 p1490 N85-19412
Laser air pollution monitoring system planned for Moscow 10 p1500 N85-19465
Pulsed excimer laser processing for cost-effective solar cells
[NASA-CR-174429] 10 p1509 N85-19517
Pulsed excimer laser processing for cost-effective solar cells
[NASA-CR-175465] 10 p1509 N85-19520

Study of microstructure of aluminum and copper alloys after processing with continuous CO2 laser beam
11 p1601 N85-20066
Laser processing of ceramics
[DE85-001184] 11 p1612 N85-20135
Functional system theory in practice
11 p1690 N85-20629
Laser studies of chemical dynamics at the gas-solid interface
[DE84-017580] 11 p1736 N85-20920
Novel photo-thermal technique for flow and spectroscopic measurements in a dense aerosol stream
[AD-A149745] 12 p1800 N85-21287
Two-dimensional measurements of OH concentration and temperature in reactive flows
[AD-A149649] 12 p1800 N85-21292
Portable remote laser sensor for methane leak detection
[NASA-CASE-NPO-15790-1] 12 p1855 N85-21631
Laser clock
[AD-D011513] 12 p1855 N85-21634
Method of and apparatus for measuring temperature and pressure — atmospheric sounding
[NASA-CASE-GSC-12558-1] 12 p1856 N85-21639
Solid propellant combustion diagnostics and automated data retrieval from holograms 13 p1998 N85-22527
A 2 x 6 Back Surface Reflection (BSR) silicon solar cell 13 p2005 N85-22570
Effect of transparent coatings on generation of laser-induced shock waves in metals
13 p2029 N85-22711
China report: Science and technology
[JPRS-CST-85-005] 13 p2052 N85-22843
Laser applications in last 10 years reviewed
13 p2052 N85-22844
Status of and outlook for producing means of transmitting units of plane angle, angular velocity and acceleration with ring lasers 13 p2074 N85-22955
Digital laser platemaker modifications
[AD-A150190] 13 p2096 N85-23074
Computer simulations of rare earth sites in glass: Experimental tests and applications to laser materials
[DE85-006156] 14 p2261 N85-24013
Laser beam shaping system with reduced objective diameter 14 p2275 N85-24095
Sphericity gauge for wavefront of laser radiation
14 p2275 N85-24096
USSR report: Machine tools and metalworking equipment
[JPRS-UMM-85-006] 14 p2283 N85-24146
Specifications of new industrial lasers reviewed
14 p2284 N85-24150
Advanced diagnostics for reacting flows
[AD-A150675] 14 p2301 N85-24246
Applications of lasers in manufacturing
14 p2308 N85-24279
Laser surface treatments 14 p2308 N85-24284
Laser welding in the manufacture of heart pacemakers
14 p2308 N85-24288
Future trends in the use of lasers in manufacturing
14 p2309 N85-24291
Ground-up-to-Space (GUTS) laser propagation code description and manual
[AD-A150783] 14 p2309 N85-24295
Lasers in the domains of ultrashort-time phenomena physics and ballistics
[ISL-CO-236/83] 14 p2310 N85-24299
Laser-assisted solar cell metallization processing
[NASA-CR-175686] 14 p2350 N85-24528
Polar motions measurement study
[AD-A150060] 14 p2372 N85-24664
Producible alternative to CdTe for epitaxy (PACE-2) of LWIR (Long Wave Infrared) HgCdTe
[AD-A150678] 14 p2428 N85-24964
Swedish equipment for automatic docking in space
15 p2489 N85-25363
Optimization of the catalytic oxidation of CO for closed-cycle CO2 laser applications
[NASA-TM-86421] 15 p2504 N85-25445
Corrosion behavior of Al4 aluminum alloy hardened by CO2 laser radiation 15 p2514 N85-25512
An experimental technique for the study of velocity profiles in a laminar jet using a pulsed nitrogen laser
[AD-A151486] 15 p2556 N85-25771
Experimental and theoretical studies of laser cooling and emittance control of neutral beams
[AD-A149215] 15 p2562 N85-25804
Bibliography of Soviet Laser Developments, Number 67, September-October 1983
[AD-A151199] 15 p2562 N85-25805
A plasma initiation-flow chamber to study CW laser beamed energy absorption in light gases
[AD-A151225] 15 p2562 N85-25806
Superfine laser position control using statistically enhanced resolution in real time
[DE85-005843] 15 p2564 N85-25817
Laser-based non-destructive testing techniques for the ultrasonic characterization of sub-surface flaws
[AERE-R-11582] 15 p2572 N85-25858
Dynamics of recrystallization and redistribution of impurities in semiconductors subjected to millisecond laser pulses 15 p2643 N85-26302
Submillimeter-band solid state distributed feedback laser 15 p2644 N85-26307
Industrial laser use expanding in the USSR
15 p2644 N85-26310
Academician Zuyev notes plans for lasers on spacecraft for atmospheric research 16 p2717 N85-26775
Application of space methods in geodesy
16 p2724 N85-26817
Impact of optical inhomogeneity in sintered interface between glasses on laser emission characteristics
16 p2763 N85-27053
USSR report: Machine tools and metalworking equipment
[JPRS-UMM-84-010] 16 p2767 N85-27071
Development, implementation of industrial lasers reviewed 16 p2767 N85-27075
Uses of laser technology described
16 p2768 N85-27080
The utilization of optical fibers in holography
[ISL-R-102/83] 16 p2787 N85-27196
Spectroscopic investigation of materials for frequency agile laser systems
[AD-A151731] 16 p2790 N85-27208
Two-dimensional beat wave acceleration simulation
[DE85-005961] 16 p2791 N85-27214
The copper vapor laser 16 p2824 N85-27417
Research and development of new instruments
16 p2824 N85-27418
Feasibility study on Laser Doppler Anemometer (LDA) wind velocity measurements using pulsed visible laser light
[ISL-CO-224/83] 16 p2836 N85-27480
The development of laser analytical methods for the characterization of solid-liquid and solid-high pressure gas interfaces
[AD-A152382] 17 p2918 N85-27966
Measurement of Franck-Condon factors for the v'=0 progression in the B-X system of PO
[AD-A152734] 17 p2919 N85-27993
X-ray crystallography of steel U8 after pulsed laser hardening
[BLL-BISI-22444-(9022.06)] 17 p2925 N85-28036
Technological apparatus for laser treatment of materials 17 p2944 N85-28174
International time transfer and portable clock evaluation using GPS timing receivers: Preliminary results
17 p2964 N85-28303
Timing of spacecraft data: Time accuracy requirements and timing facilities of the European Space Agency (ESA) 17 p2984 N85-28307
Laser measurements of distances from the ORELA neutron target to experiment stations along flight paths 1 and 6
[DE85-009457] 17 p2971 N85-28352
Presentations at the Tri-Service Cloud Modeling Workshop (2nd), held at the Naval Surface Weapons Center, White Oak, Maryland, 26-27 June 1984, volume 1
[AD-A152735] 17 p2998 N85-28522
Optical system for measuring shadowgraph data
[AD-D011642] 17 p3036 N85-28784
Recent advances in optical measurement methods in physics and chemistry
[DE85-006695] 17 p3037 N85-28792
Philips researches gallium arsenide use for lasers
18 p3087 N85-29106
Laser machining and some applications
[NHK-LABS-NOTE-307] 18 p3112 N85-29266
The application of laser resonance saturation to the development of efficient short wavelength lasers
[AD-A153951] 18 p3113 N85-29270
Definition of requirements for injection locking of pulsed UV lasers
[DE85-010126] 18 p3113 N85-29275
Institute works on modeling thermonuclear plasma processes 19 p3296 N85-30435
Specifics of laser sounding of atmosphere along horizontal and slightly slanting paths over water surface
19 p3297 N85-30441
Development of a technique for in situ detection of stratospheric nitrogen dioxide 19 p3312 N85-30534
EDS operator and control software
[DE85-010470] 19 p3340 N85-30696
Attenuated total reflection method for obtaining optical constants of powders
[AD-A154094] 19 p3367 N85-30881
Laser Schlieren crystal monitor
[NASA-CASE-MFS-28080-1] 19 p3374 N85-30932
Technical and historical overview of the study at Lawrence of porous antireflection coatings
[DE85-010925] 20 p3434 N85-31302
Velocity visualization in gaseous flows
[NASA-CR-174954] 20 p3453 N85-31445
Experimental study of laser produced ions for collective ion acceleration 20 p3460 N85-31494
Improved turbopump dynamics
[NASA-TM-86514] 20 p3462 N85-31509
Ocean tidal parameters from LAGEOS
20 p3493 N85-31716
Electronics Division research and development
[DE85-011687] 20 p3540 N85-32032
East Europe report: Science and technology
[JPRS-ESA-85-023] 21 p3572 N85-32217
Three-dimensional photochemical machining with lasers
[AD-A154711] 21 p3581 N85-32320
Laser-assisted solar-cell metallization processing
21 p3610 N85-32429
Tunable lasers with high conversion efficiency
21 p3687 N85-32906
The sound field of a moving laser-induced acoustic array (theory)
[AD-A154563] 21 p3689 N85-32961
Raman scattering studies in solids
[AD-A155528] 21 p3710 N85-33032
Cryogenic laser calorimetry for impurity analysis
[NASA-CR-176102] 22 p3743 N85-33201
Jet flows: Modeling and experiments
22 p3744 N85-33208
Simultaneous measurement of velocity and density in a turbulent nonpremixed flame 22 p3744 N85-33209
Laser sealed evacuated window glazings
[DE85-000512] 22 p3754 N85-33273
Transparent electrode for optical switch
[DE85-011618] 22 p3761 N85-33310
Electro-optic harmonic conversion to switch a laser beam out of a cavity
[DE85-011619] 22 p3790 N85-33483
Laser effects on opaque targets. Part 2C: Thermal effects of a time-variable beam intensity
[ISL-R-105/84-PT-2C] 22 p3791 N85-33486
Hole cutting in building frames by laser
[FOA-C-20589-D9] 22 p3791 N85-33487
Laser-assisted solar cell metallization processing
[NASA-CR-176124] 22 p3905 N85-33565
Flat-plate solar array project process development area process research of non-CZ silicon material
[NASA-CR-176117] 23 p3945 N85-34445
Observation of mode-converted by ion Bernstein wave by an HCN laser scattering
[IPPJ-724] 23 p3979 N85-34668

LASER BEAM DEFOCUSING
U THERMAL BLOOMING

LASER CAVITIES
Frequency stabilized laser
[AD-D011223] 01 p0063 N85-10351
External cavity diode laser sensor
[AD-D011341] 07 p0969 N85-16152
Halogen mass flow rate detection system
[AD-D011398] 08 p1166 N85-17352
Axial flow laser cavity
[AD-D011508] 12 p1855 N85-21633
Mode control and wavelength tuning in open ended Michelson interferometric semiconductor laser
13 p2095 N85-23073
Scaling blackbody laser to high powers
[NASA-TM-86395] 14 p2309 N85-24292
Internal step-up type higher harmonic light generating device
[DE85-007026] 16 p2790 N85-27213
Design and construction of a CW ND:YAG laser using a single elliptical cavity and water cooled krypton arc lamp pumping
[AD-A152657] 17 p2970 N85-28340
Spatial correlations in the decay from an unstable state in the Malthus Verhulst model — laser cavities
[NOTA-INTERNA-832] 18 p3114 N85-29280
Controlled-linewidth laser source
[AD-D011681] 19 p3274 N85-30308
Optically pumped laser system having extracavity pulse smoother
[AD-D011714] 19 p3276 N85-30319
Grazing incidence beam expander
[DE85-010784] 19 p3368 N85-30889
Generation of single nanosecond high-contrast radiation pulses (lambda=10.6 micrometers)
21 p3684 N85-32686
Influence of mirror anisotropy and Brewster window orientation on radiation characteristics of ring lasers
21 p3684 N85-32689
Electro-optic harmonic conversion to switch a laser beam out of a cavity
[DE85-011619] 22 p3790 N85-33483

LASER COMMUNICATION
U OPTICAL COMMUNICATION
LASER CUTTING
Laser Welding, Cutting and Surface Treatment
14 p2308 N85-24276
An analysis of machine tool systems suitable for laser profiling
14 p2308 N85-24282
Laser cutting: A new tool for shipbuilding
14 p2308 N85-24285
Lasers in automobile production
14 p2309 N85-24286
Lasers in the nuclear industry
14 p2309 N85-24289
Laser drilling of aeroengine components
14 p2309 N85-24290
Europe's primary producers of industrial lasers surveyed
18 p3087 N85-29101
Robot, laser tridimensional cutting technology detailed
20 p3438 N85-31335
Applications of laser technology described
21 p3572 N85-32218
LASER DAMAGE
Electronics research at the University of Texas at Austin
[AD-A146900] 07 p0947 N85-15996
Laser rupture of composite materials
10 p1444 N85-19102
Laser Hazards Bibliography, October 1984
[AD-A149534] 10 p1490 N85-19408
Time resolved Raman studies of laser induced damage in TiO2 optical coatings
[DE85-009166] 11 p1640 N85-20332
A study of low-level laser retinal damage
[AD-A150046] 12 p1905 N85-21965
Time-resolved reflectivity measurement of extrinsic silicon during pulsed laser irradiation
[AD-A150950] 13 p2159 N85-23403
Laser induced damage of zinc sulphide
[BAE-BT-13383] 15 p2582 N85-25803
Raman studies of laser damaged single and multi-layer optical coatings
[DE85-009431] 17 p2971 N85-28351
Predamage threshold electron emission from insulator and semiconductor surfaces
[DE85-008968] 19 p3377 N85-30954
Theoretical modeling of laser induced optical degradation
[AD-A155302] 21 p3582 N85-32323
LASER DOPPLER VELOCIMETERS
The development of a diode laser Doppler velocimeter for boundary layer measurements under ice: A feasibility investigation
[AD-A145076] 01 p0053 N85-10348
Hot section laser anemometry
02 p0142 N85-10962
Laser velocimeter measurements and analysis in turbulent flows with combustion. Part 3: A correction lens for laser Doppler measurements in a cylindrical tube
[AD-A146200] 03 p0366 N85-12348
Comparative review of laser Doppler and laser two-focus anemometry in turbomachinery applications
[VKI-TM-34] 03 p0367 N85-12350
Laser anemometer study of separated flow on wing profiles
[ISL-CO-214/83] 04 p0453 N85-12872
An experimental investigation of two-dimensional thrust augmenting ejectors, part 2
[NASA-CR-174110] 04 p0456 N85-12895
Laser Doppler Anemometer (LDA) wind velocity measurements: Possibilities for measurements on windpower units
05 p0668 N85-14300
A scanning laser velocimeter for turbulence research
[NASA-CR-172469] 07 p0897 N85-15686
Combustion dynamics in rockets
[AD-A148478] 08 p1114 N85-17024
Flame propagation and stabilization studies using Rayleigh scattering and laser Doppler velocimetry
[AD-A148802] 09 p1290 N85-18102
The boundary layer on compressor cascade blades
[NASA-CR-174369] 09 p1319 N85-18292
Comparison of two-dimensional laser and hot-wire velocimetry for a supersonic turbulent boundary layer
11 p1576 N85-19927
Velocity and volumetric measurement in free jets
11 p1576 N85-19931
Laser Doppler Anemometry (LDA) signal triggering and effective particle size range
[KU-SFB-210/E/5] 11 p1634 N85-20290
Projection lens scanning laser velocimeter system
[NASA-CASE-ARC-11547-1] 11 p1638 N85-20320
Solid particle receiver experiments: Velocity measurements
[DE85-000257] 12 p1853 N85-21623
Development of miniature laser Doppler anemometers
[KU-SFB-210/ET/3] 12 p1857 N85-21648
Visualization of velocity fields with Doppler images
[ISL-CO-218/83] 14 p2302 N85-24256
Measurement of the expansion velocity of an aerosol cloud during pyrotechnical dispersion
[ISL-R-125/83] 14 p2303 N85-24262
Experimental and theoretical investigation of the motion of particles in a compressible vortex
[ISL-R-129/83] 14 p2303 N85-24264
Application possibilities of laser Doppler anemometry in the investigation of the transonic interaction between shock wave and boundary layer
[ISL-R-131/83] 14 p2304 N85-24265
Interferometric velocity measurements in ballistics
[ISL-CO-239/83] 14 p2306 N85-24276
La Recherche Aerospatiale Bimonthly Bulletin, Number 1984-4, 221/July-August
[ESA-TT-884] 16 p2695 N85-26637
The development of onboard laser velocimeter at the Saint Louis Institute (France) from 1976 to 1982
[ISL-NB-402/83] 16 p2791 N85-27216
Conducting a wind sensing study
[NASA-CR-175782] 16 p2832 N85-27465
An automatic traversing system for Laser Doppler Anemometer (LDA) applications to wind tunnels and to free jets
[ISL-CO-225/83] 16 p2836 N85-27490
Formulation of a coherent light-sheet by means of a cylindrical-spherical optical system
[ISL-R-116/83] 16 p2665 N85-27674
Incident beam polarization for laser Doppler velocimetry employing a sapphire cylindrical window
[NASA-TM-87064] 17 p3037 N85-28786
Vibration-free Raman Doppler velocimeter
[NASA-CASE-LAR-13268-1] 18 p3104 N85-29216
MHD channel development
[DE85-008305] 18 p3192 N85-29796
LDV multiplexer interface
[NASA-CASE-ARC-11536-1] 19 p3258 N85-30202
Recent measurements in turbulent jet flames at Sandia Combustion Research Facility
20 p3424 N85-31254
Velocity visualization in gaseous flows
[NASA-CR-174954] 20 p3453 N85-31445
Development of a new laser Doppler velocimeter for the Ames High Reynolds Channel No. 2
[NASA-TM-86772] 20 p3458 N85-31477
Laser Doppler Anemometer (LDA) measurements in the turbulent near-wake of blunt bodies
[ISL-CO-212/84] 22 p3785 N85-33450
Measurement of velocity and concentration in free jets
[ISL-CO-215/84] 22 p3785 N85-33451
Multiparameter conditionally sampled laser velocimetry measurements during flame propagation in a spark ignition engine
[DE85-009850] 22 p3793 N85-33502
A comparison of laser Doppler anemometry and probe measurements within the boundary layer of an airfoil at subsonic flow
[ISL-CO-219/84] 23 p3895 N85-34127
Study of boundary layer separation on a supercritical profile with a spoiler by means of a laser Doppler velocimeter
[ISL-CO-225/84] 23 p3895 N85-34128
Prediction of the flow-field interference induced by the long-range laser velocimeter in the Ames 40- by 80-foot and the 80- by 120-foot wind tunnels
[NASA-TM-86763] 23 p3896 N85-34146
Nonsimultaneous coupled laser velocimeter measurement technique: Error prediction for spatially noncoincident measurements
[NASA-TM-86718] 23 p3934 N85-34379
The use of a laser Doppler velocimeter in a standard flammability tube
[NASA-CR-174960] 24 p4096 N85-35389
LASER DRILLING
Laser applications in last 10 years reviewed
13 p2052 N85-22844
Specifications of new industrial lasers reviewed
14 p2264 N85-24150
Laser Welding, Cutting and Surface Treatment
14 p2308 N85-24278
Applications of lasers in manufacturing
14 p2308 N85-24279
Laser drilling of aeroengine components
14 p2309 N85-24290
LASER FUSION
Progress in inertial confinement fusion at Lawrence Livermore National Laboratory
[DE84-016227] 04 p0588 N85-13621
Quality assurance in the Antares Laser Fusion Construction Project
[DE84-015493] 05 p0640 N85-14104
Laser program annual report 1983
[DE84-017287] 10 p1490 N85-19412
Raman sidescattering in laser-produced plasmas
[AD-A148905] 10 p1556 N85-19813
Approaches to ultrafast neutron detectors
[DE85-001206] 11 p1636 N85-20307
Modal testing and analysis of NOVA laser structures
[DE84-017599] 11 p1638 N85-20321
Operational characteristics of the OMEGA short-wavelength laser fusion facility
[DE85-002819] 11 p1640 N85-20334
Laser-induced fluorescence of metal-atom impurities in a neutral beam
[DE85-004980] 14 p2310 N85-24296
Laboratory for laser energetics report
[DE85-007235] 15 p2563 N85-25814
Design optimization of singlemain-amplifier KrF laser-fusion systems
[DE85-007680] 16 p2791 N85-27215
Sub-nanosecond cinematography in laser fusion research: Current techniques and applications at the Lawrence Livermore Laboratory
[DE85-007252] 17 p2968 N85-28334
Microwave experimental studies of laser fusion
[DE85-008327] 17 p3041 N85-28814
Rapid growth of potassium dihydrogen phosphate crystals
[DE85-007261] 17 p3045 N85-28830
KrF laser cost/performance model for ICF commercial applications
[DE85-009589] 18 p3182 N85-29726
Megajoule-class single-pulse KrF laser test facility as a logical step toward inertial fusion commercialization
[DE85-009590] 18 p3191 N85-29794
Prospects for lasers for fusion energy assessed
21 p3684 N85-32885
Energy and Technology Review
[DE85-011767] 21 p3716 N85-33061
Electro-optic harmonic conversion to switch a laser beam out of a cavity
[DE85-011619] 22 p3790 N85-33483
LASER GEODYNAMIC SATELLITE
U LAGEOS (SATELLITE)
LASER GUIDANCE
East Europe report: Science and technology
[JPRS-ESA-84-045] 06 p0815 N85-15175
Laser-guided measuring system for precisioning device
06 p0816 N85-15179
Optmizing the specifications for an air-surface laser system
16 p2696 N85-26644
LASER GYROSCOPES
Evaluation of the stochastic drift of rate-integrating gyros as preparation for the analysis of laser gyro drift measurements
[ESA-TT-827] 05 p0639 N85-14099
Flight testing of Litton laser gyro strapdown system LTN-90 for general aviation
[DFVLR-MITT-84-16] 07 p0901 N85-15709
Reflectivity measurements of laser gyro mirrors
[ESA-TT-851] 09 p1386 N85-18714
Laser gyroscope random walk determination using a fast filtering technique
16 p2696 N85-26647
Gyrolaser guidance system for medium range missiles
16 p2696 N85-26649
Autofocus motion compensation for synthetic aperture radar and its compatibility with strapdown inertial navigation sensors on highly maneuverable aircraft
[AD-A151940] 16 p2704 N85-26693
Measurements of laser gyro errors as a function of the beam path
[DFVLR-FB-85-02] 17 p2969 N85-28336
Flight testing the Litton LTN 90 laser gyro strapdown system for civil aviation
[ESA-TT-904] 20 p3392 N85-31042
Advanced (unfloated) gyros for satellite control
[ESA-CR(P)-2010] 20 p3419 N85-31222
Development of an active laser gyro for inertial rotation sensing in attitude/heading reference and inertial navigation systems, phase 1
[BMFT-FB-W-85-001] 20 p3460 N85-31489
LASER HEATING
Material degradation in heavy steel plates caused by bending with a laser
[AD-A144784] 01 p0052 N85-10343
Biform resolidification and amorphous phases in a laser and electron beam processed tantalum-iridium alloy
[DE84-013334] 02 p0184 N85-11234
Laser-assisted solar cell metallization processing
[NASA-CR-174213] 06 p0813 N85-15160
Time-resolved studies of ultrarapid solidification of highly undercooled molten silicon formed by pulsed laser irradiation
[DE84-016664] 06 p0813 N85-15164
Analysis of phase composition of products of laser destruction of metallic surfaces
11 p1600 N85-20064
Influence of laser treatment of structure and mechanical properties if MA21 alloy
13 p2029 N85-22713
Specifics of laser heat treatment of high steel tools
13 p2029 N85-22714

Structure of amorphous films of alloys based on Fe, condensed from laser erosion products
13 p2035 N85-22749
Specifications of new industrial lasers reviewed
14 p2284 N85-24150
Laser Welding, Cutting and Surface Treatment
14 p2306 N85-24278
Applications of lasers in manufacturing
14 p2308 N85-24279
Trends in laser equipment 14 p2308 N85-24280
Laser surface treatments 14 p2308 N85-24284
Dopant incorporation in silicon during nonequilibrium solidification: Comparison of 2 processes
[DE85-005568] 14 p2430 N85-24988
Investigation of basic characteristics of laser heating in thermoluminescence and of laser-stimulated luminescence
[AD-A152143] 16 p2790 N85-27212
Limiting processes laser CVD
[DE85-008846] 18 p3114 N85-29279
Development of growth techniques for electromagnetic crystals
[AD-A154089] 19 p3375 N85-30937
Quasi-steady-state melting mode during combined laser irradiation of semiconductor materials
21 p3682 N85-32874
Nonequilibrium kinetics of growth of oxide layer grains during laser heating of metals in air
21 p3689 N85-32919
Coefficient of optical absorption and scattered light capture effect 21 p3695 N85-32959
On one nonlinear problem of laser thermochemistry
21 p3697 N85-32971
Asymptotically stable solutions of some nonlinear equations 21 p3698 N85-32974
Magnetic fields in laser heated plasmas
[DE85-010715] 21 p3707 N85-33022
Laser effects on opaque targets. Part 2C: Thermal effects of a time-variable beam intensity
[ISL-R-105/84-PT-2C] 22 p3791 N85-33486

LASER INTERFEROMETRY

Real time sensing and control of out-of-plane distortion due to line heating by laser
[AD-A144773] 01 p0027 N85-10169
Effect of hydrogen on formation of energy spectrum of multiply charged and copper ions
02 p0263 N85-11720
Improved sensitivities in laser interferometers for the detection of gravitational waves
[MPQ-88] 04 p0506 N85-13232
Modular laser distance measurement system for multiaxis machine tools
[BMFT-FB-T-84-166] 05 p0641 N85-14110
Measuring large amplitudes of mechanical vibrations with laser interferometers 06 p0787 N85-15028
Turbulence measurement interferometer apparatus
[AD-D011377] 07 p0970 N85-16158
High temperature laser interferometric studies of solid electrolytes 09 p1396 N85-18785
CO2 laser interferometer array for Big Dee
[DE85-001718] 10 p1490 N85-19411
Technical support for microwave experiments on the eye lens
[AD-A149702] 12 p1933 N85-22144
Geophysical laser interferometer with 12.5 meter base
13 p2089 N85-23046
System for lower hybrid current startup
15 p2654 N85-26373
One-frequency laser interferometer using the optic fiber as a polarization-independent interference phase detector
[DE85-010544] 19 p3277 N85-30326
Applications of laser technology described
21 p3572 N85-32218
Possibility of measurement of small displacements by ring laser 21 p3687 N85-32904
Practical aspects of laser holographic interferometry in wind tunnels
[NASA-TM-86786] 23 p3933 N85-34379

LASER MATERIALS

Laser diodes for infrared spectroscopy
[BMFT-FB-T-84-131] 05 p0640 N85-14109
Position effects of laser protective materials on simulator tracking performance
[AD-A148297] 08 p1167 N85-17359
Improved solid-state laser sources, volume 2
[DE85-000759] 09 p1325 N85-18330
Picosecond laser pulse interactions with metallic and semiconductor surfaces
[AD-A149112] 10 p1490 N85-19405
Modern solid state laser materials
[DE85-003665] 10 p1490 N85-19410
Advanced crystalline laser materials
[DE85-003142] 12 p1857 N85-21647
Research progress on laser crystals in China
13 p2166 N85-23440
Studies on radiative collisional and ultraviolet lasers
[AD-A151004] 14 p2310 N85-24296
Bibliography of Soviet Laser Developments, Number 67, September-October 1983
[AD-A151199] 15 p2602 N85-25805
Spectroscopic investigation of materials for frequency agile laser systems
[AD-A151731] 16 p2790 N85-27206
Saturation effect in multilevel lasing media
21 p3686 N85-32901

LASER MICROSCOPY

Applications of laser technology described
21 p3572 N85-32218

LASER MODE LOCKING

Microcomputer controlled automatic peak locking of laser circuit 15 p2537 N85-25855
A study of mode-locked argon ion-dye laser systems
16 p2789 N85-27205
Optical injection locking of solid-state oscillators by frequency-multiplexed injection-locked, laser diodes
[AD-D011695] 19 p3275 N85-30307
Dye laser traveling wave amplifier
[NASA-CR-175969] 19 p3275 N85-30308
Choice of optimum saturating absorber for YAG passive mode-locking laser 21 p3685 N85-32893
Dynamics of emission from dye lasers employing synchronous pumping by limited picosecond pulse train
21 p3686 N85-32899

LASER MODES

Linear theory of free-electron lasers with cylindrical interaction space 02 p0262 N85-11718
Laser source of neutral atoms for collective-field particle accelerator 02 p0263 N85-11719
Space-time characteristics of radiation of single-mode injection lasers 02 p0269 N85-11756
Overview of recent advances in laser applications
05 p0725 N85-14660
Electron acceleration by laser fields in a gas
[DE85-000575] 11 p1639 N85-20323
Simplified analytical model for calculation of population inversion in channels of CW gasdynamic lasers operating at various transitions among levels pertaining to coupled upsilon 1 and upsilon 2 modes of CO2
[STN-2] 20 p3461 N85-31496
Self Q-modulation and generation of short pulses in distributed-feedback lasers 21 p3687 N85-32907

LASER OUTPUTS

Extracts from the test plan for in-flight evaluation of the NT-33A peripheral vision display
01 p0009 N85-10055
New type of unique frequency laser communications
[AD-A145128] 01 p0038 N85-10239
Free electron lasers
[AD-A145109] 01 p0053 N85-10349
Achievements in laser development
01 p0115 N85-10784
Laser speckle technique for burner liner strain measurements 02 p0142 N85-10960
High repetition rate nitrogen ion laser
02 p0201 N85-11340
Influence of radiation wavelength on elastic pulse shape during laser excitation 02 p0257 N85-11681
Biaxial-crystal laser with waveguide resonator
02 p0262 N85-11717
Linear theory of free-electron lasers with cylindrical interaction space 02 p0262 N85-11718
Laser source of neutral atoms for collective-field particle accelerator 02 p0263 N85-11719
Nonlinear symmetrization of picosecond pulses in optical fibers 02 p0264 N85-11725
Study of CW injection laser with a dispersive external cavity 02 p0270 N85-11760
Injection lasers based on AlGaAsSb/GaSb and InGaAsSb/GaSb heterostructures
02 p0270 N85-11761
Laser on copper and gold vapors with space diversity mode 02 p0270 N85-11762
Efficiency of lasing dye media in pumping high-power radiation with nanosecond pulses
02 p0270 N85-11763
Anomalies in frequency characteristics of solid-state ring laser 02 p0271 N85-11765
Optimizing CW CO2 lasers with respect to output power in different bands 02 p0271 N85-11766
Laser paint removal
[AD-P004009] 03 p0308 N85-11989
Calculation of energy characteristics of double-passage amplifier 03 p0347 N85-12236
Breakdown of porous metals by laser radiation
03 p0349 N85-12249
Heatsink requirements for coherent operation of high-power semiconductor laser arrays
[AD-A146184] 03 p0368 N85-12346
Beam profiling in gigawatt 1064-nm lasers used in research on optical materials at Livermore
[DE84-007226] 04 p0505 N85-13223
Overview of recent advances in laser applications
05 p0725 N85-14660
Storage stability of jet fuels
[AD-A146360] 06 p0773 N85-14943
Device for measuring average power of laser radiation
06 p0786 N85-15026
Laser illuminated nano-second microscope
[DE84-016200] 06 p0811 N85-15152
Laser-assisted solar cell metallization processing
[NASA-CR-174213] 06 p0813 N85-15160
Time-resolved studies of ultrarapid solidification of highly undercooled molten silicon formed by pulsed laser irradiation
[DE84-016664] 06 p0813 N85-15164
Wavelength scaling of laser plasma coupling
[DE84-014837] 06 p0896 N85-15505
RF laser array driver apparatus
[AD-D011376] 07 p0969 N85-16155
Delta wing nozzle assembly for chemical lasers
[AD-D011396] 07 p0970 N85-16156
Design and testing of a refractive laser beam homogenizer
[AD-A146997] 07 p0970 N85-16162
Visible and ultraviolet lasers based on excimer transitions in the homonuclear halogens
[AD-D011311] 07 p0971 N85-16163
Theoretical study of laser-induced surface excitations on a grating
[AD-A147855] 07 p0972 N85-16172
Measurement of high temperature strain by the laser-speckle strain gauge
[NASA-TM-77751] 07 p0977 N85-16207
Longer-scalelength plasma perturbations by an intense laser beam
[AD-A147005] 07 p1045 N85-16638
Construction, testing of 1-MW nitrogen laser
08 p1140 N85-17182
In-situ formation of a grain boundary in field ion microscopy using a laser
[AD-A148225] 08 p1166 N85-17355
Time-resolved studies of free radicals and laser-initiated chain reactions
[DE85-002100] 09 p1326 N85-18332
Laser ablation studies using RIS
[DE85-001118] 09 p1326 N85-18336
Quantum noise effects in single-mode injection lasers
[FUB-11-1984] 09 p1327 N85-18338
Multiphoton ionization of cesium atoms above and below the two-photon ionization threshold
[DE85-000976] 09 p1381 N85-18682
Determination of vapor phase content when metals are struck by laser radiation pulses of various densities
10 p1445 N85-19106
Temperature variation of laser mirror stability criteria
10 p1445 N85-19108
Experimental and theoretical study of condensation in multicomponent vapors
[DE85-000843] 10 p1485 N85-19376
A free electron laser with two-component wiggler
11 p1623 N85-20217
The noise of laser diodes with modulated injection current
[FI-465-TBR-23] 11 p1625 N85-20233
Projection lens scanning laser velocimeter system
[NASA-CASE-ARC-11547-1] 11 p1638 N85-20320
Potential of high-average-power solid state lasers
[DE85-003884] 11 p1639 N85-20329
Model calculations for a CO2 mixing laser with screen nozzle
[ESA-TT-859] 11 p1640 N85-20336
USSR report: Physics and mathematics
[JPRS-UPM-85-001] 11 p1715 N85-20798
Study of light shifts in laser pumped quantum discriminator frequency 11 p1716 N85-20798
Distortion of temporal characteristics during parametric up-conversion of ultrashort laser pulses
11 p1717 N85-20803
Spontaneous diffraction of sequence of supershort light pulses in dye solution 11 p1718 N85-20811
Electron acceleration
[DE85-002337] 11 p1725 N85-20850
Photo-thermal detection of the onset of photo-chemical nucleation (laser-snow) in vapor
[AD-A150111] 12 p1801 N85-21295
Research study of droplet sizing technology leading to the development of an advanced droplet sizing system
[NASA-CR-174839] 12 p1850 N85-21604
Transmission and reflection of laser beams propagating through aerosol clouds in space
[LA-9996-MS] 12 p1856 N85-21638
Dynamics of space charge waves in the laser beat wave accelerator
[AD-A149668] 12 p1936 N85-22163
Adequacy of metal ablation process with laser radiation and a shock-compressed plasma
13 p2028 N85-22708

Neodymium YAG laser pumped with radiation from high frequency electrodeless discharge
13 p2044 N85-22796
Comparison reference etalon of unit laser radiation power 13 p2074 N85-22957
Invariance of probability characteristics of detector to shape of optical pulse signals 13 p2090 N85-23048
Near Field/Far Field (NF/FF) energy loss in Electric Discharge Lasers (EDL's): A mode-medium interaction
[AD-A150299] 13 p2096 N85-23075
Chemical stabilization of laser dyes
[AD-A150451] 13 p2096 N85-23076
A spatially incoherent and temporally coherent source
[AD-A151281] 13 p2157 N85-23390
Ion transport in beam-plasma interactions
[AD-A150145] 13 p2161 N85-23410
Laser beam shaping system with reduced objective diameter 14 p2275 N85-24095
Sphericity gauge for wavefront of laser radiation
14 p2275 N85-24096
Trends in laser equipment 14 p2306 N85-24260
Safety with industrial manufacturing lasers
14 p2306 N85-24261
An analysis of machine tool systems suitable for laser profiling 14 p2306 N85-24262
The measurement of laser beam parameters
14 p2306 N85-24263
Laser cutting: A new tool for shipbuilding
14 p2306 N85-24265
Laser spot welding in the electronics industry
14 p2306 N85-24267
Future trends in the use of lasers in manufacturing
14 p2309 N85-24291
Scaling blackbody laser to high powers
[NASA-TM-86395] 14 p2309 N85-24292
Active dispersion control for a Doppler broadened laser
[AD-D011570] 14 p2310 N85-24297
Calorimeter for measuring high-energy optical pulses
[PB85-160695] 15 p2561 N85-25799
Bibliography of Soviet Laser Developments, Number 67, September-October 1983
[AD-A151199] 15 p2562 N85-25805
Method and apparatus for high speed, sustained recording of infrared laser beam patterns
[AD-D011585] 15 p2563 N85-25811
Discharge characteristics of high-pressure, fast-discharge XeCl excimer laser
15 p2564 N85-25820
Characteristics of laser emission discharge created by pulsed CO2-laser 15 p2643 N85-26305
Amplification of scattered induced radiation flux in high-gain laser rods 15 p2644 N85-26309
Industrial laser use expanding in the USSR
15 p2644 N85-26310
Method and apparatus for generating a structured light beam array
[AD-D011590] 15 p2652 N85-26357
LDA study of non-steady flame propagation in a constant volume duct
[DE85-007233] 16 p2746 N85-26948
Population inversion in laser-initiated vacuum arcs
[AD-A151958] 16 p2790 N85-27210
Photoionization mass spectrometry with VUV hydrogen laser source
[AD-A153362] 17 p2921 N85-29009
Operating characteristics, absorptivity/reflectivity measurements, and pulse system design of the NPS (Naval Postgraduate School) hydrogen fluoride/deuterium fluoride laser
[AD-A152712] 17 p2970 N85-26341
Low voltage free electron laser development
[AD-A152917] 17 p2970 N85-26342
Instabilities and chaotic behavior of active and passive laser systems
[AD-A153366] 17 p2971 N85-26346
Europe's primary producers of industrial lasers surveyed 18 p3087 N85-29101
Magnetically switched power supply systems for lasers
[NASA-CASE-NPO-16402-1] 18 p3112 N85-29265
Intense excitation source for high power laser
[AD-A153424] 18 p3112 N85-29267
Technique for measuring surface diffusion by laser-beam-localized surface photochemistry
[DE85-007865] 18 p3113 N85-29273
Accelerator technology working group summary
[DE85-009547] 18 p3160 N85-29717
KrF laser cost/performance model for ICF commercial applications
[DE85-009569] 18 p3162 N85-29728
Self-detecting optical sensors
[AD-D011657] 18 p3165 N85-29751
All-optical logic gates with external switching by laser and incoherent radiation 18 p3167 N85-29766
Apparatus for non-destructive inspection of blind holes
[AD-D011707] 19 p3273 N85-30295
Experiments in plasma initiation and laser absorption in flowing gases
[AD-A154903] 19 p3276 N85-30313
Development and application of a high power ND-glass laser instrument
[AD-A154366] 19 p3276 N85-30314
Optically pumped laser system having extracavity pulse smoother
[AD-D011714] 19 p3276 N85-30319
Phase and amplitude feedback control system for the Los Alamos free-electron laser
[DE85-010787] 19 p3277 N85-30325
Research with high-power short-wavelength lasers
[DE85-010329] 19 p3278 N85-30332
Clearing of polydisperse aqueous aerosol by laser radiation pulses 19 p3298 N85-30445
Development of a new laser Doppler velocimeter for the Ames High Reynolds Channel No. 2
[NASA-TM-86772] 20 p3458 N85-31477
Z-contrast imaging and electron channeling analysis of dopants in semiconductors
[DE85-011410] 21 p3562 N85-32269
The 2-D simulations of the NRL (Naval Research Laboratory) laser experiment
[AD-A154915] 21 p3592 N85-32321
Visibility and vertical structure measurements in southern Germany
[AD-A154714] 21 p3635 N85-32574
Luminescence and absorption of indium-activated potassium-borate glasses subjected to high-power excitation 21 p3681 N85-32868
Generation and amplification of radiation during stimulated Raman scattering in crystals
21 p3681 N85-32869
Absorption of 10.6 micrometer laser radiation in electron-hole condensate in germanium
21 p3681 N85-32870
Defect formation in amorphous hydrated silicon subjected to laser radiation 21 p3682 N85-32873
Establishment of steady-state power level in pulse-periodic excimer laser 21 p3685 N85-32896
The problem of brightness enhancement during laser frequency doubling 21 p3686 N85-32897
Excimer-laser generator of powerful UV picosecond pulses synchronized with picosecond pulses in visible and IR bands 21 p3686 N85-32903
Investigation of ion-acoustic plasma turbulence in field of powerful electromagnetic wave by CO2-laser radiation scattering 21 p3691 N85-32935
Characteristics of optogalvanic effect in media with inverse populations 21 p3693 N85-32944
Absorption of laser radiation in substance with absorption coefficient depending linearly upon temperature 21 p3694 N85-32953
Optical waveguide along front of exothermic reaction
21 p3694 N85-32954
Coefficient of optical absorption and scattered light capture effect 21 p3695 N85-32959
The sound field of a moving laser-induced acoustic array (theory)
[AD-A154553] 21 p3699 N85-32981
Multiphoton production and detection of atoms
[AD-A155581] 21 p3702 N85-33000
Method of characterizing critical timing paths and analyzing timing related failure modes in very large scale integrated circuits
[AD-D011731] 22 p3759 N85-33298
Sliding discharge in CO2 and excimer lasers
22 p3773 N85-33379
Device for frequency modulation of a laser output spectrum
[DE85-011634] 22 p3790 N85-33479
Lasertron simulation with a two-gap output cavity
[DE85-011213] 22 p3790 N85-33480
Picosecond-pulse damage studies of diffraction gratings
[DE85-010785] 22 p3790 N85-33481
Effects of laser radiation on surfaces and coatings
[DE85-010475] 22 p3790 N85-33484
Method and apparatus for measuring areas of photoelectric cells and photoelectric cell performance parameters
[DE85-011629] 22 p3810 N85-33599
Microcomputer controlled image processor
[AD-D011734] 22 p3833 N85-33735
Time-resolved spectroscopic studies of detonating heterogeneous explosives
[DE85-009760] 23 p3921 N85-34297
Thermal transport measurements of UV laser irradiated spherical targets
[DE85-011038] 23 p3931 N85-34365
Apparatus and method for the spectrochemical analysis of liquids using the laser spark
[DE85-006749] 23 p3935 N85-34387
Ranging system which compares an object reflected component of a light beam to a reference component of the light beam
[NASA-CASE-NPO-15885-1] 23 p3973 N85-34629
High energy plasma accelerators
[DE85-013121] 24 p4155 N85-35760
Laser and electron beam processing of semiconductors
[AD-A155914] 24 p4161 N85-35796

LASER PLASMA INTERACTIONS

Focusing effects of a laser beam in the nonresonant multiphoton ionization (MPI) of gases
[LP-207] 04 p0506 N85-13231
Role of cavitons in laser-plasma interactions
[DE85-001842] 11 p1731 N85-20666
Activities report of the Institute of Plasma Research
11 p1733 N85-20903
Increased hot-electron production at quarter-critical density in long-scalelength, laser-plasma interactions
[AD-A150519] 13 p2161 N85-23411
Ion emission from solid surfaces: Comparison of dust impact with other excitations — Giotto mission
14 p2244 N85-23912
Direct electron and ion fluid computation of high electrostatic fields in dense inhomogeneous plasma with subsequent nonlinear optical and dynamical laser interaction 15 p2656 N85-26388
Progress in inertial fusion at LLNL
[DE85-010931] 19 p3277 N85-30321

LASER PLASMAS

Optical properties of laser erosion flares in plasma
02 p0270 N85-11784
RF laser plasma measurements
[AD-A145936] 03 p0366 N85-12344
Non-LTE considerations in spectral diagnostics of thermal transport and implosion experiments
[DE84-015187] 05 p0730 N85-14689
Measurements of X-ray spectra from laser produced plasma 06 p0748 N85-14794
Wavelength scaling of laser plasma coupling
[DE84-014637] 06 p0866 N85-15505
Thermal evaporation in blast waves: A model for ansurism formation in the NRL (Naval Research Laboratory) LASER-HANE simulation experiment
[AD-A147006] 07 p0978 N85-16210
SWIR and visible atomic emission from laser-produced oxygen and nitrogen plasmas
[AD-A147528] 07 p1045 N85-16641
Proceedings on US-Japan Workshop on Tokamak Diagnostics by X-ray, VUV and Optical Radiations
[IPPJ-703] 09 p1386 N85-18719
Recent ICF research by GEKKO 12 glass layer at ILE Osaka 09 p1387 N85-18726
Soft X-ray spectroscopy of laser produced plasmas
09 p1387 N85-18727
Electron-hole plasma formation in semiconductors due to the absorption of pulsed CO2 laser light
[DE85-001559] 09 p1392 N85-18757
Raman sidescattering in laser-produced plasmas
[AD-A148905] 10 p1556 N85-19813
Parametric processes in underdense UV laser-produced plasmas
[DE85-002812] 10 p1559 N85-19830
Ion velocity distributions from spherical 1054 nm and 351 nm laser plasmas
[DE85-002816] 10 p1559 N85-19833
X-ray line broadening of a diagnostic in laser produced plasma
[DE85-001179] 10 p1560 N85-19841
Measurement of hot-electron production and microwave emission by laser-irradiated CH targets
[DE85-003139] 11 p1640 N85-20331
Plasma stalse near surface of metal irradiated by CO2 laser 11 p1719 N85-20815
Influence of shock wave front on nature of luminescence of recombining laser plasma 11 p1719 N85-20816
Coronal spectroscopy in laser plasmas
[DE85-002817] 11 p1730 N85-20880
Laser-plasma interactions for the deposition and etching of semiconductor materials
[DE85-000458] 11 p1731 N85-20885
Role of cavitons in laser-plasma interactions
[DE85-001842] 11 p1731 N85-20886
X-ray spectroscopy of laser-produced plasmas
[DE85-002170] 11 p1733 N85-20897
Development and application of low energy X-ray and electron physics
[AD-A149983] 12 p1926 N85-22099
Affect of angle of incidence on plasmas generated during laser welding
[DE85-005724] 15 p2569 N85-25852
Characteristics of laser emission discharge created by pulsed CO2-laser 15 p2643 N85-26305
Soft X-ray diagnostics of laser-produced plasmas (HALNA) 15 p2655 N85-26382

Laser plasma LINAC
[DE85-006294] 17 p2971 N85-28348
Microwave experimental studies of laser fusion
[DE85-006327] 17 p3041 N85-28814
The application of laser resonance saturation to the development of efficient short wavelength lasers
[AD-A153951] 18 p3113 N85-29270
Research with high-power short-wavelength lasers
[DE85-010329] 19 p3278 N85-30332
Strong coupling effects on bound states in plasmas
[AD-A154353] 19 p3370 N85-30905
Report of near field group
[DE85-010536] 20 p3527 N85-31940
Investigation of plasma processes in electronic transition lasers
[AD-A155598] 21 p3593 N85-32327
Selective population of N = 3 OVIII level during expansion of laser plasma in helium
21 p3688 N85-32914
CCD-based X-ray spectrometry for on-line determination of laser plasma electron temperature
21 p3692 N85-32938
Investigation of space-time structure of glow of laser plasma colliding with flat screen
21 p3693 N85-32947
Magnetic fields in laser heated plasmas
[DE85-010715] 21 p3707 N85-33022
Multiple inner shell vacancies in laser-irradiated Au plasma 23 p3981 N85-34687
Elliptical X-ray analyzer spectrograph application to a laser-produced plasma
[DE85-013790] 24 p4097 N85-35398

LASER PUMPING
Singlet delta oxygen generator
[AD-D011208] 01 p0012 N85-10072
Solar-pumped lasers: A review
02 p0261 N85-11711
Theory of free-electron lasers with focusing pumping field 02 p0262 N85-11714
Narrowband tunable dye laser with amplifier pumped by powerful nitrogen laser 02 p0262 N85-11716
Biaxial-crystal laser with waveguide resonator
02 p0262 N85-11717
Efficiency of lasing dye media in pumping high-power radiation with nanosecond pulses
02 p0270 N85-11763
Transformation of energy spread of laser pumping via phase conjugation 05 p0725 N85-14661
Highly efficient Nd:YAG lasers for free-space optical communications 10 p1463 N85-19229
Improved electron emission by use of a cloth fiber cathode
[AD-A149250] 10 p1480 N85-19340
Electron-oscillatory spectra of yttrium-erbium-aluminum garnet of crystals and their role in laser pumping
11 p1715 N85-20791
Study of light shifts in laser pumped quantum discriminator frequency 11 p1716 N85-20796
Investigation of dye lasers pumped by high-power KrF laser radiation 11 p1718 N85-20806
The effects of surface waves on RF discharge pumped lasers
[AD-A149689] 12 p1856 N85-21643
Scaling blackbody laser to high powers
[NASA-TM-86395] 14 p2309 N85-24292
Population inversion in laser-initiated vacuum arcs
[AD-A151958] 16 p2790 N85-27210
Study on a prismatic dye vat — laser systems
[CERT-2/6124-04-RO] 16 p2791 N85-27217
Experimental investigation of the pulsed photoacoustic effect produced on a solid surface
[AD-A152114] 16 p2860 N85-27640
Coherently pumped two-frequency laser-type devices
[AD-A154065] 19 p3275 N85-30311
Theoretical modeling of the discharge-pumped XeCl excimer laser 20 p3460 N85-31495
Three-dimensional photochemical machining with lasers
[AD-A154711] 21 p3591 N85-32320
A fast discharge excimer laser with symmetric geometry
[AD-A155294] 21 p3592 N85-32322
Lasing on LIF:F(-)2 - dye centers with transverse pumping 21 p3684 N85-32890
Dynamics of emission from dye lasers employing synchronous pumping by limited picosecond pulse train
21 p3686 N85-32899
Stimulated Mandelstam-Brillouin scattering with distributed feedback 21 p3686 N85-32901
Influence of spatial pumping spectrum on quality of phase conjugate reflection during 4-photon interaction
21 p3686 N85-32904
Photoionization-pumped, Ne 2, X-ray laser studies project
[DE85-012973] 23 p3936 N85-34399

LASER RADAR
U OPTICAL RADAR

LASER RANGE FINDERS
Influence of depolarization of linear polarized radiation on heterodyne detection in laser range finders
[DFVLR-FB-84-31] 10 p1491 N85-19414
Preliminary processing of laser ranging data from LAGEOS artificial Earth satellite during short merit program observation period 15 p2488 N85-25355
Influence of depolarization of linear polarized radiation on the heterodyne detection in laser range finders
[ESA-TT-903] 20 p3461 N85-31500
Contemporary plate motions from LAGEOS
20 p3489 N85-31689
Comparing SLR and VLBI geodetic parameters
20 p3491 N85-31703
Applications of laser technology described
21 p3572 N85-32218

LASER RANGER/TRACKER
Tidal dissipation in the Earth and Moon from lunar laser ranging 04 p0585 N85-13733
Specifics of polarization structure of repeated scattering background in optical laser sounding signals
14 p2342 N85-24485
Station coordinates and Earth rotation parameters from Lageos laser ranging 16 p2606 N85-27299
Theoretical and experimental analyses of the performance of two-color laser ranging systems
[NASA-CR-176159] 23 p3936 N85-34397

LASER SPECTROMETERS
Comparison of flame photometer data with total particle volume calculated from laser spectrometer particle count data
[AD-A151008] 14 p2252 N85-23958
Cryogenic laser calorimetry for impurity analysis
[NASA-CR-176102] 22 p3743 N85-33201

LASER SPECTROSCOPY
NT OPTOGALVANIC SPECTROSCOPY
Laser spectroscopy and gas-phase chemistry in CVD
[DE84-014959] 02 p0173 N85-11158
Laser spectroscopy of combustion intermediates
[DE84-016101] 02 p0173 N85-11161
Laser cooling and trapping of neutral atoms
[AD-A146048] 03 p0366 N85-12345
Bibliography of Soviet laser developments, number 65, May - June 1983
[AD-A146189] 03 p0366 N85-12347
Time-resolved spectroscopy of evanescent-wave excited fluorescence
[DE84-015213] 04 p0473 N85-13013
Intermediate results of a 1-year study of a laser spectrometer in the DOE filter test facilities
[DE84-016478] 04 p0506 N85-13228
Velocity-changing collisional effects in nonlinear atomic spectroscopy and photon echo decay in gases
[NASA-CR-174159] 04 p0559 N85-13559
Laser diodes for infrared spectroscopy
[BMFT-FB-T-84-131] 05 p0640 N85-14109
In situ analysis of corrosive and passive surfaces by laser-excited Raman spectroscopy — lead, galvanized iron, and asbestos-cement pipes
[PB84-229756] 06 p0767 N85-14904
Laser spectroscopy of alkali atom-tetrahaloethylene reactions
[AD-A147431] 07 p0923 N85-15848
Reactions of metal ions and their cluster in the gas phase using laser ionization: Ion cyclotron resonance spectroscopy
[DE84-016491] 09 p1293 N85-18120
Developments and applications of laser fluorescence spectroscopy for studies of particle behaviours in fusion plasmas 09 p1389 N85-18735
Measurements of electric fields in plasmas by using beam probe and laser fluorescence techniques
09 p1389 N85-18737
Density measurements of atomic hydrogen in NBT-IM by laser-induced fluorescence spectroscopy
09 p1389 N85-18739
Laser-induced-fluorescence-spectroscopy of atomic processes under a high magnetic field
09 p1389 N85-18740
Capabilities of laser diagnostics for combustion and flow fields
[DE85-002661] 10 p1438 N85-19084
Optical studies of dynamical processes in disordered materials
[DE85-002400] 10 p1453 N85-19158
Fundamental study of catalysts using laser Raman, infrared, auger electron spectroscopy and low energy electron diffraction
[DE85-001813] 11 p1595 N85-20033
Application of Raman, TEM and other ion based techniques to oxidation problems
[AERE-R-11447] 11 p1610 N85-20121
Computer modeling of vibrational energy levels of potential laser candidates (diatomic molecules)
[AD-A151785] 16 p2790 N85-27209
High resolution spectroscopy of C13O18 in gas mixtures
[AD-A152625] 17 p2919 N85-27991
Laser measurement techniques: Laser spectroscopy in semiconductors
[DE85-007887] 17 p2971 N85-28350
Recent advances in optical measurement methods in physics and chemistry
[DE85-006695] 17 p3037 N85-28792
Field measurements with the TAMS-2B and development of methods for measuring HCHO, HC3 and HONO in real air
[PB85-172955] 18 p3135 N85-29419
The development of new techniques in laser spectroscopy 19 p3233 N85-30041
Laser-induced fluorescence measurement of vapor concentration surrounding evaporating droplets
[DE85-009409] 19 p3277 N85-30320
Sensitive detection of tunable diode laser absorption by polarization rotation
[DE85-009821] 19 p3277 N85-30322
Applied Science Division's Environmental Research Program
[DE85-010637] 19 p3308 N85-30510
Reactions of metal ions and their clusters in the gas phase using laser ionization-ion cyclotron resonance spectroscopy
[DE85-009478] 19 p3361 N85-30838
Applications of laser technology described
21 p3572 N85-32218
Activities of the Physics Division
[DE85-000784] 21 p3702 N85-33002
Nonlinear spectroscopy
[AD-A154708] 21 p3704 N85-33010
Rapid analysis of steels using laser-based techniques
[DE85-010747] 22 p3748 N85-33232
Apparatus and method for the spectrochemical analysis of liquids using the laser spark
[DE85-005749] 23 p3935 N85-34387
The detection and study of molecular species using time resolved laser spectroscopy
[AD-A155910] 24 p4075 N85-35256
Infrared generation and wave-mixing studies in cesium
[DE85-012883] 24 p4083 N85-35304
Cryogenic laser calorimetry for impurity analysis
[NASA-CR-176179] 24 p4097 N85-35395
Atmospheric nitrogen oxides: Their detection and chemistry
[PB85-193910] 24 p4114 N85-35502

LASER STABILITY
Measurement of areal mass variation in Rayleigh-Taylor unstable targets
[AD-A145541] 02 p0198 N85-11325
Study of CW injection laser with a dispersive external cavity 02 p0270 N85-11760
Characteristics of unstable resonators in flashlamp-pumped organic-compound lasers
11 p1717 N85-20800
Stability of temporal and energy parameters of picosecond lanthanum beryllate laser
11 p1717 N85-20804
The effects of surface waves on RF discharge pumped lasers
[AD-A149689] 12 p1856 N85-21643

LASER TARGET INTERACTIONS
Measurement of areal mass variation in Rayleigh-Taylor unstable targets
[AD-A145541] 02 p0198 N85-11325
Optical properties of laser erosion flares in plasma
02 p0270 N85-11764
Simulation of the interaction of single-pulsed optical lasers with targets in a vacuum
[DE84-016476] 05 p0640 N85-14107
USSR report: Physics and mathematics
[JPRS-UPM-84-007] 05 p0723 N85-14651
Laser excitation of coupled surface electromagnetic and acoustic waves and of static structures in solids
05 p0723 N85-14652
Transformation of energy spread of laser pumping via phase conjugation 05 p0725 N85-14661
Self-generated magnetic fields and thermal flux inhibition
[AD-A147405] 07 p0971 N85-16166
Bibliography of Soviet laser developments, Number 66, July-August 1983
[AD-A149113] 10 p1490 N85-19406
KMSF X-ray laser experiments, task no. 1
[DE85-001002] 11 p1639 N85-20325
Measurement of hot-electron production and microwave emission by laser-irradiated CH targets
[DE85-003139] 11 p1840 N85-20331

Enhanced thermal coupling by a repetitively pulsed laser
[AD-A164435] 19 p0276 N85-30317
Laser effects on opaque targets. Part 2C: Thermal effects of a time-variable beam intensity
[ISL-R-105/84-PT-2C] 22 p3791 N85-33498

LASER TARGETS
Wavelength scaling of laser plasma coupling
[DE84-014837] 06 p0866 N85-15505
Soft X-ray spectroscopy of laser produced plasmas 09 p1387 N85-18727
A microchannel plate pinhole camera for 20 to 100 keV X-ray imaging
[DE85-001572] 10 p1486 N85-19396
Laser program annual report 1983
[DE84-017287] 10 p1490 N85-19412
Study of opacity effects on line radiation from pellet implosions
[DE85-000380] 10 p1491 N85-19413
Parametric processes in underdense UV laser-produced plasmas
[DE85-002812] 10 p1559 N85-19830
Modal testing and analysis of NOVA laser structures
[DE84-017699] 11 p1638 N85-20321
Use of the ORACLE DEMS in determining the response of complex scientific instrumentation
[DE85-001742] 12 p1853 N85-21621
Laboratory for laser energetics report
[DE85-007295] 15 p2563 N85-25814
Autofocus motion compensation for synthetic aperture radar and its compatibility with strapdown inertial navigation sensors on highly maneuverable aircraft
[AD-A151940] 16 p2704 N85-26693
Megajoule-class single-pulse KrF laser test facility as a logical step toward inertial fusion commercialization
[DE85-009500] 18 p3191 N85-29794
Progress in inertial fusion at LLNL
[DE85-010931] 19 p3277 N85-30321
Shifts and widths of hydrogenic ion lines
[DE85-011375] 19 p3277 N85-30323
Hybrid two-dimensional Monte-Carlo electron transport in self-consistent electromagnetic fields
[DE85-010757] 19 p3348 N85-30758
Thermal transport measurements of UV laser irradiated spherical targets
[DE85-011036] 23 p3931 N85-34365
Solid neon sources for plasma and X-ray lasers
[DE85-011947] 24 p4096 N85-35402

LASER WEAPONS
Directed energy missile defense in space
[PB84-210111] 01 p0015 N85-10095
High energy lasers: A primer on directed energy weapons for space use
[AD-A151279] 15 p2562 N85-25807

LASER WELDING
NT BRAZING
NT FUSION WELDING
NT LOW TEMPERATURE BRAZING
Features of laser welding of medium carbon steel through a cadmium coating 01 p0020 N85-10122
Overview of recent advances in laser applications 05 p0725 N85-14660
Two-dimensional modeling of conduction-mode laser welding
[DE85-001604] 09 p1327 N85-18341
Structure and mechanical characteristics of heterogeneous joints produced by laser welding 13 p2094 N85-22742
Specifications of new industrial lasers reviewed 14 p2284 N85-24150
Laser Welding, Cutting and Surface Treatment 14 p2306 N85-24278
Applications of lasers in manufacturing 14 p2306 N85-24279
Trends in laser equipment 14 p2306 N85-24280
Laser welding in the manufacture of heart pacemakers 14 p2306 N85-24286
Laser spot welding in the electronics industry 14 p2306 N85-24287
Lasers in automobile production 14 p2309 N85-24288
Lasers in the nuclear industry 14 p2309 N85-24289
Laser drilling of aeroengine components 14 p2309 N85-24290
Affect of angle of incidence on plasmas generated during laser welding
[DE85-005724] 15 p2569 N85-25852
Laser welder for fabricating neutron tubes
[DE85-009955] 17 p2974 N85-28377
Experimental and theoretical studies on transport processes in laser welding
[DE84-006572] 17 p2975 N85-28378
Laser beam interactions with vapor plumes during Nd:YAG laser welding on aluminum
[DE85-006793] 21 p3503 N85-32328
Laser welding of 6Al-4V titanium alloy
[DE85-012019] 23 p3938 N85-34413

LASER WINDOWS
Pulsed electric discharge laser technology. Electron beam window foil material
[AD-A147486] 07 p0972 N85-16171
Incident beam polarization for laser Doppler velocimetry employing a sapphire cylindrical window
[NASA-TM-87064] 17 p3037 N85-28788
Influence of mirror anisotropy and Brewster window orientation on radiation characteristics of ring lasers 21 p3684 N85-32889

LASERS
NT ARGON LASERS
NT ATMOSPHERIC LASERS
NT CARBON DIOXIDE LASERS
NT CARBON LASERS
NT CARBON MONOXIDE LASERS
NT CHEMICAL LASERS
NT CONTINUOUS WAVE LASERS
NT DF LASERS
NT DYE LASERS
NT EXCIMER LASERS
NT FREE ELECTRON LASERS
NT GALLIUM ARSENIDE LASERS
NT GAS LASERS
NT GASDYNAMIC LASERS
NT GLASS LASERS
NT HCN LASERS
NT HELIUM-NEON LASERS
NT HF LASERS
NT HIGH POWER LASERS
NT INFRARED LASERS
NT INJECTION LASERS
NT IODINE LASERS
NT KRYPTON FLUORIDE LASERS
NT METAL VAPOR LASERS
NT NEODYMIUM LASERS
NT NITROGEN LASERS
NT NOVA LASER SYSTEM
NT NUCLEAR PUMPED LASERS
NT OPTICAL RESONATORS
NT ORGANIC LASERS
NT PLASMADYNAMIC LASERS
NT PULSED LASERS
NT Q SWITCHED LASERS
NT RAMAN LASERS
NT RARE GAS-HALIDE LASERS
NT RING LASERS
NT RUBY LASERS
NT SEMICONDUCTOR LASERS
NT SOLAR-PUMPED LASERS
NT SOLID STATE LASERS
NT TEA LASERS
NT TUNABLE LASERS
NT TWO-WAVELENGTH LASERS
NT ULTRASHORT PULSED LASERS
NT ULTRAVIOLET LASERS
NT WAVEGUIDE LASERS
NT X RAY LASERS
NT XENON CHLORIDE LASERS
NT XENON FLUORIDE LASERS
NT YAG LASERS
Center for Electronics and Electrical Engineering Technical Bulletin covering center programs
[PB84-218056] 01 p0045 N85-10296
The development of a diode laser Doppler velocimeter for boundary layer measurements under ice: A feasibility investigation
[AD-A145076] 01 p0053 N85-10348
East Europe report: Science and technology
[JPRS-ESA-84-029] 01 p0115 N85-10783
Achievements in laser development 01 p0115 N85-10784
Hot section laser anemometry 02 p0142 N85-10962
Laser anemometer optimization 02 p0142 N85-10963
Evaluation of laser profile and deflection measuring system
[FAA-PM-84-24] 02 p0201 N85-11341
Parameters of geometric stability of laser mirror optical surface 02 p0273 N85-11777
Laser paint removal
[AD-P004009] 03 p0308 N85-11999
Calculation of energy characteristics of double-passage amplifier 03 p0347 N85-12238
Beam profiling in gigawatt 1064-nm lasers used in research on optical materials at Livermore
[DE84-007226] 04 p0505 N85-13223
Theory of non-linear index of refraction of compound semiconductors
[DE84-013660] 04 p0569 N85-13626
Dynamic testing of NOVA laser switchyard tower
[DE84-014460] 05 p0640 N85-14103
Quality assurance in the Antares Laser Fusion Construction Project
[DE84-015493] 05 p0640 N85-14104
Cleaning procedures of laser mirror substrates
[DFVLR-MITT-84-06] 05 p0640 N85-14106
China report: Science and technology
[JPRS-CST-84-042] 06 p0747 N85-14789
External cavity diode laser sensor
[AD-D011341] 07 p0969 N85-16152
RF laser array driver apparatus
[AD-D011375] 07 p0969 N85-16155
Laser R and D in the armed services
[AD-A146930] 07 p0970 N85-16161
Bragg cell spectrum analyzer specification
[AD-D011320] 07 p1044 N85-16829
Rayleigh and Raman scattering for density in a swirling flow combustor 08 p1120 N85-17060
In-situ formation of a grain boundary in field ion microscopy using a laser
[AD-A148225] 08 p1166 N85-17355
Theoretical issues involving traps for neutral spin-polarized atoms
[AD-A148035] 08 p1220 N85-17682
Journal of Research of the National Bureau of Standards, Volume 89, Number 1, January-February, 1984
[PB84-235530] 08 p1262 N85-17931
Laser Hazards Bibliography, October 1984
[AD-A149534] 10 p1490 N85-19406
Use of laser flow visualization techniques in reactor component thermal-hydraulic studies
[DE84-014766] 11 p1639 N85-20330
Photoacoustic effect and its applications 12 p1820 N85-21421
Flow measurement by laser Doppler anemometry in a nuclear fuel assembly
[DE85-003260] 12 p1848 N85-21592
Multiple double heterojunction buried laser device
[AD-D011519] 12 p1855 N85-21635
State-selected ion-molecule reaction dynamics
[AD-A150068] 12 p1928 N85-22115
Intensity fluctuations of focused laser beam during reflection in turbulent atmosphere 13 p2076 N85-22975
China report: Science and technology
[JPRS-CST-85-003] 13 p2166 N85-23433
InGaAs/GaAs, Strained-Layer Superlattice (SLS), junction photodetectors, LED's, injection LASER's and FET's for optoelectronic IC applications
[DE85-001940] 14 p2490 N85-24966
China report: Science and technology
[JPRS-CST-85-013] 15 p2536 N85-25652
Modified Landolt C-ring test to measure the effects of laser filters on visual acuity
[AD-A151164] 15 p2617 N85-26127
Internal step-up type higher harmonic light generating device
[DE85-007026] 16 p2790 N85-27213
Lidar ER2 (ozone). Crystal characterization for harmonic conversion — laser systems
[CERT-2/6129-00] 16 p2872 N85-27717
Photoionization mass spectrometry with VUV hydrogen laser source
[AD-A153362] 17 p2921 N85-28009
High precision materials characterization in the near millimeter wave-length range
[AD-A153267] 17 p2968 N85-28331
Instabilities and chaotic behavior of active and passive laser systems
[AD-A153366] 17 p2971 N85-28348
Support structures for optical components in the Laser Demonstration Facility
[DE85-006879] 17 p2971 N85-28349
Limiting processes laser CVD
[DE85-006846] 18 p3114 N85-29279
Self-detecting optical sensors
[AD-D011657] 18 p3185 N85-29751
Picosecond photoconductive devices for 10 Gbit/s optoelectronic switching 18 p3187 N85-29770
Current activities and background of technology transfer and exchange program at Lawrence Livermore National Laboratory
[DE85-009526] 18 p3199 N85-29843
A laser slope gauge and a spar buoy wave gauge: Tools for the validation of microwave remote sensors
[AD-A154038] 19 p3272 N85-30290
Analog frequency modulated laser using magnetostriction
[AD-D011701] 19 p3276 N85-30318
Four-photon resonant third harmonic generation
[DE85-010070] 19 p3367 N85-30883
USSR report: Life sciences. Biomedical and behavioral sciences
[JPRS-UBB-85-017] 20 p3504 N85-31785
USSR report: Physics and mathematics
[JPRS-UPM-85-004] 21 p3680 N85-32860

Inter-zone auger recombination in GaSb laser structures 21 p3662 N85-32875
The problem of brightness enhancement during laser frequency doubling 21 p3686 N85-32897
Low-threshold injection InGaAsP/GaAs double heterostructure lasers with separate limiting obtained by liquid-phase epitaxy (lambda = 0.76 divided by 0.87 microns, I sub thr = 460 A/cm 2, T = 300 K) 21 p3687 N85-32908
An attempt to detect induced neutron capture in laser radiation field 21 p3690 N85-32928
The sound field of a moving laser-induced acoustic array (theory) [AD-A154553] 21 p3699 N85-32981
Size exclusion chromatography-low angle laser light scattering photometry of lignite macromolecules [DE85-012017] 22 p3745 N85-33215
Pulsed lasers for filming color holographic film images 22 p3781 N85-33426
Metal vapor lasers and their applications [ISL-CO-218/84] 22 p3791 N85-33488
Index of laser program publications and related reports, calendar year 1984 [DE85-011663] 23 p3936 N85-34396
Laser probes of natural gas ignition chemistry [PB85-200210] 24 p4077 N85-35264
Laser and electron beam processing of semiconductors [AD-A155914] 24 p4161 N85-35796

LASING
Space-time characteristics of radiation of single-mode injection lasers 02 p0269 N85-11758
Theoretical analysis of physical processes of lasing medium degradation in semiconductor lasers 02 p0269 N85-11759
Study of CW injection laser with a dispersive external cavity 02 p0270 N85-11760
Injection lasers based on AlGaAsSb/GaSb and InGaAsSb/GaSb heterostructures 02 p0270 N85-11761
Thresholds of optical breakdown in alkali-halide crystals under pulses from CO2-laser 14 p2262 N85-24134
Spectroscopic studies of lasing transitions in the diatomic mercury halides [AD-A151553] 15 p2563 N85-25809

LASV
U F-111 AIRCRAFT

LATCH-UP
Effects of space radiation on advanced semiconductor devices. Part 3: Further cosmic ray simulation studies of single event upsets and latch-up in CMOS memories [AERE-G-3368-PT-3] 22 p3848 N85-33833

LATCHES
Materials properties, loads, and stress analysis, Spartan REM: Appendix A [NASA-CR-171092] 02 p0208 N85-11375
Computer models and output, Spartan REM: Appendix B [NASA-CR-171093] 02 p0208 N85-11376
Hemispherical latching apparatus [NASA-CASE-MFS-25837-1] 19 p3224 N85-29991
Latch assembly [DE85-011660] 22 p3792 N85-33492

LATE STARS
Observations of interstellar HI toward nearby late-type stars 06 p0874 N85-15548
Mg II spectra of late type stars used to probe the LISM 06 p0874 N85-15549
Detection of narrow C 4 and Si 4 absorption features in spectra of stars within 200 pc f the Sun 06 p0876 N85-15564
Spectrophotometry of cool stars from objective prism spectra 07 p0966 N85-16134
The Origin of Nonradiative Heating/Momentum in Hot Stars [NASA-CP-2358] 06 p1231 N85-17755
Far-infrared photometry of low-mass pre-main-sequence stars with broad CO wings 06 p1246 N85-17886
X-ray coronae of late type stars: Theoretical implications 11 p1742 N85-20953
Chromospheric activity in M giants 11 p1757 N85-21056
A progress report on the analysis of long exposure SWP high resolution spectra of cool stars 11 p1758 N85-21057
Precise measurements of radial velocities of emission lines in the far-ultraviolet spectra of late-type stars 11 p1758 N85-21062
Circumstellar shells of late-type stars: A study at millimeter and infrared wavelengths 24 p4167 N85-35836

LATENT HEAT OF FUSION
U HEAT OF FUSION

LATERAL CONTROL
Preliminary airworthiness evaluation of the Rutan Aircraft Factory (RAF), Inc. LONG-EZ airplane with external sight [AD-A145381] 02 p0138 N85-10997
Aileron controls for wind turbine applications [NASA-TM-86667] 02 p0222 N85-11458
The lateral-directional characteristics of a 74-degree Delta wing employing gothic planform vortex flaps [NASA-CR-3848] 03 p0311 N85-12009
Reflection of lateralization of sound stimuli in evoked potentials of human brain 04 p0544 N85-13483
Maximum normalized rate as a flying qualities parameter 05 p0702 N85-14503
Flight tests with a new helicopter Force Feel System (FFS) 08 p1075 N85-16818
Leading edge flap system for aircraft control augmentation [NASA-CASE-LAR-12787-2] 11 p1585 N85-19985
Relative control effectiveness technique with application to airplane control coordination [NASA-TP-2416] 14 p2218 N85-23753
Resource allocation in cerebral specialization of function: Behavioral and electrophysiological studies [AD-A155092] 21 p3664 N85-32759

LATERAL OSCILLATION
Clearance flow-generated transverse forces at the rotors of thermal turbomachines [NASA-TM-77292] 07 p0973 N85-16180
Tolerance, fatigue, physiological and performance effects of sustained and oscillating lateral accelerations 10 p1533 N85-19859

LATERAL STABILITY
Experimental investigation of lateral forces induced by flow through model labyrinth glands 05 p0643 N85-14128
Aileron effectiveness for a subsonic transport model with a high-aspect-ratio supercritical wing [NASA-TM-85674] 07 p0898 N85-15695
Operational and developmental experience with the F/A-18A digital flight control system 16 p2713 N85-26742
Experimental and theoretical determination of the wing-induced lateral wind on the tail surfaces in oscillating rolling motion. Part 2: Theoretical investigations for calculation of the lateral wind [IFD-1/84-PT-2] 18 p3061 N85-28940
The lateral distributions of charged particles of energy greater than 0.3 E sub crit in electron-photon cascades in lead and air [HE-3.6-10] 24 p4185 N85-35957
Properties of 10 (18)-10 (19)eV EAS at far core distance [HE-4.7-3] 24 p4198 N85-36054

LATERALITY
U LATERAL STABILITY

LATERALIZATION
U LATERAL CONTROL

LATEX
Preparation of large-particle-size monodisperse latexes in space: The STS-3, STS-4, and STS-7 mission results 02 p0151 N85-11021
Guayule research [GPO-29-562] 04 p0477 N85-13042
Monodisperse Latex Reactor (MLR): A materials processing space shuttle mid-deck payload [NASA-TM-86487] 12 p1782 N85-21187
Preparation of polystryene latex particles in a rotating reactor [NASA-CR-171475] 17 p2933 N85-28108

LATHES
NT TURRET LATHES
Design of a flexible machining system [CETIM-1-3E-140] 04 p0510 N85-13252
Production cells with IR 2SO robot examined 15 p2524 N85-25561
Device for preventing intrusion of a blade during vibration cutting of intermittent cutting with a lathe 16 p2794 N85-27232
Assessing the machinability of gearwheel steels during manufacture [BLL-BISI-TRANS-22343-(9902.08)] 17 p2973 N85-28365
Machining of beryllium with the LLNL precision engineering research lathe [DE85-010832] 19 p3250 N85-30149

LATITUDE
NT GEOMAGNETIC LATITUDE
Space observation of latitudinal changes in vegetation cover 02 p0164 N85-11113
A paleomagnetic study of the Prince William terrane and Nixon Fork terrane, Alaska 02 p0226 N85-11478
Computer-generated latitude and longitude templates for rapid determination of geographic positions in Alaska 04 p0516 N85-13288
Study of factors affecting an HF/VHF direct broadcasting satellite service [PB85-120889/GAR] 09 p1313 N85-18255
Simultaneous determination of the xi and eta components of vertical deflection with a prism astrolabe [SER-B-270-MITT-171] 09 p1343 N85-18450
Tactical military communications by satellite relay at high latitudes 11 p1709 N85-20756
Development of a portable zenith chamber and its use on the 47th parallel [SER-C-287] 11 p1741 N85-20946
Quaternary North Atlantic surface paleoceanography in regions of potential deep-water formation 15 p2602 N85-26036
Some evidence for high energy gamma-ray sources at large galactic latitudes [OG-2.7-5] 22 p3871 N85-33978
Latitude dependence of co-rotating shock acceleration [SH-1.5-14] 23 p3997 N85-34777
Differential measurement of cosmic-ray gradient with respect to interplanetary current sheet [SH-4.2-9] 23 p4007 N85-34847
Determination of galactic cosmic ray latitudinal gradient using Earth based detectors [SH-4.2-13] 23 p4008 N85-34851
Latitudinal gradients of cosmic rays and the polarity reversal of the heliospheric magnetic field: A preliminary evaluation [SH-4.2-16] 23 p4008 N85-34853
Comparative study of the phase of diurnal anisotropy on quiet and disturbed days on a long term basis up to recent period [SH-4.5-9] 23 p4037 N85-35027
Radial and latitudinal gradients of anomalous oxygen during 1977 - 1985 [SH-4.6-4] 23 p4039 N85-35042

LATTICE IMPERFECTIONS
U CRYSTAL DEFECTS

LATTICE PARAMETERS
Neutron scattering on the FRM double crystal spectrometer 03 p0423 N85-12704
EXAFS and Mossebauer study of small metal clusters isolated in rare-gas solids [DE84-015976] 04 p0470 N85-12994
Theory of non-linear index of refraction of compound semiconductors [DE84-013660] 04 p0569 N85-13626
Understanding the high pressure properties of molecular solids and molecular surfaces deposited on hetrogeneous substrates [NASA-CR-174262] 07 p1047 N85-16649
Tracer diffusion in an ordered alloy: Application of the path probability and Monte Carlo methods [DE85-002768] 14 p2257 N85-23986
Relationship between symmetrical tilt, twist, special, and favored grain boundaries [DE85-004024] 14 p2429 N85-24982
Hydrostatic compression of Fe1-chi 0 wustite. 15 p2508 N85-25472
Strained-layer-superlattice optoelectronic devices [DE85-009148] 19 p3377 N85-30953
Z-contrast imaging and electron channeling analysis of dopants in semiconductors [DE85-011410] 21 p3582 N85-32269
Method for preparing Pb-(beta)-aluminum ceramic [DE85-011665] 22 p3752 N85-33256
Changes in lattice cell parameter of film intermetallic compounds RT2 [BLL-M-35874-(5828.4)] 23 p3915 N85-34261
On-line model driven control of the SLC electron Damping Ring [DE85-013377] 24 p4157 N85-35772
Simulation of lattice damage due to dynamic loading [DE85-008468] 24 p4162 N85-35808

LATTICE VIBRATIONS
Anharmonic lattice effects in molecular crystals 03 p0424 N85-12709
Observation of surface vibrational resonances on (110) surfaces of FCC metals [AD-A150469] 13 p2163 N85-23419
Interaction of low energy electrons with surface lattice vibrations [DE85-005475] 14 p2429 N85-24975
The temperature dependence of diffracted beam intensities in atom-surface scattering [AD-A152762] 17 p3029 N85-28736
X-ray diffractometric measurements and calculations of limiting values of discrepancy between lattices and layer thicknesses, preventing generation of dislocations during growth of multilayer heterostructures 21 p3661 N85-32966
Doping superlattices in organometallic VPE InP [AD-A155151] 21 p3710 N85-33029

LATTICES
Aperture studies with PATRICIA and RACETRACK on simple arbices containing SSC dipoles
[DE85-004163] 11 p1724 N85-20842
Combined function lattices for a 6 GeV synchrotron light source
[DE85-010959] 19 p3367 N85-30885
LATTICES (MATHEMATICS)
NT BOOLEAN ALGEBRA
NT BOOLEAN FUNCTIONS
Gauge Theory on a Lattice, 1984: Proceedings
[DE84-014658] 02 p0291 N85-11892
Comparison of analytical and experimental steadyand unsteady-pressure distributions at Mach number 0.78 for a high-aspect-ratio supercritical wing model with oscillating control surfaces
[NASA-TM-84580] 07 p0899 N85-15697
Lattice statistics
[AD-A146962] 07 p1029 N85-16530
Eigenvalue approximation methods for quantum lattice Hamiltonians 16 p2858 N85-27627
Lattice actions improved by block-spin renormalisation group and maximally symmetric lattices
[DE85-007416] 17 p3045 N85-28841
On the definition of topological susceptibility via lattice anomalous Ward identities and its perturbative tail
[PREPRINT-416] 18 p3184 N85-29744
Nested dissection on a mesh-connected processor array
[AD-A154088] 19 p3342 N85-30711
Monte Carlo sampling strategies for lattice gauge calculations
[DE85-010756] 19 p3377 N85-30948
Adaptive identification and control of structural dynamics systems using recursive lattice filters
[NASA-TP-2371] 20 p3407 N85-31142
Lattice theory for nonspecialists, lecture notes
[NIKHEF-H/84-11] 20 p3539 N85-32019
LAUE METHOD
A new high-resolution pickup tube for live X-ray topography
[NHK-LABS-NOTE-309] 18 p3183 N85-29602
LAUNCH COMPLEXES
U LAUNCHING BASES
LAUNCH DATES
Rocket observations 01 p0014 N85-10084
Balloon observations 01 p0014 N85-10086
List of recent Soviet space launches
02 p0165 N85-11120
List of recent Soviet space launches
13 p1965 N85-22457
LAUNCH TIME
U LAUNCH WINDOWS
LAUNCH VEHICLE CONFIGURATIONS
Future launching systems, 3rd prospective phase
[SNIAS-S/DT/Y-25-063] 11 p1599 N85-19999
French CNES official describes Ariane V launcher
15 p2532 N85-25619
LAUNCH VEHICLES
NT ARIANE LAUNCH VEHICLE
NT ATLAS CENTAUR LAUNCH VEHICLE
NT CENTAUR LAUNCH VEHICLE
NT RECOVERABLE LAUNCH VEHICLES
NT REUSABLE LAUNCH VEHICLES
NT TITAN CENTAUR LAUNCH VEHICLE
NT VEGA LAUNCH VEHICLE
Second Symposium on Space Industrialization — space commercialization
[NASA-CP-2313] 02 p0149 N85-11011
Conestoga 2: A low cost commercial space transport system 02 p0153 N85-11033
Comments on the commercialization of expendable launch vehicles 02 p0153 N85-11034
International cooperation and competition in space. Introduction 02 p0295 N85-11912
LOX/LH2 propulsion system for launch vehicle upper stage, test results
[NASA-TM-77727] 03 p0324 N85-12089
Status of Stretched Rohini Satellite System (SROSS) and Augmented Satellite Launch Vehicle Project (ASLV)
04 p0459 N85-12909
The Expendable Launch Vehicle Commercialization Act
[GPO-30-838] 04 p0460 N85-12919
Commercial Space Launch Act
[GPO-30-613] 04 p0578 N85-13690
One rocket multiple satellite launch technology
[AD-A149228] 10 p1427 N85-19002
Commercial space launches
[S-REPT-98-656] 12 p1788 N85-21225
Distance-inertial guidance of launch vehicle described
12 p1820 N85-21417
Estimation of launch vehicle performance parameters
[AD-A151927] 16 p2728 N85-28639
Computer program for prediction of capture maneuver probability for an on-off reaction controlled upper stage
[NASA-CR-165937] 17 p3010 N85-28611
Proceedings of the Workshop on Identification and Control of Flexible Space Structures, volume 1
[NASA-CR-176051] 20 p3408 N85-31148
The development of staging mechanisms for the Japanese satellite launcher Mu-3SII
22 p3798 N85-33528
LAUNCH WINDOWS
The launch window of a geostationary satellite
05 p0600 N85-13822
LAUNCHERS
NT GUN LAUNCHERS
NT HYPERVELOCITY LAUNCHERS
NT MISSILE LAUNCHERS
NT MOBILE MISSILE LAUNCHERS
NT ROCKET LAUNCHERS
A feasibility study on the use of wind profilers to support Space Shuttle launches
[NASA-CR-3861] 04 p0538 N85-13423
Electromagnetic rail launcher as a circuit element
[AD-A150087] 12 p1835 N85-21516
LAUNCHING
NT AIR LAUNCHING
NT ORBITAL LAUNCHING
NT ROCKET LAUNCHING
NT SPACECRAFT LAUNCHING
Voice command weapons launching system
[AD-D011378] 07 p0937 N85-15940
Impact of activation optimization on the Vandenberg Ground Support System using Q-GERT analysis
[AD-A148448] 08 p1105 N85-16986
One rocket multiple satellite launch technology
[AD-A149228] 10 p1427 N85-19002
Guided-mode launching in a slab waveguide by way of diffraction at the edge of a conducting screen residing on one surface of the slab
[AD-A154886] 21 p3575 N85-32232
LAUNCHING BASES
NT CAPE KENNEDY LAUNCH COMPLEX
Sweden's Kiruna may be future launch site for satellites 03 p0310 N85-12000
View of Ariane countdown procedures, Kourou launch facilities 03 p0310 N85-12001
Vandenberg space shuttle launch complex
[S-HRG-98-1075] 05 p0601 N85-13833
Statement of Edward C. Aldridge, Jr., Under Secretary of the Air Force, Department of the Air Force, accompanied by Lieutenant General Robert W. Bazley, Inspector General and Brigadier General Donald J. Kutyna, Director of Space Systems and Command, Control and Communications, Deputy Chief of Staff, Research, Development and Acquisition 05 p0601 N85-13834
Statement of Honorable James M. Beggs, Administrator, National Aeronautics and Space Administration
05 p0601 N85-13835
External tank processing from barge to pad
08 p1096 N85-16927
LAUNCHING DEVICES
U LAUNCHERS
LAUNCHING PADS
Zero adhesion system
[AD-D011237] 01 p0015 N85-10093
Mechanical features of the shuttle rotating service structure 08 p1102 N85-16967
LAUNCHING SITES
NT LAUNCHING PADS
West Europe report: Science and technology
[JPRS-WST-84-004] 03 p0309 N85-11998
Sweden's Kiruna may be future launch site for satellites 03 p0310 N85-12000
Impact of activation optimization on the Vandenberg Ground Support System using Q-GERT analysis
[AD-A148448] 08 p1105 N85-16986
Natural environment analysis
[NASA-CR-171333] 10 p1428 N85-19010
Atmospheric environment for space shuttle (STS-51C) launch
[NASA-TM-86508] 19 p3315 N85-30547
LAVA
Petrology of deep crustal xenoliths from the eastern Snake River Plain, Idaho 02 p0226 N85-11477
Geomorphic classification of lava flows on Io
13 p2173 N85-23480
Characteristics of basaltic lava flows on Venus
13 p2177 N85-23508
Magmas as selective filters of volatiles between planetary mantles and surfaces
13 p2185 N85-23557
Estimates of lava eruption rates at Alba Patera, Mars
13 p2185 N85-23562
Emplacement of long lava flows on Mauna Loa (Hawaii) and Alba (Mars) 13 p2186 N85-23563
Surface structures of Hawaiian lavas
13 p2186 N85-23566
Basaltic pressure ridges: Formation and relationship to flow emplacement 13 p2186 N85-23567
Radar observations of fissure-fed basaltic lava flows, Craters of the Moon, Idaho 13 p2199 N85-23640
Preliminary results of an ALVIN dive program on active hydrothermal vents at the southern Juan de Fuca Ridge
24 p4106 N85-35454
LAW (JURISPRUDENCE)
NT AIR LAW
NT LEGAL LIABILITY
NT LIABILITIES
NT PUBLIC LAW
NT SPACE LAW
Second Symposium on Space Industrialization — space commercialization
[NASA-CP-2313] 02 p0149 N85-11011
Legal considerations and cooperative opportunities for space commercial activities 02 p0150 N85-11013
SAR maritime missions 06 p0751 N85-14813
Effective use of remote sensing products in litigation
[E85-10048] 06 p0827 N85-15250
Government contract contingent liabilities. The anti-deficiency act, and the hobgoblin of little minds
[AD-A147919] 07 p1053 N85-16684
Microcomputers and the electrical engineer
[AD-A150499] 13 p2147 N85-23325
National Aeronautics and Space Administration Authorization Act, 1986
[S-REPT-99-91] 19 p3381 N85-30978
LAWS
NT CHILD-LANGMUIR LAW
NT CLOSURE LAW
NT CONSERVATION LAWS
NT KEPLER LAWS
NT KIRCHHOFF LAW OF RADIATION
NT OHMS LAW
NT SCALING LAWS
NT STOKES LAW OF RADIATION
Some weak and strong laws of large numbers for d(0,1) - valued random variables
[AD-A144845] 01 p0111 N85-10754
LAY-UP
Fracture toughness of fibrous composite materials
[NASA-TP-2370] 02 p0170 N85-11136
LAYERS
Acoustic resonator and method of making same
[DE84-014655] 01 p0116 N85-10792
Propagation of longitudinal elastic waves in multilayered half-space 02 p0273 N85-11779
Elastodynamic stress intensity factors of an interface finite-width crack
[DE84-016908] 06 p0817 N85-15190
Determination of parameters of doped thin semiconductor layers from plasmatic minimum of reflection coefficient for infrared radiation
07 p0954 N85-16047
Antiscaling technology: Theories of surface scaling and performance of antiscaling surface coatings
[NASA-CR-174274] 07 p0991 N85-16296
TEM combined with Al/sub x/Ga/sub 1-x/ as marker layers as a technique for the study of GaAs MBE growth
[DE85-008451] 18 p3194 N85-29809
Tailored vacuum chambers for ac magnets
[DE85-010767] 21 p3501 N85-32319
LAYOUTS
JESS facility modification and environmental/power plans
[NASA-CR-175685] 14 p2227 N85-23607
LDEF
U LONG DURATION EXPOSURE FACILITY
LEACHING
Electrochemical features of the ferric sulfate leaching of CuFeS2/C aggregates
[AD-A148661] 08 p1123 N85-17061
Mod silver metallization for photovoltaics
[NASA-CR-174444] 10 p1509 N85-19518
A comparative evaluation of the effects of acid precipitation, natural acid production and harvesting of cation removal from forests
[DE85-005254] 15 p2589 N85-25961
A comparative evaluation of the effects of acid precipitation, natural acid production and harvesting on cation removal from forests
[DE85-010821] 19 p3309 N85-30511
Source-term considerations for a potential radioactive-waste repository located in unsaturated tuff
[DE85-010000] 20 p3529 N85-31953
Marine environmental quality assessment program, five-year plan (FY 1984 - 1988)
[AD-A154715] 21 p3613 N85-32459
AUTSKED: An addendum
[DE85-010410] 22 p3829 N85-33712
Effects of acid rain on forest nutrient status
[DE85-012486] 23 p3947 N85-34463

LEAD (METAL)
Mechanical properties of a leaded, resulfurized, rephosphorized steel in various thermo/mechanical conditions
[PB84-216464] 03 p0333 N85-12144
Progress in lead/uranium zircon studies of lower paleozoic rocks of the southern Alexander terrane
04 p0518 N85-13304
Behaviour of lead-silver anodes in zinc electrodeposition from sulphuric acid baths
[BLL-MINTEK-TR-1180-(5810.5758)]
06 p0784 N85-14887
Extreme incompatibility of Pb during the crystallization of magmatic iron meteorites 06 p0886 N85-15827
The growth of metastable peritectic compounds
[NASA-CR-171290] 07 p0920 N85-15825
Susceptibility of 2 1/4 Cr-1Mo steel to liquid metal induced embrittlement by lithium-lead solutions
[DE85-000897] 09 p1294 N85-18130
High temperature laser interferometric studies of solid electrolytes 09 p1396 N85-18785
Structure of transient zone in diffusion welding of TaTS-19 piezoceramic with AMg6 alloy
11 p1603 N85-20082
Effect of rhodamine-B on the electrodeposition of lead on copper, revision
[DE85-000674] 11 p1606 N85-20101
EXAFS of monolayers on silver electrodes: SSRL proposal number 717M
[AD-A150823] 13 p2018 N85-22652
Spectral evaluation of irregularity of superconducting coaxial cables 13 p2092 N85-23000
Trends of petroleum fuels
[DE85-000116] 14 p2263 N85-24023
Effects of ion bombardment on the morphology of lead films
[DE85-007232] 15 p2511 N85-25494
Comparative analysis of laboratory and fullscale experimental data for metal flow displacements and speeds
[BLL-M-36266-(5828.4)] 20 p3430 N85-31276
Lead, platinum, and other heavy elements in the primary cosmic radiation: HEAO-3 results sec wg032961 cb553097 20 p3543 N85-32048
Method for preparing Pb-(beta)-aluminum ceramic
[DE85-011665] 22 p3752 N85-33256
Environmental surveillance at Los Alamos during 1984
[DE85-011666] 22 p3811 N85-33605
Germanium and lead: Significant differences between meteoritic and photospheric abundances?
[OG-7.1-2] 23 p4012 N85-34864
Lead and uranium group abundances in cosmic rays
[OG-7.1-3] 23 p4013 N85-34865
Coupling functions for lead and lead-free neutron monitors from the latitudinal measurements performed in 1982 in the research station Academician Kurchatov
[SH-8.1-1] 23 p4044 N85-35076
Sensitivity of single and multiple cosmic ray neutrons to the surrounding medium in a lead-free monitor
[SH-8.1-10] 23 p4051 N85-35125
The neutron moderated detector and groundbased cosmic ray modulation studies
[SH-8.1-13] 23 p4052 N85-35128
The Conterminous United States Mineral Assessment Program 24 p4106 N85-35458
Estimation of the total inelasticity coefficient in interaction of greater than or equal to 20 TeV hadrons with lead
[HE-1.1-9] 24 p4171 N85-35857
LPM effect and primary energy estimations
[HE-3.6-4] 24 p4185 N85-35953
The lateral distributions of charged particles of energy greater than 0.3 E sub crit in electron-photon cascades in lead and air
[HE-3.6-10] 24 p4185 N85-35957
Result of Monte-Carlo simulation of electron-photon cascades in lead and layers of lead-scintillator
[HE-3.6-11] 24 p4185 N85-35958

LEAD ACID BATTERIES
Performance of improved lead acid batteries for electric vehicles
[DE84-015845] 04 p0495 N85-13180
Research, development, and demonstration of lead-acid batteries for electric vehicle propulsion
[DE84-017442] 05 p0832 N85-14055
Energy storage with lead acid batteries in photovoltaic systems 05 p0863 N85-14290
Performance on advanced lead-acid batteries for load-leveling applications
[DE84-015817] 06 p0805 N85-15125
Impact of temperature on cycle life of globe ISOA EV-3000 lead-acid batteries
[DE84-015840] 06 p0805 N85-15126
Composite batteries 07 p0936 N85-15932
Prospects for advanced storage battery technologies
[DE84-015706] 09 p1345 N85-18484
Electric vehicle battery test plan and results
[DE84-001972] 09 p1410 N85-18887
Electrical and thermal performance during charging and discharging a Phase 1 gel cell battery
[PB85-114312] 11 p1677 N85-20585
In-vehicle evaluation of the Globe EV 2300 lead-acid, Delco Remy 150 nickel-zinc, and Eagle-Picher NIF 270 nickel-iron battery systems
[NASA-CR-175653] 14 p2349 N85-24521
Lead shortage hastens need for improved storage batteries 15 p2481 N85-25195
Test and evaluation of the Hoppecke Model E240G144/16 electric vehicle battery charger
[DE85-000573] 17 p2955 N85-28253
Transfer of battery technology developed by the US Department of Energy
[DE85-000668] 22 p3808 N85-33588

LEAD ALLOYS
Directional solidification studies of Pb-Bi peritectic alloys
[DE84-015656] 04 p0474 N85-13016
Accuracy of preparation of three-dimensional reference grid
[BLL-M-35921-(5828.4)] 05 p0616 N85-13939
Thermodynamic properties of liquid Li-Pb, Na-Pb and K-Pb alloys: Similarities and Differences
[DE85-004074] 16 p2197 N85-29830
Counter current extraction system for tritium recovery from 17Li-83Pb
[DE85-010519] 19 p3240 N85-30090
Comparative analysis of laboratory and fullscale experimental data for metal flow displacements and speeds
[BLL-M-36266-(5828.4)] 20 p3430 N85-31276

LEAD COMPOUNDS
NT LEAD OXIDES
NT LEAD TELLURIDES
Structure of transient zone in diffusion welding of TaTS-19 piezoceramic with AMg6 alloy
11 p1603 N85-20082
Effect of traffic and meteorology on air pollution
16 p2830 N85-27452

LEAD OXIDES
Structural studies on lead dioxides
[DE84-015837] 06 p0805 N85-15127
Spectroscopic studies of lead oxide in a flow tube
[AD-A151849] 15 p2505 N85-25455
Calculation of molecular constants potential energy curves and Franck-Condon factors for lead oxide
[AD-A154521] 21 p3582 N85-32158

LEAD POISONING
Effect of traffic and meteorology on air pollution
16 p2830 N85-27452
Environmental summary for calendar year 1984
[DE85-012020] 22 p3810 N85-33604
Estimating risks of lead-induced hemoglobin decrements under conditions of uncertainty: Methodology, pilot judgments and illustrative calculations
[DE85-012293] 23 p3952 N85-34493

LEAD TELLURIDES
The behavior of Pb(1-x)Sn(x)Te semiconductor laser diodes in a magnetic field
[AD-A145431] 02 p0287 N85-11872

LEAD ZIRCONATE TITANATES
Effect of powder characteristics on microstructure and properties in alkoxide prepared PZT ceramics
[AD-A149082] 10 p1451 N85-19141
Sol-gel processing of lead zirconate titanate films
[ATR-85(8343)-2] 18 p3073 N85-29010
Materials used by industry for the production of piezoelectric transducers. The state of the art of research work performed in the field of PZT ceramics and ferroelectric polymers
[ISL-CO-211/84] 24 p4089 N85-35344
Conduction and aging of piezoelectric PZT ceramics
24 p4089 N85-35346

LEADERSHIP
Conceptual model of critical requirements for effective pilot performance in high performance aircraft
10 p1533 N85-19663
Individual characteristics and unit performance: A review of research and methods
[AD-A153145] 17 p3001 N85-28550
The effects of controversy and concurrence seeking on effective decision making
[AD-A153370] 17 p3002 N85-28555
Central problems in the management of innovation
[AD-A152598] 17 p3047 N85-28852
Symbolic and interactional perspectives on leadership: An integrative framework
[AD-A155247] 21 p3665 N85-32769

LEADING EDGE FLAPS
Leading edge flap system for aircraft control augmentation
[NASA-CASE-LAR-12787-2] 11 p1585 N85-19985
Investigation of the Vortex Tab
[NASA-CR-172586] 15 p2463 N85-25209
Simulator study of the stall departure characteristics of a light general aviation airplane with and without a wing-leading-edge modification
[NASA-TM-86309] 15 p2470 N85-25250
Application of an aerodynamic analysis method including attainable thrust estimates to low speed leading-edge flap design for supersonic cruise vehicles
[NASA-CR-165843] 19 p3212 N85-29918
Aerodynamic characteristics of a distinct wing-body configuration at Mach 6: Experiment, theory, and the hypersonic isolation principle
[NASA-TP-2467] 22 p3727 N85-33107

LEADING EDGE SLATS
Design of an airfoil leading edge slat using an inverse aerodynamic calculation method
06 p1069 N85-16777
Effects of leading-edge devices on the low-speed aerodynamic characteristics of a highly-swept arrow-wing
[NASA-CR-172531] 13 p1988 N85-22365
Pressure distribution data from tests of 2.29 M (7.5 feet) span EET high-lift transport aircraft model in the Ames 12-foot pressure tunnel
[NASA-TM-84517] 19 p3211 N85-29912
Low-speed tests of a high-aspect-ratio, supercritical-wing transport model equipped with a high-lift flap system in the Langley 4- by 7-meter and Ames 12-foot pressure tunnels
[NASA-TP-2097] 20 p3386 N85-31010
Presentation of the acoustic and aerodynamic results of the Aladin 2 concept qualification testing
[NASA-TM-77683] 24 p4060 N85-35181

LEADING EDGES
Prediction of aerodynamic characteristics of fighter wings at high angles of attack
[AD-A145107] 01 p0003 N85-10017
Force and moment measurements on a 74 deg delta wing with an apex flap
[NASA-CR-166061] 02 p0134 N85-10918
Hybrid laminar flow control study
[NASA-CR-165930] 02 p0137 N85-10933
A visual study of a delta wing in steady and unsteady motion
[AD-P004188] 09 p1264 N85-17943
Laminar separation bubble with transition: Prediction test with local interaction — airfoils
[PNR-90231] 09 p1274 N85-18008
A calculation of slender delta wing with leading-edge separation by quasi-vortex-lattice method
12 p1821 N85-21423
Energy losses at leading edge of turbine blade during multirow jet cooling 13 p2049 N85-22626
Interactions of unstable shear layers with leading edges and associated pressure fields 14 p2259 N85-24236
An exploratory study of apex fence flaps on a 74 deg delta wing
[NASA-CR-172463] 15 p2463 N85-25208
Flow past a flat plat with a vortex/sink combination
[JIAA-TR-58] 15 p2464 N85-25215
Some effects of sweep direction and strakes for wings with sharp leading edges
[CA-8421] 17 p2992 N85-27826
On the effect of wing taper and sweep direction on leading edge transition
[CA-8435] 17 p2992 N85-27827
A study of aerodynamic control in stalled flight leading-edge vortex formation analysis
[AD-A153758] 18 p3059 N85-28628
Lee-side flow over delta wings at supersonic speeds
[NASA-TP-2430] 19 p3212 N85-29921
A method for computing the core flow in three-dimensional leading-edge vortices
[NASA-TM-87489] 19 p3214 N85-29932
DC-10 winglet flight evaluation
[NASA-CR-3704] 19 p3217 N85-29949

LEAKAGE
Qualification of noninvasive systems for on-line leak detection in high pressure feed water preheaters
[CISE-2341] 04 p0558 N85-13565
Gamma-induced leakage in junction field-effect transistors
[DE84-014960] 04 p0570 N85-13634
Analysis for leakage and rotordynamic coefficients of surface roughened tapered annular gas seals
06 p0844 N85-14135
Development of a van-portable remote-sensing laser system for selective detection of natural gas leaks
[PB85-101939/GAR] 06 p0911 N85-15156
Identification of leaks: Internal acoustic method, phase 2
[PB85-101947/GAR] 07 p0936 N85-15927
Clearance flow-generated transverse forces at the rotors of thermal turbomachines
[NASA-TM-77292] 07 p0973 N85-16180

A voice-actuated wind tunnel model leak checking system
[NASA-TM-86359] 09 p1263 N85-17936
Leakage-flow induced vibrations of a chimney structure suspended in a liquid flow — nuclear reactors 09 p1339 N85-18420
Theory versus experiment for the rotordynamic coefficients of annular gas seals. Part 2: Constant clearance and convergent-tapered geometry
[NASA-CR-174413] 10 p1491 N85-19416
Theory versus experiment for the rotordynamic coefficients of annular gas seals. Part 1: Test facility and apparatus
[NASA-CR-174409] 10 p1491 N85-19417
Low leakage turbine shaft seals for advanced combined cycle systems
[AD-A149372] 10 p1492 N85-19420
Leak monitoring in high pressure preheaters by a noninvasive ultrasonic method
[CISE-2373] 11 p1650 N85-20394
Leak detection by acoustic emission monitoring in power plant high pressure preheaters
[CISE-2392] 11 p1650 N85-20395
Leakage-flow-induced vibration of a tube-in-tube slip joint
[DE84-007301] 11 p1652 N85-20406
Interactions between F-111 fuselage fuel tank sealants. Part 2: Variation in performance properties of polysulfides after contact with polyester degradation products
[AD-A149777] 12 p1812 N85-21368
Analysis of experimental shaft seal data for high-performance turbomachines, as for Space Shuttle main engines
[NASA-TM-86928] 12 p1844 N85-21569
Carbon granule probe microphone for leak detection — recovery boilers
[NASA-CASE-NPO-16027-1] 12 p1849 N85-21597
Leak detectors for organic Rankine cycle power plants: On-line and manual methods
[DE85-002792] 12 p1852 N85-21617
Portable remote laser sensor for methane leak detection
[NASA-CASE-NPO-15790-1] 12 p1855 N85-21631
Magnetic field interactions with material discontinuities
[AD-A150197] 13 p2154 N85-23373
Effect of apparent fluid masses on natural vibration frequencies of impellers of multistage centrifugal pumps 14 p2277 N85-24106
Effect of diaphragm leakage on turbine stage characteristics 14 p2286 N85-24168
New electronic measurement, control devices 14 p2289 N85-24192
Experimental simulation of the flows in front of and behind a projectile with and without gas slippage
[ISL-CO-232/83] 14 p2302 N85-24258
Hermetic sealing of nonlubricated gas seal and friction characteristics, chapter 7
[DE85-006375] 15 p2569 N85-25851
Physics effects of accidental submersion of space power reactors in water
[DE85-005020] 15 p2650 N85-26344
Management of vacuum leak-detection processes, standards and calibration
[DE85-006705] 16 p2788 N85-27202
Magnetic flux leakage inspection: Principles and applications
[BLL-BISI-TRANS-22246-(9022.06)] 17 p2975 N85-28362
Differential between crack and pseudo-crack indications by means of objective magnetic flux leakage testing
[BLL-BISI-TRANS-22033-(9022.06)] 17 p2976 N85-28386
SSME seal test program: Test results for hole-pattern damper seals
[NASA-CR-171505] 20 p3395 N85-31059
Refrigerated dynamic seal to 6.9 MPa (1000 psi)
[NASA-TM-87108] 23 p3930 N85-34356
Upgrading auxiliary facility outleakage and combustion detection
[DE85-012796] 23 p3934 N85-34386

LEAR JET AIRCRAFT
Aircraft accident report. Central Airlines flight 27, Hughes Charter Air, Gates Learjet model 25 (N51CA) Newark International Airport, Newark, New Jersey, March 30, 1983
[PB84-910411] 02 p0136 N85-10924
Safety recommendation(s), A-84-93 through -95
[REPT-3983/33] 14 p2216 N85-23746
Learjet Model 55 wing analysis with landing loads 15 p2575 N85-25683

LEARNING
NT ASTRONAUT TRAINING
NT CONDITIONING (LEARNING)
NT TRANSFER OF TRAINING
Feature discovery by competitive learning
[AD-A146052] 01 p0097 N85-10646
Memory-based expert systems
[AD-A145612] 02 p0249 N85-11626
The impact of pictorial display on operator learning and performance 05 p0706 N85-14527
Mental models of invisible logical networks 05 p0706 N85-14544
Conjunctive and disjunctive item response functions
[AD-A147615] 07 p1033 N85-16561
Training high performance skills: Fallacies and guidelines
[AD-A148574] 08 p1196 N85-17545
A theorem on the optimal allocation of effort
[AD-A148028] 08 p1211 N85-17623
Toward a model of attention and the development of automatic processing
[AD-A149348] 10 p1567 N85-19682
Learning to search. From weak methods to domain-specific heuristics
[AD-A149949] 12 p1918 N85-22045
Psychophysiological studies. 1: Performance and physiological response in learning, short-term memory and discrimination tasks
[AD-A151018] 14 p2392 N85-24731
The acquisition of procedures from text. A production-system analysis of transfer of training
[AD-A151029] 14 p2392 N85-24732
The impact of group processing on achievement in cooperative learning groups
[AD-A153168] 17 p3001 N85-28551
Oral discussion, group-to-individual transfer and achievement in cooperative learning groups
[AD-A153209] 17 p3001 N85-28552
Biofeedback and performance: An update
[AD-A153228] 17 p3001 N85-28553
Learning and self adaptation applied to the simulation of a human pilot
[ONERA-RT-24/5122-SY] 20 p3511 N85-31828
The International Cometary Explorer (ICE)wallsheet teacher's guide
[NASA-TM-87498] 23 p3988 N85-34727

LEARNING MACHINES
Decentralized control of scheduling in distributed systems
[AD-A147445] 07 p1028 N85-16523
Monte Carlo techniques for analyzing deep penetration problems
[DE85-011426] 23 p3988 N85-34598
Justified generalization: Acquiring procedures from examples
[AD-A156408] 24 p4135 N85-35626

LEARNING THEORY
The design and use of subtasks in part training and their relationship to the whole task 05 p0711 N85-14559
Oral discussion, group-to-individual transfer and achievement in cooperative learning groups
[AD-A153209] 17 p3001 N85-28552
Models for multidimensional tests and hierarchically structured training materials
[AD-A155231] 21 p3665 N85-32768

LEAST SQUARES METHOD
Harmonizable, Cramer, and Karhunen classes of processes
[AD-A144984] 01 p0113 N85-10767
Credibility approximations for Bayesian prediction of second moments
[AD-A144996] 01 p0113 N85-10768
Fast Fourier transform for unequally spaced data 01 p0128 N85-10876
Planning of navigation measurements using TD criterion for determination of movement of spacecraft by method of least squares 02 p0159 N85-11081
Determination of nonlinear viscoelasticity parameters for polymeric and composite materials by numerical methods
[AD-A145311] 02 p0185 N85-11240
An algorithm for least squares projections onto the intersection of shifted, convex cones
[AD-A145428] 02 p0251 N85-11640
Estimation in nonlinear time series model II: Some nonstationary series
[AD-A145709] 02 p0255 N85-11668
Local geoid determination in mountain regions
[AD-A145799] 03 p0384 N85-12458
Signal processing algorithms
[AD-A145748] 03 p0406 N85-12590
Least squares estimation of conditionally heteroscedastic autoregressions
[AD-A145994] 03 p0411 N85-12626
Least squares spline regression with block-diagonal variance matrices
[NPL-DITC-40/84] 04 p0554 N85-13523
Satellite orbit determination 05 p0598 N85-13613
Use of least-squares method for estimating errors of turbine blade type parts during fabrication 06 p0776 N85-14963
Parametric estimates of propulsion system maintenance manhours
[AD-A147120] 07 p0894 N85-15662
Optimization of orientation in navigation by two heavenly bodies 07 p0951 N85-16027
Splitting methods for the numerical solution of the incompressible Navier-Stokes equations
[AD-A147463] 07 p1032 N85-16554
Background detection and correction in multicomponent analysis
[AD-A148251] 08 p1212 N85-17628
On the ergodicity of bilinear time series models and some applications
[AD-A148032] 08 p1215 N85-17651
Computer programs for the adjustment of indirect observation with condition equations between the unknowns
[SER-B-268-MITT-170] 09 p1370 N85-18612
Blunder detection using a sequential least squares adjustment
[AD-A149514] 10 p1548 N85-19765
The inefficiency of least squares: Extensions of Kantorovich inequality
[AD-A149566] 10 p1549 N85-19768
Improved models for increasing wind penetration, economics and operating reliability
[NASA-CR-175536] 11 p1674 N85-20545
Sequential minimization for sum of squares of unknown functions
[DE85-004162] 11 p1707 N85-20738
New approach for solving large residual nonlinear least squares problems
[DE85-002555] 11 p1707 N85-20742
Influence of individual reflections on the precision of parameter estimates in least squares refinement
[DE85-000830] 11 p1735 N85-20909
Estimation of the impulse response of television channels from digitized waveforms
[CRC-1376] 12 p1822 N85-21429
On the accuracy of least squares methods in the presence of corner singularities
[NASA-CR-172552] 12 p1919 N85-22050
A mixed-basis band structure interpolation scheme applied to the fluorite structure compounds NiSi2, AuAl2, AuGa2 and AuIn2
[AD-A150131] 12 p1940 N85-22187
Efficiency of algorithms for gas-air channel diagnostics in gas turbine engines based on gas thermodynamic parameters 13 p2048 N85-22823
Consistency of smoothing with running linear fits
[AD-A150232] 13 p2150 N85-23349
Macro for fitting nonlinear models to Poisson distributed data
[DE84-009569] 14 p2412 N85-24871
Least squares reduction technique 14 p2437 N85-25038
Very large least squares problems and supercomputers
[AD-A151270] 15 p2623 N85-26162
Applications of Kalman filtering and recursive least-squares in river flow modelling 15 p2636 N85-26254
Statistical regularization methods in problem of navigational determination of space vehicle orbits 16 p2719 N85-26784
Solving the minimal least squares problem subject to bounds on the variables
[TRITA-NA-8215] 16 p2852 N85-27580
Symbolic Givens reduction in large sparse least squares problems
[DE85-006685] 17 p3021 N85-28681
A multiple regression technique for detecting outliers
[REPT-84-33] 17 p3025 N85-28706
On the condition number of modified moment matrices arising from least squares approximation in the complex plane
[AD-A152353] 17 p3026 N85-28714
Analytical generation of satellite orbits at the RAE (Royal Aircraft Establishment)
[AD-A152655] 17 p3053 N85-28901
Least-squares approximation to minimum chi-square estimators of location and scale parameters and their effect on the Pearson chi-square test
[AD-A153534] 18 p3169 N85-29638
Least squares inversion of Stokes profiles in the presence of velocity gradients 18 p3207 N85-29892
The effect of line damping, magneto-optics and parasitic light on the derivation of sunspot vector magnetic fields 18 p3207 N85-29895
Fast moving average recursive least mean square fit
[DE85-010036] 19 p3348 N85-30752
Description and operation of CHISQMO, INVRTS, VOIGEN, VOIGTV, SMEAR, RUFF, AND POSCAR in the Stokes Analysis Program
[PB85-180628] 19 p3364 N85-30991

Adaptive identification and control of structural dynamics systems using recursive lattice filters
[NASA-TP-2371] 20 p3407 N85-31142
Comparison of ERS-1 scatterometer Monte Carlo performance simulations using a weighted nonlinear least squares and a maximum likelihood estimation method
20 p3420 N85-31224
A guide to the statistical analysis of the results of linear and nonlinear least-squares data fitting
[NPL-DITC-53/84] 20 p3521 N85-31895
Regression metamodel summarization of model behavior
[FEW-120] 20 p3522 N85-31902
A practical approach to Karmarkar's algorithm
[AD-A155714] 21 p3673 N85-32818
On a variational approach to some parameter estimation problems
[NASA-CR-177935] 21 p3675 N85-32829
Kalman filter time series analysis of gamma-ray data from NaI(T1) detectors for the ND9620 computer
[AD-A154995] 21 p3705 N85-33014
Application of nonlinear least squares methods to the analysis of solar spectra
[NASA-CR-176122] 22 p3816 N85-33637
Two-dimensional inversion of resistivity monitoring data from the Cerro Prieto geothermal field
[DE85-012554] 24 p4113 N85-35494

LEAVES

Compilation of elemental concentration data for NBS (National Bureau of Standards) biological, geological and environmental standard reference materials, 1982
[PB84-216336] 01 p0025 N85-10158
Scattering from randomly oriented scatterers of arbitrary shape in the low-frequency limit with application to vegetation
04 p0525 N85-13362
Changes in spectral properties of detached leaves
[E85-10042] 07 p0963 N85-16243
Microwave model prediction and verifications for vegetated terrain
[E85-10102] 16 p2809 N85-27322
Light scattering by leaf layers with application to canopy reflectance modeling: The Scattering by Arbitrarily Inclined Leaves (SAIL) model
[NLR-MP-84011-U] 17 p3038 N85-28796

LECTURES

Eleven lectures on the physics of the quark-gluon plasma
[DE85-004321] 15 p2662 N85-26431

LED (DIODES)

U LIGHT EMITTING DIODES

LEE WAVES

Mesoscale lee cyclogenesis 09 p1355 N85-18527
Kinetic energy and vorticity of lee cyclones
[MITT-40] 17 p2993 N85-28502
The determination of lee circulation during the foehn wind 24 p4122 N85-35554

LEG (ANATOMY)

NT FEET (ANATOMY)
NT KNEE (ANATOMY)

Locomotion research for the analysis of the human gait and for the determination of the maximum loads of the pelvis-leg skeleton. Volume 1: Two-dimensional analysis
[BMFT-FB-T-83-167-VOL-1] 02 p0236 N85-11535
Locomotion research for the analysis of the human gait and for the determination of the maximum loads of the pelvis-leg skeleton. Volume 2: Three-dimensional analysis
[BMFT-FB-T-83-168-VOL-2] 02 p0236 N85-11536
Leg volume changes. Responses to Lower Body Negative Pressure (LBNP) during 7 days of zero-g simulation (6 deg Head-Down Tilt (HDT))
05 p0692 N85-14452
Electromyographic patterns associated with discrete limb movements 05 p0710 N85-14551
Comparison of thermal responses between rest and leg exercise in water
[AD-A146818] 07 p1015 N85-16448
Rat skeletal muscles with simulation of physiological effects of weightlessness (morphological study)
23 p3953 N85-34502
The effect of +Gx acceleration on platelet activation as determined by plasma platelet factor 4 levels
[AD-A155881] 24 p4131 N85-35608

LEGAL LIABILITY

The structures and the role of an international agency for the control of satellites
[NASA-TM-76765] 03 p0441 N85-12806
Microcomputers and the electrical engineer
[AD-A150499] 13 p2147 N85-23325

LEGENDRE CODE

U COMPUTER PROGRAMMING
U NEUTRON SCATTERING

LEGENDRE FUNCTIONS

Boundary conditions in Chebyshev and Legendre methods
[NASA-CR-172469] 02 p0250 N85-11635
Phase function, backscatter, extinction, and absorption for standard radiation atmosphere and El Chichon aerosol models at visible and near-infrared wavelengths
[NASA-TM-86379] 12 p1892 N85-21674
Object identification and manipulation using silhouette moments
[AD-A154755] 21 p3705 N85-33011

LEGENDRE POLYNOMIALS

U LEGENDRE FUNCTIONS

LEGENDRE TRANSFORMATION

U LEGENDRE FUNCTIONS

LEGIBILITY

An exploratory study of the effect of screen size and resolution on the legibility of graphics in automated job performance aids
[AD-A155669] 24 p4136 N85-35632

LEGUMINOUS PLANTS

Mutant peas as probes in the understanding of growth and gravitropism 15 p2611 N85-26068

LEMMAS

U THEOREMS

LENGTH

Estimating number, time and length; a baseline study
05 p0695 N85-14473
Signal propagation delay, wire length distribution and the efficiency of VLSI circuits
[CWI-CS-R8412] 11 p1630 N85-20266
Design of a variable-focal-length optical system
[NASA-CR-175710] 15 p2651 N85-26349
A comparison of methods of least squares adjustment of traverses
[AD-A153612] 18 p3170 N85-29645
Literature survey of discontinuous-fiber-reinforced composites with emphasis on pressure vessels
[DE85-010366] 19 p3232 N85-30038

LENS ANTENNAS

Millimeter wave antenna technology
[AD-A146694] 08 p1155 N85-17291
3-D Dome/Rotman lens antenna breadboard demonstration
[AD-A149809] 12 p1828 N85-21475
Cylindrical lens-array antenna for wideband electronic scanning
[AD-A156085] 24 p4090 N85-35350

LENS DESIGN

Optic's Institute's development of equipment for comet probe 15 p2484 N85-25333
Design of a variable-focal-length optical system
[NASA-CR-175710] 15 p2651 N85-26349
Holographic lens for optical correlator
16 p2763 N85-27052
Possibility of developing charged-particle energy analyzer based on hyperboloidal axisymmetrical lens
21 p3691 N85-32933
Electrostatic astigmatic tubular lens
21 p3695 N85-32955
Relaxation lens in inhomogeneous binary mixture
21 p3695 N85-32957
New method for correcting chromatism of mirror-lens objectives 21 p3696 N85-32965

LENSES

NT FRESNEL LENSES
NT GRAVITATIONAL LENSES
NT MAGNETIC LENSES
NT WIDE ANGLE LENSES

Fore-optics systems designed for electronic streak cameras using fiber optics
[DE84-014525] 02 p0261 N85-11830
Laser velocimeter measurements and analysis in turbulent flows with combustion. Part 3: A correction lens for laser Doppler measurements in a cylindrical tube
[AD-A146206] 03 p0366 N85-12348
Comparison of wide aperture and short residance time ion lenses
[DE84-015274] 03 p0420 N85-12685
A low-sidelobe space feed lens
[AD-A147869] 07 p0942 N85-15972
Helmet mounted telescope
[AD-D011355] 07 p1019 N85-16467
Modulation Transfer Function (MTF) measurement techniques for lenses and linear detector arrays
[NASA-TM-86168] 10 p1556 N85-19612
Technical support for microwave experiments on the eye lens
[AD-A149702] 12 p1933 N85-22144
Properties of chirped grating lenses in optical waveguides
[AD-A150023] 12 p1934 N85-22149
Positioning errors of commutating lenses and their influence on characteristics of high speed movie cameras 14 p2273 N85-24085
Laser beam shaping system with reduced objective diameter 14 p2275 N85-24095
Role of fluid lubricant-coolant in fine grinding of optical glass by diamond tool 14 p2280 N85-24125
Applications of compound eye configurations to smart sensor design
[AD-A150731] 14 p2420 N85-24935
Optic's Institute's development of equipment for comet probe 15 p2484 N85-25333
Supersonic missile seeker lens system using gradient index material for first element lens
[AD-A151476] 15 p2490 N85-25507
Dall-Null tester for spaceborne applications
[AD-A151772] 16 p2681 N85-27779
Two-degree-of-freedom linear and planar microwave array lenses
[AD-A153701] 18 p3095 N85-29156
Influence of edge effects on performance of electrooptical lens 22 p3770 N85-33366
Automatic sphericity interferometer for testing lens radii
[AD-A155736] 22 p3786 N85-33457
Theoretical and computational research on the focused transport of intense charged particle beams
[DE85-012990] 23 p3972 N85-34621

LEPTONS

NT ANTINEUTRINOS
NT CONDUCTION ELECTRONS
NT ELECTRONS
NT MUONS
NT NEUTRINOS
NT POSITRONS
NT SOLAR NEUTRINOS

Standard model and beyond
[DE85-004289] 14 p2418 N85-24819
Measurements of heavy quark and lepton lifetimes
[DE85-008321] 16 p3181 N85-29724
Deep-inelastic lepton scattering by nuclei: The pion-exchange model
[DE85-010498] 19 p3359 N85-30839
Nuclear structure problems in double beta decay
[DE85-010739] 19 p3364 N85-30859
Toward the question of multi-quark configurations in nuclei 21 p3691 N85-32929
Dependence of the average spatial and energy characteristics of the hadron-lepton cascade on the strong interaction parameters at superhigh energies
24 p4189 N85-35877
Charge 4/3 leptons in cosmic rays
[HE-8.2-14] 24 p4212 N85-36150

LESIONS

NT PULMONARY LESIONS

Neural control of the direction of covert visual orienting
[AD-A145189] 01 p0097 N85-10850
Pathology of organophosphorus-induced delayed neurotoxicity
[AD-P004024] 08 p0844 N85-15358
Application of the isoenergy principle and the A weighting to evaluate lesion risks due to noise in a military environment
[ISL-CO-231/83] 14 p2380 N85-24720
Effects of long-term low-level radiofrequency radiation exposure on rats. Volume 8: Evaluation of longevity, cause of death, and histopathological findings
[AD-A154263] 19 p3327 N85-30610

LETHALITY

Teratogenicity studies of carbaryl and malathion alone and in combination in various laboratory animals
[AD-P004034] 08 p0845 N85-15364
Theory of lethality
[DE85-000457] 11 p1721 N85-20828
Systems vulnerability and lethality in the development phase
[AD-A149737] 12 p1934 N85-22099

LETTERS (SYMBOLS)

U SYMBOLS

LEUKEMIAS

H1-NMR studies on lymphocyte membranes in human lymphoproliferative diseases 20 p3505 N85-31787

LEUKOCYTES

NT LYMPHOCYTES

LEVEL (HORIZONTAL)

NT LIQUID LEVELS

Approximation of difference in water table positions by horizontal stratum in studies of their influence on gravity
10 p1502 N85-19478
Mathematical modeling of results of geometric leveling in variable gravity field 13 p2114 N85-23170

LEVEL (QUANTITY)

NT ATOMIC ENERGY LEVELS
NT EFFECTIVE PERCEIVED NOISE LEVELS
NT ELECTRON STATES
NT ENERGY LEVELS
NT GROUND STATE
NT INTERMOLECULAR FORCES
NT MOLECULAR ENERGY LEVELS

Oscillator development
[AD-A149899] 12 p1934 N85-21509

LEVELING
Margin leveling algorithm for fully saturated satellite transponder with CDMA (Code Division Multiple Access) signalling
[AD-A151710] 15 p2543 N85-25699
Planetary surface processes: A review
22 p3955 N85-33860

LEVERS
The guidelines to design the lever turning gears in articulated vehicles
[AD-P004301] 09 p1409 N85-18878
Axial bearings with lever-type equalizer system
14 p2267 N85-24048

LEVITATION
NT ACOUSTIC LEVITATION
NBS (National Bureau of Standards): Materials measurements
[NASA-CR-174036] 03 p0332 N85-12143
The generation of rolling moments with the superconducting solenoid model
[NASA-CR-172520] 09 p1283 N85-18088
Closed loop electrostatic levitation system
[NASA-CASE-NPO-15553-1] 18 p3092 N85-29142

LEVITATION MELTING
High temperature acoustic levitator
[NASA-CASE-NPO-16022-1] 12 p1927 N85-22105

LIABILITIES
NT LEGAL LIABILITY
Government contract contingent liabilities. The anti-deficiency act, and the hobgoblin of little minds
[AD-A147910] 07 p1053 N85-16884

LIAPUNOV FUNCTIONS
Lyapunov stability of very simple steady solutions of prognostic systems 14 p2333 N85-24429
Optimal open loop and nonlinear feedback control for remote orbital capture
[AD-A151967] 16 p2732 N85-26859
Characterization of intermittency in chaotic systems
[PREPRINT-429] 18 p3173 N85-29669
Sub-optimal control of nonlinear flexible space structures 20 p3414 N85-31190

LIBRARIES
Depository librarians' views on GPO's administration of the depository library program. Report to the Chairman, Joint Committee on Printing
[PB84-212265] 01 p0126 N85-10867
An investigation of the use, cost, perceived value and social context of telecommunications tools in two-year college libraries in the southeastern United States
02 p0293 N85-11901
Collection overlap and coordinated collection development 02 p0293 N85-11902
Evaluation of the National Library of Medicine's programs in the medical behavior sciences. Coverage of the Medical Behavioral Sciences (MBS) literature in monographic databases, study 5
[PB84-230531] 03 p0439 N85-12797
Evaluation of the National Library of Medicine's programs in the medical behavior sciences. Online searchers' reactions to database and vendor capabilities in the Medical Behavioral Sciences (MBS), study 4
[PB84-230523] 03 p0439 N85-12798
Evaluation of the National Library of Medicine's programs in the medical behavior sciences. Quality of indexing: The development and testing of a methodology comparing databases covering the Medical Behavioral Sciences (MBS) literature, study 3
[PB84-230515] 03 p0439 N85-12799
Evaluation of the National Library of Medicine's programs in the medical behavior sciences. Test retrievals in five major databases covering the Medical Behavioral Sciences (MBS) literature, study 2
[PB84-230507] 03 p0440 N85-12800
Evaluation of the National Library of Medicine's programs in the medical behavior sciences. Coverage, overlaps and gaps in bibliographic databases dealing with the Medical Behavioral Sciences (MBS) literature, study 1
[PB84-230499] 03 p0440 N85-12801
Evaluation of the National Library of Medicine's program in the medical behavior sciences. An analysis of the National Library of Medicine's (NLM) handling of Medical Behavioral Sciences (MBS) literatures: Some research tests of methods for evaluating bibliographic databases, executive summary
[PB84-230481] 03 p0440 N85-12802
Automated Library Search System (ALSS) user's manual
[DE84-015952] 04 p0576 N85-13672
Some attributes of online search intermediaries that relate to search outcome 05 p0734 N85-14721
Implementation of a Zilog Z-80 base realization library for the computer systems design environment
[AD-A146359] 06 p0953 N85-15422
The UK Schmidt telescope and the facilities in Edinburgh 07 p0965 N85-16121
Implementation of an Intel 8086 microprocessor-based realization library for the control system design language
[AD-A148506] 08 p1202 N85-17589
Computer center CDC Libraries-PROCFIL (procedures)
[AD-A148633] 08 p1206 N85-17589
Computer center CDC libraries/NSRD (subprograms)
[AD-A148792] 08 p1206 N85-17593
Computer center CDC libraries/utility (programs)
[AD-A148680] 09 p1366 N85-18593
Automation of information services furnished by documentation centers and specialized libraries
[FUB-6-1984] 09 p1402 N85-18827
Computer center CDC libraries
[AD-A149005] 10 p1540 N85-19707
Provision of Federal government publication in electronic format to depository libraries
[S-PRT-98-260] 10 p1567 N85-19880
The integrated library system design concepts for a complete serials control subsystem
[AD-A149379] 10 p1568 N85-19884
Abstract and index collection
[PB85-119501] 10 p1569 N85-19892
Parallel linear algebra library for the Denelcor HEP
[DE85-004685] 12 p1917 N85-22034
Software library: A reusable software issue
[AD-A150722] 14 p2403 N85-24816
Procedures for use in compiling requirements specifications for computerized library systems
[CSTI-76] 15 p2685 N85-26446
List of serials indexed for online users, 1985
[PB85-143220] 15 p2686 N85-26455
Notes for medical catalogers, 1984
[PB85-180206] 18 p3200 N85-29853
National Archives and Records Service (NARS) twenty year preservation plan
[PB85-177640] 18 p3200 N85-29854
Local automation model software benchmarking: Test plan
[AD-A154349] 19 p3337 N85-30676
Performance and library issues for mathematical software on high performance computers
[DE85-010263] 19 p3339 N85-30690
A transportable, machine oriented library of european sky and terrain radiance distributions with contemporary radiometric and meteorological profiles
[AD-A155254] 21 p3637 N85-32590
Lopez Energy Alternatives Project
[DE85-010569] 22 p3849 N85-33837
Technology transfer system automation implementation
[PB85-177335] 22 p3849 N85-33838
NBS (National Bureau of Standards) library serial holdings, 1985
[PB85-191948] 22 p3849 N85-33839
Procedure for editing the fluxgate magnetometer data of the AFGL (Air Force Geophysics Laboratory) magnetometer network
[AD-A156331] 24 p4117 N85-35523
Source header list, supplement 3
[AD-A156100] 24 p4165 N85-35824

LIBRATION
Vibration/libration interaction dynamics during the orbiter based deployment of flexible members
20 p3411 N85-31171

LIBRATIONAL MOTION
Stability of steady motions of dynamically symmetrical solid at a triangular libration point
14 p2279 N85-24120

LICENSING
Commercial space launches
[S-REPT-98-856] 12 p1788 N85-21225
Current regulatory and licensing status for byproduct sources, facilities and applications
[DE85-010967] 22 p3842 N85-33796

LICHENS
Interactive effects of acid rain and gaseous air pollutants on natural terrestrial vegetation
[DE85-005255] 16 p2821 N85-27401

LIDAR
U OPTICAL RADAR

LIE GROUPS
NT SPINOR GROUPS
Lie-transformation action principle for classical plasma dynamics
[DE84-014576] 02 p0285 N85-11858
Unrestricted convergence for generalized Poisson integrals
[CTH-MATH-1984-13] 04 p0556 N85-13540
Covariant lie-transformed plasma action principle
[DE85-000285] 11 p1732 N85-20891
Invariant differential operators on a semisimple symmetric space and finite multiplicities in a Plancherel formula
[CWI-PM-R8409] 12 p1925 N85-22094
Asymptotic behavior of matrix coefficients related to reductive symmetric spaces
[CWI-PM-R8410] 12 p1925 N85-22095
Intertwining functions on compact Lie groups
[CWI-TRACT-5] 14 p2414 N85-24895
A convexity theorem for semisimple symmetric spaces
[CWI-PM-R8414] 14 p2415 N85-24900
Cocycles and magnetic monopole
[DE85-007797] 16 p2856 N85-27612
On the transformation of derivatives of distributions on surfaces
[PREPRINT-434] 18 p3173 N85-29670

LIFE (BIOLOGY)
U LIFE SCIENCES

LIFE (DURABILITY)
NT CARRIER LIFETIME
NT FATIGUE LIFE
NT HALF LIFE
NT SATELLITE LIFETIME
NT SERVICE LIFE
NT STORAGE STABILITY
Effect of scandium on the structure and properties of Al-Zn-Mg alloys 01 p0018 N85-10111
Influence of aluminum metallization coatings on corrosion fatigue properties of steel
01 p0018 N85-10112
Free-piston Stirling engine development
[PB84-237767] 01 p0056 N85-10369
Turbine Engine Hot Section Technology (HOST)
[NASA-TM-83022] 02 p0140 N85-10951
Nonlinear structural and life analyses of a turbine blade 02 p0141 N85-10954
Nonlinear structural and life analyses of a combustor liner 02 p0141 N85-10955
Constitutive model development for isotropic materials
02 p0144 N85-10975
Life prediction and constitutive models for anisotropic materials 02 p0144 N85-10976
Surface protection overview 02 p0144 N85-10978
Effects of surface chemistry on hot corrosion life: Overview 02 p0145 N85-10980
Life distribution properties of devices subject to deterioration
[AD-A145554] 02 p0206 N85-11358
Reliability considerations for the total strain range version of strainrange partitioning
[NASA-CR-174757] 02 p0209 N85-11380
Lifetime of excess charge carriers in weakly doped epitaxial GaAs layers 04 p0487 N85-13106
The monitoring of machines
[CETIM-15-J-041] 04 p0510 N85-13253
Potential of flywheels for spacecraft energy storage
05 p0609 N85-13890
Method for predicting the creep rupture life of nickel-base precipitation-hardened superalloys from their chemical composition
[BLL-PNR-90241-(8019.3153)]
06 p0768 N85-14910
In-flight evalution of LCF life consumption of critical rotor components subjected to high transient thermal stress
07 p0906 N85-15734
Monitoring engine thermal stresses
07 p0906 N85-15735
Accelerated Mission Endurance Testing (AMET)
07 p0906 N85-15736
Inconel 718 alloy resistance to crack propagation
07 p0907 N85-15740
Cumulative damage modeling of fatigue crack growth
07 p0907 N85-15741
Problems and possibilities for life extension in gas turbine components 07 p0907 N85-15742
Engine cyclic durability by analysis and material testing 07 p0907 N85-15744
Life prediction at high temperature under multiaxial loading 07 p0907 N85-15745
Verification of life prediction through component testing 07 p0908 N85-15748
CFM 56-2. Oligocyclic fatigue of the turbofan disk: Dimensionning and tests for verification and improvements 07 p0908 N85-15750
View of future requirements for engine cyclic durability by analysis and testing 07 p0908 N85-15751
Ensuring required metrological reliability of analog instrument channels by parametric compensation
07 p0955 N85-16050
Effective life cycle software support: A study in discipline and versatility 08 p1085 N85-16748
SSME lifetime prediction and verification, integrating environments, structures, materials: The challenge
08 p1095 N85-16918
Ada in mission critical system acquisition: A guidebook
[AD-A149271] 10 p1540 N85-19710
Ada (trademark) Joint Program Office objectives and progress through 1983
[AD-A149436] 10 p1541 N85-19713

A study of interdiffusion in beta + gamma/gamma + gamma prime Ni-Cr-Al
[NASA-CR-174852] 11 p1597 N85-20041
Method of constructing diagram of bimetal fatigue failure 11 p1599 N85-20058
Airbus fatigue tests 11 p1618 N85-20186
Emergency Locator Transmitter (ELT) batteries guidance and recommendations
[NASA-TM-87436] 11 p1624 N85-20225
Method and apparatus for measuring minority carrier lifetime in a direct band-gap semiconductor
[NASA-CASE-NPO-16337-1-] 11 p1628 N85-20251
Hyperfine structure and lifetime measurements on electronically excited long-life molecules in a beam experiment
[MPIS-11/1984] 11 p1726 N85-20655
Preliminary review of statistical treatment of S-glass/epoxy stress rupture data
[AD-A149810] 12 p1797 N85-21275
Plasticizer system for propellant compositions
[AD-D011502] 12 p1816 N85-21390
Plasticizer system for propellant compositions
[AD-D011508] 12 p1816 N85-21391
Plasticizer system for propellant compositions
[AD-D011514] 12 p1817 N85-21393
Plasticizer system for propellant compositions
[AD-D011517] 12 p1817 N85-21395
Life study of RF excited Hg arc lamps and CO_2 waveguide lasers
[AD-A149618] 12 p1856 N85-21640
Technological process effect on the carrier lifetime degradation of silicon solar cell base layer irradiated by 1 MeV electrons (boron doping case)
13 p2007 N85-22585
Low thrust bipropellant engine/redundant seat valve assembly
[AD-A150293] 13 p2013 N85-22628
Some specifics of development of fatigue and creep in heat-resistant alloys with asymmetrical multicycle loading
13 p2031 N85-22724
Developing procedures for thermomechanical processing of high-durability VT22 titanium alloy
13 p2031 N85-22726
Durability of VT16 alloy compounds obtained by diffusion welding 13 p2034 N85-22740
A state of the art assessment of turboprop transmission technology and projected needs for the next generation
14 p2220 N85-23770
Fabrication of ceramic substrate-reinforced and free forms
[NASA-TM-86994] 14 p2247 N85-23926
Clutchless mechanism for engagement of forging press 14 p2268 N85-24051
Modernization of running gear of crane
14 p2286 N85-24163
Oxygen-hydrogen thrusters for Space Station auxiliary propulsion systems
[NASA-CR-175691] 15 p2494 N85-25383
Self-sustaining low-Z coatings for fusion applications 2 - copper-lithium
[DE85-002553] 15 p2658 N85-26403
Effects of surface chemistry on hot corrosion life
[NASA-CR-174915] 16 p2708 N85-26711
Development of new materials for turbopump bearings
16 p2735 N85-26877
Bearings working group 16 p2735 N85-26878
Material for electrodes of pulsed and arc sources of light
[DE85-007453] 16 p2780 N85-27156
Life and reliability modeling of bevel gear reductions
[NASA-TM-87006] 16 p2793 N85-27227
Fatigue life analysis of a turboprop reduction gearbox
[NASA-TM-87014] 16 p2793 N85-27228
Reexamination of cumulative fatigue damage laws
17 p2914 N85-27962
Optical strain measurement system development
17 p2915 N85-27969
Heat flux sensor calibrator 17 p2915 N85-27970
Feasibility of mapping velocity flow fields in SSME powerhead by laser anemometry techniques
17 p2915 N85-27971
A test methodology for an automated and interactive software development environment
[AD-A152857] 17 p3011 N85-28618
Corrosion in civil aircraft structures
[SNIAS-851-111-105] 20 p3432 N85-31291
Propellant plasticizer
[AD-D011501] 20 p3434 N85-31306
Results of analysis on the design variable cells
20 p3445 N85-31388
Accelerated and real-time geosynchronous life cycling test performance of nickel-hydrogen batteries
20 p3448 N85-31405
Nickel-hydrogen cell test program summary
20 p3448 N85-31407
Micromechanics of high temperature deformation and failure 20 p3466 N85-31534
Improved Nominal Operating Cell Temperature (NOCT) test procedure 21 p3612 N85-32449
Corrosion management strategies for aircraft and related systems 22 p3749 N85-33239
Development of a high-efficiency, gas-fired, heat pipe, warm-air heating system
[PB85-199636] 24 p4085 N85-35318

LIFE CYCLE COSTS
Technologies for space station autonomy
[NASA-CR-174112] 04 p0458 N85-12906
Accelerated Mission Endurance Testing (AMET)
07 p0906 N85-15738
Concept and cost analysis of an orbiting lunar station
[ILR-MITT-138] 07 p0913 N85-15776
Life cycle cost management master plan for the Defense Communications Agency
[AD-A148876] 07 p1050 N85-16668
A practical example of reducing life cycle costs and increased availability 08 p1063 N85-16736
Standard Attitude Heading Reference System (SAHRS) full scale development program
08 p1073 N85-16804
Life cycle cost model for very high speed integrated circuits
[AD-A147798] 08 p1157 N85-17298
Concept paper for the development of a DOD Ada (trademark) software engineering education and training plan
[AD-A148774] 08 p1206 N85-17592
Permanent magnet motors
[DE85-000860] 10 p1482 N85-19355
Optimization of a ground coupled heat pump
[DE85-000273] 10 p1486 N85-19380
BIT/BITE tradeoff analysis model
[AD-A149345] 11 p1701 N85-20697
Life cycle costing in government procurement
[AD-A151878] 15 p2666 N85-26456
Some aspects of how to design cost-effective flight control systems 16 p2695 N85-26639
An analysis of the materiel fielding plan for the SINCGARS (Single Channel Ground and Airborne Radio System) radio
[AD-A155101] 21 p3576 N85-32236
Development of a high-efficiency, gas-fired, heat pipe, warm-air heating system
[PB85-199636] 24 p4085 N85-35318

LIFE RAFTS
Air carrier overwater emergency equipment and procedures
[PB85-917006] 21 p3553 N85-32105

LIFE SCIENCES
NT EXTRATERRESTRIAL LIFE
NT MOLECULAR BIOLOGY
National Science Foundation grants and awards for fiscal year 1983, volume 2
[PB84-212323] 01 p0125 N85-10854
Life Sciences Research in Space — conference
[ESA-SP-212] 05 p0699 N85-14425
Space station: New frontier for life sciences in space
05 p0696 N85-14477
USSR report: Life sciences. Biomedical and behavioral sciences
[JPRS-UBB-84-027] 07 p1012 N85-16426
Conference on Singlet Molecular Oxygen (COSMO 84), program and abstracts
[AD-A147281] 07 p1040 N85-16605
USSR report: Life sciences. Biomedical and behavioral sciences
[JPRS-UBB-85-001] 08 p1193 N85-17515
Research and technology, Lyndon B. Johnson Space Center
[NASA-TM-58263] 08 p1262 N85-17929
USSR report: Life sciences. Biomedical and behavioral sciences
[JPRS-UBB-85-007] 09 p1362 N85-18586
USSR report: Life sciences. Biomedical and behavioral sciences
[JPRS-UBB-85-008] 10 p1523 N85-19605
USSR report: Life sciences. Biomedical and behavioral sciences
[JPRS-UBB-85-011] 10 p1525 N85-19616
USSR report: Life sciences. Biomedical and behavioral sciences
[JPRS-UBB-85-009] 10 p1526 N85-19625
China report: Science and technology
[JPRS-CST-84-032] 11 p1621 N85-20202
China report: Science and technology
[JPRS-CST-84-040] 11 p1623 N85-20219
China report: Science and technology
[JPRS-CST-84-036] 11 p1696 N85-20661
Research and technology activities at Ames Research Center's Biomedical Research Division
[NASA-TM-86692] 12 p1899 N85-21925
Aerospace Safety Advisory Panel
[NASA-TM-87426] 13 p1970 N85-22573
China report: Science and technology
[JPRS-CST-85-003] 13 p2166 N85-23433
USSR report: Life sciences. Biomedical and behavioral sciences
[JPRS-UBB-85-012] 14 p2366 N85-24697
Research and technology
[NASA-TM-86662] 14 p2458 N85-25166
China report: Science and technology
[JPRS-CST-85-009] 15 p2530 N85-25588
China report: Science and technology
[JPRS-CST-85-013] 15 p2536 N85-25652
China report: Science and technology
[JPRS-CST-85-010] 15 p2564 N85-25819
Structural development and gravity
15 p2606 N85-26071
A search for evidence of large body Earth impacts associated with biological crisis zones in the fossil record 15 p2662 N85-26567
China report: Science and Technology
[JPRS-CST-85-012] 16 p2806 N85-27300
Life sciences flight experiments program mission science requirements document. The first life sciences dedicated Spacelab mission, part 1
[NASA-TM-87494] 21 p3559 N85-32137
USSR Space Life Sciences Digest
[NASA-CR-3922] 21 p3656 N85-32709
Search for the universal ancestors
[NASA-SP-477] 21 p3667 N85-32777
USSR report: Space
[JPRS-USP-84-006] 22 p3731 N85-33128
USSR report: Life sciences. Biomedical and behavioral sciences
[JPRS-UBB-85-021] 23 p3951 N85-34489
Effect of seeds of heavy charged particles of galactic cosmic radiation 23 p3954 N85-34505

LIFE SPAN
The role of gravity on the reproduction of arabidopsis plants 15 p2607 N85-26069

LIFE SUPPORT SYSTEMS
NT CLOSED ECOLOGICAL SYSTEMS
NT EMERGENCY LIFE SUSTAINING SYSTEMS
Aeronautical systems technology needs: Escape, rescue and survival, test facilities and test equipment and training-simulation equipment
[AD-A145059] 01 p0001 N85-10002
Conceptual design and evaluation of selected Space Station concepts, volume 2
[NASA-TM-87364] 02 p0168 N85-11130
The controlled ecological life support system
15 p2588 N85-26603
Controlled Ecological Life Support Systems (CELSS)
15 p2588 N85-26604
Controlled Ecological Life Support System. Life Support Systems in Space Travel
[NASA-CP-2378] 18 p3155 N85-29531
BLSS: A contribution to future life support
18 p3155 N85-29534
Advanced regenerative environmental control and life support systems: Air and water regeneration
18 p3155 N85-29535
Dynamic considerations for control of closed life support systems 18 p3155 N85-29537
CELSS transportation analysis
18 p3156 N85-29538
Extended mission life support systems
18 p3157 N85-29547
Space shuttle revitalization system
18 p3157 N85-29548
Space station ECLSS integration analysis: Simplified General Cluster Systems Model, ECLS System Assessment Program enhancements
[NASA-CR-176089] 21 p3570 N85-32796
Composition and dynamics of bacteriocenosis associated with algae in human life-support systems
22 p3823 N85-33684
Chemical composition of Musca domestica L. larval and pupal biomass when developing in organic waste of biological life-support system for man
22 p3824 N85-33691

LIFEBOATS
Air carrier overwater emergency equipment and procedures
[PB85-917006] 21 p3553 N85-32105

LIFETIME (DURABILITY)
U LIFE (DURABILITY)

LIFT
NT INTERFERENCE LIFT
NT ZERO LIFT
Observations from varying the lift and drag inputs to a noise prediction method for supersonic helical tip speed propellers
[NASA-TM-83797] 01 p0115 N85-10788

Lifting surface theory for a helicopter rotor in forward flight
[NASA-TM-86315] 02 p0134 N85-10916
A comparison of Wortmann airfoil computer-generated lift and drag polars with flight and wind tunnel results
[NASA-TM-86035] 04 p0452 N85-12866
A study of lift characteristics of an upper surface blown jetwing with a rectangular nozzle
05 p0591 N85-13767
Improvement of Aerodynamic Performance Through Boundary Layer Control and High Lift Systems
[AGARD-CP-365] 08 p1066 N85-16771
Recent progress of development and understanding of high lift systems 08 p1066 N85-16772
Investigations into the effects of scale and compressibility on lift and drag in the RAE 5m pressurized low-speed wind tunnel 08 p1066 N85-16773
Detailed study of the flow around a multi-element airfoil. Comparison with calculations 08 p1069 N85-16775
Turbulent bubbles behind airfoils and wings at high angle of attack 08 p1069 N85-16779
Aerodynamic issues in the design of high-lift systems for transport aircraft 08 p1069 N85-16780
An update of the Canada/USA augmentor-wing project 08 p1070 N85-16781
Preliminary results from the unsteady airfoil model USTAR2
[AD-P004171] 09 p1266 N85-17956
Icing flight research: Aerodynamic effects of ice and ice shape documentation with stereo photography
[NASA-TM-86908] 09 p1270 N85-18049
Investigations into the effects of scale and compressibility on lift and drag in the RAE 5m pressurised low-speed wind tunnel
[RAE-TM-AERO-2006] 13 p1969 N85-22372
Estimating unsteady aerodynamic forces on a cascade in a three-dimensional turbulence field
[NASA-TM-86701] 14 p2200 N85-23704
A preliminary investigation of the dynamic force-calibration of a magnetic suspension and balance system
[NASA-CR-172580] 14 p2228 N85-23806
Flow past a flat plat with a vortex/sink combination
[JIAA-TR-58] 15 p2464 N85-25215
High specific power aircraft turn maneuvers: Tradeoff of time-to-turn versus change in specific energy
[AD-A151701] 15 p2471 N85-25257
Aerodynamic performance of a wing in ground effect using the PANAIR program
[AD-A153303] 17 p2892 N85-27832
Method of calculating separation flow of subsonic gas stream around wings 17 p2942 N85-28161
A method for computing the core flow in three-dimensional leading-edge vortices
[NASA-TM-87469] 19 p3214 N85-29932
Application of two-dimensional unsteady aerodynamic to a free-tip rotor response analysis
[NASA-CR-177348] 19 p3215 N85-29933
Circulation control lift generation experiment: Hardware development 22 p3799 N85-33535

LIFT AUGMENTATION
Manufacturing report of an augmented lift, variable deflection half wing
[ONERA-RT-25/1736-AY-108-A]
05 p0591 N85-13766
Presentation of the acoustic and aerodynamic results of the Aladin 2 concept qualification testing
[NASA-TM-77865] 24 p4060 N85-35161

LIFT COEFFICIENTS
U AERODYNAMIC COEFFICIENTS
U LIFT

LIFT DEVICES
Incompressible lifting-surface aerodynamics for a rotor-stator combination
[NASA-TM-83767] 03 p0316 N85-12039
Recent progress of development and understanding of high lift systems 08 p1066 N85-16772
Three-dimensional unsteady lifting surface theory in the subsonic range
[NASA-TM-77812] 12 p1770 N85-21111
Auxiliary units for Robots 14 p2265 N85-24161
Wind tunnel wall interference
[AD-A151212] 15 p2474 N85-25273
A computational method for wings of arbitrary planform
[AD-A153788] 18 p3059 N85-28929
Unsteady transonic flow calculations for interfering lifting surface configurations
[NASA-TM-86432] 19 p3214 N85-29931
Trailing edge flow and aerodynamic sound. Part 1: Tonal pressure and velocity fluctuations. Part 2: Random pressure and velocity fluctuations
[AD-A154947] 21 p3552 N85-32097

LIFT DISTRIBUTION
U FORCE DISTRIBUTION
U LIFT

LIFT DRAG RATIO
An experimental study of the transonic equivalence rule with lift, part 2
[AR-LR-614-PT-2] 01 p0001 N85-10004
Low lift-to-drag aero-assisted orbit transfer vehicles
08 p1107 N85-16994
Moderate lift-to-drag aeroassist
08 p1107 N85-16995
Benefits of high aerodynamic efficiency to orbital transfer vehicles 08 p1107 N85-16996
Over the wing propeller
[NASA-CASE-LAR-13134-1] 11 p1584 N85-19980
Aerodynamic performance of a wing in ground effect using the PANAIR program
[AD-A153303] 17 p2892 N85-27832
Study of an efficient long-range Mach 2.7 supersonic transport configuration concept
[NASA-TM-86414] 21 p3554 N85-32110
The influence of helicopter tail shape on drag: An aerodynamic study using a low speed wind tunnel
[AD-A156304] 24 p4082 N85-35174

LIFT FORCES
U LIFT

LIFTING BODIES
NT LIFTING REENTRY VEHICLES
Lifting surface theory for a helicopter rotor in forward flight
[NASA-TM-86315] 02 p0134 N85-10916
An investigation of vortex-induced aerodynamic characteristics of supersonic cruise configurations
[NASA-CR-174299] 07 p0698 N85-15890
Comparison of analytical and experimental steadyand unsteady-pressure distributions at Mach number 0.78 for a high-aspect-ratio supercritical wing model with oscillating control surfaces
[NASA-TM-84589] 07 p0699 N85-15897
Simultaneous flow visualization and unsteady lift measurement on an oscillating lifting surface
[AD-P004157] 09 p1264 N85-17942
Genesis of unsteady separation
[AD-P004173] 09 p1266 N85-17958
Unsteady transonic flow calculations for interfering lifting surface configurations
[NASA-TM-86432] 19 p3214 N85-29931

LIFTING REENTRY VEHICLES
Aerodynamic characteristics of some lifting reentry concepts applicable to transatmospheric vehicle design studies
[NASA-TM-86331] 06 p0747 N85-14787
The application of some lifting-body reentry concepts to missile design
[NASA-TM-86394] 13 p1969 N85-22366

LIFTING ROTORS
NT BEARINGLESS ROTORS
Basic consideration of the lifting capability of stoppable rotors
[AD-A150850] 14 p2219 N85-23759
A new main rotor hub for the AS 332 Super Puma
[SNIAS-851-210-102] 20 p3393 N85-31047

LIFTING SURFACES
U LIFT DEVICES
U LIFTING BODIES
U SURFACES

LIFTS
Hoist
[AD-D011458] 10 p1493 N85-19425

LIGANDS
Chemically modified electrodes and related solution chemistry
[DE84-017110] 05 p0614 N85-13924
Correlation of electronic charge transfer transitions and electrochemical potentials. The Bipyrazine(Tetracarbonyl)Molybdenum(O) system in various solvents
[AD-A147660] 08 p1120 N85-17082
Ligand structural influences upon electrochemical reactivity: Organic substituent effects upon Carboxylatopentaamminecobalt(3) reductions at mercury and gold electrodes
[AD-A150685] 14 p2250 N85-23944
Metal complexes of some heterocyclic ligands
15 p2504 N85-25446
Metal alkoxides: Models for metal oxides. Alkoxide ligands in early transition metal organometallic chemistry
[DE85-011366] 23 p3916 N85-34269

LIGHT (VISIBLE RADIATION)
NT AIRGLOW
NT COHERENT LIGHT
NT GEOCORONAL EMISSIONS
NT LIGHT BEAMS
NT NIGHTGLOW
NT POLARIZED LIGHT
NT SKY RADIATION
NT SUNLIGHT
NT TWILIGHT GLOW
NT ZODIACAL LIGHT

Personal experience with the PVHD and opinion of situations in which a wide Field Of View (FOV) PVHD might be helpful 01 p0008 N85-10045
Proton pumping in purple membrane, appendix 1
[DE84-014601] 01 p0118 N85-10811
Characteristics of light diffraction by two acoustic waves, one with complex frequency composition
03 p0348 N85-12243
Improved radiographic viewing system
[AD-A147587] 07 p1016 N85-16456
Switchable zero order diffraction gratings as light valves
[AD-A147575] 07 p1044 N85-16833
The relative effectiveness of red and white light for subsequent dark-adaptation
[AD-A148883] 10 p1530 N85-19642
Optical guiding in a free electron laser
[DE85-003141] 11 p1639 N85-20327
Study of light shifts in laser pumped quantum discriminator frequency 11 p1716 N85-20796
Measurement of the configuration of a concave surface by the interference of reflected light
[NASA-TM-77796] 11 p1728 N85-20867
Acoustooptic cell as space-frequency filter
13 p2090 N85-23051
Measurement of the nighttime infrared luminosity of Spacelab 1 in the H- and K-bands
[NASA-TM-85972] 14 p2434 N85-25011
Raman scattering of light in epitaxial films of solid phosphide-gallium arsenide solutions
15 p2643 N85-26301
Optically triggered transferred-electron device microwave burst and single pulse generators
[AD-D011514] 16 p2778 N85-27141
Pursuit tracking performance and flash disruption: The effects of training the non-dominant eye on target reacquisition
[AD-A153404] 17 p2999 N85-28541
The touch panel system: Design and development
[AD-A153014] 17 p3008 N85-28596
System of white-light density pseudocolor encoding with three primary colors
[AD-D011651] 17 p3037 N85-28791
Light transmitting window assembly
[NASA-CASE-MSC-18417-1] 18 p3185 N85-29750
Method for the preperation of photochromic insulating crystals
[DE85-011606] 19 p3282 N85-30229
Optically pumped laser system having extracavity pulse smoother
[AD-D011714] 19 p3276 N85-30319
Haze over eastern North America. Part 1: Haze properties
[PB85-181857] 19 p3311 N85-30526
Quasioptical gyroklystron
[AD-D011666] 19 p3356 N85-30801
Radioluminescent lighting for Alaskan runway lighting and marking
[DE85-010405] 19 p3368 N85-30887
Visual phenomena produced by binocularly disparate dynamic visual noise
[AD-A154758] 21 p3683 N85-32757
Ice fog as an electro-optical obscurant
[AD-A155059] 21 p3705 N85-33015
Estimating angular position of optical radiation source when received by array of photodetectors
22 p3778 N85-33413
Self-study manual on optical radiation measurements. Part 1: Concepts. Chapter 12: Blackbodies, blackbody radiation, and temperature scales
[PB85-196303] 24 p4154 N85-35754
Study of the shower maximum depth by the method of detection of the EAS Cerenkov light pulse shape
[HE-4.4-15] 24 p4194 N85-36021
Preliminary results of the Cerenkov EAS flashes the Crimean Astrophysical Observatory
[HE-4.4-17] 24 p4194 N85-36023

LIGHT ABSORPTION
U ELECTROMAGNETIC ABSORPTION

LIGHT ADAPTATION
Effect of extreme peripheral light on dark adaptation
[AD-A148923] 10 p1528 N85-19636
Discovery regarding visual neuron adaptation applicable to robot use 20 p3504 N85-31786

LIGHT AIRCRAFT
NT CESSNA 402B AIRCRAFT
NT DO-28 AIRCRAFT
Crashworthiness of light aircraft fuselage structures: A numerical and experimental investigation
01 p0060 N85-10399
Preliminary airworthiness evaluation of the Rutan Aircraft Factory (RAF), Inc. LONG-EZ airplane with external sight
[AD-A145361] 02 p0138 N85-10937
Low power laminar aircraft structures
04 p0451 N85-12857

Contribution of the study of light aircraft propeller noise
[ESA-TT-665] 09 p1378 N85-18667
The design of sport and touring aircraft
[NASA-TM-77783] 10 p1423 N85-18975
Development and operation of a measuring data acquisition system for use in light airplanes
24 p4123 N85-35556

LIGHT ALLOYS
NT ALUMINUM ALLOYS
NT BERYLLIUM ALLOYS
NT MAGNESIUM ALLOYS
Influence of recrystallization and solution on the tenacity of the 7010 and 7475 alloys. Oligocyclic fatigue of the 7010 alloy
[ONERA-RT-19/5069-M] 20 p3432 N85-31289

LIGHT AMPLIFIERS
Fiber cable in optical system with brightness amplifier
02 p0263 N85-11724
Optical inhomogeneities in a nanosecond-pulse iodine photodissociation laser with slow UV radiation pumping
21 p3686 N85-32902

LIGHT BEAMS
Fluctuations in parameters of light beam along path with reflection in turbulent atmosphere
02 p0263 N85-11722
Optical computer studies at UK's Heriot-Watt University 09 p1309 N85-18227
Numerical investigation of propagation of radiation pulse at xxx 11 p1718 N85-20809
Spontaneous diffraction of sequence of supershort light pulses in dye solution 11 p1718 N85-20811
Intensity fluctuations of focused laser beam during reflection in turbulent atmosphere
13 p2078 N85-22975
Time spectra of intensity fluctuations along reflecting path 13 p2079 N85-22981
Method and apparatus for generating a structured light beam array
[AD-D011580] 15 p2652 N85-26357
Double window viewing chamber assembly
[NASA-CASE-MFS-28057-1] 18 p3063 N85-28951
Multiport optical detectors 18 p3167 N85-29769
Laser Schlieren crystal monitor
[NASA-CASE-MFS-28060-1] 19 p3374 N85-30932
Influence of coherent light beams on free carriers in semiconductors 21 p3681 N85-32867
Fluctuations in light intensity during backscattering in turbulent medium 21 p3695 N85-32956
Coefficient of optical absorption and scattered light capture effect 21 p3695 N85-32959
Refraction of narrow probing light beam in multilayer optical fiber 22 p3764 N85-33330
Asymmetry of diffraction orders with light diffraction at surface acoustic wave 22 p3782 N85-33431
Ranging system which compares an object reflected component of a light beam to a reference component of the light beam
[NASA-CASE-NPO-15865-1] 23 p3973 N85-34629

LIGHT BULBS
U LUMINAIRES

LIGHT COMMUNICATION
U OPTICAL COMMUNICATION

LIGHT CURVE
One to eight month X-ray light curves for active extragalactic objects 08 p1239 N85-17817
Optical and X-ray observations of 4U2129+47/V1727 CYG in a quiescent state 11 p1742 N85-20950
Recent results on the Crab Pulsar X-ray light curve
11 p1742 N85-20955
Eclipse observations of Epsilon Aurigae
11 p1755 N85-21037
Convex-profile inversion of asteroid lightcurves
13 p2176 N85-23502
Very high energy gamma rays from the Crab Nebula
[OG-2.3-3] 22 p3866 N85-33940
A new approach to evaluate gamma-ray measurements
[OG-9.5-11] 23 p4031 N85-34988
The experimental cascade curves of EAS at E sub 0 10(17) eV obtained by the method of detection of Cherenkov pulse shape
[HE-4.4-16] 24 p4194 N85-36024

LIGHT DURATION
U FLASH
U PULSE DURATION

LIGHT ELEMENTS
Calculation of Si(Li) X-ray detector efficiencies
[DE85-002732] 10 p1489 N85-19400

LIGHT EMISSION
NT BIOLUMINESCENCE
NT CATHODOLUMINESCENCE
NT CHEMILUMINESCENCE
NT ELECTROLUMINESCENCE
NT FLUORESCENCE
NT INCANDESCENCE
NT LUMINESCENCE
NT OPTICAL RESONANCE
NT PHOSPHORESCENCE
NT PHOTOLUMINESCENCE
NT RESONANCE FLUORESCENCE
NT SHOCK WAVE LUMINESCENCE
NT THERMOLUMINESCENCE
NT X RAY FLUORESCENCE
New lighting technologies, their status and impacts on power densities
[DE85-000712] 09 p1315 N85-18266
Formation of optical-line emitting regions in the jets of SS433 12 p1959 N85-22316
Optical monitoring of gamma-ray source fields
[OG-1.1-7] 22 p3861 N85-33908
Search for optical bursts from the gamma ray burst source GBS 0526-66
[OG-1.1-8] 22 p3861 N85-33909

LIGHT EMITTING DIODES
LED multifunction keyboard engineering study
[AD-A145199] 01 p0010 N85-10061
1.5 to 1.7 micrometers LEDs (Light-Emitting Diode)
[AD-A149685] 12 p1834 N85-21508
Transistor-transistor logic microcircuit tester
12 p1842 N85-21556
Focal plane array optical proximity sensor
[NASA-CASE-NPO-15155-1] 12 p1932 N85-22130
AL-124 light-emitting diode in 30 Mbit/s fiber-optic communication line 13 p2069 N85-22925
Optoacoustic receiver with semiconductor-type radiator and photodetector 14 p2274 N85-24086
Error of distance measurement by phase-type optical range finders with photoreceivers of various types
14 p2276 N85-24101
InGaAs/GaAs, Strained-Layer Superlattice (SLS), junction photodetectors, LED's, injection LASER's and FET's for optoelectronic IC applications
[DE85-001940] 14 p2430 N85-24986
Electron irradiation of light emitting diodes
[AD-A154441] 19 p3260 N85-30213
Electrochromic display device
[AD-D011733] 22 p3759 N85-33299
Transceiver test device
[AD-D011728] 22 p3786 N85-33458

LIGHT GAS GUNS
The utilization of a light-gas gun to simulate interior ballistic flow
[ISL-CO-233/83] 14 p2303 N85-24259
Experimental simulation of internal ballistic flows
[ISL-CO-208/84] 20 p3435 N85-31312

LIGHT INTENSITY
U LUMINOUS INTENSITY

LIGHT IONS
Experiments with light ions at CERN super proton synchrotron
[DE85-007625] 17 p3031 N85-28744
Heavy ion medical accelerator options
[DE85-011204] 22 p3841 N85-33784
Light ion sources for ICF
[DE85-011544] 23 p3983 N85-34702
Multidimensional analysis of data obtained in experiments with X-ray emulsion chambers and extensive air showers
[HE-3.6-2] 24 p4184 N85-35951

LIGHT MODULATION
NT ULTRASONIC LIGHT MODULATION
Transfer function of multilayered magnetooptical space-time modulator 02 p0264 N85-11726
Optical waveguide spatial filters
[AD-A145674] 02 p0280 N85-11825
The spectral distribution of field components for a sinusoidal power modulated monofrequency optical carrier source
[FI-44-TBR-84] 04 p0565 N85-13601
A picosecond population modulation study of near interband resonances in semiconductors
09 p1396 N85-18787
An electro-optic spatial light modulator for thermo-elastic generation of programmably focused ultrasound
[AD-A149078] 10 p1553 N85-19794
Switchable zero order diffraction gratings as light valves
[AD-A150129] 12 p1934 N85-22153
Space-time response characteristics of acoustooptic filter for compression of linearly frequency-modulated signal 13 p2071 N85-22937
Theory of diaphragm light modulators with electrical input signal 13 p2082 N85-23002
An electro-optic spatial light modulator for thermoelastic generation of programmably focused ultrasound
[AD-A152066] 15 p2646 N85-26323
Electron-bombarded silicon spatial light modulator
[AD-D011579] 15 p2652 N85-26355
Charge isolation in a spatial light modulator
[AD-D011581] 15 p2652 N85-26356
Construction and analysis of a PRIZ spatial light modulator exhibiting dynamic image selection
[AD-A152318] 17 p3037 N85-28787
Deformable mirror nearest neighbor optical computer
18 p3188 N85-29772
Stokes parameters modulator for birefringent filters
18 p3205 N85-29884
Differentiating spatial light modulator
[AD-D011727] 23 p3973 N85-34632

LIGHT PRESSURE
U ILLUMINANCE

LIGHT PROBES
U LIGHT BEAMS

LIGHT SCATTERING
NT HALOS
Physical-chemical properties of articulated rodlike polymers
[AD-A145549] 02 p0186 N85-11244
Characterization of atmospheric conditions along transmission paths from a remotely piloted vehicle
[AD-A145527] 02 p0232 N85-11511
Structure of vibrational spectrum and selection rules in Raman and hyper-Raman light scattering spectra of inorganic glasses 02 p0271 N85-11769
Extinction by dielectric particles at optical and infrared wavelengths
[AD-A146305] 03 p0413 N85-12640
Brillouin scattering in underdense UV laser-produced plasmas
[DE84-015184] 04 p0567 N85-13614
Storage stability of jet fuels
[AD-A146360] 06 p0773 N85-14943
Investigation of light source and scattering medium related to vapor-screen flow visualization in a supersonic wind tunnel
[NASA-TM-86290] 06 p0810 N85-15144
Research on acoustical and optical scattering, optics of bubbles, diffraction catastrophes, laser generation of sound, and shock induced cavitation
[AD-A146703] 06 p0860 N85-15466
A study of structural phase transitions using light scattering techniques
[AD-A147261] 07 p1048 N85-16654
Light scattered from polished optical surfaces: Wings of the point spread function 08 p1252 N85-17911
Journal of Research of the National Bureau of Standards, Volume 89, Number 1, January-February, 1984
[PB84-235530] 08 p1262 N85-17931
Measurement of drop-size distributions with the aid of a scattered light particle size counting analyser
[BLL-TRANS-WH-620-(9091.9F)]
09 p1317 N85-18278
Application of scattered light particle size counting analysis to the determination of wide drop size distributions
[BLL-TRANS-WH-619-(9091.9F)]
09 p1317 N85-18279
Light scattering studies of lower dimensional colloidal particle and critical fluid systems
[DE85-002087] 09 p1377 N85-18654
Theory of resonant light scattering from a rough surface 09 p1383 N85-18701
Experimental and theoretical study of condensation in multicomponent vapors
[DE85-000843] 10 p1485 N85-19376
Effect of extreme peripheral light on dark adaptation
[AD-A148923] 10 p1528 N85-19636
Experimental investigation of wavefront conjugation during Mandelstam-Brillouin scattering of focused laser beams in condensed media 11 p1716 N85-20796
Spontaneous diffraction of sequence of supershort light pulses in dye solution 11 p1718 N85-20811
Light diffraction with collective, thermal electron density fluctuation in plasmas with several ionic components
[IPF-84-5] 11 p1733 N85-20904
Subnanosecond time-resolved emission study of Cu2O and GaAs
[DE85-002070] 11 p1735 N85-20912
Research study of droplet sizing technology leading to the development of an advanced droplet sizing system
[NASA-CR-174839] 12 p1850 N85-21604
Transmission and reflection of laser beams propagating through aerosol clouds in space
[LA-9968-MS] 12 p1858 N85-21838
On the inversion of the lidar equation
[AD-A149053] 12 p1858 N85-21841
A systematic study of light scattering by irregularly shaped particles
[AD-A150192] 13 p2159 N85-23400
Nonrelativistic Kapitza-Dirac scattering
[AD-A150622] 13 p2159 N85-23405
Scattering properties of a moving dielectric object
[AD-A151974] 15 p2544 N85-25706
Application of scattering methods to the studies of the structure of polymer blends
[IFPR-13/1984] 17 p2933 N85-28104

Earth observation modeling based on layer scattering matrices
[NLR-MP-84015-U] 17 p2984 N85-28440
Studies of optical-beam phase-conjugation by nonlinear refraction
[AD-A152865] 17 p3037 N85-28788
Light scattering by leaf layers with application to canopy reflectance modeling: The Scattering by Arbitrarily Inclined Leaves (SAIL) model
[NLR-MP-84011-U] 17 p3038 N85-28796
Light scattering and spectroscopic studies of polymerization processes
[AD-A153407] 18 p3069 N85-28984
Technique to reduce scattered light in optical systems
[AD-D011597] 18 p3185 N85-29752
Laser forward and backscattering in particulate media
[AD-A154136] 19 p3275 N85-30312
Detection of internal structure by scattered light intensity: Application to kidney cell sorting
20 p3503 N85-31777
Flow cytometry of human embryonic kidney cells: A light scattering approach 20 p3503 N85-31778
Journal of Research of the National Bureau of Standards, volume 90, number 1, January - February 1985
[PB85-179083] 20 p3522 N85-31908
Phase behavior and QLS (Quasielastic Light Scattering) in potassium linoleate/n-alkanol microemulsions
[AD-A155029] 21 p3583 N85-32163
Temperature measurements on small droplets
21 p3583 N85-32660
Influence on bi-phonon states on Raman scattering of light in molecular crystals 21 p3660 N85-32665
Generation and amplification of radiation during stimulated Raman scattering in crystals
21 p3681 N85-32869
Effective brightness of zero-point fluctuations of the electromagnetic vacuum accompanying parametric scattering of light 21 p3694 N85-32951
Correlation of intensities of different scattering channels 21 p3694 N85-32952
Coefficient of optical absorption and scattered light capture effect 21 p3695 N85-32959
Stimulated Mandelstam-Brillouin scattering with distributed feedback 21 p3696 N85-32961
Influence of phonon interaction on width and form of Mandelstam-Brillouin optical scattering line
21 p3696 N85-32962
Transmission of light by disperse medium of densely packed optically soft particles 21 p3697 N85-32969
Ice fog as an electro-optical obscurant
[AD-A155059] 21 p3705 N85-33015
Calculating solar highlight and shadeless areas for scanning photographs from space and optimizing lighting conditions 22 p3736 N85-33160
Size exclusion chromatography-low angle laser light scattering photometry of lignite macromolecules
[DE85-012017] 22 p3745 N85-33215
Interrelations for the elements of the scattering matrix
22 p3855 N85-33872
High resolution Cherenkov detectors for cosmic ray isotope experiment
[OG-8.1-4] 23 p4023 N85-34930
Energy calibration of the fly's eye detector
[HE-4.4-1] 24 p4192 N85-36011

LIGHT SCATTERING METERS
Apparatus for determining the liquid water content of a gas
[AD-D011287] 07 p0922 N85-15839
Particle sizing from forward scattered light at two angles using a Variable-Focal-Length optical system
[AD-A154164] 20 p3533 N85-31960

LIGHT SOURCES
NT ILLUMINATORS
A limbus-sensing eye movement recorder
[AD-A144772] 01 p0049 N85-10323
An evaluation of flashtube signal characteristics
[AD-A149580] 10 p1423 N85-18974
Formulation of a coherent light-sheet by means of a cylindrical-spherical optical system
[ISL-R-116/83] 16 p2985 N85-27874
Electrodeless HID lamp study
[DE85-010628] 18 p3096 N85-29167
Experience with a high-brightness storage ring: The NSLS 750 MeV VUV ring
[DE85-010547] 18 p3190 N85-29787
Combined function lattices for a 6 GeV synchrotron light source
[DE85-010059] 19 p3367 N85-30665
Radioluminescent lighting for Alaskan runway lighting and marking
[DE85-010405] 19 p3368 N85-30667
Pulsed lasers for filming color holographic film images
22 p3781 N85-33426
Study of composition of cosmic rays with energy .7 E 3 Ee
[OG-8.1-7] 22 p3801 N85-34049
Electronic imaging system and technique
[DE85-005740] 23 p3935 N85-34393
Vacuum system for the Argonne 6 GeV synchrotron light source
[DE85-012286] 24 p4157 N85-35773
Background light measurements at the DUMAND site
[HE-5.2-7] 24 p4203 N85-36084

LIGHT SPEED
On the propagation speed in relativistic quantum mechanics
[CWI-AM-R8410] 17 p3046 N85-28848
Sub-luminal pulses from cosmic ray air showers
[HE-4.7-13] 24 p4200 N85-36083

LIGHT TRANSMISSION
NT HALOS
NT LIGHT SCATTERING
Collapse of cavitation bubbles between two walls in ultrasonic field 02 p0266 N85-11799
Experimental capabilities and prospects for measuring soft X-ray photoabsorption
[DE84-015486] 02 p0278 N85-11813
Atmospheric extinction in critical environments
[AD-A146102] 03 p0396 N85-12527
Free-space propagation of light pulses
[PB84-217100] 03 p0421 N85-12689
Site-specific research conducted in support of the Salton Sea Solar Pond Project, FY 1982 report
[NASA-CR-174182] 05 p0666 N85-14280
Laboratory investigations 05 p0666 N85-14281
Development and analysis of silicon solar cells near 20% efficiency 06 p0829 N85-15267
Long-term light induced changes in dark conductivity of kapton
[AD-A148791] 08 p1224 N85-17706
Development of photoconductive power switch technology
[DE85-001514] 09 p1315 N85-18270
Diffraction diffusion screen with holographically-suppressed zero-order beam
[AD-D011445] 10 p1487 N85-19387
Improvements in glazings: SERI materials research in progress
[DE84-013049] 12 p1814 N85-21378
Transmission and reflection of laser beams propagating through aerosol clouds in space
[LA-9998-MS] 12 p1856 N85-21638
Temperature-insensitive optical fibers
[AD-D011551] 12 p1933 N85-22142
Fine structure of vertical distribution of light attenuation index of sea water 13 p2109 N85-23140
Ways of optimization of light energy transformation in primary stages of photosynthesis. Optimization of lattice structure of uniform photosynthetic unit
14 p2386 N85-24701
Studies of electro-optical attenuation in the vicinity of cloud base
[AD-A151745] 15 p2653 N85-26360
Philips researches gallium arsenide use for lasers
18 p3087 N85-29106
Light transmitting window assembly
[NASA-CASE-MSC-18417-1] 18 p3185 N85-29750
Model computations of light reflection from sea surface 19 p3292 N85-30411
Comparison of 8 to 12 micrometer and 3 to 5 micrometer CVF transmissometer data with LOWTRAN calculations
[AD-A154218] 19 p3350 N85-30763
Switchable zero order diffraction gratings as light valves
[AD-A154471] 20 p3533 N85-31981
Ship-to-ship propagation: Maritime data analyses
[AD-A155484] 21 p3592 N85-32325
Transmission of light by disperse medium of densely packed optically soft particles 21 p3697 N85-32969
Energy calibration of the fly's eye detector
[HE-4.4-1] 24 p4192 N85-36011
The structure of EAS at E 0.1 EeV
[HE-4.4-2] 24 p4193 N85-36012

LIGHT VALVES
Switchable zero order diffraction gratings as light valves
[AD-A147575] 07 p1044 N85-16633
Switchable zero order diffraction gratings as light valves
[AD-A150129] 12 p1934 N85-22153
Electron-bombarded silicon spatial light modulator
[AD-D011579] 15 p2652 N85-26355
Charge isolation in a spatial light modulator
[AD-D011581] 15 p2652 N85-26356
Numerical optical computing at the Ohio State University 16 p3188 N85-29775
Switchable zero order diffraction gratings as light valves
[AD-A154471] 20 p3533 N85-31981
Liquid crystal light valve structures
[NASA-CASE-MSC-20036-1] 22 p3847 N85-33826

LIGHT WATER REACTORS
Neutron detector counting capabilities for (10) B-lined and (235) U fission chambers in high gamma-ray fluxes
[DE85-011893] 22 p3840 N85-33760
Effect of stainless steel weld overlay cladding on the structural integrity of flawed steel plates in bending, series 1
[TI85-010349] 23 p3939 N85-34418
Pressure measurements in a hydrogen combustion environment: Hydrogen-air combustion test series 1 and 2 in the FITS tank, volume 1
[TI85-009899] 24 p4076 N85-35259

LIGHTHILL METHOD
Hypersonic flow of mixture around blunt body
06 p0779 N85-14979

LIGHTING
U ILLUMINATING

LIGHTING EQUIPMENT
NT AIRCRAFT LIGHTS
NT ARC LAMPS
NT FLASH LAMPS
NT ILLUMINATORS
NT LUMINAIRES
NT MERCURY LAMPS
NT RUNWAY LIGHTS
Brightness comparison of electroluminescent versus incandescent lighting: A photometric validation
[AD-A145395] 02 p0280 N85-11822
Development of novel lamps for study of enhanced production of resonance by low-density mercury discharges
[DE84-016889] 05 p0832 N85-14053
Evaluation of arctic test of improved tritium radioluminescent lighting
[AD-A148215] 08 p1089 N85-16884
New lighting technologies, their status and impacts on power densities
[DE85-000712] 09 p1315 N85-18266
Lighting controls: The role of advanced technology; past, present and future
[DE84-015977] 09 p1384 N85-18706
Astronomy and sodium lighting
[RAND/N-2089-RC] 09 p1413 N85-18914
System of light protection of antenna-mast structures of radio-relay lines 15 p2527 N85-25563

LIGHTNING
A lightning detection system in Sweden
01 p0078 N85-10519
Nowcasting using lightning location techniques
01 p0084 N85-10568
Effects of a lightning strike on a civil defense operation center
[FOA-A-30035-A3] 02 p0232 N85-11514
Study of effects of lightning on aircraft systems stressed 03 p0310 N85-12005
NASA thunderstorm overflight program: Atmospheric electricity research. An overview report on the optical lightning detection experiment for spring and summer 1983
[NASA-TM-86468] 03 p0363 N85-12330
Tests for susceptibility to electromagnetic attack
[SNIAS-842-422-101] 04 p0494 N85-13154
Improvement of lightning arresters energy capability
[SNIAS-842-422-104] 04 p0497 N85-13172
Spring program summary, 1983
[PB84-222223] 06 p0839 N85-15330
International Aerospace and Ground Conference on Lightning and Static Electricity. 1984 technical papers. Supplement
[NASA-CP-2356] 07 p0999 N85-16343
Data and results of a laboratory investigation of microprocessor upset caused by simulated lightning-induced analog transients
07 p0999 N85-16345
Lightning research: A user's lament
07 p0999 N85-16348
A comparison of lightning and nuclear electromagnetic pulse response of a helicopter 07 p1000 N85-16349
A comparison of lightning and nuclear electromagnetic pulse response of tactical shelters
07 p1000 N85-16350
Mathematical physics approaches to lightning discharge problems
[NASA-TM-86349] 08 p1187 N85-17482
A study of the effects of triggered lightning
[AD-A148296] 08 p1189 N85-17494
Direct-strike lightning photographs, swept-flash attachment patterns, and flight conditions for storm hazards 1982
[NASA-TM-86347] 12 p1892 N85-21877
Collection and use of lightning strike data in the western US during summer 1983
[PB85-110534] 12 p1907 N85-21907

Preliminary results of associating cloud-to-ground lightning with surface convergence and radar reflectivity at Kennedy Space Center in 1983
[NASA-CR-175543] 12 p1897 N85-21910
Surge strength of symmetric cable with monolithic polyethylene insulation of quads
13 p2082 N85-23001
1981 wC-130 airborne lightning characterization program data review
[AD-A150230] 13 p2138 N85-23275
USSR report: Transportation
[JPRS-UTR-84-017] 15 p2461 N85-25196
Effects of lightning on aircraft studied at Sheremetyevo 15 p2461 N85-25199
Saturn electrostatic discharges
15 p2673 N85-26499
Lightning strikes on aircraft. The TRIP 82 experiment and 3-dimensional electromagnetic interferometry
[ONERA-RF-88/7154-PY] 16 p2703 N85-26690
Lightning-safe carbon fiber composite for Airbus tail unit 18 p3087 N85-29100
Comparison of the electromagnetic properties of lightning and EMP (Electromagnetic pulse): Results of recent lightning studies
[AD-A154325] 19 p3317 N85-30560
Investigation of the lightning vulnerability of nuclear explosive test systems at the Nevada Test Site
[DE85-011761] 24 p4124 N85-35563
Application of pulsed power in the simulation of severe natural lightning
[DE85-012866] 24 p4124 N85-35564

LIGHTS
U LUMINAIRES

LIGNITE
Some principles of plant resources evaluation using remotely sensed data 04 p0543 N85-13459
Alternative anodic reactions in water splitting
[DE85-004159] 12 p1802 N85-21300
Commercial feasibility of underground gasification of Texas lignite to produce synthetic gas
[DE85-001998] 18 p3127 N85-29361
Supercritical solvent extraction of lignite to form carbonaceous chars
[DE85-010156] 19 p3229 N85-30019
Size exclusion chromatography-low angle laser light scattering photometry of lignite macromolecules
[DE85-012017] 22 p3745 N85-33215

LIKELIHOOD RATIO
On the power functions of test statistics in order restricted inference
[AD-A147126] 07 p1035 N85-16568
The asymptotic behavior of the likelihood ratio statistic for testing a shift in mean in a sequence of independent normal variates
[AD-A149329] 10 p1550 N85-19779
Asymptotic expansions of the distribution of test statistics associated with several two parameter exponential distributions
[AD-A151908] 15 p2641 N85-26289

LIMB BRIGHTENING
Comparison of wind derived from the LIMS (Limb Infrared Monitor of the Stratosphere) satellite instrument with rocket observations
[NASA-CR-174083] 04 p0541 N85-13444
Extreme limb profiles of the Sun at far infrared and submillimeter wavelengths 08 p1244 N85-17852

LIMBS (ANATOMY)
NT ARM (ANATOMY)
NT ELBOW (ANATOMY)
NT FEET (ANATOMY)
NT FINGERS
NT HAND (ANATOMY)
NT KNEE (ANATOMY)
NT LEG (ANATOMY)
New uses for sensitivity analysis: How different movement tasks effect limb model parameter sensitivity
05 p0706 N85-14529

LIME
U CALCIUM OXIDES

LIMESTONE
Selection, procurement and description of Salem Limestone samples used to study the effects of acid rain
[PB84-231067] 04 p0484 N85-13088
Paleozoic limestones of the Crazy Mountains and vicinity, Circle quadrangle, east-central Alaska
04 p0517 N85-13298
Petrography, diagenesis and depositional models of the St. Louis limestone, valmeyeran (middle Mississippian), Illinois Basin, USA 09 p1352 N85-18508
Petrography, sedimentology, diagenesis, and reservoir characteristics of some Pennsylvanian phylloid algal limestones: Kansas and Utah, USA
09 p1352 N85-18507
Organogenic structures (submerged reefs) in Silhetian limestone of west Bengal basin
10 p1500 N85-19484
Evaluation of the Santee limestone for use in flue-gas desulfurization systems
[DE85-901277] 19 p3249 N85-30148
Deep-burial diagenesis in carbonates
[DE85-011224] 22 p3602 N85-33554

LIMITATIONS
U CONSTRAINTS

LIMITER AMPLIFIERS
Frequency selective signals-to-noise enhancer/limiter apparatus
[AD-D011583] 15 p2548 N85-25724

LIMITER CIRCUITS
Effects of monolayer coverages on substrate sputtering yields
[DE84-016312] 04 p0476 N85-13033

LIMITERS (FUSION REACTORS)
Sources, densities, and transport of impurities in neutral-beam injected Tokamaks
09 p1388 N85-18731
Magnetic divertor design for the compact reversed-field pinch reactor
[DE85-002031] 09 p1391 N85-18753
Extended abstract: Ergodic magnetic limiter experiments on TEXT with a 7/3 resonance
[DE85-001390] 09 p1391 N85-18754
Coupled plasma-neutral transport model for the scrape-off region
[DE85-007559] 16 p2668 N85-27695
New concept for pumping the edge plasma
[DE85-010180] 19 p3371 N85-30909
Limiter
[DE85-011620] 24 p4150 N85-35736
Neutral pumping rates for a next step tokamak ignition device
[DE85-012780] 24 p4157 N85-35776

LIMITS (MATHEMATICS)
Sensitivity analysis of limit state functions for probability-based plastic design
01 p0059 N85-10388
A note on two papers in dependent central limit theory
[CWI-MS-R8410] 05 p0722 N85-14638
On limit of the largest eigenvalue of the large dimensional sample covariance matrix
[AD-A150589] 13 p2151 N85-23358
Statistical techniques for signal processing
[AD-A151231] 15 p2541 N85-25690
Entire functions with spiral limits
15 p2634 N85-26241
Limiting values of stress state index after rupture of metals
[BLL-BISI-TRANS-22293-(9022.06)] 17 p2978 N85-28407

LIMNOLOGY
Automatic hydrological data collection facility using ARGOS 14 p2324 N85-24363
Microwave hydrology: A trilogy
[NASA-CR-176042] 20 p3477 N85-31603

LIMONITE
A comparison of LANDSAT thematic mapper, multispectral scanner and airborne sensors for mapping the distribution of alteration minerals: Examples from the southwestern United States 24 p4108 N85-35452

LINE OF SIGHT
Probe of the nearby interstellar medium by the vacant line of sight to Beta CMa 06 p0874 N85-15551
Kinematics of nearby gas and stars
06 p0880 N85-15591
Solar monochromatic images in magneto-sensitive spectral lines and maps of vector magnetic fields
18 p3207 N85-29697

LINE OF SIGHT COMMUNICATION
Real-time estimation of amplitude and group delay distortion in a PSK line-of-sight communications channel
[AD-A147735] 08 p1151 N85-17266
Influence of propagation in digital wireless beam, microwave links 10 p1470 N85-19277
Wideband line-of-sight channel measurements and simulation: Application to digital radio links
10 p1471 N85-19283
Design criteria for limited scan antennas at digital microwave line of sight links 10 p1471 N85-19284
Some propagation experimental results on protection techniques for line-of-sight digital systems
10 p1472 N85-19286
LOS microwave channel simulation: A survey of models, realizations and new concepts 10 p1472 N85-19291
Theoretical study of a dynamic simulator of selective fading for digital, wireless beam microwave links
10 p1473 N85-19294
A ray trace program for line-of-sight microwave communication links
[AD-A156168] 24 p4087 N85-35336
Microwave propagation studies, measurements and education in Surabaya, Indonesia
[B8484633] 24 p4089 N85-35339

LINE SHAPE
New instabilities in line driven winds
06 p1235 N85-17785
A remote source system for measuring relative positron annihilation line widths in individual slab cylindrical samples
[AERE-R-10549] 12 p1838 N85-22173
A positron annihilation Doppler broadening study of niobium
[DE85-010287] 20 p3527 N85-31936

LINE SPECTRA
NT BALMER SERIES
NT D LINES
NT ELECTRONIC SPECTRA
NT FRAUNHOFER LINES
NT H ALPHA LINE
NT H LINES
NT K LINES
NT LYMAN SPECTRA
NT RYDBERG SERIES
The X-ray spectrum and time variability of narrow emission line galaxies
[NASA-TM-83859] 03 p0446 N85-12842
Absolute transition probabilities of lines in the spectra of astrophysical atoms, molecules, and ions
[NASA-CR-174141] 04 p0580 N85-13705
Search for the radiative decay of a cosmic relic particle with IUE
[PREPRINT-410] 04 p0580 N85-13707
The IRAS galaxy 0421+040P06: An active spiral (?) galaxy with extended radio lobes
[NASA-CR-174208] 06 p0871 N85-15536
A type stars as probes of the local interstellar medium
06 p0874 N85-15550
Probe of the nearby interstellar medium by the vacant line of sight to Beta CMa 06 p0874 N85-15551
Optical emission line studies and the warm, ionized component of the local interstellar medium
06 p0875 N85-15555
A high-resolution study of local interstellar sodium
06 p0875 N85-15556
Degenerate four-wave mixing lineshapes in sodium vapor under pulsed excitation
[AD-A148211] 08 p1222 N85-17698
Departures from LTE populations versus anomalous abundances: The effects of heating
08 p1234 N85-17776
Multiline transfer and the dynamics of stellar winds
08 p1236 N85-17785
Radio Seyferts and the forbidden line region
08 p1236 N85-17793
The ultraviolet spectra of the narrow line active galaxies NGC 3081 and NGC 4507 08 p1237 N85-17799
Dueling winds: A model for broad-line regions — galactic nuclei 08 p1242 N85-17837
Theoretical studies of emission line variability in type 1 Seyfert galaxies 08 p1242 N85-17839
On the stability of broad line clouds in active galactic nuclei 08 p1243 N85-17840
Star formation in globules 08 p1247 N85-17868
Mid-infrared spectroscopy of planetary nebulae
08 p1247 N85-17872
Effect of inner subshell ionization for emission lines of OIV ion 09 p1388 N85-18729
Spectra of highly-ionized atoms for the diagnostics of the new generation of Tokamaks
09 p1388 N85-18730
X-ray line broadening of a diagnostic in laser produced plasma
[DE85-001179] 10 p1580 N85-19841
KMSF X-ray laser experiments, task no. 1
[DE85-001002] 11 p1839 N85-20325
The UV spectra of intermediate redshift quasars
11 p1746 N85-20080
Fluorescent excitation of Fe 2, Mn 2, Ti 2, H 1 lines by V 4, N 5, O 6: Emission lines in the spectra of symbiotic stars and Seyfert galaxies 11 p1746 N85-20084
IUE observations of planetary nebulae in the Magellanic Clouds 11 p1747 N85-20086
1983 observations of the eclipsing nucleus of the bipolar planetary nebula NGC 2346 11 p1747 N85-20087
The changing ultraviolet spectrum of Herbig-Haro object No. 1 11 p1747 N85-20089
Short-wavelength observations of HH-2H and HH-24A
11 p1747 N85-20090
A search for young stellar chromospheres in NGC 2264 11 p1748 N85-20093
Ultraviolet observations of circumstellar matter in Algol type binary systems 11 p1756 N85-21043
Circumstellar material in Algols and Serpentids
11 p1757 N85-21051
Chromospheric emission lines in high-resolution LWR spectra (220 - 3000 alpha) of gamma CRU (IAB 3) and alpha CRI (IA2 lab) 11 p1758 N85-21068

Precise measurements of radial velocities of emission lines in the far-ultraviolet spectra of late-type stars
11 p1758 N85-21082
Ultraviolet, radio and X-ray observations of hybrid stars
11 p1759 N85-21083
Rotational modulation of chromospheric emission in cool giants and hybrid stars
11 p1759 N85-21084
Magnetospheres and winds in the helium weak stars: Observations of C 5 in upper main sequence CP stars
11 p1759 N85-21086
IUE spectrophotometry of helium weak and silicon stars
11 p1759 N85-21087
Formation of optical-line emitting regions in the jets of SS433
12 p1959 N85-22318
NIMBUS-7 SBUV (Solar Backscatter Ultraviolet) observations of solar UV spectral irradiance variations caused by solar rotation and active-region evolution for the period November 7, 1978 - November 1, 1980
[NASA-CR-175544]
12 p1962 N85-22334
An atlas of nitrogen-broadened water vapor spectra from 500 to 5000 cm(-1), volume 1
[AD-A160527]
13 p2018 N85-22650
Chemical and localization effects in Auger lineshapes of transition metal compounds
[AD-A150865]
14 p2251 N85-23949
Further developments of CCD line array telecine
[BBC-RD-1985/3]
14 p2293 N85-24217
Documentation for the machine-readable version of A Finding List for the Multiplet Tables of NSRDS-NBS 3, Sections 1-10 (Adelman, Adelman, Fischel and Warren 1984)
[NASA-TM-87440]
14 p2438 N85-25048
The Fe XIII 10747 A and Fe XIV 5303 A coronal emission lines polarization
14 p2448 N85-25111
Experience in automation of data processing in interpretation and defining of linear elements from space photographs
15 p2486 N85-25349
Linewidth and bandwidth measurements of the q-branch of h2 using CW coherent anti-Stokes Raman spectroscopy
[AD-A151868]
15 p2506 N85-25458
User manual for IMAGER: The DREO (Defence Research Establishment Ottawa) image processing system
[AD-A151754]
15 p2653 N85-26362
A measurement of the vibrational band strength for the upsilon sub 3 band of the HO2 radical
[NASA-CR-175858]
16 p2744 N85-26936
An atlas of pure water vapor spectra from 500 to 5000/cm, Volume 2
[AD-A151757]
16 p2745 N85-26940
Mirror accessory for line straightening in diffraction spectrometers
16 p2764 N85-27054
Radio observations of comet P/Crommelin
[INPE-3480-PRE/723]
16 p2881 N85-27777
Contribution functions for Zeeman-split lines, and line formation in photospheric faculae
18 p3207 N85-29683
Effect of polarized radiative transfer on the Hanle magnetic field determination in prominences: Analysis of hydrogen H alpha line observations at Pic-du-Midi
18 p3207 N85-29684
The effect of line damping, magneto-optics and parasitic light on the derivation of sunspot vector magnetic fields
18 p3207 N85-29685
The inference of vector magnetic fields from polarization measurements with limited spectral resolution
18 p3207 N85-29686
Solar monochromatic images in magneto-sensitive spectral lines and maps of vector magnetic fields
18 p3207 N85-29687
Controlled-linewidth laser source
[AD-D011681]
19 p3274 N85-30306
Shifts and widths of hydrogenic ion lines
[DE85-011375]
19 p3277 N85-30323
The ultraviolet spectra of intermediate redshift quasars
20 p3544 N85-32056
Voigt line profile computation of infrared lines in the stratosphere and mesosphere
[AERONOMICA-ACTA-A-294-1985]
22 p3813 N85-33622
Detection of gamma-ray lines from the direction of the Crab Nebula
22 p3866 N85-33943
HEAO 3 upper limits to the expected 1634 KeV line from SS 433
[OG-2.4-9]
22 p3868 N85-33954
Search for gamma ray lines from SS433
[OG-2.4-11]
22 p3868 N85-33955
High-resolution spectrum of Cygnus X-1
[OG-2.4-12]
22 p3868 N85-33956
Search for positron annihilation line and continuum radiation from the Galactic Center
[OG-2.5-5]
22 p3869 N85-33962
Abundances from solar-flare gamma-ray line spectroscopy
[SH-2.1-13]
23 p3999 N85-34794
Solar flare gamma-ray line spectroscopy
[SH-2.1-14]
23 p3999 N85-34795
Elliptical X-ray analyzer spectrograph application to a laser-produced plasma
[DE85-013790]
24 p4097 N85-35398
Far-infrared emission lines of CO and OH in the Orion-KL molecular shock
[NASA-TM-86721]
24 p4167 N85-35832
The HEAO-2 Guest Investigator Program: Non-linear growth of instabilities in line-driven stellar winds
[NASA-CR-176168]
24 p4168 N85-35840
The ionization structure of planetary nebulae. Part 4: NGC 7662
[NASA-CR-176151]
24 p4169 N85-35844

LINEAMENT
U STRUCTURAL PROPERTIES (GEOLOGY)

LINEAR ACCELERATORS
NRL (Naval Research Laboratory) FEL (Free Electron Laser) program
[AD-A145057]
01 p0052 N85-10347
Accelerator technology program
[DE84-015052]
01 p0118 N85-10806
Methods to increase linac efficiency
[DE84-014692]
01 p0118 N85-10809
Linac quadrupole connections
[DE84-014694]
01 p0118 N85-10810
Use of magnetic compression based on amorphous alloys as a drive for induction linacs
[DE84-014524]
02 p0277 N85-11805
Use of a first-harmonic RF system in the NSLS booster
[DE84-016432]
02 p0277 N85-11806
Multipurpose 5-MeV linear induction accelerator
[DE84-014523]
02 p0278 N85-11808
Large linear colliders
[DE84-015700]
02 p0278 N85-11811
ATLAS beam properties: Some implications for target making
[DE84-006595]
02 p0278 N85-11812
SLC nomenclature for beamline components
[DE84-014776]
02 p0279 N85-11816
Accelerator development in support of the NRL (Naval research laboratory) beam dynamic program
[AD-A145976]
03 p0417 N85-12689
Cerenkov ring imaging detector development at SLAC
[DE84-015883]
04 p0560 N85-13564
Intense non-relativistic cesium ion beam
[DE84-012575]
04 p0560 N85-13566
Search for neutral, penetrating, metastable particles produced in the SLAC beam dump
[DE84-012468]
04 p0560 N85-13569
LAMPF transmition-region mechanical fabrication
[DE84-017078]
04 p0562 N85-13577
Accelerator Technology Program
[DE84-017083]
04 p0563 N85-13586
Preliminary grouping in A strong-current linear ion accelerator with a low injection energy
[DE84-017192]
04 p0563 N85-13587
Status of beam transport with the ETA and ATA accelerators
[DE84-013205]
05 p0726 N85-14670
Energy spread in SLC linac with Landau damping
[DE84-016259]
05 p0727 N85-14675
Minimizing the energy spread within a single bunch by shaping its charge distribution
[DE84-016172]
05 p0727 N85-14676
ATA probe beam experiment
[DE84-016017]
06 p0862 N85-15477
Calculated parameters for the initial part of an accelerator with high-frequency quadrupole focusing
[RAE-TRANS-2122]
07 p1040 N85-16600
Status of RF superconductivity at Argonne National Laboratory
[DE85-002145]
09 p1312 N85-18245
Experimental investigation of certain beam transport issues in a pulsed transmission line linear accelerator
[DE85-002310]
10 p1555 N85-19805
High power pulsed accelerators with potential industrial applications
[DE85-001710]
11 p1720 N85-20821
Notes on the RF system for the SLC positron source
[DE85-002628]
11 p1722 N85-20830
Low-energy, high-intensity positron beam experiments with a linac
[DE85-001048]
11 p1723 N85-20835
Calculations pertaining to the design of a prebuncher for a 150-MeV electron linear accelerator 3. Comparisons with experimental data
[DE85-002666]
11 p1724 N85-20844
Experiments on ETA comparing wire-conditioned and non-wire-conditioned beam propagation
[DE85-004451]
11 p1725 N85-20848
Look at energy compression as an assist for high power RF production
[DE85-001568]
11 p1725 N85-20851
Operating experience and construction status of ATLAS --- Argonne tandem-linac accelerator
[DE85-002741]
11 p1735 N85-20914
Enhancing the performance of a high-gain free electron laser operating at millimeter wavelengths
[DE85-000862]
12 p1857 N85-21646
Single-cavity SLED device
[DE85-002587]
12 p1929 N85-22117
Los Alamos free electron laser: Accelerator performance
[DE85-005722]
13 p2097 N85-23084
Collective acceleration of ions using high current relativistic electron beams
[DE85-004889]
13 p2157 N85-23393
Radio frequency quadrupole and alternating phase focusing methods used in proton linear accelerator technology in the USSR
[AD-A150830]
14 p2418 N85-24916
Two-beam accelerator
[DE85-004662]
15 p2649 N85-26335
Superconducting traveling wave accelerators
[DE85-006247]
15 p2661 N85-26424
Generalization of the Child-Langmuir relation for 1-dimensional time-dependent diodes
[DE85-007386]
16 p2779 N85-27152
Surveying and optical tooling technologies combined to align a skewed beamline at the LAMPF accelerator
[DE85-005902]
16 p2864 N85-27664
Laser plasma LINAC
[DE85-008294]
17 p2971 N85-28348
Measurement and interpretation of electron angle at MABE beam stop
[DE85-008583]
17 p3032 N85-28755
Phase and amplitude considerations for the 2-beam accelerator
[DE85-008455]
18 p3160 N85-29715
Calculations of beam dynamics in Sandia linear electron accelerators, 1984
[DE85-010417]
18 p3160 N85-29719
Plasma wake field accelerator
[DE85-010538]
18 p3191 N85-29791
Preliminary results on open accelerating structures
[DE85-010231]
18 p3191 N85-29793
Accelerator column models for low-current beams
[DE85-010722]
19 p3262 N85-30226
Los Alamos Free-Electron Laser (FEL) RF system
[DE85-010719]
19 p3278 N85-30329
Application of GPS in a high precision engineering survey network
[DE85-010556]
19 p3313 N85-30539
The SLC program
[DE85-011433]
19 p3357 N85-30813
Beam dynamics in MABE
[DE85-010670]
19 p3358 N85-30819
Emittance growth caused by current variation in a beam-transport channel
[DE85-010743]
19 p3363 N85-30849
Mechanical considerations in cw linacs
[DE85-010728]
19 p3363 N85-30850
Quantum effects in linear collider scaling laws
[DE85-009846]
19 p3363 N85-30851
Additional muon calculations for the SLC positron source
[DE85-011212]
19 p3363 N85-30855
Report of near field group
[DE85-010536]
20 p3527 N85-31940
Requirements for very high energy accelerators
[DE85-011173]
20 p3529 N85-31952
The 3lambda/4 post coupler for drift-tube linacs
[DE85-010753]
20 p3531 N85-31962
Lasertron simulation with a two-gap output cavity
[DE85-011213]
22 p3790 N85-33480
Control technology for radioactive emissions to the atmosphere at US Department of Energy facilities: The Los Alamos Meson Physics Facility
[DE85-011402]
22 p3811 N85-33609
Determination of DTL configurations
[DE85-010714]
22 p3830 N85-33719
The cw operation of the FMIT RFQ accelerator
[DE85-012667]
22 p3837 N85-33757
Transverse emittance of a 2.0-MeV RFQ beam with high brightness
[DE85-012718]
22 p3837 N85-33758
Proceedings of the 18th LAMPF Users Group Meeting
[DE85-011668]
22 p3839 N85-33773
Acceleration of polarized H(-) in the BNL 200 MeV linac
[DE85-011836]
22 p3840 N85-33777
Iris tilting and RF steering in the SLAC Linac
[DE85-011704]
22 p3841 N85-33783
Accelerator vibration issues
[DE85-010768]
22 p3842 N85-33791
New formulation for linear accelerator design
[DE85-011171]
22 p3842 N85-33792

Physics Division annual review, 1 April 1983 - 31 March 1984
[ANL-84-24] 23 p3969 N85-34602
RADLAC technolgy review
[DE85-011995] 23 p3982 N85-34691
Technology of magnetically driven accelerators
[DE85-011857] 23 p3983 N85-34700
Observations of accelerated high current low emittance beams in the SLC Linac
[DE85-013073] 24 p4088 N85-35211
Solid state high power amplifier for driving the SLC injector klystron
[DE85-013063] 24 p4090 N85-35356
ATA upgrade to 150 MeV
[DE85-013174] 24 p4096 N85-35404
Error message recording and reporting in the SLC control system
[DE85-013057] 24 p4140 N85-35684
Time domain reflectometry for SLC BPM system
[DE85-012389] 24 p4155 N85-35758
Four stage HELIA experiment
[DE85-012028] 24 p4156 N85-35768
High resolution beam profile monitors in the SLC
[DE85-013375] 24 p4157 N85-35774
Recent advances in remote handling at LAMPF
[DE85-012725] 24 p4157 N85-35775
SLC Energy Upgrade Program at SLAC
[DE85-014290] 24 p4160 N85-35790
Multi-channel pulser for the SLC thermionic electron source
[DE85-014222] 24 p4160 N85-35792
TOSCA calculations and measurements for the SLAC SLC damping ring dipole magnet
[DE85-014366] 24 p4160 N85-35793

LINEAR ARRAYS
NT MULTISPECTRAL LINEAR ARRAYS
On aircraft antennas and basic scattering studies
[AD-A146017] 03 p0355 N85-12282
A dynamical model for a towed linear sonar antenna
[REPT-8-84] 04 p0512 N85-13263
Synthesis of zeros in radiation pattern of linear antenna array 06 p0784 N85-15015
Modulation Transfer Function (MTF) measurement techniques for lenses and linear detector arrays
[NASA-TM-86168] 10 p1558 N85-19812
Further developments of CCD line array telecine
[BBC-RD-1985/3] 14 p2293 N85-24217
Space processing of acoustic signals in plane-parallel waveguide — antenna arrays 15 p2525 N85-25572
Design and development of a linear Fresnel lens air-cooled photovoltaic module and a stand-alone photovoltaic collector array
[DE85-006854] 16 p2819 N85-27391
The theoretical response of a vertical line array to wind-generated noise in shallow water
[AD-A151730] 16 p2860 N85-27638
Development of a second-generation linear Fresnel Photovoltaic and Thermal (PVT) concentrator array, including fabrication and installation of a 200 square meter collector field
[DE85-008473] 17 p2968 N85-28465
ECM multiple-target retrodirective antenna
[AD-D011528] 20 p3439 N85-31346

LINEAR CIRCUITS
Diakoptic calculation of characteristics for optimization of linear circuits with respect to parameters of individual branches 22 p3767 N85-33346

LINEAR ENERGY TRANSFER (LET)
Inelastic Near-Surface Interactions. Proceedings of the Werner Brandt Workshop on Penetration Phenomena
[DE85-010579] 20 p3526 N85-31928
Hit-size effectiveness theory applied to high doses of low LET radiation for pink mutations in Tradescantia
[DE85-011635] 22 p3819 N85-33657

LINEAR EQUATIONS
NT LINEAR EVOLUTION EQUATIONS
Modular design attitude control system
[NASA-CR-171182] 01 p0016 N85-10098
Parallel, iterative solution of sparse linear systems: Models and architectures
[NASA-CR-172457] 02 p0243 N85-11586
Numerical methods for solving systems of linear equations
[INPE-3240-RPE/463] 02 p0250 N85-11633
United States Air Force on research on algebraic manipulation
[AD-A145737] 02 p0253 N85-11655
Linear theory of free-electron lasers with cylindrical interaction space 02 p0262 N85-11718
Liquid payload moment equations
[AD-A145077] 03 p0362 N85-12319
An integral equation formulation for a boundary value problem of elasticity in the domain exterior to an arc
[PREPRINT-833] 03 p0413 N85-12843
Some implementations of multigrid linear system solvers
[CWI-NM-R8401] 05 p0720 N85-14626
Feedback, adaptivity and A-posterior estimates in finite elements: Aims, theory and experience
[AD-A146699] 07 p1029 N85-16531
First derivatives of flow quantities behind two-dimensional, nonuniform supersonic flow over a convex corner
[NASA-TM-86272] 08 p1077 N85-16826
Signal reconstruction from Fourier transform sign information
[AD-A146039] 08 p1211 N85-17624
A feedback finite element method with a posteriori error estimation. Part 1. The finite element method and some basic properties of the A posteriori error estimator
[AD-A148345] 08 p1212 N85-17631
Use of iterative linear and nonlinear algebraic methods for solving large stiff systems of ODEs
[AD-A146516] 08 p1213 N85-17636
On limits of applicability of linear models to dynamics of gas channels in aircraft engines 09 p1308 N85-18219
Solving large linear systems 14 p2398 N85-24759
The omni-transform in single-channel queues
[AD-A151019] 14 p2409 N85-24852
MATRIX: A program that shows how row and column orderings affect matrix fill-in
[DE85-007522] 15 p2630 N85-26213
A stability analysis of incomplete LU factorizations
[AD-A152058] 15 p2638 N85-26271
Ductility equation for porous metals and its linearization
[BLL-M-36118-(5628.4)] 16 p2748 N85-28658
Solving the minimal least squares problem subject to bounds on the variables
[TRITA-NA-8215] 16 p2852 N85-27580
Numerical methods for the solution of stiff delay differential equations 19 p3334 N85-30683
Numerical algorithms for solving linear algebra problems
[DE85-010310] 19 p3346 N85-30736
A multiple linear regression analysis of hot corrosion attack on a series of nickel base turbine alloys
[NASA-TM-87020] 20 p3431 N85-31284
A new problem in mathematical physics associated with the problem of coherent phase transformation 21 p3696 N85-32976
Implementing linear multistep formulas for solving DAES
[DE85-012400] 22 p3834 N85-33740
Stress analysis of axisymmetric sandwich shells of variable thickness 24 p4101 N85-35419
A new method for boundary value problems
[AD-A155934] 24 p4143 N85-35683

LINEAR EVOLUTION EQUATIONS
Symmetric linear multistep methods for second-order differential equations with periodic solutions
[CWI-NM-R8501] 17 p3022 N85-29698

LINEAR FILTERS
NT KALMAN FILTERS
NT REDUCED ORDER FILTERS
Robust linear filtering for multivariable stationary time series, part 3
[AD-A148169] 08 p1212 N85-17627
Piezoelectric filter with low-Q inductances 13 p2070 N85-22932
Acoustooptic cell as space-frequency filter 13 p2090 N85-23051
Linearization of digital derived rate algorithm for use in linear stability analysis
[NASA-TM-87000] 14 p2243 N85-23904
Theory and Applications of State Estimation. NRIMS Summer Seminar Series
[CSIR-SWISK-37] 15 p2635 N85-26244
The Kalman filter 15 p2635 N85-26246
Linear filtering with non-Gaussian initial conditions 15 p2635 N85-26247
State estimation with interrupted observations 15 p2635 N85-26251
Coupling of the solar wind to measures of magnetic activity
[DE85-002415] 15 p2665 N85-26580
Linear time-invariant, space-variant filters and the WKB approximation with applications to underwater acoustic signal processing
[AD-A154250] 19 p3352 N85-30775
Linear filters as a method of real-time prediction of geomagnetic activity
[DE85-010760] 22 p3860 N85-33899

LINEAR INTEGRATED CIRCUITS
NT OPERATIONAL AMPLIFIERS

LINEAR POLARIZATION
Detection of submillimeter polarization in the Orion Nebula
[NASA-TM-86013] 04 p0579 N85-13700
Polarization of radio molecular lines and mapping of magnetic field direction 06 p0878 N85-15581
Polarization transformation by single-mode fibers — optical fibers
[FI-452-TBR-59] 11 p1729 N85-20876
Coordinated ultraviolet and visual observations of Omega Orionis 1982-1983 11 p1750 N85-21007
Design and performance of etched polarization transformers for microwave frequencies
[R-NIAS-26] 14 p2297 N85-24218
Magnetic field-vector measurements in quiescent prominences via the Hanle effect: Analysis of prominences observed at Pic-du-Midi and at Sacramento Peak 18 p3208 N85-29698
Influence of depolarization of linear polarized radiation on the heterodyne detection in laser range finders
[ESA-TT-903] 20 p3461 N85-31500

LINEAR PREDICTION
Description of a semiannual selection procedure of vowel parts of the voice signal using a PDP 11/34 computer
[FUB-4-1983] 01 p0039 N85-10250
Coupling of the solar wind to measures of magnetic activity 14 p2357 N85-24565
Environmental background measurement program
[AD-A153660] 19 p3319 N85-30577

LINEAR PROGRAMMING
Interactive graphics nonlinear constrained optimization 01 p0058 N85-10387
A combined logistic regression and Zionts-Wallenius methodology for multiple criteria linear programming
[TWISK-314] 01 p0102 N85-10679
A comparative evaluation of algorithms for generalized network problems
[TWISK-299] 01 p0107 N85-10721
New labeling procedures for the basis graph in generalized networks
[AD-A146217] 03 p0407 N85-12601
A two-segment approximation algorithm for separable convex programming with linear constraints
[AD-A146215] 03 p0412 N85-12834
Boolean approach to zero-one linear programming
[DE84-016654] 04 p0550 N85-13498
Users manual for BRGLM: Interactive general linear model regression, version 3
[DE84-017366] 04 p0550 N85-13501
An iterative scheme for linear complementarity problems
[AD-A147464] 07 p1032 N85-16555
Extracting embedded generalized networks from linear programming problems
[AD-A147565] 07 p1033 N85-16558
Simple approximate variances for b-letter values. A sampling enquiry: Supplement
[DE85-001410] 09 p1376 N85-18647
Efficient algorithm for fuzzy linear programming with multiple objectives
[AD-A149012] 10 p1544 N85-19736
An exact solution to the 2 point OC (Operating-Characteristic) curve determination
[AD-A148120] 11 p1708 N85-20746
Automatic control design procedures for restructurable aircraft control
[NASA-CR-172489] 12 p1760 N85-21173
Parallel linear algebra library for the Denelcor HEP
[DE85-004685] 12 p1917 N85-22034
Needs, opportunities, and options for large scale systems research
[DE85-004642] 12 p1925 N85-22091
Approaches and algorithms for robust signal processing 13 p2062 N85-22878
Optimal allocation of components in parallel-series and series-parallel systems
[AD-A150199] 13 p2144 N85-23309
LEXICON: A structured modeling system for optimization
[AD-A150536] 13 p2147 N85-23329
Minimal cost flow in processing networks: A primal approach
[CWI-TRACT-4] 14 p2432 N85-25001
Solving set covering problems using heuristics with branch and bound
[AD-A151905] 15 p2638 N85-26269
Proposal for an extended set of FORTRAN Basic Linear Algebra subprograms
[DE85-007241] 16 p2648 N85-27562
A decomposition procedure for convex quadratic programs
[AD-A151732] 16 p2654 N85-27595
The interface with decision makers in interactive multiobjective linear programming
[REPT-84-26] 17 p3014 N85-29637
Operations research
[B8561897] 17 p3026 N85-25712
A variable-complexity norm maximization problem
[AD-A153514] 18 p3169 N85-29634

Finding the largest l(p)-ball in a polyhedral set
[AD-A153542] 16 p3170 N85-29843
Modeling water resources systems for water quality
[AD-A154266] 19 p3300 N85-30457
On the step size in Karmarkar's algorithm
[AD-A154040] 19 p3336 N85-30661
Numerical algorithms for solving linear algebra problems
[DE85-010310] 19 p3348 N85-30736
An analysis of multi-fingered hands
20 p3462 N85-31504
Symposium on Computational Mathematics-State-of-the-Art: Informal Proceedings
[DE85-008122] 20 p3516 N85-31858
Study of an efficient long-range Mach 2.7 supersonic transport configuration concept
[NASA-TM-86414] 21 p3554 N85-32110
A practical approach to Karmarkar's algorithm
[AD-A155714] 21 p3673 N85-32818
On the problem of linear programming with approximate data
21 p3698 N85-32976

LINEAR RECEIVERS
Liquid cooled, linear focus solar cell receiver
[DE84-014446] 01 p0067 N85-10448

LINEAR SYSTEMS
Design of a digital ride quality augmentation system for commuter aircraft
[NASA-CR-172419] 01 p0006 N85-10037
The rate of convergence of a class of block Jacobi schemes
[AD-A144738] 01 p0111 N85-10749
Credibility approximations for Bayesian prediction of second moments
[AD-A144996] 01 p0113 N85-10768
Singular perturbations, coherency and aggregation of dynamic systems
[DE84-014166] 01 p0114 N85-10772
Qualitative results for distributed systems with discrete damping and stiffness with application to control
[AD-A145525] 02 p0209 N85-11382
On a class of suboptimal controls for infinite-dimensional bilinear systems
[RR-258] 02 p0249 N85-11630
Linear intersecting codes -- error correction
[ENST-C-84002] 03 p0356 N85-12291
Chandrasekhar equations and computational algorithms for distributed parameter systems
[NASA-CR-172467] 03 p0402 N85-12564
Maximum likelihood estimation of parameters in linear systems from flight test data: A FORTRAN program
[AD-B087196L] 05 p0715 N85-14588
Optimal stochastic LQ control with measurements displaced in time
[OUEL-1547/84] 08 p1209 N85-17605
Improved stability and performance bounds using approximate models -- control system design
[RR-260] 08 p1209 N85-17606
Use of iterative linear and nonlinear algebraic methods for solving large stiff systems of ODEs
[AD-A148516] 08 p1213 N85-17636
Dynamics and control of general linear lumped-parameter systems 09 p1372 N85-18623
Chandrasekhar equations for infinite dimensional systems
[NASA-CR-172515] 09 p1376 N85-18651
Research in adaptive and decentralized control
[AD-A148964] 10 p1543 N85-19728
A note on the disturbance decoupling problem for retarded systems
[AD-A149045] 10 p1543 N85-19730
Linear magnetic bearings
[NASA-CASE-GSC-12582-2] 11 p1641 N85-20337
Low sidelobe phased array antenna system
[AD-D011558] 12 p1823 N85-21435
Methods of progressing waves in turbulent media with applications to acoustics
[AD-A149599] 12 p1920 N85-22055
Analysis and design of linear microwave transistor amplifiers 13 p2066 N85-23036
Synthesis of optimal controls for real-time linear digital systems 14 p2270 N85-24082
Transducer of linear displacements
14 p2281 N85-24130
Decomposition in problem of correcting inertial navigation systems 14 p2287 N85-24172
Investigation of the time history and modal responses of some simple linear and nonlinear systems
[DE85-002027] 14 p2321 N85-24344
Results of studies of wave field internal structure in prediction of geological cross section
14 p2346 N85-24504
Practical methods for the compensation and control of multivariable systems
[AD-A151047] 14 p2407 N85-24841
State estimation with interrupted observations
15 p2635 N85-26251
Fundamental equivalence of generalised state space systems
[MATHEMATICS-RESEARCH-182]
15 p2642 N85-26293
Complexity of dense linear system solution on a multiprocessor ring
[AD-A151970] 16 p2854 N85-27598
Mathematical modeling and control of a large space structure as applied to a shuttle-antenna configuration
[AD-A153269] 17 p2910 N85-27939
Generalised translation invariance and systems theory
[CRM-9501] 17 p3017 N85-28657
Efficient parallel solution of linear systems with hyperbolic rotations
[AD-A152355] 17 p3018 N85-28661
Efficient parallel solution of linear systems
[AD-A152663] 17 p3018 N85-28663
Polynomial iteration for nonsymmetric indefinite linear systems
[AD-A153094] 17 p3019 N85-28671
An interactive computer aid for the design and analysis of linear, single input/single output digital and continuous control systems
[AD-A153704] 18 p3162 N85-29589
Infinite dimensional linear systems with unbounded control and observation: A functional analytic approach
[AD-A153535] 18 p3169 N85-29639
Control and regulation of generalized linear systems
19 p3257 N85-30193
Interactive computer program for the analysis and design of linear time invariant systems
[AD-A154076] 19 p3335 N85-30664
An iterative method for indefinite systems of linear equations
[NASA-CR-172345] 19 p3345 N85-30728
Profile of a relativistic electron beam propagated through a linear wiggler and an axial guide field
[AD-A154403] 19 p3353 N85-30783
A new slab geometry radiation transport differencing scheme
[DE85-006681] 19 p3366 N85-30874
New directions in asymptotically stable finite-dimensional adaptive control of linear distributed parameter systems 20 p3412 N85-31177
An overview of latest model reduction and control methods of large flexible space structures
20 p3414 N85-31191
Frequency domain control design of large space structures: A practical approach
20 p3415 N85-31192
Sensor/actuator selection for the constrained variance control problem 20 p3415 N85-31197
Eigenvalue placement and stabilization by constrained optimization 20 p3416 N85-31198
Stable direct adaptive control of linear infinite-dimensional systems using a command generator tracker approach 20 p3416 N85-31204
Linear system structure and cone containment for bilinear systems
[RR-266] 20 p3519 N85-31879
On the choice of parameterization for identification
[OUEL-1554/84] 20 p3522 N85-31904
Routing algorithms and stochastic analysis for large communications networks
[AD-A154654] 21 p3573 N85-32225
Decomposing the joint distribution of several linear combinations of uniform spacings
[AD-A155056] 21 p3677 N85-32845
Design and development of a linear thermal actuator
22 p3796 N85-33518
Substructure coupling in the frequency domain
[NASA-CR-176140] 22 p3800 N85-33543
A graph theoretic procedure for the design of feedback patterns
[REPT-110] 24 p4142 N85-35673
A new theory for multistep discretizations of stiff ordinary differential equations: Stability with large step sizes
[NASA-CR-177941] 24 p4142 N85-35675
Spreading the control complexity in decentralized control of interconnected systems
[BU-117] 24 p4144 N85-35688
Decentralized stabilization by high gain feedback
[BU-115] 24 p4144 N85-35689

LINEAR TRANSFORMATIONS
Linear associative mapping
[ESA-TT-856] 05 p0719 N85-14611
Transformation of electromagnetic waves in plasma with randomly-heterogeneous magnetic field
07 p0953 N85-16039

LINEAR VIBRATION
Nonlinear wave propagation study
[AD-A147011] 07 p0996 N85-16329
A pole-free reduced-order characteristic determinant method for linear vibration analysis based on sub-structuring 09 p1338 N85-18412
Dynamics and control of general linear lumped-parameter systems 09 p1372 N85-18623

LINEARITY
NT COLLINEARITY
Shift-variant multidimensional systems
[AD-A144756] 01 p0111 N85-10752
Method for calculating linear shrinkage and expansion of metals and alloys
[BLL-M-35747-(5828.4)] 02 p0175 N85-11173
On the rate of mean convergence of finite linear predictors of multivariate stationary stochastic processes
[AD-A145809] 02 p0254 N85-11664
Linear conformal gravitation 02 p0265 N85-11735
A two-segment approximation algorithm for separable convex programming with linear constraints
[AD-A146215] 03 p0412 N85-12634
Structure of frequency modulated and phase-shift keyed signals reflected from ionosphere at near-critical frequencies 07 p0952 N85-16035
Digital thermometer with linearizer on slide wire
07 p0954 N85-16049
Image-to-image correspondence: Linear structure matching 07 p0986 N85-16266
SIMM1: A linearized particle code
[AD-A148627] 08 p1221 N85-17689
Effect of scattering on instabilities in line-driven stellar winds 08 p1235 N85-17784
New instabilities in line driven winds
08 p1235 N85-17785
On the role played by lines in radiatively driven stellar winds depending on the position of the stars in the HR diagram 08 p1236 N85-17787
finite element analysis of bi-material systems with applications in hydraulic fracturing
09 p1332 N85-18369
Existence, uniqueness and stability conditions for general finite element methods in linear elasticity
09 p1332 N85-18372
Improved magnetic bias and delay linearity in a magnetostatic wave delay line
[AD-D011441] 10 p1479 N85-19337
Close-to-convex functions and linear-invariant families
10 p1536 N85-19683
Smoothing with split linear fits
[AD-A149032] 10 p1545 N85-19740
Simulation of the ion-beam-driven drift instability in a magnetic trap, 2
[AD-A149452] 10 p1554 N85-19798
Method for increasing linearity of load cell
11 p1623 N85-20221
New results on the PLL false lock phenomenon
12 p1948 N85-22236
Absolute stability of unsteady movement of axisymmetrical rotating flight vehicle
13 p2044 N85-22793
Approaches and algorithms for robust signal processing 13 p2062 N85-22878
Consistency of smoothing with running linear fits
[AD-A150232] 13 p2150 N85-23349
Nonlinear 0-1 programming. 1: Linearization techniques, revision
[AD-A150960] 14 p2405 N85-24828
A 4-node bilinear isoparametric element in Rockwell NASTRAN 15 p2573 N85-25667
On geoid heights and flexure of the lithosphere at seamounts
[AD-A151220] 15 p2804 N85-26050
An evaluation of discretized conditional probability and linear regression threshold techniques in model output statistics forecasting of visibility over the north Atlantic Ocean
[AD-A151955] 16 p2857 N85-27619
Distortion functions
[DE85-007511] 16 p2862 N85-27655
Study on a flexure hinged pendulum accelerometer
[NAL-TR-844] 18 p3104 N85-29220
Linear motion valve
[NASA-CASE-MSC-20148-1] 18 p3115 N85-29284
Fixed width interval estimation in linear regression
[AD-A153633] 18 p3174 N85-29675
On the characterization of nonnegatively estimable linear combinations of variance components
[AD-A153788] 18 p3174 N85-29678
Large-time behavior of viscous surface waves
[AD-A154805] 21 p3584 N85-32278
Test evaluation of the Honeywell GG1111 Single-Degree-of-Freedom (SDF) strapdown gyroscope
[AD-A154768] 21 p3589 N85-32307
Precision linear ramp function generator
[DE85-011647] 22 p3760 N85-33304
Linear boundary detection using pressure buildup tests
[DE85-009926] 22 p3784 N85-33444
Instrumentation for sensing moisture content of material using a transient thermal pulse
[NASA-CASE-NPO-15493-2] 23 p3933 N85-34373

A new approach to linear quadtrees
23 p3961 N85-34550
Scale separation closure and Alfven wave turbulence
[DE85-013124] 24 p4095 N85-35385
The geostatistical approach to the inverse problem in two-dimensional steady state groundwater modeling
24 p4107 N85-35462

LINEARIZATION
Nonsteady motion of solid sphere in compressible viscous fluid 02 p0269 N85-11753
Quasi-three dimensional modeling of functionally-integrated elements of large-scale integrated circuits 04 p0490 N85-13122
Overview of magnetic bearing control and linearization approaches for annular magnetically suspended devices
05 p0607 N85-13872
Magnetostatic problems in nonlinear media with hysteresis
[DE85-003701] 10 p1482 N85-19358
Elastic-plastic analysis for cyclic loading using a linearized yield condition
[PB85-149607] 14 p2322 N85-24346
Non-linear methods for inertial navigation system alignment
[BAE-BT-12683] 15 p2468 N85-25232
On the equivalent bilinearization of nonlinear controlled delay systems
[RR-272] 20 p3519 N85-31880
Development and validation of a general purpose linearization program for rigid aircraft models
[NASA-TM-86737] 21 p3556 N85-32122
Realization and linearization of a hyperfrequency power amplifier implemented with bipolar transistors in class C polarization — microwave amplifiers
[CNES-NT-114] 23 p3928 N85-34348
Production of initial estimates of photogrammetric variables
[NPL-MOM-68] 23 p3943 N85-34434

LINERS
U LININGS

LINES (GEOMETRY)
NT GEODESIC LINES
A description of the Langley wireframe geometry standard (LaWGS) format
[NASA-TM-85767] 13 p1971 N85-22380
Selection of segment similarity measures for hierarchical picture segmentation 23 p3960 N85-34548

LING-TEMCO-VOUGHT AIRCRAFT
NT A-7 AIRCRAFT
NT F-8 AIRCRAFT

LINGUISTICS
NT MACHINE TRANSLATION
NT PHONEMES
NT PSYCHOLINGUISTICS
NT SEMANTICS
NT SYNTAX
NT WORDS (LANGUAGE)
Neuro-linguistic programming: Eye movements as indicators of representational systems
[AD-A147541] 07 p1016 N85-16454
Toward a principle-based parser
[AD-A147637] 08 p1202 N85-17565
Research on knowledge delivery
[AD-A149585] 10 p1538 N85-19698
Symbiosis between postgraduate training and research projects: A successful experience
[INPE-3216-PRE/569] 16 p2810 N85-27330
Artificial Intelligence in Ada (trademark): Pattern-directed processing
[AD-A156230] 24 p4141 N85-35671

LININGS
NT ROCKET LININGS
Nonlinear structural and life analyses of a combustor liner 02 p0141 N85-10955
Heat flux sensors for burner liners and turbine blades and vanes 02 p0142 N85-10961
Burner liner thermal/structural load modelling
02 p0143 N85-10970
Validation of structural analysis methods using the in-house liner cyclic rigs 02 p0146 N85-10987
HOST liner cyclic facilities: Facility description
02 p0146 N85-10988
A study of the Armstrong Whitworth swing beam engine for automotive application 04 p0508 N85-13239
Electrical resistivity technique to assess the integrity of geomembrane liners
[PB85-122414/GAR] 09 p1325 N85-18327
Polymeric liner selection for military waste impoundments
[AD-P004143] 09 p1348 N85-18479
Advanced liner-cooling techniques for gas turbine combustors
[NASA-TM-86952] 12 p1770 N85-21115
Shallow land burial technology: Humid
[DE85-004432] 12 p1932 N85-22136
Determination of wear intensity and resource of crankshafts and cylinder liners of ZIL-130 and ZMZ-53 engines
[BLL-BISI-TRANS-21393-(9022.06)]
17 p2972 N85-28355
Development of carbon based brake lining materials without asbestos content in the form of carbon-carbon composites and carbon-metal or carbon-carbide composites
[BMFT-FB-T-85-014] 18 p3082 N85-29067
Nonlinear analysis of an axisymmetric structure subjected to non-axisymmetric loading
20 p3468 N85-31549
SCAP: A Shaped Charge Analysis Program. User's manual for SCAP 1.0
[DE85-011182] 20 p3515 N85-31854
Elevated temperature crack growth
[NASA-CR-174957] 22 p3799 N85-33540
Prestressed concrete vessel according to the hot liner concept: A critical evaluation of experimental results with a prototype vessel
[OEFZS-4313] 22 p3801 N85-33550
High temperature structural insulating material
[DE85-006361] 23 p3920 N85-34291
Development of advanced high-temperature heat flux sensors. Phase 2: Verification testing
[NASA-CR-174973] 24 p4096 N85-35391

LINKAGES
Kinematic synthesis of planar cam-link mechanisms for exact path and exact motion generation
03 p0341 N85-12189
Burmester theory for 4 precision positions: An extended discourse with application to the dimensional synthesis of arbitrary planar linkages 03 p0367 N85-12351
Second seliplane project: The RP-2
04 p0468 N85-12977
Controlling rotation of elastic manipulator link
04 p0488 N85-13113
Space shuttle elevon seal panel mechanism
06 p1101 N85-16961
Vibrations of rotors connected through couplings with backlash 17 p2940 N85-28147
On the turning lozange of constant side whose vertices alternate between two fixed circles of a ring
[AD-A154803] 21 p3677 N85-32840
The balancing of complex linkage mechanisms
23 p3924 N85-34313
Conjugated symmetrical coupler curves, produced by 4-bar linkages having the same transmission angles
23 p3924 N85-34322

LINKING
U JOINING

LINKS (MATHEMATICS)
On ergodic actions whose self-joinings are graphs
[CWI-PM-R8408] 12 p1925 N85-22093

LIOUVILLE EQUATIONS
Covariant Poisson brackets for classical fields
[DE85-010085] 18 p3171 N85-29654

LIPID METABOLISM
Dynamics of some parameters of carbohydrate and lipid metabolism in recovery period following long-term hypokinesia 01 p0093 N85-10823
Effects of immobilization and high-altitude adaptation on energy metabolism in rats 22 p3820 N85-33663
Lipid hydrolysis in man during antiorthostatic hypokinesia 23 p3953 N85-34500
Lipogenesis in rat liver after flight aboard Cosmos-1129 biosatellite 23 p3954 N85-34508

LIPIDS
NT LIPOPROTEINS
Static and quasielastic neutron scattering for the investigation of structure, dynamics and transport properties of lipid layers and lipid/protein compounds
03 p0432 N85-12753
The lipid composition and its alteration during the growth stage in pathogenic fungus, epidermophyton floccosum
[NASA-TM-77440] 07 p1011 N85-16421
Liposome-encapsulated hemoglobin for emergency resuscitation
[AD-A146794] 07 p1015 N85-16448
Microalgae culture collection, 1984-1985
[DE84-013035] 11 p1690 N85-20626
Magnetically-localizable, polymerized lipid vesicles and method of disrupting same
[AD-D011686] 19 p3249 N85-30144
Rat blood serum and liver carbohydrates and lipids in recovery period after 15-day hypokinesia
19 p3326 N85-30606
The role of sulfur in osmoregulation and salinity tolerance in cyanobacteria, algae, and plants
21 p3660 N85-32736

LIPOPROTEINS
Distinctive morphological manifestations of acute stress reaction in adrenal cortex of hypokinetic rats
12 p1902 N85-21944

LIPSCHITZ CONDITION
Sensitivity analysis in generalized rational approximation with restricted denominator
[CSIR-TWISK-319] 01 p0109 N85-10734
Domains with Lipschitz mapping functions
10 p1535 N85-19575
Extension of embeddings close to isometries or similarities 15 p2634 N85-26342
Hardy spaces and the L sup P-Neumann problem for Laplace's equation in a Lipschitz domain
[CTH-MATH-1985-02] 22 p3836 N85-33749

LIQUEFACTION
NT COAL LIQUEFACTION
Bench-scale research in biomass direct liquefaction
[DE84-011881] 02 p0223 N85-11480
Biomass thermochemical conversion program
[DE84-017177] 05 p0621 N85-13872
Active cooling requirements for propellant storage
06 p1106 N85-17004
Response of saturated porous nonlinear materials to dynamic loadings
[AD-A148528] 08 p1173 N85-17394
Innovation in earthquake and natural hazards research: Determining soil liquefaction potential
[PB85-149573] 14 p2374 N85-24878

LIQUEFIED GASES
NT LIQUEFIED NATURAL GAS
NT LIQUID AIR
NT LIQUID AMMONIA
NT LIQUID HELIUM
NT LIQUID HELIUM 2
NT LIQUID HYDROGEN
NT LIQUID NITROGEN
NT LIQUID OXYGEN
Status of gaseous fuels for use in highway transportation: A 1983 perspective
[DE84-015205] 01 p0034 N85-10211
Electronics Engineering Department EE Technical Review
[UCRL-50025-84-1] 13 p2063 N85-22867
Liquid membranes for the production of oxygen-enriched air
[DE85-006056] 15 p2506 N85-25460
Hydrocarbon pool and vapor fire data analysis
[DE85-005857] 15 p2523 N85-25550

LIQUEFIED NATURAL GAS
Insulating polymer concrete
[DE84-017239] 04 p0480 N85-13057
Risks in the transport and storage of liquefied natural gas. Sub-project 5-2: Investigation into building damage
[BLL-RISLEY-TR-4608-(9091.9F)]
07 p0935 N85-15926
Penetration of the atmosphere by flammable mixtures as a result of spillage of LNG on the ground
08 p1179 N85-17432
Thermal radiation hazards from Liquified Petroleum Gas (LPG) fireballs
[VTT-304] 09 p1293 N85-18122
Mechanisms of heat and mass transfer across a double-diffusive interface
[PB85-148488] 12 p1848 N85-21504
Facility for large-scale hazardous gas testing
[DE85-011852] 21 p3564 N85-32189

LIQUID AIR
Liquid membranes for the production of oxygen-enriched air
[DE85-006056] 15 p2506 N85-25460

LIQUID ALLOYS
Electronic structure of liquid metal alloys
[DE85-000904] 09 p1295 N85-18136

LIQUID AMMONIA
Two phase discharge of liquefied gases through pipes. Field experiments with ammonia and theoretical model
[FOA-B-40139-C1] 18 p3103 N85-29209

LIQUID ATOMIZATION
Certain optimal parameters of high-velocity Venturi ejection tubes
[BLL-M-35924-(5828.4)] 05 p0634 N85-14088
Injection, atomization, ignition and combustion of liquid fuels in high-speed air streams
[AD-A154058] 19 p3251 N85-30158

LIQUID CHROMATOGRAPHY
Compound class quantitation of JP-5 jet fuels by high performance liquid chromatography-differential refractive index detection
[AD-A145754] 03 p0340 N85-12185
Supercritical fluid chromatography/supersonic jet spectroscopy
[DE84-016199] 04 p0471 N85-12988
Development of acceptance criteria for batches of silane primer for external tank thermal protection system bonding applications
[NASA-CR-171266] 04 p0478 N85-13043
Analysis and characterization of organic carbon compounds in atmospheric particulate matter
[PB84-232636] 06 p0766 N85-14903

Prediction of retention indices of polynuclear aromatic hydrocarbons. Part 1: HPLC on nitrogen containing normal phase packing materials
[DE85-001902] 10 p1436 N85-19051
Quantitative determination of compound classes in jet turbine fuels by high performance liquid Chromatography/Differential refractive index detection: Part 2
[AD-A149298] 11 p1613 N85-20144
Analysis of aldehydes and ketones in the gas phase
[PB85-181866] 20 p3426 N85-31281
Rapid estimation of concentration of aromatic classes in middledistillate fuels by high-performance liquid chromatography
[NASA-TP-2495] 20 p3434 N85-31307

LIQUID COOLED REACTORS
NT BOILING WATER REACTORS
NT EXPERIMENTAL BREEDER REACTOR 2
NT LIGHT WATER REACTORS
NT LIQUID METAL COOLED REACTORS
NT PRESSURIZED WATER REACTORS
NT WATER COOLED REACTORS
NT ZERO POWER REACTORS
Thermal hydraulic features of the TMI accident
[DE85-014569] 24 p4152 N85-35747

LIQUID COOLING
NT FILM COOLING
Thermal fluid-structure interaction: A few scaling considerations --- nuclear reactors
[GKSS-84-E-18] 01 p0048 N85-10314
Liquid cooled, linear focus solar cell receiver
[DE84-014446] 01 p0067 N85-10448
Advanced concepts liquid droplet radiator
05 p0610 N85-13899
The liquid droplet radiator - an ultralightweight heat rejection system for efficient energy conversion in space
05 p0610 N85-13900
An evaluation of liquid and two-phase cooling techniques for use in electrical machinery
[AD-A149528] 10 p1484 N85-19372
Method of calculating cooldown process in cryostat of cryogenic electric machine 12 p1843 N85-21567
Thermal state of cooled thin-walled nozzle blade
14 p2270 N85-24066
Role of fluid lubricant-coolant in fine grinding of optical glass by diamond tool 14 p2280 N85-24125
Low gravity exothermic heating/cooling apparatus
[NASA-CASE-MSC-25707-1] 18 p3104 N85-29214
Comparison of the response of shape memory alloy actuators using air-cooling and water-cooling
[AD-A155216] 21 p3567 N85-32185

LIQUID CRYSTALS
Investigation and development of multicolored liquid crystal display systems for automotive dashboard application and large format information boards
[BMFT-FB-T-84-167] 04 p0572 N85-13652
Measurement of parameters defining orientation of liquid crystals in electrooptic cells 06 p0777 N85-14971
Research on submicrometer structures
[AD-A146578] 06 p0867 N85-15508
Synthesis and characterization of unique liquid crystalline block copolyesters. A proposal for a polymer research center at the Atlanta University
[AD-A147280] 07 p0932 N85-15807
Matrix display simulation
[AD-D011371] 07 p1055 N85-16695
Improved real-time ultra-high resolution image projection display using laser-addressed liquid crystal light valve
[AD-D011414] 08 p1223 N85-17705
A brief review of the technology of microemulsions and other micellar systems
[AD-A149759] 12 p1800 N85-21289
Exploratory development of foams from liquid crystal polymers
[NASA-CR-172510] 13 p2038 N85-22754
Interaction of liquid crystals with inhomogeneous surfaces
[AD-A151557] 15 p2660 N85-26413
Nematic liquid crystals for car dashboards
[BMFT-FB-T-84-296] 16 p2872 N85-27718
InP materials
[AD-A152341] 17 p3043 N85-28828
Numerical optical computing at the Ohio State University 18 p3188 N85-29775
Electrochemical studies in liquid crystals
[AD-A154317] 19 p3234 N85-30050
Mesophase mechanisms in the formation of graphitic microstructures
[AD-A154100] 19 p3248 N85-30140
Electrochromic display device
[AD-D011733] 22 p3759 N85-33299
Liquid crystal light valve structures
[NASA-CASE-MSC-20038-1] 22 p3847 N85-33826
Differentiating spatial light modulator
[AD-D011727] 23 p3973 N85-34632

LIQUID DROPS
U DROPS (LIQUIDS)

LIQUID FILLED SHELLS
Moment induced by liquid payload during spin-up without a critical layer
[AD-A145716] 02 p0199 N85-11327
High-frequency asymptotic behavior of reflected and transmitted waves during scattering of sound by hollow elastic sphere filled with fluid 02 p0266 N85-11738
Liquid payload moment equations
[AD-A145977] 03 p0362 N85-12319
A study of the critical layer in a rotating liquid payload
[AD-A146094] 03 p0362 N85-12321
Fluid motion in a rotating and nutating container
[AD-A146175] 03 p0362 N85-12322
Modifications to SOLA-VOF for flow dynamics in spinning cylinders
[AD-A154093] 19 p3285 N85-30250

LIQUID FLOW
NT OPEN CHANNEL FLOW
NT WATER FLOW
Finite element method for a class of viscoelastic flows in deforming domains applied to jet breakup
[DE84-014571] 04 p0500 N85-13166
Magnetic inductive flowmeter for low conducting liquids
[BMFT-FB-T-84-136] 04 p0504 N85-13216
Instability of film boiling of moving liquids
[BLL-WH-603-(9091.9F)] 07 p0956 N85-16056
Leakage-flow induced vibrations of a chimney structure suspended in a liquid flow --- nuclear reactors
09 p1339 N85-18420
Liquid mass flow rate computer
13 p2075 N85-22962
Radiation-dominated snowmelt on Mars
13 p2191 N85-23582
Catalytic hydrotreatment studies with model compounds
[DE85-010187] 19 p3236 N85-30084
Instability and chaotic behavior in a free-surface flow
[AD-A154879] 21 p3584 N85-32279
Detailed validation of a liquid and heat flow code against field performance
[DE85-009901] 23 p3932 N85-34368

LIQUID FUELS
NT AIRCRAFT FUELS
NT AUTOMOBILE FUELS
NT CRYOGENIC ROCKET PROPELLANTS
NT DIESEL FUELS
NT GASOLINE
NT HYDROGEN FUELS
NT HYPERGOLIC ROCKET PROPELLANTS
NT JET ENGINE FUELS
NT JP-4 JET FUEL
NT JP-5 JET FUEL
NT JP-8 JET FUEL
NT KEROGEN
NT KEROSENE
NT LIQUID ROCKET PROPELLANTS
NT MONOPROPELLANTS
NT SLURRY PROPELLANTS
Prospectus of the utilization of leafy spurge (Euphorbia Esula L.) as a source of liquid fuel and biomass
[DE84-015203] 01 p0034 N85-10208
Converting gasoline farm tractors to run efficiently on farm-produced alcohol
[DE84-015796] 02 p0205 N85-11350
Liquid hydrocarbon fuels from syngas
[DE84-015942] 04 p0482 N85-13069
Pressure oscillations in liquid-fueled ramjet engines
05 p0596 N85-13797
Liquid-fueled Ramjet engines
07 p0918 N85-15814
A review of hazard assessment procedures for liquid gun propellants
[AD-A149470] 10 p1457 N85-19182
Numerical simulations of liquid propellant combustion instability: Onset and growth
[DE85-000743] 10 p1458 N85-19186
The influence of fuel quality upon flame-tube temperature and flame radiation in a model gas-turbine primary zone
[K233] 13 p1974 N85-22396
The influence of fuel molecular composition upon flame-tube temperature and flame radiation in a model gas-turbine primary zone
[K234] 13 p2017 N85-22646
Atmospheric dispersion of hypergolic liquid rocket fuels, volume 2
[AD-A150699] 14 p2283 N85-24020
Studies on rocket engines for future European launchers
[SEP-TPRL/K-19572/84] 15 p2495 N85-25393
CON1D: A computer program for calculating spherically symmetric droplet combustion
[DE85-005604] 15 p2507 N85-25484
Improved catalysts for liquid hydrocarbon fuels from syngas
[DE85-006569] 16 p2746 N85-26947
Technical and economic analysis of liquid fuel production from microalgae
[DE85-002926] 16 p2758 N85-27018
Liquid propellants for use in guns: A review
[AD-A153051] 17 p2937 N85-28131
Liquid hydrocarbon fuels from syngas
[DE85-009613] 19 p3228 N85-30017
Improved catalysts for liquid hydrocarbon fuels from syngas
[DE85-011062] 20 p3421 N85-31234
Biomass thermochemical conversion program
[DE85-011667] 21 p3572 N85-32213
Production of liquid fuels and chemicals by microalgae
[DE85-008780] 22 p3819 N85-33658

LIQUID HELIUM
NT LIQUID HELIUM 2
High specific heat dielectrics and Kapitza resistance at dielectric boundaries
[AD-A148476] 08 p1217 N85-17666
Acoustic microscopy at cryogenic temperatures
[AD-A148755] 09 p1384 N85-18704
Turbulence in pure superfluid flow
09 p1397 N85-18790
Shock compression of liquid helium to 56 GPa (560) kbar
13 p2184 N85-23551
A measurement of the intensity of the cosmic background radiation at 3.9 cm
13 p2206 N85-23681
NMR manometer for measuring high pressures at liquid-helium temperatures 17 p2944 N85-28171
Balloon-borne, He-cooled Fourier transform spectrometer for far infrared astronomy
[MPE-IR-41] 17 p3053 N85-28899
Cooling high intensity atomic hydrogen beams to liquid helium temperatures
[DE85-012515] 24 p4148 N85-35718

LIQUID HELIUM 2
Outlook for realization of proximity effect and Josephson direct current in helium-2 13 p2074 N85-22956
Entropy of He 2 and universality near the superfluid in He(4) 19 p3378 N85-30957

LIQUID HYDROGEN
Measurement of scattering cross sections of liquid and solid hydrogen deuterium and deuterium hydride for thermal neutrons
[DE84-014814] 05 p0727 N85-14671
Partial bleed expander cycle for low thrust LOX/LH2 rocket engine
[NAL-TR-837T] 10 p1430 N85-19018
An air-breathing ballistic space transporter for Europe
[NASA-TM-77645] 12 p1792 N85-21244
Capture of liquid hydrogen boiloff with metal hydride absorbers
[NASA-CR-175677] 14 p2249 N85-23939
Ten degree Kelvin hydride refrigerator
[NASA-CASE-NPO-16393-1-CU] 18 p3085 N85-29084
Preliminary considerations for the gasdynamic precompression of solid molecular hydrogen
[DE85-013256] 22 p3784 N85-33445

LIQUID INJECTION
NT DEEP WELL INJECTION (WASTES)
NT WATER INJECTION
Improvement of gas turbine engine performance by water injection into turbine cooling air
09 p1307 N85-18209
Effect of water injection into air for turbine cooling on economy of operation of gas turbine engine with afterburning 13 p2050 N85-22630
Vortex generating flow passage design for increased film cooling effectiveness
[NASA-CASE-LEW-14039-1] 22 p3782 N85-33433

LIQUID LEVELS
Experimental investigation of the oscillation behaviour of a liquid-filled rotor with centrifugal motion
[BLL-DOUNREAY-TR-936-(9091.9F)] 08 p1160 N85-17317

LIQUID LITHIUM
New liquid cathodes for lithium batteries. Part A: Halocarbons
[AD-A148433] 08 p1178 N85-17423

LIQUID MERCURY
U MERCURY (METAL)

LIQUID METAL COOLED REACTORS
NT EXPERIMENTAL BREEDER REACTOR 2
Analysis of the natural initiation of vapor explosions
[DE85-000188] 11 p1632 N85-20279
Technical assessment of thermal-hydraulics for high heat flux fusion components
[DE85-013176] 23 p3930 N85-34359

LIQUID METAL FAST BREEDER REACTORS
Non-isothermal irradiation creep of nickel alloys Inconel 706 and PE-16
[DE85-000842] 11 p1607 N85-20102
Use of laser flow visualization techniques in reactor component thermal-hydraulic studies
[DE84-014768] 11 p1639 N85-20330
Coolant mixing in LMFBR rod bundles and outlet plenum mixing transients
[DE85-010336] 19 p3268 N85-30268
Loss-of-flow transient characterization in carbide-fueled LMFBRs
[DE85-009552] 19 p3269 N85-30270
Analytical simulation of weld effects in creep range
20 p3468 N85-31550
Resolution of thermal striping issue downstream of a horizontal pipe elbow in stratified pipe flow
[DE85-006195] 21 p3586 N85-32292
LIQUID METALS
NT LIQUID LITHIUM
NT LIQUID POTASSIUM
NT LIQUID SODIUM
NT MERCURY (METAL)
Study of vibrational energy transfer at a liquid tin surface
[AD-A145741] 02 p0277 N85-11804
Emission mechanisms in the liquid metal ion source: A review
[AERE-R-11294] 03 p0418 N85-12675
Reproducibility of readings from oxygen concentration elements
[BLL-M-35920-(5828.4)] 05 p0616 N85-13941
Effects of temperature on the response time of thermocouples and resistance thermometers
[DE84-016855] 06 p0811 N85-15154
Extreme incompatibility of Pb during the crystallization of magmatic iron meteorites 06 p0886 N85-15627
Investigations concerning the magmatic iron meteorites: Static vs. dynamic experiments
06 p0886 N85-15629
Investigation of electric and wear phenomena of liquid metal wetted copper fiber brushes under conditions of high slip ring eccentricity
[AD-A147634] 08 p1156 N85-17295
Susceptibility of 2 1/4 Cr-1Mo steel to liquid metal induced embrittlement by lithium-lead solutions
[DE85-000997] 09 p1294 N85-18130
Electronic structure of liquid metal alloys
[DE85-000904] 09 p1295 N85-18136
Glass corrosion in liquid lithium
[DE85-002066] 09 p1299 N85-18162
Characteristics of the boat inductor for keeping liquid metal in the suspended state
[NASA-TM-77816] 12 p1851 N85-21611
Anomalies of aluminum structure and properties
13 p2026 N85-22693
Division boundary in Al-B composite material with boron in contact with solid and liquid aluminum
13 p2027 N85-22704
Electrodynamic stability of composite liquid-metal contacts 13 p2087 N85-23031
The volume change during solidification
[NASA-TM-77817] 14 p2300 N85-24243
Experimental facility for studying MHD effects in liquid metal cooled blankets
[DE85-000583] 14 p2423 N85-24943
Magneto-fluid-dynamic issues for fusion first wall and blanket systems
[DE85-004022] 14 p2424 N85-24954
Magnetohydrodynamic considerations for the design of self-cooled liquid-metal fusion reactor blankets
[DE85-000242] 14 p2425 N85-24957
Analysis of alkali liquid metal Rankine space power systems
[DE85-005089] 16 p2741 N85-26917
Flat magnetohydrodynamic induction pump
17 p2939 N85-28145
Dependence of characteristics of centrifugal magnetohydrodynamic conduction pump on electrical conductance of end walls. Part 1: Experiment
17 p2939 N85-28146
Liquid-metal transducers for strain measurement during in-pile materials testing 17 p2945 N85-28176
Automatic liquid-metal temperature monitoring with the use of immersed tranducers
[BLL-BISI-TRANS-22427-(6022.06)]
18 p3104 N85-29215
Liquid metal thermoelectric converter (LMTEC) for solar applications
[DE85-008405] 18 p3129 N85-29376
Thermodynamic properties of liquid Li-Pb, Na-Pb and K-Pb alloys: Similarities and Differences
[DE85-004074] 18 p3197 N85-29830
Arc spray fabrication of metal matrix composite monotape
[NASA-CASE-LEW-13828-1] 19 p3230 N85-30027
Liquid metal reactor programs: Safeguards and program assurance
[DE85-010821] 19 p3331 N85-30635
Rapid analysis of steels using laser-based techniques
[DE85-010747] 22 p3748 N85-33232
Key issues of fusion nuclear technology development (FINESSE)
[DE85-012599] 22 p3845 N85-33817
Electrically conductive containment vessel for molten aluminum
[DE85-006518] 23 p3930 N85-34415
LIQUID NITROGEN
Wear of anodic oxide films on aluminum alloys in cryogenic liquids
[NAL-TR-818] 06 p0766 N85-14914
New method for heat treatment of metals
10 p1446 N85-19110
Comparison of calculations and measurements of the off-axis radiation dose (SI) in liquid nitrogen as a function of radiation length
[AD-A153676] 18 p3178 N85-29704
A system for the assessment of non-thermal effects of ultrasound on cells at liquid nitrogen temperatures
20 p3523 N85-31915
A liquid nitrogen cooled composite wall hollow cathode — molecular spectroscopy
[USIP-85-07] 20 p3526 N85-31930
Basic cryogenics and materials. Phase 1
[NASA-CR-177932] 21 p3572 N85-32215
Sound speed measurements in liquid oxygen-liquid nitrogen mixtures
[NASA-TP-2464] 24 p4083 N85-35307
LIQUID OXYGEN
Numerical analysis of flow and heat transfer in the VAFB LOX storage Dewar tank
[NASA-CR-171203] 02 p0197 N85-11315
A study on dynamic characteristics of liquid oxygen pumps for rocket engines
[NAL-TR-806] 03 p0324 N85-12088
Ultrasound instrumentation for the 7 inch Mach seven tunnel
[NASA-CR-174277] 07 p1038 N85-16586
Automatic software for controlling cryogenic systems
08 p1097 N85-16932
Partial bleed expander cycle for low thrust LOX/LH2 rocket engine
[NAL-TR-837T] 10 p1430 N85-19018
An air-breathing ballistic space transporter for Europe
[NASA-TM-77645] 12 p1792 N85-21244
Nonlinear rotordynamics analysis
[NASA-CR-171425] 13 p1968 N85-22364
Flow induced vibration of the SSME LOX posts
[NASA-CR-175606] 15 p2495 N85-25391
Studies on rocket engines for future European launchers
[SEP-TPRL/K-19572/84] 15 p2495 N85-25393
Flow-induced vibration of the SSME LOX posts: Additional issues
[DE85-007339] 16 p2741 N85-26916
Flow-induced vibration of SSME main injector liquid-oxygen posts 17 p2912 N85-27951
Ignition characterization of LOX/hydrocarbon propellants
[NASA-CR-171884] 18 p3083 N85-29070
Ignition characterization of LOX/hydrocarbon propellants
[NASA-CR-171882] 18 p3083 N85-29071
Basic cryogenics and materials. Phase 1
[NASA-CR-177932] 21 p3572 N85-32215
Sound speed measurements in liquid oxygen-liquid nitrogen mixtures
[NASA-TP-2464] 24 p4083 N85-35307
LIQUID PHASE EPITAXY
Producing gallium arsenide crystals in space
02 p0151 N85-11023
Effect of liquid phase composition on thickness of epitaxial Ga sub (1-x) Al sub x As films
02 p0257 N85-11683
Symmetry of exchange interaction in crystalline magnetic films 02 p0259 N85-11694
Photoelectric effect in liquid crystals
02 p0259 N85-11695
Current controlled LPE (Liquid Phase Epitaxy) growth of semiconductors
[AD-A145536] 02 p0287 N85-11875
LPE (Liquid phase epitaxy) semiconductor material transfer method
[AD-D011250] 05 p0731 N85-14696
Tunable microwave transversal filters
[AD-A148370] 08 p1158 N85-17304
P-I-N CdTe gamma-ray detectors by Liquid Phase Epitaxy (LPE)
[DE84-012276] 09 p1323 N85-18315
Liquid-phase epitaxial growth of CdTe on HgCdTe
[AD-D011482] 10 p1561 N85-19846
Preparation of crystal growth experiments in Spacelab: Si (FSLP), CdTe (D1), ZnS (D1)
[BMFT-FB-W-84-045] 12 p1789 N85-21227
Development of solid state infrared emitters for gas detection applications
[PB85-148450] 15 p2561 N85-25800
Materials-process interactions in ternary alloy semiconductors
[AD-A153133] 17 p3043 N85-28832
Electron irradiation of light emitting diodes
[AD-A154441] 19 p3260 N85-30213
Design and operation of epitaxial reactor
[DE85-011099] 19 p3306 N85-30491
Low-threshold injection InGaAsP/GaAs double heterostructure lasers with separate limiting obtained by liquid-phase epitaxy (lambda = 0.76 divided by 0.87 microns, I sub thr = 480 A/cm 2, T = 300 K)
21 p3687 N85-32908
LIQUID PHASES
Thermodynamics of decarburization of niobium-bearing high-alloy melts
[BLL-M-35728-(5828.4)] 02 p0175 N85-11169
Deuterium diffusion in a soil-water-ice mixture
[AD-A148457] 08 p1176 N85-17415
Liquid phase methanol process development unit: Installation, operation, and support studies
[DE85-001311] 09 p1301 N85-18171
Analysis of phase composition of products of laser destruction of metallic surfaces
11 p1600 N85-20064
Denitification and deformation in the presence of a liquid phase
[DE85-005101] 13 p2038 N85-22783
Catalyst and reactor development for a liquid phase Fischer-Tropsch process
[DE85-005894] 17 p2922 N85-28014
Electrochemical studies in liquid crystals
[AD-A154317] 19 p3234 N85-30060
Modeling of chemical transformations of SO(x) and NO(x) in the polluted atmosphere: An overview of approaches and current status
[PB85-173169] 20 p3487 N85-31677
Phase behavior and QLS (Quasielastic Light Scattering) in potassium linoleate/n-alkanol microemulsions
[AD-A155028] 21 p3565 N85-32163
Liquid-phase compositions from vapor-phase analyses 2: Adaptation of the Prausnitz program to UF6 and some of its potential impurities
[DE85-011521] 21 p3673 N85-32819
The effect of liquid-liquid phase separation of glass on the properties and crystallization behavior
[NASA-TM-77890] 23 p3919 N85-34285
Chemistry of ore-forming fluids
24 p4103 N85-35436
LIQUID POTASSIUM
Operating experience with potassium systems — thermal power stations
[OEFZS-4275] 03 p0357 N85-12473
LIQUID PROPELLANT ROCKET ENGINES
NT HYDRAZINE ENGINES
NT HYDROGEN OXYGEN ENGINES
NT RL-10 ENGINES
NT SPACE SHUTTLE MAIN ENGINE
Columbium chamber fabrication study
[AD-A145230] 01 p0017 N85-10102
A study on dynamic characteristics of liquid oxygen pumps for rocket engines
[NAL-TR-806] 03 p0324 N85-12088
A study of air breathing rockets. Part 4: Direct fuel injection into a secondary combustor
[NAL-TR-832] 09 p1287 N85-18083
Partial bleed expander cycle for low thrust LOX/LH2 rocket engine
[NAL-TR-837T] 10 p1430 N85-19018
The 1984 JANNAF Propulsion Systems Hazards Subcommittee Meeting, volume 1
[AD-A148665] 10 p1454 N85-19182
Safety aspects of prepackaged liquid propellant stages for strategic missiles
[AD-P004350] 10 p1456 N85-19174
Low loss injector for liquid propellant rocket engines
[NASA-CASE-MFG-25989-1] 11 p1591 N85-20008
An integral closed loop combustion stability model-status and review 13 p2003 N85-22553
Development of a three-phase combustion code for modeling liquid rocket engines 13 p2003 N85-22564
Atomization data requirements for rocket combustor modeling 13 p2003 N85-22565
Effect of compliability of hot walls in liquid-propellant engine on low frequency instability
13 p2049 N85-22824
AFRPL (Air Force Rocket Propulsion Laboratory) technical objective document FY 85
[AD-A151369] 15 p2495 N85-25389
Materials for advanced rocket engine turbopump turbine blades 16 p2734 N85-26872

Ignition/combustion processes
16 p2740 N85-26909
A closed loop analysis of POGO instability
[AD-A153121] 17 p2937 N85-28132
Hydrazine and the F-16 20 p3511 N85-31626
Sound speed measurements in liquid oxygen-liquid nitrogen mixtures
[NASA-TP-2464] 24 p4063 N85-35307

LIQUID ROCKET PROPELLANTS
NT CRYOGENIC ROCKET PROPELLANTS
NT HYPERGOLIC ROCKET PROPELLANTS
NT MONOPROPELLANTS
NT SLURRY PROPELLANTS
Safety aspects of prepackaged liquid propellant stages for strategic missiles
[AD-P004350] 10 p1456 N85-19174
Space Transportation System (STS) propellant scavenging system study. Volume 1: Technical report
[NASA-CR-171848-VOL-1] 11 p1589 N85-20000
Fluid slosh dynamics of surface tension tanks in three axis stabilized spacecraft
[MBB-UR-E-739-84-O] 11 p1634 N85-20291
Dynamic investigations of a spherical tank structure filled with liquid using ANSYS three-dimensional fluid elements
[MBB-UR-E-737-83-O] 11 p1654 N85-20418
Feasibility of producing commodities and electricity for space shuttle operations at Vandenberg Air Force Base
[DCN-84-203-001-80-21] 12 p1789 N85-21230
Atomization data requirements for rocket combustor modeling 13 p2003 N85-22555
Low thrust bipropellant engine/redundant seat valve assembly
[AD-A150293] 13 p2013 N85-22628
Atmospheric dispersion of hypergolic liquid rocket fuels, volume 2
[AD-A150699] 14 p2263 N85-24020
Ignition/combustion processes
16 p2740 N85-26909
Application of the hydraulic system frequency response program to propellant feed systems
[AD-A151824] 16 p2741 N85-26914
A closed loop analysis of POGO instability
[AD-A153121] 17 p2937 N85-28132

LIQUID ROTATION
U ROTATING LIQUIDS

LIQUID SLOSHING
In-orbit experiments on IRAS for application to the ISO satellite
[FOK-TR-R-84-057] 03 p0322 N85-12078
Propellant transfer: Tethered depot
08 p1108 N85-17006
Fluid slosh dynamics of surface tension tanks in three axis stabilized spacecraft
[MBB-UR-E-739-84-O] 11 p1634 N85-20291
Analysis of seismic sloshing of reactor tanks considering submerged components and seismic isolation
[DE85-010490] 19 p3269 N85-30273
Further studies on liquid sloshing
[PB85-196605] 24 p4095 N85-35388

LIQUID SODIUM
Induction voidmeter
[DE84-014321] 01 p0050 N85-10329
Study of alternative system conversions for the Solar One pilot plant
[DE85-010026] 22 p3809 N85-33594

LIQUID SURFACES
NT MENISCI
Study of vibrational energy transfer at a liquid tin surface
[AD-A145741] 02 p0277 N85-11804
Free surface effects on the wake of a flat plate
[AD-A146998] 07 p0958 N85-16071
Liquid thickness gage
[NASA-CASE-LAR-13342-1] 11 p1635 N85-20297
Instability and chaotic behavior in a free-surface flow
[AD-A154879] 21 p3584 N85-32279
Surface temperature distribution along a thin liquid layer due to thermocapillary convection
[NASA-TM-87115] 23 p3930 N85-34357

LIQUID WASTES
NT URINE
NT WASTE WATER
Radioactive liquid wastes discharged to ground in the 200 areas during 1984
[DE85-010619] 19 p3310 N85-30517
Review of hazardous waste cleanup and disposal efforts at Tinker Air Force Base
[GPO-43-294] 21 p3613 N85-32457

LIQUID-GAS MIXTURES
NT AEROSOLS
NT FOG
Mathematical-cartographic model for study of distribution of hydrochemical elements in sea water (using dissolved oxygen in the Pacific Ocean as an example)
13 p2109 N85-23138

LIQUID-LIQUID INTERFACES
The behaviour of unstable surfaces: A literature review
[CFD/84/6] 02 p0199 N85-11329
Investigation of the Ostwald ripening of separated particles in liquid-liquid systems under microgravity conditions
[BMFT-FB-W-84-037] 05 p0615 N85-13927
Properties of materials using acoustic waves
[AD-A150465] 13 p2155 N85-23382
Free-surface phenomena under low- and zero-gravity conditions
[NASA-CR-175885] 17 p2907 N85-27922
Computer-aided thermohydraulic design of TEMA type E shell and tube heat exchangers for use in low pressure, liquid-to-liquid, single phase applications
[AD-A153779] 18 p3100 N85-29191
Natural convection experiments in a stratified liquid-saturated porous medium
[DE85-009003] 20 p3455 N85-31457

LIQUID-SOLID INTERFACES
Thermal fluid-structure interaction: A few scaling considerations — nuclear reactors
[GKSS-84-E-18] 01 p0048 N85-10314
Structure and kinetics of physisorption, properties of helium during reduction of the dimension
03 p0432 N85-12749
A similarity analysis of phase change heat conduction in corners 05 p0634 N85-14069
Modulated surface vibrational spectroscopies at electrode/electrolyte interfaces
[AD-A148665] 08 p1123 N85-17083
Linear and nonlinear ultrasonic interaction on liquid-solid boundaries
[AD-A148979] 10 p1553 N85-19793
Time resolved X-ray studies during pulsed laser irradiation of Ge
[DE85-005263] 13 p2097 N85-23083
Surface scattering
[AD-A150252] 13 p2153 N85-23366
The development of laser analytical methods for the characterization of solid-liquid and solid-high pressure gas interfaces
[AD-A152382] 17 p2918 N85-27988
A Navier-Stokes capillary free boundary in open boat crystal growth
[REPT-84-34] 17 p2960 N85-28283
MPS solidification model. Analysis and calculation of macrosegregation in a casting ingot
[NASA-CR-171589] 21 p3566 N85-32178
Polymer-water interaction studies
21 p3609 N85-32411
Approximate determination of the extent of the solid-liquid zone
[BLL-M-35829-(5828.4)] 23 p3914 N85-34251

LIQUID-VAPOR EQUILIBRIUM
Study of the liquid vapor equilibrium in the bromine-hydrobromic acid-water system
[NASA-TM-77787] 07 p0921 N85-15836
A study of liquid-vapor equilibria of the bromine-hydrobromic acid-water system
[NASA-TM-77748] 14 p2249 N85-23940

LIQUID-VAPOR INTERFACES
Surface scattering
[AD-A150252] 13 p2153 N85-23366
Convective instability of horizontal layer of binary mixture 14 p2338 N85-24458
The development of laser analytical methods for the characterization of solid-liquid and solid-high pressure gas interfaces
[AD-A152382] 17 p2918 N85-27988
The polar caps and the climatic evolution of Mars
22 p3854 N85-33866
Effects of ambient pressure on the instability of a liquid boiling explosively at the superheat limit
[DE85-009476] 23 p3932 N85-34370

LIQUIDS
NT CRYOGENIC FLUIDS
NT CRYOGENIC ROCKET PROPELLANTS
NT FERMI LIQUIDS
NT FERROFLUIDS
NT HYDRAULIC FLUIDS
NT HYPERGOLIC ROCKET PROPELLANTS
NT LIQUEFIED GASES
NT LIQUID AMMONIA
NT LIQUID FUELS
NT LIQUID HELIUM
NT LIQUID HYDROGEN
NT LIQUID LITHIUM
NT LIQUID METALS
NT LIQUID NITROGEN
NT LIQUID OXYGEN
NT LIQUID POTASSIUM
NT LIQUID ROCKET PROPELLANTS
NT LIQUID SODIUM
NT MERCURY (METAL)
NT MONOPROPELLANTS
NT ORGANIC LIQUIDS
NT ROTATING LIQUIDS
NT SLURRY PROPELLANTS
The analysis of tank calibration data from several runs
[DE84-015529] 02 p0200 N85-11337
Diffusive combustion of fluids with free surface
02 p0274 N85-11785
Nonlinear acoustics
[AD-A145580] 02 p0276 N85-11796
Investigation of liquid encapsulation Chochralski growth of InP
[AD-A146096] 03 p0433 N85-12760
Separation of metal species by supported liquid membranes
[DE84-014536] 04 p0470 N85-12992
Dynamics of liquid filament breakup
[DE84-016008] 04 p0500 N85-13187
Bicomponent flow problems in rheological fluid mechanics 05 p0635 N85-14073
Motion of electrons in non polar classical liquids
[DE84-013609] 05 p0727 N85-14672
Stability of rigid motions and rollers in bicomponent flows of immiscible liquids
[AD-A147302] 07 p0960 N85-16081
Convection heat transfer in the critical region of fluid mixtures
[DE85-002118] 07 p0961 N85-16088
A virial equation of state option for the TIGER computer program
[AD-A147490] 07 p1025 N85-16507
Supersonic molecular jet study of the liquid state
[AD-A147416] 09 p1379 N85-18671
Liquid thickness gage
[NASA-CASE-LAR-13342-1] 11 p1635 N85-20297
Influence of pressure on speed of sound in single-phase region of stratifying mixtures 11 p1715 N85-20768
Examination of the contact wetting angle in the vicinity of critical temperature
[BLL-T6416/BG/CRS/LR-ST735/84]
13 p2091 N85-23054
Vapor explosions in superheated liquids and fundamental studies of the physics of detonation
[AD-A151362] 15 p2504 N85-25447
Wave propagation in density stratified fluids
16 p2781 N85-27162
Liquid propellants for use in guns: A review
[AD-A153051] 17 p2937 N85-28131
An evaluation and preparation of ferromagnetic liquid composites for use at millimeter wavelengths
[AD-A153939] 18 p3089 N85-29980
Liquid sampling system
[DE85-011673] 19 p3265 N85-30248
Lost circulation in geothermal wells: Research and development status
[DE85-009836] 19 p3268 N85-30267
Seismic analysis of liquid-filled tanks with an eccentric core barrel
[DE85-010249] 19 p3269 N85-30272
Interaction of slow electrons with high-pressure gases (quasi-liquids): Synthesis of our knowledge on slow electron-molecule interactions
[DE85-010081] 19 p3355 N85-30800
Weak shock waves propagating in fluid-gas mixtures
[AD-A154759] 21 p3584 N85-32276
Thermophysical properties of fluids for the gas industry
[PB85-196471] 22 p3747 N85-33227
Apparatus and method for the spectrochemical analysis of liquids using the laser spark
[DE85-005749] 23 p3935 N85-34387
Depletion modeling of liquid dominated geothermal reservoirs
[DE85-009923] 23 p3943 N85-34437
Gas analysis of ore-forming fluids
24 p4105 N85-35447
Cationic exchange membrane for the zinc-ferricyanide battery
[DE85-013152] 24 p4112 N85-35489
Calculation of heavy-ion tracks in liquid water
[DE85-012101] 24 p4149 N85-35725

LIQUIDUS
Studies on copper alloys containing chromium on the copper side phase diagram
[NASA-TM-77752] 07 p0927 N85-15876

LISP (PROGRAMMING LANGUAGE)
MACSYMA usage at Langley
[NASA-CR-172518] 10 p1537 N85-19688
The portable LISP translation tool
[AD-A149765] 12 p1915 N85-22023

LISTS
Glossary of landscape and vegetation ecology for Alaska
[PB85-153831] 16 p2816 N85-27372

LITERATURE
NT BIOGRAPHY
NT DOCUMENTATION
European Scientific Notes, volume 38, number 12
[AD-A148713] 09 p1418 N85-18946
A network-based approach to text handling for the online scientific community 15 p2664 N85-28444
The next assignment: The state of the literature on space 23 p4057 N85-35146

LITHIUM
NT LIQUID LITHIUM
Method and apparatus for determining the content and distribution of a thermal neutron absorbing material in an object
[DE84-014319] 01 p0117 N85-10801
Lithium battery safety: A fiber-optic application for safe observation of lithium cells under severe tests
[AD-A146846] 06 p0804 N85-15119
Rechargeable lithium cell
[AD-D011302] 07 p0993 N85-16304
Pion inelastic scattering to the first three excited states of Lithium-6
[AD-A147560] 07 p1041 N85-16606
Susceptibility of 2 1/4 Cr-1Mo steel to liquid metal induced embrittlement by lithium-lead solutions
[DE85-000997] 09 p1294 N85-18130
Glass corrosion in liquid lithium
[DE85-002086] 09 p1299 N85-18162
Calculation of Si(Li) X-ray detector efficiencies
[DE85-002732] 10 p1489 N85-19400
Lithium counterdoped silicon solar cell
[NASA-CASE-LEW-14177-1] 11 p1672 N85-20535
Negative lithium emission from a tungsten surface in a plasma
[DE85-003456] 12 p1936 N85-22167
The effects of lithium counterdoping on radiation damage and annealing in n(+)p silicon solar cells
13 p2007 N85-22586
Relationship between topological and magnetic order in small metal clusters
[AD-A150547] 13 p2018 N85-22651
Hartree-Fock interaction between a helium atom and lithium-metal: A test for the effective medium theory
[AD-A150468] 13 p2156 N85-23387
Gigantic lithium deposit discovered in France
14 p2289 N85-24184
Active Magnetospheric Particle Tracing Explorers (AMPTE)
[AD-A151072] 14 p2374 N85-24674
Sodium and lithium corrosion in molybedenum heat pipes
[DE85-005561] 16 p2784 N85-27179
Investigation of the structure and dynamics of electrolytes in solvents used for primary and secondary Li-batteries
[AD-A153089] 17 p2954 N85-28240
Experimental study of dissociative attachment in optically-pumped lithium molecules
[AD-A152800] 17 p3030 N85-28738
Development of reduced activation alloys for fusion service: Draft
[DE85-007464] 18 p3074 N85-29014
British breakthrough in lightweight lithium batteries
18 p3086 N85-29092
Lithium cell reactions
[AD-A154429] 19 p3305 N85-30484
Instrumentation for particle-beams research using excited merging beams
[AD-A154155] 19 p3356 N85-30807
The production and destruction of metastable negative ions
[DE85-011056] 19 p3364 N85-30858
Improvements in safety testing of lithium cells
20 p3444 N85-31379
Design evaluation of high reliability lithium batteries
20 p3444 N85-31380
Safety of Li-SOCl2 cells 20 p3444 N85-31383
Rechargeable lithium-organic electrolyte battery having overcharge protection and method of providing overcharge protection for a lithium-organic electrolyte battery
[AD-D011738] 22 p3806 N85-33575
Evaluation of low-temperature geothermal potential in Utah and Goshen Valleys and adjacent areas, Utah. Part 2: Water temperature and chemistry
[DE85-009344] 23 p3943 N85-34438
Light ion sources for ICF
[DE85-011544] 23 p3983 N85-34702
Thermodynamics of the corrosion of chromium in molten carbonates
[DE85-011407] 24 p4079 N85-35282
Experimental lithium system
[DE85-013252] 24 p4094 N85-35382
The Conterminous United States Mineral Assessment Program 24 p4106 N85-35458

LITHIUM ALLOYS
Sea water rope batteries
[AD-A144775] 01 p0042 N85-10275
Phase equilibria of stored chemical energy reactants
[AD-A146527] 06 p0765 N85-14896
Synergistic sputtering properties of binary alloys
[DE84-017493] 09 p1297 N85-18148
Problem of pore formation mechanism in welded joints of aluminum alloys in the system aluminum-magnesium-lithium 13 p2032 N85-22732
Pechiney strategy includes development of new materials 15 p2531 N85-25607
Performance of a copper-lithium alloy as an impurity control system surface material for a fusion reactor
[DE85-006494] 15 p2657 N85-26398
Self-sustaining low-Z coatings for fusion applications 2 - copper-lithium
[DE85-002553] 15 p2658 N85-26403
Experimental studies of the electronic structure of 1-2 and 1-3 intermetallic compounds
[DE85-006978] 15 p2662 N85-26432
Investigation of the pitting potential of rapidly solidified aluminum-lithium alloys
[VTH-LR-434] 16 p2752 N85-26986
Aluminum-lithium alloys: The answer of the aluminum industry to the threat of advanced fiber-reinforced materials
[VTH-LR-406] 17 p2932 N85-28102
West Europe report: Science and technology
[JPRS-WST-84-035] 18 p3087 N85-29102
Lithium-alloy/iron sulfide battery design studies
[DE85-007991] 18 p3131 N85-29389
Self-sustaining coatings for fusion applications: Copper lithium alloys
[DE85-009740] 18 p3190 N85-29783
Thermodynamic properties of liquid Li-Pb, Na-Pb and K-Pb alloys: Similarities and Differences
[DE85-004074] 18 p3197 N85-29830
Anisotropic electron-impurity scattering in dilute AlLi: (Small) corrections to the local density approximation
[DE85-002946] 19 p3238 N85-30076
Counter current extraction system for tritium recovery from 17Li-83Pb
[DE85-010519] 19 p3240 N85-30080
Molten salt cooling/17Li-83Pb breeding blanket concept
[DE85-010522] 19 p3363 N85-30854
Current state of development and expected performance of copper-lithium alloys as an impurity control system in fusion applications
[DE85-009673] 19 p3372 N85-30917

LITHIUM BORATES
Water absorption and conductivity in poly(ethylene oxide)-lithium tetrafluoroborate films
[AD-A147969] 10 p1450 N85-19138

LITHIUM CHLORIDES
Investigation of the dissolution of CaCrO4 in molten LiCl-KCl eutectic
[DE84-016394] 04 p0469 N85-12985
High capacity inorganic oxyhalide electrochemical cell
[AD-D011321] 07 p0923 N85-15845
Synthesis and properties of Hexachloromolybdate(5) and related species
[AD-A139599] 07 p0924 N85-15852
A safe, high-power-density lithium battery
[AD-A155223] 21 p3813 N85-32454

LITHIUM COMPOUNDS
NT LITHIUM BORATES
NT LITHIUM CHLORIDES
NT LITHIUM FLUORIDES
NT LITHIUM IODATES
NT LITHIUM NIOBATES
NT LITHIUM OXIDES
NT ORGANIC LITHIUM COMPOUNDS
(Vinyloxy)fluorocyclotriphosphazenes
[AD-A147448] 07 p0924 N85-15850
Polymer electrolytes: An investigation of some poly (N-propylaziridine)/lithium salt compositions
[RAE-TR-84036] 08 p1131 N85-17130
Polymer electrolytes: An investigation of some poly (N-propylaziridine)/lithium salt compositions
[AD-A149444] 10 p1452 N85-19146
Neutron scattering studies of graphite intercalation compounds
[DE85-003079] 12 p1942 N85-22198
Ionic conduction and water diffusion in Li (BETA)-alumina
[DE85-007548] 16 p2755 N85-27005
Super hydrides
[AD-A153489] 18 p3070 N85-29966
RAY-O-VAC BR2325 lithium carbon monofluoride cell performance 20 p3444 N85-31382
An update of the JPL program to develop Li-SOCl2 cells 20 p3445 N85-31384

LITHIUM FLUORIDES
Lasing characteristics of YAG: Nd(3+)-laser with LiF passive shutter with F2 color centers
11 p1717 N85-20502
Selective radiative cooling with MgO and/or LiF layers
[DE85-011595] 19 p3262 N85-30228
Lasing on LiF:F(-)2 - dye centers with transverse pumping 21 p3684 N85-32890
In-cavity laser IR spectrum analyzer for investigating non-steady-state processes 21 p3685 N85-32894

LITHIUM IODATES
Design evaluation of high reliability lithium batteries
20 p3444 N85-31380

LITHIUM NIOBATES
Multichannel electrooptical modulators for digital information storage and processing systems
07 p0950 N85-16021

LITHIUM OXIDES
Development of the Cascade inertial-confinement-fusion reactor
[DE85-010933] 19 p3357 N85-30812

LITHIUM SULFUR BATTERIES
Research to explore the feasibility of sulfolanes as electrolytic solvents for rechargeable lithium batteries
[DE85-004345] 12 p1837 N85-21625
Sixth DOE Electrochemical Contractor's Review. Extended abstracts
[DE84-013679] 16 p2779 N85-27151
Lithium-alloy/iron sulfide battery design studies
[DE85-007991] 18 p3131 N85-29389
Lithium cell reactions
[AD-A154429] 19 p3305 N85-30484
Advances in rechargeable lithium molybdenum disulfide batteries 20 p3444 N85-31376
Geosynchronous performance of a lithium-titanium disulfide battery 20 p3444 N85-31377
Development of a lithium secondary battery separator
20 p3444 N85-31378
Transfer of battery technology developed by the US Department of Energy
[DE85-009868] 22 p3808 N85-33588

LITHOGRAPHY
NT PHOTOLITHOGRAPHY
Workshop on the Use of Future Multispectral Imaging Capabilities for Lithologic Mapping: Workshop summary
02 p0214 N85-11413
Ion beam lithography
[BMFT-FB-T-84-182] 04 p0504 N85-13219
Development of short gate FET's
[AD-A147033] 07 p0947 N85-15899
Lithography radiation effects study
[AD-A149552] 10 p1468 N85-19260
China report: Science and technology
[JPRS-CST-85-005] 13 p2052 N85-22843
X-ray lithography and VLSI circuits
13 p2052 N85-22846
Use of optical techniques in studies of wear rates of anodized aluminum and polymer coatings on aluminum
14 p2259 N85-23987
DARPA/TTO program IR binary optics
[AD-A152196] 16 p2965 N85-27672
Communications and logic systems at millimeter wave frequencies, summary 17 p3042 N85-28825

LITHOLOGY
Assessment of computer techniques for processing digital LANDSAT MSS data for lithological discrimination of Serra do Ramalho, State of Bahia
[E85-10033] 03 p0378 N85-12412
Evaluation of criteria for selecting the spectral attributes of digital LANDSAT MSS imagery for discriminating lithological units in the lower Curaca River Valley, Bahia — Brazil
[E85-10038] 03 p0379 N85-12415
Sedimentary and tectonic evolution of the western Taiwan foredeep 03 p0389 N85-12491
Newly recognized sedimentary environments in the Shelikof Formation, Alaska 04 p0516 N85-13202
A multiple approach in remote sensing for structural and lithological mapping by use Modular Optoelectronic Multispectral Scanner (MOMS)/LANDSAT/Heat Capacity Mapping Mission (HCMM) data
05 p0680 N85-14244
Some methodological aspects of study of layer associations in continents and oceans
06 p0820 N85-15205
Effect of lithology and climate on the morphology of drainage basins in northwestern Colorado
[PB84-228238] 06 p0828 N85-15258
Quantitative use of multiincidence-angle SAR for geologic mapping 08 p1145 N85-17220
Evaluation of the L-band scattering characteristics of volcanic terrain in aid of lithologic identification, assessment of SIR-B calibration, and development of planetary geomorphic analogs 08 p1146 N85-17232
Investigation of SIR-B images for lithologic mapping
08 p1148 N85-17241

Late precambrian to ordovician metamorphism and orogenesis in the Blue Ridge and western Piedmont, Virginia Appalachians 09 p1352 N85-18503
Organogenic structures (submerged reefs) in Silhetian limestone of west Bengal basin 10 p1500 N85-19464
Lithologic and environmental atlas of Berea Sandstone (Mississippian) in the Appalachian Basin [PB85-129039] 11 p1682 N85-20600
LANDSAT 4 investigations of Thematic Mapper and Multispectral Scanner applications — Drum Mountains, Utah and Tonopah, Nevada [E85-10095] 12 p1874 N85-21757
Review of problems in lithology 13 p2113 N85-23160
Geologic utility of LANDSAT-4 TM data — Death Valley, California and the Silver Bell area of southern Arizona 13 p2118 N85-23192
Lithologic and structural control on slope morphology in the Valles Marineris 13 p2201 N85-23651
Report on regional groundwater flow modeling for the Palo Duro Basin, Texas [DE85-007490] 16 p2815 N85-27370
Structural analysis of terrane accretions in the eastern Brooks Range and adjacent areas in central Alaska and Canada [DE85-008279] 17 p2993 N85-28501
Clay identification and amount measured by laboratory techniques compared to well log responses: Application to tight gas sands and shales [DE85-010411] 19 p3362 N85-30843
Reduced to pole long-wavelength magnetic anomalies of Africa and Europe 20 p3475 N85-31595
Lithology and stratigraphy of drill holes completed during 1984 in LANL use areas of Yucca Flat, Nevada Test Site, volume 6 [DE85-010695] 22 p3815 N85-33631
Geology and petroleum resources of basins in western China [DE85-013036] 23 p3948 N85-34469
Some recent deposit modeling efforts 24 p4106 N85-35453
Hydrogeology of the lower Glen Rose Aquifer, south-central Texas 24 p4108 N85-35466

LITHOSPHERE
NT EARTH CORE
NT EARTH CRUST
NT EARTH MANTLE
NT EARTH SURFACE
Lithospheric structure in the Pacific geoid [NASA-CR-174155] 04 p0526 N85-13365
Oceanic plateaus, anomalous subduction, and the accretion of buoyant features at convergent margins 05 p0686 N85-14422
Stresses and strains in lithosphere caused by Earth's thermoconvective oscillations 06 p0822 N85-15217
Basic structural features and probable mechanism of formation of the Kuril Island system 10 p1501 N85-19472
Thermal conditions and thinning of lithosphere in late cenozoic in southwestern US 10 p1501 N85-19473
Influence of scattering on Q in the lithosphere [AD-A149316] 10 p1515 N85-19563
Use of paleomagnetic data in tectonic analysis of oceanic structures 13 p2108 N85-23135
Interrelationship of earthquake magnitude and lithospheric-asthenospheric thermodynamic parameters in seismically active zones 13 p2116 N85-23183
Ic: Generation of silicate magma by shear melting at the base of a basaltic lithosphere 13 p2172 N85-23476
Formation of bright terrain bands on Ganymede by unstable lithosphere extension 13 p2173 N85-23485
Venus chasmata: A lithosphere stretching model 13 p2178 N85-23516
Elysium region, Mars: Tests of lithospheric loading models for the formation of tectonic features 13 p2200 N85-23650
On geoid heights and flexure of the lithosphere at seamounts [AD-A151220] 15 p2604 N85-26050
Altimetry data and the elastic stress tensor of subduction zones [NASA-CR-175796] 16 p2825 N85-27425
Heat flow through ocean floor and its relationship to lithosphere structure and thickness 19 p3294 N85-30422
Geometry, velocity structure and penetration depths of descending slabs in the western Pacific 19 p3319 N85-30574
Euro-African MAGSAT anomaly-tectonic observations 20 p3475 N85-31596
Intraplate crustal deformation due to continental collisions 20 p3490 N85-31693
Satellite-determined stresses in the crust of Europe with particular consideration to the Liege earthquake of November 8, 1983 20 p3490 N85-31694
Conditions during formation of the Earth 21 p3717 N85-33066
Anorthositic oceanic crust in the Archean Earth 21 p3719 N85-33077
A solid-state framework for terrestrial upper mantles 22 p3856 N85-33876
Contrasts in evolution of Venus and Earth 22 p3857 N85-33880
The non-hydrostatic figures of the terrestrial planets 22 p3858 N85-33887
Workshop Proceedings: Interpretation of Seismic Wave Propagation in Laterally Heterogeneous Structures [BMR-258] 24 p4118 N85-35530

LITTORAL CURRENTS
U COASTAL CURRENTS

LIVER
Biligenic function of white rat liver 01 p0093 N85-10624
Rat blood serum and liver carbohydrates and lipids in recovery period after 15-day hypokinesia 19 p3326 N85-30606
The 1984 environmental monitoring program report for Idaho National Engineering Laboratory site [DE85-011209] 22 p3812 N85-33611
Effects of immobilization and high-altitude adaptation on energy metabolism in rats 22 p3820 N85-33663
Lipogenesis in rat liver after flight aboard Cosmos-1129 biosatellite 23 p3954 N85-34508

LMCR (REACTORS)
U LIQUID METAL COOLED REACTORS

LMFBR
U LIQUID METAL FAST BREEDER REACTORS

LNG
U LIQUEFIED NATURAL GAS

LOAD DISTRIBUTION (FORCES)
Distributions of fatigue life and fatigue strength in notched specimens of a carbon 8-harness-satin laminate [NAL-TR-809T] 01 p0061 N85-10407
Design proposals for torsional buckling of stiffeners [AD-A144783] 01 p0062 N85-10409
Model for non-linear crack growth prediction, taking load sequence (LOSEQ) effects into consideration [BLL-RAE-TRANS-2114-(5207)] 02 p0208 N85-11371
Fatigue in composite materials 04 p0467 N85-12968
Performance on advanced lead-acid batteries for load-leveling applications [DE84-015617] 06 p0805 N85-15125
Evaluation of operational loads to verify structural design 07 p0896 N85-15677
Controlled movement of elastic manipulator with distributed parameters 13 p2048 N85-22818
The effect of center delamination on the instability of composite cylindrical panels [AD-A153494] 18 p3069 N85-28979

LOAD FACTORS
U LOADS (FORCES)

LOAD TESTING MACHINES
Locomotion research for the analysis of the human gait and for the determination of the maximum loads of the pelvis-leg skeleton. Volume 1: Two-dimensional analysis [BMFT-FB-T-83-187-VOL-1] 02 p0236 N85-11535
Influence of tire on resistance and steering forces of tires [AD-P004306] 09 p1410 N85-18883

LOAD TESTS
Composite materials characterization and development at AFWAL 04 p0464 N85-12944
Synthesis of load-time histories resulting from statistical analysis 05 p0650 N85-14171
Finite element calculation for a Y-joint and comparison of results with strain measurements [BLL-RISLEY-TR-4526-(9091.9F)] 08 p1171 N85-17361
A study of spectrum fatigue crack propagation in two aluminum alloys. 1: Spectrum simplification [NASA-TM-86929] 09 p1293 N85-18124
A study of spectrum fatigue crack propagation in two aluminum alloys. 2: Influence of microstructures [NASA-TM-86930] 09 p1294 N85-18125
Load carrying capacity of double circular arc gears 14 p2221 N85-23776
Durability calculation of wing panel element 14 p2265 N85-24159
Calibration loading of a strain-gauged diverless helicopter weapon recovery system [AD-A151486] 15 p2471 N85-25253
An improved torsional method for determining the fracture toughness of stiff materials and of adhesive joints [AD-A152091] 16 p2800 N85-27267
Composite loads spectra for select space propulsion structural components 17 p2912 N85-27953
Influence of manganese and heat treatment on structure and properties of Fe-0.1 percent-C-14 percent Cr-based steels [BLL-BISI-TRANS-22299-(9022.06)] 17 p2928 N85-28071

LOADING
Magnetic and structural properties of shock-synthesized zinc ferrite [DE85-000469] 11 p1736 N85-20915

LOADING FORCES
U LOADS (FORCES)

LOADING MOMENTS
Variable loading of elastic-plastic shells of revolution 06 p0779 N85-14861
Stability of hollow shafts under torsion 06 p0780 N85-14866
A literature survey of ground load statistics for landing gear fatigue design purposes [FFA-TN-1984-39] 09 p1260 N85-18054
Two recent cases of marker load applications on cargo/fighter aircraft fatigue tests 14 p2318 N85-24325
Generation of marker lines on fatigue fracture surfaces 14 p2319 N85-24328
Consolidation theory with consideration of frame plasticity [REPT-9/1984] 16 p2796 N85-27240
Analysis of elastoplastic grids under conditions of variable loads [REPT-16/1984] 16 p2797 N85-27242
Calculation of friction at spherical bearing journals in turbomachines 17 p2940 N85-28150
Load-induced rotordynamic instabilities in turbomachinery 19 p3280 N85-30340
Intermittent motion 23 p3925 N85-34323

LOADING OPERATIONS
Mechanical features of the shuttle rotating service structure 08 p1102 N85-16967
STS payload ground handling mechanism at John F. Kennedy Space Center 08 p1103 N85-16971
New applications for robot loaders, unloaders 08 p1139 N85-17175
Hoist [AD-D011458] 10 p1493 N85-19425
Advanced life analysis methods. Volume 2: Crack growth analysis methods for attachment lugs [AD-A150420] 13 p2103 N85-23109
Cargo handling system [AD-D011569] 14 p2219 N85-23782
Calibration loading of a strain-gauged diverless helicopter weapon recovery system [AD-A151486] 15 p2471 N85-25253
Shuttle car loading system [NASA-CASE-NPO-15949-1] 23 p3987 N85-34722

LOADING RATE
Constitutive features of solids at shock-wave loading rates [DE84-015715] 03 p0362 N85-12325
On the use of marker loads and replicas for measuring growth rates for small cracks 14 p2319 N85-24331
Modifications of flight-by-flight load sequences to provide for good fracture surface readability [NLR-MP-84012-U] 20 p3472 N85-31577

LOADING WAVES
U ELASTIC WAVES
U LOADS (FORCES)

LOADS (FORCES)
NT AERODYNAMIC LOADS
NT AXIAL COMPRESSION LOADS
NT AXIAL LOADS
NT BLAST LOADS
NT COMPRESSION LOADS
NT CRITICAL LOADING
NT CYCLIC LOADS
NT DYNAMIC LOADS
NT EDGE LOADING
NT GUST LOADS
NT IMPACT LOADS
NT LANDING LOADS
NT RANDOM LOADS
NT ROLLING CONTACT LOADS
NT SHOCK LOADS
NT STATIC LOADS
NT THRUST LOADS
NT TRANSIENT LOADS
NT VIBRATORY LOADS
NT WING LOADING
The NBS tri-directional test facility [PB84-217462] 01 p0051 N85-10334
Three programs for evaluating bending moments, deflections and shear forces in simply-supported uniform bridge decks under South African NA loading: NAB, NAD and NAS. NITRR manual P13 [ISBN-0-7988-2283-X] 01 p0102 N85-10681

Structural analysis 02 p0143 N85-10989
Atmospheric and pressurized low speed wind tunnel performance and cost comparisons
[ARL/AERO-R-160] 02 p0146 N85-11008
A study of environmental characterization of conventional and advanced aluminum alloys for selection and design. Phase 1: Literature review
[NASA-CR-172367-PHASE-1] 02 p0161 N85-11216
Evaluation of laser profile and deflection measuring system
[FAA-PM-84-24] 02 p0201 N85-11341
Materials properties, loads, and stress analysis, Spartan REM: Appendix A
[NASA-CR-171092] 02 p0206 N85-11375
Extended aeroelastic analysis for helicopter rotors with prescribed hub motion and blade appended pendulaum vibration absorbers
[NASA-CR-172455] 03 p0315 N85-12038
Evaluation of laterally loaded laminated glass units by theory and experiment
[PB84-216423] 03 p0339 N85-12179
Comparison of predicted and measured friction for a tilt-pad thrust bearing with crown and roughness under hydrodynamic and mixed lubrication
[AD-A145752] 03 p0371 N85-12371
An experimental evaluation of the J integral in 50% sidegrooved compact geometry specimens
[AERE-R-11202] 03 p0374 N85-12386
Application of the ONERA model of dynamic stall
[NASA-TP-2399] 04 p0451 N85-12662
Initial sailplane project: The RP-1
04 p0468 N85-12976
Response of ferritic steels to nonsteady loading at elevated temperatures
[DE84-014280] 04 p0513 N85-13272
Solving equations of movement with variable inertia moment
[BLL-M-35975-(5828.4)] 05 p0641 N85-14111
Analysis of dynamic characteristics of fluid force induced by labyrinth seal 05 p0643 N85-14129
Prediction of force coefficients for labyrinth seals
05 p0644 N85-14130
An Iwatsubo-based solution for labyrinth seals - comparison with experimental results
05 p0644 N85-14131
Preliminary investigation of labyrinth packing pressure drops at onset of swirl-induced rotor instability
05 p0644 N85-14132
Identification of dynamic coefficients of annular turbulent seals 05 p0644 N85-14133
Design of electromagnetic bearing for vibration control of flexible transmission shaft 05 p0645 N85-14136
Effects of fluid inertia and turbulence on force coefficients for squeeze film dampers
05 p0645 N85-14137
Conditions for assembling dies for drawing under hydrodynamic friction conditions
[BLL-M-35954-(5828.4)] 05 p0647 N85-14153
An analysis of kinetic response variability
05 p0707 N85-14533
Effects of external loads on human head movement control systems 05 p0707 N85-14534
Experimental investigation and analysis of oscillations of thin-walled spherical shell during pulse loading
05 p0725 N85-14662
Testing the antifriction properties of alloys for heavily loaded bearings 06 p0760 N85-14990
Encapsulation design analysis
06 p0829 N85-15266
Operational Loads Data
[AGARD-CP-375] 07 p0894 N85-15664
Experiences obtained from service fatigue monitoring exercises 07 p0895 N85-15672
CF-5 vertical stabilizer flight load survey
07 p0895 N85-15673
US Army helicopter operational flight loads
07 p0895 N85-15675
Helicopter data acquisition in WHL
07 p0896 N85-15676
Influence of pressure on compaction during compression of powders of iron and 40Kh and 10R6MS steels
[BLL-M-35995-(5828.4)] 07 p0926 N85-15866
Nondestructive measurement of bulk residual stresses
[AD-A147063] 07 p0978 N85-16211
Development of large wind energy power generation system
[NASA-TM-77779] 07 p0992 N85-16301
A theoretical view on the stress analysis of fully inflated parachute canopies
[AD-A148387] 08 p1078 N85-16835
Natural environment analysis
[NASA-CR-174330] 08 p1180 N85-17433
Determination of blade service life under irregular loading conditions 09 p1309 N85-18222
Mechanical and transient hygrothermal loading of multilayer orthotropic cylinders 09 p1330 N85-18359
The Shock and Vibration Bulletin 54. Part 2: Ship shock, shock and blast and ground shock
[AD-A148132] 09 p1334 N85-18388
Direct energy minimization approach to whipping analysis of pressure hulls 09 p1335 N85-18393
Water impact laboratory and flight test results for the space shuttle solid rocket booster aft skirt
09 p1335 N85-18394
Determination of shear coefficient of a general beam cross section by finite element method
09 p1338 N85-18413
A simple prediction model for soil compaction under various wheel loads and geometries as an aid to vehicle design
[AD-P004298] 09 p1409 N85-18875
Forces on undriven, angled wheels
[AD-P004303] 09 p1409 N85-18880
Influence of tire on resistance and steering forces of tires
[AD-P004306] 09 p1410 N85-18883
Detailed pressure distribution measurements obtained on several configurations of an aspect-ratio-7 variable twist wing
[NASA-TM-88306] 10 p1419 N85-18950
Integrated Technology Rotor/Flight Research Rotor (ITR/FRR) concept definition
[NASA-CR-166443] 10 p1423 N85-18978
Estimation of endurance characteristics of heat resistant materials. Report 2: Determination of endurance limit of heat resistant alloys over a broad temperature range
10 p1447 N85-19120
Methodology for stress analysis of heavy metal plate
10 p1460 N85-19203
Design procedure for the new 70-meter antenna subreflector positioner 10 p1463 N85-19232
Elevation bearing maximum load, 70-meter antenna
10 p1464 N85-19239
Hydrostatic bearing pad maximum load and overturning conditions for the 70-meter antenna
10 p1465 N85-19241
Connector/nitinol delta contact force device
[AD-D011467] 10 p1481 N85-19349
Crack problems for bonded nonhomogeneous materials under antiplane shear loading
[NASA-CR-172532] 10 p1495 N85-19438
Interaction between a crack and a soft inclusion
[NASA-CR-172533] 10 p1495 N85-19439
Evaluation of features of reinforcing fibers by testing bundles 11 p1599 N85-20059
Adjustable indicating device for load position
[NASA-CASE-MFS-28008-1] 11 p1635 N85-20300
Tether fundamentals 11 p1643 N85-20345
Techniques to analyze vehicle coastdown data
[DE85-005159] 12 p1772 N85-21127
Characterization of lubricated bearing surfaces operated under high loads
[NASA-TM-86964] 12 p1811 N85-21357
Cost comparison of small gas turbines versus electric motors in a variable load industrial application
[PB85-149763] 12 p1837 N85-21530
Ring-on-ring tests and load capacity of cladding glass
[PB85-106391] 12 p1868 N85-21717
Reliability of structural brittle materials
12 p1948 N85-22222
Study for prediction of rotor/wake/fuselage interference, part 1
[NASA-CR-177340-VOL-1] 13 p1965 N85-22346
Study for prediction of rotor/wake/fuselage interference. Part 2: Program users guide
[NASA-CR-177340-VOL-2] 13 p1966 N85-22347
Prediction of the resistance of structural materials to cavitation erosion
[BLL-DRIC-TRANS-7435-(3623.66)]
13 p2020 N85-22659
Development of a sintered shim
[DE85-006183] 13 p2025 N85-22685
Comparison of dynamic-tension and constant-load strength characteristics of heat-resistant materials
13 p2030 N85-22722
Characteristics of surface crack development in AlTiS aluminum alloy during slow-cycle loading
13 p2034 N85-22745
Steady-state reaction of three-layered cylindrical shell to effect of moving load 13 p2047 N85-22811
Axisymmetrical oscillations of shell systems subjected to impulse loads 13 p2047 N85-22814
Nonlinear behavior and stability of thin spherical shells subjected to non-axisymmetrical loading
13 p2048 N85-22821
Elysium region, Mars: Tests of lithospheric loading models for the formation of tectonic features
13 p2200 N85-23650
Advanced life analysis methods. Volume 4: Tabulated test data for attachment lugs
[AD-A151016] 14 p2219 N85-23780
Load carrying capacity of double circular arc gears
14 p2221 N85-23776
Case depth on flanks of gears for helicopter gearboxes 14 p2222 N85-23780
The observation and interpretation of gear tooth failures 14 p2224 N85-23792
A preliminary investigation of the dynamic force-calibration of a magnetic suspension and balance system
[NASA-CR-172580] 14 p2228 N85-23808
Wave motion of three-component medium under load moving on plane boundary 14 p2277 N85-24105
Computations for segmented radial bearings
14 p2286 N85-24180
Work of axial bearing under dynamic loading
14 p2288 N85-24182
Recent developments in the dynamics of advanced rotor systems
[NASA-TM-86680] 14 p2317 N85-24320
Effect of flight sequences in complex load histories on crack front marking 14 p2318 N85-24326
Generation of marker lines by means of marker loads
14 p2318 N85-24327
Generation of marker lines on fatigue fracture surfaces 14 p2319 N85-24328
Periodic loading sequences for the systematic marking of fatigue crack fracture surfaces
14 p2319 N85-24329
Modifications of flight by flight load sequences to provide for good fracture surface readability
14 p2319 N85-24330
On the use of marker loads and replicas for measuring growth rates for small cracks 14 p2319 N85-24331
On the use of marker loads for fatigue crack growth measurements 14 p2319 N85-24332
Crack propagation under constant and variable stress amplitudes: A comparison of calculations based on the Striation spacing and tests 14 p2320 N85-24336
Finite element model for creep in composite masonry
[PB85-150324] 14 p2322 N85-24347
Comets and nongravitational forces
14 p2437 N85-25038
Unsteady gas dynamics problems related to flight vehicles
[AD-A151187] 15 p2484 N85-25218
Pseudo bipolar nickel-cadmium batteries used as filter elements to pulsed current loads
[AD-A151192] 15 p2547 N85-25717
Structural development and gravity
15 p2608 N85-26071
Finite-difference computations of rotor loads
[NASA-TM-86662] 16 p2700 N85-26669
Automatic flight control modes for the AFTI/F-111 mission adaptive wing aircraft 16 p2714 N85-26758
Rotordynamics 16 p2737 N85-26866
Effects of bearing deadbands on bearing loads and rotor stability 16 p2737 N85-26889
Breakway friction and dynamic friction/wear measurements of various ceramic materials from 25 C (75 F) to 650 C (1200 F)
[NASA-CR-174803] 16 p2754 N85-26994
Experimentally determined distribution of stress around a horizontally loaded model pile in dense sand
[CE-43] 16 p2796 N85-27239
Adaptation of continuous beams and the method of optimizing the flexibility of their elastic supports. Theorem on maximal adaptation loading, supplement
[REPT-10/1984-SUPPL] 16 p2797 N85-27241
Fatigue damage and small crack growth during biaxial loading 16 p2797 N85-27247
Dynamic response of shells and plates subjected to variable magnitude traveling loads
16 p2798 N85-27250
Monitoring of turbo-machines by shaft vibration measurement
[BLL-CE-TRANS-7900-(9022.09)]
16 p2799 N85-27255
Some advances in experimentation supporting development of viscoplastic constitutive models
[NASA-CR-174855] 16 p2799 N85-27260
Structural Integrity and Durability of Reusable Space Propulsion Systems
[NASA-CP-2381] 17 p2910 N85-27941
Composite loads spectra for select space propulsion structural components: Probabilistic load model development 17 p2912 N85-27954
Dynamic creep buckling: Analysis of shell structures subjected to time-dependent mechanical and thermal loading 17 p2913 N85-27959
Overload effects on sustained load crack growth at elevated temperature
[AD-A153223] 17 p2931 N85-28091
The Mises yield condition for thin rotationally symmetric shells
[BLL-BISI-TRANS-22047-(9022.06)]
17 p2978 N85-28409

Finite element thermal-structural analysis of cable-stiffened space structures
[AD-A153622] 18 p3066 N85-28963
B-52B/DTV (Drop Test Vehicle) flight test results: Drop test missions
[NASA-CR-171530] 19 p3215 N85-29934
General Aviation Crashworthiness Project. Phase 2: Impact severity and potential injury prevention in general aviation accidents
[PB85-917002] 19 p3215 N85-29938
Aircraft rotor blade with passive tuned tab
[NASA-CASE-ARC-11444-1] 19 p3217 N85-29947
A study of the stress wave factor technique for the characterization of composite materials
[NASA-CR-174870] 19 p3231 N85-30035
Load-carrying capabilities of refractory alloys for space reactor power applications
[DE85-010586] 19 p3240 N85-30087
Fatigue resistance of VT3-1 titanium alloy related to surface cold working 19 p3245 N85-30120
Temperature and surface damage under lubricated sliding-rolling contacts 19 p3280 N85-30338
Acoustic emission study of fatigue crack extension position in a stress cycle 19 p3283 N85-30355
Residual stress distributions in (plastically) surface deformed two-phase materials 19 p3283 N85-30356
Estimation of dynamic rotor loads for the rotor systems research aircraft: Methodology development and validation
[NASA-CR-177362] 20 p3393 N85-31045
Some advances in experimentation supporting development of viscoplastic constitutive models 20 p3468 N85-31545
A comparison of smooth specimen and analytical simulation techniques for notched members at elevated temperatures 20 p3468 N85-31548
Estimation of power-law creep parameters from bend test data
[PB85-183406] 20 p3472 N85-31579
The effect of stress and hot corrosion on nickel-base superalloys
[AD-A154722] 21 p3566 N85-32181
A comparison of experimental and theoretical results for rotordynamic coefficients of four annular gas seals
[NASA-CR-176086] 21 p3596 N85-32332
Measurement and analysis of critical crack tip processes during fatigue crack growth
[NASA-CR-172597] 21 p3598 N85-32342
Analysis of long bone and vertebral failure patterns
[AD-A154798] 21 p3663 N85-32758
Pressure-shear loading of PBX-9404
[DE85-009962] 23 p3921 N85-34296
Inertial stresses and deformations in mechanisms 23 p3924 N85-34320
Tensile testing apparatus
[NASA-CASE-LAR-13243-1] 23 p3933 N85-34375
The design and analysis of single flank transmission error tester for loaded gears
[NASA-CR-176163] 23 p3937 N85-34404
Further studies on liquid sloshing
[PB85-198695] 24 p4095 N85-35366
Stress-intensity factors for circumferential surface cracks in pipes and rods under tension and bending loads
[NASA-TM-87594] 24 p4101 N85-35424
Prediction of plasticity characteristics for three-dimensional fracture specimens comparison with experiment
[AD-A156425] 24 p4102 N85-35430
Evaluation of the crack plane equilibrium model for predicting plastic fractures
[DE85-005558] 24 p4102 N85-35431
Response of a BWR Mark 2 containment vessel head to loads beyond the design basis
[DE85-010524] 24 p4103 N85-35432
Simulation of lattice damage due to dynamic loading
[DE85-008468] 24 p4162 N85-35806

LOCAL GROUP (ASTRONOMY)
NT ANDROMEDA GALAXIES
NT MILKY WAY GALAXY

LOCALIZATION
U POSITION (LOCATION)

LOCATION
U POSITION (LOCATION)

LOCI
Surfaces with canonical hyperplane sections
[CWI-TRACT-1] 14 p2410 N85-24858
Search for positron annihilation line and continuum radiation from the Galactic Center
[OG-2.5-5] 22 p3869 N85-33962

LOCKHEED AIRCRAFT
NT C-5 AIRCRAFT
NT C-141 AIRCRAFT
NT F-104 AIRCRAFT
NT L-1011 AIRCRAFT
NT P-3 AIRCRAFT
NT T-33 AIRCRAFT
NT U-2 AIRCRAFT

LOCKHEED C-5 AIRCRAFT
U C-5 AIRCRAFT

LOCKHEED U-2 AIRCRAFT
U U-2 AIRCRAFT

LOCKING
NT LASER MODE LOCKING
Storage life of thermal detents
[DE84-016934] 04 p0476 N85-13030
Hydraulic locking bolt work system
[AD-D011299] 06 p0815 N85-15174
A simulator for determining the performance of transaction manager and lock manager combinations in a database
[AD-A147827] 07 p1055 N85-16696
Elbow and knee joint for hard space suits and the like
[NASA-CASE-ARC-11610-1] 11 p1697 N85-20686
Locking of Automotive Products hydraulic selector valves
[BAE-EXPER/NOTE-459] 15 p2567 N85-25839
Self-locking mechanical center joint
[NASA-CASE-LAR-12864-1] 19 p3279 N85-30336
Dual optical mechanical position tracker
[AD-D011739] 22 p3844 N85-33811
Variable length strut with longitudinal compliance and locking capability
[NASA-CASE-MFS-25007-1] 23 p3937 N85-34401

LOCKS
An improved servo-controlled inertial clock for laboratory tests of general relativity 19 p3376 N85-30955

LOCKS (FASTENERS)
Connector/nitinol delta contact force device
[AD-D011467] 10 p1481 N85-19349
Mechanical locking between multi-layer printed wiring board conductors and through-hole plating
[AD-D011477] 10 p1481 N85-19352
Code lock with microcircuit 13 p2071 N85-22935

LOCOMOTION
NT WALKING
Influence of simulated weightlessness on the motility of the acellular slime mold Physarum polycephalum 05 p0669 N85-14430
Global optical metrics for self-motion perception
[AD-P004333] 09 p1271 N85-17987
Study of the motion of agricultural vehicles on steep grass-covered slopes
[AD-P004290] 09 p1408 N85-18867
Non-rigid body motion 23 p3964 N85-34576

LOCOMOTIVES
DELTA: An expert system for diesel electric locomotive repair
[AD-P003941] 02 p0248 N85-11621
Antenna matching device tuning for type ZhRU radiostations 06 p0785 N85-15017
Natural gas the new locomotive fuel
[DE84-901824] 09 p1302 N85-18179
Industry review: Locomotive dynamic characterization test-analysis
[NASA-CR-171467] 19 p3382 N85-30981

LOFTING
Semianalytic modeling of aerodynamic shapes
[NASA-TP-2413] 12 p1771 N85-21120

LOG PERIODIC ANTENNAS
Defocusing losses in a log periodic-fed reflector
[AD-A151616] 15 p2547 N85-25722
Frequency independent parabolic phased antenna array of log periodic antennas 22 p3774 N85-33367

LOGARITHMIC RECEIVERS
A multi-channel radar receiver
[AD-A156058] 24 p4087 N85-35333

LOGARITHMS
Applications of the simple-layer logarithmic potential 05 p0718 N85-14606
Generating positively correlated random variables from a sequence of independent random variables with symmetric logarithmically concave densities
[AD-A148436] 08 p1216 N85-17658
Applicability of log-normal model to probabilistic description of quasi-pulse interference 13 p2084 N85-23014
Parallel update of minimum spanning trees in logarithmic time
[AD-A150497] 13 p2151 N85-23357
Adiabatic thermal models for planetary bodies 22 p3857 N85-33881

LOGIC
Mental models of invisible logical networks 05 p0708 N85-14544

LOGIC CIRCUITS
NT THRESHOLD GATES
Basic EMC (Electromagnetic Compatibility) technology advancement for C3 systems, macromodeling of digital circuits, volume 2B
[AD-A146333] 03 p0359 N85-12306
Restructurable VLSI program
[AD-A148145] 08 p1157 N85-17301
Deployment sequence mode selection system for aircraft ejection seat
[AD-D011464] 10 p1422 N85-18966
Development of mass-producible line-focus tracking concentrating solar collectors. Category 2: Trackers
[DE85-002673] 10 p1512 N85-19543
Dusign of explosive logic elements
[DE84-009611] 11 p1614 N85-20148
15KW power supply development
[DE85-001057] 11 p1629 N85-20260
Transistor-transistor logic microcircuit tester 12 p1842 N85-21556
Basic EMC (electromagnetic interference) technology advancement for c3 systems. Volume 3A: Probabilistic analysis of combinational circuits with random delays
[AD-A150349] 13 p2055 N85-22866
Development of a planar heterojunction bipolar transistor for very high speed logic
[AD-A150374] 13 p2064 N85-22895
Dataflow computation
[CWI-TRACT-6] 14 p2406 N85-24833
All-optical logic gates with external switching by laser and incoherent radiation 16 p3187 N85-29766
Electro-optic techniques for VLSI interconnect 16 p3188 N85-29774
Electron lithography STAR design guidelines. Part 1: The STAR user design manual
[NASA-CR-170765] 20 p3513 N85-31840
Electron lithography STAR design guidelines. Part 2: The design of a STAR for space applications
[NASA-CR-170766] 20 p3513 N85-31841
Electron lithography STAR design guidelines. Part 3: The mosaic transistor array applied to custom microprocessors. Part 4: Stores logic arrays, SLAs implemented with clocked CMOS
[NASA-CR-170767] 20 p3514 N85-31842
Design of a sixteen-bit pipelined adder using CMOS bulk P-well technology
[AD-A155043] 21 p3560 N85-32260
Digital integrated circuits 21 p3669 N85-32787
Method of characterizing critical timing paths and analyzing timing related failure modes in very large scale integrated circuits
[AD-D011731] 22 p3759 N85-33298
Hardware realization of digital filters without multipliers 22 p3766 N85-33340
Computer simulation of integrated injection logic 22 p3767 N85-33349
Research on distributed artificial intelligence
[AD-A155356] 22 p3833 N85-33733

LOGIC DESIGN
Basic EMC (Electromagnetic Compatibility) technology advancement for C3 systems, macromodeling of digital circuits, volume 2B
[AD-A146333] 03 p0359 N85-12306
Knowledge representation and natural-language semantics
[AD-A146025] 03 p0409 N85-12615
Research on introspective systems
[AD-A146406] 06 p0870 N85-15530
Representation and refinement of visual specifications in PegaSys
[AD-A148733] 09 p1366 N85-18598
Dialog system of preparation and presentation of visual information 10 p1526 N85-19622
Logic analyzer survey and reviews
[BAE-861/ELO/1645] 15 p2621 N85-26151
Optimal design and use of retry in fault tolerant real-time computer systems
[NASA-CR-175920] 17 p3015 N85-29643
Electron lithography STAR design guidelines. Part 1: The STAR user design manual
[NASA-CR-170765] 20 p3513 N85-31840
Electron lithography STAR design guidelines. Part 2: The design of a STAR for space applications
[NASA-CR-170766] 20 p3513 N85-31841
Electron lithography STAR design guidelines. Part 3: The mosaic transistor array applied to custom microprocessors. Part 4: Stores logic arrays, SLAs implemented with clocked CMOS
[NASA-CR-170767] 20 p3514 N85-31842
Modeling of discrete devices with use of multivalued logic and nomograms 22 p3768 N85-33351
Filtration of higher harmonic components in two-level digital computing synthesizers 22 p3778 N85-33410

LOGIC NETWORKS
U LOGIC CIRCUITS

LOGIC PROGRAMMING
TCAS 2 logic performance during phase one operational evaluation
[DOT/FAA/PM-84/20] 05 p0595 N85-13793
A distributed expert system for Space Shuttle flight control 05 p0602 N85-13836

Dialog system of preparation and presentation of visual information 10 p1526 N85-19622
Characterizing the parallelism in rule-based expert systems
[DE85-002432] 12 p1919 N85-22047
Evaluation of expert systems 12 p1947 N85-22229
Execution of cellular logic operations in spatially continuous, bit slice processor 14 p2401 N85-24796
Modeling of discrete devices with use of multivalued logic and nomograms 22 p3768 N85-33351

LOGICAL ELEMENTS
Circuit engineering and technological optimization of very high speed LSI logic elements and transistor structures 03 p0347 N85-12237
The automated reasoning system ITP
[ANL-84-27] 12 p1914 N85-22016
Bipolar nonswitching logic arrays: Universal components of function expanders for computation of elementary functions 14 p2400 N85-24797
Execution of cellular logic operations in spatially continuous, bit slice processor 14 p2401 N85-24796
Development of new circuit symbols for binary logic elements
[MBB-Z-39/85-O] 17 p3014 N85-26640

LOGISTICS
NT SPACE LOGISTICS
Software engineering environments for mission critical applications: STARS alternative programmatic approaches
[AD-A145285] 02 p0241 N85-11571
An overview of the Joint Logistics Commanders Automatic Test Equipment Panel
[AD-P003916] 02 p0244 N85-11596
Constraint-based scheduling in an intelligent logistics support system: An artificial intelligence approach
[AD-A145813] 02 p0293 N85-11900
Future robotics program at San Antonio ALC (Air Logistics Center)
[AD-P004011] 03 p0309 N85-11991
Supply center processes
[AD-P004014] 03 p0309 N85-11993
Logistics support costs for the B-1B aircraft can be reduced
[AD-A145846] 03 p0309 N85-11996
Distribution and storage of aviation turbine fuel for military operations in northern Australia
[AD-A147180] 07 p0935 N85-15921
A description of a logistically ideal aircraft
[AD-A148425] 08 p1084 N85-16686
Adapting logistics models to a microcomputer for interface with computer-aided design systems
[AD-A147666] 08 p1202 N85-17566
A preliminary analysis of C-12 aircraft usage by the Navy Air Logistics System
[AD-A151921] 16 p2694 N85-26634
A Dictionary-Directory System (DDS) for the SPLICE system
[AD-A152223] 16 p2878 N85-27759
Bayesian inference and diagnostics for the 3 parameter logistic model
[AD-A153640] 18 p3175 N85-29661
EOQ (Economic Order Quantity) range model
[AD-A153709] 19 p3379 N85-30965

LOGISTICS MANAGEMENT
NT INVENTORY CONTROLS
NT INVENTORY MANAGEMENT
An overview of the Joint Logistics Commanders Automatic Test Equipment Panel
[AD-P003916] 02 p0244 N85-11596
Benefit value to the Air Force of the GIDEP (Government Industry Data Exchange Program) alert
[AD-A145470] 02 p0292 N85-11897
An update of the functional requirements of the Naval Aviation Logistics Command Management Information System (NALCOMIS)
[AD-A146565] 06 p0871 N85-15532
Managing recoverable aircraft components in the PPB and related processes: Executive summary
[AD-A146805] 07 p1050 N85-16667
Feasibility of measuring technical productivity improvements in Air Force Logistics Command depot-level maintenance using the Data Envelopment Analysis (DEA) and Constrained Facet Analysis (CFA) models
[AD-A147329] 07 p1052 N85-16676
Utilization of Increased Airlift Capability (UIAC) study
[AD-A148669] 08 p1081 N85-16847
On maximizing the expected lifetime of replaceable systems
[AD-A150003] 12 p1862 N85-21680
Managing recoverable aircraft components in the PPB (Planning, Programming and Budgeting) and related processes. Technical volume
[AD-A152014] 15 p2457 N85-25169
Improving the defense energy information system (DEIS)
[AD-A153524] 18 p3200 N85-29849
An analysis of the materiel fielding plan for the SINCGARS (Single Channel Ground and Airborne Radio System) radio
[AD-A155101] 21 p3576 N85-32238
Security controls in the Stockpoint Logistics Integrated Communications Environment (SPLICE)
[AD-A155536] 21 p3576 N85-32244
DoD Value Engineering conference report. Value Engineering (VE): A tool that benefits line management. Part 4, Workshop B: VE on spare parts
[AD-A156070] 24 p4163 N85-35813

LONG DURATION EXPOSURE FACILITY
Feasibility of long duration ballooning in Antarctica
[PB84-240571] 04 p0541 N85-13443
The heavy ions in space experiment
[OG-9.1-10] 23 p4023 N85-34936

LONG DURATION SPACE FLIGHT
USSR report: Space Biology and Aerospace Medicine, volume 18, no. 4, July - August 1984
[JPRS-USB-84-006] 01 p0091 N85-10611
Compensatory and adaptive regional hemodynamic reactions to weightlessness during long-term spaceflights 01 p0091 N85-10616
Nutritional models for space travel from chemically defined diets
[NASA-CR-3850] 03 p0402 N85-12561
NASA welding assessment program
[NASA-CR-175512] 12 p1859 N85-21661
Rat tissue opioid peptide content during long-term hypokinesia 12 p1904 N85-21954
Comments on Salyut-7 150-day flight 13 p1977 N85-22406
Research opportunities in human behavior and performance
[NASA-CR-3886] 13 p2142 N85-23299
Nutrition in space flight: Some thoughts 14 p2394 N85-24743
Fluid-electrolyte responses during prolonged space flight: A review and interpretation of significant findings
[NASA-CR-171878] 15 p2617 N85-26124
The controlled ecological life support system 15 p2668 N85-26603
Research on zero-gravity botany apparatus 16 p2723 N85-26811
Construction and functioning of extended orbital systems 16 p2724 N85-26814
BLSS: A contribution to future life support 18 p3155 N85-29534
Advanced regenerative environmental control and life support systems: Air and water regeneration 18 p3155 N85-29535
Extended mission life support systems 18 p3157 N85-29547
Cosmonauts' postural reactions after long-term missions aboard Salyut-6 orbital station 19 p3323 N85-30585
Blood serum enzyme activity following long term spaceflights 19 p3326 N85-30604
Psychological issues relevant to astronaut selection for long-duration space flight: A review of the literature
[AD-A154051] 19 p3330 N85-30627
Air Force Human Resources Laboratory research and development summary
[AD-A154310] 19 p3331 N85-30632
Living aloft: Human requirements for extended spaceflight
[NASA-SP-483] 21 p3666 N85-32772
Cosmonauts' cardiovascular system function during long-term orbital flights aboard Salyut-6 station 22 p3733 N85-33141
Fluid-electrolyte metabolism and renal function in cosmonauts following 185-day spaceflight 23 p3952 N85-34495

LONG RANGE NAVIGATION
U LORAN

LONG RANGE WEATHER FORECASTING
Illinois Climate: Trends, Impacts and Issues
[PB84-211966] 01 p0066 N85-10577
Summary of 1984 Atlantic seasonal tropical cyclone activity and verification of author's forecast 03 p0395 N85-12520
Spectral energetics diagnoses and FGGE spectral observing periods and energetics analyses of forecast experiments with GLAS GCM 05 p0683 N85-14391
Forecasting water temperature decline and freeze-up in rivers
[AD-A147068] 07 p0967 N85-16274
A weather service for agriculture 16 p2830 N85-27450
An appraisal of the duration of the recent drought in northeast Brazil and a forecast for 1985
[INPE-3477-PRE/720] 16 p2934 N85-27478
Accuracy and operational use of medium and extended range numerical atmospheric forecasts: A review
[AD-A155027] 21 p3635 N85-32579
Model projections of time-dependent response to increasing carbon dioxide
[DE85-013326] 22 p3816 N85-33641

LONG TERM EFFECTS
Long-term thermal aging of 2 graphite-polyimide composite materials
[NASA-TP-2369] 03 p0325 N85-12094
Modeling long-term changes in forested landscapes and their relation to the Earth's energy balance 05 p0653 N85-14194
Effects of prolonged hypokinesia on nervous system 08 p1194 N85-17524
Durability and behavior of prestressed concrete beams. Posttensioned concrete beam investigation, supplemental laboratory tests of beams exposed from 1981 to 1982
[AD-A148821] 09 p1304 N85-18191
Evaluation and prediction of long-term environmental effects of nonmetallic materials
[NASA-CR-171353] 10 p1450 N85-19137
Synthetic fuels policy
[GPO-34-227] 11 p1613 N85-20143
Long-range electronics program outlined 11 p1700 N85-20687
Long-term strength and fracture criteria for EI698VD alloy under complex stress conditions 13 p2030 N85-22723
Influence of annealing on cyclic and short-term strength of thin sheets of VT1-0 titanium and OT4 alloy 13 p2031 N85-22727
Effects of interactive transport and scavenging of smoke on the calculated temperature change resulting from large amounts of smoke
[DE85-006450] 14 p2378 N85-24684
Design and fabrication of a unique electromechanical machine for long-term fatigue testing
[DE85-006524] 15 p2580 N85-25912
Quaternary North Atlantic surface paleoceanography in regions of potential deep-water formation 15 p2602 N85-26036
Effects of long-term low-level radiofrequency radiation exposure on rats. Volume 7: Metabolism, growth and development
[AD-A150829] 15 p2615 N85-26112
Assessing the short- and long-term health effects of decompression sickness among US Navy divers
[AD-A151867] 15 p2618 N85-26132
The cumulative effects of long term exposure to low levels of radiofrequency radiation (RFR) 16 p2776 N85-27132
Acid precipitation in North America: 1980, 1981 and 1982 annual data summaries from acid deposition system data base
[PB85-162477] 16 p2822 N85-27410
Long term exposure of animals to antiorthostatis (-90 deg) as a model of critical homeostatic disturbances 19 p3324 N85-30592
Short term determination of the creep properties of high temperature materials
[CRIF-MT-160] 20 p3432 N85-31258
Predicting photothermal field performance 21 p3606 N85-32404
Topics in electrochemical degradation of photovoltaic modules 21 p3608 N85-32410
Voyager 0.2-lbf thruster valve assembly short pulse test report
[NASA-CR-176121] 22 p3741 N85-33185
Climatic consequences of very high CO2 levels in Earth's early atmosphere 22 p3854 N85-33865
Lipogenesis in rat liver after flight aboard Cosmos-1129 biosatellite 23 p3954 N85-34508
Long-period cosmic ray variations and their altitude dependence
[SH-6.1-19] 23 p4048 N85-35091
High temperature corrosion of ceramics
[DE85-013481] 24 p4083 N85-35303

LONG WAVE RADIATION
The Martian climate: Energy balance models with CO2/H2O atmospheres
[NASA-CR-174073] 03 p0443 N85-12849
Year-to-year variability of components of Earth's radiation budget according to satellite measurement data 16 p2725 N85-26821
Influence of phonon interaction on width and form of Mandelstam-Brillouin optical scattering line 21 p3696 N85-32962
Sporadic radio emission connected with a definite manifestation of solar activity in the near Earth space
[SH-10.1-8] 23 p4053 N85-35139

LONG WAVES (METEOROLOGY)
U PLANETARY WAVES

LONGERONS
Section 1. Method of determining mode shapes and natural frequencies of the NASA unmodified test structure. Section 2. Continuous beam closed from solution to the NASA-LSS astromast torsional vibration, appendix E
05 p0803 N85-13844
Modelling and identification of the structural properties of an astromast
[CRC-1374] 09 p1329 N85-18352
Efficient structures for geosynchronous spacecraft solar arrays
[NASA-CR-174448] 10 p1428 N85-19004
The residual strength of cracked specimens representing a section of the mirage into wing main spar
[ARL/STRUC-R-408] 12 p1865 N85-21699
Definition of ground test for verification of large space structure control
[NASA-CR-171438] 15 p2492 N85-25377
Tensile and fracture toughness properties of Mirage III spars
[AR-003-019] 15 p2578 N85-25899
Fatigue lives of specimens representing critical locations in Mirage 3 spars under Australian and Swiss test spectra
[ARL-STRUC-R-415] 24 p4064 N85-35187
LONGITUDE
Computer-generated latitude and longitude templates for rapid determination of geographic positions in Alaska
04 p0516 N85-13286
Simultaneous determination of the xi and eta components of vertical deflection with a prism astrolabe
[SER-S-270-MITT-171] 09 p1343 N85-18450
Longitudinal distribution of cosmic rays in the heliosphere
[SH-4.1-14] 23 p4006 N85-34837
LONGITUDE MEASUREMENT
Determination of the longitude differences Munich-Lissabon-San Fernando, Munich-Wettzell, and Munich-Karlsruhe-Niederrellerberg
[ASTRON-GEODAET-ARB-44]
04 p0524 N85-13353
Determination of astronomical longitude differences for the European longitude reference system for 1980. Relative right ascension corrections for 125 FK4 and FK4 Sup stars
04 p0524 N85-13354
Determination of astronomical longitude differences: Munich, Karlsruhe, Niederrellerberg in 1974
04 p0524 N85-13355
The longitudinal development of muons in cosmic ray air showers at energies 10(15) - 10(17) eV
[HE-4.3-12] 24 p4192 N85-36006
Longitudinal development of muons in large air showers studies from the arrival time distributions measured at 900m above sea level
[HE-4.7-4] 24 p4199 N85-36055
LONGITUDINAL CONTROL
Flight tests with a new helicopter Force Feel System (FFS)
08 p1075 N85-16818
A feasibility study of tree-tip rotor application as a passive cyclic control device
09 p1279 N85-18046
Remote pivot decoupler pylon: Wing/store suppression
[NASA-CASE-LAR-13173-1] 11 p1584 N85-19981
Total energy-rate feedback for automatic glide-slope tracking during wind-shear penetration
[NASA-TP-2412] 14 p2226 N85-23801
In-flight investigation of the influence of pitch damping and pitch control effectiveness on landing approach flying qualities of statically unstable transport aircraft
[DFVLR-FB-84-12] 17 p2900 N85-27880
Transonic and supersonic wind tunnel tests on control effectiveness on schematic missile configurations
[FFA-TN-1983-20] 20 p3389 N85-31020
Transonic and supersonic wind tunnel tests on control effectiveness on schematic missile configurations: Supplement
[FFA-TN-1983-20-SUPPL] 20 p3389 N85-31021
Longitudinal tune control in synchrotrons
[DE85-010745] 20 p3527 N85-31937
Analysis of flexible aircraft longitudinal dynamics and handling qualities. Volume 1: Analysis methods
[NASA-CR-177943-VOL-1] 24 p4066 N85-35202
Analysis of flexible aircraft longitudinal dynamics and handling qualities. Volume 2: Data
[NASA-CR-177943-VOL-2] 24 p4067 N85-35203
LONGITUDINAL STABILITY
Approximate neutral point of a subsonic canard aircraft
[NASA-TM-86694] 15 p2462 N85-25205
Static longitudinal stability and control characteristics of the Fokker F27 Friendship calculated by simple handbook methods
[VTH-LR-394] 16 p2711 N85-26728
Realisation of relaxed static stability on a commercial transport
17 p2903 N85-27890
Active control technology experience with the Space Shuttle in the landing regime
17 p2903 N85-27900
Contributions on the subject of longitudinal movements of aircraft in wind shears
[NASA-TM-77837] 18 p3139 N85-29432
LONGITUDINAL WAVES
NT PLANE WAVES
Generation of longitudinal acoustic waves by modulated helicon waves — nonlinear steady state waves in metals
13 p2090 N85-23049
Surface acoustic wave structure and volume waves
15 p2525 N85-25586
The longitudinal thickness of air-shower fronts
[OG-9.5-1] 23 p4030 N85-34978
LONGSHORE CURRENTS
U COASTAL CURRENTS
LOOP ANTENNAS
Impedance measurements on a VLF multi-turn loop antenna in a space plasma simulation chamber
[AD-A145104] 04 p0492 N85-13141
Tactical HF communication for military helicopters using the NVIS mode
06 p1074 N85-16807
Loop radiating elements
[AD-D011409] 08 p1158 N85-17308
Experimental measurements of the ion cyclotron antennas' coupling and RF characteristics
[DE85-011569] 23 p3982 N85-34694
LOOPS
Design and performance of sampled data loops for subcarrier and carrier tracking
05 p0623 N85-13966
Wideband phase keyers
12 p1839 N85-21544
New results on the PLL false lock phenomenon
12 p1948 N85-22236
Normal mode calculations for fuselage type intricate structures by regarding them as systems with superposed constraints
13 p2048 N85-22817
Reliability report for communication networks
[AD-A153784] 18 p3090 N85-29127
Low-profile fastener
[AD-D011667] 19 p3280 N85-30343
Quarter-inch streaming tape drive application with the Serial ASCII Instrumentation Loop (SAIL) system
[AD-A155954] 22 p3759 N85-33295
General design principles of high speed frequency synthesizers based on phase synchronization systems
22 p3779 N85-33417
Wide-band phase locked loop amplifier apparatus
[AD-D011720] 23 p3927 N85-34337
LORAN
NT LORAN C
Field tests of the real-data acquisition system for the NASA-LaRC differential absorption lidar
[NASA-CR-174020] 01 p0106 N85-10710
LORAN C
National Airspace System Plan: Facilities, equipment and associated development
16 p2704 N85-26692
The time and frequency comparisons via Loran-C and National TV Network in Yugoslavia
19 p3109 N85-29248
Experiments of a LORAN-C aided recovery system and a proposal of its application to rescue system
20 p3404 N85-31121
LORAN-C harbor and harbor entrance survey: Charleston, South Carolina
[AD-A154675] 21 p3554 N85-32106
Nonlinear digital phase-locked loops with application to Loran-C receivers
24 p4063 N85-35178
LORENTZ FORCE
Update of thermal conductivity and electrical resistivity of electrolytic iron, tungsten and stainless steel
[PB85-115814] 12 p1803 N85-21311
Variations in the small-scale galactic magnetic field and short time-scale intensity variations of extragalactic radio sources
20 p3549 N85-32084
Cerenkov counters for high energy nuclei: Some new developments
[OG-9.1-5] 23 p4023 N85-34931
On mini-cluster observed by Chacaltaya emulsion chamber experiment
[HE-3.6-12] 24 p4185 N85-35959
LORENTZ GAS
Heat flux in Lorentzian plasma
[IPPJ-704] 12 p1935 N85-22158
LORENTZ TRANSFORMATIONS
The solar dynamo and the complex Lorenz equations
14 p2447 N85-25107
Comment on quantum effects on 4-dimensional space-time symmetries
[DE85-007760] 16 p2872 N85-27722
Modulation transfer function for two-point and periodic objects using Gaussian and Lorentzian resolution functions
[PB85-167557] 19 p3368 N85-30691
Hadron thermodynamics in relativistic nuclear collisions
[HE-1.1-8] 24 p4171 N85-35858
LOS ALAMOS TURRET REACTOR
U HIGH TEMPERATURE NUCLEAR REACTORS
LOSSES
Predicted heat transfer loss in the expansion cylinder of a 2 cylinder reciprocating engine
[AD-A144831] 01 p0055 N85-10366
Voluntary dehydration and electrolyte losses during prolonged exercise in the heat
[AD-A145157] 01 p0095 N85-10639
The effect of temperature on the radiation induced losses of large diameter GPS (Germanium phosphosilicate) and GBS core optical fibers
[AD-A145409] 02 p0280 N85-11823
An improved computer model for prediction of axial gas turbine performance losses
[NASA-CR-174246] 07 p0904 N85-15724
Age life prediction of nylon 66 parachute materials. Part 1: Mechanical properties
[AD-A147698] 08 p1170 N85-17378
Current status of trailing edge loss calculation for a turbine blade
[PNR-90244] 09 p1282 N85-18061
Effects of slip on energy distribution between tyre and soil
[AD-P004263] 09 p1404 N85-18839
Kinetics of reaction of metals and non-metals during diffusion welding
11 p1602 N85-20076
Hot stars: Six years of progress
11 p1743 N85-20963
The effect of jamming/deception on decision making
[AD-A149740] 12 p1828 N85-21472
Reducing electric power losses in discharge chamber of induction plasmatron
12 p1841 N85-21553
Beam loss due to the aperture limitation resulting from intrabeam scattering
[DE85-005138] 12 p1930 N85-22124
Optical reflectometer for multimode fiber lightpipes
13 p2075 N85-22961
Effect of diaphragm leakage on turbine stage characteristics
14 p2286 N85-24166
Defocusing losses in a log periodic-fed reflector
[AD-A151616] 15 p2547 N85-25722
Finite element prediction of loss factors for structures with frequency-dependent damping treatments
15 p2576 N85-25889
Multi-access fiber optic data bus using FDM/FSK
[NASA-CR-175739] 15 p2621 N85-26152
Fuel and oxidizer turbine loss analysis
16 p2739 N85-26900
Histological and compositional responses of bone to immobilization and other experimental conditions
[NASA-CR-175837] 16 p2841 N85-27518
Electrochemical and morphological study of the effect of temperature on the restructuring and loss of capacity of alkaline battery electrodes
[DE85-006869] 18 p3129 N85-29378
Study of Kapton under simulated shuttle environment
[NASA-CR-176003] 19 p3225 N85-29997
Receiver loss study of optimized solar central receiver systems as a function of receiver thermal loss per unit area
[DE85-010631] 19 p3268 N85-30265
Important loss mechanisms in high-efficiency solar cells
21 p3610 N85-32424
Kinetic loss experiments on Mite
[DE85-012826] 24 p4158 N85-35780
LOSSLESS MATERIALS
Microwave surface resistivity of several materials at ambient temperature
10 p1463 N85-19226
LOSSY MEDIA
Joint services electronics program
[AD-A145085] 01 p0042 N85-10276
Impedance of vertical dipoles above a dissipative ground
[REPT-S-152] 02 p0192 N85-11287
General image theory for the Sommerfeld problem
[REPT-S-154] 02 p0193 N85-11288
Numerical methods for analyzing electromagnetic scattering
[NASA-CR-175507] 12 p1823 N85-21438
Normal modes in an overmoded circular waveguide coated with lossy material
[NASA-CR-176186] 24 p4085 N85-35320
LOUDNESS
Contribution of tonal components to the overall loudness, annoyance and noisiness of noise: Relation between single tones and noise spectral shape
[NASA-CR-3992] 15 p2645 N85-26317
LOUDSPEAKERS
Acoustic scaling: The development of improved instrumentation
[BBC-RD-1985/7] 24 p4145 N85-35804

LOUISIANA
The influence of the number of ground control points on the scene-to-map registration accuracy — Kansas, Louisiana, Mississipp, and Missouri
07 p0986 N85-16264
Image variance and spatial structure in remotely sensed scenes — South Dakota, California, Missouri, Kentucky, Louisiana, Tennessee, District of Columbia, and Oregon
07 p0986 N85-16265
Revised Uniform Summary of Surface Weather Observations (RUSSWO). England AFB, Alexandria, Louisiana, parts A-F
[AD-A146920] 07 p1006 N85-16391
LOUVERS
Pre-HOST high temperature crack propagation
02 p0141 N85-10956
Vertical solar louver project
[DE84-017335] 11 p1676 N85-20558
Fast shutter apparatus
[DE85-006501] 23 p3928 N85-34343
LOVE WAVES
Love and Rayleigh waves in irregular ground
04 p0523 N85-13348
Resolution of 2-dimensional seismologic problems by a finite element approximation. Application to the Love wave propagation through the Atlantic border of the Iberic Peninsula
11 p1681 N85-20594
Resolution of 2-dimensional seismologic problems by a finite element approximation. Application to the Love wave propagation through the Atlantic border of the Iberic Peninsula. Appendix: Graphs of results — Lagrange coordinates
11 p1681 N85-20595
LOW ALLOY STEELS
U HIGH STRENGTH STEELS
LOW ALTITUDE
Study of proton and neutron activation of metal samples in low Earth orbit
[NASA-CR-171183] 01 p0026 N85-10164
Magnetospheric plasma studies using data from the dynamics high and low altitude plasma instruments
[AD-A145751] 03 p0392 N85-12505
Using a limited field of view simulator to instruct high speed, low altitude flying skills
[AD-P004309] 09 p1267 N85-17963
Visual perceptual aspects of low level high speed flight and flight simulation
[AD-P004310] 09 p1267 N85-17964
Low altitude high speed flight simulation using video disc technology
[AD-P004312] 09 p1268 N85-17966
AVTS (Advanced Visual Technology System): A high fidelity visual simulator
[AD-P004336] 09 p1271 N85-17992
Personnel protection concepts for advance escape system design
10 p1532 N85-19656
Low altitude texture comparison data base and smooth shaded texture
[AD-A150342] 13 p2146 N85-23323
Safety recommendation(s), A-84-82 through -84
[REPT-3957] 14 p2217 N85-23748
Deuteron whistlers at low latitudes in the low altitude topside ionosphere
14 p2366 N85-24625
Low-latitude ducted whistlers observed at Sanya, Hainan, China
14 p2367 N85-24626
Whistler observation at Okinawa, Japan during the IMS
14 p2367 N85-24627
Multistep orbital correction algorithms for an Earth satellite using low thrust engine
15 p2479 N85-25303
Spectral characteristics of protons at low and high altitudes during geomagnetic storm of 29 July 1977
16 p2719 N85-26786
The role of simulation
18 p3058 N85-28919
LOW ASPECT RATIO
Study of controlled diffusion stator blading
[NASA-CR-167995] 09 p1281 N85-18058
Calculation of transonic steady and oscillatory pressures on a low aspect ratio model and comparison with experiment
[NASA-TM-86449] 21 p3551 N85-32092
LOW ASPECT RATIO WINGS
NT DELTA WINGS
Experimental data base for computers program assessment. Report of the Fluid Dynamics Panel Working Group 04: Addendum
[AGARD-AR-138-ADD] 01 p0004 N85-10020
LOW CARBON STEELS
Alloying specialty low carbon silicon-bearing steel with nitrogen
[BLL-M-35707-(5828.4)] 02 p0175 N85-11170
The influence of aluminum on the qualities of low and medium carbon steel
[BLL-M-35754-(5828.4)] 03 p0330 N85-12123
Nondestructive evaluation of residual stress in low-carbon steel
[NASA-CR-174157] 04 p0512 N85-13264
Nondestructive evaluation of residual stress in low-carbon steel, introduction
04 p0512 N85-13265
The influence of manganese on intercrystalline internal adsorption of arsenic in low carbon steel
[BLL-M-35965-(5828.4)] 05 p0615 N85-13931
Specifics of kinetics of polymorphous conversion upon heating of low carbon steels
13 p2030 N85-22721
The influence of melting practice and of microalloying, with rare earth metals and with boron, on the quality of low-carbon steel
[BLL-BISI-22467-(9022.06)] 17 p2925 N85-28036
Multi-phase crystallization of ferrous alloys
[BLL-BISI-TRANS-22441-(9022.06)]
17 p2925 N85-28037
Influence of preliminary cold deformation on fineness of pearlite
[BLL-BISI-TRANS-22409-(9022.06)]
17 p2927 N85-28054
Influence of thermochemical treatment on properties of low-carbon steel
[BLL-BISI-TRANS-22410-(9022.06)]
17 p2927 N85-28055
Preventing the formation of an anomalous structure in chemically sealed low carbon steel
[BLL-BISI-TRANS-22373-(9022.06)]
17 p2930 N85-28065
New method for determining stampability of sheet materials
[BLL-BISI-22486-(9022.06)] 17 p2972 N85-28360
Tendency of selected low-carbon steels to corrosion cracking in nitrates
[BLL-BISI-TRANS-22282-(9022.06)]
18 p3073 N85-29006
Continuous casting of quality steels on billet casters
[BMFT-FB-T-84-262] 18 p3078 N85-29041
Microstructure-abrasive wear characteristics of low carbon dual phase steels
[DE85-010668] 19 p3239 N85-30083
Production process for steel with decarburized surface adapted for single coating enamelling
[BMFT-FB-T-85-022] 20 p3432 N85-31292
Fractographic analysis for nonpropagating conditions of fatigue crack at high stress ratios in mild steel
23 p3905 N85-34194
Crystallographic orientation dependence of fatigue crack propagation in extremely low carbon steel
23 p3906 N85-34195
Safety and reliability of steel structural materials under random service impact loads
23 p3906 N85-34197
LOW CONCENTRATIONS
Model computations of radon, and radon decay product, concentrations in an open system; the Hewlett-Packard 41C program RNSS, version 02
[IRI-190-83-12] 17 p3035 N85-28775
LOW COST
Training effectiveness evaluation and utilization demonstration of a low cost cockpit procedures trainer
[AD-A145179] 01 p0013 N85-10078
Low cost gyrocompass
[AD-A148295] 08 p1082 N85-16857
Replaceable blade turbine and stationary specimen corrosion testing facility
[NASA-TM-86831] 09 p1294 N85-18126
An inexpensive vector thin film magnetometer
[AD-A148725] 09 p1323 N85-18310
Low cost, sprayed CuInSe2 solar cell research
[DE85-003467] 12 p1881 N85-21799
Aspects of low cost module technology — spacecraft solar arrays
13 p2011 N85-22614
Practical considerations when using water quality and structure monitoring sensors as applied to portable ARGOS satellite transmitter equipment
14 p2330 N85-24405
Development of a low cost drifting buoy
14 p2330 N85-24406
Navigation: Accounting for copy
16 p2695 N85-26641
Iron rich low cost superalloys
[NASA-CR-174900] 16 p2748 N85-26962
Performance test results of a low cost GPS time and frequency monitor
18 p3109 N85-29252
Investigation for low-cost permanent magnets
[AD-A154367] 19 p3260 N85-30212
A new large-scale, high-resolution multicolor software display concept
[AD-A155404] 22 p3827 N85-33703
LOW DENSITY GASES
U RAREFIED GASES
LOW DENSITY MATERIALS
Single-drop impact damage prediction for low density, coated ceramic materials — rain erosion
01 p0061 N85-10402
X-ray gauge measures areal density variations as small as 0.1%
[DE85-003774] 12 p1854 N85-21629
French, UK, Swedish research in powder metallurgy, HIP
18 p3068 N85-29109
New form of graphite
19 p3243 N85-30111
Method for making a low density polyethylene waste form for safe disposal of low level radioactive material
[DE85-006401] 23 p3920 N85-34292
LOW DENSITY RESEARCH
Nonequilibrium air radiation (Nequair) program: User's manual
[NASA-TM-86707] 19 p3353 N85-30780
LOW FREQUENCIES
NT VERY LOW FREQUENCIES
Scattering of plane wave on cylindrical shell in low-frequency region
02 p0256 N85-11677
Low frequency electrical properties of selected dielectrics
[DE84-016220] 05 p0632 N85-14052
Study of low-frequency sound with point source in stream with shear
06 p0825 N85-15239
Synoptic observations of the radio noise background in the frequency range 150-180 kHz to provide design data for the low frequency communications designer
[AD-A147438] 07 p0941 N85-15965
Detection of low frequency impulsive noise from large wind turbine generators
[NASA-CR-172511] 07 p1036 N85-16588
D1 LF wind measurements in the 90 to 100 km height range
08 p1185 N85-17468
Natural unsteadiness of a separation bubble behind a backward-facing step
[AD-P004176] 09 p1267 N85-17961
The wobble of the Earth and the low frequency dynamics of the ocean
09 p1358 N85-18548
Design of low loss helix circuits for interference fitted and brazed circuits
[NASA-CR-168313] 10 p1478 N85-19328
Simulation of the ion-beam-driven drift instability in a magnetic trap, 2
[AD-A149452] 10 p1554 N85-19798
Analysis of Jovian low frequency radio emissions
[NASA-CR-174449] 10 p1571 N85-19908
Autostochastic behavior of solid state ring laser with low frequency periodic loss modulation
11 p1717 N85-20805
LF. RADIO-DATA: Specification of BBC phase-modulated transmissions on long-wave
[BBC-RD-1984/19] 12 p1822 N85-21431
Method of designing digital band-pass filters with infinite memory
12 p1840 N85-21548
Effect of compliability of hot walls in liquid-propellant engine on low frequency instability
13 p2049 N85-22834
Excitation of low-frequency resonance waves by moving conductor in space plasma
13 p2067 N85-22912
The low frequency behaviour of an immersed structure at a standstill in a high density fluid with free surface
[TP-1983-31] 13 p2103 N85-23105
Shuttle payload bay dynamic environments: Summary and conclusion report for STS flights 1-5 and 9
[NASA-CR-175656] 14 p2241 N85-23896
Low-frequency oscillations of sea level and group structure of wind waves
14 p2335 N85-24441
Conjugacy of ELF-VHF emissions near L=6 — chorus phenomenon, hiss
14 p2367 N85-24629
Field of point source of low-frequency sound in atmosphere with altitudinally nonuniform wind
15 p2524 N85-25586
Long range downwind propagation of low-frequency sound
[NASA-TM-86409] 15 p2645 N85-26318
Evaluation of human exposures to low frequency fields
16 p2776 N85-27135
Biological influences of low-frequency sinusoidal electromagnetic signals alone and superimposed on RF carrier waves
[PB85-161248] 16 p2842 N85-27827
Timing accuracy of LF and TV synchronization techniques
17 p2961 N85-28288
Study of sound attenuation in sediments
[AD-A153680] 18 p3177 N85-29697
New measurement solutions for low frequency systems
20 p3437 N85-31325
Automated testing of developmental satellite communications systems and subsystems
[NASA-TM-87070] 20 p3440 N85-31348
Upward continuation of surface gravity anomalies
[AD-A154973] 21 p3631 N85-32580
Influence of phonon interaction on width and form of Mandelstam-Brillouin optical scattering line
21 p3696 N85-32962
RF stabilization of interchange-ballooning modes
[DE85-012000] 24 p4090 N85-35363
LOW FREQUENCY BANDS
NT VERY LOW FREQUENCIES
LOW GRAVITY
U REDUCED GRAVITY

LOW GRAVITY MANUFACTURING
Microgravity containerless processing in long drop tubes
02 p0153 N85-11037
Directional solidification of flake and nodular cast iron during KC-135 low-g maneuvers
02 p0154 N85-11040
Project Explorer
02 p0154 N85-11041
Critical point wetting drop tower experiment
02 p0155 N85-11045
Design and implementation of a low-gravity solidification experiment package for the F-104
02 p0156 N85-11053
The feasibility of low-G grey solidification of nodular iron in the F-104 experimental furnace package
[NASA-TM-82527] 10 p1426 N85-18996
Microgravity: A new tool for basic and applied research in space
[EP-212] 16 p2716 N85-26767
Technological experiments on high-altitude rockets
16 p2725 N85-26818
Microgravity silicon zoning investigation
[NASA-CR-171531] 20 p3397 N85-31073
Research study for gel precursors as glass and ceramic starting materials for space processing applications research
[NASA-CR-176113] 22 p3751 N85-33250
LOW LATITUDES
U TROPICAL REGIONS
LOW LEVEL TURBULENCE
Statistics from the operation of the low-level wind shear alert system (LLWAS) during the Joint Airport Weather Studies (JAWS) Project
[DOT/FAA/PM-84/32] 06 p0750 N85-14804
Adding computationally efficient realism to Monte Carlo turbulence simulation
[NASA-TP-2469] 17 p2925 N85-26708
Mean flow and turbulence in complex terrain
[AD-A155138] 21 p3636 N85-32583
LOW MASS
U MASS
LOW NOISE
Low noise multiple crystal-controlled oscillator
[AD-D011401] 07 p0948 N85-16010
Physical electronics of cooled operation of very short compound semiconductor transistors
14 p2297 N85-24223
Cryogenically-cooled, low-noise microwave receivers: Present status and future needs
14 p2298 N85-24226
Low noise polycrystalline semiconductor resistors by hydrogen passivation
[AD-D011721] 23 p3927 N85-34338
LOW PASS FILTERS
China report: Science and technology
[JPRS-CST-84-001] 04 p0557 N85-13545
Present status, future prospects of domestic acoustical instruments
04 p0557 N85-13548
An airborne infrared thermal scanning system for easy use on Navy P-3 aircraft
[AD-A149660] 12 p1933 N85-22143
Synthesis of low-pass filters using coupled lines with unmatched loads
13 p2071 N85-22938
Efficiency of digital compensator of strong non-Gaussian interference
13 p2072 N85-22942
Some studies in filtering of atmospheric turbulence
[AD-A154042] 19 p3316 N85-30557
LOW PRESSURE
NT CYCLOGENESIS
NT HIGH ALTITUDE PRESSURE
Forecasting of polar lows
01 p0075 N85-10495
Energy efficient engine. Low pressure turbine test hardware detailed design report
[NASA-CR-167956] 02 p0147 N85-10994
Semiconductor-type transducer with universal strain gauge for measurement of low pressures
04 p0469 N85-13116
Electrical properties of 10-50 nm TEOS (Tetraethoxysilane) LPCVD (Low Pressure Chemical Vapor Deposition) films
[AD-A146416] 06 p0803 N85-15111
Nitriding of titanium and its alloys by N2, NH3 or mixtures of N2 + H2 in a dc arc plasma at low pressures (or = to torr)
[NASA-TM-83803] 06 p0814 N85-15166
Cut-off lows and their influence on the weather in Switzerland
[REPT-45] 10 p1519 N85-19574
Low loss injector for liquid propellant rocket engines
[NASA-CASE-MFG-25869-1] 11 p1591 N85-20008
Non-self-maintained high-voltage low-pressure discharge
13 p2088 N85-23037
Estimating defectiveness buildup during service in metal of welded runner in low-pressure cylinder of turbine
14 p2271 N85-24070
Measurements in low pressure flow using an electronic beam detector — wind tunnel tests
16 p2701 N85-26676
Experimental testing of cooling by low pressure adsorption in a zeolite
[DE85-007509] 16 p2716 N85-26783
On development mechanisms for polar lows
20 p3495 N85-31727
The nucleation of ice at very low temperatures and pressures
21 p3641 N85-32617
Monitoring dosage of volatile compounds in tests at low barometric pressure
23 p3954 N85-34506
LOW PRESSURE CHAMBERS
U VACUUM CHAMBERS
LOW REYNOLDS NUMBER
Numerical integrations of the Navier-Stokes equations for flow over surface-mounted obstacles
05 p0583 N85-13784
The resistance and mobility functions of two equal spheres in low Reynolds number flow
[AD-A147301] 07 p0959 N85-16080
Low Reynolds number vehicles
[AGARD-AG-288] 16 p2699 N85-26666
Aerodynamic characteristics of a distinct wing-body configuration at Mach 6: Experiment, theory, and the hypersonic isolation principle
[NASA-TP-2467] 22 p3727 N85-33107
LOW SPEED
Results of winglet development studies for DC-10 derivatives
[NASA-CR-3677] 02 p0138 N85-10936
Design studies of thick laminar flow airfoils for low speed flight employing turbulent boundary layer suction over the rear part
06 p1070 N85-16786
Recent methods for calibrating the anemometry of helicopters at low speeds
06 p1074 N85-16809
Air intake efficiency at zero speed and lip suction — jet engines
[BAE-KRS-N-GEN-303] 09 p1272 N85-17966
Effects of leading-edge devices on the low-speed aerodynamic characteristics of a highly-swept arrow-wing
[NASA-CR-172531] 13 p1968 N85-22365
The use of pressure sensing taps on the aircraft wing as sensor for flight control systems
16 p2696 N85-26660
LOW SPEED STABILITY
Application of the ONERA model of dynamic stall
[NASA-TP-2399] 04 p0451 N85-12662
Low-speed stability and control wind-tunnel investigations of effects of spanwise blowing on fighter flight characteristics at high angles of attack — Langely 12-ft low-speed tunnel and 30- by 60-ft tunnel
[NASA-TP-2431] 14 p2210 N85-23706
Low-speed tests of a high-aspect-ratio, supercritical-wing transport model equipped with a high-lift flap system in the Langley 4- by 7-meter and Ames 12-foot pressure tunnels
[NASA-TP-2097] 20 p3388 N85-31010
LOW SPEED WIND TUNNELS
NT SUBSONIC WIND TUNNELS
Atmospheric and pressurized low speed wind tunnel performance and cost comparisons
[ARL/AERO-R-160] 02 p0149 N85-11008
Wall influence corrections in wind tunnels: Blockage correction according to the wall pressure signature method
[FW-FO-1613] 04 p0453 N85-12675
Comparison of options for reduction of noise in the test section of the NASA Langley 4x7m wind tunnel, including reduction of nozzle area
[NASA-CR-172446-VOL-2] 05 p0726 N85-14667
Investigations into the effects of scale and compressibility on lift and drag in the RAE 5m pressurized low-speed wind tunnel
08 p1068 N85-16773
Low-speed wind tunnel tests of the NAL fan-jet STOL research aircraft model with ground simulation by tangential blowing
[NAL-TR-828] 10 p1423 N85-18976
Investigations into the effects of scale and compressibility on lift and drag in the RAE 5m pressurised low-speed wind tunnel
[RAE-TM-AERO-2006] 13 p1969 N85-22372
China report: Science and technology
[JPRS-CST-85-005] 13 p2052 N85-22843
CARD's low-speed wind tunnel described
13 p2052 N85-22849
A numerical simulation of the NFAC (National Full-scale Aerodynamics Complex) open-return wind tunnel inlet flow
[NASA-TM-86724] 16 p2700 N85-26672
Construction 1976-1980: Design, manufacturing, calibration of the German-Dutch wind tunnel (DNW)
17 p2905 N85-27913
Background noise measurements from jet exit vanes designed to reduced flow pulsations in an open-jet wind tunnel
[NASA-TM-86383] 17 p2906 N85-27916
A computer-controlled traverse gear for the Oxford wind engineering research group's 4 metre x 2 metre wind tunnel
[OUEL-1525/84] 20 p3463 N85-31514
The influence of helicopter tail shape on drag: An aerodynamic study using a low speed wind tunnel
[AD-A156304] 24 p4062 N85-35174
LOW TEMPERATURE
NT ULTRALOW TEMPERATURES
Materials studies for magnetic fusion energy applications at low temperatures, 7
[DE84-013487] 01 p0122 N85-10637
Low temperature properties of Mo/Mi superlattices
[DE84-014729] 02 p0288 N85-11881
The extremeness of the cold front of December 31, 1978 over the CSR
[REPT-566] 03 p0377 N85-12409
Diffusion of gases in porous solids: Simulation and measurements
[DE84-016292] 04 p0500 N85-13191
Kohn anomaly in metastable fcc lanthanum at low temperatures
[DE84-015459] 04 p0569 N85-13628
Oxide charge characteristics of low temperature MOS (Metal-Oxide-Silicon) oxide films
[AD-A146447] 06 p0803 N85-15113
Charge trapping in low temperature MOS (Metal-Oxide-Silicon) oxides
[AD-A146450] 06 p0860 N85-15467
Method for making alloy additions to base metals having higher melting points
[AD-D011403] 07 p0926 N85-15884
Effects of low temperatures on the growth and unfrozen water content of an aquatic plant
[AD-A147107] 07 p1011 N85-16424
Carotid baroreceptor influences on peripheral circulatory and thermal responses during cold exposure
[AD-A146808] 07 p1015 N85-16447
Determination of the decomposition behavior of double base propellants at low temperatures
06 p1117 N85-17045
New phases and chemical reactions in solid CO under pressure
[DE85-002033] 09 p1377 N85-18055
Low temperature properties of CeOs2 in the C14 and C15 crystallographic Laves phases
[DE85-003754] 10 p1564 N85-19666
Low-temperature geothermal assessment of the Jordan Valley Salt Lake County, Utah
[DE85-000616] 11 p1670 N85-20524
Low temperature deposition of nickel films
[AD-D011568] 12 p1805 N85-21319
Oscillator development
[AD-A149699] 12 p1834 N85-21509
Experimental studies of low temperature surface interactions of atomic hydrogen using maser technique
[AD-A150216] 13 p2017 N85-22647
Low temperature calibration fixture
[DE85-003969] 13 p2094 N85-23071
Proceedings of the Cold Electronics Workshop
[NASA-CR-175662] 14 p2297 N85-24220
Cold electronics: An overview
14 p2297 N85-24221
Recent developments in semiconductor research
14 p2297 N85-24222
The effects of cooling on delay-time limits in IC's
14 p2297 N85-24224
Si MOS devices at low temperatures
14 p2297 N85-24225
Cryogenically-cooled, low-noise microwave receivers: Present status and future needs
14 p2298 N85-24226
Structural changes with one- and two-stage aging of alloys Ti-Al-Mo-Fe and Ti-Zr-V-Al-Sn
15 p2499 N85-25415
Mechanism of formation of low temperatures in nighttime Venusian thermosphere
16 p2723 N85-26807
Investigation of the requirement for auxiliary heating of Canadian forces personnel
[AD-A151950] 16 p2841 N85-27522
The fatigue properties of welds at low temperature, according to the type of steel
[BLL-BISI-TRANS-22455-(9022.06)]
17 p2978 N85-28410
Hydrogen maser oscillation at 10 K
18 p3108 N85-29241
On the low temperature chemistry preceding end gas autoignition
[DE85-010471] 19 p3252 N85-30162
Physics with low temperature antiproton
[DE85-009627] 19 p3355 N85-30796

Low-temperature positron lifetime and Doppler-broadening measurements for single-crystal nickel oxide containing cation vacancies
[DE85-010236] 19 p3376 N85-30944
Detailed studies of aviation fuel flowability
[NASA-CR-174938] 20 p3435 N85-31308
A comparison of two bench scale tests of fuel low temperature flow properties
[AD-A154477] 20 p3435 N85-31311
Polymer solution-supercritical fluid behavior
[AD-A154514] 21 p3568 N85-32192
Synthesis and properties of arylethersulfone thermoset systems
[AD-A154811] 21 p3569 N85-32198
The nucleation of ice at very low temperatures and pressures 21 p3641 N85-32617
Method for fluorination of actinide fluorides and oxyfluorides using O2F2
[DE85-011646] 22 p3743 N85-33202
Very low temperature studies of hyperfine effects in metals
[DE85-013367] 22 p3749 N85-33236
Low temperature experimental capability for use with gas guns
[DE85-010418] 22 p3801 N85-33548
Measurement and correlation of jet fuel viscosities at low temperatures
[NASA-CR-174911] 23 p3921 N85-34295
Decomposition of martensite in R6M5 and R6AM5 steels after direct immersion in liquid nitrogen
[BLL-M-36305] 24 p4077 N85-35268
Evaluation of low-temperature geothermal potential in north-central Box Elder County, Utah
[DE85-009541] 24 p4112 N85-35490
Energy from low temperature differences
[DE85-008617] 24 p4112 N85-35492

LOW TEMPERATURE BRAZING
Fatigue crack propagation characteristics and fatigue fracture toughness in 780 MPa grade high strength steel weldments at low temperature
[BLL-BISI-TRANS-22369-(9022.05)] 17 p2979 N85-26411

LOW TEMPERATURE ENVIRONMENTS
Evaluation of thermocouple junction temperature
[DE84-015159] 04 p0502 N85-13206
Effects of restricted water intake on performance in a cold environment
[AD-A146904] 07 p1015 N85-16450
Properties of filamentary sublimation residues from dispersions of clay in ice 13 p2197 N85-23629
Low Temperature Science. Series A: Physical Sciences
[ISSN-0439-3538] 15 p2581 N85-25917

LOW TEMPERATURE PHYSICS
Exothermic processes in solids under low temperatures, their physics and their cryogenic implications
[JUEL-1919] 03 p0414 N85-12651

LOW TEMPERATURE PLASMAS
U COLD PLASMAS

LOW TEMPERATURE TESTS
An evaluation of grease type ball bearing lubricants operating in various environments
[NASA-TM-86460] 02 p0185 N85-11239
Investigation of the production and properties of lattice defects induced by low temperature reactor irradiation 03 p0430 N85-12739
Geomagnetic field dynamics 13 p2116 N85-23182
Mechanical properties of Shielded Metal Arc (SMA) and Submerged Arc (SA) welded joints in a steel Raex 366 P Arctic
[VTT-339] 22 p3801 N85-33551

LOW THRUST
Low thrust bipropellant engine/redundant seat valve assembly
[AD-A150293] 13 p2013 N85-22628

LOW THRUST PROPULSION
NT ELECTROMAGNETIC PROPULSION
NT ELECTROSTATIC PROPULSION
NT ION PROPULSION
NT PLASMA PROPULSION
NT SOLAR PROPULSION
Partial bleed expander cycle for low thrust LOX/LH2 rocket engine
[NAL-TR-837T] 10 p1430 N85-19018
Design and analysis report for the RL10-2B breadboard low thrust engine
[NASA-CR-174857] 10 p1430 N85-19020
Station keeping of geostationary satellites by electric propulsion
[NASA-TM-77820] 14 p2320 N85-24337
Oxygen-hydrogen thrusters for Space Station auxiliary propulsion systems
[NASA-CR-175691] 15 p2494 N85-25383

LOW VELOCITY
U LOW SPEED

LOW VOLTAGE
Optimization of overall dimensions of enclosures for low-voltage devices and equipment 13 p2067 N85-23033
Low voltage free electron laser development
[AD-A152917] 17 p2970 N85-28342

LOW WEIGHT
Free-surface phenomena under low- and zero-gravity conditions
[NASA-CR-175835] 16 p2782 N85-27166

LOWER ATMOSPHERE
NT BIOSPHERE
NT OZONOSPHERE
NT TROPOSPHERE
Exploratory investigation of the need for and feasibility of a Lower Atmosphere Research Satellite (LARS) program
[NASA-CR-171181] 01 p0015 N85-10091
H2O profile in lower atmosphere of Venus based on effective radiation flux measurements 02 p0163 N85-11102
Characteristics of latitude effect on cosmic ray charged component in atmosphere at altitudes 3-5 KM 13 p1976 N85-22413
Influence of bubbles formed upon breaking of waves on gas exchange between ocean and atmosphere 14 p2335 N85-24439
Energy structure of atmospheric boundary layer above waves 14 p2335 N85-24442
The possibility of observing solar neutron events in the lower atmosphere
[NOTA-INTERNA-637] 18 p3209 N85-29906

LOWER BODY NEGATIVE PRESSURE
Leg volume changes. Responses to Lower Body Negative Pressure (LBNP) during 7 days of zero-g simulation (6 deg Head-Down Tilt (HDT)) 05 p0692 N85-14452
The influence of angiotensin on the maintenance of venous tone. The effect of Lower Body Negative Pressure (LBNP) and angiotensin blockade 05 p0693 N85-14457
LBNP training of crew members on main missions aboard Salyut-6 orbital station 12 p1901 N85-21938
Oxygenation and regional circulation in gingival mucosa during exposure to lower body negative pressure 23 p3953 N85-34498

LOWER CALIFORNIA (MEXICO)
Stratigraphy, petrology, and tectonic setting of the Alisitos Group, Baja California, Mexico 03 p0389 N85-12488

LOWER IONOSPHERE
NT D REGION
Behavior of charged particles in lower ionosphere with acoustical effects 02 p0161 N85-11089
Experimental results of study of artificial perturbation region in upper and lower ionosphere disturbance by the method of vertical probing 06 p0784 N85-15011
Study of lower ionosphere by pulse cross-modulation method 10 p1500 N85-19467

LOX (OXYGEN)
U LIQUID OXYGEN

LOX-HYDROGEN ENGINES
U HYDROGEN OXYGEN ENGINES

LSI
U LARGE SCALE INTEGRATION

LST
U HUBBLE SPACE TELESCOPE

LUBRICANT TESTS
Performance evaluation of automotive wheel bearing greases
[AD-A145948] 03 p0337 N85-12168
The European Space Tribology Laboratory (ESTL) activities report
[ESA-ESTL-51] 05 p0646 N85-14146
The performance of Fomblin Z25 oil in ball bearings operating in vacuum — spacecraft lubricant
[ESA-ESTL-056] 08 p1134 N85-17150
Locking of Automative Products hydraulic selector valves
[BAE-EXPER/NOTE-459] 15 p2567 N85-25839
European Space Tribology Laboratory: Facilities, services, capabilities
[ESA-BR-12] 20 p3398 N85-31080
Activities report of the European Space Tribology Laboratory
[ESA-ESTL-66] 20 p3484 N85-31653
The use of perfluoroether lubricants in unprotected space environments 22 p3797 N85-33523

LUBRICANTS
NT GAS LUBRICANTS
NT LUBRICATING OILS
NT SOLID LUBRICANTS
An evaluation of grease type ball bearing lubricants operating in various environments
[NASA-TM-86460] 02 p0185 N85-11239
Performance evaluation of automotive wheel bearing greases
[AD-A145948] 03 p0337 N85-12168
Microscopic aspects of the effect of friction reducers at the lubrication limit
[NASA-TM-77413] 03 p0367 N85-12354
Effect of lubricant extreme-pressure additives on surface fatigue life of AISI 9310 spur gears
[NASA-TP-2408] 04 p0507 N85-13234
Fluorinated aliphatic polyalkylether lubricant with an additive composed of an aromatic phosphine substituted with perfluoroalkylether groups
[AD-D011286] 06 p0770 N85-14927
Effects of silver and group 2 fluorides addition to plasma sprayed chromium carbide high temperature solid lubricant for foil gas bearing to 650 deg C
[NASA-TM-86895] 06 p0770 N85-14928
Stability of lubricant film in gas dynamic bearing 06 p0778 N85-14977
Contact angle and surface tension measurements of a five-ring polyphenyl ether
[NASA-TM-86927] 07 p0930 N85-15697
Effect of five lubricants on life of AISI 9310 spur gears
[NASA-TP-2419] 07 p0962 N85-16099
Toxic hazards research
[AD-A147857] 07 p1011 N85-16425
Structure of solids surfaces in wear situations
[AD-A148480] 08 p1168 N85-17366
Tribological properties of graphite-fiber-reinforced, partially fluorinated polyimide composites
[NASA-TM-86928] 09 p1298 N85-18153
Characterization of lubricated bearing surfaces operated under high loads
[NASA-TM-86964] 12 p1811 N85-21357
Formation of high molecular weight products from benzene during boundary lubrication
[NASA-TM-86966] 13 p2017 N85-22644
Use of ferrofluids in machining of metals 13 p2045 N85-22802
Transmission efficiency measurements and correlations with physical characteristics of the lubricant 14 p2222 N85-23781
Chemical-mechanical interaction in gears 14 p2223 N85-23785
Problems regarding the practical evaluation of efficiency of worm gears 14 p2224 N85-23793
Role of fluid lubricant-coolant in fine grinding of optical glass by diamond tool 14 p2280 N85-24125
Model of friction bearing hydrodynamics 14 p2288 N85-24178
Computations for segmented radial bearings 14 p2288 N85-24180
Thermal traction contact performance evaluation under fully flooded and starved conditions
[NASA-CR-168173] 15 p2568 N85-25848
Evaluation of used crankcase oils using computerized infrared spectrometry
[AD-A152993] 17 p2920 N85-27999
Evaluation of used crankcase oils using computerized infrared spectrometry. Appendices
[AD-A152994] 17 p2920 N85-28000
New method for determining stampability of sheet materials
[BLL-BISI-22486-(9022.06)] 17 p2972 N85-28360
Lubricant and additive effects on spur gear fatigue life
[NASA-TM-87044] 17 p2974 N85-28373
Correlation of rheological characteristics of lubricants with transmission efficiency measurements
[NASA-TM-86968] 19 p3280 N85-30042
The design and development of a spacecraft appendage tie down mechanism 22 p3797 N85-33522
The use of perfluoroether lubricants in unprotected space environments 22 p3797 N85-33523

LUBRICATING OILS
Cooperative program evaluation of NATO multigraded diesel engine oils
[AD-A146072] 03 p0337 N85-12171
A simple electronic apparatus for determining the oxidation stability of lubricants and other organic compounds
[AD-A146060] 03 p0338 N85-12172
Effect of two inner-ring oil-flow distribution schemes on the operating characteristics of a 35 millimeter bore ball bearing to 2.5 million DN
[NASA-TP-2404] 04 p0507 N85-13233
Grease versus oil lubrication of wheel bearings in Army equipment
[AD-A147548] 07 p0973 N85-16184
The performance of Fomblin Z25 oil in ball bearings operating in vacuum — spacecraft lubricant
[ESA-ESTL-056] 08 p1134 N85-17150
New technique for fluid feed in simultaneous multisurface grinding 13 p2045 N85-22800
Fine filtration: An attractive route towards lower helicopter operating costs 14 p2221 N85-23774

Design of piping for oil drain from turbine bearings
14 p2271 N85-24073
Investigation of reaction layer formation in high-load capacity lubricating oils
[MPA-83-01] 17 p2975 N85-26381
Activities report of the European Space Tribology Laboratory
[ESA-ESTL-66] 20 p3484 N85-31653

LUBRICATION
NT BOUNDARY LUBRICATION
NT SELF LUBRICATION
NT SPACECRAFT LUBRICATION
Performance evaluation of automotive wheel bearing greases
[AD-A145948] 03 p0337 N85-12168
Lubricity of well-characterized jet and broad-cut fuels by ball-on-cylinder machine
[NASA-TM-83807] 03 p0339 N85-12183
Microscopic aspects of the effect of friction reducers at the lubrication limit
[NASA-TM-77413] 03 p0367 N85-12354
Comparison of predicted and measured friction for a tilt-pad thrust bearing with crown and roughness under hydrodynamic and mixed lubrication
[AD-A145752] 03 p0371 N85-12371
Development of gas-lubricated pistons for heavy duty diesel engine technology program
[NASA-CR-174746] 03 p0441 N85-12808
Fundamental tribological properties of ceramics
[NASA-TM-86915] 07 p0930 N85-15893
Grease versus oil lubrication of wheel bearings in Army equipment
[AD-A147546] 07 p0973 N85-16184
Metallographic grinding efficiency
[DE85-001520] 09 p1304 N85-18194
Study of advanced fuel system concepts for commercial aircraft
[NASA-CR-174751] 11 p1584 N85-19978
Tribological systems as applied to aircraft engines
[NASA-TM-86985] 12 p1858 N85-21657
Lubrication and performance of high-speed rolling-element bearings
[NASA-TM-86958] 12 p1859 N85-21658
Development of a multiplane multispeed balancing system for turbine systems
[NASA-CR-174750] 13 p1976 N85-22400
Thermal and thermoelastic effects in rolling/sliding contacts
[AD-A150435] 13 p2165 N85-23429
Gears and Power Transmission Systems for Helicopters and Turboprops
[AGARD-CP-369] 14 p2220 N85-23765
Helicopter transmission lubricants
14 p2220 N85-23768
A state of the art assessment of turboprop transmission technology and projected needs for the next generation
14 p2220 N85-23770
Significant parameters of the behavior and of the surface damage of the lubricated Hertzian contact: An application to gears 14 p2222 N85-23783
Problems of elastic hydrodynamic lubrication of helicopter transmission gears 14 p2222 N85-23784
Wear reduction by lubricants in confined contacts
14 p2223 N85-23786
Experimental study of heat transfer from shaft in cooled radial bearing of GNT-25 gas turbine
14 p2270 N85-24068
Selection of bearing type for large steam turbines
14 p2271 N85-24069
Molybdenum disulphide lubrication: A continuation survey, 1981 - 1983
[REPT-84-549] 18 p3082 N85-29065
Dynamics of thin-film breakup in a constricted pore
[DE85-008442] 18 p3101 N85-29199
Mechanical interactions of rough surfaces
[DE85-005653] 18 p3118 N85-29299
Study of the chemical mechanism in lubrication
[DE85-010768] 19 p3228 N85-30013
Fast approach for calculating film thicknesses and pressures in elastohydrodynamically lubricated contacts at high loads
[NASA-TM-87032] 19 p3264 N85-30242
Temperature and surface damage under lubricated sliding-rolling contacts 19 p3280 N85-30338
Activities report of the European Space Tribology Laboratory
[ESA-ESTL-66] 20 p3484 N85-31653
Surface roughness effects in elastohydrodynamic contacts
[NASA-TP-2488] 21 p3595 N85-32329
Mechanics of a gaseous film barrier to lubricant wetting of elastohydrodynamically lubricated conjunctions
[NASA-TP-2500] 21 p3595 N85-32330
Lubrication and cooling for high speed gears
[NASA-TM-87096] 23 p3938 N85-34407
Elastohydrodynamic lubrication calculations used as a tool to study scuffing
[NASA-TM-87097] 23 p3938 N85-34408
Design and lubrication of high-speed rolling-element bearings
[NASA-TM-87107] 23 p3938 N85-34409

LUBRICATION SYSTEMS
Effect of interconnection of the ends of a sliding bearing on film thickness
[AD-A147736] 08 p1132 N85-17135
Design of piping for oil drain from turbine bearings
14 p2271 N85-24073
Study of axial bearings without oil bath with radial cooling of blocks 14 p2286 N85-24164

LUCITE (TRADEMARK)
U POLYMETHYL METHACRYLATE

LUDER BANDS
U PLASTIC DEFORMATION
U YIELD POINT

LUGS
The research of driving wheel with movable lugs of the paddy field floating tractor
[AD-P004283] 09 p1407 N85-18860
An investigation of the driving wheel thrust of paddy field tractors
[AD-P004284] 09 p1407 N85-18861
Behaviour of soil under a lugged wheel
[AD-P004287] 09 p1407 N85-18864
The analysis on the dynamic performance of a single lug
[AD-P004289] 09 p1408 N85-18866
Advanced life analysis methods. Volume 1: Cracking data survey and NDI (nondestructive inspection) assessment for attachment lugs
[AD-A150419] 13 p2103 N85-23108
Advanced life analysis methods. Volume 2: Crack growth analysis methods for attachment lugs
[AD-A150420] 13 p2103 N85-23109
Advanced life analysis methods. Volume 4: Tabulated test data for attachment lugs
[AD-A151016] 14 p2219 N85-23760
Advanced life analysis methods. Volume 5: Executive summary and damage tolerance criteria recommendations for attachment lugs
[AD-A151017] 14 p2219 N85-23761
Advanced life analysis methods. Volume 3: Experimental evaluation of crack growth analysis methods for attachment lugs
[AD-A151058] 14 p2317 N85-24319
The effect of frictional forces on fatigue crack growth in lugs
[AD-A151994] 15 p2576 N85-25898
Advanced life analysis methods. Volume 6: User's manual for LUGRO computer program to predict crack growth in attachment lugs
[AD-A151235] 15 p2628 N85-26195

LUMBERING AREAS
U FORESTS

LUMINAIRES
NT AIRCRAFT LIGHTS
NT ARC LAMPS
NT FLASH LAMPS
NT MERCURY LAMPS
NT RUNWAY LIGHTS
Determining lamp/ballast system performance with a temperature-controlled integrating chamber
[DE84-014606] 05 p0631 N85-14049
New lighting technologies, their status and impacts on power densities
[DE85-000712] 09 p1315 N85-18266
Evaluation of miniature vacuum ultraviolet lamps for stability and operating characteristics, Lyman-Alpha task
[NASA-CR-171345] 10 p1477 N85-19323
Lifetime and reliability of rubidium discharge lamps for use in atomic frequency standards
[AD-A150787] 14 p2417 N85-24915
Radioluminescent lighting for rural Alaskan runway lighting and marking
[DE85-007022] 16 p2716 N85-26764
Acceptability testing of radioluminescent lights for VFR-night air taxi operations
[DE85-007303] 16 p2716 N85-26765
Material for electrodes of pulsed and arc sources of light
[DE85-007453] 16 p2780 N85-27156
The role of long term lamp fluctuations in the random walk of frequency behavior of the rubidium frequency standard: A case study
[AD-A155336] 21 p3590 N85-32314

LUMINANCE
The Beatrice experiment and the luminance concept in Dante
[NOTA-INTERNA-823] 02 p0281 N85-11831
Approximating true radioluminance distribution from observations on aperture synthesis systems
06 p0783 N85-15003
NBS (National Bureau of Standards) daylight availability database
[PB84-245745] 07 p1054 N85-16688
Astronomy and sodium lighting
[RAND/N-2069-RC] 09 p1413 N85-18914
Electronic displays: Their strengths and weaknesses for advanced high performance aircraft
10 p1533 N85-19664
Television camera video level control system
[NASA-CASE-MSC-18578-1] 12 p1821 N85-21427
Visual simulation requirements for aircraft aspect recognition at real world distances
[AD-A151040] 14 p2228 N85-23810
Issue of sky conditions
[DE85-010590] 19 p3317 N85-30562
Sub-luminal pulses from cosmic ray air showers
[HE-4.7-13] 24 p4200 N85-36063

LUMINESCENCE
NT BIOLUMINESCENCE
NT CATHODOLUMINESCENCE
NT CHEMILUMINESCENCE
NT ELECTROLUMINESCENCE
NT FLUORESCENCE
NT OPTICAL RESONANCE
NT PHOSPHORESCENCE
NT PHOTOLUMINESCENCE
NT RESONANCE FLUORESCENCE
NT SHOCK WAVE LUMINESCENCE
NT THERMOLUMINESCENCE
NT X RAY FLUORESCENCE
Evaluation of arctic test of improved tritium radioluminescent lighting
[DE84-014887] 05 p0597 N85-13805
Photophysical studies of triplet exciton processes in pure polymer films
[DE84-016258] 05 p0620 N85-13965
Processes of smooth increase and dropoff in intensity of glow line lambda' = 5577 A with exposure of ionosphere to electron beam 06 p0822 N85-15219
International Conference on Luminescence
[AD-A148470] 08 p1223 N85-17701
Facilities for studing radiation damage in nonmetals during irradiation
[DE85-000590] 10 p1554 N85-19801
Light your runways and taxiways without electricity
[DE85-000289] 11 p1586 N85-19991
Influence of shock wave front on nature of luminescence of recombining laser plasma 11 p1719 N85-20818
Submanosecond time-resolved emission study of Cu2O and GaAs
[DE85-002070] 11 p1735 N85-20912
Examination of the feasibility for demonstration and use of radioluminescent lights for Alaskan remote runway lighting
[DE85-002503] 12 p1782 N85-21185
EXAFS of monolayers on silver electrodes: SSRL proposal number 717M
[AD-A150823] 13 p2018 N85-22652
Glow of ionospheric F-layer in Line 630 nm determined from photographs taken aboard Salyut-6 orbital station: Interpretation of results 16 p2721 N85-26799
Luminescence probe studies of ionomers. 2. Steady-state measurements from sulfonated polyethylene and teflon membranes
[AD-A152233] 16 p2755 N85-27000
Laser measurement techniques: Laser spectroscopy in semiconductors
[DE85-007887] 17 p2971 N85-28350
Luminescence probe studies of ionomers. I: Steady-state measurements from nafion membrane
[AD-A152475] 17 p3029 N85-28730
Symposium on Luminescent Radiation Receivers and Converters 19 p3295 N85-30430
Radioluminescent lighting for Alaskan runway lighting and marking
[DE85-010405] 19 p3368 N85-30887
The space shuttle glow
[AD-A154937] 21 p3559 N85-32139
Multidimensional luminescence measurements
[AD-A154950] 21 p3563 N85-32162
Luminescence and absorption of indium-activated potassium-borate glasses subjected to high-power excitation 21 p3681 N85-32868
Influence of technological factors on luminescence characteristics of InGaAsP/InP heterolasers (lambda = 1.55 microns) 21 p3688 N85-32910
Spectral-luminescence characteristics and induced emission of Nd-3(+) ion in Gd(2-x)Nd(x)(WO4)3 crystals
21 p3688 N85-32912
Plasmodynamic methods for generating powerful light puses 21 p3693 N85-32943
Optical properties of heterostructures and superlattices
[AD-A156243] 24 p4162 N85-35802

LUMINESCENT INTENSITY
U LUMINOUS INTENSITY

LUMINOSITY
NT STELLAR LUMINOSITY
Considerations regarding the choice of beam parameters and IP configuration for the SSC
[DE84-014532] 01 p0118 N85-10603
A search for low luminosity pulsars and its implications for the pulsar luminosity functions
02 p0296 N85-11919
Effects of core mixing on solar oscillation frequencies
[DE84-015540] 03 p0449 N85-12853
Continuum distributions of active galactic nuclei
05 p0742 N85-14770
Physical conditions in low-luminosity active galactic nuclei
05 p0742 N85-14771
The correlation between excitation parameter and nebular luminosity for galactic HII regions with application to regions of star formation in M83
05 p0743 N85-14773
Evidence for non-radiative activity in hot stars
06 p1231 N85-17756
Is the ratio of observed X-ray luminosity to bolometric luminosity in early-type stars really a constant?
06 p1234 N85-17777
Non-radiative energy from differential rotation in hot stars
06 p1234 N85-17778
The Orion molecular cloud at far-infrared wavelengths
06 p1245 N85-17860
The 157 micron (C II) luminosity of the galaxy
06 p1248 N85-17877
The structure and dynamics of ringed galaxies
09 p1415 N85-18926
Solid state luminescent light filters for neodymium lasers
11 p1716 N85-20799
STS atmospheric luminosities
[NASA-CR-175514] 12 p1791 N85-21240
High energy facilities advanced projects: Intrabeam scattering for a beam of gold ions
[DE85-000887] 12 p1941 N85-22192
IRAS observations of Seyfert galaxies
[NASA-CR-175557] 12 p1953 N85-22287
Plasma in the clusters of galaxies
12 p1957 N85-22298
The Feinheit method: A phase-independent formulation of the period-luminosity relation for Cephids
[NASA-CR-175708] 14 p2440 N85-25056
Atomic physics aspects of a Relativistic Nuclear Collider
[DE85-006867] 15 p2650 N85-26342
Electrodes for flash discharge lamps
[DE85-006897] 17 p2955 N85-28250
A new luminosity component in 3C48
[NASA-CR-175840] 17 p3052 N85-28694
Evolution of the luminosity function of extragalactic objects
[NASA-CR-175977] 18 p3201 N85-29860
Requirements for very high energy accelerators
[DE85-011173] 20 p3529 N85-31952
Visibility and vertical structure measurements in southern Germany
[AD-A154714] 21 p3635 N85-32574
Solar variability observed through changes in solar figure and mean diameter
[DE85-012857] 22 p3860 N85-33700
On gamma and neutrino radiation from Cyg X-3
[OG-2.1-7] 22 p3863 N85-33924
Evidence for long-term variability in the ultra high energy photon flux from Cygnus X-3
[OG-2.1-10] 22 p3863 N85-33926
The universal spectrum of AGNs and QSOs
[OG-2.7-9] 22 p3872 N85-33932
X-ray spectra of bursting neutron stars
23 p3961 N85-34686

LUMINOUS FLUX DENSITY
U LUMINOUS INTENSITY

LUMINOUS INTENSITY
NT ILLUMINANCE
NT LUMINANCE
Efficiency of lasing dye media in pumping high-power radiation with nanosecond pulses
02 p0270 N85-11783
Surface coatings for low emittance in the thermal surveillance band
[MRL-R-937] 03 p0398 N85-12158
In search of a visual-cortical describing function: A summary of work in progress
05 p0707 N85-14538
Central regulation of sensory flow in human visual system
07 p1013 N85-16435
Individual difference in chromatic brightness matching
[AD-A149882] 10 p1529 N85-19641
The relative effectiveness of red and white light for subsequent dark-adaptation
[AD-A149883] 10 p1530 N85-19642
Twilight intensity variation of the infrared hydroxyl airglow
11 p1663 N85-20481
EXOSAT observations of the 35d intensity variations of Her X-1 — X ray binary source
11 p1742 N85-20956
Research study of droplet sizing technology leading to the development of an advanced droplet sizing system
[NASA-CR-174839] 12 p1950 N85-21604
A posteriori increase of resolving power of optical system forming averaged monochromatic images
13 p2082 N85-23003
Dependence of parameters of silicon photovoltaic cells on temperature and light intensity
14 p2275 N85-24094
Pursuit tracking performance and flash disruption: The effects of training the non-dominant eye on target reacquisition
[AD-A153404] 17 p2999 N85-28541
Intense excitation source for high power laser
[AD-A153424] 18 p3112 N85-29267
Fluctuations in light intensity during backscattering in turbulent medium
21 p3695 N85-32956
Beam potential measurement of an intense H(-) beam by use of the emissive probe technique
[DE85-012871] 24 p4155 N85-35782
Connection between variations of the atmosphere temperature profile and variations of the meson component intensity
[HE-3.1-12] 24 p4178 N85-35910

LUMPED PARAMETER SYSTEMS
The analysis by the lumped parameter method of slade platform friction dampers used in the high pressure fuel turbopump on the space shuttle main engine
09 p1338 N85-18417
Basic EMC (Electromagnetic Compatibility) technology advancement for C3 systems. Volume 4E: Modeling of transmission lines. A comparison of lumped-circuit iterative models and the transmission line model
[AD-A150652] 14 p2291 N85-24201

LUMPING
Acoustic agglomeration methods and apparatus
[NASA-CASE-NPO-15468-1] 12 p1927 N85-22104

LUNA LUNAR PROBES
U LUNIK LUNAR PROBES

LUNAR ATMOSPHERE
Investigation of the daytime lunar atmosphere
[NASA-CR-175836] 14 p2440 N85-25057

LUNAR BASES
Lunar nuclear power feasibility study
[NASA-CR-171831] 07 p1041 N85-16611
Impact of lunar and planetary missions on the space station
[NASA-CR-171832] 08 p1108 N85-16988
Impact of lunar and planetary missions on the space station: Preliminary STS logistics report
[NASA-CR-171837] 09 p1285 N85-18072
In-situ rock melting applied to lunar base construction and for exploration drilling and coring on the moon
[DE85-006716] 16 p2717 N85-26770
Historical perspective on the Moon base: The British perspective
[DE85-005905] 17 p2907 N85-27925
Space ventures and society long-term perspectives
[NASA-CR-176012] 19 p3379 N85-30983

LUNAR CINEMATOGRAPHY
U LUNAR PHOTOGRAPHY

LUNAR COMPOSITION
NT LUNAR CORE
Is phosphorus predictably incompatible in igneous processes?
04 p0583 N85-13722
Megaregolith thickness, heat flow, and the bulk composition of the Moon
04 p0583 N85-13723
The bulk-Moon MgO/FeO ratio: A highlands perspective
04 p0583 N85-13724
Bulk composition of the Moon in the context of models for condensation in the solar nebula
04 p0583 N85-13725
Petrologic constraints on the origin of the Moon: Evidence from Apollo 14
04 p0583 N85-13726
Origin of the Moon: Constraints from volatile elements
04 p0584 N85-13727
Tests of the lunar hypothesis
04 p0584 N85-13730
On the origin of the Moon by rotational fission
04 p0587 N85-13746
An integrated dynamical and geochemical approach to lunar origin modelling
04 p0587 N85-13748
A circumterrestrial compositional filter
04 p0588 N85-13753
The origin of the Moon
04 p0588 N85-13754
Remote sensing analyses of localized lunar dark mantle deposits
13 p2195 N85-23616
Spectral reflectance studies of the Orientale basin
13 p2196 N85-23617
Landform identification on radar images
13 p2198 N85-23635
Mineralogical studies of lunar meteorites and their lunar analogs
15 p2563 N85-26572

LUNAR CORE
The size of the lunar core
04 p0581 N85-13713
On the Apollo subsatellite evidence for a lunar core
04 p0581 N85-13714
Implications of lunar palaeomagnetism for the origin of the Moon
04 p0582 N85-13717
Constraints on the origin of the Moon from molybdenum and other siderophile elements
04 p0582 N85-13718
Is phosphorus predictably incompatible in igneous processes?
04 p0583 N85-13722
Cosmogenic Na-22 and Al-26 in Luna-24 lunar drill core soil samples
13 p1981 N85-22427
Implications of convection in the Moon and the terrestrial planets
13 p2183 N85-23548
Modelling equilibrium and fractional crystallization in the system MgO-FeO-CaO-Al2O3-SiO2
13 p2184 N85-23552
Quenching effects on iron site partitioning in the Apollo 17 orange glass composition
13 p2184 N85-23553

LUNAR CRATERS
Physical and mechanical properties of lunar soil as function of specifics of relief and processes in vicinity of operation of Lunokhod-2
02 p0161 N85-11090
Directional properties of circular Maria: Interpretation in the context of a testable gravitational capture model for lunar origin
04 p0586 N85-13743
Moon
09 p1411 N85-18893
Monte Carlo modeling of lunar megaregolith development
13 p2197 N85-23627
Radar observations of fissure-fed basaltic lava flows, Craters of the Moon, Idaho
13 p2199 N85-23640
A comprehensive investigation of the dynamics of micron and submicron lunar ejecta in heliocentric space
19 p3384 N85-30994
Lunar and Martian impact basins: Exposed records of terrestrial bombardment?
21 p3721 N85-33090

LUNAR CRUST
Two lunar global asymmetries
04 p0585 N85-13734
Spectral reflectance studies on the orientale region of the Moon
06 p0688 N85-15839
The deep structure of lunar basins: Clues to the understanding of basin formation and modification
13 p2200 N85-23647
Primordial magmaspheres and their lasting consequences
22 p3857 N85-33982

LUNAR ECHOES
NT LUNAR RADAR ECHOES

LUNAR EFFECTS
NT LUNAR TIDES
Research directions in recent studies of the lunar geomagnetic effects
04 p0520 N85-13320
Daily magnetic variations at Ebro, Spain
04 p0520 N85-13325
Tidal dissipation in the Earth and Moon from laser ranging
04 p0585 N85-13733
Numerical simulations of fission
04 p0585 N85-13737

LUNAR ENVIRONMENT
NT LUNAR ATMOSPHERE

LUNAR EVOLUTION
Conference on the Origin of the Moon
[NASA-CR-174068] 04 p0581 N85-13709
Geophysical and geochemical constraints favoring the capture hypothesis
04 p0581 N85-13710
Lunar magma ocean and its implication for origin of the Moon
04 p0581 N85-13711
The initial thermal state of the Moon
04 p0581 N85-13712
Lunar magnetic history
04 p0582 N85-13715
Magnetic constraints on early lunar evolution revisited: Limits on accuracy imposed by methods of paleointensity measurements
04 p0582 N85-13716
Implications of lunar palaeomagnetism for the origin of the Moon
04 p0582 N85-13717
Constraints on the origin of the Moon from molybdenum and other siderophile elements
04 p0582 N85-13718
Nickel-cobalt systematics and their bearing on lunar origin
04 p0582 N85-13719
Ge abundances in the lunar mantle and implications for the origin of the Moon
04 p0582 N85-13721
Megaregolith thickness, heat flow, and the bulk composition of the Moon
04 p0583 N85-13723
The bulk-Moon MgO/FeO ratio: A highlands perspective
04 p0583 N85-13724
Bulk composition of the Moon in the context of models for condensation in the solar nebula
04 p0583 N85-13725
Petrologic constraints on the origin of the Moon: Evidence from Apollo 14
04 p0583 N85-13726
Origin of the Moon: Constraints from volatile elements
04 p0584 N85-13727

Volatile elements in and on lunar volcanic glasses: What do they tell us about lunar genesis?
04 p0584 N85-13728
Tests of the lunar hypothesis
04 p0584 N85-13730
Constraints on lunar origin: Evidence preserved in Precambrian stromatolites 04 p0584 N85-13731
Numerical simulations of fission
04 p0585 N85-13737
The dynamic fission instability and the origin of the Moon 04 p0586 N85-13738
Tidal disruption and the origin of the Moon
04 p0586 N85-13739
A numerical investigation of planetesimal collision trajectories with a Moon accumulating in Earth orbit
04 p0586 N85-13740
Stochastic does not equal ad hoc — theories of lunar origin 04 p0586 N85-13741
A testable gravitational capture model for the origin of the Earth's Moon 04 p0586 N85-13742
Directional properties of circular Maria: Interpretation in the context of a testable gravitational capture model for lunar origin 04 p0586 N85-13743
The problem of iron partition between Earth and Moon during simultaneous formation as a double planet system 04 p0587 N85-13744
Origin of the Moon 04 p0587 N85-13745
On the origin of the Moon by rotational fission
04 p0587 N85-13746
Geochemical evidence for the formation of the Moon by impact induced fission of the proto-Earth
04 p0587 N85-13747
An integrated dynamical and geochemical approach to lunar origin modelling 04 p0587 N85-13748
Lunar origin: role of giant impacts
04 p0587 N85-13749
Models of angular momentum input to a circumterrestrial swarm from encounters with heliocentric planetesimals
04 p0587 N85-13750
Capture of planetesimals into a circumterrestrial swarm 04 p0588 N85-13751
The lunar angular momentum problem
04 p0588 N85-13752
The origin of the Moon 04 p0588 N85-13754
Formation of the prelunar accretion disk
04 p0588 N85-13755
Mechanical models of close approaches and collisions of large protoplanets 04 p0588 N85-13756
Lunar origin from impact on the Earth
04 p0588 N85-13757
Moon 09 p1411 N85-18893
Lunar origin: Role of giant impacts
13 p2179 N85-23519
Implications of convection in the Moon and the terrestrial planets 13 p2183 N85-23548
Modelling equilibrium and fractional crystallization in the system MgO-FeO-CaO-Al2O3-SiO2
13 p2184 N85-23552

LUNAR EXPLORATION
Mission science value-cost savings from the Advanced Imaging Communication System (AICS)
[NASA-CR-174170] 04 p0458 N85-12905
Concept and cost analysis of an orbiting lunar station [ILR-MITT-136] 07 p0913 N85-15776
A new look at the planets — space probes
[AERONOMICA-ACTA-37-1984]
11 p1765 N85-21096
In-situ rock melting applied to lunar base construction and for exploration drilling and coring on the moon
[DE85-006716] 16 p2717 N85-26770
Surface exploration geophysics applied to the Moon
[DE85-006714] 16 p2684 N85-27793

LUNAR GEOLOGY
NT LUNAR CORE
Physical and mechanical properties of lunar soil as function of specifics of relief and processes in vicinity of operation of Lunokhod-2 02 p0161 N85-11090
Volatile elements in and on lunar volcanic glasses: What do they tell us about lunar genesis?
04 p0584 N85-13728
On the origin of the Moon by rotational fission
04 p0587 N85-13746
Moon 09 p1411 N85-18893
Why not a constant early lunar impact rate?
13 p2181 N85-23536
Correction and geological analysis of lunar 3.8 cm radar data 13 p2198 N85-23634
Closer look at lunar volcanism
[DE85-006663] 15 p2683 N85-26576
Adsorption of Hg on lunar samples
[DE85-007948] 17 p3054 N85-28906

LUNAR IONOSPHERE
U LUNAR ATMOSPHERE

LUNAR MAGNETIC FIELDS
Research directions in recent studies of the lunar geomagnetic effects 04 p0520 N85-13320
Lunar magnetic history 04 p0582 N85-13715
Magnetospheres in the solar system
12 p1954 N85-22274
Magnetic field generation in the cores of terrestrial bodies 22 p3859 N85-33694

LUNAR MANTLE
Nickel-cobalt systematics and their bearing on lunar origin 04 p0582 N85-13719
Abundancies of Ni, Cr, CO and major elements in the silicate portion of the Moon: Constraints from primary lunar magmas 04 p0582 N85-13720
Remote sensing analyses of localized lunar dark mantle deposits 13 p2195 N85-23616
The deep structure of lunar basins: Clues to the understanding of basin formation and modification
13 p2200 N85-23647

LUNAR MAPS
A unified lunar control network
13 p2203 N85-23669

LUNAR MARIA
Two lunar global asymmetries
04 p0585 N85-13734
Directional properties of circular Maria: Interpretation in the context of a testable gravitational capture model for lunar origin 04 p0586 N85-13743
Moon 09 p1411 N85-18893

LUNAR OCCULTATION
NT SOLAR ECLIPSES

LUNAR ORBITS
Implications of lunar palaeomagnetism for the origin of the Moon 04 p0582 N85-13717
Constraints on the origin of viscoelastic bodies
04 p0584 N85-13732
Tidal dissipation in the Earth and Moon from lunar laser ranging 04 p0585 N85-13733
The Moon's orbit history and inferences on its origin
04 p0585 N85-13735
A testable gravitational capture model for the origin of the Earth's Moon 04 p0586 N85-13742
Telescope in lunar orbit 15 p2682 N85-26568

LUNAR PERTURBATION
U LUNAR EFFECTS

LUNAR PHOTOGRAPHY
A unified lunar control network
13 p2203 N85-23669

LUNAR PROBES
NT LUNIK LUNAR PROBES

LUNAR PROGRAMS
NT APOLLO PROJECT

LUNAR RADAR ECHOES
Landform identification on radar images
13 p2198 N85-23635

LUNAR RADIATION
Natural interference phenomena affecting spaceborne receivers
[NASA-CR-174256] 07 p0916 N85-15796

LUNAR ROCKS
Is phosphorus predictably incompatible in igneous processes? 04 p0583 N85-13722
Megaregolith thickness, heat flow, and the bulk composition of the Moon 04 p0583 N85-13723
The bulk-Moon MgO/FeO ratio: A highlands perspective 04 p0583 N85-13724
Petrologic constraints on the origin of the Moon: Evidence from Apollo 14 04 p0583 N85-13726
Origin of the Moon: Constraints from volatile elements 04 p0584 N85-13727
The influence of gravitational body force in meteoritic chondrule and lunar glass formation
06 p0884 N85-15614
Asteroid-meteorite connection: Regolith effects implied by lunar reflectance spectra 06 p0888 N85-15640
Mineralogical investigations of lunar samples and meteorites
[NASA-CR-174291] 08 p1258 N85-17918
Quenching effects on iron site partitioning in the Apollo 17 orange glass composition 13 p2184 N85-23553
Experimental methods for quenching structures in lunar-analog silicate melts: Variations as a function of quench media and composition
13 p2184 N85-23554
Electrolysis of simulated lunar melts
15 p2681 N85-26561
Mineralogical studies of lunar meteorites and their lunar analogs 15 p2683 N85-26572
Microwave processing of lunar materials: Potential applications
[DE85-007223] 16 p2755 N85-27003
Mechanical properties of lunar materials under anhydrous, hard vacuum conditions: Applications of lunar glass structural components
[DE85-006682] 16 p2801 N85-27271

LUNAR ROTATION
The dynamic fission instability and the origin of the Moon 04 p0586 N85-13738

LUNAR ROVING VEHICLES
NT LUNOKHOD LUNAR ROVING VEHICLES

LUNAR SATELLITES
NT IMP
Concept and cost analysis of an orbiting lunar station [ILR-MITT-136] 07 p0913 N85-15776

LUNAR SCATTERING
U DIFFUSE RADIATION
U LUNAR RADAR ECHOES

LUNAR SHELTERS
In-situ rock melting applied to lunar base construction and for exploration drilling and coring on the moon
[DE85-006716] 16 p2717 N85-26770

LUNAR SOIL
Physical and mechanical properties of lunar soil as function of specifics of relief and processes in vicinity of operation of Lunokhod-2 02 p0161 N85-11090
Constraints on the origin of the Moon from molybdenum and other siderophile elements
04 p0582 N85-13718
Ge abundances in the lunar mantle and implications for the origin of the Moon 04 p0582 N85-13721
The bulk-Moon MgO/FeO ratio: A highlands perspective 04 p0583 N85-13724
Solar cosmic ray produced neon in lunar soils and their implication for gas-rich meteorite studies
06 p0887 N85-15636
Asteroid-meteorite connection: Regolith effects implied by lunar reflectance spectra 06 p0888 N85-15640
Cosmogenic Na-22 and Al-26 in Luna-24 lunar drill core soil samples 13 p1981 N85-22427
Electrolysis of simulated lunar melts
15 p2681 N85-26561
In-situ rock melting applied to lunar base construction and for exploration drilling and coring on the moon
[DE85-006716] 16 p2717 N85-26770

LUNAR SPACECRAFT
NT APOLLO SPACECRAFT
NT LUNAR SATELLITES
NT LUNIK LUNAR PROBES

LUNAR SURFACE
An error analysis for the use of presently available lunar radio flux data in broadbeam antenna-system measurements
[PB84-218361] 01 p0016 N85-10097
Geophysical and geochemical constraints favoring the capture hypothesis 04 p0581 N85-13710
Lunar magma ocean and its implication for origin of the Moon 04 p0581 N85-13711
The initial thermal state of the Moon
04 p0581 N85-13712
Moon 09 p1411 N85-18893
Why not a constant early lunar impact rate?
13 p2181 N85-23536
Morphology and mechanics of terraces in lunar craters
13 p2182 N85-23543
Quenching effects on iron site partitioning in the Apollo 17 orange glass composition 13 p2184 N85-23553
Remote sensing analyses of localized lunar dark mantle deposits 13 p2195 N85-23616
Spectral reflectance studies of the Orientale basin
13 p2195 N85-23617
Monte Carlo modeling of lunar megaregolith development 13 p2197 N85-23627
Mechanisms of basalt-plains ridge formation
13 p2199 N85-23643
On the absence of strike-slip faults from the planets and satellites 13 p2200 N85-23645
The deep structure of lunar basins: Clues to the understanding of basin formation and modification
13 p2200 N85-23647
Some new photometric data form panoramic pictures taken by Lunokhod-2 15 p2481 N85-25312
Telescope in lunar orbit 15 p2682 N85-26568
Closer look at lunar volcanism
[DE85-006663] 15 p2683 N85-26576
Lunar and Martian impact basins: Exposed records of terrestrial bombardment? 21 p3721 N85-33090
High-energy neutrinos from a lunar observatory
[HE-5.3-21] 24 p4207 N85-36112

LUNAR SURFACE VEHICLES
NT LUNOKHOD LUNAR ROVING VEHICLES

LUNAR TEMPERATURE
The initial thermal state of the Moon
04 p0581 N85-13712

LUNAR TIDES
Tidal dissipation in the Earth and Moon from lunar laser ranging 04 p0585 N85-13733
The Moon's orbit history and inferences on its origin
04 p0585 N85-13735

LUNAR TOPOGRAPHY
Monte Carlo modeling of lunar megaregolith development 13 p2197 N85-23627

LUNGS
Oxygen delivery during exercise: Limitations to maximum flow 05 p0688 N85-14424

Interaction between lung mechanics and gas exchange by low volume high frequency pulmonary ventilation in patients with respiratory failure
[AD-A146604] 06 p0846 N85-15372
Chemical characterization and toxicologic evaluation of airborne mixtures. Inhalation toxicology of diesel fuel obscurant aerosol in Sprague-Dawley rats. Phase 3. Subchronic exposures
[AD-A150100] 12 p1905 N85-21966
Aerosol deposition along the respiratory tract at zero gravity: A theoretical study
[DE85-006703] 15 p2619 N85-26136
Carcinogenesis of nitrated toluenes and benzenes skin and lung tumor assays in mice
[AD-A155723] 22 p3818 N85-33655

LUNIK LUNAR PROBES
Cosmogenic Na-22 and Al-26 in Luna-24 lunar drill core soil samples 13 p1981 N85-22427

LUNOKHOD LUNAR ROVING VEHICLES
Some new photometric data form panoramic pictures taken by Lunokhod-2 15 p2481 N85-25312

LUTETIUM
Debye temperature and static displacements in LuH sub x single crystals from energy dispersive X-ray diffraction
[DE85-010961] 19 p3376 N85-30946

LUTETIUM COMPOUNDS
Electrochemistry of rare-earth diphthalocyanines
[AD-A145813] 03 p0327 N85-12106

LYAPUNOV FUNCTIONS
U LIAPUNOV FUNCTIONS

LYMAN ALPHA RADIATION
Lyman-Alpha aurora 02 p0302 N85-11953
Temporal and spatial variations in the intensity of ultraviolet emissions from Jupiter and the Io torus
03 p0448 N85-12846
Pioneer 10 and Voyager observations of the interstellar medium in scattered emission of the He 584 A and H Lya 1216 A lines 06 p0873 N85-15541
Changes of LISM characteristics in the heliospheric interface 06 p0873 N85-15542
Observations of interstellar HI toward nearby late-type stars 06 p0874 N85-15546
Radio and UV observations of high latitude HI
06 p0879 N85-15583
Lyman alpha coronagraph research sounding rocket program
[NASA-CR-174376] 09 p1354 N85-18517
MSG-7: Atmospheric penetration of solar radiation in the range of Schumann-Runge bands
11 p1657 N85-20443
Ionospheric absorption on 1539 kHz in relation to solar ionizing radiation 11 p1659 N85-20455
Aeronomical aspects of mesospheric photodissociation: Processes resulting from the solar H Lyman alpha line
[AERONOMICA-ACTA-A-285-1984]
11 p1680 N85-20587
Analysis of white dwarf Lyman alpha profiles
11 p1752 N85-21018
The extent of the local hi halo
[NASA-CR-176115] 23 p3987 N85-34724
On the detectability of key-MeV solar protons through their nonthermal Lyman-alpha emission
[SH-1.3-5] 23 p3993 N85-34752

LYMAN SPECTRA
Lyman-Alpha aurora 02 p0302 N85-11953
Studies of hot B subdwarfs. Part 2: Energy distributions of three bright sdB/sdOB stars in the 950-5500 angstrom range
[NASA-CR-175854] 16 p2881 N85-27775

LYMPH
NT LYMPHOCYTES

LYMPHOCYTES
Experiment 1ES031 on Spacelab 1: Are cells sensitive to gravity? — lymphocyte proliferation
05 p0669 N85-14428
H1-NMR studies on lymphocyte membranes in human lymphoproliferative diseases 20 p3505 N85-31787
The DNA metabolism and poly-(ADP-ribose) synthesis in lymphocytes of persons exposed to low doses of ionizing radiation
[OEFZS-4307] 20 p3507 N85-31800
Sensitivity of human lymphocytes to microgravity in-vitro 20 p3510 N85-31820
Non-rigid body motion 23 p3964 N85-34576

LYOPHILIZATION
U COLLOIDING

LYOPHILS
U COLLOIDS

LYRA CONSTELLATION
Observations of RR Lyrae and X Arietis with the IUE satellite 11 p1754 N85-21030

LYSIMETERS
Field lysimeter facility for evaluating the performance of commercial solidified low-level waste
[DE85-003886] 11 p1727 N85-20863

M

M REGION
The distribution and dynamics of planetary nebulae in M32 and the Andromeda Galaxy
20 p3546 N85-32068
Isotopic overabundances and the energetic particle model of solar flares
[SH-2.2-1] 23 p4000 N85-34796

M STARS
NT FLARE STARS
Theoretical studies of chromospheres and winds in cool stars
[NASA-CR-174204] 06 p0880 N85-15596
Theory tested by means of the stars — viability of the alpha-omega dynamo model 06 p1233 N85-17770

M WINGS
U VARIABLE SWEEP WINGS

MAARS
U CRATERS

MACH NUMBER
Wind tunnel tests on a tube-launched missile configuration with a deflectable nose control and a novel wrap-around fin stabiliser
[AR-003-696] 01 p0001 N85-10003
Effect of upstream sidewall boundary layer removal on an airfoil test — conducted in Langley 0.3-m transonic cryogenic tunnel 03 p0313 N85-12019
Progress in wind tunnel wall interference assessment/correction procedures at the NAE
03 p0314 N85-12025
Space Shuttle Orbiter trimmed center-of-gravity extension study. Volume 8: Effects of configuration modifications on the aerodynamic characteristics of the 140 A/B Orbiter at a Mach number of 5.97
[NASA-TM-72861-VOL-8] 04 p0452 N85-12867
Comparison of analytical and experimental steadyand unsteady-pressure distributions at Mach number 0.78 for a high-aspect-ratio supercritical wing model with oscillating control surfaces
[NASA-TM-84589] 07 p0899 N85-15897
Joined wing transonic design and test validation
[AD-A148355] 08 p1078 N85-16834
Exploratory investigation of the aerodynamic characteristics of a biwing vehicle at Mach 20.3
[NASA-TM-86314] 08 p1113 N85-17021
Unsteady stall penetration of an oscillating swept wing
[AD-P004156] 09 p1264 N85-17941
Mach-10 high Reynolds number development in the NSWC (Naval Surface Weapons Center) hypervelocity facility
[AD-A151241] 15 p2474 N85-25274
Measurements of the symmetric aerodynamic coefficients for flat faced cylinders in the angle of attack regime 0 to 90 deg for transonic and supersonic speeds
[FFA-TN-1984-04] 16 p2700 N85-26875
On power effecient operation of the 2m x 2m transonic wind tunnel at the National Aerospace Laboratory
[NAL-TR-847] 18 p3084 N85-28953
Development of a temperature-compensated hot-film anemometer system for boundary-layer transition detection on high-performance aircraft
[NASA-TM-86732] 22 p3730 N85-33121
An evaluation of three helicopter rotor sections
[NASA-TM-86719] 23 p3893 N85-34115
Unsteady flow in a supersonic cascade with two in-passage shocks
[NASA-CR-3925] 24 p4060 N85-35158

MACH REFLECTION
Experimental study of Mach reflection of weak shock waves 02 p0260 N85-11703
Pseudo-stationary oblique-shock-wave reflections in a polystomic gas, sulfur hexafluoride
[UTIAS-TN-253] 12 p1845 N85-21577
Tabular and graphical solutions of regular and Mach reflections in pseudo-stationary frozen and vibrational-equilibrium flows, part 1
[UTIAS-283-PT-1] 23 p3893 N85-34117
Tabular and graphical solutions of regular and Mach reflections in pseudo-stationary frozen and vibrational-equilibrium flows, part 2
[UTIAS-283-PT-2] 23 p3894 N85-34118

MACHINE LEARNING
U LEARNING MACHINES

MACHINE LIFE
U SERVICE LIFE

MACHINE RECOGNITION
U ARTIFICIAL INTELLIGENCE

MACHINE STORAGE
U COMPUTER STORAGE DEVICES

MACHINE TOOLS
NT BORING MACHINES
NT GRINDING MACHINES
NT LATHES
NT MILLING MACHINES
NT TURRET LATHES
USSR report: Machine tools and metalworking equipment
[JPRS-UMM-84-019] 01 p0035 N85-10214
Report on high-precision jig-boring machines
01 p0035 N85-10215
The US machine tool industry and the defense industrial base
[PB84-216928] 01 p0036 N85-10225
Use of robotics in heavy machinery, equipment construction industry 04 p0485 N85-13093
USSR report: Machine tools and metalworking equipment
[JPRS-UMM-84-020] 04 p0491 N85-13126
DNC, CNC network for robotized machining cells
04 p0491 N85-13130
Advances of implementing NC machine tools discussed 04 p0491 N85-13131
Thermal shock as a carbide grade development tool
[DE84-016939] 04 p0509 N85-13251
Modular laser distance measurement system for multiaxis machine tools
[BMFT-FB-T-84-166] 05 p0641 N85-14110
Efficiency of programmed motion control systems
06 p0776 N85-14961
East Europe report: Science and technology
[JPRS-ESA-84-045] 06 p0815 N85-15175
New concepts for industrial robots outlined
06 p0815 N85-15176
Machine tools at 1984 Leipzig Spring Fair
06 p0815 N85-15177
NC programming, machine tool information
06 p0816 N85-15178
Laser-guided measuring system for precisioning device 06 p0816 N85-15179
Power of deterministic thinking in machine tool accuracy
[DE85-001751] 07 p0974 N85-16188
USSR report: Machine tools and metalworking equipment
[JPRS-UMM-84-021] 08 p1138 N85-17168
Technology planning for flexible manufacturing systems 08 p1139 N85-17170
USSR report: Machine tools and metalworking equipment
[JPRS-UMM-85-001] 08 p1139 N85-17172
Structure of solids surfaces in wear situations
[AD-A148480] 08 p1166 N85-17366
Airport ground equipment under development at Riga
09 p1278 N85-18038
Scania, ASEA of Sweden use robots for all production phases 09 p1310 N85-18229
The control of manufacturing systems for varying medium-batch production
[PNR-90236] 09 p1371 N85-18616
State and development of the machine-tool industry in Japan. Part 2: Flexible manufacturing systems
[PNR-90236-PT-2] 09 p1371 N85-18617
New method for heat treatment of metals
10 p1446 N85-19110
East Europe report: Science and technology
[JPRS-ESA-85-006] 10 p1480 N85-19200
National Machine Tools Conference slated for 1985; Conference agenda, papers 10 p1480 N85-19202
USSR report: Machine tools and metalworking equipment
[JPRS-UMM-85-003] 10 p1481 N85-19211
Armenia markets new drive motors for machine tools
10 p1481 N85-19212
Dean of Kiev State University on impact of robots
10 p1481 N85-19213
Specifications, applications of gantry robots viewed
10 p1481 N85-19215
Control system of complex CNC machining cell
10 p1482 N85-19218
Productivity gains through CAD of CNC programs
10 p1482 N85-19219
USSR report: Materials science and metallurgy
[JPRS-UMS-84-005] 11 p1597 N85-20044
East Europe report: Science and technology
[JPRS-ESA-85-009] 11 p1616 N85-20165
Institute director surveys industrial automation drive
11 p1617 N85-20167
Increased use of CNC in machine tool construction
11 p1617 N85-20170
New CNC systems described
11 p1617 N85-20172
Technological and economic assessment of advanced ceramic materials: Volume 4: A case study of integrated optic devices
[PB85-113116] 12 p1815 N85-21385
Technological and economic assessment of advanced ceramic materials. Volume 6: A case study of ceramic cutting tools
[PB85-113132] 12 p1815 N85-21387
Development of a sintered shim
[DE85-006183] 13 p2025 N85-22665

Rational use of tatanium in nonferrous metallurgy
13 p2031 N85-22726
New technique for fluid feed in simultaneous multisurface grinding
13 p2045 N85-22800
USSR report: Machine tools and metalworking equipment
[JPRS-UMM-85-005] 13 p2051 N85-22839
Diamond cutters' grinders 13 p2051 N85-22841
Machine tool vibrations: A review
13 p2102 N85-23104
USSR report: Engineering and equipment
[JPRS-UEQ-84-001] 14 p2265 N85-24094
Small-size measuring gauges for metal cutting machine tools
14 p2267 N85-24045
Fabrication of turbine parts with transportable tools
14 p2267 N85-24046
Novel drives for machine tools
14 p2268 N85-24053
Use of program controlled machine tools to automate and mechanize production processes in pipe manufacture
14 p2269 N85-24059
USSR report: Machine tools and metalworking equipment
[JPRS-UMM-85-006] 14 p2283 N85-24148
Metal waste in machine tool industry examined
14 p2283 N85-24147
New CNC turning centers described
14 p2284 N85-24148
Large CNC machining center for turbine production
14 p2284 N85-24149
Minister B. V. Balmont on status of automation drive
14 p2284 N85-24151
USSR report: Machine tools and metalworking equipment
[JPRS-UMM-85-004] 14 p2284 N85-24152
Integrated control system for FMS components
14 p2285 N85-24156
Cutting structural materials in vacuum
14 p2286 N85-24165
Automating the study of error in discrete aerodynamic fairing design
14 p2288 N85-24176
An analysis of machine tool systems suitable for laser profiling
14 p2308 N85-24282
Robotic deburring. Part 2: Evaluation of cutters and noncompliant tooling
[DE85-006152] 14 p2311 N85-24306
Electrical features of new DNC, CNC system viewed — direct numerical control
15 p2524 N85-25562
Flexible machining systems described
15 p2524 N85-25563
USSR report: Machine tools and metalworking equipment
[JPRS-UMM-84-010] 16 p2767 N85-27071
Status, prospects of computer-aided design discussed
16 p2767 N85-27073
New robotized, vertical broaching machine featured
16 p2767 N85-27074
Guidelines for optimization of robotized machining cells
16 p2767 N85-27076
East Europe report: Science and technology
[JPRS-ESA-85-019] 16 p2767 N85-27077
Extreme evaluation of reliability indices for components of metallurgical equipment
[BLL-M-36070-(5828.4)] 16 p2798 N85-27234
Steels with improved machinability
[BLL-BISI-22341-(9022.06)] 17 p2927 N85-28061
USSR report: Machine tools and metalworking equipment
[JPRS-UMM-84-014] 17 p2946 N85-28188
Applications of robots in machine tool industry reviewed
17 p2946 N85-28189
Manufacturing information system
[AD-A152715] 17 p3011 N85-28616
Spiral bevel and circular arc helical gears: Tooth contact analysis and the effect of misalignment on circular arc helical gears
[NASA-TM-87013] 20 p3395 N85-31060
USSR report: Machine tools and metalworking equipment
[JPRS-UMM-85-008] 20 p3437 N85-31329
Standard series of direct-current motors for regulated electric drives
22 p3772 N85-33375
Generation of round bores in composite structure rollguns
[DE85-011872] 22 p3793 N85-33501
Properties of tungsten-free steel for cutting tools
[BLL-M-35908-(5828.4)] 23 p3915 N85-34250
Generated spiral bevel gears: Optimal machine-tool settings and tooth contact analysis
[NASA-TM-87075] 23 p3937 N85-34405

MACHINE TRANSLATION
An operational system for subject switching between controlled vocabularies: A computational linguistics approach
[NASA-CR-3936] 02 p0293 N85-11903
Graphics translators for computer-aided drafting and design: Interface alternatives for the A/E community
[AD-A148892] 10 p1540 N85-19706
Developing an automated technique for translating a relational database into an equivalent network one
[AD-A151844] 15 p2866 N85-26451
Expressiveness and language choice
[AD-A153280] 17 p3012 N85-28623
Local automation model software benchmarking: Test plan
[AD-A154349] 19 p3337 N85-30676

MACHINE-INDEPENDENT PROGRAMS
Machine computation of delay and capacitance of transistor structures of subnanosecond large integrated circuits
04 p0460 N85-13120

MACHINING
NT CHEMICAL MACHINING
NT ELECTROCHEMICAL MACHINING
NT MILLING (MACHINING)
NT SPARK MACHINING
Three-dimensional photochemical machining with lasers
[AD-A145792] 03 p0365 N85-12342
DNC, CNC network for robotized machining cells
04 p0491 N85-13130
Design of a flexible machining system
[CETIM-1-3E-140] 04 p0510 N85-13252
USSR report: Machine tools and metalworking equipment
[JPRS-UMM-84-021] 06 p1136 N85-17168
Survey of the finish characteristics of machined optical surfaces
[DE85-001343] 09 p1385 N85-18708
National Machine Tools Conference slated for 1985: Conference agenda, papers
10 p1460 N85-19202
Production turret lathe retrofitted with robot
10 p1461 N85-19214
Evaluation of machining damage in brittle materials
[DE85-001794] 11 p1612 N85-20136
Nondestructive method for detecting machine damage in beryllium
[DE85-001074] 12 p1862 N85-21681
Use of ferrofluids in machining of metals
13 p2045 N85-22802
USSR report: Machine tools and metalworking equipment
[JPRS-UMM-85-005] 13 p2051 N85-22839
T700 cutter life improvement program
[AD-A150450] 13 p2099 N85-23089
Technology for pressure-instrumented thin airfoil models, phase 1
[NASA-CR-3891] 14 p2227 N85-23804
Group technology for working turbine drive wheel disks
14 p2269 N85-24061
An analysis of machine tool systems suitable for laser profiling
14 p2308 N85-24282
Influence of phosphorus content and heat treatment on the machinability of electroless nickel deposits
[DE85-007250] 15 p2522 N85-25548
Steels with improved machinability
[BLL-BISI-22341-(9022.06)] 17 p2927 N85-28061
Study of a simulated test for assessing the machinability of steels
[BLL-BISI-TRANS-22344-(9022.06)]
17 p2972 N85-28357
Study of a test method for assessing machinability in gear cutting operations
[BLL-BISI-TRANS-22345-(9022.06)]
17 p2972 N85-28358
Examples of application of machinability tests
[BLL-BISI-TRANS-22346-(9022.06)]
17 p2973 N85-28363
Assessing the machinability of gearwheel steels during manufacture
[BLL-BISI-TRANS-22343-(9002.06)]
17 p2973 N85-28365
Europe's primary producers of industrial lasers surveyed
18 p3087 N85-29101
Laser machining and some applications
[NHK-LABS-NOTE-307] 18 p3112 N85-29268
Machining of beryllium with the LLNL precision engineering research lathe
[DE85-010832] 19 p3250 N85-30149
Metallographic preparation of materials with various coatings
[BLL-DRIC-TRANS-7522-(3823.06)]
20 p3433 N85-31299
Machining-induced deformation in stepped specimens of PH 13-8 Mo, 18 nickel maraging steel grade 200T1 and grain-refined HP 9-4-20
[NASA-CR-172480] 21 p3585 N85-32177
Method of precisely modifying predetermined surface layers of a workpiece by cluster ion impact therewith
[DE85-006519] 23 p3884 N85-34710
Single-point diamond crushing of Zerodur with in-situ polishing and metrology on a diamond turning machine
[DE85-012918] 24 p4083 N85-35306

MACROCLIMATE
U CLIMATE

MACROMOLECULES
U MOLECULES

MACULAR VISION
U VISION

MAGELLANIC CLOUDS
Studies of extragalactic RR Lyrae stars
03 p0444 N85-12831
On the scale of distances of the galaxy
05 p0737 N85-14735
Optical studies of X-ray selected Active Galactic Nuclei (AGN) in the direction of the Large Magellanic Cloud (LMC)
06 p1237 N85-17797
Far IR observations of the Magellanic clouds
06 p1246 N85-17879
Magellanic cloud objects 11 p1744 N85-20965
Highly ionized gas associated with the small Magellanic cloud
11 p1745 N85-20976
Galactic absorption lines measured from the IUE low dispersion spectra of active galaxies
11 p1745 N85-20977
IUE observations of planetary nebulae in the Magellanic Clouds
11 p1747 N85-20986
The UV extinction laws in two very young clusters, NGC 6530 in the galaxy and NGC 2100 in the LMC
11 p1748 N85-20994
Ultraviolet studies of the young populous cluster NGC 2100 in the LMC
11 p1748 N85-20995
All-Union conference of radio astronomers
13 p1977 N85-22408
Optical pulsar in the Large Magellanic Cloud remnant 0540-69.3
[DE85-006707] 16 p2883 N85-27788

MAGMA
Lunar magma ocean and its implication for origin of the Moon
04 p0581 N85-13711
Abundancies of Ni, Cr, CO and major elements in the silicate portion of the Moon: Constraints from primary lunar magmas
04 p0582 N85-13720
Two lunar global asymmetries
04 p0585 N85-13734
Petrology and petrogenesis of Batholitic rocks, San Jacinto Mountains, southern California
05 p0673 N85-14322
Extreme incompatibility of Pb during the crystallization of magmatic iron meteorites
06 p0886 N85-15827
Correlation and petrological interpretation of abyssal and terrestrial tephra layers
09 p1353 N85-18512
Physical characterization of magma
[DE85-000568] 09 p1354 N85-18519
Vertical movements and structure formation within island systems of northeast Asia
10 p1501 N85-19471
Mesozoic magmatism of Mongolian-Okhotsk Belt and its possible geodynamic interpretation
10 p1502 N85-19481
High-resolution microseismicity study of possible magmatic intrusion in the Long Valley Caldera
[DE85-001076] 11 p1681 N85-20593
Shallow magma targets in the western US
[DE85-003274] 12 p1861 N85-21803
Magmatism in continent-ocean transition zone (development of ideas of A. N. Zavaritskiy)
13 p2113 N85-23161
Thermohydrodynamic model: Hydrothermal system, shallowly seated magma chamber
13 p2115 N85-23173
Io: Generation of silicate magma by shear melting at the base of a basaltic lithosphere
13 p2172 N85-23476
Characteristics of basaltic lava flows on Venus
13 p2177 N85-23508
Modelling equilibrium and fractional crystallization in the system MgO-FeO-CaO-Al2O3-SiO2
13 p2184 N85-23552
Magmas as selective filters of volatiles between planetary mantles and surfaces
13 p2185 N85-23557
Volcanism of the Colorado Plateau (basin and range transition): Implications for crustal processes
13 p2187 N85-23569
A silicic shield volcano in Bolivia
13 p2187 N85-23572
Hydrovolcanism 13 p2188 N85-23574
What we know about Mars (but otherwise wouldn't) if it is the shergottite parent body
15 p2662 N85-26565
Selection of promising sites for magma energy experiments
[DE85-006832] 16 p2820 N85-27393

Melt zones beneath five volcanic complexes in California: An assessment of shallow magma occurrences
[DE85-010644] 19 p3305 N85-30489
Anorthositic oceanic crust in the Archean Earth 21 p3719 N85-33077
Earth's primordial differentiation, and its after-effects 21 p3722 N85-33092
Primordial magmaspheres and their lasting consequences 22 p3857 N85-33882
Geochemical confirmation of the lunar magmasphere hypothesis 22 p3859 N85-33895
Heat transfer and brine evolution in magma-hydrothermal systems 24 p4104 N85-35441
Ore genesis at the Monterrosas deposit in the Coastal Batholith, Ica, Peru 24 p4115 N85-35510

MAGNESIUM
NT MAGNESIUM ISOTOPES
Universal binding energy relations in metallic adhesion
[NASA-TM-86889] 03 p0331 N85-12132
Strong-coupling superconductivity of Mg in proximity to Ta
[DE84-015462] 04 p0589 N85-13627
Testing of production of silicon-titanium-magnesium alloying composition
[BLL-M-35904-(5828.4)] 05 p0616 N85-13937
Observations of local interstellar Mg I and Mg II 06 p0874 N85-15547
Mg II spectra of late type stars used to probe the LISM 06 p0874 N85-15548
FeII and MgII in the nearby interstellar medium 06 p0874 N85-15549
Minor elements and cathodoluminescence of Mg-rich olivines from Murchison and Allende carbonaceous meteorites 06 p0884 N85-15619
Combustion properties of fuel-rich magnesium propellants with HTPB as binder
[FOA-C-20555-D1] 07 p0935 N85-15924
Structure of transient zone in diffusion welding of TeTS-19 piezoceramic with AMg6 alloy 11 p1603 N85-20082
Observations of Mg 1 and Mg 2 in the local ISM 11 p1748 N85-20997
Mg 2 emission of Pop. 2 long-period Cepheids 11 p1754 N85-21032
Ultraviolet, radio and X-ray observations of hybrid stars 11 p1759 N85-21063
Structural strenght of strip D16T aluminum alloy with low copper and magnesium content 13 p2025 N85-22691
New deformable secondary aluminum alloys 13 p2026 N85-22694
The effect of microalloying with calcium and magnesium on the plasticity of Poldi AKN 20 Ni-based alloy
[BLL-BISI-TRANS-2174-(9022.09)] 17 p2929 N85-28075
Effect of periodic accelerations on physiochemical properties and Ca2+ reactivity of actomyosin in white rat myocardium and skeletal muscles 19 p3324 N85-30584
Measurements of Fe and Ar fragmentation cross sections
[PAPER-OG-7.2-20] 21 p3714 N85-33047
Photoionization of alkali and alkaline earth atoms: Na and Mg
[DE85-011612] 22 p3837 N85-33755
Radiation measurements on magnesium flames
[BLL-CE-TRANS-8110-(9022.09)] 24 p4075 N85-35254

MAGNESIUM ALLOYS
Relationships between electronic structure and stability of metallic glasses
[AD-A145506] 02 p0287 N85-11874
Application of the diffraction model to amorphous magnesium zinc alloys
[AD-A147369] 07 p0928 N85-15883
Influence of excess phases on fracture toughness of cast alumun-magnesium-zinc alloy 10 p1442 N85-19091
Computation of thermal shock-free straightening conditions for aluminum-magnesium alloy welded structures 10 p1449 N85-19131
Rapid solidification processing of magnesium alloys
[AD-A150270] 13 p2022 N85-22686
Influence of laser treatment of structure and mechanical properties if MA21 alloy 13 p2029 N85-22713
Problem of pore formation mechanism in welded joints of aluminum alloys in the system aluminum-magnesium-lithium 13 p2032 N85-22732
The role of hydrogen in the stress corrosion failure of high strength Al-Zn-Mg alloys
[AD-A150891] 14 p2256 N85-23978
Temperature variation of resistivity of certain alloys based on transition and simple metals in amorphous and crystalline states 15 p2486 N85-25399
Superplasticity in a thermo-mechanically processed Aluminum-10.2%Mg-0.52%Mn alloy
[AD-A152016] 15 p2510 N85-25485
Special features of the one-sided automatic welding of structures of Al-Mg alloys 16 p2792 N85-27222
Thermal expansion effects in electrical transport in amorphous metals
[AD-A152477] 17 p2930 N85-28089
Study of phase equilibria and crystallization processes in Al-Zn-Mg alloy systems 19 p3241 N85-30068
Influence of type of processing of AK4 alloy on its surface state and strength of bonding of plasma coatings 19 p3242 N85-30103
Resistance to corrosion fatigue in aluminum alloy 1561 in sea water 19 p3243 N85-30106
Atomized magnetism-aluminum protective coatings 19 p3244 N85-30116
The effect of alloy additions on superplasticity in thermomechanically processed high magnesium aluminum-magnesium alloys
[AD-A155142] 21 p3587 N85-32184

MAGNESIUM CHLORIDES
Coexistence of antiferromagnetism and spin-glass ordering in the Ising system FeO 55MgO 45Cl2
[DE85-004164] 12 p1942 N85-22197

MAGNESIUM COMPOUNDS
NT CHLOROPHYLLS
NT DOLOMITE (MINERAL)
NT ENSTATITE
NT MAGNESIUM CHLORIDES
NT MAGNESIUM FLUORIDES
NT MAGNESIUM OXIDES
Fracture toughness of MgCr(sub)2O(sub)4-ZrO(sub)2
[DE85-007945] 17 p2917 N85-27982

MAGNESIUM FLUORIDES
Peculiarities of MgF2 film formation and optimization of MgF2 film deposition process 14 p2251 N85-24132

MAGNESIUM ISOTOPES
A 200-MeV pi(+) induced nucleon removal from 24Mg 17 p3042 N85-28821

MAGNESIUM OXIDES
The bulk-Moon MgO/FeO ratio: A highlands perspective 04 p0583 N85-13724
Surface effects of corrosive media on hardness, friction, and wear of materials
[NASA-TM-83711] 07 p0930 N85-15898
Special purpose materials for fusion application
[DE85-005346] 14 p2424 N85-24850
Selective radiative cooling with MgO and/or LiF layers
[DE85-011595] 19 p3282 N85-30228
Method for the preparation of photochromic insulating crystals
[DE85-011806] 19 p3282 N85-30229

MAGNESYN (TRADEMARK)
U SERVOMOTORS

MAGNET COILS
NT FIELD COILS
Design, construction, and operational results of an 800-A, 10-kV hot deck amplifier
[DE84-014044] 04 p0498 N85-13162
Positron flux concentrator: An update
[DE84-016280] 04 p0561 N85-13576
Two-rotor alternators with superconductor field winding 06 p0795 N85-15082
Design and test of a four channel motor for electromechanical flight control actuation
[NASA-CR-171838] 08 p1156 N85-17294
Design and construction details of the FRX-C/T device: A compact toroid plasma translation experiment
[DE85-001527] 09 p1380 N85-18749
Transient voltage oscillations in coils
[DE85-006715] 15 p2550 N85-25738
Magnetics calculations for an ELMO Bumpy Square
[DE85-011438] 21 p3707 N85-33021
Series-counterpulse repetitive-pulse inductive storage circuit
[DE85-006438] 23 p3928 N85-34342

MAGNETIC ABSORPTION
U ELECTROMAGNETIC ABSORPTION

MAGNETIC ANNULAR ARC
Development of theory of high-current high-pressure pulsed arc 15 p2645 N85-26314

MAGNETIC ANOMALIES
NT GEOMAGNETIC HOLLOW
The south-central United States magnetic anomaly
[E85-10025] 02 p0218 N85-11436
Continental and oceanic crustal magnetization modelling
[E85-10034] 03 p0378 N85-12413
Phonon anomalies in superconducting transition metal compounds --- lanthanum and niobium compounds 03 p0426 N85-12718
Petrologic model of the northern Mississippi embayment based on satellite magnetic and ground based geophysical data
[NASA-TM-85075] 04 p0533 N85-13406
Measurements of electric fields obtained by stratospheric balloons in the region of the South Atlantic anomaly
[INPE-3218-PRE/571] 06 p0675 N85-14335
Anomalous magnetic field in northwestern Pacific Ocean and Pacific Ocean plate kinematics 06 p0820 N85-15210
Correlation radius of gravitational and magnetic anomalies and methods of its determination 06 p0821 N85-15213
The mineralogy of global magnetic anomalies
[E85-10061] 07 p0987 N85-16272
Prospects and means for development of theory and practice of interpretation of gravitational and magnetic anomalies 10 p1501 N85-19474
Geological reasons for change in intensity of linear magnetic anomalies of the Kursk magnetic anomaly
[NASA-TM-77824] 10 p1514 N85-19552
Precursors for Brazilian magnetic anomalies from 1922 to 1969
[INPE-3283-PRE/605] 11 p1681 N85-20590
Structure of Iceland and ocean floor spreading 13 p2112 N85-23159
MAGSAT anomaly field data of the crustal properties of Australia
[E85-10100] 13 p2122 N85-23215
An investigation of the crustal properties of Australia and surrounding regions derived from interpretation of MAGSAT anomaly field data 13 p2122 N85-23216
Remanent magnetization model for the broken ridge satellite magnetic anomaly 13 p2123 N85-23219
System of interpretation of remote sensing data when hydrocarbons are present, volume 2
[INPE-3087-TDL/162-VOL-2] 16 p2810 N85-27326
X-ray ionenification at balloon altitudes of the South Atlantic magnetic anomaly in association with geomagnetic activity
[INPE-3469-PRE/712] 16 p2827 N85-27437
Structure of Reykjanes Ridge rift zone and Icelandic thermal anomaly 19 p3289 N85-30395
Improving the geological interpretation of magnetic and gravity satellite anomalies
[E85-10103] 20 p3473 N85-31585
MAGSAT scalar anomaly map of South America 20 p3473 N85-31586
MAGSAT satellite magnetic anomaly map over South America 20 p3474 N85-31587
Geologic analysis of averaged magnetic satellite anomalies 20 p3474 N85-31588
Statistical magnetic anomalies from satellite measurements for geologic analysis 20 p3474 N85-31589
Binning of satellite magnetic anomalies 20 p3474 N85-31590
The south-central United States magnetic anomaly 20 p3474 N85-31591
The south-central United States magnetic anomaly 20 p3475 N85-31592
A comparative study of spherical and flat-Earth geopotential modeling at satellite elevations 20 p3475 N85-31593
A comparative study of spherical and flat-Earth geopotential modeling at satellite elevations 20 p3475 N85-31594
Reduced to pole long-wavelength magnetic anomalies of Africa and Europe 20 p3475 N85-31595
Euro-African MAGSAT anomaly-tectonic observations 20 p3475 N85-31596
Long-wavelength magnetic and gravity anomaly correlations on Africa and Europe 20 p3476 N85-31597
Continental and oceanic magnetic anomalies: Enhancement through GRIM 20 p3476 N85-31598
Continental magnetic anomaly constraints on continental reconstruction 20 p3476 N85-31599
Regional magnetic anomaly constraints on continental rifting 20 p3476 N85-31600
A real time index of geomagnetic background noise for the MAD (Magnetic Anomaly Detection) frequency band
[AD-A155717] 22 p3814 N85-33827
Solar cycle variations of the anaomalous cosmic ray component
[SH-4.6-2] 23 p4039 N85-35040
Temporal variations of the anomalous oxygen component, 1977 - 1984
[SH-4.6-3] 23 p4039 N85-35041

MAGNETIC BEARINGS
Overview of magnetic bearing control and linearization approaches for annular magnetically suspended devices 05 p0607 N85-13872
Europeans active in magnetic bearing industry 08 p1141 N85-17195
Linear magnetic bearings
[NASA-CASE-GSC-12582-2] 11 p1641 N85-20337
A theoretical model for the study of nonlinear dynamics of magnetic bearings 20 p3462 N85-31505

MAGNETIC CHARGE DENSITY
New types of power supplies for ultrasonic processing equipment 12 p1843 N85-21566
MAGNETIC CIRCUITS
Lightweight cladding for magnetic circuits [AD-D011469] 10 p1481 N85-18350
MAGNETIC COILS
NT FIELD COILS
Results of prototype field measurements on SM4 [NAC-83-01] 01 p0117 N85-10797
Magnetic spin reduction system for free spinning objects [NASA-CASE-MFS-25968-1] 02 p0166 N85-11122
High-performance TF coil design for the Toroidal Fusion Core Experiment (TFCX) [DE85-001127] 08 p1159 N85-17315
Extended abstract: Ergodic magnetic limiter experiments on TEXT with a 7/3 resonance [DE85-001390] 09 p1391 N85-18754
Mathematical model of electromagnetic suspension device with two control windings 13 p2074 N85-22954
Outline of alternative design of R-Tokamak 15 p2654 N85-26371
Simultaneous phase and frequency control of a three-phase inductor-convertor bridge [DE85-006197] 18 p3096 N85-29164
Physics-magnetics trade studies for tandem mirror reactors [DE85-010043] 18 p3182 N85-29732
Recent progress in stellarator reactor conceptual design [DE85-009592] 18 p3189 N85-29760
Magnetics calculations for an ELMO Bumpy Square [DE85-010442] 18 p3191 N85-29762
Plasma engineering models of tandem mirror devices with high-field test-cell inserts [DE85-010046] 18 p3192 N85-29797
TFCX shielding optimization [DE85-010503] 19 p3359 N85-30626
MIG: MCNP Input Generator for EFFI magnet geometries [DE85-010494] 20 p3515 N85-31857
Assessment of magnetic field asymmetries in ELMO Bumpy square [DE85-011905] 22 p3846 N85-33819
High-field launch electron cyclotron heating experiments in the ELMO Bumpy Torus [DE85-012088] 22 p3848 N85-33825
Design improvements and cost reductions for a 5000 MWh superconducting Magnetic Energy Storage plant [DE85-010572] 22 p3847 N85-33830
Reversing-counterpulse repetitive-pulse inductive storage circuit [DE85-008409] 23 p3928 N85-34344
Apparatus for unilateral generation of a homogeneous magnetic field [DE86-008001] 23 p3928 N85-34345
Assessment of magnetic field asymmetries in ELMO Bumpy square [DE85-011559] 23 p3964 N85-34705
Analysis of a pulsed power system containing rotating machine [DE85-014128] 24 p4159 N85-35786
Effect of Cu4Ti compound formation on the characteristics of NbTi accelerator magnet wire [DE85-014226] 24 p4159 N85-35788
MAGNETIC COMPASSES
Impact of magnetic isolation on pointing system performance in the presence of structural flexibility [NASA-CR-172481] 16 p2732 N85-28661
MAGNETIC COMPRESSION
Use of magnetic compression based on amorphous alloys as a drive for induction linacs [DE84-014524] 02 p0277 N85-11605
Los Alamos Spheromak Program [DE85-010746] 20 p3396 N85-31077
Magnetics calculations for an ELMO Bumpy Square [DE85-011436] 21 p3707 N85-33021
MAGNETIC CONTROL
Magnetic spin reduction system for free spinning objects [NASA-CASE-MFS-25968-1] 02 p0166 N85-11122
MAGNETIC COOLING
Deceleration, cooling, and trapping of atoms [AD-A146234] 03 p0418 N85-12672
Magnetic refrigeration and heat pumping design options [DE85-003405] 13 p2092 N85-23084
MAGNETIC DIPOLES
General image theory for the Sommerfeld problem [REPT-S-154] 02 p0193 N85-11280
Comparisons of secular variation in two-dipole and spherical harmonic models with observatory data in Eurasia, 1965-1975 04 p0521 N85-13330
Advanced artificial dielectric materials for millimeter wavelength applications [AD-A148960] 10 p1431 N85-19027
Aperture studies with PATRICIA and RACETRACK on simple attices containing SSC dipoles [DE85-004163] 11 p1724 N85-20842
The ULF/ELF/VLF electromagnetic fields generated in a sea of finite depth by elevated dipole sources [AD-A149636] 12 p1828 N85-21470
Orientation and strength of Martian magnetic dipole 16 p2723 N85-26808
Possible configuration of Martian magnetosphere 16 p2723 N85-26809
Ion-acoustic double layer in a magnetic picket fence configuration [INPE-3552-PRE/764] 19 p3369 N85-30866
Numerical modeling of subsurface communication [DE85-012818] 21 p3577 N85-32249
On the influence of the heliomagnetospheric periphery on the galactic cosmic rays [SH-4.2-19] 23 p4009 N85-34856
Pulsars as cosmic ray particle accelerators: Dynamics of electrons [OG-8.2-23] 23 p4021 N85-34919
Event parameters: Fixed targets 24 p4146 N85-35702
High energy cosmic ray signature of quark nuggets [HE-6.2-11] 24 p4212 N85-36147
MAGNETIC DISKS
ADAM: An abstract database machine [RSRE-84007] 02 p0293 N85-11904
Analog disc recorder system: Operator's reference manual [DE84-016926] 04 p0509 N85-13209
MOM peripherals 08 p1141 N85-17189
Television animation store: Recording pictures on a parallel transfer magnetic disc [BBC-RD-1984/17] 10 p1482 N85-19220
Recovery of lost files from VAX/VMS disk structures: A case study [DE85-010652] 19 p3333 N85-30650
Performance and electric field limitations in inflow disk MHD generators 20 p3534 N85-31987
Conferences of quantum-radiooptics section 22 p3773 N85-33360
MAGNETIC DISPERSION
Comments on the paper by F. Pegoraro, L. Suglyama: Spatial diffusion of charged high-energy fusion products by shear Alfven perturbations [INPE-3291-PRE/606] 16 p2666 N85-27675
A method of solving the dispersion equation for electrostatic electron waves in magnetized plasma [KGI-PREPRINT-071] 16 p2669 N85-27697
High harmonic rectangular gyrotron 19 p3256 N85-30189
MAGNETIC DISTURBANCES
NT MAGNETIC STORMS
National solar-terrestrial research program [PB84-216163] 01 p0072 N85-10479
Plans for Interbol satellite experiment 13 p1977 N85-22407
Substorms in energetic radiation belt particles according to data from Meteor artificial Earth satellite 16 p2719 N85-26788
Magnetic and thermodynamic structure of the solar corona during sunspot minimum 18 p3203 N85-29873
Study of spectral exponent on quiet and disturbed days [SH-4.5-10] 23 p4037 N85-35026
The cosmic ray differential diurnal variation dependences on the zenith angle and the geomagnetic disturbance [SH-4.5-16] 23 p4038 N85-35033
MAGNETIC DOMAINS
Investigation of domain structures and walls using neutron diffraction 03 p0423 N85-12702
Neutron scattering on structural phase transitions with domain building 03 p0425 N85-12711
SEM (Scanning Electron Microscopy) studies of magnetic domains in amorphous metals [AD-A150963] 14 p2256 N85-23979
MAGNETIC EFFECTS
NT MAGNETIC RIGIDITY
Induction voldmeter [DE84-014321] 01 p0050 N85-10329
Magnetic interaction in low-dimensional systems 03 p0426 N85-12717
Effect of external magnetic field on characteristics of current-carrying steel tape 06 p0788 N85-15094
The determination of vertical sintering speed of sinter charges [BLL-M-36033-(5828.4)] 07 p0926 N85-15869
Influence of geomagnetic disturbances on cardiovascular function of athletes 08 p1193 N85-17516
Calculation of secondary-electron escape currents from inclined-spacecraft surfaces in a magnetic field 13 p1992 N85-22491
Magnetovolume effects in some Y-Ni intermetallic compounds [ISSN-0066-2003] 13 p2021 N85-22663
Mechanisms of magnetic heating of the solar corona 14 p2448 N85-25113
On the role of mother-planet magnetic field in spiral structure explanation of formation of spokes — Saturn rings 15 p2676 N85-26525
Very low temperature studies of hyperfine effects in metals [DE85-013367] 22 p3749 N85-33236
Relativistic electron in curved magnetic fields [OG-8.2-11] 22 p3890 N85-34110
Summary of activities, 1983 [LBL-18500] 23 p3969 N85-34605
Heavy cosmic ray measurement aboard Spacelab-1 [SH-10.1-7] 23 p4053 N85-35138
Injector losses on Mite [DE85-012356] 24 p4090 N85-35355
MAGNETIC ENERGY STORAGE
Repetitive pulse generation with inductive energy storage: A new technology for defense [DE84-017090] 06 p0805 N85-15122
Plasma erosion opening switch [DE85-011384] 20 p3535 N85-31998
Design improvements and cost reductions for a 5000 MWh superconducting Magnetic Energy Storage plant [DE85-010572] 22 p3847 N85-33830
Superconducting magnetic energy storage for asynchronous electrical systems [DE85-005986] 22 p3847 N85-33832
MAGNETIC EQUATOR
Magnetosonic waves and their relationship with energetic protons 14 p2368 N85-24635
Experimental check of ion transport mechanism in Earth's radiation belt with exposure to nonsteady-state electric fields 15 p2480 N85-25308
Spatial variation of cosmic rays near the heliospheric current sheet [SH-4.2-10] 23 p4007 N85-34848
Effects of a wavy neutral sheet on cosmic ray anisotropies [SH-4.2-11] 23 p4008 N85-34849
Determination of galactic cosmic ray latitudinal gradient using Earth based detectors [SH-4.2-13] 23 p4008 N85-34851
MAGNETIC FIELD CONFIGURATIONS
Plasma drift equilibrium (gyration) in toroidal systems with complex magnetic-field geometry [DE84-015627] 01 p0122 N85-10839
Elimination of stochasticity in stellarators 02 p0282 N85-11839
Relaxation of plasma rotation in a Tokamak in the presence of extraneous forces and corrugation of the magnetic field [DE84-015628] 02 p0284 N85-11854
On the annual and semiannual variation of S sub R at l'Aquila — geomagnetism 04 p0520 N85-13326
On some new features of semiannual variation of the geomagnetic field 04 p0520 N85-13327
Experimental observation of plasma neoclassical currents [DE84-015706] 04 p0568 N85-13605
Zero-current, high beta stelleration equilibria with rotational transform profile control [DE84-016835] 04 p0568 N85-13624
Compact toroidal development: Activity plan for field reversed configurations [DE84-017145] 05 p0730 N85-14695
High frequency plasma generator for ion thrusters [NASA-CR-174772] 08 p1114 N85-17023
Diffusion of particles in a slowly modulated wave [DE85-000729] 09 p1391 N85-18756
A free electron laser with a rotating quadrupole wiggler [AD-A149052] 10 p1489 N85-19404
Physical aspects of the prediction of solar flares [NASA-CR-175487] 10 p1572 N85-19915
Proposal for hollow cathode electron gun for electron cooling [DE85-002721] 11 p1630 N85-20263
Magnetic fluctuations, field reversal maintenance, and anomalous thermal transport in the reversed field pinch [DE85-003804] 11 p1732 N85-20892
Dynamics of space charge waves in the laser beat wave accelerator [AD-A149688] 12 p1936 N85-22163
Forced recognition by nonlinear MHD waves and sequential triggering of solar flares 12 p1956 N85-22291
The continuous spectrum of an axisymmetric, self-gravitating equilibrium in the presence of a poloidal magnetic field 12 p1959 N85-22315

Magnetostatic-wave propagation in a finite YIG-Loaded rectangular waveguide
[AD-A150332] 13 p2055 N85-22865
The structure and dynamics of the magnetosphere: Progress in the IMS 14 p2355 N85-24550
Magnetic field in the Earth's outer magnetosphere: Prognoz-6, -7 data 14 p2356 N85-24556
Structure of the boundary layer for steady-state magnetopause reconnection 14 p2356 N85-24561
Spline techniques for magnetic fields
[DE85-004919] 14 p2415 N85-24902
On the structure of magnetic fields in the solar convection zone 14 p2447 N85-25103
Amplification and maintenance of thin magnetic flux tubes by compressible convection — solar magnetism 14 p2447 N85-25104
A numerical simulation of the formation of solar prominences 14 p2448 N85-25112
Linear incompressible magnetoconvection in a planar layer with a nonuniform horizontal magnetic field 14 p2450 N85-25127
The continuous spectrum of an axisymmetric equilibrium with a mixed poloidal and toroidal magnetic field with gravity included 14 p2450 N85-25128
A study of the material motion into an eruptive prominence — solar prominence 14 p2453 N85-25146
Magnetic field structures of hard X-ray flares observed by HINOTORI spacecraft — solar flares 14 p2455 N85-25161
Internal field probing of translating FRCs
[DE85-003732] 15 p2657 N85-26394
On the role of mother-planet magnetic field in spiral structure explanation of formation of spokes — Saturn rings 15 p2676 N85-26525
TOKASTAR: A Tokamak stellarator hybrid with possible bean-shaped operation
[IPPJ-718] 16 p2866 N85-27680
Inherent magnetic field error measurements in ELMO Bumpy Torus
[DE85-005655] 16 p2867 N85-27685
Charge uncovering effects on flute instabilities in hot electron plasmas
[DE85-006957] 16 p2867 N85-27686
Spherical torus, compact fusion at low field
[DE85-006983] 16 p2867 N85-27689
I. F. S. (Institute for Fusion Studies) Newsletter, Volume 4, Number 1
[DE85-007917] 17 p3040 N85-28809
Theoretical and numerical studies of magnetic field line displacements in an Elmo Bumpy Torus
[DE85-008757] 17 p3041 N85-28816
Physics-magnetics trade studies for tandem mirror reactors
[DE85-010043] 18 p3182 N85-29732
Magnetics calculations for an ELMO Bumpy Square
[DE85-010442] 18 p3191 N85-29792
Plasma engineering models of tandem mirror devices with high-field test-cell inserts
[DE85-010046] 18 p3192 N85-29797
Toroidal viscosity and ambipolarity in the neoclassical transport theory of axisymmetric tori
[DE85-010822] 19 p3358 N85-30820
Magnetic probing of the solar interior
[NASA-CR-176025] 19 p3385 N85-30996
MIG: MCNP Input Generator for EFFI magnet geometries
[DE85-010494] 20 p3515 N85-31857
Magnetics calculations for an ELMO Bumpy Square
[DE85-011438] 21 p3707 N85-33021
Magnetic shielding with superconductors based on niobium-tin compounds 22 p3771 N85-33370
Electron and ion cyclotron heating calculations in the tandem-mirror
[DE85-011858] 22 p3842 N85-33797
Method and apparatus for maintaining equilibrium in a helical axis stellarator
[DE85-011626] 22 p3845 N85-33815
Elmo bumpy square plasma confinement device
[DE85-011628] 22 p3845 N85-33816
Assessment of magnetic field asymmetries in ELMO Bumpy square
[DE85-011905] 22 p3846 N85-33819
Spectral measurements of magnetic energy and magnetic helicity between 0.29 and 0.97 AU
[IFSI-85-2] 22 p3850 N85-33844
Potential effect in transport due to non-axisymmetric confining field 23 p3975 N85-34645
Activities of the RF Section 23 p3975 N85-34646
Radial transport caused by collision 23 p3976 N85-34652
Assessment of magnetic field asymmetries in ELMO Bumpy square
[DE85-011559] 23 p3984 N85-34705

MAGNETIC FIELD INTENSITY
U MAGNETIC FLUX

MAGNETIC FIELD INVERSIONS
Reversals of the Earth's magnetic field 04 p0521 N85-13332
Effects of solar magnetic field on cosmic rays
[SH-4.2-12] 23 p4008 N85-34850
On the influence of the heliomagnetospheric periphery on the galactic cosmic rays
[SH-4.2-19] 23 p4009 N85-34856
An update on the correlation between the cosmic radiation intensity and the geomagnetic AA index
[SH-4.2-24] 23 p4009 N85-34861

MAGNETIC FIELDS
NT BIOMAGNETISM
NT FORCE-FREE MAGNETIC FIELDS
NT GEOMAGNETISM
NT INTERPLANETARY MAGNETIC FIELDS
NT INTERSTELLAR MAGNETIC FIELDS
NT LUNAR MAGNETIC FIELDS
NT NONUNIFORM MAGNETIC FIELDS
NT PALEOMAGNETISM
NT PLANETARY MAGNETIC FIELDS
NT SOLAR MAGNETIC FIELD
NT STELLAR MAGNETIC FIELDS
NT TRAPPED MAGNETIC FIELDS
Natural environment design criteria for the Advanced X-ray Astrophysics Facility (AXAF) definition and preliminary design
[NASA-TM-86481] 01 p0014 N85-10089
Induction voldmeter
[DE84-014321] 01 p0050 N85-10329
NASA Geodynamics Program
[NASA-TM-87359] 01 p0063 N85-10418
Investigation of current setting procedures for sector magnets
[CSIR-NAC-83-03] 01 p0117 N85-10795
Final magnetic shimming of vacuum chamber suspension holes on the sector magnets
[CSIR-NAC-83-02] 01 p0117 N85-10796
Results of prototype field measurements on SM4
[NAC-83-01] 01 p0117 N85-10797
Magnetic spin reduction system for free spinning objects
[NASA-CASE-MFS-25966-1] 02 p0166 N85-11122
Generalized linear inversion of 2.5 - dimensional gravity and magnetic anomalies 02 p0226 N85-11480
Plane wave (EMP) incidence on a finitely conducting plane Earth with the magnetic field intensity parallel to the Earth's surface
[DE84-015364] 02 p0228 N85-11493
Polarization of ultrasound transmitted through boundary of magnetically inactive and equatorially magnetized media 02 p0257 N85-11662
Excitation of quasi-static magnetic fields with axial structure 02 p0259 N85-11696
Random processes and magnetohydrodynamic turbulence 02 p0271 N85-11767
Destruction of magnetic surfaces in three-dimensional MHD equilibria 02 p0282 N85-11838
Elimination of stochasticity in stellarators 02 p0282 N85-11839
The behavior of Pb(1-x)Sn(x)Te semiconductor laser diodes in a magnetic field
[AD-A145431] 02 p0287 N85-11872
Theory of the double critical state in type-2 superconductors
[DE84-015461] 02 p0289 N85-11886
Nonlinear electromagnetic waves in ferromagnetic conducting media 03 p0346 N85-12232
Magnetic characteristics of some volcanic rocks of the west Carpathians
[REPT-557] 03 p0376 N85-12400
Magnetospheric plasma studies using data from the dynamics high and low altitude plasma instruments
[AD-A145751] 03 p0392 N85-12505
On the cause of X-line formation in the near-Earth plasma sheet: Results of adiabatic convection of Plasma-Sheet-Plasma
[AD-A145835] 03 p0396 N85-12525
Electrical parameters in 60-Hz biological exposure systems and their measurement: A primer
[PB84-217793] 03 p0400 N85-12548
Charged particle erosion of icy satellites: Coronal atmospheres and surface redistribution 03 p0448 N85-12845
Vector magnetic field analysis of Lorentz forces acting in the solar atmosphere
[AD-A145941] 03 p0449 N85-12852
Ion thruster performance model
[NASA-CR-174810] 04 p0462 N85-12935
EXAFS and Mossebauer study of small metal clusters isolated in rare-gas solids
[DE84-015976] 04 p0470 N85-12994
Superconducting magnet for probing eddy currents in dynamic models 04 p0489 N85-13117
Human reactions to ELF (Extremely Low Frequency) electric and magnetic fields. An annotated bibliography of current literature, fourth edition
[PB84-230358] 04 p0545 N85-13472
Oscillating field current drive for reversed field pinch discharges
[DE84-015090] 04 p0567 N85-13610
Monte Carlo studies of transport in stellarators
[DE84-017833] 04 p0568 N85-13625
Magnetic constraints on early lunar evolution revisited: Limits on accuracy imposed by methods of paleointensity measurements 04 p0582 N85-13718
Magnetohydrodynamic and gasdynamic theories for planetary bow waves
[NASA-CR-174135] 04 p0589 N85-13780
The determination of eddy current losses in electrical equipment
[DE84-016340] 05 p0632 N85-14050
Particle physics
[DE84-013834] 05 p0727 N85-14673
Equations of plasma transport in a curved magnetic field
[DE84-015625] 05 p0730 N85-14690
Magnetic field calculation for ideal conductors by method of equivalent currents 06 p0786 N85-15035
Birkeland currents correlated with dc-electric fields observed during the CENTAUR BBX rocket experiments
[DRI-6-84] 06 p0834 N85-15311
A warm magnetoactive plasma in a large volume of space 06 p0878 N85-15579
Axisymmetric electromagnetic field influence on the characteristic velocity of an arc-jet
[NASA-TM-77475] 07 p0938 N85-15942
Slow surface magnetoplasma waves in oblique magnetic field 07 p0952 N85-16034
Transformation of electromagnetic waves in plasma with randomly-heterogeneous magnetic field 07 p0953 N85-16039
Amplitude mode magnetic sensors
[AD-D011335] 07 p0961 N85-16094
Self-generated magnetic fields and thermal flux inhibition
[AD-A147405] 07 p0971 N85-16166
Thermal evaporation in blast waves: A model for aneurism formation in the NRL (Naval Research Laboratory) LASER-HANE simulation experiment
[AD-A147006] 07 p0978 N85-16210
Ionospheric turbulence: Interchange instabilities and chaotic fluid behavior
[AD-A147810] 07 p0998 N85-16337
A low perturbation electron injector for cyclic accelerators
[AD-D011312] 07 p1040 N85-16604
Declinations in carbon-carbon composites
[AD-A146290] 08 p1119 N85-17052
Evaluation of interstitial gas contamination in titanium alloys using induced magnetic field analysis
[AD-P004130] 08 p1127 N85-17105
Electromagnetic inspection of wire ropes using sensor arrays
[AD-A148317] 08 p1170 N85-17379
Estimate of sound absorption due to magnetoelastic interactions
[AD-A146216] 08 p1218 N85-17671
Evidence for non-radiative activity in stars with T sub eff 10000 K 08 p1231 N85-17757
Winds from rotating, magnetic, hot stars 08 p1234 N85-17775
Current measurements by Faraday rotation in single mode optical fibers
[DE85-002025] 09 p1384 N85-18707
Beam probe spectroscopic technique for ion temperature and magnetic field measurements 09 p1389 N85-18738
Laser-induced-fluorescence-spectroscopy of atomic processes under a high magnetic field 09 p1389 N85-18740
Brief outline of analytic stability studies of magnetically insulated systems — bibliographies
[DE85-000212] 09 p1393 N85-18765
Advanced ion thruster research
[NASA-CR-174862] 10 p1430 N85-19021
Electromagnetic braking of a metallic projectile in flight
[AD-A148424] 10 p1480 N85-19345
Experience highlights from the design and manufacture of US LCT coils
[DE84-017504] 10 p1482 N85-19364
Role of multiple helicity nonlinear interaction of tearing modes in dynamo and anomalous thermal transport in the Reversed Pitch Field
[DE85-002176] 10 p1560 N85-19839
Resistive evolution of general plasma configuration
[DE85-002340] 10 p1561 N85-19843

Magnetization of very thin Ni films in epitaxial metal film sandwiches of Cu
[DE85-001640] 10 p1583 N85-19660
Development of high field Nb-Ti accelerator dipoles
[DE85-000621] 11 p1714 N85-20782
Aperture studies with PATRICIA and RACETRACK on simple attices containing SSC dipoles
[DE85-004163] 11 p1724 N85-20642
Stability of superconducting composites in a magnetic field
[DE85-002731] 11 p1734 N85-20907
Multifrequency observations of BL LAC objects and violently variable quasers 11 p1746 N85-20981
Magnetically-induced luminescence of (tr(2=phoe)(2)C10(4)
[AD-A149659] 12 p1799 N85-21286
Magentically actuated compressor
[NASA-CASE-GSC-12799-1] 12 p1818 N85-21404
Magnetic field in main gap of separator 12 p1843 N85-21563
Behavior of small ferromagnetic particles in traveling magnetic field 12 p1843 N85-21564
Rotating squid magnetometers and gradiometers
[AD-D011529] 12 p1849 N85-21600
Betatron-synchrotron detrapping in a tapered wiggler free electron laser
[AD-A149686] 12 p1856 N85-21642
Effect of long-term repeated exposure to high-intensity stationary magnetic field on adrenomedullary activity 12 p1904 N85-21955
Effect of stationary magnetic field on bleeding time 12 p1904 N85-21956
Superconducting magnet technology for accelerators
[DE85-004192] 12 p1926 N85-22102
Strong iron accelerating by collisionless magnetosonic shock wave propagating perpendicular to a magnetic field
[IPPJ-709] 12 p1935 N85-22161
Use of ferrofluids in machining of metals 13 p2045 N85-22802
Exitation of low-frequency resonance waves by moving conductor in space plasma 13 p2067 N85-22912
Magnetic noise in single-machine rotating frequency converters 13 p2077 N85-22969
Study of resolution of deep MT soundings by means of physical model 13 p2112 N85-23155
Discrimination of normal and anomalous magnetic and electric fields in geoelectromagnetic variations 13 p2114 N85-23166
1981 wC-130 airborne lightning characterization program data review
[AD-A150230] 13 p2138 N85-23275
High-field dipoles for future accelerators
[DE85-002315] 13 p2157 N85-23391
Improvement in magnetic field properties of vanadium-gallium superconductors by enhancement of spin-orbit scattering
[DE85-002893] 13 p2164 N85-23422
Design, theoretical innovations in Tokamaks systems 14 p2289 N85-24190
Applications of eddy currents 14 p2316 N85-24315
Spreading of greatly extended inhomogeneities in upper ionosphere 14 p2339 N85-24462
Experimental investigation of neutral plasma beam propagation across a magnetic field
[AD-A150944] 14 p2423 N85-24947
Cosmic ray environment model for Earth orbit
[NASA-CR-175866] 14 p2455 N85-25165
Magnetic field penetration into cometary ionosphere 15 p2477 N85-25290
Resonant rotations of satellite in polar orbit in magnetic and gravitational fields 15 p2479 N85-25302
Two interactive graphics postprocessors for NASTRAN 15 p2574 N85-25871
Forced MHD turbulence in a uniform external magnetic field
[NASA-CR-172576] 15 p2654 N85-26366
High energy beam experiment 15 p2654 N85-26376
Effects of magnetic shear on lower hybrid waves in the suprauroral region
[AD-A151980] 15 p2656 N85-26392
Evaluation of human exposures to low frequency fields 16 p2776 N85-27135
Electric field and energy transfer by magnetopause reconnection
[INPE-3448-PRE/701] 16 p2826 N85-27432
A multipole model of the observed cerebral cortex magnetic field
[AD-A152237] 16 p2842 N85-27526
High energy particle acceleration by coherent electromagnetic waves propagating across the magnetic field
[IPPJ-717] 16 p2866 N85-27679
Prospects for developing attractive magnetic fusion concepts
[DE85-006925] 16 p2867 N85-27684
Thermal and magnetic properties of neutron stars 16 p2880 N85-27774
The state of martensite after quenching in a magnetic field
[BLL-BISI-TRANS-22297-(9022.06)] 17 p2926 N85-28051
Magnetic monopoles
[DE85-008176] 17 p3027 N85-28719
Effects of level broadening on the magnetothermal oscillations in two-dimensional electron systems
[AD-A152639] 17 p3029 N85-28732
I. F. S. (Institute for Fusion Studies) Newsletter, Volume 4, Number 1
[DE85-007917] 17 p3040 N85-28809
Theoretical and numerical studies of magnetic field line displacements in an Elmo Bumpy Torus
[DE85-006757] 17 p3041 N85-28816
Central limit theorems in the area of large deviations for some dependent random variables
[AD-A153125] 17 p3043 N85-28831
Experimental research on electrical propulsion
[NASA-TM-77876] 18 p3067 N85-29069
Reciprocating magnetic refrigerator employing tandem porous matrices within a reciprocating displacer
[NASA-CASE-NPO-16257-1] 18 p3085 N85-29082
Swedish space program includes research satellites 18 p3088 N85-29113
Maser cavity servo-tuning system
[NASA-CASE-NPO-15890-1-CU] 18 p3093 N85-29143
Effects of Formvar coating and copper-nickel outer sheath on the ac losses of multi-strand subsize cables
[DE85-010413] 18 p3096 N85-29166
Optical fiber magnetic field sensor with nanosecond response time
[DE85-008409] 18 p3110 N85-29259
Intense ion beam diode diagnostics using a tunable dye laser
[DE85-008079] 18 p3113 N85-29272
Auroral zone electric fields from DE-1 and -2 at magnetic conjunctions
[NASA-CR-175974] 18 p3136 N85-29421
Wide-angle optics with strong magnetic fields for efficient generation of secondary-particle beams
[DE85-007727] 18 p3179 N85-29713
3d calculations of a fixed field alternating gradient synchrotron magnet
[DE85-002742] 18 p3183 N85-29739
Electromagnetic solitary waves in magnetized plasmas
[DE85-010084] 18 p3190 N85-29788
Inertial fusion reactors and magnetic fields
[DE85-009571] 18 p3191 N85-29789
MHD channel development
[DE85-008305] 18 p3192 N85-29796
Magnetic impurities in superconductors
[DE85-008372] 18 p3196 N85-29825
The vector structure of active magnetic fields 18 p3203 N85-29870
The Hanle effect applied to magnetic field measurements 18 p3204 N85-29878
Some design considerations for a satellite-borne magnetograph 18 p3204 N85-29879
Analysis of the new polarimeter for the Marshall Space Flight Center vector magnetograph 18 p3205 N85-29881
Inferred flows of electric currents in solar active regions 18 p3208 N85-29899
Comparisons of simultaneous vector magnetograms 18 p3208 N85-29900
Ephemeral regions versus pseudo ephemeral regions 18 p3208 N85-29901
Cosmic ray modulation and turbulent interaction regions near 11 AU
[NASA-TM-86193] 18 p3209 N85-29909
Magnetically-localizable, polymerized lipid vesicles and method of disrupting same
[AD-D011666] 19 p3249 N85-30144
An experimental study of the magnetoelastic bending of thin plates made of soft ferromagnetic material 19 p3262 N85-30352
Functions of Prognoz-10: Intercosmos' station explained 19 p3296 N85-30433
Effect of triphthesine and elenium on changes in evoked bioelectrical activity of the brain exposed to stationary magnetic field 19 p3325 N85-30601
Profile of a relativistic electron beam propagated through a linear wiggler and an axial guide field
[AD-A154403] 19 p3353 N85-30783
Trajectories of charged particles traversing a plasma sheath in an oblique magnetic field
[DE85-011070] 19 p3371 N85-30911
Fractional statistics and fractional quantized Hall effect
[DE85-007833] 19 p3375 N85-30940
Design of aggressive superconducting TFCX magnet systems
[DE85-010003] 19 p3376 N85-30943
Stability of a hot symmetric tandem mirror with thermal barrier
[DE85-010539] 19 p3377 N85-30952
Structure of the distant geotail: ISEE-3 observations 20 p3488 N85-31678
The temporal evolution of a small auroral substorm as viewed from high altitudes with Dynamics Explorer 1
[NASA-CR-176064] 20 p3493 N85-31718
Guide to the Main Ring DO overpass
[DE85-011722] 20 p3531 N85-31969
Alternating current OHMIC heating in a toroidal stellerator 20 p3534 N85-31968
Slow tearing modes: Transitions to instability 20 p3534 N85-31969
Simulating the effects of plasma disruption with a 1 MA current pulse in a coaxial test fixture
[DE85-010491] 20 p3535 N85-31998
On the role of the magnetic field strength in critical ionization velocity interaction
[TRITA-EPP-85-01] 20 p3536 N85-32003
Electrodeposition of chromium and copper in magnetic fields
[AD-A154648] 21 p3566 N85-32180
Magnetic materials
[AD-A154679] 21 p3580 N85-32256
Analysis of spacecraft data
[NASA-CR-171587] 21 p3669 N85-32789
Investigation of reproducibility of emission wavelength of helium-neon laser with external neon absorption cell (0.63 micrometers) 21 p3683 N85-32884
Solution of problem of equilibrium confinement of plasma by magnetic field in an infinite circular cylinder 21 p3692 N85-32936
The Faraday effect in ruby and corundum in strong magnetic fields 21 p3697 N85-32957
Magnetic fields in laser heated plasmas
[DE85-010715] 21 p3707 N85-33022
Very low temperature studies of hyperfine effects in metals
[DE85-013367] 22 p3749 N85-33236
Analysis of solution of Bloch's equations in time domain 22 p3771 N85-33371
Calculation of external magnetic field of a shielded transformer 22 p3771 N85-33373
Magnetic field and equivalent circuit of induction motors with shielded poles 22 p3772 N85-33378
Electron trajectories in a combined wiggler and alternating gradient quadrupole field
[DE85-010727] 22 p3842 N85-33794
Collisional transport for a superthermal ion species in a plasma
[DE85-011943] 22 p3845 N85-33818
Striation free doped silicon
[AD-A155730] 22 p3847 N85-33827
Magnetotails of the terrestrial planets: A comparative study 22 p3856 N85-33875
Virgo cluster as a high energy cosmic rays source
[OG-5.4-8] 22 p3866 N85-34065
Theoretical and Experimental Beam Plasma Physics (TEBPP) 23 p3901 N85-34166
Improved negative ion source
[DE85-006445] 23 p3912 N85-34241
Apparatus for unilateral generation of a homogeneous magnetic field
[DE85-006001] 23 p3928 N85-34345
Some physical differences between sheet plasma and multicusp plasma as volume produced H- or D- ion sources
[IPPJ-728] 23 p3974 N85-34637
Size effects of vacuum chamber for H- (D-) ion volume production by sheet plasma 1
[IPPJ-731] 23 p3974 N85-34639
Magnetohydrodynamic equilibrium and stability of spheromak with spheroidal plasma-vacuum interface
[IPPJ-732] 23 p3974 N85-34640
Radial transport phenomena for TMX-upgrade 23 p3976 N85-34647
RF induced radial diffusion in tandem mirrors 23 p3976 N85-34649
Induced azimuthal electric field effects on tandem transport and ambipolarity 23 p3976 N85-34650
Low frequency instability in a mirror field 23 p3977 N85-34657
Azimuthal uniformity and current balance study of ICRH-produced plasma in RFC-XXM 23 p3977 N85-34659
Breakdown of intrinsic ambipolarity for the radial diffusion due to a rotating RF field 23 p3977 N85-34660
Guiding center distribution function and longitudinal invariant 23 p3978 N85-34663

Simulation studies on stability of hot electron plasma
23 p3978 N85-34664
Behavior of helically-trapped fast ion orbits in heliotron E
23 p3978 N85-34666
Neoclassical diffusion including ellipticity in a heliotron-like configuration
23 p3978 N85-34667
Technology of magnetically driven accelerators
[DE85-011857] 23 p3983 N85-34700
Acceleration of ions and electrons to near-cosmic ray energies in a perpendicular shock: The January 6, 1978 event
[SH-1.5-4] 23 p3986 N85-34773
Isotopic overabundances and the energetic particle model of solar flares
[SH-2.2-1] 23 p4000 N85-34796
The dispersive evolution of charged-particle bunches in random magnetic fields
[SH-4.1-2] 23 p4004 N85-34828
Numerical descriptions of cosmic-ray transport
[SH-4.1-3] 23 p4004 N85-34829
Latitudinal gradients of cosmic rays and the polarity reversal of the heliospheric magnetic field: A preliminary evaluation
[SH-4.2-16] 23 p4008 N85-34853
Alfven wave scattering and the secondary to primary ratio
[OG-7.2-9] 23 p4015 N85-34876
The role of cosmic rays in magnetic hydrodynamics of interstellar medium
[OG-7.2-15] 23 p4015 N85-34882
On magnetic pair production above fast pulsar polar caps
[OG-8.2-13] 23 p4020 N85-34909
Cosmic rays 10Be biennal data and their relationship to aurorae and sunspots
[SH-7.1-1] 23 p4047 N85-35094
Long-time asymptotics of a system for plasma diffusion
[NASA-CR-177947] 24 p4093 N85-35375
Aeromagnetic and gravity models of the pluton below the Lake City caldera, Colorado
24 p4104 N85-35442
SLC arc transport system: Magnet design and construction
[DE85-014289] 24 p4159 N85-35789
TOSCA calculations and measurements for the SLAC SLC damping ring dipole magnet
[DE85-014366] 24 p4160 N85-35793
A new study of muons in air showers by NBU air shower array
24 p4190 N85-35997
Radio wave emitted by an extensive air showers in 10KHz to 1MHz region
[HE-4.6-15] 24 p4196 N85-36051

MAGNETIC FILMS
Symmetry of exchange interaction in crystalline magnetic films
02 p0259 N85-11604
Twisted domain wall in very thin magnetic films with perpendicular anisotropy
03 p0350 N85-12252
Development of wide band recording materials
[AD-A154961] 21 p3589 N85-32309
Changes in lattice cell parameter of film intermetallic compounds RT2
[BLL-M-35874-(5828.4)] 23 p3915 N85-34281

MAGNETIC FLUX
Induction voltmeter
[DE84-014321] 01 p0050 N85-10329
Free electron lasers
[AD-A145109] 01 p0053 N85-10349
Plane wave (EMP) incidence on a finitely conducting plane Earth with the magnetic field intensity parallel to the Earth's surface
[DE84-015364] 02 p0229 N85-11493
Flux-line pinning by the grain boundary in niobium bicrystals
[DE84-016668] 04 p0570 N85-13638
ATA probe beam experiment
[DE84-016017] 06 p0862 N85-15477
Magnetic fusion energy plasma interactive and high heat flux components. Volume 2: Technical assessment of the critical issues and problem areas in high heat flux materials and component development
[DE85-001155] 09 p1393 N85-18764
Electromagnetic inspection of wire ropes using sensor arrays
[AD-A149016] 10 p1495 N85-19436
Fermi surface study of CeSb
[DE85-002532] 10 p1584 N85-19862
Convergent spectral representation for 3-dimensional inverse MHD equilibria
[DE85-000668] 11 p1733 N85-20900
Magnetic field in main gap of separator
12 p1843 N85-21569
Ultrasensitive measuring devices
[DE85-000672] 12 p1853 N85-21622
Non-contacting electromagnetic de-spin system for Earth orbiting satellites
12 p1946 N85-22225
Equilibrium model of thin magnetic flux tubes — solar atmosphere
12 p1958 N85-22310
Observation of cosmic ray flux variations in stratosphere
13 p1981 N85-22430
Method of separately determining electrophysical properties of bulky conductor
13 p2073 N85-22951
Magnetic buoyancy instabilities in the convective overshoot zone — Sun
14 p2447 N85-25101
The photospheric temperature structure of magnetic flux tubes
14 p2447 N85-25102
On the structure of magnetic fields in the solar convection zone
14 p2447 N85-25103
Amplification and maintenance of thin magnetic flux tubes by compressible convection — solar magnetism
14 p2447 N85-25104
Nonlinear time-evolution of kink-unstable magnetic flux tubes in the convection zone of the Sun
14 p2447 N85-25105
A consideration of the solar cycle in the light of the behavior of the large active regions
14 p2452 N85-25140
Approximate closed-form expression for the electron-scattering-induced interaction between magnetic flux lines and grain boundaries
[DE85-004699] 15 p2660 N85-28417
Magnetic flux leakage inspection: Principles and applications
[BLL-BISI-TRANS-22248-(9022.06)]
17 p2975 N85-28382
Differential between crack and pseudo-crack indications by means of objective magnetic flux leakage testing
[BLL-BISI-TRANS-22033-(9022.06)]
17 p2976 N85-28386
Induction heating gun
[NASA-CASE-LAR-13161-1] 18 p3065 N85-29063
Measurements of Solar Vector Magnetic Fields
[NASA-CP-2374] 18 p3203 N85-29669
Current evolution in a numerical emerging-magnetic-flux model
18 p3204 N85-29675
Evidence for submergence of magnetic flux in a growing active region
18 p3208 N85-29902
Ballooning instabilities on a magnetic separatrix
[DE85-010855] 19 p3372 N85-30915
Flux pinning and flux flow studies in superconductors using flux flow noise technique
[DE85-010814] 19 p3376 N85-30945
Fractal structure of the interplanetary magnetic field
[NASA-TM-86212] 19 p3383 N85-30987
Structure of the distant geotail: ISEE-3 observations
20 p3488 N85-31678
Alternating current OHMIC heating in a toroidal stellerator
20 p3534 N85-31988
Spectral measurements of magnetic energy and magnetic helicity between 0.29 and 0.97 AU
[IFSI-85-2] 22 p3850 N85-33844
Neutral particle beam intensity controller
[DE85-006411] 23 p3969 N85-34804
Effect of ECH and ICH on ambipolar potential in NBT-1M
23 p3978 N85-34661
Stellarator approach to fusion plasma confinement
[DE85-011420] 23 p3984 N85-34704
Interstellar turbulence, random density variations, and scintillation measurements
[OG-7.2-13] 23 p4015 N85-34880
System expectations for Pioneer 1 foil implosion experiments
[DE85-014129] 24 p4091 N85-35359
Proposed FRX-D experiment
[DE85-012766] 24 p4158 N85-35778
The structure of Herbig-Haro object 43 and Orion dark cloud extinction
[NASA-TM-87503] 24 p4186 N85-35831

MAGNETIC FORMING
Major facility overhauls at LAMPF
[DE85-012724] 24 p4156 N85-35765

MAGNETIC INDUCTION
Multipurpose 5-MeV linear induction accelerator
[DE84-014523] 02 p0278 N85-11808
In-line beam current monitor
[DE84-014054] 04 p0560 N85-13567
Magnetic flux leakage inspection: Principles and applications
[BLL-BISI-TRANS-22248-(9022.06)]
17 p2975 N85-28382
Magnetic field and equivalent circuit of induction motors with shielded poles
22 p3772 N85-33378

MAGNETIC INDUCTION PROBES
U MAGNETIC PROBES

MAGNETIC LENSES
Fast and precise processing of material by means of an intensive electron beam
[BMFT-FB-T-84-123] 03 p0342 N85-12201

MAGNETIC MATERIALS
NT FERROFLUIDS
NT FERROMAGNETIC FILMS
NT FERROMAGNETIC MATERIALS
NT MAGNETITE
Metamagnetic systems
03 p0423 N85-12701
Anisotropy and microstructure of rare earth permanent magnet materials
[AD-A146549] 06 p0869 N85-15480
Selection of regenerator geometry for magnetic refrigerator applications
[DE84-012637] 11 p1816 N85-20160
Magnetic X-ray scattering studies of the rare Earth metal holmium
[DE85-003608] 12 p1807 N85-21305
Metrology for Electronic Technology: A bibliography of NBS (National Bureau of Standards)
[PB85-112895] 12 p1830 N85-21488
Green's function solution of the Kondo problems and universality of the thermodynamic properties
[DE85-002739] 12 p1943 N85-22208
Relationship between topological and magnetic order in small metal clusters
[AD-A150547] 13 p2018 N85-22951
SEM (Scanning Electron Microscopy) studies of magnetic domains in amorphous metals
[AD-A150963] 14 p2256 N85-22979
Practical surface methods
14 p2316 N85-24314
Tunneling in magnetic superconducting systems
[AD-A150577] 14 p2426 N85-24983
Magnetic steels with the lowest specific total losses
[BMFT-FB-T-84-263] 18 p3078 N85-29042
Magnetic materials
[AD-A154679] 21 p3580 N85-32258
Metallic glass composition
[DE85-011594] 22 p3751 N85-33253
Induction motors with minimum waste of magnetic iron
22 p3772 N85-33377

MAGNETIC MEASUREMENT
Results of prototype field measurements on SM4
[NAC-83-01] 01 p0117 N85-10797
Magnetic properties of the cobalt matrix in WC-Co compacts
02 p0177 N85-11198
Present practice for the recording of the Earth magnetic field — geophysical observatories
04 p0519 N85-13317
Analysis of the daily geomagnetic variation with the use of MAGSAT data — MAGSAT satellites
04 p0520 N85-13319
Contributions to the error analysis in the relativity gyroscope experiment
05 p0639 N85-14095
Amplitude mode magnetic sensors
[AD-D011395] 07 p0961 N85-16094
External cavity diode laser sensor
[AD-D011341] 07 p0969 N85-16152
Low power microprocessor based measurements system for determining the integrity of coatings on buried pipelines
[ERS-E.980] 09 p1324 N85-18329
Magnetization of very thin Ni films in epitaxial metal film sandwiches of Cu
[DE85-001840] 10 p1583 N85-19860
Magnetic measurements, calibrations, and standards: Report on a survey
[PB85-127827] 11 p1838 N85-20317
Solution of direct magnetometric problem on spherical Earth
13 p2116 N85-23170
Rapid advances in geological work
13 p2166 N85-23437
Metal complexes of some heterocyclic ligands
15 p2504 N85-25448
Overview of applications of SQUIDS
[DE85-009942] 20 p3458 N85-31480
A real time index of geomagnetic background noise for the MAD (Magnetic Anomaly Detection) frequency band
[AD-A155717] 22 p3614 N85-33627
Absolute measurement of Declination (D) by means of a proton magnetometer
[DMI-GEOPHYS-PAPERS-R-86]
22 p3836 N85-33751
Interplanetary magnetic field control of high-latitude electric fields and currents determined from Greenland magnetometer data
[DMI-GEOPHYS-PAPERS-R-89]
22 p3950 N85-33945

MAGNETIC METALS
U MAGNETIC MATERIALS
U METALS

MAGNETIC MIRRORS
Small, octopole-stabilized tandem mirror reactor
[DE85-002144] 10 p1580 N85-19832
Monte Carlo studies of tandem mirror plasmas interacting with waves in the Ion Cyclotron Range of Frequencies (ICRF)
[DE85-002966] 11 p1731 N85-20883

Efficient heating and confinement of ions in an axisymmetric magnetic mirror supplemented with dc electric field
[IPPJ-707] 12 p1935 N85-22160
Spectroscopic study of sources and control of impurities in TMX-U: Revision 1
[DE85-004423] 12 p1937 N85-22170
Stability of high energy particle plasmas to MHD-like modes
[DE85-007879] 17 p3039 N85-28603
Physics-magnetics trade studies for tandem mirror reactors
[DE85-010043] 18 p3182 N85-29732
Plasma engineering models of tandem mirror devices with high-field test-cell inserts
[DE85-010046] 18 p3192 N85-29797
Tritium system design for the mirror reactors FPD-1, FPD-2 and FPD-3
[DE85-010490] 19 p3363 N85-30852
Stability of a hot symmetric tandem mirror with thermal barrier
[DE86-010539] 19 p3377 N85-30952
Neutronics activities for next generation devices
[DE85-010488] 20 p3527 N85-31939
Simulation of automatic control of MFTF-B neutral beams
[DE85-010640] 20 p3530 N85-31960
Proton ring trapping in a magnetic mirror
20 p3534 N85-31990
Energy and Technology Review
[DE85-011767] 21 p3716 N85-33061
Elmo bumpy square plasma confinement device
[DE85-011628] 22 p3845 N85-33816
Proceedings of the US-Japan Workshop on Transport in Open-Ended Systems
[IPPJ-727] 23 p3975 N85-34644
Electron dynamics and transport in a mirror field
23 p3977 N85-34656
RF stabilization of interchange-ballooning modes
[DE85-012060] 24 p4080 N85-35353
Analysis of a pulsed power system containing rotating machine
[DE85-014128] 24 p4159 N85-35788

MAGNETIC MOMENTS
Electronic structure and properties of magnetic defects in Co(1+x)Al(1-x) and Fe(1+x)Al(1-x) alloys
[NASA-TM-77498] 07 p1047 N85-16648
Stochastic methods for the description of multiparticle production
[DE84-009681] 10 p1556 N85-19810
Magnetization of very thin Ni films in epitaxial metal film sandwiches of Cu
[DE85-001640] 10 p1563 N85-19860
Measurement of the induced moment magnetic form factor of a heavy fermion superconductor
[DE85-004165] 12 p1942 N85-22194
Microscopic magnetic structure of multiple bilayers of thin films of Fe and Ge
[DE85-004188] 13 p2024 N85-22682
Theoretical studies of high energy phenomenon: Analysis of models of CP and T violation
[DE85-007455] 17 p3036 N85-28782
Excited leptons contribution to muon g-2
[PREPRINT-432] 18 p3164 N85-29745
Physics with low temperature antiproton
[DE85-009827] 19 p3355 N85-30798

MAGNETIC MONOPOLES
Study for a large area underground detector made with organic scintillators for searching for magnetic monopoles
[NOTA-INTERNA-814] 02 p0201 N85-11339
An underground search for massive slow particles (hunting Grand Unified Theory (GUT) monopoles)
[NOTA-INTERNA-821] 02 p0292 N85-11864
Renewal request for high energy physics at Texas A and M University
[DE85-004469] 11 p1724 N85-20843
Superheavy magnetic monopoles and the standard cosmology
[DE85-003922] 15 p2585 N85-28587
Cocycles and magnetic monopole
[DE85-007797] 16 p2856 N85-27612
Magnetic monopoles
[DE85-008176] 17 p3027 N85-28719
A possible digital circuit able to recognize magnetic monopoles crossing a thick scintillator counter
[NOTA-INTERNA-826] 18 p3097 N85-29173
Study for a large area acrylic scintillator detector — magnetic monopoles
[NOTA-INTERNA-827] 18 p3097 N85-29174
Measurement of the attenuation length of an acrylic scintillator — magnetic monopoles
[NOTA-INTERNA-828] 18 p3097 N85-29175
Experimental performance of a digital circuit able to recognize magnetic monopole events
[NOTA-INTERNA-836] 18 p3097 N85-29176
The dimensional reduction transition
[DE85-003948] 19 p3363 N85-30990
Nineteenth International Cosmic Ray Conference. HE sessions, volume 8
[NASA-CP-2376-VOL-8] 24 p4200 N85-36066
Search for magnetic monopoles using proportional counters filled with helium gas
[HE-6.1-1] 24 p4209 N85-36127
Magnetic monopole search by 130 m(2)sr He gas proportional counter
[HE-6.1-2] 24 p4209 N85-36128
Results of a search for monopoles and tachyons in horizontal cosmic ray flux
[HE-6.1-3] 24 p4209 N85-36129
Monopole, astrophysics and cosmic ray observatory at Gran Sasso
[HE-6.1-4] 24 p4209 N85-36130
Monopole search below the Parker limit with the MACRO detector at Gran Sasso
[HE-6.1-5] 24 p4209 N85-36131
Limits on monopole fluxes from KFG experiment
[HE-6.1-6] 24 p4209 N85-36132
An experiment to detect gut monopoles
[HE-6.1-7] 24 p4210 N85-36133
Search for supermassive magnetic monopoles using mica crystals
[HE-6.1-8] 24 p4210 N85-36134
The homestake surface-underground scintillations: Description
[HE-6.1-9] 24 p4210 N85-36135
Upper limit on magnetic monopole flux from Baksan experiment
[HE-6.1-11] 24 p4210 N85-36136
Results from the UCSD magnetic monopole search
[HE-6.1-12] 24 p4210 N85-36137

MAGNETIC PERMEABILITY
Theory of near-field phased arrays for electromagnetic susceptibility testing
[PB84-217836] 01 p0042 N85-10273
Effect of annealing in transverse magnetic field on magnetic permeability of amorphous Fe5Co70Si15B10 alloy
03 p0349 N85-12247
Magnetic susceptibility, electrical resistivity, and specific heat of single crystal LaFe-4P-12
[DE84-009979] 04 p0570 N85-13833
Electronic structure and properties of magnetic defects in Co(1+x)Al(1-x) and Fe(1+x)Al(1-x) alloys
[NASA-TM-77498] 07 p1047 N85-16648
Magnetism of californium metal
[DE85-001141] 09 p1377 N85-18657
Effects of hydrogen on magnetic properties of amorphous zirconium alloys
[DE85-003303] 11 p1607 N85-20107
Investigation of electric and magnetic properties of intercalated graphite
[AD-A149801] 12 p1797 N85-21274
Method of separately determining electrophysical properties of bulky conductor 13 p2073 N85-22951
Optimum dimensions of power solenoids for magnetic suspension
[NASA-TM-77864] 17 p3026 N85-28716
Linear motion valve
[NASA-CASE-MSC-20146-1] 18 p3115 N85-29284
Advanced detectors and signal processing
[NASA-CR-176193] 24 p4088 N85-35343

MAGNETIC POLES
Magnetosphere, rings, and moons of Uranus
02 p0301 N85-11951
Development of high field Nb-Ti accelerator dipoles
[DE85-000621] 11 p1714 N85-20782
Preliminary documentation for the polar code
[AD-A154125] 19 p3336 N85-30667
Magnetic field and equivalent circuit of induction motors with shielded poles 22 p3772 N85-33378

MAGNETIC PROBES
Internal field probing of translating FRCs
[DE85-003732] 15 p2657 N85-26394
Magnetic flux leakage inspection: Principles and applications
[BLL-BISI-TRANS-22248-(8022.06)]
17 p2975 N85-28382
Magnetic probing of the solar interior
[NASA-CR-176025] 19 p3365 N85-30996

MAGNETIC PROPERTIES
NT ANTIFERROMAGNETISM
NT BIOMAGNETISM
NT CURIE TEMPERATURE
NT DIAMAGNETISM
NT FERROMAGNETISM
NT GEOMAGNETISM
NT GYROMAGNETISM
NT MAGNETIC EFFECTS
NT MAGNETIC INDUCTION
NT MAGNETIC MOMENTS
NT MAGNETIC PERMEABILITY
NT MAGNETIC RELAXATION
NT MAGNETIC RIGIDITY
NT MAGNETIC SUSPENSION
NT MAGNETOACOUSTICS
NT MAGNETOACTIVITY
NT MAGNETORESISTIVITY
NT MAGNETOSTRICTION
NT PALEOMAGNETISM
NT PARAMAGNETISM
NT POLARIZATION CHARACTERISTICS
NT SPIN-LATTICE RELAXATION
NT THERMOMAGNETIC EFFECTS
Preparation and properties of single crystals of hydrogen bis(phthalocyaninato) neodymium(3)
[AD-A144933] 01 p0123 N85-10846
Input-output stability analysis with magnetic hysteresis non-linearity: A class of multipliers
[AD-A145729] 02 p0253 N85-11654
Magnetic properties of and superfine interactions in amorphous Fe-Cr-Co-Si-B alloys
03 p0349 N85-12248
Magnetic characteristics of some volcanic rocks of the west Carpathians
[REPT-557] 03 p0376 N85-12400
Report on research results in solid state nuclear physics, 1980-1982
[JUEL-SPEZ-250] 03 p0422 N85-12696
Magnetic properties of intermetallic phases and simple systems — neutron diffraction 03 p0422 N85-12697
Investigations of magnetic phase transitions with neutron scattering 03 p0423 N85-12700
Metamagnetic systems 03 p0423 N85-12701
Neutron scattering on magnetic structures and at magnetic phase transitions 03 p0424 N85-12706
Magnetism of the rare earth compounds — intermetallic compounds 03 p0424 N85-12707
Growth and magnetic investigations of single crystals of intermetallic compounds of rare earths and uranium — magnetic properties 03 p0425 N85-12712
Magnetic interaction in low-dimensional systems
03 p0426 N85-12717
USSR report: Physics and mathematics
[JPRS-UPM-84-007] 05 p0723 N85-14651
Actinides, the narrowest bands
[DE84-016463] 05 p0733 N85-14710
Electronic and magnetic properties of transition-metal surfaces, interfaces and overlayers
[DE84-016886] 05 p0733 N85-14713
The growth of metastable perfectic compounds
[NASA-CR-171289] 07 p0920 N85-15824
Structure-property relationships in intercalated graphite
[AD-A147949] 08 p1219 N85-17660
Study of the physical properties of crystalline rocks in the southeast Voronezh anteclise
[NASA-TM-77823] 10 p1514 N85-19551
Study of magnetism at surfaces by scattering of neutrons at grazing incidence
[DE84-015850] 10 p1564 N85-19865
Magnetic measurements, calibrations, and standards: Report on a survey
[PB85-127827] 11 p1638 N85-20317
Theoretical determination of surface magnetism
[DE85-003224] 11 p1714 N85-20783
Magnetic and structural properties of shock-synthesized zinc ferrite
[DE85-000469] 11 p1736 N85-20915
Electric and magnetic properties of intercalated graphite
[AD-A149846] 12 p1798 N85-21276
Magnetic studies of Ni3Al(Fe) compounds
[DE85-005262] 13 p2025 N85-22686
Primary processing of experimental magnetovariation sounding data using spline functions
13 p2115 N85-23175
Improvement in magnetic field properties of vanadium-gallium superconductors by enhancement of spin-orbit scattering
[DE85-002693] 13 p2164 N85-23422
Mixed valence materials
[AD-A151009] 14 p2252 N85-23959
Parameters of magnetically active layers of Indian Ocean determined from deep drilling data and magnetic surveys
14 p2337 N85-24451
Transient analysis of a magnetic heat pump
15 p2576 N85-25891
Effect of nickel addition on the thermal, magnetic and magnetomechanical properties of Fe(80)B(15)Si(5)
[AD-A152281] 16 p2749 N85-26967
Paramagnetic form factors from itinerant electron theory
[DE85-005272] 16 p2750 N85-26973
Effects of wear on structure-sensitive magnetic properties of ceramic ferrite in contact with magnetic tape
[NASA-TM-87007] 16 p2753 N85-26991

Magnetic impurities in superconductors
[DE85-008372] 18 p3196 N85-29825
Flux pinning and flux flow studies in superconductors using flux flow noise techniques
[DE85-010814] 19 p3376 N85-30845
A dual spin space station design
20 p3408 N85-31152
Magnitude and range of the RKKy interaction in SmRh4B4
[DE85-012264] 23 p3985 N85-34712
ATA upgrade to 150 MeV
[DE85-013174] 24 p4098 N85-35404

MAGNETIC RECORDING

Television animation store: Recording pictures on a parallel transfer magnetic disc
[BBC-RD-1984/17] 10 p1462 N85-19220
Remote self-contained undersea monitor
[AD-D011520] 12 p1849 N85-21599
GSFC specification electronic data processing magnetic recording tape
[NASA-TM-80599] 12 p1851 N85-21609
Video animation system
[DE85-005494] 14 p2405 N85-24831
Operation of autotracking system in various video playback modes 16 p2764 N85-27055
Balloon-borne video cassette recorders for digital data storage
[OG-9.3-11] 21 p3715 N85-33050
Quarter-inch streaming tape drive application with the Serial ASCII Instrumentation Loop (SAIL) system
[AD-A155354] 22 p3759 N85-33295
Module for interfacing microprocessors and microcomputer 22 p3774 N85-33390

MAGNETIC RELAXATION

NT SPIN-LATTICE RELAXATION
Nuclear Magnetic Resonance of Polymeric Materials
[AD-A145078] 01 p0032 N85-10192
Theory of nuclear magnetic relaxation
[AD-P003911] 01 p0032 N85-10197
Anisotropy and relaxation effects of Co2+ ions in LiTi ferrite
[AD-A146550] 06 p0961 N85-15469

MAGNETIC RESONANCE

NT ELECTRON PARAMAGNETIC RESONANCE
NT FERROMAGNETIC RESONANCE
NT NUCLEAR MAGNETIC RESONANCE
NT PROTON RESONANCE
Analysis of glow discharges for understanding the process of film formation
[NASA-TM-83750] 01 p0022 N85-10138
Magnetic resonance studies of transient radicals and radical ions
[DE84-011699] 03 p0328 N85-12116
Analysis of spin echo signals in multi-pulse experiment
06 p0792 N85-15065
High switching speed electrically tuned microwave magnetic resonance devices
[AD-D011699] 19 p3260 N85-30217

MAGNETIC RIGIDITY

Absolute rigidity spectrum of protons and helium nuclei above 10 GV/c
[OG-4.1-1] 22 p3675 N85-34007
Observation of cosmic ray positrons from 5 to 25 GeV
[OG-6.2-5] 22 p3689 N85-34104
An observation of cosmic ray positrons from 10-20 GeV
[OG-6.2-6] 22 p3689 N85-34105
Diurnal effect in cosmic rays at middle latitudes according to stratospheric measurements
[SH-4.5-8] 23 p4036 N85-35026
Anomalous increase of solar anisotropy above 150GV in 1981-1983
[SH-4.5-18] 23 p4038 N85-35035
Re-evaluation of cosmic ray cutoff terminology
[SH-6.1-11] 23 p4045 N85-35084
The use of the McIlwain L-parameter to estimate cosmic ray vertical cutoff rigidities for different epochs of the geomagnetic field
[SH-6.1-12] 23 p4045 N85-35085

MAGNETIC SHIELDING

Magnetic shielding with superconductors based on niobium-tin compounds 22 p3771 N85-33370

MAGNETIC SIGNALS

The magneto-optical filter, working principles and recent progress 14 p2442 N85-25066
Fluxgate magnetometer (SSM) for the defense meteorological satellite program (DMSP) block 5D-2, flight 7
[AD-A155229] 21 p3560 N85-32143
A real time index of geomagnetic background noise for the MAD (Magnetic Anomaly Detection) frequency band
[AD-A155717] 22 p3814 N85-33627

MAGNETIC SIGNATURES

Orientation and strength of Martian magnetic dipole
16 p2723 N85-26808
Possible configuration of Martian magnetosphere
16 p2723 N85-26809
Analysis of the new polarimeter for the Marshall Space Flight Center vector magnetograph
18 p3205 N85-29681
The San Fernando Observatory video Stokes polarimeter 18 p3205 N85-29685
The new solar magnetograph for the Canary Islands Observatory THEMIS 18 p3206 N85-29686
The vector magnetograph of the Sayan Solar Observatory 18 p3206 N85-29687
Diagnostics of vector magnetic fields
18 p3206 N85-29689
Comparisons of simultaneous vector magnetograms
18 p3206 N85-29900
Ephemeral regions versus pseudo ephemeral regions
18 p3206 N85-29901
Evidence for submergencew of magnetic flux in a growing active region 18 p3206 N85-29902
Graphic displays of vector magnetograph data
18 p3209 N85-29904
Solar cycle variation of ephemeral regions
[AD-A154967] 21 p3723 N85-33097
Aeromagnetic and radiometric signatures of a possible porphyry system in the western Tusher Mountains, Utah
24 p4103 N85-35437

MAGNETIC SPECTROSCOPY

Mixed valence materials
[AD-A151009] 14 p2252 N85-23959
NMR in the 80 s: New nuclei, new pulses — nuclear magnetic resonance (NMR)
[DRIC-T-7467] 22 p3836 N85-33754
Improved negative ion source
[DE85-006445] 23 p3912 N85-34241

MAGNETIC STARS

High energy cosmic ray signature of quark nuggets
[HE-6.2-11] 24 p4212 N85-36147

MAGNETIC STORAGE

NT BUBBLE MEMORY DEVICES
NT MAGNETIC DISKS

MAGNETIC STORMS

Precipitation of protons with E sub p approximately 1 MeV near plasmopause 02 p0161 N85-11093
Behavior of the ionospheric F region in low latitudes and in the equatorial region of Brazil during strong magnetic storms in the 1978 to 1983 period
[INPE-3231-PRE/581] 05 p0675 N85-14333
Nocturnal increases of ionization in the ionospheric F region in the low latitude of Brazil during magnetic storms
[INPE-3271-PRE/596] 05 p0675 N85-14334
Hot plasma particles in the Earth's outer magnetosphere: New understandings during the IMS
[DE84-016826] 05 p0677 N85-14348
Repulsive force of magnetic clouds during solar flares and magnetospheric substorms
06 p0824 N85-15233
Influence of geomagnetic disturbances on cardiovascular function of athletes
08 p1193 N85-17516
Observation of a westward travelling surge from satellites at low, medium and high altitudes
[NASA-TM-87434] 09 p1342 N85-18442
High energy particle effects in the D region during and after geomagnetic storms 11 p1664 N85-20485
Dependence of the high latitude middle atmosphere ionization on structures in interplanetary space
11 p1664 N85-20487
Solar terrestrial influences on the D region as shown by the level of atmospheric radio noise
11 p1664 N85-20488
Latitudinal dependance of the energy input into the mesosphere by high energy electrons
11 p1664 N85-20489
Geomagnetic disturbances caused by internal atmospheric dynamics 11 p1665 N85-20491
Substorms in the Earth's atmosphere
[DE85-000854] 12 p1890 N85-21861
Periodic substorm activity in the geomagnetic tail
[NASA-CR-175629] 13 p2161 N85-23409
Diagram of nonstationary rejoining of magnetic force lines 14 p2344 N85-24492
Excitation of geomagnetic Pcl-2 and pulsations with decreasing period during microsubstorms
14 p2344 N85-24494
Observations of energetic electron and ion distributions near the magnetopause at geosynchronous orbit and related ground effects 14 p2356 N85-24560
Response of magnetospheric substorm activity to changes in the interplanetary magnetized plasma
14 p2357 N85-24563
Timing between particle injections at the geostationary orbit and particle flux decreases in the distant geomagnetic tail during substorms 14 p2358 N85-24569
Plasma sheet dynamics deduced from ISEE-1 and -2 energetic particle flux data 14 p2358 N85-24570
Streaming reversal of energetic particles in the magnetotail during a substorm 14 p2358 N85-24571
Ring current dynamics and plasma sheet sources — magnetic storms 14 p2359 N85-24577
Electrodynamics of magnetosphere-ionosphere coupling 14 p2359 N85-24579
Electron and proton precipitation in magnetic substorms — auroral substorms
14 p2360 N85-24585
Development of an auroral absorption substorm
14 p2360 N85-24586
Coordinated balloon-satellite studies of energetic electron precipitation mechanisms
14 p2360 N85-24587
Observations during a magnetospheric substorm triggered by a Storm Sudden Commencement (SSC): A case study 14 p2361 N85-24588
SAMBO-GEOS: Substorm trapped particle particle boundary movements, particle precipitation and acceleration 14 p2361 N85-24589
Auroral X-rays and equatorial electrons in the morning sector — substorm 14 p2361 N85-24590
On the location of the source for X-ray microbursts
14 p2361 N85-24591
Disturbance of midlatitude electrodynamic parameters due to the magnetospheric convection
14 p2362 N85-24593
Testing of some substorm features by multiple balloon observations 14 p2363 N85-24600
Characteristics of the electrodynamics of auroral arcs as inferred from rocket and ground-base observations during IMS 14 p2363 N85-24601
On the dynamics of the westward traveling surge
14 p2364 N85-24607
Theory and computer simulation of auroral kilometric radiation 14 p2365 N85-24617
Short-period magnetic pulsations during substorms
14 p2368 N85-24636
Substorm associated Pc 1 emission in the morning sub-cleft latitudes 14 p2368 N85-24637
Pi2 pulsations and the substorm current wedge - ground observations 14 p2370 N85-24650
Ground-satellite observations of substorm related Pi 2 pulsations and current systems
14 p2370 N85-24651
Observation of polar aurora from the Salyut-6 space station during the great geomagnetic storm of 11-13 Apr. 1981 15 p2477 N85-25291
Spectral characteristics of protons at low and high altitudes during geomagnetic storm of 29 July 1977
16 p2719 N85-26788
Correlated fluctuations of charged particle fluxes and magnetic field according to data from Intercosmos-10 satellite 16 p2722 N85-26802
Effects of Birkeland current limitation on high latitude convection patterns
[TRITA-EPP-84-10] 20 p3494 N85-31725
The longitudinal asymmetry of the interplanetary perturbation producing Forbush decreases
[IFSI-84-18] 20 p3546 N85-32065
Interplanetary disturbances during Forbush decreases
[IFSI-84-10] 20 p3547 N85-32075
Transient cosmic ray increase associated with a geomagnetic storm
[SH-5.1-8] 23 p4042 N85-35062
Study of dominating parameters of high speed solar plasma streams in relation to cosmic ray and geomagnetic storms
[SH-5.1-11] 23 p4042 N85-35064
Dynamics of the penetration boundaries of solar protons during a strong magnetic storm
[SH-6.1-16] 23 p4049 N85-35089

MAGNETIC SUBSTORMS

U MAGNETIC STORMS

MAGNETIC SURVEYS

Geological effectiveness of automated processing of highly precise aeromagnetic surveys in Caspian region
06 p0821 N85-15216
GADB: A database facility for modelling naturally occurring geophysical fields 13 p2122 N85-23217
Data selection techniques in the interpretation of MAGSAT data over Australia 13 p2123 N85-23218
Parameters of magnetically active layers of Indian Ocean determined from deep drilling data and magnetic surveys
14 p2337 N85-24451
Interpretation of directional magnetotelluric soundings by analytical continuation method
14 p2343 N85-24488
Directional analysis of wave packets of magnetotelluric field 14 p2344 N85-24495
Method for determining depth and shape of a sub-surface conductive object
[DE85-006502] 23 p3935 N85-34389
Magnetic search system
[PB85-185108] 23 p3949 N85-34477

MAGNETIC SUSCEPTIBILITY
U MAGNETIC PERMEABILITY
MAGNETIC SUSPENSION
Optimum dimensions of power solenoids for magnetic suspension 04 p0469 N85-13118
European development experience on energy storage wheels for space 05 p0605 N85-13856
Magnetically suspended reaction wheel assembly 05 p0607 N85-13870
Magnetic suspension options for spacecraft inertia-wheel applications 05 p0607 N85-13871
Overview of magnetic bearing control and linearization approaches for annular magnetically suspended devices 05 p0607 N85-13872
Magnetically suspended flywheel system study 05 p0607 N85-13873
The generation of rolling moments with the superconducting solenoid model [NASA-CR-172520] 09 p1283 N85-18068
Characteristics of the boat inductor for keeping liquid metal in the suspended state [NASA-TM-77816] 12 p1851 N85-21611
Mathematical model of electromagnetic suspension device with two control windings 13 p2074 N85-22954
A preliminary investigation of the dynamic force-calibration of a magnetic suspension and balance system [NASA-CR-172580] 14 p2228 N85-23608
Study on needs for a magnetic suspension system operating with a transonic wind tunnel [NASA-CR-3900] 16 p2715 N85-26759
Effect of superconducting solenoid model cores on spanwise iron magnet roll control [NASA-TM-86378] 17 p2905 N85-27915
Optimum dimensions of power solenoids for magnetic suspension [NASA-TM-77884] 17 p3026 N85-28716
An improved servo-controlled inertial clock for laboratory tests of general relativity 19 p3378 N85-30955
A theoretical model for the study of nonlinear dynamics of magnetic bearings 20 p3462 N85-31505
Optimization of design parameters for alternating current stabilizer based on magnetic suspension 22 p3772 N85-33374
MAGNETIC TAPE RECORDERS
U MAGNETIC RECORDING
U TAPE RECORDERS
MAGNETIC TAPES
NT COMPUTER COMPATIBLE TAPES
Documentation for the machine-readable version of A Catalogue of Extragalactic Radio Source Identifications (Veron-Cetty and Veron 1983) [NASA-TM-87373] 03 p0405 N85-12587
Documentation for the machine-readable version of The Revised AFGL Infrared Sky Survey Catalog (Price and Murdock 1983) [NASA-TM-87377] 03 p0405 N85-12588
Documentation for the machine-readable version of the MK classification extension catalogue Morris-Kennedy (1983) [NASA-TM-87372] 04 p0549 N85-13491
Effect of external magnetic field on characteristics of current-carrying steel tape 06 p0788 N85-15034
High speed magnetic tape interface for a microcomputer [CSIRO-TP-7] 06 p0847 N85-15377
Beginner's guide to blocked records on magnetic tape [DE85-001691] 06 p0855 N85-15433
EDP computer tapes described 08 p1142 N85-17203
The care and feeding of magnetic tapes [AD-A145853] 09 p1366 N85-18585
Satellite support to the Sierra Cooperative Pilot Project: 1979/80 and 1980/81 [PB85-115079] 10 p1520 N85-19583
Humidity effects on adhesion of nickel-zinc ferrite in elastic contact with magnetic tape and itself [NASA-TP-2449] 12 p1811 N85-21359
The 20:16 block code for digital recording and transmission channels [BBC-RD-1985/1] 12 p1824 N85-21443
Atmospheric handbook: Atmospheric data tables available on computer tape [PB85-109512] 12 p1891 N85-21867
Simple detonation meter 13 p2077 N85-22971
Prediction of the long term stability of polyester-based recording media [PB85-160133] 14 p2282 N85-24018
Documentation for the machine-readable version of A Finding List for the Multiplet Tables of NSRDS-NBS 3, Sections 1-10 (Adelman, Adelman, Fischel and Warren 1984) [NASA-TM-87440] 14 p2438 N85-25048
Documentation for the machine-readable version of the Cordoba Durchmusterung (CD) [NASA-TM-87441] 14 p2439 N85-25049
Catalog of the National Energy Software Center [TI85-900521] 15 p2630 N85-26209
Effects of wear on structure-sensitive magnetic properties of ceramic ferrite in contact with magnetic tape [NASA-TM-87007] 16 p2753 N85-26991
A transportable, machine oriented library of european sky and terrain radiance distributions with contemporary radiometric and meteorological profiles [AD-A155254] 21 p3637 N85-32590
Quarter-inch streaming tape drive application with the Serial ASCII Instrumentation Loop (SAIL) system [AD-A155354] 22 p3759 N85-33295
Relaxation techniques [AD-A156246] 24 p4133 N85-35621
Using an LSI-11/23 and RT-11 to digitize analog tapes [DE85-012736] 24 p4139 N85-35658
Aeronautical Systems Division Manufacturing/Quality assurance orientation [AD-A156128] 24 p4164 N85-35617
MAGNETIC TRANSDUCERS
Electromagnetic Acoustic Transducers (EMATs) for erosion monitoring [DE85-004834] 12 p1854 N85-21628
A literature review of EMATs, with stress calculations for simple EMAT geometries [AERE-R-11415] 15 p2642 N85-26295
Geomagnetic velocimeter [AD-D011672] 19 p3218 N85-29953
MAGNETIC VARIATIONS
NT GEOMAGNETIC PULSATIONS
NT NOCTURNAL VARIATIONS
Analysis of the daily geomagnetic variation with the use of MAGSAT data --- MAGSAT satellites 04 p0520 N85-13319
Research directions in recent studies of the lunar geomagnetic effects 04 p0520 N85-13320
On derivation and significance of geomagnetic equivalent amplitude indices 04 p0520 N85-13321
A directly obtained geomagnetic activity measure, J3 04 p0520 N85-13322
Daily magnetic variations at Ebro, Spain 04 p0520 N85-13325
Geomagnetic secular variation at Ebro Observatory during the past 70 years 04 p0521 N85-13331
Spectrum of geomagnetic field variations in the range of periods between 1 and 10 years 06 p0821 N85-15215
Artificial ionospheric disturbances caused by powerful radio waves [AD-A148077] 08 p1186 N85-17473
Dynamic spectra of mean monthly values of geomagnetic field elements based on spectral-time analysis data 14 p2344 N85-24496
Report of the geomagnetic and geoelectric observations, 1983 (rapid variations) [REPT-24] 15 p2581 N85-25975
Poloidal rotation of magnetic fluctuations in reversed field pinch plasma [IPPJ-715] 16 p2866 N85-27677
A study of the cyclical variations of coronal holes and their relation to open magnetic fields [AD-A155251] 21 p3723 N85-33099
Diurnal variations from muon data at Takeyama underground station [SH-4.5-13] 23 p4037 N85-35030
Long term changes in cosmic ray diurnal variations observed by ion chambers in Hong Kong and Japan [SH-4.5-14] 23 p4037 N85-35031
The modulation features of the long-period cosmic ray variations in connection with the sign change of the general magnetic field of the Sun [SH-4.5-15] 23 p4037 N85-35032
Change of cosmic ray anisotropy with solar activity [SH-4.5-20] 23 p4038 N85-35037
Magnetic fluctuation and cosmic ray diurnal variations [SH-4.5-21] 23 p4038 N85-35038
Solar cycle variations of the anomalous cosmic ray component [SH-4.6-2] 23 p4039 N85-35040
MAGNETICALLY TRAPPED PARTICLES
NT INNER RADIATION BELT
NT OUTER RADIATION BELT
NT PROTON BELTS
NT RADIATION BELTS
Asymptotic orbit theory for trapped electrons in inhomogeneous Whistler field [AD-A146178] 03 p0392 N85-12510
Longitude and pitch-angle distributions of streams of high-energy electrons under Earth's radiation belts 13 p1978 N85-22415
Correlated fluctuations of charged particle fluxes and magnetic field according to data from Intercosmos-10 satellite 16 p2722 N85-26802
System and method of operating toroidal magnetic confinement devices [DE85-011670] 22 p3845 N85-33814
MAGNETITE
Evolutionary history of CI and CM chondrites 06 p0884 N85-15615
Structure and property formation mechanism in magnetite alloy-binder composite 10 p1444 N85-19103
Some recent deposit modeling efforts 24 p4106 N85-35453
MAGNETIZATION
Determination of optimum Curie point as a function of source and sink temperatures for magnetic heat pumps [DE84-016995] 04 p0499 N85-13182
Petrologic model of the northern Mississippi embayment based on satellite magnetic and ground based geophysical data [NASA-TM-85075] 04 p0533 N85-13406
Electronic structure and properties of magnetic defects in Co(1+x)Al(1-x) and Fe(1+x)Al(1-x) alloys [NASA-TM-77498] 07 p1047 N85-16648
Replacement of Fe-3+ ions in nickel ferrites by nonmagnetic Al-3+ and Sc-3+ ions [BLL-WH-594-(9091.9F)] 08 p1125 N85-17090
Cobalt-free permanent magnet alloys [AD-A140272] 10 p1441 N85-19079
Magnetization of very thin Ni films in epitaxial metal film sandwiches of Cu [DE85-001840] 10 p1563 N85-19660
Application of hysteresis modelling to the non-destructive inspection of stress [DE85-003061] 11 p1650 N85-20393
Theoretical determination of surface magnetism [DE85-003224] 11 p1714 N85-20783
Magnetization measurements on multifilamentary Nb3Sn and NbTi conductors [DE85-001237] 11 p1737 N85-20923
Measurement of the induced moment magnetic form factor of a heavy fermion superconductor [DE85-004165] 12 p1942 N85-22194
Remanent magnetization model for the broken ridge satellite magnetic anomaly 13 p2123 N85-23219
Standing of industrial radiography in South Africa 14 p2316 N85-24311
Study of amorphous strips and microconductors by ferromagnetic resonance method 15 p2497 N85-25402
Magnetic steels with the lowest specific total losses [BMFT-FB-T-84-263] 16 p3078 N85-29042
Diffusion of strongly magnetized cosmic ray particles in a turbulent medium [OG-7.2-16] 23 p4015 N85-34883
MAGNETO-OPTICS
Guided-wave optic devices for integrated optic information processing [AD-A145695] 02 p0280 N85-11827
Characterization of III-V compound semiconductor device materials [AD-A148203] 08 p1226 N85-17719
Evaluation of a magneto-optical filter and a Fabry-Perot interferometer for the measurement of solar velocity fields from space 14 p2442 N85-25067
Optical fiber magnetic field sensor with nanosecond response time [DE85-006409] 18 p3110 N85-29259
Diagnostics of vector magnetic fields 18 p3206 N85-29689
The inference of vector magnetic fields from polarization measurements with limited spectral resolution 18 p3207 N85-29696
Magnetic materials [AD-A154679] 21 p3580 N85-32256
Development of wide band recording materials [AD-A154961] 21 p3580 N85-32309
MAGNETOACOUSTIC WAVES
Magnetosonic waves and their relationship with energetic protons 14 p2368 N85-24636
Oscillatory convection in sunspots 14 p2448 N85-25099
On running penumbral waves 14 p2453 N85-25150
MAGNETOACOUSTICS
Squid detection of acoustomagnetic effects 19 p3373 N85-30924
MAGNETOACTIVITY
NT MAGNETORESISTIVITY
Diamagnetic instability of cyclotron waves in plasma 21 p3693 N85-32948
MAGNETOELASTIC VIBRATIONS
U MAGNETOELASTIC WAVES
MAGNETOELASTIC WAVES
NT MAGNETOACOUSTIC WAVES

Influence of axial shaft load on operation of magnetoelastic torque transducer
14 p2270 N85-24065
Cyclotron absorption of fast magnetosonic wave in stellarator
21 p3993 N85-32945
Resonant ion acceleration by oblique magnetosonic shock wave in a collisionless plasma
[IPPJ-735] 23 p3975 N85-34843

MAGNETOELASTICITY
U MAGNETOSTRICTION

MAGNETOGASDYNAMICS
U MAGNETOHYDRODYNAMICS

MAGNETOGRAMS
U MAGNETIC SIGNATURES

MAGNETOHYDRODYNAMIC ACCELERATION
U PLASMA ACCELERATION

MAGNETOHYDRODYNAMIC FLOW
Solar flares and laboratory experiments on magnetic reconnection in current sheaths
02 p0162 N85-11099
Electric field and plasma energization in computer simulations of magnetotail reconnection
[DE84-014023] 02 p0285 N85-11859
The solar wind at 20-30 AU 02 p0301 N85-11960
Magnetohydrodynamic and gasdynamic theories for planetary bow waves
[NASA-CR-174132] 03 p0448 N85-12850
China report: Science and technology
[JPRS-CST-84-003] 04 p0491 N85-13132
Magnetohydrodynamic flow of two-component gas analyzed
04 p0491 N85-13133
Plasma flow in the near and distant geomagnetic tail
[DE84-014029] 04 p0534 N85-13415
Magnetohydrodynamic and gasdynamic theories for planetary bow waves
[NASA-CR-174135] 04 p0589 N85-13760
Application of the energy problem to the problem of plasma flow stability
[DE84-013359] 05 p0730 N85-14691
Magnetic effects in the heating and modification of flows in the outer stellar atmospheres with application to early type star case
08 p1235 N85-17783
On the hydrodynamical equations of astrophysical jets — active galactic nuclei
08 p1241 N85-17831
Centrifugally driven magnetohydrodynamic (MHD) winds and the nonthermal emission regions in Active Galactic Nuclei (AGN)
08 p1242 N85-17835
Macroscopic currents and wind perturbations in the frame of the wind and shock model — galactic nuclei
08 p1242 N85-17836
Simulation of thermal and electromagnetic processes in induction plasmatrons
12 p1841 N85-21552
Pressure-gradient-driven Tokamak resistive MHD instability in the banana-plateau collisionality regime
[DE85-004589] 12 p1937 N85-22171
Wakes and differential charging of large bodies in low Earth orbit
13 p1992 N85-22486
Efficiency of electric field transfer at Earth's magnetopause and flow amplitudes related to reconnection
14 p2356 N85-24557
Hydromagnetic vortices: An interpretation for dawnside events as on December 11, 1977 — magnetotail
14 p2371 N85-24653
Kinematic dynamo theory for an arbitrary mean flow
14 p2448 N85-25108
A siphon flow model for Evershed motion — sunspot regions
14 p2453 N85-25147
An interplanetary magnetic field ensemble at 1 AU
[NASA-TM-86209] 16 p2882 N85-27784
Flat magnetohydrodynamic induction pump
17 p2939 N85-28145
Dependence of characteristics of centrifugal magnetohydrodynamic conduction pump on electrical conductance of end walls. Part 1: Experiment
17 p2939 N85-28146
Reversed field pinch dynamics and transport studies
[DE85-007563] 18 p3189 N85-29778
Screening phase transitions in two-dimensional Coulomb gas
[NOTA-INTERNA-630] 18 p3192 N85-29798
Current evolution in a numerical emerging-magnetic-flux model
18 p3204 N85-29875
Thermal contraction of current flow through electrode turbulent boundary layer
21 p3690 N85-32026
Modeling the exhaust of the pulsed plasma thruster
[AD-A155344] 21 p3707 N85-33018
Time-dependent nonlinear cosmic ray shocks confirming abstract
[OG-8.1-3] 23 p4017 N85-34863
Efficiency of regular acceleration of particles by a shock wave at different injection regimes
[OG-8.1-13] 23 p4019 N85-34902

MAGNETOHYDRODYNAMIC GENERATORS
Khibiny experiment described
07 p0961 N85-16230
MHD performance demonstration experiment, FY 1974 to FY 1984
[DE85-000654] 08 p1224 N85-17709
Development of materials for open-cycle MHD
[DE84-017293] 09 p1393 N85-18770
Three-dimensional analysis of heat transfer and gas flow in a radiant furnace
[DE84-011732] 11 p1633 N85-20284
Performance of solar thermal systems with liquid metal MHD conversion
[DE85-002758] 11 p1675 N85-20555
Experimental investigations of thermal radiation from potassium atoms in magnetohydrodynamic system: Preliminary report
[DE85-003715] 12 p1936 N85-22169
Radiation heat transfer within an open-cycle MHD generator channel — mathematical models
[NLR-TR-83068-U] 14 p2304 N85-24267
Parametric study of potential early commercial power plants Task 3-A MHD cost analysis
[NASA-CR-175839] 16 p2817 N85-27377
MHD channel development
[DE85-008305] 18 p3192 N85-29796
Performance and electric field limitations in inflow disk MHD generators
20 p3534 N85-31987
MHD generator CDIF
[DE85-011389] 20 p3536 N85-32001
Thermal contraction of current flow through electrode turbulent boundary layer
21 p3690 N85-32926
Study to assess the effects of magnetohydrodynamic electromagnetic pulse on electric power systems, phase 1, volume 3
[DE85-011301] 24 p4156 N85-35771

MAGNETOHYDRODYNAMIC STABILITY
NT WEIBEL INSTABILITY
MHD instabilities in simple plasma configuration
[AD-A144936] 01 p0121 N85-10829
Experimental observation of neoclassical currents
[DE84-015113] 01 p0122 N85-10834
Means of varying conditions in the expanded boundary divertor without affecting energy confinement
[DE84-013840] 01 p0122 N85-10836
Plasma drift equilibrium (gyration) in toroidal systems with complex magnetic-field geometry
[DE84-015627] 01 p0122 N85-10839
Studies of solar flares and coronal loops
[AD-A145009] 01 p0130 N85-10896
Bremsstrahlung radiation from longitudinal plasma waves caused by subthermal electrons in plasma
02 p0264 N85-11730
Neutral beam interactions with materials
[AD-A145836] 02 p0285 N85-11857
Physics of reversed-field pinch profile sustainment
[DE84-014024] 04 p0565 N85-13602
Theoretical studies in tandem mirror physics
[DE84-015634] 04 p0566 N85-13604
Theory of resistive ballooning modes in Tokamaks
[DE84-015626] 04 p0566 N85-13606
Internal helical mode m = 1 of a Tokamak in the plateau and banana regimes
[DE84-015623] 04 p0566 N85-13607
Fusion plasma theory. Task 1: Magnetic confinement fusion plasma theory
[DE84-014941] 04 p0566 N85-13608
Fusion plasma theory. Task 3: Auxiliary heating in Tokamaks and tandem mirrors
[DE84-014940] 04 p0566 N85-13609
High-Beta Tokamak research
[DE84-016470] 04 p0568 N85-13618
High-Beta plasma theory
[DE84-016471] 04 p0568 N85-13619
Proceedings of the US-Japan Theory Workshop on 3-D MHD Studies
[DE84-012019] 04 p0568 N85-13620
Application of the energy problem to the problem of plasma flow stability
[DE84-013359] 05 p0730 N85-14691
Stabilization of the hot electron precessional mode in a symmetric tandem mirror by the axial variation of radial electric field
[DE84-016389] 05 p0730 N85-14692
Passive stabilization of vertical instability in Tokamak reactor
06 p0775 N85-14958
Limits of possible operation of the R-Tokamak due to ideal MHD instabilities
[IPPJ-694] 06 p0863 N85-15488
Theoretical investigations relevant to magnetic fusion research, April 1, 1983 - March 31, 1984
[DE85-001778] 06 p0865 N85-15498
Shear-Alfven dynamics of toroidally confined plasmas, part A
[DE85-001590] 06 p0866 N85-15502
Shear-Alfven dynamics of toroidally confined plasmas, part B
[DE85-001787] 06 p0866 N85-15504
The role of finite parallel length on the stability of barium clouds
[AD-A146972] 07 p0996 N85-16328
Asymptotic behaviour of the plasma equation
[AD-A147242] 07 p1031 N85-16549
Experimental results on Tokamak beta limits from ISX-B
[DE84-015372] 07 p1046 N85-16644
Radiatively driven winds and what they imply: A review of radiative driven instabilities and their importance in hot stars
08 p1235 N85-17782
Impurity control by additional current rise and gas puffing during ICRF heating in JIPP T-IIU Tokamak
09 p1387 N85-18725
Impact of atomic data on Tokamak modeling
09 p1390 N85-18743
The plasma assisted modified betatron
[AD-A148728] 09 p1390 N85-18748
MHD equilibrium and stability for stellarator/torsatron configurations
[DE85-001139] 09 p1391 N85-18750
Effect of alpha particles on the stability of Elmo Bumpy Torus (EBT) reactor
[DE84-017266] 09 p1392 N85-18759
Brief outline of analytic stability studies of magnetically insulated systems — bibliographies
[DE85-000212] 09 p1393 N85-18765
Effects of q and high beta on Tokamak stability
[DE84-016650] 09 p1393 N85-18767
Four phase model for turbulent instabilities calculation in plasma jets
[IPF-84-2] 09 p1394 N85-18776
Experimental investigation of certain beam transport issues in a pulsed transmission line linear accelerator
[DE85-002310] 10 p1555 N85-19805
Small, octopole-stabilized tandem mirror reactor
[DE85-002144] 10 p1559 N85-19832
Finite-(beta) optimization of tandem mirrors
[DE85-002658] 10 p1560 N85-19835
Role of multiple helicity nonlinear interaction of tearing modes in dynamo and anomalous thermal transport in the Reversed Pitch Field
[DE85-002176] 10 p1560 N85-19839
Electrodynamic interactions 11 p1643 N85-20348
Explosive instability of strong electromagnetic wave in plasma
11 p1719 N85-20817
Coronal spectroscopy in laser plasmas
[DE85-002817] 11 p1730 N85-20880
Observations of low frequency plasma fluctuations in ELMC Bumpy Torus
[DE85-003796] 11 p1732 N85-20895
Theory of resistivity-gradient-driven turbulence
[DE85-002175] 11 p1733 N85-20898
Activation of solar flares 12 p1954 N85-22276
Signatures of the coalescence instability in solar flares
12 p1958 N85-22293
Discharges on a negatively biased solar cell array in a charged-particle environment
13 p1994 N85-22499
Increased hot-electron production at quarter-critical density in long-scalelength, laser-plasma interactions
[AD-A150519] 13 p2161 N85-23411
Lower hybrid heating and current drive, and ion cyclotron heating experiments on the Alcator C and the Versator II Tokamaks
[DE85-004918] 13 p2161 N85-23412
Theoretical and observational studies of stellar activity
13 p2171 N85-23488
Magnetic instabilities — solar magnetism
14 p2449 N85-25117
Energy balance in resistive instabilities — solar prominences
14 p2454 N85-25155
Asymmetric flux generation and its relaxation in reversed field pinch
[IPPJ-712] 15 p2656 N85-26387
Effects of finite current channel width on the current convective instability
[AD-A151414] 15 p2656 N85-26389
Stability and vibrations of internal windings of high-current superconducting solenoid magnets
[AD-A151465] 15 p2656 N85-26390
Effects of magnetic shear on lower hybrid waves in the suprauroral region
[AD-A151960] 15 p2656 N85-26392
MHD fluctuations in ISX-B
[DE85-004800] 15 p2657 N85-26395
Plasma-wall interactions in tandem mirror machines
[DE85-006367] 15 p2657 N85-26399
Toroidal equilibrium with low frequency wave driven currents
[DE85-005790] 15 p2658 N85-26401
Theoretical studies of Elmo Bumpy Torus
[DE85-007202] 15 p2658 N85-26402
Finite orbit analysis for long wavelength modes in a plasma with a hot component
[DE85-006898] 15 p2658 N85-26404

Optimal control theory applied to fusion plasma thermal stabilization
[DE85-007589] 15 p2858 N85-26405
Ballooning beta limits of dee and bean shaped Tokamaks
[IPPJ-713] 16 p2866 N85-27676
Magnetohydrodynamic stability of spheromak plasma in toroidal flux conserver with rectangular cross section
[IPPJ-716] 16 p2866 N85-27678
Geophysical plasmas and atmospheric modeling
[AD-A152805] 17 p2993 N85-28467
Application of the MHD energy principle to magnetostatic atmospheres
[NASA-CR-175987] 18 p3136 N85-29420
Millimeter wave generation by relativistic electron beams
[AD-A153080] 18 p3179 N85-29708
Research with high-power short-wavelength lasers
[DE85-010329] 19 p3278 N85-30332
Two-point theory of current-driven ion-cyclotron turbulence
[DE85-010114] 19 p3372 N85-30918
Stability of a hot symmetric tandem mirror with thermal barrier
[DE85-010539] 19 p3377 N85-30952
Effects of zonal disturbances on the ionization state of the solar wind
[NASA-CR-175997] 19 p3385 N85-31000
Nuclear responses in INTOR plasma stabilization elements
[DE85-010489] 20 p3535 N85-31995
Drift anisotropy instability of a finite Beta magnetospheric plasma
[IFSI-84-12] 20 p3536 N85-32005
Diamagnetic instability of cyclotron waves in plasma
21 p3693 N85-32948
Low frequency instabilities driven by an ion temperature anisotropy
[AD-A154902] 21 p3707 N85-33016
User's manual for the FLORA equilibrium and stability code
[DE85-013182] 23 p3866 N85-34590
Magnetohydrodynamic equilibrium and stability of spheromak with spheroidal plasma-vacuum interface
[IPPJ-732] 23 p3874 N85-34640
Low frequency instability in a mirror field
23 p3877 N85-34657
ECH tokamak
[DE85-012074] 23 p3964 N85-34707
Onset of solar flares as predicted by two-dimensional MHD-models of quiescent prominences
[SH-1.3-1] 23 p3992 N85-34750
A cosmic ray driven instability
[OG-8.1-5] 23 p4018 N85-34885

MAGNETOHYDRODYNAMIC TURBULENCE
NT PLASMA TURBULENCE
Random processes and magnetohydrodynamic turbulence 02 p0271 N85-11767
Magnetohydrodynamic (MHD) turbulence in radio galaxies 12 p1958 N85-22305
Forced MHD turbulence in a uniform external magnetic field
[NASA-CR-172578] 15 p2654 N85-26368
An interplanetary magnetic field ensemble at 1 AU
[NASA-TM-86209] 16 p2862 N85-27784
Cosmic ray modulation and turbulent interaction regions near 11 AU
[NASA-TM-86193] 18 p3209 N85-29909
Fractal structure of the interplanetary magnetic field
[NASA-TM-86212] 19 p3383 N85-30987
Prompt acceleration of ions by oblique turbulent shocks in solar flares
[SH-1.1-6] 23 p3989 N85-34733
Isotopic overabundances and the energetic particle model of solar flares
[SH-2.2-1] 23 p4000 N85-34798
Diffusion of strongly magnetized cosmic ray particles in a turbulent medium
[OG-7.2-16] 23 p4015 N85-34883

MAGNETOHYDRODYNAMIC WAVES
NT ELECTROSTATIC WAVES
NT PLASMA WAVES
Precipitation of protons with E sub p approximately 1 MeV near plasmopause 02 p0181 N85-11093
Fine structure of Alfven maser radiation
06 p0624 N85-15232
Shear-Alfven dynamics of toroidally confined plasmas, part A
[DE85-001580] 06 p0666 N85-15502
A leaky waveguide model for MHD wave driven winds from coronal holes 08 p1235 N85-17781
Generation of Alfven waves due to thermal modulation of the electrical conductivity
[AD-A149369] 10 p1558 N85-19826
Driven global Alfven eigenmodes
[DE85-001056] 11 p1732 N85-20890
Forced recognition by nonlinear MHD waves and sequential triggering of solar flares
12 p1956 N85-22291
Nonlinear evolution of astrophysical Alfven waves
12 p1956 N85-22294
Hydromagnetic precursors of interplanetary plasma burst 13 p1976 N85-22414
Excitation of low-frequency plasma waves by a conducting, tethered satellite 13 p2171 N85-23470
Anisotropy of Alfven wave absorption in ionosphere
14 p2339 N85-24464
Diagram of nonstationary rejoining of magnetic force lines 14 p2344 N85-24492
Magnetosphere-ionosphere interaction through hydromagnetic waves 14 p2364 N85-24610
Contribution of the Scandinavian Twin Auroral Radar Experiment (STARE) radar to the understanding of the physical mechanisms associated with Pc5 pulsations
14 p2364 N85-24613
Propagation and amplification of Ion Cyclotron Waves (ICW's) in a multicomponent plasma. The Earth magnetosphere as a giant maser for Alfven waves
14 p2368 N85-24634
Results of ULF-wave investigations in the USSR
14 p2369 N85-24644
Magnetic pulsations recorded in northern Scandinavia during the IMS; a study of Pc 4-5 events
14 p2370 N85-24647
Implications of the global appearance of Pi2 and Pc 3 bursts 14 p2371 N85-24652
Magnetospheric wave characteristics derived from cross-spectral analysis 14 p2371 N85-24659
Nonlinear dynamos — solar activity
14 p2447 N85-25106
Observational constraints on heating processes — solar corona 14 p2449 N85-25115
Waves in inhomogeneous media — magnetohydrodynamic waves; solar atmosphere
14 p2449 N85-25116
Dynamo action of magnetostrophic waves — solar atmosphere 14 p2451 N85-25136
Coronal heating by turbulent phase mixed MHD waves — solar corona 14 p2453 N85-25148
Effects of atmospheric stratification on dissipative acoustic and Alfven waves — solar atmosphere
14 p2453 N85-25149
On running penumbral waves
14 p2453 N85-25150
Comments on the paper by F. Pegoraro, L. Suglyama: Spatial diffusion of charged high-energy fusion products by shear Alfven perturbations
[INPE-3291-PRE/606] 16 p2866 N85-27675
Solar wind observations associated with a slow forward shock wave at 0.31 AU
[MPAE-W-79-84-46] 17 p3055 N85-28909
Stability of a hot symmetric tandem mirror with thermal barrier
[DE85-010539] 19 p3377 N85-30952
Stochastic particle acceleration in solar flares
[SH-1.1-4] 23 p3989 N85-34731
Alfven wave scattering and the secondary to primary ratio
[OG-7.2-9] 23 p4015 N85-34878
Diffusion of strongly magnetized cosmic ray particles in a turbulent medium
[OG-7.2-16] 23 p4015 N85-34883
The role of cosmic rays and Alfven waves in the structure of the galactic halo
[OG-7.2-18] 23 p4016 N85-34885
A cosmic ray driven instability
[OG-8.1-5] 23 p4018 N85-34895
Relativistic transport theory for cosmic-rays
[OG-8.3-8] 23 p4022 N85-34926
Scale separation closure and Alfven wave turbulence
[DE85-013124] 24 p4095 N85-35385
Parallel fast-forward shock within 1 AU: Helios-1 and 2 observations
[MPAE-W-79-84-27] 24 p4169 N85-35847

MAGNETOHYDRODYNAMICS
NT CYLINDRICAL PLASMAS
Fluctuation spectrum for linear gyroviscous MHD
[IPP-6/237] 01 p0121 N85-10828
MHD instabilities in simple plasma configuration
[AD-A144936] 01 p0121 N85-10829
Ceramic materials for MHD electrodes
[DE84-015580] 02 p0187 N85-11250
Destruction of magnetic surfaces in three-dimensional MHD equilibria 02 p0262 N85-11838
Electric field and plasma energization in computer simulations of magnetotail reconnection
[DE84-014023] 02 p0285 N85-11859
Magnetohydrodynamic and gasdynamic theories for planetary bow waves
[NASA-CR-174132] 03 p0448 N85-12850
High-Beta plasma theory
[DE84-016471] 04 p0568 N85-13619
Proceedings of the US-Japan Theory Workshop on 3-D MHD Studies
[DE84-012019] 04 p0568 N85-13620
Special topics reports for the reference tandem mirror fusion breeder: Liquid metal MHD pressure drop effects in the packet bed blanket, volume 1
[DE85-002142] 06 p0865 N85-15500
Spicules and surges
[AD-A146785] 07 p1061 N85-16727
MHD performance demonstration experiment, FY 1974 to FY 1984
[DE85-000854] 08 p1224 N85-17709
Electromagnetic pulse (EMP) interaction with electric power systems. Power Systems Technology Program
[DE85-000166] 09 p1312 N85-18244
Normal mode analysis for linear resistive magnetohydrodynamics
[IPP-6/235] 11 p1730 N85-20878
Convergent spectral representation for 3-dimensional inverse MBD equilibria
[DE85-000866] 11 p1733 N85-20900
Strong iron accelerating by collisionless magnetoconic shock wave propagating perpendicular to a magnetic field
[IPPJ-709] 12 p1935 N85-22181
Hydrodynamics of astrophysical jets — active galactic nuclei 12 p1958 N85-22307
An analytic model for hydromagnetospheres — stellar winds; pulsars; cosmic jets 12 p1959 N85-22313
Development of a Global 3-D magnetohydrodynamic computational model for solar wind-cometary and planetary studies
[NASA-CR-175490] 12 p1962 N85-22331
Physics of the inner heliosphere: Mechanisms, models and observational signatures
[NASA-CR-175632] 13 p2205 N85-23677
Dynamics of solid body with ellipsoidal cavity containing magnetic fluid 14 p2279 N85-24116
Electromagnetic field of currents and its use to estimate total conductivity of sedimentary depoeits in Western Black Sea 14 p2334 N85-24434
Experimental facility for studying MHD effects in liquid metal cooled blankets
[DE85-000583] 14 p2423 N85-24943
Magneto-fluid-dynamic issues for fusion first wall and blanket systems
[DE85-004022] 14 p2424 N85-24954
Magnetohydrodynamic considerations for the design of self-cooled liquid-metal fusion reactor blankets
[DE85-000242] 14 p2425 N85-24957
Numerical simulations of convectively excited gravity waves 14 p2444 N85-25082
The hydromagnetics of the Sun — conference
[ESA-SP-220] 14 p2445 N85-25091
Magnetoconvection: The interaction of convection and small scale magnetic fields — photosphere
14 p2446 N85-25098
Nonlinear dynamos — solar activity
14 p2447 N85-25106
A numerical simulation of the formation of solar prominences 14 p2448 N85-25112
The possible role of electrical currents in coronal phenomena 14 p2453 N85-25151
Solar magnetohydrodynamics: Symposium review
14 p2455 N85-25162
Magnetohydrodynamics of Earth's bow shock
15 p2481 N85-25311
Development of a global 3-D magnetohydrodynamic computational model for solar wind/cometary and planetary studies
[NASA-CR-175724] 15 p2684 N85-26577
Stream dynamics between 1 AU and 2 AU: A detailed comparison of observations and theory
[NASA-TM-86066] 15 p2684 N85-26578
Asymptotic solutions of MHD equations with finite conductivity
[REPT-12/1984] 16 p2852 N85-27581
A four-field model for Tokamak plasma dynamics
[DE85-007111] 16 p2868 N85-27694
Fluid modeling of magnetized plasmas
[DE85-007679] 17 p3039 N85-28804
Electromagnetic solitary waves in magnetized plasmas
[DE85-010084] 18 p3190 N85-29788
Coal-Fired MHD Combustor Development Project, Phase 3D
[DE85-008822] 18 p3192 N85-29795
MHD channel development
[DE85-008305] 18 p3192 N85-29796
The effects of alpha particle production on the stability of an Elmo Bumpy Torus (EBT) reactor
19 p3369 N85-30895
Solar-wind magnetosphere energy input functions
[NASA-CR-176021] 19 p3385 N85-31001
Magnetohydrodynamics and the National Coal Science, Technology, and Engineering Development Acts
[S-HRG-98-1179] 20 p3535 N85-31994

Planetary Dynamos
[NASA-CR-176001] 21 p0679 N85-32857
Plasmodynamic methods for generating powerful light pulses 21 p0693 N85-32943
A system of magnetohydrodynamic-type equations 21 p0693 N85-32946
Method and apparatus for maintaining equilibrium in a helical axis stellarator
[DE85-011626] 22 p0845 N85-33815
Linear filters as a method of real-time prediction of geomagnetic activity
[DE85-010760] 22 p0860 N85-33999
Moving finite element method for ICF target implosion 23 p0980 N85-34675
Instrument to synchronize Thomson scattering diagnostic measurements with MHD activity in a Tokamak
[DE85-012082] 23 p0984 N85-34708
Onset of solar flares as predicted by two-dimensional MHD-models of quiescent prominences
[SH-1.3-1] 23 p0992 N85-34750
The role of cosmic rays in magnetic hydrodynamics of interstellar medium
[OG-7.2-15] 23 p4015 N85-34882
Some rigorous results concerning spectral theory for ideal MHD
[DE85-013427] 24 p4156 N85-35770

MAGNETOIONIC PLASMA
U PLASMAS (PHYSICS)

MAGNETOMECHANICS (PHYSICS)
Contributions to the 7th International Acoustic Emission Symposium
[AD-A145368] 02 p0275 N85-11792
Moessbauer study of amorphous Fe(67)Co(18)B(14)S(1)
[AERE-R-11526] 11 p1737 N85-20928

MAGNETOMETERS
NT VARIOMETERS
Magnetic properties of the cobalt matrix in WC-Co compacts 02 p0177 N85-11186
Present practice for the recording of the Earth magnetic field — geophysical observatories 04 p0519 N85-13317
Amplitude mode magnetic sensors
[AD-D011335] 07 p0961 N85-16094
Investigation of dynamic noise affecting geodynamics information in a tethered subsatellite
[NASA-CR-174292] 08 p1174 N85-17405
An inexpensive vector thin film magnetometer
[AD-A148725] 09 p1323 N85-18310
A preliminary study of a cryogenic equivalence principle experiment on Shuttle
[NASA-CR-171300] 10 p1426 N85-18894
Note of the dynamic behavior of a magnet system suspended by a thin fiber, with special reference to the Quartz Horizontal Magnetometer (QHM)
[DMI-GEOPHYS-PAPERS-R-70] 11 p1714 N85-20785
Rotating squid magnetometers and gradiometers
[AD-D011529] 12 p1849 N85-21600
Satellite, auroral radar and ground magnometer observations of transient ULF pulsations 14 p2369 N85-24645
Ground magnetic observations of high-latitude Pt2 pulsations: Scandinavian magnetometer array results 14 p2370 N85-24649
The use of a self-compensated magnetometer in an economical navigation system for the helicopter 16 p2697 N85-26650
A method of estimating aircraft attitude from fly by wire flight control system data 16 p2697 N85-26653
On the use of a sunward-libration-point orbiting spacecraft as an IMF monitor for magnetospheric studies
[NASA-CR-175809] 16 p2825 N85-27426
Results of the magnetic field experiments E2 and E4 onboard Helios 1 and Helios 2 — magnetometer development 16 p2885 N85-27799
Rome/Goddard Space Flight Center (GSFC) magnetic field experiment: A summary of results — flux gate magnetometer 16 p2885 N85-27800
Research relative to the development of a cryogenic microwave cavity gradiometer for orbital use
[NASA-CR-176002] 19 p3222 N85-29960
Overview of applications of SQUIDS
[DE85-009942] 20 p3458 N85-31480
Spaceborne gradiometer error analysis 20 p3492 N85-31707
Fluxgate magnetometer (SSM) for the defense meteorological satellite program (DMSP) block 5D-2, flight 7
[AD-A155229] 21 p3580 N85-32143
The Galileo spacecraft magnetometer boom 22 p3796 N85-33513
Magnetic search system
[PB85-185108] 23 p3949 N85-34477
Procedure for editing the fluxgate magnetometer data of the AFGL (Air Force Geophysics Laboratory) magnetometer network
[AD-A156331] 24 p4117 N85-35523

MAGNETOMETRY
U MAGNETIC MEASUREMENT

MAGNETOPAUSE
Magnetohydrodynamic and gasdynamic theories for planetary bow waves
[NASA-CR-174132] 03 p0448 N85-12950
Reduction and analysis of data from the plasma wave instruments on the IMP-8 and IMP-8 spacecraft
[NASA-CR-175127] 04 p0460 N85-12918
The Earth magnetosphere: A charged particle accelerator 04 p0519 N85-13315
Research relative to plasma transport across the magnetopause
[NASA-CR-174300] 07 p1046 N85-16636
Research study of space plasma boundary processes
[NASA-CR-174351] 10 p1558 N85-19823
The Earth's magnetopause — International Magnetospheric Study 14 p2355 N85-24549
Electric field and plasma observations near the magnetopause and bow shock during a rapid compression 14 p2355 N85-24553
Magnetic field observations at the dayside magnetopause: ISEE-1 and -2 contributions during the IMS 14 p2356 N85-24555
Efficiency of electric field transfer at Earth's magnetopause and flow amplitudes related to reconnection 14 p2356 N85-24557
Satellite-borne electric field measurements with spherical double probes — ISEE satellites 14 p2356 N85-24558
Energetic particle sounding at the magnetopause and implications for magnetic reconnection 14 p2356 N85-24559
Observations of energetic electron and ion distributions near the magnetopause at geosynchronous orbit and related ground effects 14 p2358 N85-24560
Structure of the boundary layer for steady-state magnetopause reconnection 14 p2358 N85-24561
Characteristics of Pc 4,5 pulsations and their source mechanisms 14 p2370 N85-24648
The structure, stability, wave transmission and energy transfer at the Earth's magnetopause 14 p2372 N85-24661
Bursts of relativistic electrons in magnetopause and in outer radiation belt 16 p2722 N85-26801

MAGNETOPLASMADYNAMICS
Convection of plasma in polar ionosphere, comparison of measurements from Cosmos-184 with model dependent on interplanetary magnetic field vector 02 p0160 N85-11066
The Earth's magnetopause — International Magnetospheric Study 14 p2355 N85-24549
The structure and dynamics of the magnetosphere: Progress in the IMS 14 p2355 N85-24550
Plasma sheet dynamics deduced from ISEE-1 and -2 energetic particle flux data 14 p2358 N85-24570

MAGNETOPLASMAS
U PLASMAS (PHYSICS)

MAGNETORESISTIVITY
Magnetoconductance in aluminum films, wires, and cylinders 19 p3374 N85-30928
Development of position sensors for microcomputer-oriented sensor systems
[BMFT-FB-T-85-021] 24 p4091 N85-35361

MAGNETOSONIC RESONANCE
Cyclotron absorption of fast magnetosonic wave in stellarator 21 p3693 N85-32945

MAGNETOSPHERE
NT GEOMAGNETIC TAIL
NT MAGNETOPAUSE
The propagation and growth of whistler mode waves generated by electron beams in Earth's bow shock
[AD-A145572] 02 p0228 N85-11492
Uranus and Neptune
[NASA-CP-2330] 02 p0298 N85-11927
Magnetospheric structures: Uranus and Neptune 02 p0301 N85-11949
Magnetosphere, rings, and moons of Uranus 02 p0301 N85-11951
Do the satellites of Uranus control its magnetosphere? 02 p0301 N85-11952
Magnetospheric plasma studies using data from the dynamics high and low altitude plasma instruments
[AD-A145751] 03 p0392 N85-12505
On the cause of X-line formation in the near-Earth plasma sheet: Results of adiabatic convection of Plasma-Sheet-Plasma
[AD-A145835] 03 p0398 N85-12525
The Earth magnetosphere: A charged particle accelerator 04 p0519 N85-13315
Hot plasma particles in the Earth's outer magnetosphere: New understandings during the IMS
[DE84-016826] 05 p0677 N85-14348
Summaries of physical research in the geosciences
[DE85-001882] 06 p0818 N85-15194
Observation of natural noise near upper hybrid resonance in terrestrial magnetosphere by Prognoz-5 satellite 06 p0822 N85-15221
Electric field in plasma layer of magnetosphere during preliminary substorm phase 06 p0824 N85-15231
Fine structure of Alfven maser radiation 06 p0824 N85-15232
Birkeland currents correlated with dc-electric fields observed during the CENTAUR BBX rocket experiments
[DRI-6-84] 06 p0834 N85-15311
Electric fields in Earth orbital space
[AD-A146448] 06 p0835 N85-15313
Region 1 birkeland currents from a global MHD simulation of the magnetosphere
[AD-A147435] 07 p0987 N85-16335
Earth's radiation belts
[AD-A147927] 07 p0988 N85-16339
Ionospheric and magnetospheric modifications caused by VLF waves
[AD-A146210] 08 p1186 N85-17475
Current carriers for the field-aligned current system
[NASA-TM-86161] 08 p1260 N85-17925
Morphology of keV-electrons in the Earth's magnetosphere as observed by GEOS 1
[DRI-3-84] 09 p1350 N85-18496
Partial penetration of IMF B(sub y) into the magnetosphere
[DRI-5-84] 10 p1514 N85-19554
Recent investigations at INPE in magnetospheric physics and geomagnetism
[INPE-3280-PRE/803] 10 p1514 N85-19555
Ionospheric research at INPE
[INPE-3279-PRE/802] 10 p1514 N85-19556
A modeling analysis program for the JPL table mountain Io sodium cloud data
[NASA-CR-175474] 10 p1572 N85-19910
High energy particle effects in the D region during and after geomagnetic storms 11 p1684 N85-20485
Application of dimensional analysis to the problem of solar wind-magnetosphere energy coupling
[DE85-002414] 11 p1674 N85-20551
A modeling analysis program for the JPL Table Mountain Io sodium cloud data
[NASA-CR-175493] 11 p1681 N85-20589
Magnetospheres and winds in the helium weak stars: Observations of C 5 in upper main sequence CP stars 11 p1759 N85-21066
Substorms in the Earth's atmosphere
[DE85-000654] 12 p1890 N85-21861
Space research and the new approach to the mechanics of fluid media in cosmos 12 p1953 N85-22271
Magnetospheres in the solar system 12 p1954 N85-22274
Particle transport in planetary magnetospheres 12 p1954 N85-22275
The axisymmetric pulsar magnetosphere 12 p1955 N85-22279
Nonlinear waves in the magnetosphere of pulsars 12 p1955 N85-22281
About static and dynamic solutions of the aligned rotator model — pulsar magnetospheres 12 p1958 N85-22306
An analytic model for hydromagnetospheres — stellar winds; pulsars; cosmic jets 12 p1959 N85-22313
Plans for Interbol satellite experiment 13 p1977 N85-22407
Aerospace spacecraft-charging guidelines document 13 p1984 N85-22501
Argon ion pollution of the magnetosphere 13 p1998 N85-22523
Excitation of low-frequency plasma waves by a conducting, tethered satellite 13 p2171 N85-23470
Interaction of the magnetospheric ions with the surfaces of the icy satellites of Saturn 13 p2174 N85-23491
Diurnal variations in terrestrial magnetic field and structure of magnetosphere 14 p2344 N85-24493
Excitation of geomagnetic Pci-2 and pulsations with decreasing period during microsubstorms 14 p2344 N85-24494
Plasma and magnetospheric research
[NASA-CR-175675] 14 p2354 N85-24543
Achievements of the International Magnetospheric Study (IMS) — conference
[ESA-SP-217] 14 p2354 N85-24544
Some contributions to knowledge of the magnetospheric plasma by ISEE-1 investigators 14 p2354 N85-24548
The structure and dynamics of the magnetosphere: Progress in the IMS 14 p2355 N85-24550

Observations of the magnetospheric boundary layers — International Magnetospheric Study
14 p2355 N85-24551
Hot plasma and energetic particles in the Earth's outer magnetosphere: New understandings during the IMS
14 p2355 N85-24552
The keV electrons and 80 keV protons in the vicinity of the high latitude magnetosphere and at the bow shock
14 p2355 N85-24554
Magnetic field in the Earth's outer magnetosphere: Prognoz-6, -7 data
14 p2356 N85-24556
The application of dimensional analysis to the problem of solar wind-magnetosphere energy coupling
14 p2357 N85-24564
Coupling of the solar wind to measures of magnetic activity
14 p2357 N85-24565
Entry of solar energetic protons into the distant plasma sheet dependence on distance from the neutral sheet
14 p2357 N85-24567
Particle sources, transport, storage and precipitation — magnetosphere
14 p2359 N85-24576
IMS advances in studies of field-aligned currents and their related electrodynamics
14 p2359 N85-24578
Electrodynamics of magnetosphere-ionosphere coupling
14 p2359 N85-24579
Achievements of the plasma composition experiment on ISEE-1 during the IMS
14 p2360 N85-24583
Observations during a magnetosphere substorm triggered by a Storm Sudden Commencement (SSC): A case study
14 p2361 N85-24588
Disturbance of midlatitude electrodynamic parameters due to the magnetospheric convection
14 p2362 N85-24593
The magnetospheric convection electric field at ionospheric altitudes: A case study based on STARE and Saint-Santin data
14 p2362 N85-24594
Results of the Langmuir-probe experiment on board Intercosmos-18 — ionosphere-magnetosphere interaction
14 p2362 N85-24596
Comparison of magnetospheric and ionospheric electric fields using different empirical mapping factors
14 p2362 N85-24597
Solar wind control of electric fields and currents in the magnetosphere and ionosphere
14 p2364 N85-24608
Ionosphere-magnetosphere coupling and convection
14 p2364 N85-24609
Magnetosphere-ionosphere interaction through hydromagnetic waves
14 p2364 N85-24610
Pc 1-2 pulsations and related phenomena: A review — geomagnetic pulsations
14 p2364 N85-24611
An evaluation of the contributions of the IMS to experimental and theoretical studies of ULF plasma
14 p2365 N85-24614
Solar wind control of magnetospheric convection
14 p2365 N85-24615
Magnetospheric effects on the upper atmosphere
14 p2365 N85-24616
ELF chorus in the Earth's outer magnetosphere
14 p2366 N85-24624
Contribution of relaxation sounding experiments to the understanding of magnetospheric processes
14 p2371 N85-24655
Contribution of mutual impedance experiments to the understanding of magnetospheric processes — GEOS satellites
14 p2371 N85-24656
The use of the spectral matrix in analyzing the propagation characteristics of electromagnetic emissions — magnetosphere
14 p2371 N85-24658
Magnetospheric wave characteristics derived from cross-spectral analysis
14 p2371 N85-24659
Advances in magnetospheric plasma-wave research during the IMS
14 p2372 N85-24662
Active Magnetospheric Particle Tracing Explorers (AMPTE)
[AD-A151072]
14 p2374 N85-24674
Dynamo action of magnetoatrophic waves — solar atmosphere
14 p2451 N85-25136
Space-time features of solar cosmic ray penetration into high latitude regions of Earth's magnetosphere based on Intercosmos-19 satellite data
15 p2481 N85-25319
Modeling longitudinal motions of thermal O+ and H+ ions in magnetic field tube convective through daytime polar cusp
15 p2481 N85-25314
Plasma and magnetospheric research
[NASA-CR-171447]
15 p2581 N85-25976
Dynamics of charged small particles — Jupiter, Saturn magnetospheres
15 p2676 N85-26522
On planetary rings as sources and sinks of magnetospheric plasmas
15 p2677 N85-26526
Electrons and cosmic ray produced protons in Saturn's inner magnetosphere
[NASA-TM-87469]
15 p2679 N85-26548
Coupling of the solar wind to measures of magnetic activity
[DE85-002415]
15 p2685 N85-26580
Substorms in energetic radiation belt particles according to data from Meteor artificial Earth satellite
16 p2719 N85-26788
Modeling plasma mantle of Earth's magnetosphere
16 p2720 N85-26790
Orientation and strength of Martian magnetic dipole
16 p2723 N85-26808
Possible configuration of Martian magnetosphere
16 p2723 N85-26809
Electric field and energy transfer by magnetopause reconnection
[INPE-3448-PRE/701]
16 p2826 N85-27432
Solar activity monitoring satellite (SAMSAT): Impact on space environment services
[PB85-165066]
16 p2888 N85-27818
IMS (International Magnetospheric Study) contributions to the understanding of auroral precipitation, transport, and particle sources
[AD-A152320]
17 p2992 N85-28492
The boundary layers as the primary transport regions of the Earth's magnetotail
[AD-A152714]
17 p2992 N85-28496
More on shock-wave studies with Prognoz-10 satellite
19 p3296 N85-30432
Functions of Prognoz-10: Intercosmos' station explained
19 p3296 N85-30433
Prognoz-10 Intercosmos' station launched to study shock waves
19 p3296 N85-30434
Magnetospheres of the outer planets
[AD-A154354]
19 p3364 N85-30996
Solar-wind magnetosphere energy input functions
[NASA-CR-176021]
19 p3385 N85-31001
The role of scientific ballooning for exploration of the magnetosphere
[TRITA-EPP-84-07]
20 p3494 N85-31724
Observations of low energy magnetospheric plasma outside the plasmasphere
[KGI-PREPRINT-075]
20 p3536 N85-32004
Drift anisotropy instability of a finite Beta magnetospheric plasma
[IFSI-84-12]
20 p3536 N85-32005
Magnetospheric response to solar wind variations
[DE85-010762]
20 p3547 N85-32074
Interaction between an interplanetary shock and the Earth's magnetosphere on 27 August 1978: ISEE-1 electric field and ISEE-2 plasma observations
[IFSI-84-15]
20 p3548 N85-32078
The radiation of the Vela pulsar
20 p3548 N85-32080
A model of pulsed radiation from the Crab pulsar
20 p3548 N85-32081
ISEE-1 data reduction and analysis plasma composition experiment
[NASA-CR-175306]
21 p3630 N85-32552
Statistical analyses in the study of solar wind-magnetosphere coupling
[DE85-008596]
22 p3859 N85-33896
Linear filters as a method of real-time prediction of geomagnetic activity
[DE85-010760]
22 p3860 N85-33899
On the emission region of gamma ray bursts
[OG-1.1-4]
22 p3861 N85-33906
Waves in Space Plasmas (WISP)
23 p3901 N85-34164
Cosmic-ray transport in the galactic magnetosphere
[OG-7.2-17]
23 p4016 N85-34884
The influence of quiet asymmetric magnetosphere on the cutoff rigidities of the main cone
[SH-6.1-10]
23 p4045 N85-35083
Penetration of solar protons into the Earth's magnetosphere on November 22, 1977
[SH-6.1-15]
23 p4046 N85-35088
Dynamics of the penetration boundaries of solar protons during a strong magnetic storm
[SH-6.1-16]
23 p4046 N85-35089
The influence of the Earth's magnetosphere on the high-energy solar protons
[SH-6.1-22]
23 p4046 N85-35093
A suggested standardized format for cosmic ray ground-level event data
[SH-6.1-15]
23 p4052 N85-35130
Observation of nuclei with energies 8-30 MeV per nucleon in the Earth's magnetosphere at the altitudes 350 KM
[SH-10.1-5]
23 p4053 N85-35136
Two-dimensional quasineutral description of particles and fields above discrete auroral arcs
[NASA-CR-176170]
24 p4116 N85-35517
High energy radiation from neutron stars
[DE85-014353]
24 p4169 N85-35843

MAGNETOSPHERIC ELECTRON DENSITY

Energetic particle sounding at the magnetopause and implications for magnetic reconnection
14 p2356 N85-24559
Morphology of 2keV-electrons observed by GEOS 1
14 p2360 N85-24581
Coordinated balloon-satellite studies of energetic electron precipitation mechanisms
14 p2360 N85-24587
Contribution of relaxation sounding experiments to the understanding of magnetospheric processes
14 p2371 N85-24655
Ionospheric electron density profile and related studies
[AD-A155257]
21 p3632 N85-32567

MAGNETOSPHERIC INSTABILITY

Cold streams of ionospheric oxygen in the plasma sheet during the CDAW-6 event of March 22, 1979
[NASA-CR-174064]
03 p0393 N85-12513
Repulsive force of magnetic clouds during solar flares and magnetospheric substorms
06 p0824 N85-15233
Long-period magnetospheric pulsations observed with an electric field experiment in the magnetosphere
14 p2369 N85-24639
Magnetospheric pulsations observed by ISEE 1 and 2 satellites
14 p2369 N85-24640
Characteristics of Pc 4,5 pulsations and their source mechanisms
14 p2370 N85-24648
Ionospheric electron density profile and related studies
[AD-A155257]
21 p3632 N85-32567
Robinson instability and beam loading
[DE85-013301]
24 p4151 N85-35737

MAGNETOSPHERIC ION DENSITY

NT MAGNETOSPHERIC PROTON DENSITY
Achievements of the plasma composition experiment on ISEE-1 during the IMS
14 p2360 N85-24583

MAGNETOSPHERIC PROTON DENSITY

Energetic particle sounding at the magnetopause and implications for magnetic reconnection
14 p2356 N85-24559
Magnetotail current sheet and energetic particles observed on ISEE-1
14 p2357 N85-24566
Magnetosonic waves and their relationship with energetic protons
14 p2368 N85-24635

MAGNETOSTATICS

Magnetostatic wave frequency analyzer apparatus
[AD-D011249]
05 p0631 N85-14044
Improved magnetic bias and delay linearity in a magnetostatic wave delay line
[AD-D011441]
10 p1479 N85-19337
Magnetostatic problems in nonlinear media with hysteresis
[DE85-003701]
10 p1482 N85-19358
Magnetostatic-wave propagation in a finite YIG-Loaded rectangular waveguide
[AD-A150332]
13 p2055 N85-22865
Axisymmetric magnetofluidstatic (MFS) equilibria of solar coronal loops: An integral equation approach
14 p2449 N85-25118

MAGNETOSTRICTION

Estimate of sound absorption due to magnetoelastic interactions
[AD-A148216]
08 p1218 N85-17671
Analog frequency modulated laser using magnetostriction
[AD-D011701]
19 p3276 N85-30318
An experimental study of the magnetoelastic bending of thin plates made of soft ferromagnetic material
19 p3282 N85-30352

MAGNETOTELLURIC PROFILING

U MAGNETIC SURVEYS

MAGNETOVARIOGRAPHS

U VARIOMETERS

MAGNETRON SPUTTERING

Compensation of dangling bonds in A-Si, GeH alloys
[DE85-002905]
15 p2662 N85-26433

MAGNETRONS

Rippled-field magnetron apparatus
[AD-D011354]
07 p0969 N85-16154
Experimental and theoretical investigation of microwave and millimeter wave radiation from hollow, rotating electron beams
[AD-A153827]
18 p3179 N85-29706
Improved negative ion source
[DE85-006445]
23 p3912 N85-34241

MAGNETS

NT CRYOGENIC MAGNETS
NT ELECTROMAGNETS
NT FERRIMAGNETS
NT SUPERCONDUCTING MAGNETS
NT WIGGLER MAGNETS
On the calculating models of permanent magnets
[AD-A145111]
01 p0115 N85-10780
Shock electromechanical energy converter with permanent magnet
[AD-D011226]
01 p0115 N85-10781
Calibration of hall probes
[CSIR-NAC-83-04]
01 p0116 N85-10794
Results of prototype field measurements on SM4
[NAC-83-01]
01 p0117 N85-10797

LAMPF transmition-region mechanical fabrication
[DE84-017078] 04 p0562 N85-13577
Anisotropy and microstructure of rare earth permanent magnet materials
[AD-A146549] 06 p0859 N85-15480
Rotary magnetic heat pump
[DE84-017017] 09 p1320 N85-18303
Cobalt-free permanent magnet alloys
[AD-A149272] 10 p1441 N85-19079
Permanent magnet motors
[DE85-000660] 10 p1482 N85-19355
Non-contacting electromagnetic de-spin system for Earth orbiting satellites 12 p1946 N85-22225
The ferrite permanent magnet AC motor: A technical and economical assessment
[DE85-002480] 13 p2066 N85-22903
Mechanization and automation of production processes in turbine building 14 p2269 N85-24057
Linear motion valve
[NASA-CASE-MSC-20148-1] 18 p3115 N85-29284
3d calculations of a fixed field alternating gradient synchrotron magnet
[DE85-002742] 18 p3183 N85-29739
Investigation for low-cost permanent magnets
[AD-A154387] 19 p3260 N85-30212
Combined function lattices for a 6 GeV synchrotron light source
[DE85-010959] 19 p3367 N85-30885
Hot isostatically pressed Sm(2)(TM)17 magnets
[AD-A155479] 21 p3582 N85-32267
Tailored vacuum chambers for ac magnets
[DE85-010767] 21 p3591 N85-32319
SLC arc transport system: Magnet design and construction
[DE85-014299] 24 p4159 N85-35789

MAGNIFICATION
Investigation into the use of the TV magnifier in the Netherlands
[HSE-TRANS-11142] 20 p3533 N85-31986

MAGNIFIERS
U MAGNIFICATION

MAGNITUDE
NT STELLAR MAGNITUDE
On the error of typhoon intensity estimation by means of IR Dvorak technique occurring when the eye is very small 12 p1894 N85-21886

MAGNONS
Symmetry of exchange interaction in crystalline magnetic films 02 p0259 N85-11664
Observation of standing spinwaves in thin Fe-films by means of Raman spectroscopy
[DE85-003036] 11 p1735 N85-20913

MAGSAT SATELLITES
Analysis of the daily geomagnetic variation with the use of MAGSAT data — MAGSAT satellites 04 p0520 N85-13319
Science Applications, part 2 11 p1843 N85-20347

MAIN SEQUENCE STARS
NT PRE-MAIN SEQUENCE STARS
Theoretical studies of chromospheres and winds in cool stars
[NASA-CR-174204] 06 p0880 N85-15596
Theory tested by means of the stars — viability of the alpha-omega dynamo model 08 p1233 N85-17770
A survey for photometric variability from space 08 p1251 N85-17897
On the progenitors of white dwarfs
[NASA-CR-174378] 09 p1413 N85-18913
Interstellar extinction in the nucleus of H PER 11 p1749 N85-21001
Main sequence B stars with strong winds 11 p1750 N85-21005
A search for the spectroscopic binary companions of Polaris using IUE spectra 11 p1757 N85-21053
The solar stellar connection in the far ultraviolet 11 p1757 N85-21055
Magnetospheres and winds in the helium weak stars: Observations of C 5 in upper main sequence CP stars 11 p1759 N85-21066

MAINE
Peat resources of Maine. Volume 1: Aroostook County
[DE85-004196] 11 p1669 N85-20519
Peat resources of Maine. Volume 4: Southern and western Maine
[DE85-004198] 11 p1670 N85-20520
Peat resources of Maine. Volume 2: Penobscot County
[DE85-004195] 11 p1670 N85-20522
Peat resources of Maine. Volume 5: Washington County
[DE85-004197] 11 p1670 N85-20523

MAINTAINABILITY
Ada (trademark) training curriculum. Software engineering for managers m101 teacher's exercise guide
[AD-A145094] 01 p0104 N85-10895
Artificial intelligence approaches to monitoring system integrity
[AD-P003930] 02 p0246 N85-11610
Design for Tactical Avionics Maintainability
[AGARD-CP-361] 08 p1063 N85-16731
Objectives in studying the maintainability of aircraft systems 08 p1063 N85-16732
Joint service design for testability program 08 p1063 N85-16733
The embedded test (BIT): Impact on the total cost of possession 08 p1063 N85-16734
ATE user's view on design for maintainability 08 p1064 N85-16737
Maintainability: An ILS effort to manipulate LCC 08 p1064 N85-16743
The production of maintainable, trustworthy, and portable software 08 p1064 N85-16744
A description of a logistically ideal aircraft
[AD-A148425] 08 p1064 N85-16986
Computer aided of maintainability design: A feasibility study
[AD-A149293] 11 p1738 N85-20932
Maintainability time standards for electronic equipment
[AD-A149664] 12 p1834 N85-21507
Reliability analysis of automatic systems
[VTT-301] 12 p1863 N85-21682
A summary and assessment of historical reliability and maintainability data for solar hot water and space conditioning systems
[DE84-004521] 12 p1876 N85-21770
Design for tactical avionics maintainability, technical evaluation report
[AGARD-AR-204] 14 p2225 N85-23798
Statistical aspects of reliability, maintainability and availability
[AD-A151226] 15 p2640 N85-26282
Space Station Engineering and Technology Development
[NASA-CR-175606] 16 p2731 N85-26851
A framework for software development
[AD-A152067] 16 p2847 N85-27551
Maintenance of long life space systems, volume 1
[MATRA-0316/DX80-VOL-1] 18 p3066 N85-29964
Maintenance of long life space systems, volume 2
[MATRA-0350/DX80-VOL-2] 18 p3066 N85-29965
Los Alamos optical materials reliability, maintainability, and exposure testing program
[DE85-011894] 21 p3613 N85-32458
Air university commander's and supervisor's guide on substance abuse
[AD-A156336] 24 p4133 N85-35822

MAINTENANCE
NT AIRCRAFT MAINTENANCE
NT FILE MAINTENANCE (COMPUTERS)
NT SPACE MAINTENANCE
NT SPACECRAFT MAINTENANCE
Hot-gas cleanup for molten carbonate fuel cells-dechlorination and soot formation
[DE84-003072] 01 p0068 N85-10450
Stochastic properties of a sequence of interfailure times under minimal repair and under revival
[AD-A145003] 01 p0113 N85-10769
Updating logical databases
[AD-A144937] 01 p0125 N85-10860
Air Force Human Resources Laboratory report: Fiscal year, 1983
[AD-A145847] 02 p0238 N85-11548
Artificial Intelligence in Maintenance: Proceedings of the Joint Services Workshop
[AD-A145349] 02 p0244 N85-11592
The need for improvements in weapon system maintenance: What can AI (Artificial Intelligence) contribute?
[AD-P003913] 02 p0244 N85-11593
Artificial intelligence applications to maintenance
[AD-P003914] 02 p0244 N85-11594
On applying AI (Artificial Intelligence) to maintenance and troubleshooting
[AD-P003915] 02 p0244 N85-11595
Overview of training and aiding
[AD-P003917] 02 p0245 N85-11597
AI (Artificial Intelligence) approaches to troubleshooting
[AD-P003918] 02 p0245 N85-11598
Diagnosis based on description of structure and function
[AD-P003919] 02 p0245 N85-11599
Designing an expert system for training automotive electrical troubleshooting
[AD-P003926] 02 p0246 N85-11606
Models of natural intelligence in fault diagnosis tasks: Implications for training and aiding of maintenance personnel
[AD-P003927] 02 p0246 N85-11607
A generalized model of fault-isolation performance
[AD-P003928] 02 p0246 N85-11608
Expert systems in maintenance diagnostics for self-repair of digital flight control systems
[AD-P003933] 02 p0247 N85-11613
Model-based probabilistic reasoning for electronics troubleshooting
[AD-P003937] 02 p0247 N85-11617
Knowledge based tools for electronic equipment maintenance
[AD-P003940] 02 p0248 N85-11620
DELTA: An expert system for diesel electric locomotive repair
[AD-P003941] 02 p0248 N85-11621
LES: (Lockheed Expert System): A model-based expert system for electronic maintenance
[AD-P003944] 02 p0248 N85-11624
The application of artificial intelligence to a maintenance and diagnostic information system
[AD-P003945] 02 p0249 N85-11625
Future robotics program at San Antonio ALC (Air Logistics Center)
[AD-P004011] 03 p0309 N85-11991
Logistics support costs for the B-1B aircraft can be reduced
[AD-A145848] 03 p0309 N85-11996
Development of a pavement maintenance management system. Volume 10: Summary of development from 1974 through 1983
[AD-A146035] 03 p0320 N85-12067
Materials for emergency repair of runways
[AD-A146139] 03 p0320 N85-12068
Development of a pavement maintenance management system. Volume 9: Development of airfield pavement performance prediction models
[AD-A146150] 03 p0321 N85-12069
Correlation and reassessment of the OTEC plant power cycle
[DE84-015467] 04 p0529 N85-13382
Minimal cut-set methodology for artificial intelligence applications
[DE84-016574] 04 p0553 N85-13518
Electric vehicle maintenance
[PB84-233352] 04 p0579 N85-13693
Prefabricated panels for rapidly runway repair and expedient airfield surfacing
[AD-D011277] 05 p0697 N85-13804
Situational interactive micro/graphic simulator system for improving maintenance performance
[AD-A146877] 06 p0757 N85-14846
Analyses to develop models to project failure rates and repair costs of electronic modules and subassemblies
[AD-A146509] 06 p0816 N85-15180
National airspace system configuration management interface control document. Maintenance processor subsystem to remote monitoring subsystems and remote monitoring subsystem concentrators
[NAS-MD-790] 07 p0900 N85-15705
System for rapid repair of damaged airfield runways
[AD-D011325] 07 p0909 N85-15754
An analysis of the technical training of enlisted minuteman missile maintenance personnel
[AD-A147078] 07 p0912 N85-15775
Grease versus oil lubrication of wheel bearings in Army equipment
[AD-A147546] 07 p0973 N85-16184
Managing recoverable aircraft components in the PPB and related processes: Executive summary
[AD-A146806] 07 p1050 N85-16667
A simulation model for Air Launched Cruise Missile engine management
[AD-A147018] 07 p1051 N85-16672
Feasibility of measuring technical productivity improvements in Air Force Logistics Command depot-level maintenance using the Data Envelopment Analysis (DEA) and Constrained Facet Analysis (CFA) models
[AD-A147329] 07 p1052 N85-16676
Maintainability: An ILS effort to manipulate LCC 08 p1064 N85-16743
A weapon system design approach to diagnostics 08 p1066 N85-16752
Planning for the on-orbit servicing of military spacecraft
[AD-A148447] 08 p1104 N85-16983
Flight service evaluation of advanced composite ailerons on the L-1011 transport aircraft
[NASA-CR-172483] 08 p1118 N85-17049
Repair of composites 08 p1120 N85-17058
Operating and maintenance guidelines for the kinergetics (trade name) environmental control system. Carbon dioxide scrubber model DH-10 and heat exchanger model CCU-01
[AD-A148107] 08 p1200 N85-17557
Performance management system enhancement and maintenance
[NASA-CR-175271] 08 p1202 N85-17564

Prematurely terminated sequential tests for MIL-STD 781C
[AD-A145417] 08 p1216 N85-17657
Liquid phase methanol process development unit: Installation, operation, and support studies
[DE85-001311] 09 p1301 N85-18171
Control and electronic subsystems for the advanced servomanipulator
[DE85-001900] 09 p1327 N85-18343
The care and feeding of magnetic tapes
[AD-A145853] 09 p1366 N85-18585
Material flow in the manufacturing system: Fault-diagnosis systems as support for the maintenance of highly automated manufacturing systems
[PNR-90236] 09 p1371 N85-18618
In situ washing procedures for the UKIRT 3.8 meter primary mirror — United Kingdom Infrared Telescope (UKIRT)
[UKIRT-20] 09 p1414 N85-18918
Adhesive joint formation under field conditions
[AD-D011478] 10 p1453 N85-19153
Monitoring the execution of plans in SIPE (System for Interactive Planning and Execution) monitoring
[AD-A149138] 10 p1544 N85-19731
Fiat introduces 1000-CC engine
11 p1616 N85-20185
Corrosion and coatings review of specifications and drawings of facilities for the Oman Military Construction Program at Masirah Island, Oman
[AD-A149739] 12 p1812 N85-21366
Operation and maintenance requirements of the Army Remotely Piloted Vehicle (RPV)
[NASA-CR-175714] 14 p2216 N85-23755
Establishment and maintenance of certification standards for helicopter and turboprop power transmission systems 14 p2224 N85-23798
Mini-Seminar on Non-Destructive Testing
[CSIR-TSD-0009/83] 14 p2316 N85-24306
Lead shortage hastens need for improved storage batteries 15 p2461 N85-25195
Pavement-marking materials: New York's experience
[PB85-153294] 15 p2523 N85-25558
Automation of serviceibility of radio-relay station equipment 15 p2527 N85-25582
Installation, maintenance and operating manual for the Lucas-type fuel injection system of the 3 B rotary engine
[NASA-TM-77872] 15 p2568 N85-25848
Graphic simulation of a machine-repairman model
[AD-A151761] 16 p2604 N85-26633
Maintaining consistency and accommodating network repair in a self-regenerative distributed database management system (a discussion of the means and cost) 16 p2698 N85-26656
Management aspects of software maintenance
[AD-A152035] 16 p2647 N85-27550
Inspection evaluation and repair of the flawed feedwater nozzle of the 50 MWe Dodewaard GKN boiling water reactor
[ISBN-90-353-0017-3] 17 p2977 N85-28394
Tokamak fusion core experiment maintenance study
[DE85-008040] 17 p3040 N85-28813
The use of flight simulators in measuring and improving training effectiveness
[AD-A153617] 18 p3084 N85-28954
Automated maintenance system test program increment VI production scheduling
[AD-A153694] 18 p3196 N85-29838
Touch-off: A method to determine the position of an object by means of a sensor-driven robot
[DE85-011178] 19 p3339 N85-30691
Fusion Power Demonstration (FPD) maintenance and disassembly considerations
[DE85-011413] 22 p3846 N85-33820
Upgrading auxiliary facility outleakage and combustion detection
[DE85-012796] 23 p3934 N85-34388
Maintenance port system
[AD-D011724] 23 p3967 N85-34594
Dissected motors-propellants motor number STM-012. Phase 15: Surveillance report, stage 1
[AD-A156088] 24 p4071 N85-35226
Quality assurance considerations for the implementation of a pulsed power R and D project
[DE85-012357] 24 p4148 N85-35720
Time domain reflectometry for SLC BPM system
[DE85-012369] 24 p4155 N85-35758

MAINTENANCE TRAINING
The psychology of technical devices and technical discourse
[AD-P003929] 02 p0246 N85-11609
AFHRL (Air Force Human Resources Laboratory) program for artificial intelligence applications to maintenance and training
[AD-P003931] 02 p0247 N85-11611
Artificial intelligence contributions to training and maintenance
[AD-P003934] 02 p0247 N85-11614
An analysis of the technical training of enlisted minuteman missile maintenance personnel
[AD-A147078] 07 p0912 N85-15775
Maintenance training simulators prime item development specification. Model specification and handbook
[AD-A154106] 19 p3330 N85-30828

MALEATES
Stabilized unsaturated polyesters
[NASA-CASE-NPO-16103-1] 18 p3078 N85-29043
Condensation of anhydrides or dicarboxylic acids with compounds containing active methylene groups. Part 1: Condensation of phthalic anhydride with acetoacetic and malonic ester
[NASA-TM-77686] 19 p3227 N85-30010

MALES
Anthropometric cockpit compatibility assessment of US Army aircraft for large and small personnel wearing a training, warm-weather clothing configuration
[AD-A145208] 01 p0099 N85-10656
Skeletal muscle metabolism during exercise is influenced by heat acclimation
[AD-A146845] 10 p1527 N85-19832
Assessment of muscle strength and prediction of lifting capacity in US Army personnel
[AD-A146846] 10 p1527 N85-19833
Hemodynamics responses to upright tilt at sea level and high altitude
[AD-A146848] 10 p1527 N85-19834
Dynamics of quantitative and qualitative changes in conditionally pathogenic microflora of the human intestine during long-term hypokinesia 12 p1903 N85-21953
Aerobic and anaerobic exercise tolerance in the heat: Effect and acclimatization 14 p2388 N85-24707
Comparative anaerobic power of males and females
[AD-A151960] 16 p2842 N85-27523
Positive Gz accelerations tolerance of individuals 41 to 58 years of age 19 p3323 N85-30588
Investigation of some aspects of amino acid metabolism in man during brief exposure to antiorthostatic hypokinesia combined with ultraviolet radiation
22 p3822 N85-33678

MALFUNCTIONS
Safety recommendation(s), A-84-65
[REPT-3908] 14 p2216 N85-23743
General Aviation Airworthiness Alerts, no. 85
[FAA-AC-43-16] 22 p3729 N85-33117

MALLEABILITY
Assessing the machinability of gearwheel steels during manufacture
[BLL-BISI-TRANS-22343-(9902.06)]
17 p2973 N85-28365

MAMMALS
NT BABOONS
NT BEARS
NT CATS
NT DEER
NT DOGS
NT DOLPHINS
NT GUINEA PIGS
NT HUMAN BEINGS
NT MICE
NT MONKEYS
NT PRIMATES
NT RABBITS
NT RATS
NT SEALS (ANIMALS)
NT SHEEP
NT WHALES
Genetic effects of microwave exposure on mammalian cells in vitro. Volume 2, Appendix A: Cytogenetics and growth kinetics data, 850 MHz
[AD-A146866] 10 p1522 N85-19599
Genetic effects of microwave exposure on mammalian cells in vitro. Volume 2, Appendix B: Cytogenetics and growth kinetics data, 1.2 GHz
[AD-A146867] 10 p1522 N85-19600
Control of mammals at airports
[AD-P004192] 11 p1560 N85-19957
Mammalian gravity receptors: Structure and metabolism 15 p2605 N85-26055
Gravitational effects on reproduction, growth and development of mammals 15 p2612 N85-26097
Quantitation of Na+, K+-ATPase enzyme activity in tissues of the mammalian vestibular system
15 p2613 N85-26102
A communications link for an implantable electrode array
[AD-A152238] 16 p2840 N85-27510
Effects of method of detachment on electrophoretic mobility of mammalian cells grown in monolayer culture
20 p3500 N85-31757
Vertebrate development in space: Gravity is a drag (and has been for eons and eons) 24 p4126 N85-35580
Report of the NASA Mammalian Developmental Biology Working Group 24 p4126 N85-35581

MAN
U HUMAN BEINGS

MAN ENVIRONMENT INTERACTIONS
The SANCOR programme on coastal processes, April 1982 - March 1988
[REPT-68] 01 p0069 N85-10455
Modeling long-term changes in forested landscapes and their relation to the Earth's energy balance
05 p0653 N85-14194
Education and training for the climate related activities in Latin America and the Caribbean
07 p1004 N85-16379
Ozone and temperature trends due to the injection of trace species in the atmosphere
[AERONOMICA-ACTA-A-288-1984]
18 p3132 N85-29399
Applied climatology — regional planning
18 p3147 N85-29486
Ozone in the 21st century: Increase or decrease
[AERONOMICA-ACTA-A-291-1984]
20 p3489 N85-31687
Meteorology and Society: Statements presented at the 9th congress under agenda item 12 — World Meteorological Organization
[WMO-643] 22 p3817 N85-33644
Agents and effects of ozone trends in the atmosphere
[AERONOMICA-ACTA-A-287-1984]
23 p3948 N85-34466

MAN MACHINE SYSTEMS
Nowcasting with Doppler radar: The forecaster-computer relationship
01 p0077 N85-10514
FRONTIERS: Progress with a system for nowcasting rain — Forecasting Rain Optimized using New Techniques of Interactively Enhanced Radar and Satellite (FRONTIERS) 01 p0062 N85-10552
Nowcasting: Advances with McIDAS 3 — Man-computer Interactive Data System System (McIDAS)
01 p0052 N85-10553
Development of nowcasting in China
01 p0083 N85-10554
Interactive computer display systems in nowcasting
01 p0063 N85-10557
MERIT: A man/computer data management and enhancement system for upper air nowcasting/forecasting in the United States — Minimum Energy Routes using Interactive Techniques (MERIT)
01 p0083 N85-10558
PROMIS 600: The pilot project for the future Swedish weather service 01 p0083 N85-10560
Robust rate control system designs for a submersible
[AD-A144792] 01 p0111 N85-10753
Effects of alternative chromatic mixed graphics displays in decision support systems
[AD-A145561] 02 p0242 N85-11578
An effective graphics user interface for rules and inference mechanisms
[AD-P003942] 02 p0248 N85-11622
Decision Support System (DSS): A survey
[NRIMS-TWISK-317] 02 p0292 N85-11896
A management workstation concept
[AD-A145617] 02 p0294 N85-11906
Use of prototyping for man-machine interface requirements definition on the AWDS (Automated Weather Distribution System) program
[AD-A146033] 03 p0396 N85-12526
Preserving the time dimension in information systems
03 p0437 N85-12784
Developments in Soviet robot technology viewed
04 p0491 N85-13127
Development, new application of Soviet robots
04 p0491 N85-13129
Rech-1 speech synthesizer for man-machine dialog
04 p0543 N85-13456
The human role in space. Volume 1: Executive summary
[NASA-CR-171223] 04 p0546 N85-13473
The Interactive Planetary Image Processing System (IPIPS): A major facility for research and teaching in remote sensing 05 p0655 N85-14203
An interactive technique for satellite-improved rainfall monitoring 05 p0658 N85-14224
A methodology for an integrated spatial data model and its application to image classification
05 p0659 N85-14234
Twentieth Annual Conference on Manual Control, volume 1
[NASA-CP-2341-VOL-1] 05 p0699 N85-14487
Time series modeling of human operator dynamics in manual control tasks 05 p0699 N85-14488
Statistical time series models of pilot control with applications to instrument discrimination
05 p0700 N85-14489

Utilization of historic information in an optimisation task 05 p0700 N85-14490
Six degrees of freedom control with each hand? 05 p0700 N85-14492
A model for the effectiveness of aircraft alerting and warning systems 05 p0702 N85-14506
Evaluation of fuzzy rulemaking for expert systems for failure detection 05 p0703 N85-14508
Psychological issues in online adaptive task allocation 05 p0704 N85-14516
Suppression of biodynamic interference by adaptive filtering 05 p0706 N85-14530
Twentieth Annual Conference on Manual Control, volume 2 [NASA-CP-2341-VOL-2] 05 p0707 N85-14535
Representing multidimensional systems using visual displays 05 p0711 N85-14560
Performance measures for aircraft landings as a function of aircraft dynamics 05 p0712 N85-14565
Measuring pilot workload in a moving-base simulator. Part 2: Building levels of workload 05 p0712 N85-14566
Multi-crew model analytic assessment of landing performance and decision-making demands 05 p0712 N85-14567
A framework for research on adaptive decision aids [AD-A138331] 05 p0734 N85-14719
Technical Workshop: Advanced Helicopter Cockpit Design [NASA-CP-2351] 06 p0750 N85-14806
Superaugmented rotorcraft program 06 p0750 N85-14807
Helicopter human factors programs and plans 06 p0751 N85-14808
Guidance and navigation programs and plans 06 p0751 N85-14809
Integrated cockpit design for the Army helicopter improvement program 06 p0751 N85-14816
Man-machine interface requirements - advanced technology 06 p0753 N85-14825
Design and analysis of an SQL (Structured Query Language) interface for a multi-backend database system [AD-A146534] 06 p0856 N85-15447
Mental status in relation to special conditions of activity 07 p1011 N85-16420
Interaction of human cognitive models and computer based models in supervisory control [AD-A142547] 07 p1020 N85-16474
Mental models and cooperative problem solving with expert systems [AD-A147843] 07 p1021 N85-16479
International aviation (selected articles) [AD-A148704] 08 p1067 N85-16762
Integrated control and display systems for helicopter battlefield mission management 08 p1073 N85-16805
A review of US Army aircrew-aircraft integration research programs 08 p1075 N85-16814
Time series analysis of closed-loop pilot vehicle dynamics 08 p1087 N85-16876
Ground man-machine interfaces for orbiter checkout 08 p1091 N85-16897
East Europe report: Science and technology [JPRS-ESA-84-048] 08 p1139 N85-17176
Man-machine communication research for robotics reported 08 p1139 N85-17177
Automatic speech recognition in severe environments [AD-A148461] 08 p1153 N85-17280
A computer aided Multi-Man-Machine Work Area Design and Evaluation System (MAWADES) [AD-A147950] 08 p1199 N85-17554
Steps towards parsing of query sequences to a database [AD-A148769] 08 p1206 N85-17590
The effects of time delay in man-machine control systems: Implications for design of flight simulator Visual-Display-Delay compensation [AD-P004329] 09 p1270 N85-17983
Role of engineering psychology 09 p1361 N85-18581
Problems of psychological support of automated organization control systems 09 p1362 N85-18571
Material flow in the manufacturing system: Fault-diagnosis systems as support for the maintenance of highly automated manufacturing systems [PNR-90238] 09 p1371 N85-18618
Dean of Kiev State University on impact of robots 10 p1461 N85-19213
Production turret lathe retrofitted with robot 10 p1461 N85-19214
Control system of complex CNC machining cell 10 p1462 N85-19218
Health standards for general vibration 10 p1523 N85-19607
Sector suite man-machine functional capabilities and performance requirements [AD-A148881] 10 p1531 N85-19647
Man-machine interaction: Operator [AD-A149075] 10 p1531 N85-19648
Human Factors Considerations in High Performance Aircraft [AGARD-CP-371] 10 p1532 N85-19653
Military pilot ergonomics 10 p1532 N85-19655
Grasp of information by the pilot in future combat aircraft 10 p1533 N85-19662
The cockpit of the year 2000: How big a step? 10 p1534 N85-19667
The multiple resources model of human performance: Implications for display design 10 p1534 N85-19669
French plans for fifth generation computer systems [AD-A149435] 10 p1544 N85-19732
Reliability of DNC system examined 11 p1617 N85-20171
Man/machine interface for a nuclear cask remote handling control station: System design requirements [DE85-000256] 11 p1697 N85-20667
Parallel input and feedback in dialogue cells [CWI-CS-R8413] 11 p1703 N85-20708
Data and information systems and decision making in large public organizations: Research agenda [DE85-003639] 11 p1736 N85-20931
Operations concept for the advanced automation system man-machine interface [AD-A149797] 12 p1774 N85-21139
Automatic speech recognition in severe environments [PB85-121697] 12 p1830 N85-21490
The man-machine interface [AD-A149971] 12 p1910 N85-21989
An interactive environment for the development of an expert system in ZOG [AD-A149954] 12 p1915 N85-22025
Design of graphic displays in computerized systems [AD-A150071] 12 p1916 N85-22027
Research and Modeling of Supervisory Control Behavior, report of a workshop [AD-A149621] 12 p1950 N85-22248
USSR report: Space [JPRS-USP-85-001] 13 p1977 N85-22403
TASS update on unmanned flight of Salyut-7 13 p1977 N85-22404
A design analysis and implementation of a user-friendly interface for the UNIX operating system [AD-A150558] 13 p2145 N85-23312
Investigation of transport operations of ergatic robot 14 p2286 N85-24166
Interference effects of vocalization on dual task performance [AD-A150687] 14 p2291 N85-24203
The acquisition of procedures from text. A production-system analysis of transfer of training [AD-A151029] 14 p2392 N85-24732
Programmer/analyst workstation evaluation report [NASA-CR-175289] 14 p2394 N85-24749
Dual-task timesharing using a projected attitude display (Malcolm horizon) [AD-A150789] 14 p2395 N85-24750
Robotic arc welding 15 p2566 N85-25830
Biotechnology in Japan [PB85-169464] 15 p2615 N85-26113
Computerized biophysical data acquisition system for motion sickness studies [AD-A151691] 15 p2618 N85-26131
Proceedings of the BAe human factors seminar [BAE-BT-11873] 15 p2620 N85-26145
Human factors department 1981 publications [BAE-BT-12685] 15 p2620 N85-26147
Activities report for FOA 53: Laboratory for man and information systems [FOA-C-53019-H] 15 p2621 N85-26150
Extension of the software development workbench to include microcomputer workstations [AD-A151903] 15 p2630 N85-26207
A description of the process of elaborating man-machine dialog in an aircraft equipped with cathode tubes: Rules and specifications of piloted simulation methods 16 p2696 N85-26658
A comparison of pictorial and speech warning messages in the modern cockpit [AD-A151917] 16 p2707 N85-26706
Fujen forges ahead in electronic production 16 p2806 N85-27301
Automation of the reporting and tracking requirements of architect-engineering type contracts [AD-A152218] 16 p2876 N85-27745
Controller requirements for uncoupled aircraft motion, volume 2 [AD-A153900] 17 p2900 N85-27879
Hand controllers for teleoperation. A state-of-the-art technology survey and evaluation [NASA-CR-175890] 17 p3002 N85-28559
Mechanizing of handling operations in drop forging with hammers and presses (conducted ergonomical examinations) [BMFT-FB-HA-84-051] 17 p3002 N85-28561
Efforts at office automation and information systems utilization at Martin Marietta Energy Systems, Incorporated [DE85-008154] 17 p3013 N85-28633
The interface with decision makers in interactive multiobjective linear programming [REPT-84-38] 17 p3014 N85-28637
General laws of development of technology 17 p3049 N85-28875
A study of user-defined searching requirements for the on-line version of the directory of DOD-sponsored R and D data bases on the Defense Gateway computer system [AD-A153000] 17 p3050 N85-28878
Man-machine tradeoff study 18 p3158 N85-29561
Some ideas and questions regarding space station design for human use 18 p3158 N85-29562
Space station automation study-satellite servicing. Volume 1: Executive summary [NASA-CR-171512] 19 p3226 N85-29699
Space station automation study-satellite servicing, volume 2 [NASA-CR-171513] 19 p3226 N85-30000
Adaptive aiding for symbiotic human-computer control: Conceptual model and experimental approach [AD-A153670] 19 p3332 N85-30644
ZOG-Vinson technology demonstration project. Volume 2: System description [AD-A153671] 19 p3333 N85-30645
ZOG/VINSON technology demonstration project system description. Volume 1 [AD-A154211] 19 p3342 N85-30713
Space Station man-machine automation trade-off analysis [NASA-CR-176046] 20 p3408 N85-31147
Manipulators in teleoperation [DE85-010563] 20 p3512 N85-31833
The blind and the paralyzed. The notion of the tool revealed and integrated in a different organization environment [SNIAS-851-422-104] 20 p3513 N85-31835
Program Manager: The journal of the defense systems management college, volume 14, number 2, March-April 1985 [AD-A154219] 20 p3540 N85-32031
Myoelectric control of a computer based expert system for flight control [AD-A154981] 21 p3557 N85-32126
Importance of automation, robotization in economy 21 p3572 N85-32219
Design guidelines for user-system interface software [AD-A154907] 21 p3671 N85-32807
A PASCAL interpreter for the functional programming language ELC (Extended lambda calculus) [AD-A155218] 21 p3672 N85-32810
Space station automation and robotics study. Operator-systems interface [NASA-CR-176095] 22 p3738 N85-33172
Space station automation study: Autonomous systems and assembly, volume 2 [NASA-CR-176092] 22 p3739 N85-33175
Machine intelligence for robotics applications [DE85-011430] 22 p3793 N85-33503
Man-vehicle systems research facility advanced aircraft flight simulator throttle mechanism 22 p3798 N85-33527
The CADME approach to the interface of solid modellers 23 p3961 N85-34554
Designing a graphics application interface 23 p3964 N85-34574
Development of NATOPS performance software for the SH-3D and SH-3H helicopters [AD-A156140] 24 p4065 N85-35192
The integrated manual and automatic control of complex flight systems [NASA-CR-176166] 24 p4066 N85-35201
An exploratory study of the effect of screen size and resolution on the legibility of graphics in automated job performance aids [AD-A155969] 24 p4136 N85-35632

MANAGEMENT

- NT CONFIGURATION MANAGEMENT
- NT CONTRACT MANAGEMENT
- NT DATA MANAGEMENT
- NT ENGINEERING MANAGEMENT
- NT ENVIRONMENT MANAGEMENT
- NT FINANCIAL MANAGEMENT
- NT FOREST MANAGEMENT
- NT INDUSTRIAL MANAGEMENT
- NT INFORMATION MANAGEMENT
- NT INVENTORY CONTROLS
- NT INVENTORY MANAGEMENT
- NT LAND MANAGEMENT

NT LOGISTICS MANAGEMENT
NT PERSONNEL MANAGEMENT
NT PROCUREMENT MANAGEMENT
NT PRODUCTION MANAGEMENT
NT PROJECT MANAGEMENT
NT RESEARCH MANAGEMENT
NT RESOURCES MANAGEMENT
NT SAFETY MANAGEMENT
NT SYSTEMS MANAGEMENT
NT WATER MANAGEMENT
Synopsis of the OTA Workshop on Cost Containment of Civilian Infrastructure (Civilian Space Station) Elements 07 p0915 N85-15790
Distribution and storage of aviation turbine fuel for military operations in northern Australia [AD-A147180] 07 p0935 N85-15921
Principles of multiobjective optimization [AD-A147520] 07 p1052 N85-16679
Technical order managers handbook: Utilization assessment [AD-A147579] 07 p1055 N85-16684
Flight Training Technology for Regional/Commuter Airline Operations: Regional Airline Association/NASA Workshop Proceedings [NASA-CP-2348] 09 p1275 N85-18009
Management training for cockpit crews at Piedmont flight 09 p1276 N85-18013
Video concepts in CRM training 09 p1276 N85-18015
Use of simplifier scenarios for CRM training 09 p1276 N85-18016
Management: A bibliography for NASA managers [NASA-SP-7500(19)] 15 p2664 N85-26439
Central problems in the management of innovation [AD-A152598] 17 p3047 N85-28852
Management of Corrosion [AGARD-LS-141] 22 p3749 N85-33236
DOD Value Engineering Conference report. Value Engineering (VE): A tool that benefits line management held at Leesburg, Virginia on 1-2 November 1984. Part 1. Executive summary [AD-A156067] 24 p4163 N85-35810
DOD Value Engineering Conference report. Value Engineering (VE): A tool that benefits line management held at Leesburg, Virginia on 1-2 November 1984. Part 2. Plenary session [AD-A156068] 24 p4163 N85-35811
DoD Value Engineering conference report. Value Engineering (VE): A tool that benefits line management. Part 5, Workshop C: VEP/VECP administration, negotiation, and implementation [AD-A156071] 24 p4163 N85-35814

MANAGEMENT ANALYSIS
Doing business in space: How to get there from here 02 p0156 N85-11057
An overview of the Joint Logistics Commanders Automatic Test Equipment Panel [AD-P003916] 02 p0244 N85-11596
Planning for the on-orbit servicing of military spacecraft [AD-A148447] 08 p1104 N85-16963
Performance management system enhancement and maintenance [NASA-CR-175271] 03 p1202 N85-17564
Aviation maintenance computerized management information systems: Perspective for the future [AD-A150637] 13 p1966 N85-22349
Food service management 14 p2393 N85-24736
Guide on workload forecasting [PB85-177632] 19 p3341 N85-30704
Program Manager: The journal of the defense systems management college, volume 14, number 2, March-April 1985 [AD-A154219] 20 p3540 N85-32031

MANAGEMENT INFORMATION SYSTEMS
Data dictionary systems and their role in information resource management [AD-A144905] 01 p0125 N85-10859
Effects of alternative chromatic mixed graphics displays in decision support systems [AD-A145561] 02 p0242 N85-11578
A management workstation concept [AD-A145617] 02 p0294 N85-11906
Primer on the registration of technical information in industry 03 p0438 N85-12766
Maintenance Management Information and Control System (MMICS): Administrative boon or burden [AD-A145762] 03 p0436 N85-12790
Executive information system [DE84-015355] 04 p0576 N85-13675
Introduction to software packages [PB84-217843] 06 p0856 N85-15441
An update of the functional requirements of the Naval Aviation Logistics Command Management Information System (NALCOMIS) [AD-A146565] 06 p0871 N85-15532
The effects of software quality control and baseline management on the acquisition of computer programs [AD-A147051] 07 p1024 N85-16502
A study of the relationship between user attitudes and the success of the MAJCOM and AFRCE work information management system [AD-A146956] 07 p1051 N85-16671
A validated methodology for determination of laboratory instrument computer interface efficacy [AD-A149338] 10 p1487 N85-19391
The evolution from data processing to information resource management [AD-A149429] 10 p1587 N85-19678
An interactive environment for the development of an expert system in ZOG [AD-A149954] 12 p1915 N85-22025
Aviation maintenance computerized management information systems: Perspective for the future [AD-A150637] 13 p1966 N85-22349
General design considerations of an Air Force information system [AD-A150611] 13 p2168 N85-23449
The design and analysis of a complete hierarchical interface for the multi-backend database system [AD-A151550] 15 p2629 N85-26203
An analysis of data dictionaries and their role in information resource management [AD-A152134] 16 p2774 N85-27121
Implementation and analysis of a microcomputer based relational database system [AD-A151770] 16 p2845 N85-27536
Data dictionary design as a stepping-stone to DBMS (Data Base Management System) implementation in the Indonesian Army Data Collecting and Processing Service [AD-A152101] 16 p2877 N85-27752
Manufacturing information system [AD-A152715] 17 p3011 N85-28616
DLA: Data/data base administration analysis [AD-A153031] 17 p3050 N85-28879
Improving the defense energy information system (DEIS) [AD-A153524] 18 p3200 N85-29849
Test and Evaluation Master Plan (TEMP) for the Navy Occupational Health Information Management System (NOHIMS). Phase 1: Appendix A through appendix U [AD-A154179] 19 p3360 N85-30067
The Human Resource Management Information Network (HRMIN): A cost comparison in accordance with Office of Management and Budget (OMB) Circular no. A-76, 5 April 1979 [AD-A154583] 21 p3713 N85-33039
Integration of office automation within computing [DE85-010021] 22 p3833 N85-33736

MANAGEMENT METHODS
NT DELPHI METHOD (FORECASTING)
NT PATTERN METHOD (FORECASTING)
NT PROFILE METHOD (FORECASTING)
Artificial Intelligence in Maintenance: Proceedings of the Joint Services Workshop [AD-A145349] 02 p0244 N85-11592
Diagnosis based on description of structure and function [AD-P003919] 02 p0245 N85-11589
Decision Support System (DSS): A survey [NRIMS-TWISK-317] 02 p0292 N85-11898
Maintenance Management Information and Control System (MMICS): Administrative boon or burden [AD-A145762] 03 p0436 N85-12790
Design of a scientific information collation and dissemination system, volumes 1 thru 3 [AD-A146002] 03 p0438 N85-12791
International comparative study of systems for the government advancement of research and development [NASA-TM-77569] 04 p0578 N85-13689
Performance evaluation of A-10 aircraft maintenance units and aircraft using constrained facet analysis [AD-A146955] 07 p0693 N85-15660
A Q-GERT network simulation model for examining pipeline time in the Navy's J-52 intermediate level jet engine repair cycle [AD-A147269] 07 p0694 N85-15663
Feasibility of measuring technical productivity improvements in Air Force Logistics Command depot-level maintenance using the Data Envelopment Analysis (DEA) and Constrained Facet Analysis (CFA) models [AD-A147329] 07 p1052 N85-16676
Effective life cycle software support: A study in discipline and versatility 08 p1065 N85-16746
Manufacturing costs, equipment needs and technological opportunities among small and medium-size manufacturers [DE85-000479] 09 p1304 N85-18193
Management challenges encountered in CAD implementation [DE85-002072] 10 p1541 N85-19716
Security of personal computer systems: A management guide [PB85-181040] 14 p2400 N85-24703
The development and implementation of advanced welding technology 15 p2585 N85-25824
Welding techniques in pressure part technology 15 p2586 N85-25835
Future information technology, 1984 telecommunications [PB85-185850] 15 p2624 N85-26173
Management communication and financial modeling 15 p2627 N85-26190
Management: A bibliography for NASA managers [NASA-SP-7500(19)] 15 p2664 N85-26439
Management aspects of software maintenance [AD-A152035] 16 p2847 N85-27550
The significance of Helios for Europe 16 p2866 N85-27808
Managerial benefits of Helios for the European industry 16 p2867 N85-27809
Helios project support 16 p2867 N85-27812
Integrating quality assurance and research and development [DE85-007974] 17 p2976 N85-28392
Future directions in operations research [REPT-84-24] 17 p3026 N85-28711
Multicriteria decision analysis as an aid to strategic planning of energy research and development [REPT-84-02] 17 p3049 N85-28870
Direct digital control study [AD-A153885] 18 p3167 N85-29621
Automated maintenance system test program increment VI production scheduling [AD-A153694] 18 p3198 N85-29838
CMP: Code Maintenance Package reference manual, version 2.0 [DE85-011396] 19 p3340 N85-30697
Guide on workload forecasting [PB85-177632] 19 p3341 N85-30704
Discrete simulation models - their role in the design, development and management of inventory control systems [PNR-90249] 23 p3988 N85-34719
Fire service emergency management handbook [AD-A155780] 24 p4084 N85-35313
DoD Value Engineering conference report. Value Engineering (VE): A tool that benefits line management. Part 6, Workshop D: VE training-orientation [AD-A156072] 24 p4164 N85-35815
Aeronautical Systems Division Manufacturing/Quality assurance orientation [AD-A156128] 24 p4164 N85-35817

MANAGEMENT PLANNING
NT PRODUCTION PLANNING
NT PROJECT PLANNING
Hydrologic and economic models for watershed evaluation and research [PB84-222371] 01 p0066 N85-10438
Development of a production order release methodology [AD-A145213] 01 p0124 N85-10852
System engineering and integration contract for implementation of the National Airspace System plan, volume 1, sections 1.0-4.0, 6.0 [AD-A145763] 03 p0317 N85-12048
Matrix organizations: Overcoming the disadvantages [AD-A145318] 03 p0436 N85-12772
Five-year plan for meeting the automatic data processing and telecommunications needs of the Federal Government. Volume 2: Major information technology systems acquisition plans of Federal executive agencies, 1984-1989 [PB84-214519] 03 p0436 N85-12778
IRM (Information Resources Management) long-range plan: Fiscal year 1984-1988 (update). Volume 2: ADP and telecommunications acquisition plan [PB84-229244] 03 p0439 N85-12796
USSR report: Machine tools and metalworking equipment [JPRS-UMM-84-020] 04 p0491 N85-13125
Development, new application of Soviet robots 04 p0491 N85-13129
Advances of implementing NC machine tools discussed 04 p0491 N85-13131
Survey relating to the implementation of cost/schedule control systems criteria within the Department of Defense and industry [AD-A146664] 06 p0670 N85-15526
Decentralized control of scheduling in distributed systems [AD-A147446] 07 p1022 N85-16487
The effects of software quality control and baseline management on the acquisition of computer programs [AD-A147051] 07 p1024 N85-16502

The management of research institutions: A look at government laboratories
[NASA-SP-481] 07 p1050 N85-16665
Life cycle cost management master plan for the Defense Communications Agency
[AD-A146676] 07 p1050 N85-16668
Acquisition planning at the Defense Communications Agency
[AD-A146677] 07 p1051 N85-16669
A study of the relationship between user attitudes and the success of the MAJCOM and AFRCE work information management system
[AD-A146956] 07 p1051 N85-16671
An evaluation of the effect of establishing a minimum Economic Order Quantity (EOQ) on the Air Force EOQ item management system
[AD-A147121] 07 p1051 N85-16673
Project manager's handbook for special projects
[AD-A147913] 07 p1053 N85-16683
Commerce Lab: Mission analysis. Payload integration study
[NASA-CR-171285] 08 p1104 N85-16982
Decentralized control of scheduling in distributed systems
[AD-A147686] 08 p1228 N85-17731
Strategic management for organizational effectiveness. The effect of human resource planning on retention and related issues, volume 1
[AD-A149398] 10 p1566 N85-19674
Strategic management for organizational effectiveness. The effect of human resource planning on retention and related issues, volume 2
[AD-A149399] 10 p1566 N85-19675
Strategic management for organizational effectiveness. The effect of human resource planning on retention and related issues, volume 3
[AD-A149400] 10 p1566 N85-19676
Strategic management for organizational effectiveness. The effect of human resource planning on retention and related issues: Methodological appendix
[AD-A149401] 10 p1566 N85-19677
Siemens, Philips megaproject to yield superchip in 5 years 11 p1592 N85-20018
Environmental Monitoring Improvement Act
[GPO-39-742] 11 p1677 N85-20568
Software management issues — space station software development 11 p1700 N85-20690
Program manager: The Journal of the Defense Systems Management College. Volume 13, Number 6, November-December 1984
[AD-A149546] 11 p1739 N85-20933
Air Force satellite position management
12 p1787 N85-21217
Computing Division two-year operational plan, FY 1984 - 1985
[LA-9978-MS] 12 p1913 N85-22006
Response to NAS plan audit report recommendations
[FAA-ES-85-1] 15 p2468 N85-25235
Manufacturing methods and technology CAD/CAM (Computer-Aided Design/Computer-Aided Manufacturing) related efforts (FY 1980 - 1985)
[AD-A151817] 16 p2846 N85-27547
Personal computer aided decision analysis
[AD-A151911] 16 p2875 N85-27743
Navy program manager's guide, 1985 edition
[AD-A151925] 16 p2876 N85-27744
Management control systems and interdependencies: An empirical study
[AD-A152280] 16 p2876 N85-27746
An examination of alternative forms of fit in contingency theory
[AD-A152602] 17 p3047 N85-28853
The concept of fit in contingency theory
[AD-A152603] 17 p3047 N85-28854
Documentation for the West German Federal Cabinet's space policy decision 17 p3051 N85-28866
Evaluation and Validation (E/V) team public report, volume 1
[AD-A153609] 18 p3161 N85-29584
Overhead management guide for aerospace procurements
[AD-A153626] 18 p3196 N85-29835
Guide on workload forecasting
[PB85-177632] 19 p3341 N85-30704
Assessment of computer resource management plan for division support weapon system
[AD-A154142] 19 p3342 N85-30712
EOQ (Economic Order Quantity) range model
[AD-A153709] 19 p3379 N85-30985
Producibility Engineering and Planning (PEP): Program management guidelines
[AD-A153730] 19 p3379 N85-30986
Quality analysis 21 p3666 N85-32785
Study to encourage and facilitate industrial investment and involvement in space
[NASA-CR-176152] 23 p3886 N85-34147
Analyzing performance of small projects using URS and PMAS, information pamphlet
[DE85-011964] 23 p3966 N85-34716
Aeronautical Systems Division Manufacturing/Quality assurance orientation
[AD-A156128] 24 p4164 N85-35817

MANAGEMENT SYSTEMS
NT FLIGHT MANAGEMENT SYSTEMS
NT MANAGEMENT INFORMATION SYSTEMS
Report of the Department of Aerospace Engineering
03 p0307 N85-11977
Development of a pavement maintenance management system. Volume 10: Summary of development from 1974 through 1983
[AD-A146035] 03 p0320 N85-12067
Development of a pavement maintenance management system. Volume 9: Development of airfield pavement performance prediction models
[AD-A146150] 03 p0321 N85-12069
An evaluation of the effect of establishing a minimum Economic Order Quantity (EOQ) on the Air Force EOQ item management system
[AD-A147121] 07 p1051 N85-16673
Technology planning for flexible manufacturing systems 08 p1139 N85-17170
Automated plant, production management system
08 p1139 N85-17171
Kernel Ada Programming Support Environment (KAPSE) interface team public report, volume 4
[AD-A147648] 08 p1205 N85-17581
GIDEP representative interaction
[DE84-016792] 09 p1401 N85-18820
Biotechnology in Japan
[PB85-169464] 15 p2615 N85-26113
National Airspace System Plan: Facilities, equipment and associated development 16 p2704 N85-26692
Management control systems and interdependencies: An empirical study
[AD-A152280] 16 p2876 N85-27746
West European report: Science and technology
[JPRS-WST-84-036] 18 p3066 N85-28960
Interactive graphics for a data analysis management system
[DE85-010977] 19 p3334 N85-30651
The economics of private sector R and D decisionmaking in aeronautics
[NASA-CR-176007] 19 p3379 N85-30962
NASA Space controls research and technology program 20 p3408 N85-31149
Evaluative report on the Institute for Computer Sciences and Technology, National Bureau of Standards, fiscal year 1984
[PB85-176097] 20 p3514 N85-31848
Determining functional requirements for NASA Goddard's command management system software design using expert systems 20 p3539 N85-32020
Symbolic and interactional perspectives on leadership: An integrative framework
[AD-A155247] 21 p3665 N85-32789
DOD Value Engineering Conference report. Value Engineering (VE): A tool that benefits line management held at Leesburg, Virginia on 1-2 November 1984. Part 1. Executive summary
[AD-A156067] 24 p4163 N85-35810
DOD Value Engineering Conference report. Value Engineering (VE): A tool that benefits line management held at Leesburg, Virginia on 1-2 November 1984. Part 2. Plenary session
[AD-A156068] 24 p4163 N85-35811

MANDELSTAM REPRESENTATION
Experimental investigation of wavefront conjugation during Mandelstam-Brillouin scattering of focused laser beams in condensed media 11 p1716 N85-20796
Stimulated Mandelstam-Brillouin scattering with distributed feedback 21 p3696 N85-32961

MANEUVERABILITY
A generalized mathematical solution for transient off tracking of single vehicles and truck combinations
[DM-2] 01 p0107 N85-10719
Performance capabilities of the C-5 and C-17 cargo aircraft
[AD-A145515] 02 p0138 N85-10939
Robotics in nondestructive inspection at Sacramento Air Logistics Center
[AD-P004012] 03 p0309 N85-11992
Details of export A-5 close-support aircraft given — Qiang-5 aircraft 06 p0748 N85-14793
Supermaneuverability
[AD-P004153] 09 p1263 N85-17936
Thrust vectoring apparatus for maneuvering missile in flight
[AD-D011693] 19 p3226 N85-30004

MANEUVERABLE SPACECRAFT
NT APOLLO SPACECRAFT
NT LIFTING REENTRY VEHICLES
NT RENDEZVOUS SPACECRAFT

MANEUVERS
NT AIRCRAFT MANEUVERS
NT EVASIVE ACTIONS
NT HOVERING
NT ORBITAL MANEUVERS
NT ORBITAL RENDEZVOUS
NT SIDESLIP
NT SPACECRAFT DOCKING
NT SPACECRAFT MANEUVERS
Helicopter pilot performance for discrete-maneuver flight tasks 06 p0702 N85-14602
Translational control of a graphically simulated robot arm by kinematic rate equations that overcome elbow joint singularity
[NASA-TP-2378] 06 p0858 N85-15446
Bifurcation theory applied to aircraft motions
[NASA-TM-86704] 14 p2210 N85-23705
Harrier 15 p2687 N85-26595
Design of robust controllers for a multiple input-multiple output control system with uncertain parameters application to the lateral and longitudinal modes of the KC-135 transport aircraft
[AD-A153100] 17 p2900 N85-27877

MANGANESE
NT MANGANESE ISOTOPES
International strategic minerals inventory. Summary report: Manganese
[GS-CIRC-930-A] 02 p0219 N85-11442
Weld metal solidification cracking in a carbon-manganese steel 03 p0330 N85-12126
The influence of manganese on intercrystalline internal adsorption of arsenic in low carbon steel
[BLL-M-35965-(5828.4)] 05 p0615 N85-13931
Manganese in recent sediments of Ukrainian SSR Black Sea shelf 06 p0819 N85-15200
The growth of metastable peritectic compounds
[NASA-CR-171289] 07 p0920 N85-15824
SPAR X technical report for experiment 76-22 directional solidification of magnetic composites
[NASA-CR-171271] 07 p0927 N85-15880
Analysis of diffusion in an ion-implanted alloy using a phenomenological model
[AERE-R-11527] 11 p1609 N85-20120
Investigation of manganese dioxide as an improved solid desiccant
[DE85-004034] 13 p2018 N85-22654
Technical and cost analyses of manganese nodule processing techniques and their significant variations
[PB85-148615] 14 p2258 N85-23092
Measurements of radiation-induced segregation and diffusion in ion irradiated alloy using implanted manganese
[AERE-R-11528] 14 p2258 N85-23094
Influence of manganese and heat treatment on structure and properties of Fe-0.1 percent-C-14 percent Cr-based steels
[BLL-BISI-TRANS-22299-(9022.06)]
17 p2928 N85-29071
Part played by non-metallic inclusions during deformation and fracture of steel with different grain sizes
[BLL-BISI-TRANS-22321-(9022.06)]
17 p2928 N85-29072
Temperature and manganese content dependences of tensile deformation in iron-high manganese binary alloys
[DE85-007656] 17 p2932 N85-29099
Solid phase reactions among manganese, potassium perchlorate and barium chromate
[HSE-TRANS-11166] 19 p3237 N85-30071
Geochemistry of manganese in ocean
19 p3291 N85-30408
Mineralogical-geochemical characteristics of ferromanganese formations in Arabian-Indian Ocean Ridge 19 p3293 N85-30416
Analysis of ferrates and ferrites of three transition metals using Mossebauer effects
[BLL-CE-TRANS-8019-(9022.09)]
20 p3430 N85-31273
Physical and chemical aerosol characteristics in extremely clean air masses at Cape Grim, Tasmania
21 p3646 N85-32655
Possible roles of manganese redox chemistry in the sulfur cycle 21 p3659 N85-32731
Precision measurements of solar energetic particle elemental composition
[PAPER-SH-2.1-4] 21 p3715 N85-33052
Environmental surveillance at Los Alamos during 1984
[DE85-011886] 22 p3811 N85-33605
Cobalt-rich ferromanganese crusts in the oceans
24 p4104 N85-35444
Applications of the mineral resources data system and the international strategic minerals inventory in mineral-resource assessments by region and commodity
24 p4105 N85-35451

MANGANESE ALLOYS
Rapid solidification of steels: Model and commercial alloys 02 p0176 N85-11184
Metallurgy Institute's developments for alloy and aircraft producers 03 p0353 N85-12268
Thermal diffusivity and conductivity of chromium-manganese alloying compositions [BLL-M-36925-(5828.4)] 05 p0616 N85-13938
Study of high performance alloy electroforming [NASA-CR-174276] 07 p0927 N85-15875
Magnetic excitation in CuMn spin glass alloy [DE85-002564] 10 p1453 N85-19159
Study of high performance alloy electroforming [NASA-CR-175741] 15 p2508 N85-25473
Superplasticity in a thermo-mechanically processed Aluminum-10.2%Mg-0.52%Mn alloy [AD-A152016] 15 p2510 N85-25485
Swelling behavior of manganese-bearing AISI 216 steel [DE85-005712] 15 p2512 N85-25495
Mechanical stabilization of austenite against epsilon martensite and its effect on deformation behavior in high manganese steels [DE85-007654] 17 p2932 N85-28067
Strength versus toughness relation in Fe-high manganese alloys [DE85-007662] 18 p3074 N85-29013
Directional solidification of an eutectic Bi-MnBi alloy [BLL-M-36270-(5828.4)] 20 p3430 N85-31275
Dynamics of the melting of chromium-manganese alloys in molten steel [BLL-M-35850-(5828.4)] 23 p3014 N85-34252

MANGANESE COMPOUNDS
NT MANGANESE OXIDES
Unsinkability of ferromanganese nodules 06 p0819 N85-15202

MANGANESE ISOTOPES
Cosmogenic Mn-53 in meteorites [SH-7.1-17] 23 p4049 N85-35107

MANGANESE OXIDES
Influence of eutectic silicate inclusions on micro-processes during deformation and fracture of 12GS steel [BLL-BISI-TRANS-22296-(9022.06)] 17 p2929 N85-28073
Carbon reduction of mixtures of MnO(2) and Fe(2)O(3) [BLL-M-36260-(5828.4)] 20 p3422 N85-31241
Iron and manganese in oxide minerals and in glasses: Preliminary consideration of Eh buffering potential at Yucca Mountain, Nevada [DE85-011662] 23 p3916 N85-34271

MANGANESE 53
U MANGANESE ISOTOPES

MANGANESE 54
U MANGANESE ISOTOPES

MANGANESE 56
U MANGANESE ISOTOPES

MANIFOLDS
Manifold insulated with knitted impregnated sleeve [AD-D011270] 06 p0814 N85-15167
Calculation of flow about posts and powerhead model --- space shuttle main engine [NASA-CR-171344] 10 p1483 N85-19362
Experimental evaluation of an advanced Space Shuttle main engine hot-gas manifold design concept 16 p2738 N85-26898
Numerical analysis of flow non-uniformity in the hot gas manifold of the Space Shuttle main engine 16 p2738 N85-26899
Investigation of the behavior of fuel in the intake manifold and its relation to SI engines, 1980 - 1983 19 p3279 N85-30337

MANIFOLDS (MATHEMATICS)
NT RIEMANN MANIFOLD
A continuous Heisen surface in R3 11 p1686 N85-20674
Supermanifolds and Berezin's new integral [DE85-001633] 11 p1706 N85-20732
Using semigroups and the Trotter product formula to solve quasi-linear systems [DE85-002041] 11 p1706 N85-20736
Special relativity of Kaluza-Klein [DE85-007638] 17 p3046 N85-28847

MANIPULATION
U MANIPULATORS

MANIPULATORS
NT REMOTE MANIPULATOR SYSTEM
Portable slotting device [AD-D011213] 01 p0033 N85-10206
United States Air Force on research on algebraic manipulation [AD-A145737] 02 p0253 N85-11655
Industrial robots and transmanipulations: Important link in setup of automated production lines 03 p0345 N85-12222
Test-bed for programmable automation research. Phase 1 [AD-A145872] 03 p0409 N85-12614
Optimization of movements of manipulators with kinematic redundancy 04 p0468 N85-13112
Controlling rotation of elastic manipulator link 04 p0488 N85-13113
USSR report: Machine tools and metalworking equipment [JPRS-UMM-84-020] 04 p0491 N85-13126
Soviet robot exhibition reviewed 04 p0491 N85-13128
Improved robotic equipment for radiological emergencies [DE84-017637] 04 p0509 N85-13240
Evaluation of automated decisionmaking methodologies and development of an integrated robotic system simulation [NASA-CR-172401] 04 p0552 N85-13516
Instantaneous kinematics and joint displacement analysis of fully-parallel robotic devices 05 p0641 N85-14113
Application of robotics in remote fuel fabrication operations [DE84-011481] 05 p0646 N85-14144
Review of teleoperator research 05 p0703 N85-14511
Translational control of a graphically simulated robot arm by kinematic rate equations that overcome elbow joint singularity [NASA-TP-2376] 06 p0856 N85-15446
Precise control of flexible manipulators [NASA-CR-174210] 07 p0973 N85-16178
Automatic camera tracking for remote manipulators [DE85-001897] 07 p0974 N85-16187
Design features, applications of new robots 08 p1139 N85-17174
The optimal control and design of a flexible manipulator arm 09 p1327 N85-18340
Control and electronic subsystems for the advanced servomanipulator [DE85-001900] 09 p1327 N85-18343
Dual arm master controller concept [DE85-001901] 09 p1327 N85-18344
Advanced remotely maintainable force-reflecting servomanipulator concept [DE85-001902] 09 p1328 N85-18345
Parallel algorithms for robot dynamics [DE84-016563] 09 p1389 N85-18605
Dean of Kiev State University on impact of robots 10 p1461 N85-19213
Planning of minimum-time trajectories for robot arms [AD-A148956] 10 p1492 N85-19418
Simplified grasping and manipulation with dextrous robot hands [AD-A148962] 10 p1492 N85-19419
Some data manipulation requirements for the exploratory analysis of large data sets [DE85-002541] 10 p1566 N85-19887
Real time algorithms for robotic control of teleoperators [DE85-001137] 11 p1647 N85-20380
A remotely controlled orbiting retriever 12 p1786 N85-21212
Impacts of robotic and flexible manufacturing technologies on manufacturing costs and employment [AD-A150060] 12 p1860 N85-21686
Mechanical properties for the grasp of a robotic hand [AD-A150062] 12 p1860 N85-21689
Sensor control of robot arc welding 12 p1948 N85-22233
Cyclic industrial robots with mechanical energy storing devices: Multipositional system with one or several degrees of freedom 13 p2045 N85-22803
Design of tightening device and calculation of forces in manipulator transmissions with base-drive mounted 13 p2046 N85-22804
Hydraulic brakes for industrial robots 13 p2046 N85-22806
Controlled movement of elastic manipulator with distributed parameters 13 p2048 N85-22818
Investigation of dynamics of manipulator with elastic sections 13 p2048 N85-22819
Optimum design of electrical motors for multilink manipulators and automated manufacturing systems 13 p2062 N85-22880
Controllable movements of elastic manipulator with three degrees of freedom 14 p2266 N85-24040
Modular design, versatility of robots viewed 14 p2284 N85-24155
Integrated control system for FMS components 14 p2285 N85-24156
Investigation of transport operations of ergatic robot 14 p2286 N85-24166
Plans, developments in robotics 14 p2289 N85-24191
Study of experimental robotized system for arc welding based on Universal-15 manipulator 15 p2500 N85-25423
Italy's Fiat uses Sweden's Asea seeing robot 15 p2536 N85-25650
Applicability of modular versus universal robots discussed 15 p2538 N85-25664
Robotic arc welding 15 p2566 N85-25830
The kinematic control of redundant manipulators 15 p2566 N85-25836
Manipulation and simulation of general robots using the zero-position description 15 p2567 N85-25838
Structural design and kinematic configuration of two-armed robots 16 p2761 N85-27037
Experience of sheet stamping robotic complexes 16 p2761 N85-27041
Automatic manipulators for forging rollers 16 p2762 N85-27042
Updating model RPD-1.25 industrial robot 16 p2762 N85-27043
Industrial robots and automatic manipulators for forging and pressing operations at Second International Exhibition 16 p2762 N85-27044
Control of motion of manipulator robots on basis of first-order kinematic algorithms 16 p2762 N85-27047
Guidelines for optimization of robotized machining cells 16 p2767 N85-27076
A general simulation program for robot manipulator arm dynamics [AD-A152121] 16 p2793 N85-27230
Kinematic rate control of simulated robot hand at or near wrist singularity [NASA-TP-2440] 16 p2851 N85-27575
Positioning of a robotic manipulator through the use of visual feedback [AD-A151933] 16 p2851 N85-27577
Precision manipulator heating and cooling apparatus for use in UHV systems with sample transfer capability [NASA-CASE-LAR-13040-1] 18 p3116 N85-29286
HERMIES-1: A mobile robot for navigation and manipulation experiments [DE85-006652] 18 p3118 N85-29301
Analysis of remote operating systems for space-based servicing operations, volume 1 [NASA-CR-171885] 19 p3225 N85-29993
Analysis of remote operating systems for space-based servicing operations. Volume 2: Study results [NASA-CR-171886] 19 p3225 N85-29994
Space station automation study-satellite servicing. Volume 1: Executive summary [NASA-CR-171512] 19 p3226 N85-29999
Space station automation study-satellite servicing, volume 2 [NASA-CR-171513] 19 p3226 N85-30000
A remote-operated manipulator vehicle [HSE-TRANS-11133] 19 p3281 N85-30349
Computer methods in manipulator kinematics, dynamics and control: A comparative study 20 p3462 N85-31506
Manipulators in teleoperation [DE85-010563] 20 p3512 N85-31633
Ultrasonic position reference systems for an autonomous sentry robot and a robot manipulator arm [AD-A155481] 21 p3596 N85-32336
East Europe report: Science and technology. Selections on CSSR computer technology [JPRS-ESA-84-017] 21 p3668 N85-32781
Robots, Manipulators 21 p3668 N85-32786
Space robot simulator vehicle [NASA-CR-176133] 22 p3739 N85-33176
Future of robots in nuclear plants and processes [DE85-011505] 22 p3793 N85-33500
Dual arm master controller development 22 p3797 N85-33526
The compliance of end effector force sensors for robot manipulator control 24 p4098 N85-35406
Testbed for sensory control of intelligent machines [DE85-012355] 24 p4099 N85-35412

MANNED ORBITAL LABORATORIES
NT MANNED ORBITAL RESEARCH LABORATORIES
NT SPACELAB
Manned space station solar array study [ESA-CR(P)-1941] 09 p1287 N85-18081
Identification and control of structures in space [NASA-CR-175790] 16 p2731 N85-26850
European utilization aspects of a US manned space station, volume 1 [ESA-CR(P)-1907-VOL-1] 17 p2907 N85-27926
European utilization aspects of a US manned space station, volume 2 [ESA-CR(P)-1907-VOL-2] 17 p2907 N85-27927
USSR report: Space [JPRS-USP-84-006] 22 p3731 N85-33128

Space Station Polar Platform: Integrating research and operational missions
[PB85-195279] 24 p4069 N85-35218
MANNED ORBITAL RESEARCH LABORATORIES
NT SPACELAB
Concept for a commercial space station laboratory
02 p0153 N85-11035
Role of Space Station: The how of space industrialization 02 p0153 N85-11036
MANNED ORBITAL SPACE STATIONS
U ORBITAL SPACE STATIONS
MANNED SPACE FLIGHT
NT SPACE SHUTTLE MISSION 31-C
NT SPACE SHUTTLE MISSION 41-B
NT SPACE SHUTTLE MISSION 41-C
NT SPACE SHUTTLE MISSION 41-G
NT SPACE SHUTTLE MISSION 51-A
NT SPACE SHUTTLE MISSION 51-C
Bone structure and microgravity
05 p0694 N85-14463
Man in Space: National Historic Landmark Theme Study
[PB85-107233/GAR] 07 p0911 N85-15768
25th anniversary of the Gagarin Cosmonaut Training Center
[NASA-TM-77644] 09 p1286 N85-18078
Biomechanics finds practical applications in aerospace research 11 p1621 N85-20205
The space flight of the Soviet-Indian crew
[NASA-TM-77615] 12 p1788 N85-21226
USSR report: Space
[JPRS-USP-85-001] 13 p1977 N85-22403
TASS update on unmanned flight of Salyut-7
13 p1977 N85-22404
Feoktistov recalls period leading to Gagarin spaceflight 13 p1985 N85-22451
Feoktistov says manned lunar, Mars flights lack justification 13 p1985 N85-22452
Research opportunities in human behavior and performance
[NASA-CR-3896] 13 p2142 N85-23299
USSR report: Space
[JPRS-USP-85-004] 16 p2717 N85-26772
Tass reports program for Salyut-7 fully completed
16 p2717 N85-26773
Living aloft: Human requirements for extended spaceflight
[NASA-SP-483] 21 p3666 N85-32772
USSR report: Space
[JPRS-USP-84-006] 22 p3731 N85-33128
Proceedings of a Scientific Meeting on the Occasion of the Inauguration of New Buildings for the DFVLR Institute for Aerospace Medicine
[ESA-TT-857] 24 p4129 N85-35595
Biophysical research in space — radiation effects
24 p4130 N85-35603
MANNED SPACECRAFT
NT APOLLO SPACECRAFT
NT LONG DURATION EXPOSURE FACILITY
NT MANNED ORBITAL LABORATORIES
NT MANNED ORBITAL RESEARCH LABORATORIES
NT ORBITAL SPACE STATIONS
NT SALYUT SPACE STATION
NT SHUTTLE DERIVED VEHICLES
NT SKYLAB 3
NT SKYLAB 4
NT SOYUZ SPACECRAFT
NT SPACE SHUTTLES
NT SPACE STATIONS
Features and uses of progress cargo ships
02 p0157 N85-11061
Tass reports launch of Progress-22
02 p0157 N85-11063
Progress-22 docks with Salyut-7
02 p0157 N85-11064
Tass reports launch of Soyuz T-12
02 p0158 N85-11070
Dynamics and controls working group summary
05 p0604 N85-13854
A historical overview of the electrical power systems in the US manned and some US unmanned spacecraft
[NASA-CR-174808] 05 p0612 N85-13910
Manned space station solar array study
[ESA-CR(P)-1941] 09 p1287 N85-18081
Keynote address 09 p1333 N85-18378
Approaches to radiation guidelines for space travel
[DE85-001248] 09 p1363 N85-18576
Space Station
[NASA-EP-211] 12 p1793 N85-21251
Descent vehicles
[NASA-TM-77654] 17 p2909 N85-27933
Some Europeans voice opposition to space station participation 18 p3066 N85-28961
MANOMETERS
NMR manometer for measuring high pressures at liquid-helium temperatures 17 p2944 N85-28171
MANPOWER
NT SCIENTISTS
Parametric estimates of propulsion system maintenance manhours
[AD-A147120] 07 p0894 N85-15682
Application of the HARDMAN methodology to the single channel ground-airborne radio system (SINCGARS)
[NASA-CR-175486] 10 p1467 N85-19259
MANTLE (EARTH STRUCTURE)
U EARTH MANTLE
MANUAL
Standard analytical procedures of the NOAA National Analytical Facility, 1984-85: Extractable toxic organic compounds
[PB85-126282] 12 p1887 N85-21840
Outside users payload model
[NASA-CR-176011] 19 p3223 N85-29986
MANUAL CONTROL
NT VISUAL CONTROL
Twentieth Annual Conference on Manual Control, volume 1
[NASA-CP-2341-VOL-1] 05 p0699 N85-14487
Time series modeling of human operator dynamics in manual control tasks 05 p0699 N85-14488
A nonlinear filter for compensating for time delays in manual control systems 05 p0700 N85-14493
Model estimation and identification of manual controller objectives in complex tracking tasks
05 p0700 N85-14494
A method for measuring the effective throughput time delay in simulated displays involving manual control
05 p0701 N85-14497
Effects of transport delays of manual control system performance 05 p0701 N85-14498
Multiloop manual control of dynamic systems
05 p0702 N85-14505
The effect of part-simulation of weightlessness on human control of bilateral teleoperation: Neuromotor considerations 05 p0703 N85-14510
Suppression of biodynamic interference by adaptive filtering 05 p0706 N85-14530
Active sticks: A new dimension in controller design
05 p0706 N85-14531
Twentieth Annual Conference on Manual Control, volume 2
[NASA-CP-2341-VOL-2] 05 p0707 N85-14535
On looking into the black box: Prospects and limits in the search for mental models 05 p0709 N85-14546
A manual control test for the detection and deterrence of impaired drivers 05 p0709 N85-14550
Manual-control analysis applied to the money-supply control task 05 p0710 N85-14553
Types of tracking errors induced by concurrent secondary manual task 05 p0711 N85-14561
Low-speed longitudinal orbiter qualities
08 p1092 N85-16905
Order picking in an aisle
[AD-A149553] 10 p1548 N85-19766
The effect of strategy in second order manual control on resource competition with a sternberg memory search task
[AD-A150865] 14 p2391 N85-24727
Docking simulation analysis of range data requirements for the orbital maneuvering vehicle
[NASA-TM-86510] 20 p3407 N85-31143
The integrated manual and automatic control of complex flight systems
[NASA-CR-176166] 24 p4066 N85-35201
MANUALS
NT INSTALLATION MANUALS
NT USER MANUALS (COMPUTER PROGRAMS)
Manual for Raman cells
[NASA-TM-77756] 01 p0052 N85-10342
Ada (trademark) training curriculum. Real-time concepts l303 teacher's guide
[AD-A145093] 01 p0104 N85-10694
Ada (trademark) training curriculum. Software engineering for managers m101 teacher's exercise guide
[AD-A145094] 01 p0104 N85-10695
Intelligent information retrieval from on-line technical documentation
[AD-P003946] 02 p0249 N85-11626
Method for evaluating petrol products corrosivity using piezoelectric crystals. Part 2: Instruction manual — jet engine corrosion tests
[FOA-C-40198-B4] 04 p0482 N85-13073
Performance management system enhancement and maintenance
[NASA-CR-175271] 08 p1202 N85-17564
NATO AC/310 activities report on NATO STANAG 4170 and Allied Ordnance Publication 7 (Manual of Tests for Qualification of Explosive Materials for Military Use)
[AD-P004341] 10 p1454 N85-19165
User's guide for the Photochemical Box Model (PBM)
[PB85-137184] 11 p1682 N85-20602
Review of US manual of clinical aviation medicine
12 p1904 N85-21957
A strain gauge manual
[AD-A151602] 16 p2787 N85-27197
DoD manual for standard data elements, part 2
[AD-A152202] 16 p2878 N85-27755
DoD manual for standard data elements, part 3
[AD-A152203] 16 p2878 N85-27756
DoD manual for standard data elements, part 4
[AD-A152204] 16 p2878 N85-27757
DoD manual for standard data elements, part 5
[AD-A152205] 16 p2878 N85-27758
Technical instructions for a control operating system of the gas flow installation for the solid fuel combustion chamber
[VTH-LR-410] 18 p3118 N85-29902
A retarding ion mass spectrometer for the Dynamics Explorer-1
[NASA-CR-171586] 21 p3589 N85-32303
Ada (trademark) training curriculum. Advanced Ada topics L305 teacher's guide exercises
[AD-A154621] 21 p3670 N85-32798
A manual of methods for the continuous flow determination of ammonia, nitrate-nitrite, phosphate and silicate in seawater
[IOS-177] 23 p3913 N85-34243
Master Fit users' guide, version 1.0
[DE85-014199] 24 p4140 N85-35857
Comet Halley returns: A teachers' guide 1985-1986
[NASA-EP-197] 24 p4168 N85-35859
MANUFACTURING
NT COMPUTER AIDED MANUFACTURING
NT LOW GRAVITY MANUFACTURING
NT SPACE MANUFACTURING
Fluorinated diamond particles bonded in a filled fluorocarbon resin matrix
[DE84-014444] 01 p0022 N85-10136
Report on high-precision jig-boring machines
01 p0035 N85-10215
Publications of Center for Manufacturing Engineering (of the National Bureau of Standards), 1976-1983
[PB84-224526] 01 p0036 N85-10226
Manufacturing methods for microwave circuits
[AD-A145237] 01 p0043 N85-10276
Microminiature coaxial cable and methods of manufacture
[DE84-014228] 01 p0044 N85-10284
RADC/NBS (Rome Air Development Center/National Bureau of Standards) Workshop. Moisture Measurement and Control for Semiconductor Devices, 3
[PB84-219559] 01 p0051 N85-10337
Advanced manufacturing development of a composite empennage component for L-1011 aircraft
[NASA-CR-165885] 02 p0170 N85-11141
Manufacturing Methods and Technology (MM/T) specifications for miniature cathode ray tube
[AD-A145597] 02 p0194 N85-11298
Industrial robots and transmanipulations: Important link in setup of automated production lines
03 p0345 N85-12222
Newer carbon fibers and their properties
04 p0485 N85-12955
Quality organization — quality control
[CNES-NT-106] 04 p0511 N85-13257
Manufacturing report of an augmented IR, variable deflection half wing
[ONERA-RT-25/1736-AY-108-A]
05 p0591 N85-13766
Influence of residual stresses resulting from manufacturing on the fatigue strength of welded joints
05 p0650 N85-14177
The relationship between radiation sensitivity and redox equilibria — glass processing variables
[AD-A147216] 07 p0932 N85-15006
Fiat, Peugeot introduce integrated robotized engine: CAD used 07 p0936 N85-15033
Flexible manufacturing system for the production of aircraft parts
[BLL-PNR-90237-(8019.3153)]
08 p1137 N85-17159
The effects of manufacturing automation on the surge and mobilization capabilities of the gas turbine engine industry
[AD-A147295] 08 p1137 N85-17162
Control systems for robotic production lines
08 p1138 N85-17169
Technology planning for flexible manufacturing systems 08 p1139 N85-17170
Summaries of press automation conference presented
08 p1139 N85-17173
New applications for robot loaders, unloaders
08 p1139 N85-17175
Specifications of bloc floppy disk drives
08 p1141 N85-17188
MOM peripherals 08 p1141 N85-17189

Europeans active in magnetic bearing industry
08 p1141 N85-17195
Ultrasonic transducers, performance variability, design, and manufacturing procedures
[AD-A148575] 08 p1158 N85-17306
Production of concentrated nitric acid
[DE84-017191] 09 p1293 N85-18121
Manufacturing costs, equipment needs and technological opportunities among small and medium-size manufacturers
[DE85-000479] 09 p1304 N85-18193
Evaluating the variability of ceramics with X-ray fluorescence
[DE85-002028] 10 p1453 N85-19155
Experience highlights from the design and manufacture of US LCT coils
[DE84-017504] 10 p1462 N85-19354
Develop and demonstrate manufacturing processes for fabricating graphite filament reinforced polymide (Gr/PI) composite structural elements
[NASA-CR-172497] 11 p1592 N85-20019
Robot production lines in operation
11 p1617 N85-20166
New PCB production for robotics application
11 p1617 N85-20169
Reliability of DNC system examined
11 p1617 N85-20171
Report of the Technology and Test Panel
11 p1646 N85-20370
Exploratory assessment of second generation robotics and sensor-based systems
[PB85-132783] 11 p1648 N85-20388
Technological and economic assessment of advanced ceramic materials. Volume 5: A case study of ceramic toxic and combustible gas sensors
[PB85-113124] 12 p1815 N85-21386
Speed and accuracy in automated manufacture
[DE85-009913] 12 p1819 N85-21410
Computer integration of engineering design and production: A national opportunity
[NASA-CR-175483] 12 p1820 N85-21414
Impacts of robotic and flexible manufacturing technologies on manufacturing costs and employment
[AD-A150060] 12 p1860 N85-21668
A 2 x 6 Back Surface Reflection (BSR) silicon solar cell 13 p2005 N85-22570
Optimum design of electrical motors for multilink manipulators and automated manufacturing systems
13 p2062 N85-22880
Use of program controlled machine tools to automate and mechanize production processes in pipe manufacture 14 p2269 N85-24059
USSR report: Machine tools and metalworking equipment
[JPRS-UMM-85-006] 14 p2283 N85-24146
Metal waste in machine tool industry examined
14 p2283 N85-24147
Specifications of new industrial lasers reviewed
14 p2284 N85-24150
Minister B. V. Balmont on status of automation drive
14 p2284 N85-24151
West Europe report: Science and technology
[JPRS-WST-85-013] 14 p2289 N85-24183
Laser Welding, Cutting and Surface Treatment
14 p2308 N85-24278
Lasers in automobile production
14 p2309 N85-24288
Future trends in the use of lasers in manufacturing
14 p2309 N85-24291
Status of the U.K. N.D.T. industry today
14 p2316 N85-24309
Fiber optics applications for MIL-STD-1760
[AD-A151113] 15 p2470 N85-25251
Powder metallurgy production problems
15 p2497 N85-25406
French robotics research at Grenoble labs
15 p2523 N85-25555
Status of French research in plastic batteries
15 p2530 N85-25603
France develops new continuous vacuum treatment method 15 p2531 N85-25611
Criteria for qualifying for FRG federal CAD/CAM subsidies 15 p2536 N85-25651
ONR (Office of Naval Research) Far East Scientific Bulletin, Volume 9, Number 4, October-December 1984
[AD-A151274] 15 p2665 N85-26448
Manufacturing and producibility technology
16 p2733 N85-26866
USSR report: Engineering and equipment
[JPRS-UEQ-84-006] 16 p2760 N85-27035
Experience with introduction of Finish perforation of precision parts for optical instruments
16 p2761 N85-27038
Calculating reliability and productivity of cold stamping robot complex as queuing system
16 p2761 N85-27039
Estimates of errors of a gyroscope stabilized platform
16 p2763 N85-27050
Physio-chemical mechanisms of the processes of the formation of globular inclusions in ball-bearing metal
[BLL-BISI-TRANS-22235-(9022.06)]
17 p2924 N85-28030
Uses of, experiences in production of custom designed IC's 17 p2945 N85-28180
Modern equipment for manufacture of IC's in Hungary
17 p2945 N85-28181
Robots, automatic devices inside VW's Wolfsburg plant 17 p2946 N85-28186
Future directions of robotics, automation in Italy
17 p2946 N85-28187
Application of 4-wire submerged arc method to welding UOE pipe
[BLL-BISI-TRANS-22417-(9022.06)]
17 p2972 N85-28358
Production of electrically welded tubes with removed internal flash
[BLL-BISI-TRANS-22382-(9022.06)]
17 p2973 N85-28367
Future of ceramic turbochargers: Promises and pitfalls
[DE85-006209] 17 p2975 N85-28380
Principal quality assurance measures in the manufacture of HF-welded high-pressure linepipe
[BLL-BISI-TRANS-21690-(9022.06)]
17 p2976 N85-28389
Component problems plague French robotics industry
18 p3085 N85-29068
Crystallization of aluminum-based alloys in weightlessness 19 p3242 N85-30101
Producibility Engineering and Planning (PEP): Program management guidelines
[AD-A153730] 19 p3379 N85-30966
Improved turbopump dynamics
[NASA-TM-86514] 20 p3462 N85-31509
Encapsulation processing and manufacturing yield analysis 21 p3611 N85-32434
GDR semiconductor parts 21 p3669 N85-32788
Structure and functions of ultra-thin films of organic compounds
[DRIC-T-7481] 22 p3741 N85-33188
Centralized surveillance of flexible workshops for the manufacturing of composite materials
[SNIAS-851-430-103] 23 p3910 N85-34227
Manufacturing process to reduce large grain growth in zirconium alloys
[DE85-011649] 23 p3915 N85-34267
A rational approach to cam design
23 p3923 N85-34311

MANY BODY PROBLEM
Capture of planetesimals into a circumterrestrial swarm 04 p0588 N85-13751
The restricted problem of 2 + N bodies
09 p1414 N85-18825
Capture of planetesimals into a circumterrestrial swarm 13 p2179 N85-23522
Ionization equilibrium and equation of state in the solar interior 14 p2445 N85-25088
Boson degrees of freedom in Fermion many-body systems
[DE85-006997] 16 p2863 N85-27660
Multi-particle quantum mechanics obeying fractional statistics
[DE85-007830] 16 p2873 N85-27723
Quantized Hall conductance as a topological invariant
[DE85-007796] 18 p3193 N85-29808
Quasiparticle excitations in valence-fluctuation materials: Effects of band structure and crystal fields
[DE85-010783] 19 p3359 N85-30824
Memory effects in dynamical many-body systems: The isomneaic (constant-memory) approximation
[AD-A154160] 20 p3520 N85-31869
Ab initio calculations of materials properties
[DE85-011167] 20 p3531 N85-31984

MANY ELECTRON EFFECTS
Many-electron effects in electron impact ionization of multiply charged ions
[DE85-005570] 15 p2649 N85-26340

MANY PARTICLE THEORY
U MANY BODY PROBLEM

MAP MATCHING GUIDANCE
SIR-B cartography and stereo topographic mapping
08 p1147 N85-17234

MAPPING
NT CADASTRAL MAPPING
NT COMPUTER AIDED MAPPING
NT ICE MAPPING
NT PHOTOMAPPING
NT PLANETARY MAPPING
NT SOIL MAPPING
NT THEMATIC MAPPING
NT THERMAL MAPPING

The inferring of preferences from indifference in multicriteria decision analysis
[CSIR-TWISK-306] 01 p0106 N85-10729
Model diagnosis in two-way tables by means of row and column Euclidean maps
[CSIR-TWISK-307] 01 p0108 N85-10730
On Bezout domains, elementary divisor rings, and pole assignability
[CSIR-TWISK-330] 01 p0110 N85-10740
Range-residuated mappings
[AD-A145148] 01 p0112 N85-10759
LANDSAT data and interactive computer mapping
02 p0152 N85-11028
Commentary on cosmonauts geological mapping, photography 02 p0158 N85-11089
Workshop on the Use of Future Multispectral Imaging Capabilities for Lithologic Mapping: Workshop summary
02 p0214 N85-11413
A preliminary study of the feasibility of detecting the floating macrophytes by means of digital processing of MSS/LANDSAT data
[E85-10005] 02 p0215 N85-11418
On complementary and independent mappings on databases
[AD-A145557] 03 p0438 N85-12788
Summary of LANDSAT quadrangle studies in Alaska
04 p0515 N85-13284
Digital elevation models improve processing of Alaskan gravity data 04 p0515 N85-13285
Cretaceous plutonic rocks, Mitkof and Kupreanof Islands, Petersburg quadrangle, southeastern Alaska
04 p0518 N85-13306
A review of seismicity in peninsular Spain
04 p0523 N85-13349
Blind zones and aspect ratio bias in acquisition of discontinuity orientation data
[DE84-002718] 04 p0533 N85-13410
An integrated LANDSAT/ancillary data classification of desert rangeland
[E85-10046] 06 p0826 N85-15248
Computer vision research and its applications to automated cartography
[AD-A146668] 06 p0828 N85-15255
AFOS (Automation of Field Operations and Services) display of MDR (Manually Digitized Radar) data on local map backgrounds
[PB84-220797] 06 p0840 N85-15338
HEAO-1 diffuse soft X-ray sky maps
06 p0877 N85-15570
Manual and automated line generalization and feature displacement: Appendixes
[AD-A143251] 07 p1054 N85-16689
Map display for helicopters 08 p1073 N85-16801
Quantitative use of multiincidence-angle SAR for geologic mapping 08 p1145 N85-17220
SIR-B cartography and stereo topographic mapping
08 p1147 N85-17234
Application and calibration of the subsurface mapping capability of SIR-B in desert regions
08 p1148 N85-17244
Analysis of SIR-B radar illumination of geometry for depth of penetration and surface feature and vegetation detection, Nevada and California
08 p1149 N85-17248
Color visual simulation applications at the Defense Mapping Agency
[AD-P004315] 09 p1268 N85-17969
Symbol structure, information content and visual form: A carto-semiotic theory of map signs
09 p1342 N85-18439
An analysis of the seasonal variations in the water vapor transport fields over the Southern Hemisphere
09 p1356 N85-18531
Application of SLF (Standard Linear Format) to digital hydrographic products
[AD-A149509] 10 p1522 N85-19596
Retinal information mapping system
[AD-D011531] 12 p1849 N85-21601
Hybrid method of mapping and photogeodetic control network densification
[PB85-133775] 12 p1876 N85-21766
Implementation of the computer program-system MOSS (Map Overlay and Statistical System) on a VAX-11 series computer under VMS
[AD-A149612] 12 p1914 N85-22019
Geological remote sensing develops rapidly, finds broad applications 13 p2052 N85-22848
Possibility of mapping active tectonic structures from mercury gas aureoles over sea surface
13 p2113 N85-23162
Possibilities of aerial electric prospecting by long cable method for detecting poorly conducting strata
13 p2115 N85-23177
China report: Science and technology
[JPRS-CST-85-003] 13 p2166 N85-23433

Development, achievements in China's cartography work 13 p2166 N85-23434
Accomplishments of Institute of Cartography summarized 13 p2166 N85-23435
Geophysical interpretation of Venus gravity data 13 p2178 N85-23513
Newly discovered Martian impact basins 13 p2182 N85-23544
Mapping and geological analysis of Mercury and Venus radar ranging data 13 p2196 N85-23633
Mars radar catalog 13 p2196 N85-23636
Late Tertiary and Quaternary river systems of the eastern Sahara as mapped on shuttle radar and LANDSAT images 13 p2199 N85-23641
Map design for computer processing: Literature review and DMA product critique
[AD-A151081] 14 p2347 N85-24513
Comparison of magnetospheric and ionospheric electric fields using different empirical mapping factors 14 p2362 N85-24597
Commercial data base management system for geonames data base
[AD-A150835] 14 p2433 N85-25007
Measurement of ocean surface currents from space with multi-frequency microwave radars 15 p2539 N85-25672
Contamination of the fetch-limited directional wave spectrum by waves emanating from an embayment
[NASA-TM-84441] 15 p2604 N85-26048
The design and analysis of a complete hierarchical interface for the multi-backend database system
[AD-A151550] 15 p2629 N85-26203
The Mars ancient cratered terrain, smooth plains boundary: Implications of Viking color data for evolution of the Amenthes Region 15 p2682 N85-26584
Study and mapping of anthropogenic effect on environment in different regions of USSR on basis of space photographs 16 p2726 N85-26624
Creating a Mobile Autonomous Robot Research System (MARRS)
[AD-A151963] 16 p2783 N85-27229
Acid precipitation in North America: 1980, 1981 and 1982 annual data summaries from acid deposition system data base
[PB85-162477] 16 p2822 N85-27410
Circulation statistics from January and July: Simulation with the NCAR (National Center for Atmospheric Research) community climate model (CCM0B)
[PB85-165837] 16 p2837 N85-27497
Comparative study of the digital analysis of areas of the Earth's surface prepared for planting using different classification algorithms
[INPE-3359-PRE/637] 16 p2846 N85-27545
Microwave responses of the western North Atlantic
[NASA-CR-175888] 17 p2946 N85-28191
Evaluation of Defense Mapping Agency level 1 second edition digital data for training simulator applications
[AD-A152444] 17 p2963 N85-28437
Boundary to constructive solid geometry mappings: A focus on 2-D issues 17 p3004 N85-28570
German contributions to the cartography of Antarctica by means of photogrammetry and remote sensing 18 p3124 N85-29342
Reports on cartography and geodesy. Series 1: Original reports, number 93
[ISSN-0469-4236] 18 p3124 N85-29343
On approximating a set-valued function locally
[AD-A153540] 18 p3170 N85-29641
Diagnostics of vector magnetic fields 18 p3206 N85-29869
A constant altitude flight survey method for mapping atmospheric ambient pressures and systematic radar errors
[NASA-TM-86733] 19 p3217 N85-29951
Discovery in earthquake forecasting and seismic zoning recorded 19 p3295 N85-30426
Space methods for geological research 19 p3295 N85-30429
Fracture detection and mapping for geothermal reservoir definition: An assessment of current technology, research, and research needs
[DE85-010827] 19 p3301 N85-30484
Defense Mapping Agency (DMA) raster-to-Vector analysis
[AD-A154153] 19 p3336 N85-30668
Defense Mapping Agency (DMA) raster-to-Vector benchmark testing
[AD-A154152] 19 p3338 N85-30683
Combined finite element meshing techniques using SUPERTAB
[DE85-011393] 19 p3340 N85-30686
Single-dish high sensitivity determination of solar limb emission at 22 and 44 GHz
[INPE-3545-PRE/758] 19 p3365 N85-30899
Video discs - what are they and where do they fit in?
[AD-A154166] 20 p3458 N85-31479
SEASAT altimetry for surface height of inland seas 20 p3493 N85-31714
Correlation analysis of 1 to 30 MeV celestial gamma rays 20 p3549 N85-32063
Mapping with QUASAT (quasar satellite) using short observation times
[AD-A155155] 21 p3559 N85-32141
The measurement of strain fields by X-ray topographic contour mapping
[AD-A154870] 21 p3599 N85-32348
Use of the synoptic view: Examples from Earth and other planets 21 p3602 N85-32371
Techniques, problems and uses of mega-geomorphological mapping 21 p3604 N85-32379
Planetary perspective. Report of Working Group Number 4 21 p3605 N85-32385
Realizing the full potential of the video disc for mapping applications
[AD-A154966] 21 p3606 N85-32391
Optical storage technology for mapping
[AD-A154969] 21 p3606 N85-32392
Fracture detection and characterization for geothermal reservoir definition
[DE85-008677] 22 p3815 N85-33630
Graph-theoretical exorcism
[DE85-011916] 23 p3955 N85-34512
A comparison of LANDSAT thematic mapper, multispectral scanner and airborne sensors for mapping the distribution of alteration minerals: Examples from the southwestern United States 24 p4106 N85-35452
Evaluation: Close-range photogrammetry for slope inventory and monitoring
[PB85-192755] 24 p4108 N85-35470

MAPS
NT ASTRONOMICAL MAPS
NT LUNAR MAPS
NT METEOROLOGICAL CHARTS
NT PHOTOMAPS
NT RADAR MAPS
NT RELIEF MAPS
Requirements and specifications for cartographic video discs
[AD-A144906] 01 p0049 N85-10325
Environmental geologic atlas of the North Carolina coastal zone: Dare, Hyde, Tyrrell and Washington Counties
[PB84-222975] 01 p0066 N85-10439
Birkhoff orbits for non-monotone twist maps
[AD-A144718] 01 p0110 N85-10747
Range-residuated mappings
[AD-A145148] 01 p0112 N85-10759
The Alaskan mineral resources assessment program: Guide to information contained in the folio of geologic and mineral-resource maps of the Medfra Quadrangle, Alaska
[GS-CIRC-928] 02 p0219 N85-11443
Diffusion and intermittency in an extended one-dimensional maps 02 p0282 N85-11834
Long time correlation and stochastic diffusion in the standard map 02 p0282 N85-11835
Mars-Earth geographical comparisons: A pictorial view
[NASA-TM-86166] 02 p0302 N85-11957
Two-dimensional modeling for lineal and areal probabilities of weather conditions
[AD-A147970] 08 p1188 N85-17486
NGC 2024: Multi-wavelength infrared and radio observations 08 p1246 N85-17865
Far-infrared photometry of low-mass pre-main-sequence stars with broad CO wings 08 p1246 N85-17866
Automatic land vehicle navigation using road map data
[DE84-017178] 09 p1278 N85-18043
Automatic map name placement system 09 p1341 N85-18438
Ground-water level data and preliminary potentiometric-surface maps, Yucca Mountain and vicinity, Nye County, Nevada
[DE85-001771] 09 p1343 N85-18448
Monthly and Seasonal Weather Outlook for November, 1984, Volume 36, Number 27, October 30, 1984
[PB85-118600] 10 p1521 N85-19686
Index to published geologic maps in the region around the potential Yucca Mountain nuclear waste repository site, southern Nye County, Nevada
[DE85-000260] 11 p1669 N85-20518
Digital and color energy maps for graphic display of hourly data
[DE85-000526] 11 p1673 N85-20543
Monthly and seasonal weather outlook for mid-October to mid-November 1984, volume 36, number 20, 13 October 1984
[PB85-113546] 11 p1687 N85-20611
Digital laser plotamaker modifications
[AD-A150190] 13 p2096 N85-23074
An investigation of the crustal properties of Australia and surrounding regions derived from interpretation of MAGSAT anomaly field data 13 p2122 N85-23218
Development, achievements in China's cartography work 13 p2166 N85-23434
Accomplishments of Institute of Cartography summarized 13 p2166 N85-23435
Hexagonal data base study
[AD-A150176] 13 p2167 N85-23448
Mars geologic mapping: A review and new concepts 13 p2202 N85-23663
The Galilean Satellite Geological Mapping Program, 1984 13 p2203 N85-23664
Map design for computer processing: Literature review and DMA product critique
[AD-A151081] 14 p2347 N85-24513
Testing of scanner-assisted revision of the topographic map 1:25,000 (TK 25) 16 p2814 N85-27359
Circulation statistics from January and July: Simulation with the NCAR (National Center for Atmospheric Research) community climate model (CCM0B)
[PB85-165837] 16 p2837 N85-27497
UTM (Universal Transverse Mercator) determinations from geographical data
[AD-A152293] 16 p2858 N85-27610
Orphans of the Valley: Abandoned surface mines in the Tennessee Valley. Volume 2: Maps
[DE85-001249] 19 p3301 N85-30485
Defense Mapping Agency (DMA) raster-to-Vector analysis
[AD-A154153] 19 p3336 N85-30668
Defense Mapping Agency (DMA) raster-to-Vector benchmark testing
[AD-A154152] 19 p3338 N85-30683
MAGSAT scalar anomaly map of South America 20 p3473 N85-31586
MAGSAT satellite magnetic anomaly map over South America 20 p3474 N85-31587
Planetary perspective. Report of Working Group Number 4 21 p3605 N85-32385
The automatic labeling of geographic maps: A problem in computer aesthetics 23 p3962 N85-34581
An experimental study of dielectric rod antennas for millimeter-wave imaging applications
[AD-A155832] 24 p4086 N85-35328
New silver resource map of the United States: Potential for increased domestic silver production 24 p4105 N85-35445
Early and middle Cenozoic volcanic synthesis 24 p4105 N85-35449
Applications of the mineral resources data system and the International strategic minerals inventory in mineral-resource assessments by region and commodity 24 p4105 N85-35451

MARAGING STEELS
A study of vacuum melting to increase the toughness of maraging steels
[AD-A145017] 01 p0028 N85-10175
Maraging steels: Structure, properties and applications 02 p0177 N85-11191
Near-threshold fatigue crack growth and crack closure in 17-4 precipitation hardening steel and 2043-T3 aluminum alloy
[FFA-TN-1984-16] 02 p0210 N85-11395
Machining-induced deformation in stepped specimens of PH 13-8 Mo, 18 nickel maraging steel grade 200T1 and grain-refined HP 9-4-20
[NASA-CR-172450] 21 p3565 N85-32177

MARANGONI CONVECTION
High Marangoni number convection in a square cavity
[NASA-CR-174283] 07 p0959 N85-16078

MARGINS
Margin leveling algorithm for fully saturated satellite transponder with CDMA (Code Division Multiple Access) signalling
[AD-A151710] 15 p2543 N85-25689

MARIA
NT LUNAR MARIA

MARINE BIOLOGY
Activities of the Coastal Research Center
[PB84-231323] 05 p0672 N85-14320
USSR report: Life sciences. Biomedical and behavioral sciences
[JPRS-UBB-84-015] 07 p1010 N85-16416
Extremely Low Frequency (ELF) Communications System Ecological Monitoring Program: Summary of 1983 progress
[AD-A147704] 08 p1161 N85-17265
Bibliography of venomous and poisonous marine animals and their toxins
[AD-A148409] 08 p1192 N85-17514
An assessment of biological processes close to the sea bed in a slope region and its significance to the assessment of sea-bed disposal of radioactive waste
[IOS-195] 09 p1360 N85-18554

Microplankton species assemblages at the Scripps Pier from March to November 1983 during the 1982-1984 El Nino event
[NASA-CR-175553] 12 p1899 N85-21926
Production and turnover of suspended organic detritus in the coastal water of the southeastern continental shelf
[DE85-003977] 13 p2140 N85-23290
An analysis of issues concerning acid rain, report to the Congress of the United States
[TI85-901070] 15 p2589 N85-25859
MARMAP survey of the continental shelf from Cape Hatteras, North Carolina to Cape Sable, Nova Scotia (1977 - 1983). Atlas 1: Summary of operations
[PB85-150985] 16 p2839 N85-27506
Towards a study of synoptic-scale variability of the California current system
[NASA-CR-175871] 17 p2997 N85-28529
Chemical, biological, and physical measurements from the subtropical western North Atlantic Ocean. Summer 1982, USNS Lynch, cruise 710-82
[AD-A153823] 18 p3201 N85-29857
Use of a two-dimensional flow model to quantify aquatic habitat
[AD-A154287] 19 p3266 N85-30253
Marine environmental quality assessment program, five-year plan (FY 1984 - 1988)
[AD-A154715] 21 p3613 N85-32459

MARINE CHEMISTRY
The marine geochemistry of the rare earth elements
[AD-A145132] 01 p0088 N85-10596
Activities of the Coastal Research Center
[PB84-231323] 05 p0672 N85-14320
Gas-liquid chemistry of natural waters, volume 1
[DE85-002603] 12 p1884 N85-21822
Operation guiding light-scientific program and field plan. The pilot field experiment for NORDA project chemical dynamics in ocean frontal areas
[AD-A153765] 18 p3150 N85-29507
Chemical, biological, and physical measurements from the subtropical western North Atlantic Ocean. Summer 1982, USNS Lynch, cruise 710-82
[AD-A153823] 18 p3201 N85-29857
Dispersal From Deep Ocean Sources: Physical and Related Scientific Processes
[DE85-010420] 20 p3497 N85-31740

MARINE ENVIRONMENTS
Mineral nutrients in Mediterranean ecosystems
[REPT-71] 01 p0069 N85-10456
Radiotracer studies of the dispersion of solid pollutants in marine and estuarial environment: Measurement of diffusion coefficients and the phenomenon of dispersion by currents
[BLL-DRIC-TRANS-7104-(3623.66)] 02 p0224 N85-11468
Evaluation of an aerosol prediction model for coastal regions using marine aerosol generation and transport data
[AD-A145443] 02 p0231 N85-11510
Experiences with a high-blockage model tested in the NASA Ames 12-foot pressure wind tunnel 03 p0315 N85-12032
Icing rate on stationary structures under marine conditions
[AD-A145795] 03 p0395 N85-12524
Newly recognized sedimentary environments in the Shelikof Formation, Alaska 04 p0516 N85-13292
Interactions of the marine phosphorus and carbon cycles 05 p0653 N85-14190
Multi-property modeling of the marine biosphere in relation to global climate and carbon cycles 05 p0678 N85-14355
An investigation of the marine boundary layer during cold air outbreak 05 p0680 N85-14368
Structure and growth of the marine boundary layer 05 p0680 N85-14369
Marine helicopter missions 06 p0751 N85-14811
SAR maritime missions 06 p0751 N85-14813
Mariners weather log, volume 28, no. 3, July-August-September 1984
[PB85-107266] 06 p0840 N85-15334
Environmental research laboratories (of the National Oceanic and Atmospheric Administration) programs and plans: FY 1983 programs and FY 1984 plans
[PB84-226729] 06 p0840 N85-15336
Experiments in forecasting atmospheric marine horizontal visibility using model output statistics with conditional probabilities of discretized parameters
[AD-A147574] 07 p1006 N85-16404
Bibliography of venomous and poisonous marine animals and their toxins
[AD-A148409] 08 p1192 N85-17514
Special features of computations of vertical distribution of concentration of suspended sediments under marine conditions 13 p2106 N85-23125
Contribution to theory of ocean-atmosphere gas exchange 13 p2108 N85-23134
The relationship between marine aerosol particles and satellite-detected radiance 13 p2131 N85-23263
Variability in constant-load-amplitude fatigue crack growth rates in marine environments
[AD-A150786] 14 p2255 N85-23975
Statistical/Trend analysis of the marine atmospheric boundary layer model
[AD-A151053] 14 p2374 N85-24673
Geophysical Fluid Dynamics Laboratory activities, FY84, plans, FY85
[PB85-147601] 15 p2558 N85-25783
The physics of the marine stratocumulus-capped mixed layer 15 p2593 N85-25979
Monitoring of marine environment 16 p2812 N85-27341
An evaluation of discretized conditional probability and linear regression threshold techniques in model output statistics forecasting of visibility over the north Atlantic Ocean
[AD-A151955] 16 p2857 N85-27619
Fatigue of synthetic fibers for marine rope applications
[MIT-R84-2] 17 p2979 N85-28414
Environmental Research Laboratories publication abstracts, FY 1984
[PB85-160594] 19 p3313 N85-30540
Environmental background measurement program
[AD-A153860] 19 p3319 N85-30577
Optimization of MCr Al coating compositions for marine gas turbines
[BR91159] 20 p3394 N85-31056
The U.S. Geological Survey in Alaska: Accomplishments during 1982
[US-GEOL-SURV-CIRC-939] 20 p3493 N85-31719
Understanding and laboratory prediction of the atmospheric corrosion behavior of steels and of non-ferrous metals and alloys
[AD-A154642] 21 p3566 N85-32179
Using ship wake patterns to evaluate SAR (Synthetic Aperture Radar) ocean wave imaging mechanisms. Joint US-Canadian Ocean Wave Investigation Project
[AD-A154633] 21 p3573 N85-32223
Marine environmental quality assessment program, five-year plan (FY 1984 - 1988)
[AD-A154715] 21 p3613 N85-32459
Forecasting atmospheric visibility over the summer north Atlantic using the principal discriminant method
[AD-A155537] 21 p3637 N85-32593
Bacterial ice nuclei of marine origin: Some recent observations 21 p3640 N85-32611
Marine aerosols at the Dutch North Sea coast: Size distributions and fractionation of trace elements 21 p3648 N85-32664
Sulfates in marine aerosols over the tropical Western Pacific Ocean 21 p3651 N85-32690
Granulometric study of the acidity and sulfate excess in marine aerosols 21 p3652 N85-32691
Sulfur diagenesis in marine sediments 21 p3658 N85-32721
Sulfur reduction in sediments of marine and evaporite environments 21 p3661 N85-32742
Submarine hydrothermal environments as sites for the origin and evolution of life 21 p3719 N85-33074
Corrosion management strategies for aircraft and related systems 22 p3749 N85-33239
Current requirements for the design and maintenance against corrosion of UK military aircraft 22 p3750 N85-33244
The development and evaluation of the creep and corrosion resistant alloy IN6201
[PNR-90253] 23 p3917 N85-34278

MARINE GEOLOGY
U HYDROGEOLOGY

MARINE METEOROLOGY
Operational use of shipboard numerical aid programs 01 p0082 N85-10546
Energy-active zones in north Atlantic as manifestation of interannual variability of radiation balance 02 p0164 N85-11106
Bibliography of climate textbooks and studies
[WCP-84] 02 p0231 N85-11505
Observational-numerical study of maritime extratropical cyclones using FGGE data 05 p0685 N85-14400
Air-sea interaction during cold air outbreaks 05 p0685 N85-14401
Mariners weather log, volume 28, no. 3, July-August-September 1984
[PB85-107266] 06 p0840 N85-15334
MIZEX. A program for mesoscale Air-Ice-Ocean interaction experiments in arctic marginal ice zones. 4: Initial results and analysis from MIZEX 83
[AD-A148255] 08 p1173 N85-17399
Development of guidance forecasts at the Royal Netherlands Meteorological Institute (KNMI). Part 2: Extreme wind speed at IJmuiden
[KNMI-TR-54-PT-2] 08 p1190 N85-17500
Annual data and verification tabulation for Eastern North Pacific tropical storms and hurricanes, 1983
[PB85-109635] 10 p1520 N85-19580
Science opportunities using the NASA scatterometer on N-ROSS
[NASA-CR-175639] 13 p2123 N85-23222
The BALSAMINE experiment 14 p2238 N85-23876
Automatic weather stations in Antarctica 14 p2324 N85-24360
The 1981 transatlantic boat race contribution for marine meteorological measurements 14 p2324 N85-24361
The development of an automated marine meteorological data system 14 p2324 N85-24362
Intermediate results of the NORDSEE experiment
[AD-A151363] 15 p2542 N85-25693
Report of the Hydrographic Service Royal Australian Navy for the year ended 30th June 1984, issue number 20
[AD-A151460] 15 p2583 N85-25932
Diagnostic verification of the GLAS (Goddard Laboratory for Atmospheric Sciences) general circulation model as applied to a case of extratropical maritime explosive cyclogenesis
[AD-A153686] 18 p3148 N85-29494
Mariners weather log, volume 29, number 1, winter 1985
[PB85-177483] 19 p3318 N85-30570
Mariners weather log, volume 28, number 4, fall 1984
[PB85-178408] 19 p3318 N85-30571
Commission for Marine Meteorology
[WMO-640] 20 p3496 N85-31735

MARINE NAVIGATION
U SURFACE NAVIGATION

MARINE PROPULSION
An analytic model of gas turbine engine installations
[AD-A148708] 09 p1281 N85-18059
USSR report: Engineering and equipment
[JPRS-UEQ-85-004] 17 p2939 N85-28142

MARINE RESOURCES
Cultivation and conversion of marine macroalgae — biomass energy production
[DE84-004522] 04 p0544 N85-13464
The use of hydrometeorological data in explaining shrimp cycles in Guyana 07 p1004 N85-16381
Contribution of the NOAA-7 and 8 and ARGOS partnership to white tuna fishing in the northeast Atlantic 16 p2813 N85-27355

MARINE TECHNOLOGY
Design proposals for torsional buckling of stiffeners
[AD-A144783] 01 p0062 N85-10409
Evaluation of an integrated mixed-layer model for single station prediction in a marine regime 01 p0080 N85-10535
Ultrafiltration as pretreatment for the preparation of drinking water by reverse osmosis onboard ships
[PML-1984-32] 01 p0096 N85-10654
High-data-rate wide-angle underwater acoustic telemetry system
[DE84-015696] 02 p0233 N85-11519
NAVAIR's (Naval air systems command) AI (Artificial intelligence) program for ATE (Automated Test Equipment)
[AD-P003935] 02 p0247 N85-11615
Navy programs on ion implantation for materials modification
[AD-P003952] 02 p0266 N85-11868
ONR (Office of Naval Research) Far east Scientific Bulletin, Volume 9, Number 2, April - June 1984
[AD-A145861] 02 p0305 N85-11974
The Lindstrom-Madden method for series systems with repeated components
[AD-A146265] 03 p0412 N85-12636
Protective coverings for fiber reinforced epoxy composites
[PB84-231059] 04 p0480 N85-13063
Naval surface weapons center technology transfer report (FY83)
[AD-A146501] 06 p0671 N85-15534
USC (University of Southern California) Sea Grant Program Directory, 1984-1985
[PB85-135051] 12 p1899 N85-21922
Research needs for artificial intelligence applications in support of C3 (Command, Control, and Communication)
[AD-A150867] 14 p2292 N85-24210
Miscellaneous ARGOS maritime applications — yacht races 14 p2327 N85-24363
A summary of the Naval Postgraduate School research program
[AD-A151721] 16 p2875 N85-27736
Recent Naval Postgraduate School publications
[AD-A151723] 16 p2875 N85-27740

The dynamics of slack marine cables
[AD-A155022] 21 p3599 N85-32349
Physical oceanography program science abstracts
[AD-A154637] 21 p3654 N85-32701
High powered epicyclic gears: Some recent development 23 p3924 N85-34316

MARINE TRANSPORTATION
USSR report: Transportation
[JPRS-UTR-85-008] 15 p2460 N85-25189
USSR report: Transportation
[JPRS-UTR-84-017] 15 p2461 N85-25196
USSR report: Transportation
[JPRS-UTR-84-014] 15 p2467 N85-25229
Review and evaluation of plans to incorporate NAVSTAR global positioning system user equipment on military sealift command ships
[AD-A153799] 18 p3060 N85-28934
The international organization of maritime search and rescue 20 p3400 N85-31089

MARINER SPACE PROBES
NT MARINER 5 SPACE PROBE
NT MARINER 9 SPACE PROBE

MARINER 5 SPACE PROBE
Evaluation of semiconductor devices for Electric and Hybrid Vehicle (EHV) ac-drive applications, volume 2
[NASA-CR-176103] 22 p3759 N85-33294

MARINER 9 SPACE PROBE
Participation in the Mars Data Analysis Program: Analysis of cloud forms in Viking and Mariner 9 images
[NASA-CR-175604] 13 p2204 N85-23673

MARISAT SATELLITES
INMARSAT: An overview 20 p3400 N85-31091
Existing and potential INMARSAT capabilities for the Future Global Maritime Distress and Safety System 20 p3402 N85-31110
The International Radio Consultative Committee (CCIR) recommended satellite Emergency Position Indicating Radio Beacon (EPIRB) system operating through geostationary satellites at 1.6 GHz 20 p3402 N85-31112
UK experience with COSPAS-SARSAT and INMARSAT distress systems 20 p3406 N85-31132
INMARSAT distress and safety communication 20 p3406 N85-31134
Future prospects for a combined INMARSAT polar communication and search and rescue satellite system 20 p3406 N85-31137

MARITIME SATELLITES
NT ERS-1 (ESA SATELLITE)
INMARSAT marine satellite organization 13 p1985 N85-22456
INMARSAT: An overview 20 p3400 N85-31091
Maritime mobile satellite techniques as an integral part of the Future Global Maritime Distress and Safety System (FGMDSS): The position of the Federal Republic of Germany 20 p3406 N85-31136
Future prospects for a combined INMARSAT polar communication and search and rescue satellite system 20 p3406 N85-31137

MARKERS
TEM combined with Al/sub x/Ga/sub 1-x/ as marker layers as a technique for the study of GaAs MBE growth
[DE85-006451] 18 p3194 N85-29809

MARKET RESEARCH
Abrasive products study
[PB84-223635] 01 p0033 N85-10205
User requirements for very-short-range weather forecasts: Some key issues 01 p0084 N85-10562
Use of short-range weather forecasts at construction sites: Some results from a user and a market test 01 p0084 N85-10563
Foreign civil aviation competition: 1976 summary and implications
[NASA-TM-X-73907] 02 p0133 N85-10907
The future of satellite remote sensing: A worldwide assessment and prediction 02 p0151 N85-11025
German domestic scheduled air transport in the year 2000
[ESA-TT-828] 05 p0595 N85-13792
Telecommunication market research processing
[ENST-83E018] 23 p3926 N85-34331

MARKETING
Abrasive products study
[PB84-223635] 01 p0033 N85-10205
Financial issues for commercial space ventures: Paying for the dreams 02 p0150 N85-11014
Subliminal communication technology
[GPO-38-833] 05 p0622 N85-13979
UK, FRG, France: R and D in sensors, related fields 08 p1142 N85-17197
French panel makes specific proposals for robotics research. Current state of French robotics 11 p1618 N85-20180
Development of computer centers, equipment described: Problems of computer centers 11 p1700 N85-20686
High-technology ceramics in Japan
[PB85-125029] 12 p1815 N85-21389
MBB cost-reduction plan for Airbus construction described 15 p2532 N85-25616
FRG journal analyzes state, prospects of airbus programs: General analysis 15 p2535 N85-25638
French firm plans recapture of domestic CAD/CAM market 15 p2535 N85-25641
Air quality benefit analysis for Los Angeles and San Francisco based on housing values and visibility
[PB85-166049] 16 p2822 N85-27409
The Ariane launch vehicle is the key of the Europeans to the space market 17 p2908 N85-27931

MARKING
NT ISOTOPIC LABELING
New labeling procedures for the basis graph in generalized networks
[AD-A146217] 03 p0407 N85-12601
Simultaneous determination of cerebral blood flow and partition coefficient with a freely diffusable tracer
[DE85-001226] 11 p1690 N85-20625
On the use of marker loads for fatigue crack growth measurements 14 p2319 N85-24332
Pavement-marking materials: New York's experience
[PB85-153294] 15 p2523 N85-25558
On the use of marker loads for fatigue crack growth measurements
[FFA-TN-1984-52] 16 p2802 N85-27277
Resource management for the tagged token dataflow architecture
[AD-A154773] 21 p3667 N85-32779

MARKOV CHAINS
Numerical studies in nonlinear filtering
[TWISK-305] 01 p0108 N85-10728
The growth and composition of supercritical branching populations on general type spaces
[CTH-MATH-1984-18] 05 p0721 N85-14031
Limiting distributions of functionals of Markov chains
[AD-A147832] 07 p1036 N85-16577
Regenerative structure of Markov chains simulated via common random numbers
[AD-A149092] 10 p1550 N85-19777
Algebraic decay in self-similar Markov chains
[DE85-003162] 11 p1707 N85-20740
Reliability bounds for fault-tolerant systems with competing responses to component failures
[NASA-TP-2409] 13 p2100 N85-23090
Regenerative simulation of non-Markovian stochastic systems
[AD-A150344] 13 p2153 N85-23367
Automatic symbolic solution of Markov chains
[AD-A150478] 13 p2153 N85-23369
Ergodicity and Steady-State-Equilibrium conditions for Markov chains
[AD-A151038] 14 p2409 N85-24854
Sensitivity of conditions for lumping finite Markov chains
[AD-A152122] 16 p2855 N85-27604
Sensitivity of the stationary distribution vector for an ergodic Markov chain
[DE85-006979] 16 p2857 N85-27621
Limit behaviour for stochastic monotonicity and applications
[AD-A153814] 18 p3170 N85-29648
Tunisian climate seen through a Markov process
[CT-585] 23 p3950 N85-34482

MARKOV PROCESSES
NT MARKOV CHAINS
Markovian control problems: Functional equations and algorithms
[MCTH-97] 01 p0107 N85-10717
Optimum replacement of a system subject to shocks
[AD-A145811] 03 p0372 N85-12374
Regenerative simulation methods for local area computer networks
[AD-A146197] 03 p0409 N85-12612
Very short range statistical forecasting of automated weather observations
[DOT/FAA/PM-84/31] 05 p0679 N85-14359
Power spectral ensity of markov texture fields 07 p0986 N85-16262
On modeling the performance and reliability of multi-mode computer systems
[AD-A148444] 08 p1208 N85-17599
A unified model for performance and reliability of Fault-Tolerant/Multi-Mode systems
[AD-A148789] 08 p1208 N85-17601
Extended Stochastic Petri Nets: Applications and analysis
[AD-A148439] 08 p1213 N85-17633
Convergence of quasi-stationary to stationary distributions for stochastically monotone Markov processes
[AD-A148041] 08 p1215 N85-17652
State estimation with interrupted observations 15 p2535 N85-25251
Inference and state estimation for stochastic point processes
[AD-A151216] 15 p2540 N85-25281
Bayesian estimation of one dimensional discrete markov random fields
[AD-A151503] 15 p2840 N85-28284
A Markov method for simulating non-Gaussian wind speed time series
[DE85-007131] 16 p2835 N85-27485
Sensitivity of conditions for lumping finite Markov chains
[AD-A152122] 16 p2855 N85-27604
An abstract specification language for Markov reliability models
[NASA-TM-86423] 16 p2857 N85-27616
An application of Markov chains to the problem of migration in inventory systems
[AD-A151954] 16 p2857 N85-27618
Theory of laser-stimulated surface process. 2: A generalized-master-equation approach to energy transfer between an IR laser, an aspecties and phonons
[AD-A153083] 17 p2970 N85-28344
On estimating transition intensities of a Markov process with aggregate data of a certain type
[CWI-MS-R8411] 17 p3025 N85-28707
Maximum flow in planar networks with exponentially distributed arc capacities
[AD-A153158] 17 p3026 N85-28710
Quantum model of dephasing-enhanced laser desorption: Master equation approach
[AD-A153769] 18 p3112 N85-29269
The completion time of a job on multi-mode systems
[AD-A154113] 19 p3336 N85-30666
Memory effects in dynamical many-body systems: The isomnesic (constant-memory) approximation
[AD-A154160] 20 p3520 N85-31989
Comprehensive radio direction finder with electronically stabilized radiation pattern 22 p3762 N85-33315
Optimal complex nonlinear processing of continuous and pulsed signals 22 p3763 N85-33323
Synthesis of optimum receiver and processor for interfering radio pulse signals 22 p3769 N85-33361
Optimal Bayesian estimators for image segmentation and surface reconstruction
[AD-A156732] 22 p3827 N85-33704

MARROW
Effect of spaceflight factors on rat bone marrow cells 01 p0092 N85-10620

MARS
Volcanic debris flows in the Elysium region of Mars 13 p2185 N85-23560
Estimates of lava eruption rates at Alba Patera, Mars 13 p2185 N85-23562

MARS (PLANET)
Mars exploration, Venus swingby and conjunction class mission modes, time period 2000 to 2045
[NASA-TM-86477] 02 p0093 N85-11961
Martian impact basins: Morphology differences and tectonic provinces
[NASA-CR-174074] 03 p0448 N85-12847
The Martian climate: Energy balance models with CO2/H2O atmospheres
[NASA-CR-174073] 03 p0448 N85-12849
A Mars dust sample return mission
[CNES-CT/PMF/APS/EMS-177] 04 p0459 N85-12915
Mars polar volatiles: Topographic and geologic setting
[NASA-CR-174089] 04 p0581 N85-13706
An autonomous roving vehicle for the planet Mars: A summary of over 15 years of research
[RPI-TR-MP-83] 07 p0973 N85-16179
The geology of the terrestrial planets
[NASA-SP-469] 09 p1410 N85-18688
Mars 09 p1411 N85-18694
A model for the climatic behavior of water on Mars 09 p1415 N85-18931
Conclusion of Viking Lander Imaging Investigation: Picture catalog of experiment data record
[NASA-RP-1137] 11 p1765 N85-21099
Viking radio science data analysis and synthesis
[NASA-CR-175831] 13 p2171 N85-23471
Study and estimation of planet-crossing asteroid populations: Discoveries and analysis 13 p2175 N85-23498
Viking radio science data analysis and synthesis 13 p2180 N85-23528
Estimates of lava eruption rates at Alba Patera, Mars 13 p2185 N85-23562
Observed changes at Viking Lander 1 13 p2188 N85-23575
Seasonal and secular variation of the Solis Lacus albedo feature: Relation to the Martian dust-transport cycle 13 p2188 N85-23576
Eolian erosion on Mars: Three scales 13 p2188 N85-23577

The origin of regional dust deposits on Mars
13 p2188 N85-23578
On the latitudinal distribution of debris in the Northern Hemisphere of Mars 13 p2188 N85-23579
Transformation of polar ice sublimate residue into Martian circumpolar sand 13 p2189 N85-23580
The effect of particle density on aeolian transport
13 p2189 N85-23581
Paleohydrologic implications of valley networks of Mars 13 p2190 N85-23585
Fluvial drainage basins and valley networks: Eastern Margaritifer Sinus, Mars 13 p2190 N85-23586
Catastrophic-flood features in Swedish Lapland as a terrestrial analog for Martian channel flows
13 p2190 N85-23587
Experiments and analyses of the formation of erosional scour marks with implications to the origin of the Martian outflow channels 13 p2190 N85-23588
Relative time-scale for channeling events within chaotic terrains, Margaritifer Sinus, Mars
13 p2190 N85-23589
Terrestrial analog studies for Martian patterned ground
13 p2190 N85-23590
Origin of Martian polygonal terrain: Preliminary results
13 p2191 N85-23591
Radiation-dominated snowmelt on Mars
13 p2191 N85-23592
Chemical weathering of soils from the dry valleys of Antarctica: A terrestrial analog of Martian weathering processes 13 p2197 N85-23636
Mars radar catalog 13 p2198 N85-23636
Statistics of Aeolian surface of Mars
13 p2199 N85-23637
Radar and the detection of liquid water on Mars
13 p2199 N85-23638
Planetary interior modeling and tectonic implications
13 p2200 N85-23649
Elysium region, Mars: Tests of lithospheric loading models for the formation of tectonic features
13 p2200 N85-23650
Mars: Stratigraphy of western highlands and polar regions 13 p2201 N85-23653
Participation in the Mars Data Analysis Program: Analysis of cloud forms in Viking and Mariner 9 images [NASA-CR-175604] 13 p2204 N85-23673
Structure and origin of Martian satellites
15 p2493 N85-25323
Distribution of gravity and plumb line deflection at Martian surface 15 p2493 N85-25324
Sixteenth Lunar and Planetary Science Conference. Press abstracts [NASA-CR-175692] 15 p2650 N85-26548
Identification of the youngest meteorites and a discussion of the possibility that they came from Mars
15 p2651 N85-26559
What we know about Mars (but otherwise wouldn't) if it is the shergottite parent body
15 p2652 N85-26565
Orientation and strength of Martian magnetic dipole
16 p2723 N85-26608
Possible configuration of Martian magnetosphere
16 p2723 N85-26609
The influence of global dust storms on the mean seasonal daily insolations at the Martian surface [AERONOMICA-ACTA-A-289-1984]
16 p3203 N85-29668
Space ventures and society long-term perspectives [NASA-CR-176012] 19 p3379 N85-30983
Mega-geomorphology: Mars vis a vis Earth
21 p3601 N85-32360
The polar caps and the climatic evolution of Mars
22 p3654 N85-33668
Volatiles on satellites of the outer solar system
22 p3654 N85-33668
Permafrost features on Earth and Mars: Similarities, differences 22 p3655 N85-33670
Venus, Earth and Mars: Present bounds on similarities and differences in bulk composition
22 p3656 N85-33676
Planning for VRM: Radar and sonar studies of volcanic terrains on Earth, Venus and Mars
22 p3657 N85-33684
What we have learned about the magnetic field of Mars 22 p3658 N85-33692
Comparisons of the North Polar Cap of Mars and the Earth's Northern Hemisphere snow cover [NASA-TM-86191] 23 p3959 N85-34728

MARS ATMOSPHERE
Clouds above the Martin Limb: Viking observations [NASA-CR-174027] 02 p0296 N85-11922
The Martian climate: Energy balance models with CO2/H2O atmospheres [NASA-CR-174073] 03 p0448 N85-12849
A Mars dust sample return mission [CNES-CT/PMF/APS/EMS-177]
04 p0459 N85-12915
Construction of a superheterodyne receiver for 10 micron waves to be put on a Cassegrain optics telescope for spectroscopic research on the Mars and Venus atmospheres [MPE-163] 06 p0872 N85-15538
Exploration of the solar system by airborne astronomy
06 p1244 N85-17851
Mars 09 p1411 N85-18894
The effect of particle density on aeolian transport
13 p2189 N85-23581
Mars: Long term changes in the state and distribution of H2O 13 p2191 N85-23593
Water-ice clouds on Mars: Location and seasonal variation 13 p2194 N85-23611
The Martian climate: Energy balance models with CO2/H2O atmospheres [NASA-CR-175722] 15 p2679 N85-26547
Dust devils on Mars 15 p2683 N85-26573
The influence of global dust storms on the mean seasonal daily insolations at the Martian surface [AERONOMICA-ACTA-A-289-1984]
16 p3203 N85-29668
Noble gas patterns in the atmospheres of Mars and Earth: A comparison via the SNC meteorites
22 p3652 N85-33653

MARS CRATERS
Martian impact basins: Morphology differences and tectonic provinces [NASA-CR-174074] 03 p0448 N85-12847
Mars 09 p1411 N85-18894
The nature of Martian flow ejecta craters
13 p2183 N85-23545
Paleohydrologic implications of valley networks of Mars 13 p2190 N85-23585
Geomorphology and geology of the Southwestern Margaritifer Sinus and Argyre regions of Mars. Part 2: Crater size-frequency distribution curves and geomorphic unit ages 13 p2192 N85-23601
Geomorphology and geology of the Southwestern Margaritifer Sinus and Argyre regions of Mars. Part 4: Flow ejecta crater distribution 13 p2193 N85-23603
Identification of the youngest meteorites and a discussion of the possibility that they came from Mars
15 p2651 N85-26559
Lunar and Martian impact basins: Exposed records of terrestrial bombardment? 21 p3721 N85-33090

MARS ENVIRONMENT
NT MARS ATMOSPHERE
Properties of filamentary sublimation residues from dispersions of clay in ice 13 p2197 N85-23629
Statistics of Aeolian surface of Mars
13 p2199 N85-23637

MARS LANDING
Mars landing sites 22 p3659 N85-33683

MARS PHOTOGRAPHS
Mars-Earth geographical comparisons: A pictorial view [NASA-TM-86186] 02 p0302 N85-11957
Conclusion of Viking Lander Imaging Investigation: Picture catalog of experiment data record [NASA-RP-1137] 11 p1765 N85-21099
Viking Lander mosaics of Mars
13 p2203 N85-23667
The control network of Mars: October 1984
13 p2203 N85-23670

MARS PROBES
NT VIKING LANDER SPACECRAFT
NT VIKING LANDER 1
NT VIKING MARS PROGRAM
NT VIKING ORBITER SPACECRAFT
NT VIKING SPACECRAFT
A Mars dust sample return mission [CNES-CT/PMF/APS/EMS-177]
04 p0459 N85-12915
Mars landing sites 22 p3659 N85-33683

MARS SURFACE
Mars-Earth geographical comparisons: A pictorial view [NASA-TM-86186] 02 p0302 N85-11957
Martian impact basins: Morphology differences and tectonic provinces [NASA-CR-174074] 03 p0448 N85-12847
The Martian climate: Energy balance models with CO2/H2O atmospheres [NASA-CR-174073] 03 p0448 N85-12849
Growth of soil bacteria in presence of Martian soil analog, carbon dioxide and hydrogen peroxide
09 p1361 N85-18560
Mars 09 p1411 N85-18894
Conclusion of Viking Lander Imaging Investigation: Picture catalog of experiment data record [NASA-RP-1137] 11 p1765 N85-21099
Physiography of the Martian west equatorial uplift
12 p1961 N85-22325
The origin and evolution of terrestrial and Martian rock labyrinths [NASA-CR-175811] 12 p1961 N85-22326
Viking radio science data analysis and synthesis
13 p2180 N85-23628
Martian terrain ages 13 p2181 N85-23637
The evolution of CO2 on Mars
13 p2185 N85-23558
Ridged plains of Lunae Planum: Thickness distribution revised 13 p2185 N85-23559
Thickness of ridged plains materials in Hesperia Planum, Mars 13 p2185 N85-23561
Observed changes at Viking Lander 1
13 p2186 N85-23575
Seasonal and secular variation of the Solis Lacus albedo feature: Relation to the Martian dust-transport cycle
13 p2188 N85-23576
Eolian erosion on Mars: Three scales
13 p2188 N85-23577
The origin of regional dust deposits on Mars
13 p2188 N85-23578
On the latitudinal distribution of debris in the Northern Hemisphere of Mars 13 p2188 N85-23579
Transformation of polar ice sublimate residue into Martian circumpolar sand 13 p2189 N85-23580
Paleohydrologic implications of valley networks of Mars 13 p2190 N85-23585
Fluvial drainage basins and valley networks: Eastern Margaritifer Sinus, Mars 13 p2190 N85-23586
Catastrophic-flood features in Swedish Lapland as a terrestrial analog for Martian channel flows
13 p2190 N85-23587
Experiments and analyses of the formation of erosional scour marks with implications to the origin of the Martian outflow channels 13 p2190 N85-23588
Mars: Long term changes in the state and distribution of H2O 13 p2191 N85-23593
Mapping structures characteristic of the highland boundary scarp on Mars 13 p2191 N85-23595
Investigations of the Mars cratered terrain: Smooth plains boundary in the eastern equatorial region
13 p2191 N85-23596
Martian fretted terrain morphometry interpreted using principal components analysis 13 p2192 N85-23597
Distribution and properties of large symmetric knobs on Mars 13 p2192 N85-23598
Enigmatic hills of the mottled plains, Mare Acidalium quadrangle (MC-4), Mars 13 p2192 N85-23599
Geomorphology and geology of the Southwestern Margaritifer Sinus and Argyre regions of Mars. Part 1: Geological and geomorphological overview
13 p2192 N85-23600
Geomorphology and geology of the Southwestern Margaritifer Sinus and Argyre regions of Mars. Part 2: Crater size-frequency distribution curves and geomorphic unit ages 13 p2192 N85-23601
Geomorphology and geology of the Southwestern Margaritifer Sinus and Argyre regions of Mars. Part 3: Valley types and distribution 13 p2193 N85-23602
Geomorphology and geology of the Southwestern Margaritifer Sinus and Argyre regions of Mars. Part 4: Flow ejecta crater distribution 13 p2193 N85-23603
Planetary analogs in Antarctica: Mars
13 p2193 N85-23604
Multispectral analysis of the Kasei Valles-Lunae Planum region of Mars 13 p2193 N85-23607
Geologic interpretation of remote sensing data for the Martian volcano, Aecraeus Mons
13 p2194 N85-23608
The search for igneous materials at the Viking landing sites 13 p2194 N85-23609
Basalts of Mars: Constraints on volatile evolution
13 p2194 N85-23610
First direct detection of clay minerals on Mars
13 p2194 N85-23612
Iron oxides of Mars: Evidence for contemporary weathering 13 p2195 N85-23613
Reassignment of the iron (3) absorption bands in the spectra of Mars 13 p2195 N85-23614
Zeolites on Mars: Prospects for remote sensing
13 p2195 N85-23615
Mars radar catalog 13 p2198 N85-23636
Statistics of Aeolian surface of Mars
13 p2199 N85-23637
Radar and the detection of liquid water on Mars
13 p2199 N85-23638
Mechanisms of basalt-plains ridge formation
13 p2199 N85-23643
On the absence of strike-slip faults from the planets and satellites 13 p2200 N85-23645
Lithologic and structural control on slope morphology in the Valles Marineris 13 p2201 N85-23651
Valles Marineris basin beds: A complex story
13 p2201 N85-23652
Kasei Vallis of Mars: Dating the interplay of tectonics and geomorphology 13 p2201 N85-23654

Mars geologic mapping: A review and new concepts
13 p2202 N85-23663
Mars planimetric mapping 13 p2203 N85-23666
The Mars ancient cratered terrain, smooth plains boundary: Implications of Viking color data for evolution of the Amenthes Region 15 p2682 N85-26564
Mars: Seasonally variable radar reflectivity
15 p2683 N85-26570
Dust devils on Mars 15 p2683 N85-26573
Geological analyses of the surface of Venus and Mars from lander spacecraft images and orbital radar observations 19 p3384 N85-30993
Lunar and Martian impact basins: Exposed records of terrestrial bombardment? 21 p3721 N85-33090

MARS VOLCANOES
Mars 09 p1411 N85-18694
Emplacement of long lava flows on Mauna Loa (Hawaii) and Alba (Mars) 13 p2186 N85-23563
Geologic interpretation of remote sensing data for the Martian volcano, Ascraeus Mons
13 p2194 N85-23608
Geologic interpretation of remote sensing data for the Martian volcano Ascraeus Mons
19 p3384 N85-30992
Geomorphic classification of Icelandic and Martian volcanoes: Limitations of comparative planetology research from LANDSAT and Viking orbiter images
21 p3603 N85-32372

MARSHES
U MARSHLANDS

MARSHLANDS
Remote sensing of coastal wetlands biomass using Thematic Mapper wavebands — Lewes, Delaware
13 p2119 N85-23198

MARTENSITE
Structural changes with one- and two-stage aging of alloys Ti-Al-Mo-Fe and Ti-Zr-V-Al-Sn
15 p2499 N85-25415
The state of martensite after quenching in a magnetic field
[BLL-BISI-TRANS-22297-(9022.06)]
17 p2926 N85-28051
The structure of carbon martensite analyzed with Mossebauer spectra
[BLL-BISI-TRANS-22402-(9022.06)]
17 p2927 N85-28082
Mechanical stabilization of austenite against epsilon martensite and its effect on deformation behavior in high manganese steels
[DE85-007654] 17 p2932 N85-28097
Fatigue crack propagation characteristics and fatigue fracture toughness in 780 MPa grade high strength steel weldments at low temperature
[BLL-BISI-TRANS-22369-(9022.06)]
17 p2979 N85-28411
Shape memory effect in uranium-niobium alloys below room temperature
[DE85-012964] 23 p3916 N85-34268
Decomposition of martensite in R6M5 and R6AM5 steels after direct immersion in liquid nitrogen
[BLL-M-36305] 24 p4077 N85-35268

MARTENSITIC STAINLESS STEELS
Microstructure and deformation aspects of some specialty steels and hard metals
02 p0176 N85-11182
Maraging steels: Structure, properties and applications 02 p0177 N85-11191
Metallurgy of a 12 percent chromium stainless steel
02 p0178 N85-11195
Mechanism of titanium impact on brittle tendency in delayed deformation of martensite-aging steels
11 p1604 N85-20087
The role of void nucleation in the swelling resistance of ferritic steel
[AERE-R-11525] 11 p1610 N85-20122

MARTENSITIC TRANSFORMATION
Fatigue crack propagation in metastable titanium alloys
[AD-A145824] 03 p0372 N85-12376
Effect of phase state of TiC-NiTi powder composite materials on nature of failure and mechanical properties
13 p2027 N85-22702
Mechanical properties of cast Martensitic high-strength multicomponent titanium alloys
15 p2514 N85-25514
Textural transformations taking place during heat and mechanical treatment in triplex steels
[BLL-BISI-TRANS-22404-(9022.06)]
17 p2927 N85-28063
Influence of structural state and alloy content of austenite on formation of martensitic phases in steels
[BLL-BISI-TRANS-22365-(9022.06)]
17 p2928 N85-28066
The mechanics of internal stress and microcrack toughening mechanisms in ceramics
[AD-A154049] 19 p3248 N85-30139
The effect of prior parent phase cold work on martensite transformation in Cu-Zn-Al shape memory alloys
[AD-A155140] 21 p3586 N85-32183
Electrical resistivity and hysteresis of the equiatomic nickel-titanium alloy near the martensitic transformation temperature 23 p3904 N85-34181
Decomposition of martensite in R6M5 and R6AM5 steels after direct immersion in liquid nitrogen
[BLL-M-36305] 24 p4077 N85-35268

MARTINGALES
Applications of functional analytic and Martingale methods
[AD-A145555] 02 p0255 N85-11672
The growth and composition of supercritical branching populations on general type spaces
[CTH-MATH-1984-18] 05 p0721 N85-14631
An on-line parameter estimation algorithm for counting process observations
[CWI-OS-R8406] 05 p0721 N85-14632
A note on two papers in dependent central limit theory
[CWI-MS-R8410] 05 p0722 N85-14636
A martingale approach to supercritical (C-M-J) branching processes
[CTH-MATH-1984-25] 05 p0722 N85-14643

MARYLAND
Erosion and sedimentation chronology of three watersheds in Maryland
[PB84-207356] 01 p0071 N85-10467

MASCONS
The non-hydrostatic figures of the terrestrial planets
22 p3858 N85-33887

MASER OUTPUTS
Software for Crimea-Pushchino radiointerferometer
06 p0783 N85-15007
Fine structure of Alfven maser radiation
06 p0824 N85-15232
Electron-cyclotron maser emission during solar and stellar flares
[NASA-CR-175883] 17 p3054 N85-26907
Hydrogen maser oscillation at 10 K
18 p3106 N85-29241

MASER RESONATORS
U MASERS

MASERS
NT HYDROGEN MASERS
NT INTERSTELLAR MASERS
NT TRAVELING WAVE MASERS
NT WATER MASERS
A new maser effect in plasma turbulence
02 p0284 N85-11852
Passive maser using timesharing for control of the cavity and control of the oscillator on the line of stimulated emission
[AD-D011326] 07 p0969 N85-16151
Technology for satellite power conversion
[NASA-CR-174335] 09 p1343 N85-18451
The superconducting cavity stability ruby maser oscillator 17 p2967 N85-28324
Maser cavity servo-tuning system
[NASA-CASE-NPO-15890-1-CU]
18 p3093 N85-29143
The system design of a rubidium maser frequency standard 18 p3106 N85-29232
Operation of a quasioptical electron cyclotron maser
[DE85-008450] 18 p3113 N85-29276
Turbulence and wave particle interactions in solar-terrestrial plasmas
[NASA-CR-175970] 18 p3209 N85-29906
Cerenkov maser and Cerenkov laser devices
[AD-A155443] 21 p3592 N85-32324
USSR report: Physics and mathematics
[JPRS-UPM-85-004] 21 p3680 N85-32860

MASKING
Spatial and temporal visual masking and visibility
[AD-A151968] 16 p2642 N85-27524
Low defect, high purity crystalline layers grown by selective deposition
[NASA-CASE-NPO-15813-1] 19 p3373 N85-30922
Basic development of a 1.5 micrometer very large scale integrated technique, part 1-4
[BMFT-FB-T-85-032-PT-1-4] 20 p3449 N85-31417
SONTRAC: A solar neutron track chamber detector
[SH-9.1-12] 23 p4052 N85-35127

MASKS
Computerized circuit designs: Realization of masks to manufacture microwave circuits
[CNES-NT-107] 04 p0496 N85-13168
Hydrogen-oxygen (hydrox) breathing at 1.3MPa
[FOA-C-58015-H1] 09 p1364 N85-18577
Lithography radiation effects study
[AD-A149552] 10 p1468 N85-19260
DARPA/TTO program IR binary optics
[AD-A152196] 16 p2665 N85-27672
A prototype test chamber for fit testing of protective masks in the field
[FOA-C-40208-C1(C2)] 20 p3512 N85-31834

MASONRY
Finite element model for creep in composite masonry
[PB85-150324] 14 p2322 N85-24347

MASS
NT CENTER OF MASS
NT CRITICAL MASS
NT ELECTRON MASS
NT PARTICLE MASS
NT STELLAR MASS
Searching for top, Higgs, and supersymmetry: The minimum invariant mass technique
[DE84-014539] 01 p0119 N85-10813
Measurement of areal mass variation in Rayleigh-Taylor unstable targets
[AD-A145541] 02 p0198 N85-11325
A method for automatic water mass classification
[AD-D011405] 08 p1191 N85-17505
Hot stars: Six years of progress
11 p1743 N85-20963
Histological and compositional responses of bone to immobilization and other experimental conditions
[NASA-CR-175837] 16 p2841 N85-27518
The role of thermal motions of air particles for fireballs
[PUBL-59] 17 p3053 N85-26900
One mechanism for generation of wave disturbances in spectra of turbulent flows near ocean surface
19 p3269 N85-30397
Physics with low temperature antiproton
[DE85-009627] 19 p3355 N85-30798
Mass-discrimination during prolonged weightlessness
20 p3509 N85-31814
Plasma mass and effective inductance in a small railgun
[AD-A154844] 21 p3569 N85-32304

MASS DISTRIBUTION
Measurement of the inertial constants of a rigid or flexible structure of arbitrary shape through a vibration test
[NASA-TM-77557] 02 p0209 N85-11381
The origin and evolution of Uranus and Neptune
02 p0296 N85-11926
Satellite masses in the Uranus and Neptune systems
[PSI-CONTRIB-198] 02 p0301 N85-11947
The influence of stellar luminosity and temperature calibration on the determination of the initial mass function 05 p0740 N85-14760
Far infrared spectroscopy of (O III) in M82
06 p1249 N85-17863
Primer for mass metrology
[PB85-121424/GAR] 09 p1305 N85-18199
Effect of hitch positions on the performance of track-grouser systems
[AD-P004277] 09 p1406 N85-18853
Mass distribution and evolutionary scheme for central stars of planetary nebulae 11 p1751 N85-21012
Dynamics of gas disks in triaxial galaxies
13 p2171 N85-23469
Greenland ice sheet mass balance
15 p2603 N85-26043
Potential climatic effects on the Greenland ice sheet
15 p2603 N85-26044
Aluminum-air power cell: The M3-3 experiment
[DE85-006878] 18 p3006 N85-29168
Design of helicopter rotor blades for optimum dynamic characteristics
[NASA-CR-176076] 20 p3393 N85-31044

MASS DRIVERS (PAYLOAD DELIVERY)
Possibilities and limits of electromagnetic acceleration in space applications
[ILR-MITT-136] 02 p0193 N85-11292

MASS FILTERS
U FLUID FILTERS

MASS FLOW
Comparison of options for reduction of noise in the test section of the NASA Langley 4x7m wind tunnel, including reduction of nozzle area
[NASA-CR-172446-VOL-2] 05 p0726 N85-14667
Flow measurement device
[AD-D011432] 08 p1168 N85-17369
Methanol vaporization: Effects on volumetric efficiency and on determination of optimum fuel delivery system
[PB84-243914] 09 p1302 N85-18181
Field validation of statistically-based acceptance plan for bituminous airport pavements. Volume 2: Statistical analysis of Marshall properties of plant-produced bituminous materials
[FAA-PM-84-12-VOL-2] 12 p1781 N85-21181
Mathematical modeling of transient performance of gas turbine engine 13 p2050 N85-22834
Turbulence measurements in shock induced flows
13 p2091 N85-23055
Effective specific impulse of secondary flow injected into a rocket nozzle
[NAL-TR-848T] 18 p3067 N85-29670

Quasi non-intrusive sampling and analysis of gases associated with the boundary layer on the tethered satellite and similar supersonic and hypersonic research vehicles
[NASA-CR-176075] 20 p3407 N85-31140
Free zone electrophoresis simulation of static column electrophoresis in microgravity on shuttle flight STS-3
20 p3502 N85-31773
Microgravity electrophoresis: A study of the factors that affect free-fluid separation 20 p3502 N85-31774
Pre-flight report on cultured human embryonic kidney cell handling and cell electrophoresis. Prepared prior to continuous-flow electrophoretic separation experiments aboard space shuttle flight STS-8
20 p3503 N85-31775
Properties of electrophoretic fractions of human embryonic kidney cells separated on space shuttle flight STS-8 20 p3503 N85-31776
Flow cytometry of human embryonic kidney cells: A light scattering approach 20 p3503 N85-31778
Heat-mass flow enhancement system for a metal hydride assembly
[DE85-010686] 22 p3783 N85-33441
The balancing of complex linkage mechanisms
23 p3924 N85-34313

MASS FLOW RATE
Finite element method for a class of viscoelastic flows in deforming domains applied to jet breakup
[DE84-014571] 04 p0500 N85-13186
Surge transient simulation in turbo-jet engine
05 p0596 N85-13796
Halogen mass flow rate detection system
[AD-D011388] 08 p1166 N85-17352
An episodic red-wing structure of SiIV, lambda 1394A, in gamma Cas 11 p1750 N85-21009
Calibration of sonic valves for the laminar flow control, leading-edge flight test
[NASA-TP-2423] 14 p2210 N85-23707
Deep water formation 15 p2601 N85-26030
Density and confinement effects on mixing characteristics of an axisymmetrical CO(2) jet
[AD-A154468] 19 p3267 N85-30258

MASS RATIOS
NT MASS TO LIGHT RATIOS
Satellite physical and orbital characteristics
16 p2604 N85-27267

MASS SPECTRA
Experimental medium energy physics
[DE84-014625] 02 p0278 N85-11607
Nitriding of titanium and its alloys by N2, NH3 or mixtures of N2 + H2 in a dc arc plasma at low pressures (or = to torr)
[NASA-TM-83803] 06 p0614 N85-15168
Mass analysis of neutral particles and ions released during electrical breakdowns on spacecraft surfaces
[NASA-CR-175585] 12 p1793 N85-21250
Analysis of biological particles by mass spectrometry
[AD-A149652] 13 p2141 N85-23291
The muon content of EAS as a function of primary energy
[OG-5.1-6] 22 p3881 N85-34050
Mass resolution optimization in a large isotopic composition experiment
[OG-9.1-6] 23 p4023 N85-34935

MASS SPECTROMETERS
Advanced mass spectrometers for hydrogen isotope analyses
[DE85-000716] 06 p0611 N85-15150
The design of an ion-neutral mass spectrometer to be used in the Shuttle environment
[AD-A148093] 08 p1114 N85-17022
A cometary ion mass spectrometer
[NASA-CR-174328] 08 p1164 N85-17343
Laser ablation studies using RIS
[DE85-001116] 09 p1326 N85-18336
Documentation for an instrument database system
[DE84-017302] 09 p1472 N85-18826
A GC/MS (Gas Chromatograph/Mass Spectrometer) data management process. Part 1: User's guide, version 1.0
[PB85-116051] 12 p1803 N85-21309
Analyses via automated mass spectrometry (MS/DS)
12 p1947 N85-22227
A computer controlled mass spectrometer system for investigating the decomposition of non-metallic materials under atmospheric conditions 12 p1948 N85-22237
Mass spectra of neutral particles released during electrical breakdown of thin polymer films
13 p1998 N85-22511
Plasma environment effects on the Giotto Ion Mass Spectrometer 14 p2245 N85-23919
Extraction of ions from solutions at atmospheric pressure, mass spectrometric analysis of bioorganic substances 14 p2387 N85-24706
Galileo 15 p2668 N85-26601
An investigation of tropospheric ions
16 p2823 N85-27412
Mass spectrometry technology at the Jet Propulsion Laboratory (JPL) 18 p3157 N85-29552
Mass spectrometer based gas permeation apparatus
[DE85-011178] 19 p3273 N85-30299
Reactions of metal ions and their clusters in the gas phase using laser ionization-ion cyclotron resonance spectroscopy
[DE85-009478] 19 p3361 N85-30836
A retarding ion mass spectrometer for the Dynamics Explorer-1
[NASA-CR-171586] 21 p3589 N85-32303
Fabrication and test of modified quadrupole mass spectrometer
[AD-A155186] 21 p3590 N85-32312
Analysis of spacecraft data
[NASA-CR-171567] 21 p3689 N85-32789
Ion composition measurements of the disturbed and quiet D-region in 1980 - 1981
[AD-A156055] 24 p4117 N85-35521

MASS SPECTROMETRY
U MASS SPECTROSCOPY

MASS SPECTROSCOPY
Supercritical fluid chromatography/supersonic jet spectroscopy
[DE84-016199] 04 p0471 N85-12998
Cardiac output measured by mass spectroscopy
05 p0692 N85-14449
Advanced mass spectrometers for hydrogen isotope analyses
[DE85-000716] 06 p0611 N85-15150
An optical and mass spectrometric study of the aluminum-oxygen flame
[AD-A147434] 07 p0923 N85-15849
Nondestructive evaluation of titanium alloys. ESCA (Electron Spectroscopy for Chemical Analysis), ISS (Ion Scattering Spectroscopy), and SIMS (Secondary Ion Mass Spectrometry) examination of titanium alloy solid surfaces
[AD-P004135] 08 p1128 N85-17110
Analysis of middle distillate fuels by high resolution field ionization mass spectrometry
[AD-A147724] 08 p1135 N85-17153
Mass spectrometry/mass spectrometry as a screening method for detecting explosive vapors
[DE85-001278] 09 p1292 N85-18110
Supersonic molecular jet study of the liquid state
[AD-A147416] 09 p1379 N85-18671
Comparative evaluation of GC/MS (Gas Chromatography/Mass Spectrometry) data analysis processing
[PB85-125684] 11 p1596 N85-20037
Instrumentation for Application Number 1: Mass spectrometric analysis of the boundary layer associated with the tethered satellite 11 p1646 N85-20372
A GC/MS (Gas Chromatograph/Mass Spectrometer) data management process. Part 2: Program documentation, version 1.0
[PB85-116069] 12 p1803 N85-21310
New high resolution scanning ion microprobe and focused ion beam applications
[AD-A149992] 12 p1852 N85-21616
Analyses via automated mass spectrometry (MS/DS)
12 p1947 N85-22227
Analysis of biological particles by mass spectrometry
[AD-A149952] 13 p2141 N85-23291
Collaborative shock tube studies of benzene pyrolysis
[DE85-006347] 14 p2253 N85-23962
Glueball candidates
[DE85-003627] 14 p2418 N85-24921
Secondary ion mass spectrometry studies of solids and surfaces
[AD-A151744] 16 p2745 N85-26939
Photoionization mass spectrometry with VUV hydrogen laser source
[AD-A153362] 17 p2921 N85-29009
Resonance ionization mass spectrometry of carbon
[DE85-009040] 17 p2923 N85-29018
Morphological stability and fluid dynamics of vapor crystal growth
[NASA-CR-175879] 17 p3042 N85-29822
Mass spectrometry technology at the Jet Propulsion Laboratory (JPL) 18 p3157 N85-29552
Selective detection of species in complex matrices by SIMS (Secondary Ion Mass Spectrometry)
[AD-D011685] 19 p3235 N85-30053
Measurement of combustion species by electron impact fluorescence
[DE85-011163] 19 p3236 N85-30065
Identification and quantification of nitropolynuclear aromatic hydrocarbons in ambient and indoor air particulate samples
[PB85-176790] 19 p3311 N85-30525
Quasi non-intrusive sampling and analysis of gases associated with the boundary layer on the tethered satellite and similar supersonic and hypersonic research vehicles
[NASA-CR-176075] 20 p3407 N85-31140
Micro-scale methods for characterization of supercritical fluid extraction and fractionation processes
[DE85-010968] 20 p3455 N85-31456
Compositional analysis of silicon
20 p3480 N85-31626
Aerosol analysis and emission spectrometry with free jets
[DE85-010676] 21 p3564 N85-32168
Determination of organobromide compounds in water by gas chromatography-negative ion chemical ionization mass spectrometry
[DRIC-T-7411] 22 p3743 N85-33199
Gas composition and molecule velocity in the detonation products of pentaerythritol tetranitrate (PETN) in expansion in a high vacuum container. Analysis by mass spectroscopy and time of flight spectrometry
[ISL-R-109/84] 22 p3747 N85-33226
Improved negative ion source
[DE85-008445] 23 p3912 N85-34241
Real time analysis of PETN detonation products
[DE85-009561] 23 p3922 N85-34303
Heats of formation of gas phase organosulfur molecules, radicals and ions measured by PEPICO and application of (17)O and (33)S NMR spectroscopy to structure determination of organosulfur compounds
[DE85-010558] 24 p4071 N85-35229
Gas analysis of ore-forming fluids
24 p4105 N85-35447
Ion composition measurements of the disturbed and quiet D-region in 1980 - 1981
[AD-A156055] 24 p4117 N85-35521

MASS TO LIGHT RATIOS
Calculation of Si(Li) X-ray detector efficiencies
[DE85-002732] 10 p1489 N85-19400
The muon content of EAS as a function of primary energy
[OG-5.1-6] 22 p3881 N85-34050

MASS TRANSFER
Second All-Union Seminar on Hydromechanics and Heat and Mass Exchange in Weightlessness, summaries of reports
[NASA-TM-77590] 01 p0047 N85-10305
The inducement of planetary boundary layer mass convergence associated with varying vorticity beneath tropospheric wind maximum 01 p0074 N85-10494
Bibliography of US patents on augmentation of convective heat and mass transfer, part 2
[DE84-014865] 04 p0498 N85-13178
Similarity considerations in 1-component 2-phase flow
[DE84-016370] 04 p0499 N85-13184
Investigation of an ejector heat pump by analytical methods
[DE84-016675] 04 p0500 N85-13189
Proposal for wall function for friction and heat transfer in the presence of roughness and mass transfer
[CFD/84/12] 04 p0501 N85-13198
Mass and momentum transport in a turbulent buoyant vertical axisymmetric jet 05 p0635 N85-14070
Development of a mass transfer machine for gas/liquid operations in the absence of gravity
[BMFT-FB-W-84-027] 05 p0637 N85-14091
Variability of short-term eddy-correlation estimates of mass exchange
[DE84-007271] 05 p0677 N85-14349
Investigation of the local mass transfer of a laminar and turbulent falling liquid film
[BLL-T6368/BG/WH792/84] 06 p0807 N85-15130
On the role played by lines in radiatively driven stellar winds depending on the position of the stars in the HR diagram 08 p1236 N85-17787
Multiline transfer and the dynamics of stellar winds
08 p1236 N85-17788
A one dimensional dynamical model of ocean/atmosphere interactions
09 p1358 N85-18545
Heat and mass exchange in a partially stratified fluid
[DE85-000528] 10 p1486 N85-19384
Formaldehyde and tracer gas transfer between airstreams in enthalpy-type air-to-air heat exchangers
[DE84-016951] 11 p1631 N85-20274
The eclipsing binary U Sagittae: Evidence for CNO processing and mass exchange in the past
11 p1757 N85-21049
Mechanisms of heat and mass transfer across a double-diffusive interface
[PB85-148408] 12 p1846 N85-21594
A survey for galactic plane ultraviolet-excess objects: Space densities for white dwarfs, subdwarfs, and cataclysmic variables 13 p2169 N85-23456
Seasonal and secular variation of the Solis Lacus albedo feature: Relation to the Martian dust-transport cycle
13 p2186 N85-23576
Eolian erosion on Mars: Three scales
13 p2186 N85-23577
The effect of particle density on aeolian transport
13 p2189 N85-23581

A comparison of terrestrial saltation flux in the laboratory and the field 13 p2189 N85-23582
Mass and heat transfer in reflux condensers of absorption heat pumps
[DFVLR-FB-83-43] 14 p2304 N85-24266
Dissolution of solid solutions in absence of internal mass transfer
[BLL-M-36092-(5828.4)] 16 p2748 N85-26959
Stefan-Maxwell relations for plasma diffusion currents in magnetic field 17 p2942 N85-28160
Transport in aqueous battery systems
[DE85-007246] 17 p2955 N85-28251
CALTECH-DOE program on numerical analysis, computing and fundamental studies of motion, energy and mass transfer in fluids
[DE85-006106] 17 p2959 N85-28274
Molten carbonate fuel cell performance model update
[DE85-003956] 17 p2966 N85-28454
Variability of short term eddy-correlation estimates of mass exchange
[PB85-172841] 18 p3136 N85-29431
Effect of multi-functional inhibitors on the electrochemistry within corrosion crack 19 p3238 N85-30075
Turbulent transport and length scale measurement experiments with confined coaxial jets
[NASA-CR-174831] 19 p3265 N85-30245
Thermomigration in porous media. Study of the development of a drying zone 20 p3456 N85-31462
Influence of spatial variability of hydraulic characteristics of soils on surface parameters obtained from remote sensing data in infrared and microwaves
[NASA-TM-77902] 20 p3477 N85-31604
Vaporization from a heated surface into a saturated stream
[DE85-010484] 20 p3530 N85-31958
New estimating procedures for surface runoff, sediment yield, and contaminant transport in Los Alamos County, New Mexico
[DE85-011690] 21 p3606 N85-32393
Vertical transport in the atmosphere: Measurement capabilities and requirements of VHF radars, part 1.6A 21 p3617 N85-32476
A new hypothesis for the observed vertical distribution of atmospheric aerosols 21 p3645 N85-32648
Size spectra for the source-enhanced coagulation with the turbulent mass transfer 21 p3645 N85-32649
Study of molecular diffusivity influence on mass transfer rate at a water-atmosphere interface 22 p3747 N85-33222
Advances in open-cycle solid desiccant cooling
[DE85-008797] 22 p3808 N85-33500
Determination of properties of zeolite/refrigerant combinations for solar refrigeration systems
[DE85-012009] 23 p3945 N85-34448
Studies in thermo-hydro-chemical transport in porous and fractured media
[DE85-012555] 23 p3949 N85-34473
Molecular and macromolecular sieving by asymmetric ultrafiltration membranes
[PB85-157706] 24 p4077 N85-35266

MASSACHUSETTS

Intraband radiometric performance of the LANDSAT 4 Thematic Mapper — Washington, DC, Arkansas, Massachusetts, Virginia, and Arizona 12 p1871 N85-21738

MASSIFS

Thematic mapping of likely target areas for the occurence of cassiterite in the Serra do Mocambo (GO) granitic massifs using LANDSAT 2 digital imaging
[E85-10027] 02 p0219 N85-11440
Earthquake activity in the Bohemian massif and in the western Carpathians
[REPT-547] 03 p0375 N85-12390
Geomorphology and geology of the Southwestern Margaritifer Sinus and Argyre regions of Mars. Part 1: Geological and geomorphological overview 13 p2192 N85-23600

MASTICATION

Characteristics of human masseter under conditions of hypokinesia 11 p1691 N85-20630

MATCHED FILTERS

Optical implementation of the synthetic discriminant function
[AD-A149562] 10 p1557 N85-19817
Fundamental limits to synchronization and tracking
[AD-A149823] 12 p1833 N85-21504
Acousto-optically addressed Fourier transform matched filters
[AD-A150298] 13 p2063 N85-22589
An investigation into generalized matched filter techniques
[BAE-BR-12971] 15 p2651 N85-26348
Rayleigh criteria resolution of optical correlations
[AD-A151711] 15 p2652 N85-26359
Compression of spread spectrum signals on an excessively dispersive channel
[AD-A155184] 21 p3576 N85-32240
Matched filtering of visual evoked potentials to detect acceleration (+Gz) induced blackout
[AD-A155912] 24 p4131 N85-35609

MATCHING

Antenna matching device tuning for type ZhRU radiostations 08 p0785 N85-15017
The combinatorics of local constraints in model-based recognition and localization
[AD-A148338] 08 p1230 N85-17748
A generalized ordering constraint for stereo correspondence
[AD-A149182] 10 p1487 N85-19390
Individual differences in chromatic brightness matching
[AD-A148882] 10 p1529 N85-19641
Some facets of the tri-index assignment polytope
[AD-A149195] 10 p1547 N85-19753
On large matchings and cycles in sparse random graphs
[AD-A149184] 10 p1550 N85-19778
Multichannel digital processing of wideband signals 12 p1840 N85-21548
Dimensions of smooth mating parts with protective coatings 14 p2280 N85-24124
The effect of set size on color matching
[AD-A150899] 14 p2368 N85-24713
On matchings and Hamiltonian cycles in random graphs
[AD-A151015] 14 p2409 N85-24851
Further study of digital matching of dissimilar images
[AD-A153112] 17 p3019 N85-28672
Generalized planar matching
[AD-A154809] 21 p3677 N85-32842
Digital matched filter 22 p3765 N85-33339
Hierarchical chamfer matching
[FOA-C-30367-E1] 22 p3802 N85-33558

MATERIAL ABSORPTION

Characterization and selection of polymer materials for binary munitions storage. Part 2: Characterization of LLDPE resins
[AD-A148324] 08 p1133 N85-17144
Influence of chemical form, feeding regimen, and animal species on the gastrointestinal absorption of plutonium
[DE85-010291] 21 p3662 N85-32751

MATERIAL BALANCE

NT WATER BALANCE
Aluminum-air power cell: The M3-3 experiment
[DE85-008878] 18 p3096 N85-29166
Measurement of uranium enrichment for gaseous uranium at low pressure
[DE85-012697] 24 p4150 N85-35733

MATERIAL REMOVAL (MACHINING)

U MACHINING

MATERIALS

Thermodynamic calculations and the chemical vapour deposition of hard materials 02 p0179 N85-11200
Electrochemical investigations of novel electrode materials
[DE84-014952] 04 p0495 N85-13158
Online directory of databases for material properties
[DE84-016511] 09 p1402 N85-18824
A DOE directory of databases for material properties
[UCAR-10124] 11 p1739 N85-20937
Topics in optical materials and device research, 3. Volume 2
[AD-A149727] 12 p1911 N85-21996
Electrostatic forming and testing of polymer films on a 16-foot diameter test fixture
[NASA-TM-86326] 13 p2083 N85-22855
Low gravity exothermic heating/cooling apparatus
[NASA-CASE-MSC-25707-1] 18 p3104 N85-29214

MATERIALS HANDLING

NT GROUND HANDLING
NT PROPELLANT TRANSFER
NT REMOTE HANDLING
DoD Robotics Application Workshop Proceedings
[AD-A145867] 03 p0307 N85-11978
Depot modernization at the Defense Logistics Agency
[AD-P004008] 03 p0308 N85-11988
Future robotics program at San Antonio ALC (Air Logistics Center)
[AD-P004011] 03 p0309 N85-11991
Supply center processes
[AD-P004014] 03 p0309 N85-11993
Field applications for robotic materiel handling
[AD-P004016] 03 p0309 N85-11995
Testing the antifriction properties of alloys for heavily loaded bearings 06 p0780 N85-14990
Multi-directional straddle-lift carrier
[AD-D011315] 07 p0973 N85-16183
Improvements in linked-spar motion-compensated lifting system
[AD-D011413] 08 p1138 N85-17165
BI-PAC F-15 external fuel tank container modification
[AD-A148836] 09 p1260 N85-18083
Control of the manufacturing process and material flow in flexible manufacturing systems
[PNR-90234] 09 p1371 N85-18615
Material flow in the manufacturing system: Fault-diagnosis systems as support for the maintenance of highly automated manufacturing systems
[PNR-90236] 09 p1371 N85-18616
A review of hazard assessment procedures for liquid gun propellants
[AD-A149470] 10 p1457 N85-19182
Simplified grasping and manipulation with dextrous robot hands
[AD-A149962] 10 p1492 N85-19419
Hoist
[AD-D011458] 10 p1493 N85-19425
Automated parts storage and retrieval system positioning device and method
[AD-D011494] 11 p1647 N85-20379
Methods/materials matrix of ultimate disposal techniques for spilled hazardous materials
[PB85-116853] 12 p1885 N85-21833
Cargo handling system
[AD-D011589] 14 p2219 N85-23782
Auxiliary units for Robots 14 p2285 N85-24161
MI-8 helicopter cargo loading experiment for Arctic shipping 14 p2332 N85-24425
Development of molten carbonate fuel cell power plant technology
[DE84-016839] 14 p2352 N85-24536
West Europe report: Science and technology
[JPRS-WST-84-014] 15 p2536 N85-25647
Technological experiments on high-altitude rockets 16 p2725 N85-26818
Technological apparatus for laser treatment of materials 17 p2944 N85-28174
West Europe report: Science and technology
[JPRS-WST-84-037] 18 p3088 N85-29108
French, UK, Swedish research in powder metallurgy, HIP 18 p3088 N85-29109
Qualitative comparison of fusion reactor materials for waste handling and disposal
[DE85-010473] 19 p3360 N85-30830
Oil tank electrostatic charging report
[DRIC-T-6967] 20 p3436 N85-31319
A systematic plan for the continued study of dimensional stability of metallic alloys considered for the fabrication of cryogenic wind tunnel models
[NASA-CR-172449] 21 p3565 N85-32172
TNT equivalency of EAK explosive
[AD-A155737] 21 p3571 N85-32211
Basic cryogenics and materials. Phase 1
[NASA-CR-177932] 21 p3572 N85-32215
Monocellane and diallene, 1984 report
[DE85-008776] 22 p3752 N85-33262
Corrosion resistant storage container for radioactive material
[DE85-011666] 22 p3838 N85-33765
Office of Civilian Radioactive Waste Management
[DE85-012585] 22 p3839 N85-33774
Container for radioactive materials
[DE85-005757] 23 p3972 N85-34626
Laboratory vibration schedules
[AD-A155858] 24 p4084 N85-35186
Radiation safety problems in handling highly active tritium targets
[DE85-014268] 24 p4151 N85-35742

MATERIALS RECOVERY

NT NUCLEAR FUEL REPROCESSING
NT WATER RECLAMATION
Research and development work on a single cation specific membrane for the recovery of raw materials with electrodialysis
[BMFT-FB-T-84-163] 03 p0329 N85-12120
Investigation of internal fields and motions, radiation damages and recovery processes using beta and gamma active probe nuclei 03 p0427 N85-12726
Flow-based analyses of metal deformation processes: An overview 06 p0796 N85-15087
Microbiological method for the desiliconization of high-silica bauxites
[BLL-MINTEK-TR-1168-(5810.5759)] 07 p0925 N85-15864
Research and development work concerning liquid membranes
[BMFT-FB-T-84-227] 06 p1124 N85-17087
Adaptation of remelting procedures for the use of recycled metal in nickel-base superalloy castings
[PNR-90232] 09 p1297 N85-18149
Treatment of wastewater (red water) resulting from TNT (trinitrotoluene) purification
[AD-P004146] 09 p1348 N85-18482
Hydrolysis of plastic wastes with the aim of recovering and reprocessing the starting components (recycling)
[BMFT-FB-T-84-250] 12 p1865 N85-21828

Lead shortage hastens need for improved storage batteries 15 p2461 N85-25195
Microwave processing of lunar materials: Potential applications
[DE85-007223] 16 p2755 N85-27003
Michelle-derived catalysts for extended Schulz-Flory
[DE85-005656] 17 p2922 N85-28012
Conservation and substitution technology for critical metals in bearings and related components for industrial equipment and opportunities for improved bearing performance
[PB85-176246] 18 p3082 N85-29089
Counter current extraction system for tritium recovery from 17Li-83Pb
[DE85-010519] 19 p3240 N85-30090
Development of processes for the inclusion of radioactive waste in glass-metal compounds and ceramic materials
[BLL-CE-TRANS-6014-(9022.09)] 20 p3526 N85-31931
Measurement of uranium enrichment for gaseous uranium at low pressure
[DE85-012897] 24 p4150 N85-35733

MATERIALS SCIENCE
Non-oxide ceramics: A new class of engineering materials 02 p0179 N85-11199
USSR report: Engineering and equipment
[JPRS-UEQ-84-007] 06 p0775 N85-14954
Encapsulation materials and processing 06 p0830 N85-15269
West Europe report: Science and technology
[JPRS-WST-84-039] 07 p0936 N85-15929
Research and technology highlights of the Lewis Research Center
[NASA-TM-86899] 08 p1261 N85-17928
USSR report: Materials science and metallurgy
[JPRS-UMS-84-008] 10 p1442 N85-19068
Metals and Ceramics Division Materials Science Program
[DE85-003795] 11 p1592 N85-20012
USSR report: Materials science and metallurgy
[JPRS-UMS-84-005] 11 p1597 N85-20044
Research in surface sciences, disordered materials, and solidification and growth
[PB85-132140] 11 p1737 N85-20927
Technological and economic assessment of advanced ceramic materials. Volume 1: Summary and conclusions
[PB85-113082] 12 p1815 N85-21383
Thermal response of aircraft cabin ceiling materials during a post-crash, external fuel-spill, fire scenario
[PB85-145647] 14 p2220 N85-23764
Material research in microgravity
[NASA-TM-77626] 14 p2226 N85-23811
USSR report: Engineering and equipment
[JPRS-UEQ-84-005] 14 p2285 N85-24157
West Europe report: Science and technology
[JPRS-WST-84-020] 15 p2534 N85-25633
Activities of Istituto Elettrotecnico Nazionale Galileo Ferraris 18 p3199 N85-29845
USSR report: Materials Science and Metallurgy
[JPRS-UMS-85-005] 19 p3241 N85-30095
Proceedings of the Twentyseventh Japan Congress on Materials Research
[ISSN-0368-3141] 23 p3903 N85-34180

MATERIALS TESTING REACTORS
U NUCLEAR RESEARCH AND TEST REACTORS

MATERIALS TESTS
Measurement of material properties to Mbar pressures using time-resolved shock wave techniques
[DE85-007319] 15 p2556 N85-25780
Evaluation methods of ceramic fiber reinforced metal matrix composite 23 p3907 N85-34208

MATHEMATICAL ANALYSIS
U APPLICATIONS OF MATHEMATICS

MATHEMATICAL LOGIC
NT ALGORITHMS
NT BOOLEAN ALGEBRA
NT BOOLEAN FUNCTIONS
NT BOREL SETS
NT EQUIVALENCE
NT FORMULAS (MATHEMATICS)
NT LATTICES (MATHEMATICS)
NT PARSING ALGORITHMS
NT SET THEORY
NT SIMPLEX METHOD
NT THRESHOLD LOGIC
Model theory for infinitely deep languages
[ISSN-0355-0087] 01 p0101 N85-10674
Research topics: Multiprocessing algorithms for computational logic
[DE84-015500] 02 p0242 N85-11583
Belief structures
[AD-A147526] 07 p1036 N85-16575
Polyfith and environments for mathematical computation
[DE85-002967] 11 p1702 N85-20704
Universal file processing program for field programmable integrated circuits
[DE85-004384] 12 p1637 N85-21526
System of microprocessor instructions 22 p3770 N85-33362

MATHEMATICAL MODELS
NT ANALOG SIMULATION
NT BIOLOGICAL MODELS (MATHEMATICS)
NT DIGITAL SIMULATION
NT PETRI NETS
NT THOMAS-FERMI MODEL
Implementation of the supersonic triplet singularity into the USTORE computer code
[CSIR-NIAST-83/47] 01 p0001 N85-10006
Prediction of aerodynamic characteristics of fighter wings at high angles of attack
[AD-A145107] 01 p0003 N85-10017
Aerodynamics of airfoils subject to 3-dimensional periodic gusts
[AD-A145149] 01 p0003 N85-10018
Modular design attitude control system
[NASA-CR-171182] 01 p0016 N85-10096
Singular asymptotic expansions in nonlinear rotordynamics
[NASA-CR-174012] 01 p0017 N85-10100
Cumulative damage model for advanced composite materials
[AD-A144840] 01 p0022 N85-10135
Computer simulation of the shock initiation of detonation in solid explosives
[PML-1984-23] 01 p0033 N85-10207
A model for grain misalignment in cylindrical port motors
[AD-A144856] 01 p0034 N85-10210
Modelling the demand for construction
[CSIR-TWISK-322] 01 p0035 N85-10218
Predictor model for seasonal variations in skid resistance. Volume 2: Comprehensive report
[PB84-226620] 01 p0037 N85-10230
Battery optimization considerations
[DE84-014759] 01 p0044 N85-10288
DYNKIN: A computer program for the description of detailed gas reactions in interaction with gas dynamics
[AD-B085364] 01 p0046 N85-10296
Single viewpoint self calibration: A contribution to field calibration of recording chambers
[SER-C-289] 01 p0049 N85-10320
Economic model of calibration improvements for automatic test equipment
[PB84-217827] 01 p0051 N85-10335
Combustion modeling of a 2 cylinder cycle reciprocating engine
[AD-A144782] 01 p0055 N85-10364
Estimation of the threshold in fatigue crack initiation models: A Bayesian approach
[AD-A144847] 01 p0062 N85-10410
Development of advanced constitutive model for reinforced concrete
[AD-A145050] 01 p0062 N85-10411
A generalized mathematical solution for transient off tracking of single vehicles and truck combinations
[DM-2] 01 p0107 N85-10719
On the calculating models of permanent magnets
[AD-A145111] 01 p0115 N85-10780
KrCl lasers for fusion
[DE84-012210] 01 p0122 N85-10835
Reduction of nonlinear problems to Schroedinger or heat equations: Formation of Kepler orbits, singular solutions for hydrodynamical equations
[REPT-72] 01 p0129 N85-10892
Structure and evolution of the large scale solar and heliospheric magnetic fields
[NASA-CR-175268] 01 p0130 N85-10897
Enhanced TCAS 2/CDTI traffic Sensor digital simulation model and program description
[NASA-CR-172445] 02 p0136 N85-10927
Advanced composite stabilizer for Boeing 737 aircraft
[NASA-CR-168451] 02 p0137 N85-10934
Quasi-steady analysis of aircraft panel flammability
[AD-A145461] 02 p0138 N85-10938
Advances in electrophoretic separations 02 p0156 N85-11054
Satellite servicing: A business opportunity? 02 p0156 N85-11056
Cumulative damage model for advanced composite materials
[AD-A145441] 02 p0171 N85-11142
A study of environmental characterization of conventional and advanced aluminum alloys for selection and design. Phase 2: The breaking load test method
[NASA-CR-172387-PHASE-2] 02 p0182 N85-11219
Direct numerical simulation of curved turbulent channel flow
[NASA-TM-85974] 02 p0197 N85-11316
A constitutive modeling technique based on a generalized rheological model to predict the response of materials 02 p0207 N85-11368
Computer models and output, Spartan REM: Appendix B
[NASA-CR-171093] 02 p0208 N85-11376
Biophysical and spectral modeling for crop identification and assessment
[E85-10006] 02 p0215 N85-11419
Study on spectral/radiometric characteristics of the Thematic Mapper for land use applications
[E85-10021] 02 p0216 N85-11434
Theoretical development of Monte Carlo codes for modeling cumulus cloud fields
[NASA-CR-174063] 02 p0230 N85-11500
Northern Hemisphere atlas of 1-minute rainfall rates
[AD-A145411] 02 p0231 N85-11508
Southern Hemisphere atlas of 1-minute rainfall rates
[AD-A145421] 02 p0231 N85-11509
Description of the software acquisition process (SWAP) model
[AD-A145413] 02 p0241 N85-11573
Parallel searching and merging on ZMOB
[AD-A145424] 02 p0241 N85-11574
Trajectory estimation using combined time-of-arrival and velocity measurements
[DE84-015872] 02 p0242 N85-11582
Diagnosis based on description of structure and function
[AD-P003919] 02 p0245 N85-11599
Weighted distributions arising out of methods of ascertainment
[AD-A145615] 02 p0252 N85-11648
Likelihood estimation for generalized mixed exponential distributions
[AD-A145675] 02 p0252 N85-11651
Dynamics of symmetry breaking: Phase coherence in finite and random systems
[NOTA-INTERNA-813] 02 p0253 N85-11658
Unified approach to sensitivity and uncertainty analysis
[DE84-014049] 02 p0255 N85-11669
A mathematical theory of command and control structures
[AD-A145608] 02 p0256 N85-11675
Method of splitting for solution of problems in semiconductor physics 02 p0265 N85-11736
A simple transport model 02 p0284 N85-11853
Fractals: From snow flakes to galactic clusters
[NOTA-INTERNA-796] 02 p0296 N85-11918
Determination of equivalent model geometry for tunnel wall interference assessment/correction 03 p0314 N85-12031
Estimation of helicopter performance using a program based on blade element analysis
[AD-A146341] 03 p0318 N85-12055
Damping synthesis for a spacecraft using substructure and component data
[CRC-1365] 03 p0323 N85-12082
Chemoviscosity modeling for thermosetting resins - I
[NASA-CR-172443] 03 p0326 N85-12096
Kinematic synthesis of planar cam-link mechanisms for exact path and exact motion generation 03 p0341 N85-12189
Autoregressive modeling and the classification of land clutter — radar signatures
[ENST-C-84003] 03 p0356 N85-12292
Second order modeling of scalar turbulent flows 03 p0360 N85-12311
Comparison of predicted and measured friction for a tilt-pad thrust bearing with crown and roughness under hydrodynamic and mixed lubrication
[AD-A145752] 03 p0371 N85-12371
Numerical simulations of compliant material response to turbulent flow, revision 1
[AD-A145801] 03 p0372 N85-12373
A decomposable algorithm for contour surface display generation
[AD-A145783] 03 p0410 N85-12619
Least squares estimation of conditionally heteroscedastic autoregressions
[AD-A145994] 03 p0411 N85-12626
Prediction and modeling of helicopter noise
[AD-A145764] 03 p0415 N85-12656
Ways to improve management of Federal funded computerized models
[LCD-75-111] 03 p0435 N85-12771
A methodology for comparing the variable costs of the continuous and periodic review models
[AD-A146351] 03 p0436 N85-12776
A stochastic model for optimizing the consumption and exploration of nonrenewable natural resources
[INPE-2770-PRE/343] 03 p0440 N85-12804

Dynamical models for radio jets
03 p0449 N85-12664
Modelling viscous flow in turbomachinery
[PNR-90220] 04 p0457 N85-12698
Review of the attributes and performance of six urban diffusion models
[PB84-236650] 04 p0484 N85-13087
Mathematical modeling of assembly processes involving use of sensitized robots 04 p0486 N85-13111
A preliminary study of numerical simulation of thermoclutal convection of interest to crystal growth
[NASA-TP-2394] 04 p0496 N85-13175
Numerical modelling of the drying of porous materials
[DE84-013056] 04 p0499 N85-13181
Comparisons of secular variation in two-dipole and spherical harmonic models with observatory data in Eurasia, 1955-1975 04 p0521 N85-13330
Reversals of the Earth's magnetic field
04 p0521 N85-13332
Scattering models in the microwave regime
[NASA-CR-174001] 04 p0525 N85-13361
Outline of a new emissions model for military and civilian aircraft facilities
[DE84-016455] 04 p0531 N85-13394
Urban aerosol modeling
[PB84-233469] 04 p0532 N85-13401
Relationship between model complexity and data base quality for complex terrain tracer experiments
[DE84-015022] 04 p0539 N85-13429
Operational numerical forecasts: Survey and verification over the period 1978-1983
[KNMI-TR-49] 04 p0540 N85-13435
Computational models of crystals
[DE84-016831] 04 p0572 N85-13647
Model reduction for control system design
05 p0596 N85-13799
Theory of kinetics of impregnation of porous bodies
[BLL-M-35917-(5828.4)] 05 p0616 N85-13942
Parametric models for signal processing: Autoregressive (AR), Moving Average (MA) and mixed autoregressive with moving average (ARMA)
[ENST-84D001] 05 p0628 N85-14028
Damping capacity of a sealed squeeze film bearing
05 p0645 N85-14139
Theoretical analysis of the dynamic behavior of structures with a passenger car as example
05 p0649 N85-14170
The upwind power plant Manzanares
05 p0669 N85-14305
Structure and growth of the marine boundary layer
05 p0680 N85-14369
Implicit numerical methods in meteorology
05 p0686 N85-14408
Statistical time series models of pilot control with applications to instrument discrimination
05 p0700 N85-14489
Model estimation and identification of manual controller objectives in complex tracking tasks
05 p0700 N85-14494
Structure errors in system identification
05 p0700 N85-14496
Use of artificial intelligence and simple mathematics to analyze a physiological model 05 p0717 N85-14597
Mathematical models for the brightness temperature of object and environment in the microwave region
[ESA-TT-829] 05 p0718 N85-14610
Some error estimates for the p-version of the finite element method
[CTH-MATH-1984-21] 05 p0719 N85-14614
A comment on Rosen's comments on activation and inhibition
[CTH-MATH-1984-24] 05 p0719 N85-14617
Relaxation times for queueing systems
[CWI-OS-R8407] 05 p0719 N85-14618
Construction of a confidence region for linear functions with unknown parameters
[CTH-MATH-1984-17] 05 p0721 N85-14630
A martingale approach to supercritical (C-M-J) branching processes
[CTH-MATH-1984-25] 05 p0722 N85-14643
Polarity principle: Foundation for parallel digital signal processes 05 p0725 N85-14669
Analysis of flat finite antenna consisting of waveguide radiators 06 p0790 N85-15048
Individual geopotential coefficients of order 15 and 30, from resonant satellite orbits
[AD-A146887] 06 p0828 N85-15256
Summary of photovoltaic performance models
06 p0832 N85-15296
Practical application of IREPS (Integrated Refractive Effects Prediction System)
[AD-A146528] 06 p0838 N85-15323
Toward an improved FIPS cost-benefit methodology. Phase 2: Descriptive models, general purpose application software development and maintenance
[PB84-226943] 06 p0870 N85-15527
Tristatic tracking filter used by the multistatic measurement system
[AD-A146885] 07 p0911 N85-15769
Efficient computation of reflector antenna aperture distributions and far field patterns
[AD-A147367] 07 p0940 N85-15962
An asymptotic analysis of a transient p-n junction model
[AD-A147270] 07 p0947 N85-16004
Ensuring required metrological reliability of analog instrument channels by parametric compensation
07 p0955 N85-16050
Trends in development of software for computer-aided analysis of large-scale integrated circuits
07 p0955 N85-16055
Analysis of the heating process of a body in a melt
[BLL-M-36014-(5828.4)] 07 p0956 N85-16057
Numerical reconstruction of part of an actual blast-wave flow field to agree with available experimental data
[UTIAS-TN-251] 07 p0958 N85-16061
Numerical studies of interacting vortices
[NASA-TM-86325] 07 p0957 N85-16062
Growth/reflectance model interface for wheat and corresponding model
[E85-10058] 07 p0987 N85-16269
Forecasting water temperature decline and freeze-up in rivers
[AD-A147068] 07 p0987 N85-16274
Water and climate, study of one case
07 p1002 N85-16369
Experiments in forecasting atmospheric marine horizontal visibility using model output statistics with conditional probabilities of discretized parameters
[AD-A147574] 07 p1008 N85-16404
Model robust response surface designs: Scaling 2-level factorials
[AD-A147494] 07 p1033 N85-16556
Conjunctive and disjunctive item response functions
[AD-A147815] 07 p1033 N85-16561
Response surface designs
[AD-A147202] 07 p1035 N85-16569
Current and current shear effects in the parabolic approximation for underwater sound channels
[AD-A147633] 07 p1039 N85-16597
Austrian contributions to fuel rod failure models shown at the International Standard Problem (ISP)-14
[OEFZS-4276] 07 p1041 N85-16613
A simulation model for Air Launched Cruise Missile engine management
[AD-A147018] 07 p1051 N85-16672
A Generalized Escape System Simulation (GESS) computer program. Volume 2: GESS programmer's manual, version 2
[AD-A148383] 08 p1081 N85-16845
Mathematical models for space shuttle ground systems 08 p1097 N85-16933
Modeling techniques used in the communications link analysis and simulation system (CLASS)
08 p1100 N85-16953
Numerical simulation of the shock detonation transition 08 p1116 N85-17039
Modelling the thermal explosion phenomenon in solid propellants: The case of fixed and variable temperatures 08 p1117 N85-17044
Numerical modeling of steady, laminar free-convective boundary layer flow beneath heated or combusting horizontal surfaces 08 p1160 N85-17318
A study of Reynolds-stress closure model
[NASA-CR-174342] 08 p1161 N85-17324
Evolution of nonlinear wave groups on water of slowly-varying depth
[AD-A147947] 08 p1162 N85-17329
Papers of the 15th International Society for Photogrammetry and Remote Sensing (ISPRS) Congress — conferences
[TRITA-FMI-9] 08 p1175 N85-17406
Mathematical aspects of digital terrain information; Report from International Society for Photogrammetry and Remote Sensing (ISPRS) working group 3:3, 1980 - 1984 — photogrammetry 08 p1175 N85-17407
A comparative test of photogrammetrically sampled digital elevation models 08 p1175 N85-17408
Multimodels increase accuracy: Summary of an experiment — photogrammetry
08 p1175 N85-17409
Sequential data processing for photogrammetric acquisition of digital elevation models
08 p1176 N85-17413
Advanced development of an active neuromusculature response to mechanical stress
[AD-A148436] 08 p1196 N85-17536
Adapting logistics models to a microcomputer for interface with computer-aided design systems
[AD-A147666] 08 p1202 N85-17566
Improved stability and performance bounds using approximate models — control system design
[RR-260] 08 p1209 N85-17606
The EM algorithm for censored data
[AD-A148136] 08 p1212 N85-17628
Background detection and correction in multicomponent analysis
[AD-A148251] 08 p1212 N85-17626
Multicomponent calibration and quantitation methods
[AD-A148252] 08 p1212 N85-17629
On the ergodicity of bilinear time series models and some applications
[AD-A148032] 08 p1215 N85-17651
Production rate variations cost models
[AD-A147706] 08 p1228 N85-17732
The calculation of theoretical chromospheric models and the interpretation of solar spectra from rockets and spacecraft
[NASA-CR-174289] 08 p1259 N85-17922
Modeling of aircraft performance from flight test results using quasi steady-state test techniques
09 p1279 N85-18047
Battery response to pulse loads: A mathematical model
[DE85-001149] 09 p1316 N85-18277
The sensitivity analysis in k-epsilon turbulence modeling applied to jet flows 09 p1318 N85-18288
Three-dimensional vortex methods
[DE85-000391] 09 p1320 N85-18299
Two-dimensional modeling of conduction-mode laser welding
[DE85-001804] 09 p1327 N85-18341
Models for shock damage to marine structural materials 09 p1336 N85-18400
Structural modifications by viscoelastic elements
09 p1337 N85-18407
World Geodetic System, 1984
[AD-A147409] 09 p1342 N85-18445
Models for mixture experiments when the response depends on the total amount
[DE85-000370] 09 p1374 N85-18637
Study of mathematical models of mutation and selection in multi-locus systems
[DE85-000673] 09 p1376 N85-18648
Control of tractors on sloping ground
[AD-P004282] 09 p1408 N85-18869
A simple prediction model for soil compaction under various wheel loads and geometries as an aid to vehicle design
[AD-P004298] 09 p1409 N85-18875
Modeling and simulation of a fin actuation system
[AD-A149443] 10 p1428 N85-19005
Mathematical modeling of wave fields by superimposition of boundary waves in reflected earthquake waves method 10 p1501 N85-19476
Predicting the performance of distributed knowledge-based systems: A modeling approach
[AD-A149021] 10 p1545 N85-19738
Modelling and residual analysis of nonlinear auto-regressive time series in exponential variables
[AD-A149047] 10 p1550 N85-19776
Rock mechanics: Issues and research needs in the disposal of wastes in hydraulic fractures
[DE85-001399] 10 p1556 N85-19809
Thermodynamics of the reactive flow model
[DE85-004405] 10 p1565 N85-19870
Compensator development and examination of performance and robustness
[NASA-CR-175470] 11 p1627 N85-20244
Theoretical and experimental analysis of vertical, concentric-tube ground-coupled heat exchangers
[DE85-000474] 11 p1633 N85-20286
The use of analytical models to interpret data properly
[ERS-E.341] 11 p1651 N85-20399
The use of analytical models to interpret measured data properly. 1. General background theory
11 p1651 N85-20400
The use of analytical models to interpret measured data properly. 2. The application to modal analysis of structures 11 p1651 N85-20401
A three-dimensional geometric-physical model for conventional geodetic observations-observables, parameter estimation, and deformation analysis
[SER-C-298] 11 p1666 N85-20493
Performance of the SERI parallel-passage dehumidifier
[DE85-000509] 11 p1672 N85-20536
Research on the basic understanding of high efficiency in silicon solar cells
[DE85-000507] 11 p1672 N85-20537
Continued research in mesoscale air pollution simulation modeling. Volume 7: Mathematical modeling of urban aerosol dynamics
[PB85-137368] 11 p1679 N85-20584

Precursors for Brazilian magnetic anomalies from 1922 to 1969
[INPE-3283-PRE/605] 11 p1681 N85-20590
Resolution of 2-dimensional seismologic problems by a finite element approximation. Application to the Love wave propagation through the Atlantic border of the Iberic Peninsula 11 p1681 N85-20594
Resolution of 2-dimensional seismologic problems by a finite element approximation. Application to the Love wave propagation through the Atlantic border of the Iberic Peninsula. Appendix: Graphs of results — Lagrange coordinates 11 p1681 N85-20595
User's guide for the Photochemical Box Model (PBM)
[PB85-137164] 11 p1682 N85-20602
A method for reduction of ambiguity in segmentation of images
[INPE-3304-TDL/186] 11 p1697 N85-20664
Digital imaging processing
[INPE-3325-PRE/624] 11 p1701 N85-20696
Investigation of the output parameters of the pulsed neutron generator NGI-5
[DE85-001823] 11 p1725 N85-20849
Theory of resistivity-gradient-driven turbulence
[DE85-002175] 11 p1733 N85-20898
Cometary atmospheres: Modeling the spatial distribution of observed neutral radicals
[NASA-CR-175485] 11 p1765 N85-21098
Deflection model of a CT4-A undercarriage
[AD-A149778] 12 p1777 N85-21156
The influence on IR emission of engine parameters for an afterburn case. A sensitivity study on NATO infrared air target model (NIRATAM) version: 0.0
[AD-B089311L] 12 p1779 N85-21171
ACOSS 17 (Active Control of Space Structures)
[AD-A150007] 12 p1793 N85-21253
A computer analysis of the RF performance of a ground-mounted, air-supported radome
[AD-P004952] 12 p1824 N85-21446
Simulation of thermal and electromagnetic processes in induction plasmatrons 12 p1841 N85-21552
An investigation of compressible flows over open cavities including sheer layer thickness effects
[AD-A150086] 12 p1847 N85-21586
A new model for thin plates with rapidly varying thickness. Part 3: Comparison of different scalings
[AD-A149748] 12 p1866 N85-21704
Numerical simulation of static and dynamic shadow patterns using an atomistic description of crack initiation and propagation
[DE85-003226] 12 p1867 N85-21715
User's guide to the TAMW wheat model as implemented on the IBM 360/195 computer
[E85-10084] 12 p1873 N85-21749
Local behavior of solutions of an elliptic-parabolic equation
[AD-A149824] 12 p1920 N85-22057
Ordinary and proper location M-estimates for ARMA models, revised
[AD-A149705] 12 p1920 N85-22061
A review of some aspects of robust inference for time series
[AD-A149706] 12 p1923 N85-22062
A note on validity generalization procedures
[AD-A150065] 12 p1924 N85-22065
Surface forward scattering and reflection
[AD-A150115] 12 p1928 N85-22112
Singular asymptotic expansions in nonlinear rotordynamics 12 p1945 N85-22218
A mathematical formulation of the problem of optimal use of ground resources for future space missions 12 p1947 N85-22232
Computational mechanics: A perspective on problems and opportunities for increasing productivity and quality of engineering
[PB85-126106] 12 p1950 N85-22252
Simple theoretical models for composite rotor blades
[NASA-CR-175620] 13 p1971 N85-22382
Model reduction for control system design
[NASA-CR-170417] 13 p1975 N85-22398
Expansion of functions describing planetary surface and gravity field 13 p1978 N85-22410
Nontraditional method for determining unperturbed orbits of unknown space objects using incomplete optical observational data 13 p1979 N85-22417
An integral closed loop combustion stability model-status and review 13 p2003 N85-22563
Improved modeling of the open circuit voltage of solar cells 13 p2011 N85-22619
Some unique features of isentropic flow of gas under high pressures 13 p2043 N85-22788
Mathematical modeling of transient performance of gas turbine engine 13 p2050 N85-22834
Research efforts in support of resonance extraction studies. Volume 1: Improvement and validation of TWFD (Thin-Wire Frequency-Domain): A thin-wire frequency-domain scattering code
[AD-A150298] 13 p2054 N85-22864
Mathematical model of discriminator for signals with fluctuations and thermal noise 13 p2072 N85-22943
Mathematical model of electromagnetic suspension device with two control windings 13 p2074 N85-22954
Problem of diffraction by wavy surface: Comparison of numerical methods of solution 13 p2079 N85-22985
Mathematical modeling of two-frequency laser sounding of scattering media 13 p2089 N85-23045
Investigation of parabolic computational techniques for internal high-speed viscous flows
[NASA-CR-172555] 13 p2091 N85-23056
Numerical experiments with simple model of ocean climate 13 p2106 N85-23123
Numerical modeling of plane stick-slip fault 13 p2111 N85-23150
Mathematical modeling of results of geometric leveling in variable gravity field 13 p2114 N85-23170
The microwave propagation and backscattering characteristics of vegetation — wheat, sorghum, soybeans and corn fields in Kansas
[E85-10088] 13 p2122 N85-23213
Remanent magnetization model for the broken ridge satellite magnetic anomaly 13 p2123 N85-23219
Estimation of regional evapotranspiration using remotely sensed land surface temperature. Part 1: Measurement of evapotranspiration at the Environmental Research Center and determination of Priestley-Taylor parameter 13 p2125 N85-23233
Estimation of regional evapotranspiration using remotely sensed land surface temperature. Part 2: Application of equilibrium evaporation model to estimate evapotranspiration by remote sensing technique — Japan 13 p2125 N85-23234
Testing an energy balance model for estimating actual evapotranspiration using remotely sensed data — Hannover, West Germany barley and wheat fields 13 p2125 N85-23236
ROSS: An object-oriented language for constructing simulations
[AD-A150556] 13 p2147 N85-23330
On a mathematical structure for an image algebra
[AD-A150228] 13 p2150 N85-23348
The design of a unified package for the solution of stochastic petri net models
[AD-A150326] 13 p2151 N85-23354
Magnetic field interactions with material discontinuities
[AD-A150197] 13 p2154 N85-23373
A model for eclipsing cataclysmic variables 13 p2171 N85-23487
Impact crater scaling laws 13 p2181 N85-23532
Planetary interior modeling and tectonic implications 13 p2200 N85-23649
Elysium region, Mars: Tests of lithospheric loading models for the formation of tectonic features 13 p2200 N85-23650
An eigensystem realization algorithm for application to modal testing 14 p2233 N85-23842
Adaptive techniques for control of large space structures
[AD-A150957] 14 p2246 N85-23923
Model of normal and erosive burning of composite propellants
[ONERA-NT-1984-3] 14 p2263 N85-24024
Determining optimum service conditions for concentrator mirrors by methods of mathematically planned experiment 14 p2274 N85-24090
Basic EMC (Electromagnetic Compatibility) technology advancement for C3 systems. Volume 4E: Modeling of transmission lines. A comparison of lumped-circuit iterative models and the transmission line model
[AD-A150852] 14 p2291 N85-24201
Radiation heat transfer within an open-cycle MHD generator channel — mathematical models
[NLR-TR-83068-U] 14 p2304 N85-24267
Developement of a theoretical model to describe the interaction between electric discharge and supersonic flow of a pulsed CO laser
[DFVLR-FB-84-45] 14 p2310 N85-24301
Seismic analysis of rotating mechanical systems
[PB85-149599] 14 p2311 N85-24307
Interpretation of directional magnetotelluric soundings by analytical continuation method 14 p2343 N85-24488
Determination of crust and upper mantle density based on deep seismic sounding and gravimetry data, part 1 14 p2345 N85-24498
Modelling of photodegradation in solar cell modules of substrate and superstrate design made with ethylene-vinyl acetate as potent material
[NASA-CR-175690] 14 p2350 N85-24527
Adjustment of the national dispersion model for air pollution from elevated sources
[KNMI-TR-57] 14 p2353 N85-24540
The dawn-dusk asymmetry of particles near the neutral sheet of geomagnetotail 14 p2358 N85-24574
A study of terrain reductions, density anomalies and geophysical inversion methods in gravity field modelling
[AD-A150788] 14 p2373 N85-24668
Visual recognition of simple objects by a connection network
[AD-A151043] 14 p2389 N85-24718
Potential models — Earth gravity 14 p2396 N85-24764
Orbit reconstitution — satellite orbits 14 p2396 N85-24765
The generation of three-dimensional body-fitted coordinate systems for viscous flow problems
[AD-A150861] 14 p2408 N85-24848
Macro for fitting nonlinear models to Poisson distributed data
[DE84-006569] 14 p2412 N85-24871
Application of far-field models to the disposal of nuclear waste in geologic formations
[DE85-005489] 14 p2420 N85-24932
A fast ray tracing routine for laterally inhomogeneous media
[AD-A150984] 14 p2421 N85-24938
A system-level mathematical model for evaluation of power train performance of load-leveled electric-vehicles
[NASA-CR-175652] 14 p2434 N85-25009
Solar inverse theory 14 p2441 N85-25063
Numerical simulations of convectively excited gravity waves 14 p2444 N85-25082
Cosmic ray environment model for Earth orbit
[NASA-CR-175666] 14 p2455 N85-25165
Automatic Dynamic Aircraft Modeler (ADAM), volume 1
[AD-A151410] 15 p2471 N85-25252
Multi-rate digital autopilot modeling methodology
[AD-A152044] 15 p2474 N85-25272
Mathematical modeling of the AEDC (Arnold Engineering Development Center) propulsion wind tunnel (16T)
[AD-A151293] 15 p2475 N85-25275
Mathematical model for rollout of planet roving vehicle from landing craft 15 p2484 N85-25334
Local elastoplastic fracture of fibrous composite materials 15 p2497 N85-25405
The accuracy of approximate solutions in the analysis of fracture of composites
[NASA-CR-175738] 15 p2503 N85-25437
Mathematical aspect of welding technology research discussed 15 p2538 N85-25663
CSMP (Continuous System Modeling Program) modeling of brushless DC motors
[AD-A152043] 15 p2549 N85-25731
On coupling factors of explosion 15 p2551 N85-25747
A critical evaluation of various turbulence models as applied to internal fluid flows
[NASA-TP-2474] 15 p2554 N85-25757
Turbulence effects on a glow discharge as derived from continuity and energy considerations
[AD-A151838] 15 p2557 N85-25775
NPLOT: An interactive plotting program for NASTRAN finite element models 15 p2573 N85-25869
Ritz procedure for COSMIC/NASTRAN 15 p2575 N85-25877
Analysis of shell type structures subjected to time dependent mechanical and thermal loading
[NASA-CR-175747] 15 p2577 N85-25896
Modeling and optimization of a multiple-cell photovoltaic converter system 15 p2585 N85-25934
Operational methods for calculating atmospheric dispersion
[BLL-CE-TRANS-8040-(9022.09)] 15 p2588 N85-25955
Field validation of 6-particle puff model
[DE85-004073] 15 p2589 N85-25962
Numerical experiments of jet streak ageostrophic circulations using pseudo-geostrophic initialization and perspectives 15 p2590 N85-25969
A simulation experiment on the impact of geostationary temperature retrievals in numerical models 15 p2597 N85-26005
Numerical simulation of North Atlantic Sea ice variability, 1951 - 1980 15 p2603 N85-26040
Origin of the Greenland ice sheet 15 p2604 N85-26046
On geoid heights and flexure of the lithosphere at seamounts
[AD-A151220] 15 p2604 N85-26050

Description, validation, and modification of the Guyton model for space-flight applications. Part A. Guyton model of circulatory, fluid and electrolyte control. Part B. Modification of the Guyton model for circulatory, fluid and electrolyte control
[NASA-CR-171676] 15 p2616 N85-26122
Mathematical models relating to human thermoregulation: Basic assumptions, validation, and application. Parts A and B
[AD-A151556] 15 p2618 N85-26130
An MRTD-compatible bar pattern response model for TV and direct view sighting systems
[BAE-BT-12060] 15 p2620 N85-26146
The modeling and simulation of feedback control systems
[NASA-CR-171675] 15 p2632 N85-26225
On failure modeling, revised
[AD-A151411] 15 p2637 N85-26263
Lectures on probability and statistics
[DE85-007079] 15 p2641 N85-26291
Numerical modeling of gas dynamic phenomena during supersonic flow of viscous gas in channel with electrical flow discharge 15 p2643 N85-26304
Fundamental studies of structure borne noise for advanced turboprop applications
[NASA-CR-175737] 15 p2646 N85-26320
An application of the Rayleigh distribution to contract cost data
[AD-A151551] 15 p2664 N85-26441
The investigation of tethered satellite system dynamics
[NASA-CR-175855] 16 p2731 N85-26854
The effect of inaccuracies in structural models on the control of large space structures
[AD-A151794] 16 p2732 N85-26858
Evaluation of human exposures to low frequency fields 16 p2776 N85-27135
Theoretical and experimental comparisons of nearfield electrogalvanic fields due to nonlinear polarization layers
[AD-A152085] 16 p2779 N85-27149
Studies of structure and modeling in turbulent shear flows
[AD-A151807] 16 p2782 N85-27170
Two-d heat transfer through porous media with heat generation
[AD-A151965] 16 p2783 N85-27173
The development of a computational model for a two-dimensional turbulent flow. Part 1: Mathematical background --- solid fuel combustion
[VTH-LR-438-PT-1] 16 p2785 N85-27188
Optimal modeling with a minimum of local distortion
[REPT-18/1984] 16 p2797 N85-27243
Topex Gravity Model Development Team activities during fiscal year 1984
[NASA-TM-86208] 16 p2804 N85-27285
Atmospheric density model 16 p2805 N85-27297
Use of forest modeling to project acid rain effects
[DE85-005251] 16 p2821 N85-27400
Fluid-dynamic model of a downburst
[UTIAS-271] 16 p2829 N85-27441
General continuous formulations of atmospheric energy laws 16 p2830 N85-27448
A modeling analysis program for the JPL table mountain lo sodium cloud
[NASA-CR-175851] 16 p2833 N85-27468
Intercomparison of Radiation Codes in Climate Models (ICRCCM)
[DE85-007251] 16 p2835 N85-27487
Comparison of a diffusion model with dye dispersion measurements to study turbulence in coastal waters
[INPE-3492-PRE/729] 16 p2836 N85-27504
Sensitivity of conditions for lumping finite Markov chains
[AD-A152122] 16 p2855 N85-27804
An application of Markov chains to the problem of migration in inventory systems
[AD-A151954] 16 p2857 N85-27818
Sensitivity of the stationary distribution vector for an ergodic Markov chain
[DE85-006979] 16 p2857 N85-27821
Refinements in the computation of collision probabilities
[DE85-006118] 16 p2864 N85-27863
Kinetic theory and simulation of multi-species plasmas in Tokamaks excited with ICRF microwaves
[DE85-008119] 16 p2868 N85-27891
Polycrystalline semiconductor heterojunction modelling (CdS/CuInSe(sub)2)
[DE85-002913] 16 p2871 N85-27713
Inflation from extra dimensions
[DE85-007834] 16 p2883 N85-27787
An introduction to vortex breakdown and vortex core bursting
[NAE-AN-28] 17 p2892 N85-27829
Parameter identification results of tests in nonsteady symmetric flight with the Hawker Hunter Mk 7
[NLR-TR-83042-U] 17 p2897 N85-27860
Mathematical modeling and control of a large space structure as applied to a shuttle-antenna configuration
[AD-A153289] 17 p2910 N85-27939
Composite loads spectra for select space propulsion structural components: Probabilistic load model development 17 p2912 N85-27954
Hydrogen embrittlement of high-strength steel
[B6580075] 17 p2933 N85-28103
Navier-Stokes computational study of axisymmetric transonic turbulent flows with a two-equation model of turbulence
[AD-A152653] 17 p2958 N85-28265
Coherent structure reflective turbulent viscous flow modeling
[AD-A153086] 17 p2958 N85-28267
Statistical models used in analyzing the quality of welded tubes
[BLL-BISI-TRANS-22232-(9022.06)] 17 p2976 N85-28384
Earth observation modeling based on layer scattering matrices
[NLR-MP-84015-U] 17 p2984 N85-28440
Simplified analysis of Stirling engines and heat pumps
[DE85-008753] 17 p2986 N85-28457
Two-dimensional inverse kinematic problem: Application to the Saudi Arabian refraction profile 17 p2990 N85-28478
Crustal structure of the Red Sea-Arabian Shield transition 17 p2990 N85-28479
A crustal section for the Arabian Shield and adjacent Red Sea margin derived from first-arrival data 17 p2990 N85-28480
A seismic refraction profile across the Arabian Shield 17 p2990 N85-28481
A preliminary examination of the 1978 refraction profiles in Saudi Arabia 17 p2990 N85-28482
A comparison of crustal sections: Arabian Shield to the Red Sea 17 p2992 N85-28491
Solar radiance models for determination of ERBE scanner filter factor
[NASA-CR-172595] 17 p2995 N85-28513
Presentations at the Tri-Service Cloud Modeling Workshop (2nd), held at the Naval Surface Weapons Center, White Oak, Maryland, 26-27 June 1984, volume 1
[AD-A152735] 17 p2996 N85-28522
Parameterization of subgrid-scale fluxes in mesoscale meteorological models
[AD-A153016] 17 p2996 N85-28523
Mathematical modeling and simulation of climate and climatic change
[DE85-006974] 17 p2997 N85-28526
A new technique for system-to-system transfer of surface data 17 p3007 N85-28589
Optical phenomena in computer vision
[AD-A152970] 17 p3008 N85-28595
A discussion of adaptive grids and their applicability in numerical hydrodynamic modeling
[AD-A151843] 17 p3017 N85-28658
Deconvolution methods for multi-sensors
[AD-A152351] 17 p3018 N85-28660
Echo-response from crack-like two-dimensional reflectors in focused ultrasonic fields 17 p3027 N85-28724
Kirchhoff modeling via wave equation datuming
[AD-A152399] 17 p3028 N85-28727
Light scattering by leaf layers with application to canopy reflectance modeling: The Scattering by Arbitrarily Inclined Leaves (SAIL) model
[NLR-MP-84011-U] 17 p3038 N85-28796
Analysis of nonlinear parabolic equations modeling plasma diffusion across a magnetic field
[DE85-007883] 17 p3040 N85-28807
Continous chemical reaction chromatography
[DE85-006812] 18 p3072 N85-29098
Time-averaged and time-dependent computations of isothermal flowfields in a centerbody combustor
[AD-A153682] 18 p3100 N85-29189
Kalman filter modeling 18 p3107 N85-29237
Relationship between Allan variances and Kalman Filter parameters 18 p3107 N85-29238
Description and illustration of the use of CRACKS IV
[AD-A153543] 18 p3121 N85-29325
Conceptual hydrologic model of flow in the unsaturated zone, Yucca Mountain, Nevada
[DE85-006346] 18 p3125 N85-29350
F-cell: The Aspen fuel cell model
[DE85-001975] 18 p3131 N85-29383
Thermal performance testing and mathematically modeling of integral collector storage solar hot water systems
[PB85-186006] 18 p3132 N85-29396
Vertical redistribution of a pollutant tracer due to cumulus convection
[PB85-172971] 18 p3134 N85-29415
Wave-theoretical approach to seismic modeling problems (WELMOD)
[BMFT-FB-T-84-258] 18 p3137 N85-29429
High-latitude filtering in a global grid-point model using model normal modes 18 p3140 N85-29442
A numerical study of the Pacific polar low
[AD-A153777] 18 p3149 N85-29495
Utilization of the SEASAT scatterometer winds for ocean mixed layer modeling
[AD-A153748] 18 p3150 N85-29506
Image processing: Mathematics, engineering or art
[DE85-007666] 18 p3154 N85-29527
Atmosphere behavior in gas-closed mouse-algal systems: An experimental and modelling study 18 p3155 N85-29536
Distribution of mathematical software via electronic mail
[DE85-009664] 18 p3166 N85-29617
The role of ellipticity and normality assumptions in formulating live-boundary conditions in elasticity
[AD-A153475] 18 p3166 N85-29630
Bayesian full rank marginalization for 2-way contingency tables
[AD-A153841] 18 p3171 N85-29649
Monotonicity preserving bicubic interpolation
[DE85-004206] 18 p3172 N85-29657
Nonparametric renewal function estimation
[AD-A153474] 18 p3173 N85-29672
A robust estimator of location using an adaptive spline model
[AD-A153662] 18 p3174 N85-29676
An extended two-target differential game model for medium-range air combat game analysis
[NASA-CR-175868] 18 p3175 N85-29687
Further studies of the NRL collective particle accelerator via numerical modeling with the MAGIC code
[AD-A153563] 18 p3176 N85-29703
Electron multiple, plural and single scattering
[DE85-010325] 18 p3181 N85-29721
Plasma engineering models of tandem mirror devices with high-field test-cell inserts
[DE85-010048] 18 p3192 N85-29797
Numerical simulations of the effect of floor and ceiling venting on fire and smoke spread in aircraft cabins
[PB85-178333] 19 p3216 N85-29939
Outside users payload model
[NASA-CR-176011] 19 p3223 N85-29986
On the accuracy of modeling the dynamics of large space structures 19 p3225 N85-29995
Accelerator column models for low-current beams
[DE85-010722] 19 p3262 N85-30226
Turbulent transport and length scale measurement experiments with confined coaxial jets
[NASA-CR-174831] 19 p3265 N85-30245
Use of a two-dimensional flow model to quantify aquatic habitat
[AD-A154287] 19 p3266 N85-30253
A method for predicting additive drag reduction from small-diameter pipe flows
[AD-A154411] 19 p3266 N85-30254
Thermal performance and design of a solid particle cavity receiver
[DE85-010830] 19 p3274 N85-30300
Laser forward and backscattering in particulate media
[AD-A154138] 19 p3275 N85-30312
A mathematical model of reciprocating combustion engine dynamics for the diagnosis of deficient energy conversion 19 p3280 N85-30339
Computational methods in advanced stress and durability analyses
[AD-A154119] 19 p3286 N85-30375
Plane Tsunami wave caused by elastic oscillations of ocean floor 19 p3290 N85-30403
Model computations of light reflection from sea surface 19 p3292 N85-30411
Method for computing evolution of random hydrodynamic fields on basis of adjoint equations 19 p3292 N85-30412
Mathematical model of global processes in the biosphere 19 p3295 N85-30431
Institute works on modeling thermonuclear plasma processes 19 p3296 N85-30435
Using PVFORM, a systems performance model, to determine optimum mounting configurations for flat-plate photovoltaic modules
[DE86-011191] 19 p3306 N85-30495
F-CAP documentation
[DE86-003369] 19 p3307 N85-30503
Qualitative and quantitative examination of the performance of regional air quality models representing different modeling approaches
[DE85-010508] 19 p3310 N85-30518

MELSAR: A mesoscale air quality model for complex terrain. Volume 2: Appendices
[DE85-010991] 19 p3310 N85-30519
Analysis of leachate production in closed hazardous waste landfills
[DE85-010978] 19 p3310 N85-30520
Synthetic rainfall and its use in hydrologic modeling
19 p3314 N85-30542
A probabilistic forecasting model of tropical cyclone-generated storm surge for a straight coastline
19 p3314 N85-30544
Atmospheric planetary wave response to external forcing
[NASA-CR-176000] 19 p3315 N85-30548
A global low order spectral model designed for climate sensitivity studies
[NASA-CR-176099] 19 p3316 N85-30549
Effects of relative humidity gradients on the evaluation of submicron aerosol flux measurements in the atmospheric surface layer
[DE85-010510] 19 p3316 N85-30555
Effect of vertical shear on regional-scale trajectories in near-frontal conditions
[DE85-007554] 19 p3317 N85-30561
Examination of the time and spatial scales appropriate for the carbon dioxide climate change issue
[DE85-009852] 19 p3317 N85-30563
Geometry, velocity structure and penetration depths of descending slabs in the western Pacific
19 p3319 N85-30574
Evolution of the oceanic upper mantle and effects on sea floor subsidence geoid height and heat flow
19 p3319 N85-30575
An approach to modeling database activity
19 p3332 N85-30642
Estimating ability with the wrong model
[AD-A154071] 19 p3335 N85-30663
High gain adaptive control of decentralized systems
[DE85-010040] 19 p3339 N85-30688
Performance and library issues for mathematical software on high performance computers
[DE85-010269] 19 p3339 N85-30690
Identification of a mathematical model 1: Goodness of fit criterion
[HSE-TRANS-11109] 19 p3341 N85-30703
Expanding expertise by use of an expert system
[DE85-010759] 19 p3344 N85-30723
One-dimensional hybrid code for FRM dynamics
[DE85-010667] 19 p3361 N85-30840
Modulation transfer function for two-point and periodic objects using Gaussian and Lorentzian resolution functions
[PB85-167557] 19 p3368 N85-30891
Perspectives of nonlinear dynamics
[IFPJ-723] 19 p3370 N85-30902
Plasma radiation sources. Quasi-adiabatic theory and numerical modeling in the electro-diffusive approximation
[AD-A154375] 19 p3370 N85-30906
Steady-state spheromak reactor studies
[DE85-009666] 19 p3372 N85-30916
A study on the control of third generation spacecraft
20 p3415 N85-31196
An Eigensystem Realization Algorithm (ERA) for modal parameter identification and model reduction
20 p3418 N85-31212
Ion thruster performance model
20 p3420 N85-31226
Conditional modeling in turbulent shear flows
20 p3424 N85-31250
Computer-controlled carburizing
[BLL-OA-TRANS-5204-(6196.300)]
20 p3429 N85-31268
Scattering models in signal processing
20 p3439 N85-31339
Modeling taper charge with a non-linear equation
20 p3445 N85-31390
Informatics Division 20 p3449 N85-31416
Numerical and experimental investigation of turbomachinery rotor flow fields
20 p3451 N85-31429
Turbulence modeling in a two-dimensional wake
20 p3452 N85-31431
Natural convection experiments in a stratified liquid-saturated porous medium
[DE85-009009] 20 p3455 N85-31457
Intermittent gas-liquid flow modeling in horizontal or weakly inclined pipes
[EME-132] 20 p3466 N85-31465
A theoretical model for the study of nonlinear dynamics of magnetic bearings 20 p3462 N85-31505
Theoretical modelling of the electro-chemistry in a corrosion fatigue crack. Part 2: Mathematical aspects of associated unsteady reaction equations
[NPL-DMA(A)-100-PT-2] 20 p3465 N85-31529
Numerical considerations in the development and implementation of constitutive models
20 p3467 N85-31541
On numerical integration and computer implementation of viscoplastic models 20 p3467 N85-31542
Numerical study of tensile fracture in plane stress
[ONERA-RT-22/7169-RY-070-R]
20 p3470 N85-31563
Mathematical model of the nitrogen cycle in a nonsaturated area of cultivated soil
20 p3478 N85-31610
Current status of one- and two-dimensional numerical models: Successes and limitations
20 p3482 N85-31636
Update on the evolution of the LAGEOS orbit
20 p3491 N85-31698
Error spectrum of Goddard satellite models for the gravity field 20 p3491 N85-31704
On development mechanisms for polar lows
20 p3495 N85-31727
Benthic boundary layer modelling studies
[IOS-161] 20 p3497 N85-31742
A systems analysis of the erythropoietic responses to weightlessness. Volume 1: Mathematical model simulations of the erythropoietic responses to weightlessness
[NASA-CR-171880] 20 p3506 N85-31794
A systems analysis of the erythropoietic responses to weightlessness. Volume 2: Description of the model of erythropoiesis regulation. Part A: Model for regulation of erythropoiesis. Part B: Detailed description of the model for regulation of erythropoiesis
[NASA-CR-171891] 20 p3506 N85-31795
Distributed implementation of functional program evaluation
[DE85-009573] 20 p3514 N85-31844
Exponential order statistic models of software reliability growth
[NASA-CR-3909] 20 p3515 N85-31852
SCAP: A Shaped Charge Analysis Program. User's manual for SCAP 1.0
[DE85-011182] 20 p3515 N85-31854
Time-implicit Monte-Carlo collision algorithm for particle-in-cell electron transport models
[DE85-010768] 20 p3521 N85-31900
Propagation and reflection of a finite amplitude ultrasonic beam including harmonic content: A numeric model
20 p3523 N85-31914
Source-term considerations for a potential radioactive-waste repository located in unsaturated tuff
[DE85-010090] 20 p3529 N85-31953
Aerodynamic characteristics of the standard dynamics model in coning motion at Mach 0.6
[NASA-TM-86717] 21 p3552 N85-32094
Development of reduced order models for control system design using the OPTSYSX program
[AD-A154552] 21 p3556 N85-32124
Injection of drag reducing additives into turbulent water flows: Two-component velocity measurements and mixing length model predictions
[AD-A154604] 21 p3583 N85-32274
Theoretical modeling of laser induced optical degradation
[AD-A155302] 21 p3592 N85-32323
A continuous damage model based on stepwise-stress creep rupture tests
[NASA-CR-174941] 21 p3597 N85-32341
Modelling and parameter estimation for distributed vibratory systems
[AD-A154518] 21 p3598 N85-32344
Development of improved dynamic failure models
[AD-A155586] 21 p3600 N85-32354
A new global geomorphology?
21 p3601 N85-32358
Modeling of the silane FBR system
21 p3609 N85-32415
Comprehensive silicon solar-cell computer modeling
21 p3609 N85-32421
Emergency modeling of hazardous air pollutants
[AD-A155441] 21 p3614 N85-32461
The Norwegian seismic array (NORSAR)
[AD-A154751] 21 p3631 N85-32555
The diurnal variation of the neutral sodium species in the upper atmosphere: A model study
[AD-A154986] 21 p3631 N85-32561
Development of ultrasonic modeling techniques for the study of crustal inhomogeneities
[AD-A155206] 21 p3632 N85-32565
Diagnostics of severe convection and subsynoptic scale ageostrophic circulations
[NASA-CR-171581] 21 p3634 N85-32571
Scavenging of submicron aerosol particles by snow crystals: Theory and experiments
21 p3648 N85-32667
A probabilistic method for particle size analysis of aerosols 21 p3648 N85-32669
A simple model to investigate the activation process in watercloude 21 p3649 N85-32675
Numerical modeling of sea ice dynamics and ice thickness characteristics
[AD-A154800] 21 p3654 N85-32700
Carbon and sulfur cycling through geologic time
21 p3658 N85-32720
An error-dependent model of instrument-scanning behavior in commercial airline pilots
[NASA-CR-3908] 21 p3665 N85-32765
Optimal low thrust transfer using a first-order perturbation model
[AD-A154781] 21 p3676 N85-32835
Theory of soliton waves
[AD-A154784] 21 p3676 N85-32837
Identification of unsteady aerodynamics and aeroelastic integro-differential systems
[NASA-TM-86749] 21 p3678 N85-32851
Diamagnetic instability of cyclotron waves in plasma
21 p3683 N85-32948
Asymptotically stable solutions of some nonlinear equations 21 p3686 N85-32974
Iteration solution for a submerged force-driven finite cylinder
[AD-A154567] 21 p3699 N85-32982
Overground Excess Sound Attenuation (ESA). Volume 3: Application of ESA data in NOISEFILE
[AD-A154820] 21 p3699 N85-32984
Lateral attenuation of aircraft flight noise
[AD-A154958] 21 p3700 N85-32986
Modeling the exhaust of the pulsed plasma thruster
[AD-A155344] 21 p3707 N85-33018
Feasibility of applications of Competition Decision Assist Package (CDAP) to spare parts
[AD-A154716] 21 p3712 N85-33036
Discrimination of linear contour elements of space photographs based on visual perception model
22 p3736 N85-33161
Modeling granular explosive detonations with shear band concepts
[DE85-011823] 22 p3754 N85-33271
Model that predicts pulse charged gas switching breakdown phenomena
[DE85-013119] 22 p3761 N85-33313
Method of estimating convergence of Haar coefficients in message compression problems
22 p3769 N85-33358
Analysis of crosstalk in nonhomogeneous multiconductor lines 22 p3769 N85-33360
Estimating optimum technical and economic indicators of data transmission systems 22 p3777 N85-33406
Pulsed hydrojet propulsion
[DE85-010771] 22 p3784 N85-33446
The calculation of two-dimensional buoyant surface jets with the k-W model of turbulence — kinetic energy-vorticity fluctuations (k-W)
[CFD/84/21] 22 p3785 N85-33449
Current internal-dosimetry practices at US Department of Energy facilities
[DE85-011718] 22 p3787 N85-33466
Numerical experiment of elastic wave propagation by framework model
[DRIC-T-7462] 22 p3795 N85-33511
Stochastic groundwater flow modeling using the second-order method
[DE85-011250] 22 p3802 N85-33556
Theory of cellwise optimization for solar central receiver system
[DE85-012586] 22 p3807 N85-33579
Estimation of Sr90 and Cs137 activity introduced and accumulation in the Po basin until 1963
[CISE-2515] 22 p3813 N85-33617
Model projections of time-dependent response to increasing carbon dioxide
[DE85-013326] 22 p3816 N85-33641
Data Base Workshop: Availability-Reliability Modeling
[DE85-011570] 22 p3829 N85-33713
Presentation of numerical simulation work in terminal ballistics using a few examples. Applications of the calculation model Program for Elastoplastic Simulation of Impacts (PEPSI) of the Franco-German Research Institute Saint Louis (ISL)
[ISL-CO-209/84] 22 p3834 N85-33741
A formulation and analysis of combat games
[NASA-TP-2487] 22 p3835 N85-33745
New formulation for linear accelerator design
[DE85-011171] 22 p3842 N85-33792
Late-stage planetesimals: How big?
22 p3852 N85-33857
Component-specific modeling
[NASA-CR-174765] 23 p3897 N85-34140
On high strain rate fragmentation of a closed vessel
23 p3904 N85-34187

Experimental evaluation of the thermodynamic properties of concentrated aqueous potassium hydroxide solutions
[DE85-010629] 23 p3912 N85-34238
Pressure-shear loading of PBX-9404
[DE85-009962] 23 p3921 N85-34298
Modeling heterogeneous high explosive burn with an explicit hot-spot process
[DE85-009593] 23 p3922 N85-34300
Three-dimensional hydrodynamic hot-spot model
[DE85-009587] 23 p3922 N85-34301
Detonation of condensed explosives: Evolution of knowledge in the last 40 years
[ISL-CO-228/84] 23 p3923 N85-34307
Finding the roots of the transcendental equations in problems in determining the thermal conductivity of spheres with heterogeneous boundary conditions
[BLL-M-35878-(5828.4)] 23 p3929 N85-34347
Preliminary SPR thermal model description and results for WH-11 and BM-4
[DE85-013171] 23 p3931 N85-34360
Detailed validation of a liquid and heat flow code against field performance
[DE85-009901] 23 p3932 N85-34368
Mathematical modeling of ultimate heat sink cooling ponds
[TI85-009747] 23 p3932 N85-34369
Modeling of geothermal systems
[DE85-012553] 23 p3943 N85-34439
Ocean thermal energy conversion
[DE85-012291] 23 p3946 N85-34456
Evaluation of source strength and dispersion model predications with data from large nitrogen tetroxide field experiments
[DE85-011855] 23 p3947 N85-34465
Graph-theoretical exorcism
[DE85-011916] 23 p3955 N85-34512
Computer analysis techniques for the temporal evaluation of cardiac wall motion
23 p3958 N85-34530
A user-friendly computer-aided construction of boundaries 23 p3962 N85-34564
Numerical solutions of the Vlasov equation
23 p3979 N85-34672
Cubic interpolated pseudo-particle method (CIP) for solving hyperbolic-type equation
23 p3979 N85-34673
Numerical simulation in astrophysics: Smoothed particle methods 23 p3979 N85-34674
Moving finite element method for ICF target implosion
23 p3980 N85-34675
Dissipation terms in one-dimensional hydrodynamic code for ICF target 23 p3980 N85-34677
Simulation of instability of cylindrically converging shock waves 23 p3980 N85-34679
On the heat flux derived by the moment method in Lorentzian plasma between hot and cold walls
23 p3980 N85-34682
Observation of helical sawtooth oscillations in a tokamak
[DE85-012062] 23 p3983 N85-34703
The 1973-1984 solar modulation of cosmic ray nuclei
[SH-4.1-16] 23 p4006 N85-34838
Evidence for regions of negligible cosmic-ray modulation in the inner heliosphere (10 AU)
[SH-4.1-21] 23 p4006 N85-34840
Drift and observations in cosmic-ray modulation, 2
[SH-4.2-5] 23 p4007 N85-34843
Electron capture decay of cosmic rays: A model of the inhomogeneous interstellar medium
[OG-7.1-10] 23 p4014 N85-34871
The model-independence of cosmic ray source determinations
[OG-7.2-1] 23 p4014 N85-34873
Explanation of the secondary to primary ratio within the continuous Fermi accelerator model
[OG-8.3-2] 23 p4021 N85-34921
Empirical model for the Earth's cosmic ray shadow at 400 KM: Prohibited cosmic ray access
[SH-6.1-14] 23 p4046 N85-35087
Chemoviscosity modeling for thermosetting resins, 2
[NASA-CR-177958] 24 p4073 N85-35243
An analytical and numerical model of radiation heat transfer in direct injection-type diesel combustion
24 p4092 N85-35368
Studies on effects of boundary conditions in confined turbulent flow predictions
[NASA-CR-3929] 24 p4093 N85-35371
Transient three-phase three-component systems. Part 1: Formulation of the system of differential equations
[DE85-013267] 24 p4095 N85-35384
Development of a mathematical model for predicting the percentage fatigue life increase resulting from shot peened components
[AD-A155774] 24 p4101 N85-35425
An atmospheric boundary layer model forced by the operational ECMWF-model
[WSR-3] 24 p4120 N85-35541
A mechanical model of the human body and its application 24 p4129 N85-35598
Benchmark evaluation of PC almacript
[AD-A156133] 24 p4138 N85-35651
Algorithmic approaches in sets of good answers in inverse problems
[PM/84/18] 24 p4142 N85-35677
Constrained stiffness matrix adjustment using mode data
[AD-A155988] 24 p4143 N85-35685
Model robust response surface designs: Scaling two-level factorials
[AD-A156218] 24 p4143 N85-35686
Acoustic resonances in cylinder bundles oscillating in a compressible fluid
[DE85-004066] 24 p4145 N85-35699
A lead glass tubing drift calorimeter
24 p4147 N85-35711
Use of a minimum-ellipse criterion in the study of ion-beam extraction systems
[DE85-012670] 24 p4148 N85-35721
Applications and misapplications of the channel-capture formalism of direct neutron capture
[DE85-013992] 24 p4152 N85-35748
On-line model driven control of the SLC electron Damping Ring
[DE85-013377] 24 p4157 N85-35772

MATHEMATICAL PROGRAMMING
NT DYNAMIC PROGRAMMING
NT LINEAR PROGRAMMING
NT NONLINEAR PROGRAMMING
NT QUADRATIC PROGRAMMING
Sensitivity analysis in generalized rational approximation with restricted denominator
[CSIR-TWISK-319] 01 p0109 N85-10734
On the formal development of graph theoretical algorithms by transformation
[TUM-I8403] 04 p0553 N85-13522
Monotone operators in mathematical programming
[AD-A147309] 07 p1025 N85-16506
Fast arithmetic for microcomputers
08 p1140 N85-17180
Relative performance of micro and mainframe computers
[AD-A149281] 10 p1538 N85-19695
Description of 8048 microcomputer operation published 11 p1700 N85-20685
An approach for user controlled reinforced concrete design optimization 15 p2627 N85-26187
Mathematical software for hyperbolic equations and two point boundary value problems
[AD-A151982] 15 p2638 N85-26270
Mathematical programming in computer network design
[AD-A152275] 16 p2848 N85-27558
H-sets, convex programming and constrained approximation
[TRITA-NA-8308] 16 p2853 N85-27587
The essence of investy
[CSIR-TWISK-321] 16 p2858 N85-27626
A global optimization algorithm using stochastic differential equations
[AD-A153526] 18 p3161 N85-29583
The origin of the binary-search paradigm
[AD-A154367] 19 p3337 N85-30877
Mathematical programming in the Netherlands
[REPT-ARW-03-THE-BDK/ORS/83/10]
20 p3517 N85-31866
New developments on the core function for efficient implementation of the difficult residue number system operations
[AD-A154678] 21 p3676 N85-32834
Necessary and sufficient conditions for single-extremum and convex problems of mathematical programming
21 p3698 N85-32977
A geometric modeller for turbomachinery applications
23 p3962 N85-34556

MATHEMATICAL TABLES
Log linear model applications
[AD-A149620] 08 p0658 N85-15457
Tables for distributions of quadratic forms
[AD-A154084] 19 p3347 N85-30745

MATHEMATICS
USSR report: Physics and mathematics
[JPRS-UPM-84-006] 02 p0258 N85-11676
Emergency Mathematics and Science Education Act
[GPO-29-561] 03 p0435 N85-12770
Experimental mathematics
[CWI-PM-R8411] 12 p1925 N85-22096
Ada (trademark) training curriculum. Advanced Ada topics L305 teacher's guide exercises
[AD-A154621] 21 p3670 N85-32796

MATRICES (CIRCUITS)
A study of reflex optoelectronic switching matrices and their derivatives
[CRC-TN-720] 19 p3253 N85-30169
Charge Injection Device (CID) used as a photodector: Implementation and performance. Application to light source tracking (stars, lasers)
[CNES-83/CT/DRT/TIT/OE/148]
20 p3533 N85-31983

MATRICES (MATHEMATICS)
NT ADJOINTS
NT CANONICAL FORMS
NT EIGENVALUES
NT EIGENVECTORS
NT JORDAN FORM
NT STIFFNESS MATRIX
Calculations of optical properties of transition metals
[BLL-M-35744-(5828.4)] 02 p0175 N85-11175
Seminar on Principal Components Analysis in the Atmospheric and Earth Sciences
[CSIR-S-334] 02 p0211 N85-11389
Principal components: A review
02 p0211 N85-11390
Description of a data matrix structure and model diagnosis by means of row and column Euclidean maps
02 p0211 N85-11392
A fast, compact assignment algorithm
[NRIMS-TWISK-331] 02 p0250 N85-11632
Numerical methods for solving systems of linear equations
[INPE-3240-RPE/483] 02 p0250 N85-11633
Pointwise iterations of finite element modeling of advection-diffusion equations
[DE84-015284] 02 p0253 N85-11656
Evaluating A(T) *D*A for sparse matrices: Analysis
[AD-A145916] 03 p0411 N85-12625
Bulletin of the Faculty of Engineering, Hokkaido University, no. 123
[ISSN-0386-602-X] 04 p0482 N85-13075
Implication structures for generalized implication matrix in ISM 04 p0483 N85-13079
Least squares spline regression with block-diagonal variance matrices
[NPL-DITC-40/84] 04 p0554 N85-13523
Effects of changing the signs of rows and columns of a matrix and the hyperbolic transpose
[DE84-014651] 04 p0555 N85-13530
Electrooptical matrix multiplication using the twos complement arithmetic for improved accuracy
[AD-D011252] 05 p0728 N85-14662
Advanced cube processor
[AD-D011262] 05 p0729 N85-14663
Algebraic techniques in systolic array design
[AD-A146417] 06 p0857 N85-15451
On a random difference equation for matrices and a characterization of the gamma distribution
[AD-A146858] 07 p1029 N85-16529
Lattice statistics
[AD-A146862] 07 p1029 N85-16530
Continuity of the null space basis and constrained optimization
[AD-A147038] 07 p1030 N85-16538
A complete characterization of triply balanced matrices with applications to survey sampling
[AD-A147083] 07 p1031 N85-16542
Extracting embedded generalized networks from linear programming problems
[AD-A147565] 07 p1033 N85-16558
Sequential and parallel matrix computations
[AD-A147871] 07 p1034 N85-16562
Structural optimization and other large-scale processes
[AD-A147895] 07 p1034 N85-16564
An optimal parallel processing method for inverting sparse matrices 09 p1367 N85-18588
Modeling relationships using groups and items
09 p1367 N85-18591
On the connection between multigrid and cyclic reduction
[NASA-TM-86020] 09 p1373 N85-18629
Investigation of three-dimensional mesh generation with precise controls
[AD-A148759] 09 p1374 N85-18636
Methods of computer-aided analysis of non-Gaussian noise and application to robust adaptive detection, part 2
[AD-A148879] 10 p1539 N85-19704
The inefficiency of least squares: Extensions of Kantorovich inequality
[AD-A149568] 10 p1549 N85-19788
On the probability density of signal-to-noise ratio in an improved adaptive detector, part 1
[AD-A148858] 10 p1550 N85-19772
Triple matrix product optical processors using combined time-and-space integration
[AD-D011483] 10 p1557 N85-19820

Complex symmetric matrices with strongly stable iterates
[NASA-CR-172542] 11 p1706 N85-20731
Differentiating matrices for arbitrarily spaced grid points
[NASA-CR-172556] 12 p1919 N85-22051
On the limiting empirical distribution function of the eigenvalues of a multivariate F matrix
[AD-A149618] 12 p1921 N85-22065
Direct secant updates of sparse matrix factors
[DE85-004008] 12 p1922 N85-22073
Asymptotic behavior of matrix coefficients related to reductive symmetric spaces
[CWI-PM-R8410] 12 p1925 N85-22095
Implementation of some concurrent algorithms
[DE85-004667] 13 p2148 N85-23334
On limit of the largest eigenvalue of the large dimensional sample covariance matrix
[AD-A150589] 13 p2151 N85-23358
Algorithm for singular decomposition
[DE85-016488] 13 p2152 N85-23361
Sparse matrix computations
[DE85-004780] 13 p2152 N85-23362
Modal synthesis of multidimensional PI-regulators for objects with inertial sections 14 p2270 N85-24084
On positive vectors, positive matrices and the specialization ordering
[CWI-PM-R8407] 14 p2414 N85-24899
MATRIX: A program that shows how row and column orderings affect matrix fill-in
[DE85-007522] 15 p2630 N85-26213
Investigation of the numerical method of moments for digital computer determination of differential equations
[AD-A151696] 15 p2638 N85-26268
Explicit construction of contractivity matrices
[TRITA-NA-8309] 16 p2652 N85-27586
Finite elements and the method of conjugate gradients on a concurrent processor
[NASA-CR-175812] 16 p2653 N85-27588
Formulas for updating the generalized inverse of a symmetric matrix perturbed by a symmetric rank 2 matrix composed of 2 nonsymmetric DYADS
[AD-A151736] 16 p2658 N85-27629
Computing the singular value decomposition of a product of two matrices
[DE85-006977] 16 p2659 N85-27631
A method to calculate the parameters of wings of arbitrary planform
[AD-A152699] 17 p2692 N85-27831
Discrete mathematics for communications systems
[AD-A152814] 17 p3018 N85-28664
Robust tests of mean vector in symmetrical multivariate distributions
[AD-A153116] 17 p3020 N85-28674
Symbolic Givens reduction in large sparse least squares problems
[DE85-006695] 17 p3021 N85-28681
On the condition number of modified moment matrices arising from least squares approximation in the complex plane
[AD-A152353] 17 p3026 N85-28714
Kalman filter modeling 18 p3107 N85-29237
Studies in quality improvement. Part 1: Dispersion effects from fractional designs, revised
[AD-A153516] 18 p3119 N85-29308
Pipelined Givens method for computing the QR factorization of a sparse matrix
[DE85-009772] 18 p3171 N85-29653
High accuracy digital acousto-optic matrix computer
[AD-D011692] 19 p3343 N85-30716
An iterative method for indefinite systems of linear equations
[NASA-CR-172345] 19 p3345 N85-30726
Monte Carlo sampling strategies for lattice gauge calculations
[DE85-010786] 19 p3377 N85-30948
Matrix transfer function design for flexible structures: An application 20 p3416 N85-31199
Fast eigenvector methods for digital signal processing 20 p3439 N85-31341
Method to render second order beam optics programs symplectic
[DE85-010631] 20 p3515 N85-31855
Detection of and search for faults in programmable logic arrays 22 p3778 N85-33409
Determination of low chloride values in Rocky Flats scrub alloy solutions and other complex matrices
[DE85-011506] 23 p3911 N85-34234
Invariant tests and likelihood ratio tests for multivariate elliptically contoured distributions
[AD-A155844] 24 p4142 N85-35679

MATRIX ANALYSIS
U MATRICES (MATHEMATICS)

MATRIX MATERIALS
High performance fibers for structurally reliable metal and ceramic composites — advanced gas turbine engine materials
[NASA-TM-86878] 03 p0325 N85-12095
Matrix resin characterization in cured graphite composites using diffuse reflectance-FTIR 04 p0466 N85-12969
Solvent resistant thermoplastic composite matrices 04 p0466 N85-12960
Aliphatic-aromatic heterocyclics as potential thermoplastics for composite matrices 04 p0466 N85-12962
Constituent properties and interrelationships 04 p0467 N85-12964
Matrix synthesis and characterization 04 p0467 N85-12965
Work hardening of simple two phase composites
[DE84-014629] 04 p0468 N85-12978
Carbon fibre reinforced aluminum matrix composites: A critical review
[AD-A146367] 06 p0764 N85-14883
Fine-grained millimeter-sized objects in type 3 ordinary chondrites and their relation to chondrules and matrix 06 p0862 N85-15603
Chondrule rims and interchondrule matrix in UOC 06 p0862 N85-15604
The influence of porosity on the deformation and fracture of alloys
[AD-A148766] 08 p1130 N85-17124
Development of a heterogeneous laminating resin system
[NASA-CR-172459] 09 p1268 N85-18089
Proceedings of Colloquium/Workshop on Composite Materials and Structures, Standardization, Qualification, Certification held at washington, D.C. on 8-10 May 1984
[AD-A149039] 10 p1432 N85-19029
Quantitative estimate of compatibility of fiber composite material components 10 p1444 N85-19099
Structure and property formation mechanism in magnetite alloy-binder composite 10 p1444 N85-19103
Fiber composite materials with titanium matrix 10 p1445 N85-19105
Chemical approach for controlling nadimide cure temperature and rate with maleimide
[NASA-CASE-LEW-13770-3] 12 p1809 N85-21350
Chemical approach for controlling nadimide cure temperature and rate with maleimide
[NASA-CASE-LEW-13770-4] 12 p1810 N85-21351
Method and apparatus for detecting acoustic emissions from metal matrix wire
[AD-D011556] 12 p1927 N85-22107
Development of epoxy matrices for filament-wound graphite structures
[DE85-003674] 13 p2015 N85-22642
Monitoring of laminate cure with microdielectrometry
[AD-A150863] 14 p2248 N85-23934
In-plane shear properties of graphite Fibre/Epoxy composites for aerospace applications: Evaluation of test methods by the decision analysis technique
[AD-A151599] 15 p2503 N85-25440
Mechanics of polymers and composites: Research opportunities
[DE85-007052] 15 p2503 N85-25442
Development of a new faster process for the fabrication of ceramic fiber-reinforced ceramic composites by chemical vapor infiltration
[DE85-007550] 16 p2758 N85-27007
Polymer matrix and graphite fiber interface study
[NASA-CR-177357] 19 p3232 N85-30036
Chemical approach for controlling nadimide cure temperature and rate
[NASA-CASE-LEW-13770-6] 19 p3232 N85-30039
Features of the interaction between fibers and matrix in production of aluminum-boron composite material 19 p3244 N85-30117
Matrix fracture in fiber-reinforced ceramics
[AD-A154704] 21 p3569 N85-32197
Apparatus and method for identification of matrix materials in which transuranic elements are embedded using thermal neutron capture gamma-ray emission
[DE85-011659] 22 p3786 N85-33454
Development of solid thorium-232 reference materials
[DE85-011453] 22 p3841 N85-33785
Impact fracture mechanism of polymer plates containing a heavy inner material 23 p3908 N85-34215
Mechanical properties of SiC fiber-reinforced reaction-bonded SiN4 composites
[NASA-TM-87085] 23 p3909 N85-34223
Viscoelastic behavior of short-fiber composite materials
[DE85-011233] 23 p3910 N85-34225

MATRIX METHODS
A routine to find the lowest few eigenvalues and vectors for the generalised sparse symmetric eigenproblem
[NPL-DITC-43/84] 05 p0722 N85-14841
The use of analytical models to interpret measured data properly. 1. General background theory 11 p1651 N85-20400
The use of analytical models to interpret measured data properly. 2. The application to modal analysis of structures 11 p1651 N85-20401
Adaptive filtering for large space structures: A closed-form solution 20 p3417 N85-31206

MATRIX STRESS CALCULATION
U MATRIX METHODS

MATRIX THEORY
A T-matrix theory of galactic heavy-ion fragmentation
[NASA-TP-2363] 06 p1221 N85-17690

MATTER (PHYSICS)
Galaxy and cluster formation in a universe dominated by cold dark matter
[DE84-015879] 04 p0580 N85-13706
Space charge, interfacial kinetics, and electrical response of condensed matter
[AD-A146364] 06 p0765 N85-14893
Theoretical studies relating to the interaction of radiation with matter: Atomic collision processes occurring in the presence of radiation fields
[AD-A146854] 07 p1040 N85-16602
Propagation of sound in matter
[AD-A151052] 14 p2416 N85-24906
Particle physics: Recent successes and future prospects
[DE85-008175] 17 p3033 N85-28765
Proceedings of the 1984 Workshop on High-Energy Excitations in Condensed Matter, volume 2
[DE85-007395] 19 p3357 N85-30609
Characterization of the optical and thermal properties of matter by photothermal technique
[DE85-012607] 24 p4078 N85-35260

MATTS (SYSTEMS)
User's manual of the BNDSCO computer program for solving constrained optimal control problems
[DFVLR-MITT-85-05] 20 p3516 N85-31865

MATURING
U GROWTH

MAXIMA
Attainable rates of convergence of maxima
[AD-A150838] 14 p2408 N85-24847
Large deviations for the maxima of some random fields
[AD-A155909] 24 p4143 N85-35681

MAXIMUM ENTROPY METHOD
Autoregressive modeling and the classification of land clutter — radar signatures
[ENST-C-84003] 03 p0356 N85-12292
On maximum entropy signal analysis
[AD-A144374] 03 p0410 N85-12618
Fundamental limitations in antenna resolution by maximum entropy methods
[DE84-017052] 04 p0493 N85-13145
Local geomagnetic characteristics of solar activity (Dourbes 1960-1978) 04 p0521 N85-13328
Relative-entropy minimization with uncertain constraints--theory and application to spectrum analysis
[AD-A149192] 10 p1546 N85-19752
Space and time variations and turbopause dynamical structure 11 p1663 N85-20483
Simulation of estimating periodicity of seasonally stationary time series
[DE85-003517] 11 p1706 N85-20748
Determination of experimental Tokamak plasma properties using maximum entropy analysis
[DE85-001723] 12 p1936 N85-22165
Application of the maximum entropy/optimal projection control design approach for large space structures 14 p2234 N85-23849
Maximum entropy spectral analysis
[LEOK-TR-1984-06] 14 p2299 N85-24235

MAXIMUM LIKELIHOOD ESTIMATES
A Monte Carlo comparison of the recovery of winds near upwind and downwind from the SASS-1 model function by means of the sum of squares algorithm and a maximum likelihood estimator
[NASA-CR-3639] 01 p0084 N85-10421
Nonparametric maximum penalized likelihood estimation of a density from arbitrarily right-censored observations
[AD-A145589] 02 p0251 N85-11644
Likelihood estimation for generalized mixed exponential distributions
[AD-A145675] 02 p0252 N85-11651
Maximum likelihood estimation of the survival functions of N stochastically ordered random variables
[AD-A145429] 02 p0254 N85-11662
The ML (Maximum Likelihood) method for frequency estimation of real sinusoids in noise
[AD-A146053] 03 p0411 N85-12628

Maximum likelihood and Bayesian parameter estimation in item response theory
[AD-A145775] 03 p0413 N85-12844
A very efficient transfer function bounding technique on bit error rate for Viterbi decoded, rate 1/N convolutional codes 05 p0624 N85-13991
Maximum likelihood estimation of parameters in linear systems from flight test data: A FORTRAN program
[AD-B087186L] 05 p0715 N85-14588
Estimating a monotone density
[CWI-MS-R8403] 05 p0721 N85-14633
More than you want to know about maximum likelihood estimation
[NASA-TM-85905] 07 p0909 N85-15752
Improved digital baseband transmission by application of maximum likelihood decoding to an 8-level signal generated by convolution and block coding
[FI-44-TBR-83] 07 p0942 N85-15973
Bayesian estimation of normal mixture parameters 07 p0985 N85-16255
Local likelihood estimation
[AD-A147317] 07 p1035 N85-16571
Improved estimation procedures for item response functions
[AD-A147677] 08 p1215 N85-17648
Statistical aspects of shear fracture propagation
[ERS-E.398] 09 p1341 N85-18434
User's guide to MIX: A computer code for fitting mixture distributions to data
[DE85-001451] 09 p1369 N85-18603
Estimating the scale parameter of an exponential distribution from a sample of time-censored r-th order statistics
[AD-A148080] 09 p1375 N85-18644
Adaptive signal processing for radio communications 10 p1473 N85-19295
The likelihood displacement: A unifying principle for influence measures
[AD-A149456] 10 p1551 N85-19783
Identification of dynamic systems, theory and formulation
[NASA-RP-1138] 10 p1551 N85-19784
On the application of compatibility checking techniques to dynamic flight test data
[ARL/AERO-R-161] 12 p1776 N85-21151
Ordinary and proper location M-estimates for ARMA models, revised
[AD-A149705] 12 p1920 N85-22061
Accuracy of approximation of Bayes estimates in presence of noninformative parameters 13 p2064 N85-23015
Reception of signal with unknown amplitude and duration submerged in white noise 13 p2064 N85-23016
Why do noninvertible estimated moving averages occur?
[AD-A150366] 13 p2153 N85-23368
Better bootstrap confidence intervals
[AD-A150798] 14 p2408 N85-24846
Nonparametric estimation of density and hazard rate functions when samples are censored
[AD-A150948] 14 p2411 N85-24868
Censored observations, repeated measures and mixed effects models: An approach using the EM algorithm and normal errors
[MATHEMATICS-RESEARCH-183] 15 p2636 N85-26256
Validation of the ERBE scanner scene identification methodology: Analysis with Nimbus-7 ERB data
[NASA-CR-172596] 16 p2832 N85-27466
Topics in time delay estimation
[AD-A152231] 16 p2855 N85-27607
Multivariate statistical modelling and its application 16 p2857 N85-27617
Local likelihood estimation
[DE85-007238] 16 p2857 N85-27620
Nonsmooth analysis and Frechet differentiability of M-functionals
[AD-A152932] 17 p3019 N85-28668
Extraction of aerodynamic parameters for aircraft at extreme flight conditions
[NASA-TM-86730] 18 p3175 N85-29886
Maximum likelihood estimation with emphasis on aircraft flight data 20 p3417 N85-31206
A residuals approach to filtering, smoothing and identification for static distributed systems 20 p3418 N85-31213
Numerical experimentation with maximum likelihood identification in static distributed systems 20 p3418 N85-31214
Comparison of ERS-1 scatterometer Monte Carlo performance simulations using a weighted nonlinear least squares and a maximum likelihood estimation method 20 p3420 N85-31224
On the confidence limits for Weibull reliability and quantiles: The case of maximum likelihood estimation from small size censored samples
[REPT-84-RR-345] 20 p3521 N85-31898
Robust detection and classification of regional seismic signals using a two mode/two stage cascaded adaptive arma (CAARMA) model
[AD-A154710] 21 p3630 N85-32554
On a variational approach to some parameter estimation problems
[NASA-CR-177935] 21 p3675 N85-32829
Weibull distribution based on maximum likelihood with interval inspection data
[NASA-TM-86515] 21 p3678 N85-32847
Invariant tests and likelihood ratio tests for multivariate elliptically contoured distributions
[AD-A155844] 24 p4142 N85-35879
A new method of differential structural analysis of gamma-family basic parameters
[HE-3.6-3] 24 p4184 N85-35952
Study of the time-differentiated particle flux density at various distances from EAS axis
[HE-4.7-15] 24 p4200 N85-36065

MAXWELL EQUATION
Theoretical study of laser-induced surface excitations on a grating
[AD-A147855] 07 p0972 N85-16172
The liner package: An incipient MHD capability for CCUBE
[LA-9969-MS] 12 p1913 N85-22007
An iteration method for complex scattering problems
[AD-A150038] 12 p1934 N85-22151
Nonlinear waves in the magnetosphere of pulsars 12 p1955 N85-22281
Explosive transverse electric field and particle acceleration during magnetic collapse --- cosmic plasma 12 p1956 N85-22292
Solutions of field equations in General Relativity with spinor connection 15 p2663 N85-26436
Cavityless optical bistability in systems of two-level atoms 18 p3186 N85-29764
Modeling solar magnetic structures 18 p3203 N85-29872
Trends in measurement of solar vector magnetic fields using the Zeeman effect 18 p3204 N85-29877
Laser forward and backscattering in particulate media
[AD-A154136] 19 p3275 N85-30312
Equations of motion for electromagnetic waves in 4-dimensional Euclidian space 21 p3697 N85-32970
Analysis of the nonlinear equations describing the elastic, thermal, and electromagnetic behavior of solids: Existence of solutions of semi-inverse problems 24 p4100 N85-35415
Relation between field energy and RMS emittance in intense particle beams
[DE85-012655] 24 p4159 N85-35784

MAXWELL FLUIDS
Dynamics of liquid filament breakup
[DE84-016006] 04 p0500 N85-13187
Existence of slow steady flows of viscoelastic fluids with differential constitutive equations
[AD-A147240] 07 p0959 N85-16077

MAXWELL-BOLTZMANN DENSITY FUNCTION
High resolution hard X-ray spectra of solar and cosmic sources 14 p2455 N85-25163
Attenuated total reflection method for obtaining optical constants of powders
[AD-A154094] 19 p3367 N85-30881
The electric current densities beneath thunderstorms 20 p3494 N85-31726
Effect of ECH and ICH on ambipolar potential in NBT-1M 23 p3978 N85-34661

MAXWELLIAN DISTRIBUTION (DENSITY)
U MAXWELL-BOLTZMANN DENSITY FUNCTION

MAYPOLE ANTENNAS
Combined state and parameter estimation for a static model of the Maypole (Hoop-Column) antenna suface 20 p3417 N85-31210

MCDONNELL AIRCRAFT
NT DC 10 AIRCRAFT
NT RF-4 AIRCRAFT

MCDONNELL DOUGLAS AIRCRAFT
NT DC 8 AIRCRAFT
NT DC 9 AIRCRAFT
NT DC 10 AIRCRAFT
NT F-18 AIRCRAFT
NT RF-4 AIRCRAFT

MEADOWLANDS
U GRASSLANDS

MEAN
On the rate of mean convergence of finite linear predictors of multivariate stationary stochastic processes
[AD-A145609] 02 p0254 N85-11684
Estimating the scale parameter of an exponential distribution from a sample of time-censored r-th order statistics
[AD-A148080] 09 p1375 N85-18644
The asymptotic behavior of the likelihood ratio statistic for testing a shift in mean in a sequence of independent normal variates
[AD-A149329] 10 p1550 N85-19779
Asymptotic distributions of the sample mean, autocovariances and autocorrelations of long-memory time series
[AD-A149409] 10 p1551 N85-19781
Motion of symmetrical satellite with flexible viscoelastic rods about center of mass in circular orbit 13 p1979 N85-22420
Microcomputer: Controlled statistics analyzer
[BLL-CE-TRANS-7971-(9022.09)] 13 p2144 N85-23306
The worldwide distribution of the seasonal cycle of mean sea level
[IOS-190] 20 p3497 N85-31743
The mean ionic charge of silicon in 3HE-rich solar flares
[SH-2.2-6] 23 p4000 N85-34603

MEAN FREE PATH
Anomalon search --- heavy cosmic ray interactions
[NOTA-INTERNA-825] 02 p0305 N85-11970
Arc-evaporated carbon films: Optical properties and electron mean free paths
[DE85-001246] 08 p0987 N85-15510
Statistical theory of fragmentation processes
[DE85-002206] 11 p1653 N85-20414
Mean free paths, viscosity, and the limitations of perfect fluid hydrodynamics in the description of the quark-gluon plasma
[DE85-005501] 15 p2649 N85-26339
Monte Carlo techniques for analyzing deep penetration problems
[DE85-011426] 23 p3998 N85-34598
Calculation of heavy-ion tracks in liquid water
[DE85-012101] 24 p4149 N85-35725
Penetrative nature of high energy showers observed in Chacaltaya emulsion chamber
[HE-3.3-5] 24 p4180 N85-35923
On mini-cluster observed by Chacaltaya emulsion chamber experiment
[HE-3.6-12] 24 p4185 N85-35959
Search for anomalons using plastic nuclear track detectors
[HE-6.2-12] 24 p4212 N85-36148
Search for acoustic signals from high energy cascades
[HE-7.1-1] 24 p4213 N85-36155

MEAN SQUARE VALUES
A complete characterization of triply balanced matrices with applications to survey sampling
[AD-A147083] 07 p1031 N85-16542
A note on the prediction error for small time lags into the future
[AD-A148221] 08 p1215 N85-17654
Fast moving average recursive least mean square fit
[DE85-010036] 19 p3348 N85-30752

MEANDERS
The gulf stream deflection and meander energetics experiment. Current meter and bottom pressure gauge data report for the September, 1981 to April, 1982 mooring period
[AD-A144977] 01 p0066 N85-10585

MEASURE AND INTEGRATION
NT BOREL SETS
NT INTEGRAL CALCULUS
NT J INTEGRAL
NT NUMERICAL INTEGRATION
NT RUNGE-KUTTA METHOD
NT WEIGHTING FUNCTIONS
Measure determining classes of balls in Banach space
[CTH-MATH-1984-14] 04 p0556 N85-13541
A limit theorem for the superposition of renewal processes
[CWI-MS-R8408] 05 p0722 N85-14636
Generalized predictor-corrector methods of high order for the time integration of parabolic differential equations
[CWI-NM-R8402] 08 p1214 N85-17644
A conformal mapping suitable for problems involving interaction between given geometries and known far fields
[AD-A149050] 10 p1545 N85-19744
Developments in microelectronics: Past and future 15 p2530 N85-25587
Relaxation methods for hyperbolic equations
[REPT-84-20] 17 p3021 N85-28667
State Weights and Measures Laboratories: Program handbook
[PB85-183358] 18 p3111 N85-29263
Some properties of Loeb-Sobolev spaces
[CTH-MATH-1985-01] 22 p3835 N85-33748

MEASURE THEORY
U MEASURE AND INTEGRATION
MEASUREMENT
Measurement assurance programs. Part 2: Development and implementation
[PB84-217676] 01 p0051 N85-10338
Measurement assurance programs. Part 1: General introduction
[PB84-217668] 01 p0051 N85-10339
Water resources data for Michigan, water year 1983
[PB84-225176] 01 p0066 N85-10442
Method for measuring haze in transparencies
[AD-D011233] 01 p0120 N85-10823
Quantization study for ERS-1 wave mode
[DFVLR-FB-84-39] 11 p1625 N85-20234
State measurement laboratories: Program description (part 1). Directory (part 2)
[PB85-137651] 11 p1739 N85-20935
In situ thin film measurements
[AD-A151379] 15 p2652 N85-26353
Principles of quality assurance of chemical measurements
[PB85-177947] 18 p3072 N85-28997
Use of the VAD technique and measurements of momentum flux in the stratosphere at Aercibo, part 4.3A
21 p3622 N85-32505
Measurement control for plutonium isotopic measurements using gamma-ray spectrometry
[DE85-013394] 24 p4097 N85-35397
MEASURES
Invariant measures and the equicontinuous structure relation 1
[CWI-PM-R8403] 05 p0723 N85-14645
Invariant measures and the equicontinuous structure relation 2: The relative case
[CWI-PM-R8404] 05 p0723 N85-14646
MEASURING
U MEASUREMENT
MEASURING INSTRUMENTS
NT ACCELEROMETERS
NT ACTINOMETERS
NT ALTIMETERS
NT AMMETERS
NT ANALYZERS
NT ANEMOMETERS
NT APPROACH INDICATORS
NT ASTROLABES
NT ATOMIC CLOCKS
NT ATTITUDE INDICATORS
NT AUTONOMOUS SPACECRAFT CLOCKS
NT BALLOON-BORNE INSTRUMENTS
NT BAROMETERS
NT BATHYMETERS
NT BATHYTHERMOGRAPHS
NT BOLOMETERS
NT CALORIMETERS
NT CERENKOV COUNTERS
NT CHRONOMETERS
NT CLOCKS
NT CLOUD HEIGHT INDICATORS
NT COMPARATORS
NT COMPASSES
NT COULOMETERS
NT COUNTERS
NT CYCLOTRON RESONANCE DEVICES
NT DENSIMETERS
NT DENSITOMETERS
NT DIFFRACTOMETERS
NT DISTANCE MEASURING EQUIPMENT
NT DOSIMETERS
NT DYNAMOMETERS
NT ELECTRICAL CONDUCTIVITY METERS
NT ELECTROMETERS
NT ELECTRON PROBES
NT ELECTROPHOTOMETERS
NT ELECTROSTATIC PROBES
NT ELLIPSOMETERS
NT ENGINE ANALYZERS
NT ENGINE MONITORING INSTRUMENTS
NT ERGOMETERS
NT EXTENSOMETERS
NT FABRY-PEROT INTERFEROMETERS
NT FABRY-PEROT SPECTROMETERS
NT FIELD INTENSITY METERS
NT FLAME PROBES
NT FLIGHT LOAD RECORDERS
NT FLIR DETECTORS
NT FLOW DIRECTION INDICATORS
NT FLOWMETERS
NT FUEL GAGES
NT GALVANOMETERS
NT GAMMA RAY SPECTROMETERS
NT GAS METERS
NT GONIOMETERS
NT GRAVITY GRADIOMETERS
NT GYRO HORIZONS
NT GYROCOMPASSES
NT HELIOMETERS
NT HODOSCOPES
NT HOT-FILM ANEMOMETERS
NT HOT-WIRE ANEMOMETERS
NT HOT-WIRE FLOWMETERS
NT HYGROMETERS
NT IMPEDANCE PROBES
NT INDICATING INSTRUMENTS
NT INFRARED DETECTORS
NT INFRARED INSTRUMENTS
NT INFRARED INTERFEROMETERS
NT INFRARED RADIOMETERS
NT INFRARED SCANNERS
NT INFRARED SPECTROMETERS
NT INFRARED SPECTROPHOTOMETERS
NT INTERFEROMETERS
NT ION PROBES
NT IONIZATION GAGES
NT IONOSONDES
NT LASER ANEMOMETERS
NT LASER DOPPLER VELOCIMETERS
NT LASER RANGE FINDERS
NT LASER SPECTROMETERS
NT LIGHT SCATTERING METERS
NT MAGNETIC PROBES
NT MAGNETOMETERS
NT MANOMETERS
NT MASS SPECTROMETERS
NT METEOROLOGICAL INSTRUMENTS
NT MICHELSON INTERFEROMETERS
NT MICROBALANCES
NT MICRODENSITOMETERS
NT MICROWAVE INTERFEROMETERS
NT MICROWAVE PROBES
NT MICROWAVE RADIOMETERS
NT MICROWAVE REFLECTOMETERS
NT MICROWAVE SENSORS
NT MICROWAVE SPECTROMETERS
NT MOISTURE METERS
NT MONOCHROMATORS
NT MULTISPECTRAL BAND SCANNERS
NT NEPHELOMETERS
NT NEUTRON COUNTERS
NT NEUTRON SPECTROMETERS
NT OCULOMETERS
NT OMEGA NAVIGATION SYSTEM
NT OPTICAL MEASURING INSTRUMENTS
NT OPTICAL RANGE FINDERS
NT OPTICAL SCANNERS
NT OSCILLOGRAPHS
NT OXYGEN ANALYZERS
NT PARTICLE TELESCOPES
NT PASSIVE L-BAND RADIOMETERS
NT PENETROMETERS
NT PHOTOGONIOMETERS
NT PHOTOMETERS
NT PIEZOELECTRIC GAGES
NT PLAN POSITION INDICATORS
NT PLASMA PROBES
NT POLARIMETERS
NT POSITION INDICATORS
NT POTENTIOMETERS (INSTRUMENTS)
NT PRESSURE GAGES
NT PROFILOMETERS
NT PROPORTIONAL COUNTERS
NT PYRANOMETERS
NT PYROHELIOMETERS
NT PYROMETERS
NT QUANTUM COUNTERS
NT RADIATION COUNTERS
NT RADIATION DETECTORS
NT RADIATION MEASURING INSTRUMENTS
NT RADIO ALTIMETERS
NT RADIO DIRECTION FINDERS
NT RADIO INTERFEROMETERS
NT RADIOMETERS
NT RADIOSONDES
NT RAIN GAGES
NT RANGE FINDERS
NT RAWINSONDES
NT REFLECTOMETERS
NT RESISTANCE THERMOMETERS
NT RESONANCE PROBES
NT RHEOMETERS
NT RIOMETERS
NT SATELLITE-BORNE INSTRUMENTS
NT SCATTEROMETERS
NT SCINTILLATION COUNTERS
NT SEISMOGRAPHS
NT SIGNAL ANALYZERS
NT SILICON RADIATION DETECTORS
NT SMOKE DETECTORS
NT SOLAR SPECTROMETERS
NT SONDES
NT SPACECRAFT POSITION INDICATORS
NT SPARK CHAMBERS
NT SPECTROHELIOGRAPHS
NT SPECTROMETERS
NT SPECTROPHOTOMETERS
NT SPECTRORADIOMETERS
NT SPEED INDICATORS
NT SPUTTERING GAGES
NT STRAIN GAGE ACCELEROMETERS
NT STRAIN GAGES
NT TACHOMETERS
NT TEMPERATURE MEASURING INSTRUMENTS
NT TEMPERATURE PROBES
NT TENSIOMETERS
NT THEODOLITES
NT THERMOCOUPLE PYROMETERS
NT THERMOMETERS
NT THRESHOLD DETECTORS (DOSIMETERS)
NT TILTMETERS
NT TIME MEASURING INSTRUMENTS
NT TIME OF FLIGHT SPECTROMETERS
NT TIMING DEVICES
NT TORQUEMETERS
NT TRANSMISSOMETERS
NT TURBULENCE METERS
NT ULTRAVIOLET SPECTROMETERS
NT ULTRAVIOLET SPECTROPHOTOMETERS
NT VARIOMETERS
NT VIBRATION METERS
NT VOLTMETERS
NT WATTMETERS
NT WEATHER DATA RECORDERS
NT WEIGHT INDICATORS
NT WIND VANES
Pavement friction measurements on nontangent sections of roadways, vol. 1
[PB84-219732] 01 p0036 N85-10227
Aspects and applications of SAR (Synthetic Aperture Radar) imagery for mensuration
[AD-A146301] 03 p0358 N85-12290
Method for evaluating petrol products corrosivity using piezoelectric crystals. Part 2: Instruction manual — jet engine corrosion tests
[FOA-C-40198-B4] 04 p0482 N85-13073
Portable instrument for the detection and identification of air pollutants
[DE84-014767] 05 p0672 N85-14316
Assessment of Techniques for Measuring Tropospheric H sub x O sub y
[NASA-CP-2332] 05 p0675 N85-14336
Assessment of Techniques for Measuring Tropospheric H sub x O sub y: Summary 05 p0675 N85-14337
Experimentation and measurement
[PB84-233659] 06 p0812 N85-15157
East Europe report: Science and technology
[JPRS-ESA-84-045] 06 p0815 N85-15175
Laser-guided measuring system for precisioning device 06 p0816 N85-15179
Advanced fatigue monitoring on service aircraft
07 p0895 N85-15671
The determination of vertical sintering speed of sinter charges
[BLL-M-36033-(5828.4)] 07 p0926 N85-15869
Gallium arsenide compounds tested nondestructively with X-rays 07 p0936 N85-15934
Performance characteristics of a battery charger and state-of-charge indicator
[NASA-CR-174273] 07 p0948 N85-15992
Ensuring required metrological reliability of analog instrument channels by parametric compensation
07 p0955 N85-16050
High temperature thermocouple and heat flux gauge using a unique thin film-hardware hot juncture
[NASA-TM-86898] 07 p0962 N85-16096
A narrow band pulsed eddy current instrument for materials testing
[AERE-R-11229] 07 p0968 N85-16149
Data acquisition, measurement devices at 1984 Leipzig Spring Fair 09 p1378 N85-16861
Radiation response of optical fibers in a nuclear reactor
[DE84-017221] 09 p1385 N85-16710
Electromagnetic compatibility of measurement and control equipment in nuclear installations
[BLL-WH-607-(8091.9F)] 11 p1623 N85-20222
Liquid thickness gage
[NASA-CASE-LAR-13342-1] 11 p1635 N85-20297
Precision volume measuring system
[DE85-002589] 11 p1636 N85-20305
In-situ detection of micron-sized dust particles in near-Earth space 12 p1785 N85-21205
Transistor-transistor logic microcircuit tester
12 p1842 N85-21556
Program for controlling electrical measuring contact instrument on glow-discharge indicator panel
12 p1842 N85-21558

Self-charging metering and dispensing device for fluids
[NASA-CASE-MSC-20275-1] 12 p1848 N85-21595
Dielectric measurements in intralow-frequency band
13 p2067 N85-23034
Proceedings of the Geoscience Instrumentation Workshop
[DE85-004359] 13 p2132 N85-23268
Monitoring of laminate cure with microdielectrometry
[AD-A150663] 14 p2248 N85-23934
New electronic measurement, control devices
14 p2289 N85-24192
An atlas of pure water vapor spectra from 500 to 5000/cm, volume 1
[AD-A151756] 15 p2505 N85-25454
Instrument for measuring dispersional distortions in optical fibers and cables 15 p2530 N85-25595
Advanced smoke meter development survey and analysis
[NASA-CR-166287] 15 p2560 N85-25792
Development and diffusion of automated clinical chemistry analyzers
[PB85-150696] 15 p2561 N85-25796
Three new fiber-optic components
[DE85-006260] 15 p2653 N85-26364
Study of acceptance criteria for joint densities in bituminous airport pavements
[FAA-PM-85-5] 16 p2715 N85-26761
Free-surface phenomena under low- and zero-gravity conditions
[NASA-CR-175835] 16 p2782 N85-27168
A transduction path method of solid state sensor analysis and investigation
[AD-A152123] 16 p2870 N85-27707
Uniaxial angular accelerometers
17 p2944 N85-28173
Apparatus for measuring velocity of sound in fluids
17 p2944 N85-28175
Technique for measuring the effective source reflection coefficient of 2-resistor power splitters
[DE85-009984] 17 p2958 N85-28256
Theoretical and experimental studies of the mechanics of viscoelastic liquids
[AD-A153505] 18 p3070 N85-28987
Oscillating pressure device for dynamic calibration of pressure transducers
[NASA-CASE-LAR-13094-1] 18 p3104 N85-29217
State Weights and Measures Laboratories: Program handbook
[PB85-183358] 18 p3111 N85-29263
A simple power meter for high energy pulsed lasers
[AD-D011661] 18 p3113 N85-29271
Ultrasonic testing of tubes
[BLL-BISI-TRANS-22337-(9022.06)]
18 p3119 N85-29304
Electrodynamic transducers for ultrasonic reception
18 p3119 N85-29306
Rapid rate-kinetic turbidometric assay for quantitation of antiviral complement-fixing antibodies
[AD-A153844] 18 p3152 N85-29516
Multiport optical detectors 18 p3167 N85-29769
A laser slope gauge and a spar buoy wave gauge: Tools for the validation of microwave remote sensors
[AD-A154038] 19 p3272 N85-30290
Transport and relaxation processes in supercritical fluids
[DE85-010554] 19 p3358 N85-30816
Proceedings of the Electronic Test Equipment Division's Annual Program Review of Electronic Test Equipment Industry Response to Emerging Defense Requirements
[AD-A154455] 20 p3436 N85-31320
New measurement solutions in the microwave industry
20 p3437 N85-31324
An overview of measurement solutions for digital systems 20 p3437 N85-31326
Solid surface characterization by contact angle measurements
[FOA-C-40209-C,82] 20 p3459 N85-31483
Improved coordinate measuring machine calibration and control
[DE85-012053] 21 p3580 N85-32315
Digital tachometer 22 p3779 N85-33416
Capacitance measuring device
[DE85-011643] 22 p3787 N85-33460
Electrochemical methane sensor
[DE85-011663] 22 p3787 N85-33464
On-line temperature sensor
[DE85-011641] 22 p3787 N85-33465
Evaluation of coordinate measuring machines
[DE85-011712] 22 p3788 N85-33467
Development of a prototype energy meter
[PB85-196430] 22 p3789 N85-33479
Instrumentation for sensing moisture content of material using a transient thermal pulse
[NASA-CASE-NPO-15493-2] 23 p3933 N85-34373
Apparatus and method for the spectrochemical analysis of liquids using the laser spark
[DE85-005749] 23 p3935 N85-34387
Improved flow cytometer measurement of binding assays
[DE85-006407] 23 p3935 N85-34390
Hydrology
[PB85-182954] 23 p3944 N85-34440
Measurement of low energy cosmic rays aboard Spacelab-1
[SH-10.1-6] 23 p4053 N85-35137
Analyzer, flight line
[AD-A155777] 24 p4067 N85-35207
Development of advanced high-temperature heat flux sensors. Phase 2: Verification testing
[NASA-CR-174973] 24 p4096 N85-35391
Atmospheric nitrogen oxides: Their detection and chemistry
[PB85-193910] 24 p4114 N85-35502
Development of an NBS (National Bureau of Standards) polymer gage for dynamic soil stress measurement
[PB85-208494] 24 p4116 N85-35526

MECHANICAL DEVICES
Stimulus factors in motion perception and spatial orientation 01 p0008 N85-10049
On the computer analysis of structures and mechanical systems 01 p0061 N85-10404
Materials properties, loads, and stress analysis, Spartan REM: Appendix A
[NASA-CR-171092] 02 p0208 N85-11375
Computer models and output, Spartan REM: Appendix B
[NASA-CR-171093] 02 p0208 N85-11376
Kinematic synthesis of planar cam-link mechanisms for exact path and exact motion generation
03 p0341 N85-12189
Soviet robot exhibition reviewed
04 p0491 N85-13128
Swing-arm beam erector (SABER) concept for single astronaut assembly of space structure
[NASA-TP-2379] 10 p1429 N85-19015
Planning of minimum-time trajectories for robot arms
[AD-A148956] 10 p1492 N85-19418
Hoist
[AD-D011458] 10 p1493 N85-19425
Extended moment arm anti-spin device
[NASA-CASE-LAR-12979-1] 12 p1776 N85-21147
Maintainability time standards for electronic equipment
[AD-A149684] 12 p1834 N85-21507
Connection system — insuring against loss of a tool component without using multiple tethers
[NASA-CASE-MSC-20319-1] 12 p1857 N85-21649
Mechanical properties for the grasp of a robotic hand
[AD-A150062] 12 p1860 N85-21669
Cyclic industrial robots with mechanical energy storing devices: Principles of drive design
13 p2046 N85-22907
Optimum design and automated dynamic analysis of flexible mechanisms
[AD-A150152] 13 p2099 N85-23088
Stabilization of steady motion of mechanical systems
14 p2280 N85-24122
Auxiliary units for Robots 14 p2285 N85-24161
Preliminary technology utilization assessment of the robotic fruit harvester
[NASA-CR-175834] 16 p2844 N85-27532
Apparatus for mounting a field emission cathode
[NASA-CASE-LEW-14108-1] 18 p3094 N85-29149
Hoop/column antenna deployment mechanism overview 22 p3796 N85-33514
The properties of thin-section, four-point-contact ball bearings in space 22 p3797 N85-33521
The design and development of a spacecraft appendage tie down mechanism 22 p3797 N85-33522
The balancing of complex linkage mechanisms
23 p3924 N85-34313
A versatile computer package for mechanism analysis
23 p3924 N85-34314
A versatile computer package for mechanism analysis, part 2: Dynamics and balance
23 p3924 N85-34315

MECHANICAL DRAWINGS
U ENGINEERING DRAWINGS

MECHANICAL DRIVES
NT HELICOPTER PROPELLER DRIVE
NT TRANSMISSIONS (MACHINE ELEMENTS)
Vibrational power transmission of an idealised gearbox
[ISVR-TR-124] 02 p0204 N85-11348
Nitinol devices, phase 2, integration of slip ring system and tracking mechanism with memory drive
[BMFT-FB-W-84-032] 05 p0619 N85-13059
Torque sensor
[AD-D011276] 05 p0639 N85-14096
Space shuttle rudder/speedbrake actuation subsystem
06 p1102 N85-16965
Specifications of bloc floppy disk drives
08 p1141 N85-17188
MOM peripherals 08 p1141 N85-17189
Acoustic radiation from single and double ribbed circular cylindrical shells
[AD-A148771] 08 p1219 N85-17676
Precision measurement of torsional oscillations induced by gear errors 09 p1338 N85-18416
Adjustment structure
[AD-D011481] 10 p1459 N85-19193
Armenia markets new drive motors for machine tools
10 p1461 N85-19212
Antenna azis drive torques for the 70-meter antenna
10 p1464 N85-19237
Characteristics of the elevation drive suspension of the 64-meter antennas 10 p1464 N85-19240
Seven-year thermal-vacuum real-life test of a solar array drive mechanism manufactured by Marconi Space and Defence Systems (Model No. 002)
[ESA-ESTL-82] 11 p1616 N85-20161
Design of tightening device and calculation of forces in manipulator transmissions with base-drive mounted
13 p2046 N85-22904
Cyclic industrial robots with mechanical energy storing devices: Principles of drive design
13 p2046 N85-22907
Assembly robot control algorithms
13 p2046 N85-22908
Summary of drive-train component technology in helicopters 14 p2220 N85-23768
Special power train requirements for the next generation of rotary-wing aircraft 14 p2220 N85-23769
Pneumohydraulic drive 14 p2268 N85-24050
Novel drives for machine tools
14 p2268 N85-24053
Manufacture of drive wheel vanes for hydraulic turbines on program controlled machine tools
14 p2269 N85-24058
Solid state compressor
[AD-A150790] 14 p2311 N85-24302
Thermal traction contact performance evaluation under fully flooded and starved conditions
[NASA-CR-168173] 15 p2569 N85-25848
A description of the 64-meter antenna elevation drive gears and their strange wear 16 p2771 N85-27107
AC powertrain for an electric vehicle, phase 2 and phase 3
[NASA-CR-175760] 16 p2880 N85-27771
Vibrations of rotors connected through couplings with backlash 17 p2940 N85-28147
Remotely operable peristaltic pump
[NASA-CASE-MFS-29059-1] 18 p3116 N85-29268
Study of meshing of beveled gears with normally decreasing arc teeth
[NASA-TM-77866] 18 p3117 N85-29293
Improvement of conditions for meshing spiral bevel gears
[NASA-TM-77867] 18 p3117 N85-29294
Observations of high resistance on slip-rings employing Ag/MoS2/Cu brushes — solar array drives
[ESA-ESTL-70] 18 p3123 N85-29333
Department of Energy gear drive unit final prototype testing and design evaluation
[DE85-003296] 22 p3793 N85-33489
Nineteenth Aerospace Mechanisms Symposium
[NASA-CP-2371] 22 p3795 N85-33512
Drag-compensated, precision-powered hinge system
22 p3796 N85-33517
The design and development of a constant-speed solar array drive 22 p3796 N85-33519
Application of traction drives as servo mechanisms
22 p3797 N85-33520
Features of the solar array drive mechanism for the space telescope 22 p3796 N85-33532
Dual optical mechanical position tracker
[AD-D011739] 22 p3844 N85-33811
High powered epicyclic gears: Some recent development 23 p3924 N85-34316
State-of-the-art of solid-state motor controllers
[TIB5-009674] 24 p4182 N85-35808

MECHANICAL ENGINEERING
National Science Foundation grants and awards for fiscal year 1983, volume 2
[PB84-212323] 01 p0125 N85-10854
Activities report of the Department of Engineering
03 p0342 N85-12202
Heavy duty precision pan and tilt head
[AD-A148669] 04 p0509 N85-13248
Activities report in technology
[ISBN-951-38-1998-1] 04 p0577 N85-13881
BAe antenna hardware technology for current satellite projects 05 p0628 N85-14011
Hemispherical antenna pointing mechanism — satellite antennae 05 p0627 N85-14021
Machine tools at 1984 Leipzig Spring Fair
08 p0815 N85-15177

A summary of the foundation research program
[AD-A146524] 06 p0891 N85-15856
Research and technology, 1984 report
[NASA-TM-83986] 07 p1061 N85-16730
Eigenvalues of rotating machinery 08 p1167 N85-17361
The analysis of kinematic restraint and freedom using point contacts
[RR-154/03/75/02] 08 p1169 N85-17372
The synthesis of kinematic restraint and freedom using point contacts
[RR-154/03/75/03] 08 p1169 N85-17373
Technical data on new engineering products 10 p1460 N85-19201
Flexible applications robot used in Moscow training course 10 p1462 N85-19217
Design and qualification testing of the Olympus solar array blanket 13 p2009 N85-22600
The Olympus solar array structure and mechanisms 13 p2012 N85-22623
Advances in cutting tool technology surveyed 13 p2051 N85-22840
The design and validation of software for dimensional metrology
[NPL-DITC-50/84] 15 p2521 N85-25542
Compilation of abstracts of theses submitted by candidates for degrees
[AD-A151722] 16 p2675 N85-27739
Micro-CAE mechanical engineering software development at Lawrence Livermore National Laboratory and participating universities and technology transfer
[DE85-006660] 18 p3163 N85-29597
Special tools used by cosmonauts in EVA 22 p3731 N85-33129
Proceedings of the Mechanisms Conference, volume 1 23 p3923 N85-34309
Proceedings of the Mechanisms Conference, volume 2 23 p3924 N85-34318
An introduction to finite elements 23 p3924 N85-34319
Inertial stresses and deformations in mechanisms 23 p3924 N85-34320
Optimization in the computer aided design of mechanisms 23 p3924 N85-34321

MECHANICAL MEASUREMENT
NT DISPLACEMENT MEASUREMENT
NT DRAG MEASUREMENT
NT FLOW MEASUREMENT
NT FRICTION MEASUREMENT
NT PRESSURE MEASUREMENT
NT STRESS MEASUREMENT
NT THRUST MEASUREMENT
NT VELOCITY MEASUREMENT
NT VIBRATION MEASUREMENT
NT WIND MEASUREMENT
NT WIND VELOCITY MEASUREMENT
Measuring and control tasks in OPTIWA 05 p0669 N85-14304
Viscosity measurements for thick-film pastes 06 p0831 N85-15280
Application of the unloading compliance methods in fracture toughness measurements of a quenched and tempered steel
[BLL-CE-TRANS-7953-(9022.09)] 20 p3465 N85-31523
A versatile computer package for mechanism analysis 23 p3924 N85-34314

MECHANICAL OSCILLATORS
NT PENDULUMS
Measurement of blood and plasma density with the mechanical oscillator technique 05 p0693 N85-14456
Quality control in soil compaction by behaviours of exciter
[AD-P004295] 09 p1408 N85-18872
Precise bearing support dithever
[AD-D011470] 10 p1493 N85-19428
Investigation of the time history and modal responses of some simple linear and nonlinear systems
[DE85-002027] 14 p2321 N85-24344
Method for controlling the viscosity of siloxane oils
[DE85-011586] 23 p3909 N85-34221

MECHANICAL PROPERTIES
NT ABRASION RESISTANCE
NT AEROELASTICITY
NT BRITTLENESS
NT BULK MODULUS
NT COMPRESSIBILITY
NT COMPRESSIVE STRENGTH
NT CREEP PROPERTIES
NT CREEP RUPTURE STRENGTH
NT CREEP STRENGTH
NT DIMENSIONAL STABILITY
NT DUCTILITY
NT DYNAMIC MODULUS OF ELASTICITY
NT EARTHQUAKE RESISTANCE
NT ELASTIC PROPERTIES
NT ELASTOPLASTICITY
NT ELECTROSTRICTION
NT FATIGUE LIFE
NT FIBER STRENGTH
NT FLEXIBILITY
NT FRACTURE STRENGTH
NT HARDNESS
NT HIGH STRENGTH
NT HYDROELASTICITY
NT IMPACT STRENGTH
NT KNOOP HARDNESS
NT MAGNETOSTRICTION
NT MALLEABILITY
NT MICROHARDNESS
NT MICROYIELD STRENGTH
NT MODULAR RATIOS
NT MODULUS OF ELASTICITY
NT NOTCH SENSITIVITY
NT NOTCH STRENGTH
NT PHOTOELASTICITY
NT PHOTOPLASTICITY
NT PHOTOVISCOELASTICITY
NT PIEZOELECTRICITY
NT PLASTIC PROPERTIES
NT POISSON RATIO
NT PROPORTIONAL LIMIT
NT RESILIENCE
NT SHEAR CREEP
NT SHEAR PROPERTIES
NT SHEAR STRENGTH
NT SHELL STABILITY
NT STEADY STATE CREEP
NT STIFFNESS
NT STRESS CYCLES
NT STRESS RATIO
NT STRESS RELAXATION
NT STRUCTURAL STABILITY
NT SUPERPLASTICITY
NT TENSILE CREEP
NT TENSILE PROPERTIES
NT TENSILE STRENGTH
NT THERMAL RESISTANCE
NT THERMOELASTICITY
NT THERMOPLASTICITY
NT THERMOVISCOELASTICITY
NT TOUGHNESS
NT VISCOELASTICITY
NT VISCOPLASTICITY
NT WELD STRENGTH
NT YIELD POINT
NT YIELD STRENGTH
Development of new and improved polymer matrix resin systems, phase 1
[NASA-CR-166595] 01 p0017 N85-10104
Effect of scandium on the structure and properties of Al-Zn-Mg alloys 01 p0018 N85-10111
Heat treatment of welded joints in OT4 and VT20 titanium alloys 01 p0020 N85-10119
Influence of nitrogen on the sensitization, corrosion, mechanical, and microstructural properties of austenitic stainless steels
[DE84-015134] 01 p0028 N85-10177
Fabrication and characterization of Si3N4 ceramics without additives by high pressure hot pressing
[NASA-TM-77724] 01 p0031 N85-10189
Diblock copolymers of polystyrene/1,2 polybutadiene and polystyrene/polybutene-1: Molecular structure, morphology and mechanical properties
[AD-A144960] 01 p0033 N85-10201
Electrically conductive rigid polyurethane foam
[DE84-014490] 01 p0033 N85-10203
Broadband transverse field interaction continuous beam amplifier
[AD-D011229] 01 p0043 N85-10279
Ultrasonic nondestructive evaluation, microstructure, and mechanical property interrelations
[NASA-TM-86876] 01 p0056 N85-10371
Materials studies for magnetic fusion energy applications at low temperatures, 7
[DE84-013467] 01 p0122 N85-10837
Laser speckle technique for burner liner strain measurements 02 p0142 N85-10960
Microstructural design in low alloy steels 02 p0176 N85-11179
Toughness in high speed steels and hard metals 02 p0176 N85-11181
The constitution as the basis for recent and future developments of wear resistant materials 02 p0179 N85-11205
Physical-chemical properties of articulated rodlike polymers
[AD-A145549] 02 p0186 N85-11244
Silicon nitride joining
[AD-A145668] 02 p0187 N85-11248
Method of making a porous carbon cathode: A porous carbon cathode so made, and electrochemical cell including the porous carbon cathode
[AD-D011243] 02 p0195 N85-11301
Materials properties, loads, and stress analysis, Spartan REM: Appendix A
[NASA-CR-171092] 02 p0208 N85-11375
Use of magnetic compression based on amorphous alloys as a drive for induction linacs
[DE84-014524] 02 p0277 N85-11805
Optical waveguide spatial filters
[AD-A145674] 02 p0280 N85-11825
Materials modification by ion beam mixing
[AD-P003948] 02 p0286 N85-11864
Review of the University of Manchester Ion Implantation Conference
[AD-P003950] 02 p0286 N85-11866
Mechanical properties of a leaded, resulfurized, rephosphorized steel in various thermo/mechanical conditions
[PB84-216464] 03 p0333 N85-12144
Guide to the selection of rubbers
[AMTE(N)-TM-84301] 03 p0336 N85-12164
USSR report: Materials science and metallurgy
[JPRS-UMS-84-007] 03 p0348 N85-12244
Causes of strength reduction in welded titanium-steel joints 03 p0352 N85-12262
Reinforcement of molybdenum disilicide with nematic crystals of aluminum oxide 03 p0353 N85-12269
Constitutive features of solids at shock-wave loading rates
[DE84-015715] 03 p0362 N85-12325
Static and dynamic characteristics of materials with beam-microstructure 03 p0370 N85-12361
Review: Role of refractory metal alloys in fusion reactor applications
[AERE-R-11317] 03 p0422 N85-12695
Morphology and dynamic mechanical properties of diglycidyl ether of bisphenol-A toughened with carboxyl-terminated butadiene-acrylonitrile 04 p0456 N85-12958
Matrix synthesis and characterization 04 p0457 N85-12965
Experimental and theoretical studies of moisture and temperature effects on the mechanical properties of graphite/epoxy laminates and neat resins 04 p0467 N85-12969
High temperature mechanical properties of ceramics
[DE84-016492] 04 p0480 N85-13058
Nondestructive determination of mechanical properties — aluminum alloys 04 p0512 N85-13266
Arctic ice island and sea ice movements and mechanical properties
[DE84-016323] 04 p0542 N85-13450
Investigation of the relations between neat resin and advanced composite mechanical properties. Volume 1: Results
[NASA-CR-172303] 05 p0612 N85-13911
Characterization of stressed metals using acoustic shear waves 05 p0648 N85-14159
Theoretical methods for the study of transition metals in crystals
[DE84-015606] 05 p0732 N85-14709
Investigation of the relations between resin and advanced composite mechanical properties. Volume 2: Appendices
[NASA-CR-172303-VOL-2] 06 p0763 N85-14880
The metallurgical processes during the soft soldering of copper and copper alloys and the strength characteristics of soldered joints
[BLL-T6366/BG/WH903/84] 06 p0767 N85-14908
Effect of substituted phenylnadimides on processing and properties of PMR polyimide composites
[NASA-TM-86902] 06 p0770 N85-14929
Effects of surface interactions and mechanical properties of PBXs (plastic bonded explosives) on explosive sensitivity
[AD-A146368] 06 p0773 N85-14944
A nonnoble front metallization process 06 p0830 N85-15279
Size dependence of chondrule textural types 06 p0882 N85-15606
Titanium Matrix/Continuous Fiber/Continuous fiber composite interface interactions and their influence on mechanical properties
[AD-A147504] 07 p0920 N85-15829
Austenitic stainless steel for high temperature and pressure applications
[BLL-RISLEY-TR-4527-(9091.9F)] 07 p0925 N85-15880
Design of ordered intermetallic alloys for high-temperature structural use
[DE85-000897] 07 p0928 N85-15885
Gradient polymers
[AD-A146836] 07 p0931 N85-15900

Thermal and mechanical properties of polyurethane foams and a survey of insulating concretes at cryogenic temperatures
[PB85-100949/GAR] 07 p0934 N85-15916
Determination of the decomposition behavior of double base propellants at low temperatures
08 p1117 N85-17045
Effects of high energy radiation on the mechanical properties of epoxy-graphite fiber reinforced composites
[NASA-CR-174314] 08 p1118 N85-17047
ESR (Electroslag Refining) technology in Australia: Laboratory research and industrial development
[AD-A147776] 08 p1129 N85-17114
Mechanical properties and microstructure of centrifugally cast alloy 718
[AD-A147800] 08 p1129 N85-17116
Review of the mechanical properties of SMC and GRP materials
[NPL-DMA(A)-88] 08 p1131 N85-17128
Field test results of experimental EPDM (Ethylene Propylene Diene Monomer) and PUF (Polyurethane Foam) roofing
[AD-A147897] 08 p1132 N85-17133
Process development for the production of technically high quality monocrystalline diamond grits
[BMFT-FB-T-84-204] 08 p1136 N85-17166
Effect of iron on the performance of IN 625 weld deposits
[BR91456] 08 p1169 N85-17376
Age life prediction of nylon 66 parachute materials. Part 1: Mechanical properties
[AD-A147698] 08 p1170 N85-17378
The Shock and Vibration Digest, volume 16, no. 10
[AD-A147588] 09 p1331 N85-18361
Physical characterization of magma
[DE85-000568] 09 p1354 N85-18519
Magnetic fusion energy plasma interactive and high heat flux components. Volume 2: Technical assessment of the critical issues and problem areas in high heat flux materials and component development
[DE85-001155] 09 p1393 N85-18764
Online directory of databases for material properties
[DE84-016511] 09 p1402 N85-18824
Mechanics of composite materials
[DE85-003611] 10 p1432 N85-19031
Mechanical properties of Be-Al composite
10 p1443 N85-19094
Quantitative estimate of compatibility of fiber composite material components 10 p1444 N85-19099
Influence of laser hardening on mechanical properties of type 45 steel with various preliminary heat treatments
10 p1446 N85-19111
Kinetics of joint formation during diffusion welding of VT5 titanium alloys 10 p1448 N85-19125
Modern solid state laser materials
[DE85-003665] 10 p1490 N85-19410
Mechanical interactions of rough surfaces
[DE85-000814] 10 p1494 N85-19434
Study of the physical properties of crystalline rocks in the southeast Voronezh anteclise
[NASA-TM-77823] 10 p1514 N85-19551
Strength properties of unidirectionally reinforced hybrid composites 11 p1599 N85-20056
Effect of silicon and titanium properties on Ni9Co9Mo5Ti steel 11 p1601 N85-20069
Dependence of mechanical properties of large VT3-1 alloy forgings on microstructure parameters
11 p1602 N85-20072
Effect of macrostructure on durability of polycrystalline graphite 11 p1605 N85-20091
Method for increasing linearity of load cell
11 p1623 N85-20221
Report of the Technology and Test Panel
11 p1648 N85-20370
Requirements of quantitative NDE in developing fracture control plans
[DE85-003147] 11 p1654 N85-20415
Magnetic and structural properties of shock-synthesized zinc ferrite
[DE85-000469] 11 p1736 N85-20915
A DOE directory of databases for material properties
[UCAR-10124] 11 p1739 N85-20937
Composite structural materials
[NASA-CR-175515] 12 p1796 N85-21268
Effect of reduction of strategic Columbium addition in 718 Alloy on the structure and properties
[NASA-CR-174841] 12 p1805 N85-21320
Effects of chromium and aluminum on mechanical and oxidation properties of iron-nickel-base superalloys based on CG-27
[NASA-TP-2443] 12 p1805 N85-21323
Elastomer toughened polyimide adhesives — bonding metal and composite material structures for aircraft and spacecraft
[NASA-CASE-LAR-12775-2] 12 p1809 N85-21349
Broadband thermoplastic radomes
[AD-P004369] 12 p1827 N85-21483
A new model for thin plates with rapidly varying thickness. Part 3: Comparison of different scalings
[AD-A149748] 12 p1866 N85-21704
Summary of recent research on mechanical behavior of polycrystalline solids
[DE85-004601] 12 p1942 N85-22199
Research Reports: 1984 NASA/ASEE Summer Faculty Fellowship Program
[NASA-CR-171317] 12 p1944 N85-22210
Investigation of the effects of NaOH dopant level on the physical and mechanical properties of carbon/phenolic composite material 12 p1945 N85-22213
Solid Rocket Motor Case (SRMC) dynamic sensitivity to changes in composite properties
12 p1948 N85-22236
Kapton charging characteristics: Effects of material thickness and electron-energy distribution
13 p1996 N85-22513
Influence of external electric field on structural-mechanical properties of powdered materials
13 p2013 N85-22630
Rapid solidification processing of magnesium alloys
[AD-A150270] 13 p2022 N85-22668
Mechanical properties of electrodeposited nickel and copper
[DE85-005321] 13 p2023 N85-22677
Influence of laser treatment of structure and mechanical properties if MA21 alloy 13 p2029 N85-22713
Influence of annealing on cyclic and short-term strength of thin sheets of VT1-0 titanium and OTR4 alloy
13 p2031 N85-22727
Method of calculating strength of joint produced by cold welding of aluminum under discrete loading
13 p2034 N85-22743
Effect of moisture in inert gases on density of seam metal and on mechanical characteristics of welded joints of aluminum and aluminum alloys
13 p2034 N85-22744
Characteristics of surface crack development in ATtsS aluminum alloy during slow-cycle loading
13 p2034 N85-22745
Research program on the effect of pressure on the mechanical properties of polymers, part 2
[DE85-000995] 13 p2037 N85-22761
Diamond cutters' grinders 13 p2051 N85-22841
The ferrite permanent magnet AC motor: A technical and economical assessment
[DE85-002480] 13 p2066 N85-22903
The Shock and Vibration Digest, volume 16, no. 12
[AD-A150594] 13 p2102 N85-23102
Significant parameters of the behavior and of the surface damage of the lubricated Hertzian contact: An application to gears 14 p2222 N85-23783
Extreme precision antenna reflector study results
14 p2232 N85-23830
NASA space materials research
14 p2232 N85-23831
Fracture toughness of HY-130 steel weld metals
[AD-A150841] 14 p2255 N85-23976
Outlook for polymer composite materials
15 p2497 N85-25403
Research, development of composite materials described 15 p2497 N85-25404
Local elastoplastic fracture of fibrous composite materials 15 p2497 N85-25405
Ways of improving level and stability of mechanical characteristics of diffusion-welded joints of OT4 titanium alloy 15 p2499 N85-25417
Structure and mechanical properties of dispersion-hardened nickel alloy joints welded by diffusion 15 p2500 N85-25422
Influence of oxygen traces on the properties of tungsten heavy metals
[BLL-RARDE-TR-1177-(7291.7965)]
15 p2508 N85-25470
Mechanical properties of TiN deposits obtained by PVD and TiN, TiC, TiC + TiN obtained by CVD
[BLL-RISLEY-TR-6007-(9091.9F)]
15 p2508 N85-25471
Study of high performance alloy electroforming
[NASA-CR-175741] 15 p2508 N85-25473
Summary of recent investigations of the mechanical properties of polycrystalline solids
[DE85-006778] 15 p2511 N85-25492
Oxidation of nickel-aluminum and iron-aluminum alloys
[DE85-006930] 15 p2512 N85-25497
USSR report: Materials science and metallurgy
[JPRS-UMS-85-004] 15 p2513 N85-25503
Hardening of titanium alloy electric-arc welded joints
15 p2514 N85-25513
Mechanical properties of cast Martensitic high-strength multicomponent titanium alloys
15 p2514 N85-25514
Thermal stability of titanium alloys after cold plastic deformation 15 p2515 N85-25515
Structure and properties of VT20L titanium alloy with 0.1-0.3 percent content 15 p2515 N85-25517
Effect of initial structure on texture of pressed titanium alloy bars 15 p2515 N85-25518
Mechanical aspects of interfaces and surfaces in ceramic containing systems
[AD-A151978] 15 p2519 N85-25530
Titanium alloys, products, standards listed
15 p2533 N85-25626
A Gimbal sizing analysis for an IPACS rotating assembly
[NASA-CR-172524] 16 p2741 N85-28913
Pulsed electrodeposition
[DE85-007057] 16 p2747 N85-28950
Effect of nickel addition on the thermal, magnetic and magnetomechanical properties of Fe(80)B(15)Si(5)
[AD-A152261] 16 p2749 N85-28967
New materials and techniques for aircraft structures
[B8580074] 17 p2897 N85-27861
Mechanical properties of polycrystalline alpa titanium
[BLL-BISI-TRANS-21923-(9022.06)]
17 p2924 N85-28029
Thermomechanical treatment aimed at the protection of type 316 stainless steel from IGC and IGSCC
[BLL-BISI-TRANS-22498-(9022.06)]
17 p2925 N85-28040
The synergistic actions of stress corrosion cracking and corrosion fatigue
[BLL-BISI-TRANS-22334-(9022.06)]
17 p2926 N85-28045
Improving the properties of copper and copper alloys through heat treatment and alloying
[BLL-BISI-TRANS-21939-(9022.06)]
17 p2926 N85-28047
Steels with improved machinability
[BLL-BISI-22341-(9022.06)] 17 p2927 N85-28061
Microstructure and mechanical properties of rare-earths-microalloyed high-speed tool steel
[BLL-BISI-TRANS-22043-(9022.06)]
17 p2928 N85-28064
Physical properties of steels and their temperature dependence
[BLL-BISI-TRANS-22285-(9022.06)]
17 p2928 N85-28065
Influence of composition on the microstructural evolution and mechanical properties of irradiated Fe-Ni-Cr ternaries
[DE85-007462] 17 p2931 N85-28094
USSR report: Engineering and equipment
[JPRS-UEQ-85-004] 17 p2939 N85-28142
Conformational and mechanical properties at high strain rates
[AD-A153401] 17 p2958 N85-28272
Examination of the regions of the joint of sheets bonded by the explosive welding technique
[BLL-BISI-TRANS-22352-(9022.06)]
17 p2973 N85-28370
Tests of low-cycle fatigue of elected steels of class 11
[BLL-BISI-TRANS-22039-(9022.06)]
17 p2978 N85-28404
Radiation damage experiments and lifetime estimates for beryllium components in fusion systems
[DE85-008038] 17 p3040 N85-28811
Mechanical properties of adhesively bonded aluminum structures protected with hydration inhibitors
[AD-A153755] 18 p3079 N85-29047
Statistical fracture theories for brittle materials
[AD-A153530] 18 p3121 N85-29324
Measurement and calculation of the mechanical response of a highly fractured rock
[DE85-008421] 18 p3127 N85-29362
Influence of microstructure on mechanical properties in cemented tungsten-carbides 19 p3230 N85-30029
Possible causes of modification and strengthening of aluminum by scandium 19 p3241 N85-30099
Properties of heat resistant Ni-Al-Nb alloys with unidirectional eutectic structure
19 p3247 N85-30123
Mechanical protection of DLC films on fused silica slides
[NASA-TM-87058] 19 p3248 N85-30138
On design of off-axis specimens
[AD-A154328] 19 p3286 N85-30379
Numerical simulation of chemical and physical properties of cumulus clouds
[DE85-009744] 19 p3317 N85-30584
Special materials: Carbons
[SNIAS-851-551-104] 20 p3421 N85-31235
Activities report of the Laboratory of Mechanics and Energetics 20 p3437 N85-31329
Improved materials for composite and adhesive joints
[AD-A155085] 21 p3562 N85-32153
Basic cryogenics and materials. Phase 1
[NASA-CR-177932] 21 p3572 N85-32215

Effects of environment on spacecraft materials
22 p3733 N85-33144
Filament wound structures in PSP carbon composite [RV10/84424] 22 p3743 N85-33196
Rationale in the selection of corrosion protective coating systems 22 p3750 N85-33242
Geologic, technical, and economic sensitivity analysis in support of the GRI (Gase Research Institute) tight gas reservoirs project area [PB85-192276] 22 p3802 N85-33659
Mechanical properties of SiC fiber-reinforced reaction-bonded Si3N4 composites [NASA-TM-87085] 23 p3909 N85-34223
Proceedings of the Mechanisms Conference, volume 1 23 p3923 N85-34309
A versatile computer package for mechanism analysis, part 2: Dynamics and balance 23 p3924 N85-34315
Proceedings of the Mechanisms Conference, volume 2 23 p3924 N85-34316
Generated spiral bevel gears: Optimal machine-tool settings and tooth contact analysis [NASA-TM-87075] 23 p3937 N85-34405
Contribution to the properties of carbon fiber reinforced composites — structural mechanics [ESA-TT-849] 24 p4074 N85-35246
Interaction of trace elements and welding parameters on GTA weld shape [DE85-004046] 24 p4080 N85-35294
Development and characterization of carbon-bonded carbon fiber insulation for radioisotope space power systems [DE85-013385] 24 p4082 N85-35229
User's guide: A computer program for strength analysis of non-hydraulic concrete structural elements. Report 1. Concrete General Strength Investigation (CGSI) [AD-A156392] 24 p4102 N85-35428

MECHANICAL RESONANCE
U RESONANT VIBRATION

MECHANICAL SHOCK
NT HYDRAULIC SHOCK
Shock capturing finite difference algorithms for supersonic flow past fighter and missile type configurations [NASA-CR-174081] 02 p0134 N85-10913
The Shock and Vibration Digest, volume 16, no. 9 [AD-A146779] 07 p0976 N85-16200
Reflections on trends in dynamics: The Navy's perspective 09 p1334 N85-16382
Acceleration responses of typical LRU's subjected to bench handling and installation shock 09 p1334 N85-16385
The Shock and Vibration Bulletin 54. Part 2: Ship shock, shock and blast and ground shock [AD-A148132] 09 p1334 N85-16386
Two-dimensional shock response of a mass on energy-absorbing shock mounts 09 p1334 N85-16389
Optimum design for nonlinear shock mounts for transient inputs 09 p1334 N85-16390
Alternative shock characterizations for consistent shock test specifications 09 p1335 N85-16396
Shock response analysis by personal computer using the extended IFT algorithm 09 p1335 N85-16397
A study of the effect of mass loading on the shock environment 09 p1336 N85-16401
The Shock and Vibration Bulletin 54. Part 3: Structural dynamics, machinery dynamics and vibration problems [AD-A148133] 09 p1337 N85-16406
The Shock and Vibration Digest, volume 16, no. 12 [AD-A150594] 13 p2102 N85-23102
Recovery of pyroshock data from distorted acceleration records [NASA-TP-2494] 20 p3407 N85-31141
Short-time spectroscopic measurement of the temperature of solids [ISL-CO-302/84] 20 p3459 N85-31486
A mechanical model of the human body and its application 24 p4129 N85-35508

MECHANICS (PHYSICS)
USSR report: Physics and mathematics [JPRS-UPM-84-006] 02 p0258 N85-11676
Computational mechanics: A perspective on problems and opportunities for increasing productivity and quality of engineering [PB85-128106] 12 p1950 N85-22252
User's and programmer's guide to the mechanics of moving finite element code [DE85-006165] 13 p2152 N85-23365

MECHANIZATION
Economic model of calibration improvements for automatic test equipment [PB84-217827] 01 p0051 N85-10335
Automation of assembly of electrical products 03 p0346 N85-12228
Automation and robotics in welding 15 p2586 N85-25831
USSR report: Science and technology policy [JPRS-UST-85-008] 17 p3049 N85-26872
Importance of automation, robotization in economy 21 p3572 N85-32219
Re-designing a mechanism for higher speed: A case history from textile machinery 23 p3923 N85-34310

MECHANORECEPTORS
Effects of tasks on responses of human skin mechanoreceptors 11 p1691 N85-20635
Gravity perception in a Cladoceran-Zooplankter: Anatomy of antennal socket setae of Daphnia magna 15 p2605 N85-26057

MEDIA
NT ANISOTROPIC MEDIA
NT ELASTIC MEDIA
NT INTERGALACTIC MEDIA
NT INTERPLANETARY DUST
NT INTERPLANETARY MEDIUM
NT ZODIACAL DUST
Thermomechanical cracking in layered media from moving friction load [AD-A146022] 03 p0373 N85-12379
Localization of waves in a disordered medium 19 p3373 N85-30926
Toward the propagation of waves in unsteady media 21 p3683 N85-32851

MEDIAN (STATISTICS)
A multiple regression technique for detecting outliers [REPT-84-33] 17 p3025 N85-26706

MEDICAL ELECTRONICS
Bioengineering and rehabilitation: Windows of opportunity past, present and future [NASA-EP-216] 16 p2841 N85-27516

MEDICAL EQUIPMENT
NT PROSTHETIC DEVICES
NT RESPIRATORS
NT X RAY APPARATUS
NT X RAY TUBES
Military vital sign monitor [AD-A147257] 07 p1016 N85-16452
Improved radiographic viewing system [AD-A147587] 07 p1016 N85-16456
Functional system theory in practice 11 p1690 N85-20629
Medical planning criteria for implementation of clinical hyperbaric facilities [AD-A151001] 14 p2389 N85-24715
Bioengineering and rehabilitation: Windows of opportunity past, present and future [NASA-EP-216] 16 p2841 N85-27516
Gas analysis techniques for human physiological measurements in space — Spacelab [A/6537] 20 p3507 N85-31603
Heavy ion medical accelerator options [DE85-011204] 22 p3841 N85-33784
New technologies at the forefront of industrial developments 24 p4061 N85-35168
Dental multi-purpose slowspeed handpiece test and evaluation [AD-A155784] 24 p4130 N85-35606

MEDICAL PERSONNEL
Efforts to improve aviation medical examiner performance through continuing medical education and annual performance reports [AD-A148078] 06 p1195 N85-17531

MEDICAL SCIENCE
NT ANESTHESIOLOGY
NT DENTISTRY
NT ENDOCRINOLOGY
NT EPIDEMIOLOGY
NT HISTOLOGY
NT HUMAN PATHOLOGY
NT IMMUNOLOGY
NT NEUROLOGY
NT NEUROPSYCHIATRY
NT NUCLEAR MEDICINE
NT OPHTHALMOLOGY
NT PATHOLOGY
NT RADIOBIOLOGY
NT RADIOLOGY
Evaluation of the National Library of Medicine's programs in the medical behavior sciences. Coverage of the Medical Behavioral Sciences (MBS) literature in monographic databases, study 5 [PB84-230531] 03 p0439 N85-12787
Evaluation of the National Library of Medicine's programs in the medical behavior sciences. Online searchers' reactions to database and vendor capabilities in the Medical Behavioral Sciences (MBS), study 4 [PB84-230523] 03 p0439 N85-12796
Evaluation of the National Library of Medicine's programs in the medical behavior sciences. Quality of indexing: The development and testing of a methodology comparing databases covering the Medical Behavioral Sciences (MBS) literature, study 3 [PB84-230515] 03 p0439 N85-12799
Evaluation of the National Library of Medicine's programs in the medical behavior sciences. Test retrievals in five major databases covering the Medical Behavioral Sciences (MBS) literature, study 2 [PB84-230507] 03 p0440 N85-12800
Evaluation of the National Library of Medicine's programs in the medical behavior sciences. Coverage, overlaps and gaps in bibliographic databases dealing with the Medical Behavioral Sciences (MBS) literature, study 1 [PB84-230499] 03 p0440 N85-12801
Evaluation of the National Library of Medicine's program in the medical behavior sciences. An analysis of the National Library of Medicine's (NLM) handling of Medical Behavioral Sciences (MBS) literatures: Some research tests of methods for evaluating bibliographic databases, executive summary [PB84-230481] 03 p0440 N85-12802
The application of basic control laws to human medicine [DFVLR-MITT-84-13] 05 p0697 N85-14482
USSR report: Life sciences. Biomedical and behavioral sciences [JPRS-UBB-85-001] 06 p1193 N85-17515
USSR report: Life sciences. Biomedical and behavioral sciences [JPRS-UBB-85-007] 09 p1362 N85-19586
USSR report: Life sciences. Biomedical and behavioral sciences [JPRS-UBB-85-008] 10 p1523 N85-19605
USSR report: Life sciences. Biomedical and behavioral sciences [JPRS-UBB-85-010] 11 p1690 N85-20628
Symposium on Military Aviation Medicine summarized 11 p1696 N85-20663
Research and technology activities at Ames Research Center's Biomedical Research Division [NASA-TM-86692] 12 p1899 N85-21925
Armed forces special Symposium on Medicine of Altitudes 13 p2166 N85-23441
China report: Science and technology [JPRS-CST-84-012] 14 p2283 N85-24140
Advances in study of cold injury in Army 14 p2283 N85-24145
China report: Science and technology [JPRS-CST-85-011] 15 p2551 N85-25746
Alterations/corrections to the BRASS Program [NASA-CR-171674] 15 p2616 N85-26121
New technologies to improve laboratory testing [DE85-008151] 18 p3110 N85-29257
Applications of aerospace technology in biology and medicine [NASA-CR-166100] 19 p3328 N85-30619
USSR Space Life Sciences Digest [NASA-CR-3922] 21 p3656 N85-32709
Structural changes in thyroid due to high-altitude adaptation in Kirghizia 22 p3820 N85-33666
Electroanesthesia as a means of controlling cold stress of local hypothermia 22 p3823 N85-33687
USSR report: Life sciences. Biomedical and behavioral sciences [JPRS-UBB-85-021] 23 p3951 N85-34489
USSR report: Space Biology and Aerospace Medicine, vol. 19, no. 3, May - June 1985 [JPRS-USB-85-005] 23 p3952 N85-34494
Tolerance to +Gz and +Gx accelerations of individuals in older age groups in good health and with early signs of arteriosclerosis 23 p3952 N85-34496
Proceedings of the 14th Army Science Conference. Volume 2: Principal authors I through O [AD-A149201] 24 p4144 N85-35690

MEDICAL SERVICES
Bioengineering and rehabilitation: Windows of opportunity past, present and future [NASA-EP-216] 16 p2841 N85-27516
Test and Evaluation Master Plan (TEMP) for the Navy Occupational Health Information Management System (NOHIMS). Phase 1: Appendix A through appendix U [AD-A154179] 19 p3360 N85-30957

MEDITERRANEAN SEA
Mineral nutrients in Mediterranean ecosystems [REPT-71] 01 p0069 N85-10456
SEASAT altimeter data over the Mediterranean: Implications for ERS-1 03 p0362 N85-12443
The altimeter as a support to the scatterometer in the representation of winds and derived wave fields in coastal waters and enclosed seas: A research at its onset 03 p0383 N85-12453
Hydrologic characteristics of the Mediterranean and Black Sea 07 p0961 N85-16228

Bio-optical variability in the Alboran Sea as assessed by Nimbus-7 coastal zone color scanner
[AD-A147909] 07 p0969 N85-16281
Preliminary report on the results of hydrological measurements in the southern Tyrrhenian Sea, in the Messina strait and in the western Ionian sea
[PREPRINT-433] 14 p2362 N85-24693
Variability of air humidity profiles over ocean determined by lidar sounding 19 p3296 N85-30436
Seasonal variability and spatial non-uniformity of bioluminescence in the Mediterranean Sea
[DRIC-T-7545] 24 p4125 N85-35572

MEETINGS
U CONFERENCES

MEISSNER EFFECT
U DIAMAGNETISM
U SUPERCONDUCTIVITY

MELT SPINNING
Rapidly solidified NiAl and FeAl
[NASA-TM-86941] 11 p1597 N85-20042
Rapid solidification processing of magnesium alloys
[AD-A150270] 13 p2022 N85-22868
Apparatus for producing amorphous and microcrystalline metal powders 13 p2030 N85-22720
Microstructures in rapidly solidified Ni-Mo alloys
[NASA-TM-87100] 23 p3915 N85-34266

MELTING
NT FUSION (MELTING)
NT LEVITATION MELTING
NT VACUUM MELTING
Time resolved calorimetry of 30 nm Te-films during laser annealing
[AD-A145047] 01 p0052 N85-10346
Design and implementation of a low-gravity solidification experiment package for the F-104
02 p0156 N85-11053
Studies of laser melting and rapid solidification using amorphous silicon
[DE84-014737] 02 p0202 N85-11345
Abundances of Ni, Cr, CO and major elements in the silicate portion of the Moon: Constraints from primary lunar magmas 04 p0562 N85-13720
Fractionation of siderophiles in cosmic spherules and its implications 06 p0884 N85-15613
Influence of temperatures of reactants on nature of product of solid-phase reactions
[BLL-M-36019-(5828.4)] 07 p0921 N85-15632
Procedure for investigating high-temperature properties of iron-ore materials
[BLL-M-36020-(5828.4)] 07 p0926 N85-15688
Diurnal freeze-thaw frequencies in selected regions of the high latitudes
[AD-A147276] 07 p1007 N85-16400
Adaptation of remelting procedures for the use of recycled metal in nickel-base superalloy castings
[PNR-90232] 09 p1297 N85-18149
Comparison of property regeneration techniques and life prediction procedures applied to laboratory tested and service exposed Ni-Cr alloys
[NPL-DMA(A)-91] 09 p1333 N85-18374
Stabilization of contaminated soils by in situ vitrification
[AD-P004144] 09 p1348 N85-18490
Influence of melting conditions on strength of transition zone between steel and composite material
10 p1450 N85-19133
Development of media for dynamic latent heat storage for the low-temperature range. Part 1: Thermal analyses of selected salt hydrate systems
[NASA-TM-77776] 10 p1507 N85-19510
Analysis of phase composition of products of laser destruction of metallic surfaces
11 p1600 N85-20064
Hot melt adhesive attachment pad
[NASA-CASE-LAR-12894-1] 11 p1610 N85-20125
Initial velocity of the emerging free boundary in a two-phase Stefan problem with imposed flux
[DE85-003613] 11 p1631 N85-20272
SI-on-insulator formation using a line-source electron beam
[DE85-003449] 11 p1737 N85-20925
Experimental and numerical analysis of electric currents and electromagnetic blunting of cracks in thin plates
[AD-A150418] 13 p2022 N85-22869
Determining degree of partial melting of asthenosphere from seismic data 13 p2107 N85-23127
Hydrovolcanism 13 p2166 N85-23574
Radiation-dominated snowmelt on Mars
13 p2191 N85-23592
North Atlantic Deep Water formation: Information from ice cores 15 p2602 N85-26035
In-situ rock melting applied to lunar base construction and for exploration drilling and coring on the moon
[DE85-006716] 16 p2717 N85-28770
The influence of melting practice and of microalloying, with rare earth metals and with boron, on the quality of low-carbon steel
[BLL-BISI-22467-(9022.06)] 17 p2925 N85-28036
Influence of temperature in melting and casting on quality of medium-alloy steel
[BLL-BISI-TRANS-22310-(9902.06)]
17 p2938 N85-28137
Modern sedimentation in the northern Barents Sea: Input, dispersal and deposition of suspended sediments from glacial meltwater
[AD-A152520] 17 p2997 N85-28530
Preparation of heavy metal fluoride glasses in the bulk form
[AD-A153784] 18 p3079 N85-29049
Feasibility of melt casting strontium fluoride to produce high-density heat sources
[DE85-009429] 18 p3130 N85-29381
Determination of the vacancy formation enthalpy in chromium by positron annihilation
[DE85-010286] 19 p3239 N85-30084
A study of freezing and melting with eutectic interactions 19 p3378 N85-30956
The nature of the anomalies on the polytherms of the properties of molten metallic alloys
[BLL-M-36265-(5828.4)] 20 p3430 N85-31277
Method for determining Wagner parameters of interaction of first and second orders
[BLL-M-36261-(5828.4)] 20 p3430 N85-31278
Quasi-steady-state melting mode during combined laser irradiation of semiconductor materials
21 p3682 N85-32874
Experimental studies of glass refining
[NASA-CR-176130] 22 p3751 N85-33248
Laser effects on opaque targets. Part 2C: Thermal effects of a time-variable beam intensity
[ISL-R-105/84-PT-2C] 22 p3791 N85-33486
Technology of off-gas treatment for liquid-fed ceramic melters
[DE85-012467] 22 p3812 N85-33610
Dynamic compaction of a monosized spherical tungsten powder
[DE85-014806] 24 p4080 N85-35289
Analysis of reactor material experiments investigating oxide fuel crust stability and heat transfer in jet impingement flow
[DE85-012097] 24 p4151 N85-35739

MELTING POINTS
Sealing ceramic material in low melting point glass
[NASA-TM-77599] 01 p0031 N85-10190
Evaluation of thermocouple junction temperature
[DE84-015159] 04 p0502 N85-13206
Kinetics of saturation of porous titanium with low melting point metals 10 p1446 N85-19114
Study of advanced fuel system concepts for commercial aircraft and engines
[NASA-CR-174752] 10 p1456 N85-19176
Jet fuel property changes and their effect on producibility and cost in the U.S., Canada, and Europe
[NASA-CR-174840] 16 p2757 N85-27012
Fuel freeze point investigations
[AD-A152801] 17 p2937 N85-28129
Radar study of the melting layer
[ESA-CR(P)-1974] 17 p2997 N85-28527
High performance mixed bisimide resins and composites based thereon
[NASA-CASE-ARC-11538-1-SB]
19 p3231 N85-30033
Processable and stable conductive polymers
[AD-D011684] 19 p3249 N85-30143
Development of low-melting fused salts 8: Formation of molybdenum film from molten ammonium formate bath
[BLL-OA-TRANS-3195-(8196.300)]
20 p3429 N85-31264
Ice-forming efficiency of the soluble and insoluble portions of dust contained in snow
21 p3643 N85-32631
Measurement and correlation of jet fuel viscosities at low temperatures
[NASA-CR-174911] 23 p3921 N85-34295

MELTS (CRYSTAL GROWTH)
NT CONTAINERLESS MELTS
NT IMPACT MELTS
NT MELT SPINNING
New metallurgical processes based on high-speed crystallization and diffusion of metals
01 p0021 N85-10126
Nuclear Magnetic Resonance of Polymeric Materials
[AD-A145078] 01 p0032 N85-10192
Dynamics of polymers in solution and melts
[AD-P003907] 01 p0032 N85-10193
NMR (Nuclear Magnetic Resonance) and macromolecular migration in a melt or in concentrated solutions
[AD-P003908] 01 p0032 N85-10194
Producing semiconductor materials by superfast cooling of melt 03 p0354 N85-12274
Neutron scattering on macromolecular solid state materials, solutions and melts 03 p0431 N85-12747
Dynamic crystallization of silicate melts
[NASA-CR-174103] 05 p0743 N85-14774
Calculation of energy of atomization in silicate tetrahedron Si4(4-)
[BLL-M-36000-(5828.4)] 07 p1040 N85-16589
The growth of large diameter single crystals by vertical solidification of the melt
[AD-A148756] 09 p1397 N85-18792
Method for synthesizing indium phosphide
[AD-D011475] 10 p1563 N85-19865
Total immersion crystal growth
[NASA-CASE-NPO-15800-2] 12 p1939 N85-22173
Experimental methods for quenching structures in lunar-analog silicate melts: Variations as a function of quench media and composition
13 p2184 N85-23554
The volume change during solidification
[NASA-TM-77817] 14 p2300 N85-24243
Impurity studies
[DE85-006235] 15 p2661 N85-26423
A Navier-Stokes capillary free boundary in open boat crystal growth
[REPT-84-34] 17 p2960 N85-28283
Crystallization of aluminum-based alloys in weightlessness 19 p3242 N85-30101
Conditions for formation of paragenesses containing kyanite-orthoclase in region of Mount Provender and Pratt Peak (Shackleton Range, Antarctica)
19 p3298 N85-30447
Ribbon growing method and apparatus
[NASA-CASE-NPO-16306-1-CU]
19 p3375 N85-30934
Temperature field around a spherical, cylindrical, and needle-shaped crystal, growing in a pre-cooled melt
[NASA-TM-77869] 20 p3537 N85-32011
Silicon dendritic web growth 21 p3611 N85-32435
Temperature-stress modeling
21 p3611 N85-32436
Silicon ribbon stress-strain activities
21 p3611 N85-32437

MEMBRANE ANALOGY
U MEMBRANE STRUCTURES
U STRUCTURAL ANALYSIS

MEMBRANE STRUCTURES
NT SKIN (STRUCTURAL MEMBER)
Development of a preprototype timex wastewater recovery subsystem, addendum
[NASA-CR-171823] 07 p1019 N85-16488
Ion transporting composite membranes. 1: Nafion impregnated gore-tex
[AD-A151020] 14 p2252 N85-23990
Evaluation of developmental membranes for the mixed reactant iron-chromium redox system
[NASA-TM-87074] 23 p3944 N85-34443

MEMBRANE THEORY
U STRUCTURAL ANALYSIS

MEMBRANES
NT ION EXCHANGE MEMBRANE ELECTROLYTES
NT MEMBRANE STRUCTURES
NT SKIN (STRUCTURAL MEMBER)
Operating experiences of reverse osmosis plants treating Rand Water Board (RWB) water: Pitfalls and problems 01 p0023 N85-10142
Control of the dynamic response of a damped membrane by distributed forces
[CSIR-TWISK-312] 01 p0061 N85-10406
Proton pumping in purple membrane, appendix 1
[DE84-014601] 01 p0118 N85-10811
Neutron small angle scattering of the free and membrane-bound ATPase — adenosine triphosphate (ATP) 03 p0431 N85-12746
Separation of metal species by supported liquid membranes
[DE84-014536] 04 p0470 N85-12992
Field/cell interaction model
[DE84-011914] 04 p0544 N85-13465
DOE supported research in alcohol fuel technology development
[DE84-007696] 06 p0774 N85-14948
Data appendix: F-number = 1.0 EMR with a flexible back electrode
[NASA-CR-172477] 07 p0946 N85-15894
Workshop on membrane biophysics
[AD-A148238] 08 p1192 N85-17512
Mechanisms of gas permeation through polymer membranes
[DE84-017423] 09 p1293 N85-18117
The Shock and Vibration Digest, volume 16, no. 10
[AD-A147588] 09 p1331 N85-18361
A review of approximate methods for determining the vibrational modes of membranes
09 p1331 N85-18363

Effect of air cavity on the vibration analysis of loaded drums 09 p1339 N85-18422
ECUT, Energy Conversion and Utilization Technologies program: Isothermal separation processes update [NASA-CR-175463] 10 p1433 N85-19033
Bioelectrochemistry 2: Membrane phenomena [AD-A149132] 10 p1522 N85-19802
The effect of inert gases on ion transport across the erythrocyte membrane [AD-A148899] 10 p1527 N85-19835
Investigation of structure-permeability relationships of silicone polymer membranes [PB85-148476] 11 p1596 N85-20036
Supported liquid membrane battery separators [DE85-001031] 12 p1836 N85-21519
Interaction of metals and metalloids with biomembranes [DE85-004902] 13 p2141 N85-23293
Ion transporting composite membranes. 1: Nafion impregnated gore-tex [AD-A151020] 14 p2252 N85-23960
Liquid membranes for the production of oxygen-enriched air [DE85-006056] 15 p2506 N85-25460
Luminescence probe studies of ionomers. 2. Steady-state measurements from sulfonated polyethylene and teflon membranes [AD-A152233] 16 p2755 N85-27000
Interactions between electromagnetic fields [AD-A153796] 18 p3091 N85-29129
Threshold effects and cellular recognition [DE85-010816] 19 p3327 N85-30614
A system for the assessment of non-thermal effects of ultrasound on cells at liquid nitrogen temperatures 20 p3523 N85-31915
Silicon dendritic web growth 21 p3611 N85-32435
Temperature-stress modeling 21 p3611 N85-32436
Silicon ribbon stress-strain activities 21 p3611 N85-32437
Analysis of stress-strain relationships in silicon ribbon 21 p3611 N85-32438
Stress and buckling analysis 21 p3611 N85-32439
Stress and efficiency studies in EFG 21 p3611 N85-32440
Silicon sheet surface studies 21 p3611 N85-32441
Edge-defined film-fed growth of thin silicon sheets 21 p3612 N85-32443
The investigation of natural and artificial ice nuclei by the improved membrane filter method 21 p3642 N85-32626
Development and demonstration of a spiral-wound thin-film composite membrane system for the economical production of oxygen-enriched air, phase 4 [DE85-012260] 23 p3920 N85-34268
Membrane reinforcement in concrete shells: Design versus nonlinear behavior 24 p4084 N85-35312
Development and evaluation of sulfonated polysulfone membranes for the zinc-ferricyanide battery [DE85-009104] 24 p4090 N85-35357
Cationic exchange membrane for the zinc-ferricyanide battery [DE85-013152] 24 p4112 N85-35489

MEMORY

The effects of feedback and predictability of human judgment [AD-A145744] 02 p0237 N85-11542
Measuring workload differences between short-term memory and long-term memory scenarios in a simulated flight environment 05 p0703 N85-14513
Visual attention to radar displays 05 p0704 N85-14514
Subjective workload assessment and voluntary control of effort in a tracking task 05 p0708 N85-14540
The representation of action plans in long term memory 05 p0709 N85-14545
Effects of individual mnemonic characteristics on problem solving 07 p1010 N85-16419
Problems of psychological support of automated organization control systems 09 p1362 N85-18570
Stereotype traits can be processed automatically [AD-A150947] 14 p2391 N85-24725
The effect of strategy in second order manual control on resource competition with a sternberg memory search task [AD-A150985] 14 p2391 N85-24727
The role of prior knowledge in operating equipment from written instructions [AD-A151007] 14 p2392 N85-24730
Psychophysiological studies. 1: Performance and physiological response in learning, short-term memory and discrimination tasks [AD-A151018] 14 p2392 N85-24731
Skilled memory [AD-A152063] 15 p2620 N85-26143
The levels of processing conceptualization of human memory: Some empirical and theoretical issues [AD-A152321] 17 p3000 N85-28544
Distributed memory [AD-A153364] 17 p3001 N85-28554
The effect of set size on time to recall color coded information [AD-A155013] 21 p3665 N85-32767

MEMORY (COMPUTERS)

Microcomputers in Hungary 01 p0115 N85-10786
Analysis of dynamic characteristics and ways of development of bipolar main memory with miniaturization of integrated circuit elements 04 p0490 N85-13123
Memory hierarchies for Directly Executed Language microprocessors 05 p0713 N85-14570
Improving the Spacelab mass memory unit tape layout with a simulation model [NASA-TM-86483] 05 p0713 N85-14571
Electrical characterization of VLSI (Very Large Scale Integration) memories [AD-A147657] 08 p1156 N85-17296
Programmable realtime interface between a block floating point processor and memory [AD-D011431] 08 p1203 N85-17571
Vector computer memory bank contention [NASA-CR-177342] 09 p1376 N85-18649
Automatic multi-banking of memory for microprocessors [NASA-CASE-NPO-15295-1] 12 p1911 N85-21992
Trends in computational capabilities for fluid dynamics 15 p2457 N85-25172
Signal flow model for sequential logic built from combinational logic elements and its implementation in Prolog [DE85-005792] 15 p2549 N85-25734
Microstore: The Stanford analog memory unit [DE85-005534] 18 p3095 N85-29160
Performance of the butterfly processor-memory interconnection in a vector environment [DE85-007931] 19 p3261 N85-30224
Development and evaluation of a fault-tolerant multiprocessor (FTMP) computer. Volume 1: FTMP principles of operation [NASA-CR-166071] 19 p3341 N85-30705
Fault-tolerant computing research [AD-A154082] 19 p3342 N85-30710
Digital matched filter 22 p3765 N85-33339
Basic features of personal computers 22 p3766 N85-33344
Design of digital bandpass filters with finite memory 22 p3775 N85-33392
Spatial trees: A fast access method for unstructured graphical data 23 p3958 N85-34533
Analysis of transient radiation upset in a 16K SRAM [DE85-009442] 23 p3965 N85-34586
Error-correcting codes for computer memories 24 p4136 N85-35636

MENSCI

Advanced radiator concepts [NASA-TM-87008] 14 p2300 N85-24245
Effects of thermal fluctuations on systems with small surface tension [PREPRINT-437] 18 p3152 N85-29520

MENTAL HEALTH

Job and family stress as predictors of pilot health, job satisfaction and performance [AD-A142176] 07 p1016 N85-16464

MENTAL PERFORMANCE

Primate equilibrium performance and diazepam: A behavioral tolerance effect [AD-A145158] 01 p0094 N85-10634
A representation for the functioning of devices that supports compilation of expert problem solving structures: An extended summary [AD-P003921] 02 p0245 N85-11601
Cognitive coordinate systems: Accounts of mental rotation and individual differences in spatial ability [AD-A146149] 03 p0401 N85-12557
The role of knowledge structures in fault diagnosis 05 p0703 N85-14509
POPCORN: A supervisory control simulation for workload and performance research 05 p0704 N85-14515
ERPS to monitor non-conscious mentation 05 p0707 N85-14536
Decision tree rating scales for workload estimation: Theme and variations 05 p0708 N85-14541
Mental models of invisible logical networks 05 p0708 N85-14544
The Sternberg task as a workload metric in flight handling qualities research 05 p0712 N85-14568
Mental status in relation to special conditions of activity 07 p1011 N85-16420
Cognitive performance during successive sustained physical work episodes [AD-A149061] 08 p1200 N85-17556
Methods of monitoring mental work efficiency, emotional activity 10 p1526 N85-19627
Improvement of workload estimation techniques in piloting tasks [NASA-CR-174374] 10 p1531 N85-19648
Qualitative process theory [AD-A146967] 10 p1543 N85-19729
Human cognition and intelligence: Towards an integrated theoretical perspective [CSIR-SR-PERS-350] 13 p2143 N85-23300
Perceived heterogeneity and its effect on various types of tasks [AD-A151003] 14 p2392 N85-24729
Space brain research in China reported 15 p2537 N85-25657
A portable battery for objective, non-obstrusive measures of human performances [NASA-CR-171868] 15 p2586 N85-25942
Skilled memory [AD-A152063] 15 p2620 N85-26143
Effects of dehydration or cold exposure and restricted fluid intake upon cognitive performance [AD-A151973] 16 p2842 N85-27525
Performance Evaluation Tests for Environmental Research (PETER) evaluation of 112 measures [AD-A152317] 17 p2999 N85-28543
The levels of processing conceptualization of human memory: Some empirical and theoretical issues [AD-A152321] 17 p3000 N85-28544
Oral discussion, group-to-individual transfer and achievement in cooperative learning groups [AD-A153209] 17 p3001 N85-28552
A task battery for applied human performance assessment research [AD-A153677] 18 p3154 N85-29530
Equipercentile test equating: The effects of preamoothing and postsmoothing on the magnitude of sample-dependent errors [AD-A154110] 19 p3347 N85-30746
Design and implementation of an intelligence database [AD-A154095] 19 p3381 N85-30973
Manual and computer-aided sequential diagnostic inference [AD-A156229] 24 p4133 N85-35620

MENTAL STRESS

U STRESS (PSYCHOLOGY)

MERCAPTAN

U THIOLS

MERCAPTO COMPOUNDS

U THIOLS

MERCATOR PROJECTION

UTM (Universal Transverse Mercator) determinations from geographical data [AD-A152293] 16 p2856 N85-27610

MERCURY (METAL)

Measurement of magnetic sublevel differential scattering cross sections for potassium and mercury [MPIS-10/1983] 01 p0119 N85-10815
Mercury health effects update: Health issue assessment [PB85-123925] 10 p1528 N85-19639
Ligand structural influences upon electrochemical reactivity: Organic substituent effects upon Carboxylatopentaamminecobalt(3) reductions at mercury and gold electrodes [AD-A150685] 14 p2250 N85-23944
Intramolecular electron transfer at metal surfaces. Part 5: Pendant substituent effects upon thiocarboxylate-bridged Cobalt (3) reduction kinetics at mercury and gold electrodes [AD-A150847] 14 p2254 N85-23971
Spectroscopic studies of lasing transitions in the diatomic mercury halides [AD-A151553] 15 p2563 N85-25609
Adsorption of Hg on lunar samples [DE85-007948] 17 p3054 N85-28906
Environmental surveillance at Los Alamos during 1984 [DE85-011886] 22 p3811 N85-33605

MERCURY (PLANET)

The geology of the terrestrial planets [NASA-SP-469] 09 p1410 N85-18688
Mercury 09 p1411 N85-18690
Mercury radar altimetry: A preliminary analysis 13 p2198 N85-23631
Mapping and geological analysis of Mercury and Venus radar ranging data 13 p2198 N85-23633
Mechanisms of basalt-plains ridge formation 13 p2199 N85-23643
Questions about Mercury's role in comparative planetary geophysics 22 p3853 N85-33861

MERCURY ARCS

Investigation of light source and scattering medium related to vapor-screen flow visualization in a supersonic wind tunnel [NASA-TM-86290] 06 p0610 N85-15144

MERCURY CADMIUM TELLURIDES
Effect of an underlayer of cadmium telluride on the reflection-reducing properties of zinc sulfide on mercury cadmium telluride
[AD-A146195] 03 p0414 N85-12649
HgCdTe surface and defect study program
[AD-A146343] 03 p0434 N85-12764
Liquid-phase epitaxial growth of CdTe on HgCdTe
[AD-D011482] 10 p1561 N85-19846
Method for the preparation of epitaxial films of mercury cadmium telluride
[AD-D011532] 12 p1938 N85-22175
Theoretical interpretation of thermal arrest data from differential thermal analysis measurements
12 p1949 N85-22241
Producible alternative to CdTe for epitaxy (PACE-2) of LWIR (Long Wave Infrared) HgCdTe
[AD-A150678] 14 p2426 N85-24964
Laser annealing of ion implanted HgCdTe
[AD-A150675] 14 p2427 N85-24966
Properties of defects in Hg(1-x)Cd(x)Te
[AD-A153243] 17 p3044 N85-28835
Interface chemistry of Hg(1-x)Cd(x)Te
[AD-A154878] 21 p3563 N85-32161
Mosaic Infrared Sensor for Space Astronomy (MIRSSA)
[NASA-CR-176154] 22 p3786 N85-33456
HgCdTe surface and defect study program
[AD-A156079] 24 p4161 N85-35799

MERCURY COMPOUNDS
NT MERCURY TELLURIDES
Mercuric iodide photodetectors for scintillation spectroscopy
[DE85-001437] 10 p1437 N85-19056
New and revised methods of purifying mercuric iodide
[DE85-011684] 22 p3749 N85-33237

MERCURY ION ENGINES
Development of the Engineering Test Satellite-3 (ETS-3) ion engine system
[NASA-TM-77536] 01 p0017 N85-10101
Ion thruster system (8-cm) cyclic endurance test
[NASA-CR-174745] 04 p0463 N85-12937
Ion thruster project
[NASA-TM-77726] 07 p0917 N85-15805
Analysis of orbit transfer vehicles for GPS Block 3 satellites
[AD-A152021] 16 p2732 N85-26860

MERCURY LAMPS
Optical radiation emissions from selected sources. Part 2: High intensity discharge lamps
[PB85-149136] 15 p2523 N85-25551
Electrodeless HID lamp study
[DE85-010626] 18 p3096 N85-29167

MERCURY TELLURIDES
Quaternary narrow-band semiconductors (HgTe)x (InSb)1-x for far-infrared detectors
[AD-A149350] 10 p1582 N85-19852

MERIDIONAL FLOW
Global scale diagnoses of FGGE data
[NASA-CR-174356] 09 p1356 N85-18533
The modelling of latitudinal gradients in the solar wind in the outer solar system 12 p1947 N85-22231
Azimuthal and meridional asymmetries of the solar wind and quasiperiodic variations of intensity of Galactic Cosmic Rays (GCR)
[SH-4.4-20] 23 p4035 N85-35016

MEROMORPHIC FUNCTIONS
NT ELLIPTIC FUNCTIONS
Annuals of the Finnish Academy of Sciences, series A. 1: Mathematica, volume 6, part 2
[ISSN-0066-1953] 10 p1535 N85-19673
On the spherical derivative of a meromorphic function with a Nevanlinna deficient value
10 p1535 N85-19676
Locally univalent functions in the unit disk
10 p1536 N85-19680
Contribution of the cup-product of Milnor's fiber with /1/ sup 2 lambda poles 11 p1698 N85-20672
Annals of the Scientific Academy of Finland, series A. 1: Mathematica, volume 9
[ISSN-0066-1953] 15 p2633 N85-26229
On meromorphic functions continuous on the Stollow boundary 15 p2633 N85-26232
On the length of asymptotic paths of meromorphic functions of order zero 15 p2633 N85-26234

MESFETS
U FIELD EFFECT TRANSISTORS

MESH
Image theory for a vertical electric dipole above a wire grid with square cells
[REPT-6-150] 02 p0192 N85-11286
Numerical simulations of fuel droplet flows using a Lagrangian triangular mesh
[AD-A146067] 03 p0362 N85-12320
Diffraction diffusion screen with holographically-suppressed zero-order beam
[AD-D011445] 10 p1487 N85-19387
WRAP-RIB antenna technology development
14 p2231 N85-23824
Diffraction analysis of mesh deployable reflector antennas 14 p2235 N85-23854
Determination of electromagnetic properties of mesh material using advanced radiometer techniques
14 p2235 N85-23855
Synthetic acceleration of coarse-mesh S/sub n/ transport calculations
[DE84-014721] 14 p2409 N85-24855
Flow through very porous inclined screens
[NASA-TM-86979] 15 p2555 N85-25781
Isoparametric 3-D finite element mesh generation using interactive computer graphics 15 p2574 N85-25873
On the interconnection of incompatible solid finite element meshes using multipoint constraints
15 p2575 N85-25879
Use of COSMIC NASTRAN in a design department
15 p2575 N85-25881
An incremental multigrid strategy for the fluid dynamics equations
[AD-A151953] 16 p2783 N85-27172
Monotonicity preserving bicubic interpolation, revision 1
[DE85-007976] 17 p3021 N85-28683
Study of meshing of beveled gears with normally decreasing arc teeth
[NASA-TM-77866] 18 p3117 N85-29293
Application of closed-form solutions to a mesh point field in silicon solar cells 20 p3482 N85-31637
Adaptive rezoner in a two-dimensional Lagrangian hydrodynamic code
[DE85-010108] 24 p4094 N85-35381

MESH (MATHEMATICS)
U COMPUTATIONAL GRIDS

MESOMETEOROLOGY
Rocket measurements of mesospheric ionization irregularities
[NASA-CR-176056] 20 p3494 N85-31721

MESONS
NT HYPERONS
NT KAONS
NT MUONS
NT PIONS
NT VECTOR MESONS
Searching for top, Higgs, and supersymmetry: The minimum invariant mass technique
[DE84-014539] 01 p0119 N85-10813
Proposal for the systematic naming of mesons and baryons
[DE85-008453] 17 p3035 N85-28773
A comprehensive study of psi meson production
[DE85-009094] 18 p3180 N85-29718
Control technology for radioactive emissions to the atmosphere at US Department of Energy facilities: The Los Alamos Meson Physics Facility
[DE85-011402] 22 p3811 N85-33809
Proceedings of the 18th LAMPF Users Group Meeting
[DE85-011868] 22 p3839 N85-33773
The SCR flare of 16 February 1984 as recorded by the Sayan spectrograph
[SH-1.3-17] 23 p3994 N85-34781
The phi-meson and Chiral-mass-meson production in heavy-ion collisions as potential probes of quark-gluon-plasma and Chiral symmetry transitions
24 p4175 N85-35884
Forward particle production in inelastic Ne-22 InteVractions in emulsion at 4.1 A Ge/c
[HE-1.4-7] 24 p4176 N85-35895
Meson multiplicity in nucleus-nucleus collisions above 4 GeV/amu
[HE-1.4-10] 24 p4177 N85-35897
Connection between variations of the atmosphere temperature profile and variations of the meson component intensity
[HE-3.1-12] 24 p4178 N85-35910

MESOPAUSE
Radiation transport in the Earth atmosphere
04 p0522 N85-13341
Cold Arctic Mesopause Project (CAMP): Scientific objectives 11 p1656 N85-20433
Large scale winter time disturbances in meteor winds over central and eastern Europe
11 p1661 N85-20467
Coupling between the thermosphere and the stratosphere: The role of nitric oxide
11 p1662 N85-20472
Meteor wind results from Atlanta, USA, and Ramey, Puerto Rico 11 p1662 N85-20474
Basic features of global circulation in the mesopause lower thermosphere region 11 p1662 N85-20475
The nucleation of ice at very low temperatures and pressures 21 p3641 N85-32617

MESOSCALE PHENOMENA
NT JET STREAMS (METEOROLOGY)
Nowcasting 2. Mesoscale Observations and Very-Short-Range Weather Forecasting — conference
[ESA-SP-208] 01 p0073 N85-10487
The mesoscale-beta-scale evolution of mid-latitude meso-alpha-scale convective complexes
01 p0073 N85-10488
Generation of deep convective clouds along mesoscale storm outflow boundaries 01 p0074 N85-10490
Automated analysis and nowcasting of mesoscale convective systems 01 p0074 N85-10492
Three-dimensional mesoscale analysis of aerial soundings 01 p0074 N85-10493
Layered sloping mesoscale structures and rainbands in atmospheric frontal regions and their relation to symmetric instability 01 p0075 N85-10497
About the influence of nonadiabatic processes on frontogenesis near the ground 01 p0075 N85-10498
Some mesoscale weather effects and the very short-range forecasting impact of variable snow cover
01 p0075 N85-10499
Detailed analysis of the structure of local wind systems in Canterbury, New Zealand 01 p0075 N85-10501
Test results from RAINSAT 01 p0076 N85-10508
VHF/UHF radar and its application in nowcasting
01 p0078 N85-10518
Analysis strategies for field dependent estimation and network design — mesoscale modeling
01 p0078 N85-10520
Evaluation of surface sensible heat flux effects on the generation and modification of mesoscale circulations
01 p0079 N85-10527
Predicability of mesoscale phenomena
01 p0079 N85-10528
The initialization of mesoscale models
01 p0079 N85-10529
Applications of a finite-element regional model to very-short-range forecasting 01 p0080 N85-10531
Application of mesoscale numerical model to local weather prediction 01 p0080 N85-10532
The United Kingdom Meteorological Office mesoscale forecasting system 01 p0080 N85-10533
A local dynamical interpretation method of numerical weather forecasting 01 p0080 N85-10536
A one-level mesoscale model suitable for nowcasting and short-term forecasting in regions of complex terrain
01 p0081 N85-10541
Short-term forecasting using a REMOS approach — regime model output statistics (REMOS)
01 p0081 N85-10544
Experiment on nowcasting of heavy rainfall and severe storms in central China in 1979-1981
01 p0081 N85-10545
Simple methods in very short-range forecasting based on data from a mesoscale network of automatic stations (ANETZ) and from satellite (Meteosat) and radar — Swiss Alps 01 p0082 N85-10548
Development of an operational system for Very-Short-Range Forecasting (VSRF) at Swedish Meteorological and Hydrological Institute (SMHI)
01 p0083 N85-10559
Use of short-range weather forecasts at construction sites: Some results from a user and a market test
01 p0084 N85-10563
Benefits resulting from tailored very-short-range forecasts in Sweden 01 p0084 N85-10564
The arc cloud complex: A case study
[AD-A145384] 02 p0231 N85-11507
Mesoscale and convective-scale characteristics of mature hurricanes 03 p0394 N85-12516
Recent examples of mesoscale numerical forecasts of severe weather events along the east coast
[NASA-TM-86172] 03 p0395 N85-12523
Investigations of severe/tornadic thunderstorm development and evolution based on satellite and AVE/SESAME/VAS data
[NASA-CR-174154] 04 p0538 N85-13424
Weather research program report; FY 1983
[PB84-236894] 04 p0541 N85-13440
Dynamics of coupled ice-ocean system in the marginal ice zone: Study of the mesoscale processes and of constitutive equations for sea ice
[NASA-CR-174171] 04 p0542 N85-13448
Conditional symmetric instability and mesoscale rainbands 05 p0679 N85-14358
An investigation of the marine boundary layer during cold air outbreak 05 p0680 N85-14368
Convective scale weather analysis and forecasting
[NASA-CR-174185] 06 p0839 N85-15320
Simple mesoscale models for operational use in regions of topographic and thermal forcing: Development and evaluation
[AD-A148667] 06 p0839 N85-15325

Precipitation characteristics of a dual mesoscale convective complex
[PB84-226711] 06 p0840 N85-15337
An evaluation of an advection fog prediction model
[AD-A147436] 07 p1008 N85-16403
Interactions between mean flow and finite-amplitude mesoscale eddies in a barotropic ocean
[AD-A147249] 07 p1009 N85-16413
Studies of coastal mesoscale winds using SIR-B
08 p1147 N85-17236
The use of principal components analysis techniques Nimbus-7 coastal zone color scanner data to define mesoscale ocean features through a warm humid atmosphere
[AD-A148567] 08 p1176 N85-17416
Sea breeze-induced mesoscale systems and severe weather
[NASA-CR-174317] 08 p1187 N85-17480
A method for determining mesoscale dynamic topography
[AD-D011412] 08 p1191 N85-17506
Mesoscale lee cyclogenesis 09 p1355 N85-18527
The rationale and suggested approaches for research geosynchronous satellite measurements for severe storm and mesoscale investigations
[NASA-TM-86185] 09 p1356 N85-18532
The influence of soil moisture distribution on the severe-storm environment of the southern Great Plains: A numerical study of the SESAME 4 case
09 p1357 N85-18534
Mesoscale storm and dry period parameters from hourly precipitation data: Program documentation
[DE85-001366] 09 p1357 N85-18538
Rain volume estimation over areas using satellite and radar data
[NASA-CR-174434] 10 p1518 N85-19508
Continued research in mesoscale air pollution simulation modeling. Volume 5: Refinements in numerical analysis, transport, chemistry, and pollutant removal
[PB85-137362] 11 p1680 N85-20585
Mesoscale studies of flow regimes and fluxes of particulate matter in coastal waters
[DE85-003625] 11 p1689 N85-20620
Continued research in mesoscale air pollution simulation modeling. Volume 6: Further studies in the modeling of microscale phenomena
[PB85-137370] 12 p1887 N85-21844
Digital processing of mesoscale analysis and space sensor data
[NASA-CR-171429] 13 p2146 N85-23319
Mountain barrier baroclinity effects on surface winds along the Alaskan Arctic coast 14 p2238 N85-23577
Variational mesoscale satellite data assimilation and initialization
[NASA-CR-175704] 14 p2378 N85-24880
Mesoscale Atmospheric Processes Research Program Science Review
[NASA-TM-87485] 15 p2594 N85-25987
Modeling of midwest severe thunderstorms
15 p2596 N85-25995
Satellite detection of severe thunderstorms
15 p2596 N85-25996
Mesoscale analysis and modeling group
15 p2596 N85-26001
Recent VAS imaging/sounding research
15 p2597 N85-26004
A simulation experiment on the impact of geostationary temperature retrievals in numerical models
15 p2597 N85-26005
VAS/model impact study 15 p2597 N85-26006
Role of jet streaks and boundary layer processes in organizing a pre-convective environment
15 p2597 N85-26008
Role of frontal circulations and gravity waves in initiating convective storm systems 15 p2598 N85-26010
Sea breeze-induced mesoscale systems and severe weather 15 p2598 N85-26012
The sensitivity of mesoscale cyclogenesis forecasts to detailed three-dimensional isentropic initial analyses and varied vertical model resolution
15 p2598 N85-26015
Influence of coherent mesoscale structures on satellite-based Doppler lidar wind measurements
[NASA-CR-175853] 16 p2833 N85-27467
MARMAP survey of the continental shelf from Cape Hatteras, North Carolina to Cape Sable, Nova Scotia (1977 - 1983). Atlas 1: Summary of operations
[PB85-150985] 16 p2839 N85-27506
Convective storm downdraft outflows detected by NASA/MSFC's Airborne 10.6 micron pulsed Doppler Lidar System
[NASA-CR-3698] 17 p2995 N85-28511
Arctic mixed layer dynamics
[AD-A153582] 18 p3150 N85-29505
MELSAR: A mesoscale air quality model for complex terrain. Volume 2: Appendices
[DE85-010991] 19 p3310 N85-30519
Approximate factorization method for computation of nonhydrostatic mesoscale flows
[DE85-007259] 19 p3313 N85-30537
System enhancements of Mesoscale Analysis and Space Sensor (MASS) computer system
[NASA-CR-171483] 19 p3342 N85-30708
Global mean sea surface based upon a combination of the GEOS-3 and SEASAT altimeter data
20 p3492 N85-31710
Diagnostics of severe convection and subsynoptic scale ageostrophic circulations
[NASA-CR-171581] 21 p3634 N85-32571
Dynamics of Mesoscale Weather Systems: 1984 Summer Colloquium
[PB85-168266] 22 p3817 N85-33649
Airborne Investigations of Mesoscale Convective Systems (AIMCS), 1984: Operational summary and data inventory
[PB85-187904] 24 p4125 N85-35571

MESOSPHERE

Ground-based measurements of mesosphere temperatures by optical means
08 p1183 N85-17453
Incoherent scatter radar studies of the mesosphere
08 p1184 N85-17483
PMP-2: Equatorial wave dynamics
11 p1655 N85-20422
Variation of derived mesospheric nitric oxide in relation to wind and temperature in winter
11 p1658 N85-20452
Seasonal characteristics of mesospheric plasma and their transitions 11 p1660 N85-20464
VHF radar observations in the stratosphere and mesosphere during a stratospheric warming
11 p1661 N85-20468
Latitudinal dependence of the energy input into the mesosphere by high energy electrons
11 p1664 N85-20489
Aeronomical aspects of mesospheric photodissociation: Processes resulting from the solar H Lyman alpha line
[AERONOMICA-ACTA-A-285-1984]
11 p1680 N85-20587
Experiment for measuring electric fields within the sounding rocket project Energy Budget
[BMFT-FB-W-84-048] 12 p1891 N85-21866
Wave dynamics and transport in the stratosphere
[NASA-CR-175789] 16 p2823 N85-27413
Circulation and transport in the middle atmosphere: Mesosphere and lower thermosphere
18 p3148 N85-29492
Gravity waves from the stratosphere to the mesosphere, part 1.3B 21 p3616 N85-32471
A numerical analysis of transient planetary waves and the vertical structure in a meso-strato-troposphere model, part 1.4A 21 p3617 N85-32473
Morphology of the scattering targets: Fresnel and turbulent mechanisms, part 2.1A
21 p3618 N85-32481
Observations of mesospheric turbulence by rocket probe and VHF radar, part 2.4A 21 p3619 N85-32484
Interpretation of radar returns from the mesosphere, part 2.3A 21 p3619 N85-32485
Radar echoes at 2.66 and 40.92 MHz from the mesosphere, part 2.6A 21 p3619 N85-32486
Antenna induced range smearing in MST radars
21 p3620 N85-32495
Effects of line-of-sight velocity on spaced-antenna measurements, part 3.5A 21 p3621 N85-32496
Mesospheric measurements of irregularity patches using a 3-antenna interferometer, part 3.6B
21 p3621 N85-32498
Spectral measurements of turbulence and gravity waves, part 4.2A 21 p3622 N85-32501
Relationship of isolated turbulent regions to the general turbulent background, part 4.4A
21 p3623 N85-32506
Estimation of vertical diffusion from observations of Atmospheric turbulence layers, part 4.4B
21 p3623 N85-32507
Momentum flux measurements: Techniques and needs, part 4.5A 21 p3623 N85-32508
Sample interchange of MST radar data from the Urbana radar 21 p3627 N85-32531
Urbana radar systems: Possibilities and limitations
21 p3628 N85-32540
Progress and plans for the Colorado Wind Profiler Network 21 p3628 N85-32542
Voigt line profile computation of infrared lines in the stratosphere and mesosphere
[AERONOMICA-ACTA-A-294-1985]
22 p3613 N85-33622

MESSAGE PROCESSING

Reserve and authentication in Integrated Services Distributed Networks (ISDN) networks
[FUB-37-1983] 01 p0041 N85-10262
Pluribus satellite IMP (Interface Message Provision) development mobile access terminal network
[AD-A145348] 02 p0190 N85-11269
Real-time Ada (trademark)
[AD-A146258] 03 p0407 N85-12603
Crew communication as a factor in aviation accidents
05 p0710 N85-14555
Selecting a leader in a clique in O(N log N) messages
[AD-A146581] 06 p0857 N85-15453
Implementation of a constraint machine for prism - A parallel problem solver
[AD-A147844] 07 p1026 N85-16512
Benchmarking database systems in multiple backend configurations
[AD-A148191] 08 p1202 N85-17568
EGP (Exterior Gateway Protocol) gateway under Berkeley UNIX 4.2
[AD-A148056] 08 p1208 N85-17597
Performance evaluation of a database system in multiple backend configurations
[AD-A148192] 08 p1229 N85-17743
Extracting digital data from a bus and multiplexing it with a video signal
[AD-D011491] 11 p1636 N85-20302
Distributed asynchronous deterministic and stochastic gradient optimization algorithms: Revision
[AD-A149997] 12 p1921 N85-22068
A perspective on multiaccess channels
[AD-A150183] 13 p2146 N85-23322
Orphan detection in the Argus system
[AD-A150562] 13 p2148 N85-23331
Distributed matchmaking for processes in computer networks
[CWI-CS-R8421] 17 p3016 N85-28652
Assured information flow capping architecture
[AD-A155392] 22 p3756 N85-33283
Pluribus satellite IMP (Interface Message Processors) development mobile access terminal network
[AD-A155754] 24 p4069 N85-35216

MESSAGES

Comparative review of single-line and multiline optical character readers used in mail processing
[PB84-234624] 04 p0548 N85-13489
Selecting a leader in a clique in O(N log N) messages
[AD-A146581] 06 p0857 N85-15453
Experimental satellite system for determining coordinates of maritime distress
09 p1308 N85-18216
Study of terrestrial mobile systems for personal communications
[MCS-8436] 20 p3441 N85-31357

METABOLIC WASTES

NT FECES
NT HUMAN WASTES
NT URINE
BLSS: A contribution to future life support
18 p3155 N85-29534

METABOLISM

NT ADRENAL METABOLISM
NT CALCIUM METABOLISM
NT CARBOHYDRATE METABOLISM
NT ELECTROLYTE METABOLISM
NT ENZYME ACTIVITY
NT FERMENTATION
NT HORMONE METABOLISMS
NT LIPID METABOLISM
NT MINERAL METABOLISM
NT NITROGEN METABOLISM
NT OXYGEN METABOLISM
NT PHOSPHORUS METABOLISM
NT PROTEIN METABOLISM
Vitamin metabolism in cosmonauts following short-term flights 01 p0091 N85-10615
Functional capacities of elderly subjects exposed to simulated spaceflight factors 01 p0091 N85-10617
Skeletal muscle metabolism in hypokinetic rats
[NASA-CR-174059] 02 p0233 N85-11520
Toxicology and metabolism of nickel compounds
[DE84-014919] 05 p0696 N85-14478
Chemistry and metabolism of delayed neurotoxic organophosphorus esters
[AD-P004023] 06 p0844 N85-15357
Comparison of thermal responses between rest and leg exercise in water
[AD-A146818] 07 p1015 N85-16448
Influence of hyperthermia on body temperature and content of catecholamines in white rat hypothalamus
10 p1524 N85-19615
Skeletal muscle metabolism during exercise is influenced by heat acclimation
[AD-A148845] 10 p1527 N85-19632

Effects of hyperthermia on free amino acids in rat brain and in subcellular fractions 11 p1691 N85-20631
Effects of hypothermia on brain metabolism 11 p1692 N85-20636
USSR report: Space Biology and Aerospace Medicine, volume 18, no. 6, November - December 1984 [JPRS-USB-85-002] 12 p1900 N85-21931
Cosmonauts' blood plasma free amino acid levels during preflight training 12 p1901 N85-21937
Fluid metabolism of monkeys during two-week antiorthostatic hypokinesia 12 p1902 N85-21943
NASA Space Biology Program: 9th Annual Symposium [NASA-CP-2336] 15 p2605 N85-26054
Constant fiber number during skeletal muscle atrophy and modified arachidonate metabolism during hypertrophy 15 p2609 N85-26078
Gravity, body mass and composition, and metabolic rate 15 p2610 N85-26084
Differential effect of denervation on free radical scavenging enzymes in slow and fast muscle of rat [NASA-CR-175719] 15 p2614 N85-26110
Research opportunities in loss of red blood cell mass in space flight [NASA-CR-175808] 16 p2841 N85-27517
Changes in pentose and glucuronate pathway dehydrogenases in rat brains following single or multiple hypothermic episodes 20 p3505 N85-31790
The role of sulfur in osmoregulation and salinity tolerance in cyanobacteria, algae, and plants 21 p3660 N85-32736
Sulfur cycling and metabolism of phototrophic and filamentous sulfur bacteria 21 p3660 N85-32737
Anaerobic reduction of elemental sulfur by Chromatium vinosum and Beggiatoa alba 21 p3660 N85-32739
Interactions among sulfide-oxidizing bacteria 21 p3661 N85-32741
Studies of circulatory and metabolic changes during ketamine narcosis [AD-A154512] 21 p3663 N85-32756
Microwave radiation and thermoregulation [AD-A155718] 22 p3818 N85-33654
Investigation of some aspects of amino acid metabolism in man during brief exposure to antiorthostatic hypokinesia combined with ultraviolet radiation 22 p3822 N85-33678
Response of amino acids in hindlimb muscles to recovery from hypogravity and unloading by tail-cast suspension [NASA-CR-176183] 24 p4128 N85-35589

METABOLITES
Effect of 1,25-dihydroxycholecalciferol and 24,25 dihydroxycholecalciferol on growth and alteration of rat bones during hypokinesa (histomorphometric study) 01 p0092 N85-10622

METAGALAXY
U UNIVERSE

METAL BONDING
NT METAL-METAL BONDING
Bondability of Al-Si thin film in thermosonic gold wire bonding — integrated circuits [NASA-TM-77795] 10 p1439 N85-19071
Study of character of adhesive interaction and breaking of polyimid-aluminum foil junction during process of hardening 13 p2014 N85-22637
Technology for pressure-instrumented thin airfoil models, phase 1 [NASA-CR-3891] 14 p2227 N85-23804
Diffusion vacuum welding 15 p2499 N85-25416
Fracture surface analysis in composite and titanium bonding: Part 1: Titanium bonding [NASA-CR-175750] 15 p2502 N85-25434
Development of acceptance criteria for batches of silane primer for external tank thermal protection system bonding applications [NASA-CR-175850] 16 p2754 N85-26995
New process for production of bimetal with corrosion-resistant cladding layer [BLL-BISI-TRANS-22371-(9022.06)] 17 p2927 N85-29056
Fatigue resistance of homogeneous and heterogeneous welded joints of TS5 titanium alloy 19 p3248 N85-30126
Advanced thermal barrier system bond coatings for use on Ni, Co-, and Fe-base alloy substrates [NASA-TM-87062] 20 p3431 N85-31283
Determination of deformation speed during high-speed deformation of cylindrical shells [BLL-M-36290-(5828.4)] 20 p3465 N85-31527
Study of an ultrasonic detection method to inspect bonding effects in light alloy bonded structures, test report no. 43-854/F — aircraft structures [PV-43-854/F] 22 p3795 N85-33510

METAL COATINGS
NT ALUMINUM COATINGS
NT GOLD COATINGS
NT NICKEL COATINGS
NT ZINC COATINGS
Features of laser welding of medium carbon steel through a cadmium coating 01 p0020 N85-10122
Methods for producing platinum-group metal coatings from molten alkali cyanides [PB84-225994] 01 p0029 N85-10181
USSR report: Materials science and metallurgy [JPRS-UMS-84-007] 03 p0348 N85-12244
Electrochemical behaviour of TiCl4 solutions in low melting point organic media [BLL-OA-TRANS-3174-(6196.3)] 06 p0764 N85-14886
Plasma deposition of amorphous metal alloys [DE85-000768] 09 p1295 N85-18132
Effects of MAR-M247 substrate (modified) composition on coating oxidation coating/substrate interdiffusion — protective coatings for hot section components of gas turbine engines [NASA-CR-174851] 10 p1440 N85-19073
The role of silver in self-lubricating coatings for use at extreme temperatures [NASA-TM-86943] 11 p1611 N85-20127
Low temperature deposition of nickel films [AD-D011568] 12 p1805 N85-21319
Metallic and metallocermic coating by thermal decomposition [NASA-TM-86992] 13 p2096 N85-22755
Film and interstitial formation of metals in plasma-sprayed ceramics [NASA-TM-86993] 13 p2096 N85-22758
Gear-cutting tools made of ultra high speed steel coated with TiN [BLL-RISLEY-TR-5109-(9091.9F)] 15 p2567 N85-25637
Self-sustaining low-Z coatings for fusion applications 2 - copper-lithium [DE85-002553] 15 p2656 N85-26403
Effects of surface chemistry on hot corrosion life [NASA-CR-174915] 16 p2708 N85-26711
Vacuum plasma coatings for turbine blades 16 p2734 N85-26869
Solid state hydrogen pumping and storage material [AD-D011610] 16 p2757 N85-27011
Forming of coating protection system: Mechanism of paint-coating anti-corrosion protection of steel [BLL-BISI-TRANS-22061-(9022.06)] 17 p2925 N85-29033
Corrosion resistant coating [NASA-CASE-NPO-15928-1] 18 p3073 N85-29005
Atomized magnetism-aluminum protective coatings 19 p3244 N85-30116
East Europe report: Science and technology [JPRS-ESA-85-021] 21 p3568 N85-32190
Tests on zirconium nitride coatings applied to SW 18 steel using the chemical vapor deposition method 24 p4078 N85-35271

METAL COMBUSTION
Status of boron combustion research 13 p1998 N85-22528
Ignition phenomena of bulk aluminum alloy as a function of oxygen pressure 13 p1999 N85-22531
Review of zirconium-zircaloy pyrophoricity [DE85-011169] 23 p3918 N85-34270

METAL COMPOUNDS
Macrocyclic poly(tertiary) phosphines for the attachment of metals to surfaces of photodevices [DE84-015552] 05 p0617 N85-13946
Structure-property relationships in intercalated graphite [AD-A147949] 08 p1219 N85-17680
Metal-support interactions: The effect of catalyst preparation on catalytic activity [DE84-017425] 09 p1293 N85-18118
Phthalocyanine polymers [NASA-CASE-ARC-11413-1] 12 p1809 N85-21348

METAL CORROSION
U CORROSION

METAL CRYSTALS
New metallurgical processes based on high-speed crystallization and diffusion of metals 01 p0021 N85-10126
Raman scattering from metastable GaSb(1-x) Ge(2x) alloys [AD-A145897] 03 p0327 N85-12106
Back stress in dislocation creep. Part 1: Basic concepts and measuring techniques [NASA-TM-77773] 07 p0977 N85-16206
Magnetism of californium metal [DE85-001141] 09 p1377 N85-18657
Studies of the kinetics and mechanisms of ammonia synthesis and hydrodesulfurization on metal single crystal surfaces [DE85-001650] 11 p1595 N85-20030
Summary of recent research on mechanical behavior of polycrystalline solids [DE85-004601] 12 p1942 N85-22189
Observation of surface vibrational resonances on (110) surfaces of FCC metals [AD-A150469] 13 p2163 N85-23419
Measurements of radiation-induced segregation and diffusion in ion irradiated alloy using implanted manganese [AERE-R-11528] 14 p2258 N85-23904
Summary of recent investigations of the mechanical properties of polycrystalline solids [DE85-006776] 15 p2511 N85-25492
The precipitation mechanism in a metallic solid solution crystal: Case of the aluminum-copper and aluminum-silver systems [DE85-009981] 18 p3077 N85-29032

METAL CUTTING
New titanium carbide grade for metal cutting 02 p0181 N85-11214
Specifications, applications of gantry robots viewed 10 p1461 N85-19215
Productivity gains through CAD of CNC programs 10 p1462 N85-19219
Small-size measuring gauges for metal cutting machine tools 14 p2267 N85-24045
Group technology for working turbine drive wheel disks 14 p2269 N85-24061
USSR report: Machine tools and metalworking equipment [JPRS-UMM-85-006] 14 p2283 N85-24146
Large CNC machining center for turbine production 14 p2284 N85-24149
Laser cutting: A new tool for shipbuilding 14 p2308 N85-24295
USSR report: Machine tools and metalworking equipment [JPRS-UMM-84-010] 16 p2767 N85-27071
New robotized, vertical broaching machine featured 16 p2767 N85-27074
Development, implementation of industrial lasers reviewed 16 p2767 N85-27075
Study of a test method for assessing machinability in gear cutting operations [BLL-BISI-TRANS-22345-(9022.06)] 17 p2972 N85-28359
Very high speed lap with negative lift effect [AD-D011711] 19 p3281 N85-30345
Mechanical properties of plasma arc cut steel 23 p3905 N85-34188

METAL DRAWING
Prediction of forming limit diagrams for deep drawing 06 p0795 N85-15089
Gel drawn fibers of poly(vinyl alcohol) [AD-A149062] 10 p1435 N85-19040
New method for determining stampability of sheet materials [BLL-BISI-22486-(9022.06)] 17 p2972 N85-28360
Durability of reinforced hard-alloy draw plates [BLL-M-36278-(5826.4)] 20 p3466 N85-31529

METAL FATIGUE
The inter-relation of microstructure, toughness and fatigue crack growth behaviour in WC-Co hardmetals 02 p0177 N85-11189
New titanium carbide grade for metal cutting 02 p0181 N85-11214
Reliability considerations for the total strain range version of strainrange partitioning [NASA-CR-174757] 02 p0209 N85-11380
Near-threshold fatigue crack growth and crack closure in 17-4 precipitation hardening steel and 2043-T3 aluminum alloy [FFA-TN-1984-16] 02 p0210 N85-11385
Acoustic emission monitoring of fatigue in 7010 aluminum alloys [AERE-R-11167] 03 p0334 N85-12152
Fatigue crack propagation in metastable titanium alloys [AD-A145824] 03 p0372 N85-12376
Constitutive modeling of engine materials [AD-A146830] 06 p0817 N85-15189
Modelling of deformation and fracture in high-temperature structural materials [DE84-016906] 06 p0818 N85-15191
Cumulative damage modeling of fatigue crack growth 07 p0907 N85-15741
Thermal-mechanical fatigue crack growth in Inconel X-750 [NASA-CR-174740] 07 p0927 N85-15877
A study of spectrum fatigue crack propagation in two aluminum alloys. 1: Spectrum simplification [NASA-TM-86929] 09 p1293 N85-18124

A study of spectrum fatigue crack propagation in two aluminum alloys. 2: Influence of microstructures
[NASA-TM-86930] 09 p1294 N85-16125
Ti-6Al-4V alloy castings prepared in zircon sand molds and the effect of hot isostatic pressing
[PB85-100932/GAR] 09 p1296 N85-16150
Development of surface cracks in AMg6 alloy under low-cycle loading conditions 10 p1442 N85-19089
Fractographic features of titanium alloy fatigue failure under repeated static stress and high frequency vibration 11 p1601 N85-20070
Effect of hydrogen on fatigue of VT6 alloy 11 p1601 N85-20071
Effect of stress concentration fatigue resistance of refractory nickel alloys under asymmetrical multicycle loading, communication 1 11 p1604 N85-20096
Fatigue crack growth in Aramid Reinforced Aluminum Laminates (ARALL): Mechanisms and predictions
[DFVLR-FB-84-37] 11 p1609 N85-20116
Structural strenght of strip D16T aluminum alloy with low copper and magnesium content 13 p2025 N85-22691
Fatigue life, crack initiation, and propagation of 304 stainless steel with non-proportional axial/torsional strain-paths 13 p2101 N85-23094
A study of fatigue crack growth in 2 1/4 Cr1Mo steel. Part 1: The influences of environment and material condition
[AERE-R-11472] 14 p2258 N85-23993
Study of fatigue strength of shafts with segmented channels 14 p2282 N85-24138
Fatigue crack propagation and fracture in 7050 and 7091 aluminum alloy forgings 14 p2316 N85-24324
Fatigue crack topography and crack growth analysis — wrought and cast aluminum 14 p2319 N85-24333
Crack propagation under constant and variable stress amplitudes: A comparison of calculations based on the Striation spacing and tests 14 p2320 N85-24336
Fatigue strength of alpha-titanium alloys under cophasal action of variable normal and tangential stresses 15 p2498 N85-25407
On the use of marker loads for fatigue crack growth measurements
[FFA-TN-1984-52] 16 p2802 N85-27277
Reaction-bonded and fiber-reinforced SiC static and dynamic gas turbine components
[BMFT-FB-T-84-302] 17 p2899 N85-27874
Role of hydrogen and structure on CMSX-2 17 p2915 N85-27967
The synergistic actions of stress corrosion cracking and corrosion fatigue
[BLL-BISI-TRANS-22334-(9022.06)] 17 p2926 N85-28045
X-ray diffraction study of changes in stress-strain distributions during fatigue of a 2-phase alloy
[AD-A152367] 17 p2930 N85-28067
Development of high temperature resistant, noncorrosible, non-metallic ceramic materials, especially silicon nitride in gas turbine application
[BMFT-FB-T-85-015] 17 p2936 N85-28125
Development of high temperature resistant noncorrodible silicon carbide components for gas turbine applications, follow-up report
[BMFT-FB-T-85-016] 17 p2936 N85-28126
The fatigue properties of welds at low temperature, according to the type of steel
[BLL-BISI-TRANS-22455-(9022.06)] 17 p2978 N85-28410
Fractographic analysis for nonpropagating conditions of fatigue crack at high stress ratios in mild steel 23 p3905 N85-34194
Crystallographic orientation dependence of fatigue crack propagation in extremely low carbon steel 23 p3906 N85-34195
Fatigue crack retardation phenomenon caused by single-multiple overloads in 2017-T3 aluminum alloy 23 p3906 N85-34196
The stress pattern analysis of coarse grain titanium specimens
[PNR-90250] 23 p3942 N85-34433

METAL FIBERS
Investigation of electric and wear phenomena of liquid metal wetted copper fiber brushes under conditions of high slip ring eccentricity
[AD-A147634] 08 p1156 N85-17295
Influence of volumetric fiber content on some matrix damage factors during thermal cycling of tungsten-El 765 composite 10 p1443 N85-19097
Theoretical and experimental investigation of mechanically fastened composites
[AD-A150961] 14 p2248 N85-23935
Production and compaction of amorphous metal powders
[BLL-BISI-TRANS-22367-(9022.06)] 17 p2929 N85-28060
Research on design of cryotransformers and its prospects for the future
[AD-A152400] 17 p2952 N85-28230

METAL FILMS
Research on large, highly accurate, inflatable reflectors
[AD-A145060] 01 p0016 N85-10099
Platinum thin film resistors as accurate and stable temperature sensors
[NASA-TM-77728] 01 p0049 N85-10322
Composition of metal films on gallium arsenide surface 02 p0257 N85-11685
Calculation of critical temperature for Nb-Cu multilayer film superconductor
[AD-A144321] 02 p0274 N85-11788
Formation of subsurface Al2O3 layers in aluminum by oxygen ion implantation
[DE84-015599] 04 p0474 N85-13020
Effects of monolayer coverages on substrate sputtering yields 06 p0865 N85-15496
Synergestic sputtering properties of binary alloys 06 p0865 N85-15497
Method for bonding insulator to insulator
[AD-D011340] 07 p0929 N85-15891
Structural studies of amorphous Mo-Ge alloys using synchrotron radiation
[DE85-002061] 08 p1131 N85-17125
Short range order-long range order in superconducting materials
[AD-A148764] 08 p1227 N85-17724
Bondability of Al-Si thin film in thermosonic gold wire bonding — integrated circuits
[NASA-TM-77795] 10 p1439 N85-19071
Picosecond laser pulse interactions with metallic and semiconductor surfaces
[AD-A149112] 10 p1490 N85-19405
Magnetization of very thin Ni films in epitaxial metal film sandwiches of Cu
[DE85-001840] 10 p1563 N85-19660
Quasi-thermodynamic prediction of hydrogen reemission behavior from titanium films
[DE85-003667] 10 p1564 N85-19664
Structural studies of sputtered Ni-As-O films
[DE85-003229] 11 p1605 N85-20095
Effect of interfacial characteristics of metal clad polymeric substrates on electrical high frequency interconnection performance
[NASA-TM-86948] 11 p1624 N85-20223
Observation of standing spinwaves in thin Fe-films by means of Raman spectroscopy
[DE85-003036] 11 p1735 N85-20913
Reaction of amorphous NiNb films with crystalline metal overlayers
[DE85-005483] 13 p2024 N85-22680
Study of 1/f noise in solids
[AD-A151069] 14 p2428 N85-24972
Effects of ion bombardment on the morphology of lead films
[DE85-007232] 15 p2511 N85-25494
The replacement of precious metal thick film inks using conductive polymer technology
[AD-A152002] 16 p2749 N85-26965
Sol-gel processing of lead zirconate titanate films
[ATR-85(8343)-2] 18 p3073 N85-29010
The determination of optical constants of thin metal films by surface plasma techniques 19 p3373 N85-30925
Amorphous metallic films in silicon metallization systems 21 p3610 N85-32427

METAL FINISHING
NT ELECTROPOLISHING
NT SHOT PEENING
Advanced high-efficiency concentrator cells
[DE84-013020] 09 p1344 N85-18459
Kinetics of the formation of a complex alloyed boride coating on iron and its properties
[BLL-BISI-TRANS-22303-(9022.06)] 17 p2930 N85-28064

METAL FLUORIDES
NT BERYLLIUM FLUORIDES
NT CADMIUM FLUORIDES
NT CALCIUM FLUORIDES
NT LITHIUM FLUORIDES
NT MAGNESIUM FLUORIDES
NT STRONTIUM FLUORIDES
NT URANIUM FLUORIDES
Preparation of heavy metal fluoride glasses in the bulk form
[AD-A153784] 18 p3079 N85-29049

METAL FOILS
Zero adhesion system
[AD-D011237] 01 p0015 N85-10093
Formation of subsurface Al2O3 layers in aluminum by oxygen ion implantation
[DE84-015599] 04 p0474 N85-13020
Pulsed electric discharge laser technology. Electron beam window foil material
[AD-A147488] 07 p0972 N85-16171
Confinement of low-energy electrons near metallic surfaces for plasmon generation
[DE85-001119] 09 p1381 N85-18688
Study of character of adhesive interaction and breaking of polyimid-aluminum foil junction during process of hardening 13 p2014 N85-22637
Conversions in amorphous zirconium-vanadium alloy 15 p2496 N85-25400
The effects of water and hydrogen on materials used in integrated circuit packages
[AD-A151893] 15 p2518 N85-25529
Determination of local deformation during explosive welding
[BLL-M-36279-(5828.4)] 20 p3462 N85-31503

METAL FORGING
U FORGING

METAL FORMING
U FORMING TECHNIQUES
U METAL WORKING

METAL GRINDING
Very high speed lap with negative lift effect
[AD-D011711] 19 p3281 N85-30345
Study on the correlation between grinding conditions and residual stresses in ground surface of steel by the X-ray method 23 p3907 N85-34203

METAL HALIDES
NT ALKALI HALIDES
NT ALUMINUM CHLORIDES
NT BERYLLIUM FLUORIDES
NT CADMIUM FLUORIDES
NT CALCIUM CHLORIDES
NT CALCIUM FLUORIDES
NT CESIUM IODIDES
NT COPPER CHLORIDES
NT IRON CHLORIDES
NT LITHIUM CHLORIDES
NT LITHIUM FLUORIDES
NT MAGNESIUM FLUORIDES
NT POTASSIUM CHLORIDES
NT SILVER CHLORIDES
NT SILVER HALIDES
NT SILVER IODIDES
NT SODIUM CHLORIDES
NT SODIUM IODIDES
NT STRONTIUM FLUORIDES
NT TITANIUM CHLORIDES
NT URANIUM FLUORIDES
NT ZINC CHLORIDES
Combustion kinetics of metal oxide and halide radicals
[AD-A150924] 14 p2251 N85-23952

METAL HARDENING
U HARDENING (MATERIALS)

METAL HYDRIDES
Gas chromatographic separation of hydrogen isotopes using metal hydrides
[DE84-014455] 04 p0469 N85-12983
Paramagnetic impurity effects in NMR determinations of hydrogen diffusion and electronic structure in metal hydrides. Cerium in YH-2 and LaH-2.25
[DE84-014127] 04 p0472 N85-13005
Thermodynamical characteristics of heat storage reactors using metal hydrides
[NAL-TR-822] 06 p0869 N85-15524
Properties and thermal stabilities of amorphous transition metal hydrides
[DE85-002117] 11 p1607 N85-20104
Capture of liquid hydrogen boiloff with metal hydride absorbers
[NASA-CR-175677] 14 p2249 N85-23939
Heat-mass flow enhancement system for a metal hydride assembly
[DE85-010698] 22 p3783 N85-33441

METAL INSULATOR SEMICONDUCTORS
U MIS (SEMICONDUCTORS)

METAL IONS
NT FERRIC IONS
Repetitively pulsed metal ion beams for ion implantation
[DE84-014065] 05 p0732 N85-14704
Anisotropy and relaxation effects of Co2+ ions in LiTi ferrite
[AD-A146550] 06 p0861 N85-15469
Homogeneous reaction involving components of different redox couples. 1: Theoretical considerations and digital simulation
[AD-A148666] 08 p1124 N85-17084
Research and development work concerning liquid membranes
[BMFT-FB-T-84-227] 08 p1124 N85-17087
Reactions of metal ions and their cluster in the gas phase using laser ionization: Ion cyclotron resonance spectroscopy
[DE84-016491] 09 p1293 N85-18120

Negative lithium emission from a tungsten surface in a plasma
[DE85-003456] 12 p1936 N85-22167
International Conference on Coordination Chemistry (23rd) held at Boulder, Colorado on 29 July - 3 August, 1984
[AD-A150980] 14 p2252 N85-23956
Laser-induced fluorescence of metal-atom impurities in a neutral beam
[DE85-004960] 14 p2310 N85-24298
Reactions of metal ions and their clusters in the gas phase using laser ionization-ion cyclotron resonance spectroscopy
[DE85-009478] 19 p3361 N85-30638
Interpretation of 119 Sn isomer shifts and 3d 5/2-core-level shifts based on Dirac-Slater calculations on a number of ionic states
[USIP-85-06] 20 p3532 N85-31973

METAL JOINTS
NT SOLDERED JOINTS
NT SPOT WELDS
NT WELDED JOINTS
Fatigue behavior of bolted joints made of carbon fiber reinforced epoxy resins 05 p0650 N85-14173
Recommended aluminum pipe welding procedures for corps of engineers construction
[AD-A146712] 06 p0815 N85-15172
Durability calculation of wing panel element 14 p2285 N85-24159
Joining of sintered composite TiC-steel materials by welding
[BLL-M-36253-(5828.4)] 20 p3461 N85-31502
Moire interferometric measurement of relative displacements in dovetail joints
[OUEL-1563/85] 20 p3471 N85-31566
Negative flexural behavior of precase composite slabs with steel joint 23 p3904 N85-34163

METAL MATRIX COMPOSITES
High performance fibers for structurally reliable metal and ceramic composites — advanced gas turbine engine materials
[NASA-TM-86878] 03 p0325 N85-12095
Composite structural materials
[NASA-CR-174077] 04 p0467 N85-12966
Fatigue behavior of continuous fiber silicon-carbide-aluminum composites
[NASA-TM-86332] 06 p0763 N85-14879
Titanium Matrix/Continuous Fiber/Continuous fiber composite interface interactions and their influence on mechanical properties
[AD-A147504] 07 p0920 N85-15829
The response of metallic structures to dynamic loading 08 p1172 N85-17389
Spreading upon compacting of fiber composite materials with porous metal matrix 10 p1443 N85-19096
Structure and property formation mechanism in magnetite alloy-binder composite 10 p1444 N85-19103
Evaluation and prediction of long-term environmental effects of nonmetallic materials
[NASA-CR-171353] 10 p1450 N85-19137
Effect of operating medium on cyclic durability of AD33-W composite 13 p2029 N85-22716
MMCIAC (Metal Matrix Composites Information Analysis Center)
[AD-A150654] 14 p2248 N85-23933
The effect of notch acuity on the fracture toughness of silicon carbide/aluminum metal matrix composites
[AD-A150970] 14 p2246 N85-23936
Localized corrosion currents from graphite/aluminum and welded SiC/Al metal matrix composites
[AD-A150966] 14 p2256 N85-23960
Mechanical aspects of interfaces and surfaces in ceramic containing systems
[AD-A151978] 15 p2519 N85-25530
On residual stresses and stress intensity factors in composite materials 15 p2572 N85-25859
Nonlinear structural analysis for fiber-reinforced superalloy turbine blades 16 p2737 N85-26987
Microscopic study of the influence of impurities on interface bonding
[AD-A151725] 16 p2743 N85-26928
Titanium metal-matrix composites
[AD-D011643] 17 p2930 N85-28066
Localized ionic currents from a corroding iron-copper galvanic couple
[AD-A153627] 18 p3074 N85-29011
Development of carbon based brake lining materials without asbestos content in the form of carbon-carbon composites and carbon-metal or carbon-carbide composites
[BMFT-FB-T-85-014] 18 p3082 N85-29067
Fatigue behavior of unidirectional FP-Al composites with circular holes
[AD-A153468] 18 p3121 N85-29322
Arc spray fabrication of metal matrix composite monotape
[NASA-CASE-LEW-13828-1] 19 p3230 N85-30027
Effect of matrix composition on steel fiber reinforced concrete properties 19 p3230 N85-30028
Three body abrasive wear in various metal combinations 23 p3906 N85-34200
X-ray measurement of thermal stresses in tungsten fiber-copper composites 23 p3907 N85-34205
Evaluation methods of ceramic fiber reinforced metal matrix composite 23 p3907 N85-34206
Fracture behavior of aluminum composites reinforced with fiber 23 p3907 N85-34207
Rotating bending fatigue strength of silicon carbide and alumina-fiber reinforced aluminum 23 p3907 N85-34208

METAL OXIDE SEMICONDUCTORS
NT CHARGE COUPLED DEVICES
NT CHARGE INJECTION DEVICES
NT CHARGE TRANSFER DEVICES
NT CMOS
Metal oxide semiconductors power transistors
[CNES-84/QPE/FT/190] 04 p0486 N85-13166
NMOS test chip for a course in semiconductor parameter measurements
[PB84-216506] 04 p0497 N85-13174
Power MOS fast switching techniques
[DE84-015046] 05 p0732 N85-14707
Optics of solids (surface related) and effect of surface roughness on MOS
[AD-A146883] 07 p0946 N85-15996
Design of self-checking N-MOS (H-MOS) integrated circuits 08 p1084 N85-16742
Silicon superlattices. 2: Si-Ge heterostructures and MOS systems
[NASA-CR-174267] 08 p1224 N85-17711
Comparison of ionizing radiation and hot electron effects in MOS structures
[DE84-016766] 09 p1400 N85-18809
The Si/SiO2 intrinsic states and interface charges. Chapter 1: Origin, properties, models, impact
[HMI-B-413] 09 p1400 N85-18812
Qualitative of analysis of MOS circuits
[AD-A149267] 10 p1480 N85-19341
Variational calculation of the 2D H2 molecule
[INPE-3304-PRE/615] 10 p1554 N85-19796
Study of metal oxide semiconductor structures by capacitive transient spectroscopy
[ENST-84E011] 11 p1737 N85-20926
Factors affecting SOS (Silicon-On-Sapphire) yield and reliability
[AD-A150004] 12 p1835 N85-21515
Metal-semiconductor phase transition and its application
[DRIC-T-7149] 13 p2021 N85-22665
Electrical overstress protection of submicron devices
[AD-A150334] 13 p2064 N85-22892
Algorithm in Walsh function basis for analysis of integrated microcircuits on MOS-structures 13 p2063 N85-23006
SI MOS devices at low temperatures 14 p2297 N85-24225
Studies in electron phenomena in MOS structures: The pulsed C-V method 15 p2659 N85-26407
Completely consumed carbide: A new process for dielectric isolation
[AD-A152379] 17 p2918 N85-27987
Self-scanning MDS-integrated photosensor strip 17 p2940 N85-28151
Goals, achievements of microelectronics program 17 p2945 N85-28179
VLSI workshop and project: February - November 1982
[WSRL-0374-TR] 17 p2951 N85-28223
Random access memory technologies
[AD-A153069] 17 p3008 N85-28597
System design of multi-layer (3-dimensional) integrated circuits
[AD-A153468] 18 p3094 N85-29154
Microstore: The Stanford analog memory unit
[DE85-005534] 18 p3095 N85-29160
Electronic states in silicon and on its interfaces
[AD-A153664] 18 p3193 N85-29807
Electron spin resonance study of interface states induced by electron injection in metal-oxide-semiconductor devices
[DE85-009502] 18 p3195 N85-29817
Photoeffects of semiconductor electrolyte interfaces
[AD-A154163] 20 p3449 N85-31411
Electron lithography STAR design guidelines. Part 1: The STAR user design manual
[NASA-CR-170765] 20 p3513 N85-31840
Electron lithography STAR design guidelines. Part 2: The design of a STAR for space applications
[NASA-CR-170766] 20 p3513 N85-31841
Electron lithography STAR design guidelines. Part 3: The mosaic transistor array applied to custom microprocessors. Part 4: Stores logic arrays, SLAs implemented with clocked CMOS
[NASA-CR-170767] 20 p3514 N85-31842
Synthesis of tests for programmable logic arrays 22 p3777 N85-33408

METAL OXIDES
NT ALKALINE EARTH OXIDES
NT ALUMINUM OXIDES
NT BARIUM OXIDES
NT BERYLLIUM OXIDES
NT BISMUTH OXIDES
NT CALCIUM OXIDES
NT CERIUM OXIDES
NT CHROMITES
NT CHROMIUM OXIDES
NT COBALT OXIDES
NT COPPER OXIDES
NT IRON OXIDES
NT LEAD OXIDES
NT LITHIUM OXIDES
NT MAGNESIUM OXIDES
NT MAGNETITE
NT MANGANESE OXIDES
NT MOLYBDENUM OXIDES
NT NICKEL OXIDES
NT NIOBIUM OXIDES
NT PLUTONIUM OXIDES
NT POTASSIUM OXIDES
NT RUTILE
NT SAPPHIRE
NT TIN OXIDES
NT TITANIUM OXIDES
NT VANADIUM OXIDES
NT YTTRIUM OXIDES
NT ZINC OXIDES
NT ZIRCONIUM OXIDES
An investigation of the role of sintering in gas-solid interactions
[DE84-015481] 02 p0288 N85-11884
The electrochemical deoxidation of molten oxide substances
[BLL-M-35982-(5828.4)] 05 p0614 N85-13920
Charge trapping in low temperature MOS (Metal-Oxide-Silicon) oxides
[AD-A146450] 06 p0880 N85-15467
Combustion kinetics of metal oxide and halide radicals
[AD-A148521] 08 p1122 N85-17076
Adhesive joint formation under field conditions
[AD-D011478] 10 p1453 N85-19153
Thermal barrier coating system
[NASA-CASE-LEW-13324-2] 12 p1786 N85-21286
Characterization of high temperature electrically conducting oxides
[DE85-004296] 12 p1803 N85-21307
Combustion kinetics of metal oxide and halide radicals
[AD-A150924] 14 p2251 N85-23952
High-temperature oxidation of reaction-roasted silicon nitride with various additives 19 p3244 N85-30114
Molecular orbital studies in oxidation: Sulfate formation and metal-metal oxide adhesion
[NASA-CR-176070] 21 p3585 N85-32174
A study of adherent oxide scales
[AD-A155554] 21 p3587 N85-32188
Long-term research in Japan: Amorphous metals, metal oxide varistors, high-power semiconductors and superconducting generators
[DE85-010827] 22 p3748 N85-33230
Composite desiccant structure
[DE85-006400] 23 p3910 N85-34226
Metal alkoxides: Models for metal oxides. Alkoxide ligands in early transition metal organometallic chemistry
[DE85-011368] 23 p3916 N85-34269

METAL PARTICLES
NT METAL POWDER
NT POWDERED ALUMINUM
Breakdown of porous metals by laser radiation 03 p0349 N85-12249
Sample introduction methods for improving the particle detection capability of the spectrometric oil analysis program
[AD-A150139] 13 p2158 N85-23369
Particulate and whisker toughened alumina composites
[DE85-005239] 16 p2743 N85-26930
The enhancement of molecular fluorescence and photochemistry by small metal particles
[AD-A152740] 17 p2919 N85-27994
Spectral characteristics of grinding sparks used for identification of scrap metals
[PB85-198570] 24 p4090 N85-35290

METAL PLATES
Material degradation in heavy steel plates caused by bending with a laser
[AD-A144784] 01 p0052 N85-10343

Characterization of aluminum alloy 7010 in moderate width plate and T651 and T7651 metallurgical states
[REPT-44-606/F] 05 p0619 N85-13981
Copper-nickel sheathing study, phase 2. Two-year service performance of test panels on the ARCO TEXAS
[PB84-242411] 06 p0775 N85-14952
NDE (Nondestructive Evaluation) of oxygen contaminated titanium alloys and weldments
[AD-P004121] 08 p1126 N85-17098
Feasibility study to demonstrate detection of low levels of oxygen contaminant in titanium using eddy current and ultrasonic NDE (Nondestructive Evaluation) techniques
[AD-P004129] 08 p1127 N85-17104
East Europe report: Science and technology
[JPRS-ESA-85-008] 10 p1460 N85-19200
Methodology for stress analysis of heavy metal plate
10 p1460 N85-19203
Bending two-layer metal-polymer plates
11 p1604 N85-20085
Numerical results of acoustic radiation, transmission and reflection of steel plate in water
[AMTE(N)-TM-84037] 13 p2155 N85-23378
Ultrasonic SH wave velocity in textured aluminum plates
[AERE-R-11516] 15 p2509 N85-25475
Angular dependence of the Rayleigh-surface wave velocity in polycrystalline metals with small anisotropy
[AERE-R-11595] 15 p2509 N85-25476
Compositional control of plate steels
15 p2565 N85-25826
Ultrafast holography using optical fibers
[ISL-CO-238/83] 16 p2768 N85-27204
Formation of a fine structure during shock wave welding
[BLL-BISI-TRANS-22401-(9022.06)]
17 p2973 N85-29368
Brittle fracture behaviour of cold formed, welded 10mm to 20 mm thick plate manufactured from plain carbon structural steels
[BLL-BISI-TRANS-21678-(9022.06)]
18 p3120 N85-29311
A clamped rectangular plate containing a crack
[NASA-CR-177925] 20 p3469 N85-31552
Stresses and strains in a plate resulting from two closely-spaced interference-fit fasteners
[ARL/STRUC-TM-409] 23 p3941 N85-34429
Strain measurement using point recognition picture processing
[DRIC-T-7407] 24 p4101 N85-35421

METAL POLISHING
NT ELECTROPOLISHING
Metallographic preparation of materials with various coatings
[BLL-DRIC-TRANS-7522-(9623.66)]
20 p3433 N85-31299

METAL POWDER
NT POWDERED ALUMINUM
Silicon carbide ceramic production
[NASA-TM-77568] 01 p0035 N85-10220
Mechanochemical reactions of elastomers with metals
[AD-A145657] 02 p0186 N85-11246
Tests and modeling for sintering theory
[DE84-016110] 04 p0473 N85-13012
Influence of pressure on compaction during compression of powders of iron and 40Kh and 10R6M5 steels
[BLL-M-35095-(5828.4)] 07 p0926 N85-15686
Application of diffusion welding of nickel based metals and application of electron beam welding of hot isostatically pressed nickel based powdered metals
08 p1169 N85-17375
Improving operational properties of titanium alloys by diffusion siliciding
11 p1602 N85-20075
Preparation and study of highly reactive metal powders
[AD-A150026] 12 p1808 N85-21331
Slip casting and nitridation of silicon powder
[NASA-TM-77809] 12 p1818 N85-21406
Structural distortions of ultra-dispersed titanium nitride powders
13 p2029 N85-22717
Degassification of silicon nitride powders of various origins
13 p2030 N85-22718
Apparatus for producing amorphous and microcrystalline metal powders
13 p2030 N85-22720
Research on products obtained by powder metallurgy
16 p2768 N85-27081
Electrodes for flash discharge lamps
[DE85-006807] 17 p2955 N85-28250
Powder metallurgy forged gear development
[NASA-TM-87463] 18 p3117 N85-29295
Distribution of density in closed-impression die forging of axisymmetrical products from metal powders
19 p3245 N85-30118
Sintering studies project
[AD-A154750] 21 p3572 N85-32218
Influence of technology of atomization of naturally alloyed iron on grain-size characteristics of powder material
[BLL-M-35810-(5828.4)] 23 p3914 N85-34257
Chromium-base powder alloys for welding cladding layer of bimetal
[BLL-M-35776-(5828.4)] 23 p3915 N85-34260
Synthesis of ultrafine ceramic and metallic powders in a thermal argon rf plasma
[DE85-009634] 23 p3953 N85-34696

METAL SHEETS
Prediction of forming limit diagrams for deep drawing
08 p0796 N85-15099
Study of superplastic alloys based on Al-Zn-Ca
10 p1442 N85-19092
Method for continuously casting
[AD-D011481] 10 p1459 N85-19195
High strength steel sheet with dual phase structure
[BMFT-FB-T-84-219] 12 p1808 N85-21342
Auxiliary units for Robots 14 p2265 N85-24161
Effectiveness of use of heat-dissipating clamps to reduce deformation during argon arc welding of thin sheets of AMg6 alloy
15 p2501 N85-25427
Experience of sheet stamping robotic complexes
16 p2761 N85-27041
Examination of the regions of the joint of sheets bonded by the explosive welding technique
[BLL-BISI-TRANS-22352-(9022.06)]
17 p2973 N85-28370
Inhibited anticorrosion protection of automotive steel strip in the NLMK
[BLL-M-36250-(5828.4)] 20 p3430 N85-31274
A theory of electromagnetic shielding with applications to MIL-STD-285, IEEE-299, and EMP simulation
[AD-A154905] 21 p3575 N85-32233

METAL SHELLS
Dynamic creep buckling: Analysis of shell structures subjected to time-dependent mechanical and thermal loading
17 p2913 N85-27959

METAL SPINNING
Microstructural and electronic characteristics of metallic spin glasses
[AD-A149959] 12 p1813 N85-21371

METAL SPRAYING
Conversions in amorphous zirconium-vanadium alloy
15 p2496 N85-25400

METAL STRIPS
High strength steel sheet with dual phase structure
[BMFT-FB-T-84-219] 12 p1808 N85-21342
High tensile strength, punchable, hot rolled strips with good plasticity
[BMFT-FB-T-84-256] 18 p3078 N85-29040

METAL SURFACES
Metrological consequences of the hard optical boundary assumption
[PB84-223577] 01 p0121 N85-10627
Erosion of sintered WC-Co alloys
02 p0179 N85-11201
Parameters of geometric stability of laser mirror optical surface
02 p0273 N85-11777
The modification of metallic corrosion by ion implantation: Engineering applications and fundamentals studies
[AD-P003954] 02 p0286 N85-11870
Intramolecular electron transfer at metal surfaces. 4: Dependence of tunneling probability upon donor-acceptor separation distance
[AD-A145611] 02 p0287 N85-11876
Characterization of amorphous surface layers in Fe implanted with Ti and C
[DE84-014960] 02 p0289 N85-11885
Fast and precise processing of material by means of an intensive electron beam
[BMFT-FB-T-84-123] 03 p0342 N85-12201
Dispersion forces of solids under stress. Chemisorption under stress
[AD-A145171] 03 p0373 N85-12380
Electronic and magnetic properties of transition-metal surfaces, interfaces and overlayers
[DE84-016866] 05 p0733 N85-14713
A review of metallic surface treatments for corrosion mitigation
[AD-A145701] 06 p0769 N85-14918
Surface effects of corrosive media on hardness, friction, and wear of materials
[NASA-TM-83711] 07 p0930 N85-15696
Cryogenic glass-to-metal seal
[AD-D011370] 07 p0933 N85-15911
Arc erosion of metal in current interval of 1-10 amperes
07 p0963 N85-16042
Low and moderate temperature oxidation of atomically clean nickel, chromium and Ni-Cr alloys
[DE84-017350] 09 p1295 N85-18131
Ion beam studies of hydrogen in metals
[DE84-017422] 09 p1297 N85-18145
Fundamental aspects on ion-beam surface modification: Defect production and migration processes
[DE85-000093] 09 p1399 N85-18804
Characterization of erosion of metallic materials under cavitation attack in a mineral oil
[NASA-TM-86634] 10 p1440 N85-19075
Role of hydrogen in processes of deformation and fracture of metals 10 p1449 N85-19132
Influence of melting conditions on strength of transition zone between steel and composite material
10 p1450 N85-19133
Picosecond laser pulse interactions with metallic and semiconductor surfaces
[AD-A149112] 10 p1490 N85-19405
Effect of implantation species on the tribological response of stainless steel surfaces
[DE85-003530] 10 p1493 N85-19432
Analysis of phase composition of products of laser destruction of metallic surfaces
11 p1600 N85-20064
Study of microstructure of aluminum and copper alloys after processing with continuous CO2 laser beam
11 p1601 N85-20066
Theoretical determination of surface magnetism
[DE85-003224] 11 p1714 N85-20783
Plasma states near surface of metal irradiated by CO2 laser 11 p1719 N85-20815
Classical rainbow scattering of alkali ions on metal surfaces. Application to the investigation of unknown surface structures
[MPIS-10/1984] 11 p1728 N85-20854
Mass analysis of neutral particles and ions released during electrical breakdowns on spacecraft surfaces
[NASA-CR-175585] 12 p1793 N85-21250
Adsorption thermodynamics and surface transport of metal catalyst poisons
[DE85-003750] 12 p1802 N85-21301
Ion-beam nitriding of steels
[NASA-CASE-LEW-14104-1] 12 p1805 N85-21324
Effects of B, Ti and Ta implantation on the wear resistance of Fe and Ni-plated Fe
[AD-A149947] 12 p1806 N85-21330
Chemisorption theory: Adsorption on copper-nickel alloys and titanium surface embrittlement
[DE85-001815] 12 p1807 N85-21334
Evaluation of Epoxo 300-C nonskid coating for use on bridge decks
[PB85-108843] 12 p1819 N85-21412
Formation of alumina layers on iron-base alloys
[BLL-T6418/BG/LRS/LRST737/84]
13 p2020 N85-22657
Study of the effects of implantation on the high Fe-Ni-Cr and Ni-Cr-Al alloys
[NASA-CR-175625] 13 p2021 N85-22661
Hydrogen on impurity-covered iron surfaces
14 p2254 N85-23968
Intramolecular electron transfer at metal surfaces. Part 5: Pendant substituent effects upon thiocarboxylate-bridged Cobalt (3) reduction kinetics at mercury and gold electrodes
[AD-A150647] 14 p2254 N85-23971
Electroreflectance spectroscopy as a probe of the electronic structure at the metal-electronic interface
[DE85-003541] 14 p2428 N85-24976
Material for protection of metal surfaces against corrosion by molten salts
[DE85-007714] 16 p2750 N85-26968
Characteristics of polyacrylic acid-complexed zinc phosphate conversion films deposited on metal surfaces
[DE85-004057] 16 p2750 N85-26974
Surface degradation of ductile metal in elevated temperature gas-particle streams
[DE85-008428] 18 p3074 N85-29017
Micro-reactions of metal contacts on various types of GaAs surfaces
[AD-A153650] 18 p3193 N85-29606
Resolvability of defect ensembles with positron annihilation studies
[DE85-010041] 18 p3196 N85-29623
Mechanical modification of friction surfaces of aluminum alloys by friction transfer 19 p3241 N85-30097
Machining of beryllium with the LLNL precision engineering research lathe
[DE85-010832] 19 p3250 N85-30149
Spontaneous emission by two atoms with different resonance frequencies near a metal surface
[AD-A154115] 19 p3353 N85-30781
Fluorescence quenching by metal semiconductor and insulator surfaces 19 p3374 N85-30929
An investigation of cementation and carbonitriding by means of ionic bombardment
[BLL-OA-TRANS-3203-(6196.300)]
20 p3429 N85-31285
Why CO bonds side-on at low coverage and both side-on and upright at high coverage on the Cr(110) surface
[NASA-CR-176071] 21 p3585 N85-32173

Nonradiative damping of molecular electronic excited states by metal surfaces
[AD-A154619] 21 p3701 N85-32994
The effect of metal overlayers of thermionic dispenser cathodes
[AD-A154795] 21 p3701 N85-32995
Materials characterization with intense positron beams
[DE85-011850] 22 p3839 N85-33769
Study on the correlation between grinding conditions and residual stresses in ground surface of steel by the X-ray method 23 p3907 N85-34203
Method for preparing hydride configurations and reactive metal surface
[DE85-006443] 23 p3917 N85-34274
Electronic structure and lattice dynamics of dimensionally constrained and disordered solids
[AD-A155927] 24 p4161 N85-35797

METAL VAPOR LASERS
Numerical analysis of parameters of self-heating copper vapor lasers 02 p0260 N85-11704
High power metal vapor laser
[AD-D011271] 06 p0813 N85-15159
Measurement of elements in the stratosphere
[NASA-CR-175891] 16 p2823 N85-27414
High efficiency transverse dc electron beams
[AD-A152036] 16 p2862 N85-27851
Infrared generation and wave-mixing studies in cesium
[DE85-012863] 24 p4083 N85-35304

METAL VAPORS
NT SODIUM VAPOR
Laser on copper and gold vapors with space diversity media 02 p0270 N85-11762
Metal vapor arc switch electromagnetic accelerator technology
[NASA-CR-174380] 09 p1314 N85-18259
Analysis of the dissipation mechanism within an instationary cathode spot of metal vapor arcs
[AD-A149258] 10 p1558 N85-19825
Combustion kinetics of metal atoms and metallic radicals over wide temperature ranges 13 p1999 N85-22530
Response of steam-water mixtures to pressure transients
[DE85-010798] 19 p3267 N85-30262
Passive Q-modulation of optical cavities by KCl crystals containing OH(-) -ions 21 p3688 N85-32915
Metal vapor lasers and their applications
[ISL-CO-218/84] 22 p3791 N85-33488

METAL WHISKER REINFORCEMENT
U WHISKER COMPOSITES

METAL WORKING
NT CLADDING
NT EXPLOSIVE FORMING
NT FORGING
NT MAGNETIC FORMING
NT METAL DRAWING
NT METAL SPINNING
NT SIZING (SHAPING)
USSR report: Machine tools and metalworking equipment
[JPRS-UMM-84-019] 01 p0035 N85-10214
Microstructural design in low alloy steels 02 p0176 N85-11179
USSR report: Machine tools and metalworking equipment
[JPRS-UMM-84-020] 04 p0491 N85-13126
Process Modeling Applied to Metal Forming and Thermomechanical Processing
[AGARD-LS-137] 06 p0796 N85-15086
Flow-based analyses of metal deformation processes: An overview 06 p0796 N85-15087
Prediction of forming limit diagrams for deep drawing 06 p0796 N85-15089
Numerical methods in metalforming 06 p0797 N85-15092
Finite element simulation of forging processes 06 p0797 N85-15093
Computer-aided design of extrusion dies by metal-flow simulation 06 p0797 N85-15094
Modeling microstructural changes during hot rolling of steels 06 p0796 N85-15096
Heliostat tested 07 p0904 N85-16318
Materials of the fourth scientific-technical Conference on Questions of the Extrusion of Metals (Selected articles)
[AD-A148578] 08 p1130 N85-17121
USSR report: Machine tools and metalworking equipment
[JPRS-UMM-84-021] 08 p1138 N85-17168
Control systems for robotic production lines 08 p1138 N85-17169
USSR report: Machine tools and metalworking equipment
[JPRS-UMM-85-001] 08 p1139 N85-17172
USSR report: Machine tools and metalworking equipment
[JPRS-UMM-85-003] 10 p1461 N85-19211
Developments in GDR metal forming technology assessed 11 p1617 N85-20168
Use of ferrofluids in machining of metals 13 p2045 N85-22802
USSR report: Machine tools and metalworking equipment
[JPRS-UMM-85-005] 13 p2051 N85-22839
Advances in cutting tool technology surveyed 13 p2051 N85-22840
New tooling for plasma cutting technology 13 p2051 N85-22842
Metal waste in machine tool industry examined 14 p2283 N85-24147
USSR report: Machine tools and metalworking equipment
[JPRS-UMM-85-004] 14 p2284 N85-24152
Powder metallurgy production problems 15 p2497 N85-25406
Optimizing hot workability and controlling microstructures in difficult to process high strength and high temperature materials
[AD-D011586] 15 p2510 N85-25482
Production of shaped parts of NITINOL alloys by solid-state sintering
[AD-A152089] 16 p2749 N85-26966
Experience with introduction of Finish perforation of precision parts for optical instruments 16 p2761 N85-27038
USSR report: Machine tools and metalworking equipment
[JPRS-UMM-84-010] 16 p2767 N85-27071
New robotized, vertical broaching machine featured 16 p2767 N85-27074
Development, implementation of industrial lasers reviewed 16 p2767 N85-27075
USSR report: Machine tools and metalworking equipment
[JPRS-UMM-84-014] 17 p2946 N85-28188
New method for determining stampability of sheet materials
[BLL-BISI-22486-(9022.06)] 17 p2972 N85-28360
State of stress and penetration of plastic deformation in forming
[BLL-BISI-22199-(9022.06)] 17 p2977 N85-28396
Strain fields for aluminum at different tooling temperatures and extrusion ratios
[DE85-008257] 18 p3075 N85-29020
The fabrication, microstructure, and strengthening behavior of heavily cold-worked in situ composites 19 p3231 N85-30031
USSR report: Machine tools and metalworking equipment
[JPRS-UMM-85-008] 20 p3437 N85-31329
Thermomechanical deformation in the presence of metallurgical changes 20 p3466 N85-31533
Study on the correlation between grinding conditions and residual stresses in ground surface of steel by the X-ray method 23 p3907 N85-34203
Algorithm for calculation of strain state from measurements of node coordinates of arbitrary curvilinear grid
[BLL-M-36304-(5828.4)] 23 p3940 N85-34422

METAL-INSULATOR-METAL DIODES
U MIM DIODES

METAL-INSULATOR-METAL SEMICONDUCTORS
U MIM (SEMICONDUCTORS)

METAL-METAL BONDING
Influence of aluminum oxide film on thermocompression bonding of gold wire to evaporated aluminum film
[NASA-TM-77503] 03 p0330 N85-12127
Causes of strength reduction in welded titanium-steel joints 03 p0352 N85-12262
Investigation of the creep behaviour of soft soldered joints with solder L-SnAg5 at ambient temperature
[BLL-T9383/BG/WH796/84] 07 p0926 N85-15865
Comparative studies on the electronic structures of W2(O2CH)4 and W2(O2CH)4-(CH3)2 by the relativistic X Alpha-SW method: A d3-d3 metal dimer with a quadruple metal-metal bond?
[AD-A148814] 09 p1397 N85-18793
Microscopic study of the influence of impurities on interface bonding
[AD-A151725] 16 p2743 N85-26926
Solid state bonding of molybdenum and TZM
[BLL-T8439/BG/LRS/LRST751/85] 16 p2792 N85-27220
New examples of clusters, extended metal-metal bonding and interstitial derivatives
[DE85-005926] 17 p3044 N85-28837
Molecular orbital studies in oxidation: Sulfate formation and metal-metal oxide adhesion
[NASA-CR-176070] 21 p3565 N85-32174
Anti wear property of two phasic metal composite 23 p3906 N85-34199

METALLIC GLASSES
Relationships between electronic structure and stability of metallic glasses
[AD-A145141] 01 p0028 N85-10176
Kinetics of short-range ordering in metallic glasses: Analysis of the crossover effect
[DE84-015524] 02 p0187 N85-11251
Use of magnetic compression based on amorphous alloys as a drive for induction linacs
[DE84-014524] 02 p0277 N85-11805
Relationships between electronic structure and stability of metallic glasses
[AD-A145506] 02 p0287 N85-11874
Re-evaluation of phase separation in Ti-Zr-Be metallic glasses
[DE84-015603] 03 p0338 N85-12176
Evidence for d-band conduction in metallic glasses containing transition metal elements
[DE84-014822] 04 p0570 N85-13685
Structural relaxation and isoconfigurational flow of a metallic glass near equilibrium
[AD-A147868] 07 p0933 N85-15915
Electronic properties of intercalated graphite and amorphous metals
[AD-A147664] 08 p1225 N85-17716
Electrical resistivity and structural changes upon relaxation and crystallization of (Mo/sub 0.6/Ru/sub 0.4)sub 100-x/B/sub x/ metallic glasses
[DE84-017281] 09 p1299 N85-18160
Study of the mechanism for annealing embrittlement of an iron-based metallic glass
[DE84-016856] 09 p1300 N85-18184
Amorphous Ni-Ti alloys: A new method of synthesis
[DE85-002744] 11 p1605 N85-20094
Properties and thermal stabilities of amorphous transition metal hydrides
[DE85-002117] 11 p1607 N85-20104
Effects of hydrogen on magnetic properties of amorphous zirconium alloys
[DE85-003303] 11 p1607 N85-20107
Microstructural and electronic characteristics of metallic spin glasses
[AD-A149959] 12 p1813 N85-21371
Quenching effects on iron site partitioning in the Apollo 17 orange glass composition 13 p2184 N85-23553
Surface composition, properties and thermal stability of massive and fine metallic glasses 15 p2513 N85-25506
Effect of nickel addition on the thermal, magnetic and magnetomechanical properties of Fe(80)B(15)Si(5)
[AD-A152261] 16 p2749 N85-26967
Vibrational spectra of a-Fe(.78)P(.22) by inelastic neutron scattering
[DE85-008298] 17 p2922 N85-28016
Theoretical studies on the structures of insulating and metallic glasses
[DE85-010022] 18 p3194 N85-29814
Metallic glass composition
[DE85-011594] 22 p3751 N85-33253

METALLIC HYDROGEN
Experiments with phase transitions at very high pressure
[NASA-CR-174029] 02 p0172 N85-11148

METALLIC PLASMAS
Synthesis of ultrafine ceramic and metallic powders in a thermal argon rf plasma
[DE85-009634] 23 p3983 N85-34696

METALLIC STARS
Lessons from the globular cluster NGC 5466 05 p0739 N85-14749
Ultraviolet observations of Population 2 Cepheids 11 p1754 N85-21034

METALLIZING
Influence of aluminum metallization coatings on corrosion fatigue properties of steel 01 p0018 N85-10112
MOD silver metallization for photovoltaics
[NASA-CR-174011] 01 p0026 N85-10163
Laser-assisted solar cell metallization processing
[NASA-CR-174213] 06 p0813 N85-15160
Amorphous metallic layers in Si metallization systems 06 p0830 N85-15277
A nonnoble front metallization process 06 p0830 N85-15279
Laser-assisted solar-cell metallization processing 06 p0831 N85-15282
Ion cluster beam deposition research 06 p0831 N85-15283
Mod silver metallization for photovoltaics
[NASA-CR-174444] 10 p1509 N85-19518
MOD silver metallization for photovoltaics
[NASA-CR-175460] 10 p1510 N85-19526
A process to produce fine line metallic collection patterns on semiconductors devices
[NASA-CASE-NPO-16413-1] 12 p1805 N85-21325

Electrostatic forming and testing of polymer films on a 16-foot diameter test fixture
[NASA-TM-86328] 13 p2063 N85-22885
Laser-assisted solar cell metallization processing
[NASA-CR-175686] 14 p2350 N85-24528
Structure of condensed aluminum thin film metallizations 15 p2512 N85-25501
Ink jet printing of silver metallization for photovoltaics
[NASA-CR-175709] 15 p2586 N85-25943
Metallurgical means of preventing the corrosion of metal
[BLL-BISI-TRANS-22320-(9022.06)] 17 p2929 N85-28082
Micro-reactions of metal contacts on various types of GaAs surfaces
[AD-A153650] 18 p3193 N85-29606
Metallographic preparation of materials with various coatings
[BLL-DRIC-TRANS-7522-(3623.66)] 20 p3433 N85-31299
High reflective surfaces for millimeter RF waves, phase A — satellite antenna reflectors
[HRS-FR-01] 20 p3442 N85-31366
High temperature electronics technology: Life test report
[AD-A154681] 21 p3580 N85-32257
Amorphous metallic films in silicon metallization systems 21 p3610 N85-32427
Laser-assisted solar-cell metallization processing 21 p3610 N85-32429
A non-noble front metallization process 21 p3611 N85-32430
Pulsed excimer laser processing for cost-effective solar cells 21 p3611 N85-32432
Laser-assisted solar cell metallization processing
[NASA-CR-176124] 22 p3805 N85-33565
Ink jet printing of silver metallization for photovoltaics
[NASA-CR-176054] 22 p3805 N85-33569
Development of metallization process: FSA project, cells and module formation research area
[NASA-CR-176138] 23 p3945 N85-34447

METALLOGRAPHY
Electrolytic lapping technique for vanadium
[DE84-014710] 02 p0183 N85-11227
Bilform resolidification and amorphous phases in a laser and electron beam processed tantalum-iridium alloy
[DE84-013334] 02 p0184 N85-11234
Metallography of Kovar/glass/thermite interfaces
[DE84-015247] 02 p0195 N85-11302
A metallographic investigation of rotating bands for 7.5 cm artillery projectiles
[FOA-C-20551-D2] 07 p0929 N85-15868
Metallographic grinding efficiency
[DE85-001520] 09 p1304 N85-18194
Properties and microstructures for dual alloy combinations of three superalloys with alloy 901
[NASA-TM-86987] 16 p2749 N85-26963
Ce-Ga, Sr-Ga and Ba-Ga binary systems
[DE85-006454] 16 p2751 N85-26980
Full statistical characteristics of microdeformation
[BLL-M-36076-(5828.4)] 16 p2796 N85-27254
Physic-chemical mechanisms of the processes of the formation of globular inclusions in ball-bearing metal
[BLL-BISI-TRANS-22235-(9022.06)] 17 p2924 N85-28030
Quality testing to the specifications of the Stahl-Eisen-Prueflblatt 1570/71 using an automatic image analysis system
[BLL-BISI-TRANS-22253-(9022.06)] 17 p2976 N85-28385
Metallographic preparation of materials with various coatings
[BLL-DRIC-TRANS-7522-(3623.66)] 20 p3433 N85-31299
The effect of stress and hot corrosion on nickel-base superalloys
[AD-A154722] 21 p3566 N85-32181
Proceedings of the Twentyseventh Japan Congress on Materials Research
[ISSN-0368-3141] 23 p3903 N85-34180
Characterization of modified 9 r-1 Mo steel sand castings
[DE85-012057] 24 p4060 N85-35267

METALLOIDS
NT ANTIMONY
NT ARSENIC
NT BORON
NT BORON 10
NT GERMANIUM
NT GERMANIUM ISOTOPES
NT SILICON
NT SILICON ISOTOPES
NT TELLURIUM
Measurement of state and dynamic solid state properties in nonmetals using excited probe nuclei on the Erlanger 12 MeV tandem accelerator 03 p0429 N85-12730
Interaction of metals and metalloids with biomembranes
[DE85-004902] 13 p2141 N85-23293
Pressure-dependence of TiS(2) and TiSe(2) bandstructures
[AD-A151200] 15 p2659 N85-26410
Method of production of metals by cathodic solution of their compounds in electrolytic cells
[BLL-OA-TRANS-3207-(6196.300)] 20 p3429 N85-31266

METALLORGANIC COMPOUNDS
U ORGANOMETALLIC COMPOUNDS

METALLURGY
Metalurgy of a 12 percent chromium stainless steel 02 p0178 N85-11195
The metallurgical processes during the soft soldering of copper and copper alloys and the strength characteristics of soldered joints
[BLL-T6368/BG/WH803/84] 06 p0787 N85-14908
Machine tools at 1984 Leipzig Spring Fair 06 p0815 N85-15177
Method for making alloy additions to base metals having higher melting points
[AD-D011403] 07 p0928 N85-15884
USSR report: Materials science and metallurgy
[JPRS-UMS-84-006] 10 p1442 N85-19088
USSR report: Materials science and metallurgy
[JPRS-UMS-84-005] 11 p1597 N85-20044
USSR report: Materials science and metallurgy
[JPRS-UMS-85-001] 15 p2496 N85-25395
Estimation of the depth of a spherical cap in an hydraulic drawing test for some simple conditions of loss of stability
[REPT-4/1984] 16 p2748 N85-26956
Extreme evaluation of reliability indices for components of metallurgical equipment
[BLL-M-36070-(5828.4)] 16 p2796 N85-27234
Metallurgical means of preventing the corrosion of metal
[BLL-BISI-TRANS-22320-(9022.06)] 17 p2929 N85-28082
The thermal calculation of opaque heat screens
[BLL-M-36273-(5828.4)] 20 p3450 N85-31421

METALS
NT ACTINIDE SERIES
NT ALKALI METALS
NT ALKALINE EARTH METALS
NT ALUMINUM
NT ALUMINUM COATINGS
NT ALUMINUM ISOTOPES
NT ALUMINUM 26
NT AMERICIUM
NT AMERICIUM ISOTOPES
NT AMERICIUM 241
NT BARIUM
NT BERYLLIUM
NT BERYLLIUM ISOTOPES
NT BERYLLIUM 7
NT BERYLLIUM 9
NT BERYLLIUM 10
NT BISMUTH
NT CADMIUM
NT CALCIUM
NT CALCIUM ISOTOPES
NT CALIFORNIUM ISOTOPES
NT CERIUM
NT CERIUM 144
NT CESIUM
NT CESIUM ISOTOPES
NT CESIUM 134
NT CESIUM 137
NT CHROMIUM
NT CHROMIUM ISOTOPES
NT COBALT
NT COBALT 60
NT CURIUM
NT CURIUM 244
NT ERBIUM
NT FERROUS METALS
NT GADOLINIUM
NT GALLIUM
NT GOLD
NT GOLD COATINGS
NT HAFNIUM
NT HOLMIUM
NT INDIUM
NT IRIDIUM
NT IRON
NT IRON ISOTOPES
NT IRON 59
NT LANTHANUM
NT LEAD (METAL)
NT LIQUID LITHIUM
NT LIQUID METALS
NT LIQUID POTASSIUM
NT LIQUID SODIUM
NT LITHIUM
NT LUTETIUM
NT MAGNESIUM
NT MAGNESIUM ISOTOPES
NT MANGANESE
NT MANGANESE ISOTOPES
NT MERCURY (METAL)
NT METAL COATINGS
NT METAL CRYSTALS
NT METAL FILMS
NT METAL FOILS
NT METAL MATRIX COMPOSITES
NT METAL POWDER
NT METAL VAPORS
NT MOLYBDENUM
NT NEODYMIUM
NT NEODYMIUM ISOTOPES
NT NICKEL
NT NICKEL COATINGS
NT NICKEL ISOTOPES
NT NIOBIUM
NT NOBLE METALS
NT NONFERROUS METALS
NT OSMIUM
NT OSMIUM ISOTOPES
NT PALLADIUM
NT PLATINUM
NT PLUTONIUM
NT PLUTONIUM ISOTOPES
NT PLUTONIUM 238
NT PLUTONIUM 239
NT POTASSIUM
NT POTASSIUM 40
NT POWDERED ALUMINUM
NT PRASEODYMIUM
NT RADIUM
NT RARE EARTH ELEMENTS
NT REFRACTORY METALS
NT RHENIUM
NT RHODIUM
NT RUBIDIUM
NT RUBIDIUM ISOTOPES
NT RUTHENIUM
NT SAMARIUM
NT SCANDIUM
NT SCANDIUM ISOTOPES
NT SILVER
NT SINTERED ALUMINUM POWDER
NT SODIUM
NT SODIUM ISOTOPES
NT SODIUM VAPOR
NT STRONTIUM 90
NT TANTALUM
NT TECHNETIUM
NT THALLIUM
NT THORIUM
NT THORIUM ISOTOPES
NT TIN
NT TITANIUM
NT TRANSITION METALS
NT TRANSURANIUM ELEMENTS
NT TUNGSTEN
NT URANIUM
NT URANIUM ISOTOPES
NT URANIUM 235
NT VANADIUM
NT YTTERBIUM
NT YTTRIUM
NT ZINC
NT ZINC COATINGS
NT ZIRCONIUM
Study of proton and neutron activation of metal samples in low Earth orbit
[NASA-CR-171183] 01 p0026 N85-10164
The driving-force dependence of electrochemical rate parameters: Origins of anodic-cathodic asymmetries for metal aquo redox couples
[AD-A145605] 02 p0172 N85-11153
Method for calculating linear shrinkage and expansion of metals and alloys
[BLL-M-35747-(5828.4)] 02 p0175 N85-11173
Microstructural basis of strength and toughness in hardmetals 02 p0177 N85-11185
The constitution as the basis for recent and future developments of wear resistant materials 02 p0179 N85-11206
Application of positron annihilation in materials science
[DE84-014733] 02 p0288 N85-11883
Universal binding energy relations in metallic adhesion
[NASA-TM-86869] 03 p0331 N85-12132
Structure and properties of titanium alloys after isothermal deformation at low speeds 03 p0351 N85-12260

Photoelectrochemistry with chemically modified electrodes
[DE84-016798] 04 p0471 N85-12997
A bibliography of publications on corrosion and oxidation from UK government laboratories at Teddington, 1924 - 1983
[NPL-DMA(A)-82] 04 p0472 N85-13004
Effect of humidity on fretting wear of several pure metals
[NASA-TP-2403] 04 p0472 N85-13006
Effect of barrier height on friction behavior of the semiconductors silicon and gallium arsenide in contact with pure metals
[NASA-TP-2405] 04 p0478 N85-13044
Structure and properties of grain boundaries
[DE84-014368] 04 p0570 N85-13636
Distribution of oxygen between metal and basic slags
[BLL-M-35932-(5828.4)] 05 p0616 N85-13935
Characterization of stressed metals using acoustic shear waves 05 p0648 N85-14159
Modelling of deformation and fracture in high-temperature structural materials
[DE84-016906] 06 p0818 N85-15191
Inclined dislocation emission at a shielded crack tip
[DE84-016703] 06 p0818 N85-15192
Polymer-metal interface bond stability 06 p0830 N85-15272
JPL in-house fluidized-bed reactor research 06 p0832 N85-15291
Analysis of the heating process of a body in a melt
[BLL-M-36014-(5828.4)] 07 p0956 N85-16057
Measurement of high temperature strain by the laser-speckle strain gauge
[NASA-TM-77751] 07 p0977 N85-16207
Ion microscopy of metals and semiconductors
[AD-A147118] 07 p1043 N85-16626
Application of electricity to the reheating of metals prior to forming. Forging, lamination, induction
[BLL-TR-T6399/BG/MRS14903/84] 08 p1137 N85-17160
Lidar studies of the alkali metals 08 p1184 N85-17460
Electronic properties of intercalated graphite and amorphous metals
[AD-A147664] 08 p1225 N85-17716
Metal-support interactions: Their effects upon adsorption, electronics, and activity/selectivity properties of cobalt in hydrogenation
[DE85-003316] 09 p1292 N85-18113
Resistivity of alloys
[DE85-000906] 09 p1296 N85-18138
Ion beam studies of hydrogen in metals
[DE84-017422] 09 p1297 N85-18145
A metal-catalyzed rearrangement of alkene-alkynes and the stereochemistry of metallacyclobutene ring opening
[AD-A149084] 10 p1435 N85-19042
Characterization of erosion of metallic materials under cavitation attack in a mineral oil
[NASA-TM-86934] 10 p1440 N85-19075
Determination of vapor phase content when metals are struck by laser radiation pulses of various densities 10 p1445 N85-19106
Excitation modes and parameters of stress waves in metal exposed to single laser pulses 10 p1446 N85-19100
Removal of heavy metals by artificial wetlands
[PB85-116127] 10 p1513 N85-19548
Kinetics of reaction of metals and non-metals during diffusion welding 11 p1602 N85-20078
Electron-plastic effect in metals 11 p1605 N85-20089
Insulation bonding test system
[NASA-CASE-MFS-25662-1] 11 p1610 N85-20126
Computer simulation of grain-boundary properties in ionic crystals and metals
[DE85-000577] 11 p1734 N85-20908
Studies of silicon-refractory metal interfaces: Photoemission study of interface formation and compound nucleation
[AD-A150075] 12 p1800 N85-21293
Properties of supported metal catalysts
[DE85-003627] 12 p1802 N85-21303
Method and apparatus for detecting acoustic emissions from metal matrix wire
[AD-D011558] 12 p1927 N85-22107
Effects of scatterer spacing statistics on ultrasonic backscatter signal spectra
[DE85-003259] 12 p1928 N85-22114
Experimental determination of systems suitable for study as monotectic binary metallic alloy solidification models 12 p1948 N85-22235
Characteristics of EMI generated by negative metal-positive dielectric voltage stresses due to spacecraft charging 13 p1965 N85-22505
Adequacy of metal ablation process with laser radiation and a shock-compressed plasma 13 p2028 N85-22706
Effect of transparent coatings on generation of laser-induced shock waves in metals 13 p2028 N85-22711
Generation of longitudinal acoustic waves by modulated helicon waves --- nonlinear steady state waves in metals 13 p2090 N85-23049
Characterization of atomic defects and their aggregates using positron annihilation spectroscopy
[DE85-006206] 14 p2418 N85-24918
Monte Carlo lattice models for adsorbed polymer conformation
[NASA-TP-2453] 14 p2426 N85-24981
USSR report: Materials science and metallurgy
[JPRS-UMS-85-001] 15 p2496 N85-25395
Study of amorphous strips and microconductors by ferromagnetic resonance method 15 p2497 N85-25402
C2H(n) fragments on metal surfaces
[AD-A151474] 15 p2505 N85-25449
Sweden develops new rapid solidification process 15 p2531 N85-25610
Electronic properties of new organic conductors
[DE85-005590] 15 p2549 N85-25736
Experimental and theoretical study of the infrared reflectance of thin oxide films on metals
[DE85-005799] 15 p2553 N85-26366
Pressure-dependence of TiS(2) and TiSe(2) bandstructures
[AD-A151200] 15 p2559 N85-26410
Ignition of metals in high pressure oxygen 16 p2735 N85-26874
Ductility equation for porous metals and its linearization
[BLL-M-36118-(5828.4)] 16 p2748 N85-26958
Electrical resistivity in amorphous metals: Consequences of phonon ineffectiveness in the diffraction model
[AD-A152130] 16 p2779 N85-27150
Thermal expansion effects in electrical transport in amorphous metals
[AD-A152477] 17 p2930 N85-28069
Electrons and grain boundary energies in metals
[DE85-006530] 17 p2932 N85-28099
Limiting values of stress state index after rupture of metals
[BLL-BISI-TRANS-22293-(9022.06)] 17 p2978 N85-28407
The effect of ion-bombardment-induced atomic mixing on depth-profiling of interfaces
[AD-A153199] 17 p3044 N85-28834
Thermodynamic calculations of equilibrium states in metal-carbon-hydrogen-oxygen system
[BLL-BISI-TRANS-22092-(9022.06)] 17 p3045 N85-28844
Field theory of the metal-insulator transitions in restricted symmetries
[NOTA-INTERNA-829] 18 p3196 N85-29826
Multiaxial fatigue and fracture: A literature review
[ARL/STRUC-R-410] 19 p3285 N85-30370
Polyethylene imine-metal salt solid electrolyte
[AD-D011678] 19 p3305 N85-30485
Spectrographic investigation of low-voltage arc discharge in argon atmosphere
[BLL-M-36276-(5828.4)] 20 p3422 N85-31242
Study of solute segregation at interfaces using Auger electron spectroscopy
[DE85-005709] 20 p3423 N85-31247
Method of production of metals by cathodic solution of their compounds in electrolytic cells
[BLL-OA-TRANS-3207-(8196.300)] 20 p3429 N85-31266
The nature of the anomalies on the polytherms of the properties of molten metallic alloys
[BLL-M-36265-(5828.4)] 20 p3430 N85-31277
Influence of error of determination of moire isotach orders on the stability of their approximation
[BLL-M-36277-(5828.4)] 20 p3450 N85-31423
Viscoplasticity based on overstress with a differential growth law for the equilibrium stress 20 p3466 N85-31532
On the use of internal state variables in thermoviscoplastic constitutive equations 20 p3466 N85-31536
On numerical integration and computer implementation of viscoplastic models 20 p3467 N85-31542
Simulation model of acoustic emission due to microscopic fracture in metals
[BLL-BISI-TRANS-22267-(9022.06)] 20 p3523 N85-31909
Development of processes for the inclusion of radioactive waste in glass-metal compounds and ceramic materials
[BLL-CE-TRANS-8014-(9022.09)] 20 p3526 N85-31931
Metal-insulator-metal models of tunneling 20 p3536 N85-32006
Study of proton and neutron activation of metal samples in low Earth orbit
[NASA-CR-171596] 21 p3558 N85-32130
High-frequency furnace
[DE85-011210] 21 p3586 N85-32291
On one nonlinear problem of laser thermochemistry 21 p3607 N85-32971
The effect of metal overlayers of thermionic dispenser cathodes
[AD-A154795] 21 p3701 N85-32995
Long-term research in Japan: Amorphous metals, metal oxide varistors, high-power semiconductors and superconducting generators
[DE85-010827] 22 p3748 N85-33230
Proceedings of the Twentyseventh Japan Congress on Materials Research
[ISSN-0368-3141] 23 p3903 N85-34180
Method for extracting lanthanides and actinides from acid solutions by modification of Purex solvent
[DE85-005763] 23 p3909 N85-34220
Direct determination of metals in organic matrices by Inductively Coupled Plasma-Atomic Emission Spectrometry (ICP-AES)
[DE85-012015] 23 p3911 N85-34233

METAMORPHISM (GEOLOGY)
Petrology of deep crustal xenoliths from the eastern Snake River Plain, Idaho 02 p0226 N85-11477
Geology and geochemistry of early Tertiary submarine volcanic rocks of the Aleutian Islands, and their bearing on the development of the Aleutian Island Arc 03 p0389 N85-12493
Metamorphic petrology of the Table Mountain area, Circle quadrangle, Alaska 04 p0516 N85-13295
Structural observations in the Circle quadrangle, Yukon-Tanana Upland, Alaska 04 p0517 N85-13298
The northern coast plutonic-metamorphic complex, southeastern Alaska and northwestern British Columbia 04 p0518 N85-13305
Cretaceous plutonic rocks, Mitkof and Kupreanof Islands, Petersburg quadrangle, southeastern Alaska 04 p0518 N85-13306
Late oligocene gabbro near Ketchikan, southeastern Alaska 04 p0518 N85-13307
A tectonic and metamorphic history of the north-central Klamath Mountains, California 05 p0673 N85-14323
Late precambrian to ordovician metamorphism and orogenesis in the Blue Ridge and western Piedmont, Virginia Appalachians 09 p1352 N85-18503
Conditions for formation of paragneisses containing kyanite-orthoclase in region of Mount Provender and Pratt Peak (Shackleton Range, Antarctica) 19 p3298 N85-30447
Hydrothermal alteration in the 3.5 b.y. old Onverwacht Group of South Africa 21 p3718 N85-33071
The 3.5 b.y. old Onverwacht Group: A remnant of ancient oceanic crust 21 p3718 N85-33073
Bedrock geology of the Brattleboro Quadrangle, Vermont-New Hampshire
[DE85-011027] 22 p3815 N85-33834
Structural development of the west-central Grant Range, Nye County, Nevada 24 p4115 N85-35508

METASTABILITY
U METASTABLE STATE

METASTABLE ATOMS
Infrared emission and atomic transitions
[AD-A147840] 07 p1041 N85-16607

METASTABLE STATE
Metastable phase formation in ion implanted metals
[DE84-014945] 02 p0183 N85-11229
Raman scattering from metastable GaSb(1-x) Ge(2x) alloys
[AD-A145697] 03 p0327 N85-12108
Fatigue crack propagation in metastable titanium alloys
[AD-A145824] 03 p0372 N85-12376
Formation of superconductive Al(GeSi) alloys by low temperature laser quenching methods
[DE84-016887] 04 p0474 N85-13021
Search for neutral, penetrating, metastable particles produced in the SLAC beam dump
[DE84-012468] 04 p0560 N85-13569
Kohn anomaly in metastable fcc lanthanum at low temperatures
[DE84-015459] 04 p0569 N85-13628
Electron spin polarization effects in low energy electron diffraction, ion neutralization and metastable atom deexcitation at solid surfaces
[DE84-016560] 04 p0572 N85-13649

The growth of metastable peritectic compounds
[NASA-CR-171289] 07 p0920 N85-15824
The growth of metastable peritectic compounds
[NASA-CR-171290] 07 p0920 N85-15825
An experimental and theoretical investigation of optogalvanic effects
[AD-A148456] 08 p1223 N85-17700
Effect of inner subshell ionization for emission lines of OIV ion 09 p1388 N85-18729
Alloy development, processing and characterization of devitrified titanium base microcrystalline alloys
[AD-A149609] 12 p1806 N85-21327
Specifics of structure and mechanical properties of metastable beta-titanium alloys after deformation and aging 13 p2032 N85-22731
Theoretical and experimental studies of stabilized metastable helium
[AD-A150706] 14 p2417 N85-24913
Effect of inner subshell ionization on emission lines OIV ions
[IPPJ-719] 19 p3370 N85-30903
Theoretical investigation of material characteristics of semiconductor superlattices
[AD-A154128] 19 p3375 N85-30938
Globally-asynchronous locally-synchronous systems
[AD-A154634] 21 p3573 N85-32222
Detection of excited states by laser-induced fluorescence
[AD-A155558] 21 p3592 N85-32326
Modulated voltage metastable ionization detector
[NASA-CASE-ARC-11503-1] 23 p3933 N85-34374

METAZOA
U ANIMALS

METEOR BURSTS
U METEOROID SHOWERS

METEOR CRATERS
U CRATERS

METEOR HAZARDS
U METEOROID HAZARDS

METEOR TRAILS
Scattering of radio waves on magnitized meteor trail 03 p0344 N85-12221
Discovery of nuclear tracks in interplanetary dust 06 p0689 N85-15647
Influence of Faraday effect in ionosphere on nonmutuality of meteor radio channel 07 p0952 N85-16037
MWR, Meteor Wind Radars 08 p1164 N85-17462
Calculation of amplitude-phase characteristics of signal scattered obliquely on meteor trail 13 p2073 N85-22948
Ionization coefficient for atomic collisions in meteor trail 16 p2720 N85-26792
Interpolation problems in meteor radar analysis, part 7.8A 21 p3626 N85-32528
MENTOR: Adding an outlying receiver to an ST radar for meteor-wind measurement 21 p3628 N85-32538

METEORITE COLLISIONS
Impact phenomena as factors in the evolution of the Earth
[NASA-CR-174015] 01 p0072 N85-10474

METEORITE COMPRESSION TESTS
U COMPRESSION TESTS
U MECHANICAL PROPERTIES
U METEORITES

METEORITE CRATERS
Martian terrain ages 13 p2161 N85-23537
Interaction of Martian flow ejecta blankets with pre-existing impact craters: Morphological observations 13 p2183 N85-23546
The Mars ancient cratered terrain, smooth plains boundary: Implications of Viking color data for evolution of the Amenthes Region 15 p2682 N85-26564
A search for evidence of large body Earth impacts associated with biological crisis zones in the fossil record 15 p2682 N85-26567
Large arcuate scars: A geological legacy of the Earth's accretionary past 21 p3721 N85-33089

METEORITES
NT ALLENDE METEORITE
NT CARBONACEOUS CHONDRITES
NT CARBONACEOUS METEORITES
NT CHONDRITES
NT IRON METEORITES
NT MICROMETEORITES
NT PANTAR CHONDRITES
NT STONY METEORITES
NT TEKTITES
The origin of the Moon 04 p0586 N85-13754
Atmospheric heating of meteorites: Results from nuclear track studies 06 p0682 N85-15607
Solar cosmic ray produced neon in lunar soils and their implication for gas-rich meteorite studies 06 p0687 N85-15636
Meteorite concentrations in Antarctica: How complete is the picture? 06 p0689 N85-15644
Discovery of nuclear tracks in interplanetary dust 06 p0689 N85-15647
Mineralogical investigations of lunar samples and meteorites
[NASA-CR-174291] 08 p1258 N85-17918
Lunar sample analysis — Allende meteorite
[NASA-CR-171851] 10 p1572 N85-19911
Antarctic Meteorite Newsletter, volume 8, number 1
[NASA-CR-175587] 12 p1961 N85-22328
Sixteenth Lunar and Planetary Science Conference. Press abstracts
[NASA-CR-175692] 15 p2680 N85-26548
Evidence in meteorites for an active early Sun 15 p2680 N85-26550
Nd-isotopic evidence for the origin of the Sudbury complex by meteoritic impact 15 p2680 N85-26554
Identification of the youngest meteorites and a discussion of the possibility that they came from Mars 15 p2681 N85-26559
What we know about Mars (but otherwise wouldn't) If it is the shergottite parent body 15 p2682 N85-26565
The impact ejection of living organisms into space 15 p2682 N85-26566
Mineralogical studies of lunar meteorites and their lunar analogs 15 p2683 N85-26572
The role of thermal motions of air particles for fireballs
[PUBL-59] 17 p3053 N85-28600
MENTOR: Adding an outlying receiver to an ST radar for meteor-wind measurement 21 p3628 N85-32538
Explosion in flight 21 p3683 N85-32883
Terrestrial Planets: Comparative Planetology
[NASA-CR-176093] 22 p3851 N85-33849
Noble gas patterns in the atmospheres of Mars and Earth: A comparison via the SNC meteorites 22 p3852 N85-33853
Ultraheavy cosmic ray tracks in meteorites: A reappraisal, based on calibrations with relativistic ions
[OG-4.4-10] 22 p3860 N85-34041
Cosmic-ray exposure records and origins of meteorites
[SH-7.1-7] 23 p4047 N85-35099
Depth and size effects on cosmogenic nuclide production in meteorites
[SH-7.1-9] 23 p4048 N85-35101
Clusters and cycles in the cosmic ray age distributions of meteorites
[SH-7.1-11] 23 p4048 N85-35103
The read-out system of spatial distribution of thermoluminescence in meteorites
[SH-9.1-16] 23 p4052 N85-35131

METEORITIC COMPOSITION
Size dependence of chondrule textural types 06 p0682 N85-15606
Neutron activation analysis of stoney spherules from a marine sediment sample 06 p0683 N85-15608
Oxygen isotopes in deep sea spherules 06 p0683 N85-15609
Minor elements in relict olivine grains of deep-sea spheres: Match with Mg-rich olivines from C2 meteorites 06 p0683 N85-15610
The Colony meteorite and the possible existence of a new chemical subgroup of CO3 chondrites 06 p0685 N85-15621
X-radiography of slices of the Allende Meteorite 06 p0685 N85-15622
A study of tetrataenite 06 p0685 N85-15623
Mossbauer spectroscopy and X-ray diffraction of samples from the Santa Catharina iron meteorite 06 p0685 N85-15624
Structural development in the Santa Catharina meteorite 06 p0686 N85-15625
Low temperature diffusion coefficients in the Fe-Ni and FeNiP systems: Application to meteorite cooling rates 06 p0686 N85-15626
Extreme incompatibility of Pb during the crystallization of magmatic iron meteorites 06 p0686 N85-15627
Experimental and theoretical study of the formation of the 2AB, 3AB, and 9A meteorite chemical groups from the parent liquid 06 p0866 N85-15628
Investigations concerning the magmatic iron meteorites: Static vs. dynamic experiments 06 p0886 N85-15629
Boron cosmochemistry 06 p0888 N85-15642
Differentiated meteorites and the components of chondrites
[NASA-CR-174201] 06 p0890 N85-15649
Hibonite: Crystal chemistry and origin of blue coloration in meteoritic assemblages 13 p2184 N85-23555
Crystal chemistry of meteoritic hibonites 13 p2185 N85-23556
Evidence in meteorites for an active early Sun 15 p2680 N85-26550
A spectacular nitrogen isotope anomaly in Bencubbin 15 p2683 N85-26569
Origin and evolution of ordinary chondrite meteorites 15 p2683 N85-26571
Mineralogical studies of lunar meteorites and their lunar analogs 15 p2683 N85-26572
Origin of mesosiderites as a natural consequence of planet formation 15 p2683 N85-26574
Ionization coefficient for atomic collisions in meteor trail 16 p2720 N85-26792
Cosmic-ray exposure records and origins of meteorites
[SH-7.1-7] 23 p4047 N85-35099
Accelerator experiments on the contribution of secondary particles to the production of cosmogenic nuclides in meteorites
[SH-7.1-8] 23 p4048 N85-35100
Depth and size effects on cosmogenic nuclide production in meteorites
[SH-7.1-9] 23 p4048 N85-35101
Spallogenic origin of nuclei in meteorites
[SH-7.1-10] 23 p4048 N85-35102

METEORITIC DAMAGE
Directional properties of circular Maria: Interpretation in the context of a testable gravitational capture model for lunar origin 04 p0586 N85-13743
Origin of the Moon 04 p0587 N85-13745
Grainsize evolution and differential comminution in an experimental regolith 06 p0688 N85-15638
Spectral reflectance studies on the orientale region of the Moon 06 p0688 N85-15639
Periodic cometary showers: Real or imaginary? 15 p2680 N85-26555
A search for evidence of large body Earth impacts associated with biological crisis zones in the fossil record 15 p2682 N85-26567

METEORITIC DUST
U MICROMETEOROIDS

METEORITIC IONIZATION
U ATMOSPHERIC IONIZATION
U METEOR TRAILS

METEORITIC MICROSTRUCTURES
X-radiography of slices of the Allende Meteorite 06 p0685 N85-15622
Mossbauer spectroscopy and X-ray diffraction of samples from the Santa Catharina iron meteorite 06 p0685 N85-15624
Speculations on the formation of metallic meteorite phases 06 p0689 N85-15648
Antarctic Meteorite Newsletter, volume 8, number 1
[NASA-CR-175587] 12 p1961 N85-22328
Crystal chemistry of meteoritic hibonites 13 p2185 N85-23556
Evidence in meteorites for an active early Sun 15 p2680 N85-26550

METEOROID CRATERS
U METEORITE CRATERS

METEOROID DUST CLOUDS
NT ZODIACAL DUST

METEOROID HAZARDS
Manmade orbital debris studies at NASA Langley 12 p1783 N85-21192
Periodic cometary showers: Real or imaginary? 15 p2680 N85-26555

METEOROID PROTECTION
Manmade orbital debris studies at NASA Langley 12 p1783 N85-21192
Hypervelocity impact investigations and meteoroid shielding experience related to Apollo and Skylab 12 p1785 N85-21206
Space debris protection for a reusable orbital transfer vehicle 12 p1786 N85-21208
Parametric analysis: SOC meteoroid and debris protection 12 p1786 N85-21209

METEOROID SHOWERS
NT ARIETID METEOROIDS
NT ORIONID METEOROIDS
Periodic cometary showers: Real or imaginary? 15 p2680 N85-26555

METEOROID TECHNOLOGY SATELLITE
U EXPLORER 46 SATELLITE

METEOROIDS
NT ARIETID METEOROIDS
NT MICROMETEOROIDS
NT ORIONID METEOROIDS
NT RADIO METEORS
NT ZODIACAL DUST
Natural environment design criteria for the Advanced X-ray Astrophysics Facility (AXAF) definition and preliminary design
[NASA-TM-86481] 01 p0014 N85-10089
Interaction of large meteoroids with the atmosphere 11 p1656 N85-20431
The global meteor observation system (GLOBMET) 11 p1656 N85-20432
Middle Atmosphere Program. Handbook for MAP, volume 7
[NASA-CR-175479] 11 p1656 N85-20437

Global meteor observation system (GLOBMET)
11 p1656 N85-20438
Atmospheric profile imprint in firewall ablation coefficient
11 p1662 N85-20473
Survivable propagation
[AD-A150070] 12 p1829 N85-21478
Improvement of VHF(MB) model
[AD-A150087] 12 p1829 N85-21480
Plasma production by meteoroid impact
13 p2174 N85-23492
The evolution of meteor streams
15 p2678 N85-26539
Examination of returned solar-max surfaces for impacting orbital debris and meteoroids
15 p2681 N85-26560
A study of the chemistry of alkali metals in the upper atmosphere
[AD-A156349] 24 p4117 N85-35524

METEOROLOGICAL BALLOONS
NT JIMSPHERE BALLOONS
Feasibility of long duration ballooning in Antarctica
[PB84-240571] 04 p0541 N85-13443
Meteorological Sounding System (MSS) standard operating procedures
[AD-A149513] 10 p1519 N85-19578
Location and data collection for long stratospheric balloon flights
14 p2326 N85-24377
Development of an adjustable buoyancy balloon tracer of atmospheric motion. Phase 1: Systems design and demonstration of feasibility
[PB85-165817] 22 p3817 N85-33648

METEOROLOGICAL CHARTS
The 500 millibar sign frequency teleconnection charts: Winter
[PB85-106276/GAR] 07 p1009 N85-16410
Use and interpretation of isentropic analyses
[PB85-132694] 11 p1688 N85-20618
Investigations of micro-turbulence in the bottom of the boundary layer
[AD-A149823] 12 p1896 N85-21897
Digital processing of mesoscale analysis and space sensor data
[NASA-CR-171429] 13 p2146 N85-23319
Development of a graphic system: Example using the outline of synoptic charts
[INPE-3296-PRE/611] 16 p2810 N85-27327
A graphic system for drawing synoptic maps by computer
[INPE-3215-PRE/568] 16 p2834 N85-27474
SINOGRAFO: A system for influencing and forecasting weather
[INPE-3349-PRE/628] 16 p2834 N85-27475
Monthly and seasonal weather outlook for mid-February to mid-March 1985, volume 30, number 4, February 14, 1985
[PB85-164580] 18 p3149 N85-29500

METEOROLOGICAL FLIGHT
Airborne research meteorological data collected by the National Hurricane Research Laboratory (Hurricane Research Division/AOML) during the 1982-1983 hurricane seasons: Inventory and availability
[PB85-163681] 17 p2997 N85-28528
Proceedings of Meteorological Motor Glider (MEMO) Workshop '84
[DFVLR-MITT-85-04] 24 p4121 N85-35542
Motor glider meteorology
24 p4121 N85-35543
Typical and historical aspects of motor gliders as meteorological measuring aircraft
24 p4121 N85-35544
Determination of vertical air velocity using measurements of the aircraft motion
24 p4121 N85-35545
A comparison between Falcon data and motor glider data
24 p4121 N85-35547
Case studies for flux measurements along a low-flying route to the south of Munich
24 p4121 N85-35548
Environmental-physical measurements and determination of atmospheric turbulence with the ASK-16 motor glider
24 p4122 N85-35549
Partitioning of the vertical turbulent energy transport into positive and negative contributions — meteorology
24 p4122 N85-35551
Aircraft measurements during the Bonn Experiment (BONEX 1) — meteorology
24 p4122 N85-35552
Meteorological measurements with motor gliders in Poland
24 p4122 N85-35555
The principles of wind measurement with the help of aircraft
24 p4123 N85-35556

METEOROLOGICAL INSTRUMENTS
NT BAROMETERS
NT CLOUD HEIGHT INDICATORS
NT IONOSONDES
NT RADIOSONDES
NT RAIN GAGES
NT RAWINSONDES
NT WEATHER DATA RECORDERS
NT WIND VANES
An evaluation of wind measurements by four Doppler sodars
[PB85-115301] 10 p1520 N85-19586
ADAPS (Airborne Data Acquisition and Processing System) operation and maintenance manual
[AD-A149297] 11 p1585 N85-19983
Instructor's handbook on meteorological instrumentation
[PB85-105930] 11 p1688 N85-20615
Cabauw (Netherlands) meteorological data tapes 1973-1984: Description of instrumentation and data processing for continuous measurements
[KNMI-WR-84-6] 14 p2379 N85-24685
SCPP (Sierra Cooperative Pilot Project) Forecasting Support
16 p2837 N85-27493
Snow Scale/Rate meter
[AD-D011648] 17 p2994 N85-28605
Notes on atmospheric stability, turbulence, and its measurements
[AD-A155230] 21 p3637 N85-32588
Verification of Doppler sodar measurements — atmospheric boundary layer
[KNMI-WR-85-2] 22 p3817 N85-33645

METEOROLOGICAL PARAMETERS
Pavement friction measurements on nontangent sections of roadways, vol. 1
[PB84-219732] 01 p0036 N85-10227
The SANCOR programme on coastal processes, April 1982 - March 1988
[REPT-66] 01 p0069 N85-10455
The development of objective forecast techniques based on advection of surface weather parameters
01 p0078 N85-10522
Synthesis of current measurements in Puget Sound, Washington. Volume 1: Index to current measurements made in Puget Sound from 1906-1980 with daily and record averages for selected measurements
[PB84-214105] 01 p0089 N85-10603
A principal component analysis of eastern Transvaal seasonal rainfall, 1950 to 1981
02 p0212 N85-11395
Arctic haze: Meteorological aspects of long-range transport
02 p0230 N85-11409
Southern Hemisphere atlas of 1-minute rainfall rates
[AD-A145421] 02 p0231 N85-11509
STS natural environment analysis
[NASA-CR-171221] 03 p0322 N85-12079
Achievements in development of space meteorology
03 p0343 N85-12212
GASP cloud- and particle-encounter statistics and their application to LFC aircraft studies. Volume 2: Appendixes
[NASA-TM-85835-VOL-2] 03 p0395 N85-12522
Closely spaced independent parallel runway simulation
[DOT/FAA/CT-84/45] 04 p0457 N85-12902
Acquisition and storage of Cabauw measurements: A system proposal
[KNMI-TR-48] 04 p0540 N85-13434
Operational numerical forecasts: Survey and verification over the period 1978-1983
[KNMI-TR-49] 04 p0540 N85-13435
Atmospheric environment for Space Shuttle (STS-41D) launch
[NASA-TM-86484] 05 p0679 N85-14358
Investigation of satellite measurements in the presence of clouds, forcing influences on clouds and feedback to the large scale following convection
05 p0682 N85-14381
ECMWF/NMC/GLAS joint simulation study
05 p0682 N85-14385
Epidemiologic methods applied to the study of the relationship between climate and human health
05 p0687 N85-14418
Spring program summary, 1983
[PB84-222223] 06 p0839 N85-15330
Climate applications: General
07 p1001 N85-16355
Meteorological aspects of the 1982-83 El Nino/southern oscillation episode
07 p1001 N85-16356
Climate and water quality
07 p1002 N85-16368
Revised Uniform Summary of Surface Weather Observations (RUSSWO). Shemya AFB, Alaska, parts A-F
[AD-A146917] 07 p1005 N85-16388
Revised Uniform Summary of Surface Weather Observations (RUSSWO). Pope AFB, Fayetteville, North Carolina, parts A-F
[AD-A146918] 07 p1005 N85-16389
Revised Uniform Summary of Surface Weather Observations (RUSSWO). Sondestrom AB, Greenland, parts A-F
[AD-A146919] 07 p1005 N85-16390
Revised Uniform Summary of Surface Weather Observations (RUSSWO). England AFB, Alexandria, Louisiana, parts A-F
[AD-A146920] 07 p1006 N85-16391
Revised Uniform Summary of Surface Weather Observations (RUSSWO). Parts A-F: Homestead AFB, Florida
[AD-A147203] 07 p1007 N85-16396
Limited surface observations climatic summary (LISOCS). Camp Casey, Tong Du Chon, Korea
[AD-A147204] 07 p1007 N85-16397
Limited surface observations climatic summary (LISOCS). Aneback AHP, Germany
[AD-A147205] 07 p1007 N85-16398
Revised Uniform Summary of Surface Weather Observations (RUSSWO). O'Hare International Airport, Chicago, parts A-F
[AD-A147206] 07 p1007 N85-16399
Interrelationship of atmospheric parameters in Honduras
[AD-A147371] 07 p1007 N85-16401
Guidelines for atmospheric measurements in support of electro-optical systems testing
[AD-A146090] 08 p1186 N85-17474
The visibility climatology of McMurdo Sound-Williams Field, Antarctica
[AD-A148108] 08 p1189 N85-17492
An automatic weather station network for low-altitude wind shear investigations
[AD-A148139] 08 p1189 N85-17493
Meteorological factors responsible for high CO (carbon monoxide) levels in Alaskan cities
[PB85-115137/GAR] 09 p1350 N85-18493
Mesoscale storm and dry period parameters from hourly precipitation data: Program documentation
[DE85-001366] 09 p1357 N85-18538
Weather data for simplified energy calculation methods. Volume 4: United States, WYEC data
[DE85-000491] 09 p1357 N85-18539
Weather data for simplified energy calculation methods. Volume 3: Western United States: TRY data
[DE85-000495] 09 p1358 N85-18540
Weather data for simplified energy calculation methods. Volume 1: Eastern United States: TRY data
[DE85-000493] 09 p1358 N85-18541
PATHFINDER: A trajectory prediction system for the Great Lakes
[PB85-115335] 10 p1508 N85-19506
Equations and algorithms for meteorological applications in air weather service
[AD-A146894] 10 p1519 N85-19575
Meteorological Sounding System (MSS) standard operating procedures
[AD-A149513] 10 p1519 N85-19578
MIZEX (Marginal Ice Zone Program): A program for mesoscale air-ice-ocean interaction experiments in Arctic marginal ice zones. 5. MIZEX 84. Summer experiment PI (Principal Investigator) preliminary reports
[AD-A148986] 10 p1521 N85-19594
Middle Atmosphere Program. Handbook for MAP. Volume 12: Coordinated Study of the Behavior of the Middle Atmosphere in Winter (PMP-1) Workshops
[NASA-CR-175475] 11 p1665 N85-20492
Weather data for simplified energy calculation methods. Volume 2: Middle United States. TRY data
[DE85-000494] 11 p1667 N85-20608
International list of selected, supplementary and auxiliary ships — WMO
[WMO-47-ED-84] 11 p1667 N85-20609
Instructor's handbook on meteorological instrumentation
[PB85-105930] 11 p1688 N85-20615
Use and interpretation of isentropic analyses
[PB85-132694] 11 p1688 N85-20618
Civil weather satellite systems
11 p1711 N85-20766
Meteorological and oceanographic support during the Falklands conflict
11 p1712 N85-20769
Practical applications of satellite-derived meteorological and oceanographic data in Naval operations
11 p1712 N85-20771
Sector analysis of relevant meteorological parameters for long range transport of air pollutants
[NR-27] 12 p1893 N85-21882
Navy tactical applications guide. Volume 4. Part 1. Eastern North Pacific weather analysis and forecast applications
[AD-A150097] 12 p1896 N85-21900
Slow motions in the tropical troposphere
13 p2131 N85-23262
Summary of Meteorological Observations, Surface (SMOS) Camp Pendleton, California
[AD-A150482] 13 p2136 N85-23277
Summary of Meteorological Observations, Surface (SMOS), Bermuda
[AD-A150537] 13 p2138 N85-23278

Summary of Meteorological Observations Surface (SMOS), Sigonella, Sicily/Navy
[AD-A150539] 13 p2138 N85-23280
Summary of Meteorological Observations, Surface (SMOS), Alameda, California
[AD-A150609] 13 p2138 N85-23281
The experience of the Swedish Meteorological and Hydrological Institute (SMHI) with the ARGOS system
[PM-U1/81] 14 p2240 N85-23892
Meteorological buoys developed at the EERM laboratory 14 p2326 N85-24374
The Tropical Ocean and Global Atmosphere program (TOGA) 14 p2330 N85-24411
An overview of NDBC drifting buoy development programs — NOAA Data Buoy Center (DBC)
14 p2332 N85-24422
Cabauw (Netherlands) meteorological data tapes 1973-1984: Description of instrumentation and data processing for continuous measurements
[KNMI-WR-84-6] 14 p2379 N85-24685
Meteorological conditions affecting electromagnetic propagation on the Arabian Peninsula
[AD-A152019] 15 p2544 N85-25708
East coast snowstorm survey
15 p2598 N85-26013
Model sensitivity studies of major east coast storms
15 p2598 N85-26016
Three-dimensional/perspective display techniques for meteorological data sets 15 p2599 N85-26018
General meteorological package (GEMPAK)
15 p2599 N85-26019
Meteorological factors in Earth-Satellite propagation
[NASA-CR-175764] 16 p2769 N85-27089
EHF attenuation derived from emission temperatures in light rain
[AD-A151166] 16 p2772 N85-27110
Routine wave and meteorological measurements in offshore areas using ARGOS data surveillance
16 p2812 N85-27344
Forecast of Atlantic seasonal hurricane activity for 1985 16 p2833 N85-27470
Summary of Meteorological Observations, Surface (SMOS), Dallas, Texas
[AD-A150599] 16 p2835 N85-27480
Hurricane Research Division, fiscal year 1984 programs, fiscal year 1985 projections 16 p2836 N85-27491
Investigation of air pollution impact in Eastern Bavaria: Measurement results from August and September, 1984
[DFVLR-FB-85-03] 17 p2968 N85-28471
Functional and performance requirements of the next NOAA-Kansas City computer system
17 p2994 N85-28510
Air Weather Service (AWS) climatic briefs: Europe
[AD-A152526] 17 p2996 N85-28519
Radar study of the melting layer
[ESA-CR(P)-1974] 17 p2997 N85-28527
Contributions on the subject of longitudinal movements of aircraft in wind shears
[NASA-TM-77837] 18 p3139 N85-29432
Environmental Research Laboratories publication abstracts, FY 1984
[PB85-180594] 19 p3313 N85-30540
Atmospheric environment for space shuttle (STS-51C) launch
[NASA-TM-86508] 19 p3315 N85-30547
Workshop on objective analysis: Analysis strategies for field-dependent estimation
[PB85-179901] 19 p3318 N85-30569
Experimental investigation of properties of ice-forming reagents 21 p3639 N85-32602
Solar energy meteorological research and training program: Region 4
[DE85-011783] 22 p3816 N85-33640
Development of an adjustable buoyancy balloon tracer of atmospheric motion. Phase 1: Systems design and demonstration of feasibility
[PB85-185617] 22 p3817 N85-33648
Description of a test site for large-scale heavy gas dispersion and combustion experiments
[DE85-004987] 23 p3911 N85-34231
Incorporating meteorological data into receptor analysis: RAPS (Regional Air Pollution Study) revisited
[PB85-188944] 24 p4114 N85-35503
An atmospheric boundary layer model forced by the operational ECMWF-model
[WSR-3] 24 p4120 N85-35541
Meteorological data from the OPTOMA (Ocean Prediction Through Observations, Modeling and Analysis) program OPTOMA 2, leg D2. 30 Jun. - 10 Jul. 1984
[AD-A156134] 24 p4123 N85-35580

METEOROLOGICAL PROBES
U SONDES

METEOROLOGICAL RADAR
Operational evaluation of 5 cm Doppler radar. Two contributions: Review of WSR-74C Doppler radar operations at WSO Montgomery, Alabama (April 1982 - August 1983). The Johnson-Effect resolving ambiguous Doppler velocities
[PB84-207521] 01 p0041 N85-10269
Combining radar and satellite data for the localization and identification of summer convection
01 p0077 N85-10509
A multipurpose weather radar network
01 p0077 N85-10510
Remote sensing of atmospheric particulates: Technological innovation and physical limitations in applications to short-range weather prediction
[NSF ATM-82-09684] 01 p0077 N85-10511
The use of dual polarisation radar for observing and predicting convective activity 01 p0077 N85-10512
The PROMIS Doppler radar system; design and operational experience 01 p0077 N85-10513
Nowcasting with Doppler radar: The forecaster-computer relationship
01 p0077 N85-10514
Doppler radar analysis of a frontal zone prior to convective development 01 p0077 N85-10515
VHF/UHF radar and its application in nowcasting
01 p0078 N85-10516
The potential use of atmospheric profilers in short-range prediction 01 p0078 N85-10518
Preliminary assessment of very short term forecasting of rain from single radar data 01 p0078 N85-10523
Optimum parameters for determining the motion of radar field by cross-correlation method
01 p0079 N85-10524
Digital radar data as an aid in nowcasting in Hong Kong 01 p0079 N85-10525
Simple methods in very short-range forecasting based on data from a mesoscale network of automatic stations (ANETZ) and from satellite (Meteosat) and radar — Swiss Alps 01 p0082 N85-10548
Operational precipitation observation system using digitized radar and rain gages 01 p0082 N85-10549
The French weather radar network: A status report
01 p0082 N85-10550
PROMIS 600: The pilot project for the future Swedish weather service 01 p0083 N85-10560
Project COST 72 (The European weather radar project) today 01 p0084 N85-10561
Utilization of SAGE aerosol profiles in the analysis of Mauna Loa stratospheric lidar data
[NASA-CR-174198] 05 p0675 N85-14332
Rain volume estimation over areas using satellite and radar data 05 p0686 N85-14406
Simultaneous ocean cross-section and rainfall measurements from space with a nadir-pointing radar
[NASA-TM-86167] 07 p0967 N85-16273
MWR, Meteor Wind Radars 08 p1184 N85-17462
The potential of the NEXRAD radar system for warning of bird hazards
[AD-P004210] 11 p1583 N85-19977
Digital controller for the Wave Propagation Laboratory's VHF and UHF wind-profiling radars
[PB85-112142] 11 p1626 N85-20238
Prospective investigations with DFVLR radar of possible relevance in the assessment of radio interference due to scattering from precipitations — meteorological radar
[DFVLR-FB-84-42] 12 p1830 N85-21485
Radioacoustic system for remote synchronous measurements of wind speed, temperature and its fluctuations 13 p2110 N85-23145
Experimental study of anisotropy of scattering of radar signals by clouds and precipitation
14 p2340 N85-24473
Observation of precipitating clouds by a vertically pointing radar at Morino in the Iburi District, Hokkaido, Japan 15 p2582 N85-25922
Hurricane structure and dynamics from stereoscopic and infrared satellite observations and radar data
15 p2594 N85-25968
Contamination of the fetch-limited directional wave spectrum by waves emanating from an embayment
[NASA-TM-84441] 15 p2604 N85-26048
The development and application of volume scan and cell tracking capabilities for the analysis of convective cloud systems 16 p2830 N85-27451
The use of radar in determining precipitation processes in the BEWMEX area 16 p2831 N85-27455
Conducting a wind sensing study
[NASA-CR-175782] 16 p2832 N85-27465
Statistical comparison of radar echoes of convective precipitation between the northern Alps and its foreland
[DFVLR-FB-85-07] 17 p2950 N85-28215
Weather radar studies
[AD-A152563] 17 p2996 N85-28521
Radar study of the melting layer
[ESA-CR(P)-1974] 17 p2997 N85-28527
Progress in radar meteorology
18 p3148 N85-29488
Use of radar with frequency modulation for studying atmospheric boundary layer 19 p3296 N85-30437
Middle Atmosphere Program. Handbook for MAP. Volume 14: URSI/SCOSTEP Workshop on Technical Aspects of MST Radar
[NASA-CR-176085] 21 p3615 N85-32466
Meteorological and aeronomical requirements for MST radar networks (keynote paper), part 1
21 p3615 N85-32467
Tropospheric-stratospheric exchange, part 1.1A
21 p3615 N85-32468
Gravity waves from the stratosphere to the mesosphere, part 1.3B 21 p3616 N85-32471
The suppression of convective wavebreaking by radiative transfer processes, part 1.3C
21 p3616 N85-32472
General circulation of the middle atmosphere, part 1.4B 21 p3617 N85-32474
Performance of the Colorado wind-profiling network, part 1.5A 21 p3617 N85-32475
Vertical transport in the atmosphere: Measurement capabilities and requirements of VHF radars, part 1.6A
21 p3617 N85-32476
Comparison of tropopause altitude determination by the Platteville Radar, Sunset Radar and the NWS Rawinsonde 21 p3617 N85-32477
Synoptic-scale dynamics with vertical velocity, part 1.8A 21 p3617 N85-32478
Practical use of a tropopause height determination algorithm on an MST radar data set, part 1.8B
21 p3618 N85-32479
Morphology of the scattering targets: Fresnel and turbulent mechanisms, part 2.1A
21 p3618 N85-32481
Usefulness of multifrequency MST radar measurements, part 2.6B 21 p3619 N85-32487
Anisotropy of the permittivity field inferred from aspect-sensitive radar echoes 21 p3620 N85-32492
Accuracy of velocity and power determination by the Doppler method 21 p3620 N85-32493
Determination of billows and other turbulent structures, part 4.1A 21 p3621 N85-32500
Spectral measurements of turbulence and gravity waves, part 4.2A 21 p3622 N85-32501
Gravity-wave spectra in the atmosphere observed by MST radar, part 4.2B 21 p3622 N85-32502
Momentum flux measurements: Techniques and needs, part 4.5A 21 p3623 N85-32508
Tropospheric gravity waves observed by three closely spaced ST radars 21 p3623 N85-32509
Determination of horizontal and vertical wavelengths of gravity waves in the mesosphere by spaced wind measurements 21 p3623 N85-32510
Criteria for site selection and frequency allocation (keynote paper), part 5 21 p3623 N85-32511
Frequency and site selection criteria for MST radars, part 5.1A 21 p3624 N85-32512
Summary of session on optimum transmitter and antenna configuration for MST radar, part 6
21 p3624 N85-32514
Practicality of electronic beam steering for MST/ST radars, part 6.2A 21 p3624 N85-32516
Testing and optimizing MST coaxial collinear arrays, part 6.4A 21 p3625 N85-32518
Overview of on-line data processing for MST radars (keynote paper), part 7 21 p3625 N85-32519
Coding schemes for improving MST radar performance, part 7.1A 21 p3625 N85-32520
Elimination of range-aliased echoes in the VHF radars
21 p3625 N85-32521
Sidelobe reduction of Barker codes, part 7.1C
21 p3625 N85-32522
A high-speed digital signal processor for atmospheric radar, part 7.3A 21 p3626 N85-32525
Hardware schemes for fast Fourier transform, part 7.4A 21 p3626 N85-32526
Criteria and algorithms for spectrum parameterization of MST radar signals 21 p3626 N85-32527
Interpolation problems in meteor radar analysis, part 7.6A 21 p3626 N85-32528
Data base management: MSTRAC (keynote paper), part 8 21 p3626 N85-32530
Sample interchange of MST radar data from the Urbana radar 21 p3627 N85-32531
MST radar data management
21 p3627 N85-32532
Data base for the Colorado profiling network
21 p3627 N85-32533
Further developments of EISCAT as an MST radar
21 p3627 N85-32534
Status of the Jicamarca radar
21 p3627 N85-32535
Recent results at the Sunset radar
21 p3627 N85-32536

The Boot Lake MF imaging radar
21 p3628 N85-32537
MENTOR: Adding an outlying receiver to an ST radar for meteor-wind measurement 21 p3628 N85-32538
Summary of progress at the Poker Flat Observatory in Alaska 21 p3628 N85-32539
Urbana radar systems: Possibilities and limitations
21 p3628 N85-32540
The Sondrestrom radar: Progress and proposed upgrades for ST work 21 p3628 N85-32541
Progress and plans for the Colorado Wind Profiler Network 21 p3628 N85-32542
The MU radar now partly in operation
21 p3628 N85-32543
Network ST radar and related measurements at Pennsylvania State University 21 p3629 N85-32544
A note on the proposed UK VHF radar
21 p3629 N85-32545
The Adelaide VHF radar: Capabilities and future plans
21 p3629 N85-32546
The Proust radar 21 p3629 N85-32547
Millstone Hill radar: Capabilities for S/T observations
21 p3629 N85-32548
The Ponape ST radar 21 p3629 N85-32549
Measurements of vertical velocity over flat terrain by ST radar and other related uses of the radar data set
21 p3630 N85-32550
Automated cell detection as a mesocyclone precursor tool
[AD-A154952] 21 p3635 N85-32577
Method and apparatus for four-beam radar
[PB85-181477] 22 p3757 N85-33289
A multi-channel radar receiver
[AD-A156058] 24 p4087 N85-35333
Polarization diversity addition to the 10 centimeter Doppler weather radar
[AD-A156062] 24 p4087 N85-35334

METEOROLOGICAL RESEARCH AIRCRAFT
NOAA (National Oceanic and Atmospheric Administration) Aircraft Satellite Data Link (ASDL)
[PB84-243773] 07 p0942 N85-15976
Three powered sailplanes as meteorological instrumentation for atmospheric boundary layer studies at DFVLR
[DFVLR-FB-84-50] 17 p2887 N85-27862
DFVLR measuring system for the determination of the spatial distribution of environmental parameters of the atmosphere by means of mobile instrumented platforms
[DFVLR-FB-85-09] 17 p2989 N85-28472
Airborne research meteorological data collected by the National Hurricane Research Laboratory (Hurricane Research Division/AOML) during the 1982-1983 hurricane seasons: Inventory and availability
[PB85-163681] 17 p2997 N85-28526
A preliminary intercomparison between numerical upper wind forecasts and research aircraft measurements of jet streams
[NASA-CR-167884] 24 p4120 N85-35539

METEOROLOGICAL ROCKETS
U SOUNDING ROCKETS

METEOROLOGICAL SATELLITES
NT AEROS SATELLITE
NT ARC CLOUDS
NT DMSP SATELLITES
NT METEOSAT SATELLITE
NT NIMBUS SATELLITES
NT NIMBUS 5 SATELLITE
NT NIMBUS 7 SATELLITE
NT NOAA SATELLITES
NT NOAA 6 SATELLITE
NT NOAA 7 SATELLITE
NT NOAA 8 SATELLITE
NT SIRS B SATELLITE
NT TIROS N SERIES SATELLITES
NT TIROS SATELLITES
Satellite reconnaissance
[AD-B085034] 01 p0015 N85-10094
The past, present, and anticipated future contributions of geosynchronous satellites to short range prediction
01 p0076 N85-10503
A system for meteorological satellite, radar, conventional data and model analysis 01 p0082 N85-10551
Atlas of polar cap energetic particle observations. Volume 1: TIROS-N, 1 January 1979 - 28 February 1981
[PB84-233402] 04 p0535 N85-13419
Frost nowcasting in the agricultural area of Valencia (Spain) — meteorological satellites
05 p0658 N85-14225
Use of photographs of meteorologic satellites in synoptic analysis
[SESIT-5] 05 p0679 N85-14357
Applications of sequential estimation to numerical weather prediction 05 p0681 N85-14374
Weather and climate parameters from Tiros-N
05 p0681 N85-14377
Weather satellite products in the Flight Service Automation System (FSAS)
[AD-A146520] 06 p0759 N85-14855
Satellite definition of the bio-optical and thermal variation of coastal eddies associated with the African current
[AD-A147910] 07 p0969 N85-16282
An auroral X-ray imaging spectrometer
[AD-A147756] 08 p1185 N85-17489
The rationale and suggested approaches for research geosynchronous satellite measurements for severe storm and mesoscale investigations
[NASA-TM-86185] 09 p1356 N85-18532
Technical evaluation report on the 46th Symposium of the Avionics Panel on Space System Applications to Tactical Operations
[AGARD-AR-203] 10 p1425 N85-18988
Processing of Global Area Coverage (GAC) data of the TIROS-N/NOAA series polar orbiters
[AD-A148992] 10 p1519 N85-19576
Defense Meteorological Satellite Program (DMSP)
11 p1711 N85-20766
Military applications of meteorological satellite (METSAT) data 11 p1711 N85-20767
Development of satellite data presentation for environmental forecasting 11 p1712 N85-20770
Meteorological Satellite Center Technical Note No. 10, 1984
[MSC-TN-10] 12 p1894 N85-21884
An analysis of the data obtained by a simultaneous observation of GMS and GMS-2: A study of the difference between the brightness temperatures by GMS and those by GMS-2 12 p1894 N85-21886
GMS operational calibration procedure and status
12 p1895 N85-21893
Remote sensing used for study of forest resources
13 p1983 N85-22440
Research on atmospheric dust formations using satellite observation data 15 p2485 N85-25339
NOAA satellite operations: Programs briefing — Environmental satellites, LANDSAT, and space station polar platform 15 p2599 N85-26020
Recent failures of weather satellites
[S-HRG-98-1070] 16 p2731 N85-26855
Aerospace technology determines forest-fire danger
19 p3295 N85-30427
Six mechanisms used on the SSM/I radiometer
22 p3798 N85-33534

METEOROLOGICAL SERVICES
A summary of operational developments in nowcasting and short-range forecasting techniques on the Canadian West Coast 01 p0082 N85-10547
The French weather radar network: A status report
01 p0082 N85-10550
Development of nowcasting in China
01 p0083 N85-10554
PROFS: An approach to improved operational weather services — Program for Regional Observing and Forecasting Services (PROFS) 01 p0083 N85-10555
A subjective evaluation of the PROFS operational workstation based upon a real-time forecasting experiment in summer 1983 — Program for Regional Observing and Forecasting Services (PROFS) 01 p0083 N85-10556
PROMIS 600: The pilot project for the future Swedish weather service 01 p0083 N85-10560
Use of short-range weather forecasts at construction sites: Some results from a user and a market test
01 p0084 N85-10563
Benefits resulting from tailored very-short-range forecasts in Sweden 01 p0084 N85-10564
Some aspects of matching nowcasting and Very-Short-Range Forecasting (VSRF) products with the need of a multilingual community of a mountainous country — Swiss Alps 01 p0084 N85-10566
Videotex and weather services: Finnish applications
01 p0084 N85-10567
Acquisition and storage of Cabauw measurements: A system proposal
[KNMI-TR-48] 04 p0540 N85-13434
Weather satellite products in the Flight Service Automation System (FSAS)
[AD-A146520] 06 p0759 N85-14855
Climate and climate data. Report on the workshop held in Brasilia (Argentina) from 11-15 April 1983
07 p1001 N85-16357
Requirements for training in climate-related subjects
07 p1004 N85-16378
Equations and algorithms for meteorological applications in air weather service
[AD-A148694] 10 p1519 N85-19575
AFOS (Automation of Field Operations and Services)-ERA forecast verification, September 1984
[PB85-137578] 12 p1897 N85-21912
Project PAPA: The integration of drifting buoy data into an operational meteorological service
14 p2238 N85-23874
The ARGOS communications performance trials
14 p2326 N85-24376
Collecting meteorological reports with the ARGOS system 14 p2329 N85-24398
A weather service for agriculture
16 p2830 N85-27450
Meteorology and food production: The theme of the 16 meteorology day
[AD-A152372] 17 p2996 N85-28518
J. P. Finley: The first severe storms forecaster
[PB85-17453] 19 p3318 N85-30566
150 years of meteorology in Belgium
22 p3817 N85-33642

METEOROLOGICAL STATIONS
U WEATHER STATIONS

METEOROLOGY
NT AEROLOGY
NT AGROMETEOROLOGY
NT ALPINE METEOROLOGY
NT BIOMETEOROLOGY
NT HYDROMETEOROLOGY
NT LONG RANGE WEATHER FORECASTING
NT MARINE METEOROLOGY
NT MESOMETEOROLOGY
NT MICROMETEOROLOGY
NT NOWCASTING
NT NUMERICAL WEATHER FORECASTING
NT POLAR METEOROLOGY
NT RADIO METEOROLOGY
NT STATISTICAL WEATHER FORECASTING
NT SYNOPTIC METEOROLOGY
NT TROPICAL METEOROLOGY
NT WEATHER FORECASTING
Research study: Studies in atmospheric processes from Space Platforms
[NASA-CR-171176] 01 p0072 N85-10473
The climate of Denmark. Summaries of observations from light vessels. 3: Sea temperature
[ISBN-87-7478-215-0] 01 p0073 N85-10481
Photon and electron dosimetry at the Physikalische-Technische Bundesanstalt in Brunswick
[PTB-DOS-9] 01 p0119 N85-10814
Seminar on Principal Components Analysis in the Atmospheric and Earth Sciences
[CSIR-S-334] 02 p0211 N85-11386
Application of correspondence analysis to meteorological data 02 p0211 N85-11393
Statistical interpretation of NWP model output: An overview of techniques used and results achieved
[REPT-551.509.313] 02 p0231 N85-11503
Bibliography of climate textbooks and studies
[WCP-84] 02 p0231 N85-11505
Southern Hemisphere atlas of 1-minute rainfall rates
[AD-A145421] 02 p0231 N85-11509
Atmospheric tracer experiments in a deep narrow valley
[PB84-234590] 04 p0532 N85-13402
Report on United States Antarctic research activities, February 1983 - October 1984 and United States Antarctic research activities planned for October 1984 - September 1985
[PB84-231265] 05 p0677 N85-14352
Atmospheric environment for Space Shuttle (STS-41D) launch
[NASA-TM-86484] 05 p0679 N85-14358
Implicit numerical methods in meteorology
05 p0686 N85-14408
A comparison of evaporation duct models for IREPS (Integrated Refractive Effects Prediction System)
[AD-A146471] 06 p0799 N85-15103
USSR report: Earth sciences
[JPRS-UES-84-007] 06 p0819 N85-15196
The 47th Annual Meteorlical Society Meeting
[NASA-CR-174071] 06 p0881 N85-15599
A summary of the foundation research program
[AD-A146624] 06 p0891 N85-15656
USSR report: Earth sciences
[JPRS-UES-84-008] 07 p0960 N85-16223
Atmospheric acidification chemistry: A review
[PB84-215490] 09 p1350 N85-18495
Natural environment analysis
[NASA-CR-171333] 10 p1428 N85-19010
USSR report: Earth sciences
[JPRS-UES-85-003] 10 p1497 N85-19446
Frozen precipitation and concurrent weather: A case study for Munchen-Riem, West Germany
[AD-A149227] 10 p1519 N85-19577
Instructor's handbook on meteorological instrumentation
[PB86-105830] 11 p1688 N85-20615
Isentropic objective analysis
[PB85-112167] 11 p1688 N85-20617
Use and interpretation of isentropic analyses
[PB85-132694] 11 p1688 N85-20618

Communications software for Olympics Micromation Computer System
[PB85-109610] 11 p1704 N85-20723
Space Shuttle interactive meteorological data system study
[NASA-CR-171418] 12 p1892 N85-21876
On the relative motion of typhoons: In the case of Typhoon 8305 and Typhoons 8306 and 8307
12 p1894 N85-21885
On the error of typhoon intensity estimation by means of IR Dvorak technique occurring when the eye is very small 12 p1894 N85-21886
SAOSUM: A short summary of observations
[PB85-120384] 12 p1897 N85-21909
Earth radiation budget experiment software development
[NASA-CR-172567] 12 p1912 N85-22002
USSR report: Earth sciences
[JPRS-UES-85-002] 13 p2105 N85-23116
Mean flow and turbulence in complex terrain NPS (Naval Postgraduate School)/Vandenberg measurement system
[AD-A150184] 13 p2138 N85-23274
Environmental satellites 14 p2328 N85-24392
USSR report: Earth sciences
[JPRS-UES-85-004] 14 p2332 N85-24424
Possible multiple atmospheric thermal modes with time scale on order of one month 14 p2333 N85-24430
Variational mesoscale satellite data assimilation and initialization
[NASA-CR-175704] 14 p2378 N85-24680
An introduction to USAFETAC (USAF Environmental Technical Applications Center)
[AD-A150971] 14 p2378 N85-24682
Geophysical Fluid Dynamics Laboratory activities, FY84, plans, FY85
[PB85-147601] 15 p2558 N85-25783
Low Temperature Science. Series A: Physical Sciences
[ISSN-0438-9536] 15 p2581 N85-25917
Operational methods for calculating atmospheric dispersion
[BLL-CE-TRANS-8040-(9022.08)] 15 p2586 N85-25955
General meteorological package (GEMPAK)
15 p2599 N85-26019
Oceanographic variations in recent decades and their impact on the fertility of the Iceland Sea
15 p2602 N85-26034
USSR report: Earth sciences
[JPRS-UES-85-005] 16 p2607 N85-27307
Review and annotated bibliography of benthic studies in coastal and estuarine areas of Florida with a selected compilation of worldwide benthic methodological references and southeastern United States benthic taxonomic reference
[PB85-151041] 16 p2622 N85-27405
Study of the functions of similarity of the planetary boundary layer. Part 1: Theory
[INPE-3129-PRE/520-PT-1] 16 p2626 N85-27428
Symposium on Atmospheric Sciences in South Africa
[CSIR-S-331] 16 p2629 N85-27442
Hurricane Research Division, fiscal year 1984 programs, fiscal year 1985 projections 16 p2636 N85-27491
Comparison of circulation statistics based on FGGE (First GARP Global Experiment) level 3-B analyses produced by GFDL (Geophysics Fluid Dynamics Laboratory) and ECMWF (European Centre for Medium Range Weather Forecasts) for special observing periods
[PB85-153946] 16 p2636 N85-27492
Compilation of abstracts of theses submitted by candidates for degrees
[AD-A151722] 16 p2875 N85-27739
Developments in the area of air traffic control systems and the relation with meteorology
[NLR-MP-84029-U] 17 p2895 N85-27848
Air Weather Service (AWS) climatic briefs: Europe
[AD-A152539] 17 p2996 N85-28519
Airborne research meteorological data collected by the National Hurricane Research Laboratory (Hurricane Research Division/AOML) during the 1982-1983 hurricane seasons: Inventory and availability
[PB85-163691] 17 p2997 N85-28528
Improved cloud and surface fields derived from HIRS2/MSU 18 p3140 N85-29439
Hellmut Berg Issue — meteorology
[MITT-39] 18 p3147 N85-29483
Numerical meteorology 18 p3147 N85-29484
Regional meteorology of the Bering Sea during MIZEX-West, February and March 1983
[PB85-173690] 18 p3150 N85-29503
Middle Atmosphere Program. Handbook for MAP. Volume 14: URSI/SCOSTEP Workshop on Technical Aspects of MST Radar
[NASA-CR-176085] 21 p3615 N85-32466
Generation of available potential energy and the energy cycle during the global weather experiment
[NASA-CR-175301] 21 p3634 N85-32572
Meteorological weapons
[AD-A154735] 21 p3635 N85-32575
A transportable, machine oriented library of european sky and terrain radiance distributions with contemporary radiometric and meteorological profiles
[AD-A155254] 21 p3637 N85-32590
Medium range atmospheric forecast system: Evaluation plan
[AD-A155623] 21 p3638 N85-32595
Meteorology and Society: Statements presented at the 9th congress under agenda item 12 — World Meteorological Organization
[WMO-643] 22 p3817 N85-33644
METEORS
U METEOROIDS
METEOSAT SATELLITE
Short period forecasts in West Africa using Meteosat data 01 p0079 N85-10526
The METEOSAT exploitation project, operational use of a remote sensing system 05 p0658 N85-14223
Conceptual ideas for a second generation METEOSAT system 05 p0658 N85-14228
METERS
U MEASURING INSTRUMENTS
METHACRYLATE RESINS
U ACRYLIC RESINS
METHANATION
An infrared study of isotopic exchange during methanation over supported rhodium catalysts; an inverse spillover effect
[AD-A149990] 10 p1435 N85-19046
An infrared study of the hydrogenation of carbon dioxide on supported rhodium catalysts
[AD-A149477] 10 p1436 N85-19049
Characterization of supported metal catalysts by imaging, microdiffraction and microanalysis techniques
[DE85-005567] 14 p2253 N85-23961
METHANE
Plasma deposited diamondlike carbon on GaAs and InP
[NASA-TM-86870] 01 p0123 N85-10844
Raman and fluorescence spectroscopy in a methane-nitrous oxide laminar flame
[AD-A146092] 03 p0328 N85-12111
Methane heat transfer investigation
[NASA-CR-171199] 03 p0362 N85-12318
Study of catalysts and mechanisms in syntheses reactions
[DE84-015025] 04 p0470 N85-12990
Methane-fueled vehicle RD and D
[GPO-37-926] 04 p0481 N85-13064
Diffusion of gases in porous solids: Simulation and measurements
[DE84-016292] 04 p0500 N85-13191
Biomass thermochemical conversion program
[DE84-017177] 05 p0621 N85-13972
The structure of dilute combusting sprays
[NASA-CR-174838] 07 p0905 N85-15728
The abundance of deuterium in the outer solar system from ground-based measurements of monodeuterated methane 07 p1060 N85-16725
Liquid phase methanol process development unit: Installation, operation, and support studies
[DE85-001311] 09 p1301 N85-18171
Mechanisms and reaction dynamics related to methane combustion
[PB85-129690] 10 p1436 N85-19065
Dissociated methanol ciation
[DE85-000505] 10 p1458 N85-19166
Test report for Getty Synthetic Fuels, Inc., Calumet City, Illinois
[PB85-119493] 10 p1459 N85-19191
Kinetics of nitric oxide formation in laminar and turbulent methane combustion
[PB85-149698] 12 p1804 N85-21313
Mechanisms of heat and mass transfer across a double-diffusive interface
[PB85-148468] 12 p1848 N85-21594
Portable remote laser sensor for methane leak detection
[NASA-CASE-NPO-15790-1] 12 p1855 N85-21631
Ignition of mixtures of SiH sub 4, CH sub 4, O sub 2, and Ar or N sub 2 behind reflected shock waves
[NASA-TP-2415] 13 p1974 N85-22395
Anaerobic digestion of biomass: status summary and research development needs, 1983
[PB85-161925] 13 p2040 N85-22772
Optical properties of hydrogenated amorphous carbon films grown from methane plasma
[NASA-TM-86695] 15 p2658 N85-26406
Modeling the role of radicals in the ignition of and flame propagation in hydrogen-air and methane-air mixtures
16 p2744 N85-26935
Low pressure storage of methane on interlayered clays for potential vehicular applications
[DE85-006949] 16 p2758 N85-27017
Studies related to the deep Earth gas: 1983
[PB85-171114] 16 p2816 N85-27373
Monodeuterated methane in the outer solar system. 2. Its detection on Uranus at 1.6 microns
[NASA-CR-175762] 16 p2882 N85-27782
Fatty and aromatic acid catabolizing bacteria from methanogenic ecosystems
[DE85-008133] 17 p2998 N85-28537
Heat of mixing experiments for liquified gases
[PB85-163697] 18 p3084 N85-29061
Optical waveguide sensor for methane gas
[AD-D011691] 19 p3273 N85-30294
Flash pyrolysis of biomass with reactive and non-reactive gases
[DE85-010962] 19 p3306 N85-30496
Atmospheric chlorofluromethanes as tracers of ocean circulation and mixing: Measurement and calibration techniques and studies in the Greenland and Norwegian Seas 19 p3319 N85-30573
Rayleigh scattering for density measurements in premixed flames: One point, time series data
20 p3424 N85-31253
Mechanistic and kinetic studies of the elementary processes in catalytic combustion of methane
[PB85-188308] 20 p3435 N85-31314
Elementary processes in the catalytic combustion of methane (mechanism, intermediates, and controlling reactions)
[PB85-188357] 20 p3436 N85-31316
Electrochemical methane sensor
[DE85-011663] 22 p3787 N85-33464
Measurements of the fragmentation of (40)Ar, (28)Si and (12)C in CH2C and H targets between 300 and 1500 MeV/nuc at the Bevalac
[OG-7.2-19] 23 p4016 N85-34666
Microbiological and biochemical studies towards optimization of substrate utilization by methanogenic bacteria
[PB85-188332] 24 p4084 N85-35310
METHIONINE
Blood amino acids of cosmonauts before and after 211-day spaceflight 12 p1900 N85-21933
METHOD OF CHARACTERISTICS
Modeling of propulsive jet plumes—extension of modeling capabilities by utilizing wall curvature effects
[AD-A146262] 03 p0362 N85-12324
High altitude chemically reacting gas particle mixtures. Volume 1: A theoretical analysis and development of the numerical solution — rocket nozzle and orbital plume flow fields
[NASA-CR-171826] 07 p0916 N85-15801
The split-coefficient matrix method for supersonic three dimensional flow 12 p1821 N85-21425
METHOD OF MOMENTS
Variational and moment method solutions of the fields in a parallel-plate waveguide-aperture system
[DE85-006268] 13 p2057 N85-22576
Analysis of waveguide discontinuities by the method of moments
[AD-A151499] 15 p2547 N85-25721
Investigation of the numerical method of moments for digital computer determination of differential equations
[AD-A151696] 15 p2636 N85-26268
Analysis of systems of waveguide discontinuities by the method of moments 19 p3253 N85-30171
Random vibration of nonlinear, parametrically excited systems 19 p3282 N85-30351
Calculation of mixed depth for some metal-Si systems
[DE85-011907] 23 p3971 N85-34616
METHODOLOGY
Method for making alloy additions to base metals having higher melting points
[AD-D011403] 07 p0928 N85-15884
Use of iterative linear and nonlinear algebraic methods for solving large stiff systems of ODEs
[AD-A146516] 08 p1213 N85-17636
Software and its relationship to methods
[DE85-004784] 14 p2405 N85-24829
METHODS
U METHODOLOGY
U PROCEDURES
METHOXY SYSTEMS
Preparations of methoxynitrophenazines and their photoconductivities
[NASA-TM-77775] 14 p2247 N85-23929
METHYL ALCOHOLS
Advanced concepts for methanol fuel vehicles
[DE84-013612] 04 p0482 N85-13071
Dissociated methanol vehicle test results
[DE84-004507] 04 p0509 N85-13248
Impact of alcohol fuels on urban air pollution: Methanol photochemistry study
[DE84-012950] 04 p0531 N85-13397

Methanol vaporization: Effects on volumetric efficiency and on determination of optimum fuel delivery system
[PB84-243914] 09 p1302 N85-18181
Volatility of in-use gasoline and gasoline-methanol blends
[PB85-117976] 10 p1459 N85-19189
Engine wear and cold startability of methanol fueled engines.
[DE85-001208] 11 p1647 N85-20381
Methanol adsorption on Pt(111)
[DE85-006802] 17 p2923 N85-28017
Conversion of methanol to gasoline: Engineering and construction of the demonstration plant
[DE85-003237] 17 p2937 N85-28133
Investigation of the flame speeds of propane/methanol gas mixtures
[DE85-012817] 23 p3912 N85-34239

METHYL CHLORIDE
The synthesis and characterization of Poly(Oxy(2-Methyl-1,3-Phenylene) Methyl-1,3 -Phenylene) Oxyterephthaloyl)Oxy
[AD-A148269] 08 p1133 N85-17143

METHYL COMPOUNDS
NT METHYL POLYSILOXANE
Interactions of ketones and hexacarbons
[AD-P004019] 06 p0843 N85-15353
Characterization and selection of polymer materials for binary munitions storage. Part 2: Characterization of LLDPE resins
[AD-A148324] 08 p1133 N85-17144
Properties of ultra-violet cured poly(dimethylsiloxane)-urea acrylates
[AD-A148570] 08 p1134 N85-17146
Poly(dimethylsiloxane)-polyurethane elastomers: Synthesis and properties of segmented copolymers and related zwitterionomers
[AD-A148571] 08 p1134 N85-17147
Crystallization behavior of poly(3,3-bis(Ethoxymethyl) oxentane) and poly(3,3-bis(Azidomethyl) oxetane)
[AD-A148271] 08 p1226 N85-17720
Improved lithium-intercalation cathode material
[AD-A149319] 10 p1435 N85-19043
Stable polymeric carbon radicals. Part 2: Attempts at the preparation of polyradicals of the triphenylmethyl type linked by P-phenylene units
[NASA-TM-77799] 10 p1450 N85-19134
Process for producing tris s(n-methylamino) methylsilane
[NASA-CASE-MFS-25721-1] 12 p1799 N85-21280
Electrochemical reduction of titanium in dimethyl sulphoxide
[BLL-OA-TRANS-3225-(6196.300)] 20 p3429 N85-31267

METHYL POLYSILOXANE
Neutron scattering on polysiloxanes
03 p0432 N85-12751

METHYLENE
Electrically conducting complexes of poly(3,6-n-methylcarbazolyl methylene)
[AD-A147884] 07 p0933 N85-15914
The effect of occupational exposure and the body weight to height ratio on exhaled methylene chloride breath concentration in females at one, eighteen and sixty-six hours post exposure 14 p2388 N85-24708
Mechanical properties of adhesively bonded aluminum structures protected with hydration inhibitors
[AD-A153755] 18 p3079 N85-29047
Condensation of anhydrides or dicarboxylic acids with compounds containing active methylene groups. Part 1: Condensation of phthalic anhydride with acetoacetic and malonic ester
[NASA-TM-77886] 19 p3227 N85-30010

METHYLENE BLUE
The electrochemistry of azine, oxazine and thiazine dyes
[AD-A152394] 17 p2918 N85-27990

METRIC CONVERSION
U METRICATION

METRIC PHOTOGRAPHY
Metric camera experiment: Spacelab 1 mission
05 p0658 N85-14229
The photogrammetric camera experiment on Spacelab 1 05 p0658 N85-14230
Metric evaluation of SAR-580 optical images for cartographic purposes 05 p0659 N85-14231

METRIC SPACE
NT HILBERT SPACE
On two concepts of fundamental matching
[CSIR-TWISK-335] 01 p0110 N85-10743
Extension of embeddings close to isometries or similarities 15 p2834 N85-26242
The definition and computation of a metric on plane curves. The meaning of a face on a geometric model
17 p3004 N85-28571
Performance measurement of OSI (Open System Interconnection) class 4 transport implementations
[PB85-177657] 18 p3161 N85-29582
Synthesis of metrico-topological model for layout of topology of large-scale-integration arrays
22 p3781 N85-33427

METRICATION
Performance measurement of OSI (Open System Interconnection) class 4 transport implementations
[PB85-177657] 18 p3161 N85-29582

METROLOGY
Force standard machines of the National Institutes for Metrology, vol. 2
[PTB-ME-62-VOL-2] 01 p0038 N85-10224
Center for Electronics and Electrical Engineering Technical Bulletin covering center programs with 1984 CEEE events calendar
[PB84-223684] 01 p0045 N85-10293
Center for Electronics and Electrical Engineering Technical Bulletin covering center programs
[PB84-219716] 01 p0045 N85-10295
Metrological consequences of the hard optical boundary assumption
[PB84-223577] 01 p0121 N85-10827
Center for Electronic and Electrical Engineering Technical Progress Bulletin, January - March 1983, no. 2
[PB84-231224] 03 p0360 N85-12306
Error and uncertainty — metrology
[NPL-DPMA-2] 08 p1137 N85-17161
Guidelines for atmospheric measurements in support of electro-optical systems testing
[AD-A148090] 08 p1186 N85-17474
Primer for mass metrology
[PB85-121424/GAR] 09 p1305 N85-18199
Modeling turbulent flow in compressible fluids: Metrological aspects — conferences
11 p1575 N85-19928
Metrology for Electronic Technology: A bibliography of NBS (National Bureau of Standards)
[PB85-112895] 12 p1830 N85-21486
The design and validation of software for dimensional metrology
[NPL-DITC-50/84] 15 p2521 N85-25542
New sensor for industrial metrology developed
15 p2538 N85-25665
Measurement capabilities of the Bendix Metrology Organization
[DE85-005795] 16 p2760 N85-27029
NBS physical measurement services
[NBSIR-84-2875] 16 p2859 N85-27633
Methods for optimal recursive estimation of non-stationary time series, applications to atomic time and frequency metrology 17 p2965 N85-28312
Activities of Istituto Elettrotecnico Nazionale Galileo Ferraris 18 p3199 N85-29845
Activities report in energy technology
[OEFZS-4302] 18 p3199 N85-29846
The 1982 National Measurement Requirements Survey
[NMRC-83-01-SUMM] 20 p3436 N85-31321
Recommendations for the design and equipping of engineering metrology laboratories
[NPL-MOM-22] 23 p3898 N85-34145

METROPOLITAN AREAS
U CITIES

MEXICO
Socio-economic impact of climate — Mexico
07 p1003 N85-16372
Geology of the Batopilas mining district, Chihuahua, Mexico, volumes 1 and 2 09 p1351 N85-18498
SIR-A imagery in geologic studies of the Sierra Madre Oriental, northeastern Mexico. Part 1 (Regional stratigraphy): The use of morphostratigraphic units in remote sensing mapping
[NASA-CR-175457] 10 p1505 N85-19497
Analysis of the Gran Desierto, Pinacte Region, Sonora, Mexico, via shuttle imaging radar
[NASA-CR-175711] 15 p2582 N85-25927

MICA
NT BIOTITE
Structural morphology and associated strain within parts of the US section of the Kootenay Arc, NE, Washington
09 p1352 N85-18505
Search for supermassive magnetic monopoles using mica crystals
[HE-8.1-8] 24 p4210 N85-36134

MICE
Effects of simulated weightlessness on mammalian development. Part 2: Meiotic maturation of mouse oocytes during clinostat rotation 15 p2612 N85-26094
Effects on in vivo and in vitro exposure to excess gravity on growth and differentiation of mammalian embryos
15 p2612 N85-26095
The controlled ecological life support system
15 p2668 N85-26603
Radioprotective efficacy of ATP and adenosine with exposure to high energy protons
19 p3325 N85-30602
Mouse oocyte killing by neutrons: Target considerations
[DE85-011362] 19 p3328 N85-30624
Differences in susceptibility of inbred mice to bacillus anthracis
[AD-A155646] 21 p3662 N85-32750

MICHELSON INTERFEROMETERS
Development of a measuring procedure for the automatic evaluation of the flatness of reflective surfaces
[BMFT-FB-T-84-168] 03 p0421 N85-12686
Improved sensitivities in laser interferometers for the detection of gravitational waves
[MPQ-86] 04 p0506 N85-13232
Geophysical laser interferometer with 12.5 meter base
13 p2089 N85-23046
Mode control and wavelength tuning in open ended Michelson interferometric semiconductor laser
13 p2095 N85-23073
Special topics in infrared interferometry — Michelson interferometer development
[NASA-TM-87472] 17 p3038 N85-28794
Wide Angle Michelson Doppler Imaging Interferometer (WAMDII) 23 p3902 N85-34172

MICHIGAN
Water resources data for Michigan, water year 1983
[PB84-225176] 01 p0066 N85-10442
Compilation of annual reports of the Navy ELF (Extremely Low Frequency) communications system ecological monitoring program. Volume 1: Tabs A-E
[AD-A148326] 08 p1152 N85-17272
Compilation of annual reports of the Navy ELF (Extremely Low Frequency) communications system ecological monitoring program (1983). Volume 2: Tabs F-J
[AD-A148327] 08 p1152 N85-17273
Diagenesis of niagaran (middle silurian) pinnacle reefs, northwest Michigan 09 p1352 N85-18508

MICROANALYSIS
Secondary fluorescence effects on X-ray microanalysis
[DE84-016800] 05 p0618 N85-13951
Transmission electron microscopy of inorganic materials
[DE85-000708] 09 p1291 N85-18107
K and L-shell cross-sections for X-ray microanalysis in an AEM
[DE85-002733] 11 p1721 N85-20822
Characterization of supported metal catalysts by imaging, microdiffraction and microanalysis techniques
[DE85-005567] 14 p2253 N85-23961
Secondary fluorescence effects on X-ray microanalysis
[DE85-005565] 15 p2508 N85-25457
Z-contrast imaging and electron channeling analysis of dopants in semiconductors
[DE85-011410] 21 p3582 N85-32260
Cyanobacterial mats: Microanalysis of community metabolism 21 p3661 N85-32743
Microanalysis of dissolved iron and phosphate in pore waters of hypersaline sediment
21 p3661 N85-32744

MICROBALANCES
Data analysis for lidar and quartz crystal microbalance systems
[NASA-CR-172601] 21 p3615 N85-32464

MICROBALLOONS
Microshell (trademark)-tipped optical fibers as sensors of high-pressure pulses in adverse environments
[DE84-015520] 03 p0365 N85-12336
Development of the sonic pump levitator
[NASA-CR-171382] 12 p1782 N85-21186

MICROBE
U MICROORGANISMS

MICROBIOLOGY
NT BACTERIOLOGY
Evaluation of survival straws (pocket purifier)
[AD-A148240] 03 p0328 N85-12114
Microbiological method for the desiliconization of high-silica bauxites
[BLL-MINTEK-TR-1168-(5810.5759)] 07 p0925 N85-15864
USSR report: Life sciences. Biomedical and behavioral sciences
[JPRS-UBB-84-015] 07 p1010 N85-16416
USSR report: Life sciences. Biomedical and behavioral sciences
[JPRS-UBB-85-002] 09 p1360 N85-18559
USSR report: Space Biology and Aerospace Medicine, volume 18, no. 6, November - December 1984
[JPRS-USB-85-002] 12 p1900 N85-21831
Results of sanitary-microbiological studies aboard Cosmos-1129 biosatellites 12 p1903 N85-21852

Dynamics of quantitative and qualitative changes in conditionally pathogenic microflora of the human intestine during long-term hypokinesia 12 p1903 N85-21953
USSR report: Life sciences. Biomedical and behavioral sciences
[JPRS-UBB-85-012] 14 p2386 N85-24697
Flow through bacteria detection system
[NASA-CASE-LAR-12571-1] 18 p3104 N85-29218
Development annd testing of electrophoresis solutions. Task I.1: Development of optimal buffer system 20 p3500 N85-31755
The global sulfur cycle
[NASA-TM-87570] 21 p3656 N85-32710
Results of microbiological studies conducted during operation of Salyut-6 orbital station 22 p3623 N85-33662
USSR report: Space Biology and Aerospace Medicine, vol. 19, no. 3, May - June 1985
[JPRS-USB-85-005] 23 p3952 N85-34494
Microbiological and biochemical studies towards optimization of substrate utilization by methanogenic bacteria
[PB86-186332] 24 p4084 N85-35310
Literature search for new physical methods for biological aerosol detection
[AD-A155863] 24 p4128 N85-35582

MICROCALORIMETERS
U CALORIMETERS

MICROCHANNEL PLATES
Fine grained hodoscopes based on scintillating optical fibers
[DE84-014840] 01 p0120 N85-10825
A microchannel plate streak camera
[DE84-016836] 06 p0811 N85-15153
Photometry with Multi-Anode Microchannel Arrays (MAMAs) and Charge Injection Devices (CIDs) 08 p1252 N85-17909
Improved performance for large area triple layer microchannel plate detector for a neutral spectrometer in Doublet III
[DE85-001719] 10 p1488 N85-19395
Development of high resolution imaging detectors for X-ray astronomy
[NASA-CR-175505] 12 p1953 N85-22266
Utilization of microchannel plates in the flash X-ray technique
[ISL-CO-228/83] 14 p2308 N85-24275
Microchannel plate streak camera
[DE85-011604] 20 p3458 N85-31481

MICROCHANNELS
The development and test of ultra-large-format multi-anode microchannel array detector systems
[NASA-CR-174247] 07 p1043 N85-16622

MICROCIRCUITS
U MICROELECTRONICS

MICROCLIMATOLOGY
Bibliography of climate textbooks and studies
[WCP-94] 02 p0231 N85-11505

MICROCOMPUTERS
NT PERSONAL COMPUTERS
Composite laminate optimization program suitable for microcomputers 01 p0059 N85-10399
A microcomputer aided measurement equipment for monitoring performance in digital radio relay systems
[FUB-4-1984] 01 p0101 N85-10688
Floating-point function generation routines for 16-bit microcomputers
[NASA-TM-83783] 01 p0102 N85-10683
Microcomputer management guidelines
[PB84-212174] 01 p0105 N85-10704
Analysis of three database system architectures using benchmarks
[PB84-217512] 01 p0105 N85-10706
Microcomputers in Hungary 01 p0115 N85-10786
Systems analysis for microcomputer acquisitions
[AD-A145447] 02 p0239 N85-11556
East Europe report, science and technology. Czechoslovakia: System of small electronic computers
[JPRS-ESA-84-040] 02 p0239 N85-11558
Development of a microcomputer coupled atmospheric and oceanic boundary layer prediction model
[AD-A146334] 03 p0397 N85-12530
An inexpensive microcomputer for laboratory data acquisition and test equipment control
[AD-A146085] 03 p0403 N85-12567
Information Center handbook
[PB84-211341] 03 p0439 N85-12795
A control scheme for microcomputers being used in multiprocessor arrays
[DE84-014590] 04 p0547 N85-13479
Microcomputer control of a residential photovoltaic power conditioning system
[DE84-013867] 04 p0547 N85-13480
Hardware multiplier processor
[DE84-006174] 05 p0713 N85-14574
How to implement the welcome program in compatible microcomputers such as Apple 2
[INPE-3114-PRE/511] 05 p0715 N85-14586
Machine tools at 1984 Leipzig Spring Fair 06 p0815 N85-15177
High speed magnetic tape interface for a microcomputer
[CSIRO-TP-7] 06 p0847 N85-15377
A standard operating system interface for microcomputer software development
[AD-A146584] 06 p0854 N85-15428
Control system design language implementation of a gas turbine starting controller
[AD-A147696] 07 p0905 N85-15732
Development of a 2 micrometer silicon-gate-CMOS-technology for microcomputer oriented VLSI circuits with a supply voltage range between 1.5 and 5 V
[BMFT-FB-T-84-203] 07 p0949 N85-16012
Microcomputer control of a residential photovoltaic power conditioning system
[DE84-014774] 07 p1022 N85-16488
Possibilities and impossibilities of microcomputer systems
[AD-1984-904] 07 p1028 N85-16522
Ultrasound instrumentation for the 7 inch Mach seven tunnel
[NASA-CR-174277] 07 p1038 N85-16586
Fast arithmetic for microcomputers 08 p1140 N85-17180
Specifications of bloc floppy disk drives 08 p1141 N85-17188
Adapting logistics models to a microcomputer for interface with computer-aided design systems
[AD-A147666] 08 p1202 N85-17566
MINDS: A microcomputer interactive data system for 8086-based controllers
[NASA-TP-2378] 08 p1204 N85-17576
Guide to personal desktop computing at ANL
[DE85-001438] 08 p1206 N85-17594
Data acquisition, measurement devices at 1984 Leipzig Spring Fair 09 p1378 N85-18681
Linear, position-sensitive X-ray detector used for real-time calculations of small-angle scattering parameters with submillisecond resolution
[DE85-002530] 10 p1489 N85-19401
A decision model for selection of microcomputers and operating systems
[AD-A149078] 10 p1538 N85-19694
Relative performance of micro and mainframe computers
[AD-A149281] 10 p1538 N85-19695
Microcomputers in transit: A hardware handbook
[PB85-113660] 10 p1538 N85-19700
Order picking in an aisle
[AD-A149553] 10 p1548 N85-19766
ESOP expert system model described 11 p1619 N85-20187
Guidepost routing algorithm for distributed computer networks 11 p1622 N85-20210
East Europe report: Scientific affairs
[JPRS-ESA-84-006] 11 p1700 N85-20684
Description of 8048 microcomputer operation published 11 p1700 N85-20685
A functional vehicle for autonomous mobile robot research
[AD-A150052] 12 p1860 N85-21666
Selection and use of general-purpose programming-language: Program examples, volume 2
[PB85-122000] 12 p1917 N85-22039
Selection and use of general-purpose programming language: Overview, volume 1
[PB85-122018] 12 p1917 N85-22040
Microcomputers in transit: A software handbook
[PB85-136414] 12 p1918 N85-22042
Microcomputer: Controlled statistics analyzer
[BLL-CE-TRANS-7971-(9022.00)] 13 p2144 N85-23306
Exploiting parallel computing with limited program changes using a network of microcomputers
[NASA-TM-86367] 13 p2146 N85-23318
Microcomputers and the electrical engineer
[AD-A150499] 13 p2147 N85-23325
An improved battery state-of-charge indicator
[NASA-CR-175701] 14 p2298 N85-24227
Arithmetic and elementary functions on mini and microcomputers 14 p2396 N85-24761
Evaluating the appropriateness of microcomputers for litigation document management using the analytic hierarchy process 14 p2399 N85-24788
USSR report: Cybernetics, computers, and automation technology
[JPRS-UCC-85-002] 14 p2400 N85-24794
The problem of creating a standardized series of personal computers 14 p2400 N85-24795
Automation of development of software for switching units that are implemented in the form of multiprocessor systems on a microcomputer base 14 p2401 N85-24802
Microcomputer application of aerospace asset surface search planning
[AD-A151633] 15 p2467 N85-25227
Czech institute develops microcomputer for satellites 15 p2484 N85-25331
Using a single-board computer to maintain constant voltage, current sources 15 p2551 N85-25749
Recent advances in arc welding equipment and their application 15 p2566 N85-25832
The design and implementation of a syntax directed editor for a space constrained microcomputer
[AD-A151313] 15 p2623 N85-26163
An extension of a microcomputer based system for analysis of line drawing quantization schemes
[AD-A152008] 15 p2624 N85-26171
Mini- and microcomputer local control network architecture and design principles 15 p2625 N85-26179
Extension of the software development workbench to include microcomputer workstations
[AD-A151903] 15 p2630 N85-26207
Investigation of the numerical method of moments for digital computer determination of differential equations
[AD-A151696] 15 p2638 N85-26266
System design of automated VLSI (Very Large Scale Integrated) test station and implementation of selected system aspects
[AD-A151981] 16 p2778 N85-27147
Design and construction of a computer controlled microthermocouple probe for the study of buoyant jets
[AD-A152224] 16 p2788 N85-27199
China report: Science and Technology
[JPRS-CST-85-012] 16 p2808 N85-27300
Implementation and analysis of a microcomputer based relational database system
[AD-A151770] 16 p2845 N85-27536
Detailed design of an object oriented, multiprogramming, multitasking operating system for sixteen-bit microcomputers
[AD-A152088] 16 p2847 N85-27552
Numerical optimization algorithm for engineering problems using microcomputer
[AD-A152135] 16 p2847 N85-27554
Computer assisted flight schedule optimization
[AD-A151689] 16 p2856 N85-27623
A portable pulse analyzer for nuclear geophysics using a Sinclair-TK microcomputer
[INPE-3278-PRE/601] 16 p2864 N85-27666
Automation of the reporting and tracking requirements of architect-engineering type contracts
[AD-A152218] 16 p2876 N85-27745
Design of an interface to an information retrieval network 16 p2877 N85-27750
Ultrasonic flaw detector with microcomputer interpretation
[BMFT-FB-T-84-272] 17 p2977 N85-28395
Microcomputer-controlled system for measuring atmospheric particle fluxes
[DE85-007910] 17 p2988 N85-28469
Microprocessor controlled temperature chassis
[DE85-006362] 17 p3009 N85-28602
A programming system for a modular flexible multimicrocomputer system for the automatic control of automated test equipment
[JUEL-1962] 17 p3014 N85-28641
A task battery for applied human performance assessment research
[AD-A153677] 18 p3154 N85-29530
Safety system with microcomputer
[OEFZS-4294] 18 p3166 N85-29618
Deployable Core Automated Maintenance System (DCAMS)
[AD-A153695] 18 p3196 N85-29839
Fracture mechanics formulas on microcomputers
[NASA-TM-77650] 19 p3284 N85-30362
Graceful fault tolerance in large networks of microcomputers 19 p3332 N85-30643
ZOG-Vinson technology demonstration project. Volume 2: System description
[AD-A153671] 19 p3333 N85-30645
Demonstration project: Putting the bioastronautics data book on line
[NASA-CR-178424] 19 p3335 N85-30659
ZOG/VINSON technology demonstration project system description. Volume 1
[AD-A154211] 19 p3342 N85-30713
Implementation of a serial communication process for a fault tolerant, real time, multitransputer operating system
[AD-A154237] 19 p3343 N85-30714

Forth system for coherent-scatter radar data acquisition and processing
[NASA-CR-178055] 20 p3494 N85-31720
Visualization of computation results. Definition of a graphics satellite computer
[ONERA-RT-2/3587-CY] 20 p3514 N85-31845
PIPE-1000: An implementation of piping on an HP-1000 minicomputer
[PB85-191955] 20 p3514 N85-31847
DHC: A diurnal heat capacity program for microcomputers
[DE85-009545] 20 p3516 N85-31859
Microcomputers in transportation: Software and source book, February 1985
[PB85-181022] 20 p3517 N85-31868
Microcomputer processing of LANDSAT Thematic Mapper data for the acquisition of military tactical terrain data
[AD-A154781] 21 p3605 N85-32389
Robots, Manipulators 21 p3668 N85-32786
An automated quality assurance surveillance plan for ADP (Automated Data Processing) operations under the Navy's commercial activities program
[AD-A154767] 21 p3671 N85-32802
A comparison and analysis of Vinit's global routing algorithm with the Lee routing algorithm in two-layer printed circuit boards
[AD-A155600] 21 p3673 N85-32816
Development of a dedicated speech work station
[AD-A155465] 21 p3674 N85-32824
Microcomputer network: Investigation and implementation
[AD-A155631] 21 p3674 N85-32826
Art of programming programmable microcalculators: Calculation of response from current values of action
22 p3767 N85-33348
Module for interfacing microprocessors and microcomputer 22 p3774 N85-33390
Art of programming programmable microcalculators, part 4: errors of calculations 22 p3778 N85-33411
Microcomputer controlled image processor
[AD-D011734] 22 p3833 N85-33735
An innovative user interface for microcomputer-based computer-aided design 23 p3961 N85-34555
Recording system for the solar neutron monitoring at Mt. Norikura
[SH-9.1-8] 23 p4051 N85-35123
Development of position sensors for microcomputer-oriented sensor systems
[BMFT-FB-T-85-021] 24 p4091 N85-35361
Materials and process development for microcomputer-compatible pressure, temperature, and position sensors
[BMFT-FB-T-85-024] 24 p4097 N85-35399
Expert systems research in regional resource evaluation: Experiences in the application of microcomputer technologies 24 p4105 N85-35450
DSS/MIS (Decision Support Systems/Management Information Systems) design and implementation for LAMPS Mk 3 utilizing a microcomputer and a maintenance personnel assignment program
[AD-A155652] 24 p4135 N85-35629
A quickly tested Pascal random number generator for microcomputers
[AD-A156059] 24 p4136 N85-35633
A research program to reduce the interior noise in general aviation aircraft, index and summary
[NASA-CR-176178] 24 p4145 N85-35695
Application of thermoluminescence for detection of cascade shower 1: Hardware and software of reader system
[HE-7.1-8] 24 p4213 N85-36160
Spatial distribution read-out system for thermoluminescence sheets
[HE-7.1-7] 24 p4213 N85-36161

MICROCRACKS

Salt action on concrete
[AD-A147812] 07 p0933 N85-15912
Fundamentals of microcrack nucleation mechanics
[NASA-CR-3851] 07 p0975 N85-16195
Influence of constant amplitude and variable amplitude loading on crack initiation and micro crack propagation in Al 2024-T3
[DFVLR-FB-84-29] 07 p0979 N85-16220
Experimental and analytical study of ceramic-coated turbine-tip shroud seals for small turbine engines
[NASA-TM-86881] 09 p1281 N85-18057
Evaluation of machining damage in brittle materials
[DE85-001794] 11 p1612 N85-20136
Change in microstructure of heat-resistant nickel alloys upon thermal cycling in a current of gas
13 p2031 N85-22725
On Rayleigh waves and Rayleigh wave extension of surface micro-cracks 15 p2572 N85-25860
Mechanical properties of high performance carbon fibers 16 p2742 N85-26922
The mechanics of internal stress and microcrack toughening mechanisms in ceramics
[AD-A154049] 19 p3248 N85-30139
Mechanics of near tip microcracking in brittle material
[AD-A154684] 21 p3598 N85-32346

MICROCRYSTALS

Basic ice nucleation mechanisms on mono and microcrystals and ice forming nuclei. Theoretical analysis and experimental results achieved in the laboratory over the past ten years: Review paper
21 p3642 N85-32629
Size and shape dependence of CO adsorption sites on sapphire supported Fe microcrystals
[NASA-CR-176171] 24 p4160 N85-35794

MICRODENSITOMETERS

Recent developments on the COSMOS plate-scanning machine — microdensitometer 07 p0966 N85-16128
Plate measurements and reductions at Muenster — astronomical photography 07 p0966 N85-16129
First tests on the astrometric performance of the new PDS1010G at Hamburg Observatory — grante microdensitometer 07 p0966 N85-16135
Astrometric applications of the Mt. Stromlo PDS 1010A — microdensitometer 07 p0967 N85-16136

MICROELECTRONICS

NT LARGE SCALE INTEGRATION
Manufacturing methods for microwave circuits
[AD-A145237] 01 p0043 N85-10278
Moving object detection system using infrared scanning
[AD-D011222] 01 p0120 N85-10822
Energy deposition in microvolumes of silicon from high energy proton reactions
[AD-A144713] 01 p0123 N85-10845
Cosmic ray effects on microelectronics. Part 3: Propagation of cosmic rays in the atmosphere
[AD-A145028] 01 p0131 N85-10902
Fundamental electronic properties of donor-type graphite intercalated compounds
[AD-A146146] 03 p0326 N85-12099
West Europe report: Science and technology, no. 166
[JPRS-84845] 03 p0341 N85-12190
French firms develop artificial intelligence robot
03 p0341 N85-12192
Swiss firm improves method for soldering printed circuits 03 p0341 N85-12193
Integrated circuits, MBM's, form focus of work at French LETI 03 p0341 N85-12194
East Europe report: Scientific affairs, no. 791
[JPRS-84624] 03 p0341 N85-12195
Problems in CEMA microelectronic cooperation noted
03 p0341 N85-12196
East Europe report: Science and technology
[JPRS-ESA-84-038] 03 p0343 N85-12210
USSR report: Electronics and electrical engineering
[JPRS-UEE-84-014] 03 p0344 N85-12215
Chemical derivatization of an array of three gold microelectrodes with polypyrrole: Fabrication of a molecule-based transistor
[AD-A146221] 03 p0359 N85-12304
Contamination problems during surface cleaning for thermocompression bonding
[DE84-013066] 04 p0475 N85-13023
Procedures for precap visual inspection
[NASA-RP-1122] 04 p0486 N85-13156
The effect of aircraft generated electromagnetic interference (EMI) on future avionics systems: A compendium
[AD-A146380] 06 p0799 N85-15101
East Europe report: Science and technology
[JPRS-ESA-84-045] 06 p0815 N85-15175
Facility safety study
[NASA-CR-174280] 07 p0910 N85-15759
Improvement of electromechanical systems by utilization of microelectronic technology 07 p0955 N85-16053
Solid state research
[NASA-CR-174285] 07 p1048 N85-16656
The construction and behaviour of ultramicroelectrodes: Investigations of novel electrochemical systems
[AD-A146658] 08 p1123 N85-17079
Robotics application in construction industry assessed
08 p1139 N85-17178
Telecommunications equipment at 1984 Leipzig Spring Fair 08 p1140 N85-17179
Electronics component R and D, production capability reviewed 08 p1140 N85-17181
Researchers on third generation robotics development
08 p1140 N85-17184
Flexible manufacturing system concept features cache memory 08 p1140 N85-17186
West Europe report: Science and technology
[JPRS-WST-85-001] 09 p1141 N85-17190
East Europe report: Science and technology
[JPRS-ESA-84-043] 08 p1142 N85-17198
Chemical, material electronics studies established
08 p1142 N85-17200
General assessment of GDR microelectronics industry, applications 08 p1142 N85-17202
Solid state research
[AD-A147640] 08 p1225 N85-17714
Gallium arsenide/AlGaAs multilayer structures with special doping profiles for microwave and optoelectronic devices
[BMFT-FB-T-84-207] 08 p1227 N85-17725
The planned expansion of microelectronics capability at Sandia National Laboratory
[TI85-004326] 09 p1314 N85-18260
Semiconductors at Leipzig Spring Fair
09 p1377 N85-18660
West Europe report: Science and technology
[JPRS-WST-85-004] 10 p1460 N85-19204
Researchers, projects at French intelligent machine center 10 p1460 N85-19207
MOD silver metallization for photovoltaics
[NASA-CR-175460] 10 p1510 N85-19526
East Europe report: Science and technology
[JPRS-ESA-85-009] 11 p1616 N85-20165
Institute director surveys industrial automation drive
11 p1617 N85-20167
New CNC systems described
11 p1617 N85-20172
West Europe report: Science and technology
[JPRS-WST-85-008] 11 p1617 N85-20174
CAD/CAM systems for printed circuit design, manufacture 11 p1619 N85-20188
Electronics Engineering Department: EE technical review
[DE85-004360] 11 p1629 N85-20259
Description of 8048 microcomputer operation published 11 p1700 N85-20685
Long-range electronics program outlined
11 p1700 N85-20687
USSR report: Electronics and electrical engineering
[JPRS-UEE-85-004] 12 p1837 N85-21531
Transistor-transistor logic microcircuit tester
12 p1842 N85-21556
Redundancy of codes for detection and correction of unidirectional errors 12 p1842 N85-21557
New high resolution scanning ion microprobe and focused ion beam applications
[AD-A149992] 12 p1852 N85-21616
Investigation of device and electronic interactions in GaAs device processing
[AD-A149747] 12 p1940 N85-22182
Electrical overstress protection of submicron devices
[AD-A150334] 13 p2064 N85-22892
Code lock with microcircuit 13 p2071 N85-22935
Recommendation on use of series K157UL1 microcircuits 13 p2071 N85-22936
Application of K176-series microcircuits
13 p2077 N85-22973
Parallel test method for LSI (Large Scale Integration) microprocessors
[AD-A150237] 13 p2144 N85-23310
USSR report: Machine tools and metalworking equipment
[JPRS-UMM-85-004] 14 p2284 N85-24152
China report: Science and technology
[JPRS-CST-85-009] 15 p2530 N85-25586
Developments in microelectronics: Past and future
15 p2530 N85-25597
West Europe report: Science and technology
[JPRS-WST-84-007] 15 p2530 N85-25600
Phase-locked loop design with MHB4046
15 p2534 N85-25631
West Europe report: Science and technology
[JPRS-WST-84-009] 15 p2535 N85-25639
West Europe report: Science and technology
[JPRS-WST-84-010] 15 p2535 N85-25644
West Europe report: Science and technology
[JPRS-WST-84-014] 15 p2536 N85-25647
CaD systems for electronic component design reviewed 15 p2537 N85-25660
New designs from electronics R and D center
15 p2538 N85-25666
Recent advances in arc welding equipment and their application 15 p2566 N85-25832
East Europe report: Science and technology
[JPRS-ESA-85-019] 16 p2767 N85-27077
Bond test data acquisition and analysis system
[DE86-007021] 16 p2780 N85-27158
China report: Science and Technology
[JPRS-CST-85-012] 16 p2806 N85-27300
NBS (National Bureau of Standards) research reports
[PB85-127421] 16 p2879 N85-27764
East Europe report: Science and technology
[JPRS-ESA-85-017] 17 p2945 N85-28177
Goals, achievements of microelectronics program
17 p2945 N85-28179
West Europe report: Science and technology
[JPRS-WST-84-024] 17 p2945 N85-28183

Present status of physics research in Spain: Some impressionistic remarks
[AD-A153455] 17 p3027 N85-28718
West European report: Science and technology
[JPRS-WST-84-036] 18 p3086 N85-29060
West Europe report: Science and technology
[JPRS-WST-84-031] 18 p3086 N85-29089
West Europe report: Science and technology
[JPRS-WST-84-032] 18 p3086 N85-29095
West Europe report: Science and technology
[JPRS-WST-84-035] 18 p3087 N85-29102
Method for ultrasonic bonding to soft microelectronic substrates
[NASA-CASE-NPO-16087-1] 18 p3094 N85-29151
Laser machining and some applications
[NHK-LABS-NOTE-307] 18 p3112 N85-29268
West Europe report: Science and technology
[JPRS-WST-85-020] 20 p3438 N85-31333
France's LETI reports 1983 electronic components research 20 p3438 N85-31336
Leading-edge microelectronics research at Sweden's Chalmers 20 p3438 N85-31337
Swedish program for sensor research, development 20 p3438 N85-31338
Resistance of polyaniline films as a function of electrochemical potential and the fabrication of polyaniline-based microelectronic devices
[AD-A154699] 21 p3569 N85-32201
East Europe report: Science and technology
[JPRS-ESA-85-023] 21 p3572 N85-32217
High temperature electronics technology: Life test report
[AD-A154661] 21 p3580 N85-32257
Selections on CSSR computer technology 21 p3668 N85-32782
GDR semiconductor parts 21 p3669 N85-32788
Prospects for a new kind of synthesis: Assembly of molecular components to achieve functions
[AD-A155023] 21 p3702 N85-32997
Solid state research
[AD-A154783] 21 p3709 N85-33025
Electrotransport in thin films
[AD-A155584] 21 p3710 N85-33034
Space station automation study. Automation requirements derived from space manufacturing concepts. Volume 1: Executive summary
[NASA-CR-176099] 22 p3736 N85-33170
Space Station automation study. Automation requirements derived from space manufacturing concepts. Volume 2: Technical report
[NASA-CR-176100] 22 p3736 N85-33171
Photothyristor optrons and optron microcircuits, part 1 22 p3781 N85-33424

MICROFILMS
Facsimile transmission of microforms
[AD-A144855] 01 p0038 N85-10236

MICROGRAPHY
U PHOTOMICROGRAPHY

MICROGRAVITY
U REDUCED GRAVITY

MICROGRAVITY APPLICATIONS
Monodisperse Latex Reactor (MLR): A materials processing space shuttle mid-deck payload
[NASA-TM-86487] 12 p1782 N85-21187

MICROHARDNESS
Study of deformation and fracture of AMg6N weldable aluminum alloy by method of acoustic emission 03 p0352 N85-12266
Nitriding of titanium and its alloys by N2, NH3 or mixtures of N2 + H2 in a dc arc plasma at low pressures (or = to torr)
[NASA-TM-85803] 06 p0814 N85-15188
Surface effects of corrosive media on hardness, friction, and wear of materials
[NASA-TM-83711] 07 p0930 N85-15896
Estimation of endurance characteristics of heat resistant materials. Report 2: Determination of endurance limit of heat resistant alloys over a broad temperature range 10 p1447 N85-19120
Ion-beam nitriding of steels
[NASA-CASE-LEW-14104-1] 12 p1805 N85-21324
Structure and mechanical characteristics of heterogeneous joints produced by laser welding 13 p2034 N85-22742
Frictional and structural characterization of ion-nitrided low and high chromium steels
[NASA-TM-86991] 13 p2098 N85-23085
Pulsed electrodeposition
[DE85-007057] 16 p2747 N85-26950

MICROINDENTATION
U MICROHARDNESS

MICROMANOMETERS
U MANOMETERS

MICROMECHANICS
Investigation of toughened neat resins and their relations to advanced composite mechanical properties 04 p0464 N85-12949
Numerical investigation of the micromechanics of composite fracture 04 p0467 N85-12970
Investigation of the relations between resin and advanced composite mechanical properties. Volume 2: Appendices
[NASA-CR-172303-VOL-2] 06 p0763 N85-14880
Some aspects of the micromechanics of hot spot formation in energetic materials
[AD-P004348] 10 p1456 N85-19172
Delamination micromechanics analysis
[NASA-CR-172596] 20 p3422 N85-31237
Micromechanics of high temperature deformation and failure 20 p3468 N85-31534

MICROMETEORITES
The micrometeorite experiment on Helice — Inner solar system 16 p2885 N85-27797

MICROMETEOROIDS
NT ZODIACAL DUST
Hypervelocity impacts on Skylab 4/Apollo windows 12 p1785 N85-21202
Survey of probable micrometer-sized Earth-orbital debris fragments in the NASA-JSC cosmic dust sample collection 12 p1785 N85-21203
Impacts on Explorer 46 from an Earth orbiting population 12 p1785 N85-21204
In-situ detection of micron-sized dust particles in near-Earth space 12 p1785 N85-21205
The Jovian ring 15 p2672 N85-26492
The gravito-electrodynamics of charged dust in planetary ring systems 15 p2677 N85-26531

MICROMETEOROLOGY
Bibliography of climate textbooks and studies
[WCP-94] 02 p0231 N85-11505
Eddy correlation measurements of energy partition for Amazonian forest
[INPE-3195-PRE/559] 06 p0827 N85-15252
The micrometeorology of an Amazonian rainforest
[INPE-3515-PRE/740] 19 p3315 N85-30551
Investigations of micro-turbulence in the bottom of the boundary layer
[AD-A155148] 21 p3636 N85-32585

MICROMETEORS
U MICROMETEOROIDS

MICROMINIATURIZATION
NT LARGE SCALE INTEGRATION
Qualitative of analysis of MOS circuits
[AD-A149267] 10 p1480 N85-19341
Checking microcode algebraically
[AD-A149441] 10 p1547 N85-19759
The use of ultrasound to monitor incipient failure of rolling element bearings 23 p3924 N85-34317

MICROMOTORS
Semiconductors at Leipzig Spring Fair 09 p1377 N85-18660

MICROORGANISMS
NT AEROBES
NT ANAEROBES
NT BACILLUS
NT BACTERIA
NT CLOSTRIDIUM BOTULINUM
NT ESCHERICHIA
NT PROTOZOA
NT PSEUDOMONAS
NT STAPHYLOCOCCUS
NT VIRUSES
Lagging development of biotechnology described 01 p0115 N85-10787
Spacelab 1 experiment: Microorganisms in space hard environment 05 p0691 N85-14443
DOE supported research in alcohol fuel technology development
[DE84-007686] 06 p0774 N85-14948
A biological sensor for the detection of toxicants
[AD-D011304] 07 p0967 N85-16141
Distinctions of SPF rats used in experiments aboard biosatellites 07 p1012 N85-16427
Growth of soil bacteria in presence of Martian soil analog, carbon dioxide and hydrogen peroxide 09 p1361 N85-18560
Dynamics of quantitative and qualitative changes in conditionally pathogenic microflora of the human intestine during long-term hypokinesia 12 p1903 N85-21953
Analysis of biological particles by mass spectrometry
[AD-A149952] 13 p2141 N85-23291
The impact ejection of living organisms into space 15 p2662 N85-26566
Flow through bacteria detection system
[NASA-CASE-LAR-12871-1] 18 p3104 N85-29218
Equipment development for rapid detection of microorganisms in air and water
[FOA-A-40046-B2] 18 p3134 N85-29410
A basic study to assess the potential usefulness of resonance Raman spectroscopy as a means of rapidly detecting and identifying bacteria and other microorganisms
[AD-A153549] 18 p3152 N85-29513
Influence of underwater volcanic mountains of Atlantic on microplankton distribution 19 p3294 N85-30424
Microbial ecology of extreme environments: Antarctic yeasts and growth in substrate-limited habitats
[NASA-CR-176005] 19 p3326 N85-30609
Biocatalysis project
[NASA-CR-176044] 20 p3496 N85-31744
Efficiency tests of samplers for microbiological aerosols, a review
[FOA-C-40199-B1] 20 p3504 N85-31783
Protocyanobacteria: Oxygenic and Anoxygenic photosynthesis in mat-forming bacteria 21 p3657 N85-32714
Sulfur transformations at the hydrogen sulfide/oxygen interface in stratified waters and in cyanobacterial mats 21 p3657 N85-32715
Microbiology of solar salt ponds 21 p3658 N85-32724
Some thoughts on GAIA and the sulfur cycle 21 p3658 N85-32727
From microbial communities to cells 21 p3659 N85-32728
Microbial colonization and growth on metal sulfides and other mineral surfaces 21 p3662 N85-32747
Sulfur Cycle 21 p3662 N85-32748
Results of microbiological studies conducted during operation of Salyut-6 orbital station 22 p3823 N85-33682
Distinctions in formation of microflora on construction materials used in habitable pressurized compartments 22 p3823 N85-33683
Screening and characterizing oleaginous microalgal species from the southeastern United States
[DE85-009787] 23 p3951 N85-34488
Microorganisms in space flight 23 p3951 N85-34490
Production of butanol by fermentation in the presence of cocultures of clostridium
[NASA-CASE-NPO-16203-1] 24 p4071 N85-35227
Biodegradation of jet fuel by aquatic microbial communities
[PB85-191971] 24 p4084 N85-35311
Report of the Microbial Development Working Group 24 p4127 N85-35586

MICROPARTICLES
Monodisperse Latex Reactor (MLR): A materials processing space shuttle mid-deck payload
[NASA-TM-86487] 12 p1782 N85-21187

MICROPHONES
Determination of the pressure sensitivity of 1 inch condenser microphones
[PTB-AK-26] 05 p0633 N85-14058
Carbon granule probe microphone for leak detection — recovery boilers
[NASA-CASE-NPO-16027-1] 12 p1849 N85-21597
Recording of acoustic wave in gaseous medium with thin-film pyroelectric transducers 15 p2525 N85-25571
Spectral methods for the estimation of acoustic intensity, energy density, and surface velocity using a multimicrophone probe 20 p3524 N85-31916
A theoretical appraisal of the use of ground-plane microphones for aircraft noise measurements
[NPL-AC-103] 22 p3836 N85-33752
Acoustic scaling: The development of improved instrumentation
[BBC-RD-1985/7] 24 p4145 N85-35694

MICROPHOTOMETERS
U PHOTOMETERS

MICROPOROSITY
Design and use of nonstandard tensile specimens for irradiated materials testing
[DE85-001071] 11 p1652 N85-20408
Predicting microfracture in ceramics via a microcontact model
[DE85-005654] 18 p3081 N85-29060

MICROPROCESSORS
A relational approach to the development of expert diagnostic systems
[NASA-TM-86288] 01 p0099 N85-10658
Evaluating a scientific workstation computer
[DE84-014764] 01 p0100 N85-10663
The application of microprocessors in the command and control of satellites by the MECB stations
[INPE-3282-RPE/466] 02 p0239 N85-11553
The microprocessor control of a motor-alternator
[RAE-TM-NAV-ENG-1023(L)] 02 p0244 N85-11591
Functional checking of microprocessors and microprocessor systems 03 p0347 N85-12236
Microprocessor implementation of algorithms of nonlinear filtration 04 p0486 N85-13104

Revision of signal and interference space-time processing algorithms for implementation by microprocessors 04 p0487 N85-13105
Portable microprocessor-controlled instrument for sensing, identifying and monitoring gaseous chemicals [DE84-013431] 04 p0504 N85-13214
Fiber optic, Fabry-Perot high temperature sensor [NASA-CR-174712] 04 p0564 N85-13594
A new physical Lagrangian tracer [DE84-016212] 05 p0667 N85-14419
Memory hierarchies for Directly Executed Language microprocessors 05 p0713 N85-14570
Hardware multiplier processor [DE84-006174] 05 p0713 N85-14574
Internal structure of microprocessor 06 p0785 N85-15020
Peculiarities of microprocessor implementation of algorithms for processing radio signals and noise in large antenna arrays 06 p0792 N85-15059
Workshop on Computer Architecture [AD-A146455] 06 p0847 N85-15378
Implementation of a Zilog Z-80 base realization library for the computer systems design environment [AD-A146350] 06 p0853 N85-15423
Control system design language implementation of a gas turbine starting controller [AD-A147696] 07 p0905 N85-15732
A microprocessor data system for developing countries --- climatology 07 p1003 N85-16377
Functional built-in-test in a pipelined image processor 08 p1064 N85-16740
Data stimulated on-line-checking (IROLD) 08 p1066 N85-16754
Automatic error detection and recovery techniques in onboard intelligent units for space and avionic application 08 p1096 N85-16786
Microprocessors in geophysical instruments discussed 08 p1142 N85-17199
Implementation of an Intel 8086 microprocessor-based realization library for the control system design language [AD-A146508] 08 p1202 N85-17569
MC68CR3X cross-assembler users manual [AD-A148031] 08 p1205 N85-17584
Design description of a microprocessor based Engine Monitoring and Control unit (EMAC) for small turboshaft [NASA-TM-86860] 09 p1263 N85-17935
Software for event oriented processing on multiprocessor systems [DE84-016720] 09 p1370 N85-18607
Computer equipment at 1984 Leipzig Spring Fair 09 p1378 N85-18662
A microprocessor controlled parallel model with FDPSK 10 p147a N85-19304
Advanced inverter technology [AD-A149335] 10 p1480 N85-19343
Linear, position-sensitive X-ray detector used for real-time calculations of small-angle scattering parameters with submillisecond resolution [DE85-002530] 10 p1489 N85-19401
Microprocessor-based monitoring and control project, phase 1 [DE84-001974] 10 p1538 N85-19699
Personal desktop computing in a research and development laboratory [DE85-002765] 11 p1705 N85-20728
Synthesis of digital control for object with lag 12 p1843 N85-21562
Remote self-contained undersea monitor [AD-D011520] 12 p1849 N85-21599
Microprocessor-controlled anodic stripping voltammeter for trace metal analysis in tap water [DE85-002781] 12 p1852 N85-21619
Microprocessor-controlled rotating shadowband radiometer [DE85-003693] 12 p1854 N85-21630
Second generation USAFSAM (United States Air Force School of Aerospace Medicine) microprocessor audiometer [AD-A149936] 12 p1905 N85-21963
Automatic multi-banking of memory for microprocessors [NASA-CASE-NPO-15295-1] 12 p1911 N85-21992
Variable data base generator apparatus [AD-D011515] 12 p1911 N85-21993
NDE methods for green ceramics [DE85-004019] 13 p2038 N85-22766
The audiomat: An automatic audiometer for use in occupational audiometry [DRIC-T-7136] 13 p2142 N85-23294
Research on CAD/CAM support for microprocessor development surveyed 14 p2290 N85-24189
Automatic hydrological data collection facility using ARGOS 14 p2324 N85-24363
Bipolar nonswitching logic arrays: Universal components of function expanders for computation of elementary functions 14 p2400 N85-24797
Systems design and application of computers with flexible architecture 14 p2401 N85-24800
Implementation of an inertial navigation algorithm using a limited wordlength microprocessor for a strapdown navigation computer [BAE-BT-12792] 15 p2468 N85-25234
Structurization of programs for real-time microprocessor arrays 15 p2529 N85-25592
China report: Science and technology [JPRS-CST-85-007] 15 p2533 N85-25621
Microprocessor controlled storage sampling oscilloscope 15 p2533 N85-25622
Effective microinstruction pipeline organization in a high-capacity microprocessor 15 p2625 N85-26178
Optimal control of electric drive with simultaneous control inputs for motor current and flux 16 p2763 N85-27049
Creating a Mobile Autonomous Robot Research System (MARRS) [AD-A151983] 16 p2793 N85-27229
Development of a microprocessor controlled communication system for ships [BMFT-FB-T-84-275] 17 p2950 N85-28216
VLSI (Very large scale integrated circuits) device reliability models [AD-A153288] 17 p2954 N85-28245
Microprocessor controlled temperature chassis [DE85-006392] 17 p3009 N85-28602
Development of a multiprocessor system, using the MOTORLA microprocessor 6809, with the aim of providing maximum flexibility in the design of individual control devices [BMFT-FB-T-84-270] 17 p3010 N85-28607
The AFTI/F16 terrain-aided navigation system [DE85-008411] 18 p3060 N85-28935
Development of a butterfly multiprocessor test bed description of butterfly components [AD-A153892] 18 p3095 N85-29155
A variable frequency control for three-phase induction motors 19 p3258 N85-30190
Development and evaluation of a fault-tolerant multiprocessor (FTMP) computer. Volume 1: FTMP principles of operation [NASA-CR-166071] 19 p3341 N85-30705
Apollo multiplexer operations manual [DE85-011293] 19 p3343 N85-30719
Control system for parabolic dish concentrator No. 1 [NASA-CR-176045] 20 p3463 N85-31510
Production verification of the acoustic emission weld monitor [AD-A154168] 20 p3464 N85-31519
Microprocessor AirborneData Acquisition and Replay (MADAR) system [AD-A151728] 20 p3514 N85-31843
A microprocessor based multiscaling data acquisition system for Mossbauer spectroscopy [USIP-85-01] 20 p3518 N85-31875
Microprocessor control design for a low-head crossflow turbine [AD-A155477] 21 p3556 N85-32121
A microprocessor-controlled, multichannel fluorimeter for analysis of sea water [AD-A154998] 21 p3560 N85-32310
Ultrasonic position reference systems for an autonomous sentry robot and a robot manipulator arm [AD-A155481] 21 p3566 N85-32336
The 8080 emulator 21 p3568 N85-32783
Basic features of personal computers 22 p3766 N85-33344
System of microprocessor instructions 22 p3770 N85-33362
Module for interfacing microprocessors and microcomputer 22 p3774 N85-33390
Developmental trends in radio receiver design 22 p3777 N85-33407
Optical-fiber/microprocessor-based remote velocity sensor [DE85-010071] 22 p3788 N85-33470
Magnetic search system [PB85-185109] 23 p3949 N85-34477
Hardware math for the 6502 microprocessor [NASA-TM-86517] 23 p3955 N85-34511
New technologies at the forefront of industrial developments 24 p4061 N85-35168
Design for MISP: A multiple instruction stream shared pipeline processor [AD-A156314] 24 p4136 N85-35635
Error message recording and reporting in the SLC control system [DE85-013057] 24 p4140 N85-35664
Report on the SLC control system [DE85-013076] 24 p4148 N85-35722
Investigation of cosmic rays in very short time scales [HE-4.6-7] 24 p4197 N85-36044
Microprocessor-based single particle calibration of scintillation counter [HE-4.6-13] 24 p4198 N85-36049
A mini-array for large air showers [HE-4.7-10] 24 p4199 N85-36061
Study of the time-differentiated particle flux density at various distances from EAS axis [HE-4.7-15] 24 p4200 N85-36065

MICROPROGRAMMING
S-MICRO: A system for simulating a microprogrammed control unit [INPE-3224-PRE/575] 06 p0715 N85-14585
Data stimulated on-line-checking (IROLD) 08 p1066 N85-16754
Development and analysis of a global compaction technique of microprograms 19 p3334 N85-30654
Implementation of a proposed system for automated microcode generation [AD-A154235] 19 p3336 N85-30671
Evaluation and implementation of a functional microprogram generator [AD-A155184] 21 p3674 N85-32823
Design of a microprogram control unit with concurrent error detection [AD-A156447] 24 p4139 N85-35655

MICRONOCKET ENGINES
NT ORBIT MANEUVERING ENGINE (SPACE SHUTTLE)
The highly underexpanded exhaust plume from nozzles with boundary layers [DFVLR-FB-85-10] 20 p3421 N85-31230

MICROSCALES
U MICROBALANCES

MICROSCOPES
NT ACOUSTIC MICROSCOPES
NT ELECTRON MICROSCOPES
NT ION MICROSCOPES
NT OPTICAL MICROSCOPES
Laser illuminated nano-second microscope [DE84-016200] 06 p0811 N85-15152
Photoacoustic microscopy of oxygen contaminated titanium alloys [AD-P004127] 08 p1127 N85-17102
Microscopic identification of feathers in order to improve birdstrike statistics [AD-P004187] 11 p1579 N85-19950
Method of examining microcircuit patterns [NASA-CASE-NPO-16299-1] 11 p1628 N85-20250
Operation of the Zeiss cytopherometer with Zn/ZnSO4 electrode system of Tenforde et al 20 p3499 N85-31752

MICROSCOPY
NT ELECTRON MICROSCOPY
NT LASER MICROSCOPY
NT ULTRAVIOLET MICROSCOPY
Ion contrasting chamber for discrimination of grains and textures [BMFT-FB-T-84-151] 04 p0477 N85-13036
Acoustic microscopy at cryogenic temperatures [AD-A148755] 09 p1384 N85-18704
Application of optical and electron microscopic techniques in the fractographic determination of fatigue crack growth rates 14 p2320 N85-24334
Measuring: The quantifying art 14 p2437 N85-25035
A micrographic and gravimetric study of intercalation and deintercalation of graphite fibers [NASA-TM-87026] 17 p2934 N85-28110
Modification of the grain size of sputtered copper with additions of oxygen, krypton, silver, or yttrium [DE85-010975] 21 p3567 N85-32189

MICROSEISMS
Wave-wave interactions, microseisms, and infrasonic ambient noise in the ocean [AD-A146529] 06 p0839 N85-15463
Microseism level, time variations at Turkmen seismic stations studied 07 p0961 N85-16231
A seismic ARGOS data collection platform 16 p2813 N85-27350

MICROSTRIP TRANSMISSION LINES
The study of microstrip antenna arrays and related problems [NASA-CR-174054] 02 p0189 N85-11265
Microstrip directional filters [INPE-3127-PRE/518] 02 p0194 N85-11293
Green function in theory of microstrip antennas 06 p0790 N85-15050
A transistor oscillator-doubler [AD-D011408] 08 p1158 N85-17307
Effect of interfacial characteristics of metal clad polymeric substrates on electrical high frequency interconnection performance [NASA-TM-86948] 11 p1824 N85-20223
An experimental investigation of microstrip properties on soft substrates from 2 to 40 GHz [NASA-TM-86961] 11 p1824 N85-20224

Distributed Gunn effect devices; a numerical analysis of microstrip circuits on thin active GaAs substrates
[FOA-C-30363-E] 12 p1837 N85-21527
A generalized solution to a class of printed circuit antennas 13 p2062 N85-22862
Synthesis of optimum smooth transition in microstrip through line on microwave integrated circuit 13 p2089 N85-23041
Microstrip comb array design
[R-NIAS-24] 14 p2290 N85-24195
A study of computational techniques for noncanonical microstrip antennas and arrays
[AD-A152216] 16 p2774 N85-27123
Mutual coupling analysis for conformal microstrip antennas
[AD-A154292] 19 p3259 N85-30210
Dielectric resonator stabilized microstrip oscillator
[AD-D011708] 19 p3261 N85-30219
Mutual coupling analysis for conformal microstrip antennas 20 p3439 N85-31343
Calculating dominant (quasi-t) mode group velocity in shielded microstrip line 22 p3780 N85-33422
Multidiode integrated-circuit protective device 22 p3781 N85-33425
Perturbation-iteration theory for analyzing microwave striplines
[NASA-CR-176186] 24 p4065 N85-35321
Characterization of microstrip discontinuities in the time and frequency domains
[NASA-CR-176190] 24 p4068 N85-35342

MICROSTRUCTURE
NT METEORITIC MICROSTRUCTURES
Results of the technical exchange agreement between NASA and DuPont on the containerless drop tube solidification of NiAl3
[NASA-TM-86473] 01 p0014 N85-10087
Effects of cobalt, boron, and zirconium on the microstructure of Udimet 738
[NASA-CR-174762] 01 p0027 N85-10168
The effects of seven alloying elements on the microstructure and stress-rupture behavior of nickle-base superalloys
[NASA-TM-83791] 01 p0027 N85-10168
Influence of nitrogen on the sensitization, corrosion, mechanical, and microstructural properties of austenitic stainless steels
[DE84-015134] 01 p0028 N85-10177
Ceramic microstructure and adhesion
[NASA-TM-83804] 01 p0031 N85-10186
Ultrasonic nondestructive evaluation, microstructure, and mechanical property interrelations
[NASA-TM-86876] 01 p0056 N85-10371
The effect of overload on three different kinds of steel 02 p0174 N85-11165
Effect of microstructure and trapping on the hydrogen embrittlement susceptibility of a titanium bearing HSLA steel 02 p0174 N85-11166
International Conference on Recent Developments in Specialty Steels and Hard Materials. Conference abstracts
[CSIR-S-258] 02 p0176 N85-11177
Microstructural design and control of sintered hard materials 02 p0176 N85-11180
Microstructure and deformation aspects of some specialty steels and hard metals 02 p0176 N85-11182
Rapid solidification of steels: Model and commercial alloys 02 p0176 N85-11184
Microstructural basis of strength and toughness in hardmetals 02 p0177 N85-11185
The inter-relation of microstructure, toughness and fatigue crack growth behaviour in WC-Co hardmetals 02 p0177 N85-11186
An investigation into the superhardening effect in molybdenum-free steel with specific reference to alloy substitution 02 p0180 N85-11209
The structure of rapidly solidified nickel-base alloys 02 p0181 N85-11215
Microstructure and creep behaviour at elevated temperature of unidirectionally solidified eutectic nickel base superalloys 02 p0181 N85-11216
Metastable phase formation in ion implanted metals
[DE84-014945] 02 p0183 N85-11229
Review: The influence of short circuit diffusion on the oxidation of nickel, chromium and nickel/chromium alloys
[AERE-R-11311] 02 p0185 N85-11237
Plastic deformation and microstructural transformations of metals under shock waves 02 p0272 N85-11775
Internal friction, microstructure and radiation effects
[DE84-013905] 02 p0286 N85-11880
Application of positron annihilation in materials science
[DE84-014733] 02 p0288 N85-11883
Characterization of amorphous surface layers in Fe implanted with Ti and C
[DE84-014960] 02 p0289 N85-11885
Structure of silane coupling agents adsorbed on silicon powder
[AD-A145803] 03 p0327 N85-12105
Effect of rhenium on the structure and properties of the weld metal of a molybdenum alloy
[NASA-TM-77491] 03 p0330 N85-12128
Effects of tin on microstructure and mechanical behavior of inconel 718
[NASA-TM-86866] 03 p0330 N85-12129
Application of solidification theory to rapid solidification processing
[AD-A145953] 03 p0331 N85-12136
Effects of prior austenite and ferrite grain size on fracture properties of a plain carbon steel
[AD-A146276] 03 p0332 N85-12138
The effects of microstructure on the temper embrittlement susceptibility of a Cr-2-1/4 1Mo forging
[AERE-R-11110] 03 p0334 N85-12151
A study of precipitation and boron distribution in 20 Cr 25Ni base stainless steels
[AERE-M-3353] 03 p0334 N85-12154
Microstructure and properties of ceramics
[NASA-TM-77416] 03 p0335 N85-12155
Microstructure of ceramics fabricated by unidirectional solidification
[NASA-TM-77423] 03 p0336 N85-12157
Ceramic powder for sintering materials
[NASA-TM-77434] 03 p0336 N85-12160
Ceramic microstructure development
[AD-A145753] 03 p0337 N85-12166
Microstructure development in polymers
[AD-A145980] 03 p0337 N85-12170
Structure of two-phase titanium alloys with different microstructures 03 p0351 N85-12257
Constitutive features of solids at shock-wave loading rates
[DE84-015715] 03 p0362 N85-12325
Static and dynamic characteristics of materials with beam-microstructure 03 p0370 N85-12361
Stress relief cracking studies of 2 1/4Cr1Mo steel
[AERE-R-11111] 03 p0374 N85-12388
Effect of a thermal gradient applied to a sinusoidal surface profile
[DE84-015649] 03 p0434 N85-12765
Development and fabrication of refractory bodies for gas turbine engines
[BMFT-FB-T-84-160] 04 p0457 N85-12899
The chemical nature of the fiber/resin interface in composite materials 04 p0465 N85-12963
Subgrains, dislocations and the elevated-temperature strength of type 304 stainless steel
[DE84-001233] 04 p0473 N85-13014
The Al-Be system: The effects of RSP on structure and phase relating
[DE84-015604] 04 p0474 N85-13019
Ion contrasting chamber for discrimination of grains and textures
[BMFT-FB-T-84-151] 04 p0477 N85-13036
Microstructural effects in abrasive wear
[DE84-016155] 04 p0509 N85-13247
Nondestructive determination of mechanical properties — aluminum alloys 04 p0512 N85-13266
Imaging of surfaces and defects of crystals
[DE84-016449] 04 p0570 N85-13632
Study of the reactive-element effect in oxidation of Fe-Cr alloys using transverse section analytical electron microscopy
[DE84-016237] 04 p0571 N85-13641
The microstructural characteristics of revert superalloys — for turbine blades 05 p0617 N85-13945
Application of solidification theory to rapid solidification processing
[AD-A146619] 06 p0769 N85-14917
Microstructure of rapidly quenched type 308 stainless steel weld filler metal and its implications on rapid solidification processes
[DE85-000930] 06 p0769 N85-14920
Development and characterization of ductile Long-Range-Ordered (LRO) alloys (Fe,Co, Ni)3V for high-temperature structural use
[DE84-016750] 06 p0769 N85-14921
Microstructural origins of hot spots in RDX explosive and a reference inert material
[AD-A146685] 06 p0774 N85-14947
Process Modeling Applied to Metal Forming and Thermomechanical Processing
[AGARD-LS-137] 06 p0796 N85-15086
Microstructure, texture and formability of thin aluminium sheets 06 p0796 N85-15088
The role of microstructure in the modelling of plastic flow in P/M superalloys at forging temperatures and strain rate 06 p0796 N85-15090
Control of microstructure during hot working of Ti-6242 06 p0797 N85-15091
Modeling microstructural changes during hot rolling of steels 06 p0798 N85-15096
Structural studies on lead dioxides
[DE84-015837] 06 p0805 N85-15127
Investigation of structural and electrical properties of low-angle silicon sheet 06 p0831 N85-15288
Anisotropy and microstructure of rare earth permanent magnet materials
[AD-A146549] 06 p0859 N85-15460
Oxygen isotopes in deep sea spherules 06 p0883 N85-15609
Aqueous alteration of meteorite parent bodies: Possible role of unfrozen water and the Antarctic meteorite analogy 06 p0884 N85-15617
The growth of metastable peritectic compounds
[NASA-CR-171289] 07 p0920 N85-15824
The formation of isolated phase precipitates during the decomposition of high-coercive force Fe-Cr-Co alloys
[BLL-M-36028-(5828.4)] 07 p0924 N85-15855
Studies on copper alloys containing chromium on the copper side phase diagram
[NASA-TM-77752] 07 p0927 N85-15876
Fundamentals of microcrack nucleation mechanics
[NASA-CR-3851] 07 p0975 N85-16195
Effects of oxygen on the microstructure and properties of titanium 6211 alloys
[AD-P004122] 08 p1126 N85-17097
Effects of oxygen-contamination-induced microstructural changes on the reverberation of ultrasound in Ti-6211 alloys
[AD-P004124] 08 p1126 N85-17099
Ultrasonic evaluation of titanium contamination with correlation techniques
[AD-P004126] 08 p1126 N85-17101
High resolution acoustic microstructural characterization of titanium with interstitial contamination
[AD-P004128] 08 p1127 N85-17103
Grain refining and microstructural modification during solidification
[AD-A147705] 08 p1128 N85-17111
Mechanical properties and microstructure of centrifugally cast alloy 718
[AD-A147800] 08 p1129 N85-17116
Rapid solidification processing and powder metallurgy of Al alloys
[AD-A148427] 08 p1130 N85-17120
Effect of microstructure and trapping on the hydrogen embrittlement susceptibility of a Ti-bearing HSLA steel
[AD-A148610] 08 p1130 N85-17122
Structural studies of amorphous Mo-Ge alloys using synchrotron radiation
[DE85-002061] 08 p1131 N85-17125
Research on nondestructive testing
[AD-A148375] 08 p1171 N85-17380
A study of spectrum fatigue crack propagation in two aluminum alloys. 2: Influence of microstructures
[NASA-TM-86930] 09 p1294 N85-18125
The effect of tantalum on the structure/properties of two polycrystalline nickel-base superalloys: B-1900 + Hf MAR-M247
[NASA-CR-174847] 09 p1294 N85-18127
Alloying effects and microstructure of iron aluminides
[DE85-000903] 09 p1295 N85-18137
Ti-6Al-4V alloy castings prepared in zircon sand molds and the effect of hot isostatic pressing
[PB85-109932/GAR] 09 p1298 N85-18150
Mechanisms of elevated temperature rupture in single phase ceramics
[DE85-000697] 09 p1299 N85-18156
The feasibility of low-G grey solidification of nodular iron in the F-104 experimental furnace package
[NASA-TM-82527] 10 p1426 N85-18998
Mechanics of composite materials
[DE85-003611] 10 p1432 N85-19031
Creep-rupture behavior of iron superalloys in high-pressure hydrogen
[NASA-CR-174411] 10 p1441 N85-19078
Impact toughness of composites with layered microstructure of OT4 titanium alloy 10 p1445 N85-19104
Effect of powder characteristics on microstructure and properties in alkoxide prepared PZT ceramics
[AD-A149082] 10 p1451 N85-19141
Microstructural analysis of ion containing polymers
[DE85-001594] 10 p1453 N85-19157
Reliability studies of ceramic capacitors
[AD-A149126] 10 p1479 N85-19338
The effect of filler wire and flux compositions on the microstructure and properties of microalloyed steel weld metal
[AD-A149529] 10 p1492 N85-19423

Internal Gravity Waves and Small-Scale Turbulence: Proceedings of the 2nd 'Aha Huliko'a Hawaiian Winter Workshop
[AD-A149510] 10 p1522 N85-19597

Application of layered synthetic microstructures to high temperature plasma diagnostics
[DE85-002095] 10 p1559 N85-19628

Effect of ingot structure of failure ductility of pressed semifinished products of high-durability aluminum alloys 11 p1597 N85-20045

Study of microstructure of aluminum and copper alloys after processing with continuous CO2 laser beam 11 p1601 N85-20066

Dependence of mechanical properties of large VT3-1 alloy forgings on microstructure parameters 11 p1602 N85-20072

Electron-diffraction structural examination of amorphous iron-tin alloys 11 p1604 N85-20084

Effect of microstructure on solid particle erosion in multiphase materials
[DE85-000426] 11 p1608 N85-20109

Weldability and mechanical property characterization of weld clad alloy 600H tubesheet forging
[DE85-001737] 11 p1609 N85-20116

The role of void nucleation in the swelling resistance of ferritic steel
[AERE-R-11525] 11 p1610 N85-20122

Design and use of nonstandard tensile specimens for irradiated materials testing
[DE85-001071] 11 p1652 N85-20408

Transverse microstructure of an oxide scale formed on a 20 % Cr/25 % Ni niobium stabilized stainless steel
[AERE-R-11034] 12 p1804 N85-21315

Method for refining microstructures of cast titanium articles
[AD-D011518] 12 p1804 N85-21318

Effect of reduction of strategic Columbium addition in 718 Alloy on the structure and properties
[NASA-CR-174841] 12 p1805 N85-21320

Stress corrosion cracking and oxidation characteristics of boride-strengthened microcrystalline iron and nickel based alloys
[AD-A149805] 12 p1806 N85-21328

Microstructural and electronic characteristics of metallic spin glasses
[AD-A149959] 12 p1813 N85-21371

Micromechanical modeling of microstructural damage in creeping alloys
[DE85-003925] 13 p2022 N85-22671

TEM/FIM study of modulated microstructures in the Fe-Be system
[DE85-005379] 13 p2023 N85-22678

Influence of laser treatment of structure and mechanical properties if MA21 alloy 13 p2029 N85-22713

Electrodynamic stability of composite liquid-metal contacts 13 p2067 N85-23031

Microstructural study on the processing and properties of high-field A15 superconducting materials
[DE85-004652] 13 p2164 N85-23423

Non-steady combustion of composite solid propellants
[AD-A150827] 14 p2250 N85-23947

Synthesis and properties of elevated temperature P/M aluminum alloys
[AD-A151031] 14 p2256 N85-23981

Microstructure and properties of ferrous alloy weldments
[DE85-005582] 14 p2257 N85-23987

Laser surface treatments 14 p2308 N85-24284

Investigation of the MBE growth of InSb and novel quantum well structures
[AD-A151014] 14 p2427 N85-24969

Study of amorphous strips and microconductors by ferromagnetic resonance method 15 p2497 N85-25402

Effect of aluminum on nature of titanium alloy failure 15 p2498 N85-25411

Hydrogen resistance of VT1-0 titanium under 150 MPa pressure at room temperature 15 p2499 N85-25414

Structural changes with one- and two-stage aging of alloys Ti-Al-Mo-Fe and Ti-Zr-V-Al-Sn 15 p2499 N85-25415

Ways of improving level and stability of mechanical characteristics of diffusion-welded joints of OT4 titanium alloy 15 p2499 N85-25417

Microstructural characteristics during the controlled solidification of a binary system
[DE85-005200] 15 p2507 N85-25461

Application of solidification theory to rapid solidification processing
[AD-A151251] 15 p2509 N85-25480

Optimizing hot workability and controlling microstructures in difficult to process high strength and high temperature materials
[AD-D011586] 15 p2510 N85-25482

Mossbauer spectrometry: Testing of a new computer based system and its application to a study of an aluminum-iron-cerium alloy
[AD-A151626] 15 p2510 N85-25483

Metallurgical characterization of aluminum powder consolidation
[AD-A151990] 15 p2510 N85-25484

Structure of condensed aluminum thin film metallizations 15 p2512 N85-25501

Dependence of plasticity of VT1-00 titanium alloy on microstructure 15 p2515 N85-25516

Transformation toughened ceramics: A potential material for light diesel engine application
[AD-A151421] 15 p2518 N85-25526

Mammalian gravity receptors: Structure and metabolism 15 p2605 N85-26055

Radiation effects on structural materials
[DE85-007032] 15 p2649 N85-26338

Relationships between microstructure and microfissuring in alloy 718 16 p2735 N85-26976

Microstructures and properties of rapidly solidified alloys
[NASA-CR-172377] 16 p2748 N85-26981

Properties and microstructures for dual alloy combinations of three superalloys with alloy 901
[NASA-TM-86967] 16 p2749 N85-26983

Hydrogen induced crack growth in Grade-12 Titanium
[BNL-NUREG-35598] 16 p2751 N85-26976

Microwave processing of lunar materials: Potential applications
[DE85-007223] 16 p2755 N85-27003

Multiple scattering of electromagnetic waves in discrete random media
[AD-A151766] 16 p2772 N85-27112

Full statistical characteristics of microdeformation
[BLL-M-36076-(5828.4)] 16 p2798 N85-27254

Constitutive cyclic deformation behavior in single-crystal and directionally solidified SSME high-pressure fuel turbopump airfoil materials 17 p2914 N85-27965

Study of self-propagating condensed phase reactions TiB(2) synthesis
[AD-A153198] 17 p2921 N85-29006

Powder-metallurgy alloys and steels
[BLL-BISI-TRANS-22239-(9022.06)] 17 p2926 N85-29050

Textural transformations taking place during heat and mechanical treatment in triplex steels
[BLL-BISI-TRANS-22404-(9022.06)] 17 p2927 N85-29063

Microstructure and mechanical properties of rare-earths-microalloyed high-speed tool steel
[BLL-BISI-TRANS-22043-(9022.06)] 17 p2928 N85-29064

Preventing the formation of an anomalous structure in chemically sealed low carbon steel
[BLL-BISI-TRANS-22373-(9022.06)] 17 p2930 N85-29085

Influence of composition on the microstructural evolution and mechanical properties of irradiated Fe-Ni-Cr ternaries
[DE85-007462] 17 p2931 N85-29094

Properties of nitrogen containing stainless alloy designed for high resistance to pitting
[DE85-006262] 17 p2931 N85-29095

Mechanical stabilization of austenite against epsilon martensite and its effect on deformation behavior in high manganese steels
[DE85-007654] 17 p2932 N85-29097

Microstructure-mechanical property relationships in transformation-toughened ceramics
[DE85-009722] 17 p2935 N85-29117

Submerged arc welding of new Czechoslovak micro-alloy steels
[BLL-BISI-TRANS-22193-(9022.06)] 17 p2972 N85-29356

Formation of a fine structure during shock wave welding
[BLL-BISI-TRANS-22401-(9022.06)] 17 p2973 N85-29368

Preliminary results of the Inconel 617 optimization program. Advanced gas cooled reactor materials program
[DE85-008235] 18 p3075 N85-29024

Sintering reactions, structure and properties of a cobalt free nonconventional hard material
[DE85-007704] 18 p3076 N85-29025

Evaluation of 7XXX-series aluminum alloys for the W87 aft support ring
[DE85-008687] 18 p3076 N85-29027

Predicting microfracture in ceramics via a microcontract model
[DE85-005654] 18 p3081 N85-29060

Study of the influence of metallurgical factors on fatigue and fracture of aerospace structural materials
[AD-A153913] 18 p3122 N85-29329

Influence of microstructure on mechanical properties in cemented tungsten-carbides 19 p3230 N85-30029

The fabrication, microstructure, and strengthening behavior of heavily cold-worked in situ composites 19 p3231 N85-30031

The physical and mechanical properties of near-equiatomic titanium-nickel 19 p3237 N85-30072

Internal structure of GP zones in dilute Al-Cu alloys 19 p3238 N85-30073

Microstructures and mechanical properties of microalloyed medium carbon steels 19 p3238 N85-30074

Microstructure-abrasive wear characteristics of low carbon dual phase steels
[DE85-010098] 19 p3239 N85-30083

The microstructural state of Nb3Sn in a multifilamentary titanium doped bronze-process wire
[DE85-010979] 19 p3240 N85-30089

Weldability/microstructure relationships of high nickel alloys for header applications
[DE85-009337] 19 p3241 N85-30094

Specifics of fine structure of pressed aluminum alloys manufactured by plasma atomization 19 p3242 N85-30102

Effect of matrix plasticity on durability of fibrous composition materials 19 p3243 N85-30107

Mesophase mechanisms in the formation of graphitic microstructures
[AD-A154100] 19 p3248 N85-30140

Superconducting electronic film structures
[AD-A154196] 19 p3259 N85-30207

Investigation for low-cost permanent magnets
[AD-A154387] 19 p3260 N85-30212

Microstructural analysis of Pacific Ocean and Indian Ocean ultrabasites 19 p3291 N85-30405

Grain structure identification by ultrasound frequency averaging and deconvolution
[AD-A154332] 19 p3352 N85-30777

The microstructure approach to conserved scalar pdf models 20 p3424 N85-31251

Phase size distribution in WC/Co hardmetal
[NPL-DMA(A)-93] 20 p3431 N85-31281

Structure and chemistry of sol-gel derived transparent silica aerogel
[DE85-009002] 20 p3434 N85-31303

Metallurgical origins of fracture toughness and microstructure and fracture toughness of an HSLA (High-Strength/Low-Alloy) steel
[AD-A155530] 21 p3567 N85-32187

Fundamental investigations of failure during superplastic forming process
[AD-A154647] 21 p3588 N85-32194

The variability of aerosol microstructure in continental and oceanic surface layers of the atmosphere in anticyclones 21 p3647 N85-32660

Variation of the submicron aerosol structure 21 p3647 N85-32661

Microstructure-mechanical property relationships in the transformation-toughened ceramics
[DE85-011946] 22 p3752 N85-33261

Investigation of the microstructure and photovoltaic properties of semicrystalline silicon 22 p3806 N85-33573

Manufacturing process to reduce large grain growth in zirconium alloys
[DE85-011649] 23 p3915 N85-34267

Experimental attempt to achieve microstructure variations through temperature/time permutations for a nonwrought powder metallurgy uranium-6 niobium alloy
[DE85-013160] 23 p3916 N85-34272

Influence of particle erosion on the microstructural changes in metals and alloys
[TI85-901364] 23 p3917 N85-34276

High resolution electron microscopic characterization of interfaces in ceramics
[DE85-011207] 23 p3920 N85-34289

Near-threshold fatigue: An overview of the role of microstructure and environment
[DE85-009903] 23 p3941 N85-34431

Analytical ultrasonics for structural materials
[TI85-006132] 23 p3968 N85-34800

Effect of thermal ageing on the mechanical properties of PWR pressure vessel steels and weldments
[AERE-R-11460] 24 p4078 N85-35275

Effect of prior warm rolling on the retained austenite content and hardening response of VIM-VAR (vacuum-induction melted-vacuum-arc remelted) AISI M-50 steel
[AD-A156145] 24 p4079 N85-35281

Effect of microstructure on the fatigue behavior of Fe-C-X alloys
[DE85-011749] 24 p4080 N85-35285

MICROTRONS
Performance of an RF beam monitor on the NBS-Los Alamos racetrack microtron
[DE85-010725] 19 p3262 N85-30232

MICROWAVE AMPLIFIERS
NT CYCLOTRON RESONANCE DEVICES
Linear wideband microwave amplifiers for monolithic integrated microcircuits 07 p0955 N85-16051
Combined microwave parallel amplifier-RF attenuator/modulator
[AD-D011536] 12 p1833 N85-21499
Analysis and design of linear microwave transistor amplifiers 13 p2066 N85-23036
Proceedings of the Cold Electronics Workshop
[NASA-CR-175662] 14 p2297 N85-24220
Cryogenically-cooled, low-noise microwave receivers: Present status and future needs
14 p2296 N85-24226
Design and testing of gyrotystron amplifiers
[AD-A151038] 14 p2296 N85-24231
The design of megawatt gyrotrons
[DE85-007662] 17 p3032 N85-26754
Proposal for continuation of research on megawatt gyrotrons for the period January 1, 1985 through December 31, 1985
[DE85-009062] 18 p3110 N85-29260
Design and fabrication of monolithic broadband microwave GaAs low noise FET amplifiers
20 p3443 N85-31370
Thirty GHz low noise GaAs FET amplifiers — satellite-ground communication
[CD.8500666] 20 p3449 N85-31413
140 GHz gyrotron development program
[DE85-010348] 20 p3537 N85-32013
Clarke Stations and mercurian mass-drivers: Energy for large-scale transportation systems
[DE85-009807] 21 p3580 N85-32145
High-power solid-state rf source for accelerator cavities
[DE85-012872] 22 p3761 N85-33309
Study of nonlinear distortion in microwave amplifiers using Schottky gate field effect transistors
22 p3780 N85-33423
Realization and linearization of a hyperfrequency power amplifier implemented with bipolar transistors in class C polarization — microwave amplifiers
[CNES-NT-114] 23 p3926 N85-34346

MICROWAVE ANTENNAS
NT HORN ANTENNAS
NT LENS ANTENNAS
NT RECTENNAS
NT SLOT ANTENNAS
NT SPACETENNAS
Mark IVA DSN 26-meter subnet
05 p0624 N85-13995
64-meter to 70-meter antenna extension
05 p0624 N85-13996
Antenna microwave subsystem
05 p0625 N85-13997
Characterization of MMIC devices for active array antennas
[NASA-TM-86907] 07 p0913 N85-15779
The 20 GHz proof-of-concept test model results for a multiple scan beam dual reflector antenna
[NASA-CR-174288] 07 p0938 N85-15944
A low-sidelobe space feed lens
[AD-A147863] 07 p0942 N85-15972
Power transfer from natural emitters to collection apertures at microwave wavelengths
[NASA-CR-174275] 07 p0945 N85-15989
Microwave surface resistivity of several materials at ambient temperature 10 p1463 N85-19226
The effects of mode impurity of Ka-band system performance 10 p1463 N85-19227
Comparison of measured and calculated mutual coupling in the near field between microwave antennas
[PB85-105963] 11 p1625 N85-20237
Orbiting multi-beam microwave radiometer for soil moisture remote sensing 14 p2230 N85-23618
Low-frequency microwave radiometer for N-ROSS
14 p2230 N85-23619
Development of the microwave antenna range of the national antenna test facility at Pasadefontein
[R-NIAS-21] 15 p2539 N85-25869
ECM multiple-target retrodirective antenna
[AD-D011528] 20 p3439 N85-31346

MICROWAVE ATTENUATION
Attenuation experimental data bank in the COST 205 project. Structure and management of the final supports
[FUB-5-1983] 01 p0126 N85-10965
Absorption of radiation by water vapor in windows of relative transparency of 95-145 micrometer range
13 p2076 N85-22966
The microwave propagation and backscattering characteristics of vegetation — wheat, sorghum, soybeans and corn fields in Kansas
[E85-10068] 13 p2122 N85-23213
Precision microwave attenuation measurement by time interval ratio
[RSRE-85005] 22 p3755 N85-33280

MICROWAVE CIRCUITS
Manufacturing methods for microwave circuits
[AD-A145237] 01 p0043 N85-10278
Computerized circuit designs: Realization of masks to manufacture microwave circuits
[CNES-NT-107] 04 p0496 N85-13166
Interface structures for millimeter-wave circuits
[AD-A146557] 06 p0804 N85-15118
Characterization of MMIC devices for active array antennas
[NASA-TM-86907] 07 p0913 N85-15779
Slow wave circuit with shaped dielectric substrate
[AD-D011385] 07 p0945 N85-15986
Investigation of planar waveguides and components for millimeter-wave integrated circuits
[AD-A147360] 07 p0948 N85-16005
Configuration study for a 30 GHz monolithic receive array, volume 1
[NASA-CR-174697-VOL-1] 09 p1311 N85-18239
Monolithic thin film SAW (Surface Acoustic Wave) structures
[AD-A149762] 12 p1835 N85-21511
Reduction of amplitude-phase distortions of movable microwave coupling circuit for antenna field measurements 13 p2068 N85-22920
Measurement methods for accurate microwave characterization and modeling of MESFET chips
[AD-A152360] 17 p2952 N85-26227
Communications and logic systems at millimeter wave frequencies
[NASA-CR-175859] 17 p3042 N85-26824
Microwave semiconductor research: Materials, devices and circuits and gallium arsenide ballistic electron transistors
[AD-A154666] 21 p3709 N85-33024
Software for frequency analysis of microwave circuits
22 p3768 N85-33352

MICROWAVE COUPLING
NT COUPLING CIRCUITS
A transistor oscillator-doubler
[AD-D011406] 08 p1156 N85-17307
Effect of resonant microwave power on a PIG ion source
[DE85-001396] 09 p1379 N85-18673
Phenomenology of microwave coupling, part 1
[DE85-003097] 11 p1624 N85-20229
Reduction of amplitude-phase distortions of movable microwave coupling circuit for antenna field measurements 13 p2068 N85-22920
Synthesis of multistep directional couplers with nonminimum-phase characteristics
13 p2079 N85-22986
Maser cavity servo-tuning system
[NASA-CASE-NPO-15890-1-CU]
18 p3093 N85-29143
Mutual coupling analysis for conformal microstrip antennas 20 p3439 N85-31343

MICROWAVE EMISSION
Power transfer from natural emitters to collection apertures at microwave wavelengths
[NASA-CR-174275] 07 p0945 N85-15989
Microwave emissions from snow
[E85-10085] 08 p1174 N85-17403
Data report on variations in the composition of sea ice during MIZEX/East'83 with the Nimbus-7 SMMR
[NASA-TM-86170] 09 p1342 N85-18443
Measurement of hot-electron production and microwave emission by laser-irradiated CH targets
[DE85-003139] 11 p1640 N85-20331
Remote Sensing of Snow and Evapotranspiration
[NASA-CP-2363] 13 p2123 N85-23223
Microwave radiometer observations of snowpack properties and comparison of U.S. Japanese results — Hokkaido, Japan and Vermont and North Dakota test sites 13 p2125 N85-23230
Microwave remote sensing of soil moisture
13 p2125 N85-23235
Modeling of radiothermal radiation of rain by Monte-Carlo method 14 p2341 N85-24476
Technical development to improve satellite sounding over radiatively complex terrain
[NASA-CR-175746] 15 p2583 N85-25629
Microwave emission from relativistic electron beams
[AD-A151472] 15 p2648 N85-26333
Microwave emission from Saturn's rings
15 p2670 N85-26475
Experiments in microwave exposure in the rat: Body temperature, serum chemistry and the use of chemical restraint
[PB85-156634] 16 p2840 N85-27512

MICROWAVE EQUIPMENT
NT COLD CATHODE TUBES
NT GYRATORS
NT HELITRONS
NT HORN ANTENNAS
NT KLYSTRONS
NT LENS ANTENNAS
NT MAGNETRONS
NT MICROWAVE AMPLIFIERS
NT MICROWAVE ANTENNAS
NT MICROWAVE FILTERS
NT MICROWAVE INTERFEROMETERS
NT MICROWAVE OSCILLATORS
NT MICROWAVE PROBES
NT MICROWAVE RADIOMETERS
NT MICROWAVE TUBES
NT PHOTOMULTIPLIER TUBES
NT RECTENNAS
NT SLOT ANTENNAS
NT SPACETENNAS
NT THERMICONS
NT THYRATRONS
NT TRAVELING WAVE TUBES
NT VIDICONS
Linear theory of free-electron lasers with cylindrical interaction space 02 p0262 N85-11718
Target detection using microwave irradiances from natural sources: A passive, local and global surveillance system
[NASA-CR-174260] 07 p0946 N85-15991
USSR report: Electronics and electrical engineering
[JPRS-UEE-84-017] 07 p0951 N85-16025
Investigation of the ice dynamics in the marginal ice zone
[AD-A146729] 07 p1009 N85-16411
Microwave resonator using lateral excitation
[AD-D011374] 07 p1039 N85-16596
Transient response of a small-signal microwave GaAs FET to X-rays
[DE85-000066] 09 p1315 N85-18285
The impact of propagation effects on the design of high capacity digital microwave links in the 18 GHz frequency band 10 p1470 N85-19278
Improved electron emission by use of a cloth fiber cathode
[AD-A149250] 10 p1480 N85-19340
Planar ferroelectric microcapacitors for microwave devices 13 p2087 N85-23032
Demonstration of feasibility of depositing semiconductor layers using microwave enhanced plasma technique
[NASA-CR-174392] 13 p2163 N85-23421
Equipment for hot-to-serve foods
14 p2393 N85-24741
Study of 1/f noise in solids
[AD-A151069] 14 p2428 N85-24972
Future prospects of China's microwave semiconductor technology 15 p2530 N85-25598
In situ microwave measurements of dielectric properties and moisture in materials
[DE85-003622] 16 p2747 N85-26953
Microwave processing of lunar materials: Potential applications
[DE85-007223] 16 p2755 N85-27003
Hardware test program for evaluation of baseline range-range rate sensor concept
[NASA-CR-175794] 16 p2787 N85-27193
An inexpensive radar-responding relocation device for drifting oceanographic instruments
[AD-A152170] 16 p2836 N85-27505
Design of the waveguide for microwave heating of solid lithium ceramic blankets
[DE85-009776] 17 p2935 N85-28120
Technique for measuring the effective source reflection coefficient of 2-resistor power splitters
[DE85-009964] 17 p2956 N85-28256
VULTURE manual
[DE85-006873] 17 p3013 N85-29031
Research relative to the development of a cryogenic microwave cavity gradiometer for orbital use
[NASA-CR-176002] 19 p3222 N85-29990
New measurement solutions in the microwave industry
20 p3437 N85-31324
Microwave semiconductor research: Materials, devices and circuits and gallium arsenide ballistic electron transistors
[AD-A154666] 21 p3709 N85-33024
USSR report: Electronics and electrical engineering
[JPRS-UEE-84-003] 22 p3773 N85-33361
Instrumentation for sensing moisture content of material using a transient thermal pulse
[NASA-CASE-NPO-15493-2] 23 p3933 N85-34373

MICROWAVE FILTERS
Microstrip directional filters
[INPE-3127-PRE/518] 02 p0194 N85-11293
Dual mode directionally coupled band reject filter apparatus
[AD-D011359] 07 p0945 N85-15984
Tunable microwave transversal filters
[AD-A148370] 08 p1158 N85-17304
Synthesis of low-pass filters using coupled lines with unmatched loads 13 p2071 N85-22938
Investigation of bimodal paramagnetic filter 13 p2083 N85-23007
Microwave bandstop filter
[AD-D011716] 19 p3261 N85-30222
Receive shaping filter manufacture — QPSK uplinks
[ESA-CR(P)-1998] 20 p3449 N85-31412
MICROWAVE FREQUENCIES
NT C BAND
NT EXTREMELY HIGH FREQUENCIES
NT SUPERHIGH FREQUENCIES
Spectral noise density and random errors of pulse frequency characteristic meters 03 p0346 N85-12231
Improvement of the accuracy of reflection factor measurements by a computer 05 p0629 N85-14033
Realization of noise power in the microwave range by thermal noise standards 05 p0629 N85-14034
Calculations of high-current characteristics of silicon diodes at microwave frequencies
[AD-A147406] 09 p1314 N85-18261
Spectrum resource assessment of the frequency bands from 17.7-40.5 GHz
[PB85-125748] 10 p1469 N85-19267
Spectrum resource assessment of the 1530-1660.5 MHz band
[NTIA/REPT-84/160] 10 p1469 N85-19268
Spectrum resource assessment of the fixed and mobile services in the 947-17,700 MHz band, phase 1
[PB85-126288] 11 p1626 N85-20243
Study of laminated dielectric behavior at microwave and millimeter-wave frequencies
[AD-P004358] 12 p1825 N85-21452
Process for making a heterojunction source-drain insulated gate field-effect transistors utilizing diffusion to form the lattice
[AD-D011536] 12 p1939 N85-22176
Design and performance of etched polarization transformers for microwave frequencies
[R-NIAS-26] 14 p2297 N85-24218
Frequency and time standards based on stored ions 18 p3105 N85-29223
Effects of hydrometeors on electromagnetic wave propagation
[AD-A155379] 22 p3759 N85-33297
Recording small frequency drifts of microwave oscillators 22 p3771 N85-33372
Strongly coupled millimeter-band waveguide directional couplers 22 p3779 N85-33418
Microwave properties of a quiet sea
[NASA-CR-176199] 24 p4085 N85-35322
MICROWAVE HOLOGRAPHY
Detection of cracks in a plastics pipe joint by reflection holography
[NPL-DMA(A)-87/MOM-70] 04 p0502 N85-13202
MICROWAVE IMAGERY
The interpretation of SIR-B imagery of surface waves and other oceanographic features using in-situ, meteorological satellite, and infrared satellite data 08 p1143 N85-17212
Microwave and optical remote sensing of forest vegetation 08 p1146 N85-17228
Development and evaluation of techniques for using combined microwave and optical image data for vegetation studies 08 p1148 N85-17240
Automatic terrain elevation mapping and registration 08 p1148 N85-17242
Resolution enhancement of multichannel microwave imagery from the Nimbus-7 SMMR for maritime rainfall analysis
[NASA-CR-174367] 10 p1462 N85-19221
Earth resources research using the Shuttle Imaging Radar system 11 p1713 N85-20779
Digital processing of passive Ka-band microwave images for sea-ice classification
[AD-A150666] 14 p2347 N85-24511
Microwave responses of the western North Atlantic
[NASA-CR-175868] 17 p2946 N85-28191
Microwave hydrology: A trilogy
[NASA-CR-176042] 20 p3477 N85-31603
MICROWAVE INTERFEROMETERS
Direct reading fast microwave interferometer for EBT
[DE85-000183] 11 p1636 N85-20306
System for lower hybrid current startup 15 p2654 N85-26373
MICROWAVE LANDING SYSTEMS
Flight tests of the Digital Integrated Automatic Landing System (DIALS)
[NASA-CR-3859] 04 p0457 N85-12900
Developments in the area of air traffic control systems and the relation with meteorology
[NLR-MP-84029-U] 17 p2895 N85-27848
Evaluation of a fault tolerant system for an integrated avionics sensor configuration with TSRV flight data
[NASA-CR-172589] 18 p3062 N85-28941
Microwave landing systems for heliport operators, owners and users
[FAA-PM-85-7] 19 p3216 N85-29940
MICROWAVE OSCILLATORS
Planning of hybrid integrated circuits for microwave-band oscillators 04 p0490 N85-13124
Low frequency noise in oscillator with limited space-charge accumulation 06 p0766 N85-15024
Device for frequency stabilization of microwave oscillators 06 p0768 N85-15033
Coherent array of Josephson oscillators with external bias leads
[AD-D011367] 08 p1156 N85-17293
An integrated varactor tuned coaxial gunn oscillator for 60 GHz operation
[AD-D011439] 10 p1479 N85-19335
Filter reflection image guide oscillator and solid state line scanning device
[AD-D011440] 10 p1479 N85-19336
The 60 GHz gyrotron development program
[DE85-000599] 12 p1836 N85-21522
Effect of space-charge field on output characteristics of O-type oscillators with distributed interaction 13 p2089 N85-23043
Dielectric resonator
[AD-D011573] 14 p2299 N85-24233
Deterministic and random phase noise of oscillators — synthetic aperture radar
[ESA-TT-848] 20 p3449 N85-31415
Recording small frequency drifts of microwave oscillators 22 p3771 N85-33372
MICROWAVE PROBES
Multiple reflection theory for microwave measurement of solid propellant burning rates 13 p2002 N85-22549
MICROWAVE RADIATION
U MICROWAVES
MICROWAVE RADIOMETERS
Use of ground based microwave radiometers for nowcasting 01 p0078 N85-10517
The potential use of atmospheric profilers in short-range prediction 01 p0078 N85-10518
Multispectral passive microwave correlations with an antecedent precipitation index using the Nimbus 7 SMMR
[AD-A145419] 02 p0200 N85-11334
Feasibility study of a satellite-borne 90 GHz radiometer 04 p0459 N85-12914
Restoration of multichannel microwave radiometric images
[NASA-CR-174115] 04 p0554 N85-13527
Basic investigation concerning the applicability of multispectral radiation data from microwave radiometry measurements to geoscientific objectives of remote sensing
[ESA-TT-846] 05 p0628 N85-14027
Studies of atmospheric water in storms with the Nimbus 7 scanning multichannel microwave radiometer 05 p0682 N85-14382
Mathematical models for the brightness temperature of object and environment in the microwave region
[ESA-TT-829] 05 p0718 N85-14610
Microstrip antenna for multichannel radiometer 06 p0791 N85-15058
Support for the Naval Research Laboratory Passive Microwave Clutter Analysis Program
[AD-A146771] 07 p0939 N85-15951
Spaceborne receivers: Basic principles
[NASA-CR-174269] 07 p0946 N85-15990
Spaceborne microwave radiometers: Background and technology requirements
[LD-R-267] 08 p1165 N85-17350
Microwave radiometric studies of composition and structure 08 p1183 N85-17458
The 13.9 GHz radiometer design
[AD-A149637] 12 p1851 N85-21613
Studies on physical properties of snow based on multi channel microwave radiometer 13 p2125 N85-23231
Orbiting multi-beam microwave radiometer for soil moisture remote sensing 14 p2220 N85-23818
Low-frequency microwave radiometer (N-ROSS 14 p2230 N85-23819
Determination of electromagnetic properties of mesh material using advanced radiometer techniques 14 p2235 N85-23855
Determination of temperature and degree of roughness of sea and land surfaces by microwave radiometric polarization measurements 14 p2334 N85-24432
Aerospace technology determines forest-fire danger 19 p3295 N85-30427
MIZEX, 1984, NASA CV-990 flight report
[NASA-TM-86216] 19 p3299 N85-30451
Radiometry: A useful prediction tool — atmospheric attenuation
[ESA-SP-1071] 20 p3399 N85-31084
Preliminary investigations concerning a 90 GHz radiometer satellite experiment
[ESA-TT-860] 20 p3420 N85-31225
High reflective surfaces for millimeter RF waves, phase A — satellite antenna reflectors
[HRS-FR-01] 20 p3442 N85-31386
Network ST radar and related measurements at Pennsylvania State University 21 p3629 N85-32544
Six mechanisms used on the SSM/1 radiometer 22 p3796 N85-33534
MICROWAVE REFLECTOMETERS
Implementing waveguide bandwidth six-port reflectometer circuits at millimetric wavelengths
[RSRE-MEMO-3678] 04 p0495 N85-13155
Comparing different theoretical designs of six-port reflectometer junctions
[AD-A149419] 13 p2054 N85-22861
MICROWAVE RESONANCE
High switching speed electrically tuned microwave magnetic resonance devices
[AD-D011699] 19 p3260 N85-30217
Laboratory evaluation and application of microwave absorption properties under simulated conditions for planetary atmospheres
[NASA-CR-176078] 22 p3851 N85-33847
MICROWAVE SCATTERING
Numerical investigation of diffraction models of microwave integrated circuits 03 p0347 N85-12233
Scattering models in the microwave regime
[NASA-CR-174001] 04 p0525 N85-13361
Scattering of H10-mode wave by narrow conducting plate inside rectangular waveguide 06 p0788 N85-15036
Research in image understanding as applied to 3-D tomographic imaging with near optical resolution
[AD-A150098] 12 p1829 N85-21483
The microwave propagation and backscattering characteristics of vegetation — wheat, sorghum, soybeans and corn fields in Kansas
[E85-10088] 13 p2122 N85-23213
Modeling the backscattering and transmission properties of vegetation canopies
[E85-10099] 16 p2809 N85-27320
Microwave model prediction and verifications for vegetated terrain
[E85-10102] 16 p2809 N85-27322
MICROWAVE SENSORS
The investigation of selected oceanographic applications of spaceborne synthetic-aperture radar 08 p1146 N85-17233
Passive microwave remote sensing for sea ice research
[NASA-CR-175570] 12 p1874 N85-21758
Evaluation of OMV ranging and docking systems 12 p1947 N85-22230
Short-range radiotechnical point sensor 13 p2081 N85-22996
Cryogenically-cooled, low-noise microwave receivers: Present status and future needs 14 p2298 N85-24226
Ion sensor signal fluctuations during operation of spacecraft reaction engines 16 p2724 N85-26815
Wideband disturbance accomodation in precision flexible space structures 20 p3415 N85-31194
Influence of spatial variability of hydraulic characteristics of soils on surface parameters obtained from remote sensing data in infrared and microwaves
[NASA-TM-77902] 20 p3477 N85-31604
MICROWAVE SOUNDING
Research relative to high spatial resolution passive microwave sounding systems 05 p0681 N85-14380
Investigation of satellite measurements in the presence of clouds, forcing influences on clouds and feedback to the large scale following convection 05 p0682 N85-14381
Experimental results of temperature-wind soundings of the atmosphere by the radio acoustical method 14 p2340 N85-24471
MICROWAVE SPECTRA
A review of the millimeter and centimeter observations of Uranus 02 p0299 N85-11935
Cosmology . 07 p1056 N85-16701
Laboratory evaluation and application of microwave absorption properties under simulated conditions for planetary atmospheres
[NASA-CR-176078] 22 p3851 N85-33847

MICROWAVE SPECTROMETERS
Virtual cathode oscillator study
[AD-A149269] 10 p1480 N85-19342
MICROWAVE SWITCHING
Wave guide branchings (n-port) types of representation of linear, time-independent and sourceless n-ports
[NASA-TM-77770] 01 p0037 N85-10233
MICROWAVE TRANSMISSION
NT MANDELSTAM REPRESENTATION
Interference experiment with the Sirio-OTS satellites
[FUB-17-1983] 01 p0040 N85-10254
The pluviometric recording stations in the 11 GHz radio link at Involotella Monte S. Pancrazio — Italy
[FUB-6-1983] 01 p0086 N85-10575
Real-time estimation of amplitude and group delay distortion in a PSK line-of-sight communications channel
09 p1311 N85-18237
Digital data communications over microwave radio channels 10 p1469 N85-19272
Influence of propagation in digital wireless beam, microwave links 10 p1470 N85-19277
Theoretical study of a dynamic simulator of selective fading for digital, wireless beam microwave links
10 p1473 N85-19294
Millimeter-wave range masers: A review
13 p2089 N85-23042
High switching speed electrically tuned microwave magnetic resonance devices
[AD-D011699] 19 p3260 N85-30217
Study of the interferences of 2 GHz radio beams with a DORIS system — precise low orbit determination system (DORIS)
[CNES-CT/DRT/TIT/RL-84/140-T]
20 p3442 N85-31382
Utilization of microwave measuring systems for the automation of composite materials manufacturing
[SNIAS-851-430-102] 22 p3742 N85-33197
New directional couplers for multimode circular waveguides applied to intense pulsed microwave systems
[DE85-011753] 23 p3926 N85-34330
Perturbation-iteration theory for analyzing microwave striplines
[NASA-CR-176189] 24 p4085 N85-35321
Microwave propagation studies, measurements and education in Surabaya, Indonesia
[B8404833] 24 p4088 N85-35339
MICROWAVE TUBES
NT COLD CATHODE TUBES
NT HELITRONS
NT KLYSTRONS
NT MAGNETRONS
NT MICROWAVE OSCILLATORS
NT PHOTOMULTIPLIER TUBES
NT THERMICONS
NT THYRATRONS
NT TRAVELING WAVE TUBES
Millimeter-wave traveling-wave IMPATT diode
[AD-A146545] 06 p0804 N85-15117
Research relative to the development of a cryogenic microwave cavity gradiometer for orbital use
[NASA-CR-174249] 07 p0962 N85-16095
Microwave tubes: Literature survey no. 5 comprising year 1983
[FOA-C-30377-E] 15 p2550 N85-25739
MICROWAVES
NT CENTIMETER WAVES
NT DECIMETER WAVES
NT MICROWAVE EMISSION
NT MILLIMETER WAVES
A coaxial noise standard for the 1 GHz to 12.4 GHz frequency range
[PB84-217864] 01 p0042 N85-10272
Transverse field interaction multibeam amplifier
[AD-D011241] 01 p0043 N85-10282
Conversion of microwave signals by superconducting films in the resistive state
[NASA-TM-77595] 01 p0123 N85-10843
The Bellkt experiment 02 p0159 N85-11079
Radiofrequency and microwave radiation
[AD-A145402] 02 p0191 N85-11274
Microwave susceptibility experiments
[DE84-016186] 02 p0192 N85-11281
Harmonic emission from high power gyrotron oscillators
[AD-A145821] 02 p0200 N85-11335
Active microwave measurements of sea ice under fall conditions: The RADARSAT/FIREX fall experiment — in the Canadian Arctic
[E85-10019] 02 p0217 N85-11432
Laboratory evaluation of microwave absorption properties under simulated conditions for planetary atmospheres
[NASA-CR-174060] 02 p0303 N85-11960
Numerical investigation of diffraction models of microwave integrated circuits 03 p0347 N85-12233
Generation of superpowerful microsecond electromagnetic radiation pulses
03 p0347 N85-12234
Determination of bound water in biological tissue and energy dissipated in bound water by low level microwaves
[AD-A143101] 03 p0399 N85-12547
Research activities of the Illinois University Coordinated Science Laboratory
[AD-A145589] 03 p0449 N85-12856
Ceramic/ceramic seals by microwave heating
[DE84-007486] 04 p0479 N85-13050
Microwave measurement of the complex dielectric tensor of anisotropic slab materials
[DE84-017050] 04 p0493 N85-13144
Thermoregulatory consequences of long-term microwave exposure at controlled ambient temperatures
[PB84-236603] 05 p0697 N85-14484
New measurements of the spectrum of the cosmic microwave background
[DE84-016055] 05 p0746 N85-14785
A new leaky wave antenna for millimeter waves based on the groove guide
[AD-A146428] 06 p0799 N85-15102
Natural interference phenomena affecting spaceborne receivers
[NASA-CR-174256] 07 p0916 N85-15796
Support for the Naval Research Laboratory Passive Microwave Clutter Analysis Program
[AD-A146771] 07 p0939 N85-15951
Micro-waveguide transformers of coherent optical signals 07 p0950 N85-16022
Effect of microwave radiation on local blood circulation and oxygenation of brain tissue
07 p1012 N85-16431
Electromagnetic processing of materials
[AD-A146604] 09 p1311 N85-18241
Microwave discharge in a supersonic flow for the excitation of a gas dynamic CO laser
[ESA-TT-833] 09 p1326 N85-18337
Resonant activation of a Josephson junction
[DE85-000702] 10 p1583 N85-19857
Effect of interfacial characteristics of metal clad polymeric substrates on electrical high frequency interconnection performance
[NASA-TM-86948] 11 p1624 N85-20223
Precision tunable resonant microwave cavity
[NASA-CASE-LEW-13935-1] 11 p1628 N85-20248
Evaluation of resonant modes in isolated dielectric resonators using a surface integral equation formulation
[PB85-110831] 12 p1837 N85-21528
Analysis and computations of microwave-atmospheric interactions
[AD-A149666] 12 p1889 N85-21854
Technical support for microwave experiments on the eye lens
[AD-A149702] 12 p1933 N85-22144
Microwave blackbodies for spaceborne receivers
[NASA-CR-175847] 13 p2094 N85-23068
Calculations of microwave brightness temperature of rough soil surfaces: Bare field
[NASA-TM-86200] 13 p2123 N85-23221
Design considerations for high-altitude, long-endurance, microwave-powered aircraft
[NASA-TM-86403] 14 p2218 N85-23751
Microwave methods for paving
[DE85-004194] 14 p2265 N85-24032
Determining atmosphere moisture content from differences in two-frequency microwave radiation measurements 14 p2341 N85-24474
A survey of radar ECM and ECCM
15 p2536 N85-25653
Measurement of ocean surface currents from space with multi-frequency microwave radars
15 p2539 N85-25672
Microwave tubes: Literature survey no. 5 comprising year 1983
[FOA-C-30377-E] 15 p2550 N85-25739
Effects of long-term low-level radiofrequency radiation exposure on rats. Volume 7: Metabolism, growth and development
[AD-A150829] 15 p2615 N85-26112
Thermal consequences of localized SAR from RFR exposures 16 p2775 N85-27130
The medical results of human exposures to radio frequency radiation 16 p2776 N85-27133
Development and application of new radiofrequency radiation safety standards 16 p2777 N85-27137
Active and passive remote sensing of ice
[AD-A151741] 16 p2815 N85-27369
Hydrogen recovery from extraterrestrial materials using microwave energy
[DE85-006717] 16 p2883 N85-27789
A synchrotron/inverse Compton interpretation of a solar burst producing fast pulses at lambda 3 mm and hard X-rays 16 p2887 N85-27815
Microwaves and hard X-rays ultrafast time structures at the impulsive phase of solar bursts
[INPE-3478-PRE/721] 16 p2888 N85-27816
Microwave responses of the western North Atlantic
[NASA-CR-175888] 17 p2946 N85-28191
Microwave experimental studies of laser fusion
[DE85-008327] 17 p3041 N85-28814
Low density inorganic foams fabricated using microwaves
[DE85-007706] 18 p3080 N85-29051
Beam forming network
[NASA-CASE-NPO-15743-1] 18 p3089 N85-29118
Two-degree-of-freedom linear and planar microwave array lenses
[AD-A153701] 18 p3095 N85-29156
Measurement of permittivity and permeability of microwave materials
[AD-D011656] 18 p3176 N85-29688
Experimental and theoretical investigation of microwave and millimeter wave radiation from hollow, rotating electron beams
[AD-A153627] 18 p3179 N85-29706
Multiport optical detectors 18 p3187 N85-29799
Preliminary results on open accelerating structures
[DE85-010231] 18 p3191 N85-29793
High switching speed electrically tuned microwave magnetic resonance devices
[AD-D011699] 19 p3260 N85-30217
Use of Omega radio navigation system in geophysical work in Antarctica 19 p3298 N85-30448
Effects of long-term low-level radiofrequency radiation exposure on rats. Volume 8: Evaluation of longevity, cause of death, and histopathological findings
[AD-A154283] 19 p3327 N85-30610
New measurement solutions in the microwave industry
20 p3437 N85-31324
New concepts in free electron lasers
20 p3460 N85-31483
Microwave SAW (Surface Acoustic Wave) monochromator
[AD-D011718] 21 p3590 N85-32311
Microwave-enhanced thin-film deposition
21 p3611 N85-32431
Form factor effects on microwave Cerenkov radiation
[AD-A154577] 21 p3701 N85-32993
Sodium nitrate containing mixture for producing ceramic-glass-ceramic seal by microwave heating
[DE85-011610] 22 p3751 N85-33254
Vacuum ultraviolet laser
[DE85-011632] 22 p3790 N85-33478
Six mechanisms used on the SSM/1 radiometer
22 p3798 N85-33534
Microwave radiation and thermoregulation
[AD-A155718] 22 p3818 N85-33654
Quantitative analysis of flare accelerated electrons through their hard X-ray and microwave radiation
[SH-1.2-7] 23 p3901 N85-34742
Feasibility study of radar-transmitting materials
[AD-A155839] 24 p4087 N85-35329
A ray trace program for line-of-sight microwave communication links
[AD-A156168] 24 p4087 N85-35336
Literature search for new physical methods for biological aerosol detection
[AD-A155883] 24 p4128 N85-35592
Electromagnetic compatibility conference features biological interactions
[AD-A155813] 24 p4144 N85-35682
MICROWEIGHING
U WEIGHT MEASUREMENT
MICROYIELD STRENGTH
Dependence of microplasticity of beryllium on grain size and heat treatment 03 p0353 N85-12273
MIDAIR COLLISIONS
NT BIRD-AIRCRAFT COLLISIONS
TCAS II: Design and validation of the high-traffic-density surveillance subsystem
[DOT/FAA/PM-84/5] 13 p1970 N85-22375
MIDDLE ATMOSPHERE
NT MESOPAUSE
NT MESOSPHERE
NT OZONOSPHERE
NT STRATOSPHERE
National solar-terrestrial research program
[PB84-216183] 01 p0072 N85-10479
Middle atmospheric ionization. Observations and chemistry 04 p0522 N85-13340
Middle Atmosphere program. Handbook for MAP. Volume 13: Ground-based techniques
[NASA-CR-174345] 06 p1183 N85-17452
Microwave radiometric studies of composition and structure 06 p1183 N85-17456
Lidar systems for aerosol studies: An outline
06 p1183 N85-17457

Active optical sounding of ozone and minor constituents in the middle atmosphere: A review of ground-based lidar measurements 08 p1183 N85-17458
Lidar studies of temperature and density using Rayleigh scattering 08 p1184 N85-17459
Middle Atmosphere Program. Handbook for MAP, volume 4 [NASA-CR-175482] 11 p1654 N85-20420
PMP-1: A coordinated study of the behavior of the middle atmosphere in winter 11 p1654 N85-20421
French activities relevant to middle atmosphere research 11 p1655 N85-20423
MAP in India 11 p1655 N85-20424
MAP in Japan: Organization and projects 11 p1655 N85-20425
UK participation in the Middle Atmosphere Programme 11 p1655 N85-20426
MAP-related activities in the United States 11 p1655 N85-20427
Soviet National Middle Atmosphere Program 11 p1655 N85-20428
The Middle Atmosphere Program: Winter in Northern Europe (MAP/WINE) 11 p1655 N85-20429
The Middle Atmosphere Program: A special project for the Antarctic Middle Atmosphere (AMA) 11 p1656 N85-20430
Interaction of large meteoroids with the atmosphere 11 p1656 N85-20431
Middle Atmosphere Program. Handbook for MAP, volume 6 [NASA-CR-175480] 11 p1656 N85-20436
Winter in Northern Europe (WINE) project 11 p1657 N85-20439
MAP activities in Hungary 11 p1657 N85-20440
PMP-2 report: Equatorial wave dynamics 11 p1657 N85-20442
MSG-7: Atmospheric penetration of solar radiation in the range of Schumann-Runge bands 11 p1657 N85-20443
Middle Atmosphere Program. Handbook for MAP, volume 8 [NASA-CR-175478] 11 p1657 N85-20445
The first winter of MAP-dynamics, 1982-1983: A winter with three different warming periods 11 p1657 N85-20446
MSG-7: Molecular absorption processes related to the penetration of ultraviolet solar radiation into the middle atmosphere 11 p1658 N85-20449
Middle Atmosphere Program. Handbook for MAP, volume 10 [NASA-CR-175477] 11 p1658 N85-20450
Neutral atmosphere properties determining D-region electron densities 11 p1658 N85-20451
Middle atmosphere temperature and dynamics as revealed from D-region observations 11 p1659 N85-20453
A model of the influence of neutral air dynamics on the seasonal variation in the low ionosphere 11 p1660 N85-20462
Midwinter disturbances in the middle atmosphere 11 p1661 N85-20465
Spring changeover of the middle atmosphere circulation compared with rocket wind data up to 80 km 11 p1661 N85-20466
Some aspects of general circulation and tides in the middle atmosphere 11 p1661 N85-20470
Atmospheric profile imprint in firewall ablation coefficient 11 p1662 N85-20473
Winds and waves (4 min - 11 yrs) in the upper middle atmosphere (80-110 km) at Saskatoon, Canada (52 deg N, 107 deg W): MF radar (2.2 MHz) soundings 1973 - 1983 11 p1662 N85-20476
Dependence of the high latitude middle atmosphere ionization on structures in interplanetary space 11 p1664 N85-20487
Middle Atmosphere Program. Handbook for MAP. Volume 12: Coordinated Study of the Behavior of the Middle Atmosphere in Winter (PMP-1) Workshops [NASA-CR-175475] 11 p1665 N85-20492
Middle atmosphere NO and NO2 observed by means of the Spacelab one grille spectrometer [AERONOMICA-ACTA-A-293-1984] 11 p1680 N85-20588
An improved rocket-borne electric field meter for the middle atmosphere [NASA-CR-175510] 12 p1668 N85-21851
Middle Atmosphere Program. Handbook for MAP. Volume 14: URSI/SCOSTEP Workshop on Technical Aspects of MST Radar [NASA-CR-176065] 21 p3615 N85-32468
Excerpts from the paper: Research Status and Recommendation from the Alaska Workshop on Gravity Waves and Turbulence in the Middle Atmosphere, part 1.3A 21 p3616 N85-32470
General circulation of the middle atmosphere, part 1.4B 21 p3617 N85-32474
Sample interchange of MST radar data from the Urbana radar 21 p3627 N85-32531
The MU radar now partly in operation 21 p3628 N85-32543
Middle Atmosphere Program. Handbook for MAP, volume 11 [NASA-CR-176107] 22 p3614 N85-33625

MIDLATITUDE ATMOSPHERE
The mesoscale-beta-scale evolution of mid-latitude meso-alpha-scale convective complexes 01 p0073 N85-10488
Model of atmospheric ozone for middle latitudes 02 p0161 N85-11091
Medium- and large-scale wave disturbances and heterogeneities of electron concentration in outer ionosphere in middle and low latitudes 06 p0625 N85-15241
Winter anomaly of the lower ionosphere and its possible causes 11 p1660 N85-20459
Structure and energetics of medium-scale atmospheric waves in the Southern Hemisphere 20 p3489 N85-31685

MIDLATITUDES
U TEMPERATE REGIONS

MIE SCATTERING
NT RAYLEIGH SCATTERING
Investigation of light source and scattering medium related to vapor-screen flow visualization in a supersonic wind tunnel [NASA-TM-86290] 06 p0610 N85-15144
Novel photo-thermal technique for flow and spectroscopic measurements in a dense aerosol stream [AD-A149745] 12 p1800 N85-21287
A systematic study of light scattering by irregularly shaped particles [AD-A150192] 13 p2159 N85-23400
Macrostructure and microphysics of Saturn's E-ring 15 p2677 N85-26528
A comprehensive investigation of the dynamics of micron and submicron lunar ejecta in heliocentric space 19 p3364 N85-30994
Journal of Research of the National Bureau of Standards, volume 90, number 1, January - February 1985 [PB85-179063] 20 p3522 N85-31606
Ice fog as an electro-optical obscurant [AD-A155059] 21 p3705 N85-33015
Calculation of the diffusion of light by aerosols: Description of the MIELOR software and results obtained [REPT-80] 24 p4137 N85-35838

MIE THEORY
U MIE SCATTERING

MIG AIRCRAFT
China has developed a new version of fighter aircraft [AD-A155293] 21 p3685 N85-32118

MIGRATION
The use of small mobile radars to detect, monitor, and quantify bird movements [AD-P004188] 11 p1580 N85-19051
Plasticizer system for propellant compositions [AD-D011514] 12 p1817 N85-21393
Transatlantic migration study of the leathery turtle using the ARGOS system. Transatlantic turtle race 14 p2326 N85-24379
An application of Markov chains to the problem of migration in inventory systems [AD-A151954] 16 p2857 N85-27618
Propellant plasticizer [AD-D011501] 20 p3434 N85-31306
Microgravity electrophoresis: A study of the factors that affect free-fluid separation 20 p3502 N85-31774
Thermally induced chemical migration: A natural analog approach [DE85-012308] 23 p3949 N85-34474

MILANKOVITCH THEORY
U CLIMATOLOGY

MILITARY AIR FACILITIES
DoD Robotics Application Workshop Proceedings [AD-A145867] 03 p0307 N85-11978
Air force engine repair - Oklahoma City Air Logistics Center, Propulsion Division [AD-P003999] 03 p0307 N85-11980
Air force landing gear repair - Ogden Air Logistics Center Industrial Products and Landing Gear Division [AD-P004001] 03 p0307 N85-11982
Depot modernization at the Defense Logistics Agency [AD-P004008] 03 p0308 N85-11988
Future robotics program at San Antonio ALC (Air Logistics Center) [AD-P004011] 03 p0309 N85-11991
Supply center processes [AD-P004014] 03 p0309 N85-11993
Development of a pavement maintenance management system. Volume 2: Development of airfield pavement performance prediction models [AD-A146150] 03 p0321 N85-12069
Visibility monitoring in the southern California desert for the Department of Defense: Research on operations-limiting visual extinction, RESOLVE protocol [AD-A146617] 06 p0636 N85-15315
Installation restoration program. Phase 2: Stage 1 problem confirmation study, Duluth International Airport Duluth, Minnesota [AD-A148318] 08 p1089 N85-16885
Environmental and energy audits of Air Force government owned-contractor operated installations [AD-P004138] 09 p1347 N85-18474
Staff assistance to bases for bird hazards [AD-P004205] 11 p1583 N85-19972
Bird strike avoidance system for Dover AFB, Delaware [AD-P004206] 11 p1583 N85-19973
Mean conditions and turbulence statistics at Vandenberg AFB, California [AD-A151386] 15 p2665 N85-26449
Review of hazardous waste cleanup and disposal efforts at Tinker Air Force Base [GPO-49-294] 21 p3613 N85-32467

MILITARY AIRCRAFT
Determining training device requirements in Army aviation systems 05 p0711 N85-14558
The Air Force stock fund and aircraft availability [AD-A149853] 08 p1087 N85-16761
Mission-oriented requirements for updating MIL-H-8501. Volume 1: STI proposed structure --- military rotorcraft [NASA-CR-177331-VOL-1] 08 p1088 N85-16877
Mission-oriented requirements for updating MIL-H-8501. Volume 2: STI background and rationale --- military rotorcraft [NASA-CR-177331-VOL-2] 08 p1088 N85-16878
Using the control system design environment in the design of a data link receiver unit for the Coast Guard HH-65A helicopter [AD-A148624] 08 p1088 N85-16880
Reliability predictions for military avionics. Royal Signals and Radar Establishment reliability prediction method no. 250 [BR89221] 13 p1973 N85-22366
High specific power aircraft turn maneuvers: Tradeoff of time-to-turn versus change in specific energy [AD-A151701] 15 p2471 N85-25257
Generation of flight paths using heuristic search [AD-A151949] 16 p2704 N85-26694
Operations research [B8561897] 17 p3026 N85-28712

MILITARY AVIATION
Determining training device requirements in Army aviation systems 05 p0711 N85-14558
Keeping up with operational loads in the French Air Force: Defining new equipment 07 p0896 N85-15681
Development of NATOPS (Naval Air Training and Operating Procedure Standardization) performance software for the H-46D helicopter [AD-A156088] 24 p4064 N85-35190

MILITARY HELICOPTERS
NT CH-47 HELICOPTER
NT UH-1 HELICOPTER
NT UH-60A HELICOPTER
Airworthiness and flight characteristics test of the JOH-6A light combat helicopter configured with a wire strike protection system [AD-A144660] 01 p0006 N85-10036
Airworthiness and Flight Characteristics (A and FC) test of the EH - 1X/EH - 1H helicopter configurations [AD-A144981] 01 p0007 N85-10039
US Army helicopter operational flight loads 07 p0895 N85-15675
Speed benefits of tilt-rotor designs for LHX [NASA-CR-166437] 07 p0902 N85-15717
A digital piloting system for the combat helicopter 08 p1074 N85-16806
Tactical HF communication for military helicopters using the NVIS mode 08 p1074 N85-16807
Evaluation of nose, roof, and mast mounted sensor platforms for piloting and sighting, integrated in future combat helicopters 08 p1074 N85-16808
The design and development of an integrated core system for battlefield helicopters 08 p1074 N85-16811
Evolution toward a multi-bus architecture for Army helicopter avionic systems 08 p1074 N85-16812
A review of US Army aircrew-aircraft integration research programs 08 p1075 N85-16814
A simulator for studying helicopter weapons systems 08 p1075 N85-16816
Preliminary airworthiness evaluation AH-1S (MC) helicopter with external fuel tanks installed [AD-A149091] 08 p1084 N85-16865
Aircrew-aircraft integration issues in future US Army helicopters 10 p1535 N85-19672

Proceedings of the 14th Army Science Conference. Volume 1: Principal Authors A through H
[AD-A149200] 10 p1573 N85-19920
Cost-estimating relationships for tactical combat aircraft
[AD-A151575] 15 p2471 N85-25255
Piloted simulation of one-on-one helicopter air combat at NOE flight levels
[NASA-TM-86686] 16 p2710 N85-26720
A new main rotor hub for the AS 332 Super Puma
[SNIAS-851-210-102] 20 p3393 N85-31047
Research Flight Simulator for Helicopters (RFSH): Description and application to fire control system design
[SNIAS-851-210-106] 20 p3393 N85-31050

MILITARY OPERATIONS
NT COMBAT
NT ELECTRONIC WARFARE
Command control group behaviors. Objective 1: A methodology for and identification of command control group behaviors
[AD-A145890] 02 p0191 N85-11279
On applying AI (Artificial Intelligence) to maintenance and troubleshooting
[AD-P003915] 02 p0244 N85-11595
Overview of training and aiding
[AD-P003917] 02 p0245 N85-11597
AFHRL (Air Force Human Resources Laboratory) program for artificial intelligence applications to maintenance and training
[AD-P003931] 02 p0247 N85-11611
Artificial intelligence applications to automatic test equipment
[AD-P003936] 02 p0247 N85-11616
Model-based probabilistic reasoning for electronics troubleshooting
[AD-P003937] 02 p0247 N85-11617
The structures and the role of an international agency for the control of satellites
[NASA-TM-76765] 03 p0441 N85-12806
Army aviation today and tomorrow
06 p0751 N85-14810
Marine helicopter missions 06 p0751 N85-14811
Attack helicopter (AH-1T) cockpit systems integration
06 p0753 N85-14826
Distribution and storage of aviation turbine fuel for military operations in northern Australia
[AD-A147160] 07 p0935 N85-15921
The Air Force can improve its forecasts of aircraft spare parts requirements
[AD-A147911] 07 p1053 N85-16682
Estimating wartime support resource requirements. Statistical and related policy issues
[AD-A147923] 07 p1053 N85-16685
Operational requirements versus technological capabilities 08 p1072 N85-16798
Automatic briefing and mission management systems for battlefield support 08 p1073 N85-16799
Standard Attitude Heading Reference System (SAHRS) full scale development program
08 p1073 N85-16804
Integrated control and display systems for helicopter battlefield mission management
08 p1073 N85-16805
Evaluation of nose, roof, and mast mounted sensor platforms for piloting and sighting, integrated in future combat helicopters 08 p1074 N85-16808
Design of an evaluation system to measure performance degradation due to continuous operations
[AD-A148188] 08 p1200 N85-17558
Military applications of the Singer Link-Miles IMAGE visual system
[AD-P004337] 09 p1271 N85-17991
Assessment of environmental costs at ordnance activities
[AD-P004140] 09 p1347 N85-18476
Personnel protection concepts for advance escape system design 10 p1532 N85-19658
Space System Applications to Tactical Operations
[AGARD-CP-344] 11 p1709 N85-20751
Tactical operations and space applications
11 p1709 N85-20752
EHF MILSATCOM systems for tactical users
11 p1709 N85-20755
Tactical military communications by satellite relay at high latitudes 11 p1709 N85-20756
The Ferranti Tactical SHF SATCOM station (MANSAT) 11 p1710 N85-20759
Tactical satellite terminals for land and airborne C3 applications 11 p1710 N85-20760
The Global Positioning System (GPS): Program status update 11 p1710 N85-20761
Potential impact of Navstar GPS on NATO tactical operations 11 p1711 N85-20763
Tactical applications of GPS user equipment
11 p1711 N85-20765
Practical applications of satellite-derived meteorological and oceanographic data in Naval operations
11 p1712 N85-20771
Dual band radome wall design
[AD-P004357] 12 p1825 N85-21451
Base communications issues for the 1980s
[AD-A149764] 12 p1828 N85-21474
Statistics of french Armee de l'air ejections 1970 - 1980 12 p1906 N85-21971
Testing of the digital flight control system of the German CCV fighter experimental aircraft
13 p1968 N85-22361
SPARTEN (Scientific Program of Aerobic and Resistance Training Exercise in the Navy): A total body fitness program for health and physical readiness
[AD-A150669] 14 p2366 N85-24711
Exercise-heat strain during hypohydration: Interaction with heat acclimation and aerobic fitness
[AD-A151023] 14 p2389 N85-24717
Nutritional criteria for military rations and effects of prolonged feeding on acceptability
14 p2394 N85-24742
Fiber optics applications for MIL-STD-1760
[AD-A151113] 15 p2470 N85-25251
A database design for the Brazilian Air Force Flying Unit Operational Control System
[AD-A151848] 15 p2666 N85-26452
The evolution of active control technology systems for the 1990's helicopter 16 p2715 N85-26756
US said to seek military advantage in space
16 p2727 N85-26831
Military journal on US intelligence satellites
16 p2727 N85-26832
Development of a persistent chemical agent simulation system
[NASA-CR-175780] 16 p2745 N85-26937
The NAVTAG (Naval Tactical Game) system and its modification to include the SH-60B helicopter
[AD-A152004] 16 p2858 N85-27624
A Dictionary-Directory System (DDS) for the SPLICE system
[AD-A152223] 16 p2878 N85-27759
Soviet space programs, 1976-1980 (with supplementary data through 1983). Part 3: Unmanned space activities
[S-PRT-98-235-PT-3] 16 p2879 N85-27765
Future of V/STOL aircraft systems: A survey of opinions
[NASA-TM-86689] 18 p3061 N85-28937
US restrictions on technology transfer reviewed
18 p3088 N85-29115
Introduction to European air traffic control
[AD-A156328] 24 p4062 N85-35176
A guide to USAF helicopter instrument flight procedures
[AD-A156102] 24 p4063 N85-35182
RAFTS: A T-38 replacement for the 21st century
[AD-A156103] 24 p4065 N85-35191
Next generation gunship
[AD-A156361] 24 p4065 N85-35193
Air university commander's and supervisor's guide on substance abuse
[AD-A156336] 24 p4133 N85-35622

MILITARY SPACECRAFT
NT DMSP SATELLITES
NT RECONNAISSANCE SPACECRAFT
NT VELA SATELLITES
Autonomous navigation of USAF spacecraft
03 p0321 N85-12074
Planning for the on-orbit servicing of military spacecraft
[AD-A148447] 09 p1104 N85-16983
US MILSATCOM: Present and future
11 p1709 N85-20753
UK Skynet 4 communications satellites
11 p1710 N85-20757
Minimization of system vulnerability in Naval satellite communication networks 11 p1710 N85-20758
Militarization of space activity in United States
15 p2468 N85-25360
New ESA director on space station, military space
18 p3066 N85-28962

MILITARY TECHNOLOGY
Directed energy missile defense in space
[PB84-210111] 01 p0015 N85-10095
Frequency stabilized laser
[AD-D011223] 01 p0053 N85-10351
The application of artificial intelligence to a maintenance and diagnostic information system
[AD-P003945] 02 p0249 N85-11625
Air Force Materials Laboratory plans/projects
[AD-P004010] 03 p0308 N85-11990
Field applications for robotic material handling
[AD-P004016] 03 p0309 N85-11995
Wideband integrated voice/data technology
[AD-A146054] 03 p0355 N85-12283
Naval surface weapons center technology transfer report (FY83)
[AD-A146501] 06 p0871 N85-15534
Laser R and D in the armed services
[AD-A146930] 07 p0970 N85-16161
Documentation and separate test program development is most important for test/maintenance
08 p1065 N85-16745
Helicopter Guidance and Control Systems for Battlefield Support
[AGARD-CP-359] 08 p1072 N85-16797
The changing vibration simulation for military ground vehicles 09 p1334 N85-18367
A rig for testing the soft soil performance of track systems
[AD-P004272] 09 p1405 N85-18848
Technical evaluation report on the 46th Symposium of the Avionics Panel on Space System Applications to Tactical Operations
[AGARD-AR-203] 10 p1425 N85-19068
Narrowband spread spectrum systems
10 p1475 N85-19307
Tire deflation mechanism
[AD-D011460] 10 p1493 N85-19427
Phenomenology of microwave coupling, part 1
[DE85-003097] 11 p1624 N85-20229
Symposium on Military Aviation Medicine summarized
11 p1696 N85-20663
U.S., Soviet space program aims contrasted
13 p1965 N85-22455
Low-bit rate speech encoders based on Line-Spectrum Frequencies (LSF)
[AD-A150518] 13 p2056 N85-22871
Current approaches for the biophysical and physiological evaluation of combat clothing for environmental extremes
[AD-A151012] 14 p2395 N85-24752
Some critical factors that limit the effectiveness of machine intelligence technology in military systems applications
[AD-A150684] 14 p2407 N85-24838
Artificial intelligence applications to testability
[AD-A150694] 14 p2407 N85-24839
Personal computer aided decision analysis
[AD-A151911] 16 p2875 N85-27743
Science and Technology in the Soviet Union
[AD-A152828] 17 p3047 N85-28856
Soviet weapons development and the scientific community
[AD-P004562] 17 p3047 N85-28857
Technology and technical efficiency in the Soviet Union: Dominant patterns of constrained optimization in a noncompetitive economic regime
[AD-P004567] 17 p3048 N85-28862
The revolution in military affairs and the Soviet system
[AD-P004568] 17 p3048 N85-28863
Program Manager: The journal of the defense systems management college, volume 14, number 2, March-April 1985
[AD-A154219] 20 p3540 N85-32031
Meteorological weapons
[AD-A154735] 21 p3635 N85-32575
Air Force Office of Scientific Research (AFOSR). Technical report summaries: First quarter (CY)
[AD-A154757] 21 p3713 N85-33041
Military hydrology. Report 9: State-of-the-art review and annotated bibliography of dam-breach flood forecasting
[AD-A155363] 22 p3801 N85-33553
Proceedings of the 14th Army Science Conference. Volume 2: Principal authors I through O
[AD-A149201] 24 p4144 N85-35690
Proceedings of the 14th Army Science Conference. Volume 3: Principal authors P through Z
[AD-A149202] 24 p4144 N85-35691

MILKY WAY GALAXY
Constraints to the radiative lifetime of a light neutral fermion in the galactic halo from IUE
[NOTA-INTERNA-817] 02 p0279 N85-11820
Distribution and properties of molecular clouds in the galaxy 03 p0442 N85-12810
The number and distribution of molecular clouds in the inner galaxy 03 p0442 N85-12811
IRAS observations of galactic star formation
03 p0442 N85-12813
A large scale height galactic component of the diffuse 2-60 keV background
[NASA-TM-83637] 03 p0446 N85-12841
Cosmic ray propagation in the local superbubble
[NASA-TM-85030] 03 p0449 N85-12855
Far-infrared line emission from the galaxy
[NASA-CR-174166] 04 p0580 N85-13702
Local galactic kinematics 05 p0741 N85-14765
Molecular clouds within 100 pc
06 p0877 N85-15573

A wide latitude CO survey of molecular clouds in the northern Milky Way
08 p0877 N85-15574
Dark cloud and globule distribution for galactic longitudes 230 to 360 degrees
08 p0878 N85-15575
The z-dependence of the spin temperature of HI
08 p0878 N85-15580
The galaxy scene and QUASAT — VLBI satellite
07 p1056 N85-16703
Airborne Astronomy Symposium. A symposium commemorating the tenth anniversary of operations of the Kuiper Airborne Observatory
[NASA-CP-2353] 08 p1244 N85-17848
Far infrared observations of molecular clouds in the outer galaxy
08 p1247 N85-17869
Far infrared continuum emission from the galactic center
08 p1248 N85-17876
The 157 micron (C II) luminosity of the galaxy
08 p1248 N85-17877
Variation of oxygen and nitrogen abundances in the galaxy
08 p1248 N85-17878
The color excesses of classical cepheids and the structure of our galaxy
13 p2169 N85-23459
The structure of galactic HI in directions of low total column density
[NASA-CR-175709] 16 p2882 N85-27785
A high energy X-ray study of the galactic center
[AD-A153652] 18 p3202 N85-29662
The 6.3 and 12.4 micron imaging of the Galactic Center source complex with the Goddard infrared array camera
[NASA-TM-86225] 19 p3382 N85-30962
Cosmic-ray transport in the galactic magnetosphere
[OG-7.2-17] 23 p4016 N85-34884

MILLIMETER WAVES

Atmospheric channel performance measurements at 10 to 100 GHz
[PB84-211325] 01 p0042 N85-10271
Scattering from snow backgrounds at 35, 98, and 140 GHz
[AD-A145798] 03 p0355 N85-12280
Modeling rain polarization effects to millimeter wave frequencies
[PB84-231042] 03 p0357 N85-12296
Millimeter-wave propagation and remote sensing of the atmosphere
[AD-A146339] 03 p0393 N85-12512
Anglo-German millimeter wave backscatter measurements on snow, environmental data report
[REPT-7-84] 04 p0492 N85-13136
Implementing waveguide bandwidth six-port reflectometer circuits at millimetric wavelengths
[RSRE-MEMO-3678] 04 p0495 N85-13155
The UK and Netherlands millimetre-wave telescope — Netherlands (NL)
05 p0625 N85-14003
A new leaky wave antenna for millimeter waves based on the groove guide
[AD-A146428] 06 p0799 N85-15102
Millimeter-wave travelling-wave IMPATT diode
[AD-A146545] 06 p0804 N85-15117
Interface structures for millimeter-wave circuits
[AD-A146557] 06 p0804 N85-15118
MMIC devices for active phased array antennas
[NASA-CR-174281] 07 p0938 N85-15843
A quasi-optical method for measuring the complex permittivity of materials
[AD-A147483] 07 p0941 N85-15966
Investigation of planar waveguides and components for millimeter-wave integrated circuits
[AD-A147390] 07 p0948 N85-16005
Low-loss flexible dielectric waveguide for millimeter-wave transmission and its application to devices
[AD-A147846] 07 p0948 N85-16006
Development of a 30 GHz/1 kW broadband traveling wave tube with suppression of band edge oscillations
[BMFT-FB-W-84-035] 07 p0948 N85-16011
Rippled-field magnetron apparatus
[AD-D011354] 07 p0969 N85-16154
A new free electron laser using a relativistic beam with spiralling electron
[AD-D011318] 07 p0971 N85-16165
Millimeter wave antenna technology
[AD-A148694] 08 p1156 N85-17291
Multi-spectral observations of the star formation: The role of far infrared photometry
08 p1245 N85-17859
Instrumentation for submillimeter polarimetry
08 p1250 N85-17869
High power millimeter-wave mode converters in overmoded circular waveguides using periodic wall perturbations
[IPF-84-6] 09 p1305 N85-18780
Advanced artificial dielectric materials for millimeter wavelength applications
[AD-A148960] 10 p1431 N85-19027
An electronically controlled array for simulation of passive target/background signatures at millimeter wavelengths
[AD-D011456] 10 p1468 N85-19263
Effective millimeter wave transmission under severe multipath conditions
10 p1475 N85-19308
Image line voltage controlled oscillator with replaceable components
[AD-D011436] 10 p1479 N85-19333
An integrated varactor tuned coaxial gunn oscillator for 60 GHz operation
[AD-D011439] 10 p1479 N85-19335
Virtual cathode oscillator study
[AD-A149268] 10 p1480 N85-19342
Millimeter wave dielectric property measurement of gyrotron window materials
[DE85-004430] 12 p1802 N85-21304
Study of laminated dielectric behavior at microwave and millimeter-wave frequencies
[AD-P004358] 12 p1825 N85-21452
A millimeter wave apparatus for free-space measurement of dielectric constants at high temperatures
[AD-P004361] 12 p1826 N85-21455
Design and calibration of a 35GHz dielectrometer
[AD-P004363] 12 p1826 N85-21457
Exploration of new methods to produce efficient sources of coherent near millimeter wave radiation
[AD-A150094] 12 p1829 N85-21481
Effect of space-charge field on output characteristics of O-type oscillators with distributed interaction
13 p2089 N85-23043
Millimeter-wave diffraction devices and materials
[AD-A150876] 14 p2418 N85-24617
Monolithic planar doped barrier limiter
[AD-D011578] 15 p2548 N85-25723
Microwave emission from relativistic electron beams
[AD-A151472] 15 p2648 N85-26333
EHF attenuation derived from emission temperatures in light rain
[AD-A151166] 16 p2772 N85-27110
Calibration methods in millimeter-wave radioastronomy
[INPE-3481-PRE/724] 16 p2881 N85-27778
Radiometer integrated into a communication terminal
[AD-A151746] 17 p2947 N85-28195
A transport theory of millimeter wave propagation in woods and forests
[AD-A151883] 17 p2947 N85-28196
High precision materials characterization in the near millimeter wave-length range
[AD-A153267] 17 p2968 N85-28331
Communications and logic systems at millimeter wave frequencies
[NASA-CR-175859] 17 p3042 N85-28824
An evaluation and preparation of ferromagnetic liquid composites for use at millimeter wavelengths
[AD-A153039] 18 p3058 N85-28960
Some further aspects of the influence of raindrop-size distributions on millimeter-wave propagation
[PB85-168334] 18 p3092 N85-29138
Two-degree-of-freedom linear and planar microwave array lenses
[AD-A153701] 18 p3095 N85-29156
Atmospheric probing by active millimeter wave system
[AD-A153550] 18 p3136 N85-29422
Experimental and theoretical investigation of microwave and millimeter wave radiation from hollow, rotating electron beams
[AD-A153627] 18 p3179 N85-29706
Millimeter wave generation by relativistic electron beams
[AD-A153980] 18 p3179 N85-29708
A comparison of millimeter wave, direct detect and heterodyne laser intersatellite links
[AD-A151964] 20 p3461 N85-31496
Millimetre wave pulse technology — satellite mapping
[ESA-CR(P)-2004] 20 p3478 N85-31611
A multiplying slot array
[AD-A155670] 21 p3576 N85-32245
Effects of hydrometeors on electromagnetic wave propagation
[AD-A155379] 22 p3759 N85-33297
Examination of anisotropic films by resonance method
22 p3778 N85-33412
Strongly coupled millimeter-band waveguide directional couplers
22 p3779 N85-33418
Waveguide dielectric millimeter band filter with enhanced selectivity
22 p3780 N85-33421
An experimental study of dielectric rod antennas for millimeter-wave imaging applications
[AD-A155832] 24 p4086 N85-35328
Millimeter-wave propagation in moist air: Model versus path data
[AD-A156040] 24 p4087 N85-35331

MILLING (MACHINING)

Manufacturing methods for microwave circuits
[AD-A145237] 01 p0043 N85-10278
Structural changes during milling of aluminum oxide powders
[NASA-TM-77486] 04 p0472 N85-13008
Electropulse chemical machining
[DE84-016693] 04 p0484 N85-13084
Inclusion formation during solidification of steels with improved machinability
[BMFT-FB-T-84-160] 05 p0619 N85-13957
Technology reports of the Yamaguchi University, volume 3, no. 3
[ISSN-0388-3493] 09 p1302 N85-18182
Method of testing carbide inserts for premature fracture by face milling of cylindrical workpieces
09 p1303 N85-18183
Flexible manufacturing system for machining axially symmetric workpieces
[PNR-90229] 09 p1305 N85-18196
Factors influencing the ball milling of Si3N4 in water
[NASA-TM-86932] 10 p1450 N85-19136
Parametric evaluation of ball milling of SiC in water
[NASA-TM-86974] 12 p1811 N85-21956
Milling of spherical zones in parts
14 p2286 N85-24041
Milling machine with numerical programmed control for cutting teeth
14 p2286 N85-24052
Re-designing a mechanism for higher speed: A case history from textile machinery
23 p3923 N85-34310
Method for measuring surface activity of silicon nitride powder
[NASA-TM-77906] 24 p4073 N85-35242

MILLING (MIXING)

U COMPOUNDING

MILLING MACHINES

New tooling for plasma cutting technology
13 p2051 N85-22942
T700 cutter life improvement program
[AD-A150450] 13 p2089 N85-23089
Microstructure and mechanical properties of rare-earths-microalloyed high-speed tool steel
[BLL-BISI-TRANS-22043-(9022.06)]
17 p2928 N85-28084
The application of numerical control (NC) in manufacturing wind tunnel models
[B8580078] 17 p2939 N85-28140

MIM (SEMICONDUCTORS)

EMC (Electromagnetic compatibility) spec criteria in Voltaire systems
[AD-A147859] 08 p1151 N85-17269

MIM DIODES

Research and developmental study on MIS thin film solar cells of amorphous hydrogenated silicon, part 2
[BMFT-FB-T-84-290] 17 p2968 N85-28467

MINE DETECTORS

The PINGUIN B3: A remotely piloted vehicle for mine identification and disposal
[MBB-UM-1/84-O] 16 p2874 N85-27735

MINERAL DEPOSITS

International strategic minerals inventory. Summary report: Manganese
[GS-CIRC-930-A] 02 p0219 N85-11442
Petrology and genesis of carbonate-hosted Pb-Zn-Ag, San Cristobal District, Department of Junin, Peru
03 p0389 N85-12487
Lacustrine and eolian deposits of Wisconsin age at Riverside Bluff in the upper Tanana River valley, Alaska
04 p0517 N85-13289
Geology and geochemical evolution of the Lost River, Alaska, tin deposit
04 p0533 N85-13405
Alabama Tin Belt: Metallogenesis and mineral resource evaluation. Year-end report
[DE84-001335] 07 p0969 N85-16283
Geology of the Batopilas mining district, Chihuahua, Mexico, volumes 1 and 2
09 p1351 N85-18498
Types of placer formation of eastern Arctic shelf
10 p1498 N85-19452
Silver metallogeny in Earth's Pacific Ocean segment
10 p1498 N85-19455
Relationship of gold content to gravity fields in Far East
10 p1501 N85-19475
Geological reasons for change in intensity of linear magnetic anomalies of the Kursk magnetic anomaly
[NASA-TM-77824] 10 p1514 N85-19552
Radioactive waste isolation in salt: Peer review of the Office of Nuclear Waste Isolation's report on the organic geochemistry of deep groundwaters from the Palo Duro Basin, Texas
[DE85-001439] 10 p1558 N85-19811
LANDSAT 4 investigations of Thematic Mapper and Multispectral Scanner applications — Drum Mountains, Utah and Tonopath, Nevada
[E85-10095] 12 p1874 N85-21757
Geologic utility of LANDSAT-4 TM data — Death Valley, California and the Silver Bell area of southern Arizona
13 p2118 N85-23192
Characteristics of alunyte deposits discussed
13 p2166 N85-23438

Technical and cost analyses of manganese nodule processing techniques and their significant variations
[PB85-148615] 14 p2258 N85-23992
Gigantic lithium deposit discovered in France
14 p2269 N85-24184
Influence of phosphorus content and heat treatment on the machinability of electroless nickel deposits
[DE85-007250] 15 p2522 N85-26548
Nd-isotopic evidence for the origin of the Sudbury complex by meteoritic impact 15 p2680 N85-26554
Yearbook of the Bureau of Mineral Resources, Geology and Physics: Geoscientific research, resource assessment, and database development, 1 Jul. 1983 to 30 Jun. 1984
[BMR-84] 17 p2989 N85-28474
Ash contents of Costa Rican peat deposits
[DE85-010734] 19 p3301 N85-30462
Orphans of the Valley: Abandoned surface mines in the Tennessee Valley. Volume 2: Maps
[DE85-901249] 19 p3301 N85-30465
Petroleum and mineral resources of Antarctica
[US-GEOL-SURV-CIRC-909] 20 p3477 N85-31605
Comparative study of fracture planes computed from topography and lineaments from imagery with structures and mineralization in the magnetic belt of Washington State
[DE85-010972] 20 p3477 N85-31608
The U.S. Geological Survey in Alaska: Accomplishments during 1982
[US-GEOL-SURV-CIRC-939] 20 p3493 N85-31719
Geomorphology, tectonics, and exploration
21 p3601 N85-32365
Sulfur reduction in sediments of marine and evaporite environments 21 p3661 N85-32742
The United States Geological Survey in Alaska: Accomplishments during 1983
[USGS-CIRC-945] 23 p3948 N85-34468
USGS research on mineral resources, 1985
[CIRC-949] 24 p4103 N85-35435
Chemistry of ore-forming fluids
24 p4103 N85-35436
Aeromagnetic and radiometric signatures of a possible porphyry system in the western Tushar Mountains, Utah
24 p4103 N85-35437
Some geophysical guides to ore in southern and southwestern Alaska 24 p4103 N85-35438
Marine phosphorite deposits model for exploration, with emphasis on deposits in the US Atlantic coastal plain
24 p4104 N85-35439
The role of regional subsurface geochemistry in resource assessment in the central United States
24 p4104 N85-35440
Aeromagnetic and gravity models of the pluton below the Lake City caldera, Colorado
24 p4104 N85-35442
Origin of sedimentary humic acids, potential carriers of ore-forming elements 24 p4104 N85-35443
Cobalt-rich ferromanganese crusts in the oceans
24 p4104 N85-35444
New silver resource map of the United States: Potential for increased domestic silver production
24 p4105 N85-35445
Massive sulfide deposits from the southern Juan de Fuca Ridge 24 p4105 N85-35446
Gas analysis of ore-forming fluids
24 p4105 N85-35447
Mineral deposit models: Theory and practice
24 p4105 N85-35448
Expert systems research in regional resource evaluation: Experiences in the application of microcomputer technologies 24 p4105 N85-35450
Applications of the mineral resources data system and the international strategic minerals inventory in mineral-resource assessments by region and commodity
24 p4105 N85-35451
A comparison of LANDSAT thematic mapper, multispectral scanner and airborne sensors for mapping the distribution of alteration minerals: Examples from the southwestern United States 24 p4106 N85-35452
Some recent deposit modeling efforts
24 p4106 N85-35453
Processing of LANDSAT imagery to map surface mineral alteration on the Alaska Peninsula, Alaska
24 p4106 N85-35455
Mineral resources programs 24 p4106 N85-35456
The development of assessment techniques program
24 p4106 N85-35457
The Conterminous United States Mineral Assessment Program 24 p4106 N85-35458
Federal Mineral Land Information System
24 p4106 N85-35459
The Alaska Mineral Resources Assessment Program
24 p4107 N85-35460
Hydrogeology of the lower Glen Rose Aquifer, south-central Texas 24 p4108 N85-35466
Ore genesis at the Monterrosas deposit in the Coastal Batholith, Ica, Peru 24 p4115 N85-35510

MINERAL EXPLORATION

The feasibility of satellite remote sensing as a technique for evaluating coal mine surface features
02 p0213 N85-11401
Remote sensing as a mineral prospecting technique
[E85-10010] 02 p0216 N85-11423
Thematic mapping of likely target areas for the occurence of caselterite in the Serra do Mocambo (GO) granitic massifs using LANDSAT 2 digital imaging
[E85-10027] 02 p0219 N85-11440
Development of a method for exploring low-reflectance areas through the combined use of different geophysical methods taking the north-west German basin as an example
[BMFT-FB-T-83-180] 02 p0220 N85-11450
Methods for correlating geological, geochemical and geophysical data with satellite imagery in central Ireland
05 p0655 N85-14208
USSR report: Earth sciences
[JPRS-UES-84-008] 07 p0980 N85-16223
Maritime prospecting, mining discussed
07 p0980 N85-16226
Exploring ocean's mineral wealth
07 p0980 N85-16227
Microprocessors in geophysical instruments discussed
08 p1142 N85-17199
Analysis of SIR-B radar illumination of geometry for depth of penetration and surface feature and vegetation detection, Nevada and California
08 p1149 N85-17248
Depositional modeling of tetrahedrite in the Coeur d'Alene district, Idaho 08 p1182 N85-17448
Deep seabed stable reference areas
[PB84-241470] 09 p1360 N85-18555
Arctic-North Atlantic rift megasystem
13 p2105 N85-23117
Possibilities of aerial electric prospecting by long cable method for detecting poorly conducting strata
13 p2115 N85-23177
Evaluation of Thematic Mapper performance as applied to hydrocarbon exploration — Ontario, Canada; Cement, Oklahoma; and Death Valley, California
13 p2118 N85-23191
China report: Science and technology
[JPRS-CST-84-012] 14 p2283 N85-24140
Investigative report on using geological research to promote prospecting 14 p2283 N85-24142
Organizing geological work tasks for 1985 outlined
16 p2606 N85-27303
Comparative study of fracture planes computed from topography and lineaments from imagery with structures and mineralization in the magnetic belt of Washington State
[DE85-010972] 20 p3477 N85-31608
Geomorphology, tectonics, and exploration
21 p3601 N85-32365
Use of space photographs for analysis of structural and dynamic conditions of formation of ancient phlogopite and apatite deposits 22 p3735 N85-33153
USGS research on mineral resources, 1985
[CIRC-949] 24 p4103 N85-35435
Aeromagnetic and radiometric signatures of a possible porphyry system in the western Tushar Mountains, Utah
24 p4103 N85-35437
Some geophysical guides to ore in southern and southwestern Alaska 24 p4103 N85-35438
Marine phosphorite deposits model for exploration, with emphasis on deposits in the US Atlantic coastal plain
24 p4104 N85-35439
The role of regional subsurface geochemistry in resource assessment in the central United States
24 p4104 N85-35440
Aeromagnetic and gravity models of the pluton below the Lake City caldera, Colorado
24 p4104 N85-35442
Massive sulfide deposits from the southern Juan de Fuca Ridge 24 p4105 N85-35446
Gas analysis of ore-forming fluids
24 p4105 N85-35447
Mineral deposit models: Theory and practice
24 p4105 N85-35448
Early and middle Cenozoic volcanic synthesis
24 p4105 N85-35449
Mineral resources programs 24 p4106 N85-35456
The Conterminous United States Mineral Assessment Program 24 p4106 N85-35458
Federal Mineral Land Information System
24 p4106 N85-35459
The Alaska Mineral Resources Assessment Program
24 p4107 N85-35460

MINERAL METABOLISM

Effect of 1,25-dihydroxycholecalciferol and 24,25 dihydroxycholecalciferol on growth and alteration of rat bones during hypokinesa (histomorphometric study)
01 p0092 N85-10622
Alterations in gut transport of minerals and in binding proteins during simulated weightlessness
[NASA-CR-175537] 14 p2388 N85-24709
The role of vitamin D in the bone changes associated with simulated weightlessness 15 p2606 N85-26072
Changes in bone structure and metabolism during simulated weightlessness: Endocrine and dietary factors
[NASA-CR-175961] 18 p3153 N85-29521
Fluid-electrolyte metabolism and renal function in cosmonauts following 185-day spaceflight
23 p3952 N85-34495

MINERAL OILS

Characterization of erosion of metallic materials under cavitation attack in a mineral oil
[NASA-TM-86934] 10 p1440 N85-19075

MINERALOGY

Petrology and genesis of carbonate-hosted Pb-Zn-Ag, San Cristobal District, Department of Junin, Peru
03 p0389 N85-12487
Peculiar spherules from Antarctica and their origin
06 p0863 N85-15612
Hydrothermal alteration of CM carbonaceous chondrites: Implications of the identification of tochilinite as one type of meteoritic PCP 06 p0884 N85-15616
The mineralogy of global magnetic anomalies
[E85-10061] 07 p0987 N85-16272
Alabama Tin Belt: Metallogenesis and mineral resource evaluation. Year-end report
[DE84-901335] 07 p0989 N85-16283
A wind-tunnel study of the saltation of heterogeneous (size, density) sands 08 p1182 N85-17449
Mineralogical investigations of lunar samples and meteorites
[NASA-CR-174291] 08 p1258 N85-17918
Diagenesis of niagaran (middle silurian) pinnacle reefs, northwest Michigan 09 p1352 N85-18508
Research and development related to the Nevada nuclear waste storage investigations
[DE85-002303] 12 p1932 N85-22138
Characteristics of alumyte deposits discussed
13 p2166 N85-23438
The olivine asteroids: Discovery, mineralogy, and relationship to palasites 13 p2175 N85-23500
Crystal chemistry of meteoritic hibonites
13 p2185 N85-23556
Determining mineral types and abundances from reflectance measurements 13 p2196 N85-23622
Determination of mineral type, abundance, and grain size with remotely obtained reflectance spectra
13 p2196 N85-23623
Quantitative analyses of planetary reflectance spectra
13 p2197 N85-23625
Analysis of SMIRR data for volcanic and sedimentary terrains of the trans-Pecos region, Texas
13 p2197 N85-23626
Mineralogical-geochemical characteristics of ferromanganese formations in Arabian-Indian Ocean Ridge 19 p3293 N85-30416
Petrologic and geochemical characterization of the Topopah Spring Member of the Paintbrush Tuff: Outcrop samples used in waste package experiments
[DE85-010449] 19 p3302 N85-30470
Physical and chemical changes to rock near electrically heated boreholes at Spent Fuel Test-Climax
[DE85-010834] 19 p3302 N85-30472
Mineralogy and chemistry of the Earth
22 p3856 N85-33877

MINERALS

NT ASBESTOS
NT BERYL
NT BIOTITE
NT CALCITE
NT CHROMITES
NT DOLOMITE (MINERAL)
NT ENSTATITE
NT FELDSPARS
NT FLUORITE
NT GARNETS
NT GRAPHITE
NT IRON ORES
NT LIMONITE
NT MAGNETITE
NT MICA
NT OLIVINE
NT PEROVSKITES
NT PYRITES
NT PYROXENES
NT QUARTZ
NT SERPENTINE

NT SIDERITES
NT SPINEL
NT TROILITE
Operating experiences of reverse osmosis plants treating Rand Water Board (RWB) water: Pitfalls and problems 01 p0023 N85-10142
Compilation of elemental concentration data for NBS (National Bureau of Standards) biological, geological and environmental standard reference materials, 1982
[PB84-218336] 01 p0025 N85-10158
Mineral nutrients in Mediterranean ecosystems
[REPT-71] 01 p0069 N85-10456
Middle infrared spectral studies of geologic materials in their natural state using photothermal beam deflection spectroscopy
[AD-A144894] 01 p0120 N85-10820
The Alaskan mineral resources assessment program: Guide to information contained in the folio of geologic and mineral-resource maps of the Medfra Quadrangle, Alaska
[GS-CIRC-928] 02 p0219 N85-11443
Late oligocene gabbro near Ketchikan, southeastern Alaska 04 p0518 N85-13307
Atmospheric heating of meteorites: Results from nuclear track studies 06 p0882 N85-15607
A study of tetrataenite 06 p0885 N85-15623
Structural development in the Santa Catharina meteorite 06 p0886 N85-15625
New data on presence of ores in salt dome structures of Dnieper-Donets Basin 07 p0961 N85-16234
Geostatistics for resource and reserve estimation
[PB85-105761/GAR] 07 p0989 N85-16286
A study of structural phase transitions using light scattering techniques
[AD-A147261] 07 p1048 N85-16654
Depositional modeling of tetrahedrite in the Coeur d'Alene district, Idaho 08 p1182 N85-17448
Impact and collisional processes in the solar system
[NASA-CR-174297] 08 p1255 N85-17914
Evaluating the variability of ceramics with X-ray fluorescence
[DE85-002028] 10 p1453 N85-19155
Review of problems in lithology 13 p2113 N85-23160
Rapid advances in geological work 13 p2166 N85-23437
Characteristics of alunyte deposits discussed 13 p2166 N85-23438
Impact and collisional processes in the solar system 13 p2180 N85-23530
First direct detection of clay minerals on Mars 13 p2194 N85-23612
Iron oxides of Mars: Evidence for contemporary weathering 13 p2195 N85-23613
Zeolites on Mars: Prospects for remote sensing 13 p2195 N85-23615
Temperature anomalies above ore bodies 14 p2345 N85-24500
Hydrostatic compression of Fe1-chi O wustite. 15 p2508 N85-25472
Spectral reflectance of carbonate minerals and rocks in the visible and near infrared (0.35 - 2.55 microns) and its applications in carbonate petrology
[NASA-CR-175763] 15 p2501 N85-25973
Effects of temperature on remotely sensed mafic mineral absorption features 16 p2800 N85-27323
Review of national emission standards for mercury
[PB85-153906] 16 p2822 N85-27406
Process for clarification of water
[DE85-007864] 17 p2923 N85-28023
Space-flight simulations of calcium metabolism using a mathematical model of calcium regulation
[NASA-CR-171863] 19 p3328 N85-30621
Mineral aerosols and source identification 21 p3646 N85-32654
Microbial colonization and growth on metal sulfides and other mineral surfaces 21 p3662 N85-32747
The effects of prolonged feeding meal, ready-to-eat (MRE) operational rations
[AD-A154763] 21 p3666 N85-32773
Quantitative determination of mineral composition by powder X-ray diffraction
[DE85-011654] 22 p3760 N85-33301
Chemistry of ore-forming fluids 24 p4103 N85-35436

MINES (EXCAVATIONS)
Land use/land cover 02 p0214 N85-11410
Mapping land use changes in the carboniferous region of Santa Catarina, report 2
[E85-10017] 02 p0217 N85-11430
Interactive system for the interpretation of coal deposit data as a basis of future mine planning systems
[BMFT-FB-T-83-115] 02 p0220 N85-11449
Effect of lithology and climate on the morphology of drainage basins in northwestern Colorado
[PB84-228236] 06 p0828 N85-15258
Geology of the Batoplias mining district, Chihuahua, Mexico, volumes 1 and 2 09 p1351 N85-18498
Stability indicators for front end loaders
[AD-P004293] 09 p1408 N85-18870
Effect of water vapor and water droplets on the RAM-1 (Real-Time Aerosol Monitor): Preliminary results
[PB85-109429] 11 p1637 N85-20313
China report: Science and technology
[JPRS-CST-84-036] 11 p1696 N85-20661
Comparative techniques used to evaluate Thematic Mapper data for land cover classification in Logan County, West Virginia 13 p2121 N85-23209
Rapid advances in geological work 13 p2166 N85-23437
Development of a stationary carbon monoxide detector
[BMFT-FB-T-84-253] 18 p3134 N85-29413
Orphans of the Valley: Abandoned surface mines in the Tennessee Valley. Volume 2: Maps
[DE85-901249] 19 p3301 N85-30465
New silver resource map of the United States: Potential for increased domestic silver production 24 p4105 N85-35445
Regular synthesis of pairs of phase-keyed binary minimax signals 13 p2069 N85-22823
Federal Mineral Land Information System 24 p4106 N85-35459
The homestake surface-underground scintillations: Description
[HE-6.1-9] 24 p4210 N85-36135

MINIATURE ELECTRONIC EQUIPMENT
A miniature urethane molded acoustic transducer
[AD-A146459] 06 p0804 N85-15114
Miniature electrooptical air flow sensor
[NASA-CASE-LAR-13065-1] 11 p1635 N85-20295
A miniature tactical Rb frequency standard 16 p3106 N85-29229
Miniature infra-red data acquisition and telemetry system
[NASA-CR-177953] 24 p4096 N85-35390

MINIATURIZATION
NT MICROMINIATURIZATION
Microminiature coaxial cable and methods of manufacture
[DE84-014228] 01 p0044 N85-10284
Manufacturing Methods and Technology (MM/T) specifications for miniature cathode ray tube
[AD-A145597] 02 p0194 N85-11298
Guided-wave optic devices for integrated optic information processing
[AD-A145695] 02 p0260 N85-11827
Development of miniature laser Doppler anemometers
[KU-SFB-210/ET/3] 12 p1857 N85-21648
Miniature two-mode filters 22 p3775 N85-33394

MINICOMPUTERS
East Europe report: Science and technology
[JPRS-ESA-84-030] 01 p0101 N85-10670
Analysis of three database system architectures using benchmarks
[PB84-217512] 01 p0105 N85-10706
East Europe report, science and technology. Czechoslovakia: System of small electronic computers
[JPRS-ESA-84-040] 02 p0239 N85-11558
Use of minicomputers for the formation of hydrological data banks 07 p1001 N85-16358
Specifications of bloc floppy disk drives 08 p1141 N85-17188
Design and analysis of an access control system for a multi-backend database system
[AD-A148750] 09 p1367 N85-18586
Proposal for a small scheme implementation
[AD-A148707] 09 p1368 N85-18595
The integrated library system design concepts for a complete serials control subsystem
[AD-A149379] 10 p1568 N85-19884
Arithmetic and elementary functions on mini and microcomputers 14 p2396 N85-24761
Computer technology advances exhibited 15 p2625 N85-26175
Mini- and microcomputer local control network architecture and design principles 15 p2625 N85-26179
Management considerations for an information center
[AD-A151774] 16 p2875 N85-27742
Program DISAS: A computer program to obtain hard-copy plots of an image displayed on a vector graphics device in a local-area-network
[AD-A153643] 18 p3162 N85-29586
Visualization of computation results. Definition of a graphics satellite computer
[ONERA-RT-2/3587-CY] 20 p3514 N85-31845
Electronic file system on an SM 90 minicomputer: The SARDE project
[ENST-84E018] 22 p3828 N85-33705
User's operating procedures. Volume 3: Projects directorate information programs
[NASA-CR-177950] 23 p3956 N85-34520
Procedure for editing the fluxgate magnetometer data of the AFGL (Air Force Geophysics Laboratory) magnetometer network
[AD-A156331] 24 p4117 N85-35523
Optimize computer throughput using array processors
[AD-A155643] 24 p4135 N85-35628

MINIMAL SURFACES
Lectures on generalized solutions to the minimal surface equation
[DE84-016882] 05 p0722 N85-14642

MINIMAX TECHNIQUE
Minimax optimal control in the reentry of a space glider 02 p0167 N85-11124
Nonlinear regression with emphasis on spline methods
[AD-A146192] 03 p0412 N85-12833
An H-infinity-minimax approach to the design of robust control systems
[OUEL-1537/84] 05 p0717 N85-14600
Minimax multiple t-tests for comparing k normal populations with a control
[AD-A148306] 08 p1215 N85-17858
On maximizing the expected lifetime of replaceable systems
[AD-A150003] 12 p1682 N85-21680

MINIMIZATION
U OPTIMIZATION

MINIMUM ENTROPY METHOD
An overview of latest model reduction and control methods of large flexible space structures 20 p3414 N85-31191

MINIMUM VARIANCE ORBIT DETERMINATION
Satellite orbit determination 05 p0698 N85-13813
Heliosynchronism and phasing. Application to the SPOT orbit 05 p0800 N85-13826
Orbit reconstitution — satellite orbits 14 p2396 N85-24786

MINING
Geostatistics for resource and reserve estimation
[PB85-105761/GAR] 07 p0989 N85-16286
China report: Science and technology
[JPRS-CST-85-003] 13 p2166 N85-23438
Rapid advances in geological work 13 p2166 N85-23437
Technical and cost analyses of manganese nodule processing techniques and their significant variations
[PB85-148615] 14 p2258 N85-23892
Gigantic lithium deposit discovered in France 14 p2299 N85-24184
Mining cosmic dust from the blue ice lakes of Greenland 15 p2682 N85-26583
An analysis of alternate hydrogen sources for lunar manufacture
[DE85-007234] 16 p2884 N85-27792
Shuttle car loading system
[NASA-CASE-NPO-16949-1] 23 p3967 N85-34722

MINIVAR ORBIT DETERMINATION
U MINIMUM VARIANCE ORBIT DETERMINATION

MINKOWSKI SPACE
Special relativity of Kaluza-Klein
[DE85-007839] 17 p3048 N85-28947

MINOR PLANET 1221
U AMOR ASTEROID

MINORITIES
Companies participating in the Department of Defense Subcontracting Program, first three quarters fiscal year 1984
[AD-A146137] 03 p0436 N85-12775
NASA initiatives with historically black colleges and universities
[NASA-EP-210] 19 p3379 N85-30960

MINORITY CARRIERS
Studies in electron phenomena in MOS structures: The pulsed C-V method 15 p2659 N85-26407
High efficiency large area polysilicon solar cells 20 p3482 N85-31639
High-purity silicon crystal growth 21 p3612 N85-32444

MINUTEMAN ICBM
An analysis of the technical training of enlisted minuteman missile maintenance personnel
[AD-A147078] 07 p0912 N85-15775

MINUTEMAN MISSILES
U MINUTEMAN ICBM

MIRAGE AIRCRAFT
NT MIRAGE 3 AIRCRAFT
Aeroelastic analysis and the identification of flight loads — Mirage 2000 aircraft 07 p0896 N85-15679

Map display for helicopters 08 p1073 N85-16801
A comparison of fatigue lives under a complex and a much simplified flight-by-flight testing sequence — Mirage 3 aircraft
[ARL/STRUC-TM-388] 09 p1280 N85-18052
Unsteady aerodynamic characterization of a military aircraft in vertical gusts
[NASA-TM-77810] 12 p1770 N85-21110
Calculation of unsteady transonic flow around a high swept wing 15 p2459 N85-25184

MIRAGE 3 AIRCRAFT
Fatigue crack propagation in mirage 1110 wing main spar specimens and the effects of spectrum truncation on life
[ARL/STRUC-R-405] 12 p1776 N85-21152
Tensile and fracture toughness properties of Mirage III spars
[AR-003-019] 15 p2578 N85-25899
Further investigations to improve the fatigue life of the Mirage 1110 wing main span
[ARL/STRUC-TM-397] 16 p3061 N85-28058

MIRANDA SATELLITE
Satellite masses in the Uranus and Neptune systems
[PSI-CONTRIB-196] 02 p0301 N85-11947

MIRROR FUSION
Theoretical studies in tandem mirror physics
[DE84-016634] 04 p0566 N85-13604
Fusion plasma theory. Task 3: ECRH and transport modeling in tandem mirrors and divertor physics
[DE84-014939] 04 p0567 N85-13612
EBT electron energy confinement experiments
[DE84-015402] 04 p0567 N85-13613
Stabilization of the hot electron precessional mode in a symmetric tandem mirror by the axial variation of radial electric field
[DE84-016389] 05 p0730 N85-14692
Theoretical investigations relevant to magnetic fusion research, April 1, 1983 - March 31, 1984
[DE85-001778] 06 p0665 N85-15498
Special topics reports for the reference tandem mirror fusion breeder: Liquid metal MHD pressure drop effects in the packet bed blanket, volume 1
[DE85-002142] 06 p0665 N85-15500
Long-pulse beamlines for the mirror fusion test facility
[DE84-017091] 09 p1302 N85-18760
Heat transfer and mechanical interactions in fusion nuclear systems
[DE84-016233] 09 p1302 N85-18761
Electronics Engineering Department: EE technical review
[DE85-004360] 11 p1629 N85-20259
Mirror fusion progress
[DE85-001187] 11 p1731 N85-20868
Plasma-wall interactions in tandem mirror machines
[DE85-006887] 15 p2657 N85-26399
Stability of high energy particle plasmas to MHD-like modes
[DE85-007670] 17 p3039 N85-28803
An Impurity Control Test Facility (ICTF) for the study of fusion reactor/plasma edge materials
[DE85-007946] 17 p3040 N85-28810
Energy and Technology Review
[DE85-004358] 17 p3049 N85-28868
Physics-magnetics trade studies for tandem mirror reactors
[DE85-010043] 18 p3182 N85-29732
Test cell modeling and optimization for FPD-2
[DE85-010536] 19 p3358 N85-30821
Stability of a hot symmetric tandem mirror with thermal barrier
[DE85-010539] 19 p3377 N85-30952
Neutronics activities for next generation devices
[DE85-010488] 20 p3527 N85-31939
Modeling and optimization of a test-cell upgrade for MFTF-B operating in the high neutron wall loading mode
[DE85-009997] 20 p3528 N85-31946
Simulation of automatic control of MFTF-B neutral beams
[DE85-010640] 20 p3530 N85-31960
Energy and Technology Review
[DE85-011787] 21 p3716 N85-33061
Proceedings of the US-Japan Workshop on Transport in Open-Ended Systems
[IPPJ-727] 23 p3975 N85-34644
Plug and thermal barrier potential formation in Gamma 10 23 p3976 N85-34648
RF induced radial diffusion in tandem mirrors 23 p3976 N85-34649
Induced azimuthal electric field effects on tandem transport and ambipolarity 23 p3976 N85-34650
Recent experiments in Gamma-10 23 p3976 N85-34651
Radial transport caused by collision 23 p3976 N85-34652
Transport issues in Phaedrus-type plasmas 23 p3976 N85-34653
Possibility of potential generation by lower hybrid wave 23 p3977 N85-34654
Bounce resonance heating and radial transport of electrons 23 p3977 N85-34655
Electron dynamics and transport in a mirror field 23 p3977 N85-34656
Low frequency instability in a mirror field 23 p3977 N85-34657
Model of azimuthal non-uniformities induced by RF heating in RFC-XXM 23 p3977 N85-34658
Azimuthal uniformity and current balance study of ICRH-produced plasma in RFC-XXM 23 p3977 N85-34659
Advanced Toroidal Facility (ATF)
[DE85-011567] 23 p3983 N85-34699
Perspective on the next ten years in plasma physics
[DE85-011849] 23 p3984 N85-34706
Analysis of a pulsed power system containing rotating machine
[DE85-014128] 24 p4159 N85-35786

MIRRORS
NT FRESNEL REFLECTORS
NT MAGNETIC MIRRORS
NT PARABOLOID MIRRORS
NT ROTATING MIRRORS
Parameters of geometric stability of laser mirror optical surface 02 p0273 N85-11777
Development of a measuring procedure for the automatic evaluation of the flatness of reflective surfaces
[BMFT-FB-T-84-168] 03 p0421 N85-12688
Dynamic testing of NOVA laser switchyard tower
[DE84-014450] 05 p0640 N85-14103
Cleaning procedures of laser mirror substrates
[DFVLR-MITT-84-06] 05 p0640 N85-14108
Design of two-mirror scanner with axes of rotation not in plane of mirrors 06 p0777 N85-14989
High energy laser mirror
[AD-D011255] 06 p0812 N85-15156
Dual-secondary mirror Cassegrain optical system
[AD-D011273] 06 p0862 N85-15478
Plasma-surface interactions in large tandem mirror devices, MFTF-B
[DE85-001753] 06 p0665 N85-15499
Theoretical investigations relevant to magnetic fusion research
[DE85-001777] 06 p0666 N85-15503
Evaluation of colorless polyimide film for thermal control coating applications
[NASA-TM-86341] 07 p0930 N85-15894
Reverse wave suppression in unstable ring resonator
[AD-A146825] 07 p0939 N85-15952
Unstable optical resonator with cancelling edge waves
[AD-D011379] 07 p1042 N85-16618
Mirror actuator control system
[AD-D011383] 07 p1042 N85-16619
Light scattered from polished optical surfaces: Wings of the point spread function 08 p1252 N85-17911
Calculation and computer simulation of the Paraboloidal Mirror Analyzer (PMA)
[DE85-001417] 09 p1364 N85-18705
Reflectivity measurements of laser gyro mirrors
[ESA-TT-851] 09 p1366 N85-18714
Procedures for the bonding of the E.M.C. mirror onto its INVAR mirror flange — United Kingdom Infrared Telescope
[UKIRT-19] 09 p1414 N85-18917
In situ washing procedures for the UKIRT 3.8 meter primary mirror — United Kingdom Infrared Telescope (UKIRT)
[UKIRT-20] 09 p1414 N85-18918
Temperature variation of laser mirror stability criteria 10 p1445 N85-19106
Fine figuring actuator
[AD-D011476] 10 p1557 N85-19819
Solar optical telescope primary mirror controller
[NASA-CR-174416] 10 p1570 N85-19903
Characteristics of unstable resonators in flashlamp-pumped organic-compound lasers 11 p1717 N85-20800
Four-wave hypersonic reversing mirrors in saturated mode 11 p1719 N85-20812
Optimization of piezoceramic optical deflector 11 p1719 N85-20813
Wide-angle flat field telescope
[NASA-CASE-GSC-12625-1] 11 p1728 N85-20868
An analysis of the high frequency vibrations in early Thematic Mapper scenes 12 p1872 N85-21742
Three-mirror open resonator for millimeter wave band 13 p2077 N85-22972
ROSA: A computer model for optical power ratio calculations
[DE85-005174] 13 p2129 N85-23251
Innovative research in the design and operation of large telescopes for space: Aspects of giant telescopes in space
[NASA-CR-175826] 13 p2170 N85-23462
Measurement of sensitivity of shadowgraphic instruments with spherical autocollimating mirror 14 p2274 N85-24087
Multilayer reflecting systems based on glassy chalcogenides for infrared lasers 14 p2274 N85-24089
Determining optimum service conditions for concentrator mirrors by methods of mathematically planned experiment 14 p2274 N85-24090
Vibration isolator actuator
[AD-D011574] 14 p2321 N85-24343
Angular error of position of RATAN-600 screens during radial displacement 15 p2476 N85-25286
Mirror accessory for line straightening in diffraction spectrometers 16 p2764 N85-27054
Software for reflectivity calculations of X-ray mirrors, revision 1
[DE85-006842] 16 p2967 N85-27688
Downdraw extrusion of ULE(TM) glass
[AD-A153763] 16 p3079 N85-29048
Thin layered interference mirrors to reduce radiation damage
[DE85-009763] 16 p3185 N85-29756
Optically bistable devices using InSb 16 p3186 N85-29758
Deformable mirror nearest neighbor optical computer 16 p3188 N85-29772
Optically pumped laser system having extracavity pulse smoother
[AD-D011714] 19 p3276 N85-30319
Measurements of folded path optical scintillation using a corner cube, a cat's eye and a flat mirror reflector
[AD-A154044] 19 p3367 N85-30879
Silicon nitride protective coatings for silvered glass mirrors
[DE85-011637] 20 p3433 N85-31300
Influence of mirror anisotropy and Brewster window orientation on radiation characteristics of ring lasers 21 p3684 N85-32680
Mirror reflection of charged particles from +amorphous and polycrystalline surfaces 21 p3690 N85-32927
Comparison of findings of theories describing reflection from real surface with experiments in region of ultrasoft X-radiation 21 p3694 N85-32950
Dielectric mirror with ferromagnetic substrate 21 p3696 N85-32956
Mean intensity of wave reflected by wavefront reversing mirror in turbulent medium 22 p3782 N85-33432
Method of bonding silver to glass and mirrors produced according to this method
[DE85-011642] 22 p3792 N85-33495
Electron and ion cyclotron heating calculations in the tandem-mirror
[DE85-011658] 22 p3842 N85-33797
Role of ECRH in potential formation for tandem mirrors
[DE85-011659] 22 p3848 N85-33834
Effect of ECH and ICH on ambipolar potential in NBT-1M 23 p3978 N85-34661
Fokker-Planck calculation of hot electron formation in the thermal barrier region of tandem mirror Gamma-10
[IPPJ-726] 23 p3979 N85-34669
A method to improve observations of gamma-ray sources near 10 (15) eV
[OG-9.5-5] 23 p4030 N85-34982
Single-point diamond crushing of Zerodur with in-situ polishing and metrology on a diamond turning machine
[DE85-012918] 24 p4083 N85-35305
A normal incidence X-ray telescope sounding rocket payload
[NASA-CR-176169] 24 p4153 N85-35749

MIS (SEMICONDUCTORS)
Novel techniques for the fabricating and characterization of GaAs MIS (Metal Insulator Semiconductor) structures
[AD-A145766] 03 p0358 N85-12301
Aluminum nitride insulator for 3-5 MIS (Metal-Insulator-Semiconductor) applications
[AD-A147842] 07 p1049 N85-16662

MISALIGNMENT
Gyrodynamic fixture for measuring thrust force components
[AD-D011258] 08 p0760 N85-14860
Study of energy versus misorientation for grain boundaries in gold by crystallite rotation method. 1: 001 twist boundaries
[DE85-004598] 12 p1943 N85-22201
Dependence of properties of optical cavity on misalignment 14 p2276 N85-24099

MISCIBILITY
U SOLUBILITY

MISFETS
U FIELD EFFECT TRANSISTORS

MISMATCH (ELECTRICAL)
Nonlinearity and spectral mismatch problems of solar cells 13 p2010 N85-22605
MISORIENTATION
U MISALIGNMENT
MISS DISTANCE
Methodology improvement program for the second generation miss distance radar (MIDI 2)
[AD-A148467] 08 p1153 N85-17281
MISSILE ANTENNAS
Hardwire missile receiver coupler
[AD-D011350] 07 p0937 N85-15936
Dual mode radio frequency-infrared frequency system
[AD-D011402] 08 p1081 N85-16850
MISSILE BODIES
Empirical formulas for the prediction of the base pressure of missile bodies at subsonic velocities
[DFVLR-FB-84-23] 03 p0316 N85-12044
Empirical formulas for the prediction of the base pressure of missile bodies at subsonic velocities
[ESA-TT-893] 20 p3399 N85-31082
Flow modeling at the base region of missiles
[SNIAS-851-320-101] 20 p3420 N85-31228
MISSILE CASES
U MISSILE BODIES
MISSILE COMPONENTS
NT MISSILE ANTENNAS
NT MISSILE BODIES
Zero adhesion system
[AD-D011237] 01 p0015 N85-10093
Hardwire missile receiver coupler
[AD-D011350] 07 p0937 N85-15936
Modeling and simulation of a fin actuation system
[AD-A149443] 10 p1428 N85-19005
Dual band radome wall design
[AD-P004357] 12 p1825 N85-21451
Hot radome boresight error measurements
[AD-P004364] 12 p1826 N85-21458
Supersonic missile seeker lens system using gradient index material for first element lens
[AD-A151476] 15 p2490 N85-25367
MISSILE CONFIGURATIONS
Wind tunnel tests on a tube-launched missile configuration with a deflectable nose control and a novel wrap-around fin stabiliser
[AR-003-696] 01 p0001 N85-10003
Shock capturing finite difference algorithms for supersonic flow past fighter and missile type configurations
[NASA-CR-174051] 02 p0134 N85-10913
An overview of some monoplanar missile programs
[NASA-TM-86330] 06 p0747 N85-14786
MISSILE CONTROL
Application of modern guidance control theory to a bank-to-turn missile
[AD-A145646] 02 p0166 N85-11123
Polaris guidance system
[AD-D011324] 07 p0900 N85-15704
Prediction of cruciform all-movable control characteristics at transonic speeds
[AD-A147291] 09 p1078 N85-16832
Optical data processing for missile guidance
[AD-A149346] 10 p1422 N85-18972
Space interception guidance with uncertain factors
13 p2042 N85-22781
Multi-rate digital autopilot modeling methodology
[AD-A152044] 15 p2474 N85-25272
Optical flow-patterns of image velocity and their potential use in guidance and image interpretation
[BAE-BT-12091] 15 p2551 N85-26347
Cost-effective missile guidance through distributed architecture and standard processes
16 p2696 N85-26662
Computer simulation of a cruise missile using brushless dc motor fin control
[AD-A156935] 24 p4089 N85-35349
MISSILE DEFENSE
Directed energy missile defense in space
[PB84-210111] 01 p0015 N85-10095
About ambiguity and Q-functions
[AD-A145293] 02 p0250 N85-11636
MISSILE DESIGN
Tactical missiles technologies. Research and prospectives
[SNIAS-841-320-101] 04 p0461 N85-12925
Proceedings of the 17th Symposium on Electromagnetic Windows, part 1
[AD-A149185] 10 p1466 N85-19253
The application of some lifting-body reentry concepts to missile design
[NASA-TM-86394] 13 p1969 N85-22366
Simulation: A tool for cost-effective systems design and live test reduction 16 p2696 N85-26657
Cost-effective missile guidance through distributed architecture and standard processes
16 p2696 N85-26662
Flow modeling at the base region of missiles
[SNIAS-851-320-101] 20 p3420 N85-31228
MISSILE DETECTION
NT RADAR DETECTION
MISSILE ENGINE CASES
U ROCKET ENGINE CASES
MISSILE GUIDANCE
U MISSILE CONTROL
MISSILE LAUNCHERS
NT MOBILE MISSILE LAUNCHERS
Wind tunnel tests on a tube-launched missile configuration with a deflectable nose control and a novel wrap-around fin stabiliser
[AR-003-696] 01 p0001 N85-10003
Zero adhesion system
[AD-D011237] 01 p0015 N85-10093
Hardwire missile receiver coupler
[AD-D011350] 07 p0937 N85-15936
Lateral support system for canister-launched missile
[AD-D011369] 08 p1108 N85-16987
Missile launcher integral shock isolation and running gear system
[AD-D011490] 11 p1589 N85-19998
MISSILE SILOS
Invited papers: DNA ICBM technical R and D program 09 p1333 N85-18379
Empirical development of ground acceleration, velocity and displacement for accidental explosions at J5 or the proposed large altitude rocket cell at Arnold Engineering Development Center
[DE85-008324] 16 p2758 N85-27020
MISSILE STABILIZATION
U MISSILE CONTROL
U STABILIZATION
MISSILE STORAGE
Safety aspects of prepackaged liquid propellant stages for strategic missiles
[AD-P004350] 10 p1456 N85-19174
MISSILE SYSTEMS
Tactical missiles technologies. Research and prospectives
[SNIAS-841-320-101] 04 p0461 N85-12925
Some dynamical aspects of Army missile systems
09 p1333 N85-18380
Simulation: A tool for cost-effective systems design and live test reduction 16 p2696 N85-26657
MISSILE TRAJECTORIES
Fast response impulse generator
[AD-D011263] 06 p0759 N85-14853
Technical manual: Description and operation Slaved Tracking System
[DE85-004807] 13 p2094 N85-23070
Estimation of launch vehicle performance parameters
[AD-A151927] 16 p2728 N85-26839
MISSILE VIBRATION
Some dynamical aspects of Army missile systems
09 p1333 N85-18380
MISSILES
NT AIR TO SURFACE MISSILES
NT ANTIMISSILE MISSILES
NT BALLISTIC MISSILES
NT CRUISE MISSILES
NT INTERCONTINENTAL BALLISTIC MISSILES
NT MINUTEMAN ICBM
NT POLARIS MISSILES
NT RAMJET MISSILES
NT SIDEWINDER MISSILES
NT SURFACE TO SURFACE MISSILES
Ramjet and Ramrocket Propulsion Systems for Missiles
[AGARD-LS-136] 07 p0917 N85-15809
Some aspects of engine and airframe integration for Ramjet and Ramrocket powered missiles
07 p0918 N85-15812
Special problems of Ramjet with solid fuel
07 p0918 N85-15815
Solid propellant Ramrockets 07 p0918 N85-15816
Air Force space technology center space technology: Emphasis 84 09 p1333 N85-18381
The 1984 JANNAF Propulsion Systems Hazards Subcommittee Meeting, volume 1
[AD-A148865] 10 p1454 N85-19162
Preventing explosive propagation in racks or containers of tactical missiles
[AD-P004342] 10 p1455 N85-19166
Fiscal year 1986 technical objective document
[AD-A151039] 14 p2432 N85-25000
Gyrolaser guidance system for medium range missiles
16 p2696 N85-26649
A simulation study of jammer nulling trade-offs in a reactively steered adaptive array
[AD-A153461] 18 p3090 N85-29124
An extended two-target differential game model for medium-range air combat game analysis
[NASA-CR-175068] 18 p3175 N85-29687
Thrust vectoring apparatus for maneuvering missile in flight
[AD-D011693] 19 p3226 N85-30004
Transonic and supersonic wind tunnel tests on control effectiveness on schematic missile configurations
[FFA-TN-1983-20] 20 p3389 N85-31020
Transonic and supersonic wind tunnel tests on control effectiveness on schematic missile configurations: Supplement
[FFA-TN-1983-20-SUPPL] 20 p3389 N85-31021
MISSION PLANNING
Information Science Panel joint meeting with Imaging Science Panel 02 p0214 N85-11415
Mars exploration, Venus swingby and conjunction class mission modes, time period 2000 to 2045
[NASA-TM-86477] 02 p0303 N85-11961
Proceedings of a Workshop on Applications of Tethers in Space, Executive Summary
[NASA-CR-171195] 03 p0322 N85-12075
Lessons from the SEASAT and GEOS-3 altimeters data projects 03 p0364 N85-12457
Status of Stretched Rohini Satellite System (SROSS) and Augmented Satellite Launch Vehicle Project (ASLV) 04 p0459 N85-12909
A Mars dust sample return mission
[CNES-CT/PMF/APS/EMS-177] 04 p0459 N85-12915
Interstellar mission 04 p0459 N85-12916
Definition of technology development missions for early Space Station satellite servicing. Volume 2: Technical
[NASA-CR-171229] 04 p0461 N85-12923
The human role in space. Volume 1: Executive summary
[NASA-CR-171223] 04 p0546 N85-13473
The satellite maneuvers determination department 05 p0599 N85-13820
Missions/planning panel 05 p0609 N85-13886
Sample return from a comet flyby 06 p0689 N85-15646
Commerce Laboratory: Mission analysis payload integration study
[NASA-CR-171298] 07 p0911 N85-15764
Results of principal NASA studies on space station uses and functional requirements 07 p0914 N85-15787
Acquisition planning at the Defense Communications Agency
[AD-A146577] 07 p1051 N85-16669
QUASAT: A VLBI observatory in space — conference
[ESA-SP-213] 07 p1056 N85-16700
Automatic briefing and mission management systems for battlefield support 08 p1073 N85-16790
A Computer-generated topographic display system for navigation and mission planning in helicopters 08 p1073 N85-16800
Descent guidance and mission planning for space shuttle 08 p1092 N85-16902
Commerce Lab: Mission analysis and payload integration study
[NASA-CR-171272] 08 p1104 N85-16981
Commerce Lab: Mission analysis. Payload integration study
[NASA-CR-171285] 08 p1104 N85-16982
Impact of lunar and planetary missions on the space station
[NASA-CR-171832] 08 p1106 N85-16988
Space Station needs, attributes, and architectural option study
[NASA-CR-174316] 08 p1109 N85-17011
The SIR-B science investigations plan
[NASA-CR-174282] 08 p1143 N85-17208
Space Station engineering and technology development
[NASA-CR-174383] 09 p1287 N85-18079
Air Force space technology center space technology: Emphasis 84 09 p1333 N85-18381
Data Requirement (DR) MA-03: Payload missions integration — Spacelab payloads
[NASA-CR-171331] 10 p1428 N85-19009
CNES, INRA do joint remote-sensing research 10 p1477 N85-19321
Human Factors Considerations in High Performance Aircraft
[AGARD-CP-371] 10 p1532 N85-19853
Satellite module design 11 p1642 N85-20344
A mathematical formulation of the problem of optimal use of ground resources for future space missions 12 p1947 N85-22232
Activities of the Jet Propulsion Laboratory, 1 January - 31 December 1983
[NASA-CR-175555] 13 p2167 N85-23447
National Space Transportation Systems Program mission report
[NASA-TM-87454] 14 p2242 N85-23899
NASA plans for a space station
14 p2293 N85-24735

Shuttle operational test and scientific investigations
14 p2394 N85-24748
Mission analysis and orbit control of the helioesynchronous satellite SPOT
14 p2397 N85-24773
Towards the Halley Comet 14 p2399 N85-24783
The development of a performance and mission planning program for the A-7E aircraft
[AD-A151717] 15 p2471 N85-25258
Definition of technology development missions for early space stations: Large space structures
[NASA-CR-171446] 15 p2476 N85-25281
Automatic rendezvous and docking systems functional and performance requirements
[NASA-CR-171866] 15 p2482 N85-25376
Calendar of Ariane launches 1984 - 1987
15 p2523 N85-25554
European space science horizon 2000
[ESA-SP-1070] 16 p2717 N85-26771
A SLAM II simulation model for analyzing space station mission processing requirements
[NASA-CR-175894] 16 p2731 N85-26853
Tethered nuclear power for the Space Station
[NASA-TM-87023] 16 p2740 N85-26912
Component-specific modeling
[NASA-CR-174795] 16 p2799 N85-27261
Shuttle-tethered satellite system definition study extension
[NASA-CR-171473] 17 p2807 N85-27923
Mission requirements and handling qualities
18 p3057 N85-28918
Customer and mission influence on space station architecture 18 p3150 N85-29587
Space station automation study. Volume 2: Technical report. Autonomous systems and assembly
[NASA-CR-171615] 19 p3228 N85-30001
An artificial intelligence based framework for planning air launched cruise missile missions
[AD-A154486] 19 p3244 N85-30722
Mission analysis of solar powered aircraft
[NASA-CR-172583] 20 p3397 N85-31072
Maritime search and rescue cooperation and planning
20 p3400 N85-31090
X-ray satellite
[NASA-TM-77662] 20 p3407 N85-31145
Space Station reference configuration description
[NASA-TM-87403] 20 p3408 N85-31146
Studies toward a manned space station: Participation of European industry in NASA space station (MSS)
[SNIAS-S/DT-Y-25-212] 20 p3418 N85-31217
Life sciences flight experiments program mission science requirements document. The first life sciences dedicated Spacelab mission, part 1
[NASA-TM-87494] 21 p3550 N85-32137
Space station automation study. Automation requirements derived from space manufacturing concepts. Volume 1: Executive summary
[NASA-CR-176090] 22 p3738 N85-33170
Space Station automation study. Automation requirements derived from space manufacturing concepts. Volume 2: Technical report
[NASA-CR-176100] 22 p3738 N85-33171
Space Station Engineering and Technology Development: Proceedings of the Panel on In-Space Engineering Research and Technology Development
[NASA-CR-176110] 23 p3899 N85-34153

MISSIONS
Search for proton decay in the Frejus experiment
[HE-6.2-2] 24 p4210 N85-36138
Data acquisition system for phase-2 KGF proton decay experiment
[HE-6.2-4] 24 p4211 N85-36140

MISSISSIPPI
Water resources data, Mississippi, water year 1982
[PB84-224559] 01 p0065 N85-10434
Remote sensing applications program
[E85-10022] 02 p0218 N85-11435
Petrologic model of the northern Mississippi embayment based on satellite magnetic and ground based geophysical data
[NASA-TM-86075] 04 p0533 N85-13406
The influence of the number of ground control points on the scene-to-map registration accuracy — Kansas, Louisiana, Mississippi, and Missouri
07 p0986 N85-16264

MISSISSIPPI DELTA (LA)
Geological, structural, and geomorphological analyses from SIR-B 08 p1145 N85-17226

MISSISSIPPI RIVER (US)
Use of a two-dimensional flow model to quantify aquatic habitat
[AD-A154287] 19 p3266 N85-30253

MISSOURI
The influence of the number of ground control points on the scene-to-map registration accuracy — Kansas, Louisiana, Mississippi, and Missouri
07 p0986 N85-16264
Image variance and spatial structure in remotely sensed scenes — South Dakota, California, Missouri, Kentucky, Louisiana, Tennessee, District of Columbia, and Oregon
07 p0986 N85-16265

MISSOURI RIVER BASIN (US)
Water resources data for Colorado, water year 1983. Volume 1: Missouri River Basin, Arkansas River Basin and Rio Grande Basin
[PB85-123859] 11 p1671 N85-20528

MIST
Mist flammability studies of candidate fire-resistant hydraulic fluids
[AD-A146572] 08 p1134 N85-17146
Description of a technique to measure spray distribution in an air stream
[AD-A149780] 12 p1771 N85-21122

MITOCHONDRIA
Effects of hyperthermia on free amino acids in rat brain and in subcellular fractions 11 p1691 N85-20631
Effects of immobilization and high-altitude adaptation on energy metabolism in rats 22 p3820 N85-33663

MIXED CRYSTALS
Structural phase transitions in doped hexahalogen metallates 03 p0426 N85-12721

MIXED FLOW
U MULTIPHASE FLOW

MIXERS
On selecting bypass mixers for turbofan engines
09 p1306 N85-18207
Flameholder with integrated air mixer
[AD-D011549] 12 p1778 N85-21161
Switching mixer
[AD-D011602] 16 p2777 N85-27139

MIXING
NT COLLOIDING
NT COMPOUNDING
NT DISSOLVING
NT HOMOGENIZING
NT SIGNAL MIXING
NT TURBULENT MIXING
Materials modification by ion beam mixing
[AD-P003948] 02 p0286 N85-11664
Nonlinear optical studies of rydberg atoms using degenerate four-wave mixing
[AD-A146827] 07 p1043 N85-16823
An experimental study on the instability of a mixing-layer with laminar wake as the initial condition
08 p1076 N85-16824
Effects of a periodic disturbance on structure and mixing in turbulent shear layers and wakes
[AD-A149278] 10 p1484 N85-19370
Convergence rates in the strong law for bounded mixing sequences
[CWI-MS-R8412] 12 p1922 N85-22076
Constraints of observations of solar oscillations on solar models with mixing by turbulent diffusion
[DE85-003741] 13 p2205 N85-23678
Influences of thermal spikes in ion beam mixing
[DE85-008130] 14 p2419 N85-24924
Mixing in the solar interior 14 p2446 N85-25095
Ion beam mixing of marker layers in Al and Si
[DE85-006227] 15 p2511 N85-25490
North Atlantic Deep Water Formation
[NASA-CP-2367] 15 p2601 N85-26026
North Atlantic Deep Water and the world ocean
15 p2602 N85-26033
Glacial-to-interglacial changes in NADW fluxes?
15 p2602 N85-26037
Evaluation of experimental epoxy monomers
[NASA-TM-87476] 16 p2754 N85-26996
Holoewitch, phase 1
[AD-A152212] 16 p2787 N85-27196
The seasonal cycle of atmospheric CO in the Southern Hemisphere 16 p2830 N85-27447
Surface modification of solids
[DE85-007543] 16 p2871 N85-27715
A bilaterally deterministic rho-mixing stationary random sequence
[AD-A152856] 17 p3019 N85-28666
The effect of ion-bombardment-induced atomic mixing on depth-profiling of interfaces
[AD-A153199] 17 p3044 N85-28834
Experimental determination of the mixing frequency parameter for coalescence/dispersion modeling of turbulent combustion
[DE85-011466] 19 p3270 N85-30260
Large eddy structures in transitional and turbulent flames
[AD-A154520] 21 p3562 N85-32157
Numerical solution of the Navier-Stokes equations for 3-D internal flows: An emerging capability
21 p3588 N85-32300
Survey of mixing in metal/insulator systems
[DE85-011938] 23 p3985 N85-34714
Holoewitch
[AD-A155841] 24 p4096 N85-35392

MIXING CIRCUITS
Conversion of microwave signals by superconducting films in the resistive state
[NASA-TM-77505] 01 p0123 N85-10643
Coherent receiver phase and amplitude alignment circuit
[AD-D011487] 10 p1468 N85-19265
Detection of angular modulated electromagnetic signals
[AD-D011563] 12 p1823 N85-21437
High-speed digital baseband mixer
16 p2771 N85-27103
Switching mixer
[AD-D011602] 16 p2777 N85-27139
Communications and logic systems at millimeter wave frequencies, summary 17 p3042 N85-28625
Multiport optical detectors 18 p3187 N85-29769

MIXING DEPTH
U MIXING HEIGHT

MIXING HEIGHT
Mean maximum mixing heights for northern Asia for the winter of 1976
[DE84-015960] 05 p0672 N85-14315

MIXING LENGTH FLOW THEORY
Model calculations for a CO2 mixing laser with screen nozzle
[ESA-TT-859] 11 p1640 N85-20336
Contribution to the theory of stationary separation areas
[NASA-TM-77825] 14 p2300 N85-24244

MIXTURES
NT ADMIXTURES
NT AEROSOLS
NT AQUEOUS SOLUTIONS
NT BINARY MIXTURES
NT COLLOIDS
NT DISPERSIONS
NT EMULSIONS
NT EUTECTIC ALLOYS
NT EUTECTICS
NT EXPIRED AIR
NT FOG
NT GAS MIXTURES
NT LIQUID-GAS MIXTURES
NT METAL MATRIX COMPOSITES
NT NUCLEAR EMULSIONS
NT PHOTOGRAPHIC EMULSIONS
NT SIALON
NT SLURRIES
NT SMOKE
NT SOLID SOLUTIONS
NT SOLID SUSPENSIONS
NT SOLUTIONS
Equation of state study for polar fluids
[PB84-222801] 01 p0025 N85-10157
Factor analysis applied to a silane coupling agent on E-glass fiber system
[AD-A145687] 02 p0187 N85-11249
Small angle neutron scattering (SANS) on polymer-oligomer mixtures and on deformed polyethylene melts 03 p0432 N85-12750
Thermite and Fe/KClO4: Some thermodynamic calculations
[DE84-016945] 04 p0573 N85-13653
Pharmacokinetic interactions of mixtures
[AD-P004032] 06 p0844 N85-15382
The toxicity of complex mixtures
[AD-P004033] 06 p0844 N85-15383
Aspects of solvent toxicity in mixtures
[AD-P004036] 06 p0845 N85-15386
Properties of miscible polymer blends
[AD-A147090] 07 p0931 N85-15003
Convection heat transfer in the critical region of fluid mixtures
[DE85-002118] 07 p0961 N85-16088
Background detection and correction in multicomponent analysis
[AD-A148251] 08 p1212 N85-17628
Compressive strength-maturity relationships of mortar containing fly ash
[AD-A148705] 09 p1339 N85-18423
User's guide to MIX: A computer code for fitting mixture distributions to data
[DE85-001451] 09 p1369 N85-18603
Models for mixture experiments when the response depends on the total amount
[DE85-000370] 09 p1374 N85-18637
User's manual for GRIZZLY
[DE85-001405] 11 p1702 N85-20702

Influence of pressure on speed of sound in single-phase region of stratifying mixtures 11 p1715 N85-20788
Wavecode constitutive models: Nonhomogeneous mixtures
[DE85-000836] 12 p1796 N85-21278
Process for producing tris s(n-methylamino) methylsilane
[NASA-CASE-MFS-25721-1] 12 p1799 N85-21280
PSA, Renault work on all fuel automobile engine 15 p2531 N85-25604
Modeling the role of radicals in the ignition of and flame propagation in hydrogen-air and methane-air mixtures 16 p2744 N85-29935
Equation of state and two-body correlations for fluids of non-spherical molecules
[AD-A151969] 16 p2783 N85-27174
Application of scattering methods to the studies of the structure of polymer blends
[IFPR-13/1984] 17 p2933 N85-28104
High performance mixed bismide resins and composites based thereon
[NASA-CASE-ARC-11538-1-SB] 19 p3231 N85-30033
An experimental apparatus to study nucleate pool boiling of R-114 and oil mixtures
[AD-A154077] 19 p3265 N85-30249
Antistarshapedness, dispersiveness and mixtures
[AD-A155583] 21 p3678 N85-32849
Sodium nitrate containing mixture for producing ceramic-glass-ceramic seal by microwave heating
[DE85-011610] 22 p3751 N85-33254
Development of a prototype energy meter
[PB85-198430] 22 p3789 N85-33476
Equation of state study for polar fluids
[PB85-204345] 24 p4076 N85-35262
Nitrogen analysis by chemiluminescence
[AD-A156197] 24 p4083 N85-35308

MLA
U MULTISPECTRAL LINEAR ARRAYS

MMS
U MULTIMISSION MODULAR SPACECRAFT

MNEMONICS
Effects of individual mnemonic characteristics on problem solving 07 p1010 N85-16419

MOBILE COMMUNICATION SYSTEMS
NT LAND MOBILE SATELLITE SERVICE
Defense Meteorological Satellite Program (DMSP) 11 p1711 N85-20766
Spread spectrum mobile radio communications
[AD-A149936] 12 p1829 N85-21477
Concepts and cost trade-offs for land vehicle antennas in satellite mobile communications
[NASA-CR-175731] 15 p2540 N85-25680
Measurement results from a balloon experiment simulating land mobile satellite transmissions
[NASA-CR-175740] 15 p2540 N85-25683
Moon bounce communications to small terminals
[AD-A153297] 17 p2950 N85-28212
Personal mobile communications by satellite
[REPT-15-4572] 18 p3091 N85-29135
Preliminary investigation of the performance of repeater technology for satellite sound broadcasting
[SSP/017/82] 18 p3092 N85-29137
Study of terrestrial mobile systems for personal communications
[MCS-8436] 20 p3441 N85-31357
Pluribus satellite IMP (Interface Message Processors) development mobile access terminal network
[AD-A155754] 24 p4069 N85-35218

MOBILE MISSILE LAUNCHERS
Invited papers: DNA ICBM technical R and D program 09 p1333 N85-18379

MOBILITY
NT CARRIER MOBILITY
NT ELECTRON MOBILITY
NT HOLE MOBILITY
NT IONIC MOBILITY
Diffusion mechanisms and point defects in transition-metal oxides
[DE84-016238] 04 p0571 N85-13839
Electron distribution function and mobility in 3-5 compounds for high and low fields
[AD-A147447] 07 p1048 N85-16858
Grouser effect studies
[AD-P004278] 09 p1406 N85-18854
Mobility of the small combine (track type) on soft ground-relationship between the position of the center of gravity and the mobility
[AD-P004285] 09 p1407 N85-18862
Determination of functional mobility of human nervous system with the PNN-3 instrument 10 p1525 N85-19618
Robotics at Savannah River site: Activity report
[DE85-003657] 11 p1648 N85-20383
Hall mobility in fluid argon
[DE85-007288] 17 p3045 N85-28840
The position and mobility of the shoulder, spinal column and pelvis in seated subjects
[AD-A153751] 18 p3153 N85-29524
Effects of coating rectangular microscopic electrophoresis chamber with methylcellulose 20 p3498 N85-31748
Theoretical prediction of stationary positions in the rectangular chamber during asymmetric electroosmotic flow 20 p3499 N85-31750
Summary electrophoretic data base on human embryonic kidney cell strain 8514 20 p3501 N85-31768

MODAL RESPONSE
The Shock and Vibration Digest, volume 16, no. 6
[AD-A145653] 02 p0208 N85-11372
Hardware and software selection for experimental modal analysis 02 p0208 N85-11373
F-8 refueling boom ground vibration test
[NASA-TM-84914] 07 p0902 N85-15713
Elias Klein memorial lecture: Modal testing, a critical review 09 p1334 N85-18383
The use of analytical models to interpret data properly
[ERS-E.341] 11 p1651 N85-20399
The use of analytical models to interpret measured data properly. 1. General background theory 11 p1651 N85-20400
The use of analytical models to interpret measured data properly. 2. The application to modal analysis of structures 11 p1651 N85-20401
Multishaker modal testing
[NASA-CR-176139] 22 p3800 N85-33544
A modal parameter extraction procedure applicable to linear time-invariant dynamic systems
[NASA-CR-176120] 22 p3835 N85-33747
Automated dynamic analytical model improvement for damped structures
[NASA-CR-177945] 23 p3941 N85-34425

MODE (STATISTICS)
Normal mode analysis for linear resistive magnetohydrodynamics
[IPP-6/235] 11 p1730 N85-20878

MODE COUPLING
U COUPLED MODES

MODE OF VIBRATION
U VIBRATION MODE

MODE SHAPES
U MODAL RESPONSE

MODE TRANSFORMERS
Design and construction of a mode converter from rectangular TE 10 to circular TE 11
[REPT-84-158] 05 p0833 N85-14084
Transformation of mode composition of circular optical waveguide 07 p0950 N85-16023
High power millimeter-wave mode converters in overmoded circular waveguides using periodic wall perturbations
[IPF-84-6] 09 p1395 N85-18780
Design of mode converters from TE circular om modes in circular waveguides to TE rectangular mo modes in rectangular waveguides for high power applications in the frequency range 1 to 30 GHz
[IPF-84-7] 09 p1395 N85-18781

MODELS
NT AIRCRAFT MODELS
NT ANALOG SIMULATION
NT ASTRONOMICAL MODELS
NT ATMOSPHERIC MODELS
NT BIOLOGICAL MODELS (MATHEMATICS)
NT BREADBOARD MODELS
NT DENSITY WAVE MODEL
NT DIGITAL SIMULATION
NT DYNAMIC MODELS
NT ENVIRONMENT MODELS
NT HYDROLOGY MODELS
NT MATHEMATICAL MODELS
NT NUCLEAR MODELS
NT OCEAN MODELS
NT REFERENCE ATMOSPHERES
NT SCALE MODELS
NT SPACECRAFT MODELS
NT STELLAR MODELS
NT THOMAS-FERMI MODEL
NT WIND TUNNEL MODELS
Development of the Antares electron gun
[DE84-014043] 01 p0053 N85-10352
Retardation analytical model to extend service life
[NASA-CR-171177] 01 p0057 N85-10376
Effects of surface chemistry on hot corrosion life: Overview 02 p0145 N85-10980
Simulation study of a new inverse-pinch high Coulomb transfer switch
[NASA-CR-172420] 02 p0184 N85-11294
Evaluation of an aerosol prediction model for coastal regions using marine aerosol generation and transport data
[AD-A145443] 02 p0231 N85-11510
SMP: A solid modeling program
[NASA-CR-172473] 02 p0241 N85-11570
Models of natural intelligence in fault diagnosis tasks: Implications for training and aiding of maintenance personnel
[AD-P003927] 02 p0248 N85-11607
A generalized model of fault-isolation performance
[AD-P003928] 02 p0248 N85-11608
Estimation in nonlinear time series model II: Some nonstationary series
[AD-A145709] 02 p0255 N85-11668
Numerical investigation of diffraction models of microwave integrated circuits 03 p0347 N85-12233
A topological approach to database theory 03 p0437 N85-12781
Digital elevation models improve processing of Alaskan gravity data 04 p0515 N85-13285
Resonance model of Pc3 in subtropical regions — geomagnetism 04 p0520 N85-13323
Models of angular momentum input to a circumterrestrial swarm from encounters with heliocentric planetesimals 04 p0587 N85-13750
Mechanical models of close approaches and collisions of large protoplanets 04 p0586 N85-13756
Analytical modeling of spacecraft power systems 05 p0610 N85-13897
Modelling the aerodynamics in a system of continuous channels and experimentation procedure
[BLL-M-35923-(5828.4)] 05 p0634 N85-14067
Mental models of invisible logical networks 05 p0706 N85-14544
On looking into the black box: Prospects and limits in the search for mental models 05 p0709 N85-14548
A comparison of evaporation duct models for IREPS (Integrated Refractive Effects Prediction System)
[AD-A146471] 06 p0799 N85-15103
A hydrogen partitioning model for hydrogen assisted crack growth
[AD-A147385] 07 p0978 N85-16214
General model of earthquake and the place of warnings in it 07 p0981 N85-16232
Model of team organization and behavior and team description method
[AD-A147540] 07 p1053 N85-16690
Ballistic/detonic transition of propellants 08 p1117 N85-17041
Depositional modeling of tetrahedrite in the Coeur d'Alene district, Idaho 08 p1182 N85-17448
Crystalline structure of urea ice sheets used in modeling experiments in the CRREL test basin
[AD-A148434] 08 p1226 N85-17722
Designing off-road vehicles with good ride behaviour
[AD-P004267] 09 p1405 N85-18843
A decision model for selection of microcomputers and operating systems
[AD-A149076] 10 p1538 N85-19694
LSS 2018: A double-lined spectroscopic binary central star with an extremely large reflection effect
[NASA-CR-175503] 11 p1762 N85-21082
A study of transonic flutter of a two-dimensional airfoil using the U-g and p-k methods
[LR-615] 12 p1771 N85-21121
Modeling of transient heat pipe operation
[NASA-CR-175496] 12 p1844 N85-21571
Flow measurement by laser Doppler anemometry in a nuclear fuel assembly
[DE85-003280] 12 p1846 N85-21592
Evaluation of complex terrain air quality simulation models
[PB85-119485] 12 p1886 N85-21835
Protons with energies above 30 KeV in Earth's radiation belt at low altitudes during magnetically quiet time close to geomagnetic equator 13 p1980 N85-22423
Auroral-polar cap environment and its impact on spacecraft plasma interactions 13 p1991 N85-22484
Three-dimensional calculation of shuttle charging in polar orbit 13 p1992 N85-22486
Acoustic energy balance method 13 p2000 N85-22537
Measurement requirements for the detection of ozone trends 13 p2105 N85-23115
Study of resolution of deep MT soundings by means of physical model 13 p2112 N85-23155
LEXICON: A structured modeling system for optimization
[AD-A150536] 13 p2147 N85-23329
Monte Carlo modeling of lunar regolith development 13 p2197 N85-23627
Analyses of radar images of small craters 13 p2199 N85-23642
Terrestrial analogs for planetary wrinkle ridges 13 p2199 N85-23644
Mixing, chemical reaction and flow field development in ducted rockets
[DE85-004093] 14 p2247 N85-23928

A model for the compressive buckling of extended chain polymers
[AD-A151025] 14 p2260 N85-24006
Thermocouple modeling
[DE85-005172] 14 p2306 N85-24273
The retrieval expert model of information retrieval 14 p2433 N85-25003
Near-nucleus studies of Comet Halley 14 p2435 N85-25018
Temperature, velocity, and species mapping in an induction plasma
[DE85-004005] 15 p2512 N85-25499
Heavy doping effects in high efficiency silicon solar cells
[NASA-CR-175681] 15 p2586 N85-25940
Management communication and financial modeling 15 p2627 N85-26190
Harnessing computional power: Distributed combinator reduction
[DE85-005967] 15 p2631 N85-26216
Feasibility analysis of moving bank multiple model adaptive estimation and control algorithms
[AD-A152015] 15 p2641 N85-26292
SU(N,1) inflation
[DE85-003952] 15 p2669 N85-26469
Study of longitudinal landing flying qualities evaluation using pilot model theory
[AD-A152194] 16 p2706 N85-26702
Metal armatures for railguns
[AD-A152129] 16 p2728 N85-26838
Model reduction techniques applied to the control of large space structures
[AD-A151784] 16 p2731 N85-26857
Liquid rocket combustor computer code development 16 p2740 N85-26910
Laser Schlieren and ultraviolet diagnostics of rocket combustion 16 p2740 N85-26911
Mechanical properties of high performance carbon fibers 16 p2742 N85-26922
Optical best arc RMS test results 16 p2804 N85-27290
The selection of the starting field: General versus tailored model 16 p2805 N85-27294
A wind-bivane/microprocessor system for on-line prediction and display of pollutant distributions 16 p2830 N85-27449
A multipole model of the observed cerebral cortex magnetic field
[AD-A152237] 16 p2842 N85-27526
A general purpose scatter storage subsystem and a comparison of hashing methods
[NASA-CR-175814] 16 p2945 N85-27542
Multivariable statistical modelling and its application 16 p2957 N85-27617
Airport and airway system cost allocation model. Volume 7: User's manual
[AD-A152877] 17 p2906 N85-27917
Composite loads spectra for select space propulsion structural components 17 p2912 N85-27953
One-dimensional velocity-depth functions determined for the Arabian Shield and the southwestern Red Sea: A comparison of models 17 p2992 N85-28490
The definition and computation of a metric on plane curves. The meaning of a face on a geometric model 17 p3004 N85-28571
Improving the effectiveness of integral property calculation in a CSG solid modeling system by exploiting predictability 17 p3006 N85-28586
Generation and display apparatus
[AD-D011639] 17 p3008 N85-28599
The design of megawatt gyrotrons
[DE85-007892] 17 p3032 N85-28754
Experimental methods of heavy quark detection
[DE85-006316] 17 p3036 N85-28781
Mockups and human productivity studies 18 p3159 N85-29570
The fabrication, microstructure, and strengthening behavior of heavily cold-worked in situ composites 19 p3231 N85-30031
Pressure recovery in a cylindrical heat pipe at high radial Reynolds numbers and at high Mach numbers
[DE85-010718] 19 p3269 N85-30274
Optimization of single and multi-component analytical techniques
[HSE-TRANS-10987] 19 p3347 N85-30744
Experimental level-structure determination in odd-odd actinide nuclei
[DE85-010476] 19 p3360 N85-30835
Primordial inflation and supergravity
[DE85-008538] 19 p3383 N85-30969
Venus thermospheric circulation
[PB85-180420] 19 p3384 N85-30997
An overview of latest model reduction and control methods of large flexible space structures 20 p3414 N85-31191
New adatom model for Si(11) 7X7 and Si(111)Ge 5X5 reconstructed surfaces 20 p3460 N85-31625
Modeling of chemical transformations of SO(x) and NO(x) in the polluted atmosphere: An overview of approaches and current status
[PB85-173169] 20 p3487 N85-31677
MPS solidification model. Analysis and calculation of macrosegregation in a casting ingot
[NASA-CR-171589] 21 p3566 N85-32176
Numerical modeling of subsurface communication
[DE85-012818] 21 p3577 N85-32249
Numerical solutions of turbulent models for flow over a flat plate with angle of attack
[DE85-010380] 21 p3585 N85-32286
A modified Fresnel scattering model for the parameterization of Fresnel returns, part 2.3A 21 p3618 N85-32483
Review of the psychological issues relating to the effectiveness of structured programming
[AD-A154503] 21 p3665 N85-32766
On the dependence of the convergence of Gummel's algorithm on the regularity of the solution
[AD-A154626] 21 p3675 N85-32832
Cosmic ray He3 measurements
[OG-4.2-3] 21 p3714 N85-33045
Sandia Cooperative Group on the Aerothermochemistry of Turbulent Combustion. Discussion record of the second meeting
[DE85-007493] 22 p3743 N85-33203
Second order modelling in non-constant density flows 22 p3744 N85-33206
Jet flows: Modelling and experiments 22 p3744 N85-33208
A model for predicting propagation-related DSCS (Defense Communications Engineering Center) margin requirements
[AD-A155355] 22 p3756 N85-33281
Development of a chemical kinetic mechanism for the US EPA (Environmental Protection Agency) regional oxidant model
[PB85-185858] 22 p3813 N85-33618
Modeling of auto exhaust smog chamber data for EKMA development
[PB85-186492] 22 p3813 N85-33619
Model building and practical aspects of nonlinear programming
[AD-A155720] 22 p3829 N85-33711
Role of ECRH in potential formation for tandem mirrors
[DE85-011859] 22 p3848 N85-33834
Models of planetary structure and evolution: The case of Io 22 p3855 N85-33874
On galactic origin of cosmic rays with energy up to 10(19) eV
[OG-5.4-15] 22 p3887 N85-34091
Halo of NGC 4631 and models of cosmic-ray transport
[OG-6.2-3] 22 p3889 N85-34103
Detonation in tungsten-loaded HMX
[DE85-009606] 23 p3922 N85-34299
Mathematical modeling of ultimate heat sink cooling ponds
[TI85-009747] 23 p3932 N85-34389
The impact of supercomputers on experimentation: A view from a national laboratory
[NASA-TM-86822] 23 p3955 N85-34510
Spatial trees: A fast access method for unstructured graphical data 23 p3958 N85-34533
3D computer animation: More an evolution problem than a motion problem 23 p3959 N85-34536
Using dynamic analysis to animate articulated bodies such as humans and robots 23 p3959 N85-34537
Simulation studies on stability of hot electron plasma 23 p3978 N85-34684
Perspective on the next ten years in plasma physics
[DE85-011849] 23 p3984 N85-34706
The influence of nonstationarity of the solar activity and general solar field on modulation of cosmic rays
[SH-4.2-17] 23 p4008 N85-34854
Spatial distribution of cosmic rays in magnetic cycles of the Sun
[SH-4.2-20] 23 p4009 N85-34857
Diurnal anisotropy during solar activity cycle twenty and diffusion-convection model
[SH-4.5-7] 23 p4036 N85-35025
FAA requirements for model to support capacity, delay, noise and energy programs
[AD-A155815] 24 p4063 N85-35179
Elliptical X-ray analyzer spectrograph application to a laser-produced plasma
[DE85-013790] 24 p4097 N85-35398
Linear absorption and scattering of laser beams
[AD-A156167] 24 p4098 N85-35401
Investment justification of robotic technology in aerospace manufacturing. User's manual
[AD-A156193] 24 p4099 N85-35410
Expert systems research in regional resource evaluation: Experiences in the application of microcomputer technologies 24 p4105 N85-35450
The development of assessment techniques program 24 p4106 N85-35457
Comparative analysis of operational forecasts versus actual weather conditions in airline flight planning, volume 2
[NASA-CR-167863] 24 p4119 N85-35535
Comparative analysis of operational forecasts versus actual weather conditions in airline flight planning: Summary report
[NASA-CR-167866] 24 p4120 N85-35538
On-line model driven control of the SLC electron Damping Ring
[DE85-013377] 24 p4157 N85-35772
Circumstellar shells of late-type stars: A study at millimeter and infrared wavelengths 24 p4167 N85-35836
Gamma-hadron families and scaling violation
[HE-3.4-7] 24 p4182 N85-35935
On the halo events observed by Mount Fuji and Mount Kanbala Emulsion Chamber Experiments
[HE-3.4-9] 24 p4182 N85-35937
Multidimensional analysis of data obtained in experiments with X-ray emulsion chambers and extensive air showers
[HE-3.6-2] 24 p4184 N85-35951
Experimental basis for the models of cascade propagation in atmosphere
[HE-3.6-6] 24 p4185 N85-35954
Relation between gamma-ray family and EAS core: Monte-Carlo simulation of EAS core
[HE-3.6-7] 24 p4185 N85-35955
A comparative analysis of gamma and hadron families at the superhigh energies recorded in experiment Pamir
[HE-3.7-1] 24 p4185 N85-35960
Electrons, muons and hadrons in extensive air showers and how do they depend on nuclear interaction model, part 2 24 p4187 N85-35969
The maximum depth of shower with E sub 0 larger than 10(17) eV on average characteristics of EAS different components 24 p4188 N85-35981
Sensitivity of depth of maximum and absorption depth of EAS to hadron production mechanism 24 p4188 N85-35982
The capability of the existing network of installations for detecting the antineutrino burst from collapsing stars
[HE-5.3-13] 24 p4208 N85-36107
A search for cosmic sources of high energy neutrinos with small underground detectors
[HE-5.3-16] 24 p4208 N85-36110

MODEMS
Adaptive signal processing for radio communications 10 p1473 N85-19295
Fast synchronization model for UHF spread-spectrum communication system 10 p1473 N85-19296
A modem with pseudo-orthogonal codes: Experimental results 10 p1474 N85-19302
Error correction coding for a self-adaptive modem: Theoretical and experimental results 10 p1474 N85-19303
A microprocessor controlled parallel model with FDPSK 10 p1475 N85-19304
Serial data transmission with large output on the HF channel 10 p1475 N85-19305
Comparative architectures for a multiple function speech processor
[AD-A150873] 14 p2292 N85-24211

MODERATION (ENERGY ABSORPTION)
NT THERMALIZATION (ENERGY ABSORPTION)

MODERATORS
Radiation damage experiments and lifetime estimates for beryllium components in fusion systems
[DE85-008038] 17 p3040 N85-28811

MODES
NT AXIAL MODES
NT BALLOONING MODES
NT COUPLED MODES
NT FAILURE MODES
NT LASER MODES
NT MODES (STANDING WAVES)
NT PROPAGATION MODES
NT PUSHBROOM SENSOR MODES
NT VIBRATION MODE
Resonant frequencies and mode shapes for single and double cylindrical shells
[AD-A144778] 01 p0062 N85-10408
MHD instabilities in simple plasma configuration
[AD-A144936] 01 p0121 N85-10829
Influence of mode noise suppression in multimode fiber optic light guides 03 p0348 N85-12242
Normal mode initialization 05 p0660 N85-14372
Buildup of oscillations in two-mode gyrotron 06 p0788 N85-15037

Nonlocal and nonlinear effects on solar oscillations
09 p1416 N85-18934
Calculation of mode field in electron beam welding of VT6 titanium alloy
10 p1449 N85-19129
The effects of internal waves on acoustic normal modes
[AD-A150235] 13 p2155 N85-23379
Development and application of a unified balancing approach with multiple constraints
15 p2737 N85-26891
Miniature two-mode filters 22 p3775 N85-33394

MODES (STANDING WAVES)
Implications of observed frequencies of solar P modes
14 p2443 N85-25073
The vertical structure of global rotational normal modes 18 p3144 N85-29464

MODIFICATION
U REVISIONS

MODULAR RATIOS
Modular photovoltaic array field
[SAND-83-7028] 02 p0222 N85-11454

MODULARITY
Modular design, versatility of robots viewed
14 p2284 N85-24155
A modular dissimilar redundant computer designed for high integrity control 17 p2904 N85-27904

MODULATED CONTINUOUS RADIATION
Dynamics of growth of surface periodic structures when intense light acts on condensed media
02 p0268 N85-11748

MODULATION
NT AMPLITUDE MODULATION
NT FREQUENCY MODULATION
NT FREQUENCY SHIFT KEYING
NT INTERMODULATION
NT LIGHT MODULATION
NT PHASE MODULATION
NT PHASE SHIFT KEYING
NT PULSE AMPLITUDE MODULATION
NT PULSE CODE MODULATION
NT PULSE DURATION MODULATION
NT PULSE FREQUENCY MODULATION
NT PULSE MODULATION
NT PULSE POSITION MODULATION
NT PULSE TIME MODULATION
NT TRAVELING WAVE MODULATION
NT ULTRASONIC LIGHT MODULATION
NT VELOCITY MODULATION
Investigation of several aspects of LANDSAT 4/5 data quality
[E85-10038] 04 p0525 N85-13357
Reduction of signal modulation caused by polarization in visible optical scanning systems
[AD-D011389] 07 p1042 N85-16820
Noise jammer discrimination by noise modulation bandwidth
[AD-D011473] 10 p1468 N85-19264
Infrared modulation of photoluminescence in glow discharge amorphous silicon
[DE85-016993] 11 p1737 N85-20922
Fundamental limits to synchronization and tracking
[AD-A149623] 12 p1833 N85-21504
Generation of longitudinal acoustic waves by modulated helicon waves — nonlinear steady state waves in metals
13 p2080 N85-23049
Modulation of light energy transduction in photosynthesis
[DE85-004711] 13 p2141 N85-23292
Rational pulse-shaping filters for almost MSK-like modulation
[AD-A153065] 17 p2949 N85-28208
Moon bounce communications to small terminals
[AD-A153297] 17 p2950 N85-28212
Cosmic ray modulation and turbulent interaction regions near 11 AU
[NASA-TM-86193] 18 p3209 N85-29909
Modulated voltage metastable ionization detector
[NASA-CASE-ARC-11503-1] 23 p0933 N85-34374
Longitudinal distribution of cosmic rays in the heliosphere
[SH-4.1-14] 23 p4006 N85-34837
Effects of solar magnetic field on cosmic rays
[SH-4.2-12] 23 p4008 N85-34850
The influence of nonstationarity of the solar activity and general solar field on modulation of cosmic rays
[SH-4.2-17] 23 p4008 N85-34854
The effect of the neutral sheet structure of the interplanetary magnetic field on cosmic ray distribution in space
[SH-4.2-18] 23 p4008 N85-34855
On the influence of the heliomagnetospheric periphery on the galactic cosmic rays
[SH-4.2-19] 23 p4009 N85-34856
Spatial distribution of cosmic rays in magnetic cycles of the Sun
[SH-4.2-20] 23 p4009 N85-34857
11- and 22-year variations of the cosmic ray density and of the solar wind speed
[SH-4.2-21] 23 p4009 N85-34858
The dependence of solar modulation on the sign of the cosmic ray particle charge
[SH-4.2-23] 23 p4009 N85-34860
An update on the correlation between the cosmic radiation intensity and the geomagnetic AA index
[SH-4.2-24] 23 p4009 N85-34861
Long-term modulation of cosmic rays during solar cycle 21
[SH-4.4-10] 23 p4034 N85-35008
Role of solar flare index in long term modulation of cosmic ray intensity
[SH-4.4-12] 23 p4034 N85-35009
A study of periodicities and recurrences in solar activity and cosmic ray modulation
[SH-4.4-14] 23 p4034 N85-35010

MODULATION TRANSFER FUNCTION
The spectral distribution of field components for a sinusoidal power modulated monofrequency optical carrier source
[FI-44-TBR-84] 04 p0585 N85-13601
Spaceborne receivers: Basic principles
[NASA-CR-174269] 07 p0848 N85-15890
LANDSAT-4 Thematic Mapper Modulation Transfer Function (MFT) evaluation — California and New Mexico
[E85-10055] 07 p0984 N85-16250
Modulation Transfer Function (MTF) measurement techniques for lenses and linear detector arrays
[NASA-TM-86169] 10 p1556 N85-19812
Infrared material optical damage by rain
[AD-P004372] 12 p1827 N85-21486
MTF analysis of LANDSAT-4 Thematic Mapper
12 p1871 N85-21737
An investigation of several aspects of LANDSAT-5 data quality — Palmer County, Shelby, mt; White sands, NM; Great Salt Lake, UT; San Mateo Bridge and Sacramento, California
[E85-10096] 13 p2122 N85-23214
Modulation transfer function for two-point and periodic objects using Gaussian and Lorentzian resolution functions
[PB85-187557] 19 p3368 N85-30891

MODULATORS
NT MODEMS
Frequency shifting in multimode fiber optic phase modulation devices 03 p0347 N85-12239
Advanced infrared laser modulator development
[NASA-CR-172479] 06 p0662 N85-15479
Multichannel electrooptical modulators for digital information storage and processing systems
07 p0950 N85-16021
Miniature high performance pulsed modulator apparatus
[AD-D011427] 08 p1158 N85-17310
Battery charger
[AD-D011420] 08 p1178 N85-17425
Multiplex gas chromatography for use in space craft
[NASA-TM-86668] 09 p1290 N85-18097
An electro-optic spatial light modulator for thermo-elastic generation of programmably focused ultrasound
[AD-A149078] 10 p1553 N85-19794
Development of a 20 GHz modulator for the payload of a satellite for propagation and transmission experiments, including the required converters of the test equipment
[BMFT-FB-W-84-044] 11 p1590 N85-20004
Detection of angular modulated electromagnetic signals
[AD-D011563] 12 p1823 N85-21437
An electro-optic spatial light modulator for thermoelastic generation of programmably focused ultrasound
[AD-A152066] 15 p2548 N85-26323
Spatial light modulator having a capacitively coupled photoconductor
[AD-D011646] 17 p3037 N85-28790
Optical modulators and bistable devices using molecular gases 18 p3186 N85-29761
Stokes parameters modulator for birefringent filters
18 p3205 N85-29884
SLC Energy Upgrade Program at SLAC
[DE85-014290] 24 p4160 N85-35790

MODULATORS-DEMODULATORS
U MODEMS

MODULES
NT CHEMICAL RELEASE MODULES
NT ELECTRONIC MODULES
NT SPACECRAFT MODULES
Modular detonator device
[AD-D011232] 03 p0340 N85-12184
Thermal characterization of photovoltaic modules in natural environments 06 p0832 N85-15296
Demonstration of transparent solar array module design
[NASA-CR-174257] 07 p0992 N85-16302
Application of large eddy interaction model to channel flow
[NASA-TM-86691] 12 p1844 N85-21572
Test results of an organic Rankine-cycle power module for a small community solar thermal power experiment
[NASA-CR-175698] 14 p2350 N85-24584
Intermediate load modules for test and evaluation
[NASA-CR-175697] 14 p2350 N85-24526
On localization of injective modules
[CSIR-TWISK-342] 14 p2413 N85-24678
Module performance and failure analysis area: Flat-plate solar array project
[NASA-CR-175699] 15 p2585 N85-25936
Operating characteristics of a 0.87 kW-hr flywheel energy storage module
[NASA-TM-87036] 17 p2974 N85-28371
CAMAC 488 module: 68000 based GPIB interface module
[DE85-006367] 17 p3014 N85-28635

MODULUS OF ELASTICITY
NT DYNAMIC MODULUS OF ELASTICITY
The theory of elastic modulus of fabric composites and its examination by experiments
[NAL-TR-808] 01 p0022 N85-10133
Detection of hydrogen assisted crack growth by measurement of modulus changes and acoustic emission
[DE84-015752] 02 p0184 N85-11236
Effective moduli of elasticity of unidirectional fibrous composite 02 p0265 N85-11793
Evaluation of moduli and thicknesses of pavement systems by spectral-analysis-of-surface-waves method
[PB84-219112] 03 p0342 N85-12205
Transformation toughened ceramics for the heavy duty diesel engine technology program
[NASA-CR-174699] 07 p1055 N85-16908
Solid Rocket Motor Case (SRMC) dynamic sensitivity to changes in composite properties
12 p1948 N85-22238
Development and study of two-matrix glass fiber composite with increased transverse deformation
13 p2027 N85-22700
Fracture mechanics evaluation of GaAs
[NASA-CR-175857] 13 p2102 N85-23101
High resistance and raised modulus carbon fibers
[NASA-TM-76884] 15 p2502 N85-25436
Compressive strength of epoxy resin chocks subjected to elevated temperatures
[AD-A152018] 15 p2519 N85-25532
Natural vibrations of reinforced spherical shells
17 p2943 N85-28185
A concept for the intrinsic dielectric strength of electrical insulation materials
[NASA-CR-176040] 20 p3448 N85-31410
Rolling, slip and traction measurements on low modulus materials
[NASA-CR-174909] 22 p3791 N85-33491
Effects of temperature on the tensile strength and elastic modulus of composite material
[AD-A156112] 24 p4075 N85-35251

MOHAWK AIRCRAFT
U OV-1 AIRCRAFT

MOHR CIRCLES
U FRACTURE MECHANICS

MOIRE EFFECTS
A comparison of electronic heterodyne moire deflectometry and electronic heterodyne holographic interferometry for flow measurements
[NASA-TM-87071] 21 p3568 N86-32302

MOIRE FRINGES
Holographic FLI for detection of defects
[AD-A148339] 08 p1184 N85-17345
Influence of error of determination of moire isotach orders on the stability of their approximation
[BLL-M-36277-(5823.4)] 20 p3460 N85-31423
Modular digital holographic fringe data processing system
[NASA-CR-177952] 23 p0933 N85-34375
Experiments and discussions on the analysis of interferograms with closed-loop fringes
[NPL-MOM-68] 23 p3956 N85-34515

MOIRE INTERFEROMETRY
Holographic FLI for detection of defects
[AD-A148339] 08 p1184 N85-17345
Moire interferometric measurement of relative displacements in dovetail joints
[OUEL-1563/85] 20 p3471 N85-31566
Experiments and discussions on the analysis of interferograms with closed-loop fringes
[NPL-MOM-68] 23 p3956 N85-34515

MOISTURE
NT SOIL MOISTURE
Experimental and theoretical studies of moisture and temperature effects on the mechanical properties of graphite/epoxy laminates and neat resins
04 p0467 N85-12969

Thermal properties of soils and soils testing
[DE84-015312] 04 p0525 N85-13360
An evaluation and comparison of vertical profile data from the VISSR Atmospheric Sounder (VAS)
[NASA-TP-2425] 07 p1000 N85-16351
Thermal stress-dependent dilation of concrete
[DE84-014668] 11 p1653 N85-20412
The evolution of CO2 on Mars
13 p2185 N85-23558
Wave motion of three-component medium under load moving on plane boundary 14 p2277 N85-24106
Experimental study of the effect of moist environments on epoxy resin chocks
[AD-A152052] 15 p2568 N85-25849
Bound and free moisture studies of solid materials by FTNMR
[DE85-003227] 16 p2747 N85-26952
In situ microwave measurements of dielectric properties and moisture in materials
[DE85-003622] 16 p2747 N85-26953
Trace water sensor
[NASA-CASE-NPO-15722-1] 18 p3103 N85-29212
Flight-service program for advanced composite rudders on transport aircraft
[NASA-CR-174537] 19 p3217 N85-29950
Metabolic mechanisms of plant growth at low water potentials 19 p3327 N85-30812
Upgrading auxiliary facility outleakage and combustion detection
[DE85-012796] 23 p3934 N85-34388

MOISTURE CONTENT
NT ATMOSPHERIC MOISTURE
Surface soil moisture measurements of the White Sands, New Mexico
[NOAA-TM-NESDIS-7] 02 p0219 N85-11441
Determination of the conservation state of long conservation agricultural products by means of capacitive sensors
[NOTA-INTERNA-799] 02 p0220 N85-11447
Operational test of three instruments for measuring liquid water content in laboratory and from aircraft
[DFVLR-MITT-84-08] 03 p0397 N85-12531
The areal pattern of latent and sensible heat fluxes: The combination of soil physics and remotely sensed data 05 p0956 N85-14213
Apparatus for determining the liquid water content of a gas
[AD-D011297] 07 p0922 N85-15839
Effects of low temperatures on the growth and unfrozen water content of an aquatic plant
[AD-A147107] 07 p1011 N85-16424
The effects of soil moisture on bistatic clutter power
[AD-A147636] 08 p1150 N85-17261
LX-10 and LX-17 moisture content and release
[DE84-016579] 09 p1301 N85-18173
Development and evaluation of a procedure for the rapid analysis of fresh concrete
[AD-A149741] 12 p1866 N85-21703
Human lung fluid content during 7-day head-down tilt 12 p1902 N85-21941
Effect of moisture in inert gases on density of seam metal and on mechanical characteristics of welded joints of aluminum and aluminum alloys
13 p2034 N85-22744
Dependence of combustion of homogeneous kerosene-air mixtures on humidity of air
13 p2061 N85-22835
Distribution of snow and maximum snow water equivalent obtained by LANDSAT data and degree day method 13 p2124 N85-23229
Microwave radiometer observations of snowpack properties and comparison of U.S. Japanese results — Hokkaido, Japan and Vermont and North Dakota test sites 13 p2125 N85-23230
Studies on physical properties of snow based on multi channel microwave radiometer
13 p2125 N85-23231
Determination of electromagnetic properties of mesh material using advanced radiometer techniques
14 p2235 N85-23855
Measurement of water equivalent of mountain snow cover — ARGOS system 14 p2327 N85-24366
Determination of total moisture content in cloud-free atmosphere by relative radio emission measurements
14 p2340 N85-24472
Determining atmosphere moisture content from differences in two-frequency microwave radiation measurements 14 p2341 N85-24474
High-frequency microwave observations of convective precipitation 15 p2506 N85-26000
Recent VAS imaging/sounding research
15 p2507 N85-26004
Impact of soil moisture in organizing a severe storm outbreak 15 p2597 N85-26009
Luminescence probe studies of ionomers. 2. Steady-state measurements from sulfonated polyethylene and teflon membranes
[AD-A152233] 16 p2755 N85-27000
Moisture content and gas sampling device
[NASA-CASE-MSC-18666-1] 18 p3103 N85-29213
Aerospace technology determines forest-fire danger
19 p3295 N85-30427
Fiber optic moisture sensor
[DE85-011651] 22 p3787 N85-33462
Effect of substrate moisture on growth and structure of corn leaf 22 p3824 N85-33692
Instrumentation for sensing moisture content of material using a transient thermal pulse
[NASA-CASE-NPO-15493-2] 23 p3933 N85-34373

MOISTURE DETECTORS
U MOISTURE METERS

MOISTURE METERS
NT HYGROMETERS
Determination of the conservation state of long conservation agricultural products by means of capacitive sensors
[NOTA-INTERNA-799] 02 p0220 N85-11447
Operational test of three instruments for measuring liquid water content in laboratory and from aircraft
[DFVLR-MITT-84-08] 03 p0397 N85-12531
Microstrip antenna for multichannel radiometer
06 p0791 N85-15058
Fiber optic moisture sensor
[DE85-011651] 22 p3787 N85-33462
Instrumentation for sensing moisture content of material using a transient thermal pulse
[NASA-CASE-NPO-15493-2] 23 p3933 N85-34373

MOISTURE RESISTANCE
The water vapor resistances of some clothing assemblies used by flying personnel of the Swedish Armed Forces: A series of model studies
[FOA-C-59011-H1] 02 p0238 N85-11551
Process for improving moisture resistance of epoxy resins by addition of chromium ions
[NASA-CASE-LAR-13226-1] 23 p3919 N85-34282

MOJAVE DESERT (CA)
Visibility monitoring in the southern California desert for the Department of Defense: Research on operations-limiting visual extinction, RESOLVE protocol
[AD-A146617] 06 p0635 N85-15315

MOL (ORBITAL LABORATORIES)
U MANNED ORBITAL LABORATORIES

MOLDING MATERIALS
Sealing ceramic material in low melting point glass
[NASA-TM-77599] 01 p0031 N85-10190
General studies on composite materials. Evaluation of auxiliary products of national origin
[SNIAS-2500/DCI-PR/84] 03 p0326 N85-12101
Review of the mechanical properties of SMC and GRP materials
[NPL-DMA(A)-88] 08 p1131 N85-17126
Exploratory development of foams from liquid crystal polymers
[NASA-CR-172510] 13 p2036 N85-22754
New material, process spins off from Volvo LCP 2000 program 15 p2536 N85-25648

MOLDS
Sintered silicon carbide molded body and method for its production
[NASA-TM-77646] 14 p2259 N85-23999
Method and apparatus for casting conductive and semi-conductive materials
[DE85-011655] 22 p3792 N85-33494

MOLECULAR ABSORPTION
Middle Atmosphere Program. Handbook for MAP, volume 8
[NASA-CR-175478] 11 p1657 N85-20445
MSG-7: Molecular absorption processes related to the penetration of ultraviolet solar radiation into the middle atmosphere 11 p1658 N85-20449
Absorption of ozone molecules in strong field of tea CO2 injection laser 11 p1718 N85-20906
Carbon monoxide adsorption on a platinum electrode studied by polarization modulated FT-IRRAS (Fourier Transform-IR Reflections Adsorption Spectroscopy). Part 1: CO adsorbed in the double layer potential region and its oxidation in acids
[AD-A149751] 12 p1800 N85-21268

MOLECULAR BEAM EPITAXY
Silicon sheet with molecular beam epitaxy for high efficiency solar cells
[NASA-CR-174022] 02 p0222 N85-11459
Pulsed irradiation of optimized, MBE grown, AlGaAs/GaAs radiation hardened photodiodes
[DE84-014984] 04 p0569 N85-13631
High-efficiency silicon solar cell research
06 p0829 N85-15261
MBE growth for high-efficiency silicon solar cells
06 p0829 N85-15265
Strained-layer superlattice emitter and detector structures using modulation-doped active regions
[DE85-000064] 06 p0857 N85-15511
Development of short gate FET's
[AD-A147033] 07 p0947 N85-15989
Aluminum nitride insulator for 3-5 MIS (Metal-Insulator-Semiconductor) applications
[AD-A147842] 07 p1049 N85-16662
Gallium arsenide/AlGaAs multilayer structures with special doping profiles for microwave and optoelectronic devices
[BMFT-FB-T-84-207] 08 p1227 N85-17725
Some investigations of molecular beam epitaxial growth of 3-5 semiconductor films via Monte-Carlo computer simulations, carrier tunneling and spectroscopic ellipsometry
[AD-A149465] 10 p1563 N85-19854
Characterization of high purity Si-doped molecular beam epitaxial GaAs
[AD-A149651] 12 p1939 N85-22181
AlN insulator for 3-5 MIS applications
[AD-A150674] 14 p2426 N85-24962
Producible alternative to CdTe for epitaxy (PACE-2) of LWIR (Long Wave Infrared) HgCdTe
[AD-A150676] 14 p2426 N85-24964
Investigation of the MBE growth of InSb and novel quantum well structures
[AD-A151014] 14 p2427 N85-24969
Fabrication and I-V characterization of AlGaAs/GaAs MODFETs with P-type surface layers grown by molecular beam epitaxy
[AD-A151695] 15 p2660 N85-26415
A study of Ga(.47)In(.53)As and Al(.48)In(.52)As for very high frequency device applications
[AD-A151996] 16 p2870 N85-27706
TEM investigation of polar-on-nonpolar epitaxy: GaAs-AlGaAs on (100) Ge
[DE85-007613] 16 p2871 N85-27714
Communications and logic systems at millimeter wave frequencies, summary 17 p3042 N85-28825
Leading-edge microelectronics research at Sweden's Chalmers 20 p3436 N85-31337
Determination of kinetic parameters of molecular beam epitaxy
[AD-A155222] 21 p3710 N85-33030
Sixty GHz IMPATT diode development
[NASA-CR-174969] 22 p3758 N85-33293
Investigations of the molecular beam epitaxial growth and characteristics of external excitation induced non-equilibrium phases of immiscible 3-5 compound semiconductors
[AD-A156325] 24 p4162 N85-35804

MOLECULAR BEAMS
Molecular beam scattering 03 p0417 N85-12666
Instrumentation for particle-beams research using laser excited merging beams
[AD-A147966] 08 p1220 N85-17681
Hyperfine structure and lifetime measurements on electronically excited long-life molecules in a beam experiment
[MPIS-11/1984] 11 p1726 N85-20855
Measurements of integral yields of charged secondary particles using neutral beams simulating a cometary fly-by — Giotto mission 14 p2244 N85-23906
Development of an apparatus for obtaining molecular beams in the energy range from 2 to 200 eV
[NASA-TM-77835] 15 p2647 N85-26326
TEM combined with Al/sub x/Ga/sub 1-x/ as marker layers as a technique for the study of GaAs MBE growth
[DE85-008451] 18 p3194 N85-29809
Measurement of combustion species by electron impact fluorescence
[DE85-011163] 19 p3236 N85-30065
Instrumentation for particle-beams research using excited merging beams
[AD-A154155] 19 p3356 N85-30807
Shuttle Molecular Gunc Smog. Potential experiment for the electrodynamic Tethered Satellite System (TSS) mission
[IFSI-84-17] 20 p3419 N85-31221
Interrelations for the elements of the scattering matrix
22 p3855 N85-33872
High-resolution spectroscopy and dynamics of multiphoton processes in atoms and molecules
[AD-A155862] 24 p4147 N85-35714
Investigations of the molecular beam epitaxial growth and characteristics of external excitation induced non-equilibrium phases of immiscible 3-5 compound semiconductors
[AD-A156325] 24 p4162 N85-35804

MOLECULAR BIOLOGY
The cosmic history of the biogenic elements and compounds
[NASA-SP-476] 17 p3003 N85-28562
Institute works on modeling thermonuclear plasma processes 19 p3296 N85-30435

Molecular biology of environmental aromatic hydrocarbons
[DE85-015036] 24 p4128 N85-35593
MOLECULAR BONDS
U CHEMICAL BONDS
MOLECULAR CHAINS
Nuclear Magnetic Resonance of Polymeric Materials
[AD-A145078] 01 p0032 N85-10192
NMR (Nuclear Magnetic Resonance) and macromolecular migration in a melt or in concentrated solutions
[AD-P003908] 01 p0032 N85-10194
Deuteron NMR (Nuclear Magnetic Resonance) in relation to the glass transition in polymers
[AD-P003910] 01 p0032 N85-10196
MOLECULAR CLOUDS
Star Formation Workshop
[ROE-OR-13] 03 p0441 N85-12809
Distribution and properties of molecular clouds in the galaxy 03 p0442 N85-12810
The number and distribution of molecular clouds in the inner galaxy 03 p0442 N85-12811
Far-infrared observations of some regions of star formation 03 p0442 N85-12814
Relation of core structure to high velocity outflow in G35.2-0.74 and other molecular clouds 03 p0443 N85-12818
Time-dependent chemistry of molecular clouds 03 p0443 N85-12822
The significance of comets for star formation 03 p0443 N85-12824
Molecules in external galaxies 03 p0444 N85-12828
Future theoretical needs in studies of star formation 03 p0444 N85-12829
The fragmentation of molecular clouds and the IMF 05 p0740 N85-14759
Molecular clouds within 100 pc 06 p0877 N85-15573
A wide latitude CO survey of molecular clouds in the northern Milky Way 06 p0877 N85-15574
The Draco Nebula, a molecular cloud associated with a high velocity cloud? 06 p0878 N85-15577
Nearby molecular hydrogen 06 p0879 N85-15582
The Orion molecular cloud at far-infrared wavelengths 06 p1245 N85-17860
First results of submillimeter polarimetry 06 p1246 N85-17861
Far-infrared photometry of low-mass pre-main-sequence stars with broad CO wings 06 p1246 N85-17866
Star formation in globules 06 p1247 N85-17868
Far infrared observations of molecular clouds in the outer galaxy 06 p1247 N85-17869
Boundary conditions for the paleoenvironment: Chemical and physical processes in the pre-solar nebula — molecular clouds, interstellar matter, and abundance
[NASA-CR-174370] 10 p1570 N85-19001
Mechanical energy release by protostars to molecular clouds 12 p1957 N85-22302
The Formation of preplanetary disks from the collapse of rotating molecular cloud cores 13 p2180 N85-23526
Radio counterparts of galactic gamma-ray sources 20 p3549 N85-32085
Galactic gamma-ray sources, SNOBs, and giant H2 regions
[OG-2.5-4] 22 p3869 N85-33961
The galactic gamma-ray distribution and the radial cosmic ray gradient
[OG-3.1-4] 22 p3873 N85-33992
Cosmic ray secondary nuclei and the structure of the galaxy
[OG-7.2-4] 23 p4014 N85-34878
Alfven wave scattering and the secondary to primary ratio
[OG-7.2-9] 23 p4015 N85-34879
Giant molecular clouds as regions of particle acceleration 23 p4020 N85-34913
Far-infrared emission lines of CO and OH in the Orion-KL molecular shock
[NASA-TM-86721] 24 p4167 N85-35832
MOLECULAR COLLISIONS
Collisional excitation cross sections
[AD-A145196] 01 p0117 N85-10800
Energy transfer in atom-molecule scattering experiments in the 1eV region with SF6-Ar, CF4-Ne and Xe-CO2 systems as examples
[REPT-11/1983] 04 p0563 N85-13588
Rotational inelastic scattering of He-atoms at HF-, HCl-, CF4-, SF6-, C2H6- and C2F6-molecules
[MPIS-9/1984] 04 p0564 N85-13590
Laboratory studies of atomic collision processes of importance in planetary atmospheres
[NASA-CR-174142] 04 p0589 N85-13758
Chaos near the Coulomb Barrier: Nuclear molecules
[DE85-001260] 07 p1041 N85-16606
Collisional energy exchange in polyatomic molecules
[AD-A147710] 08 p1219 N85-17679
Atomic and molecular collision processes
[DE85-001604] 09 p1382 N85-18690
Quantum mechanical and semiclassical approaches to molecular dynamics
[DE85-003458] 10 p1555 N85-19603
Studies of collisional and nonlinear radiative process for development of coherent UV and XUV sources
[AD-A152001] 16 p2665 N85-27670
Large, energetic cluster impacts on surfaces
[DE85-006559] 17 p3034 N85-28789
Interaction of slow electrons with high-pressure gases (quasi-liquids): Synthesis of our knowledge on slow electron-molecule interactions
[DE85-010081] 19 p3355 N85-30600
Inelastic Near-Surface Interactions. Proceedings of the Werner Brandt Workshop on Penetration Phenomena
[DE85-010579] 20 p3526 N85-31928
MOLECULAR DIFFUSION
The role of molecular diffusion in the adhesion of elastomers
[AD-A145576] 02 p0186 N85-11245
Contribution to theory of ocean-atmosphere gas exchange 13 p2108 N85-23134
Current understanding of point defects and diffusion processes in silicon 20 p3481 N85-31632
Vortex dynamics simulation of conserved scalar dissipation 22 p3745 N85-33210
MOLECULAR DISSOCIATION
U DISSOCIATION
MOLECULAR ELECTRONICS
NT LARGE SCALE INTEGRATION
Investigation of several low-lying levels of X doublet pi state of NCO using argon laser excited fluorescence
[AD-A153693] 18 p3071 N85-28994
MOLECULAR ENERGY LEVELS
NT INTERMOLECULAR FORCES
Electronic and redox properties of stacked-ring silicon phthalocyanines from molecular orbital theory
[AD-A147161] 07 p0922 N85-15844
Pion inelastic scattering to the first three excited states of Lithium-6
[AD-A147560] 07 p1041 N85-16606
Sequential excitation preparation of molecular energy levels with special structural and chemical properties
[AD-A150301] 13 p2156 N85-23386
Noncontinuum solvent effects upon the intrinsic free-energy barrier for electron-transfer reactions
[AD-A150662] 14 p2250 N85-23943
Intermolecular energy transfer between the individual zero-field levels of triplet traps in an orientationally disordered solid
[AD-A150751] 14 p2417 N85-24914
Computer modeling of vibrational energy levels of potential laser candidates (diatomic molecules)
[AD-A151765] 16 p2790 N85-27209
A method to estimate the self-consistency effects on electronic structure calculations
[INPE-3536-PRE/752] 19 p3375 N85-30936
MOLECULAR EXCITATION
Collisional excitation cross sections
[AD-A145196] 01 p0117 N85-10800
Electronic-to-vibrational energy transfer studies of singlet molecular oxygen and hydrogen halides
[AD-A145567] 02 p0277 N85-11802
Theoretical studies in molecular fragmentation: Processes, energetics and diagnostics
[AD-A146310] 03 p0418 N85-12673
Quantum Monte Carlo for molecules
[AD-A146159] 06 p1227 N85-17727
Photoionization of excited molecular states
[DE84-017454] 09 p1291 N85-18103
Hyperfine structure and lifetime measurements on electronically excited long-life molecules in a beam experiment
[MPIS-11/1984] 11 p1726 N85-20855
Direct measurement of the temperature dependence of the velocity of the reaction of deuterium atoms with vibration-excited hydrogen molecules
[MPIS-12/1984] 11 p1726 N85-20856
Threshold double photoionization of argon with synchrotron radiation
[AD-A150615] 13 p2157 N85-23389
Transverse periodic boundary conditions in molecular dynamics with unsteady strain shock waves
[DE85-006497] 16 p2663 N85-27656
Studies of collisional and nonlinear radiative process for development of coherent UV and XUV sources
[AD-A152001] 16 p2665 N85-27670
Electronically excited alkaline earth oxides: Chemical production and collisional energy transfer processes
[AD-A153172] 17 p3044 N85-28833
Nonradiative damping of molecular electronic excited states by metal surfaces
[AD-A154619] 21 p3701 N85-32994
The detection and study of molecular species using time resolved laser spectroscopy
[AD-A155910] 24 p4075 N85-35256
High-resolution spectroscopy and dynamics of multiphoton processes in atoms and molecules
[AD-A155662] 24 p4147 N85-35714
MOLECULAR FLOW
NT TRANSITION FLOW
Bipolar molecular outflows: T Tauri stars and Herbig-Haro objects 03 p0446 N85-12837
Structure of amorphous films of alloys based on Fe, condensed from laser erosion products 13 p2035 N85-22749
Cone drag in the transition from continuum to free molecular flow
[OUEL-1536/84] 20 p3380 N85-31023
Variations in the small-scale galactic magnetic field and short time-scale intensity variations of extragalactic radio sources 20 p3549 N85-32084
MOLECULAR GASES
NT DIATOMIC GASES
NT POLAR GASES
Electron collision processes in molecular gases
[AD-A146078] 03 p0418 N85-12671
Conference on Singlet Molecular Oxygen (COSMO 84), program and abstracts
[AD-A147281] 07 p1040 N85-16605
Understanding the high pressure properties of molecular solids and molecular surfaces deposited on hetrogeneous substrates
[NASA-CR-174262] 07 p1047 N85-16649
Optical modulators and bistable devices using molecular gases 18 p3186 N85-29781
Participation of singlet oxygen in photodestruction of air-saturated solutions of coumarin dyes 21 p3685 N85-32891
The possibilities of remote analysis of atmospheric gases based on Raman scattering spectroscopy 21 p3685 N85-32892
Preliminary considerations for the gasdynamic precompression of solid molecular hydrogen
[DE85-013256] 22 p3784 N85-33445
Far-infrared observations of young clusters embedded in the R Coronae Australnae and RHO Ophiuchi dark clouds
[NASA-TM-86681] 24 p4167 N85-35834
MOLECULAR INTERACTIONS
NT INTERSTELLAR CHEMISTRY
NT MOLECULAR COLLISIONS
Molecular mechanisms of n-hexane neurotoxicity
[AD-P004020] 06 p0843 N85-15354
Vibrational spectroscopy of chemisorption phenomena on model catalyst surfaces
[AD-A146753] 07 p0922 N85-15840
Applications of molecular dynamics to the study of shock-induced chemistry
[AD-A148017] 08 p1121 N85-17066
USSR report: Physics and mathematics
[JPRS-UPM-85-001] 11 p1715 N85-20766
In situ monitoring of electrochemical reactions by surface enhanced Raman scattering
[PB85-149789] 12 p1803 N85-21312
Bibliography of atomic and molecular processes, 1983
[DE85-000662] 12 p1929 N85-22121
Theoretical study of near-threshold electron-molecule scattering
[DE85-004530] 12 p1930 N85-22126
Combustion kinetics of metal atoms and metallic radicals over wide temperature ranges 13 p1999 N85-22530
Molecular dynamics of propellant gases, part 2 13 p2002 N85-22552
Molecular dynamics studies of energy transfer processes in crystal systems
[AD-A150161] 13 p2163 N85-23416
Intermolecular energy transfer between the individual zero-field levels of triplet traps in an orientationally disordered solid
[AD-A150751] 14 p2417 N85-24914
USSR report: Physics and mathematics
[JPRS-UPM-85-003] 15 p2642 N85-26300
Finite-perturbation intermediate neglect of differential overlap molecular orbital calculations of nuclear magnetic resonance spin-spin coupling constants for polycyclic aromatic hydrocarbons and aromatic nitrogen heterocyclics
[NASA-TM-87498] 20 p3525 N85-31927
USSR report: Physics and mathematics
[JPRS-UPM-85-004] 21 p3680 N85-32960
Intermolecular explosives
[DE85-009809] 23 p3921 N85-34296
MOLECULAR IONS
Electronics research at the University of Texas at Austin
[AD-A146900] 07 p0947 N85-15998
State-selected ion-molecule reaction dynamics
[AD-A150068] 12 p1928 N85-22115

Multiparticle 3D imaging technique to study the structure of molecular ions
[DE85-001843] 12 p1929 N85-22122
Extraction of ions from solutions at atmospheric pressure, mass spectrometric analysis of bioorganic substances 14 p2387 N85-24706
Hydrogen vibrational population distributions and negative ion generation in tandem high-density hydrogen discharges
[DE85-006764] 16 p2863 N85-27657
Imaging Spectrometric Observatory (ISO)
23 p3902 N85-34169
Negative ion sources equipped with continuous annular and spherical geometry surface ionizers
[DE85-011939] 23 p3971 N85-34619

MOLECULAR ORBITALS
Application of quantum chemistry of atmospheric chemistry
[AD-A147035] 07 p0922 N85-15943
Electronic and redox properties of stacked-ring silicon phthalocyanines from molecular orbital theory
[AD-A147161] 07 p0922 N85-15844
Why CO bonds side-on at low coverage and both side-on and upright at high coverage on the Cr(110) surface
[NASA-CR-176071] 21 p3565 N85-32173
Molecular orbital studies in oxidation: Sulfate formation and metal-metal oxide adhesion
[NASA-CR-176070] 21 p3565 N85-32174

MOLECULAR OSCILLATIONS
Electronic-to-vibrational energy transfer studies of singlet molecular oxygen and hydrogen halides
[AD-A145667] 02 p0277 N85-11802
High temperature gas energy transfer
[AD-A146134] 03 p0328 N85-12113
Phase-dissipative mechanisms for laser-induced surface desorption-dissociation processes
[AD-A147961] 08 p1121 N85-17065
Supersonic molecular jet study of the liquid state
[AD-A147416] 09 p1379 N85-18671
Sequential excitation preparation of molecular energy levels with special structural and chemical properties
[AD-A150301] 13 p2156 N85-23366
Rotational energy transfer in highly vibrationally excited hydrogen fluoride and deuterium fluoride
[AD-A152003] 16 p2862 N85-27650
Vibrational overtone excitation of diatomic molecules
[AD-A154827] 21 p3701 N85-32096

MOLECULAR OSCILLATORS
Construction techniques of a molecular hydrogen laser
[AD-A152928] 17 p2970 N85-28343

MOLECULAR PHYSICS
The 2nd European Conference on Atomic and Molecular Physics
[AD-A155863] 24 p4148 N85-35715

MOLECULAR PUMPS
Optimum geometry of interblade passages in impellers of thermomolecular vacuum pump
16 p2764 N85-27058
Impurity and particle control systems for tokamak reactor experiments
[DE85-006124] 19 p3366 N85-30673

MOLECULAR RELAXATION
Collisional excitation cross sections
[AD-A145198] 01 p0117 N85-10800
Anomalies in frequency characteristics of solid-state ring laser 02 p0271 N85-11765
Low-frequency sound absorption measurements in air
[NASA-RP-1120] 02 p0275 N85-11789
Phase-dissipative mechanisms for laser-induced surface desorption-dissociation processes
[AD-A147961] 08 p1121 N85-17065
Transport relaxation processes in supercritical fluids
[DE85-002076] 09 p1398 N85-18796
Saturation kinetics of active medium of oxygen-iodine laser 11 p1718 N85-20607
Vibrational relaxation in H-2 molecules by wall collisions: Applications to negative ion source processes
[DE85-000852] 11 p1721 N85-20828
Theory of relaxation processes in decomposing polymer materials during high-intensity convective heating
13 p2028 N85-22710
Quantum statistical theory of vibrational dynamics in a laser-driven admolecule-surface system
[AD-A152022] 16 p2872 N85-27719
Some amplification by relaxation processes in nitrogen and mixtures of nitrogen with helium and hydrogen
[AD-A153620] 18 p3071 N85-29892
Laser-stimulated vibrational excitation of an adspecies studied by a generalized master equation: Neutral atomic hydrogen on hydrated KCl(001)
[AD-A153965] 18 p3112 N85-29286
Theoretical modeling of the discharge-pumped XeCl excimer laser 20 p3480 N85-31495

MOLECULAR ROTATION
Calculation of the scattering function of rotating molecules with emphasis on the tunnel spectra of absorbed molecules 03 p0427 N85-12725
Rotational inelastic scattering of He-atoms at HF-, HCl-, CF4-, SF6-, C2H6- and C2F6-molecules
[MPIS-9/1984] 04 p0564 N85-13590
Detection of the J-10 manifold of the pure rotational band of phosphine on Saturn 08 p1245 N85-17855
Far-infrared spectroscopy of interstellar gas
08 p1245 N85-17858
Photoionization of excited molecular states
[DE84-017454] 09 p1291 N85-18103
Two-dimensional measurements of OH concentration and temperature in reactive flows
[AD-A149849] 12 p1800 N85-21292
Rotational energy transfer in highly vibrationally excited hydrogen fluoride and deuterium fluoride
[AD-A152003] 16 p2862 N85-27650
Rotational relaxation studies of hydrogen fluoride
[AD-A152711] 17 p3029 N85-28734

MOLECULAR SIEVES
U ABSORBENTS

MOLECULAR SPECTRA
NT ELECTRONIC SPECTRA
NT RAMAN SPECTRA
NT VIBRATIONAL SPECTRA
On the content of nitrogen in atmospheres of late giants derived from molecular bands on NH in the UV spectral range 05 p0740 N85-14761
Starbursts in galaxies: Implications of molecular and far-infrared observations 08 p1248 N85-17861
The fluorescence of cometary OH and CN
09 p1411 N85-18806
Mass analysis of neutral particles and ions released during electrical breakdowns on spacecraft surfaces
[NASA-CR-175585] 12 p1793 N85-21250

MOLECULAR SPECTROSCOPY
NT RAMAN SPECTROSCOPY
The 248 nm - new short wavelength for pumping lasers employing vapors of complex molecules
02 p0261 N85-11705
Vibrational spectroscopy of chemisorption phenomena on model catalyst surfaces
[AD-A146753] 07 p0922 N85-15840
Development of an airborne measuring system for remote sensing of Earth surface and atmosphere, spectroscopic investigations
[BMFT-FB-W-84-029] 08 p1178 N85-17420
Study of metal oxide semiconductor structures by capacitive transient spectroscopy
[ENST-84E011] 11 p1737 N85-20926
A liquid nitrogen cooled composite wall hollow cathode — molecular spectroscopy
[USIP-85-07] 20 p3526 N85-31930

MOLECULAR STRUCTURE
Diblock copolymers of polystyrene/1,2 polybutadiene and polystyrene/polybutene-1: Molecular structure, morphology and mechanical properties
[AD-A144980] 01 p0033 N85-10201
Proton pumping in purple membrane, appendix 1
[DE84-014601] 01 p0118 N85-10811
Physical-chemical properties of articulated rodlike polymers
[AD-A145549] 02 p0186 N85-11244
Computer molecular dynamics of 2-D water (ice) structures under shock
[AD-A145818] 03 p0372 N85-12375
Stable isotope studies
[DE84-016752] 04 p0562 N85-13583
Structure and properties of grain boundaries
[DE84-014368] 04 p0570 N85-13636
Synthesis of film-forming electron-accepting polymers
[AD-A146430] 06 p0771 N85-14931
Structure and functions of fungal cell surfaces
[NASA-TM-77439] 06 p0842 N85-15347
Structure determination of molecular adsorbates with dynamical LEED and HREELS
[DE85-002007] 06 p0861 N85-15473
Catalytic oxidation by transition metal ions in zeolites
[AD-A146828] 07 p0922 N85-15842
Quantum Monte Carlo for molecules
[AD-A148159] 08 p1227 N85-17727
Isomer enumeration in polytertiary phosphines and related compounds
[AD-A148058] 09 p1290 N85-18099
Supersonic molecular jet study of the liquid state
[AD-A147416] 09 p1379 N85-18671
Metal atom diffusion in amorphous silica and at the silica surface
[DE84-017351] 09 p1380 N85-18674
Compilation of atomic data for diagnostics of Tokamak
09 p1390 N85-18744
Compositional, structural, and physical studies of some graphite hexafluoroarsenates and their relatives
[DE85-000855] 10 p1432 N85-19030
On shrinkage and molecular extension
[AD-A149100] 10 p1451 N85-19144
Characterization of acetylene-terminated resin cure states
[AD-A149483] 10 p1452 N85-19148
Application of Monte Carlo and molecular dynamics methods to the calculation of thermodynamic properties of molten salts
[AD-A148697] 10 p1585 N85-19869
Characterization of the network structure of a hardened epoxy resin (TGMDA/DDS system)
[ONERA-RT-3/3348-M] 11 p1613 N85-20140
Multiparticle 3D imaging technique to study the structure of molecular ions
[DE85-001843] 12 p1929 N85-22122
The crystal and molecular structure of a new propellant compound: Triaminoguanidium Azide Nitrate (TAZN)
13 p2002 N85-22551
The chemistry of RDX and HMX cluster ions
13 p2004 N85-22561
The influence of fuel molecular composition upon flame-tube temperature and flame radiation in a model gas-turbine primary zone
[K234] 13 p2017 N85-22648
Sequential excitation preparation of molecular energy levels with special structural and chemical properties
[AD-A150301] 13 p2156 N85-23366
Bonding information from Auger spectroscopy
[AD-A150864] 14 p2251 N85-23948
Extraction of ions from solutions at atmospheric pressure, mass spectrometric analysis of bioorganic substances 14 p2387 N85-24706
Metal complexes of some heterocyclic ligands
15 p2504 N85-25448
Studies of photosynthetic Energy Conversion
[DE85-005973] 15 p2586 N85-25844
Equation of state and two-body correlations for fluids of non-spherical molecules
[AD-A151969] 16 p2783 N85-27174
Periodic cluster simulation of a disordered impurity system
[INPE-3453-PRE/705] 16 p2858 N85-27628
An investigation of molecular structure of copolymers using positron annihilation spectroscopy
[NASA-TM-86431] 17 p2916 N85-27977
Detailed chemical kinetic study of the effect of molecular structure on autoignition of fuel-air mixtures
[DE85-004424] 17 p2921 N85-28010
Electroweak interactions in nuclei
[DE85-007811] 17 p3033 N85-28762
Exploratory study of coal conversion chemistry
[DE85-010393] 19 p3229 N85-30018
Molecular toxicology of chromatin: The role of Poly(ADP-Ribose) in gene control
[AD-A154415] 19 p3327 N85-30611
Activities of Rutgers - The State University Department of Mathematics
[AD-A154158] 19 p3370 N85-30904
A method to estimate the self-consistency effects on electronic structure calculations
[INPE-3536-PRE/752] 19 p3375 N85-30936
Interaction of solutes with stretched polymers
[AD-A154662] 21 p3569 N85-32196
Polymerizable ultraviolet stabilizers
21 p3608 N85-32406
Insights into the phylogenetic positions of photosynthetic bacteria obtained from 5S rRNA and 16S rRNA sequence data 21 p3658 N85-32719
X-ray diffractometric measurements and calculations of limiting values of discrepancy between lattices and layer thicknesses, preventing generation of dislocations during growth of multilayer heterostructures
21 p3681 N85-32866
Three-dimensional reconstruction and data display of chromosome structure studied by electron microscope tomography
[DE85-011562] 22 p3825 N85-33697
On the potential link equation of a spot centre with relative deformation for a semi-infinite molecular crystal
[BLL-M-35795-(5828.4)] 23 p3965 N85-34711
The detection and study of molecular species using time resolved laser spectroscopy
[AD-A155910] 24 p4075 N85-35256

MOLECULAR THEORY
Flow and plasticity via nonequilibrium molecular dynamics
[DE85-001011] 10 p1555 N85-19804
Simulation of brittle fracture via molecular dynamics
[DE85-001081] 11 p1653 N85-20410
Atomic, Molecular and Solid-State Theory, and Computational Quantum Chemistry, part 1
[DE85-009401] 20 p3526 N85-31929
Equation of state study for polar fluids
[PB85-204345] 24 p4076 N85-35262

MOLECULAR WEIGHT
Physical-chemical properties of articulated rodlike polymers
[AD-A145549] 02 p0186 N85-11244
Thermoplastic/melt-processable polyimides
04 p0466 N85-12961
Determination of the decomposition behavior of double base propellants at low temperatures
08 p1117 N85-17045
Characterization and adhesive bonding of poly(etheretherketone) resins and composites
[DE85-002526] 11 p1593 N85-20023
Structural basis for the mechanical properties of polyethenes
[PB85-149771] 11 p1613 N85-20142
Synthesis and thermomechanical properties of new AT-Phenylene R systems
[AD-A149861] 12 p1813 N85-21372
Extraction of ions from solutions at atmospheric pressure, mass spectrometric analysis of bioorganic substances 14 p2367 N85-24706
High performance size exclusion chromatography (IX) bulk and component analysis of silanol groups in polydimethylsiloxanes: Process development endeavor
[DE85-006853] 15 p2506 N85-25458
A soluble linear Schiff-base coordination polymer containing eight-coordinate zirconium(4)
[AD-A151446] 15 p2518 N85-25527
Formulation/cure technology for ultrahigh molecular weight silphenylene-siloxane polymers
[NASA-TP-2476] 16 p2753 N85-26990
Relationship of isolated turbulent regions to the general turbulent background, part 4.4A
21 p3823 N85-32506
Size exclusion chromatography-low angle laser light scattering photometry of lignite macromolecules
[DE85-012017] 22 p3745 N85-33215
Molecular and macromolecular sieving by asymmetric ultrafiltration membranes
[PB85-157766] 24 p4077 N85-35266

MOLECULES
NT DIATOMIC MOLECULES
NT POLYATOMIC MOLECULES
Spectrophotometric studies of iodine complexes in an aluminum chloride - butylpyridinium chloride ionic liquid
[AD-A145074] 01 p0024 N85-10150
Nuclear Magnetic Resonance of Polymeric Materials
[AD-A145078] 01 p0032 N85-10192
Theory of nuclear magnetic relaxation
[AD-P003911] 01 p0032 N85-10197
A perturbation solution for rigid dumbbell suspensions in steady shear flow
[AD-A144876] 01 p0111 N85-10755
Chemical derivatization of an array of three gold microelectrodes with polypyrrole: Fabrication of a molecule-based transistor
[AD-A146221] 03 p0359 N85-12304
Neutron scattering on macromolecular solid state materials, solutions and melts 03 p0431 N85-12747
Physico-chemical investigation of some areas of fundamental significance to biophysics
[DE84-016385] 04 p0471 N85-12999
Loeb solutions of the Boltzmann equation with initial boundary values and external forces
[CTH-MATH-1984-23] 05 p0719 N85-14616
Electronically excited atomic and molecular oxygen
[AD-A147732] 08 p1121 N85-17084
Time-of-flight spectroscopy of ionic and metastable fragments from dissociating molecules
[AD-A148068] 08 p1220 N85-17683
Quantum Monte Carlo for molecules
[AD-A148159] 08 p1227 N85-17727
Microscopic study of fluid flow
09 p1317 N85-18280
Supersonic molecular jet study of the liquid state
[AD-A147416] 09 p1379 N85-18671
Molecular hydrogen and thermal phases in astrophysics 09 p1414 N85-18822
Polymers and macromolecules
[DE85-003176] 10 p1454 N85-19160
Dynamical studies of molecular systems
[DE85-003053] 11 p1594 N85-20028
Electrostatic potentials: A new method for interpreting and predicting molecular reactivities and for designing synthetic pathways. Applications to nitroaromatics, nitraminse and nitrated
[AD-A150120] 12 p1801 N85-21296
Some unique aspects of fouling on copper as compared to titanium or nickel
[AD-A150072] 12 p1806 N85-21332
Mean delta-ray energies in ion molecule collisions
[DE85-005524] 13 p2157 N85-23395
O. F. Mossotti and the physics of molecules
[NOTA-INTERNA-822] 14 p2420 N85-24931
Spectroscopy of quasimolecular X-rays with H-like decelerated ions
[DE85-006565] 15 p2649 N85-26337
Experimental study of dissociative attachment in optically-pumped lithium molecules
[AD-A152600] 17 p3030 N85-28738
Spectroscopy of surface adsorbed molecules
[DE85-009452] 17 p3034 N85-28768
Space shuttle molecular and wake vacuum measurements
[NASA-TM-86509] 19 p3222 N85-29978
Determining partial molar volume of hydrogen in titanium alloys 19 p3245 N85-30119
Activities of Rutgers - The State University Department of Mathematics
[AD-A154158] 19 p3370 N85-30804
Photoabsorption and photodissociation of molecules important in the interstellar medium
[NASA-CR-175918] 19 p3383 N85-30986
Size exclusion chromatography-low angle laser light scattering photometry of lignite macromolecules
[DE85-012017] 22 p3745 N85-33215
Preparation and use of very pure o-D2
[DE85-009415] 22 p3843 N85-33800
Electron density distribution analysis for nitroguanidine
[DE85-009596] 23 p3969 N85-34603
Solar modulation of cosmic ray intensity and solar flare events inferred from (14)C contents in dated tree rings
[SH-7.1-2] 23 p4047 N85-35095

MOLIERE FORMULA
U COSMIC RAY SHOWERS
U SECONDARY COSMIC RAYS
U SPATIAL DISTRIBUTION

MOLTEN SALT ELECTROLYTES
Hot-gas cleanup for molten carbonate fuel cells-dechlorination and soot formation
[DE84-003072] 01 p0068 N85-10450
Physico-chemical investigations on the electronic partial conductivity of molten electrolytes, especially of the eutectic mixture LiCl-KCl
[BMFT-FB-T-84-205] 05 p0633 N85-14063
Polymer electrolytes: An investigation of some poly (N-propylaziridine)/lithium salt compositions
[RAE-TR-84036] 08 p1131 N85-17130
Electrolyte resevoir for carbonate fuel cells
[DE85-005736] 23 p3847 N85-34480

MOLTEN SALTS
Effects of H2S on molten carbonate fuel cells
[DE84-015186] 02 p0195 N85-11307
Thermal energy storage at 900 deg C
[DE84-004589] 04 p0530 N85-13387
Measurement of oxide ion concentration in NaCl-ZnCl2 molten salt and several applications
[BLL-AWRE-TRANS-74-(9091.9F)]
06 p0764 N85-14886
Electrochemical behaviour of TiCl4 solutions in low melting point organic media
[BLL-OA-TRANS-3174-(8196.3)]
06 p0764 N85-14886
Advanced latent heat storage media for high-temperature industrial applications
[DE85-000907] 09 p1345 N85-18481
Application of Monte Carlo and molecular dynamics methods to the calculation of thermodynamic properties of molten salts
[AD-A148897] 10 p1586 N85-19869
Direct contact heat recovery from molten salt
[DE85-002830] 11 p1674 N85-20550
Electrochemistry and electrochemical methodology in molten salts
[AD-A149813] 12 p1799 N85-21294
Cathode materials for molten carbonate fuel cells
[DE85-004078] 13 p2130 N85-23254
Exploratory corrosion tests on alloys in molten salts at 900(0)C
[DE85-000511] 14 p2257 N85-23983
Exploratory corrosion tests on materials and fluids for advanced high-temperature molten-salt storage
[DE85-002911] 14 p2258 N85-23991
Material for protection of metal surfaces against corrosion by molten salts
[DE85-007714] 16 p2750 N85-26968
High temperature sensible heat storage options
[DE85-000534] 18 p3129 N85-29375
Development of molten carbonate fuel cell power plant, volume 1
[DE85-008743] 18 p3131 N85-29384
Mechanism of strength degradation for hot corrosion of alpha-SiC
[NASA-TM-87052] 19 p3248 N85-30135
Molten salt cooling/17Li-83Pb breeding blanket concept
[DE85-010522] 19 p3363 N85-30854
Development of low-melting fused salts 6: Formation of molybdenum film from molten ammonium formate bath
[BLL-OA-TRANS-3195-(8196.300)]
20 p3429 N85-31254
Design of a helium-cooled molten salt fusion breeder
[DE85-010474] 20 p3528 N85-31943
The effect of stress and hot corrosion on nickel-base superalloys
[AD-A154722] 21 p3586 N85-32181
Recent advances in d-c relaxation techniques for the measurement of kinetics of fast electrode reactions
[DE85-005029] 22 p3745 N85-33216
Molten carbonate fuel cell separator
[DE85-011615] 22 p3806 N85-33577
Study of alternative system conversions for the Solar One pilot plant
[DE85-010026] 22 p3809 N85-33594
Thermodynamics of the corrosion of chromium in molten carbonates
[DE85-011407] 24 p4079 N85-35262

MOLYBDATES
Additives for heat engine coal slurry fuels
[DE84-016434] 05 p0621 N85-13971
Synthesis and properties of Hexachloromolybdates(5) and related species
[AD-A139599] 07 p0924 N85-15852

MOLYBDENUM
The effect of replacing molybdenum with vanadium on the corrosion resistant properties of stainless steels
02 p0176 N85-11197
Recent developments on the role of molybdenum in irons and steels 02 p0180 N85-11206
Swaged Mo-5 percent W alloy and recrystallized commercially pure molybdenum
02 p0180 N85-11208
The influence of rare Earth elements on the temper embrittlement behaviour and mechanical properties of a low alloy steel 02 p0180 N85-11210
The role of molybdenum as an alloy element in adhesive wear resistance 02 p0181 N85-11212
Corrosion in alkali metal/molybdenum heat pipes
[DE84-014039] 02 p0184 N85-11233
Review: Role of refractory metal alloys in fusion reactor applications
[AERE-R-11317] 03 p0422 N85-12695
Constraints on the origin of the Moon from molybdenum and other siderophile elements
04 p0582 N85-13718
Autenite transformation in powder-compacted chromium-nickel-molybdenum steels during continuous cooling
[BLL-M-35981-(5828.4)] 05 p0615 N85-13933
Special features of the deformation of molybdenum at high temperatures
[BLL-M-36027-(5828.4)] 07 p0924 N85-15856
Investigation of granules of molybdenum-base alloys obtained with pulsed discharges
[BLL-M-36012-(5828.4)] 07 p0926 N85-15871
Identification of spectra of highly ionized Mo, Nb, Zr and Y atoms 09 p1390 N85-18745
WRAP-RIB antenna technology development
14 p2231 N85-23824
Molybdenum solar neutrino experiment
[DE85-003747] 14 p2445 N85-25090
Corrosion inhibitor formulation for molybdenum, tungsten and other metals
[AD-D011593] 15 p2510 N85-25488
Electronic transport in Mo/Ni superlattice
[DE85-006835] 15 p2661 N85-26425
Sodium and lithium corrosion in molybdenum heat pipes
[DE85-005561] 16 p2784 N85-27179
Solid state bonding of molybdenum and TZM
[BLL-T6439/BG/LRS/LRST751/85]
16 p2792 N85-27220
Influence of heat treatment parameters on the properties of induction hardened Ni-Cr-Mo steels
[BLL-BISI-TRANS-2499-(9022.06)]
17 p2926 N85-28053
Influence of temperature in melting and casting on quality of medium-alloy steel
[BLL-BISI-TRANS-22310-(9902.06)]
17 p2936 N85-28137
Study of a simulated test for assessing the machinability of steels
[BLL-BISI-TRANS-22344-(9022.06)]
17 p2972 N85-28357
Elevated temperature erosion corrosion of 9Cr1Mo steel
[DE85-008445] 18 p3074 N85-29016
Surface degradation of ductile metal in elevated temperature gas-particle streams
[DE85-008428] 18 p3074 N85-29017

The effect of temperature on the corrosion-erosion of 9Cr1Mo steel
[DE85-008607] 18 p3076 N85-29030
Structural transformation of a 9% Cr - 2%Mo steel (type Z10CDNbV 09-02) for use in steam generators for fast neutron reactors
[BLL-CE-TRANS-7943-(9022.09)] 20 p3430 N85-31271
The effect of pre-heating on the structure and properties of chromium-molybdenum steels
[BLL-M-35897-(5828.4)] 23 p3914 N85-34255
Development of metallization process: FSA project, cells and module formation research area
[NASA-CR-176136] 23 p3945 N85-34447
Some recent deposit modeling efforts 24 p4106 N85-35453
The Conterminous United States Mineral Assessment Program 24 p4106 N85-35458

MOLYBDENUM ALLOYS
NT RENE 95
Effect of rhenium on the structure and properties of the weld metal of a molybdenum alloy
[NASA-TM-77491] 03 p0330 N85-12128
The formation of isolated phase precipitates during the decomposition of high-coercive force Fe-Cr-Co alloys
[BLL-M-36028-(5828.4)] 07 p0824 N85-15855
Susceptibility of 2 1/4 Cr-1Mo steel to liquid metal induced embrittlement by lithium-lead solutions
[DE85-000697] 09 p1294 N85-18130
Effect of tempering on the strength and toughness of 2 1/4 Cr-1 Mo steel weldments
[DE85-003618] 09 p1296 N85-18140
Electrical resistivity and structural changes upon relaxation and crystallization of (Mo/sub 0.6/Ru/sub 0.4/)sub 100-x/B/sub x/ metallic glasses
[DE84-017281] 09 p1299 N85-18160
Assessment of the need for an advanced high-strength chromium-molybdenum steel for construction of third-generation gasifier pressure vessels
[DE85-002865] 11 p1608 N85-20097
Ferromagnetic resonance in a Ni-Mo superlattice
[DE85-003039] 11 p1735 N85-20911
Partial replacement of chromium in austenitic stainless steels by molybdenum, copper, and vanadium, report of investigations 1884
[PB86-116508] 12 p1809 N85-21346
Solution softening in molybdenum-rhenium alloys
[DE85-006706] 16 p2750 N85-26972
Study to optimize Cr-Mo steels to resist hydrogen and temper embrittlement
[DE85-005492] 17 p2932 N85-28096
Corrosion-erosion rates/mechanisms of 9Cr1Mo steel
[DE85-008506] 18 p3076 N85-29029
Fatigue behavior of HY-130 steel weldments containing fabrication discontinuities
[AD-A153630] 18 p3122 N85-29326
Fatigue-crack growth and ductile fracture toughness behavior of ASTM A387 Grade 91 steel
[DE85-006495] 20 p3431 N85-31286
Reliability of welds to repair defects in cast components made from CrMoV steel
[BLL-CE-TRANS-8054-(9022.09)] 20 p3461 N85-31501
Application of the unloading compliance methods in fracture toughness measurements of a quenched and tempered steel
[BLL-CE-TRANS-7953-(9022.09)] 20 p3465 N85-31523
Fatigue behavior of chromium-containing ferritic steels at elevated temperature
[DE85-012309] 22 p3748 N85-33231
Microstructures in rapidly solidified Ni-Mo alloys
[NASA-TM-87100] 23 p3915 N85-34256
Characterization of modified 9 Cr Mo steel extruded pipe
[DE85-012056] 23 p3941 N85-34430
Characterization of modified 9 r-1 Mo steel sand castings
[DE85-012057] 24 p4060 N85-35287

MOLYBDENUM COMPOUNDS
NT MOLYBDATES
NT MOLYBDENUM DISULFIDES
NT MOLYBDENUM OXIDES
Reinforcement of molybdenum disilicide with nematic crystals of aluminum oxide 03 p0353 N85-12269
Preparation and electronic properties of MoS(2) and WS(2) single crystals grown in the presence of cobalt
[AD-A146508] 06 p0866 N85-15506
The mechanisms of phenylacetylene polymerization by molybdenum and titanium initiators
[AD-A150993] 14 p2290 N85-24007

MOLYBDENUM DISULFIDES
Structural studies of sputtered MOS(2) films by angle-resolved photoelectron spectroscopy
[AD-A146052] 03 p0433 N85-12759
Molybdenum disulphide lubrication: A continuation survey, 1981 - 1983
[REPT-84-549] 18 p3082 N85-29065
Advances in rechargeable lithium molybdenum disulfide batteries 20 p3444 N85-31376

MOLYBDENUM OXIDES
Butene oxidation by molybdenum crystallographic shear compounds
[DE84-013910] 05 p0614 N85-13923
Correlation of electronic charge transfer transitions and electrochemical potentials. The Bipyrazine(Tetracarbonyl)Molybdenum(O) system in various solvents
[AD-A147660] 06 p1120 N85-17062
Development of low-melting fused salts 8: Formation of molybdenum film from molten ammonium formate bath
[BLL-OA-TRANS-3195-(6196.300)] 20 p3429 N85-31264

MOLYBDENUM SULFIDES
NT MOLYBDENUM DISULFIDES

MOMENT DISTRIBUTION
Force and moment measurements on a 74 deg delta wing with an apex flap
[NASA-CR-166061] 02 p0134 N85-10918
Mathematical modeling of assembly processes involving use of sensitized robots 04 p0488 N85-13111
Experimentally determined distribution of stress around a horizontally loaded model pile in dense sand
[CE-43] 16 p2796 N85-27239
Moment-method formulation of the cavity-probe aperture antenna
[DE85-013264] 24 p4088 N85-35338

MOMENTS
NT BENDING MOMENTS
NT DIPOLE MOMENTS
NT DISTRIBUTION MOMENTS
NT ELECTRIC MOMENTS
NT LOADING MOMENTS
NT MAGNETIC MOMENTS
NT MEAN
NT MOMENTS OF INERTIA
NT ORTHOGONALITY
NT PITCHING MOMENTS
NT ROLLING MOMENTS
NT STABILITY DERIVATIVES
NT STANDARD DEVIATION
NT TORQUE
NT YAWING MOMENTS
Experimental trim drag values and flow-field measurements for a wide-body transport model with conventional and supercritical wings
[NASA-TP-2071] 02 p0135 N85-10920
Determination of moments of initial estimate during linear approximation of distribution of ejected impurity 07 p0964 N85-16045
Magnetic and structural properties of shock-synthesized zinc ferrite
[DE85-000469] 11 p1736 N85-20915
A moment solution for an arbitrary configuration of partly shielded wires above a ground plane
[AD-A149762] 12 p1828 N85-21473
Stability of functionals determined by moment conditions
[TRITA-NA-8310] 16 p2852 N85-27585
Moments in particle-in-cell simulations
[DE85-010792] 19 p3356 N85-30803
The use of moments of momentum to account for crystal habits
[NASA-CR-3907] 20 p3421 N85-31232
Object identification and manipulation using silhouette moments
[AD-A154755] 21 p3705 N85-33011

MOMENTS OF INERTIA
Solving equations of movement with variable inertia moment
[BLL-M-35975-(5828.4)] 05 p0641 N85-14111
Inertial analysis of the Charpy test
[OUEL-1571/85] 20 p3471 N85-31570
Inertial stresses and deformations in mechanisms 23 p3924 N85-34320

MOMENTUM
NT ANGULAR MOMENTUM
Turbulent boundary layers over rough surfaces hypersonic flow
[AD-A145040] 01 p0003 N85-10016
Review of some vortex relations
[NASA-CR-172452] 01 p0046 N85-10302
Searching for top, Higgs, and supersymmetry: The minimum invariant mass technique
[DE84-014539] 01 p0119 N85-10813
Autonomous momentum management for space station, exhibit A
[NASA-CR-171256] 04 p0462 N85-12933
Turbulent drag reduction research 08 p1071 N85-16788
The Origin of Nonradiative Heating/Momentum in Hot Stars
[NASA-CP-2358] 08 p1231 N85-17755
Theoretical investigation of dynamic stall using a momentum integral method
[AD-P004170] 09 p1286 N85-17955
The Fermi surface and momentum space densities of ferromagnetic Gd using the Positron technique 09 p1396 N85-18768
Aspects of planetary wave transports in the middle atmosphere 11 p1661 N85-20471
Mathematical modeling of transient performance of gas turbine engine 13 p2050 N85-22834
Investigation of potential and viscous flow effects contributing to dynamic stall
[AD-A151696] 15 p2557 N85-25773
Coherent state description of non-topological solitons and momentum projection
[DE85-007814] 17 p3033 N85-28761
Multiple equilibria of the barotropic vorticity equation on a sphere 18 p3146 N85-29475
An experimental investigation of curvature and freestream turbulence effects on heat transfer and fluid mechanics in transitional boundary layer flows 19 p3264 N85-30240
The use of moments of momentum to account for crystal habits
[NASA-CR-3907] 20 p3421 N85-31232
Techniques for the study of gravity waves and turbulence (keynote paper), part 4 21 p3621 N85-32499
Momentum flux measurements: Techniques and needs, part 4.5A 21 p3623 N85-32508
Electron loss process and cross section of multiply charged ions by neutral atoms 23 p3981 N85-34685
1Single particle momentum and angular distributions in hadron-hadron collisions at ultrahigh energies
[HE-1.2-1] 24 p4171 N85-35860

MOMENTUM ENERGY
U KINETIC ENERGY

MOMENTUM THEORY
Phase space factors in multiparticle processes 24 p4175 N85-35888

MOMENTUM TRANSFER
Mass and momentum transport in a turbulent buoyant vertical axisymmetric jet 05 p0635 N85-14070
Analysis of diabatic heating during FGGE 05 p0683 N85-14393
Momentum distributions in superfluid helium: Bose condensate fraction
[DE84-014676] 05 p0731 N85-14700
Corotating interaction regions in stellar winds: Particle acceleration and non-thermal radio emission in hot stars 08 p1234 N85-17773
Synchrotron emission from chaotic stellar winds 08 p1234 N85-17774
A one dimensional dynamical model of ocean/atmosphere interactions 09 p1358 N85-18545
Studies of P-shell nuclei by large momentum transfer electron scattering
[DE84-016803] 09 p1381 N85-18686
Momentum and heat transfers in a complex, but well-defined turbulent fluid flow
[DE85-002857] 10 p1486 N85-19381
UK participation in the Middle Atmosphere Programme 11 p1655 N85-20426
Recent progress in electron scattering at SLAC
[DE85-002718] 11 p1723 N85-20840
Physics of the inner heliosphere: Mechanisms, models and observational signatures
[NASA-CR-175632] 13 p2205 N85-23677
Circulation and transport in the middle atmosphere: Troposphere and lower atmosphere 18 p3148 N85-29491
Circulation and transport in the middle atmosphere: Mesosphere and lower thermosphere 18 p3148 N85-29492
Magnetic scattering and polarized neutrons
[DE85-009623] 19 p3355 N85-30794
Transverse momentum distribution of pion dog in the fragmentation region of super high energy interactions 24 p4190 N85-35921

MONEL (TRADEMARK)
The use of sustenitic stainless steel versus monel (Ni-cu) alloy in pressurized Gaseous Oxygen (GOX) life support systems
[AD-A156305] 24 p4134 N85-35625

MONGE-AMPERE EQUATION
New methods for numerical solution of one class of strongly nonlinear partial differential equations with applications in hydrodynamics
[AD-A149026] 10 p1545 N85-19739

MONITORS
NT INFRARED RADIOMETERS

User experience of existing corrosion monitoring techniques and the development of Thin Layer Activation (TLA) for corrosion monitoring
[AERE-R-11248] 01 p0029 N85-10183
A microcomputer aided measurement equipment for monitoring performance in digital radio relay systems
[FUB-4-1984] 01 p0101 N85-10668
The structures and the role of an international agency for the control of satellites
[NASA-TM-76765] 03 p0441 N85-12806
System status display information
[NASA-CR-172347] 04 p0455 N85-12889
Comparison of wind derived from the LIMS (Limb Infrared Monitor of the Stratosphere) satellite instrument with rocket observations
[NASA-CR-174083] 04 p0541 N85-13444
Qualification of noninvasive systems for on-line leak detection in high pressure feed water preheaters
[CISE-2341] 04 p0558 N85-13555
In-line beam current monitor
[DE84-014054] 04 p0560 N85-13567
Use of monitors in FORTRAN: A tutorial on the barrier, self-scheduling DO-loop and Askfor monitors
[DE84-016506] 05 p0715 N85-14587
Tornado: Structural Usage Monitoring System (SUMS)
07 p0896 N85-15860
Battery control and fault detection method
[AD-D011384] 07 p0993 N85-16307
Military vital sign monitor
[AD-A147257] 07 p1016 N85-16452
Interactive color-graphics interface for energy monitoring and control systems
[AD-A147538] 07 p1025 N85-16509
Monitoring cure of epoxy resins using a microdielectrometer
[AD-A148618] 08 p1119 N85-17054
The use of microdielectrometry in monitoring the cure of resins and composites
[AD-A148619] 08 p1119 N85-17055
Battery charger
[AD-D011420] 08 p1178 N85-17425
Design description of a microprocessor based Engine Monitoring and Control unit (EMAC) for small turboshaft
[NASA-TM-86860] 09 p1263 N85-17935
Effect of water vapor and water droplets on the RAM-1 (Real-Time Aerosol Monitor): Preliminary results
[PB85-109429] 11 p1637 N85-20313
Development of a low cost electrochemical CO monitor based on anodic scanning voltammetry in nonaqueous electrolyte
[PB85-113488] 11 p1637 N85-20314
Continuous measurement of zircaloy corrosion in air with an ultrasonic corrosion monitor
[DE85-003663] 12 p1807 N85-21337
Remote self-contained undersea monitor
[AD-D011520] 12 p1849 N85-21599
Applications of vibration analysis to the condition monitoring of rolling element bearings
[ARL/AERO-R-163] 12 p1859 N85-21663
Focal plane array optical proximity sensor
[NASA-CASE-NPO-15155-1] 12 p1932 N85-22139
Invariant system of technological preparation of production
14 p2268 N85-24056
An improved battery state-of-charge indicator
[NASA-CR-175701] 14 p2296 N85-24227
Computer controlled acquistion of corrosion rate data from multiple sensors
[PB85-157378] 15 p2524 N85-25559
Continued development of a data base management system performance monitor, volume 2
[AD-A151714] 15 p2623 N85-26167
Signal analysis techniques for incipient failure detection in turbomachinery
16 p2736 N85-26884
Reusable rocket engine turbopump condition monitoring
16 p2740 N85-26907
Equipment for monitoring low concentrations of volatile substances in gases or liquid metals
[BLL-DOUNREAY-TR-949-(9091.9F)]
16 p2786 N85-27190
Results from radiation monitoring equipment experiment on STS-8
[AD-A153241] 17 p3055 N85-28911
Retinally stabilized differential resolution television display
[NASA-CASE-NPO-15432-1] 18 p3089 N85-29117
Laser Schlieren crystal monitor
[NASA-CASE-MFS-28060-1] 19 p3374 N85-30632
Heat transfer monitor for measurements of fouling of industrial heat exchangers
[DE85-010257] 20 p3455 N85-31455
Production verification of the acoustic emission weld monitor
[AD-A154166] 20 p3464 N85-31519
Results from radiation monitoring equipment experiments on STS-41C, 41D, 41G and 51A
[AD-A154676] 21 p3580 N85-32142
Monitoring dosage of volatile compounds in tests at low barometric pressure
23 p3954 N85-34506
Evaluation: Close-range photogrammetry for slope inventory and monitoring
[PB85-192755] 24 p4108 N85-35470

MONKEYS
Primate equilibrium performance and diazepam: A behavioral tolerance effect
[AD-A145158] 01 p0094 N85-10634
Specific absorption rate in a sitting rhesus model at 225, 1290, and 5950 MHz for E, H, and K polarizations
[AD-A145435] 02 p0234 N85-11524
Susceptibility of cat and squirrel monkey to motion sickness induced by visual stimulation: Correlation with susceptibility to vestibular stimulation
11 p1694 N85-20650
Histological and compositional responses of bone to immobilization and other experimental conditions
[NASA-CR-175837] 16 p2841 N85-27518
Encapsulation and packaging of a semiconductor multielectrode array for cortical implantation
[AD-A153180] 17 p2986 N85-28535
Primate adrenal reactions to antiorthostatic hypokinesia
19 p3324 N85-30591
Analysis of long bone and vertebral failure patterns
[AD-A154796] 21 p3663 N85-32758
Morphological study of antiorthostatic hypokinesia in monkeys
22 p3822 N85-33680

MONOCHROMATIC RADIATION
Analysis of data entry performance: Chromatic versus monochromatic
[AD-A145568] 03 p0438 N85-12789
Application of tunable monochromatic synchrotron radiation to the quantitative determination of trace elements
[DE85-001271] 09 p1291 N85-18106
Design of VUV monochromator systems
09 p1388 N85-18733
Kinetic energies of fragment ions produced by dissociative photoionization of NO
[NASA-CR-175721] 15 p2647 N85-26327

MONOCHROMATIZATION
A posteriori increase of resolving power of optical system forming averaged monochromatic images
13 p2062 N85-23003

MONOCHROMATORS
A normal-incidence monochromator branch line on the FEL-undulator for experimental studies in the 5 to 30 eV region
[DE84-014379] 04 p0505 N85-13225
Design of VUV monochromator systems
09 p1388 N85-18733
In situ thin film measurement
[AD-A151365] 15 p2659 N85-26411
Optical 3-D signature device for detecting chemical agents
[AD-D011669] 19 p3272 N85-30293
Microwave SAW (Surface Acoustic Wave) monochromator
[AD-D011718] 21 p3590 N85-32311

MONOCRYSTALS
U SINGLE CRYSTALS

MONOLITHIC CIRCUITS
U INTEGRATED CIRCUITS

MONOMERS
Implantation of ionized monomer into aluminum alloy 6061 for marine corrosion protection
[AD-A144874] 01 p0028 N85-10172
Vinyl citrates from citric acid as new monomers
[BMFT-FB-T-83-256] 03 p0338 N85-12178
Chemical modification of the surface of high modulus carbon fibers
04 p0467 N85-12967
Conduction in polymerized polyfunctional diacetylenes
[AD-A149104] 10 p1451 N85-19145
Process for preparing highly optically transparent-colorless aromatic polyimide film
[NASA-CASE-LAR-13351-1] 12 p1811 N85-21360
Chiral polymers
[AD-A150366] 13 p2037 N85-22760
Evaluation of experimental epoxy monomers
[NASA-TM-87476] 16 p2754 N85-26996
Light scattering and spectroscopic studies of polymerization processes
[AD-A153407] 18 p3089 N85-29084
Processable and stable conductive polymers
[AD-D011684] 19 p3249 N85-30143
Graphite/PMR polyimide composites with improved toughness
[NASA-TM-87081] 21 p3561 N85-32148

MONOMOLECULAR FILMS
Interaction of UV-laser radiation with molecular surface-films
[AD-A146311] 03 p0388 N85-12349

MONOPLANES
NT A-7 AIRCRAFT
NT B-70 AIRCRAFT
NT BOEING 737 AIRCRAFT
NT BOEING 767 AIRCRAFT
NT C-135 AIRCRAFT
NT C-141 AIRCRAFT
NT CESSNA 402B AIRCRAFT
NT CL-41 AIRCRAFT
NT CV-990 AIRCRAFT
NT DC 8 AIRCRAFT
NT DH 115 AIRCRAFT
NT DHC 2 AIRCRAFT
NT DO-28 AIRCRAFT
NT F-8 AIRCRAFT
NT F-17 AIRCRAFT
NT F-27 AIRCRAFT
NT F-104 AIRCRAFT
NT F-106 AIRCRAFT
NT JET PROVOST AIRCRAFT
NT MIRAGE AIRCRAFT
NT MIRAGE 3 AIRCRAFT
NT OV-1 AIRCRAFT
NT P-3 AIRCRAFT
NT RF-4 AIRCRAFT
NT T-33 AIRCRAFT
NT U-2 AIRCRAFT
An overview of some monoplanar missile programs
[NASA-TM-86330] 08 p0747 N85-14786

MONOPOLE ANTENNAS
NT WHIP ANTENNAS
Compact wideband multiple conductor monopole antenna
[AD-D011331] 07 p0944 N85-15881
Surface wave excitation study
[DE85-005301] 13 p2056 N85-22875
Parameterization of a transient electromagnetic facility and test antennas from transient data
[DE85-006231] 15 p2545 N85-25710

MONOPOLES
NT MAGNETIC MONOPOLES
Slowly rotating pulsed radiation source
02 p0258 N85-11678

MONOPROPELLANTS
Liquid propellants for use in guns: A review
[AD-A153051] 17 p2937 N85-28131

MONOPULSE ANTENNAS
Phase only adaptive nulling in a monopulse antenna
[AD-D011289] 05 p0626 N85-14026
Inherent angular tracking error in an amplitude comparison monopulse radar
[AD-A154212] 19 p3255 N85-30185

MONOPULSE RADAR
Phase only adaptive nulling in a monopulse antenna
[AD-D011289] 05 p0626 N85-14026
Conformal phased array antenna pattern corrector
[AD-D011489] 10 p1488 N85-19266
A radome for air traffic control SSR radar systems
[AD-P004373] 12 p1827 N85-21467
Ziv-Zakai bound applied to an amplitude-comparison monopulse radar
[AD-A151937] 16 p2773 N85-27118
Angular tracking error in A phase comparison monopulse tracking radar: A critical review and extension of the phase front distortion approach
[AD-A152628] 17 p2949 N85-28205
Inherent angular tracking error in an amplitude comparison monopulse radar
[AD-A154212] 19 p3255 N85-30185

MONOSACCHARIDES
NT RIBOSE

MONOTONE FUNCTIONS
Estimating a monotone density
[CWI-MS-R8403] 05 p0721 N85-14833
A monotonicity property of the power function of multivariate tests
[CWI-MS-R8406] 05 p0721 N85-14835
Stable monotone variational inequalities
[AD-A147123] 07 p1031 N85-16544
Convergence of quasi-stationary to stationary distributions for stochastically monotone Markov processes
[AD-A148041] 08 p1215 N85-17652
On functions with a finite or locally bounded Dirichlet integral
15 p2635 N85-26243
When is a Bernstein-Bezier curve the graph of a function?
17 p3003 N85-28568
Limit behaviour for stochastic monotonicity and applications
[AD-A153814] 18 p3170 N85-29648

MONSOONS
Investigation of satellite measurements in the presence of clouds, forcing influences on clouds and feedback to the large scale following convection
05 p0682 N85-14381

Relationship of Indian monsoon intensity to time of onset 13 p2106 N85-23120
The BALSAMINE experiment 14 p2238 N85-23876
Radiative forcing of the southwest summer monsoon (a satellite perspective) 15 p2593 N85-25981
Influence of land surface processes on the Indian monsoon: A numerical study 18 p3146 N85-29478
On the interannual variability of the Indian monsoon and the Southern Oscillation 20 p3495 N85-31728

MONTANA
Geology of selected migmatite zones within the bitterroot lobe of the Idaho batholith, Idaho and Montana 03 p0389 N85-12489
Chronologic and climatic control on soil development, northern Bighorn Basin, Wyoming and Montana 06 p1181 N85-17443
Depositional systems and coal occurrence in the Fort Union Formation (Paleocene), Powder River Basin, Wyoming and Montana 24 p4114 N85-35505

MONTE CARLO METHOD
A Monte Carlo comparison of the recovery of winds near upwind and downwind from the SASS-1 model function by means of the sum of squares algorithm and a maximum likelihood estimator
[NASA-CR-3839] 01 p0064 N85-10421
SANDYL radiation transport code at the Naval Research Laboratory
[AD-A144890] 01 p0117 N85-10799
Theoretical development of Monte Carlo codes for modeling cumulus cloud fields
[NASA-CR-174063] 02 p0230 N85-11600
Design and implementation of a modular program system for statistical analyses
[IKE-4-114] 04 p0551 N85-13503
Risk analysis without Monte Carlo methods 04 p0556 N85-13537
Approximating the percentage points of Greenwood's statistic with Cornish-Fisher expansions
[CWI-MS-R8405] 05 p0721 N85-14634
Binaries and evolution of globular clusters 05 p0736 N85-14744
Efficient scores, variance decompositions and Monte Carlo swindles
[AD-A146573] 06 p0858 N85-15458
The effect of assumptions about cost element probability distributions on operating and support cost risk analysis
[AD-A147553] 07 p1036 N85-16576
Validation of the communications link analysis and simulation system (CLASS) 08 p1100 N85-16954
The extension of an invertible coniferous forest canopy reflectance model using SIR-B and LANDSAT data 08 p1149 N85-17246
Two-dimensional modeling for lineal and areal probabilities of weather conditions
[AD-A147970] 08 p1188 N85-17486
A modified Monte-Carlo technique for the simulation of satellite communication systems
[AD-A148669] 08 p1214 N85-17641
Quantum Monte Carlo for molecules
[AD-A148159] 08 p1227 N85-17727
Multiline transfer and the dynamics of stellar winds 08 p1236 N85-17788
Turbulent premixed flame study
[DE85-003220] 09 p1292 N85-18112
Generation of radiation transport geometry from computer-generated design data — monte carlo solution of the neutron transport equation
[DE84-017380] 09 p1370 N85-18606
Small-sample properties of kernel density estimators from randomly right-censored data
[AD-A148752] 09 p1374 N85-18634
A kernel type estimator of a quantile function from right-censored data
[AD-A148753] 09 p1374 N85-18635
Monte Carlo simulation of electron thermalization in rare gases
[NAL-TR-834T] 09 p1375 N85-18643
Monte Carlo simulation of gas Cerenkov detectors
[DE85-002422] 10 p1488 N85-19394
Some investigations of molecular beam epitaxial growth of 3-5 semiconductor films via Monte-Carlo computer simulations, carrier tunneling and spectroscopic ellipsometry
[AD-A149485] 10 p1583 N85-19854
Application of Monte Carlo and molecular dynamics methods to the calculation of thermodynamic properties of molten salts
[AD-A148897] 10 p1585 N85-19868
MCNP code
[DE85-002585] 11 p1702 N85-20705
ITS: The Integrated TIGER Series of coupled electron/photon Monte Carlo transport codes
[DE85-003719] 11 p1725 N85-20847
Monte Carlo studies of tandem mirror plasmas interacting with waves in the Ion Cyclotron Range of Frequencies (ICRF)
[DE85-002988] 11 p1731 N85-20883
Simulating supersymmetry at the SSC
[DE85-000699] 11 p1736 N85-20917
Cometary atmospheres: Modeling the spatial distribution of observed neutral radicals
[NASA-CR-175491] 11 p1765 N85-21097
A model for the evolution of on-orbit manmade debris environment 12 p1784 N85-21196
Ordinary and proper location M-estimates for ARMA models, revised
[AD-A149705] 12 p1920 N85-22061
Jet topologies in hadron-hadron collisions
[DE85-001328] 12 p1929 N85-22119
A Monte Carlo sampling plan for estimating network reliability
[AD-A150511] 13 p2065 N85-22898
Introduction to combinatorial geometry
[DE85-003266] 13 p2152 N85-23364
Problems in recovering crater production functions 13 p2182 N85-23539
Monte Carlo modeling of lunar megaregolith development 13 p2197 N85-23627
Tracer diffusion in an ordered alloy: Application of the path probability and Monte Carlo methods
[DE85-002766] 14 p2257 N85-23986
Modeling of radiothermal radiation of rain by Monte-Carlo method 14 p2341 N85-24476
Research in theoretical nuclear physics
[DE85-006172] 14 p2418 N85-24920
Monte Carlo lattice models for adsorbed polymer conformation
[NASA-TP-2453] 14 p2426 N85-24961
Soliton energetics in extended Peierls-Hubbard models: A quantum Monte Carlo study
[DE85-005409] 14 p2429 N85-24981
Lattice Monte Carlo calculations of finite temperature QCD
[DE85-004035] 14 p2431 N85-24992
Multiple scattering of electromagnetic waves in discrete random media
[AD-A151766] 16 p2772 N85-27112
A mathematical model for calculating detection probability of a diffusion target
[AD-A152026] 16 p2854 N85-27601
An overview of stochastic signal modeling
[AD-A152144] 16 p2855 N85-27605
The statistical analysis of initial imperfection measurements — shell profiles
[VTH-LR-442] 16 p2857 N85-27622
Energy reflection coefficient for H+ ions at energies between 10 and 60 keV
[DE85-007547] 16 p2863 N85-27662
LIGHT: A ray tracing code to simulate light collection in scintillation spectrometers and light pipes
[DE85-007213] 16 p2865 N85-27673
Adding computationally efficient realism to Monte Carlo turbulence simulation
[NASA-TP-2469] 17 p3025 N85-28706
Incorporation of Monte Carlo electron interface studies into photon general cavity theory
[DE85-007674] 17 p3034 N85-28772
Lattice actions improved by block-spin renormalisation group and maximally symmetric lattices
[DE85-007416] 17 p3045 N85-28841
Diffusion of gases in porous solids: Simulation and measurements
[DE85-006870] 18 p3101 N85-29196
Fast electromagnetic (EM) shower simulation
[NOTA-INTERNA-831] 18 p3175 N85-29683
Monte Carlo simulation of thermalization of subexcitation electrons in He, Ne, Ar, Kr and Xe
[NAL-TR-843T] 18 p3178 N85-29702
Comparison of calculations and measurements of the off-axis radiation dose (SI) in liquid nitrogen as a function of radiation length
[AD-A153676] 18 p3178 N85-29704
SPECTER: Neutron damage calculations for materials irradiations
[DE85-005791] 18 p3180 N85-29716
Mathematics of oil production
[DE85-011235] 19 p3267 N85-30261
SABRINA: An interactive solid geometry modeling program for Monte Carlo
[DE85-010796] 19 p3339 N85-30692
MECA: A multiprocessor concept specialized to Monte Carlo
[DE85-010791] 19 p3346 N85-30737
MCNP variance reduction overview
[DE85-010765] 19 p3346 N85-30741
A comparison of four Monte Carlo methods for estimating the probability OF S=T connectedness
[AD-A154264] 19 p3348 N85-30749
MCNP: A general Monte Carlo code for neutron and photon transport
[DE85-010764] 19 p3348 N85-30753
Low-discrepancy point sets in transport codes
[DE85-010768] 19 p3348 N85-30755
Hybrid two-dimensional Monte-Carlo electron transport in self-consistent electromagnetic fields
[DE85-010757] 19 p3348 N85-30756
Monte Carlo alpha calculation
[DE85-010720] 19 p3349 N85-30758
Surface effects on sputtered atoms and their angular and energy dependence
[DE85-010506] 19 p3354 N85-30790
High-energy particle Monte Carlo at Los Alamos
[DE85-010716] 19 p3363 N85-30856
Monte Carlo electron/photon transport
[DE85-010799] 19 p3364 N85-30861
Monte Carlo simulations of fermion systems: The determinant method
[DE85-010708] 19 p3376 N85-30947
Monte Carlo sampling strategies for lattice gauge calculations
[DE85-010756] 19 p3377 N85-30948
Comparison of ERS-1 scatterometer Monte Carlo performance simulations using a weighted nonlinear least squares and a maximum likelihood estimation method 20 p3420 N85-31224
Direct simulation techniques for the Boltzmann equation
[DFVLR-FB-85-13] 20 p3457 N85-31470
MIG: MCNP Input Generator for EFFI magnet geometries
[DE85-010494] 20 p3515 N85-31857
Monte Carlo: In the beginning and some great expectations
[DE85-010789] 20 p3518 N85-31872
Monte-Carlo treatment of nonlinear collisional effects in charged-particle transport
[DE85-010755] 20 p3521 N85-31897
Methods of Monte Carlo electron transport in particle-in-cell codes
[DE85-010702] 20 p3521 N85-31898
Time-implicit Monte-Carlo collision algorithm for particle-in-cell electron transport models
[DE85-010758] 20 p3521 N85-31900
Forecasting of tropical cyclone motion using an EOF (Empirical Orthogonal Function) representation of wind forcing
[AD-A155034] 21 p3636 N85-32580
Monte Carlo studies of H2O layers adsorbed on a model basal face of AgI 21 p3643 N85-32633
Radiation transport
[DE85-010333] 21 p3703 N85-33005
Power density and threshold control strategies for radar track initiation
[AD-A155357] 22 p3756 N85-33262
MORSE-CGA: A Monte Carlo radiation transport code with array geometry capability
[DE85-012063] 22 p3830 N85-33718
Monte Carlo learning-biasing experiment with intelligent random numbers
[DE85-010713] 22 p3834 N85-33742
Implicit Monte Carlo methods and non-equilibrium Marshak wave radiative transport
[DE85-010711] 22 p3835 N85-33743
Nuclear data for MCNP
[DE85-010794] 22 p3840 N85-33782
Digital characterization of particle tracks for microdosimetry
[DE85-012898] 22 p3846 N85-33822
Energy spectrum of extragalactic gamma-ray sources
[OG-2.7-13] 22 p3872 N85-33986
Long term variability of the cosmic ray intensity
[OG-3.1-11] 22 p3874 N85-33990
Arrival directions of cosmic rays of E .4 EeV
[OG-5.3-4] 22 p3884 N85-34071
Coupled electron-photon transport calculations using the method of discrete ordinates
[DE85-009444] 23 p3967 N85-34597
Monte Carlo techniques for analyzing deep penetration problems
[DE85-011426] 23 p3968 N85-34598
CYLTRAN calculations of electron effects on XD detectors
[LA-10264-MS] 23 p3969 N85-34601
Low-energy sputterings with the Monte Carlo Program ACAT
[IPPJ-AM-40] 23 p3982 N85-34690
Monte Carlo calculations of relativistic solar proton propagation in interplanetary space
[SH-3.2-11] 23 p4004 N85-34826
Modeling a high energy gamma-ray telescope
[OG-9.2-5] 23 p4025 N85-34944
A position sensitive phoswich hard X-ray detector system
[OG-9.3-12] 23 p4026 N85-34957

On the statistical significance of excess events: Remarks of caution and the need for a standard method of calculation
[OG-9.5-10] 23 p4031 N85-34867
Additional flux of particles and albedo-electrons in upper atmosphere
[SH-6.1-6] 23 p4045 N85-35080
Monte Carlo calibration of the SMM gamma ray spectrometer for high energy gamma rays and neutrons
[SH-9.1-6] 23 p4051 N85-35121
Two-dimensional numerical modeling of ion implanted GaAs MESFET devices 24 p4088 N85-35341
Calculation of heavy-ion tracks in liquid water
[DE85-012101] 24 p4149 N85-35725
EAS accompanied by gamma-families at Mt. Norikura and comparison with Monte Carlo simulation
[HE-3.3-10] 24 p4181 N85-35928
Relation between gamma-ray family and EAS core: Monte-Carlo simulation of EAS core
[HE-3.6-7] 24 p4185 N85-35955
The lateral distributions of charged particles of energy greater than 0.3 E sub crit in electron-photon cascades in lead and air
[HE-3.6-10] 24 p4185 N85-35957
Result of Monte-Carlo simulation of electron-photon cascades in lead and layers of lead-scintillator
[HE-3.6-11] 24 p4185 N85-35958
Hadrons registration in emulsion chamber with carbon block
[HE-3.7-3] 24 p4186 N85-35962
New analysis of nuclear interaction observed by Mt. Kanbara emulsion chamber experiment
[HE-3.7-4] 24 p4186 N85-35963
Intensities of high-energy cosmic rays at Mount Kanbala
[HE-3.7-5] 24 p4186 N85-35964
Ultra high energy events in ECHOS series and primary energy spectrum
[HE-3.7-9] 24 p4186 N85-35966
Theoretical study of EAS hadronic structure
24 p4189 N85-35991
Particle distributions in approximately 10(13) - 10(16) eV air shower cores at mountain altitude and comparison with Monte Carlo simulations
[HE-4.2-18] 24 p4190 N85-35994
The longitudinal development of muons in cosmic ray air showers at energies 10(15) - 10(17) eV
[HE-4.3-12] 24 p4192 N85-36006
Topological aspects of age parameter
[HE-4.3-13] 24 p4192 N85-36007
Monte Carlo simulation of EAS generated by 10(14) - 10(16) eV protons
[HE-4.3-14] 24 p4192 N85-36008
A three-dimensional Monte Carlo calculation of the photon initiated showers and Kiel result
[HE-4.5-13] 24 p4196 N85-36035
Multimuons events and primary composition
[HE-5.1-5] 24 p4201 N85-36070
The spectrum of cosmic ray muons obtained with 100-ton scintillation detector underground and the analysis of recent experimental data
[HE-5.1-6] 24 p4201 N85-36071
A new world survey expression for cosmic ray vertical intensity vs. depth in standard rock
[HE-5.1-10] 24 p4201 N85-36073
Muon groups and primary composition at 10 to the 13th power to 10 to the 15th power eV
[HE-5.1-12] 24 p4201 N85-36074

MONTEREY BAY (CA)
Coastal erosion along Monterey Bay
[AD-A155810] 21 p3855 N85-32707

MOON
Magnetosphere, rings, and moons of Uranus
02 p0301 N85-11951
Conference on the Origin of the Moon
[NASA-CR-174068] 04 p0581 N85-13709
Geophysical and geochemical constraints favoring the capture hypothesis 04 p0581 N85-13710
Lunar magma ocean and its implication for origin of the Moon 04 p0581 N85-13711
The initial thermal state of the Moon
04 p0581 N85-13712
Lunar magnetic history 04 p0582 N85-13715
The I-Pu-Xe age of the Moon
04 p0584 N85-13729
Constraints on the origin of viscoelastic bodies
04 p0584 N85-13732
Tidal disruption and the origin of the Moon
04 p0585 N85-13739
A numerical investigation of planetesimal collision trajectories with a Moon accumulating in Earth orbit
04 p0586 N85-13740
Stochastic does not equal ad hoc — theories of lunar origin 04 p0586 N85-13741
A testable gravitational capture model for the origin of the Earth's Moon 04 p0586 N85-13742
Directional properties of circular Maria: Interpretation in the context of a testable gravitational capture model for lunar origin 04 p0586 N85-13743
The problem of iron partition between Earth and Moon during simultaneous formation as a double planet system 04 p0587 N85-13744
Origin of the Moon 04 p0587 N85-13745
Geochemical evidence for the formation of the Moon by impact induced fission of the proto-Earth
04 p0587 N85-13747
Catalogue of observations of total occultations of stars by the Moon for the years 1972 to 1980 and of grazing occultations for the years 1963 to 1980
[BULL-192] 05 p0741 N85-14768
Spectral reflectance studies on the orientale region of the Moon 06 p0868 N85-15839
The geology of the terrestrial planets
[NASA-SP-469] 09 p1410 N85-18868
Moon 09 p1411 N85-18883
Herstmonceux observations of the Sun, planets and Moon, 1957 - 1982
[BULL-193] 11 p1762 N85-21087
A new look at the planets — space probes
[AERONOMICA-ACTA-37-1984]
11 p1765 N85-21096
Giant planets and their satellites: Cosmochemistry, evolution and structure 13 p2175 N85-23494
A circum-terrestrial compositional filter
13 p2179 N85-23520
Models of angular momentum input to a circum-terrestrial swarm from encounters with heliocentric planetesimals 13 p2179 N85-23521
Landform identification on radar images
13 p2198 N85-23635
Radar observations of fissure-fed basaltic lava flows, Craters of the Moon, Idaho 13 p2199 N85-23640
Relationship between seismic status of Earth and relative position of bodies in sun-earth-moon system
14 p2345 N85-24499
Neutrino measurements on the Moon
[DE85-007700] 16 p2884 N85-27791
An analysis of alternate hydrogen sources for lunar manufacture
[DE85-007234] 16 p2884 N85-27792
Surface exploration geophysics applied to the Moon
[DE85-008714] 16 p2884 N85-27793
Moon bounce communications to small terminals
[AD-A153297] 17 p2950 N85-28212
Analytical generation of satellite orbits at the RAE (Royal Aircraft Establishment)
[AD-A152655] 17 p3053 N85-28901
Adsorption of Hg on lunar samples
[DE85-007948] 17 p3054 N85-28906
Geochemical confirmation of the lunar magmasphere hypothesis 22 p3859 N85-33895

MOORING
The long term upper ocean study (LOTUS). Cruise summary and hydrographic data report, OCEANUS 154, May 1984
[AD-A147908] 07 p1009 N85-16414
The body burden of organic vapors in artificial air trial measurements aboard a moored submarine
[AD-A149698] 12 p1910 N85-21988

MOORINGS
U MOORING

MORAINES
U GLACIAL DRIFT

MORL
U MANNED ORBITAL RESEARCH LABORATORIES

MORNING
Substorm associated Pc 1 emission in the morning sub-cleft latitudes 14 p2366 N85-24637

MORPHOLOGY
NT GEOMORPHOLOGY
NT ISOMORPHISM
NT POLYMORPHISM
Morphological changes of gamma prime precipitates in nickel-base superalloy single crystals
[NASA-TM-83698] 01 p0026 N85-10185
Morphology and dynamic mechanical properties of diglycidyl ether of bisphenol-A toughened with carboxyl-terminated butadiene-acrylonitrile
04 p0486 N85-12958
Effect of lithology and climate on the morphology of drainage basins in northwestern Colorado
[PB84-228236] 06 p0828 N85-15258
Structure and functions of fungal cell surfaces
[NASA-TM-77439] 06 p0842 N85-15347
Rubber-modified epoxies. 1: Cure, transitions, and morphology
[AD-A147377] 07 p0932 N85-15908
Effects of body mass and morphology on thermal responses in water
[AD-A147558] 07 p1016 N85-16455
Rubber-modified epoxies. Part 2: Morphology, transitions, and mechanical properties
[AD-A147962] 08 p1132 N85-17137
Australian Multiexperimental Assessment of SIR-B (AMAS) 08 p1148 N85-17243
Morphology and optical polarization of the 3C 273 jet — radio jet 08 p1238 N85-17803
Tribological properties of graphite-fiber-reinforced, partially fluorinated polyimide composites
[NASA-TM-86926] 09 p1298 N85-18153
Influence of the amorphous-crystalline interface morphology on dislocation nucleation in pre-amorphized silicon
[DE85-002068] 09 p1398 N85-18800
Microstructural analysis of ion containing polymers
[DE85-001594] 10 p1453 N85-19157
Mechanism and pattern of fatigue crack growth in aluminum alloys 11 p1697 N85-20047
Morphological study of monkeys submitted to antiorthostatic hypokinesia 12 p1902 N85-21942
Effect of long-term repeated exposure to high-intensity stationary magnetic field on adrenomedullary activity
12 p1904 N85-21955
On the morphology of spiral modes — disk galaxies
12 p1955 N85-22283
Origin of Martian polygonal terrain: Preliminary results
13 p2191 N85-23591
Morphology of 2keV-electrons observed by GEOS 1
14 p2380 N85-24581
Effects of ion bombardment on the morphology of lead films
[DE85-007232] 15 p2511 N85-25494
Induced changes in the cholinergic system of sciatic nerve and slow and fast twitch muscle of rats
15 p2609 N85-26061
Percutaneous connectors
[NASA-CR-175627] 16 p2839 N85-27508
The state of martensite after quenching in a magnetic field
[BLL-BISI-TRANS-22297-(9022.06)]
17 p2926 N85-29051
Application of scattering methods to the studies of the structure of polymer blends
[IFPR-13/1984] 17 p2933 N85-28104
Morphological stability and fluid dynamics of vapor crystal growth
[NASA-CR-175879] 17 p3042 N85-28822
Morphological stability and fluid dynamics of vapor crystal growth
[NASA-CR-175880] 17 p3042 N85-28823
The structure of ion plated films in relation to coating properties
[NASA-TM-87055] 18 p3085 N85-29085
Electrochemical and morphological study of the effect of temperature on the restructuring and loss of capacity of alkaline battery electrodes
[DE85-006869] 18 p3129 N85-29378
Method for growth of crystals by pressure reduction of supercritical or subcritical solution
[NASA-CASE-NPO-15772-1] 18 p3192 N85-29800
Morphological study of primate hypothalamus and hypophysis after experiment with antiorthostatic hypokinesia 19 p3325 N85-30803
A study of freezing and melting with eutectic interactions 19 p3378 N85-30956
Measurement and analysis of two-phase flow through low permeability media, task 3
[PB85-186373] 20 p3435 N85-31313
Identification and quantitation of morphological cell types in electrophoretically separated human embryonic kidney cell cultures 20 p3501 N85-31764
Milliarcsecond morphology of the twin quasar 0957 + 56A,B: The view through a gravitational lens
20 p3544 N85-32054
Understanding and laboratory prediction of the atmospheric corrosion behavior of steels and of non-ferrous metals and alloys
[AD-A154642] 21 p3566 N85-32179
Enrichments for phototrophic bacteria and characterization by morphology and pigment analysis
21 p3660 N85-32738

MORPHOTROPISM
U ISOMORPHISM

MORTALITY
Morbidity and mortality associated with exposure to Otto Fuel II in the U.S. Navy 1966-1979
[AD-A148726] 09 p1383 N85-18574
Response of unmanaged forests to CO2-induced climate change: Available information, initial tests and data requirements
[DOE/NBB-0063] 12 p1883 N85-21817

MORTARS (MATERIAL)
Compressive strength-maturity relationships of mortar containing fly ash
[AD-A148705] 09 p1339 N85-18423

Experimental characterization and stability of salt- and nonsalt-containing grouts and mortars (BCT-1F- and BCT-1FF-related)
[DE85-012339] 22 p3753 N85-33263

MOS (JAPANESE SPACECRAFT)
U JAPANESE SPACECRAFT

MOS (SEMICONDUCTORS)
U METAL OXIDE SEMICONDUCTORS

MOSAICS
Viking Lander mosaics of Mars
13 p2203 N85-23667
Voyager cartography 13 p2203 N85-23668
Mosaic Infrared Sensor for Space Astronomy (MIRSSA)
[NASA-CR-176154] 22 p3786 N85-33456

MOSCOW
Laser air pollution monitoring system planned for Moscow 10 p1500 N85-19465

MOSFET
U FIELD EFFECT TRANSISTORS

MOSS (SPACE STATIONS)
U ORBITAL SPACE STATIONS

MOSSBAUER EFFECT
Mossbauer spectroscopic investigations of the diffusion and correlation of lattice defects (complementary to neutron spectroscopic investigations)
03 p0429 N85-12736
Mossbauer effect and contactless conductivity studies of superconducting actinides intermetallics and hydrides. Mossbauer high pressure studies
03 p0430 N85-12743
Mossbauer spectroscopy and X-ray diffraction of samples from the Santa Catherina iron meteorite
06 p0685 N85-15824
Theoretical determination of surface magnetism
[DE85-003224] 11 p1714 N85-20783
Mossebauer study of amorphous Fe(67)Co(18)B(14)Si(1)
[AERE-R-11526] 11 p1737 N85-20928
Inelastic scattering in condensed matter with high intensity Moessbauer radiation
[DE85-003531] 12 p1854 N85-21627
Quenching effects on iron site partitioning in the Apollo 17 orange glass composition 13 p2184 N85-23553
Hibonite: Crystal chemistry and origin of blue coloration in meteoritic assemblages 13 p2184 N85-23555
Mossbauer spectrometry: Testing of a new computer based system and its application to a study of an aluminum-iron-cerium alloy
[AD-A151826] 15 p2510 N85-25483
The structure of carbon martensite analyzed with Moessbauer spectra
[BLL-BISI-TRANS-22402-(9022.06)]
17 p2927 N85-28062
Highly dispersed metal atoms in zeolites
[DE85-010515] 19 p3354 N85-30792
Analysis of ferrates and ferrites of three transition metals using Moessbauer effects
[BLL-CE-TRANS-8019-(9022.06)]
20 p3430 N85-31273
In situ Moessbauer investigation of bimetallic catalysts on a base: FeRu, FeRh, FePd, FeIr, and FePt on SiO2
[B8563200] 20 p3432 N85-31293
A microprocessor based multiscaling data acquisition system for Moessbauer spectroscopy
[USIP-85-01] 20 p3518 N85-31875
Noble metals as incipient transition metals
[DE85-013283] 24 p4080 N85-35288

MOTILITY
U LOCOMOTION

MOTION
A control model: Interpretation of Fitts' law
05 p0706 N85-14526
Modeling of human motion by computer considering measurement errors in initial data
07 p1012 N85-16429
More limit theory for the sample correlation function of moving averages
[AD-A148975] 10 p1550 N85-19773
Television animation store: Digital chroma, key and mixer units
[BBC-RD-1984/16] 12 p1824 N85-21442
3D computer animation: More an evolution problem than a motion problem 23 p3959 N85-34536
Using dynamic analysis to animate articulated bodies such as humans and robots 23 p3959 N85-34537
Towards an integrated view of 3-D computer character animation 23 p3959 N85-34538
Research issues in generating graphical explanations
23 p3959 N85-34539

MOTION AFTEREFFECTS
Thresholds for detection of linear oscillation following prolonged weightlessness 20 p3508 N85-31810

MOTION EQUATIONS
U EQUATIONS OF MOTION

MOTION PERCEPTION
Theory underlying the peripheral vision horizon device
01 p0008 N85-10048
Stimulus factors in motion perception and spatial orientation 01 p0008 N85-10049
The peripheral visual cue assessment facility at Ames Research Center 01 p0008 N85-10050
Evaluation of the Malcolm horizon in a moving-base flight simulator 01 p0008 N85-10051
Thresholds of perception of whole body linear oscillation: Modification by spaceflight 05 p0694 N85-14467
Visual-vestibular interaction in human motion perception 05 p0695 N85-14471
Use of linear perspective scene cues in a simulated height regulation task 05 p0704 N85-14517
Mean and random errors of visual roll rate perception from central and peripheral visual displays
05 p0704 N85-14519
Direction judgement errors in perspective displays
05 p0705 N85-14520
The interaction of focused attention with flow-field sensitivity 05 p0705 N85-14521
Accuracy of system step response roll magnitude estimation from central and peripheral visual displays and simulator cockpit motion 05 p0705 N85-14522
Automatic determination of motion in an image sequence. The interest for interpretation
[ENST-84E012] 05 p0716 N85-14592
Spatiotemporal characteristics of visual localization
[AD-A148013] 08 p1200 N85-17555
Optical flow and texture variables useful in detecting decelerating and accelerating self-motion
[AD-A148718] 09 p1384 N85-18703

MOTION PICTURES
Positioning errors of commutating lenses and their influence on characteristics of high speed movie cameras 14 p2273 N85-24085
Pulsed lasers for filming color holographic film images
22 p3781 N85-33426

MOTION SICKNESS
The adaptation of vestibulo-spinal reflexes as a function of spaceflight and their relationship to space motion sickness 05 p0694 N85-14468
Proceedings of a Workshop on Research Issues in Simulator Sickness
[AD-A148543] 08 p1196 N85-17538
Simulator sickness: Sensorimotor disturbances induced in flight simulators
[AD-P004334] 09 p1271 N85-17986
Management of vibration sickness in coal mines by hyperbaric oxygenation 10 p1523 N85-19609
Comparative assessment of different treatment modalities in miners with vibration- and noise-induced disease 10 p1524 N85-19610
Modulated sinusoidal currents in management of vibration sickness 10 p1524 N85-19612
Motion Sickness: Mechanisms, Prediction, Prevention and Treatment
[AGARD-CP-372] 11 p1693 N85-20642
Neurophysiological correlates of motion sickness: Role of vestibulocerebellum and 'vomiting center' reanalyzed
11 p1693 N85-20643
Influence of gravitoinertial force level on apparent magnitude of coriolis cross-coupled angular accelerations and motion sickness 11 p1693 N85-20644
Vestibular and oculomotor function during Gz variations 11 p1693 N85-20645
Prediction of the space adaptation syndrome
11 p1693 N85-20646
Prediction of seasickness susceptibility
11 p1693 N85-20647
Laboratory tests of motion sickness susceptibility
11 p1694 N85-20648
Results of a longitudinal study of airsickness incidence during Naval flight officer training
11 p1694 N85-20649
Susceptibility of cat and squirrel monkey to motion sickness induced by visual stimulation: Correlation with susceptibility to vestibular stimulation
11 p1694 N85-20650
Susceptability to kinetoses and the amplitude perceived from sensory illusions 11 p1694 N85-20651
Preflight and postflight motion sickness testing of the Spacelab 1 crew 11 p1694 N85-20652
Simulator sickness: Reaction to a transformed perceptual world. 6: Preliminary site surveys
11 p1694 N85-20653
Space motion sickness monitoring experiment: Spacelab 1 11 p1695 N85-20654
Space adaptation syndrome: Incidence and operational implications for the space transportation system program
11 p1695 N85-20655
Analysis of head motion during simulated, rough water operation of a 2200 ton surface effect ship
11 p1695 N85-20656
A double blind comparative trial of powdered ginger root, hyoscine hydrobromide, and cinnarizine in the prophylaxis of motion sickness induced by cross coupled stimulation
11 p1695 N85-20657
The current status of the RAF programme of desensitisation for motion sick aircrew
11 p1695 N85-20658
Psychological components in the development and prevention of air sickness 11 p1695 N85-20659
Biofeedback treatment of airsickness: A review
11 p1696 N85-20660
Results of a longitudinal study of airsickness during naval flight officer training: Executive summary
[AD-A150857] 14 p2388 N85-24712
Shuttle operational test and scientific investigations
14 p2394 N85-24748
Sensory and motor properties of the cerebellar uvula and modulus 15 p2613 N85-26104
Anatomy of the vestibulo-automatic outflow to the gut
15 p2614 N85-26106
Airsickness control using biofeedback to self-regulate psychophysiological responses
[AD-A151167] 15 p2617 N85-26128
Computerized biophysical data acquisition system for motion sickness studies
[AD-A151691] 15 p2618 N85-26131
What is being done to control motion sickness?
15 p2687 N85-26599
Mission operations requirements document for D-1 Experiment 102, Vestibular Experiments in Spacelab
[NASA-TM-87495] 21 p3557 N85-32129
USSR report: Space Biology and Aerospace Medicine, volume 19, no. 2, March - April 1985
[JPRS-USB-85-004] 22 p3820 N85-33667
Labyrinthine and extralabyrinthine mechanisms of development of motion sickness in weightlessness
22 p3821 N85-33668
Effect of experimental motion sickness on postrotory nystagmus and counterrotation illusion
22 p3824 N85-33690
A review of motion sickness with special reference to simulator sickness
[AD-A155975] 24 p4131 N85-35611

MOTION SICKNESS DRUGS
Management of microcirculatory disorders in vibration sickness 10 p1524 N85-19611
A double blind comparative trial of powdered ginger root, hyoscine hydrobromide, and cinnarizine in the prophylaxis of motion sickness induced by cross coupled stimulation
11 p1695 N85-20657

MOTION SIMULATION
Motion sensor evaluation using simulation
[DE84-014989] 01 p0050 N85-10331
Models for the effects of G-seat cuing on roll-axis tracking performance 05 p0707 N85-14532
Method for prompt modeling of quasiperiodic movement of solid near-axisymmetrical body in atmosphere
13 p2043 N85-22790
A systematic determination of skill and simulator requirements for airline transport pilot certification
[AD-A154135] 19 p3330 N85-30630
Docking simulation analysis of range data requirements for the orbital maneuvering vehicle
[NASA-TM-86510] 20 p3407 N85-31143

MOTION SIMULATORS
Suppression of biodynamic interference by adaptive filtering 05 p0706 N85-14530

MOTION STABILITY
NT AERODYNAMIC STABILITY
NT AIRCRAFT STABILITY
NT ATTITUDE STABILITY
NT BOUNDARY LAYER STABILITY
NT DIRECTIONAL STABILITY
NT FLAME STABILITY
NT FLOW STABILITY
NT GYROSCOPIC STABILITY
NT LATERAL STABILITY
NT LONGITUDINAL STABILITY
NT LOW SPEED STABILITY
NT MAGNETOHYDRODYNAMIC STABILITY
NT ROTARY STABILITY
NT SPACECRAFT STABILITY
NT WEIBEL INSTABILITY
Improvements in linked-spar motion-compensated lifting system
[AD-D011413] 08 p1138 N85-17165
Translating rudder pedal system
[AD-D011510] 12 p1780 N85-21172
Absolute stability of unsteady movement of axisymmetrical rotating flight vehicle
13 p2044 N85-22793
Electronics Engineering Department EE Technical Review
[UCRL-50025-84-1] 13 p2083 N85-22887

Linearization of digital derived rate algorithm for use in linear stability analysis
[NASA-TM-87000] 14 p2243 N85-23904
Stability of steady modes of motion by axis of rotating wheel in nonlinear bearings 14 p2279 N85-24117
Stability of steady motions of dynamically symmetrical solid at a triangular libration point 14 p2279 N85-24120
Investigation of dynamic noise affecting geodynamics information in a tethered subsatellite
[NASA-CR-176031] 20 p3476 N85-31602

MOTIVATION
NT CONTRACT INCENTIVES
Analysis of team performance in a programmed environment
[NASA-CR-175634] 14 p2392 N85-24728
Effect of triphthalsine and elenium on changes in evoked bioelectrical activity of the brain exposed to stationary magnetic field 19 p3325 N85-30601
Air university commander's and supervisor's guide on substance abuse
[AD-A156336] 24 p4133 N85-35622

MOTOR SYSTEMS (BIOLOGY)
U EFFERENT NERVOUS SYSTEMS

MOTOR VEHICLES
NT AUTOMOBILES
NT ELECTRIC AUTOMOBILES
NT ELECTRIC MOTOR VEHICLES
NT TANK TRUCKS
NT TRACKED VEHICLES
NT TRACTORS
NT TRUCKS
Size specific total particulate emission factors for mobile sources
[PB84-226653] 01 p0071 N85-10471
Vehicle-to-vehicle connection mechanism
[AD-D011267] 05 p0845 N85-14142
The changing vibration simulation for military ground vehicles 09 p1334 N85-18387
Study of the motion of agricultural vehicles on steep grass-covered slopes
[AD-P004290] 09 p1408 N85-18667
Alternative fuels for buses: Current assessment and future perspectives
[PB85-116325] 10 p1459 N85-19190
USSR report: Transportation
[JPRS-UTR-84-008] 14 p2208 N85-23694
USSR report: Transportation
[JPRS-UTR-84-015] 15 p2460 N85-25192
USSR report: Transportation
[JPRS-UTR-84-014] 15 p2467 N85-25229
An electron microscopic study of urban aerosol 21 p3651 N85-32689

MOTORS
NT ASYNCHRONOUS MOTORS
NT ELECTRIC MOTORS
NT INDUCTION MOTORS
NT MICROMOTORS
NT SERVOMOTORS
NT SYNCHRONOUS MOTORS
NT TORQUE MOTORS
Solving equations of movement with variable inertia moment
[BLL-M-35975-(5828.4)] 05 p0841 N85-14111
Dual optical mechanical position tracker
[AD-D011739] 22 p3844 N85-33811

MOUNTAINS
NT ALPS MOUNTAINS (EUROPE)
NT ANDES MOUNTAINS (SOUTH AMERICA)
NT APPALACHIAN MOUNTAINS (NORTH AMERICA)
NT BIGHORN MOUNTAINS (MT-WY)
NT CARPATHIAN MOUNTAINS (EUROPE)
NT CASCADE RANGE (CA-OR-WA)
NT COASTAL RANGES (CA)
NT HIMALAYAS
NT PYRENEES MOUNTAINS (EUROPE)
NT ROCKY MOUNTAINS (NORTH AMERICA)
NT SIERRA NEVADA MOUNTAINS (CA)
Fungi of Mt. Babia Gora. 2: Indicative value of macromycetes in forest associations. A: Initial considerations
[NASA-TM-77485] 01 p0094 N85-10632
Fungi of Mount Babia Gora. 3: The indicating value of macromycetes in the forest associations
[NASA-TM-77486] 01 p0094 N85-10633
The effect of naproxen on acute mountain sickness and vascular responses to hypoxia
[AD-A145144] 01 p0095 N85-10638
Local geoid determination in mountain regions
[AD-A145799] 03 p0384 N85-12458
Stratigraphy, petrology, and structure of the Pingston terrane, Mount Hayes C-5 and C-6 quadrangles, eastern Alaska Range, Alaska 04 p0517 N85-13301
Paleogene volcanic rocks of the Matanuska Valley area and the displacement history of the Castle Mountain fault 04 p0518 N85-13303
Effect of mountain wave dynamics on orographic storms
[DE84-014713] 04 p0540 N85-13433
A tectonic and metamorphic history of the north-central Klamath Mountains, California 05 p0673 N85-14323
Petrology and structure of Pwemain to Jurassic rocks near Yreka, Klamath Mountains, California 05 p0673 N85-14325
Sedimentation, structure and tectonics of the Umpqua group (paleocene to early eocene), southwestern Oregon 05 p0678 N85-14354
Tectonic, volcanic, and climatic geomorphology study of the Sierras Pampeanas Andes, northwestern Argentina 06 p1144 N85-17215
Post-Laramide history of North Central Wyoming 06 p1161 N85-17444
Sedimentary petrology and provenance of the upper Jackforth Sandstone (Morrowan) Ouachita Mountains, Arkansas, USA 06 p1182 N85-17447
Stratigraphy of early ordovician El Paso group of the southern Hueco Mountains, Hudspeth County, Texas 09 p1353 N85-18510
Preliminary photomaps of Venus surface in the Maxwell Mountains and adjacent areas 13 p1982 N85-22438
The geology of Mt. Hope, a silicic volcanic center in West Central Arizona 13 p2187 N85-23571
Geomorphology and geology of the Southwestern Margaritifer Sinus and Argyre regions of Mars. Part 1: Geological and geomorphological overview 13 p2192 N85-23600
Mountain barrier baroclinity effects on surface winds along the Alaskan Arctic coast 14 p2238 N85-23677
Hydrological data collection from Swedish mountain areas 14 p2327 N85-24366
Structural analysis of terrane accretions in the eastern Brooks Range and adjacent areas in central Alaska and Canada
[DE85-006279] 17 p2993 N85-28501
Implications about in situ stress at Yucca Mountain
[DE85-008068] 18 p3126 N85-29356
Influence of underwater volcanic mountains of Atlantic on microplankton distribution 19 p3294 N85-30424
The Terrain-Responsive Atmospheric Code (TRAC) for plume growth and dispersion in complex terrain
[DE85-010541] 19 p3309 N85-30513
Possible use of the COSPAS/SARSAT system within the Swedish mountain rescue organization 20 p3401 N85-31100
The 1984 biotic studies of Yucca Mountain, Nevada test site, Nye County, Nevada
[DE85-011715] 23 p3951 N85-34487
Aeromagnetic and radiometric signatures of a possible porphyry system in the western Tushar Mountains, Utah 24 p4103 N85-35437

MOUNTING
NT RIGID MOUNTING
Mounting construction for turbine vane assembly
[AD-D011395] 07 p0904 N85-15723
Recommended improvements for second generation 121.5/243 MHz ELT's
[NASA-CR-175274] 08 p1080 N85-16841
Gear case vibration isolation in a geared turbine generator 09 p1336 N85-18414
Advanced life analysis methods. Volume 1: Cracking data survey and NDI (nondestructive inspection) assessment for attachment lugs
[AD-A150419] 13 p2103 N85-23106
Advanced life analysis methods. Volume 2: Crack growth analysis methods for attachment lugs
[AD-A150420] 13 p2103 N85-23109
Precise mounting of instruments in universal suspension with skewed axes 14 p2273 N85-24083
Support structures for optical components in the Laser Demonstration Facility
[DE85-006879] 17 p2971 N85-28349
Using PVFORM, a systems performance model, to determine optimum mounting configurations for flat-plate photovoltaic modules
[DE85-011191] 19 p3306 N85-30485

MOUNTS
U SUPPORTS

MOVEMENT
U MOTION

MOVING TARGET INDICATORS
Moving object detection system using infrared scanning
[AD-D011222] 01 p0120 N85-10822
Optimization of moving-target selection radar devices for nonGaussian signals for stationary targets 08 p0799 N85-15043
Algorithm for tracking manuevering object with ambiguous measurements 06 p0791 N85-15057
Adaptive MTI (Moving Target Indicator) system
[AD-D011361] 07 p0937 N85-15937
Dual mode scanner-tracker
[AD-D011417] 08 p1113 N85-17016
Hybrid state estimation approach to multiobject tracking for airborne surveillance radars
[AD-A148459] 08 p1153 N85-17279
Pulse heterodyne equipment for measurements of range and velocity of moving targets-pulse radar
[ESA-TT-845] 09 p1312 N85-18248
MTI system simulation and clutter output statistics
[AD-A149193] 10 p1467 N85-19255
Method and means for providing frequency agile operation of MTI (Moving Target Indicator) radar
[AD-D011561] 12 p1823 N85-21436
Moving target detection 13 p2067 N85-22915
Eye movement in response to single and multiple targets
[AD-A151115] 15 p2617 N85-28128
Interference suppressor for radar MTI
[AD-D011606] 16 p2769 N85-27086
Techniques for operating Charge Coupled Devices (CCD's) in very high speed framing mode
[AD-A152878] 17 p2953 N85-28238
Atmospheric probing by active millimeter wave system
[AD-A153550] 18 p3136 N85-29422
Characteristics of digital range finder with stroboscopic discretization 22 p3762 N85-33319

MRCA AIRCRAFT
Tornado: Structural Usage Monitoring System (SUMS) 07 p0896 N85-15680
Flight parameters recording for structure fatigue life monitoring 07 p0896 N85-15682
Study and realisation of a 3rd level maintenance center based on ATE systems utilization 09 p1063 N85-16735

MSAT
Propagation considerations in land mobile satellite transmission
[NASA-CR-175733] 15 p2540 N85-25684
Combined trellis coding with asymmetric MPSK modulation: An MSAT-X report
[NASA-CR-176039] 20 p3440 N85-31347
Second-generation mobile satellite system. A conceptual design and trade-off study
[NASA-CR-176195] 24 p4086 N85-35325

MTF
U MODULATION TRANSFER FUNCTION

MTI RADAR
U MOVING TARGET INDICATORS

MUSES (SCANNERS)
U MULTIPLE BEAM INTERVAL SCANNERS

MUFFLERS
Technology reports of the Yamaguchi University, volume 3, no. 3
[ISSN-0386-3433] 09 p1302 N85-18182
Studies on reactive mufflers. Part 2: Mufflers with air flow 09 p1303 N85-18184

MULLITES
Transformation toughened ceramics for the heavy duty diesel engine technology program
[NASA-CR-174689] 07 p1055 N85-16698

MULTI-ANODE MICROCHANNEL ARRAYS
The multi-anode microchannel array detector system: Current status and future prospects 11 p1781 N85-21080

MULTI-ROLE COMBAT AIRCRAFT
U MRCA AIRCRAFT

MULTIBEAM ANTENNAS
Configuration study for a 30 GHz monolithic receive array: Technical assessment
[NASA-CR-174697] 09 p1311 N85-18238
Configuration study for a 30 GHz monolithic receive array, volume 1
[NASA-CR-174697-VOL-1] 09 p1311 N85-18239
Shuttle S-band high gain switched beam breadboard antennas
[NASA-CR-171852] 10 p1478 N85-19327
3-D Dome/Rotman lens antenna breadboard demonstration
[AD-A149809] 12 p1826 N85-21475
Synthesis of multistep directional couplers with nonminimum-phase characteristics 13 p2079 N85-22986
Orbiting multi-beam microwave radiometer for soil moisture remote sensing 14 p2230 N85-23818
Design, fabrication and testing of a multibeam forming network
[NASA-CR-175695] 14 p2298 N85-24228

MULTICHANNEL COMMUNICATION
Guided-wave optic devices for integrated optic information processing
[AD-A145695] 02 p0280 N85-11827
Analysis of a coded, M-ary orthogonal input optical channel with random-gain photomultiplier detection 05 p0624 N85-13990
Synthesis of systems for coherent weighted signal processing against background of correlated interference 06 p0790 N85-15045

Multiwavelength bidirectional coupler-decouplers
[AD-A147009] 07 p1043 N85-16625
Equipment for multiplexing multichannel radio-relay lines of communication
[AD-A148402] 08 p1153 N85-17276
Error probability during optimal noncoherent reception of binary signals in multibeam channel
13 p2069 N85-22922
Asymptotically optimum multialternative sequential procedures for discernment of processes minimizing average length of observations
13 p2084 N85-23012
A perspective on multiaccess channels
[AD-A150183] 13 p2146 N85-23322
MULTICHANNEL PLATES
U MICROCHANNEL PLATES
MULTILAYER INSULATION
System design of multi-layer (3-dimensional) integrated circuits
[AD-A153468] 16 p3094 N85-29154
MULTILAYER STRUCTURES
U LAMINATES
MULTILOOP SYSTEMS
U CASCADE CONTROL
MULTIMISSION MODULAR SPACECRAFT
Satellite module design 11 p1642 N85-20344
Multimission advanced configurations study — telecommunication satellites
[MATRA-DM.51/CC/FL/0151.83]
12 p1790 N85-21237
MULTIMODE RESONATORS
Transformation of mode composition of circular optical waveguide 07 p0950 N85-16023
Coupled-cavity gyrotrons with mode conversion
13 p2076 N85-22987
Investigation of generation of oscillations using anomalous Doppler effect 13 p2078 N85-22980
MULTIPATH TRANSMISSION
Digital radio link: Comparison of the resistance of two different 4-phase modulation forms to multipath propagation
[FOA-C-30362-E] 02 p0193 N85-11291
Limits of the propagation medium with respect to digital signal transmission 10 p1469 N85-19270
Propagation influences on the performance of a reduced bandwidth quadrature phase shift keyed digital radio system 10 p1470 N85-19274
A review of atmospheric multipath measurements and digital system performance 10 p1470 N85-19279
Multipath and Doppler observations during transatlantic digital HF propagation experiments
10 p1471 N85-19281
An ionospheric mode detection system for HF communications application 10 p1471 N85-19282
Wideband line-of-sight channel measurements and simulation: Application to digital radio links
10 p1471 N85-19283
Design criteria for limited scan antennas at digital microwave line of sight links 10 p1471 N85-19284
Measurements and predictions of multipath dispersion for troposcatter links 10 p1472 N85-19289
Asynchronous transmission with strong spectral spread 10 p1474 N85-19300
Fast data and voice transmission for mobile services with high immunity against multipath and co-channel interference 10 p1475 N85-19306
Effective millimeter wave transmission under severe multipath conditions 10 p1475 N85-19308
Accurate baseline determination by radio interferometry on NAVSTAR GPS satellite transmissions
[AD-A150881] 14 p2291 N85-24202
Distributed control of circuits in multiuser communication networks with circuit precedence and path suitability criteria using failsafe routing concepts
[AD-A151825] 16 p2772 N85-27113
Development of a modified time delay spectrometry technique for underwater acoustic measurements in a multipath environment
[AD-A152111] 16 p2860 N85-27639
A comparison of multipath arrival structures observed in the presence of a surface duct with predictions obtained using classical ray techniques and the parabolic equation method
[AD-A156024] 24 p4145 N85-35606
MULTIPHASE FLOW
NT TWO PHASE FLOW
Investigation of phase separation models in RELAP 4/MOD 6
[OEFZS-4286] 05 p0638 N85-14093
Modelling the local interstellar medium as a supernova remnant in a multiphase gas 06 p0879 N85-15585
Combustion in high speed air flows
[AD-A148371] 09 p1122 N85-17070
Investigation of condensing, three-phase, two-component, flow through porous media
09 p1317 N85-18283
Development of a three-phrase combustion code for modeling liquid rocket engines 13 p2003 N85-22554
The physics of the marine stratocumulus-capped mixed layer 15 p2593 N85-25979
An experimental study of plane mixing layer development
[NASA-TM-86698] 19 p3221 N85-29971
An investigation of hydraulic transients in combination free surface and pressurized flows
19 p3264 N85-30239
Mathematics of oil production
[DE85-011235] 19 p3267 N85-30261
PHOENICS 84: A multi-dimensional multi-phase general-purpose computer simulator for fluid flow, heat transfer and combustion: 36 lecture panels
[CFD/84/18] 20 p3457 N85-31468
Progress in the development of a two-fluid model of turbulence: A set of 42 lecture panels
[CFD/84/20] 20 p3457 N85-31469
Experimental study of free and mixed convective flow of air in a heated cavity
[DE85-012538] 24 p4094 N85-35360
MULTIPHOTON ABSORPTION
Laser ablation studies using RIS
[DE85-001116] 09 p1326 N85-18336
Generation of stimulated emission in the soft X-ray range by nonlinear processes with excimer lasers
[DE85-012465] 24 p4096 N85-35403
MULTIPLE ACCESS
NT CODE DIVISION MULTIPLE ACCESS
NT DEMAND ASSIGNMENT MULTIPLE ACCESS
NT FREQUENCY DIVISION MULTIPLE ACCESS
NT TIME DIVISION MULTIPLE ACCESS
Throughput characteristics of Carrier Sense Multiple Access (CSMA) networks
[FUB-25-1983] 01 p0106 N85-10713
A perspective on multiaccess channels
[AD-A146608] 06 p0799 N85-15105
Analysis of the performance of multiaccess networks of the bus type
[FUB-47-1983] 09 p1313 N85-18249
A perspective on multiaccess channels
[AD-A150183] 13 p2146 N85-23322
On the throughput of channel access algorithms with limited sensing
[AD-A151984] 15 p2630 N85-26206
High performance asynchronous limited sensing algorithms for CSMA and CSMA-CD channels
[AD-A153919] 18 p3171 N85-29650
MULTIPLE BEAM INTERVAL SCANNERS
The 20 GHz proof-of-concept test model results for a multiple scan beam dual reflector antenna
[NASA-CR-174286] 07 p0936 N85-15944
Digital controller for the Wave Propagation Laboratory's VHF and UHF wind-profiling radars
[PB85-112142] 11 p1626 N85-20236
Feed system design considerations for large space antenna systems. Part 1: Multiple apertures with non-overlapping feeds 14 p2234 N85-23652
Feed system design considerations for large space antenna systems. Part 2: Single aperture with overlapping feeds 14 p2235 N85-23653
Offset reflector with horn feed array, used as an experimental sensor for radiometric measurements
[ESA-TT-830] 20 p3443 N85-31369
Method and apparatus for four-beam radar
[PB85-181477] 22 p3757 N85-33289
MULTIPLE TARGET TRAJECTORY SYSTEMS
U MATTS (SYSTEMS)
MULTIPLETS
U FINE STRUCTURE
MULTIPLEX TRANSMISSION
U MULTIPLEXING
MULTIPLEXERS
U MULTIPLEXING
MULTIPLEXING
NT FREQUENCY DIVISION MULTIPLEXING
NT TIME DIVISION MULTIPLEXING
NT WAVELENGTH DIVISION MULTIPLEXING
A total dose characterization of five commercial analog multiplexers
[AD-A146886] 07 p0946 N85-15997
Electro-optical target detection
[AD-D011395] 07 p1042 N85-16617
Equipment for multiplexing multichannel radio-relay lines of communication
[AD-A148402] 08 p1153 N85-17276
Integrated digital networks
[AD-A150605] 13 p2056 N85-22873
Interference immunity of fiber-optic communication lines with spectral multiplexing of channels
13 p2069 N85-22924
Interactive communication channel
[AD-D011580] 15 p2542 N85-25695
Wavelength multiplexer-demultiplexer
[AD-D011606] 16 p2777 N85-27140
Channel multiplexers for broadcast satellite transponders in the 12 GHz band
[NHK-LABS-NOTE-310] 18 p3090 N85-29122
LDV multiplexer interface
[NASA-CASE-ARC-11536-1] 19 p3258 N85-30202
Apollo multiplexer operations manual
[DE85-011293] 19 p3343 N85-30719
MULTIPLICATION
VLSI architectures for the multiplication of integers modulo a Fermat number 05 p0624 N85-13993
Electrooptical matrix multiplication using the twos complement arithmetic for improved accuracy
[AD-D011252] 05 p0728 N85-14682
Advanced cube processor
[AD-D011262] 05 p0729 N85-14683
Triple matrix product optical processors using combined time-and-space integration
[AD-D011483] 10 p1557 N85-19820
High accuracy digital acousto-optic matrix computer
[AD-D011692] 19 p3343 N85-30716
MULTIPLIER PHOTOTUBES
U PHOTOMULTIPLIER TUBES
MULTIPLIERS
NT CHANNEL MULTIPLIERS
Input-output stability analysis with magnetic hysteresis non-linearity: A class of multipliers
[AD-A145729] 02 p0253 N85-11654
Application of a silicon compiler to VLSI (Very Large Scale Integrated circuits) design of digital pipelined multipliers
[AD-A146328] 03 p0403 N85-12569
Developments of optical fast-gated imaging systems
[DE84-016170] 04 p0502 N85-13204
Hardware multiplier processor
[DE84-006174] 05 p0713 N85-14574
Efficiency of digital compensator of strong non-Gaussian interference 13 p2072 N85-22942
Numerical optical computing at the Ohio State University 18 p3186 N85-29775
Hardware realization of digital filters without multipliers
22 p3766 N85-33340
MULTIPOLAR FIELDS
Small, octopole-stabilized tandem mirror reactor
[DE85-002144] 10 p1559 N85-19832
MULTIPOLES
Structures of ordered linear dislocation multipoles in Cu-Al alloys
[ISSN-0379-6906] 13 p2021 N85-22664
A multipole model of the observed cerebral cortex magnetic field
[AD-A152237] 16 p2842 N85-27526
MULTIPROCESSING (COMPUTERS)
NT PIPELINING (COMPUTERS)
The FLEX/32 multicomputing environment
01 p0057 N85-10378
Application of concurrent processing to structural dynamic response computations
01 p0057 N85-10380
Hardware for a real-time multiprocessor simulator
[NASA-TM-83805] 01 p0099 N85-10659
Activities of the MIT Laboratory for Computer Science
[AD-A145134] 01 p0100 N85-10661
DISCUS multiprocessor enhancements — Distributed Control Microprocessor System (DISCUS)
[RSRE-MEMO-3591] 02 p0239 N85-11554
Criteria for the optimization of processing flow in a model of an incremental computer with multiprocessing resources
[INPE-3046-TDL/158] 02 p0240 N85-11560
Parallel searching and merging on ZMOB
[AD-A145424] 02 p0241 N85-11574
Research topics: Multiprocessing algorithms for computational logic
[DE84-015500] 02 p0242 N85-11583
Fault tolerant computing research
[AD-A145640] 02 p0244 N85-11590
The design and performance analysis of an arbiter for a multi-processor shared-memory system
[AD-A146074] 03 p0403 N85-12566
A building blocks approach to statistical databases
03 p0437 N85-12782
A control scheme for microcomputers being used in multiprocessor arrays
[DE84-014580] 04 p0547 N85-13479
Development of the NLTSS operating system
[DE84-013702] 05 p0714 N85-14576
Concurrency in parallel processing systems
05 p0714 N85-14581
Local area network evaluation by MICROSS extensions
[AD-A146773] 07 p1027 N85-16521
Evolution toward a multi-bus architecture for Army helicopter avionic systems 08 p1074 N85-16812
Operating system for a real-time multiprocessor propulsion system simulator. User's manual
[NASA-TP-2426] 08 p1207 N85-17596

Software for event oriented processing on multiprocessor systems
[DE84-016720] 09 p1370 N85-18607
Multitasking kernel for the C and FORTRAN programming languages
[DE85-001799] 09 p1370 N85-18609
Where are the parallel algorithms?
[NASA-CR-172516] 09 p1373 N85-18627
The feasibility of a multiprocessor architecture for real-time contour surface display generation
[AD-A149427] 10 p1538 N85-19697
Methodology investigation software testing of multiprocessor systems
[AD-A149446] 10 p1541 N85-19714
Domain decomposition techniques for solving elliptic partial differential equations on multiprocessors
[DE85-004448] 10 p1549 N85-19769
A quality control experiment in a real time multiprocessor operating system: The Mara 800 — software testing
11 p1702 N85-20707
Solving partial differential equations on multiprocessors
[DE85-000745] 11 p1706 N85-20734
RAPIDbus: Design of an extensible multiprocessor structure
[AD-A150061] 12 p1912 N85-21998
Exploiting multiprocessors: Issues and options
[DE85-003144] 13 p2145 N85-23313
Synthesis of tree-structured computing systems through use of closures
[AD-A150502] 13 p2147 N85-23326
Use of function processors in multiprocessor systems
14 p2400 N85-24796
Organization of conveyor processing of vector commands in multiprocessor computer systems with a reorganizable structure 14 p2401 N85-24799
Automation of development of software for switching units that are implemented in the form of multiprocessor systems on a microcomputer base
14 p2401 N85-24802
The EGPA multiprocessor system and its possible application for pattern recognition tasks — computer architecture 15 p2622 N85-26156
Backend control processor for a multi-processor relational database computer system
[AD-A151892] 15 p2624 N85-26169
ADA (trademark) tasking and exceptions: A formal definition
[AD-A151618] 15 p2629 N85-26204
Reentrancy and multitasking on CRAY computers
[DE85-007256] 15 p2630 N85-26211
Communication complexity of the Gaussian elimination algorithm on multiprocessors
[AD-A151891] 15 p2636 N85-26257
A modular dissimilar redundant computer designed for high integrity control 16 p2714 N85-26751
Reports on cartography and geodesy. Series 1: Original reports, no. 94
[ISSN-0469-4236] 16 p2814 N85-27357
Realization of cartographic tasks on the multiprocessor system EGPA — image processing
16 p2814 N85-27360
Multigrid algorithms on the hypercube multiprocessor
[AD-A152200] 16 p2847 N85-27558
Parallel computation of multiple-scale problems
[DE85-007230] 16 p2849 N85-27563
Local uniform mesh refinement on loosely-coupled parallel processors
[AD-A152199] 16 p2850 N85-27571
Complexity of dense linear system solution on a multiprocessor ring
[AD-A151970] 16 p2854 N85-27596
Multiple array processors for ocean acoustic problems
[AD-A152174] 16 p2860 N85-27641
A modular dissimilar redundant computer designed for high integrity control 17 p2904 N85-27904
Development of a multiprocessor system, using the MOTORLA microprocessor 6809, with the aim of providing maximum flexibility in the design of individual control devices
[BMFT-FB-T-84-270] 17 p3010 N85-28607
Real-Time Multiprocessor Programming Language (RTMPL) user's manual
[NASA-TP-2422] 17 p3010 N85-28610
Parallel Cholesky factorization on a multiprocessor
[DE85-008762] 17 p3021 N85-28682
Development of a butterfly multiprocessor test bed description of butterfly components
[AD-A153692] 18 p3095 N85-29155
Tradeoffs among portability, complexity, and efficiency in multiprocessing environments
[DE85-007690] 18 p3161 N85-29580
Performance measurement of OSI (Open System Interconnection) class 4 transport implementations
[PB85-177857] 18 p3161 N85-29582
Introduction to programming multiple-processor computers
[DE85-010274] 18 p3164 N85-29599
The multiple processor machine for image processing, volume 5
[ESA-CR(P)-1976-VOL-5] 18 p3164 N85-29603
Solving elliptic partial differential equations on the hypercube multiprocessor
[AD-A153464] 18 p3166 N85-29629
Performance of the butterfly processor-memory interconnection in a vector environment
[DE85-007931] 19 p3261 N85-30224
Multigrid method for multiprocessors
[DE85-007929] 19 p3333 N85-30647
The BLAZE language: A parallel language for scientific programming
[NASA-CR-172615] 19 p3334 N85-30656
A parallelized point successive over-relaxation method on a multiple instruction multiple data stream computer
[AD-A154377] 19 p3337 N85-30679
Development and evaluation of a fault-tolerant multiprocessor (FTMP) computer. Volume 1: FTMP principles of operation
[NASA-CR-166071] 19 p3341 N85-30705
Development and evaluation of a Fault-Tolerant Multiprocessor (FTMP) computer. Volume 2: FTMP software
[NASA-CR-166072] 19 p3341 N85-30706
Development and evaluation of a Fault-Tolerant Multiprocessor (FTMP) computer. Volume 3: FTMP test and evaluation
[NASA-CR-166073] 19 p3341 N85-30707
Proceedings of the Argonne Workshop on Programming the Next Generation of Supercomputers
[DE85-006348] 19 p3343 N85-30718
MECA: A multiprocessor concept specialized to Monte Carlo
[DE85-010791] 19 p3346 N85-30737
Work in Amsterdam on local intelligence — artificial intelligence
[NIKHEF-H/84-9] 20 p3518 N85-31877
Performance and evaluation of real-time multicomputer control systems
[NASA-CR-176098] 21 p3673 N85-32821
Concurrent implementation of the Crank-Nicolson method for heat transfer analysis
[NASA-TM-86448] 21 p3674 N85-32822
Use of monitors in Pascal on the Lemur: A tutorial on the barrier, self-scheduling FOR-loop, and askfor monitors
[ANL-84-53] 22 p3828 N85-33706
Parallel Cholesky factorization in message-passing multiprocessor environments
[DE85-012079] 22 p3830 N85-33717
Modeling and measurement of fault-tolerant multiprocessors
[NASA-CR-3920] 22 p3833 N85-33732
Some ideas for decomposing the domain of elliptic partial differential equations in the Schwarz process
[DE85-011844] 22 p3834 N85-33739

MULTIPROGRAMMING
PROGEN: An incremental programming environment
[NRIMS-TWISK-315] 02 p0241 N85-11568
ES devices at fair 08 p1141 N85-17187
Exploiting multiprocessors: Issues and options
[DE85-003144] 13 p2145 N85-23313
Structurization of programs for real-time microprocessor arrays 15 p2529 N85-25592
Detailed design of an object oriented, multiprogramming, multitasking operating system for sixteen-bit microcomputers
[AD-A152086] 16 p2847 N85-27552
Research in computer science
[NASA-CR-175922] 17 p3010 N85-28612

MULTIPROPELLANTS
U ROCKET PROPELLANTS

MULTIRADAR TRACKING
U RADAR NETWORKS

MULTISENSOR APPLICATIONS
Multisensor satellite data integration for sea surface wind speed and direction determination
[NASA-CR-174162] 04 p0542 N85-13446

MULTISPECTRAL BAND CAMERAS
An overview of Multispectral Electro-Optical Stereo Scanner (MEOSS) mission 04 p0458 N85-12908
Modular Optoelektronischer Multispektraler Scanner (MOMS), interpretation and evaluation of the MOMS image Arica, West Coast of South America — STS-7 flight
05 p0657 N85-14222
The Bressex multispectral camera: Preliminary characteristics
[INPE-3424-PRE/667] 16 p2787 N85-27195

MULTISPECTRAL BAND SCANNERS
Direction dependent radiation behavior in the classification of multispectral aircraft remote sensing data
[SER-C-290] 01 p0083 N85-10419
The application of principal components analysis to LANDSAT MSS data 02 p0212 N85-11396
The feasibility of satellite remote sensing as a technique for evaluating coal mine surface features
02 p0213 N85-11401
Imaging Science Panel. Multispectral Imaging Science Working Group joint meeting with Information Science Panel: Introduction 02 p0213 N85-11406
The Monocular Electro-Optical Stereo Scanner Experiment (MEOSS) 04 p0459 N85-12910
LANDSAT instruments characterization
[E85-10032] 04 p0524 N85-13356
Investigation of several aspects of LANDSAT 4/5 data quality
[E85-10038] 04 p0525 N85-13357
Basic investigation concerning the applicability of multispectral radiation data from microwave radiometry measurements to geoscientific objectives of remote sensing
[ESA-TT-848] 05 p0628 N85-14027
LANDSAT instruments characterization
[E85-10030] 05 p0654 N85-14199
Characterizing the scientific potential of satellite sensors
[E85-10031] 05 p0654 N85-14200
Integrative investigation on forest damage detection based on airborne Multispectral Scanner data
05 p0656 N85-14215
Integration of multispectral data obtained at different view angles for vegetation analysis
05 p0657 N85-14218
The use of Thematic Mapper data for land cover survey 05 p0657 N85-14220
Multispectral remote sensing of inland wetlands in South Carolina: Selecting the appropriate sensor
[DE84-013951] 05 p0661 N85-14247
Electronic satellite imaging system MOMS-ESA
[BMFT-FB-W-84-033] 05 p0661 N85-14248
Studies of atmospheric water in storms with the Nimbus 7 scanning multichannel microwave radiometer
05 p0662 N85-14382
Characterizing the scientific potential of satellite sensors — San Francisco, California
[E85-10053] 07 p0984 N85-16249
Study of spectral/radiometric characteristics of the Thematic Mapper for land use applications
[E85-10057] 07 p0987 N85-16268
Thematic Mapper. Volume 1: Calibration report flight model, LANDSAT 5
[E85-10059] 07 p0987 N85-16270
Thematic Mapper. Volume 2: Flight model preshipment review
[E85-10060] 07 p0987 N85-16271
Enhancement of multispectral scanner images by digital filtering
[ESA-TT-824] 07 p0989 N85-16284
Forest area estimates from LANDSAT MSS and forest inventory plot data
[PB85-105617/GAR] 07 p0990 N85-16290
Spectroradiometric calibration of the Thematic Mapper and Multispectral Scanner system
[E85-10077] 10 p1504 N85-19491
LANDSAT-4 Science Characterization Early Results. Volume 1: Multispectral Scanner (MSS)
[E85-10067] 11 p1666 N85-20496
Spectral characterization of the LANDAT-4 MSS sensors 11 p1666 N85-20499
Investigation of radiometric properties of LANDSAT-4 MSS — California, North Carolina, South Carolina, and New England 11 p1666 N85-20500
LANDSAT scene-to-scene registration accuracy assessment 11 p1667 N85-20502
Geometric accuracy of LANDSAT-4 MSS image data
11 p1667 N85-20503
Impact of LANDSAT MSS sensor differences on change detection analysis — New Mexico, San Francisco, CA, New Hampshire, and Connecticut
11 p1667 N85-20506
Spectral characterization of the LANDSAT Thematic Mapper sensors 11 p1669 N85-20514
Prelaunch absolute radiometric calibration of the reflective bands on the LANDSAT-4 protoflight Thematic Mapper 11 p1669 N85-20515
The spot operational remote sensing satellite system: Current status and perspectives
11 p1713 N85-20778
In-progress absolute radiometric inflight calibration of the LANDSAT-4 sensors — New Mexico
12 p1870 N85-21733
LANDSAT-4 Thematic Mapper calibration and atmospheric correction 12 p1870 N85-21734

Thematic Mapper spectral dimensionality and data structure 12 p1871 N85-21736
Intraband radiometric performance of the LANDSAT 4 Thematic Mapper — Washington, DC, Arkansas, Massachusetts, Virginia, and Arizona 12 p1871 N85-21738
The use of linear feature detection to investigate Thematic Mapper data performance and processing 12 p1872 N85-21740
Geodetic accuracy of LANDSAT 4 Multispectral Scanner and Thematic Mapper data 12 p1873 N85-21746
Preliminary comparisons of the information content and utility of TM versus MSS data 13 p2120 N85-23202
The use of Thematic Mapper data for land cover discrimination: Preliminary results from the UK SATMaP programme 13 p2121 N85-23207
Calculation of image shift in panoramic photography 15 p2488 N85-25357
Modular Optoelectronic Multispectral Scanner (MOMS) for Earth observation. First results of STS-7 mission [MBB-UR-717/83-O] 16 p2574 N85-27732
Thermal Infrared Multispectral Scanner (TIMS): An investigator's guide to TIMS data [NASA-CR-175875] 17 p2981 N85-29286
An assessment of the potential role of multispectral imagery in bathymetric charting [AD-A153460] 17 p2984 N85-29436
Dynamic rectification of airborne scanner digital image recordings 18 p3124 N85-29344
Nimbus 7 Coastal Zone Color Scanner (CZCS). Level 2 data product users' guide [NASA-TM-86202] 19 p3299 N85-30452
Nimbus 7 Coastal Zone Color Scanner (CZCS). Level 1 data product users' guide [NASA-TM-86203] 19 p3299 N85-30453
Spectroradiometric calibration of the Thematic Mapper and Multispectral Scanner system [E85-10104] 20 p3476 N85-31601
Stripe filters on multispectral linear arrays [NASA-CR-175305] 21 p3579 N85-32252
Use of spaceborne imaging radar in regional geomorphic studies 21 p3603 N85-32377
Quantitative geomorphologic studies from spaceborne platforms 21 p3604 N85-32381
Calculating solar highlight and shadeless areas for scanning photographs from space and optimizing lighting conditions 22 p3736 N85-33160
Comprehensive mapping of arid territories of Arizona using space photography 22 p3737 N85-33164

MULTISPECTRAL LINEAR ARRAYS
Imaging Science Panel. Multispectral Imaging Science Working Group joint meeting with Information Science Panel: Introduction 02 p0213 N85-11406
An overview of Multispectral Electro-Optical Stereo Scanner (MEOSS) mission 04 p0458 N85-12908
Chemometric analysis of multisensor arrays [AD-A153805] 18 p3174 N85-29880
Nimbus 7 Coastal Zone Color Scanner (CZCS). Level 1 data product users' guide [NASA-TM-86203] 19 p3299 N85-30453
Stripe filters on multispectral linear arrays [NASA-CR-175305] 21 p3579 N85-32252
The application of bispectral analyses to aeroelastic phenomena 24 p4080 N85-35157

MULTISPECTRAL PHOTOGRAPHY
NT COLOR INFRARED PHOTOGRAPHY
NT INFRARED PHOTOGRAPHY
NT RADAR PHOTOGRAPHY
Space observation of latitudinal changes in vegetation cover 02 p0164 N85-11113
The Multispectral Imaging Science Working Group. Volume 1: Executive summary [E85-10001] 02 p0213 N85-11404
The Multispectral Imaging Science Working Group. Volume 2: Working group reports [E85-10002] 02 p0213 N85-11405
Botanical sciences team 02 p0214 N85-11407
Noise removal in multichannel images [NASA-CR-174116] 04 p0554 N85-13526
Evaluation of SPOT simulation data of the S GEOS campaign of the EEC by data of the test sites Freiburg and Staubing (West Germany) 05 p0659 N85-14237
Combining Heat Capacity Mapping Mission (HCMM) LANDSAT and thematic map information into a unique high precision merged multichannel system — climatology 05 p0660 N85-14239
Microwave and optical remote sensing of forest vegetation 08 p1146 N85-17228
Feature extraction assessment study [AD-A150189] 13 p2126 N85-23239
Comprehensive, integrated, remote sensing at DOE sites [DE85-004867] 13 p2126 N85-23240
Multispectral analysis of the Kasei Valle-Lunae Planum region of Mars 13 p2193 N85-23607
Studies in parallel image processing 14 p2399 N85-24789
Efficient contextual measures for classification of multispectral image data 14 p2433 N85-25005
Relative geological information yield from small-scale multizonal space images (example of Fergana depression and its mountainous margins) 15 p2485 N85-25343
Identifying land use structures of multizonal aerospace photographs using digital data processing 15 p2486 N85-25348
Lidar and radiometer observations of thunderstorm tops 15 p2595 N85-25994
Interpretation of multiband photographs made during Telefoto-80 experiment for the purpose of discriminating agricultural crops 22 p3735 N85-33152
Cataloging the spectral brightness coefficients of the forested region of the European territory of the USSR 22 p3735 N85-33155
Regression analysis of aircraft and ground measurement data on vegetation cover 22 p3735 N85-33156
Direct regression analysis of remote sensing data (using example of grass cover) 22 p3736 N85-33157

MULTISPECTRAL RADAR
Multispectral (X and C band) crop classification with synthetic aperture radar (SAR-580) optical data 05 p0657 N85-14217
Digital controller for the Wave Propagation Laboratory's VHF and UHF wind-profiling radars [PB85-112142] 11 p1626 N85-20238

MULTISPECTRAL RESOURCE SAMPLER
A comparison of LANDSAT thematic mapper, multispectral scanner and airborne sensors for mapping the distribution of alteration minerals: Examples from the southwestern United States 24 p4106 N85-35452

MULTISTAGE COMPRESSORS
U TURBOCOMPRESSORS

MULTISTAGE ROCKET VEHICLES
NT ARIANE LAUNCH VEHICLE
NT ATLAS CENTAUR LAUNCH VEHICLE
NT VEGA LAUNCH VEHICLE
Conestoga 2: A low cost commercial space transport system 02 p0153 N85-11033
An experimental study on the induced normal force on tail-fins due to wing-tail interference [NAL-TR-814] 03 p0018 N85-12051
The development of staging mechanisms for the Japanese satellite launcher Mu-3SII 22 p3798 N85-33528

MULTISTATIC RADAR
Tristatic tracking filter used by the multistatic measurement system [AD-A146885] 07 p0911 N85-15769
Bistatic coherent radar receiving system [AD-D011447] 10 p1466 N85-19252
High time-resolution studies of the auroral ionosphere [AD-A150045] 14 p2409 N85-24850
Multi-bistatic radar for short range surveillance [BAE-BT-10603] 15 p2539 N85-25673
Phase synchronizing large antenna arrays using the spatial correlation properties of radar clutter 20 p3439 N85-31344
Potential coordinate estimate accuracy estimation accuracy by multiposition radar systems 22 p3763 N85-33322

MULTITEMPORAL ANALYSIS
U TEMPORAL RESOLUTION

MULTIVARIATE STATISTICAL ANALYSIS
NT BIVARIATE ANALYSIS
NT COVARIANCE
NT DISCRETE FUNCTIONS
NT ORTHOGONALITY
NT REGRESSION ANALYSIS
MICROSCOPE: A software system for multivariate analysis [AD-A144720] 01 p0103 N85-10688
Testing of inequality hypotheses in linear models using the Bayes method [SER-C-292] 01 p0112 N85-10761
Total positivity. A review [AD-A145205] 01 p0114 N85-10771
The information in the minor principal components 02 p0211 N85-11391
Asymptotically optimal adaptive control [AD-A145666] 02 p0249 N85-11629
On the rate of mean convergence of finite linear predictors of multivariate stationary stochastic processes [AD-A145609] 02 p0254 N85-11664
Computer equipment for research in statistics [AD-A145755] 03 p0406 N85-12591
Return difference feedback design for robust uncertainty tolerance in stochastic multivariable control systems [AD-A145861] 03 p0411 N85-12624
Multivariate analyses of sedimentological data at two early Bronze age sites, Bab edh-Dhra and Numeira, southeast Dead Sea Graben, Jordan 05 p0674 N85-14326
A monotonicity property of the power function of multivariate tests [CWI-MS-R8406] 05 p0721 N85-14635
Asymptotic distributions of estimators for posterior probabilities in a classification model with both continuous and discrete variables [CWI-MS-R8409] 05 p0722 N85-14637
Log linear model applications [AD-A146620] 06 p0858 N85-15457
The stable evaluation of multivariate b-splines [AD-A147386] 07 p1032 N85-16551
The symmetry group and exponents of operator stable probability measures [AD-A147187] 07 p1035 N85-16568
A factor analysis for time series [AD-A147495] 07 p1036 N85-16574
Tail behaviour for suprema of empirical processes [AD-A147629] 08 p1210 N85-17613
Robust linear filtering for multivariable stationary time series, part 3 [AD-A148169] 08 p1212 N85-17627
Multicomponent calibration and quantitation methods [AD-A148252] 08 p1212 N85-17629
Methods and applications of time series analysis. Part 2: Linear stochastic models [AD-A147292] 08 p1214 N85-17645
Generating positively correlated random variables from a sequence of independent random variables with symmetric logarithmically concave densities [AD-A148438] 08 p1216 N85-17658
Methods of computer-aided analysis of non-Gaussian noise and application to robust adaptive detection, part 2 [AD-A148879] 10 p1539 N85-19704
Dual adaptive control based upon sensitivity functions [NASA-CR-169331] 10 p1543 N85-19727
Controlled approximation and a characterization of the local approximation order [AD-A149095] 10 p1546 N85-19750
Looking at multivariate data through fuzzy sets [DE85-000684] 11 p1702 N85-20706
On the limiting empirical distribution function of the eigenvalues of a multivariate F matrix [AD-A149618] 12 p1921 N85-22065
An asymptotically optimal subclass of BTIB designs for comparisons with a control [AD-A149619] 12 p1921 N85-22066
Draftsman displays: A graphical technique for exploratory data analysis [AD-A150515] 13 p2041 N85-22775
Effects of assuming independent component failure times, if they are actually dependent, in a series system [AD-A150582] 13 p2101 N85-23092
Multivariate analysis and its applications [AD-A150324] 13 p2151 N85-23352
On limit of the largest eigenvalue of the large dimensional sample covariance matrix [AD-A150589] 13 p2151 N85-23358
The integration of information from an analog-visual display: The role of dimensional integrality [AD-A150756] 14 p2404 N85-24820
Practical methods for the compensation and control of multivariable systems [AD-A151047] 14 p2407 N85-24841
Ergodicity and Steady-State-Equilibrium conditions for Markov chains [AD-A151038] 14 p2409 N85-24854
Classification and multiple regression through projection pursuit [AD-A150797] 14 p2411 N85-24867
Convolution of the IFRA (Increasing Failure Rate Average) scaled-mins class [AD-A151070] 14 p2411 N85-24870
Construction of efficient algorithms for the estimation of multivariate probability densities [AD-A151509] 15 p2640 N85-26285
On limiting empirical distribution function of the eigenvalues of a multivariate F matrix, revised [AD-A151885] 15 p2641 N85-26288
On asymptotic joint distribution of the eigenvalues of the noncentral manova matrix for nonnormal populations [AD-A151886] 15 p2642 N85-26294
The statistical analysis of initial imperfection measurements — shell profiles [VTH-LR-442] 16 p2857 N85-27622
Analysis of control system from a viewpoint of desired pole placement and desired degree of robustness [AD-A152627] 17 p2899 N85-27676
An empirical comparison of the accuracy of univariate and multivariate corrections for range restriction [AD-A153071] 17 p3019 N85-29570
Detection of multivariate outliers with dispersion slippage in elliptically symmetric distributions [AD-A153785] 18 p3174 N85-29677

Robust control of multivariable and large space systems
[AD-A155117] 21 p3559 N85-32140
Computer graphics for multivariate data
23 p3958 N85-34528
Invariant tests and likelihood ratio tests for multivariate elliptically contoured distributions
[AD-A155844] 24 p4142 N85-35679
MULTIVIBRATORS
NT FLIP-FLOPS
MUON SPIN ROTATION
Spin dynamics of rare Earth ions in crystal fields probed by muon spin rotation
[DE84-013606] 02 p0278 N85-11810
Activities of the Solid State Physics Research Institute
[NASA-CR-175890] 17 p3042 N85-28818
Muon spin rotation studies 17 p3042 N85-28819
Proportional drift tubes for large area muon detectors
[HE-5.2-11] 24 p4203 N85-36087
MUONS
Uniaxial stress induced symmetry breaking for muon sites in Fe 17 p3042 N85-28820
Early study of muons and muon decay
[NOTA-INTERNA-835] 18 p3184 N85-29742
Excited leptons contribution to muon g-2
[PREPRINT-432] 18 p3184 N85-29745
Additional muon calculations for the SLC positron source
[DE85-011212] 19 p3363 N85-30655
Search for gamma rays of energy 10(15) eV from Cygnus X-3
[OG-2.1-1] 22 p3862 N85-33919
Observation of an excess of cosmic ray muons of energies 2 TeV from the direction of Cygnus X-3
[OG-2.1-3] 22 p3863 N85-33920
Muon content of gamma ray induced EAS from Cygnus X-3
[OG-2.1-4] 22 p3863 N85-33921
Observations of Cygnus X-3 above 10(15) eV from 1979 - 1984
[OG-2.1-6] 22 p3863 N85-33923
Evidence for long-term variability in the ultra high energy photon flux from Cygnus X-3
[OG-2.1-10] 22 p3863 N85-33926
Constraints on cosmic-ray observation of Cygnus X-3
[OG-2.2-3] 22 p3864 N85-33930
Search for excess showers from Crab Nebula
[OG-2.3-2] 22 p3866 N85-33939
Search for ultra high energy gamma-rays from various sources
[OG-2.6-7] 22 p3870 N85-33969
The muon content of EAS as a function of primary energy
[OG-5.1-8] 22 p3881 N85-34050
Estimation of composition of cosmic rays with E sub zero approximately equals 10(17) - 10(18) eV
[OG-5.1-14] 22 p3882 N85-34055
All particle energy spectrum of cosmic rays in 10 to the 15th power - 10 to the 20th power eV region
[OG-5.1-15] 22 p3882 N85-34056
Composition of primary cosmic rays near the bend from a study of hadrons in air showers at sea level
[OG-5.2-2] 22 p3883 N85-34059
The composition of cosmic rays near the Bend (10 to the 15th power eV) from a study of muons in air showers at sea level
[OG-5.2-3] 22 p3883 N85-34060
EAS fluctuation approach to primary mass composition investigation
[OG-5.2-5] 22 p3883 N85-34062
The primary composition beyond 10 to the 5th power GeV as deduced from high energy hadrons and muons in air showers
[OG-5.2-6] 22 p3883 N85-34063
High-energy multiple muons and heavy primary cosmic-rays
[OG-5.2-9] 22 p3883 N85-34065
Composition of primary cosmic rays near the knee
[OG-5.2-10] 22 p3884 N85-34066
Anisotropy of cosmic rays of energy 10 (15) eV to 10 (17) eV observed at Akeno
[OG-5.3-3] 22 p3884 N85-34070
The sidereal anisotropy of cosmic rays around 3 x 10 (15) eV observed at a middle north latitude
[OG-5.3-6] 22 p3884 N85-34072
Cosmic ray intensity variations at primary rigidities near 1900 GV
[OG-5.3-9] 22 p3885 N85-34075
Corrected sidereal anisotropy for underground muons
[SH-4.4-7] 23 p4033 N85-35005
Long-term modulation of galactic cosmic rays in high-energy region
[SH-4.4-22] 23 p4035 N85-35018
The cosmic ray differential diurnal variation dependences on the zenith angle and the geomagnetic disturbance
[SH-4.5-16] 23 p4036 N85-35033
Anomalous increase of solar anisotropy above 150GV in 1981-1983
[SH-4.5-18] 23 p4038 N85-35035
Atmospheric effects on the underground muon intensity
[SH-6.1-3] 23 p4044 N85-35078
Burst size distributions in the digitized data of the ion chambers t Mt. Norikura and sea level stations
[SH-9.1-9] 23 p4051 N85-35124
Plastic scintillators in coincidence for the study of multi-particle production of sea level cosmic rays in dense medium
[SH-9.1-11] 23 p4052 N85-35126
New Matsushiro underground cosmic ray station (220 M.W.E. in depth)
[SH-9.1-14] 23 p4052 N85-35129
Neutrino production of like sign dimuons
[DE85-013594] 24 p4151 N85-35741
Electrons, muons and hadrons in extensive air showers and how do they depend on nuclear interaction model, part 2 24 p4187 N85-35969
Analysis of equi-intensity curves and NU distribution of EAS 24 p4187 N85-35970
A new study of shower age distribution in near vertical showers by EAS air shower array
24 p4190 N85-35996
A new study of muons in air showers by NBU air shower array 24 p4190 N85-35997
Study of muons near shower cores at sea level using the E594 neutrino detector 24 p4191 N85-36000
Correlation of high energy muons with primary composition in extensive air shower
[HE-4.3-7] 24 p4191 N85-36001
Measurement of energy muons in EAS at energy region larger thean 10(17) eV
[HE-4.3-8] 24 p4191 N85-36002
Muon fluctuation studies of EAS 10(17) eV
[HE-4.3-9] 24 p4191 N85-36003
Average features of the muon component of EAS or = 10(17) eV
[HE-4.3-10] 24 p4191 N85-36004
Measurement of shower electrons and muons using a small air shower array
[HE-4.3-11] 24 p4192 N85-36005
The longitudinal development of muons in cosmic ray air showers at energies 10(15) - 10(17) eV
[HE-4.3-12] 24 p4192 N85-36006
Lateral distribution of high energy muons in EAS of sizes Ne approximately equals 10(5) and Ne approximately equals 10(6)
[HE-4.3-16] 24 p4192 N85-36010
The identification of gamma ray induced EAS
[HE-4.5-1] 24 p4195 N85-36026
Muons in gamma showers
[HE-4.5-3] 24 p4195 N85-36027
Muon spectrum in air showers initiated by gamma rays
[HE-4.5-4] 24 p4195 N85-36028
Development of electromagnetic cascades in the atmosphere including the Landau-Pomeranchuk-Migdal effect
[HE-4.5-5] 24 p4195 N85-36029
Electromagnetic and muonic structure of showers initiated by gamma-rays and by hadrons
[HE-4.5-6] 24 p4195 N85-36030
The muon content of gamma-ray showers
[HE-4.5-7] 24 p4195 N85-36031
Simulation of gamma-initiated showers
[HE-4.5-10] 24 p4195 N85-36033
An underground cosmic ray muon telescope for observation of cosmic ray anisotropy
24 p4196 N85-36037
Nuclear cascades in electromagnetic showers produced by primary gamma-quanta in the atmosphere
[HE-4.5-16] 24 p4196 N85-36038
On the possibilities of large-scale radio and fiber optics detectors in cosmic rays
[HE-4.6-2] 24 p4196 N85-36039
A possible EAS array above the Soudan 2 detector
[HE-4.8-9] 24 p4197 N85-36046
Samarkand complex setup for investigation of cosmic ray variation in the energy range of 7 10 (9) - 10 (15) eV
[HE-4.8-14] 24 p4198 N85-36050
Longitudinal development of muons in large air showers studies from the arrival time distributions measured at 900m above sea level
[HE-4.7-4] 24 p4199 N85-36055
Arrival time distributions of electrons in air showers with primary energies above 10 (18)eV observed at 900m above sea level
[HE-4.7-5] 24 p4199 N85-36056
A note on some statistical properties of rise time parameters used in muon arrival time measurements
[HE-4.7-12] 24 p4199 N85-36062
Sub-luminal pulses from cosmic ray air showers
[HE-4.7-13] 24 p4200 N85-36063
Nineteenth International Cosmic Ray Conference. HE sessions, volume 8
[NASA-CP-2376-VOL-8] 24 p4200 N85-36065
Preliminary results on underground muon bundles observed in the Frejus proton-decay detector
[HE-5.1-1] 24 p4200 N85-36067
Muon and neutrino results from KGF experiment at a depth of 7000 hg/square cm
[HE-5.1-2] 24 p4200 N85-36068
Relevance of multiple muons detected underground to the mass composition of primary cosmic rays
[HE-5.1-4] 24 p4201 N85-36069
Multimuons events and primary composition
[HE-5.1-5] 24 p4201 N85-36070
The spectrum of cosmic ray muons obtained with 100-ton scintillation detector underground and the analysis of recent experimental data
[HE-5.1-6] 24 p4201 N85-36071
A large area cosmic muon detector located at Ohya stone mine
[HE-5.1-7] 24 p4201 N85-36072
A new world survey expression for cosmic ray vertical intensity vs. depth in standard rock
[HE-5.1-10] 24 p4201 N85-36073
Muon groups and primary composition at 10 to the 13th power to 10 to the 15th power eV
[HE-5.1-12] 24 p4201 N85-36074
On muon energy spectrum in muon groups underground
[HE-5.1-14] 24 p4201 N85-36076
Energy spectrum of cascades generated by muons in Baksan underground scintillation telescope
[HE-5.1-15] 24 p4202 N85-36077
Underwater measurements of muon intensity
[HE-5.1-16] 24 p4202 N85-36078
Multiple muons in MACRO
[HE-5.2-1] 24 p4202 N85-36079
The Nagoya cosmic-ray muon spectrometer 3, part 1: Preliminary observations
[HE-5.2-2] 24 p4202 N85-36080
The Nagoya cosmic-ray muon spectrometer 3, part 2: Track detector
[HE-5.2-3] 24 p4202 N85-36081
The Nagoya cosmic-ray muon spectrometer 3, part 3: Automatic film scanning equipment
[HE-5.2-4] 24 p4202 N85-36082
The Nagoya cosmic-ray muon spectrometer 3, part 4: Track reconstruction method
[HE-5.2-5] 24 p4202 N85-36083
Background light measurements at the DUMAND site
[HE-5.2-7] 24 p4203 N85-36084
Hybrid TLC-pair meter for the Sphinx Project
[HE-5.2-10] 24 p4203 N85-36086
Proportional drift tubes for large area muon detectors
[HE-5.2-11] 24 p4203 N85-36087
An upper limit of muon flux of energies above 100 TeV determined from horizontal air showers observed at Akeno
[HE-5.2-12] 24 p4203 N85-36088
Comments on the measurements of multiple muon phenomena
[HE-5.2-13] 24 p4203 N85-36089
Energy spectrum of cascade showers induced by cosmic ray muons in the range from 50 GeV to 5 TeV
[HE-5.2-14] 24 p4203 N85-36090
Measurement of muon intensity by Cerenkov method
[HE-5.2-15] 24 p4204 N85-36091
Analytical calculation of muon intensities under deep sea-water
[HE-5.2-16] 24 p4204 N85-36092
Photo nuclear energy loss term for muon-nucleus interactions based on xi scaling model of QCD
[HE-5.2-17] 24 p4204 N85-36093
On method of muon spectrum measurements by the scintillation detectors of a large thickness T4t sub o
[HE-5.2-18] 24 p4204 N85-36094
Range fluctuations of high energy muons passing through matter
[HE-5.2-19] 24 p4204 N85-36095
The research program of the Liquid Scintillation Detector (LSD) in the Mont Blanc Laboratory
[HE-5.3-6] 24 p4205 N85-36100
Atmospheric neutrinos observed in underground detectors
[HE-5.3-8] 24 p4205 N85-36102
Measurement of neutrino oscillations in MACRO experiment
[HE-5.3-10] 24 p4206 N85-36104
High energy neutrino astronomy with MACRO
[HE-5.3-12] 24 p4206 N85-36106

Angular distribution of muons produced by cosmic ray neutrinos in rock
[HE-5.3-24] 24 p4207 N85-36115
Multiple muons of conventional and exotic origin in DUMAND
[HE-5.4-4] 24 p4207 N85-36117
Atmospheric muons and neutrinos, and the neutrino-induced muon flux underground
[HE-5.4-7] 24 p4207 N85-36118
Analysis of the electron component of EAS at observational level 700 g x cm(-2) with a scale breaking interaction model and gammaisation hypothesis
[HE-5.4-8] 24 p4208 N85-36119
Relationship of sea level muon charge ratio to primary composition including nuclear target effects
[HE-5.4-10] 24 p4208 N85-36121
Study of photonuclear muon interactions at Baksan underground scintillation telescope
[HE-5.4-10] 24 p4208 N85-36122
Calculation of intensity of high energy muon groups observed deep underground
[HE-5.4-13] 24 p4208 N85-36123
Modular detector for deep underwater registration of muons and muon groups
[HE-5.4-15] 24 p4208 N85-36125
Results of investigation of muon fluxes of superhigh energy cosmic rays with X-ray emulsion chambers
[HE-5.4-16] 24 p4208 N85-36126
Energetic delayed hadrons in large air showers observed at 5200m above sea level
[HE-6.2-9] 24 p4211 N85-36145
Muon and neutrino fluxes
[HE-6.2-18] 24 p4213 N85-36154

MUSCLE RELAXANTS
Smith predictor and self-tuning control of muscle relaxant drug administration
[RR-257] 02 p0235 N85-11534

MUSCLES
NT MYOCARDIUM
Skeletal muscle metabolism in hypokinetic rats
[NASA-CR-174059] 02 p0233 N85-11520
Modulation of the cytosolic androgen receptor in striated muscle by sex steroids
[NASA-CR-174173] 04 p0545 N85-13468
An analysis of kinetic response variability
05 p0707 N85-14533
Electromyographic patterns associated with discrete limb movements 05 p0710 N85-14551
Alterations in skeletal muscle with disuse atrophy
[NASA-CR-174195] 06 p0843 N85-15349
Effect of disuse on sarcoplasmic reticulum in fast and slow skeletal muscle
[NASA-CR-174337] 09 p1191 N85-17508
Acid phosphatase and protease activities in immobilized rat skeletal muscles
[NASA-CR-174340] 08 p1192 N85-17509
A comparison of rat myosin from fast and slow skeletal muscle and the effect of disuse
[NASA-CR-174339] 08 p1192 N85-17510
Neural compensation, muscle load distribution and muscle function in control of biped models
09 p1314 N85-18257
Application of the system identification technique to goal-directed saccades
[AD-A150132] 12 p1906 N85-21967
Aerobic and anaerobic exercise tolerance in the heat: Effect and acclimatization 14 p2368 N85-24707
SPARTEN (Scientific Program of Aerobic and Resistance Training Exercise in the Navy): A total body fitness program for health and physical readiness
[AD-A150869] 14 p2368 N85-24711
Is fast fiber innervation responsible for increased acetylcholinesterase activity in reinnervating soleus muscles?
[NASA-CR-175716] 15 p2614 N85-26106
Differential effect of denervation on free radical scavenging enzymes in slow and fast muscle of rat
[NASA-CR-175719] 15 p2614 N85-26110
Effect of periodic accelerations on physiochemical properties and Ca2+ reactivity of actomyosin in white rat myocardium and skeletal muscles
19 p3324 N85-30594
The 1984 environmental monitoring program report for Idaho National Engineering Laboratory site
[DE85-011209] 22 p3812 N85-33611
Response of amino acids in hindlimb muscles to recovery from hypogravity and unloading by tail-cast suspension
[NASA-CR-176183] 24 p4128 N85-35589
Relaxation techniques
[AD-A158248] 24 p4133 N85-35621

MUSCULAR FATIGUE
The effects of helicopter vibration on the spinal system
[AD-A148274] 03 p0402 N85-12562
Responses of skeletal muscle to unloading, a review
[NASA-CR-176177] 24 p4128 N85-35594

MUSCULAR FUNCTION
USSR report: Space Biology and Aerospace Medicine, volume 18, no. 4, July - August 1984
[JPRS-USB-84-006] 01 p0091 N85-10611
Change in energetics of muscular contraction as a result of hyperoxia 01 p0093 N85-10629
Effects of muscle atrophy on motor control: Cage size effects 15 p2609 N85-26080
Induced changes in the cholinergic system of sciatic nerve and slow and fast twitch muscle of rats
15 p2609 N85-26081
Regional circulation during testing on isokinetic dynamometer following 14-day bedrest
19 p3323 N85-30590
Postural adjustments associated with arm movements in weightlessness 20 p3509 N85-31813
Muscle protein and glycogen responses to recovery from hypogravity and unloading by tail-cast suspension
[NASA-CR-176181] 24 p4128 N85-35591

MUSCULAR STRENGTH
Assessment of muscle strength and prediction of lifting capacity in US Army personnel
[AD-A148846] 10 p1527 N85-19633
Comparative analysis of effects of weightlessness and its models on velocity and strength properties and tone of human skeletal muscles 12 p1901 N85-21936
Use and disuse and the control of acetylcholinesterase activity in fast and slow twitch muscle of rat
[NASA-CR-175717] 15 p2614 N85-26109
Rat skeletal muscles with simulation of physiological effects of weightlessness (morphological study)
23 p3953 N85-34502
Responses of skeletal muscle to unloading, a review
[NASA-CR-176177] 24 p4128 N85-35594

MUSCULAR TONUS
Comparative analysis of effects of weightlessness and its models on velocity and strength properties and tone of human skeletal muscles 12 p1901 N85-21936

MUSCULOSKELETAL SYSTEM
NT BONES
NT CEREBRUM
NT ELBOW (ANATOMY)
NT FEMUR
NT JOINTS (ANATOMY)
NT KNEE (ANATOMY)
NT MARROW
NT PELVIS
NT SCIATIC REGION
NT SKULL
NT VERTEBRAE
NT VERTEBRAL COLUMN
NT WRIST
Non-invasive techniques for determining musculoskeleton body composition
[DE84-015718] 04 p0545 N85-13470
Evaluation of the musculoskeletal diseases program
[PB84-230648] 07 p1017 N85-16461
Skeletal muscle metabolism during exercise is influenced by heat acclimation
[AD-A148845] 10 p1527 N85-19632
Characteristics of human masseter under conditions of hypokinesia 11 p1691 N85-20630
Alterations in gut transport of minerals and in binding proteins during simulated weightlessness
[NASA-CR-175637] 14 p2368 N85-24709
Nutrition in space flight: Some thoughts
14 p2394 N85-24743
Constant fiber number during skeletal muscle atrophy and modified arachidonate metabolism during hypertrophy 15 p2609 N85-26078
Gravity, body mass and composition, and metabolic rate 15 p2610 N85-26084
Changes in bone structure and metabolism during simulated weightlessness: Endocrine and dietary factors
[NASA-CR-175961] 18 p3153 N85-29521
Results and prospects of physiological research during spaceflights 22 p3732 N85-33139
Formation of new microvessels in skeletal muscles of rats exposed to hypobaric hypoxia for one week
22 p3820 N85-33662
Morphological study of antiorthostatic hypokinesia in monkeys 22 p3822 N85-33680
Fluid-electrolyte metabolism and renal function in cosmonauts following 185-day spaceflight
23 p3952 N85-34495
Responses of skeletal muscle to unloading, a review
[NASA-CR-176177] 24 p4128 N85-35594

MUTAGENS
Toxicology of natural and man-made toxicants in drinking water
[AD-P004035] 06 p0845 N85-15365

MUTATIONS
Effect of spaceflight factors on rat bone marrow cells
01 p0092 N85-10620
Study of mathematical models of mutation and selection in multi-locus systems
[DE85-000873] 09 p1376 N85-18648
Toxicity, mutagenesis and aging due to endogenous oxygen radicals
[AD-A150121] 12 p1900 N85-21928
Mutant peas as probes in the understanding of growth and gravitropism 15 p2611 N85-26088
Genetics in methylotrophic bacteria
[DE85-011460] 19 p3327 N85-30615
Mouse oocyte killing by neutrons: Target considerations
[DE85-011362] 19 p3328 N85-30624
Organization of the R region in maize
[DE85-011273] 20 p3504 N85-31780
Hit-size effectiveness theory applied to high doses of low LET radiation for pink mutations in Tradescantia
[DE85-011835] 22 p3819 N85-33657

MYOCARDIAL INFARCTION
Morbidity and mortality associated with exposure to Otto Fuel II in the U.S. Navy 1966-1979
[AD-A148726] 09 p1363 N85-18574
Longitudinal study of cardiovascular disease in US Navy pilots
[AD-A154331] 19 p3328 N85-30623

MYOCARDIUM
Morphological study of monkeys submitted to antiorthostatic hypokinesia 12 p1902 N85-21942
Preventive effect of acute heat factors during hypokinesia 12 p1902 N85-21945
Effects of blood volume overload on myocardial ultrastructure in relation to adaptation to high altitude hypoxia 22 p3820 N85-33664

MYOPIA
Test and evaluation of the 2.4-micron photorefractor ocular screening system
[NASA-TM-86492] 15 p2615 N85-26115

N

N-P JUNCTIONS
U P-N JUNCTIONS

N-TYPE SEMICONDUCTORS
Composition of metal films on gallium arsenide surface 02 p0257 N85-11685
Novel transport and recombination processes in semiconductors
[AD-A145969] 03 p0433 N85-12757
High temperature thermoelectric energy conversion
05 p0610 N85-13894
Photoluminescent and electroluminescent properties of Cd sub 0.95 Mn sub 0.05 Se electrodes
[AD-A146775] 07 p0946 N85-15995
Diffusion barrier for long wavelength laser diodes
[AD-D011390] 07 p0970 N85-16157
Surface and interfacial properties of Ga(0.47) In(0.53)As alloys
[AD-A148891] 10 p1582 N85-19849
Multiple double heterojunction buried laser device
[AD-D011519] 12 p1855 N85-21635
Thermally stimulated conductivity in semi-insulating gallium arsenide 13 p2088 N85-23036
Fabrication and I-V characterization of AlGaAs/GaAs MODFETs with P-type surface layers grown by molecular beam epitaxy
[AD-A151695] 15 p2660 N85-26415
Electrical properties of bulk grown nitrogen doped silicon
[AD-A155471] 21 p3581 N85-32266
TEMO and TEB thermoelectronic devices
22 p3779 N85-33415

NACELLES
Energy efficient engine ICLS Nacelle detail design report
[NASA-CR-167870] 02 p0146 N85-10993
Installed nacelle drag-improvement tests of an M = 0.8 turboprop transport configuration
[NASA-TM-84302] 07 p0902 N85-15716
Some aspects of engine and airframe integration for Ramjet and Ramrocket powered missiles
07 p0918 N85-15812
Over the wing propeller
[NASA-CASE-LAR-13134-1] 11 p1584 N85-19960
Hover test results of a small-scale twin-tilt nacelle model
[NASA-TM-86665] 14 p2210 N85-23706
Low-speed wind-tunnel tests of an advanced eight-bladed propeller
[NASA-TM-86364] 19 p3214 N85-29928
Calculation of transonic flows around an aircraft configuration with motorized nacelle
[SNIAS-851-111-106] 20 p3387 N85-31008

An experimental investigation of propfan installations on an upswept supercritical wing at transonic Mach numbers
[NASA-CR-172605] 20 p3366 N85-31013
Design of the nacelle for the A-320 aircraft
[SNIAS-851-111-111] 20 p3393 N85-31048

NAMIBIA
An evaluation of the electrodialysis reversal process (Edr) for the desalination of brackish water from the Omaruru delta (SWA/Namibia)
01 p0023 N85-10141

NAMING
NT NORMS
Commercial data base management system for geonames data base
[AD-A150835] 14 p2433 N85-25007
Proposal for the systematic naming of mesons and baryons
[DE85-006453] 17 p3035 N85-28773
Distributed name management
[AD-A154785] 21 p3712 N85-33037
The automatic labeling of geographic maps: A problem in computer aesthetics 23 p3962 N85-34561

NAP-OF-THE-EARTH NAVIGATION
Guidance and navigation programs and plans
06 p0751 N85-14609
Integrated cockpit design for the Army helicopter improvement program 06 p0751 N85-14616
Assessment of simulation fidelity using measurements of piloting technique in flight 06 p1075 N85-16817
Ground evaluation of helicopter air-to-air warfare
13 p1967 N85-22360
Piloted simulation of one-on-one helicopter air combat at NOE flight levels
[NASA-TM-86686] 16 p2710 N85-26720

NAPHTHALENE
Supercritical fluid chromatography/supersonic jet spectroscopy
[DE84-016199] 04 p0471 N85-12998
Intermolecular energy transfer between the individual zero-field levels of triplet traps in an orientationally disordered solid
[AD-A150751] 14 p2417 N85-24914
Transport and relaxation processes in supercritical fluids
[DE85-010554] 19 p3358 N85-30818

NAPPES
U FOLDS (GEOLOGY)

NARROWBAND
Improvement of the narrowband linear predictive coder. Part 2: Synthesis improvements
[AD-A145031] 01 p0036 N85-10237
Digital radio receivers and problems of analog-to-digital conversion of narrow-band signals
04 p0486 N85-13101
The adaptive spectrum analyser
05 p0622 N85-13978
A narrow band pulsed eddy current instrument for materials testing
[AERE-R-11229] 07 p0988 N85-18149
Survey of narrow band vocoder technology
[AD-A151919] 16 p2773 N85-27114

NASA PROGRAMS
NT ACEE PROGRAM
NT APOLLO APPLICATIONS PROGRAM
NT APOLLO PROJECT
NT EARTH RESOURCES PROGRAM
NT GALILEO PROJECT
NT HELIOS PROJECT
NT NASTRAN
NT PROJECT SETI
NT SCOUT PROJECT
NT SKYLAB PROGRAM
NT SUPERSONIC CRUISE AIRCRAFT RESEARCH
NT TIROS PROJECT
NT VIKING MARS PROGRAM
NT VOYAGER PROJECT
Department of Housing and Urban Development, and certain independent agencies appropriations for fiscal year 1985, part 2
[S-REPT-98-888-PT-2] 01 p0127 N85-10870
National Aeronautics and Space Administration
01 p0127 N85-10871
Workshop on Automated Space Station
01 p0127 N85-10873
Project Explorer 02 p0154 N85-11041
Initiatives to promote space commercialization
[GPO-37-551] 02 p0156 N85-11058
Statement of Hon. James M. Beggs, Administrator, NASA, Washington, DC 02 p0156 N85-11059
Research and technology
[NASA-TM-86321] 02 p0305 N85-11873
Proceedings of a Workshop on Applications of Tethers in Space, Executive Summary
[NASA-CR-171195] 03 p0322 N85-12075
Proceedings of a Workshop on the Applications of Tethers in Space, Volume 1
[NASA-CR-171196] 03 p0322 N85-12076
Review of Space Shuttle requirements, operations, and future plans
[GPO-39-101] 04 p0461 N85-12927
The 1984 NASA/ASEE summer faculty fellowship program
[NASA-TM-87392] 04 p0574 N85-13662
The 1984 ASEE-NASA summer faculty fellowship program (aeronautics and research)
[NASA-TM-87393] 04 p0575 N85-13664
NASA-Ames vertical gun 04 p0579 N85-13696
NASA's SESAC report on research and analysis in space and Earth sciences 04 p0579 N85-13697
Space telescope cost, schedule, and performance review, 1984
[GPO-39-085] 04 p0579 N85-13698
Resident research associateships. Postdoctoral and senior research awards
[NASA-TM-87399] 05 p0734 N85-14717
Issues and findings 07 p0914 N85-15782
Financing considerations and Federal budget impacts
07 p0915 N85-15792
A research in support of NASA's space science
[NASA-CR-174267] 08 p1227 N85-17728
Summary of activities of Aeronautics and Space Engineering Board
[NASA-CR-174294] 08 p1228 N85-17729
Scientific and technical information output of the Langley Research Center for calendar year 1984
[NASA-TM-86336] 08 p1229 N85-17740
United Kingdom report on space research
08 p1231 N85-17752
Chronology of KSC and KSC related events for 1983
[NASA-TM-87400] 09 p1261 N85-17927
Manned space station solar array study
[ESA-CR(P)-1941] 09 p1287 N85-18061
NASA new technology identification and evaluation
[NASA-CR-174368] 09 p1403 N85-18832
Resident research associateships. Postdoctoral and senior research awards: Opportunities for research at the Jet Propulsion Laboratory
[NASA-CR-174343] 09 p1418 N85-18045
Aerospace Safety Advisory Panel
[NASA-TM-87428] 12 p1774 N85-21135
NASA/MSFC ground experiment for large space structure control verification
[NASA-TM-86496] 12 p1792 N85-21248
Bibliography of Lewis Research Center technical publications announced in 1983
[NASA-TM-83693] 12 p1951 N85-22255
Summary of activities of the Committee on Science and Technology
[H-REPT-99-1169] 12 p1964 N85-22341
U.S., Soviet space program aims contrasted
13 p1995 N85-22455
NASA photovoltaic research and technology development program for space applications
13 p2011 N85-22617
NASA's land remote sensing plans for the 1990's
13 p2124 N85-23224
Small business innovation research: Abstracts of 1984. Phase 1 awards
[NASA-TM-87427] 13 p2165 N85-23431
NASA Patent Abstracts Bibliography. A continuing bibliography. Section 2: Indexes
[NASA-SP-7039(28)] 13 p2187 N85-23445
Authorizing appropriations to the National Aeronautics and Space Administration for fiscal year 1986
[H-REPT-99-32] 13 p2188 N85-23452
NASA space materials research
14 p2232 N85-23631
Precision space structures 14 p2232 N85-23633
NASA Thesaurus supplement, a three part cumulative supplement to the 1982 edition of the NASA Thesaurus
[NASA-SP-7051(SUPPL-3)] 14 p2432 N85-25002
Technology for large space systems: A bibliography with indexes, supplement 11
[NASA-SP-7046(11)] 15 p2475 N85-25277
Militarization of space activity in United States
15 p2488 N85-25380
Study on the extension of experiment resources in the MAUS project
[BMFT-FB-W-84-051] 15 p2650 N85-26343
Management: A bibliography for NASA managers
[NASA-SP-7500(19)] 15 p2664 N85-26439
The 1985 long-range program plan
[NASA-TM-87464] 15 p2664 N85-26440
NASA photography index
[NASA-TM-87457] 15 p2665 N85-26445
NASA Ames Summer High School Apprenticeship Research Program
[NASA-TM-86606] 15 p2666 N85-26590
The search for extraterrestrial intelligence
15 p2669 N85-26609
Activities of the Aeronautics and Space Engineering Board
[NASA-CR-175825] 16 p2691 N85-28810
Spacestation: The next logical step
[NASA-EP-213] 16 p2730 N85-28847
Bioengineering and rehabilitation: Windows of opportunity past, present and future
[NASA-EP-216] 16 p2841 N85-27916
Department of Housing and Urban Development-independent agencies appropriations for 1986. Part 6: National Aeronautics and Space Administration
[GPO-47-235] 16 p2879 N85-27768
European utilization aspects of a US manned space station, volume 1
[ESA-CR(P)-1967-VOL-1] 17 p2907 N85-27926
European utilization aspects of a US manned space station, volume 2
[ESA-CR(P)-1967-VOL-2] 17 p2907 N85-27927
Summer High School Apprenticeship Research Program (SHARP) of the National Aeronautics and Space Administration
[NASA-CR-175791] 17 p3046 N85-29849
National Aeronautics and Space Administration Authorization Act, 1986
[S-REPT-99-91] 17 p3051 N85-28885
Space station study
[BL-6167] 18 p3066 N85-28959
NASA initiatives with historically black colleges and universities
[NASA-EP-210] 19 p3379 N85-30960
National Aeronautics and Space Administration Authorization Act, 1986
[S-REPT-99-91] 19 p3381 N85-30978
Studies toward a manned space station: Participation of European industry in NASA space station (MSS)
[SNIAS-S/DT-Y-25-212] 20 p3418 N85-31217
NASA authorization, 1986, volume 1
[GPO-46-365] 20 p3541 N85-32039
Life sciences flight experiments program mission science requirements document. The first life sciences dedicated Spacelab mission, part 1
[NASA-TM-87494] 21 p3559 N85-32137
Testimony of Robert A. Frosch before the Subcommittee on HUD and Independent Agencies of the Senate Committee on Appropriations
[NASA-TM-87496] 22 p3736 N85-33173
NASA patent abstracts bibliography: A continuing bibliography. Section 1: Abstracts (supplement 27)
[NASA-SP-7039(27)-SECTION-1] 22 p3949 N85-33840
Department of Housing and Urban Development Independent Agencies Appropriation Bill, 1986
[S-REPT-99-129] 23 p3987 N85-34720
National Aeronautics and Space Administration research and development: Program description
23 p3987 N85-34721
A spacefaring people: Perspectives on early spaceflight
[NASA-SP-4405] 23 p4056 N85-35142
Management of large-scale technology
23 p4057 N85-35145
NASA patent abstracts bibliography, a continuing bibliography. Section 2: Indexes (supplement 27)
[NASA-SP-7039(27)-SECTION-2] 24 p4164 N85-35820

NASA SPACE PROGRAMS
NT APOLLO APPLICATIONS PROGRAM
NT APOLLO PROJECT
NT EARTH RESOURCES PROGRAM
NT GALILEO PROJECT
NT HELIOS PROJECT
NT PROJECT SETI
NT SCOUT PROJECT
NT SKYLAB PROGRAM
NT TIROS PROJECT
NT VOYAGER PROJECT

NASA STRUCTURAL ANALYSIS PROGRAM
U NASTRAN

NASTRAN
Comparison of free component mode synthesis techniques using MSC/NASTRAN
[DE84-014451] 04 p0514 N85-13278
Investigation of the HPFTP first stage impeller crack
[NASA-CR-171281] 07 p0977 N85-16208
Thirteenth NASTRAN Users' Colloquium
[NASA-CP-2373] 15 p2573 N85-25863
New enhancements in April 85 NASTRAN release
15 p2573 N85-25864
Improved accuracy in solid isoparametric elements using selectively reduced integration 15 p2573 N85-25865
Crack elements for COSMIC/NASTRAN
15 p2573 N85-25866
A 4-node bilinear isoparametric element in Rockwell NASTRAN 15 p2573 N85-25867

Layered composite analysis capability
15 p2573 N85-25868
NPLOT: An interactive plotting program for NASTRAN finite element models 15 p2573 N85-25869
COSMIC/NASTRAN-PATRAN interface
15 p2574 N85-25870
Two interactive graphics postprocessors for NASTRAN 15 p2574 N85-25871
An unusual application of NASTRAN contour plotting capability 15 p2574 N85-25872
A new NASTRAN capability for data reduction
15 p2574 N85-25874
Automatic Dynamic Aircraft Modeler (ADAM) for the computer program NASTRAN 15 p2574 N85-25875
Ritz procedure for COSMIC/NASTRAN
15 p2575 N85-25877
Symmetric composite laminate stress analysis
15 p2575 N85-25878
NASTRAN's application in agricultural engineering
15 p2575 N85-25880
Use of COSMIC NASTRAN in a design department
15 p2575 N85-25881
An elastic analysis of a plated bone to determine fracture gap motion 15 p2575 N85-25882
Learjet Model 55 wing analysis with landing loads
15 p2575 N85-25883
Fillet weld stress using finite element methods
15 p2576 N85-25884
The structural finite element model of the C-5A
15 p2576 N85-25885
Using NASTRAN to model missile inertia loads
15 p2576 N85-25886
Experience with free bodies 15 p2576 N85-25887
NASTRAN analysis comparison to shock tube tests used to simulate nuclear overpressures
15 p2576 N85-25888
Finite element prediction of loss factors for structures with frequency-dependent damping treatments
15 p2576 N85-25889
Direct transient analysis of a fuze assembly by axisymmetric solid elements 15 p2576 N85-25890
Transient analysis of a magnetic heat pump
15 p2576 N85-25891
NASTRAN-based software for the structural dynamic analysis of vertical and horizontal axis wind turbines
[DE85-001712] 15 p2580 N85-25911
Structural analysis of electronic assembly housing
[DE85-005794] 15 p2580 N85-25913

NATIONAL AIRSPACE SYSTEM
National airspace review 02 p0136 N85-10926
System engineering and integration contract for implementation of the National Airspace System Plan. Volume 2: Section 5.0
[AD-A145710] 02 p0137 N85-10929
System engineering and integration contract for implementation of the National Airspace System plan, volume 1, sections 1.0-4.0, 6.0
[AD-A145763] 03 p0317 N85-12048
National airspace system configuration management interface control document. Maintenance processor subsystem to remote monitoring subsystems and remote monitoring subsystem concentrators
[NAS-MD-790] 07 p0900 N85-15705
National airspace review: Airport radar service area operational confirmation report
[DOT/FAA/AT-84/2] 07 p0901 N85-15707
National airspace review enhancement plan, revision 3
[AD-A150743] 08 p1082 N85-16552
National airspace system: Operational requirements
[AD-A149349] 10 p1422 N85-19973
Response to NAS plan audit report recommendations
[FAA-ES-85-1] 15 p2466 N85-25235
National Airspace System Plan: Facilities, equipment and associated development 16 p2704 N85-26692
National airspace review, change 1
[AD-A152369] 17 p2894 N85-27844

NATIONAL AIRSPACE UTILIZATION SYSTEM
National airspace review 02 p0136 N85-10926
National airspace system configuration management interface control document. Maintenance processor subsystem to remote monitoring subsystems and remote monitoring subsystem concentrators
[NAS-MD-790] 07 p0900 N85-15705

NATIONAL AVIATION SYSTEM
Satellite navigation
[S-HRG-98-856] 08 p1082 N85-16851
Thirty years' activities for aircraft safety
20 p3391 N85-31033

NATIONAL OCEANIC SATELLITE SYSTEM
Ocean services user needs assessment. Volume 1: Survey results, conclusions and recommendations
[NASA-CR-174104] 04 p0541 N85-13445

NATIONAL PARKS
Inventory and monitoring of national park landscapes — remote sensing 05 p0660 N85-14245

NATIONS
NT ALABAMA
NT ALASKA
NT ARGENTINA
NT ARIZONA
NT ARKANSAS
NT AUSTRALIA
NT AUSTRIA
NT BANGLADESH
NT BELGIUM
NT BOLIVIA
NT BRAZIL
NT BRITISH COLUMBIA
NT BULGARIA
NT CALIFORNIA
NT CANADA
NT CHILE
NT CHINA
NT COLOMBIA
NT COLORADO
NT CONNECTICUT
NT COSTA RICA
NT CUBA
NT CZECHOSLOVAKIA
NT DELAWARE
NT DENMARK
NT EAST GERMANY
NT EGYPT
NT ENGLAND
NT FINLAND
NT FLORIDA
NT FRANCE
NT GEORGIA
NT GUATEMALA
NT GUYANA
NT HAWAII
NT HONDURAS
NT HUNGARY
NT ICELAND
NT IDAHO
NT ILLINOIS
NT INDIA
NT INDIANA
NT INDONESIA
NT IOWA
NT IRAN
NT ISRAEL
NT ITALY
NT JAPAN
NT KANSAS
NT KENTUCKY
NT KENYA
NT LOUISIANA
NT MAINE
NT MARYLAND
NT MASSACHUSETTS
NT MEXICO
NT MICHIGAN
NT MISSISSIPPI
NT MISSOURI
NT MONTANA
NT NEBRASKA
NT NETHERLANDS
NT NEVADA
NT NEW HAMPSHIRE
NT NEW JERSEY
NT NEW MEXICO
NT NEW YORK
NT NEW ZEALAND
NT NIGERIA
NT NORTH CAROLINA
NT NORTH DAKOTA
NT NORWAY
NT OHIO
NT OKLAHOMA
NT OREGON
NT PENNSYLVANIA
NT PERU
NT POLAND
NT REPUBLIC OF SOUTH AFRICA
NT SAUDI ARABIA
NT SOUTH CAROLINA
NT SOUTH DAKOTA
NT SPAIN
NT SUDAN
NT SWEDEN
NT SWITZERLAND
NT TAIWAN
NT TENNESSEE
NT TEXAS
NT THAILAND
NT TUNISIA
NT TURKEY
NT U.S.S.R.
NT UNITED KINGDOM
NT UNITED STATES
NT UTAH
NT VIRGINIA
NT WASHINGTON
NT WEST GERMANY
NT WISCONSIN
NT WYOMING
NT YUGOSLAVIA

NATURAL FREQUENCIES
U RESONANT FREQUENCIES

NATURAL GAS
NT LIQUEFIED NATURAL GAS
Status of gaseous fuels for use in highway transportation: A 1983 perspective
[DE84-015205] 01 p0034 N85-10211
State of knowledge of environmental concerns related to natural gas-fueled vehicles
[DE84-015894] 01 p0070 N85-10461
US energy for the rest of the century, 1984 edition
[PB84-207406] 04 p0531 N85-13393
Development of a van-portable remote-sensing laser system for selective detection of natural gas leaks
[PB85-101939/GAR] 06 p0811 N85-15158
Analysis of gases in the Earth's crust
[PB85-113397/GAR] 07 p0990 N85-16267
USSR report: Energy
[JPRS-UEN-84-039] 07 p0994 N85-16312
Natural gas the new locomotive fuel
[DE84-901824] 09 p1302 N85-18179
The influence of modern control techniques on the gas industry
[ERS-E.395] 09 p1325 N85-18326
Measurement of gas compressibility factor data for natural gas and synthetic gas components and their mixtures
[PB85-129047] 11 p1614 N85-20151
Solar-gas systems impact analysis study
[PB85-129068] 11 p1616 N85-20163
Combustion gas properties. 2: Natural gas fuel and dry air
[NASA-TP-2435] 12 p1779 N85-21166
New method of reconstructing conditions of recent differentiation of oil and gas in the Amudarya Basin (based on results of interpretation of space photographs)
13 p1984 N85-22446
Low pressure storage of methane on interlayered clays for potential vehicular applications
[DE85-006949] 16 p2758 N85-27017
Deep source gas
[DE85-001984] 18 p3126 N85-29358
Natural gas anomaly in bottom waters of South China Sea 19 p3290 N85-30399
Development of improved capabilities for computation of gas supercompressibility factors and other properties
[PB85-188316] 20 p3436 N85-31315
Ultrasonic flowmetering with reflected pulses
[PB85-179665] 20 p3460 N85-31492
Environmental concerns related to natural gas vehicles
[DE85-010246] 20 p3486 N85-31666
State of knowledge of environmental concerns related to natural-gas-fueled vehicles
[DE85-009746] 20 p3486 N85-31667
Development of a prototype energy meter
[PB85-196430] 22 p3789 N85-33476
Geologic, technical, and economic sensitivity analysis in support of the GRI (Gase Research Institute) tight gas reservoirs project area
[PB85-192276] 22 p3802 N85-33559
Laser probes of natural gas ignition chemistry
[PB85-200210] 24 p4077 N85-35264
Assessment of metal heating technologies for ferrous forging: A pilot study of the form value of natural gas
[PB85-204394] 24 p4084 N85-35314
High Temperature Heating System (HTHS)
[PB85-186340] 24 p4084 N85-35316

NATURAL GAS EXPLORATION
New method of reconstructing conditions of recent differentiation of oil and gas in the Amudarya Basin (based on results of interpretation of space photographs)
13 p1984 N85-22446
Evaluation of Thematic Mapper performance as applied to hydrocarbon exploration — Ontario, Canada; Cement, Oklahoma; and Death Valley, California
13 p2118 N85-23191
Western gas sands
[DE85-001985] 18 p3126 N85-29360
Pacific index, April 1983 - October 1984
[TI85-901335] 19 p3320 N85-30582
Using remote photographs in prospecting for hydrocarbons on the Kerch Peninsula
22 p3735 N85-33154

NATURAL LANGUAGE (COMPUTERS)
On the requirements of expert systems for fault isolation
[AD-P003947] 02 p0249 N85-11627

Research in knowledge representation for natural language understanding
[AD-A145807] 03 p0409 N85-12813
Knowledge representation and natural-language semantics
[AD-A146025] 03 p0409 N85-12815
Interpretation of natural language database queries using optimization methods 05 p0735 N85-14723
Toward a principle-based parser
[AD-A147837] 08 p1202 N85-17585
Ada (trademark) Joint Program Office objectives and progress through 1983
[AD-A149436] 10 p1541 N85-19713
French plans for fifth generation computer systems
[AD-A149435] 10 p1544 N85-19732
The four forms of omega
[AD-A149994] 12 p1915 N85-22020
Infinite computing
[AD-A151437] 15 p2628 N85-26197
Research in knowledge representation for natural language understanding
[AD-A152260] 16 p2851 N85-27579
Language design, computers and brains
[AD-A152819] 17 p3006 N85-28594
Experience with omega: Implementation of a prototype programming environment: Part 1
[AD-A155438] 21 p3672 N85-32811
Research on distributed artificial intelligence
[AD-A155356] 22 p3833 N85-33733
EPALIT: A data management system applied to the control and retrieval of technical reports
[PB85-193068] 24 p4166 N85-35828

NATURAL LASERS
U LASERS

NATURAL SATELLITES
NT CALLISTO
NT CHARON
NT DEIMOS
NT ENCELADUS
NT EUROPA
NT GALILEAN SATELLITES
NT GANYMEDE
NT IO
NT JUPITER SATELLITES
NT MOON
NT SATURN SATELLITES
NT TITAN
NT TRITON
Origin and evolution of the Uranian and Neptunian satellites: Some dynamical considerations
02 p0300 N85-11943
Composition, structure and evolution of Uranian and Neptunian satellites 02 p0300 N85-11944
Physical properties of the Uranian satellites
02 p0300 N85-11946
Do the satellites of Uranus control its magnetosphere?
02 p0301 N85-11952
The rheology of icy satellites
[NASA-CR-174024] 02 p0302 N85-11959
Charged particle erosion of icy satellites: Coronal atmospheres and surface redistribution
03 p0448 N85-12845
Impact and collisional processes in the solar system
[NASA-CR-174297] 08 p1255 N85-17914
Interaction of the magnetospheric ions with the surfaces of the icy satellites of Saturn 13 p2174 N85-23491
Origin and evolution of the Saturn system
13 p2175 N85-23493
Studies of icy bodies: Uranian satellites and cometary nuclei 13 p2175 N85-23496
Small solar system bodies 13 p2175 N85-23499
Impact and collisional processes in the solar system
13 p2180 N85-23530
How a shepherd guides a sheep herd — satellite-planetary ring interaction
15 p2674 N85-26503
Effects of shepherd conjunctions on Saturn's F-ring
15 p2675 N85-26511
Applications of three-body resonances to satellites and planetary rings 15 p2676 N85-26518
Extended atmospheres of outer planet satellites and comets
[NASA-CR-176137] 22 p3851 N85-33848
What determines the location of satellites and planets? 22 p3853 N85-33858
Volatiles on satellites of the outer solar system
22 p3854 N85-33868
Interpretation of photometric measurements of airless bodies 22 p3855 N85-33871

NAUTICAL CHARTS
Advanced technology for hydrographic mapping
[FOA-C-30371-E1] 08 p1176 N85-17418

NAVIER-STOKES EQUATION
Accelerated convergence for incompressible flow calculations
[NASA-TM-86863] 02 p0140 N85-10949
The CMC/3DPNS computer program for prediction of three-dimensional, subsonic, turbulent aerodynamic juncture region flow. Volume 3: Programmers' manual
[NASA-CR-165996] 02 p0197 N85-11318
Further development of a transonic cascade analysis
[AD-A145410] 02 p0198 N85-11319
Moment induced by liquid payload during spin-up without a critical layer
[AD-A145716] 02 p0199 N85-11327
Navier-Stokes solution of 3-dimensional hypersonic afterbody flowfields over capsule-type vehicles
[NAL-TR-819] 03 p0311 N85-12010
Model equation for simulating flows in multistage turbomachinery
[NASA-TM-86869] 03 p0315 N85-12036
Physics on aircraft wakes
[NASA-CR-174105] 04 p0453 N85-12871
Numerical integrations of the Navier-Stokes equations for flow over surface-mounted obstacles
05 p0593 N85-13784
Navier-Stokes computational study of axisymmetric transonic turbulent flows with a two-equation model of turbulence 05 p0634 N85-14068
Numerical investigations into the parabolized Navier-Stokes equations 05 p0635 N85-14075
Reducing numerical diffusion for incompressible flow calculations
[NASA-TM-83621] 06 p0756 N85-14840
A second-order accurate parabolized Navier-Stokes algorithm for internal flows
[NASA-CR-174258] 07 p0956 N85-16059
Computational analysis of scramjet dual mode operation
[NASA-CR-174250] 07 p0956 N85-16060
Numerical studies of interacting vortices
[NASA-TM-86325] 07 p0957 N85-16062
Development of a Navier-Stokes rotor and stator analysis
[AD-A146967] 07 p0958 N85-16070
Splitting methods for the numerical solution of the incompressible Navier-Stokes equations
[AD-A147463] 07 p1032 N85-16554
Analysis of a penalty finite element approximation of the Navier Stokes equations 08 p1161 N85-17321
Numerical solution of the Navier-Stokes equations for unsteady separated flows
[AD-P004161] 09 p1265 N85-17946
A Navier-Stokes calculation of the airfoil dynamic stall process
[AD-P004163] 09 p1265 N85-17948
Researched applied to transonic compressors in numerical fluid mechanics of inviscid flow and viscous flow
[NASA-CR-174353] 09 p1319 N85-18291
A free shear layer prediction of the turbulent wake of a flat plate towed below a free surface
[AD-A146899] 09 p1319 N85-18293
A series expansion study of the Navier-Stokes equations
[DFVLR-FB-84-34] 09 p1321 N85-18306
Evaluation of inviscid/boundary layer and parabolized Navier-Stokes solutions for design of reentry vehicles
[DE84-014329] 10 p1428 N85-19006
Thrust chamber performance using Navier-Stokes solution — space shuttle main engine viscous nozzle calculation
[NASA-CR-171348] 10 p1430 N85-19019
A multistage time-stepping scheme for the Navier-Stokes equations
[NASA-CR-172527] 10 p1483 N85-19385
Algorithms for the Euler and Navier-Stokes equations for supercomputers
[NASA-CR-172543] 10 p1539 N85-19701
Experimental approach to terms within grids — turbulent flow calculations 11 p1576 N85-19930
A new method for calculating the flow field in a dump combustor
[AD-A149305] 11 p1631 N85-20271
Pseudospectral calculations of two-dimensional transonic flow (Task 1). Numerical investigation of VTOL aerodynamics (Task 2)
[AD-A150123] 12 p1772 N85-21126
Numerical study of large-eddy breakup and its effect on the drag characteristics of boundary layers
[NASA-CR-3884] 12 p1797 N85-21272
Surface-slip equations for multicomponent nonequilibrium air flow
[NASA-TM-85820] 12 p1845 N85-21573
Solution of the three-dimensional Navier-Stokes equations for a steady laminar horseshoe vortex flow
[AD-A149851] 12 p1846 N85-21582
Hydrodynamic stability problem formulated by numerical solutions of the Navier-Stokes equations
12 p1946 N85-22223
Internal fluid mechanism of solid propellant rocket motors 13 p2001 N85-22544
Liquid moment on a filled coning cylinder during spin-up: Ad hoc model
[AD-A150280] 13 p2092 N85-23060
Significance of the thin-layer Navier-Stokes approximation
[DE85-002630] 13 p2092 N85-23063
Wave motion of three-component medium under load moving on plane boundary 14 p2277 N85-24105
Block-implicit multigrid solution of Navier-Stokes equations in primitive variables
[DE85-004071] 14 p2301 N85-24250
A 3-dimensional Navier-Stokes-Euler code for blunt-body flow computations
[NASA-TM-58266] 15 p2463 N85-25211
A finite element, Navier-Stokes study of the confined, laminar flow over a downstream facing step
15 p2553 N85-25754
Numerical simulation of boundary layer excitation by surface heating/cooling
[NASA-CR-172575] 15 p2554 N85-25756
Computational models of the viscous sublayer and limiting behavior of turbulence near a wall
[AD-A151198] 15 p2556 N85-25767
Unsteady Navier-Stokes calculations in an accelerated reference frame
[AD-A151751] 15 p2557 N85-25774
Flow over a biconic configuration with an afterbody compression flap
[AD-A151882] 15 p2557 N85-25778
Viscous effects on blast wave flowfields
[AD-A152013] 15 p2558 N85-25779
Numerical solutions of 3-dimensional Navier-Stokes equations for closed blunt-bodies
[NASA-CR-175755] 15 p2636 N85-26255
Numerical analyses in aerodynamic design of aero-engine fan 16 p2692 N85-26618
Navier-Stokes solution of hypersonic blunt-nosed body flowfields 16 p2693 N85-26624
Recent progress in computational aerodynamics
16 p2693 N85-26626
LU methods for the compressible Navier-Stokes equations 16 p2761 N85-27160
Theoretical investigation of three-dimensional shock wave turbulent boundary layer interactions. Part 3
[AD-A152251] 16 p2783 N85-27177
Users manual for coordinate generation code CRDSRA
[NASA-CR-172584] 17 p2891 N85-27824
User's manual for airfoil flow field computer code SRAIR
[NASA-CR-172585] 17 p2891 N85-27825
Use of quaternions in flight mechanics
[AD-A152616] 17 p2899 N85-27875
Navier-Stokes computational study of axisymmetric transonic turbulent flows with a two-equation model of turbulence
[AD-A152653] 17 p2958 N85-28265
Proceedings of the 9th US Air Force and the Federal Republic of Germany Data Exchange Agreement Meeting, Viscous and Interacting Flow Field Effects
[AD-A153020] 17 p2958 N85-28266
A Navier-Stokes capillary free boundary in open boat crystal growth
[REPT-84-34] 17 p2960 N85-28283
Numerical computation of space shuttle orbiter flow field
[NASA-CR-175912] 18 p3058 N85-28821
Numerical simulation of unsteady motion in a turbulent mixing layer
[NAL-TR-849T] 18 p3099 N85-29183
Two approaches for the prediction of plume-induced separation
[AD-A154098] 19 p3215 N85-29935
Application of computational fluid dynamics to complex inlet ducts
[NASA-TM-87060] 19 p3265 N85-30247
A numerical solution of a nonisothermal wall using the two-dimensional Navier-Stokes equations
[AD-A154467] 19 p3286 N85-30257
On spectral multigrid methods for the time-dependent Navier-Stokes equations
[NASA-CR-172613] 19 p3344 N85-30725
Superconvergence of finite element approximation for Navier-Stokes equations 19 p3345 N85-30732
Turbulent solutions of equations of fluid motion
20 p3453 N85-31441
An implicit finite-difference code for a two-equation turbulence model for three-dimensional flows
[NASA-TM-86752] 20 p3454 N85-31448
High Re separated flow solutions using the Navier-Stokes and approximate equations
[AD-A152252] 20 p3454 N85-31451
The calculation of fully three dimensional flow through any type of turbomachine blade row
21 p3587 N85-32294

Performance evaluation of flow in turbomachinery blade rows
21 p3587 N85-32299
Calculation of steady and unsteady airfoil flow fields via the Navier-Stokes equations
[NASA-CR-3899] 22 p3727 N85-33105
Jet flows: Modelling and experiments
22 p3744 N85-33208
A mixed pseudospectral/finite difference method for a thermally driven fluid in a nonuniform gravitational field
[NASA-TM-87581] 22 p3763 N85-33456
A three-dimensional viscous flow analysis for the helicopter tip vortex generation problem
[NASA-CR-3906] 23 p3993 N85-34114
Comments on the prediction of dynamic stall
[GU-AERO-6501] 23 p3994 N85-34125
A curvilinear coordinate method for the solutions of initial value problems using the third-order upwind differencing scheme
[IPPJ-734] 23 p3975 N85-34642

NAVIGATION
NT AIR NAVIGATION
NT ALL-WEATHER AIR NAVIGATION
NT AREA NAVIGATION
NT ASTRONAVIGATION
NT CELESTIAL NAVIGATION
NT DEAD RECKONING
NT DIGITAL NAVIGATION
NT DOPPLER NAVIGATION
NT HYBRID NAVIGATION SYSTEMS
NT INERTIAL NAVIGATION
NT INTERPLANETARY NAVIGATION
NT LORAN
NT LORAN C
NT NAP-OF-THE-EARTH NAVIGATION
NT OMEGA NAVIGATION SYSTEM
NT RADAR NAVIGATION
NT RADIO NAVIGATION
NT SPACE NAVIGATION
NT SURFACE NAVIGATION
NT TACAN
NT VHF OMNIRANGE NAVIGATION
Operational requirements - system concepts
08 p0752 N85-14823
Certification of advanced systems
08 p0753 N85-14829
Integrated navigation systems: Where are we headed?
[AD-A146425] 06 p0753 N85-14832
Map display for helicopters 08 p1073 N85-16801
Development of a Helicopter Integrated navigation system 08 p1073 N85-16802
High accuracy Doppler navigation employing optimum integrated position fix information
08 p1073 N85-16803
Standard Attitude Heading Reference System (SAHRS) full scale development program
08 p1073 N85-16804
Integrated control and display systems for helicopter battlefield mission management
08 p1073 N85-16805
Shuttle navigation status 08 p1092 N85-16801
Space Shuttle Technical Conference, part 2
[NASA-CP-2342-PT-2] 08 p1096 N85-16837
Three position estimation procedures
[AD-A146748] 09 p1276 N85-18042
Automatic land vehicle navigation using road map data
[DE84-017178] 09 p1278 N85-18043
USSR report: Engineering and equipment
[JPRS-UEQ-85-001] 09 p1305 N85-18200
Using the global positioning system (GPS) phase observable for relative geodesy: Modeling, processing, and results 09 p1341 N85-18437
The use of synthetic aperture radar imagery to detect hazards to navigation
[AD-A149324] 10 p1422 N85-19971
The Telecommunications and Data Acquisition Report
[NASA-CR-174366] 10 p1462 N85-19224
Space System Applications to Tactical Operations
[AGARD-CP-344] 11 p1709 N85-20751
Dynamic world modeling for an intelligent mobile robot using a rotating ultra-sonic ranging device
[AD-A149979] 12 p1775 N85-21143
Investigation of a failure detection/identification system for a tactical aircraft navigation system
[AD-A151846] 15 p2469 N85-25240
A cost-efficient control procedure for the benefit of all airspace users 16 p2697 N85-26651
Avionics data base
[AD-A152415] 17 p2897 N85-27863
Time transfer techniques: Historical overview, current practices and future capabilities
18 p3108 N85-29245
HERMIES-1: A mobile robot for navigation and manipulation experiments
[DE85-006652] 18 p3118 N85-29301
LORAN-C harbor and harbor entrance survey: Charleston, South Carolina
[AD-A154875] 21 p3554 N85-32106
The potential of the NAVSTAR global positioning system for the Corps of Engineers, civil works
[AD-A154913] 21 p3554 N85-32109
Nonlinear digital phase-locked loops with application to Loran-C receivers 24 p4083 N85-35178

NAVIGATION AIDS
NT COMPASSES
NT GYROCOMPASSES
NT MAGNETIC COMPASSES
NT NAVIGATION INSTRUMENTS
NT RADAR BEACONS
NT RADIO BEACONS
NT RADIO DIRECTION FINDERS
Peripheral vision displays: The future
01 p0009 N85-10058
A production peripheral vision display system
01 p0010 N85-10059
Use of microprocessor techniques and new antenna systems to improve the navigation aids very high frequency omnidirectional radar (VOR), Doppler VOR and Instrument Landing System (ILS)
[BMFT-FB-W-84-026] 02 p0137 N85-10930
Autonomous navigation of USAF spacecraft
03 p0321 N85-12074
Integrated navigation systems: Where are we headed?
[AD-A146425] 06 p0753 N85-14832
Technology development for unmanned untethered submersible vehicle systems
[AD-A148794] 09 p1304 N85-18190
The susceptibility of aeronautical navigational aids to interference from adjacent-band broadcast transmissions
[BBC-RD-1984/12] 09 p1311 N85-18234
An evaluation of flashtube signal characteristics
[AD-A149569] 10 p1423 N85-18974
Navigation for an intelligent mobile robot
[AD-A150061] 12 p1775 N85-21144
Reference systems for the evaluation of dead-reckoning navigation equipment 13 p1967 N85-22358
Operational experience with ion concentration sensors in orientation systems 13 p1980 N85-22422
USSR report: Engineering and equipment
[JPRS-UEQ-84-001] 14 p2265 N85-24034
Combinatorial performance/cost analysis of an autonomous navigation system for aircraft
16 p2695 N85-26640
Prequidance and piloting with the aid of composite inertial sensors 16 p2696 N85-26648
The use of a self-compensated magnetometer in an economical navigation system for the helicopter
16 p2697 N85-26650
A method of estimating aircraft attitude from fly by wire flight control system data 16 p2697 N85-26653
Terrain following without use of forward looking sensors 16 p2698 N85-26659
Low cost two gimbal inertial platform and its system integration 16 p2698 N85-26661
Navigation and flight director guidance for the NASA/FAA helicopter MLS curved approach flight test program
[NASA-CR-177350] 16 p2704 N85-26691
Observability in problem of correction of inertial navigation systems using additional information from artificial Earth satellite 16 p2719 N85-26785
Avionics data base
[AD-A152415] 17 p2897 N85-27863
The AFTI/F16 terrain-aided navigation system
[DE85-006411] 18 p3060 N85-29035
The DREO (Defence Research Establishment Ottawa) Inertial Navigation Laboratory: Development and test capabilities
[AD-A154425] 19 p3216 N85-29945
LORAN-C harbor and harbor entrance survey: Charleston, South Carolina
[AD-A154875] 21 p3554 N85-32108

NAVIGATION INSTRUMENTS
NT ATTITUDE INDICATORS
NT COMPASSES
NT GYRO HORIZONS
NT GYROCOMPASSES
NT MAGNETIC COMPASSES
NT RADIO ALTIMETERS
NT RADIO DIRECTION FINDERS
Evaluation of air and ground launched cruise missile navigational element containers
[AD-A149654] 12 p1774 N85-21138
Reference systems for the evaluation of dead-reckoning navigation equipment 13 p1967 N85-22358
Navigation and flight director guidance for the NASA/FAA helicopter MLS curved approach flight test program
[NASA-CR-177350] 16 p2704 N85-26691

NAVIGATION SATELLITES
NT NAVSTAR SATELLITES
NT TRANSIT SATELLITES
The motion of the Earth by Doppler observing campaign (MEDOC) 05 p0601 N85-13831
A replenishment phase study for the NAVSTAR global positioning system
[AD-A152030] 16 p2704 N85-26695
Observability in problem of correction of inertial navigation systems using additional information from artificial Earth satellite 16 p2719 N85-26785
Analysis of orbit transfer vehicles for GPS Block 3 satellites
[AD-A152021] 16 p2732 N85-26860
Scintillation using NNSS satellites
[AD-A152804] 17 p2949 N85-28207
Rescue satellite COSPAS 20 p3401 N85-31103

NAVIGATORS
International flight planning handbook
[AD-A156330] 24 p4062 N85-35177

NAVSTAR SATELLITES
Simulation of the performance of adaptively controlled Navstar antennas in battlefield scenarios
10 p1472 N85-19292
Potential impact of Navstar GPS on NATO tactical operations 11 p1711 N85-20763
Coverage and buildup of the Navstar constellation
11 p1711 N85-20764
Optimization of guidance and control using function minimization and NAVSTAR/GPS
[AD-A149956] 12 p1775 N85-21141
Program INNAVSAT: Global Positioning System (GPS): Test and demonstration program
[BMFT-FB-W-84-047] 12 p1775 N85-21145
Accurate baseline determination by radio interferometry on NAVSTAR GPS satellite transmissions
[AD-A150681] 14 p2291 N85-24202
Real-time position determinations using the GPS TI4100/GEOSTAR receiver
[AD-A152551] 17 p2894 N85-27845
Kalman filter estimates of the NAVSTAR satellite clock parameters 17 p2965 N85-28315
Review and evaluation of plans to incorporate NAVSTAR global positioning system user equipment on military sealift command ships
[AD-A153799] 18 p3060 N85-29034
On-orbit frequency stability analysis of the GPS NAVSTAR-1 quartz clock and the NAVSTARs-6 and -8 rubidium clocks 18 p3105 N85-29227
Rubidium and cesium frequency standards status and performance on the GPS program
18 p3106 N85-29228
The NAVSTAR Global Positioning System (GPS) receiver development program, phase 1
[BMFT-FB-W-85-002] 20 p3399 N85-31085

NAVY
Don't fowl out
[AD-P004179] 11 p1578 N85-19941
Practical applications of satellite-derived meteorological and oceanographic data in Naval operations
11 p1712 N85-20771
Navy tactical applications guide. Volume 4. Part 1. Eastern North Pacific weather analysis and forecast applications
[AD-A150097] 12 p1896 N85-21900
A review of neck injury and impaired consciousness associated with US Navy ejections 1 January 1969 - 31 December 1979 12 p1906 N85-21973
An airborne infrared thermal scanning system for easy use on Navy P-3 aircraft
[AD-A149690] 12 p1933 N85-22143
SPARTEN (Scientific Program of Aerobic and Resistance Training Exercise in the Navy): A total body fitness program for health and physical readiness
[AD-A150669] 14 p2368 N85-24711
A preliminary analysis of C-12 aircraft usage by the Navy Air Logistics System
[AD-A151921] 16 p2694 N85-26634
Recent Naval Postgraduate School publications
[AD-A151723] 16 p2875 N85-27740
Navy program manager's guide, 1985 edition
[AD-A151925] 16 p2876 N85-27744
Navy geothermal plan
[AD-A152478] 17 p2965 N85-28450
Test and Evaluation Master Plan (TEMP) for the Navy Occupational Health Information Management System (NOHIMS). Phase 1: Appendix A through appendix U
[AD-A154179] 19 p3380 N85-30967
Development of NATOPS (Naval Air Training and Operating Procedure Standardization) performance software for the H-46D helicopter
[AD-A156089] 24 p4084 N85-35190
Solar pond technology for Navy applications
[AD-A155877] 24 p4112 N85-35488

NEAR FIELDS
Case study of sample spacing in planar near-field measurement of high gain antennas
[NASA-TM-86872] 01 p0037 N85-10234
System of equations for finding antenna radiation pattern from near-field samples 06 p0791 N85-15054
Comparison of measured and calculated mutual coupling in the near field between microwave antennas
[PB85-105963] 11 p1625 N85-20237
Near Field/Far Field (NF/FF) energy loss in Electric Discharge Lasers (EDL's): A mode-medium interaction
[AD-A150299] 13 p2096 N85-23075
Analytical studies and experimental measurements of amplitude and phase of near-field range antenna probes
[AD-A150922] 14 p2293 N85-24212
Theoretical and experimental comparisons of nearfield electromagnetic fields due to nonlinear polarization layers
[AD-A152085] 16 p2779 N85-27149
High precision materials characterization in the near millimeter wave-length range
[AD-A153267] 17 p2968 N85-28931
An experimental study of plane mixing layer development
[NASA-TM-86698] 19 p3221 N85-29971
Transient dynamic solutions of some half space problems by the boundary element method
19 p3283 N85-30360
Report of near field group
[DE85-010536] 20 p3527 N85-31940
NEAR INFRARED RADIATION
A high resolution spectroscopic study of the oxygen molecule
[NASA-CR-174061] 02 p0172 N85-11150
Variation in spectral response of soybeans with respect to illumination, view, and canopy geometry
[E85-10040] 07 p0982 N85-16241
Detection of the J-10 manifold of the pure rotational band of phosphine on Saturn 08 p1245 N85-17855
The 1.5 - 3.5 micron spectroscopy of the Orion H2 source 08 p1246 N85-17864
The BRESEX multispectral camera: Preliminary characteristics
[INPE-3357-PRE/635] 10 p1487 N85-19386
The Feinheit method: A phase-independent formulation of the period-luminosity relation for Cephids
[NASA-CR-175708] 14 p2440 N85-25056
Space methods in oceanology
[NASA-TM-77652] 15 p2604 N85-26047
In situ thin film measurements
[AD-A151379] 15 p2652 N85-26353
INPE's line imaging camera: Preliminary results
[INPE-3478-PRE/719] 16 p2787 N85-27194
The ISAVF opto-mechanical test bed
[NASA-TM-87505] 24 p4067 N85-35206
NEAR WAKES
A study of the effect of wake-passing on turbine blades
[OUEL-1515/84] 03 p0363 N85-12326
Wake flow behind bluff bodies
05 p0593 N85-13783
Unsteady flow characteristics in the near-wake of a two-dimensional obstacle
[NASA-TM-77762] 07 p0897 N85-15684
Free surface effects on the wake of a flat plate
[AD-A146988] 07 p0958 N85-16071
Giotto plasmasheath and wake charging near Halley's Comet: Revised parameters 14 p2245 N85-23915
Experimental investigations of prismatic cylinders in flow with harmonic pulsations
[KU-SFB-210/E/4] 16 p2785 N85-27186
Wake effects of the aerodynamic performance of horizontal axis wind turbines 19 p3211 N85-29915
Laser Doppler Anemometer (LDA) measurements in the turbulent near-wake of blunt bodies
[ISL-CO-212/84] 22 p3785 N85-33450
NEARSHORE WATER
NT COASTAL WATER
Activities of the Coastal Research Center
[PB84-231323] 05 p0672 N85-14320
Slope water intrusions within the nearshore waters off Long Island, New York
[DE85-001366] 09 p1359 N85-18549
NEBRASKA
Revised Uniform Summary of Surface Weather Observations (RUSSWO). Offutt AFB, Nebraska, parts A-F
[AD-A147183] 07 p1006 N85-16394
NEBULAE
NT CASSIOPEIA A
NT CRAB NEBULA
NT ORION NEBULA
NT PLANETARY NEBULAE
Far-infrared observations of some regions of star formation 03 p0442 N85-12814
Open cluster formation — stellar evolution
03 p0442 N85-12815
An infrared study of the bi-polar outflow region GGD 12-15
[NASA-TM-86655] 03 p0445 N85-12835
Bulk composition of the Moon in the context of models for condensation in the solar nebula
04 p0583 N85-13725
The distribution of dust in the region of the Rosette Nebula and MON OB2 association
05 p0739 N85-14753
The correlation between excitation parameter and nebular luminosity for galactic HII regions with application to regions of star formation in M83
05 p0743 N85-14773
Dark cloud and globule distribution for galactic longitudes 230 to 360 degrees 06 p0878 N85-15575
A neutral gas jet in a low velocity shock front at the boundary of the Draco Nebula 06 p0878 N85-15576
The Draco Nebula, a molecular cloud associated with a high velocity cloud? 06 p0878 N85-15577
Bipolar ejection of matter from hot stars
08 p1233 N85-17767
Fragmentation and turbulence in collapsing gas clouds
[DE85-003745] 11 p1633 N85-20282
Future of Ultraviolet Astronomy Based on Six Years of IUE Research
[NASA-CP-2349] 11 p1743 N85-20961
IUE spectroscopy of extragalactic H II regions
11 p1745 N85-20974
Structure of the Seyfert broad line region and absorption region of NGC 4151 11 p1746 N85-20978
A model for the variable continuum of the Seyfert 1 galaxy NGC 5548 11 p1747 N85-20985
Dust in the region of Herbig-Haro objects: The case of NGC 1999 11 p1747 N85-20991
Ultraviolet studies of the young populous cluster NGC 2100 in the LMC 11 p1748 N85-20995
IUE and ESO observations of the P Cyg star AG Carinae and its ring nebula 11 p1750 N85-21006
The electron spectra in the synchrotron nebula of the supernova remnant G 29.7-0.3
[OG-6.2-10] 22 p3880 N85-34109
Far-infrared observations of young clusters embedded in the R Coronae Australinae and RHO Ophiuchi dark clouds
[NASA-TM-86681] 24 p4167 N85-35834
The nature and geometry of infrared reflection nebulae 24 p4167 N85-35835
NECK (ANATOMY)
The clinical and radiological assessment of cervical injury, Annex A 12 p1907 N85-21976
NEEL TEMPERATURE
Coexistence of antiferromagnetism and spin-glass ordering in the Ising system FeO 55MgO 45Cl2
[DE85-004184] 12 p1942 N85-22197
NEGATIVE CONDUCTANCE
Circuit transients due to negative bias arcs on a high-voltage solar array in low Earth orbit
[NASA-TP-2407] 06 p0760 N85-14868
NEGATIVE FEEDBACK
Playback amplifier with high interference immunity
13 p2077 N85-22970
NEGATIVE IONS
Surface production of negative hydrogen ions
[AD-A145437] 02 p0277 N85-11601
Vibrational relaxation in H-2 molecules by wall collisions: Applications to negative ion source processes
[DE85-000852] 11 p1721 N85-20628
Hydrogen vibrational population distributions and negative ion generation in tandem high density hydrogen discharges
[DE85-001207] 11 p1722 N85-20634
Reconsideration of sheath related to negative ion extraction
[IPPJ-706] 12 p1935 N85-22159
Negative lithium emission from a tungsten surface in a plasma
[DE85-003456] 12 p1936 N85-22167
Theoretical studies of kinetic mechanisms of negative ion formation in plasmas
[AD-A150820] 14 p2423 N85-24848
A study of excitations during collisionally-induced electron detachment of negative ions
[AD-A152879] 17 p3030 N85-28739
Generation of intense negative ion beams
[NASA-CASE-NPO-16061-1-CU]
18 p3178 N85-29701
Maximum current densities from tandem high density systems
[DE85-006966] 18 p3180 N85-29720
One- and two-electron transfer processes in ion-surface scattering
[AD-A154206] 19 p3353 N85-30782
The production and destruction of metastable negative ions
[DE85-011056] 19 p3364 N85-30868
Improved negative ion source
[DE85-006445] 23 p3912 N85-34241
Negative ion acurces equipped with continuous annular and spherical geometry surface ionizers
[DE85-011939] 23 p3971 N85-34619
NEGATRONS
An observation of cosmic ray positrons from 10-20 GeV
[OG-6.2-6] 22 p3869 N85-34105
NEODYMIUM
Structural, morphological and optical characteristics of KGd(WO4)2 crystals 14 p2280 N85-24126
Investigation for low-cost permanent magnets
[AD-A154387] 19 p3260 N85-30212
Spectral-luminescence characteristics and induced emission of Nd-3(+) ion in Gd(2-x)Nd(x)(WO4)3 crystals
21 p3688 N85-32912
NEODYMIUM ALLOYS
Anisotropy and microstructure of rare earth permanent magnet materials
[AD-A146549] 06 p0859 N85-15460
NEODYMIUM COMPOUNDS
Preparation and properties of single crystals of hydrogen bis(phthalocyaninato) neodymium(3)
[AD-A144933] 01 p0123 N85-10846
NEODYMIUM ISOTOPES
Constraints on the development of the early continental crust from isotopic data 21 p3719 N85-33076
NEODYMIUM LASERS
Pulsed neodymium glass laser system for investigating nonlinear optical phenomena in gases
03 p0348 N85-12241
Laser balancing system for high material removal rates
[NASA-CR-174731] 03 p0365 N85-12341
Design and testing of a refractive laser beam homogenizer
[AD-A146987] 07 p0970 N85-16162
Highly efficient Nd:YAG lasers for free-space optical communications 10 p1483 N85-19229
Solid state luminescent light filters for neodymium lasers 11 p1716 N85-20799
Lasing characteristics of YAG: Nd(3+)-laser with LiF passive shutter with F2 color centers
11 p1717 N85-20802
Stability of temporal and energy parameters of picosecond lanthanum beryllate laser
11 p1717 N85-20804
Autostochastic behavior of solid state ring laser with low frequency periodic loss modulation
11 p1717 N85-20805
Neodymium YAG laser pumped with radiation from high frequency electrodeless discharge
13 p2044 N85-22796
Research, development of laser glasses in China
13 p2166 N85-23439
Amplification of scattered induced radiation flux in high-gain laser rods 15 p2644 N85-26509
Conducting a wind sensing study
[NASA-CR-175782] 16 p2832 N85-27465
Development and application of a high power ND-glass laser instrument
[AD-A154366] 19 p3276 N85-30314
Laser beam interactions with vapor plumes during Nd:YAG laser welding on aluminum
[DE85-009793] 21 p3593 N85-32328
Luminescence and absorption of indium-activated potassium-borate glasses subjected to high-power excitation 21 p3681 N85-32868
Defect formation in amorphous hydrated silicon subjected to laser radiation 21 p3682 N85-32873
Selective population of N = 3 OVIII level during expansion of laser plasma in helium
21 p3889 N85-32914
Passive Q-modulation of optical cavities by KCl crystals containing OH(-) -ions 21 p3888 N85-32915
Switching power supply
[DE85-005993] 22 p3761 N85-33312
Infrared generation and wave-mixing studies in cesium
[DE85-012983] 24 p4083 N85-35304
Elliptical X-ray analyzer spectrograph application to a laser-produced plasma
[DE85-013790] 24 p4087 N85-35398
NEON
NT NEON ISOTOPES
Study of opacity effects on line radiation from pellet implosions
[DE85-000380] 10 p1491 N85-19413
Time dependent Hartree-Fock theory of ion-atom collisions: Application to F(9+) + He
[DE85-003083] 11 p1723 N85-20639
Hydrogen maser oscillation at 10 K
18 p3108 N85-29241
Initial results from the Caltech/DSRI balloon-borne isotope experiment
[OG-4.3-8] 21 p3714 N85-33048

Solar cycle variations of the anomalous cosmic ray component
[PAPER-SH-4.6-2] 21 p3715 N85-33057
Recombination and ionization in a nitrogen plasma
[AD-A155428] 22 p3845 N85-33813
A new analysis of cosmic ray isotopes at 3 GeV/n from HEA03-C2 data
[OG-4.3-6] 22 p3879 N85-34031
Photoionization-pumped, Ne 2, X-ray laser studies project
[DE85-012973] 23 p3936 N85-34399

NEON ISOTOPES
Solar cosmic ray produced neon in lunar soils and their implication for gas-rich meteorite studies
06 p0887 N85-15636
The (20)Ne interaction in extended matter
[NASA-TM-86312] 07 p1061 N85-16728
The energy dependance of the neon-22 excess in the cosmic radiation
[OG-4.3-7] 22 p3879 N85-34032
Forward particle production in inelastic Ne-22 interactions in emulsion at 4.1 A Ge/c
[HE-1.4-7] 24 p4176 N85-35895

NEON 19
U NEON ISOTOPES

NEOPLASMS
NT CANCER
NT LEUKEMIAS

NEOPRENES
U CHLOROPRENE RESINS

NEPHANALYSIS
A new NASA/MSFC mission analysis global cloud cover data base
[NASA-TP-2448] 12 p1693 N85-21878

NEPHELOMETERS
Chemical, biological, and physical measurements from the subtropical western North Atlantic Ocean. Summer 1982, USNS Lynch, cruise 710-82
[AD-A153823] 18 p3201 N85-29857

NEPTUNE (PLANET)
Uranus and Neptune
[NASA-CP-2330] 02 p0296 N85-11927
The origin and evolution of Uranus and Neptune
02 p0296 N85-11928
Atmospheres of Uranus and Neptune
02 p0296 N85-11929
Aeronomy 02 p0296 N85-11930
Temperature structures and infrared-derived properties of the atmosphere of Uranus and Neptune
02 p0298 N85-11931
Rotational properties of Uranus and Neptune
02 p0299 N85-11940
Oblatenesses of Uranus and Neptune
02 p0300 N85-11941
Physical properties of Neptune and Triton inferred from the Orbit of Triton 02 p0300 N85-11942
Origin and evolution of the Uranian and Neptunian satellites: Some dynamical considerations
02 p0300 N85-11943
Composition, structure and evolution of Uranian and Neptunian satellites 02 p0300 N85-11944
Physical properties of the satellites of Neptune
02 p0300 N85-11945
Satellite masses in the Uranus and Neptune systems
[PSI-CONTRIB-198] 02 p0301 N85-11947
Magnetospheric structures: Uranus and Neptune
02 p0301 N85-11949
The structure of the Uranian rings and the search for rings around Neptune 02 p0302 N85-11954
The structure and composition of Uranus and Neptune
13 p2175 N85-23495
Rings around Neptune? 15 p2672 N85-26491
Sixteenth Lunar and Planetary Science Conference. Press abstracts
[NASA-CR-175892] 15 p2680 N85-26548
Occultation detection of a Neptune ring segment
15 p2681 N85-26558
The 1986 National Aeronautics and Space Administration authorization
[GPO-47-635] 24 p4166 N85-35829

NEPTUNE ATMOSPHERE
Properties of the upper tropospheres of Uranus and Neptune derived from observations at visible to near-infrared wavelengths 02 p0298 N85-11933
Near infrared imaging of Uranus and Neptune
02 p0299 N85-11934
Atmospheric dynamics of Uranus and Neptune: Theoretical considerations 02 p0299 N85-11936
Variability of Neptune 02 p0299 N85-11938
Ultraviolet observations of Uranus and Neptune below 3000 A 11 p1760 N85-21071
Possible period of Jovian activity and possibility of seasons 16 p2723 N85-26810

NEPTUNIUM COMPOUNDS
Volume compressibilities of transuranium elements compounds, especially of neptunium compounds
03 p0431 N85-12744

NERNST HEAT THEOREM
U NERNST-ETTINGSHAUSEN EFFECT

NERNST-ETTINGSHAUSEN EFFECT
Magnetic fields in laser heated plasmas
[DE85-010715] 21 p3707 N85-33022

NERVES
Dynamics of morphological changes in articulation nervous system under hypokinetic conditions as a model of a spaceflight factor 01 p0092 N85-10621
Pathology of organophosphorus-induced delayed neurotoxicity
[AD-P004024] 06 p0844 N85-15356
Natural electrical activity of human sympathetic nerve fibers, recorded from body surface
07 p1013 N85-16433
Is fast fiber innervation responsible for increased acetylcholinesterase activity in reinnervating soleus muscles?
[NASA-CR-175716] 15 p2614 N85-26108
Differential effect of denervation on free radical scavenging enzymes in slow and fast muscle of rat
[NASA-CR-175719] 15 p2614 N85-26110

NERVOUS SYSTEM
NT AUTONOMIC NERVOUS SYSTEM
NT BRAIN
NT BRAIN STEM
NT CENTRAL NERVOUS SYSTEM
NT CEREBELLUM
NT CEREBRAL CORTEX
NT CEREBRAL VENTRICLES
NT CEREBRUM
NT EFFERENT NERVOUS SYSTEMS
NT NERVES
NT NEURONS
NT PERIPHERAL NERVOUS SYSTEM
NT SPINAL CORD
NT SPINE
NT SYMPATHETIC NERVOUS SYSTEM
NT SYNAPSES
NT THALAMUS
Effects of prolonged hypokinesia on nervous system
06 p1194 N85-17524
Neural compensation, muscle load distribution and muscle function in control of biped models
09 p1314 N85-18257
Determination of functional mobility of human nervous system with the PNN-3 instrument
10 p1525 N85-19618
Mercury health effects update: Health issue assessment
[PB85-123925] 10 p1528 N85-19639
Selecting one among the many: A simple network implementing shifts in selective visual attention
[AD-A148999] 10 p1530 N85-19644

NETHERLANDS
Fokker wants to start new Netherlands space program
03 p0310 N85-11999
Synoptical observations of snow depths at Dutch meteorological stations, 1956 - 1977
[KNMI-TR-51] 07 p1008 N85-16407
On the altitudinal distribution of birds and bird strikes in the Netherlands
[AD-P004189] 11 p1580 N85-19952
Task and future of the Large Institutes of Technology (LIT)
[B8474720] 11 p1741 N85-20945
Wind observation station description for Den Helder (period 1843-1972) and De Kooy (period 1955-1980)
[KNMI-TR-42] 14 p2379 N85-24666
Rotterdam Airport and the Common Market
17 p2894 N85-27840
Water quantity and quality research for the Rhine Meuse estuary
[PUBL-325] 17 p2966 N85-28470
Observations of surface water temperature in the Netherlands since 1860: Statistics
[KNMI-WR-84-3] 17 p2997 N85-28531
Observations of surface water temperature in the Netherlands since 1860: Tables for light vessels
[KNMI-WR-84-4] 17 p2998 N85-28532
Observations of surface water temperature in the Netherlands since 1860: Series from KNMI-RWS
[KNMI-WR-84-5] 17 p2998 N85-28533
OWEMA report: A project study concerning the possibilities and the desirability of a east-west runway for Maastricht Airport (Netherlands) as a Euro-regional air freight center
[B8476490] 18 p3064 N85-28955
Climatological data of stations in the Netherlands No. 11: Frequency tables and tables with runs according to measurements at principal climatological stations 1961-1980, sunshine stations 1956-1980, precipitation stations 1951-1980
[KNMI-150-11] 18 p3149 N85-29499
Wind energy in the north Netherlands region
20 p3485 N85-31661
Wind turbines and environment management
[CP-MEMO-1983-11] 20 p3485 N85-31662
Mathematical programming in the Netherlands
[REPT-ARW-03-THE-BDK/ORS/83/10] 20 p3517 N85-31666
Microwave propagation studies, measurements and education in Surabaya, Indonesia
[B8464633] 24 p4088 N85-35339

NETS
NT NEURAL NETS
NT PETRI NETS
Spline curves, wire frames and B-value
17 p3006 N85-28587

NETWORK ANALYSIS
NT CRITICAL PATH METHOD
Interaction of voice and data traffic in a packet switching communication network and virtual circuit
[FUB-83-1982] 01 p0039 N85-10249
Broadband local distribution networks: Problems and prospects in Italy
[FUB-18-1983] 01 p0040 N85-10255
End-to-end performance in local area networks of interconnected token rings
[FUB-42-1983] 01 p0107 N85-10714
A comparative evaluation of algorithms for generalized network problems
[TWISK-289] 01 p0107 N85-10721
Parametric analysis for generalized network flow problems
[AD-A145556] 02 p0243 N85-11589
Study on the conversion and test of protocols
[ENST-84E005] 03 p0356 N85-12293
The application of queueing theory to communications networks: A review
[AD-A146660] 04 p0492 N85-13140
Relaxation times for queueing systems
[CWI-OS-R8407] 05 p0719 N85-14618
The transient behavior of networks with infinite server nodes
[CWI-OS-R8408] 05 p0722 N85-14640
Local area network evaluation by MICROSS extensions
[AD-A146773] 07 p1027 N85-16521
EGP (Exterior Gateway Protocol) gateway under Berkeley UNIX 4.2
[AD-A148056] 08 p1208 N85-17597
Distributed asynchronous relaxation methods for convex network flow problems
[AD-A148027] 08 p1211 N85-17622
Beyond fault trees to fault graphs
[DE84-017022] 09 p1370 N85-18608
Coordination in a distributed problem solving network
[AD-A148925] 10 p1565 N85-19872
Vertical solar louver project
[DE84-017335] 11 p1676 N85-20558
A fully distributed approach to the design of a 16 K bit/sec VHF packet radio network
[AD-A141282] 13 p2054 N85-22959
Research using a DISCUS based network emulator
[AD-A141294] 13 p2149 N85-23338
Evaluating computer-communication networks with simulation techniques
[AD-A151852] 15 p2632 N85-26222
Developing an automated technique for translating a relational database into an equivalent network one
[AD-A151844] 15 p2666 N85-26451
Algebra of communicating processes
[CWI-CS-R8421] 17 p2950 N85-28214
Defense data network support concept analysis
[AD-A153214] 17 p3016 N85-28649
Numerical methods for stiff ordinary and elliptic partial differential equations
[AD-A153247] 17 p3020 N85-28675
Maximum flow in planar networks with exponentially distributed arc capacities
[AD-A153158] 17 p3026 N85-28710
Harold Hazen and the theory and design of servomechanism
[RR-270] 22 p3794 N85-33506

NETWORK CONTROL
Communications protocols for a fault tolerant, integrated local area network for Space Station applications
[NASA-TM-86304] 01 p0106 N85-10711
Proceedings of the 5th LAN-Transport Workshop
[PB84-232667] 01 p0107 N85-10715
Performance evaluation and control of distributed computer communication networks
[AD-A148103] 08 p1208 N85-17598

Process algebra with asynchronous communication mechanisms
[CWI-CS-R8410] 11 p1625 N85-20235
System dynamics and network control
[AD-A149420] 13 p2054 N85-22863
Distributed control of circuits in multiuser communication networks with circuit precedence and path suitability criteria using failsafe routing concepts
[AD-A151625] 16 p2772 N85-27113
Distributed elections in a ring of processors using Archimedean time
[CWI-CS-R8416] 17 p3016 N85-29853
LAN (Local Area Network) interoperability study of protocols needed for distributed command and control
[AD-A154033] 19 p3255 N85-30182
A study of the ESA-NAVSAT control segment
[ESA-CR(P)-2000] 20 p3366 N85-31079

NETWORK SYNTHESIS
Stuttgart Interconnection Network Project from PIX to NICS
[NASA-TM-77802] 06 p0870 N85-15528
Design, fabrication and testing of a multibeam forming network
[NASA-CR-175695] 14 p2296 N85-24228
Regional seismic wave propagation
[AD-A150801] 14 p2373 N85-24671
Corrective-predictive systems
[BLL-M-36063-(5826.4)] 16 p2851 N85-27573

NETWORKS
Extracting embedded generalized networks from linear programming problems
[AD-A147585] 07 p1033 N85-16558
Selecting one among the many: A simple network implementing shifts in selective visual attention
[AD-A148989] 10 p1530 N85-19644
Design of the National Trends Network for monitoring the chemistry of atmospheric precipitation
[GS-CIRC-864] 20 p3486 N85-31684
Procedure for editing the fluxgate magnetometer data of the AFGL (Air Force Geophysics Laboratory) magnetometer network
[AD-A156331] 24 p4117 N85-35523

NEUMANN PROBLEM
Integral equation formulations in two dimensions
05 p0718 N85-14605
Three-dimensional, direct and vectorized elliptic solvers for various boundary conditions
[AD-B088266L] 08 p1206 N85-17595
On the connection between multigrid and cyclic reduction
[NASA-TM-86020] 09 p1373 N85-18629
Neumann type boundary conditions for Hamilton-Jacobi equations
[AD-A149069] 10 p1546 N85-19746
The low frequency behaviour of an immersed structure at a standstill in a high density fluid with free surface
[TP-1983-31] 13 p2103 N85-23105
Adaptive detection of noise signal according to Neumann-Pearson criterion 15 p2527 N85-25580
Sobolev-Poincare's inequality and the Neumann problem for u sub t = divergence of the absolute value of the gradient u to the p-2 power x the gradient u
[AD-A154788] 21 p3575 N85-32839
Hardy spaces and the L sup P-Neumann problem for Laplace's equation in a Lipschitz domain
[CTH-MATH-1985-02] 22 p3836 N85-33749

NEURAL NETS
Feature discovery by competitive learning
[AD-A145052] 01 p0097 N85-10648
Direct assessment of synaptic modification rules
[AD-A148376] 08 p1196 N85-17534
Biological investigations of adaptive networks. Neuronal control of conditioned responding
[AD-A150959] 14 p2385 N85-24695
Semantic networks and neural nets
[AD-A150750] 14 p2407 N85-24840
Distributed memory
[AD-A153364] 17 p3001 N85-29554

NEUROLOGY
Cognitive science program. A framework for relating cognitive to neural systems
[AD-A145185] 01 p0097 N85-10649
Neural control of the direction of covert visual orienting
[AD-A145189] 01 p0097 N85-10650
Inhibition of return: Neural basis and function
[AD-A145242] 01 p0098 N85-10652
Proceedings of the 14th Conference on Environmental Toxicology
[AD-A146400] 06 p0843 N85-15350
Neurotoxicology: A new scientific challenge
[AD-P004017] 06 p0843 N85-15351
Interactions of ketones and hexacarbons
[AD-P004019] 06 p0843 N85-15353
Molecular mechanisms of n-hexane neurotoxicity
[AD-P004020] 06 p0843 N85-15354
Pathology and axonal transport in hexacarbon neuropathies
[AD-P004021] 06 p0843 N85-15355
Organophosphorus-induced delayed neurotoxicity: Syndrome and experimental models
[AD-P004022] 06 p0844 N85-15356
Chemistry and metabolism of delayed neurotoxic organophosphorus esters
[AD-P004023] 06 p0844 N85-15357
Pathology of organophosphorus-induced delayed neurotoxicity
[AD-P004024] 06 p0844 N85-15358
Electrophysiologic changes in organophosphorus-induced delayed neurotoxicity
[AD-P004025] 06 p0844 N85-15359
Biochemistry and pathogenic hypotheses of organophosphorus-induced delayed neurotoxicity
[AD-P004026] 06 p0844 N85-15360
Multiple resources and brain laterality
[AD-A148912] 10 p1530 N85-19643
USSR report: Life sciences. Biomedical and behavioral sciences
[JPRS-UBB-85-010] 11 p1690 N85-20628
Biological investigations of adaptive networks. Neuronal control of conditioned responding
[AD-A150959] 14 p2385 N85-24695
A model for generalization and specification by single neurons
[AD-A150871] 14 p2391 N85-24724
Neural mechanism by which gravitational stimulus and stress affect the secretion of renin and other hormones
15 p2610 N85-26083
Academician Ovchinnikov on future of bioorganic chemistry 17 p3049 N85-29874

NEUROMUSCULAR TRANSMISSION
The effect of part-simulation of weightlessness on human control of bilateral teleoperation: Neuromotor considerations 05 p0709 N85-14510
Advanced development of an active neuromusculature response to mechanical stress
[AD-A148436] 08 p1196 N85-17536
Neural compensation, muscle load distribution and muscle function in control of biped models
09 p1314 N85-18257
Investigation of adaptive distinctions of mechanism of controlled glycemia in Macaca rhesus monkeys
12 p1902 N85-21948
Application of the system identification technique to goal-directed saccades
[AD-A150132] 12 p1906 N85-21957
Induced changes in the cholinergic system of sciatic nerve and slow and fast twitch muscle of rats
15 p2609 N85-26081
Changes in the cholinergic system of rat sciatic nerve and skeletal muscle following suspension induced disuse
[NASA-CR-175718] 15 p2615 N85-26111
Physical chemical state of water in living cells
[AD-A154566] 21 p3662 N85-32749

NEURON TRANSMISSION
U BIOELECTRICITY

NEURONS
Cognitive science program. A framework for relating cognitive to neural systems
[AD-A145185] 01 p0097 N85-10649
Biological investigations of adaptive networks. Neuronal control of conditioned responding
[AD-A150959] 14 p2385 N85-24695
A model for generalization and specification by single neurons
[AD-A150871] 14 p2391 N85-24724
Cell death, neuronal plasticity and functional loading in the development of the central nervous system
15 p2612 N85-26096
Sensory and motor properties of the cerebellar uvula and nodulus 15 p2613 N85-26104
Anatomy of the vestibulo-automatic outflow to the gut
15 p2614 N85-26106
Discovery regarding visual neuron adaptation applicable to robot use 20 p3504 N85-31786

NEUROPHYSIOLOGY
Dynamics of morphological changes in articulation nervous system under hypokinetic conditions as a model of a spaceflight factor 01 p0092 N85-10621
Organophosphorus-induced delayed neurotoxicity: Syndrome and experimental models
[AD-P004022] 06 p0844 N85-15356
Aspects of solvent toxicity in mixtures
[AD-P004036] 06 p0845 N85-15366
Lateral specifics of visual perception
07 p1013 N85-16436
Change in relationship of biopotentials of brain zones for various levels of working capacity
07 p1013 N85-16438
Vision by man and machine: How the brain processes visual information may be suggested by studies in computer vision (and vice versa)
[AD-A147690] 07 p1017 N85-16458
Effects of partial deprivation of slow-wave sleep on sleep-wakefulness cycles 10 p1524 N85-19613
USSR report: Life sciences. Biomedical and behavioral sciences
[JPRS-UBB-85-010] 11 p1690 N85-20628
Characteristics of human masseter under conditions of hypokinesia 11 p1691 N85-20630
Topography of human brain electric potentials and dominance 11 p1691 N85-20633
Functional significance of some EEG parameters and dominant principle 11 p1691 N85-20634
Neurophysiological correlates of motion sickness: Role of vestibulocerebellum and 'vomiting center' reanalyzed
11 p1693 N85-20643
Circadian rhythm control: Neurophysiological investigations 15 p2612 N85-26099
Airsickness control using biofeedback to self-regulate psychophysiological responses
[AD-A151167] 15 p2617 N85-26128
Functional impairment and structural cervical injuries in human surrogates
[PB85-167436] 15 p2619 N85-26137

NEUROPSYCHIATRY
Toward a computational neuropsychology of high-level vision
[AD-A145711] 02 p0236 N85-11540
Psychometric evaluation of head injury among fliers referred to the AF School of Aerospace Medicine
[AD-A151479] 15 p2617 N85-26129

NEUROSCIENCE
U NEUROLOGY

NEUROTRANSMITTERS
USSR report: Life sciences. Biomedical and behavioral sciences
[JPRS-UBB-85-010] 11 p1690 N85-20629
Use and disuse and the control of acetylcholinesterase activity in fast and slow twitch muscle of rat
[NASA-CR-175717] 15 p2614 N85-26109

NEUTRAL ATMOSPHERES
Neutral atmosphere properties determining D-region electron densities 11 p1658 N85-20451
A model of the influence of neutral air dynamics on the seasonal variation in the low ionosphere
11 p1660 N85-20462
The diurnal variation of the neutral sodium species in the upper atmosphere: A model study
[AD-A154988] 21 p3691 N85-32561

NEUTRAL ATOMS
Plasma surface interactions in magnetic fusion systems
[DE84-015255] 01 p0123 N85-10842
Laser cooling and trapping of neutral atoms
[AD-A146048] 03 p0366 N85-12345
Forces on neutral atoms due to electromagnetic fields
[AD-A146984] 07 p1040 N85-16803
Theoretical issues involving traps for neutral spin-polarized atoms
[AD-A146035] 08 p1220 N85-17682
Numerical model for swirl cooling in high-heat-flux particle beam targets and the design of a swirl-flow-based plasma limiter
[DE85-003824] 11 p1732 N85-20694
Secondary ion mass spectrometry studies of solids and surfaces
[AD-A151744] 16 p2745 N85-28939

NEUTRAL BEAMS
NT MOLECULAR BEAMS
NT NEUTRON BEAMS
Neutral beam interactions with materials
[AD-A146836] 02 p0295 N85-11857
Low energy ion-molecule reaction dynamics and chemionization kinetics
[DE84-015861] 04 p0559 N85-13582
Alpha-particle diagnostics with high energy neutral beams
[IPPJ-895] 06 p0883 N85-15485
The role of fast electrons for the performance characteristics of hydrogen ion sources
09 p1303 N85-18189
Sources, densities, and transport of impurities in neutral-beam injected Tokamaks
09 p1388 N85-18731
Beam probe spectroscopic technique for ion temperature and magnetic field measurements
09 p1389 N85-18738
Long-pulse beamlines for the mirror fusion test facility
[DE84-017091] 09 p1392 N85-18760
All solid state high voltage power supply for neutral beam sources
[DE85-002531] 11 p1629 N85-20257

Collisional pumping for the production of intense spin-polarized, neutral beams: Target considerations
[DE85-003459] 11 p1723 N85-20841
Neutral beam injector oxygen impurity measurements and concentration reduction via gettering processes
[DE85-000861] 12 p1836 N85-21521
Spectroscopic study of sources and control of impurities in TMX-U: Revision 1
[DE85-004423] 12 p1937 N85-22170
Measurements of integral yields of charged secondary particles using neutral beams simulating a cometary fly-by — Giotto mission 14 p2244 N85-23906
Laser-induced fluorescence of metal-atom impurities in a neutral beam
[DE85-004960] 14 p2310 N85-24298
Experimental and theoretical studies of laser cooling and emittance control of neutral beams
[AD-A149215] 15 p2562 N85-25804
Development of an apparatus for obtaining molecular beams in the energy range from 2 to 200 eV
[NASA-TM-77935] 15 p2647 N85-26326
Development of RF plasma generators for neutral beams
[DE85-004125] 15 p2658 N85-26400
Simulation of automatic control of MFTF-B neutral beams
[DE85-010640] 20 p3530 N85-31960
Recent experiments in Gamma-10 23 p3976 N85-34651
Considerations on collective ion acceleration as an intense ion injector
[DE85-012706] 24 p4155 N85-35757

NEUTRAL CURRENTS
Neutral-current x-distributions
[DE84-016522] 09 p1382 N85-18691
Plasma waves at and near the neutral sheet 14 p2358 N85-24572

NEUTRAL GASES
Absorption line studies and the distribution of neutral gas in the local interstellar medium 06 p0873 N85-15544
Synthesis of data on the local interstellar medium 06 p0874 N85-15545
A neutral gas jet in a low velocity shock front at the boundary of the Draco Nebula 06 p0878 N85-15576
Radio and UV observations of high latitude HI 06 p0879 N85-15583
Seasonal characteristics of mesospheric plasma and their transitions 11 p1660 N85-20464
Electrostatic charging of the Giotto spacecraft due to neutral gas impact 14 p2244 N85-23913
Digital image analysis of four-frame holographic plasma and neutral gas interferograms
[DE85-006397] 16 p2788 N85-27200
The structure of galactic HI in directions of low total column density
[NASA-CR-175709] 16 p2882 N85-27785
On the anomalous component
[SH-4,6-6] 23 p4039 N85-35044

NEUTRAL PARTICLES
NT COLD NEUTRONS
NT FAST NEUTRONS
NT NEUTRONS
NT THERMAL NEUTRONS
Emission mechanisms in the liquid metal ion source: A review
[AERE-R-11294] 09 p0418 N85-12675
Search for neutral, penetrating, metastable particles produced in the SLAC beam dump
[DE84-012468] 04 p0560 N85-13569
Gas pressure and electron density in the active zone level of hollow cathode arc discharges
[NASA-TM-77468] 07 p0945 N85-15986
Improved performance for large area triple layer microchannel plate detector for a neutral spectrometer in Doublet III
[DE85-001719] 10 p1488 N85-19395
Mass analysis of neutral particles and ions released during electrical breakdowns on spacecraft surfaces
[NASA-CR-175585] 12 p1793 N85-21250
User's guide for TWOHEX: A code package for two-dimensional, neutral-particle transport in equilateral triangular meshes
[DE85-004482] 12 p1930 N85-22125
Mass spectra of neutral particles released during electrical breakdown of thin polymer films 13 p1996 N85-22511
Measurement of charged secondary particle emission under ion and neutral impact — Giotto mission 14 p2243 N85-23906
Cometary atmospheres: Modeling the spatial distribution of observed neutral radicals
[NASA-CR-175852] 16 p2882 N85-27781
Neutral particle beam intensity controller
[DE85-006411] 23 p3969 N85-34804
Behavior of helically-trapped fast ion orbits in heliotron E 23 p3978 N85-34666
Neutral pion production in solar flares
[SH-1.4-7] 23 p3995 N85-34767
Strategic defense initiative
[DE85-012778] 24 p4150 N85-35735

NEUTRAL SHEETS
Cosmic ray intensity and the tilt of the neutral sheet
[SH-4.2-8] 23 p4007 N85-34846
Effects of a wavy neutral sheet on cosmic ray anisotropies
[SH-4.2-11] 23 p4008 N85-34849
Difference between even and odd 11-year cycles in cosmic ray intensity
[SH-4.2-22] 23 p4009 N85-34859
Influence of the neutral sheet on the Swinson's type north-south anisotropy of cosmic rays
[SH-4.3-10] 23 p4032 N85-34995
The sidereal semi-diurnal variation observed at high zenith angles at Mawson, 1968-1984, and the polarity of the solar main field
[SH-4.4-6] 23 p4033 N85-35004

NEUTRALIZERS
Development anmd testing of electrophoresis solutions. Task I.1: Development of optimal buffer system 20 p3500 N85-31755

NEUTRINO BEAMS
AGS broad band neutrino beam
[DE85-010954] 19 p3366 N85-30875
On gamma and neutrino radiation from Cyg X-3
[OG-2.1-7] 22 p3863 N85-33924

NEUTRINOS
NT SOLAR NEUTRINOS
Results on weak current from CHARM collaboration — neutrino interactions
[NOTA-INTERNA-810] 02 p0279 N85-11817
Search for the radiative decay of a cosmic relic particle with IUE
[PREPRINT-410] 04 p0580 N85-13707
Iron core collapse models of Type 2 supernovae
[DE84-013909] 05 p0743 N85-14775
Neutrino measurements on the Moon
[DE85-007700] 16 p2884 N85-27791
Did bosonic sneutrino stars ever exist
[PREPRINT-421] 18 p3202 N85-29657
Search for proton decay
[DE85-006283] 19 p3353 N85-30786
Search for neutrino oscillations at the Brookhaven AGS
[DE85-009766] 20 p3530 N85-31957
Neutrino-antineutrino annihilation around collapsing star
[OG-1.1-10] 22 p3861 N85-33911
Detection of 10 (1) GeV cosmic neutrinos with a space station
[OG-9.4-10] 23 p4030 N85-34977
Neutrino production from the solar atmosphere
[SH-8.1-9] 23 p4050 N85-35114
Solar cosmic ray bursts and solar neutrino fluxes
[SH-8.1-10] 23 p4050 N85-35115
Three dimensional calculation of flux of low energy atmospheric neutrinos
[SH-8.1-11] 23 p4050 N85-35116
Neutrino production of like sign dimuons
[DE85-013694] 24 p4151 N85-35741
High energy physics at Tufts University
[DOE/ER-40095/7] 24 p4152 N85-35744
Nineteenth International Cosmic Ray Conference. HE sessions, volume 8
[NASA-CP-2376-VOL-8] 24 p4200 N85-36066
Muon and neutrino results from KGF experiment at a depth of 7000 hg/square cm
[HE-5.1-2] 24 p4200 N85-36068
Background light measurements at the DUMAND site
[HE-5.2-7] 24 p4203 N85-36084
Hybrid TLC-pair meter for the Sphinx Project
[HE-5.2-10] 24 p4203 N85-36086
A study of atmospheric neutrinos with the IMB detector
[HE-5.3-7] 24 p4205 N85-36101
Atmospheric neutrinos observed in underground detectors
[HE-5.3-8] 24 p4205 N85-36102
Geophysical searches for three-neutrino oscillations
[HE-5.3-9] 24 p4205 N85-36103
Measurement of neutrino oscillations in MACRO experiment
[HE-5.3-10] 24 p4206 N85-36104
The capability of the existing network of installations for detecting the antineutrino burst from collapsing stars
[HE-5.3-13] 24 p4206 N85-36107
Energy spectra of high energy atmospheric neutrinos
[HE-5.3-14] 24 p4206 N85-36108
A standard source for high energy neutrino astronomy
[HE-5.3-15] 24 p4206 N85-36109
A search for cosmic sources of high energy neutrinos with small underground detectors
[HE-5.3-16] 24 p4206 N85-36110
Neutrino astronomy and the atmospheric background
[HE-5.3-17] 24 p4207 N85-36111
High-energy neutrinos from a lunar observatory
[HE-5.3-21] 24 p4207 N85-36112
Characteristics of slow particles emitted in the charged current interactions of neutrinos with emulsion nuclei
[HE-5.3-22] 24 p4207 N85-36113
QCD analysis of neutrino charged current structure function F2 in deep inelastic scattering
[HE-5.3-23] 24 p4207 N85-36114
Angular distribution of muons produced by cosmic ray neutrinos in rock
[HE-5.3-24] 24 p4207 N85-36115
Atmospheric muons and neutrinos, and the neutrino-induced muon flux underground
[HE-5.4-7] 24 p4207 N85-36116
Nucleon decay and atmospheric neutrinos in the Mont Blanc experiment
[HE-6.2-6] 24 p4211 N85-36142
Muon and neutrino fluxes
[HE-6.2-18] 24 p4213 N85-36154
Experimental investigation of radiative-acoustic effects in the water by the thermodynamical conditions of Dumand
[HE-7.1-2] 24 p4213 N85-36156

NEUTRON ABSORBERS
Method and apparatus for determining the content and distribution of a thermal neutron absorbing material in an object
[DE84-014319] 01 p0117 N85-10601
Time-integrated yield for the Joint European Torus (JET), April - September 1984
[AERE-M-3449] 17 p3038 N85-28797

NEUTRON ACTIVATION ANALYSIS
In vivo neutron activation analysis: Body composition studies in health and disease
[DE84-014092] 05 p0696 N85-14480
JPL in-house fluidized-bed reactor research 06 p0832 N85-15291
Neutron activation analysis of stoney spherules from a marine sediment sample 06 p0883 N85-15608
Proceedings of the 2nd Workshop on Nondestructive Evaluation (NDE) of Titanium Alloys
[AD-A147626] 08 p1125 N85-17095
Measurement of oxygen contamination in titanium alloy ingots by fast neutron activation analysis
[AD-P004133] 08 p1128 N85-17108
Neutron activation analysis of titanium with oxygen contamination
[AD-P004134] 08 p1128 N85-17109
Investigation of the output parameters of the pulsed neutron generator NGI-5
[DE85-001623] 11 p1725 N85-20849
Multiple element neutron-activation analysis of atmospheric aerosols with X-ray and gamma-spectrometric recording of radionuclides formed 13 p2013 N85-22631
Time-integrated yield for the Joint European Torus (JET), April - September 1984
[AERE-M-3449] 17 p3038 N85-28797
Quantitative analysis of defects in silicon-characterization of UCP, HAMCO, and microcrystalline material
[NASA-CR-175986] 18 p3079 N85-29046
Proceedings of the Fifth International Conference on Nuclear Methods in Environmental and Energy Research
[DE84-017348] 19 p3310 N85-30521
Sulfur activation at the Little Boy-Comet Critical Assembly: A replica of the Hiroshima bomb
[DE85-010261] 20 p3527 N85-31936
Determination of the average neutron activation cross section with an annular-shaped 241 Am/Be neutron source and a NaI(T1) detector for the 27 Al (n,p)27 Mg-reaction
[REPT-4/1984] 20 p3532 N85-31975
Activation analysis of natural water using neutrons of various energies 21 p3690 N85-32924
Rhodium-103 and Indium-115 inelastic scattering reactions for fission neutron dosimetry 21 p3703 N85-33004

NEUTRON BEAMS
Performing (p vector,)c)n), (d vector, n) and (n vector, n) measurements with a rotating magnet beam swinger
[DE84-017003] 04 p0562 N85-13562
Paramagnetic scattering from Ni
[DE85-004207] 12 p1942 N85-22198
Magnetic scattering and polarized neutrons
[DE85-006823] 19 p3355 N85-30794
Measurement and evaluation of selected 14-MeV neutron cross sections for fusion
[DE85-010295] 19 p3365 N85-30867
Cosmic ray north-south anisotropy 1961 - 1983
[SH-4.2-6] 23 p4007 N85-34844

NEUTRON COUNTERS
NT NEUTRON SPECTROMETERS
Method and apparatus for determining the content and distribution of a thermal neutron absorbing material in an object
[DE84-014319] 01 p0117 N85-10601
Approaches to ultrafast neutron detectors
[DE85-001206] 11 p1636 N85-20307
Ultrahigh-sensitivity threshold neutron detector for plasma diagnostics
[DE85-005270] 13 p2161 N85-23413
Neutron detector counting capabilities for (10) B-lined and (235) U fission chambers in high gamma-ray fluxes
[DE85-011893] 22 p3840 N85-33780
Spectra of solar proton ground level events using neutron monitor and neutron moderated detector recordings
[SH-1.3-14] 23 p3994 N85-34759
Determination of galactic cosmic ray latitudinal gradient using Earth based detectors
[SH-4.2-13] 23 p4008 N85-34851
An update on the correlation between the cosmic radiation intensity and the geomagnetic AA index
[SH-4.2-24] 23 p4009 N85-34861
Cosmic ray sidereal diurnal variation of galactic origin observed by neutron monitors
[SH-4.4-2] 23 p4033 N85-35000
Observations of cosmic-ray modulations in the fall, 1954
[SH-5.1-16] 23 p4043 N85-35069
Frequency spectra of short-period variations of cosmic ray
[SH-5.1-17] 23 p4043 N85-35070
Coupling functions for lead and lead-free neutron monitors from the latitudinal measurements performed in 1982 in the research station Academician Kurchatov
[SH-5.1-1] 23 p4044 N85-35076
On the solar cycle variation in the barometer coefficients of high latitude neutron monitors
[SH-5.1-2] 23 p4044 N85-35077
Recording system for the solar neutron monitoring at Mt. Norikura
[SH-9.1-8] 23 p4051 N85-35123
Sensitivity of single and multiple cosmic ray neutrons to the surrounding medium in a lead-free monitor
[SH-9.1-10] 23 p4051 N85-35125
SONTRAC: A solar neutron track chamber detector
[SH-9.1-12] 23 p4052 N85-35127
The neutron moderated detector and groundbased cosmic ray modulation studies
[SH-9.1-13] 23 p4052 N85-35128
New Matsushiro underground cosmic ray station (220 M.W.E. in depth)
[SH-9.1-14] 23 p4052 N85-35129
A suggested standardized format for cosmic ray ground-level event data
[SH-9.1-15] 23 p4052 N85-35130
The influences of the galactic cosmic ray on the atmospheric ozone
[SH-10.1-1] 23 p4053 N85-35133

NEUTRON CROSS SECTIONS
SPECTER: Neutron damage calculations for materials irradiations
[DE85-005791] 18 p3180 N85-29716
Chemical spectroscopy
[DE85-009594] 18 p3191 N85-29790
Measurement and evaluation of selected 14-MeV neutron cross sections for fusion
[DE85-010295] 19 p3365 N85-30957
An attempt to detect induced neutron capture in laser radiation field
21 p3690 N85-32928
Rhodium-103 and Indium-115 inelastic scattering reactions for fission neutron dosimetry
21 p3703 N85-33004
Radiation transport
[DE85-010333] 21 p3703 N85-33005
The effects of newly measured cross sections in hydrogen on the production of secondary nuclei during the propagation of cosmic rays through interstellar H
[OG-7.2-2] 23 p4014 N85-34874
(NAT)Fe(n,n'x) spectra at 65.5 MeV
[AD-A155778] 24 p4150 N85-35730

NEUTRON DECAY
High energy neutron and gamma-radiation generated during the solar flares
[SH-1.4-8] 23 p3995 N85-34768

NEUTRON DETECTORS
U NEUTRON COUNTERS

NEUTRON DIFFRACTION
Diffraction by the time-of-flight technique at pulsed neutron sources
[DE84-015839] 03 p0418 N85-12674
Magnetic properties of intermetallic phases and simple systems — neutron diffraction 03 p0422 N85-12697
Fine structure analysis with thermal neutrons and development and construction of a multidetector system
03 p0422 N85-12698
Investigation of domain structures and walls using neutron diffraction 03 p0423 N85-12702
Construction of a neutron single crystal diffractometer
03 p0427 N85-12723
Measurement of scattering cross sections of liquid and solid hydrogen deuterium and deuterium hydride for thermal neutrons
[DE84-014814] 05 p0727 N85-14671
Momentum distributions in superfluid helium: Bose condensate fraction
[DE84-014676] 05 p0731 N85-14700
Neutron diffraction studies of the hydrogen bonding and water molecules in zeolites
[DE84-016431] 06 p0766 N85-14900
SANS and TEM studies of carbide precipitation and creep damage in type 304 stainless steel
[DE85-000933] 09 p1296 N85-18139
Study of magnetism at surfaces by scattering of neutrons at grazing incidence
[DE84-015850] 10 p1584 N85-19885
Microscopic magnetic structure of multiple bilayers of thin films of Fe and Ge
[DE85-004188] 13 p2024 N85-22662
Ultrasonic SH wave velocity in textured aluminum plates
[AERE-R-11516] 15 p2509 N85-25475
High resolution powder diffraction
[DE85-008267] 17 p2922 N85-28015
Magnetism at interfaces and surfaces, as probed by neutron scattering
[DE85-007967] 18 p3176 N85-29690
Structural and physical studies on a new class of low-dimensional conducting material: FeOCl intercalated with TTF and related molecules
[DE85-009701] 18 p3196 N85-29824
Magnetic scattering and polarized neutrons
[DE85-009823] 19 p3355 N85-30794
Determination of the intramolecular potential flow from a neutron diffraction experiment
[88563199] 20 p3532 N85-31978

NEUTRON EMISSION
Nuclear moments and nuclear structure
[DE84-015847] 04 p0561 N85-13573
Performing (p vector, pc)n), (d vector, n) and (n vector, n) measurements with a rotating magnet beam swinger
[DE84-017003] 04 p0562 N85-13582
Neutron and gamma-ray signatures for particle acceleration in solar flares 12 p1954 N85-22278
Refinements in the computation of collision probabilities
[DE85-006118] 16 p2664 N85-27663
Fast-neutron-spectrum measurements for the thick-target (9)Be(d/ — 7 MeV
[DE85-010481] 18 p3183 N85-29735
Investigation of thick-target neutron emission from Be-9(d,n)B-10 at E(d) — 7 MeV for angles other than zero degrees
[DE85-010254] 20 p3528 N85-31947
Methodology for evaluating P sub nu distributions: Results to date
[DE85-007286] 20 p3530 N85-31958
Magnetically insulated diode for generating pulsed neutron and gamma ray emissions
[DE85-011658] 22 p3760 N85-33306
Apparatus and method for identification of matrix materials in which transuranic elements are embedded using thermal neutron capture gamma-ray emission
[DE85-011659] 22 p3766 N85-33454
Measurement of radionuclides in waste packages
[DE85-011674] 22 p3838 N85-33766
Calculated neutron-induced cross sections for /sup 63,65/Cu/sup 58,60/Ni and (52) Cr from 1 to 20 MeV and comparisons with experiments
[DE85-011928] 22 p3844 N85-33805
Helios 1 energetic particle observations of the solar gamma ray flare events of 7, 21 June 1980 and 3 June 1982
[SH-1.3-8] 23 p3993 N85-34755
Source energy spectra from demodulation of solar particle data by interplanetary and coronal transport
[SH-1.3-13] 23 p3994 N85-34758
On the angular and energy distribution of solar neutrons generated in P-P reactions
[SH-1.4-9] 23 p3995 N85-34769
Recording system for the solar neutron monitoring at Mt. Norikura
[SH-9.1-8] 23 p4051 N85-35123
Sensitivity of single and multiple cosmic ray neutrons to the surrounding medium in a lead-free monitor
[SH-9.1-10] 23 p4051 N85-35125
The neutron moderated detector and groundbased cosmic ray modulation studies
[SH-9.1-13] 23 p4052 N85-35128
Neutron production by Ne and Si ions on a thick Cu target at 670 MeV/A with application to radiation protection
[DE86-014526] 24 p4152 N85-35748

NEUTRON FLUX
U FLUX (RATE)

NEUTRON FLUX DENSITY
Monte Carlo alpha calculation
[DE85-010720] 19 p3349 N85-30758
Study of proton and neutron activation of metal samples in low Earth orbit
[NASA-CR-171596] 21 p3558 N85-32130
Neutron flux, spectrum and dose equivalent measurements for a 4500-W(th) 236 PuO2 general purpose heat source
[DE85-011361] 22 p3841 N85-33788
Solar modulation of cosmic ray intensity and solar flare events inferred from (14)C contents in dated tree rings
[SH-7.1-2] 23 p4047 N85-35095
Neutronic calculations for a new high flux reactor
[DE85-011551] 24 p4150 N85-35734
Samarkand complex setup for investigation of cosmic ray variation in the energy range of 7 10 (9) - 10 (15) eV
[HE-4.6-14] 24 p4198 N85-36050

NEUTRON IRRADIATION
Review: Role of refractory metal alloys in fusion reactor applications
[AERE-R-11317] 03 p0422 N85-12695
Neutron irradiation of semiconductors — lattice defects, electron irradiation 03 p0428 N85-12732
Sputtering of gold irradiated with thermal neutrons
03 p0429 N85-12736
Investigation of the production and properties of lattice defects induced by low temperature reactor irradiation
03 p0430 N85-12739
Spectroscopic investigations on neutron induced impurity atoms and radiation defects
03 p0430 N85-12742
Evaluation of ferritic alloy Fe-2 1/4Cr-1Mo after neutron irradiation: Irradiation creep and swelling
[DE84-014647] 04 p0474 N85-13022
Effect of neutron irradiation on the high temperature operation of injection laser diodes
[DE85-000068] 09 p1326 N85-18333
Radiation effects in Strain-Layer Superlattice (SLS) structures
[DE85-001713] 09 p1398 N85-18799
Major facilities for materials research and related disciplines
[PB85-106850] 11 p1739 N85-20934
Effects of neutron irradiation on the fracture properties of HT-9 weld
[DE85-001068] 12 p1807 N85-21339
Effects of neutron irradiation at 450(0)C and 16 dpa on the properties of various commercial copper alloys
[DE85-005716] 13 p2024 N85-22664
Effect of elevated-temperature neutron irradiation on fracture toughness of ceramics
[DE85-000652] 14 p2261 N85-24010
Measurement and evaluation of selected 14-MeV neutron cross sections for fusion
[DE85-010295] 19 p3365 N85-30957
Study of proton and neutron activation of metal samples in low Earth orbit
[NASA-CR-171596] 21 p3558 N85-32130
The 1983 international intercomparison of nuclear accident dosimetry systems at Oak Ridge National Laboratory
[DE85-011303] 23 p3934 N85-34362
Rapid annealing of temperature-compensated, precision voltage references following fast-neutron irradiation
[DE85-009821] 23 p3970 N85-34609

NEUTRON PHYSICS
Neutronics activities for next generation devices
[DE85-010488] 20 p3527 N85-31939
Nuclear data for MCNP
[DE85-010794] 22 p3840 N85-33782

NEUTRON RADIOGRAPHY
Tomographic reconstruction of neutron radiograph images
[AD-A145682] 02 p0290 N85-11826
Robotics in nondestructive inspection at Sacramento Air Logistics Center
[AD-P004012] 03 p0309 N85-11992
Mobile accelerator neutron radiography system
[AD-A148608] 09 p1323 N85-18911
NBS (National Bureau of Standards) reactor: Summary of activities Jul. 1983 through Jun. 1984
[PB85-184836] 20 p3522 N85-31907

NEUTRON SCATTERING
Report on research results in solid state nuclear physics, 1980-1982
[JUEL-SPEZ-250] 03 p0422 N85-12696
Investigations of magnetic phase transitions with neutron scattering 03 p0423 N85-12700

Crystal chemistry and real structure of crystals
03 p0423 N85-12703
Neutron scattering on the FRM double crystal spectrometer
03 p0423 N85-12704
Neutron interferometry and double diffractometer for condensed matter
03 p0424 N85-12705
Neutron scattering on magnetic structures and at magnetic phase transitions
03 p0424 N85-12706
Diffuse elastic and inelastic neutron scattering of disorder transitions and boundaries. Phase determination of structure factors
03 p0424 N85-12708
Development and utilization of advanced methods of neutron scattering
03 p0424 N85-12710
Neutron scattering on structural phase transitions with domain building
03 p0425 N85-12711
Inelastic neutron scattering on crystals for the clarification of structure and semiconductor properties
03 p0425 N85-12714
Measurements on the triple axis spectrometer UNIDAS for the investigation of dynamic processes in crystals using inelastic neutron scattering
03 p0426 N85-12716
Quasielastic neutron scattering on single crystals of solid ionic conductor
03 p0426 N85-12719
X-ray and neutron scattering and X-ray spectroscopy for the study of defects in solid state materials
03 p0430 N85-12741
Neutron small angle scattering of the free and membrane-bound ATPase — adenosine triphosphate (ATP)
03 p0431 N85-12746
Neutron scattering on macromolecular solid state materials, solutions and melts
03 p0431 N85-12747
Description and characterization of deuterated polymers for the analysis with neutron scattering
03 p0431 N85-12748
Small angle neutron scattering (SANS) on polymer-oligomer mixtures and on deformed polyethylene melts
03 p0432 N85-12750
Neutron scattering on polysiloxanes
03 p0432 N85-12751
Neutron scattering for the investigation of solid state materials, utilization in chemical structures
03 p0432 N85-12752
Static and quasielastic neutron scattering for the investigation of structure, dynamics and transport properties of lipid layers and lipid/protein compounds
03 p0432 N85-12753
Performing (p vector,)(c)n), (d vector, n) and (n vector, n) measurements with a rotating magnet beam swinger
[DE84-017003] 04 p0562 N85-13562
Journal of Research of the National Bureau of Standards, Volume 89, Number 1, January-February, 1984
[PB84-235530] 08 p1262 N85-17931
The Fermi surface and momentum space densities of ferromagnetic Gd using the Positron technique
09 p1396 N85-18788
On shrinkage and molecular extension
[AD-A149100] 10 p1451 N85-19144
Study of magnesium at surfaces by scattering of neutrons at grazing incidence
[DE84-015850] 10 p1564 N85-19665
SANS studies of polymers
[DE85-002471] 11 p1612 N85-20134
Major facilities for materials research and related disciplines
[PB85-108850] 11 p1739 N85-20934
Neutron scattering studies of graphite intercalation compounds
[DE85-003079] 12 p1942 N85-22196
Paramagnetic form factors from itinerant electron theory
[DE85-005272] 16 p2750 N85-26973
Discrete foundation for physics and experience
[DE85-006172] 16 p2872 N85-27720
Vibrational spectra of a-Fe(.78)P(.22) by inelastic neutron scattering
[DE85-006296] 17 p2922 N85-28018
Neutron scattering and reactions on 59Co from 1 to 20 MeV
[AERE-R-11439] 17 p3028 N85-28729
An examination of the use of wave packets for the calculation of atom diffraction by surface
[AD-A152760] 17 p3029 N85-28735
Magnetism at interfaces and surfaces, as probed by neutron scattering
[DE85-007867] 18 p3176 N85-29690
Chemical spectroscopy
[DE85-009594] 18 p3191 N85-29790
Magnetic scattering and polarized neutrons
[DE85-009823] 19 p3355 N85-30794
Neutron scattering study of the heavy fermion system UBe-13
[DE85-010955] 19 p3358 N85-30804
Investigation of thick-target neutron emission from Be-9(d,n)B-10 at E(d) = 7 MeV for angles other than zero degrees
[DE85-010254] 20 p3528 N85-31947
Toward a theory of excitation of atoms during nuclear and magnetic neutron scattering
21 p3689 N85-32918
Scientific Opportunities with Advanced Facilities for Neutron Scattering
[DE85-012113] 22 p3839 N85-33770
Capture in the 1.15-keV iron resonance
[DE85-011913] 23 p3970 N85-34612
Some nuclear data needs in astrophysics
[DE85-012916] 24 p4168 N85-35842

NEUTRON SOURCES
Diffraction by the time-of-flight technique at pulsed neutron sources
[DE84-015839] 03 p0418 N85-12674
Construction of a cold neutron source at FRM, Munich
03 p0427 N85-12722
Investigation of special facilities for a spallation neutron source
03 p0427 N85-12724
Fast neutron capture with a white neutron source
[DE84-016799] 04 p0562 N85-13560
Preliminary grouping in A strong-current linear ion accelerator with a low injection energy
[DE84-017192] 04 p0563 N85-13587
Investigation of the output parameters of the pulsed neutron generator NGI-5
[DE85-001823] 11 p1725 N85-20649
3d calculations of a fixed field alternating gradient synchrotron magnet
[DE85-002742] 18 p3183 N85-29739
High-energy particle Monte Carlo at Los Alamos
[DE85-010716] 19 p3363 N85-30656
Determination of the average neutron activation cross section with an annular-shaped 241 Am/Be neutron source and a NaI(T1) detector for the 27 Al (n,p)27 Mg-reaction
[REPT-4/1964] 20 p3532 N85-31975
Radiation transport
[DE85-010333] 21 p3703 N85-33005
Scientific Opportunities with Advanced Facilities for Neutron Scattering
[DE85-012113] 22 p3839 N85-33770
Nuclear physics in the 10 to 300 MeV energy range using a pulsed white neutron source
[DE85-003713] 22 p3839 N85-33775
Time extended production of neutrons during a solar flare
[SH-1.4-1] 23 p3994 N85-34782
Pulsed-neutron-source models for the astrophysical s-process
[DE85-012927] 24 p4151 N85-35740
Los Alamos high-current proton storage ring
[DE85-012684] 24 p4158 N85-35779

NEUTRON SPECTRA
Nuclear moments and nuclear structure
[DE84-015847] 04 p0561 N85-13573
The effect of the choice or response matrix on unfolded bonner sphere spectra
[AD-A150462] 13 p2159 N85-23404
Fast-neutron-spectrum measurements for the thick-target (t)Be(d/ = 7 MeV
[DE85-010481] 18 p3183 N85-29735
High-energy particle Monte Carlo at Los Alamos
[DE85-010716] 19 p3363 N85-30656
Paired ion chamber constants for fission gamma-neutron fields
[AD-A155069] 21 p3702 N85-32999
Neutron flux, spectrum and dose equivalent measurements for a 4500-W(th) 238 PuO2 general purpose heat source
[DE85-011361] 22 p3841 N85-33786
Microdosimetric spectra measurements of JANUS neutrons
[DE85-012108] 22 p3843 N85-33801
SONTRAC: A solar neutron track chamber detector
[SH-9.1-12] 23 p4052 N85-35127
The neutron moderated detector and groundbased cosmic ray modulation studies
[SH-9.1-13] 23 p4052 N85-35128

NEUTRON SPECTROMETERS
Neutron scattering on the FRM double crystal spectrometer
03 p0423 N85-12704
Development and utilization of advanced methods of neutron scattering
03 p0424 N85-12710
Construction, putting into operation, and utilization of a triple axis neutron spectrometer
03 p0425 N85-12715
Measurements on the triple axis spectrometer UNIDAS for the investigation of dynamic processes in crystals using inelastic neutron scattering
03 p0426 N85-12716
The effect of the choice or response matrix on unfolded bonner sphere spectra
[AD-A150462] 13 p2159 N85-23404
Observations on (3)He neutron spectrometry
[DE85-010731] 23 p3970 N85-34608

NEUTRON STARS
NT PULSARS
Transport properties of the outer crust of magnetic neutron stars
09 p1415 N85-18927
A spectroscopic study of LMC X-4
[NASA-CR-174414] 10 p1571 N85-19905
X-ray bursts: Observation versus theory
[NASA-CR-174415] 10 p1573 N85-19916
Old and new neutron stars
[DE85-002716] 11 p1762 N85-21085
Cooling of neutron stars with hyperons
[DE85-004641] 13 p2171 N85-23472
Extragalactic origin or gamma-ray bursts, revision 1
[DE85-005622] 15 p2686 N85-26588
Thermal and magnetic properties of neutron stars
16 p2880 N85-27774
Axion mass limits from pulsar X-rays
[DE85-010634] 18 p3202 N85-29865
Annihilation radiation in cosmic gamma-ray bursts
[OG-1.1-3] 22 p3861 N85-33905
On the emission region of gamma ray bursts
[OG-1.1-4] 22 p3861 N85-33906
Observations of Cygnus X-3 above 10(15) eV from 1979 - 1984
[OG-2.1-6] 22 p3863 N85-33923
On gamma and neutrino radiation from Cyg X-3
[OG-2.1-7] 22 p3863 N85-33924
500 TeV gamma rays from Hercules X-1
[OG-2.2-7] 22 p3865 N85-33933
A model for the UHE gamma-rays from Hercules X-1
[OG-2.2-8] 22 p3865 N85-33934
High-resolution spectroscopic observation of Vela X-1 in the hard X-ray energy range
[OG-2.2-10] 22 p3865 N85-33936
Observation of gamma-rays from LMC X-4 above 10(16) eV
[OG-2.6-10] 22 p3870 N85-33972
Investigations of the cyclotron resonance effects in the X ray spectrum of the neutron star Hercules X-1
[MPE-191] 22 p3890 N85-34112
X-ray spectra of bursting neutron stars
23 p3981 N85-34866
Quasiperiodic oscillations in bright galactic-bulge X-ray sources
[NASA-CR-176138] 23 p3987 N85-34723
A very important process of nucleosynthesis in stars
[OG-7.1-11] 23 p4014 N85-34872
High energy radiation from neutron stars
[DE85-014953] 24 p4169 N85-35843
High energy cosmic ray signature of quark nuggets
[HE-6.2-11] 24 p4212 N85-36147

NEUTRON TRANSMUTATION
U NUCLEAR REACTIONS

NEUTRONS
NT COLD NEUTRONS
NT FAST NEUTRONS
NT THERMAL NEUTRONS
Study of proton and neutron activation of metal samples in low Earth orbit
[NASA-CR-171183] 01 p0026 N85-10164
Study of structure of nuclei with neutrons and nuclear data measurements for MFE
[DE84-015128] 01 p0117 N85-10802
Effects of irradiation fluence and creep on fracture toughness of 347/348 stainless steel
[DE84-016091] 05 p0618 N85-13953
Generation of radiation transport geometry from computer-generated design data — monte carlo solution of the neutron transport equation
[DE84-017360] 09 p1370 N85-18606
Instrumental background in balloon-borne gamma-ray spectrometers and techniques for its reduction
[NASA-TM-86162] 00 p1413 N85-18911
MCNP code
[DE85-002565] 11 p1702 N85-20705
Finite element method for solving neutron transport problems
[DE85-001075] 11 p1722 N85-20829
A linear characteristic-nodal transport method for the two-dimensional (X,Y)-geometry multigroup discrete ordinates equations over an arbitrary triangle mesh
[LA-10092-T] 12 p1913 N85-22008
Cyclic changes in barometric coefficient of cosmic ray neutron component
15 p2478 N85-25293
Space radiation monitor observations from Salyut-4 orbital station
15 p2482 N85-25317
Nuclear radiation induced absorption in optical materials
[DE85-007128] 15 p2649 N85-26336
Physics effects of accidental submersion of space power reactors in water
[DE85-005020] 15 p2650 N85-26344
Nonlinear DSA difference schemes for radiative transfer applications
[DE85-005729] 16 p2856 N85-27611
Laser welder for fabricating neutron tubes
[DE85-009985] 17 p2974 N85-28377

Axion mass limits from pulsar X-rays
[DE85-010634] 18 p3202 N85-29865
The possibility of observing solar neutron events in the lower atmosphere
[NOTA-INTERNA-837] 18 p3209 N85-29908
Mouse oocyte killing by neutrons: Target considerations
[DE85-011362] 19 p3328 N85-30624
MCNP: A general Monte Carlo code for neutron and photon transport
[DE85-010764] 19 p3348 N85-30753
Low-discrepancy point sets in transport codes
[DE85-010786] 19 p3348 N85-30755
Modeling and optimization of a test-cell upgrade for MFTF-B operating in the high neutron wall loading mode
[DE85-009997] 20 p3528 N85-31946
Solid-state track recorder neutron dosimetry in the Three-Mile Island Unit-2 reactor cavity
[DE85-011360] 20 p3531 N85-31966
Detection of solar neutrons by ground based neutron monitors
[IFSI-84-11] 20 p3547 N85-32076
Multiple collision solutions for time-dependent neutron transport in slabs of finite thickness
[OEFZS-4312] 22 p3838 N85-33762
Novette diagnostic support
[DE85-012937] 23 p3934 N85-34383
Application of evaluated fission-product delayed-neutron precursor data in reactor kinetics calculations
[DE85-012728] 23 p3972 N85-34624
The SCR flare of 16 February 1984 as recorded by the Sayan spectrograph
[SH-1.3-17] 23 p3994 N85-34761
Further observations of protons resulting from the decay of neutrons ejected by solar flares
[SH-1.4-2] 23 p3994 N85-34763
Suggestions for improving the efficiency of ground-based neutron monitors for detecting solar neutrons
[SH-1.4-3] 23 p3995 N85-34764
Search for solar neutrons using NM-64 equipment
[SH-1.4-5] 23 p3995 N85-34765
A search for solar neutrons on a long duration balloon flight
[SH-1.4-6] 23 p3995 N85-34766
High energy neutron and gamma-radiation generated during the solar flares
[SH-1.4-8] 23 p3995 N85-34768
Energetic particle observations of the solar-gamma ray/neutron flare events of 3 Jun 1982 and 21 June 1980 isotopic and chemical composition
[SH-2.1-3] 23 p3998 N85-34784
Exponential anisotropy of solar cosmic rays
[SH-3.2-1] 23 p4002 N85-34817
Neutron-rich nuclei in cosmic rays and Wolf-Rayet stars
[OG-8.2-6] 23 p4019 N85-34906
An approach of reducing the background induced by neutrons
[OG-9.3-5] 23 p4027 N85-34960
Neutron-induced 2.2 MeV background in gamma ray telescopes
[OG-9.3-6] 23 p4027 N85-34961
Characteristics of cosmic ray pole-equator anisotropy derived from spherical harmonic analysis of neutron monitor data
[SH-4.3-12] 23 p4032 N85-34996
First zonal harmonic component of cosmic ray neutron intensity
[SH-4.3-13] 23 p4032 N85-34997
Monte Carlo calibration of the SMM gamma ray spectrometer for high energy gamma rays and neutrons
[SH-9.1-6] 23 p4051 N85-35121
Comparisons of monthly mean cosmic ray counting rates observes from worldwide network of neutron monitors
[SH-9.1-7] 23 p4051 N85-35122
(NAT)Fe(n,n'x) spectra at 65.5 MeV
[AD-A155776] 24 p4150 N85-35730
Neutron production by Ne and Si ions on a thick Cu target at 670 MeV/A with application to radiation protection
[DE85-014526] 24 p4152 N85-35746
Applications and misappli-ations of the channel-capture formalism of direct neutron capture
[DE85-013902] 24 p4152 N85-35748
Los Alamos high-current proton storage ring
[DE85-012864] 24 p4158 N85-35779
Some nuclear data needs in astrophysics
[DE85-012916] 24 p4186 N85-35842
Determination of the cross section of the proton, pion and neutron inelastic interaction with lead and carbon nuclei at 0.5 - 5.0 TeV energies (PION experiment)
[HE-1.1-5] 24 p4170 N85-35853
The spectrum of neutrons at 60 hg m(-2)
[HE-5.2-20] 24 p4204 N85-36006

NEVADA
Hydrogeochemical investigation of thermal springs in the Black Canyon-Hoover Dam area, Nevada and Arizona
[PB84-202472] 01 p0064 N85-10426
Post-Sonoman conodont biofacies of the Triassic of northwestern Nevada 03 p0390 N85-12497
Classification of vegetation communities in the Battle Mountain SE quadrangle, Nevada with MSS digital data
[E85-10043] 06 p0826 N85-15246
Analysis of SIR-B radar illumination of geometry for depth of penetration and surface feature and vegetation detection, Nevada and California
06 p1149 N85-17248
Index to published geologic maps in the region around the potential Yucca Mountain nuclear waste repository site, southern Nye County, Nevada
[DE85-000260] 11 p1669 N85-20518
Research and development related to the Nevada nuclear waste storage investigations
[DE85-002303] 12 p1932 N85-22138
Summary of Meteorological Observations, Surface (SMOS), Fallon, Nevada
[AD-A150481] 13 p2138 N85-23276
Preliminary assessment of climatic change during late Wisconsin time, southwest Great Basin and vicinity, Arizona, California and Nevada
[DE85-008343] 16 p2836 N85-27486
Analysis of the elastic and strength properties of Yucca Mountain tuff, Nevada
[DE85-008975] 19 p3300 N85-30480
Petrologic and geochemical characterization of the Topopah Spring Member of the Paintbrush Tuff: Outcrop samples used in waste package experiments
[DE85-010449] 19 p3302 N85-30470
Structural and tectonic history of the Goldonda allochton, southern Tolyabe Range, Nevada
19 p3312 N85-30529
Comparison of survey and photogrammetry methods to position gravity data, Yucca Mountain, Nevada
[DE85-011685] 21 p3590 N85-32316
A 1984 environmental summary: Sandia National Laboratories Tonopah Test Range, Tonopah, Nevada
[DE85-011145] 22 p3812 N85-33612
Iron and manganese in oxide minerals and in glasses: Preliminary consideration of Eh buffering potential at Yucca Mountain, Nevada
[DE85-011892] 23 p3916 N85-34271
Simulated effects of increased recharge on the ground-water flow system of Yucca Mountain and vicinity, Nevada-California
[DE85-012985] 24 p4106 N85-35469

NEW ENGLAND (US)
Investigation of radiometric properties of LANDSAT-4 MSS — California, North Carolina, South Carolina, and New England 11 p1666 N85-20500
East coast snowstorm survey
15 p2598 N85-26013
Model sensitivity studies of major east coast storms
15 p2598 N85-26016
Justification and plan for participation in GALE
15 p2599 N85-26017

NEW HAMPSHIRE
Potential for acidification of six remote ponds in the White Mountains of New Hampshire
[PB84-207349] 02 p0225 N85-11475
Climate at CRREL (Cold Regions Research and Engineering Laboratory) Hanover, New Hampshire
[AD-A148400] 08 p1189 N85-17495
Impact of LANDSAT MSS sensor differences on change detection analysis — New Mexico, San Francisco, CA, New Hampshire, and Connecticut
11 p1667 N85-20506

NEW JERSEY
Soil formation on tertiary landsurfaces of the New Jersey coastal plain 08 p1181 N85-17441

NEW MEXICO
Spectroradiometric calibration of the Thematic Mapper and Multispectral Scanner system
[E85-10026] 02 p0216 N85-11439
Surface soil moisture measurements of the White Sands, New Mexico
[NOAA-TM-NESDIS-7] 02 p0219 N85-11441
Solar energy resource assessment in Eastern New Mexico and solar and wind energy resource assessment in Eastern New Mexico
[DE84-901511] 04 p0527 N85-13370
LANDSAT instruments characterization
[E85-10026] 05 p0654 N85-14197
LANDSAT-4 Thematic Mapper Modulation Transfer Function (MFT) evaluation — California and New Mexico
[E85-10055] 07 p0964 N85-16250
Spectroradiometric calibration of the Thematic Mapper and Multispectral Scanner system
[E85-10077] 10 p1504 N85-19491
Impact of LANDSAT MSS sensor differences on change detection analysis — New Mexico, San Francisco, CA, New Hampshire, and Connecticut
11 p1667 N85-20506
In-progress absolute radiometric inflight calibration of the LANDSAT-4 sensors — New Mexico
12 p1870 N85-21733
Evaluation of geothermal potential of Rio Grande rift and Basin and Range province, New Mexico
[DE85-901360] 19 p3301 N85-30466
Remote sensing of hydrologic transport processes using spot simulation data
[DE85-012412] 24 p4108 N85-35467

NEW YORK
Major institutional arrangements affecting ground water in New York state
[PB84-202506] 01 p0065 N85-10429
Slope water intrusions within the nearshore waters off Long Island, New York
[DE85-001386] 09 p1359 N85-18549
Analysis of flow within the coastal boundary layer off Long Island, New York
[DE85-001384] 09 p1359 N85-18550
Pavement-marking materials: New York's experience
[PB85-153294] 15 p2523 N85-25558

NEW ZEALAND
Detailed analysis of the structure of local wind systems in Canterbury, New Zealand 01 p0075 N85-10501
New Zealand SIR-B science investigations
08 p1144 N85-17218

NEWS MEDIA
Origin, processing, and dissemination of scientific news, with examples from 20 research institutes
[JUEL-1940] 17 p3050 N85-26882

NEWTON THEORY
Quasi-three dimensional modeling of functionally-integrated elements of large-scale integrated circuits 04 p0490 N85-13122
Elements of celestial mechanics
14 p2396 N85-24782
Finite axisymmetric deformation of a thin shell of revolution 16 p2798 N85-27251

NEWTON-RAPHSON METHOD
A solution method for large deformation contact problems
[AD-A149842] 12 p1866 N85-21707
Direct secant updates of sparse matrix factors
[DE85-004008] 12 p1922 N85-22073
A numerical procedure on three-dimensional parabolic flow in duct 16 p2892 N85-28820
X-ray spectra of bursting neutron stars
23 p3981 N85-34686

NEWTONIAN FLUIDS
Trapping for Newtonian diffusion processes
[REPT-73] 01 p0130 N85-10893
Dynamics of liquid filament breakup
[DE84-016008] 04 p0500 N85-13187
Numerical experiments and theoretical analysis of the flow of an elastic liquid of the Maxwell-Oldroyd type in the presence of geometrical singularities
[WTHD-164] 08 p1183 N85-17340
Practical real-time quality control of antimisting kerosene
[DE/FAA/CT-85/1] 18 p3083 N85-29072
On the importance of viscous dissipation in Io
22 p3885 N85-33873

NICKEL
NT NICKEL ISOTOPES
The effects of seven alloying elements on the microstructure and stress-rupture behavior of nickle-base superalloys
[NASA-TM-83791] 01 p0027 N85-10168
Thermodynamics of reactions of deoxidation of nickel melts
[BLL-M-35729-(5828.4)] 02 p0175 N85-11168
The reactions of cobalt, iron and nickel in SO-2 atmospheres: Similarities and differences
[NASA-TM-86868] 02 p0181 N85-11217
Environment-induced embrittlement: Effect of impurity segregation and state of stress
[DE84-015436] 02 p0184 N85-11235
Review: The influence of short circuit diffusion on the oxidation of nickel, chromium and nickel/chromium alloys
[AERE-R-11311] 02 p0185 N85-11237
Characterization of ion implanted deuterium traps in nickel by equilibration with deuterium gas
[DE84-014958] 02 p0298 N85-11879
Electroforming of nickel
[SNIAS-841-501-101] 04 p0484 N85-13085
Nickel-cobalt systematics and their bearing on lunar origin 04 p0582 N85-13719
Abundancies of Ni, Cr, CO and major elements in the silicate portion of the Moon: Constraints from primary lunar magmas 04 p0582 N85-13720

Austenite transformation in powder-compacted chromium-nickel-molybdenum steels during continuous cooling
[BLL-M-35981-(5828.4)] 05 p0615 N85-13933
Mechanisms of impurity diffusion in rutile
[DE84-014741] 06 p0766 N85-14902
Comparison between the properties of conventional wrought and powder metallurgical alloys for turbine disc applications 07 p0906 N85-15739
Optimization of the NiCrAl-Y/ZrO-Y2O3 thermal barrier system
[NASA-TM-86905] 07 p0927 N85-15878
Surface effects of corrosive media on hardness, friction, and wear of materials
[NASA-TM-83711] 07 p0930 N85-15896
Defective nature of the crystalline lattice of nickel ferrite-based solid solutions
[BLL-WH-595-(8091.9F)] 07 p1048 N85-16645
Hydrogen embrittlement of nickel
[AD-A148322] 08 p1129 N85-17119
The influence of strain rate and porosity on the deformation and fracture of titanium and nickel
[AD-A149670] 08 p1130 N85-17123
Stability of amorphous metals on semiconductor substrates
[DE84-017256] 09 p1295 N85-18134
Production method of nickel electrode
[NASA-TM-76948] 10 p1439 N85-19069
Method of producing nickel electrode
[NASA-TM-76944] 10 p1440 N85-19077
Radiation-induced compositional redistribution and local phase transformation in irradiated alloys
[DE85-000080] 10 p1441 N85-19082
Antifriction properties of gas thermal coatings of clad carbine powders 10 p1447 N85-19115
Magnetization of very thin Ni films in epitaxial metal film sandwiches of Cu
[DE85-001840] 10 p1583 N85-19860
Analysis of diffusion in an ion-implanted alloy using a phenomenological model
[AERE-R-11527] 11 p1609 N85-20120
Semiconductor electrochemistry approach to the study of oxide films on nickel electrodes
[DE85-003042] 11 p1630 N85-20264
Low temperature deposition of nickel films
[AD-D011566] 12 p1805 N85-21319
Humidity effects on adhesion of nickel-zinc ferrite in elastic contact with magnetic tape and itself
[NASA-TP-2449] 12 p1811 N85-21350
Paramagnetic scattering from Ni
[DE85-004207] 12 p1942 N85-22196
Mechanical properties of electrodeposited nickel and copper
[DE85-006321] 13 p2023 N85-22677
Role of segregated P and S in intergranular stress corrosion cracking of nickel
[DE85-004547] 13 p2024 N85-22679
Apparatus for producing amorphous and microcrystalline metal powders 13 p2030 N85-22720
Molten carbonate fuel cell performance model update, draft
[DE85-005423] 13 p2129 N85-23252
Adsorption site, adsorption energy and normal vibration frequency of H/Ni(100) via total energy calculations
[AD-A150555] 13 p2156 N85-23386
Observation of surface vibrational resonances on (110) surfaces of FCC metals
[AD-A150469] 13 p2163 N85-23419
Dipole active surface vibrational resonances on clean and hydrogen covered Ni(110)
[AD-A150546] 13 p2163 N85-23420
Characterization of supported metal catalysts by imaging, microdiffraction and microanalysis techniques
[DE85-005867] 14 p2253 N85-23981
Microstructure and properties of ferrous alloy weldments
[DE85-005582] 14 p2257 N85-23987
The effects of water and hydrogen on materials used in integrated circuit packages
[AD-A151883] 15 p2518 N85-25529
Influence of phosphorus content and heat treatment on the machinability of electroless nickel deposits
[DE85-007250] 15 p2522 N85-25548
Crack closure characteristics considering center cracked and compact tension specimens
[AD-A151702] 15 p2579 N85-25907
Electronic transport in Mo/Ni superlattice
[DE85-008835] 15 p2661 N85-26425
Nd-isotopic evidence for the origin of the Sudbury complex by meteoritic impact 15 p2660 N85-26554
Effect of nickel addition on the thermal, magnetic and magnetomechanical properties of Fe(80)B(15)Si(5)
[AD-A152281] 16 p2749 N85-26967
Low dose irradiation creep of pure nickel
[DE85-006320] 16 p2751 N85-26975
Influence of manganese and heat treatment on structure and properties of Fe-0.1 percent-C-14 percent Cr-based steels
[BLL-BISI-TRANS-22299-(9022.06)] 17 p2926 N85-28071
The physical and mechanical properties of near-equiatomic titanium-nickel 19 p3237 N85-30072
State variable theories based on Hart's formulation
[DE85-009474] 19 p3239 N85-30082
Thermodynamics of high temperature materials
[AD-A154269] 19 p3378 N85-30958
Analysis of ferrates and ferrites of three transition metals using Moessbauer effects
[BLL-CE-TRANS-8019-(9022.08)] 20 p3430 N85-31273
Defect production and recovery in FCC metals irradiated at 4.2 K
[DE85-010477] 20 p3536 N85-32014
The effect of diffusive hydrogen segregation on fracture of polycrystalline nickel
[AD-A155238] 21 p3567 N85-32186
Relative abundances of sub-iron to iron nuclei in low energy (50-250 MeV/N) cosmic rays as observed in the Skylab experiment
[CG-4.1-4] 22 p3876 N85-34010
Calculating the interatomic pair potential allowing for resonance interaction in titanium, nickel and vanadium
[BLL-M-35843-(5828.4)] 23 p3913 N85-34249
Metal (2) 4,4',4',4'' phthalocyanine tetramines as curing agents for epoxy resins
[NASA-CASE-ARC-11424-1] 23 p3919 N85-34281
Oxidation resistant slurry coating for carbon-based materials
[NASA-CASE-LEW-13923-1] 24 p4077 N85-35267
X-ray fluorescence analysis of 304L stainless steel
[DE85-013254] 24 p4080 N85-35288
Applications of the mineral resources data system and the international strategic minerals inventory in mineral-resource assessments by region and commodity 24 p4105 N85-35451
The Conterminous United States Mineral Assessment Program 24 p4106 N85-35458

NICKEL ALLOYS

NT HASTELLOY (TRADEMARK)
NT INCONEL (TRADEMARK)
NT MONEL (TRADEMARK)
NT NITINOL ALLOYS
NT RENE 95
NT UDIMET ALLOYS
NT WASPALOY

Results of the technical exchange agreement between NASA and DuPont on the containerless drop tube solidification of NiAl3
[NASA-TM-86473] 01 p0014 N85-10087
Weldability of aged heat resistant nickel alloys 01 p0021 N85-10125
Morphological changes of gamma prime precipitates in nickel-base superalloy single crystals
[NASA-TM-83666] 01 p0026 N85-10165
Containerless drop tube solidification and grain refinement of NiAl3 02 p0154 N85-11042
Determining the optimum heating parameters for precision alloys — iron-nickel alloys
[BLL-M-35718-(5824.4)] 02 p0174 N85-11167
Thermodynamics of decarburization of niobium-bearing high-alloy melts
[BLL-M-35728-(5828.4)] 02 p0175 N85-11169
Rapid solidification of steels: Model and commercial alloys 02 p0176 N85-11184
The structure of rapidly solidified nickel-base alloys 02 p0181 N85-11215
Microstructure and creep behaviour at elevated temperature of unidirectionally solidified eutectic nickel base superalloys 02 p0181 N85-11216
The transient oxidation of single crystal NiAl+Zr
[NASA-CR-174756] 02 p0182 N85-11221
The effect of tantalum and carbon on the structure/properties of a single crystal nickel-base superalloy
[NASA-CR-174770] 02 p0182 N85-11223
Studies on the hot corrosion of a nickel-base superalloy, Udimet 700
[NASA-TM-86882] 02 p0183 N85-11224
Review: The influence of short circuit diffusion on the oxidation of nickel, chromium and nickel/chromium alloys
[AERE-R-11311] 02 p0185 N85-11237
Plastic strain localization in superalloy single crystals
[AD-A145705] 02 p0298 N85-11878
The effects of Cr, Co, Al, Mo and Ta on the cyclic oxidation behavior of a prototype cast Ni-base superalloy based on a 2(5) composite statistically designed experiment
[NASA-TM-83784] 03 p0331 N85-12131
The effect of orientation on fatigue growth in a nickel-based single crystal superalloy
[PNR-90207] 03 p0332 N85-12141
Structural stability of nickel heat resistant alloys at high temperatures 03 p0350 N85-12251
Radiation effects in amorphous metallic alloys
[DE84-014302] 04 p0475 N85-13025
The effect of trace elements on the properties at high temperature of a Ni-Cr-base alloy 05 p0617 N85-13944
Method for predicting the creep rupture life of nickel-base precipitation-hardened superalloys from their chemical composition
[BLL-PNR-90241-(8019.3153)] 06 p0768 N85-14910
Application of solidification theory to rapid solidification processing
[AD-A146819] 06 p0769 N85-14917
Metallographic evaluation of the reactions between boronated graphite and Fe-Ni-Cr alloys
[DE84-015374] 06 p0769 N85-14922
A study of tetrataenite 06 p0885 N85-15623
Low temperature diffusion coefficients in the Fe-Ni and FeNiP systems: Application to meteorite cooling rates 06 p0886 N85-15626
Speculations on the formation of metallic meteorite phases 06 p0889 N85-15648
Problems and possibilities for life extension in gas turbine components 07 p0907 N85-15742
Study of high performance alloy electroforming
[NASA-CR-174276] 07 p0927 N85-15875
Design of ordered intermetallic alloys for high-temperature structural use
[DE85-000897] 07 p0928 N85-15885
Recommendations for the use of Ni-Cr-base alloy extensometers for measurement of creep strain
[NPL-DMA(A)-81] 08 p1164 N85-17342
The effect of tantalum on the structure/properties of two polycrystalline nickel-base superalloys: B-1900 + Hf MAR-M247
[NASA-CR-174847] 09 p1294 N85-18127
Low and moderate temperature oxidation of atomically clean nickel, chromium and Ni-Cr alloys
[DE84-017350] 09 p1295 N85-18131
Plasma deposition of amorphous metal alloys
[DE85-000768] 09 p1295 N85-18132
Adaptation of remelting procedures for the use of recycled metal in nickel-base superalloy castings
[PNR-90232] 09 p1297 N85-18149
Laser-initiated combustion studies on metallic alloys in pressurized oxygen
[PB85-128114] 10 p1438 N85-19066
Low cycle fatigue of MAR-M 200 single crystals at 760 and 870 deg C
[NASA-TM-86933] 10 p1440 N85-19074
Influence of volumetric fiber content on some matrix damage factors during thermal cycling of tungsten-Et 765 composite 10 p1443 N85-19097
Influence of gaseous hydrogen on strength and ductility of nickel heat-resistant alloys 10 p1447 N85-19119
Diffusion welding with forced deformation of heat-resistant nickel-based dispersion hardened alloy 10 p1449 N85-19130
Effect of stress concentration fatigue resistance of refractory nickel alloys under asymmetrical multicycle loading, communication 1 11 p1604 N85-20088
Effect of form memory in alloys based on Cu-Al systems 11 p1604 N85-20088
Amorphous Ni-Ti alloys: A new method of synthesis
[DE85-002744] 11 p1605 N85-20094
Structural studies of sputtered Ni-As-O films
[DE85-003229] 11 p1605 N85-20095
Heavy ion induced crystallization in amorphous phases
[DE85-003114] 11 p1606 N85-20098
Non-isothermal irradiation creep of nickel alloys Inconel 706 and PE-16
[DE85-000842] 11 p1607 N85-20102
Initial development of nickel and nickel-iron aluminides for structural uses
[DE84-016641] 11 p1608 N85-20108
Ferromagnetic resonance in a Ni-Mo superlattice
[DE85-003039] 11 p1735 N85-20911
Stress corrosion cracking and oxidation characteristics of boride-strengthened microcrystalline iron and nickel based alloys
[AD-A149805] 12 p1806 N85-21328
Sputter-induced compositional modifications in a Ni-Au alloy
[DE85-002771] 12 p1807 N85-21333
Chemisorption theory: Adsorption on copper-nickel alloys and titanium surface embrittlement
[DE85-001815] 12 p1807 N85-21334

Performance of Chromel versus Alumel and Nicrosil versus Nisil thermocouple assemblies in vacuum and argon between 1000 deg C and 1200 deg C
[DE85-000810] 12 p1853 N85-21624
Study of the effects of implantation on the high Fe-Ni-Cr and Ni-Cr-Al alloys
[NASA-CR-175825] 13 p2021 N85-22661
Thermodynamics of copper-nickel alloys containing aluminum, silicon, titanium, and chromium relative to their use in ceramic brazing
[DE85-004787] 13 p2023 N85-22674
Reaction of amorphous NiNb films with crystalline metal overlayers
[DE85-005483] 13 p2024 N85-22680
Effect of phase state of TiC-NiTi powder composite materials on nature of failure and mechanical properties
13 p2027 N85-22702
Long-term strength and fracture criteria for EI868VD alloy under complex stress conditions
13 p2030 N85-22723
Change in microstructure of heat-resistant nickel alloys upon thermal cycling in a current of gas
13 p2031 N85-22725
The cyclic stress-strain behavior of nickel-base superalloy poly- and single crystals
14 p2254 N85-23969
Local phase transformation in alloys during charged-particle irradiation
[DE85-005012] 14 p2258 N85-23990
Structure and mechanical properties of dispersion-hardened nickel alloy joints welded by diffusion
15 p2500 N85-25422
Contact point and seam welding of heat-resistant alloys
15 p2501 N85-25429
Study of high performance alloy electroforming
[NASA-CR-175741] 15 p2508 N85-25473
Effects of primary recoil energy on the production rate of mobile defects during elevated temperature irradiation
[DE85-006218] 15 p2511 N85-25489
Design of ductile polycrystaline Ni3Al alloys
[DE85-005572] 15 p2511 N85-25491
Weldability of Ni3Al-type aluminide alloys
[DE85-006932] 15 p2512 N85-25496
Studies of ferritic filler metals for welding 9 percent nickel steel
15 p2565 N85-25825
Fatigue life extension 16 p2733 N85-26864
Ignition of metals in high pressure oxygen
16 p2735 N85-26874
Relationships between microstructure and microfissuring in alloy 718 16 p2735 N85-26876
Structural inhomogeneities in amorphous nickel-phosphorus alloy
[BLL-M-36103-(5828.4)] 16 p2748 N85-26960
Role of hydrogen and structure on CMSX-2
17 p2915 N85-27957
The behaviour of nitride inclusions in nickel-base alloys
[BLL-BISI-TRANS-22396-(9022.06)]
17 p2927 N85-28058
The effect of microalloying with calcium and magnesium on the plasticity of Poldi AKN 20 Ni-based alloy
[BLL-BISI-TRANS-2174-(9022.06)]
17 p2929 N85-28075
Kinetics of the formation of a complex alloyed boride coating on iron and its properties
[BLL-BISI-TRANS-22303-(9022.06)]
17 p2930 N85-28084
Sintering reactions, structure and properties of a cobalt free nonconventional hard material
[DE85-007704] 18 p3076 N85-29025
Study of the influence of metallurgical factors on fatigue and fracture of aerospace structural materials
[AD-A153913] 18 p3122 N85-29328
Weldability/microstructure relationships of high nickel alloys for header applications
[DE85-006937] 19 p3241 N85-30094
Effect of prolonged high temperature on durability of coated high-temperature nickel alloys
19 p3243 N85-30105
On compounding nickel alloys as defense against sulfide-oxide corrosion 19 p3243 N85-30109
Properties of heat resistant Ni-Al-Nb alloys with unidirectional eutectic structure
19 p3247 N85-30133
concentration variation of work function of alloys in the system nickel-titanium-aluminum
19 p3247 N85-30134
Investigation for low-cost permanent magnets
[AD-A154367] 19 p3260 N85-30212
A study of the effect of a mismatch in gamma and gamma prime phase lattice spacings on the high temperature strength characteristics of dispersion-hardened nickel alloys
[BLL-CE-TRANS-8048-(9022.09)]
20 p3430 N85-31279
Mechanical behavior of Ni-Cr-base superalloys in forms and conditions representative of service
[NPL-DMA(A)-94] 20 p3431 N85-31282
A multiple linear regression analysis of hot corrosion attack on a series of nickel base turbine alloys
[NASA-TM-87020] 20 p3431 N85-31284
Long range ordered alloys modified by addition of niobium and cerium
[DE85-011661] 20 p3431 N85-31285
Experimental studies of the geometric and electronic structure of chemisorption bonding
[PB85-192250] 22 p3747 N85-33228
Metallic glass composition
[DE85-011594] 22 p3751 N85-33253
Electrical resistivity and hysteresis of the equiatomic nickel-titanium alloy near the martensitic transformation temperature 23 p3904 N85-34181
Microstructures in rapidly solidified Ni-Mo alloys
[NASA-TM-87100] 23 p3915 N85-34266
The development and evaluation of the creep and corrosion resistant alloy IN6201
[PNR-90253] 23 p3917 N85-34278
Microshrink, tensile properties, and the detection of microshrink
[AD-A155875] 24 p4079 N85-35278
Deposition of nickel-cobalt alloys by controlled-potential electrolysis
[PB85-196562] 24 p4081 N85-35291

NICKEL CADMIUM BATTERIES
Positive electrodes of nickel-cadmium batteries
[NASA-TM-77808] 10 p1478 N85-19330
Nickel-cadmium battery cell reversal from resistive network effects
[AD-A149628] 12 p1834 N85-21505
Pseudo bipolar nickel-cadmium batteries used as filter elements to pulsed current loads
[AD-A151192] 15 p2547 N85-25717
Analysis and testing of the thermal properties of space battery cells, phase B, draft
[ESA-CR(P)-1971] 15 p2550 N85-25741
Proposed energy systems for the Brazilian data collection satellite
[INPE-3393-PRE/664] 16 p2731 N85-26856
Investigation of pseudo bi-polar nickel cadmium batteries as filter elements for pulsed power loads
[AD-A152112] 16 p2819 N85-27389
Nickel-cadmium cell design variable program data analysis
[NASA-TM-86198] 19 p3258 N85-30203
The 1984 Goddard Space Flight Center Battery Workshop
[NASA-CP-2382] 20 p3443 N85-31371
RCA's planned test program to compare the performance and life of NiCd cells containing Pellon 2536 in contrast with Pellon 2505 separator material
20 p3445 N85-31385
Failure modes experienced on spacecraft NiCd batteries 20 p3445 N85-31386
Nickel cadmium cell design variable program data analysis 20 p3445 N85-31387
Results of analysis on the design variable cells
20 p3445 N85-31388
Fundamental algorithms of the Goddard battery model
20 p3445 N85-31389
Modeling taper charge with a non-linear equation
20 p3445 N85-31390
High discharge rate characteristics of nickel-cadmium batteries for pulse load filtering
20 p3446 N85-31391
Nickel-cadmium battery cell reversal from resistive network effects 20 p3446 N85-31392
LEO life testing with different charge control
20 p3446 N85-31393
A 34 ampere-hour nickel-cadmium minimum trickle charge testing 20 p3446 N85-31394
AUSSAT battery life test program
20 p3446 N85-31395
Flight experience of Solar Mesosphere Explorer's two nickel-cadmium batteries 20 p3446 N85-31396
Deep reconditioning of batteries during DSCS 3 flight operations 20 p3446 N85-31397

NICKEL COATINGS
USSR report: Materials Science and Metallurgy
[JPRS-UMS-85-005] 19 p3241 N85-30095

NICKEL COMPOUNDS
NT NICKEL OXIDES
The alpha-form of the hydroxides of bivalent metals
[NASA-TM-77509] 04 p0473 N85-13009
Toxicology and metabolism of nickel compounds
[DE84-014919] 05 p0896 N85-14478
Vaporization behavior, phase equilibria, and thermodynamic stabilities of nickel phosphides
[AD-A146663] 06 p0785 N85-14697
Replacement of Fe-3+ ions in nickel ferrites by nonmagnetic Al-3+ and Sc-3+ ions
[BLL-WH-504-(9091.9F)] 08 p1125 N85-17090
Liquid phase methanol process development unit: Installation, operation, and support studies
[DE85-001311] 09 p1301 N85-18171
Defective nature of the crystalline lattice of nickel ferrite-based solid solutions
[BLL-TRANS-WH-595-(9091.9F)]
10 p1439 N85-19068
Alloys based on NiAl for high temperature applications
[NASA-TM-86976] 12 p1805 N85-21322
Magnetovolume effects in some Y-Ni intermetallic compounds
[ISSN-0066-2003] 13 p2021 N85-22663
Raman structural studies of the nickel electrode
[NASA-CR-175619] 13 p2162 N85-23414

NICKEL HYDROGEN BATTERIES
Advanced nickel-hydrogen cell configuration study
[NASA-CR-174775] 01 p0067 N85-10444
Design and development of a sealed 100-Ah nickel-hydrogen battery
[DE84-016935] 06 p0805 N85-15128
Prospects for advanced storage battery technologies
[DE84-015708] 09 p1345 N85-18484
Multikilowatt hydrogen-nickel oxide battery system
[DE85-003339] 15 p2550 N85-25737
Analysis and testing of the thermal properties of space battery cells, phase B, draft
[ESA-CR(P)-1971] 15 p2550 N85-25741
Initial performance of advanced designs for IPV nickel-hydrogen cells
[NASA-TM-87029] 17 p2984 N85-28444
Life cycle test results of a bipolar nickel hydrogen battery
[NASA-TM-87048] 19 p3304 N85-30480
The 1984 Goddard Space Flight Center Battery Workshop
[NASA-CP-2382] 20 p3443 N85-31371
Multikilowatt hydrogen-nickel oxide battery system
20 p3443 N85-31373
Design principles for nickel hydrogen cells and batteries 20 p3447 N85-31398
Improved specific energy Ni-H2 cell
20 p3447 N85-31399
Bipolar nickel-hydrogen battery design
20 p3447 N85-31400
Nickel-hydrogen spacecraft module configurations study 20 p3447 N85-31401
Nickel hydrogen bipolar battery electrode design
20 p3447 N85-31402
Nickel-cadmium cell life test 20 p3447 N85-31403
Initial performance of advanced designs for IPV nickel-hydrogen cells 20 p3448 N85-31404
Accelerated and real-time geosynchronous life cycling test performance of nickel-hydrogen batteries
20 p3448 N85-31405
Life cycle test results of a bipolar nickel hydrogen battery 20 p3448 N85-31406
Nickel-hydrogen cell test program summary
20 p3448 N85-31407
The failure mechanism of a nickel electrode in a nickel-hydrogen cell 20 p3448 N85-31408
An industry and government survey: A nickel-hydrogen testing data base 20 p3448 N85-31409
Design principles for nickel-hydrogen cells and batteries
[NASA-TM-87037] 20 p3483 N85-31846

NICKEL ISOTOPES
Fusion reactions at low energy
[DE85-010561] 20 p3528 N85-31944

NICKEL OXIDES
Design and development of a sealed 100-Ah nickel-hydrogen battery
[DE84-016935] 06 p0805 N85-15128
Grain boundary structure in NiO
[DE84-016242] 06 p0868 N85-15519
Semiconductor electrochemistry approach to the study of oxide films on nickel electrodes
[DE85-003042] 11 p1630 N85-20264
Grain boundaries in NiO
[DE85-006129] 13 p2025 N85-22687
Tilt grain boundaries in NiO
[DE85-006839] 16 p2751 N85-26978
Low-temperature positron lifetime and Doppler-broadening measurements for single-crystal nickel oxide containing cation vacancies
[DE85-010238] 19 p3376 N85-30944
Multikilowatt hydrogen-nickel oxide battery system
20 p3443 N85-31373
Adsorption of O2, SO2, and SO3 on nickel oxide. Mechanism for sulfate formation
[NASA-CR-176072] 21 p3565 N85-32175

NICKEL STEELS
A study of precipitation and boron distribution in 20 Cr 25Ni base stainless steels
[AERE-M-3353] 03 p0334 N85-12154

The corrosion resistance of chromium-nickel steel containing rare-earth metals
[BLL-BISI-TRANS-22477-(9022.06)] 17 p2925 N86-28041
Influence of heat treatment parameters on the properties of induction hardened Ni-Cr-Mo steels
[BLL-BISI-TRANS-2499-(9022.06)] 17 p2926 N86-28053
Obtaining oxide films on surface of tubes of chromium-nickel steels
[BLL-BISI-TRANS-22479-(9022.06)] 17 p2929 N86-28076
Influence of temperature in melting and casting on quality of medium-alloy steel
[BLL-BISI-TRANS-22310-(9002.06)] 17 p2936 N86-28137
The fatigue properties of welds at low temperature, according to the type of steel
[BLL-BISI-TRANS-22455-(9022.06)] 17 p2978 N86-28410
Fatigue behavior of HY-130 steel weldments containing fabrication discontinuities
[AD-A153630] 18 p3122 N86-29326
Application of the unloading compliance methods in fracture toughness measurements of a quenched and tempered steel
[BLL-CE-TRANS-7953-(9022.09)] 20 p3465 N86-31523
Effects of residual stresses and distortion on the nickel 200 and stainless steel 304 weldments
[DE86-011886] 22 p3748 N86-33233

NICKEL ZINC BATTERIES
Research, development, and demonstration of nickel-iron batteries for electric vehicle propulsion
[DE84-017430] 05 p0632 N85-14054
Supported liquid membrane battery separators
[DE85-001031] 12 p1836 N85-21519
In-vehicle evaluation of the Globe EV 2300 lead-acid, Delco Remy 160 nickel-zinc, and Eagle-Picher NIF 270 nickel-iron battery systems
[NASA-CR-175653] 14 p2349 N85-24521
Transfer of battery technology developed by the US Department of Energy
[DE85-009666] 22 p3808 N86-33568

NIGERIA
Geophysical investigations of the central part of Niger State, Nigeria 03 p0390 N85-12496

NIGHT
Two-level model for formation of night ionosphere of Venus from radio occulation experiments 02 p0162 N85-11100
HH-60D night hawk helicopter 06 p0752 N85-14817
Mechanism of formation of low temperatures in nighttime Venusian thermosphere 16 p2723 N86-29807
Turbulent structure of stably stratified nocturnal slope flows
[AD-A155845] 24 p4123 N86-35559

NIGHT AIRGLOW
U NIGHTGLOW

NIGHT E LAYER
U E REGION
U NIGHT SKY

NIGHT F LAYER
U F REGION
U NIGHT SKY

NIGHT FLIGHTS (AIRCRAFT)
Peripheral vision horizon display on the single seat night attack A-10 01 p0009 N85-10053
Civil law enforcement missions 06 p0751 N85-14812
Some thoughts on the implementation of pilot night vision devices for helicopters 06 p0751 N85-14814
Flight research on visual aids and navigation equipment for helicopter low-level flight at night 06 p1076 N85-16820

NIGHT SKY
Inference of equatorial field-line integrated electron density values using whistlers
[AD-A145822] 03 p0392 N85-12507
The Malin effect in stellar photography 07 p0868 N85-16131

NIGHT VISION
Dark focus: Intersubject variation, intrasubject stability, and relationship to near retinoscopy
[AD-A145469] 02 p0235 N85-11530
Some thoughts on the implementation of pilot night vision devices for helicopters 06 p0751 N85-14814
Effect of extreme peripheral light on dark adaptation
[AD-A146923] 10 p1526 N85-19636
The relative effectiveness of red and white light for subsequent dark-adaptation
[AD-A146883] 10 p1530 N85-19642
Immediate visibility after red and white adaptation
[AD-A156271] 24 p4132 N86-35618

NIGHTGLOW
Upper atmosphere research at INPE
[INPE-3281-PRE/604] 10 p1515 N85-19557
First sodium nightglow results for Natal
[INPE-3397-PRE/666] 10 p1515 N85-19560
Increase in hydrogen emission of upper atmosphere following launches of space vehicles 13 p1981 N85-22431
Fabry-Perot interferometer and skymapping photometer determinations of midlatitude f-region neutral winds and temperatures and airglow enhancement/depletions
[AD-A150730] 14 p2373 N85-24668

NIMBUS SATELLITES
NT NIMBUS 5 SATELLITE
NT NIMBUS 7 SATELLITE
Severe storm detection with passive 37 GHz observations 15 p2596 N85-25997
Satellites and politics: Weather, communications, and earth resources 23 p4057 N85-35144

NIMBUS 5 SATELLITE
Analysis of selective chopper radiometer data
[NASA-CR-175157] 12 p1895 N85-21894

NIMBUS 7 SATELLITE
Coastal Zone Color Scanner (CZCS): Imagery of near-surface phytoplankton pigment concentrations from the first coastal ocean dynamics experiment (CODE-1), March - July 1981
[NASA-CR-174169] 04 p0542 N85-13447
Bio-optical variability in the Alboran Sea as assessed by Nimbus-7 coastal zone color scanner
[AD-A147809] 07 p0989 N85-16281
Data report on variations in the composition of sea ice during MIZEX/East'83 with the Nimbus-7 SMMR
[NASA-TM-86170] 09 p1342 N85-18443
Atlas of relectance patterns for uniform earth and cloud surfaces (NIMBUS-7ERB-81 days)
[PB85-116382] 12 p1891 N85-21870
NIMBUS-7 SBUV (Solar Backscatter Ultraviolet) observations of solar UV spectral irradiance variations caused by solar rotation and active-region evolution for the period November 7, 1978 - November 1, 1980
[NASA-CR-175544] 12 p1962 N85-22334
Validation of the ERBE scanner scene identification methodology: Analysis with Nimbus-7 ERB data
[NASA-CR-172596] 16 p2832 N85-27466
MIZEX, 1984, NASA CV-990 flight report
[NASA-TM-86216] 19 p3290 N85-30451

NIMPHE (ENGINE)
U HYDRAZINE ENGINES

NIOBATES
NT LITHIUM NIOBATES

NIOBIUM
Columbium chamber fabrication study
[AD-A145230] 01 p0017 N85-10102
The oxidation behaviour of a 20 percent Cr/25 percent Ni/Nb stabilized stainless steel in carbon dioxide at high temperatures and its improvement by cerium and yttrium
[AERE-R-11228] 01 p0029 N85-10182
Review: Role of refractory metal alloys in fusion reactor applications
[AERE-R-11317] 03 p0422 N85-12695
Flux-line pinning by the grain boundary in niobium bicrystals
[DE84-016668] 04 p0570 N85-13638
Surface studies of Nb, its compounds, and coatings
[DE84-017353] 06 p0868 N85-15516
Stability of amorphous metals on semiconductor substrates
[DE84-017256] 09 p1295 N85-18134
Transverse microstructure of an oxide scale formed on a 20 % Cr/25 % Ni niobium stabilized stainless steel
[AERE-R-11034] 12 p1804 N85-21315
Spectral evaluation of irregularity of superconducting coaxial cables 13 p2062 N85-23000
Studies of deformation in niobium by X-ray topographic methods
[AD-A150726] 14 p2427 N85-24965
Positron annihilation studies of vacancy formation in tungsten, chromium, and niobium
[DE85-006837] 16 p2871 N85-27710
Submerged arc welding of new Czechoslovak micro-alloy steels
[BLL-BISI-TRANS-22193-(9022.06)] 17 p2972 N85-28356
Microstructures and mechanical properties of microalloyed medium carbon steels 19 p3238 N85-30074
Long range ordered alloys modified by addition of niobium and cerium
[DE85-011661] 20 p3431 N85-31285
A positron annihilation Doppler broadening study of niobium
[DE85-010287] 20 p3527 N85-31936
Evaluated nuclear-data file for niobium
[DE85-012095] 21 p3704 N85-33009
Shape memory effect in uranium-niobium alloys below room temperature
[DE85-012964] 23 p3916 N85-34266
Fast-neutron interaction with niobium
[DE85-011471] 24 p4150 N85-35731

NIOBIUM ALLOYS
Thermodynamics of decarburization of niobium-bearing high-alloy melts
[BLL-M-35726-(5828.4)] 02 p0175 N85-11169
Calculation of critical temperature for Nb-Cu multilayer film superconductor
[AD-A144321] 02 p0274 N85-11766
Characterization of Nb-8 wt % Al wires by analytical electron microscopy
[DE85-002726] 10 p1442 N85-19086
Effect of reduction of strategic Columbium addition in 718 Alloy on the structure and properties
[NASA-CR-174841] 12 p1805 N85-21320
Reaction of amorphous NiNb films with crystalline metal overlayers
[DE85-005483] 13 p2024 N85-22680
Decomposition of VTAN alloy solid solution upon irradiation and thermal aging 13 p2029 N85-22712
High temperature antifriction properties of Ti sub 1-sub xNb sub x C sub 0.5N sub 0.5 alloys 13 p2029 N85-22715
Effect of oxygen on mechanical properties of Nb-V alloy
[DE85-002681] 14 p2256 N85-23982
Special purpose materials for fusion application
[DE85-006346] 14 p2424 N85-24950
Effect of protective atmosphere composition on durability of welded joints of niobium alloys 15 p2502 N85-25432
The microstructural state of Nb3Sn in a multifilamentary titanium doped bronze-process wire
[DE85-010079] 19 p3240 N85-30089
Critical current density and microstructural state of an internal tin multifilamentary superconducting wire
[DE85-009666] 22 p3761 N85-33308
Experimental attempt to achieve microstructure variations through temperature/time permutations for a nonwrought powder metallurgy uranium-6 niobium alloy
[DE85-013166] 23 p3916 N85-34272

NIOBIUM CARBIDES
Possibility of producing monolithic composite materials based on niobium carbide 13 p2028 N85-22707

NIOBIUM COMPOUNDS
NT NIOBIUM CARBIDES
NT NIOBIUM OXIDES
NT NIOBIUM STANNIDES
Phonon anomalies in superconducting transition metal compounds --- lanthanum and niobium compounds 03 p0426 N85-12716
Surface studies of Nb, its compounds, and coatings
[DE84-017353] 06 p0868 N85-15516
Short range order-long range order in superconducting materials
[AD-A148764] 08 p1227 N85-17724
Application of NbN films to the development of very high field superconducting magnets
[DE85-002729] 10 p1585 N85-19867
Magnetization measurements on multifilamentary Nb3Sn and NbTi conductors
[DE85-001237] 11 p1737 N85-20923
Critical current measurements on an NbTi superconducting wire standard reference material
[PB85-116594] 13 p2066 N85-22906
Thin films properties of sputtered niobium silicide on SiO2, Si3N4 and on n+ poly-Si
[AD-A152378] 17 p2952 N85-28228

NIOBIUM OXIDES
Electrochromic and thermochromic materials for solar energy applications with emphasis on niobium and vanadium oxides
[DE85-010630] 19 p3249 N85-30147

NIOBIUM STANNIDES
Properties of Ti alloyed multifilamentary Nb3Sn wires by internal tin process
[DE85-003212] 12 p1941 N85-22191

NITINOL ALLOYS
Nitinol devices, phase 2, integration of slip ring system and tracking mechanism with memory drive
[BMFT-FB-W-84-032] 05 p0619 N85-13959
Production of shaped parts of NITINOL alloys by solid-state sintering
[AD-A152089] 16 p2749 N85-26966

NITRAMINE PROPELLANTS
Transition to detonation from rapid-compression (ramp-waves) generated in a burning porous bed
[AD-P004345] 10 p1455 N85-19169
Chemical kinetics of gas phase decomposition products of nitramine propellants 13 p2003 N85-22559
Kinetics of mechanism of the thermal decomposition of dimethylnitramine and dimethylnitrosamine 13 p2004 N85-22560

Study on the combustion of nitramine propulsion powder up to 1500 MPa and comparison of the performance with that of classical propulsion powders
[ISL-CO-203/83] 14 p2264 N86-24025
Analysis of deflagration to detonation transition in high-energy solid propellants 16 p2757 N86-27010

NITRATE ESTERS
Morbidity and mortality associated with exposure to Otto Fuel II in the U.S. Navy 1966-1979
[AD-A148726] 09 p1363 N85-18574

NITRATES
NT AMMONIUM NITRATES
NT CELLULOSE NITRATE
NT DINITRATES
NT HYDRAZINE NITRATE
NT PETN
NT SODIUM NITRATES
Denitrification-efficiencies of alternate carbon sources
[AD-A148029] 08 p1119 N85-17050
Meteorological support for the 1983 Deep Creek, Maryland experiment
[DE85-002816] 11 p1678 N85-20575
Applicability of laboratory kinetics studies to the evaluation of aqueous phase atmospheric oxidation of sulfur-4
[DE85-000586] 12 p1883 N85-21819
The crystal and molecular structure of a new propellant compound: Triaminoguanidium Azide Nitrate (TAZN)
13 p2002 N85-22551
Geographic variation in the relationships of temperature, salinity or sigma sub t versus plant nutrient concentrations in the world ocean --- silicic acid, nitrate, and phosphate concentration
[NASA-CR-175621] 13 p2140 N85-23267
Influence of preliminary thermomechanical treatment on depth and hardness of nitrided layers
[BLL-BISI-TRANS-22488-(9022.06)]
17 p2929 N85-28078
Tendency of selected low-carbon steels to corrosion cracking in nitrates
[BLL-BISI-TRANS-22282-(9022.06)]
18 p3073 N85-29006
Environmental surveillance at Los Alamos during 1984
[DE85-011886] 22 p3811 N85-33605
Throughfall rate and chemistry studies: Whiteface Mountain
[DE85-012407] 23 p3947 N85-34484

NITRATION
The nitrogen cycle: Atmosphere interactions
05 p0653 N85-14191
Mononitration of durene
[NASA-TM-77774] 06 p0765 N85-14892
Nitrolysis of the CN single bond and related chemistry of nitro and nitroso groups
[AD-A151753] 15 p2505 N85-25453

NITRIC ACID
Production of concentrated nitric acid
[DE84-017191] 09 p1293 N85-18121
Stratospheric concentration of nitric acid, ozone and carbonyl sulfide: Measurement of nitric acid absorption in the Q branch of the V4 band as a function of temperature
[ESA-TT-864] 09 p1355 N85-18524
Meteorological support for the 1983 Deep Creek, Maryland experiment
[DE85-002816] 11 p1678 N85-20575
Studies of the mechanisms and rates with which nitrogen species are incorporated into cloud water and precipitation
[PB85-144360] 12 p1898 N85-21914
An analysis of issues concerning acid rain, report to the Congress of the United States
[TI85-901070] 15 p2589 N85-25959
Analysis and model/data comparisons of large-scale releases of nitrogen tetroxide
[DE85-009989] 18 p3133 N85-29406
Determination of the association constant for pertechnetic acid
[DE85-010224] 19 p3235 N85-30057

NITRIC OXIDE
Stability evaluation of sulfur dioxide nitric oxide and carbon monoxide gases in cylinders
11 p1648 N85-20387
Variation of derived mesospheric nitric oxide in relation to wind and temperature in winter
11 p1658 N85-20452
Coupling between the thermosphere and the stratosphere: The role of nitric oxide
11 p1662 N85-20472
Middle atmosphere NO and NO2 observed by means of the Spacelab one grille spectrometer
[AERONOMICA-ACTA-A-293-1984]
11 p1680 N85-20588
Laser studies of chemical dynamics at the gas-solid interface
[DE84-017590] 11 p1736 N85-20920
Kinetics of nitric oxide formation in laminar and turbulent methane combustion
[PB85-149696] 12 p1804 N85-21313
The source of stratospheric NO and N2O
[NASA-CR-175713] 15 p2586 N85-25956
An analysis of issues concerning acid rain, report to the Congress of the United States
[TI85-901070] 15 p2589 N85-25959
Slow chemistry effects in a turbulent mixing layer
20 p3424 N85-31252
Static high pressure study of nitric oxide chemistry: Proposed mechanism for nitric oxide detonation
[DE85-010795] 22 p3746 N85-33220
The 1984 environmental monitoring program report for Idaho National Engineering Laboratory site
[DE85-011209] 22 p3812 N85-33611
Dissociative and double photoionization cross sections of NO from threshold to 120 A
[NASA-CR-176185] 24 p4147 N85-35713

NITRIDES
NT ALUMINUM NITRIDES
NT BORON NITRIDES
NT SILICON NITRIDES
NT TITANIUM NITRIDES
NT ZIRCONIUM NITRIDES
Corrosion resistance of nitrided low-alloy steels
[PB84-235027] 04 p0477 N85-13040
Application of NbN films to the development of very high field superconducting magnets
[DE85-002729] 10 p1565 N85-19867
The behaviour of nitride inclusions in nickel-base alloys
[BLL-BISI-TRANS-22396-(9022.06)]
17 p2927 N85-28058
Technological apparatus for laser treatment of materials 17 p2944 N85-28174
Thermodynamic data for mineral technology
[PB85-184331] 22 p3803 N85-33560

NITRIDING
Change in the nitrogen content when nitrided alloys are heated
[BLL-M-35946-(5828.4)] 05 p0615 N85-13929
Nitriding of titanium and its alloys by N2, NH3 or mixtures of N2 + H2 in a dc arc plasma at low pressures (or = to torr)
[NASA-TM-83803] 06 p0814 N85-15168
Ion-beam nitriding of steels
[NASA-CASE-LEW-14104-1] 12 p1805 N85-21324
Slip casting and nitridation of silicon powder
[NASA-TM-77609] 12 p1816 N85-21406
Thermodynamic analysis of the plasma nitriding of ferrovanadium
[BLL-BISI-TRANS-22237-(9022.06)]
17 p2924 N85-28032
An investigation of cementation and carbonitriding by means of ionic bombardment
[BLL-OA-TRANS-3203-(6196.300)]
20 p3429 N85-31265
Nitridation of SiO2 for surface passivation
20 p3480 N85-31627
Nitriding of super alloys for enhancing physical properties
[DE85-005782] 23 p3917 N85-34275

NITRILES
NT ACRYLONITRILES
Development of nitrile rubbers and foams having a high static modulus and low creep
[BR91465] 14 p2259 N85-24001
Microstructural characteristics during the controlled solidification of a binary system
[DE85-005200] 15 p2507 N85-25461
Processable and stable conductive polymers
[AD-D011664] 19 p3249 N85-30143

NITRO COMPOUNDS
NT NITROBENZENES
NT NITROGUANIDINE
NT NITROPROPANE
NT TRINITROTOLUENE
Acute oral toxicity (LD50) of 4-nitrophenyl monochloromethyl (Phenyl) phosphinate (TA009) in male rats
[AD-A148337] 08 p1192 N85-17513
Preparations of methoxynitrophenazines and their photoconductivities
[NASA-TM-77775] 14 p2247 N85-23929
Electrochemistry of Hexanitrosobenzene (HNAB)
[DE85-010807] 21 p3585 N85-32171
Sensitivity and performance characterization of DINGU
[DE85-010750] 22 p3754 N85-33269
Experimental studies of chemical reactivity during shock initiation of hexanitrostilbene
[DE85-011726] 22 p3754 N85-33270
Ethylenediamine salt of 5-nitrotetrazole and preparation
[DE85-005736] 23 p3923 N85-34306

NITROBENZENES
NT TRINITROTOLUENE
Hazardous air pollutants: Wet removal rates and mechanisms
[PB85-138626] 12 p1887 N85-21842
Single-pulse Raman and photoacoustic spectroscopy studies of Triaminotrinitrobenzene (TATB) and related compounds
[DE85-010072] 18 p3084 N85-29078
Electrochemistry of Hexanitrosobenzene (HNAB)
[DE85-010807] 21 p3585 N85-32171

NITROCELLULOSE
U CELLULOSE NITRATE

NITROGEN
NT LIQUID NITROGEN
NT NITROGEN IONS
NT NITROGEN ISOTOPES
NT NITROGEN 15
Treating silicon carbide sinter by heating in nitrogen
[NASA-TM-77601] 01 p0021 N85-10130
Influence of nitrogen on the sensitization, corrosion, mechanical, and microstructural properties of austenitic stainless steels
[DE84-015134] 01 p0028 N85-10177
Electron energy loss rates in N-2, O-2 and air
[AD-A145158] 01 p0072 N85-10476
Feasibility of the electrochemical method of determining nitrogen content in metallic melts
[BLL-M-35730-(5828.4)] 03 p0330 N85-12124
Lubricity of well-characterized jet and broad-cut fuels by ball-on-cylinder machine
[NASA-TM-83807] 03 p0339 N85-12183
Diffusion of gases in porous solids: Simulation and measurements
[DE84-016292] 04 p0500 N85-13191
Effects of acid rain on plant microbial associations in California
[PB84-242122] 04 p0532 N85-13404
Change in the nitrogen content when nitrided alloys are heated
[BLL-M-35946-(5828.4)] 05 p0615 N85-13929
The nitrogen cycle: Atmosphere interactions
05 p0653 N85-14191
Terrestrial nitrogen cycles: Some unanswered questions 05 p0653 N85-14192
Recent studies of the ocean nitrogen cycle
05 p0653 N85-14193
Shock testing of a nitrogen tank (Cryo diffusion type 220 VLR) on the middle weight shock stand
[NASA-TM-77747] 06 p0817 N85-15183
The low-energy secondary cosmic ray flux: Detectors in iron meteorites 06 p0887 N85-15835
Flow of nitrogen-pressurized Halon 1301 in fire extinguishing systems
[NASA-CR-174271] 07 p0900 N85-15701
Nitrogen flushing during exposure of large Schmidt telescope plates 07 p0963 N85-16109
Variation of oxygen and nitrogen abundances in the galaxy 08 p1248 N85-17878
Effects of heteroatom substituents on the properties of 1,2-dioxetanes
[AD-A146727] 09 p1290 N85-18100
The reaction of oxygen-nitrogen mixtures with granular activated carbons below the spontaneous ignition temperature
[AD-A149041] 10 p1434 N85-19009
Growth and reflectance characteristics of winter wheat canopies
[E85-10080] 10 p1505 N85-19494
Role of nitrogen in improving resistance to localized corrosion in austenitic stainless steels
11 p1609 N85-20115
Stability evaluation of sulfur dioxide nitric oxide and carbon monoxide gases in cylinders
11 p1648 N85-20387
Nitrogen control of photosynthetic protein synthesis
[DE85-003513] 11 p1690 N85-20623
Comments on the origins and variations of carbon and nitrogen in the ISM of galaxies as evident from IUE spectroscopy of H 2 regions 11 p1745 N85-20973
Molecular dynamics of propellant gases, part 2
13 p2002 N85-22552
An atlas of nitrogen-broadened water vapor spectra from 500 to 5000 cm(-1), volume 1
[AD-A150527] 13 p2018 N85-22850
Statistical comparison of pooled nitrogen washout data of various altitude decompression response groups
[NASA-TM-58285] 15 p2839 N85-26275
A comprehensive strategy for saturation decompression with nitrogen-oxygen
[AD-A151800] 16 p2841 N85-27520
Systematic nomenclature of the nitrogen, oxygen and sulfur functional polycyclic aromatic hydrocarbons
[DE85-007426] 17 p2916 N85-27974

Some amplification by relaxation processes in nitrogen and mixtures of nitrogen with helium and hydrogen
[AD-A153620] 18 p3071 N85-28962
Heat of mixing experiments for liquified gases
[PB85-183697] 18 p3084 N85-29081
Screening Prosopis (mesquite) species for biofuel production on semi-arid lands
[DE85-010048] 19 p3302 N85-30471
Flash pyrolysis of biomass with reactive and non-reactive gases
[DE85-010962] 19 p3306 N85-30496
Calculation of the propagation constant in a rectangular waveguide containing an inhomogeneous longitudinally magnetized plasma
[DE85-012072] 21 p3577 N85-32250
Biogeochemical cycling and remote sensing
21 p3659 N85-32733
Solar cycle variations of the anomalous cosmic ray component
[PAPER-SH-4.6-2] 21 p3715 N85-33057
Carbon and nitrogen in the deep Earth
21 p3721 N85-33085
Electrode erosion in arc discharges at atmospheric pressure
[NASA-TM-87067] 23 p3903 N85-34178
Oxygen analyzer
[DE85-006002] 23 p3935 N85-34392
Determination of individual tolerance in hyperbaric oxygen 23 p3954 N85-34507
Nitrogen analysis by chemiluminescence
[AD-A156197] 24 p4083 N85-35308
Detection threshold energy of high energy cascade showers using thermoluminescence PTFE-sheet and hot-gas reader
[HE-7.1-5] 24 p4213 N85-36159

NITROGEN COMPOUNDS
NT ALUMINUM NITRIDES
NT AMIDES
NT AMMONIA
NT AMMONIUM NITRATES
NT ATROPINE
NT AZIDES (INORGANIC)
NT AZIDES (ORGANIC)
NT AZO COMPOUNDS
NT BORON NITRIDES
NT CELLULOSE NITRATE
NT CYANO COMPOUNDS
NT DIISOCYANATES
NT DINITRATES
NT HYDRAZINE NITRATE
NT IMIDES
NT IMINES
NT ISOCYANATES
NT LIQUID AMMONIA
NT NITRATE ESTERS
NT NITRATES
NT NITRIC ACID
NT NITRIC OXIDE
NT NITRIDES
NT NITRO COMPOUNDS
NT NITROBENZENES
NT NITROGEN DIOXIDE
NT NITROGEN OXIDES
NT NITROGEN TETROXIDE
NT NITROGUANIDINE
NT NITROPROPANE
NT NITROSO COMPOUNDS
NT NITROUS OXIDES
NT PETN
NT POLYIMIDES
NT QUINOLINE
NT RDX
NT SILICON NITRIDES
NT SODIUM NITRATES
NT THIAZINE (TRADEMARK)
NT TITANIUM NITRIDES
NT TRIAMINOGUANIDINIUM AZIDE
NT TRINITROTOLUENE
NT TRYPTOPHAN
NT UREAS
NT ZIRCONIUM NITRIDES

Theoretical studies in molecular fragmentation: Processes, energetics and diagnostics
[AD-A146310] 03 p0418 N85-12673
Boron-nitrogen polymers. 1: Mechanistic studies of borazine pyrolyses
[AD-A146470] 06 p0771 N85-14933
Non-photochemical interactions of sulfur and nitrogen compounds in acid deposition
[DE84-016141] 10 p1513 N85-19548
Electrostatic potentials: A new method for interpreting and predicting molecular reactivities and for designing synthetic pathways. Applications to nitroaromatics, nitramines and nitrated
[AD-A150120] 12 p1801 N85-21298
Gas-liquid chemistry of natural waters, volume 2
[DE85-002457] 12 p1864 N85-21823
Adsorption behaviour of nitrogen compounds on to porous polymer beads and applications to atmospheric sampling
[BLL-DRIC-TRANS-7399-(3623.68)]
13 p2036 N85-22753
Preparation of nitrocompounds
[AD-A153687] 18 p3071 N85-28993
Mathematical model of the nitrogen cycle in a nonsaturated area of cultivated soil
20 p3478 N85-31610
Synthesis of energetic materials
[AD-A154687] 21 p3571 N85-32210

NITROGEN DIOXIDE
Short-term human respiratory effects of nitrogen dioxide: Determination of quantitative dose-response profiles. Phase 2: Exposure of asthmatic volunteers to 4 PPM NO2
[PB85-104388/GAR] 07 p1017 N85-16462
National Performance Audit Program ambient air audits of analytical proficiency
[PB85-138204] 11 p1680 N85-20588
Middle atmosphere NO and NO2 observed by means of the Spacelab one grille spectrometer
[AERONOMICA-ACTA-A-293-1984]
11 p1680 N85-20588
Research and development of new instruments
16 p2824 N85-27418
Lidar system using polarization discrimination techniques for molecular air pollution monitoring
19 p3308 N85-30504
Development of a technique for in situ detection of stratospheric nitrogen dioxide 19 p3312 N85-30534
Facility for large-scale hazardous gas testing
[DE85-011852] 21 p3564 N85-32169
The 1984 environmental monitoring program report for Idaho National Engineering Laboratory site
[DE85-011209] 22 p3812 N85-33611

NITROGEN FIXATION
U NITROGENATION

NITROGEN IONS
Oxygen-nitrogen interactions in ion-implanted silicon
[DE85-010091] 18 p3195 N85-29819
Electrical properties of bulk grown nitrogen doped silicon
[AD-A155471] 21 p3581 N85-32266

NITROGEN ISOTOPES
NT NITROGEN 15
Evidence for pairing of implanted nitrogen in silicon
[DE84-015822] 06 p0968 N85-15517
A spectacular nitrogen isotope anomaly in Bencubbin
15 p2683 N85-26569
Control technology for radioactive emissions to the atmosphere at US Department of Energy facilities: The Los Alamos Meson Physics Facility
[DE85-011402] 22 p3811 N85-33609
Implications of new measurements of O-16 + p + C-12,13, N-14,15 for the abundances of C, N isotopes at the cosmic ray source
[OG-4.3-2] 22 p3878 N85-34027

NITROGEN LASERS
High repetition rate nitrogen ion laser
02 p0201 N85-11340
Formation of lattice defects by nitrogen laser exposure in A2B6 semiconductors with wide forbidden band
02 p0258 N85-11682
Construction, testing of 1-MW nitrogen laser
06 p1140 N85-17182
An experimental technique for the study of velocity profiles in a laminar jet using a pulsed nitrogen laser
[AD-A151496] 15 p2556 N85-25771
Investigation of influence of gas exit modes on characteristics of N2O - N2 - He discharge laser
21 p3684 N85-32868

NITROGEN METABOLISM
Effect of high ammonia content in closed environment on some parameters of human nitrogen and carbohydrate metabolism against background of a controlled diet
12 p1903 N85-21948

NITROGEN OXIDES
NT NITRIC OXIDE
NT NITROGEN DIOXIDE
NT NITROGEN TETROXIDE
NT NITROUS OXIDES
Future scenarios and ozone change
[DE84-014781] 01 p0085 N85-10573
Estimation of the potential and probable source regions for acid precipitation
[DE84-015119] 02 p0225 N85-11472
A 2-dimensional description of potential perturbations to the ozone layer due to NOx and H-2-O aircraft emissions
[AD-A146292] 03 p0392 N85-12511
Direct measurements of nitrous acid, nitrogen dioxide and formaldehyde in auto exhaust by differential optical absorption spectroscopy
[PB84-229269] 06 p0767 N85-14905
NOx emissions near a heat pump with gas motor
[BLL-WH-782-(9091.9F)] 07 p0995 N85-16311
Impact of aircraft emissions on air quality in the vicinity of airports. Volume 4. Nitrogen dioxide and hydrocarbons
[AD-A148253] 08 p1180 N85-17436
Optical studies of nitrogen oxides in the stratosphere
08 p1183 N85-17455
Evaluation of the particulate levels occurring under 1.0/1.2 g/mi nitrogen oxide standards for light duty diesel vehicles and light duty diesel trucks
[PB85-115939/GAR] 09 p1350 N85-18494
MAP/GLOBUS campaign 1983
11 p1658 N85-20447
Evaluation of recent SO/sub x/ and NO/sub x/ emission inventories
[DE85-002649] 11 p1677 N85-20570
National Acid Precipitation Assessment Program. Report to the President and Congress (1983)
[PB85-116713] 11 p1679 N85-20581
Results of recent large-scale NH3 and N2O4 dispersion experiments
[DE85-004968] 15 p2589 N85-25980
Kinetic energies of fragment ions produced by dissociative photoionization of NO
[NASA-CR-175721] 15 p2647 N85-26327
Is there more than one steady state for NOx?
15 p2687 N85-26593
Transformation of nitrogen oxides while sampling combustion products
[AD-A152184] 16 p2746 N85-28945
Absolute calibrations of SO2 and NO analyzers by photographic methods
[DFVLR-MITT-85-02] 17 p2994 N85-29504
Analysis and model/data comparisons of large-scale releases of nitrogen tetroxide
[DE85-009989] 18 p3133 N85-29406
Investigation of the reaction system NOX/ClOX/HOX under tropospheric and stratospheric conditions
[BPT-11/84] 18 p3137 N85-29427
Assessment of the role of nitrogen oxides in nonurban ozone formation
[PB85-173680] 19 p3311 N85-30524
Historic emissions of sulfur and nitrogen oxides in the U.S. from 1900 to 1980. Volume 1: Results
[PB85-191195] 20 p3487 N85-31674
Historic emissions of sulfur and nitrogen oxides in the U.S. from 1900 to 1980. Volume 2: Data
[PB85-191203] 20 p3487 N85-31675
Emergency modeling of hazardous air pollutants
[AD-A155441] 21 p3614 N85-32461
Technology of off-gas treatment for liquid-fed ceramic melters
[DE85-012467] 22 p3812 N85-33610
Atmospheric reaction products from hazardous air pollutant degradation
[PB85-185841] 22 p3813 N85-33620
Forecasting future industrial SO2 and NC/sub x/ emissions, revised 23 p3947 N85-34461
Review of US NOx abatement technology
[PB85-193522] 24 p4114 N85-35501
Atmospheric nitrogen oxides: Their detection and chemistry
[PB85-193910] 24 p4114 N85-35502
The measurement of nitrogen oxide (NO, NO2) exchange over plant/soil surfaces
[CSIRO-DAR-TP-8] 24 p4127 N85-35587

NITROGEN PLASMA
SWIR and visible atomic emission from laser-produced oxygen and nitrogen plasmas
[AD-A147528] 07 p1045 N85-16841
A 50-kW electric-discharge CO2 laser
[AD-A149779] 12 p1857 N85-21644
Frictional and structural characterization of ion-nitrided low and high chromium steels
[NASA-TM-86991] 13 p2098 N85-23065
Thermodynamic analysis of the plasma nitriding of ferrovanadium
[BLL-BISI-TRANS-22237-(9022.06)]
17 p2924 N85-29032
Recombination and ionization in a nitrogen plasma
[AD-A155426] 22 p3845 N85-33813

NITROGEN TETROXIDE
Atmospheric dispersion of hypergolic liquid rocket fuels, volume 1
[AD-A149597] 12 p1817 N85-21399
Evaluation of source strength and dispersion model predications with data from large nitrogen tetroxide field experiments
[DE85-011855] 23 p3947 N85-34465

NITROGEN 15
Stable isotope studies
[DE84-016752] 04 p0582 N85-13583
Evidence for pairing of implanted nitrogen in silicon
[DE84-015822] 06 p0858 N85-15517
NITROGENATION
Alloying specialty low carbon silicon-bearing steel with nitrogen
[BLL-M-35707-(5828.4)] 02 p0175 N85-11170
Recent studies of the ocean nitrogen cycle
05 p0653 N85-14193
Effects of acid rain on forest nutrient status
[DE85-012486] 23 p3947 N85-34463
NITROGUANIDINE
Electron density distribution analysis for nitroguanidine
[DE85-009598] 23 p3989 N85-34603
NITROLYSIS
Nitrolysis of the CN single bond and related chemistry of nitro and nitroso groups
[AD-A151753] 15 p2505 N85-25453
NITROPROPANE
Multiple product channels in the collision free UV photodissociation of 2-nitropropane
[AD-A150886] 14 p2251 N85-23951
NITROSO COMPOUNDS
Nitrolysis of the CN single bond and related chemistry of nitro and nitroso groups
[AD-A151753] 15 p2505 N85-25453
NITROUS OXIDES
Raman and fluorescence spectroscopy in a methane-nitrous oxide laminar flame
[AD-A146092] 03 p0328 N85-12111
Continued research in mesoscale air pollution simulation modeling. Volume 5: Refinements in numerical analysis, transport, chemistry, and pollutant removal
[PB85-137362] 11 p1680 N85-20585
Non-precipitating cumulus cloud study
[DE85-002352] 12 p1896 N85-21902
Modeling of chemical transformations of SO(x) and NO(x) in the polluted atmosphere: An overview of approaches and current status
[PB85-173169] 20 p3487 N85-31677
Review of US NOx abatement technology
[PB85-193522] 24 p4114 N85-35501
The measurement of nitrogen oxide (NO, NO2) exchange over plant/soil surfaces
[CSIRO-DAR-TP-8] 24 p4127 N85-35587
NMR
U NUCLEAR MAGNETIC RESONANCE
NOAA E
U NOAA 8 SATELLITE
NOAA SATELLITES
NT NOAA 6 SATELLITE
NT NOAA 7 SATELLITE
NT NOAA 8 SATELLITE
Report of the First Session of the International Working Group on Data Management for the International Satellite Cloud Climatology Project (ISCCP)
[WCP-42] 01 p0073 N85-10483
Cloud cover sampling capability of various satellite combinations for ISCCP 01 p0073 N85-10484
Monitoring and mapping global vegetation cover using data from meteorological satellites
05 p0656 N85-14211
An interactive technique for satellite-improved rainfall monitoring 05 p0658 N85-14224
Environmental data inventory for the antarctic area
[PB85-107944] 06 p0819 N85-15195
Civil weather satellite systems
11 p1711 N85-20768
The development of image processing of NOAA AVHRR data and its application to sea surface temperature
12 p1895 N85-21891
Scientific requirements for ozone measurements
13 p2105 N85-23113
The ARGOS system status report after 2 years operation 14 p2237 N85-23870
System performance, data distribution and technical files — ARGOS project 14 p2237 N85-23871
The ARGOS system status report
14 p2239 N85-23884
Automatic weather stations in Antarctica
14 p2324 N85-24360
The ARGOS system after 3 years operation
14 p2325 N85-24368
The use of TOMS data in evaluating and improving the total ozone from TOVS measurements
[NOAA-TR-NESDIS-23] 22 p3814 N85-33626
NOAA 6 SATELLITE
Image texture study for the operational meteorological satellites NOAA 6 and NOAA 7 and its variation with time. Application to the Beauce region
[ENST-84E009] 05 p0661 N85-14249
Observation of a westward travelling surge from satellites at low, medium and high altitudes
[NASA-TM-87434] 09 p1342 N85-18442
The ARGOS system main characteristics — satellite based localization 14 p2325 N85-24367
The ARGOS program — satellite based localization
14 p2397 N85-24775
Location and data collection satellite system ARGOS. User's guide — satellite based localization
16 p2816 N85-27371
First results of oceanography utilization of infrared high resolution picture transmission images
[KNMI-TR-59] 16 p3151 N85-29511
NOAA 7 SATELLITE
Image texture study for the operational meteorological satellites NOAA 6 and NOAA 7 and its variation with time. Application to the Beauce region
[ENST-84E009] 05 p0661 N85-14249
The ARGOS system main characteristics — satellite based localization 14 p2325 N85-24367
The ARGOS program — satellite based localization
14 p2397 N85-24775
Availability of the ARGOS system based on the orbital characteristics of the TIROS-N satellites — oceanographic/meteorological data
16 p2813 N85-27352
Contribution of the NOAA-7 and 8 and ARGOS partnership to white tuna fishing in the northeast Atlantic
16 p2813 N85-27355
Location and data collection satellite system ARGOS. User's guide — satellite based localization
16 p2816 N85-27371
Information relative to cartography and geodesy. Series 2: Translations, number 42, volume 1
[ISSN-0469-4244] 16 p3123 N85-29338
Digital image mapping of Antarctica using NOAA-7 AVHRR imagery 16 p3124 N85-29340
First results of oceanography utilization of infrared high resolution picture transmission images
[KNMI-TR-59] 16 p3151 N85-29511
NOAA 8 SATELLITE
Availability of the ARGOS system based on the orbital characteristics of the TIROS-N satellites — oceanographic/meteorological data
16 p2813 N85-27352
Contribution of the NOAA-7 and 8 and ARGOS partnership to white tuna fishing in the northeast Atlantic
16 p2813 N85-27355
First results of oceanography utilization of infrared high resolution picture transmission images
[KNMI-TR-59] 16 p3151 N85-29511
SARSAT 121.5/243 MHz technical evaluation
20 p3405 N85-31126
NOBLE GASES
U RARE GASES
NOBLE METALS
NT GOLD
NT RUTHENIUM
NT SILVER
Conductor structure for thick film electrical device
[AD-D011240] 01 p0043 N85-10281
The replacement of precious metal thick film inks using conductive polymer technology. Phase 1: Feasibility study
[AD-A147814] 07 p0933 N85-15913
Comparisons between computed and observed grain boundary structures and properties in metals
[DE85-002596] 10 p1442 N85-19085
Noble metals as incipient transition metals
[DE85-013263] 24 p4060 N85-35286
NOCTILUCENCE
U LUMINESCENCE
NOCTILUCENT CLOUDS
Interaction of large meteoroids with the atmosphere
11 p1656 N85-20431
Cold Arctic Mesopause Project (CAMP): Scientific objectives 11 p1656 N85-20433
NOCTURNAL VARIATIONS
Relationship between model complexity and data base quality for complex terrain tracer experiments
[DE84-015022] 04 p0539 N85-13429
Comparison between tracer measurements and model calculations for nighttime drainage flows in complex terrain
[DE84-014709] 04 p0539 N85-13431
Atmospheric studies in complex terrain
[DE84-006553] 05 p0676 N85-14345
Statistical relationships between meteorological data stations and implications to diagnostic models in complex terrain
[DE84-014360] 06 p0839 N85-15328
On the formation of the nocturnal coastal surface wind speed maximum 09 p1356 N85-18528
Categorization of nocturnal drainage flows within the Brush Creek valley in western Colorado and the variability of sigma theta in complex terrain
[DE85-011291] 19 p3300 N85-30461
VALMET: A valley air pollution model
[DE85-010820] 21 p3614 N85-32483
NODULES
Unsinkability of ferromanganese nodules
06 p0819 N85-15202
Exploring ocean's mineral wealth
07 p0960 N85-16227
NOE NAVIGATION
U NAP-OF-THE-EARTH NAVIGATION
NOISE
Study on spectral/radiometric characteristics of the Thematic Mapper for land use applications
[E85-10021] 02 p0218 N85-11434
NBS (National Bureau of Standards) and WR82 and WR90 reference noise standards
[PB84-235704] 07 p0942 N85-15977
Investigation of dynamic noise affecting geodynamics information in a tethered subsatellite
[NASA-CR-176031] 20 p3476 N85-31602
Visual phenomena produced by binocularly disparate dynamic visual noise
[AD-A154758] 21 p3683 N86-32757
NOISE (SOUND)
NT AERODYNAMIC NOISE
NT AIRCRAFT NOISE
NT ENGINE NOISE
NT JET AIRCRAFT NOISE
NT SONIC BOOMS
NT THERMAL NOISE
Study of annoyance due to urban automobile traffic
[NASA-TM-77514] 01 p0069 N85-10458
Response measurements for two building structures excited by noise from a large horizontal axis wind turbine generator
[NASA-CR-172482] 04 p0556 N85-13552
Wave-wave interactions, microseisms, and infrasonic ambient noise in the ocean
[AD-A146529] 06 p0859 N85-15463
Detection of low frequency impulsive noise from large wind turbine generators
[NASA-CR-172511] 07 p1036 N85-16588
Investigation of dynamic noise affecting geodynamics information in a tethered subsatellite
[NASA-CR-174292] 08 p1174 N85-17405
Computation of noise radiation from a free jet perpendicular to its axis via laser anemometry measurements
[ESA-TT-870] 09 p1379 N85-18669
Effects of overall vibration and noise on operational personnel 10 p1523 N85-19606
Further comparison of wind tunnel and airplane acoustic data for advanced design high speed propeller models
[NASA-TM-86935] 12 p1927 N85-22108
Machine tool vibrations: A review
13 p2102 N85-23104
Transmission of gear noise to aircraft interiors prediction methods 14 p2223 N85-23788
Several specific and nonspecific responses of the human and animal body to ship noise
[NASA-TM-77483] 15 p2615 N85-26116
Contribution of tonal components to the overall loudness, annoyance and noisiness of noise: Relation between single tones and noise spectral shape
[NASA-CR-3892] 15 p2645 N85-26317
Vortex studies relating to boundary layer turbulence and noise
[NASA-TM-87475] 16 p2782 N85-27189
The theoretical response of a vertical line array to wind-generated noise in shallow water
[AD-A151730] 16 p2960 N85-27838
Acoustic noise associated with the MOD-1 wind turbine: Its source, impact, and control
[DE85-002947] 18 p3178 N85-29700
A study of interior noise levels, noise sources and transmission paths in light aircraft
[NASA-CR-172152] 19 p3350 N85-30766
Operational noise data for the LACV-30 air cushion vehicle
[AD-A154063] 19 p3351 N85-30773
Aviation noise effects
[AD-A154319] 19 p3352 N85-30776
Noise in stages and in interstage couplings of various transistor circuits 22 p3765 N85-33334
Some problems in high speed gears and gearing
23 p3923 N85-34312
Generated spiral bevel gears: Optimal machine-tool settings and tooth contact analysis
[NASA-TM-87075] 23 p3937 N85-34405
NOISE ATTENUATION
U NOISE REDUCTION
NOISE ELIMINATION
U NOISE REDUCTION
NOISE GENERATORS
Calibration of noise power transfer standards, measurement uncertainties and long term stability
05 p0650 N85-14095

The development of a 90 GHz solid state noise source
[CD.6600666] 05 p0733 N85-14715
NOISE HAZARDS
U HAZARDS
U NOISE (SOUND)
NOISE INJURIES
Application of the isoenergy principle and the A weighting to evaluate lesion risks due to noise in a military environment
[ISL-CO-231/83] 14 p2390 N85-24720
Auditory impairment and the onset of disability and handicap in noise-induced hearing loss
[ISVR-TR-126] 20 p3507 N85-31801
Noise reduction in the automotive test cell of the Motor Institute of Naples
[REPT-85-RR-361] 20 p3524 N85-31917
NOISE INTENSITY
Human response to vibroacoustic environments of space vehicles
[NASA-TM-86316] 01 p0116 N85-10789
Rules for post-detector detection of weak signals in non-Gaussian noise of unknown power
03 p0344 N85-12218
Investigation on experimental techniques to detect, locate and quantify gear noise in helicopter transmissions
[NASA-CR-3847] 08 p1217 N85-17667
Noise in stages and in interstage couplings of various transistor circuits 22 p3765 N85-33334
NOISE MEASUREMENT
Analysis of noise measured from a propeller in a wake
[NASA-TP-2358] 02 p0274 N85-11788
Airport noise impact prediction and measurement
03 p0367 N85-12476
Study of annoyance due to urban automobile traffic. Annex 4: A catalog of the characteristics of noise at different measuring points
[NASA-TM-77516] 03 p0367 N85-12478
Patterns of behavior in lodgings exposed to traffic noise
[NASA-TM-77750] 03 p0367 N85-12479
Total area of diffusion elements in a reverberation chamber and measured degree of sound absorption
[NRC/CNR-TT-2110] 03 p0415 N85-12653
Evaluation of the Langley 4- by 7-meter tunnel for propeller noise measurements
[NASA-TM-85721] 04 p0558 N85-13553
Coaxial noise measurement circuits
05 p0630 N85-14036
Helicopter noise survey performed at Las Vegas, Nevada, 19-21 January, 1984
[AD-A147392] 07 p1039 N85-16583
Noise measurement flight test: Data-analyses aerospatiale AS-355F TwinStar helicopter
[AD-A147497] 07 p1039 N85-16595
Noise measurement flight test for Boeing Vertol 234/CH 47-d helicopter: Data/analyses
[AD-A148172] 08 p1218 N85-17670
Noise measurement flight test: Data-analyses Aerospatiale AS 350D AStar helicopter
[AD-A148496] 08 p1218 N85-17672
Noise measurement flight test: Data-analyses, Sikorsky S-76A helicopter
[AD-A148525] 08 p1218 N85-17673
A preliminary assessment of environmental noise from large Wind Energy Conversion Systems (WECS) based on experiences from Swedish prototypes
[FFA-TN-1984-48] 09 p1379 N85-18668
Statistical study of anthropogenic seismic noise with IVK-7 computer system 10 p1503 N85-19483
Noise measurement flight test: Data/Analyses, hughes 500 D/E helicopter
[AD-A148110] 14 p2219 N85-23758
Transmission error measurements in gearbox development 14 p2224 N85-23794
Sound propagation studies for a large horizontal axis wind turbine
[NASA-CR-172564] 14 p2415 N85-24904
An experimental study of the noise generated by vaporous cavitation in turbulent shear flows produced by confined orifice plates 15 p2645 N85-26316
Contribution of tonal components to the overall loudness, annoyance and noisiness of noise: Relation between single tones and noise spectral shape
[NASA-CR-3692] 15 p2645 N85-26317
Contribution to the study of equivalent noise source identification in fast cold jets
[ISL-R-114/83] 16 p2661 N85-27645
Analyses of orderly structures in jets and the relationship with emitted noise
[ISL-R-117/83] 16 p2661 N85-27646
Prediction of free-field noise levels from aircraft flyover measurements
[VTH-LR-427] 16 p2661 N85-27647
Measured noise performance of a new method of frequency hopping
[AD-A152679] 17 p2953 N85-28234
A study of interior noise levels, noise sources and transmission paths in light aircraft
[NASA-CR-172152] 19 p3350 N85-30766
Design of a freestanding noise measurement and recording system to predict the intensity and location of electromagnetic radiation from earthquakes
[AD-A155070] 21 p3632 N85-32563
FAA/GAMA (Federal Aviation Administration/General Aviation Manufacturer's Association) propeller aircraft noise test program, Salina Municipal Airport, Salina, Kansas
[AD-A154818] 21 p3699 N85-32983
Overground Excess Sound Attenuation (ESA). Volume 3: Application of ESA data in NOISEFILE
[AD-A154820] 21 p3699 N85-32984
Helicopter noise survey for selected cities in the contiguous US
[AD-A154893] 21 p3699 N85-32985
A theoretical appraisal of the use of ground-plane microphones for aircraft noise measurements
[NPL-AC-103] 22 p3836 N85-33752
A Programmable Automatic Noise Data and Other Related parameter Acquisition system (PANDORA) — wind energy converters 24 p4111 N85-35479
NOISE POLLUTION
Study of annoyance due to urban automobile traffic
[NASA-TM-77514] 01 p0069 N85-10458
Study of annoyance due to urban automobile traffic. Annex 4: A catalog of the characteristics of noise at different measuring points
[NASA-TM-77516] 03 p0367 N85-12478
Patterns of behavior in lodgings exposed to traffic noise
[NASA-TM-77750] 03 p0367 N85-12479
NOISEMAP 4.4 computer program update, operator's manual, addendum 1
[AD-A147091] 07 p1025 N85-16503
Construction and application of a questionnaire for the social scientific investigation of environmental noise effects
[NASA-TM-75492] 10 p1512 N85-19544
Development of guidelines for setting physiological and hygienic standards for noise levels in aerospace medicine 19 p3323 N85-30584
The timing of noise-sensitive activities in residential areas
[NASA-CR-177937] 20 p3524 N85-31918
Statistical methods for efficient design of community surveys of response to noise: Random coefficients regression models
[NASA-CR-177933] 21 p3696 N85-32979
GROWIAN: First observations of the environmental impact at the GROWIAN site — wind energy converter 24 p4110 N85-35476
NOISE PREDICTION
On the application of a hairpin vortex model of wall turbulence to trailing edge noise prediction
[NASA-CR-177938] 22 p3728 N85-33109
Wind turbine noise: Prediction tools and design parameter dependence 24 p4110 N85-35477
NOISE PREDICTION (AIRCRAFT)
Observations from varying the lift and drag inputs to a noise prediction method for supersonic helical tip speed propellers
[NASA-TM-83797] 01 p0115 N85-10788
Airport noise impact prediction and measurement
03 p0367 N85-12476
Prediction and modeling of helicopter noise
[AD-A145764] 03 p0415 N85-12656
Contribution of the study of light aircraft propeller noise
[ESA-TT-865] 09 p1378 N85-18667
Wind tunnel acoustic study of a propeller installed behind an airplane empennage: Data report
[NASA-CR-177335] 13 p2154 N85-23377
Transmission of gear noise to aircraft interiors prediction methods 14 p2223 N85-23788
A study of the methods for evaluating the noise impact of a proposed airport on a community
15 p2586 N85-25957
Prediction of free-field noise levels from aircraft flyover measurements
[VTH-LR-427] 16 p2661 N85-27647
Design of sidewall treatment of cabin noise control of a twin engine turboprop aircraft
[NASA-CR-172245] 19 p3351 N85-30771
Some problems in high speed gears and gearing
23 p3923 N85-34312
Optimally designed propellers constrained by noise
24 p4065 N85-35196
NOISE PROPAGATION
A preliminary assessment of environmental noise from large Wind Energy Conversion Systems (WECS) based on experiences from Swedish prototypes
[FFA-TN-1984-48] 09 p1379 N85-18668
Computation of noise radiation from a free jet perpendicular to its axis via laser anemometry measurements
[ESA-TT-870] 09 p1379 N85-18669
Noise transmission loss of a rectangular plate in an infinite baffle
[NASA-TP-2398] 12 p1927 N85-22109
Gear noise origins 14 p2224 N85-23791
Long range downwind propagation of low-frequency sound
[NASA-TM-86409] 15 p2645 N85-26318
An evaluation of proposed acoustic treatments for the NASA LaRC 4 x 7 meter wind tunnel
[NASA-CR-172577] 15 p2646 N85-26319
Interaction of finite-amplitude sound with air-filled porous materials
[NASA-CR-174885] 16 p2660 N85-27637
Aircraft cabin noise prediction and optimization
[NASA-CR-175982] 19 p3350 N85-30768
Design of sidewall treatment of cabin noise control of a twin engine turboprop aircraft
[NASA-CR-172245] 19 p3351 N85-30771
Overground Excess Sound Attenuation (ESA). Volume 3: Application of ESA data in NOISEFILE
[AD-A154820] 21 p3699 N85-32984
Some problems in high speed gears and gearing
23 p3923 N85-34312
NOISE REDUCTION
Noise isolation system for high-speed circuits
[DE84-014229] 01 p0043 N85-10283
Conversion of microwave signals by superconducting films in the resistive state
[NASA-TM-77595] 01 p0123 N85-10843
Highlights of the Institute of Sound and Vibration Research 01 p0131 N85-10905
Jet noise suppression by porous plug nozzles
[NASA-CR-3613] 02 p0275 N85-11790
Noise reduction of the exhaust from pneumatic tools
[BMFT-FB-HA-83-021] 02 p0276 N85-11799
Influence of mode noise suppression in multimode fiber optic light guides 03 p0348 N85-12242
Numerical simulations of compliant material response to turbulent flow, revision 1
[AD-A145801] 03 p0372 N85-12373
Commercial aircraft noise
[PNR-90206] 03 p0417 N85-12665
Tap noise-pressure fluctuations. Study of the acoustic behavior of hydraulic equipment in buildings as a function of the temperature
[CETIM-11-H-337] 04 p0502 N85-13201
A.A.D. engine noise evaluation
04 p0508 N85-13241
Experimental investigation of shock-cell noise reduction for dual-stream nozzles in simulated flight
[NASA-CR-3846] 04 p0557 N85-13549
Experimental investigation of shock-cell noise reduction for single stream nozzles in simulated flight
[NASA-CR-3645] 04 p0557 N85-13550
Noise in small portable motocompressors. Experiments on limited-cost acoustic treatments to obtain progressive improvements
[CETIM-11-H-445] 04 p0558 N85-13557
Vibroacoustic control diagnostics of selected machines based on research on the slide bearing of an automobile engine and the alternator
[ISSN-0208-5658] 05 p0641 N85-14112
LANDSAT instruments characterization
[E85-10029] 05 p0654 N85-14196
Detailed performance calculations: Goddard Group, appendix D 05 p0676 N85-14341
Sources, paths, and concepts for reduction of noise in the test section of the NASA Langley 4x7m wind tunnel
[NASA-CR-172446-VOL-1] 05 p0726 N85-14666
Comparison of options for reduction of noise in the test section of the NASA Langley 4x7m wind tunnel, including reduction of nozzle area
[NASA-CR-172446-VOL-2] 05 p0726 N85-14667
Studies on reactive mufflers. Part 2: Mufflers with air flow 09 p1303 N85-18184
Acoustic tomographic reconstrution of anomalies in three-dimensional bodies
[DE84-017035] 09 p1378 N85-18666
One-dimensional processing for adaptive image restoration
[AD-A149314] 10 p1557 N85-19815
Noise constraints effecting optimal propeller designs
[NASA-TM-86967] 11 p1575 N85-19923
Comparator with noise suppression
[NASA-CASE-LAR-13151-1] 11 p1627 N85-20247
Abatement of noise and vibration in pipelines of hydro systems 14 p2276 N85-24102

A study of the methods for evaluating the noise impact of a proposed airport on a community
15 p2588 N85-25957
An evaluation of proposed acoustic treatments for the NASA LaRC 4 x 7 meter wind tunnel
[NASA-CR-172577] 15 p2648 N85-26319
Interaction of finite-amplitude sound with air-filled porous materials
[NASA-CR-174885] 16 p2860 N85-27837
Fan noise suppression in turbofan engines
[B8580076] 17 p2898 N85-27872
A simplified GPS C/A reciever front end with low noise performance 18 p3109 N85-29251
Reports on cartography and geodesy. Series 1: Original reports, number 93
[ISSN-0469-4236] 18 p3124 N85-29343
An information theoretical method for automatic noise elimination in digital image processing
18 p3124 N85-29345
Effects of propeller rotation direction on airplane interior noise levels
[NASA-TP-2444] 19 p3350 N85-30767
Aircraft cabin noise prediction and optimization
[NASA-CR-175982] 19 p3350 N85-30768
Design of sidewall treatment of cabin noise control of a twin engine turboprop aircraft
[NASA-CR-172245] 19 p3351 N85-30771
Noise reduction in the automotive test cell of the Motor Institute of Naples
[REPT-85-RR-361] 20 p3524 N85-31917
Models for describing active noise control in ducts
[ISVR-TR-127] 20 p3525 N85-31922
Sound-insulating enclosures — machine noise
[BMFT-FB-HA-85-005] 20 p3525 N85-31925
FAA/GAMA (Federal Aviation Administration/General Aviation Manufacturer's Association) propeller aircraft noise test program, Salina Municipal Airport, Salina, Kansas
[AD-A154818] 21 p3699 N85-32983
Discussion of the paper, Some Aspects of Propulsion for the Augmenter-Wing Concept, by D. C. Whittley
[NASA-TM-77884] 22 p3727 N85-33106
Some problems in high speed gears and gearing
23 p3923 N85-34312
Langley aeronautics and space test highlights, 1984
[NASA-TM-87585] 23 p4057 N85-35151
Optimally designed propellers constrained by noise
24 p4065 N85-35196
A research program to reduce the interior noise in general aviation aircraft, index and summary
[NASA-CR-176178] 24 p4145 N85-35695

NOISE SPECTRA
Noise jammer discrimination by noise spectral bandwidth
[AD-D011224] 01 p0038 N85-10242
Noise analysis of the Coarse Optical Power Spectrum Estimator (COPSE) data acquisition system
[AD-A145918] 03 p0419 N85-12677
Study of the velocity-acoustic pressure correlation in a cold jet, centered on the sign and the amplitude of the velocity fluctuations
[ISL-R-124/83] 04 p0501 N85-13193
Detection of low frequency impulsive noise from large wind turbine generators
[NASA-CR-172511] 07 p1038 N85-16588
Quantum noise effects in single-mode injection lasers
[FUB-11-1984] 09 p1327 N85-18338
Effects of vane/blade ratio and spacing on fan noise, volume 1
[NASA-CR-174864] 10 p1553 N85-19791
Effects of vane/blade ratio and spacing on fan noise. Volume 2: Data supplement
[NASA-CR-174885] 10 p1553 N85-19792
Shuttle electrical environment
13 p1990 N85-22475
Noise characteristics of sulfur-doped silicon diodes
13 p2073 N85-22952
Flux pinning and flux flow studies in superconductors using flux flow noise techniques
[DE85-010814] 19 p3376 N85-30945
Overview of applications of SQUIDS
[DE85-009942] 20 p3458 N85-31480
Overground Excess Sound Attenuation (ESA). Volume 3: Application of ESA data in NOISEFILE
[AD-A154820] 21 p3699 N85-32984
Lateral attenuation of aircraft flight noise
[AD-A154958] 21 p3700 N85-32986
A comparison of calculated and measured background noise rates in hard X-ray telescopes at balloon altitude
[OG-9.3-7] 23 p4026 N85-34962

NOISE SUPPRESSORS
U NOISE REDUCTION

NOISE TEMPERATURE
A coaxial noise standard for the 1 GHz to 12.4 GHz frequency range
[PB84-217884] 01 p0042 N85-10272
Superconducting NbTi and Pb(Cu) bandpass filters
05 p0623 N85-13986
The dc SQUID as a tuned radiofrequency amplifier
[DE85-000701] 08 p0805 N85-15123
Preliminary investigation into using the sun as a source for G/T (Gain to System Noise Temperature) measurements
[PB85-126148] 12 p1952 N85-22265

NOISE THRESHOLD
Robust detection of fading narrow-band signals in non-Gaussian noise
[AD-A152262] 16 p2774 N85-27124

NOISE TOLERANCE
Study of annoyance due to urban automobile traffic
[NASA-TM-77514] 01 p0069 N85-10458
Airport noise impact prediction and measurement
03 p0367 N85-12476
NOISEMAP 4.4 computer program update, operator's manual, addendum 1
[AD-A147091] 07 p1025 N85-16503
Construction and application of a questionnaire for the social scientific investigation of environmental noise effects
[NASA-TM-75492] 10 p1512 N85-19544
Investigation of influence of communications link and synchronization error on noise tolerance of group transmission of binary information based on orthogonal Walsh function 13 p2086 N85-23026
A community survey of helicopter noise annoyance conducted under controlled noise exposure conditions
[NASA-TM-86400] 13 p2154 N85-23374
Disturbance to the population due to flight operations at landing fields. Questionnaire on community reaction to non-commercial and sporting aviation
[NASA-TM-76531] 14 p2353 N85-24537
Effect of broad-band constant noise on some systems of animal body 14 p2387 N85-24705

NOMENCLATURES
Fungi of Mt. Babia Gora. 1: Mycoflora of forests
[NASA-TM-77484] 02 p0234 N85-11522
SLC nomenclature for beamline components
[DE84-014776] 02 p0279 N85-11816
DoD manual for standard data elements, part 2
[AD-A152202] 16 p2878 N85-27755
DoD manual for standard data elements, part 3
[AD-A152203] 16 p2878 N85-27756
DoD manual for standard data elements, part 4
[AD-A152204] 16 p2878 N85-27757
DoD manual for standard data elements, part 5
[AD-A152205] 16 p2878 N85-27758
Systematic nomenclature of the nitrogen, oxygen and sulfur functional polycyclic aromatic hydrocarbons
[DE85-007426] 17 p2916 N85-27974
Coping with computer terminology
[DE85-008076] 18 p3161 N85-29579

NOMINAL VALUES
U APPROXIMATION

NOMOGRAMS
U NOMOGRAPHS

NOMOGRAPHS
Nomographs for estimating the levelized cost of energy from flat-plate and concentrator photovoltaic systems
[NASA-CR-176048] 20 p3483 N85-31645
Modeling of discrete devices with use of multivalued logic and nomograms 22 p3768 N85-33351

NONADIABATIC PROCESSES
U HEAT TRANSFER

NONADIABATIC THEORY
Nonlocal and nonadiabatic expression for the ponderomotive force near cyclotron resonance
[IPPJ-736] 23 p3974 N85-34636

NONAQUEOUS ELECTROLYTES
Voltammetry and coulometry with immersed thin layer electrodes. Part 1: Model for effects of solution resistivity in linear sweep voltammetry
[AD-A148655] 08 p1159 N85-17313
Development of a low cost electrochemical CO monitor based on anodic scanning voltammetry in nonaqueous electrolyte
[PB85-113488] 11 p1637 N85-20314
Electrochemical reduction of titanium in dimethyl sulphoxide
[BLL-OA-TRANS-3225-(6196.300)] 20 p3429 N85-31267

NONCONDENSABLE GASES
Theoretical analysis of condensation in the presence of noncondensable gases as applied to open cycle OTEC condensers
[DE84-015809] 11 p1675 N85-20556

NONCONDUCTORS
U ELECTRICAL INSULATION

NONCONSERVATIVE FORCES
Satellite physical and orbital characteristics
16 p2804 N85-27287

NONDESTRUCTIVE TESTS
NT NEUTRON RADIOGRAPHY
NT STATIC FIRING
Nonlinear ultrasonic characterization of oxygen impurities in titanium, 2
[AD-A144857] 01 p0027 N85-10171
Electromagnetic-acoustic-transducer e system for thick-weld inspection
[PB84-219492] 01 p0051 N85-10336
Ultrasonic nondestructive evaluation, microstructure, and mechanical property interrelations
[NASA-TM-86876] 01 p0056 N85-10371
Evaluation of interfacial stresses from the amplitude of reflected ultrasonic signal
[DE84-015472] 02 p0276 N85-11798
Robotics in nondestructive inspection at Sacramento Air Logistics Center
[AD-P004012] 03 p0309 N85-11992
Acoustic emission monitoring of fatigue in 7010 aluminum alloys
[AERE-R-11167] 03 p0334 N85-12152
Evaluation of moduli and thicknesses of pavement systems by spectral-analysis-of-surface-waves method
[PB84-219112] 03 p0342 N85-12205
Research in quantitative NDE techniques
[AD-A145090] 03 p0369 N85-12358
Technical activities 1983, Office of Nondestructive Evaluation
[PB84-217074] 03 p0370 N85-12360
Microwave measurement of the complex dielectric tensor at anisotropic slab materials
[DE84-017050] 04 p0493 N85-13144
Defect detection threshold in riveted joints, test report no.44-833/F — in aircraft 04 p0511 N85-13280
Nondestructive evaluation of residual stress in low-carbon steel
[NASA-CR-174157] 04 p0512 N85-13284
Nondestructive evaluation of residual stress in low-carbon steel, introduction 04 p0512 N85-13285
Nondestructive determination of mechanical properties — aluminum alloys 04 p0512 N85-13286
CuInSe2-based photoelectrochemical cells: Their use in characterization of thin CuInSe2 films, and as photovoltaic cells per se
[DE84-004514] 04 p0529 N85-13379
Impact of NDE unreliability on pressure vessel fracture predictions
[DE84-015586] 05 p0647 N85-14151
Measuring the corrosion rate of reinforcing steel in concrete
[PB84-244532] 06 p0770 N85-14925
Synthesis study of nondestructive testing devices for use in overlay thickness design of flexible pavements
[PB84-218060] 06 p0774 N85-14950
Pulse-echo method for flaw detection in concrete
[PB84-234509] 06 p0775 N85-14963
Nondestructive deceleration of a rocket sled — target penetration tests
[FOA-C-20549-D3] 07 p0912 N85-15771
Gallium arsenide compounds tested nondestructively with X-rays 07 p0936 N85-15934
A narrow band pulsed eddy current instrument for materials testing
[AERE-R-11229] 07 p0968 N85-16149
Comparison of the sensitivities of ultrasonic, radiographic and acoustic emission test methods for the examination of a thick weld
[BLL-RISLEY-TR-4547-(9091.9F)]
07 p0975 N85-16194
Nondestructive inspection: Improved capabilities of technicians
[AD-A147388] 07 p0975 N85-16196
Nondestructive tests and fracture mechanics investigations in the Component Integrity Research Programme
[BLL-RISLEY-TR-4541-(9091.9F)]
07 p0976 N85-16199
Nondestructive measurement of bulk residual stresses
[AD-A147063] 07 p0978 N85-16211
Ultrasonic measurements, X-ray photographs and image processing
[BLL-RISLEY-TR-4586-(9091.9F)]
07 p1037 N85-16583
Proceedings of the 2nd Workshop on Nondestructive Evaluation (NDE) of Titanium Alloys
[AD-A147628] 08 p1125 N85-17095
NDE (Nondestructive Evaluation) of oxygen contaminated titanium alloys and weldments
[AD-P004121] 08 p1126 N85-17096
Effects of oxygen-contamination-induced microstructural changes on the reverberation of ultrasound in Ti-6211 alloys
[AD-P004124] 08 p1126 N85-17099
Acoustical characterization of Ti-6211 weldments and oxygen contamination Ti-6211 plate
[AD-P004125] 08 p1126 N85-17100

Feasibility study to demonstrate detection of low levels of oxygen contaminant in titanium using eddy current and ultrasonic NDE (Nondestructive Evaluation) techniques
[AD-P004129] 08 p1127 N85-17104
Electromagnetic NDE of interstitial contamination in titanium alloy weldments
[AD-P004131] 08 p1127 N85-17106
Evaluation of the thermoelectric method for determination of interstitial gases in titanium
[AD-P004132] 08 p1127 N85-17107
Measurement of oxygen contamination in titanium alloy ingots by fast neutron activation analysis
[AD-P004133] 08 p1128 N85-17108
Neutron activation analysis of titanium with oxygen contamination
[AD-P004134] 08 p1128 N85-17109
Nondestructive evaluation of titanium alloys. ESCA (Electron Spectroscopy for Chemical Analysis), ISS (Ion Scattering Spectroscopy), and SIMS (Secondary Ion Mass Spectrometry) examination of titanium alloy solid surfaces
[AD-P004135] 08 p1128 N85-17110
Ultrasonic transducers, performance variability, design, and manufacturing procedures
[AD-A148575] 08 p1158 N85-17306
Research on nondestructive testing
[AD-A148375] 08 p1171 N85-17380
Exploratory development of advanced surface flaw detection methods
[AD-A148757] 09 p1281 N85-18060
Evaluation of laterally loaded laminated glass units by theory and experiment
[PB85-111532/GAR] 09 p1300 N85-18166
Nondestructive characterization of semiconductor surfaces and interfaces 09 p1329 N85-18349
Experimental verification of eddy-current flaw theory
[DE85-001288] 09 p1329 N85-18350
Emerging technology of synthetic aperture focusing for ultrasonic testing
[DE85-000373] 09 p1378 N85-18664
Develop and demonstrate manufacturing processes for fabricating graphite filament reinforced polyimide (Gr/PI) composite structural elements
[NASA-CR-172497] 11 p1592 N85-20019
Insulation bonding test system
[NASA-CASE-MFS-25882-1] 11 p1610 N85-20126
Method and apparatus for measuring minority carrier lifetime in a direct band-gap semiconductor
[NASA-CASE-NPO-16337I-1] 11 p1628 N85-20251
NDE for heat engine ceramics
[NASA-TM-86949] 11 p1649 N85-20369
Stress waves in an isotropic elastic plate excited by a circular transducer
[NASA-CR-3677] 11 p1650 N85-20390
Infrared-thermal wave scanner for NDE of naval thermal spray coatings
[DE85-002237] 11 p1650 N85-20391
Application of hysteresis modelling to the non-destructive inspection of stress
[DE85-003081] 11 p1650 N85-20393
Aerostructure nondestructive evaluation by thermal field detection. Phase 2: Technique refinement and quantitative determination of flaw detection capabilities
[AD-A149622] 12 p1777 N85-21155
Quantitative non-destructive evaluation of damage in composite materials using transmitted and reflected ultrasound
[NASA-CR-175550] 12 p1796 N85-21269
Method and apparatus for mapping the distribution of chemical elements in an extended medium
[NASA-CASE-GSC-12808-1] 12 p1798 N85-21279
The role of dislocations in ultrasonic attenuation
[AERE-R-11384] 12 p1804 N85-21317
Nondestructive testing of stainless steel to improve quality and output efficiency of the processing of ingot and continuous casting
[BMFT-FB-T-84-240] 12 p1808 N85-21345
Eddy current test probe with circumferential segments and method of testing material surrounding fastener holes
[AD-D011554] 12 p1850 N85-21603
A new NDE (Non-Destructive Evaluation) capability for thin-shelled structures
[AD-A149625] 12 p1862 N85-21678
Nondestructive method for detecting machine damage in beryllium
[DE85-001074] 12 p1862 N85-21681
Defect characterisation and monitoring by acoustic emission
[AERE-R-11409] 12 p1863 N85-21683
The measurement of residual stresses using ultrasonics
[AERE-R-11415] 12 p1868 N85-21722
Investigation of steel structures using ultrasonic waves
[BR93258] 13 p2101 N85-23091
Magnetic field interactions with material discontinuities
[AD-A150197] 13 p2154 N85-23373
Mini-Seminar on Non-Destructive Testing
[CSIR-TSD-0009/83] 14 p2316 N85-24306
Status of the U.K. N.D.T. industry today
14 p2316 N85-24309
Ultrasonic non-destructive testing technique
14 p2316 N85-24313
Applications of eddy currents
14 p2316 N85-24315
Flash radiography 14 p2317 N85-24316
New developments in industrial radiography
14 p2317 N85-24317
Acoustic emission of semiconductor devices
15 p2529 N85-25593
Nondestructive equipment study
[NASA-CR-171865] 15 p2571 N85-25853
Laser-based non-destructive testing techniques for the ultrasonic characterization of sub-surface flaws
[AERE-R-11562] 15 p2572 N85-25856
System for NDH of thermal spray coating bonds
[DE85-007463] 15 p2572 N85-25858
Spectral reflectance of carbonate minerals and rocks in the visible and near infrared (0.35 - 2.55 microns) and its applications in carbonate petrology
[NASA-CR-175763] 15 p2591 N85-25973
An electro-optic spatial light modulator for thermoelastic generation of programmably focused ultrasound
[AD-A152066] 15 p2646 N85-26323
Ultrasonic characterization of porosity: Theory
[DE85-005922] 15 p2646 N85-26325
Optical monitoring of photo-acoustic pulse propagation in silicon wafers
[AD-A151333] 15 p2651 N85-26352
Nondestructive tests of ceramic components for aircraft turbines 16 p2700 N85-26718
Initial quality of advanced joining concepts
[AD-A152241] 16 p2759 N85-27027
Echo-response from crack-like two-dimensional reflectors in focused ultrasonic fields. Ultrasonic crack tip method for the determination of crack depth
[BLL-BISI-22062-(9022.06)] 16 p2796 N85-27236
Structural Integrity and Durability of Reusable Space Propulsion Systems
[NASA-CP-2361] 17 p2910 N85-27941
Differential between crack and pseudo-crack indications by means of objective magnetic flux leakage testing
[BLL-BISI-TRANS-22033-(9022.06)]
17 p2976 N85-28386
Non-destructive testing of HF-welded pipe
[BLL-BISI-TRANS-22162-(9022.06)]
17 p2976 N85-28388
Detecting and analyzing crack defects
[BLL-BISI-TRANS-22062-(9022.06)]
17 p3027 N85-28723
Echo-response from crack-like two-dimensional reflectors in focused ultrasonic fields
17 p3027 N85-28724
Compact L-edge densitometer for uranium concentration assay
[DE85-010344] 18 p3110 N85-29281
Investigation on the application of the pulsed eddy current method of non-destructive testing using controlled signals (CS-technique)
[BLL-BISI-TRANS-22249-(9022.06)]
18 p3119 N85-29303
Ultrasonic testing of plates containing edge cracks
[NASA-CR-3904] 18 p3119 N85-29307
A study of the stress wave factor technique for the characterization of composite materials
[NASA-CR-174870] 19 p3231 N85-30035
Apparatus for non-destructive inspection of blind holes
[AD-D011707] 19 p3273 N85-30295
Optical beam deflection detection of thermal waves in opaque solids 19 p3374 N85-30827
Production verification of the acoustic emission weld monitor
[AD-A154168] 20 p3464 N85-31519
Description of an holographic interferometry nondestructive test installation: Application to bond tests
[SNIAS-851-430-101] 20 p3464 N85-31521
Philosophy of nondestructive control in aeronautics quality control. Knowledge of and improvements to nondestructive test safety
[SNIAS-851-551-101] 20 p3465 N85-31522
Modifications of flight-by-flight load sequences to provide for good fracture surface readability
[NLR-MP-84012-U] 20 p3472 N85-31577
NBS (National Bureau of Standards) reactor: Summary of activities Jul. 1983 through Jun. 1984
[PB85-184836] 20 p3522 N85-31907
Solid-state track recorder neutron dosimetry in the Three-Mile Island Unit-2 reactor cavity
[DE85-011360] 20 p3531 N85-31968
Experimental and theoretical assessment of a new technique for the non-destructive evaluation of laminated panels
[AD-A155622] 21 p3582 N85-32155
Reliability of void detection in structural ceramics using scanning laser acoustic microscopy
[NASA-TM-87035] 21 p3597 N85-32337
Acoustic emission during transformation of austenite in 38KhN3MF steel
[BLL-M-35825-(5828.4)] 23 p3914 N85-34258
Quantitative non-destructive evaluation of composite materials based on ultrasonic wave propagation
[NASA-CR-176176] 24 p4074 N85-35244
Ultrasonic inspection of carbon fiber reinforced plastic by means of sample-recognition methods
[NASA-TM-77896] 24 p4074 N85-35245
Methods for nondestructive tests of CFRP laminates
24 p4074 N85-35246
Fatigue damage detection in steels by optical correlation
[AD-A155830] 24 p4079 N85-35277
Subcritical fracture propagation in rocks: An examination using the methods of fracture mechanics and non-destructive testing 24 p4116 N85-35516

NONEQUILIBRIUM CONDITIONS
Nonequilibrium air radiation (Nequair) program: User's manual
[NASA-TM-86707] 19 p3353 N85-30780
Non-equilibrium effects in turbulent diffusion flames
20 p3425 N85-31258
Implicit Monte Carlo methods and non-equilibrium Marshak wave radiative transport
[DE85-010711] 22 p3835 N85-33743
Calculations of heavy ion charge state distributions for nonequilibrium conditions
[SH-2.1-12] 23 p3999 N85-34793

NONEQUILIBRIUM DRAG
U FRICTION DRAG

NONEQUILIBRIUM FLOW
Computation of the nonequilibrium flow in a gasdynamic laser
[AD-A141022] 04 p0505 N85-13224
Flow and plasticity via nonequilibrium molecular dynamics
[DE85-001011] 10 p1555 N85-19804
Hypersonic nonequilibrium gas flow past zero-aspect wing 16 p2765 N85-27063
Some amplification by relaxation processes in nitrogen and mixtures of nitrogen with helium and hydrogen
[AD-A153620] 18 p3071 N85-28992
Transient three-phase three-component systems. Part 1: Formulation of the system of differential equations
[DE85-013287] 24 p4095 N85-35384

NONEQUILIBRIUM IONIZATION
Non equilibrium ionization in the local hot bubble
06 p0879 N85-15587
Stromgren trails of hot white dwarfs
06 p0879 N85-15589

NONEQUILIBRIUM PLASMAS
Excitation of impurities by heavy particles and radiative losses of thermonuclear plasma
11 p1719 N85-20616
Plasma processing of materials
[AD-A152398] 17 p3039 N85-28600

NONEQUILIBRIUM RADIATION
Nonequilibrium air radiation (Nequair) program: User's manual
[NASA-TM-86707] 19 p3353 N85-30780

NONEUCLIDIAN GEOMETRY
U DIFFERENTIAL GEOMETRY

NONFERROUS METALS
Testing the antifriction properties of alloys for heavily loaded bearings 06 p0780 N85-14990
A computer controlled mass spectrometer system for investigating the decomposition of non-metallic materials under atmospheric conditions 12 p1948 N85-22237
Rational use of tatanium in nonferrous metallurgy
13 p2031 N85-22726
Inoculation of non-metallic inclusions in steel 17GS
[BLL-BISI-TRANS-22431-(9022.06)]
17 p2925 N85-28042

NONFLAMMABLE MATERIALS
Flame-resistant materials for use in pyrotechnic safety clothing
[AD-A146857] 07 p0931 N85-15001
(Vinyloxy)chlorocyclotriphosphazenes
[AD-D011471] 10 p1453 N85-19152
High performance mixed bismide resins and composites based thereon
[NASA-CASE-ARC-11536-1-SB]
19 p3231 N85-30033
Investigation of experimental lightweight firewall materials for A/C engine bay applications
[AD-A155765] 24 p4062 N85-35175

NONHOMOGENEITY
U INHOMOGENEITY

NONISOTHERMAL PROCESSES
A numerical solution of a nonisothermal wall using the two-dimensional Navier-Stokes equations
[AD-A154467] 19 p3266 N85-30257
Thermomechanical deformation in the presence of metallurgical changes 20 p3466 N85-31533
NONISOTROPIC PLATES
U ANISOTROPIC PLATES
NONISOTROPY
U ANISOTROPY
NONLIFTING VEHICLES
U BALLISTIC VEHICLES
NONLINEAR EQUATIONS
NT MONGE-AMPERE EQUATION
NT NONLINEAR EVOLUTION EQUATIONS
NT QUADRATIC EQUATIONS
Quasi-Newton algorithms for large scale nonlinear systems 02 p0206 N85-11370
Inverse problems, optimization and algorithms
[AD-A145397] 02 p0250 N85-11638
Supersymmetric Yang-Mills fields as an integrable system and connections with other non-linear systems
[DE84-013231] 04 p0556 N85-13539
A lumped mass finite element method with quadrature for a nonlinear parabolic problem
[CTH-MATH-1984-22] 05 p0719 N85-14615
Trust region methods for minimization
[AD-A147073] 07 p1030 N85-16540
Self similar solutions for a degenerate Cauchy problem
[AD-A147241] 07 p1031 N85-16548
Nonlinear wave propagation
[AD-A148114] 08 p1152 N85-17269
On solving nonlinear problems of aircraft structural mechanical design 09 p1309 N85-18223
Nonlocal and nonlinear effects on solar oscillations 09 p1416 N85-18934
New methods for numerical solution of one class of strongly nonlinear partial differential equations with applications in hydrodynamics
[AD-A149026] 10 p1545 N85-19739
Hamilton-Jacobi equations in infinite dimensions. Part 1. Uniqueness of viscosity solutions
[AD-A149094] 10 p1546 N85-19749
Construction of solutions for two-dimensional Riemann problems
[DE85-003136] 10 p1549 N85-19770
Triple layer system for numerical integration of equations of gas dynamics and nonlinear heat conduction equation
[DE85-000297] 11 p1632 N85-20277
Local strain redistribution corrections for a simplified inelastic analysis procedure based on an elastic finite-element analysis
[NASA-TP-2421] 11 p1651 N85-20396
Algebraic decay in self-similar Markov chains
[DE85-003162] 11 p1707 N85-20740
Time marching numerical solution of the dynamic response of nonlinear systems
[NAF-AN-25] 12 p1885 N85-21896
Local behavior of solutions of an elliptic-parabolic equation
[AD-A149624] 12 p1920 N85-22057
A method of calculating periodic solutions of second order dynamical systems
[AD-A149634] 12 p1920 N85-22058
Nonlinear partial differential equations and related problems of Pade approximations
[AD-A149650] 12 p1920 N85-22059
Nonlinear sigma-models and integration methods
[DE85-004447] 12 p1922 N85-22071
Direct secant updates of sparse matrix factors
[DE85-004008] 12 p1922 N85-22073
Influence of internal gravity waves on F layer 14 p2336 N85-24460
Solution of coupled system of PDE by the transistorized multigrid method
[DE85-006377] 15 p2639 N85-26276
An approximation theory for nonlinear evolution equations and single conservation laws 16 p2691 N85-26614
Internal resonance in nonlinear vibrating systems
[REPT-15/1984] 16 p2797 N85-27245
A split explicit model for short-term numerical weather prediction 16 p2831 N85-27480
Fundamentals of plasma simulation
[DE85-007699] 16 p2867 N85-27683
Large scale electricity production scheduling via nonlinear optimization
[REPT-84-07] 17 p3017 N85-28655
Convergence of Newton's method for a single real equation
[NASA-TP-2469] 17 p3017 N85-28656
On the algebraic equations in implicit Runge-Kutta methods
[CWI-NM-R8413] 17 p3022 N85-28696
Coherent state description of non-topological solitons and momentum projection
[DE85-007814] 17 p3033 N85-28761
Sensitivity analysis of initial value problems with mixed ode's and algebraic equations
[AD-A153528] 18 p3169 N85-29637
Quantized Hall effect in two-dimensional electron systems
[AD-A154347] 19 p3259 N85-30211
Large deflections of a cantilever beam under arbitrarily directed tip load
[NASA-TM-86442] 19 p3284 N85-30383
Use of adjoint equations in problems of evaluating state of random hydrodynamic fields 19 p3289 N85-30398
A global low order spectral model designed for climate sensitivity studies
[NASA-CR-175999] 19 p3315 N85-30549
Perspectives of nonlinear dynamics
[IPPJ-723] 19 p3370 N85-30902
Automatic assembly of space stations 20 p3409 N85-31153
Modeling taper charge with a non-linear equation 20 p3445 N85-31390
Approximate solution to the problem of heating massive bodies by radiation
[BLL-M-36272-(5828.4)] 20 p3450 N85-31422
Construction of constraint equation for stresses and strains
[BLL-M-36239-(5828.4)] 20 p3465 N85-31524
Viscoplasticity based on overstress with a differential growth law for the equilibrium stress 20 p3466 N85-31532
Constitutive modeling of superalloy single crystals and directionally solidified materials 20 p3466 N85-31535
Non-model based estimation with applications to sensor calibration using multiple sensors
[AD-A154736] 21 p3589 N85-32306
Numerical model of a pulse combustor
[DE85-011717] 23 p3912 N85-34240
A review of spectral methods
[NASA-CR-172502] 23 p3929 N85-34350
Nonlinear flap-lag-extensional vibrations of rotating, pretwisted, preconed beams including Coriolis effects
[NASA-TM-87102] 23 p3941 N85-34427
DISPL1: A software package for one and two spatially dimensioned kinetics-diffusion problems
[ANL-84-56] 23 p3958 N85-34516
Identification and control of structures in space
[NASA-CR-176175] 24 p4089 N85-35214
Long-time asymptotics of a system for plasma diffusion
[NASA-CR-177947] 24 p4093 N85-35375
Analysis of the nonlinear equations describing the elastic, thermal, and electromagnetic behavior of solids: Existence of solutions of semi-inverse problems 24 p4100 N85-35415
NONLINEAR EVOLUTION EQUATIONS
Step-by-step stability in the numerical solution of partial differential equations
[CWI-NW-161/83] 05 p0720 N85-14623
Lax-pair operators for squared-sum and squared-difference eigenfunctions
[AD-B089083L] 09 p1386 N85-18718
Recent developments and open problems in the mathematical theory of viscoelasticity
[AD-A149043] 10 p1545 N85-19742
Nonlinear evolution of astrophysical Alfven waves 12 p1956 N85-22294
A fast implementation of explicit time stepping algorithms with the finite element method for a class of nonlinear evolution problems
[REPT-84-03] 17 p3021 N85-28686
Spectral transform approach to Backlund transformations
[PREPRINT-420] 18 p3172 N85-29663
Reduction techniques for infinite-dimensional Hamiltonian systems: Some ideas and applications
[PREPRINT-424] 18 p3173 N85-29666
NONLINEAR FEEDBACK
Optimal open loop and nonlinear feedback control for remote orbital capture
[AD-A151967] 16 p2732 N85-26859
NONLINEAR FILTERS
Numerical studies in nonlinear filtering
[TWISK-305] 01 p0108 N85-10728
Microprocessor implementation of algorithms of nonlinear filtration 04 p0486 N85-13104
A nonlinear filter for compensating for time delays in manual control systems 05 p0700 N85-14493
Numerical methods and approximation and modelling problems in stochastic control theory
[AD-A146827] 07 p1029 N85-16533
Digital imaging processing
[INPE-3325-PRE/624] 11 p1701 N85-20696
Synthesis of optimum receiver and processor for signal packet of radio pulses 12 p1839 N85-21541
Prefiltration in Kalman filter with a priori indeterminacy 13 p2071 N85-22939
Assessment of a nonlinear method of INS alignment — inertial navigation systems (INS)
[BAE-BT-12684] 15 p2466 N85-25233
Theory and Applications of State Estimation. NRIMS Summer Seminar Series
[CSIR-SWISK-37] 15 p2635 N85-26244
Nonlinear estimation 15 p2635 N85-26245
Truncated nonlinear filters 15 p2635 N85-26249
Recursive nonlinear filtering through complete linearization
[AD-A155029] 21 p3677 N85-32844
Comprehensive radio direction finder with electronically stabilized radiation pattern 22 p3762 N85-33318
Optimal complex nonlinear processing of continuous and pulsed signals 22 p3763 N85-33323
Nonlinear filtration of clutter 22 p3777 N85-33404
NONLINEAR OPTICS
Self-induced nonlinear effects in optical fibers: A unified approach
[FUB-67-1982] 09 p1385 N85-18713
Chaos and order in an optical ring cavity
[CWI-AM-R8416] 17 p3036 N85-28795
Optically nonlinear and bistable behaviour of direct gap semiconductors 18 p3186 N85-29759
An experimental nonlinear optical waveguide device 18 p3186 N85-29762
Prospects for parallel nonlinear optical signal processing using GaAs etalons and ZnS interference filters 18 p3187 N85-29765
Applications and investigations of second harmonic generation 19 p3367 N85-30878
Edge detection and geometric methods in computer vision
[AD-A155873] 24 p4135 N85-35830
NONLINEAR PROGRAMMING
Composite laminate optimization program suitable for microcomputers 01 p0059 N85-10389
ADS: A FORTRAN program for automated design synthesis, version 1.00
[NASA-CR-172460] 01 p0102 N85-10684
A sequential quadratic programming algorithm for solving large, sparse nonlinear programs
[AD-A145854] 03 p0407 N85-12587
Optimization of moving-target selection radar devices for nonGaussian signals for stationary targets 06 p0769 N85-15043
Generalized convex functions: Properties, optimality and duality
[DE85-001553] 09 p1378 N85-18652
Large scale electricity production scheduling via nonlinear optimization
[REPT-84-07] 17 p3017 N85-28655
Recent developments in nonlinear normal mode initialization 18 p3142 N85-29451
Computable numerical bounds for Lagrange multipliers of stationary points of nonconvex differentiable nonlinear programs
[AD-A153513] 18 p3169 N85-29633
Expected utility, penalty functions, and duality in stochastic nonlinear programming, revised
[AD-A154034] 19 p3335 N85-30680
User's manual of the BNDSCO computer program for solving constrained optimal control problems
[DFVLR-MITT-85-05] 20 p3516 N85-31865
Local epi-continuity and local optimization
[AD-A154812] 21 p3677 N85-32843
Optimization of design parameters for alternating current stabilizer based on magnetic suspension 22 p3772 N85-33374
Model building and practical aspects of nonlinear programming
[AD-A155720] 22 p3829 N85-33711
NONLINEAR SYSTEMS
Non-Gaussian approach for parametric random vibration of non-linear structures 01 p0060 N85-10395
Development of advanced constitutive model for reinforced concrete
[AD-A145050] 01 p0062 N85-10411
Determination of the input-output characteristics of time-invariant memoryless nonlinear devices
[FUB-41-1983] 01 p0100 N85-10687
Time invariant memoryless nonlinear systems identification method
[FUB-9-1983] 01 p0114 N85-10773
Aeroelastic stability analysis with interacting structural nonlinearities 02 p0207 N85-11384
Linear and bilinear infinite-dimensional representations of finite-dimensional nonlinear systems
[RR-259] 02 p0254 N85-11681
Nonlinear acoustics
[AD-A145580] 02 p0276 N85-11796

N-frequency quasiperiodicity and chaos in dissipative dynamical systems 02 p0282 N85-11840
Nonlinear system identification methodology development based on F-4S flight test data analysis [AD-A146289] 03 p0318 N85-12053
Forced oscillations theory for resonant extended interaction electron devices [PR-206] 03 p0358 N85-12298
Non-linear systems in infinite dimensional state spaces [AD-A145828] 03 p0410 N85-12623
Filtering and prediction performance for a class of systems with uncertain parameters [AD-A146145] 03 p0411 N85-12630
Formulation and solution methods for classical problems of static buckling [CETIM-101010] 04 p0514 N85-13280
Nonlinear deformation and static linear buckling of structures under pressure [CETIM-11-E-350] 04 p0514 N85-13281
Fly's eye sensor nonlinear signal processing [AD-D011290] 05 p0729 N85-14684
Iterative method of calculating strength of airframe members using finite element method 06 p0775 N85-14955
Techniques for nonlinear random vibration problems 07 p0977 N85-16201
Nonlinear ultrasonic characterization of oxygen impurities in titanium [AD-P004123] 08 p1126 N85-17098
EMC (Electromagnetic compatibility) spec criteria in Volterra systems [AD-A147659] 08 p1151 N85-17263
On a general nonlinear theory of plates and shells: Formulation and applications 08 p1172 N85-17387
A nonlinear technique for high-resolution data processing [AD-D011415] 08 p1203 N85-17570
On the global asymptotic stabilization of nonlinear systems [PREPRINT-838] 08 p1209 N85-17604
The practical identification of systems with nonlinearities [RR-264] 08 p1209 N85-17607
Use of iterative linear and nonlinear algebraic methods for solving large stiff systems of ODEs [AD-A148516] 08 p1213 N85-17636
Research in stochastic processes [AD-A148622] 08 p1216 N85-17660
Nonlinear real-time optical signal processing [AD-A148293] 08 p1222 N85-17699
Nonlinear analysis of composite laminates 09 p1288 N85-18087
Modal analysis of structural systems involving nonlinear coupling 09 p1337 N85-18409
A program design for an adaptive, non-linear finite element solver [AD-A148680] 10 p1539 N85-19705
On the application of compatibility checking techniques to dynamic flight test data [ARL/AERO-R-161] 12 p1776 N85-21151
Time marching numerical solution of the dynamic response of nonlinear systems [NAF-AN-25] 12 p1865 N85-21696
Nonlinear rotordynamics analysis [NASA-CR-171425] 13 p1968 N85-22364
Nonlinear interactions between vortices and acoustic waves in a rocket combustion chamber 13 p1999 N85-22533
A model for large sparse contingency tables [AD-A150320] 13 p2151 N85-23350
Investigation of the time history and modal responses of some simple linear and nonlinear systems [DE85-002027] 14 p2321 N85-24344
System theoretic description of physical systems [CWI-TRACT-3] 14 p2414 N85-24894
Statistical techniques for signal processing [AD-A151231] 15 p2541 N85-25690
Effect of internal pressure on flexibility and stress intensification factors for pipe elbows analyzed by the finite element method [AD-A151161] 15 p2578 N85-25901
Computer program TRAMP: Inclusion of state space facilities and the analysis of non-linear elements [BAE-BT-12643] 15 p2626 N85-26161
Application of CFD techniques toward the validation of nonlinear aerodynamic models [NASA-TM-86715] 16 p2700 N85-26671
Alternatives for jet engine control [NASA-CR-175831] 16 p2709 N85-26713
Alternatives for jet engine control [NASA-CR-175832] 16 p2709 N85-26714
Alternatives for jet engine control [NASA-CR-175833] 16 p2709 N85-26715
Observations, theoretical ideas and modeling of turbulent flows: Past, present and future [NASA-TM-86679] 16 p2782 N85-27167
An analytical investigation of dynamic coupling in nonlinear, geared rotor systems 16 p2792 N85-27216
Numerical methods for stiff ordinary and elliptic partial differential equations [AD-A153247] 17 p3020 N85-28675
Scalar modal control of a nonlinear system using time varying gain [AD-A153252] 17 p3020 N85-28676
Estimating random integrals from noisy observations: Sampling designs and their performance [AD-A152926] 17 p3025 N85-28702
Evaluation of a fault tolerant system for an integrated avionics sensor configuration with TSRV flight data [NASA-CR-172589] 18 p3062 N85-29941
A numerical study of the Pacific polar low [AD-A153777] 18 p3149 N85-29495
On design of off-axis specimens [AD-A154326] 19 p3286 N85-30379
Excitation of turbulence by density waves [NASA-CR-3905] 19 p3314 N85-30546
Sub-optimal control of nonlinear flexible space structures 20 p3414 N85-31190
A nonlinear dual-adaptive control strategy for identification and control of flexible structures 20 p3416 N85-31203
A theoretical model for the study of nonlinear dynamics of magnetic bearings 20 p3462 N85-31505
Dynamical study of flat plates by nonlinear elasticity theory [STN-6] 20 p3471 N85-31572
On the equivalent bilinearization of nonlinear controlled delay systems [RR-272] 20 p3519 N85-31880
An overview of nonlinear systems identification [RR-271] 20 p3520 N85-31894
Aerodynamic characteristics of the standard dynamics model in coning motion at Mach 0.6 [NASA-TM-86717] 21 p3552 N85-32094
On the dependence of the convergence of Gummel's algorithm on the regularity of the solution [AD-A154626] 21 p3675 N85-32832
Theory of soliton waves [AD-A154784] 21 p3676 N85-32837
The application of bispectral analyses to aeroelastic phenomena 24 p4060 N85-35157

NONLINEARITY

Nonlinear propagation in a depth-dependent ocean [AD-A145079] 01 p0116 N85-10791
Nonlinear oscillations of 2 body system relative to center of mass in elliptical orbit 02 p0159 N85-11062
Optimal nonlinear feedback control of spacecraft attitude maneuvers 02 p0167 N85-11126
Determination of nonlinear viscoelasticity parameters for polymeric and composite materials by numerical methods [AD-A145311] 02 p0185 N85-11240
A nonlinear theory for gyro-devices [AD-A145297] 02 p0200 N85-11333
Model for non-linear crack growth prediction, taking load sequence (LOSEQ) effects into consideration [BLL-RAE-TRANS-2114-(5207)] 02 p0206 N85-11371
Weak shocks and steady waves in a nonlinear elastic rod or granular material [AD-A145715] 02 p0209 N85-11383
Statistical Plasma Physics. Proceedings of the Workshop of the US-Japan Joint Institute for Fusion Theory Program [IPPJ-689] 02 p0282 N85-11832
Stochasticity and transport in Hamiltonian systems 02 p0282 N85-11836
Pulsed neodymium glass laser system for investigating nonlinear optical phenomena in gases 03 p0348 N85-12241
Self-study manual on optical radiation measurements. Part 1: Concepts. Chapter 11: Linearity considerations and calibrations [PB84-218346] 03 p0421 N85-12690
Simulation of a transmission circuit composed of slightly nonlinear elements. Computation of the intermodulation on signals composed of N carriers [CNES-NT-105] 04 p0496 N85-13167
Numerical improvement of asymptotic solutions and nonlinear shell analysis 05 p0648 N85-14158
PROGRAM VSAERO: A computer program for calculating the non-linear aerodynamic characteristics of arbitrary configurations: User's manual [NASA-CR-166476] 06 p0749 N85-14602
Perceptibility of nonlinear distortions in power amplifier 06 p0789 N85-15041
Supersonic nonlinear potential analysis [NASA-CR-172456] 07 p0897 N85-15685
An investigation of vortex-induced aerodynamic characteristics of supersonic cruise configurations [NASA-CR-174299] 07 p0898 N85-15690
Nonlinear semigroups and evolution governed by accretive operators [AD-A147556] 07 p1033 N85-16557
Nonlinear optical studies of rydberg atoms using degenerate four-wave mixing [AD-A146827] 07 p1043 N85-16623
Prediction of dynamic stall characteristics using advanced non-linear panel methods [AD-A148453] 08 p1078 N85-16836
The pressure deflagration limit of solid rocket propellants 08 p1117 N85-17046
Nonlinear finite element analysis of elastic and elastic-plastic buckling of cylinders under complex combined loads 09 p1332 N85-18373
Generation and evolution of diabatic planetary waves in continuously stratified atmosphere with Ekman dissipation 09 p1354 N85-18515
On the interaction of a sound pulse with the shear layer of an axisymmetric jet. Part 3: Nonlinear effects [NASA-CR-172512] 09 p1378 N85-18663
Magnetostatic problems in nonlinear media with hysteresis [DE85-003701] 10 p1482 N85-19358
Finite element analysis of nonlinear oscillations and flutter of shells of revolution [AD-A149071] 10 p1496 N85-19440
Nonlinear seismology 10 p1503 N85-19482
Symmetry breaking for a class of semi-linear elliptic problems [AD-A149093] 10 p1546 N85-19748
Modelling and residual analysis of nonlinear auto-regressive time series in exponential variables [AD-A149047] 10 p1550 N85-19776
New approach for solving large residual nonlinear least squares problems [DE85-002555] 11 p1707 N85-20742
Nonlinear analysis for high-temperature multilayered fiber composite structures — turbine blades [NASA-TM-83754] 12 p1797 N85-21273
Control of nonlinear objects 12 p1842 N85-21561
On local total strain redistribution using a simplified cyclic inelastic analysis based on an elastic solution [NASA-TM-86913] 12 p1864 N85-21690
Nonlinear analysis of layered composite plates and shells [PB85-127181] 12 p1868 N85-21719
Mesh effects on the computation of non-linear gravity waves of arbitrary discharge [COLL-AERON-8501] 12 p1888 N85-21848
Seismic waves and dispersion relations 13 p2116 N85-23181
Bifurcation theory applied to aircraft motions [NASA-TM-86704] 14 p2210 N85-23705
Macro for fitting nonlinear models to Poisson distributed data [DE84-008569] 14 p2412 N85-24871
Nonlinear problems in flight dynamics involving aerodynamic bifurcations [NASA-TM-86706] 15 p2462 N85-25206
Uniqueness and stability in nonlinear elasticity and viscoelasticity [AD-A151470] 15 p2637 N85-26264
The nonlinear analysis of thick composite plates using a cubic spline function 16 p2796 N85-27252
Studies of collisional and nonlinear radiative process for development of coherent UV and XUV sources [AD-A152001] 16 p2865 N85-27670
Method of calculating separation flow of subsonic gas stream around wings 17 p2942 N85-28161
Numerical solution of one-dimensional nonlinear problems of statics for elastic beams and shells under rigid constraints 17 p2943 N85-28166
How a swing behaves [DE85-006280] 17 p3027 N85-28720
Nonlinear problems in continuum mechanics [AD-A153387] 17 p3046 N85-28846
Hyperbolic phenomena in the flow of viscoelastic fluids [AD-A153533] 18 p3099 N85-29186
Nonlinear plasma reactions on the antenna impedance of high transmission power satellites [BMFT-FB-W-84-053] 18 p3192 N85-29799
The stability and dynamics of elastic structures and fluid flows [AD-A154188] 19 p3268 N85-30252
On the stability of collocated controllers in the presence or uncertain nonlinearities and other perils 20 p3416 N85-31201
Basic EMC (Electromagnetic Compatibility) technology advancement for C3 systems. Volume 1B: Demodulation radio frequency interference effects in operational amplifier circuits [AD-A154121] 20 p3440 N85-31350

Nonlinear Constitutive Relations for High Temperature Application, 1984
[NASA-CP-2369] 20 p3465 N85-31530
Nonlinear analysis of an axisymmetric structure subjected to non-axisymmetric loading
20 p3468 N85-31549
Strongly nonlinear dynamics of baroclinic waves
20 p3488 N85-31681
Nonlinear dynamics: A personal perspective
[DE85-010962] 20 p3521 N85-31899
Hubble space telescope: Pointing error effects on nonlinear ball joints
[NASA-TM-86511] 20 p3545 N85-32058
New approximations and findings of theory of nonlinear acoustic beams 21 p3680 N85-32863
Toward the propagation of waves in unsteady media
21 p3683 N85-32881
Nonlinear spectroscopy
[AD-A154708] 21 p3704 N85-33010
Study of nonlinear distortion in microwave amplifiers using Schottky gate field effect transistors
22 p3780 N85-33423
Nonlinear response and failure characteristics of internally pressurized composite cylindrical panels
[NASA-CR-176148] 22 p3800 N85-33546
Application of nonlinear least squares methods to the analysis of solar spectra
[NASA-CR-176122] 22 p3816 N85-33637
Refractive indices and thermo-optic coefficients of nonlinear crystals isomorphic to KH2PO4
[DE85-012968] 22 p3847 N85-33831
Elastohydrodynamic lubrication calculations used as a tool to study scuffing
[NASA-TM-87097] 23 p3938 N85-34408
Nonlinear adhesive behavior effects in a cracked orthotropic sheet stiffened by a semi-infinite orthotropic sheet
[NASA-TM-87584] 23 p3941 N85-34426
Nonlinear digital phase-locked loops with application to Loran-C receivers 24 p4063 N85-35178
Membrane reinforcement in concrete shells: Design versus nonlinear behavior 24 p4084 N85-35312
Generation of stimulated emission in the soft X-ray range by nonlinear processes with excimer lasers
[DE85-012465] 24 p4098 N85-35403
Analysis of the nonlinear equations describing the elastic, thermal, and electromagnetic behavior of solids: Existence of solutions of semi-inverse problems
24 p4100 N85-35415
Width of nonlinear difference resonances
[DE85-013026] 24 p4148 N85-35719
The HEAO-2 Guest Investigator Program: Non-linear growth of instabilities in line-driven stellar winds
[NASA-CR-176166] 24 p4168 N85-35840

NONNEWTONIAN FLOW
A two phase flow model at the level of a narrowing section — blood flow 20 p3507 N85-31799

NONNEWTONIAN FLUIDS
Vertical channel free convection for a power law fluid with a constant heat flux
[DE84-014551] 01 p0047 N85-10311
Nonnewtonian, unsteady flow in a convergent divergent duct 20 p3456 N85-31483

NONOSCILLATORY ACTION
Uniformly high-order accurate non-oscillatory schemes, 1
[NASA-CR-175768] 16 p2853 N85-27589

NONPARAMETRIC STATISTICS
Nonparametric maximum penalized likelihood estimation of a density from arbitrarily right-censored observations
[AD-A148589] 02 p0251 N85-11644
Nonparametric analysis of Minnesota spruce and aspen tree data and LANDSAT data 07 p0984 N85-16253
Bootstrap confidence intervals
[AD-A147572] 07 p1033 N85-16559
A kernel type estimator of a quantile function from right-censored data
[AD-A148753] 09 p1374 N85-18635
Nonparametric estimation of density and hazard rate functions when samples are censored
[AD-A150948] 14 p2411 N85-24868
Generation and termination of binary decision trees for nonparametric multiclass classification
[AD-A151361] 15 p2640 N85-26283
Construction of efficient algorithms for the estimation of multivariate probability densities
[AD-A151509] 15 p2640 N85-26285
A non-parametric probability density estimator and some applications
[AD-A151653] 15 p2641 N85-26287
Confidence intervals based on interpolated order statistics
[AD-A152607] 17 p3025 N85-28701
Nonparametric renewal function estimation
[AD-A153474] 18 p3173 N85-29672
Nonparametric estimation of the probability of ruin
[AD-A153523] 18 p3174 N85-29674
A new approach to evaluate gamma-ray measurements
[OG-9.5-11] 23 p4031 N85-34988
Multidimensional analysis of data obtained in experiments with X-ray emulsion chambers and extensive air showers
[HE-3.6-2] 24 p4184 N85-35951

NONPOINT SOURCES
Algorithm for astronomical, extended source, signal-to-noise radio calculations
[NASA-TP-2396] 03 p0445 N85-12833

NONREFLECTION
U ENERGY ABSORPTION

NONRELATIVISTIC ELECTRONS
U ELECTRONS

NONRIGIDITY
U FLEXIBILITY

NONSTABILIZED OSCILLATION
Coupled acoustic and hydrodynamic wave instabilities
13 p2000 N85-22538
Nonlinear problems in flight dynamics involving aerodynamic bifurcations
[NASA-TM-86706] 15 p2462 N85-25206

NONUNIFORM FLOW
Laminar flow heat exchangers. Viscosity induced non-uniform flow
[AD-A144777] 01 p0047 N85-10307
First derivatives of flow quantities behind two-dimensional, nonuniform supersonic flow over a convex corner
[NASA-TM-86272] 08 p1077 N85-16828
Studies on the interference of wings and propeller slipstreams
[NASA-CR-175753] 15 p2463 N85-25210
Effect of nonuniform size on internal stresses in a rapid, simple shear flow of granular materials. Part 1: Two grain sizes
[AD-A154045] 19 p3285 N85-30372

NONUNIFORM MAGNETIC FIELDS
Geological reasons for change in intensity of linear magnetic anomalies of the Kursk magnetic anomaly
[NASA-TM-77824] 10 p1514 N85-19552
Fermi surface study of CeSb
[DE85-002532] 10 p1564 N85-19662
Velocity space diffusion of high energy ions induced by a lower hybrid wave in a nonuniform magnetic field
[IPPJ-714] 16 p2968 N85-27681
Electrostatic ion cyclotron instability due to a nonuniform electric field perpendicular to the external magnetic field
[AD-A155474] 21 p3707 N85-33019

NONUNIFORM PLASMAS
Diffraction of plane TM-wave on continuously irregular elliptical plasma 13 p2067 N85-22914

NONUNIFORMITY
Spectral evaluation of irregularity of superconducting coaxial cables 13 p2082 N85-23000
Gradient scaling for nonuniform meshes
[DE85-009625] 22 p3784 N85-33443

NONVISCOUS FLOW
U INVISCID FLOW

NOREPINEPHRINE
Does a 50-cycle alternating field have central nervous effects?
[BLL-CE-TRANS-8083-(9022.09)] 16 p2839 N85-27507

NORMAL DENSITY FUNCTIONS
The performance of variable sampling plans when the normal distribution is truncated
[AD-A147717] 08 p1215 N85-17649
A new method of approximating normal and t-tail areas
[AD-A148457] 10 p1548 N85-19761
Comparison of MESOI atmospheric dispersion estimates with data and estimates from other models
[DE85-002372] 11 p1678 N85-20572
Full statistical characteristics of microdeformation
[BLL-M-36078-(5828.4)] 16 p2798 N85-27254
Analysis and model/data comparisons of large-scale release of nitrogen tetroxide
[DE85-009869] 18 p3133 N85-29406
A robust estimator of location using an adaptive spline model
[AD-A153662] 18 p3174 N85-29676
Bayesian inference and diagnostics for the 3 parameter logistic model
[AD-A153840] 18 p3175 N85-29681
Evaluation of densities and distributions via hermite and generalized laguerre series employing high-order expansion coefficients determined recursively via moments or cumulants
[AD-A153950] 18 p3175 N85-29682
Decay of a coherent scalar disturbance in a turbulent flow
[NASA-TM-86700] 19 p3284 N85-30244
Bayesian factor analysis
[AD-A154184] 19 p3347 N85-30747
Comments on estimating quantiles for Gaussian functionals by simulation
[AD-A154302] 19 p3348 N85-30750
The distribution of the number of empty cells in a generalized random allocation scheme
[AD-A154808] 21 p3677 N85-32841
The dispersive evolution of charged-particle bunches in random magnetic fields
[SH-4.1-2] 23 p4004 N85-34828
On the statistical significance of excess events: Remarks of caution and the need for a standard method of calculation
[OG-9.5-10] 23 p4031 N85-34987
Large deviations for the maxima of some random fields
[AD-A155909] 24 p4143 N85-35881

NORMAL DISTRIBUTIONS
U NORMAL DENSITY FUNCTIONS

NORMAL FORCE DISTRIBUTION
U FORCE DISTRIBUTION

NORMAL SHOCK WAVES
Effect of the Basset term on particle relaxation behind normal shock waves
[AD-A145446] 02 p0196 N85-11320
Dispersion curves for normal waves in cylindrical shell and conditions for spatial coincidence in vicinity of critical frequencies 06 p0778 N85-14973
Calculation of an unsteady transonic flow with shock waves and separation in Laval nozzles
[MPIS-14/1984] 14 p2213 N85-23729
Parallel fast-forward shock within 1 AU: Helios-1 and 2 observations
[MPAE-W-79-84-27] 24 p4169 N85-35847

NORMALITY
More limit theory for the sample correlation function of moving averages
[AD-A148975] 10 p1550 N85-19773

NORMALIZING (STATISTICS)
Renormalization theory in four dimensional scalar fields
[NOTA-INTERNA-624] 02 p0292 N85-11895
Probability distribution density of normalized radar range 04 p0485 N85-13098
Development of computer aided database design and maintenance tools
[AD-A151782] 16 p2845 N85-27537
The distribution and dynamics of planetary nebulae in M32 and the Andromeda Galaxy
20 p3546 N85-32068

NORMS
On the distribution of integral and prime divisors with equal norms 11 p1688 N85-20689
A variable-complexity norm maximization problem
[AD-A153514] 18 p3169 N85-29634
Dosimetry and limit values for internal contamination with radionuclides: From (International Commission on Radioactive Protection) ICRP-2 to ICRP-30
[IRI-190-84-03] 20 p3507 N85-31804

NORTH AMERICA
Tectonic history of a continent: Island arc boundary, west-central Idaho 05 p0673 N85-14324
Simulating responses to expected climate change in eastern North America: Applications to decision-making in the forest industry
[DE85-001272] 07 p1008 N85-16408
North American vegetation patterns observed with the NOAA-7 advanced very high resolution radiometer — North America
[E85-10082] 08 p1174 N85-17400
Monthly and seasonal weather outlook for January 1985, volume 39, number 1
[PB85-148799] 12 p1898 N85-21915
Arctic-North Atlantic rift megasystem
13 p2105 N85-23117
El Nino, the capricious child 13 p2108 N85-23121
Acid precipitation in North America: 1980, 1981 and 1982 annual data summaries from acid deposition system data base
[PB86-162477] 16 p2822 N85-27410
Monthly and seasonal weather outlook for mid-January to mid-February 1985, volume 39, number 2, January 15, 1985
[PB85-164572] 16 p2837 N85-27500
Monthly and seasonal weather outlook for February 1985, volume 39, number 3, January 30, 1985
[PB85-159424] 16 p2838 N85-27502
Monthly and seasonal weather outlook for mid-February to mid-March 1985, volume 39, number 4, February 14, 1985
[PB85-164580] 19 p3149 N85-29500
Use of 121.5/243.0 MHz COSPAS-SARSAT data by North American SAR agencies — search and rescue (SAR) 20 p3405 N85-31127

NORTH AMERICAN AIRCRAFT
NT B-1 AIRCRAFT
NT B-70 AIRCRAFT
NT X-15 AIRCRAFT
NORTH ATLANTIC TREATY ORGANIZATION (NATO)
Hazard Studies for Solid Propellant Rocket Motors
[AGARD-CP-367] 08 p1114 N85-17025
Aims and requirements of NATO group AC/310
08 p1114 N85-17026
NORTH CAROLINA
Environmental geologic atlas of the North Carolina coastal zone: Dare, Hyde, Tyrrell and Washington Counties
[PB84-222975] 01 p0068 N85-10439
Revised Uniform Summary of Surface Weather Observations (RUSSWO). Pope AFB, Fayetteville, North Carolina, parts A-F
[AD-A146918] 07 p1005 N85-16389
Control technology for fiber reinforced plastics industry at AMF Hatteras Yachts, New Bern Division, New Bern, North Carolina
[PB85-109015] 10 p1460 N85-19198
Investigation of radiometric properties of LANDSAT-4 MSS — California, North Carolina, South Carolina, and New England 11 p1686 N85-20500
NORTH DAKOTA
Geothermal resource assessment for North Dakota
[DE84-016128] 04 p0526 N85-13367
NORTH POLAR SPUR (ASTRONOMY)
The nature of the soft X-ray emitting region in the direction of the North Polar spur
06 p0677 N85-15568
Excess gamma rays from the Loop I supernova remnant
[OG-3.1-10] 22 p3874 N85-33998
NORTH SEA
Effects of the oceans on polar motion: Continued investigations
[E85-10037] 03 p0379 N85-12416
Impact of ERS-1 observations on wave forecasting in the North Sea 03 p0381 N85-12437
Determination of the altimetric geoid and gravity anomalies in the North Sea: Implications for a solution of the general circulation problem using ERS-1 data
03 p0382 N85-12446
The structure of the Iceland-Faeroe ridge, derived from geophysical measurements
[DRIC-T-7255] 03 p0397 N85-12535
Measurements on the diffusion of hydrogen chloride in the waste gas plume of incineration ships in the North Sea. Part 1: Methodology, instrumentation and presentation of data
[GKSS-84-E-23-PT-1] 05 p0672 N85-14319
Intrusion of radioactive industrially polluted water from North Sea into central Baltic Sea
10 p1498 N85-19454
NORTHERN HEMISPHERE
NT ARCTIC REGIONS
Climate of the Northern Hemisphere, 1851 - 1900 compared to contemporary climate
[DE84-016368] 04 p0539 N85-13426
Interannual variations of the winter circulation in the Northern Hemisphere and in the southern oscillation (meridian) and their possible connections with the climate of Northeast Brazil
[INPE-3333-TDL/182] 10 p1519 N85-19573
Middle Atmosphere Program. Handbook for MAP, volume 5
[NASA-CR-175481] 11 p1656 N85-20434
A catalogue of dynamic parameters describing the variability of the middle stratosphere during the northern winters 11 p1656 N85-20435
Middle Atmosphere Program. Handbook for MAP, volume 7
[NASA-CR-175479] 11 p1656 N85-20437
Workshop on Comparison of Data and Derived Dynamical Quantities During Northern Hemisphere (PMP-1) Winters 11 p1657 N85-20444
Middle Atmosphere Program. Handbook for MAP. Volume 12: Coordinated Study of the Behavior of the Middle Atmosphere in Winter (PMP-1) Workshops
[NASA-CR-175475] 11 p1665 N85-20492
The 500 millibar sign frequency teleconnection charts: Fall
[PB85-110930] 11 p1667 N85-20612
The 500 millibar sign frequency teleconnection charts: Summer
[PB85-111359] 11 p1668 N85-20613
The 500 millibar sign frequency teleconnection charts: Spring
[PB85-111367] 11 p1668 N85-20614
A new NASA/MSFC mission analysis global cloud cover data base
[NASA-TP-2448] 12 p1893 N85-21678
Moisture variation in northern hemisphere temperate latitudes 13 p2105 N85-23119
Optimization of system for observing Northern Hemisphere atmospheric pressure field
15 p2485 N85-25338
Numerical simulation of North Atlantic Sea ice variability, 1951 - 1980 15 p2603 N85-26040
Climatic impact of a change in North Atlantic Deep Water formation 15 p2603 N85-26045
Full shadow phenomenon in Earth's upper atmosphere 16 p2808 N85-27316
A climatic data bank for Northern Hemisphere land areas, 1851-1980
[DE85-007863] 16 p2835 N85-27486
The contrasting Northern Hemisphere winters of 1980-81 and 1981-82 18 p3144 N85-29468
On the global distribution of three-dimensional Eliassen-Palm fluxes by stationary waves
18 p3145 N85-29469
Transient eddies in the UCLA GCM
18 p3145 N85-29470
Troposphere-stratosphere (surface-55 km) monthly general circulation statistics for the Northern Hemisphere-four year averages
[NASA-TM-86182] 20 p3495 N85-31730
All sky Northern Hemisphere 10(15) EV gamma-ray survey
[OG-2.6-3] 22 p3870 N85-33968
NORTHERN SKY
The structure of galactic HI in directions of low total column density
[NASA-CR-175709] 16 p2882 N85-27785
All sky Northern Hemisphere 10(15) EV gamma-ray survey
[OG-2.6-3] 22 p3870 N85-33968
NORTHROP AIRCRAFT
NT F-18 AIRCRAFT
NORWAY
Space research in Norway
[SAD-110-T] 03 p0321 N85-12072
Deployment of a regional array in Norway
[AD-A147032] 07 p0997 N85-16330
Finnair, LOT, SAS reps in USSR on present operations, plans 09 p1278 N85-18035
The national Search and Rescue (SAR) needs and organization in Norway 20 p3401 N85-31099
The COSPAS/SARSAT local user terminal in Tromso, Norway. Special considerations and experience with high latitude location (69 deg, 43 min N)
20 p3402 N85-31109
The COSPAS-SARSAT system evaluation in Norway
20 p3406 N85-31133
NOSE
Re-design of ARL/HLF (Heated Laminar Flow) body nose region
[AD-A150063] 12 p1846 N85-21585
NOSE CAPS
U NOSE CONES
NOSE CONES
Laminar heat-transfer distributions on biconics at incidence in hypersonic-hypervelocity flows
[NASA-TP-2213] 07 p0957 N85-16065
Structure of SYLDA double launch system for Ariane
17 p2946 N85-26185
Applied research and development for falling-sphere air density measuring systems
[AD-A155227] 21 p3552 N85-32099
The development of staging mechanisms for the Japanese satellite launcher Mu-3SII
22 p3798 N85-33528
NOSE FINS
Wind tunnel tests on a tube-launched missile configuration with a deflectable nose control and a novel wrap-around fin stabiliser
[AR-003-696] 01 p0001 N85-10003
NOSES (FOREBODIES)
NT NOSE CONES
Automated radome testing
[AD-P004362] 12 p1826 N85-21456
Development of the F-20 nose radome
[AD-P004374] 12 p1827 N85-21468
Nose and inlet duct radomes for the firebolt aerial target
[AD-P004375] 12 p1827 N85-21469
Transonic merging separated flows
[AD-A150667] 14 p2213 N85-23724
Development of a fuselage forward section in Carbon Fiber Reinforced Plastic (CFRP) type of construction
[MBB/LFA34/CFK/PUB/008] 17 p2895 N85-27851
Wind tunnel drag evaluations of helicopter nose sections
[AD-A155489] 21 p3553 N85-32100
NOTATION
U CODING
NOTCH SENSITIVITY
The effect of notch acuity on the fracture toughness of silicon carbide/aluminum metal matrix composites
[AD-A150970] 14 p2248 N85-23936
Creep-fatigue interaction of notched 304 stainless steel bars 16 p2798 N85-27249
Initiation, growth and coalescence of small fatigue cracks
[AD-A151799] 16 p2800 N85-27265
NOTCH STRENGTH
Preliminary report on tests of tensile specimens with a part-through surface notch for a filament wound graphite/epoxy material
[NASA-CR-172545] 10 p1431 N85-19026
Tendency of selected low-carbon steels to corrosion cracking in nitrates
[BLL-BISI-TRANS-22262-(9022.06)]
18 p3073 N85-29006
Finite element analysis of notch behavior using a state variable constitutive equation 20 p3488 N85-31548
Damage mechanisms in damaged CFRP laminates
24 p4074 N85-35249
NOTCH TESTS
NT CHARPY IMPACT TEST
A discussion of problems encountered in the dynamic fracture toughness testing of materials
[OUEL-1524/84] 08 p1173 N85-17397
Effect of tempering on the strength and toughness of 2 1/4 Cr-1 Mo steel weldments
[DE85-003816] 09 p1296 N85-18140
Finite element analysis of notch behavior using a state variable constitutive equation 20 p3488 N85-31548
Effect of strain rate on the initial failure of notched GRP laminates 23 p3908 N85-34214
NOTCHED METALS
U NOTCH TESTS
NOTCHES
Weldability of micro-alloy steels as reaction of structure and inclusions
[BLL-BISI-TRANS-22196-(9022.06)]
17 p2924 N85-28027
NOVA LASER SYSTEM
Modal testing and analysis of NOVA laser structures
[DE84-017569] 11 p1636 N85-20321
Technical and historical overview of the study at Lawrence of porous antireflection coatings
[DE85-010925] 20 p3434 N85-31302
NOVAE
NT DWARF NOVAE
NT HERCULES NOVA
The abundances of the elements -carbon to silicon- in Nova Corona Australa 1981 11 p1753 N85-21024
Hydrodynamic simulations of recurrent novae
11 p1753 N85-21025
Strong earthquakes, novae and cosmic ray environment
[SH-10.1-3] 23 p4053 N85-35135
NOWCASTING
Nowcasting 2. Mesoscale Observations and Very-Short-Range Weather Forecasting — conferences
[ESA-SP-208] 01 p0073 N85-10487
On the nowcasting of mountain-generated thunderstorm systems 01 p0074 N85-10489
Generation of deep convective clouds along mesoscale storm outflow boundaries 01 p0074 N85-10490
Automated analysis and nowcasting of mesoscale convective systems 01 p0074 N85-10492
Forecasting of polar lows 01 p0075 N85-10495
Rain bands and symmetric instability
01 p0075 N85-10496
Some mesoscale weather effects and the very short-range forecasting impact of variable snow cover
01 p0075 N85-10499
Frontal motion in mountainous terrain: Analysis and implications for 0 to 12 hour forecasts
01 p0076 N85-10502
The past, present, and anticipated future contributions of geosynchronous satellites to short range prediction
01 p0076 N85-10503
Use of satellite soundings and imagery for nowcasting and very-short-range forecasting
01 p0076 N85-10504
NESDIS operational precipitation estimation technique 01 p0076 N85-10505
A scheme for the delineation and extrapolation of thunderstorms from GOES satellite data
01 p0076 N85-10507
Test results from RAINSAT 01 p0076 N85-10508
The use of dual polarisation radar for observing and predicting convective activity 01 p0077 N85-10512
The PROMIS Doppler radar system; design and operational experience 01 p0077 N85-10513
Nowcasting with Doppler radar: The forecaster-computer relationship
01 p0077 N85-10514
Doppler radar analysis of a frontal zone prior to convective development 01 p0077 N85-10515
VHF/UHF radar and its application in nowcasting
01 p0078 N85-10516

Use of ground based microwave radiometers for nowcasting 01 p0078 N85-10517
The potential use of atmospheric profilers in short-range prediction 01 p0078 N85-10518
Analysis strategies for field dependent estimation and network design — mesoscale modeling 01 p0078 N85-10520
Application of automatic pattern methods in very-short-range forecasting 01 p0078 N85-10521
The development of objective forecast techniques based on advection of surface weather parameters 01 p0078 N85-10522
Preliminary assessment of very short term forecasting of rain from single radar data 01 p0078 N85-10523
Optimum parameters for determining the motion of radar field by cross-correlation method 01 p0079 N85-10524
Digital radar data as an aid in nowcasting in Hong Kong 01 p0079 N85-10525
Short period forecasts in West Africa using Meteosat data 01 p0079 N85-10526
Predicability of mesoscale phenomena 01 p0079 N85-10528
The initialization of mesoscale models 01 p0079 N85-10529
Applications of a finite-element regional model to very-short-range forecasting 01 p0080 N85-10531
Application of mesoscale numerical model to local weather prediction 01 p0080 N85-10532
The United Kingdom Meteorological Office mesoscale forecasting system 01 p0080 N85-10533
An operational forecasting system for stratus and fog with sodar 01 p0081 N85-10539
Preperation steps for the use of one-dimensional interpretation models for nowcasting purposes in the German weather net 01 p0081 N85-10540
A one-level mesoscale model suitable for nowcasting and short-term forecasting in regions of complex terrain 01 p0081 N85-10541
A short-term forecast model for thunderstorm rotation 01 p0081 N85-10542
Experiment on nowcasting of heavy rainfall and severe storms in central China in 1979-1981 01 p0081 N85-10545
A summary of operational developments in nowcasting and short-range forecasting techniques on the Canadian West Coast 01 p0082 N85-10547
Simple methods in very short-range forecasting based on data from a mesoscale network of automatic stations (ANETZ) and from satellite (Meteosat) and radar — Swiss Alps 01 p0082 N85-10548
FRONTIERS: Progress with a system for nowcasting rain — Forecasting Rain Optimized using New Techniques of Interactively Enhanced Radar and Satellite (FRONTIERS) 01 p0082 N85-10552
Nowcasting: Advances with McIDAS 3 — Man-computer Interactive Data System System (McIDAS) 01 p0082 N85-10553
Development of nowcasting in China 01 p0083 N85-10554
Interactive computer display systems in nowcasting 01 p0083 N85-10557
MERIT: A man/computer data management and enhancement system for upper air nowcasting/forecasting in the United States — Minimum Energy Routes using Interactive Techniques (MERIT) 01 p0083 N85-10558
Development of an operational system for Very-Short-Range Forecasting (VSRF) at Swedish Meteorological and Hydrological Institute (SMHI) 01 p0083 N85-10559
PROMIS 600: The pilot project for the future Swedish weather service 01 p0083 N85-10560
User requirements for very-short-range weather forecasts: Some key issues 01 p0084 N85-10562
Use of short-range weather forecasts at construction sites: Some results from a user and a market test 01 p0084 N85-10563
Benefits resulting from tailored very-short-range forecasts in Sweden 01 p0084 N85-10564
Some aspects of matching nowcasting and Very-Short-Range Forecasting (VSRF) products with the need of a multilingual community of a mountainous country — Swiss Alps 01 p0084 N85-10566
Nowcasting using lightning location techniques 01 p0084 N85-10568
Frost nowcasting in the agricultural area of Valencia (Spain) — meteorological satellites 05 p0658 N85-14225
TAF verification (airport weather forecasts) [GEOPHYSBDBW-FM-205] 05 p0667 N85-14420
Agricultural weather report for the Ijsselmeer polders in the 1984 summer season; a verification report [KNMI-TR-61] 20 p3498 N85-31737

NOXIOUS MATERIALS
U CONTAMINANTS

NOZZLE COEFFICIENT
U NOZZLE FLOW

NOZZLE DESIGN
Jet noise suppression by porous plug nozzles [NASA-CR-3613] 02 p0275 N85-11790
Experimental investigation of shock-cell noise reduction for single stream nozzles in simulated flight [NASA-CR-3845] 04 p0557 N85-13550
Delta wing nozzle assembly for chemical lasers [AD-D011396] 07 p0970 N85-16158
Some aspects of the design of a fly-by-wire flying control system for a supersonic V/STOL fighter aircraft [COLL-AERON-8413] 12 p1780 N85-21175
Characteristics of a confined jet thrust vector control nozzle [AD-A153087] 17 p2958 N85-28268
Convoluted nozzle design for the RL10 derivative 2B engine [NASA-CR-174953] 19 p3220 N85-29965
Analytical simulation of weld effects in creep range 20 p3468 N85-31550

NOZZLE EFFICIENCY
Static internal performance of single-expansion-ramp nozzles with various combinations of internal geometric parameters [NASA-TM-86270] 06 p0749 N85-14797
Advanced OTV engine concepts 08 p1108 N85-17001
Mixing characteristics of an underexpanded multiple jet ejector [AD-A149557] 10 p1485 N85-19375
Modifications to the nozzle test chamber to extend nozzle static-test capability [NASA-TM-86368] 15 p2464 N85-25216

NOZZLE FLOW
Local stability analysis for a planar shock wave [NASA-TP-2387] 04 p0452 N85-12864
Experimental investigation of shock-cell noise reduction for single stream nozzles in simulated flight [NASA-CR-3845] 04 p0557 N85-13550
Transonic jets: A numerical approach in the hodograph plane 05 p0592 N85-13774
Flow of nitrogen-pressurized Halon 1301 in fire extinguishing systems [NASA-CR-174271] 07 p0900 N85-15701
A computer program for the performance analysis of scarfed nozzles [AD-A147370] 07 p0905 N85-15730
Delta wing nozzle assembly for chemical lasers [AD-D011396] 07 p0970 N85-16158
Critical flashing flow of subcooled fluids in nozzles with contour discontinuities [DE84-017229] 09 p1319 N85-18296
Static internal performance of a two-dimensional convergent nozzle with thrust-vectoring capability up to 60 deg [NASA-TP-2391] 10 p1419 N85-18951
SSME thrust chamber simulation using Navier-Stokes equations [NASA-CR-171349] 10 p1430 N85-19017
Preliminary analysis of selected gas dynamic problems — space shuttle main engine main combustion transients and IUS nozzle flow [NASA-CR-171343] 10 p1483 N85-19361
Mixing characteristics of an underexpanded multiple jet ejector [AD-A149557] 10 p1485 N85-19375
Characteristics of flow of oscillatory-relaxing gas in nozzles with constant cross-sections in throat region 11 p1716 N85-20794
An experimental study of spray thruster [REPT-613] 12 p1845 N85-21578
Calculation of an unsteady transonic flow with shock waves and separation in Laval nozzles [MPIS-14/1984] 14 p2213 N85-23728
Thermal state of cooled thin-walled nozzle blade 14 p2270 N85-24066
Effect of drag behind nozzle array on its force and energy characteristics 14 p2277 N85-24107
Modifications to the nozzle test chamber to extend nozzle static-test capability [NASA-TM-86368] 15 p2464 N85-25216
An experimental study of clustered, two-dimensional rocket nozzles [AD-A151889] 15 p2495 N85-25390
Nozzle wall roughness effects on free-stream noise and transition in the pilot low-disturbance tunnel [NASA-TM-86369] 23 p3930 N85-34355

NOZZLE GEOMETRY
Density distribution in supersonic jet discharged into vacuum from nozzle with bevel tip 02 p0269 N85-11757
An experimental investigation of two-dimensional thrust augmenting ejectors, part 1 [NASA-CR-174111] 04 p0458 N85-12894
A study of lift characteristics of an upper surface blown jetwing with a rectangular nozzle 05 p0591 N85-13767
Certain optimal parameters of high-velocity Venturi ejection tubes [BLL-M-35924-(5828.4)] 05 p0634 N85-14068
Comparison of options for reduction of noise in the test section of the NASA Langley 4x7m wind tunnel, including reduction of nozzle area [NASA-CR-172446-VOL-2] 05 p0726 N85-14667
Multiple steady states for characteristic initial value problems [NASA-CR-172486] 06 p0749 N85-14800
Preliminary analysis of tone-excited two-stream jet velocity decay [NASA-TM-86951] 12 p1770 N85-21114
Some unique features of isentrophic flow of gas under high pressures 13 p2043 N85-22768
Thermal state of cooled thin-walled nozzle blade 14 p2270 N85-24066
Effect of drag behind nozzle array on its force and energy characteristics 14 p2277 N85-24107
Nonnewtonian, unsteady flow in a convergent divergent duct 20 p3456 N85-31483
Investigation of influence of gas exit modes on characteristics of N2O - N2 - He discharge laser 21 p3684 N85-32868

NOZZLE INSERTS
Thermal state of cooled thin-walled nozzle blade 14 p2270 N85-24066

NOZZLE THRUST COEFFICIENTS
Static internal performance of a two-dimensional convergent nozzle with thrust-vectoring capability up to 60 deg [NASA-TP-2391] 10 p1419 N85-18951

NOZZLE WALLS
A curved test section for research on transonic shock wave-boundary layer interaction [VTH-LR-414] 16 p2701 N85-26682

NOZZLES
Turbine test report, addendum [DE84-015130] 02 p0205 N85-11353
Investigation of an ejector heat pump by analytical methods [DE84-016675] 04 p0500 N85-13189
Pressure drop and coefficients of internal heat transfer necessary for transpiration cooling 13 p2050 N85-22831
Discussion of the paper, Some Aspects of Propulsion for the Augmenter-Wing Concept, by D. C. Whitley [NASA-TM-77884] 22 p3727 N85-33108

NUCLEAR AUXILIARY POWER UNITS
NT SNAP
NT SPACE POWER REACTORS
NT SPACE POWER UNIT REACTORS
Spaceborne power systems preference analyses. Volume 1: Summary [NASA-CR-175844] 14 p2349 N85-24517
Spaceborne power systems preference analyses. Volume 2: Decision analysis [NASA-CR-175845] 14 p2349 N85-24518

NUCLEAR CAPTURE
NT ELECTRON CAPTURE
Activities of the Solid State Physics Research Institute [NASA-CR-175899] 17 p3042 N85-28818
A 200-MeV pi(+) induced nucleon removal from 24Mg 17 p3042 N85-28821
An attempt to detect induced neutron capture in laser radiation field 21 p3690 N85-32928
Evaluated nuclear-data file for niobium [DE85-012095] 21 p3704 N85-33009
Applications and misapplications of the channel-capture formalism of direct neutron capture [DE85-013992] 24 p4152 N85-35748

NUCLEAR CHEMISTRY
Fundamental molecular physics and chemistry, part 1 [DE84-009127] 04 p0561 N85-13571
Activities in nuclear physics and high energy physics 11 p1728 N85-20866

NUCLEAR DEFORMATION
Trapping model analysis of annihilation line narrowing in some plastically deformed metals and alloys [AERE-R-10599] 14 p2258 N85-23995

NUCLEAR ELECTRIC POWER GENERATION
NT NUCLEAR AUXILIARY POWER UNITS
NT NUCLEAR POWER PLANTS
NT NUCLEAR POWER REACTORS
NT SNAP
NT SPACE POWER REACTORS
NT SPACE POWER UNIT REACTORS
NT THERMONUCLEAR POWER GENERATION
USSR report: Engineering and equipment [JPRS-UEQ-84-007] 08 p0775 N85-14954
Technology transfer to the Middle East [PB85-127744] 12 p1952 N85-22264

USSR report: Engineering and equipment
[JPRS-UEQ-85-004] 17 p2939 N85-26142
East Europe report: Science and technology
[JPRS-ESA-85-023] 21 p3572 N85-32217
Magnetic Fusion Program plan
[DE85-009881] 22 p3846 N85-33823
NUCLEAR ELECTRIC PROPULSION
Rendezvous with Saturn's rings 15 p2679 N85-26543
Tethered nuclear power for the Space Station
[NASA-TM-87023] 16 p2740 N85-26912
An evaluation of oxygen-hydrogen propulsion systems for the Space Station
[NASA-TM-87059] 18 p3087 N85-28971
NUCLEAR EMULSIONS
The inner granulometric density of the tracks in nuclear emulsions and its application to determine the chemical spectrum of primary cosmic ray nuclidi
[OG-4.3-9] 22 p3879 N85-34034
Abundance of low energy (50-150 MeV) antiprotons in cosmic rays
[OG-6.1-1] 22 p3887 N85-34092
A survey of multiplicities and rapidity densities from existing emission data on hadron-nucleus nucleus-nucleus collisions 24 p4146 N85-35706
On a possibility of inelasticity partial coefficient K sub gamma determination in pi C and pi Pb interactions at 10 to the 14th power eV (experiment PAMIR 1)
[HE-1.1-12] 24 p4171 N85-35859
Anugiar distribution of shower particles produced in the collisions of 20-GeV/c and 300-GeV negative pions with emulsion nuclei 24 p4172 N85-35868
Stopping relativistic Xe, Ho, Au and U nuclei in nuclear emulsions 24 p4173 N85-35876
Heavy nucleus collisions between 20 and 60 GeV/nucleon
[HE-1.4-2] 24 p4175 N85-35890
Characteristics of central collision events in Fe-nucleus interactions for 20 - 60 GeV/nucleon
[HE-1.4-3] 24 p4176 N85-35891
Nucleus-nucleus interaction above several hundred GeV/n
[HE-1.4-4] 24 p4176 N85-35892
Observation of direct hadronic pairs in nucleus-nucleus collisions in JACEE emulsion chambers
[HE-1.4-5] 24 p4176 N85-35893
Excessive production of electron pairs by soft photons in low multiplicity ion interactions
[HE-1.4-6] 24 p4176 N85-35894
On the mechanism of anomalous nucleus-nucleus interactions at energies above 1 TeV/nucleon
[HE-1.4-8] 24 p4177 N85-35896
Meson multiplicity in nucleus-nucleus collisions above 4 GeV/amu
[HE-1.4-10] 24 p4177 N85-35897
Inclusive angular distribution of alpha and Li fragments produced in the Fe-C and Fe-Pb collisions at 1.88 GeV/u
[HE-1.4-11] 24 p4177 N85-35898
Experiment Pamir-3. Coplanar emission of high energy gamma-quanta at interaction of hadrons with nuclei of air atoms at energies above 10 to the 7th power GeV
[HE-1.4-12] 24 p4177 N85-35899
The effect of the relative nuclear size on the nucleus-nucleus interactions
[HE-1.4-13] 24 p4177 N85-35900
Japan - USSR joint emulsion chamber experiment at Pamir
[HE-3.1-1] 24 p4177 N85-35901
Intensities of high-energy cosmic rays at Mount Kanbala
[HE-3.1-2] 24 p4177 N85-35902
High energy gamma-rays and hadrons at Mount Fuji
[HE-3.1-3] 24 p4177 N85-35903
On the characteristics of emulsion chamber family events produced in low heights
[HE-3.1-6] 24 p4178 N85-35904
Some characteristic cosmic ray events and an attempt at their explanation
[HE-3.1-8] 24 p4178 N85-35906
Energy spectra of proton and nuclei of primary cosmic rays in energy region 10 TeV/particle
[HE-3.1-10] 24 p4178 N85-35908
Jets in air-jet family
[HE-3.2-1] 24 p4179 N85-35912
Search for anomalous C-jets in Chacaltaya emulsion chamber experiment
[HE-3.2-5] 24 p4179 N85-35913
Exotic interactions among C-jets and Pb-jets
[HE-3.2-6] 24 p4179 N85-35914
Characteristics of anomalously high multiplicity cosmic ray interactions
[HE-3.3-1] 24 p4180 N85-35920
Transverse momentum distribution of pion deg in the fragmentation region of super high energy interactions 24 p4180 N85-35921
Study of hadron bundles observed in Chacaltaya two-story emulsion chamber
[HE-3.3-4] 24 p4180 N85-35922
Atmospheric interactions detected in both the upper and the lower chambers at Chacaltaya
[HE-3.3-7] 24 p4180 N85-35925
NUCLEAR ENERGY
Advancement of remote technology: Past perspectives and future plans
[DE85-000934] 09 p1327 N85-18342
Proceedings of the Fifth International Conference on Nuclear Methods in Environmental and Energy Research
[DE84-017348] 19 p3310 N85-30521
NUCLEAR EXPLOSION EFFECT
EMP injection on conduit entries, type Brattberg — electromagnetic pulse (EMP) injection
[FOA-E-30001-A3] 02 p0193 N85-11290
Electromagnetic pulse and the electric power network
[DE84-015403] 04 p0493 N85-13143
Tests for susceptibility to electromagnetic attack
[SNIAS-842-422-101] 04 p0494 N85-13154
Evaluation of nuclear detonation location capability under high attack scenario
[AD-A155761] 24 p4149 N85-35729
NUCLEAR EXPLOSIONS
NT THERMONUCLEAR EXPLOSIONS
Seismology 1983: Nuclear test ban verification, earthquake and Earth resource investigation
[FOA-C-20537-T1] 02 p0229 N85-11495
Theoretical and observed dispersion of acoustic-gravity waves in atmosphere 04 p0557 N85-13547
High-bandwidth multichannel fiber optic system for measuring gamma rays
[DE84-014526] 04 p0564 N85-13596
China report: Science and technology
[JPRS-CST-84-025] 11 p1620 N85-20197
Micro-deformation of quartz under dynamic action and its applications 11 p1620 N85-20201
Attenuation of seismic waves at regional distances
[AD-A150198] 13 p2132 N85-23267
NASTRAN analysis comparison to shock tube tests used to simulate nuclear overpressures 15 p2576 N85-25888
Elastic-workhardening SDF (Single-Degree-of-Freedom) system subjected to random blast excitations
[AD-A151668] 15 p2579 N85-25909
Three new fiber-optic components
[DE85-006269] 15 p2653 N85-26364
A multiphase continuum model to describe dynamic loading effects in nonlinear porous media
[DE85-010102] 19 p3301 N85-30463
Seismic discrimination
[AD-A154167] 20 p3494 N85-31722
Marine Sample Exploitation Project: Estimates regarding the sensitivity and technology for the detection of nuclear explosion debris in the marine environment
[DE85-013176] 23 p3947 N85-34462
Investigation of the lightning vulnerability of nuclear explosive test systems at the Nevada Test Site
[DE85-011761] 24 p4124 N85-35563
Evaluation of nuclear detonation location capability under high attack scenario
[AD-A155761] 24 p4149 N85-35729
Ground motion measurements for the QUESO nuclear event
[DE85-014808] 24 p4151 N85-35743
Heavy flavours production in quark-gluon plasma formed in high energy nuclear reactions 24 p4175 N85-35886
NUCLEAR FISSION
Energy-advanced nuclear data: Measurements and physical interpretations
[DE85-006196] 19 p3366 N85-30872
Design of a helium-cooled molten salt fusion breeder
[DE85-010474] 20 p3528 N85-31943
Liquid uranium alloy-helium fission reactor
[DE85-006511] 23 p3970 N85-34607
A very important process of nucleosynthesis in stars
[OG-7.1-11] 23 p4014 N85-34872
Neutronic calculations for a new high flux reactor
[DE85-011551] 24 p4150 N85-35734
NUCLEAR FUEL ELEMENTS
Technology status of thermionic fuel elements for space nuclear power 05 p0610 N85-13893
Austrian contributions to fuel rod failure models shown at the International Standard Problem (ISP)-14
[OEFZS-4276] 07 p1041 N85-16613
Evacuate and backfill apparatus and method
[DE85-006018] 23 p3938 N85-34411
Thermal hydraulic features of the TMI accident
[DE85-014569] 24 p4152 N85-35747
NUCLEAR FUEL REPROCESSING
Advancement of remote systems technology: Past perspectives and future plans
[DE84-016710] 04 p0509 N85-13250
Inquiry into disintegration control of irradiated low enrichment uranium for high temperature gas cooled reactors
[OEFZS-7281] 07 p1042 N85-16615
Advancement of remote technology: Past perspectives and future plans
[DE85-000934] 09 p1327 N85-18342
Control and electronic subsystems for the advanced servomanipulator
[DE85-001900] 09 p1327 N85-18343
Dual arm master controller concept
[DE85-001901] 09 p1327 N85-18344
Advanced remotely maintainable force-reflecting servomanipulator concept
[DE85-001902] 09 p1328 N85-18345
Flow measurement by laser Doppler anemometry in a nuclear fuel assembly
[DE85-003260] 12 p1848 N85-21592
Consolidated fuel reprocessing program
[DE85-010591] 19 p3358 N85-30818
Analytical methods in the purex process
[BLL-DOUNREAY-TR-952(9091.9F)] 24 p4149 N85-35727
NUCLEAR FUELS
NT CERAMIC NUCLEAR FUELS
NT SPENT FUELS
USSR report: Energy
[JPRS-UEN-84-038] 07 p0994 N85-16312
Irradiation effects on fuels for space reactors
[DE84-016460] 12 p1931 N85-22134
Tritium catalyzed deuterium Tokamaks
[DE85-004825] 12 p1936 N85-22166
Feasibility study of a fission-suppressed Tokamak fusion breeder
[DE85-009099] 18 p3190 N85-29786
Experimental program to determine maximum temperatures for dry storage of spent fuel
[DE85-010307] 19 p3236 N85-30060
Mixtures experiment where the amount of the mixture is a factor under study
[DE85-010974] 19 p3250 N85-30153
Response of steam-water mixtures to pressure transients
[DE85-010798] 19 p3267 N85-30262
A review of the SIMMER-2 analyses of liquid-metal-cooled fast breeder reactor core-disruptive accident fuel escape
[DE85-010803] 19 p3366 N85-30876
Solid-state track recorder neutron dosimetry in the Three-Mile Island Unit-2 reactor cavity
[DE85-011360] 20 p3531 N85-31966
East Europe report: Science and technology
[JPRS-ESA-85-021] 21 p3568 N85-32190
Reaction of uranium and the fluorocarbon FC-75
[DE85-012322] 22 p3843 N85-33802
Liquid uranium alloy-helium fission reactor
[DE85-006511] 23 p3970 N85-34607
Separation of uranium from technetium in recovery of spent nuclear fuel
[DE85-006499] 23 p3972 N85-34627
NUCLEAR FUSION
NT CONTROLLED FUSION
Study of structure of nuclei with neutrons and nuclear data measurements for MFE
[DE84-015128] 01 p0117 N85-10602
Fusion and its future in Illinois
[DE84-014686] 01 p0122 N85-10633
Materials studies for magnetic fusion energy applications at low temperatures, 7
[DE84-013487] 01 p0122 N85-10637
Report on solar neutrino experiments
[DE84-014567] 01 p0131 N85-10699
Statistical Plasma Physics. Proceedings of the Workshop of the US-Japan Joint Institute for Fusion Theory Program
[IPPJ-689] 02 p0282 N85-11832
Chlorine and bromine solar neutrino experiments
[DE84-015720] 02 p0304 N85-11969
Fusion plasma theory. Task 3: Auxiliary heating in Tokamaks and tandem mirrors
[DE84-014940] 04 p0566 N85-13609
Theoretical investigations relevant to magnetic fusion research
[DE85-001777] 06 p0866 N85-15503
Multihole couplers for overmoded waveguide systems
[IPF-83-8] 09 p1394 N85-18773
Short mode selective directional couplers
[IPF-83-9] 09 p1394 N85-18774
Improved directional couplers for overmoded waveguide systems
[IPF-84-1] 09 p1394 N85-18775
Lidar-Thomson scattering — Joint European Torus
[IPF-84-3] 09 p1394 N85-18777
Two phases of neutron production in the POSEIDON plasma focus
[IPF-84-10] 09 p1395 N85-18783

A proposed method for fast determination of plasma parameters
[IPP-1/228] 11 p1730 N85-20877
Light diffraction with collective, thermal electron density fluctuation in plasmas with several ionic components
[IPF-84-5] 11 p1733 N85-20904
Plasma and nuclear processes in solar matter
12 p1954 N85-22277
Opacity determinations for Inertial Confinement Fusion (ICF) materials using an average atom model
12 p1957 N85-22295
Slowing down of charged particles by the bound electrons in a plasma — ion beams, nuclear fusion
[LP-209] 14 p2419 N85-24829
Glossary of fusion energy
[DE84-017180] 14 p2425 N85-24958
A new approach to quasr differential equations
[AD-A149321] 15 p2638 N85-26272
Plasma theory and computations
15 p2655 N85-26384
Prospects for developing attractive magnetic fusion concepts
[DE85-006925] 16 p2667 N85-27684
Fusion-power-core design of a Compact Reversed-Field Pinch Reactor (CRFPR)
[DE85-007710] 16 p2668 N85-27692
Experimental plasma research: Plasma summaries
[DE85-008116] 17 p3039 N85-28805
Tokamak fusion core experiment maintenance study
[DE85-008040] 17 p3040 N85-28813
Current activities and background of technology transfer and exchange program at Lawrence Livermore National Laboratory
[DE85-009526] 18 p3199 N85-29843
LINE: A code which simulates spectral line shapes for fusion reaction products generated by various speed distributions
[DE85-010833] 19 p3341 N85-30702
Magnetic fusion 1985: What next?
[DE85-009953] 19 p3365 N85-30868
Energy-advanced nuclear data: Measurements and physical interpretations
[DE85-006198] 19 p3366 N85-30872
Fusion reactions at low energy
[DE85-010561] 20 p3526 N85-31944
Nuclear responses in INTOR plasma stabilization elements
[DE85-010469] 20 p3535 N85-31995
Nuclear data needs for fusion energy development
[DE85-010445] 20 p3536 N85-32000
Prospects for lasers for fusion energy assessed
21 p3684 N85-32885
Infrared laser holography used in fusion plasma studies
21 p3687 N85-32905
Tritium technology review
[DE85-010504] 21 p3703 N85-33006
Gamma-ray line emission from Al-26 produced by Wolf-Rayet stars
[OG-3.2-5] 22 p3875 N85-34003
Diffuse galactic annihilation radiation from supernova nucleosynthesis
[OG-3.2-8] 22 p3875 N85-34004
Numerical solutions of the Vlasov equation
23 p3979 N85-34672
Dissipation terms in one-dimensional hydrodynamic code for ICF target
23 p3980 N85-34677
Stability of implosion dynamics
23 p3980 N85-34680
Nucleosynthesis in the terrestrial and solar atmospheres
[SH-2.2-2] 23 p4000 N85-34797
Propagation and nucleosynthesis of ultraheavy cosmic rays
[OG-7.1-5] 23 p4013 N85-34867
A very important process of nucleosynthesis in stars
[OG-7.1-11] 23 p4014 N85-34872
Results of ultra-low level 71ge counting for application in the Gallex-solar neutrino experiment at the Gran Sasso Underground Physics Laboratory
[SH-8.1-2] 23 p4049 N85-35108
Gamma-ray production cross sections for alpha-particle induced reactions on F-19 and Na-23
[DE85-012603] 24 p4150 N85-35732
Operations considerations in designing a high speed multi-channel data acquisition system
[DE85-012640] 24 p4154 N85-35758
Some nuclear data needs in astrophysics
[DE85-012916] 24 p4168 N85-35842

NUCLEAR INTERACTIONS
NT ELECTRON CAPTURE
NT NUCLEAR CAPTURE
NT SPIN-ORBIT INTERACTIONS
NT STRONG INTERACTIONS (FIELD THEORY)
NT WEAK INTERACTIONS (FIELD THEORY)

Chaos near the Coulomb Barrier: Nuclear molecules
[DC85-001280] 07 p1041 N85-16608
Workshop on Nuclear Dynamics 3
[INC-40007-24] 12 p1931 N85-22130
Theoretical aspects of electroweak and other interactions in medium-energy nuclear physics
[DE85-003821] 13 p2157 N85-23392
Nuclear spectroscopic studies
[DE85-006894] 16 p2662 N85-27652
Study of proton and neutron activation of metal samples in low Earth orbit
[NASA-CR-171596] 21 p3558 N85-32130
Contributions to the 19th International Cosmic Ray Conference
[NASA-CR-176060] 21 p3714 N85-33044
Gamma ray line production from cosmic ray spallation reactions
22 p3875 N85-34005
Abundance of low energy (50-150 MeV) antiprotons in cosmic rays
[OG-6.1-1] 22 p3887 N85-34092
Search for heavy antinuclei in the cosmic radiation
[OG-6.1-2] 22 p3887 N85-34093
Nineenth International Cosmic Ray Conference. OG sessions, volume 3
[NASA-CP-2376-VOL-3] 23 p4012 N85-34862
Cosmic ray secondary nuclei and the structure of the galaxy
[OG-7.2-4] 23 p4014 N85-34876
Observations of accelerated high current low emittance beams in the SLC Linac
[DE85-013073] 24 p4068 N85-35211
Proceedings of the Workshop on Detectors for Relativistic Nuclear Collisions
[LBL-18225] 24 p4146 N85-35700
Detectors for relativistic nuclear collisions (report from the Fixed-Target Hadron Group)
24 p4146 N85-35701
Event parameters: Fixed targets
24 p4146 N85-35702
Working group on penetrating probes at fixed target facilities
24 p4146 N85-35703
A survey of multiplicities and rapidity densities from existing emission data on hadron-nucleus nucleus-nucleus collisions
24 p4146 N85-35706
A simulation of ultra-relativistic nucleus-nucleus collisions
24 p4146 N85-35707
Some remarks about simulation of cosmic ray phenomena with use of nuclear interaction models based on the current SPS proton-antiproton data
[HE-1.2-6] 24 p4172 N85-35864
Low P sub T hadron-nucleus interactions
[HE-1.2-7] 24 p4172 N85-35865
The response of a scintillation counter below an emulsion chamber to heavy nucleus interactions in the chamber
24 p4175 N85-35889
Characteristics of central collision events in Fe-nucleus interactions for 20 - 60 GeV/nucleon
[HE-1.4-3] 24 p4176 N85-35891
Nucleus-nucleus interaction above several hundred GeV/n
[HE-1.4-4] 24 p4176 N85-35892
Observation of direct hadronic pairs in nucleus-nucleus collisions in JACEE emulsion chambers
[HE-1.4-5] 24 p4176 N85-35893
Excessive production of electron pairs by soft photons in low multiplicity ion interactions
[HE-1.4-6] 24 p4176 N85-35894
Meson multiplicity in nucleus-nucleus collisions above 4 GeV/amu
[HE-1.4-10] 24 p4177 N85-35897
Inclusive angular distribution of alpha and Li fragments produced in the Fe-C and Fe-Pb collisions at 1.88 GeV/u
[HE-1.4-11] 24 p4177 N85-35898
The effect of the relative nuclear size on the nucleus-nucleus interactions
[HE-1.4-13] 24 p4177 N85-35900
Japan - USSR joint emulsion chamber experiment at Pamir
[HE-3.1-1] 24 p4177 N85-35901
On the characteristics of emulsion chamber family events produced in low heights
[HE-3.1-5] 24 p4178 N85-35904
Search for anomalous C-jets in Chacaltaya emulsion chamber experiment
[HE-3.2-5] 24 p4179 N85-35913
Exotic interactions among C-jets and Pb-jets
[HE-3.2-6] 24 p4179 N85-35914
Scaling violation in hadron-nucleus interaction
[HE-3.2-8] 24 p4179 N85-35916
The model of independent particles emission in the multiparticle production theory
[HE-3.2-10] 24 p4179 N85-35918
Study of hadron bundles observed in Chacaltaya two-story emulsion chamber
[HE-3.3-4] 24 p4180 N85-35922
Anomalous correlation between hadron and electromagnetic particles in hadron and gamma-ray families
[HE-3.3-6] 24 p4180 N85-35924
Atmospheric interactions detected in both the upper and the lower chambers at Chacaltaya
[HE-3.3-7] 24 p4180 N85-35925
Lateral distribution of high energy hadrons and gamma ray in air shower cores observed with emulsion chambers
[HE-3.3-8] 24 p4180 N85-35926
Size distributions of air showers accompanied with high energy gamma ray bundles observed at Mt. Chacaltaya
[HE-3.3-9] 24 p4181 N85-35927
A halo event created at 200 m above the Chacaltaya emulsion chamber
[HE-3.4-5] 24 p4182 N85-35933
A binocular-type atmospheric interaction generating sequential exotic features
[HE-3.4-6] 24 p4182 N85-35934
Gamma-hadron families and scaling violation
[HE-3.4-7] 24 p4182 N85-35935
Super-family P2 C-96-125 observed by Japan-URSS Joint Emulsion Chamber Experiment
[HE-3.4-8] 24 p4182 N85-35936
On the halo events observed by Mount Fuji and Mount Kanbala Emulsion Chamber Experiments
[HE-3.4-9] 24 p4182 N85-35937
Experiment Pamir-2. Fianit: A giant super-family with halo (Epsilon sub 0 at approximately 10(17) eV)
[HE-3.4-10] 24 p4182 N85-35938
Experiment Pamir-4: Analysis of superfamily with halo of electromagnetic nature detected in deep XEC
[HE-3.4-11] 24 p4183 N85-35939
Particle interactions at energies over 1000 TeV inferred from gamma-families observed at Mount Fuji
[HE-3.5-1] 24 p4183 N85-35940
A search for mini-clusters in Japan-USSR Joint Experiment at Pamir
[HE-3.5-2] 24 p4183 N85-35941
Mini-clusters
[HE-3.5-3] 24 p4183 N85-35942
Structure of super-families
[HE-3.5-7] 24 p4183 N85-35944
Extremely high energy hadron and gamma-ray families(3). Core structure of the halo of superfamily
[HE-3.5-8] 24 p4183 N85-35945
Numerical analysis of electromagnetic cascades in emulsion chambers
[HE-3.5-9] 24 p4184 N85-35946
New analysis of nuclear interaction observed by Mt. Kanbara emulsion chamber experiment
[HE-3.7-4] 24 p4186 N85-35963
Structured events in Pamir carbon X-ray chambers
[HE-3.7-7] 24 p4186 N85-35965
Electrons, muons and hadrons in extensive air showers and how do they depend on nuclear interaction model, part 2
24 p4187 N85-35969
Electrons, muons and hadrons in extensive air showers and how do they depend on nuclear interaction model, part 1
24 p4187 N85-35972
Takhra-Takaro complex intended for the investigations of EAS spatial characteristics near axis
24 p4190 N85-35995
Correlation of high energy muons with primary composition in extensive air shower
[HE-4.3-7] 24 p4191 N85-36001
The longitudinal development of muons in cosmic ray air showers at energies 10(15) - 10(17) eV
[HE-4.3-12] 24 p4192 N85-36006
Simulation of gamma-initiated showers
[HE-4.5-10] 24 p4195 N85-36033
Delayed particles in EAS at Akeno
[HE-6.2-6] 24 p4211 N85-36144

NUCLEAR MAGNETIC RESONANCE
NT PROTON RESONANCE

Studies of hydrogenated amorphous silicon
[DE84-013038] 01 p0067 N85-10443
Electronic structure and lattice dynamics of solid state substances from gamma nuclear resonance absorption and angular correlation measurements
03 p0427 N85-12728
Paramagnetic impurity effects in NMR determinations of hydrogen diffusion and electronic structure in metal hydrides. Cerium in YH-2 and LaH-2.25
[DE84-014127] 04 p0472 N85-13005
Development program: Nuclear magnetic resonance gyroscope (NMR-gyro). Phase 1: Development of an experimental model
[BMFT-FB-W-84-041] 05 p0639 N85-14101
Polarization in chemically doped hydrogen-rich glasses
[DE84-017486] 06 p0771 N85-14936
The 13C nuclear magnetic resonance in graphite intercalation compounds
[NASA-CR-174261] 07 p1040 N85-16601

NMR study on rotational fluctuation in solid hydrogen and deuterium 09 p1289 N85-18093
Advanced NMR characterization of zeolite catalysts [DE85-000456] 09 p1291 N85-18104
Transport and relaxation processes in supercritical fluids [DE85-002079] 09 p1308 N85-18797
Theoretical determination of surface magnetism [DE85-003224] 11 p1714 N85-20763
Proton NMR and susceptibility measurements in TiCoH/sub x [DE85-003309] 12 p1807 N85-21336
Synthesis and thermomechanical properties of new AT-Phenylene R systems [AD-A149961] 12 p1813 N85-21372
Phase separation in polyurethanes: A deuterium NMR study [AD-A151515] 15 p2505 N85-25451
Electronic properties of new organic conductors [DE85-005590] 15 p2549 N85-25736
Bound and free moisture studies of solid materials by FTNMR [DE85-003227] 16 p2747 N85-26952
Ion and polymer chain motion in a superionic sodium-poly(ethylene oxide) complex [AD-A152290] 16 p2755 N85-27001
NMR manometer for measuring high pressures at liquid-helium temperatures 17 p2944 N85-28171
Characteristics of charge transfer in the dispersed phase of electrorheological suspensions [RAE-TRANS-2125] 19 p3233 N85-30040
Biology and Medicine Division [DE85-010696] 19 p3327 N85-30613
NMR investigation of crystalline electric field effect on spin-spin relaxation in (Y(1-x)RE(x))Rh4B4 [DE85-010512] 19 p3357 N85-30814
Advanced NMR characterization of zeolite catalysts [DE85-010143] 19 p3363 N85-30853
H1-NMR studies on lymphocyte membranes in human lymphoproliferative diseases 20 p3505 N85-31787
An EPR (Electron-Paramagnetic-Resonance) and ENDOR (Electron-Nuclear-Double-Resonance) study of ferroelectric ammonium sulfate [AD-A155580] 21 p3710 N85-33033
NMR in the 80 s: New nuclei, new pulses — nuclear magnetic resonance (NMR) [DRIC-T-7467] 22 p3836 N85-33754
Nuclear magnetic resonance study of the intramolecular rearrangement of 2-(5-cyanotetrazolato)pentaammine cobalt (III) perchlorate [DE85-010810] 22 p3839 N85-33772
Apparatus for unilateral generation of a homogeneous magnetic field [DE85-006001] 23 p3928 N85-34345

NUCLEAR MEDICINE
NT RADIOBIOLOGY
Isotopes in day to day life [IAEA/PI/A.6E-84-00824] 03 p0417 N85-12068
Applications of CdTe to nuclear medicine [DE85-011877] 23 p3952 N85-34482

NUCLEAR MODELS
Particle physics: Recent successes and future prospects [DE85-006175] 17 p3033 N85-28765
Many-body processes in atomic and molecular physics [DE85-009750] 19 p3354 N85-30791
Proceedings of the 1984 Workshop on High-Energy Excitations in Condensed Matter, volume 2 [DE85-007395] 19 p3357 N85-30809
Soliton matter as a model of dense nuclear matter [DE85-009937] 19 p3359 N85-30825
Heavy quarks and CP: Moriond 1985 [DE85-010553] 22 p3841 N85-33790
Quark structure of nuclei [DE85-010781] 22 p3842 N85-33795

NUCLEAR PARTICLES
NT ALPHA PARTICLES
NT ANTINEUTRINOS
NT ANTINUCLEONS
NT ANTIPARTICLES
NT ANTIPROTONS
NT BETA PARTICLES
NT BOSONS
NT HYPERONS
NT KAONS
NT MESONS
NT MUONS
NT NUCLEONS
NT PHOTOELECTRONS
NT PHOTONS
NT PIONS
NT POSITRONS
NT VECTOR MESONS
A numerical study of the mean trajectory approximation in a non-adiabatic process [AD-A152763] 17 p3030 N85-28737
Possibilities for studying short-lived nuclei produced at LAMPF [DE85-010740] 19 p3365 N85-30864
Plastic scintillator detectors for the study of transfer and breakup reactions at intermediate energies [DE85-009945] 20 p3528 N85-31945
Abundances from solar-flare gamma-ray line spectroscopy [SH-2.1-13] 23 p3999 N85-34794
The heavy ions in space experiment [OG-9.1-10] 23 p4023 N85-34936
Cherenkov-dE/dx-range measurements on cosmic ray iron group nuclei [OG-9.1-12] 23 p4024 N85-34937
The response of ionization chambers to relativistic heavy nuclei [OG-9.1-13] 23 p4024 N85-34938

NUCLEAR PHYSICS
NT REACTOR PHYSICS
USSR report: Physics and mathematics [JPRS-UPM-84-006] 02 p0256 N85-11676
Experimental medium energy physics [DE84-014625] 02 p0278 N85-11807
ATLAS beam properties: Some implications for target making [DE84-006595] 02 p0278 N85-11812
Solid state investigations with nuclear physics methods 03 p0428 N85-12731
Activities report in nuclear physics 05 p0728 N85-14680
Experimental investigations in particle physics at intermediate energies [DE85-001481] 11 p1722 N85-20832
Renewal request for high energy physics at Texas A and M University [DE85-004469] 11 p1724 N85-20843
Activities in nuclear physics and high energy physics 11 p1728 N85-20866
Theoretical nuclear physics [DE85-003466] 12 p1932 N85-22135
Research in theoretical nuclear physics [DE85-004349] 12 p1932 N85-22137
Theoretical aspects of electroweak and other interactions in medium-energy nuclear physics [DE85-009621] 13 p2157 N85-23392
Research in theoretical nuclear physics [DE85-006172] 14 p2418 N85-24920
Breakthrough in container confinement of ultracold neutrons 15 p2644 N85-26311
Heavy ion physics at BNL, the AGS and RHIC [DE85-005951] 17 p3033 N85-28760
High energy gamma rays from complex particle collisions [DE85-007871] 17 p3036 N85-28783
Research activities of the Physics Division [DE85-006958] 19 p3357 N85-30811
Work in Amsterdam on local intelligence — artificial intelligence [NIKHEF-H/84-9] 20 p3518 N85-31877
Current experiments in elementary particle physics, revision 1-85 [DE85-011513] 20 p3529 N85-31950
Activities report in nuclear physics and particle acceleration 20 p3532 N85-31977
USSR report: Physics and mathematics [JPRS-UPM-85-004] 21 p3680 N85-32960
High-energy Physics Institute building 3-trillion-ev accelerator 21 p3691 N85-32934
Activities of the Physics Division [DE85-000784] 21 p3702 N85-33002
Proceedings of the 16th LAMPF Users Group Meeting [DE85-011666] 22 p3839 N85-33773
Nuclear physics in the 10 to 300 MeV energy range using a pulsed white neutron source [DE85-003713] 22 p3839 N85-33775
Physics Division annual review, 1 April 1983 - 31 March 1984 [ANL-84-24] 23 p3969 N85-34602
Forty-five years of e(+)e(-) annihilation physics: 1956 to 2001 [DE85-013052] 24 p4149 N85-35723

NUCLEAR POTENTIAL
K(-) hydrogen bound and continuum states in momentum space [DE85-010429] 22 p3841 N85-33789

NUCLEAR POWER GENERATION
U NUCLEAR ELECTRIC POWER GENERATION

NUCLEAR POWER PLANTS
A pilot study of future research on seismic hazards in Sweden [FOA-C-20644-T1] 02 p0229 N85-11496
Control and electronic subsystems for the advanced servomanipulator [DE85-001900] 09 p1327 N85-18343
Electromagnetic compatibility of measurement and control equipment in nuclear installations [BLL-WH-607-(9091.9F)] 11 p1623 N85-20222
Assuring structural integrity in Army systems [NASA-CR-175492] 11 p1651 N85-20398
Computer-generated display system guidelines. Volume 1: Display design [DE85-000679] 11 p1701 N85-20699
Lasers in the nuclear industry 14 p2309 N85-24289
Application of new welding technology in the fabrication of nuclear power plant 15 p2566 N85-25829
Information presentation in power plant control rooms [VTT-320] 16 p2864 N85-27668
Corrosion test on high-alloy steels [BLL-BISI-TRANS-21627-(9022.06)] 17 p2926 N85-28046
Investigation on the application of the pulsed eddy current method of non-destructive testing using controlled signals (CS-technique) [BLL-BISI-TRANS-22249-(9022.06)] 18 p3119 N85-29303
A remote-operated manipulator vehicle [HSE-TRANS-11133] 19 p3281 N85-30349
Seismic pipe support construction practices [DE85-901315] 19 p3287 N85-30386
Advanced ultrasonic imaging of piping in Dresden and Vermont Yankee reactors [TI85-010049] 20 p3464 N85-31520
Airborne cloud tracking measurements during the Three Mile Island nuclear station accident, Middletown, Pennsylvania. Date of survey: March - June 1979 [DE85-012080] 22 p3816 N85-33638
SMACS: A system of computer programs for probabilistic seismic analysis of structures and subsystems. Volume 1: User's manual [DE85-011853] 22 p3830 N85-33724
State-of-the-art of solid-state motor controllers [TI85-006674] 24 p4162 N85-35806

NUCLEAR POWER REACTORS
NT SPACE POWER REACTORS
NT SPACE POWER UNIT REACTORS
Acoustic imaging in a water filled metallic pipe — monitoring heat exchangers in nuclear power reactors [DE84-016051] 09 p1378 N85-18665
Graphic display development program, volume 1 [DE85-011076] 19 p3333 N85-30649
ASME performance test on TVA Sequoyah unit 1 [DE85-901316] 19 p3358 N85-30815
Magnetic fusion 1985: What next? [DE85-009953] 19 p3365 N85-30866
Applicability of 100kWe-class of space reactor power systems to NASA manned space station missions [NASA-CR-174696] 24 p4149 N85-35728

NUCLEAR PROPULSION
NT NUCLEAR ELECTRIC PROPULSION

NUCLEAR PUMPED LASERS
Estimate of nuclear-pumped X-ray laser mechanism 06 p0748 N85-14795

NUCLEAR RADIATION
NT BETA PARTICLES
NT FAST NEUTRONS
NT GAMMA RAY BEAMS
NT GAMMA RAY BURSTS
NT GAMMA RAYS
NT NEUTRON BEAMS
NT SPALLATION
NT THERMAL NEUTRONS
Inquiry into disintegration control of irradiated low enrichment uranium for high temperature gas cooled reactors [OE/ZS-7251] 07 p1042 N85-16615
Nuclear radiation induced absorption in optical materials [DE85-007128] 15 p2649 N85-26336
Space radiation studies — Spacelab 2 Payload [NASA-CR-171410] 15 p2665 N85-26584
MATADOR (Methods for the Analysis of Transport And Deposition Of Radionuclides) code description and user's manual [TI85-901402] 23 p3966 N85-34592
Abundances from solar-flare gamma-ray line spectroscopy [SH-2.1-13] 23 p3999 N85-34794

NUCLEAR RADIATION SPECTROSCOPY
Investigations of vacuum ultraviolet and soft X-ray lasers [AD-A148277] 06 p1167 N85-17358
Moessbauer study of amorphous Fe(67)Co(18)B(14)Si(1) [AERE-R-11526] 11 p1737 N85-20928
NMR in the 80 s: New nuclei, new pulses — nuclear magnetic resonance (NMR) [DRIC-T-7467] 22 p3836 N85-33754

NUCLEAR REACTIONS
NT ALPHA DECAY
NT ANNIHILATION REACTIONS
NT CONTROLLED FUSION
NT ELECTRON CAPTURE
NT ELECTRON SCATTERING
NT HIGH ENERGY INTERACTIONS
NT NEUTRON EMISSION
NT NEUTRON SCATTERING
NT NUCLEAR CAPTURE
NT NUCLEAR FISSION
NT NUCLEAR FUSION
NT NUCLEAR INTERACTIONS
NT NUCLEAR SCATTERING
NT PHOTONUCLEAR REACTIONS
NT PHOTOPRODUCTION
NT POSITRON ANNIHILATION
NT PROTON SCATTERING
NT PROTON-PROTON REACTIONS
NT RADIOACTIVE DECAY
NT RESONANCE SCATTERING
NT SPALLATION
NT SPIN-ORBIT INTERACTIONS
NT THERMONUCLEAR REACTIONS
Engineering Physics Division
[DE84-007778] 02 p0274 N85-11787
Solar neutrino spectroscopy
[DE84-015518] 02 p0304 N85-11968
A study of defects in neutron transmutation doped silicon: Gallium by hall effect analysis
[AD-A148047] 03 p0433 N85-12758
Tables of nuclear cross sections for galactic cosmic rays: Absorption cross sections
[NASA-RP-1134] 16 p2964 N85-27665
Activities report in nuclear physics and high energy physics
[JF40026] 17 p3095 N85-28777
New approaches to functionalized fluorocarbons
[AD-A154205] 19 p3248 N85-30141
Multiple collision solutions for time-dependent neutron transport in slabs of finite thickness
[OEFZS-4312] 22 p3838 N85-33762
Bibliography and index for nuclear reactions among light charged particles, volume 26
[DE85-011482] 22 p3838 N85-33766
Pairing correction of particle-hole state densities for two kinds of fermions
[DE85-011549] 23 p3971 N85-34620
Some nuclear data needs in astrophysics
[DE85-012916] 24 p4168 N85-35842
Heavy flavours production in quark-gluon plasma formed in high energy nuclear reactions
24 p4175 N85-35886
Preliminary results on underground muon bundles observed in the Frejus proton-decay detector
[HE-5.1-1] 24 p4200 N85-36067

NUCLEAR REACTOR CONTROL
Instrumentation and controls evaluation for space nuclear power systems
[DE85-000983] 09 p1383 N85-18695
Tritium technology review
[DE85-010504] 21 p3703 N85-33006

NUCLEAR REACTORS
NT BOILING WATER REACTORS
NT BREEDER REACTORS
NT EXPERIMENTAL BREEDER REACTOR 2
NT FAST NUCLEAR REACTORS
NT FAST TEST REACTORS
NT FUSION REACTORS
NT GAS COOLED REACTORS
NT HEALTH PHYSICS RESEARCH REACTOR
NT HIGH TEMPERATURE GAS COOLED REACTORS
NT HIGH TEMPERATURE NUCLEAR REACTORS
NT JANUS REACTOR
NT LIGHT WATER REACTORS
NT LIQUID COOLED REACTORS
NT LIQUID METAL COOLED REACTORS
NT LIQUID METAL FAST BREEDER REACTORS
NT NUCLEAR POWER REACTORS
NT NUCLEAR RESEARCH AND TEST REACTORS
NT PRESSURIZED WATER REACTORS
NT SPACE POWER REACTORS
NT SPACE POWER UNIT REACTORS
NT SPHEROMAKS
NT TOKAMAK DEVICES
NT WATER COOLED REACTORS
NT ZERO POWER REACTORS
The reactor dynamic code RETRANS: Structure and users guide
[OEFZS-4287] 07 p1041 N85-16614
Something in the air at Windscale — radioactive contaminants from the Sellafield nuclear Complex for reprocessing and storing irradiated fuel
[BLL-RISLEY-TR-4998-(9091.9F)]
08 p1179 N85-17429
Leakage-flow induced vibrations of a chimney structure suspended in a liquid flow — nuclear reactors
09 p1339 N85-18420
Radiation response of optical fibers in a nuclear reactor
[DE84-017221] 09 p1365 N85-18710
Proceedings of the 1984 DOE Nuclear Reactor and Facility Safety Conference, volume 1
[DE84-012130] 12 p1931 N85-22132
Proceedings of the DOE Nuclear Reactor and Facility Safety Conference, volume 2
[DE84-012694] 12 p1931 N85-22133
Comprehensive, integrated, remote sensing at DOE sites
[DE85-004667] 13 p2126 N85-23240
USSR report: Engineering and equipment
[JPRS-UEQ-84-001] 14 p2265 N85-24034
The gamma thermometer: A new type of fixed internal instrumentation developed by EDF
[BLL-CE-TRANS-6060-(9022.09)]
15 p2560 N85-25791
Analysis of orbit transfer vehicles for GPS Block 3 satellites
[AD-A152021] 16 p2732 N85-26860
High thermal power density heat transfer apparatus providing electrical isolation at high temperature using heat pipes
[NASA-CASE-LEW-12950-2] 18 p3096 N85-29179
Jet pump-drive system for heat removal
[NASA-CASE-NPO-16494-1-CU]
18 p3099 N85-29182
Flow visualization study of inverted annular flow of post dryout heat transfer region
[DE85-010482] 19 p3269 N85-30275
Development of the Cascade inertial-confinement-fusion reactor
[DE85-010933] 19 p3357 N85-30812
Simulation and operation of the EBR-2 automatic control rod drive system
[DE85-010262] 19 p3360 N85-30832
Source Term Experiments Project (STEP): Aerosol characterization system
[DE85-010248] 19 p3361 N85-30839
Solid-state track recorder neutron dosimetry in the Three-Mile Island Unit-2 reactor cavity
[DE85-011360] 20 p3531 N85-31966
Experimental method for measuring positronium reflection from surfaces
[DE85-010949] 20 p3531 N85-31967
Operation of solid state lasers exposed to electron beam
21 p3685 N85-32895
On-line temperature sensor
[DE85-011641] 22 p3787 N85-33465
Data Base Workshop: Availability-Reliability Modeling
[DE85-011570] 22 p3829 N85-33713
Neutronic calculations for a new high flux reactor
[DE85-011551] 24 p4150 N85-35734

NUCLEAR RELAXATION
Nuclear Magnetic Resonance of Polymeric Materials
[AD-A145078] 01 p0032 N85-10192
Theory of nuclear magnetic relaxation
[AD-P003911] 01 p0032 N85-10197

NUCLEAR RESEARCH
Engineering Physics Division
[DE84-007778] 02 p0274 N85-11787
China report: Science and technology
[JPRS-CST-84-025] 11 p1620 N85-20197
USSR report: Engineering and equipment
[JPRS-UEQ-85-004] 17 p2939 N85-28142

NUCLEAR RESEARCH AND TEST REACTORS
NT EXPERIMENTAL BREEDER REACTOR 2
NT HEALTH PHYSICS RESEARCH REACTOR
NT HIGH TEMPERATURE NUCLEAR REACTORS
NT JANUS REACTOR
Lidar-Thomson scattering — nuclear fusion
[IPP-1/299] 08 p1221 N85-17693
Lidar-Thomson scattering — Joint European Torus
[IPF-84-3] 09 p1394 N85-18777
NBS (National Bureau of Standards) reactor: Summary of activities Jul. 1983 through Jun. 1984
[PB85-184836] 20 p3522 N85-31907
Scientific Opportunities with Advanced Facilities for Neutron Scattering
[DE85-012113] 22 p3839 N85-33770

NUCLEAR SCATTERING
NT NEUTRON SCATTERING
NT RESONANCE SCATTERING
Bremsstrahlung from nuclear scattering at low energy near a resonance
[DE84-014852] 04 p0561 N85-13572
Toward the question of multi-quark configurations in nuclei
21 p3691 N85-32929
A unification of the interactions and the diffractive processes
24 p4173 N85-35870
On mini-cluster observed by Chacaltaya emulsion chamber experiment
[HE-3.6-12] 24 p4185 N85-35959

NUCLEAR SHIELDING
U RADIATION SHIELDING

NUCLEAR SPIN
Nuclear Magnetic Resonance of Polymeric Materials
[AD-A145078] 01 p0032 N85-10192
NMR (Nuclear Magnetic Resonance) and macromolecular migration in a melt or in concentrated solutions
[AD-P003908] 01 p0032 N85-10194
Collisional pumping for the production of intense spin-polarized, neutral beams: Target considerations
[DE85-003459] 11 p1723 N85-20841
Remarks on nucleon-nucleon hard scattering
[NIKHEF-H/84-14] 20 p3532 N85-31979

NUCLEAR STRUCTURE
Comment on the validity of an L2 treatment of the center of mass problem
[CSIR-TWISK-324] 01 p0114 N85-10779
Study of structure of nuclei with neutrons and nuclear data measurements for MFE
[DE84-015128] 01 p0117 N85-10802
Dirac single particle wave functions in inelastic electron scattering
[DE84-015129] 02 p0279 N85-11814
Studies of P-shell nuclei by large momentum transfer electron scattering
[DE84-016803] 09 p1381 N85-18688
Investigations of the structure and electromagnetic interactions of few-body systems
[DE85-002854] 11 p1721 N85-20824
Nuclear spectroscopic studies
[DE85-006894] 16 p2962 N85-27652
Extension of the consistent Q formalism to odd-A nuclei in the W-Pt region
[DE85-006284] 17 p3034 N85-28770
High energy gamma rays from complex particle collisions
[DE85-007871] 17 p3036 N85-28783
A 200-MeV pi(+) induced nucleon removal from 24Mg
17 p3042 N85-28821
S-matrix theory of nuclear forces
[DE85-007833] 18 p3179 N85-29710
Boson-fermion symmetries in the W-Pt region
[DE85-009755] 19 p3362 N85-30845
Nuclear structure problems in double beta decay
[DE85-010739] 19 p3364 N85-30859

NUCLEAR TEST REACTORS
U NUCLEAR RESEARCH AND TEST REACTORS

NUCLEAR WASTES
U RADIOACTIVE WASTES

NUCLEAR WEAPONS
Directed energy missile defense in space
[PB84-210111] 01 p0015 N85-10095
US said to seek military advantage in space
16 p2727 N85-26831
Military journal on US intelligence satellites
16 p2727 N85-26832
Surveillance program for the dissection and analysis of explosive and pyrotechnic components
[DE85-006105] 16 p2757 N85-27016
Nuclear thermal transmittance in the atmosphere using LOWTRAN-6 computer code
[AD-A154869] 21 p3630 N85-32583
Evaluation of nuclear detonation location capability under high attack scenario
[AD-A155761] 24 p4149 N85-35729

NUCLEATE BOILING
Subcooled flow boiling at high heat flux
[OUEL-1540/84] 08 p1163 N85-17338
An experimental apparatus to study nucleate pool boiling of R-114 and oil mixtures
[AD-A154077] 19 p3265 N85-30249

NUCLEATION
NT CLOUD SEEDING
Experimental and theoretical study of condensation in multicomponent vapors
[DE84-015810] 02 p0174 N85-11184
Dynamic crystallization of silicate melts
[NASA-CR-174103] 05 p0743 N85-14774
Homogeneous condensation of gaseous mixtures of Si, Fe, O, N, and C in relative cosmic abundance and implications for astronomical condensation
06 p0887 N85-15632
Fundamentals of microcrack nucleation mechanics
[NASA-CR-3851] 07 p0975 N85-16195
Influence of the amorphous-crystalline interface morphology on dislocation nucleation in pre-amorphized silicon
[DE85-002068] 09 p1398 N85-18800
Experimental and theoretical study of condensation in multicomponent vapors
[DE85-000843] 10 p1485 N85-19378

The role of void nucleation in the swelling resistance of ferritic steel
[AERE-R-11525] 11 p1610 N85-20122
A computer simulation of thin film nucleation and growth: The Volmer-Weber case
[NASA-TM-86968] 12 p1796 N85-21264
Photo-thermal detection of the onset of photo-chemical nucleation (laser-snow) in vapor
[AD-A150111] 12 p1801 N85-21295
Ionic mechanisms of soot formation in flames
[AD-A150119] 12 p1801 N85-21297
Nucleation of phase transitions in the vicinity of phase boundary. Part 1: Comparison of various idolated mechanisms. Part 2: Coupled cluster growth processes
[N-0808-5658] 12 p1938 N85-22174
Theory of oriented nucleation with asymmetric single elements. 2: Effects of rotational diffusion
[IFTR-32/1984] 12 p1939 N85-22179
Research on the kinetics of phase changes in solids
[AD-A152307] 17 p2918 N85-27989
Experimental and theoretical study of condensation in multicomponent vapors
[DE85-009357] 17 p2923 N85-28021
Interfacial segregation and fracture
[DE85-009779] 18 p3075 N85-29019
Flow field effects on nucleation in a reacting mixing layer
[ARL/AERO-R-165] 19 p3263 N85-30237
Amorphous alloys of ion-implanted Fe-Ti-C
[DE85-010856] 19 p3360 N85-30834
Ice nucleation by silver iodine particles with nearly critical size 21 p3636 N85-32600
The nucleation of ice crystals during the freezing of large supercooled drops 21 p3640 N85-32606
Concentrations of ice nuclei of different modes of activities 21 p3641 N85-32616
The nucleation of ice at very low temperatures and pressures 21 p3641 N85-32617
Ice nucleating characteristics of Capparis Aphylla, an Indian herb 21 p3641 N85-32619
The capture of ice nucleating and non ice-nucleating aerosols by ice phase precipitation 21 p3641 N85-32620
Supersaturation obtained in a condensation nucleus counter 21 p3642 N85-32624
Basic ice nucleation mechanisms on mono and microcrystals and ice forming nuclei. Theoretical analysis and experimental results achieved in the laboratory over the past ten years: Review paper 21 p3642 N85-32629
Ice nucleation of single water droplet by silver iodide: A laboratory observation 21 p3643 N85-32630
Ice-forming efficiency of the soluble and insoluble portions of dust contained in snow 21 p3643 N85-32631
Critical supersaturations with respect to water for fast condensation-freezing ice nucleation 21 p3643 N85-32632
Concentration and source areas of ice nuclei in the Alaskan atmosphere 21 p3643 N85-32634
Cloud droplet nucleation and initial growth derived from lidar depolarization studies 21 p3644 N85-32635
Eleventh International Conference on Atmospheric Aerosols, Condensation and Ice Nuclei, volume 1
[PB85-182400] 21 p3644 N85-32636
The first condensation nucleus conference 21 p3644 N85-32637
The influence of Brownian coagulation on the size distributions of atmospheric aerosols 21 p3645 N85-32643
Measurements of giant salt nuclei from inland in east China 21 p3648 N85-32668
Cloud condensation on insoluble particles 21 p3648 N85-32670
The measured rate of condensation nucleation to droplets using the techniques of chemical kinetics 21 p3652 N85-32684
Effect of ions on cloud formation and its role in solar terrestrial relationship 21 p3653 N85-32697
Modeling granular explosive detonations with shear band concepts
[DE85-011629] 22 p3754 N85-33271
Interrelationships among the terrestrial planets 22 p3953 N85-33859
The effect of liquid-liquid phase separation of glass on the properties and crystallization behavior
[NASA-TM-77880] 23 p3919 N85-34285
Size and shape dependence of CO adsorption sites on sapphire supported Fe microcrystals
[NASA-CR-176171] 24 p4100 N85-35794

NUCLEI

Arcsecond positions for millisecond VLBI nuclei of extragalactic radio sources. Part 3: 74 sources 10 p1463 N85-19225
A thermal diffusion chamber for the measurement of cloud condensation nuclei 21 p3642 N85-32627
Breakdown of helium nuclei in matter processed near black holes
[OG-8.2-20] 23 p4021 N85-34916

NUCLEI (NUCLEAR PHYSICS)

NT ALPHA PARTICLES
NT DEUTERONS
NT EVEN-EVEN NUCLEI
NT HEAVY NUCLEI
NT HYPERNUCLEI
NT ODD-EVEN NUCLEI
NT ODD-ODD NUCLEI

Study of structure of nuclei with neutrons and nuclear data measurements for MFE
[DE84-015128] 01 p0117 N85-10802
Energy deposition in microvolumes of silicon from high energy proton reactions
[AD-A144713] 01 p0123 N85-10845
Investigations of the structure and electromagnetic interactions of few-body systems
[DE85-002854] 11 p1721 N85-20824
Recent progress in electron scattering at SLAC
[DE85-002718] 11 p1723 N85-20840
Shell-model Lanczos-method studies of the Gamow-Teller strength function in astrophysics
[DE85-004205] 11 p1763 N85-21093
Solar cycle variations of the anomalous cosmic ray component
[PAPER-SH-4.6-2] 21 p3715 N85-33057
Radial and latitudinal gradients of anomalous oxygen during 1977 - 1985
[PAPER-SH-4.6-4] 21 p3716 N85-33058
NMR in the 80 s: New nuclei, new pulses — nuclear magnetic resonance (NMR)
[DRIC-T-7467] 22 p3836 N85-33754
Nineteenth International Cosmic Ray Conference. OG sessions, volume 2
[NASA-CP-2376-VOL-2] 22 p3875 N85-34006
Absolute rigidity spectrum of protons and helium nuclei above 10 GV/c
[OG-4.1-1] 22 p3875 N85-34007
Charge and energy dependence of the residence time of cosmic ray nuclei below 15 GeV/nucleon
[OG-4.1-3] 22 p3876 N85-34009
Relative abundances of sub-iron to iron nuclei in low energy (50-250 MeV/N) cosmic rays as observed in the Skylab experiment
[OG-4.1-4] 22 p3876 N85-34010
Cosmic ray charge and energy spectrum measurements using a new large area Cerenkov x dE/dx telescope
[OG-4.1-5] 22 p3876 N85-34011
Energy spectrum of cosmic-ray iron nucleus observed with emulsion chamber
[OG-4.1-10] 22 p3877 N85-34016
Measurement of the iron spectrum from 60 to 200 GeV per nucleon
[OG-4.1-11] 22 p3877 N85-34017
Cosmic ray nuclei of energy 50 GeV/NUC
[OG-4.1-12] 22 p3877 N85-34018
Composition and energy spectra of cosmic ray nuclei above 500 GeV/nucleon from the JACEE emulsion chambers
[OG-4.1-13] 22 p3877 N85-34019
Charge composition and energy spectral of cosmic ray primary particles for energies higher than 1 TeV
[OG-4.1-14] 22 p3877 N85-34020
Measurements of galactic hydrogen and helium isotopes from 1978 through 1983
[OG-4.2-2] 22 p3877 N85-34022
Primary cosmic ray spectrum in the 10 to the 12th power - 10 to the 16th power eV energy range from the NUSEX experiment
[OG-5.1-5] 22 p3881 N85-34047
Observation of arrival times of EAS with energies or = 6 x 10 (14) eV
[OG-5.3-8] 22 p3885 N85-34074
Search for heavy antinuclei in the cosmic radiation
[OG-6.1-2] 22 p3887 N85-34093
Analysis of experimental data on interstellar antiprotons in the light of measurements of high-energy electrons and He-3 nuclei
[OG-6.1-6] 22 p3888 N85-34097
Study of photon emission by electron capture during solar nuclei acceleration, 1: Temperature-dependent cross section for charge changing processes
[SH-1.1-8] 23 p3990 N85-34735
Study of photon emission by electron capture during solar nuclei acceleration. 2: Delimitation of conditions for charge transfert establishment
[SH-1.1-9] 23 p3990 N85-34736
Observation of the fluxes of nuclei with energies 10-20 MEV per nucleon during the solar flare of April 26, 1984
[SH-2.1-1] 23 p3998 N85-34783
Measurements of the fragmentation of (40)Ar, (28)Si and (12)C in CH2C and H targets between 300 and 1500 MeV/nuc at the Bevalac
[OG-7.2-19] 23 p4016 N85-34886
Cross sections for the production of fragments with Z greater than or equal to 8 by fragmentation of Z greater than or equal to 9 and less than or equal to 26 nuclei
[OG-7.2-22] 23 p4016 N85-34889
Calculation of improved spallation cross sections
[OG-7.2-23] 23 p4017 N85-34890
Cerenkov counters for high energy nuclei: Some new developments
[OG-9.1-5] 23 p4023 N85-34931
Detector calibration of the Indian cosmic ray experiment (IONS) in Space-Shuttle Spacelab-13
[SH-9.1-2] 23 p4050 N85-35117
Observation of nuclei with energies 8-30 MeV per nucleon in the Earth's magnetosphere at the altitudes 350 KM
[SH-10.1-5] 23 p4053 N85-35136
Nineteenth International Cosmic Ray Conference. HE Sessions, volume 6
[NASA-CP-2376-VOL-6] 24 p4170 N85-35848
On total cross sections and slopes at superhigh energies
[HE-1.1-4] 24 p4170 N85-35852
Measurement of interaction cross section of cosmic ray Fe nuclei (E4 GeV/N) with Al target
[HE-1.1-7] 24 p4170 N85-35855
Empirical description of the hadron-hadron and hadron-nucleus interaction at the accelerator energy range
[HE-1.2-4] 24 p4171 N85-35862
Low P sub T hadron-nucleus interactions
[HE-1.2-7] 24 p4172 N85-35865
Angular distribution of shower particles produced in the collisions of 20-GeV/c and 300-GeV negative pions with emulsion nuclei 24 p4172 N85-35868
Determination of primary energy in nucleus-nucleus collisions and the high P(sub)T tail of alpha-particles 24 p4173 N85-35875
Stopping relativistic Xe, Ho, Au and U nuclei in nuclear emulsions 24 p4173 N85-35876
Physical meaning of the multiplicities of emitted nucleons in hadron-nucleus collisions 24 p4174 N85-35877
How are particle production, nucleon emission and target fragment evaporation processes interrelated in hadron-nucleus collisions? 24 p4174 N85-35878
Experimental evidence of the decrease of kinetic energy of hadrons in passing through atomic nuclei 24 p4174 N85-35880
Energy-range relations for hadrons in nuclear matter 24 p4174 N85-35881
Scattering and stopping of hadrons in nuclear matter 24 p4174 N85-35882
Measurements of hadron mean free path for the particle-producing collisions in nuclear matter 24 p4174 N85-35883
The phi-meson and Chiral-mass-meson production in heavy-ion collisions as potential probes of quark-gluon-plasma and Chiral symmetry transitions 24 p4175 N85-35884
Experimental basis for the models of cascade propagation in atmosphere
[HE-3.6-6] 24 p4185 N85-35954
A study of gamma-families generated in nucleon-nucleus (NA) and pion-nucleus (pi A) interactions
[HE-3.7-2] 24 p4186 N85-35961
Dependence of the average spatial and energy characteristics of the hadron-lepton cascade on the strong interaction parameters at superhigh energies 24 p4186 N85-35977
A facility for investigation of multiple hadrons at cosmic-ray energies
[HE-4.6-8] 24 p4197 N85-36045
Photo nuclear energy loss term for muon-nucleus interactions based on xi scaling model of QCD
[HE-5.2-17] 24 p4204 N85-36093

NUCLEIC ACIDS

NT DEOXYRIBONUCLEIC ACID
NT RIBONUCLEIC ACIDS

NUCLEON-NUCLEON INTERACTIONS

Theoretical aspects of the nucleon-nucleon workshop
[DE85-003740] 14 p2420 N85-24933
Nonrelativistic theory of heavy-ion collisions
[DE85-007536] 17 p3031 N85-28747
Nucleon-nucleon program at TRIUMF
[DE85-000430] 17 p3032 N85-28756
S-matrix theory of nuclear forces
[DE85-007633] 18 p3179 N85-29710
Development of the relativistic impulse approximation
[DE85-008505] 18 p3179 N85-29711
Intermediate energy nuclear theory
[DE85-010440] 18 p3182 N85-29731
Summary of the discussion of the theory of radiative processes
[DE85-007612] 19 p3371 N85-30914
Antiproton-nucleus inelastic scattering and the spin-isospin dependence of the N anti N interaction
[DE85-010546] 20 p3526 N85-31935

The nucleon intensity in the atmosphere and the Pt distribution
[HE-3.1-9] 24 p4176 N85-35907
New aspects in nucleon-nucleus collisions and EAS properties around 10(6) GeV 24 p4187 N85-35974
Small air showers and collider physics
[HE-4.1-9] 24 p4187 N85-35975
Primary chemical composition from simultaneous recording of muons induced cascades and accompanying muon group underground
[HE-5.1-13] 24 p4201 N85-36075
NUCLEON-NUCLEON SCATTERING
Remarks on nucleon-nucleon hard scattering
[NIKHEF-H/84-14] 20 p3532 N85-31979
Comparison of big event with calculations of the air shower development
[HE-3.6-8] 24 p4165 N85-35956
NUCLEONS
Bremsstrahlung from nuclear scattering at low energy near a resonance
[DE84-014852] 04 p0561 N85-13572
Solar He-3-rich events and non-relativistic electron events: A new association
[NASA-TM-86179] 06 p0890 N85-15652
Neutral-current x-distributions
[DE84-016522] 09 p1382 N85-18691
A 200-MeV pi(+) induced nucleon removal from 24Mg
17 p3042 N85-28821
Soliton matter as a model of dense nuclear matter
[DE85-009937] 19 p3359 N85-30825
Deep-inelastic lepton scattering by nuclei: The pion-exchange model
[DE85-010498] 19 p3359 N85-30828
Discussion session: Nucleon- and antinucleon-nucleus inelastic scattering and charge exchange
[DE85-010723] 19 p3364 N85-30860
Cosmic ray He3 measurements
[OG-4.2-3] 21 p3714 N85-33045
Initial results from the Caltech/DSRI balloon-borne isotope experiment
[OG-4.3-8] 21 p3714 N85-33046
K(-) hydrogen bound and continuum states in momentum space
[DE85-010429] 22 p3841 N85-33789
New calorimetric all-particle energy spectrum
[OG-5.1-4] 22 p3861 N85-34048
Observation of nuclei with energies 8-30 MeV per nucleon in the Earth's magnetosphere at the altitudes 350 KM
[SH-10.1-5] 23 p4053 N85-35136
Heavy cosmic ray measurement aboard Spacelab-1
[SH-10.1-7] 23 p4053 N85-35138
Proceedings of the Workshop on Detectors for Relativistic Nuclear Collisions
[LBL-18225] 24 p4146 N85-35700
High energy physics at Tufts University
[DOE/ER-40085/7] 24 p4152 N85-35744
Nucleon-nucleus interactions from JACEE
24 p4173 N85-35869
Is the inelastic charge-exchange contribution constant at the large X and superhigh energies? Qaut 01Kuchin, I. A.
24 p4173 N85-35871
Propagation of cosmic rays through the atmosphere in the quark-gluon strings model 24 p4173 N85-35873
Scaling violation in the fragmentation region of inclusive nucleon spektrum 24 p4173 N85-35874
Physical meaning of the multiplicities of emitted nucleons in hadron-nucleus collisions 24 p4174 N85-35877
How are particle production, nucleon emission and target fragment evaporation processes interrelated in hadron-nucleus collisions? 24 p4174 N85-35878
Experimental study of the space-time development of the particle production process in hadron-nucleon collisions, using massive target nucleus as a detector
24 p4174 N85-35879
Measurements of hadron mean free path for the particle-producing collisions in nuclear matter
24 p4174 N85-35883
Ringlike inelastic events in cosmic rays and accelerators 24 p4175 N85-35887
Experimental basis for the models of cascade propagation in atmosphere
[HE-3.6-6] 24 p4165 N85-35954
On mini-cluster observed by Chacaltaya emulsion chamber experiment
[HE-3.6-12] 24 p4165 N85-35959
A study of gamma-families generated in nucleon-nucleus (NA) and pion-nucleus (pi A) interactions
[HE-3.7-2] 24 p4166 N85-35961
New aspects in nucleon-nucleus collisions and EAS properties around 10(6) GeV 24 p4187 N85-35974
Small air showers and collider physics
[HE-4.1-9] 24 p4187 N85-35975
Sub-luminal pulses from cosmic ray air showers
[HE-4.7-13] 24 p4200 N85-36063
A study of atmospheric neutrinos with the IMB detector
[HE-5.3-7] 24 p4205 N85-36101
Limits on monopole fluxes from KFG experiment
[HE-6.1-6] 24 p4209 N85-36132
Search for proton decay in the Frejus experiment
[HE-6.2-2] 24 p4210 N85-36136
Results on nucleon life-time from the Kolar gold field experiment
[HE-6.2-3] 24 p4211 N85-36139
Construction of the Soudan 2 detector
[HE-6.2-5] 24 p4211 N85-36141
Nucleon decay and atmospheric neutrinos in the Mont Blanc experiment
[HE-6.2-6] 24 p4211 N85-36142
Energetic delayed hadrons in large air showers observed at 5200m above sea level
[HE-6.2-9] 24 p4211 N85-36145
NUCLEOSIDES
NT ADENOSINE DIPHOSPHATE
NT ADENOSINE TRIPHOSPHATE
NT ADENOSINES
The DNA metabolism and poly-(ADP-ribose) synthesis in lymphocytes of persons exposed to low doses of ionizing radiation
[OEFZS-4307] 20 p3507 N85-31800
NUCLEOSYNTHESIS
U NUCLEAR FUSION
NUCLEOTIDES
NT ADENOSINE DIPHOSPHATE
NT ADENOSINE TRIPHOSPHATE
NT ADENOSINES
NUCLIDES
NT ALUMINUM ISOTOPES
NT ALUMINUM 26
NT AMERICIUM
NT AMERICIUM ISOTOPES
NT AMERICIUM 241
NT ARGON ISOTOPES
NT BERYLLIUM ISOTOPES
NT BERYLLIUM 7
NT BERYLLIUM 9
NT BERYLLIUM 10
NT BORON 10
NT BROMINE ISOTOPES
NT CALCIUM ISOTOPES
NT CALIFORNIUM ISOTOPES
NT CARBON ISOTOPES
NT CARBON 12
NT CARBON 13
NT CARBON 14
NT CERIUM 144
NT CESIUM ISOTOPES
NT CESIUM 134
NT CESIUM 137
NT CHROMIUM ISOTOPES
NT COBALT 60
NT CURIUM
NT CURIUM 244
NT DEUTERIUM
NT GERMANIUM ISOTOPES
NT HELIUM ISOTOPES
NT HYDROGEN ISOTOPES
NT IODINE ISOTOPES
NT IRON ISOTOPES
NT IRON 59
NT ISOTOPES
NT KRYPTON ISOTOPES
NT KRYPTON 85
NT LUTETIUM
NT MANGANESE ISOTOPES
NT NEODYMIUM ISOTOPES
NT NEON ISOTOPES
NT NICKEL ISOTOPES
NT NITROGEN ISOTOPES
NT NITROGEN 15
NT OXYGEN ISOTOPES
NT PLUTONIUM
NT PLUTONIUM ISOTOPES
NT PLUTONIUM 238
NT PLUTONIUM 239
NT POTASSIUM 40
NT RADIOACTIVE ISOTOPES
NT RADON ISOTOPES
NT RUBIDIUM ISOTOPES
NT SCANDIUM ISOTOPES
NT SODIUM ISOTOPES
NT STRONTIUM 90
NT TELLURIUM
NT THORIUM ISOTOPES
NT TRANSURANIUM ELEMENTS
NT TRITIUM
NT URANIUM ISOTOPES
NT URANIUM 235
NT XENON ISOTOPES
NT XENON 129
The low-energy secondary cosmic ray flux: Detectors in iron meteorites 06 p0867 N85-15635
International program to improve decay data for transactinium nuclides
[DE85-011258] 20 p3529 N85-31954
The isotopic composition of cosmic ray chlorine
[OG-4.3-3] 22 p3878 N85-34028
Cosmic ray isotope measurements with a new Cerenkov X total energy telescope
[OG-4.3-4] 22 p3878 N85-34029
The inner granulometric density of the tracks in nuclear emulsions and its application to determine the chemical spectrum of primary cosmic ray nuclid
[OG-4.3-9] 22 p3879 N85-34034
Variations in the propagation of UH-nuclei
[OG-7.1-1] 23 p4012 N85-34863
Cosmogenic-nuclide production by primary cosmic-ray protons
[SH-7.1-6] 23 p4047 N85-35098
The detection and study of molecular species using time resolved laser spectroscopy
[AD-A155910] 24 p4075 N85-35256
NULL HYPOTHESIS
Continuity of the null space basis and constrained optimization
[AD-A147038] 07 p1030 N85-16538
On the power functions of test statistics in order restricted inference
[AD-A147126] 07 p1035 N85-16566
A new approach to evaluate gamma-ray measurements
[OG-9.5-11] 23 p4091 N85-34989
NULL ZONES
Parallel processor configuration for adaptive antenna arrays
[AD-D011347] 07 p0942 N85-15970
Null generation using discs on a reflector
[AD-A151897] 15 p2544 N85-25703
Adaptive nulling at HF using a compact array of active parasitic antennas
[AD-A152582] 17 p2948 N85-28203
Effect of some estimators on a large sample approximation to the non-null distribution of the pearson chi-square statistic
[AD-A153515] 18 p3173 N85-29673
Null synthesis with phase and amplitude controls at the subarray outputs
[AD-A155167] 21 p3578 N85-32241
Reconciling Bayesian and frequentist evidence in the one-sided testing program
[AD-A156603] 21 p3678 N85-32850
A planar version of a 4.0 gigahertz reactively steered adaptive array
[AD-A156029] 24 p4087 N85-35330
NUMBER THEORY
NT ARITHMETIC
NT CONGRUENCES
NT DIVIDING (MATHEMATICS)
NT FIXED POINT ARITHMETIC
NT FLOATING POINT ARITHMETIC
NT INDUCTION (MATHEMATICS)
NT INTEGERS
NT MULTIPLICATION
Disproof of the Mertens conjecture
[CWI-NM-R8412] 14 p2414 N85-24898
A convexity theorem for semisimple symmetric spaces
[CWI-PM-R8414] 14 p2415 N85-24900
NUMERICAL ANALYSIS
NT APPROXIMATION
NT BORN APPROXIMATION
NT CHEBYSHEV APPROXIMATION
NT COMPUTATIONAL CHEMISTRY
NT COMPUTATIONAL FLUID DYNAMICS
NT CONJUGATE GRADIENT METHOD
NT DIFFERENCE EQUATIONS
NT EDDINGTON APPROXIMATION
NT ERROR ANALYSIS
NT FINITE DIFFERENCE THEORY
NT FINITE ELEMENT METHOD
NT FINITE VOLUME METHOD
NT HARTREE APPROXIMATION
NT INTERPOLATION
NT ITERATION
NT ITERATIVE SOLUTION
NT LEAST SQUARES METHOD
NT MEAN SQUARE VALUES
NT MONTE CARLO METHOD
NT NEWTON-RAPHSON METHOD
NT NOMOGRAPHS
NT NUMERICAL DIFFERENTIATION
NT NUMERICAL INTEGRATION
NT PADE APPROXIMATION
NT PARTICLE IN CELL TECHNIQUE
NT RELAXATION METHOD (MATHEMATICS)

NT RITZ AVERAGING METHOD
NT RUNGE-KUTTA METHOD
NT TRUNCATION ERRORS
Numerical analysis of the 3-dimensional inviscid hypersonic flow around capsule-type bodies by the alternate directional implicit method
[NAL-TR-799] 01 p0002 N85-10012
Comparison of numerical techniques for integration of stiff ordinary differential equations arising in combustion chemistry
[NASA-TP-2372] 01 p0011 N85-10065
Radiation effects on structural materials
[DE84-014771] 01 p0029 N85-10178
Numerical analysis of some problems related to the mechanics of pneumatic tires: Finite deformation/rolling contact of a viscoelastic cylinder and finite deformation of cord-reinforced rubber composites
01 p0060 N85-10397
Effect of the Basset term on particle relaxation behind normal shock waves
[AD-A145446] 02 p0196 N85-11320
Numerical analysis of parameters of self-healing copper vapor lasers 02 p0260 N85-11704
Difference schemes for equations of Schrodinger type
[AD-A145812] 03 p0410 N85-12622
Application of summability methods to Jackson theorems for splines
[AD-A146256] 03 p0412 N85-12635
The Lindstrom-Madden method for series systems with repeated components
[AD-A146265] 03 p0412 N85-12636
The development of new methods for solving the target identification or inverse scattering problem for time-harmonic acoustic and electromagnetic waves
[AD-A145821] 03 p0415 N85-12657
Analyses of energy extraction efficiency of unstable resonators
[AD-A146391] 06 p0813 N85-15161
Research in applied mathematics, numerical analysis, and computer science
[NASA-CR-172505] 07 p1021 N85-16480
Use of coordinate functions to calculate deformation fields
[BLL-M-36010-(5828.4)] 07 p1028 N85-16524
An efficient numerical solution technique for wave propagation in horizontally stratified ocean environments
[AD-A148537] 08 p1190 N85-17502
Utilization of numerical optimization techniques in the design of robust multi-input, multi-output control systems
[AD-A148269] 08 p1212 N85-17630
A numerical study of several supersonic flows
09 p1272 N85-17995
The analysis by the lumped parameter method of slade platform friction dampers used in the high pressure fuel turbopump on the space shuttle main engine
09 p1338 N85-18417
Exact simultaneous confidence intervals for pairwise comparisons of three normal means
[AD-A148751] 09 p1375 N85-18645
Study on steerability of articulated tracked vehicles
[AD-P004308] 09 p1410 N85-18865
Computable real analysis
[AD-A149079] 10 p1546 N85-19747
A new method of approximating normal and t-tail areas
[AD-A149457] 10 p1548 N85-19761
Numerical simulation of turbulent reacting flows
[DE84-016777] 11 p1632 N85-20278
Numerical investigation of propagation of radiation pulse at xxx 11 p1716 N85-20809
Measurement of the configuration of a concave surface by the interference of reflected light
[NASA-TM-77796] 11 p1726 N85-20867
Evaluation of resonant modes in isolated dielectric resonators using a surface integral equation formulation
[PB85-110831] 12 p1837 N85-21528
Interaction of part-through cracks in a flat plate
[NASA-CR-175586] 12 p1864 N85-21692
Intensification of tropical instabilities
[AD-A149965] 12 p1896 N85-21899
Cumulative reports and publications through December 31, 1984
[NASA-CR-172569] 12 p1911 N85-21991
A linear characteristic-nodal transport method for the two-dimensional (X,Y)-geometry multigroup discrete ordinates equations over an arbitrary triangle mesh
[LA-10092-T] 12 p1913 N85-22006
A method of calculating periodic solutions of second order dynamical systems
[AD-A149934] 12 p1920 N85-22058
Statistics for the maximum of several positive random variables with application to networking
[AD-A150005] 12 p1922 N85-22069
Approximation order from certain spaces of smooth bivariate splines on a 3-direction mesh
[AD-A149633] 12 p1925 N85-22092
Hydrodynamic stability problem formulated by numerical solutions of the Navier-Stokes equations
12 p1946 N85-22223
China report: Science and technology
[JPRS-CST-84-008] 13 p1972 N85-22384
Elasticity solution of an adhesively bonded joint
[NASA-CR-175591] 13 p2101 N85-23097
Evolution of set of Rossby waves toward anisotropic equilibrium state 13 p2109 N85-23141
Two-dimensional numerical model of sensible and latent heat transport in an irrigated field under advective conditions 13 p2131 N85-23261
Second thoughts on the mathematical software effort: A perspective
[DE85-004831] 13 p2148 N85-23333
Computations of two-dimensional airfoil-vortex interactions — helicopter rotor flowfields
[NASA-CR-3885] 14 p2210 N85-23709
Analysis of slabs-on-grade for a variety of loading and support conditions
[AD-A150865] 14 p2264 N85-24030
Flow around axisymmetric bodies with uniform-velocity zones 14 p2276 N85-24103
An analytical and numerical study of the interaction of rarefaction waves with area changes in ducts. Part 2: Area enlargements
[UTIAS-273] 14 p2300 N85-24242
On the influence of turbulent motions on non-radial oscillations 14 p2444 N85-25083
Mathematical aspect of welding technology research discussed 15 p2536 N85-25663
Unsteady Navier-Stokes calculations in an accelerated reference frame
[AD-A151751] 15 p2557 N85-25774
Frequency/period estimation and adaptive rejection of periodic disturbances
[AD-A149229] 15 p2632 N85-26226
Numerical analysis of supersonic reactive flow in wake of reverse step 15 p2643 N85-26303
Forced MHD turbulence in a uniform external magnetic field
[NASA-CR-172576] 15 p2654 N85-26368
Proceedings of the NAL Symposium on Aircraft Computational Aerodynamics
[NAL-SP-1] 16 p2691 N85-26611
Progress of computational fluid dynamics in the world
16 p2691 N85-26612
Numerical analyses in aerodynamic design of aero-engine fan 16 p2692 N85-26618
Numerical simulation of inviscid compressible flow through three-dimensional cascade
16 p2692 N85-26619
A numerical procedure on three-dimensional parabolic flow in duct 16 p2692 N85-26620
Nonlinear structural analysis for fiber-reinforced superalloy turbine blades 16 p2737 N85-26887
Numerical analysis of flow non-uniformity in the hot gas manifold of the Space Shuttle main engine
16 p2738 N85-26899
A study of computational techniques for noncanonical microstrip antennas and arrays
[AD-A152216] 16 p2774 N85-27123
An incremental multigrid strategy for the fluid dynamics equations
[AD-A151953] 16 p2783 N85-27172
In plane stress analysis
[NASA-CR-175775] 16 p2799 N85-27259
A decomposition procedure for convex quadratic programs
[AD-A151732] 16 p2854 N85-27595
Evaluation of an algorithm for the solution of the time-dependent Euler equations
[AD-A151993] 16 p2854 N85-27600
Multiple array processors for ocean acoustic problems
[AD-A152174] 16 p2860 N85-27641
Kinetic theory and simulation of multi-species plasmas in Tokamaks excited with ICRF microwaves
[DE85-006119] 16 p2866 N85-27691
On the choice of coordinates for semiconductor simulation
[AD-A152214] 16 p2870 N85-27706
Numerical solution of one-dimensional nonlinear problems of statics for elastic beams and shells under rigid constraints 17 p2943 N85-28166
Kolmogorov and scalar spectral regimes in numerical turbulence
[NASA-TM-86899] 17 p2957 N85-28264
CALTECH-DOE program on numerical analysis, computing and fundamental studies of motion, energy and mass transfer in fluids
[DE85-006106] 17 p2959 N85-28274
Spectral decomposition and verification of NOGAPS 500MB medium-range forecasts
[AD-A152550] 17 p2996 N85-28520
Software for estimating sparse Hessian matrices
[DE85-008121] 17 p3013 N85-28629
A discussion of adaptive grids and their applicability in numerical hydrodynamic modeling
[AD-A151843] 17 p3017 N85-28659
Numerical methods for stiff ordinary and elliptic partial differential equations
[AD-A153247] 17 p3020 N85-28675
Numerical evaluation of low frequency sound propagation in layered media
[AD-A152690] 17 p3028 N85-28728
Fluid modeling of magnetized plasmas
[DE85-007679] 17 p3039 N85-28804
Numerical analysis of end effects in symmetric laminated plates
[NAL-TR-850] 18 p3088 N85-28977
Time-averaged and time-dependent computations of isothermal flowfields in a centerbody combustor
[AD-A153662] 18 p3100 N85-29189
Laser-stimulated vibrational excitation of an adspecies studied by a generalized master equation: Neutral atomic hydrogen on hydrated KCl(001)
[AD-A153665] 18 p3112 N85-29268
A numerical study of the Pacific polar low
[AD-A153777] 18 p3149 N85-29495
Computable numerical bounds for Lagrange multipliers of stationary points of nonconvex differentiable nonlinear programs
[AD-A153513] 18 p3169 N85-29633
Numerical solutions of the potential distribution within the vacuum region of the FEATRON
[AD-A153683] 18 p3178 N85-29705
Evaluation of the eigenvalue method in the solution of transient heat conduction problems
[AD-A154434] 19 p3266 N85-30256
Computational methods in advanced stress and durability analyses
[AD-A154119] 19 p3288 N85-30375
Foundations of data envelopment analysis for Pareto-Koopmans efficient empirical productions functions
[AD-A154244] 19 p3346 N85-30735
Mathematics of surfaces
[DE85-010439] 19 p3346 N85-30742
Effect of diffusely-reflected sunlight on the orbit of LAGEOS 20 p3491 N85-31700
Compressible Lagrangian hydrodynamics without Lagrangian cells
[DE85-009597] 20 p3520 N85-31891
Numerical modeling of subsurface communication
[DE85-012818] 21 p3577 N85-32249
Numerical solutions of turbulent models for flow over a flat plate with angle of attack
[DE85-010380] 21 p3585 N85-32286
A numerical analysis of transient planetary waves and the vertical structure in a meso-strato-troposphere model, part 1.4A 21 p3617 N85-32473
Circulation analysis of two snowstorms during the SNOW-TWO program
[AD-A155225] 21 p3637 N85-32587
Numerical simulations of the response of intense ocean currents to atmospheric forcing
[AD-A155161] 21 p3655 N85-32704
Overlap integrals for atom-metal surface interactions
[AD-A155038] 21 p3702 N85-32998
Method of and apparatus for generating an interstitial point in a data stream having an even number of data points
[NASA-CASE-MFS-25319-1] 22 p3827 N85-33701
QKPLT users guide, version 2.0
[L-10094-M] 22 p3828 N85-33707
Implementing linear multistep formulas for solving DAES
[DE85-012400] 22 p3834 N85-33740
Three-dimensional hydrodynamic hot-spot model
[DE85-009587] 23 p3922 N85-34301
Modeling of geothermal systems
[DE85-012553] 23 p3943 N85-34439
The impact of supercomputers on experimentation: A view from a national laboratory
[NASA-TM-86822] 23 p3955 N85-34510
Analytic and numerical calculations of the ambipolar electric field in a stellarator 23 p3978 N85-34665
Numerical simulation in astrophysics: Smoothed particle methods 23 p3979 N85-34674
Numerical calculations on shock loaded materials
23 p3980 N85-34676
Two-dimensional simulation of LIB target implosion
23 p3980 N85-34678
Effects of a wavy neutral sheet on cosmic ray anisotropies
[SH-4.2-11] 23 p4008 N85-34849
The influence of nonstationarity of the solar activity and general solar field on modulation of cosmic rays
[SH-4.2-17] 23 p4008 N85-34854
Time-dependent nonlinear cosmic ray shock: confirming abstract
[OG-8.1-3] 23 p4017 N85-34893

Algorithmic approaches in sets of good answers in inverse problems
[PM/84/18] 24 p4142 N85-35677
Invariant tests and likelihood ratio tests for multivariate elliptically contoured distributions
[AD-A155844] 24 p4142 N85-35679
Constrained stiffness matrix adjustment using mode data
[AD-A155966] 24 p4143 N85-35685
Relation between field energy and RMS emittance in intense particle beams
[DE85-012655] 24 p4159 N85-35784
Analytical-numerical methods of calculations of energy and three-dimensional particle distributions in electromagnetic cascades
[HE-3.5-13] 24 p4184 N85-35950

NUMERICAL CONTROL

Publications of Center for Manufacturing Engineering (of the National Bureau of Standards), 1978-1983
[PB84-224526] 01 p0036 N85-10226
The NBS tri-directional test facility
[PB84-217462] 01 p0051 N85-10334
Autonomous Attitude Determination System (AADS). Volume 1: System description
[NASA-TM-87385] 02 p0240 N85-11559
Experimental study with parameter variations on a hydraulic positioning servo with computer implemented observer
[FOA-C-20645-E3] 02 p0256 N85-11673
Development of a modular multicoordinate measuring system with continuous-path microprocessor control
[BMFT-FB-T-84-158] 03 p0408 N85-12606
Advances of implementing NC machine tools discussed 04 p0491 N85-13131
Portable microprocessor-controlled instrument for sensing, identifying and monitoring gaseous chemicals
[DE84-013431] 04 p0504 N85-13214
Design of a flexible machining system
[CETIM-1-3E-140] 04 p0510 N85-13252
A unified method for evaluating real-time computer controllers: A case study — aircraft control
[NASA-CR-174168] 04 p0547 N85-13478
Optical characterization of radiation-resistant fibers
[DE84-015248] 05 p0620 N85-13964
Programming and application of numerical controlled measuring machines (NCMES)
[BMFT-FB-T-84-153] 05 p0717 N85-14589
Efficiency of programmed motion control systems 06 p0776 N85-14961
NC programming, machine tool information 06 p0816 N85-15178
Performance characteristics of a battery charger and state-of-charge indicator
[NASA-CR-174273] 07 p0946 N85-15992
Passive maser using timesharing for control of the cavity and control of the oscillator on the line of stimulated emission
[AD-D011326] 07 p0969 N85-16151
Shuttle avionics software trials, tribulations and success 08 p1090 N85-16691
Man-machine interface and control of the shuttle digital flight system 08 p1091 N85-16694
Space shuttle main engine hardware simulation 08 p1091 N85-16695
Flexible manufacturing system for the production of aircraft parts
[BLL-PNR-90237-(8019.3153)] 08 p1137 N85-17159
New applications for robot loaders, unloaders 08 p1139 N85-17175
Utilization of numerical optimization techniques in the design of robust multi-input, multi-output control systems
[AD-A148289] 08 p1212 N85-17630
Design description of a microprocessor based Engine Monitoring and Control unit (EMAC) for small turboshaft
[NASA-TM-86980] 09 p1263 N85-17935
Design and realization of a multirader tracking system for air traffic control
[ENST-84E010] 09 p1279 N85-18044
Flexible manufacturing system for machining axially symmetric workpieces
[PNR-90229] 09 p1305 N85-18196
The control of manufacturing systems for varying medium-batch production
[PNR-90235] 09 p1371 N85-18618
Strategy planning by an intelligent machine
[DE84-016609] 09 p1372 N85-18624
Electric vehicle battery test plan and results
[DE84-001972] 09 p1410 N85-18867
Armenia markets new drive motors for machine tools 10 p1461 N85-19212
Productivity gains through CAD of CNC programs 10 p1462 N85-19219
A microprocessor controlled parallel model with FDPSK 10 p1475 N85-19304
The F-18: A new era for human factors 10 p1534 N85-19671
Reliability of DNC system examined 11 p1617 N85-20171
New CNC systems described 11 p1617 N85-20172
Digital temperature and velocity control of mach 0.3 atmospheric pressure durability testing burner rigs in long time, unattended cyclic testing
[NASA-TM-86969] 12 p1805 N85-21321
Synthesis of digital control for object with lag 12 p1843 N85-21562
SIMULA: Digital controller simulation package
[PB85-134492] 12 p1917 N85-22041
Sensor control of robot arc welding 12 p1948 N85-22233
A computer controlled mass spectrometer system for investigating the decomposition of non-metallic materials under atmospheric conditions 12 p1948 N85-22237
Research and Modeling of Supervisory Control Behavior, report of a workshop
[AD-A149821] 12 p1950 N85-22248
Reliability of robotized welding apparatus 13 p2034 N85-22741
Assembly robot control algorithms 13 p2046 N85-22906
Manufacturing perspective in the design of bevel gearing 14 p2221 N85-23777
Milling machine with numerical programmed control for cutting teeth 14 p2268 N85-24052
Mechanization and automation of production processes in turbine building 14 p2289 N85-24057
Manufacture of drive wheel vanes for hydraulic turbines on program controlled machine tools 14 p2289 N85-24058
Use of program controlled machine tools to automate and mechanize production processes in pipe manufacture 14 p2289 N85-24059
USSR report: Machine tools and metalworking equipment
[JPRS-UMM-85-006] 14 p2293 N85-24146
New CNC turning centers described 14 p2294 N85-24148
Large CNC machining center for turbine production 14 p2294 N85-24149
Minister B. V. Belmont on status of automation drive 14 p2294 N85-24151
Robots for application in forge-press operation 14 p2294 N85-24154
Integrated control system for FMS components 14 p2295 N85-24156
Automating the study of error in discrete aerodynamic fairing design 14 p2298 N85-24176
French work toward flexible software workshops 14 p2299 N85-24187
Investigation of doubly-fed machine in variable speed application
[DE85-004378] 14 p2299 N85-24234
Czech institute develops microcomputer for satellites 15 p2484 N85-25331
Selection of optimal control program for solar cell panels of Earth satellites 15 p2484 N85-25335
Electrical features of new DNC, CNC system viewed — direct numerical control 15 p2524 N85-25562
Microcomputer controlled image acquisition system 15 p2537 N85-25654
Microcomputer controlled automatic peak locking of laser circuit 15 p2537 N85-25655
Using a single-board computer to maintain constant voltage, current sources 15 p2551 N85-25749
Development of robots and application to industrial processes
[NASA-CR-175754] 15 p2567 N85-25840
Application of AFTI/F-16 task-tailored control modes in advanced multirole fighters 16 p2712 N85-26735
X-29A digital flight control system design 16 p2712 N85-26736
Some flight test results with redundant digital flight control systems 16 p2712 N85-26739
An update on experience on the fly by wire Jaguar equipped with a full-time digital flight control system 16 p2712 N85-26740
Optimal control of electric drive with simultaneous control inputs for motor current and flux 16 p2763 N85-27049
Development, implementation of industrial lasers reviewed 16 p2767 N85-27075
Guidelines for optimization of robotized machining cells 16 p2767 N85-27076
The development and application of volume scan and cell tracking capabilities for the analysis of convective cloud systems 16 p2830 N85-27451
Corrective-predictive systems
[BLL-M-36062-(5629.4)] 16 p2951 N85-27573
The application of numerical control (NC) in manufacturing wind tunnel models
[B8580078] 17 p2939 N85-28140
Automation of Precise Time Reference Stations (PTRS) 17 p2962 N85-28291
Adapting shape parameters for cubic Bezier curves 17 p3004 N85-28576
Triangular Berstein-Bezier patches, a survey and new results 17 p3005 N85-28577
A uniform subdivision method for triangular Bezier patches 17 p3005 N85-28578
Microprocessor controlled temperature chassis
[DE85-008392] 17 p3009 N85-28602
Automatic volume calibration system
[DE85-008955] 18 p3102 N85-29204
An interactive computer aid for the design and analysis of linear, single input/single output digital and continuous control systems
[AD-A153704] 18 p3162 N85-29589
Space station automation study. Volume 1: Executive summary. Autonomous systems and assembly
[NASA-CR-171514] 19 p3226 N85-30002
MELCOR Accident Consequence Code System (MACCS)
[DE85-009712] 19 p3339 N85-30669
Computer-controlled carburizing
[BLL-OA-TRANS-3204-(8196.300)] 20 p3429 N85-31268
Drag soldering process control
[DE85-010853] 20 p3433 N85-31301
Flight control system for a computer controlled aircraft with limited sensors
[AD-A155107] 21 p3555 N85-32115
Speech understanding research
[AD-A155462] 21 p3700 N85-32990
Standard series of direct-current motors for regulated electric drives 22 p3772 N85-33375
Project management using graphics 23 p3982 N85-34560
The automatic labeling of geographic maps: A problem in computer aesthetics 23 p3982 N85-34561
Design and construction of an advanced power conditioning subsystem for small photovoltaic applications
[DE85-013940] 24 p4113 N85-35495
Optimizing data access in the LAMPF control system
[DE85-012653] 24 p4140 N85-35663
Distribution of computer functionality for accelerator control at the Brookhaven AGS
[DE85-012520] 24 p4141 N85-35669
On-line model driven control of the SLC electron Damping Ring
[DE85-013377] 24 p4157 N85-35772

NUMERICAL DIFFERENTIATION

Methods for numerical differentiation
[AD-A145058] 01 p0112 N85-10758
On edge detection
[AD-A148573] 08 p1223 N85-17703

NUMERICAL FLOW VISUALIZATION

Numerical methods for bluff body aerodynamics 05 p0593 N85-13782
Developments in the simulation of compressible inviscid and viscous flow on supercomputers
[NASA-TM-86674] 11 p1575 N85-19924
Calculation of an unsteady transonic flow with shock waves and separation in Laval nozzles
[MPIS-14/1984] 14 p2213 N85-23728
Calculation of transonic flows around an aircraft configuration with motorized nacelle
[SNIAS-851-111-106] 20 p3387 N85-31008

NUMERICAL INTEGRATION

NT RUNGE-KUTTA METHOD
Oscillatory integrals by Hermite interpolatory rules
[CSIR-TWISK-301] 01 p0108 N85-10725
Conservation laws and the numerical solution of ODEs
[DE84-016206] 04 p0555 N85-13531
Orbit extrapolation — satellite orbits 05 p0598 N85-13811
Calculation of cumulative distributions and detection probabilities in communications and optics
[AD-A147761] 08 p1215 N85-17650
Contribution to the study of a numerical implicit method for solving the Euler equations
[ESA-TT-872] 10 p1549 N85-19771
Triple layer system for numerical integration of equations of gas dynamics and nonlinear heat conduction equation
[DE85-000297] 11 p1632 N85-20277
Evaluation of two numerical integrator schemes
[PB85-138196] 11 p1683 N85-20603
A comparison of the efficiency of numerical methods for integrating chemical kinetic rate equations
[NASA-TM-83500] 12 p1778 N85-21162
Nonlinear sigma-models and integration methods
[DE85-004447] 12 p1922 N85-22071

Problem of diffraction by wavy surface: Comparison of numerical methods of solution
13 p2079 N85-22985
Improved accuracy in solid isoparametric elements using selectively reduced integration 15 p2573 N85-25865
Numerical integration through force discontinuities: Solar radiation pressure 16 p2805 N85-27298
Sensitivity analysis of initial value problems with mixed ode's and algebraic equations
[AD-A153526] 18 p3169 N85-29637
Bayesian inference and diagnostics for the 3 parameter logistic model
[AD-A153840] 18 p3175 N85-29681
Numerical optical computing at the Ohio State University 18 p3188 N85-29775
Application of closed-form solutions to a mesh point field in silicon solar cells 20 p3482 N85-31637
Reliability prediction of the series system with spares subject to Weibull failure 24 p4100 N85-35413

NUMERICAL STABILITY
On explicit difference schemes for hyperbolic systems with variable coefficient 2
[PREPRINT-808] 03 p0413 N85-12641
Convergence of method of lines approximations to partial differential equations
[CWI-NM-R8404] 05 p0720 N85-14627
Stability results for discrete Volterra equations: Numerical experiments
[CWI-NM-R8409] 11 p1707 N85-20743
Lyapunov stability of very simple steady solutions of prognostic systems 14 p2333 N85-24429
On the stability of predictor-corrector methods for parabolic equations with delay
[CWI-NM-R8410] 14 p2410 N85-24860
A stability analysis of incomplete LU factorizations
[AD-A152058] 15 p2636 N85-26271
Squeezing the most out of Eigenvalue solvers on high-performance computers
[DE85-007569] 16 p2649 N85-27565
Stability of functionals determined by moment conditions
[TRITA-NA-8310] 16 p2652 N85-27585
Compressor and turbine models - numerical stability and other aspects
[AD-A153811] 18 p3063 N85-28948
Evaluation of the eigenvalue method in the solution of transient heat conduction problems
[AD-A154434] 19 p3266 N85-30256
A numerical and analytical investigation of lee cyclogenesis
[AD-A155607] 21 p3636 N85-32594

NUMERICAL WEATHER FORECASTING
Rain bands and symmetric instability
01 p0075 N85-10496
Test results from RAINSAT 01 p0076 N85-10508
The potential use of atmospheric profilers in short-range prediction 01 p0078 N85-10518
A simulation experiment of a rapidly developed medium scale cyclone 01 p0079 N85-10530
Application of mesoscale numerical model to local weather prediction 01 p0080 N85-10532
The United Kingdom Meteorological Office mesoscale forecasting system 01 p0080 N85-10533
Numerical forecast of pressure field by considering the mutual influence of orography, thermal nonhomogeneity and surface friction 01 p0080 N85-10534
Evaluation of an integrated mixed-layer model for single station prediction in a marine regime
01 p0080 N85-10535
A local dynamical interpretation method of numerical weather forecasting 01 p0080 N85-10536
An operational numerical model for prediction of fog and stratus 01 p0080 N85-10537
Operational use of shipboard numerical aid programs
01 p0082 N85-10546
A system for meteorological satellite, radar, conventional data and model analysis 01 p0082 N85-10551
Development of an operational system for Very-Short-Range Forecasting (VSRF) at Swedish Meteorological and Hydrological Institute (SMHI)
01 p0083 N85-10559
The extremeness of the cold front of December 31, 1978 over the CSR
[REPT-506] 03 p0377 N85-12409
Impact of ERS-1 observations on wave forecasting in the North Sea 03 p0381 N85-12437
Recent examples of mesoscale numerical forecasts of severe weather events along the east coast
[NASA-TM-86172] 03 p0395 N85-12523
Operational numerical forecasts: Survey and verification over the period 1976-1983
[KNMI-TR-49] 04 p0540 N85-13435
Orographic effects in atmospheric circulation
05 p0679 N85-14362
Spectral general circulation model development
05 p0679 N85-14363
Numerical modeling of the atmosphere
05 p0680 N85-14370
Comparison of optimum interpolation and Cressman analyses 05 p0680 N85-14371
Normal mode initialization 05 p0680 N85-14372
Forecast impact of components of the FGGE observing system 05 p0681 N85-14373
Applications of sequential estimation to numerical weather prediction 05 p0681 N85-14374
Some new mathematical methods for variational objective analysis 05 p0681 N85-14375
Extended range forecasting 05 p0681 N85-14376
Weather and climate parameters from Tiros-N
05 p0681 N85-14377
Applications of TOMS ozone data and clustering techniques in satellite soundings
05 p0681 N85-14379
Research relative to high spatial resolution passive microwave sounding systems 05 p0681 N85-14380
ECMWF/NMC/GLAS joint simulation study
05 p0682 N85-14385
The use of available potential energy to evaluate two GLAS FGGE data sets 05 p0682 N85-14387
Comparison of forecast and observed energetics
05 p0683 N85-14389
Energy diagnostics and impact studies of FGGE global data sets and GLAS GCM simulations
05 p0683 N85-14390
Spectral energetics diagnoses and FGGE spectral observing periods and energetics analyses of forecast experiments with GLAS GCM 05 p0683 N85-14391
Jet stream errors and tropospheric-stratospheric interactions in the GLAS general circulation model
05 p0683 N85-14392
Theoretical modeling for numerical weather prediction
05 p0684 N85-14395
Numerical prediction of the president's day cyclone
05 p0684 N85-14396
Development of guidance forecasts at the Royal Netherlands Meteorological Institute (KNMI). Part 1: General information
[KNMI-TR-54-PT-1] 08 p1190 N85-17499
Velocity inversion using a stratified reference
[AD-A150082] 12 p1889 N85-21858
Summary of Meteorological Observations, Surface (SMOS), Bermuda
[AD-A150537] 13 p2136 N85-23278
Summary of Meteorological Observations, Surface (SMOS), Beaufort, South Carolina
[AD-A150538] 13 p2136 N85-23279
Lyapunov stability of very simple steady solutions of prognostic systems 14 p2333 N85-24429
Utilization of satellite data in mesoscale modeling of severe weather 15 p2597 N85-26007
Meso-8 scale numerical simulations of the jet streak adjustments which organized the Carolina tornado outbreak and the subsequent explosive coastal cyclogenesis 15 p2598 N85-26011
Numerical studies of frontal dynamics
15 p2598 N85-26014
Wind modelling for increased aircraft operational efficiency 16 p2697 N85-26652
Data from BOC-yachts: A significant input to Southern Hemisphere analysis 16 p2814 N85-27356
A split explicit model for short-term numerical weather prediction 16 p2831 N85-27460
Statistical interpretation of the ECMWF model using MOS to predict surface wind and temperature
[WSR-2] 17 p2995 N85-28515
The impact of scatterometer data on limited-area model predictions of the QE 2 storm 18 p3130 N85-29436
A factored implicit scheme for numerical weather prediction with small factorization error
18 p3141 N85-29447
Comparison of optimum interpolation and Cressman analyses 18 p3141 N85-29448
Recent developments in nonlinear normal mode initialization 18 p3142 N85-29451
Comparison of two orographical data sets for the GLAS Fourth Order GCM 18 p3142 N85-29452
Development and testing of the variable vertical resolution Fourth Order GCM 18 p3142 N85-29453
Development of an optimum interpolation analysis method for the CYBER 205 18 p3143 N85-29456
Model development highlight for 1984: The GLA Fourth Order GCM 18 p3143 N85-29457
Response of winter forecasts made with the GLA Fourth Order GCM to Changes in the horizontal grid resolution
18 p3143 N85-29458
Comparison of forecast and observed energetics
18 p3143 N85-29459
Error growth in operational 10-day forecasts
18 p3143 N85-29460
Numerical meteorology 18 p3147 N85-29484
A numerical study of the Pacific polar low
[AD-A153777] 18 p3149 N85-29495
Monthly and seasonal weather outlook for mid-February to mid-March 1985, volume 39, number 4, February 14, 1985
[PB85-164580] 18 p3149 N85-29500
A probabilistic forecasting model of tropical cyclone-generated storm surge for a straight coastline
19 p3314 N85-30544
Utilization of satellite data and regional scale numerical models in short range weather forecasting
[NASA-CR-175980] 19 p3314 N85-30545
Examination of the time and spatial scales appropriate for the carbon dioxide climate change issue
[DE85-009852] 19 p3317 N85-30563
AEV local verification for aviation, precipitation, and temperature programs: AV, REL, TEM
[PB85-179125] 19 p3318 N85-30568
Accuracy and operational use of medium and extended range numerical atmospheric forecasts: A review
[AD-A155027] 21 p3635 N85-32579
Medium range atmospheric forecast system: Evaluation plan
[AD-A155623] 21 p3636 N85-32595

NUSSELT NUMBER
Numerical solutions of turbulent models for flow over a flat plate with angle of attack
[DE85-010380] 21 p3585 N85-32286

NUTATION
Transient optical nutation in CO2 laser
02 p0261 N85-11709
Active nutation control of spacecraft using a magnetic bearing momentum wheel with Vernier gimballing capability
[NAL-TR-8201] 06 p0759 N85-14857
Attitude data consistence check of rocket payloads
[BMFT-FB-W-84-049] 12 p1790 N85-21239
Earth rotation and polar wandering
14 p2399 N85-24785
The Earth's wobble and associated ocean motions
20 p3490 N85-31698

NUTATIONAL OSCILLATION
U NUTATION

NUTRIENTS
Characterization of heat transfer in nutrient materials — space flight feeding
[NASA-CR-171841] 06 p1199 N85-17551
Effects of acid rain on forest nutrient status
[DE85-012486] 23 p3947 N85-34463

NUTRITION
Nutritional models for space travel from chemically defined diets
[NASA-CR-3850] 03 p0402 N85-12561
Feasibility of producing a range of food products from a limited range of undifferentiated major food components
[NASA-CR-177329] 07 p1020 N85-16473
Food Service and Nutrition for the Space Station
[NASA-CP-2370] 14 p2393 N85-24733
The context for food service and nutrition in the space station 14 p2393 N85-24734
Preparation methods: Past and potential methods of food preparation for space 14 p2393 N85-24736
Nutritional criteria for military rations and effects of prolonged feeding on acceptability
14 p2394 N85-24742
Nutrition in space flight: Some thoughts
14 p2394 N85-24743
Food service and nutritional needs
14 p2394 N85-24744
Psychobiology and food perception
14 p2394 N85-24745
Diet of first Soviet expedition on Mount Everest
19 p3323 N85-30586
Chemolithotrophy and physiology of bacterial nutrient limitation 21 p3659 N85-32730
Influence of chemical form, feeding regimen, and animal species on the gastrointestinal absorption of plutonium
[DE85-010291] 21 p3662 N85-32751

NUTRITIONAL REQUIREMENTS
NT CALORIC REQUIREMENTS
Mineral nutrients in Mediterranean ecosystems
[REPT-71] 01 p0069 N85-10456
Problems associated with the utilization of algae in bioregenerative life support systems
[NASA-CR-166615] 07 p1019 N85-16469
Diet of first Soviet expedition on Mount Everest
19 p3323 N85-30586

NUTS (FASTENERS)
Tube coupling device
[NASA-CASE-MFS-25964-1] 11 p1647 N85-20378

NYLON (TRADEMARK)
Temperature dependence of the crystal structures of Nylon 11
[AD-A147563] 07 p1049 N85-16861
Piezoelectric transducer using electrically poled gamma-phase Nylon 11
[AD-D011552] 12 p1850 N85-21602

The effects of sea water and concentrated salt solutions on the fatigue of nylon 6,6 fibers
17 p2979 N85-28416
Solid-state co-extrusion of nylon 6 gel
[AD-A156167] 24 p4082 N85-35296

NYLON RESINS
U POLYAMIDE RESINS

NYQUIST DIAGRAM
On the relationship between Lehtomaki's robustness test and an inverse Nyquist based test
[QUEL-1526/84] 03 p0409 N85-12616
Approximate models in multivariable process control: An inverse Nyquist array and robust tuning regulator interpretation
[RR-261] 08 p1216 N85-17663

NYSTAGMUS
NT VESTIBULAR NYSTAGMUS
Stimulus factors in motion perception and spatial orientation 01 p0006 N85-10049
Influence of limboreticular complex on some reactions of rabbits 19 p3326 N85-30607
The European vestibular experiments of the Spacelab-1 mission 20 p3508 N85-31808
Some results of the European vestibular experiments in the Spacelab-1 mission 20 p3509 N85-31809

O

O RING SEALS
Analysis of experimental shaft seal data for high-performance turbomachines, as for Space Shuttle main engines
[NASA-TM-86926] 12 p1844 N85-21569
Experimental stiffness of tapered bore seals
[NASA-TM-86976] 15 p2566 N85-25847

O STARS
Observations of the O-type subdwarf eclipsing binary system LB 3459 (AA Dor) 01 p0128 N85-10881
Spectroscopic observations of selected stellar systems
[NASA-CR-174288] 08 p1255 N85-17915
A spectroscopic study of LMC X-4
[NASA-CR-174414] 10 p1571 N85-19905
UV observations and results on pre-main sequence stars 11 p1744 N85-20970
Stellar winds in the young galactic cluster NGC 6530 11 p1750 N85-21004
IUE and Voyager observations of very hot O-type subdwarfs 11 p1751 N85-21010
Statistical classification of IUE low-dispersion stellar spectra: Progress report 11 p1760 N85-21075
Possible origin of the anomalous component of cosmic rays
[SH-4.6-7] 23 p4039 N85-35045

OAO
NT OAO 3

OAO 3
Absorption line studies and the distribution of neutral gas in the local interstellar medium 06 p0873 N85-15544
Synthesis of data on the local interstellar medium 06 p0874 N85-15545
Observations of interstellar HI toward nearby late-type stars 06 p0874 N85-15546
Observations of local interstellar Mg I and Mg II 06 p0874 N85-15547
IUE absorption line studies of highly ionized interstellar gas 11 p1743 N85-20962
MU Sagittarii and Beta Lyrae: Combined IUE/Voyager observations 11 p1757 N85-21052

OAO-C
U OAO 3

OATS
Multi crop area estimation in Idaho using EDITOR
[E85-10054] 06 p0827 N85-15251

OBLATE SPHEROIDS
Oblatenesses of Uranus and Neptune 02 p0300 N85-11941

OBLIQUE SHOCK WAVES
Oblique shock wave-turbulent boundary layer interaction on a porous wall with suction 08 p1072 N85-16794
Tabular and graphical solutions of regular and Mach reflections in pseudo-stationary frozen and vibrational-equilibrium flows, part 1
[UTIAS-283-PT-1] 23 p3893 N85-34117
Tabular and graphical solutions of regular and Mach reflections in pseudo-stationary frozen and vibrational-equilibrium flows, part 2
[UTIAS-283-PT-2] 23 p3894 N85-34118

OBSCURATION
U OCCULTATION

OBSERVABILITY (SYSTEMS)
A three-dimensional geometric-physical model for conventional geodetic observations-observables, parameter estimation, and deformation analysis
[SER-C-298] 11 p1665 N85-20493
State estimation with interrupted observations
15 p2635 N85-26251
Observability in problem of correction of inertial navigation systems using additional information from artificial Earth satellite 16 p2719 N85-26785

OBSERVATION
NT EARTH OBSERVATIONS (FROM SPACE)
NT SATELLITE OBSERVATION
NT SPACE OBSERVATIONS (FROM EARTH)
NT SPOT (FRENCH SATELLITE)
NT VISUAL OBSERVATION
Exploring the solar system with stellar occultations
08 p1245 N85-17857
Observations of mesospheric turbulence by rocket probe and VHF radar, part 2.4A 21 p3619 N85-32484
Analysis of unreplicated factorials allowing for possibly faulty observations
[AD-A154813] 21 p3678 N85-32848

OBSERVATION AIRCRAFT
NT MIRAGE AIRCRAFT
NT MIRAGE 3 AIRCRAFT
NT OV-1 AIRCRAFT
NT RF-4 AIRCRAFT
NT U-2 AIRCRAFT
Investigation of air pollution impact in Eastern Bavaria: Measurement results from August and September, 1984
[DFVLR-FB-85-03] 17 p2988 N85-28471
Motor glider meteorology 24 p4121 N85-35543

OBSERVATORIES
NT ASTRONOMICAL OBSERVATORIES
NT ASTRONOMICAL SATELLITES
NT GAMMA RAY OBSERVATORY
NT GEOPHYSICAL OBSERVATORIES
NT HEAO
NT HEAO 1
NT HEAO 2
NT HEAO 3
NT HUBBLE SPACE TELESCOPE
NT INFRARED ASTRONOMY SATELLITE
NT IUE
NT OAO 3
NT OGO
NT QUASAT
NT ROSAT MISSION
NT SOLAR OBSERVATORIES
NT SPACE INFRARED TELESCOPE FACILITY
NT SPARTAN SATELLITES
Recent results on the Crab Pulsar X-ray light curve
11 p1742 N85-20955
Monopole, astrophysics and cosmic ray observatory at Gran Sasso
[HE-6.1-4] 24 p4209 N85-36130

OBSTACLE AVOIDANCE
LPI-radar for helicopter obstacle warning
08 p1074 N85-16810

OBSTACLES
U BARRIERS

OBSTRUCTING
U BLOCKING

OCCLUSION
Reaction of cerebral ventricles to antiorthostatic position and occlusion of jugular veins 01 p0093 N85-10826
Dynamic occlusion analysis in optical flow fields
[AD-A145805] 03 p0406 N85-12594

OCCULTATION
NT RADIO OCCULTATION
NT SOLAR ECLIPSES
NT STELLAR OCCULTATION
The structure of the Uranian rings and the search for rings around Neptune 02 p0302 N85-11954
Ice fog as an electro-optical obscurant
[AD-A155059] 21 p3705 N85-33015
Application of nonlinear least squares methods to the analysis of solar spectra
[NASA-CR-176122] 22 p3916 N85-33637

OCCUPATION
Cognitive asymmetry and occupation. Computer programmers, students, and bank personnel, part 1 and part 2
[AD-A147125] 09 p1197 N85-17540
Success in learning occupation of chemical production technician as function of certain personality traits and development of psychophysiological functions
09 p1362 N85-18568

OCEAN BOTTOM
Seafloor geosciences division: Missions, technical specialties, accomplishments, and activities, calendar year 1983
[AD-A144849] 01 p0087 N85-10532
The gulf stream deflection and meander energetics experiment. Current meter and bottom pressure gauge data report for the September, 1981 to April, 1982 mooring period
[AD-A144977] 01 p0088 N85-10595
Marine geological and geophysical investigations of the Antarctic Continental Margin, 1984
[GS-CIRC-935] 02 p0212 N85-11400
On gravity from SST, geoid from Seasat, and plate age and fracture zones in the Pacific
[E85-10020] 02 p0217 N85-11433
A comparison of seismic properties of young and mature oceanic crust 02 p0226 N85-11479
Submarine sand ridges: Geology and development, New Jersey, USA 02 p0227 N85-11482
A study of highly energetic near-bottom ocean flow at the base of the Scotian Rise 02 p0233 N85-11515
One-year records of current and bottom pressure in the strait between Nordaustlandet and Kvitoeya and Svalbard, 1980 - 1981
[AD-A145594] 02 p0233 N85-11518
Continental and oceanic crustal magnetization modelling
[E85-10034] 03 p0378 N85-12413
The structure of the Iceland-Faeroe ridge, derived from geophysical measurements
[DRIC-T-7255] 03 p0397 N85-12535
Uninkability of ferromanganese nodules
06 p0819 N85-15202
Some methodological aspects of study of layer associations in continents and oceans
06 p0820 N85-15205
Some trends in the modern Earth sciences — plate tectonics and Earth's crust 06 p0820 N85-15207
Boundary velocities of mohorovicic discontinuity and upper mantle structure of Pacific Ocean bed
06 p0821 N85-15211
Platinum group nuggets in deep sea sediments
06 p0883 N85-15611
Exploring ocean's mineral wealth
07 p0980 N85-16227
Satellite photographs suggest arctic volcano
07 p0982 N85-16239
Research of inverse methods to describe the structure of the earth and ocean bottom
[AD-A147082] 07 p1030 N85-16541
Ocean acoustics
[AD-A147082] 07 p1038 N85-16591
Arctic marine acoustics
[AD-A147492] 07 p1039 N85-16594
Late Quaternary deep-water paleoceanography of the eastern equatorial Indian Ocean: Evidence from Bethnic foraminifera, carbonate dissolution, and stable isotopes
08 p1182 N85-17446
Detailed oceanic crustal modeling
[AD-A148589] 08 p1191 N85-17507
A broadband matching network
[AD-D011406] 08 p1219 N85-17675
Preliminary post-emplacement safety analysis of the subseabed disposal of high-level nuclear waste
[DE84-011162] 08 p1221 N85-17682
Technology development for unmanned untethered submersible vehicle systems
[AD-A148794] 09 p1304 N85-18190
Measurements of sediment temperatures, conductivity and heat flow in the North Atlantic and their relevance to radioactive waste disposal
[IOS-172] 09 p1359 N85-18551
Benthic boundary layer, IOS observational programme: Discovery Gap measurements, March 1984 — Institute of Oceanographic Sciences (IOS)
[ISO-180] 09 p1359 N85-18552
The use of in-situ photography in studies of the deep-sea benthos at IOS — Institute of Oceanographic Sciences (IOS)
[IOS-182] 09 p1360 N85-18553
An assessment of biological processes close to the sea bed in a slope region and its significance to the assessment of sea-bed disposal of radioactive waste
[IOS-185] 09 p1360 N85-18554
Deep seabed stable reference areas
[PB84-241470] 09 p1360 N85-18555
Propagation of electromagnetic fields along the sea/sea-bed interface
[AD-A149523] 10 p1487 N85-19257
New data on structure of Shirshov Ridge (Bering Sea)
10 p1498 N85-19459
Specifics of backscattering of sound by bottom of bank in open sea 10 p1499 N85-19460
Aluminum in biogenic cycle and forms of its occurence in ocean 10 p1499 N85-19463
Research on ocean floor electrical surveys
[AD-A149831] 12 p1899 N85-21920
Determining degree of partial melting of asthenosphere from seismic data 13 p2107 N85-23127

Determining adsorption of surface-active substances by sea bottom deposits 13 p2107 N85-23128
Use of paleomagnetic data in tectonic analysis of oceanic structures 13 p2108 N85-23135
More precise curve of dependence between density and velocity of longitudinal waves in consolidated crust and top of mantle in oceanic structures 13 p2110 N85-23143
Crustal and upper mantle density model of Owen fault zone 13 p2110 N85-23144
Structure of Iceland and ocean floor spreading 13 p2112 N85-23159
Assessing LANDSAT TM and MSS data for detecting submerged plant communities 13 p2120 N85-23203
Remanent magnetization model for the broken ridge satellite magnetic anomaly 13 p2123 N85-23219
Submarine volcanic eruptions and potential analogs for Venus 13 p2187 N85-23573
The Deep Drifter Program — deep ocean sensors 14 p2329 N85-24400
Automation of radiometric measurements in nuclear oceanology 14 p2337 N85-24452
Most important geochemical barrier zones in ocean (with example of Atlantic Ocean basin) 14 p2343 N85-24491
Water wave propagation over uneven bottoms [AD-A151460] 15 p2556 N85-25769
The effect of the Benthic Boundary Layer on the physics of intense mesoscale eddies [AD-A153193] 17 p2958 N85-28270
Geoacoustic models: Washington state continental margin [AD-A153781] 18 p3177 N85-29899
Concretization of high level radioactive source in marine sediment [AD-D011703] 19 p3249 N85-30146
Natural gas anomaly in bottom waters of South China Sea 19 p3290 N85-30399
Ultramicroscopic study of structure of phosphorites from Sea of Japan floor 19 p3290 N85-30400
Plane Tsunami wave caused by elastic oscillations of ocean floor 19 p3290 N85-30403
Heat flow through ocean floor and its relationship to lithosphere structure and thickness 19 p3294 N85-30422
Density characteristics of asthenosphere in Atlantic Ocean 19 p3294 N85-30423
Influence of underwater volcanic mountains of Atlantic on microplankton distribution 19 p3294 N85-30424
Evolution of the oceanic upper mantle and effects on sea floor subsidence geoid height and heat flow 19 p3310 N85-30575
Environmental background measurement program [AD-A153860] 19 p3310 N85-30577
Dispersal From Deep Ocean Sources: Physical and Related Scientific Processes [DE85-010420] 20 p3497 N85-31740
Benthic boundary layer modelling studies [IOS-181] 20 p3497 N85-31742
Global geomorphology 21 p3601 N85-32359
Deep sea mega-geomorphology: Progress and problems 21 p3602 N85-32360
Sulfur and carbon cycling in organic-rich marine sediments 21 p3659 N85-32729
A random layer model for reflection from ocean bottom sediments [AD-A155019] 21 p3700 N85-32988
Understanding coherence losses incurred by bottom-retained signals [AD-A155559] 21 p3701 N85-32992
The 3.5 b.y. old Onverwacht Group: A remnant of ancient oceanic crust 21 p3718 N85-33073
Anorthositic oceanic crust in the Archean Earth 21 p3719 N85-33077
Subduction zone tectonic studies to develop concepts for the occurrence of sediment subduction [DE85-011794] 22 p3815 N85-33632
Arctic and offshore research [DE85-001995] 22 p3818 N85-33653
Research at the Institute of Oceanographic Sciences related to the possible disposal of radioactive waste on or beneath the seafloor [IOS-204] 23 p3973 N85-34628
Marine phosphorite deposits model for exploration, with emphasis on deposits in the US Atlantic coastal plain 24 p4104 N85-35439
Massive sulfide deposits from the southern Juan de Fuca Ridge 24 p4105 N85-35446
Background light measurements at the DUMAND site [HE-5.2-7] 24 p4203 N85-36084
Measurements of light background at large depth in the ocean [HE-5.2-8] 24 p4203 N85-36085

OCEAN COLOR SCANNER
Characteristic vector analysis of inflection ratio spectra: New technique for analysis of ocean color data [NASA-TP-2428] 13 p2126 N85-23237

OCEAN CURRENTS
NT COASTAL CURRENTS
NT EL NINO
NT GULF STREAM
An improved analytical theory of Rossby wave driven Eulerian and Lagrangian mean flows along non-zonal barriers with application to the Hawaiian Ridge [AD-A144051] 01 p0088 N85-10593
The gulf stream deflection and meander energetics experiment. Current meter and bottom pressure gauge data report for the September, 1981 to April, 1982 mooring period [AD-A144977] 01 p0088 N85-10595
A description and discussion of FREDDEX oceanographic measurements [AD-A145032] 01 p0088 N85-10596
Observations of the vertical structure of the eddy field in the Kuroshio extension [AD-A145178] 01 p0089 N85-10599
Analysis and interpretation of current measurements from the Beaufort Sea [AD-A145197] 01 p0089 N85-10600
Numerical studies of mesoscale eddies using quasigeostrophic and primitive equation ocean models [PB84-214048] 01 p0089 N85-10602
Radiotracer studies of the dispersion of solid pollutants in marine and estuarial environment: Measurement of diffusion coefficients and the phenomenon of dispersion by currents [BLL-DRIC-TRANS-7104-(3623.66)] 02 p0224 N85-11468
A study of highly energetic near-bottom ocean flow at the base of the Scotian Rise 02 p0233 N85-11515
One-year records of current and bottom pressure in the strait between Nordaustlandet and Kvitoeya and Svalbard, 1980 - 1981 [AD-A145594] 02 p0233 N85-11518
Eddy detection in the Norwegian, Greenland, and Barents Seas with a radar altimeter 03 p0382 N85-12442
Determination of the altimetric geoid and gravity anomalies in the North Sea: Implications for a solution of the general circulation problem using ERS-1 data 03 p0382 N85-12448
The POSEIDON altimeter description 03 p0383 N85-12454
The Long Term Upper Ocean Study (LOTUS). Cruise summary [AD-A145767] 03 p0397 N85-12536
Dynamics of coupled ice-ocean system in the marginal ice zone: Study of the mesoscale processes and of constitutive equations for sea ice [NASA-CR-174171] 04 p0542 N85-13448
Tide tables 1985, high and low water predictions, central and western Pacific Ocean and Indian Ocean [PB84-236393] 04 p0542 N85-13451
Recent observations of tides and tidal currents from the northeastern Bering Sea shelf [PB84-241785] 04 p0543 N85-13452
Sigma code testing [AD-A146548] 06 p0841 N85-15340
Bio-optical variability in the Alboran Sea as assessed by Nimbus-7 coastal zone color scanner [AD-A147909] 07 p0969 N85-16281
Satellite definition of the bio-optical and thermal variation of coastal eddies associated with the African current [AD-A147910] 07 p0969 N85-16282
The problem of climate and climate variation 07 p1001 N85-16353
Meteorological aspects of the 1982-83 El Nino/southern oscillation episode 07 p1001 N85-16356
Ocean and climate, an example. The interannual variability of the tropical Pacific Ocean 07 p1002 N85-16365
The El Nino phenomenon and its agrometeorological implications 07 p1004 N85-16382
A compilation of moored current meter and wind recorder data. Volume 35: Long-Term Upper Ocean Study (LOTUS) (Moorings 764, 765, 766, 767, 770), May 1982 - April 1983 [AD-A147103] 07 p1009 N85-16412
The long term upper ocean study (LOTUS). Cruise summary and hydrographic data report, OCEANUS 154, May 1984 [AD-A147908] 07 p1009 N85-16414
Current and current shear effects in the parabolic approximation for underwater sound channels [AD-A147833] 07 p1039 N85-16597
Use of SIR-B multiincidence-angle imagery to study iceberg detectability and offshore ocean feature extraction 08 p1145 N85-17225
MIZEX. A program for mesoscale Air-Ice-Ocean interaction experiments in arctic marginal ice zones. 4: Initial results and analysis from MIZEX 83 [AD-A146255] 08 p1173 N85-17399
Bibliography update on the California current system and related mesoscale ocean modeling [AD-A146546] 08 p1190 N85-17503
Deep water mass circulation in the Western Alboran Basin: Measurements in July and September 1980 (Alboran I experiment) [AD-A146566] 08 p1191 N85-17504
Surface currents of the Indian Ocean (to 25 deg S., 100 deg E.) [IOS-167] 10 p1521 N85-19503
Atlas of the Beaufort Sea [AD-A149545] 11 p1689 N85-20619
Intensification of tropical instabilities [AD-A149965] 12 p1898 N85-21899
Circulation and internal waves in a cold Gulf Stream wave [AD-A149704] 12 p1898 N85-21918
Preliminary results of the oceanographic cruise of USCGC NORTHWIND to the Greenland Sea [AD-A149802] 12 p1898 N85-21919
Microplankton species assemblages at the Scripps Pier from March to November 1983 during the 1982-1984 El Nino event [NASA-CR-175553] 12 p1899 N85-21926
Calculation of level surface in problems of large-scale ocean circulation 13 p2108 N85-23136
Double and inverse Taylor-Hogg vortices in a stratified ocean 13 p2108 N85-23137
Circulation pattern of the North Atlantic, part of the warmwater sphere research effort at Kiel University 14 p2239 N85-23668
Surface currents in the tropical Pacific during 1979-1980 using drifting buoys 14 p2323 N85-24354
The Indian Ocean surface dynamics experiment (SINODE) 14 p2325 N85-24370
The ARGOS contribution to the First GARP Global Experiment (FGGE) study of drifting buoys 14 p2325 N85-24371
Main features of Antarctic Ocean circulation as revealed by satellite tracking of icebergs 14 p2325 N85-24372
The Deep Drifter Program — deep ocean sensors 14 p2329 N85-24400
Frontal nature of Cromwell Current 14 p2336 N85-24445
Local mechanism of equatorial countercurrents 14 p2336 N85-24446
Modeling evolution of unstable geostropic eddies in barotropic ocean 14 p2336 N85-24447
A study of the turbulent layer in the water at an air-water interface 14 p2378 N85-24679
Observations of the California countercurrent [AD-A150781] 14 p2362 N85-24691
Some preliminary results concerning deep northern-boundary currents in the North Pacific [AD-A151021] 14 p2362 N85-24692
Measurement of ocean surface currents from space with multi-frequency microwave radars 15 p2539 N85-25672
Chemical signatures associated with the freshening of Northern Atlantic waters between 1972 and 1981 15 p2601 N85-26032
North Atlantic Deep Water and the world ocean 15 p2602 N85-26033
Glacial-to-interglacial changes in NADW fluxes? 15 p2602 N85-26037
Changes in the high-latitude ocean as possible causes of atmosphere CO2 variations 15 p2602 N85-26038
Possible sea ice impacts on oceanic deep convection 15 p2603 N85-26041
Development of a Lagrangian drifting buoy 16 p2811 N85-27338
Long term drifting float for measuring mean oceanic circulation using ARGOS system 16 p2811 N85-27339
ARGOS-tracked drifters in the Rockall Trough 16 p2812 N85-27340
Results of an initial trial of a satellite telemetering buoy measuring near surface current 16 p2812 N85-27345
Towards a study of synoptic-scale variability of the California current system [NASA-CR-175871] 17 p2997 N85-28529
Rip in White Sea 19 p3290 N85-30401
Study of drift currents in initial stage of generation of wind waves by laser Doppler anemometer 19 p3291 N85-30408
Dynamic theory of polar tide 19 p3292 N85-30414
Sand dispersion from an ephemeral river delta on the wave-dominated central California coast [AD-A154352] 19 p3300 N85-30458

Northeast Brazil droughts and Atlantic SST anomalies
[INPE-3538-PRE/754] 19 p3316 N85-30553
Atmospheric chlorofluromethanes as tracers of ocean circulation and mixing: Measurement and calibration techniques and studies in the Greenland and Norwegian Seas 19 p3319 N85-30573
Experiments using atmospheric forcing from a FGGE analysis to drive an upper ocean model
[INPE-3503-PRE/738] 19 p3319 N85-30576
Error spectrum of Goddard satellite models for the gravity field 20 p3491 N85-31704
Ocean circulation studies 20 p3492 N85-31712
Dispersal From Deep Ocean Sources: Physical and Related Scientific Processes
[DE85-010490] 20 p3497 N85-31740
Horizontal and vertical structure of velocity, potential vorticity and energy in the gulf stream
[AD-A154753] 21 p3655 N85-32702
Hydrographic data from the OPTOMA (Ocean Prediction Through Observations, Modeling and Analysis) program: OPTOMA15, 24 January to 23 February 1985
[AD-A155012] 21 p3655 N85-32703
Numerical simulations of the response of intense ocean currents to atmospheric forcing
[AD-A155161] 21 p3655 N85-32704
Method and apparatus for Delta Kappa synthetic aperture radar measurement of ocean current
[NASA-CASE-NPO-15704-1] 23 p3925 N85-34327
Meteorological data from the OPTOMA (Ocean Prediction Through Observations, Modeling and Analysis) program OPTOMA 2, leg D2. 30 Jun. - 10 Jul. 1984
[AD-A156134] 24 p4123 N85-35560

OCEAN DATA ACQUISITIONS SYSTEMS

Sea ice data buoys in the Weddell Sea
[AD-A144953] 01 p0088 N85-10594
High-data-rate wide-angle underwater acoustic telemetry system
[DE84-015696] 02 p0233 N85-11519
Ocean wave parameters extraction using satellite short-pulse radar altimeters 03 p0360 N85-12425
The impact of satellite altimeter data on wave research 03 p0360 N85-12427
The NASA/JPL pilot ocean data system 03 p0361 N85-12433
NODC/1983: National Oceanographic Data Center report
[PB84-222231] 04 p0542 N85-13449
Advanced technology for hydrographic mapping
[FOA-C-30371-E1] 08 p1176 N85-17418
The use of in-situ photography in studies of the deep-sea benthos at IOS — Institute of Oceanographic Sciences (IOS)
[IOS-182] 09 p1360 N85-18553
International list of selected, supplementary and auxiliary ships — WMO
[WMO-47-ED-84] 11 p1687 N85-20609
Remote self-contained undersea monitor
[AD-D011520] 12 p1849 N85-21509
Method of measuring sea surface water temperature with a satellite including wideband passive synthetic-aperture multichannel receiver
[NASA-CASE-NPO-15651-1] 12 p1869 N85-21723
Project PAPA: The integration of drifting buoy data into an operational meteorological service 14 p2238 N85-23874
Automatic buoys to assist the tuna fishery off the Azores 14 p2238 N85-23879
Operational experiences with the ARGOS system in oceanography and oil spill emergency planning. Future plans for the use of the ARGOS system as a component in offshore data collection system 14 p2239 N85-23887
Some experience from ARGOS stations in the open sea 14 p2240 N85-23891
Proceedings of the ARGOS Users Conference on Data Collection and Location by Satellite 14 p2322 N85-24348
The development of Platform Transmitter Terminal (PTT) and its application for drifting buoys 14 p2323 N85-24353
US programs using the ARGOS data collection and platform location system 14 p2323 N85-24355
Inferences of future operations drawn from past and present applications of drifting buoys 14 p2323 N85-24356
US program in anchored data buoy and the other fixed observation platforms 14 p2324 N85-24358
One thousand days in the brine — platform transmitter terminals 14 p2324 N85-24359
Data Collection and Platform Location by Satellite: ARGOS Users' Conference 14 p2325 N85-24366
The ARGOS system main characteristics — satellite based localization 14 p2325 N85-24367
Meteorological buoys developed at the EERM laboratory 14 p2326 N85-24374
The ARGOS contribution to the successful dredging of a deep moored current meter 14 p2327 N85-24381
Data Collection and Platform Location by Satellite: ARGOS users' Conference 14 p2328 N85-24391
Collecting meteorological reports with the ARGOS system 14 p2329 N85-24398
The French Ocean Climate in Equatorial Atlantic (FOCAL) Drifter Program, 1983-1984 14 p2329 N85-24399
The Deep Drifter Program — deep ocean sensors 14 p2329 N85-24400
US programs using the ARGOS data collection and platform location system 14 p2329 N85-24401
Telemetered meteorological and engineering data from a deep sea moored body in the Long Term Upper Ocean Study (LOTUS) 14 p2329 N85-24402
Practical considerations when using water quality and structure monitoring sensors as applied to portable ARGOS satellite transmitter equipment 14 p2330 N85-24405
Drifting buoy development and future programs — Japanese ARGOS program 14 p2330 N85-24406
Development of a low cost drifting buoy 14 p2330 N85-24408
Data Collection and Platform Location by Satellite: ARGOS Users' Conference 14 p2330 N85-24409
US program using the ARGOS data collection and platform location system 14 p2330 N85-24410
A report on the DRIFTERS program — buoys 14 p2331 N85-24413
Drifting buoys on the Labrador shelf 14 p2331 N85-24415
A new versatile ARGOS PTT for oceanographic applications — Platform Transmit Terminal (PTT) 14 p2331 N85-24417
Overview of data processing at AES local user terminals — Canadian Atmospheric Environment Service (AES) 14 p2331 N85-24418
An overview of NDBC drifting buoy development programs — NOAA Data Buoy Center (DBC) 14 p2332 N85-24422
Preliminary report on the results of hydrological measurements in the southern Tyrrhenian Sea, in the Messina strait and in the western Ionian sea
[PREPRINT-433] 14 p2362 N85-24693
Survey of remote sensing techniques for wave measurement
[NASA-TM-84429] 15 p2583 N85-25928
Ocean circulation and meteorology off the Georgia coast. Part 1: Real-time telemetry system for data collection
[PB85-155935] 15 p2605 N85-26052
Data Collection and Platform Location by Satellite: ARGOS Users' Conference 16 p2611 N85-27333
DB2 and DB3: The next generation — buoys 16 p2611 N85-27337
Development of a Lagrangian drifting buoy 16 p2611 N85-27338
Long term drifting float for measuring mean oceanic circulation using ARGOS system 16 p2611 N85-27339
Monitoring of marine environment 16 p2612 N85-27341
Routine wave and meteorological measurements in offshore areas using ARGOS data surveillance 16 p2612 N85-27344
Results of an initial trial of a satellite telemetering buoy measuring near surface current 16 p2612 N85-27345
An operational buoy network collecting meteorological data 16 p2613 N85-27351
Availability of the ARGOS system based on the orbital characteristics of the TIROS-N satellites — oceanographic/meteorological data 16 p2613 N85-27352
Contribution of the NOAA-7 and 8 and ARGOS partnership to white tuna fishing in the northeast Atlantic 16 p2613 N85-27355
First results of oceanography utilization of infrared high resolution picture transmission images
[KNMI-TR-59] 16 p3151 N85-29511
ERS economic impace study
[ESA-CR(P)-1979] 18 p3199 N85-29847
Chemical, biological, and physical measurements from the subtropical western North Atlantic Ocean. Summer 1982, USNS Lynch, cruise 710-82
[AD-A153823] 18 p3201 N85-29857
Tropical Ocean and Global Atmosphere (TOGA) heat exchange project: A summary report
[NASA-CR-176036] 20 p3498 N85-31738
Large-scale sea surface temperature variability from satellite and shipboard measurements
[NASA-CR-176123] 22 p3818 N85-33651

OCEAN DATA PLATFORMS

U OCEAN DATA ACQUISITIONS SYSTEMS

OCEAN DATA STATIONS

U OCEAN DATA ACQUISITIONS SYSTEMS

OCEAN DYNAMICS

Large-scale ocean-atmosphere interactions in the mid-latitudes and equatorial regions: A literature review
[CSIR-T/SEA-8302] 01 p0073 N85-10482
Observations of the vertical structure of the eddy field in the Kuroshio extension
[AD-A145178] 01 p0089 N85-10599
Return wave heights off South Uist estimated from seven years of data
[IOS-164] 01 p0089 N85-10601
Numerical studies of mesoscale eddies using quasigeostrophic and primitive equation ocean models
[PB84-214048] 01 p0089 N85-10602
Synthesis of current measurements in Puget Sound, Washington. Volume 1: Index to current measurements made in Puget Sound from 1906-1980 with daily and record averages for selected measurements
[PB84-214105] 01 p0089 N85-10603
A study of highly energetic near-bottom ocean flow at the base of the Scotian Rise 02 p0233 N85-11515
Monitoring of the tidal dynamics of the Dutch Waddensea by SIR-B 08 p1147 N85-17235
A one dimensional dynamical model of ocean/atmosphere interactions 09 p1358 N85-18545
Characteristic vector analysis of inflection ratio spectra: New technique for analysis of ocean color data
[NASA-TP-2428] 13 p2126 N85-23237
The Indian Ocean surface dynamics experiment (SINODE) 14 p2325 N85-24370
The ARGOS contribution to the First GARP Global Experiment (FGGE) study of drifting buoys 14 p2325 N85-24371
A large-scale air sea interaction project over the Pacific basin 14 p2326 N85-24373
Review of North Atlantic source waters 15 p2601 N85-26029
Deep water formation 15 p2601 N85-26030
Temporal and spatial scales of Labrador Sea water formation 15 p2601 N85-26031
Chemical signatures associated with the freshening of Northern Atlantic waters between 1972 and 1981 15 p2601 N85-26032
North Atlantic Deep Water and the world ocean 15 p2602 N85-26033
Oceanographic variations in recent decades and their impact on the fertility of the Iceland Sea 15 p2602 N85-26034
Quaternary North Atlantic surface paleoceanography in regions of potential deep-water formation 15 p2602 N85-26036
First results of oceanography utilization of infrared high resolution picture transmission images
[KNMI-TR-59] 16 p3151 N85-29511
Destruction of density jumps in ocean by turbulence 19 p3291 N85-30407
Study of drift currents in initial stage of generation of wind waves by laser Doppler anemometer 19 p3291 N85-30408
Frequency of recurrence and critical conditions for generation of Langmuir circulations 19 p3291 N85-30409
Dynamic theory of polar tide 19 p3292 N85-30414
Atmospheric chlorofluromethanes as tracers of ocean circulation and mixing: Measurement and calibration techniques and studies in the Greenland and Norwegian Seas 19 p3319 N85-30573
Research, progress and the mark A box model for physical, biological and chemical transports
[DE85-010574] 19 p3320 N85-30581
Physical oceanography program science abstracts
[AD-A154637] 21 p3654 N85-32701
Air-sea interaction with SSM/I and altimeter
[NASA-CR-176105] 22 p3818 N85-33650
Large-scale sea surface temperature variability from satellite and shipboard measurements
[NASA-CR-176123] 22 p3818 N85-33651

OCEAN MODELS

Numerical studies of mesoscale eddies using quasigeostrophic and primitive equation ocean models
[PB84-214048] 01 p0089 N85-10602
MIZEX. A program for mesoscale air-ice-ocean interaction experiments in arctic marginal ice zones. III: Modeling the marginal ice zone
[AD-A145351] 02 p0233 N85-11517
Intercomparison of GEOS 3/SEASAT wave data and wave model data 03 p0361 N85-12436
Simulation of wavefronts returned by realistic surfaces 03 p0363 N85-12448
Parameterizing extreme still water levels and waves in design level studies
[IOS-183] 03 p0366 N85-12542

NUTSATSEA: An on line data reduction program linking a Chemlab continuous flow analyser to a Commodore PET microcomputer
[IOS-176] 03 p0403 N85-12570
Sigma code testing
[AD-A146548] 06 p0841 N85-15340
Interactions between mean flow and finite-amplitude mesoscale eddies in a barotropic ocean
[AD-A147249] 07 p1009 N85-16413
Research of inverse methods to describe the structure of the earth and ocean bottom
[AD-A147082] 07 p1030 N85-16541
Bibliography update on the California current system and related mesoscale ocean modeling
[AD-A148548] 08 p1190 N85-17503
A critical analysis of ocean thermal analysis models in operation at FNOC (Fleet Numerical Oceanography Centers)
[AD-A148731] 09 p1359 N85-18547
Stochastic convective-dispersive transport model for wastes disposed at the 106-mile ocean disposal site
[PB85-116176] 12 p1885 N85-21631
Intensification of tropical instabilities
[AD-A149985] 12 p1898 N85-21899
Calculation of level surface in problems of large-scale ocean circulation 13 p2108 N85-23138
Mathematical-cartographic model for study of distribution of hydrochemical elements in sea water (using dissolved oxygen in the Pacific Ocean as an example)
13 p2109 N85-23138
Sea-ice motion in response to geostrophic winds
14 p2323 N85-24357
Influence of bubbles formed upon breaking of waves on gas exchange between ocean and atmosphere
14 p2335 N85-24439
Representation of temperature and salinity fields using statistically orthogonal functions (in example of polymode data) 14 p2337 N85-24449
Sensitivity analysis of a coupled atmospheric-oceanic boundary layer model
[AD-A150760] 14 p2382 N85-24690
Ocean modeling of the North Atlantic
15 p2602 N85-26039
Ocean tide models for Topex analysis
16 p2805 N85-27291
Tropical Oceans-Global Atmosphere (TOGA) experiment planning for the Brazilian participation in TOGA global climate program
[INPE-3499-PRE/735] 16 p2834 N85-27477
Comparison of a diffusion model with dye dispersion measurements to study turbulence in coastal waters
[INPE-3492-PRE/729] 16 p2836 N85-27504
Research Review, 1983
[NASA-TM-86219] 18 p3139 N85-29433
On Fofonoff's mode 18 p3145 N85-29471
Utilization of the SEASAT scatterometer winds for ocean mixed layer modeling
[AD-A153748] 18 p3150 N85-29506
Parametric description of cold film on ocean surface
19 p3292 N85-30410
Dynamic theory of polar tide 19 p3292 N85-30414
Experiments using atmospheric forcing from a FGGE analysis to drive an upper ocean model
[INPE-3503-PRE/736] 19 p3319 N85-30578
One-dimensional model hindcasts of warm anomalies in the North Pacific Ocean
[AD-A154128] 19 p3320 N85-30579
Research, progress and the mark A box model for physical, biological and chemical transports
[DE85-010574] 19 p3320 N85-30581
Dispersal From Deep Ocean Sources: Physical and Related Scientific Processes
[DE85-010420] 20 p3497 N85-31740
Benthic boundary layer modelling studies
[IOS-181] 20 p3497 N85-31742
Anorthositic oceanic crust in the Archean Earth
21 p3719 N85-33077

OCEAN SURFACE

Large-scale ocean-atmosphere interactions in the mid-latitudes and equatorial regions: A literature review
[CSIR-T/SEA-8302] 01 p0073 N85-10482
The Marine Resources Experiment Program (MAREX)
[NASA-TM-87368] 01 p0086 N85-10580
Return wave heights off South Uist estimated from seven years of data
[IOS-164] 01 p0089 N85-10601
Energy-active zones in north Atlantic as manifestation of interannual variability of radiation balance
02 p0164 N85-11108
A radar sea clutter model for atmospheric ducting conditions
[AD-A145321] 02 p0190 N85-11268
Theory of radio wave propagation over the ocean
02 p0259 N85-11696
SEASAT altimeter data over the Mediterranean: Implications for ERS-1 03 p0382 N85-12443
Satellite altimetry for sea-surfacing topography determination and geoid improvement
03 p0382 N85-12444
Development of a microcomputer coupled atmospheric and oceanic boundary layer prediction model
[AD-A146334] 03 p0397 N85-12530
Simple prediction of convergence zone propagation in waters around australia
[AD-A145986] 03 p0416 N85-12659
Multisensor satellite data integration for sea surface wind speed and direction determination
[NASA-CR-174162] 04 p0542 N85-13446
Components of the time variation of sea surface height from SEASAT altimeter data 05 p0658 N85-14227
Statistical analysis of visual wave observations and gage/radar measurements
[AD-A146358] 06 p0798 N85-15100
Energy active areas of ocean
06 p0820 N85-15204
Studies of the ocean surface and the coupling between the sea and the atmosphere
[AD-A146546] 06 p0841 N85-15339
The interpretation of SIR-B imagery of surface waves and other oceanographic features using in-situ, meteorological satellite, and infrared satellite data
08 p1143 N85-17212
Remote sensing of rice fields and sea pollution by SIR-B 08 p1145 N85-17222
The investigation of selected oceanographic applications of spaceborne synthetic-aperture radar
08 p1146 N85-17233
The use of synthetic aperture radar imagery to detect hazards to navigation
[AD-A149324] 10 p1422 N85-18971
Surface currents of the Indian Ocean (to 25 deg S., 100 deg E.)
[IOS-187] 10 p1521 N85-19593
Drifting buoy data from equatorial Pacific Ocean, 31 Aug. 1980 - 30 Apr. 1982
[PB85-120046] 10 p1522 N85-19598
Oceanographic and meteorological research based on the data products of SEASAT
[E85-10091] 12 p1874 N85-21753
Calculation of level surface in problems of large-scale ocean circulation 13 p2108 N85-23138
Possibility of mapping active tectonic structures from mercury gas aureoles over sea surface
13 p2113 N85-23162
Surface currents in the tropical Pacific during 1979-1980 using drifting buoys 14 p2323 N85-24354
The Indian Ocean surface dynamics experiment (SINODE) 14 p2325 N85-24370
Possible multiple atmospheric thermal modes with time scale on order of one month 14 p2333 N85-24430
Influence of bubbles formed upon breaking of waves on gas exchange between ocean and atmosphere
14 p2335 N85-24439
Low-frequency oscillations of sea level and group structure of wind waves 14 p2335 N85-24441
Energy structure of atmospheric boundary layer above waves 14 p2335 N85-24442
Frontal nature of Cromwell Current
14 p2336 N85-24445
Parameterization of apparent and latent heat fluxes above water surface in calm weather under natural conditions 14 p2337 N85-24454
Measurement of ocean surface currents from space with multi-frequency microwave radars
15 p2539 N85-25672
Survey of remote sensing techniques for wave measurement
[NASA-TM-84429] 15 p2583 N85-25928
Quaternary North Atlantic surface paleoceanography in regions of potential deep-water formation
15 p2602 N85-26036
Changes in the high-latitude ocean as possible causes of atmosphere CO2 variations 15 p2602 N85-26038
Sea ice, climate and Fram Strait
15 p2603 N85-26042
Ocean circulation and meteorology off the Georgia coast. Part 1: Real-time telemetry system for data collection
[PB85-155935] 15 p2605 N85-26052
Sound propagation through directional internal wave fields
[AD-A151168] 15 p2646 N85-26321
Topex Gravity Model Development Team activities during fiscal year 1984
[NASA-TM-86208] 16 p2804 N85-27285
Results of an initial trial of a satellite telemetering buoy measuring near surface current
16 p2812 N85-27345
Atmospheric frontal zone studies
[NASA-CR-175293] 16 p2833 N85-27469
On the 1983 drought in northeast Brazil
[INPE-3412-PRE/678] 16 p2834 N85-27476
Simulation of a synchronously coupled atmosphere-ocean prediction model
[AD-A152020] 16 p2835 N85-27482
Analysis of ocean surface wind fields using SEASAT-A scatterometer data 18 p3139 N85-29434
Intercomparison of sea-surface temperature anomaly fields 18 p3140 N85-29440
A GCM study of the atmospheric response to tropical SST anomalies 18 p3146 N85-29477
One mechanism for generation of wave disturbances in spectra of turbulent flows near ocean surface
19 p3289 N85-30397
Study of drift currents in initial stage of generation of wind waves by laser Doppler anemometer
19 p3291 N85-30408
Frequency of recurrence and critical conditions for generation of Langmuir circulations
19 p3291 N85-30409
Parametric description of cold film on ocean surface
19 p3292 N85-30410
Model computations of light reflection from sea surface 19 p3292 N85-30411
Sea surface radio emission at wavelengths 0.86 and 1.3 cm near Brewster angle 19 p3293 N85-30418
Specifics of laser sounding of atmosphere along horizontal and slightly slanting paths over water surface
19 p3297 N85-30441
A survey of the turbulence in the marine surface layer for the operation of low-Reynolds number aircraft
[AD-A154133] 19 p3316 N85-30558
A study of the turbulent layer in the water at an air-water interface
[AD-A154117] 19 p3319 N85-30578
One-dimensional model hindcasts of warm anomalies in the North Pacific Ocean
[AD-A154128] 19 p3320 N85-30579
Geodynamics Branch research program
[NASA-TM-86223] 20 p3489 N85-31688
Global mean sea surface based upon a combination of the GEOS-3 and SEASAT altimeter data
20 p3492 N85-31710
Using ship wake patterns to evaluate SAR (Synthetic Aperture Radar) ocean wave imaging mechanisms. Joint US-Canadian Ocean Wave Investigation Project
[AD-A154633] 21 p3573 N85-32223
Numerical simulations of the response of intense ocean currents to atmospheric forcing
[AD-A155161] 21 p3655 N85-32704
Simulation of the coupled atmospheric and oceanic boundary layer model during MILDEX
[AD-A155166] 21 p3655 N85-32705
Basic properties and interpretation of synthesized radar images of sea waves with long synthetization time
22 p3773 N85-33364
Large-scale sea surface temperature variability from satellite and shipboard measurements
[NASA-CR-176123] 22 p3818 N85-33651
Microwave properties of a quiet sea
[NASA-CR-176199] 24 p4085 N85-35322
Sea surface and remotely sensed temperatures off Cape Mendocino, California
[NASA-TM-86712] 24 p4125 N85-35573

OCEAN TEMPERATURE

NT SEA SURFACE TEMPERATURE

The gulf stream deflection and meander energetics experiment. Current meter and bottom pressure gauge data report for the September, 1981 to April, 1982 mooring period
[AD-A144977] 01 p0088 N85-10595
Ocean and climate, an example. The interannual variability of the tropical Pacific Ocean
07 p1002 N85-16365
The ocean and the dynamics of the tropical atmosphere; Its possible predictability 07 p1002 N85-16366
A compilation of moored current meter and wind recorder data. Volume 35: Long-Term Upper Ocean Study (LOTUS) (Moorings 764, 765, 766, 767, 770), May 1982 - April 1983
[AD-A147103] 07 p1009 N85-16412
Measurements of sediment temperatures, conductivity and heat flow in the North Atlantic and their relevance to radioactive waste disposal
[IOS-172] 09 p1359 N85-18551
Drifting buoy data from equatorial Pacific Ocean, 31 Aug. 1980 - 30 Apr. 1982
[PB85-120046] 10 p1522 N85-19598
Hydrographic data collected in 1982 and 1983 for EPOCS (Equatorial Pacific Ocean Climate Studies)
[PB85-110799] 12 p1876 N85-21765
Oceanic role in terrestrial climate
[DE85-004422] 12 p1896 N85-21904
Horizontal coherence of temperature microstructure in upper ocean layer 13 p2109 N85-23139

Geographic variation in the relationships of temperature, salinity or sigma sub t versus plant nutrient concentrations in the world ocean — silicic acid, nitrate, and phosphate concentration
[NASA-CR-175621] 13 p2140 N85-23287
Dynamic stochastic model of long-period variability of ocean surface temperature 14 p2334 N85-24437
Representation of temperature and salinity fields using statistically orthogonal functions (in example of polymode data) 14 p2337 N85-24449
North Atlantic Deep Water Formation
[NASA-CP-2367] 15 p2601 N85-26028
Review of North Atlantic source waters 15 p2601 N85-26029
Deep water formation 15 p2601 N85-26030
Temporal and spatial scales of Labrador Sea water formation 15 p2601 N85-26031
North Atlantic Deep Water and the world ocean 15 p2602 N85-26033
Oceanographic variations in recent decades and their impact on the fertility of the Iceland Sea 15 p2602 N85-26034
Quaternary North Atlantic surface paleoceanography in regions of potential deep-water formation 15 p2602 N85-26036
Glacial-to-interglacial changes in NADW fluxes? 15 p2602 N85-26037
Real-time enhancement of a climatology or forecast of ocean thermal structure using observed ocean temperatures
[AD-A151118] 15 p2604 N85-26049
Ocean circulation and meteorology off the Georgia coast. Part 1: Real-time telemetry system for data collection
[PB85-155935] 15 p2605 N85-26052
On the 1983 drought in northeast Brazil
[INPE-3412-PRE/678] 16 p2834 N85-27478
Intercomparison of sea-surface temperature anomaly fields 16 p3140 N85-29440
A GCM study of the atmospheric response to tropical SST anomalies 16 p3146 N85-29477
Publications of the Jet Propulsion Laboratory 1983
[NASA-CR-175979] 16 p3199 N85-29648
Parametric description of cold film on ocean surface 19 p3292 N85-30410
Air-sea interaction with SSM/I and altimeter
[NASA-CR-176105] 22 p3618 N85-33650
Large-scale sea surface temperature variability from satellite and shipboard measurements
[NASA-CR-176123] 22 p3618 N85-33651

OCEAN THERMAL ENERGY CONVERSION

Biofouling and corrosion studies at the Seacoast Test Facility in Hawaii
[DE84-014643] 01 p0029 N85-10180
Ocean energy systems at the Johns Hopkins University Applied Physics Laboratory
[PB84-225705] 03 p0397 N85-12474
Research approaches to qualify aluminum for Ocean Thermal Energy Conversion (OTEC) systems
[DE84-013007] 04 p0476 N85-13034
Correlation and reassessment of the OTEC plant power cycle
[DE84-015467] 04 p0529 N85-13382
Open cycle OTEC thermal-hydraulic systems analysis and parametric studies
[DE84-013011] 04 p0530 N85-13391
NOAA OTEC CWP (National Oceanic and Atmospheric Administration Ocean Thermal Energy Conversion Cold Water Pipe) at-sea test. Volume 3, part 1: Tabulation of the power spectra for selected channels
[PB84-236955] 09 p1346 N85-18467
NOAA OTEC CWP (National Oceanic and Atmospheric Administration Ocean Thermal Energy Conversion Cold Water Pipe) at-sea test. Volume 3: Additional tabulation of the power spectra, part 2
[PB84-236997] 09 p1346 N85-18468
Conceptual design of a 10 MW shore-based OTEC plant
[DE84-015808] 10 p1511 N85-19532
OTEC (Ocean Thermal Energy Conversion) Cold Water Pipe At-Sea Test Program. Phase 2: Suspended pipe test
[PB85-119931] 10 p1512 N85-19542
Theoretical analysis of condensation in the presence of noncondensable gases as applied to open cycle OTEC condensers
[DE84-015809] 11 p1675 N85-20556
Ocean energy systems
[PB85-110856] 11 p1676 N85-20564
Experimental study of steam condensation on water in countercurrent flow in presence of inert gases
[DE84-013028] 12 p1661 N85-21800
Temperature sensors for OTEC applications
[DE85-009607] 18 p3110 N85-29254
Numerical techniques for steady two-dimensional transcritical stratified flow problems, with an application to the intermediate field dynamics of ocean thermal energy conversion plants
[DE85-008347] 18 p3151 N85-29609
Renewable technologies program summaries
[DE85-001509] 19 p3307 N86-30500
Heat transfer monitor for measurements of fouling of industrial heat exchangers
[DE85-010257] 20 p3455 N85-31455
Solar energy education. Renewable energy: A background text
[DE85-010366] 23 p3946 N85-34452
Ocean thermal energy conversion
[DE85-012291] 23 p3946 N85-34456
Energy from low temperature differences
[DE85-008617] 24 p4112 N85-35492

OCEANOGRAPHIC PARAMETERS

NT OCEAN TEMPERATURE
Sea ice data buoys in the Weddell Sea
[AD-A144953] 01 p0068 N85-10584
A description and discussion of FREDDEX oceanographic measurements
[AD-A145032] 01 p0068 N85-10596
Analysis and interpretation of current measurements from the Beaufort Sea
[AD-A145197] 01 p0069 N85-10600
Active remote sensing of ocean parameters, an engineering study 02 p0213 N85-11403
One-year records of current and bottom pressure in the strait between Nordaustlandet and Kvitoeya and Svalbard, 1980 - 1981
[AD-A145594] 02 p0233 N85-11518
Archiving and exchange of a computerized marine seismic database: The ROSE (Rivera Ocean Seismic Experiment) data archive system
[AD-A145858] 02 p0204 N85-11908
Ocean wave parameters extraction using satellite short-pulse radar altimeters 03 p0360 N85-12425
Physical oceanography report. Helicopter-based STD data from MIZEX 83 (Marginal Ice zone experiment)
[AD-A145848] 03 p0398 N85-12538
An introduction to the MIAS conversion system
[IOS-184] 03 p0403 N85-12571
Multisensor satellite data integration for sea surface wind speed and direction determination
[NASA-CR-174162] 04 p0542 N85-13446
The long term upper ocean study (LOTUS). Cruise summary and hydrographic data report, OCEANUS 154, May 1984
[AD-A147906] 07 p1009 N85-16414
Smoothing with split linear fits
[AD-A149032] 10 p1545 N85-19740
Atlas of the Beaufort Sea
[AD-A149545] 11 p1699 N85-20619
Advanced 2-frequency ocean sensing radar using high resolution antenna beams 14 p2230 N85-23821
The Tropical Ocean and Global Atmosphere program (TOGA) 14 p2330 N85-24411
Observations of the California countercurrent
[AD-A150781] 14 p2362 N85-24691
Ocean modeling of the North Atlantic 15 p2602 N85-26039
Space methods in oceanology
[NASA-TM-77652] 15 p2604 N85-26047
Tenth Conference of Working Group of Socialist Countries on Remote Sensing of Earth under Intercosmos Program 16 p2725 N85-26620
Function of remote sensing in Brazil
[INPE-3314-PRE/621] 16 p2810 N85-27329
Diffusion coefficients for coastal water determined from aerial photographs
[INPE-3413-PRE/679] 16 p2810 N85-27331
Symposium on Atmospheric Sciences in South Africa
[CSIR-S-331] 16 p2829 N85-27442
Air flow of the western coastal boundary of South Africa and its influence on the ocean 16 p2831 N85-27459
NASA Oceanic Processes Program annual review
[NASA-TM-87565] 16 p2836 N85-27503
Towards a study of synoptic-scale variability of the California current system
[NASA-CR-175871] 17 p2997 N85-28529
Intercomparison of sea-surface temperature anomaly fields 18 p3140 N85-29440
Geological-geophysical and gas-biochemical studies in Bering Sea 19 p3291 N85-30404
Geochemistry of manganese in ocean 19 p3291 N85-30406
Environmental background measurement program
[AD-A153860] 19 p3319 N85-30677
Research, progress and the mark A box model for physical, biological and chemical transports
[DE85-010574] 19 p3320 N85-30681
Tropical Ocean and Global Atmosphere (TOGA) heat exchange project: A summary report
[NASA-CR-179008] 20 p3496 N85-31736
The worldwide distribution of the seasonal cycle of mean sea level
[IOS-190] 20 p3497 N85-31743
Hydrographic data from the OPTOMA (Ocean Prediction Through Observations, Modeling and Analysis) program: OPTOMA15, 24 January to 23 February 1985
[AD-A155012] 21 p3655 N85-32703
Basic properties and interpretation of synthesized radar images of sea waves with long synthetization time 22 p3773 N85-33384
Salinity driven oceanographic upwelling
[DE85-011664] 22 p3618 N85-33652

OCEANOGRAPHY

Satellite reconnaissance
[AD-B085034] 01 p0015 N85-10094
The development of a diode laser Doppler velocimeter for boundary layer measurements under ice: A feasibility investigation
[AD-A145076] 01 p0053 N85-10348
Estuaries of the Cape. Part 2: Synopses of available information on individual systems. Report no. 17: Lourens (CSW 7)
[CSIR-RR-416-PT-2] 01 p0067 N85-10586
Estuaries of the Cape. Part 2: Synopses of available information on individual systems. Report no. 19: Groot (WES) (CMS 23) and Sout (CMS 22)
[CSIR-RR-418] 01 p0067 N85-10588
Sea-level in the world ocean. Part 6: The South Atlantic and South Pacific Oceans, a catalogue of measurements
[CSIR-T/SEA-8303-6] 01 p0067 N85-10590
Sea-level in the world ocean. Part 7: The Indian Ocean, a catalogue of measurements
[CSIR-T/SEA-8303-7] 01 p0067 N85-10591
Seafloor geosciences division: Missions, technical specialties, accomplishments, and activities, calendar year 1983
[AD-A144849] 01 p0067 N85-10592
Applications of remote sensing techniques to oceanography and sea ice
[FOA-B-60004-M7] 02 p0220 N85-11448
Radiotracer studies of the dispersion of solid pollutants in marine and estuarial environment: Measurement of diffusion coefficients and the phenomenon of dispersion by currents
[BLL-DRIC-TRANS-7104-(3623.66)] 02 p0224 N85-11488
Bibliography of climate textbooks and studies
[WCP-84] 02 p0231 N85-11505
A study of highly energetic near-bottom ocean flow at the base of the Scotian Rise 02 p0233 N85-11515
Physical oceanography report. Helicopter-based STD data from MIZEX 83 (Marginal ice zone experiment)
[AD-A145848] 03 p0398 N85-12538
Abstracts of papers submitted in 1983 for publication
[PB84-217579] 03 p0398 N85-12543
Coastal Zone Color Scanner (CZCS): Imagery of near-surface phytoplankton pigment concentrations from the first coastal ocean dynamics experiment (CODE-1), March - July 1981
[NASA-CR-174169] 04 p0542 N85-13447
Contributions to remote sensing : Applications of thermal infrared
[COMMUN-34/1984] 05 p0654 N85-14198
Activities of the Coastal Research Center
[PB84-231323] 05 p0672 N85-14320
USSR report: Earth sciences
[JPRS-UES-84-007] 06 p0819 N85-15196
A summary of the foundation research program
[AD-A146524] 06 p0891 N85-15656
USSR report: Earth sciences
[JPRS-UES-84-008] 07 p0980 N85-16223
Exploring ocean's mineral wealth 07 p0980 N85-16227
Ocean and climate, an example. The interannual variability of the tropical Pacific Ocean 07 p1002 N85-16365
Oceanographic data for development of the US exclusive economic zone
[PB85-106458/GAR] 07 p1010 N85-16415
The interpretation of SIR-B imagery of surface waves and other oceanographic features using in-situ, meteorological satellite, and infrared satellite data 08 p1143 N85-17212
The spatial evolution of t he directional wave spectrum in the Southern Ocean: Its relation to extreme waves in Agulhas Current 08 p1144 N85-17213
Evaluation of SIR-B imagery for geologic and geomorphic mapping, hydrology, and oceanography in Australia 08 p1146 N85-17229
SEASAT 3 and 4
[AD-A148343] 08 p1152 N85-17274
Altimetry, orbits and tides
[E85-10066] 08 p1174 N85-17404

The use of principal components analysis techniques Nimbus-7 coastal zone color scanner data to define mesoscale ocean features through a warm humid atmosphere
[AD-A148557] 09 p1176 N85-17416
Late Quaternary deep-water paleoceanography of the eastern equatorial Indian Ocean: Evidence from Bethnic foraminifera, carbonate dissolution, and stable isotopes
08 p1182 N85-17446
Bibliography update on the California current system and related mesoscale ocean modeling
[AD-A148546] 08 p1190 N85-17503
A critical analysis of ocean thermal analysis models in operation at FNOC (Fleet Numerical Oceanography Centers)
[AD-A148731] 09 p1359 N85-18547
USSR report: Earth sciences
[JPRS-UES-85-003] 10 p1497 N85-19446
Nautical charting with remotely sensed imagery, volume 1
[AD-A149361] 10 p1506 N85-19503
Practical applications of satellite-derived meteorological and oceanographic data in Naval operations
11 p1712 N85-20771
Hydrographic data collected in 1982 and 1983 for EPOCS (Equatorial Pacific Ocean Climate Studies)
[PB85-110799] 12 p1876 N85-21765
USC (University of Southern California) Sea Grant Program Directory, 1984-1985
[PB85-135051] 12 p1899 N85-21922
Biological processes in the water column of the South Atlantic Bight. Volume 1: Published manuscripts
[DE85-004610] 12 p1900 N85-21929
An airborne infrared thermal scanning system for easy use on Navy P-3 aircraft
[AD-A149690] 12 p1933 N85-22143
USSR report: Earth sciences
[JPRS-UES-85-002] 13 p2105 N85-23116
World ocean level oscillations and their relationship to change in inflow of continental waters
13 p2108 N85-23133
Fine structure of vertical distribution of light attenuation index of sea water 13 p2109 N85-23140
Science opportunities using the NASA scatterometer on N-ROSS
[NASA-CR-175639] 13 p2123 N85-23222
USSR report: Earth sciences
[JPRS-UES-85-004] 14 p2332 N85-24424
Determination of temperature and degree of roughness of sea and land surfaces by microwave radiometric polarization measurements 14 p2334 N85-24432
One physical mechanism of formation of fine structure of ocean waters 14 p2334 N85-24436
Two-cycle mechanism of dissipation of tidal energy in ocean 14 p2335 N85-24438
Automation of radiometric measurements in nuclear oceanology 14 p2337 N85-24452
Most important geochemical barrier zones in ocean (with example of Atlantic Ocean basin)
14 p2343 N85-24491
Remote sensing of directional wave spectra using the surface contour radar
[NASA-TM-84440] 14 p2347 N85-24510
Preliminary report on the results of hydrological measurements in the southern Tyrrhenian Sea, in the Messina strait and in the western Ionian sea
[PREPRINT-433] 14 p2362 N85-24693
Geophysical Fluid Dynamics Laboratory activities, FY84, plans, FY85
[PB85-147601] 15 p2558 N85-25783
Real-time enhancement of a climatology or forecast of ocean thermal structure using observed ocean temperatures
[AD-A151118] 15 p2604 N85-26049
ONR (Office of Naval Research) Far East Scientific Bulletin, Volume 9, Number 4, October-December 1984
[AD-A151274] 15 p2665 N85-26448
China's integrated circuit production
16 p2806 N85-27302
USSR report: Earth sciences
[JPRS-UES-85-005] 16 p2807 N85-27307
An inexpensive radar-responding relocation device for drifting oceanographic instruments
[AD-A152170] 16 p2838 N85-27505
The effect of the Benthic Boundary Layer on the physics of intense mesoscale eddies
[AD-A153193] 17 p2958 N85-28270
Low-rate discharge of various electrochemical batteries for use with oceanographic instruments
[AD-A153965] 18 p3095 N85-29159
Environmental Research Laboratories (of the National Oceanic and Atmospheric Administration) programs and plans: FY 1984 programs and FY 1985 plans
[PB85-171494] 18 p3149 N85-29501
Arctic mixed layer dynamics
[AD-A153582] 18 p3150 N85-29505
Utilization of the SEASAT scatterometer winds for ocean mixed layer modeling
[AD-A153748] 18 p3150 N85-29506
Metrology and Oceanology Institutes' underwater acoustics R and D 19 p3289 N85-30394
Geological-geophysical and gas-biochemical studies in Bering Sea 19 p3291 N85-30404
Sixth All-Union Marine Geology School
19 p3294 N85-30420
Environmental Research Laboratories publication abstracts, FY 1984
[PB85-180594] 19 p3313 N85-30540
Environmental background measurement program
[AD-A153860] 19 p3319 N85-30577
The application of computer imaging techniques to ocean topography and geophysical data
20 p3492 N85-31711
Ocean circulation studies 20 p3492 N85-31712
The time averaged circulation of the oceans from satellite altimetry 20 p3493 N85-31713
Ocean tidal parameters from LAGEOS
20 p3493 N85-31716
Offshore oceanographic and environmental monitoring services for the Strategic Petroleum Reserve, volume 3
[DE85-009907] 20 p3497 N85-31741
Physical oceanography program science abstracts
[AD-A154637] 21 p3654 N85-32701
Climate modeling: A retrospective-prospective view with consideration for the atmospheric carbon dioxide-climate issue
[DE85-011532] 23 p3950 N85-34481
Noiseless coding for the Gamma Ray spectrometer
[NASA-CR-176201] 24 p4069 N85-35219
Microwave properties of a quiet sea
[NASA-CR-176199] 24 p4085 N85-35322
Sea surface and remotely sensed temperatures off Cape Mendocino, California
[NASA-TM-86712] 24 p4125 N85-35573

OCEANS
NT ARCTIC OCEAN
NT ATLANTIC OCEAN
NT INDIAN OCEAN
NT PACIFIC OCEAN
The Marine Resources Experiment Program (MAREX)
[NASA-TM-87368] 01 p0066 N85-10580
Nonlinear propagation in a depth-dependent ocean
[AD-A145079] 01 p0116 N85-10791
Prediction of wave height of wind-generated seas in finite water depth
[AD-A145996] 03 p0398 N85-12539
Plans for the NRL/NORDA (Naval Research Laboratory-Naval Ocean Research and Development Activity) fine-scale variability experiment - 1984 (FVX-84)
[AD-A146041] 03 p0398 N85-12540
Recent studies of the ocean nitrogen cycle
05 p0653 N85-14193
Energy diagnostics and impact studies of FGGE global data sets and GLAS GCM simulations
05 p0683 N85-14390
Internal waves in ocean 06 p0819 N85-15201
Wave-wave interactions, microseisms, and infrasonic ambient noise in the ocean
[AD-A146529] 06 p0859 N85-15463
Interactions between mean flow and finite-amplitude mesoscale eddies in a barotropic ocean
[AD-A147249] 07 p1009 N85-16413
New Zealand SIR-B science investigations
08 p1144 N85-17218
Theoretical and experimental analyses of laser altimeters for barometric measurements over the ocean
08 p1165 N85-17351
An efficient numerical solution technique for wave propagation in horizontally stratified ocean environments
[AD-A148537] 08 p1190 N85-17502
ONR (Office of Naval Research) Far East Scientific Bulletin, volume 9, number 3, July to September 1984
[AD-A147282] 08 p1262 N85-17930
The wobble of the Earth and the low frequency dynamics of the ocean 09 p1358 N85-18548
Field studies of run-up generated by wind waves on dissipative beaches
[AD-A148793] 09 p1359 N85-18548
Evolution of sedimentation basins in Earth's history
10 p1497 N85-19451
Tectonic position and formation of young alkaline provinces of continents and oceans
10 p1502 N85-19480
Mercury health effects update: Health issue assessment
[PB85-123925] 10 p1526 N85-19639
Earth observations and the polar platform
[NOAA-TR-NESDIS-18] 11 p1669 N85-20517
Along-track deflection of the vertical from SEASAT: GEBCO (General Bathymetric Chart of the Oceans) overlays
[PB85-129641] 12 p1876 N85-21767
Carbonate chemistry of the Weddell Sea
[DOE/EV-110611/4] 12 p1896 N85-21916
Numerical experiments with simple model of ocean climate 13 p2106 N85-23123
Boundary velocities of longitudinal seismic waves and lateral inhomogeneities of upper ocean mantle
13 p2113 N85-23165
Assessing LANDSAT TM and MSS data for detecting submerged plant communities 13 p2120 N85-23203
Luminescence in the ocean
[AD-B089136L] 13 p2140 N85-23288
Internal waves in layers of Earth's upper mantle
16 p2807 N85-27312
Reconstruction of past atmospheric CO/sub 2/ contents from the chemistry of the contemporary ocean: An evaluation
[DE85-008426] 16 p3133 N85-29401
Specification of surface roughness over oceans in the GLAS Fourth Order GCM 16 p3142 N85-29455
Environmental Research Laboratories (of the National Oceanic and Atmospheric Administration) programs and plans: FY 1984 programs and FY 1985 plans
[PB85-171494] 18 p3149 N85-29501
Operation guiding light-scientific program and field plan. The pilot field experiment for NORDA project chemical dynamics in ocean frontal areas
[AD-A153765] 18 p3150 N85-29507
Sixth All-Union Marine Geology School
19 p3294 N85-30420
Use of stereographic projection in marine geodesy
19 p3294 N85-30421
MIZEX, 1984, NASA CV-990 flight report
[NASA-TM-86216] 19 p3299 N85-30451
Satellite measurements of atmospheric aerosols
[AD-A153807] 19 p3316 N85-30556
Linear time-invariant, space-variant filters and the WKB approximation with applications to underwater acoustic signal processing
[AD-A154250] 19 p3352 N85-30775
Maritime search and rescue cooperation and planning
20 p3400 N85-31093
Continental and oceanic magnetic anomalies: Enhancement through GRM 20 p3476 N85-31598
Global Mega-Geomorphology
[NASA-CP-2312] 21 p3600 N85-32357
The variability of aerosol microstructure in continental and oceanic surface layers of the atmosphere in anticyclones 21 p3647 N85-32660
Some thoughts on GAIA and the sulfur cycle
21 p3658 N85-32727
Global environmental transport models for tritium
[DE85-011497] 22 p3816 N85-33639
Two dimensional CO2-ocean model including the biological processes
[DE85-012341] 23 p3950 N85-34483
Cobalt-rich ferromanganese crusts in the oceans
24 p4104 N85-35444

OCTANE NUMBER
Trends of petroleum fuels
[DE85-000116] 14 p2263 N85-24023

OCULOMETERS
Eye movement in response to single and multiple targets
[AD-A151115] 15 p2617 N85-26126
Electrooculographic measurement, fatigue and variability of performance in simulated aircraft flight
19 p3217 N85-29948

OCULOMOTOR NERVES
Sensory and motor properties of the cerebellar uvula and nodulus 15 p2613 N85-26104

ODAS
U OCEAN DATA ACQUISITIONS SYSTEMS

ODD-EVEN NUCLEI
Extension of the consistent Q formalism to odd-A nuclei in the W-Pt region
[DE85-008284] 17 p3034 N85-28770
Boson-fermion symmetries in the W-Pt region
[DE85-009755] 19 p3362 N85-30845

ODD-ODD NUCLEI
Experimental level-structure determination in odd-odd actinide nuclei
[DE85-010476] 19 p3360 N85-30835

OFF-ON CONTROL
Time-optimal bang-bang slew of rigidized SCOLE configuration 20 p3410 N85-31164

OFFGASSING
Technology of off-gas treatment for liquid-fed ceramic melters
[DE85-012467] 22 p3812 N85-33610

OFFSHORE PLATFORMS
High-data-rate wide-angle underwater acoustic telemetry system
[DE84-015696] 02 p0233 N85-11519
Icing rate on stationary structures under marine conditions
[AD-A145795] 03 p0395 N85-12524

Full load testing in the platform module prior to tow-out: A case history of subsynchronous instability
05 p0642 N85-14117
A crew exposure study. Volume 1: Offshore
[AD-A146884] 07 p1015 N85-16449
Defect tolerance in pipeline girth welds
[ERS-E.353] 09 p1328 N85-18347

OFT
U SPACE TRANSPORTATION SYSTEM FLIGHTS

OFT 1
U SPACE TRANSPORTATION SYSTEM 1 FLIGHT

OFT 3
U SPACE TRANSPORTATION SYSTEM 3 FLIGHT

OFT 4
U SPACE TRANSPORTATION SYSTEM 4 FLIGHT

OGEE WINGS
U VARIABLE SWEEP WINGS

OGO
The downshift of electron plasma oscillations in the electron foreshock region
[NASA-CR-175633] 14 p2423 N85-24945

OHIO
Interlobate comparison of glacial-depositional style as evidenced by small-relief glacial landscape features in Illinois, Indiana, and Ohio, utilizing SIR-B
06 p1146 N85-17231
Lithologic and environmental atlas of Berea Sandstone (Mississippian) in the Appalachian Basin
[PB85-129039] 11 p1682 N85-20600

OHMIC DISSIPATION
Alternating current OHMIC heating in a toroidal stellerator
20 p3534 N85-31988

OHMS LAW
Mathematical physics approaches to lightning discharge problems
[NASA-TM-86349] 08 p1187 N85-17482

OIL EXPLORATION
A stochastic model for optimizing the consumption and exploration of nonrenewable natural resources
[INPE-2770-PRE/343] 03 p0440 N85-12804
Geological effectiveness of automated processing of highly precise aeromagnetic surveys in Caspian region
06 p0821 N85-15216
New method of reconstructing conditions of recent differentiation of oil and gas in the Amudarya Basin (based on results of interpretation of space photographs)
13 p1984 N85-22446
Evaluation of Thematic Mapper performance as applied to hydrocarbon exploration — Ontario, Canada; Cement, Oklahoma; and Death Valley, California
13 p2118 N85-23191
Use of space information in petroleum- and gas-prospecting work (example of Southern Mangyshlak)
15 p2485 N85-25341
Pacific Index, April 1983 - October 1984
[TIB5-901335] 19 p3320 N85-30582
Using remote photographs in prospecting for hydrocarbons on the Kerch Peninsula
22 p3735 N85-33154
The transient electromagnetic depth sounding technique applied to hydrocarbons and geothermal exploration
[MITT-42] 23 p3949 N85-34476

OIL FIELDS
New method of reconstructing conditions of recent differentiation of oil and gas in the Amudarya Basin (based on results of interpretation of space photographs)
13 p1984 N85-22446
Steamflood pilots in the O'Connell Ranch field and the T-4 Ranch field
[DE85-001363] 24 p4109 N85-35468

OIL POLLUTION
Drifting ice as mechanical factor in purifying and polluting hydrosphere
13 p2108 N85-23132
Operational experiences with the ARGOS system in oceanography and oil spill emergency planning. Future plans for the use of the ARGOS system as a component in offshore data collection system
14 p2239 N85-23667
Arabian gulf circulation — pollution monitoring
14 p2331 N85-24412

OIL RECOVERY
Investigation of condensing, three-phase, two-component, flow through porous media
09 p1317 N85-18283
Synthesis and characterization of novel polymers from non-petroleum sources for use in enhanced oil recovery
[DE85-010922] 19 p3250 N85-30151

OIL SLICKS
Internal waves in ocean
06 p0819 N85-15201

OILS
NT CRUDE OIL
NT FUEL OILS
NT LUBRICATING OILS
NT MINERAL OILS
NT SHALE OIL
Computations for segmented radial bearings
14 p2288 N85-24180
Aviation turbine fuels from tar sands bitumen and heavy oils. Part 1: Process analysis
[AD-A151319] 15 p2521 N85-25539
Oil resistant silicone elastomers
[AD-131523] 16 p2753 N85-26987
Combustion and micro-explosion of water/oil emulsions in high pressure environments
[AD-A152980] 17 p2919 N85-27997
An experimental apparatus to study nucleate pool boiling of R-114 and oil mixtures
[AD-A154077] 19 p3265 N85-30249
Mathematics of oil production
[DE85-011235] 19 p3267 N85-30261
The influence of oil contamination on the nucleate pool-boiling behavior of R-114 from a structured surface
[AD-A155609] 21 p3585 N85-32284
Method of distributing liquefaction catalysts in solid carbonaceous material
[DE85-005759] 23 p3909 N85-34218
Method for controlling the viscosity of siloxane oils
[DE85-011586] 23 p3909 N85-34221
Further studies on liquid sloshing
[PB85-199695] 24 p4095 N85-35388
Steamflood pilots in the O'Connell Ranch field and the T-4 Ranch field
[DE85-001363] 24 p4109 N85-35468

OKLAHOMA
Post-carboniferous tectonics in the Anadarko Basin, Oklahoma: Evidence from side-looking radar imagery
[NASA-CR-175458] 10 p1505 N85-19496

OLEFINS
U ALKENES

OLIVINE
Mechanisms of electrical conductivity in olivine
[DE84-014333] 04 p0495 N85-13159
Is phosphorus predictably incompatible in igneous processes?
04 p0583 N85-13722
Minor elements in relict olivine grains of deep-sea spheres: Match with Mg-rich olivines from C2 meteorites
06 p0883 N85-15610
Minor elements and cathodoluminescence of Mg-rich olivines from Murchison and Allende carbonaceous meteorites
06 p0884 N85-15619
Strain analysis of the Leoville chondrite and conditions in asteroidal interiors
06 p0885 N85-15620
The olivine asteroids: Discovery, mineralogy, and relationship to palasites
13 p2175 N85-23500

OMS
U ORBIT MANEUVERING ENGINE (SPACE SHUTTLE)

OMEGA NAVIGATION SYSTEM
Error analysis of wind determined using a VLF Omega sonde
[WSRL-0361-TM] 06 p0838 N85-15321
Use of three omega radionavigation system position lines for solving problems in marine geodesy
13 p2107 N85-23131

OMNIDIRECTIONAL ANTENNAS
NT MONOPOLE ANTENNAS
NT WHIP ANTENNAS

OMNIRANGE NAVIGATION
U VHF OMNIRANGE NAVIGATION

ON-LINE SYSTEMS
On line digitizer software
[AD-A146249] 03 p0403 N85-12566
Maintenance Management Information and Control System (MMICS): Administrative boon or burden
[AD-A145762] 03 p0438 N85-12790
User behavior upon introduction of a network help system
[DE84-016466] 04 p0552 N85-13515
International information networks for material properties
[DE84-013836] 04 p0576 N85-13676
Some attributes of online search intermediaries that relate to search outcome
05 p0734 N85-14721
Electrooptical sensor for automatic detection of objects
06 p0789 N85-15040
Workshop on Computer Architecture
[AD-A146455] 06 p0847 N85-15378
Research activities of the Norwegian seismic array (NORSAR)
[AD-A146778] 07 p0996 N85-16326
Data stimulated on-line-checking (IROLD)
08 p1088 N85-16754
Real-time estimation of amplitude and group delay distortion in a PSK line-of-sight communications channel
[AD-A147735] 08 p1151 N85-17266
Pilot climate data system
[NASA-CR-174321] 08 p1187 N85-17481
CIG (Computer image generation) data bases in an instance: Bits and pieces
[AD-P004318] 09 p1269 N85-17972
Online database search strategies and thesaural relationship models
09 p1402 N85-18822
Commentary on start of scientific data transmissions with USSR
10 p1476 N85-19319
Provision of Federal government publication in electronic format to depository libraries
[S-PRT-98-260] 10 p1567 N85-19880
A DOE directory of databases for material properties
[UCAR-10124] 11 p1739 N85-20937
Base communications issues for the 1990s
[AD-A149764] 12 p1828 N85-21474
Calculation and display of stack departure times for aircraft inbound to Heathrow Airport
[AD-A151991] 15 p2469 N85-25241
A network-based approach to text handling for the online scientific community
15 p2664 N85-26444
Document retrieval from a relational database management system: An investigation of multiple-line query formulation using SEQUEL
15 p2665 N85-26447
List of serials indexed for online users, 1985
[PB85-143220] 15 p2666 N85-26455
Retrieval performance in a full text journal article database
16 p2877 N85-27747
A study of user-defined searching requirements for the on-line version of the directory of DOD-sponsored R and D data bases on the Defense Gateway computer system
[AD-A153000] 17 p3050 N85-28878
Distribution of mathematical software via electronic mail
[DE85-009664] 18 p3166 N85-29617
SAFEORD: Safety of explosive ordnance databank
[AD-A154058] 19 p3360 N85-30972
Individual differences in online search behavior: The effect of learning styles and cognitive abilities on process and outcome
20 p3541 N85-32037
Interactive on-line conference
[AD-A154723] 21 p3574 N85-32227
Overview of on-line data processing for MST radars (keynote paper), part 7
21 p3625 N85-32519
On-line model driven control of the SLC electron Damping Ring
[DE85-013377] 24 p4157 N85-35772

ONBOARD COMPUTERS
U AIRBORNE/SPACEBORNE COMPUTERS

ONBOARD DATA PROCESSING
Overview of Autonomous Payload Control Experiment
04 p0459 N85-12911
Keeping up with operational loads in the French Air Force: Defining new equipment
07 p0896 N85-15681
Automatic error detection and recovery techniques in onboard intelligent units for space and avionic application
08 p1066 N85-16756
Designer on Aeroflot automated COMMO system development
08 p1067 N85-16766
On-board processing for linescan sensors in miniature unmanned aircraft
[RAE-TM-SPACE-327] 08 p1085 N85-16870
Integration of ground and on-board system for terminal count
08 p1092 N85-16899
Automation of checkout for the shuttle operations era
08 p1092 N85-16900
Air Force space technology center space technology: Emphasis 84
09 p1333 N85-18381
Spaceborne automatic data processing
14 p2397 N85-24769
DORIS: Prediction in Doppler measurement — satellite onboard measurement
[CNES-CT/DTI/MS/AE/170] 16 p2729 N85-26843
Piloted simulation of an algorithm for onboard control of time-optimal intercept
[NASA-TP-2445] 18 p3063 N85-28949
In orbit infrastructure
[DM-51/CC-FL-044-83] 18 p3066 N85-29066
Investigation and construction of the Mini Remote Terminal Unit (mRTU-M) Analog Processor Module (AP-M), volume 1
[MR-DS-01-VOL-1] 18 p3166 N85-29619
Investigation and construction of the Mini Remote Terminal Unit (mRTU-M), Analog Processor Module (AP-M), volume 2
[MR-DS-01-VOL-2] 18 p3166 N85-29620
Standard Generic approach for Spacecraft Autonomy and Automation, phase 2 (SGASA-2). Volume 1: Executive summary
[ESA053-1-VOL-1] 18 p3167 N85-29623
Standard Generic Approach for Spacecraft Autonomy and Automation, phase 2 (SGASA-2). Volume 2: Technical report
[ESA053-1-VOL-2] 18 p3167 N85-29624
Standard Generic Approach for Spacecraft Autonomy and Automation, phase 2 (SGASA-2). Volume 3: Appendices
[ESA053-1-VOL-3] 18 p3167 N85-29625

Evolution of 406 MHz Search and Rescue (SAR) processor 20 p3403 N85-31116
Study of the applicability of higher order languages for on-board satellite software production
[ESA-CR(P)-2024] 20 p3516 N85-31884
Implications of artificial intelligence on the design of future onboard systems
[SFENA-DPS/C/SS/84252A] 23 p3967 N85-34596
ONBOARD EQUIPMENT
NT AIRBORNE EQUIPMENT
NT AIRBORNE/SPACEBORNE COMPUTERS
NT AIRCRAFT EQUIPMENT
NT BOMBING EQUIPMENT
NT SPACECRAFT ELECTRONIC EQUIPMENT
NT SPACECRAFT EQUIPMENT
Study of effects of lightning on aircraft systems stressed 03 p0310 N85-12005
Improvements in linked-spar motion-compensated lifting system
[AD-D011413] 08 p1138 N85-17165
The value and utility of inflight onboard simulation
[AD-A148033] 08 p1198 N85-17543
On-board Computer Image Generator (CIG) applications
[AD-P004335] 09 p1271 N85-17989
Dynamic training devices in CRM training 09 p1276 N85-18018
Use of airplanes for loft training 09 p1276 N85-18019
Cockpit resources management and the theory of the situation 09 p1276 N85-18022
Cockpit resource management training 09 p1276 N85-18023
Telemetry systems of Interkosmos satellites 11 p1617 N85-20173
Adaptive control of airborne radar antennas 13 p2080 N85-22989
The development of onboard laser velocimeter at the Saint Louis Institute (France) from 1976 to 1982
[ISL-NB-402/83] 16 p2791 N85-27216
Data from BOC-yachts: A significant input to Southern Hemisphere analysis 16 p2814 N85-27356
Results of the magnetic field experiments E2 and E4 onboard Helios 1 and Helios 2 — magnetometer development 16 p2885 N85-27799
Rome/Goddard Space Flight Center (GSFC) magnetic field experiment: A summary of results — flux gate magnetometer 16 p2885 N85-27800
Flight control system for a computer controlled aircraft with limited sensors
[AD-A155107] 21 p3555 N85-32115
SCRIBE data of October 23, 1963 flight
[AD-A154864] 21 p3705 N85-33012
Comprehensive radio direction finder with electronically stabilized radiation pattern 22 p3762 N85-33316
ONE DIMENSIONAL FLOW
ICARUS: A general one-dimensional heat conduction code
[DE84-016125] 01 p0047 N85-10310
One-dimensional two-phase constant lag flow in combustion chamber of solid propellant rocket motors
[AD-A145679] 02 p0173 N85-11157
The overall reaction concept in premixed, laminar, steady-state flames. 2: Initial temperatures and pressures
[AD-A152132] 16 p2748 N85-26944
Evaluation of an algorithm for the solution of the time-dependent Euler equations
[AD-A151993] 16 p2854 N85-27600
Explosion in flight 21 p3683 N85-32983
Unsteady flow in a supersonic cascade with two in-passage shocks
[NASA-CR-3925] 24 p4060 N85-35158
ONISOTROPY
U ANISOTROPY
ONTOGENESIS
U ONTOGENY
ONTOGENY
General description of experiment dealing with rat ontogenesis aboard Cosmos-1514 biosatellite 22 p3822 N85-33679
NASA Developmental Biology Workshop: A summary
[NASA-TM-86756] 24 p4126 N85-35578
OOCYTES
U GAMETOCYTES
OPACITY
The smallest sizes of diffuse interstellar clouds 08 p0878 N85-15578
Study of opacity effects on line radiation from pellet implosions
[DE85-000380] 10 p1491 N85-19413
X-ray line broadening of a diagnostic in laser produced plasma
[DE85-001179] 10 p1560 N85-19841
Opacity determinations for Inertial Confinement Fusion (ICF) materials using an average atom model 12 p1957 N85-22295
Opacity control technique for jet engine test cells
[AD-D011668] 19 p3220 N85-29068
Frequent observations of extragalactic compact sources at 24 GHz 19 p3366 N85-31003
Implicit Monte Carlo methods and non-equilibrium Marshak wave radiative transport
[DE85-010711] 22 p3835 N85-33743
X-ray spectra of bursting neutron stars 23 p3981 N85-34686
OPEN CHANNEL FLOW
Technology reports of the Yamaguchi University, volume 3, no. 3
[ISSN-0386-3433] 09 p1302 N85-18182
On the virtual wall height in open channel flow with large relative roughness 09 p1303 N85-18188
Calculation of oscillating turbulent flows in open channels
[KU-SFB-80/T/228] 11 p1633 N85-20289
Behavior of turbulent gas jets in an axisymmetric confinement
[NASA-CR-174829] 15 p2473 N85-25265
Monogroove heat pipe design: Insulated liquid channel with bridging wick
[NASA-CASE-MSC-20497-1] 18 p3096 N85-29180
OPEN CIRCUIT VOLTAGE
Avalanche photodiode statistics in triggered-avalanche detection mode 05 p0623 N85-13987
Improved modeling of the open circuit voltage of solar cells 13 p2011 N85-22619
New high-efficiency silicon solar cells
[NASA-CR-175643] 13 p2128 N85-23244
OPENINGS
NT APERTURES
NT PORTS (OPENINGS)
NT SLITS
NT SYNTHETIC APERTURES
A buckling analysis for rectangular orthotropic plates with centrally located cutouts
[NASA-TM-86263] 04 p0513 N85-13268
Optimum geometry of interblade passages in impellers of thermomolecular vacuum pump 16 p2764 N85-27058
Strength and failure analysis of composite laminates with holes at room and elevated temperatures
[AD-A153263] 17 p2917 N85-27961
OPERATING COSTS
Energy efficient engine flight propulsion system preliminary analysis and design report
[NASA-CR-174701] 02 p0140 N85-10947
Energy efficient engine component development and integration program
[NASA-CR-168496] 02 p0146 N85-10989
Energy efficient engine. Volume 1: Component development and integration program
[NASA-CR-173084] 02 p0146 N85-10992
Activities report of the aerospace industry in West Germany
[ISSN-0722-3838] 07 p1053 N85-16666
Activities report of the aerospace industry in West Germany
[ISSN-0722-3838] 07 p1054 N85-16667
OPERATING SYSTEMS (COMPUTERS)
New YeS 1056 unified system computer model described 04 p0485 N85-13092
Development of the NLTSS operating system
[DE84-013702] 05 p0714 N85-14576
Requirements and overview of the LINCS distributed operating system architecture
[DE84-013721] 05 p0714 N85-14577
Operating system versus programming environment, for example the UNIX
[SWA-84/037] 07 p1027 N85-16516
EGP (Exterior Gateway Protocol) gateway under Berkeley UNIX 4.2
[AD-A148058] 08 p1208 N85-17597
A unified model for performance and reliability of Fault-Tolerant/Multi-Mode systems
[AD-A148789] 08 p1208 N85-17601
A decision model for selection of microcomputers and operating systems
[AD-A149076] 10 p1538 N85-19694
Structurization of programs for real-time microprocessor arrays 15 p2529 N85-25592
Detailed design of an object oriented, multiprogramming, multitasking operating system for sixteen-bit microcomputers
[AD-A152066] 16 p2847 N85-27552
Multicomputer operating systems and applications
[AD-A153205] 17 p3016 N85-28648
The design of a capability-based distributed operating system
[CWI-CS-R8418] 17 p3016 N85-28650
Distributed systems management in wide area networks
[CWI-CS-R8419] 17 p3016 N85-28651
A new taxonomy for distributed computer systems based upon operating system structure
[NASA-TM-86438] 19 p3342 N85-30709
A distributed real-time operating system
[NIKHEF-H/84-8] 20 p3518 N85-31876
User's operating procedures. Volume 1: Scout project information programs
[NASA-CR-177948] 23 p3956 N85-34518
OPERATING TEMPERATURE
Electromagnetic Acoustic Transducers (EMATs) for erosion monitoring
[DE85-004834] 12 p1854 N85-21628
Proceedings of the Cold Electronics Workshop
[NASA-CR-175662] 14 p2297 N85-24220
Cold electronics: An overview 14 p2297 N85-24221
SI MOS devices at low temperatures 14 p2297 N85-24225
Stressed-strained state of tightening buckles in sectional runners of gas turbines 17 p2940 N85-28149
Status of high-efficiency module design and fabrication 21 p3612 N85-32446
OPERATIONAL AMPLIFIERS
Semiconductors at Leipzig Spring Fair 09 p1377 N85-18660
A circuit grammar for operational amplifier design
[AD-A149566] 10 p1481 N85-19346
Development of thin film hybrid IC active filter for video band use
[NHK-LABS-NOTE-312] 18 p3094 N85-29153
OPERATIONAL HAZARDS
Radio Frequency Radiation (RFR) measurements in operational settings 16 p2777 N85-27138
OPERATIONAL PROBLEMS
Results of Space Shuttle Flight 41-C
[GPO-36-092] 04 p0461 N85-12928
Statement of Captain Robert L. Crippen, USN, Commander of Space Shuttle Flight 41-C; Francis R. Scobee, pilot; Doctor George D. Nelson, Mission Specialist; Terry J. Hart, Mission Specialist; and Doctor James D. Van Hoften, Mission Specialist; accompanied by Frank Cepollina, Solar Maximum Repair Mission Project Manager, Goddard Space Flight Center 04 p0461 N85-12929
Statement of Frank Cepollina, Solar Maximum Repair Mission Project Manager, Goddard Space Flight Center 04 p0461 N85-12930
Operational problems with radiation survey meters: The university and accelerator
[DE84-015703] 06 p0811 N85-15151
Electric and hybrid vehicle demonstration project
[DE84-014622] 06 p0871 N85-15535
Design evolution of the orbiter reaction control subsystem 06 p1099 N85-16944
Electric and hybrid vehicle demonstration project
[DE85-003939] 13 p2169 N85-23455
Gas turbines: Operating conditions, material selection and development
[NLR-MP-83046-U] 20 p3395 N85-31062
OPERATIONS
Optimum performance parameters for ski-jump operations of USAF fighter aircraft
[AD-A148532] 06 p1084 N85-16867
OPERATIONS RESEARCH
NT DYNAMIC PROGRAMMING
NT LINEAR PROGRAMMING
NT MATHEMATICAL PROGRAMMING
NT NONLINEAR PROGRAMMING
NT QUADRATIC PROGRAMMING
Interactive graphics nonlinear constrained optimization 01 p0058 N85-10387
Optimizing search with positive information feedback
[CSIR-TWISK-313] 01 p0125 N85-10855
A summary of the foundation research program
[AD-A148524] 08 p0891 N85-15856
Principles of multiobjective optimization
[AD-A147520] 07 p1052 N85-16679
Distributed asynchronous relaxation methods for convex network flow problems
[AD-A148027] 08 p1211 N85-17622
European scientific notes. Volume 38, number 11
[AD-A148228] 08 p1230 N85-17745
European Scientific Notes, volume 38, number 12
[AD-A148713] 09 p1418 N85-18948
A proposed integration among organizational information requirements, media richness and structural design
[AD-A149317] 10 p1567 N85-19681
European Scientific Notes. Volume 39, number 2
[AD-A148994] 10 p1573 N85-19919
Control of nonlinear objects 12 p1842 N85-21561

Statistics for the maximum of several positive random variables with application to networking
[AD-A150006] 12 p1922 N85-22069
A decision support methodology for space technology advocacy
[AD-A151895] 15 p2476 N85-25283
Management control systems and interdependencies: An empirical study
[AD-A152280] 16 p2876 N85-27746
A greedy algorithm for the transhipment along a single road problem
[AD-A152343] 17 p3025 N85-28709
Future directions in operations research
[REPT-84-24] 17 p3026 N85-28711
Operations research
[B8561897] 17 p3026 N85-28712
A new taxonomy for distributed computer systems based upon operating system structure
[NASA-TM-86438] 19 p3342 N85-30709
The priming effect in task design research
[AD-A154589] 21 p3679 N85-32852
Necessary and sufficient conditions for single-extremum and convex problems of mathematical programming
21 p3696 N85-32977
Design and implementation of an interactive route editor 23 p3962 N85-34559

OPERATOR PERFORMANCE

Human engineering data base for design and selection of cathode ray tube and other display systems
[AD-A145704] 02 p0236 N85-11549
The human operator and system effectiveness
[AD-A146326] 03 p0402 N85-12563
Analysis of data entry performance: Chromatic versus monochromatic
[AD-A145568] 03 p0438 N85-12789
Defect detection threshold in riveted joints, test report no.44-833/F — in aircraft 04 p0511 N85-13260
Six degrees of freedom control with each hand?
05 p0700 N85-14492
Effects of control stick parameters on human controller response 05 p0701 N85-14496
Effects of transport delays of manual control system performance 05 p0701 N85-14498
The effect of part-simulation of weightlessness on human control of bilateral teleoperation: Neuromotor considerations 05 p0703 N85-14510
Visual attention to radar displays
05 p0704 N85-14514
POPCORN: A supervisory control simulation for workload and performance research
05 p0704 N85-14515
Psychological issues in online adaptive task allocation
05 p0704 N85-14516
The impact of pictorial display on operator learning and performance 05 p0706 N85-14527
A manual control test for the detection and deterrence of impaired drivers 05 p0709 N85-14550
The effects of task structure on time-sharing efficiency and resource allocation optimality
05 p0711 N85-14562
Multi-crew model analytic assessment of landing performance and decision-making demands
05 p0712 N85-14567
Speech-action interrelationships in operational work
07 p1010 N85-16418
Work physiology of operating personnel at power plants in arid regions 10 p1523 N85-19606
The effect of jamming/deception on decision making
[AD-A149740] 12 p1828 N85-21472
The role of prior knowledge in operating equipment from written instructions
[AD-A151007] 14 p2392 N85-24730
Shape with and without redundant colour as coding mechanism for simulated radar displays in a time-extended simple vigilance task
[AD-A151683] 16 p2844 N85-27533
Operator's functional comfort zone when controlling moving object 22 p3821 N85-33670
Manual and computer-aided sequential diagnostic inference
[AD-A156229] 24 p4133 N85-35620

OPERATORS (MATHEMATICS)

Scattering theory by Enss' method for operator valued matrices: Dirac operator in an electric field
[REPT-84] 01 p0045 N85-10290
On the commutant of an irreducible set of operators in real Hilbert space
[TUM-M8316] 01 p0114 N85-10774
Quasistable parametric optimization without compact level sets
[AD-A144716] 01 p0114 N85-10776
Boundary conditions in Chebyshev and Legendre methods
[NASA-CR-172460] 02 p0250 N85-11635
Linear and bilinear infinite-dimensional representations of finite-dimensional nonlinear systems
[RR-259] 02 p0254 N85-11661
An introduction to multilinear formula score theory
[AD-A145696] 02 p0254 N85-11667
Model equation for simulating flows in multistage turbomachinery
[NASA-TM-86869] 03 p0315 N85-12035
Application of summability methods to Jackson theorems for splines
[AD-A146256] 03 p0412 N85-12835
On the theory of coercitive linear partial differential operators
[ISSN-0355-0087] 03 p0414 N85-12846
Molarity principle: Foundation for parallel digital signal processes 05 p0725 N85-14683
Monotone operators in mathematical programming
[AD-A147309] 07 p1025 N85-16506
An operator method for computing the asymptotics of a collision resolution interval
[AD-A148837] 07 p1028 N85-16528
Nonlinear semigroups and evolution governed by accretive operators
[AD-A147556] 07 p1033 N85-16557
The symmetry group and exponents of operator stable probability measures
[AD-A147187] 07 p1035 N85-16568
Boundary conditions for artificial dissipation operators — convection
[FFA-TN-1984-53] 09 p1375 N85-18642
Lax-pair operators for squared-sum and squared-difference eigenfunctions
[AD-B089063L] 09 p1386 N85-18718
Annuals of the Finnish Academy of Sciences, series A. 1: Mathematica, volume 8, part 2
[ISSN-0066-1953] 10 p1535 N85-19573
Towards the construction of periodic solutions of pseudodifferential equations with the aid of algebraic operators 10 p1535 N85-19574
A non-hypoelliptic Dirichlet problem from stochastics
10 p1537 N85-19667
Annals of the Fourier Institute, volume 34, no. 4
11 p1666 N85-20666
Classic Fourier microdistributions in the real analytic case 11 p1666 N85-20673
The eigenvalues of the pseudospectral Fourier approximation to the operator sin (2x) d/dx
[NASA-CR-172538] 11 p1706 N85-20729
Normal mode analysis for linear resistive magnetohydrodynamics
[IPP-6/235] 11 p1730 N85-20876
Invariant differential operators on a semisimple symmetric space and finite multiplicities in a Plancherel formula
[CWI-PM-R8409] 12 p1925 N85-22094
Asymptotic construction of a procedure for plane-wave synthesis and migration
[AD-A150969] 14 p2374 N85-24672
On an assymetric choice for a cluster expansion of the three-body problem
[CSIR-TWISK-339] 14 p2408 N85-24844
A new implicit plus minus splitting method for the solution of the Euler equations in the transonic flow regime
15 p2461 N85-25200
Analysis of spectral operators in one-dimensional domains
[NASA-CR-172573] 15 p2633 N85-26228
Deconvolution methods for multi-sensors
[AD-A152351] 17 p3018 N85-28660
A note on integral operators
[REPT-83-26] 17 p3021 N85-28688
About product formulas with variable step-size
[AD-A153527] 18 p3169 N85-29636
Infinite dimensional linear systems with unbounded control and observation: A functional analytic approach
[AD-A153535] 18 p3169 N85-29639
Some applications of a convenient finite-dimensional matrix representation of the differential operator
[PREPRINT-418] 18 p3172 N85-29661
Numerical tests of a novel technique to compute the eigenvalues of differential operators
[PREPRINT-427] 18 p3173 N85-29667
Spectral Theory of Sturm-Liouville Differential Operators: Proceedings of the 1984 Workshop
[DE85-009893] 20 p3520 N85-31800
Aspects of SAR image segmentation
[AD-A154985] 21 p3575 N85-32236
Edge detection and geometric methods in computer vision
[AD-A155873] 24 p4135 N85-35630
Some rigorous results concerning spectral theory for ideal MHD
[DE85-013427] 24 p4156 N85-35770

OPERATORS (PERSONNEL)

NT AIRCRAFT PILOTS
NT PILOTS (PERSONNEL)

Random pattern tracking acceleration tolerance tester
[AD-D011404] 07 p1017 N85-16459
Work capacity of heat and electric power plant operations working 12 hour day and night shifts
09 p1362 N85-18587
Study of bodily functional status and quality of controlling action of power unit operators with various intensities of labor 09 p1362 N85-18589
Ride comfort of off-road vehicles
[AD-P004279] 09 p1406 N85-18855
Man-machine interaction: Operator
[AD-A149075] 10 p1531 N85-19648
Research and Modeling of Supervisory Control Behavior, report of a workshop
[AD-A149621] 12 p1950 N85-22248
Streamlined Test Reporting And Planning (STRAP): Computerized human factors questionnaire
[AD-A150611] 14 p2395 N85-24751
A comparison of numeric data entry with touch-sensitive and conventional numeric keypads
[AD-A153276] 17 p3008 N85-28598
Adaptive aiding for symbiotic human-computer control: Conceptual model and experimental approach
[AD-A153670] 19 p3332 N85-30644
Computer center policy
[AD-A154416] 19 p3338 N85-30681
Robot environment expert system
[NASA-CR-3915] 23 p3967 N85-34593

OPHTHALMOLOGY

Investigation into the use of the TV magnifier in the Netherlands
[HSE-TRANS-11142] 20 p3533 N85-31966

OPIK THEORY

The study of the physics of cometary nuclei
[NASA-CR-175917] 17 p3054 N85-28905

OPTICAL ABSORPTION

U ELECTROMAGNETIC ABSORPTION
U LIGHT TRANSMISSION

OPTICAL AMPLIFIERS

U LIGHT AMPLIFIERS

OPTICAL BISTABILITY

Digital Optical Circuit Technology
[AGARD-CP-362] 18 p3185 N85-29757
Optically bistable devices using InSb
18 p3186 N85-29758
Optically nonlinear and bistable behaviour of direct gap semiconductors 18 p3186 N85-29759
Optical bistability in Cd(x)Hg(1-x)Te
18 p3186 N85-29760
Optical modulators and bistable devices using molecular gases 18 p3186 N85-29761
An experimental nonlinear optical waveguide device
18 p3186 N85-29762
Stationary properties and switching characteristics of dispersive optical bistability in CuCl
18 p3186 N85-29763
Cavityless optical bistability in systems of two-level atoms 18 p3186 N85-29764
All-optical logic gates with external switching by laser and incoherent radiation 18 p3187 N85-29766

OPTICAL COMMUNICATION

New type of unique frequency laser communications
[AD-A145128] 01 p0038 N85-10230
Timing performance of phase-locked loops in optical pulse position modulation communication systems
[AD-A145403] 02 p0190 N85-11271
Low-threshold injection lasers on grown GaInPAs/InP heterostructures (1.2-1.6 micrometers wavelengths)
02 p0258 N85-11693
Optical recording of information on paper by CO2 and YAG-lasers 02 p0261 N85-11710
Regenerators of binary pulses for optical communication systems 04 p0485 N85-13099
Simulation of optical configurations and signal processing methods in Anger-type neutron-position scintillation detector
[DE84-012095] 04 p0503 N85-13210
Analysis of a coded, M-ary orthogonal input optical channel with random-gain photomultiplier detection
05 p0024 N85-13090
A single optical fiber telephone system
[AD-D011293] 06 p0799 N85-15107
Holographic directional coupler for fiber optic systems
[AD-D011365] 07 p0937 N85-15939
Micro-waveguide transformers of coherent optical signals 07 p0950 N85-16022
Nonlinear processing of optical pulse signals
07 p0951 N85-16026
Analysis of threshold effects during estimation of arrival time of optical signals 07 p0951 N85-16030
Potential effectiveness of spatial processing in detecting signals against background of interfering reflections
07 p0952 N85-16032
Spacecraft system study: A study to define the impact of laser communication systems on their host spacecraft
[NASA-CR-175272] 07 p0970 N85-16159

RF fiber optic link
[AD-A148679] 08 p1155 N85-17290
Two-photon coherent state light - its generation and potential applications
[AD-A148245] 08 p1166 N85-17358
Optical wave propagation and imaging in the atmosphere 08 p1222 N85-17694
Matrix-matrix multiplication using an electrooptical systolic-engagement array processing architecture
[AD-D011410] 08 p1223 N85-17704
Quantum noise effects in single-mode injection lasers
[FUB-11-1984] 09 p1327 N85-18336
The Telecommunications and Data Acquisition Report
[NASA-CR-174366] 10 p1462 N85-19224
Detection and symbol synchronization for multiple-bit per photon optical communications 10 p1463 N85-19228
Highly efficient Nd:YAG lasers for free-space optical communications 10 p1463 N85-19229
Optical fiber communications link design in compliance with systems performance standards
[PB85-111037] 12 p1830 N85-21469
The future of lightwave technology
[PB85-109759] 12 p1935 N85-22155
Optimization of number of pulses in detection of fluctuating optical signals 13 p2081 N85-22993
Technical Digest: Symposium on Optical Fiber measurements, 1984
[PB85-114700] 13 p2160 N85-23407
Spatial acquisition algorithms and systems for intersatellite optical communication links
[AD-A150794] 14 p2292 N85-24207
The effects of atmospheric turbulence on an air-to-air optical communication link
[AD-A151640] 15 p2543 N85-25700
Length dependent, optical time delay/filter device for electrical signals
[AD-D011594] 15 p2549 N85-25732
Mode dependent, optical time delay system for electrical signals
[AD-D011596] 15 p2553 N85-26383
Optical non-line-of-sight covert, secure high data communication system
[AD-D011607] 16 p2769 N85-27067
Photon detection with cooled avalanche photodiodes: Theory and preliminary experimental results 16 p2770 N85-27096
The development and implementation of an optical communications laboratory
[AD-A151662] 16 p2772 N85-27111
The weighting function for scintillation on a folded path
[AD-A152659] 17 p2949 N85-28206
Philips researches gallium arsenide use for lasers 18 p3087 N85-29106
Rifa of Sweden conducts research in 3-5 materials 18 p3088 N85-29107
Multiport optical detectors 18 p3187 N85-29769
Picosecond photoconductive devices for 10 Gbit/s optoelectronic switching 18 p3187 N85-29770
Optical techniques for signal distribution and control in advanced radar and communication systems 18 p3188 N85-29773
A study of reflex optoelectronic switching matrices and their derivatives
[CRC-TN-720] 19 p3253 N85-30169
Thin film phase transition materials development program
[AD-A154260] 19 p3259 N85-30209
Fiber optic expanded beam connector
[AD-A154057] 19 p3367 N85-30680
Phase-locked loops for optical homodyne detection, volume 1 — spaceborne receivers
[ESA-CR(P)-2029-VOL-1] 20 p3442 N85-31367
Phase locked loops for optical homodyne detection, volume 2 — spaceborne receivers
[ESA-CR(P)-2029-VOL-2] 20 p3442 N85-31368
A comparison of millimeter wave, direct detect and heterodyne laser intersatellite links
[AD-A151664] 20 p3461 N85-31496
Intersatellite optical links: The point ahead angle
[CNES-83/DRT/TIT/TR/150] 20 p3533 N85-31984
Optical receivers using rough reflectors
[NASA-CR-176200] 24 p4154 N85-35750

OPTICAL COMPUTERS
West Europe report: Science and technology
[JPRS-WST-85-003] 09 p1309 N85-18224
Optical computer studies at UK's Heriot-Watt University 09 p1309 N85-18227
Triple matrix product optical processors using combined time-and-space integration
[AD-D011483] 10 p1557 N85-19820
Technical evaluation report on Avionics Panel Specialists' Meeting on Digital Optical Circuit Technology
[AGARD-AR-202] 15 p2653 N85-26367
Methods for the optical processing of signals
[DRIC-T-7439] 22 p3844 N85-33809

OPTICAL CORRECTION PROCEDURE
Fast Hartmann method for problems in astronomical adaptive optics 02 p0161 N85-11094
Holographic corrector in objective with compound main mirror 17 p2941 N85-28153
New method for correcting chromatism of mirror-lens objectives 21 p3696 N85-32985

OPTICAL COUPLING
Multiwavelength bidirectional coupler-decouplers
[AD-A147009] 07 p1043 N85-16825
Dimensions of smooth mating parts with protective coatings 14 p2280 N85-24124
Multi-access fiber optic data bus using FDM/FSK
[NASA-CR-175739] 15 p2621 N85-26152
Spatial light modulator having a capacitively coupled photoconductor
[AD-D011646] 17 p3037 N85-28790
Optical fiber coupling method and apparatus
[NASA-CASE-NPO-15464-1] 18 p3184 N85-29749

OPTICAL DATA PROCESSING
NT SCENE ANALYSIS
Standards for commercially emerging technologies: A preliminary cost-benefit assessment for the Optical Digital data disk (OD3) technology for mass data storage applications
[PB84-223593] 01 p0101 N85-10669
Guided-wave optic devices for integrated optic information processing
[AD-A145695] 02 p0260 N85-11627
LANDAT-4/5 image data quality analysis
[E85-10039] 03 p0379 N85-12417
Multi-disciplinary techniques for understanding time-varying space-based imagery
[AD-A144357] 05 p0726 N85-14681
Electrooptical matrix multiplication using the twos complement arithmetic for improved accuracy
[AD-D011252] 05 p0728 N85-14682
Advanced cube processor
[AD-D011262] 05 p0729 N85-14683
Wavelength coded image transmission and holographic optical elements
[AD-A146490] 06 p0810 N85-15147
Two-dimensional signal processing and storage and theory and applications of electromagnetic measurements. Supplemental appendix
[AD-A146848] 07 p0939 N85-15953
Modern signal processing and reconnaissance — conferences
[FOA-C-30374-E1] 07 p0942 N85-15975
White-light optical information processing and holography
[AD-A146836] 07 p0967 N85-16136
Development and evaluation of techniques for using combined microwave and optical image data for vegetation studies 08 p1148 N85-17240
Nonlinear real-time optical signal processing
[AD-A148293] 08 p1222 N85-17699
Optical data processing for missile guidance
[AD-A149346] 10 p1422 N85-18972
Optical implementation of the synthetic discriminant function
[AD-A149562] 10 p1557 N85-19817
Triple matrix product optical processors using combined time-and-space integration
[AD-D011483] 10 p1557 N85-19820
Optical eigenvector
[AD-A149550] 11 p1729 N85-20871
Topics in optical materials and device research, 3: Volume 1
[AD-A149726] 12 p1933 N85-22145
Switchable zero order diffraction gratings as light valves
[AD-A150129] 12 p1934 N85-22153
Electronic generation of text for television
[BBC-RD-1984/14] 13 p2053 N85-22856
Two-dimensional signal processing and storage and theory and applications of electromagnetic measurements
[AD-A150590] 13 p2065 N85-22899
Optical memory research and its application to digital optical processing 13 p2158 N85-23397
Optical processing in radon space
[AD-A150289] 13 p2159 N85-23402
Space-variant optical systems
[AD-A151032] 14 p2421 N85-24939
Evaluating radiation distortions of optical image of Earth's surface in horizontally inhomogeneous atmosphere 15 p2486 N85-25345
Optical flow-patterns of image velocity and their potential use in guidance and image interpretation
[BAE-BT-12091] 15 p2651 N85-26347
An investigation into generalised matched filter techniques
[BAE-BR-12971] 15 p2651 N85-26348
Feasibility studies of optical processing of image bandwidth compression schemes
[AD-A151254] 15 p2651 N85-26350
Electron-bombarded silicon spatial light modulator
[AD-D011579] 15 p2652 N85-26355
Technical evaluation report on Avionics Panel Specialists' Meeting on Digital Optical Circuit Technology
[AGARD-AR-202] 15 p2653 N85-26367
La Recherche Aerospatiale Bimonthly Bulletin, Number 1984-4, 221/July-August
[ESA-TT-884] 16 p2695 N85-26837
SVIT complex for analysis of space photography 16 p2725 N85-26819
China's integrated circuit production 16 p2806 N85-27302
Optical phenomena in computer vision
[AD-A152970] 17 p3008 N85-28595
Studies of optical-beam phase-conjugation by nonlinear refraction
[AD-A152665] 17 p3037 N85-28786
Spatial light modulator having a capacitively coupled photoconductor
[AD-D011646] 17 p3037 N85-28790
The prospects of the digital optical computer 18 p3186 N85-29771
Deformable mirror nearest neighbor optical computer 18 p3188 N85-29772
Numerical optical computing at the Ohio State University 18 p3188 N85-29775
Thin film phase transition materials development program
[AD-A154260] 19 p3259 N85-30209
High accuracy digital acousto-optic matrix computer
[AD-D011692] 19 p3343 N85-30716
Digital holographic synthesis of pattern-forming transparencies for ring antenna arrays 22 p3763 N85-33326
Characteristics of optical information-measurement channels with utilization of scattering effects 22 p3781 N85-33429
A general purpose image processing package 23 p3961 N85-34549

OPTICAL DATA STORAGE MATERIALS
Proceedings of the National Bureau of Standards and National Security Agency Workshop on Standardization Issues for Optical Data Disk (OD3) Technology
[PB84-217785] 06 p0848 N85-15383
Multichannel electrooptical modulators for digital information storage and processing systems 07 p0950 N85-16021
West Europe report: Science and technology
[JPRS-WST-84-026] 15 p2532 N85-25617
Philips tested new materials for optical data storage 15 p2532 N85-25620
Conference of quantum-radiooptics section 22 p3773 N85-33380

OPTICAL DENSITY
The calibration of photographic and spectroscopic films: A densitometric analysis of IIaO film flown aboard the Space Shuttle 3
[NASA-CR-174278] 07 p0962 N85-16101
NGC 2024: Multi-wavelength infrared and radio observations 08 p1246 N85-17865
SAM 2 measurements of the polar stratospheric aerosol, volume 5
[NASA-RP-1140] 15 p2590 N85-25970
Use of Goudrian model in studying laws of reflection in vegetation-soil system in optical range. 2: Influence of illumination conditions on spectral brightness coefficients 16 p2726 N85-26827
Projections of plasma cloud structures and their spectra
[AD-A153608] 18 p3189 N85-29776
Laser Schlieren crystal monitor
[NASA-CASE-MFS-29080-1] 19 p3374 N85-30932
Hadrons registration in emulsion chamber with carbon block
[HE-3.7-3] 24 p4166 N85-35662
Structured events in Pamir carbon X-ray chambers
[HE-3.7-7] 24 p4166 N85-35665

OPTICAL DEPOLARIZATION
Influence of depolarization of linear polarized radiation on heterodyne detection in laser range finders
[DFVLR-FB-84-31] 10 p1491 N85-19414

OPTICAL DISKS
Role of optical disk at computing centers
[DE85-005124] 13 p2145 N85-23314
Conference of quantum-radiooptics section 22 p3773 N85-33380

OPTICAL EMISSION
U LIGHT EMISSION

OPTICAL EMISSION SPECTROSCOPY
NT LASER SPECTROSCOPY
Optical and UV emission of active galactic nuclei 08 p1236 N85-17791

Optical studies of X-ray selected Active Galactic Nuclei (AGN) in the direction of the Large Magellanic Cloud (LMC) 08 p1237 N85-17797
Spatially resolved optical spectroscopy of the radio jet of the X-ray galaxy NGC 2110 08 p1238 N85-17804
Observational constraints on heating processes — solar corona 14 p2449 N85-25115

OPTICAL EQUIPMENT
NT ASTRONOMICAL TELESCOPES
NT BALLISTIC CAMERAS
NT CAMERAS
NT COLLIMATORS
NT DIFFRACTOMETERS
NT ELECTROPHOTOMETERS
NT ELLIPSOMETERS
NT FRAMING CAMERAS
NT HELIOMETERS
NT HIGH SPEED CAMERAS
NT IMAGE CONVERTERS
NT INFRARED SPECTROMETERS
NT INFRARED SPECTROPHOTOMETERS
NT LASER DOPPLER VELOCIMETERS
NT LIGHT SCATTERING METERS
NT MICRODENSITOMETERS
NT MICROWAVE REFLECTOMETERS
NT MULTISPECTRAL BAND CAMERAS
NT MULTISPECTRAL BAND SCANNERS
NT NEPHELOMETERS
NT OPTICAL GYROSCOPES
NT OPTICAL MEASURING INSTRUMENTS
NT OPTICAL MICROSCOPES
NT OPTICAL RADAR
NT OPTICAL RANGE FINDERS
NT OPTICAL SCANNERS
NT PANORAMIC CAMERAS
NT PERISCOPES
NT PHOTOGONIOMETERS
NT PHOTOMETERS
NT PINHOLE CAMERAS
NT POLARIMETERS
NT PRISMATIC BARS
NT PRISMS
NT PYROHELIOMETERS
NT REFLECTOMETERS
NT SCHMIDT CAMERAS
NT SPECTROHELIOGRAPHS
NT SPECTROPHOTOMETERS
NT SPECTROSCOPIC TELESCOPES
NT STREAK CAMERAS
NT STROBOSCOPES
NT TELEVISION CAMERAS
NT THEODOLITES
NT THERMICONS
NT TRANSMISSOMETERS
NT ULTRAVIOLET SPECTROMETERS
NT ULTRAVIOLET SPECTROPHOTOMETERS
NT WIDE ANGLE LENSES
NT X RAY TELESCOPES
Programmable optical sensor
[AD-D011244] 02 p0281 N85-11829
Direct view helmet mounted telescope
[AD-D011291] 06 p0755 N85-14839
Effect of aberration in optical system on illuminance distribution over image of strip in semicoherent light 06 p0777 N85-14970
Optics and opto-electronic systems
[AD-A147277] 07 p1044 N85-16630
LPI-radar for helicopter obstacle warning 08 p1074 N85-16810
Air combat visual simulation using a head slaved projector
[AD-P004327] 09 p1270 N85-17981
Survey of the finish characteristics of machined optical surfaces
[DE85-001343] 09 p1385 N85-18706
Monte Carlo simulation of gas Cerenkov detectors
[DE85-002422] 10 p1488 N85-19394
Optical mark reader
[AD-D011462] 10 p1557 N85-19818
Airborne remote sensing CCD imaging system 11 p1623 N85-20220
Topics in optical materials and device research, 3. Volume 2
[AD-A149727] 12 p1911 N85-21996
High resolution diffraction grating
[AD-D011541] 12 p1933 N85-22141
Topics in optical materials and device research, 3: Volume 1
[AD-A149726] 12 p1933 N85-22145
Optical system
[NASA-CASE-NPO-15801-1] 13 p2158 N85-23396
Equipment for performing surfaces of optical parts 14 p2268 N85-24043
Color-selective coating for viewfinder in optical instruments 14 p2276 N85-24066
Transducer of linear displacements 14 p2281 N85-24130
Three-dimensional sensing and interpretation
[AD-A150890] 14 p2311 N85-24304
Space-variant optical systems
[AD-A151032] 14 p2421 N85-24939
Instrument for measuring dispersional distortions in optical fibers and cables 15 p2530 N85-25595
ACT applied to helicopter flight control 16 p2712 N85-26738
USSR report: Engineering and equipment
[JPRS-UEQ-84-006] 16 p2760 N85-27035
Experience with introduction of Finish perforation of precision parts for optical instruments 16 p2761 N85-27038
The utilization of optical fibers in holography
[ISL-R-102/83] 16 p2787 N85-27196
Formulation of a coherent light-sheet by means of a cylindrical-spherical optical system
[ISL-R-116/83] 16 p2665 N85-27674
Acoustooptic pulse-echo transducer system
[NASA-CR-175919] 17 p2951 N85-28224
Instabilities and chaotic behavior of active and passive laser systems
[AD-A153366] 17 p2971 N85-28346
Support structures for optical components in the Laser Demonstration Facility
[DE85-008879] 17 p2971 N85-28349
Spatial light modulator having a capacitively coupled photoconductor
[AD-D011646] 17 p3037 N85-28790
Technique to reduce scattered light in optical systems
[AD-D011597] 18 p3185 N85-29752
High-pressure optical cell
[AD-A153639] 18 p3185 N85-29754
Digital Optical Circuit Technology
[AGARD-CP-382] 18 p3185 N85-29757
Optically bistable devices using InSb 18 p3186 N85-29758
An experimental nonlinear optical waveguide device 18 p3186 N85-29762
Multiport optical detectors 18 p3187 N85-29769
Optical 3-D signature device for detecting chemical agents
[AD-D011669] 19 p3272 N85-30293
Optical multiplexing on monomode fibers
[ENST-83E016] 20 p3533 N85-31982
Space optics
[CNES-84/105/T/CT/DRT/TIT/10] 20 p3533 N85-31985
Optical storage technology for mapping
[AD-A154969] 21 p3606 N85-32392
Microwave semiconductor research: Materials, devices and circuits and gallium arsenide ballistic electron transistors
[AD-A154696] 21 p3709 N85-33024
Conferences of quantum-radiooptics section 22 p3773 N85-33380
Fundamentals of radio optical theory of resonant and directional quasi-optical devices 22 p3780 N85-33420
Single-point diamond crushing of Zerodur with in-situ polishing and metrology on a diamond turning machine
[DE85-012918] 24 p4083 N85-35305

OPTICAL FILTERS
NT BIREFRINGENT FILTERS
Single crystal semiconductor multilayers for electrically active optical interference filters
[DE84-015614] 04 p0571 N85-13640
Position effects of laser protective materials on simulator tracking performance
[AD-A148297] 08 p1157 N85-17359
Filter and passband problems 08 p1252 N85-17910
Solid state luminescent light filters for neodymium lasers 11 p1716 N85-20799
Lasing characteristics of YAG: Nd(3+)-laser with LiF passive shutter with F2 color centers 11 p1717 N85-20802
Imaging apparatus for transverse electrode electro-optic tunable filter
[AD-D011524] 12 p1832 N85-21497
The magneto-optical filter, working principles and recent progress 14 p2442 N85-25066
Length dependent, optical time delay/filter device for electrical signals
[AD-D011594] 15 p2549 N85-25732
Modified Landolt C-ring test to measure the effects of laser filters on visual acuity
[AD-A151164] 15 p2617 N85-26127
Mode dependent, optical time delay system for electrical signals
[AD-D011596] 15 p2653 N85-26363
Three new fiber-optic components
[DE85-006269] 15 p2653 N85-26364
Prospects for parallel nonlinear optical signal processing using GaAs etalons and ZnS interference filters 16 p3187 N85-29765
Filter induced errors in laser anemometer measurements using counter processors
[NASA-TM-87047] 19 p3272 N85-30288

OPTICAL GENERATORS
U LASER CAVITIES

OPTICAL GYROSCOPES
Analysis of fiber-gyroscopes discussed 13 p2052 N85-22845

OPTICAL HETERODYNING
Measuring large amplitudes of mechanical vibrations with laser interferometers 06 p0787 N85-15028
A 150 micron heterodyne spectrometer for airborne astronomy 08 p1249 N85-17887
Tunable heterodyne receiver from 100 micron to 1,000 micron for airborne observations 08 p1249 N85-17888
Influence of depolarization of linear polarized radiation on heterodyne detection in laser range finders
[DFVLR-FB-84-31] 10 p1491 N85-19414
Multiport optical detectors 18 p3187 N85-29769
Phase locked loops for optical homodyne detection, volume 2 — spaceborne receivers
[ESA-CR(P)-2029-VOL-2] 20 p3442 N85-31368
A comparison of millimeter wave, direct detect and heterodyne laser intersatellite links
[AD-A151984] 20 p3481 N85-31496
Influence of depolarization of linear polarized radiation on the heterodyne detection in laser range finders
[ESA-TT-903] 20 p3481 N85-31500

OPTICAL IMAGES
U IMAGES

OPTICAL MASER MODULATION
U LIGHT MODULATION

OPTICAL MASERS
U LASERS

OPTICAL MEASUREMENT
NT ASTRONOMICAL PHOTOMETRY
NT COLORIMETRY
NT ELECTROPHOTOMETRY
NT INFRARED PHOTOMETRY
NT PHOTOMETRY
NT POLARIMETRY
NT SPECTROPHOTOMETRY
NT STELLAR SPECTROPHOTOMETRY
NT ULTRAVIOLET PHOTOMETRY
NT VISUAL PHOTOMETRY
Model study of the interaction of a blast wave with the superstructure of ships. Part 5: Application of optical measurement methods to the study of blast interaction
[PML-1984-12-PT-5] 01 p0057 N85-10375
Metrological consequences of the hard optical boundary assumption
[PB84-223577] 01 p0121 N85-10827
Predicting optical image displacement velocity in survey of Earth's surface 02 p0165 N85-11116
Methods for determining atmospheric optical parameters using results of space survey of Earth's surface 02 p0165 N85-11117
Checking optical-polarization measurements at interfaces 02 p0271 N85-11770
Development of optical techniques for Earth rotational measurements
[AD-A145859] 03 p0364 N85-12333
Energy parameters of optical radiation space research systems 06 p0791 N85-15058
Channel constructed to provide well defined boundary layers for vorticity optical probe measurements
[AD-A146879] 06 p0809 N85-15140
An experimental and theoretical investigation of optogalvanic effects
[AD-A148456] 08 p1223 N85-17700
S-11 and S-20 photocathode research activity, revision 1
[DE84-017164] 09 p1326 N85-18335
Modulation Transfer Function (MTF) measurement techniques for lenses and linear detector arrays
[NASA-TM-86168] 10 p1556 N85-19812
Preliminary design of an Earth-based debris detection system using current technology and existing installations 12 p1784 N85-21199
Parameters of amplitude-modulated signal upon reflections 13 p2078 N85-22366
In situ thin film measurement
[AD-A151365] 15 p2659 N85-26411
Recent advances in optical measurement methods in physics and chemistry
[DE85-006695] 17 p3037 N85-28792
Remote Sensing Technology: Symposium Proceedings
[DE85-010212] 20 p3477 N85-31606
New optical satellite data 20 p3492 N85-31705
Optical beat arc RMS test results 20 p3492 N85-31706

Simulation model of acoustic emission due to microscopic fracture in metals
[BLL-BISI-TRANS-22367-(8022.06)] 20 p0523 N85-31909
SCRIBE data of October 23, 1983 flight
[AD-A154884] 21 p3705 N85-33012
The ISAVF opto-mechanical test bed
[NASA-TM-87506] 24 p4087 N85-35206
Self-study manual on optical radiation measurements. Part 1: Concepts. Chapter 12: Blackbodies, blackbody radiation, and temperature scales
[PB85-196303] 24 p4154 N85-35754
Energy calibration of the fly's eye detector
[HE-4.4-1] 24 p4192 N85-36011

OPTICAL MEASURING INSTRUMENTS
NT DIFFRACTOMETERS
NT ELECTROPHOTOMETERS
NT ELLIPSOMETERS
NT INFRARED SPECTROMETERS
NT INFRARED SPECTROPHOTOMETERS
NT LIGHT SCATTERING METERS
NT MICRODENSITOMETERS
NT MICROWAVE REFLECTOMETERS
NT MULTISPECTRAL BAND SCANNERS
NT NEPHELOMETERS
NT OCULOMETERS
NT OPTICAL RANGE FINDERS
NT OPTICAL SCANNERS
NT PHOTOGONIOMETERS
NT PHOTOMETERS
NT POLARIMETERS
NT REFLECTOMETERS
NT SPECTROPHOTOMETERS
NT THEODOLITES
NT TRANSMISSOMETERS
NT ULTRAVIOLET SPECTROMETERS
NT ULTRAVIOLET SPECTROPHOTOMETERS
Programmable optical sensor
[AD-D011244] 02 p0251 N85-11829
Sensor technology for second, third generation industrial robots. Optical sensor applications 03 p0342 N85-12196
Formation of reference signals in laser-type gas analyzers with mechanical switching of optical channels 06 p0787 N85-15027
Optical method of measuring velocity of shear waves 06 p0787 N85-15029
Facilities for studing radiation damage in nonmetals during irradiation
[DE85-000590] 10 p1554 N85-19801
Operating time meter for tape recorder 12 p1838 N85-21537
Design of an optical proximity sensor using multiple cones of light for measuring surface shape — application to a robot manipulator
[AD-A150060] 12 p1934 N85-22152
Small-size measuring gauges for metal cutting machine tools 14 p2267 N85-24045
OMEGA: An optronic device to measure the incidence angle of a projectile
[ISL-CO-207/83] 14 p2306 N85-24274
First- and second-order charged particle optics
[DE85-006310] 14 p2421 N85-24940
Application of infrared radiometers for airborne detection of clear air turbulence and low level wind shear, airborne infrared low level wind shear detection test
[NASA-CR-175725] 15 p2594 N85-25985
Method and apparatus for generating a structured light beam array
[AD-D011590] 15 p2652 N85-26357
Surveying and optical tooling technologies combined to align a skewed beamline at the LAMPF accelerator
[DE85-005902] 16 p2864 N85-27664
Optical strain measurement system development 17 p2915 N85-27969
Optical system for measuring shadowgraph data
[AD-D011642] 17 p3036 N85-28784
Vibration-free Raman Doppler velocimeter
[NASA-CASE-LAR-13288-1] 18 p3104 N85-29216
Optical fiber magnetic field sensor with nanosecond response time
[DE85-008409] 18 p3110 N85-29259
Self-detecting optical sensors
[AD-D011657] 18 p3165 N85-29751
Fiber optic sensors operating at dc
[AD-D011674] 19 p3271 N85-30283
Apparatus for non-destructive inspection of blind holes
[AD-D011707] 19 p3273 N85-30295
Method of measuring spherical aberration and apparatus therefor
[AD-D011708] 19 p3367 N85-30682
Wideband disturbance accomodation in precision flexible space structures 20 p3415 N85-31184
A simple optical extensometer achieving high accuracy
[NPL-DMA(A)-95] 20 p3458 N85-31474
New method for compensating and measuring any motion of three-dimensional objects in holographic interferometry
[ISL-CO-216/84] 22 p3789 N85-33474
Redefining the scratch standards
[PB85-194736] 24 p4154 N85-35755

OPTICAL MEMORY (DATA STORAGE)
Acousto-optically addressed Fourier transform matched filters
[AD-A150298] 13 p2063 N85-22889
Two-dimensional signal processing and storage and theory and applications of electromagnetic measurements
[AD-A150590] 13 p2065 N85-22899
Realizing the full potential of the video disc for mapping applications
[AD-A154985] 21 p3606 N85-32391
Optical storage technology for mapping
[AD-A154969] 21 p3606 N85-32392

OPTICAL METHODS
U OPTICS

OPTICAL MICROSCOPES
Polarisation insensitive achromatic cube beamsplitter — binocular microscopes
[NPL-MOM-72] 23 p3973 N85-34630

OPTICAL MODULATION
U LIGHT MODULATION

OPTICAL PATHS
Measurement of the configuration of a concave surface by the interference of reflected light
[NASA-TM-77796] 11 p1728 N85-20867
Time spectra of intensity fluctuations along reflecting path 13 p2079 N85-22981
Mean free path lenght of photons with broken cloud cover 14 p2338 N85-24455
Arctic acoustic tomography MIZEX 84
[AD-A154426] 19 p3320 N85-30580
Microcomputer controlled image processor
[AD-D011734] 22 p3833 N85-33735

OPTICAL POLARIZATION
Morphology and optical polarization of the 3C 273 jet — radio jet 08 p1238 N85-17803
Research in image understanding as applied to 3-D tomographic imaging with near optical resolution
[AD-A150096] 12 p1829 N85-21483
The Saturn ring particles from optical reflectance polarimetry 15 p2571 N85-26484

OPTICAL PROPERTIES
NT ABSORPTANCE
NT ABSORPTIVITY
NT BIREFRINGENCE
NT BRIGHTNESS
NT BRIGHTNESS DISTRIBUTION
NT COLOR
NT DICHROISM
NT LUMINOSITY
NT OPACITY
NT OPTICAL BISTABILITY
NT OPTICAL REFLECTION
NT PHOSPHORESCENCE
NT PHOTOCONDUCTIVITY
NT PHOTOELECTRIC EFFECT
NT PHOTOELECTRIC EMISSION
NT PHOTOIONIZATION
NT PHOTOVISCOELASTICITY
NT PHOTOVOLTAIC EFFECT
NT RADIANCE
NT REFLECTANCE
NT REFRACTIVITY
NT SKY BRIGHTNESS
NT SOLAR GRANULATION
NT SPECTRAL REFLECTANCE
NT STELLAR LUMINOSITY
NT STIGMATISM
NT TRANSLUCENCE
NT TRANSMISSIVITY
NT TRANSMITTANCE
NT TRANSPARENCE
NT TURBIDITY
NT WATER COLOR
The two modes of visual processing: Implications for spatial orientation 01 p0008 N85-10047
Investigating compression failure mechanisms in composite laminates with a transparent fiberglass-epoxy birefringent materials
[NASA-TM-86306] 02 p0170 N85-11137
Trivalent ion exchange in beta alumina
[AD-A145373] 02 p0172 N85-11151
Calculations of optical properties of transition metals
[BLL-M-35744-(5826.4)] 02 p0175 N85-11175
Optical properties of laser erosion flares in plasma 02 p0270 N85-11764
Checking optical-polarization measurements at interfaces 02 p0271 N85-11770
Using fiber-optics light guides in diagnosing intense shock waves 02 p0272 N85-11773
Pulsed neodymium glass laser system for investigating nonlinear optical phenomena in gases 03 p0348 N85-12241
NASA thunderstorm overflight program: Atmospheric electricity research. An overview report on the optical lightning detection experiment for spring and summer 1983
[NASA-TM-86468] 03 p0363 N85-12330
Dynamic occlusion analysis in optical flow fields
[AD-A145805] 03 p0406 N85-12584
Dielectric and optical properties of sputtered thin films
[AD-A146210] 03 p0420 N85-12681
Self-study manual on optical radiation measurements. Part 1: Concepts. Chapter 11: Linearity considerations and calibrations
[PB84-218346] 03 p0421 N85-12690
Concentrator optical characterization using computer mathematical modelling and point source testing
[NASA-CR-174109] 04 p0528 N85-13375
Optical characterization of radiation-resistant fibers
[DE84-015248] 05 p0820 N85-13964
Photoluminescence studies of Ga(As,P) strained-layer superlattices
[DE84-015709] 05 p0731 N85-14701
Analysis of optical and electrical performance of a TCP-coated solar cell 06 p0832 N85-15293
Optical polarization as a probe of the local interstellar medium 06 p0875 N85-15560
Optical properties of composite materials
[AD-A146768] 07 p0920 N85-15828
Multiple scattering effects on transmission through the atmosphere
[AD-A147527] 07 p0941 N85-15969
Comparison measurements on optical particle counters
[BLL-DOUNREAY-TR-934-(9091.9F)] 07 p0961 N85-16092
Bio-optical variability in the Alboran Sea as assessed by Nimbus-7 coastal zone color scanner
[AD-A147909] 07 p0989 N85-16281
Optical RF downconverter
[AD-D011336] 07 p1042 N85-16616
Nonlinear optical studies of rydberg atoms using degenerate four-wave mixing
[AD-A146827] 07 p1043 N85-16623
Multiwavelength bidirectional coupler-decouplers
[AD-A147009] 07 p1043 N85-16625
Quantum noise and excess noise in optical homodyne and heterodyne receivers
[AD-A148296] 08 p1157 N85-17303
International Conference on Luminescence
[AD-A148470] 08 p1223 N85-17701
Optical computer studies at UK's Heriot-Watt University 09 p1309 N85-18227
Survey of the finish characteristics of machined optical surfaces
[DE85-001343] 09 p1385 N85-18708
Effective antireflection coatings of transparent polymeric materials by gas-phase surface fluorination
[DE84-013027] 09 p1385 N85-18711
High temperature laser interferometric studies of solid electrolytes 09 p1396 N85-18785
Infrared horizon sensor modeling for attitude determination and control: Analysis and mission experience
[NASA-TM-86181] 10 p1429 N85-19016
Calculation of optical characteristics of shelf ecological system based on its mathematical model 10 p1498 N85-19453
Ab initio calculations of the optical properties of ions in glass
[DE85-001008] 11 p1612 N85-20133
Optically bistable devices using semiconductor materials
[AD-A149551] 11 p1628 N85-20253
Subnanosecond time-resolved emission study of Cu2O and GaAs
[DE85-002070] 11 p1735 N85-20912
Novel photo-thermal technique for flow and spectroscopic measurements in a dense aerosol stream
[AD-A149745] 12 p1800 N85-21257
Control of electronic, magnetic and optical properties of doped polyacetylene conductors
[AD-A150117] 12 p1814 N85-21375
Investigation of the optical properties of solar elements 12 p1879 N85-21766
Multiple resolution representation and probabilistic matching of 2-D gray-scale shapes
[AD-A149861] 12 p1933 N85-22147
Time-resolved ellipsometry and reflectivity measurements of the optical properties of silicon during pulsed excimer laser irradiation
[DE85-005091] 13 p2096 N85-23079
Assessing LANDSAT TM and MSS data for detecting submerged plant communities 13 p2120 N85-23203

Research in the optical sciences
[AD-A150196] 13 p2159 N85-23401
Power control of induction equipment for founding optical glass in array of platinum crucibles
14 p2267 N85-24044
Dependence of properties of optical cavity on misalignment 14 p2276 N85-24099
Water-resistance and some other properties of polyalkali fluorophosphate glasses 14 p2281 N85-24133
Thresholds of optical breakdown in alkali-halide crystals under pulses from CO2-laser 14 p2282 N85-24134
Classification of atmospheric aerosol for evaluation of its effect on climate 14 p2333 N85-24428
Stress and efficiency studies
[NASA-CR-175668] 14 p2351 N85-24531
First- and second-order charged particle optics
[DE85-006310] 14 p2421 N85-24940
Particle curtain generator for optical property measurements of solid particles
[DE85-005784] 15 p2560 N85-25797
Optical monitoring of photo-acoustic pulse propagation in silicon wafers
[AD-A151333] 15 p2651 N85-26352
In situ thin film measurements
[AD-A151379] 15 p2652 N85-26353
Experimental and theoretical study of the infrared reflectance of thin oxide films on metals
[DE85-005799] 15 p2653 N85-26386
Optical properties of hydrogenated amorphous carbon films grown from methane plasma
[NASA-TM-86995] 15 p2658 N85-26406
Interaction of liquid crystals with inhomogeneous surfaces
[AD-A151557] 15 p2660 N85-26413
Optical pulsar in the Large Magellanic Cloud remnant 0540-69.3
[DE85-006707] 16 p2683 N85-27788
USSR report: Engineering and equipment
[JPRS-UEQ-85-004] 17 p2939 N85-28142
Materials-process interactions in ternary alloy semiconductors
[AD-A153139] 17 p3043 N85-28632
Electrochromic and thermochromic materials for solar energy applications with emphasis on niobium and vanadium oxides
[DE85-010830] 19 p3249 N85-30147
Machining of beryllium with the LLNL precision engineering research lathe
[DE85-010832] 19 p3250 N85-30149
Optical effects of thin film adhesives in multijunction solar cells
[DE85-010120] 19 p3305 N85-30486
Opticals constant at X-ray wavelengths
[DE85-009743] 19 p3355 N85-30795
Application of single and multiple scattering techniques to optical properties of dielectric media
19 p3366 N85-30877
Failure analysis of thin-film amorphous-silicon solar-cell modules 21 p3613 N85-32452
Properties of aerosol particles detected by satellites in coastal regions 21 p3641 N85-32622
Radiative-collision generation of sound in gases subjected to single-pulse optical excitation
21 p3689 N85-32920
Nonlinear spectroscopy
[AD-A154708] 21 p3704 N85-33010
Optical output stabilization method for direct current arc lamps
[AD-A154987] 21 p3705 N85-33013
Impact of fluctuations in optical properties of atmosphere on the ratio of spectral brightness from remote sensing of agricultural land 22 p3734 N85-33149
Hercules X-1: Pulsed gamma-rays detected above 150 GeV
[OG-2.2-9] 22 p3885 N85-33935
Theoretical and experimental analyses of the performance of two-color laser ranging systems
[NASA-CR-176159] 23 p3936 N85-34397
Characterization of the optical and thermal properties of matter by photothermal techniques
[DE85-012607] 24 p4076 N85-35260
Los Alamos free-electron laser
[DE85-012606] 24 p4098 N85-35405
Optical properties of heterostructures and superlattices
[AD-A156243] 24 p4162 N85-35802
Ionic crystals
[DE85-009482] 24 p4163 N85-35809

OPTICAL PUMPING

NT LASER PUMPING

Synchronously pumped mode-locked semiconductor platelet laser
[AD-D011214] 01 p0051 N85-10340
Tunable CW semiconductor platelet laser
[AD-D011215] 01 p0052 N85-10341
Intense excitation source of blue-green laser
[AD-A147450] 07 p0971 N85-16166
High-power radiating plasma
[NASA-TM-77784] 07 p1045 N85-16637
Optical studies of dynamical processes in disordered materials
[DE85-002400] 10 p1453 N85-19158
Optically pumped iodine monofluoride laser
[AD-D011555] 12 p1855 N85-21637
High precision materials characterization in the near millimeter wave-length range
[AD-A153267] 17 p2968 N85-28331
Design and construction of a CW ND:YAG laser using a single elliptical cavity and water cooled krypton arc lamp pumping
[AD-A152657] 17 p2970 N85-28340
Experimental study of dissociative attachment in optically-pumped lithium molecules
[AD-A152800] 17 p3030 N85-28738
Diode laser 87Rb optical pumping in an evacuated wall-coated cell 18 p3105 N85-29226
Optically pumped laser system having extracavity pulse smoother
[AD-D011714] 19 p3276 N85-30319
Electron-atom collision studies using optically state selected beams
[DE85-010848] 19 p3368 N85-30868
Fiber optics interface for a dye laser oscillator and method
[DE85-005765] 23 p3973 N85-34633
Infrared generation and wave-mixing studies in cesium
[DE85-012883] 24 p4083 N85-35304
Generation of stimulated emission in the soft X-ray range by nonlinear processes with excimer lasers
[DE85-012465] 24 p4098 N85-35403

OPTICAL RADAR

Shipboard measurement of cloud bases and average surface visibility with an eye-safe lidar
[AD-A144889] 01 p0052 N85-10345
Field tests of the real-data acquisition system for the NASA-LaRC differential absorption lidar
[NASA-CR-174020] 01 p0106 N85-10710
Multifrequency lidar based on dye laser
02 p0262 N85-11715
Measurement of range-resolved water vapor concentration by coherent CO2 differential absorption lidar
[PB84-236892] 04 p0535 N85-13420
Utilization of SAGE aerosol profiles in the analysis of Mauna Loa stratospheric lidar data
[NASA-CR-174198] 05 p0675 N85-14332
Detailed performance calculations: Wayne State University and Ford Motor Company, appendix C
05 p0676 N85-14340
Lidar measurements of structural characteristics of atmospheric turbulence 06 p0824 N85-15229
Dual mode scanner-tracker
[AD-D011417] 08 p1113 N85-17018
NASA three-laser airborne differential absorption lidar system electronics
[NASA-CR-174293] 08 p1166 N85-17353
Lidar systems for aerosol studies: An outline
08 p1183 N85-17457
Active optical sounding of ozone and minor constituents in the middle atmosphere: A review of ground-based lidar measurements 08 p1183 N85-17458
Lidar studies of temperature and density using Rayleigh scattering 08 p1184 N85-17459
Lidar studies of the alkali metals
08 p1184 N85-17460
Lidar-Thomson scattering — nuclear fusion
[IPP-1/299] 08 p1221 N85-17693
Pulse heterodyne equipment for measurements of range and velocity of moving targets-pulse radar
[ESA-TT-845] 09 p1312 N85-18246
Carbon dioxide laser radar for monitoring atmospheric transmittance and atmospheric aerosol
09 p1354 N85-18516
Development and operation of a real-time data acquisition system for the NASA-LaRC differential absorption lidar
[NASA-CR-174394] 09 p1366 N85-18583
Investigations relating to the simultaneous use of Combined Optical Adaptive Techniques (COAT) and angle-tracking
[ESA-TT-844] 09 p1385 N85-18712
Lidar-Thomson scattering — Joint European Torus
[IPF-84-3] 09 p1394 N85-18777
Airborne lidar measurements of El Chichon stratospheric aerosols, October 1982 to November 1982
[NASA-RP-1136] 10 p1514 N85-19550
Lidar observations of stratospheric aerosol over Mauna Loa Observatory, 1974 - 1981
[PB85-115061] 11 p1682 N85-20597
In situ orbital debris experiment concepts
12 p1784 N85-21198
On the inversion of the lidar equation
[AD-A149653] 12 p1856 N85-21641
Observational study of transport in the free troposphere
[PB85-144145] 12 p1867 N85-21848
Analysis of the NASA/MSFC Airborne Doppler Lidar results from San Gorgonio Pass, California
[NASA-CR-171355] 12 p1892 N85-21873
Time spectra of intensity fluctuations along reflecting path 13 p2079 N85-22981
Picosecond lidar techniques in laboratory and field diagnostics
[AD-A150755] 14 p2309 N85-24294
3D (Three-Dimensional) sensor for adaptive suspension vehicle
[AD-A150921] 14 p2311 N85-24305
Specifics of polarization structure of repeated scattering background in optical laser sounding signals
14 p2342 N85-24485
Interference immunity of optical radar system with phased antenna array 15 p2526 N85-25578
Lidar and radiometer observations of thunderstorm tops 15 p2595 N85-25994
High-frequency microwave observations of convective precipitation 15 p2596 N85-26000
Utilization of remote sensing data in the evaluation of air pollution characteristics in the south coast/Southeast Desert Air Basin
[PB85-162063] 16 p2822 N85-27407
Analysis of the NASA/MSFC airborne Doppler lidar results from San Gorgonio Pass, California
[NASA-CR-3901] 16 p2832 N85-27463
Conducting a wind sensing study
[NASA-CR-175782] 16 p2832 N85-27465
Influence of coherent mesoscale structures on satellite-based Doppler lidar wind measurements
[NASA-CR-175853] 16 p2833 N85-27467
Geophysical monitoring for climatic change, number 12
[PB85-172278] 16 p2837 N85-27496
Test of lidar inversion algorithm sensitivity to atmospheric backscatter and extinction parameters, revision A
[AD-A152082] 16 p2865 N85-27671
Lidar ER2 (ozone). Crystal characterization for harmonic conversion — laser systems
[CERT-2/6129-00] 16 p2872 N85-27717
Convective storm downdraft outflows detected by NASA/MSFC's Airborne 10.6 micron pulsed Doppler Lidar System
[NASA-CR-3898] 17 p2995 N85-28511
Thin film phase transition materials development program
[AD-A154290] 19 p3259 N85-30209
Technology assessment of high pulse energy CO(2) lasers for remote sensing from satellites
[NASA-TM-86415] 19 p3275 N85-30309
Lidar techniques for search and rescue
[DE85-009586] 19 p3278 N85-30327
Variability of air humidity profiles over ocean determined by lidar sounding 19 p3296 N85-30436
Specifics of laser sounding of atmosphere along horizontal and slightly slanting paths over water surface
19 p3297 N85-30441
Lidar system using polarization discrimination techniques for molecular air pollution monitoring
19 p3308 N85-30504
Comparison of wind and turbulence measurements from Doppler lidar and instrumented aircraft
[NASA-CR-171535] 20 p3495 N85-31729
Data analysis for lidar and quartz crystal microbalance systems
[NASA-CR-172601] 21 p3615 N85-32484
Visibility and vertical structure measurements in southern Germany
[AD-A154714] 21 p3635 N85-32574
Cloud droplet nucleation and initial growth derived from lidar depolarization studies 21 p3644 N85-32635
Laser Elektronika-01 for air pollution control lidar
21 p3684 N85-32887
Participation of singlet oxygen in photodestruction of air-saturated solutions of coumarin dyes
21 p3685 N85-32891

OPTICAL RANGE FINDERS

NT LASER RANGE FINDERS

Error of distance measurement by phase-type optical range finders with photoreceivers of various types
14 p2276 N85-24101

OPTICAL REFLECTION

Metrological consequences of the hard optical boundary assumption
[PB84-223577] 01 p0121 N85-10827
Polarized electron cyclotron emission in the Tokapole 2 Tokamak
[DE84-014953] 01 p0122 N85-10838

Space environment simulation to test satellite thermal control coatings, volume 1
[CERT-4128-VOL-1] 08 p1109 N85-17012
Space environment simulation to test satellite thermal control coatings. Volume 2: Annex 1
[ESA-CR(P)-1870-VOL-2] 08 p1109 N85-17013
Space environment simulation to test satellite thermal control coatings. Volume 2: Annexes 2, 3, 4
[ESA-CR(P)-1870-VOL-3] 08 p1109 N85-17014
Transmission and reflection of laser beams propagating through aerosol clouds in space
[LA-9998-MS] 12 p1858 N85-21638
Parameters of amplitude-modulated signal upon reflections 13 p2076 N85-22968
Time spectra of intensity fluctuations along reflecting path 13 p2079 N85-22981
Performance estimate of a reflecting light pipe for infrared detectors
[AD-A141269] 13 p2158 N85-23398
Diffuse reflection of light from turbid conservative medium of finite thickness with incidence of beam on surface of scattering glancing 14 p2342 N85-24481
Determining characteristics of optical radiation reflectors based on results of remote sensing 15 p2488 N85-25358
Apparatus for non-destructive inspection of blind holes
[AD-D011707] 19 p3273 N85-30295
Model computations of light reflection from sea surface 19 p3292 N85-30411
Attenuated total reflection method for obtaining optical constants of powders
[AD-A154094] 19 p3367 N85-30681
Influence of spatial pumping spectrum on quality of phase conjugate reflection during 4-photon interaction 21 p3696 N85-32964

OPTICAL RELAY SYSTEMS
Facilities for studing radiation damage in nonmetals during irradiation
[DE85-000590] 10 p1554 N85-19601
Experimental demonstration of an optoelectronic switch matrix for satellite-switched TDMA signals in the 0.3-4.0 GHz band
[CRC-TN-717] 19 p3253 N85-30170

OPTICAL RESONANCE
Optical studies of dynamical processes in disordered materials
[DE85-002400] 10 p1453 N85-19158
Resonance identifications in Saturn's rings 15 p2674 N85-26504
Saturation effect in multilevel lasing media 21 p3686 N85-32901

OPTICAL RESONATORS
Unstable optical resonator with cancelling edge waves
[AD-D011379] 07 p1042 N85-16618
Reflectivity measurements of laser gyro mirrors
[ESA-TT-851] 09 p1386 N85-18714
Characteristics of unstable resonators in flashlamp-pumped organic-compound lasers 11 p1717 N85-20800
Resonator optical designs for free electron lasers
[DE85-007678] 17 p2971 N85-28347
Optical modulators and bistable devices using molecular gases 18 p3186 N85-29761

OPTICAL SCANNERS
NT MULTISPECTRAL BAND SCANNERS
Moving object detection system using infrared scanning
[AD-D011222] 01 p0120 N85-10622
DoD Robotics Application Workshop Proceedings
[AD-A145867] 03 p0307 N85-11978
Air Force honeycomb shaping at SM-ALC (Sacramento Air Logistics Center)
[AD-P004005] 03 p0308 N85-11985
Mapping of mammalian arrhythmias with the cardiac laser scanner 03 p0390 N85-12545
Design of two-mirror scanner with axes of rotation not in plane of mirrors 06 p0777 N85-14969
Electrooptical sensor for automatic detection of objects 06 p0789 N85-15040
Reduction of signal modulation caused by polarization in visible optical scanning systems
[AD-D011389] 07 p1042 N85-16620
Dual mode scanner-tracker
[AD-D011417] 08 p1113 N85-17018
Design and analysis of airborne scanning optical systems 11 p1623 N85-20218
A scanning optical microprobe for infrared detector measurement
[AD-A151748] 15 p2653 N85-26361
Testing of scanner-assisted revision of the topographic map 1:25,000 (TK 25) 16 p2814 N85-27359
Applied computer graphics in a geographic information system: Problems and successes 23 p3962 N85-34563

OPTICAL SENSORS
U OPTICAL MEASURING INSTRUMENTS

OPTICAL SIGNALS
U OPTICAL COMMUNICATION

OPTICAL SPECTRUM
U LIGHT (VISIBLE RADIATION)
U SPECTRA

OPTICAL THICKNESS
Some statistical characteristics of atmospheric optical thickness in visible spectral range 02 p0164 N85-11109
Pair production at moderate optical depths — galactic nuclei X ray spectra 06 p1241 N85-17830
Saturn's rings resolved by the VLA — Very Larg Array (VLA) 15 p2670 N85-26476
Impact of fluctuations in optical properties of atmosphere on the ratio of spectral brightness from remote sensing of agricultural land 22 p3734 N85-33149

OPTICAL TRACKING
Optical seam tracking of robotic arc welding
[VTT-272] 01 p0055 N85-10368
Position effects of laser protective materials on simulator tracking performance
[AD-A148297] 06 p1167 N85-17359
Optical flow and texture variables useful in detecting decelerating and accelerating self-motion
[AD-A148718] 09 p1384 N85-18703
Investigations relating to the simultaneous use of Combined Optical Adaptive Techniques (COAT) and angle-tracking
[ESA-TT-844] 09 p1385 N85-18712
NORAD operational system 12 p1783 N85-21189
History of satellite break-ups in space 12 p1783 N85-21190
Modified Landolt C-ring test to measure the effects of laser filters on visual acuity
[AD-A151164] 15 p2617 N85-26127
Optical flow-patterns of image velocity and their potential use in guidance and image interpretation
[BAE-BT-12091] 15 p2651 N85-26347
Rayleigh criteria resolution of optical correlations
[AD-A151711] 15 p2652 N85-26359
An automatic traversing system for Laser Doppler Anemometer (LDA) applications to wind tunnels and to free jets
[ISL-CO-225/83] 16 p2836 N85-27490
M-BLASER: A device to study pursuit tracking in the rhesus monkey
[AD-A152986] 17 p2998 N85-28534
Pursuit tracking performance and flash disruption: The effects of training the non-dominant eye on target reacquisition
[AD-A153404] 17 p2999 N85-28541
Retinally stabilized differential resolution television display
[NASA-CASE-NPO-15432-1] 18 p3089 N85-29117

OPTICAL TRANSFER FUNCTION
Infrared material optical damage by rain
[AD-P004372] 12 p1827 N85-21466
DARPA/TTO program IR binary optics
[AD-A152196] 16 p2865 N85-27672

OPTICAL WAVEGUIDES
Guided-wave optic devices for integrated optic information processing
[AD-A145695] 02 p0280 N85-11827
Influence of mode noise suppression in multimode fiber optic light guides 03 p0348 N85-12242
Integration of detectors with optical waveguide structures
[AD-A146278] 03 p0420 N85-12682
Qualitative and quantitative compositional analysis of shale derived by gas chromatography and combined gas Chromatography/Mass spectrometry. Executive summary
[AD-A148389] 07 p0924 N85-15851
Precision electrooptical deflector based on corrugated light guide 07 p0950 N85-16020
Transformation of mode composition of circuler optical waveguide 07 p0950 N85-16023
General theory and design considerations for optical waveguide chemical vapor sensors
[AD-A148505] 08 p1223 N85-17702
Self-induced nonlinear effects in optical fibers: A unified approach
[FUB-67-1982] 09 p1385 N85-18713
Betegeuse at maximum luminosity 11 p1758 N85-21061
Properties of chirped grating lenses in optical waveguides
[AD-A150023] 12 p1934 N85-22149
Dispersion characteristics of small-mode gradient optical fibers 13 p2082 N85-23004
Integrated optical components utilizing acoustooptic and electrooptic diffraction in micro-waveguides 13 p2089 N85-23044
Acoustooptic demodulation of frequency-modulated signals 13 p2090 N85-23050
Technical Digest: Symposium on Optical Fiber measurements, 1984
[PB85-114700] 13 p2160 N85-23407
Investigation of semiconductor clad optical waveguides
[NASA-CR-175870] 17 p3036 N85-28785
Optical waveguide characterization using grating couplers
[AD-A153063] 17 p3037 N85-28789
An experimental nonlinear optical waveguide device 18 p3186 N85-29762
The potential of semiconductors for optical integrated circuits 18 p3187 N85-29768
A study of reflex optoelectronic switching matrices and their derivatives
[CRC-TN-720] 19 p3253 N85-30169
Optical waveguide sensor for methane gas
[AD-D011691] 19 p3273 N85-30294
Optical waveguide along front of exothermic reaction 21 p3694 N85-32954
Methods for measuring and analyzing dispersion properties of multimode fiber optic lightpipes (a review) 21 p3695 N85-32960
Photothyristor optrons and optron microcircuits, part 1 22 p3781 N85-33424

OPTICS
Technical activities 1983, Office of Nondestructive Evaluation
[PB84-217074] 03 p0370 N85-12360
Focussing and confinement
[DE84-016181] 05 p0640 N85-14106
The use of an optical data acquisition system for bladed disk vibration analysis
[NASA-TM-86891] 06 p0817 N85-15184
Theory and applications of two-photon quantum optics
[AD-A147382] 07 p1044 N85-16631
Ill-posed problems and regularization analysis in early vision
[AD-A147753] 08 p1222 N85-17696
High-pressure optical cell
[AD-A153639] 18 p3185 N85-29754
Wideband disturbance accomodation in precision flexible space structures 20 p3415 N85-31194
Summary of activities, 1983
[LBL-18500] 23 p3969 N85-34605

OPTIMAL CONTROL
NT TIME OPTIMAL CONTROL
On the Pontryagin principle for stochastic optimal control
[TWISK-328] 01 p0112 N85-10762
Application of modern guidance control theory to a bank-to-turn missile
[AD-A145646] 02 p0166 N85-11123
Minimax optimal control in the reentry of a space glider 02 p0167 N85-11124
Asymptotically optimal adaptive control
[AD-A145666] 02 p0249 N85-11629
On a class of suboptimal controls for infinite-dimensional bilinear systems
[RR-258] 02 p0249 N85-11630
Control and performance of a photovoltaic-thermal energy system 03 p0397 N85-12475
Chandrasekhar equations and computational algorithms for distributed parameter systems
[NASA-CR-172467] 03 p0402 N85-12564
Utilization of historic information in an optimization task 05 p0700 N85-14490
Algorithm for tracking manuevering object with ambiguous measurements 06 p0791 N85-15057
Research on optimal control, stabilization and computational algorithms for aerospace applications
[NASA-CR-174318] 08 p1209 N85-17603
Optimal stochastic LQ control with measurements displaced in time
[OUEL-1547/84] 08 p1209 N85-17605
SUBOPT: A CAD program for suboptimal linear regulators
[NASA-CR-172536] 10 p1539 N85-19702
Optimal symmetric flight studies
[NASA-CR-172508] 12 p1780 N85-21176
An asymptotically optimal subclass of BTIB designs for comparisons with a control
[AD-A149819] 12 p1921 N85-22066
Synthesis of quasi-optimum two-level signal discriminator with level changing at unknown point 13 p2083 N85-23010
Approximation in optimal control and identification of large space structures
[AD-A150323] 13 p2151 N85-23351
Optimal designs for comparisons between two sets of treatments
[AD-A150621] 13 p2152 N85-23360
Total energy-rate feedback for automatic glide-slope tracking during wind-shear penetration
[NASA-TP-2412] 14 p2226 N85-23801

Application of the maximum entropy/optimal projection control design approach for large space structures
14 p2234 N85-23849
Synthesis of optimal controls for real-time linear digital systems
14 p2270 N85-24062
Optimal space trajectories
14 p2306 N85-24756
Selection of optimal control program for solar cell panels of Earth satellites
15 p2484 N85-25335
Optimal control theory applied to fusion plasma thermal stabilization
[DE85-007599] 15 p2658 N85-26405
Application of linear optimal control theory to the design of the elevator control system of the DHC-2 Beaver experimental aircraft
[VTH-LR-411] 16 p2711 N85-28729
The effect of inaccuracies in structural models on the control of large space structures
[AD-A151794] 16 p2732 N85-28658
Optimal control of electric drive with simultaneous control inputs for motor current and flux
16 p2763 N85-27049
Development of graphical pole-zero, root-locus, Bode, Nyquist, and Nichols responses using the OPTSYSX program
[AD-A152146] 16 p2847 N85-27555
Development of graphical time response using the OPTSYSX program
[AD-A152221] 16 p2848 N85-27557
Some new results on the discrete-time Riccati Equation and their use in the design of optimal regulators and observer-estimators
[AD-A151934] 16 p2854 N85-27597
Research on optimal control, stabilization and computational algorithms for aerospace applications
[NASA-CR-172528] 19 p3221 N85-29970
Some asymptotic problems in the optimal control of distributed systems
20 p3412 N85-31175
A factorization approach to the linear regulator quadratic cost problem
20 p3413 N85-31178
An integrated control and minimum mass structural optimization algorithm for large space structures
20 p3413 N85-31183
Optimization of controlled structures
20 p3414 N85-31186
Robust control design for large space structures
20 p3416 N85-31200
User's manual of the BNDSCO computer program for solving constrained optimal control problems
[DFVLR-MITT-85-05] 20 p3516 N85-31865

OPTIMIZATION
NT FLIGHT OPTIMIZATION
NT OPTIMAL CONTROL
NT TIME OPTIMAL CONTROL
NT TRAJECTORY OPTIMIZATION
Study to optimize Cr-Mo steels to resist hydrogen and temper embrittlement. A study of carbides formed in low alloy Cr-Mo steels
[DE84-015206] 01 p0029 N85-10179
Combustion modeling of a 2 cylinder cycle reciprocating engine
[AD-A144782] 01 p0055 N85-10364
Interactive graphics nonlinear constrained optimization
01 p0058 N85-10367
Composite laminate optimization program suitable for microcomputers
01 p0059 N85-10369
Hydrologic and economic models for watershed evaluation and research
[PB84-222371] 01 p0066 N85-10438
Manual of phosphoric acid fuel cell power plant optimization model and computer program
[NASA-CR-174721] 01 p0067 N85-10445
ADS: A FORTRAN program for automated design synthesis, version 1.00
[NASA-CR-172460] 01 p0102 N85-10684
Some concepts in multi-criteria optimization
[CSIR-TWISK-299] 01 p0108 N85-10722
On the commutant of an irreducible set of operators in real Hilbert space
[TUM-M8316] 01 p0114 N85-10774
Quasistable parametric optimization without compact level sets
[AD-A144710] 01 p0114 N85-10776
Optimizing search with positive information feedback
[CSIR-TWISK-313] 01 p0125 N85-10855
Fitting aerodynamic forces in the Laplace domain: An application of a nonlinear nongradient technique to multilevel constrained optimization
[NASA-TM-86317] 02 p0134 N85-10917
Energy efficient engine. High pressure compressor detail design report
[NASA-CR-165558] 02 p0147 N85-10996
Asymptotically optimal adaptive control
[AD-A145668] 02 p0249 N85-11629
Inverse problems, optimization and algorithms
[AD-A145397] 02 p0250 N85-11636
Constrained optimization using iterated partial Kuhn-Tucker vectors
[AD-A145478] 02 p0251 N85-11641
Rapidly convergent algorithms for nonsmooth optimization
[AD-A145556] 02 p0251 N85-11643
Minimization of anomalous errors in measuring systems employing search and testing devices
03 p0344 N85-12219
Circuit engineering and technological optimization of very high speed LSI logic elements and transistor structures
03 p0347 N85-12237
Evaluating A(T) *D*A for sparse matrices: Analysis
[AD-A146916] 03 p0411 N85-12625
The Lindstrom-Madden method for series systems with repeated components
[AD-A146265] 03 p0412 N85-12636
A methodology for supporting views in relational databases
03 p0437 N85-12783
Optimization of movements of manipulators with kinematic redundancy
04 p0486 N85-13112
Boolean approach to zero-one linear programming
[DE84-016654] 04 p0550 N85-13498
Utilization of historic information in an optimisation task
05 p0700 N85-14490
Interpretation of natural language database queries using optimization methods
05 p0735 N85-14723
A self-organizing database system: A different approach to query optimization
05 p0735 N85-14725
Optimization of the die entrance shape for polymeric extrusion
[DE85-001588] 06 p0772 N85-14937
Optimization of moving-target selection radar devices for nonGaussian signals for stationary targets
06 p0789 N85-15043
A nonnoble front metallization process
06 p0830 N85-15279
Performance of Bayes-optimal angle-of-arrival estimators
[AD-A146594] 06 p0856 N85-15454
An improved computer model for prediction of axial gas turbine performance losses
[NASA-CR-174246] 07 p0904 N85-15724
Predicted performance benefits of an adaptive digital engine control system of an F-15 airplane
[NASA-TM-85916] 07 p0905 N85-15729
Optimization of the NiCrAl-Y/ZrO-Y2O3 thermal barrier system
[NASA-TM-86905] 07 p0927 N85-15878
Charge domain filters for enhanced monolithic signal processing
[AD-A147428] 07 p0941 N85-15984
Analysis of effectiveness of partial optimization of spatial processing systems
07 p0952 N85-16031
Reduction method for thermal analysis of complex aerospace structures
[NASA-TP-2373] 07 p0957 N85-16066
Continuity of the null space basis and constrained optimization
[AD-A147038] 07 p1030 N85-16538
Trust region methods for minimization
[AD-A147073] 07 p1030 N85-16540
Some applications of penalty functions in mathematical programming
[AD-A147443] 07 p1032 N85-16552
Structural optimization and other large-scale processes
[AD-A147895] 07 p1034 N85-16564
Pari-mutuel as a system of aggregation of information
[AD-A147210] 07 p1035 N85-16570
Principles of multiobjective optimization
[AD-A147520] 07 p1052 N85-16679
Efficient computation of optimal time for transaction processing in a database system
[AD-A147568] 07 p1054 N85-16693
An optimization method for the preliminary design of interplanetary aerobraking missions
08 p1076 N85-16822
Impact of activation optimization on the Vandenberg Ground Support System using Q-GERT analysis
[AD-A148448] 08 p1105 N85-16986
Finite element computation of structural design sensitivity analysis
09 p1330 N85-18353
Design oriented identification of critical points in transient response
09 p1330 N85-18357
Treatment of general boundary conditions and point-wise state variable constraints in optimum design for static and dynamic response
09 p1330 N85-18358
Optimization of vibrating beams including the effects of coupled bending and torsional modes
09 p1331 N85-18364
Optimization of design and control strategies for geothermal space heating systems
[DE85-000496] 09 p1344 N85-18458
Partial evaluation as a means of language extensibility
[AD-A148730] 09 p1368 N85-18596
Generalized convex functions: Properties, optimality and duality
[DE85-001553] 09 p1376 N85-18652
GaAlAs Sb APD optimization
[AD-A149406] 10 p1480 N85-19344
Optimization of a ground coupled heat pump
[DE85-000273] 10 p1486 N85-19360
Identification of dynamic systems, theory and formulation
[NASA-RP-1138] 10 p1551 N85-19784
Improving engineering system design by formal decomposition, sensitivity analysis, and optimization
[NASA-TM-86377] 10 p1551 N85-19785
Finite-(beta) optimization of tandem mirrors
[DE85-002658] 10 p1560 N85-19835
Noise constraints effecting optimal propeller designs
[NASA-TM-86967] 11 p1575 N85-19923
Sequential minimization for sum of squares of unknown functions
[DE85-004162] 11 p1707 N85-20738
Space nuclear-power reactor design based on combined neutronic and thermal-fluid analyses
[DE85-002433] 11 p1727 N85-20864
On maximizing the expected lifetime of replaceable systems
[AD-A150003] 12 p1862 N85-21660
Towards the generation of efficient code from verified programs
[TR-40] 12 p1914 N85-22017
Rates of convergence of semistochastic approximation procedures for solving stochastic optimization problems
12 p1924 N85-22066
A mathematical formulation of the problem of optimal use of ground resources for future space missions
12 p1947 N85-22232
Preliminary development of an approximation procedure for supercritical wing design optimization applications
[AD-A150177] 13 p1972 N85-22383
China report: Science and technology
[JPRS-CST-84-008] 13 p1972 N85-22384
Optimal design efforts in Shanghai described
13 p1972 N85-22386
Model reduction for control system design
[NASA-CR-170417] 13 p1975 N85-22398
Analysis and optimization of parameters of tanned surface acoustic wave transducers
13 p2070 N85-22934
Optimization of number of pulses in detection of fluctuating optical signals
13 p2081 N85-22903
Asymptotically optimum multialternative sequential procedures for discernment of processes minimizing average length of observations
13 p2084 N85-23012
Shape optimization for minimal stress concentration
13 p2101 N85-23093
Optimal allocation of components in parallel-series and series-parallel systems
[AD-A150166] 13 p2144 N85-23309
Relative control effectiveness technique with application to airplane control coordination
[NASA-TP-2416] 14 p2218 N85-23753
Software for designing teeth for reduction gears and transmissions
14 p2221 N85-23773
Manufacturing perspective in the design of bevel gearing
14 p2221 N85-23777
An optimization study to minimize surface distortions of a hoop-column antenna
14 p2232 N85-23837
Some optimization problems in static aeroelasticity for wings made of composite materials
14 p2277 N85-24104
Some problems in optimally designing shells of revolution
14 p2278 N85-24114
Ways of optimization of light energy transformation in primary stages of photosynthesis. Optimization of lattice structure of uniform photosynthetic unit
14 p2398 N85-24701
Optimal control and optimization
14 p2395 N85-24755
An expert system for choosing the best combination of options in a general-purpose program for automated design synthesis
[NASA-TM-86329] 14 p2402 N85-24807
Software and its relationship to methods
[DE85-004784] 14 p2405 N85-24829
Optimization of the catalytic oxidation of CO for closed-cycle CO2 laser applications
[NASA-TM-86421] 15 p2504 N85-25445
Mercedes-Benz auto 2000 achieves low drag coefficient
15 p2530 N85-25602
Receiver optimization for detection in doubly spread communication channels
[AD-A151226] 15 p2541 N85-25689

Design of shear deformable antisymmetric angle-ply laminates to maximize the fundamental frequency and frequency separation
[CSIR-TWISK-333] 15 p2577 N85-35882
Solving set covering problems using heuristics with branch and bound
[AD-A151905] 15 p2636 N85-26369
Design and implementation of the digital engineering laboratory distributed database management system
[AD-A151694] 15 p2685 N85-26450
Optimizing the specifications for an air-surface laser system 16 p2696 N85-26644
Alternatives for jet engine control
[NASA-CR-175831] 16 p2709 N85-26713
Alternatives for jet engine control
[NASA-CR-175833] 16 p2709 N85-26715
ESP (External-Stores Program): A pilot computer program for determining flutter-critical external-store configurations. Volume 1: User's manual
[AD-A152266] 16 p2710 N85-26725
Probabilistic computer model of optimal runway turnoffs
[NASA-CR-172549] 16 p2715 N85-26760
Optimum rotation of solid body with 1 axis of symmetry 16 p2718 N85-26781
Hybrid bearings for LH2 and LO2 turbopumps
16 p2736 N85-26880
Rotordynamics 16 p2737 N85-26886
Advanced energy storage systems
[AD-A152244] 16 p2741 N85-26915
Adaptation of continuous beams and the method of optimizing the flexibility of their elastic supports. Theorem on maximal adaptation loading, supplement
[REPT-10/1984-SUPPL] 16 p2797 N85-27241
Development and application of optimum sensitivity analysis of structures
[NASA-CR-175857] 16 p2799 N85-27257
Parallel computing in optimization
[AD-A151812] 16 p2850 N85-27568
H-sets, convex programming and constrained approximation
[TRITA-NA-8308] 16 p2853 N85-27587
The essence of invexity
[CSIR-TWISK-321] 16 p2858 N85-27626
Incorporating control into the optimal structural design of large flexible space structures
[AD-A152858] 17 p2900 N85-27937
Digital methods of the optimum processing of radar signals
[AD-A152469] 17 p2948 N85-28202
Optimally robust redundancy relations for failure in uncertain systems
[NASA-CR-175953] 17 p2976 N85-28391
The construction of curves and surfaces using numerical optimization techniques 17 p3003 N85-28585
Large scale electricity production scheduling via nonlinear optimization
[REPT-84-07] 17 p3017 N85-28655
The role of duality in optimization problems involving entropy functionals, with applications to information theory
[AD-A152336] 17 p3026 N85-28713
Optimum dimensions of power solenoids for magnetic suspension
[NASA-TM-77864] 17 p3026 N85-28716
The method of residual minimization in compressible steady flows
[AD-A153924] 18 p3100 N85-29193
Optimization of axially compressed carbon fiber reinforced plastic (CFRP) cylinders
18 p3121 N85-29318
Comparison of optimum interpolation and Cressman analyses 18 p3141 N85-29448
A global optimization algorithm using stochastic differential equations
[AD-A153526] 18 p3161 N85-29583
A quadratic programming algorithm
[AD-A153476] 18 p3166 N85-29631
Detection of multivariate outliers with dispersion slippage in elliptically symmetric distributions
[AD-A153785] 18 p3174 N85-29677
Adaptive signal detection and other topics in real time signal processing
[AD-A154139] 19 p3255 N85-30184
Receiver loss study of optimized solar central receiver systems as a function of receiver thermal loss per unit area
[DE85-010831] 19 p3268 N85-30265
High-efficiency, low-cost, passively-cooled PV concentrator module
[DE85-010013] 19 p3305 N85-30490
Identification of a mathematical model 1: Goodness of fit criterion
[HSE-TRANS-11109] 19 p3341 N85-30703
Optimization of single and multi-component analytical techniques
[HSE-TRANS-10987] 19 p3347 N85-30744
Evaluation of curve-smoothing techniques
[HSE-TRANS-11108] 19 p3349 N85-30759
TFCK shielding optimization
[DE85-010503] 19 p3359 N85-30826
Design of helicopter rotor blades for optimum dynamic characteristics
[NASA-CR-176076] 20 p3393 N85-31044
Interactive aircraft flight control and aeroelastic stabilization
[NASA-CR-176035] 20 p3396 N85-31064
An integrated control and minimum mass structural optimization algorithm for large space structures
20 p3413 N85-31183
Characteristic elastic systems of time-limited optimal maneuvers 20 p3413 N85-31184
A control concept for large flexible spacecraft using order reduction techniques 20 p3415 N85-31193
Wideband disturbance accomodation in precision flexible space structures 20 p3415 N85-31194
Sensor/actuator selection for the constrained variance control problem 20 p3415 N85-31197
Eigenvalue placement and stabilization by constrained optimization 20 p3416 N85-31198
Optimal sensor locations for structural identification
20 p3417 N85-31209
An Eigensystem Realization Algorithm (ERA) for modal parameter identification and model reduction
20 p3418 N85-31212
Drag soldering process control
[DE85-010853] 20 p3433 N85-31301
The design of Direct Injection (DI) diesel engines. Injection system by a numerical optimization technique
[REPT-84-RR-346] 20 p3462 N85-31508
Design of simulation experiments
[FEW-123] 20 p3519 N85-31885
Modeling and optimization of a test-cell upgrade for MFTF-B operating in the high neutron wall loading mode
[DE85-009997] 20 p3526 N85-31946
Globally-asynchronous locally-synchronous systems
[AD-A154624] 21 p3573 N85-32222
Application of adaptive noise cancellation to Coast Guard voice communications
[AD-A154798] 21 p3574 N85-32230
Testing and optimizing MST coaxial collinear arrays, part 6.4A 21 p3625 N85-32518
The Norwegian seismic array (NORSAR)
[AD-A154751] 21 p3631 N85-32555
New developments on the core function for efficient implementation of the difficult residue number system operations
[AD-A154678] 21 p3676 N85-32834
Optimal low thrust transfer using a first-order perturbation model
[AD-A154761] 21 p3676 N85-32835
Generalized planar matching
[AD-A154809] 21 p3677 N85-32842
Local epi-continuity and local optimization
[AD-A154812] 21 p3677 N85-32843
Optimization of sampling in statistical physics experiments 21 p3698 N85-32975
Necessary and sufficient conditions for single-extremum and convex problems of mathematical programming
21 p3698 N85-32977
Diakoptic calculation of characteristics for optimization of linear circuits with respect to parameters of individual branches 22 p3767 N85-33346
Optimization of radioelectronic circuits with software for modeling of integrated circuits on unified system computer 22 p3768 N85-33354
Determination of sensitivity functions for discrete dynamic systems from results of function modeling on digital computer 22 p3769 N85-33359
Synthesis of optimum receiver and processor for interfering radio pulse signals 22 p3769 N85-33361
Optimization of design parameters for alternating current stabilizer based on magnetic suspension
22 p3772 N85-33374
Gradiental adaptive corrector with optimum tuning step 22 p3776 N85-33403
Synthesis of system with nonideal components for optimal processing of radio signal
22 p3777 N85-33405
Estimating optimum technical and economic indicators of data transmission systems 22 p3777 N85-33406
Theory of cellwise optimization for solar central receiver system
[DE85-012586] 22 p3807 N85-33579
Blanket optimization studies for Cascade
[DE85-010002] 22 p3846 N85-33824
High pressure compressor component performance report
[NASA-CR-168245] 23 p3897 N85-34138
Re-designing a mechanism for higher speed: A case history from textile machinery 23 p3923 N85-34310
Optimization in the computer aided design of mechanisms 23 p3924 N85-34321
Mass resolution optimization in a large isotopic composition experiment
[OG-9.1-9] 23 p4023 N85-34935
An automated technique for encasing specific payloads with low-drag fairings 24 p4063 N85-35183
Energy management of three-dimensional minimum-time intercept
[NASA-CR-176174] 24 p4084 N85-35186
An evaluation of a class of practical optimization techniques for structural dynamics applications
[PB85-195786] 24 p4103 N85-35434
Optimizing data access in the LAMPF control system
[DE85-012653] 24 p4140 N85-35683
Two methods of global data assimilation
[AD-A155981] 24 p4143 N85-35684
Beryllium production
[DE85-013360] 24 p4148 N85-35716

OPTIMUM CONTROL
U OPTIMAL CONTROL

OPTOGALVANIC SPECTROSCOPY
An experimental and theoretical investigation of optogalvanic effects
[AD-A148456] 08 p1223 N85-17700

OR-GATES
U GATES (CIRCUITS)

ORBIT CALCULATION
NT MINIMUM VARIANCE ORBIT DETERMINATION
Satellite motion: Lectures and exercises on space mechanics
[ISBN-2-85428-114-4] 05 p0598 N85-13807
Orbit extrapolation — satellite orbits
05 p0598 N85-13811
Measurements in satellite orbit tracing
05 p0598 N85-13812
Spatial mechanics formulas and exercises
05 p0601 N85-13832
On the origin of Triton and Pluto
13 p2175 N85-23497
Location and synchronization — space-time coordinates 14 p2397 N85-24768
The work on Comet Halley's orbit at ESOC
14 p2438 N85-25041
Use of atmospheric models in predicting artificial Earth satellite motion 15 p2478 N85-25296
Using velocity vector in determining Keplerian orbit of geodectic satellite 15 p2478 N85-25297
Autonomous state determination for an Earth orbiting satellite using horizon and star sensors
[AD-A151827] 15 p2493 N85-25379
Flight Experiment Demonstration System (FEDS) functional description and interface document
[NASA-CR-175290] 16 p2717 N85-26769
Accuracy in predicting orbital motion of artificial Earth satellite 16 p2720 N85-26793
DORIS: Prediction in Doppler measurement — satellite onboard measurement
[CNES-CT/DTI/MS/AE/170] 16 p2729 N85-26843
Topex Gravity Model Development Team activities during fiscal year 1984
[NASA-TM-86208] 16 p2804 N85-27285
Satellite physical and orbital characteristics
16 p2804 N85-27287
Gravity model development software status
16 p2804 N85-27289
Radial orbit error spectrum for Topex
16 p2805 N85-27292
An algorithm for the influence numbers in the expansion of the lumped gravitational potential coefficients in the presence of resonant inclination variation
[AD-A154229] 19 p3336 N85-30669
Study of the interferences of 2 GHz radio beams with a DORIS system — precise low orbit determination system (DORIS)
[CNES-CT/DRT/TIT/RL-84/140-T]
20 p3442 N85-31362
Effect of solar eclipses on the LAGEOS semimajor axis 20 p3491 N85-31699
Geodyn systems development
20 p3492 N85-31708

ORBIT DECAY
Natural atmospheric reentry — satellite orbit decay
05 p0600 N85-13829
Orbital Debris
[NASA-CP-2360] 12 p1783 N85-21188
History of satellite break-ups in space
12 p1783 N85-21190
Manmade orbital debris studies at NASA Langley
12 p1783 N85-21192
NASA/JSC orbital debris study: Debris model
12 p1783 N85-21193
Proposed preliminary design criteria model environment for the 1990's 12 p1784 N85-21194

The long term behaviour of Earth orbits and the implications for debris control 12 p1786 N85-21213
Natural reentry of satellites 14 p2397 N85-24774
Examination of returned solar-max surfaces for impacting orbital debris and meteoroids 15 p2681 N85-26560
Update on the evolution of the LAGEOS orbit 20 p3491 N85-31698

ORBIT EQUATIONS
U ORBITAL MECHANICS

ORBIT MANEUVERING ENGINE (SPACE SHUTTLE)
Orbital Maneuvering system design evolution 08 p1096 N85-16943
Space station systems technology study (add-on task). Volume 1: Executive summary [NASA-CR-171415] 13 p1966 N85-22459
Selected tether applications in space: Phase 2. Executive summary [NASA-CR-171421] 13 p1967 N85-22462
Selected tether applications in space: Phase 2 [NASA-CR-171422] 13 p1967 N85-22463

ORBIT PERTURBATION
NT SATELLITE PERTURBATION
Deformations of two-dimensional dissipative maps — orbit perturbation [REPT-89] 01 p0129 N85-10891
Theory of the orbital motion of an artificial Earth satellite [NAL-TR-807] 06 p0758 N85-14847
SIMM1: A linearized particle code [AD-A146627] 08 p1221 N85-17669
A semianalytical, artificial satellite orbit propagation procedure based on optimal parameter estimation [INPE-3301-PRE/613] 10 p1427 N85-18997
Selection of a model of Earth's albedo radiation, practical calculation of its effect on the trajectory of a satellite [NASA-TM-77870] 15 p2591 N85-25072
The 6 pi-periodic solutions of plane restricted elliptical 3-body problem in neighborhood of libration points 16 p2716 N85-26779
Stability of periodic satellite motions relative to center of mass in circular orbit 16 p2716 N85-26780
Simulation of a low orbit restitution. Covariance analysis of the position-velocity by Doppler and accelerometer measurements [CNES-CT/DTI/MS/AE/166] 16 p2728 N85-26836
Analytical generation of satellite orbits at the RAE (Royal Aircraft Establishment) [AD-A152855] 17 p3053 N85-29001
Effect of solar eclipses on the LAGEOS semimajor axis 20 p3491 N85-31699
Effect of diffusely-reflected sunlight on the orbit of LAGEOS 20 p3491 N85-31700
Optical beat arc RMS test results 20 p3492 N85-31706

ORBIT SPECTRUM UTILIZATION
The international environment UNISPACE '82 and the ITU: A relationship between orbit-spectrum resource allocation and orbital debris 12 p1787 N85-21215
Transmission and orbital constraints in space-related programs: Briefing summary 12 p1787 N85-21216
Engineering calculations for communications satellite systems planning [NASA-CR-175552] 12 p1789 N85-21233

ORBIT TRANSFER VEHICLES
Possibilities and limits of electromagnetic acceleration in space applications [ILR-MITT-136] 02 p0193 N85-11282
Boundary layer simulator improvement [NASA-CR-174199] 05 p0597 N85-13802
Advanced concepts liquid droplet radiator 05 p0610 N85-13899
Impact of lunar and planetary missions on the space station [NASA-CR-171832] 08 p1106 N85-16968
OTV Propulsion Issues [NASA-CP-2347] 08 p1106 N85-16969
NASA OAST perspective 08 p1106 N85-16970
Space station task force perspective 08 p1106 N85-16982
Performance assessment of aero-assisted orbital transfer vehicles 08 p1106 N85-16983
Low lift-to-drag aero-assisted orbit transfer vehicles 08 p1107 N85-16984
Moderate lift-to-drag aeroassist 08 p1107 N85-16985
Benefits of high aerodynamic efficiency to orbital transfer vehicles 08 p1107 N85-16986
OTV propulsion tecnology programmatic overview 08 p1107 N85-16987
Drives and benefits overview 08 p1107 N85-16988
Aerojet advanced engine concept 08 p1107 N85-16989
Advanced OTV engines and issues 08 p1108 N85-17000
Advanced OTV engine concepts 08 p1108 N85-17001
Earth-to-orbit propellant transportation overview 08 p1108 N85-17002
Active cooling requirements for propellant storage 08 p1108 N85-17004
Propellant transfer: Attached depot 08 p1108 N85-17005
Propellant transfer: Tethered depot 08 p1108 N85-17006
OTV fluid mangement systems 08 p1108 N85-17007
Vehicle/engine integration — orbit transfer vehicles 08 p1109 N85-17008
Orbital transfer vehicle propulsion issues 08 p1109 N85-17009
Space based OTV servicing 08 p1109 N85-17010
Design and analysis report for the RL10-2B breadboard low thrust engine [NASA-CR-174857] 10 p1430 N85-19020
The servicing vehicle of Columbus [MBB-UR-E-750-84-O] 11 p1588 N85-19997
Orbital Debris [NASA-CP-2360] 12 p1783 N85-21188
Environment definition, small particles, diameter less than or equal to 1 MM 12 p1788 N85-21223
Design study of an integrated aerobraking orbital transfer vehicle [NASA-TM-58264] 12 p1795 N85-21262
Space station systems technology study (add-on task). Volume 1: Executive summary [NASA-CR-171415] 13 p1966 N85-22459
Selected tether applications in space: Phase 2. Executive summary [NASA-CR-171421] 13 p1967 N85-22462
Selected tether applications in space: Phase 2 [NASA-CR-171422] 13 p1967 N85-22463
Space Station technology planning 13 p1969 N85-22471
Space station systems technology study (add-on task). Volume 2: Trade study and technology selection [NASA-CR-171416] 15 p2475 N85-25279
Analysis of orbit transfer vehicles for GPS Block 3 satellites [AD-A152021] 16 p2732 N85-26980
Convoluted nozzle design for the RL10 derivative 2B engine [NASA-CR-174953] 19 p3220 N85-29965
Nonequilibrium air radiation (Nequair) program: User's manual [NASA-TM-86707] 19 p3353 N85-30780
A review of shock waves around aeroassisted orbital transfer vehicles [NASA-TM-86769] 22 p3739 N85-33177
A dual, fault-tolerant aerospace actuator 22 p3796 N85-33530
Design of a dual fault tolerant space shuttle payload deployment actuator 22 p3796 N85-33531
Status of advanced orbital transfer propulsion [NASA-TM-87069] 24 p4071 N85-35225

ORBITAL ASSEMBLY
Swing-arm beam erector (SABER) concept for single astronaut assembly of space structure [NASA-TP-2379] 10 p1429 N85-19015
Verification for large space structures 14 p2232 N85-23836
Assembly Concept for Construction of Erectible Space Structure (ACCESS) neutral buoyancy testing results 14 p2236 N85-23862
Construction in space [NASA-TM-77630] 15 p2492 N85-25374
Construction and functioning of extended orbital systems 16 p2724 N85-26814
NASA space station automation: AI-based technology review [NASA-CR-176094] 21 p3558 N85-32134
NASA space station automation: AI-based technology review. Executive summary [NASA-CR-176096] 21 p3558 N85-32135
A modular docking mechanism for in-orbit assembly and spacecraft servicing 22 p3796 N85-33516

ORBITAL ELEMENTS
Theory of the orbital motion of an artificial Earth Satellite [NAL-TR-807] 09 p1285 N85-18075
History of satellite break-ups in space 12 p1783 N85-21190
Some numerical estimates of perturbation of orbital elements of artificial Earth satellite with total dynamic symmetry about rotating aspherical Earth 15 p2478 N85-25294
Systematic and random deformations of orbits of long-period comets 15 p2479 N85-25299
Multistep orbital correction algorithms for an Earth satellite using low thrust engine 15 p2479 N85-25303
Orbital elements of Saturn's F ring and its shepherding satellites 15 p2675 N85-26815
Gravity model development software status 16 p2804 N85-27289
Optical best arc RMS test results 16 p2804 N85-27290
An algorithm for the influence numbers in the expansion of the lumped gravitational potential coefficients in the presence of resonant inclination variation [AD-A154229] 19 p3336 N85-30669
An introduction to satellite orbits [RAE-TM-SPACE-344] 20 p3397 N85-31076
Geodyn systems development 20 p3492 N85-31708
Insolation changes on Pluto caused by orbital element variations [AERONOMICA-ACTA-A-290-1984] 20 p3548 N85-32070

ORBITAL FLIGHT TEST 1 (SHUTTLE)
U SPACE TRANSPORTATION SYSTEM 1 FLIGHT

ORBITAL FLIGHT TEST 3 (SHUTTLE)
U SPACE TRANSPORTATION SYSTEM 3 FLIGHT

ORBITAL FLIGHT TEST 4 (SHUTTLE)
U SPACE TRANSPORTATION SYSTEM 4 FLIGHT

ORBITAL FLIGHT TESTS (SHUTTLE)
U SPACE TRANSPORTATION SYSTEM FLIGHTS

ORBITAL LAUNCHING
Analysis of orbit transfer vehicles for GPS Block 3 satellites [AD-A152021] 16 p2732 N85-26980

ORBITAL LIFETIME
Natural atmospheric reentry — satellite orbit decay 05 p0600 N85-13829
The long term behaviour of Earth orbits and the implications for debris control 12 p1786 N85-21213
Natural reentry of satellites 14 p2397 N85-24774

ORBITAL MANEUVERING VEHICLES
The servicing vehicle of Columbus [MBB-UR-E-750-84-O] 11 p1588 N85-19997
Evaluation of OMV ranging and docking systems 12 p1947 N85-22230
Space station systems technology study (add-on task). Volume 2: Trade study and technology selection [NASA-CR-171416] 15 p2475 N85-25279
Automatic rendezvous and docking systems functional and performance requirements [NASA-CR-171866] 15 p2492 N85-25376
Docking simulation analysis of range data requirements for the orbital manauvering vehicle [NASA-TM-86510] 20 p3407 N85-31143
NASA space station automation: AI-based technology review [NASA-CR-176094] 21 p3558 N85-32134
NASA space station automation: AI-based technology review. Executive summary [NASA-CR-176096] 21 p3558 N85-32135
Space station automation and robotics study. Operator-systems interface [NASA-CR-176095] 22 p3738 N85-33172
Hardware test program for evaluation of baseline range-range rate sensor concept [NASA-CR-176143] 23 p3933 N85-34377
Status of advanced orbital transfer propulsion [NASA-TM-87069] 24 p4071 N85-35225

ORBITAL MANEUVERS
USSR report: Space [JPRS-USP-84-005] 02 p0158 N85-11060
Features and uses of progress cargo ships 02 p0157 N85-11061
Orbital maneuvers with finite thrust. Volume 1: Mathematical formulation, numerical methods, catalog concept [ESA-CR(P)-1910-VOL-1] 06 p0758 N85-14848
Orbit maneuvers with finite thrust. Volume 2: Reference manual, part 1 [ESA-CR(P)-1910-VOL-2-PT-1] 06 p0758 N85-14849
Orbit maneuvers with finite thrust. Volume 3: User's guide, part 2 [ESA-CR(P)-1910-VOL-3-PT-2] 06 p0758 N85-14850
Orbit maneuvers with finite thrust. Volume 3: Reference catalog, parts 1 and 2 [ESA-CR(P)-1910-VOL-3-PT-1/2] 06 p0758 N85-14851
Orbit maneuvers with finite thrust. Volume 3: Reference catalog, part 3 [ESA-CR(P)-1910-VOL-3-PT-3] 06 p0758 N85-14852
Shuttle-tethered satellite system definition study extension [NASA-CR-171473] 17 p2907 N85-27923
Docking simulation analysis of range data requirements for the orbital maneuvering vehicle [NASA-TM-86510] 20 p3407 N85-31143

ORBITAL MECHANICS
NT KEPLER LAWS
NT MINIMUM VARIANCE ORBIT DETERMINATION
Deformations of two-dimensional dissipative maps — orbit perturbation
[REPT-69] 01 p0129 N85-10891
USSR report: Space
[JPRS-USP-84-005] 02 p0156 N85-11080
Tass reports launch of Soyuz T-12
02 p0158 N85-11070
Some considerations on elliptic hallocentric orbits
[INPE-3217-PRE/570] 02 p0297 N85-11828
A testable gravitational capture model for the origin of the Earth's Moon 04 p0598 N85-13742
Satellite motion: Lectures and exercises on space mechanics
[ISBN-2-85428-114-4] 05 p0598 N85-13807
Orbit perturbation — satellites
05 p0598 N85-13810
Orbit extrapolation — satellite orbits
05 p0598 N85-13811
The CDC: Facilities on offer from the CNES computing center for space mathematics (a look at the capacities of CDC computers) 05 p0599 N85-13818
JPL highlights
[NASA-CR-175517] 11 p1767 N85-21102
Orbital Debris
[NASA-CP-2360] 12 p1783 N85-21188
History of satellite break-ups in space
12 p1783 N85-21190
NORAD's PARCS small satellite tests (1976 and 1978) 12 p1783 N85-21191
NASA/JSC orbital debris study: Debris model
12 p1783 N85-21193
The long term behaviour of Earth orbits and the implications for debris control 12 p1786 N85-21213
Debris in the geostationary orbit ring, the endless shooting gallery: The necessity for a disposal policy
12 p1786 N85-21214
Algorithm for determining optimal three impulse point-to-orbit transfer with limited transfer time
13 p1979 N85-22419
Satellite oscillations in elliptical orbit
13 p1981 N85-22429
Satellite-to-satellite orbit determination using minimum, discrete range and range-rate data only
13 p1985 N85-22458
Halley's Comet, a bibliography
[LC-84-600109] 13 p2204 N85-23674
Motion of satellite with total dynamic symmetry around rotating aspherical Earth 14 p2287 N85-24174
Orbit perturbation. Extrapolation of perturbed orbits
14 p2396 N85-24763
Modeling needed for the design and definition of spacecraft attitude and orbit control systems
14 p2397 N85-24766
Attitude measurements and determination
14 p2397 N85-24767
Mission analysis and orbit control of the helioynchronous satellite SPOT
14 p2397 N85-24773
Some numerical estimates of perturbation of orbital elements of artificial Earth satellite with total dynamic symmetry about rotating aspherical Earth
15 p2478 N85-25294
Using velocity vector in determining Keplerian orbit of geodectic satellite 15 p2478 N85-25297
Resonance identifications in Saturn's rings
15 p2674 N85-26504
Dense but collisionless orbiting rings — Saturn rings
15 p2675 N85-26517
The asteroid ring 15 p2678 N85-26536
Integrable cases of restricted doubly averaged 3-body problem 16 p2718 N85-26778
Optimal relative data weights
16 p2905 N85-27296
Numerical integration through force discontinuities: Solar radiation pressure 16 p2905 N85-27298
Shuttle-tethered satellite system definition study extension
[NASA-CR-171473] 17 p2907 N85-27923
Maximizing the semi-major axis for a freely coning solar sailcraft
[AD-A153175] 17 p2909 N85-27938
How a swing behaves
[DE85-008280] 17 p3027 N85-28720
An introduction to satellite orbits
[RAE-TM-SPACE-344] 20 p3397 N85-31076
Effect of diffusely-reflected sunlight on the orbit of LAGEOS 20 p3491 N85-31700
Structural dynamics model and response of the deployable reference configuration space station
[NASA-TM-86386] 22 p3799 N85-33539
Target observability for satellite-based sensors
[AD-A156139] 24 p4069 N85-35217

ORBITAL MOTION
U ORBITS
ORBITAL POSITION ESTIMATION
Planning of navigation measurements using TD criterion for determination of movement of spacecraft by method of least squares 02 p0159 N85-11081
Satellite orbit determination 05 p0598 N85-13813
The performance of differential VLBI delay during interplanetary cruise 05 p0623 N85-13984
Shuttle navigation status 08 p1092 N85-16901
A semianalytical, artificial satellite orbit propagation procedure based on optimal parameter estimation
[INPE-3301-PRE/613] 10 p1427 N85-18997
Air Force satellite position management
12 p1787 N85-21217
Use of atmospheric models in predicting artificial Earth satellite motion 15 p2478 N85-25296
Minimax problem of estimating trajectory parameters in continuous formulation 15 p2479 N85-25301
Inference and state estimation for stochastic point processes
[AD-A151216] 15 p2640 N85-26281
Accuracy in predicting orbital motion of artificial Earth satellite 16 p2720 N85-26793
Simulation of a low orbit restitution. Covariance analysis of the position-velocity by Doppler and accelerometer measurements
[CNES-CT/DTI/MS/AE/166] 16 p2728 N85-26836
Optical best arc RMS test results
16 p2804 N85-27290
Self-tuning adaptive-controller using online frequency identification 20 p3417 N85-31205
Combined state and parameter estimation for a static model of the Maypole (Hoop-Column) antenna suface
20 p3417 N85-31210

ORBITAL RENDEZVOUS
Optimal multiple-impulse nonlinear orbital rendezvous
08 p1105 N85-16984
Docking simulation analysis of range data requirements for the orbital maneuvering vehicle
[NASA-TM-86510] 20 p3407 N85-31143

ORBITAL SERVICING
Tass reports launch of Soyuz T-12
02 p0158 N85-11070
Magnetic spin reduction system for free spinning objects
[NASA-CASE-MFS-25966-1] 02 p0166 N85-11122
Definition of technology development missions for early Space Station satellite servicing. Volume 1: Executive summary
[NASA-CR-171228] 04 p0460 N85-12922
Definition of technology development missions for early Space Station satellite servicing. Volume 2: Technical
[NASA-CR-171229] 04 p0461 N85-12923
OTV propulsion tecnology programmatic overview
08 p1107 N85-16997
Space based OTV servicing 08 p1109 N85-17010
The servicing vehicle of Columbus
[MBB-UR-E-750-84-O] 11 p1586 N85-19997
Applications of Tethers in Space, volume 1
[NASA-CP-2364] 11 p1642 N85-20339
Orbital Debris
[NASA-CP-2360] 12 p1783 N85-21188
Satellite services and orbital retrieval
12 p1786 N85-21211
Utilization of space station by the large deployment reflector 14 p2235 N85-23857
Analysis of remote operating systems for space-based servicing operations, volume 1
[NASA-CR-171885] 19 p3225 N85-29993
Analysis of remote operating systems for space-based servicing operations. Volume 2: Study results
[NASA-CR-171886] 19 p3225 N85-29994
Space station automation study-satellite servicing. Volume 1: Executive summary
[NASA-CR-171512] 19 p3226 N85-29999
Space station automation study-satellite servicing, volume 2
[NASA-CR-171513] 19 p3226 N85-30000
A modular docking mechanism for in-orbit assembly and spacecraft servicing 22 p3798 N85-33516

ORBITAL SIMULATORS
U SPACE SIMULATORS
ORBITAL SPACE STATIONS
NT EOSS
NT LONG DURATION EXPOSURE FACILITY
NT ORBITING LUNAR STATIONS
NT SALYUT SPACE STATION
NT SKYLAB 3
NT SKYLAB 4
Definition of technology development missions for early space stations: Large space structures
[NASA-CR-171209] 03 p0323 N85-12084
Definition of technology development missions for early Space Station satellite servicing. Volume 1: Executive summary
[NASA-CR-171228] 04 p0460 N85-12922
Advanced and nontraditional concepts working group report 05 p0612 N85-13909
Space station: New frontier for life sciences in space
05 p0696 N85-14477
Engineering model system study for a regenerative fuel cell: Study report
[NASA-CR-174601] 07 p0991 N85-18292
Drives and benefits overview
08 p1107 N85-16996
Manned space station solar array study
[ESA-CR(P)-1941] 09 p1267 N85-18081
Preliminary concepts of candidate elements for a potential European participation in a manned space station
[MBB-UR-E-749-84-O] 11 p1587 N85-19996
The servicing vehicle of Columbus
[MBB-UR-E-750-84-O] 11 p1588 N85-19997
Earth observations and the polar platform
[NOAA-TR-NESDIS-18] 11 p1669 N85-20517
Space Station Software Issues
[NASA-CP-2361] 11 p1700 N85-20689
Software management issues — space station software development 11 p1700 N85-20690
Software development environment issues — space station software development 11 p1700 N85-20691
Software standards issues — space station software development 11 p1701 N85-20692
Information systems issues 11 p1701 N85-20693
Parametric analysis: SOC meteoroid and debris protection 12 p1786 N85-21209
Natural environment design criteria for the Space Station definition and preliminary design
[NASA-TM-86498] 12 p1789 N85-21232
Computer integration of engineering design and production: A national opportunity
[NASA-CR-175483] 12 p1820 N85-21414
Debris impact on Earth-orbiting spacecraft
12 p1948 N85-22234
The intelligent database machine
12 p1949 N85-22242
Concentrator technologies evaluation for large solar arrays and their application for space stations/platforms
13 p2010 N85-22609
Space Station solar array 13 p2010 N85-22610
Analysis of space station operations in the space debris environment
[AD-A151872] 15 p2493 N85-25380
Manrating orbital transfer vehicle propulsion
[NASA-TM-87019] 15 p2494 N85-25385
Space methods in oceanology
[NASA-TM-77652] 15 p2604 N85-26047
European utilization aspects of a US manned space station, volume 1
[ESA-CR(P)-1967-VOL-1] 17 p2907 N85-27926
European utilization aspects of a US manned space station, volume 2
[ESA-CR(P)-1967-VOL-2] 17 p2907 N85-27927
Space station study
[BL-6167] 18 p3066 N85-28959
Some Europeans voice opposition to space station participation 18 p3066 N85-28961
New ESA director on space station, military space
18 p3066 N85-28962
ESA presents plans for European manned space station 18 p3085 N85-29087
Space station automation study-satellite servicing. Volume 1: Executive summary
[NASA-CR-171512] 19 p3226 N85-29999
Space station automation study-satellite servicing, volume 2
[NASA-CR-171513] 19 p3226 N85-30000
Space ventures and society long-term perspectives
[NASA-CR-176012] 19 p3379 N85-30963
Multivariable control of a soft coupled space station
20 p3408 N85-31151
Studies toward a manned space station: Participation of European industry in NASA space station (MSS)
[SNIAS-S/DT-Y-25-212] 20 p3418 N85-31217
Comparative study on data system architectures — spacecraft data processing
[ESA-CR(P)-2015] 21 p3575 N85-32828
Applicability of 100kWe-class of space reactor power systems to NASA manned space station missions
[NASA-CR-174696] 24 p4149 N85-35728

ORBITAL TEST SATELLITE (ESA)
U OTS (ESA)
ORBITAL TRANSFER
U TRANSFER ORBITS
ORBITAL VELOCITY
Using velocity vector in determining Keplerian orbit of geodectic satellite 15 p2478 N85-25297

Simulation of a low orbit restitution. Covariance analysis of the position-velocity by Doppler and accelerometer measurements
[CNES-CT/DTI/MS/AE/166] 16 p2728 N85-26836
ORBITALS
NT ELECTRON ORBITALS
NT MOLECULAR ORBITALS
Vacancy-rearrangement theory in the first Magnus approximation
[DE85-004435] 12 p1930 N85-22123
ORBITING GEOPHYSICAL OBSERVATORY
U OGO
ORBITING LUNAR STATIONS
Concept and cost analysis of an orbiting lunar station
[ILR-MITT-138] 07 p0913 N85-15776
ORBITING SATELLITES
U ARTIFICIAL SATELLITES
ORBITS
NT CIRCULAR ORBITS
NT EARTH ORBITS
NT ECCENTRIC ORBITS
NT ELLIPTICAL ORBITS
NT GEOSYNCHRONOUS ORBITS
NT INTERPLANETARY TRANSFER ORBITS
NT LUNAR ORBITS
NT PARKING ORBITS
NT PERIGEES
NT PERIHELIONS
NT PLANETARY ORBITS
NT POLAR ORBITS
NT SATELLITE ORBITS
NT SOLAR ORBITS
NT SPACECRAFT ORBITS
NT STATIONARY ORBITS
NT TRANSFER ORBITS
Birkhoff orbits for non-monotone twist maps
[AD-A144718] 01 p0110 N85-10747
Shape of power spectrum of intermittent chaos
02 p0283 N85-11841
Physical properties of Neptune and Triton inferred from the Orbit of Triton 02 p0300 N85-11942
Origin and evolution of the Uranian and Neptunian satellites: Some dynamical considerations
02 p0300 N85-11943
The asteroidal source region of ordinary chondrites
06 p0981 N85-16800
An optimization method for the preliminary design of interplanetary aerobraking missions
06 p1076 N85-16822
Improvement in magnetic field properties of vanadium-gallium superconductors by enhancement of spin-orbit scattering
[DE85-002893] 13 p2164 N85-23422
The orbits of Comets Halley and Giacobini-Zinner
14 p2437 N85-25039
The orbital motion of Comet Halley
14 p2437 N85-25040
Systematic and random deformations of orbits of long-period comets 15 p2479 N85-25299
Indications of twist in the Epsilon rings of Uranus
15 p2672 N85-26490
Construction and functioning of extended orbital systems 16 p2724 N85-26814
Multiple time-scale methods in particle simulations of plasmas
[DE85-007519] 17 p3040 N85-28806
Tenth-order expansion formulae for the orbital eccentricity function K (sub lpq)(e) obtained using a symbolic algebraic manipulation system
[AD-A153754] 18 p3170 N85-29647
An algorithm for the influence numbers in the expansion of the lumped gravitational potential coefficients in the presence of resonant inclination variation
[AD-A154229] 19 p3336 N85-30669
Guide to the Main Ring DO overpass
[DE85-011722] 20 p3531 N85-31983
Estimating the change in asymptotic direction due to secular changes in the geomagnetic field
[SH-6.1-13] 23 p4045 N85-35086
ORDER-DISORDER TRANSFORMATIONS
Static and dynamic disordering in amorphous magnets and crystals 03 p0422 N85-12699
Diffuse elastic and inelastic neutron scattering of disorder transitions and boundaries. Phase determination of structure factors 03 p0424 N85-12706
The disordering process in an L1sub2 ordered alloy
[DE84-016599] 04 p0475 N85-13029
Development and characterization of ductile Long-Range-Ordered (LRO) alloys (Fe,Co, Ni)3V for high-temperature structural use
[DE84-016750] 06 p0769 N85-14821
Phase diagram of polymer blends containing block copolymers
[AD-A147706] 06 p1132 N85-17134
Phase formation and stability in the pseudobinary Ni3Al-Ni3V alloy system
[DE85-001117] 09 p1296 N85-18143
First principles theory of Fermi-surface driven concentration waves in Cu/sub c/Pd/sub 1-c/ alloys
[DE85-005367] 13 p2024 N85-22681
On the feasibility of Ab Initio calculations of ordering alloy phase diagrams
[DE85-007073] 16 p2751 N85-26979
The disordering process in an L12 ordered alloy
[DE85-006152] 17 p2931 N85-28093
Local density theory of heats of formation and short-range order parameters in substitutionally disordered alloys
[DE85-009611] 18 p3075 N85-29021
Electronic structure and lattice dynamics of dimensionally constrained and disordered solids
[AD-A155927] 24 p4161 N85-35797
ORDNANCE
Evolution of the NWC (Naval Weapons Center) thermal standard. Part 5: Thermal standard development and applications
[AD-A146173] 03 p0364 N85-12334
Safing and arming mechanism
[AD-D011261] 05 p0621 N85-13969
Assessment of environmental costs at ordnance activities
[AD-P004140] 09 p1347 N85-18476
The remote detection of polynuclear aromatic hydrocarbons using laser-induced fluorescence
[AD-A152294] 16 p2757 N85-27013
Voltammetric analysis of ordnance materials. Part 2: A portable digital voltammeter for use with a silver wire working electrode
[AD-A152480] 17 p2967 N85-28325
SAFEORD: Safety of explosive ordnance databank
[AD-A154058] 19 p3380 N85-30972
Development of improved dynamic failure models
[AD-A155586] 21 p3600 N85-32354
OREGON
Image variance and spatial structure in remotely sensed scenes — South Dakota, California, Missouri, Kentucky, Louisiana, Tennessee, District of Columbia, and Oregon
07 p0966 N85-16265
Mesoscale studies of flow regimes and fluxes of particulate matter in coastal waters
[DE85-003825] 11 p1689 N85-20620
ORES
U MINERALS
ORGANIC CHARGE TRANSFER SALTS
Synthesis of film-forming electron-accepting polymers
[AD-A146430] 06 p0771 N85-14931
ORGANIC CHEMISTRY
Biocatalyzed processes for production of commodity chemicals: Assessment of future research advances for N-butanol production
[NASA-CR-174264] 07 p0919 N85-15819
A study of organic chemical reactions in microemulsions
[AD-A150083] 12 p1796 N85-21265
Abstracts of the 36th Southeastern Regional Meeting of the American Chemical Society
[AD-A151506] 15 p2496 N85-25394
Systematic nomenclature of the nitrogen, oxygen and sulfur functional polycyclic aromatic hydrocarbons
[DE85-007426] 17 p2916 N85-27974
Academician Ovchinnikov on future of bioorganic chemistry 17 p3049 N85-28874
Biocatalysis project
[NASA-CR-176044] 20 p3498 N85-31744
Studies in photochemical smog chemistry. 1: Atmospheric chemistry of toulene. 2: Analysis of chemical reaction mechanisms for photochemical smog
24 p4113 N85-35497
ORGANIC COMPOUNDS
NT ADENOSINE DIPHOSPHATE
NT ADENOSINE TRIPHOSPHATE
NT ADENOSINES
NT ALANINE
NT AMINO ACIDS
NT ASPARTATES
NT ASPARTIC ACID
NT CARBON TETRAFLUORIDE
NT CHOLINE
NT CYCLIC COMPOUNDS
NT FATS
NT FATTY ACIDS
NT FLUORINE ORGANIC COMPOUNDS
NT FLUOROCARBONS
NT FLUOROHYDROCARBONS
NT GLUTAMINE
NT GLUTATHIONE
NT GLYCINE
NT METHIONINE
NT ORGANIC CHARGE TRANSFER SALTS
NT ORGANIC LIQUIDS
NT ORGANIC SULFUR COMPOUNDS
NT OXIDASE
NT PEPTIDES
NT PERFLUOROALKANE
NT PHOSPHAZENE
NT POLYNUCLEAR ORGANIC COMPOUNDS
NT POLYPEPTIDES
NT PROPARGYL GROUPS
NT QUINOLINE
NT TETRAHYDROFURAN
NT TRYPTOPHAN
A simple electronic apparatus for determining the oxidation stability of lubricants and other organic compounds
[AD-A146080] 03 p0338 N85-12172
Organic aerosol formation: OH(hydroxyl radical) versus ozone oxidation pathways
[PB84-219660] 03 p0389 N85-12484
Time-resolved spectroscopy of evanescent-wave excited fluorescence
[DE84-015213] 04 p0473 N85-13013
VOC emissions from volatile organic liquid storage tanks: Background information for proposed standards
[PB84-237320] 04 p0532 N85-13403
Determination of halogens and sulfur in organic compounds and polymers by combustion-ion chromatography
[DE84-016186] 05 p0614 N85-13921
Gas chromatographic determination of content of harmful substances in air of industrial locations
06 p0761 N85-14866
Study of effectiveness of fire-resistant activity of antipyrenes for fibers of aromatic polyamides
06 p0762 N85-14874
Electrochemical behaviour of TiCl4 solutions in low melting point organic media
[BLL-OA-TRANS-5174-(6196.3)]
06 p0764 N85-14888
Pathology and axonal transport in hexacarbon neuropathies
[AD-P004021] 06 p0843 N85-15355
Solar wind and cosmic ray irradiation of grains and ices - application to erosion and synthesis of organic compounds in the solar system
06 p0888 N85-15837
Continuous organic electrochemical synthesis
[DE85-001400] 10 p1437 N85-19057
A study of organic chemical reactions in microemulsions
[AD-A150083] 12 p1796 N85-21265
Gas-liquid chemistry of natural waters, volume 1
[DE85-002603] 12 p1884 N85-21822
Standard analytical procedures of the NOAA National Analytical Facility, 1984-85: Extractable toxic organic compounds
[PB85-126282] 12 p1887 N85-21840
The body burden of organic vapors in artificial air trial measurements aboard a moored submarine
[AD-A149888] 12 p1910 N85-21988
One mechanism of formation of organic fraction in atmospheric aerosol 13 p2014 N85-22632
Analysis of biological particles by mass spectrometry
[AD-A149052] 13 p2141 N85-23291
Literature review for development of the master analytical scheme for organic compounds in water
[PB85-152674] 15 p2507 N85-25468
Thermally modulated electron affinity detector for priority pollutant analysis
[PB85-158145] 15 p2508 N85-25469
Procedure for certifying quantity of volatile organic compounds emitted by paint, ink and other coatings
[PB85-159044] 15 p2520 N85-25637
Philips tested new materials for optical data storage
15 p2532 N85-25620
Electronic properties of new organic conductors
[DE85-005590] 15 p2549 N85-25736
Carbon isotopes in bulk carbonaceous chondrites
15 p2661 N85-26557
Analytical methods for determination of POHC (Principal Organic Hazardous Constituents) in combustion products
[PB85-161576] 16 p2747 N85-26955
Role of natural dissolved organic compounds in determining the concentrations of americium in natural waters
[DE85-010266] 19 p3229 N85-30022
Technical and administrative activities of the Analytical Chemistry Laboratory (ACL)
[DE85-010150] 19 p3236 N85-30083
Thermodynamic study of CO2-organic compound interaction at high pressures and temperatures
[DE85-010699] 19 p3268 N85-30298
Sea water photoluminescence
19 p3292 N85-30415

Speciation of hazardous inorganic compounds by Fourier transform infrared (FTIR) spectroscopy
[PB85-189969] 20 p3426 N85-31262
Aerosol analysis and emission spectrometry with free jets
[DE85-010576] 21 p3584 N85-32168
Distribution and abundance of organic thiols
21 p3657 N85-32717
Development of a chemical kinetic mechanism for the US EPA (Environmental Protection Agency) regional oxidant model
[PB85-185958] 22 p3813 N85-33618
Anaerobic microbial transformations in subsurface environments
[DE85-012790] 22 p3819 N85-33659
Atmospheric modeling of organics for risk assessment: A Chemist's view
[DE85-009770] 23 p3909 N85-34217
Aspects of high-resolution gas chromatography as applied to the analysis of hydrocarbon fuels and other complex organic mixtures. Volume 1
[AD-A156154] 24 p4076 N85-35257

ORGANIC FLUORINE COMPOUNDS
U FLUORINE ORGANIC COMPOUNDS

ORGANIC LASERS
NT DYE LASERS
Characteristics of unstable resonators in flashlamp-pumped organic-compound lasers
11 p1717 N85-20800

ORGANIC LIQUIDS
Turbulent shear fields for dispersion of aqueous drops in organic liquids and application to gel-sphere processes
[DE84-016562] 06 p0909 N85-15141

ORGANIC LITHIUM COMPOUNDS
(Vinyloxy)chlorocyclotriphosphazenes
[AD-D011471] 10 p1453 N85-19152

ORGANIC MATERIALS
NT PEAT
Production and turnover of suspended organic detritus in the coastal water of the southeastern continental shelf
[DE85-003977] 13 p2140 N85-23290
West Europe report: Science and technology
[JPRS-WST-85-013] 14 p2289 N85-24183
Corrosion control through a better understanding of the metallic substrate-organic coating-interface
[AD-A151236] 15 p2509 N85-25479
Comparison of TT-F-1098 solvent-thinned block fillers with water-thinnable block fillers
[AD-A154207] 19 p3249 N85-30142
Changes in the organic material in lakes in the blast zone of Mount St. Helens, Washington: Hydrologic effects of the eruptions
[GS-CIRC-850-1] 21 p3630 N85-32551
Rechargeable lithium-organic electrolyte battery having overcharge protection and method of providing overcharge protection for a lithium-organic electrolyte battery
[AD-D011736] 22 p3806 N85-33575

ORGANIC NITRATES
NT CELLULOSE NITRATE
NT PETN

ORGANIC PEROXIDES
Chemical transformation in acid rain. Volume 1: New methodologies for sampling and analysis of gas-phase peroxide
[PB85-173425] 19 p3311 N85-30527

ORGANIC PHOSPHORUS COMPOUNDS
NT PHOSPHAZENE
Macrocyclic poly(tertiary) phosphines for the attachment of metals to surfaces of photodevices
[DE84-015552] 05 p0617 N85-13946
Proceedings of the 14th Conference on Environmental Toxicology
[AD-A146400] 06 p0843 N85-15350
Organophosphorus-induced delayed neurotoxicity: Syndrome and experimental models
[AD-P004022] 06 p0844 N85-15356
Chemistry and metabolism of delayed neurotoxic organophosphorus esters
[AD-P004023] 06 p0844 N85-15357
Pathology of organophosphorus-induced delayed neurotoxicity
[AD-P004024] 06 p0844 N85-15358
Electrophysiologic changes in organophosphorus-induced delayed neurotoxicity
[AD-P004025] 06 p0844 N85-15359
Biochemistry and pathogenic hypotheses of organophosphorus-induced delayed neurotoxicity
[AD-P004026] 06 p0844 N85-15360
Critical overview of hexacarbons and organophosphates
[AD-P004027] 06 p0844 N85-15361
Isolation, concentration and subsequent analysis by capillary gas chromatography of trace amounts of organophosphorus compounds from aqueous samples
[AD-B069301L] 12 p1803 N85-21308
USSR report: Chemistry
[JPRS-UCH-85-001] 13 p2013 N85-22629
Measurement of Franck-Condon factors for the v'=0 progression in the B-X system of PO
[AD-A152734] 17 p2919 N85-27993
TRU decontamination of high-level PUREX waste by solvent extraction using a mixed octyl(phenyl)-N,N-diisobutyl-carbamoyl methylphosphine oxide/TBP/NPH (TRUEX) solvent
[DE85-010251] 19 p3235 N85-30054

ORGANIC SEMICONDUCTORS
Study of application of organic semiconductors to electronic components
[BMFT-FB-T-84-142] 02 p0269 N85-11890
Optimizing conductive polymer compounds
[BMFT-FB-T-84-145] 03 p0336 N85-12177
Research on submicrometer structures
[AD-A146578] 06 p0867 N85-15508
Studies on organic semiconductors. 16: Effects of the substituents on the photoconductivities of substituted anthracenes
[NASA-TM-77768] 08 p1225 N85-17712
Transport studies of several novel organic conductors
[DE85-003950] 14 p2429 N85-24979
Structure and functions of ultra-thin films of organic compounds
[DRIC-T-7481] 22 p3741 N85-33188

ORGANIC SILICON COMPOUNDS
Structural and synthetic organosilicon chemistry
[AD-A147101] 07 p0919 N85-15820
Preparation of silicon carbide-silicon nitride fibers by the pyrolysis of polycarbosilazane precursors
[NASA-TM-86505] 17 p2933 N85-28107

ORGANIC SULFUR COMPOUNDS
Heats of formation of gas phase organosulfur molecules, radicals and ions measured by PEPICO and application of (17)O and (33)S NMR spectroscopy to structure determination of organosulfur compounds
[DE85-010558] 24 p4071 N85-35229

ORGANISMS
Recent studies of the ocean nitrogen cycle
05 p0653 N85-14193
Aluminum in biogenic cycle and forms of its occurance in ocean
10 p1499 N85-19463

ORGANIZATIONS
NT EUROPEAN SPACE AGENCY
NT ISRO
NT NORTH ATLANTIC TREATY ORGANIZATION (NATO)
NT WORLD METEOROLOGICAL ORGANIZATION
National Science Foundation, fiscal year 1983, volume 1
[PB84-212315] 01 p0124 N85-10853
EPA (Environmental Protection Agency) environmental data base and model directory, volume 1
[PB84-207562] 01 p0126 N85-10868
A mathematical theory of command and control structures
[AD-A145606] 02 p0256 N85-11675
Matrix organizations: Overcoming the disadvantages
[AD-A145316] 03 p0436 N85-12772
International coordination in scientific research
04 p0519 N85-13311
Sunset of the Civil Aeronautics Board
[S-HRG-98-940] 09 p1403 N85-16829
Strategic management for organizational effectiveness. The effect of human resource planning on retention and related issues, volume 1
[AD-A148396] 10 p1566 N85-19674
Strategic management for organizational effectiveness. The effect of human resource planning on retention and related issues, volume 2
[AD-A148399] 10 p1566 N85-19675
Strategic management for organizational effectiveness. The effect of human resource planning on retention and related issues, volume 3
[AD-A148400] 10 p1566 N85-19676
Strategic management for organizational effectiveness. The effect of human resource planning on retention and related issues: Methodological appendix
[AD-A148401] 10 p1566 N85-19677
A proposed integration among organizational information requirements, media richness and structural design
[AD-A149317] 10 p1567 N85-19681
Calendar of selected aeronautical and space meetings
[AGARD-CAL-84/2] 10 p1573 N85-19917
MAP-related activities in the United States
11 p1655 N85-20427
Model research: The National Advisory Committee for Aeronautics, 1915-1958, volume 1
[NASA-SP-4103-VOL-1] 14 p2207 N85-23683
Model research, the National Advisory Committee for Aeronautics, 1915-1958, volume 2
[NASA-SP-4103-VOL-2] 14 p2207 N85-23684
Measurement capabilities of the Bendix Metrology Organization
[DE85-005795] 16 p2760 N85-27029
SELPER (Latin American Society of Remote Sensory Specialists)
[INPE-3315-PRE/622] 16 p2810 N85-27328
National Telecommunications and Information Administration authorization
[GPO-38-660] 16 p2879 N85-27766
An examination of alternative forms of fit in contingency theory
[AD-A152602] 17 p3047 N85-28853
The concept of fit in contingency theory
[AD-A152603] 17 p3047 N85-28854
Worldwide directory of national Earth-science agencies and related international organizations
[GS-CIRC-934] 21 p3605 N85-32386
The flow of scientific and technical information in the US Army Research Laboratories
[AD-A155050] 21 p3713 N85-33043

ORGANIZING
Quality organization — quality control
[CNES-NT-108] 04 p0511 N85-13257
A self-organizing database system: A different approach to query optimization
05 p0735 N85-14725
Model of team organization and behavior and team description method
[AD-A147540] 07 p1053 N85-16680
Automation of information services furnished by documentation centers and specialized libraries
[FUB-6-1984] 09 p1402 N85-16827
Navy information systems: Planning, policy, organization, and management
[PB85-176113] 20 p3541 N85-32036

ORGANOMETALLIC COMPOUNDS
NT CHLOROPHYLLS
NT HEMOGLOBIN
NT ORGANIC LITHIUM COMPOUNDS
NT OXYHEMOGLOBIN
USSR report: Chemistry
[JPRS-UCH-84-012] 06 p0761 N85-14865
Metallo-Organic Decomposition (MOD) silver metallization for photovoltaics
06 p0830 N85-15278
Mod silver metallization for photovoltaics
[NASA-CR-174444] 10 p1509 N85-19518
Preparation and study of highly reactive metal powders
[AD-A150026] 12 p1808 N85-21331
Synthesis, static and reactive characterization of supported organometallics
[DE85-004285] 12 p1808 N85-21340
Synthesis of phenols from metal-carbynes and diynes
[AD-A151913] 16 p2754 N85-26997
The spectroscopy and reaction kinetics of coordinated unsaturated metal carbonyls
[AD-A153079] 17 p2920 N85-28003
Metallophthalocyanine dimers incorporating five atom covalent bridges
[AD-A154365] 19 p3234 N85-30051
New approaches to functionalized fluorocarbons
[AD-A154205] 19 p3248 N85-30141
Multilayer capacitor dielectrics produced from metallo-organic precursors
[AD-A154592] 21 p3580 N85-32254
Marine environmental quality assessment program, five-year plan (FY 1984 - 1988)
[AD-A154715] 21 p3613 N85-32459
Doping superlattices in organometallic VPE InP
[AD-A155151] 21 p3710 N85-33029
Research study for gel precursors as glass and ceramic starting materials for space processing applications research
[NASA-CR-176113] 22 p3751 N85-33250
Metal alkoxides: Models for metal oxides. Alkoxide ligands in early transition metal organometallic chemistry
[DE85-011366] 23 p3916 N85-34259

ORGANOMETALLIC POLYMERS
(Vinyloxy)chlorocyclotriphosphazenes
[AD-D011471] 10 p1453 N85-19152

ORGANS
NT BLADDER
NT KIDNEYS
NT LIVER
NT LUNGS
NT PITUITARY GLAND
NT SPLEEN
Gravity, body mass and composition, and metabolic rate
15 p2610 N85-26084

ORIENTATION
Determining object orientation from a single image using multiple information sources
[AD-A149990] 12 p1933 N85-22146

Parametric stability of analytical close-range photogrammetry 24 p4107 N85-35461
ORIFICE FLOW
Calibration and use of filter test facility orifice plates [DE84-016851] 04 p0500 N85-13190
Buckling and eccentricity effects on orifice metering accuracy — gas meters [ERS-E.350] 09 p1324 N85-18321
Experiments in dilution jet mixing effects of multiple rows and non-circular orifices [NASA-TM-86996] 15 p2473 N85-25266
An experimental study of the noise generated by vaporous cavitation in turbulent shear flows produced by confined orifice plates 15 p2645 N85-26316
Flow rate and pressure profiles for 1 to 4 axially aligned orifice inlets [NASA-TP-2460] 16 p2782 N85-27165
ORIFICES
Flow rate and pressure profiles for 1 to 4 axially aligned orifice inlets [NASA-TP-2460] 16 p2782 N85-27165
ORION AIRCRAFT
U P-3 AIRCRAFT
ORION CONSTELLATION
NT ORION NEBULA
The unidentified emission features: A study of the Orion Bar and planetary nebulae 08 p1246 N85-17862
The 1.5 - 3.5 micron spectroscopy of the Orion H2 source 08 p1246 N85-17864
ORION NEBULA
Detection of submillimeter polarization in the Orion Nebula [NASA-TM-86013] 04 p0579 N85-13700
Proper motions and kinematical properties of Orion trapezium type stellar systems 05 p0739 N85-14755
Water maser outburst 07 p1058 N85-16720
The Orion molecular cloud at far-infrared wavelengths 08 p1245 N85-17860
First results of submillimeter polarimetry 08 p1246 N85-17861
Photoionization structure of the Orion Nebula 08 p1246 N85-17863
Molecular spectroscopy from the Kuiper Airborne Observatory [NASA-CR-175748] 16 p2882 N85-27783
The structure of Herbig-Haro object 43 and Orion dark cloud extinction [NASA-TM-87503] 24 p4186 N85-35831
Far-infrared emission lines of CO and OH in the Orion-KL molecular shock [NASA-TM-86721] 24 p4187 N85-35832
Observations of far-infrared transitions between excited states of OH [NASA-TM-86722] 24 p4187 N85-35833
ORIONID METEOROIDS
Refractory inclusions in the Omans C30 chondrite 15 p2680 N85-26553
ORNITHOPTER AIRCRAFT
U RESEARCH AIRCRAFT
OROGRAPHIC CLOUDS
U CAP CLOUDS
OROGRAPHY
Numerical forecast of pressure field by considering the mutual influence of orography, thermal nonhomogeneity and surface friction 01 p0080 N85-10534
Sedimentary and tectonic evolution of the western Taiwan foredeep 03 p0389 N85-12491
Effect of mountain wave dynamics on orographic storms [DE84-014713] 04 p0540 N85-13433
Orographic effects in atmospheric circulation 05 p0679 N85-14362
Fully implicit numerical methods for the baroclinic primitive equations 05 p0679 N85-14365
Ground-based snow and ice crystal observation system used in Sierra Nevada winter orographic storms [PB85-115343] 10 p1520 N85-19584
Orographic disturbances of upper atmosphere emissions 11 p1663 N85-20480
Comparison of observations of orographic disturbances in the troposphere and upper atmosphere 14 p2341 N85-24479
Theory and modeling of the interaction between subgrid scale orography and large scale flow [DM-43] 16 p2827 N85-27440
Statistical comparison of radar echoes of convective precipitation between the northern Alps and its foreland [DFVLR-FB-85-07] 17 p2950 N85-28215
On Long's solution to hydrostatic flow over mountains [DFVLR-MITT-84-02] 17 p2994 N85-28503
Comparison of two orographical data sets for the GLAS Fourth Order GCM 18 p3142 N85-29452
Some recent developments in numerical modelling at ECMWF 18 p3147 N85-29481
Project Skywater, 1983-84 SCPP (Sierra Cooperative Pilot Project) data inventory [PB85-187052] 24 p4124 N85-35585
ORRERIES
U ASTRONOMICAL MODELS
ORTHOGONAL FUNCTIONS
NT WALSH FUNCTION
Application of large eddy interaction model to channel flow [NASA-TM-86691] 12 p1844 N85-21572
Noise tolerance of digital demodulator for complex signal system employing binary quantization 13 p2070 N85-22929
Representation of temperature and salinity fields using statistically orthogonal functions (in example of polymode data) 14 p2337 N85-24449
Natural vibrations of reinforced spherical shells 17 p2943 N85-28186
Symbolic Givens reduction in large sparse least squares problems [DE85-006685] 17 p3021 N85-28581
ORTHOGONAL MULTIPLEXING THEORY
A modem with pseudo-orthogonal codes: Experimental results 10 p1474 N85-19302
ORTHOGONALITY
Orthogonal polynomials and rigged Hilbert space [TUM-M8313] 03 p0414 N85-12647
Multiple channel adaptive filtering using a fast orthogonalization network: An application to efficient pulsed Doppler radar processing [AD-A147929] 08 p1211 N85-17619
Numerical generation of orthogonal and nonorthogonal coordinates in two dimensional simply and doubly connected regions [VKI-TN-161] 08 p1216 N85-17662
Initial fracture stages of orthogonally reinforced composite material 11 p1599 N85-20055
Orthogonalizer for inphase and quadrature digital data [AD-D011679] 19 p3254 N85-30174
Generation of three-dimensional body-fitted coordinates using hyperbolic partial differential equations [NASA-TM-86753] 20 p3519 N85-31667
ORTHONORMAL FUNCTIONS
Some families of near-orthonormal analytic and harmonic functions [AD-A144722] 01 p0110 N85-10748
Effects of changing the signs of rows and columns of a matrix and the hyperbolic transpose [DE84-014651] 04 p0555 N85-13530
Canonical analysis of the fermion sector in higher-derivative supergravity [DE85-007628] 16 p2859 N85-27635
ORTHOPHOTOGRAPHY
What does digital image processing perform in the production of orthophotomaps 16 p2815 N85-27368
The significance of orthophoto maps for developing countries 18 p3124 N85-29341
ORTHOSTATIC TOLERANCE
Circulatory orthostatic instability: Role of deconditioning of resistive vessels 01 p0091 N85-10612
Aviation-related cardiorespiratory effects of blood donation in female pilots [AD-A148045] 08 p1195 N85-17529
Investigation of adaptive distinctions of mechanism of controlled glycemia in Macaca rheesus monkeys 12 p1902 N85-21946
Computer simulation studies in fluid and calcium regulation and orthostatic intolerance [NASA-CR-171869] 15 p2616 N85-26117
Analysis of head-down tilt as an analog of weightlessness using a mathematical simulation model [NASA-CR-171870] 15 p2616 N85-26118
Predictions of cardiovascular responses during STS reentry using mathematical models [NASA-CR-171871] 15 p2616 N85-26119
Effect of 120-day antiorthostatic bedrest on gas exchange and pulmonary circulation in man 19 p3323 N85-30589
Primate adrenal reactions to antiorthostatic hypokinesia 19 p3324 N85-30591
Long term exposure of animals to antiorthostatis (-90 deg) as a model of critical homeostatic disturbances 19 p3324 N85-30592
Changes in nephron and juxtaglomerular system of primate kidneys under the effect of antiorthostatic hypokinesia 19 p3326 N85-30606
Typological characteristics of hemodynamic states of healthy subjects in orthostatic position 22 p3821 N85-33673
Cardiovascular responses to orthostatism and weightlessness 24 p4130 N85-35601
ORTHOTROPIC CYLINDERS
Mechanical and transient hygrothermal loading of multilayer orthotropic cylinders 09 p1330 N85-18359
Stability of anisotropic cylindrical sandwich shells 16 p2766 N85-27066
ORTHOTROPIC PLATES
Stress analysis of pin-loaded orthotropic plates using orthotropic photoelasticity 02 p0207 N85-11366
A buckling analysis for rectangular orthotropic plates with centrally located cutouts [NASA-TM-86263] 04 p0513 N85-13258
Stresses in pin-loaded orthotropic plates using photoelasticity [NASA-CR-172486] 07 p0977 N85-16204
Fracture analysis of notched composites [NASA-CR-172563] 11 p1593 N85-20020
The effects of pin elasticity, clearance, and friction on the stresses in a pin-loaded orthotropic plate [NASA-CR-175816] 16 p2743 N85-26927
An approximation to the problem of a pin-loaded hole in an orthotropic plate [VTH-LR-366] 16 p2802 N85-27276
Biaxial buckling of specially orthotropic, symmetric composite rectangular plates [AD-A152958] 17 p2979 N85-28417
A cracked orthotropic sheet stiffened by a semi-infinite orthotropic sheet [NASA-TP-2455] 21 p3587 N85-32339
The stress distribution in pin-loaded orthotropic plates [NASA-CR-176146] 22 p3800 N85-33547
Nonlinear adhesive behavior effects in a cracked orthotropic sheet stiffened by a semi-infinite orthotropic sheet [NASA-TM-87584] 23 p3941 N85-34426
ORTHOTROPIC SHELLS
An analysis for axially compressed orthotropic shells with a multimode imperfection representation [VTH-LR-422] 16 p2803 N85-27281
Stress analysis of axisymmetric sandwich shells of variable thickness 24 p4101 N85-35419
ORTHOTROPISM
Stress analysis of pin-loaded orthotropic plates using orthotropic photoelasticity 02 p0207 N85-11366
Shear-stress distribution and shear stiffness in the case represented by a non-homogeneous cross-section, of any shape, but composed of an orthotropic material, when subjected to a shear force [DRIC-T-7430] 20 p3469 N85-31554
OSCILLATING CYLINDERS
Some important problems in unsteady boundary layers including separation. 1: Nature of singularity on oscillating airfoils [AD-A147897] 07 p0960 N85-16087
OSCILLATING FLOW
Development and applications of algorithms for calculating the transonic flow about harmonically oscillating wings [NASA-CR-172376] 01 p0002 N85-10007
Planar jets impinging on various obstacles and some modes of flow oscillation [MPIS-MITT-78] 01 p0048 N85-10317
Numerical studies of unsteady transonic flow over an oscillating airfoil [NASA-TM-86011] 03 p0361 N85-12316
An organ-pipe oscillation — PHOENICS code [PDR/CFDU-IC/14] 04 p0501 N85-13199
Float zone experiments in space [NASA-CR-171284] 07 p0911 N85-15766
Calculation of oscillating turbulent flows in open channels [KU-SFB-80/T/228] 11 p1633 N85-20289
Large amplitude forcing of a high speed 2-dimensional jet [NASA-CR-175846] 13 p1974 N85-22393
The role of convective perturbations in supercritical inlet oscillations 13 p2004 N85-22583
Stability of an oscillating boundary layer [NASA-TM-77827] 14 p2299 N85-24238
Numerical studies of unsteady transonic flow over oscillating airfoil 15 p2458 N85-25174
A supersonic potential gradient method for the calculation of unsteady aerodynamic pressures on harmonically oscillating wings [DFVLR-FB-85-11] 20 p3360 N85-31026
Development of artificially produced perturbations in supersonic boundary layer 21 p3663 N85-32879
OSCILLATION DAMPERS
Control of the dynamic response of a damped membrane by distributed forces [CSIR-TWISK-312] 01 p0061 N85-10406
Investigation of current setting procedures for sector magnets [CSIR-NAC-83-03] 01 p0117 N85-10795
Controlled movement of elastic manipulator with distributed parameters 13 p2049 N85-22819
A study of transonic flutter of a two-dimensional airfoil using the U-g and p-k methods [AD-A151463] 15 p2473 N85-25269
Variable force, eddy-current or magnetic damper [NASA-CASE-LEW-13717-1] 19 p3279 N85-30233

OSCILLATIONS
NT ELECTRON OSCILLATIONS
NT HARMONIC OSCILLATION
NT MOLECULAR OSCILLATIONS
NT NONOSCILLATORY ACTION
NT NONSTABILIZED OSCILLATION
NT PLASMA OSCILLATIONS
NT PRESSURE OSCILLATIONS
NT SELF OSCILLATION
NT SOLAR OSCILLATIONS
NT STABLE OSCILLATIONS
NT STELLAR OSCILLATIONS
NT TRANSIENT OSCILLATIONS
NT TRANSVERSE OSCILLATION
NT WING OSCILLATIONS
Oscillatory integrals by Hermite interpolatory rules
[CSIR-TWISK-301] 01 p0108 N85-10725
Upwind compact finite difference schemes
[CSIR-TWISK-334] 01 p0110 N85-10742
Periodic oscillation of gyrostat-satellite about its center of mass in an elliptical orbit 02 p0159 N85-11080
Laminar-to-turbulent flow transition under influence of acoustic oscillations 02 p0260 N85-11701
Forced oscillations theory for resonant extended interaction electron devices
[PR-206] 03 p0356 N85-12298
Wear and corrosion of components under stress and subjected to motion
[AD-A145781] 03 p0372 N85-12372
Experimental investigation and analysis of oscillations of thin-walled spherical shell during pulse loading 05 p0725 N85-14682
Limits of applicability of long wave theory in studies of oscillations of n-layer fluid 06 p0824 N85-15234
Studies of the wall shear stress in a turbulent pulsating pipe flow
[AD-A146772] 07 p0957 N85-16068
Experimental investigation of the oscillation behaviour of a liquid-filled rotor with centrifugal motion
[BLL-DOUNREAY-TR-038-(9091.9F)] 08 p1160 N85-17317
Electronic properties of intercalated graphite and amorphous metals
[AD-A147664] 08 p1225 N85-17716
A Navier-Stokes calculation of the airfoil dynamic stall process
[AD-P004163] 09 p1265 N85-17948
Leading edge separation criterion for an oscillating airfoil
[AD-P004175] 09 p1267 N85-17960
Combustion driven oscillation of ducted diffusion flame 09 p1299 N85-18094
Thermal striping downstream of a horizontal elbow under thermally stratified transient flow conditions
[DE84-014687] 09 p1320 N85-18302
One-electron capture processes by highly charged ions from helium: Present status of HICE-IPP 09 p1380 N85-18736
Vacuum ultraviolet electronic properties of liquids
[DE85-000306] 10 p1583 N85-19856
PMP-2: Equatorial wave dynamics 11 p1658 N85-20422
Resonance between betatron and synchrotron oscillations in a free electron laser: A 3-D numerical study
[AD-A150059] 12 p1857 N85-21645
Space shuttle pilot-induced-oscillation research testing 13 p1986 N85-22351
Satellite oscillations in elliptical orbit 13 p1991 N85-22429
Measurements of distributed combustion 13 p2001 N85-22542
Distributed combustion: A mechanism of acoustic suppression 13 p2001 N85-22543
Interaction of cylindrical shell with concentrated mass moving along its inner surface 13 p2047 N85-22810
Stereo decoder without subcarrier restoration 13 p2068 N85-22921
Machine analysis of resonance characteristics of plate-type radio electronic equipment constructions 13 p2065 N85-23018
Regions of propagation of short-wave perturbations in spherical layer of rotating fluid 13 p2107 N85-23130
Observation of long-period oscillations of Earth 13 p2110 N85-23149
Nature of seismic images with amplitude and time fluctuations of recorded oscillations 13 p2112 N85-23156
Oscillations of gas turbine installation rotors under operating conditions 14 p2272 N85-24077
Study of dynamic characteristics of prefabricated gas turbine compressor rotor 14 p2272 N85-24078
Considering zonal wind in semidiurnal tide problem 14 p2335 N85-24440
Low-frequency oscillations of sea level and group structure of wind waves 14 p2335 N85-24441
Determining geometrical divergence using seismic observation data 14 p2343 N85-24489
Chaotic dynamics of instabilities in solids
[DE85-004909] 14 p2429 N85-24978
Frequency/period estimation and adaptive rejection of periodic disturbances
[AD-A149229] 15 p2632 N85-26226
Application of the hydraulic system frequency response program to propellant feed systems
[AD-A151824] 16 p2741 N85-26914
Analysis of combustion oscillations in heterogeneous systems
[AD-A151999] 16 p2745 N85-26942
Internal resonance in nonlinear vibrating systems
[REPT-15/1984] 16 p2797 N85-27245
Wing tunnel investigation of dynamic stall of an NACA 0018 airfoil oscillating in pitch
[NAE-AN-27] 17 p2892 N85-27830
Buildup of oscillation of bodies in stratified fluid 17 p2941 N85-28157
Acoustic oscillations of rods and plates 17 p2944 N85-28170
Effects of level broadening on the magnetothermal oscillations in two-dimensional electron systems
[AD-A152639] 17 p3029 N85-28732
Turbulence structure in the boundary layers of an oscillating airfoil
[AD-A153631] 18 p3059 N85-28926
Calculations of beam dynamics in Sandia linear electron accelerators, 1984
[DE85-010417] 18 p3180 N85-29719
Gyrotron traveling-wave device including quarter wavelength anti-reflective dielectric layer to enhance microwave absorption
[AD-D011690] 19 p3271 N85-30265
Ballooning instabilities on a magnetic separatrix
[DE85-010855] 19 p3372 N85-30915
Data set 8: ZKP wing, oscillating aileron 20 p3390 N85-31029
Frequency domain control design of large space structures: A practical approach 20 p3415 N85-31192
An examination of the Southern Oscillation in the upper tropospheric tropical and subtropical wind field 20 p3488 N85-31660
Thresholds for detection of linear oscillation following prolonged weightlessness 20 p3508 N85-31810
Search for neutrino oscillations at the Brookhaven AGS
[DE85-009766] 20 p3530 N85-31957
A simple model for testing the effects of gravity-wave-produced vertical oscillations of scattering irregularities on spaced-antenna, horizontal drift measurements 21 p3619 N85-32489
Saturation of a longitudinal instability due to nonlinearity of the wake field
[DE85-012514] 22 p3637 N85-33761
Robinson instability and beam loading
[DE85-013301] 24 p4151 N85-35737
Relation between field energy and RMS emittance in intense particle beams
[DE85-012655] 24 p4159 N85-35784
Geophysical searches for three-neutrino oscillations
[HE-5.3-9] 24 p4205 N85-36103
Measurement of neutrino oscillations in MACRO experiment
[HE-5.3-10] 24 p4206 N85-36104

OSCILLATOR STRENGTHS
What formulas are good for representing dipole and generalized oscillator-strength spectra
[DE84-014641] 02 p0278 N85-11609
Notes for lectures in China: The Bethe theory of inelastic collisions of fast charged particles with atoms and molecules
[DE84-017487] 09 p1380 N85-18678
Applications and investigations of second harmonic generation 19 p3367 N85-30678

OSCILLATORS
NT CATHODE RAY TUBES
NT CRYSTAL OSCILLATORS
NT GAS DISCHARGE TUBES
NT HARMONIC OSCILLATORS
NT HELITRONS
NT MAGNETRONS
NT MECHANICAL OSCILLATORS
NT MICROWAVE OSCILLATORS
NT MICROWAVE TUBES
NT MOLECULAR OSCILLATORS
NT PENDULUMS
NT PICTURE TUBES
NT VOLTAGE CONTROLLED OSCILLATORS
Isolated load switching with surge suppression
[AD-D011218] 01 p0042 N85-10274
Power flow between non-conservatively coupled oscillators
[ISVR-TR-125] 02 p0209 N85-11377
Behavior orbits of two coupled oscillators 02 p0282 N85-11833
Oscillator strengths for OII ions
[NASA-CR-174153] 04 p0559 N85-13558
Transmission line biased coherent array of Josephson oscillators
[AD-D011323] 07 p0944 N85-15979
Low noise multiple crystal-controlled oscillator
[AD-D011401] 07 p0948 N85-16010
New construction principles for oscillator power summing devices 07 p0949 N85-16016
Silent discharge carbon dioxide gas laser machining facility
[BLL-CTO-2267-(9091.9F)] 07 p0969 N85-16150
Passive maser using timesharing for control of the cavity and control of the oscillator on the line of stimulated emission
[AD-D011326] 07 p0969 N85-16151
Phased locked array laser systems
[AD-D011317] 07 p0971 N85-16164
NBS frequency measurement system from a user's viewpoint
[DE84-016782] 09 p1315 N85-18268
A coaxial cavity gunn oscillator using probe coupled microstrip
[AD-D011437] 10 p1479 N85-19334
Integrated circuit tunable cavity oscillator
[AD-D011474] 10 p1481 N85-19351
Oscillator development
[AD-A149699] 12 p1834 N85-21509
Design considerations for a 100 kW CW, 140 GHz gyrotron oscillator
[DE85-005262] 13 p2066 N85-22904
Square-pulse generator 13 p2075 N85-22959
Experimental study of high-stability oscillator with surface-acoustic-wave resonator in feedback loop 13 p2090 N85-23053
Injection controlled laser transmitter with twin local oscillators
[AD-D011577] 15 p2563 N85-25810
The measurement of linear frequency drift in oscillators 17 p2966 N85-28316
The superconducting cavity stability ruby maser oscillator 17 p2967 N85-28324
VULTURE manual
[DE85-006873] 17 p3013 N85-28631
How a swing behaves
[DE85-008280] 17 p3027 N85-28720
Submillimeter local oscillators for spaceborne heterodyne applications
[NASA-RP-1147] 19 p3228 N85-30005
Temperature sensitive oscillator
[NASA-CASE-GSC-12958-1] 19 p3258 N85-30201
Dielectric resonator stabilized microstrip oscillator
[AD-D011708] 19 p3261 N85-30219
Development and application of a high power ND-glass laser instrument
[AD-A154366] 19 p3276 N85-30314
High-brightness photoemitter development for electron accelerator injectors
[DE85-009548] 19 p3355 N85-30796
A multiplying slot array
[AD-A155570] 21 p3576 N85-32245
Generation of single nanosecond high-contrast radiation pulses (lambda=10.6 micrometers) 21 p3684 N85-32886
Fiber optics interface for a dye laser oscillator and method
[DE85-005765] 23 p3973 N85-34833
Los Alamos free-electron laser
[DE85-012666] 24 p4096 N85-35405

OSCILLOGRAMS
U OSCILLOGRAPHS

OSCILLOGRAPHS
Automatic correction of static characteristics of measurement channel of digital oscillograph 06 p0795 N85-15083

OSCILLOSCOPES
An optically coupled sampling system with 4 GHz bandwith
[AD-A148057] 09 p1384 N85-18702
China report: Science and technology
[JPRS-CST-85-007] 15 p2533 N85-25621
Microprocessor controlled storage sampling oscilloscope 15 p2533 N85-25622
The structure of the shower disk observed at Mt. Norikura
[HE-4.7-1] 24 p4198 N85-36052
Sub-luminal pulses from cosmic ray air showers
[HE-4.7-13] 24 p4200 N85-36083

OSMIUM
NT OSMIUM ISOTOPES
Low temperature properties of CaOs2 in the C14 and C15 crystallographic Laves phases
[DE85-003754] 10 p1564 N85-19998

Current status of the Os-191 yields Ir-191m generator
[DE85-006306] 23 p3971 N85-34614
OSMIUM ISOTOPES
Identification of vibrational-rotational transitions of Os-192O4 within frequency tuning limits of high pressure CO2 waveguide laser 21 p3689 N85-32917
OSMOSIS
NT REVERSE OSMOSIS
Evaluation of hollow fiber ultrafiltration as a pretreatment for reverse osmosis desalination of seawater
[PB84-212408] 01 p0026 N85-10160
GAMPHI: A database of activity and osmotic coefficients for aqueous electrolyte solutions
[PB85-163390] 18 p3072 N85-29002
Kidney cell electrophoresis
[NASA-CR-171899] 20 p3498 N85-31745
A gel-halo sample pellet: The best of both worlds? Stubby zones without a constricted sample gate
20 p3502 N85-31770
Results of computer calculations for a simulated distribution of kidney cells 20 p3502 N85-31771
Evaluation of results of cell electrophoresis experiments on space shuttle STS-3 including pre-flight and post-flight laboratory experiments 20 p3502 N85-31772
Condensation properties of atmospheric aerosol
21 p3649 N85-32672
The role of sulfur in osmoregulation and salinity tolerance in cyanobacteria, algae, and plants
21 p3660 N85-32736
OSMOTIC PRESSURE
U OSMOSIS
OSS-1 PAYLOAD
Vibroacoustic study of the NASA Goddard Space Flight Center OSS-1 payload
[NASA-CR-175320] 13 p1968 N85-22465
Vehicle charging on STS-3 Mission
13 p1969 N85-22473
OSTEOPOROSIS
Actual and simulated weightlessness inhibit osteogenesis in long bone metaphysis by different mechanisms 15 p2908 N85-26074
Mechanisms of osteodystrophy in weightlessness
22 p3733 N85-33143
OTF
U OPTICAL TRANSFER FUNCTION
OTOLITH ORGANS
The adaptation of vestibulo-spinal reflexes as a function of spaceflight and their relationship to space motion sickness 05 p0894 N85-14468
Problems of space biology. Volume 50: Nystagmometry for evaluation of the status of the vestibular function
[NASA-TM-77616] 14 p2365 N85-24694
Reinterpretation of otolith input as a primary factor in space motion sickness 20 p3509 N85-31812
Effect of experimental motion sickness on postrotary nystagmus and counterrotation illusion
22 p3824 N85-33690
OTS (ESA)
Interference experiment with the Sirio-OTS satellites
[FUB-17-1983] 01 p0040 N85-10254
OTTO CYCLE
Analysis and simulation of the I C engine Otto cycle using the second law of thermodynamics
02 p0291 N85-11691
OTV
U ORBIT TRANSFER VEHICLES
OUTCROPS
Concordant bands of augen gneiss within metasedimentary rocks in the Big Delta C-2 quadrangle, east-central Alaska 04 p0516 N85-13294
Paleozoic limestones of the Crazy Mountains and vicinity, Circle quadrangle, east-central Alaska
04 p0517 N85-13296
Petrology and petrogenesis of Batholitic rocks, San Jacinto Mountains, southern California
05 p0673 N85-14322
OUTER RADIATION BELT
Electron flux with electron energies above 40 MeV at altitudes of about 500 km in region where capture is possible and outside it when L is 3 or greater
15 p2481 N85-25315
Bursts of relativistic electrons in magnetopause and in outer radiation belt 16 p2722 N85-26801
OUTER SPACE TREATY
The structures and the role of an international agency for the control of satellites
[NASA-TM-76765] 03 p0441 N85-12808
U.S., Soviet space program aims contrasted
13 p1965 N85-22455
OUTGASSING
Where is the Earth's missing xenon?
06 p0988 N85-15841
Ambient air contamination: Characterization and detection techniques 18 p3157 N85-29546
OUTLET FLOW
Continuous laminar smoke generator
[NASA-CASE-LAR-13014-1] 12 p1781 N85-21178
effect of gas stream sweeping past the effluent of a perforated plate on heat transfer inside the perforations
13 p2051 N85-22836
Development of an artificial boundary layer for different outlet flows 14 p2212 N85-23719
OUTLETS
NT VENTS
Heat exchanger
[DE84-014299] 01 p0047 N85-10309
Investigation of influence of gas exit modes on characteristics of N2O - N2 - He discharge laser
21 p3684 N85-32888
OUTLETS (GEOLOGY)
U ESTUARIES
OUTLIERS (STATISTICS)
The information in the minor principal components
[CSIR-TWISK-320] 01 p0109 N85-10735
Influential observations in time series
[AD-A144719] 01 p0112 N85-10783
Some new estimation methods for weighted regression when there are possible outliers
[AD-A152104] 16 p2654 N85-27602
A multiple regression technique for detecting outliers
[REPT-84-33] 17 p3025 N85-28706
OUTPUT
NT LASER OUTPUTS
NT MASER OUTPUTS
A limbus-sensing eye movement recorder
[AD-A144772] 01 p0049 N85-10323
Determination of the input-output characteristics of time-invariant memoryless nonlinear devices
[FUB-41-1983] 01 p0100 N85-10667
Cardiac output measured by mass spectroscopy
05 p0692 N85-14449
Cardiac output measurement with soluble gases
05 p0692 N85-14450
Experiments in forecasting atmospheric marine horizontal visibility using model output statistics with conditional probabilities of discretized parameters
[AD-A147574] 07 p1008 N85-16404
MTI system simulation and clutter output statistics
[AD-A149193] 10 p1467 N85-19255
Adaptive regulation of transmitter radiation power in radio lines during delays of control signals
12 p1841 N85-21551
Confidence intervals using the regenerative method for simulation output analysis
[AD-A150147] 13 p2149 N85-23343
Design and testing of gyrotdyetron amplifiers
[AD-A151026] 14 p2298 N85-24231
Multivariate statistical modelling and its application
16 p2857 N85-27617
Semicrystalline casting process development and verification
[DE85-007695] 18 p3081 N85-29058
Probabilistic analysis of combinational circuits with random delays 19 p3257 N85-30192
Microwave SAW (Surface Acoustic Wave) monochromator
[AD-D011718] 21 p3500 N85-32311
Optical output stabilization method for direct current arc lamps
[AD-A154987] 21 p3705 N85-33013
Raster functionality for a VDI
[DE85-006734] 24 p4097 N85-35396
Optimize computer throughput using array processors
[AD-A155843] 24 p4135 N85-35628
Software maintenance relating to the input translator and z-80 realization volume of the computer systems design environment
[AD-A155849] 24 p4138 N85-35648
Beryllium production
[DE85-013360] 24 p4148 N85-35716
OV-1 AIRCRAFT
Preliminary airworthiness evaluation of a National Aeronautics and Space Administration automated stall warning system for an OV-1 aircraft
[AD-A152010] 16 p2707 N85-26706
OVER-THE-HORIZON RADAR
Skywave radar detectability of volcanic aerosols
[AD-A151448] 15 p2542 N85-25694
OVERCAST
U CLOUD COVER
OVERPRESSURE
Experimental investigation of the electric breakdown in SF6
[BLL-CE-TRANS-7987-(9022.09)]
15 p2546 N85-25714
NASTRAN analysis comparison to shock tube tests used to simulate nuclear overpressures
15 p2576 N85-25888
TNT equivalency of EAK explosive
[AD-A155737] 21 p3571 N85-32211
BLAF: A blast field reconstruction program from pressure histories
[AD-A155300] 21 p3585 N85-32283
OVERTONES
U HARMONICS
OVERVOLTAGE
Advanced metal oxide varistor concepts
[DE84-016677] 09 p1316 N85-18276
Power quality and protection of electric distribution systems with small, dispersed generation devices
[DE85-000990] 09 p1344 N85-18453
Stability of highly nonlinear oxide-zinc resistors under continuous voltage of industrial frequency
13 p2087 N85-23030
Requirements placed on information processing equipment
[BLL-CE-TRANS-7983-(9022.09)]
13 p2144 N85-23307
OXAZOLE
Infrared spectroscopy study of the SP-250 epoxy resin system
[AD-A145880] 03 p0337 N85-12167
Chiral polymers
[AD-A150366] 13 p2037 N85-22780
OXIDASE
Galactose oxidase in stereospecific oxidation of primary alcohols
[AD-A154059] 19 p3234 N85-30048
OXIDATION
NT ELECTROCHEMICAL OXIDATION
NT PHOTOOXIDATION
NT RUSTING
The oxidation behaviour of a 20 percent Cr/25 percent Ni/Nb stabilized stainless steel in carbon dioxide at high temperatures and its improvement by cerium and yttrium
[AERE-R-11228] 01 p0029 N85-10162
Determining the optimum heating parameters for precision alloys — iron-nickel alloys
[BLL-M-35719-(5824.4)] 02 p0174 N85-11167
The transient oxidation of single crystal NiAl+Zr
[NASA-CR-174756] 02 p0182 N85-11221
Review: The influence of short circuit diffusion on the oxidation of nickel, chromium and nickel/chromium alloys
[AERE-R-11311] 02 p0185 N85-11237
Analysis techniques for tracer studies of oxidation
[NASA-CR-174796] 03 p0336 N85-12162
A simple electronic apparatus for determining the oxidation stability of lubricants and other organic compounds
[AD-A146080] 03 p0338 N85-12172
Effect of oxidizing medium and heat treatment on stoichiometry of ZnSe crystal surface
03 p0353 N85-12272
Organic aerosol formation: OH(hydroxyl radical) versus ozone oxidation pathways
[PB84-219980] 03 p0388 N85-12484
Structural studies of sputtered MOS(2) films by angle-resolved photoelectron spectroscopy
[AD-A146052] 03 p0433 N85-12759
A bibliography of publications on corrosion and oxidation from UK government laboratories at Teddington, 1924 - 1983
[NPL-DMA(A)-82] 04 p0472 N85-13004
Study of the reactive-element effect in oxidation of Fe-Cr alloys using transverse section analytical electron microscopy
[DE84-016237] 04 p0571 N85-13641
Butene oxidation by molybdenum crystalographic shear compounds
[DE84-013910] 05 p0814 N85-13923
Distribution of oxygen between metal and basic slags
[BLL-M-35932-(5828.4)] 05 p0816 N85-13935
Solid state, surface and catalytic properties of oxides
[DE85-002096] 06 p0867 N85-15512
Platinum group nuggets in deep sea sediments
06 p0883 N85-15811
Corrosion study on zirconium refractory coatings. 1: Oxidation of zirconium nitride coatings by oxygen
[BLL-RISLEY-TR-5044-(9091.9F)]
07 p0925 N85-15857
Optimization of the NiCrAl-Y/ZrO-Y2O3 thermal barrier system
[NASA-TM-86905] 07 p0927 N85-15878
The mineralogy of global magnetic anomalies
[E85-10081] 07 p0987 N85-16272
Biochemical evaluation of bodily influence of high and low temperatures 07 p1014 N85-16441
Low and moderate temperature oxidation of atomically clean nickel, chromium and Ni-Cr alloys
[DE84-017350] 09 p1295 N85-18131
An infrared study of the oxidation of carbon monoxide over supported rhodium catalysts
[AD-A149478] 10 p1436 N85-19050
Continuous organic electrochemical synthesis
[DE85-001400] 10 p1437 N85-19057

Kinetics of oxidation of titanium alloy upon heating to 1000 deg C
10 p1448 N85-19122
Fuels combustion research
[AD-A149106] 10 p1457 N85-19178
Electron oxidation of graphite by fluorospecies
[DE85-001196] 11 p1595 N85-20034
Structure-phase state and properties of high-durability VALS alloy
11 p1597 N85-20048
Weldability of alloy ABM1 to alloy 1201
11 p1603 N85-20060
Initial development of nickel and nickel-iron aluminides for structural uses
[DE84-016641] 11 p1606 N85-20108
Application of Raman, TEM and other ion based techniques to oxidation problems
[AERE-R-11447] 11 p1610 N85-20121
Effects of chromium and aluminum on mechanical and oxidation properties of iron-nickel-base superalloys based on CG-27
[NASA-TP-2443] 12 p1805 N85-21323
Stress corrosion cracking and oxidation characteristics of boride-strengthened microcrystalline iron and nickel based alloys
[AD-A149805] 12 p1806 N85-21326
Oxidation and hot corrosion of hot-pressed SI3N4 at 1000 deg C
[NASA-TM-86977] 12 p1811 N85-21358
The use of hydrazine as an alternate source of energy
[NASA-CR-175535] 12 p1817 N85-21397
Oxidation and gum formation in jet fuels
[AD-A149934] 12 p1818 N85-21401
Applicability of laboratory kinetics studies to the evaluation of aqueous phase atmospheric oxidation of sulfur-4
[DE85-000588] 12 p1883 N85-21819
Combustion kinetics of metal atoms and metallic radicals over wide temperature ranges
13 p1999 N85-22530
Combustion of zirconium carbide
13 p1999 N85-22532
Interaction of metals and metalloids with biomembranes
[DE85-004902] 13 p2141 N85-23293
Improvement by cerium and yttrium ion implantation of oxidation behaviour of stabilised stainless steel in carbon dioxide
[AERE-R-11523] 14 p2259 N85-23996
Study of oxidized surface coating on titanium after annealing
15 p2498 N85-25412
Shock tube study of the fuel structure effects on the chemical kinetic mechanisms responsible for soot formation, part 2
[NASA-CR-174860] 15 p2504 N85-25444
Optimization of the catalytic oxidation of CO for closed-cycle CO2 laser applications
[NASA-TM-86421] 15 p2504 N85-25445
Oxidation of nickel-aluminum and iron-aluminum alloys
[DE85-006930] 15 p2512 N85-25497
Effects of surface chemistry on hot corrosion life
[NASA-CR-174915] 16 p2708 N85-26711
Elementary reactions of importance in oxidation, combustion ignition and flame inhibitions
[AD-A153139] 17 p2921 N85-28004
Oxygen isotopic study of the oxidation of SO2 by H2O2 in the atmosphere
[DE85-004017] 17 p2988 N85-28488
Chemical transformation modules for Eulerian acid deposition models. Volume 1: The gas-phase chemistry
[PB85-173714] 18 p3072 N85-29001
Corrosion Research Center of the University of Minnesota
[DE85-009418] 18 p3075 N85-29022
Corrosion-erosion rates/mechanisms of 9Cr1Mo steel
[DE85-008606] 18 p3076 N85-29029
High-temperature oxidation of alloys in mixed oxidants
[DE85-009708] 18 p3077 N85-29035
Methods for simulating gas phase SO2 oxidation in atmospheric models
[PB85-173110] 18 p3135 N85-29418
Burner rig corrosion of SiC at 1000 deg C
[NASA-TM-87061] 19 p3227 N85-30011
Novel analytical approaches to coal beneficiation
[DE85-010437] 19 p3229 N85-30021
Galactose oxidase in stereospecific oxidation of primary alcohols
[AD-A154059] 19 p3234 N85-30048
Experimental program to determine maximum temperatures for dry storage of spent fuel
[DE85-010307] 19 p3236 N85-30060
Physical-mechanical characteristics and wear resistance of coatings applied by microarc oxidation
19 p3242 N85-30104
Changes of structure of EP648-VI alloy as a result of high-temperature gas corrosion
19 p3243 N85-30110
Effect of thermochemical processing on fatigue resistance of titanium alloys
19 p3244 N85-30112
Ion beam sputter-deposited thin film coatings for protection of spacecraft polymers in low Earth orbit
[NASA-TM-87051] 19 p3248 N85-30137
Fuel-rich catalytic combustion: A soot-free technique for in situ hydrogen-like enrichment
[NASA-TP-2498] 20 p3423 N85-31244
Current understanding of point defects and diffusion processes in silicon
20 p3481 N85-31632
Shock tube measurements of growth constants in the branched-chain ethane-carbon monoxide-oxygen system
[NASA-TM-87068] 21 p3562 N85-32156
Basic research in novel inorganic reagents and fluorocarbon chemistry
[AD-A155340] 21 p3564 N85-32165
Molecular orbital studies in oxidation: Sulfate formation and metal-metal oxide adhesion
[NASA-CR-176070] 21 p3565 N85-32174
A study of adherent oxide scales
[AD-A155554] 21 p3567 N85-32188
Aerobic sulfur-oxidizing bacteria: Environmental selection and diversification
21 p3656 N85-32712
Some thoughts on GAIA and the sulfur cycle
21 p3658 N85-32727
Possible roles of manganese redox chemistry in the sulfur cycle
21 p3659 N85-32731
Sulfate-reducing bacteria: Microbiology and physiology
21 p3659 N85-32732
Structure and physiology of Beggiatoa and Thiothrix
21 p3659 N85-32734
Interactions among sulfide-oxidizing bacteria
21 p3661 N85-32741
Nonequilibrium kinetics of growth of oxide layer grains during laser heating of metals in air
21 p3689 N85-32919
Raman scattering studies in solids
[AD-A155528] 21 p3710 N85-33032
Method for removing chlorine compounds from hydrocarbon mixtures
[DE85-011606] 22 p3742 N85-33191
Oxidation of formaldehyde solutions used for the preservation of reverse osmosis membranes
[PB85-185585] 22 p3742 N85-33194
Rechargeable lithium-organic electrolyte battery having overcharge protection and method of providing overcharge protection for a lithium-organic electrolyte battery
[AD-D011738] 22 p3806 N85-33575
Effects of immobilization and high-altitude adaptation on energy metabolism in rats
22 p3820 N85-33663
Process for improving the quality of epitaxial silicon films grown on insulating substrates
[AD-D011730] 22 p3847 N85-33828
Oxidation states of iron in the terrestrial planets: Evidence and implications for accretion models
22 p3852 N85-33854
Electrolytic synthesis of colored eta alumina film
23 p3906 N85-34201
An X-ray diffraction study of titanium oxidation
[NASA-CR-176263] 23 p3915 N85-34264
Aluminum work function: Effect of oxidation, mechanical scraping and ion bombardment
[NASA-TM-87079] 23 p3915 N85-34265
Gas shielding apparatus
[DE85-005992] 23 p3939 N85-34418
The preparation of TEM specimens showing oxide scales in transverse cross-section
[AERE-R-11579] 24 p4076 N85-35276
High temperature corrosion of ceramics
[DE85-013481] 24 p4083 N85-35303
Development and evaluation of sulfonated polysulfone membranes for the zinc-ferricyanide battery
[DE85-009104] 24 p4090 N85-35357

OXIDATION RESISTANCE

The effects of Cr, Co, Al, Mo and Ta on the cyclic oxidation behavior of a prototype cast Ni-base superalloy based on a 2(5) composite statistically designed experiment
[NASA-TM-83784] 03 p0331 N85-12131
Oxidation resistance of silicon ceramics
[NASA-TM-77429] 07 p0931 N85-15898
Effects of MAR-M247 substrate (modified) composition on coating oxidation coating/substrate interdiffusion — protective coatings for hot section components of gas turbine engines
[NASA-CR-174851] 10 p1440 N85-19073
Oxidation of PT-7M and OT4-1 titanium alloys in air
11 p1600 N85-20063
Investigation of the development possibilities of a ferritic creep and oxidation-resistant steel for application under creep conditions above 650 deg C
[BMFT-FB-T-84-244] 12 p1806 N85-21344
Oxidation resistant materials for hot gas turbines and jet engines
[AD-B087399L] 13 p1973 N85-22369
High-temperature oxidation of reaction-roasted silicon nitride with various additives
19 p3244 N85-30114
Thermal barrier coating system
[NASA-CASE-LEW-14057-1] 24 p4072 N85-35233

OXIDATION-REDUCTION REACTIONS

The driving-force dependence of electrochemical rate parameters: Origins of anodic-cathodic asymmetries for metal aquo redox couples
[AD-A145605] 02 p0172 N85-11153
The oxidation of transition-metal ions by molecular oxygen
[BLL-M-29593-(5828.4)] 02 p0175 N85-11172
Electrochemistry of rare-earth diphthalocyanines
[AD-A145813] 03 p0327 N85-12106
NASA Redox Storage System Development Project
[NASA-TM-83677] 03 p0385 N85-12465
Chemically modified electrodes and related solution chemistry
[DE84-017110] 05 p0614 N85-13924
Catalytic oxidation by transition metal ions in zeolites
[AD-A146828] 07 p0922 N85-15842
Correlation of electronic charge transfer transitions and electrochemical potentials. The Bipyrazine(Tetracarbonyl)Molybdenum(O) system in various solvents
[AD-A147660] 08 p1120 N85-17082
Preparation and study of highly reactive metal powders
[AD-A150026] 12 p1806 N85-21331
Intramolecular electron transfer at metal surfaces. Part 5: Pendant substituent effects upon thiocarboxylate-bridged Cobalt (3) reduction kinetics at mercury and gold electrodes
[AD-A150647] 14 p2254 N85-23971
Cycling performance of the iron-chromium redox energy storage system
[NASA-TM-87034] 16 p2819 N85-27387
The electronic spectra of phthalocyanine radical anions and cations
[AD-A152328] 17 p2918 N85-27986
Electrochemical studies in liquid crystals
[AD-A154317] 19 p3234 N85-30050
Diffusion welding of incompatible materials
19 p3245 N85-30121
Anaerobic reduction of elemental sulfur by Chromatium vinosum and Beggiatoa alba
21 p3660 N85-32739
Microscopic control of semiconductor surface oxidation
[AD-A154799] 21 p3709 N85-33026
Isotopic Biogeochemistry
[NASA-CR-176128] 22 p3741 N85-33189
A kinetic model for predicting oxidative degradation rates in combined radiation-thermal environments
[TI85-002529] 24 p4100 N85-35414

OXIDE FILMS

Influence of parameters of aluminum alloy anodizing process on oxide coating thickness
01 p0018 N85-10113
Non-oxide ceramics: A new class of engineering materials
02 p0179 N85-11199
Optimized conditions for the formation of buried insulating layers in Si by high dose implantation of oxygen
[DE84-015369] 02 p0288 N85-11882
Electrochemistry of rare-earth diphthalocyanines
[AD-A145813] 03 p0327 N85-12106
Influence of aluminum oxide film on thermocompression bonding of gold wire to evaporated aluminum film
[NASA-TM-77503] 03 p0330 N85-12127
Transport processes during the growth of oxide films at elevated temperature
[AERE-R-11293] 03 p0434 N85-12766
Oxygen diffusion from anodic surface oxide films on titanium subhydride studies by auger electron spectroscopy and electron energy loss spectroscopy
[DE84-016942] 04 p0572 N85-13648
Anti-reflection coatings materials and models
05 p0665 N85-14278
Hydrogen production employing high-temperature solid oxide cells
[DE84-014559] 06 p0768 N85-14901
Wear of anodic oxide films on aluminum alloys in cryogenic liquids
[NAL-TR-818] 06 p0768 N85-14914
Recording holograms on thin films of titanium dioxide
06 p0769 N85-15039
Electrical properties of 10-50 nm TEOS (Tetraethoxysilane) LPCVD (Low Pressure Chemical Vapor Deposition) films
[AD-A148416] 06 p0803 N85-15111
Oxide charge characteristics of low temperature MOS (Metal-Oxide-Silicon) oxide films
[AD-A148447] 06 p0803 N85-15113
Charge trapping in low temperature MOS (Metal-Oxide-Silicon) oxides
[AD-A148450] 06 p0860 N85-15467

Characterization of thermally treated gallium arsenide by laser-Raman and Auger spectroscopy
[AD-A148414] 08 p1226 N85-17721
Photon scattering and interaction analysis of interfacial corrosion and catalysis
[DE85-002534] 11 p1608 N85-20114
Semiconductor electrochemistry approach to the study of oxide films on nickel electrodes
[DE85-003042] 11 p1630 N85-20264
Time resolved Raman studies of laser induced damage in TiO2 optical coatings
[DE85-003186] 11 p1640 N85-20332
The characterisation of oxide films on treated aluminium alloys
[MQAD-R-849] 13 p2022 N85-22667
Experimental and theoretical study of the infrared reflectance of thin oxide films on metals
[DE85-005799] 15 p2653 N85-26366
Obtaining oxide films on surface of tubes of chromium-nickel steels
[BLL-BISI-TRANS-22478-(9022.06)] 17 p2929 N85-28076
Technology development for thin-film-trace humidity sensors
[BMFT-FB-T-84-266] 17 p2969 N85-28338
Influence of type of processing of AK4 alloy on its surface state and strength of bonding of plasma coatings 19 p3242 N85-30103
Ion beam sputter-deposited thin film coatings for protection of spacecraft polymers in low Earth orbit
[NASA-TM-87051] 19 p3248 N85-30137
Development of low-melting fused salts 8: Formation of molybdenum film from molten ammonium formate bath
[BLL-OA-TRANS-3195-(6196.300)] 20 p3429 N85-31264
Electrolytic synthesis of colored eta alumina film 23 p3906 N85-34201
Features of behavior of gas bubbles in molten oxide films during enameling: Communication 2
[BLL-M-35781-(5828.4)] 23 p3919 N85-34283
Thermal barrier coating system
[NASA-CASE-LEW-14057-1] 24 p4072 N85-35233

OXIDES
NT ALKALINE EARTH OXIDES
NT ALUMINUM OXIDES
NT ANHYDRIDES
NT BARIUM OXIDES
NT BERYLLIUM OXIDES
NT BISMUTH OXIDES
NT BORON OXIDES
NT CALCIUM OXIDES
NT CARBON DIOXIDE
NT CARBON MONOXIDE
NT CERIUM OXIDES
NT CHLORINE OXIDES
NT CHROMITES
NT CHROMIUM OXIDES
NT COBALT OXIDES
NT COPPER OXIDES
NT DIOXIDES
NT ENSTATITE
NT GERMANIUM OXIDES
NT HYDROGEN PEROXIDE
NT INORGANIC PEROXIDES
NT IRON OXIDES
NT LEAD OXIDES
NT LITHIUM OXIDES
NT MAGNESIUM OXIDES
NT MAGNETITE
NT MANGANESE OXIDES
NT METAL OXIDES
NT MOLYBDENUM OXIDES
NT NICKEL OXIDES
NT NIOBIUM OXIDES
NT NITRIC OXIDE
NT NITROGEN DIOXIDE
NT NITROGEN OXIDES
NT NITROGEN TETROXIDE
NT NITROUS OXIDES
NT ORGANIC PEROXIDES
NT PEROXIDES
NT PLUTONIUM OXIDES
NT POTASSIUM OXIDES
NT PYROXENES
NT QUARTZ
NT RUTILE
NT SAPPHIRE
NT SILICON DIOXIDE
NT SILICON OXIDES
NT SULFUR DIOXIDES
NT SULFUR OXIDES
NT TIN OXIDES
NT TITANIUM OXIDES
NT VANADIUM OXIDES
NT YTTRIUM OXIDES
NT ZINC OXIDES
NT ZIRCONIUM OXIDES
Observation of oxide skin in powder metallurgy aluminum alloys
[AD-A145919] 03 p0331 N85-12135
Effect of oxide coated thickness on thermal ignition of titanium-based pyrotechnics
[DE84-013061] 04 p0481 N85-13065
Measurement of oxide ion concentration in NaCl-ZnCl2 molten salt and several applications
[BLL-AWRE-TRANS-74-(9091.9F)] 06 p0764 N85-14886
Effects of heteroatom substituents on the properties of 1,2-dioxetanes
[AD-A148727] 09 p1290 N85-18100
Transverse microstructure of an oxide scale formed on a 20 % Cr/25 % Ni niobium stabilized stainless steel
[AERE-R-11034] 12 p1804 N85-21315
Gasification of boron oxide drops and boron slurry agglomerates in combustion gases 13 p1999 N85-22529
Electrical and thermal transport property studies of high-temperature thermoelectric materials
[AD-A150167] 13 p2163 N85-23417
An investigation of the structure and high temperature mechanical properties of oxide dispersion strengthened alloys
[AD-A151107] 15 p2509 N85-25477
Quality testing to the specifications of the Stahl-Eisen-Pruefblatt 1570/71 using an automatic image analysis system
[BLL-BISI-TRANS-22253-(9022.06)] 17 p2976 N85-28385
Chemical transformation modules for Eulerian acid deposition models. Volume 1: The gas-phase chemistry
[PB85-173714] 18 p3072 N85-29001
Thermodynamic systematics of oxides of americium, curium and neighboring elements
[DE85-009704] 18 p3197 N85-29831
Effect of heating temperature in a vacuum on state of surface layers of welded OT4 titanium alloy 19 p3245 N85-30123
Method for production of ceramic oxide and carbide bodies by polymer inclusion and decomposition
[DE85-011668] 19 p3250 N85-30152
Process and design considerations for high-efficiency solar cells 20 p3482 N85-31641
The effect of stress and hot corrosion on nickel-base superalloys
[AD-A154722] 21 p3566 N85-32181
The diurnal variation of the neutral sodium species in the upper atmosphere: A model study
[AD-A154966] 21 p3631 N85-32581
Thermodynamic data for mineral technology
[PB85-184331] 22 p3803 N85-33560

OXIDIZERS
NT LIQUID OXYGEN
NT PHOTOCHEMICAL OXIDANTS
Atmospheric dispersion of hypergolic liquid rocket fuels, volume 1
[AD-A149597] 12 p1817 N85-21399
Process for improving the quality of epitaxial silicon films grown on insulating substrates
[AD-D011730] 22 p3847 N85-33828

OXIMETRY
Oxygen uptake as an indicator of animal adaptation to altitude hypoxia 19 p3324 N85-30595

OXYALKYLATION
U ALKYLATION

OXYFLUORIDES
Method for fluorination of actinide fluorides and oxyfluorides using O2F2
[DE85-011646] 22 p3743 N85-33202

OXYGEN
NT LIQUID OXYGEN
NT OXYGEN ATOMS
NT OXYGEN IONS
NT OXYGEN ISOTOPES
NT OXYGEN PLASMA
NT OZONE
Singlet delta oxygen generator
[AD-D011208] 01 p0012 N85-10072
Nonlinear ultrasonic characterization of oxygen impurities in titanium, 2
[AD-A144857] 01 p0027 N85-10171
Electron energy loss rates in N-2, O-2 and air
[AD-A145158] 01 p0072 N85-10476
Effect of maximum physical load on oxygen-transport properties of blood 01 p0093 N85-10627
Change in energetics of muscular contraction as a result of hyperoxia 01 p0093 N85-10629
A high resolution spectroscopic study of the oxygen molecule
[NASA-CR-174081] 02 p0172 N85-11150
Electrocatalysis of fuel cell reactions: Investigation of alternate electrolytes
[NASA-CR-174753] 02 p0222 N85-11455
Electronic-to-vibrational energy transfer studies of singlet molecular oxygen and hydrogen halides
[AD-A145587] 02 p0277 N85-11802
The rheology of icy satellites
[NASA-CR-174024] 02 p0302 N85-11959
Study of singlet oxygen-pentavalent phosphorus reactions
[AD-A145896] 03 p0327 N85-12107
Oscillator strengths for OII ions
[NASA-CR-174153] 04 p0559 N85-13558
Oxygen diffusion from anodic surface oxide films on titanium subhydride studies by auger electron spectroscopy and electron energy loss spectroscopy
[DE84-016942] 04 p0572 N85-13648
Reproducibility of readings from oxygen concentration elements
[BLL-M-35920-(5828.4)] 05 p0616 N85-13941
Oxygen delivery during exercise: Limitations to maximum flow 05 p0686 N85-14424
Measuring EUV line emission from the hot interstellar medium 06 p0860 N85-15595
Conference on Singlet Molecular Oxygen (COSMO 84), program and abstracts
[AD-A147281] 07 p1040 N85-16805
Proceedings of the 2nd Workshop on Nondestructive Evaluation (NDE) of Titanium Alloys
[AD-A147626] 08 p1125 N85-17095
Effects of oxygen on the microstructure and properties of titanium 6211 alloys
[AD-P004122] 08 p1126 N85-17097
Nonlinear ultrasonic characterization of oxygen impurities in titanium
[AD-P004123] 08 p1126 N85-17098
Effects of oxygen-contamination-induced microstructural changes on the reverberation of ultrasound in Ti-6211 alloys
[AD-P004124] 08 p1126 N85-17099
Acoustical characterization of Ti-6211 weldments and oxygen contamination Ti-6211 plate
[AD-P004125] 08 p1126 N85-17100
Ultrasonic evaluation of titanium contamination with correlation techniques
[AD-P004126] 08 p1126 N85-17101
Photoacoustic microscopy of oxygen contaminated titanium alloys
[AD-P004127] 08 p1127 N85-17102
High resolution acoustic microstructural characterization of titanium with interstitial contamination
[AD-P004128] 08 p1127 N85-17103
Feasibility study to demonstrate detection of low levels of oxygen contaminant in titanium using eddy current and ultrasonic NDE (Nondestructive Evaluation) techniques
[AD-P004129] 08 p1127 N85-17104
Evaluation of interstitial gas contamination in titanium alloys using induced magnetic field analysis
[AD-P004130] 08 p1127 N85-17105
Electromagnetic NDE of interstitial contamination in titanium alloy weldments
[AD-P004131] 08 p1127 N85-17106
Neutron activation analysis of titanium with oxygen contamination
[AD-P004134] 08 p1128 N85-17109
Nondestructive evaluation of titanium alloys. ESCA (Electron Spectroscopy for Chemical Analysis), ISS (Ion Scattering Spectroscopy), and SIMS (Secondary Ion Mass Spectrometry) examination of titanium alloy solid surfaces
[AD-P004135] 08 p1128 N85-17110
Variation of oxygen and nitrogen abundances in the galaxy 08 p1248 N85-17878
Blood viscosity responses to acute exercise and aerobic conditioning in women 09 p1363 N85-18573
Hydrogen-oxygen (hydrox) breathing at 1.3MPa
[FOA-C-58015-H1] 09 p1364 N85-18577
Metal atom diffusion in amorphous silica and at the silica surface
[DE84-017351] 09 p1380 N85-18674
The reaction of oxygen-nitrogen mixtures with granular activated carbons below the spontaneous ignition temperature
[AD-A149041] 10 p1434 N85-19039
Artificial photosynthesis with algal and reconstituted systems
[DE85-002557] 10 p1523 N85-19804
Orographic disturbances of upper atmosphere emissions 11 p1663 N85-20480
Saturation kinetics of active medium of oxygen-iodine laser 11 p1718 N85-20807
Comments on the origins and variations of carbon and nitrogen in the ISM of galaxies as evident from IUE spectroscopy of H 2 regions 11 p1745 N85-20973
Carbon, silicon, and oxygen in the white dwarf star GD 40 11 p1752 N85-21017

Toxicity, mutagenesis and aging due to endogenous oxygen radicals
[AD-A150121] 12 p1900 N85-21828
Characterization of material surfaces exposed to atomic oxygen on space shuttle missions
12 p1946 N85-22220
Ignition phenomena of bulk aluminum alloy as a function of oxygen pressure 13 p1999 N85-22531
Sulfur oxygen processes on Io
13 p2173 N85-23481
Diagrams of chemical and electrochemical equilibria in the presence of oxygen and sulphur
[AD-A150929] 14 p2251 N85-23953
Effect of oxygen on mechanical properties of Nb-V alloy
[DE85-002661] 14 p2256 N85-23982
Study of oxidized surface coating on titanium after annealing 15 p2498 N85-25412
Ignition of metals in high pressure oxygen
16 p2795 N85-26874
Hazards in welding due to oxygen changes in the workplace atmosphere
[BLL-WI-TRANS-684-(9312.57)]
16 p2792 N85-27224
Systematic nomenclature of the nitrogen, oxygen and sulfur functional polycyclic aromatic hydrocarbons
[DE85-007428] 17 p2916 N85-27974
Oxygen evolution on NiCo2O4 electrodes
17 p2924 N85-28028
Thermodynamic calculations of equilibrium states in metal-carbon-hydrogen-oxygen system
[BLL-BISI-TRANS-22092-(9022.06)]
17 p3045 N85-28644
Chemical, biological, and physical measurements from the subtropical western North Atlantic Ocean. Summer 1982, USNS Lynch, cruise 710-82
[AD-A153823] 18 p3201 N85-29857
Study of Kapton under simulated shuttle environment
[NASA-CR-176003] 19 p3225 N85-29997
Light-weight oxygen delivery hood assembly for hyperbaric chamber
[AD-D011708] 19 p3331 N85-30834
Oxygen and carbon impurities and related defects in silicon 20 p3461 N85-31631
Infrared absorption of oxygen complexes in electron-irradiated silicon
[FOA-C-30378-E1,E2,E3,E4] 20 p3538 N85-32015
Shock tube measurements of growth constants in the branched-chain ethane-carbon monoxide-oxygen system
[NASA-TM-87066] 21 p3562 N85-32156
Modification of the grain size of sputtered copper with additions of oxygen, krypton, silver, or yttrium
[DE85-010975] 21 p3567 N85-32189
Studies of oxygen- and carbon-related defects in high-efficiency silicon solar cells
21 p3609 N85-32420
Sulfur transformations at the hydrogen sulfide/oxygen interface in stratified waters and in cyanobacterial mats
21 p3657 N85-32715
Distribution and abundance of organic thiols
21 p3657 N85-32717
Evolution of the atmosphere 21 p3658 N85-32725
Microbial communities and microprofiles of sulfide and oxygen of alum rock sulfur springs
21 p3661 N85-32746
Changes in the energy spectrum of anomalous oxygen and helium during 1977 - 1985
[PAPER-SH-4.6-1] 21 p3715 N85-33056
Solar cycle variations of the anomalous cosmic ray component
[PAPER-SH-4.6-2] 21 p3715 N85-33057
Radial and latitudinal gradients of anomalous oxygen during 1977 - 1985
[PAPER-SH-4.6-4] 21 p3716 N85-33058
Stress and efficiency studies in EFG
[NASA-CR-176125] 22 p3751 N85-33251
Durability of oxygen sensors
[PB85-183089] 22 p3789 N85-33477
Oxygen analyzer
[DE85-006002] 23 p3935 N85-34392
Increase of total CO2 in the World ocean
[DE85-007756] 23 p3950 N85-34484
Determination of individual tolerance in hyperbaric oxygen 23 p3954 N85-34507
Changes in the energy spectrum of anomalous oxygen and helium during 1977-1985
[SH-4.6-1] 23 p4039 N85-35039
Temporal variations of the anomalous oxygen component, 1977 - 1984
[SH-4.6-3] 23 p4039 N85-35041
Radial and latitudinal gradients of anomalous oxygen during 1977 - 1985
[SH-4.6-4] 23 p4039 N85-35042
Thermodynamics of the corrosion of chromium in molten carbonates
[DE85-011407] 24 p4079 N85-35282

OXYGEN ANALYZERS
Halogen mass flow rate detection system
[AD-D011398] 08 p1166 N85-17352
OXYGEN ATOMS
Electronically excited atomic and molecular oxygen
[AD-A147732] 08 p1121 N85-17064
The source of stratospheric NO and N2O
[NASA-CR-175713] 15 p2586 N85-25956
Adsorption of O2, SO2, and SO3 on nickel oxide. Mechanism for sulfate formation
[NASA-CR-176072] 21 p3565 N85-32175
OXYGEN COMPOUNDS
Gas phase ion-molecule chemistry of carbon, nitrogen and oxygen compounds
[AD-A152876] 17 p2919 N85-27996
OXYGEN CONSUMPTION
Manned testing of two closed-circuit oxygen underwater breathing apparatus: US Navy Emerson Rig and Fenzy PO.68
[AD-A148300] 08 p1200 N85-17560
The energy cost of women walking and running in shoes and boots
[AD-A151022] 14 p2389 N85-24716
Relationship between the Army two mile run test and maximal oxygen uptake
[AD-A153914] 18 p3154 N85-29526
Oxygen uptake as an indicator of animal adaptation to altitude hypoxia 19 p3324 N85-30595
An analysis of aerobic capacity in a large United States population
[AD-A156200] 24 p4132 N85-35614
OXYGEN DEFICIENCY
U HYPOXIA
OXYGEN DETECTORS
U OXYGEN ANALYZERS
OXYGEN IONS
Optimized conditions for the formation of buried insulating layers in Si by high dose implantation of oxygen
[DE84-015369] 02 p0288 N85-11882
Cold streams of ionospheric oxygen in the plasma sheet during the CDAW-6 event of March 22, 1979
[NASA-CR-174064] 03 p0393 N85-12513
Studies of the chemistry of vibrationally and electronically excited species in planetary upper atmospheres
[NASA-CR-174134] 03 p0449 N85-12851
Effect of inner subshell ionization for emission lines of OIV ion 09 p1388 N85-18729
Neutral beam injector oxygen impurity measurements and concentration reduction via gettering processes
[DE85-000881] 12 p1836 N85-21521
Three-dimensional calculation of shuttle charging in polar orbit 13 p1992 N85-22486
The ionospheric O+ streams in the magnetotail between 22 RE and 6 RE 14 p2360 N85-24582
Oxygen-nitrogen interactions in ion-implanted silicon
[DE85-010091] 16 p3196 N85-29819
ISEE-1 data reduction and analysis plasma composition experiment
[NASA-CR-175306] 21 p3630 N85-32552
Observation of nuclei with energies 8-30 MeV per nucleon in the Earth's magnetosphere at the altitudes 350 KM
[SH-10.1-5] 23 p4053 N85-35136
OXYGEN ISOTOPES
Size dependence of chondrule textural types
06 p0662 N85-15606
Oxygen isotopes in deep sea spherules
06 p0663 N85-15609
Control technology for radioactive emissions to the atmosphere at US Department of Energy facilities: The Los Alamos Meson Physics Facility
[DE85-011402] 22 p3611 N85-33809
Implications of new measurements of O-16 + p + C-12,13, N-14,15 for the abundances of C, N isotopes at the cosmic ray source
[OG-4.3-2] 22 p3878 N85-34027
Nucleosynthesis in the terrestrial and solar atmospheres
[SH-2.2-2] 23 p4000 N85-34797
OXYGEN METABOLISM
Respiratory chain of alkalophilic bacteria
[DE84-012568] 09 p1390 N85-18556
OXYGEN PLASMA
SWIR and visible atomic emission from laser-produced oxygen and nitrogen plasmas
[AD-A147528] 07 p1045 N85-16641
OXYGEN PRODUCTION
Development and demonstration of a spiral-wound thin-film composite membrane system for the economical production of oxygen-enriched air, phase 4
[DE85-012380] 23 p3920 N85-34288
OXYGEN RECOMBINATION
Electronically excited atomic and molecular oxygen
[AD-A147732] 08 p1121 N85-17064

OXYGEN SPECTRA
Forbidden lines of oxygen in comet spectra
02 p0163 N85-11105
OXYGEN SUPPLY EQUIPMENT
Ultralightweight oxygen container
[PB84-220730] 01 p0036 N85-10226
Slow opening valve — valve design for shuttle portable oxygen system
[NASA-CASE-MSC-20112-1] 11 p1842 N85-20338
Light-weight oxygen delivery hood assembly for hyperbaric chamber
[AD-D011709] 19 p3331 N85-30834
Improved oxygen sources for breathing apparatus
[NASA-TM-86671] 24 p4134 N85-35623
OXYGEN SYSTEMS
U OXYGEN SUPPLY EQUIPMENT
OXYGEN TENSION
NT HYPOXEMIA
Effect of microwave radiation on local blood circulation and oxygenation of brain tissue
07 p1012 N85-16431
OXYGEN TOXICITY
U HYPEROXIA
OXYGENATION
Pulmonary blood flow and oxygenation of arterial blood in a healthy subject upon 7 days hypokinesia
07 p1014 N85-16439
Management of vibration sickness in coal mines by hyperbaric oxygenation 10 p1523 N85-19609
Hydrographic data collected in 1982 and 1983 for EPOCS (Equatorial Pacific Ocean Climate Studies)
[PB85-110799] 12 p1876 N85-21765
Mathematical-cartographic model for study of distribution of hydrochemical elements in sea water (using dissolved oxygen in the Pacific Ocean as an example)
13 p2109 N85-23138
Chemical signatures associated with the freshening of Northern Atlantic waters between 1972 and 1981
15 p2601 N85-26032
Jet fuel instability mechanisms
[NASA-CR-175856] 17 p2936 N85-28127
Modeling of auto exhaust smog chamber data for EKMA development
[PB85-186492] 22 p3813 N85-33619
Biological modulation of planetary atmospheres: The early Earth scenario 22 p3854 N85-33867
Oxygenation and regional circulation in gingival mucosa during exposure to lower body negative pressure
23 p3953 N85-34498
OXYHALIDES
High capacity inorganic oxyhalide electrochemical cell
[AD-D011321] 07 p0923 N85-15645
OXYHEMOGLOBIN
Liposome-encapsulated hemoglobin for emergency resuscitation
[AD-A146794] 07 p1015 N85-16446
OZONE
Future scenarios and ozone change
[DE84-014761] 01 p0065 N85-10573
Organic aerosol formation: OH(hydroxyl radical) versus ozone oxidation pathways
[PB84-219680] 03 p0388 N85-12484
Analysis of Santa Barbara oxidant study
[PB84-229277] 03 p0388 N85-12486
A 2-dimensional description of potential perturbations to the ozone layer due to NOx and H-2-O aircraft emissions
[AD-A146292] 03 p0392 N85-12511
Trends in ozone and temperature structure: Comparison of theory and measurements
[DE84-016201] 04 p0539 N85-13428
Aspects of the comparison of stratospheric trace species measurements with photochemical models
[DE84-017028] 05 p0672 N85-14317
Detailed performance calculations: Wayne State University and Ford Motor Company, appendix C
05 p0676 N85-14340
Applications of TOMS ozone data and clustering techniques in satellite soundings
05 p0861 N85-14379
Active optical sounding of ozone and minor constituents in the middle atmosphere: A review of ground-based lidar measurements 08 p1163 N85-17458
Stratospheric concentration of nitric acid, ozone and carbonyl sulfide: Measurement of nitric acid absorption in the Q branch of the V4 band as a function of temperature
[ESA-TT-864] 09 p1355 N85-18524
Upper atmosphere research at INPE
[INPE-3281-PRE/604] 10 p1515 N85-19557
Aerosol limb absorption — stratosphere
[NASA-TM-77733] 10 p1515 N85-19562
Health assessment document for carbon tetrachloride
[PB85-124196] 10 p1528 N85-19638
Soviet National Middle Atmosphere Program
11 p1655 N85-20429

MAP/GLOBUS campaign 1983
11 p1658 N85-20447
MSG-7: Molecular absorption processes related to the penetration of ultraviolet solar radiation into the middle atmosphere 11 p1658 N85-20449
Changes in the ozone content over central Europe during reversals of stratospheric circulation in late winter 11 p1661 N85-20469
Ozone measurements in the mesosphere during a solar proton event 11 p1665 N85-20490
Air quality for ozone and other photochemical oxidants. External review draft, volume 1
[PB85-126035] 11 p1679 N85-20582
Air quality criteria for ozone and other photochemical oxidants. External review draft, volume 5
[PB85-126076-VOL-5] 11 p1679 N85-20583
Continued research in mesoscale air pollution simulation modeling. Volume 5: Refinements in numerical analysis, transport, chemistry, and pollutant removal
[PB85-137362] 11 p1680 N85-20585
Absorption of ozone molecules in strong field of tea CO2 injection laser 11 p1718 N85-20808
Gas-liquid chemistry of natural waters, volume 1
[DE85-002603] 12 p1884 N85-21822
Gas-liquid chemistry of natural waters, volume 2
[DE85-002457] 12 p1884 N85-21823
Air quality criteria for ozone and other photochemical oxidants. External review draft, volume 2
[PB85-126043] 12 p1886 N85-21836
Air quality criteria for ozone and other photochemical oxidants, external review draft, volume 3
[PB85-126050] 12 p1886 N85-21837
Air quality criteria for ozone and other photochemical oxidants. External review draft, volume 4
[PB85-126068] 12 p1886 N85-21838
Simultaneous cabin and ambient ozone measurements on two Boeing 747 airplanes. Volume 3: October 1978 - July 1979
[NASA-TM-86683] 12 p1892 N85-21872
Non-precipitating cumulus cloud study
[DE85-002352] 12 p1896 N85-21902
Ozone Correlative Measurements Workshop
[NASA-CP-2362] 13 p2105 N85-23112
Scientific requirements for ozone measurements 13 p2105 N85-23113
Method for determining the number of correlative measurements required to validate the SBUV/2 ozone retrievals 13 p2105 N85-23114
Measurement requirements for the detection of ozone trends 13 p21C5 N85-23115
A theoretical study of the ozone quasi-biennial oscillation in the tropical stratosphere 13 p2132 N85-23264
Cumulus cloud venting of mixed layer ozone
[NASA-TM-87429] 13 p2132 N85-23269
Study of integral and spectral direct solar radiation over Atlantic 14 p2341 N85-24475
Development of algorithms for using satellite meteorological data sets to study global transport of stratospheric aerosols and ozone
[NASA-CR-172540] 15 p2591 N85-25974
Impact of ozone on vegetation
[PB85-159697] 16 p2621 N85-27403
Free radicals in the stratosphere: A new observational technique 16 p2624 N85-27415
Research and development of new instruments 16 p2624 N85-27418
In-situ stratospheric ozone measurements: Recent results and their implications 16 p2624 N85-27419
Role and fate of ozone in the atmosphere 16 p2624 N85-27421
Geophysical monitoring for climatic change, number 12
[PB85-172278] 16 p2637 N85-27496
Ozone and temperature trends due to the injection of trace species in the atmosphere
[AERONOMICA-ACTA-A-286-1984] 16 p3132 N85-29399
Impact of alcohol fuels on urban air pollution: Methanol photochemistry study
[DE85-009539] 16 p3133 N85-29403
Conceptual Design for a Gulf Coast Oxidant Transport and Transformation Experiment: Workshop proceedings and recommendations
[PB85-173769] 16 p3135 N85-29417
Improvement of the basic knowledge of the climatology of the vertical ozone layer by enhanced balloon sounding
[BPT-6/84] 16 p3137 N85-29426
Photochemical processes in the lower stratosphere (ozone layer) 16 p3148 N85-29490
Assessment of the role of nitrogen oxides in nonurban ozone formation
[PE85-173690] 19 p3311 N85-30524
Chemical transformation in acid rain. Volume 1: New methodologies for sampling and analysis of gas-phase peroxide
[PB85-173425] 19 p3311 N85-30527
Development of a technique for in situ detection of stratospheric nitrogen dioxide 19 p3312 N85-30534
Tropical ozone: Seasonal variations in the troposphere at 6 deg S
[INPE-3555-PRE/766] 19 p3313 N85-30535
Annual environmental monitoring report, January-December 1984
[DE85-011689] 20 p3486 N85-31665
Ozone in the 21st century: Increase or decrease
[AERONOMICA-ACTA-A-291-1984] 20 p3489 N85-31687
Modeling of auto exhaust smog chamber data for EKMA development
[PB85-186492] 22 p3813 N85-33619
Atmospheric reaction products from hazardous air pollutant degradation
[PB85-185841] 22 p3813 N85-33620
The use of TOMS data in evaluating and improving the total ozone from TOVS measurements
[NOAA-TR-NESDIS-23] 22 p3814 N85-33626
Agents and effects of ozone trends in the atmosphere
[AERONOMICA-ACTA-A-287-1984] 23 p3946 N85-34466
The influences of the galactic cosmic ray on the atmospheric ozone
[SH-10.1-1] 23 p4053 N85-35133
Space Station Polar Platform: Integrating research and operational missions
[PB85-195279] 24 p4089 N85-35218
A study of the chemistry of alkali metals in the upper atmosphere
[AD-A156349] 24 p4117 N85-35524

OZONOMETRY
Model of atmospheric ozone for middle latitudes 02 p0161 N85-11091
One approach to remote sensing of total ozone content 16 p2725 N85-26822
Improvement of the basic knowledge of the climatology of the vertical ozone layer by enhanced balloon sounding
[BPT-6/84] 16 p3137 N85-29426
Ozone during sudden stratospheric warming: A three-dimensional simulation
[AERONOMICA-ACTA-A-292-1984] 22 p3813 N85-33621

OZONOSPHERE
Solar radiation in the ozone layer 04 p0522 N85-13342
Plant responses to solar UV-B radiation 05 p0690 N85-14436
Photochemical processes in the lower stratosphere (ozone layer) 16 p3148 N85-29490

P

P WAVES
Transport properties of Topopah Spring tuff
[DE85-010448] 19 p3270 N85-30278

P-I-N DIODES
U DIODES
U P-I-N JUNCTIONS

P-I-N JUNCTIONS
Allowable surge currents and failure mechanisms in semiconductor power devices in various modes of operation 08 p0795 N85-15080
EMC enhanced constant Z modulator
[AD-A147715] 08 p1157 N85-17297
P-I-N CdTe gamma-ray detectors by Liquid Phase Epitaxy (LPE)
[DE84-012276] 09 p1323 N85-18315
Radiation effects induced in pin photodiodes by 40- and 85-MeV protons
[NASA-CR-175678] 14 p2426 N85-24960

P-N JUNCTIONS
Radiation measuring system using transistor flux sensors
[AD-D011239] 01 p0050 N85-10328
Spectral distribution of radiation in n junctions of GaAs during avalanche breakdown 02 p0258 N85-11688
Novel transport and recombination processes in semiconductors
[AD-A145969] 03 p0433 N85-12757
An asymptotic analysis of a transient p-n junction model
[AD-A147270] 07 p0947 N85-16004
Dependence of breakdown voltage for p-n junction on parameters of ion implantation and semiconductor heat treatment 07 p0954 N85-16046
Improved modeling of the open circuit voltage of solar cells 13 p2011 N85-22619
A second order difference scheme for transient semiconductor device simulation
[AD-A154824] 21 p3709 N85-33027
A review of the physics and response models for burnout of semiconductor devices
[AD-A155031] 21 p3709 N85-33028

P-N-P JUNCTIONS
Method for the fabrication of dielectric isolated junction field effect transistor and PNP transistor
[AD-D011500] 12 p1832 N85-21494
KT3127A, KT3128A transistors 22 p3779 N85-33414

P-N-P-N JUNCTIONS
Integrated power devices with three-dimensional connection for automation systems 06 p0794 N85-15077
Dependence of parameters of silicon photovoltaic cells on temperature and light intensity 14 p2275 N85-24094

P-TYPE SEMICONDUCTORS
Novel transport and recombination processes in semiconductors
[AD-A145969] 03 p0433 N85-12757
A study of defects in neutron transmutation doped silicon: Gallium by hall effect analysis
[AD-A146047] 03 p0433 N85-12758
High temperature thermoelectric energy conversion 05 p0610 N85-13894
Electrically conducting complexes of poly(3,6-n-methylcarbazolyl methylene)
[AD-A147884] 07 p0933 N85-15914
Photoelectrochemical reduction of carbon dioxide
[PB85-129054] 11 p1596 N85-20036
Multiple double heterojunction buried laser device
[AD-D011519] 12 p1855 N85-21635
Thin film cadmium telluride and zinc phosphide solar cells
[DE85-002904] 15 p2587 N85-25950
Fabrication and I-V characterization of AlGaAs/GaAs MODFETs with P-type surface layers grown by molecular beam epitaxy
[AD-A151605] 15 p2660 N85-25415
TEMO and TEB thermoelectronic devices 22 p3779 N85-33415

P-84 AIRCRAFT
U JET PROVOST AIRCRAFT

P-3 AIRCRAFT
An analysis of constraints to coordinated tactical crew interaction in the P-3C aircraft
[AD-A147220] 07 p1021 N85-16478
An airborne infrared thermal scanning system for easy use on Navy P-3 aircraft
[AD-A149690] 12 p1933 N85-22143

P-531 HELICOPTER
Wind-tunnel evaluation of a 21-percent-scale powered model of a prototype advanced scout helicopter
[NASA-TP-2420] 18 p3058 N85-28923

PACIFIC ISLANDS
NT JAPAN
NT KURILE ISLANDS
NT NEW ZEALAND
Vertical movements and structure formation within island systems of northeast Asia 10 p1501 N85-19471

PACIFIC NORTHWEST (US)
Ecology of estuarine channels of the pacific northwest coast: A community profile
[PB84-209709] 01 p0070 N85-10464
Pacific Northwest and Alaska bioenergy program glossary
[DE85-011740] 22 p3808 N85-33591

PACIFIC OCEAN
Sea-level in the world ocean. Part 5: The North-East Pacific and Arctic Oceans, a catalogue of measurements
[CSIR-T/SEA-8303-5] 01 p0087 N85-10589
Sea-level in the world ocean. Part 6: The South Atlantic and South Pacific Oceans, a catalogue of measurements
[CSIR-T/SEA-8303-6] 01 p0087 N85-10590
On gravity from SST, geoid from Seasat, and plate age and fracture zones in the Pacific
[E85-10020] 02 p0217 N85-11433
A comparison of seismic properties of young and mature oceanic crust 02 p0225 N85-11479
Lithospheric structure in the Pacific geoid
[NASA-CR-174155] 04 p0526 N85-13365
Tide tables 1985, high and low water predictions, central and western Pacific Ocean and Indian Ocean
[PB84-236393] 04 p0542 N85-13451
Archiving and exchange of a computerized marine seismic database: The ROSE data archive system
[DE84-901453] 04 p0576 N85-13677
Earthquakes and tectonics of Pacific Ocean margins 08 p0820 N85-15206
Anomalous magnetic field in northwestern Pacific Ocean and Pacific Ocean plate kinematics 08 p0820 N85-15210

Boundary velocities of mohorovicic discontinuity and upper mantle structure of Pacific Ocean bed
06 p0821 N85-15211
Tides and tidal currents of the inland waters of Western Washington
[PB84-237379] 06 p0842 N85-15346
Ocean and climate, an example. The interannual variability of the tropical Pacific Ocean
07 p1002 N85-16365
Oceanographic data for development of the US exclusive economic zone
[PB85-106458/GAR] 07 p1010 N85-16415
The spatial evolution of t he directional wave spectrum in the Southern Ocean: Its relation to extreme waves in Agulhas Current 06 p1144 N85-17213
Bibliography update on the California current system and related mesoscale ocean modeling
[AD-A146548] 06 p1190 N85-17503
Preliminary post-emplacement safety analysis of the subseabed disposal of high-level nuclear waste
[DE84-011162] 06 p1221 N85-17692
Silver metallogeny in Earth's Pacific Ocean segment
10 p1496 N85-19455
Annual data and verification tabulation for Eastern North Pacific tropical storms and hurricanes, 1983
[PB85-109635] 10 p1520 N85-19580
Tropical cyclone data tape for the Eastern and Central North Pacific Basins, 1949-1983: Contents, limitations and uses
[PB85-110054] 10 p1520 N85-19585
Drifting buoy data from equatorial Pacific Ocean, 31 Aug. 1980 - 30 Apr. 1982
[PB85-120046] 10 p1522 N85-19598
Mesoscale studies of flow regimes and fluxes of particulate matter in coastal waters
[DE85-003625] 11 p1689 N85-20620
Hydrographic data collected in 1982 and 1983 for EPOCS (Equatorial Pacific Ocean Climate Studies)
[PB85-110799] 12 p1676 N85-21705
Varying structure and intensity change characteristics of 4 Western North Pacific tropical cyclones
[AD-A149628] 12 p1695 N85-21805
Microplankton species assemblages at the Scripps Pier from March to November 1983 during the 1982-1984 El Nino event
[NASA-CR-176553] 12 p1699 N85-21826
El Nino, the capricious child 13 p2106 N85-23121
Absolute movement of Pacific Ocean plate during last 120 million years 13 p2107 N85-23126
Mathematical-cartographic model for study of distribution of hydrochemical elements in sea water (using dissolved oxygen in the Pacific Ocean as an example)
13 p2109 N85-23136
Surface currents in the tropical Pacific during 1979-1980 using drifting buoys 14 p2323 N85-24354
A large-scale air sea interaction project over the Pacific basin 14 p2326 N85-24373
The transpacific experimental sailing by YASEIGO 3
14 p2327 N85-24380
Applications of ARGOS measurements in equatorial Pacific Ocean-atmosphere interaction studies
14 p2331 N85-24414
Absolute movement of Pacific Ocean plate based on paleoclimatic and paleomagnetic data and trajectory of hot spots during last 120 million years
14 p2334 N85-24435
Some preliminary results concerning deep northern-boundary currents in the North Pacific
[AD-A151021] 14 p2382 N85-24692
Glacial-to-interglacial changes in NADW fluxes?
15 p2602 N85-26037
The ARGOS system used for tracking gray whales
16 p2812 N85-27347
Tectonic structure features of some deep faults in Atlantic and Pacific Oceans (according to deep seismic sounding-reflected waves method data)
19 p3295 N85-30426
Mariners weather log, volume 28, number 4, fall 1984
[PB85-178408] 19 p3318 N85-30571
One-dimensional model hindcasts of warm anomalies in the North Pacific Ocean
[AD-A154129] 19 p3320 N85-30579
Pacific Index, April 1983 - October 1984
[TIB5-901335] 19 p3320 N85-30582
Sulfates in marine aerosols over the tropical Western Pacific Ocean 21 p3651 N85-32690
Meteorological data from the OPTOMA (Ocean Prediction Through Observations, Modeling and Analysis) program OPTOMA 2, leg D2. 30 Jun. - 10 Jul. 1984
[AD-A156134] 24 p4123 N85-35560

PACKAGES
NT INSTRUMENT PACKAGES

PACKAGING
NT ELECTRONIC PACKAGING
Safety aspects of prepackaged liquid propellant stages for strategic missiles
[AD-P004350] 10 p1456 N85-19174
Evaluation of air and ground launched cruise missile navigational element containers
[AD-A149654] 12 p1774 N85-21138
Synchronously deployable tetrahedral truss reflector
14 p2231 N85-23827
Packaging's contribution for the effectiveness of the space station's food service operation
14 p2394 N85-24748
Packaging for food service 14 p2394 N85-24747
Encapsulation and packaging of a semiconductor multielectrode array for cortical implantation
[AD-A153180] 17 p2998 N85-28535
Sintering studies project
[AD-A154750] 21 p3572 N85-32216

PACKET SWITCHING
Interaction of voice and data traffic in a packet switching communication network and virtual circuit
[FUB-63-1982] 01 p0039 N85-10249
Voice communication handling in X 25 packet switching networks
[FUB-30-1983] 01 p0040 N85-10260
Throughput characteristics of Carrier Sense Multiple Access (CSMA) networks
[FUB-25-1983] 01 p0106 N85-10713
Contribution to the study and realization of the CARTHAGE multiservice local network
[ENST-84E006] 05 p0716 N85-14595
Voice data processing in packet switching modes
[FUB-44-1983] 09 p1312 N85-18248
Analysis of the performance of multiaccess networks of the bus type
[FUB-47-1983] 09 p1313 N85-18249
Asymptotic analysis of Markovian access control computer communication networks
09 p1372 N85-18619
A concatenated coding scheme for error control
[NASA-CR-175504] 12 p1912 N85-22001
Satellite channels in packet-switching networks
13 p2067 N85-22909
Onboard demand scheduling of a multibeam SS/TDMA satellite with integrated circuit and packet switching
14 p2229 N85-23812
Mathematical programming in computer network design
[AD-A152275] 16 p2848 N85-27558
A study of topologies and protocols for fiber optic local area network
[NASA-CR-175771] 16 p2864 N85-27699
High performance asynchronous limited sensing algorithms for CSMA and CSMA-CD channels
[AD-A153919] 18 p3171 N85-29650
A graphics interface for interactive simulation of packet-switched networks 23 p3982 N85-34558

PACKET TRANSMISSION
NT PACKET SWITCHING
Asymptotic analysis of Markovian access control computer communication networks
09 p1372 N85-18619
Multicomputer communication system
[NASA-CASE-NPO-15433-1] 12 p1822 N85-21428
Spread spectrum mobile radio communications
[AD-A149936] 12 p1829 N85-21477
A fully distributed approach to the design of a 16 K bit/sec VHF packet radio network
[AD-A141282] 13 p2054 N85-22859
Wideband integrated voice/data technology
[AD-A152329] 17 p2947 N85-28197

PACKETS (COMMUNICATION)
Throughput increase in frequency hopped multiple access channels by means of discrimination against partially overlapping interference
[AD-A145540] 02 p0191 N85-11275
Transmission scheduling to reduce convex delay costs in packet networks
[AD-A148451] 06 p1153 N85-17276
Synthesis of optimum receiver and processor for signal packet of radio pulses 12 p1839 N85-21541
Satellite channels in packet-switching networks
13 p2067 N85-22909

PACKING DENSITY
System design of multi-layer (3-dimensional) integrated circuits
[AD-A153466] 18 p3094 N85-29154

PACKINGS (SEALS)
Inhibited anticorrosion protection of automotive steel strip in the NLMK
[BLL-M-36250-(5828.4)] 20 p3430 N85-31274

PAD
Factor analysis applied to a silane coupling agent on E-glass fiber system
[AD-A145687] 02 p0187 N85-11249

PADE APPROXIMATION
Mesh effects on the computation of non-linear gravity waves of arbitrary discharge
[COLL-AERON-8501] 12 p1886 N85-21848
Nonlinear partial differential equations and related problems of Pade approximations
[AD-A149850] 12 p1920 N85-22059
Pade tables of a class of entire functions
[CSIR-TWISK-337] 14 p2413 N85-24877
Approximate inverse spectral transform for the Korteweg-de Vries equation
[PREPRINT-411] 16 p3172 N85-29658
Well-posedness of one-way wave equations and absorbing boundary conditions
[NASA-CR-172619] 19 p3345 N85-30727

PAINTS
Laser paint removal
[AD-P004009] 03 p0308 N85-11989
Progress on solar absorber selective paint research
[DE84-015536] 04 p0480 N85-13059
Application of electrochemical engineering methods and theory to solving corrosion and adhesion problems with organic coatings
[AD-A147799] 08 p1129 N85-17115
East Europe report: Science and technology
[JPRS-ESA-85-008] 10 p1460 N85-19200
Hydrogen embrittlement of cadmium-plated ultra-high strength steels in paint strippers
[ARL/MAT-R-117] 12 p1806 N85-21326
Contactless determination of the conductivity of the white paint PCB-Z — Giotto spacecraft thermal control coating 14 p2243 N85-23907
Impact ionization from gold, aluminum and PCB-Z — Giotto spacecraft paint PCB-Z 14 p2244 N85-23910
Investigation of the influence of some paint systems and water displacing corrosion inhibitors on anodic undermining corrosion of aluminum 2024 clad alloy — aircraft structures
[VTH-LR-443] 16 p2756 N85-27009
Forming of coating protection system: Mechanism of paint-coating anti-corrosion protection of steel
[BLL-BISI-TRANS-22061-(9022.06)]
17 p2925 N85-28033
Diffusely reflecting paints including polytetrafluoroethylene and method of manufacture
[NASA-CASE-GSC-12883-1] 18 p3079 N85-29044
Comparison of TT-F-1098 solvent-thinned block fillers with water-thinnable block fillers
[AD-A154207] 19 p3249 N85-30142
Thickness-insensitive selective surface paint
[DE85-010568] 19 p3250 N85-30150
Working with flammable solvents, thinners, paints and adhesives
[HSE-TRANS-11066] 19 p3250 N85-30154
Land vehicle corrosion management
22 p3750 N85-33246
Space shuttle SRB TPS protective paint test and evaluation in NASA Hot Gas Facility and AEDC Tunnel C
[NASA-CR-170884] 24 p4081 N85-35294

PAIR PRODUCTION
Power law X- and gamma-ray emission from relativistic thermal plasmas 08 p1241 N85-17829
Pair production at moderate optical depths — galactic nuclei X ray spectra 08 p1241 N85-17830
Electron-positron pair equilibrium in strongly magnetized plasmas 12 p1957 N85-22296
Electron-positron pairs in a mildly relativistic plasma in active galactic nuclei 12 p1957 N85-22297
Atomic physics aspects of a Relativistic Nuclear Collider
[DE85-006867] 15 p2650 N85-26342
Photon-photon collisions
[DE85-008056] 17 p3030 N85-28742
Physics of (very) high energy e(+)-e(-) colliders
[DE85-006177] 17 p3036 N85-28760
Measurements of heavy quark and lepton lifetimes
[DE85-008321] 18 p3181 N85-29724
The radiation of the Vela pulsar
20 p3548 N85-32060
Paired ion chamber constants for fission gamma-neutron fields
[AD-A155068] 21 p3702 N85-32999
Secondary antiproton production in relativistic plasmas
[OG-8.1-4] 22 p3988 N85-34095
Calculating the interatomic pair potential allowing for resonance interaction in titanium, nickel and vanadium
[BLL-M-35843-(5828.4)] 23 p3913 N85-34249
Neutral pion production in solar flares
[SH-1.4-7] 23 p3985 N85-34767
On magnetic pair production above fast pulsar polar caps
[OG-8.2-13] 23 p4020 N85-34909
Neutron-induced 2.2 MeV background in gamma ray telescopes
[OG-9.3-6] 23 p4027 N85-34961

Observation of direct hadronic pairs in nucleus-nucleus collisions in JACEE emulsion chambers
[HE-1.4-5] 24 p4176 N85-35893
Excessive production of electron pairs by soft photons in low multiplicity ion interactions
[HE-1.4-6] 24 p4176 N85-35894
LPM effect and primary energy estimations
[HE-3.6-4] 24 p4185 N85-35953
Result of Monte-Carlo simulation of electron-photon cascades in lead and layers of lead-scintillator
[HE-3.6-11] 24 p4185 N85-35958
Missing energies at pair creation
[HE-4.4-8] 24 p4193 N85-36016

PALEOBIOLOGY
Constraints on lunar origin: Evidence preserved in Precambrian stromatolites 04 p0584 N85-13731
Paleoclimatologists use past to predict weather patterns 06 p0819 N85-15197
Precambrian evolution and the rock record 21 p3656 N85-32711

PALEOMAGNETISM
A paleomagnetic study of the Prince William terrane and Nixon Fork terrane, Alaska 02 p0226 N85-11478
Paleomagnetic latitude of paleocene volcanic rocks of the Cantwell Formation, central Alaska 04 p0517 N85-13302
Implications of lunar paleomagnetism for the origin of the Moon 04 p0582 N85-13717
Use of paleomagnetic data in tectonic analysis of oceanic structures 13 p2108 N85-23135
Geomagnetic field dynamics 13 p2116 N85-23182
Absolute movement of Pacific Ocean plate based on paleoclimatic and paleomagnetic data and trajectory of hot spots during last 120 million years 14 p2334 N85-24435

PALEONTOLOGY
Paleohydrology and geomorphology of selected reaches of the upper Wabash Valley, Indiana 02 p0226 N85-11481
Paleoenvironmental interpretation of the upper cretaceous Point Lookout sandstone: Implications for shoreline progradation and basin tectonic history, San Juan basin, New Mexico 02 p0227 N85-11486
Post-Sonoman conodont biofacies of the Triassic of northwestern Nevada 03 p0390 N85-12497
Geographic and stratigraphic distribution of Miocene palynomorphs in north Idaho 03 p0390 N85-12498
Metamorphic petrology of the Table Mountain area, Circle quadrangle, Alaska 04 p0516 N85-13295
Late Paleozoic and early Mesozoic radiolarians in the Circle quadrangle, east-central Alaska 04 p0517 N85-13297
Magnetic constraints on early lunar evolution revisited: Limits on accuracy imposed by methods of paleointensity measurements 04 p0582 N85-13716
Late Quaternary deep-water paleoceanography of the eastern equatorial Indian Ocean: Evidence from Bethnic foraminifers, carbonate dissolution, and stable isotopes 06 p1182 N85-17446
Global paleoclimatic data base for 6000 years BP [DE85-006828] 15 p2600 N85-26024
Global Mega-Geomorphology [NASA-CP-2312] 21 p3600 N85-32357
Some observations on paleogeomorphology 21 p3601 N85-32363
Paleoenvironmental investigations at seed cave (Windust cave H-45FR46), Franklin County, Washington [AD-A154777] 21 p3635 N85-32576
Precambrian evolution and the rock record 21 p3656 N85-32711

PALLADIUM
Surface chemistry of palladium [DE84-014572] 02 p0173 N85-11163
Electron energy loss investigation of the electronic and structural properties of palladium [NOTA-INTERNA-903] 02 p0289 N85-11886
Study of catalysts and mechanisms in synthesis reactions [DE84-015025] 04 p0470 N85-12990
Transition metal catalyzed transformations of unsaturated molecules [DE85-009531] 16 p3080 N85-29055
FTIR studies of hydrocarbon synthesis on Pd/ZSM5 catalysts [DE85-012430] 24 p4071 N85-35230
Characterization of catalysts with metal-support effects and of the species adsorbed on their surfaces [DE85-012254] 24 p4096 N85-35394

PALLADIUM ALLOYS
Surface segregation of sulfur during oscillatory pin-on-plate wear studies of precious metal electrical contact alloys. 1: Friction and electrical contact resistance [DE84-006662] 02 p0195 N85-11303
First principles theory of Fermi-surface driven concentration waves in Cu/sub c/Pd/sub 1-c/ alloys [DE85-005367] 13 p2024 N85-22661
Study of the kinetics and thermodynamics of hydrogen in Pd-based alloys [DE85-007341] 16 p2750 N85-26069
Electrical conductivity and phase diagram of binary alloys. 21: The system palladium-chromium [NASA-TM-77863] 18 p3073 N85-29009

PALLADIUM COMPOUNDS
Electrical conductivity and phase diagram of binary alloys. 21: The system palladium-chromium [NASA-TM-77863] 18 p3073 N85-29009

PAM (MODULATION)
U PULSE AMPLITUDE MODULATION

PANCREAS
Endocrine responses to hypotensive gravitational stress: Catecholamines, pancreatic polypeptide, and vasopressin 05 p0693 N85-14480
Lipid hydrolysis in man during antiorthostatic hypokinesia 23 p3953 N85-34500

PANEL METHOD (FLUID DYNAMICS)
PAN AIR: A computer program for predicting subsonic or supersonic linear potential flows about arbitrary configurations using a higher order panel method. Volume 3: Case manual (version 1.0) [NASA-CR-3253] 02 p0135 N85-10922
Viscous-Inviscid aerodynamic analysis of two-dimensional thrust augmentors [NASA-CR-177321] 04 p0451 N85-12661
Prediction of dynamic stall characteristics using advanced non-linear panel methods [AD-A148453] 08 p1078 N85-16836
Application of the vortex-lattice concept to flows with smooth-surface separation 08 p1160 N85-17320
Numerical approach for the aerodynamic analysis if airfoils with laminar separation [NASA-CR-172496] 09 p1273 N85-18001
Calculation of the flow around thick wings with separation vortices 12 p1821 N85-21424
Application of time-linearized methods to oscillating wings in transonic flow and flutter 15 p2459 N85-25182
A study of aerodynamic control in stalled flight leading-edge vortex formation analysis [AD-A153758] 18 p3059 N85-28928
Shock waves in adjacent engine inlets [ISL-R-104/84] 20 p3396 N85-31068
A panel method study of vortex sheets with special emphasis on sheets of axisymmetric geometry [NASA-CR-177366] 21 p3552 N85-32095
Calculation of compressible flow about three-dimensional inlets with auxiliary inlets, slots and vanes by means of a panel method [NASA-CR-174975] 24 p4060 N85-35162

PANELS
NT CURVED PANELS
NT RECTANGULAR PANELS
NT WING PANELS
Composite laminate optimization program suitable for microcomputers 01 p0059 N85-10369
Quasi-steady analysis of aircraft panel flammability [AD-A145401] 02 p0138 N85-10838
Features of new solar panels on Salyut-7 02 p0157 N85-11062
Tensile strength of composite sheets with unidirectional stringers and crack-like damage: A brief report [NASA-TM-86310] 02 p0170 N85-11139
Effect of stress concentrations in composite structures [NASA-CR-173976] 02 p0170 N85-11140
Performance of two transonic airfoil wind tunnels utilizing limited ventilation 03 p0313 N85-12020
Long-term thermal aging of 2 graphite-polyimide composite materials [NASA-TP-2369] 03 p0325 N85-12094
Prefabricated panels for rapidly runway repair and expedient airfield surfacing [AD-D011277] 05 p0597 N85-13804
Design procedures for fiber composite structural components: Panels subjected to combined in-plane loads [NASA-TM-86909] 07 p0919 N85-15823
Preliminary evaluation of an improved flammability test method for aircraft materials [FAA-CT-84-22] 08 p1080 N85-16840
Challenges in the development of the orbiter radiator system 08 p1096 N85-16925
Space shuttle elevon seal panel mechanism 08 p1101 N85-16961
Composite repair of aircraft structures 08 p1120 N85-17059
A simple engineering treatment of center cracked tension panels in the regime of nonlinear fracture mechanics under plane stress conditions [GKSS-84-E-36] 08 p1173 N85-17396
A safety evaluation of the relocation of the ACM (Air Combat Maneuver) panel in the F-14 ( )/AIP (Avionics Integration Program) [AD-A149598] 12 p1777 N85-21158
Temperature responses of composite panels [AD-A150063] 12 p1798 N85-21277
Power from the Sun: Light at night [PB85-124097] 12 p1883 N85-21814
Aircraft safety improvement 15 p2688 N85-26602
The touch panel system: Design and development [AD-A153014] 17 p3008 N85-28598
Resistance to corrosion fatigue in aluminum alloy 1561 in sea water 19 p3243 N85-30108
The thermal calculation of opaque heat screens [BLL-M-36273-(6828.4)] 20 p3450 N85-31421
Experimental and theoretical assessment of a new technique for the non-destructive evaluation of laminated panels [AD-A155622] 21 p3562 N85-32155
An investigation into the comparisons of the underwater shock effects on a stiffened flat plate to the predictive nature of a computer model [AD-A155612] 21 p3600 N85-32355
Joint design for improved fatigue life of diffusion-bonded box-stiffened panels [NASA-TP-2480] 22 p3799 N85-33537
Nonlinear response and failure characteristics of internally pressurized composite cylindrical panels [NASA-CR-176148] 22 p3800 N85-33548
A new large-scale, high-resolution multicolor software display concept [AD-A155404] 22 p3827 N85-33703
Removable cleanable antireflection shield [AD-D011735] 22 p3844 N85-33810
A research program to reduce the interior noise in general aviation aircraft, index and summary [NASA-CR-176178] 24 p4145 N85-35895

PANORAMIC CAMERAS
Calculation of image shift in panoramic photography 15 p2488 N85-25357

PANTAR CHONDRITES
Solar cosmic ray produced neon in lunar soils and their implication for gas-rich meteorite studies 06 p0887 N85-15636

PAPER (MATERIAL)
Optical mark reader [AD-D011462] 10 p1557 N85-19818

PARABOLAS
Constrained parabolic approximation of curves in the finite element method [CSIR-TWISK-340] 14 p2408 N85-24843
The nonlinear analysis of thick composite plates using a cubic spline function [AD-A152115] 16 p2801 N85-27268
Curved finite elements and curve approximation 17 p3007 N85-28590

PARABOLIC ANTENNAS
Parabolic tapers for overmoded waveguides [DE84-014237] 01 p0039 N85-10247
Dual offset reflector antenna systems with rotationally symmetric aperture distributions [AD-A147346] 07 p0940 N85-15961
Efficient computation of reflector antenna aperture distributions and far field patterns [AD-A147367] 07 p0940 N85-15962
Image lobe analysis for large radomes [AD-P004359] 12 p1825 N85-21453
Experimental verification of beam deflection from hybrid reflector antenna within wide-angle sector 13 p2079 N85-22984
Null generation using discs on a reflector [AD-A151697] 15 p2544 N85-25703
Frequency independent parabolic phased antenna array of log periodic antennas 22 p3774 N85-33367

PARABOLIC BODIES
Scattering by a parabolic cylinder: A uniform asymptotic expansion [AD-A145988] 02 p0252 N85-11652
Progress in solar thermal distributed receiver technology [DE85-009066] 18 p3128 N85-29372

PARABOLIC DIFFERENTIAL EQUATIONS
Time discretization of parabolic problems by the discontinuous Galerkin method [CTH-MATH-1984-19] 04 p0558 N85-13543
Numerical investigations into the parabolized Navier-Stokes equations 05 p0695 N85-14075
A lumped mass finite element method with quadrature for a nonlinear parabolic problem [CTH-MATH-1984-22] 05 p0719 N85-14915
Generalized predictor-corrector methods of high order for the time integration of parabolic differential equations [CWI-NM-R8402] 08 p1214 N85-17644
On the local behaviour of solutions of degenerate parabolic equations with measurable coefficients [AD-A147412] 09 p1373 N85-18631

Spectral methods in time for parabolic problems
[NASA-CR-172539] 11 p1706 N85-20730
Local behavior of solutions of an elliptic-parabolic equation
[AD-A149624] 12 p1920 N85-22057
Brownian motion with a parabolic drift and Airy functions
[CWI-MS-R8413] 12 p1925 N85-22097
On the stability of predictor-corrector methods for parabolic equations with delay
[CWI-NM-R8410] 14 p2410 N85-24880
On the shift parameter in the backward beam method for parabolic problems for preceding times
[CWI-NM-R8411] 14 p2410 N85-24881
Water wave propagation over uneven bottoms
[AD-A151450] 15 p2556 N85-25769
Recent progress in the development and application of the parabolic equation
[AD-A151475] 15 p2637 N85-26265
Analysis of nonlinear parabolic equations modeling plasma diffusion across a magnetic field
[DE86-007663] 17 p3040 N85-26807
Numerical and experimental investigation of turbomachinery rotor flow fields
20 p3451 N85-31429
Sobolev-Poincare's inequality and the Neumann problem for u sub t = divergence of the absolute value of the gradient u to the p-2 power x the gradient u
[AD-A154788] 21 p3676 N85-32839
FEMALE: Finite Element Method for Arbitrary Lagrangian and Eulerian elements
23 p3979 N85-34671
Long-time asymptotics of a system for plasma diffusion
[NASA-CR-177947] 24 p4093 N85-35375

PARABOLIC REFLECTORS
NT PARABOLOID MIRRORS
Liquid cooled, linear focus solar cell receiver
[DE84-014446] 01 p0067 N85-10448
RF characteristics of the hoop column antenna for the land mobile satellite system mission
[NASA-CR-3842] 02 p0189 N85-11284
Analytical thermal formulations for antenna dishes — satellite antennas 05 p0627 N85-14017
Joint Indo-German program on solar energy: Parabolic dish program, step 1
[BMFT-FB-T-84-175] 05 p0670 N85-14312
Efficient computation of reflector antenna aperture distributions and far field patterns
[AD-A147367] 07 p0940 N85-15962
BBC receiving terminal for the European orbital test satellite
[BBC-RD-1984/15] 06 p1142 N85-17205
Calculation and computer simulation of the Paraboloidal Mirror Analyzer (PMA)
[DE85-001417] 09 p1384 N85-18705
Innovative solar thermal dish technology development
[DE85-002787] 11 p1673 N85-20539
Value of PV systems experiments. Volume 1: A preliminary assessment of the lessons learned from nine intermediate-size systems
[DE85-001494] 11 p1674 N85-20546
Axial focusing of signal from distant point radiator reflected twice in deep paraboloid
13 p2078 N85-22979
Synchronously deployable tetrahedral truss reflector
14 p2231 N85-23827
Electromagnetic analysis for surface tolerance effects on large space antennas 14 p2234 N85-23850
Prime-focus parabolic reflector antenna: Theory and measurement
[R-NIAS-20] 14 p2291 N85-24199
Development and testing of Parabolic Dish Concentrator No. 1
[NASA-CR-175851] 14 p2350 N85-24522
A study of structural concepts for ultralightweight spacecraft
[NASA-CR-175765] 16 p2730 N85-26848
A bibliography of reports of the Sandia solar thermal distributed receiver systems project
[SAND-84-0313] 16 p2817 N85-27378
Manufacturing cost analysis of a parabolic dish concentrator (General Electric design) for solar thermal electric power systems in selected production volumes
[NASA-CR-175772] 16 p2818 N85-27380
Activity and accomplishments of dish/Stirling electric power system development
[NASA-CR-175841] 17 p2985 N85-29445
Parabolic dish test site: History and operating experience
[NASA-CR-175882] 17 p2985 N85-29447
A program for the calculation of paraboloidal-dish solar thermal power plant performance
[NASA-CR-175874] 17 p2985 N85-29449
Shenandoah parabolic dish solar collector
[DE85-008326] 17 p2987 N85-29460
DOE/Sandia point-focus concentrator program, draft
[DE85-008209] 17 p3038 N85-26793
Progress in solar thermal distributed receiver technology
[DE85-008066] 18 p3126 N85-29372
Liquid metal thermoelectric converter (LMTEC) for solar applications
[DE85-008405] 18 p3129 N85-29376
High reflective surfaces for millimeter RF waves, phase A — satellite antenna reflectors
[HRS-FR-01] 20 p3442 N85-31366
View-limiting shrouds for insolation radiometers
[NASA-CR-176041] 20 p3458 N85-31476
Control system for parabolic dish concentrator No. 1
[NASA-CR-176045] 20 p3463 N85-31510
Optical analysis of parabolic dish concentrators for solar dynamic power systems in space
[NASA-TM-87080] 23 p3903 N85-34176

PARABOLOID MIRRORS
Influence of strut cross-section on strut radiation of reflector antennas
[FI-455-TBR-39] 03 p0357 N85-12295
Holographic corrector in objective with compound main mirror 17 p2941 N85-28153

PARABOLOIDS
U PARABOLIC BODIES

PARACHUTE DESCENT
Parachute expedition to Arctic
07 p0962 N85-16240
Tactical deployment of satellite-reporting drifting data buoys for environmental data acquisition
14 p2332 N85-24423
Processing methods of rawinsonde measurements at the descent by parachute
[KNMI-WR-84-7] 18 p3149 N85-29498

PARACHUTE FABRICS
Age life prediction of nylon 66 parachute materials. Part 1: Mechanical properties
[AD-A147698] 08 p1170 N85-17378

PARACHUTES
NT DRAG CHUTES
NT RECOVERY PARACHUTES
60,000 pound capacity extraction system
[AD-A145841] 03 p0318 N85-12052
A theoretical view on the stress analysis of fully inflated parachute canopies
[AD-A145387] 08 p1078 N85-16835
Deployment sequence mode selection system for aircraft ejection seat
[AD-D011464] 10 p1422 N85-18988
Airspeed sensing pressure valve system
[AD-D011472] 10 p1425 N85-18987
Parachute inflation dynamics
11 p1715 N85-20792
Parachute extraction device for ultralight gliders
[CH-643499-A5] 16 p2699 N85-26663
Dual towline spin-recovery device
[NASA-CASE-LAR-13076-1] 24 p4066 N85-35200

PARACHUTING
U PARACHUTE DESCENT

PARADOXES
The automated reasoning system ITP
[ANL-84-27] 12 p1914 N85-22016

PARAFFINS
Catalytic conversion of C3-C4 paraffins to gasoline
[DE85-004181] 10 p1458 N85-19187

PARAGLIDERS
NT FLEXIBLE WINGS

PARALLAX
NT STELLAR PARALLAX
Measurement of pulsar parallax by Very Long Baseline Interferometry 03 p0444 N85-12830
The parallax of pulsar 0950+08 and the local free electron density 06 p0879 N85-15584
Ranging system which compares an object reflected component of a light beam to a reference component of the light beam
[NASA-CASE-NPO-15865-1] 23 p3973 N85-34629

PARALLEL COMPUTERS
Workshop on Computer Architecture
[AD-A146455] 06 p0847 N85-15378
Solution of partial differential equations on vector and parallel computers
[NASA-CR-172500] 07 p1026 N85-16525

PARALLEL FLOW
NT PIPE FLOW
NT THREE DIMENSIONAL FLOW
Parallel flow diffusion battery
[DE84-005964] 05 p0631 N85-14047
Long range effect of turbulent pressure pulsations in plane-parallel flows at different velocities with various flame fronts 09 p1308 N85-18220
Diffusion deposition in fibrous filters for parallel and transverse flow models
[DE85-008149] 13 p2093 N85-23066
On spectral multigrid methods for the time-dependent Navier-Stokes equations
[NASA-CR-172613] 19 p3344 N85-30725

PARALLEL PLATES
Diffraction of plane electromagnetic waves on seminfinite grid of parallel conductors arranged at angle to its edge 03 p0344 N85-12217
An indirect measure of below-ground electric field, conductivity, and dielectric constant
[AD-A146516] 06 p0804 N85-15115
Variational and moment method solutions of the fields in a parallel-plate waveguide-aperture system
[DE85-006288] 13 p2057 N85-22876
Aberration characteristics of plane-parallel compensator plate 14 p2276 N85-24100
Analysis of the electromagnetic scattering from an inlet geometry with lossy walls
[NASA-CR-175743] 15 p2541 N85-25686
Colloidal particle transport with simultaneous birth, growth and capture
[DE85-010386] 19 p3235 N85-30055
Nickel cadmium cell design variable program data analysis 20 p3445 N85-31367

PARALLEL PROCESSING (COMPUTERS)
Aerospatiale's experimentations of vectorization on supercomputers for aircraft structural problems
01 p0007 N85-10041
Initial experience with distributing structural calculations among computers operating in parallel
01 p0058 N85-10381
Hardware for a real-time multiprocessor simulator
[NASA-TM-83805] 01 p0099 N85-10659
Function algorithms for MPP scientific subroutines, volume 1
[NASA-CR-175246] 01 p0102 N85-10678
Numerical algorithms and parallel tasking
[AD-A145090] 01 p0104 N85-10693
Design and descriptive tools for systolic architectures
[DE84-015521] 02 p0239 N85-11557
Criteria for the optimization of processing flow in a model of an incremental computer with multiprocessing resources
[INPE-3046-TDL/158] 02 p0240 N85-11560
Parallel triangularization of substructured finite element problems
[NASA-CR-172466] 02 p0241 N85-11569
Parallel, iterative solution of sparse linear systems: Models and architectures
[NASA-CR-172457] 02 p0243 N85-11586
Intelligent information retrieval from on-line technical documentation
[AD-P003946] 02 p0249 N85-11626
Real-time Ada (trademark)
[AD-A146258] 03 p0407 N85-12603
Analysis and design methodology for VLSI computing networks
[AD-A146030] 03 p0409 N85-12611
A decomposable algorithm for contour surface display generation
[AD-A145783] 03 p0410 N85-12619
Automatic recognition and turbuling objects
[AD-A145908] 03 p0419 N85-12676
Comparison analysis of algorithm for construction of functional tests for combined large-scale integrated circuits 04 p0490 N85-13121
Parallel processing of numerical transport algorithms
[DE84-016625] 04 p0555 N85-13534
Instantaneous kinematics and joint displacement analysis of fully-parallel robotic devices
05 p0641 N85-14113
Massively parallel processor 05 p0680 N85-14366
Research in computer science
[NASA-CR-174068] 05 p0713 N85-14572
Concurrency in parallel processing systems
05 p0714 N85-14581
Workshop on Computer Architecture
[AD-A146455] 06 p0847 N85-15378
Parallel processor configuration for adaptive antenna arrays
[AD-D011347] 07 p0942 N85-15970
Future database machine architectures
[AD-A146786] 07 p1022 N85-16481
Implementation of a constraint machine for prism - A parallel problem solver
[AD-A147844] 07 p1026 N85-16512
What a parallel programming language has to let you say
[AD-A147854] 07 p1026 N85-16513
Sequential and parallel matrix computations
[AD-A147871] 07 p1034 N85-16562
An optimal parallel processing method for inverting sparse matrices 09 p1367 N85-18585
Parallel algorithms for robot dynamics
[DE84-016563] 09 p1369 N85-18605
System software for the finite element machine
[NASA-CR-3870] 09 p1372 N85-18622

Where are the parallel algorithms?
[NASA-CR-172516] 09 p1373 N85-18627
Domain decomposition techniques for solving elliptic partial differential equations on multiprocessors
[DE85-004448] 10 p1549 N85-19769
Parallel processing experiences on the Denelcor HEP computer
[DE85-000853] 11 p1702 N85-20703
PISCES: An environment for parallel scientific computation
[NASA-CR-172544] 12 p1913 N85-22004
Interface specifications for SCR (Software Cost Reduction) (A-7E) extended computer module, revised
[AD-A149948] 12 p1915 N85-22024
Very-high level concurrent programming
[AD-A150009] 12 p1916 N85-22026
Characterizing the parallelism in rule-based expert systems
[DE85-002432] 12 p1919 N85-22047
Parallel processing of encoded bit strings
[AD-A149612] 12 p1921 N85-22064
Optimal allocation of components in parallel-series and series-parallel systems
[AD-A150169] 13 p2144 N85-23309
Exploiting parallel computing with limited program changes using a network of microcomputers
[NASA-TM-86367] 13 p2146 N85-23318
Parallel processing for computational continuum dynamics
[AD-A150513] 13 p2147 N85-23327
Studies in parallel image processing
14 p2399 N85-24789
The enhancement of concurrent processing through functional programming languages
[AD-A150771] 14 p2404 N85-24822
Workshop on Parallel Computer Architectures in Pattern Recognition and Image Processing
[BMFT-FB-DV-84-006] 15 p2622 N85-26154
Posing of the problem, status, and future of parallel computer architecture for image processing
15 p2622 N85-26155
Recognition of objects in their natural environment — parallel processing 15 p2622 N85-26158
ADA (trademark) tasking and exceptions: A formal definition
[AD-A151618] 15 p2629 N85-26204
Harnessing computional power: Distributed combinator reduction
[DE85-005987] 15 p2631 N85-26216
Parallel time O(log N) acceptance of deterministic CFLs
[AD-A152255] 16 p2845 N85-27539
Parallel computation of multiple-scale problems
[DE85-007230] 16 p2849 N85-27563
Parallel computing in optimization
[AD-A151612] 16 p2850 N85-27568
Local uniform mesh refinement on loosely-coupled parallel processors
[AD-A152199] 16 p2850 N85-27571
Complexity of dense linear system solution on a multiprocessor ring
[AD-A151970] 16 p2854 N85-27596
Computational plasma physics and supercomputers, revision 1
[DE85-007228] 16 p2867 N85-27687
Language design, computers and brains
[AD-A152819] 17 p3008 N85-28594
Introduction to the IEEE-488 bus
[INPE-3316-NTE/227] 17 p3010 N85-28613
Efficient parallel solution of linear systems with hyperbolic rotations
[AD-A152355] 17 p3018 N85-28661
Efficient parallel solution of linear systems
[AD-A152683] 17 p3018 N85-28663
Torus data flow for parallel computation of misaized matrix problems
[DE85-006761] 17 p3026 N85-28715
Development of a butterfly multiprocessor test bed description of butterfly components
[AD-A153692] 18 p3095 N85-29155
Tradeoffs among portability, complexity, and efficiency in multiprocessing environments
[DE85-007699] 18 p3161 N85-29580
Parallel computation of multiple-scale problems, revision 1
[DE85-009447] 18 p3164 N85-29598
The prospects of the digital optical computer
18 p3168 N85-29771
A parallelized point successive over-relaxation method on a multiple instruction multiple data stream computer
[AD-A154377] 19 p3337 N85-30679
VLSI structures for numerical and digital signal processing computations 20 p3439 N85-31340
Methods for design and evaluation of integrated hardware-software systems for concurrent computation
[NASA-CR-176066] 20 p3515 N85-31651
Study of new computing algorithms for supercomputers. Application to parallel processing computation
[SNIAS-440-070/84] 20 p3516 N85-31660
Parallel simulation of digital LSI circuits
[AD-A154745] 21 p3580 N85-32258
Tight bounds on the complexity of parallel sorting
[AD-A154726] 21 p3667 N85-32778
Optimum predistortion of digital signals for transmission over parallel channels 22 p3776 N85-33397
Parallel processing on the Livermore VAX 11/780-4 parallel processor system with compatability to Cray Research, Inc. (CRI) multitasking, version 1
[DE85-011856] 23 p3967 N85-34585
PARALLEL PROGRAMMING
On the formal description and derivation of temporal proof rules for program properties
[TUM-I8405] 01 p0101 N85-10875
What a parallel programming language has to let you say
[AD-A147854] 07 p1028 N85-18513
Parallel input and feedback in dialogue cells
[CWI-CS-R8413] 11 p1703 N85-20708
PASLIB programmer's guide for the finite element machine, revision 2.1-A
[NASA-CR-172281] 11 p1705 N85-20727
Parallel linear algebra library for the Denelcor HEP
[DE85-004885] 12 p1917 N85-22034
Implementation of some concurrent algorithms
[DE85-004887] 13 p2148 N85-23334
Optical memory research and its application to digital optical processing 13 p2158 N85-23397
Use of function processors in multiprocessor systems
14 p2400 N85-24796
Dataflow computation
[CWI-TRACT-6] 14 p2408 N85-24833
Parallel programmable charge domain device
[AD-D011599] 15 p2549 N85-25733
Recent trends in software technology for vector processors 16 p2691 N85-26815
Recent advances in supercomputers
16 p2693 N85-26825
Reliability models for dataflow computer systems
[NASA-CR-175813] 16 p2846 N85-27543
Research in computer science
[NASA-CR-175822] 17 p3010 N85-28612
Tradeoffs among portability, complexity, and efficiency in multiprocessing environments
[DE85-007699] 18 p3161 N85-29580
The BLAZE language: A parallel language for scientific programming
[NASA-CR-172615] 19 p3334 N85-30656
Parallel Cholesky factorization in message-passing multiprocessor environments
[DE85-012079] 22 p3830 N85-33717
Reordering computations for parallel execution
[NASA-CR-177961] 23 p3957 N85-34522
PARALLEL STRIP LINES
U MICROSTRIP TRANSMISSION LINES
PARALLELEPIPEDS
Closely spaced independent parallel runway simulation
[DOT/FAA/CT-84/45] 04 p0457 N85-12902
Building an octree from a set of parallelepipeds
23 p3964 N85-34572
PARAMAGNETIC AMPLIFIERS
U MASERS
PARAMAGNETIC RESONANCE
NT ELECTRON PARAMAGNETIC RESONANCE
PARAMAGNETISM
High specific heat dielectrics and Kapitza resistance at dielectric boundaries
[AD-A148476] 08 p1217 N85-17666
Paramagnetic scattering from Ni
[DE85-004207] 12 p1942 N85-22198
Investigation of bimodal paramagnetic filter
13 p2063 N85-23007
Paramagnetic form factors from itinerant electron theory
[DE85-005272] 16 p2750 N85-26973
An EPR (Electron-Paramagnetic-Resonance) and ENDOR (Electron-Nuclear-Double-Resonance) study of ferroelectric ammonium sulfate
[AD-A155580] 21 p3710 N85-33033
PARAMETER IDENTIFICATION
Optimum parameters for determining the motion of radar field by cross-correlation method
01 p0079 N85-10524
List of recent Soviet space launches
02 p0165 N85-11120
Simulation study of a new inverse-pinch high Coulomb transfer switch
[NASA-CR-173420] 02 p0194 N85-11294
Control and identification of time varying systems
[AD-A145636] 02 p0252 N85-11849
CVD parameter study using strategy of experimentation
[DE84-015900] 04 p0473 N85-13011
Parametric models for signal processing: Autoregressive (AR), Moving Average (MA) and mixed autoregressive with moving average (ARMA)
[ENST-84D001] 05 p0628 N85-14026
Model estimation and identification of manual controller objectives in complex tracking tasks
05 p0700 N85-14494
Effects of control stick parameters on human controller response 05 p0701 N85-14496
A search for possible members of open clusters among known Ap stars 05 p0737 N85-14740
The Lund catalogue of open cluster parameters
05 p0738 N85-14742
Quality control of integrated circuits by parametric identification methods 06 p0798 N85-15085
Aeroelastic analysis and the identification of flight loads — Mirage 2000 aircraft 07 p0896 N85-15679
More than you want to know about maximum likelihood estimation
[NASA-TM-85905] 07 p0900 N85-15752
Estimating location parameters in a mixture
07 p0984 N85-16252
Bayesian estimation of normal mixture parameters
07 p0985 N85-16255
Snow characterization measurements from SNOW-TWO/Smoke Week 6
[AD-A147423] 07 p1008 N85-16402
Identification and parameter estimation of phosphate balance models in drinking water reservoirs
[PUBL-313] 08 p1161 N85-17439
Identification of vibration parameters of flexible structures 09 p1331 N85-18360
Dynamics and control of general linear lumped-parameter systems 09 p1372 N85-18623
Initialization of Thompson-Pisarenko's algorithm — sinusoidal signal parameter estimation
[FUB-46-1983] 09 p1375 N85-18641
A method for estimating the rolling moment due to spin rate for arbitrary planform wings
[NASA-TM-86365] 10 p1425 N85-18990
A semianalytical, artificial satellite orbit propagation procedure based on optimal parameter estimation
[INPE-3301-PRE/613] 10 p1427 N85-18997
Measurements of propagation at 900 MHz in an urban zone for establishing a digital radiomobile system
10 p1472 N85-19288
Identification of dynamic systems, theory and formulation
[NASA-RP-1138] 10 p1551 N85-19784
A three-dimensional geometric-physical model for conventional geodetic observations-observables, parameter estimation, and deformation analysis
[SER-C-296] 11 p1685 N85-20493
A proposed method for fast determination of plasma parameters
[IPP-1/228] 11 p1730 N85-20877
Determination of physical parameters of jets in radio galaxies 12 p1958 N85-22304
Air combat simulation: Methods, models, trends
13 p1967 N85-22359
Determination of aerodynamic and propulsion parameters of general aviation aircraft using steady state flight test data 13 p1971 N85-22377
Use of Walsh functions for calculating characteristics of digital filters with impulse response of finite duration
13 p2093 N85-23011
An eigensystem realization algorithm for application to model testing 14 p2233 N85-23842
Peculiarities of MgF2 film formation and optimization of MgF2 film deposition process 14 p2281 N85-24132
Determination of directional gyro parameters
14 p2287 N85-24171
Results of studies of wave field internal structure in prediction of geological cross section
14 p2346 N85-24504
Observation model and parameter partials for the JPL VLBI parameter estimation software MASTERFIT-F 2.0
[NASA-CR-175840] 14 p2347 N85-24509
Parameter estimation in stochastic dynamic systems
14 p2395 N85-24754
Identification of dynamic systems
[AGARD-AG-300-VOL-2] 15 p2470 N85-25249
Minimax problem of estimating trajectory parameters in continuous formulation 15 p2479 N85-25301
Predischarge parameters of SF6-CO2 determined by laser 15 p2564 N85-25821
Estimation theory applied to improving dynamic structural models
[DE85-004148] 15 p2630 N85-26210
Theoretical investigation of lasing in 4.3 micron region in CO2 laser 15 p2643 N85-26306
Optimum parameters of aerogyroscopic satellite orientation system 16 p2718 N85-26782
Development and application of optimum sensitivity analysis of structures
[NASA-CR-175857] 16 p2799 N85-27257

Parameter identification results of tests in nonsteady symmetric flight with the Hawker Hunter Mk 7
[NLR-TR-83042-U] 17 p2897 N85-27860
Identification of gust input and gust response characteristics from Do 28 TNT flight test data
[DFVLR-FB-84-46] 17 p2900 N85-27861
Heating parameter estimation using coaxial thermocouple gages in wind tunnel test articles
[AD-A153039] 17 p2966 N85-28328
Robust regression through robust covariances
[AD-A153301] 17 p3020 N85-29577
Thermophysical properties correlations and pseudocomponent characterization parameter estimation for fossil fluids
[DE85-009297] 19 p3230 N85-30024
Expanding expertise by use of an expert system
[DE85-010759] 19 p3344 N85-30723
Vibration control experiment design for the 15-m hoop/column antenna 20 p3409 N85-31159
A nonlinear dual-adaptive control strategy for identification and control of flexible structures
20 p3416 N85-31203
Stable direct adaptive control of linear infinite-dimensional systems using a command generator tracker approach 20 p3416 N85-31204
Maximum likelihood estimation with emphasis on aircraft flight data 20 p3417 N85-31208
Optimal sensor locations for structural identification
20 p3417 N85-31209
Combined state and parameter estimation for a static model of the Maypole (Hoop-Column) antenna suface
20 p3417 N85-31210
Experimental verification of identification algorithms for control of flexible structures 20 p3418 N85-31211
An Eigensystem Realization Algorithm (ERA) for modal parameter identification and model reduction
20 p3418 N85-31212
A residuals approach to filtering, smoothing and identification for static distributed systems
20 p3418 N85-31213
Numerical experimentation with maximum likelihood identification in static distributed systems
20 p3418 N85-31214
Geodyn systems development
20 p3492 N85-31706
An overview of nonlinear systems identification
[RR-271] 20 p3520 N85-31894
On the choice of parameterization for identification
[OUEL-1554/84] 20 p3522 N85-31904
Modelling and parameter estimation for distributed vibratory systems
[AD-A154518] 21 p3596 N85-32344
Physics of heavily doped silicon and solar-cell parameter measurement 21 p3609 N85-32418
Measuring bulk recombination rates and boundary recombination velocities 21 p3609 N85-32419
Synthesis of adaptive filters for tracking radio systems
22 p3763 N85-33325
Real-time multiparameter pulse processing with decision tables
[DE85-011663] 23 p3966 N85-34589
The effect of instrumentation system parameters on the results of a flight mechanical system identification
24 p4061 N85-35170
Aspects of input signal design for order and parameter estimation in linear dynamical systems
[ER-83/05] 24 p4091 N85-35362
A strategy for calibrating atmospheric transport models
[CSIRO-DAR-TP-9] 24 p4116 N85-35518
Recursive partitioning estimation
24 p4141 N85-35670

PARAMETERIZATION
NT PARAMETER IDENTIFICATION
Qualitative results for distributed systems with discrete damping and stiffness with application to control
[AD-A145525] 02 p0209 N85-11382
Parametric analysis for generalized network flow problems
[AD-A145558] 02 p0243 N85-11589
Asymptotically optimal adaptive control
[AD-A145686] 02 p0249 N85-11629
Fluctuations in parameters of light beam along path with reflection in turbulent atmosphere
02 p0263 N85-11722
Parameterizing extreme still water levels and waves in design level studies
[IOS-163] 03 p0398 N85-12542
Maximum likelihood and Bayesian parameter estimation in item response theory
[AD-A145775] 03 p0413 N85-12844
Priority rewrite systems — computer programming
[CWI-CS-R8407] 05 p0720 N85-14621
Construction of a confidence region for linear functions with unknown parameters
[CTH-MATH-1984-17] 05 p0721 N85-14630
An on-line parameter estimation algorithm for counting process observations
[CWI-OS-R8406] 05 p0721 N85-14632
The effects of long-periodic forcing in a zero-dimensional climate model 07 p1002 N85-16363
Development of a mixed scanning interactive system for decision support
[AD-A146995] 07 p1051 N85-16670
Radiation parameterization programs for use in general circulation models
[AD-A148015] 08 p1188 N85-17488
On the ergodicity of bilinear time series models and some applications
[AD-A148032] 08 p1215 N85-17651
Speech analysis by parametric methods: A survey
[ENST-84C004] 09 p1313 N85-18251
Stress waves in an isotropic elastic plate excited by a circular transducer
[NASA-CR-3877] 11 p1650 N85-20390
The use of analytical models to interpret measured data properly. 1. General background theory
11 p1651 N85-20400
Contribution to the study of perturbational stabilization
[ONERA-NT-1984-1] 11 p1714 N85-20781
A proposed method for fast determination of plasma parameters
[IPP-1/228] 11 p1730 N85-20877
Spatial resolution estimation of LANDSAT-4 Thematic Mapper data 12 p1872 N85-21741
Statistics for the maximum of several positive random variables with application to networking
[AD-A150005] 12 p1922 N85-22069
Polynomial parameterization in inverse gravimetric problem 13 p2115 N85-23174
Parameterization of a transient electromagnetic facility and test antennas from transient data
[DE85-006231] 15 p2545 N85-25710
Parameterization of subgrid-scale fluxes in mesoscale meteorological models
[AD-A153016] 17 p2996 N85-28523
Free-form design in solid modelling
17 p3004 N85-28569
Adapting shape parameters for cubic Bezier curves
17 p3004 N85-28576
Parameterization in grid generation
17 p3005 N85-28581
The static aeroelasticity of a composite wing
18 p3121 N85-29321
Parameterization of surface fluxes in the VVR Fourth Order GCM 18 p3142 N85-29454
Error growth in operational 10-day forecasts
18 p3143 N85-29460
Preliminary GCM results with a new radiation parameterization 18 p3145 N85-29474
A new CO2 transmittance parameterization and its impact on the GLA GCM 18 p3146 N85-29476
Control and regulation of generalized linear systems
19 p3257 N85-30193
Approximation techniques for parameter estimation and feedback control for distributed models of large flexible structures 20 p3413 N85-31179
Robust control design for large space structures
20 p3416 N85-31200
Errors and parameterizations of sub-grid scale processes in regional-scale atmospheric models
20 p3468 N85-31682
On the choice of parameterization for identification
[OUEL-1554/84] 20 p3522 N85-31904
Assessment of the performance of an in-field Gaussian plume/puff model for overwater use
[AD-A155435] 21 p3614 N85-32460
A modified Fresnel scattering model for the parameterization of Fresnel returns, part 2.3A
21 p3618 N85-32483
Criteria and algorithms for spectrum parameterization of MST radar signals 21 p3626 N85-32527
On a variational approach to some parameter estimation problems
[NASA-CR-177635] 21 p3675 N85-32629
A modal parameter extraction procedure applicable to linear time-invariant dynamic systems
[NASA-CR-176120] 22 p3835 N85-33747
Parametrized energy spectrum of cosmic-ray protons with kinetic energies down to 1 GeV
[OG-4.2-11] 22 p3878 N85-34025
Application of a turbulent closure model to the parameterization of the vertical diffusion of heat, momentum, and humidity in the ECMWF model — European Center for Medium Term Weather Forecasting (ECMWF)
[MITT-41] 24 p4095 N85-35387
A new method of differential structural analysis of gamma-family basic parameters
[HE-3.6-3] 24 p4184 N85-35952
Multiple muons in MACRO
[HE-5.2-1] 24 p4202 N85-36079

PARAMETERS
U INDEPENDENT VARIABLES
PARAMETRIC AMPLIFIERS
Millimeter-wave range masers: A review
13 p2089 N85-23042
PARAMETRIC FREQUENCY CONVERTERS
Principles of designing digital compensating accelerometers 17 p2944 N85-28172
PARAMETRIC OSCILLATORS
U PARAMETRIC AMPLIFIERS
PARATHYROID GLAND
The salutary effect of dietary calcium on bone mass in a rat model of simulated weightlessness
15 p2606 N85-26073
PARITY
Spurious center of mass effects in a dynamically determined basis
[CSIR-TWISK-310] 01 p0109 N85-10732
Parity and time-reversal non-conversation in atoms
[DE84-016924] 04 p0562 N85-13581
Selected topics from J/psi decays
[DE85-010537] 18 p3183 N85-29736
Spatial parity violation in elastic neutron-nuclei interaction channel 21 p3691 N85-32932
PARKING ORBITS
The international environment UNISPACE '82 and the ITU: A relationship between orbit-spectrum resource allocation and orbital debris 12 p1787 N85-21215
PARKINSON DISEASE
Influence of activation of ASFS-2 on human emotional status 08 p1194 N85-17522
PARKS
NT NATIONAL PARKS
PARSING ALGORITHMS
Toward a principle-based parser
[AD-A147637] 08 p1202 N85-17565
Steps towards parsing of query sequences to a database
[AD-A148769] 08 p1206 N85-17590
An algorithm for generating abstract syntax trees
[NASA-CR-172541] 12 p1912 N85-22003
Construction of a menu-based system
[NASA-CR-172560] 13 p2146 N85-23321
Evaluating syntactic constraints to speech recognition in a fighter aircraft environment
[AD-A152117] 16 p2773 N85-27119
Speech understanding research
[AD-A155462] 21 p3700 N85-32990
Project management using graphics
23 p3962 N85-34560
Artificial intelligence in Ada (trademark): Pattern-directed processing
[AD-A156230] 24 p4141 N85-35671
PARTIAL DIFFERENTIAL EQUATIONS
NT BIHARMONIC EQUATIONS
NT BURGER EQUATION
NT ELLIPTIC DIFFERENTIAL EQUATIONS
NT EULER-CAUCHY EQUATIONS
NT FOKKER-PLANCK EQUATION
NT GAUSS EQUATION
NT HELMHOLTZ VORTICITY EQUATION
NT LIOUVILLE EQUATIONS
NT MONGE-AMPERE EQUATION
NT PARABOLIC DIFFERENTIAL EQUATIONS
NT VLASOV EQUATIONS
The approximation of nonsmooth solutions of hyperbolic partial differential equations
[CSIR-TWISK-297] 01 p0108 N85-10723
Qualitative results for distributed systems with discrete damping and stiffness with application to control
[AD-A145525] 02 p0209 N85-11382
Approximation of discontinuous solutions of hyperbolic partial differential equations
[NRIMS-TWISK-302] 02 p0250 N85-11631
Numerical methods for singularly perturbed differential equations with applications
[AD-A145639] 02 p0252 N85-11650
A pseudospectral Legendre method for hyperbolic equations with an improved stability condition
[NASA-CR-172475] 03 p0410 N85-12617
Convergence of SIP (Strongly Implicit Procedure)
[AD-A145810] 03 p0410 N85-12621
Moving finite elements in 2-D
[AD-A146268] 03 p0412 N85-12637
Solution generating technique for the Einstein equations 03 p0435 N85-12768
Step-by-step stability in the numerical solution of partial differential equations
[CWI-NW-161/83] 05 p0720 N85-14623
Convergence of method of lines approximations to partial differential equations
[CWI-NM-R8404] 05 p0720 N85-14627
Viscosity solutions of Hamilton-Jacobi equations at the boundary
[AD-A147444] 07 p1032 N85-16553

Splitting methods for the numerical solution of the incompressible Navier-Stokes equations
[AD-A147483] 07 p1032 N85-16554
On existence and uniqueness of solutions of Hamilton-Jacobi equations
[AD-A147597] 07 p1033 N85-16560
Composites with a periodic structure, mathematical analysis and numerical treatment
[AD-A148301] 08 p1119 N85-17053
Thermal-stress analysis for a wood composite blade
[NASA-CR-174794] 08 p1178 N85-17421
Three-dimensional, direct and vectorized elliptic solvers for various boundary conditions
[AD-B088286L] 08 p1206 N85-17595
A moving finite element method for time dependent partial differential equations with error estimation and refinement
[AD-A147719] 08 p1210 N85-17617
A local refinement finite element method for time dependent partial differential equations
[AD-A147943] 08 p1211 N85-17620
A feedback finite element method with a posteriori error estimation. Part 1. The finite element method and some basic properties of the A posteriori error estimator
[AD-A148345] 08 p1212 N85-17631
Generation of 3-dimensional body fitted coordinates using hyperbolic partial differential equations
[AD-A148059] 09 p1274 N85-18006
Designing the profile of turbine blades using an iteration technique 09 p1305 N85-18201
Accuracy of the finite analytic method for scalar transport calculations
[DE85-001474] 09 p1320 N85-18300
The implementation of irregular grid systems for the finite difference solution of partial differential equations
[LU-MATH-RES-181] 09 p1373 N85-18630
Solution of the h-equation for a single point source excitation of magnitude K
[DE84-017874] 09 p1374 N85-18638
Annuals of the Finnish Academy of Sciences, series A. 1: Mathematics, volume 8, part 2
[ISSN-0066-1953] 10 p1535 N85-19673
Towards the construction of periodic solutions of pseudodifferential equations with the aid of algebraic operators 10 p1535 N85-19674
Analytical foundations of the theory of quasiconformal mappings in Rn 10 p1536 N85-19679
A non-hypoelliptic Dirichlet problem from stochastics 10 p1537 N85-19687
New methods for numerical solution of one class of strongly nonlinear partial differential equations with applications in hydrodynamics
[AD-A149026] 10 p1545 N85-19739
Vectorization and implementation of an efficient multigrid algorithm for the solution of elliptic partial differential equations
[AD-A149049] 10 p1545 N85-19743
Neumann type boundary conditions for Hamilton-Jacobi equations
[AD-A149069] 10 p1546 N85-19746
Symmetry breaking for a class of semi-linear elliptic problems
[AD-A149093] 10 p1546 N85-19748
Hamilton-Jacobi equations in infinite dimensions. Part 1. Uniqueness of viscosity solutions
[AD-A149094] 10 p1546 N85-19749
Evaluation of time integrators for the shallow water equations
[CWI-NM-R8406] 11 p1634 N85-20292
Solving partial differential equations on multiprocessors
[DE85-000745] 11 p1706 N85-20734
Transverse vibration and buckling of a cantilevered beam with tip body under constant axial base acceleration
[NASA-CR-175567] 12 p1864 N85-21694
Numerical methods for tracking interfaces
[LA-9917-MS] 12 p1919 N85-22052
Effect of compliability of hot walls in liquid-propellant engine on low frequency instability 13 p2049 N85-22824
Models of discontinous random fields 13 p2079 N85-22983
A mathematical formulation of the Scole control problem, part 1
[NASA-CR-172581] 14 p2242 N85-23900
Implementation of a C1 triangular element based on the p-version of the finite element method
[AD-A150904] 14 p2404 N85-24825
The generation of three-dimensional body-fitted coordinate systems for viscous flow problems
[AD-A150961] 14 p2408 N85-24848
Application of adaptive grids in solving the partial differential equations governing fluid flow
[AD-A151175] 15 p2555 N85-25786
Pseudo-unsteady systems for steady inviscid flows
[ESA-TT-877] 15 p2558 N85-25782
Very large least squares problems and supercomputers
[AD-A151270] 15 p2623 N85-26162
Analysis of spectral operators in one-dimensional domains
[NASA-CR-172573] 15 p2633 N85-26228
Solution of coupled system of PDE by the transistorized multigrid method
[DE85-006377] 15 p2639 N85-26276
Analysis of combustion oscillations in heterogeneous systems
[AD-A151999] 16 p2745 N85-26942
A split explicit model for short-term numerical weather prediction 16 p2831 N85-27460
Local uniform mesh refinement on loosely-coupled parallel processors
[AD-A152199] 16 p2850 N85-27571
Uniformly high-order accurate non-oscillatory schemes, 1
[NASA-CR-175768] 16 p2853 N85-27589
On the choice of coordinates for semiconductor simulation
[AD-A152214] 16 p2870 N85-27708
Natural vibrations of reinforced spherical shells 17 p2943 N85-28185
Parameterization in grid generation 17 p3005 N85-28581
A survey of composite grid generation for general three-dimensional sections 17 p3006 N85-28584
Solving elliptic partial differential equations on the hypercube multiprocessor
[AD-A153464] 18 p3168 N85-29629
The Cauchy problem for u sub t = Delta u(m) when O m 1
[AD-A153521] 18 p3169 N85-29635
Well-posedness of one-way wave equations and absorbing boundary conditions
[NASA-CR-172619] 19 p3345 N85-30727
An iterative method for indefinite systems of linear equations
[NASA-CR-172345] 19 p3345 N85-30728
Finite control in underdamped distributed parameter systems 20 p3412 N85-31178
Proceedings of the 1st Workshop for the Design of Expert System Partial Differential Equation Solvers
[AD-A154192] 20 p3515 N85-31853
Generation of three-dimensional body-fitted coordinates using hyperbolic partial differential equations
[NASA-TM-86753] 20 p3519 N85-31887
A derivation of relativistic effects in satellite tracking
[AD-A154620] 21 p3558 N85-32132
A variable node finite element method applied to the gas dynamics equations
[AD-A155211] 21 p3584 N85-32291
On a variational approach to some parameter estimation problems
[NASA-CR-177935] 21 p3675 N85-32829
A review of spectral methods
[NASA-CR-172502] 23 p3929 N85-34350
Transient three-phase three-component systems. Part 1: Formulation of the system of differential equations
[DE85-013267] 24 p4095 N85-35384
Analysis of the nonlinear equations describing the elastic, thermal, and electromagnetic behavior of solids: Existence of solutions of semi-inverse problems 24 p4100 N85-35415
Stress analysis of axisymmetric sandwich shells of variable thickness 24 p4101 N85-35419

PARTIAL PRESSURE
NT HYPOXEMIA
NT OXYGEN TENSION
Variations with time of the carbon dioxide partial pressure in central and south Atlantic surface waters
[AD-A145825] 03 p0398 N85-12537
Reconstruction of past atmospheric CO/sub 2/ contents from the chemistry of the contemporary ocean: An evaluation
[DE85-008426] 18 p3133 N85-29401
Determination of kinetic parameters of molecular beam epitaxy
[AD-A155222] 21 p3710 N85-33030
Thermodynamics of the corrosion of chromium in molten carbonates
[DE85-011407] 24 p4078 N85-35282

PARTICLE ACCELERATION
High energy-resolution inelastic X-ray scattering
[DE84-014585] 01 p0118 N85-10804
Notes on NAC report NAC-83-05: Beam Pulse Length Determination by Spectral Analysis
[CSIR-NAC-83-06] 01 p0119 N85-10818
Long time correlation and stochastic diffusion in the standard map 02 p0262 N85-11835
Electric field and plasma energization in computer simulations of magnetotail reconnection
[DE84-014023] 02 p0285 N85-11859
Particle acceleration in two-ribbon flares — solar flares 04 p0519 N85-13314
The Earth magnetosphere: A charged particle accelerator 04 p0519 N85-13315
Particle physics
[DE84-013834] 05 p0727 N85-14673
Electromagnetic acceleration of macroparticles to hypervelocities in axisymmetric geometry
[IPPJ-696] 06 p0863 N85-15484
Corotating interaction regions in stellar winds: Particle acceleration and non-thermal radio emission in hot stars 06 p1234 N85-17773
Synchrotron emission from chaotic stellar winds 06 p1234 N85-17774
Collimated winds from active galactic nuclei 06 p1241 N85-17832
Observation of a westward travelling surge from satellites at low, medium and high altitudes
[NASA-TM-87434] 09 p1342 N85-18442
Review of polarized proton beam techniques and a report on the workshop on polarized beams
[DE85-004390] 12 p1930 N85-22127
Strong iron accelerating by collisionless magnetosonic shock wave propagating perpendicular to a magnetic field
[IPPJ-709] 12 p1935 N85-22161
Neutron and gamma-ray signatures for particle acceleration in solar flares 12 p1954 N85-22276
Self-similar modified shock structures — cosmic rays 12 p1956 N85-22290
Explosive transverse electric field and particle acceleration during magnetic collapse — cosmic plasma 12 p1956 N85-22292
Signatures of the coalescence instability in solar flares 12 p1956 N85-22293
Hydrodynamics of astrophysical jets — active galactic nuclei 12 p1958 N85-22307
Streaming reversal of energetic particles in the magnetotail during a substorm 14 p2358 N85-24571
SAMBO-GEOS: Substorm trapped particle particle boundary movements, particle precipitation and acceleration 14 p2361 N85-24589
High energy particle acceleration by coherent electromagnetic waves propagating across the magnetic field
[IPPJ-717] 16 p2866 N85-27679
Fundamentals of plasma simulation
[DE85-007699] 16 p2867 N85-27683
IMS (International Magnetospheric Study) contributions to the understanding of auroral precipitation, transport, and particle sources
[AD-A152320] 17 p2992 N85-28482
Wide-angle optics with strong magnetic fields for efficient generation of secondary-particle beams
[DE85-007727] 18 p3179 N85-29713
Activities report of the Werner-Heisenberg Institute for Physics
[ISSN-0173-8258] 18 p3184 N85-29748
Time-resolved energy spectrum of the ion beam generated in the plasma focus 19 p3369 N85-30892
Experimental study of laser produced ions for collective ion acceleration 20 p3460 N85-31494
Publications from the Department of Plasma Physics and the Unit of Accelerator Technology, index and abstracts, 1984
[TRITA-EPP-84-13] 20 p3534 N85-31991
500 TeV gamma rays from Hercules X-1
[OG-2.2-7] 22 p3865 N85-33933
Physics Division annual review, 1 April 1983 - 31 March 1984
[ANL-84-24] 23 p3969 N85-34602
Nineteenth International Cosmic Ray Conference. SH sessions, volume 4
[NASA-CP-2376-VOL-4] 23 p3989 N85-34729
Stochastic particle acceleration in solar flares
[SH-1.1-4] 23 p3989 N85-34731
First-order shock acceleration in solar flares
[SH-1.1-5] 23 p3989 N85-34732
Prompt acceleration of ions by oblique turbulent shocks in solar flares
[SH-1.1-6] 23 p3989 N85-34733
Study of photon emission by electron capture during solar nuclei acceleration, 1: Temperature-dependent cross section for charge changing processes
[SH-1.1-8] 23 p3990 N85-34735
Study of photon emission by electron capture during solar nuclei acceleration. 2: Delimitation of conditions for charge transfert establishment
[SH-1.1-9] 23 p3990 N85-34736
Study of non-thermal photon production under different scenarios in solar flares. 2: The Compton inverse and Bremsstrahlung models and fittings
[SH-1.2-3] 23 p3991 N85-34739
Quantitative analysis of flare accelerated electrons through their hard X-ray and microwave radiation
[SH-1.2-7] 23 p3991 N85-34742

Two classes of solar energetic particle events associated with impulsive and long duration soft X-ray flares
[SH-1.2-12] 23 p3992 N85-34747
The energy spectra of solar flare electrons
[SH-1.2-14] 23 p3992 N85-34749
The starting conditions for an optically small solar gamma ray flare
[SH-1.3-2] 23 p3993 N85-34751
Observations of solar flare gamma-rays and protons
[SH-1.3-6] 23 p3993 N85-34753
Energetic protons from a disappearing solar filament
[SH-1.3-7] 23 p3993 N85-34754
Helios 1 energetic particle observations of the solar gamma ray flare events of 7, 21 June 1980 and 3 June 1982
[SH-1.3-8] 23 p3993 N85-34755
Shock and statistical acceleration of energetic particles in the interplanetary medium
[SH-1.5-1] 23 p3996 N85-34771
Particle acceleration due to shocks in the interplanetary field: High time resolution data and simulation results
[SH-1.5-5] 23 p3996 N85-34774
Spatial dependence of the local diffusion coefficient measured upstream of the November 12, 1978 interplanetary traveling shock
[SH-1.5-12] 23 p3996 N85-34776
Latitude dependance of co-rotating shock acceleration
[SH-1.5-14] 23 p3997 N85-34777
Elemental abundances in corotating events
[SH-1.5-15] 23 p3997 N85-34778
Cosmic ray acceleration by stellar wind. Simulation for heliosphere
[SH-1.5-17] 23 p3997 N85-34780
On the retention of high-energy protons and nuclei with charges Z or equal to 2 in large solar flares after the process of their acceleration
[SH-2.1-8] 23 p3998 N85-34789
Type 3 solar radio bursts and 3HE-rich events
[SH-2.2-3] 23 p4000 N85-34796
Elemental abundance differences between nuclei accelerated in CIR shocks and solar flares
[SH-2.2-6] 23 p4000 N85-34801
On the connection between the 3HE-enrichment and spectral index of solar energetic particles
[SH-2.2-9] 23 p4001 N85-34804
The plasma mechanism for preferential acceleration of heavy ions
[SH-2.2-10] 23 p4001 N85-34805
Nineteenth International Cosmic Ray Conference. OG sessions, volume 3
[NASA-CP-2376-VOL-3] 23 p4012 N85-34862
Sources of the ultraheavy cosmic rays
[OG-7.1-7] 23 p4013 N85-34868
Self-similar time dependent shock structures
[OG-8.1-4] 23 p4017 N85-34894
The central engine of quasars and AGNs: A relativistic proton radiative shock
[OG-8.1-7] 23 p4018 N85-34897
A model for the origin of high-energy cosmic rays
[OG-8.1-8] 23 p4018 N85-34898
Onion-shell model for cosmic ray electrons and radio synchrotron emission in supernova remnants
[OG-8.1-10] 23 p4018 N85-34900
Approximate supernova remnant dynamics with cosmic ray production
[OG-8.1-12] 23 p4019 N85-34901
Efficiency of regular acceleration of particles by a shock wave at different injection regimes
[OG-8.1-13] 23 p4019 N85-34902
The nucleosynthesis of deturium and helium-3
[OG-8.2-18] 23 p4020 N85-34914
Pulsars as cosmic ray particle accelerators: Proton orbits
[OG-8.2-21] 23 p4021 N85-34917
Pulsars as cosmic ray accelerators: Energy development of protons
[OG-8.2-22] 23 p4021 N85-34918
Propagation of injected cosmic rays under distributed reacceleration
[OG-8.3-3] 23 p4021 N85-34922
Secondary to primary ratio and the continuous acceleration
[OG-8.3-4] 23 p4022 N85-34923
Propagation of cosmic rays and new evidence for distributed acceleration
[OG-8.3-5] 23 p4022 N85-34924
Exact solutions for sporadic acceleration of cosmic rays
[OG-8.3-7] 23 p4022 N85-34925
Stochastic particle acceleration in flaring stars
[OG-8.3-9] 23 p4022 N85-34927
On the anomalous component
[SH-4.6-6] 23 p4039 N85-35044
Possible origin of the anomalous component of cosmic rays
[SH-4.6-7] 23 p4039 N85-35045

PARTICLE ACCELERATOR TARGETS
Experimental medium energy physics
[DE84-014825] 02 p0276 N85-11807
ATLAS beam properties: Some implications for target making
[DE84-006595] 02 p0278 N85-11812
Long-pulse beamlines for the mirror fusion test facility
[DE84-017091] 09 p1392 N85-18760
Proceedings of the Workshop on Polarized Targets in Storage Rings
[DE85-002704] 16 p2862 N85-27653
Laser measurements of distances from the ORELA neutron target to experiment stations along flight paths 1 and 6
[DE85-009457] 17 p2971 N85-28352
Mouse oocyte killing by neutrons: Target considerations
[DE85-011362] 19 p3328 N85-30624
Fixed-target physics at Fermilab
[DE85-010141] 20 p3528 N85-31942
Nuclear physics in the 10 to 300 MeV energy range using a pulsed white neutron source
[DE85-003713] 22 p3839 N85-33775
Light ion sources for ICF
[DE85-011544] 23 p3983 N85-34702
Interactions of heavy nuclei, Kr, Xe and Ho, in light targets
[OG-7.2-21] 23 p4016 N85-34866
Event parameters: Fixed targets
24 p4146 N85-35702
Working group on penetrating probes at fixed target facilities
24 p4146 N85-35703
Summary of the working group on penetrating probes in collider experiments. 1: The collider environment
24 p4146 N85-35704
(NAT)Fe(n,n'x) spectra at 65.5 MeV
[AD-A155776] 24 p4150 N85-35730
Radiation safety problems in handling highly active tritium targets
[DE85-014266] 24 p4151 N85-35742
Neutron production by Ne and Si ions on a thick Cu target at 670 MeV/A with application to radiation protection
[DE85-014526] 24 p4152 N85-35746
Major facility overhauls at LAMPF
[DE85-012724] 24 p4156 N85-35765
Recent advances in remote handling at LAMPF
[DE85-012725] 24 p4157 N85-35775
How are particle production, nucleon emission and target fragment evaporation processes interrelated in hadron-nucleus collisions?
24 p4174 N85-35878

PARTICLE ACCELERATORS
NT BETATRONS
NT CYCLIC ACCELERATORS
NT CYCLOTRONS
NT ELECTRON ACCELERATORS
NT ION ACCELERATORS
NT LINEAR ACCELERATORS
NT MICROTRONS
NT STORAGE RINGS (PARTICLE ACCELERATORS)
NT SYNCHROTRONS
Accelerator technology program
[DE84-015052] 01 p0118 N85-10606
Engineering Physics Division
[DE84-007778] 02 p0274 N85-11787
Diffraction by the time-of-flight technique at pulsed neutron sources
[DE84-015839] 03 p0418 N85-12574
Utilization of a tandem accelerator for the investigation of solid state properties by means of heavy ions
03 p0429 N85-12733
Laser-driven particle accelerators
[DE84-015053] 04 p0506 N85-13227
Fast neutron capture with a white neutron source
[DE84-016799] 04 p0562 N85-13580
Accelerator Technology Program
[DE84-017063] 04 p0583 N85-13586
A proton laser accelerator by means of the inverse free electron laser mechanism
[DE85-000231] 06 p0813 N85-15163
Electron beam propagation along charged foils
[DE85-002137] 06 p0861 N85-15472
Fermilab research program workbook
[DE84-012568] 06 p0862 N85-15476
Bunch coalescing in the main ring to form intense proton and antiproton bunches without RF counterphasing
[DE85-001364] 09 p1382 N85-18692
High energy pulsed particle accelerator
[AD-A149247] 10 p1554 N85-19797
IREB (Intense Relativistic Electron Beam) converter to ac pulses
[AD-D011479] 10 p1554 N85-19800
Simulation of space charge effects in particle accelerators
[DE85-001828] 12 p1929 N85-22120
Variable flexing device for targets in internal beams of charged particle accelerators 13 p2044 N85-22797
Experimental studies of elementary particle interactions at high energies
[DE85-004795] 13 p2157 N85-23394
Explosive emission cathode plasmas in intense relativistic electron beam diodes
[AD-A150669] 14 p2417 N85-24912
Radio frequency quadrupole and alternating phase focusing methods used in proton linear accelerator technology in the USSR
[AD-A150830] 14 p2418 N85-24916
Standard model and beyond
[DE85-004289] 14 p2418 N85-24919
Summaries of FY 1984 research in high energy physics
[DE85-005641] 14 p2420 N85-24934
Beam trapping in high current cyclic accelerators with strong focusing fields
[AD-A151382] 15 p2648 N85-26331
Modified betatron accelerator studies
[AD-A151420] 15 p2648 N85-26332
Development of RF plasma generators for neutral beams
[DE85-004125] 15 p2658 N85-26400
Space station as quark matter factory
[DE85-004606] 15 p2685 N85-26585
Two-dimensional beat wave acceleration simulation
[DE85-005661] 16 p2791 N85-27214
Experiments and detectors for high energy heavy ion colliders
[DE85-007827] 17 p3031 N85-28748
Report of the Working Group on Other Acceleration Schemes
[DE85-008447] 17 p3033 N85-28764
Activities report in nuclear physics and high energy physics
[JF40026] 17 p3035 N85-28777
Accelerator technology working group summary
[DE85-009547] 18 p3180 N85-29717
A collective interaction klystron specification
[AD-D011704] 19 p3255 N85-30186
Research activities of the Physics Division
[DE85-008958] 19 p3357 N85-30811
Possibilities for studying short-lived nuclei produced at LAMPF
[DE85-010740] 19 p3365 N85-30864
Development of a resistive load for PBFA 2 rimfire gas switch simultaneity and laser triggering tests
[DE85-011080] 19 p3365 N85-30869
Method to render second order beam optics programs symplectic
[DE85-010631] 20 p3515 N85-31855
Fixed-target physics at Fermilab
[DE85-010141] 20 p3528 N85-31942
Plastic scintillator detectors for the study of transfer and breakup reactions at intermediate energies
[DE85-009945] 20 p3528 N85-31945
Current experiments in elementary particle physics, revision 1-85
[DE85-011513] 20 p3529 N85-31950
Activities report in nuclear physics and particle acceleration 20 p3532 N85-31977
An absolute calibration of the solid state detectors in the narrow band neutrino beam at CERN
[NIKHEF-H/84-10] 20 p3538 N85-32017
Vacuum interface flashover with bipolar electric fields
[DE85-012027] 22 p3755 N85-33275
Model that predicts pulse charged gas switching breakdown phenomena
[DE85-013119] 22 p3761 N85-33313
PMEXA: Diagnostic filtering program for the PBFA-1 performance monitoring and evaluation system
[DE85-013179] 22 p3831 N85-33725
Supermile vacuum interface design
[DE85-012861] 22 p3837 N85-33759
Rf program for LAMPF 2
[DE85-012693] 22 p3837 N85-33760
Summary of activities, 1983
[LBL-16500] 23 p3969 N85-34605
Repetitive pulse accelerator technology for light ion inertial confinement fusion
[DE85-012030] 23 p3982 N85-34693
Distribution of computer functionality for accelerator control at the Brookhaven AGS
[DE85-012520] 24 p4141 N85-35689
Width of nonlinear difference resonances
[DE85-013026] 24 p4148 N85-35719
Quality assurance considerations for the implementation of a pulsed power R and D project
[DE85-012357] 24 p4148 N85-35720

Operations considerations in designing a high speed multi-channel data acquisition system
[DE85-012840] 24 p4154 N85-35756
High vacuum portable pumping station suitable for accelerator use
[DE85-011840] 24 p4155 N85-35759
Ion source development for the Los Alamos heavy ion fusion injector
[DE85-012662] 24 p4156 N85-35766
Surface discharges as intense photon sources in the extreme ultraviolet
[DE85-012593] 24 p4158 N85-35782
SLC arc transport system: Magnet design and construction
[DE85-014289] 24 p4159 N85-35789

PARTICLE BEAMS
NT ATOMIC BEAMS
NT ELECTRON BEAMS
NT ION BEAMS
NT MOLECULAR BEAMS
NT NEUTRAL BEAMS
NT NEUTRINO BEAMS
NT NEUTRON BEAMS
NT PION BEAMS
NT PROTON BEAMS
NT RELATIVISTIC ELECTRON BEAMS
Visible wavelength interferometer for high speed electron density diagnostics
[AD-A145686] 02 p0277 N85-11803
Antiproton source beam position system
[DE84-016716] 09 p1380 N85-18679
Force balance limiting current for charged particle beams
[DE84-016976] 09 p1381 N85-18685
Computerized study of several electrostatic, surface-ionization ion-source configurations
[DE85-001512] 11 p1721 N85-20823
Theory of lethality
[DE85-000457] 11 p1721 N85-20826
Low-energy, high-intensity positron beam experiments with a linac
[DE85-001048] 11 p1723 N85-20835
Numerical model for swirl cooling in high-heat-flux particle beam targets and the design of a swirl-flow-based plasma limiter
[DE85-003824] 11 p1732 N85-20894
Statistical phenomena in particle beams
[DE85-001050] 12 p1929 N85-22118
Suppression of tilting instability of a compact torus by energetic particle beams
[IPPJ-705] 12 p1935 N85-22157
High energy facilities advanced projects: Intrabeam scattering for a beam of gold ions
[DE85-000887] 12 p1941 N85-22192
Experimental investigation of neutral plasma beam propagation across a magnetic field
[AD-A150944] 14 p2423 N85-24947
Noninductive current drive in Tokamaks
[DE85-005427] 14 p2424 N85-24951
Sound emission by particle beam passing through hole in rigid shield 15 p2525 N85-25570
Modified betatron accelerator studies
[AD-A151420] 15 p2648 N85-26332
A proportional-plus-integral controller for a particle beam weapon
[AD-A153213] 17 p3035 N85-28778
Comparison of simulation with experiment in an RFQ
[DE85-010770] 19 p3349 N85-30757
Optical beam deflection detection of thermal waves in opaque solids 19 p3374 N85-30927
Permanent magnets for production and use of high energy particle beams
[DE85-009934] 20 p3522 N85-31905
Fixed-target physics at Fermilab
[DE85-010141] 20 p3526 N85-31942
Current experiments in elementary particle physics, revision 1-85
[DE85-011513] 20 p3529 N85-31950
Requirements for very high energy accelerators
[DE85-011173] 20 p3529 N85-31952
Studies in mixed species charged particle beam dynamics
[OUEL-1545/84] 20 p3531 N85-31969
Injection of hydrogen macroparticles into T-10 tokamak 21 p3692 N85-32937
Model that predicts pulse charged gas switching breakdown phenomena
[DE85-013119] 22 p3781 N85-33313
PMEXA: Diagnostic filtering program for the PBFA-1 performance monitoring and evaluation system
[DE85-013179] 22 p3831 N85-33725
Rf program for LAMPF 2
[DE85-012693] 22 p3837 N85-33760
Polarization of fast particle beams by collisional pumping
[DE85-011621] 22 p3838 N85-33764
Accelerator vibration issues
[DE85-010766] 22 p3842 N85-33791
Interrelations for the elements of the scattering matrix 22 p3855 N85-33872
Space Experiments with Particle Accelerators (SEPAC) 23 p3901 N85-34165
Recoverable Plasma Diagnostics Package (RPDP) 23 p3902 N85-34167
Neutral particle beam intensity controller
[DE85-006411] 23 p3969 N85-34604
Theoretical and computational research on the focused transport of intense charged particle beams
[DE85-012960] 23 p3972 N85-34621
Depth and size effects on cosmogenic nuclide production in meteorites
[SH-7.1-9] 23 p4048 N85-35101
Observations of accelerated high current low emittance beams in the SLC Linac
[DE85-013073] 24 p4068 N85-35211
Operations considerations in designing a high speed multi-channel data acquisition system
[DE85-012840] 24 p4154 N85-35756
Synchronous timing of multi-energy fast beam extraction during a single AGS cycle
[DE85-011829] 24 p4158 N85-35781
Relation between field energy and RMS emittance in intense particle beams
[DE85-012655] 24 p4160 N85-35784
Accelerator physics measurements at the damping ring
[DE85-013373] 24 p4159 N85-35785

PARTICLE COLLISIONS
Large linear colliders
[DE84-015700] 02 p0278 N85-11811
Report of the reference designs study group on the superconducting super collider
[DE84-015567] 04 p0589 N85-13630
Waves and instabilities in collisionless shocks
[AD-A146589] 06 p0881 N85-15597
Theoretical studies relating to the interaction of radiation with matter: Atomic collision processes occurring in the presence of radiation fields
[AD-A146854] 07 p1040 N85-16602
SU(2) x U(1) vacuum and the Centauro events
[NASA-TM-86082] 08 p1260 N85-17926
Very high energy probes of the quark-gluon plasma
[DE84-016992] 09 p1392 N85-18763
Quantum mechanical and semiclassical approaches to molecular dynamics
[DE85-003458] 10 p1555 N85-19803
Correlated 2 electron effects in collisions of multiply charged Au ions with He
[DE85-003064] 11 p1723 N85-20837
Simulating supersymmetry at the SSC
[DE85-000899] 11 p1736 N85-20917
Theoretical study of near-threshold electron-molecule scattering
[DE85-004530] 12 p1930 N85-22126
Adequacy of metal ablation process with laser radiation and a shock-compressed plasma 13 p2028 N85-22708
Future accelerator studies of high energy heavy ion collisions
[DE85-005885] 15 p2650 N85-26346
Evolution of collisional systems — planetary disks 15 p2674 N85-26505
Size distribution in collisional systems — planetary rings 15 p2674 N85-26506
Comments on collision mechanics in ring systems — planetary rings
[PSI-CONTRIB-186] 15 p2675 N85-26510
Tables of nuclear cross sections for galactic cosmic rays: Absorption cross sections
[NASA-RP-1134] 16 p2864 N85-27665
Measuring structure functions at SSC energies
[DE85-007515] 17 p3031 N85-28746
Cluster production and entropy
[DE85-007626] 17 p3032 N85-28752
New experimental results in two photon physics
[NIKHEF-H/84-16] 17 p3035 N85-28776
Physics of (very) high energy e(+)-e(-) colliders
[DE85-008177] 17 p3036 N85-28780
High energy gamma rays from complex particle collisions
[DE85-007871] 17 p3098 N85-28783
Excited state populations and charge-exchange of fast ions in solids
[DE85-009362] 18 p3160 N85-29714
Present and future directions of atomic physics research with multiply-charged ions at Brookhaven National Laboratory
[DE85-010960] 19 p3354 N85-30788
Proceedings of the 1984 Workshop on High-Energy Excitations in Condensed Matter, volume 2
[DE85-007395] 19 p3357 N85-30809
Pion production and the nuclear equation of state
[DE85-009941] 19 p3365 N85-30870
Multiple collision solutions for time-dependent neutron transport in slabs of finite thickness
[OEFZS-4312] 22 p3838 N85-33762
Gamma ray line production from cosmic ray spallation reactions 22 p3875 N85-34005
Radial transport caused by collision 23 p3976 N85-34852
Electron loss process and cross section of multiply charged ions by neutral atoms 23 p3981 N85-34885
Low-energy sputterings with the Monte Carlo Program ACAT
[IPPJ-AM-40] 23 p3982 N85-34890
Cross sections for the production of fragments with Z greater than or equal to 8 by fragmentation of Z greater than or equal to 9 and less than or equal to 26 nuclei
[OG-7.2-22] 23 p4016 N85-34889
The response of ionization chambers to relativistic heavy nuclei
[OG-9.1-13] 23 p4024 N85-34939
Plastic scintillators in coincidence for the study of multi-particle production of sea level cosmic rays in dense medium
[SH-9.1-11] 23 p4052 N85-35126
The use of austenitic stainless steel versus monel (Ni-cu) alloy in pressurized Gaseous Oxygen (GOX) life support systems
[AD-A158905] 24 p4134 N85-35625
Working group on penetrating probes at fixed target facilities 24 p4146 N85-35703
Summary of the working group on penetrating probes in collider experiments. 1: The collider environment 24 p4146 N85-35704
Report of working group on detectors for hadrons and event parameters at colliders 24 p4146 N85-35705
A survey of multiplicities and rapidity densities from existing emission data on hadron-nucleus nucleus-nucleus collisions 24 p4146 N85-35706
A simulation of ultra-relativistic nucleus-nucleus collisions 24 p4146 N85-35707
Very high energy probes of the quark-gluon plasma 24 p4147 N85-35708
A holographic streamer chamber for relativistic nucleus-nucleus collision experiments 24 p4147 N85-35710
SLC arc transport system: Magnet design and construction
[DE85-014289] 24 p4159 N85-35789
Design considerations for personnel access penetrations for the superconducting super collider
[DE85-013027] 24 p4162 N85-35807
Measurement of interaction cross section of cosmic ray Fe nuclei (E4 GeV/N) with Al target
[HE-1.1-7] 24 p4170 N85-35855
Hadron thermodynamics in relativistic nuclear collisions
[HE-1.1-8] 24 p4171 N85-35856
1Single particle momentum and angular distributions in hadron-hadron collisions at ultrahigh energies
[HE-1.2-1] 24 p4171 N85-35860
Low P sub T hadron-nucleus interactions
[HE-1.2-7] 24 p4172 N85-35865
A test of the Feynman scaling in the fragmentation region
[HE-1.2-9] 24 p4172 N85-35867
Angular distribution of shower particles produced in the collisions of 20-GeV/c and 300-GeV negative pions with emulsion nuclei 24 p4172 N85-35868
Determination of primary energy in nucleus-nucleus collisions and the high P[sub]T tail of alpha-particles 24 p4173 N85-35875
Physical meaning of the multiplicities of emitted nucleons in hadron-nucleus collisions 24 p4174 N85-35877
How are particle production, nucleon emission and target fragment evaporation processes interrelated in hadron-nucleus collisions? 24 p4174 N85-35878
Experimental study of the space-time development of the particle production process in hadron-nucleon collisions, using massive target nucleus as a detector 24 p4174 N85-35879
Energy-range relations for hadrons in nuclear matter 24 p4174 N85-35881
Scattering and stopping of hadrons in nuclear matter 24 p4174 N85-35882
Measurements of hadron mean free path for the particle-producing collisions in nuclear matter 24 p4174 N85-35883
SU(2) x U(1) vacuum and the Centauro events 24 p4175 N85-35885
The multiplicity and the spectra of secondaries correlated with the leading particle energy
[HE-3.2-11] 24 p4179 N85-35919
A study of gamma-families generated in nucleon-nucleus (NA) and pion-nucleus (pi A) interactions
[HE-3.7-2] 24 p4196 N85-36061

The muon content of gamma-ray showers
[HE-4.5-7] 24 p4185 N85-36031
Fast scintillation counter preamplifier for the observation of Linsley effect
[HE-4.7-9] 24 p4199 N85-36060
A mini-array for large air showers
[HE-4.7-10] 24 p4199 N85-36061
A note on some statistical properties of rise time parameters used in muon arrival time measurements
[HE-4.7-12] 24 p4199 N85-36062

PARTICLE COUNTERS
U RADIATION COUNTERS

PARTICLE DECAY
U RADIOACTIVE DECAY

PARTICLE DENSITY (CONCENTRATION)
NT CARRIER DENSITY (SOLID STATE)
NT ELECTRON DENSITY (CONCENTRATION)
NT ELECTRON DENSITY PROFILES
NT ELECTRON DISTRIBUTION
NT ION DENSITY (CONCENTRATION)
NT IONOSPHERIC ELECTRON DENSITY
NT IONOSPHERIC ION DENSITY
NT MAGNETOSPHERIC ELECTRON DENSITY
NT MAGNETOSPHERIC ION DENSITY
NT MAGNETOSPHERIC PROTON DENSITY
NT PLASMA DENSITY
NT PROTON DENSITY (CONCENTRATION)
Dynamics of the Uranian rings
02 p0302 N85-11956
Mesoscale studies of flow regimes and fluxes of particulate matter in coastal waters
[DE85-003625] 11 p1669 N85-20620
Properties of materials using acoustic waves
[AD-A150465] 13 p2155 N85-23382
Electrophoretic mobilities of cultured human embryonic kidney cells in various buffers 20 p3501 N85-31761
The composition of cosmic rays near the Bend (10 to the 15th power eV) from a study of muons in air showers at sea level
[OG-5.2-3] 22 p3883 N85-34060
Composition of primary cosmic rays at energies 10(15) to approximately 10(16) eV
[OG-5.2-4] 22 p3883 N85-34061
Observation of cosmic ray positrons from 5 to 25 GeV
[OG-6.2-5] 22 p3899 N85-34104
Second-order Compton-Getting effect on arbitrary intensity distribution
[SH-3.1-10] 23 p4002 N85-34814
The expected cosmic ray density and stream distributions at the heliolatitudinal asymmetry of solar wind
[SH-4.2-14] 23 p4008 N85-34852
Angular resolution of air-shower array-telescopes
[OG-9.5-6] 23 p4030 N85-34983
Hadrons registration in emulsion chamber with carbon block
[HE-3.7-3] 24 p4186 N85-35962
Peculiarities of gamma-quanta distribution at 20 TeV energy
[HE-3.7-10] 24 p4186 N85-35967
Core structure of EAS in 10(15) to 10(17) eV
24 p4189 N85-35989
Particle distributions in approximately 10(14) 10(16) eV air shower cores at sea level 24 p4189 N85-35990
Monte Carlo simulations of electron lateral distributions in the core region of 10(13) - 10(16) eV air showers
24 p4190 N85-35992
Comparison of simulation results with sea-level experimental data on 10(14) - 10(16) air shower cores
24 p4190 N85-35993
A new study of shower age distribution in near vertical showers by EAS air shower array
24 p4190 N85-35996
A new study of muons in air showers by NBU air shower array 24 p4190 N85-35997
Lateral distribution of electrons of air showers
24 p4191 N85-35998
Detailed studies of the electron lateral distribution in extensive air showers with energies around 10(16) eV
24 p4191 N85-35999
Measurement of energy muons in EAS at energy region larger thean 10(17) eV
[HE-4.3-6] 24 p4191 N85-36002
Muon fluctuation studies of EAS 10(17) eV
[HE-4.3-9] 24 p4191 N85-36003
Measurement of shower electrons and muons using a small air shower array
[HE-4.3-11] 24 p4192 N85-36005
The system of EAS time analysis
[HE-4.4-10] 24 p4193 N85-36016
Properties of 10 (18)-10 (19)eV EAS at far core distance
[HE-4.7-3] 24 p4198 N85-36054
The thickness of the shower disc as observed in showers produced by primaries above 10 (19)eV
[HE-4.7-6] 24 p4199 N85-36057
Expected rates with mini-arrays for air showers
[HE-4.7-8] 24 p4199 N85-36059
Thickness of the particle swarm in cosmic ray air showers
[HE-4.7-14] 24 p4200 N85-36064
Progress report on a new search for free e/3 quarks in the cores of 10(15) - 10(16) eV air showers
[HE-6.2-15] 24 p4212 N85-36151

PARTICLE DETECTORS
U RADIATION COUNTERS

PARTICLE DIFFUSION
NT ELECTRON DIFFUSION
NT IONIC DIFFUSION
Performance deterioration of cascades exposed to solid particles 03 p0319 N85-12057
Paramagnetic impurity effects in NMR determinations of hydrogen diffusion and electronic structure in metal hydrides. Cerium in YH-2 and LaH-2.25
[DE84-014127] 04 p0472 N85-13005
Synergisms in hydrogen recycling, session summary
06 p0864 N85-15491
Steady state hydrogen transport in solids
06 p0864 N85-15492
Synergistic effects related to surface composition, session summary 06 p0865 N85-15495
Theory of oriented nucleation with asymmetric single elements. 2: Effects of rotational diffusion
[IFTR-32/1984] 12 p1939 N85-22179
Boundary of modulation diffusion and stochastic instability of high energy protons in inner radiation belt
15 p2462 N85-25316
Diffusion of dust around a central body — Keplerian orbits 15 p2676 N85-26523
Nonlinear DSA difference schemes for radiative transfer applications
[DE85-005729] 16 p2858 N85-27611
Colloidal particle transport with simultaneous birth, growth and capture
[DE85-010386] 19 p3235 N85-30055
Propagation and secondary production of low energy antiprotons in the atmosphere
[OG-6.1-3] 22 p3887 N85-34094
Guiding center distribution function and longitudinal invariant 23 p3978 N85-34663
Diffusion in the chromosphere and the composition of the solar corona and energetic particles
[SH-2.1-9] 23 p3990 N85-34790
Coronal propagation of solar flare particles observed by satellite
[SH-3.1-2] 23 p4001 N85-34807
Investigation of cosmic ray propagation in interplanetary space
[SH-3.2-9] 23 p4004 N85-34824
Diffusion-convection function of cosmic rays
[SH-3.2-10] 23 p4004 N85-34825
Numerical descriptions of cosmic-ray transport
[SH-4.1-3] 23 p4004 N85-34829
Numerical and analytic descriptions of cosmic-ray transport
[SH-4.1-4] 23 p4005 N85-34830
Diffusion of strongly magnetized cosmic ray particles in a turbulent medium
[OG-7.2-16] 23 p4015 N85-34883
Calculation of the diffusion of light by aerosols: Description of the MIELOR software and results obtained
[REPT-80] 24 p4137 N85-35638
Atmospheric muons and neutrinos, and the neutrino-induced muon flux underground
[HE-5.4-7] 24 p4207 N85-36118

PARTICLE EMISSION
NT ELECTRON EMISSION
NT FIELD EMISSION
NT ION EMISSION
NT NEUTRON EMISSION
NT PHOTOELECTRIC EMISSION
NT SECONDARY EMISSION
NT THERMIONIC EMISSION
Centrifugally driven magnetohydrodynamic (MHD) winds and the nonthermal emission regions in Active Galactic Nuclei (AGN) 08 p1242 N85-17835
Theoretical studies of high energy phenomenon: Analysis of models of CP and T violation
[DE85-007455] 17 p3036 N85-28782
Production of stable embryo particles in dense ion tracks of alpha particle emissions in the atmosphere
21 p3644 N85-32636
Application of Particle Induced X-ray Emission analysis (PIXE) to aerosol long range transport studies
21 p3648 N85-32665
On some problems of gamma-astronomy
[OG-2.7-15] 22 p3873 N85-33988
Multicomponent analysis of total COS-B gamma-ray data at intermediate latitudes
[OG-3.1-3] 22 p3873 N85-33991
Forecasting future industrial SO2 and NC/sub x/ emissions, revised 23 p3947 N85-34461
Study of photon emission by electron capture during solar nuclei acceleration, 1: Temperature-dependent cross section for charge changing processes
[SH-1.1-8] 23 p3990 N85-34735
Study of photon emission by electron capture during solar nuclei acceleration. 2: Delimitation of conditions for charge transfert establishment
[SH-1.1-9] 23 p3990 N85-34736
Study of photon emission by electron capture during solar nuclei acceleration. 3: Photon production evaluations
[SH-1.1-10] 23 p3990 N85-34737
Solar neutrinos, solar flares, solar activity cycle and the proton decay
[SH-8.1-8] 23 p4049 N85-35113
Physical meaning of the multiplicities of emitted nucleons in hadron-nucleus collisions 24 p4174 N85-35877
How are particle production, nucleon emission and target fragment evaporation processes interrelated in hadron-nucleus collisions? 24 p4174 N85-35878
Experimental evidence of the decrease of kinetic energy of hadrons in passing through atomic nuclei
24 p4174 N85-35880
Energy-range relations for hadrons in nuclear matter
24 p4174 N85-35881
The model of independent particles emission in the multiparticle production theory
[HE-3.2-10] 24 p4179 N85-35918
A study of atmospheric neutrinos with the IMB detector
[HE-5.3-7] 24 p4205 N85-36101
Study of photonuclear muon interactions at Baksan underground scintillation telescope
[HE-5.4-10] 24 p4206 N85-36122
Collimated groups of particles as possible manifestation of heavy meson production
[HE-5.4-14] 24 p4206 N85-36124
Limits on monopole fluxes from KFG experiment
[HE-6.1-6] 24 p4209 N85-36132
An experiment to detect gut monopoles
[HE-6.1-7] 24 p4210 N85-36133
Construction of the Soudan 2 detector
[HE-6.2-5] 24 p4211 N85-36141
Nucleon decay and atmospheric neutrinos in the Mont Blanc experiment
[HE-6.2-6] 24 p4211 N85-36142

PARTICLE ENERGY
NT ELECTRON ENERGY
NT ELECTRON STATES
NT PROTON ENERGY
Dynamics of the Uranian rings
02 p0302 N85-11956
Calculation of energy of atomization in silicate tetrahedron Si4(4-)
[BLL-M-36000-(5826.4)] 07 p1040 N85-16599
Experimental investigations in particle physics at intermediate energies
[DE85-001461] 11 p1722 N85-20832
Development of an apparatus for obtaining molecular beams in the energy range from 2 to 200 eV
[NASA-TM-77835] 15 p2647 N85-26326
Secondary ion mass spectrometry studies of solids and surfaces
[AD-A151744] 16 p2745 N85-26939
Particle physics: Recent successes and future prospects
[DE85-008175] 17 p3033 N85-28765
On some problems of gamma-astronomy
[OG-2.7-15] 22 p3873 N85-33988
All particle energy spectrum of cosmic rays in 10 to the 15th power - 10 to the 20th power eV region
[OG-5.1-15] 22 p3882 N85-34056
Abundance of low energy (50-150 MeV) antiprotons in cosmic rays
[OG-6.1-1] 22 p3887 N85-34092
Evidence for a dynamical halo around the edge-on galaxy NGC 4631
[OG-6.2-1] 22 p3889 N85-34102
Source energy spectra from demodulation of solar particle data by interplanetary and coronal transport
[SH-1.3-13] 23 p3994 N85-34758
the role of shock waves in modulation of galactic cosmic rays
[SH-4.1-7] 23 p4005 N85-34831
SONTRAC: A solar neutron track chamber detector
[SH-9.1-12] 23 p4052 N85-35127
The model of independent particles emission in the multiparticle production theory
[HE-3.2-10] 24 p4179 N85-35918
The multiplicity and the spectra of secondaries correlated with the leading particle energy
[HE-3.2-11] 24 p4179 N85-35919

PARTICLE FLUX
U FLUX (RATE)

PARTICLE FLUX DENSITY
NT ELECTRON FLUX DENSITY
NT NEUTRON FLUX DENSITY
NT PROTON FLUX DENSITY
SCATHA (spacecraft charging at high altitudes) plasma interaction experiment: SC-3 high energy particle spectrometer; SC-6 energetic ion composition experiment
[AD-A149728] 12 p1793 N85-21252
Rocket observations of the ionosphere during the eclipse of 26 February 1979
[NASA-CR-175513] 12 p1868 N85-21850
Timing between particle injections at the geostationary orbit and particle flux decreases in the distant geomagnetic tail during substorms 14 p2358 N85-24569
Plasma sheet dynamics deduced from ISEE-1 and -2 energetic particle flux data 14 p2358 N85-24570
Correlated fluctuations of charged particle fluxes and magnetic field according to data from Intercosmos-10 satellite 16 p2722 N85-26902
Helios 1 energetic particle observations of the solar gamma ray flare events of 7, 21 June 1980 and 3 June 1982
[SH-1.3-8] 23 p3993 N85-34755
The dispersive evolution of charged-particle bunches in random magnetic fields
[SH-4.1-2] 23 p4004 N85-34828
Observation of pick-up ions in the solar wind: Evidence for the source of the anomalous cosmic ray component?
[SH-4.6-5] 23 p4039 N85-35043
Cosmogenic-nuclide production by primary cosmic-ray protons
[SH-7.1-6] 23 p4047 N85-35098
Accelerator experiments on the contribution of secondary particles to the production of cosmogenic nuclides in meteorites
[SH-7.1-8] 23 p4048 N85-35100
Spallogenic origin of nuclei in meteorites
[SH-7.1-10] 23 p4048 N85-35102
The 4He/1H ratios in the chemical compositions of solar flare particles and the primordial solar nebula
[SH-7.1-12] 23 p4048 N85-35104
A mini-array for large air showers
[HE-4.7-10] 24 p4199 N85-36061
A note on some statistical properties of rise time parameters used in muon arrival time measurements
[HE-4.7-12] 24 p4199 N85-36062
Study of the time-differentiated particle flux density at various distances from EAS axis
[HE-4.7-15] 24 p4200 N85-36065
The capability of the existing network of installations for detecting the antineutrino burst from collapsing stars
[HE-5.3-13] 24 p4206 N85-36107

PARTICLE IN CELL TECHNIQUE
Simulations of satellite-plasma interaction, including electron space charges --- Giotto mission
14 p2245 N85-23916
Time-implicit Monte-Carlo collision algorithm for particle-in-cell electron transport models
[DE85-010758] 20 p3521 N85-31900

PARTICLE INTERACTIONS
NT ELECTRON CAPTURE
NT ELEMENTARY PARTICLE INTERACTIONS
NT INTERSTELLAR CHEMISTRY
NT ION ATOM INTERACTIONS
NT MOLECULAR COLLISIONS
NT MOLECULAR INTERACTIONS
NT NUCLEAR CAPTURE
NT NUCLEAR INTERACTIONS
NT NUCLEON-NUCLEON INTERACTIONS
NT PLASMA-PARTICLE INTERACTIONS
NT SPIN-ORBIT INTERACTIONS
NT STRONG INTERACTIONS (FIELD THEORY)
NT WEAK ENERGY INTERACTIONS
NT WEAK INTERACTIONS (FIELD THEORY)
Measurement of magnetic sublevel differential scattering cross sections for potassium and mercury
[MPIS-10/1983] 01 p0119 N85-10815
Energy deposition in microvolumes of silicon from high energy proton reactions
[AD-A144713] 01 p0123 N85-10845
On the co-variant formulation of the law of motion of passive particles in a field of turbulence
[REPT-564] 03 p0377 N85-12407
Tune shifts for coasting beams crossing at small angles
[DE84-017174] 04 p0562 N85-13579
Fermilab research program workbook
[DE84-012568] 06 p0862 N85-15476
Calculation of energy of atomization in silicate tetrahedron SiH(4-)
[BLL-M-38000-(5628.4)] 07 p1040 N85-16589
Theoretical studies relating to the interaction of radiation with matter: Atomic collision processes occurring in the presence of radiation fields
[AD-A146654] 07 p1040 N85-16602
Stochastic methods for the description of multiparticle production
[DE84-009981] 10 p1556 N85-19810
Bibliography of atomic and molecular processes, 1983
[DE85-000662] 12 p1929 N85-22121
Ion transport in beam-plasma interactions
[AD-A150145] 13 p2161 N85-23410
Summaries of FY 1984 research in high energy physics
[DE85-005641] 14 p2420 N85-24934
Introduction to LINE: A Feynman diagram graphic operator
[DE85-009299] 17 p3013 N85-29632
Implications for supersymmetry of the CERN monojets
[DE85-008178] 17 p3030 N85-28741
Photon-photon collisions
[DE85-008056] 17 p3030 N85-28742
Measuring structure functions at SSC energies
[DE85-007515] 17 p3031 N85-28746
Electroweak interactions in nuclei
[DE85-007811] 17 p3033 N85-28762
Possible indication of an A-dependence of R in deep-inelastic electron scattering from nuclei
[DE85-008174] 17 p3033 N85-28763
Physics of (very) high energy e(+)-e(-) colliders
[DE85-008177] 17 p3036 N85-28780
Oxygen-nitrogen interactions in ion-implanted silicon
[DE85-010091] 18 p3195 N85-29819
Gravitational properties of antimatter
[DE85-009801] 18 p3197 N85-29832
One- and two-electron transfer processes in ion-surface scattering
[AD-A154208] 19 p3353 N85-30782
Theory of high energy collision processes
[DE85-010183] 19 p3362 N85-30848
Free-zone electrophoresis of animal cells. 1: Experiments on cell-cell interactions
20 p3499 N85-31754
Plastic scintillator detectors for the study of transfer and breakup reactions at intermediate energies
[DE85-009945] 20 p3528 N85-31945
Current experiments in elementary particle physics, revision 1-85
[DE85-011513] 20 p3529 N85-31950
Interactions of heavy nuclei, Kr, Xe and Ho, in light targets 20 p3544 N85-32050
Wave/particle interactions in the plasma sheet
[NASA-CR-171537] 20 p3547 N85-32072
Interacting Boson approximation
[DE85-009016] 22 p3837 N85-33756
Polarization of fast particle beams by collisional pumping
[DE85-011621] 22 p3838 N85-33764
Proceedings of the 18th LAMPF Users Group Meeting
[DE85-011886] 22 p3839 N85-33773
Cosmic ray composition between 10 to the 15th power - 10 to the 17th power eV obtained by air shower experiments
[OG-5.1-12] 22 p3862 N85-34053
Space Experiments with Particle Accelerators (SEPAC) 23 p3901 N85-34165
Electron loss process and cross section of multiply charged ions by neutral atoms 23 p3981 N85-34685
Multiple inner shell vacancies in laser-irradiated Au plasma 23 p3981 N85-34687
Cosmic ray modulation in a random anisotropic magnetic field
[SH-4.1-20] 23 p4006 N85-34839
Interactions of heavy nuclei, Kr, Xe and Ho, in light targets
[OG-7.2-21] 23 p4016 N85-34888
A cosmic ray driven instability
[OG-8.1-5] 23 p4018 N85-34895
Plastic scintillators in coincidence for the study of multi-particle production of sea level cosmic rays in dense medium
[SH-9.1-11] 23 p4062 N85-35126
A suggested standardized format for cosmic ray ground-level event data
[SH-9.1-15] 23 p4062 N85-35130
Detector requirements for intensity interferometry measurements 24 p4147 N85-35709
A holographic streamer chamber for relativistic nucleus-nucleus collision experiments
24 p4147 N85-35710
Fractional charge resolution in music
24 p4147 N85-35712
Neutrino production of like sign dimuons
[DE85-013594] 24 p4151 N85-35741
High energy physics at Tufts University
[DOE/ER-40085/7] 24 p4152 N85-35744
Studies of relativistic heavy ion collisions
[DE85-014666] 24 p4152 N85-35745
Resonance localization in tokamaks excited with ICRF waves
[DE85-014559] 24 p4160 N85-35791
Some nuclear data needs in astrophysics
[DE85-012916] 24 p4168 N85-35842
Nineteenth International Cosmic Ray Conference. HE Sessions, volume 6
[NASA-CP-2376-VOL-6] 24 p4170 N85-35848
On total cross sections and slopes at superhigh energies
[HE-1.1-4] 24 p4170 N85-35852
Determination of the cross section of the proton, pion and neutron inelastic interaction with lead and carbon nuclei at 0.5 - 5.0 TeV energies (PION experiment)
[HE-1.1-5] 24 p4170 N85-35853
Measurement of interaction cross section of cosmic ray Fe nuclei (E4 GeV/N) with Al target
[HE-1.1-7] 24 p4170 N85-35855
QCD-motivated description of very high energy particle interactions
[HE-1.2-2] 24 p4171 N85-35861
Empirical description of the hadron-hadron and hadron-nucleus interaction at the accelerator energy range
[HE-1.2-4] 24 p4171 N85-35862
Low P sub T hadron-nucleus interactions
[HE-1.2-7] 24 p4172 N85-35865
Angular distribution and multiplicity of backward hadrons in hFe interactions at 0.5-5.0 TeV energies (PION Experiment)
[HE-1.2-8] 24 p4172 N85-35866
A test of the Feynman scaling in the fragmentation region
[HE-1.2-9] 24 p4172 N85-35867
A unification of the interactions and the diffractive processes 24 p4173 N85-35870
Propagation of cosmic rays through the atmosphere in the quark-gluon strings model 24 p4173 N85-35873
Experimental evidence of the decrease of kinetic energy of hadrons in passing through atomic nuclei
24 p4174 N85-35880
The phi-meson and Chiral-mese-meson production in heavy-ion collisions as potential probes of quark-gluon-plasma and Chiral symmetry transitions
24 p4175 N85-35884
Ringlike inelastic events in cosmic rays and accelerators 24 p4175 N85-35887
Few-particles generation channels in inelastic hadron-nuclear interactions at energy approximately equals 400 GeV
[HE-3.2-9] 24 p4179 N85-35917
The multiplicity and the spectra of secondaries correlated with the leading particle energy
[HE-3.2-11] 24 p4179 N85-35919
Characteristics of anomalously high multiplicity cosmic ray interactions
[HE-3.3-1] 24 p4180 N85-35920
Analytical-numerical methods of calculations of energy and three-dimensional particle distributions in electromagnetic cascades
[HE-3.5-13] 24 p4184 N85-35950
Relation between gamma-ray family and EAS core: Monte-Carlo simulation of EAS core
[HE-3.6-7] 24 p4185 N85-35955
A study of gamma-families generated in nucleon-nucleus (NA) and pion-nucleus (pi A) interactions
[HE-3.7-2] 24 p4186 N85-35961
High energy hadrons in extensive air showers
24 p4187 N85-35976
Electromagnetic and muonic structure of showers initiated by gamma-rays and by hadrons
[HE-4.5-6] 24 p4195 N85-36030
A facility for investigation of multiple hadrons at cosmic-ray energies
[HE-4.6-8] 24 p4197 N85-36045
Arrival time distributions of electrons in air showers with primary energies above 10 (10)eV observed at 900m above sea level
[HE-4.7-5] 24 p4199 N85-36058
Methods for roof-top mini-arrays
[HE-4.7-7] 24 p4199 N85-36059
Photo nuclear energy loss term for muon-nucleus interactions based on xi scaling model of QCD
[HE-5.2-17] 24 p4204 N85-36093
The spectrum of neutrons at 60 hg m(-2)
[HE-5.2-20] 24 p4204 N85-36096
Limits on deeply penetrating particles in the 10(17) eV cosmic ray flux
[HE-5.3-1] 24 p4205 N85-36098
A study of atmospheric neutrinos with the IMB detector
[HE-5.3-7] 24 p4205 N85-36101
Atmospheric neutrinos observed in underground detectors
[HE-5.3-8] 24 p4205 N85-36102
High energy neutrino astronomy with MACRO
[HE-5.3-12] 24 p4206 N85-36106

Characteristics of slow particles emitted in the charged current interactions of neutrinos with emulsion nuclei
[HE-5.3-22] 24 p4207 N85-36113
Nucleon decay and atmospheric neutrinos in the Mont Blanc experiment
[HE-6.2-6] 24 p4211 N85-36142
Energetic delayed hadrons in large air showers observed at 5200m above sea level
[HE-6.2-9] 24 p4211 N85-36145
Search for long-lived massive particles in extensive air showers
[HE-6.2-10] 24 p4212 N85-36146
Search for anomalons using plastic nuclear track detectors
[HE-6.2-12] 24 p4212 N85-36148
Observation of genetic relation among new phenomena Geminion, Chiron and mini-Centauro
[HE-6.2-16] 24 p4212 N85-36152
Tien-Shan effect and charmed particles
[HE-6.2-17] 24 p4212 N85-36153
Muon and neutrino fluxes
[HE-6.2-18] 24 p4213 N85-36154

PARTICLE LADEN JETS
Influence of turbulence on erosion by a particle-laden fluid jet
[DE84-014365] 09 p1320 N85-18301
Jets in air-jet family
[HE-3.2-1] 24 p4179 N85-35912
Search for anomalous C-jets in Chacaltaya emulsion chamber experiment
[HE-3.2-5] 24 p4179 N85-35913
Exotic interactions among C-jets and Pb-jets
[HE-3.2-6] 24 p4179 N85-35914

PARTICLE MASS
NT ELECTRON MASS
Free energy and effective mass of the polaron at finite temperatures
[TUM-M8401] 03 p0417 N85-12667
Search for neutrino oscillations at the Brookhaven AGS
[DE85-009766] 20 p3530 N85-31957
Systematics of quark mass matrices in the Standard Electroweak Model
[USIP-85-05] 20 p3532 N85-31972
Aerosol analysis and emission spectrometry with free jets
[DE85-010676] 21 p3564 N85-32168
Does low-energy physics depend on the potential of a heavy Higgs-particle
[NIKHEF-H/85-1] 22 p3838 N85-33783
Observation of cosmic ray positrons from 5 to 25 GeV
[OG-6.2-5] 22 p3889 N85-34104

PARTICLE MOTION
A covariant derivation of the ponderomotive force
[AD-A145054] 01 p0121 N85-10830
Response of propellants to high dynamic stresses: The uses of gun launch techniques
[DE84-013223] 02 p0168 N85-11259
Green River air quality model development: Meteorological and tracer data, July/August 1982. Field study in Brush Valley, Colorado
[DE84-014975] 02 p0225 N85-11474
Long-time tail in the two-wave model
02 p0262 N85-11837
Stable distribution and Levy process in fractal turbulence 02 p0263 N85-11848
Lie-transformation action principle for classical plasma dynamics
[DE84-014576] 02 p0265 N85-11858
Wall effects on the slow steady motion of a particle in a viscous incompressible fluid
[PREPRINT-828] 03 p0363 N85-12327
Dynamic compression and volatile release of carbonates
[NASA-CR-174076] 03 p0391 N85-12504
Particle entrainment in a compressible vortex
[ISL-CO-230/83] 04 p0500 N85-13192
MC2969 escapement study
[DE84-014542] 05 p0845 N85-14143
Surging as a potential response of ice sheets to CO2-induced changes in the polar environment (SPICAE)
[DE84-016472] 06 p0841 N85-15341
Earth's radiation belts
[AD-A147927] 07 p0998 N85-16339
Simulation of the ion-beam-driven drift instability in a magnetic trap, 1
[AD-A149451] 10 p1452 N85-19147
Dynamical studies of molecular systems
[DE85-009053] 11 p1594 N85-20026
Determination of the drag of free flying particles in supersonic flow with a pulsed laser
12 p1773 N85-21129
Particle transport in planetary magnetospheres
12 p1954 N85-22275
Experimental and theoretical investigation of the motion of particles in a compressible vortex
[ISL-R-129/83] 14 p2303 N85-24264
Dynamics of charged small particles -- Jupiter, Saturn magnetospheres 15 p2676 N85-26522
CALTECH-DOE program on numerical analysis, computing and fundamental studies of motion, energy and mass transfer in fluids
[DE85-006106] 17 p2959 N85-28274
Stability in dynamical systems
[DE85-006898] 17 p3034 N85-28766
Forced structural response using component mode synthesis
[DE85-008479] 19 p3267 N85-30383
Electrophoretic mobility of cells in a vertical Ficoll gradient 20 p3499 N85-31753
Free-zone electrophoresis of animal cells. 1: Experiments on cell-cell interactions
20 p3499 N85-31754
Development anmd testing of electrophoresis solutions. Task I.1: Development of optimal buffer system
20 p3500 N85-31755
Electrophoretic mobilities of erythrocytes in various buffers 20 p3500 N85-31756
Effects of method of detachment on electrophoretic mobility of mammalian cells grown in monolayer culture
20 p3500 N85-31757
Preparative electrophoresis of cultured human cells: Effect of cell cycle phase 20 p3500 N85-31758
The role of cell size in density gradient electrophoretic separation of mouse leukemia cells according to position in the cell cycle 20 p3500 N85-31760
Electrophoretic mobilities of cultured human embryonic kidney cells in various buffers 20 p3501 N85-31761
Effect of passage number on electrophoretic mobility distributions of cultured human embryonic kidney cells
20 p3501 N85-31762
Monte-Carlo treatment of nonlinear collisional effects in charged-particle transport
[DE85-010755] 20 p3521 N85-31897
Longitudinal tune control in synchrotrons
[DE85-010745] 20 p3527 N85-31937
Properties of the reflected beams from the Earth's bow shock: A simple model
[IFSI-84-14] 20 p3549 N85-32068
Relativistic electron in curved magnetic fields
[OG-6.2-11] 22 p3890 N85-34110
Pulsars as cosmic ray particle accelerators: Proton orbits
[OG-8.2-21] 23 p4021 N85-34917
Mini and super mini arrays for the study of highest energy cosmic rays
[OG-9.4-9] 23 p4029 N85-34976
The cosmic ray differential diurnal variation dependences on the zenith angle and the geomagnetic disturbance
[SH-4.5-16] 23 p4038 N85-35033
Changes in the energy spectrum of anomalous oxygen and helium during 1977-1985
[SH-4.6-1] 23 p4039 N85-35039
Two-dimensional quasineutral description of particles and fields above discrete auroral arcs
[NASA-CR-176170] 24 p4116 N85-35517
Peculiarities of gamma-quanta distribution at 20 TeV energy
[HE-3.7-10] 24 p4186 N85-35967

PARTICLE PRECIPITATION
NT ELECTRON PRECIPITATION
NT PROTON PRECIPITATION
Relations between the particle precipitation events in mid-latitudes, the ring current intensity and the polarity of the interplanetary magnetic field
04 p0519 N85-13316
Current carriers for the field-aligned current system
[NASA-TM-86161] 08 p1260 N85-17925
Ionospheric research at INPE
[INPE-3279-PRE/602] 10 p1514 N85-19556
Upper atmosphere research at INPE
[INPE-3281-PRE/604] 10 p1515 N85-19557
Ozone measurements in the mesosphere during a solar proton event 11 p1665 N85-20490
Particle sources, transport, storage and precipitation -- magnetosphere 14 p2359 N85-24576
SAMBO-GEOS: Substorm trapped particle particle boundary movements, particle precipitation and acceleration 14 p2361 N85-24589
The IMS contributions to the understanding of auroral precipitation, transport and particle sources
14 p2372 N85-24660
A study of the generation mechanisms of high latitude and equatorial F-region irregularities using DE-2 data
[NASA-CR-175745] 16 p2825 N85-27423
IMS (International Magnetospheric Study) contributions to the understanding of auroral precipitation, transport, and particle sources
[AD-A152320] 17 p2992 N85-28492
Characteristics and sources of E-region ionization in the continuous aurora
[AD-A155018] 21 p3632 N85-32562
Helios 1 energetic particle observations of the solar gamma ray flare events of 7, 21 June 1980 and 3 June 1982
[SH-1.3-8] 23 p3993 N85-34755

PARTICLE PRODUCTION
NT PAIR PRODUCTION
Emission mechanisms in the liquid metal ion source: A review
[AERE-R-11294] 03 p0418 N85-12675
Nuclear moments and nuclear structure
[DE84-015847] 04 p0561 N85-13573
Two phases of neutron production in the POSEIDON plasma focus
[IPF-84-10] 09 p1395 N85-18783
Stochastic methods for the description of multiparticle production
[DE84-009981] 10 p1556 N85-19810
Simulating supersymmetry at the SSC
[DE85-000899] 11 p1736 N85-20917
The IMS contributions to the understanding of auroral precipitation, transport and particle sources
14 p2372 N85-24660
Resonances in photon-photon scattering
[DE85-004607] 14 p2419 N85-24926
Preparation of polystyrene latex particles in a rotating reactor
[NASA-CR-171475] 17 p2933 N85-28106
Implications for supersymmetry of the CERN monojets
[DE85-008178] 17 p3030 N85-28741
Photon-photon collisions
[DE85-008056] 17 p3030 N85-28742
Experiments with light ions at CERN super proton synchrotron
[DE85-007625] 17 p3031 N85-28744
Cluster production and entropy
[DE85-007626] 17 p3032 N85-28752
Heavy quark production processes in QCD
[DE85-007240] 17 p3036 N85-28779
Experimental methods of heavy quark detection
[DE85-006316] 17 p3036 N85-28781
Some comments on SSC physics
[DE85-008444] 18 p3179 N85-29712
A comprehensive study of psi meson production
[DE85-008094] 18 p3180 N85-29718
Intermediate energy nuclear theory
[DE85-010440] 18 p3182 N85-29731
Selected topics from J/psi decays
[DE85-010537] 18 p3183 N85-29736
Topics in intermediate vector boson physics
[NOTA-INTERNA-841] 18 p3184 N85-29743
Pion production and the nuclear equation of state
[DE85-009941] 19 p3365 N85-30670
The dimensional reduction transition
[DE85-003948] 19 p3383 N85-30990
A model of pulsed radiation from the Crab pulsar
20 p3548 N85-32081
Formation of particles in the air of the humid tropical forests 21 p3644 N85-32639
Some evidence for large gravitational redshift in Seyfert galaxy NGC 4151
[OG-2.7-11] 22 p3872 N85-33984
Inverse-Compton gamma rays in the galaxy
[OG-3.1-2] 22 p3873 N85-33990
Propagation and secondary production of low energy antiprotons in the atmosphere
[OG-8.1-3] 22 p3887 N85-34094
Observed antiprotons and energy dependent confinement of cosmic rays: A conflict?
[OG-8.1-7] 22 p3888 N85-34096
Reestimation of the production spectra of cosmic ray secondary positrons and electrons in the ISM
[OG-8.2-8] 22 p3889 N85-34107
Study of non-thermal photon production under different scenarios in solar flares. 1: Scenarios and formulations
[SH-1.2-2] 23 p3991 N85-34736
Study of non-thermal photon production under different scenarios in solar flares. 2: The Compton inverse and Bremsstrahlung models and fittings
[SH-1.2-3] 23 p3991 N85-34739
The starting conditions for an optically small solar gamma ray flare
[SH-1.3-2] 23 p3993 N85-34751
Time extended production of neutrons during a solar flare
[SH-1.4-1] 23 p3994 N85-34762
Relativistic cosmic ray spectra in the full non-linear theory of shock acceleration
[OG-8.1-6] 23 p4018 N85-34896
Secondary gamma-ray production in a coded aperture mask
[OG-9.2-6] 23 p4025 N85-34945
Spallogenic origin of nuclei in meteorites
[SH-7.1-10] 23 p4048 N85-35102

Neutrino production from the solar atmosphere
[SH-8.1-9] 23 p4050 N85-35114
Solar cosmic ray bursts and solar neutrino fluxes
[SH-8.1-10] 23 p4050 N85-35115
High energy physics at Tufts University
[DOE/ER-40085/7] 24 p4152 N85-35744
Studies of relativistic heavy ion collisions
[DE85-014666] 24 p4152 N85-35745
Nineteenth International Cosmic Ray Conference. HE Sessions, volume 6
[NASA-CP-2376-VOL-6] 24 p4170 N85-35848
QCD-motivated description of very high energy particle interactions
[HE-1.2-2] 24 p4171 N85-35861
Multiplicity distributions in interaction models used for cascade simulations
[HE-1.2-5] 24 p4172 N85-35863
Is the inelastic charge-exchange contribution constant at the large X and superhigh energies? Qaut 01Kuchin, I. A. 24 p4173 N85-35871
General consequences of the violated Feynman scaling 24 p4173 N85-35872
How are particle production, nucleon emission and target fragment evaporation processes interrelated in hadron-nucleus collisions? 24 p4174 N85-35878
Experimental study of the space-time development of the particle production process in hadron-nucleon collisions, using massive target nucleus as a detector 24 p4174 N85-35879
Energy-range relations for hadrons in nuclear matter 24 p4174 N85-35881
Scattering and stopping of hadrons in nuclear matter 24 p4174 N85-35882
Measurements of hadron mean free path for the particle-producing collisions in nuclear matter 24 p4174 N85-35883
The phi-meson and Chiral-meso-meson production in heavy-ion collisions as potential probes of quark-gluon-plasma and Chiral symmetry transitions 24 p4175 N85-35884
Heavy flavours production in quark-gluon plasma formed in high energy nuclear reactions 24 p4175 N85-35886
Forward particle production in inelastic Ne-22 interactions in emulsion at 4.1 A Ge/c
[HE-1.4-7] 24 p4176 N85-35895
High energy gamma-rays and hadrons at Mount Fuji
[HE-3.1-3] 24 p4177 N85-35903
Some characteristic cosmic ray events and an attempt at their explanation
[HE-3.1-9] 24 p4178 N85-35906
The model of independent particles emission in the multiparticle production theory
[HE-3.2-10] 24 p4179 N85-35918
Experimental basis for the models of cascade propagation in atmosphere
[HE-3.6-6] 24 p4185 N85-35954
Atmospheric neutrinos observed in underground detectors
[HE-5.3-8] 24 p4206 N85-36102
Collimated groups of particles as possible manifestation of heavy meson production
[HE-5.4-14] 24 p4208 N85-36124

PARTICLE SIZE DISTRIBUTION

Milling of Si3N4 with Si3N4 hardware
[NASA-TM-86664] 01 p0031 N85-10191
Preparation of large-particle-size monodisperse latexes in space: The STS-3, STS-4, and STS-7 mission results 02 p0151 N85-11021
Aerosol sampling bias from differential electrostatic charge and particle size 02 p0224 N85-11467
Particle size distribution on surfaces in clean rooms
[AD-A146057] 03 p0328 N85-12109
Characteristics of aerosol volume distributions measured at Meppen, W. Germany
[AD-A146138] 03 p0396 N85-12528
Intermediate results of a 1-year study of a laser spectrometer in the DOE filter test facilities
[DE84-016478] 04 p0508 N85-13228
Parallel flow diffusion battery
[DE84-005864] 05 p0831 N85-14047
Influence of grain size distribution on the undrained dynamic properties of saturated sand
[PB85-102362/GAR] 09 p1305 N85-18197
Investigation of fuel additive effects on sooting flames
[AD-A149154] 10 p1457 N85-19179
Study of submicron particle size distributions by laser Doppler measurement of Brownian motion
[AD-A149139] 10 p1457 N85-19366
Condensational transformation of atmospheric aerosol particle distribution functions 10 p1500 N85-19466
Solar fuel synthesis based on colloidal and particulate semiconductors
[PB85-129104] 11 p1614 N85-20152
Laser Doppler Anemometry (LDA) signal triggering and effective particle size range
[KU-SFB-210/E/5] 11 p1634 N85-20290
Particle size, number, composition and velocity from solid rocket motors 12 p1785 N85-21201
Environment definition, large particles 12 p1787 N85-21220
Measurements 12 p1787 N85-21222
Environment definition, small particles, diameter less than or equal to 1 MM 12 p1788 N85-21223
Research study of droplet sizing technology leading to the development of an advanced droplet sizing system
[NASA-CR-174839] 12 p1850 N85-21604
Microstructure of Venus cloud layer based on spectrophotometric data from Venera-11 spacecraft 13 p1982 N85-22436
Solid propellant combustion diagnostics and automated data retrieval from holograms 13 p1998 N85-22527
Characterization of heterogeneity of composite propellants and its effects on combustion behavior 13 p2000 N85-22539
Recent trends in particle size analysis techniques
[NASA-TM-77735] 13 p2017 N85-22645
Size and velocity distributions of particles and droplets in spray combustion systems
[AD-A150355] 13 p2017 N85-22648
Laser diagnostic analyses of sooting flames
[AD-A150478] 13 p2017 N85-22649
Infrared aerosol absorption index 13 p2110 N85-23147
Potential bedforms on Venus: Wind tunnel simulations 13 p2189 N85-23583
Quantitative analyses of planetary reflectance spectra 13 p2197 N85-23625
Qualification of the T2 wind tunnel in cryogenic operation. B: Flow fluctuations, particle detection and qualification
[NASA-TM-77782] 14 p2227 N85-23806
Comparison of flame photometer data with total particle volume calculated from laser spectrometer particle count data
[AD-A151008] 14 p2252 N85-23958
Characterization of supported metal catalysts by imaging, microdiffraction and microanalysis techniques
[DE85-005567] 14 p2253 N85-23961
An apparatus for sizing particulate matter in solid rocket motors
[AD-A151282] 15 p2495 N85-25368
Particle shape characterization
[AD-A151981] 15 p2544 N85-25707
Particle curtain generator for optical property measurements of solid particles
[DE85-005784] 15 p2560 N85-25787
Case studies of snow clouds by means of snow crystal sondes 15 p2581 N85-25921
Size distributions of elemental carbon in atmospheric aerosols
[PB85-153534] 15 p2589 N85-25963
Physical properties of Saturn's rings 15 p2672 N85-26493
A simple model of Saturn's rings revisited 15 p2674 N85-26506
Size distribution in collisional systems — planetary rings 15 p2674 N85-26508
Diffusion instability in a bimodal disc — planetary rings 15 p2675 N85-26513
Macrostructure and microphysics of Saturn's E-ring 15 p2677 N85-26529
Ultrasonic dispersion of soils for routine particle size analysis: Recommended procedures
[DE85-005530] 16 p2861 N85-27843
An investigation into the soot production processes in a gas turbine engine
[AD-A152710] 17 p2919 N85-27992
Effect of nonuniform size on internal stresses in a rapid, simple shear flow of granular materials. Part 1: Two grain sizes
[AD-A154045] 19 p3285 N85-30372
Effect of nonuniform size on internal stresses in a rapid, simple shear flow of granular materials. Part 2: Multiple grain sizes
[AD-A154046] 19 p3285 N85-30373
Phase size distribution in WC/Co hardmetal
[NPL-DMA(A)-93] 20 p3431 N85-31281
Size and DNA distributions of electrophoretically separated cultured human kidney cells 20 p3500 N85-31759
The role of cell size in density gradient electrophoretic separation of mouse leukemia cells according to position in the cell cycle 20 p3500 N85-31760
Journal of Research of the National Bureau of Standards, volume 90, number 1, January - February 1985
[PB85-179083] 20 p3522 N85-31908
Particle sizing from forward scattered light at two angles using a Variable-Focal-Length optical system
[AD-A154184] 20 p3533 N85-31980
Large eddy structures in transitional and turbulent flames
[AD-A154520] 21 p3582 N85-32157
Photoinduced active sites on ice nucleating aerosol of silver iodide 21 p3639 N85-32601
Experimental investigation of properties of ice-forming reagents 21 p3639 N85-32602
The effect of supersaturation, temperature and particle size on ice-nucleating ability of atmospheric aerosol 21 p3639 N85-32604
Multi-channel electric aerosol spectrometer 21 p3642 N85-32623
Formation of particles in the air of the humid tropical forests 21 p3644 N85-32639
The influence of Brownian coagulation on the size distributions of atmospheric aerosols 21 p3645 N85-32643
A new hypothesis for the observed vertical distribution of atmospheric aerosols 21 p3645 N85-32646
On the mechanisms responsible for the formation of typical size spectra and vertical distribution of tropospheric aerosol particles 21 p3645 N85-32647
Our knowledge about the atmospheric aerosol 21 p3646 N85-32650
Characteristics of aerosol composition in a nonurban area, north China 21 p3646 N85-32651
Variation of the submicron aerosol structure 21 p3647 N85-32661
Variability of rural aerosols under stable weather conditions 21 p3647 N85-32663
Marine aerosols at the Dutch North Sea coast: Size distributions and fractionation of trace elements 21 p3648 N85-32664
A probabilistic method for particle size analysis of aerosols 21 p3648 N85-32669
An electron microscopic study of urban aerosol 21 p3651 N85-32699
Composition of primary cosmic rays near the knee
[OG-5.2-10] 22 p3684 N85-34066
Review of zirconium-zircaloy pyrophoricity
[DE85-011168] 23 p3916 N85-34270
Synthesis of ultrafine ceramic and metallic powders in a thermal argon rf plasma
[DE85-009634] 23 p3963 N85-34666
Size distributions of air showers accompanied with high energy gamma ray bundles observed at Mt. Chacaltaya
[HE-3.3-9] 24 p4181 N85-35927
Comparison of absolute intensity between EAS with gamma-families and general EAS at Mount Norikura
[HE-3.3-11] 24 p4181 N85-35929
Photo nuclear energy loss term for muon-nucleus interactions based on xi scaling model of QCD
[HE-5.2-17] 24 p4204 N85-36083

PARTICLE SPIN

NT ELECTRON SPIN
NT NUCLEAR SPIN

Spin dynamics of rare Earth ions in crystal fields probed by muon spin rotation
[DE84-013805] 02 p0278 N85-11810
A geometrical theory of spin motion
[DE84-016537] 04 p0574 N85-13958
Muon spin rotation studies 17 p3042 N85-28819
Spin physics at BNL
[DE85-009766] 20 p3529 N85-31955
Cooling high intensity atomic hydrogen beams to liquid helium temperatures
[DE85-012515] 24 p4148 N85-35718

PARTICLE TELESCOPES

Plastic scintillator detectors for the study of transfer and breakup reactions at intermediate energies
[DE85-009945] 20 p3528 N85-31945
The energy spectrum of Jovian electrons in interplanetary space
[SH-1.5-16] 21 p3715 N85-33051
Secondary gamma-ray production in a coded aperture mask
[OG-9.2-6] 23 p4025 N85-34945
Operating characteristics of a prototype high energy gamma-ray telescope
[OG-9.2-7] 23 p4025 N85-34946
High energy gamma ray balloon instrument
[OG-9.2-12] 23 p4026 N85-34951
Results of a study to build a gamma-ray telescope in an external tank
[OG-9.3-3] 23 p4027 N85-34958
An approach of reducing the background induced by neutrons
[OG-9.3-5] 23 p4027 N85-34960
Astrophysical applications of high angular resolution array-telescopes
[OG-9.5-7] 23 p4031 N85-34984
Sidereal variations deep underground in Tasmania
[SH-4.4-4] 23 p4033 N85-35002
Corrected sidereal anisotropy for underground muons
[SH-4.4-7] 23 p4033 N85-35005

Cosmic ray intensity variations observed at Matsushiro (220 M.W.E. in depth)
[SH-4.4-9] 23 p4034 N85-35007
Study of cosmic ray scintillations from 5-minute data of the scintillations telescope Izmiran and world-wide network stations
[SH-5.1-18] 23 p4043 N85-35071
Coupling functions for lead and lead-free neutron monitors from the latitudinal measurements performed in 1982 in the research station Academician Kurchatov
[SH-6.1-1] 23 p4044 N85-35076
Atmospheric effects on the underground muon intensity
[SH-6.1-3] 23 p4044 N85-35078
Observation of energy spectrum of electron albedo in low latitude region at Hyderabad, India
[SH-6.1-7] 23 p4045 N85-35081
A silicon surface barrier telescope for solar particles identification
[SH-9.1-3] 23 p4050 N85-35118
A bi-directional charged particle telescope to observe flux, energy spectrum and angular distribution of relativistic and non-relativistic particles
[SH-9.1-4] 23 p4050 N85-35119
An underground cosmic ray muon telescope for observation of cosmic ray anisotropy
24 p4196 N85-36037

PARTICLE THEORY
The search for proton decay: Introduction
[DE84-014349] 01 p0131 N85-10904
Solar neutrino spectroscopy
[DE84-015518] 02 p0304 N85-11968
Parity and time-reversal non-conversation in atoms
[DE84-016924] 04 p0562 N85-13581
Toward unification of elementary particle physics and cosmology in 10-dimensions
[DE84-013950] 05 p0727 N85-14674
On the nature of the baryon asymmetry
[NASA-TM-86156] 05 p0746 N85-14784
Ultraviolet divergences and supersymmetric theories
[DE85-001649] 11 p1729 N85-20875
A systematic study of light scattering by irregularly shaped particles
[AD-A150192] 13 p2159 N85-23400
Particle sources, transport, storage and precipitation — magnetosphere 14 p2359 N85-24576
Inflation from extra dimensions
[DE85-007834] 16 p2883 N85-27787
Spectrographic investigation of low-voltage arc discharge in argon atmosphere
[BLL-M-36276-(5828.4)] 20 p3422 N85-31242
Vector calculation of particle code
23 p3981 N85-34888
Relativistic cosmic ray spectra in the full non-linear theory of shock acceleration
[OG-8.1-6] 23 p4018 N85-34896

PARTICLE TRACKS
Green River air quality model development: Meteorological and tracer data, July/August 1982. Field study in Brush Valley, Colorado
[DE84-014975] 02 p0225 N85-11474
Climatological variability in modeling of long-term regional transport and deposition of air pollutants
[DE84-014726] 04 p0539 N85-13430
Scintillator-fiber charged particle track-imaging detector
[NASA-CR-174160] 04 p0559 N85-13560
Aspects of the comparison of stratospheric trace species measurements with photochemical models
[DE84-017028] 05 p0672 N85-14317
Use of ground radar to detect reentering debris
12 p1784 N85-21200
Digital characterization of particle tracks for microdosimetry
[DE85-012606] 22 p3846 N85-33822
Ultraheavy cosmic ray tracks in meteorites: A reappraisal, based on calibrations with relativistic ions
[OG-4.4-10] 22 p3860 N85-34041
Cross sections for the production of fragments with Z greater than or equal to 6 by fragmentation of Z greater than or equal to 9 and less than or equal to 26 nuclei
[OG-7.2-22] 23 p4016 N85-34889
SONTRAC: A solar neutron track chamber detector
[SH-9.1-12] 23 p4052 N85-35127
Observation of nuclei with energies 8-30 MeV per nucleon in the Earth's magnetosphere at the altitudes 350 KM
[SH-10.1-5] 23 p4053 N85-35136
Measurement of low energy cosmic rays aboard Spacelab-1
[SH-10.1-6] 23 p4053 N85-35137
Heavy cosmic ray measurement aboard Spacelab-1
[SH-10.1-7] 23 p4053 N85-35138
Elemental tracers of source regions of contaminants in precipitation
[DE85-012658] 24 p4113 N85-35499
Calculation of heavy-ion tracks in liquid water
[DE85-012101] 24 p4149 N85-35725
Experimental basis for the models of cascade propagation in atmosphere
[HE-3.6-6] 24 p4185 N85-35954
Search for supermassive magnetic monopoles using mica crystals
[HE-6.1-5] 24 p4210 N85-36134
Spatial distribution read-out system for thermoluminescence sheets
[HE-7.1-7] 24 p4213 N85-36161

PARTICLE TRAJECTORIES
NT ELECTRON TRAJECTORIES
Focusing beam of 1-GeV protons with volumetric capture to the mode of channeling by bent single crystal
02 p0268 N85-11750
Performance deterioration of cascades exposed to solid particles 03 p0319 N85-12057
Averaging effects in models of three-dimensional two-phase flows
[AD-A149313] 10 p1484 N85-19371
A free electron laser with a rotating quadrupole wiggler
[AD-A149052] 10 p1489 N85-19404
PATHFINDER: A trajectory prediction system for the Great Lakes
[PB85-115395] 10 p1506 N85-19506
Cometary atmospheres: Modeling the spatial distribution of observed neutral radicals
[NASA-CR-175491] 11 p1765 N85-21097
The dawn-dusk asymmetry of particles near the neutral sheet of geomagnetotail 14 p2358 N85-24574
Development and validation of a new fallout transport method using variable spectral winds
[AD-A151871] 15 p2599 N85-26022
A numerical study of the mean trajectory approximation in a non-adiabatic process
[AD-A152763] 17 p3030 N85-28737
Trajectories of charged particles traversing a plasma sheath in an oblique magnetic field
[DE85-011070] 19 p3371 N85-30911
Observation of cosmic ray positrons from 5 to 25 GeV
[OG-6.2-5] 22 p3869 N85-34104
Pulsars as cosmic ray particle accelerators: Proton orbits
[OG-8.2-21] 23 p4021 N85-34917
Bevalac calibration of the SOFIE range and hodoscope detectors
[OG-9.1-7] 23 p4023 N85-34933
Cherenkov-dE/dx-range measurements on cosmic ray iron group nuclei
[OG-9.1-12] 23 p4024 N85-34937
The response of ionization chambers to relativistic heavy nuclei
[OG-9.1-13] 23 p4024 N85-34939
Twenty-two-year cycle of the upper limiting rigidity of Daly waves
[SH-4.5-5] 23 p4036 N85-35023
Re-evaluation of cosmic ray cutoff terminology
[SH-6.1-11] 23 p4045 N85-35084
Estimating the change in asymptotic direction due to secular changes in the geomagnetic field
[SH-6.1-13] 23 p4045 N85-35086
Strategic defense initiative
[DE85-012778] 24 p4150 N85-35735
The structure of EAS at E 0.1 EeV
[HE-4.4-2] 24 p4193 N85-36012
Transition effect of air shower particles in plastic scintillators
[HE-4.4-9] 24 p4193 N85-36017
The Nagoya cosmic-ray muon spectrometer 3, part 4: Track reconstruction method
[HE-5.2-5] 24 p4202 N85-36083
Comments on the measurements of multiple muon phenomena
[HE-5.2-13] 24 p4203 N85-36089

PARTICLES
NT AEROSOLS
NT ALPHA PARTICLES
NT ANIONS
NT ANTINEUTRINOS
NT ANTINUCLEONS
NT ANTIPARTICLES
NT ANTIPROTONS
NT ARGON PLASMA
NT BARYONS
NT BETA PARTICLES
NT BOSONS
NT BOUNDARY LAYER PLASMAS
NT CATIONS
NT CHARGED PARTICLES
NT COLD NEUTRONS
NT COLD PLASMAS
NT COLLISIONAL PLASMAS
NT COLLISIONLESS PLASMAS
NT CONDUCTION ELECTRONS
NT CORPUSCULAR RADIATION
NT COSMIC PLASMA
NT CYCLOTRON RADIATION
NT CYLINDRICAL PLASMAS
NT DENSE PLASMAS
NT DEUTERIUM PLASMA
NT DEUTERONS
NT DROPS (LIQUIDS)
NT ELECTRON BEAMS
NT ELECTRON PLASMA
NT ELECTRON PRECIPITATION
NT ELECTRON RADIATION
NT ELECTRONS
NT ELEMENTARY PARTICLES
NT ELLIPTICAL PLASMAS
NT ENERGETIC PARTICLES
NT EVEN-EVEN NUCLEI
NT FAST NEUTRONS
NT FERMIONS
NT FERRIC IONS
NT FINES
NT FOG
NT FREE ELECTRONS
NT GLUONS
NT HADRONS
NT HEAVY NUCLEI
NT HELIUM PLASMA
NT HIGH ENERGY ELECTRONS
NT HIGH TEMPERATURE PLASMAS
NT HOT ELECTRONS
NT HYDROGEN PLASMA
NT HYPERNUCLEI
NT HYPERONS
NT INNER RADIATION BELT
NT ION CYCLOTRON RADIATION
NT KAONS
NT LASER PLASMAS
NT LEPTONS
NT LIGHT BEAMS
NT MAGNETIC MONOPOLES
NT MAGNETICALLY TRAPPED PARTICLES
NT MESONS
NT METAL IONS
NT METAL PARTICLES
NT METALLIC PLASMAS
NT MICROPARTICLES
NT MIST
NT MUONS
NT NEGATIVE IONS
NT NEGATRONS
NT NEUTRAL PARTICLES
NT NEUTRINOS
NT NEUTRONS
NT NITROGEN PLASMA
NT NONEQUILIBRIUM PLASMAS
NT NONUNIFORM PLASMAS
NT NUCLEAR PARTICLES
NT NUCLEI (NUCLEAR PHYSICS)
NT NUCLEONS
NT ODD-EVEN NUCLEI
NT ODD-ODD NUCLEI
NT OUTER RADIATION BELT
NT OXYGEN PLASMA
NT PHOTOELECTRONS
NT PHOTONS
NT PIONS
NT PLASMA CLOUDS
NT PLASMA FOCUS
NT PLASMA JETS
NT PLASMA LAYERS
NT PLASMA SHEATHS
NT PLASMAS (PHYSICS)
NT POLARONS
NT POLLEN
NT POSITRONS
NT POWDER (PARTICLES)
NT POWDERED ALUMINUM
NT PRIMARY COSMIC RAYS
NT PROTON BELTS
NT PROTONS
NT QUARKS
NT RADIATION BELTS
NT RELATIVISTIC ELECTRON BEAMS
NT RELATIVISTIC PARTICLES
NT RELATIVISTIC PLASMAS
NT ROTATING PLASMAS
NT SEMICONDUCTOR PLASMAS
NT SOLAR CORPUSCULAR RADIATION
NT SOLAR COSMIC RAYS
NT SOLAR ELECTRONS
NT SOLAR NEUTRINOS
NT SOLAR PROTONS
NT SOLAR WIND
NT SOOT
NT SPACE PLASMAS
NT SPHERICAL PLASMAS

NT STELLAR WINDS
NT STRONGLY COUPLED PLASMAS
NT TACHYONS
NT THERMAL NEUTRONS
NT THERMAL PLASMAS
NT TOROIDAL PLASMAS
NT TRAPPED PARTICLES
NT VECTOR MESONS
Fluorinated diamond particles bonded in a filled fluorocarbon resin matrix
[DE84-014444] 01 p0022 N85-10136
Technical Review of the Solid Particle Receiver Program
[DE84-015181] 01 p0068 N85-10451
Size specific total particulate emission factors for mobile sources
[PB84-226653] 01 p0071 N85-10471
Effect of the Basset term on particle relaxation behind normal shock waves
[AD-A145446] 02 p0198 N85-11320
A finite element projection method for the solution of particle transport problems with anisotropic scattering
[AD-A145382] 02 p0250 N85-11637
Algebra of hydrodynamic flows of an ideal fluid and the prediction of the behaviour of a system of particles of a passive admixture on Riemann surfaces with a variable curvature
[REPT-565] 03 p0377 N85-12408
Extinction by dielectric particles at optical and infrared wavelengths
[AD-A146305] 03 p0413 N85-12540
Recent heavy particle decay in a matter dominated universe
[NASA-CR-175501] 11 p1764 N85-21095
Solid particle environment and protection for the Galileo Orbiter 12 p1786 N85-21207
A method for determining in situ the absorption coefficient of particulate media using pulsed laser technique
[AD-D011548] 12 p1799 N85-21281
Improved silicon grinding method and apparatus
[NASA-CASE-NPO-16336-1-CU] 12 p1819 N85-21407
Solid particle receiver experiments: Velocity measurements
[DE85-000257] 12 p1853 N85-21623
The orientation distribution of nonspherical aerosol particles within a cloud
[AD-A150600] 13 p2092 N85-23061
Sample introduction methods for improving the particle detection capability of the spectrometric oil analysis program
[AD-A150139] 13 p2158 N85-23399
The effect of particle density on aeolian transport 13 p2189 N85-23581
A review of radar observations of Saturn's rings 15 p2670 N85-26474
Saturn's E ring 15 p2671 N85-26481
The Saturn ring particles from optical reflectance polarimetry 15 p2671 N85-26484
Solved und unsolved problems in planetary ring dynamics 15 p2674 N85-26502
Physical and geological nature of Saturn's larger ring particles 15 p2674 N85-26509
Dynamics of neutral small particles --- in the solar system 15 p2676 N85-26521
Multivalued electrostatic potentials; chance or necessity for the charge of solid particles near Saturn? 15 p2677 N85-26529
Preparation of polystyrene latex particles in a rotating reactor
[NASA-CR-171475] 17 p2933 N85-28108
Surface degradation of ductile metal in elevated temperature gas-particle streams
[DE85-008428] 18 p3074 N85-29017
Chemical, biological, and physical measurements from the subtropical western North Atlantic Ocean. Summer 1982, USNS Lynch, cruise 710-82
[AD-A153823] 18 p3201 N85-29857
Colloidal particle transport with simultaneous birth, growth and capture
[DE85-010388] 19 p3235 N85-30055
Scattering by distributions of small thin particles 19 p3253 N85-30172
Thermal performance and design of a solid particle cavity receiver
[DE85-010830] 19 p3274 N85-30300
Acoustic particle separation
[NASA-CASE-NPO-155559-1] 19 p3350 N85-30765
Wall effect on lateral migration of spherical particles in a linear shear flow 20 p3452 N85-31432
Absorption and scattering properties of aerosols of aggregated particles in the infrared spectral region
[AD-A155475] 21 p3637 N85-32591
Ice-forming efficiency of the soluble and insoluble portions of dust contained in snow 21 p3643 N85-32631
Study of the formation of particles from natural hydrocarbons released by vegetation 21 p3644 N85-32640
A study of time transformation of natural photochemical aerosols 21 p3645 N85-32644
Measurements of the critical supersaturation of 0.029 to 0.035 micron radius particles at Washington, District of Columbia 21 p3649 N85-32676
Integrated current collector and catalyst support
[DE85-011616] 22 p3781 N85-33311
Drying of pulverized material with heated condensible vapor
[DE85-011656] 22 p3783 N85-33438
Influence of particle erosion on the microstructural changes in metals and alloys
[TI85-901384] 23 p3917 N85-34276
Acoustic cross-correlation flowmeter for solid-gas flow
[DE85-005988] 23 p3935 N85-34391
The influence of nonstationarity of the solar activity and general solar field on modulation of cosmic rays
[SH-4.2-17] 23 p4008 N85-34854
Search for proton decay in the Frejus experiment
[HE-6.2-2] 24 p4210 N85-36138
Results on nucleon life-time from the Kolar gold field experiment
[HE-6.2-3] 24 p4211 N85-36139
Data acquisition system for phase-2 KGF proton decay experiment
[HE-6.2-4] 24 p4211 N85-36140
Search for long-lived massive particles in extensive air showers
[HE-6.2-10] 24 p4212 N85-36146
PARTICULATE FILTERS
U FLUID FILTERS
PARTICULATE SAMPLING
Remote sensing of atmospheric particulates: Technological innovation and physical limitations in applications to short-range weather prediction
[NSF ATM-82-09684] 01 p0077 N85-10511
Aerosol sampling bias from differential electrostatic charge and particle size 02 p0224 N85-11467
Analysis and characterization of organic carbon compounds in atmospheric particulate matter
[PB84-232636] 06 p0766 N85-14903
Sample return from a comet flyby 06 p0889 N85-15646
Evaluation of the particulate levels occurring under 1.0/1.2 g/mi nitrogen oxide standards for light duty diesel vehicles and light duty diesel trucks
[PB85-115939/GAR] 09 p1350 N85-18484
Solar fuel synthesis based on colloidal and particulate semiconductors
[PB85-129104] 11 p1614 N85-20152
National Performance Audit Program ambient air audits of analytical proficiency
[PB85-138204] 11 p1680 N85-20586
Diesel engine emissions of particulates and associated organic matter
[PB85-154425] 15 p2590 N85-25964
Microcomputer-controlled system for measuring atmospheric particle fluxes
[DE85-007910] 17 p2988 N85-28469
Role of natural dissolved organic compounds in determining the concentrations of americium in natural waters
[DE85-010266] 19 p3229 N85-30022
Sources of copper air emissions
[PB85-191136] 19 p3310 N85-30523
Identification and quantification of nitropolynuclear aromatic hydrocarbons in ambient and indoor air particulate samples
[PB85-176790] 19 p3311 N85-30525
Fuel-rich catalytic combustion: A soot-free technique for in situ hydrogen-like enrichment
[NASA-TP-2408] 20 p3423 N85-31244
Particulate contamination control in clean rooms by particle fallout (PFO) measurements
[ESA-PSS-01-204-ISSUE-1] 20 p3487 N85-31673
Physical and chemical aerosol characteristics in extremely clean air masses at Cape Grim, Tasmania 21 p3646 N85-32655
Technology of off-gas treatment for liquid-fed ceramic melters
[DE85-012467] 22 p3812 N85-33610
A study of the control of particulate emissions from turbine engine test cells 24 p4067 N85-35205
PARTITIONS (MATHEMATICS)
Parallel triangularization of substructured finite element problems
[NASA-CR-172486] 02 p0241 N85-11589
Some facets of the tri-index assignment polytope
[AD-A149195] 10 p1547 N85-19753
PASCAL (PROGRAMMING LANGUAGE)
PASCAL-MP algebraic and numerical manipulator for polynomials
[INPE-3229-TDL/178] 02 p0240 N85-11582
Programmer's guide for ASKF 77: A tool for programming of dialogs in FORTRAN and PASCAL
[FOA-C-30368-E1] 02 p0243 N85-11585
The automated reasoning system ITP
[ANL-84-27] 12 p1914 N85-22018
Computer Performance Modeling Tool (CPMT)
[AD-A154436] 19 p3336 N85-30682
A PASCAL interpreter for the functional programming language ELC (Extended lambda calculus)
[AD-A155218] 21 p3672 N85-32810
Use of monitors in Pascal on the Lemur: A tutorial on the barrier, self-scheduling FOR-loop, and askfor monitors
[ANL-84-53] 22 p3828 N85-33706
A prototype PASCAL program validation system
[NPL-DITC-57/85] 23 p3956 N85-34513
A quickly tested Pascal random number generator for microcomputers
[AD-A156059] 24 p4136 N85-35833
PASSAGEWAYS
NT STRAITS
Vortex-generating coolant-flow-passage design for increased film-cooling effectiveness and surface coverage
[NASA-TP-2388] 03 p0381 N85-12314
PASSENGER AIRCRAFT
NT A-310 AIRCRAFT
NT A-320 AIRCRAFT
NT BO-105 HELICOPTER
NT BOEING 727 AIRCRAFT
NT BOEING 737 AIRCRAFT
NT BOEING 747 AIRCRAFT
NT BOEING 767 AIRCRAFT
NT CESSNA 402B AIRCRAFT
NT CH-47 HELICOPTER
NT CV-990 AIRCRAFT
NT DC 8 AIRCRAFT
NT DC 10 AIRCRAFT
NT DO-28 AIRCRAFT
NT EUROPEAN AIRBUS
NT F-27 AIRCRAFT
NT L-1011 AIRCRAFT
Aircraft accident report, Scandinavian Airlines System, Flight 901, McDonnell Douglas DC-10-30, John F. Kennedy International Airport, Jamaica, New York, February 28, 1984
[PB84-910415] 05 p0594 N85-13788
A preliminary analysis of C-12 aircraft usage by the Navy Air Logistics System
[AD-A151921] 16 p2694 N85-26834
FAA regulation of 9-seat and under passenger aircraft
[GPO-42-703] 20 p3301 N85-31032
MBB demonstrates new research aircraft ATTAS 20 p3438 N85-31334
PASSENGERS
High-speed intercity rail passenger service
[GPO-35-896] 10 p1570 N85-19897
Air traffic: Instruments, airports, companies, post, cargo and passengers 18 p3080 N85-28932
Aviation safety (aircraft passenger survivability and cabin safety)
[GPO-39-847] 23 p3895 N85-34130
PASSES
U GAPS (GEOLOGY)
PASSIVATION
U PASSIVITY
PASSIVE L-BAND RADIOMETERS
Study of the improvement in analyzing passive microwave remote sensing data by integrated use of ground data 05 p0658 N85-14226
PASSIVE SATELLITES
NT LAGEOS (SATELLITE)
Tactical applications of GPS user equipment 11 p1711 N85-20765
A study of structural concepts for ultralightweight spacecraft
[NASA-CR-175765] 16 p2730 N85-26948
PASSIVITY
Hydrogen passivation of electrically active defects in crystalline silicon solar cells
[DE84-004590] 02 p0223 N85-11461
Research relative to high spatial resolution passive microwave sounding systems 05 p0661 N85-14380
Influence of the mechanical and electrochemical characteristics of austenitic and austenoferritic steels on the propagation rate and morphology of stress corrosion cracking
[BLL-RISLEY-TR-4545-(9091.9F)] 06 p0767 N85-14906
Passive storage technologies 06 p1108 N85-17003

Surface and allied studies in silicon solar cells
[NASA-CR-174447] 11 p1671 N85-20531
Role of passive surface films on corrosion fatigue crack initiation
[DE86-000438] 14 p2257 N85-23985
Investigation of silicon surface passivation by silicon nitride film deposition
[NASA-CR-176883] 15 p2585 N85-25938
Corrosion characteristics of some steels produced through a self-cleaning rotating electrode
[BLL-BISI-TRANS-22048-(9022.06)] 17 p2925 N85-28034
Passivation on high Q acoustic strain sensor for accelerometer
[AD-A153565] 18 p3177 N85-29695
Nitridation of SiO2 for surface passivation 20 p 480 N85-31627
Surface passivation and junction formation using low energy hydrogen implants 20 p3480 N85-31628
EBIC characterization and hydrogen passivation in silicon sheet 20 p3481 N85-31634
Silicon surface passivation by silicon nitride deposition 21 p3610 N85-32423
The development and evaluation of point defect models for the growth of passive films on single crystal, polycrystalline, and amorphous metal surfaces
[AD-A154665] 21 p3709 N85-33023
Low noise polycrystalline semiconductor resistors by hydrogen passivation
[AD-D011721] 23 p3927 N85-34338

PASTE (CONSISTENCY)
Development of metallization process: FSA project, cells and module formation research area
[NASA-CR-176136] 23 p3945 N85-34447

PASTES
Viscosity measurements for thick-film pastes 06 p0831 N85-15280

PATENT APPLICATIONS
Charge depletion meter
[AD-D011484] 10 p1488 N85-19393
Flying objects
[CH-634516-A5] 15 p2469 N85-25242
Airfoil wing with flap
[CH-634787-A5] 15 p2469 N85-25243
Helicopter rotor
[CH-637890-A5] 15 p2470 N85-25245
Aircraft
[CH-642598-A5] 15 p2470 N85-25246
Satellite structure
[CH-642922-A5] 15 p2492 N85-25373
Dual optical mechanical position tracker
[AD-D011739] 22 p3844 N85-33811
NASA patent abstracts bibliography: A continuing bibliography. Section 1: Abstracts (supplement 27)
[NASA-SP-7039(27)-SECTION-1] 22 p3849 N85-33840

PATENT POLICY
NASA Patent Abstracts Bibliography. A continuing bibliography. Section 2: Indexes
[NASA-SP-7039(26)] 13 p2167 N85-23445
NASA patent abstracts bibliography, a continuing bibliography. Section 2: Indexes (supplement 27)
[NASA-SP-7039(27)-SECTION-2] 24 p4164 N85-35820

PATENTS
Summary of trends in photovoltaic patent activity
[DE84-015757] 01 p0068 N85-10452
Bibliography of US patents on augmentation of convective heat and mass transfer, part 2
[DE84-014885] 04 p0498 N85-13178
The Uniform Science and Technology Research and Development Utilization Act
[GPO-36-327] 04 p0577 N85-13685
Uniform Science and Technology Research and Development Utilization Act
[H-REPT-98-983-PT-1] 04 p0577 N85-13686
Flying objects
[CH-634516-A5] 15 p2469 N85-25242
Airfoil wing with flap
[CH-634787-A5] 15 p2469 N85-25243
Aircraft structure for application to training aircraft
[CH-635298-A5] 15 p2469 N85-25244
Aircraft
[CH-642598-A5] 15 p2470 N85-25246
System for radio remote control of dropping bombs
[CH-639935-A5] 15 p2491 N85-25371
Jinc-trap resonator
[AD-D011650] 17 p2970 N85-28339
Orthogonalizer for inphase and quadrature digital data
[AD-D011679] 19 p3254 N85-30174
NASA patent abstracts bibliography: A continuing bibliography. Section 1: Abstracts (supplement 27)
[NASA-SP-7039(27)-SECTION-1] 22 p3849 N85-33840

PATHOGENESIS
Pathogenesis and treatment of cerebral air embolism and associated disorders
[AD-A146723] 07 p1014 N85-16443
Distinctions in formation of microflora on construction materials used in habitable pressurized compartments 22 p3823 N85-33883

PATHOLOGICAL EFFECTS
Pathophysiological study of poisoning due to thermal degradation of materials — aircraft cabins
[CERMA-84-15] 11 p1692 N85-20640

PATHOLOGY
NT HUMAN PATHOLOGY
Pathology and axonal transport in hexacarbon neuropathies
[AD-P004021] 06 p0843 N85-15355
Pathology of organophosphorus-induced delayed neurotoxicity
[AD-P004024] 06 p0844 N85-15358
Effects of long-term low-level radiofrequency radiation exposure on rats. Volume 6: Evaluation of longevity, cause of death, and histopathological findings
[AD-A154283] 19 p3327 N85-30610

PATIENTS
Interaction between lung mechanics and gas exchange by low volume high frequency pulmonary ventilation in patients with respiratory failure
[AD-A146604] 06 p0846 N85-15372

PATTERN DISTRIBUTION
U DISTRIBUTION (PROPERTY)

PATTERN METHOD (FORECASTING)
Quasi stationary states in the Southern Hemisphere 18 p3144 N85-29485

PATTERN RECOGNITION
NT CHARACTER RECOGNITION
Content, variety, and augmentation of simulated visual scenes for teaching air-to-ground attack
[AD-A145218] 01 p0013 N85-10080
Application of automatic pattern methods in very-short-range forecasting 01 p0078 N85-10521
Fundamental remote sensing science research program. Part 1: Status report of the mathematical pattern recognition and image analysis project
[E85-10004] 02 p0215 N85-11417
Hypothesis on the origin of lineaments in the LANDSAT and SLAR images of precambrian soil in the low Contas River Valley (southern Bahia)
[E85-10007] 02 p0215 N85-11420
Failure detection processes by pattern recognition and expert systems
[AD-P003924] 02 p0246 N85-11604
An investigation into fuzzy clustering and classification
[AD-A145571] 02 p0251 N85-11645
Design of edge detectors for reduced images
[AD-A145700] 02 p0252 N85-11653
Automatic recognition and turbuling objects
[AD-A145908] 03 p0419 N85-12576
Fidelity of satellite soundings 05 p0682 N85-14383
Experiences with digital processing of images at INPE
[E85-10045] 06 p0826 N85-15247
Proceedings of the Second Annual Symposium on Mathematical Pattern Recognition and Image Analysis Program
[E85-10056] 07 p0984 N85-16251
Multivariate spline methods in surface fitting 07 p0985 N85-16257
Calibration or inverse regression: Which is appropriate for crop surveys using LANDSAT data?
07 p0985 N85-16260
Power spectral ensity of markov texture fields 07 p0986 N85-16262
Rectification of single and multiple frames of satellite scanner imagery using points and edges as control 07 p0986 N85-16263
The influence of the number of ground control points on the scene-to-map registration accuracy — Kansas, Louisiana, Mississipp, and Missouri 07 p0986 N85-16264
Image variance and spatial structure in remotely sensed scenes — South Dakota, California, Missouri, Kentucky, Louisiana, Tennessee, District of Columbia, and Oregon 07 p0986 N85-16265
Image-to-image correspondence: Linear structure matching 07 p0986 N85-16266
Analysis of subpixel registration 07 p0986 N85-16267
An automatic pattern recognition apparatus
[AD-D011319] 07 p1043 N85-16626
Rule-based evidence accrual system for image understanding
[AD-A147835] 07 p1044 N85-16634
Analysis of terrestrial conditions and dynamics
[E85-10063] 08 p1174 N85-17401
Direct assessment of synaptic modification rules
[AD-A148376] 08 p1196 N85-17534
Discriminability of signals from noise in a dynamic stereoscopic space
[AD-A148406] 08 p1196 N85-17535
Extraction of feature information from 3-dimensional CAD data 08 p1203 N85-17573
Recognition of complex 3-dimensional objects using 3-dimensional moment invariants
[AD-A148119] 08 p1212 N85-17025
Neurocognitive pattern analysis of an auditory and visual numeric motor control task. Part 1: Development of methods
[AD-A148809] 09 p1364 N85-18578
Optical data processing for missile guidance
[AD-A149348] 10 p1422 N85-18972
Multi target tracking by dynamic scene analysis
[AD-A148922] 10 p1456 N85-19250
Application of SIMCA (Soft Independent Modeling of Class Analogy) pattern recognition to air pollutant analytical data
[PB85-124883] 10 p1513 N85-19549
Image Understanding: Proceedings of the 15th Workshop
[AD-A149496] 10 p1557 N85-19816
Optical implementation of the synthetic discriminant function
[AD-A149562] 10 p1557 N85-19817
Method of multivariant intraclass pattern recognition
[AD-D011548] 12 p1816 N85-21405
Assessment of Thematic Mapper band-to-band registration by the block correlation method 12 p1872 N85-21743
A computer-based gaming system for assessing recognition performance (RECOG)
[AD-A149752] 12 p1915 N85-22022
Technical support for creating an artificial intelligence system for feature extraction and experimental design
[NASA-CR-175286] 12 p1916 N85-22044
Multiple resolution representation and probabilistic matching of 2-D gray-scale shape
[AD-A149981] 12 p1933 N85-22147
Acousto-optically addressed Fourier transform matched filters
[AD-A150296] 13 p2083 N85-22860
Electroacoustical imaging technique for encoding incoherent radiance fields as Gabor elementary signals
[NASA-TM-86372] 13 p2094 N85-23067
Preliminary evaluation of Thematic Mapper image data quality 13 p2118 N85-23194
Comparative techniques used to evaluate Thematic Mapper data for land cover classification in Logan County, West Virginia 13 p2121 N85-23200
Relative accuracy assessment of LANDSAT-4 MSS and TM data for level 1 land cover inventory — Washington, D.C. 13 p2122 N85-23212
Feature extraction assessment study
[AD-A150189] 13 p2126 N85-23239
Multivariate analysis and its applications
[AD-A150324] 13 p2151 N85-23352
Terrestrial analog studies for Martian patterned ground 13 p2190 N85-23500
Basic research in electronics (JSEP)
[AD-A151002] 14 p2298 N85-24230
Three-dimensional sensing and interpretation
[AD-A150690] 14 p2311 N85-24304
Geological information content of reflected wave record form 14 p2345 N85-24502
Visual recognition of simple objects by a connection network
[AD-A151043] 14 p2389 N85-24718
Perceptual organization and visual recognition
[AD-A150626] 14 p2391 N85-24723
Feasibility of optical instruments based on multiaperture optics
[AD-A150998] 14 p2421 N85-24936
Evaluating identifiability in remote sensing problems 15 p2488 N85-25347
Identifying land use structures of multizonal aerospace photographs using digital data processing 15 p2488 N85-25348
Interpretation of space photolineaments 15 p2487 N85-25353
Vision algorithms and psychophysics
[AD-A151888] 15 p2620 N85-26142
Workshop on Parallel Computer Architectures in Pattern Recognition and Image Processing
[BMFT-FB-DV-84-006] 15 p2622 N85-26154
The EGPA multiprocessor system and its possible application for pattern recognition tasks — computer architecture 15 p2622 N85-26156
Industrial applications of pattern recognition and image processing 15 p2622 N85-26157
Recognition of objects in their natural environment — parallel processing 15 p2622 N85-26158
Influence and possibilities of Very Large Scale Integration (VLSI) in pattern recognition and image processing 15 p2622 N85-26160

Computer architecture for image processing and pattern recognition in the Federal Republic of Germany. Status 1983, a review 15 p2623 N85-26161
Scene analysis using recursive frequency domain correlation with energy normalization
[AD-A151777] 16 p2854 N85-27596
An IKBS approach to image understanding
[AD-A151902] 16 p2854 N85-27599
Ultrasonic testing of carbon fiber reinforced plastics (CFRP) using pattern recognition methods
[MBB-BB-563/84-0] 16 p2873 N85-27726
Pattern selection and instability in nonlinear wave equation: An aspect of soliton and chaos
[DE85-009578] 18 p3101 N85-29197
Air photo analysis, photo interpretation logic, and feature extraction
[AD-A153926] 18 p3124 N85-29347
Applications of fuzzy set theory to satellite soundings 18 p3141 N85-29445
Approaches to digital image registration and recognition 19 p3257 N85-30197
Adaptive aiding for symbiotic human-computer control: Conceptual model and experimental approach
[AD-A153870] 19 p3332 N85-30644
Texture perception and shape from texture
[AD-A154276] 19 p3336 N85-30672
Target discrimination using infrared techniques: Theoretical considerations
[AD-A154070] 19 p3350 N85-30762
A cluster analysis method for identification of subpopulations of cells in flow cytometric list-mode arrays 20 p3503 N85-31779
Automated cell detection as a mesocyclone precursor tool
[AD-A154952] 21 p3635 N85-32577
Object identification and manipulation using silhouette moments
[AD-A154755] 21 p3705 N85-33011
Recognition and clear representation of handwritten electronic diagrams 23 p3960 N85-34541
A star camera aspect system suitable for use in balloon experiments
[OG-9.3-10] 23 p4028 N85-34965
Artificial intelligence in Ada (trademark): Pattern-directed processing
[AD-A156230] 24 p4141 N85-35671
A holographic streamer chamber for relativistic nucleus-nucleus collision experiments 24 p4147 N85-35710

PATTERN REGISTRATION
Multi-disciplinary techniques for understanding time-varying space-based imagery
[AD-A144357] 05 p0726 N85-14681
The influence of the number of ground control points on the scene-to-map registration accuracy — Kansas, Louisiana, Mississipp, and Missouri 07 p0986 N85-16254
Analysis of subpixel registration 07 p0986 N85-16257
The use of image registration technique in Brasilia's urban growth monitoring
[INPE-3302-PRE/614] 10 p1568 N85-19896
Investigation of TM band-to-band registration using the JSC registration processor 12 p1872 N85-21745
Geodetic accuracy of LANDSAT 4 Multispectral Scanner and Thematic Mapper data 12 p1873 N85-21746
Technical support for creating an artificial intelligence system for feature extraction and experimental design
[NASA-CR-175286] 12 p1918 N85-22044
Study of the urban evolution of Brasilia with the use of LANDSAT data
[E85-10101] 16 p2909 N85-27321
Approaches to digital image registration and recognition 19 p3257 N85-30197
Repetition of dense cloud cover above Indian Ocean from generalized satellite data 22 p3737 N85-33165
The design, development, testing, fabrication, calibration and integration of a High Resolution Imager (HRI) for the Roentgen Satellite (ROSAT)
[NASA-CR-175302] 22 p3741 N85-33184
Depth dimension compression of 3-D images 22 p3764 N85-33332

PATTERNS
Multiple resolution representation and probabilistic matching of 2-D gray-scale shape
[AD-A149981] 12 p1933 N85-22147
Multi-robot assembly of IC's 23 p3964 N85-34577

PAVEMENTS
Pavement friction measurements on nontangent sections of roadways, vol. 1
[PB84-219732] 01 p0035 N85-10227
Predictor model for seasonal variations in skid resistance. Volume 2: Comprehensive report
[PB84-226620] 01 p0037 N85-10230
A study of bituminous pavements to determine a correlation between pavement structure designs and tripping of asphalt cement
[PB84-217751] 01 p0037 N85-10231
Evaluation of laser profile and deflection measuring system
[FAA-PM-84-24] 02 p0201 N85-11341
Development of a pavement maintenance management system. Volume 10: Summary of development from 1974 through 1983
[AD-A146035] 03 p0320 N85-12067
Development of a pavement maintenance management system. Volume 9: Development of airfield pavement performance prediction models
[AD-A146150] 03 p0321 N85-12069
Experimental AC (Asphalt Concrete) overlays of PCC pavement
[PB84-218171] 03 p0342 N85-12203
Evaluation of moduli and thicknesses of pavement systems by spectral-analysis-of-surface-waves method
[PB84-219112] 03 p0342 N85-12205
Skid resistance of bituminous surfaces in Ohio
[PB84-234491] 04 p0484 N85-13086
Prefabricated panels for rapidly runway repair and expedient airfield surfacing
[AD-D011277] 05 p0597 N85-13804
Synthesis study of nondestructive testing devices for use in overlay thickness design of flexible pavements
[PB84-218080] 06 p0774 N85-14950
System for rapid repair of damaged airfield runways
[AD-D011325] 07 p0909 N85-15754
Development of a preliminary ALRS stabilized material pavement analysis system (SPAS)
[AD-A147116] 07 p0910 N85-15760
Aeroprojekt develops improved runway surfacing 08 p1066 N85-16770
Runway rubber removal specification development field evaluation procedures development
[FAA-PM-84-27] 12 p1781 N85-21179
Field validation of statistically-based acceptance plan for bituminous airport pavements. Volume 1: Correlation analysis of Marshall properties of laboratory-compacted specimens
[FAA-PM-84-12-VOL-1] 12 p1781 N85-21180
Field validation of statistically-based acceptance plan for bituminous airport pavements. Volume 2: Statistical analysis of Marshall properties of plant-produced bituminous materials
[FAA-PM-84-12-VOL-2] 12 p1781 N85-21181
Field validation of statistically-based acceptance plan for bituminous airport pavements. Volume 3: Statistical analysis of 3 methods for determining maximum specific gravity of bituminous concrete mixtures
[FAA-PM-84-12-VOL-3] 12 p1781 N85-21182
Field validation of statistically-based acceptance plan for bituminous airport pavements. Volume 4: Computer simulation of multiple acceptance criteria
[FAA-PM-84-12-VOL-4] 12 p1782 N85-21183
Field validation of statistically-based acceptance plan for bituminous airport pavements. Volume 5: Summary of validation studies
[FAA-PM-84-12-VOL-5] 12 p1782 N85-21184
Evaluation of Epoxo 300-C nonskid coating for use on bridge decks
[PB85-108843] 12 p1819 N85-21412
Stress-relieving interlayers for bituminous resurfacings
[PB85-136885] 12 p1820 N85-21415
Analysis of slabs-on-grade for a variety of loading and support conditions
[AD-A150965] 14 p2264 N85-24030
Microwave methods for paving
[DE85-004194] 14 p2265 N85-24032
Overlays for plain jointed concrete pavements
[PB85-156297] 15 p2523 N85-25557
Pavement-marking materials: New York's experience
[PB85-153294] 15 p2523 N85-25558
Study of acceptance criteria for joint densities in bituminous airport pavements
[FAA-PM-85-5] 16 p2715 N85-26761
Review of rigid pavement design for vehicular parking areas
[AD-A154284] 19 p3222 N85-29975

PAYLOAD CONTROL
Commerce Laboratory: Mission analysis payload integration study
[NASA-CR-171298] 07 p0911 N85-15784
Sounding rocket program Aeronomie. The payload M-I in the project MAP-WINE
[BMFT-FB-W-84-046] 12 p1790 N85-21236
A normal incidence X-ray telescope sounding rocket payload
[NASA-CR-176169] 24 p4153 N85-35749

PAYLOAD DELIVERY (STS)
Selected tether applications in space: An analysis of five selected concepts
[NASA-CR-171222] 04 p0460 N85-12921
Advanced OTV engine concepts 08 p1108 N85-17001
Satellite services and orbital retrieval 12 p1786 N85-21211
A dual, fault-tolerant aerospace actuator 22 p3798 N85-33530
Design of a dual fault tolerant space shuttle payload deployment actuator 22 p3798 N85-33531

PAYLOAD DEPLOYMENT & RETRIEVAL SYSTEM
NT REMOTE MANIPULATOR SYSTEM
Tethers open new space options 11 p1642 N85-20340
Tethered satellite system project overview 11 p1642 N85-20341
Shuttle tethered satellite system program overview 11 p1642 N85-20342
Transportation applications, part 1 11 p1643 N85-20349
Space science and applications 11 p1644 N85-20362
Report of the Transportation Panel 11 p1645 N85-20364
Report of the Artificial Gravity Panel 11 p1645 N85-20365
Satellite services and orbital retrieval 12 p1786 N85-21211
A dual, fault-tolerant aerospace actuator 22 p3798 N85-33530
Design of a dual fault tolerant space shuttle payload deployment actuator 22 p3798 N85-33531
Appendange deployment mechanism for the Hubble Space Telescope program 22 p3798 N85-33533
The role of tethers on space station
[NASA-TM-86519] 23 p3900 N85-34154

PAYLOAD INTEGRATION
Commerce Laboratory: Mission analysis payload integration study
[NASA-CR-171298] 07 p0911 N85-15784
Commerce Lab: Mission analysis and payload integration study
[NASA-CR-171272] 08 p1104 N85-16981
Commerce Lab: Mission analysis. Payload integration study
[NASA-CR-171285] 08 p1104 N85-16982
Commerce lab: Mission analysis and payload integration study
[NASA-CR-174381] 10 p1426 N85-18993
Commerce Lab: Mission analysis payload integration study. Appendix A: Data bases
[NASA-CR-176018] 19 p3224 N85-29988

PAYLOAD INTEGRATION PLAN
Commerce Laboratory: Mission analysis payload integration study
[NASA-CR-171298] 07 p0911 N85-15784
Data Requirement (DR) MA-03: Payload missions integration — Spacelab payloads
[NASA-CR-171331] 10 p1428 N85-19009

PAYLOAD RETRIEVAL (STS)
Satellite services and orbital retrieval 12 p1786 N85-21211
A remotely controlled orbiting retriever 12 p1786 N85-21212
The investigation of tethered satellite system dynamics
[NASA-CR-175855] 16 p2731 N85-26854

PAYLOAD STATIONS
Small Payload Flight Systems (SPFS) 02 p0152 N85-11030

PAYLOAD TRANSFER
Transportation applications, part 2 11 p1643 N85-20350
Satellite services and orbital retrieval 12 p1786 N85-21211
Ignition, separation of boosters, stages in Ariane 3 14 p2289 N85-24185

PAYLOADS
NT ATMOSPHERIC GENERAL CIRCULATION EXPERIMENT
NT EARTH RADIATION BUDGET EXPERIMENT
NT OSS-1 PAYLOAD
NT PLASMA INTERACTION EXPERIMENT
NT SHUTTLE IMAGING RADAR
NT SPACE SHUTTLE PAYLOADS
NT SPACEBORNE EXPERIMENTS
NT SPACELAB
NT SPACELAB PAYLOADS
NT STARLAB
NT X RAY ASTROPHYSICS FACILITY
A study of the critical layer in a rotating liquid payload
[AD-A146094] 03 p0362 N85-12321
A normal incidence, high resolution X-ray telescope for solar coronal observations
[NASA-CR-174145] 04 p0579 N85-13899
On-orbit support of DARPA-301 payload
[AD-A146897] 07 p0911 N85-15787

Artificial gravity: Tethers and containers
11 p1645 N85-20367
Rail accelerator technology and applications
[NASA-TM-86947] 12 p1794 N85-21258
Assessment of candidate-expendable launch vehicles for large payloads
[NASA-CR-175540] 14 p2237 N85-23867
Get Away Special (GAS) thermal design summary
[X-732-83-8] 15 p2475 N85-25276
Costs, payload of Ariane, US Space Shuttle compared
15 p2530 N85-25601
Space station trace contaminant control
18 p3157 N85-29550
Outside users payload model
[NASA-CR-176011] 19 p3223 N85-29986
German payloads for EURECA 1
[BMFT-FB-W-85-003] 20 p3419 N85-31223
Brush and commutator segment torquer motor
[AD-D011728] 23 p3927 N85-34340
Research of advanced techniques for X-ray detectors and telescopes with applications to rockets and the LAMAR facility
[NASA-CR-176181] 23 p4054 N85-35141
An automated technique for encasing specific payloads with low-drag fairings 24 p4083 N85-35183

PCB
U POLYCHLORINATED BIPHENYLS

PCM (MATERIALS)
U PHASE CHANGE MATERIALS

PCM (MODULATION)
U PULSE CODE MODULATION

PCM TELEMETRY
Telemetry (TM)/telecommand (TC) processor study
[ESA-CR(P)-1915] 03 p0323 N85-12061

PDM (MODULATION)
U PULSE DURATION MODULATION

PDP COMPUTERS
NT PDP 11 COMPUTER
NT PDP 11/70 COMPUTER

PDP 11 COMPUTER
A procedure for communications with PDP-10 and PDP-11 (IS/1 UNIX) type computers through use of CPT word processing equipment, revision 1
[DE85-007586] 16 p2845 N85-27540
Data processing on the rotor test stand at DFVLR in Brunswick: Microprogrammable interfaces and array processor as key components in a PDP 11 real time data acquisition and processing system
[DFVLR-MITT-85-03] 17 p2906 N85-27921

PDP 11/70 COMPUTER
Specification of a transport protocol for computer communications. Volume 1: Overview and Services. Volume 2: Class 2 protocol. Volume 3: Class 4 protocol
[PB84-222050] 06 p0848 N85-15380
Specification of a transport protocol for computer communications. Volume 4: Service specifications. Volume 5: Guidance for the implementor. Volume 6: Guidance for implementation selection
[PB84-222068] 06 p0848 N85-15385
Specification of a transport protocol for computer communications. Volume 7: Testing OSI protocols, a compendium of papers. Volume 8: User's guide to the testing system for implementations of the ICST transport protocol. Volume 9: A test suite for implementations of the ICST transport protocol. Volume 10: Specification of a remote scenario interpreter for implementations of the ICST transport protocol
[PB84-222076] 06 p0848 N85-15386

PEARLITE
Influence of preliminary cold deformation on fineness of pearlite
[BLL-BISI-TRANS-22408-(9022.06)]
17 p2927 N85-28054
Effects of hot deformation on the kinetics of the pearlite transformation in eutectoid steel
[BLL-M-35844-(5828.4)] 23 p3913 N85-34250

PEARSON DISTRIBUTIONS
Adaptive detection of noise signal according to Neumann-Pearson criterion 15 p2527 N85-25580
Least-squares approximation to minimum chi-square estimators of location and scale parameters and their effect on the Pearson chi-square test
[AD-A153534] 18 p3169 N85-29638
Effect of some estimators on a large sample approximation to the non-null distribution of the pearson chi-square statistic
[AD-A153515] 18 p3173 N85-29673

PEAT
Versatility of peat emphasized
07 p0994 N85-16316
Peat resources of Maine. Volume 1: Aroostook County
[DE85-004196] 11 p1669 N85-20519
Peat resources of Maine. Volume 4: Southern and western Maine
[DE85-004198] 11 p1670 N85-20520
Peat resources of Maine. Volume 2: Penobscot County
[DE85-004195] 11 p1670 N85-20522
Peat resources of Maine. Volume 5: Washington County
[DE85-004197] 11 p1670 N85-20523
Ash contents of Costa Rican peat deposits
[DE85-010734] 19 p3301 N85-30462

PECULIAR STARS
NT SYMBIOTIC STARS
The spectroscopic antics of S 18/SMC
11 p1750 N85-21008

PEDIMENTS
U PIEDMONTS

PEDIPLAINS
U PIEDMONTS

PEDOLOGY
U SOIL SCIENCE

PEELING
A study of bituminous pavements to determine a correlation between pavement structure designs and tripping of asphalt cement
[PB84-217751] 01 p0037 N85-10231
Finger materials for air cushion vehicles. Volume 2: Base fabrics for finger materials
[AD-A149701] 12 p1819 N85-21408

PEENING
NT SHOT PEENING

PELLETS
Thermal conductivity of iron/potassium perchlorate heat powder
[DE84-017071] 04 p0476 N85-13035
Study of opacity effects on line radiation from pellet implosions
[DE85-006380] 10 p1491 N85-19413
Robotic thermal battery pellet fabrication
[DE85-007755] 16 p2779 N85-27154
Ion beam-plasma interactions
[DE85-010202] 19 p3371 N85-30813
A gel-halo sample pellet: The best of both worlds? Stubby zones without a constricted sample gate
20 p3502 N85-31770
Burn front velocity as a function of pellet density in iron-potassium perchlorate heat powders
[DE85-011448] 21 p3572 N85-32214

PELTIER EFFECTS
Peltier heat of a small polaron in a magnetic semiconductor
[DE85-000470] 14 p2430 N85-24983

PELVIS
Locomotion research for the analysis of the human gait and for the determination of the maximum loads of the pelvis-leg skeleton. Volume 1: Two-dimensional analysis
[BMFT-FB-T-83-187-VOL-1] 02 p0236 N85-11535
Locomotion research for the analysis of the human gait and for the determination of the maximum loads of the pelvis-leg skeleton. Volume 2: Three-dimensional analysis
[BMFT-FB-T-83-188-VOL-2] 02 p0236 N85-11536
The position and mobility of the shoulder, spinal column and pelvis in seated subjects
[AD-A153751] 18 p3153 N85-29524

PENALTY FUNCTION
Some applications of penalty functions in mathematical programming
[AD-A147443] 07 p1032 N85-16552
Analysis of a penalty finite element approximation of the Navier Stokes equations 06 p1161 N85-17321

PENDULUMS
Soil tilt measurement: First results of the comparative analysis of the response of two different tiltmeters
[NOTA-INTERNA-818] 02 p0226 N85-11494
Structure-property relationships in polymeric matrix materials
[AD-A153929] 18 p3060 N85-29050
Study on a flexure hinged pendulum accelerometer
[NAL-TR-844] 18 p3104 N85-29220

PENETRANTS
Technical activities 1983, Office of Nondestructive Evaluation
[PB84-217074] 03 p0370 N85-12360

PENETRATING PARTICLES
U CORPUSCULAR RADIATION

PENETRATION
Penetrator/armour interactions: Background to Australian work
[MRL-R-936] 03 p0367 N85-12353
Application and calibration of the subsurface mapping capability of SIR-B in desert regions
06 p1146 N85-17244
Ground truth for SIR-B images obtained by SIR system 8 impulse radar 06 p1149 N85-17251
Tractor power selection with compaction constraints
[AD-P004300] 09 p1409 N85-18677
Evaluation of the birdstrike threat to the F-15 present fleet, rapid deployment force, and dual role fighter transparencies
[AD-A148954] 10 p1421 N85-18966
Aircraft skin penetrator and agent applicator. Volume 1: Working model development and construction
[AD-A150496] 13 p1970 N85-22374
Aircraft skin penetrator and agent applicator. Volume 2: Test and evaluation
[AD-A151609] 15 p2466 N85-25225
Magnetic field penetration into cometary ionosphere
15 p2477 N85-25290
Study of intermediate velocity penetration of steel spheres into deep aluminum targets
[DE85-010419] 19 p3287 N85-30365
Geometry, velocity structure and penetration depths of descending slabs in the western Pacific
19 p3319 N85-30574
The effect of stress and hot corrosion on nickel-base superalloys
[AD-A154722] 21 p3566 N85-32181
Ice fog as an electro-optical obscurant
[AD-A155059] 21 p3705 N85-33015
Multiaxial stress analysis taking account of penetration depth of X-rays. A solution by means of polynomial approximation 23 p3907 N85-34204
Monte Carlo techniques for analyzing deep penetration problems
[DE85-011426] 23 p3968 N85-34596
Dynamics of the penetration boundaries of solar protons during a strong magnetic storm
[SH-8.1-16] 23 p4046 N85-35089
Experimental data for characterizing perforating impacts: Fragmentation processes
[AD-A156370] 24 p4102 N85-35427

PENETRATION BALLISTICS
U TERMINAL BALLISTICS

PENETROMETERS
Physical and mechanical properties of lunar soil as function of specifics of relief and processes in vicinity of operation of Lunokhod-2 02 p0161 N85-11090

PENNSYLVANIA
LANDSAT instruments characterization
[E85-10028] 05 p0654 N85-14197
Remote sensing of hydrologic transport processes using spot simulation data
[DE85-012412] 24 p4108 N85-35467

PENTACHLORIDES
U CHLORIDES

PENTAERYTHRITOL TETRANITRATE
U PETN

PENTANES
Thermodynamic properties of isobutane-isopentane mixtures from -40 to +600(0)F and up to 1000 psia
[DE84-015137] 01 p0124 N85-10650
Multiphoton ionization of benzene in solution
[DE85-000693] 06 p0766 N85-14699
Thermophysical properties of working fluids for binary geothermal cycles
[DE85-000385] 12 p1661 N85-21604

PENTOSE
NT RIBOSE
Changes in pentose and glucuronate pathway dehydrogenases in rat brains following single or multiple hypothermic episodes 20 p3505 N85-31790

PENUMBRAS
On running penumbral waves
14 p2453 N85-25150

PEOPLES DEMOCRATIC REPUBLIC OF GERMANY
U EAST GERMANY

PEPTIDES
NT POLYPEPTIDES
Effect of short-term hypokinesia on rat opioid system reaction 01 p0093 N85-10625
Rat tissue opioid peptide content during long-term hypokinesia 12 p1904 N85-21954

PERCENTAGE
U RATIOS

PERCEPTION
NT AUDITORY PERCEPTION
NT BINAURAL HEARING
NT CONSCIOUSNESS
NT MOTION PERCEPTION
NT PROPRIOCEPTION
NT SENSORY PERCEPTION
NT SOUND LOCALIZATION
NT SPACE PERCEPTION
NT TACTILE DISCRIMINATION
NT TOUCH
NT VERTICAL PERCEPTION
NT VISUAL DISCRIMINATION
NT VISUAL PERCEPTION

The psychology of technical devices and technical discourse
[AD-P003929] 02 p0246 N85-11609
Subliminal communication technology
[GPO-38-633] 05 p0622 N85-13979
Experiment 1E9031 on Spacelab 1: Are cells sensitive to gravity? — lymphocyte proliferation
05 p0689 N85-14428
Observation of the contractile vacuolar system of Paramecium caudatum on the fast running clinostat
05 p0689 N85-14431
Gravity and cell differentiation in lentil roots
05 p0690 N85-14433
The use of horizontal clinostats in studies of plant statocyte development 05 p0690 N85-14435
Twentieth Annual Conference on Manual Control, volume 1
[NASA-CP-2341-VOL-1] 05 p0699 N85-14487
Subjective workload assessment and voluntary control of effort in a tracking task 05 p0708 N85-14540
Assessing the subjective workload of directional orientation tasks 05 p0708 N85-14542
Classification systems for individual differences in multiple-task performance and subjective estimates of workload 05 p0708 N85-14543
Military pilot ergonomics 10 p1532 N85-19655
Grasp of information by the pilot in future combat aircraft 10 p1533 N85-19662
Annals of the New York Academy of Sciences, Volume 423 — timing and time perception
[AD-A150031] 12 p1909 N85-21981
Mass-discrimination during prolonged weightlessness
20 p3509 N85-31814
Resource allocation in cerebral specialization of function: Behavioral and electrophysiological studies
[AD-A155092] 21 p3664 N85-32759
The effects of prolonged feeding meal, ready-to-eat (MRE) operational rations
[AD-A154763] 21 p3666 N85-32773

PERCEPTRONS
U SELF ORGANIZING SYSTEMS

PERCHLORATES
NT AMMONIUM PERCHLORATES
NT POTASSIUM PERCHLORATES
CP DDT detonators. 4: Thermal aging
[DE85-011172] 19 p3251 N85-30160
Nuclear magnetic resonance study of the intramolecular rearrangement of 2-(5-cyanotetrazolato)pentaammine cobalt (III) perchlorate
[DE85-010810] 22 p3839 N85-33772

PERCOLATION
Determining deep heat flow and rate of horizontal percolation from temperature measurements in aquifer
13 p2116 N85-23180
Non-equilibrium effects in turbulent diffusion flames
20 p3425 N85-31256

PERCUSSION
Effect of air cavity on the vibration analysis of loaded drums 09 p1339 N85-18422

PERFECT GAS
U IDEAL GAS

PERFLUORO COMPOUNDS
NT PERFLUOROALKANE
Cross-Appalachian Tracer Experiment (CAPTEX '83)
[PB84-238641] 06 p0834 N85-15307
The use of perfluoroether lubricants in unprotected space environments 22 p3797 N85-33523

PERFLUOROALKANE
Design and chemical synthesis of iodine-containing molecules for application to solar-pumped I* lasers
[NASA-CR-176010] 19 p3275 N85-30310

PERFORATED PLATES
Stresses in pin-loaded orthotropic plates using photoelasticity
[NASA-CR-172496] 07 p0977 N85-16204
Mechanical locking between multi-layer printed wiring board conductors and through-hole plating
[AD-D011477] 10 p1481 N85-19352
Stresses in a half-plane containing either a pressurized hole or an interference-fit disc
[ARL/STRUC-R-409] 12 p1865 N85-21700
Elastic response of a half-plane to a bonded interference-fit disc of the same material
[ARL/STRUC-R-408] 12 p1865 N85-21701
effect of gas stream sweeping past the effluent of a perforated plate on heat transfer inside the perforations
13 p2051 N85-22836
Sound emission by particle beam passing through hole in rigid shield 15 p2525 N85-25570

PERFORATING
Experience with introduction of Finish perforation of precision parts for optical instruments
16 p2761 N85-27036
Some asymptotic problems in the optimal control of distributed systems 20 p3412 N85-31175

PERFORATION
Wind tunnel wall interference
[AD-A151212] 15 p2474 N85-25273

PERFORMANCE
A generalized model of fault-isolation performance
[AD-P003926] 02 p0246 N85-11608
Optimum performance parameters for ski-jump operations of USAF fighter aircraft
[AD-A148532] 08 p1084 N85-16867
Electric vehicle demonstration project
[DE85-003124] 11 p1741 N85-20944
Experimental and theoretical study of fatigue crack initiation in metals 19 p3283 N85-30357
Life cycle test results of a bipolar nickel hydrogen battery
[NASA-TM-87046] 19 p3304 N85-30480

PERFORMANCE PREDICTION
NT PREDICTION ANALYSIS TECHNIQUES
Primate equilibrium performance and diazepam: A behavioral tolerance effect
[AD-A145156] 01 p0094 N85-10634
End-to-end performance in local area networks of interconnected token rings
[FUB-42-1983] 01 p0107 N85-10714
Phosphoric acid fuel cell power plant system performance model and computer program
[NASA-CR-174638] 02 p0222 N85-11456
Individual differences in automatic and controlled information processing
[AD-A146245] 03 p0401 N85-12559
Design and off-design performance prediction of high pressure ratio centrifugal compressors
05 p0636 N85-14062
Synthesis of load-time histories resulting from statistical analysis 05 p0650 N85-14171
Measurement-technical problems in the investigation of wind energy units 05 p0666 N85-14295
Hollings hungry mantid model for the invertebrate functional response considered as a Markov process. Part 3: Mathematical elaborations
[CWI-AM-R8407-PT-3] 05 p0722 N85-14836
Predicting changes in reliability characteristics of gas turbine engines during operation
06 p0776 N85-14964
The influence of fastener flexibility on load transfer and fatigue life predictions for multirow bolted and riveted joints — aircraft structures
[LBF-FB-172/84] 07 p0979 N85-16219
What should DOE do to help establish voluntary consensus standards for measuring and rating the performance of PV modules?
[NASA-CR-174265] 07 p0992 N85-16297
Technical performance measurement handbook
[AD-A147314] 07 p1052 N85-16575
Performance prediction of pneumatic tyres on sand
[AD-P004262] 09 p1404 N85-18838
Sample size and precision in communication performance measurements
[PB85-1143270] 12 p1830 N85-21488
Aerodynamic research efforts at SERI Wind Energy Research Center at Rocky Flats
[DE85-000529] 12 p1861 N85-21805
Surface wave excitation study
[DE85-006301] 13 p2056 N85-22875
Investigations of the high frequency performance of impact avalanche transit-time diodes
13 p2063 N85-22884
Boundary layer control by transition fixing — conference
[DFVLR-MITT-84-17] 14 p2211 N85-23712
Parameters of symmetric rhombic drive mechanism for single-cylinder Stirling engine 14 p2271 N85-24072
Introduction to methods of evaluating the operational reliability of complex systems: Application to satellite control ground support 14 p2397 N85-24771
A system-level mathematical model for evaluation of power train performance of load-leveled electric-vehicles
[NASA-CR-175652] 14 p2434 N85-25009
Performance of a copper-lithium alloy as an impurity control system surface material for a fusion reactor
[DE85-006494] 15 p2657 N85-26398
Simulation: A tool for cost-effective systems design and live test reduction 16 p2696 N85-26657
Analytical fuel property effects--small combustors
[NASA-CR-174738] 16 p2708 N85-26709
Technical overview structural dynamics
16 p2736 N85-26883
Solar elements with distributed parameters
16 p2760 N85-27036
Calculation of viscous compressible flows in small gas turbines 17 p2912 N85-27950
Flat magnetohydrodynamic induction pump
17 p2939 N85-28145
A program for the calculation of paraboloidal-dish solar thermal power plant performance
[NASA-CR-175874] 17 p2985 N85-28449
Mission requirements and handling qualities
18 p3057 N85-28918
Establishment of a methodology for predicting lifetimes in active solar systems
[DE85-006629] 18 p3130 N85-29383
Aerodynamic analysis of a horizontal axis wind turbine by use of helical vortex theory. Volume 1: Theory
[NASA-CR-168054] 19 p3212 N85-29916
Onset of freezing in residential air-to-air heat exchangers
[DE85-009980] 19 p3267 N85-30259
Analytical model for predicting emergency shutdown of a two-bladed horizontal axis wind turbine
[NASA-TM-83472] 19 p3303 N85-30476
Performance comparison between NACA 23024 and NACA 64(3)-618 airfoil configurated rotors for horizontal-axis wind turbines
[NASA-TM-83471] 19 p3303 N85-30477
Ion thruster performance model
20 p3420 N85-31226
Galileo battery testing and the impact of test automation 20 p3444 N85-31361
Fundamental algorithms of the Goddard battery model
20 p3445 N85-31399
Environmental factors in corrosion and deterioration of materials 22 p3750 N85-33241
Design and development of a linear thermal actuator
22 p3766 N85-33518
PMEXA: Diagnostic filtering program for the PBFA-1 performance monitoring and evaluation system
[DE85-013179] 22 p3831 N85-33725
Assessment of metal heating technologies for ferrous forging: A pilot study of the form value of natural gas
[PB85-204394] 24 p4084 N85-35314
Wind turbine noise: Prediction tools and design parameter dependence 24 p4110 N85-35477

PERFORMANCE TESTS
Evaluation of the Malcolm horizon in a moving-base flight simulator 01 p0008 N85-10051
Peripheral vision horizon display testing in RF-4C aircraft 01 p0009 N85-10054
A preliminary flight evaluation of the peripheral vision display using the NT-33A aircraft
[AD-A145123] 01 p0010 N85-10060
Cylinder power fault diagnosis in military diesel engines
[TT-8405] 01 p0053 N85-10354
Rotordynamic analysis of the SSME turbopumps using reduced models
[NASA-CR-171170] 01 p0054 N85-10355
Performance of the h, p and h-p versions
01 p0058 N85-10383
Advanced blade tip seal system, volume 2
[NASA-CR-167851] 02 p0147 N85-10999
The Palmqvist test and its applications in WC-Co alloys 02 p0177 N85-11187
Alternate fuels combustion research
[AD-A145891] 02 p0188 N85-11258
Radar, target and ranging
[AD-A145407] 02 p0190 N85-11272
15 kW general purpose frequency changer performance improvement
[AD-A145503] 02 p0194 N85-11297
The IMX double direct process
[AD-A146250] 03 p0340 N85-12188
Construction, putting into operation, and utilization of a triple axis neutron spectrometer
03 p0425 N85-12715
Performance of improved lead acid batteries for electric vehicles
[DE84-015845] 04 p0495 N85-13160
Space telescope cost, schedule, and performance review, 1984
[GPO-39-066] 04 p0579 N85-13698
Technical support services for space and terrestrial systems programs
[DE84-009031] 05 p0597 N85-13806
Test signal generator for coherent air-to-ground radars
[AD-D011278] 05 p0628 N85-14025
Realized field tests — solar generators
05 p0664 N85-14271
Implementation assessment of a network service. The test responder exerciser specification
[NPL-DITC-44/84] 05 p0716 N85-14594
Procedural aspects of testing aerodynamic models with combustion in high-enthalpy transient-mode installations
05 p0725 N85-14658
Choice of criteria for rejection of insulating components in high-voltage surge equipment
06 p0785 N85-15021
Encapsulation design analysis
06 p0829 N85-15268
Qualification of an electrothermal hydrazine thruster with a vacuum thrust of 0.5 to 2.0 N
[BMFT-FB-W-84-043] 07 p0917 N85-15808

Special problems of Ramjet with solid fuel
07 p0916 N85-15815
Bearing tester fit analysis
[NASA-CR-171282] 07 p0973 N85-16181
Demonstration of transparent solar array module design
[NASA-CR-174257] 07 p0992 N85-16302
Evaluation of the measured energy performance of four solar systems
[AD-A147912] 07 p0993 N85-16306
Comparative investigation of three commercial radiosonde systems
[KNMI-TR-53] 07 p1009 N85-16409
Design of self-checking N-MOS (H-MOS) integrated circuits 08 p1064 N85-16742
Construction, testing of 1-MW nitrogen laser
08 p1140 N85-17182
Ultrasonic transducers, performance variability, design, and manufacturing procedures
[AD-A148575] 08 p1158 N85-17306
Ceramic fabric material testing
[DE84-012014] 09 p1300 N85-18165
FORTRAN 77 computer program for test procedure calculations of vented heaters
[PB85-109627/GAR] 09 p1305 N85-18198
Operational characteristics of a 1000 MVA superconducting power transmission system
[DE85-000232] 09 p1314 N85-18283
Fiat introduces 1000-CC engine
11 p1618 N85-20185
Spectral characterization of the LANDAT-4 MSS sensors 11 p1668 N85-20499
A system simulator for the solar generator of artificial satellites
[INPE-3320-TDL/180] 11 p1672 N85-20534
Wind generator for Solar Office Complex, Luna Vocational Technical Institute, Las Vegas, New Mexico
[DE85-000103] 11 p1674 N85-20547
Electrical and thermal performance during charging and discharging a Phase 1 gal cell battery
[PB85-114312] 11 p1677 N85-20565
BIT/BITE tradeoff analysis model
[AD-A149345] 11 p1701 N85-20697
GPS system field testing 11 p1711 N85-20762
Coverage and buildup of the Navstar constellation
11 p1711 N85-20764
Tailored airfoils for vertical axis wind turbines
[DE85-004628] 12 p1772 N85-21128
Landing control centrals
[AD-A149800] 12 p1775 N85-21140
Field validation of statistically-based acceptance plan for bituminous airport pavements. Volume 4: Computer simulation of multiple acceptance criteria
[FAA-PM-84-12-VOL-4] 12 p1782 N85-21163
Performance assessment of Class 1E pressure transmitters subjected to environmental stresses
[DE85-001623] 12 p1854 N85-21626
The Olympus solar array development and test program 13 p2009 N85-22599
Surge strength of symmetric cable with monolithic polyethylene insulation of quads
13 p2082 N85-23001
Algorithm in Walsh function basis for analysis of integrated microcircuits on MOS-structures
13 p2083 N85-23006
Laboratory tests of reciprocating internal combustion engines
[AD-A150143] 13 p2098 N85-23087
Thermal state of cooled thin-walled nozzle blade
14 p2270 N85-24066
Optimization of combined convective and film cooling of perforated baffle blades in gas turbines
14 p2270 N85-24067
Selection of bearing type for large steam turbines
14 p2271 N85-24069
Work of axial bearing under dynamic loading
14 p2286 N85-24182
Advanced life analysis methods. Volume 3: Experimental evaluation of crack growth analysis methods for attachment lugs
[AD-A151058] 14 p2317 N85-24319
Experimental report on a fiber optic light guide made by Galileo Electro-Optics Corporation
[DE85-006161] 14 p2421 N85-24941
Performance testing and system characterization. DOE hybrid test vehicle, phase 3
[NASA-CR-175868] 14 p2434 N85-25010
US Army Aviation Engineering Flight Activity (USAAEFA) report bibliography update 1983 - 1984
[AD-A151381] 15 p2457 N85-25168
Space station propulsion: The advanced development program at Lewis
[NASA-TM-86999] 15 p2494 N85-25386
Evaluation of adequacy pf JP54 protection level for large electric machines 15 p2528 N85-25588
France develops new continuous vacuum treatment method 15 p2531 N85-25611
Space reactor ground tests, assessment of facility needs
[DE85-006814] 15 p2550 N85-26345
Field use of electric vehicles compared to prototype tests
[DE85-006887] 15 p2567 N85-26458
The series 2000: A miniature gas bearing DTG for low cost strapdown guidance and control
16 p2686 N85-26648
High-pressure hydrogen testing of single crystal superalloys for advanced rocket engine turbopump turbine blades 16 p2735 N85-26875
Instrumentation technology overview
16 p2739 N85-26903
Operational test results of a prototype superconducting power transmission system and their extrapolation to the performance of a large system
[DE85-006731] 16 p2779 N85-27153
Management of vacuum leak-detection processes, standards and calibration
[DE85-006705] 16 p2786 N85-27202
Documentation and solar cell modules
[NASA-CR-175769] 16 p2818 N85-27384
Effect of precipitation on wind turbine performance
[NASA-TM-86988] 16 p2818 N85-27385
Shape with and without redundant colour as coding mechanism for simulated radar displays in a time-extended simple vigilance task
[AD-A151683] 16 p2844 N85-27533
Distance Measuring Equipment (DME), general
[AD-A152585] 17 p2895 N85-27846
An assessment of the suitability of the BHGA structural test rig for aerodynamic testing of hang gliders
[CA-8505] 17 p2896 N85-27853
Rotorcraft research testing in the National Full-Scale Aerodynamics Complex at NASA Ames Research Center
[NASA-TM-86687] 17 p2896 N85-27854
Testing of materials and coatings for jet engine components under simulated operational conditions
[B8580073] 17 p2899 N85-27873
Evaluation of used crankcase oils using computerized infrared spectrometry. Appendices
[AD-A152994] 17 p2920 N85-28000
MM2 LRSLA testing stage 3 propellant
[AD-A152540] 17 p2937 N85-28128
Performance evaluation of fiber-optic converters
17 p2941 N85-28154
Performance analysis of the DSN baseband assembly (Bba) Real-Time Combiner (RTC)
[NASA-CR-175878] 17 p2946 N85-28190
Baseline cycle testing of a 500-kWh zinc chloride battery at the Battery Energy Storage Test (BEST) Facility
[DE85-006948] 17 p2955 N85-28249
Test and evaluation of the Hoppecke Model E240G144/16 electric vehicle battery charger
[DE85-900573] 17 p2955 N85-28253
International time transfer and portable clock evaluation using GPS timing receivers: Preliminary results
17 p2964 N85-28303
Field test report of the Department of Energy's 100-kW vertical axis wind turbine
[DE85-006475] 17 p2967 N85-28458
Shenandoah parabolic dish solar collector
[DE85-006326] 17 p2967 N85-28460
Test plan for acceptance, verification and performance testing of the Bedford Lucas Chloride Electric Van. Part 1: Acceptance and verification testing at EG and G Automotive Research. Part 2: INEL performance testing, revision 1
[DE85-005157] 17 p3051 N85-28886
The attitude control model tests for the Infrared Astronomical Satellite (IRAS)
[B8580071] 18 p3067 N85-29067
A simplified GPS C/A reciever front end with low noise performance 18 p3109 N85-29251
Performance test results of a low cost GPS time and frequency monitor 18 p3109 N85-29252
Thermal performance testing and mathematically modeling of integral collector storage solar hot water systems
[PB85-186906] 18 p3132 N85-29398
Automated Weather Observing System (AWOS) demonstration program
[AD-A153463] 18 p3148 N85-29493
A task battery for applied human performance assessment research
[AD-A153677] 18 p3154 N85-29530
Specification of software quality attributes. Volume 3: Software quality evaluation guidebook
[AD-A153990] 18 p3163 N85-29595
Performance evaluation of stochastic timed decision-free Petri Nets
[AD-A153967] 18 p3171 N85-29652
Operation of HFTF to test the MIT 12 T coil
[DE85-010409] 18 p3195 N85-29821
Low-speed wind-tunnel tests of an advanced eight-bladed propeller
[NASA-TM-86364] 19 p3214 N85-29928
Traffic alert and collision avoidance system: Operational simulation
[FAA-PM-85-10] 19 p3216 N85-29941
Inertial navigation system - LAS II for SGT YORK testing
[AD-A154204] 19 p3216 N85-29944
The DREO (Defence Research Establishment Ottawa) Inertial Navigation Laboratory: Development and test capabilities
[AD-A154425] 19 p3216 N85-29945
Split-cross-bridge resistor for testing for proper fabrication of integrated circuits
[NASA-CASE-NPO-16021-1] 19 p3256 N85-30187
Recent results of the Los Alamos free-electron laser oscillator experiment
[DE85-010736] 19 p3277 N85-30324
Free-piston Stirling engine/linear alternator 1000-hour endurance test
[NASA-CR-174771] 19 p3304 N85-30481
Develop and test fuel cell powered on-site integrated total energy systems. Phase 3: Full-scale power plant development
[NASA-CR-168338] 19 p3304 N85-30483
Performance envelopes and optimal appropriateness measurement
[AD-A154129] 19 p3330 N85-30629
Ada compiler validation summary report: University of Karlsruhe-GMD/German MOD VAX 11 compiler, version v1.0
[AD-A154370] 19 p3337 N85-30676
The CCIR satellite EPIRB coordinated trials programme --- Emergency Position Indicating Radio Beacon (EPIRB); International Radio Consultative Committee (CCIR) 20 p3402 N85-31111
A 406 MHz geostationary satellite SARSAT experiment 20 p3403 N85-31113
SARSAT 121.5/243 MHz technical evaluation
20 p3405 N85-31126
RCA's planned test program to compare the performance and life of NiCd cells containing Pellon 2536 in contrast with Pellon 2505 separator material
20 p3445 N85-31385
A 34 ampere-hour nickel-cadmium minimum trickle charge testing 20 p3446 N85-31394
Nickel-hydrogen cell test program summary
20 p3448 N85-31407
An industry and government survey: A nickel-hydrogen testing data base 20 p3448 N85-31409
Recommendations and calculations concerning physical characteristics of the EEVT apparatus
20 p3502 N85-31769
MHD generator CDIF
[DE85-011389] 20 p3536 N85-32001
Fin-line horn antennas
[AD-A154597] 21 p3560 N85-32255
Fabrication and test of modified quadrupole mass spectrometer
[AD-A155186] 21 p3590 N85-32312
Module Hipot and ground continuity test results
21 p3612 N85-32447
Sensitivity and performance characterization of DINGU
[DE85-010750] 22 p3754 N85-33269
Partial discharges in and electric strength of high-voltage polymer insulation at cryogenic temperatures
22 p3770 N85-33364
Beta response of selected instruments
[DE85-013278] 22 p3788 N85-33469
Rolling, slip and traction measurements on low modulus materials
[NASA-CR-174909] 22 p3791 N85-33491
Failure testing of active solar energy system components
[DE84-013024] 22 p3804 N85-33561
Block 5 documentation and solar modules
[NASA-CR-176134] 22 p3805 N85-33564
Method and apparatus for measuring areas of photoelectric cells and photoelectric cell performance parameters
[DE85-011629] 22 p3810 N85-33599
Effect of interference on the performance of a minimum TCAS 2
[FAA-PM-84-33] 23 p3895 N85-34131
Test plan for performance testing of the Eaton AC-3 electric vehicle
[DE85-011954] 23 p3927 N85-34341
Circuit approaches to increasing SRAM performance in total dose environments
[DE85-009441] 23 p3966 N85-34586
Planetary-gear-support bearing test rig design
[NASA-CR-174927] 24 p4064 N85-35185

Development of NATOPS (Naval Air Training and Operating Procedure Standardization) performance software for the H-46D helicopter
[AD-A156089] 24 p4064 N85-35190
Dissected motors-propellants motor number STM-012. Phase 15: Surveillance report, stage 1
[AD-A156088] 24 p4071 N85-35226
Solid state high power amplifier for driving the SLC injector klystron
[DE85-013063] 24 p4090 N85-35356
Dental multi-purpose slowspeed handpieces test and evaluation
[AD-A155764] 24 p4130 N85-35606
Four stage HELIA experiment
[DE85-012026] 24 p4156 N85-35766
PERFUSION
U DIFFUSION
PERIDOTITE
The mineralogy of global magnetic anomalies
[E85-10061] 07 p0967 N85-16272
PERIGEES
The long term behaviour of Earth orbits and the implications for debris control 12 p1786 N85-21213
PERIHELIONS
Comet thermal modeling 13 p2176 N85-23505
Photometric study of Pluto near perihelion. Part 2: Refinement of rotation period: Color indices 15 p2483 N85-25325
PERIOD EQUATIONS
U PERIODIC FUNCTIONS
PERIODIC FUNCTIONS
NT TANGENTS
Dynamics of growth of surface periodic structures when intense light acts on condensed media 02 p0268 N85-11748
Propagation of acoustic shear waves through active periodic structure 04 p0490 N85-13125
An analytical model of periodic waves in shallow water
[AD-A147501] 07 p0960 N85-16085
An analytical model of periodic waves in shallow water
[AD-A147502] 07 p0960 N85-16086
Periodic solutions of prescribed energy for a class of Hamiltonian systems
[AD-A149487] 10 p1548 N85-19764
Application of perturbation theory to problem in orbital theory 15 p2537 N85-25656
On the accuracy of the Poincare-Lindstedt method
[REPT-84-37] 17 p3022 N85-28690
Symmetric linear multistep methods for second-order differential equations with periodic solutions
[CWI-NM-R8501] 17 p3022 N85-28696
Interpolation and differentiation for periodic functions
[PREPRINT-419] 18 p3172 N85-29662
On the convergence of an iterative formulation of the electromagnetic scattering from an infinite grating of thin wires 24 p4085 N85-35319
PERIODIC ORBITS
U ORBITS
PERIODIC PROCESSES
U CYCLES
PERIODIC VARIATIONS
NT ANNUAL VARIATIONS
NT DIURNAL VARIATIONS
NT NOCTURNAL VARIATIONS
NT SECULAR VARIATIONS
Periodic oscillation of gyrostat-satellite about its center of mass in an elliptical orbit 02 p0159 N85-11080
Analysis of the Frascati and Geneva gravitational wave antenna background exhibiting the one half sidereal day period
[NOTA-INTERNA-801] 02 p0192 N85-11283
N-frequency quasiperiodicity and chaos in dissipative dynamical systems 02 p0252 N85-11840
Thermal effects in stellar pulsations 02 p0297 N85-11925
Extraction of wave period from altimeter data 03 p0382 N85-12439
Global maps of foF2 derived from observations and theoretical values
[AD-A145866] 03 p0392 N85-12509
Variations with time of the carbon dioxide partial pressure in central and south Atlantic surface waters
[AD-A145825] 03 p0398 N85-12537
On derivation and significance of geomagnetic equivalent amplitude indices 04 p0520 N85-13321
Atlas of polar cap energetic particle observations. Volume 1: TIROS-N, 1 January 1979 - 28 February 1981
[PB84-233402] 04 p0535 N85-13419
Generation of available potential energy and other diagnostic studies during FGGE 05 p0683 N85-14388
A modified unit commitment and generation control for utilities with large wind generation penetrations
[DE84-015362] 06 p0806 N85-15129
Nature of short-period variations of cosmic rays in stratosphere 06 p0823 N85-15224
Microseism level, time variations at Turkmen seismic stations studied 07 p0981 N85-16231
The effects of long-periodic forcing in a zero-dimensional climate model 07 p1002 N85-16363
Composites with a periodic structure, mathematical analysis and numerical treatment
[AD-A148301] 08 p1119 N85-17053
Potential applications of forced unsteady flows
[AD-P004155] 09 p1264 N85-17940
Gamma-ray burster recurrence timescales
[NASA-TM-86157] 09 p1417 N85-18942
Effects of a periodic disturbance on structure and mixing in turbulent shear layers and wakes
[AD-A149278] 10 p1484 N85-19370
Simulation of estimating periodicity of seasonally stationary time series
[DE85-003517] 11 p1708 N85-20748
Search for millisecond rotational periods in some low-mass X-ray binaries observed by EXOSAT 11 p1741 N85-20949
EXOSAT observations of the galactic bulge X-ray source GX17+2 — X ray binary star 11 p1742 N85-20951
An episodic red-wing structure of SiIV, lambda 1394A, in gamma Cas 11 p1750 N85-21009
Multi-year and possibly periodic variations in the UV spectrum of 56 Pegasi 11 p1756 N85-21046
Observations of current pulsations of characteristics in atmosphere with period of about 1.5 hours 14 p2341 N85-24480
Relationship between seismic status of Earth and relative position of bodies in sun-earth-moon system 14 p2345 N85-24499
Ten years observations of long-period oscillations of the Sun 14 p2450 N85-25123
Variability of the quiet photospheric network 14 p2452 N85-25144
Elementary sunspot energy model 15 p2476 N85-25287
Cyclic changes in barometric coefficient of cosmic ray neutron component 15 p2478 N85-25293
Annual cycle. Part 1: The annual variation of surface temperatures over the United States and Canada
[PB85-147676] 15 p2600 N85-26026
North Atlantic Deep Water Formation
[NASA-CP-2367] 15 p2601 N85-26028
Changes in the high-latitude ocean as possible causes of atmosphere CO2 variations 15 p2602 N85-26036
The 6 pi-periodic solutions of plane restricted elliptical 3-body problem in neighborhood of libration points 16 p2718 N85-26779
Stability of periodic satellite motions relative to center of mass in circular orbit 16 p2718 N85-26780
Periodicity of variations in galactic cosmic ray fluxes and solar activity parameters near 20th cycle minimum 16 p2720 N85-26791
Variations in intensity of secondary cosmic radiation observed on 10-11 August 1981 16 p2721 N85-26796
Possible period of Jovian activity and possibility of seasons 16 p2723 N85-26810
Precipitable water in the atmosphere, determined from surface dewpoint values 16 p2831 N85-27457
Influence of coherent mesoscale structures on satellite-based Doppler lidar wind measurements
[NASA-CR-175853] 16 p2833 N85-27457
Qualitative and quantitative examination of the performance of regional air quality models representing different modeling approaches
[DE85-010508] 19 p3310 N85-30518
Southern oscillation/El Nino excitation of the Earth's Chandler wobble 20 p3490 N85-31695
Solar-geophysical data no. 485, January 1985. Part 1 (prompt reports): Data for December 1984, November 1984 and late data
[PB85-181360] 20 p3548 N85-32079
On gamma and neutrino radiation from Cyg X-3
[OG-2.1-7] 22 p3863 N85-33924
1000 GeV gamma rays from Cygnus X-3: An update
[OG-2.1-8] 22 p3863 N85-33925
Secondary periodicities of microbursts of TeV gamma rays from the Crab pulsar
[OG-2.3-5] 22 p3866 N85-33942
The 1000 GeV gamma rays from ms pulsars
[OG-2.3-12] 22 p3867 N85-33948
Periodic gamma-ray emissions from Geminga at or = 10(12) eV
[OG-2.4-2] 22 p3867 N85-33949
Search for periodicities near 59 s in the COS-B gamma-ray data of 2CG195+04 (Geminga)
[OG-2.4-3] 22 p3867 N85-33950
Search for gamma-rays above 400 GeV from Geminga
[OG-2.4-4] 22 p3867 N85-33951
Observations on TeV gamma rays from Geminga and PSR 0950+08
[OG-2.4-6] 22 p3868 N85-33953
Search for gamma ray lines from SS433
[OG-2.4-11] 22 p3868 N85-33955
Propagation of the phase of solar modulation
[SH-4.1-12] 23 p4005 N85-34835
Nineteenth International Cosmic Ray Conference. SH sessions, volume 5
[NASA-CP-2376-VOL-5] 23 p4031 N85-34991
Cosmic ray power spectral variations. 3: Solar rotation periodicities
[SH-4.4-16] 23 p4034 N85-35012
Variations of the cosmic ray general component in Antarctica
[SH-4.4-17] 23 p4035 N85-35013
Cosmic ray variations with the period close to 27 days and their connection with solar activity longitudinal distribution
[SH-4.4-19] 23 p4035 N85-35015
Azimuthal and meridional asymmetries of the solar wind and quasiperiodic variations of intensity of Galactic Cosmic Rays (GCR)
[SH-4.4-20] 23 p4035 N85-35016
Dynamics of two-year cosmic ray variations inferred from the data of spacecraft and stratospheric measurements and from the neutron monitor data in 1958-1981
[SH-4.4-21] 23 p4035 N85-35017
Formulation of cosmic-ray solar daily variation and its seasonal variation, produced from generalized stationary anisotropy of solar origin
[SH-4.5-2] 23 p4036 N85-35020
Temporal variations of the anomalous oxygen component, 1977 - 1984
[SH-4.6-3] 23 p4039 N85-35041
A relation between the short time variations of cosmic rays and geomagnetic field change
[SH-5.1-14] 23 p4043 N85-35067
Observations of cosmic-ray modulations in the fall, 1984
[SH-5.1-16] 23 p4043 N85-35069
Frequency spectra of short-period variations of cosmic ray
[SH-5.1-17] 23 p4043 N85-35070
Long-period cosmic ray variations and their altitude dependence
[SH-6.1-19] 23 p4046 N85-35091
Solar modulation of cosmic ray intensity and solar flare events inferred from (14)C contents in dated tree rings
[SH-7.1-2] 23 p4047 N85-35095
When did the average cosmic ray flux increase?
[SH-7.1-4] 23 p4047 N85-35097
Radiocarbon content in the annual tree rings during last 150 years and time variation of cosmic rays
[SH-7.1-15] 23 p4048 N85-35106
PERIODICALS
Center for Electronics and Electrical Engineering Technical Bulletin covering center programs
[PB84-218058] 01 p0045 N85-10298
The integrated library system design concepts for a complete serials control subsystem
[AD-A149379] 10 p1588 N85-19884
Sourcebook: Gaining access to US government information on the environment and natural resources
[DE84-017419] 11 p1740 N85-20941
D-1 report: The first German spacelab mission
[NASA-TM-77637] 13 p1977 N85-22402
Lopez Energy Alternatives Project
[DE85-010589] 22 p3849 N85-33837
NBS (National Bureau of Standards) library serial holdings, 1985
[PB85-191948] 22 p3849 N85-33839
PERIODICITY
U PERIODIC VARIATIONS
PERIODICITY (BIOLOGY)
U RHYTHM (BIOLOGY)
PERIPHERAL EQUIPMENT (COMPUTERS)
NT BUFFER STORAGE
NT COMPUTER COMPATIBLE TAPES
NT COMPUTER STORAGE DEVICES
NT MAGNETIC TAPES
NT OPTICAL DISKS
NT RANDOM ACCESS MEMORY
NT READ-ONLY MEMORY DEVICES
NT REGISTERS (COMPUTERS)
FCC (Federal Communication Commission) methods of measurement of radio noise emissions from computing devices
[PB84-243501] 06 p0649 N85-15387
Generation and display apparatus
[AD-D011639] 17 p3008 N85-28599
PERIPHERAL NERVOUS SYSTEM
Is fast fiber innervation responsible for increased acetylcholinesterase activity in reinnervating soleus muscles?
[NASA-CR-175716] 15 p2614 N85-26108

PERIPHERAL VISION
Peripheral Vision Horizon Display (PVHD)
[NASA-CP-2306] 01 p0008 N85-10044
Personal experience with the PVHD and opinion of situations in which a wide Field Of View (FOV) PVHD might be helpful 01 p0008 N85-10045
The two modes of visual processing: Implications for spatial orientation 01 p0008 N85-10047
Theory underlying the peripheral vision horizon device 01 p0008 N85-10048
The peripheral visual cue assessment facility at Ames Research Center 01 p0008 N85-10050
Evaluation of the Malcolm horizon in a moving-base flight simulator 01 p0008 N85-10051
Peripheral vision horizon display on the single seat night attack A-10 01 p0009 N85-10053
Peripheral vision horizon display testing in RF-4C aircraft 01 p0009 N85-10054
Extracts from the test plan for in-flight evaluation of the NT-33A peripheral vision display 01 p0009 N85-10055
NASA Ames-Dryden T-37 demonstration comments 01 p0009 N85-10056
Early Air Force Flight Test Center (AFFTC) experience with Peripheral Vision Horizon Displays (PVHD) 01 p0009 N85-10057
Peripheral vision displays: The future 01 p0009 N85-10058
A production peripheral vision display system 01 p0010 N85-10059
A preliminary flight evaluation of the peripheral vision display using the NT-33A aircraft
[AD-A145123] 01 p0010 N85-10060
Bulletin of the Faculty of Engineering, Hokkaido University, no. 123
[ISSN-0385-802-X] 04 p0482 N85-13075
A mathematical model of visual perception regarding peripheral vision and its application to the Hermann's illusion 04 p0483 N85-13080
Mean and random errors of visual roll rate perception from central and peripheral visual displays 05 p0704 N85-14519
Accuracy of system step response roll magnitude estimation from central and peripheral visual displays and simulator cockpit motion 05 p0705 N85-14522
Dual-task timesharing using a projected attitude display (Malcolm horizon)
[AD-A150789] 14 p2396 N85-24750
Perception of roll rate from an artificial horizon and peripheral displays
[VTH-LR-403] 17 p3002 N85-28557
PERIPHERIES
U BOUNDARIES
PERISCOPES
Immediate visibility after red and white adaptation
[AD-A156271] 24 p4132 N85-35616
PERMAFROST
Geothermal studies in Alaska: Conditions at Prudhoe Bay 04 p0516 N85-13290
Pulse transmission through frozen silt
[AD-A147108] 07 p0940 N85-15958
Deuterium diffusion in a soil-water-ice mixture
[AD-A148457] 08 p1176 N85-17415
Permafrost and subsurface ice in the solar system 13 p2191 N85-23584
Permafrost, seasonally frozen ground, snow cover and vegetation in the USSR
[AD-A153628] 18 p3124 N85-29346
Permafrost features on Earth and Mars: Similarities, differences 22 p3855 N85-33870
PERMEABILITY
NT DIELECTRIC PERMEABILITY
Separation of metal species by supported liquid membranes
[DE84-014536] 04 p0470 N85-12992
Influence of inter-layer effect on charge gas-permeability
[BLL-M-35919-(5828.4)] 05 p0616 N85-13940
Effect of water on hydrogen permeability — Stirling engines
[NASA-TM-86904] 06 p0761 N85-14864
Influence of size grading of sintering ore on the sintering process
[BLL-M-36004-(5828.4)] 07 p0924 N85-15854
Investigation of structure-permeability relationships of silicone polymer membranes
[PB85-148476] 11 p1596 N85-20038
Effect of host-rock dissolution and precipitation on permeability in a nuclear waste repository in tuff
[DE85-000675] 11 p1727 N85-20860
Practical surface methods 14 p2316 N85-24314
Applications of eddy currents 14 p2316 N85-24315
Variational bounds on Darcy's constant
[DE85-000638] 15 p2580 N85-25016
An experimental study of brine upward migration in thin sea ice 15 p2582 N85-25923
Ionic conduction and water diffusion in Li (BETA)-alumina
[DE85-007548] 16 p2755 N85-27005
Variational bounds on Darcy's constant
[DE85-008959] 18 p3101 N85-29195
Measurement of permittivity and permeability of microwave materials
[AD-D011656] 18 p3176 N85-29688
Mass spectrometer based gas permeation apparatus
[DE85-011176] 19 p3273 N85-30299
Tables of generalized hydrogen diffusion profiles and permeating fluxes for fusion applications
[DE85-006876] 19 p3372 N85-30919
Measurement and analysis of two-phase flow through low permeability media, task 3
[PB85-188373] 20 p3435 N85-31313
Permeation of mixed penetrants through glassy polymer membranes
[AD-A155605] 21 p3570 N85-32207
WIPP horizon in situ permeability measurements
[DE85-012687] 22 p3802 N85-33557
Geologic, technical, and economic sensitivity analysis in support of the GRI (Gase Research Institute) tight gas reservoirs project area
[PB85-192276] 22 p3802 N85-33559
Organic solvent alteration of hydraulic properties of sedimentary rocks of low permeability: A review
[DE85-012537] 22 p3815 N85-33635
Development and evaluation of sulfonated polysulfone membranes for the zinc-ferricyanide battery
[DE85-009104] 24 p4090 N85-35357
PERMEATING
Theory of kinetics of impregnation of porous bodies
[BLL-M-35917-(5828.4)] 05 p0616 N85-13942
Steady state hydrogen transport in solids 06 p0864 N85-15492
Mechanisms of gas permeation through polymer membranes
[DE84-017423] 09 p1293 N85-18117
PERMITTIVITY
Calculations of optical properties of transition metals
[BLL-M-35744-(5828.4)] 02 p0175 N85-11175
Plane wave (EMP) incidence on a finitely conducting plane Earth with the magnetic field intensity parallel to the Earth's surface
[DE84-015364] 02 p0228 N85-11493
Apparatus for measuring dielectric characteristics of polymer materials in millimetric range of wavelengths at 4.2-300 K temperatures 06 p0788 N85-15032
An indirect measure of below-ground electric field, conductivity, and dielectric constant
[AD-A146518] 06 p0804 N85-15115
A quasi-optical method for measuring the complex permittivity of materials
[AD-A147483] 07 p0941 N85-15966
The effects of soil moisture on bistatic clutter power
[AD-A147636] 08 p1150 N85-17261
An experimental investigation of microstrip properties on soft substrates from 2 to 40 GHz
[NASA-TM-86961] 11 p1624 N85-20224
Study of laminated dielectric behavior at microwave and millimeter-wave frequencies
[AD-P004356] 12 p1825 N85-21452
A millimeter wave apparatus for free-space measurement of dielectric constants at high temperature
[AD-P004361] 12 p1826 N85-21455
Determining distribution of complex dielectric permittivity over cylindrical body of intricate cross section from electromagnetic field measurement 12 p1842 N85-21559
Electric field effects on ion currents in satellite wakes 13 p1991 N85-22485
Extraction of surface-wave energy from plasma waveguide 13 p2077 N85-22974
Change of electrical characteristics of radio-frequency cables under thermal effect 13 p2081 N85-22999
Dielectric measurements in infralow-frequency band 13 p2067 N85-23034
Microwave remote sensing of soil moisture 13 p2125 N85-23235
Mars radar catalog 13 p2198 N85-23636
Chemical interpretation of the relaxed permittivity during epoxy resin cure
[AD-A150955] 14 p2260 N85-24005
Determination of temperature and degree of roughness of sea and land surfaces by microwave radiometric polarization measurements 14 p2334 N85-24432
Measurement of permittivity and permeability of microwave materials
[AD-D011656] 18 p3176 N85-29688
Transversely reinforced piezoelectric composites
[AD-D011676] 19 p3260 N85-30214
The determination of optical constants of thin metal films by surface plasma techniques 19 p3373 N85-30925
Examination of anisotropic films by resonance method 22 p3778 N85-33412
PEROVSKITES
Piezoelectric and electrostrictive materials for transducer applications
[AD-A145115] 01 p0043 N85-10277
Peculiar spherules from Antarctica and their origin 06 p0883 N85-15612
Integrated current collector and catalyst support
[DE85-011616] 22 p3761 N85-33311
PEROXIDES
NT HYDROGEN PEROXIDE
NT INORGANIC PEROXIDES
NT ORGANIC PEROXIDES
Evaluation of the alkaline peroxide pre-bond surface treatment for titanium
[AD-A147352] 07 p0928 N85-15881
Chemical transformations in acid rain. Volume 2: Investigation of kinetics and mechanism of aqueous-phase peroxide formation
[PB85-173433] 18 p3135 N85-29416
PERSONAL COMPUTERS
How to implement the welcome program in compatible microcomputers such as Apple 2
[INPE-3114-PRE/511] 05 p0715 N85-14586
Possibilities and impossibilities of microcomputer systems
[AD-1984-904] 07 p1028 N85-16522
Guide to personal desktop computing at ANL
[DE85-001436] 08 p1206 N85-17594
Personal desktop computing in a research and development laboratory
[DE85-002765] 11 p1705 N85-20728
ZTL: A subroutine package for the IBM personal computer to support the Ziatech ZT1488 IEEE-488 controller
[LA-10141-MS] 12 p1913 N85-22010
HGRAPH: A subroutine package for the IBM personal computer to support the Hercules Graphic Card
[LA-10144-MS] 12 p1914 N85-22013
ZTLCK: A subroutine package for the IBM personal computer to support the Ziatech ZT1488 real time clock
[LA-10146-MS] 12 p1914 N85-22014
TRANIC: A subroutine package for the IBM personal computer to support the transfer 6002 CAMAC crate controller
[LA-10145-MS] 12 p1914 N85-22015
The performance of a type-insensitive Runge-Kutta code on a personal computer
[TUM-I8410] 12 p1919 N85-22048
Two degree-of-freedom flutter solution for a personal computer
[NASA-TM-86381] 13 p1971 N85-22379
Personal computer aided decision analysis
[AD-A151911] 16 p2875 N85-27743
Benchmark evaluation of PC simscript
[AD-A156133] 24 p4138 N85-35651
PERSONALITY
The Reports of Aeromedical Laboratory, volume 25, no. 1/2
[ISSN-0023-2858] 01 p0090 N85-10605
The relationship between emotional tension scale and psychological uneasiness of JASDF pilots in flying situations 01 p0090 N85-10606
Classification systems for individual differences in multiple-task performance and subjective estimates of workload 05 p0706 N85-14543
Success in learning occupation of chemical production technician as function of certain personality traits and development of psychophysiological functions 09 p1362 N85-18568
Individual characteristics and unit performance: A review of research and methods
[AD-A153145] 17 p3001 N85-28550
The relationship between personality and performance 24 p4129 N85-35600
PERSONALITY TESTS
Psychological testing on the computer
[R/PERS-618] 01 p0097 N85-10645
Rapid determination of cadet discipline by projective tests 22 p3821 N85-33871
PERSONNEL
NT AIR TRAFFIC CONTROLLERS (PERSONNEL)
NT AIRCRAFT PILOTS
NT ASTRONAUTS
NT COSMONAUTS
NT CREWS
NT FLIGHT CREWS
NT FLYING PERSONNEL
NT INSTRUCTORS
NT MEDICAL PERSONNEL
NT NAVIGATORS
NT OPERATORS (PERSONNEL)
NT PILOTS (PERSONNEL)
NT POLICE

NT PROGRAMMERS
NT SCIENTISTS
NT SPACECREWS
Models of natural intelligence in fault diagnosis tasks: Implications for training and aiding of maintenance personnel
[AD-P003927] 02 p0246 N85-11607
The role of physical and physiological capacities and their modification on the tolerance to various stress experienced by Air Force personnel
[AD-A145779] 03 p0400 N85-12550
Cardiovascular disease among U.S. Navy pilots
[AD-A145871] 03 p0400 N85-12552
Maintenance Management Information and Control System (MMICS): Administrative boon or burden
[AD-A145762] 03 p0438 N85-12790
The human role in space. Volume 2: Research analysis and technology report
[NASA-CR-171224] 04 p0546 N85-13474
An analysis of the technical training of enlisted minuteman missile maintenance personnel
[AD-A147078] 07 p0912 N85-15775
Model of team organization and behavior and team description method
[AD-A147540] 07 p1053 N85-16680
Project manager's handbook for special projects
[AD-A147913] 07 p1053 N85-16683
Solid rocket booster retrieval operations
08 p1096 N85-16928
Interagency program on space nuclear power: Directory of participants in the SP-100 program
[DE85-026339] 08 p1221 N85-17691
Success in learning occupation of chemical production technician as function of certain personality traits and development of psychophysiological functions
09 p1362 N85-18568
European Scientific Notes, volume 38, number 12
[AD-A148713] 09 p1418 N85-18946
Robotic safety
[DE85-002314] 10 p1493 N85-19431
Application of the Hardman methodology to the Single Channel Ground-Airborne Radio System (SINCGARS)
[NASA-CR-175894] 14 p2218 N85-23756
SPARTEN (Scientific Program of Aerobic and Resistance Training Exercise in the Navy): A total body fitness program for health and physical readiness
[AD-A150669] 14 p2368 N85-24711
Investigation of the requirement for auxiliary heating of Canadian forces personnel
[AD-A151950] 16 p2841 N85-27522
Summary of Research, Academic Departments, 1983 - 1984
[AD-A151724] 16 p2875 N85-27741
Predictors of transfer adjustment: A longitudinal study
[AD-A152462] 17 p3000 N85-28548
An empirical comparison of the accuracy of univariate and multivariate corrections for range restriction
[AD-A153071] 17 p3019 N85-28670
Evaluation and Validation (E/V) team public report, volume 1
[AD-A153609] 18 p3161 N85-29584
Assessment of computer resource management plan for division support weapon system
[AD-A154142] 19 p3342 N85-30712
U.S. Civil airmen statistics for calender year 1984
[AD-A156326] 24 p4059 N85-35153
Data processing professionals and DP application users' perceptions and expectations of operational roles of persons working in a DP/application user interface group 24 p4165 N85-35821
PERSONNEL DEVELOPMENT
Nondestructive inspection: Improved capabilities of technicians
[AD-A147368] 07 p0975 N85-16198
Efforts to improve aviation medical examiner performance through continuing medical education and annual performance reports
[AD-A148078] 08 p1195 N85-17531
Training guide for scientific and engineering trainees 1984
[AD-A147983] 08 p1198 N85-17542
Improvements in personnel needed for better flight safety 14 p2208 N85-23693
Administration chief on air traffic control improvements 15 p2450 N85-25193
Guidelines of the Federal Minister of Transportation for the formation and examination of airline personnel, part 4 17 p3002 N85-28556
PERSONNEL MANAGEMENT
Air Force Human Resources Laboratory report: Fiscal year, 1983
[AD-A145647] 02 p0238 N85-11548
Performance evaluation of A-10 aircraft maintenance units and aircraft using constrained facet analysis
[AD-A146955] 07 p0893 N85-15660
Interaction of human cognitive models and computer based models in supervisory control
[AD-A142547] 07 p1020 N85-16474
Communications skills for CRM training
09 p1276 N85-18017
Bibliography of unclassified reports, FY 1984
[AD-A148838] 09 p1401 N85-18819
Strategic management for organizational effectiveness. The effect of human resource planning on retention and related issues, volume 1
[AD-A149396] 10 p1566 N85-19674
Strategic management for organizational effectiveness. The effect of human resource planning on retention and related issues, volume 2
[AD-A149399] 10 p1566 N85-19675
Strategic management for organizational effectiveness. The effect of human resource planning on retention and related issues, volume 3
[AD-A149400] 10 p1566 N85-19676
Strategic management for organizational effectiveness. The effect of human resource planning on retention and related issues: Methodological appendix
[AD-A149401] 10 p1566 N85-19677
PERSONNEL SELECTION
NT PILOT SELECTION
The construction of auditive tests of attention and spatial orientation and their factorial structure
[DFVLR-FB-84-21] 05 p0699 N85-14485
Cognitive asymmetry and occupation. Computer programmers, students, and bank personnel, part 1 and part 2
[AD-A147125] 08 p1197 N85-17540
Automated CPX support system preliminary design phase
[NASA-CR-175784] 16 p2769 N85-27091
Construction of a job-oriented test for the selection of air traffic controllers
[DFVLR-FB-84-51] 17 p3002 N85-28558
Psychological issues relevant to astronaut selection for long-duration space flight: A review of the literature
[AD-A154051] 19 p3330 N85-30627
PERSPIRATION
Peripheral changes in regional sweating responses to exercise in hypobaric environments
[AD-A150757] 14 p2388 N85-24710
Preparing Alberto Salazar for the heat of the 1984 Olympic Marathon
[AD-A150942] 14 p2389 N85-24714
PERT
Statistics for the maximum of several positive random variables with application to networking
[AD-A150005] 12 p1922 N85-22069
PERTURBATION
NT ORBIT PERTURBATION
NT SATELLITE PERTURBATION
N-frequency quasiperiodicity and chaos in dissipative dynamical systems 02 p0262 N85-11840
Chaotic behavior induced by solitons in perturbed integrable systems 02 p0263 N85-11844
Two- and three-dimensional model and wall data from a flexible-walled transonic test section
03 p0312 N85-12015
Investigations of flow field perturbations induced on slotted transonic-tunnel walls 03 p0312 N85-12016
A study of the critical layer in a rotating liquid payload
[AD-A146094] 03 p0362 N85-12321
A 2-dimensional description of potential perturbations to the ozone layer due to NOx and H-2-O aircraft emissions
[AD-A146292] 03 p0392 N85-12511
Dynamic stiffness characteristics of high eccentricity ratio bearings and seals by perturbation testing
05 p0645 N85-14141
Some aspects of understanding changes in the global carbon cycle 05 p0652 N85-14186
Artificial defocusing lens in ionosphere
05 p0724 N85-14654
Excitation of spiral patterns in responsible density wave theory 05 p0740 N85-14764
Comparison of uniform perturbation solutions and numerical solutions for some potential flows past slender bodies
[NASA-CR-172485] 06 p0749 N85-14799
Phase problem in aperture synthesis systems
06 p0782 N85-15002
Analysis of spin echo signals in multi-pulse experiment
06 p0792 N85-15065
Longer-scalelength plasma perturbations by an intense laser beam
[AD-A147005] 07 p1045 N85-16638
Tropospheric and ionospheric phase perturbations and Doppler frequency shift effects
[AD-A148579] 08 p1154 N85-17283
Exploratory development of advanced surface flaw detection methods
[AD-A148757] 09 p1291 N85-18060
Perturbation of a multiple eigenvalue in the Benard problem for two fluid layers
[AD-A149068] 10 p1546 N85-19745
Resonant activation of a Josephson junction
[DE85-000702] 10 p1563 N85-19857
Geomagnetic disturbances caused by internal atmospheric dynamics 11 p1665 N85-20491
Three-dimensional baroclinic instability of a Hadley cell for small Richardson number
[NASA-TP-2450] 11 p1687 N85-20605
21 Layer troposphere-stratosphere climate model
[NASA-TM-86183] 12 p1892 N85-21871
Pressure-gradient-driven Tokamak resistive MHD instability in the banana-plateau collisionality regime
[DE85-004566] 12 p1937 N85-22171
A study of the compatibility of an existing CFD package with a broader class of material constitutions
12 p1945 N85-22219
Flutter taming: A new tool for the aeroelastic designer
[AD-A150834] 14 p2228 N85-23802
Investigation and optimization of fuel production using dye-based transition metal complexes as charge-transfer intermediates
[PB85-161941] 14 p2264 N85-24029
Flow around axisymmetric bodies with uniform-velocity zones 14 p2276 N85-24103
Improvement and extension of a numerical procedure for the three dimensional unsteady transonic flows
15 p2459 N85-25181
Turbulence effects on a glow discharge as derived from continuity and energy considerations
[AD-A151838] 15 p2557 N85-25775
Method for evaluating perturbation in algorithms for solving navigational problems 16 p2718 N85-26783
Identification and control of structures in space
[NASA-CR-175790] 16 p2731 N85-26850
Formulas for updating the generalized inverse of a symmetric matrix perturbed by a symmetric rank 2 matrix composed of 2 nonsymmetric DYADS
[AD-A151736] 16 p2858 N85-27829
Analysis of control system from a viewpoint of desired pole placement and desired degree of robustness
[AD-A152627] 17 p2899 N85-27876
Maximizing the semi-major axis for a freely coning solar sailcraft
[AD-A153175] 17 p2909 N85-27936
Experiments on sorption characteristics of solid desiccant materials for solar desiccant cooling systems
[DE85-000542] 17 p2923 N85-28019
Supersonic flow around blunt wedge
17 p2942 N85-28158
The polar caps and the climatic evolution of Mars
22 p3854 N85-33866
Longitudinal dependence of the interplanetary perturbation produced by energetic type 4 solar flares and of the associated cosmic ray modulation
[SH-5.1-5] 23 p4042 N85-35059
Short perturbations of cosmic ray intensity and electric field in atmosphere
[SH-6.1-18] 23 p4048 N85-35090
DEPTH-CHARGE static and time-dependent perturbation/sensitivity system for nuclear reactor core analysis, revision 1
[DE85-013103] 24 p4139 N85-35859
Acoustic resonances in cylinder bundles oscillating in a compressible fluid
[DE85-004086] 24 p4145 N85-35889
PERTURBATION THEORY
A perturbation solution for rigid dumbbell suspensions in steady shear flow
[AD-A144876] 01 p0111 N85-10755
Singular perturbations, coherency and aggregation of dynamic systems
[DE84-014166] 01 p0114 N85-10772
Quasistable parametric optimization without compact level sets
[AD-A144716] 01 p0114 N85-10776
Numerical methods for singularly perturbed differential equations with applications
[AD-A145839] 02 p0252 N85-11850
Random processes and magnetohydrodynamic turbulence 02 p0271 N85-11767
Electrons in a disordered medium
[NOTA-INTERNA-816] 02 p0279 N85-11819
Mixed defect correction (iteration) for the solution of a singular perturbation problem
[MC-NW-182/83] 05 p0720 N85-14624
Scattering of electromagnetic waves by surface with small asperities 06 p0784 N85-15013
Theory of the orbital motion of an artificial Earth Satellite.
[NAL-TR-807] 09 p1285 N85-18075
Geometric Hamiltonian structures and perturbation theory
[DE85-002005] 11 p1707 N85-20737

Velocity inversion using a stratified reference
[AD-A150082] 12 p1889 N85-21858
Thermal stability of static coronal loops: Part 1: Effects of boundary conditions
[NASA-CR-175495] 12 p1961 N85-22330
Surface scattering
[AD-A150252] 13 p2153 N85-23366
Nonrelativistic Kapitza-Dirac scattering
[AD-A150822] 13 p2159 N85-23405
Parton dynamics in hadronic processes
[DE85-006072] 14 p2418 N85-24922
Resonances in photon-photon scattering
[DE85-004607] 14 p2419 N85-24926
Perturbations of Kalman filtering process
15 p2460 N85-25305
Application of perturbation theory to problem in orbital theory 15 p2537 N85-25656
Lattice overview
[DE85-007282] 15 p2662 N85-26427
Eleven lectures on the physics of the quark-gluon plasma
[DE85-004321] 15 p2662 N85-26431
Sensitivity of the stationary distribution vector for an ergodic Markov chain
[DE85-006079] 16 p2857 N85-27621
The temperature dependence of diffracted beam intensities in atom-surface scattering
[AD-A152762] 17 p3029 N85-28736
Photon structure function: Theory
[DE85-008064] 17 p3031 N85-28745
Stability in dynamical systems
[DE85-006698] 17 p3034 N85-28766
Theoretical and numerical studies of magnetic field line displacements in an Elmo Bumpy Torus
[DE85-008757] 17 p3041 N85-28816
Numerical simulation of the transient by the unstable state in a Lotka-Volterra model
[NOTA-INTERNA-833] 18 p3175 N85-29684
Perturbative treatment of quasi-resonant proton neutralization at alkali-halide surfaces
[AD-A154143] 19 p3356 N85-30606
A theory of quasi-conical solutions of noninteger degree — flow fields on supersonic wings
[UTH-LR-420] 20 p3390 N85-31024
An overview of latest model reduction and control methods of large flexible space structures
20 p3414 N85-31191
Wave propagation and methods of solution of the wave equation for moving disturbances sources
[ESA-TT-824] 20 p3522 N85-31906
Finite-perturbation intermediate neglect of differential overlap molecular orbital calculations of nuclear magnetic resonance spin-spin coupling constants for polycyclic aromatic hydrocarbons and aromatic nitrogen heterocyclics
[NASA-TM-87486] 20 p3525 N85-31927
Some dynamic electronic properties of semiconductor surfaces and interfaces 20 p3537 N85-32007
Calculation of the propagation constant in a rectangular waveguide containing an inhomogeneous longitudinally magnetized plasma
[DE85-012072] 21 p3577 N85-32250
Reflection of acoustic beam from inhomogeneous boundary 21 p3680 N85-32864
Identification and control of structures in space
[NASA-CR-176175] 24 p4069 N85-35214
Perturbation-iteration theory for analyzing microwave striplines
[NASA-CR-176189] 24 p4085 N85-35321
Two-point closure study of covariance budgets for turbulent Rayleigh-Benard convection
[PB85-189108] 24 p4124 N85-35566
Multiple vacancy production by high energy heavy ions
[DE85-004428] 24 p4162 N85-35805

PERU
Petrology and genesis of carbonate-hosted Pb-Zn-Ag, San Cristobal District, Department of Junin, Peru
03 p0389 N85-12487
Climate and fisheries: A Peruvian case study
07 p1003 N85-16373
The El Nino phenomenon and its agrometeorological implications 07 p1004 N85-16382

PESTICIDES
USSR report: Chemistry
[JPRS-UCH-84-012] 06 p0761 N85-14865
Teratogenicity studies of carbaryl and malathion alone and in combination in various laboratory animals
[AD-P004034] 06 p0845 N85-15364
Installation restoration program. Phase 2: Stage 1 problem confirmation study, Duluth International Airport Duluth, Minnesota
[AD-A148318] 08 p1089 N85-16885
EPA (Environmental Protection Agency) research program guide, FY-1985, October 1, 1984 - September 30, 1985
[PB85-181681] 20 p3487 N85-31676

PETN
Deformation, fracture and explosive properties of reactive materials
[AD-A146396] 06 p0774 N85-14945
Development of a PETN DDT detonator
[DE84-016944] 09 p1302 N85-18178
Nonprimary-explosive, hot-wire detonator
[DE85-005195] 12 p1816 N85-21403
X-ray photoelectron spectroscopy study of the compatibility of the explosive PETN with candidate plastic bonding materials
[DE85-010604] 19 p3251 N85-30161
Static high pressure study of nitric oxide chemistry: Proposed mechanism for nitric oxide detonation
[DE85-010795] 22 p3746 N85-33220
Gas composition and molecule velocity in the detonation products of pentaerythritol tetranitrate (PETN) in expansion in a high vacuum container. Analysis by mass spectroscopy and time of flight spectrometry
[ISL-R-109/84] 22 p3747 N85-33226
Time-resolved spectroscopic studies of detonating heterogeneous explosives
[DE85-000760] 23 p3921 N85-34297
Effect of precipitation variables on the specific surface and explosion characteristics of pentaerythritol tetranitrate
[DE85-009620] 23 p3922 N85-34302
Real time analysis of PETN detonation products
[DE85-009581] 23 p3922 N85-34303
Friction, impact, and electrostatic discharge sensitivities of energetic materials
[DE85-013321] 24 p4083 N85-35309

PETRI NETS
Extended Stochastic Petri Nets: Applications and analysis
[AD-A148439] 08 p1213 N85-17633
The design of a unified package for the solution of stochastic petri net models
[AD-A150325] 13 p2151 N85-23354
Regenerative stochastic Petri nets
[AD-A150343] 13 p2151 N85-23355
Performance evaluation of stochastic timed decision-free Petri Nets
[AD-A153987] 18 p3171 N85-29652
Petcon: A software instrument for the analysis of Petri networks, oriented towards communication protocols
[FUB-50-1983] 22 p3756 N85-33286

PETROGRAPHY
Petrography, diagenesis and depositional models of the St. Louis limestone, valmeyeran (middle Mississippian), Illinois Basin, USA 09 p1352 N85-18506
Study of the physical properties of crystalline rocks in the southeast Voronezh anteclise
[NASA-TM-77823] 10 p1514 N85-19551
Assessment of computer based geologic mapping of rock units in the LANDSAT-4 scene of northern Death Valley, California 13 p2119 N85-23185
Geological information content of reflected wave record form 14 p2345 N85-24502
Location of continental Permian volcanites of central Asia and its tectonic interpretation
14 p2346 N85-24505
Structural analysis of terrane accretions in the eastern Brooks Range and adjacent areas in central Alaska and Canada
[DE85-008279] 17 p2993 N85-28501
Clay identification and amount measured by laboratory techniques compared to well log responses: Application to tight gas sands and shales
[DE85-010411] 19 p3362 N85-30643
Chemistry of ore-forming fluids
24 p4103 N85-35436

PETROLEUM
U CRUDE OIL

PETROLEUM PRODUCTS
NT ASPHALT
NT BUTANES
NT DIESEL FUELS
NT GASOLINE
NT GREASES
NT LUBRICATING OILS
NT NATURAL GAS
User experience of existing corrosion monitoring techniques and the development of Thin Layer Activation (TLA) for corrosion monitoring
[AERE-R-11248] 01 p0029 N85-10183
Studies related to the deep Earth gas: 1983
[PB85-171114] 16 p2816 N85-27373
Improving the defense energy information system (DEIS)
[AD-A153524] 18 p3200 N85-29849
Influence of surface films of petroleum products on conditions for absorption of solar radiation by upper water layer 19 p3299 N85-30398
Protection products for the conductors of high voltage overhead lines
[BLL-OA-TRANS-3219-(6196.300)] 20 p3429 N85-31269
Biodegradation of jet fuel by aquatic microbial communities
[PB85-191971] 24 p4084 N85-35311

PETROLOGY
NT PETROGRAPHY
Petrology of deep crustal xenoliths from the eastern Snake River Plain, Idaho 02 p0226 N85-11477
The petrology and geochemistry of high cascade volcanics in southern Washington: Mount Saint Helens volcano and the Indian Heaven basalt field
02 p0227 N85-11487
Petrology and genesis of carbonate-hosted Pb-Zn-Ag, San Cristobal District, Department of Junin, Peru
03 p0389 N85-12487
Stratigraphy, petrology, and tectonic setting of the Alisitos Group, Baja California, Mexico
03 p0389 N85-12488
Geology of selected migmatite zones within the bitterroot lobe of the Idaho batholith, Idaho and Montana
03 p0389 N85-12489
Geology and geochemistry of early Tertiary submarine volcanic rocks of the Aleutian Islands, and their bearing on the development of the Aleutian Island Arc
03 p0389 N85-12493
Franciscan and related rocks of southern Humboldt County, northern California coast ranges: Analysis of structure, tectonics, sedimentary petrology, paleogeography, depositional history, and thermal maturity 03 p0390 N85-12495
Metamorphic petrology of the Table Mountain area, Circle quadrangle, Alaska 04 p0516 N85-13295
Stratigraphy, petrology, and structure of the Pingston terrane, Mount Hayes C-5 and C-6 quadrangles, eastern Alaska Range, Alaska 04 p0517 N85-13301
Report of the field work performed in the Basins of the Quebra Osso and Tanque Petro Rivers in the Catas Altas quadrangle, Minas Gerais
[INPE-3268-NTE/225] 04 p0525 N85-13359
Petrologic model of the northern Mississippi embayment based on satellite magnetic and ground based geophysical data
[NASA-TM-85075] 04 p0533 N85-13406
Petrologic constraints on the origin of the Moon: Evidence from Apollo 14 04 p0583 N85-13726
Petrology and petrogenesis of Batholitic rocks, San Jacinto Mountains, southern California
05 p0673 N85-14322
Petrology and structure of Pwemain to Jurassic rocks near Yreka, Klamath Mountains, California
05 p0673 N85-14325
Geology, petrology, and tectonic setting of the Mafic rocks of the 1480 Ma old granite-rhyolite terrane of Missouri, USA 05 p0674 N85-14327
Evolutionary history of CI and CM chondrites
06 p0684 N85-15615
Aqueous alteration of meteorite parent bodies: Possible role of unfrozen water and the Antarctic meteorite analogy 06 p0684 N85-15617
High pressure physics research focusing on composite materials 08 p1140 N85-17185
Sedimentary petrology and provenance of the upper Jackforth Sandstone (Morrowan) Quachita Mountains, Arkansas, USA 08 p1182 N85-17447
Part 1. Stratigraphy, structure and petrology of the Peterborough 1.5-minute quadrangle, New Hampshire and part 2. Graphite textural and isotropic variations in plutonic rocks, south-central New Hampshire
09 p1353 N85-18511
Correlation and petrological interpretation of abyssal and terrestrial tephra layers 09 p1353 N85-18512
Research and development related to the Nevada nuclear waste storage investigations
[DE85-002303] 12 p1932 N85-22138
Antarctic Meteorite Newsletter, volume 8, number 1
[NASA-CR-175587] 12 p1961 N85-22328
Reports of the Planetary Geology and Geophysics Program, 1984
[NASA-TM-87563] 13 p2172 N85-23474
Io: Generation of silicate magma by shear melting at the base of a basaltic lithosphere
13 p2172 N85-23476
Modelling equilibrium and fractional crystallization in the system MgO-FeO-CaO-Al2O3-SiO2
13 p2184 N85-23552
Quenching effects on iron site partitioning in the Apollo 17 orange glass composition 13 p2184 N85-23553
Petrologic and geochemical characterization of the Topopah Spring Member of the Paintbrush Tuff: Outcrop samples used in waste package experiments
[DE85-010449] 19 p3302 N85-30470

Some relations among directions of curves at an invariant point on a thermodynamic phase diagram
19 p3312 N85-30530
Dating Archean zircon by ion microprobe: New light on an old problem 21 p3722 N85-33094
Bedrock geology of the Brattleboro Quadrangle, Vermont-New Hampshire
[DE85-011027] 22 p3815 N85-33634

PFM (MODULATION)
U PULSE FREQUENCY MODULATION

PH
Potential for acidification of six remote ponds in the White Mountains of New Hampshire
[PB84-207349] 02 p0225 N85-11475
Sequential precipitation chemistry sampling program at Brookhaven National Laboratory with an analytical summary of 1976-1982 data
[DE85-002788] 10 p1513 N85-19545
Acid rain: Towards automated monitoring
16 p2829 N85-27444
Evaluation of methods used for the determination of acidity in acid rain samples
[PB85-178309] 19 p3237 N85-30070
Increase of total CO2 in the World ocean
[DE85-007756] 23 p3950 N85-34484

PH FACTOR
Investigation of chemical durability mechanisms in fluoride glasses
[AD-A145420] 02 p0186 N85-11241
A biological sensor for the detection of toxicants
[AD-D011304] 07 p0967 N85-16141
Respiratory chain of alkalophilic bacteria
[DE84-012558] 09 p1360 N85-18558
Physiochemically controlled scour jet array system
[AD-D011688] 19 p3308 N85-30505
Method for determining the point of zero zeta potential of semiconductor
[NASA-CASE-LAR-12893-1] 19 p3373 N85-30923
Environmental surveillance at Los Alamos during 1984
[DE85-011886] 22 p3811 N85-33605
Throughfall rate and chemistry studies: Whiteface Mountain
[DE85-012407] 23 p3947 N85-34464
Increase of total CO2 in the World ocean
[DE85-007756] 23 p3950 N85-34484

PHARMACOLOGY
East Europe report: Science and technology
[JPRS-ESA-84-029] 01 p0115 N85-10783
Jet lag prevention: Physiological mechanisms and pharmacological therapy
[AD-A145444] 02 p0235 N85-11529
Bioprocessing in space 05 p0690 N85-14438
Pharmacokinetic interactions of mixtures
[AD-P004032] 06 p0844 N85-15362
USSR report: Life sciences. Biomedical and behavioral sciences
[JPRS-UBB-84-015] 07 p1010 N85-16416
An atropinized heat-stressed rat model: Dose response effects and pharmacokinetics
[AD-A146851] 07 p1011 N85-16423
Review of US guide on medication and flying
12 p1904 N85-21958
East Europe report: Science and technology
[JPRS-ESA-85-023] 21 p3572 N85-32217
Interaction of opiate and phencyclidine derivatives with the acetylcholine receptor
[AD-A155119] 21 p3684 N85-32761
USSR report: Life sciences. Biomedical and behavioral sciences
[JPRS-UBB-85-018] 22 p3819 N85-33660
Effect of dibazol on parameters of nonspecific resistance of subjects in pressurized cabins
23 p3954 N85-34504

PHASE ANGLE
U PHASE SHIFT

PHASE CHANGE MATERIALS
Investigation of the Ostwald ripening of separated particles in liquid-liquid systems under microgravity conditions
[BMFT-FB-W-84-037] 05 p0615 N85-13927
Numerical investigation of phase change heat transfer in a horizontal cylinder including effects of natural convection 09 p1318 N85-18286
Advanced latent heat storage media for high-temperature industrial applications
[DE85-000907] 09 p1345 N85-18461
Development of media for dynamic latent heat storage for the low-temperature range. Part 1: Thermal analyses of selected salt hydrate systems
[NASA-TM-77778] 10 p1507 N85-19510
Evaluation of etringite and related compounds for use in solar energy storage
[DE85-003249] 12 p1882 N85-21609
Natural convection during heat accumulation by substances with change of aggregate state
13 p2043 N85-22787
Latent heat storage in cooling systems
[DE85-005355] 13 p2129 N85-23248
Overview of latent storage for passive solar applications
[DE85-005354] 13 p2129 N85-23249
Effects of the phase compositions of cast low-pearlite steels micro-alloyed with vanadium and titanium of their structure and properties
[BLL-BISI-TRANS-22301-(9022.06)]
17 p2926 N85-28067
High temperature composite thermal storage systems
[DE85-005073] 17 p2986 N85-28455
Materials research for passive solar systems: Solid-state phase-change materials
[DE85-008779] 18 p3132 N85-29395
The interactions of composition and stress in crystalline solids
[PB85-179075] 20 p3473 N85-31583

PHASE COHERENCE
Dynamics of symmetry breaking: Phase coherence in finite and random systems
[NOTA-INTERNA-813] 02 p0253 N85-11658
Coherent array of Josephson oscillators with external bias leads
[AD-D011367] 08 p1156 N85-17293
Comparative analysis of noise tolerance of quasi-coherent phase shift keying signal demodulators
13 p2072 N85-22946
Reception noise immunity of multiposition signals
13 p2085 N85-23023
Study of the coupling between average, coherent and turbulent fields in a circular excited free jet
[ISL-R-115/83] 16 p2785 N85-27184

PHASE CONJUGATION
Two novel plasma diagnostic tools: Fiber sensors and phase conjugation
[DE84-014033] 01 p0123 N85-10840
Influence of spatial pumping spectrum on quality of phase conjugate reflection during 4-photon interaction
21 p3686 N85-32964

PHASE CONTRAST
Ion contrasting chamber for discrimination of grains and textures
[BMFT-FB-T-84-151] 04 p0477 N85-13036
Synthesis of multistep directional couplers with nonminimum-phase characteristics
13 p2079 N85-22956
Resolution at its current limit: Applications of the Berkeley ARM
[DE85-009959] 19 p3274 N85-30301

PHASE CONTROL
Determination of row-and-column control principle of phase antenna array from amplitude-phase distribution of field in aperture 07 p0952 N85-16033
Coherent receiver phase and amplitude alignment circuit
[AD-D011487] 10 p1468 N85-19265
Method and apparatus for self-calibration and phasing of array antenna
[NASA-CASE-NPO-15920-1] 12 p1832 N85-21493
Transient processes in tuned amplifier during phase-shift keying with smooth phase variation
15 p2527 N85-25561
Simultaneous phase and frequency control of a three-phase inductor-convertor bridge
[DE85-006197] 18 p3096 N85-29164
Wide-band phase locked loop amplifier apparatus
[AD-D011720] 23 p3927 N85-34337

PHASE DEMODULATORS
Interference immunity of binary systems with second-order phase-difference modulation in various reception modes 13 p2072 N85-22944
Comparative analysis of noise tolerance of quasi-coherent phase shift keying signal demodulators
13 p2072 N85-22946

PHASE DETECTORS
Double reference pulsed phase locked loop (DRP-2L-2)
[NASA-CASE-LAR-13310-1] 12 p1824 N85-21441
Wideband phase keyers 12 p1839 N85-21544
Maser cavity servo-tuning system
[NASA-CASE-NPO-15890-1-CU]
18 p3093 N85-29143
Fiber optic gyroscope with alternating output signal
[AD-D011669] 19 p3271 N85-30284
One-frequency laser interferometer using the optic fiber as a polarization-independent interference phase detector
[DE85-010544] 19 p3277 N85-30326

PHASE DEVIATION
Error in compensating phase fluctuations of wave field by means of adaptive reflectors with continuous or compound surface 13 p2080 N85-22988
Investigation of bimodal paramagnetic filter
13 p2083 N85-23007

PHASE DIAGRAMS
An investigation of the solubility and diffusivity of chromium in gallium arsenide
[AD-A144949] 01 p0024 N85-10148
Metamagnetic systems 03 p0423 N85-12701
Neutron scattering on magnetic structures and at magnetic phase transitions 03 p0424 N85-12706
Thermodynamics and phase equilibria in the vanadium-silicon system
[AD-A145870] 03 p0435 N85-12769
Critical evaluation of binary rare Earth diagrams
[DE84-014880] 04 p0470 N85-12991
Mathematical models for the boiling diagram of the ideal two-component mixture
[DFVLR-FB-84-22] 04 p0471 N85-13000
Critical evaluation of binary rare earth phase diagrams
[DE84-015057] 05 p0614 N85-13922
Phase diagrams of organic superconductors
[DE84-016219] 05 p0731 N85-14669
Phase equilibria of stored chemical energy reactants
[AD-A146527] 06 p0765 N85-14896
Phase diagram of polymer blends containing block copolymers
[AD-A147706] 08 p1132 N85-17134
Application of computer methods for calculation of multicomponent phase diagrams of high temperature structural ceramics
[AD-A148138] 09 p1133 N85-17140
Electronic structure of liquid metal alloys
[DE85-000904] 09 p1295 N85-18136
New phases and chemical reactions in solid CO under pressure
[DE85-002033] 09 p1377 N85-18655
Quasi-thermodynamic prediction of hydrogen reemission behavior from titanium films
[DE85-003667] 10 p1564 N85-19664
Research on microemulsions for storage and conversion of solar energy
[DE85-000181] 12 p1882 N85-21807
Separating polymer solutions using high pressure LCST Lower Critical Solution Temperature) phenomena
[AD-A151538] 15 p2518 N85-25528
High pressure cosmochemistry applied to major planetary interiors: Experimental studies
[NASA-CR-175715] 15 p2579 N85-26544
On the feasibility of Ab Initio calculations of ordering alloy phase diagrams
[DE85-007073] 16 p2751 N85-26979
Ca-Ga, Sr-Ga and Ba-Ga binary systems
[DE85-006454] 16 p2751 N85-26980
Activities report of the Institute of Astronomy and Astrophysics 17 p3052 N85-28692
Electrical conductivity and phase diagram of binary alloys. 21: The system palladium-chromium
[NASA-TM-77863] 18 p3073 N85-29009
Local density theory of heats of formation and short-range order parameters in substitutionally disordered alloys
[DE85-009811] 18 p3075 N85-29021
Binary phase diagram determinations
[DE85-010856] 19 p3235 N85-30056
Some relations among directions of curves at an invariant point on a thermodynamic phase diagram
19 p3312 N85-30530
Phase behavior and QLS (Quasielastic Light Scattering) in potassium linoleate/n-alkanol microemulsions
[AD-A155028] 21 p3583 N85-32163
Cluster variation study of coherent ordering in FCC and BCC solid solutions
[AD-A156039] 24 p4079 N85-35280

PHASE ERROR
The Statistical Loop Analyzer (SLA)
08 p1100 N85-16955
Analytical studies and experimental measurements of amplitude and phase of near-field range antenna probes
[AD-A150922] 14 p2293 N85-24212
Angular tracking error in A phase comparison monopulse tracking radar: A critical review and extension of the phase front distortion approach
[AD-A152628] 17 p2949 N85-28205
Modulation using four phase levels. Theoretical study of the degradation caused by a spurious phase modulation
[CNES-83/219/CT/DRT/TIT/TR]
20 p3441 N85-31360

PHASE LOCK DEMODULATORS
Phase-locked loops for optical homodyne detection, volume 1 — spaceborne receivers
[ESA-CR(P)-2029-VOL-1] 20 p3442 N85-31367
Phase locked loops for optical homodyne detection, volume 2 — spaceborne receivers
[ESA-CR(P)-2029-VOL-2] 20 p3442 N85-31368

PHASE LOCKED SYSTEMS
Timing performance of phase-locked loops in optical pulse position modulation communication systems
[AD-A145403] 02 p0190 N85-11271

Design and performance of sampled data loops for subcarrier and carrier tracking 05 p0623 N85-13988
Device for frequency stabilization of microwave oscillators 06 p0788 N85-15033
Transmission line biased coherent array of Josephson oscillators
[AD-D011323] 07 p0944 N85-15979
Phased locked array laser systems
[AD-D011317] 07 p0971 N85-16164
Processing circuit with asymmetry corrector and convolutional encoder for digital data
[NASA-CASE-MSC-20187-1] 11 p1628 N85-20249
Double reference pulsed phase locked loop (DRP-2L-2)
[NASA-CASE-LAR-13310-1] 12 p1824 N85-21441
Phase function, backscatter, extinction, and absorption for standard radiation atmosphere and El Chichon aerosol models at visible and near-infrared wavelengths
[NASA-TM-86379] 12 p1662 N85-21874
New results on the PLL false lock phenomenon
12 p1948 N85-22236
Stereo decoder without subcarrier restoration
13 p2068 N85-22921
Study of phase radiogeodetic systems with phase-locked loops 13 p2115 N85-23172
System of phase-lock automatic frequency control with acoustoelectronic convolver 15 p2526 N85-25573
MHB4046 phase-lock circuit 15 p2533 N85-25629
Phase-locked loop design with MHB4046
15 p2534 N85-25631
Additional PLL designs 15 p2534 N85-25632
Digital filters for digital phase-locked loops
16 p2771 N85-27104
Phase-lock fiber optic interferometer
[AD-D011603] 16 p2786 N85-27191
Experimental performance of a frequency measurement circuit
[AD-A152951] 17 p2953 N85-28239
Atmospheric probing by active millimeter wave system
[AD-A153550] 18 p3136 N85-29422
Phase locked loop synchronization for direct detection optical PPM communication systems
[NASA-CR-176026] 19 p3254 N85-30178
Dielectric resonator stabilized microstrip oscillator
[AD-D011708] 19 p3261 N85-30219
Phase-locked loops for optical homodyne detection, volume 1 — spaceborne receivers
[ESA-CR(P)-2029-VOL-1] 20 p3442 N85-31367
Phase locked loops for optical homodyne detection, volume 2 — spaceborne receivers
[ESA-CR(P)-2029-VOL-2] 20 p3442 N85-31368
A phase-locked frequency multiplier for the signal averaging of the vibration of the Wessex helicopter input spiral bevel pinion
[AD-A154914] 21 p3555 N85-32113
Practicality of electronic beam steering for MST/ST radars, part 6.2A 21 p3624 N85-32516
General design principles of high speed frequency synthesizers based on phase synchronization systems
22 p3779 N85-33417
Wide-band phase locked loop amplifier apparatus
[AD-D011720] 23 p3927 N85-34337
Nonlinear digital phase-locked loops with application to Loran-C receivers 24 p4063 N85-35178

PHASE MATCHING

Huffman-coded pulse compression waveforms
[AD-A155322] 21 p3576 N85-32243

PHASE MODULATION

NT PHASE SHIFT KEYING
Digital radio link: Comparison of the resistance of two different 4-phase modulation forms to multipath propagation
[FOA-C-30362-E] 02 p0193 N85-11291
Visible wavelength interferometer for high speed electron density diagnostics
[AD-A145696] 02 p0277 N85-11603
Frequency shifting in multimode fiber optic phase modulation devices 03 p0347 N85-12239
Influence of mode noise suppression in multimode fiber optic light guides 03 p0348 N85-12242
Micro-waveguide transformers of coherent optical signals 07 p0950 N85-16022
L.F. RADIO-DATA: Specification of BBC phase-modulated transmissions on long-wave
[BBC-RD-1984/19] 12 p1622 N85-21431
Interference immunity of binary systems with second-order phase-difference modulation in various reception modes 13 p2072 N85-22944
Synthesis of optimum single-channel discrete signals and filters 13 p2080 N85-22960
Reception noise immunity of multiposition signals
13 p2085 N85-23023
The latitudinal variation of geomagnetic pulsation amplitude and phase 14 p2370 N85-24646
A phase modulation evaluation procedure for an ARGOS type signal 16 p2811 N85-27936
Experimental evaluation of a new form of M-ary (M = 8) phase shift keying including design of the transmitter and receiver
[AD-A155103] 21 p3576 N85-32239
A new description of combined trellis coding with asymmetric modulation
[NASA-CR-176197] 24 p4086 N85-35323

PHASE SHIFT

High frequency phase-noise in semiconductor lasers
[FUB-20-1983] 01 p0053 N85-10353
Metrological consequences of the hard optical boundary assumption
[PB84-223577] 01 p0121 N85-10827
Dynamics of growth of surface periodic structures when intense light acts on condensed media
02 p0268 N85-11748
Dust properties determined from backscattering in the interplanetary and interstellar medium
03 p0446 N85-12836
Extended X-ray absorption fine structure (Exafs) studies of the actinides
[DE84-015833] 04 p0559 N85-13561
Infralow-frequency digital phase meter
06 p0787 N85-15031
Tropospheric and ionospheric phase perturbations and Doppler frequency shift effects
[AD-A148579] 08 p1154 N85-17283
CO2 laser interferometer array for Big Dee
[DE85-001718] 10 p1490 N85-19411
Method and apparatus for measuring minority carrier lifetime in a direct band-gap semiconductor
[NASA-CASE-NPO-163371-1] 11 p1628 N85-20251
Double reference pulsed phase locked loop (DRP-2L-2)
[NASA-CASE-LAR-13310-1] 12 p1824 N85-21441
Combined microwave parallel amplifier-RF attenuator/modulator
[AD-D011535] 12 p1833 N85-21499
Wideband phase keyers 12 p1839 N85-21544
Use of electronic coding-frequency meters to measure parameters of pulsed radio signals
13 p2076 N85-22964
Change of electrical characteristics of radio-frequency cables under thermal effect 13 p2081 N85-22999
Calculation of image shift in panoramic photography
15 p2488 N85-25357
Relationship between Allan variances and Kalman Filter parameters 18 p3107 N85-29238
Thin film phase transition materials development program
[AD-A154260] 19 p3259 N85-30209
High switching speed electrically tuned microwave magnetic resonance devices
[AD-D011699] 19 p3260 N85-30217
Design of a jamming simulator for a binary communication system
[AD-A154617] 21 p3573 N85-32221
Solid state high power amplifier for driving the SLC injector klystron
[DE85-013063] 24 p4090 N85-35356
Analysis of two-parameter constant background born inversion for acoustic synthetic data
[AD-A156394] 24 p4145 N85-35698

PHASE SHIFT CIRCUITS

NT CIRCULATORS (PHASE SHIFT CIRCUITS)
Coplanar Schottky variable phase shifter
[AD-A146304] 03 p0359 N85-12305
Phase only adaptive nulling in a monopulse antenna
[AD-D011289] 05 p0628 N85-14026
Fast switching driver for inductive load, such as a phase shifter
[AD-D011368] 08 p1143 N85-17207
Low sidelobe phased array antenna system
[AD-D011558] 12 p1823 N85-21435
USSR report: Electronics and electrical engineering
[JPRS-UEE-85-002] 13 p2066 N85-22907
Wavelength multiplexer-demultiplexer
[AD-D011606] 16 p2777 N85-27140
High switching speed electrically tuned microwave magnetic resonance devices
[AD-D011699] 19 p3260 N85-30217
Dielectric resonator oscillators with digital temperature compensation
[AD-D011715] 19 p3261 N85-30221
East Europe report: Science and technology
[JPRS-ESA-85-021] 21 p3568 N85-32190

PHASE SHIFT KEYING

A transmission analysis for the use of 2-4 PSK modulation in satellite broadcasting
[ESA-STM-231] 04 p0494 N85-13151
Structure of frequency modulated and phase-shift keyed signals reflected from ionosphere at near-critical frequencies 07 p0952 N85-16035
AWOPSK: An optimum modulation technique for spread spectrum communication 09 p1311 N85-18235
A microprocessor controlled parallel model with FDPSK 10 p1475 N85-19304
Development of a 20 GHz modulator for the payload of a satellite for propagation and transmission experiments, including the required converters of the test equipment
[BMFT-FB-W-84-044] 11 p1580 N85-20004
Wideband phase keyers 12 p1839 N85-21544
Optimal discrete filtration of intricate phase-keyed signals 12 p1840 N85-21550
Regular synthesis of pairs of phase-keyed binary minimax signals 13 p2069 N85-22923
Dispersion of phase-shift keyed systems with fixed number of blocks 13 p2070 N85-22928
Analysis of characteristics of digital discriminators for phase-shift keyed signals 13 p2070 N85-22930
Combined processing method and matched filter for discrete composite frequency phase-shift keyed signal
13 p2070 N85-22931
Ionospheric distortions of digital signals with wideband modulation 13 p2072 N85-22945
Comparative analysis of noise tolerance of quasi-coherent phase shift keying signal demodulators
13 p2072 N85-22946
Transient processes in tuned amplifier during phase-shift keying with smooth phase variation
15 p2527 N85-25581
Analysis of space diversity techniques for EHF (Extremely High Frequency) satellite downlinks
[AD-A151900] 15 p2544 N85-25705
Bit error rate of coherent M-ary PSK
16 p2770 N85-27098
Serial Minimum Shift Keying (SMSK) follow-on study — spacecraft communication
[ESA-CR(P)-2026] 20 p3399 N85-31083
Modulation using four phase levels. Theoretical study of the degradation caused by a spurious phase modulation
[CNES-83/219/CT/DRT/TIT/TR]
20 p3441 N85-31360
Study of a limited band signal transmission chain
[CNES-CT/DRT/TIT/TR-83/221]
20 p3442 N85-31361
Receive shaping filter manufacture — QPSK uplinks
[ESA-CR(P)-1998] 20 p3449 N85-31412
Experimental evaluation of a new form of M-ary (M = 8) phase shift keying including design of the transmitter and receiver
[AD-A155103] 21 p3576 N85-32239
Transformation of spectrum of phase-code keyed signal for scanning in time 22 p3765 N85-33336
A new description of combined trellis coding with asymmetric modulation
[NASA-CR-176197] 24 p4086 N85-35323
DMSK: A practical 2400-bps receiver for the mobile satellite service: An MSAT-X Report
[NASA-CR-176194] 24 p4086 N85-35324
Necessary bandwidth and spectral properties of digital modulation
[PB85-185387] 24 p4088 N85-35340

PHASE TRANSFORMATIONS

NT BOILING
NT COAL LIQUEFACTION
NT EVAPORATION
NT EVAPOTRANSPIRATION
NT FILM BOILING
NT FLASHING (VAPORIZING)
NT FREEZING
NT FUSION (MELTING)
NT LEVITATION MELTING
NT LIQUEFACTION
NT MARTENSITIC TRANSFORMATION
NT MELTING
NT NUCLEATE BOILING
NT PROPELLANT EVAPORATION
NT SUBLIMATION
NT TRANSPIRATION
NT VACUUM MELTING
NT VAPORIZING
NT ZONE MELTING
Fabrication and characterization of Si3N4 ceramics without additives by high pressure hot pressing
[NASA-TM-77724] 01 p0031 N85-10189
Fundamental studies of structure property relationship in transformation toughened ceramics
[DE84-015344] 01 p0033 N85-10204
ICARUS: A general one-dimensional heat conduction code
[DE84-016125] 01 p0047 N85-10310
Influence of 5f electrons on structures and bonding in the actinide-hydrogen intermetallics
[DE84-013803] 01 p0118 N85-10807
Research program in theoretical high-energy physics
[DE84-013717] 01 p0119 N85-10817
Experiments with phase transitions at very high pressure
[NASA-CR-174029] 02 p0172 N85-11148

Alloying effects of reactive elements in ferritic stainless steels 02 p0178 N85-11196
The role of molybdenum as an alloy element in adhesive wear resistance 02 p0181 N85-11212
Metastable phase formation in ion implanted metals [DE84-014945] 02 p0183 N85-11229
Kinetics of short-range ordering in metallic glasses: Analysis of the crossover effect [DE84-015524] 02 p0187 N85-11251
Phase transition which exhibits 1/omega-spectrum: A rigorous result 02 p0283 N85-11842
High pressure cosmochemistry applied to major planetary interiors: Experimental studies [NASA-CR-174032] 02 p0302 N85-11958
Synthesis of stereoisomeric - metal complexes using phase-transfer catalysis and photochemical transforms [AD-A145787] 03 p0331 N85-12134
Microstructure development in polymers [AD-A145980] 03 p0337 N85-12170
Re-evaluation of phase separation in Ti-Zr-Be metallic glasses [DE84-015603] 03 p0338 N85-12176
Effect of heat treatment on phase composition and crystal structure of thin WSi2 films on silicon substrates 03 p0350 N85-12253
Structural recrystallization in titanium 03 p0351 N85-12258
Constitutive features of solids at shock-wave loading rates [DE84-015715] 03 p0362 N85-12325
Non-linear systems in infinite dimensional state spaces [AD-A145828] 03 p0410 N85-12623
Investigations of magnetic phase transitions with neutron scattering 03 p0423 N85-12700
Neutron scattering on structural phase transitions with domain building 03 p0425 N85-12711
Phase transformations of AlPO4 with SiO2 structures 03 p0425 N85-12713
Structural phase transitions in doped hexahalogen metallates 03 p0426 N85-12721
Center for dielectric studies [AD-A146183] 03 p0434 N85-12761
The 6th International Summer Institute in Surface Science 1983) [AD-A146253] 03 p0434 N85-12762
Thermodynamics and phase equilibria in the vanadium-silicon system [AD-A145870] 03 p0435 N85-12769
CVD parameter study using strategy of experimentation [DE84-015900] 04 p0473 N85-13011
Nonthermal mechanism for laser annealing of semiconductors and formation of super structure 04 p0487 N85-13109
Deterministic sensitivity analysis of two-phase flow systems: Forward and adjoint methods [DE84-016276] 04 p0499 N85-13185
Geology and geochemical evolution of the Lost River, Alaska, tin deposit 04 p0533 N85-13405
Zero-flux planes and flux reversals in multicomponent diffusion [DE84-015212] 05 p0618 N85-13950
A similarity analysis of phase change heat conduction in corners 05 p0634 N85-14069
Electrochemistry in near-critical and supercritical fluids. I. Ammonia [AD-A146429] 06 p0765 N85-14894
Phase equilibria of stored chemical energy reactants [AD-A146527] 06 p0765 N85-14896
Control of microstructure during hot working of Ti-6242 06 p0797 N85-15091
Reciprocal solubility of phases in multi-component systems [BLL-M-36003-(5828.4)] 07 p0926 N85-15870
A study of structural phase transitions using light scattering techniques [AD-A147261] 07 p1048 N85-16854
Passive storage technologies 08 p1108 N85-17003
Transient combustion: An important consideration in deflagration-to-detonation transition 08 p1116 N85-17037
The DDT process for high energy propellants 08 p1116 N85-17038
Phase-dissipative mechanisms for laser-induced surface desorption-dissociation processes [AD-A147961] 08 p1121 N85-17065
Research in phase transfer catalysis [AD-A148296] 08 p1121 N85-17068
Grain refining and microstructural modification during solidification [AD-A147705] 08 p1128 N85-17111
Phase diagram of polymer blends containing block copolymers [AD-A147706] 08 p1132 N85-17134
Structure-property relationships in thermoplastic elastomers. Part 1: Segmented polyether-polyurethanes [AD-A148043] 08 p1133 N85-17138
Structure-property relationships in intercalated graphite [AD-A147949] 08 p1219 N85-17680
Phase formation and stability in the pseudobinary Ni3Al-Ni3V alloy system [DE85-001117] 09 p1296 N85-18143
Radiation-induced compositional redistribution and local phase transformation in irradiated alloys [DE85-000080] 10 p1441 N85-19082
Determination of vapor phase content when metals are struck by laser radiation pulses of various densities 10 p1445 N85-19106
Study of the volumetric changes in VT23 alloy upon heating 10 p1448 N85-19123
Metal-nonmetal transitions in N-doped many-valley Si and Ge [INPE-3358-PRE/636] 10 p1562 N85-19848
A study of interdiffusion in beta + gamma/gamma + gamma prime Ni-Cr-Al [NASA-CR-174852] 11 p1597 N85-20041
Structure-phase state and properties of high-durability VAL8 alloy 11 p1597 N85-20046
Study of phase composition of Al-B plasma coatings 11 p1598 N85-20050
Phase transformations in vanadium alloys of titanium during quenching and tempering 11 p1602 N85-20073
Electric and magnetic properties of intercalated graphite [AD-A149648] 12 p1798 N85-21276
Hydrogen flame acceleration and transition to detonation [DE85-000611] 12 p1802 N85-21299
Alloy development, processing and characterization of devitrified titanium base microcrystalline alloys [AD-A149809] 12 p1806 N85-21327
Generalized radome BSE (radome boresight error) characterization using superposition techniques [AD-P004354] 12 p1825 N85-21448
Phase change thermal energy storage and the model building codes [PB85-111201] 12 p1883 N85-21813
Experimental determination of systems suitable for study as monotectic binary metallic alloy solidification models 12 p1948 N85-22235
Metal-semiconductor phase transition and its application [DRIC-T-7149] 13 p2021 N85-22665
Influence of hydrogen bonding in block copolymers and their blends 13 p2036 N85-22752
Local phase transformation in alloys during charged-particle irradiation [DE85-005012] 14 p2258 N85-23990
Dynamic shock studies of PZT 95/5 ferroelectric ceramic [DE85-006137] 14 p2261 N85-24015
The volume change during solidification [NASA-TM-77817] 14 p2300 N85-24243
Conversions in amorphous zirconium-vanadium alloy 15 p2496 N85-25400
Phase separation in polyurethanes: A deuterium NMR study [AD-A151515] 15 p2505 N85-25451
Eleven lectures on the physics of the quark-gluon plasma [DE85-004321] 15 p2662 N85-26431
Transformation of nitrogen oxides while sampling combustion products [AD-A152184] 16 p2746 N85-26945
Models of long-period superstructure [DE85-007659] 16 p2751 N85-26981
Research on the kinetics of phase changes in solids [AD-A152387] 17 p2918 N85-27989
Study of self-propagating condensed phase reactions TiB(2) synthesis [AD-A153198] 17 p2921 N85-28006
Microstructure-mechanical property relationships in transformation-toughened ceramics [DE85-009722] 17 p2935 N85-28117
Preparation of nitrocompounds [AD-A153687] 18 p3071 N85-29093
Chemical transformation modules for Eulerian acid deposition models. Volume 1: The gas-phase chemistry [PB85-173714] 18 p3072 N85-29001
Ten degree Kelvin hydride refrigerator [NASA-CASE-NPO-16393-1-CU] 18 p3085 N85-29084
Screening phase transitions in two-dimensional Coulomb gas [NOTA-INTERNA-830] 18 p3192 N85-29798
Pseudopotentials and total energy calculations: Applications to crystal stability, vibrational properties, phase transformations, and surface structures [DE85-007657] 18 p3194 N85-29810
Solid phase reactions among manganese, potassium perchlorate and barium chromate [HSE-TRANS-11166] 19 p3237 N85-30071
Fundamental studies of beta phase decomposition modes in titanium alloys [AD-A154122] 19 p3238 N85-30078
Study of phase equilibria and crystallization processes in Al-Zn-Mg alloy systems 19 p3241 N85-30098
High temperature Raman studies of phase transitions in thin film dielectrics [DE85-010973] 19 p3263 N85-30234
Clearing of polydisperse aqueous aerosol by laser radiation pulses 19 p3286 N85-30445
Comparison of the response of shape memory alloy actuators using air-cooling and water-cooling [AD-A155216] 21 p3567 N85-32185
The shearing contribution in transformation toughening of brittle materials [AD-A154858] 21 p3568 N85-32195
Aerobic sulfur-oxidizing bacteria: Environmental selection and diversification 21 p3656 N85-32712
Sulfur transformations at the hydrogen sulfide/oxygen interface in stratified waters and in cyanobacterial mats 21 p3657 N85-32715
The Konstantinov effect and absorption of sound in inhomogeneous media 21 p3680 N85-32961
An EPR (Electron-Paramagnetic-Resonance) and ENDOR (Electron-Nuclear-Double-Resonance) study of ferroelectric ammonium sulfate [AD-A155560] 21 p3710 N85-33033
Microstructure-mechanical property relationships in the transformation-toughened ceramics [DE85-011946] 22 p3752 N85-33261
Phase transformations taking place in austenitic steel during deformation at different rates [BLL-M-35875-(5828.4)] 23 p3914 N85-34254
Shape memory effect in uranium-niobium alloys below room temperature [DE85-012964] 23 p3916 N85-34268
Transient three-phase three-component systems. Part 1: Formulation of the system of differential equations [DE85-013267] 24 p4095 N85-35364

PHASE VELOCITY
Wave phase velocity in a wind gradient — gravity waves 04 p0523 N85-13343
Experimental determination of propagation rate of ELF signals employed by Omega radio navigation system for phase measurements 06 p0793 N85-15066
The development of a transducer system for the accurate measurement of ultrasonic phase delay of SH plate waves [AERE-R-11506] 15 p2559 N85-25790

PHASE-SPACE INTEGRAL
Phase space factors in multiparticle processes 24 p4175 N85-35888

PHASED ARRAYS
Reflector antenna having sidelobe suppression elements [AD-D011227] 01 p0039 N85-10244
Theory of near-field phased arrays for electromagnetic susceptibility testing [PB84-217836] 01 p0042 N85-10273
Phase only adaptive nulling in a monopulse antenna [AD-D011289] 05 p0628 N85-14028
Characteristics of circular-polarized printed radiators in planar phased antenna array 06 p0790 N85-15049
Investigation of characteristics of phased antenna array considering interaction between radiators and properties of power divider 06 p0790 N85-15051
MMIC devices for active phased array antennas [NASA-CR-174261] 07 p0936 N85-15943
Determination of row-and-column control principle of phase antenna array from amplitude-phase distribution of field in aperture 07 p0952 N85-16033
Short period guided waves over oceanic and continental paths [AD-A147053] 07 p0997 N85-16331
Configuration study for a 30 GHz monolithic receive array: Technical assessment [NASA-CR-174697] 09 p1311 N85-18238
Configuration study for a 30 GHz monolithic receive array, volume 1 [NASA-CR-174697-VOL-1] 09 p1311 N85-18239
Conformal phased array antenna pattern corrector [AD-D011489] 10 p1468 N85-19298
Design criteria for limited scan antennas at digital microwave line of sight links 10 p1471 N85-19284
Use of ground radar to detect reentering debris 12 p1784 N85-21200
Low sidelobe phased array antenna system [AD-D011558] 12 p1823 N85-21435

Method and apparatus for self-calibration and phasing of array antenna
[NASA-CASE-NPO-15920-1] 12 p1832 N85-21493
Wide angle phased array dome lens antenna with a reflection/transmission switch
[AD-D011562] 12 p1833 N85-21502
Phased antenna array for wind profiling applications
[PB85-132584] 12 p1837 N85-21529
Design considerations for high-altitude, long-endurance, microwave-powered aircraft
[NASA-TM-86403] 14 p2216 N85-23751
Interference immunity of optical radar system with phased antenna array 15 p2526 N85-25575
Cophasal horizontal wideband array antennas for transmitting with asymmetric output 15 p2526 N85-25576
Optical techniques for signal distribution and control in advanced radar and communication systems 16 p3188 N85-29773
Dual sense, circularly polarized helical antenna
[AD-D011690] 19 p3254 N85-30175
MMIC devices for active phased array antennas
[NASA-CR-176015] 19 p3254 N85-30177
New concepts in free electron lasers 20 p3460 N85-31493
Null synthesis with phase and amplitude controls at the subarray outputs
[AD-A155167] 21 p3576 N85-32241
Evaluation of the effects of roll angle on the natural convection heat transfer from an array of cylindrical spines
[AD-A154594] 21 p3583 N85-32273
Most desirable terrain, e.g., flat vs valley location, part 5.1B 21 p3624 N85-32513
Adaptive synthesis of antennas with separation of signals by direction of arrival 22 p3764 N85-33328
Frequency independent parabolic phased antenna array of log periodic antennas 22 p3774 N85-33387

PHENOLIC RESINS
Investigation of the effects of NaOH dopant level on the physical and mechanical properties of carbon/phenolic composite material 12 p1945 N85-22213
Mechanical modification of friction surfaces of aluminum alloys by friction transfer 19 p3241 N85-30097
Long-term strength of glass fibre/phenolic resin composites
[NPL-DMA(A)-98] 22 p3742 N85-33195
Poly-functional building material from fiberglass (its fabrication and properties) 23 p3908 N85-34209

PHENOLOGY
NOAA-AISC user's guide for implementing CERES maize model for large area yield estimation
[E85-10083] 12 p1873 N85-21748
User's guide to the TAMW wheat model as implemented on the IBM 360/195 computer
[E85-10084] 12 p1873 N85-21749
NOAA-AISC user's guide for implementing CERES wheat model for large area yield estimation
[E85-10085] 12 p1873 N85-21750
Estimating solar radiation for plant simulation models
[E85-10086] 12 p1873 N85-21751

PHENOLS
Preliminary evaluation of an improved flammability test method for aircraft materials
[FAA-CT-84-22] 08 p1080 N85-16840
Synthesis of phenols from metal-carbynes and diynes
[AD-A151913] 16 p2754 N85-26097
SRB attach ring phenolic TPS fishtail seal evaluation tests
[NASA-CR-170697] 24 p4096 N85-35407

PHENOMENOLOGY
NT MESOSCALE PHENOMENA
NT PHENOLOGY
An internally consistent gamma ray burst time history phenomenology
[OG-1.2-6] 22 p3862 N85-33916

PHENYLS
NT POLYCHLORINATED BIPHENYLS
NT POLYPHENYLS
NT TRIPHENYLS
Effect of substituted phenylnadimides on processing and properties of PMR polyimide composites
[NASA-TM-88902] 06 p0770 N85-14929
Polymerization and halogen scrambling behavior of phenyl-substituted cyclotriphosphazenes
[AD-A146366] 06 p0771 N85-14930
The synthesis and characterization of Poly(Oxy(2-Methyl-1,3-Phenylene) Methyl-1,3 -Phenylene) Oxyterephthaloyl)Oxy
[AD-A146269] 06 p1133 N85-17143
Acute oral toxicity (LD50) of 4-nitrophenyl monochloromethyl (Phenyl) phosphinate (TA009) in male rats
[AD-A148337] 08 p1192 N85-17513
Ideal gas thermodynamic properties for the phenyl, phenoxy, and o-biphenyl radicals
[NASA-TM-83800] 12 p1943 N85-22204
Preparations of methoxynitrophenazines and their photoconductivities
[NASA-TM-77775] 14 p2247 N85-23929
Substituent effects on the electrical conductivities of the phenazine derivatives
[NASA-TM-77792] 14 p2249 N85-23938

PHILOSOPHY
NT PARADOXES
Outer space law: A problem of astronautics
[NASA-TM-77760] 07 p1055 N85-16697
Discovery refutation and verification refutation: The proposals of Von Neumann and Wiener in the development of 20th century physics
[NOTA-INTERNA-840] 14 p2431 N85-24993
The Impact of Science on Society
[NASA-SP-482] 14 p2431 N85-24994
The legacy of science 14 p2432 N85-24995

PHOBIAS
NT FEAR OF FLYING

PHOBOS
Structure and origin of Martian satellites 15 p2483 N85-25323

PHONEMES
Vowel phoneme identification in speech
[FUB-26-1983] 01 p0040 N85-10257
Comparative analysis of the clustering of the LPC coefficients in phoneme recognition
[FUB-39-1983] 01 p0041 N85-10264
Research in continuous speech recognition
[AD-A150474] 13 p2055 N85-22868
Implementation of a real-time, interactive, continuous speech recognition system
[AD-A151936] 16 p2773 N85-27117
Evaluating syntactic constraints to speech recognition in a fighter aircraft environment
[AD-A152117] 16 p2773 N85-27119
Study to determine potential flight applications and human factors design guidelines for voice recognition and synthesis systems
[NASA-CR-172590] 20 p3440 N85-31349
Phonetic transcription statistics: Constitution and statistical utilization
[ENST-85D001] 22 p3756 N85-33285

PHONETICS
Voice phonetic coding and decoding processes
[FUB-29-1983] 01 p0040 N85-10259
Research in continuous speech recognition
[AD-A150474] 13 p2055 N85-22868
Automation of the process of speech signal segmentation in an analogic-numeric system
[REPT-5/1984] 16 p2768 N85-27082
Phonetic transcription statistics: Constitution and statistical utilization
[ENST-85D001] 22 p3756 N85-33285

PHONOCARDIOGRAPHY
NT ECHOCARDIOGRAPHY

PHONONS
Phonon anomalies in superconducting transition metal compounds — lanthanum and niobium compounds 03 p0426 N85-12718
Folded acoustic and quantized optic phonons in semiconductor superlattices
[AD-A145935] 03 p0433 N85-12756
Phonon-impurity relaxation and acoustic wave absorption in yttrium-aluminum garnet crystals with impurities 11 p1715 N85-20790
Effect of impurities on absorption in semiconductors and lasing of semiconductor lasers 11 p1716 N85-20797
Electrical and thermal transport property studies of high-temperature thermoelectric materials
[AD-A150900] 14 p2427 N85-24967
Infrared nonlinear processes in semiconductors
[AD-A150986] 14 p2427 N85-24968
Raman studies of surface temperature in laser-heated semiconductors
[AD-A151377] 15 p2659 N85-26412
Theory of laser-stimulated surface process. 2: A generalized-master-equation approach to energy transfer between an IR laser, an aspecties and phonons
[AD-A153083] 17 p2970 N85-28344
Localization of waves in a disordered medium 19 p3373 N85-30926
Influence on bi-phonon states on Raman scattering of light in molecular crystals 21 p3680 N85-32865
Influence of phonon interaction on width and form of Mandelstam-Brillouin optical scattering line 21 p3696 N85-32962
Calculating the interatomic pair potential allowing for resonance interaction in titanium, nickel and vanadium
[BLL-M-35843-(5826.4)] 23 p3913 N85-34249

PHOSPHATES
NT ADENOSINE DIPHOSPHATE
NT ADENOSINE TRIPHOSPHATE
NT CALCIUM PHOSPHATES
NT INDIUM PHOSPHATES
NT POTASSIUM PHOSPHATES
Identification and parameter estimation of phosphate balance models in drinking water reservoirs
[PUBL-313] 08 p1181 N85-17439
Geographic variation in the relationships of temperature, salinity or sigma sub t versus plant nutrient concentrations in the world ocean --- silicic acid, nitrate, and phosphate concentration
[NASA-CR-175621] 13 p2140 N85-23287
Water-resistance and some other properties of polyalkali fluorophosphate glasses 14 p2281 N85-24133
Addendum to the STCAL and LTCAL user's guide
[NASA-CR-171880] 15 p2628 N85-26184
Characteristics of polyacrylic acid-complexed zinc phosphate conversion films deposited on metal surfaces
[DE85-004057] 16 p2750 N85-26974
Characteristics of charge transfer in the dispersed phase of electrorheological suspensions
[RAE-TRANS-2125] 19 p3233 N85-30040
Design of micelles as dephosphorylating agents
[AD-A155589] 21 p3564 N85-32166
Microanalysis of dissolved iron and phosphate in pore waters of hypersaline sediment 21 p3661 N85-32744
Applications of the mineral resources data system and the international strategic minerals inventory in mineral-resource assessments by region and commodity 24 p4105 N85-35451

PHOSPHAZENE
Polymerization and halogen scrambling behavior of phenyl-substituted cyclotriphosphazenes
[AD-A146366] 06 p0771 N85-14930
(Vinyloxy)fluorocyclotriphosphazenes
[AD-A147448] 07 p0924 N85-15850
Polyphosphazene solid electrolytes
[AD-A147008] 07 p0931 N85-15902
New synthesis of phosphazene polymers
[AD-A147567] 07 p0933 N85-15910
(Vinyloxy)chlorocyclotriphosphazenes
[AD-D011471] 10 p1453 N85-19152
The synthesis and structure of polyphosphazenes
[AD-A153134] 17 p2934 N85-28112

PHOSPHIDES
NT GALLIUM PHOSPHIDES
NT INDIUM PHOSPHIDES
Vaporization behavior of chromium phosphides. The solid 2-phase regions CrP-Cr12P7, Cr12P7-Cr3P, and Cr3P-Cr
[AD-A145481] 02 p0172 N85-11152
Magnetic susceptibility, electrical resistivity, and specific heat of single crystal LaFe-4P-12
[DE84-009979] 04 p0570 N85-13633
Vaporization behavior, phase equilibria, and thermodynamic stabilities of nickel phosphides
[AD-A146863] 06 p0765 N85-14897
The UFe4P12 and CeFe4P12: Non-metallic isotopes of superconducting LaFe4P12
[DE85-003724] 12 p1942 N85-22195
Thin film cadmium telluride and zinc phosphide solar cells
[DE85-002904] 15 p2587 N85-25950
Photoelectronic properties of zinc phosphide crystals and heterojunctions
[DE85-006777] 19 p3307 N85-30501

PHOSPHINES
Macrocyclic poly(tertiary) phosphines for the attachment of metals to surfaces of photodevices
[DE84-015552] 05 p0617 N85-13946
Fluorinated aliphatic polyalkylether lubricant with an additive composed of an aromatic phosphine substituted with perfluoroalkylether groups
[AD-D011266] 06 p0770 N85-14927
New synthesis of phosphazene polymers
[AD-A147567] 07 p0933 N85-15910
Detection of the J-10 manifold of the pure rotational band of phosphine on Saturn 08 p1245 N85-17855
Isomer enumeration in polytertiary phosphines and related compounds
[AD-A148058] 09 p1290 N85-18099
Phosphorus-containing imide resins
[NASA-CASE-ARC-11368-2] 12 p1809 N85-21347

PHOSPHORESCENCE
Intermolecular energy transfer between the individual zero-field levels of triplet traps in an orientationally disordered solid
[AD-A150751] 14 p2417 N85-24914
Photophysical studies of triplet exciton processes in pure polymer films
[DE85-008571] 18 p3080 N85-29056
Beam tests of phosphorescent screens
[DE85-009843] 18 p3097 N85-29170

PHOSPHORIC ACID
Electrochemical behavior of amorphous alloys based on iron, cobalt and nickel in H3PO4 solutions alone and mixed with HF 15 p2513 N85-25505
Mechanical properties of adhesively bonded aluminum structures protected with hydration inhibitors [AD-A153755] 18 p3079 N85-29047
Improved acid electrolytes for fuel cells [PB85-176053] 18 p3132 N85-29397
System for the continuous generation of phosphorous aerosols from red phosphorus-butyl rubber [DE85-013527] 24 p4072 N85-35232

PHOSPHORIC ACID FUEL CELLS
Manual of phosphoric acid fuel cell power plant optimization model and computer program [NASA-CR-174721] 01 p0067 N85-10445
Manual of phosphoric acid fuel cell stack three-dimensional model and computer program [NASA-CR-174722] 01 p0067 N85-10447
Electrocatalysis of fuel cell reactions: Investigation of alternate electrolytes [NASA-CR-174753] 02 p0222 N85-11455
Phosphoric acid fuel cell power plant system performance model and computer program [NASA-CR-174638] 02 p0222 N85-11456
Gas cooled fuel cell systems technology development [NASA-CR-174732] 07 p0991 N85-16291
Electric utility acid fuel cell stack technology advancement [NASA-CR-174804] 08 p1178 N85-17422
Preparation and evaluation of advanced catalysts for phosphoric acid fuel cells [NASA-CR-168223] 10 p1508 N85-19511
Develop and test fuel cell powered on-site integrated total energy systems. Phase 3: Full-scale power plant development [NASA-CR-174887] 15 p2586 N85-25941
F-cell: The Aspen fuel cell model [DE85-001975] 18 p3131 N85-29393
New catalysts and new electrolytes for acid fuel cells [DE85-009940] 19 p3307 N85-30498

PHOSPHORS
Research on electroluminescence in thin film yttrium oxysulfide [AD-A146909] 07 p1037 N85-16582
Applications of pulsed-laser techniques and thermographic phosphors to dynamic thermometry of rotating surfaces [DE85-000403] 11 p1639 N85-20328
Investigation of basic characteristics of laser heating in thermoluminescence and of laser-stimulated luminescence [AD-A152143] 16 p2790 N85-27212
Streak tube characterization [DE85-009874] 17 p2956 N85-28255

PHOSPHORUS
Mechanical properties of a leaded, resulfurized, rephosphorized steel in various thermo/mechanical conditions [PB84-216464] 03 p0333 N85-12144
Is phosphorus predictably incompatible in igneous processes? 04 p0583 N85-13722
Global carbon - nitrogen - phosphorus cycle interactions: A key to solving the atmospheric CO2 balance problem? 05 p0652 N85-14188
Interactions of the marine phosphorus and carbon cycles 05 p0653 N85-14190
Plasma deposition of amorphous metal alloys [DE85-000768] 09 p1295 N85-18132
Study of processes of modification of Al-Si alloys 13 p2026 N85-22695
Determination of symmetry of immediate surroundings in amorphous Co-P alloys 15 p2496 N85-25396
Influence of phosphorus content and heat treatment on the machinability of electroless nickel deposits [DE85-007250] 15 p2522 N85-25548
Addendum to the STCAL and LTCAL user's guide [NASA-CR-171860] 15 p2628 N85-26194
Multiphoton production and detection of atoms [AD-A155561] 21 p3702 N85-33000
Precision measurements of solar energetic particle elemental composition [PAPER-SH-2.1-4] 21 p3715 N85-33052
Fire-resistant phosphorus containing polyimides and copolyimides [NASA-CASE-ARC-11522-2] 23 p3918 N85-34280
Marine phosphorite deposits model for exploration, with emphasis on deposits in the US Atlantic coastal plain 24 p4104 N85-35439

PHOSPHORUS COMPOUNDS
NT ADENOSINE DIPHOSPHATE
NT ADENOSINE TRIPHOSPHATE
NT CALCIUM PHOSPHATES
NT GALLIUM PHOSPHIDES
NT INDIUM PHOSPHATES
NT INDIUM PHOSPHIDES
NT ORGANIC PHOSPHORUS COMPOUNDS
NT PHOSPHATES
NT PHOSPHIDES
NT PHOSPHINES
NT PHOSPHORIC ACID
NT PHOSPHORUS POLYMERS
NT POTASSIUM PHOSPHATES
The effect of temperature on the radiation induced losses of large diameter GPS (Germanium phosphosilicate) and GBS core optical fibers [AD-A145409] 02 p0280 N85-11823
Study of singlet oxygen-pentavalent phosphorus reactions [AD-A145898] 03 p0327 N85-12107
USSR report: Chemistry [JPRS-UCH-84-012] 06 p0761 N85-14865
Magnetically-induced luminescence of (Ir(2=phos)(2)C10(4) [AD-A149659] 12 p1799 N85-21286
Structural inhomogeneities in amorphous nickel-phosphorus alloy [BLL-M-36103-(5826.4)] 16 p2748 N85-26960
Zn3P2 as an improved semiconductor for photovoltaic solar cells [DE85-008772] 18 p3097 N85-29171
Improved acid electrolytes for fuel cells [PB85-176053] 18 p3132 N85-29397

PHOSPHORUS METABOLISM
The role of 1,25-dihydroxyvitamin D in the inhibition of bone formation induced by skeletal unloading [NASA-TM-87460] 18 p3153 N85-29622

PHOSPHORUS POLYMERS
Phosphorus-containing imide resins [NASA-CASE-ARC-11368-2] 12 p1809 N85-21347

PHOSPHORYLATION
Design of micelles as dephosphorylating agents [AD-A155589] 21 p3584 N85-32166

PHOTOABSORPTION
Experimental capabilities and prospects for measuring soft X-ray photoabsorption [DE84-015488] 02 p0276 N85-11813
Electron-hole plasma formation in semiconductors due to the absorption of pulsed CO2 laser light [DE85-001559] 09 p1392 N85-18757
Workshop report on new directions in soft X-ray photoabsorption [DE85-006150] 14 p2419 N85-24923
Heliocentric sail problem with variable gravity field reduction 16 p2724 N85-26816
Quantitative studies for photoabsorption and fluorescence of HCl [NASA-CR-175965] 19 p3233 N85-30043
Photoabsorption and photodissociation of molecules important in the interstellar medium [NASA-CR-175916] 19 p3383 N85-30986
High-resolution spectroscopy and dynamics of multiphoton processes in atoms and molecules [AD-A155662] 24 p4147 N85-35714

PHOTOACOUSTIC MICROSCOPY
Photoacoustic microscopy of oxygen contaminated titanium alloys [AD-P004127] 08 p1127 N85-17102
Photoacoustic imaging [AD-A150823] 14 p2416 N85-24905

PHOTOACOUSTIC SPECTROSCOPY
Optoacoustic spectroscopy [AD-A145995] 03 p0419 N85-12679
Physico-chemical investigation of some areas of fundamental significance to biophysics [DE84-016385] 04 p0471 N85-12999
High resolution photoacoustic and photothermal imaging 05 p0723 N85-14849
Investigations of photochemistry using holography and photoacoustic spectroscopy [AD-A146837] 06 p0810 N85-15149
A study of the chemical interaction of gases with activated carbon [AD-A147342] 07 p0923 N85-15848
Photoacoustic microscopy of oxygen contaminated titanium alloys [AD-P004127] 08 p1127 N85-17102
Photoacoustic spectroscopy at electrode-solution interface [DE85-001872] 09 p1292 N85-18111
Photoacoustic effect and its applications 12 p1820 N85-21421
Experimental investigation of the pulsed photoacoustic effect produced on a solid surface [AD-A152114] 16 p2960 N85-27640
Single-pulse Raman and photoacoustic spectroscopy studies of Triaminotrinitrobenzene (TATB) and related compounds [DE85-010072] 18 p3084 N85-29078
Photo-acoustic effect in finite-dimensional semiconductors 21 p3682 N85-32876

PHOTOCATHODES
Programmable optical sensor [AD-D011244] 02 p0281 N85-11829
Fore-optics systems designed for electronic streak cameras using fiber optics [DE84-014625] 02 p0281 N85-11830
A microchannel plate streak camera [DE84-016536] 06 p0811 N85-15153
S-11 and S-20 photocathode research activity, revision 1 [DE84-017164] 09 p1326 N85-18335
Development and application of low energy X-ray and electron physics [AD-A149963] 12 p1925 N85-22099
High-resolution SIT TV tube for subnanosecond image shuttering [DE85-005189] 13 p2065 N85-23072
Streak tube characterization [DE85-009874] 17 p2956 N85-28255
Microchannel plate streak camera [DE85-011604] 20 p3458 N85-31481
On the possibilities of large-scale radio and fiber optics detectors in cosmic rays [HE-4.6-2] 24 p4196 N85-36039

PHOTOCELLS
U PHOTOELECTRIC CELLS

PHOTOCHEMICAL OXIDANTS
Air quality for ozone and other photochemical oxidants. External review draft, volume 1 [PB85-126035] 11 p1679 N85-20582
Air quality criteria for ozone and other photochemical oxidants. External review draft, volume 5 [PB85-126076-VOL-5] 11 p1679 N85-20583
Air quality criteria for ozone and other photochemical oxidants. External review draft, volume 2 [PB85-126043] 12 p1886 N85-21836
Air quality criteria for ozone and other photochemical oxidants, external review draft, volume 3 [PB85-126050] 12 p1886 N85-21837
Evaluation of chemical reaction mechanisms for photochemical smog. Part 2: Quantitative evaluation of the mechanisms, revised [PB85-166060] 16 p2822 N85-27406
Development of a chemical kinetic mechanism for the US EPA (Environmental Protection Agency) regional oxidant model [PB85-185858] 22 p3813 N85-33618

PHOTOCHEMICAL REACTIONS
NT PHOTOCHROMISM
NT PHOTODECOMPOSITION
NT PHOTOLYSIS
NT PHOTOSYNTHESIS
NT RADIOLYSIS
A determination of the photochemical quantum yields from 2 excited triplet states of biacetyl using holography [AD-A145091] 01 p0050 N85-10326
Research on photoelectrochemical cells based on CdSe, CdSe/sub 1-x/te/sub x and other photoelectrode materials [DE84-004527] 02 p0224 N85-11466
Aeronomy 02 p0298 N85-11930
Synthesis of stereoisomeric - metal complexes using phase-transfer catalysis and photochemical transforms [AD-A145787] 03 p0331 N85-12134
Three-dimensional photochemical machining with lasers [AD-A145792] 03 p0365 N85-12342
Interaction of UV-laser radiation with molecular surface-films [AD-A145311] 03 p0366 N85-12349
A 2-dimensional description of potential perturbations to the ozone layer due to NOx and H-2-O aircraft emissions [AD-A146292] 03 p0392 N85-12511
Regional-scale (1000 KM) model of photochemical air pollution. Part 2: Input processor network design [PB84-232651] 04 p0532 N85-13400
The nitrogen cycle: Atmosphere interactions 05 p0653 N85-14191
Aspects of the comparison of stratospheric trace species measurements with photochemical models [DE84-017028] 05 p0672 N85-14317
Determination of Toluene's degradation products under simulated atmospheric conditions 05 p0674 N85-14331
Investigations of photochemistry using holography and photoacoustic spectroscopy [AD-A146837] 06 p0810 N85-15149
Production of hydrogen by cyanobacteria [PB85-113421/GAR] 07 p0935 N85-15925
Photochemistry and kinetics of the O*2-HI system [AD-A147433] 07 p0971 N85-16167
Variation in photosynthesis with light level for model with two photochemical reactions 07 p1012 N85-16430

Conference on Singlet Molecular Oxygen (COSMO 84), program and abstracts
[AD-A147281] 07 p1040 N85-16605
Atmospheric photochemical modeling of turbine engine fuels. Phase 1: Experimental studies. Volume 2: Environmental chamber data tabulations
[AD-A147786] 08 p1185 N85-17470
Dynamics and mechanisms of catalytic processes and hot chemistry
[DE85-002899] 09 p1292 N85-18114
Hydrogen from solar energy
[DE85-001914] 10 p1437 N85-19055
Non-photochemical interactions of sulfur and nitrogen compounds in acid deposition
[DE84-016141] 10 p1513 N85-19546
Photosynthesis of ammonia
[DE85-001482] 11 p1595 N85-20029
Middle Atmosphere Program. Handbook for MAP, volume 4
[NASA-CR-175462] 11 p1654 N85-20420
The Middle Atmosphere Program: Winter in Northern Europe (MAP/WINE) 11 p1655 N85-20429
Energy transfer and photochemistry in biomimetic solar conversion
[PB85-129112] 11 p1677 N85-20566
User's guide for the Photochemical Box Model (PBM)
[PB85-137164] 11 p1682 N85-20602
Primary light harvesting system: The relationship of phycobiliosmes to photosystem 1 and 2
[DE85-003075] 11 p1689 N85-20622
Photo-thermal detection of the onset of photo-chemical nucleation (laser-snow) in vapor
[AD-A150111] 12 p1801 N85-21295
Gas-liquid chemistry of natural waters, volume 1
[DE85-002603] 12 p1884 N85-21822
Gas-liquid chemistry of natural waters, volume 2
[DE85-002457] 12 p1884 N85-21823
Air quality criteria for ozone and other photochemical oxidants. External review draft, volume 4
[PB85-126068] 12 p1886 N85-21838
Chemical kinetics and photochemical data for use in stratospheric modeling. Evaluation number 6
[NASA-CR-175564] 12 p1888 N85-21849
Chemical stabilization of laser dyes
[AD-A150451] 13 p2096 N85-23076
Composition and photochemical reactivity of turbine engine exhaust
[AD-A150559] 13 p2130 N85-23256
A theoretical study of the ozone quasi-biennial oscillation in the tropical stratosphere 13 p2132 N85-23264
Investigation and optimization of fuel production using dye-based transition metal complexes as charge-transfer intermediates
[PB85-161941] 14 p2264 N85-24029
One-dimensional nonstationary model of photochemical transformations of gas impurities in stratosphere 14 p2342 N85-24484
Sensitization and quenching in the conversion of light energy into chemical energy
[DE85-006301] 14 p2351 N85-24535
Applications of photoinduced electron transfer and hydrogen abstraction reactions to chemical and electrochemical conversion processes
[DE85-006068] 15 p2506 N85-25459
Eight DOE Solar Photochemistry Research Conference: Proceedings
[DE85-005094] 15 p2587 N85-25948
Measurement of elements in the stratosphere
[NASA-CR-175891] 16 p2823 N85-27414
Free radicals in the stratosphere: A new observational technique 16 p2824 N85-27415
Effect of traffic and meteorology on air pollution 16 p2830 N85-27452
The enhancement of molecular fluorescence and photochemistry by small metal particles
[AD-A152740] 17 p2919 N85-27904
Photochemical ignition studies. 1: Laser ignition of flowing premixed gases
[AD-A153046] 17 p2920 N85-28002
Photochemistry of coordination complexes: The phthalocyanines
[DE85-007693] 17 p2923 N85-28022
Technique for measuring surface diffusion by laser-beam-localized surface photochemistry
[DE85-007895] 18 p3113 N85-29273
Impact of alcohol fuels on urban air pollution: Methanol photochemistry study
[DE85-009639] 18 p3133 N85-29403
Kinetics and intensity of photochemical processes in the atmosphere
[BPT-10/84] 18 p3134 N85-29411
Investigation of the reaction system NOX/ClOX/HOX under tropospheric and stratospheric conditions
[BPT-11/84] 18 p3137 N85-29427
Photochemical processes in the lower stratosphere (ozone layer) 18 p3148 N85-29490
Radiation damage and repair in cells and cell components. Part 2: Physical radiations and biological significance
[DE85-008934] 18 p3152 N85-29516
The diurnal variation of the neutral sodium species in the upper atmosphere: A model study
[AD-A154988] 21 p3631 N85-32561
Photochemical aerosol formation in polluted atmosphere 21 p3644 N85-32642
A study of time transformation of natural photochemical aerosols 21 p3645 N85-32644
Process for functionalizing alkanes
[DE85-006420] 23 p3909 N85-34219
Electron photoejection in carbanions
[DE85-011747] 23 p3911 N85-34230
Electron photoejection in carbanions
[DE85-011748] 23 p3912 N85-34237
The photodissociation of acetylene at 193.3 NM
[AD-A155775] 24 p4075 N85-35255
Vectorial electron transfer on designed surfaces
[PB85-204600] 24 p4076 N85-35263
Studies in photochemical smog chemistry. 1: Atmospheric chemistry of toulene. 2: Analysis of chemical reaction mechanisms for photochemical smog 24 p4113 N85-35497

PHOTOCHEMISTRY
U PHOTOCHEMICAL REACTIONS

PHOTOCHROMISM
Method for the preparation of photochromic insulating crystals
[DE85-011606] 19 p3262 N85-30229

PHOTOCLINOMETRY
U PHOTOGRAMMETRY

PHOTOCONDUCTIVE CELLS
Magnetic and photoconductive repetitive rail-gun opening switches
[DE84-017080] 04 p0496 N85-13163
A general purpose image processing package 23 p3961 N85-34549

PHOTOCONDUCTIVITY
Effect of light pulses on film of chalcogenide vitreous semiconductors 02 p0258 N85-11687
Photoconductivity and emission from the impurity excited states in silicon
[DE84-015563] 04 p0479 N85-13052
Advanced amorphous materials for photovoltaic conversion
[DE84-017198] 04 p0529 N85-13384
Real-time analysis of space characteristics of microwave electromagnetic pulse fields by means of controllable layer structures 07 p0955 N85-16052
Density of states and recombination in amorphous silicon (a-Si:H)
[BMFT-FB-T-84-216] 08 p1135 N85-17151
Studies on organic semiconductors. 15: Effects of the substituents on the photoconductivities of substituted anthracenes
[NASA-TM-77788] 08 p1225 N85-17712
Development of photoconductive power switch technology
[DE85-001514] 09 p1315 N85-18270
Optical memory research and its application to digital optical processing 13 p2158 N85-23397
Preparations of methoxynitrophenazines and their photoconductivities
[NASA-TM-77775] 14 p2247 N85-23929
Substituent effects on the electrical conductivities of the phenazine derivatives
[NASA-TM-77792] 14 p2249 N85-23936
Investigation of the MBE growth of InSb and novel quantum well structures
[AD-A151014] 14 p2427 N85-24969
Properties of defects in Hg(1-x)Cd(x)Te
[AD-A153243] 17 p3044 N85-28835
Picosecond photoconductive devices for 10 Gbit/s optoelectronic switching 18 p3187 N85-29770
Drift mobilities by time-of-flight methods and time-dependent phototransport in the nanosecond regime in amorphous semiconductors
[DE85-008729] 18 p3194 N85-29815
A study of Co and Mn in ZnO varistors
[DE85-011193] 19 p3263 N85-30233
Photoeffects of semiconductor electrolyte interfaces
[AD-A154163] 20 p3449 N85-31411
Electron irradiation of N type cadmium telluride
[AD-A156117] 24 p4161 N85-35801

PHOTOCONDUCTORS
Photocopiers: Do they pose a health hazard?
[P83-1E] 02 p0234 N85-11527
Effect of an underlayer of cadmium telluride on the reflection-reducing properties of zinc sulfide on mercury cadmium telluride
[AD-A146195] 03 p0414 N85-12649
Physics and design of advanced infrared bolometers and photoconductors
[DE84-016883] 04 p0503 N85-13213
Development of high responsivity Ge:Ga photoconductors
[DE84-016902] 04 p0571 N85-13643
Development of photoconductive power switch technology
[DE85-001514] 09 p1315 N85-18270
Picosecond photoconductive devices for 10 Gbit/s optoelectronic switching 18 p3187 N85-29770
Photoconductive pulse power switches: A review
[DE85-014125] 24 p4091 N85-35360

PHOTOCURRENTS
U ELECTRIC CURRENT
U PHOTOELECTRIC EMISSION

PHOTODECOMPOSITION
The detection and study of molecular species using time resolved laser spectroscopy
[AD-A155910] 24 p4075 N85-35256

PHOTODETACHMENT
Characterization of multiphoton ionization processes in the ultraviolet
[AD-A151427] 15 p2652 N85-26354

PHOTODETECTORS
U PHOTOMETERS

PHOTODIODES
A concept for a hadron calorimeter with photodiode readout
[MPI-PAE/EXP-E1-130] 01 p0050 N85-10332
Improvements in photodiode readout for small CsI (Tl) crystals
[MPI-PAE/EXP-E1-131] 01 p0051 N85-10333
Fine grained hodoscopes based on scintillating optical fibers
[DE84-014849] 01 p0120 N85-10825
Pulsed irradiation of optimized, MBE grown, AlGaAs/GaAs radiation hardened photodiodes
[DE84-014984] 04 p0569 N85-13631
Avalanche photodiode statistics in triggered-avalanche detection mode 05 p0623 N85-13987
Study in spurious sensitivity of electronics in space
[AD-A148386] 08 p1158 N85-17305
The use of self-scanned silicon photodiode arrays for astronomical spectrophotometry 08 p1252 N85-17907
Photodiodes for astronomical stellar radiometry 08 p1252 N85-17908
GaAlAs Sb APD optimization
[AD-A149406] 10 p1480 N85-19344
Linear, position-sensitive X-ray detector used for real-time calculations of small-angle scattering parameters with submillisecond resolution
[DE85-002530] 10 p1489 N85-19401
Focal plane array optical proximity sensor
[NASA-CASE-NPO-15155-1] 12 p1932 N85-22139
Optoacoustic receiver with semiconductor-type radiator and photodetector 14 p2274 N85-24086
OMEGA: An optronic device to measure the incidence angle of a projectile
[ISL-CO-207/83] 14 p2306 N85-24274
Photon detection with cooled avalanche photodiodes: Theory and preliminary experimental results 16 p2770 N85-27096
Self-scanning MDS-integrated photosensor strip 17 p2940 N85-28151
Rita of Sweden conducts research in 3-5 materials 18 p3088 N85-29107
Development of photodetectors
[AD-A153773] 18 p3095 N85-29158
Summary of recent studies on AlGaAs/GaAs radiation hardened photodiodes
[DE85-009501] 18 p3194 N85-29812
Noise characteristics of an avalanche photodiode
[AD-A154096] 19 p3258 N85-30205
Particle sizing from forward scattered light at two angles using a Variable-Focal-Length optical system
[AD-A154164] 20 p3533 N85-31980
Application of photodiodes to the detection of electromagnetic bursts 24 p4189 N85-35988

PHOTODISSOCIATION
Solar radiation in the ozone layer 04 p0522 N85-13342
Theoretical studies of highly ionized species
[DE84-016797] 04 p0561 N85-13574
Laboratory studies of atomic collision processes of importance in planetary atmospheres
[NASA-CR-174142] 04 p0589 N85-13758
Excimer laser photofragmentation of organophosphonates. 1: Detection of the PO radical from dimethyl methyl phosphonate (DMMP)
[AD-A149471] 10 p1490 N85-19407
Aeronomical aspects of mesospheric photodissociation: Processes resulting from the solar H Lyman alpha line
[AERONOMICA-ACTA-A-285-1984] 11 p1680 N85-20587
Multiple product channels in the collision free UV photodissociation of 2-nitropropane
[AD-A150886] 14 p2251 N85-23951

The source of stratospheric NO and N2O
[NASA-CR-175713] 15 p2588 N85-25956
Atmospheric chemistry
[INPE-3190-PRE/554] 16 p2826 N85-27430
Cometary atmospheres: Modeling the spatial distribution of observed neutral radicals
[NASA-CR-175852] 16 p2882 N85-27781
Crossed molecular beam studies of the reactions of oxygen and fluorine atoms
[AD-A153302] 17 p2921 N85-28008
Adiabatic approach in the theory of polyatomic photodissociation: Application to C2N2
[DE85-008515] 18 p3071 N85-28996
Quantitative studies for photoabsorption and fluorescence of HCl
[NASA-CR-175965] 19 p3233 N85-30043
Photoabsorption and photodissociation of molecules important in the interstellar medium
[NASA-CR-175918] 19 p3383 N85-30986
Radiative augmented combustion
[AD-A154137] 20 p3423 N85-31246
Optical inhomogeneities in a nanosecond-pulse iodine photodissociation laser with slow UV radiation pumping
21 p3686 N85-32902
Multiphoton production and detection of atoms
[AD-A155561] 21 p3702 N85-33000
Photofragment fluorescence as a sensitive probe for gas-phase alkali compounds and their photochemistry
[DE85-010707] 22 p3746 N85-33219
The photodissociation of acetylene at 193.3 NM
[AD-A155775] 24 p4075 N85-35255
High-resolution spectroscopy and dynamics of multiphoton processes in atoms and molecules
[AD-A155862] 24 p4147 N85-35714

PHOTOELASTICITY
NT PHOTOVISCOELASTICITY
Stress analysis of pin-loaded orthotropic plates using orthotropic photoelasticity 02 p0207 N85-11366
CFM 56-2. Oligocyclic fatigue of the turbofan disk: Dimensionning and tests for verification and improvements 07 p0906 N85-15750
Stresses in pin-loaded orthotropic plates using photoelasticity
[NASA-CR-172498] 07 p0977 N85-16204
Stress concentration due to axial tension of loaded nonsymmetric-shaped grooves
[AD-A149425] 10 p1496 N85-19442
Root stresses in conformal gears-strain gauge and photoelastic investigations 14 p2223 N85-23787
Stress concentration in the elastoplastic state and residual stress after unloading
[AD-A155628] 21 p3600 N85-32956

PHOTOELECTRIC CELLS
NT PHOTOCONDUCTIVE CELLS
NT PHOTOVOLTAIC CELLS
Photoelectric effect in liquid crystals
02 p0259 N85-11695
Efficiency of photoelectric conversion of short radiation pulses 03 p0348 N85-12240
CuInSe2-based photoelectrochemical cells: Their use in characterization of thin CuInSe2 films, and as photovoltaic cells per se
[DE84-004514] 04 p0529 N85-13379
A two photoelectrode solid-state photoelectrochemical cell
[AD-A148982] 10 p1434 N85-19038
Small aperture analysis of the dual TEM (transverse electromagnetic) cell and an investigation of test object scattering in a single TEM cell
[PB85-159952] 14 p2306 N85-24277
Applications of photoinduced electron transfer and hydrogen abstraction reactions to chemical and electrochemical conversion processes
[DE85-006068] 15 p2506 N85-25459
Performance evaluation of fiber-optic converters
17 p2941 N85-28154
High-pressure optical cell
[AD-A153639] 18 p3185 N85-29754
Polymer blends for use in photoelectrochemical cells for conversion of solar energy to electricity
[DE85-011602] 22 p3752 N85-33258
Method and apparatus for measuring areas of photoelectric cells and photoelectric cell performance parameters
[DE85-011629] 22 p3810 N85-33599

PHOTOELECTRIC EFFECT
NT PHOTOIONIZATION
Photoelectric effect in liquid crystals
02 p0259 N85-11695
Determining composition in surface region of semiconductor crystals by method of sudden changes in X-ray photoelectric effect 02 p0267 N85-11746
Fundamental molecular physics and chemistry, part 1
[DC84-009127] 04 p0561 N85-13571
Test results from a comparative evaluation of a condensation nuclei fire detector
[NASA-CR-3874] 12 p1862 N85-21675
Transducer of linear displacements
14 p2281 N85-24130

PHOTOELECTRIC EMISSION
Photocurrent oscillations in Bi12GeO20 metal-semiconductor-metal structures
02 p0266 N85-11741
Investigation of effect of photocurrent amplification in meta-dielectric-semiconductor structures based on silicon 04 p0488 N85-13110
Surface structure determination with ARPEFS
[DE84-016904] 04 p0571 N85-13644
Supercell band structure calculations of the two peak photo-and inverse photoemission spectra in Ce and Pr compounds
[DE84-017485] 06 p0867 N85-15513
Study in molecular lasers
[AD-A148246] 08 p1166 N85-17357
Photoemission, vibrational and stimulated desorption studies of metal-semiconductor interfaces and of chemisorbed atoms and molecules
[AD-A147709] 08 p1225 N85-17717
A statistical evaluation of the limitations of single-channel intermediate-band photoelectric stellar photometry 08 p1251 N85-17900
S-11 and S-20 photocathode research activity, revision 1
[DE84-017164] 09 p1326 N85-18335
Temperature-dependent surface states and transitions of Si(111)-7x7
[AD-A149158] 10 p1562 N85-19650
Ion implanted lateral in 2Ga 8As/GaAs strained-layer superlattice photodector
[DE85-001365] 10 p1583 N85-19859
Operating time meter for tape recorder
12 p1836 N85-21537
Angle-resolved photoemission study of AuGa2 and AuIn2 intermetallic compounds
[AD-A150000] 12 p1940 N85-22183
Multiport optical detectors 18 p3187 N85-29769
Dual optical mechanical position tracker
[AD-D011739] 22 p3844 N85-33811
Noble metals as incipient transition metals
[DE85-013283] 24 p4080 N85-35286
Exit channels of autoionization resonances in atoms
[DE85-012299] 24 p4149 N85-35726
Ionic crystals
[DE85-009482] 24 p4163 N85-35809

PHOTOELECTRIC GENERATORS
Space power plants 18 p2724 N85-26813

PHOTOELECTRIC MATERIALS
Increased voltage photovoltaic cell
[NASA-CASE-NPO-16155-1] 19 p3303 N85-30475
High-brightness photoemitter development for electron accelerator injectors
[DE85-009548] 19 p3355 N85-30796
Practical aspects of photovoltaic technology, applications and cost (revised)
[NASA-CR-174983] 24 p4110 N85-35472

PHOTOELECTRIC PHOTOMETERS
U ELECTROPHOTOMETERS

PHOTOELECTROCHEMICAL DEVICES
Research on photoelectrochemical cells based on CdSe, CdSe/sub 1-x/te/sub x and other photoelectrode materials
[DE84-004527] 02 p0224 N85-11466
CuInSe2-based photoelectrochemical cells: Their use in characterization of thin CuInSe2 films, and as photovoltaic cells per se
[DE84-004514] 04 p0529 N85-13379
Method for determining the point of zero zeta potential of semiconductor
[NASA-CASE-LAR-12693-1] 19 p3373 N85-30923

PHOTOELECTROCHEMISTRY
Research on photoelectrochemical cells based on CdSe, CdSe/sub 1-x/te/sub x and other photoelectrode materials
[DE84-004527] 02 p0224 N85-11466
Photoelectrochemistry with chemically modified electrodes
[DE84-016798] 04 p0471 N85-12997
Luminescent properties of graded cadmium sulfoselenide electrodes prepared from cadmium sulfide substrates
[AD-A146710] 06 p0766 N85-14898
A two photoelectrode solid-state photoelectrochemical cell
[AD-A148982] 10 p1434 N85-19038
Photoelectrochemical reduction of carbon dioxide
[PB85-129054] 11 p1596 N85-20036
Solar-assisted hydrogen generation by photoelectrocatalysis
[PB85-149706] 12 p1804 N85-21314
The electrochemistry of azine, oxazine and thiazine dyes
[AD-A152394] 17 p2918 N85-27990
Photoeffects of semiconductor electrolyte interfaces
[AD-A154183] 20 p3449 N85-31411

PHOTOELECTROMAGNETIC DETECTORS
U PHOTOELECTROMAGNETIC EFFECTS
U RADIATION MEASURING INSTRUMENTS

PHOTOELECTROMAGNETIC EFFECTS
Photoelectric effect in liquid crystals
02 p0259 N85-11695

PHOTOELECTRON SPECTROSCOPY
The effect of thin-film growth mode on XPS/UPS/AES intensities
[AD-A146284] 03 p0434 N85-12763
Electron spectrometry experiments with the use of synchrotron radiation
[DE85-001266] 07 p1041 N85-16610
Photoionization of excited molecular states
[DE84-017454] 09 p1291 N85-18103
Characterization of CO binding sites on Rh(111) and Rh(331) surfaces by XPS and LEED (Low Energy Electron Diffraction): Comparison to EELS (Electron Energy Loss Spectroscopy) results
[AD-A149331] 10 p1435 N85-19044
Studies of silicon-refractory metal interfaces: Photoemission study of interface formation and compound nucleation
[AD-A150075] 12 p1800 N85-21293
Some unique aspects of fouling on copper as compared to titanium or nickel
[AD-A150072] 12 p1806 N85-21332
The Valence- and conduction-band structure of the sapphire (1102) surface
[AD-A150001] 12 p1940 N85-22184
Workshop report on new directions in soft X-ray photoabsorption
[DE85-006150] 14 p2419 N85-24923
Spectroscopy of surface adsorbed molecules
[DE85-009452] 17 p3034 N85-28766
Materials-process interactions in ternary alloy semiconductors
[AD-A153133] 17 p3043 N85-28832
The photochemical oxidation of GaAs
[AD-A153689] 19 p3233 N85-30045
Chemical structure of interfaces
20 p3480 N85-31629
Photoelectron studies of autoionizing Rydberg states in HCl
[DE85-011813] 21 p3702 N85-33001
Experimental studies of the geometric and electronic structure of chemisorption bonding
[PB85-192250] 22 p3747 N85-33228
Heats of formation of gas phase organosulfur molecules, radicals and ions measured by PEPICO and application of (17)O and (33)S NMR spectroscopy to structure determination of organosulfur compounds
[DE85-010558] 24 p4071 N85-35229

PHOTOELECTRONICS
U ELECTRONICS

PHOTOELECTRONS
Ionospheric electron density profile and related studies
[AD-A155257] 21 p3632 N85-32587

PHOTOEMISSION
U PHOTOELECTRIC EMISSION

PHOTOEMISSIVITY
U EMISSIVITY
U PHOTOELECTRIC EMISSION

PHOTOEMITTERS
U PHOTOELECTRIC MATERIALS

PHOTOGEOLOGY
Seismotectonic nature of some annular photoanomalies registered by remote methods 02 p0184 N85-11110
Predicting fracturing zones in Caspian depression subsalt deposits on basis of space information and geological-geophysical data 02 p0184 N85-11111
Assessment of computer techniques for processing digital LANDSAT MSS data for lithological discrimination of Serra do Ramalho, State of Bahia
[E85-10093] 03 p0378 N85-12412
Report of the field work performed in the Basins of the Quebra Osso and Tanque Petro Rivers in the Catas Altas quadrangle, Minas Gerais
[INPE-3266-NTE/225] 04 p0525 N85-13359
A preliminary evaluation of LANDSAT-4 Thematic Mapper data for their geometric and radiometric accuracies 12 p1871 N85-21739
LANDSAT 4 investigations of Thematic Mapper and Multispectral Scanner applications — Drum Mountains, Utah and Tonopath, Nevada
[E85-10095] 12 p1874 N85-21757
Evaluation of Thematic Mapper performance as applied to hydrocarbon exploration — Ontario, Canada; Cement, Oklahoma; and Death Valley, California
13 p2118 N85-23191

Geologic utility of LANDSAT-4 TM data — Death Valley, California and the Silver Bell area of southern Arizona
13 p2118 N85-23192
Assessment of computer based geologic mapping of rock units in the LANDSAT-4 scene of northern Death Valley, California 13 p2119 N85-23195
Geologic interpretation of remote sensing data for the Martian volcano, Ascraeus Mons
13 p2194 N85-23606
The deep structure of lunar basins: Clues to the understanding of basin formation and modification
13 p2200 N85-23647
Mars geologic mapping: A review and new concepts
13 p2202 N85-23663
Example of joint use of data from surface studies and space photographs in investigating dynamics of zone of North Zeravshan seismogenic faults
15 p2485 N85-25342
Relative geological information yield from small-scale multizonal space images (example of Fergana depression and its mountainous margins) 15 p2485 N85-25343
Function of remote sensing in Brazil
[INPE-3314-PRE/621] 16 p2610 N85-27329
Space methods for geological research
19 p3295 N85-30429
Geologic interpretation of remote sensing data for the Martian volcano Ascraeus Mons
19 p3364 N85-30992
Quantitative geomorphologic studies from spaceborne platforms 21 p3604 N85-32381
Use of space photographs for analysis of structural and dynamic conditions of formation of ancient phlogopite and apatite deposits 22 p3735 N85-33153
Using remote photographs in prospecting for hydrocarbons on the Kerch Peninsula
22 p3735 N85-33154
Geology and geomorphology of the Roraima group, southeastern Venezuela 24 p4115 N85-35511

PHOTOGONIOMETERS
Influence of geometric conditions on the indicatrix of reflection of the perfect reflecting diffuser
[PTB-OPT-16] 03 p0420 N85-12686
Status of and outlook for producing means of transmitting units of plane angle, angular velocity and acceleration with ring lasers 13 p2074 N85-22955

PHOTOGRAMMETRY
Single viewpoint self calibration: A contribution to field calibration of recording chambers
[SER-C-269] 01 p0049 N85-10320
Initial feasibility ground test of a proposed photogrammetric system for measuring the shapes of ice accretions on helicopter rotor blades during forward flight
[NASA-TM-87391] 04 p0455 N85-12867
The photogrammetric camera experiment on Spacelab 1 05 p0658 N85-14230
Papers of the 15th International Society for Photogrammetry and Remote Sensing (ISPRS) Congress — conference
[TRITA-FMI-9] 08 p1175 N85-17408
Mathematical aspects of digital terrain information; Report from International Society for Photogrammetry and Remote Sensing (ISPRS) working group 3:3, 1980 - 1984 — photogrammetry 08 p1175 N85-17407
A comparative test of photogrammetrically sampled digital elevation models 08 p1175 N85-17408
Multimodels increase accuracy: Summary of an experiment — photogrammetry
08 p1175 N85-17409
Hierarchical data structures and algorithms for digital stereoscopical mensuration 08 p1175 N85-17410
An efficient algorithm for the computation of the inverse in bundle adjustment systems — photogrammetry
08 p1175 N85-17411
Digital elevation model computation using fast Poisson solutions 08 p1175 N85-17412
Sequential data processing for photogrammetric acquisition of digital elevation models
08 p1176 N85-17413
Processing of underwater photographs
10 p1499 N85-19482
Earth resources: A continuing bibliography with indexes
[NASA-SP-7041(44)] 10 p1503 N85-19484
Radar calibration using direct measurement equipment and oblique photometry
[AD-D011530] 12 p1822 N85-21433
Hybrid method of mapping and photogeodetic control network densification
[PB85-133775] 12 p1876 N85-21766
Evaluating accuracy in orientation of topographic photograph and satellite-centered direction from star photograph 13 p1983 N85-22442
A unified lunar control network
13 p2203 N85-23669
The control network of Mars: October 1984
13 p2203 N85-23670
The control networks of the satellites of Jupiter and Saturn 13 p2204 N85-23671
Shape of Io 13 p2204 N85-23672
One aspect of determination of direction of space survey base from photographs of planetary surface and star sky
15 p2487 N85-25352
Minimizing influence of Earth's curvature in projective rectification of space photographs into photoplans and photomaps 16 p2727 N85-26829
Use of vector processors in cartographic raster data processing, with special regard to the AP-120B vector processor 16 p2814 N85-27358
Standards and specifications for geodetic control networks
[PB85-166478] 16 p2816 N85-27374
Investigations of the accuracy of the Digital Photogrammetry System (DPS), a rigorous three-dimensional compilation process for pushbroom imagery
[MSB-UA-753/83-O] 16 p2874 N85-27734
German contributions to the cartography of Antarctica by means of photogrammetry and remote sensing
18 p3124 N85-29342
Comparison of survey and photogrammetry methods to position gravity data, Yucca Mountain, Nevada
[DE85-011665] 21 p3590 N85-32316
Coastal erosion along Monterey Bay
[AD-A155610] 21 p3655 N85-32707
Production of initial estimates of photogrammetric variables
[NPL-MOM-66] 23 p3943 N85-34434
Parametric stability of analytical close-range photogrammetry 24 p4107 N85-35461
Evaluation: Close-range photogrammetry for slope inventory and monitoring
[PB85-192755] 24 p4108 N85-35470

PHOTOGRAPH INTERPRETATION
U PHOTOINTERPRETATION

PHOTOGRAPHIC EMULSIONS
NT NUCLEAR EMULSIONS
Astronomical photography 1984 — conference
[ROE-OR-14] 07 p0962 N85-16102
A spectrosensitometer with an absolute calibration
07 p0963 N85-16106
Comparison of the fine grain compensation hypersensitization (FAH) process with gas hypersensitizing techniques — astronomical photography plates
07 p0963 N85-16107
The results of hydrogen hypersensitization of photoemulsions — astronomical photography
07 p0963 N85-16108
The most effective astronomical photographic emulsions for recording of faint and low-contrast objects
07 p0963 N85-16110
Astronomical applications of new infrared films
07 p0964 N85-16111
The 3a-F emulsion and the quasar redshift cut-off
07 p0964 N85-16112
Microspots on spectroscopic plates — astronomical photography 07 p0964 N85-16113
Where to next in astronomical photography? — tabular grain emulsions 07 p0964 N85-16114
What do we want: Increased speed, resolution, contrast or DQE? — astronomical photography
07 p0964 N85-16115
The Malin effect in stellar photography
07 p0966 N85-16131
A quantitative image evaluation study of a concurrent photon amplification treated emulsion
[AD-A151631] 15 p2560 N85-25796

PHOTOGRAPHIC EQUIPMENT
NT BALLISTIC CAMERAS
NT CAMERAS
NT FRAMING CAMERAS
NT HIGH SPEED CAMERAS
NT MULTISPECTRAL BAND CAMERAS
NT PANORAMIC CAMERAS
NT PHOTOGRAPHIC PROCESSING EQUIPMENT
NT PINHOLE CAMERAS
NT SCHMIDT CAMERAS
NT STREAK CAMERAS
NT TELEVISION CAMERAS
Vapor-screen technique for flow visualization in the Langley Unitary Plan Wind Tunnel
[NASA-TM-86364] 19 p3214 N85-29929

PHOTOGRAPHIC FILM
NT MICROFILMS
The calibration of photographic and spectroscopic films: A densitometric analysis of IIaO film flown aboard the Space Shuttle 3
[NASA-CR-174278] 07 p0962 N85-16101
FLACS: A new sensitometer for measurement of extreme low intensity reciprocity in a controlled environment — X-ray films 07 p0963 N85-16104
Astronomical applications of new infrared films
07 p0964 N85-16111
Infrared presensitization photography
[AD-A146968] 07 p0967 N85-16139
S-11 and S-20 photocathode research activity, revision 1
[DE84-017164] 09 p1326 N85-18335
Development and application of low energy X-ray and electron physics
[AD-A149983] 12 p1926 N85-22099
Prediction of the long term stability of polyester-based recording media
[PB85-160133] 14 p2262 N85-24019
Astrometry of comets using hypersensitized type 2415 film 14 p2435 N85-25021
Electronic detection and concealment of film dirt
[BSC-RD-1985/4] 15 p2536 N85-25867
Method and apparatus for high speed, sustained recording of infrared laser beam patterns
[AD-D011585] 15 p2563 N85-25811
Infrared presensitization photography
16 p2786 N85-27189
High sensitive X-ray films to detect electron showers in 100 GeV region
[HE-3.1-13] 24 p4178 N85-35911
X-ray film chamber with carbon target of Tien-Shan complex array 24 p4179 N85-35915
The Nagoya cosmic-ray muon spectrometer 3, part 3: Automatic film scanning equipment
[HE-5.2-4] 24 p4202 N85-36062

PHOTOGRAPHIC MEASUREMENT
NT PHOTOGRAMMETRY
Spectroscopic data for globular cluster giants. 1: Stars of the red giant tip 01 p0128 N85-10885
Variability of Neptune 02 p0299 N85-11938
Holographic assembly for measuring velocity fields of supersonic ballistic splinters at a large distance
[ISL-CO-203/84] 20 p3459 N85-31487

PHOTOGRAPHIC PLATES
SENSIT.FOR: A program for sensitometric reduction
07 p0963 N85-16105
Nitrogen flushing during exposure of large Schmidt telescope plates 07 p0963 N85-16109
Microspots on spectroscopic plates — astronomical photography 07 p0964 N85-16113
Using a Gossen light meter to produce enlarged interpositive film copies from glass plates — astronomical photography 07 p0964 N85-16118
Processing of photographic observing material at the National Astronomical Observatory Rozhen
07 p0965 N85-16120
The UK Schmidt telescope and the facilities in Edinburgh 07 p0965 N85-16121
An investigation into the fidelity of reproduction of UKST original objective prism plates on to film — United Kingdom Schmidt Telescope (UKST) 07 p0965 N85-16123
Extending magnitude standards to faint stars with a sub-beam prism 07 p0965 N85-16124
Astronomers' problems with the calibration of Schmidt plates 07 p0965 N85-16126
Power spectrum analysis of astronomical photographs digitised with small apertures 07 p0965 N85-16127
Plate measurements and reductions at Muenster — astronomical photography 07 p0966 N85-16129
The Malin effect in stellar photography
07 p0966 N85-16131
Stellar photographic photometry using a double wedge technique with a focal reducer system
07 p0966 N85-16133
Spectrophotometry of cool stars from objective prism spectra 07 p0966 N85-16134
Digital laser platemaker modifications
[AD-A150190] 13 p2096 N85-23074
Astrometric plates obtained at the primary focus of large aperture reflectors 14 p2436 N85-25022
The astrometry network of observers in USSR
14 p2436 N85-25029
Least squares reduction technique
14 p2437 N85-25036
Reduction of astrometric plates
14 p2437 N85-25037

PHOTOGRAPHIC PROCESSING
Comparison of the fine grain compensation hypersensitization (FAH) process with gas hypersensitizing techniques — astronomical photography plates
07 p0963 N85-16107
The results of hydrogen hypersensitization of photoemulsions — astronomical photography
07 p0963 N85-16108
Nitrogen flushing during exposure of large Schmidt telescope plates 07 p0963 N85-16109
Some aspects of photography with a small Schmidt camera — astronomical photography
07 p0964 N85-16116

Using a Gossen light meter to produce enlarged interpositive film copies from glass plates — astronomical photography 07 p0964 N85-16118
Unsharp masking at the enlarger — astronomical photography 07 p0964 N85-16119
Processing of photographic observing material at the National Astronomical Observatory Rozhen 07 p0965 N85-16120
The work of the photolabs at the Royal Observatory, Edinburgh — astronomical photography 07 p0965 N85-16122
Cometary astrometry with Schmidt cameras 14 p2435 N85-25020

PHOTOGRAPHIC PROCESSING EQUIPMENT
Photo-reconnaissance system [AD-D011287] 06 p0826 N85-15245
Processing of photographic observing material at the National Astronomical Observatory Rozhen 07 p0965 N85-16120
The work of the photolabs at the Royal Observatory, Edinburgh — astronomical photography 07 p0965 N85-16122

PHOTOGRAPHIC RECORDING
Single viewpoint self calibration: A contribution to field calibration of recording chambers [SER-C-289] 01 p0049 N85-10320
Preliminary results using a rapid photographic wake traverse system — in a wind tunnel [RAE-TM-AERO-1967] 02 p0200 N85-11332
Recording holograms on thin films of titanium dioxide 06 p0789 N85-15099

PHOTOGRAPHS
NT MARS PHOTOGRAPHS
NT MOTION PICTURES
NT PHOTOMICROGRAPHS
Problem of determining highly accurate coordinates of artificial satellites by photographic methods 02 p0162 N85-11096
Initial feasibility ground test of a proposed photogrammetric system for measuring the shapes of ice accretions on helicopter rotor blades during forward flight [NASA-TM-87391] 04 p0455 N85-12887
Direct-strike lightning photographs, swept-flash attachment patterns, and flight conditions for storm hazards 1982 [NASA-TM-86347] 12 p1892 N85-21877
Near-nucleus studies of Comet Halley 14 p2435 N85-25018
NASA photography index [NASA-TM-87457] 15 p2665 N85-26445
Vapor-screen technique for flow visualization in the Langley Unitary Plan Wind Tunnel [NASA-TM-86384] 19 p3214 N85-29829
Cultural data base implementation study and computer-aided scene modeling system users manual [AD-A154232] 19 p3333 N85-30646

PHOTOGRAPHY
NT ACOUSTICAL HOLOGRAPHY
NT AERIAL PHOTOGRAPHY
NT ALL SKY PHOTOGRAPHY
NT ASTRONOMICAL PHOTOGRAPHY
NT AUTORADIOGRAPHY
NT BLACK AND WHITE PHOTOGRAPHY
NT CINEMATOGRAPHY
NT CLOUD PHOTOGRAPHY
NT COLOR INFRARED PHOTOGRAPHY
NT COLOR PHOTOGRAPHY
NT ELECTRO-OPTICAL PHOTOGRAPHY
NT FRACTOGRAPHY
NT HIGH SPEED PHOTOGRAPHY
NT HOLOGRAPHY
NT INFRARED IMAGERY
NT INFRARED PHOTOGRAPHY
NT LUNAR PHOTOGRAPHY
NT METRIC PHOTOGRAPHY
NT MICROWAVE HOLOGRAPHY
NT MULTISPECTRAL PHOTOGRAPHY
NT ORTHOPHOTOGRAPHY
NT PHOTOMICROGRAPHY
NT RADAR PHOTOGRAPHY
NT SATELLITE-BORNE PHOTOGRAPHY
NT SCHLIEREN PHOTOGRAPHY
NT SHADOWGRAPH PHOTOGRAPHY
NT SPACEBORNE PHOTOGRAPHY
NT STEREOPHOTOGRAPHY
NT STEREOSCOPY
NT STREAK PHOTOGRAPHY
NT ULTRAVIOLET PHOTOMETRY
NT UNDERWATER PHOTOGRAPHY
NT WHITE LIGHT HOLOGRAPHY
Geophysical experiments, photography aboard Salyut-7 02 p0157 N85-11068
Commentary on cosmonauts geological mapping, photography 02 p0158 N85-11069
Study of delamination cracking under static and cyclic loads of carbon-epoxy composite materials [REPT-42-727/F] 03 p0327 N85-12102
Studies of ignition and combustion wave propagation in exothermic systems using high-speed photography [DE84-016482] 04 p0471 N85-12995
Chemical and photographic evaluation of rigid explosive transfer lines [AD-A149303] 11 p1613 N85-20145
Photorefractor ocular screening system [NASA-CASE-MFS-26011-1SB] 11 p1662 N85-20639
Relationship between brightness spectrum of photographic image and spectrum of rises on a water surface with waves 13 p2115 N85-23171
Some new photometric data form panoramic pictures taken by Lunokhod-2 15 p2461 N85-25312
Test and evaluation of the 2.4-micron photorefractor ocular screening system [NASA-TM-86492] 15 p2615 N85-26115
USSR report: Engineering and equipment [JPRS-UEQ-85-004] 17 p2939 N85-28142

PHOTOINTERPRETATION
Method for interpreting soil cover of flowed fields using spectral brightnesses measured from space photographs 02 p0164 N85-11112
Utilization of LANDSAT orbital imagery in the soil survey processes at Rio Grande do Norte state [E85-10009] 02 p0216 N85-11422
Executive report: Results of the IRGA-CNPq/INPE experimental project [E85-10011] 02 p0216 N85-11424
Development and testing of a rural credit supervision system at the level of counties and rural properties utilizing remote sensing techniques [E85-10018] 02 p0217 N85-11431
Remote sensing for landforms and soils in the arid southwest United States 03 p0378 N85-12410
Integrated analysis of remote sensing products from basic geological surveys — Brazil [E85-10052] 07 p0984 N85-16248
Evidence accumulation for spatial reasoning 07 p0985 N85-16261
Forest area estimates from LANDSAT MSS and forest inventory plot data [PB85-105617/GAR] 07 p0990 N85-16290
Assessment of LANDSAT for rangeland mapping, Rush Valley, Utah [E85-10072] 10 p1503 N85-19486
LANDSAT 4 investigation of Thematic Mapper and Multispectral Scanner applications [E85-10076] 10 p1504 N85-19490
Method for approximating autocorrelation functions for describing areal photoimage features 13 p1963 N85-22443
Experience in automated interpretation of aerospace photographs 13 p1963 N85-22444
Geoindication method for interpreting aerial and space photographs: Status and prospects 13 p1964 N85-22445
Experience in combined special mapping using space information 13 p1964 N85-22449
Combined analysis of the dynamics of complex ecosystems based on repeated remote measurements 13 p1965 N85-22450
Overview of TM applications research reports 13 p2117 N85-23187
Preliminary study of information extraction of LANDSAT TM data for a suburban/regional test site 13 p2121 N85-23208
Identifying land use structures of multizonal aerospace photographs using digital data processing 15 p2486 N85-25348
Interpretation of space photolineaments 15 p2487 N85-25353
Shuttle imaging radar-B (SIR-B) data analysis for identifying rainfall event occurrence and intensity [NASA-CR-175712] 15 p2594 N85-25966
Documentation of PHOTO: A user's manual for the analysis of photographic and X-ray negatives [AD-A152968] 17 p2967 N85-28327
Airphoto interpretation of vegetation and landforms for soil mapping 17 p2983 N85-28436
Air photo analysis, photo interpretation logic, and feature extraction [AD-A153926] 18 p3124 N85-29347
Geologic interpretation of remote sensing data for the Martian volcano Ascraeus Mons 19 p3384 N85-30992
Handbook for obtaining and using aerial photography to map aquatic plant distribution [AD-A154584] 21 p3605 N85-32388

PHOTOIONIZATION
Magnetic resonance studies of transient radicals and radical ions [DE84-011690] 03 p0328 N85-12116
Physico-chemical investigation of some areas of fundamental significance to biophysics [DE84-016385] 04 p0471 N85-12999
Multiphoton ionization of benzene in solution [DE85-000693] 06 p0766 N85-14899
Photoionization structure of the Orion Nebula 06 p1246 N85-17963
Photoionization of excited molecular states [DE84-017454] 09 p1291 N85-18103
Time-resolved studies of free radicals and laser-initiated chain reactions [DE85-002100] 09 p1326 N85-18332
Multiphoton ionization of atomic cesium [DE85-001286] 09 p1360 N85-18678
Multiphoton ionization of cesium atoms above and below the two-photon ionization threshold [DE85-000976] 09 p1361 N85-18682
Effects of dc electric fields on multiphoton ionization spectra in cesium [DE85-001542] 09 p1361 N85-18684
State-selected ion-molecule reaction dynamics [AD-A150068] 12 p1928 N85-22115
Threshold double photoionization of argon with synchrotron radiation [AD-A150815] 13 p2157 N85-23369
Workshop report on new directions in soft X-ray photoabsorption [DE85-006150] 14 p2419 N85-24923
Experimental and theoretical studies of laser cooling and emittance control of neutral beams [AD-A149215] 15 p2582 N85-25804
Kinetic energies of fragment ions produced by dissociative photoionization of NO [NASA-CR-175721] 15 p2647 N85-26327
Characterization of multiphoton ionization processes in the ultraviolet [AD-A151427] 15 p2652 N85-26354
Photoionization mass spectrometry with VUV hydrogen laser source [AD-A153982] 17 p2921 N85-28009
An ultrasensitive and element specific photoionization detection system for environmental analysis [AD-A153985] 17 p2966 N85-28332
Experimental study of dissociative attachment in optically-pumped lithium molecules [AD-A152800] 17 p3030 N85-28738
Development of a technique for in situ detection of stratospheric nitrogen dioxide 19 p3312 N85-30534
Many-body processes in atomic and molecular physics [DE85-009750] 19 p3354 N85-30791
Ionospheric electron density profile and related studies [AD-A155257] 21 p3632 N85-32567
Activities of the Physics Division [DE85-000784] 21 p3702 N85-33002
Photoionization of alkali and alkaline earth atoms: Na and Mg [DE85-011812] 22 p3837 N85-33755
Photoionization-pumped, Ne 2, X-ray laser studies project [DE85-012973] 23 p3936 N85-34399
Heats of formation of gas phase organosulfur molecules, radicals and ions measured by PEPICO and application of (17)O and (33)S NMR spectroscopy to structure determination of organosulfur compounds [DE85-010558] 24 p4071 N85-35229
Dissociative and double photoionization cross sections of NO from threshold to 120 A [NASA-CR-176185] 24 p4147 N85-35713
High-resolution spectroscopy and dynamics of multiphoton processes in atoms and molecules [AD-A155862] 24 p4147 N85-35714
Exit channels of autoionization resonances in atoms [DE85-012299] 24 p4149 N85-35726

PHOTOLITHOGRAPHY
Low-threshold injection lasers on grown GaInPAs/InP heterostructures (1.2-1.6 micrometers wavelengths) 02 p0258 N85-11693
Exposure modelling of particle beam lithography [AD-A147849] 08 p1219 N85-17678
Thin film transistors for addressing flat panel displays [BMFT-FB-T-84-210] 08 p1227 N85-17726
Basic development of a 1.5 micrometer very large scale integrated technique, part 1-4 [BMFT-FB-T-85-032-PT-1-4] 20 p3449 N85-31417

PHOTOLUMINESCENCE
NT X RAY FLUORESCENCE
Photoluminescent properties of epitaxial p-GaSb 02 p0267 N85-11745
Advanced amorphous materials for photovoltaic conversion [DE84-017198] 04 p0529 N85-13384
Photoluminescence studies of Ga(As,P) strained-layer superlattices [DE84-015709] 05 p0731 N85-14701

Luminescent properties of graded cadmium sulfoselenide electrodes prepared from cadmium sulfide substrates
[AD-A146710] 06 p0766 N85-14898
Characterization of III-V compound semiconductor device materials
[AD-A148203] 06 p1226 N85-17719
Infrared modulation of photoluminescence in glow discharge amorphous silicon
[DE85-016663] 11 p1737 N85-20922
Investigation of the MBE growth of InSb and novel quantum well structures
[AD-A151014] 14 p2427 N85-24869
Electrogenerated chemiluminescence
[AD-A153547] 19 p3070 N85-29990
Sea water photoluminescence
19 p3292 N85-30415
A theory of exciton photoluminescence for two types of neutral acceptors in silicon. A study of the systems Si:(B, In), Si:(Al), (Si), Si:(Ga, In), Si:(B, Al), Si:(B, Ga), and Si:(Al, GA)
[AD-A155452] 21 p3710 N85-33031

PHOTOLUMINESCENT BANDS
Formation of lattice defects by nitrogen laser exposure in A2B6 semiconductors with wide forbidden band
02 p0258 N85-11682

PHOTOLYSIS
NT RADIOLYSIS
Laser-assisted solar-cell metallization processing
06 p0831 N85-15262
Synthesis, static and reactive characterization of supported organometallics
[DE85-004285] 12 p1806 N85-21340
Multiple product channels in the collision free UV photodissociation of 2-nitropropane
[AD-A150896] 14 p2251 N85-23951
The source of stratospheric NO and N2O
[NASA-CR-175713] 15 p2588 N85-26056
In-situ stratospheric ozone measurements: Recent results and their implications 16 p2824 N85-27419
Water vapor 16 p2824 N85-27420
Photochemical ignition studies. 1: Laser ignition of flowing premixed gases
[AD-A153048] 17 p2920 N85-28002
The spectroscopy and reaction kinetics of coordinated unsaturated metal carbonyls
[AD-A153079] 17 p2920 N85-28003
Kinetics of hydrolysis and products of hydrolysis and photolysis of tetryl
[AD-A153144] 17 p2921 N85-28005
Study of the formation of sulfuric acid aerosols
[DE85-008102] 17 p2922 N85-28011
Kinetics and intensity of photochemical processes in the atmosphere
[BPT-10/84] 18 p3134 N85-29411
Lifetime and quenching measurements of C2H emission produced by vacuum ultraviolet photolysis of C2H2
[DE85-010769] 19 p3276 N85-30330
Photofragment fluorescence as a sensitive probe for gas-phase alkali compounds and their photochemistry
[DE85-010707] 22 p3748 N85-33219

PHOTOMAPPING
Choice of cartographic projection for space system data bank used in studying natural resources
02 p0165 N85-11119
Study of Volga river delta using space photosurvey materials 15 p2485 N85-25340
Use of space photographic information to map plant cover 15 p2488 N85-25359
Minimizing influence of Earth's curvature in projective rectification of space photographs into photoplans and photomaps 16 p2727 N85-26829
Information relative to cartography and geodesy. Series 2: Translations, number 42, volume 1
[ISSN-0469-4244] 18 p3123 N85-29336
Two satellite image maps of Central Europe
18 p3123 N85-29339
Digital image mapping of Antarctica using NOAA-7 AVHRR imagery 18 p3124 N85-29340
The significance of orthophoto maps for developing countries 18 p3124 N85-29341
Mapping of dynamics of deltas by space photography
22 p3737 N85-33169
Comprehensive mapping of arid territories of Arizona using space photography 22 p3737 N85-33184

PHOTOMAPS
Preliminary photomaps of Venus surface in the Maxwell Mountains and adjacent areas 13 p1982 N85-22436
What does digital image processing perform in the production of orthophotomaps 16 p2815 N85-27368
Information relative to cartography and geodesy. Series 2: Translations, Number 42, Volume 2 — maps
[ISSN-0469-4244] 18 p3123 N85-29337

PHOTOMASKS
Unsharp masking at the enlarger — astronomical photography 07 p0964 N85-16119
Mask aligner for solar cell fabrication
[AD-D011450] 10 p1510 N85-19529
Basic development of a 1.5 micrometer very large scale integrated technique, part 1-4
[BMFT-FB-T-85-032-PT-1-4] 20 p3449 N85-31417

PHOTOMETERS
NT ELECTROPHOTOMETERS
NT ULTRAVIOLET SPECTROMETERS
NT ULTRAVIOLET SPECTROPHOTOMETERS
Integration of detectors with optical waveguide structures
[AD-A146276] 03 p0420 N85-12682
Electrooptical matrix multiplication using the twos complement arithmetic for improved accuracy
[AD-D011252] 05 p0728 N85-14682
Energy parameters of optical radiation space research systems 06 p0791 N85-15058
Apparatus for determining the liquid water content of a gas
[AD-D011297] 07 p0922 N85-15839
Using a Gossen light meter to produce enlarged interpositive film copies from glass plates — astronomical photography 07 p0964 N85-16118
Two-photon coherent state light - its generation and potential applications
[AD-A148245] 08 p1166 N85-17356
Semiconductor superlattice photodetectors
[NASA-CR-174347] 09 p1397 N85-18791
Mercuric iodide photodetectors for scintillation spectroscopy
[DE85-001437] 10 p1437 N85-19056
Ion implanted lateral in 2Ga 8As/GaAs strained-layer superlattice photodector
[DE85-001365] 10 p1563 N85-19859
Effect of variance of photoreceiver frequency characteristics on characteristics of measuring instruments 13 p2076 N85-22985
Invariance of probability characteristics of detector to shape of optical pulse signals 13 p2090 N85-23048
Fabry-Perot interferometer and skymapping photometer determinations of midlatitude f-region neutral winds and temperatures and airglow enhancement/depletions
[AD-A150730] 14 p2373 N85-24666
Measurements with an auroral spectrometer in the Energy Budget Campaign
[BMFT-FB-W-84-050] 14 p2374 N85-24677
InGaAs/GaAs, Strained-Layer Superlattice (SLS), junction photodetectors, LED's, injection LASER's and FET's for optoelectronic IC applications
[DE85-001940] 14 p2430 N85-24966
Research and development of new instruments
16 p2824 N85-27418
The vector magnetograph of the Sayan Solar Observatory 18 p3206 N85-29887
Phase locked loop synchronization for direct detection optical PPM communication systems
[NASA-CR-176026] 19 p3254 N85-30178
The temporal evolution of a small auroral substorm as viewed from high altitudes with Dynamics Explorer 1
[NASA-CR-176064] 20 p3493 N85-31718
Charge Injection Device (CID) used as a photodector: Implementation and performance. Application to light source tracking (stars, lasers)
[CNES-83/CT/DRT/TIT/OE/148] 20 p3533 N85-31983
Color evolution in high redshift galaxies
20 p3544 N85-32055
Sahara Desert dust transport to the south
21 p3648 N85-32666
Comparative characteristics of optical multiposition pulse signals with intersymbol distortion
22 p3764 N85-33329
Estimating angular position of optical radiation source when received by array of photodetectors
22 p3778 N85-33413
Hadrons registration in emulsion chamber with carbon block
[HE-9.7-3] 24 p4186 N85-35962

PHOTOMETRY
NT ASTRONOMICAL PHOTOMETRY
NT ELECTROPHOTOMETRY
NT INFRARED PHOTOMETRY
NT SPECTROPHOTOMETRY
NT STELLAR SPECTROPHOTOMETRY
NT ULTRAVIOLET PHOTOMETRY
NT VISUAL PHOTOMETRY
UBV photometry of E region stars: Some intercomparisons 01 p0128 N85-10860
Theoretical elements of photometry
[BLL-RISLEY-TR-5022-(9091.9F)] 02 p0279 N85-11821
The present state of the International Star Cluster Photometry Programme 05 p0737 N85-14741
On the most probable number of flare stars in the Pleiades field 05 p0739 N85-14756
Determining grasp points using photometric stereo and the PRISM binocular stereo system
[AD-A147782] 08 p1222 N85-17697
Far infrared and submillimeter observations of the giant planets 08 p1245 N85-17856
Multi-spectral observations of the star formation: The role of far infrared photometry 08 p1245 N85-17859
Far-infrared photometry of low-mass pre-main-sequence stars with broad CO wings 08 p1246 N85-17866
High sensitivity, high angular resolution far-infrared photometry from the KAO 08 p1246 N85-17867
Proceedings of the Workshop on Improvements to Photometry
[NASA-CP-2350] 08 p1250 N85-17892
History of photometric precision
08 p1250 N85-17893
Photometric precision needed for planetary detection
08 p1250 N85-17894
A survey for photometric variability from space
08 p1251 N85-17897
The ground based photometric limitations to the search for light variations due to 5-minute solar-type oscillations in other stars 08 p1251 N85-17898
Atmospheric limitations in stellar seismology: Should one measure radial velocity or brightness fluctuations?
08 p1251 N85-17899
The atmospheric extinction problem
08 p1251 N85-17901
Gain instabilities in photomultipliers: How accurate are photon counting measurements?
08 p1251 N85-17903
CCDs: Their cause and cure
08 p1252 N85-17905
Astronomy and sodium lighting
[RAND/N-2089-RC] 09 p1413 N85-18914
Individual differences in chromatic brightness matching
[AD-A148882] 10 p1529 N85-19641
Physical models for the UV continua of symbiotic stars
11 p1756 N85-21048
Planetary cartography in the next decade (1984 - 1994)
[NASA-SP-475] 12 p1960 N85-22323
Photometric analysis of Jupiter-illuminated images of Io 13 p2196 N85-23620
Comparison of flame photometer data with total particle volume calculated from laser spectrometer particle count data
[AD-A151008] 14 p2252 N85-23958
Some new photometric data form panoramic pictures taken by Lunokhod-2 15 p2481 N85-25312
Jupiter/Voyager data analysis
[NASA-CR-175723] 15 p2579 N85-26545
Absolute calibrations of SO2 and NO analyzers by photographic methods
[DFVLR-MITT-85-02] 17 p2994 N85-28504
Activities of Istituto Elettrotecnico Nazionale Galileo Ferraris 18 p3199 N85-29845
Size exclusion chromatography-low angle laser light scattering photometry of lignite macromolecules
[DE85-012017] 22 p3745 N85-33215
Interpretation of photometric measurements of airless bodies 22 p3855 N85-33871
A cosmic ray super high multicore family event. 1: Experiment and general features
[HE-3.4-1] 24 p4181 N85-35930

PHOTOMICROGRAPHS
Automatic analysis of speckle photographs by microcomputer
[NPL-DITC-47/84] 09 p1322 N85-18308

PHOTOMICROGRAPHY
Micrographic and fractographic examination of alloys 2214 and 2024 for conditions which would cause burning of the metal on being put into solution, trial 17/175
[DGT-23.419] 11 p1609 N85-20117
Method of examining microcircuit patterns
[NASA-CASE-NPO-16299-1] 11 p1628 N85-20250

PHOTOMULTIPLIER TUBES
Fine grained hodoscopes based on scintillating optical fibers
[DE84-014849] 01 p0120 N85-10825
Preliminary evaluation of RCA C83036E prototype photomultiplier
[DE84-016894] 04 p0496 N85-13165
Simulation of optical configurations and signal processing methods in Anger-type neutron-position scintillation detector
[DE84-012095] 04 p0503 N85-13210
Analysis of a coded, M-ary orthogonal input optical channel with random-gain photomultiplier detection
05 p0624 N85-13990
Study in spurious sensitivity of electronics in space
[AD-A148366] 08 p1158 N85-17305
Gain instabilities in photomultipliers: How accurate are photon counting measurements?
08 p1251 N85-17903

Improved Gonda's circuit described
15 p2551 N85-35748
Microchannel plate streak camera
[DE85-011604] 20 p3458 N85-31481
Evidence for long-term variability in the ultra high energy photon flux from Cygnus X-3
[OG-2.1-10] 22 p3863 N85-33926
Improved method for the stabilization of NaI-photomultiplier gamma detectors against thermal and other drift
[DE85-011830] 23 p3970 N85-34613
The angular resolution of air shower gamma ray telescopes
[OG-9.5-14] 23 p4031 N85-34990
The read-out system of spatial distribution of thermoluminescence in meteorites
[SH-9.1-16] 23 p4052 N85-35131
Air fluorescence detection of large air showers below the horizon
[HE-4.6-6] 24 p4197 N85-36043
The structure of the shower disk observed at Mt. Norikura
[HE-4.7-1] 24 p4198 N85-36052
Structure of air shower disc near the core
[HE-4.7-2] 24 p4198 N85-36053
Arrival time distributions of electrons in air showers with primary energies above 10 (18)eV observed at 900m above sea level
[HE-4.7-5] 24 p4199 N85-36056
Methods for roof-top mini-arrays
[HE-4.7-7] 24 p4199 N85-36058
Fast scintillation counter preamplifier for the observation of Linsley effect
[HE-4.7-9] 24 p4199 N85-36060
A mini-array for large air showers
[HE-4.7-10] 24 p4199 N85-36061
Detection threshold energy of high energy cascade showers using thermoluminescence PTFE-sheet and hot-gas reader
[HE-7.1-5] 24 p4213 N85-36159

PHOTON ABSORPTIOMETRY
Experimental capabilities and prospects for measuring soft X-ray photoabsorption
[DE84-015488] 02 p0278 N85-11813
Techniques for measuring intercepted and absorbed PAR in corn canopies
[E85-10081] 10 p1505 N85-19495

PHOTON BEAMS
NT LIGHT BEAMS
Photon and electron dosimetry at the Physikalische-Technische Bundesanstalt in Brunswick
[PTB-DOS-9] 01 p0119 N85-10814
Stationary properties and switching characteristics of dispersive optical bistability in CuCl
18 p3186 N85-29763
Evidence for long-term variability in the ultra high energy photon flux from Cygnus X-3
[OG-2.1-10] 22 p3863 N85-33926
X-ray spectra of bursting neutron stars
23 p3981 N85-34696
Breeding new light into old machines (and new)
[DE85-013055] 24 p4155 N85-35763

PHOTON DENSITY
Low-energy gamma rays from Cygnus X-1
[OG-2.4-13] 22 p3868 N85-33957
Some evidence for large gravitational redshift in Seyfert galaxy NGC 4151
[OG-2.7-11] 22 p3872 N85-33984
A new measurement of the cosmic ray energy spectrum between 3 x 10 to the 15th power eV and 3 x 10 to the 16th power eV
[OG-5.1-6] 22 p3881 N85-34048

PHOTON-ELECTRON INTERACTION
An inverse Compton model of the X-ray emission in Seyfert galaxies 08 p1241 N85-17827
CYLTRAN calculations of electron effects on XD detectors
[LA-10264-MS] 23 p3969 N85-34601
A new method of differential structural analysis of gamma-family basic parameters
[HE-3.6-3] 24 p4184 N85-35952
Samarkand complex setup for investigation of cosmic ray variation in the energy range of 7 10 (9) - 10 (15) eV
[HE-4.8-14] 24 p4196 N85-36050

PHOTONICS
Influence of spatial pumping spectrum on quality of phase conjugate reflection during 4-photon interaction
21 p3696 N85-32984

PHOTONS
NT LIGHT BEAMS
Avalanche photodiode statistics in triggered-avalanche detection mode 05 p0623 N85-13987
Theory and applications of two-photon quantum optics
[AD-A147382] 07 p1044 N85-16631
Two-photon coherent state light - its generation and potential applications
[AD-A148245] 08 p1166 N85-17356
Gain instabilities in photomultipliers: How accurate are photon counting measurements?
08 p1251 N85-17903
CCDs: Their cause and cure
08 p1252 N85-17905
Multiphoton ionization of cesium atoms above and below the two-photon ionization threshold
[DE85-000976] 09 p1381 N85-19682
Physics of nonmagnetic relativistic thermal plasmas
09 p1396 N85-18715
Detection and symbol synchronization for multiple-bit per photon optical communications
10 p1463 N85-19228
Photonic methods of high speed analog data recording
[DE84-016723] 11 p1637 N85-20308
MCNP code
[DE85-002565] 11 p1702 N85-20705
ITS: The Integrated TIGER Series of coupled electron/photon Monte Carlo transport codes
[DE85-003719] 11 p1725 N85-20847
Exploration of new methods to produce efficient sources of coherent near millimeter wave radiation
[AD-A150094] 12 p1829 N85-21481
Mean free path lenght of photons with broken cloud cover 14 p2238 N85-24455
A quantitative image evaluation study of a concurrent photon amplification treated emulsion
[AD-A151831] 15 p2560 N85-25796
Characterization of multiphoton ionization processes in the ultraviolet
[AD-A151427] 15 p2652 N85-26354
Photon detection with cooled avalanche photodiodes: Theory and preliminary experimental results
16 p2770 N85-27096
Photon-photon collisions
[DE85-006056] 17 p3030 N85-28742
Photon structure function: Theory
[DE85-006064] 17 p3031 N85-28745
Incorporation of Monte Carlo electron interface studies into photon general cavity theory
[DE85-007674] 17 p3034 N85-28772
New experimental results in two photon physics
[NIKHEF-H/84-16] 17 p3035 N85-28776
Adiabatic approach in the theory of polyatomic photodissociation: Application to C2N2
[DE85-006515] 18 p3071 N85-28966
The prospects of the digital optical computer
18 p3188 N85-29771
Method of reducing impurity and antisite defects in semiconductor crystal materials, and device and apparatus respectively produced from and utilizing same
[AD-D011696] 19 p3280 N85-30216
Coherently pumped two-frequency laser-type devices
[AD-A154085] 19 p3275 N85-30311
MCNP: A general Monte Carlo code for neutron and photon transport
[DE85-010764] 19 p3348 N85-30753
Double photon excitation of high-Rydberg atoms as a long-lived submillimeter detector
[NASA-CASE-NPO-16372-1] 19 p3352 N85-30779
Monte Carlo electron/photon transport
[DE85-010799] 19 p3364 N85-30881
Four-photon resonant third harmonic generation
[DE85-010070] 19 p3367 N85-30883
Photon-counting image sensors for the ultraviolet
[NASA-CR-176062] 20 p3458 N85-31478
The possibility of observing and exploiting the generation of high-energy photons by electrons in the field of an intense electromagnetic wave 21 p3691 N85-32931
Influence of spatial pumping spectrum on quality of phase conjugate reflection during 4-photon interaction
21 p3696 N85-32984
Implicit Monte Carlo methods and non-equilibrium Marshak wave radiative transport
[DE85-010711] 22 p3835 N85-33743
Reduction of reabsorption effects in scintillators by employing solutes with large Stokes shifts
[DE85-011645] 22 p3836 N85-33767
Unthermalized plasma in bursts sources
[OG-1.1-5] 22 p3881 N85-33907
A search in the COS-B data base for correlated time variability in regions containing objects of interest
[OG-2.5-9] 22 p3869 N85-33964
Search for ultra high energy gamma-rays from various sources
[OG-2.8-7] 22 p3870 N85-33969
The universal spectrum of AGNs and QSOs
[OG-2.7-9] 22 p3872 N85-33982
Low-excitation Herbig-Haro objects and interstellar extinction
[NASA-CR-176142] 23 p3968 N85-34726
Study of photon emission by electron capture during solar nuclei acceleration, 1: Temperature-dependent cross section for charge changing processes
[SH-1.1-8] 23 p3990 N85-34735
Study of photon emission by electron capture during solar nuclei acceleration. 2: Delimitation of conditions for charge transfert establishment
[SH-1.1-9] 23 p3990 N85-34736
Study of photon emission by electron capture during solar nuclei acceleration. 3: Photon production evaluations
[SH-1.1-10] 23 p3990 N85-34737
Study of non-thermal photon production under different scenarios in solar flares. 1: Scenarios and formulations
[SH-1.2-2] 23 p3991 N85-34738
Study of non-thermal photon production under different scenarios in solar flares. 2: The Compton inverse and Bremsstrahlung models and fittings
[SH-1.2-3] 23 p3991 N85-34739
Observations of solar flare photon energy spectra from 20 keV to 7 MeV
[SH-1.2-9] 23 p3992 N85-34744
On the detectability of kay-MeV solar protons through their nonthermal Lyman-alpha emission
[SH-1.3-5] 23 p3993 N85-34752
A coded aperture imaging system optimized for hard X-ray and gamma ray astronomy
[OG-9.2-3] 23 p4024 N85-34942
Secondary gamma-ray production in a coded aperture mask
[OG-9.2-6] 23 p4025 N85-34945
The final COS-B database now publicly available
[OG-9.3-8] 23 p4028 N85-34963
Generation of stimulated emission in the soft X-ray range by nonlinear processes with excimer lasers
[DE85-012465] 24 p4096 N85-35403
Status of the zeta(8.3)
[DE85-013070] 24 p4149 N85-35724
Calibration of a high-level photon irradiation
[DE85-013044] 24 p4151 N85-35736
Surface discharges as intense photon sources in the extreme ultraviolet
[DE85-012593] 24 p4158 N85-35782
Circumstellar shells of late-type stars: A study at millimeter and infrared wavelengths
24 p4187 N85-35836
Nucleon-nucleus interactions from JACEE
24 p4173 N85-35869
An experimental study of correlations in the development of the electron-photon cascades
[HE-3.5-10] 24 p4184 N85-35947
Electrons, muons and hadrons in extensive air showers and how do they depend on nuclear interaction model, part 1
24 p4187 N85-35972
The identification of gamma ray induced EAS
[HE-4.5-1] 24 p4195 N85-36028
Electromagnetic and muonic structure of showers initiated by gamma-rays and by hadrons
[HE-4.5-6] 24 p4195 N85-36030
The hump in the Cerenkov lateral distribution of gamma ray showers
[HE-4.5-9] 24 p4195 N85-36032
A three-dimensional Monte Carlo calculation of the photon initiated showers and Kiel result
[HE-4.5-13] 24 p4196 N85-36035
Study of photonuclear muon interactions at Baksan underground scintillation telescope
[HE-5.4-10] 24 p4206 N85-36122

PHOTONUCLEAR REACTIONS
Investigations of the structure and electromagnetic interactions of few-body systems
[DE85-002654] 11 p1721 N85-20824
Reduction of reabsorption effects in scintillators by employing solutes with large Stokes shifts
[DE85-011645] 22 p3836 N85-33767
Nuclear data for MCNP
[DE85-010794] 22 p3840 N85-33782
Longitudinal development of muons in large air showers studies from the arrival time distributions measured at 900m above sea level
[HE-4.7-4] 24 p4199 N85-36055
Study of the time-differentiated particle flux density at various distances from EAS axis
[HE-4.7-15] 24 p4200 N85-36065

PHOTOOXIDATION
Determination of Toluene's degradation products under simulated atmospheric conditions
05 p0574 N85-14331
Modelling of photodegradation in solar cell modules of substrate and superstrate design made with ethylene-vinyl acetate as pottant material
[NASA-CR-175690] 14 p2350 N85-24527
Formation and fate of toxic chemicals in California's atmosphere
[PB85-172609] 18 p3134 N85-29414

The photochemical oxidation of GaAs
[AD-A153699] 19 p3233 N85-30045
Atmospheric nitrogen oxides: Their detection and chemistry
[PB85-193910] 24 p4114 N85-35502

PHOTOPEAK
Intercomparison of the calculated absolute efficiency values between true coaxial and true closed-end coaxial Ge (Li) and NaI detectors
[REPT-5-1984] 20 p3532 N85-31976

PHOTOPLASTICITY
State of stress and penetration of plastic deformation in forming
[BLL-BISI-22199-(9022.06)] 17 p2977 N85-28396

PHOTOPRODUCTION
Muons in gamma showers
[HE-4.5-3] 24 p4195 N85-36027

PHOTORECEPTORS
Gravistimulus production in roots of corn
15 p2607 N85-26066
Mutant peas as probes in the understanding of growth and gravitropism 15 p2611 N85-26068
Differentiating spatial light modulator
[AD-D011727] 23 p3973 N85-34632

PHOTORECONNAISSANCE
Photo-reconnaissance system
[AD-D011287] 06 p0626 N85-15245

PHOTOREDUCTION
U PHOTOCHEMICAL REACTIONS

PHOTORESISTIVITY
U PHOTOCONDUCTIVITY

PHOTORESISTORS
U PHOTOCONDUCTORS

PHOTOSENSITIVITY
NT LIGHT ADAPTATION
NT PHOTOTROPISM
Cerenkov ring imaging detector development at SLAC
[DE84-015883] 04 p0560 N85-13584
FLACS: A new sensitometer for measurement of extreme low intensity reciprocity in a controlled environment — X-ray films 07 p0963 N85-16104
Comparison of the fine grain compensation hypersensitization (FAH) process with gas hypersensitizing technique — astronomical photography plates
07 p0963 N85-16107
Investigation and optimization of fuel production using dye-based transition metal complexes as charge-transfer intermediates
[PB85-161941] 14 p2264 N85-24029
The electrochemistry of azine, oxazine and thiazine dyes
[AD-A152394] 17 p2918 N85-27990
Three-dimensional photochemical machining with lasers
[AD-A154711] 21 p3501 N85-32320
An enhanced photoresponse at dislocation subgrain boundaries revealed by X-ray topography of polysilicon solar cells 22 p3806 N85-33572
Liquid crystal light valve structures
[NASA-CASE-MSC-20036-1] 22 p3847 N85-33826
Electron photoejection in carbanions
[DE85-011747] 23 p3911 N85-34230
Screening and characterizing oleaginous microalgal species from the southeastern United States
[DE85-006787] 23 p3951 N85-34488
High sensitive X-ray films to detect electron showers in 100 GeV region
[HE-3.1-13] 24 p4178 N85-35911

PHOTOSENSORS
U RADIATION MEASURING INSTRUMENTS

PHOTOSPHERE
NT SOLAR GRANULATION
Structure and evolution of the large scale solar and heliospheric magnetic fields
[NASA-CR-175266] 01 p0130 N85-10897
Vector magnetic field analysis of Lorentz forces acting in the solar atmosphere
[AD-A145941] 03 p0449 N85-12852
Elemental abundances of mercury-manganese stars and the population 2 type star HD 109995
[NASA-CR-174296] 08 p1255 N85-17913
Energy release in solar flares
[NASA-CR-174302] 08 p1259 N85-17924
Ultraviolet spectroscopy of the interacting binary U Sagittae 11 p1755 N85-21042
Betageuse at maximum luminosity
11 p1758 N85-21061
Sensitivity of inferred subphotospheric velocity field to mode selection, analysis technique and noise
14 p2442 N85-25065
Magnetoconvection: The interaction of convection and small scale magnetic fields — photosphere
14 p2446 N85-25098
The photospheric temperature structure of magnetic flux tubes 14 p2447 N85-25102
A model for the dynamics of the deep photosphere
14 p2450 N85-25129
Solar cycle variations of sunspot temperatures
14 p2452 N85-25141
Solar cycle variation of ephemeral active regions
14 p2452 N85-25142
Variability of the quiet photospheric network
14 p2452 N85-25144
Measurements of Solar Vector Magnetic Fields
[NASA-CP-2374] 16 p3203 N85-29669
The vector structure of active magnetic fields
16 p3203 N85-29670
Current evolution in a numerical emerging-magnetic-flux model 16 p3204 N85-29675
Stokes parameters modulator for birefringent filters
16 p3205 N85-29684
Magnetic probing of the solar interior
[NASA-CR-176025] 19 p3385 N85-30998
Single-dish high sensitivity determination of solar limb emission at 22 and 44 GHz
[INPE-3545-PRE/758] 19 p3385 N85-30999
Solar photospheric and coronal abundances from solar energetic particle measurements
[NASA-CR-176029] 20 p3547 N85-32073
Contributions to the 19th International Cosmic Ray Conference
[NASA-CR-176060] 21 p3714 N85-33044
Solar coronal and photospheric abundances from solar energetic particle measurements
[PAPER-SH-2.1-5] 21 p3715 N85-33053
Heating of the deep chromosphere during solar flares
[AD-A155258] 21 p3723 N85-33100
Helios 1 energetic particle observations of the solar gamma ray flare events of 7, 21 June 1980 and 3 June 1982
[SH-1.3-8] 23 p3993 N85-34755
Precision measurements of solar energetic particle elemental composition
[SH-2.1-4] 23 p3998 N85-34785
Solar Coronal and photospheric abundances from solar energetic particle measurements
[SH-2.1-5] 23 p3998 N85-34786
Diffusion in the chromosphere and the composition of the solar corona and energetic particles
[SH-2.1-9] 23 p3999 N85-34790
Abundances from solar-flare gamma-ray line spectroscopy
[SH-2.1-13] 23 p3999 N85-34794
The HEAO-2 Guest Investigator Program: Non-linear growth of instabilities in line-driven stellar winds
[NASA-CR-176168] 24 p4168 N85-35840

PHOTOSYNTHESIS
The Marine Resources Experiment Program (MAREX)
[NASA-TM-87368] 01 p0066 N85-10580
Proton pumping in purple membrane, appendix 1
[DE84-014601] 01 p0118 N85-10811
Terrestrial nitrogen cycles: Some unanswered questions 05 p0653 N85-14192
Spectral estimators of absorbed photosynthetically active radiation in corn canopies
[E85-10041] 07 p0983 N85-16242
Variation in photosynthesis with light level for model with two photochemical reactions 07 p1012 N85-16430
Workshop on membrane biophysics
[AD-A148238] 08 p1192 N85-17512
Techniques for measuring intercepted and absorbed PAR in corn canopies
[E85-10081] 10 p1505 N85-19495
Artificial photosynthesis with algal and reconstituted systems
[DE85-002557] 10 p1523 N85-19604
Photosynthesis of ammonia
[DE85-001462] 11 p1595 N85-20029
Energy transfer and photochemistry in biomimetic solar conversion
[PB85-129112] 11 p1677 N85-20566
Effect of elevated atmospheric CO2 on plant communities
[DE85-001810] 11 p1678 N85-20576
Primary light harvesting system: The relationship of phycobilisomes to photosystem 1 and 2
[DE85-003075] 11 p1689 N85-20622
Nitrogen control of photosynthetic protein synthesis
[DE85-003513] 11 p1690 N85-20623
Photosynthetic water splitting
[DE85-002460] 11 p1690 N85-20627
Modulation of light energy transduction in photosynthesis
[DE85-004711] 13 p2141 N85-23292
Ways of optimization of light energy transformation in primary stages of photosynthesis. Necessity of optimization of photosynthetic unit structure and method for calculating efficiency 14 p2366 N85-24700
Ways of optimization of light energy transformation in primary stages of photosynthesis. Optimization of lattice structure of uniform photosynthetic unit
14 p2366 N85-24701
Bioenergy, solar biotech research in France, Europe
15 p2536 N85-25646
Studies of photosynthetic Energy Conversion
[DE85-005973] 15 p2586 N85-25944
Eight DOE Solar Photochemistry Research Conference: Proceedings
[DE85-005094] 15 p2587 N85-25948
Photosynthetic acclimation of Acer saccharum
[DE85-006247] 17 p2998 N85-28536
Atmosphere behavior in gas-closed mouse-algal systems: An experimental and modelling study
18 p3155 N85-29538
Metabolic mechanisms of plant growth at low water potentials 19 p3327 N85-30612
Protocyanobacteria: Oxygenic and Anoxygenic photosynthesis in mat-forming bacteria
21 p3657 N85-32714
Cytochromes and iron sulfur proteins in sulfur metabolism of phototrophic bacteria
21 p3657 N85-32718
Insights into the phylogenetic positions of photosynthetic bacteria obtained from 5S rRNA and 16S rRNA sequence data 21 p3658 N85-32719
Ecophysiology of phototrophic sulfur bacteria in lakes: Vertical distribution of planktonic populations
21 p3658 N85-32722
Anaerobic reduction of elemental sulfur by Chromatium vinoeum and Begglatoa alba 21 p3660 N85-32739
Interactions among sulfide-oxidizing bacteria
21 p3661 N85-32741
Cyanobacterial mats: Microanalysis of community metabolism 21 p3661 N85-32743
Microanalysis of dissolved iron and phosphate in pore waters of hypersaline sediment
21 p3661 N85-32744
Glutathione in cyanobacteria
21 p3661 N85-32745
Microbial communities and microprofiles of sulfide and oxygen of alum rock sulfur springs
21 p3661 N85-32746
Biological modulation of planetary atmospheres: The early Earth scenario 22 p3854 N85-33867

PHOTOTHERMAL CONVERSION
Control and performance of a photovoltaic-thermal energy system 03 p0387 N85-12475
High resolution photoacoustic and photothermal imaging 05 p0723 N85-14649
Photothermal degradation of encapsulants
06 p0630 N85-15270
Short duration winter-time performances of different passive solar systems
[DE85-000850] 11 p1675 N85-20557
Photoacoustic imaging
[AD-A150823] 14 p2416 N85-24905
High-altitude testing of selective optical coatings for solar radiators and collectors 17 p2939 N85-28143
Selective coatings for solar heat converters
17 p2939 N85-28144
Characterization of the optical and thermal properties of matter by photothermal techniques
[DE85-012607] 24 p4076 N85-35260

PHOTOTHERMOTROPISM
U ANISOTROPY
U PHOTOTROPISM
U TEMPERATURE EFFECTS

PHOTOTRANSISTORS
High-temperature optically activated GaAs power switching for aircraft digital electronic control
[NASA-CR-174711] 04 p0457 N85-12901
The touch panel system: Design and development
[AD-A153014] 17 p3008 N85-28596

PHOTOTROPISM
The global sulfur cycle
[NASA-TM-87570] 21 p3656 N85-32710
Phototrophic bacteria and their role in the biogeochemical sulfur cycle 21 p3660 N85-32735
Sulfur cycling and metabolism of phototrophic and filamentous sulfur bacteria 21 p3660 N85-32737
Enrichments for phototrophic bacteria and characterization by morphology and pigment analysis
21 p3660 N85-32738
Buoyant densities of phototrophic sulfur bacteria and cyanobacteria 21 p3660 N85-32740
Interactions among sulfide-oxidizing bacteria
21 p3661 N85-32741
Cyanobacterial mats: Microanalysis of community metabolism 21 p3661 N85-32743
Glutathione in cyanobacteria
21 p3661 N85-32745

PHOTOTUBES
NT PHOTOMULTIPLIER TUBES

PHOTOVISCOELASTICITY
Influence of cyclic thermal loading on internal stress in casted epoxy resin
23 p3908 N85-34211
PHOTOVOLTAGES
Safety requirements for wiring systems and connectors for photovoltaic systems
[NASA-CR-174431] 10 p1477 N85-19324
PHOTOVOLTAIC CELLS
MOD silver metallization for photovoltaics
[NASA-CR-174011] 01 p0026 N85-10163
Summary of trends in photovoltaic patent activity
[DE84-015757] 01 p0068 N85-10452
DOE/SERI polycrystalline thin-film photovoltaic research
[DE84-004516] 02 p0223 N85-11464
Cascaded solar photovoltaic cells based on InP-GaInPAs and InP-CdS heterostructures
02 p0268 N85-11749
Control aspects of the Schuchuli Village stand-alone photovoltaic power system
[NASA-TM-83790] 04 p0495 N85-13157
Evaluation of some photovoltaic concentrator solar cell-heat sink coupling materials
[DE84-016027] 04 p0529 N85-13378
Silicon for solar cells
[DE84-004503] 04 p0529 N85-13381
Microcomputer control of a residential photovoltaic power conditioning system
[DE84-013667] 04 p0547 N85-13480
Trends in space photovoltaic technology
05 p0609 N85-13668
Information package on photovoltaics
05 p0661 N85-14250
Material models and device structures for GaAs solar cells, introduction
05 p0665 N85-14276
Comparison of SCAPID/GaAs to experiment
05 p0665 N85-14279
Encapsulation design analysis
06 p0829 N85-15268
Photothermal degradation of encapsulants
06 p0830 N85-15270
Polymer-polymer interface bond stability
06 p0830 N85-15271
Predicting electrochemical breakdown in terrestrial photovoltaic modules
06 p0830 N85-15273
Module flammability research
06 p0830 N85-15274
Process research of non-Cz silicon material
06 p0830 N85-15275
Thermal characterization of photovoltaic modules in natural environments
06 p0832 N85-15296
Summary of photovoltaic performance models
06 p0832 N85-15298
Characterization of bicrystal grain boundary properties using device structures
[DE84-004509] 06 p0869 N85-15523
Antisoiling technology: Theories of surface soiling and performance of antisoiling surface coatings
[NASA-CR-174274] 07 p0991 N85-16296
What should DOE do to help establish voluntary consensus standards for measuring and rating the performance of PV modules?
[NASA-CR-174295] 07 p0992 N85-16297
Microcomputer control of a residential photovoltaic power conditioning system
[DE84-014774] 07 p1022 N85-16466
Compilation of Sandia papers contributed to the 17th IEEE Photovoltaic Specialists Conference
[DE84-017456] 09 p1315 N85-18257
Signal Hill solar-powered repeater report and recommendations
[DE85-000467] 09 p1316 N85-18273
Diodes in photovoltaic modules and arrays
[NASA-CR-175454] 10 p1508 N85-19513
Mod silver metallization for photovoltaics
[NASA-CR-174444] 10 p1509 N85-19518
Investigation of accelerated stress factors and failure/degradation mechanisms in terrestrial solar cells
[NASA-CR-175469] 10 p1510 N85-19524
Analysis of inverter models and harmonic propagation. Part 3: Transient processes in inverter models
[DE85-000191] 10 p1510 N85-19530
Overview of photovoltaic concentrator technology
[DE84-016790] 10 p1512 N85-19539
Surface and allied studies in silicon solar cells
[NASA-CR-174447] 11 p1671 N85-20631
Research on the basic understanding of high efficiency in silicon solar cells
[DE85-000607] 11 p1672 N85-20637
GaAs and 3-5 compound solar cells status and prospects for use in space
[NASA-TM-86960] 12 p1705 N85-21281
Power from the Sun: Light at night
[PB85-124097] 12 p1893 N85-21814
History and future views on solar cells of Japanese scientific satellites
13 p2005 N85-22566
Thin and ultrathin silicon solar cells for space use
13 p2005 N85-22567
Space solar cells: Adjusting to new demands
13 p2005 N85-22568
The high voltage silicon cell: A comparative analysis
13 p2005 N85-22569
A 2 x 6 Back Surface Reflection (BSR) silicon solar cell
13 p2005 N85-22570
Experiences with Implanted Back Surface Field (BSF) solar cells
13 p2005 N85-22571
A low cost approach with larger diameter silicon wafer — solar cells
13 p2006 N85-22572
Bifacial light sensitive space solar cell
13 p2006 N85-22573
Gallium arsenide arrays versus silicon arrays for space application
13 p2006 N85-22574
Space qualified AlGaAs/GaAs solar cells
13 p2006 N85-22575
Availability of AlGaAs/GaAs solar cells in space
13 p2006 N85-22576
Comparative study of GaAs solar cell potentialities for space applications
13 p2006 N85-22577
Investigation of high output gallium arsenide solar cells
13 p2006 N85-22578
Development of very thin large area GaAs solar cells for space application
13 p2006 N85-22579
GaAs and 3-5 compound solar cells status and prospects for use in space
13 p2007 N85-22580
GaAlAs-GaAs solar cell development: Prospective for space applications under concentration
13 p2007 N85-22581
Investigation of the degradation of GaAs photovoltaic cells by proton and electron irradiation
13 p2008 N85-22587
Electrical design of the Intelsat 6 solar generator
13 p2008 N85-22592
Survival testing of silicon solar modules
13 p2009 N85-22602
Calibration of solar cells outside the atmosphere
13 p2009 N85-22603
Inverse behavior of silicon photovoltaic cells
13 p2010 N85-22604
NASA photovoltaic research and technology development program for space applications
13 p2011 N85-22617
High output photovoltaic conversion: The quadrispectral project — spacecraft power supplies
13 p2012 N85-22626
Operational performance of the photovoltaic-powered grain mill and water pump at Tangaye, Burkina Faso (formerly Upper Volta)
[NASA-TM-86970] 13 p2126 N85-23243
Photovoltaic cells of InP-CdS heterojunction type and their temperature characteristics under A-M illumination
14 p2275 N85-24092
Dependence of parameters of silicon photovoltaic cells on temperature and light intensity
14 p2275 N85-24094
Silicon-sheet and thin-film cell and module technology potential: Issue study
[NASA-CR-175654] 14 p2349 N85-24520
Intermediate load modules for test and evaluation
[NASA-CR-175697] 14 p2350 N85-24526
Modeling and optimization of a multiple-cell photovoltaic converter system
15 p2585 N85-25934
Electrical research on solar cells and photovoltaic materials
[NASA-CR-175699] 15 p2585 N85-25935
Ink jet printing of silver metallization for photovoltaics
[NASA-CR-175798] 15 p2586 N85-25943
Solar elements with distributed parameters
16 p2760 N85-27036
Photovoltaic cell reliability research: Investigation of accelerated stress factors and failure-degradation mechanisms in terrestrial solar cells
[NASA-CR-175815] 16 p2819 N85-27388
Design and development of a linear Fresnel lens air-cooled photovoltaic module and a stand-alone photovoltaic collector array
[DE85-008864] 16 p2819 N85-27391
Electrical research on solar cells and photovoltaic materials
[NASA-CR-175897] 17 p2986 N85-28452
Terrestrial photovoltaic power systems with sunlight concentration
[DE85-006398] 17 p2987 N85-28464
SERI photovoltaic advanced research and development project: FY 1984 accomplishments
[DE85-002939] 18 p3128 N85-29368
Airport solar photovoltaic concentrator phase 3
[DE85-006773] 18 p3128 N85-29370
Dynamic simulation of dispersed, grid-connected photovoltaic power systems: System studies
[DE85-011179] 19 p3262 N85-30231
Increased voltage photovoltaic cell
[NASA-CASE-NPO-16155-1] 19 p3303 N85-30475
Current status of silicon materials research for photovoltaic applications
[DE85-008799] 19 p3304 N85-30482
Block 5 documentation and solar modules
[NASA-CR-176009] 19 p3306 N85-30494
Using PVFORM, a systems performance model, to determine optimum mounting configurations for flat-plate photovoltaic modules
[DE85-011191] 19 p3306 N85-30495
Electricity from sunlight: The emergence of photovoltaics, revised edition
[DE85-002920] 19 p3307 N85-30502
Historical perspective of barriers to achieving high-efficiency silicon solar cells
20 p3479 N85-31616
User handbook for block 5 silicon solar cell modules
[NASA-CR-176043] 20 p3483 N85-31644
Photovoltaic concentrator research status
[DE85-010119] 20 p3483 N85-31647
Gallium arsenide arrays versus silicon arrays for space application
[SNIAS-851-440-104] 20 p3485 N85-31657
Photovoltaic solar devices
[BMFT-FB-T-84-288] 20 p3485 N85-31660
High-efficiency crystalline silicon technology development
21 p3607 N85-32395
Flat-plate module efficiency versus cost tradeoffs
21 p3607 N85-32396
Georgetown University Photovoltaic Higher Education National Exemplar Facility (PHENEF)
21 p3607 N85-32400
Photothermal degradation studies of encapsulants
21 p3608 N85-32403
Topics in electrochemical degradation of photovoltaic modules
21 p3608 N85-32410
Polymer-water interaction studies
21 p3609 N85-32411
Encapsulation processing and manufacturing yield analysis
21 p3611 N85-32434
Photovoltaic module spread-of-flame testing
21 p3612 N85-32448
Development of high-efficiency solar cells on silicon web
[NASA-CR-176101] 22 p3805 N85-33568
Photovoltaics technical information guide
[DE85-002924] 22 p3806 N85-33585
Photovoltaic industry progress through 1984
[DE85-013029] 22 p3809 N85-33598
Federal export assistance programs applicable to the US photovoltaic industry
[NASA-CR-176114] 22 p3849 N85-33841
Thermionic photovoltaic energy converter
[NASA-CASE-LEW-14077-1] 23 p3944 N85-34441
Practical aspects of photovoltaic technology, applications and cost (revised)
[NASA-CR-174863] 24 p4110 N85-35472
Monolithic photovoltaic series array for an energy coupler
[BMFT-FB-T-85-023] 24 p4113 N85-35496
PHOTOVOLTAIC CONVERSION
Control and performance of a photovoltaic-thermal energy system
03 p0397 N85-12475
Advanced amorphous materials for photovoltaic conversion
[DE84-017198] 04 p0529 N85-13384
National Photovoltaics Program Annual Review Meeting, abstracts
[DE84-013003] 04 p0530 N85-13390
Health and environmental effects document for photovoltaic energy systems, 1983
[DE84-017179] 04 p0532 N85-13399
Photovoltaic working group report
05 p0611 N85-13902
Information package on photovoltaics
05 p0661 N85-14250
Stimulation of technologies towards photovoltaic energy conversion
05 p0661 N85-14251
Photovoltaic power supply units
05 p0662 N85-14252
Development and construction of a prototype photovoltaic energy supply unit
05 p0662 N85-14254
Fundamentals of solar energy conversion based on fluorescence collectors
05 p0662 N85-14258
Energy storage with lead acid batteries in photovoltaic systems
05 p0663 N85-14260
The 15 photovoltaic pilot projects of the European Communities
05 p0663 N85-14263
Photovoltaic 100 kWp pilot plant on the Greek island Kythnos
05 p0664 N85-14266
Mains-connected photovoltaic system for a house
05 p0664 N85-14267
Photovoltaic pump systems
05 p0664 N85-14269
Utilization possibilities of photovoltaics in the private sector
05 p0664 N85-14272

Considerations on the dimensioning of photovoltaic supply systems in the low power range
05 p0665 N85-14273
Solar energy conversion based on the principle of fluorescent collectors. Installation of a test collector to deliver several Watts power
[BMFT-FB-T-84-192] 07 p0993 N85-16308
Solar energy conversion based on the principle of fluorescent collectors
[BMFT-FB-T-84-193] 07 p0994 N85-16309
MOD silver metallization for photovoltaics
[NASA-CR-175460] 10 p1510 N85-19526
Photovoltaic Systems Development and Evaluation Projects Integration Meeting
[DE84-006530] 11 p1673 N85-20542
International Congress Centrum Berlin report on photovoltaics 12 p1877 N85-21773
Crystallization methods for solar cell silicon
12 p1877 N85-21774
Development and prototype construction of photovoltaic energy supply units 12 p1878 N85-21781
Photovoltaic solar components
12 p1878 N85-21782
Photovoltaic roofing tile systems
12 p1878 N85-21783
Investigation of the optical properties of solar elements 12 p1879 N85-21786
Development of high-efficiency economic systems for photovoltaics 12 p1880 N85-21795
Photovoltaic Generators in Space — conferences
[ESA-SP-210] 13 p2005 N85-22565
NASA photovoltaic research and technology development program for space applications
13 p2011 N85-22617
Study of concentration for space photovoltaic generators 13 p2011 N85-22618
High output photovoltaic conversion: The quadrispectral project — spacecraft power supplies
13 p2012 N85-22626
Module performance and failure analysis area: Flat-plate solar array project
[NASA-CR-175669] 15 p2585 N85-25936
Documents of the JPL Photovoltaics Program Analysis and Integration Center: An annotated bibliography
[NASA-CR-175873] 17 p2985 N85-28448
Development of a second-generation linear Fresnel Photovoltaic and Thermal (PVT) concentrator array, including fabrication and installation of a 200 square meter collector field
[DE85-006473] 17 p2988 N85-28465
Investigation of a Si and related semiconductors as materials for photovoltaic conversion
[DE85-002932] 18 p3096 N85-29163
Research recommendations for ac interfacing between electric utility transmission and distribution systems and wind, photovoltaics, and OTEC energy systems
[DE85-002942] 18 p3096 N85-29169
Photovoltaic Systems Development Project: An activity summary
[DE85-009994] 18 p3129 N85-29379
Electricity from sunlight: The emergence of photovoltaics, revised edition
[DE85-002920] 19 p3307 N85-30502
Nomographs for estimating the levelized cost of energy from flat-plate and concentrator photovoltaic systems
[NASA-CR-176048] 20 p3483 N85-31645
Study of concentration for space photovoltaic generators
[SNIAS-851-440-105] 20 p3485 N85-31658
Investigation of the microstructure and photovoltaic properties of semicrystalline silicon
22 p3506 N85-33573
Photovoltaic energy systems
[DE85-011630] 22 p3507 N85-33581
Photovoltaics technology program summary
[DE85-013098] 24 p4112 N85-35493
Design and construction of an advanced power conditioning subsystem for small photovoltaic applications
[DE85-013940] 24 p4113 N85-35495

PHOTOVOLTAIC EFFECT
MOD silver metallization for photovoltaics
[NASA-CR-174011] 01 p0026 N85-10163
Automated installation methods for photovoltaic arrays 2
[SAND-84-7095] 02 p0222 N85-11453
Modular photovoltaic array field
[SAND-83-7028] 02 p0222 N85-11454
Research on gallium arsenide diffused junction solar cells
[NASA-CR-174057] 02 p0222 N85-11457
Research directions and progress in the SERI advanced high efficiency concept program
[DE84-004582] 02 p0223 N85-11462
Five year research plan, 1984-1988. Photovoltaics: Electricity from sunlight
[DE84-013009] 04 p0528 N85-13377
Trends in space photovoltaic technology
05 p0609 N85-13688
Information package on photovoltaics
05 p0661 N85-14250
What should DOE do to help establish voluntary consensus standards for measuring and rating the performance of PV modules?
[NASA-CR-174265] 07 p0992 N85-16297
The 35 kilowatt peak power photovoltaic system
[DE85-000189] 10 p1511 N85-19537
Study of low energy density photovoltaic applications under varying rate structures
[DE85-000185] 10 p1511 N85-19538
Value of PV systems experiments. Volume 1: A preliminary assessment of the lessons learned from nine intermediate-size systems
[DE85-001494] 11 p1674 N85-20548
Abstracts of 6th Annual Review Meeting on Photovoltaic Advanced Research and Development
[DE84-013047] 13 p2128 N85-23246
MOD silver metallization for photovoltaics
[NASA-CR-175773] 16 p2818 N85-27361
Maintenance of photovoltaic power systems
[AD-A152299] 16 p2819 N85-27390
Study of the degradation of short-circuit current and the open-circuit tension of spatial solar cells as a function of the fluency of 1MeV electrons
[INPE-3356-PRE/634] 16 p2887 N85-27814
Relative potentials of concentrating and two-axis tracking flat-plate photovoltaic arrays for central-station applications
[NASA-CR-175889] 17 p2985 N85-28446
Research recommendations for ac interfacing between electric utility transmission and distribution systems and wind, photovoltaics, and OTEC energy systems
[DE85-002942] 18 p3096 N85-29169
Photovoltaic Systems Development Project: An activity summary
[DE85-009994] 18 p3129 N85-29379
Some practical considerations for economical back contact formation on high efficiency solar cells
20 p3479 N85-31620
High efficiency solar cell research for space applications 20 p3480 N85-31624
Structural defects in crystalline silicon
20 p3481 N85-31630
Air Force Federal Photovoltaic Utilization Program
[DE85-010812] 20 p3484 N85-31648
Predicting photothermal field performance
21 p3606 N85-32404
Micromolecular modeling 21 p3606 N85-32405
Silicon refinement by chemical vapor transport
21 p3609 N85-32412
MOD silver metallization for photovoltaics
21 p3610 N85-32428
Ink jet printing of silver metallization for photovoltaics
[NASA-CR-176054] 22 p3505 N85-33569
Investigation of the microstructure and photovoltaic properties of semicrystalline silicon
22 p3506 N85-33573
Photovoltaic industry progress through 1984
[DE85-013029] 22 p3509 N85-33596
Thermionic photovoltaic energy converter
[NASA-CASE-LEW-14077-1] 23 p3944 N85-34441
Investigation of test methods, material properties, and processes for solar cell encapsulants
[NASA-CR-176132] 23 p3945 N85-34446

PHTHALATES
The synthesis and characterization of Poly(Oxy(2-Methyl-1,3-Phenylene) Methyl-1,3 -Phenylene) Oxyterephthaloyl)Oxy
[AD-A146209] 08 p1133 N85-17143
Crystallization behavior of poly(3,3-bis(Ethoxymethyl) oxetane) and poly(3,3-bis(Azidomethyl) oxetane)
[AD-A146271] 08 p1226 N85-17720
Stabilized unsaturated polyesters
[NASA-CASE-NPO-16103-1] 18 p3078 N85-29043
Condensation of anhydrides or dicarboxylic acids with compounds containing active methylene groups. Part 19: Condensation of phthalic and substituted phthalic anhydrides with benzoylacetic ester
[NASA-TM-77885] 19 p3227 N85-30009
Condensation of anhydrides or dicarboxylic acids with compounds containing active methylene groups. Part 1: Condensation of phthalic anhydride with acetoacetic and malonic ester
[NASA-TM-77886] 19 p3227 N85-30010
Processable and stable conductive polymers
[AD-D011684] 19 p3249 N85-30143

PHTHALOCYANIN
Two silicon phthalocyanines and a silicon naphthalocyanine: Synthesis, electrochemistry and electrogenerated chemiluminescence
[AD-A144760] 01 p0023 N85-10145
A silicon phthalocyanine and a silicon naphthalocyanine: Synthesis, electrochemistry, and electrogenerated chemiluminescence
[AD-A146441] 06 p0765 N85-14895
Electronic and redox properties of stacked-ring silicon phthalocyanines from molecular orbital theory
[AD-A147161] 07 p0922 N85-15844
Phthalocyanine polymers
[NASA-CASE-ARC-11413-1] 12 p1809 N85-21348
The production of copper phthalocyanine and/or its derivatives
[NASA-TM-77629] 17 p2917 N85-27963
The electronic spectra of phthalocyanine radical anions and cations
[AD-A152326] 17 p2918 N85-27966
Photochemistry of coordination complexes: The phthalocyanines
[DE85-007693] 17 p2923 N85-28022
Metallophthalocyanine dimers incorporating five atom covalent bridges
[AD-A154365] 19 p3234 N85-30051
Metal (2) 4,4',4',4'' phthalocyanine tetraamines as curing agents for epoxy resins
[NASA-CASE-ARC-11424-1] 23 p3919 N85-34281

PHUGOID OSCILLATIONS
U OSCILLATIONS
U OSCILLATORS
U PITCH (INCLINATION)

PHYLLOQUINONE
Vitamin K and the metabolic state of bone
05 p0694 N85-14485

PHYSICAL CHEMISTRY
NT QUANTUM CHEMISTRY
National Science Foundation grants and awards for fiscal year 1983, volume 2
[PB84-212323] 01 p0125 N85-10854
Physico-chemical investigation of some areas of fundamental significance to biophysics
[DE84-016385] 04 p0471 N85-12999
Surface physics instrumentation
[AD-A149304] 11 p1728 N85-20869
Physical-chemical investigations of copper sulfides for use in CdS/Cu2S solar cells 12 p1880 N85-21794
Estimating degree of development of physical-chemical interaction among components in Al-B fiber composite material 13 p2027 N85-22705
Physical chemistry of exothermic gas-aerosol calorimetry
[AD-A150872] 14 p2251 N85-23950
Abstracts of the 36th Southeastern Regional Meeting of the American Chemical Society
[AD-A151506] 15 p2496 N85-25394
Atmosphere behavior in gas-closed mouse-algal systems: An experimental and modelling study
18 p3155 N85-29536
Chemistry division report
[DE85-010586] 24 p4071 N85-35228

PHYSICAL CONSTANTS TESTING REACTOR
U NUCLEAR RESEARCH AND TEST REACTORS
U WATER COOLED REACTORS

PHYSICAL ENDURANCE
U PHYSICAL FITNESS

PHYSICAL EXAMINATIONS
Health examination findings among active civil airmen
[AD-A148325] 08 p1195 N85-17533

PHYSICAL EXERCISE
NT HYPERKINESIA
The Reports of Aeromedical Laboratory, volume 25, no. 1/2
[ISSN-0023-2858] 01 p0090 N85-10605
The effects of isotonic training on +Gz tolerance
01 p0090 N85-10607
Effect of maximum physical load on oxygen-transport properties of blood 01 p0093 N85-10627
Oxygen delivery during exercise: Limitations to maximum flow 05 p0688 N85-14424
The effect of propranolol on the training response to endurance exercise in normal human adults
05 p0696 N85-14479
A machine for weight-lift testing
[AD-A148816] 07 p0973 N85-16182
Change in relationship of biopotentials of brain zones for various levels of working capacity
07 p1013 N85-16438
Encephalographic correlates of autogenous change in human functional state 08 p1193 N85-17518
Effect of prolonged hunger during experimental hikes
11 p1692 N85-20837
Sleep deprivation and exercise tolerance
[AD-A150180] 13 p2142 N85-23295

Sleep deprivation and exercise tolerance
[AD-A150586] 13 p2142 N85-23296
Sleep deprivation and exercise tolerance
[AD-A150826] 13 p2142 N85-23297
Peripheral changes in regional sweating responses to exercise in hypobaric environments
[AD-A150757] 14 p2388 N85-24710
Heat injury: Prevention is the key
[AD-A153734] 19 p3328 N85-30822
Cosmonauts' cardiovascular system function during long-term orbital flights aboard Salyut-6 station
22 p3733 N85-33141
Cardiorespiratory function and work performance during adaptation to industrial labor in midalpine conditions
22 p3820 N85-33665

PHYSICAL FACTORS
Critical assessment of low fluence irradiation creep mechanisms
[DE84-015578] 02 p0184 N85-11232
Glucose tolerance in trained and untrained subjects during head-down tilt (6 deg) 05 p0693 N85-14461
Physical dimensions of humans, values, envelope curves in different postures
[HSE-TRANS-10869] 20 p3513 N85-31838

PHYSICAL FITNESS
A machine for weight-lift testing
[AD-A146816] 07 p0973 N85-16182
Human factors and training research in military organizations and systems
[AD-A146832] 07 p1020 N85-16475
Assessment of muscle strength and prediction of lifting capacity in US Army personnel
[AD-A148846] 10 p1527 N85-19633
SPARTEN (Scientific Program of Aerobic and Resistance Training Exercise in the Navy): A total body fitness program for health and physical readiness
[AD-A150869] 14 p2388 N85-24711
Relationship between the Army two mile run test and maximal oxygen uptake
[AD-A153914] 18 p3154 N85-29526
Physical training and G tolerance
20 p3511 N85-31824
Centrifuge operations and training in the Royal Netherlands Air Force 20 p3511 N85-31825
An analysis of aerobic capacity in a large United States population
[AD-A156200] 24 p4132 N85-35614
Relaxation techniques
[AD-A156248] 24 p4133 N85-35621

PHYSICAL OPTICS
An analysis of physical optics models for rough surface scattering
[AD-A154960] 21 p3575 N85-32235

PHYSICAL PROPERTIES
Properties of polycaproamide fibers modified by grafted polyacrylonitrile 06 p0761 N85-14867
Special soft solder TK-3 (L-SnCu 3 - DIN 1707)
[BLL-T6384/BG/WH799/84(9022.48)]
06 p0767 N85-14907
Online directory of databases for material properties
[DE84-016511] 09 p1402 N85-18624
Study of the physical properties of crystalline rocks in the southeast Voronezh anteclise
[NASA-TM-77823] 10 p1514 N85-19551
The physical and mechanical properties of near-equiatomic titanium-nickel
19 p3237 N85-30072

PHYSICAL SCIENCES
National Science Foundation grants and awards for fiscal year 1983, volume 2
[PB84-212323] 01 p0125 N85-10854
Effect of physical work and sleep loss on recovery sleep
[AD-A146062] 03 p0401 N85-12554

PHYSICAL WORK
Psychological issues in the design of expert systems
[AD-A146081] 03 p0436 N85-12792
Factors determining effectiveness of voluntary decrease in ventilation during muscular work using instrumented feedback 06 p1193 N85-17520
Cognitive performance during successive sustained physical work episodes
[AD-A148081] 06 p1200 N85-17556

PHYSICS
Overview of the physics issues at the SSC
[DE85-007074] 16 p2659 N85-27634
Proceedings of the 19th Annual Conference of the Finnish Physical Society
[REPT-104] 20 p3532 N85-31974
Solar energy education: Renewable energy activities for chemistry and physics
[DE85-010371] 23 p3946 N85-34455

PHYSIOCHEMISTRY
Review on physiological and medical problems related to climates ranging from altitude to sub-tropics
05 p0687 N85-14417
Physio-chemical mechanisms of the processes of the formation of globular inclusions in ball-bearing metal
[BLL-BISI-TRANS-22235-(9022.06)]
17 p2924 N85-28030
Physical-chemical model for the mechanism of glass corrosion with particular consideration of simulated radioactive waste glasses
[DE85-007713] 17 p2935 N85-28121
Effect of heating temperature in a vacuum on state of surface layers of welded OT4 titanium alloy
19 p3245 N85-30123
Physiochemically controlled scour jet array system
[AD-D011686] 19 p3308 N85-30505
Zinc: Biological effects. Facts and fiction
[USIP-84-12] 20 p3507 N85-31796
Activities report in nuclear physics and particle acceleration 20 p3532 N85-31977
Ecophysiology of phototrophic sulfur bacteria in lakes: Vertical distribution of planktonic populations
21 p3658 N85-32722
Tests on zirconium nitride coatings applied to SW 18 steel using the chemical vapor deposition method
24 p4078 N85-35271

PHYSIOGRAPHY
U GEOMORPHOLOGY

PHYSIOLOGICAL ACCELERATION
Problems of aviation and space medicine and psychology discussed at 14th Gagarin lectures
23 p3954 N85-34509

PHYSIOLOGICAL EFFECTS
NT HEMODYNAMIC RESPONSES
NT PHYSIOLOGICAL RESPONSES
A study of fatigue of shiftworkers in air traffic control and weather service groups in JASDF
01 p0090 N85-10610
Circulatory orthostatic instability: Role of deconditioning of resistive vessels 01 p0091 N85-10612
Hemopoiesis in rats submitted to weightlessness
01 p0091 N85-10613
Frequency and nature of electrocardiographic disturbances in dogs during single and repeated exposure to +G sub z accelerations 01 p0092 N85-10619
Dynamics of morphological changes in articulation nervous system under hypokinetic conditions as a model of a spaceflight factor 01 p0092 N85-10621
Effect of 1,25-dihydroxycholecalciferol and 24,25 dihydroxycholecalciferol on growth and alteration of rat bones during hypokinesa (histomorphometric study)
01 p0092 N85-10622
Dynamics of some parameters of carbohydrate and lipid metabolism in recovery period following long-term hypokinesa 01 p0093 N85-10623
Biligenic function of white rat liver
01 p0093 N85-10624
Effect of short-term hypokinesis on rat opioid system reaction 01 p0093 N85-10625
Reaction of cerebral ventricles to antiorthostatic position and occlusion of jugular veins 01 p0093 N85-10626
Effect of maximum physical load on oxygen-transport properties of blood 01 p0093 N85-10627
Effect of hyperoxia and increased gas atmosphere density on contractile function of the right ventricle
01 p0093 N85-10628
Change in energetics of muscular contraction as a result of hyperoxia 01 p0093 N85-10629
Hemodynamics and neurodynamics of the human brain during exposure to moderate hypoxic hypoxia
01 p0094 N85-10630
Proton pumping in purple membrane, appendix 1
[DE84-014601] 01 p0118 N85-10811
The effect of sleep loss on the human visual event-related potential
[AD-A145364] 02 p0234 N85-11526
Mechanisms of oxygen toxicity and methods of protection
[AD-A145830] 03 p0400 N85-12551
The effects of helicopter vibration on the spinal system
[AD-A146274] 03 p0402 N85-12562
A survey of space biology and space medicine
[ESA-BR-17] 04 p0545 N85-13486
Review on physiological and medical problems related to climates ranging from altitude to sub-tropics
05 p0687 N85-14417
Pharmacokinetic interactions of mixtures
[AD-P004032] 06 p0844 N85-15362
Aspects of solvent toxicity in mixtures
[AD-P004036] 06 p0845 N85-15366
The epidemiology and toxicology of Agent Orange
[AD-P004038] 06 p0845 N85-15368
Human reactions to transient electric currents, volume 12
[PB84-231463] 06 p0846 N85-15374
Pulmonary blood flow and oxygenation of arterial blood in a healthy subject upon 7 days hypokinesis
07 p1014 N85-18439
Testing changes in visual function due to orbital environment
[AD-A147259] 07 p1016 N85-18453
Tolerance endpoint for evaluating the effects of heat stress in dogs
[AD-A148104] 08 p1192 N85-17511
Encephalographic correlates of autogenous change in human functional state 08 p1193 N85-17518
Dynamics of external respiration and gas metabolism under combined effect of hypoxia and hypercapnia
08 p1193 N85-17519
Influence of activation of ASFS-2 on human emotional status 08 p1194 N85-17522
Effects of prolonged hypokinesis on nervous system
08 p1194 N85-17524
The effect of beta adrenergic blockade on ratings of perceived exertion
[AD-A148053] 08 p1195 N85-17530
Effects of pyridostigmine on psychomotor and visual performance
[AD-A148553] 08 p1196 N85-17539
Gravity and biological systems: Emphasis on human physiology
[ESA-SR-21] 09 p1360 N85-18558
Effect of modulated ultrahigh frequency field on behavior and hormone level in female rats under emotional stress
09 p1361 N85-18562
Study of bodily functional status and quality of controlling action of power unit operators with various intensities of labor 09 p1362 N85-18569
Construction and application of a questionnaire for the social scientific investigation of environmental noise effects
[NASA-TM-75492] 10 p1512 N85-19544
Genetic effects of microwave exposure on mammalian cells in vitro, volume 2
[AD-A149347] 10 p1523 N85-19603
Work physiology of operating personnel at power plants in arid regions 10 p1523 N85-19606
Effects of overall vibration and noise on operational personnel 10 p1523 N85-19608
Management of vibration sickness in coal mines by hyperbaric oxygenation 10 p1523 N85-19609
Influence of hyperthermia on body temperature and content of catecholamines in white rat hypothalamus
10 p1524 N85-19615
Aircraft noise effects: An interdisciplinary study of the effects of aircraft noise on man. Part 1: Basic report
[NASA-TM-75819] 10 p1526 N85-19629
Aircraft noise effects: An interdisciplinary study of the effect of aircraft noise on man. Part 2: Appendix
[NASA-TM-75818] 10 p1527 N85-19630
Aircraft noise effects: An inter-disciplinary study of the effect of aircraft noise on man. Part 3: Supplementary analyses of the social-scientific portion of the study on aircraft noise conducted by the DFG
[NASA-TM-75802] 10 p1527 N85-19631
Health assessment document for carbon tetrachloride
[PB85-124196] 10 p1528 N85-19638
Mercury health effects update: Health issue assessment
[PB85-123925] 10 p1528 N85-19639
Heat stress and personal protective equipment
[DE85-009552] 10 p1532 N85-19652
Observations of physiological and psychological effects of terrain following flight based on in-flight test experience 10 p1532 N85-19657
Tolerance, fatigue, physiological and performance effects of sustained and oscillating lateral accelerations
10 p1533 N85-19659
Biomechanics finds practical applications in aerospace research 11 p1621 N85-20205
Physiological considerations of artificial gravity
11 p1643 N85-20351
Physiological considerations of artificial gravity
11 p1645 N85-20366
USSR report: Life sciences. Biomedical and behavioral sciences
[JPRS-USB-85-010] 11 p1690 N85-20628
Functional system theory in practice
11 p1690 N85-20629
Effects of hyperthermia on free amino acids in rat brain and in subcellular fractions 11 p1691 N85-20631
Effects of hypothermia on brain metabolism
11 p1692 N85-20636
Effect of prolonged hunger during experimental hikes
11 p1692 N85-20637
Laboratory tests of motion sickness susceptibility
11 p1694 N85-20648
Simulator sickness: Reaction to a transformed perceptual world. 6: Preliminary site surveys
11 p1694 N85-20653
Analysis of head motion during simulated, rough water operation of a 2200 ton surface effect ship
11 p1695 N85-20656

The current status of the RAF programme of desensitisation for motion sick aircrew
11 p1695 N85-20658
Symposium on Military Aviation Medicine summarized
11 p1696 N85-20663
Air quality criteria for ozone and other photochemical oxidants. External review draft, volume 2
[PB85-126043] 12 p1896 N85-21836
Research and technology activities at Ames Research Center's Biomedical Research Division
[NASA-TM-86692] 12 p1899 N85-21925
USSR report: Space Biology and Aerospace Medicine, volume 18, no. 6, November - December 1984
[JPRS-USB-85-002] 12 p1900 N85-21951
Distinctive morphological manifestations of acute stress reaction in adrenal cortex of hypokinetic rats
12 p1902 N85-21944
Multiple regression method used to assess animal adaptation to hypoxic hypoxia 12 p1902 N85-21947
Results of sanitary-microbiological studies aboard Cosmos-1129 biosatellites 12 p1903 N85-21952
Rat tissue opioid peptide content during long-term hypokinesia 12 p1904 N85-21954
Effect of long-term repeated exposure to high-intensity stationary magnetic field on adrenomedullary activity
12 p1904 N85-21955
Effect of stationary magnetic field on bleeding time
12 p1904 N85-21956
High pressure environmental conditioning systems and chamber rehabilitation
[AD-A150039] 12 p1905 N85-21964
Effect of broad-band constant noise on some systems of animal body 14 p2367 N85-24705
Aerobic and anaerobic exercise tolerance in the heat: Effect and acclimatization 14 p2368 N85-24707
Effects of muscle atrophy on motor control: Cage size effects 15 p2609 N85-26080
Neural mechanism by which gravitational stimulus and stress affect the secretion of renin and other hormones
15 p2610 N85-26083
Homeostasis in primates in the hyperdynamic environment — circadian timekeeping and effects of lower body positive pressure on sleep
15 p2610 N85-26085
Predictions of cardiovascular responses during STS reentry using mathematical models
[NASA-CR-171671] 15 p2616 N85-26119
Description, validation, and modification of the Guyton model for space-flight applications. Part A. Guyton model of circulatory, fluid and electrolyte control. Part B. Modification of the Guyton model for circulatory, fluid and electrolyte control
[NASA-CR-171676] 15 p2616 N85-26122
Mathematical modeling of fluid-electrolyte alterations during weightlessness
[NASA-CR-171661] 15 p2617 N85-26125
Assessing the short- and long-term health effects of decompression sickness among US Navy divers
[AD-A151667] 15 p2618 N85-26132
A brief description of the two primate experiments to be carried out on SL-4 15 p2667 N85-26597
Cardiovascular effects of weightlessness
15 p2668 N85-26607
Percutaneous connectors
[NASA-CR-175627] 16 p2839 N85-27508
Biological and human health effects of extremely low frequency electromagnetic fields. Post-1977 literature review
[AD-A152731] 17 p2999 N85-28539
Mechanizing of handling operations in drop forging with hammers and presses (conducted ergonomical examinations)
[BMFT-FB-HA-84-051] 17 p3002 N85-28561
Internal contamination issues
18 p3156 N85-29543
Ambient air contamination: Characterization and detection techniques 18 p3157 N85-29546
Internal contamination in the space station
18 p3157 N85-29549
Alloy development for irradiation performance
[DE85-010454] 19 p3240 N85-30091
Cosmonauts' postural reactions after long-term missions aboard Salyut-6 orbital station 19 p3323 N85-30565
Effect of triphthasine and elenium on changes in evoked bioelectrical activity of the brain exposed to stationary magnetic field 19 p3325 N85-30601
Aviation noise effects
[AD-A154319] 19 p3352 N85-30776
Phenomenon of universal rosette-forming cell stimulation by extreme stress 20 p3505 N85-31789
Changes in pentose and glucuronate pathway dehydrogenases in rat brains following single or multiple hypothermic episodes 20 p3505 N85-31790
Anatomy of stress 20 p3505 N85-31791
Zinc: Biological effects. Facts and fiction
[USIP-84-12] 20 p3507 N85-31798
Gas analysis techniques for human physiological measurements in space — Spacelab
[A/95371] 20 p3507 N85-31803
Results of Space Experiments in Physiology and Medicine and Informal Briefings by the F-16 Medical Working Group
[AGARD-CP-377] 20 p3507 N85-31805
Evaluation of Results of Space Experiments in Physiology and Medicine and Informal Briefings by the F-16 Medical Working Group 20 p3508 N85-31806
Postural adjustments associated with arm movements in weightlessness 20 p3509 N85-31813
Cardiovascular research in space: Problems and results 20 p3510 N85-31817
G-induced Loss of Consciousness (GLC)
20 p3510 N85-31823
Study of requirements for and method of multidimensional acoustic imaging — spaceborne experiments
[ESA-CR(P)-2020] 20 p3525 N85-31924
Results and prospects of physiological research during spaceflights 22 p3732 N85-33139
Antihypertensive neutral lipid
[DE85-011625] 22 p3819 N85-33656
Effects of immobilization and high-altitude adaptation on energy metabolism in rats 22 p3820 N85-33663
Mammalian tissue sensitivity to long-term exposure to high-intensity stationary magnetic fields
22 p3823 N85-33686
Rat skeletal muscles with simulation of physiological effects of weightlessness (morphological study)
23 p3953 N85-34502
Proceedings of a Scientific Meeting on the Occasion of the Inauguration of New Buildings for the DFVLR Institute for Aerospace Medicine
[ESA-TT-857] 24 p4129 N85-35595
The deep diving simulator TITAN: Physiological problems associated with staying in great depths of water 24 p4130 N85-35604
Genetic and physiological control of protective antigen synthesis by bacillus anthracis
[AD-A156324] 24 p4133 N85-35617

PHYSIOLOGICAL FACTORS
NT PHYSICAL FACTORS
Experiments with hydrox at 1.3 MPa (13 atm) — for divers
[FOA-C-58014-H1] 04 p0545 N85-13471
Use of artificial intelligence and simple mathematics to analyze a physiological model 05 p0717 N85-14597
Results of the carbon monoxide study in Washington, D.C. and Denver, Colorado, in the winter of 1982-83
[PB84-230069] 06 p0834 N85-15309
Psychological and physiological basis of stereophonic effect 15 p2526 N85-25574
Selection procedures for F-16 pilots in the Belgian Air Force 20 p3510 N85-31822
Electroanesthesia as a means of controlling cold stress of local hypothermia 22 p3823 N85-33687

PHYSIOLOGICAL RESPONSES
NT HEMODYNAMIC RESPONSES
Jet lag prevention: Physiological mechanisms and pharmacological therapy
[AD-A145444] 02 p0235 N85-11529
An investigation of the use of steady-state evoked potentials for human performance and workload assessment and control
[AD-A145727] 02 p0237 N85-11541
Visually evoked responses from non-occipital areas of the human cortex
[AD-A146079] 03 p0400 N85-12553
Evidence for multiple areas in the human auditory cortex
[AD-A146086] 03 p0401 N85-12555
Proceedings of the 14th Conference on Environmental Toxicology
[AD-A146400] 06 p0843 N85-15350
Distinctions of SPF rats used in experiments aboard biosatellites 07 p1012 N85-16427
Effect of microwave radiation on local blood circulation and oxygenation of brain tissue
07 p1012 N85-16431
Carotid baroreceptor influences on peripheral circulatory and thermal responses during cold exposure
[AD-A146808] 07 p1015 N85-16447
Neuro-linguistic programming: Eye movements as indicators of representational systems
[AD-A147541] 07 p1016 N85-16454
Effect of disuse on sarcoplasmic reticulum in fast and slow skeletal muscle
[NASA-CR-174337] 08 p1191 N85-17508
Acid phosphatase and protease activities in immobilized rat skeletal muscles
[NASA-CR-174340] 08 p1192 N85-17509
A comparison of rat myosin from fast and slow skeletal muscle and the effect of disuse
[NASA-CR-174339] 08 p1192 N85-17510
Workshop on membrane biophysics
[AD-A146238] 08 p1192 N85-17512
Thermoregulatory responses during exercise at graded hypohydration levels
[AD-A147733] 08 p1195 N85-17528
Advanced development of an active neuromusculature response to mechanical stress
[AD-A148436] 08 p1196 N85-17536
The physiology of ultradian rhythms and their role in affecting disease resistance
[AD-A148842] 09 p1363 N85-18575
Hemodynamics responses to upright tilt at sea level and high altitude
[AD-A146848] 10 p1527 N85-19634
Multiple resources and brain laterality
[AD-A148012] 10 p1530 N85-19643
Chemical characterization and toxicologic evaluation of airborne mixtures. Inhalation toxicology of diesel fuel obscurant aerosol in Sprague-Dawley rats. Phase 3. Subchronic exposures
[AD-A150100] 12 p1905 N85-21966
Sleep deprivation and exercise tolerance
[AD-A150180] 13 p2142 N85-23295
Sleep deprivation and exercise tolerance
[AD-A150565] 13 p2142 N85-23296
Sleep deprivation and exercise tolerance
[AD-A150626] 13 p2142 N85-23297
Effect of broad-band constant noise on some systems of animal body 14 p2367 N85-24705
A model for generalization and specification by single neurons
[AD-A150871] 14 p2391 N85-24724
Psychophysiological studies. 1: Performance and physiological response in learning, short-term memory and discrimination tasks
[AD-A151018] 14 p2392 N85-24731
Current approaches for the biophysical and physiological evaluation of combat clothing for environmental extremes
[AD-A151012] 14 p2395 N85-24752
Several specific and nonspecific responses of the human and animal body to ship noise
[NASA-TM-77483] 15 p2615 N85-26116
Eye movement in response to single and multiple targets
[AD-A151115] 15 p2617 N85-26126
Physiological differences between men and women in exercise-heat tolerance and heat acclimation
[AD-A152048] 15 p2618 N85-26135
Plasma hormonal responses at graded hypohydration levels during exercise/heat stress
[AD-A153681] 18 p3153 N85-29523
An integrated analysis of the physiological effects of space flight: Executive summary
[NASA-CR-171892] 20 p3506 N85-31796
Empirical methods for predicting eutrophication in impoundments. Report 3. Phase 2. Model refinements
[AD-A155483] 21 p3614 N85-32482
USAFSAM review and analysis of radiofrequency radiation bioeffects literature
[AD-A155113] 21 p3664 N85-32760
Microwave radiation and thermoregulation
[AD-A155718] 22 p3818 N85-33654
Cardiovascular responses to orthostatism and weightlessness 24 p4130 N85-35601
Physiological responses to unvarying (steady) and 2-2-1 shifts: Miami International Flight Service Station
[AD-A155751] 24 p4133 N85-35619

PHYSIOLOGICAL TESTS
NT BODY SWAY TEST
NT VESTIBULAR TESTS
Variability of cardiac rhythm during information loading
10 p1525 N85-19619
Space motion sickness monitoring experiment: Spacelab 1 11 p1695 N85-20654
Chemical characterization and toxicologic evaluation of airborne mixtures. Inhalation toxicology of diesel fuel obscurant aerosol in Sprague-Dawley rats. Phase 3. Subchronic exposures
[AD-A150100] 12 p1905 N85-21966

PHYSIOLOGY
NT AUDIOLOGY
NT ELECTROPHYSIOLOGY
NT EXERCISE PHYSIOLOGY
NT GRAVITATIONAL PHYSIOLOGY
NT HEMATOPOIETIC SYSTEM
NT NEUROPHYSIOLOGY
NT PSYCHOPHYSIOLOGY
NT RESPIRATORY PHYSIOLOGY
NT UNDERWATER PHYSIOLOGY
NT WORKLOADS (PSYCHOPHYSIOLOGY)
USSR report: Life sciences. Biomedical and behavioral sciences
[JPRS-UBB-85-008] 10 p1523 N85-19605
Morphological study of monkeys submitted to antiorthostatic hypokinesia 12 p1902 N85-21942

Problems of space biology. Volume 50: Nystagmometry for evaulation of the statue of the vestibular function
[NASA-TM-77616] 14 p2365 N85-24694
Principal patterns of functional changes of human respiratory system in adaptation to high pressure
14 p2367 N85-24704
Development of guidelines for settling physiological and hygienic standards for noise levels in aerospace medicine 19 p3323 N85-30584
Chemolithotrophy and physiology of bacterial nutrient limitation 21 p3659 N85-32730
Structure and physiology of Beggiatoa and Thiothrix
21 p3659 N85-32734
Sulfur cycling and metabolism of phototrophic and filamentous sulfur bacteria 21 p3660 N85-32737
USSR report: Life sciences. Biomedical and behavioral sciences
[JPRS-UBB-85-018] 22 p3819 N85-33660

PHYTOTRONS
Plant growth in space 05 p0691 N85-14444

PICKLING (METALLURGY)
Picking of stainless steels: A review
[PB85-111979] 10 p1442 N85-19087

PICKOFFS
U SENSORS

PICKUPS
U SENSORS

PICOSECOND PULSES
Nonlinear symmetrization of picosecond pulses in optical fibers 02 p0264 N85-11725
Coherent amplification of ultrasonic pulses in activated crystals 05 p0724 N85-14653
Transformation of energy spread of laser pumping via phase conjugation 05 p0725 N85-14661
Optically induced intervalence-band transitions in germanium by the absorption of 1.06 micrometers picosecond pulses
[DE85-000946] 09 p1399 N85-18803
Picosecond laser pulse interactions with metallic and semiconductor surfaces
[AD-A149112] 10 p1490 N85-19405
Picosecond photoconductive devices for 10 Gbit/s optoelectronic switching 18 p3187 N85-29770
Dynamics of emission from dye lasers employing synchronous pumping by limited picosecond pulse train
21 p3686 N85-32899

PICTURE TUBES
Plans, developments in robotics
14 p2289 N85-24191

PIEDMONTS
Late precambrian to ordovician metamorphism and orogenesis in the Blue Ridge and western Piedmont, Virginia Appalachians 09 p1352 N85-18503

PIEZOELECTRIC CERAMICS
NT LEAD ZIRCONATE TITANATES
Optimization of piezoceramic optical deflector
11 p1719 N85-20813
Elasticity formulas for thin-walled shells with piezoceramic layers 13 p2047 N85-22816
Reaction of piezoceramic shell to concentrated forces
14 p2279 N85-24115
Effect of axisymmetric vibration modes on sensitivity and directivity characteristics of piezoceramic sphere — hydrophones 15 p2525 N85-25569
Scattering of sounds by piezoceramic cylindrical shell near rigid surface 17 p2943 N85-28168
Experiments on the influence of active walls on the initial amplitudes and growths of instability waves
[AD-A154630] 21 p3583 N85-32275
Materials used by industry for the production of piezoelectric transducers. The state of the art of research work performed in the field of PZT ceramics and ferroelectric polymers
[ISL-CO-211/84] 24 p4089 N85-35344
Piezoelectric transducers, state of research
24 p4089 N85-35345
Conduction and aging of piezoelectric PZT ceramics
24 p4089 N85-35346

PIEZOELECTRIC CRYSTALS
Piezoelectric and electrostrictive materials for transducer applications
[AD-A145115] 01 p0043 N85-10277
Method for evaluating petrol products corrosivity using piezoelectric crystals. Part 2: Instruction manual — jet engine corrosion tests
[FOA-C-40198-B4] 04 p0482 N85-13073
Microwave resonator using lateral excitation
[AD-D011374] 07 p1039 N85-16596
Normal coordinate monolithic crystal filter
[AD-D011496] 12 p1941 N85-22188
Stress compensation crystal device
[AD-D011497] 12 p1941 N85-22189
Adjustment of the frequency-temperature characteristics of crystal oscillators
[AD-D011586] 15 p2548 N85-25726
Suppression of vibration effects on piezoelectric crystal resonators
[AD-D011625] 16 p2778 N85-27142
Acceleration resistant combination of opposite-handed piezoelectric crystals
[AD-D011626] 16 p2778 N85-27143
Dual species ion implantation of ternary compounds based on In-Ga-As
[AD-D011617] 16 p2869 N85-27608
Power generation efficiency of piezoelectric crystals
20 p3537 N85-32008
Materials used by industry for the production of piezoelectric transducers. The state of the art of research work performed in the field of PZT ceramics and ferroelectric polymers
[ISL-CO-211/84] 24 p4089 N85-35344

PIEZOELECTRIC GAGES
Development of components for micro-C oriented sensor systems
[BMFT-FB-T-84-126] 04 p0504 N85-13215

PIEZOELECTRIC TRANSDUCERS
NT PIEZOELECTRIC GAGES
Piezoelectric and electrostrictive materials for transducer applications
[AD-A145115] 01 p0043 N85-10277
An automated immittance measuring system for electroacoustic transducers
[AD-A145701] 02 p0200 N85-11336
Development of a polymer pressure gage with temperature compensation 03 p0365 N85-12340
Analysis of piezoelectric disks and cylinders using finite element method
[AD-A146323] 03 p0414 N85-12650
Optimization piezoelectric transducer width of acousto-optical devices 07 p0950 N85-16024
Lightweight, broadband Rayleigh wave transducer
[AD-D011345] 07 p1037 N85-16584
Piezoelectric stress transducer used for measurements of explosions in hard rock 11 p1638 N85-20316
Piezoelectric transducer using electrically poled gamma-phase Nylon 11
[AD-D011552] 12 p1850 N85-21602
Piezoelectric filter with low-Q inductances
13 p2070 N85-22932
Piezoelectric and electroetatic polymeric transducers for acoustic emission detection
[AD-A150883] 14 p2306 N85-24272
Recording of acoustic wave in gaseous medium with thin-film pyroelectric transducers
15 p2525 N85-25571
The development of a transducer system for the accurate measurement of ultrasonic phase delay of SH plate waves
[AERE-R-11598] 15 p2559 N85-25790
A study of gas solid reactions using coated piezoelectric detectors
[AD-A153047] 17 p2920 N85-28001
Microwave SAW (Surface Acoustic Wave) monochromator
[AD-D011718] 21 p3590 N85-32311
Materials used by industry for the production of piezoelectric transducers. The state of the art of research work performed in the field of PZT ceramics and ferroelectric polymers
[ISL-CO-211/84] 24 p4089 N85-35344
Piezoelectric transducers, state of research
24 p4089 N85-35345
Ferroelectric homopolymer PVF2 and P (VDF-TrFe) copolymers 24 p4089 N85-35347

PIEZOELECTRICITY
Piezoelectric and electrostrictive materials for transducer applications
[AD-A145115] 01 p0043 N85-10277
Acoustic emission linear pulse holography
[DE84-014519] 01 p0050 N85-10330
Saint Venant conditions in theory of piezoelastic shells
06 p0780 N85-14987
Switchable zero order diffraction gratings as light valves
[AD-A147575] 07 p1044 N85-16633
Switchable zero order diffraction gratings as light valves
[AD-A150129] 12 p1934 N85-22153
Piezoelectric plastics — polyvinyl fluoride
[ISL-CO-202/83] 14 p2262 N85-24017
Compensation of acoustic wave devices
[AD-D011582] 15 p2546 N85-25322
Applications of piezoelectric and pyroelectric thin films: Opportunities for Langmuir-Blodgett technology
[AD-A149239] 15 p2559 N85-25408
Piezoelectric and pyroelectric polymers
16 p2758 N85-27008
Transversely reinforced piezoelectric composites
[AD-D011676] 19 p3260 N85-30214
Microwave bandstop filter
[AD-D011716] 19 p3261 N85-30222
Some dynamic electronic properties of semiconductor surfaces and interfaces 20 p3537 N85-32007
Power generation efficiency of piezoelectric crystals
20 p3537 N85-32008
Device for frequency modulation of a laser output spectrum
[DE85-011634] 22 p3790 N85-33479
Non-bonded ultrasonic transducer
[DE85-011005] 22 p3794 N85-33504

PIEZORESISTIVE TRANSDUCERS
NT PIEZOELECTRIC GAGES
Technology of thin silicon foils for the fabrication of monolithic integrated sensors
[BMFT-FB-T-84-209] 12 p1943 N85-22202
An advanced solid state pressure transducer for high reliability SSME application 16 p2739 N85-26905
Research pressure instrumentation for NASA space shuttle main engine
[NASA-CR-176014] 19 p3227 N85-30006

PIGMENTS
NT CAROTENE
NT CHLOROPHYLLS
NT CYTOCHROMES
Proton pumping in purple membrane, appendix 1
[DE84-014601] 01 p0118 N85-10811
The structure and function of fungal cells
[NASA-TM-77443] 06 p0642 N85-15348
Process for preparation of crosslinked poly(tri-n-butyltin) methacrylate with simultaneous particle size reduction
[AD-D011313] 07 p0932 N85-15905
Primary light harvesting system: The relationship of phycobiliosmes to photosystem 1 and 2
[DE85-003075] 11 p1689 N85-20622

PILE FOUNDATIONS
Experimentally determined distribution of stress around a horizontally loaded model pile in dense sand
[CE-43] 16 p2796 N85-27239

PILOT ERROR
A model for the effectiveness of aircraft alerting and warning systems 05 p0702 N85-14506
Direction judgement errors in perspective displays
05 p0705 N85-14520
Safety recommendation(s), A-84-93 through -95
[REPT-3983/33] 14 p2216 N85-23748
Investigation of technology needs for avoiding helicopter pilot error related accidents
[NASA-CR-3895] 15 p2465 N85-25220
Safety recommendation(s), A-84-96
[REPT-3983A/217] 15 p2466 N85-25223

PILOT PERFORMANCE
A mathematical simulation model of the CH-47B helicopter, volume 1
[NASA-TM-84351-VOL-1] 01 p0006 N85-10033
The Malcolm horizon: History and future
01 p0006 N85-10046
Content, variety, and augmentation of simulated visual scenes for teaching air-to-ground attack
[AD-A145218] 01 p0013 N85-10080
Workload demand and CNS depressant stressor effects on spatial orientation information processing
[AD-A145211] 01 p0096 N85-10651
Aircraft accident report. Central Airlines flight 27, Hughes Charter Air, Gates Learjet model 25 (N51CA) Newark International Airport, Newark, New Jersey, March 30, 1983
[PB84-910411] 02 p0136 N85-10924
Integrated Application of Active Controls (IAAC) technology to an advanced subsonic transport project-longitudinal handling qualities study of a relaxed-stability airplane
[NASA-CR-3680] 02 p0148 N85-11005
An in-flight investigation of a twin fuselage configuration in approach and landing
[NASA-CR-172306] 05 p0586 N85-13801
Investigation of pilot behavior in flight tests with a rate command/attitude hold control system
[DFVLR-FB-84-25] 05 p0699 N85-14486
Statistical time series models of pilot control with applications to instrument discrimination
05 p0700 N85-14489
Measurements of pilot time delay as influenced by controller characteristics and vehicles time delays
05 p0701 N85-14500
Helicopter pilot performance for discrete-maneuver flight tasks 05 p0702 N85-14502
Measuring workload differences between short-term memory and long-term memory scenarios in a simulated flight environment 05 p0703 N85-14513
Use of linear perspective scene cues in a simulated height regulation task 05 p0704 N85-14517
Cockpit window edge proximity effects on judgements of horizon vertical displacement
05 p0704 N85-14518
Mean and random errors of visual roll rate perception from central and peripheral visual displays
05 p0704 N85-14519

Accuracy of system step response roll magnitude estimation from central and peripheral visual displays and simulator cockpit motion 05 p0705 N85-14522
Twentieth Annual Conference on Manual Control, volume 2
[NASA-CP-2341-VOL-2] 05 p0707 N85-14535
Assessing the subjective workload of directional orientation tasks 05 p0708 N85-14542
A full mission simulator study of aircrew performances: The measurement of crew coordination and decisionmaking factors and their relationships to flight task performances 05 p0710 N85-14556
Measuring pilot workload in a moving-base simulator. Part 2: Building levels of workload 05 p0712 N85-14566
The Sternberg task as a workload metric in flight handling qualities research 05 p0712 N85-14568
Supersugmented rotorcraft program 06 p0750 N85-14807
Some thoughts on the implementation of pilot night vision devices for helicopters 06 p0751 N85-14814
Intelligent interfaces for tactical airborne platforms 06 p0752 N85-14820
Operational requirements - system concepts 06 p0752 N85-14823
Mental status in relation to special conditions of activity 07 p1011 N85-16420
Job and family stress as predictors of pilot health, job satisfaction and performance
[AD-A142176] 07 p1016 N85-16464
Practice makes perfect
[AD-A147124] 07 p1019 N85-16466
Assessment of simulation fidelity using measurements of piloting technique in flight 06 p1075 N85-16817
Effects of pyridostigmine on psychomotor and visual performance
[AD-A148553] 06 p1196 N85-17539
Improvement of workload estimation techniques in piloting tasks
[NASA-CR-174374] 10 p1531 N85-19646
Tolerance, fatigue, physiological and performance effects of sustained and oscillating lateral accelerations 10 p1533 N85-19658
Impact of future aircombat characteristics on pilot performance and cockpit design 10 p1533 N85-19661
Conceptual model of critical requirements for effective pilot performance in high performance aircraft 10 p1533 N85-19663
The cockpit of the year 2000: How big a step? 10 p1534 N85-19667
Pilot workload, performance and aircraft control automation 10 p1534 N85-19670
Aviation medicine's role in modern airforce discussed 11 p1696 N85-20662
Close air support mission: Development of a unitary measure of pilot performance
[AD-A149265] 11 p1697 N85-20665
Space shuttle pilot-induced-oscillation research testing 13 p1966 N85-22351
Air combat simulation: Methods, models, trends 13 p1967 N85-22359
Complex program of ergonomic studies Pilot described 14 p2366 N85-24668
Mental workload measurement: Event-related potentials and ratings of workload and fatigue
[NASA-CR-177354] 15 p2619 N85-26139
Correlations between selection ratings and success as army aviators
[FOA-C-53020-H2] 15 p2620 N85-26144
A comparison of pictorial and speech warning messages in the modern cockpit
[AD-A151917] 16 p2707 N85-26706
Development factors and field dependence-independence
[AD-A152337] 17 p3000 N85-28545
Technical evaluation of the Naval Automated Pilot Aptitude Measurement System (NAPAMS)
[AD-A152361] 17 p3000 N85-28547
Stabilizing force feedback in bio-actuated control systems
[AD-D011634] 17 p3002 N85-28560
The use of flight simulators in measuring and improving training effectiveness
[AD-A153817] 18 p3064 N85-28954
Electrooculographic measurement, fatigue and variability of performance in simulated aircraft flight 19 p3217 N85-29948
Psychophysiological nature of aircraft feel 19 p3323 N85-30587
The value of DMT in the selection of pilots
[RAE-TRANS-2127] 19 p3330 N85-30626
A systematic determination of skill and simulator requirements for airline transport pilot certification
[AD-A154135] 19 p3330 N85-30630
Selection procedures for F-16 pilots in the Belgian Air Force 20 p3510 N85-31822
G-Induced Loss of Consciousness (GLC) 20 p3510 N85-31823
Physical training and G tolerance 20 p3511 N85-31824
An error-dependent model of instrument-scanning behavior in commercial airline pilots
[NASA-CR-3908] 21 p3665 N85-32765
Human performance in continuous/sustained operations and the demands of extended work/rest schedules. An annotated bibliography
[AD-A155619] 21 p3666 N85-32771

PILOT PLANTS
The 15 photovoltaic pilot projects of the European Communities 05 p0663 N85-14263
Photovoltaic 100 kWp pilot plant on the Greek island Kythnos 05 p0664 N85-14266
Development and prototype construction of photovoltaic energy supply units 12 p1878 N85-21781
10 MWe Solar Thermal Central Receiver Pilot Plant total capitol costs
[DE85-009113] 18 p3131 N85-29390
Study of alternative system conversions for the Solar One pilot plant
[DE85-010026] 22 p3809 N85-33594

PILOT SELECTION
Correlations between selection ratings and success as army aviators
[FOA-C-53020-H2] 15 p2620 N85-26144
Selection procedures for F-16 pilots in the Belgian Air Force 20 p3510 N85-31822
Rapid determination of cadet discipline by projective tests 22 p3821 N85-33671

PILOT TRAINING
Training effectiveness evaluation and utilization demonstration of a low cost cockpit procedures trainer
[AD-A146179] 01 p0013 N85-10078
Content, variety, and augmentation of simulated visual scenes for teaching air-to-ground attack
[AD-A145218] 01 p0013 N85-10080
Determining training device requirements in Army aviation systems 05 p0711 N85-14558
Analysis of the flow field about a T-45 using PANAIR
[AD-A146811] 07 p0899 N85-15699
Directions of the West German Ministry of Transport for education and control of airline personnel (section 3, chapters 2 and 12) 08 p1081 N85-16848
Directions of the West German Ministry of Transport for education and control or airline personnel, Report 6; chapters 3/A and 3/B 08 p1081 N85-16849
Using a limited field of view simulator to instruct high speed, low altitude flying skills
[AD-P004309] 09 p1267 N85-17983
Visual perceptual aspects of low level high speed flight and flight simulation
[AD-P004310] 09 p1267 N85-17984
On-board Computer Image Generator (CIG) applications
[AD-P004335] 09 p1271 N85-17989
CIG (Computer Image Generator) goes to war: The tactical illusion
[AD-P004336] 09 p1271 N85-17990
Flight Training Technology for Regional/Commuter Airline Operations: Regional Airline Association/NASA Workshop Proceedings
[NASA-CP-2348] 09 p1275 N85-18009
Flight crew training technology: A review 09 p1275 N85-18010
Low-cost training technology 09 p1275 N85-18011
Captain development training at US Air 09 p1275 N85-18012
Management training for cockpit crews at Piedmont flight 09 p1276 N85-18013
Use of simplifier scenarios for CRM training 09 p1276 N85-18016
Safety awareness, pilot education, and incident reporting programs 09 p1276 N85-18020
The aviation safety reporting system 09 p1276 N85-18021
Simulation of aircraft behaviour on and close to the ground
[NASA-TM-87460] 14 p2218 N85-23754
Visual simulation requirements for aircraft aspect recognition at real world distances
[AD-A151040] 14 p2228 N85-23810
Technical evaluation of the Naval Automated Pilot Aptitude Measurement System (NAPAMS)
[AD-A152361] 17 p3000 N85-28547
Guidelines of the Federal Minister of Transportation for the formation and examination of airline personnel, part 4 17 p3002 N85-28556
Human factors in cockpit automation: A field study of flight crew transition
[NASA-CR-177333] 19 p3215 N85-29937
The value of DMT in the selection of pilots
[RAE-TRANS-2127] 19 p3330 N85-30626
Selection procedures for F-16 pilots in the Belgian Air Force 20 p3510 N85-31822
G-Induced Loss of Consciousness (GLC) 20 p3510 N85-31823
Physical training and G tolerance 20 p3511 N85-31824
Centrifuge operations and training in the Royal Netherlands Air Force 20 p3511 N85-31825
Advanced simulator for pilot training and helmet-mounted visual display configuration comparisons
[AD-A155326] 21 p3667 N85-32776
Rapid determination of cadet discipline by projective tests 22 p3821 N85-33671
RAFTS: A T-38 replacement for the 21st century
[AD-A156103] 24 p4065 N85-35191

PILOTED CENTRIFUGES
U HUMAN CENTRIFUGES

PILOTLESS AIRCRAFT
Visual systems for remotely controlled vehicles 05 p0703 N85-14512
On-board processing for linescan sensors in miniature unmanned aircraft
[RAE-TM-SPACE-327] 08 p1085 N85-16870

PILOTS (PERSONNEL)
NT AIRCRAFT PILOTS
Anthropometric cockpit compatibility assessment of US Army aircraft for large and small personnel wearing a training, warm-weather clothing configuration
[AD-A145208] 01 p0099 N85-10658
Decision tree rating scales for workload estimation: Theme and variations
[NASA-CR-174062] 02 p0237 N85-11544
Cardiovascular disease among U.S. Navy pilots
[AD-A145871] 03 p0400 N85-12552
Differences in health risks by aircraft model among US Navy pilots
[AD-A146147] 03 p0401 N85-12556
Measurements of pilot time delay as influenced by controller characteristics and vehicles time delays 05 p0701 N85-14500
Multiloop manual control of dynamic systems 05 p0702 N85-14505
A model for the effectiveness of aircraft alerting and warning systems 05 p0702 N85-14506
Human factors survey: C-5 pilots
[AD-A147108] 07 p1020 N85-16477
Evaluation of arctic test of improved tritium radioluminescent lighting
[AD-A148215] 08 p1089 N85-16884
Aviation-related cardiorespiratory effects of blood donation in female pilots
[AD-A148045] 08 p1195 N85-17529
Health examination findings among active civil airmen
[AD-A148325] 08 p1195 N85-17533
An investigation of spinal injury potential from the use of the ACES 2 ejection seat by lower weight female pilots
[AD-A148449] 08 p1196 N85-17537
Development of an electro-pneumatic anti-G valve for high performance fighter aircraft
[AD-A148468] 08 p1201 N85-17561
Global optical metrics for self-motion perception
[AD-P004333] 09 p1271 N85-17987
Simulator sickness: Sensorimotor disturbances induced in flight simulators
[AD-P004334] 09 p1271 N85-17988
Communications skills for CRM training 09 p1276 N85-18017
Pilot education and safety awareness programs 09 p1277 N85-18026
Innovative approaches to recurrent training 09 p1277 N85-18028
Medically disqualified airline pilots
[AD-A149454] 10 p1528 N85-19637
Crewstation assessment of reach as applied to the OH-58A helicopter
[AD-A149413] 10 p1531 N85-19650
Military pilot ergonomics 10 p1532 N85-19655
Biofeedback treatment of airsickness: A review 11 p1696 N85-20660
US Army Aviation Engineering Flight Activity (USAAEFA) report bibliography update 1963 - 1984
[AD-A151391] 15 p2457 N85-25168
Airsickness control using biofeedback to self-regulate psychophysiological responses
[AD-A151167] 15 p2617 N85-26128
Psychometric evaluation of head injury among fliers referred to the AF School of Aerospace Medicine
[AD-A151479] 15 p2617 N85-26129
Aspects of application of ACT systems for pilot workload alleviation 16 p2712 N85-26734
Aspects of application of ACT systems for pilot workload alleviation 17 p2901 N85-27887

Development factors and field dependence-independence
[AD-A152337] 17 p3000 N85-28545
Operation guiding light-scientific program and field plan. The pilot field experiment for NORDA project chemical dynamics in ocean frontal areas
[AD-A153765] 18 p3150 N85-29507
Longitudinal study of cardiovascular disease in US Navy pilots
[AD-A154391] 19 p3328 N85-30623
The value of DMT in the selection of pilots
[RAE-TRANS-2127] 19 p3330 N85-30626
U.S. Civil airmen statistics for calendar year 1984
[AD-A156326] 24 p4059 N85-35153
International flight planning handbook
[AD-A156390] 24 p4062 N85-35177

PINCH EFFECT
NT PLASMA PINCH
NT REVERSE FIELD PINCH
NT THETA PINCH
NT ZETA PINCH

PINHOLE CAMERAS
A microchannel plate pinhole camera for 20 to 100 keV X-ray imaging
[DE85-001572] 10 p1488 N85-19396
Sequentially-framing soft X-ray pinhole camera for Tokamak plasma studies
[DE85-001717] 10 p1489 N85-19399
Three-dimensional and tomographic imaging device for X-ray and gamma-ray emitting objects
[NASA-CASE-GSC-12851-1] 19 p3271 N85-30281

PINHOLES
Double pinhole spatial phase correlator apparatus
[AD-D011495] 11 p1729 N85-20872

PINNING
NT FLUX PINNING

PINS
Extractor for spring-lock pin connectors
[AD-D011235] 01 p0043 N85-10280
Stress analysis of pin-loaded orthotropic plates using orthotropic photoelasticity 02 p0207 N85-11366
Connector/nitinol delta contact force device
[AD-D011467] 10 p1481 N85-19349
The effects of pin elasticity, clearance, and friction on the stresses in a pin-loaded orthotropic plate
[NASA-CR-175816] 16 p2743 N85-26927
An approximation to the problem of a pin-loaded hole in an orthotropic plate
[VTH-LR-386] 16 p2802 N85-27278
Printed wiring board circuit isolator tool
[AD-D011638] 17 p2968 N85-28333
The stress distribution in pin-loaded orthotropic plates
[NASA-CR-176146] 22 p3800 N85-33547
Evacuate and backfill apparatus and method
[DE85-006018] 23 p3938 N85-34411
Verification of the SRB motor case pin retainer band tips
[NASA-CR-170662] 24 p4070 N85-35220

PION BEAMS
Study of hadron bundles observed in Chacaltaya two-story emulsion chamber
[HE-3.3-4] 24 p4180 N85-35922
Experimental basis for the models of cascade propagation in atmosphere
[HE-3.6-6] 24 p4185 N85-35954

PIONEER F SPACE PROBE
U PIONEER 10 SPACE PROBE

PIONEER G SPACE PROBE
U PIONEER 11 SPACE PROBE

PIONEER SATURN SPACECRAFT
U PIONEER 11 SPACE PROBE

PIONEER SPACE PROBES
NT PIONEER 10 SPACE PROBE
NT PIONEER 11 SPACE PROBE
Charged particle erosion of icy satellites: Coronal atmospheres and surface redistribution
03 p0448 N85-12845
Interpretation of Venus gravitational anomalies
15 p2483 N85-25322

PIONEER VENUS SPACECRAFT
Analysis and interpretation of observations of airglow at 297 nm in the Venus thermosphere
13 p2172 N85-23473
Venus gravity: Global field results
13 p2177 N85-23512
Geophysical interpretation of Venus gravity data
13 p2178 N85-23513
Venus chasmata: A lithosphere stretching model
13 p2178 N85-23516
Programming for Pioneer 12
15 p2668 N85-26606

PIONEER 12 SPACE PROBE
U PIONEER VENUS SPACECRAFT

PIONEER 10 SPACE PROBE
Pioneer 10 and Voyager observations of the interstellar medium in scattered emission of the He 584 A and H Lya 1216 A lines
08 p0873 N85-15541

PIONEER 11 SPACE PROBE
Investigations of planetary ring phenomena
13 p2174 N85-23487
Electrons and cosmic ray produced protons in Saturn's inner magnetosphere
[NASA-TM-87469] 15 p2679 N85-26546

PIONS
Experimental medium energy physics
[DE84-014625] 02 p0278 N85-11807
Skyrmions and vector mesons: A symmetric approach
[DE84-015297] 04 p0563 N85-13584
Pion inelastic scattering to the first three excited states of Lithium-6
[AD-A147560] 07 p1041 N85-16606
A 1-2 GeV/c beam line for hypernuclear and kaon research
[DE85-007623] 16 p2663 N85-27659
Deep-inelastic lepton scattering by nuclei: The pion-exchange model
[DE85-010498] 19 p3359 N85-30628
Pion production and the nuclear equation of state
[DE85-009941] 19 p3365 N85-30670
AGS broad band neutrino beam
[DE85-010954] 19 p3366 N85-30675
Neutral pion production in solar flares
[SH-1.4-7] 23 p3995 N85-34767
Determination of the cross section of the proton, pion and neutron inelastic interaction with lead and carbon nuclei at 0.5 - 5.0 TeV energies (PION experiment)
[HE-1.1-5] 24 p4170 N85-35883
Angular distribution and multiplicity of backward hadrons in hFe interactions at 0.5-5.0 TeV energies (PION Experiment)
[HE-1.2-8] 24 p4172 N85-35886
Anuglar distribution of shower particles produced in the collisions of 20-GeV/c and 300-GeV negative pions with emulsion nuclei 24 p4172 N85-35888
Is the inelastic charge-exchange contribution constant at the large X and superhigh energies? Cast 01Kuchin, I. A. 24 p4173 N85-35871
Energy-range relations for hadrons in nuclear matter 24 p4174 N85-35881
Measurements of hadron mean free path for the particle-producing collisions in nuclear matter 24 p4174 N85-35883
On mini-cluster observed by Chacaltaya emulsion chamber experiment
[HE-3.6-12] 24 p4185 N85-35959
A study of gamma-families generated in nucleon-nucleus (NA) and pion-nucleus (pi A) interactions
[HE-3.7-2] 24 p4186 N85-35961
Study of photonuclear muon interactions at Baksan underground scintillation telescope
[HE-5.4-10] 24 p4208 N85-36122
Observation of genetic relation among new phenomena Geminion, Chiron and mini-Centauro
[HE-6.2-16] 24 p4212 N85-36152
Tien-Shan effect and charmed particles
[HE-6.2-17] 24 p4212 N85-36153

PIPE FLOW
Classical free-streamline flow over a polygonal obstacle
[NASA-CR-172448] 01 p0046 N85-10301
Thermal fluid-structure interaction: A few scaling considerations — nuclear reactors
[GKSS-84-E-18] 01 p0048 N85-10314
Void fraction measurements performed in a vertical large diameter tube compared to different predicting correlations
[GKSS-84-E-24] 01 p0048 N85-10315
Visualization of the diverging two-phase flow pattern in a horizontal T-junction with vertical branch
[GKSS-84-E-25] 01 p0048 N85-10316
Fluid layer between infinite elastic plates II. Distribution of power flow
[AD-A146890] 03 p0361 N85-12312
An organ-pipe oscillation — PHOENICS code
[PDR/CFDU-IC/14] 04 p0501 N85-13199
Wave propagation in compliant tubes containing a heat-conducting viscous fluid
[WTHD-163] 05 p0638 N85-14094
Flow of nitrogen-pressurized Halon 1301 in fire extinguishing systems
[NASA-CR-174271] 07 p0900 N85-15701
Studies of the wall shear stress in a turbulent pulsating pipe flow
[AD-A146772] 07 p0957 N85-16066
The stability of an infinite elastic pipe with uniform mean flow
[AD-A146686] 08 p1161 N85-17326
Computation of flow and heat transfer in flow around a 180 deg bend
[AD-A146085] 08 p1162 N85-17330
Thermal striping downstream of a horizontal elbow under thermally stratified transient flow conditions
[DE84-014687] 09 p1320 N85-18302
The influence of modern control techniques on the gas industry
[ERS-E.395] 09 p1325 N85-18326
Design of piping for oil drain from turbine bearings
14 p2271 N85-24073
Unsteady flows in a tube with combustion reaction
[ISL-R-116/83] 14 p2303 N85-24261
Behavior of turbulent gas jets in an axisymmetric confinement
[NASA-CR-174829] 15 p2473 N85-25265
Heat transfer in pipes
[NASA-TM-77838] 17 p2957 N85-28262
Steady, incompressible, inviscid flow through a finite collapsible tube under longitudinal tension
[REPT-84-01] 17 p2959 N85-28278
Flow through finite collapsible tubes: A branching problem
[REPT-84-29] 17 p2960 N85-28281
Monogroove heat pipe design: Insulated liquid channel with bridging wick
[NASA-CASE-MSC-20497-1] 18 p3098 N85-29180
Transport characteristics of slurries in pipelines: Flow regimes and pressure drop
[DE85-009453] 18 p3101 N85-29198
Dynamic stability of a spinning tube conveying a flowing fluid
[DE85-007583] 18 p3102 N85-29207
Experimental investigations of the unsteady turbulent friction behavior with pressure impulses in a circular pipe
[IWAWI-MITT-102] 18 p3103 N85-29210
A method for predicting additive drag reduction from small-diameter pipe flows
[AD-A154411] 19 p3266 N85-30254
Droplet deposition in vertical two-phase flow
[CFD/84/22] 20 p3456 N85-31460
Intermittent gas-liquid flow modeling in horizontal or weakly inclined pipes
[EME-132] 20 p3456 N85-31465
Resolution of thermal striping issue downstream of a horizontal pipe elbow in stratified pipe flow
[DE85-006195] 21 p3586 N85-32292
Computer and water-model simulation of flow through poppet valves
[CFD/85/2] 22 p3785 N85-33449
Experimental simulation of in-bore flows using a high pressure shock tube
[ISL-CO-217/84] 22 p3785 N85-33452

PIPELINES
NT SEWERS
Low power microprocessor based measurements system for determining the integrity of coatings on buried pipelines
[ERS-E.360] 09 p1324 N85-18323
Defect tolerance in pipeline girth welds
[ERS-E.353] 09 p1328 N85-18347
Hydrogen induced cracking in pipeline steels
[ERS-E.327] 09 p1340 N85-18429
Mechanism of hydrogen induced cracking in pipeline steels
[ERS-E.349] 09 p1340 N85-18430
The influence of mechanical damage on transmission pipeline integrity
[ERS-E.351] 09 p1340 N85-18431
Recent studies of the significance of mechanical damage in pipelines
[ERS-E.367] 09 p1341 N85-18433
Statistical aspects of shear fracture propagation
[ERS-E.368] 09 p1341 N85-18434
The effect of an elastic foundation and of dissipative forces on the stability of fluid conveying pipes
[TAE-563] 12 p1863 N85-21668
Abatement of noise and vibration in pipelines of hydro systems 14 p2276 N85-24102
Underwater pipeline: Welding by high frequency induction
[BLL-WI-TRANS-682-(9312.57)] 16 p2792 N85-27221
Effect of the agressive action of soil on metallic pipelines. New possibilities for the passive and active corrosion protection
[BLL-BISI-TRANS-21630-(9022.06)] 17 p2928 N85-28070
Hydrogen degradation of pipeline steels
[DE85-009930] 17 p2932 N85-28101
Model documentation of the gas analysis modeling system. Volume 1: Model overview
[DE85-010652] 20 p3515 N85-31656

PIPELINING (COMPUTERS)
Solution of partial differential equations on vector and parallel computers
[NASA-CR-172500] 07 p1028 N85-16525
Siemens introduces fast computer with pipeline architecture 11 p1618 N85-20178
Exploiting multiprocessors: Issues and options
[DE85-003144] 13 p2145 N85-23313

Implementation of some concurrent algorithms
[DE85-004687] 13 p2148 N85-23334
Effective microinstruction pipeline organization in a high-capacity microprocessor 15 p2625 N85-26170
Squeezing the most out of Eigenvalue solvers on high-performance computers
[DE85-007569] 16 p2849 N85-27565
Pipelined programmable charge domain device
[AD-D011596] 17 p2951 N85-28225
Pipelined Givens method for computing the QR factorization of a sparse matrix
[DE85-009772] 18 p3171 N85-29653
VLSI structures for numerical and digital signal processing computations 20 p3439 N85-31340

PIPES (TUBES)
NT GAS PIPES
Lightweight composite launcher pod
[AD-D011236] 01 p0015 N85-10092
Bilouting and corrosion studies at the Seacoast Test Facility in Hawaii
[DE84-014643] 01 p0029 N85-10180
Heat exchanger
[DE84-014299] 01 p0047 N85-10309
Void fraction measurements performed in a vertical large diameter tube compared to different predicting correlations
[GKSS-84-E-24] 01 p0048 N85-10315
Method and apparatus for determining the content and distribution of a thermal neutron absorbing material in an object
[DE84-014319] 01 p0117 N85-10801
Directional nature of strengthening during thermomechanical treatment
[BLL-M-35746-(5828.4)] 02 p0175 N85-11174
Recent developments on the role of molybdenum in irons and steels 02 p0180 N85-11206
Modernization of IDTs-6 ultrasonic installation
[BLL-M-35716-(5828.4)] 02 p0206 N85-11356
Polycyclic aromatic hydrocarbons on the inner surfaces of copper tubing
[AD-A145879] 03 p0337 N85-12169
Corrosion of brass in potable water service
[CETIM-100390] 04 p0477 N85-13037
Detection of cracks in a plastics pipe joint by reflection holography
[NPL-DMA(A)-87/MOM-70] 04 p0502 N85-13202
Field installed brazed thermocouple feedthroughs for high vacuum experiments
[DE84-013556] 04 p0503 N85-13207
Ultrasonic and metallurgical examination of a cracked type 304 stainless steel BWR pipe weldment
[TI84-014966] 04 p0511 N85-13254
Wave propagation in compliant tubes containing a heat-conducting viscous fluid
[WTHD-163] 05 p0636 N85-14084
In situ analysis of corrosive and passive surfaces by laser-excited Raman spectroscopy — lead, galvanized iron, and asbestos-cement pipes
[PB84-229756] 06 p0767 N85-14904
Recommended aluminum pipe welding procedures for corps of engineers construction
[AD-A146712] 06 p0815 N85-15172
Identification of leaks: Internal acoustic method, phase 2
[PB85-101947/GAR] 07 p0936 N85-15927
Studies of the wall shear stress in a turbulent pulsating pipe flow
[AD-A146772] 07 p0957 N85-16068
Heat transfer due to film condensation on vertical fluted tubes
[AD-A147258] 07 p0959 N85-16079
Method for non contacting gauging of the wall thickness of tubes by backscattering radiation
[OEFZS-4274] 07 p0968 N85-16144
Improvement of gas-tightness of OTTG and TBO-5 threaded pipe couplings
[BLL-M-35693-(5828.4)] 07 p0972 N85-16175
Damping capacity of multilayer tube during torsion
[BLL-M-36011-(5828.4)] 07 p0977 N85-16202
Convective heat transfer coefficients for pipe flow with curvature induced secondary motion
09 p1318 N85-18265
Development of the GASCOPACT (R) pipe and cable tracer
[ERS-E.340] 09 p1324 N85-18320
GASCOPACT: A new approach to pipe and cable location
[ERS-E.363] 09 p1325 N85-18324
NOAA OTEC CWP (National Oceanic and Atmospheric Administration Ocean Thermal Energy Conversion Cold Water Pipe) at-sea test. Volume 3, part 1: Tabulation of the power spectra for selected channels
[PB84-238955] 09 p1346 N85-18467
NOAA OTEC CWP (National Oceanic and Atmospheric Administration Ocean Thermal Energy Conversion Cold Water Pipe) at-sea test. Volume 5: Additional tabulation of the power spectra, part 2
[PB84-238997] 09 p1346 N85-18468
Acoustic imaging in a water filled metallic pipe — monitoring heat exchangers in nuclear power reactors
[DE84-016051] 09 p1378 N85-18665
Conceptual design of a 10 MW shore-based OTEC plant
[DE84-015806] 10 p1511 N85-19532
OTEC (Ocean Thermal Energy Conversion) Cold Water Pipe At-Sea Test Program. Phase 2: Suspended pipe test
[PB85-119931] 10 p1512 N85-19542
Evaluation of 7010 aluminium alloy extruded tube in the T76 condition
[BR92019] 11 p1596 N85-20039
Ultrasonic large-diameter pipe weld testing installations 11 p1603 N85-20081
Structural basis for the mechanical properties of polyethlenes
[PB85-149771] 11 p1613 N85-20142
Leakage-flow-induced vibration of a tube-in-tube slip joint
[DE84-007301] 11 p1652 N85-20406
Simplified theory for the behaviour of buried flexible cylinders under the influence of uniform hoop compression
[PB85-116531] 11 p1654 N85-20419
Characterization and optimization of polyethylene resins and gas pipe
[PB85-118511] 12 p1815 N85-21382
The effect of an elastic foundation and of dissipative forces on the stability of fluid conveying pipes
[TAE-563] 12 p1863 N85-21688
Steam generator tube vibration tests
[DE85-003599] 12 p1867 N85-21712
Behavior of buried flexible cylinders under the influence of nonuniform hoop compression
[PB85-116523] 12 p1868 N85-21718
Influence of welding defects at melting boundary on static strength of welded joint in large-diameter pipe
13 p2033 N85-22735
Cooling performance improvement of a horizontal ground coupled heat pump
[DE85-002470] 13 p2093 N85-23065
Measurement of damping of graphite epoxy materials
[NASA-CR-175663] 14 p2248 N85-23931
Use of program controlled machine tools to automate and mechanize production processes in pipe manufacture 14 p2269 N85-24059
Problem of reduction to ideal tube in experimental aerodynamics 14 p2268 N85-24179
Fluid mechanics and heat transfer spirally fluted tubing
[AD-A150774] 14 p2301 N85-24247
Flow induced vibration of the SSME LOX posts
[NASA-CR-175606] 15 p2495 N85-25391
Pressure welding of corrosion-resistant steel with AMg6 aluminum 15 p2501 N85-25426
Soviet Institute director on GDR-USSR welding technology 15 p2538 N85-25662
Effect of internal pressure on flexibility and stress intensification factors for pipe elbows analyzed by the finite element method
[AD-A151161] 15 p2578 N85-25901
Filmwise condensation of steam on low integral-finned tubes
[AD-A152220] 16 p2783 N85-27176
Magnetic method of inspecting mechanical properties of general purpose tubes
[BLL-M-36084-(5828.4)] 16 p2796 N85-27235
Local heat treatment of welded joints of pipes and rotary vessels 17 p2924 N85-28028
Obtaining oxide films on surface of tubes of chromium-nickel steels
[BLL-BISI-TRANS-22478-(9022.06)]
17 p2929 N85-28076
Removal of longitudinal internal flash from electrically welded tubes
[BLL-BISI-TRANS-22380-(9022.06)]
17 p2936 N85-28136
Local heat treatment of welded joints of pipes and rotary vessels
[BLL-BISI-TRANS-22197-(9022.06)]
17 p2972 N85-28354
Application of 4-wire submerged arc method to welding UOE pipe
[BLL-BISI-TRANS-22417-(9022.06)]
17 p2972 N85-28358
Production of thin-walled electricity welded tubes with reduced internal flash
[BLL-BISI-TRANS-22361-(9022.06)]
17 p2973 N85-28364
High-speed longitudinal welding of pipes by automatic submerged arc process
[BLL-BISI-TRANS-22340-(9002.06)]
17 p2973 N85-28366
Production of electrically welded tubes with removed internal flash
[BLL-BISI-TRANS-22362-(9022.06)]
17 p2973 N85-28367
Steel Tubes
[BLL-BISI-TRANS-22064-(9022.06)]
17 p2973 N85-28369
Statistical models used in analyzing the quality of welded tubes
[BLL-BISI-TRANS-22232-(9022.06)]
17 p2976 N85-28384
Non-destructive testing of HF-welded pipe
[BLL-BISI-TRANS-22182-(9022.06)]
17 p2976 N85-28388
Principal quality assurance measures in the manufacture of HF-welded high-pressure linepipe
[BLL-BISI-TRANS-21690-(9022.06)]
17 p2976 N85-28389
DOE/ANL/HTRI heat exchanger tube vibration data bank: Addendum 5
[DE85-007730] 17 p2980 N85-28425
Properties of polyethylene gas piping materials
[PB85-187045] 18 p3082 N85-29068
Dynamic stability of a spinning tube conveying a flowing fluid
[DE85-007583] 18 p3102 N85-29207
Ultrasonic testing of tubes
[BLL-BISI-TRANS-22337-(9022.06)]
18 p3119 N85-29304
Characteristic features of testing equipment: Application to the ultrasonic inspection of tubes
18 p3119 N85-29305
Measurement of turbofan-turbojet thrust from tailpipe static pressure
[AD-A154036] 19 p3220 N85-29987
A method for predicting additive drag reduction from small-diameter pipe flows
[AD-A154411] 19 p3268 N85-30254
Improved fluid flow meter for measuring the rate of fluid flow in a conduit
[NASA-CASE-MFS-28030-1] 19 p3271 N85-30286
Seismic pipe support construction practices
[DE85-901315] 19 p3287 N85-30386
SHAPS-2: A three-dimensional computer program for linear/non-linear, static/dynamic analyses of piping systems
[DE85-010500] 19 p3335 N85-30658
Elastomers used in aeronautics industry
[SNIAS-851-551-103] 20 p3434 N85-31304
Viscous flows in rotating pipes with internal cavities and related vortex breakdowns
[NASA-TM-86761] 20 p3454 N85-31447
Film condensation of steam on externally finned horizontal tubes
[AD-A155842] 21 p3585 N85-32285
Resolution of thermal striping issue downstream of a horizontal pipe elbow in stratified pipe flow
[DE85-006195] 21 p3586 N85-32292
Process and device for forming imprints on ceramic tubes
[DE85-013137] 22 p3753 N85-33264
Stresses and deformations in cross-ply composite tubes subjected to a uniform temperature change: Elasticity and Approximate Solutions
[NASA-CR-176147] 22 p3800 N85-33545
Mechanical ratcheting behaviors of a steel pipe under combined cyclic axial load and internal pressure
23 p3904 N85-34184
Experimental study of collapse of thick-walled tube under external pressure and axial force
23 p3904 N85-34186
Forced convective, nonequilibrium, post-CHF heat transfer experiment data and correlation comparison report
[TI85-009331] 23 p3932 N85-34371
Calculations on the feasibility of ultrasonic inspection of steam generator tubing in pressurized water reactors
[AERE-R-10960] 23 p3940 N85-34419
Characterization of modified 9 Cr Mo steel extruded pipe
[DE85-012056] 23 p3941 N85-34430
Stress-intensity factors for circumferential surface cracks in pipes and rods under tension and bending loads
[NASA-TM-87594] 24 p4101 N85-35424
Evaluation of the crack plane equilibrium model for predicting plastic fractures
[DE85-005558] 24 p4102 N85-35431

PISTON ENGINES
NT DIESEL ENGINES

Predicted heat transfer loss in the expansion cylinder of a 2 cylinder reciprocating engine
[AD-A144831] 01 p0055 N85-10366
The KZD-85 engine test. Engine type: 1 cylinder, 2 stroke motor 2100 Husquarna
[FWE-FO-1717] 02 p0205 N85-11354
A study of the Armstrong Whitworth swing beam engine for automotive application 04 p0508 N85-13239
Long term technology development program 04 p0508 N85-13244
Evaluation of heat engine for hybrid vehicle application
[NASA-CR-174163] 04 p0508 N85-13245
Linear harmonic analysis of Stirling engine thermodynamics
[DE84-016648] 04 p0574 N85-13657
Stirling engine development, state of the art, possible engine applications and suitability in comparison to established plants and systems
[BMFT-FB-T-84-195] 05 p0648 N85-14149
Some characteristics of automotive gasolines and their performance in a light aircraft engine
[FAA-CT-84-12] 07 p0934 N85-15919
Birds and aviation
[AD-P004177] 11 p1578 N85-19939
Gas-fired duplex free-piston Stirling refrigerator 12 p1819 N85-21413
Overview of the 1985 NASA Lewis Research Center SP-100 free-piston Stirling engine activities
[NASA-TM-87028] 16 p2880 N85-27769
A mathematical model of reciprocating combustion engine dynamics for the diagnosis of deficient energy conversion 19 p3290 N85-30339
Reciprocating Brayton cycle motor
[REPT-84-RR-336] 20 p3462 N85-31507

PISTONS
Cylinder power fault diagnosis in military diesel engines
[TT-8405] 01 p0053 N85-10354
Liquid-piston Stirling machines
[DE84-014255] 02 p0205 N85-11351
Development of gas-lubricated pistons for heavy duty diesel engine technology program
[NASA-CR-174746] 03 p0441 N85-12808
Laminar flame propagation/quench for a parallel-wall duct
[DE84-009773] 04 p0470 N85-12993
Roller crosshead analysis 04 p0507 N85-13238
Improved apparatus and techniques for high temperature and pressure deformation of crystalline materials
[DE84-016049] 04 p0669 N85-13629
Pneumatic clamping device
[AD-D011544] 12 p1858 N85-21856
Sliding seal materials for adiabatic engines
[NASA-CR-174693] 13 p2037 N85-22757
Effect of form and clearance of a piston launched in a tube on the boundary layer and the heat transfer
[ISL-CO-216/83] 14 p2302 N85-24255
Compression waves in front of and behind a piston launched in a shock tube
[ISL-R-101/83] 14 p2303 N85-24260
Active control landing gear for ground loads alleviation 16 p2714 N85-26749
Lightweight piston
[NASA-CASE-LAR-13150-1] 18 p3068 N85-28975
Thermo-electric valve
[AD-D011682] 19 p3252 N85-30165
A device to detect Top Dead Center (TDC) position in motored engines
[REPT-84-RR-347] 20 p3458 N85-31475
Fast shutter apparatus
[DE85-006501] 23 p3928 N85-34343

PITCH (INCLINATION)
Development and flight evaluation of an augmented stability active controls concept: Executive summary
[NASA-CR-166009] 02 p0149 N85-11008
Cockpit window edge proximity effects on judgements of horizon vertical displacement 05 p0704 N85-14518
Integrated Application of Active Controls (IAAC) technology to an advanced subsonic transport project. ACT/Control/Guidance System study, volume 1
[NASA-CR-165963-VOL-1] 06 p0754 N85-14837
Integrated Application of Active Controls (IAAC) technology to an advanced subsonic transport project. ACT/Control/Guidance System study. Volume 2: Appendices
[NASA-CR-165963-VOL-2] 06 p0754 N85-14838
Pitch angle scattering and particle precipitation in a pulsating aurora: An experimental study
[KGI-185] 09 p1355 N85-18523
Inviscid analysis of unsteady blade tip flow correlation studies
[NASA-CR-172506] 10 p1420 N85-18958
Some effects of display format variables on the perception of aircraft spatial orientation 10 p1534 N85-19666
Directivity of Bremsstrahlung radiation from relativistic beams and the Gamma-Rays from solar flares
[NASA-CR-174433] 10 p1572 N85-19913
Generation of a pair of symmetric eddies behind a slender axisymmetric body with pitch angle
[ISL-R-121/83] 11 p1577 N85-19934
Protons with energies above 30 KeV in Earth's radiation belt at low altitudes during magnetically quiet time close to geomagnetic equator 13 p1980 N85-22423
Investigation of potential and viscous flow effects contributing to dynamic stall
[AD-A151696] 15 p2557 N85-25773
Inclinations of the Uranian rings 15 p2672 N85-26487
Wing tunnel investigation of dynamic stall of an NACA 0018 airfoil oscillating in pitch
[NAE-AN-27] 17 p2992 N85-27830
Proposals for the determination of necessary elevator handling characteristics of sailplanes in high speed range
[DFVLR-FB-84-52] 17 p2900 N85-27862
Conceptual design of a fixed-pitch wind turbine generator system rated at 400 kilowatts
[NASA-CR-174877] 18 p3127 N85-29363
New concept for a wall detector for alpha particles
[DE85-009037] 18 p3183 N85-29740
Compendium of unsteady aerodynamic measurements, addendum 1
[AGARD-R-702-ADD-1] 20 p3390 N85-31028
Data set 9: LANN wing. Pitching oscillation 20 p3390 N85-31030
In-flight evaluation of pure time delays in pitch and roll
[NASA-TM-86744] 21 p3556 N85-32123
Fokker-Planck calculation of hot electron formation in the thermal barrier region of tandem mirror Gamma-10
[IPPJ-726] 23 p3979 N85-34669
Pitch angle distributions of 35-1000 keV protons at quasi-perpendicular interplanetary shocks
[SH-1.5-6] 23 p3996 N85-34775
Diagnostic of electromagnetic conditions in space using cosmic rays
[SH-4.5-19] 23 p4036 N85-35036
Magnetic fluctuation and cosmic ray diurnal variations
[SH-4.5-21] 23 p4038 N85-35038

PITCH ANGLES
U PITCH (INCLINATION)

PITCH ATTITUDE CONTROL
U LONGITUDINAL CONTROL

PITCHING MOMENTS
An evaluation of three helicopter rotor sections
[NASA-TM-86719] 23 p3993 N85-34115

PITOT TUBES
Mixing characteristics of an underexpanded multiple jet ejector
[AD-A149557] 10 p1485 N85-19375
A comparison of laser Doppler anemometry and probe measurements within the boundary layer of an airfoil at subsonic flow
[ISL-CO-219/84] 23 p3995 N85-34127

PITTING
The influence of metallurgical aspects on the pitting corrosion behaviour of high alloy stainless steels 02 p0179 N85-11202
Electrochemical pitting evaluation of aluminum alloy 7075 in machining coolant
[DE84-016844] 04 p0475 N85-13026
Stochastic models of pitting corrosion of stainless steels. Part 1: Modelling of the initiation and growth of pits at constant potential
[AERE-R-11146-PT-1] 09 p1298 N85-18151
Local electrochemistry of pitting corrosion in stainless steels
[DE85-005207] 13 p2023 N85-22673
Studies of the initiation of pitting corrosion on stainless steels
[AERE-M-3400] 14 p2254 N85-23967
The design and construction of a flow channel and rig for corrosion studies
[AERE-M-3455] 15 p2506 N85-25474
Investigation of the pitting potential of rapidly solidified aluminum-lithium alloys
[VTH-LR-434] 16 p2752 N85-26986
Effects of gamma-ray irradiation on dislocations in sodium nitrate single crystals
[DE85-006291] 18 p3195 N85-29618
Mechanism of strength degradation for hot corrosion of alpha-SiC
[NASA-TM-87052] 19 p3248 N85-30135
Pitting corrosion of ferrous alloys
[AERE-R-11490] 24 p4078 N85-35273

PITUITARY GLAND
Regulation of physical activity in anforthostatic position by acting on adrenosympathetic and hypophysec-adrenocortical systems 22 p3824 N85-33889

PITUITARY HORMONES
NT ADRENOCORTICOTROPIN (ACTH)

PIX
U PLASMA INTERACTION EXPERIMENT

PL/1
Selection and use of general-purpose programming-language: Program examples, volume 2
[PB85-122000] 12 p1917 N85-22039
Selection and use of general-purpose programming language: Overview, volume 1
[PB85-122018] 12 p1917 N85-22040

PLAGES (FACULAE)
U FACULAE

PLAINS
NT COASTAL PLAINS
NT FLOOD PLAINS
NT TUNDRA
Petrology of deep crustal xenoliths from the eastern Snake River Plain, Idaho 02 p0226 N85-11477
Thickness of ridged plains materials in Hesperia Planum, Mars 13 p2185 N85-23561
Investigations of the Mare cratered terrain: Smooth plains boundary in the eastern equatorial region 13 p2191 N85-23598
Enigmatic hills of the mottled plains, Mare Acidalium quadrangle (MC-4), Mars 13 p2192 N85-23599
Geomorphology and geology of the Southwestern Margaritifer Sinus and Argyre regions of Mars. Part 1: Geological and geomorphological overview 13 p2192 N85-23600
Mechanisms of basalt-plains ridge formation 13 p2199 N85-23643

PLAN POSITION INDICATORS
Influence of a perspective cockpit traffic display format on pilot avoidance maneuvers 10 p1534 N85-19666

PLANAR STRUCTURES
Burmester theory for 4 precision positions: An extended discourse with application to the dimensional synthesis of arbitrary planar linkages 03 p0367 N85-12351
Autonomous momentum management for space station
[NASA-CR-174085] 04 p0462 N85-12931
Axial representations of shape
[AD-A150387] 13 p2151 N85-23356
The structure and composition of Uranus and Neptune 13 p2175 N85-23495
Linear incompressible magnetoconvection in a planar layer with a nonuniform horizontal magnetic field 14 p2450 N85-25127
Two-degree-of-freedom linear and planar microwave array lenses
[AD-A153701] 18 p3096 N85-29166
LSI/VLSI ion implanted planar GaAs IC processing
[AD-A155110] 21 p3581 N85-32362
Generalized planar matching
[AD-A154809] 21 p3677 N85-32842
A planar version of a 4.0 gigahertz reactively steered adaptive array
[AD-A156029] 24 p4067 N85-35330

PLANCKS CONSTANT
X-ray spectra of bursting neutron stars 23 p3981 N85-34668

PLANE STRAIN
Crack tip opening displacement for work hardening materials
[GKSS-84-E-28] 01 p0083 N85-10415
Free-edge failures of composite laminates 04 p0467 N85-12971
Multiaxial yield behavior of 1100 aluminum following various magnitudes of prestrain
[DE84-013004] 05 p0617 N85-13949
Fundamentals of microcrack nucleation mechanics
[NASA-CR-3851] 07 p0975 N85-16195
Modeling of large-scale accretionary wedge and thin-skinned trust-and-fold belt mechanics 08 p1161 N85-17442
Strain-controlled creep rupture in non-isothermal materials 09 p1332 N85-18368
Elastic wave scattering from an interface crack in a layered half space 13 p2101 N85-23095
Elasticity solution of an adhesively bonded joint
[NASA-CR-175591] 13 p2101 N85-23097
Numerical study of ductile rupture in plane deformations
[ONERA-RT-23/7169-RY-072-R] 20 p3469 N85-31557
Numerical study of tensile fracture in plane stress
[ONERA-RT-22/7169-RY-070-R] 20 p3470 N85-31560

A cracked orthotropic sheet stiffened by a semi-infinite orthotropic sheet
[NASA-TP-2455] 21 p3597 N85-32339

PLANE WAVES

Theory of near-field phased arrays for electromagnetic susceptibility testing
[PB84-217636] 01 p0042 N85-10273

Finitely conducting, infinitely long, cylindrical wire in the presence of a plane wave (EMP)
[DE84-015363] 02 p0192 N85-11282

Plane wave (EMP) incidence on a finitely conducting plane Earth with the magnetic field intensity parallel to the Earth's surface
[DE84-015364] 02 p0228 N85-11493

Scattering of plane wave on cylindrical shell in low-frequency region 02 p0256 N85-11677

Parameters of detonation waves excited in gas during concentrated release of energy 02 p0268 N85-11751

Diffraction of plane polarized waves by noncircular cylindrical cavity 02 p0269 N85-11754

Dispersion curves for normal waves in cylindrical shell and conditions for spatial coincidence in vicinity of critical frequencies 06 p0778 N85-14973

Bulk cavitation caused by a plane shock wave
[AD-A147031] 07 p0958 N85-18072

Multiple parallel wires above a finitely conducting plane earth in the presence of a plane wave (EMP)
[DE85-001116] 11 p1625 N85-20231

A mixed-basis band structure interpolation scheme applied to the fluorite structure compounds NiSi2, AuAl2, AuGa2 and AuIn2
[AD-A150131] 12 p1940 N85-22187

Interpretation of directional magnetotelluric soundings by analytical continuation method 14 p2343 N85-24488

Asymptotic construction of a procedure for plane-wave synthesis and migration
[AD-A150969] 14 p2374 N85-24672

Analysis of the electromagnetic scattering from an inlet geometry with lossy walls
[NASA-CR-175743] 15 p2541 N85-25686

Kirchhoff modeling via wave equation detuning
[AD-A152399] 17 p3028 N85-28727

Guided-mode launching in a slab waveguide by way of diffraction at the edge of a conducting screen residing on one surface of the slab
[AD-A154886] 21 p3575 N85-32232

Transient analysis of electromagnetic reflection from dispersive materials
[PB86-200186] 24 p4154 N85-35753

PLANET EPHEMERIDES

Relating the planetary ephemerides and the radio reference frame 16 p2770 N85-27095

PLANET ORIGINS

U PLANETARY EVOLUTION

PLANETARY ATMOSPHERES

NT HELIUM HYDROGEN ATMOSPHERES
NT JUPITER ATMOSPHERE
NT MARS ATMOSPHERE
NT NEPTUNE ATMOSPHERE
NT SATURN ATMOSPHERE
NT URANUS ATMOSPHERE
NT VENUS ATMOSPHERE

Atmospheres of Uranus and Neptune 02 p0298 N85-11929

Temperature structures and infrared-derived properties of the atmosphere of Uranus and Neptune 02 p0298 N85-11931

Laboratory studies of atomic collision processes of importance in planetary atmospheres
[NASA-CR-174142] 04 p0589 N85-13758

Effects of the solar and extraterrestrial environments on space power systems 05 p0610 N85-13886

The Interactive Planetary Image Processing System (IPIPS): A major facility for research and teaching in remote sensing 05 p0655 N85-14203

Shock-induced CO2 loss from CaCO3: Implications for early planetary atmospheres
[NASA-CR-174197] 05 p0745 N85-14777

Studies of radiative transfer in planetary atmospheres
[NASA-CR-174194] 05 p0745 N85-14778

Far infrared and submillimeter observations of the giant planets 08 p1245 N85-17856

Exploring the solar system with stellar occultations 08 p1245 N85-17857

Impact and collisional processes in the solar system
[NASA-CR-174297] 08 p1255 N85-17914

A modeling analysis program for the JPL table mountain Io sodium cloud data
[NASA-CR-175474] 10 p1572 N85-19910

Solar system studies with the IUE: 1982 - 1984 11 p1744 N85-20964

Radio scintillations observed during atmospheric occultations of Voyager: Internal gravity waves at Titan and magnetic field orientations at Jupiter and Saturn
[NASA-CR-175554] 12 p1961 N85-22327

Impact and collisional processes in the solar system 13 p2180 N85-23530

Magmas as selective filters of volatiles between planetary mantles and surfaces 13 p2185 N85-23557

Approximate analytic method of calculating trajectories of movement of a flight vehicle in the atmosphere 14 p2279 N85-24121

Development of a global 3-D magnetohydrodynamic computational model for solar wind/cometary and planetary studies
[NASA-CR-175724] 15 p2684 N85-26577

An experimental investigation of the angular scattering and backscattering behaviors of the simulated clouds of the outer planets
[NASA-CR-175909] 17 p3052 N85-28896

Magnetospheres of the outer planets
[AD-A154354] 19 p3384 N85-30996

Hadley circulation in planetary atmospheres 20 p3546 N85-32067

Aeolian geomorphology from the global perspective 21 p3603 N85-32373

Impact processes and their implications for planetary formation and early evolution 22 p3653 N85-33860

Origin of the atmosphere and hydrosphere of the terrestrial planets 22 p3853 N85-33863

An impact-induced terrestrial atmosphere and iron-water reactions during accretion of the Earth 22 p3854 N85-33864

Biological modulation of planetary atmospheres: The early Earth scenario 22 p3854 N85-33867

Volatiles on satellites of the outer solar system 22 p3854 N85-33868

Interrelations for the elements of the scattering matrix 22 p3855 N85-33872

PLANETARY BASES

Impact of lunar and planetary missions on the space station: Preliminary STS logistics report
[NASA-CR-171837] 09 p1285 N85-18072

PLANETARY BOUNDARY LAYER

The inducement of planetary boundary layer mass convergence associated with varying vorticity beneath tropospheric wind maximum 01 p0074 N85-10494

Numerical forecast of pressure field by considering the mutual influence of orography, thermal nonhomogeneity and surface friction 01 p0080 N85-10534

A diagnostic approach to obtaining planetary boundary layer winds using satellite-derived thermal data 05 p0674 N85-14330

A vertically resolved planetary boundary layer 05 p0680 N85-14367

Large-eddy simulation. Guidelines for its application to planetary boundary layer research
[AD-A146361] 06 p0890 N85-15651

Observations of the magnetospheric boundary layers — International Magnetospheric Study 14 p2355 N85-24551

The behavior of the atmosphere in the desert planetary boundary layer
[AD-A151286] 15 p2592 N85-25977

Study of the functions of similarity of the planetary boundary layer. Part 1: Theory
[INPE-3129-PRE/520-PT-1] 16 p2826 N85-27428

Study of the functions of similarity of the planetary boundary layer. Part 2: Results
[INPE-3130-PRE/521-VOL-2] 16 p2826 N85-27429

Large-eddy simulation in planetary boundary-layer research 18 p3147 N85-29482

Reports from the German Meteorological Service. No. 167: Results of aerological soundings in the model area upper Rhine: Heat release project upper Rhine area, part 3
[ISBN-3-88148-216-4] 23 p3950 N85-34479

Application of a turbulent closure model to the parameterization of the vertical diffusion of heat, momentum, and humidity in the ECMWF model — European Center for Medium Term Weather Forecasting (ECMWF)
[MITT-41] 24 p4095 N85-35387

PLANETARY COMPOSITION

High pressure cosmochemistry applied to major planetary interiors: Experimental studies
[NASA-CR-174032] 02 p0302 N85-11956

Detection of the J-10 manifold of the pure rotational band of phosphine on Saturn 08 p1245 N85-17855

Venus 09 p1411 N85-18691

Near infrared modeling of the equatorial regions of Jupiter and Saturn 09 p1415 N85-18930

Multispectral analysis of the Kasei Valle-Lunae Planum region of Mars 13 p2193 N85-23607

The search for igneous materials at the Viking landing sites 13 p2194 N85-23609

Basalts of Mars: Constraints on volatile evolution 13 p2194 N85-23610

First direct detection of clay minerals on Mars 13 p2194 N85-23612

Iron oxides of Mars: Evidence for contemporary weathering 13 p2195 N85-23613

Reassignment of the iron (3) absorption bands in the spectra of Mars 13 p2195 N85-23614

Zeolites on Mars: Prospects for remote sensing 13 p2195 N85-23615

High pressure cosmochemistry applied to major planetary interiors: Experimental studies
[NASA-CR-175715] 15 p2679 N85-26544

Workshop on the Early Earth: The Interval from Accretion to the Older Archean
[NASA-CR-176037] 21 p3717 N85-33062

Conditions during formation of the Earth 21 p3717 N85-33066

Early evolution of the crust-mantle system 21 p3717 N85-33067

Was core formation violent enough to homogenize the early mantle? 21 p3718 N85-33068

The problem of the Earth's CO2 content and the iron core 21 p3718 N85-33069

A review of noble gas geochemistry in relation to early Earth history 21 p3720 N85-33081

Carbon and nitrogen in the deep Earth 21 p3721 N85-33085

Chemical evolution of the Earth: Equilibrium or disequilibrium process? 21 p3721 N85-33086

Thermal, dynamic and compositional aspects of the core-forming Earth 21 p3722 N85-33091

Earth's primordial differentiation, and its after-effects 21 p3722 N85-33092

Terrestrial Planets: Comparative Planetology
[NASA-CR-176093] 22 p3851 N85-33849

Noble gas patterns in the atmospheres of Mars and Earth: A comparison via the SNC meteorites 22 p3852 N85-33853

Venus, Earth and Mars: Present bounds on similarities and differences in bulk composition 22 p3856 N85-33876

Mineralogy and chemistry of the Earth 22 p3856 N85-33877

PLANETARY CORES

NT EARTH CORE

Interior structure of Uranus 02 p0299 N85-11939

Planetary reorientation by surface loads 22 p3858 N85-33866

Geochemical confirmation of the lunar magmasphere hypothesis 22 p3859 N85-33895

PLANETARY CRATERS

NT MARS CRATERS

Geological, structural, and geomorphological analyses from SIR-B 08 p1145 N85-17226

Mercury 09 p1411 N85-18690

Impact cratering calculation 13 p2180 N85-23531

Impact crater scaling laws 13 p2181 N85-23532

Problems in recovering crater production functions 13 p2182 N85-23539

Examination of returned solar-max surfaces for impacting orbital debris and meteoroids 15 p2681 N85-26560

Considerations of large scale impact and the early Earth 21 p3718 N85-33070

PLANETARY ENTRY

U ATMOSPHERIC ENTRY

PLANETARY ENVIRONMENTS

NT HELIUM HYDROGEN ATMOSPHERES
NT JUPITER ATMOSPHERE
NT MARS ATMOSPHERE
NT MARS ENVIRONMENT
NT NEPTUNE ATMOSPHERE
NT PLANETARY ATMOSPHERES
NT SATURN ATMOSPHERE
NT URANUS ATMOSPHERE
NT VENUS ATMOSPHERE

The dynamic fission instability and the origin of the Moon 04 p0586 N85-13736

Far infrared and submillimeter observations of the giant planets 08 p1245 N85-17856

Exploring the solar system with stellar occultations 08 p1245 N85-17857

Ganymede and Callisto: Beauty is only skin deep 15 p2680 N85-26552

Activities at the Lunar and Planetary Institute
[NASA-CR-175914] 18 p3201 N85-29859

Microbial ecology of extreme environments: Antarctic yeasts and growth in substrate-limited habitats
[NASA-CR-176006] 19 p3326 N85-30609

Activities report of the Laboratory of Stellar and Planetary Physics
[G-127] 20 p3544 N85-32052

The global sulfur cycle
[NASA-TM-87570] 21 p3656 N85-32710

Impact processes and their implications for planetary formation and early evolution 22 p3853 N85-33860
Questions about Mercury's role in comparative planetary geophysics 22 p3853 N85-33861
PLANETARY EVOLUTION
Impact phenomena as factors in the evolution of the Earth
[NASA-CR-174015] 01 p0072 N85-10474
The origin and evolution of Uranus and Neptune 02 p0298 N85-11928
Interior structure of Uranus 02 p0299 N85-11939
The problem of iron partition between Earth and Moon during simultaneous formation as a double planet system 04 p0587 N85-13744
The geology of the terrestrial planets
[NASA-SP-469] 09 p1410 N85-18888
Asteroids, comets and planet formation 09 p1410 N85-18889
Mercury 09 p1411 N85-18890
Earth 09 p1411 N85-18892
Evolution of sedimentation basins in Earth's history 10 p1497 N85-19451
Planetary geology in the 1980s
[NASA-SP-467] 13 p2169 N85-23457
Studies of planetary rings 13 p2174 N85-23488
Origin and evolution of the Saturn system 13 p2175 N85-23493
Giant planets and their satellites: Cosmochemistry, evolution and structure 13 p2175 N85-23494
The structure and composition of Uranus and Neptune 13 p2175 N85-23495
On the origin of Triton and Pluto 13 p2175 N85-23497
The Formation of preplanetary disks from the collapse of rotating molecular cloud cores 13 p2180 N85-23526
The evolution of CO2 on Mars 13 p2185 N85-23558
Three-layer generic Ganymedes: Structure and evolution 13 p2202 N85-23657
Structure and origin of Martian satellites 15 p2483 N85-25323
Evolution of collisional systems -- planetary disks 15 p2574 N85-26505
The formation of spokes in Saturn's rings 15 p2576 N85-26524
The E-ring of Saturn 15 p2577 N85-26527
Formation of the solar system 15 p2577 N85-26532
The formation of the terrestrial planets from lunar sized planetesimals 15 p2578 N85-26533
Statistical theory of planet growth 15 p2578 N85-26534
Tidal breakup and origin of the Uranian ring system 15 p2578 N85-26535
Asteroid compositional rings: Clues to the compositions of primordial planetesimals in the middle solar system 15 p2578 N85-26537
Sixteenth Lunar and Planetary Science Conference. Press abstracts
[NASA-CR-175692] 15 p2680 N85-26548
Chondrule-like particles provide evidence of early Archean meteorite impacts, South Africa and western Australia 15 p2682 N85-26562
What we know about Mars (but otherwise wouldn't) if it is the shergottite parent body 15 p2682 N85-26565
Geologic interpretation of remote sensing data for the Martian volcano Ascraeus Mons 19 p3384 N85-30992
Global geomorphology: Report of Working Group Number 1 21 p3604 N85-32362
Landscape inheritance: Report of Working Group Number 2 21 p3604 N85-32363
Protocyanobacteria: Oxygenic and Anoxygenic photosynthesis in mat-forming bacteria 21 p3657 N85-32714
Workshop on the Early Earth: The Interval from Accretion to the Older Archean
[NASA-CR-176037] 21 p3717 N85-33062
Conditions during formation of the Earth 21 p3717 N85-33066
Early evolution of the crust-mantle system 21 p3717 N85-33067
Was core formation violent enough to homogenize the early mantle? 21 p3718 N85-33068
Considerations of large scale impact and the early Earth 21 p3718 N85-33070
Noble gases and the early history of the Earth: Inappropriate paradigms and assumptions inhibit research and communication 21 p3719 N85-33075
A review of noble gas geochemistry in relation to early Earth history 21 p3720 N85-33081
Archean sedimentary systems and crustal evolution 21 p3720 N85-33082
Crustal radiogenic heat production and the selective survival of ancient continental crust 21 p3721 N85-33086
Large arcuate scars: A geological legacy of the Earth's accretionary past 21 p3721 N85-33089
Thermal, dynamic and compositional aspects of the core-forming Earth 21 p3722 N85-33091
Comments on RS-17 X-ray telescope 22 p3731 N85-33132
Terrestrial Planets: Comparative Planetology
[NASA-CR-176093] 22 p3851 N85-33849
Relationships between chondritic meteorites and planets 22 p3851 N85-33851
Interrelationships among the terrestrial planets 22 p3853 N85-33859
Questions about Mercury's role in comparative planetary geophysics 22 p3853 N85-33861
Volatile loss following very large impacts 22 p3853 N85-33862
Origin of the atmosphere and hydrosphere of the terrestrial planets 22 p3853 N85-33863
An impact-induced terrestrial atmosphere and iron-water reactions during accretion of the Earth 22 p3854 N85-33864
Climatic consequences of very high CO2 levels in Earth's early atmosphere 22 p3854 N85-33865
The polar caps and the climatic evolution of Mars 22 p3854 N85-33866
Biological modulation of planetary atmospheres: The early Earth scenario 22 p3854 N85-33867
Volatiles on satellites of the outer solar system 22 p3854 N85-33868
Planetary surface processes: A review 22 p3855 N85-33869
Interpretation of photometric measurements of airless bodies 22 p3855 N85-33871
Models of planetary structure and evolution: The case of Io 22 p3855 N85-33874
Mineralogy and chemistry of the Earth 22 p3856 N85-33877
Crustal development in the terrestrial planets 22 p3856 N85-33879
Contrasts in evolution of Venus and Earth 22 p3857 N85-33880
Primordial magmaspheres and their lasting consequences 22 p3857 N85-33882
Thermal evolution of coastal California with implications for hydrocarbon maturation 24 p4115 N85-35509
The ionization structure of planetary nebulae. Part 4: NGC 7662
[NASA-CR-176151] 24 p4169 N85-35844
PLANETARY EXPLORATION
U SPACE EXPLORATION
PLANETARY GEOLOGY
NT MARS VOLCANOES
A bibliography of planetary geology and geophysics principal investigators and their associates, 1983 - 1984
[NASA-TM-87361] 01 p0127 N85-10874
Mars-Earth geographical comparisons: A pictorial view
[NASA-TM-86166] 02 p0302 N85-11957
The geology of the terrestrial planets
[NASA-SP-469] 09 p1410 N85-18888
Mars 09 p1411 N85-18894
The origin and evolution of terrestrial and Martian rock labyrinths
[NASA-CR-175511] 12 p1961 N85-22326
Planetary geology in the 1980s
[NASA-SP-467] 13 p2169 N85-23457
Reports of the Planetary Geology and Geophysics Program, 1984
[NASA-TM-87563] 13 p2172 N85-23474
A statistical treatment of the regional slope characteristics of Venus and Earth 13 p2178 N85-23517
Centrifuge impact cratering experiments 13 p2181 N85-23533
Progress on Experimental impact studies 13 p2181 N85-23534
Progress on studies of early intense cratering 13 p2181 N85-23535
Why not a constant early lunar impact rate? 13 p2181 N85-23536
Martian terrain ages 13 p2181 N85-23537
Impacts in Ice: Commissions of solar system crater population 13 p2181 N85-23538
Problems in recovering crater production functions 13 p2182 N85-23539
A parmetric study of crater-saturation simulation 13 p2182 N85-23540
Average spacing for rings of individual multi-ring basins is 2.0(0.5)D 13 p2182 N85-23541
Ring-diameter ratios for multi-ring basins average 2.0(0.5)D 13 p2182 N85-23542
Morphology and mechanics of terraces in lunar craters 13 p2182 N85-23543
Newly discovered Martian impact basins 13 p2182 N85-23544
The nature of Martian flow ejecta craters 13 p2183 N85-23545
Interaction of Martian flow ejecta blankets with pre-existing impact craters: Morphological observations 13 p2183 N85-23546
Ripple ring basins on Ganymede and Callisto 13 p2183 N85-23547
Implications of convection in the Moon and the terrestrial planets 13 p2183 N85-23548
High pressure cosmochemistry of major planetary interiors: Laboratory studies of the water-rich region of the system ammonia-water 13 p2183 N85-23549
Modelling equilibrium and fractional crystallization in the system MgO-FeO-CaO-Al2O3-SiO2 13 p2184 N85-23552
Ridged plains of Lunae Planum: Thickness distribution revised 13 p2185 N85-23559
Volcanic debris flows in the Elysium region of Mars 13 p2185 N85-23560
Thickness of ridged plains materials in Hesperia Planum, Mars 13 p2185 N85-23561
Mapping structures characteristic of the highland boundary scarp on Mars 13 p2191 N85-23595
Investigations of the Mars cratered terrain: Smooth plains boundary in the eastern equatorial region 13 p2191 N85-23596
Martian fretted terrain morphometry interpreted using principal components analysis 13 p2192 N85-23597
Enigmatic hills of the mottled plains, Mare Acidalium quadrangle (MC-4), Mars 13 p2192 N85-23599
Geomorphology and geology of the Southwestern Margaritifer Sinus and Argyre regions of Mars. Part 1: Geological and geomorphological overview 13 p2192 N85-23600
Geomorphology and geology of the Southwestern Margaritifer Sinus and Argyre regions of Mars. Part 2: Crater size-frequency distribution curves and geomorphic unit ages 13 p2192 N85-23601
Geomorphology and geology of the Southwestern Margaritifer Sinus and Argyre regions of Mars. Part 3: Valley types and distribution 13 p2193 N85-23602
Geomorphology and geology of the Southwestern Margaritifer Sinus and Argyre regions of Mars. Part 4: Flow ejecta crater distribution 13 p2193 N85-23603
Multispectral analysis of the Kasei Valle-Lunae Planum region of Mars 13 p2193 N85-23607
Io: Precise comparison of Voyager spectral curves with laboratory measurements 13 p2196 N85-23619
Determining mineral types and abundances from reflectance measurements 13 p2196 N85-23622
Determination of mineral type, abundance, and grain size with remotely obtained reflectance spectra 13 p2196 N85-23623
Quantitative analyses of planetary reflectance spectra 13 p2197 N85-23625
Terrestrial analogs for planetary wrinkle ridges 13 p2199 N85-23644
On the absence of strike-slip faults from the planets and satellites 13 p2200 N85-23645
Lunar mascon loading: An example of the importance of fault initiation depth on fault type predictions from stresses on planetary surfaces 13 p2200 N85-23646
Planetary interior modeling and tectonic implications 13 p2200 N85-23649
Elysium region, Mars: Tests of lithospheric loading models for the formation of tectonic features 13 p2200 N85-23650
Lithologic and structural control on slope morphology in the Valles Marineris 13 p2201 N85-23651
Valles Marineris basin beds: A complex story 13 p2201 N85-23652
Mars: Stratigraphy of western highlands and polar regions 13 p2201 N85-23653
Kasei Valls of Mars: Dating the interplay of tectonics and geomorphology 13 p2201 N85-23654
Creep of ice: Further studies 13 p2201 N85-23655
Fault offsets and lateral crustal movement on Europa 13 p2201 N85-23656
Three-layer generic Ganymedes: Structure and evolution 13 p2202 N85-23657
Lineaments on Ganymede: New evidence for late tectonic activity 13 p2202 N85-23658
Global tectonics on Ganymede 13 p2202 N85-23659
Tectonics of the Galileo Regio on Ganymede 13 p2202 N85-23660
Importance of the tectonic motions on Ganymede 13 p2202 N85-23661
Tectonics of the Valhalla structure on Callisto 13 p2202 N85-23662
Mars geologic mapping: A review and new concepts 13 p2202 N85-23663

Physical and geological nature of Saturn's larger ring particles 15 p2674 N85-26509
Ganymede and Callisto: Beauty is only skin deep 15 p2680 N85-26552
Geologic interpretation of remote sensing data for the Martian volcano Ascraeus Mons 19 p3384 N85-30992
Geological analyses of the surface of Venus and Mars from lander spacecraft images and orbital radar observations 19 p3384 N85-30993
The problem of scale in planetary geomorphology 21 p3603 N85-32375
Landscape inheritance: Report of Working Group Number 2 21 p3604 N85-32383
Questions about Mercury's role in comparative planetary geophysics 22 p3863 N85-33851

PLANETARY GRAVITATION
Rotational properties of Uranus and Neptune 02 p0299 N85-11940
Research relative to the development of a cryogenic microwave cavity gradiometer for orbital use [NASA-CR-174249] 07 p0962 N85-16085
Gravity anomaly map of Mars and Moon and analysis of Venus gravity field: New analysis procedures [NASA-CR-174295] 08 p1258 N85-17919
Expansion of functions describing planetary surface and gravity field 13 p1978 N85-22410
Viking radio science data analysis and synthesis 13 p2180 N85-23528
Gravity field of the Jovian system from Pioneer and Voyager tracking data 13 p2180 N85-23529
Evolution of collisional systems — planetary disks 15 p2674 N85-26505
The non-hydrostatic figures of the terrestrial planets 22 p3858 N85-33887
Admittance functions from Venus vertical gravity and modes of topographic support 22 p3858 N85-33889

PLANETARY LANDING
Mathematical model for rollout of planet roving vehicle from landing craft 15 p2484 N85-25334

PLANETARY LIMB
Clouds above the Martin Limb: Viking observations [NASA-CR-174027] 02 p0296 N85-11922

PLANETARY MAGNETIC FIELDS
Magnetospheric structures: Uranus and Neptune 02 p0301 N85-11949
Effects of the solar and extraterrestrial environments on space power systems 06 p0810 N85-13698
Magnetospheres in the solar system 12 p1954 N85-22274
Particle transport in planetary magnetospheres 12 p1954 N85-22275
Hydromagnetic precursors of interplanetary plasma burst 13 p1978 N85-22414
Dynamics of charged small particles — Jupiter, Saturn magnetospheres 15 p2676 N85-26522
On the role of mother-planet magnetic field in spiral structure explanation of formation of spokes — Saturn rings 15 p2676 N85-26525
The gravito-electrodynamics of charged dust in planetary ring systems 15 p2677 N85-26531
What we know about Mars (but otherwise wouldn't) if it is the shergottite parent body 15 p2682 N85-26565
Orientation and strength of Martian magnetic dipole 16 p2723 N85-26808
Possible configuration of Martian magnetosphere 16 p2723 N85-26809
Planetary Dynamos [NASA-CR-176001] 21 p3679 N85-32857
The magnetic field of planets 22 p3856 N85-33691
What we have learned about the magnetic field of Mars 22 p3856 N85-33692
Magnetic field generation in the cores of terrestrial bodies 22 p3859 N85-33894

PLANETARY MANTLES
NT EARTH MANTLE
Magmas as selective filters of volatiles between planetary mantles and surfaces 13 p2165 N85-23557
A solid-state framework for terrestrial upper mantles 22 p3856 N85-33878
Crustal development in the terrestrial planets 22 p3856 N85-33879
The non-hydrostatic figures of the terrestrial planets 22 p3858 N85-33887
Dynamic compensation of Venus's geoid: A comparison with Earth 22 p3858 N85-33888

PLANETARY MAPPING
Planetary cartography in the next decade (1984 - 1994) [NASA-SP-475] 12 p1960 N85-22323
Visualization of radar altimetry data for Venus 13 p1982 N85-22437
Mapping structures characteristic of the highland boundary scarp on Mars 13 p2191 N85-23595
Tectonics of the Galileo Regio on Ganymede 13 p2202 N85-23660
Mars geologic mapping: A review and new concepts 13 p2202 N85-23663
The Galilean Satellite Geological Mapping Program, 1984 13 p2203 N85-23664
Geology of the Ganymede quadrangle Jg7 13 p2203 N85-23665
Mars planimetric mapping 13 p2203 N85-23666
Viking Lander mosaics of Mars 13 p2203 N85-23667
Voyager cartography 13 p2203 N85-23668
The control network of Mars: October 1984 13 p2203 N85-23670
The control networks of the satellites of Jupiter and Saturn 13 p2204 N85-23671
Distribution of gravity and plumb line deflection at Martian surface 15 p2483 N85-25324

PLANETARY MOTION
U SOLAR ORBITS

PLANETARY NEBULAE
The unidentified emission features: A study of the Orion Bar and planetary nebulae 08 p1246 N85-17862
Mid-infrared spectroscopy of planetary nebulae 08 p1247 N85-17872
Spectral characteristics of dust in planetary nebulae 08 p1247 N85-17873
Variation of oxygen and nitrogen abundances in the galaxy 08 p1248 N85-17876
Ultraviolet spectroscopy of selected astronomical sources [NASA-CR-174379] 09 p1413 N85-18912
On the progenitors of white dwarfs [NASA-CR-174378] 09 p1413 N85-18913
Far-infrared line observations of planetary nebulae. 1: The O 3 spectrum [NASA-TM-86870] 10 p1570 N85-19900
IUE observations of planetary nebulae in the Magellanic Clouds 11 p1747 N85-20986
1983 observations of the eclipsing nucleus of the bipolar planetary nebula NGC 2346 11 p1747 N85-20987
Mass distribution and evolutionary scheme for central stars of planetary nebulae 11 p1751 N85-21012
The central star of NGC 40 11 p1751 N85-21013
LSS 2018: A double-lined spectroscopic binary central star with an extremely large reflection effect [NASA-CR-175503] 11 p1782 N85-21082
The distribution and dynamics of planetary nebulae in M32 and the Andromeda Galaxy 20 p3546 N85-32068
The ionization structure of planetary nebulae. Part 4: NGC 7662 [NASA-CR-176151] 24 p4169 N85-35844

PLANETARY ORBITS
Some considerations on elliptic heliocentric orbits [INPE-3217-PRE/570] 02 p0297 N85-11926
Venus 09 p1411 N85-18891
Small solar system bodies 13 p2175 N85-23499
The coorbital hypothesis 22 p3858 N85-33890

PLANETARY RADIATION
Infrared thermal radiation of Venus 02 p0163 N85-11101
Ultraviolet observations of Uranus and Neptune below 3000 Angstrom 02 p0298 N85-11932
Properties of the upper tropospheres of Uranus and Neptune derived from observations at visible to near-infrared wavelengths 02 p0298 N85-11933
Microwave emission from Saturn's rings 15 p2670 N85-26475
Saturn's E-ring in the red spectral region 15 p2671 N85-26480

PLANETARY RINGS
NT JUPITER RINGS
NT SATURN RINGS
NT URANUS RINGS
Uranus and Neptune [NASA-CP-2330] 02 p0298 N85-11927
The origin and evolution of Uranus and Neptune 02 p0298 N85-11928
Exploration of the solar system by airborne astronomy 08 p1244 N85-17851
Investigations of planetary ring phenomena 13 p2174 N85-23487
Studies of planetary rings 13 p2174 N85-23488
Dynamical studies of Saturn's rings 13 p2174 N85-23489
Meteoroidal impacts, plasma, fine structure of ringlets and spokes on Saturn's ring B 13 p2174 N85-23490
Plasma production by meteoroid impact 13 p2174 N85-23492
Origin and evolution of the Saturn system 13 p2175 N85-23493
Planetary Rings. Colloquium 75 — conferences [ISBN-2-85428-100-4] 15 p2670 N85-26473
Rings around Neptune? 15 p2672 N85-26491
How a shepherd guides a sheep herd — satellite-planetary ring interaction 15 p2674 N85-26503
Evolution of collisional systems — planetary disks 15 p2674 N85-26505
Size distribution in collisional systems — planetary rings 15 p2674 N85-26508
Comments on collision mechanics in ring systems — planetary rings [PSI-CONTRIB-186] 15 p2675 N85-26510
On the radial structure of planetary rings 15 p2675 N85-26512
Diffusion instability in a bimodal disc — planetary rings 15 p2675 N85-26513
Stochastic modeling of planetary ring systems 15 p2675 N85-26516
Applications of three-body resonances to satellites and planetary rings 15 p2676 N85-26518
Dynamics of neutral small particles — in the solar system 15 p2676 N85-26521
Diffusion of dust around a central body — Keplerian orbits 15 p2676 N85-26523
On the electric charge carried by dust grain excitation of violent discharge — planetary rings 15 p2677 N85-26530
The gravito-electrodynamics of charged dust in planetary ring systems 15 p2677 N85-26531
Future observations of planetary rings from ground-based observatories and Earth-orbiting satellites 15 p2678 N85-26540
Occultation detection of a Neptune ring segment 15 p2681 N85-26558

PLANETARY ROTATION
The origin and evolution of Uranus and Neptune 02 p0296 N85-11928
Rotational properties of Uranus and Neptune 02 p0299 N85-11940
On the origin of the Moon by rotational fission 04 p0587 N85-13746
Venus 09 p1411 N85-18891
Viking radio science data analysis and synthesis [NASA-CR-175631] 13 p2171 N85-23471
Viking radio science data analysis and synthesis 13 p2180 N85-23528
Motion of satellite with total dynamic symmetry around rotating aspherical Earth 14 p2287 N85-24174
Construction of conditionally periodic solutions of problem of reciprocating motion of axially symmetric satellite of triaxial planet 15 p2480 N85-25304
Photometric study of Pluto near perihelion. Part 2: Refinement of rotation period: Color indices 15 p2483 N85-25325
The vertical structure of global rotational normal modes 18 p3144 N85-29464

PLANETARY SATELLITES
U NATURAL SATELLITES

PLANETARY SPACE FLIGHT
U INTERPLANETARY FLIGHT

PLANETARY SPACECRAFT
U INTERPLANETARY SPACECRAFT

PLANETARY STRUCTURE
Atmospheres of Uranus and Neptune 02 p0298 N85-11929
Oblatenesses of Uranus and Neptune 02 p0300 N85-11941
Giant planets and their satellites: Cosmochemistry, evolution and structure 13 p2175 N85-23494
Studies of icy bodies: Uranian satellites and cometary nuclei 13 p2175 N85-23496
Viking radio science data analysis and synthesis 13 p2180 N85-23528
Planetary surface processes: A review 22 p3855 N85-33869
Models of planetary structure and evolution: The case of Io 22 p3855 N85-33874
Planetary reorientation by surface loads 22 p3858 N85-33886
The non-hydrostatic figures of the terrestrial planets 22 p3858 N85-33887
Dynamic compensation of Venus's geoid: A comparison with Earth 22 p3858 N85-33888
Applications of the Galerkin formalism in the coupling of the earth's free oscillations 24 p4116 N85-35514

PLANETARY SURFACES
NT MARS SURFACE
NT VENUS SURFACE
Grainsize evolution and differential comminution in an experimental regolith 06 p0888 N85-15636
Mercury 09 p1411 N85-18890
Expansion of functions describing planetary surface and gravity field 13 p1978 N85-22410
Evaluating accuracy in orientation of topographic photograph and satellite-centered direction from star photograph 13 p1983 N85-22442

Planetary geology in the 1980s
[NASA-SP-467] 13 p2169 N85-23457
A parmetric study of crater-saturation simulation
13 p2182 N85-23540
Relative time-scale for channeling events within chaotic terrains, Margaritifer Sinus, Mars
13 p2190 N85-23589
Permafrost and subsurface ice in the solar system
13 p2191 N85-23594
Terrestrial analogs for planetary wrinkle ridges
13 p2199 N85-23644
Lunar mascon loading: An example of the importance of fault initiation depth on fault type predictions from stresses on planetary surfaces
13 p2200 N85-23646
Results on volcanism, surface geology from Venera-15, -16 15 p2482 N85-25321
Distribution of gravity and plumb line deflection at Martian surface 15 p2483 N85-25324
One aspect of determination of direction of space survey base from photographs of planetary surface and star sky
15 p2487 N85-25352
Ganymede and Callisto: Beauty is only skin deep
15 p2680 N85-26552
Considerations of large scale impact and the early Earth 21 p3718 N85-33070
Origin of the atmosphere and hydrosphere of the terrestrial planets 22 p3853 N85-33863
An impact-induced terrestrial atmosphere and iron-water reactions during accretion of the Earth
22 p3854 N85-33864
Biological modulation of planetary atmospheres: The early Earth scenario 22 p3854 N85-33867
Planetary surface processes: A review
22 p3855 N85-33869
Permafrost features on Earth and Mars: Similarities, differences 22 p3855 N85-33870
Interpretation of photometric measurements of airless bodies 22 p3855 N85-33871
Planetary reorientation by surface loads
22 p3858 N85-33886

PLANETARY TEMPERATURE
Seasonal variations in Triton's atmospheric mass and composition 02 p0301 N85-11948
Planetary fluids He and NH3 at high shock pressures and temperatures
[DE85-011851] 22 p3859 N85-33896

PLANETARY WAVES
An improved analytical theory of Rossby wave driven Eulerian and Lagrangian mean flows along non-zonal barriers with application to the Hawaiian Ridge
[AD-A144951] 01 p0088 N85-10593
Quasi-stationary atmospheric responses to large-scale forcing 02 p0227 N85-11484
Global Scale Atmospheric Processes Research Program Review
[NASA-CP-2344] 05 p0679 N85-14360
Global scale diagnosis of FGGE data
05 p0683 N85-14394
Large scale rossby waves during FGGE
05 p0684 N85-14396
Limits of applicability of long wave theory in studies of oscillations of n-layer fluid 06 p0824 N85-15234
Interactions between mean flow and finite-amplitude mesoscale eddies in a barotropic ocean
[AD-A147249] 07 p1009 N85-18413
Generation and evolution of diabatic planetary waves in continuously stratified atmosphere with Ekman dissipation 09 p1354 N85-18515
Global scale diagnoses of FGGE data
[NASA-CR-174356] 09 p1356 N85-18533
Combined effects of baroclinic and barotropic instability in a nonlinear low order model
[DM-41] 09 p1358 N85-18544
PMP-2 report: Equatorial wave dynamics
11 p1657 N85-20442
Midwinter disturbances in the middle atmosphere
11 p1661 N85-20465
Aspects of planetary wave transports in the middle atmosphere 11 p1661 N85-20471
Winds and waves (4 min - 11 yrs) in the upper middle atmosphere (60-110 km) at Saskatoon, Canada (52 deg N, 107 deg W): MF radar (2.2 MHz) soundings 1973 - 1983 11 p1662 N85-20476
21 Layer troposphere-stratosphere climate model
[NASA-TM-86183] 12 p1892 N85-21871
Numerical investigation of evolution of energy spectrum of slightly nonlinear Rossby waves
13 p2106 N85-23124
Long nonlinear waves in layers of sudden changes in wind velocity 14 p2340 N85-24470
Forced MHD turbulence in a uniform external magnetic field
[NASA-CR-172576] 15 p2654 N85-26366
Wave dynamics and transport in the stratosphere
[NASA-CR-175789] 16 p2823 N85-27413
Mechanistic experiments to determine the origin of Southern Hemisphere stationary waves
18 p3143 N85-29461
Quasi stationary states in the Southern Hemisphere
18 p3144 N85-29465
On the global distribution of three-dimensional Eliassen-Palm fluxes by stationary waves
18 p3145 N85-29469
Finite amplitude stability of a Rossby wave in a channel 19 p3314 N85-30543
Atmospheric planetary wave response to external forcing
[NASA-CR-176000] 19 p3315 N85-30548
Sensitivity of planetary waves to initial conditions and forcing
[AD-A154111] 19 p3345 N85-30734
A numerical analysis of transient planetary waves and the vertical structure in a meso-strato-troposphere model, part 1.4A 21 p3617 N85-32473

PLANETISMALS
U PROTOPLANETS

PLANETOCENTRIC COORDINATES
NT GEOCENTRIC COORDINATES

PLANETOLOGY
Activities at the Lunar and Planetary Institute
[NASA-CR-174069] 04 p0579 N85-13694
Activities at the Lunar and Planetary Institute, introduction 04 p0579 N85-13695
A new look at the planets — space probes
[AERONOMICA-ACTA-37-1984] 11 p1765 N85-21096
USSR report: Space
[JPRS-USP-85-003] 15 p2476 N85-25284
Jupiter's ring system resolved: Physical properties inferred from the Voyager images
20 p3546 N85-32069
Geomorphic classification of Icelandic and Martian volcanoes: Limitations of comparative planetology research from LANDSAT and Viking orbiter images
21 p3603 N85-32372
Spacecraft-aided research discussed at geology Congress 22 p3734 N85-33147
Terrestrial Planets: Comparative Planetology
[NASA-CR-176093] 22 p3851 N85-33849

PLANETS
NT EARTH (PLANET)
NT GAS GIANT PLANETS
NT JUPITER (PLANET)
NT MARS (PLANET)
NT MERCURY (PLANET)
NT NEPTUNE (PLANET)
NT PLUTO (PLANET)
NT SATURN (PLANET)
NT TERRESTRIAL PLANETS
NT URANUS (PLANET)
NT URANUS RINGS
NT VENUS (PLANET)
High pressure cosmochemistry applied to major planetary interiors: Experimental studies
[NASA-CR-174032] 02 p0302 N85-11958
Magnetohydrodynamic and gasdynamic theories for planetary bow waves
[NASA-CR-174135] 04 p0589 N85-13760
Astrometric applications of the Mt. Stromlo PDS 1010A — microdensitometer 07 p0967 N85-16136
Photometric precision needed for planetary detection
08 p1250 N85-17894
Impact and collisional processes in the solar system
[NASA-CR-174297] 08 p1255 N85-17914
Herstmonceux observations of the Sun, planets and Moon, 1957 - 1982
[BULL-193] 11 p1762 N85-21087
A new look at the planets — space probes
[AERONOMICA-ACTA-37-1984] 11 p1765 N85-21096
Impact and collisional processes in the solar system
13 p2180 N85-23530
Astometry at La Silla 14 p2436 N85-25025
Activities at the Lunar and Planetary Institute
[NASA-CR-175914] 18 p3201 N85-29859

PLANFORMS
NT DELTA WINGS
NT RECTANGULAR PANELS
NT RECTANGULAR PLANFORMS
NT RECTANGULAR PLATES
NT RECTANGULAR WINGS
NT SWEPT FORWARD WINGS
NT SWEPTBACK WINGS
NT VARIABLE SWEEP WINGS
NT WING PLANFORMS

PLANIGRAPHY
U TOMOGRAPHY

PLANKTON
Calculation of optical characteristics of shelf ecological system based on its mathematical model
10 p1498 N85-19453
Microplankton species assemblages at the Scripps Pier from March to November 1983 during the 1982-1984 El Nino event
[NASA-CR-175563] 12 p1899 N85-21926
Biological processes in the water column of the South Atlantic Bight. Volume 1: Published manuscripts
[DE85-004810] 12 p1900 N85-21929
Possible role of ocean biota in global carbon balance — phytoplankton production 13 p2107 N85-23129
Geographic variation in the relationships of temperature, salinity or sigma sub t versus plant nutrient concentrations in the world ocean — silicic acid, nitrate, and phosphate concentration
[NASA-CR-175621] 13 p2140 N85-23267
Production and turnover of suspended organic detritus in the coastal water of the southeastern continental shelf
[DE85-003977] 13 p2140 N85-23290
Global paleoclimatic data base for 6000 years BP
[DE85-006628] 15 p2600 N85-26024
Ecology of Pamlico River, North Carolina: An estuarine profile
[PB85-155703] 16 p2822 N85-27404
MARMAP survey of the continental shelf from Cape Hatteras, North Carolina to Cape Sable, Nova Scotia (1977 - 1983). Atlas 1: Summary of operations
[PB85-150965] 16 p2839 N85-27506
Influence of underwater volcanic mountains of Atlantic on microplankton distribution 19 p3294 N85-30424
Properties of forest derived cloud condensation nuclei
21 p3650 N85-32662
Ecophysiology of phototrophic sulfur bacteria in lakes: Vertical distribution of planktonic populations
21 p3658 N85-32722
Marine Sample Exploitation Project: Estimates regarding the sensitivity and technology for the detection of nuclear explosion debris in the marine environment
[DE85-013176] 23 p3947 N85-34462
Seasonal variability and spatial non-uniformity of bioluminescence in the Mediterranean Sea
[DRIC-T-7545] 24 p4125 N85-35572

PLANKTON BLOOM
U PLANKTON

PLANNING
NT AIRPORT PLANNING
NT MANAGEMENT PLANNING
NT MISSION PLANNING
NT PRODUCTION PLANNING
NT PROJECT PLANNING
NT REGIONAL PLANNING
NT URBAN PLANNING
Air Force Materials Laboratory plans/projects
[AD-P004010] 03 p0308 N85-11990
The Air Force can improve its forecasts of aircraft spare parts requirements
[AD-A147911] 07 p1053 N85-16652
Developing double sampling plans for attributes to meet sample size criteria
[AD-A148144] 08 p1205 N85-17587
Strategy planning by an intelligent machine
[DE84-016809] 09 p1372 N85-18624
On motion planning with uncertainty: Revised
[AD-A149521] 10 p1492 N85-19421
A computer system for generating single and double sampling plans for attributes data
[AD-A149548] 11 p1701 N85-20696
FAA aviation forecasts: Fiscal years 1985-1996
[AD-A151050] 14 p2216 N85-23747
An approach to planning in the inflight emergency domain
[AD-A151869] 15 p2467 N85-25228
Artificial intelligence based control of a sensor-driven machine
[DE85-006972] 15 p2633 N85-26227
Historical perspective on the Moon base: The British perspective
[DE85-005905] 17 p2907 N85-27925
Experiments with stored heavy ions
[DE85-009976] 19 p3358 N85-30902
Report to the Working Group on Technology, Growth and Employment
[DE85-010320] 19 p3372 N85-30920
Navy information systems: Planning, policy, organization, and management
[PB85-176113] 20 p3541 N85-32038
Quality assurance considerations for the implementation of a pulsed power R and D project
[DE85-012367] 24 p4148 N85-35720

PLANOTRONS
NT HELITRONS
NT THERMICONS
NT THYRATRONS

PLANT DESIGN
Conceptual design of a 10 MW shore-based OTEC plant
[DE84-015808] 10 p1511 N85-19532

Some plant location problems — computer networks
[FUB-14-1984] 22 p0835 N85-33746

PLANT ROOTS
Gravity and cell differentiation in lentil roots
05 p0690 N85-14433
Comparative effects of auxin and abscisic acid on growth, hydrogen ion efflux and gravitropism in primary roots of maize
[NASA-CR-174355] 09 p1342 N85-18444
Amyloplast sedimentation kinetics in corn roots
15 p2606 N85-26059
Calcium and calmodulin localization in gravitropically-responding plant organs
15 p2606 N85-26061
The interaction of calcium and auxin in the gravitropic response of roots 15 p2606 N85-26062
Transduction of the root gravitropic stimulus: Can apical calcium regulate auxin distribution?
15 p2606 N85-26063
Role of Ca++ in shoot gravitropism — avena
15 p2607 N85-26065
Gravistimulus production in roots of corn
15 p2607 N85-26066
Differential wall growth in gravistimulated corn roots: Its timing and regulation 15 p2614 N85-26105

PLANT STRESS
Remote sensing of plant stress and diseases
05 p0657 N85-14216
Attempts to localize and identify the gravity sensing device of plant seedlings 15 p2607 N85-26064
The role of gravity on the reproduction of arabidopsis plants 15 p2607 N85-26069
Importance of gravity for plant growth and behavior
15 p2606 N85-26070

PLANTS (BOTANY)
NT ALFALFA
NT AQUATIC PLANTS
NT BARLEY
NT BRUSH (BOTANY)
NT CONIFERS
NT CORN
NT DECIDUOUS TREES
NT FOLIAGE
NT GRASSES
NT GUAYULE
NT LEAVES
NT LICHENS
NT OATS
NT SUGAR CANE
NT TOBACCO
NT TREES (PLANTS)
Prospectus of the utilization of leafy spurge (Euphorbia Esula L.) as a source of liquid fuel and biomass
[DE84-015203] 01 p0034 N85-10206
Estuaries of the Cape. Part 2: Synopses of available information on individual systems. Report 13: Silvermine (CSW 9)
[CSIR-RR-412-PT-2] 01 p0086 N85-10582
Estuaries of the Cape. Part 2: Synopses of available information on individual systems. Report no. 17: Lourens (CSW 7)
[CSIR-RR-416-PT-2] 01 p0087 N85-10586
A preliminary study of the feasibility of detecting the floating macrophytes by means of digital processing of MSS/LANDSAT data
[E85-10005] 02 p0215 N85-11418
Effects of acid rain on plant microbial associations in California
[PB84-242122] 04 p0532 N85-13404
Some principles of plant resources evaluation using remotely sensed data 04 p0543 N85-13459
Carbon cycle: Terrestrial interactions
05 p0652 N85-14187
The use of horizontal clinostats in studies of plant statocyte development 05 p0690 N85-14435
Plant responses to solar UV-B radiation
05 p0690 N85-14436
Preliminary results of advanced Biostack experiments with plant seeds and spores — cosmic ray effects
05 p0691 N85-14441
Plant growth in space 05 p0691 N85-14444
Controlled ecological life support system higher plant flight experiments
[NASA-CR-177323] 07 p1020 N85-18471
Calculation of optical characteristics of shelf ecological system based on its mathematical model
10 p1498 N85-19453
Vegetation analysis for arid lands geobotany
[NASA-CR-175455] 10 p1506 N85-19500
Effect of elevated atmospheric CO2 on plant communities
[DE85-001810] 11 p1678 N85-20576
Process development for commercial production of natural rubber from Guayule
[PB85-124958] 12 p1815 N85-21386
Estimating solar radiation for plant simulation models
[E85-10069] 12 p1873 N85-21751
Assessing LANDSAT TM and MSS data for detecting submerged plant communities 13 p2120 N85-23203
NASA Space Biology Program: 9th Annual Symposium
[NASA-CP-2336] 15 p2605 N85-26054
Polyamines as possible modulators of gravity induced calcium transport in plants 15 p2606 N85-26060
A possible explanation of why gravitropic growth is detected earlier than straight growth
15 p2607 N85-26067
Daylily as a system to study effects of space flight on plant development 15 p2607 N85-26068
The role of gravity on the reproduction of arabidopsis plants 15 p2607 N85-26069
Importance of gravity for plant growth and behavior
15 p2608 N85-26070
Gravitropism in leafy dicot stems
15 p2610 N85-26086
Mechanical stress regulation of plant growth and development 15 p2610 N85-26087
Plant growth biophysics: The basis for growth asymmetry induced by gravity 15 p2611 N85-26089
An indirect role for ethylene in shoot-inversion release of apical dominance in Pharbitis nil
15 p2611 N85-26090
Participation of ethylene in two modes of gravistimulation of shoots 15 p2613 N85-26101
Isolation of hybridomas for golgi-associated proteins and a plant calmodulin 15 p2613 N85-26103
A search for evidence of large body Earth impacts associated with biological crisis zones in the fossil record 15 p2682 N85-26567
The controlled ecological life support system
15 p2688 N85-26603
Research on zero-gravity botany apparatus
16 p2723 N85-26811
Ecology of Pamlico River, North Carolina: An estuarine profile
[PB85-155703] 16 p2822 N85-27404
Genetic engineering of plants: Agricultural research opportunities and policy concerns
[DE85-006771] 16 p2840 N85-27513
Photosynthetic acclimation of Acer saccharum
[DE85-006247] 17 p2998 N85-28536
Organization of the R region in maize
[DE85-011273] 20 p3504 N85-31780
Ice nucleating characteristics of Capparis Aphylla, an Indian herb 21 p3641 N85-32619
The role of sulfur in osmoregulation and salinity tolerance in cyanobacteria, algae, and plants
21 p3660 N85-32736
Hydroponics developments for spaceship garden
21 p3663 N85-32754
The 1984 environmental monitoring report, Sandia National Laboratories, Albuquerque, New Mexico
[DE85-011175] 22 p3811 N85-33607
Effect of substrate moisture on growth and structure of corn leaf 22 p3824 N85-33692
The 1984 biotic studies of Yucca Mountain, Nevada test site, Nye County, Nevada
[DE85-011715] 23 p3951 N85-34487
Mineral deposit models: Theory and practice
24 p4105 N85-35448
The measurement of nitrogen oxide (NO, NO2) exchange over plant/soil surfaces
[CSIRO-DAR-TP-8] 24 p4127 N85-35587

PLANTS (INDUSTRIES)
U INDUSTRIAL PLANTS

PLASMA ACCELERATION
Transverse electron resonance accelerator
[DE85-008289] 17 p3032 N85-28758
Report of the Working Group on Other Acceleration Schemes
[DE85-008447] 17 p3033 N85-28764
High energy plasma accelerators
[DE85-013121] 24 p4155 N85-35760

PLASMA ACCELERATORS
NT COAXIAL PLASMA ACCELERATORS
Electromagnetic acceleration of macroparticles to hypervelocities in axisymmetric geometry
[IPPJ-696] 06 p0863 N85-15484
Explosive emission cathode plasmas in intensive relativistic electron beam diodes
[AD-A147917] 07 p1048 N85-16642
Space Experiments with Particle Accelerators (SEPAC) 23 p3901 N85-34165
High energy plasma accelerators
[DE85-013121] 24 p4155 N85-35760

PLASMA ARC CUTTING
USSR report: Machine tools and metalworking equipment
[JPRS-UMM-85-005] 13 p2051 N85-22839
New tooling for plasma cutting technology
13 p2051 N85-22842
Mechanical properties of plasma arc cut steel
23 p3905 N85-34168

PLASMA ARC SPRAYING
U ARC SPRAYING

PLASMA ARC WELDING
The variable polarity plasma arc welding process: Its application to the Space Shuttle external tank
[NASA-TM-86482] 05 p0641 N85-14115
Cobalt-free permanent magnet alloys
[AD-A149272] 10 p1441 N85-19079
The strength and characteristics of VPPA welded 2219-T87 aluminum alloy 12 p1946 N85-22224
Weldability/microstructure relationships of high nickel alloys for heater applications
[DE85-009337] 19 p3241 N85-30094
Plasma arc welding, equipment, installation and process control
[DE85-008481] 19 p3373 N85-30921
Mechanical properties of Shielded Metal Arc (SMA) and Submerged Arc (SA) welded joints in a steel Raex 386 P Arctic
[VTT-339] 22 p3801 N85-33551

PLASMA ARCS
U PLASMA JETS

PLASMA BUBBLES
Irregularity decay in an isolated plasma bubble
[AD-A145782] 03 p0392 N85-12506
Observations of plasma bubbles and their zonal drift using polarimeters
[INPE-3219-PRE/572] 05 p0729 N85-14868

PLASMA CHEMISTRY
The plasma assisted modified betatron
[AD-A148728] 09 p1390 N85-18748
Spatial resolution of small particles in silane discharge
[AD-A150953] 14 p2423 N85-24948

PLASMA CLOUDS
Repulsive force of magnetic clouds during solar flares and magnetospheric substorms
06 p0824 N85-15233
The role of finite parallel length on the stability of barium clouds
[AD-A148972] 07 p0996 N85-16326
Giotto residual ionization 14 p2244 N85-23909
A model of plasma cloud expansion generated by a dust particle impact — Giotto mission
14 p2245 N85-23914
Dependence of equatorial F-region plasma bubble rise velocity and dynamo electric field on solar cycle
[INPE-3439-PRE/696] 16 p2626 N85-27434
Projections of plasma cloud structures and their spectra
[AD-A153608] 18 p3169 N85-29776
Influence of magnetic clouds on cosmic ray intensity variations
[SH-5.1-12] 23 p4042 N85-35065

PLASMA COMPOSITION
ISEE-1 data reduction and analysis plasma composition experiment
[NASA-CR-175306] 21 p3630 N85-32552
Diffusion in the chromosphere and the composition of the solar corona and energetic particles
[SH-2.1-9] 23 p3999 N85-34790

PLASMA COMPRESSION
Adequacy of metal ablation process with laser radiation and a shock-compressed plasma
13 p2028 N85-22706
Electric field and plasma observations near the magnetopause and bow shock during a rapid compression 14 p2355 N85-24553
Strong coupling effects on bound states in plasmas
[AD-A154353] 19 p3370 N85-30905
Numerical studies of high current beam compression in heavy ion fusion
[DE85-011874] 24 p4158 N85-35783

PLASMA CONDUCTIVITY
Impact of atomic data on Tokamak modeling
09 p1390 N85-18743
Excitation of low-frequency resonance waves by moving conductor in space plasma 13 p2067 N85-22912
Asymmetric flux generation and its relaxation in reversed field pinch
[IPPJ-712] 15 p2656 N85-26387
Current enhancement in a conducting channel
[AD-A155418] 22 p3845 N85-33812

PLASMA CONFINEMENT
U PLASMA CONTROL

PLASMA CONTROL
Means of varying conditions in the expanded boundary divertor without affecting energy confinement
[DE84-013840] 01 p0122 N85-10636
Study of plasma convection and wall interactions in magnetic confinement systems
[DE84-013959] 03 p0421 N85-12692
Fusion plasma theory. Task 1: Magnetic confinement fusion plasma theory
[DE84-014941] 04 p0566 N85-13608

EBT electron energy confinement experiments
[DE84-015402] 04 p0567 N85-13813
Application of the energy problem to the problem of plasma flow stability
[DE84-013359] 05 p0730 N85-14691
Compact toroidal development: Activity plan for field reversed configurations
[DE84-017145] 05 p0730 N85-14695
Passive stabilization of vertical instability in Tokamak reactor 06 p0775 N85-14958
The origin of plasma rotation in the early phase of an FRC produced by a reversed field theta pinch
[IPPJ-698] 06 p0863 N85-15482
Theoretical investigations relevant to magnetic fusion research, April 1, 1983 - March 31, 1984
[DE85-001778] 06 p0865 N85-15498
Plasma-surface interactions in large tandem mirror devices, MFTF-B
[DE85-001753] 06 p0865 N85-15499
Shear-Alfven dynamics of toroidally confined plasmas, part A
[DE85-001580] 06 p0866 N85-15502
Shear-Alfven dynamics of toroidally confined plasmas, part B
[DE85-001787] 06 p0866 N85-15504
A propagator expansion method for solving linearized plasma kinetic equations with collisions
[AD-A147524] 07 p1045 N85-16840
Sources, densities, and transport of impurities in neutral-beam injected Tokamaks 09 p1388 N85-18731
Effect of alpha particles on the stability of Elmo Bumpy Torus (EBT) reactor
[DE84-017266] 09 p1392 N85-18759
CTR plasma engineering studies
[DE84-017447] 09 p1392 N85-18762
Small, octopole-stabilized tandem mirror reactor
[DE85-002144] 10 p1559 N85-19832
Finite-(beta) optimization of tandem mirrors
[DE85-002658] 10 p1560 N85-19835
Entrop production determination of the ambipolar solution nearest equilibrium
[DE85-003049] 10 p1560 N85-19836
FRC translation dynamics and plasma confinement properties in FRX-C/T
[DE85-002366] 10 p1560 N85-19842
Thermal barrier confinement experiments in TMX-U tandem mirror, revision 1
[DE84-017029] 10 p1561 N85-19844
TMX-U neutral pressure measurement diagnostic systems
[DE85-000746] 11 p1730 N85-20881
Mirror fusion progress
[DE85-001187] 11 p1731 N85-20888
Observations of low frequency plasma fluctuations in ELMO Bumpy Torus
[DE85-003796] 11 p1732 N85-20895
Plasma performance of TFCX and jet with sawtoothing
[DE85-003335] 12 p1936 N85-22166
Opacity determinations for Inertial Confinement Fusion (ICF) materials using an average atom model 12 p1957 N85-22295
Winding insulation in electromagnetic systems for Tokamak reactor plants 13 p2087 N85-23005
Confinement properties of high energy density plasmas in the Wisconsin levitated octupole 13 p2161 N85-23408
Lower hybrid heating and current drive, and ion cyclotron heating experiments on the Alcator C and the Versator II Tokamaks
[DE85-004918] 13 p2161 N85-23412
Breakthrough in container confinement of ultracold neutrons 15 p2644 N85-26311
Nagoya bumpy torus 15 p2655 N85-26377
High beta pinch plasma (STP-L) 15 p2655 N85-26381
Plasma theory and computations 15 p2655 N85-26384
Heavy ion beam study of potential formation in bumpy torus plasma
[IPPJ-711] 15 p2656 N85-26388
Internal field probing of translating FRCs
[DE85-003732] 15 p2657 N85-26394
MHD fluctuations in ISX-B
[DE85-004600] 15 p2657 N85-26395
Plasma-wall interactions in tandem mirror machines
[DE85-006387] 15 p2657 N85-26399
Magnetohydrodynamic stability of spheromak plasma in toroidal flux conserver with rectangular cross section
[IPPJ-716] 16 p2666 N85-27678
TOKASTAR: A Tokamak stellerator hybrid with possible bean-shaped operation
[IPPJ-718] 16 p2666 N85-27680
Spherical torus, compact fusion at low field
[DE85-006983] 16 p2667 N85-27689
Time-resolving electron temperature diagnostic for ALCATOR C
[DE85-004916] 16 p2668 N85-27690
Stability of high energy particle plasmas to MHD-like modes
[DE85-007879] 17 p3039 N85-28803
An Impurity Control Test Facility (ICTF) for the study of fusion reactor/plasma edge materials
[DE85-007946] 17 p3040 N85-28810
Comparison study of toroidal-field divertors for a compact reversed-field pinch reactor
[DE85-009591] 18 p3189 N85-29781
Whist code calculations of ignition margin in an ignition Tokamak
[DE85-009507] 18 p3190 N85-29784
Radiation-cooled helicity-injecting reversed field pinch formed with relativistic electrons
[IPPJ-721] 19 p3370 N85-30901
New concept for pumping the edge plasma
[DE85-010180] 19 p3371 N85-30909
Los Alamos Spheromak Program
[DE85-010748] 20 p3396 N85-31077
System and method of operating toroidal magnetic confinement devices
[DE85-011670] 22 p3845 N85-33814
Method and apparatus for maintaining equilibrium in a helical axis stellerator
[DE85-011626] 22 p3845 N85-33815
Elmo bumpy square plasma confinement device
[DE85-011628] 22 p3845 N85-33816
Confinement and heating of high beta plasma with emphasis on compact toroids. Compact toroid research
[DE85-011463] 22 p3846 N85-33821
Collisional relaxation of electron tail distribution
[IPPJ-729] 23 p3974 N85-34635
Proceedings of the US-Japan Workshop on Transport in Open-Ended Systems
[IPPJ-727] 23 p3975 N85-34644
Potential effect in transport due to non-adsymmetric confining field 23 p3975 N85-34645
Activities of the RF Section 23 p3975 N85-34646
Radial transport phenomena for TMX-upgrade 23 p3976 N85-34647
Plug and thermal barrier potential formation in Gamma 10 23 p3976 N85-34648
Induced azimuthal electric field effects on tandem transport and ambipolarity 23 p3976 N85-34650
Recent experiments in Gamma-10 23 p3976 N85-34651
Azimuthal uniformity and current balance study of ICRH-produced plasma in RFC-XXM 23 p3977 N85-34659
Moving finite element method for ICF target implosion 23 p3980 N85-34675
Stability of implosion dynamics 23 p3980 N85-34680
On the heat flux derived by the moment method in Lorentzian plasma between hot and cold walls 23 p3980 N85-34682
Integral representation for nonlinear heat transport 23 p3981 N85-34683
Advanced Toroidal Facility (ATF)
[DE85-011567] 23 p3983 N85-34699
Stellarator approach to fusion plasma confinement
[DE85-011420] 23 p3984 N85-34704
Limiter
[DE85-011620] 24 p4150 N85-35736
Confinement and heating of high beta plasmas with emphasis on compact toroids
[DE85-011459] 24 p4155 N85-35761
Analysis of a pulsed power system containing rotating machine
[DE85-014128] 24 p4159 N85-35786
Diagnostics for Pioneer 1 imploding plasma experiments
[DE85-014120] 24 p4159 N85-35787

PLASMA CURRENTS
Fast waves near the lower hybrid frequency
[DE84-015217] 01 p0123 N85-10841
Numerical investigation of characteristics of current flow for different methods of obtaining discharge in high speed lasers. Mechanism underlying current flow in positive glow discharge column 02 p0264 N85-11728
Experimental observation of plasma neoclassical currents
[DE84-015706] 04 p0566 N85-13805
Generation of suprathermal electrons during plasma current startup by lower hybrid waves in a Tokamak
[IPPJ-697] 06 p0863 N85-15483
The anode mechanism of a thermal argon arc
[NASA-TM-77754] 07 p0921 N85-15835
Current measurements by Faraday rotation in single mode optical fibers
[DE85-002025] 09 p1384 N85-18707
Diffusion driven plasma current with turbulent dynamo
[IPPJ-700] 09 p1386 N85-18716
Wave absorption and transport studies on Electron Cyclotron Resonance (ECR) heated stellerator plasmas in W 7-A
[IPF-84-9] 09 p1395 N85-18782
Observations of bulk electron heating due to return current in a tokamak discharge started up by lower hybrid waves
[IPPJ-706] 12 p1937 N85-22172
Direct measurements of severe spacecraft charging in auroral ionosphere 13 p1991 N85-22480
Ram-wake effects on plasma current collection of the PIX 2 Langmuir probe 13 p1993 N85-22496
Entry of solar energetic protons into the distant plasma sheet dependence on distance from the neutral sheet 14 p2357 N85-24567
Estimate of the amplitude of transient electric fields in the magnetotail 14 p2358 N85-24568
Plasma sheet dynamics deduced from ISEE-1 and -2 energetic particle flux data 14 p2358 N85-24570
Current distribution in a plasma erosion opening switch
[AD-A150987] 14 p2424 N85-24949
Noninductive current drive in Tokamaks
[DE85-005427] 14 p2424 N85-24951
The possible role of electrical currents in coronal phenomena 14 p2453 N85-25151
High energy beam experiment 15 p2654 N85-26376
High beta pinch plasma (STP-3(M)) 15 p2655 N85-26380
Alternating current CHMIC heating in a toroidal stellerator 20 p3534 N85-31998
Simulating the effects of plasma disruption with a 1 MA current pulse in a coaxial test fixture
[DE85-010491] 20 p3535 N85-31999
Current enhancement in a conducting channel
[AD-A155418] 22 p3845 N85-33812
Size effects of vacuum chamber for H- (D-) ion volume production by sheet plasma 1
[IPPJ-731] 23 p3974 N85-34639
Langmuir probe on ISX-B
[DE85-012066] 23 p3983 N85-34697

PLASMA CYLINDERS
NT CYLINDRICAL PLASMAS
Scattering of radio waves on magnitized meteor trail 03 p0344 N85-12221
Diffraction of plane TM-wave on continuously irregular elliptical plasma 13 p2057 N85-22914

PLASMA DENSITY
Precipitation of protons with E sub p approximately 1 MeV near plasmopause 02 p0161 N85-11093
The solar wind at 20-30 AU 02 p0301 N85-11950
Irregularity decay in an isolated plasma bubble
[AD-A145782] 03 p0392 N85-12506
Overview of recent advances in laser applications 06 p0725 N85-14680
Longer-scalelength plasma perturbations by an intense laser beam
[AD-A147005] 07 p1045 N85-16838
Electrostatic wave observation during a space simulation Beam-Plasma-Discharge (SPD)
[NASA-CR-174288] 07 p1045 N85-16839
Far-infrared laser diagnostic on EBT and extreme far-forward laser scattering on ISX
[DE85-001788] 07 p1046 N85-16843
Artificial ionospheric disturbances caused by powerful radio waves
[AD-A148077] 08 p1186 N85-17473
Far-infrared interferometry/polarimetry on the ISX-B Tokamak
[DE84-015401] 10 p1558 N85-19827
Ion quadrupole effects in spectral line broadening
[DE85-001504] 11 p1730 N85-20879
Transient waveform acquisition system for the ELMO Bumpy Torus
[DE85-000154] 11 p1733 N85-20901
Hollow cathode apparatus
[NASA-CASE-NPO-15560-1] 12 p1832 N85-21491
Plasmachemical evaporation and doping of amorphous silicon 12 p1879 N85-21790
Electrostatic confinement in a bumpy torus
[DE85-003794] 12 p1936 N85-22164
Determination of experimental Tokamak plasma properties using maximum entropy analysis
[DE85-001723] 12 p1936 N85-22165
Vehicle charging on STS-3 Mission 13 p1989 N85-22473
Ram-wake effects on plasma current collection of the PIX 2 Langmuir probe 13 p1993 N85-22496
NASCAP simulation of PIX 2 experiments 13 p1993 N85-22497
Confinement properties of high energy density plasmas in the Wisconsin levitated octupole 13 p2161 N85-23408

Increased hot-electron production at quarter-critical density in long-scalelength, laser-plasma interactions
[AD-A150519] 13 p2161 N85-23411
Theoretical studies of kinetic mechanisms of negative ion formation in plasmas
[AD-A150820] 14 p2423 N85-24946
Chaotic dynamics of instabilities in solids
[DE85-004909] 14 p2429 N85-24978
Affect of angle of incidence on plasmas generated during laser welding
[DE85-005724] 15 p2569 N85-25852
Internal field probing of translating FRCs
[DE85-009732] 15 p2657 N85-26394
Direct evidence for solar wind control of Jupiter's hectometer-wavelength radio emission
[NASA-TM-86073] 16 p2883 N85-27790
Heating of electrons in a high density tokamak by a micro-wave near second harmonic frequency
[DE85-010682] 19 p3359 N85-30822
Effects of a radial electric field on tokamak edge turbulence
[DE85-010401] 19 p3371 N85-30910
Thermal ion heating in the vicinity of the plasmapause
[NASA-CR-176030] 20 p3535 N85-31993
Theoretical and Experimental Beam Plasma Physics (TEBPP) 23 p3901 N85-34166
Breakdown of intrinsic ambipolarity for the radial diffusion due to a rotating RF field 23 p3977 N85-34660
Simulation studies on stability of hot electron plasma 23 p3978 N85-34664
Current interruption by density depression
[DE85-013120] 24 p4169 N85-35846

PLASMA DIAGNOSTICS

Rocket observations 01 p0014 N85-10064
SEPAC (space experiments with particle accelerators) 01 p0014 N85-10065
Analysis of glow discharges for understanding the process of film formation
[NASA-TM-83750] 01 p0022 N85-10138
Fluctuation spectrum for linear gyroviscous MHD
[IPP-6/237] 01 p0121 N85-10828
Experimental observation of neoclassical currents
[DE84-015113] 01 p0122 N85-10834
Two novel plasma diagnostic tools: Fiber sensors and phase conjugation
[DE84-014033] 01 p0123 N85-10840
Physics of the inner heliosphere 1-10R sub O plasma diagnostics and models
[NASA-CR-174010] 02 p0304 N85-11964
A high transmission, 20 channel polychromator for the Thomson scattering diagnostic of TORTUR 3 — plasma diagnostics
[REPT-84-158] 03 p0422 N85-12604
High-Beta Tokamak research
[DE84-016470] 04 p0566 N85-13618
Non-LTE considerations in spectral diagnostics of thermal transport and implosion experiments
[DE84-015187] 05 p0730 N85-14689
Imaging polarimeter-interferometer arrays for Tokamak measurements
[DE84-015916] 05 p0730 N85-14693
Nitriding of titanium and its alloys by N2, NH3 or mixtures of N2 + H2 in a dc arc plasma at low pressures (or = to torr)
[NASA-TM-83803] 06 p0814 N85-15168
Alpha-particle diagnostics with high energy neutral beams
[IPPJ-886] 06 p0863 N85-15485
Measurement of proton autoneutralization potential
[DE85-001752] 06 p0865 N85-15501
Far-infrared laser diagnostic on EBT and extreme far-forward laser scattering on ISX
[DE85-001788] 07 p1046 N85-16643
Advanced diagnostics for reacting flows
[AD-A148479] 08 p1162 N85-17334
Feasibility of alpha particle measurement by CO2 laser Thomson scattering
[DE85-001784] 09 p1326 N85-18334
Current measurements by Faraday rotation in single mode optical fibers
[DE85-002025] 09 p1384 N85-18707
Proceedings on US-Japan Workshop on Tokamak Diagnostics by X-ray, VUV and Optical Radiations
[IPPJ-703] 09 p1386 N85-18719
X-rays spectroscopy on the PLT and TFTR Tokamaks 09 p1386 N85-18720
Present status of Heliotron E experiment 09 p1387 N85-18721
Spectroscopic measurement on Heliotron E 09 p1387 N85-18722
Radial profiles of high resolution X-ray spectra from the Alcator C Tokamak 09 p1387 N85-18723
Recent activities on JIPP T-IIU Tokamak 09 p1387 N85-18724
Spectroscopic instrumentation for Tokamak diagnostics 09 p1388 N85-18732
Determination of ion temperature and rotation velocity profiles by visible, UV and X-ray spectroscopy on Doublet 3 09 p1388 N85-18734
Measurements of electric fields in plasmas by using beam probe and laser fluorescence techniques 09 p1389 N85-18737
Beam probe spectroscopic technique for ion temperature and magnetic field measurements 09 p1389 N85-18738
Compilation of atomic data for diagnostics of Tokamak 09 p1390 N85-18744
The coordinated research program at IAEA on atomic collision data for plasma diagnostics 09 p1390 N85-18747
Cookbook for determining essential transmission characteristics of spherical section electrostatic analyzers
[DE85-001404] 09 p1391 N85-18751
Experimental investigations of driven Alfven wave resonances in a Tokamak plasma using carbon dioxide laser interferometry
[DE85-001049] 09 p1392 N85-18758
Background calculations for the measurement of the ion temperature in a deuterium plasma
[DE84-016546] 09 p1393 N85-18768
Lidar-Thomson scattering — Joint European Torus
[IPF-84-3] 09 p1394 N85-18777
Improved performance for large area triple layer microchannel plate detector for a neutral spectrometer in Doublet III
[DE85-001719] 10 p1488 N85-19395
Sequentially-framing soft X-ray pinhole camera for Tokamak plasma studies
[DE85-001717] 10 p1489 N85-19399
Bibliography of Soviet laser developments, Number 66, July-August 1983
[AD-A149113] 10 p1490 N85-19406
CO2 laser interferometer array for Big Dee
[DE85-001718] 10 p1490 N85-19411
Far-infrared interferometry/polarimetry on the ISX-B Tokamak
[DE84-015401] 10 p1558 N85-19827
Application of layered synthetic microstructures to high temperature plasma diagnostics
[DE85-002035] 10 p1559 N85-19828
Space-time statistics of the turbulence in a Tokamak edge plasma
[DE85-002667] 10 p1559 N85-19834
X-ray line broadening of a diagnostic in laser produced plasma
[DE85-001179] 10 p1560 N85-19841
Direct reading fast microwave interferometer for EBT
[DE85-000183] 11 p1636 N85-20306
Electrodynamic interactions 11 p1643 N85-20348
Applications of Tethers in Space, volume 2
[NASA-CP-2365] 11 p1644 N85-20361
Novel probe for determining the size and position of a relativistic electron beam
[DE85-001044] 11 p1723 N85-20836
A proposed method for fast determination of plasma parameters
[IPP-1/228] 11 p1730 N85-20877
Ion quadrupole effects in spectral line broadening
[DE85-001504] 11 p1730 N85-20879
TMX-U neutral pressure measurement diagnostic systems
[DE85-000746] 11 p1730 N85-20881
Mirror fusion progress
[DE85-001187] 11 p1731 N85-20888
X-ray spectroscopy of laser-produced plasmas
[DE85-002170] 11 p1733 N85-20897
Transient waveform acquisition system for the ELMO Bumpy Torus
[DE85-000154] 11 p1733 N85-20901
Edge diagnostics for tandem mirror machines
[DE85-001209] 11 p1733 N85-20902
Activities report of the Institute of Plasma Research 11 p1733 N85-20903
Intensified CCD camera system for plasma diagnostics
[DE85-002252] 12 p1853 N85-21620
Arc-driven rail gun research
[NASA-CR-174816] 12 p1859 N85-21662
Determination of experimental Tokamak plasma properties using maximum entropy analysis
[DE85-001723] 12 p1936 N85-22165
X-ray astronomy and plasma astrophysics 12 p1956 N85-22288
Plans for interbol satellite experiment 13 p1977 N85-22407
Suprathermal plasma observed on STS-3 Mission by plasma diagnostics package 13 p1989 N85-22472
Vehicle charging on STS-3 Mission 13 p1989 N85-22473
Electron and ion density depletions measured in the STS-3 orbiter wake 13 p1989 N85-22474
Measured electron contribution to Shuttle plasma environment: Abbreviated update 13 p1990 N85-22478
Ram-wake effects on plasma current collection of the PIX 2 Langmuir probe 13 p1993 N85-22496
Feasibility of alpha particle measurement by CO2 laser Thomson scattering
[DE85-004938] 13 p2097 N85-23081
Confinement properties of high energy density plasmas in the Wisconsin levitated octupole 13 p2161 N85-23408
Ion transport in beam-plasma interactions
[AD-A150145] 13 p2161 N85-23410
Ultrahigh-sensitivity threshold neutron detector for plasma diagnostics
[DE85-006270] 13 p2161 N85-23413
Physics of the inner heliosphere: Mechanisms, models and observational signatures
[NASA-CR-175632] 13 p2205 N85-23677
An impact plasma monitor for cometary missions — Giotto , VEGA 14 p2245 N85-23918
Advanced diagnostics for reacting flows
[AD-A150875] 14 p2301 N85-24248
Advances in magnetospheric plasma diagnosis by active experiments — IMS satellites 14 p2371 N85-24654
Contribution of mutual impedance experiments to the understanding of magnetospheric processes — GEOS satellites 14 p2371 N85-24656
Plasma-edge studies using carbon resistance probes
[DE85-005589] 14 p2424 N85-24955
Annual Review, April 1983 - March 1984
[ISSN-0547-1567] 15 p2654 N85-26369
System for lower hybrid current startup 15 p2654 N85-26373
Preparatory experiments. 1: JIPP T-IIU 15 p2654 N85-26374
Nagoya bumpy torus 15 p2655 N85-26377
Soft X-ray diagnostics of laser-produced plasmas (HALNA) 15 p2655 N85-26382
Diagnostics of a glow discharge used to produce hydrogenated amorphous silicon films
[DE85-002914] 15 p2661 N85-26420
Sub-nanosecond cinematography in laser fusion research: Current techniques and applications at the Lawrence Livermore Laboratory
[DE85-007252] 17 p2968 N85-28334
Experimental plasma research: Plasma summaries
[DE85-008116] 17 p3039 N85-28805
Accelerator-based plasma-wall interaction studies on the TEXTOR Tokamak
[DE85-007540] 17 p3040 N85-28806
Electron temperature measurements from induced toroidal current in ELMO Bumpy Torus scale
[DE85-008549] 18 p3189 N85-29779
Experiments in plasma initiation and laser absorption in flowing gases
[AD-A154303] 19 p3276 N85-30313
Research activities of the Physics Division
[DE85-006958] 19 p3357 N85-30811
Research support for plasma diagnostics on Elmo Bumpy Torus: Diamagnetic measurements and data analysis and development of ring models for realistic representation of fields near the plasma
[DE85-010035] 19 p3371 N85-30912
Thomson scattering on Elmo Bumpy Torus
[DE85-010584] 20 p3527 N85-31941
Global effects of double layers — plasma layers
[TRITA-EPP-84-12] 20 p3536 N85-32002
Observations of low energy magnetospheric plasma outside the plasmasphere
[KGI-PREPRINT-075] 20 p3536 N85-32004
Space Experiments with Particle Accelerators (SEPAC) 23 p3901 N85-34165
Recoverable Plasma Diagnostics Package (RPDP) 23 p3902 N85-34167
Magnetospheric multiprobes: MMP/CHEMSAT 23 p3902 N85-34171
Novette diagnostic support
[DE85-012937] 23 p3934 N85-34383
Langmuir probe on ISX-B
[DE85-012066] 23 p3983 N85-34697
Instrument to synchronize Thomson scattering diagnostic measurements with MHD activity in a Tokamak
[DE85-012082] 23 p3984 N85-34708
Diagnostics for Pioneer 1 imploding plasma experiments
[DE85-014120] 24 p4159 N85-35787

PLASMA DIFFUSION

Asymptotic behaviour of the plasma equation
[AD-A147242] 07 p1031 N85-16549
Velocity space diffusion of high energy ions induced by a lower hybrid wave in a nonuniform magnetic field
[IPPJ-714] 16 p2886 N85-27681
Stefan-Maxwell relations for plasma diffusion currents in magnetic field 17 p2942 N85-29160

Influence of type of processing of AK4 alloy on its surface state and strength of bonding of plasma coatings
19 p3242 N85-30103
Plasma radiation sources. Quasi-adiabatic theory and numerical modeling in the electro-diffusive approximation
[AD-A154375] 19 p3370 N85-30906
Schottky theory of three component plasmas
[AD-A154461] 19 p3371 N85-30907
RF induced radial diffusion in tandem mirrors
23 p3976 N85-34649
Guiding center distribution function and longitudinal invariant
23 p3976 N85-34663
The plasma mechanism for preferential acceleration of heavy ions
[SH-2.2-10] 23 p4001 N85-34805
Long-time asymptotics of a system for plasma diffusion
[NASA-CR-177947] 24 p4093 N85-35375

PLASMA DIODES
Explosive emission cathode plasmas in intensive relativistic electron beam diodes
[AD-A147917] 07 p1046 N85-16642
Theoretical study of collective ion acceleration in the Luce diode
[AD-A150107] 12 p1929 N85-22116
Electrochromic display device
[AD-D011733] 22 p3759 N85-33290

PLASMA DISCHARGES
U PLASMA JETS

PLASMA DISPERSION
U PLASMA DIFFUSION

PLASMA DISPLAY DEVICES
Frictional and structural characterization of ion-nitrided low and high chromium steels
[NASA-TM-86991] 13 p2098 N85-23085
Electrochromic display device
[AD-D011733] 22 p3759 N85-33290

PLASMA DRIFT
Plasma drift equilibrium (gyration) in toroidal systems with complex magnetic-field geometry
[DE84-015627] 01 p0122 N85-10839
Integral of wave kinetic equation of drift waves
02 p0283 N85-11848
Plasma drift towards a plane equipotential surface
[TRITA-EPP-84-01] 02 p0285 N85-11860
Fusion plasma theory. Task 3: ECRH and transport modelling in tandem mirrors and divertor physics
[DE84-014939] 04 p0567 N85-13612
Observations of plasma bubbles and their zonal drift using polarimeters
[INPE-3219-PRE/572] 05 p0729 N85-14668
The role of finite parallel length on the stability of barium clouds
[AD-A146972] 07 p0998 N85-16328
Ionospheric turbulence: Interchange instabilities and chaotic fluid behavior
[AD-A147810] 07 p0998 N85-16337
Fusion Energy Division
[DE85-001701] 11 p1731 N85-20884
Electrostatic confinement in a bumpy torus
[DE85-003794] 12 p1936 N85-22164
Heavy ion beam study of potential formation in bumpy torus plasma
[IPPJ-711] 15 p2658 N85-26386
Coupled plasma-neutral transport model for the scrape-off region
[DE85-007559] 16 p2868 N85-27695
Drift anisotropy instability of a finite Beta magnetospheric plasma
[IFSI-84-12] 20 p3536 N85-32005

PLASMA DYNAMICS
Long-time tail in the two-wave model
02 p0282 N85-11837
Lie-transformation action principle for classical plasma dynamics
[DE84-014576] 02 p0285 N85-11858
Magnetospheric plasma studies using data from the dynamics high and low altitude plasma instruments
[AD-A145751] 03 p0392 N85-12505
Solar wind dynamics at small distances from the sun
06 p0823 N85-15227
Shear-Alfven dynamics of toroidally confined plasmas, part B
[DE85-001787] 06 p0866 N85-15504
Spark column plasma dynamics model (a first principles model for laser triggered spark gaps)
[AD-A147954] 08 p1166 N85-17354
Four-fluid description of turbulent plasma focus dynamics
[IPF-84-4] 09 p1395 N85-18778
Ionospheric research at INPE
[INPE-3279-PRE/602] 10 p1514 N85-19556
Rail accelerator technology and applications
[NASA-TM-86947] 12 p1794 N85-21258
Theoretical study of collective ion acceleration in the Luce diode
[AD-A150107] 12 p1929 N85-22116
Ring current dynamics and plasma sheet sources — magnetic storms
14 p2359 N85-24577
The structure, stability, wave transmission and energy transfer at the Earth's magnetopause
14 p2372 N85-24681
Laboratory for laser energetics report
[DE85-007235] 15 p2563 N85-25814
Poloidal rotation of magnetic fluctuations in reversed field pinch plasma
[IPPJ-715] 16 p2866 N85-27677
A four-field model for Tokamak plasma dynamics
[DE85-007111] 16 p2868 N85-27694
Application of the MHD energy principle to magnetostatic atmospheres
[NASA-CR-175967] 18 p3136 N85-29420
Projections of plasma cloud structures and their spectra
[AD-A153608] 18 p3189 N85-29778
Plasmodynamic methods for generating powerful light pulses
21 p3693 N85-32943
Workshop report on Simulation Techniques for Shock Wave Phenomena and Characteristics of Plasmas in Inertial Confinement Fusion
[IPPJ-725] 23 p3979 N85-34670

PLASMA ELECTRODES
Space-time characteristics of field in longitudinal pulse-period discharge typical in pumping of self-terminating lasers
21 p3687 N85-32909

PLASMA ENGINES
Modeling the exhaust of the pulsed plasma thruster
[AD-A155344] 21 p3707 N85-33018

PLASMA EQUILIBRIUM
Plasma drift equilibrium (gyration) in toroidal systems with complex magnetic-field geometry
[DE84-015627] 01 p0122 N85-10839
Destruction of magnetic surfaces in three-dimensional MHD equilibria
02 p0282 N85-11838
Zero-current, high beta stellaration equilibria with rotational transform profile control
[DE84-016635] 04 p0568 N85-13624
Electric field in plasma layer of magnetosphere during preliminary substorm phase
06 p0824 N85-15231
Resistive evolution of general plasma configuration
[DE85-002340] 10 p1561 N85-19643
Monte Carlo studies of tandem mirror plasmas interacting with waves in the Ion Cyclotron Range of Frequencies (ICRF)
[DE85-002988] 11 p1731 N85-20883
Convergent spectral representation for 3-dimensional inverse MHD equilibria
[DE85-000686] 11 p1733 N85-20900
The continuous spectrum of an axisymmetric, self-gravitating equilibrium in the presence of a poloidal magnetic field
12 p1959 N85-22315
Modified betatron accelerator studies
[AD-A151420] 15 p2648 N85-26332
Toroidal equilibrium with low frequency wave driven currents
[DE85-005790] 15 p2658 N85-26401
Reversed field pinch dynamics and transport studies
[DE85-007553] 18 p3189 N85-29778
Solution of problem of equilibrium confinement of plasma by magnetic field in an infinite circular cylinder
21 p3692 N85-32936
Recombination and ionization in a nitrogen plasma
[AD-A155426] 22 p3845 N85-33813
User's manual for the FLORA equilibrium and stability code
[DE85-013182] 23 p3966 N85-34590
Magnetohydrodynamic equilibrium and stability of spheromak with spheroidal plasma-vacuum interface
[IPPJ-732] 23 p3974 N85-34640

PLASMA ETCHING
Basic development of a 1.5 micrometer very large scale integrated technique, part 1-4
[BMFT-FB-T-85-032-PT-1-4] 20 p3449 N85-31417

PLASMA FLOW
U MAGNETOHYDRODYNAMIC FLOW

PLASMA FLUX MEASUREMENT
Confinement and heating of high beta plasmas with emphasis on compact toroids
[DE85-011459] 24 p4155 N85-35761

PLASMA FOCUS
Intense excitation source of blue-green laser
[AD-A147450] 07 p0971 N85-16168
Four-fluid description of turbulent plasma focus dynamics
[IPF-84-4] 09 p1395 N85-18778
Two phases of neutron production in the POSEIDON plasma focus
[IPF-84-10] 09 p1395 N85-18783
Activities report of the Institute of Plasma Research
11 p1733 N85-20903
Restrike particle beam experiments on a dense plasma focus. Opening switch research on a dense plasma focus
[AD-A152991] 17 p3039 N85-29802
Time-resolved energy spectrum of the ion beam generated in the plasma focus
19 p3389 N85-30892
Plasmodynamic methods for generating powerful light pulses
21 p3693 N85-32943
The electromagnetic ram action of the plasma focus as a paradigm for the generation of cosmic rays and the gigantic jets in active galaxies
[OG-8.2-14] 23 p4020 N85-34910

PLASMA FREQUENCIES
Spatial resolution of small particles in silane discharge
[AD-A150953] 14 p2423 N85-24948
Experimental measurements of the ion cyclotron antennas' coupling and RF characteristics
[DE85-011569] 23 p3982 N85-34694

PLASMA GENERATION
U PLASMA GENERATORS

PLASMA GENERATORS
NT PLASMA GUNS
NT PLASMATRONS
NT TOKAMAK DEVICES
K-shell yield scaling law for conventional PRS loads
[AD-A145155] 01 p0121 N85-10831
High frequency plasma generator for ion thrusters
[NASA-CR-174772] 08 p1114 N85-17023
Bibliography of Soviet laser developments, Number 98, July-August 1983
[AD-A149113] 10 p1490 N85-19406
Characteristics of multiarc plasma devices
12 p1841 N85-21554
EMI characteristics of a potential control system
13 p1904 N85-22502
Explosive emission cathode plasmas in intense relativistic electron beam diodes
[AD-A150669] 14 p2417 N85-24912
Experimental investigation of neutral plasma beam propagation across a magnetic field
[AD-A150944] 14 p2423 N85-24947
Radio frequency containment
15 p2654 N85-26375
Basic studies. 1: Basic experiments in plasma physics
15 p2655 N85-26378
Development of RF plasma generators for neutral beams
[DE85-004125] 15 p2658 N85-26400
Experimental research on electrical propulsion. Note 2: Experimental research on a plasma jet with vortex type stabilization for propulsion
[NASA-TM-77874] 18 p3067 N85-29868
Time-resolved energy spectrum of the ion beam generated in the plasma focus
19 p3389 N85-30892

PLASMA GUNS
Hot hollow cathode gun assembly
[DE84-014312] 01 p0121 N85-10832
Steady-state spheromak reactor studies
[DE85-009585] 19 p3372 N85-30916

PLASMA HEATING
NT ELECTRON CYCLOTRON HEATING
Fast waves near the lower hybrid frequency
[DE84-015217] 01 p0123 N85-10841
Fusion plasma theory. Task 3: Auxiliary heating in Tokamaks and tandem mirrors
[DE84-014940] 04 p0568 N85-13609
Oscillating field current drive for reversed field pinch discharges
[DE84-015090] 04 p0567 N85-13610
Elmo Bumpy Torus physics
[DE84-015909] 05 p0730 N85-14694
High frequency plasma generator for ion thrusters
[NASA-CR-174772] 08 p1114 N85-17023
Heating in the solar mantle
08 p1233 N85-17769
The role of fast electrons for the performance characteristics of hydrogen ion sources
09 p1303 N85-18180
Slow wave antenna coupling to ion Bernstein waves for plasma heating in ICRF
[AD-B089084L] 09 p1386 N85-18717
Impurity control by additional current rise and gas puffing during ICRF heating in JIPP T-IIU Tokamak
09 p1387 N85-18725
Long-pulse beamline for the mirror fusion test facility
[DE84-017091] 09 p1392 N85-18760
The energy spectra of slowed-down neutrals from the heating beams in ASDEX — tokamak
[REPT-84-157] 09 p1394 N85-18772
Improved directional couplers for overmoded waveguide systems
[IPF-84-1] 09 p1394 N85-18775
Design of mode converters from TE circular om modes in circular waveguides to TE rectangular mo modes in rectangular waveguides for high power applications in the frequency range 1 to 30 GHz
[IPF-84-7] 09 p1395 N85-18781

Generation of Alfven waves due to thermal modulation of the electrical conductivity
[AD-A149389] 10 p1558 N85-19825
Thermal barrier confinement experiments in TMX-U tandem mirror, revision 1
[DE84-017029] 10 p1561 N85-19844
Electron bounce resonance heating in a bumpy cylinder
[DE85-001732] 10 p1561 N85-19845
Observations of bulk electron heating due to return current in a tokamak discharge started up by lower hybrid waves
[IPPJ-706] 12 p1937 N85-22172
Ruby wavefront-conjugation laser for obtaining high temperature plasma 13 p2044 N85-22795
Lower hybrid heating and current drive, and ion cyclotron heating experiments on the Alcator C and the Versator II Tokamaks
[DE85-004918] 13 p2161 N85-23412
Design, theoretical innovations in Tokamaks systems 14 p2269 N85-24190
Modeling longitudinal motions of thermal O+ and H+ ions in magnetic field tube convective through daytime polar cusp 15 p2481 N85-25314
Annual Review, April 1983 - March 1984
[ISSN-0547-1567] 15 p2654 N85-26369
High beta pinch plasma (STP-L) 15 p2655 N85-26381
Theoretical studies of Elmo Bumpy Torus
[DE85-007202] 15 p2658 N85-26402
Determining effective rate of plasma heating in outer equatorial ionosphere using data from ISIS-1 and ISIS-2 satellites 16 p2721 N85-26797
Velocity space diffusion of high energy ions induced by a lower hybrid wave in a nonuniform magnetic field
[IPPJ-714] 16 p2866 N85-27681
Tokamak systems code
[DE85-006147] 16 p2869 N85-27696
The effects of alpha particle production on the stability of an Elmo Bumpy Torus (EBT) reactor 19 p3369 N85-30695
Hard X-ray measurements of the hot electron rings in Nagoya BUMPY TORUS (NBT-1M)
[IPPJ-720] 19 p3370 N85-30699
Alternating current OHMIC heating in a toroidal stellerator 20 p3534 N85-31988
Self-consistent models for the X-ray emission from supernova remnants 20 p3548 N85-32082
Confinement and heating of high beta plasma with emphasis on compact toroids. Compact toroid research
[DE85-011463] 22 p3848 N85-33821
Computational study on excitation, propagation and 3 omega -heating due to the ion Bernstein wave
[IPPJ-733] 23 p3975 N85-34841
On the heat flux derived by the moment method in Lorentzian plasma between hot and cold walls 23 p3980 N85-34882
Integral representation for nonlinear heat transport 23 p3981 N85-34883
Scale separation closure and Alfven wave turbulence
[DE85-013124] 24 p4095 N85-35365
Confinement and heating of high beta plasmas with emphasis on compact toroids
[DE85-011459] 24 p4155 N85-35761
Proposed FRX-D experiment
[DE85-012766] 24 p4158 N85-35778

PLASMA INSTABILITY
U MAGNETOHYDRODYNAMIC STABILITY

PLASMA INTERACTION EXPERIMENT
SCATHA (spacecraft charging at high altitudes) plasma interaction experiment: SC-3 high energy particle spectrometer; SC-8 energetic ion composition experiment
[AD-A149728] 12 p1793 N85-21252
The PIX-2 experiment: An overview 13 p1993 N85-22494
Plasma interaction experiment 2 (PIX 2): Laboratory and flight results 13 p1993 N85-22495
Ram-wake effects on plasma current collection of the PIX 2 Langmuir probe 13 p1993 N85-22496

PLASMA INTERACTIONS
NT LASER PLASMA INTERACTIONS
NT PLASMA-ELECTROMAGNETIC INTERACTION
NT PLASMA-PARTICLE INTERACTIONS
Plasma surface interactions in magnetic fusion systems
[DE84-015255] 01 p0123 N85-10842
The effect of plasma on solar cell array arc characteristics
[NASA-TM-86887] 02 p0169 N85-11133
The effect of heat treatment on wear resistance of gas-plasma eutectic coatings
[BLL-M-35756-(5828.4)] 03 p0329 N85-12122
Study of plasma convection and wall interactions in magnetic confinement systems
[DE84-013959] 03 p0421 N85-12692
Brillouin scattering in underdense UV laser-produced plasmas
[DE84-015184] 04 p0567 N85-13614
Effects of the solar and extraterrestrial environments on space power systems 05 p0610 N85-13896
Proceedings of Workshop on Synergistic Effects in Surface Phenomena Related to Plasma-Wall Interactions
[IPPJ-AM-35] 06 p0864 N85-15488
Synergistic effects in fusion machines, session summary 06 p0864 N85-15489
Plasma surface interaction processes and possible synergisms 06 p0864 N85-15490
Synergisms in hydrogen recycling, session summary 06 p0864 N85-15491
Steady state hydrogen transport in solids 06 p0864 N85-15492
Synergisms in surface erosion, session summary 06 p0864 N85-15493
Synergism in materials erosion due to multispecies impact 06 p0864 N85-15494
Synergistic effects related to surface composition, session summary 06 p0865 N85-15495
Effects of monolayer coverages on substrate sputtering yields 06 p0865 N85-15496
Synergestic sputtering properties of binary alloys 06 p0865 N85-15497
Longer-scalelength plasma perturbations by an intense laser beam
[AD-A147005] 07 p1045 N85-16638
The environment of active galactic nuclei 07 p1057 N85-16712
Hydrogen trapping, diffusion, and recombination in austenitic stainless steels
[DE85-001871] 09 p1294 N85-18129
Developments and applications of laser fluorescence spectroscopy for studies of particle behaviours in fusion plasmas 09 p1389 N85-18735
Studies on impurity control and hydrogen pumping with chromium gettering in ISX-B
[DE85-001696] 09 p1394 N85-18771
Hydrodynamic response of a radiating Al plasma excited by a proton beam
[AD-A148904] 10 p1558 N85-19824
Plans for Interbol satellite experiment 13 p1977 N85-22407
Spacecraft Environmental Interactions Technology, 1983
[NASA-CP-2359] 13 p1989 N85-22470
Measured electron contribution to Shuttle plasma environment: Abbreviated update 13 p1990 N85-22476
Self-consistent simulation of plasma interactions with secondary-emitting insulators 13 p1993 N85-22492
Surface interactions and high-voltage current collection 13 p1993 N85-22493
The PIX-2 experiment: An overview 13 p1993 N85-22494
Plasma interaction experiment 2 (PIX 2): Laboratory and flight results 13 p1993 N85-22495
Discharges on a negatively biased solar cell array in a charged-particle environment 13 p1994 N85-22499
Spacecraft environmental interactions: A joint Air Force and NASA research and technology program 13 p1997 N85-22517
Space test program of high-voltage solar array-space plasma interactions 13 p1997 N85-22519
The Giotto spacecraft impact-induced plasma environment
[ESA-SP-224] 14 p2243 N85-23905
Measurements of integral yields of charged secondary particles using neutral beams simulating a cometary fly-by — Giotto mission 14 p2244 N85-23908
Simulations of satellite-plasma interaction, including electron space charges — Giotto mission 14 p2245 N85-23916
Anticipated impact plasma problems for the COPERNIC-RPA experiment in the cometary environment — Giotto mission 14 p2245 N85-23917
Spacecraft environment during the Giotto-Halley encounter: A summary 14 p2246 N85-23921
Preparatory experiments. 1: JIPP T-IIU 15 p2654 N85-26374
Discrete foundation for physics and experience
[DE85-008172] 16 p2872 N85-27720
Examination of a method for predicting the properties of railgun plasmas
[AR-004-322] 17 p3039 N85-28799
Microwave experimental studies of laser fusion
[DE85-008327] 17 p3041 N85-28814
Nonlinear plasma reactions on the antenna impedance of high transmission power satellites
[BMFT-FB-W-84-053] 18 p3192 N85-29799
Shocks in the solar wind between 1 and 8.5 AU: Voyager 1 observations
[NASA-CR-175911] 18 p3209 N85-29905
Cosmic ray modulation and turbulent interaction regions near 11 AU
[NASA-TM-86193] 18 p3209 N85-29909
Ion beam-plasma interactions
[DE85-010202] 19 p3371 N85-30913
On the role of the magnetic field strength in critical ionization velocity interaction
[TRITA-EPP-85-01] 20 p3536 N85-32003
Vehicle Charging And Potential (VCAP) 23 p3902 N85-34173
Latitude variation of recurrent fluxes in the outer solar system
[SH-4.1-13] 23 p4006 N85-34836
Beam potential measurement of an intense H(-) beam by use of the emissive probe technique
[DE85-012671] 24 p4155 N85-35762

PLASMA JETS
The effect of plasma on solar cell array arc characteristics
[NASA-TM-86887] 02 p0169 N85-11133
Investigation of heat exchange on models in subsonic jets of induction plasmatron 02 p0269 N85-11756
Dynamical models for radio jets 03 p0449 N85-12854
Laboratory electron beam simulation of cosmic radio jets
[DE84-016179] 04 p0590 N85-13764
The discharge mechanism of the high-temperature arc
[NASA-TM-77794] 07 p0922 N85-15837
Investigation of granules of molybdenum-base alloys obtained with pulsed discharges
[BLL-M-36012-(5828.4)] 07 p0926 N85-15871
Morphology and optical polarization of the 3C 273 jet — radio jet 08 p1238 N85-17803
On the hydrodynamical equations of astrophysical jets — active galactic nuclei 08 p1241 N85-17831
Four phase model for turbulent instabilities calculation in plasma jets
[IPF-84-2] 09 p1394 N85-18776
Cobalt-free permanent magnet alloys
[AD-A149272] 10 p1441 N85-19079
Electrodynamic interactions 11 p1643 N85-20348
Characteristics of multiarc plasma devices 12 p1841 N85-21554
Plasma performance of TFCX and jet with sawtoothing
[DE85-003335] 12 p1936 N85-22168
Determination of physical parameters of jets in radio galaxies 12 p1958 N85-22304
Hydrodynamics of astrophysical jets — active galactic nuclei 12 p1958 N85-22307
Viscous jets — extragalactic jets 12 p1958 N85-22308
Jets in galaxies 12 p1958 N85-22309
Development of theory of high-current high-pressure pulsed arc 15 p2645 N85-26314
Thermodynamic analysis of the plasma nitriding of ferrovanadium
[BLL-BISI-TRANS-22237-(9022.06)] 17 p2924 N85-28032
Implications for supersymmetry of the CERN monojets
[DE85-008178] 17 p3030 N85-28741
Examination of a method for predicting the properties of railgun plasmas
[AR-004-322] 17 p3039 N85-28799
Experimental research on electrical propulsion. Note 2: Experimental research on a plasma jet with vortex type stabilization for propulsion
[NASA-TM-77874] 18 p3067 N85-28968
Cavitation erosion of plasma sprayed alloys
[DE85-009542] 18 p3077 N85-29036
Ion-acoustic double layer in a magnetic picket fence configuration
[INPE-3552-PRE/764] 19 p3369 N85-30698
Plasma arc welding, equipment, installation and process control
[DE85-006481] 19 p3373 N85-30921
Limits on the Doppler factor in relativistic jets by means of gamma-ray observations
[OG-2.7-12] 22 p3872 N85-33985
Jets in air-jet family
[HE-3.2-1] 24 p4179 N85-35912
Search for anomalous C-jets in Chacaltaya emulsion chamber experiment
[HE-3.2-5] 24 p4179 N85-35913

PLASMA LAYERS
NT PLASMA SHEATHS
Plasma variables and tribological properties of coatings in low pressure (0.1 - 10.0 torr) plasma systems
[NASA-TM-83798] 02 p0169 N85-11261
Cold streams of ionospheric oxygen in the plasma sheet during the CDAW-6 event of March 22, 1979
[NASA-CR-174064] 03 p0393 N85-12513
On the cause of X-line formation in the near-Earth plasma sheet: Results of adiabatic convection of Plasma-Sheet-Plasma
[AD-A145835] 03 p0396 N85-12525

Electric field in plasma layer of magnetosphere during preliminary substorm phase 06 p0824 N85-15231
Development and application of low energy X-ray and electron physics
[AD-A149983] 12 p1926 N85-22099
Modeling plasma mantle of Earth's magnetosphere 16 p2720 N85-26790
The transport of neutral H, D, T and He and O in the boundary layers of a Tokamak plasma
[REPT-84-153] 17 p3041 N85-28817
Double layer formation due to contact of different temperature plasmas
[IPPJ-722] 19 p3370 N85-30900
Global effects of double layers — plasma layers
[TRITA-EPP-84-12] 20 p3536 N85-32002

PLASMA LOSS

Excitation of impurities by heavy particles and radiative losses of thermonuclear plasma 11 p1719 N85-20816
Numerical model for swirl cooling in high-heat-flux particle beam targets and the design of a swirl-flow-based plasma limiter
[DE85-003824] 11 p1732 N85-20894

PLASMA OSCILLATIONS

Hamiltonian and Lagrangian theory of gyrokinetic equations 02 p0283 N85-11845
Application of the energy problem to the problem of plasma flow stability
[DE84-013359] 05 p0730 N85-14691
Mechanism of damping of plasma oscillations in initial stage of injection of electron beams from spacecraft into ionosphere in active experiments 06 p0823 N85-15225
Waves and instabilities in collisionless shocks
[AD-A146689] 06 p0881 N85-15597
Longer-scalelength plasma perturbations by an intense laser beam
[AD-A147005] 07 p1045 N85-16838
Spacecraft-environment interaction: The environmental plasma aspect 13 p1990 N85-22479
The downshift of electron plasma oscillations in the electron foreshock region
[NASA-CR-175633] 14 p2423 N85-24945
Effects of finite current channel width on the current convective instability
[AD-A151414] 15 p2656 N85-26389
Stefan-Maxwell relations for plasma diffusion currents in magnetic field 17 p2942 N85-28160
Strong coupling effects on bound states in plasmas
[AD-A154353] 19 p3370 N85-30905
Low frequency instabilities driven by an ion temperature anisotropy
[AD-A154902] 21 p3707 N85-33016
Instrument to synchronize Thomson scattering diagnostic measurements with MHD activity in a Tokamak
[DE85-012062] 23 p3984 N85-34708
High energy plasma accelerators
[DE85-013121] 24 p4155 N85-35760

PLASMA PERTURBATION

U PLASMA OSCILLATIONS

PLASMA PHYSICS

Plasma drift equilibrium (gyration) in toroidal systems with complex magnetic-field geometry
[DE84-015627] 01 p0122 N85-10839
Fast waves near the lower hybrid frequency
[DE84-015217] 01 p0123 N85-10841
Plasma deposited diamondlike carbon on GaAs and InP
[NASA-TM-86870] 01 p0123 N85-10844
USSR report: Physics and mathematics
[JPRS-UPM-84-006] 02 p0256 N85-11676
Statistical Plasma Physics. Proceedings of the Workshop of the US-Japan Joint Institute for Fusion Theory Program
[IPPJ-689] 02 p0282 N85-11832
Behavior orbits of two coupled oscillators 02 p0282 N85-11833
Stochastic property of K-dV solitons perturbed by random forces — Korteweg-Devries equation 02 p0283 N85-11843
Chaotic behavior induced by solitons in perturbed integrable systems 02 p0283 N85-11844
Hamiltonian and Lagrangian theory of gyrokinetic equations 02 p0283 N85-11845
A simple transport model 02 p0284 N85-11853
Design, construction, and operational results of an 800-A, 10-kV hot deck amplifier
[DE84-014044] 04 p0496 N85-13162
Activities report in Earth and planetary environments physics
[CRPE-NT-134] 05 p0734 N85-14720
Proceedings on US-Japan Workshop on Tokamak Diagnostics by X-ray, VUV and Optical Radiations
[IPPJ-703] 09 p1386 N85-18719
Sources, densities, and transport of impurities in neutral-beam injected Tokamaks 09 p1388 N85-18731
Computational plasma physics and supercomputers
[DE85-001739] 09 p1393 N85-18766
Science Applications, part 1 11 p1643 N85-20346
Summary presentation of the Electrodynamics Interactions Panel 11 p1644 N85-20356
Fluctuations and transport in fusion plasmas
[DE85-003612] 11 p1732 N85-20893
Activities report of the Institute of Plasma Research 11 p1733 N85-20903
Simulation of thermal and electromagnetic processes in induction plasmatrons 12 p1841 N85-21552
Pressure-gradient-driven Tokamak resistive MHD instability in the banana-plateau collisionality regime
[DE85-004568] 12 p1937 N85-22171
University of Cambridge Institute of Astronomy report of activities 13 p2170 N85-23464
Evolution of strong inhomogeneities in ionospheric plasma, part 1 14 p2339 N85-24463
Slowing down of charged particles by the bound electrons in a plasma — ion beams, nuclear fusion
[LP-209] 14 p2419 N85-24929
Glossary of fusion energy
[DE84-017180] 14 p2425 N85-24958
USSR report: Physics and mathematics
[JPRS-UPM-85-003] 15 p2642 N85-26300
Annual Review, April 1983 - March 1984
[ISSN-0547-1567] 15 p2654 N85-26369
Scientific activities. A: Reacting plasma physics. 1: Introduction and overview 15 p2654 N85-26370
Preparatory experiments. 1: JIPP T-IIU 15 p2654 N85-26374
Basic studies. 1: Basic experiments in plasma physics 15 p2655 N85-26378
Plasma theory and computations 15 p2655 N85-26384
Propagation of wave packet in a dissipative dielectric medium
[IPPJ-710] 15 p2655 N85-26385
Optimizing computational efficiency and user convenience in plasma simulation codes
[DE85-007661] 16 p2666 N85-27682
Computational plasma physics and supercomputers, revision 1
[DE85-007228] 16 p2667 N85-27687
A four-field model for Tokamak plasma dynamics
[DE85-007111] 16 p2668 N85-27694
Plasma processing of materials
[AD-A152398] 17 p3039 N85-28600
Experimental plasma research: Plasma summaries
[DE85-008116] 17 p3039 N85-28605
Millimeter wave generation by relativistic electron beams
[AD-A153960] 18 p3179 N85-29706
ICRF antenna coupling and wave propagation in a tokamak plasma 19 p3369 N85-30893
The effects of weak turublence on parametric processes in an unmagnetized plasma 19 p3369 N85-30896
Perspectives of nonlinear dynamics
[IPPJ-723] 19 p3370 N85-30902
Effect of inner subshell ionization on emission lines OIV ions
[IPPJ-719] 19 p3370 N85-30903
Schottky theory of three component plasmas
[AD-A154461] 19 p3371 N85-30907
Slow tearing modes: Transitions to instability 20 p3534 N85-31989
Publications from the Department of Plasma Physics and the Unit of Accelerator Technology, index and abstracts, 1984
[TRITA-EPP-84-13] 20 p3534 N85-31991
USSR report: Physics and mathematics
[JPRS-UPM-85-004] 21 p3680 N85-32860
Modeling the exhaust of the pulsed plasma thruster
[AD-A155344] 21 p3707 N85-33018
Data Base Workshop: Availability-Reliability Modeling
[DE85-011570] 22 p3829 N85-33713
Electron and ion cyclotron heating calculations in the tandem-mirror
[DE85-011858] 22 p3842 N85-33797
Magnetic Fusion Program plan
[DE85-009661] 22 p3846 N85-33823
Waves in Space Plasmas (WISP) 23 p3901 N85-34184
Theoretical and Experimental Beam Plasma Physics (TEBPP) 23 p3901 N85-34186

PLASMA PINCH

NT THETA PINCH
NT ZETA PINCH
K-shell yield scaling law for conventional PRS loads
[AD-A145155] 01 p0121 N85-10831
Proceedings of the US-Japan Theory Workshop on 3-D MHD Studies
[DE84-012019] 04 p0568 N85-13620
Compact toroidal development: Activity plan for field reversed configurations
[DE84-017145] 05 p0730 N85-14695
Intense excitation source of blue-green laser
[AD-A147450] 07 p0971 N85-16168
High-power radiating plasma
[NASA-TM-77784] 07 p1045 N85-16837
Diffusion driven plasma current with turbulent dynamo
[IPPJ-700] 09 p1386 N85-18718
High beta pinch plasma (STP-3(M)) 15 p2655 N85-26380
High beta pinch plasma (STP-L) 15 p2655 N85-26381
Poloidal rotation of magnetic fluctuations in reversed field pinch plasma
[IPPJ-715] 16 p2666 N85-27677

PLASMA POTENTIALS

Anomalously high potentials observed on ISEE 13 p1994 N85-22509
Screening phase transitions in two-dimensional Coulomb gas
[NOTA-INTERNA-830] 18 p3192 N85-29798
Space-time characteristics of field in longitudinal pulse-period discharge typical in pumping of self-terminating lasers 21 p3687 N85-32909
Model of azimuthal non-uniformities induced by RF heating in RFC-XXM 23 p3977 N85-34658

PLASMA POWER SOURCES

NT PLASMA ENGINES

PLASMA PROBES

NT ELECTROSTATIC PROBES
Novel probe for determining the size and position of a relativistic electron beam
[DE85-001044] 11 p1723 N85-20836
Vehicle Charging And Potential (VCAP) 23 p3902 N85-34173

PLASMA PROPULSION

Ring-cusp ion thruster with shell anode
[NASA-CASE-LEW-13881-1] 12 p1794 N85-21256

PLASMA PUMPING

Oscillating field current drive for reversed field pinch discharges
[DE84-015090] 04 p0567 N85-13610
Investigation of silicon surface passivation by silicon nitride deposition 06 p0829 N85-15266
High-power radiating plasma
[NASA-TM-77784] 07 p1045 N85-16837
Impurity and particle control systems for tokamak reactor experiments
[DE85-006124] 19 p3366 N85-30873
Radiation-cooled helicity-injecting reversed field pinch formed with relativistic electrons
[IPPJ-721] 19 p3370 N85-30901
New concept for pumping the edge plasma
[DE85-010180] 19 p3371 N85-30909
Space-time characteristics of field in longitudinal pulse-period discharge typical in pumping of self-terminating lasers 21 p3687 N85-32909
Transport issues in Phaedrus-type plasmas 23 p3976 N85-34653
Fokker-Planck calculation of hot electron formation in the thermal barrier region of tandem mirror Gamma-10
[IPPJ-726] 23 p3979 N85-34669

PLASMA RADIATION

Optical properties of laser erosion flares in plasma 02 p0270 N85-11764
A new maser effect in plasma turbulence 02 p0284 N85-11852
Imploding plasma radiation sources: Basic concepts
[AD-A145542] 02 p0284 N85-11858
High-power radiating plasma
[NASA-TM-77784] 07 p1045 N85-16837
Hydrodynamic response of a radiating Al plasma excited by a proton beam
[AD-A148904] 10 p1556 N85-19824
Influence of shock wave front on nature of luminescence of recombining laser plasma 11 p1719 N85-20818
Arguments for fundamental emission by the parametric process L yields T + S in interplanetary type III bursts — langmuir, electromagnetic, ion acoustic waves (L, T, S) 12 p1958 N85-22311
An Impurity Control Test Facility (ICTF) for the study of fusion reactor/plasma edge materials
[DE85-007946] 17 p3040 N85-28610
Plasma radiation sources. Quasi-adiabatic theory and numerical modeling in the electro-diffusive approximation
[AD-A154375] 19 p3370 N85-30908
Plasmodynamic methods for generating powerful light puses 21 p3693 N85-32943
Characteristics of optogalvanic effect in media with inverse populations 21 p3693 N85-32944
Investigation of space-time structure of glow of laser plasma colliding with flat screen 21 p3693 N85-32947

Beam potential measurement of an intense H(-) beam by use of the emissive probe technique
[DE85-012971] 24 p4155 N85-35762
PLASMA RENIN ACTIVITY
U IMMUNOASSAY
PLASMA RESONANCE
Excitation of low-frequency resonance waves by moving conductor in space plasma 13 p2067 N85-22912
Scattering of electromagnetic waves by charged particles 13 p2067 N85-22913
The application of laser resonance saturation to the development of efficient short wavelength lasers
[AD-A153951] 18 p3113 N85-29270
The determination of optical constants of thin metal films by surface plasma techniques 19 p3373 N85-30825
Influence of ECR-heating on MHD activity of plasma in tokamak-10 installation 21 p3694 N85-32949
Cyclotron resonance in a nonneutral plasma
[AD-A155348] 21 p3707 N85-33017
Nonlocal and nonadiabatic expression for the ponderomotive force near cyclotron resonance
[IPPJ-736] 23 p3974 N85-34836
Computational study on excitation, propagation and 3 omega -heating due to the Ion Bernstein wave
[IPPJ-733] 23 p3975 N85-34841
Bounce resonance heating and radial transport of electrons 23 p3977 N85-34855
The heavy ion composition in 3HE-rich solar flares
[SH-2.2-7] 23 p4000 N85-34802
PLASMA RINGS
U TOROIDAL PLASMAS
PLASMA SHEATHS
Sun-aligned polar cap auroral arcs
[AD-A146052] 08 p1185 N85-17472
Reconsideration of sheath related to negative ion extraction
[IPPJ-706] 12 p1935 N85-22159
Direct measurements of severe spacecraft charging in auroral ionosphere 13 p1991 N85-22480
Polar plasmas as observed by Dynamics Explorers 1 and 2 13 p1991 N85-22483
Sheath ionization model of beam emissions from large spacecraft 13 p1992 N85-22489
The Giotto spacecraft impact-induced plasma environment
[ESA-SP-224] 14 p2243 N85-23905
Giotto plasmasheath and wake charging near Halley's Comet: Revised parameters 14 p2245 N85-23915
Anticipated impact plasma problems for the COPERNIC-RPA experiment in the cometary environment — Giotto mission 14 p2245 N85-23917
An impact plasma monitor for cometary missions — Giotto , VEGA 14 p2245 N85-23918
Plasma environment effects on the Giotto Ion Mass Spectrometer 14 p2245 N85-23919
Spacecraft environment during the Giotto-Halley encounter: A summary 14 p2246 N85-23921
Plasma and magnetospheric research
[NASA-CR-175675] 14 p2354 N85-24543
Research on thermionic plasmas
[AD-A150663] 14 p2423 N85-24944
Ionospheric effects on antenna impedance
[BMFT-FB-W-84-052] 17 p2950 N85-28217
Nonlinear plasma reactions on the antenna impedance of high transmission power satellites
[BMFT-FB-W-84-053] 18 p3192 N85-29799
Ion-acoustic double layer in a magnetic picket fence configuration
[INPE-3552-PRE/764] 19 p3369 N85-30898
Trajectories of charged particles traversing a plasma sheath in an oblique magnetic field
[DE85-011070] 19 p3371 N85-30911
Wave/particle interactions in the plasma sheet
[NASA-CR-171537] 20 p3547 N85-32072
PLASMA SOUND WAVES
U MAGNETOHYDRODYNAMIC WAVES
U PLASMA WAVES
PLASMA SPECTRA
High-power radiating plasma
[NASA-TM-77784] 07 p1045 N85-16637
Spectroscopic studies of a railgun muzzle flash
[MRL-R-952] 16 p2728 N85-26837
Projections of plasma cloud structures and their spectra
[AD-A153608] 18 p3189 N85-29776
PLASMA SPRAYING
Energy efficient engine high pressure turbine ceramic shroud support technology report
[NASA-CR-168036] 02 p0147 N85-10996
Mechanism of brittle heat fracture of inhomogeneous solids by high temperature gas jets
02 p0265 N85-11731
Air force plasma spray at SA-ALC (San Antonio Air Logistics Center)
[AD-P004004] 03 p0308 N85-11984
High-temperature erosion of plasma-sprayed, yttria-stabilized zirconia in a simulated turbine environment
[NASA-TP-2406] 04 p0478 N85-13045
Study of phase composition of Al-B plasma coatings
11 p1598 N85-20060
Film and interstitial formation of metals in plasma-sprayed ceramics
[NASA-TM-86993] 13 p2036 N85-22756
Vacuum plasma coatings for turbine blades
16 p2734 N85-26869
Plasma spray screen repair method
[AD-D011713] 19 p3281 N85-30346
Thermal barrier coating system
[NASA-CASE-LEW-14057-1] 24 p4072 N85-35233
PLASMA STABILITY
U MAGNETOHYDRODYNAMIC STABILITY
PLASMA TEMPERATURE
Overheated open coronal regions
08 p1234 N85-17772
Modeling thermal plasma material processing experiments
[DE85-001551] 10 p1560 N85-19838
Heat flux in Lorentzian plasma
[IPPJ-704] 12 p1935 N85-22158
Radio frequency containment
15 p2654 N85-26375
Study of a constricted electric arc cooled by transpiration
[NASA-TM-77846] 17 p3038 N85-28798
A numerical solution technique for multitemperature plasma hydrodynamics
[AD-A152701] 17 p3039 N85-28801
Low plasma edge temperatures for the self-pumped limiter
[DE85-010155] 18 p3189 N85-29782
Theoretical and Experimental Beam Plasma Physics (TEBPP) 23 p3901 N85-34166
PLASMA THEORY
U PLASMA PHYSICS
PLASMA TURBULENCE
Stable distribution and Levy process in fractal turbulence 02 p0283 N85-11846
Strong Langmuir turbulence 02 p0284 N85-11851
A new maser effect in plasma turbulence
02 p0284 N85-11852
Relaxation of plasma rotation in a Tokamak in the presence of extraneous forces and corrugation of the magnetic field
[DE84-015628] 02 p0284 N85-11854
The flow of plasma in the solar terrestrial environment
[NASA-CR-174301] 08 p1224 N85-17707
Diffusion driven plasma current with turbulent dynamo
[IPPJ-700] 09 p1366 N85-18716
Four phase model for turbulent instabilities calculation in plasma jets
[IPF-84-2] 09 p1394 N85-18776
Space-time statistics of the turbulence in a Tokamak edge plasma
[DE85-002667] 10 p1559 N85-19834
Cosmic ray generation by plasma turbulence: Development of a new paradigm in physics
12 p1955 N85-22256
Arguments for fundamental emission by the parametric process L yields T + S in interplanetary type III bursts — langmuir, electromagnetic, ion acoustic waves (L, T, S)
12 p1958 N85-22311
Heating of coronal loops by tearing turbulence
14 p2448 N85-25114
Coronal heating by turbulent phase mixed MHD waves — solar corona 14 p2453 N85-25148
Turbulence and wave particle interactions in solar-terrestrial plasmas
[NASA-CR-175970] 18 p3209 N85-29906
Effects of a radial electric field on tokamak edge turbulence
[DE85-010401] 19 p3371 N85-30910
Runaway electrons and plasma turbulence in current ramping by lower hybrid waves in tokamak plasmas
[DE85-011390] 20 p3535 N85-31997
Caviton collapse of SRS by SBS
[DE85-009605] 20 p3535 N85-31999
Interplanetary plasma turbulence and the Doppler detection of a gravitational background radiation
[IFSI-85-1] 20 p3546 N85-32066
Investigation of ion-acoustic plasma turbulence in field of powerful electromagnetic wave by CO2-laser radiation scattering 21 p3691 N85-32935
The propagation of solar flare particles in a turbulent coronal loop
[SH-1.1-3] 23 p3989 N85-34730
PLASMA WAVES
NT ELECTROSTATIC WAVES
Bremsstrahlung radiation from longitudinal plasma waves caused by subthermal electrons in plasma
02 p0264 N85-11730
Strong Langmuir turbulence 02 p0284 N85-11851
A new maser effect in plasma turbulence
02 p0284 N85-11852
Reduction and analysis of data from the plasma wave instruments on the IMP-6 and IMP-8 spacecraft
[NASA-CR-175127] 04 p0460 N85-12918
Wave absorption and transport studies on Electron Cyclotron Resonance (ECR) heated stellarator plasmas in W 7-A
[IPF-84-9] 09 p1395 N85-18782
Role of cavitons in laser-plasma interactions
[DE85-001842] 11 p1731 N85-20686
Dynamics of space charge waves in the laser beat wave accelerator
[AD-A149668] 12 p1936 N85-22163
On the spectrum of longitudinal waves in the hot degenerate plasma 12 p1955 N85-22280
Nonlinear waves in the magnetosphere of pulsars
12 p1955 N85-22281
Achievements of the International Magnetospheric Study (IMS) — conference
[ESA-SP-217] 14 p2354 N85-24544
Plasma waves at and near the neutral sheet
14 p2358 N85-24572
Pc 1-2 pulsations and related phenomena: A review — geomagnetic pulsations 14 p2364 N85-24611
Spatial characteristics of ULF pulsations and their modification by the ionosphere: IMS results
14 p2364 N85-24612
An evaluation of the contributions of the IMS to experimental and theoretical studies of ULF plasma
14 p2365 N85-24614
Observations of the MF-HF plasma wave emissions in active auroras by the sounding rocket experiments at Sycwa station 14 p2366 N85-24620
VLF wave-particle interaction experiments by EXOS-B/Siple station transmissions
14 p2366 N85-24622
Energetic electron anisotropy and ELF waves onboard GEOS. How does quasi-linear diffusion work
14 p2366 N85-24623
The structure, stability, wave transmission and energy transfer at the Earth's magnetopause
14 p2372 N85-24661
Advances in magnetospheric plasma-wave research during the IMS 14 p2372 N85-24662
Active Magnetospheric Particle Tracing Explorers (AMPTE)
[AD-A151072] 14 p2374 N85-24674
Ionosphere effects may replace some communications satellites 15 p2484 N85-25337
Propagation of wave packet in a dissipative dielectric medium
[IPPJ-710] 15 p2655 N85-26365
Effects of finite current channel width on the current convective instability
[AD-A151414] 15 p2656 N85-26369
Two-dimensional beat wave acceleration simulation
[DE85-005961] 16 p2791 N85-27214
Plasma waves in the solar wind: Ten years of Helios observations 16 p2865 N85-27801
Plasma wake field accelerator
[DE85-010538] 18 p3191 N85-29791
Preliminary results on open accelerating structures
[DE85-010231] 18 p3191 N85-29793
More on shock-wave studies with Prognoz-10 satellite
19 p3296 N85-30432
Prognoz-10 intercosmos' station launched to study shock waves 19 p3296 N85-30434
Caviton collapse of SRS by SBS
[DE85-009605] 20 p3535 N85-31999
Analysis of spacecraft data
[NASA-CR-171587] 21 p3689 N85-32789
PLASMA-ELECTROMAGNETIC INTERACTION
NT LASER PLASMA INTERACTIONS
Theory of pondermotive forces
02 p0283 N85-11847
Plasma drift towards a plane equipotential surface
[TRITA-EPP-84-01] 02 p0265 N85-11860
An experimental and theoretical investigation of optogalvanic effects
[AD-A148089] 08 p1157 N85-17299
Effect of resonant microwave power on a PIG ion source
[DE85-001396] 09 p1379 N85-18673
Plasma states near surface of metal irradiated by CO2 laser 11 p1719 N85-20615
Explosive instability of strong electromagnetic wave in plasma 11 p1719 N85-20617
Monte Carlo studies of tandem mirror plasmas interacting with waves in the Ion Cyclotron Range of Frequencies (ICRF)
[DE85-002968] 11 p1731 N85-20883
Hydromagnetic precursors of interplanetary plasma burst 13 p1978 N85-22414

Report on final recommendations for IMPS engineering-science payload
[NASA-CR-175659] 13 p1988 N85-22464
Spacecraft-environment interaction: The environmental plasma aspect 13 p1990 N85-22479
Scattering of electromagnetic waves by charged particles 13 p2067 N85-22913
Diffraction of plane TM-wave on continuously irregular elliptical plasma 13 p2067 N85-22914
Basic experiments in plasma physics (TPL) 15 p2655 N85-26379
Direct electron and ion fluid computation of high electrostatic fields in dense inhomogeneous plasma with subsequent nonlinear optical and dynamical laser interaction 15 p2656 N85-26386
The formation of spokes in Saturn's rings 15 p2676 N85-26524
Millimeter wave generation by relativistic electron beams
[AD-A153980] 18 p3179 N85-29708

PLASMA-PARTICLE INTERACTIONS
Strong Langmuir turbulence 02 p0284 N85-11851
Spacecraft-environment interaction: The environmental plasma aspect 13 p1990 N85-22479
On-off characteristics of auroral pulsations 14 p2363 N85-24604
VLF wave-particle interaction experiments by EXOS-B/Siple station transmissions 14 p2366 N85-24622
Slowing down of charged particles by the bound electrons in a plasma — ion beams, nuclear fusion
[LP-209] 14 p2419 N85-24929
Modified betatron accelerator studies
[AD-A151420] 15 p2648 N85-26332
Selfsimilar time dependent shock structures
[OG-8.1-4] 23 p4017 N85-34894
A cosmic ray driven instability
[OG-8.1-5] 23 p4018 N85-34895

PLASMADYNAMIC LASERS
Metal vapor lasers and their applications
[ISL-CO-218/84] 22 p3791 N85-33488

PLASMAGUIDES
Multihole couplers for overmoded waveguide systems
[IPF-83-8] 09 p1394 N85-18773
Short mode selective directional couplers
[IPF-83-9] 09 p1394 N85-18774
Improved directional couplers for overmoded waveguide systems
[IPF-84-1] 09 p1394 N85-18775
Pc 1 pulsation source regions and their relationship to the plasma pause 14 p2368 N85-24638

PLASMAPAUSE
Precipitation of protons with E sub p approximately 1 MeV near plasmopause 02 p0161 N85-11093
Magnetohydrodynamic and gasdynamic theories for planetary bow waves
[NASA-CR-174132] 03 p0448 N85-12850
Observation of natural noise near upper hybrid resonance in terrestrial magnetosphere by Prognoz-5 satellite 06 p0822 N85-15221
Correlation of ring current and ionospheric gap in morning and evening hours 14 p2339 N85-24466
Whistler mode waves near the plasmapause: Results from the IMS VLF experiment at Halley, Antarctica 14 p2367 N85-24628
Pc 1 pulsation source regions and their relationship to the plasma pause 14 p2368 N85-24638
Plasma and magnetospheric research
[NASA-CR-171447] 15 p2591 N85-25976
Thermal ion heating in the vicinity of the plasmapause
[NASA-CR-176030] 20 p3535 N85-31993

PLASMAS (PHYSICS)
NT ARGON PLASMA
NT BETA PARTICLES
NT BOUNDARY LAYER PLASMAS
NT COLD PLASMAS
NT COLLISIONAL PLASMAS
NT COLLISIONLESS PLASMAS
NT COSMIC PLASMA
NT CYLINDRICAL PLASMAS
NT DENSE PLASMAS
NT DEUTERIUM PLASMA
NT ELECTRON PLASMA
NT ELLIPTICAL PLASMAS
NT HELIUM PLASMA
NT HIGH TEMPERATURE PLASMAS
NT HYDROGEN PLASMA
NT LASER PLASMAS
NT METALLIC PLASMAS
NT NITROGEN PLASMA
NT NONEQUILIBRIUM PLASMAS
NT NONUNIFORM PLASMAS
NT OXYGEN PLASMA
NT PLASMA FOCUS
NT RELATIVISTIC PLASMAS
NT ROTATING PLASMAS
NT SEMICONDUCTOR PLASMAS
NT SOLAR WIND
NT SPACE PLASMAS
NT SPHERICAL PLASMAS
NT STELLAR WINDS
NT STRONGLY COUPLED PLASMAS
NT THERMAL PLASMAS
NT TOROIDAL PLASMAS
MHD instabilities in simple plasma configuration
[AD-A144936] 01 p0121 N85-10829
Polarized electron cyclotron emission in the Tokapole 2 Tokamak
[DE84-014953] 01 p0122 N85-10838
Plasma variables and tribological properties of coatings in low pressure (0.1 - 10.0 torr) plasma systems
[NASA-TM-83798] 02 p0189 N85-11261
Numerical investigation of characteristics of current flow for different methods of obtaining discharge in high speed lasers. Mechanism underlying current flow in positive glow discharge column 02 p0264 N85-11728
Scattering of electromagnetic waves by plasma half-space after initiation of motion 02 p0264 N85-11729
Neutral beam interactions with materials
[AD-A145836] 02 p0285 N85-11857
In-line beam current monitor
[DE84-014054] 04 p0560 N85-13567
Theory of resistive ballooning modes in Tokamaks
[DE84-015626] 04 p0566 N85-13606
Internal helical mode m = 1 of a Tokamak in the plateau and banana regimes
[DE84-015623] 04 p0566 N85-13607
Rotation of a tenuous plasma with a high toroidal velocity in a Tokamak
[DE84-012990] 04 p0567 N85-13615
High-Beta plasma theory
[DE84-016471] 04 p0568 N85-13619
Magnetic helicity in the solar corona 05 p0745 N85-14780
Estimate of nuclear-pumped X-ray laser mechanism 06 p0748 N85-14795
The origin of plasma rotation in the early phase of an FRC produced by a reversed field theta pinch
[IPPJ-898] 06 p0863 N85-15482
A nonlocal expression for the ponderomotive potential
[IPPJ-899] 06 p0864 N85-15487
Plasma-surface interactions in large tandem mirror devices, MFTF-B
[DE85-001753] 06 p0865 N85-15499
Slow surface magnetoplasma waves in oblique magnetic field 07 p0952 N85-16034
Research relative to plasma transport across the magnetopause
[NASA-CR-174300] 07 p1045 N85-16636
The flow of plasma in the solar terrestrial environment
[NASA-CR-174301] 08 p1224 N85-17707
A research proposal for the theoretical study of the thermodynamic and transport properties of dense plasmas
[AD-A148040] 08 p1224 N85-17708
Diffusion driven plasma current with turbulent dynamo
[IPPJ-700] 09 p1386 N85-18716
MHD equilibrium and stability for stellarator/torsatron configurations
[DE85-001139] 09 p1391 N85-18750
Very high energy probes of the quark-gluon plasma
[DE84-016992] 09 p1392 N85-18763
Brief outline of analytic stability studies of magnetically insulated systems — bibliographies
[DE85-000212] 09 p1393 N85-18765
Optically induced intervalence-band transitions in germanium by the absorption of 1.06 micrometers picosecond pulses
[DE85-000946] 09 p1399 N85-18803
1984 AFOSR Research Meeting on Diagnostics of Reacting Flow held at New Haven, Connecticut on 21-22 March 1984
[AD-A149023] 10 p1484 N85-19367
Magnetic fusion energy plasma interactive and high heat flux components. Volume 3: Strategy for international collaborations in the areas of plasma materials interactions and high heat flux materials and components development
[DE85-001145] 10 p1559 N85-19829
Small, octopole-stabilized tandem mirror reactor
[DE85-002144] 10 p1559 N85-19832
Space-time statistics of the turbulence in a Tokamak edge plasma
[DE85-002667] 10 p1559 N85-19834
Finite-(beta) optimization of tandem mirrors
[DE85-002658] 10 p1560 N85-19835
Entrop production determination of the ambipolar solution nearest equilibrium
[DE85-003049] 10 p1560 N85-19836
Nonlinear saturation of stimulated Raman scattering in homogeneous plasma
[DE85-003120] 10 p1560 N85-19837
Role of multiple helicity nonlinear interaction of tearing modes in dynamo and anomalous thermal transport in the Reversed Pitch Field
[DE85-002176] 10 p1560 N85-19839
The 1984 review of the Applied Plasma Physics Program
[DE85-002136] 10 p1560 N85-19840
FRC translation dynamics and plasma confinement properties in FRX-C/T
[DE85-002366] 10 p1560 N85-19842
Resistive evolution of general plasma configuration
[DE85-002340] 10 p1561 N85-19843
Thermal barrier confinement experiments in TMX-U tandem mirror, revision 1
[DE84-017029] 10 p1561 N85-19844
A modeling analysis program for the JPL Table Mountain Io sodium cloud data
[NASA-CR-175493] 11 p1681 N85-20589
TMX-U neutral pressure measurement diagnostic systems
[DE85-000746] 11 p1730 N85-20881
Mirror fusion progress
[DE85-001187] 11 p1731 N85-20888
Covariant lie-transformed plasma action principle
[DE85-000285] 11 p1732 N85-20891
Design, construction and initial evaluation of an absolute, time-integrating/time-resolving spectrometer for the diagnostics of pulsed, high temperature plasma X-ray sources in the 100-10,000 eV region
[DE85-003526] 11 p1732 N85-20896
Edge diagnostics for tandem mirror machines
[DE85-001209] 11 p1733 N85-20902
Hollow cathode apparatus
[NASA-CASE-NPO-15560-1] 12 p1832 N85-21491
Investigation of plasma processes in electronic transition lasers
[AD-A149682] 12 p1834 N85-21506
The 60 GHz gyrotron development program
[DE85-000599] 12 p1836 N85-21522
Analysis and computations of microwave-atmospheric interactions
[AD-A149666] 12 p1869 N85-21854
Plasma mass and effective inductance in a small rainbow
[MRL-R-947] 12 p1936 N85-22162
Negative lithium emission from a tungsten surface in a plasma
[DE85-003456] 12 p1936 N85-22167
Spectroscopic study of sources and control of impurities in TMX-U: Revision 1
[DE85-004423] 12 p1937 N85-22170
Use of markets to elucidate reacting sputtering processes
[DE85-005723] 13 p2018 N85-22655
System for forming and focusing high current beam of deuterium ions 13 p2045 N85-22798
Calculation of amplitude-phase characteristics of signal scattered obliquely on meteor trail 13 p2073 N85-22948
Domain of applicability of asymptotic description of radio pulse fields near critical frequency 13 p2073 N85-22949
Meteoroidal impacts, plasma, fine structure of ringlets and spokes on Saturn's ring B 13 p2174 N85-23490
Interaction of the magnetospheric ions with the surfaces of the icy satellites of Saturn 13 p2174 N85-23491
Plasma production by meteoroid impact 13 p2174 N85-23492
Solar and stellar coronal plasmas
[NASA-CR-175623] 13 p2205 N85-23676
Numberical simulation of the effects of radially injected barium plasma in the ionosphere
[NASA-CR-175638] 14 p2354 N85-24542
Research on thermionic plasmas
[AD-A150863] 14 p2423 N85-24944
Current distribution in a plasma erosion opening switch
[AD-A150987] 14 p2424 N85-24949
ANTENA user guide
[DE85-004961] 14 p2424 N85-24953
Ionization equilibrium and equation of state in the solar interior 14 p2445 N85-25086
Plasma and magnetospheric research
[NASA-CR-171447] 15 p2591 N85-25976
Mean free paths, viscosity, and the limitations of perfect fluid hydrodynamics in the description of the quark-gluon plasma
[DE85-005501] 15 p2649 N85-26339
Finite orbit analysis for long wavelength modes in a plasma with a hot component
[DE85-006896] 15 p2658 N85-26404

Optimal control theory applied to fusion plasma thermal stabilization
[DE85-007599] 15 p2658 N85-28405
Eleven lectures on the physics of the quark-gluon plasma
[DE85-004321] 15 p2662 N85-28431
Space station as quark matter factory
[DE85-004606] 15 p2685 N85-28585
Digital image analysis of four-frame holographic plasma and neutral gas interferograms
[DE85-006387] 16 p2788 N85-27200
Equatorial F-region irregularity latitudinal extension and dynamo electric field
[INPE-3494-PRE/731] 16 p2828 N85-27433
Fundamentals of plasma simulation
[DE85-007699] 16 p2867 N85-27683
High efficiency ionizer using a hollow cathode discharge plasma
[DE85-006690] 16 p2868 N85-27693
The decomposition of gas phase formaldehyde by plasma discharge
[AD-A153202] 17 p2921 N85-28007
Geophysical plasmas and atmospheric modeling
[AD-A152805] 17 p2993 N85-28497
Time-integrated yield for the Joint European Torus (JET), April - September 1984
[AERE-M-3449] 17 p3036 N85-28797
Plasma processing of materials
[AD-A152398] 17 p3039 N85-28800
A numerical solution technique for multitemperature plasma hydrodynamics
[AD-A152701] 17 p3039 N85-28801
Multiple time-scale methods in particle simulations of plasmas
[DE85-007519] 17 p3040 N85-28808
Nonlinear plasma reactions on the antenna impedance of high transmission power satellites
[BMFT-FB-W-84-053] 18 p3192 N85-29799
Experiments in plasma initiation and laser absorption in flowing gases
[AD-A154303] 19 p3276 N85-30313
Plasma spray screen repair method
[AD-D011713] 19 p3281 N85-30346
Institute works on modeling thermonuclear plasma processes 19 p3296 N85-30435
Angle averaged Compton cross sections for degenerate electron gases
[AD-A154484] 19 p3371 N85-30908
New concept for pumping the edge plasma
[DE85-010180] 19 p3371 N85-30909
Publications from the Department of Plasma Physics and the Unit of Accelerator Technology, index and abstracts, 1984
[TRITA-EPP-84-13] 20 p3534 N85-31991
Nuclear responses in INTOR plasma stabilization elements
[DE85-010489] 20 p3535 N85-31995
Plasma erosion opening switch
[DE85-011384] 20 p3535 N85-31998
The space shuttle glow
[AD-A154937] 21 p3559 N85-32139
The plasma erosion opening switch
[AD-A154942] 21 p3580 N85-32259
Plasma mass and effective inductance in a small railgun
[AD-A154644] 21 p3589 N85-32304
Microwave-enhanced thin-film deposition 21 p3611 N85-32431
In-cavity laser IR spectrum analyzer for investigating non-steady-state processes 21 p3685 N85-32994
Infrared laser holography used in fusion plasma studies 21 p3687 N85-32995
Operational window for a plasma erosion opening switch used for voltage multiplication on pulsed power generators
[AD-A155482] 21 p3707 N85-33020
Research in particles and fields
[NASA-CR-176069] 21 p3724 N85-33103
Electron and ion cyclotron heating calculations in the tandem-mirror
[DE85-011658] 22 p3842 N85-33797
Confinement and heating of high beta plasma with emphasis on compact toroids. Compact toroid research
[DE85-011463] 22 p3846 N85-33821
Waves in Space Plasmas (WISP) 23 p3901 N85-34164
Theoretical and Experimental Beam Plasma Physics (TEBPP) 23 p3901 N85-34165
Electrodynamic tether 23 p3902 N85-34166
Magnetospheric multiprobes: MMP/CHEMSAT 23 p3902 N85-34171
Electronic imaging system and technique
[DE85-005740] 23 p3935 N85-34393
Some physical differences between sheet plasma and multicusp plasma as volume produced H- or D- ion sources
[IPPJ-728] 23 p3974 N85-34637
Effect of ECH and ICH on ambipolar potential in NBT-1M 23 p3978 N85-34661
Transports studies of ECH and ICRH-heated bumpy torus plasma in NBT-1M 23 p3978 N85-34662
Stability of ion distribution in strong ion shock structure 23 p3980 N85-34681
On the heat flux derived by the moment method in Lorentzian plasma between hot and cold walls 23 p3980 N85-34682
The role of cosmic rays and Alfven waves in the structure of the galactic halo
[OG-7.2-18] 23 p4016 N85-34885
Stochastic particle acceleration in flaring stars
[OG-8.3-9] 23 p4022 N85-34927
Very high energy probes of the quark-gluon plasma 24 p4147 N85-35708
Kinetic loss experiments on Mirte
[DE85-012826] 24 p4158 N85-35780
The phi-meson and Chiral-mass-meson production in heavy-ion collisions as potential probes of quark-gluon-plasma and Chiral symmetry transitions 24 p4175 N85-35884
Heavy flavours production in quark-gluon plasma formed in high energy nuclear reactions 24 p4175 N85-35886
The maximum depth of shower with E sub 0 larger than 10(17) eV on average characteristics of EAS different components 24 p4188 N85-35961

PLASMASPHERE
Magnetospheric plasma studies using data from the dynamics high and low altitude plasma instruments
[AD-A145751] 03 p0392 N85-12505
On the cause of X-line formation in the near-Earth plasma sheet: Results of adiabatic convection of Plasma-Sheet-Plasma
[AD-A145835] 03 p0396 N85-12525
Plasma and magnetospheric research
[NASA-CR-175675] 14 p2354 N85-24543
Electric fields in the plasma sheet and plasma sheet boundary layer 14 p2357 N85-24562
VLF emissions observed by ISIS Satellites during the IMS 14 p2366 N85-24621
Plasma and magnetospheric research
[NASA-CR-171447] 15 p2591 N85-25976
Images of the Earth's aurora and geocorona from the Dynamics Explorer Mission
[NASA-CR-175983] 18 p3136 N85-29423

PLASMATRONS
Investigation of heat exchange on models in subsonic jets of induction plasmatron 02 p0269 N85-11756
Simulation of thermal and electromagnetic processes in induction plasmatrons 12 p1841 N85-21552
Reducing electric power losses in discharge chamber of induction plasmatron 12 p1841 N85-21553

PLASMOIDS
U PLASMAS (PHYSICS)

PLASMONS
Brillouin scattering in underdense UV laser-produced plasmas
[DE84-015184] 04 p0567 N85-13614
Confinement of low-energy electrons near metallic surfaces for plasmon generation
[DE85-001119] 09 p1381 N85-18688
Inelastic tunnel diodes
[NASA-CASE-LEW-13833-1] 12 p1832 N85-21492
Solar energy converter using surface plasma waves
[NASA-CASE-LEW-13827-1] 12 p1876 N85-21768
The Valence- and conduction-band structure of the sapphire (1102) surface
[AD-A150001] 12 p1940 N85-22184
Research in the optical sciences
[AD-A150196] 13 p2159 N85-23401
Charge transfer, polarization and relaxation effects in the Auger lineshapes of Si
[AD-A150938] 14 p2252 N85-23954

PLASTIC COATINGS
Process for preparing highly optically transparent-colorless armomatic polyimide film
[NASA-CASE-LAR-13351-1] 12 p1811 N85-21380
X-ray photoelectron spectroscopy study of the compatibility of the explosive PETN with candidate plastic bonding materials
[DE85-010804] 19 p3251 N85-30161
New corrosion protection concept for very high voltage line towers
[BLL-OA-TRANS-2691-(6196.300)] 20 p3429 N85-31270

PLASTIC DEFORMATION
Evaluation of the role of diffusion creep in superplastic deformation 01 p0021 N85-10127
Fundamental studies of structure property relationship in transformation toughened ceramics
[DE84-015344] 01 p0033 N85-10204
Shear deformation plate continua of large double-layered space structures 01 p0059 N85-10391
Swaged Mo-5 percent W alloy and recrystallized commercially pure molybdenum 02 p0180 N85-11208
Plastic deformation and microstructural transformations of metals under shock waves 02 p0272 N85-11775
Features of plastic deformation and fracture of EP 741 nickel alloy under thermal strain 03 p0349 N85-12250
An experimental evaluation of the J integral in 50% sidegrooved compact geometry specimens
[AERE-R-11202] 03 p0374 N85-12386
Fast ions as probes in solid state research 03 p0430 N85-12740
Accuracy of preparation of three-dimensional reference grid
[BLL-M-35921-(5828.4)] 05 p0616 N85-13939
Iterative method for determining the distortion of elastic-plastic frames
[ISSN-0208-5658] 05 p0647 N85-14156
Compression of a band made of elastic, ideally Coulomb plastic material
[ISSN-0208-5658] 05 p0648 N85-14157
Use of coordinate functions to calculate deformation fields
[BLL-M-36010-(5828.4)] 07 p1028 N85-16524
The fundamentals of dislocation transport of hydrogen in bcc iron
[AD-A148143] 08 p1129 N85-17117
A study of constitutive relations for polycrystalline aluminum during finite dynamic plastic deformation 08 p1172 N85-17368
Determination of the elastic constants of inhomogeneous materials with X-ray diffraction
[AD-A148469] 08 p1173 N85-17393
Creep deformation of compacted decomposed granite soils 09 p1303 N85-18187
Study of influence of cold plastic deformation on aging of VT30 alloy 10 p1448 N85-19124
Diffusion welding with forced deformation of heat-resistant nickel-based dispersion hardened alloy 10 p1449 N85-19130
Role of hydrogen in processes of deformation and fracture of metals 10 p1449 N85-19132
Influence of plastic deformation on structural stability of nichrome-tungsten composite materials 11 p1599 N85-20060
Effect of temperature and deformation rate on hardness of copper 11 p1605 N85-20090
Stress corrosion cracking behavior of tungsten heavy alloys
[AD-A149843] 12 p1806 N85-21329
An orthogonal grid technique for studying internal deformation and energy absorption in target penetration
[AD-A149969] 12 p1860 N85-21665
Critical events in inelastic deformation of glassy polymers in adsorptive medium 13 p2014 N85-22634
Development and study of two-matrix glass fiber composite with increased transverse deformation 13 p2027 N85-22700
Fatigue life, crack initiation, and propagation of 304 stainless steel with non-proportional axial/torsional strain-paths 13 p2101 N85-23094
Studies of deformation in niobium by X-ray topographic methods
[AD-A150726] 14 p2427 N85-24965
Thermal stability of titanium alloys after cold plastic deformation 15 p2515 N85-25515
Plastic deformation of crystalline polymers
[AD-A152090] 16 p2755 N85-26999
Multinomial form of the solution of problems of the statistics of elastic rectangular disks
[REPT-17/1984] 16 p2797 N85-27244
Determination of failure characteristics of materials and structures
[AD-A152073] 16 p2800 N85-27266
Thermomechanical softening treatment for bearing and tool steels
[BLL-BISI-TRANS-22432-(9022.06)] 17 p2925 N85-28035
Influence of eutectic silicate inclusions on micro-processes during deformation and fracture of 12GS steel
[BLL-BISI-TRANS-22296-(9022.06)] 17 p2929 N85-28073
New method for determining stampability of sheet materials
[BLL-BISI-22486-(9022.06)] 17 p2972 N85-28360

State of stress and penetration of plastic deformation in forming
[BLL-BISI-22199-(9022.06)] 17 p2977 N85-28396
Effects of the structural state in thermo-bimetals on their resistance to microscopic plastic deformation
[BLL-BISI-TRANS-22403-(9022.06)] 17 p2979 N85-28412
Critical conditions for failure in materials subjected to high rates of loading
[AD-A153135] 17 p2980 N85-28420
Studies on surface processes during friction and wear
[AD-A153509] 18 p3117 N85-29296
State variable theories based on Hart's formulation
[DE85-009474] 19 p3239 N85-30082
Mechanical modification of friction surfaces of aluminum alloys by friction transfer 19 p3241 N85-30097
The initiation and growth of adiabatic shear bands
[AD-A154459] 19 p3287 N85-30382
Microstructural analysis of Pacific Ocean and Indian Ocean ultrabasites 19 p3291 N85-30405
On elastic-plastic fracture criterion 20 p3465 N85-31528
Fundamental investigations of failure during superplastic forming process
[AD-A154647] 21 p3568 N85-32194
Dynamic fracture of concrete and other heterogeneous materials
[AD-A154513] 21 p3598 N85-32343
The measurement of strain fields by X-ray topographic contour mapping
[AD-A154870] 21 p3599 N85-32348
Presentation of numerical simulation work in terminal ballistics using a few examples. Applications of the calculation model Program for Elastoplastic Simulation of Impacts (PEPSI) of the Franco-German Research Institute Saint Louis (ISL)
[ISL-CO-209/84] 22 p3834 N85-33741
Prediction of plasticity characteristics for three-dimensional fracture specimens comparison with experiment
[AD-A156425] 24 p4102 N85-35430

PLASTIC FILMS
U POLYMERIC FILMS

PLASTIC FLOW
NT TRESCA FLOW
Multiaxial yield behavior of 1100 aluminum following various magnitudes of prestrain
[DE84-013904] 05 p0617 N85-13949
The perfecting of the method of experimental-analytic solution of the problem of stationary plastic flow
[BLL-M-35838-(5828.4)] 05 p0634 N85-14065
The role of microstructure in the modelling of plastic flow in P/M superalloys at forging temperatures and strain rate 06 p0796 N85-15090
Flow and plasticity via nonequilibrium molecular dynamics
[DE85-001011] 10 p1555 N85-19804
Dependence of superplastic flow on state of grain boundaries 13 p2025 N85-22869
Influence of short-range order on deformation mechanisms in solid solutions
[DE85-006374] 14 p2258 N85-23869
On the accurate representation of large strain non-proportional plastic flow in ductile materials
[DE85-007106] 16 p2801 N85-27273
Conformational and mechanical properties at high strain rates
[AD-A153401] 17 p2959 N85-28272

PLASTIC MATERIALS
U PLASTICS

PLASTIC MEMORY
Effect of form memory in alloys based on Cu-Al systems 11 p1604 N85-20088
Production of shaped parts of NITINOL alloys by solid-state sintering
[AD-A152089] 16 p2749 N85-26986

PLASTIC PROPELLANTS
Effects of surface interactions and mechanical properties of PBXs (plastic bonded explosives) on explosive sensitivity
[AD-A146368] 06 p0773 N85-14944

PLASTIC PROPERTIES
NT ELASTOPLASTICITY
NT PHOTOPLASTICITY
NT SUPERPLASTICITY
NT THERMOPLASTICITY
NT VISCOPLASTICITY
NT YIELD POINT
Sensitivity analysis of limit state functions for probability-based plastic design 01 p0059 N85-10388
High temperature low-cycle fatigue mechanisms in single crystals of nickel-based superalloy Mar-M 200
[NASA-CR-174739] 03 p0331 N85-12130
Dependence of microplasticity of beryllium on grain size and heat treatment 03 p0353 N85-12273
Eta values for compact geometry specimens to calculate the J integral
[AERE-R-11126] 03 p0374 N85-12385
Numerical methods in metalforming 06 p0797 N85-15092
Finite element simulation of forging processes 06 p0797 N85-15093
Ultrahigh carbon steel
[AD-A147762] 08 p1128 N85-17113
Modeling of large-scale accretionary wedge and thin-skinned trust-and-fold belt mechanics 08 p1161 N85-17442
Nonlinear finite element analysis of elastic and elastic-plastic buckling of cylinders under complex combined loads 09 p1332 N85-18373
Influence of gaseous hydrogen on strength and ductility of nickel heat-resistant alloys 10 p1447 N85-19119
Flow and plasticity via nonequilibrium molecular dynamics
[DE85-001011] 10 p1555 N85-19804
Structure-phase state and properties of high-durability VAL8 alloy 11 p1597 N85-20046
Electron-plastic effect in metals 11 p1605 N85-20089
A remote source system for measuring relative positron annihilation line widths in individual slab cylindrical samples
[AERE-R-10549] 12 p1938 N85-22173
Some problems of optimum journal design for disk-drum rotors under antisymmetric loading 14 p2286 N85-24167
Effect of annealing procedures on structure and properties of VT6 alloy with initial large-grained structure 15 p2498 N85-25410
Effect of zirconium on forming ultrafine-grained structure in Al-Mg-Zr alloy 15 p2513 N85-25504
Dependence of plasticity of VT1-00 titanium alloy on microstructure 15 p2515 N85-25516
Predicting fully plastic mode 2 crack growth from an asymmetric defect
[AD-A152227] 16 p2801 N85-27269
Numerical resolution calculation for elastic-plastic impact problems
[AD-A152292] 16 p2801 N85-27270
On the accurate representation of large strain non-proportional plastic flow in ductile materials
[DE85-007106] 16 p2801 N85-27273
Properties of corrosion resistant stabilized ferritic steels
[BLL-BISI-TRANS-22519-(9022.06)] 17 p2925 N85-28039
The effect of microalloying with calcium and magnesium on the plasticity of Poldi AKN 20 Ni-based alloy
[BLL-BISI-TRANS-2174-(9022.06)] 17 p2929 N85-28075
The Shock and Vibration Digest, volume 17, no. 2
[AD-A153129] 17 p2977 N85-28400
Recent progress in the dynamic plastic behaviour of structures, part 4 17 p2978 N85-28402
Cyclic torsion of a circular cylinder and its residual stress distribution
[AD-A153347] 17 p2980 N85-28424
High tensile strength, punchable, hot rolled strips with good plasticity
[BMFT-FB-T-84-256] 18 p3078 N85-29040
Fatigue behavior of unidirectional FP-Al composites with circular holes
[AD-A153466] 18 p3121 N85-29322
Study of the influence of metallurgical factors on fatigue and fracture of aerospace structural materials
[AD-A153913] 18 p3122 N85-29328
Construction of constraint equation for stresses and strains
[BLL-M-36239-(5828.4)] 20 p3465 N85-31524
A numerical algorithm for endochronic plasticity and comparison with experiment 20 p3467 N85-31539

PLASTIC YIELDING
U PLASTIC DEFORMATION

PLASTICITY
U PLASTIC PROPERTIES

PLASTICIZERS
1-Fluoro-1,1,5-Trinitro-3-Oxa-5-Azahexane and method of preparation
[AD-D011421] 08 p1136 N85-17158
Plasticizer system for propellant compositions
[AD-D011502] 12 p1816 N85-21390
Plasticizer system for propellant compositions
[AD-D011508] 12 p1816 N85-21391
Azido nitramino ether containing solid propellants
[AD-D011511] 12 p1816 N85-21392
Plasticizer system for propellant compositions
[AD-D011514] 12 p1817 N85-21393
Plasticizer system for propellant compositions
[AD-D011516] 12 p1817 N85-21394
Plasticizer system for propellant compositions
[AD-D011517] 12 p1817 N85-21395
Propellant plasticizer
[AD-D011601] 20 p3434 N85-31306
Synthesis of energetic materials
[AD-A154887] 21 p3571 N85-32210
Polymer-water interaction studies 21 p3609 N85-32411
A new drawing technique for nylon 6 by reversible plasticization with iodine
[AD-A156272] 24 p4162 N85-35803

PLASTICS
NT ACRYLIC RESINS
NT CARBON FIBER REINFORCED PLASTICS
NT EPOXY RESINS
NT KEVLAR (TRADEMARK)
NT NYLON (TRADEMARK)
NT PHENOLIC RESINS
NT POLYAMIDE RESINS
NT POLYBUTADIENE
NT POLYESTER RESINS
NT POLYETHER RESINS
NT POLYETHYLENE TEREPHTHALATE
NT POLYETHYLENES
NT POLYISOBUTYLENE
NT POLYMETHYL METHACRYLATE
NT POLYPROPYLENE
NT POLYSTYRENE
NT POLYTETRAFLUOROETHYLENE
NT POLYVINYL ALCOHOL
NT POLYVINYL CHLORIDE
NT POLYVINYL FLUORIDE
NT REINFORCED PLASTICS
NT SYNTHETIC RESINS
NT TEFLON (TRADEMARK)
NT THERMOPLASTIC FILMS
NT THERMOPLASTIC RESINS
NT THERMOSETTING RESINS
NT VINYL COPOLYMERS
Comparison study of analytical methods for the determination of fluoride, chloride, and bromide in plastics
[DE84-015008] 04 p0470 N85-12999
Detection of cracks in a plastics pipe joint by reflection holography
[NPL-DMA(A)-87/MOM-70] 04 p0502 N85-13202
Method for forming electromagnetic-wave-screening composite 07 p0936 N85-15930
Polymer blends as high explosive binders
[DE85-001210] 11 p1611 N85-20131
Hydrolysis of plastic wastes with the aim of recovering and reprocessing the starting components (recycling)
[BMFT-FB-T-84-250] 12 p1885 N85-21828
Mechanism of strengthening plastics with rubbers 13 p2014 N85-22836
Chain dynamics and structure property relation in high impact strength polycarbonate plastic
[AD-A152011] 15 p2519 N85-25531
Status of French research in plastic batteries 15 p2530 N85-25603
Natural and accelerated aging of plastics 17 p2936 N85-28123
Qualitative and quantitative determination of aging by mechanical tests — plastics 17 p2977 N85-28393
Conservation and substitution technology for critical metals in bearings and related components for industrial equipment and opportunities for improved bearing performance
[PB85-178346] 18 p3082 N85-29069
Silvered polymer reflectors
[DE85-008782] 18 p3130 N85-29364
Plastic heliostat enclosure analysis
[DE85-009112] 18 p3130 N85-29367
X-ray photoelectron spectroscopy study of the compatibility of the explosive PETN with candidate plastic bonding materials
[DE85-010804] 19 p3251 N85-30161
Standard procedures to be used in specifying basic properties of plastics and polymers
[NPL-DMA(A)-99] 20 p3433 N85-31295

PLASTISOLS
NT SMOKE

PLATE (METAL)
U METAL PLATES

PLATE THEORY
On a general nonlinear theory of plates and shells: Formulation and applications 08 p1172 N85-17387
Numerical results of acoustic radiation, transmission and reflection of steel plate in water
[AMTE(N)-TM-84037] 13 p2155 N85-23378

PLATEAUS
NT PIEDMONTS
Oceanic plateaus, anomalous subduction, and the accretion of buoyant features at convergent margins 05 p0668 N85-14422
Basaltic pressure ridges: Formation and relationship to flow emplacement 13 p2186 N85-23567

Volcanism of the Colorado Plateau (basin and range transition): Implications for crustal processes
13 p2187 N85-23569

PLATELETS

The effect of +Gx acceleration on platelet activation as determined by plasma platelet factor 4 levels
[AD-A155881] 24 p4131 N85-35608

PLATES

An inverse source problem for elastic waves
03 p0371 N85-12368

Investigation of electromagnetic launcher behavior for impact fusion
[DE84-017401] 04 p0563 N85-13585

Modeling localized stress fields in composite laminates
[AD-A149630] 08 p1120 N85-17056

Large deformations of a nonlinear elastic solid and the diffusion of an ideal fluid treated as interacting continua
09 p1330 N85-18356

Coriolis effects on the vibrations of rotating beams, plates and shells 09 p1331 N85-18366

PLATES (STRUCTURAL MEMBERS)

NT ANISOTROPIC PLATES
NT CANTILEVER PLATES
NT CIRCULAR PLATES
NT ELASTIC PLATES
NT METAL PLATES
NT ORTHOTROPIC PLATES
NT PERFORATED PLATES
NT POROUS PLATES
NT RECTANGULAR PLATES
NT REINFORCED PLATES

Shear deformation plate continua of large double-layered space structures
01 p0059 N85-10391

Calculation of the optimum conditions for the forging of plates
[BLL-M-35757-(5828.4)] 02 p0169 N85-11260

Modeling the stress field in laminated composite plates near discontinuities
[PB84-219237] 03 p0327 N85-12103

The effects of microstructure on the temper embrittlement susceptibility of a Cr-2-1/4 1Mo forging
[AERE-R-11110] 03 p0334 N85-12151

Experimental study on transonic flutter characteristics of sweptback wing with core composite plates having different fiber orientations
[NAL-TR-827] 06 p0756 N85-14842

Evaluation of laterally loaded laminated glass units by theory and experiment
[PB85-111532/GAR] 09 p1300 N85-18166

Experimental verification of eddy-current flaw theory
[DE85-001288] 09 p1329 N85-18350

The problem of protecting the structure of a packet composite of optimal thinwall elements
10 p1444 N85-19101

Simple higher-order theory for laminated composite plates
[NASA-CR-174421] 10 p1496 N85-19445

Bending two-layer metal-polymer plates
11 p1604 N85-20085

Stress waves in an isotropic elastic plate excited by a circular transducer
[NASA-CR-3977] 11 p1650 N85-20390

Geometrically nonlinear analysis of laminated elastic structures
[NASA-CR-175609] 12 p1866 N85-21720

Machine analysis of resonance characteristics of plate-type radio electronic equipment constructions
13 p2085 N85-23018

Acoustic radiation from bilaminar plates
14 p2415 N85-24903

Symmetric composite laminate stress analysis
15 p2575 N85-25878

An elastic analysis of a plated bone to determine fracture gap motion
15 p2575 N85-25882

Design of shear deformable antisymmetric angle-ply laminates to maximize the fundamental frequency and frequency separation
[CSIR-TWISK-333] 15 p2577 N85-25892

Model for computing late detonations initiated in propellants by impact (XDT reactions)
[DE85-007377] 16 p2758 N85-27019

Dynamic response of shells and plates subjected to variable magnitude traveling loads
16 p2798 N85-27250

The nonlinear analysis of thick composite plates using a cubic spline function 16 p2798 N85-27252

Stress analysis of the space telescope focal plane structure joint
[NASA-CR-176797] 16 p2803 N85-27284

Solution to eigenvalue problems of antisymmetric cross-ply and antisymmetric angle-ply laminated plates using affine transformations
[AD-A165040] 17 p2917 N85-27990

Acoustic oscillations of rods and plates
17 p2944 N85-28170

Numerical analysis of end effects in symmetric laminated plates
[NAL-TR-850] 18 p3068 N85-28977

Ultrasonic testing of plates containing edge cracks
[NASA-CR-3904] 18 p3119 N85-29307

A control concept for large flexible spacecraft using order reduction techniques 20 p3415 N85-31193

Durability of reinforced hard-alloy draw plates
[BLL-M-36278-(5828.4)] 20 p3465 N85-31526

PLATES (TECTONICS)

On gravity from SST, geoid from Seasat, and plate age and fracture zones in the Pacific
[E85-10020] 02 p0217 N85-11433

Seismic studies in southern Alaska
04 p0515 N85-13286

A computational study of two possible intraplate earthquake triggering mechanisms
05 p0674 N85-14329

Oceanic plateaus, anomalous subduction, and the accretion of buoyant features at convergent margins
05 p0688 N85-14422

Summaries of physical research in the geosciences
[DE85-001882] 06 p0818 N85-15194

Some trends in the modern Earth sciences — plate tectonics and Earth's crust 06 p0820 N85-15207

Anomalous magnetic field in northwestern Pacific Ocean and Pacific Ocean plate kinematics
06 p0820 N85-15210

Delineation of major geologic structures in Turkey using SIR-B data 08 p1149 N85-17249

Basic structural features and probable mechanism of formation of the Kuril Island system
10 p1501 N85-19472

Tectonic position and formation of young alkaline provinces of continents and oceans
10 p1502 N85-19480

Tectonic lineaments in the cenozoic volcanics of southern Guatemala: Evidence for a broad continental plate boundary zone
[NASA-CR-175456] 10 p1505 N85-19499

Science Applications, part 2 11 p1643 N85-20347

Absolute movement of Pacific Ocean plate during last 120 million years 13 p2107 N85-23126

Crustal dynamics studies in China
[NASA-CR-175617] 13 p2132 N85-23265

A tectonic model of an incipient spreading center and its margins: The Northern Red Sea and the Dead Sea rift 13 p2140 N85-23266

Absolute movement of Pacific Ocean plate based on paleoclimatic and paleomagnetic data and trajectory of hot spots during last 120 million years
14 p2334 N85-24435

Lateral inhomogeneity of mantle surface in western Eurasia 14 p2344 N85-24497

Density characteristics of asthenosphere in Atlantic Ocean 19 p3204 N85-30423

Geometry, velocity structure and penetration depths of descending slabs in the western Pacific
19 p3319 N85-30574

Geodynamics Branch research program
[NASA-TM-86223] 20 p3489 N85-31688

Contemporary plate motions from LAGEOS
20 p3489 N85-31689

Intraplate crustal deformation due to continental collisions 20 p3490 N85-31693

New stations supporting crustal dynamics project VLBI measurements 20 p3491 N85-31701

Global geomorphology 21 p3601 N85-32359

Techniques, problems and uses of mega-geomorphological mapping
21 p3604 N85-32378

Planetary perspective. Report of Working Group Number 4 21 p3605 N85-32385

The Aravalli sequence of Rajasthan, India: A Precambrian continental margin?
21 p3720 N85-33084

Subduction zone tectonic studies to develop concepts for the occurrence of sediment subduction
[DE85-011794] 22 p3815 N85-33832

Scaling differences between large interplate and intraplate earthquakes
[NASA-CR-176149] 23 p3948 N85-34467

Thermal evolution of coastal California with implications for hydrocarbon maturation 24 p4115 N85-35509

A dynamic model of Venus's gravity field
[NASA-CR-176173] 24 p4169 N85-35845

PLATFORMS

Orbiter processing facility: Access platforms Kennedy Space Center, Florida, from challenge to achievement
08 p1102 N85-16968

Analysis of interaction of dynamically adjustable gyroscopes on elastic platform by finite-element method
13 p2048 N85-22822

PLATING

NT ELECTROPLATING
NT ION PLATING

Mechanical locking between multi-layer printed wiring board conductors and through-hole plating
[AD-D011477] 10 p1461 N85-19352

Study of high performance alloy electroforming
[NASA-CR-175494] 11 p1596 N85-20040

Trace metal determinations in nickel-plating baths by polarographic methods
[DE85-007084] 15 p2511 N85-25488

Plating density standards
[DE85-010014] 21 p3591 N85-32318

Towards the development of technological processes for the preparation of cadmium plated steel articles
[BLL-M-36315-(5828.4)] 23 p3913 N85-34248

PLATINUM

Methods for producing platinum-group metal coatings from molten alkali cyanides
[PB84-225994] 01 p0029 N85-10181

Platinum thin film resistors as accurate and stable temperature sensors
[NASA-TM-77726] 01 p0049 N85-10322

Platinum group nuggets in deep sea sediments
06 p0883 N85-15611

Dispersed metal-toughened ceramics and ceramic brazing
[NASA-CR-174284] 07 p0933 N85-15916

Subtractively normalized interfacial Fourier transform infrared spectroscopy of difluorobenzene adsorbed at polycrystalline platinum electrodes
[AD-A148660] 08 p1123 N85-17080

Metal atom diffusion in amorphous silica and at the silica surface
[DE84-017351] 09 p1360 N85-18674

Response time correlations for platinum resistance thermometers in flowing fluids
[NASA-CR-172523] 12 p1850 N85-21606

Advanced thin film thermocouples
[NASA-CR-175541] 12 p1850 N85-21607

Power control of induction equipment for founding optical glass in array of platinum crucibles
14 p2267 N85-24044

C2H(n) fragments on metal surfaces
[AD-A151474] 15 p2505 N85-25449

Methanol adsorption on Pt(111)
[DE85-006802] 17 p2923 N85-28017

New catalysts and new electrolytes for acid fuel cells
[DE85-009940] 19 p3307 N85-30498

Opticals constant at X-ray wavelengths
[DE85-009743] 19 p3355 N85-30795

Defect production and recovery in FCC metals irradiated at 4.2 K
[DE85-010477] 20 p3536 N85-32014

Lead, platinum, and other heavy elements in the primary cosmic radiation: HEAO-3 results sec wg032961 cb553097 20 p3543 N85-32048

Characterization of catalysts with metal-support effects and of the species adsorbed on their surfaces
[DE85-012254] 24 p4096 N85-35394

Applications of the mineral resources data system and the international strategic minerals inventory in mineral-resource assessments by region and commodity
24 p4105 N85-35451

PLATINUM ALLOYS

Compatibility experiments of facilities, materials, and propellants for electrothermal thrusters
[NASA-TM-86956] 12 p1795 N85-21260

CO adsorption on (111) and (100) surfaces of the Pt sub 3 Ti alloy. Evidence for parallel binding and strong activation of CO
[NASA-CR-176077] 21 p3565 N85-32176

PLATINUM COMPOUNDS

Interactions between corrosion and creep of uncoated and coated superalloys in sulfate melts
04 p0477 N85-13038

PLAYBACKS

Playback amplifier with high interference immunity
13 p2077 N85-22970

Operation of autotracking system in various video playback modes 16 p2764 N85-27055

PLETHYSMOGRAPHY

Vascular mechanisms of adaptation to antiorthostatic position 22 p3822 N85-33675

PLEXIGLASS (TRADEMARK)

U POLYMETHYL METHACRYLATE

PLIES

U LAYERS

PLOTTERS

SPLOT: A plot program for finite element data, function versus distance
[DE85-007129] 15 p2638 N85-26273

Isotropic plotter
[PB85-175651] 18 p3150 N85-29504

Defense Mapping Agency (DMA) raster-to-Vector analysis
[AD-A154153] 19 p3336 N85-30668
Defense Mapping Agency (DMA) raster-to-Vector benchmark testing
[AD-A154152] 19 p3338 N85-30663
Applied computer graphics in a geographic information system: Problems and successes
23 p3962 N85-34563

PLOTTING
Severe weather statistics STADTS decoder (SXW) and plotter (SWY)
[PB84-213693] 01 p0066 N85-10576
Plotting TDL coastal wind forecasts
[PB84-220789] 03 p0397 N85-12533
Computer-generated latitude and longitude templates for rapid determination of geographic positions in Alaska
04 p0516 N85-13288
A program to produce standard shewhart control charts for the statistics X-bar and R or S, P, NP, C, or U
[AD-A146971] 07 p1024 N85-16501
PLOT3D: An interactive graphics code for 3-dimensional plots
[AD-A147887] 07 p1026 N85-16514
Two-dimensional modeling for lineal and areal probabilities of weather conditions
[AD-A147970] 08 p1188 N85-17486
A FORTRAN plotting package for graphic VDUs
[AD-A148489] 08 p1204 N85-17577
User's manual: Menu-driven data graphing program for the Tektronix 7912AD and 7612D transient digitizer system
[DE85-002151] 09 p1370 N85-18810
Hurricane plotting program
[PB85-121432] 10 p1521 N85-19592
Plotfile appender
[PB85-109502] 11 p1688 N85-20616
Implementation of the computer program-system MOSS (Map Overlay and Statistical System) on a VAX-11 series computer under VMS
[AD-A149612] 12 p1914 N85-22019
Easyplot: An interactive, user-friendly graphics program
[AD-A150779] 14 p2404 N85-24824
NPLOT: An interactive plotting program for NASTRAN finite element models 15 p2573 N85-25869
Two interactive graphics postprocessors for NASTRAN 15 p2574 N85-25871
An unusual application of NASTRAN contour plotting capability 15 p2574 N85-25872
The interactive plotting program: GRAPH
[AD-A151371] 15 p2623 N85-26165
A heuristic solution to the spacing problem: Maximizing the minimum Euclidean distance among N points in a convex region
[AD-A152116] 16 p2855 N85-27603
Looking at more than three dimensions
[DE85-007764] 17 p3009 N85-29600
Computer program for plotting and fairing wind-tunnel data
[NASA-TM-86848] 20 p3387 N85-31009
A device-independent 2D plotting package written in FORTRAN
[RSRE-MEMO-3776] 23 p3956 N85-34514

PLOTTING INSTRUMENTS
U PLOTTERS

PLOWED FIELDS
U FARMLANDS

PLOWING
Prediction accuracy of the torques for rotary tillage by an analog tool
[AD-P004288] 09 p1406 N85-18865

PLUG NOZZLES
Jet noise suppression by porous plug nozzles
[NASA-CR-3613] 02 p0275 N85-11790
Experimental investigation of shock-cell noise reduction for dual-stream nozzles in simulated flight
[NASA-CR-3846] 04 p0557 N85-13549
Experimental investigation of shock-cell noise reduction for single stream nozzles in simulated flight
[NASA-CR-3845] 04 p0557 N85-13550
Thrust vectoring apparatus for maneuvering missile in flight
[AD-D011693] 19 p3226 N85-30004

PLUGS
Superconducting gyroscope research
[NASA-CR-171406] 15 p2560 N85-25795
Vapor-liquid phase separator studies
[NASA-CR-166545] 21 p3583 N85-32272

PLUMAGE
Microscopic identification of feathers in order to improve birdstrike statistics
[AD-P004187] 11 p1579 N85-19950

PLUMBANE
U LEAD COMPOUNDS
U METAL HYDRIDES

PLUMES
NT ROCKET EXHAUST
Collisional excitation cross sections
[AD-A145196] 01 p0117 N85-10600
Observed rate of tropospheric diffusion
[DE84-016047] 02 p0224 N85-11470
Modeling of propulsive jet plumes--extension of modeling capabilities by utilizing wall curvature effects
[AD-A148262] 03 p0362 N85-12324
Development of computational fluid dynamics at NASA Ames Research Center
[NASA-TM-86021] 04 p0452 N85-12866
Review of the attributes and performance of six urban diffusion models
[PB84-236850] 04 p0484 N85-13087
HS and E environmental sciences
[DE84-016183] 05 p0672 N85-14314
Measurements on the diffusion of hydrogen chloride in the waste gas plume of incineration ships in the North Sea. Part 1: Methodology, instrumentation and presentation of data
[GKSS-84-E-23-PT-1] 05 p0672 N85-14319
The properties of a round turbulent buoyant jet
[NAL-TR-826] 08 p0906 N85-15136
Shuttle system ascent aerodynamic and plume heating 08 p1103 N85-16975
Carbon vaporization/condensation effects
[NASA-TM-87430] 10 p1436 N85-19048
Meteorological support for the 1983 Deep Creek, Maryland experiment
[DE85-002616] 11 p1678 N85-20575
Preliminary analysis of tone-excited two-stream jet velocity decay
[NASA-TM-86951] 12 p1770 N85-21114
The influence on IR emission of engine parameters for an afterburn case. A sensitivity study on NATO infrared air target model (NIRATAM) version: 0.0
[AD-B089311L] 12 p1779 N85-21171
Hazardous air pollutants: Wet removal rates and mechanisms
[PB85-136626] 12 p1887 N85-21842
Time and space variability of turbulent concentration fluctuations
[AD-A149963] 12 p1896 N85-21898
Stagnation zone impaction on a simple terrain feature in stable flow 13 p2130 N85-23255
Deep water formation 15 p2501 N85-26030
A method for simulating 3-D aircraft flow fields with jet plume effects
[NASA-CR-175802] 16 p2699 N85-26564
The Terrain-Responsive Atmospheric Code (TRAC) for plume growth and dispersion in complex terrain
[DE85-010541] 19 p3309 N85-30513
Mechanisms of exhaust pollutants and plume formation in continuous combustion
[AD-A154169] 20 p3435 N85-31310
Manual for the computer program for the Gaussian plume model with percentile calculations
[KNMI-TR-60] 20 p3517 N85-31867
Laser beam interactions with vapor plumes during Nd:YAG laser welding on aluminum
[DE85-009793] 21 p3593 N85-32328
Assessment of the performance of an in-field Gaussian plume/puff model for overwater use
[AD-A155435] 21 p3614 N85-32480
VALMET: A valley air pollution model
[DE85-010820] 21 p3614 N85-32483
Modeling the exhaust of the pulsed plasma thruster
[AD-A155344] 21 p3707 N85-33018
Turbulence modelling for the prediction of turbulent jets: Wakes and plumes
[CFD/84/5] 22 p3784 N85-33447
Airborne cloud tracking measurements during the Three Mile Island nuclear station accident, Middletown, Pennsylvania. Date of survey: March - June 1979
[DE85-012080] 22 p3816 N85-33636
A dynamic model of Venus's gravity field
[NASA-CR-176173] 24 p4169 N85-35845

PLUNGERS
Design of inductive shift transducers
22 p3771 N85-33368

PLUTO (PLANET)
Research in planetary studies and operation of Mauna Kea Observatory
[NASA-CR-175618] 13 p2169 N85-23480
On the origin of Triton and Pluto
13 p2175 N85-23497
Photometric study of Pluto near perihelion. Part 2: Refinement of rotation period: Color indices
15 p2483 N85-25325
Magnetospheres of the outer planets
[AD-A154354] 19 p3384 N85-30996
Lightcurve CCD spectrophotometry of Pluto
20 p3545 N85-32057
Insolation changes on Pluto caused by orbital element variations
[AERONOMICA-ACTA-A-290-1984] 20 p3546 N85-32070

PLUTONIUM
NT PLUTONIUM ISOTOPES
NT PLUTONIUM 238
NT PLUTONIUM 239
General-purpose heat source development: Safety test program. Postimpact evaluation, design iteration test 5
[LA-10232-SR] 12 p1931 N85-22129
General-purpose heat source development: Safety test program. Postimpact evaluation, design iteration test 1
[LA-9880-SR] 12 p1931 N85-22131
Distribution of radium and plutonium in human bone
[DE85-005025] 13 p2142 N85-23298
Expected behavior of plutonium in the IFR fuel cycle
[DE85-006225] 18 p3181 N85-29725
Plutonium metal preparation and purification at Los Alamos, 1984
[DE85-010732] 19 p3239 N85-30085
Influence of chemical form, feeding regimen, and animal species on the gastrointestinal absorption of plutonium
[DE85-010291] 21 p3662 N85-32751
Measurement control for plutonium isotopic measurements using gamma-ray spectrometry
[DE85-013394] 24 p4097 N85-35397

PLUTONIUM COMPOUNDS
NT PLUTONIUM OXIDES

PLUTONIUM ISOTOPES
NT PLUTONIUM 238
NT PLUTONIUM 239
The I-Pu-Xe age of the Moon
04 p0584 N85-13729
Power flattening techniques for radioisotopic thermoelectric generators
[AD-A146365] 06 p0833 N85-15299
General-purpose heat source development: Safety test program. Postimpact evaluation, design iteration test
[LA-10034-SR] 23 p3969 N85-34606

PLUTONIUM OXIDES
Space nuclear safety program
[DE84-015074] 04 p0483 N85-12939
Space nuclear safety program
[DE84-015064] 04 p0483 N85-12940
Long-term exposure of pressed plutonium oxide heat sources to aquatic environments
[DE85-007365] 15 p2495 N85-25362
General-purpose heat source development: Safety test program. Postimpact evaluation, design iteration test
[LA-10034-SR] 23 p3969 N85-34606

PLUTONIUM 238
Environmental surveillance at Los Alamos during 1984
[DE85-011898] 22 p3811 N85-33606
Long-term exposure of (238) PuO2 to a terrestrial environment, volume 3
[DE85-011896] 22 p3840 N85-33781
Neutron flux, spectrum and dose equivalent measurements for a 4500-W(th) 238 PuO2 general purpose heat source
[DE85-011361] 22 p3841 N85-33786

PLUTONIUM 239
Historical review of californium-252 discovery and development
[DE85-010223] 19 p3362 N85-30844
The 1984 environmental monitoring program report for Idaho National Engineering Laboratory site
[DE85-011209] 22 p3812 N85-33611

PLUVIOGRAPHS
U RAIN GAGES
U RECORDING INSTRUMENTS

PLY ORIENTATION
Design sensitivity analysis of an antisymmetric angle-ply laminate
[CSIR-TWISK-316] 01 p0021 N85-10128
Design of shear deformable antisymmetric angle-ply laminates to maximize the fundamental frequency and frequency separation
[CSIR-TWISK-333] 15 p2577 N85-25862

PLYWOOD
Self-heating to ignition measurements and computation of critical size for solar energy collector materials
[PB85-183374] 20 p3485 N85-31883

PNEUMATIC CONTROL
Development of an electro-pneumatic anti-G valve for high performance fighter aircraft
[AD-A148468] 08 p1201 N85-17561

PNEUMATIC EQUIPMENT
NT GAS VALVES
Noise reduction of the exhaust from pneumatic tools
[BMFT-FB-HA-83-021] 02 p0276 N85-11799
Pneumatic turbulators: A device for drag reduction at Reynolds numbers below 5 million
08 p1071 N85-16791
Tire inflation/deflation system
[AD-D011459] 10 p1493 N85-19426

Pneumatic clamping device
[AD-D011544] 12 p1858 N85-21856
Pneumohydraulic drive 14 p2268 N85-24050
Dynamic response of fluid transmission lines
[AD-A151926] 16 p2782 N85-27171
Thermo-electric valve
[AD-D011682] 19 p3252 N85-30165

PNEUMATIC RESET
U PNEUMATIC CONTROL

PNEUMATICS
Acoustic cross-correlation flowmeter for solid-gas flow
[DE85-005988] 23 p3935 N85-34391

POCKELS EFFECT
U BIREFRINGENCE

PODS (EXTERNAL STORES)
Equipment for preflight test of an Electronic Countermeasures (ECM) avionic system
07 p0939 N85-15949

POGO EFFECTS
STS-1 Pogo analysis
[NASA-TM-87433] 11 p1591 N85-20007

POIKILOTHERMIA
NT AMPHIBIA
NT FROGS
NT TURTLES

POINCARE PROBLEM
Stability of periodic satellite motions relative to center of mass in circular orbit 16 p2718 N85-26780

POINCARE SPHERES
Behavior orbits of two coupled oscillators
02 p0282 N85-11833

POINT DEFECTS
NT VACANCIES (CRYSTAL DEFECTS)
Radiation effects on structural materials
[DE84-014771] 01 p0029 N85-10178
Complex formation and temperature stability of electrophysical properties of GaAs seminsulating single crystals 02 p0256 N85-11689
Diffusion mechanisms and point defects in transition-metal oxides
[DE84-016238] 04 p0571 N85-13639
Analysis of diffusion in an ion-implanted alloy using a phenomenological model
[AERE-R-11527] 11 p1609 N85-20120
Oxidation of nickel-aluminum and iron-aluminum alloys
[DE85-008930] 15 p2512 N85-25497
Current understanding of point defects and diffusion processes in silicon 20 p3481 N85-31632
Thin-film reliability and engineering overview
21 p3612 N85-32450
The development and evaluation of point defect models for the growth of passive films on single crystal, polycrystalline, and amorphous metal surfaces
[AD-A154685] 21 p3709 N85-33023
Defect interactions at high concentrations in solid oxide electrolytes
[DE85-011824] 22 p3807 N85-33560
Formation of amorphous silicon by light ion damage
[DE85-012605] 23 p3972 N85-34623

POINT MATCHING METHOD (MATHEMATICS)
U BOUNDARY VALUE PROBLEMS

POINT SOURCES
Algorithm for astronomical, point source, signal to noise ratio calculations
[NASA-TP-2397] 03 p0445 N85-12834
Concentrator optical characterization using computer mathematical modelling and point source testing
[NASA-CR-174109] 04 p0526 N85-13375
Selection of parameters for image decomposition by television system for recognition of group of point sources 06 p0785 N85-15016
Study of low-frequency sound with point source in stream with shear 05 p0625 N85-15239
Analysis of processing 09 p1412 N85-18905
Sky coverage, confusion, completeness and reliability
09 p1412 N85-18906
Consolidation around a point heat source
[PB85-116549] 11 p1682 N85-20601
Electrical line source and point source interactions with anomalies in the ground
[DE85-009777] 18 p3095 N85-29161
Source characterization of point-like and distributed sources of acoustic emission 20 p3523 N85-31910
Mean intensity of wave reflected by wavefront reversing mirror in turbulent medium 22 p3782 N85-33432
Nineteenth International Cosmic Ray Conference. OG sessions, volume 1
[NASA-CP-2376-VOL-1] 22 p3860 N85-33902
A search for gamma-ray point sources with the Carpet shower array
[OG-2.1-12] 22 p3864 N85-33928
Detection of gamma-ray lines from the direction of the Crab Nebula 22 p3866 N85-33943
All sky Northern Hemisphere 10(15) EV gamma-ray survey
[OG-2.6-3] 22 p3870 N85-33968
Search for ultra high energy gamma-rays from various sources
[OG-2.6-7] 22 p3870 N85-33969
Diffusion-convection function of cosmic rays
[SH-3.2-10] 23 p4004 N85-34825
The cosmic ray composition as viewed from the chemical abundances of the solar system
[OG-7.1-8] 23 p4013 N85-34869
Electron capture decay of cosmic rays: A model of the inhomogeneous interstellar medium
[OG-7.1-10] 23 p4014 N85-34871
The model-independence of cosmic ray source determinations
[OG-7.2-1] 23 p4014 N85-34873
The effects of newly measured cross sections in hydrogen on the production of secondary nuclei during the propagation of cosmic rays through interstellar H
[OG-7.2-2] 23 p4014 N85-34874
A Cerenkov imaging telescope for high energy gamma rays
[OG-9.3-13] 23 p4028 N85-34968
A new ultra high energy gamma ray telescope at Ohya mine
[OG-9.4-3] 23 p4029 N85-34970
The Buckland Park air shower array
[OG-9.4-4] 23 p4029 N85-34971
An EAS experiment at mountain altitude for the detection of gamma-ray sources
[OG-9.4-5] 23 p4029 N85-34972
A new array for the study of ultra high energy gamma-ray sources
[OG-9.4-7] 23 p4029 N85-34974
Cerenkov light images of EAS produced by primary gamma
[OG-9.5-3] 23 p4030 N85-34979
A method to improve observations of gamma-ray sources near 10 (15) eV
[OG-9.5-5] 23 p4030 N85-34982
Note on the detection of high energy primary cosmic gamma rays by air shower observation
[OG-9.5-9] 23 p4031 N85-34986
Expected rates with mini-arrays for air showers
[HE-4.7-8] 24 p4199 N85-36050
A large area cosmic muon detector located at Ohya stone mine
[HE-5.1-7] 24 p4201 N85-36072
A study of atmospheric neutrinos with the IMB detector
[HE-5.3-7] 24 p4205 N85-36101

POINT SPREAD FUNCTIONS
Light scattered from polished optical surfaces: Wings of the point spread function 06 p1252 N85-17911
Improved continuum definition in high-background IUE images 11 p1761 N85-21078
Spatial resolution estimation of LANDSAT-4 Thematic Mapper data 12 p1872 N85-21741

POINTING CONTROL SYSTEMS
The design, fabrication and delivery of a spacelab neutral buoyancy Instrument Pointing System (IPS) mockup — underwater training simulator
[NASA-CR-171233] 04 p0462 N85-12934
Heavy duty precision pan and tilt head
[AD-A146869] 04 p0509 N85-13248
Attempts to contruct two-dimensional image of Sun from observations made with RATAN-600 radiotelescope by relay race method 06 p0783 N85-15005
Pointing and control system design study for the space infrared telescope facility (SIRTF)
[NASA-CR-166612] 07 p0915 N85-15795
Precise control of flexible manipulators
[NASA-CR-174210] 07 p0973 N85-16178
The UKIRT centre section structural investigation — United Kingdom Infrared Telescope (UKIRT)
[UKIRT-22] 09 p1414 N85-18920
Summary presentation of the Constellations Panel
11 p1644 N85-20359
Modal control of structural systems
[AD-A149734] 12 p1790 N85-21235
Impact of magnetic isolation on pointing system performance in the presence of structural flexibility
[NASA-CR-172481] 16 p2732 N85-26861
Modeling and analysis of pinhole occulter experiment: Initial study phase
[NASA-CR-175978] 19 p3272 N85-30287
Antenna pointing of large flexible telecommunications spacecraft 20 p3409 N85-31156
Design and evaluation of control systems for large communications satellites 20 p3409 N85-31157
Wideband disturbance accomodation in precision flexible space structures 20 p3415 N85-31194
Hubble space telescope: Pointing error effects on nonlinear ball joints
[NASA-TM-86511] 20 p3545 N85-32058

POINTS
Point processes associated with extreme value theory
[AD-A151211] 15 p2640 N85-26260
Inference and state estimation for stochastic point processes
[AD-A151216] 15 p2640 N85-26261
On the exceedance point process for a stationary sequence
[AD-A152627] 17 p3018 N85-29665

POINTS (MATHEMATICS)
NT FIXED POINTS (MATHEMATICS)
NT INFLECTION POINTS
NT POINT SPREAD FUNCTIONS
Spacefilling curves and the planar travelling salesman problem
[AD-A149337] 10 p1551 N85-19788
A description of the Langley wireframe geometry standard (LaWGS) format
[NASA-TM-85767] 13 p1971 N85-22380
A comparison of methods of least squares adjustment of traverses
[AD-A153612] 18 p3170 N85-29645
Method of and apparatus for generating an interstitial point in a data stream having an even number of data points
[NASA-CASE-MFS-25319-1] 22 p3827 N85-33701

POISEUILLE FLOW
U LAMINAR FLOW

POISONING (REACTION INHIBITION)
Effects of H2S on molten carbonate fuel cells
[DE84-015166] 02 p0195 N85-11307

POISONING (TOXICOLOGY)
U TOXIC DISEASES

POISONS
NT DDT
NT PESTICIDES
NT URETHANES
Bibliography of venomous and poisonous marine animals and their toxins
[AD-A148409] 08 p1192 N85-17514
Toxic hazards tests for vehicles and other equipment
[AD-A149164] 20 p3506 N85-31797
Emergency modeling of hazardous air pollutants
[AD-A155441] 21 p3614 N85-32461

POISSON DENSITY FUNCTIONS
Reversals of the Earth's magnetic field
04 p0521 N85-13332
A note on two papers in dependent central limit theory
[CWI-MS-R8410] 05 p0722 N85-14638
Distribution of atmospheric radio interference
06 p0792 N85-15063
Limiting distributions of functionals of Markov chains
[AD-A147832] 07 p1036 N85-16577
Digital elevation model computation using fast Poisson solutions 08 p1175 N85-17412
Inequalities for the M/G/Infinity queue and related shot noise processes
[AD-A149015] 10 p1545 N85-19737
A note on equivalent random theory
[CWI-OS-R8410] 14 p2412 N85-24872
Point processes associated with extreme value theory
[AD-A151211] 15 p2640 N85-26260
Inference and state estimation for stochastic point processes
[AD-A151216] 15 p2640 N85-26261
Poisson and multinomial shadowing processes
[AD-A151600] 15 p2640 N85-26266
On the exceedance point process for a stationary sequence
[AD-A152627] 17 p3018 N85-29665
Upward continuation of surface gravity anomalies
[AD-A154973] 21 p3631 N85-32560
On the statistical significance of excess events: Remarks of caution and the need for a standard method of calculation
[OG-9.5-10] 23 p4031 N85-34987

POISSON EQUATION
Optimum replacement of a system subject to shocks
[AD-A145811] 03 p0372 N85-12374
Unrestricted convergence for generalized Poisson integrals
[CTH-MATH-1984-13] 04 p0556 N85-13540
On the connection between multigrid and cyclic reduction
[NASA-TM-86020] 09 p1373 N85-18629
Twisting of segmental shafts
14 p2279 N85-24119
Macro for fitting nonlinear models to Poisson distributed data
[DE84-008599] 14 p2412 N85-24871
Investigation of the numerical method of moments for digital computer determination of differential equations
[AD-A151886] 15 p2638 N85-26268
Polycrystalline semiconductor heterojunction modelling (CdS/CuInSe(sub)2)
[DE85-002913] 16 p2871 N85-27713
Covariant Poisson brackets for classical fields
[DE85-010085] 18 p3171 N85-29654

Poisson formula for radon transformation and numerical image reconstruction algorithm
21 p3697 N85-32973
Admissible convergence of Poisson integrals in symmetric spaces
[CTH-MATH-1985-04] 22 p3836 N85-33750
POISSON PROCESS
U POISSON DENSITY FUNCTIONS
U STOCHASTIC PROCESSES
POISSON RATIO
The effect of pressure on the mechanical properties of polymers. Part 2: Measurement of the time-dependent Poisson's ratio
[DE85-002139] 06 p0772 N85-14938
Development and study of two-matrix glass fiber composite with increased transverse deformation
13 p2027 N85-22700
Research program on the effect of pressure on the mechanical properties of polymers, part 2
[DE85-000995] 13 p2037 N85-22761
Limiting values of stress state index after rupture of metals
[BLL-BISI-TRANS-22293-(9022.06)]
17 p2978 N85-28407
POLAND
Fungi of Mt. Babia Gora. 2: Indicative value of macromycetes in forest associations. A: Initial considerations
[NASA-TM-77485] 01 p0094 N85-10832
Fungi of Mount Babia Gora. 3: The indicating value of macromycetes in the forest associations
[NASA-TM-77486] 01 p0094 N85-10833
Development, production, application of robots assessed
03 p0343 N85-12211
Fiber optics development, prospects assessed
03 p0343 N85-12214
Polar research in Earth sciences described
08 p1142 N85-17204
Finnair, LOT, SAS reps in USSR on present operations, plans
09 p1278 N85-18035
National Machine Tools Conference slated for 1985: Conference agenda, papers
10 p1460 N85-19202
Automation of the process of speech signal segmentation in an analogic-numeric system
[REPT-5/1984] 16 p2768 N85-27082
Meteorological measurements with motor gliders in Poland
24 p4122 N85-35555
POLAR AURORAS
U AURORAS
POLAR CAPS
Seasonal variations in Triton's atmospheric mass and composition
02 p0301 N85-11948
Magnetospheric plasma studies using data from the dynamics high and low altitude plasma instruments
[AD-A145751] 03 p0392 N85-12505
Atlas of polar cap energetic particle observations. Volume 1: TIROS-N, 1 January 1979 - 28 February 1981
[PB84-233402] 04 p0535 N85-13419
Polar rain: Solar coronal electrons in the Earth's magnetosphere
[NASA-TM-86150] 07 p1060 N85-16726
Sun-aligned polar cap auroral arcs
[AD-A146052] 08 p1185 N85-17472
An atlas of polar cap energetic particle observations. Volume 2: NOAA-6, 8 July 1979 to 10 May 1983
[PB85-109072] 12 p1891 N85-21868
Polar cap formation on Ganymede
13 p2174 N85-23486
Properties of filamentary sublimation residues from dispersions of clay in ice
13 p2197 N85-23629
Afternoon radar aurora and polar cap convection pattern
14 p2381 N85-24592
The polar caps and the climatic evolution of Mars
22 p3654 N85-33866
Comparisons of the North Polar Cap of Mars and the Earth's Northern Hemisphere snow cover
[NASA-TM-86191] 23 p3969 N85-34728
On magnetic pair production above fast pulsar polar caps
[OG-8.2-13] 23 p4020 N85-34909
POLAR CUSPS
Birkeland currents correlated with dc-electric fields observed during the CENTAUR BBX rocket experiments
[DRS-6-84] 06 p0634 N85-15311
POLAR GASES
Equation of state study for polar fluids
[PB85-204345] 24 p4076 N85-35282
POLAR METEOROLOGY
On development mechanisms for polar lows
20 p3495 N85-31727
POLAR ORBITS
Tracking requirements for precise ERS-1 orbit determination
03 p0380 N85-12431
Ice sheets as invariant surfaces for radar altimeter calibration and orbit determination
03 p0383 N85-12449
S3-3 ONR-116 data analysis
[AD-A149725] 12 p1889 N85-21855
Direct measurements of severe spacecraft charging in auroral ionosphere
13 p1991 N85-22480
Charging of DMSP/F6 spacecraft in aurora on 10 January 1983
13 p1991 N85-22481
Average and worst-case specifications of precipitating auroral electron environment
13 p1991 N85-22482
Auroral-polar cap environment and its impact on spacecraft plasma interactions
13 p1991 N85-22484
Three-dimensional calculation of shuttle charging in polar orbit
13 p1992 N85-22486
Polar orbit electrostatic charging of objects in shuttle wake
13 p1992 N85-22487
Utilization of the polar platform of NASA's Space Station Program for operational Earth observations
[PB85-152502] 14 p2240 N85-23895
Universal time effects in polar ionosphere
14 p2338 N85-24481
Resonant rotations of satellite in polar orbit in magnetic and gravitational fields
15 p2479 N85-25302
Availability of the ARGOS system based on the orbital characteristics of the TIROS-N satellites — oceanographic/meteorological data
16 p2813 N85-27352
The space station polar platform: NOAA systems considerations and requirements
[NOAA-TR-NESDIS-22] 22 p3740 N85-33182
Space Station Polar Platform: Integrating research and operational missions
[PB85-195279] 24 p4069 N85-35218
POLAR REGIONS
NT ANTARCTIC REGIONS
NT ARCTIC REGIONS
NT ROSS ICE SHELF
Convection of plasma in polar ionosphere, comparison of measurements from Cosmos-184 with model dependent on interplanetary magnetic field vector
02 p0160 N85-11066
Electric conductivities, currents and energy dissipation in the polar ionosphere
02 p0227 N85-11483
Occurrences of the polar slant E condition (SEC) at Narssarssuaq, Godhavn, Thule 1982
03 p0393 N85-12514
Mars polar volatiles: Topographic and geologic setting
[NASA-CR-174089] 04 p0581 N85-13708
Polar regions and climatic change
[PB84-237023] 05 p0688 N85-14421
Distribution of the K-corona over the polar regions of the solar disk: 1965-1983
[PB84-230077] 06 p0835 N85-15317
Region 1 birkeland currents from a global MHD simulation of the magnetosphere
[AD-A147435] 07 p0997 N85-16335
Diurnal freeze-thaw frequencies in selected regions of the high latitudes
[AD-A147276] 07 p1007 N85-16400
Polar research in Earth sciences described
08 p1142 N85-17204
Polar regions and climatic change: Appendix
[PB85-122679] 10 p1521 N85-19590
PMP-1 report: The fourth winter of PMP-1, 1981 - 1982: A winter with several interesting features
11 p1657 N85-20441
Passive microwave remote sensing for sea ice research
[NASA-CR-175570] 12 p1874 N85-21758
An atlas of polar cap energetic particle observations. Volume 2: NOAA-6, 8 July 1979 to 10 May 1983
[PB85-109072] 12 p1891 N85-21868
Carbonate chemistry of the Weddell Sea
[DOE/EV-110611/4] 12 p1898 N85-21916
Polar plasmas as observed by Dynamics Explorers 1 and 2
13 p1991 N85-22483
Mars: Stratigraphy of western highlands and polar regions
13 p2201 N85-23653
New directions in ARGOS instrumentation at Polar Research Lab (PRL)
14 p2323 N85-24350
Polar motions measurement study
[AD-A150890] 14 p2372 N85-24684
Space-time features of solar cosmic ray penetration into high latitude regions of Earth's magnetosphere based on Intercosmos-19 satellite data
15 p2481 N85-25310
SAM 2 measurements of the polar stratospheric aerosol, volume 5
[NASA-RP-1140] 15 p2590 N85-25970
A study of the generation mechanisms of high latitude and equatorial F-region irregularities using DE-2 data
[NASA-CR-175745] 16 p2825 N85-27423
Electron and ion distributions at high latitudes as measured by the Air Force polar orbiting satellites
[AD-A153242] 17 p2993 N85-28500
Preliminary documentation for the polar code
[AD-A154125] 19 p3336 N85-30887
Future prospects for a combined INMARSAT polar communication and search and rescue satellite system
20 p3406 N85-31137
Effects of Birkeland current limitation on high latitude convection patterns
[TRITA-EPP-84-10] 20 p3494 N85-31725
Airborne measurements of the vertical distribution of Arctic haze
21 p3647 N85-32657
Interplanetary magnetic field control of high-latitude electric fields and currents determined from Greenland magnetometer data
[DMI-GEOPHYS-PAPERS-R-69]
22 p3850 N85-33845
Comparisons of the North Polar Cap of Mars and the Earth's Northern Hemisphere snow cover
[NASA-TM-86191] 23 p3969 N85-34728
The influence of the Earth's magnetosphere on the high-energy solar protons
[SH-6.1-22] 23 p4046 N85-35093
The NORDA/FNOC (Naval Ocean Research and Development Activity's/Fleet Numerical Oceanography Center) Polar Ice Prediction System (PIPS)-Arctic: A technical description
[AD-A156332] 24 p4126 N85-35577
POLAR SUBSTORMS
Distribution of electric field near westward propagating bend in aurora
06 p0823 N85-15222
POLAR WANDERING (GEOLOGY)
Effects of the oceans on polar motion: Continued investigations
[E85-10037] 03 p0379 N85-12416
Earth rotation and polar wandering
14 p2399 N85-24785
Southern oscillation/El Nino excitation of the Earth's Chandler wobble
20 p3490 N85-31695
The Earth's wobble and associated ocean motions
20 p3490 N85-31696
POLARIMETERS
Imaging polarimeter-interferometer arrays for Tokamak measurements
[DE84-015916] 05 p0730 N85-14693
Far-infrared interferometry/polarimetry on the ISX-B Tokamak
[DE84-015401] 10 p1558 N85-19827
FIR interferometer/polarimeter system on ISX-B Tokamak
[DE85-001129] 11 p1731 N85-20867
Effects of focusing on HRS focal-plane polarimeter measurements
[DE85-004627] 13 p2160 N85-23406
Ultraviolet Spectrometer and Polarimeter (UVSP) software development and hardware tests for the solar maximum mission
[NASA-CR-175279] 14 p2305 N85-24271
X-ray polarimetry: The measurement of the polarization of solar flare X-rays and the design of a Compton polarimeter
14 p2441 N85-25059
Polarimetric image recorder
[AD-D011605] 16 p2787 N85-27192
Measurements of vector fields with diode array
18 p3204 N85-29880
Analysis of the new polarimeter for the Marshall Space Flight Center vector magnetograph
18 p3205 N85-29881
The solar vector magnetograph of the Okayama Astrophysical Observatory
18 p3205 N85-29882
Vector magnetic field observations with the Haleakala polarimeter
18 p3205 N85-29883
Program for observations of Halley's comet
22 p3732 N85-33138
POLARIMETRY
Observations of plasma bubbles and their zonal drift using polarimeters
[INPE-3219-PRE/572] 05 p0729 N85-14688
Optical polarization as a probe of the local interstellar medium
06 p0875 N85-15560
First results of submillimeter polarimetry
08 p1246 N85-17861
Instrumentation for submillimeter polarimetry
08 p1250 N85-17889
Ultraviolet and optical spectroscopy and polarimetry of the helium weak star HD 21699: Evidence for a magnetically controlled stellar wind
11 p1759 N85-21085
Modern problems in polarimetry of solid surfaces of cosmic bodies
13 p1977 N85-22409
The Saturn ring particles from optical reflectance polarimetry
15 p2571 N85-26484
The San Fernando Observatory video Stokes polarimeter
18 p3205 N85-29885
The new solar magnetograph for the Canary Islands Observatory THEMIS
18 p3205 N85-29886
Diagnostics of vector magnetic fields
18 p3206 N85-29889

The nature and geometry of infrared reflection nebulae 24 p4167 N85-35835

POLARIS MISSILES

Polaris guidance system
[AD-D011324] 07 p0900 N85-15704

POLARITONS

NT PLASMONS

Splitting of surface polariton spectrum by holographic grating 02 p0272 N85-11771

POLARITY

Response of the F2 layer to the polarity of the interplanetary magnetic field
[REPT-561] 03 p0377 N85-12404

Relations between the particle precipitation events in mid-latitudes, the ring current intensity and the polarity of the interplanetary magnetic field 04 p0519 N85-13316

Characteristics of EMI generated by negative metal-positive dielectric voltage stresses due to spacecraft charging 13 p1995 N85-22505

A multipole model of the observed cerebral cortex magnetic field
[AD-A152237] 16 p2642 N85-27526

Luminescence probe studies of ionomers. I: Steady-state measurements from nafion membrane
[AD-A152475] 17 p3029 N85-28730

Effects of a wavy neutral sheet on cosmic ray anisotropies
[SH-4.2-11] 23 p4008 N85-34849

Latitudinal gradients of cosmic rays and the polarity reversal of the heliospheric magnetic field: A preliminary evaluation
[SH-4.2-16] 23 p4008 N85-34853

Isotropic intensity waves and features of their occurrence
[SH-4.3-8] 23 p4032 N85-34993

Cosmic ray sidereal diurnal variation of galactic origin observed by neutron monitors
[SH-4.4-2] 23 p4033 N85-35000

The sidereal semi-diurnal variation observed at high zenith angles at Mawson, 1968-1984, and the polarity of the solar main field
[SH-4.4-6] 23 p4033 N85-35004

POLARIZATION

Dust properties determined from backscattering in the interplanetary and interstellar medium 03 p0446 N85-12838

POLARIZATION (CHARGE SEPARATION)

NT DIELECTRIC POLARIZATION
NT ELECTROLYTIC POLARIZATION

Giacobini-Zinner comet: Polarimetric and physical observations
[NASA-TM-77771] 01 p0130 N85-10694

Simulation of the electrochemical machining process
[DE85-003797] 11 p1616 N85-20159

Stress corrosion cracking behavior of tungsten heavy alloys
[AD-A148943] 12 p1806 N85-21329

Theoretical and experimental comparisons of nearfield electrogalvanic fields due to nonlinear polarization layers
[AD-A152085] 16 p2779 N85-27149

The Hanle effect applied to magnetic field measurements 18 p3204 N85-29678

Applications and investigations of second harmonic generation 19 p3367 N85-30678

Equation of state study for polar fluids
[PB85-204345] 24 p4076 N85-35262

POLARIZATION (SPIN ALIGNMENT)

Performing (p vector,)(c)n), (d vector, n) and (n vector, n) measurements with a rotating magnet beam swinger
[DE84-017003] 04 p0562 N85-13582

Electron spin polarization effects in low energy electron diffraction, ion neutralization and metastable atom deexcitation at solid surfaces
[DE84-016550] 04 p0572 N85-13649

Magnetic alignment theory and the interpretation of polarization 06 p0880 N85-15590

Review of polarized proton beam techniques and a report on the workshop on polarized beams
[DE85-004390] 12 p1930 N85-22127

Effects of focusing on HRS focal-plane polarimeter measurements
[DE85-004627] 13 p2160 N85-23406

Theoretical and experimental studies of stabilized metastable helium
[AD-A150708] 14 p2417 N85-24913

Proceedings of the Workshop on Polarized Targets in Storage Rings
[DE85-002704] 16 p2662 N85-27653

Spin-polarized quantum systems
[DE85-006914] 16 p2664 N85-27667

Polarized internal target apparatus
[DE85-011611] 19 p3354 N85-30793

Polarization of fast particle beams by collisional pumping
[DE85-011621] 22 p3838 N85-33764

POLARIZATION (WAVES)

NT CIRCULAR POLARIZATION
NT CROSS POLARIZATION
NT LINEAR POLARIZATION

Polarization of ultrasound transmitted through boundary of magnetically inactive and equatorially magnetized media 02 p0257 N85-11682

Diffraction of plane polarized waves by noncircular cylindrical cavity 02 p0269 N85-11754

Nonlinear electromagnetic waves in ferromagnetic conducting media 03 p0346 N85-12232

Computer molecular dynamics of 2-D water (ice) structures under shock
[AD-A145818] 03 p0372 N85-12375

X-ray polarization in highly oriented pyrolytic graphite
[DE84-015573] 05 p0613 N85-13917

Detailed performance calculations: Goddard Group, appendix D 05 p0676 N85-14341

Polarization in chemically doped hydrogen-rich glasses
[DE84-017486] 06 p0771 N85-14936

Characteristics of polarization grids made of parallel metal strips during hemispherical scanning 06 p0792 N85-15062

Optical polarization as a probe of the local interstellar medium 06 p0875 N85-15560

Intrinsic polarization basis of radar target observed by system employing diversity reception 07 p0949 N85-16015

Reduction of signal modulation caused by polarization in visible optical scanning systems
[AD-D011389] 07 p1042 N85-16620

Nonlinear optical studies of rydberg atoms using degenerate four-wave mixing
[AD-A146827] 07 p1043 N85-16623

Instrumentation for submillimeter polarimetry 08 p1250 N85-17889

Analysis of Jovian decametric data: Study of radio emission mechanisms
[NASA-CR-174206] 08 p1258 N85-17917

Polarization angles of linearly polarized antennas and radio waves in satellite communications
[PB85-131613] 11 p1626 N85-20240

Generalized radome BSE (radome boresight error) characterization using superposition techniques
[AD-P004354] 12 p1825 N85-21448

Modern problems in polarimetry of solid surfaces of cosmic bodies 13 p1977 N85-22409

Interference flux during reflection of heterogeneous waves 13 p2078 N85-22977

Specifics of polarization structure of repeated scattering background in optical laser sounding signals 14 p2342 N85-24485

Holoswitch, phase 1
[AD-A152212] 16 p2787 N85-27198

Results of simultaneous measurements of absorption and polarization of radio waves reflected from ionosphere 16 p2807 N85-27313

Incident beam polarization for laser Doppler velocimetry employing a sapphire cylindrical window
[NASA-TM-87064] 17 p3037 N85-28786

Magnetism at interfaces and surfaces, as probed by neutron scattering
[DE85-007987] 18 p3176 N85-29690

The San Fernando Observatory video Stokes polarimeter 18 p3205 N85-29685

The new solar magnetograph for the Canary Islands Observatory THEMIS 18 p3205 N85-29686

The vector magnetograph of the Sayan Solar Observatory 18 p3206 N85-29687

Sensitive detection of tunable diode laser absorption by polarization rotation
[DE85-009821] 19 p3277 N85-30322

Lidar system using polarization discrimination techniques for molecular air pollution monitoring 19 p3306 N85-30504

Description and operation of CHISQMO, INVRTS, VOIGEN, VOIGTV, SMEAR, RUFF, AND POSCAR in the Stokes Analysis Program
[PB85-180628] 19 p3384 N85-30991

The Faraday effect in ruby and corundum in strong magnetic fields 21 p3697 N85-32967

Preparation and use of very pure o-D2
[DE85-009415] 22 p3843 N85-33800

Transient analysis of electromagnetic reflection from dispersive materials
[PB85-200186] 24 p4154 N85-35753

POLARIZATION CHARACTERISTICS

Checking optical-polarization measurements at interfaces 02 p0271 N85-11770

Measurements of polarization characteristics of radiation field of on-board aircraft antennas 03 p0348 N85-12230

Modeling rain polarization effects to millimeter wave frequencies
[PB84-231042] 03 p0357 N85-12296

Collisional pumping for the production of intense spin-polarized, neutral beams: Target considerations
[DE85-003459] 11 p1723 N85-20841

Modern problems in polarimetry of solid surfaces of cosmic bodies 13 p1977 N85-22409

The Fe XIII 10747 A and Fe XIV 5303 A coronal emission lines polarization 14 p2448 N85-25111

Spin physics at BNL
[DE85-009768] 20 p3529 N85-31955

Influence of mirror anisotropy and Brewster window orientation on radiation characteristics of ring lasers 21 p3684 N85-32886

Analysis of Jovian decametric data: Study of radio emission mechanisms
[NASA-CR-176057] 22 p3851 N85-33848

POLARIZATION CHARTS

U GRAPHS (CHARTS)
U POLARIZATION (WAVES)

POLARIZED ELECTROMAGNETIC RADIATION

NT POLARIZED LIGHT
NT SYNCHROTRON RADIATION

Specific absorption rate in a sitting rhesus model at 225, 1290, and 5950 MHz for E, H, and K polarizations
[AD-A145435] 02 p0234 N85-11524

Detection of submillimeter polarization in the Orion Nebula
[NASA-TM-86013] 04 p0579 N85-13700

Relation between polarization of artificial low frequency radiation and parameters of auroral ionosphere 06 p0785 N85-15016

Explosive instability of strong electromagnetic wave in plasma 11 p1719 N85-20817

Modern problems in polarimetry of solid surfaces of cosmic bodies 13 p1977 N85-22409

Small aperture analysis of the dual TEM (transverse electromagnetic) cell and an investigation of test object scattering in a single TEM cell
[PB85-159952] 14 p2306 N85-24277

POLARIZED LIGHT

The Saturn ring particles from optical reflectance polarimetry 15 p2671 N85-26484

Holoswitch, phase 1
[AD-A152212] 16 p2787 N85-27198

Bandpass filter formed by serial gratings operating in a wood's anomaly region
[AD-D011660] 18 p3093 N85-29148

Polarized internal target apparatus
[DE85-011611] 19 p3354 N85-30793

POLARIZED RADIATION

NT POLARIZED ELECTROMAGNETIC RADIATION
NT POLARIZED LIGHT
NT SYNCHROTRON RADIATION

Considerations for upgrading modifications to the Marshall Space Flight Center's X-ray calibration facility 12 p1946 N85-22226

The ultraviolet excess of quasars 3: The highly polarized quasars PKS 0736+017 and PKS 1510-089
[NASA-CR-175576] 12 p1953 N85-22268

Generation and transfer of polarized radiation in the solar atmosphere: Physical mechanisms and magnetic-field diagnostics 18 p3206 N85-29690

Dynamic models of flux tubes in the interpretation of polarization measurements 18 p3206 N85-29691

Contribution functions for Zeeman-split lines, and line formation in photospheric faculae 18 p3207 N85-29693

Effect of polarized radiative transfer on the Hanle magnetic field determination in prominences: Analysis of hydrogen H alpha line observations at Pic-du-Midi 18 p3207 N85-29694

The inference of vector magnetic fields from polarization measurements with limited spectral resolution 18 p3207 N85-29696

Dual sense, circularly polarized helical antenna
[AD-D011680] 19 p3254 N85-30175

Commissioning the polarized beam in the AGS
[DE85-010958] 22 p3841 N85-33788

POLARIZERS

Characteristics of polarization grids made of parallel metal strips during hemispherical scanning 06 p0792 N85-15062

Polarization diversity addition to the 10 centimeter Doppler weather radar
[AD-A156062] 24 p4087 N85-35334

POLAROGRAPHS

U POLAROGRAPHY

POLAROGRAPHY

Homogeneous reaction involving components of different redox couples. 2: Polarographic studies of the interactions of alkali metal cations with anthracene and fluoranthene dianions in N,N-dimethylformamide and acetonitrile
[AD-A148687] 08 p1124 N85-17085

Trace metal determinations in nickel-plating baths by polarographic methods
[DE85-007084] 15 p2511 N85-25488

Electrochemical reduction of titanium in dimethyl sulphoxide
[BLL-OA-TRANS-3225-(6196.300)] 20 p3429 N85-31267

POLARONS
Free energy and effective mass of the polaron at finite temperatures
[TUM-M8401] 03 p0417 N85-12867
Peltier heat of a small polaron in a magnetic semiconductor
[DE85-000470] 14 p2430 N85-24983

POLICE
Civil law enforcement missions 06 p0751 N85-14812

POLICIES
NT ENERGY POLICY
NT PATENT POLICY
Polychlorinated biphenyls (PCBs) in transit system electrical equipment
[PB84-222207] 01 p0045 N85-10291
Acid rain and transported air pollutants: Implications for public policy
[PB84-222967] 01 p0071 N85-10469
Second Symposium on Space Industrialization — space commercialization
[NASA-CP-2313] 02 p0149 N85-11011
Legal considerations and cooperative opportunities for space commercial activities 02 p0150 N85-11013
Emergency Mathematics and Science Education Act
[GPO-29-561] 03 p0435 N85-12770
Federal Telecommunications Privacy Act of 1984
[H-REPT-98-815] 03 p0441 N85-12807
Aircraft navigation and landing technology: Status of implementation
[GPO-38-615] 04 p0454 N85-12883
The Expendable Launch Vehicle Commercialization Act
[GPO-30-838] 04 p0460 N85-12919
Review of Space Shuttle requirements, operations, and future plans
[GPO-39-101] 04 p0461 N85-12927
Assessing erosion on US cropland: Land management and physical features
[PB84-219252] 04 p0526 N85-13366
Publications of the Executive Office of the President: January 20, 1981 - June 30, 1984
[PB84-230671] 06 p0871 N85-15533
Issues and findings 07 p0914 N85-15782
An evaluation of the effect of establishing a minimum Economic Order Quantity (EOQ) on the Air Force EOQ item management system
[AD-A147121] 07 p1051 N85-16673
Evaluation of the effectiveness of the weighted guidelines to induce contractor's investment in cost reducing facilities equipment
[AD-A147586] 07 p1053 N85-16681
Technical order managers handbook: Utilization assessment
[AD-A147579] 07 p1055 N85-16684
National airspace review enhancement plan, revision 3
[AD-A150743] 08 p1082 N85-16852
An analysis of production competition and award methodology
[AD-A147775] 08 p1228 N85-17733
International cooperation and competition in civilian space activities
[OTA-ISC-240] 08 p1231 N85-17750
Deep seabed stable reference areas
[PB84-241470] 09 p1360 N85-18555
Commission operation. National Low-Level Radioactive Waste Management Program
[DOE/LLW-33T] 09 p1383 N85-18699
Worldwide report: Telecommunications policy, research and development
[JPRS-TTP-85-002] 10 p1475 N85-19309
Worldwide report: Telecommunications policy, research and development
[JPRS-TTP-85-006] 10 p1478 N85-19314
Communications satellite needs examined 10 p1476 N85-19317
Strategic management for organizational effectiveness. The effect of human resource planning on retention and related issues, volume 3
[AD-A149400] 10 p1566 N85-19876
Strategic management for organizational effectiveness. The effect of human resource planning on retention and related issues: Methodological appendix
[AD-A149401] 10 p1566 N85-19877
FAA policy regarding solid waste disposal facilities
[AD-P004196] 11 p1581 N85-19983
Synthetic fuels policy
[GPO-34-227] 11 p1613 N85-20143
French research minister on policy, technology transfer 11 p1618 N85-20182
Debris in the geostationary orbit ring, the endless shooting gallery: The necessity for a disposal policy 12 p1786 N85-21214
Orbital debris policy issues: Battelle involvement and some personal observations 12 p1787 N85-21218
Considerations for policy on man-made debris propagation control 12 p1787 N85-21219
Spacecraft hazard and shielding requirements 12 p1788 N85-21224
Systems research on China in year 2000 12 p1820 N85-21418
Oversight review of the five-year outlook report on science and technology
[GPO-41-058] 12 p1949 N85-22243
1984 science and technology posture hearing with the director of the Office of Science and Technology Policy
[GPO-41-060] 12 p1949 N85-22244
USSR report: Space
[JPRS-USP-85-001] 13 p1977 N85-22403
INMARSAT marine satellite organization 13 p1985 N85-22458
USSR report: Science and technology policy
[JPRS-UST-85-002] 13 p2167 N85-23442
Militarization of space activity in United States 15 p2486 N85-25360
West Europe report: Science and technology
[JPRS-WST-84-014] 15 p2536 N85-25647
USSR report: Space
[JPRS-USP-85-004] 16 p2717 N85-26772
West Europe report: Science and technology
[JPRS-WST-84-024] 17 p2945 N85-28183
Social and political problems in Soviet basic research
[AD-P004565] 17 p3048 N85-28860
New ESA director on Ariane, space station, future trends 18 p3066 N85-29096
Inventory policy for high backorder items
[AD-A153696] 18 p3198 N85-29840
Computer center policy
[AD-A154416] 19 p3338 N85-30681
Methodology for assessing benefits and costs of government information collection
[DE85-010594] 19 p3381 N85-30975
FAA regulation of 9-seat and under passenger aircraft
[GPO-42-703] 20 p3391 N85-31032
West Europe report: Science and technology
[JPRS-WST-85-020] 20 p3438 N85-31333
Navy information systems: Planning, policy, organization, and management
[PB85-176113] 20 p3541 N85-32038
Opportunities for policy historians: The evolution of the US civilian space program 23 p4057 N85-35147
A guide for new environmental coordinators
[AD-A156327] 24 p4113 N85-35498

POLISHED METALS
U METAL POLISHING

POLISHING
NT ELECTROPOLISHING
NT METAL POLISHING
Development of a measuring procedure for the automatic evaluation of the flatness of reflective surfaces
[BMFT-FB-T-84-168] 03 p0421 N85-12686
Fabrication of monocrystalline GaAs solar cells utilizing NaCl sacrificial substrates
[DE84-013016] 11 p1673 N85-20544

POLITICS
International cooperation and competition in space
[GPO-38-001] 02 p0295 N85-11911
Statement of Otho E. Eskin, Director, Office of Advanced Technology, Department of State 02 p0295 N85-11914
Area handbook series. Honduras: A country study
[AD-A146510] 06 p0827 N85-15253
Outer space law: A problem of astronautics
[NASA-TM-77760] 07 p1055 N85-16697
Social and political problems in Soviet basic research
[AD-P004565] 17 p3048 N85-28860
Technology and Soviet political choices
[AD-P004566] 17 p3048 N85-28861
U.S.-China conference on science policy
[PB85-176345] 19 p3360 N85-30971
Satellites and politics: Weather, communications, and earth resources 23 p4057 N85-35144

POLLEN
Geographic and stratigraphic distribution of Miocene palynomorphs in north Idaho 03 p0390 N85-12498
Global paleoclimatic data base for 6000 years BP
[DE85-006828] 15 p2600 N85-26024

POLLUTANTS
U CONTAMINANTS

POLLUTION
NT AIR POLLUTION
NT ENVIRONMENT POLLUTION
NT GLOBAL AIR POLLUTION
NT INDOOR AIR POLLUTION
NT NOISE POLLUTION
NT OIL POLLUTION
NT WATER POLLUTION
Practical application of earth resistivity methods in phase 2 of the installation restoration program
[AD-P004148] 09 p1348 N85-18484
Acid rain: Towards automated monitoring 16 p2829 N85-27444
The seasonal cycle of atmospheric CO in the Southern Hemisphere 16 p2830 N85-27447
Protective systems and maintenance policies for marine environments 22 p3750 N85-33345
Solar energy meteorological research and training program: Region 4
[DE85-011783] 22 p3816 N85-33640

POLLUTION CONTROL
Operating experiences of reverse osmosis plants treating Rand Water Board (RWB) water: Pitfalls and problems 01 p0023 N85-10142
Demonstrating air quality improvements: A review of alternatives
[DE84-014274] 01 p0070 N85-10462
Acid rain and transported air pollutants: Implications for public policy
[PB84-222967] 01 p0071 N85-10469
Fabric filter system study
[PB84-229749] 03 p0342 N85-12206
Electrostatic augmentation of fabric filtration: Reverse-air pilot unit experience
[PB84-230002] 03 p0343 N85-12207
Effect of sealants of the sound absorption coefficients of acoustical friable insulating materials
[AD-A148541] 08 p1218 N85-17674
Proceedings of the Environmental Systems Symposium (13th) held at Bethesda, Md., 20-22 March 1984
[AD-A148194] 09 p1346 N85-18471
The application of emissions trading to DoD installations
[AD-P004136] 09 p1346 N85-18472
Compatible goals: Defense and environmental protection
[AD-P004137] 09 p1347 N85-18473
Environmental and energy audits of Air Force government owned-contractor operated installations
[AD-P004138] 09 p1347 N85-18474
Assessment of environmental costs at ordnance activities
[AD-P004140] 09 p1347 N85-18476
Protocol for aquifer cleanup decision making at military installations
[AD-P004151] 09 p1349 N85-18487
Versator divertor experiment: Preliminary designs
[DE84-017159] 09 p1393 N85-18769
Experimental investigation of a pulse combustor: Flow visualization by Schlieren photography
[DE85-002662] 11 p1636 N85-20304
Considerations for policy on man-made debris propagation control 12 p1787 N85-21219
Role of biological assessment in effluent control
[PB85-116101] 12 p1885 N85-21830
Papers from the Symposium on Emissions: The Value of Incentives and Guidelines for Control
[S-336] 15 p2590 N85-25957
Analytical methods for determination of POHC (Principal Organic Hazardous Constituents) in combustion products
[PB85-161578] 16 p2747 N85-26955
Environmental management needs
[DE85-007859] 18 p3133 N85-29405
Space station trace contaminant control 18 p3157 N85-29550
Control of acid deposition precursors through dry scrubbing
[DE85-010281] 19 p3235 N85-30058
Reduction of pollutant formation in combustion processes
[DE85-010181] 19 p3309 N85-30512
Technical guide for estimating fugitive dust impacts from coal handling operations, volume 2
[DE85-010939] 19 p3309 N85-30514
Technical guide for estimating fugitive dust impacts from coal handling operations. Volume 1: Project summary
[DE85-010948] 19 p3309 N85-30515
Third US/USSR Symposium on Particulate Control
[PB85-190890] 19 p3310 N85-30522
Sources of copper air emissions
[PB85-191138] 19 p3310 N85-30523
State-of-the-art of aquifer restoration. Volume 1: Sections 1 through 8
[PB85-161071] 20 p3478 N85-31612
State-of-the-art of aquifer restoration. Volume 2: Appendices A through G
[PB85-161089] 20 p3478 N85-31613
Historic emissions of sulfur and nitrogen oxides in the U.S. from 1900 to 1980. Volume 1: Results
[PB85-191195] 20 p3487 N85-31674

Historic emissions of sulfur and nitrogen oxides in the U.S. from 1900 to 1980. Volume 2: Data
[PB85-191203] 20 p3457 N85-31675
EPA (Environmental Protection Agency) research program guide, FY-1985, October 1, 1984 - September 30, 1985
[PB85-181881] 20 p3457 N85-31676
Environmental monitoring at Lawrence Livermore National Laboratory: 1984 report
[DE85-011583] 22 p3811 N85-33606
Technology of off-gas treatment for liquid-fed ceramic melters
[DE85-012467] 22 p3812 N85-33610
A guide for new environmental coordinators
[AD-A156327] 24 p4113 N85-35496
Review of US NOx abatement technology
[PB85-193522] 24 p4114 N85-35501

POLLUTION MONITORING
Mobile source exposure estimation
[PB84-224518] 01 p0095 N85-10643
Water resources by orbital remote sensing: Examples of applications
[E85-10015] 02 p0217 N85-11428
Analysis of Santa Barbara oxidant study
[PB84-229277] 03 p0388 N85-12486
Development and evaluation of cloud water collectors
[PB84-232529] 04 p0540 N85-13437
Portable instrument for the detection and identification of air pollutants
[DE84-014767] 05 p0672 N85-14316
Gas chromatographic determination of content of harmful substances in air of industrial locations
06 p0761 N85-14866
Measurement and analysis of ambient carbon monoxide concentrations for project-level air quality impact studies
[PB85-104602/GAR] 09 p1350 N85-18492
Laser air pollution monitoring system planned for Moscow
10 p1500 N85-19465
Comparative evaluation of GC/MS (Gas Chromatography/Mass Spectrometry) data analysis processing
[PB85-125664] 11 p1596 N85-20037
Research in environmental biology reviewed
11 p1622 N85-20211
Solid sorbent air sampler
[NASA-CASE-MSC-20663-1] 11 p1636 N85-20301
Development of a low cost electrochemical CO monitor based on stripping voltammetry
[PB85-113470] 11 p1637 N85-20312
User's guide for the Photochemical Box Model (PBM)
[PB85-137164] 11 p1662 N85-20602
Role of biological assessment in effluent control
[PB85-116101] 12 p1885 N85-21830
Evaluation of complex terrain air quality simulation models
[PB85-116485] 12 p1886 N85-21835
Atlantic Coast Unique Regional Atmospheric Tracer Experiment (ACURATE)
[PB85-128460] 12 p1886 N85-21839
Arabian gulf circulation — pollution monitoring
14 p2331 N85-24412
Utilization of remote sensing data in the evaluation of air pollution characteristics in the south coast/Southeast Desert Air Basin
[PB85-162063] 16 p2622 N85-27407
Symposium on Atmospheric Sciences in South Africa
[CSIR-S-331] 16 p2629 N85-27442
Elemental analysis of aerosols in Tranvaal urban and power-producing areas using time and size-resolved samples 16 p2629 N85-27443
Acid rain: Towards automated monitoring
16 p2629 N85-27444
A wind-bivane/microprocessor system for on-line prediction and display of pollutant distributions
16 p2630 N85-27449
A study of gas solid reactions using coated piezoelectric detectors
[AD-A153047] 17 p2920 N85-29001
Elemental tracers of source regions of contaminants in precipitation
[DE85-007366] 18 p3133 N85-29407
Application of climatological analysis to minimize air pollution impacts in California
[PB85-172663] 18 p3149 N85-29502
Atmosphere monitoring requirements
18 p3156 N85-29553
Contamination control for increased crew productivity
18 p3158 N85-29555
Sources of copper air emissions
[PB85-191136] 19 p3310 N85-30523
Analysis of aldehydes and ketones in the gas phase
[PB85-181665] 20 p3426 N85-31261
VALMET: A valley air pollution model
[DE85-010820] 21 p3614 N85-32463
Laser Elektronika-01 for air pollution control lidar
21 p3664 N85-32667
Chemoreception and detection of micropollutants by means of a telemetric bionic detector
[DRIC-T-7460] 22 p3810 N85-33600
Environmental monitoring at Lawrence Livermore National Laboratory: 1984 report
[DE85-011593] 22 p3811 N85-33606
Modeling of auto exhaust smog chamber data for EKMA development
[PB85-188492] 22 p3813 N85-33619
Airborne cloud tracking measurements during the Three Mile Island nuclear station accident, Middletown, Pennsylvania. Date of survey: March - June 1979
[DE85-012060] 22 p3816 N85-33638

POLLUTION TRANSPORT
Space Shuttle Environmental Effects: The First 5 Flights
[NASA-CR-171812] 01 p0069 N85-10457
Solution of contaminant transport equations using an orthogonal-upstream finite element scheme
[DE84-014266] 01 p0070 N85-10463
The use of fixed-bed adsorber models to predict the fluxes of toxic substances in groundwaters and soil environments
[PB84-202563] 01 p0071 N85-10468
Acid rain and transported air pollutants: Implications for public policy
[PB84-222967] 01 p0071 N85-10469
Arctic haze: Meteorological aspects of long-range transport 02 p0230 N85-11499
Review of the attributes and performance of six urban diffusion models
[PB84-236650] 04 p0484 N85-13087
Transformation processes and wet deposition on the urban scale
[DE84-015294] 04 p0539 N85-13432
Spatial and temporal interpolation of NEROS radiosonde winds
[PB84-232545] 04 p0540 N85-13436
Calms processor (CALMPRO) user's guide
[PB84-229467] 04 p0540 N85-13439
Mean maximum mixing heights for northern Asia for the winter of 1978
[DE84-015960] 05 p0672 N85-14315
Cross-Appalachian Tracer Experiment (CAPTEX '83)
[PB84-236641] 06 p0834 N85-15307
NOx emissions near a heat pump with gas motor
[BLL-WH-782-(9091.6F)] 07 p0995 N85-16319
Climate and water quality 07 p1002 N85-16368
Installation restoration program. Phase 2: Stage 1 problem confirmation study, Duluth International Airport Duluth, Minnesota
[AD-A148318] 08 p1089 N85-16885
Determination of the laws governing the changes in the standard deviations of the distribution of pollution based on observations of the atmospheric turbulence spectrum and the possibility of simulating it in the laboratory
[BLL-TR-T6373/BG/MRS14663/84]
08 p1179 N85-17431
Penetration of the atmosphere by flammable mixtures as a result of spillage of LNG on the ground
08 p1179 N85-17432
Modeling of turbulent dispersion of neutral and buoyant contaminants released from two dimensional sources — air pollution
[VKI-TN-150] 08 p1180 N85-17436
Preliminary post-emplacement safety analysis of the subseabed disposal of high-level nuclear waste
[DE84-011162] 08 p1221 N85-17692
Meteorological factors responsible for high CO (carbon monoxide) levels in Alaskan cities
[PB85-115137/GAR] 09 p1350 N85-18493
TRAN-STAT: Statistics for environmental studies
[DE85-000829] 10 p1513 N85-19547
Study of pollutant dispersion in an urban street canyon
[DE85-002648] 11 p1677 N85-20571
Comparison of MESOI atmospheric dispersion estimates with data and estimates from other models
[DE85-002372] 11 p1678 N85-20572
Models and parameters for environmental radiological assessments
[DE81-027154] 11 p1678 N85-20573
Meteorological support for the 1983 Deep Creek, Maryland experiment
[DE85-002816] 11 p1678 N85-20575
Turbulence parameters impacting dispersion in an urban convection boundary layer
[PB85-116036] 11 p1682 N85-20598
Atmospheric dispersion of hypergolic liquid rocket fuels, volume 1
[AD-A149597] 12 p1817 N85-21399
ELECT groundwater transport research code
[DE85-003284] 12 p1884 N85-21824
Air quality criteria for ozone and other photochemical oxidants. External review draft, volume 2
[PB85-126043] 12 p1886 N85-21836
Hazardous air pollutants: Wet removal rates and mechanisms
[PB85-139626] 12 p1887 N85-21842
Continued research in mesoscale air pollution simulation modeling. Volume 6. Further studies in the modeling of microscale phenomena
[PB85-137370] 12 p1887 N85-21844
Observational study of transport in the free troposphere
[PB85-144145] 12 p1887 N85-21845
Sector analysis of relevant meteorological parameters for long range transport of air pollutants
[NR-27] 12 p1893 N85-21882
Drifting ice as mechanical factor in purifying and polluting hydrosphere 13 p2106 N85-23132
Arabian gulf circulation — pollution monitoring
14 p2331 N85-24412
PLUVIUS: A generalized 1-dimensional model of reactive pollutant behavior, including dry deposition, precipitation formation, and wet removal, 2nd edition
[DE85-005542] 14 p2353 N85-24538
Adjustment of the national dispersion model for air pollution from elevated sources
[KNMI-TR-57] 14 p2353 N85-24540
Operational methods for calculating atmospheric dispersion
[BLL-CE-TRANS-8040-(9022.09)]
15 p2586 N85-25955
Field validation of 6-particle puff model
[DE85-004073] 15 p2589 N85-25962
Analytical methods for determination of POHC (Principal Organic Hazardous Constituents) in combustion products
[PB85-161578] 16 p2747 N85-26955
Limiting profiles in contaminant transport through porous media — ground water pollution
[REPT-84-31] 17 p2960 N85-28282
Quality assurance for RESOLVE (Research on Operations-Limiting Visual Extinction). A visibility study in the California desert
[AD-A152383] 17 p2992 N85-28494
Vertical redistribution of a pollutant tracer due to cumulus convection
[PB85-172971] 18 p3134 N85-29415
Diffusion of trace gases in the ground level boundary layer 18 p3148 N85-29489
Global model of transport of pollutants in atmosphere
19 p3297 N85-30439
MELSAR: A mesoscale air quality model for complex terrain. Volume 2: Appendices
[DE85-010991] 19 p3310 N85-30519
Effect of vertical shear on regional-scale trajectories in near-frontal conditions
[DE85-007554] 19 p3317 N85-30561
Preliminary investigation of dispersion of pollutants in model building wake flows using bipolar space charge
[IC-AERO-84-04] 20 p3487 N85-31671
Modeling of chemical transformations of SO(x) and NO(x) in the polluted atmosphere: An overview of approaches and current status
[PB85-173169] 20 p3487 N85-31677
Errors and parameterizations of sub-grid scale processes in regional-scale atmospheric models
20 p3488 N85-31682
VALMET: A valley air pollution model
[DE85-010820] 21 p3614 N85-32463
Application of Particle Induced X-ray Emission analysis (PIXE) to aerosol long range transport studies
21 p3648 N85-32665
Sahara Desert dust transport to the south
21 p3648 N85-32666
Measurements of giant salt nuclei from inland in east China 21 p3648 N85-32668
on the transport of large condensation nuclei in the atmosphere at various altitudes over the territory of the USSR 21 p3653 N85-32696
MELSAR: A mesoscale air quality model for complex terrain. Volume 1: Overview, technical description and user's guide
[DE85-010943] 22 p3811 N85-33608
Airborne cloud tracking measurements during the Three Mile Island nuclear station accident, Middletown, Pennsylvania. Date of survey: March - June 1979
[DE85-012060] 22 p3816 N85-33638
Studies in thermo-hydro-chemical transport in porous and fractured media
[DE85-012555] 23 p3949 N85-34473
User's guide to the MATHEW/ADPIC models
[DE85-012952] 23 p3966 N85-34587
MATADOR (Methods for the Analysis of Transport And Deposition Of Radionuclides) code description and user's manual
[TR85-901402] 23 p3966 N85-34592

POLOIDAL FLUX
Versator divertor experiment: Preliminary designs
[DE84-017159] 09 p1393 N85-18769

The continuous spectrum of an axisymmetric, self-gravitating equilibrium in the presence of a poloidal magnetic field 12 p1959 N85-22315
The continuous spectrum of an axisymmetric equilibrium with a mixed poloidal and toroidal magnetic field with gravity included 14 p2450 N85-25128
Comparison study of toroidal-field divertors for a compact reversed-field pinch reactor [DE85-009591] 18 p3189 N85-29781
Poloidal variations in toroidal fusion reactor wall power loadings [DE85-009505] 19 p3362 N85-30648
Observation of helical sawtooth oscillations in a tokamak [DE85-012062] 23 p3963 N85-34703

POLYACETYLENE
Control of electronic, magnetic and optical properties of doped polyacetylene conductors [AD-A150117] 12 p1814 N85-21375
Polymeric electrolytes for ambient temperature lithium batteries [DE85-001032] 12 p1835 N85-21518
Electron-donor dopant, method of improving conductivity of polymers by doping therewith, and a polymer so treated [DE85-011640] 22 p3752 N85-33257
Electrically conductive doped block copolymer of polyacetylene and polyisoprene [DE85-006500] 24 p4082 N85-35301

POLYACRYLATES
U ACRYLIC RESINS

POLYAMIDE RESINS
NT KEVLAR (TRADEMARK)
NT NYLON (TRADEMARK)
Thermoset-thermoplastic aromatic polyamide containing N-propargyl groups [NASA-CASE-LAR-12723-1] 11 p1610 N85-20123
Process for preparing highly optically transparent-colorless aromatic polyimide film [NASA-CASE-LAR-13351-1] 12 p1811 N85-21360
Fire and heat resistant laminating resins based on maleimido and citraconimido substituted 1-(diorgano oxyphosphonyl)methyl-2,4- and 2,6-diaminobenzenes [NASA-CASE-ARC-11533-1] 12 p1812 N85-21364
Determination of the viscosity number of thermoplastics in dilute solution; polyamides (PA) [NASA-TM-77673] 24 p4081 N85-35296

POLYATOMIC GASES
NT DIATOMIC GASES

POLYATOMIC MOLECULES
NT DIATOMIC MOLECULES
Collisional energy exchange in polyatomic molecules [AD-A147710] 08 p1219 N85-17679
Identification and properties of molecular systems of potential use in solar-pumped lasers [NASA-CR-175804] 16 p2769 N85-27207
Crossed molecular beam studies of the reactions of oxygen and fluorine atoms [AD-A153302] 17 p2921 N85-29008

POLYBUTADIENE
Diblock copolymers of polystyrene/1,2 polybutadiene and polystyrene/polybutene-1: Molecular structure, morphology and mechanical properties [AD-A144960] 01 p0033 N85-10201
Synthesis and characterization of a 1,4 Polybutadiene/isotactic polypropylene block copolymer [AD-A148199] 08 p1133 N85-17142
Deuterium isotope effect on the compatibility between polystyrene and polybutadiene [AD-A148551] 00 p1134 N85-17145
LL-100: A new polybutadiene (resin system for radome applications) [AD-P004368] 12 p1826 N85-21462
Effects of triazine components on physicochemical properties of polybutadiene: urethane block copolymers 13 p2014 N85-22635

POLYCARBONATES
Properties of miscible polymer blends [AD-A147090] 07 p0931 N85-15903
Development of a heterogeneous laminating resin system [NASA-CR-172459] 09 p1288 N85-18089
Chain dynamics and structure property relation in high impact strength polycarbonate plastic [AD-A152011] 15 p2519 N85-25531
Laminated thermoplastic radome [AD-D011664] 18 p3079 N85-29045

POLYCHLORINATED BIPHENYLS
Polychlorinated biphenyls (PCBs) in transit system electrical equipment [PB84-222207] 01 p0045 N85-10291
Soil extraction kit [AD-D011736] 22 p3742 N85-33190

POLYCRYSTALS
Life prediction and constitutive models for anisotropic materials 02 p0144 N85-10976
Surface chemistry of palladium [DE84-014572] 02 p0173 N85-11183
The current status of diamond and cubic boron nitride composites 02 p0178 N85-11194
DOE/SERI polycrystalline thin-film photovoltaic research [DE84-004516] 02 p0223 N85-11464
High temperature deformation of hot-pressed polycrystalline orthoenstatite [NASA-CR-174026] 02 p0285 N85-11861
Development of a polysilicon process based on chemical vapor deposition of dichlorosilane in an advanced Siemen's reactor [NASA-CR-174148] 04 p0483 N85-13083
Elastic wave propagation through polycrystals [DE84-016772] 04 p0558 N85-13554
Process research of polycrystalline silicon material (PROPSM) [NASA-CR-174130] 05 p0619 N85-13982
Electron channeling and EBIC studies of polycrystalline silicon sheets [DE84-004515] 05 p0670 N85-14309
Analysis of spin echo signals in multi-pulse experiment 06 p0792 N85-15065
Process Research On Polycrystalline Silicon Material (PROPSM) 06 p0830 N85-15276
Subtractively normalized interfacial Fourier transform infrared spectroscopy of difluorobenzene adsorbed at polycrystalline platinum electrodes [AD-A148660] 08 p1123 N85-17080
The fundamentals of dislocation transport of hydrogen in bcc iron [AD-A148143] 08 p1129 N85-17117
The effect of tantalum on the structure/properties of two polycrystalline nickel-base superalloys: B-1900 + Hf MAR-M247 [NASA-CR-174847] 09 p1294 N85-18127
Process Research on Polycrystalline Silicon Material (PROPSM) [NASA-CR-175461] 10 p1509 N85-19523
Quaternary narrow-band semiconductors (HgTe)x (InSb)1-x for far-infrared detectors [AD-A149350] 10 p1562 N85-19852
Effect of macrostructure on durability of polycrystalline graphite 11 p1605 N85-20091
Development of a polysilicon process based on chemical vapor deposition of dichlorosilane in an advanced Siemen's reactor [NASA-CR-174445] 11 p1672 N85-20532
Summary of recent research on mechanical behavior of polycrystalline solids [DE85-004601] 12 p1942 N85-22199
Texture independent determination of residual stress in polycrystalline aggregates using Rayleigh waves [AERE-R-11483] 12 p1943 N85-22203
High sheet resistance, arsenic implanted polycrystalline silicon for integrated circuit resistors [DE85-004355] 13 p2065 N85-22902
The cyclic stress-strain behavior of nickel-base superalloy poly- and single crystals 14 p2254 N85-23969
Solar cells based on polycrystalline silicon with isothermal potential barriers along grain boundaries 14 p2275 N85-24091
Angular dependence of the Rayleigh-surface wave velocity in polycrystalline metals with small anisotropy [AERE-R-11595] 15 p2509 N85-25476
Design of ductile polycrystaline N3Al alloys [DE85-005572] 15 p2511 N85-25491
Summary of recent investigations of the mechanical properties of polycrystalline solids [DE85-005776] 15 p2511 N85-25492
An analysis of the economics of turning titanium alloys with polycrystalline diamond tools 15 p2567 N85-25841
Process Research on Polycrystalline Silicon Material (PROPSM) [NASA-CR-175761] 15 p2587 N85-25951
Thin-film polycrystalline silicon research [DE85-002906] 15 p2593 N85-26434
Secondary ion mass spectrometry studies of solids and surfaces [AD-A151744] 16 p2745 N85-26939
Mechanical properties of polycrystalline alpa titanium [BLL-BISI-TRANS-21923-(9022.09)] 17 p2924 N85-29029
Semicrystalline casting process development and verification [DE85-007665] 18 p3081 N85-29058
Electrohydrodynamic process for the production of large area polycrystalline silicon sheet [DE85-006761] 19 p3261 N85-30225
Photoelectronic properties of zinc phosphide crystals and heterojunctions [DE85-006777] 19 p3307 N85-30501
Neutron scattering study of the heavy fermion system UBe-13 [DE85-010955] 19 p3358 N85-30604
Compositional analysis of silicon 20 p3480 N85-31626
Surface passivation and junction formation using low energy hydrogen implants 20 p3480 N85-31628
The effect of diffusive hydrogen segregation on fracture of polycrystalline nickel [AD-A155238] 21 p3567 N85-32186
Electrical and mechanical properties of intercalated graphite fibers [AD-A155560] 21 p3570 N85-32205
Thermoelectric properties of beta-boron and some boron compounds [DE85-011976] 21 p3582 N85-32270
Basic ice nucleation mechanisms on mono and microcrystals and ice forming nuclei. Theoretical analysis and experimental results achieved in the laboratory over the past ten years: Review paper 21 p3642 N85-32629
Mirror reflection of charged particles from +amorphous and polycrystalline surfaces 21 p3690 N85-32927
The development and evaluation of point defect models for the growth of passive films on single crystal, polycrystalline, and amorphous metal surfaces [AD-A154685] 21 p3709 N85-33023
Method for preparing Pb-(beta)-aluminum ceramic [DE85-011685] 22 p3752 N85-33256
Aluminum work function: Effect of oxidation, mechanical scraping and ion bombardment [NASA-TM-87079] 23 p3915 N85-34265
Low noise polycrystalline semiconductor resistors by hydrogen passivation [AD-D011721] 23 p3927 N85-34338
Noise in sodium beta alumina crystals [AD-A156025] 24 p4161 N85-35798

POLYESTER RESINS
System for rapid repair of damaged airfield runways [AD-D011325] 07 p0909 N85-15754
Properties of miscible polymer blends [AD-A147090] 07 p0931 N85-15903
The synthesis and characterization of Poly(Oxy(2-Methyl-1,3-Phenylene) Methyl-1,3 -Phenylene) Oxyterephthaloyl)Oxy [AD-A148269] 08 p1133 N85-17143
Interactions between F-111 fuselage fuel tank sealants. Part 2: Variation in performance properties of polysulfides after contact with polyester degradation products [AD-A149777] 12 p1812 N85-21368
Scale-up of vanadium trineodecanoate [AD-A149935] 12 p1813 N85-21370
Fluorinated polyesters [AD-D011611] 16 p2753 N85-26988

POLYESTERS
Synthesis and characterization of unique liquid crystalline block copolyesters. A proposal for a polymer research center at the Atlanta University [AD-A147280] 07 p0932 N85-15907
Stabilized unsaturated polyesters [NASA-CASE-NPO-16103-1] 19 p3078 N85-29043
Polyesters: A review of the literature on products of combustion and toxicity [NBSIR-85-3139] 20 p3439 N85-31298
Polymerizable ultraviolet stabilizers 21 p3606 N85-32406
Impact fracture mechanism of polymer plates containing a heavy inner material 23 p3908 N85-34215

POLYETHER RESINS
NT POLYMETHYL METHACRYLATE
Optimization of the injection process for thermostatic polyether-ether-ketone (Peek) thermoplastics reinforced with short carbon fibers [SNIAS-842-422-102] 04 p0480 N85-13082
Structure-property relationships in thermoplastic elastomers. Part 1: Segmented polyether-polyurethanes [AD-A148043] 08 p1133 N85-17138
Characterization of novel binders based on energetic thermoplastic elastomers [AD-A148993] 10 p1451 N85-19139
Crystallinity determination by curvefit procedure for a semi-crystalline polymer [NASA-TM-86412] 15 p2517 N85-25520
Phenoxy resins containing pendent ethynyl groups and cured resins obtained therefrom [NASA-CASE-LAR-13282-1] 19 p3068 N85-29973
Mechanical properties of aligned short carbon fiber reinforced PES and PI laminates [ESA-TT-868] 20 p3422 N85-31240

POLYETHYLENE TEREPHTHALATE
Description and characterization of deuterated polymers for the analysis with neutron scattering 03 p0431 N85-12748

Prediction of the long term stability of polyester-based recording media
[PB85-160133] 14 p2262 N85-24019

POLYETHYLENES
NT POLYETHYLENE TEREPHTHALATE
Nuclear Magnetic Resonance of Polymeric Materials
[AD-A145078] 01 p0032 N85-10192
13C and 1H NMR (Nuclear Magnetic Resonance) studies of solid polyolefines
[AD-P003909] 01 p0032 N85-10195
Equibiaxial extension of two polymer melts: Polystyrene and low density polyethylene
[AD-A144893] 01 p0032 N85-10200
Small angle neutron scattering (SANS) on polymer-oligomer mixtures and on deformed polyethylene melts 03 p0432 N85-12750
Apparatus for measuring dielectric characteristics of polymer materials in millimetric range of wavelengths at 4.2-300 K temperatures 06 p0788 N85-15032
Characterization of porosity in porous polymer implant materials
[PB85-119960] 10 p1454 N85-19161
Structural basis for the mechanical properties of polyethlenes
[PB85-149771] 11 p1613 N85-20142
Characterization and optimization of polyethylene resins and gas pipe
[PB85-118511] 12 p1815 N85-21382
Characterization of poly(ethylene oxide) drawn by solid state extrusion
[AD-A150967] 14 p2260 N85-24006
Uniaxial orientation of linear low density polyethylene
[AD-A151037] 14 p2261 N85-24009
Plastic deformation of crystalline polymers
[AD-A152080] 16 p2755 N85-26999
Properties of polyethylene gas piping materials
[PB85-187045] 18 p3082 N85-29068
Polyethylene imino-metal salt solid electrolyte
[AD-D011678] 19 p3305 N85-30485
Orientation and strength of semi-crystalline polymers 20 p3432 N85-31294
Interaction of solutes with stretched polymers
[AD-A154662] 21 p3569 N85-32196
Electron-donor dopant, method of improving conductivity of polymers by doping therewith, and a polymer so treated
[DE85-011640] 22 p3752 N85-33257
Polyethylene solidification of low-level wastes
[DE85-012568] 22 p3843 N85-33799
Method for making a low density polyethylene waste form for safe disposal of low level radioactive material
[DE85-006401] 23 p3920 N85-34292
Sensitivity of single and multiple cosmic ray neutrons to the surrounding medium in a lead-free monitor
[SH-9.1-10] 23 p4051 N85-35125
Structure and properties of polyethylene films used in heavy lift balloons
[NASA-CR-176227] 24 p4083 N85-35306

POLYGONS
NT RECTANGLES
Classical free-streamline flow over a polygonal obstacle
[NASA-CR-172448] 01 p0048 N85-10301
Origin of Martian polygonal terrain: Preliminary results 13 p2191 N85-23591
Chemical applications of topology and group theory. 17: An information theoretical approach to polyhedral symmetry
[AD-A152821] 17 p2919 N85-27995
Fourier coding and reconstruction of complicated contours
[REPT-84-39] 17 p3022 N85-28691
Shadow volumes for non-planar polygons 23 p3965 N85-34580
Reachable grasps on a polygon: The convex rope algorithm
[AD-A155913] 24 p4138 N85-35647

POLYHEDRONS
NT PARALLELEPIPEDS
NT PYRAMIDS

POLYIMIDE RESINS
Thermal deformation measurements of heat-resistant structural materials for aircraft by electro optical displacement transducer
[NAL-TR-810] 03 p0325 N85-12092
Polyimide resin characteristics, test
[DOT-24.322] 04 p0479 N85-13049
Flame resistant fibrous materials development
[NASA-CR-167817] 07 p0820 N85-15827
Phosphorus-containing imide resins
[NASA-CASE-ARC-11368-2] 12 p1809 N85-21347
Chemical approach for controlling nadimide cure temperature and rate with maleimide
[NASA-CASE-LEW-13770-3] 12 p1809 N85-21350
Chemical approach for controlling nadimide cure temperature and rate with maleimide
[NASA-CASE-LEW-13770-4] 12 p1810 N85-21351
Chemical approach for controlling nadimide cure temperature and rate
[NASA-CASE-LEW-13770-5] 12 p1810 N85-21352
Development and study of two-matrix glass fiber composite with increased transverse deformation 13 p2027 N85-22700
Adsorption behaviour of nitrogen compounds on to porous polymer beads and applications to atmospheric sampling
[BLL-DRIC-TRANS-7399-(3623.66)] 13 p2036 N85-22753
The effects of water and hydrogen on materials used in integrated circuit packages
[AD-A151893] 15 p2516 N85-25529
Chemical control of nadimide cure temperature and rate
[NASA-CASE-LEW-13770-2] 18 p3069 N85-28982
Chemical approach for controlling nadimide cure temperature and rate
[NASA-CASE-LEW-13770-6] 19 p3232 N85-30039
Adhesive evaluation of LARC-TPI and a water-soluble version of LARC-TPI
[NASA-TM-86428] 19 p3248 N85-30136
Graphite/PMR polyimide composites with improved toughness
[NASA-TM-87061] 21 p3561 N85-32148
Permeation of mixed penetrants through glassy polymer membranes
[AD-A155605] 21 p3570 N85-32207
Rigid zeolite containing polyurethane foams
[DE85-006406] 23 p3919 N85-34286

POLYIMIDES
NT KAPTON (TRADEMARK)
Thermoplastic/melt-processable polyimides 04 p0466 N85-12961
Effect of substituted phenylnadimides on processing and properties of PMR polyimide composites
[NASA-TM-86902] 06 p0770 N85-14929
Evaluation of colorless polyimide film for thermal control coating applications
[NASA-TM-86341] 07 p0930 N85-15894
The wear of small polyacetal and polyimide gears in vacuum — spacecraft gears
[ESA-ESTL-058] 08 p1169 N85-17374
Tribological properties of graphite-fiber-reinforced, partially fluorinated polyimide composites
[NASA-TM-86926] 09 p1298 N85-18153
Characterization of a thermoplastic polyimidesulfone
[NASA-TM-86358] 10 p1450 N85-19135
Process for preparing solvent resistant, thermoplastic aromatic poly(imidesulfone)
[NASA-CASE-LAR-12858-2] 11 p1610 N85-20124
Process for preparing essentially colorless polyimide film containing phenoxy-linked diamines
[NASA-CASE-LAR-13353-1] 11 p1611 N85-20128
Oxidation protection coatings for polymers
[NASA-CASE-LEW-14072-1] 11 p1611 N85-20129
Elastomer toughened polyimide adhesives — bonding metal and composite material structures for aircraft and spacecraft
[NASA-CASE-LAR-12775-2] 12 p1809 N85-21349
Fire resistant polymers based on 1-(diorgano oxyphosphonyl)methyl-2,4- and 2,6-diamino benzenes
[NASA-CASE-ARC-11512-2] 12 p1811 N85-21362
Study of character of adhesive interaction and breaking of polyimid-aluminum foil junction during process of hardening 13 p2014 N85-22637
Spectroscopic analysis of radiation-generated changes in tensile properties of a polyetherimide film
[NASA-TP-2429] 15 p2502 N85-25435
Ion beam sputter-deposited thin film coatings for protection of spacecraft polymers in low Earth orbit
[NASA-TM-87051] 19 p3248 N85-30137
Mechanical properties of aligned short carbon fiber reinforced PES and PI laminates
[ESA-TT-898] 20 p3422 N85-31240
Synthesis and characterization of copolyimides with varying flexibilizing groups
[NASA-TM-86416] 20 p3433 N85-31296
STPI/LARC: A 200 deg C polyimide adhesive
[NASA-TM-86447] 20 p3433 N85-31297
Graphite/PMR polyimide composites with improved toughness
[NASA-TM-87061] 21 p3561 N85-32148
Fire-resistant phosphorus containing polyimides and copolyimides
[NASA-CASE-ARC-11522-2] 23 p3918 N85-34280

POLYISOBUTYLENE
The role of molecular diffusion in the adhesion of elastomers
[AD-A145576] 02 p0186 N85-11245

POLYISOPRENES
Plastic deformation of crystalline polymers
[AD-A152090] 16 p2755 N85-26999
Orientation and strength of semi-crystalline polymers 20 p3432 N85-31294

POLYMER CHEMISTRY
Method of obtaining polybenzimidazopyrrolones
[AD-A145140] 01 p0018 N85-10108
Method of obtaining heterocyclic polymers
[AD-A145127] 01 p0033 N85-10202
A new heat-resistant polymer from dimer diamine bismaleimide. Part 1: Preparation and free radical cure of dimer diamine bismaleimide
[AD-A145664] 02 p0186 N85-11247
The concept of solid solvent as processing aid
[AD-A146556] 06 p0771 N85-14934
Polyphosphazene solid electrolytes
[AD-A147008] 07 p0931 N85-15902
Rubber-modified epoxies. 1: Cure, transitions, and morphology
[AD-A147377] 07 p0932 N85-15908
Polymer electrolytes: An investigation of some poly (N-propylaziridine)/lithium salt compositions
[RAE-TR-84036] 08 p1131 N85-17130
Elastomers and other organic composites
[AD-A147624] 08 p1131 N85-17131
Stable polymeric carbon radicals. Part 2: Attempts at the preparation of polyradicals of the triphenylmethyl type linked by P-phenylene units
[NASA-TM-77799] 10 p1450 N85-19134
Polymer electrolytes: An investigation of some poly (N-propylaziridine)/lithium salt compositions
[AD-A149444] 10 p1452 N85-19146
Polymers and macromolecules
[DE85-003176] 10 p1454 N85-19160
USSR report: Chemistry
[JPRS-UCH-85-001] 13 p2013 N85-22629
Effect of alternative aging and accident simulations on polymer properties
[DE85-002642] 13 p2037 N85-22762
Abstracts of the 36th Southeastern Regional Meeting of the American Chemical Society
[AD-A151506] 15 p2496 N85-25394
Separating polymer solutions using high pressure LCST Lower Critical Solution Temperature) phenomena
[AD-A151538] 15 p2516 N85-25528
Polyaromatic ether-sulfone-keytones with fluoro-substituted-p-cyclophane units as cross-linking sites
[AD-D011649] 17 p2933 N85-28105
New polymers for composites: A summary of research on polystyrylpyridines
[NASA-CR-175886] 17 p2933 N85-28106
The synthesis and structure of polyphosphazenes
[AD-A153134] 17 p2934 N85-28112
Model for the growth of fractal silica polymers
[DE85-007884] 17 p2935 N85-28115
Chemical approach for controlling nadimide cure temperature and rate
[NASA-CASE-LEW-13770-6] 19 p3232 N85-30039
Mechanical modification of friction surfaces of aluminum alloys by friction transfer 19 p3241 N85-30097
Method for production of ceramic oxide and carbide bodies by polymer inclusion and decomposition
[DE85-011668] 19 p3250 N85-30152
Electrophoretic mobility of cells in a vertical Ficoll gradient 20 p3499 N85-31753
Bubble dynamics in polymer solutions undergoing shear
[AD-A154575] 21 p3568 N85-32193
Importance and significance of transition temperatures
[AD-A154871] 21 p3569 N85-32199

POLYMER MATRIX COMPOSITES
Development of new and improved polymer matrix resin systems, phase 1
[NASA-CR-166595] 01 p0017 N85-10104
Friction and wear of polymers and polymer composite materials 01 p0054 N85-10361
Tough Composite Materials
[NASA-CP-2334] 04 p0463 N85-12941
Characterization of interlaminar crack growth in composites with the double cantilever beam specimen 04 p0463 N85-12942
Composite materials characterization and development at AFWAL 04 p0464 N85-12944
Investigation of toughened neat resins and their relations to advanced composite mechanical properties 04 p0464 N85-12949
Effect of polymer matrix on properties of fibers obtained by caking polymer dispersions 06 p0782 N85-14878
Investigation of the relations between resin and advanced composite mechanical properties. Volume 2: Appendices
[NASA-CR-172303-VOL-2] 06 p0783 N85-14880

Unidirectional fibers and polyurethane elastomer matrix based composites synthesis and properties
[NASA-TM-77501] 07 p0920 N85-15826
Characterization and selection of polymer materials for binary munitions storage. Part 2: Characterization of LLDPE resins
[AD-A146324] 06 p1133 N85-17144
New method for studying surface crack growth in laminated polymer composite materials
11 p1598 N85-20051
Electrical conduction in polymer dielectrics
13 p1995 N85-22514
Interlaminar fracture toughness in resin matrix composites
[AD-A150565] 13 p2015 N85-22640
Outlook for polymer composite materials
15 p2497 N85-25403
Research, development of composite materials described
15 p2497 N85-25404
Effect of counterface material type and its topography on the tribological properties of polyimide composites
[NASA-TM-87036] 16 p2754 N85-26993
Accuracy of the calculated stress field around a craze
[DE85-005520] 16 p2801 N85-27272
Experiments and micromechanical models for creep-rupture in polymer matrix composites
[DE85-009533] 17 p2935 N85-28118
Structure-property relationships in polymeric matrix materials
[AD-A153929] 18 p3080 N86-29050
Transversely reinforced piezoelectric composites
[AD-D011676] 19 p3260 N85-30214
Implementation of polymer impregnation as a bridge deck sealant
[PB85-186718] 22 p3753 N85-33265
Conductor-polymer composite electrode materials
[DE85-005766] 23 p3920 N85-34293

POLYMER PHYSICS
Equibiaxial extension of two polymer melts: Polystyrene and low density polyethylene
[AD-A144893] 01 p0032 N85-10200
Transport properties of multiphase systems
[DE84-015560] 02 p0173 N85-11159
Electrically conducting complexes of poly(3,6-n-methylcarbazolyl methylene)
[AD-A147884] 07 p0933 N85-15914
Critical events in inelastic deformation of glassy polymers in adsorptive medium
13 p2014 N85-22634
Effects of triazine components on physicochemical properties of polybutadiene: urethane block copolymers
13 p2014 N85-22635
Theory of relaxation processes in decomposing polymer materials during high-intensity convective heating
13 p2028 N85-22710
High performance mixed bismide resins and composites based thereon
[NASA-CASE-ARC-11538-1-SB]
19 p3231 N85-30033
Importance and significance of transition temperatures
[AD-A154871] 21 p3569 N85-32199

POLYMERIC FILMS
NT KAPTON (TRADEMARK)
Optical constant determination of thin polymer films in the infrared
[AD-A145889] 02 p0287 N85-11877
Photophysical studies of triplet exciton processes in pure polymer films
[DE84-016258] 05 p0820 N85-13065
Synthesis of film-forming electron-accepting polymers
[AD-A146430] 06 p0771 N85-14931
The replacement of precious metal thick film inks using conductive polymer technology. Phase 1: Feasibility study
[AD-A147814] 07 p0933 N85-15913
Estimation of the rate of electron transfers between 2 contacting polymer surfaces
[AD-A148416] 08 p1122 N85-17072
Potential dependence of electrical conductivity and chemical charge storage of poly(pyrrole) films on electrodes
[AD-A148513] 08 p1122 N85-17075
Electrochemistry of polymer films. Applications to chemical analysis and energy conversion
[AD-A147737] 08 p1132 N85-17136
The kinetics of electron transfer reactions in and at films of electroactive polymers
[AD-A148597] 08 p1134 N85-17149
Mechanisms of gas permeation through polymer membranes
[DE84-017423] 09 p1293 N85-18117
Evaluation and prediction of long-term environmental effects of nonmetallic materials
[NASA-CR-171359] 10 p1450 N85-19137
Water absorption and conductivity in poly(ethylene oxide)-lithium tetrafluoroborate films
[AD-A147969] 10 p1450 N85-19138
Process for preparing essentially colorless polyimide film containing phenoxy-linked diamines
[NASA-CASE-LAR-13353-1] 11 p1611 N85-20128
Effect of interfacial characteristics of metal clad polymeric substrates on electrical high frequency interconnection performance
[NASA-TM-86948] 11 p1624 N85-20223
Mass analysis of neutral particles and ions released during electrical breakdowns on spacecraft surfaces
[NASA-CR-175585] 12 p1793 N85-21250
Process for preparing highly optically transparent-colorless aromatic polyimide film
[NASA-CASE-LAR-13351-1] 12 p1811 N85-21360
Effect of ultraviolet radiation on transparent polymer films as determined using in situ FTIR-RA spectroscopy. Volume 1: Photodegradation of transparent polymer films
[DE84-013039] 12 p1814 N85-21377
Polymeric electrolytes for ambient temperature lithium batteries
[DE85-001032] 12 p1835 N85-21518
Optimal design efforts in Shanghai described
13 p1972 N85-22366
Mass spectra of neutral particles released during electrical breakdown of thin polymer films
13 p1996 N85-22511
Study of character of adhesive interaction and breaking of polyimid-aluminum foil junction during process of hardening
13 p2014 N85-22637
Electrostatic forming and testing of polymer films on a 16-foot diameter test fixture
[NASA-TM-86328] 13 p2063 N85-22885
Uniaxial orientation of linear low density polyethylene
[AD-A151037] 14 p2261 N85-24009
Piezoelectric and electrostatic polymeric transducers for acoustic emission detection
[AD-A150883] 14 p2306 N85-24272
Monte Carlo lattice models for adsorbed polymer conformation
[NASA-TP-2453] 14 p2426 N85-24961
Investigation of the MBE growth of InSb and novel quantum well structures
[AD-A151014] 14 p2427 N85-24969
Finger materials for air cushion vehicles. Volume 1: Flexible coatings for finger materials
[AD-A151498] 15 p2522 N85-25545
Electrochemistry of polymer films not immersed in solution: Electron transfer on an ion budget
[AD-A152989] 17 p2920 N85-27998
Photophysical studies of triplet exciton processes in pure polymer films
[DE85-008571] 18 p3080 N85-29056
Silvered polymer reflectors
[DE85-006762] 18 p3130 N85-29384
Mass spectrometer based gas permeation apparatus
[DE85-011176] 19 p3273 N85-30299
Inhibited anticorrosion protection of automotive steel strip in the NLMK
[BLL-M-36250-(5828.4)] 20 p3430 N85-31274
Radiation-hardened polymeric films
[DE85-011636] 22 p3752 N85-33259
Development and demonstration of a spiral-wound thin-film composite membrane system for the economical production of oxygen-enriched air, phase 4
[DE85-012380] 23 p3920 N85-34288
Structure and properties of polyethylene films used in heavy lift balloons
[NASA-CR-176227] 24 p4083 N86-35306

POLYMERIZATION
NT COPOLYMERIZATION
NT VINYL COPOLYMERS
Method of obtaining polychalcones
[AD-A146051] 01 p0018 N85-10107
Preparation of large-particle-size monodisperse latexes in space: The STS-3, STS-4, and STS-7 mission results
02 p0151 N85-11021
The concept of doping of conducting polymers. The role of reduction potentials
[AD-A145480] 02 p0186 N85-11243
Microstructure development in polymers
[AD-A145980] 03 p0337 N85-12170
Aliphatic-aromatic heterocyclics as potential thermoplastics for composite matrices
04 p0488 N85-12982
Constituent properties and interrelationships
04 p0467 N85-12984
Influence of relaxation on the mechanical characteristics of a carbon-epoxy composite. Report no. 45.427/1
04 p0488 N85-12980
USSR report: Chemistry
[JPRS-UCH-84-012] 06 p0761 N85-14865
Polymerization and halogen scrambling behavior of phenyl-substituted cyclotriphosphazenes
[AD-A146366] 06 p0771 N85-14930
Boron-nitrogen polymers. 1: Mechanistic studies of borazine pyrolyses
[AD-A146470] 06 p0771 N85-14933
The concept of solid solvent as processing aid
[AD-A146556] 06 p0771 N85-14934
Preparation of polymers of functionalized acetylenes
[AD-D011296] 06 p0771 N85-14935
Optimization of the die entrance shape for polymeric extrusion
[DE85-001568] 06 p0772 N85-14937
Instruments for characterization of carbon black and polymers
[AD-A145475] 06 p0810 N85-15148
Pseudo-p-1,2,2,9,9,10,10-octofluoro (2,2)-p-cyclophane bis-acid chloride
[AD-D011393] 07 p0919 N85-15818
Gradient polymers
[AD-A146836] 07 p0931 N85-15900
Synthesis and characterization of unique liquid crystalline block copolyesters. A proposal for a polymer research center at the Atlanta University
[AD-A147280] 07 p0932 N85-15907
New synthesis of phosphazene polymers
[AD-A147567] 07 p0933 N85-15910
Elastomers and other organic composites
[AD-A147624] 08 p1131 N85-17131
Study of reaction kinetics and development of elastic properties in network polymerization systems by the impulse technique
[AD-A148187] 08 p1133 N85-17141
Applicability of linear elastic fracture mechanics to fatigue in polymers and short-fiber composites
09 p1298 N85-18152
Mechanism and process of flocculation by polymeric flocculant
09 p1303 N85-18185
Electromagnetic processing of materials
[AD-A148804] 09 p1311 N85-18241
Stable polymeric carbon radicals. Part 2: Attempts at the preparation of polyradicals of the triphenylmethyl type linked by P-phenylene units
[NASA-TM-77799] 10 p1450 N85-19134
Method for making heterocyclic block copolymers
[AD-D011446] 10 p1451 N85-19143
Characterization of acetylene-terminated resin cure states
[AD-A149463] 10 p1452 N85-19148
(Vinyloxy)chlorocyclotriphosphazenes
[AD-D011471] 10 p1453 N85-19152
SANS studies of polymers
[DE85-002471] 11 p1612 N85-20134
Characterization of the network structure of a hardened epoxy resin (TGMDA/DDS system)
[ONERA-RT-3/3348-M] 11 p1613 N85-20140
Status of specific FRG high tech research funded by BMFT
11 p1618 N85-20161
A brief review of the technology of microemulsions and other micellar systems
[AD-A149759] 12 p1800 N85-21289
Phthalocyanine polymers
[NASA-CASE-ARC-11413-1] 12 p1809 N85-21348
Fire resistant polymers based on 1-(diorgano oxyphosphonyl)methyl-2,4- and 2,6-diamino benzenes
[NASA-CASE-ARC-11512-2] 12 p1811 N85-21362
Fire and heat resistant laminating resins based on maleimido and citraconimido substituted 1-(diorgano oxyphosphonyl)methyl-2,4- and 2,6-diaminobenzenes
[NASA-CASE-ARC-11533-1] 12 p1812 N85-21364
Rheology of dissemination
[AD-A150006] 12 p1813 N85-21373
Plasticizer system for propellant compositions
[AD-D011516] 12 p1817 N85-21394
Amine salts as bonding agents
[AD-D011543] 12 p1817 N85-21396
LL-100: A new polybutadiene resin system for radome applications)
[AD-P004368] 12 p1826 N85-21462
Synthesis and characterization of poly(vinylidene fluoride)
[AD-A150291] 13 p2037 N85-22759
Chiral polymers
[AD-A150366] 13 p2037 N85-22760
The mechanism of phenylacetylene polymerization by molybdenum and titanium initiators
[AD-A150993] 14 p2260 N85-24007
Compressive strength of epoxy resin chocks subjected to elevated temperatures
[AD-A152018] 15 p2519 N85-25532
Electrical research on solar cells and photovoltaic materials
[NASA-CR-175699] 15 p2585 N85-25935
Oil resistant silicone elastomers
[AD-131523] 16 p2753 N85-26987

Formulation/cure technology for ultrahigh molecular weight silphenylene-siloxane polymers
[NASA-TP-2476] 16 p2753 N85-26990
Synthesis of phenols from metal-carbynes and diynes
[AD-A151913] 16 p2754 N85-26997
Theoretical studies of solar-pumped lasers
[NASA-CR-175801] 16 p2789 N85-27206
NBS (National Bureau of Standards) research reports
[PB85-127421] 16 p2879 N85-27764
Polyaromatic ether-sulfone-ketones with fluoro-substituted-p-cyclophane units as cross-linking sites
[AD-D011649] 17 p2933 N85-28105
Preparation of polystyrene latex particles in a rotating reactor
[NASA-CR-171475] 17 p2933 N85-28108
Model for the growth of fractal silica polymers
[DE85-007884] 17 p2935 N85-28115
Light scattering and spectroscopic studies of polymerization processes
[AD-A153407] 18 p3069 N85-29084
Stabilized unsaturated polyesters
[NASA-CASE-NPO-16103-1] 18 p3078 N85-29043
Processable and stable conductive polymers
[AD-D011684] 19 p3249 N85-30143
Magnetically-localizable, polymerized lipid vesicles and method of disrupting same
[AD-D011686] 19 p3249 N85-30144
Molecular toxicology of chromatin: The role of Poly(ADP-Ribose) in gene control
[AD-A154415] 19 p3327 N85-30611
Development of a lithium secondary battery separator
20 p3444 N85-31378
Graphite/PMR polyimide composites with improved toughness
[NASA-TM-87081] 21 p3561 N85-32148
Introduction of structural variations into oxide polymers and their effect on sintering and crystallization
[AD-A155597] 21 p3570 N85-32206
Three-dimensional photochemical machining with lasers
[AD-A154711] 21 p3591 N85-32320
Polymerizable ultraviolet stabilizers
21 p3606 N85-32406

POLYMERS
Method of obtaining polychalcones
[AD-A145051] 01 p0016 N85-10107
Nuclear Magnetic Resonance of Polymeric Materials
[AD-A145078] 01 p0032 N85-10192
Dynamics of polymers in solution and melts
[AD-P003907] 01 p0032 N85-10193
NMR (Nuclear Magnetic Resonance) and macromolecular migration in a melt or in concentrated solutions
[AD-P003908] 01 p0032 N85-10194
13C and 1H NMR (Nuclear Magnetic Resonance) studies of solid polyolefines
[AD-P003909] 01 p0032 N85-10195
A determination of the photochemical quantum yields from 2 excited triplet states of biacetyl using holography
[AD-A145091] 01 p0060 N85-10326
An investigation of the suitability of using a Slegleff-McKelvey high shear rate melt rheometer for the measurement of low viscosity polymer solutions
[AD-A146275] 03 p0338 N85-12174
Optimizing conductive polymer compounds
[BMFT-FB-T-84-145] 03 p0338 N85-12177
Insulating polymer concrete
[DE84-017239] 04 p0480 N85-13057
Determination of halogens and sulfur in organic compounds and polymers by combustion-ion chromatography
[DE84-016186] 05 p0614 N85-13921
USSR report: Chemistry
[JPRS-UCH-84-012] 06 p0761 N85-14865
Low temperature synthesis of polycaproamide copolymers grafted with polydimethylaminothylmethacrylate
06 p0761 N85-14866
Synthesis of reinforced composite threads based on polymer mixtures 06 p0761 N85-14869
Polymer-carbon black interaction in electrically conducting fiber-forming composites
06 p0762 N85-14875
Effect of polymer matrix on properties of fibers obtained by caking polymer dispersions 06 p0762 N85-14876
Encapsulation materials and processing
06 p0830 N85-15269
Polymer-metal interface bond stability
06 p0830 N85-15272
Pseudo-p-1,2,2,9,9,10,10-octofluoro (2,2)-p-cyclophane bis-acid chloride
[AD-D011393] 07 p0919 N85-15818
Moisture absorbing anti-arcing coating and method for applying same
[AD-D011310] 07 p0932 N85-15904
New synthesis of phosphazene polymers
[AD-A147567] 07 p0933 N85-15910
Electrically conducting complexes of poly(3,6-n-methylcarbezolyl methylene)
[AD-A147884] 07 p0933 N85-15914
Mechanisms of gas permeation through polymer membranes
[DE84-017423] 09 p1293 N85-18117
Tribological properties of graphite-fiber-reinforced, partially fluorinated polyimide composites
[NASA-TM-86926] 09 p1298 N85-18153
Effective antireflection coatings of transparent polymeric materials by gas-phase surface fluorination
[DE84-013027] 09 p1385 N85-18711
On shrinkage and molecular extension
[AD-A149100] 10 p1451 N85-19144
Microstructural analysis of ion containing polymers
[DE85-001594] 10 p1453 N85-19157
Overview of major Swedish institutions in polymer research 11 p1592 N85-20014
Low temperature deposition of nickel films
[AD-D011568] 12 p1805 N85-21319
Control of electronic, magnetic and optical properties of doped polyacetylene conductors
[AD-A150117] 12 p1814 N85-21375
Polymer intermediates from limonene (follow-up project)
[BMFT-FB-T-84-243] 12 p1814 N85-21380
Research program on the effect of pressure on the mechanical properties of polymers, part 2
[DE85-000985] 13 p2037 N85-22761
HREELS and Auger studies of conducting polymers
[DE85-004541] 13 p2038 N85-22764
The replacement of precious metal thick film inks using conductive polymer technology
[AD-A152002] 16 p2749 N85-26965
Process for clarification of water
[DE85-007864] 17 p2923 N85-28023
Application of scattering methods to the studies of the structure of polymer blends
[IFPR-13/1984] 17 p2933 N85-28104
Development of concrete polymer materials
[DE85-005957] 17 p2934 N85-28114
Experiments and micromechanical models for creep-rupture in polymer matrix composites
[DE85-009633] 17 p2935 N85-28118
Polymer Research at Synchrotron Radiation Sources: Symposium Proceedings
[DE85-008488] 18 p3061 N85-29062
Synthesis and characterization of novel polymers from non-petroleum sources for use in enhanced oil recovery
[DE85-010922] 19 p3250 N85-30151
Polyethylene imine-metal salt solid electrolyte
[AD-D011678] 19 p3305 N85-30485
Orientation and strength of semi-crystalline polymers
20 p3432 N85-31294
Standard procedures to be used in specifying basic properties of plastics and polymers
[NPL-DMA(A)-99] 20 p3433 N85-31295
Synthesis and characterization of copolyimides with varying flexibilizing groups
[NASA-TM-86416] 20 p3433 N85-31296
EVA-glass interface bond stability
21 p3606 N85-32406
Process for improving moisture resistance of epoxy resins by addition of chromium ions
[NASA-CASE-LAR-13228-1] 23 p3919 N85-34282
Degradation mechanisms and accelerated aging test design
[TI85-003251] 23 p3940 N85-34420
Development of an NBS (National Bureau of Standards) polymer gage for dynamic soil stress measurement
[PB85-208494] 24 p4118 N85-35526

POLYMETHYL METHACRYLATE
Mechanochemical reactions of polymethyl methacrylate and polystyrene at high pressure
[DRIC-T-7307] 03 p0337 N85-12165
Gradient polymers
[AD-A146836] 07 p0931 N85-15900
Theory of relaxation processes in decomposing polymer materials during high-intensity convective heating
13 p2028 N85-22710
Light scattering and spectroscopic studies of polymerization processes
[AD-A153407] 18 p3069 N85-29084
A model for the combustion of polymethyl methacrylate in air in a laminar diffusion flame
[VTH-LR-439] 18 p3165 N85-29606

POLYMORPHISM
Synthesis and characterization of poly(vinylidene fluoride)
[AD-A150291] 13 p2037 N85-22759

POLYNOMIALS
NT BINOMIALS
NT HERMITIAN POLYNOMIAL
Simultaneous rational approximation of a function and its derivatives in the complex plane
[CSIR-TWISK-311] 01 p0109 N85-10733
Polynomial and power series FGS-rings have trivial coefficient rings
[TWISK-326] 01 p0109 N85-10737
A weighted polynomial inequality
[CSIR-TWISK-332] 01 p0110 N85-10741
Partitions of unity and approximation
[AD-A144717] 01 p0110 N85-10746
A trivariate Clough-Tocher scheme for tetrahedral data
[AD-A144740] 01 p0111 N85-10751
Methods for numerical differentiation
[AD-A145058] 01 p0112 N85-10758
Time invariant memoryless nonlinear systems identification method
[FUB-9-1983] 01 p0114 N85-10773
Estimates of Freud-Christoffel functions for some weights with the whole real line as support
[CSIR-TWISK-323] 01 p0114 N85-10775
PASCAL-MP algebraic and numerical manipulator for polynomials
[INPE-3229-TDL/176] 02 p0240 N85-11582
Control and identification of time varying systems
[AD-A145838] 02 p0252 N85-11649
Orthogonal polynomials and rigged Hilbert space
[TUM-M8313] 03 p0414 N85-12647
On the weak limits of elementary symmetric polynomials
[CWI-MS-R8407] 05 p0719 N85-14620
Orthogonal polynomials and a Dirichlet problem related to the Hilbert transform
[CWI-PM-R8406] 05 p0723 N85-14647
Performance of the h, p and h-p versions of the finite element method
[AD-A146940] 07 p1029 N85-16535
Probabilistic analysis of algorithms for NP-Complete problems
[AD-A148207] 08 p1215 N85-17653
On the quadratic mean radius of a polynomial in Cz
[AD-A149189] 10 p1546 N85-19751
On the spans of polynomials and the spans of a Laguerre-Polya-Schur sequence of polynomials
[AD-A149384] 10 p1547 N85-19754
Some qualitative properties of bivariate Euler-Frobenius polynomials
[AD-A149408] 10 p1547 N85-19755
A note on the use of polynomial transformations in evaluating singular integrals
[MATHEMATICS-RESEARCH-165]
12 p1920 N85-22053
Approximate perturbing part of geopotential by polynomials of stipulated form 13 p1984 N85-22448
Polynomial parameterization in inverse gravimetric problem 13 p2115 N85-23174
Squares of Gegenbauer polynomials and Milin type inequalities
[CWI-PM-R8412] 14 p2410 N85-24862
A fast ray tracing routine for laterally inhomogeneous media
[AD-A150984] 14 p2421 N85-24936
Entire functions with spiral limits
15 p2634 N85-26241
Multinomial form of the solution of problems of the statistics of elastic rectangular disks
[REPT-17/1984] 16 p2797 N85-27244
Quadratic spaces over discrete Hodge algebras
16 p2853 N85-27593
Polynomial approaches for the characteristic velocity and flame temperature as a function of mixing compounding and pressure for the systems PMMA/O2, PMMA/air, PE/O2, PE/air, PS/O2 and PS/air
[VTH-LR-421] 17 p2924 N85-28024
Comparison of two algebraic methods for curve/curve intersection 17 p3007 N85-28591
Polynomial iteration for nonsymmetric indefinite linear systems
[AD-A153094] 17 p3019 N85-28671
A class of polynomials related to those of Laguerre
[CWI-AM-R8411] 17 p3022 N85-28693
Determinal representations of polynomials satisfying linear Ordinary Differential Equations (ODEs) or linear recurrence relations
[PREPRINT-417] 18 p3172 N85-29660
Evaluation of densities and distributions via hermite and generalized laguerre series employing high-order expansion coefficients determined recursively via moments or cumulants
[AD-A153950] 18 p3175 N85-29662
An algorithm for the generation of primitive polynomials
[FUB-17-1984] 22 p3831 N85-33730

POLYNUCLEAR ORGANIC COMPOUNDS
Analysis and characterization of organic carbon compounds in atmospheric particulate matter
[PB84-232636] 06 p0766 N85-14903

Prediction of retention indices of polynuclear aromatic hydrocarbons. Part 1: HPLC on nitrogen containing normal phase packing materials
[DE85-001302] 10 p1436 N85-19051
Desorption efficiences of vapor phase polynuclear aromatic compounds on solid adsorbents
[DE85-001303] 10 p1436 N85-19052
Prediction of retention indices of polynuclear aromatic hydrocarbons. Part 2: Capillary gas chromatography
[DE85-001301] 10 p1437 N85-19053
Diesel engine emissions of particulates and associated organic matter
[PB85-154425] 15 p2500 N85-25964
Identification and quantification of nitropolynuclear aromatic hydrocarbons in ambient and indoor air particulate samples
[PB85-176790] 19 p3311 N85-30525
The interaction of polynuclear aromatic hydrocarbons PAH's with water vapor and their role as condensation nuclei in the formation of haze and fog
21 p3652 N85-32695

POLYPEPTIDES
Endocrine responses to hypotensive gravitational stress: Catecholamines, pancreatic polypeptide, and vasopressin 05 p0693 N85-14480
Primary light harvesting system: The relationship of phycobiliomes to photosystem 1 and 2
[DE85-003075] 11 p1689 N85-20622

POLYPHENYL ETHER
Contact angle and surface tension measurements of a five-ring polyphenyl ether
[NASA-TM-86927] 07 p0930 N85-15897
Formation of high molecular weight products from benzene during boundary lubrication
[NASA-TM-86966] 13 p2017 N85-22644

POLYPHENYLS
NT TRIPHENYLS
Stable polymeric carbon radicals. Part 2: Attempts at the preparation of polyradicals of the triphenylmethyl type linked by P-phenylene units
[NASA-TM-77799] 10 p1450 N85-19134
The mechanisms of phenylacetylene polymerization by molybdenum and titanium initiators
[AD-A150993] 14 p2260 N85-24007

POLYPROPYLENE
Nuclear Magnetic Resonance of Polymeric Materials
[AD-A145078] 01 p0032 N85-10192
13C and 1H NMR (Nuclear Magnetic Resonance) studies of solid polyolefines
[AD-P003909] 01 p0032 N85-10195
Synthesis and characterization of a 1,4 Polybutadiene/Isotactic polypropylene block copolymer
[AD-A148199] 08 p1133 N85-17142
Determination of threshold and maximum operating electric stresses for selected high voltage insulation. Task 3: Investigation of high voltage capacitor insulation
[DE84-017051] 09 p1316 N85-18274
Rep rated long life capacitor development: Phase 1 and 2
[DE85-000719] 11 p1629 N85-20256
Separating polymer solutions using high pressure LCST Lower Critical Solution Temperature) phenomena
[AD-A151538] 15 p2518 N85-25528
Polymer blends for use in photoelectrochemical cells for conversion of solar energy to electricity
[DE85-011602] 22 p3752 N85-33258
Strength properties of glassfiber reinforced thermoplastics 23 p3908 N85-34212

POLYQUINOXALINES
Fracture surface analysis in composite and titanium bonding: Part 1: Titanium bonding
[NASA-CR-175750] 15 p2502 N85-25434

POLYSACCHARIDES
NT CELLULOSE
NT GLYCOGENS
NT STARCHES

POLYSTATION DOPPLER TRACKING SYSTEM
Fundamental limits to synchronization and tracking
[AD-A149623] 12 p1833 N85-21504

POLYSTYRENE
Nuclear Magnetic Resonance of Polymeric Materials
[AD-A145078] 01 p0032 N85-10192
Deuteron NMR (Nuclear Magnetic Resonance) in relation to the glass transition in polymers
[AD-P003910] 01 p0032 N85-10196
Equibiaxial extension of two polymer melts: Polystyrene and low density polyethylene
[AD-A144893] 01 p0032 N85-10200
Diblock copolymers of polystyrene/1,2 polybutadiene and polystyrene/polybutene-1: Molecular structure, morphology and mechanical properties
[AD-A144980] 01 p0033 N85-10201
Mechanochemical reactions of polymethyl methacrylate and polystyrene at high pressure
[DRIC-T-7307] 03 p0337 N85-12165
Photophysical studies of triplet exciton processes in pure polymer films
[DE84-016258] 05 p0620 N85-13965
The effect of pressure on the mechanical properties of polymers. Part 2: Measurement of the time-dependent Poisson's ratio
[DE85-002139] 06 p0772 N85-14938
Deuterium isotope effect on the compatibility between polystyrene and polybutadiene
[AD-A148551] 08 p1134 N85-17145
Monodisperse Latex Reactor (MLR): A materials processing space shuttle mid-deck payload
[NASA-TM-86487] 12 p1782 N85-21187
Development of a polystyrene insulation system
[DE85-009950] 16 p2784 N85-27180
Preparation of polystryene latex particles in a rotating reactor
[NASA-CR-171475] 17 p2933 N85-28108
Ac field-induced order in dense colloidal systems
[DE85-009107] 17 p2935 N85-28119
Polymer solution-supercritical fluid behavior
[AD-A154514] 21 p3568 N85-32192

POLYSULFIDES
Interactions between F-111 fuselage fuel tank sealants. Part 2: Variation in performance properties of polysulfides after contact with polyester degradation products
[AD-A149777] 12 p1812 N85-21368

POLYTETRAFLUOROETHYLENE
Bending two-layer metal-polymer plates
11 p1604 N85-20085
Diffusely reflecting paints including polytetrafluoroethylene and method of manufacture
[NASA-CASE-GSC-12883-1] 18 p3079 N85-29044
Detection threshold energy of high energy cascade showers using thermoluminescence PTFE-sheet and hot-gas reader
[HE-7.1-5] 24 p4219 N85-36159

POLYTOPES
Some facets of the tri-index assignment polytope
[AD-A149195] 10 p1547 N85-19753

POLYURETHANE FOAM
Electrically conductive rigid polyurethane foam
[DE84-014490] 01 p0033 N85-10203
Polyimide-glass multilayer printed wiring boards
[DE84-015092] 05 p0631 N85-14048
Thermal and mechanical properties of polyurethane foams and a survey of insulating concretes at cryogenic temperatures
[PB85-100949/GAR] 07 p0934 N85-15918
Field test results of experimental EPDM (Ethylene Propylene Diene Monomer) and PUF (Polyurethane Foam) roofing
[AD-A147697] 08 p1132 N85-17133
Pathophysiological study of poisoning due to thermal degradation of materials — aircraft cabins
[CERMA-84-15] 11 p1692 N85-20640
X-ray gauge measures areal density variations as small as 0.1%
[DE85-003774] 12 p1854 N85-21629
Damage caused to polyurethane foams by aging, simulated sunlight exposure, heat and fire
[AD-A152040] 16 p2754 N85-28068
Buildup of electric charge in foil dielectrics during gamma irradiation 22 p3770 N85-33363
Rigid zeolite containing polyurethane foams
[DE85-006406] 23 p3919 N85-34266

POLYURETHANE RESINS
Aircraft surface coatings
[NASA-CR-3861] 02 p0137 N85-10935
Description and characterization of deuterated polymers for the analysis with neutron scattering
03 p0431 N85-12748
Protective coverings for fiber reinforced epoxy composites
[PB84-231059] 04 p0480 N85-13063
Unidirectional fibers and polyurethane elastomer matrix based composites synthesis and properties
[NASA-TM-77501] 07 p0920 N85-15828
Structure-property relationships in thermoplastic elastomers. Part 1: Segmented polyether-polyurethanes
[AD-A148043] 08 p1133 N85-17138
Poly(dimethylsiloxane)-polyurethane elastomers: Synthesis and properties of segmented copolymers and related zwitterionomers
[AD-A148571] 08 p1134 N85-17147
Fluorinated polyurethanes
[AD-D011526] 12 p1810 N85-21353
Phase separation in polyurethanes: A deuterium NMR study
[AD-A151515] 15 p2505 N85-25451
Finger materials for air cushion vehicles. Volume 1: Flexible coatings for finger materials
[AD-A151436] 15 p2522 N85-25545
Structure-property relationships in thermoplastic elastomers. Part 3: Segmented polyacetal-polyurethanes
[AD-A154897] 21 p3569 N85-32200

POLYVINYL ALCOHOL
Gel drawn fibers of poly(vinyl alcohol)
[AD-A149062] 10 p1435 N85-19040

POLYVINYL CHLORIDE
New corrosion protection concept for very high voltage line towers
[BLL-OA-TRANS-2691-(6196.300)]
20 p3429 N85-31270
Organic air pollutants during manufacturing and handling of PVC floor tiles
[FOA-E-40018] 20 p3487 N85-31669

POLYVINYL FLUORIDE
Preliminary study for an IR-vidicon for the 8 to 14 micron range, phase 1
[BMFT-FB-W-84-025] 05 p0633 N85-14057
Effect of ultraviolet radiation on transparent polymer films as determined using in situ FTIR-RA spectroscopy. Volume 2: Photophysics of poly(vinylidene fluoride) films
[DE84-013040] 09 p1299 N85-18159
Piezoelectric plastics — polyvinyl fluoride
[ISL-CO-202/83] 14 p2262 N85-24017
Piezoelectric and pyroelectric polymers
16 p2756 N85-27009
Ferroelectric homopolymer PVF2 and P (VDF-TrFe) copolymers 24 p4089 N85-35347

PONDEROMOTIVE FORCES
A covariant derivation of the ponderomotive force
[AD-A145054] 01 p0121 N85-10830
Theory of ponderomotive forces
02 p0293 N85-11847
A nonlocal expression for the ponderomotive potential
[IPPJ-699] 06 p0864 N85-15487
Direct electron and ion fluid computation of high electrostatic fields in dense inhomogeneous plasma with subsequent nonlinear optical and dynamical laser interaction 15 p2656 N85-26368
Nonlocal and nonadiabatic expression for the ponderomotive force near cyclotron resonance
[IPPJ-736] 23 p3974 N85-34636
Transport issues in Phaedrus-type plasmas
23 p3976 N85-34653

PONDS
Potential for acidification of six remote ponds in the White Mountains of New Hampshire
[PB84-207349] 02 p0225 N85-11475
Solar pond research at the Los Alamos National Laboratory
[DE85-008631] 18 p3128 N85-29366
Salt-gradient solar ponds
[DE85-008626] 18 p3129 N85-29380
Stable density stratification solar pond
[NASA-CASE-NPO-15419-2] 19 p3303 N85-30474
Production of liquid fuels and chemicals by microalgae
[DE85-008780] 22 p3819 N85-33658
Solar pond technology for Navy applications
[AD-A155877] 24 p4112 N85-35488

PONTRYAGIN PRINCIPLE
On the Pontryagin principle for stochastic optimal control
[TWISK-328] 01 p0112 N85-10782

POPULATION INVERSION
Imploding plasma X-ray laser research
[DE85-000057] 09 p1326 N85-18331
Optimization of silicon-nitride-inversion layer solar cells
12 p1878 N85-21784
Population inversion in laser-initiated vacuum arcs
[AD-A151958] 16 p2790 N85-27210
Coherently pumped two-frequency laser-type devices
[AD-A154085] 19 p3275 N85-30311
Simplified analytical model for calculation of population inversion in channels of CW gasdynamic lasers operating at various transitions among levels pertaining to coupled upsilon 1 and upsilon 2 modes of CO2
[STN-2] 20 p3461 N85-31498
Expansion ratio influence on population inversion in CO2/Ar CW gasdynamic lasers operating at various transitions within coupled upsilon 1 and upsilon 2 modes of CO2
[STN-4] 22 p3790 N85-33485

POPULATION THEORY
Maximum likelihood estimation of the survival functions of N stochastically ordered random variables
[AD-A145429] 02 p0254 N85-11662
The growth and composition of supercritical branching populations on general type spaces
[CTH-MATH-1984-18] 05 p0721 N85-14631
On the power functions of test statistics in order restricted inference
[AD-A147126] 07 p1035 N85-16566
Empirical Bayes rules for selecting good binomial populations
[AD-A147614] 08 p1214 N85-17646

Improved estimation procedures for item response functions
[AD-A147677] 08 p1215 N85-17648
Minimax multiple t-tests for comparing k normal populations with a control
[AD-A148306] 08 p1215 N85-17656
Study of mathematical models of mutation and selection in multi-locus systems
[DE85-000873] 09 p1376 N85-18648
On asymptotic joint distribution of the eigenvalues of the noncentral manova matrix for nonnormal populations
[AD-A151886] 15 p2642 N85-26294
The dynamical behavior of the age-size-distribution of a cell population
[CWI-AM-R8414] 17 p2998 N85-28538
A formal analysis of the evolution of cooperation
[AD-A152536] 17 p3018 N85-28602
Confidence intervals based on interpolated order statistics
[AD-A152607] 17 p3025 N85-28701
Spatial correlations in the decay from an unstable state in the Malthus Verhulst model — laser cavities
[NOTA-INTERNA-832] 18 p3114 N85-29280
Numerical simulation of the transient by the unstable state in a Lotka-Volterra model
[NOTA-INTERNA-833] 18 p3175 N85-29684

POPULATIONS
Response of algal populations to changes in stream water quality
[PB84-202464] 01 p0070 N85-10465
Results of the carbon monoxide study in Washington, D.C. and Denver, Colorado, in the winter of 1982-83
[PB84-230069] 06 p0634 N85-16309
NAAQS (National Ambient Air Quality Standards) Exposure Model (NEM) applied to carbon monoxide
[PB84-242551] 06 p0634 N85-16310
Hurricane experience levels of coastal county populations: Texas to Maine
[PB85-111383] 10 p1520 N85-19581
The use of image registration technique in Brasilia's urban growth monitoring
[INPE-3308-PRE/614] 10 p1569 N85-19886
Blackbirds and starlings: Population ecology and habits related to airport environments
[AD-P004190] 11 p1580 N85-19953
Feoktistov discusses need for space colonization
13 p1965 N85-22454
Study and estimation of planet-crossing asteroid populations: Discoveries and analysis
13 p2175 N85-23486

PORES
U POROSITY

POROSITY
NT MICROPOROSITY
Suppressing porosity in weld joints of 1420 aluminum alloy 01 p0020 N85-10123
Definition of global dispersion coefficients — aquifers
[PSE-83/4-B] 01 p0064 N85-10426
Study of the pore structure of ceramics prepared by the slip casting method
[NASA-TM-77486] 04 p0478 N85-13048
The variable polarity plasma arc welding process: Its application to the Space Shuttle external tank
[NASA-TM-86482] 05 p0841 N85-14115
Effect of polymer matrix on properties of fibers obtained by casing polymer dispersions 06 p0762 N85-14876
The influence of strain rate and porosity on the deformation and fracture of titanium and nickel
[AD-A148670] 08 p1130 N85-17123
The influence of porosity on the deformation and fracture of alloys
[AD-A148768] 08 p1130 N85-17124
Regularity of the free boundary for the porous medium equation
[AD-A147299] 08 p1210 N85-17611
Mechanisms of elevated temperature rupture in single phase ceramics
[DE85-000897] 09 p1299 N85-18156
Kinetics of saturation of porous titanium with low melting point metals 10 p1446 N85-19114
Behavior and specifics of fracture of porous fiber materials in extension 10 p1447 N85-19118
Collapse and removal of discontinuities in joint zone during diffusion welding 11 p1602 N85-20077
Effect of host-rock dissolution and precipitation on permeability in a nuclear waste repository in tuff
[DE85-000675] 11 p1727 N85-20660
Slip casting and nitridation of silicon powder
[NASA-TM-77809] 12 p1818 N85-21408
Problem of pore formation mechanism in welded joints of aluminum alloys in the system aluminum-magnesium-lithium 13 p2032 N85-22732
NDE methods for green ceramics
[DE85-004019] 13 p2038 N85-22786
Variational bounds on Darcy's constant
[DE85-006938] 15 p2580 N85-25916
Ultrasonic characterization of porosity: Theory
[DE85-005922] 15 p2646 N85-25325
Investigation to optimize the passive shock wave/boundary layer control for supercritical airfoil drag reduction
[NASA-CR-175788] 16 p2699 N85-26865
Continued development and testing of tungsten controlled porosity dispenser cathodes
[AD-A152596] 17 p2931 N85-28090
Detection of pores in hot continuously cast rounds
[BMFT-FB-T-85-007] 18 p3072 N85-29000
Variational bounds on Darcy's constant
[DE85-006950] 18 p3101 N85-29195
Interim rock mass properties and conditions for analyses of a repository in crystalline rock
[DE85-010700] 18 p3125 N85-29352
Analysis of the elastic and strength properties of Yucca Mountain tuff, Nevada
[DE85-006975] 19 p3300 N85-30460
A multiphase continuum model to describe dynamic loading effects in nonlinear porous media
[DE85-010102] 19 p3301 N85-30463
Measurement and analysis of two-phase flow through low permeability media, task 3
[PB85-186373] 20 p3435 N85-31313
Gas sensing with surface acoustic wave devices
[DE85-009125] 20 p3524 N85-31921
MPS solidification model. Analysis and calculation of macrosegregation in a casting ingot
[NASA-CR-171589] 21 p3566 N85-32178
KRAK: A computer program for two-phase two-component porous flow and fracture
[LA-9703] 22 p3782 N85-33434
Deep-burial diagenesis in carbonates
[DE85-011224] 22 p3802 N85-33554
WIPP horizon in situ permeability measurements
[DE85-012687] 22 p3802 N85-33557
The character of observed porosity and its possible effects on rolling contact fatigue life of M-50 steel
[AD-A155930] 24 p4079 N85-35279
Development and evaluation of sulfonated polysulfone membranes for the zinc-ferricyanide battery
[DE85-009104] 24 p4090 N85-35357
Simplified procedures for the evaluation of settlements in sands due to earthquake shaking
[PB85-197887] 24 p4118 N85-35527

POROUS BOUNDARY LAYER CONTROL
Progress in wind tunnel wall interference assessment/correction procedures at the NAE
03 p0314 N85-12025
Development of thermoconvective instabilities in porous media. Influence of boundary conditions
20 p3456 N85-31461

POROUS MATERIALS
Method of making a porous carbon cathode: A porous carbon cathode so made, and electrochemical cell including the porous carbon cathode
[AD-D011243] 02 p0195 N85-11301
Surface diffusion of high temperature vapors in porous alumina
[DE84-015968] 04 p0479 N85-13053
Numerical modelling of the drying of porous materials
[DE84-013056] 04 p0499 N85-13181
Theory of kinetics of impregnation of porous bodies
[BLL-M-35917-(5828.4)] 05 p0816 N85-13942
Characteristic impedance of a porous center during transmission of quasi-static sinusoidal vibrations
[ISSN-0208-5658] 05 p0847 N85-14155
Fatigue strength of different sintered steels and design criteria for porous material (PM) parts
[LBF-FB-170/84] 07 p0928 N85-15886
The influence of porosity on the deformation and fracture of alloys
[AD-A148768] 08 p1130 N85-17124
Response of saturated porous nonlinear materials to dynamic loadings
[AD-A148528] 08 p1173 N85-17394
Investigation of condensing, three-phase, two-component, flow through porous media
09 p1317 N85-18283
Natural convection experiments about a finite-length cylindrical heat source in a liquid-saturated porous medium
[DE84-012657] 09 p1320 N85-18296
Characterization of porosity in porous polymer implant materials
[PB85-119980] 10 p1454 N85-19161
Transition to detonation from rapid-compression (ramp-waves) generated in a burning porous bed
[AD-P004345] 10 p1455 N85-19169
Thermophysical properties of porous fiber materials
11 p1601 N85-20068
Adsorption behaviour of nitrogen compounds on to porous polymer beads and applications to atmospheric sampling
[BLL-DRIC-TRANS-7399-(3623.66)]
13 p2036 N85-22753
Molten carbonate fuel cell performance model update, draft
[DE85-005423] 13 p2129 N85-23252
Impact crater scaling laws 13 p2181 N85-23532
Model for high rate gas flows in deformable and reactive porous beds
[DE85-006140] 14 p2253 N85-23964
Flow through very porous inclined screens
[NASA-TM-86979] 15 p2555 N85-25761
Variational bounds on Darcy's constant
[DE85-006938] 15 p2580 N85-25916
Ductility equation for porous metals and its linearization
[BLL-M-36118-(5828.4)] 16 p2748 N85-26958
Two-d heat transfer through porous media with heat generation
[AD-A151985] 16 p2783 N85-27173
Interaction of finite-amplitude sound with air-filled porous materials
[NASA-CR-174885] 16 p2860 N85-27637
Numerical study of porous airfoils in transonic flow
[NASA-TM-86713] 17 p2892 N85-27828
Limiting profiles in contaminant transport through porous media — ground water pollution
[REPT-84-31] 17 p2960 N85-28262
High temperature composite thermal storage systems
[DE85-005073] 17 p2966 N85-28455
Variational bounds on Darcy's constant
[DE85-006959] 18 p3101 N85-29195
Diffusion of gases in porous solids: Simulation and measurements
[DE85-006870] 18 p3101 N85-29196
Dynamics of thin-film breakup in a constricted pore
[DE85-006442] 18 p3101 N85-29199
Distribution of density in closed-impression die forging of axisymmetrical products from metal powders
19 p3245 N85-30118
Technical and historical overview of the study at Lawrence of porous antireflection coatings
[DE85-010925] 20 p3434 N85-31302
Natural convection experiments in a stratified liquid-saturated porous medium
[DE85-009003] 20 p3455 N85-31457
Development of thermoconvective instabilities in porous media. Influence of boundary conditions
20 p3456 N85-31461
Thermomigration in porous media. Study of the development of a drying zone 20 p3456 N85-31462
Vapor-liquid phase separator studies
[NASA-CR-166545] 21 p3583 N85-32272
Combustion-deflagration-detonation transition
[ISL-CO-221/84] 22 p3747 N85-33225
Detailed validation of a liquid and heat flow code against field performance
[DE85-009901] 23 p3932 N85-34368
Studies in thermo-hydro-chemical transport in porous and fractured media
[DE85-012555] 23 p3949 N85-34473
Method of preparing thin porous sheets of ceramic material
[DE85-006399] 24 p4082 N85-35300

POROUS PLATES
Behavior of the porous bed in a combustion-deflagration-detonation transition
[ISL-CO-220/84] 22 p3747 N85-33224

POROUS WALLS
Numerical simulation of natural convection in porous media — heat transfer
[CFD/84/10] 02 p0199 N85-11330
Jet noise suppression by porous plug nozzles
[NASA-CR-3613] 02 p0275 N85-11790
Investigations of reactive and non reactive acoustic boundary layers in porous walled ducts
13 p2000 N85-22535

PORPHYRINS
NT CHLOROPHYLLS
Three-dimensional photochemical machining with lasers
[AD-A145792] 03 p0365 N85-12342
Photoelectrochemistry with chemically modified electrodes
[DE84-016798] 04 p0471 N85-12997
Chemically modified electrodes and related solution chemistry
[DE84-017110] 05 p0814 N85-13924
Investigation and optimization of fuel production using dye-based transition metal complexes as charge-transfer intermediates
[PB85-161941] 14 p2264 N85-24029

PORTABLE EQUIPMENT
Portable slotting device
[AD-D011213] 01 p0033 N85-10206
Evaluation of survival straws (pocket purifier)
[AD-A146240] 03 p0328 N85-12114
Portable real-time clock
[AD-A146218] 03 p0364 N85-12336
Improved robotic equipment for radiological emergencies
[DE84-017637] 04 p0509 N85-13249
Noise in small portable motocompressors. Experiments on limited-cost acoustic treatments to obtain progressive improvements
[CETIM-11-H-445] 04 p0558 N85-13557
Portable instrument for the detection and identification of air pollutants
[DE84-014767] 05 p0672 N85-14316
Testing of a field portable GPS (Global Positioning System) geodetic receiver
[AD-A148336] 08 p1082 N85-16859
Mobile accelerator neutron radiography system
[AD-A148808] 09 p1323 N85-18311
Location of volatile buried wastes by field portable instrumentation
[AD-P004147] 09 p1348 N85-18483
Fast data and voice transmission for mobile services with high immunity against multipath and co-channel interference 10 p1475 N85-19306
The use of small mobile radars to detect, monitor, and quantify bird movements
[AD-P004186] 11 p1580 N85-19951
Portable pellet weighing apparatus
[NASA-CASE-GSC-12789-1] 11 p1635 N85-20294
Development of a portable zenith chamber and its use on the 47th parallel
[SER-C-287] 11 p1741 N85-20948
Portable remote laser sensor for methane leak detection
[NASA-CASE-NPO-15790-1] 12 p1855 N85-21631
Portable electrochemical cell interrogator
[DE85-005186] 13 p2065 N85-22901
Technical manual: Description and operation Slaved Tracking System
[DE85-004807] 13 p2094 N85-23070
A concept for a mobile remote manipulator system 14 p2236 N85-23859
Fabrication of turbine parts with transportable tools 14 p2267 N85-24048
Deployable Core Automated Maintenance System (DCAMS)
[AD-A153695] 18 p3198 N85-29639
Expedient runway surfacing with post tensioning system for expeditionary airfields
[AD-D011677] 19 p3222 N85-29976
Field testing of a lightweight relocatable structure in a temperate environment
[AD-A155171] 21 p3599 N85-32350

PORTS (OPENINGS)
Wave guide branchings (n-port) types of representation of linear, time-independent and sourceless n-ports
[NASA-TM-77770] 01 p0037 N85-10233
Integral boost, heat protection, port covers and transition 07 p0918 N85-15813
Comparing different theoretical designs of six-port reflectometer junctions
[AD-A149419] 13 p2054 N85-22661
A preliminary human factors planning and design outline of parameters related to space station windows and CCTV monitoring 18 p3158 N85-29559

POSITION (LOCATION)
NT SOLAR POSITION
Drift characteristics of northeastern Bering Sea ice during 1982
[PB84-213982] 01 p0089 N85-10604
A trivariate Clough-Tocher scheme for tetrahedral data
[AD-A144740] 01 p0111 N85-10751
Problem of determining highly accurate coordinates of artificial satellites by photographic methods 02 p0162 N85-11096
The 7-Amino-4,6-Dinitrobenzofuroxan, an insensitive high explosive
[AD-A145665] 02 p0188 N85-11257
Estimation of target positioning using planar arrays
[RSRE-MEMO-3675] 02 p0189 N85-11266
Fungi of Mt. Babia Gora. 1: Mycoflora of forests
[NASA-TM-77484] 02 p0234 N85-11522
Interactions in localization
[NOTA-INTERNA-815] 02 p0279 N85-11818
Electrons in a disordered medium
[NOTA-INTERNA-816] 02 p0279 N85-11819
Realistic localizer courses for aircraft instrument landing simulators
[NASA-CR-172333] 04 p0455 N85-12885
Documentation for the machine-readable version of the Perth 75: A Catalogue of Positions of 2589 FK4 and FK4S Stars (Nikoloff and Hog 1982)
[NASA-TM-87376] 04 p0549 N85-13492
Documentation for the machine-readable version of the AGK3 Star Catalogue of Positions and Proper Motions North of -2 deg .5 declination (Dieckvoss and Collaborators 1975)
[NASA-TM-87378] 04 p0549 N85-13493
Terrestrial locating — of buoys from space 05 p0599 N85-13816
Documentation of earthquake algorithms
[PB84-235324] 05 p0677 N85-14351
High accuracy Doppler navigation employing optimum integrated position fix information 08 p1073 N85-16803
Data analysis techniques for vehicle attitudinal, positional and experimental measurements
[AD-A147752] 08 p1188 N85-17484
Spatiotemporal characteristics of visual localization
[AD-A148013] 08 p1200 N85-17555
The combinatorics of local constraints in model-based recognition and localization
[AD-A148336] 08 p1230 N85-17746
Three position estimation procedures
[AD-A148748] 09 p1278 N85-18042
Localization of destruction process 10 p1500 N85-19470
Fine figuring actuator
[AD-D011476] 10 p1557 N85-19819
Adjustable indicating device for load position
[NASA-CASE-MFS-29008-1] 11 p1635 N85-20300
Geodetic accuracy of LANDSAT 4 Multispectral Scanner and Thematic Mapper data — Washington, DC, California, Alabama, South Dakota, and Illinois 11 p1667 N85-20504
Performance of time-position discriminator of composite signal 13 p2072 N85-22941
Use of three omega radionavigation system position lines for solving problems in marine geodesy 13 p2107 N85-23131
Data Collection and Platform Location by Satellite: ARGOS Users' Conference 14 p2237 N85-23869
System performance, data distribution and technical files — ARGOS project 14 p2237 N85-23871
The ARGOS system status report 14 p2239 N85-23884
Three-dimensional sensing and interpretation
[AD-A150890] 14 p2311 N85-24304
Proceedings of the ARGOS Users Conference on Data Collection and Location by Satellite 14 p2322 N85-24348
Data Collection and Platform Location by Satellite: ARGOS Users' Conference 14 p2325 N85-24366
The ARGOS system main characteristics — satellite based localization 14 p2325 N85-24367
The ARGOS system after 3 years operation 14 p2325 N85-24368
The SARSAT program 14 p2327 N85-24385
Data Collection and Platform Location by Satellite: ARGOS users' Conference 14 p2328 N85-24391
Data Collection and Platform Location by Satellite: ARGOS Users' Conference 14 p2330 N85-24409
Location and synchronization — space-time coordinates 14 p2397 N85-24768
The ARGOS program — satellite based localization 14 p2397 N85-24775
The SARSAT/COSPAS system for assisting satellite based search and rescue 14 p2396 N85-24776
The TRANSIT and Global Positioning System (GPS) systems. Precision navigation and localization 14 p2398 N85-24777
Kitt Peak measurements of P/Halley positions 14 p2436 N85-25023
Measuring: The quantifying art 14 p2437 N85-25035
The orbital motion of Comet Halley 14 p2437 N85-25040
Documentation for the machine readable version of the Yale Catalogue of the Positions and Proper Motions of Stars between Declinations -60 deg and -70 deg (Fallon 1983)
[NASA-TM-87443] 14 p2439 N85-25051
Microcomputer application of aerospace asset surface search planning
[AD-A151833] 15 p2457 N85-25227
A FORTRAN program for deep space sensor analysis
[AD-A151700] 15 p2489 N85-25366
Low-resolution target classification from a staring infrared sensor
[AD-A151690] 15 p2852 N85-26358
Data Collection and Platform Location by Satellite: ARGOS Users' Conference 16 p2811 N85-27333
Location and data collection satellite system ARGOS. User's guide — satellite based localization 16 p2816 N85-27371
Real-time position determinations using the GPS TI4100/GEOSTAR receiver
[AD-A152561] 17 p2894 N85-27845
A comparison of methods of least squares adjustment of traverses
[AD-A153612] 18 p3170 N85-29645
A robust estimator of location using an adaptive spline model
[AD-A153662] 18 p3174 N85-29676
Ephemeral regions versus pseudo ephemeral regions 18 p3208 N85-29901
Use of Omega radio navigation system in geophysical work in Antarctica 19 p3296 N85-30448
The location of stress in clothing
[AD-A154423] 19 p3331 N85-30633
Touch-off: A method to determine the position of an object by means of a sensor-driven robot
[DE85-011178] 19 p3339 N85-30691
COSPAS/SARSAT: An overview 20 p3400 N85-31092
The COSPAS-SARSAT system 20 p3401 N85-31101
Comparing SLR and VLBI geodetic parameters 20 p3491 N85-31703
New optical satellite data 20 p3492 N85-31705
The potential of the NAVSTAR global positioning system for the Corps of Engineers, civil works
[AD-A154913] 21 p3554 N85-32109
Parameter estimation in communication system tracking satellite observations
[AD-A155137] 21 p3636 N85-32582
Estimating angular position of optical radiation source when received by array of photodetectors 22 p3778 N85-33413
Evaluation of coordinate measuring machines
[DE85-011712] 22 p3788 N85-33487
Dual optical mechanical position tracker
[AD-D011739] 22 p3844 N85-33811
What determines the location of satellites and planets? 22 p3863 N85-33858
Initial placement of STO instruments 23 p3902 N85-34174
Visual position determination for autonomous vehicle navigation
[AD-A156007] 24 p4063 N85-35181
Development of position sensors for microcomputer-oriented sensor systems
[BMFT-FB-T-85-021] 24 p4091 N85-35361
Materials and process development for microcomputer-compatible pressure, temperature, and position sensors
[BMFT-FB-T-85-024] 24 p4097 N85-35369
Evaluation of nuclear detonation location capability under high attack scenario
[AD-A155761] 24 p4149 N85-35729

POSITION ERRORS
NT BORESIGHT ERROR
Predictions of cockpit simulator experimental outcome using system models 05 p0702 N85-14504
A discussion of coning errors exhibited by inertial navigation systems
[RAE-TM-RAD-NAV-243] 08 p1082 N85-16854
Ordinary and proper location M-estimates for ARMA models, revised
[AD-A149705] 12 p1920 N85-22061
Positioning errors of commutating lenses and their influence on characteristics of high speed movie cameras 14 p2273 N85-24085
Angular error of position of RATAN-600 screens during radial displacement 15 p2476 N85-25286
Studies into location accuracy — ARGOS system 16 p2811 N85-27334
Positioning accuracy of the ARGOS system in operational use 16 p2811 N85-27335
An evaluation of the performance of a new storm tracking methodology
[AD-A152234] 16 p2835 N85-27484
Simulations of strapdown-system errors and error compensation methods — transport aircraft navigation
[DFVLR-MITT-84-22] 20 p3392 N85-31040
Search and rescue satellite (SARSAT) error analysis of the 406 MHz system 20 p3403 N85-31118

POSITION INDICATORS
NT ASTROLABES
NT PLAN POSITION INDICATORS
NT RADIO DIRECTION FINDERS
NT SPACECRAFT POSITION INDICATORS
Improved legislated emergency locating transmitters and emergency position indicating radio beacons
[NASA-CASE-GSC-12892-1] 11 p1624 N85-20226
Short-range radiotechnical point sensor 13 p2081 N85-22998
Enhancements to the TTS-502 time transfer system 17 p2963 N85-28296

High temperature position sensors based on monolithic GaAs Hall IC
[BMFT-FB-T-84-206] 17 p2969 N85-26337
A study of the application of differential techniques to the global positioning system for a helicopter precision approach
[NASA-CR-177326] 20 p3391 N85-31036
A device to detect Top Dead Center (TDC) position in motored engines
[REPT-84-RR-347] 20 p3458 N85-31475
POSITION SENSING
A position sensitive phoswich hard X-ray detector system
[OG-9.9-12] 23 p4026 N85-34967
POSITIONING
Linac quadrupole connections
[DE84-014694] 01 p0116 N85-10810
The facilities of the Calculation Center and Real Time Room for satellite positioning 05 p0599 N85-13819
Laser-guided measuring system for precisioning device 06 p0816 N85-15179
Recent development in astronomic position determinations
[AD-A148335] 08 p1062 N85-16858
Navigation for an intelligent mobile robot
[AD-A150051] 12 p1775 N85-21144
Orbital positioning and stationkeeping of geostationary satellites 14 p2397 N85-24772
Criteria for the classification of hydrographic positioning data
[AD-A152283] 16 p2705 N85-26697
Positioning of a robotic manipulator through the use of visual feedback
[AD-A151933] 16 p2851 N85-27577
Global positioning system carrier phase: Description and use
[PB85-174126] 19 p3216 N85-29946
Spillover minimization: An approach for actuators and sensors placement in distributed parameter study
[INPE-3625-PRE/746] 19 p3272 N85-30289
Optimal sensor locations for structural identification 20 p3417 N85-31209
The Galileo spacecraft magnetometer boom 22 p3796 N85-33513
Time domain reflectometry for SLC BPM system
[DE85-012369] 24 p4155 N85-35758
POSITIONING DEVICES (MACHINERY)
NT BOOMS (EQUIPMENT)
NT CAMS
NT JIGS
Experimental study with parameter variations on a hydraulic positioning servo with computer implemented observer
[FOA-C-20545-E3] 02 p0256 N85-11673
Vehicle anchoring system
[AD-D011282] 06 p0815 N85-15173
Multi-directional straddle-lift carrier
[AD-D011315] 07 p0973 N85-16183
The space shuttle orbiter remote manipulator positioning mechanism 08 p1102 N85-16963
Design procedure for the new 70-meter antenna subreflector positioner 10 p1463 N85-19232
Automated parts storage and retrieval system positioning device and method
[AD-D011494] 11 p1647 N85-20379
POSITIVE IONS
Meson delta-ray energies in ion molecule collisions
[DE85-005534] 13 p2157 N85-23395
Quantitation of Na+, K+-ATPase enzyme activity in tissues of the mammalian vestibular system 15 p2613 N85-26102
POSITRON ANNIHILATION
Application of positron annihilation in materials science
[DE84-014733] 02 p0286 N85-11683
The Fermi surface and momentum space densities of ferromagnetic Gd using the Positron technique 09 p1396 N85-18788
A remote source system for measuring relative positron annihilation line widths in individual slab cylindrical samples
[AERE-R-10548] 12 p1936 N85-22173
Trapping model analysis of annihilation line narrowing in some plastically deformed metals and alloys
[AERE-R-10593] 14 p2258 N85-23965
Characterization of atomic defects and their aggregates using positron annihilation spectroscopy
[DE85-006206] 14 p2418 N85-24918
Positron annihilation studies of vacancy formation in tungsten, chromium, and niobium
[DE85-006837] 16 p2871 N85-27710
An investigation of molecular structure of copolymers using positron annihilation spectroscopy
[NASA-TM-86431] 17 p2916 N85-27977
Measurements of heavy quark and lepton lifetimes
[DE85-006321] 18 p3181 N85-29724
Theory of positron annihilation in vacancies in concentrated disordered alloys
[DE85-010267] 18 p3183 N85-29734
Study of the equilibrium vacancy ensemble in aluminum using 1D- and 2D-angular correlation of annihilation radiation
[DE85-008967] 18 p3194 N85-29813
Electron-proton collider option for the superconducting super collider
[DE85-010146] 18 p3196 N85-29822
Resolvability of defect ensembles with positron annihilation studies
[DE85-010041] 18 p3196 N85-29823
Determination of the vacancy formation enthalpy in chromium by positron annihilation
[DE85-010266] 19 p3239 N85-30084
PAS determination of the vacancy formation enthalpy in tungsten
[DE85-010263] 19 p3240 N85-30086
Low-temperature positron lifetime and Doppler-broadening measurements for single-crystal nickel oxide containing cation vacancies
[DE85-010238] 19 p3376 N85-30944
Reduction of the trapping of positrons in dislocated single crystals of iron when charged with hydrogen
[DE85-010235] 19 p3377 N85-30950
A positron annihilation Doppler broadening study of niobium
[DE85-010287] 20 p3527 N85-31938
Positron measurements in 2H-TaSe2 crystals
[DE85-010507] 20 p3529 N85-31949
Materials characterization with intense positron beams
[DE85-011850] 22 p3839 N85-33769
Search for positron annihilation line and continuum radiation from the Galactic Center
[OG-2.5-5] 22 p3869 N85-33962
Some evidence for large gravitational redshift in Seyfert galaxy NGC 4151
[OG-2.7-11] 22 p3872 N85-33964
On some problems of gamma-astronomy
[OG-2.7-15] 22 p3873 N85-33966
A coded aperture imaging system optimized for hard X-ray and gamma ray astronomy
[OG-9.2-3] 23 p4024 N85-34942
Forty-five years of e(+)e(-) annihilation physics: 1958 to 2001
[DE85-013052] 24 p4149 N85-35723
POSITRONIUM
Experimental method for measuring positronium reflection from surfaces
[DE85-010949] 20 p3531 N85-31967
POSITRONS
Positron ring system using Anger-type detectors
[DE84-016788] 04 p0503 N85-13212
Positron flux concentrator: An update
[DE84-016260] 04 p0561 N85-13576
Notes on the RF system for the SLC positron source
[DE85-002628] 11 p1722 N85-20830
Low-energy, high-intensity positron beam experiments with a linac
[DE85-001048] 11 p1723 N85-20835
Electron-positron pair equilibrium in strongly magnetized plasmas 12 p1957 N85-22296
Electron-positron pairs in a mildly relativistic plasma in active galactic nuclei 12 p1957 N85-22297
Theory of positron annihilation in vacancies in concentrated disordered alloys
[DE85-010267] 18 p3183 N85-29734
Additional muon calculations for the SLC positron source
[DE85-011212] 19 p3363 N85-30855
Reduction of the trapping of positrons in dislocated single crystals of iron when charged with hydrogen
[DE85-010235] 19 p3377 N85-30950
Materials characterization with intense positron beams
[DE85-011850] 22 p3839 N85-33769
Advanced instrumentation for Positron Emission Tomography
[DE85-011147] 22 p3840 N85-33779
Observation of cosmic ray positrons from 5 to 25 GeV
[OG-6.2-5] 22 p3869 N85-34104
An observation of cosmic ray positrons from 10-20 GeV
[OG-6.2-6] 22 p3869 N85-34105
Reestimation of the production spectra of cosmic ray secondary positrons and electrons in the ISM
[OG-6.2-8] 22 p3869 N85-34107
Electrons and positrons from expanding supernova envelopes in dense clouds
[OG-6.2-9] 22 p3869 N85-34108
Possible detection of flare-generated positrons by Helios 1 on 3 Jun 1982
[SH-1.4-10] 23 p3996 N85-34770
Pulsed-neutron-source models for the astrophysical s-process
[DE85-012927] 24 p4151 N85-35740
Vacuum system for the Argonne 6 GeV synchrotron light source
[DE85-012296] 24 p4157 N85-35773
Missing energies at pair creation
[HE-4.4-8] 24 p4193 N85-36016
POST BOOST PROPULSION SYSTEM
Combined cycle ramjet engine
[AD-D011247] 06 p0760 N85-14859
POSTMISSION ANALYSIS (SPACECRAFT)
Results of Space Shuttle Flight 41-C
[GPO-36-092] 04 p0461 N85-12928
Statement of Captain Robert L. Crippen, USN, Commander of Space Shuttle Flight 41-C; Francis R. Scobee, pilot; Doctor George D. Nelson, Mission Specialist; Terry J. Hart, Mission Specialist; and Doctor James D. Van Hoften, Mission Specialist; accompanied by Frank Capollina, Solar Maximum Repair Mission Project Manager, Goddard Space Flight Center 04 p0461 N85-12929
National Space Transportation Systems Program mission report
[NASA-TM-87456] 14 p2241 N85-23698
POSTURE
Establishment of posture and working movements of pilot in air crash enquiries 07 p1010 N85-16417
Human body dimensions: Body outlines and envelope curves at different normal positions and movements
[HSE-TRANS-10666] 19 p3332 N85-30640
Postural adjustments associated with arm movements in weightlessness 20 p3509 N85-31613
POTABLE LIQUIDS
NT POTABLE WATER
POTABLE WATER
Reverse osmosis treatment to control inorganic and volatile organic contamination
[PB84-223528] 01 p0071 N85-10470
Ultrafiltration as pretreatment for the preparation of drinking water by reverse osmosis onboard ships
[PML-1984-32] 01 p0098 N85-10654
Corrosion of brass in potable water service
[CETIM-100390] 04 p0477 N85-13037
Tap noise-pressure fluctuations. Study of the acoustic behavior of hydraulic equipment in buildings as a function of the temperature
[CETIM-11-H-337] 04 p0502 N85-13201
Toxicology of natural and man-made toxicants in drinking water
[AD-P004035] 06 p0845 N85-15365
Closed-loop concepts for the Army: Water conservation, recycle, and reuse
[AD-A148839] 09 p1365 N85-18581
Literature review for development of the master analytical scheme for organic compounds in water
[PB85-152674] 15 p2507 N85-25486
Radiation-induced degradation of trichloroethylene and tetrachloroethylene in drinking water
[OEFZS-4298] 18 p3134 N85-29409
The degradation of pollutants in water and waste water by means of electron or gamma irradiation
[OEFZS-4317] 22 p3812 N85-33615
Experimental validation of allowable concentrations of sodium and potassium in recycled drinking water 22 p3823 N85-33665
POTASSIUM
NT LIQUID POTASSIUM
NT POTASSIUM 40
Measurement of magnetic sublevel differential scattering cross sections for potassium and mercury
[MPIS-10/1983] 01 p0119 N85-10815
Investigation on K (4 2P3/2) Hg interaction at collision energies from 0.5 to 5.7 eV
[MPIS-15/1983] 04 p0563 N85-13589
Titanium-potassium heat pipe corrosion studies
[DE84-015526] 05 p0637 N85-14090
Scattering experiments on interactions of excited atoms: Differential cross sections of the system Na (3P)+K(4S)
[MPIS-8/1984] 05 p0728 N85-14677
Calorimetric investigation into the possibility of a charge density wave ground state in alkali metals
[DE85-002006] 09 p1397 N85-18795
U, Th, K content, heat production and thermal conductivity of Sao Paulo, Brazil continental shelf sediments: A reconnaissance work
[INPE-3401-PRE/670] 10 p1515 N85-19558
Experimental investigations of thermal radiation from potassium atoms in magnetohydrodynamic system: Preliminary report
[DE85-003715] 12 p1936 N85-22169
Structural, morphological and optical characteristics of KGd(WO4)2 crystals 14 p2260 N85-24126
Performance characteristics of gravity-assisted potassium heat pipes
[DE85-010717] 19 p3287 N85-30367
Circadian dynamics of potassium excretion in urine as related to working on one and two shifts 19 p3325 N85-30598

Passive Q-modulation of optical cavities by KCl crystals containing OH(-) -ions 21 p3688 N85-32915
Measurements of Fe and Ar fragmentation cross sections
[PAPER-OG-7.2-20] 21 p3714 N85-33047
Precision measurements of solar energetic particle elemental composition
[PAPER-SH-2.1-4] 21 p3715 N85-33052
Thermodynamics of the corrosion of chromium in molten carbonates
[DE85-011407] 24 p4079 N85-35282
POTASSIUM ALLOYS
Thermodynamic properties of liquid Li-Pb, Na-Pb and K-Pb alloys: Similarities and Differences
[DE85-004074] 18 p3197 N85-29830
POTASSIUM CHLORIDES
Investigation of the dissolution of CaCrO4 in molten LiCl-KCl eutectic
[DE84-016394] 04 p0469 N85-12985
Passive Q-modulation of optical cavities by KCl crystals containing OH(-) -ions 21 p3688 N85-32915
POTASSIUM COMPOUNDS
NT POTASSIUM CHLORIDES
NT POTASSIUM HYDROXIDES
NT POTASSIUM OXIDES
NT POTASSIUM PERCHLORATES
NT POTASSIUM PHOSPHATES
Phase behavior and QLS (Quasielastic Light Scattering) in potassium linoleate/n-alkanol microemulsions
[AD-A155028] 21 p3563 N85-32163
Luminescence and absorption of indium-activated potassium-borate glasses subjected to high-power excitation 21 p3681 N85-32668
Ames Laboratory measurements of alkali levels in the Curtiss-Wright PFBC gas stream
[DE85-011357] 22 p3745 N85-33214
Throughfall rate and chemistry studies: Whiteface Mountain
[DE85-012407] 23 p3947 N85-34484
POTASSIUM HYDROXIDES
Effects of additives and KOH electrolyte concentration on dissolution of iron electrodes
[DE84-014840] 02 p0173 N85-11162
Experimental evaluation of the thermodynamic properties of concentrated aqueous potassium hydroxide solutions
[DE85-010828] 23 p3912 N85-34238
POTASSIUM ISOTOPES
NT POTASSIUM 40
POTASSIUM OXIDES
Improved oxygen sources for breathing apparatus
[NASA-TM-86671] 24 p4134 N85-35623
POTASSIUM PERCHLORATES
Thermal conductivity of iron/potassium perchlorate heat powder
[DE84-017071] 04 p0476 N85-13035
Solid phase reactions among manganese, potassium perchlorate and barium chromate
[HSE-TRANS-11166] 19 p3237 N85-30071
Burn front velocity as a function of pellet density in iron-potassium perchlorate heat powders
[DE85-011448] 21 p3572 N85-32214
Friction, impact, and electrostatic discharge sensitivities of energetic materials
[DE85-013321] 24 p4083 N85-35309
POTASSIUM PHOSPHATES
Chemical engineering principles of constant temperature-constant supersaturation growth of potassium dihydrogen phosphate (KDP) crystals
[DE84-017081] 04 p0571 N85-13645
Rapid growth of potassium dihydrogen phosphate crystals
[DE85-007261] 17 p3045 N85-28839
Refractive indices and thermo-optic coefficients of nonlinear crystals isomorphic to KH2PO4
[DE85-012968] 22 p3847 N85-33831
POTASSIUM 40
Investigation of the daytime lunar atmosphere
[NASA-CR-175636] 14 p2440 N85-25057
POTATOES
Multi crop area estimation in Idaho using EDITOR
[E85-10054] 06 p0827 N85-15251
Alcohol: An alternate energy resource for community use
[DE85-007731] 18 p3084 N85-29075
Use of gamma radiation as a form of preservation of sweet potatoes
[DE85-011998] 22 p3841 N85-33787
POTENTIAL ENERGY
NT BIOELECTRIC POTENTIAL
NT COULOMB POTENTIAL
NT ELECTRIC POTENTIAL
NT GEOPOTENTIAL HEIGHT
NT IONIZATION POTENTIALS
NT LOW VOLTAGE
NT NUCLEAR POTENTIAL
NT OPEN CIRCUIT VOLTAGE
NT PHOTOVOLTAGES
NT PLASMA POTENTIALS
NT QUANTUM WELLS
Theoretical studies in molecular fragmentation: Processes, energetics and diagnostics
[AD-A146310] 03 p0418 N85-12673
Theoretical studies of highly ionized species
[DE84-016797] 04 p0561 N85-13574
The use of available potential energy to evaluate two GLAS FGGE data sets 05 p0662 N85-14387
Generation of available potential energy and other diagnostic studies during FGGE
05 p0683 N85-14388
Analysis of diabatic heating during FGGE
05 p0683 N85-14389
Potential at atomic boundaries in the TF (or TFD) model and equations of states 12 p1820 N85-21419
Translational and extensional energy release rates (the J- and M-integrals) for a crack layer in thermoelasticity
[NASA-CR-174872] 12 p1863 N85-21685
Theoretical studies of kinetic mechanisms of negative ion formation in plasmas
[AD-A150820] 14 p2423 N85-24946
Electronically excited alkaline earth oxides: Chemical production and collisional energy transfer processes
[AD-A153172] 17 p3044 N85-28833
Variational transition state theory
[DE85-010685] 19 p3235 N85-30059
Calculation of Franck-Condon factors for diatomic molecules
[AD-A154463] 19 p3353 N85-30784
Determination of the intramolecular potential flow from a neutron diffraction experiment
[B8563199] 20 p3532 N85-31978
Generation of available potential energy and the energy cycle during the global weather experiment
[NASA-CR-175301] 21 p3634 N85-32572
Horizontal and vertical structure of velocity, potential vorticity and energy in the gulf stream
[AD-A154753] 21 p3655 N85-32702
POTENTIAL FLOW
NT EQUIPOTENTIALS
PAN AIR: A computer program for predicting subsonic or supersonic linear potential flows about arbitrary configurations using a higher order panel method. Volume 3: Case manual (version 1.0)
[NASA-CR-3253] 02 p0135 N85-10922
Comparison of uniform perturbation solutions and numerical solutions for some potential flows past slender bodies
[NASA-CR-172485] 06 p0749 N85-14799
Supersonic nonlinear potential analysis
[NASA-CR-172456] 07 p0897 N85-15685
Inviscid compressible flow past a multi-element aerofoil 08 p1089 N85-16776
Spectral modeling of a potential vorticity equation for a barotropic flow on a beta-plane
[CWI-AM-R8408] 08 p1186 N85-17478
Potential applications of forced unsteady flows
[AD-P004155] 09 p1264 N85-17940
Numerical approach for the aerodynamic analysis if airfoils with laminar separation
[NASA-CR-172496] 09 p1273 N85-18001
A frozen vorticity approach to the axisymmetric strong interaction problem
[AD-A149101] 10 p1484 N85-19369
Numerical integration of the unsteady full-potential equation with applications to transonic flow about a two-dimensional airfoil
[NLR-MP-84022-U] 12 p1773 N85-21130
Robust calculation of three-dimensional transonic potential flow based on the nonlinear gas multigrid method and a mixed incomplete lower upper decomposition/strongly implicit procedure (ILU/SIP) algorithm
[NLR-MP-84003-U] 12 p1848 N85-21593
Comparison of measured and computed boundary layers at the tail-end of an axisymmetric body in an air-jet
[AMTE(N)-TM-83053] 14 p2209 N85-23700
Wind tunnel wall interference
[AD-A151212] 15 p2474 N85-25273
An experimental study of hairpin-type vortices as a potential flow structure of turbulent boundary layers
15 p2553 N85-25751
Investigation of potential and viscous flow effects contributing to dynamic stall
[AD-A151666] 15 p2557 N85-25773
A counterpart of Faxen's formula in potential flow
[REPT-84-09] 17 p2980 N85-28279
A study of aerodynamic control in stalled flight long laminar separation bubble analysis
[AD-A153950] 19 p3059 N85-29930
A first-order time-domain Green's function approach to supersonic unsteady flow
[NASA-CR-172208] 19 p3214 N85-29930
Floating shock-fitting in transonic potential flow calculations 20 p3367 N85-31007
Fuselage upwash effects on RSRA rotor systems
[NASA-CR-177349] 20 p3388 N85-31015
Numerical simulation of potential flow in transonic steady regimes 20 p3389 N85-31016
Vortex sheet modeling with higher order curved panels
20 p3451 N85-31428
The calculation of fully three dimensional flow through any type of turbomachine blade row
21 p3587 N85-32294
On the limiting configuration of interfacial gravity waves
[AD-A154821] 21 p3631 N85-32557
Calculation of compressible flow about three-dimensional inlets with auxiliary inlets, slats and vanes by means of a panel method
[NASA-CR-174975] 24 p4060 N85-35162
POTENTIAL GRADIENTS
Ohmic potential drop and gas bubble radius distribution in alkaline water electrolysis 17 p2924 N85-28025
Double layer formation due to contact of different temperature plasmas
[IPPJ-722] 19 p3370 N85-30900
A supersonic potential gradient method for the calculation of unsteady aerodynamic pressures on harmonically oscillating wings
[DFVLR-FB-85-11] 20 p3390 N85-31026
Influence of edge effects on performance of electrooptical lens 22 p3770 N85-33366
Possibility of potential generation by lower hybrid wave 23 p3977 N85-34654
Fokker-Planck calculation of hot electron formation in the thermal barrier region of tandem mirror Gamma-10
[IPPJ-726] 23 p3979 N85-34669
POTENTIAL THEORY
Self potentials of an electron ring in a torus for large ring displacement from the minor axis
[AD-A146088] 03 p0421 N85-12691
Boundary element methods in potential theory: Four lectures
[NPL-DITC-46/84] 05 p0718 N85-14604
Applications of the simple-layer logarithmic potential
05 p0718 N85-14606
Applications of Green's boundary formula
05 p0718 N85-14607
Three-dimensional and axisymmetric problems
05 p0718 N85-14608
A comparative study of the nonuniqueness problem of the potential equation
[NASA-TP-2385] 07 p0899 N85-15694
A fast algorithm of the finite difference method for computation of the transonic flow past an arbitrary airfoil with the conservative full-potential equation
11 p1619 N85-20191
Field theory analysis using the finite element method to determine the deliberation curves of three dimensional fracture mechanics specimens with a semicircular surface crack applying the electrical direct current potential method for crack depth measurement
[GKSS-84-E-53] 17 p2982 N85-28434
Nonlinear potential analysis techniques for supersonic-hypersonic configuration design
[NASA-CR-166078] 19 p3212 N85-29917
Computer simulation of elastic waves by a new mass-point system with potentials
[DRIC-T-7274] 20 p3469 N85-31583
POTENTIOMETERS (INSTRUMENTS)
A simple, low cost potentiostat for corrosion studies
[NPL-DMA(A)-47] 04 p0502 N85-13203
Ground-water level data and preliminary potentiometric-surface maps, Yucca Mountain and vicinity, Nye County, Nevada
[DE85-001771] 09 p1343 N85-18448
Development and testing of a spacecraft surface potential monitor 13 p2007 N85-22582
Using a single-board computer to maintain constant voltage, current sources 15 p2551 N85-25749
POTENTIOMETERS (RESISTORS)
The measurement of high value resistances at the NPL — electrical resistance
[NPL-DES-81] 22 p3758 N85-33291
POTTING COMPOUNDS
Electrical research on solar cells and photovoltaic materials
[NASA-CR-175889] 15 p2585 N85-25935
Electrical research on solar cells and photovoltaic materials
[NASA-CR-175897] 17 p2966 N85-28452
POWDER (PARTICLES)
NT FINES
NT METAL POWDER
NT POWDERED ALUMINUM

Powder containing 2H-type silicon carbide produced by reacting silicon dioxide and carbon powder in nitrogen atmosphere in the presence of aluminum
[NASA-TM-77597] 01 p0027 N85-10167
Processing ceramics
[NASA-TM-77603] 01 p0031 N85-10168
Milling of Si3N4 with SiSN4 hardware
[NASA-TM-86864] 01 p0031 N85-10191
Structure of silane coupling agents adsorbed on silicon powder
[AD-A145803] 03 p0327 N85-12105
Sintering behavior of ultrafine silicon carbide powders obtained by vapor phase reaction
[NASA-TM-77422] 03 p0336 N85-12161
Ceramic microstructure development
[AD-A145753] 03 p0337 N85-12166
Preparation of sinter-active silicon carbide powders
[BMFT-FB-T-84-189] 04 p0469 N85-12982
Structural changes during milling of aluminum oxide powders
[NASA-TM-77466] 04 p0472 N85-13008
Thermal conductivity of iron/potassium perchlorate heat powder
[DE84-017071] 04 p0476 N85-13035
Infrared thermography of burn front propagation in heat powders
[DE85-003307] 10 p1438 N85-19060
Factors influencing the ball milling of Si3N4 in water
[NASA-TM-86932] 10 p1450 N85-19136
Effect of powder characteristics on microstructure and properties in alkoxide prepared PZT ceramics
[AD-A149062] 10 p1451 N85-19141
Dynamic compaction of powders
[DE85-001062] 11 p1612 N85-20137
Influence of external electric field on structural-mechanical properties of powdered materials
13 p2013 N85-22630
Recent trends in particle size analysis techniques
[NASA-TM-77735] 13 p2017 N85-22645
A comprehensive review of black powder
[AD-A150455] 13 p2039 N85-22769
Comparative sinterability of combustion synthesized and commercial titanium carbides
[DE85-006255] 15 p2512 N85-25498
Interfacial and colloidal aspects of aqueous suspension containing oxidic powders
[DE85-005972] 15 p2519 N85-25534
Sintering phenomena of non-oxide silicon compounds
[DE85-006676] 15 p2520 N85-25535
Test and modeling for sintering theory
[DE85-007761] 16 p2755 N85-27004
High resolution powder diffraction
[DE85-008287] 17 p2922 N85-28015
Attenuated total reflection method for obtaining optical constants of powders
[AD-A154094] 19 p3367 N85-30881
Multilayer capacitor dielectrics produced from metallo-organic precursors
[AD-A154592] 21 p3580 N85-32254
Combustion-deflagration-detonation transition in a confined spherical powder
[ISL-R-108/84] 22 p3747 N85-33223
Quantitative determination of mineral composition by powder X-ray diffraction
[DE85-011654] 22 p3760 N85-33301
Method for removing oxide contamination from silicon carbide powders
[DE85-011648] 23 p3919 N85-34287
Dynamic compaction of a monosized spherical tungsten powder
[DE85-014808] 24 p4080 N85-35289
Computational methods for the explosive and impact compaction of powders
[AD-A156219] 24 p4139 N85-35653

POWDER METALLURGY
USSR report: Materials science and metallurgy, no. 93
[JPRS-84810] 01 p0018 N85-10110
Development of powder metallurgy in various sections of USSR 01 p0019 N85-10116
Fabrication and characterization of Si3N4 ceramics without additives by high pressure hot pressing
[NASA-TM-77724] 01 p0031 N85-10189
Microstructural design and control of sintered hard materials 02 p0176 N85-11180
Development of powder metallurgy 2XXX series Al alloys for high temperature aircraft structural applications
[NASA-CR-172408] 02 p0182 N85-11220
Hot isostatically pressed manufacture of high strength MERL 76 disk and seal shapes
[NASA-CR-165550] 02 p0183 N85-11225
Observation of oxide skin in powder metallurgy aluminum alloys
[AD-A145819] 03 p0331 N85-12135
USSR report: Materials science and metallurgy
[JPRS-UMS-84-007] 03 p0348 N85-12244
Breakdown of porous metals by laser radiation
03 p0349 N85-12249
Comparison between the properties of conventional wrought and powder metallurgical alloys for turbine disc applications 07 p0906 N85-15739
Influence of temperatures of reactants on nature of product of solid-phase reactions
[BLL-M-36019-(5828.4)] 07 p0921 N85-15832
Influence of pressure on compaction during compression of powders of iron and 40Kh and 10R6MS steels
[BLL-M-35995-(5828.4)] 07 p0926 N85-15866
Investigation of granules of molybdenum-base alloys obtained with pulsed discharges
[BLL-M-36012-(5828.4)] 07 p0926 N85-15871
Solid-phase sintering of tantalum carbide
[BLL-M-36013-(5828.4)] 07 p0926 N85-15872
Fatigue strength of different sintered steels and design criteria for porous material (PM) parts
[LBF-FB-170/84] 07 p0928 N85-15886
Rapid solidification processing and powder metallurgy of Al alloys
[AD-A148427] 08 p1130 N85-17120
Application of diffusion welding of nickel based metals and application of electron beam welding of hot isostatically pressed nickel based powdered metals
08 p1169 N85-17375
Deformation and fracture of P/M (Powder/Metallurgy) titanium alloys
[AD-A148672] 09 p1294 N85-18128
Sub-eutectic densification and second phase formation in Al2O3 - CaO
[DE85-002065] 09 p1398 N85-18796
Research on rapidly solidified alloys
[AD-A149380] 10 p1441 N85-19080
Characterization of Nb-8 wt % Al wires by analytical electron microscopy
[DE85-002726] 10 p1442 N85-19086
Alloys based on NiAl for high temperature applications
[NASA-TM-86976] 12 p1805 N85-21322
Stress corrosion cracking behavior of tungsten heavy alloys
[AD-A149643] 12 p1806 N85-21329
USSR report: Materials science and metallurgy
[JPRS-UMS-85-002] 13 p2025 N85-22688
Effect of phase state of TiC-NiTi powder composite materials on nature of failure and mechanical properties
13 p2027 N85-22702
Apparatus for producing amorphous and microcrystalline metal powders 13 p2030 N85-22720
Fabrication of ceramic substrate-reinforced and free forms
[NASA-TM-86994] 14 p2247 N85-23926
Pressure-density behavior for AlN, Al2O3, SiO2, TiB2, and TiC powders up to 3.5 GPa
[DE85-006146] 14 p2261 N85-24012
Powder metallurgy production problems
15 p2497 N85-25406
Mechanisms of corrosion fatigue in high strength I/M (ingot Metallurgy) and P/M (Powder Metallurgy) aluminum alloys
[AD-A151177] 15 p2509 N85-25478
Metallurgical characterization of aluminum powder consolidation
[AD-A151990] 15 p2510 N85-25484
Interfacial and colloidal aspects of aqueous suspension containing oxidic powders
[DE85-005972] 15 p2519 N85-25534
Powder metallurgy bearings for advanced rocket engines 16 p2736 N85-26861
Microstructures and properties of rapidly solidified alloys
[NASA-CR-172377] 16 p2748 N85-26961
East Europe report: Science and technology
[JPRS-ESA-85-019] 16 p2767 N85-27077
Research on products obtained by powder metallurgy
16 p2768 N85-27081
Powder-metallurgy alloys and steels
[BLL-BISI-TRANS-22239-(9022.06)]
17 p2926 N85-28050
Sintering and properties of metal-ceramic alloys of the Kovar type
[BLL-BISI-TRANS-21622-(9022.06)]
17 p2927 N85-28060
Production and compaction of amorphous metal powders
[BLL-BISI-TRANS-22367-(9022.06)]
17 p2929 N85-28080
Dispersion-strengthened powder-metallurgical chromium steels
[BLL-BISI-TRANS-22323-(9022.06)]
17 p2929 N85-28081
Preparation of sinteractive silicon nitride powders
[BMFT-FB-T-84-303] 18 p3082 N85-29066
French, UK, Swedish research in powder metallurgy, HIP 18 p3088 N85-29109
Powder metallurgy forged gear development
[NASA-TM-87483] 18 p3117 N85-29295
USSR report: Materials Science and Metallurgy
[JPRS-UMS-85-005] 19 p3241 N85-30095
Hot isostatically pressed Sm(2)(TM)17 magnets
[AD-A155479] 21 p3582 N85-32257
Experimental attempt to achieve microstructure variations through temperature/time permutations for a nonwrought powder metallurgy uranium-6 niobium alloy
[DE85-013166] 23 p3916 N85-34272
The read-out system of spatial distribution of thermoluminescence in meteorites
[SH-9.1-16] 23 p4052 N85-35131
Method for measuring surface activity of silicon nitride powder
[NASA-TM-77906] 24 p4073 N85-35242
Oxidation resistant slurry coating for carbon-based materials
[NASA-CASE-LEW-13923-1] 24 p4077 N85-35267

POWDERED ALUMINUM
Observation of oxide skin in powder metallurgy aluminum alloys
[AD-A145919] 03 p0331 N85-12135
Non-steady combustion of composite solid propellants
[AD-A150827] 14 p2250 N85-23947
A fundamental study of liquid phase particle breakup. Revision
[AD-A150791] 14 p2301 N85-24249
Means for reducing hydrogen concentration upon surfacing of antifriction aluminum alloys with powder electrode 19 p3247 N85-30132

POWDERED METALS
U METAL POWDER

POWER
Circuit engineering and technological optimization of very high speed LSI logic elements and transistor structures 03 p0347 N85-12237

POWER AMPLIFIERS
Development of the Antares electron gun
[DE84-014043] 01 p0053 N85-10352
Spectrally matched modulation of radiation of injection laser in traveling-wave amplifier below 2 GHz
02 p0262 N85-11712
Metal oxide semiconductors power transistors
[CNES-84/QPE/FT/190] 04 p0496 N85-13166
Perceptibility of nonlinear distortions in power amplifier
06 p0789 N85-15041
Dual-gate MESFET variable gain constant output power amplifier
[AD-D011334] 07 p0945 N85-15982
Semiconductors at Leipzig Spring Fair
09 p1377 N85-19660
Combined microwave parallel amplifier-RF attenuator/modulator
[AD-D011535] 12 p1833 N85-21499
Proposal for continuation of research on megawatt gyrotrons for the period January 1, 1985 through December 31, 1986
[DE85-009962] 18 p3110 N85-29260
Methods of reliability design of semiconductor power devices 22 p3770 N85-33365
Research on gyrotrons
[AD-A154032] 23 p3934 N85-34360

POWER CONDITIONING
Multipurpose 5-MeV linear induction accelerator
[DE84-014523] 02 p0278 N85-11808
Space know-how, twenty years' space experience
04 p0461 N85-12926
Microcomputer control of a residential photovoltaic power conditioning system
[DE84-013867] 04 p0547 N85-13480
An Assessment of Integrated Flywheel System Technology
[NASA-CP-2346] 05 p0604 N85-13850
Microcomputer control of a residential photovoltaic power conditioning system
[DE84-014774] 07 p1022 N85-16488
Compilation of Sandia papers contributed to the 17th IEEE Photovoltaic Specialists Conference
[DE84-017456] 09 p1315 N85-18267
Variable speed generator technology options for wind turbine generators
[RR-84-4] 10 p1478 N85-19331
Inelastic tunnel diodes
[NASA-CASE-LEW-13833-1] 12 p1832 N85-21492
Autonomous uninterruptable power supply apparatus
[AD-D011571] 14 p2298 N85-24232
Advanced energy storage systems
[AD-A152244] 16 p2741 N85-26915
The plasma erosion opening switch
[AD-A154942] 21 p3580 N85-32259
Design and construction of an advanced power conditioning subsystem for small photovoltaic applications
[DE85-013940] 24 p4113 N85-35495

POWER DENSITY (ELECTROMAGNETIC)
U RADIANT FLUX DENSITY
POWER EFFICIENCY
Cylinder power fault diagnosis in military diesel engines
[TT-8405] 01 p0053 N85-10354
Measurements of satellite refrigeration compressor power consumption and efficiency
[DE84-016724] 05 p0632 N85-14056
High-power gate turn-off thyristors
06 p0793 N85-15071
New methods of fast switching of high power by means of semiconductor devices 06 p0794 N85-15075
Use of braking stages for control of turbine speed
09 p1306 N85-18215
Study of low energy density photovoltaic applications under varying rate structures
[DE85-000185] 10 p1511 N85-19538
Thermionic converter for space reactor described
11 p1621 N85-20208
The relevance of averaging period to wind power measurements and efficiency of Wind Energy Conversion Systems (WECS)
[GKSS-84-E-35] 11 p1676 N85-20562
Estimation of gas turbine engine boost provided by injecting water behind compressor
13 p2051 N85-22938
The ferrite permanent magnet AC motor: A technical and economical assessment
[DE85-002480] 13 p2066 N85-22903
Effect of diaphragm leakage on turbine stage characteristics 14 p2266 N85-24158
The effects of cooling on delay-time limits in IC's
14 p2297 N85-24224
The measurement of laser beam parameters
14 p2306 N85-24283
Aspects of CSSR CMOS integrated circuits discussed
15 p2533 N85-25827
Advanced energy storage systems
[AD-A152244] 16 p2741 N85-26915
Effect of precipitation on wind turbine performance
[NASA-TM-86998] 16 p2816 N85-27365
Commercialization of the power factor controller
[NASA-CR-171500] 17 p2951 N85-28221
On power efficient operation of the 2m x 2m transonic wind tunnel at the National Aerospace Laboratory
[NAL-TR-847] 18 p3064 N85-28953
Intense excitation source for high power laser
[AD-A153424] 18 p3112 N85-29287
Wind tunnel results of advanced high speed propellers in the takeoff, climb and landing operating regimes
[NASA-TM-87054] 19 p3213 N85-29925
Increased voltage photovoltaic cell
[NASA-CASE-NPO-16155-1] 19 p3303 N85-30475
Free-piston Stirling engine/linear alternator 1000-hour endurance test
[NASA-CR-174771] 19 p3304 N85-30481
A new large-scale, high-resolution multicolor software display concept
[AD-A155404] 22 p3827 N85-33703
Determination of DTL configurations
[DE85-010714] 22 p3830 N85-33719
Technology of magnetically driven accelerators
[DE85-011657] 23 p3983 N85-34700
Wingtip vortex propeller
[NASA-CASE-LAR-13019-1] 24 p4085 N85-35194
POWER FACTOR CONTROLLERS
Solar powered actuator with continuously variable auxiliary power control
[NASA-CASE-MFS-25637-1] 12 p1876 N85-21769
Power control for ac motor
[NASA-CASE-MFS-25681-1] 13 p2062 N85-22877
Commercialization of the power factor controller
[NASA-CR-171500] 17 p2951 N85-28221
POWER GENERATORS
U ELECTRIC GENERATORS
POWER LIMITERS
Monolithic planar doped barrier limiter
[AD-D011578] 15 p2548 N85-25723
POWER LINES
EMP injection on conduit entries, type Brattberg — electromagnetic pulse (EMP) injection
[FOA-E-30001-A3] 02 p0193 N85-11290
Pulsed-power system diagnostics: Electromagnetic data interpretation along pulse lines
[AD-A146607] 08 p0810 N85-15148
The ac power line protection for an IEEE 587 Class B environment 07 p1000 N85-16347
Adaptation of an air-dielectric RF cable for use as an oil-filled high voltage pulse transmission line
[DE84-017414] 11 p1630 N85-20265
Electromagnetic pulse (EMP) injection on cable entries, type ERA; EMP memo no. 10
[FOA-E-30003-A3] 12 p1830 N85-21484
Study of electric field and ion effects on HVDC lines
[DE85-002975] 12 p1833 N85-21503
Numerical Electromagnetics Code (NEC)
[DE85-004999] 13 p2056 N85-22874
Operational test results of a prototype superconducting power transmission system and their extrapolation to the performance of a large system
[DE85-006731] 16 p2779 N85-27153
Unalloyed and alloyed line wires of improved properties
[BLL-BISI-TRANS-21930-(9022.00)]
18 p3073 N85-29008
Effects of Formvar coating and copper-nickel outer sheath on the ac losses of multi-strand subsize cables
[DE85-010413] 18 p3098 N85-29166
Protection products for the conductors of high voltage overhead lines
[BLL-OA-TRANS-3219-(6196.300)]
20 p3429 N85-31269
New corrosion protection concept for very high voltage line towers
[BLL-OA-TRANS-2691-(6196.300)]
20 p3429 N85-31270
Injector losses on Mite
[DE85-012356] 24 p4090 N85-35355
RFQ modeling computer program
[DE85-012665] 24 p4140 N85-35661
POWER PLANTS
Combustion chamber floatwall panel attachment arrangement
[AD-D011358] 07 p1047 N85-16647
Leak detectors for organic Rankine cycle power plants: On-line and manual methods
[DE85-002792] 12 p1852 N85-21617
A model for the economic assessment of solar power plants
[DE85-009355] 19 p3381 N85-30977
POWER PROCESSING SYSTEMS
U POWER CONDITIONING
POWER REACTORS
In-situ stress relief of expanded alloy 600 steam generator tubing
[DE84-014560] 04 p0513 N85-13273
A new rheological model for concrete structural analysis
[DE84-014743] 11 p1653 N85-20413
Development of the Cascade inertial-confinement-fusion reactor
[DE85-010933] 19 p3357 N85-30612
Transient three-phase three-component systems. Part 1: Formulation of the system of differential equations
[DE85-013267] 24 p4095 N85-35384
DEPTH-CHARGE static and time-dependent perturbation/sensitivity system for nuclear reactor core analysis, revision 1
[DE85-013103] 24 p4139 N85-35659
Applicability of 100kWe-class of space reactor power systems to NASA manned space station missions
[NASA-CR-174696] 24 p4149 N85-35728
POWER SERIES
NT TAYLOR SERIES
Polynomial and power series FGS-rings have trivial coefficient rings
[TWISK-326] 01 p0109 N85-10737
A simple and efficient algorithm to compute tail probabilities from transforms
[AD-A150928] 14 p2409 N85-24849
Use of REDUCE 2 for symbolic programming
[INPE-3955-PRE/633] 16 p2846 N85-27544
POWER SPECTRA
The average power density spectra of additive scrambler signals and their versions in AMI code
[FUB-27-1983] 01 p0040 N85-10258
Shape of power spectrum of intermittent chaos
02 p0283 N85-11841
Phase transition which exhibits 1/omega-spectrum: A rigorous result 02 p0283 N85-11842
Using measured variance of skywave radar sea-echo power spectra to estimate ionospheric Doppler broadening of mean spectra
[PB84-214071] 03 p0399 N85-12544
Noise analysis of the Coarse Optical Power Spectrum Estimator (COPSE) data acquisition system
[AD-A145918] 03 p0419 N85-12677
On syntheses of the X-ray background with power-law sources
[NASA-TM-82173] 03 p0446 N85-12940
Flight test technique for evaluation of gust load alleviation analysis methodology
[NASA-TM-86344] 06 p0754 N85-14833
Power spectrum analysis of astronomical photographs digitized with small apertures 07 p0965 N85-16127
Power spectral analysis of markov texture fields
07 p0966 N85-16262
Electrostatic wave observation during a space simulation Beam-Plasma-Discharge (BPD)
[NASA-CR-174266] 07 p1045 N85-16639
A nonlinear technique for high-resolution data processing
[AD-D011415] 08 p1203 N85-17570
NOAA OTEC CWP (National Oceanic and Atmospheric Administration Ocean Thermal Energy Conversion Cold Water Pipe) at-sea test. Volume 3, part 1: Tabulation of the power spectra for selected channels
[PB84-236955] 09 p1346 N85-18467
MTF analysis of LANDSAT-4 Thematic Mapper
12 p1871 N85-21737
The use of the spectral matrix in analyzing the propagation characteristics of electromagnetic emissions — magnetosphere 14 p2371 N85-24888
Evaluation of a magneto-optical filter and a Fabry-Perot interferometer for the measurement of solar velocity fields from space 14 p2442 N85-25067
Detection of solar gravity mode oscillations
14 p2442 N85-25070
Solar gravity modes from ACRIM-SWM irradiance data
14 p2443 N85-25071
Implications of observed frequencies of solar P modes
14 p2443 N85-25073
The effects of a nearly 100% duty cycle in observations of solar oscillations 14 p2443 N85-25078
Spectral information from gapped data. A comparison of technique 14 p2444 N85-25080
The stability of the low-degree 5-minute solar oscillations 14 p2444 N85-25084
An excitation mechanism for solar 5-minute oscillation of intermediate and high degree
14 p2444 N85-25085
Rational pulse-shaping filters for almost MSK-like modulation
[AD-A153065] 17 p2949 N85-28208
Projections of plasma cloud structures and their spectra
[AD-A153608] 18 p3189 N85-29776
Estimate of signal-to-interference energy ratio in discrete-data transmission 22 p3776 N85-33398
Cosmic ray biannual variation
[SH-4.4-15] 23 p4034 N85-35011
Cosmic ray power spectral variations. 3: Solar rotation periodicities
[SH-4.4-16] 23 p4034 N85-35012
A relation between the short time variations of cosmic rays and geomagnetic field change
[SH-5.1-14] 23 p4043 N85-35057
Pressure cross spectra in turbulent boundary layers in water
[AD-A156153] 24 p4094 N85-35378
Noise in sodium beta alumina crystals
[AD-A156025] 24 p4161 N85-35798
POWER SUPPLIES
DC switching regulated power supply for driving an inductive load
[DE84-014238] 01 p0044 N85-10295
Design, construction, and operational results of an 800-A, 10-kV hot deck amplifier
[DE84-014044] 04 p0496 N85-13182
Distributed energy store railguns experiment and analysis 09 p1313 N85-18258
All solid state high voltage power supply for neutral beam sources
[DE85-002531] 11 p1629 N85-20257
Photovoltaic industry progress through 1984
[DE85-013029] 22 p3809 N85-33596
POWER SUPPLY CIRCUITS
Isolated load switching with surge suppression
[AD-D011218] 01 p0042 N85-10274
Control aspects of the Schuchuli Village stand-alone photovoltaic power system
[NASA-TM-83780] 04 p0495 N85-13157
Developments in space power components for power management and distribution 05 p0808 N85-13877
Fuse status indicator system
[AD-D011294] 06 p0804 N85-15121
High-voltage, high-power, solid-state remote power controllers for aerospace applications
[NASA-TP-2437] 12 p1795 N85-21283
Erosion of electrodes due to switching of capacitor-bank discharge circuits
[AD-A151207] 15 p2547 N85-25718
China report: Science and technology
[JPRS-CST-85-011] 15 p2551 N85-25746
Improved Gonda's circuit described
15 p2551 N85-25748
Using a single-board computer to maintain constant voltage, current sources 15 p2551 N85-25749
POWER TRANSMISSION
Vibrational power transmission of an idealized gearbox
[ISVR-TR-124] 02 p0204 N85-11348
Operational characteristics of a 1000 MVA superconducting power transmission system
[DE85-000232] 09 p1314 N85-18283

Superconducting magnetic energy storage for asynchronous electrical systems
[DE85-005986] 22 p3847 N85-33832

POWER TRANSMISSION (LASERS)
Technology for satellite power conversion
[NASA-CR-174335] 09 p1343 N85-18451

POWERED LIFT AIRCRAFT
Future of V/STOL aircraft systems: A survey of opinions
[NASA-TM-86699] 18 p3061 N85-25937

POYNTING THEOREM
Theoretical approach to evolution of solar magnetic field 18 p3204 N85-29874

PPI (POSITION INDICATORS)
U PLAN POSITION INDICATORS

PPM (MODULATION)
U PULSE POSITION MODULATION

PRACTICES
U PROCEDURES

PRAESEPE STAR CLUSTERS
The behaviour of brighter binaries and yellow giants in open clusters 05 p0737 N85-14738

PRAIRIES
U GRASSLANDS

PRANDTL NUMBER
Influence of Prandtl number on natural convection heat transfer correlations
[DE84-013006] 05 p0637 N85-14089
High Marangoni number convection in a square cavity
[NASA-CR-174263] 07 p0959 N85-16078
Internal forced convection to low Prandtl number gas mixtures
[AD-A148932] 10 p1484 N85-19366
Contribution to the theory of stationary separation areas
[NASA-TM-77825] 14 p2300 N85-24244

PRANDTL-MEYER EXPANSION
The highly underexpanded exhaust plume from nozzles with boundary layers
[DFVLR-FB-85-10] 20 p3421 N85-31230

PRASEODYMIUM
Supercell band structure calculations of the two peak photo-and inverse photoemission spectra in Ce and Pr compounds
[DE84-017485] 06 p0667 N85-15513
Very low temperature studies of hyperfine effects in metals
[DE85-013367] 22 p3749 N85-33236

PRE-MAIN SEQUENCE STARS
Molecular hydrogen emission associated with high velocity flows. A tracer for low velocity shocks
03 p0443 N85-12819
X-ray activity in pre-main sequence stars
06 p1233 N85-17764
Active phenomena in the pre-main sequence star AB AUR 06 p1233 N85-17765
A search for young stellar chromospheres in NGC 2264 11 p1748 N85-20993

PREAMPLIFIERS
New preamplifier for particle detectors
[DE85-004115] 12 p1836 N85-21524
Tubes and transistors in audio amplifiers
12 p1837 N85-21532
Recommendation on use of series K157UL1 microcircuits 13 p2071 N85-22936
Fast scintillation counter preamplifier for the observation of Linsley effect
[HE-4.7-9] 24 p4199 N85-36060
A mini-array for large air showers
[HE-4.7-10] 24 p4199 N85-36061

PREBURNERS
Analysis of physical-chemical processes governing SSME internal fluid flows
[NASA-CR-174245] 06 p0760 N85-14682
An investigation of space shuttle main engine shutdown chugging instability 12 p1946 N85-22221
Fiber optic Raman thermometer for Space Shuttle main engine preburner profiling 16 p2730 N85-26904
SSME fuel preburner two-dimensional analysis
17 p2911 N85-27943

PRECAMBRIAN PERIOD
Archean sedimentation and tectonics in southern Africa
[NASA-CR-174156] 04 p0533 N85-13408
Constraints on lunar origin: Evidence preserved in Precambrian stromatolites 04 p0584 N85-13731
Synthesis of proterozoic data as a prerequisite for tectonic and thermal modeling
[NASA-CR-174252] 07 p0995 N85-16323
SIR-B analysis of the Precambrian shield of Sudan and Egypt: Penetration studies and subsurface mapping
08 p1145 N85-17219
Structural investigation of the Canadian Shield by orbital radar and LANDSAT 08 p1147 N85-17238
Late precambrian to ordovician metamorphism and orogenesis in the Blue Ridge and western Piedmont, Virginia Appalachians 09 p1352 N85-18503
Precambrian evolution and the rock record
21 p3656 N85-32711
Use of space photographs for analysis of structural and dynamic conditions of formation of ancient phlogopite and apatite deposits 22 p3735 N85-33153

PRECAUTIONS
U ACCIDENT PREVENTION

PRECESSION
NT QUENCHING (ATOMIC PHYSICS)
Earth rotation and polar wandering
14 p2399 N85-24785

PRECIOUS METALS
U NOBLE METALS

PRECIPITATION
Monthly and seasonal weather outlook for October 1984, volume 38, number 19, 29 September 1984
[PB85-113538] 11 p1687 N85-20610
Monthly and seasonal weather outlook for January 1985, volume 39, number 1
[PB85-146799] 12 p1898 N85-21915

PRECIPITATION (CHEMISTRY)
The X-ray Absorption Coefficient Fine Structure (EXAFS) study on precipitates in AlCu
[DESY-SR-84-15] 01 p0025 N85-10153
Rapid solidification processing and the control of structure/property relationships
02 p0176 N85-11178
A study of precipitation and boron distribution in 20 Cr 25Ni base stainless steels
[AERE-M-3353] 03 p0334 N85-12154
Investigation of the isothermal precipitation behavior of nickel-base alloys using electrochemical phase extraction
[JUEL-1903] 05 p0819 N85-13958
Microstructure, texture and formability of thin aluminium sheets 06 p0796 N85-15088
Clusters of defects in semiconductors
[AD-A147426] 07 p1048 N85-16655
Effect of powder characteristics on microstructure and properties in alkoxide prepared PZT ceramics
[AD-A149082] 10 p1451 N85-19141
Geothermal injection treatment: Process chemistry, field experiences, and design options
[DE85-002873] 11 p1675 N85-20554
Microstructural study on the processing and properties of high-field A15 superconducting materials
[DE85-004652] 13 p2164 N85-23423
MAP3S precipitation chemistry network
[DE85-006324] 14 p2353 N85-24539
An investigation of the structure and high temperature mechanical properties of oxide dispersion strengthened alloys
[AD-A151107] 15 p2509 N85-25477
A comparative evaluation of the effects of acid precipitation, natural acid production and harvesting of cation removal from forests
[DE85-005254] 15 p2589 N85-25961
Thermal annealing of Fe implanted Al2O3 in oxidizing and reducing environment: Revised version
[DE85-007546] 16 p2752 N85-26983
The precipitation mechanism in a metallic solid solution crystal: Case of the aluminum-copper and aluminum-silver systems
[DE85-009981] 18 p3077 N85-29032
North American acid deposition data base system (ADS) and its use in spatial analysis
[PB85-173235] 18 p3201 N85-29856
Electrochemical reduction of titanium in dimethyl sulphoxide
[BLL-OA-TRANS-3225-(6196.300)] 20 p3429 N85-31267
A study of the effect of a mismatch in gamma and gamma prime phase lattice spacings on the high temperature strength characteristics of dispersion-hardened nickel alloys
[BLL-CE-TRANS-8048-(9022.09)] 20 p3430 N85-31279
Effect of precipitation variables on the specific surface and explosion characteristics of penteerythritol tetranitrate
[DE85-009620] 23 p3922 N85-34302

PRECIPITATION (METEOROLOGY)
NT ACID RAIN
NT RAIN
NT SNOW
NT SNOW COVER
Geostationary satellite cloud and precipitation analysis using an interactive computer system
01 p0076 N85-10506
Test results from RAINSAT 01 p0076 N85-10508
A tropical cyclone precipitation estimation technique using geostationary satellite data
[PB84-226703] 01 p0086 N85-10579
The identification of rain-bearing synoptic systems through principal component analysis
02 p0212 N85-11394
The application of principal component analysis in a study of rainfall 02 p0212 N85-11396
Spatial relationships in stream flow residuals
02 p0212 N85-11397
Forecast of the northeastern drought by the method of periodicities: Use and abuses
[INPE-3109-PRE/508] 02 p0230 N85-11502
Heat sources in the tropics and large scale flow anomalies associated with precipitation anomalies in northeast Brazil
[INPE-3211-TDL/175] 04 p0538 N85-13421
Weather research program report; FY 1983
[PB84-236694] 04 p0541 N85-13440
Studies of atmospheric water in storms with the Nimbus 7 scanning multichannel microwave radiometer
05 p0682 N85-14362
Trends in skill and accuracy of National Weather Service pop forecasts
[PB84-229053] 06 p0840 N85-15335
Precipitation characteristics of a dual mesoscale convective complex
[PB84-226711] 06 p0840 N85-15337
Revised Uniform Summary of Surface Weather Observations (RUSSWO). Aconbury RAF United Kingdom, parts A-F
[AD-A146913] 07 p1004 N85-16384
Revised Uniform Summary of Surface Weather Observations (RUSSWO). McChord AFB, Washington, parts A-F
[AD-A146914] 07 p1005 N85-16385
Revised Uniform Summary of Surface Weather Observations (RUSSWO). Mildenhall RAF, United Kingdom, parts A-F
[AD-A146915] 07 p1005 N85-16386
Revised Uniform Summary of Surface Weather Observations (RUSSWO). Dobbins AFB, Georgia, parts A-F
[AD-A146916] 07 p1005 N85-16387
Revised Uniform Summary of Surface Weather Observations (RUSSWO). Shemya AFB, Alaska, parts A-F
[AD-A146917] 07 p1005 N85-16388
Revised Uniform Summary of Surface Weather Observations (RUSSWO). Pope AFB, Fayetteville, North Carolina, parts A-F
[AD-A146918] 07 p1005 N85-16389
Revised Uniform Summary of Surface Weather Observations (RUSSWO). Sondestrom AB, Greenland, parts A-F
[AD-A146919] 07 p1005 N85-16390
Revised Uniform Summary of Surface Weather Observations (RUSSWO). England AFB, Alexandria, Louisiana, parts A-F
[AD-A146920] 07 p1006 N85-16391
Revised Uniform Summary of Surface Weather Observations (RUSSWO). Parts A-F: Homestead AFB, Florida
[AD-A147203] 07 p1007 N85-16396
Limited surface observations climatic summary (LISOCS). Camp Casey, Tong Du Chon, Korea
[AD-A147204] 07 p1007 N85-16397
Limited surface observatins climatic summary (LISOCS). Ansbeck AHP, Germany
[AD-A147205] 07 p1007 N85-16398
Revised Uniform Summary of Surface Weather Observations (RUSSWO). O'Hare International Airport, Chicago, parts A-F
[AD-A147206] 07 p1007 N85-16399
Methodology for the collection and analysis of trace metals in atmospheric precipitation
[CM-67] 09 p1350 N85-18491
Revised Uniform Summary of Surface Weather Observations (RUSSWO). Parts A-F Zweibrucken AB, Germany
[AD-A147165] 09 p1357 N85-18536
Mesoscale storm and dry period parameters from hourly precipitation data: Program documentation
[DE85-001366] 09 p1357 N85-18538
Sequential precipitation chemistry sampling program at Brookhaven National Laboratory with an analytical summary of 1976-1982 data
[DE85-002788] 10 p1513 N85-19545
Large scale circulation anomalies and prediction of northeast Brazil droughts
[INPE-3405-PRE/674] 10 p1518 N85-19571
Interannual variations of the winter circulation in the Northern Hemisphere and in the southern oscillation (meridian) and their possible connections with the climate of Northeast Brazil
[INPE-3333-TDL/182] 10 p1519 N85-19573
Frozen precipitation and concurrent weather: A case study for Munchen-Riem, West Germany
[AD-A149227] 10 p1519 N85-19577

Precipitation gage network operations for wintertime research in the Central Sierra Nevada
[PB85-115020] 10 p1520 N85-19582
Computer-assisted data processing and analysis system for ground-based meteorological data collection, report on the Sierra Cooperative Pilot Project
[PB85-115350] 10 p1520 N85-19587
Monthly and Seasonal Weather Outlook for November, 1984, Volume 38, Number 27, October 30, 1984
[PB85-118800] 10 p1521 N85-19588
Monthly and seasonal weather outlook for mid-October to mid-November 1984, volume 38, number 20, 13 October 1984
[PB85-113546] 11 p1667 N85-20611
Prospective investigations with DFVLR radar of possible relevance in the assessment of radio interference due to scattering from precipitations — meteorological radar
[DFVLR-FB-84-42] 12 p1830 N85-21485
Combined effects of atmospheric deposition, internal acid production, and harvesting on nutrient gains and losses from forest ecosystems
[DE85-002325] 12 p1884 N85-21821
OSCAR experiment high-density network data report
[DE85-004907] 12 p1884 N85-21826
Hazardous air pollutants: Wet removal rates and mechanisms
[PB85-138626] 12 p1887 N85-21842
On the wind error of the Finnish raingauge
[REPT-37] 12 p1893 N85-21883
Moisture variation in northern hemisphere temperate latitudes 13 p2105 N85-23119
Relationship of Indian monsoon intensity to time of onset 13 p2106 N85-23120
Summary of Meteorological Observations, Surface (SMOS), Bermuda
[AD-A150537] 13 p2138 N85-23278
Summary of Meteorological Observations, Surface (SMOS), Beaufort, South Carolina
[AD-A150538] 13 p2138 N85-23279
Summary of Meteorological Observations Surface (SMOS), Sigonella, Sicily/Navy
[AD-A150539] 13 p2138 N85-23280
Summary of Meteorological Observations, Surface (SMOS), Alameda, California
[AD-A150609] 13 p2138 N85-23281
MAP3S precipitation chemistry network
[DE85-005324] 14 p2353 N85-24539
Experimental investigation of annular air curtain domes
[UTIAS-286] 15 p2521 N85-25543
An analysis of issues concerning acid rain, report to the Congress of the United States
[TI85-901070] 15 p2589 N85-25959
Shuttle imaging radar-B (SIR-B) data analysis for identifying rainfall event occurrence and intensity
[NASA-CR-175712] 15 p2594 N85-25986
Severe storm detection with passive 37 GHz observations 15 p2596 N85-25997
High-frequency microwave observations of convective precipitation 15 p2596 N85-26000
Model sensitivity studies of major east coast storms 15 p2598 N85-26018
Characteristics of precipitation regimes during first global atmospheric research project global experiments
[AD-A151572] 15 p2599 N85-26021
Annual cycle. Part 2: The annual variation of precipitation over the United States and Canada
[PB85-147664] 15 p2600 N85-26027
Cloud-seeding for regulating precipitation in Moscow area 16 p2807 N85-27308
Regularities in recent changes in surface air temperature and atmospheric precipitation fields 16 p2807 N85-27311
Effect of precipitation on wind turbine performance
[NASA-TM-86986] 16 p2818 N85-27365
Precipitable water in the atmosphere, determined from surface dewpoint values 16 p2831 N85-27457
Summary of Meteorological Observations, Surface (SMOS), Dallas, Texas
[AD-A150599] 16 p2835 N85-27480
A climatic data bank for Northern Hemisphere land areas, 1851-1980
[DE85-007863] 16 p2835 N85-27486
SCPP (Sierra Cooperative Pilot Project) data collection and analysis. Volume 1: Executive summary
[PB85-156085] 16 p2837 N85-27494
Monthly and seasonal weather outlook for mid-January to mid-February 1985, volume 39, number 2, January 15, 1985
[PB85-164572] 16 p2837 N85-27500
Monthly and seasonal weather outlook for February 1985, volume 39, number 3, January 30, 1985
[PB85-159424] 16 p2838 N85-27502
Precipitation and snow cover data, 1977
[ISBN-951-697-215-2] 17 p2995 N85-28514
Environmental Research Division report: Atmospheric physics
[DE85-009659] 18 p3133 N85-29404
Elemental tracers of source regions of contaminants in precipitation
[DE85-007366] 18 p3133 N85-29407
Cloud physics 18 p3147 N85-29485
Areal coverage of storm precipitation
[NASA-CR-176013] 19 p3315 N85-30550
Precipitation estimation using collocated GOES satellite and surface data
[AD-A154248] 19 p3317 N85-30559
Monthly and seasonal weather outlook for mid-March to mid-April 1985, March 14, 1985, volume 39, no. 6
[PB85-174751] 19 p3317 N85-30565
Measurements of giant salt nuclei from inland in east China 21 p3648 N85-32668
Monthly and seasonal weather outlook for April 1985, March 30, 1985, volume 39, no. 7
[PB85-183604] 22 p3817 N85-33648
Throughfall rate and chemistry studies: Whiteface Mountain
[DE85-012407] 23 p3947 N85-34464

PRECIPITATION HARDENING

Strain hardening and strain aging in Fe-Al-Mn alloys 02 p0178 N85-11198
The effect of potential on the corrosion fatigue behavior of a precipitation hardened aluminum alloy
[AD-A146537] 06 p0768 N85-14918
Anomalies of aluminum structure and properties 13 p2026 N85-22683
Age hardening and atomic structure of an aluminum-6 at. % silver alloy
[DE85-009977] 18 p3077 N85-29031
Influence of gamma-phase on magnetic properties and structure of KhK15YuB alloy during strain-aging
[BLL-M-36281-(5626.4)] 20 p3431 N85-31280
Thermomechanical deformation in the presence of metallurgical changes 20 p3466 N85-31533
The dynamic strain ageing of A533B class 1 nuclear pressure vessel steel
[AERE-R-11485] 24 p4078 N85-35274

PRECIPITATION PARTICLE MEASUREMENT

Experimental study of anisotropy of scattering of radar signals by clouds and precipitation 14 p2340 N85-24473
Modeling of radiothermal radiation of rain by Monte-Carlo method 14 p2341 N85-24476
Experimental and theoretical investigations of open resonators — precipitation measurement
[DFVLR-FB-85-12] 20 p3449 N85-31414

PRECIPITATORS

NT ELECTROSTATIC PRECIPITATORS
Acoustic agglomeration methods and apparatus
[NASA-CASE-NPO-15466-1] 12 p1927 N85-22104

PRECISION

Publications of Center for Manufacturing Engineering (of the National Bureau of Standards), 1978-1983
[PB84-224526] 01 p0036 N85-10226
East Europe report: Science and technology
[JPRS-ESA-84-045] 05 p0815 N85-15175
Power of deterministic thinking in machine tool accuracy
[DE85-001751] 07 p0974 N85-16188
Proceedings of the Workshop on Improvements to Photometry
[NASA-CP-2350] 08 p1250 N85-17892
History of photometric precision 08 p1250 N85-17893
Photometric precision needed for planetary detection 08 p1250 N85-17894
Reduction to outside the atmosphere and statistical tests used in Geneva photometry 08 p1251 N85-17902
Operational experience with ion concentration sensors in orientation systems 13 p1980 N85-22422
Method for determining the number of correlative measurements required to validate the SBUV/2 ozone retrievals 13 p2105 N85-23114
Precision linear ramp function generator
[DE85-011647] 22 p3760 N85-33304
Analyzer, flight line
[AD-A155777] 24 p4067 N85-35207

PREDICTION ANALYSIS TECHNIQUES

Aerodynamics of airfoils subject to 3-dimensional periodic gusts
[AD-A145149] 01 p0003 N85-10018
The use of fixed-bed adsorber models to predict the fluxes of toxic substances in groundwaters and soil environments
[PB84-202563] 01 p0071 N85-10468
Prediction of deflections of the vertical by gravimetric methods
[PB84-213727] 01 p0072 N85-10478
On probability forecasts for temperature 01 p0084 N85-10565
Automated aircraft icing forecast technique
[AD-A144853] 01 p0085 N85-10571
A tropical cyclone precipitation estimation technique using geostationary satellite data
[PB84-228703] 01 p0086 N85-10579
The prediction of observer responses from photometric data on smoke screens; an analysis of the Oldebroek 2 trials, May 1981
[IZF-1984-21] 01 p0095 N85-10642
Credibility approximations for Bayesian prediction of second moments
[AD-A144996] 01 p0113 N85-10768
KrCl lasers for fusion
[DE84-012210] 01 p0122 N85-10835
Structure and evolution of the large scale solar and heliospheric magnetic fields
[NASA-CR-175269] 01 p0130 N85-10897
VORCOR: A computer program for calculating characteristics of wings with edge vortex separation by using a vortex-filament and-core model
[NASA-CR-165902] 02 p0135 N85-10921
Nonlinear structural and life analyses of a turbine blade 02 p0141 N85-10954
Nonlinear structural and life analyses of a combustor liner 02 p0141 N85-10955
Gas side heat transfer: 2-D flow 02 p0142 N85-10985
Gas flow environment and heat transfer nonrotating 3D program 02 p0142 N85-10986
Life prediction and constitutive behavior: Overview 02 p0143 N85-10973
Validation of structural analysis methods using the in-house liner cyclic rig 02 p0146 N85-10987
Three dimensional separation and vortex formation 02 p0196 N85-11308
A constitutive modeling technique based on a generalized rheological model to predict the response of materials 02 p0207 N85-11368
Reliability considerations for the total strain range version of strainrange partitioning
[NASA-CR-174757] 02 p0209 N85-11380
Statistical interpretation of NWP model output: An overview of techniques used and results achieved
[REPT-551.509.313] 02 p0231 N85-11503
An algorithm for least squares projections onto the intersection of shifted, convex cones
[AD-A145428] 02 p0251 N85-11640
An asymptotic theory for logistic regression when some predictors are measured with error
[AD-A145673] 02 p0254 N85-11666
Energetic electrons in impulsive solar flares 02 p0303 N85-11962
Estimation of helicopter performance using a program based on blade element analysis
[AD-A146341] 03 p0316 N85-12065
Development of a pavement maintenance management system. Volume 9: Development of airfield pavement performance prediction models
[AD-A146150] 03 p0321 N85-12069
Fatigue-impact studies in laminated composites
[AD-A142841] 03 p0326 N85-12097
Modeling of propulsive jet plumes--extension of modeling capabilities by utilizing wall curvature effects
[AD-A146262] 03 p0362 N85-12324
Laser velocimeter measurements and analysis in turbulent flows with combustion. Part 3: A correction lens for laser Doppler measurements in a cylindrical tube
[AD-A146206] 03 p0366 N85-12348
Ballpark reliability estimation techniques
[AD-A145971] 03 p0369 N85-12357
Computer molecular dynamics of 2-D water (ice) structures under shock
[AD-A145818] 03 p0372 N85-12375
Recent examples of mesoscale numerical forecasts of severe weather events along the east coast
[NASA-TM-86172] 03 p0395 N85-12523
Development of a microcomputer coupled atmospheric and oceanic boundary layer prediction model
[AD-A146334] 03 p0397 N85-12530
Prediction of wave height of wind-generated seas in finite water depth
[AD-A145996] 03 p0398 N85-12539
Filtering and prediction performance for a class of systems with uncertain parameters
[AD-A146145] 03 p0411 N85-12630
Simple prediction of convergence zone propagation in waters around australia
[AD-A145986] 03 p0416 N85-12659
Vertical coherence along a macroray path in an inhomogeneous anisotropic ocean
[AD-A145992] 03 p0416 N85-12660
Prediction of long term strength of glass reinforced plastics in wet environments
[NPL-DMA(A)-80] 04 p0477 N85-13041

Non-linear data fitting for the analysis of creep rupture data on GRP materials in aggressive environments — glass reinforced plastics (GRP)
[NPL-DMA(A)-79] 04 p0512 N85-13261
Weather research program report; FY 1983
[PB84-236694] 04 p0541 N85-13440
Computer programs to predict induced effects of jets exhausting into a crossflow
[NASA-CR-166591] 05 p0592 N85-13776
Prediction of force coefficients for labyrinth seals
05 p0644 N85-14130
Critical evaluation of methods to calculate fatigue life
05 p0649 N85-14165
Sequence of effects in the crack initiation and crack propagation phase 05 p0649 N85-14168
Very short range statistical forecasting of automated weather observations
[DOT/FAA/PM-84/31] 05 p0679 N85-14359
Some new mathematical methods for variational objective analysis 05 p0681 N85-14375
Extended range forecasting 05 p0681 N85-14376
The period of orbit as a test of the general theory of relativity 05 p0742 N85-14772
Method for predicting the creep rupture life of nickel-base precipitation-hardened superalloys from their chemical composition
[BLL-PNR-80241-(8019.3153)]
06 p0768 N85-14910
A comparison of evaporation duct models for IREPS (Integrated Refractive Effects Prediction System)
[AD-A146471] 06 p0799 N85-15103
Analyses to develop models to project failure rates and repair costs of electronic modules and subassemblies
[AD-A146509] 06 p0816 N85-15180
Modelling of deformation and fracture in high-temperature structural materials
[DE84-016906] 06 p0818 N85-15191
Predicting electrochemical breakdown in terrestrial photovoltaic modules 06 p0830 N85-15273
Probable maximum flood estimation - Eastern United States
[AD-A146536] 06 p0839 N85-15324
Environmental research laboratories (of the National Oceanic and Atmospheric Administration) programs and plans: FY 1983 programs and FY 1984 plans
[PB84-226729] 06 p0840 N85-15336
Prediction of percent body fat for U.S. Navy women from body circumferences and height
[AD-A146456] 06 p0845 N85-15370
Parametric estimates of propulsion system maintenance manhours
[AD-A147120] 07 p0894 N85-15662
Experiences with the material bevaviour and high temperature low cycle fatigue life prediction of the IN 738 blading alloy 07 p0906 N85-15746
View of future requirements for engine cyclic durability by analysis and testing 07 p0908 N85-15761
Exploring the use of structural models to improve remote sensing agricultural estimates 07 p0965 N85-16259
Evidence accumulation for spatial reasoning
07 p0965 N85-16261
An evaluation of an advection fog prediction model
[AD-A147436] 07 p1008 N85-16403
Experiments in forecasting atmospheric marine horizontal visibility using model output statistics with conditional probabilities of discretized parameters
[AD-A147574] 07 p1008 N85-16404
Robust prediction and interpolation for vector stationary processes, part 3
[AD-A147660] 07 p1036 N85-16579
Prediction of cruciform all-movable control characteristics at transonic speeds
[AD-A147291] 08 p1078 N85-16832
Prediction of dynamic stall characteristics using advanced non-linear panel methods
[AD-A148453] 08 p1078 N85-16836
The development and application of aerodynamic uncertainties: And flight test verification for the space shuttle orbiter 08 p1083 N85-16910
Model for prediction of the elastic response of composite materials over wide ranges of concentration
[AD-A148186] 08 p1119 N85-17051
Analysis of deflagration to detonation transition in high-energy solid propellants
[AD-A148302] 08 p1135 N85-17156
The role of nuclei size in transient cavitation threshold measurements
[AD-A148334] 08 p1162 N85-17332
Age life prediction of nylon 66 parachute materials. Part 1: Mechanical properties
[AD-A147698] 08 p1170 N85-17378
Atmospheric photochemical modeling of turbine engine fuels. Phase 1: Experimental studies. Volume 2: Environmental chamber data tabulations
[AD-A147786] 08 p1185 N85-17470
Estimations of diabatic heating for an explosively-developing maritime cyclone
[AD-A147678] 08 p1188 N85-17483
A scheme for short-term prediction of hydrometeors using advection and physical forcing
[AD-A148011] 08 p1188 N85-17487
An application of discriminant analysis to the selection of software cost estimating models
[AD-A147632] 08 p1204 N85-17580
Probable cause: A decision making framework
[AD-A147642] 08 p1210 N85-17614
A variable span smoother
[AD-A148241] 08 p1215 N85-17655
On estimating the cost growth of weapon systems
[AD-A147297] 08 p1230 N85-17749
Synthesized airfoil data method for prediction of dynamic stall and unsteady airloads
[NASA-CR-3672] 09 p1274 N85-18005
Theory of wing rock 09 p1282 N85-18064
Fracture mechanics analysis and prediction of delamination growth in composite structures
[FFA-TN-1984-45] 09 p1289 N85-18092
Statistical aspects of shear fracture propagation
[ERS-E.368] 09 p1341 N85-18434
Contribution of the study of light aircraft propeller noise
[ESA-TT-865] 09 p1378 N85-18867
A comparison between a conventional method and an improved method for predicting tracked vehicle performance
[AD-P004276] 09 p1406 N85-18852
A simple prediction model for soil compaction under various wheel loads and geometries as an aid to vehicle design
[AD-P004298] 09 p1409 N85-18875
Mechanics of composite materials
[DE85-003611] 10 p1432 N85-19031
A comparison between predicted and measured propagation loss in the VHF/UHF range in rugged terrain 10 p1471 N85-19285
Fluidelastic instability in shell and tube heat exchangers: A framework for a prediction method
[DE84-006518] 10 p1496 N85-19444
Earthquake-modeling experiment using unique press
10 p1500 N85-19469
Large scale circulation anomalies and prediction of northeast Brazil droughts
[INPE-3405-PRE/674] 10 p1518 N85-19571
Assessment of muscle strength and prediction of lifting capacity in US Army personnel
[AD-A148848] 10 p1527 N85-19633
Predicting the performance of distributed knowledge-based systems: A modeling approach
[AD-A149021] 10 p1545 N85-19738
Physical aspects of the prediction of solar flares
[NASA-CR-175487] 10 p1572 N85-19915
Predicting stability of full-scale composite constructions of the basis of stiffness 11 p1589 N85-20054
Improvement of VHF(MB) model
[AD-A150087] 12 p1829 N85-21480
Numerical studies of fluid spin-up from rest in a partially-filled cylinder
[AD-A150079] 12 p1847 N85-21586
NASA: Model development for human factors interfacing
[NASA-CR-175584] 12 p1910 N85-21985
Predicting a future response using rank predictive probabilities
[MATHEMATICS-RESEARCH-166]
12 p1923 N85-22077
Method for the prediction of the installation aerodynamics of a propfan at subsonic speeds
[NASA-CR-3667] 13 p1969 N85-22369
Reliability predictions for military avionics. Royal Signals and Radar Establishment reliability prediction method no. 250
[BR80221] 13 p1973 N85-22386
Snowmelt runoff model in Japan
13 p2124 N85-23227
Thermal and thermoelastic effects in rolling/sliding contacts
[AD-A150435] 13 p2165 N85-23429
Advanced life analysis methods. Volume 4: Tabulated test data for attachment lugs
[AD-A151016] 14 p2219 N85-23760
Shuttle payload bay dynamic environments: Summary and conclusion report for STS flights 1-5 and 9
[NASA-CR-175656] 14 p2241 N85-23896
Ordered carbon metal alloys for extraterrestrial power systems
[AD-A150881] 14 p2255 N85-23977
Basic EMC (Electromagnetic Compatibility) technology advancement for C3 systems: Model revision for IEMCAP (Intrasystem Electromagnetic Compatibility Analysis Program)
[AD-A150795] 14 p2292 N85-24206
Effect of flight sequences in complex load histories on crack front marking 14 p2318 N85-24326
Generation of marker lines by means of marker loads
14 p2318 N85-24327
Results of studies of wave field internal structure in prediction of geological cross section
14 p2346 N85-24504
Characteristics and behavior of atmospheric aerosols; application to prediction of infrared extinction
[AD-A150691] 14 p2372 N85-24665
Sensitivity analysis of a coupled atmospheric-oceanic boundary layer model
[AD-A150760] 14 p2382 N85-24690
Prediction of vortex-induced loads on wind-tunnel turning vanes
[NASA-TM-86578] 15 p2462 N85-25204
Crack growth direction in unidirectional off-axis graphite epoxy
[NASA-CR-175752] 15 p2502 N85-25433
Optimizing hot workability and controlling microstructures in difficult to process high strength and high temperature materials
[AD-D011586] 15 p2510 N85-25482
Deepwater wind wave growth with fetch and duration
[AD-A151604] 15 p2604 N85-26051
On failure modeling, revised
[AD-A151411] 15 p2637 N85-26263
Confined turbulent swirling recirculating flow predictions
[NASA-CR-174917] 16 p2709 N85-26716
Thrust chamber life prediction
16 p2733 N85-26885
Elevated temperature biaxial fatigue
[NASA-CR-175795] 16 p2800 N85-27263
The practical and theoretical significance of small cracks: An evaluation
[VTH-LR-432] 16 p2803 N85-27283
An appraisal of the duration of the recent drought in northeast Brazil and a forecast for 1985
[INPE-3477-PRE/720] 16 p2834 N85-27476
Predictions and measurements of isothermal flowfields in axisymmetric combustor geometries
[NASA-CR-174916] 17 p2896 N85-27867
SRB filament wound case material property study
[NASA-CR-171469] 17 p2910 N85-27940
Reexamination of cumulative fatigue damage laws
17 p2914 N85-27962
VLSI (Very large scale integrated circuits) device reliability models
[AD-A153268] 17 p2954 N85-28245
Spectral decomposition and verification of NOGAPS 500MB medium-range forecasts
[AD-A152550] 17 p2996 N85-28520
Electronically excited alkaline earth oxides: Chemical production and collisional energy transfer processes
[AD-A153172] 17 p3044 N85-28833
Improved statistical analysis method for prediction of maximum inlet distortion
[AD-A153767] 18 p3063 N85-28947
Time-averaged and time-dependent computations of isothermal flowfields in a centerbody combustor
[AD-A153662] 18 p3100 N85-29189
Turbulent wake of a submerged flat plate
[AD-A153776] 18 p3100 N85-29190
Numerical techniques for steady two-dimensional transcritical stratified flow problems, with an application to the intermediate field dynamics of ocean thermal energy conversion plants
[DE85-006347] 18 p3151 N85-29509
Wake effects of the aerodynamic performance of horizontal axis wind turbines 19 p3211 N85-29915
Nonlinear potential analysis techniques for supersonic-hypersonic configuration design
[NASA-CR-166078] 19 p3212 N85-29917
Fault detection and accommodation testing on an F100 engine in an F-15 airplane
[NASA-TM-86735] 19 p3219 N85-29962
Experimental and theoretical study of fatigue crack initiation in metals 19 p3283 N85-30357
Strain-path modeling for geo-materials
[AD-A154378] 19 p3286 N85-30380
Mathematical model of global processes in the biosphere 19 p3295 N85-30431
Flood-runoff forecasting with HEC1F
[AD-A154286] 19 p3300 N85-30456
Analytical model for predicting emergency shutdown of a two-bladed horizontal axis wind turbine
[NASA-TM-83472] 19 p3303 N85-30476
Workshop on objective analysis: Analysis strategies for field-dependent estimation
[PB85-179601] 19 p3316 N85-30589
Measurements of folded path optical scintillation using a corner cube, a cat's eye and a flat mirror reflector
[AD-A154044] 19 p3367 N85-30679

Radiometry: A useful prediction tool — atmospheric attenuation
[ESA-SP-1071] 20 p3399 N85-31084
Short term determination of the creep properties of high temperature materials
[CRIF-MT-160] 20 p3432 N85-31288
Prediction of lifetime for ceramic materials in the elastic and viscoelastic region by fracture mechanical methods
[ESA-TT-825] 20 p3434 N85-31305
Vortex sheet modeling with higher order curved panels
20 p3451 N85-31426
Heat transfer and fluid mechanics measurements in transitional boundary layer flows
20 p3453 N85-31439
A review and analysis of boundary layer transition data for turbine application 20 p3453 N85-31440
A comparison of millimeter wave, direct detect and heterodyne laser intersatellite links
[AD-A151984] 20 p3461 N85-31496
A comparison of two contemporary creep-fatigue life prediction methods 20 p3467 N85-31538
Two simplified procedures for predicting cyclic material response from a strain history 20 p3467 N85-31543
Creep crack growth predictions in INCO 718 using a continuum damage model 20 p3469 N85-31551
In-service supervision of a pressurized concrete pressure vessel
[OEFZS-4308] 20 p3470 N85-31564
The three-dimensional J-integral. An investigation into its use for post-yield fracture safety assessment
[WTHD-167] 20 p3472 N85-31578
An overview of nonlinear systems identification
[RR-271] 20 p3520 N85-31694
Wall flames and implications for upward flame spread
[FAA-CT-85-2] 21 p3553 N85-32103
Injection of drag reducing additives into turbulent water flows: Two-component velocity measurements and mixing length model predictions
[AD-A154604] 21 p3583 N85-32274
Assessment of the performance of an in-field Gaussian plume/puff model for overwater use
[AD-A155435] 21 p3614 N85-32460
Accuracy and operational use of medium and extended range numerical atmospheric forecasts: A review
[AD-A155027] 21 p3635 N85-32579
Forecasting of tropical cyclone motion using an EOF (Empirical Orthogonal Function) representation of wind forcing
[AD-A155034] 21 p3636 N85-32580
An evaluation of discretized conditional probability and linear regression threshold techniques in model output statistics forecasting of cloud amount and ceiling over the North Atlantic Ocean
[AD-A155100] 21 p3636 N85-32581
Medium range atmospheric forecast system: Evaluation report
[AD-A155240] 21 p3637 N85-32589
Forecasting atmospheric viability over the summer north Atlantic using the principal discriminant method
[AD-A155537] 21 p3637 N85-32593
A numerical and analytical investigation of lee cyclogenesis
[AD-A155807] 21 p3638 N85-32594
Simulation of the coupled atmospheric and oceanic boundary layer model during MILDEX
[AD-A155166] 21 p3655 N85-32705
On the problem of linear programming with approximate data 21 p3696 N85-32978
A model for predicting propagation-related DSCS (Defense Communications Engineering Center) margin requirements
[AD-A155355] 22 p3756 N85-33281
Predicting electrical performance parameters of underwater cables 22 p3775 N85-33391
Finite element methods for viscoelastic flow
[AD-A154877] 22 p3783 N85-33437
The use of TOMS data in evaluating and improving the total ozone from TOVS measurements
[NOAA-TR-NESDIS-23] 22 p3814 N85-33626
Global environmental transport models for tritium
[DE85-011437] 22 p3816 N85-33639
Comments on the prediction of dynamic stall
[GU-AERO-8501] 23 p3894 N85-34125
Prediction of the flow-field interference induced by the long-range laser velocimeter in the Ames 40- by 80-foot and the 80- by 120-foot wind tunnels
[NASA-TM-86763] 23 p3898 N85-34146
Nonsimultaneous coupled laser velocimeter measurement technique: Error prediction for spatially noncoincident measurements
[NASA-TM-86718] 23 p3934 N85-34379
Lubrication and cooling for high speed gears
[NASA-TM-87096] 23 p3938 N85-34407
Forecasting future industrial SO2 and NC/sub x/ emissions, revised 23 p3947 N85-34461
Cerenkov radiation from periodic electron bunches for finite emission length in air
[AD-A156156] 24 p4090 N85-35352
Development and application of a unified viscoelastic constitutive model for the prediction of material response under thermomechanical loading
24 p4101 N85-35420
Development of a mathematical model for predicting the percentage fatigue life increase resulting from shot peened components
[AD-A155774] 24 p4101 N85-35425
Evaluation of the crack plane equilibrium model for predicting plastic fractures
[DE85-005558] 24 p4102 N85-35431
Meteorological data from the OPTOMA (Ocean Prediction Through Observations, Modeling and Analysis) program OPTOMA 2, leg D2. 30 Jun. - 10 Jul. 1984
[AD-A156134] 24 p4123 N85-35560
The NORDA/FNOC (Naval Ocean Research and Development Activity's/Fleet Numerical Oceanography Center) Polar Ice Prediction System (PIPS)-Arctic: A technical description
[AD-A156332] 24 p4126 N85-35577
Models for assessing workload of aircrews on long distance flights 24 p4129 N85-35599
SASSYS-1 computer code verification with EBR-2 test data
[DE85-012119] 24 p4139 N85-35657
A comparison of multipath arrival structures observed in the presence of a surface duct with predictions obtained using classical ray techniques and the parabolic equation method
[AD-A156024] 24 p4145 N85-35696

PREDICTIONS
NT FLOOD PREDICTIONS
NT IMPACT PREDICTION
NT LINEAR PREDICTION
NT NOISE PREDICTION
NT NOISE PREDICTION (AIRCRAFT)
NT PERFORMANCE PREDICTION
Predictor model for seasonal variations in skid resistance, volume 1
[PB84-226612] 01 p0036 N85-10229
Predictability of mesoscale phenomena
01 p0079 N85-10528
Estimating sunspot number
[NASA-TM-86471] 01 p0130 N85-10896
Effects of surface chemistry on hot corrosion life: Overview 02 p0145 N85-10980
Evaluation of an aerosol prediction model for coastal regions using marine aerosol generation and transport data
[AD-A145443] 02 p0231 N85-11510
Unified approach to sensitivity and uncertainty analysis
[DE84-014049] 02 p0255 N85-11689
On-line fatigue life prediction under stochastic loading by the time series modeling 03 p0370 N85-12362
Seismology today 04 p0523 N85-13346
Geothermal resource assessment for North Dakota
[DE84-016128] 04 p0526 N85-13367
Weather research program report; FY 1983
[PB84-236694] 04 p0541 N85-13440
Tide tables 1985, high and low water predictions, central and western Pacific Ocean and Indian Ocean
[PB84-238393] 04 p0542 N85-13451
Long-range predictive control using weighting-sequence models
[OUEL-1542/84] 04 p0553 N85-13521
Investigation of the relations between neat resin and advanced composite mechanical properties. Volume 1: Results
[NASA-CR-172303] 05 p0612 N85-13911
Evaluation of the crack initiation life behavior of fatigue loaded automotive components made from high strength aluminium alloys
[ESA-TT-733] 05 p0651 N85-14181
Predictions of cockpit simulator experimental outcome using system models 05 p0702 N85-14504
Practical application of IREPS (Integrated Refractive Effects Prediction System)
[AD-A146526] 06 p0836 N85-15323
Two-dimensional lake wave prediction system
[PB84-231034] 06 p0841 N85-15342
General model of earthquakes and the place of warnings in it 07 p0981 N85-16232
The problem of climate and climate variation
07 p1001 N85-16353
Meteorological aspects of the 1982-83 El Nino/southern oscillation episode 07 p1001 N85-16356
The ocean and the dynamics of the tropical atmosphere; its possible predictability 07 p1002 N85-16366
Prediction of cruciform all-movable control characteristics at transonic speeds
[AD-A147291] 08 p1078 N85-16832
Air traffic management concepts for the UK in the 1990's: A review of recent RSRE work
[AD-A147850] 08 p1082 N85-16853
Generalized predictor-corrector methods of high order for the time integration of parabolic differential equations
[CWI-NM-R8402] 08 p1214 N85-17644
A note on the prediction error for small time lags into the future
[AD-A148221] 08 p1215 N85-17654
Design of mismatched Smith predictors using plant step data
[RR-263] 08 p1217 N85-17664
Flame propagation and stabilization studies using Rayleigh scattering and laser Doppler velocimetry
[AD-A148802] 09 p1290 N85-18102
A free shear layer prediction of the turbulent wake of a flat plate towed below a free surface
[AD-A148699] 09 p1319 N85-18293
Prediction of in-sand tire and wheeled vehicle drawbar performance
[AD-P004295] 09 p1404 N85-18841
Prediction accuracy of the torques for rotary tillage by an analog tool
[AD-P004286] 09 p1408 N85-18865
Nonlocal and nonlinear effects on solar oscillations
09 p1416 N85-18934
Low energy antiproton interaction studies at Brookhaven
[DE85-001228] 11 p1720 N85-20820
Modeling 12 p1787 N85-21221
Minister B. V. Balmont on status of automation drive
14 p2284 N85-24151
Study of earthquake preparation processes from distribution of weak tremor epicenters
14 p2345 N85-24501
COSPAS-SARSAT satellite orbit predictor, volume 5
[NASA-TM-85015-VOL-5] 14 p2439 N85-25052
Shuttle fleet operations: A simulation analysis
[AD-A151383] 15 p2491 N85-25370
Significant parameters for predicting flame spread
[PB85-178002] 16 p2760 N85-27034
Use of forest modeling to project acid rain effects
[DE85-006251] 16 p2821 N85-27400
A study of the effect of gently varying terrain on atmospheric flow near the surface
16 p2823 N85-27411
Basic EMC technology advancement for C3 systems. Volume 4F: Prediction of crosstalk in flatpack coaxial cables
[AD-A153111] 17 p2954 N85-28242
Improving the effectiveness of integral property calculation in a CSG solid modeling system by exploiting predictability 17 p3006 N85-28586
Ozone and temperature trends due to the injection of trace species in the atmosphere
[AERONOMICA-ACTA-A-288-1984] 18 p3132 N85-29399
The impact of scatterometer data on limited-area model predictions of the QE 2 storm 18 p3139 N85-29436
SANDRAG: A computer code for predicting drag of bodies of revolution at zero angle of attack in incompressible flow
[DE85-011170] 19 p3338 N85-30684
Ozone in the 21st century: Increase or decrease
[AERONOMICA-ACTA-A-291-1984] 20 p3489 N85-31687
Understanding and laboratory prediction of the atmospheric corrosion behavior of steels and of non-ferrous metals and alloys
[AD-A154642] 21 p3586 N85-32179
Resource management for the tagged token dataflow architecture
[AD-A154773] 21 p3667 N85-32779
Oxidation states of iron in the terrestrial planets: Evidence and implications for accretion models
22 p3852 N85-33854
Comparison of experimental data on detonation velocity and Chapman-Jougat pressure vs initial HE density with predictions from Ree's model equation of state
[DE85-007296] 23 p3922 N85-34304
Evaluation of source strength and dispersion model predications with data from large nitrogen tetroxide field experiments
[DE85-011855] 23 p3947 N85-34485
System expectations for Pioneer 1 foil implosion experiments
[DE85-014129] 24 p4091 N85-35359
Calculation of trajectories of detached wind turbine blades and prediction of site risk levels associated with failures of HAWT's 24 p4110 N85-35475

PREDICTORS
U PREDICTIONS

PREFLIGHT ANALYSIS
Oral presentation of first year final report, appendix A
05 p0602 N85-13840

PREFLIGHT OPERATIONS
NT COUNTDOWN
PREFORMS
Equipment for performing surfaces of optical parts
14 p2266 N85-24043
Negative flexural behavior of precase composite slabs with steel joint 23 p3904 N85-34183
PREHEATERS
U HEATING EQUIPMENT
PREHEATING
U HEATING
PREIMPREGNATION
Quality assurance of composite materials, test report no. 45-649/F 04 p0469 N85-12981
Parametric study of the P9 HT glass fiber finish (Fatigue resistance). Lot no. 1: Report on the microfatigue tests [CS-794] 05 p0620 N85-13968
PRELAUNCH PROBLEMS
Results of tests of K5NA and a revised formulation of EPDM/cork patch material in MSFC Hot Gas Facility [NASA-CR-170900] 24 p4073 N85-35238
PRELAUNCH TESTS
NT STATIC FIRING
PRELOADING
U PRESTRESSING
PREMIXED FLAMES
Further developments of a nongradient theory of premixed turbulent flames
[NAL-TR-802T] 01 p0023 N85-10143
Gravitational effects on premixed particle cloud flames 02 p0171 N85-11144
Analysis of pressure gradient-velocity correlation in turbulent, premixed flames 09 p1272 N85-17994
Turbulent premixed flame study
[DE85-003220] 09 p1292 N85-18112
Asymptotic methods especially in combustion
[AD-A151505] 15 p2505 N85-25450
The overall reaction concept in premixed, laminar, steady-state flames. 2: Initial temperatures and pressures
[AD-A152132] 16 p2746 N85-26944
On the analytic calculation of premixed flames
[VTH-LR-417] 16 p2747 N85-26954
Flame acceleration mechanisms under conditions of partial confinement
[PB85-184083] 18 p3073 N85-29004
Vortex simulation of v-shaped flame 20 p3425 N85-31259
Comments on two matters related to turbulent combustion 22 p3743 N85-33204
Simultaneous measurement of velocity and density in a turbulent nonpremixed flame 22 p3744 N85-33209
Modeling of turbulent recirculating combusting flows 22 p3745 N85-33212
PREPARATION
NT PRESTRESSING
NT PRETREATMENT
Preparation of silicon carbide fibers
[DE84-014691] 01 p0022 N85-10137
1-Fluoro-1,1,5-Trinitro-3-Oxa-5-Azahexane and method of preparation
[AD-D011421] 08 p1136 N85-17158
Preparation methods: Past and potential methods of food preparation for space 14 p2393 N85-24736
A robotic system for preparing reagent and dilution vials
[DE85-006262] 16 p2793 N85-27231
Preparation of sinteractive silicon nitride powders
[BMFT-FB-T-84-303] 18 p3062 N85-29086
Plutonium metal preparation and purification at Los Alamos, 1984
[DE85-010732] 19 p3239 N85-30085
Improved process for the preparation of fiber-reinforced ceramic composites by chemical vapor deposition
[DE85-011584] 22 p3752 N85-33255
PREPOLYMERS
NT DIMERS
NT TRIMERS
Properties of ultra-violet cured poly(dimethylsiloxane)-urea acrylates
[AD-A148570] 08 p1134 N85-17146
PREPREGS
Development of new and improved polymer matrix resin systems, phase 1
[NASA-CR-166595] 01 p0017 N85-10104
Aliphatic-aromatic heterocyclics as potential thermoplastics for composite matrices 04 p0466 N85-12962
Evaluation of failure criterion for graphite/epoxy fabric laminates
[NASA-CR-172547] 10 p1431 N85-19025
Investigation of the effects of NaOH dopant level on the physical and mechanical properties of carbon/phenolic composite material 12 p1945 N85-22213
Development of an impact- and solvent-resistant thermoplastic composite matrix, phase 3
[NASA-CR-172568] 20 p3422 N85-31239
PREPROCESSING
Noise removal in multichannel images
[NASA-CR-174116] 04 p0554 N85-13526
Adaptive preprocessing system
[AD-D011327] 07 p0937 N85-15935
Scientific experiments. Preprocessing of scientific data — spaceborne experiments 14 p2398 N85-24779
A study of aerodynamic control in stalled flight leading-edge vortex formation analysis
[AD-A153758] 18 p3059 N85-28928
PRESELECTORS
U PREAMPLIFIERS
PRESERVING
Alternative food preservation techniques, new technology in food preparation and appropriateness of food supply for the permanently manned space station 14 p2393 N85-24739
Characterization-curing-property studies of HBRF 55A resin formulations
[NASA-CR-175836] 16 p2753 N85-26989
Use of gamma radiation as a form of preservation of sweet potatoes
[DE85-011996] 22 p3841 N85-33787
PRESIDENTIAL REPORTS
Publications of the Executive Office of the President: January 20, 1981 - June 30, 1984
[PB84-230671] 06 p0871 N85-15533
National Acid Precipitation Assessment Program. Report to the President and Congress (1983)
[PB85-116713] 11 p1679 N85-20581
President's private sector survey on cost control, report on research and development
[PB84-173269] 12 p1951 N85-22253
National aeronautical R and D goals: Technology for America's future 19 p3379 N85-30964
PRESINTERING
U SINTERING
PRESSES
Earthquake-modeling experiment using unique press 10 p1500 N85-19469
Automatic multi-layer welding of thick cylindrical structures under flux 13 p2035 N85-22748
Experience with introduction of Finish perforation of precision parts for optical instruments 16 p2761 N85-27038
PRESSING (FORMING)
NT STAMPING
Prediction of forming limit diagrams for deep drawing 06 p0796 N85-15089
Making high explosive bodies for shaped charges by casting or pressing. Shaped charge research at Research Institute of National Defence (FOA) in 1972 - 1983, part 1
[FOA-C-20554-D4-PT-1] 07 p0935 N85-15923
Summaries of press automation conference presented 08 p1139 N85-17173
Consolidation of thermites by pressing and sintering
[DE84-016943] 09 p1297 N85-18146
Robotized blanks loader for new forge press 10 p1461 N85-19216
Experience in use of optical theodolite for machine construction 14 p2267 N85-24049
Clutchless mechanism for engagement of forging press 14 p2268 N85-24051
USSR report: Machine tools and metalworking equipment
[JPRS-UMM-85-004] 14 p2284 N85-24152
Automated, robotized forge-press systems viewed 14 p2284 N85-24153
Robots for application in forge-press operation 14 p2284 N85-24154
Method of selecting robotized system design for pressing process 16 p2761 N85-27040
Industrial robots and automatic manipulators for forging and pressing operations at Second International Exhibition 16 p2762 N85-27044
Mechanizing of handling operations in drop forging with hammers and presses (conducted ergonomical examinations)
[BMFT-FB-HA-84-051] 17 p3002 N85-28561
Specifics of fine structure of pressed aluminum alloys manufactured by plasma atomization 19 p3242 N85-30102
PRESSURE
NT ATMOSPHERIC PRESSURE
NT BASE PRESSURE
NT BLOOD PRESSURE
NT CRITICAL PRESSURE
NT DENSIFICATION
NT DYNAMIC PRESSURE
NT FLUID PRESSURE
NT GAS PRESSURE
NT HIGH ALTITUDE PRESSURE
NT HIGH PRESSURE
NT HIGH VACUUM
NT HYDROSTATIC PRESSURE
NT HYPOXEMIA
NT ILLUMINANCE
NT IMPACT LOADS
NT INLET PRESSURE
NT INTERNAL PRESSURE
NT INTRAOCULAR PRESSURE
NT ISOSTATIC PRESSURE
NT LOW PRESSURE
NT LUMINANCE
NT LUMINOUS INTENSITY
NT OVERPRESSURE
NT OXYGEN TENSION
NT PARTIAL PRESSURE
NT RADIATION PRESSURE
NT SOUND PRESSURE
NT STAGNATION PRESSURE
NT STATIC PRESSURE
NT SUPERCRITICAL PRESSURES
NT TRANSIENT PRESSURES
NT TRANSITION PRESSURE
NT ULTRAHIGH VACUUM
NT VACUUM
NT VAPOR PRESSURE
NT WALL PRESSURE
NT WATER PRESSURE
NT WIND PRESSURE
Thermodynamic properties of isobutane-isopentane mixtures from -40 to +600(0)F and up to 1000 psia
[DE84-015137] 01 p0124 N85-10850
An alternative to reduction of surface pressure to sea level
[NASA-CR-174174] 04 p0538 N85-13422
Homogeneous condensation of gaseous mixtures of Si, Fe, O, N, and C in relative cosmic abundance and implications for astronomical condensation 06 p0887 N85-15632
Analysis of the surface load and radiated sound of a vibrating airfoil with application to the experiment of Brooks
[NASA-CR-3864] 07 p1038 N85-16580
Pressure tests in soil below tires of agricultural vehicles
[AD-P004294] 09 p1408 N85-18671
Flotation tires and subsurface compaction
[AD-P004299] 09 p1409 N85-18676
Airspeed sensing pressure valve system
[AD-D011472] 10 p1425 N85-18967
Electron storage ring beam lifetime dependence on pressure and pumping speed
[DE85-003208] 11 p1724 N85-20845
The sensitivity of solar eigenfrequencies to the treatment of the equation of state 14 p2445 N85-25089
Pressure-dependence of TiS(2) and TiSe(2) bandstructures
[AD-A151200] 15 p2859 N85-26410
Sources of improvement in quality of contact butt welding of wire
[BLL-M-36085-(5828.4)] 16 p2793 N85-27225
A study of aerodynamic control in stalled flight leading-edge vortex formation analysis
[AD-A153758] 18 p3059 N85-28928
Oscillating pressure device for dynamic calibration of pressure transducers
[NASA-CASE-LAR-13094-1] 18 p3104 N85-29217
An experimental study of the pressure in a fast bottom beneath the apex of an overlying fluid wedge
[AD-A153616] 18 p3177 N85-29696
An investigation of hydraulic transients in combination free surface and pressurized flows 19 p3264 N85-30239
Computation of three-dimensional, inviscid, rotational flows 21 p3587 N85-32296
X-ray spectroscopy of solids under pressure
[DE85-011486] 22 p3745 N85-33213
Finite element methods for viscoelastic flow
[AD-A154877] 22 p3783 N85-33437
Linear boundary detection using pressure buildup tests
[DE85-009926] 22 p3784 N85-33444
Adiabatic thermal models for planetary bodies 22 p3857 N85-33861
PRESSURE BREATHING
Hyperbaric physiology (status and prospects) 08 p1194 N85-17521
Manned testing of two closed-circuit oxygen underwater breathing apparatus: US Navy Emerson Rig and Fenzy PO.68
[AD-A148300] 08 p1200 N85-17560
PRESSURE CABINS
U PRESSURIZED CABINS
PRESSURE CHAMBERS
NT HYPERBARIC CHAMBERS
NT VACUUM CHAMBERS

Folker wants to start new Netherlands space program
03 p0310 N85-11999
Small animal hypobaric chamber
[AD-A146196] 03 p0364 N85-12335
Pressure chamber simulation of 450-meter dive
20 p3505 N85-31786
Diving simulation experiment with pressure chambers
20 p3506 N85-31793

PRESSURE DEPENDENCE
A hydrogen partitioning model for hydrogen assisted crack growth
[AD-A147385] 07 p0978 N85-16214
Electrical resistance measurements of metals to 40 GPa in the diamond cell
[DE85-001009] 11 p1629 N85-20262
Dynamic shock studies of PZT 95/5 ferroelectric ceramic
[DE85-006137] 14 p2261 N85-24015
X-ray spectroscopy of solids under pressure
[DE85-006939] 15 p2507 N85-25465
Electronic properties of new organic conductors
[DE85-005590] 15 p2549 N85-25736
Dynamics of vapor explosions
[DE85-008845] 18 p3101 N85-29194

PRESSURE DISTRIBUTION
Integral equation of lifting surfaces in Laplace domain and analytic continuation of its pressure kernel
[NAL-TR-795T] 01 p0002 N85-10009
A study of aerodynamic characteristics of wing-body combinations. Part 2: Low-wing airplane
[NAL-TR-796] 01 p0002 N85-10010
Pressure distributions measured on research wing M100 mounted on an axisymmetric body
01 p0004 N85-10023
Pressure distributions measured on research wing M86 mounted on an axisymmetric body
01 p0004 N85-10024
Pressure distribution on a swept wing aircraft in flight
01 p0004 N85-10025
Effect of combined pressure and temperature distortion orientation on high-bypass-ratio turbofan engine stability
[NASA-TM-83771] 01 p0011 N85-10067
Visualization of the diverging two-phase flow pattern in a horizontal T-junction with vertical branch
[GKSS-84-E-25] 01 p0048 N85-10316
Transonic flow analysis for rotors. Part 1: Three-dimensional quasi-steady, full-potential calculation
[NASA-TP-2375-PT-1] 02 p0134 N85-10914
Effect of upstream sidewall boundary layer removal on an airfoil test — conducted in Langley 0.3-m transonic cryogenic tunnel
03 p0313 N85-12019
Performance of two transonic airfoil wind tunnels utilizing limited ventilation
03 p0313 N85-12020
Tunnel constraint for a jet in crossflow
03 p0314 N85-12027
Structure and properties of titanium alloys after isothermal deformation at low speeds
03 p0351 N85-12260
Internal heat transfer and pressure drop measurements in a variously baffled shell and tube heat exchanger
03 p0360 N85-12310
Summary of 1984 Atlantic seasonal tropical cyclone activity and verification of author's forecast
03 p0395 N85-12520
Investigations of boundary layers in the Emmen Federal Aircraft works transonic tunnel, Switzerland
[FW-FO-1641] 04 p0453 N85-12877
Flight and wind-tunnel comparisons of the inlet-airframe interaction of the F-15 airplane
[NASA-TP-2374] 04 p0455 N85-12884
Model equations describing unsteady fluid motion
[ESA-TT-850] 04 p0501 N85-13194
Experiments on the structure of turbulent reattaching flow
05 p0635 N85-14074
Static internal performance of single-expansion-ramp nozzles with various combinations of internal geometric parameters
[NASA-TM-86270] 06 p0749 N85-14797
A theoretical design method for 3-dimensional transonic wings
[NAL-TR-830] 06 p0754 N85-14834
Analysis of the flow field about a T-45 using PANAIR
[AD-A146811] 07 p0899 N85-15899
Some important problems in unsteady boundary layers including separation. 2: Unsteady boundary layers close to the stagnation region of slender bodies
[AD-A146964] 07 p0958 N85-16089
Analysis of the surface load and radiated sound of a vibrating airfoil with application to the experiment of Brooks
[NASA-CR-3864] 07 p1038 N85-16590
The NYU inverse swept wing code
[NASA-CR-3862] 08 p1077 N85-16830
A comparison of measured and predicted unsteady pressure on a fan blade in unstalled supersonic flutter
[PNR-90223] 08 p1079 N85-16839
An improved source model for aircraft interior noise studies
[NASA-CR-172517] 08 p1217 N85-17668
Acceleration of an electron ring in a modified betatron with transverse pressure
[AD-A148626] 08 p1221 N85-17688
Can the singularity be removed in time-dependent flows?
[AD-P004185] 09 p1265 N85-17950
Convective heat transfer coefficients for pipe flow with curvature induced secondary motion
09 p1316 N85-18295
Analysis of ground pressure distribution beneath tracked model with respect to external loading
[AD-P004275] 09 p1406 N85-18851
Detailed pressure distribution measurements obtained on several configurations of an aspect-ratio-7 variable twist wing
[NASA-TM-86308] 10 p1419 N85-18950
Transonic pressure distribution computations of a flexible wing
11 p1622 N85-20213
Measured unsteady transonic aerodynamic characteristics of an elastic supercritical wing with an oscillating control surface
[NASA-TM-86376] 12 p1771 N85-21116
An experimental investigation of flap turbulent heat transfer and pressure characteristics in hypersonic flow
12 p1821 N85-21426
Re-design of ARL/HLF (Heated Laminar Flow) body nose region
[AD-A150063] 12 p1846 N85-21585
Recent transonic unsteady pressure measurements at the NASA Langley Research Center
[NASA-TM-86406] 14 p2210 N85-23710
The influence of transition strips on the pressure distribution on transonic profiles
14 p2212 N85-23718
Problems of elastic hydrodynamic lubrication of helicopter transmission gears 14 p2222 N85-23784
Technology for pressure-instrumented thin airfoil models, phase 1
[NASA-CR-3891] 14 p2227 N85-23804
Some problems in improving reliability and accuracy of regulators with hydraulic amplifiers in main channel of power turbine 14 p2271 N85-24071
Interactions of unstable shear layers with leading edges and associated pressure fields 14 p2299 N85-24236
The photospheric temperature structure of magnetic flux tubes 14 p2447 N85-25102
Transonic pressure distributions on a two-dimensional 0012 and supercritical MBB-A3 profile oscillating in heave and pitch 15 p2457 N85-25173
Mathematical modeling of the AEDC (Arnold Engineering Development Center) propulsion wind tunnel (16T)
[AD-A151293] 15 p2475 N85-25275
Investigation to optimize the passive shock wave/boundary layer control for supercritical airfoil drag reduction
[NASA-CR-175788] 16 p2699 N85-26665
Flow rate and pressure profiles for 1 to 4 axially aligned orifice inlets
[NASA-TP-2460] 16 p2782 N85-27165
Aerodynamic research in preparation for a new Dutch transport aircraft with supercritical wings
[B8580077] 17 p2893 N85-27836
Proceedings of the 9th US Air Force and the Federal Republic of Germany Data Exchange Agreement Meeting, Viscous and Interacting Flow Field Effects
[AD-A153020] 17 p2958 N85-28266
Characteristics of a confined jet thrust vector control nozzle
[AD-A153067] 17 p2958 N85-28268
Transport characteristics of slurries in pipelines: Flow regimes and pressure drop
[DE85-009453] 18 p3101 N85-29196
Pressure distribution data from tests of 2.29 M (7.5 foot) span EET high-lift transport aircraft model in the Ames 12-foot pressure tunnel
[NASA-TM-84517] 19 p3211 N85-29912
Transient combustion dynamics
[AD-A154430] 19 p3235 N85-30052
An experimental investigation of propfan installations on an upswept supercritical wing at transonic Mach numbers
[NASA-CR-172605] 20 p3388 N85-31013
Calculation of flow around the SF 310 airplane using a full potential equation method
[FFA-TN-1984-63] 20 p3389 N85-31022
Data set 8: ZKP wing, oscillating aileron
20 p3390 N85-31029
Trailing edge flow and aerodynamic sound. Part 1: Tonal pressure and velocity fluctuations. Part 2: Random pressure and velocity fluctuations
[AD-A154947] 21 p3552 N85-32097
Generation by conformal mappings of aerofoil sections and of certain other simple shapes suitable for both aerodynamic and stress-concentration problems
[AD-A154901] 22 p3729 N85-33112
Experimental study of collapse of thick-walled tube under external pressure and axial force
23 p3904 N85-34186
Pressure cross spectra in turbulent boundary layers in water
[AD-A156153] 24 p4094 N85-35378

PRESSURE DRAG
NT INTERFERENCE DRAG
NT WAVE DRAG

PRESSURE DROP
Heat transfer and pressure drop in blade cooling channels with turbulence promoters
[NASA-CR-3837] 03 p0361 N85-12315
Special topics reports for the reference tandem mirror fusion breeder: Liquid metal MHD pressure drop effects in the packed bed blanket, volume 1
[DE85-002142] 06 p0865 N85-15500
Determination of total pressure losses in stepped annular diffusers with curvilinear outer walls and uniform velocity field at inlet 09 p1306 N85-18203

PRESSURE EFFECTS
A thermodynamic surface for the critical region of ethylene
[PB84-217860] 01 p0025 N85-10159
Interpolation formulas for viscosity of six gases: Air, nitrogen, carbon dioxide, helium, argon and oxygen
[PB84-217801] 01 p0026 N85-10161
Calculation of the optimum conditions for the forging of plates
[BLL-M-35757-(5828.4)] 02 p0189 N85-11260
Nonlinear deformation and static linear buckling of structures under pressure
[CETIM-11-E-350] 04 p0514 N85-13281
The effect of temperature and pressure on the composition density of alkaline metals
[BLL-M-35940-(5828.4)] 05 p0616 N85-13834
Vityaz specialists study human adaptability to ocean depths 07 p0960 N85-16225
Investigation of the pressure-and velocity-coupled responses of solid propellants using impedance tube method 09 p1300 N85-18168
Studies on seismic earth pressure of cohesive backfill
09 p1303 N85-18186
Ignition phenomena of bulk aluminum alloy as a function of oxygen pressure 13 p1999 N85-22531
Pressure-density behavior for AlN, Al2O3, SiO2, TiB2, and TiC powders up to 3.5 GPa
[DE85-006146] 14 p2261 N85-24012
Stability of turbine runners in sliding bearings under external circulation forces 14 p2272 N85-24074
A numerical study of nonspherical black hole accretion 16 p2681 N85-27780
Thermal expansion effects in electrical transport in amorphous metals
[AD-A152477] 17 p2930 N85-28089
Stability of cylindrical shells with variable thickness under external pressure 17 p2943 N85-28184
A second-order pressure-correction method for viscous incompressible flow
[REPT-84-15] 17 p2960 N85-28280
Dynamics of vapor explosions
[DE85-008845] 18 p3101 N85-29194
Fast approach for calculating film thicknesses and pressures in elastohydrodynamically lubricated contacts at high loads
[NASA-TM-87032] 19 p3264 N85-30242
Interaction of slow electrons with high-pressure gases (quasi-liquids): Synthesis of our knowledge on slow electron-molecule interactions
[DE85-010081] 19 p3355 N85-30900
Pressure-shear loading of PBX-9404
[DE85-009982] 23 p3921 N85-34298

PRESSURE FIELDS
U PRESSURE DISTRIBUTION

PRESSURE GAGES
NT BAROMETERS
NT IONIZATION GAGES
NT MANOMETERS
NT PIEZOELECTRIC GAGES
Development of a polymer pressure gage with temperature compensation 03 p0365 N85-12340
Dynamic polymer pressure transducer with temperature compensation
[AD-D011373] 07 p0857 N85-16142
Performance assessment of Class 1E pressure transmitters subjected to environmental stresses
[DE85-001623] 12 p1854 N85-21626
Detonation velocity measurements of the explosives Detasheet C and Amatol
[AD-A152298] 16 p2757 N85-27015
A strain gauge manual
[AD-A151802] 16 p2787 N85-27197

PRESSURE GRADIENTS
Approximate solution of a laminar flow over a flat plate with suction and pressure gradient
[AD-A145482] 02 p0106 N85-11321
Numerical calculation of steady turbulent flows in adverse pressure gradients
[CFD/83/9] 04 p0501 N85-13195
Operational numerical forecasts: Survey and verification over the period 1978-1983
[KNMI-TR-49] 04 p0540 N85-13435
Drag reduction due to boundary-layer control by combined blowing and suction 08 p1070 N85-16785
On the relaxation of a turbulent boundary layer after an encounter with a forward facing step
08 p1071 N85-16789
Analysis of pressure gradient-velocity correlation in turbulent, premixed flames 09 p1272 N85-17994
Calculating secondary nonviscous gas flows in spatial cascades of turbines 09 p1305 N85-18202
Shock propagation in the exhaust gas handling system of the proposed large altitude rocket cell: Methods and preliminary analysis
[DE85-003055] 11 p1591 N85-20010
Nested subcritical flows within supercritical systems
[NASA-TM-86980] 12 p1845 N85-21574
Re-design of ARL/HLF (Heated Laminar Flow) body nose region
[AD-A150063] 12 p1846 N85-21585
Fine structure of vertical distribution of light attenuation index of sea water 13 p2109 N85-23140
Some problems in improving reliability and accuracy of regulators with hydraulic amplifiers in main channel of power turbine 14 p2271 N85-24071
Wind tunnel wall interference
[AD-A151212] 15 p2474 N85-25273
Two-phase fluid thermal transport for spacecraft
[AD-A151316] 15 p2493 N85-25378
A four-field model for Tokamak plasma dynamics
[DE85-007111] 16 p2666 N85-27694
The effects of microbubbles on turbulent boundary layer skin friction 20 p3451 N85-31425
Pressure correlations in turbulent reacting flows
22 p3744 N85-33205
Second order modelling in non-constant density flows
22 p3744 N85-33206
A design procedure to modify the trailing edge upper surface pressure gradient of a given aerofoil
[GU-AERO-8408] 23 p3894 N85-34120
Refrigerated dynamic seal to 6.9 MPa (1000 psi)
[NASA-TM-87106] 23 p3930 N85-34356
A three-dimensional turbulent boundary layer undergoing transverse strain and streamwise pressure gradient
[NASA-TM-86708] 23 p3930 N85-34358
Adverse pressure gradient and separating turbulent boundary-layer flows: The effect of disequilibrium in initial conditions 24 p4059 N85-35155
Computer code calculations of the TMI-2 accident: Initial and boundary conditions
[DE85-012613] 24 p4140 N85-35666

PRESSURE HEADS
Low-head hydroelectric power demonstration project: City of Gonzales, Texas
[DE85-010403] 22 p3809 N85-33595

PRESSURE ICE
Kinetic friction coefficient of ice
[AD-A155035] 21 p3680 N85-32659

PRESSURE MEASUREMENT
Inlet and airframe compatibility for a V/STOL fighter/attack aircraft with top-mounted inlets
[NASA-TM-84252] 01 p0003 N85-10015
Pressure distributions measured on research wing M100 mounted on an axisymmetric body
01 p0004 N85-10023
Pressure distributions measured on research wing M98 mounted on an axisymmetric body
01 p0004 N85-10024
Measurement and analysis of spark ignition engine pressure data to determine heat release profiles
[AD-A144770] 01 p0055 N85-10363
Turbine test report, addendum
[DE84-015130] 02 p0205 N85-11353
Spectroradiometric calibration of the Thematic Mapper and Multispectral Scanner system
[E85-10026] 02 p0218 N85-11439
Wind tunnel wall interference correction for aircraft models 03 p0314 N85-12029
Adaptation of a four-wall interference assessment/correction procedure for airfoil tests in the 0.3-m TCT 03 p0315 N85-12035
Internal heat transfer and pressure drop measurements in a variously baffled shell and tube heat exchanger
03 p0360 N85-12310
Microshell (trademark)-tipped optical fibers as sensors of high-pressure pulses in adverse environments
[DE84-015520] 03 p0365 N85-12338
Development of a polymer pressure gage with temperature compensation 03 p0365 N85-12340
Semiconductor-type transducer with universal strain gauge for measurement of low pressures
04 p0489 N85-13116
Development of components for micro-C oriented sensor systems
[BMFT-FB-T-84-126] 04 p0504 N85-13215
Unsteady pressure measurements on a biconvex airfoil in a transonic oscillating cascade
[NASA-TM-86914] 07 p0898 N85-15689
Steady- and unsteady-pressure measurements on a supercritical-wing model with oscillating control surfaces at subsonic and transonic speeds
[NASA-TM-84543] 08 p1077 N85-16831
Comparison of techniques to measure the low wavenumber wall pressure spectrum of a turbulent boundary layer
[AD-A148074] 08 p1162 N85-17331
Flow quality of NAL 2-dimensional transonic wind tunnel. Part 2: Extensive and systematic pressure fluctuations study in the settling chamber, test section and second throat of the NAL 2-D transonic wind tunnel
[NAL-TR-836-PT2] 09 p1263 N85-18066
Detailed pressure distribution measurements obtained on several configurations of an aspect-ratio-7 variable twist wing
[NASA-TM-86308] 10 p1419 N85-18950
Unsteady transonic pressure measurements on a semispan wind-tunnel model of a transport-type supercritical wing (Lann model). Part 2: Pressure distributions (plotted) and plots of the vibration modes
[AD-A130488] 10 p1421 N85-18965
Dynamic pressure test unit-ratio method
[AD-D011466] 10 p1468 N85-19392
Precision volume measuring system
[DE85-002589] 11 p1636 N85-20305
Unsteady transonic pressure measurements on a semi-span wind-tunnel model of a transport-type supercritical wing (Lann model). Part 2: Pressure distributions (plotted) and plots of the vibration modes
[AD-A130488] 12 p1846 N85-21579
The seven-hole pressure probe
[AD-A149799] 12 p1852 N85-21615
Method of and apparatus for measuring temperature and pressure — atmospheric sounding
[NASA-CASE-GSC-12558-1] 12 p1856 N85-21639
Seismic observation of infrasonic signals
[AD-A149574] 12 p1889 N85-21853
MFTF sensor verification computer program
[DE85-004452] 12 p1916 N85-22029
Liquid moment on a filled coning cylinder during spin-up: Ad hoc model
[AD-A150280] 13 p2092 N85-23060
Recent transonic unsteady pressure measurements at the NASA Langley Research Center
[NASA-TM-86406] 14 p2210 N85-23710
Transition detection using surface pressure holes
14 p2212 N85-23722
Surface pressure produced by Space Transportation System flight 41B
[AD-A150793] 14 p2242 N85-23901
Analysis of unsteady pressure measurements on a supercritical airfoil with a harmonically oscillating trailing edge flap at subsonic and transonic speeds
[DFVLR-FB-84-49] 17 p2893 N85-27837
Pressure measurement: Short course
[DE85-006644] 16 p3102 N85-29205
Measurement of turbofan-turbojet thrust from tailpipe static pressure
[AD-A154036] 19 p3220 N85-29957

PRESSURE OSCILLATIONS
An experimental investigation of combustion pressure oscillations in solid fuel ramjets
[AD-A144870] 01 p0024 N85-10147
Similarity criteria of spectra of pressure pulsations of turbulent boundary layer near wall
02 p0256 N85-11679
Pressure oscillations in liquid-fueled ramjet engines
05 p0596 N85-13797
Steady- and unsteady-pressure measurements on a supercritical-wing model with oscillating control surfaces at subsonic and transonic speeds
[NASA-TM-84543] 08 p1077 N85-16831
Effect of jet exit vanes on flow pulsations in an open-jet wind tunnel
[NASA-TM-86299] 09 p1273 N85-17999
Turbulent buoyant flow and pressure variations around a circular cylinder in a cross uniform flow near the ground 09 p1318 N85-18287
Measured unsteady transonic aerodynamic characteristics of an elastic supercritical wing with an oscillating control surface
[NASA-TM-86376] 12 p1771 N85-21116
An investigation of space shuttle main engine shutdown chugging instability 12 p1946 N85-22221
Nonlinear interactions between vortices and acoustic waves in a rocket combustion chamber
13 p1999 N85-22533
Comparisons of solid propellant with instability predictions and motor firing experience
13 p2001 N85-22541
Transonic pressure distributions on a two-dimensional 0012 and supercritical MBB-A3 profile oscillating in heave and pitch 15 p2457 N85-25173
Parametric study of autooscillation upon flow of supersonic jet into cylindrical cavity
16 p2785 N85-27060
Atmospherically forced, coastally trapped, long period gravity waves off the south coast of southern Africa
16 p2832 N85-27461

PRESSURE PROBES
U PRESSURE SENSORS

PRESSURE PULSES
Microshell (trademark)-tipped optical fibers as sensors of high-pressure pulses in adverse environments
[DE84-015520] 03 p0365 N85-12338
Long range effect of turbulent pressure pulsations in plane-parallel flows at different velocities with various flame fronts 09 p1308 N85-18220
Flow dynamic environment data base development for the SSME 16 p2736 N85-26885
Pulsed hydrojet propulsion
[DE85-010771] 22 p3784 N85-33448

PRESSURE RATIO
Design and off-design performance prediction of high pressure ratio centrifugal compressors
05 p0636 N85-14082
Mixing characteristics of an underexpanded multiple jet ejector
[AD-A149557] 10 p1485 N85-19375
Calibration of sonic valves for the laminar flow control, leading-edge flight test
[NASA-TP-2423] 14 p2210 N85-23707
Optimum geometry of interblade passages in impellers of thermomolecular vacuum pump
16 p2764 N85-27058
High pressure compressor component performance report
[NASA-CR-168245] 23 p3897 N85-34138

PRESSURE RECOVERY
Pressure recovery in a cylindrical heat pipe at high radial Reynolds numbers and at high Mach numbers
[DE85-010718] 19 p3269 N85-30274

PRESSURE REDUCTION
Internal heat transfer and pressure drop measurements in a variously baffled shell and tube heat exchanger
03 p0360 N85-12310
Pressure loss due to the tip clearance of impeller blades in centrifugal and axial blowers
05 p0636 N85-14083
Preliminary investigation of labyrinth packing pressure drops at onset of swirl-induced rotor instability
05 p0644 N85-14132
Safe decompression schedules for caisson workers
[PB85-103612/GAR] 07 p1017 N85-16463
Low loss injector for liquid propellant rocket engines
[NASA-CASE-MFG-25989-1] 11 p1591 N85-20008
Statistical comparison of pooled nitrogen washout data of various altitude decompression response groups
[NASA-TM-58265] 15 p2639 N85-26278
A feasibility study for using low boiling point fluids to change aircraft tire deflection
[AD-A152096] 16 p2706 N85-26701
A comprehensive strategy for saturation decompression with nitrogen-oxygen
[AD-A151800] 16 p2841 N85-27520
Method for growth of crystals by pressure reduction of supercritical or subcritical solution
[NASA-CASE-NPO-15772-1] 18 p3192 N85-29800
Diving simulation experiment with pressure chambers
20 p3506 N85-31783

PRESSURE REGULATORS
Simulation in the design of gas pressure control equipment
[ERS-E.352] 09 p1324 N85-18322

PRESSURE RIDGES
U PRESSURE ICE

PRESSURE SENSORS
Development of a floating element wall shear transducer
[AD-A144794] 01 p0049 N85-10324
Microshell (trademark)-tipped optical fibers as sensors of high-pressure pulses in adverse environments
[DE84-015520] 03 p0365 N85-12338
Development of a polymer pressure gage with temperature compensation 03 p0365 N85-12340
Semiconductor-type transducer with universal strain gauge for measurement of low pressures
04 p0489 N85-13116

Development of components for micro-C oriented sensor systems
[BMFT-FB-T-84-126] 04 p0504 N85-13215
Aero-optics experimental techniques
[AD-A148755] 07 p0957 N85-16067
Dynamic polymer pressure transducer with temperature compensation
[AD-D011373] 07 p0967 N85-16142
Ultrasound instrumentation for the 7 inch Mach seven tunnel
[NASA-CR-174277] 07 p1038 N85-16586
Development of a pressure transducer for usage in high-temperature and vibration environments. Phase 1: Feasibility investigation
[AD-A148695] 08 p1165 N85-17349
Pressure measurements in a hydrogen combustion environment: An evaluation of 3 pressure transducers
[TI85-003645] 09 p1323 N85-18312
A probe for direct measurement of flow direction
[ESA-TT-853] 11 p1637 N85-20310
Heat pipe cooled probe
[NASA-CASE-LAR-12588-1] 12 p1844 N85-21568
The seven-hole pressure probe
[AD-A149799] 12 p1852 N85-21615
Performance assessment of Class 1E pressure transmitters subjected to environmental stresses
[DE85-001623] 12 p1854 N85-21626
An advanced solid state pressure transducer for high reliability SSME application 16 p2739 N85-26905
Oscillating pressure device for dynamic calibration of pressure transducers
[NASA-CASE-LAR-13094-1] 18 p3104 N85-29217
Fluidic angular velocity sensor
[NASA-CASE-NPO-16479-1-CU] 18 p3104 N85-29219
Research pressure instrumentation for NASA space shuttle main engine
[NASA-CR-176014] 19 p3227 N85-30006
Materials and process development for microcomputer-compatible pressure, temperature, and position sensors
[BMFT-FB-T-85-024] 24 p4097 N85-35399

PRESSURE SUITS
NT SPACE SUITS
The Reports of Aeromedical Laboratory, volume 25, no. 1/2
[ISSN-0023-2858] 01 p0090 N85-10805
Assessment of the inflating characteristics of the modified anti-G suit 01 p0090 N85-10809
Acceptance-testing procedures for air-line supplied-air suits
[DE84-016860] 05 p0712 N85-14569
Development of an electro-pneumatic anti-G valve for high performance fighter aircraft
[AD-A148468] 08 p1201 N85-17561
Servo operated anti-G suit pressurization system
[AD-D011466] 10 p1531 N85-19851
Analysis of the transient response of temporal artery blood flow data relative to various anti-G suit pressure schedules 10 p1533 N85-19860
Simulation of high +Gz onset in the dynamic environment simulator
[AD-A155983] 24 p4131 N85-35610

PRESSURE TRANSDUCERS
U PRESSURE SENSORS

PRESSURE VESSEL DESIGN
Advanced nickel-hydrogen cell configuration study
[NASA-CR-174775] 01 p0067 N85-10444
Reactor pressure vessel steels ASME SA533B and SA508 C 1.2
[VTT-340] 22 p3794 N85-33507

PRESSURE VESSELS
NT PREBURNERS
Ultralightweight oxygen container
[PB84-220730] 01 p0036 N85-10226
Detection of hydrogen assisted crack growth by measurement of modulus changes and acoustic emission
[DE84-015752] 02 p0184 N85-11236
Stress corrosion of pressure vessel steel A533-B in high temperature water
[BLL-RISLEY-TR-4600-(9091.9F)] 03 p0330 N85-12125
Field installed brazed thermocouple feedthroughs for high vacuum experiments
[DE84-013556] 04 p0503 N85-13207
Response of ferritic steels to nonsteady loading at elevated temperatures
[DE84-014280] 04 p0513 N85-13272
Impact of HDE unreliability on pressure vessel fracture predictions
[DE84-015586] 05 p0647 N85-14151
Static and dynamic fracture toughness characterization of SA508 forging and SA533B welded plate — pressure vessel steels
[CISE-2258] 08 p1131 N85-17127
Effect of temperature on the stress-relaxation response of a pressure vessel steel
[TI85-003588] 09 p1339 N85-18424
Assessment of the need for an advanced high-strength chromium-molybdenum steel for construction of third-generation gasifier pressure vessels
[DE85-002865] 11 p1606 N85-20097
Optimization of pressure vessels with standard intercepting spheres
[INPE-3276-PRE/600] 11 p1651 N85-20397
Effect of input distributions on the probabilistic fracture mechanics analysis of reactor pressure vessels
[DE85-000632] 11 p1652 N85-20403
Mechanical properties and brittle fracture resistance of welded multilayer elements for high pressure vessels 13 p2033 N85-22736
Welding technology: Japan — Conference
[ISBN-0-85300177-4] 15 p2565 N85-25823
Nondestructive equipment study
[NASA-CR-171886] 15 p2571 N85-25853
Sizing capability of automated ultrasonic time-of-flight diffraction in thick section steel and aspects of reliable inspection in practice
[AERE-R-11548] 15 p2571 N85-25855
Fatigue strength of Inconel 625 plate and weldments used in the DIII-D configuration vacuum vessel
[DE85-008276] 17 p2981 N85-28427
Initial performance of advanced designs for IPV nickel-hydrogen cells
[NASA-TM-87029] 17 p2984 N85-28444
Feasibility of electrolytic hydrogen production in the Pacific Northwest
[DE85-009856] 18 p3084 N85-29080
Ten year environmental test of glass fiber/epoxy pressure vessels
[NASA-TM-87058] 19 p3231 N85-30034
Literature survey of discontinuous-fiber-reinforced composites with emphasis on pressure vessels
[DE85-010386] 19 p3232 N85-30038
Initial performance of advanced designs for IPV nickel-hydrogen cells 20 p3448 N85-31404
In-service supervision of a prestressed concrete pressure vessel
[OEFZS-4306] 20 p3470 N85-31584
Solid-state track recorder neutron dosimetry in the Three-Mile Island Unit-2 reactor cavity
[DE85-011360] 20 p3531 N85-31966
Slideline verification for multilayer pressure vessels and piping analysis including strain hardening
[DE85-005616] 22 p3801 N85-33549
Prestressed concrete vessel according to the hot liner concept: A critical evaluation of experimental results with a prototype vessel
[OEFZS-4313] 22 p3801 N85-33550
Effect of stainless steel weld overlay cladding on the structural integrity of flawed steel plates in bending, series 1
[TI85-010349] 23 p3939 N85-34418
The dynamic strain ageing of A533B class 1 nuclear pressure vessel steel
[AERE-R-11485] 24 p4078 N85-35274

PRESSURE WAVES
U ELASTIC WAVES

PRESSURE WELDING
NT DIFFUSION WELDING
NT EXPLOSIVE WELDING
NT ULTRASONIC WELDING
Pressure welding of corrosion-resistant steel with AMg6 aluminum 15 p2501 N85-25428
Thermocompression welding of parts made from AMts and VT1 alloys 15 p2501 N85-25430
Welding techniques in pressure part technology 15 p2566 N85-25835
Solid state bonding of molybdenum and TZM
[BLL-T8439/BG/LRS/LRST751/85] 16 p2792 N85-27220
Low pressure arc butt welding of dissimilar metals 19 p3246 N85-30128
Welding of steel-aluminum cooling panels for the holds of refrigerator vessels 19 p3248 N85-30129
Solid-state resistance welding cylinders and spheres
[DE85-010064] 20 p3469 N85-31555

PRESSURIZED CABINS
Aircraft cabin pressurization control system tester
[AD-D011225] 01 p0013 N85-10061
Distinctions in formation of microflora on construction materials used in habitable pressurized compartments 22 p3823 N85-33693
Effect of dibazol on parameters of nonspecific resistance of subjects in pressurized cabins 23 p3954 N85-34504

PRESSURIZED WATER REACTORS
Thermal fluid-structure interaction: A few scaling considerations — nuclear reactors
[GKSS-84-E-18] 01 p0048 N85-10314
The detection and assessment of defects in automatic ultrasonic inspection
[BLL-RISLEY-TR-4597-(9091.9F)] 05 p0647 N85-14150
Application of new welding technology in the fabrication of nuclear power plant 15 p2566 N85-25829
Information presentation in power plant control rooms
[VTT-320] 16 p2864 N85-27668
Calculations on the feasibility of ultrasonic inspection of steam generator tubing in pressurized water reactors
[AERE-R-10960] 23 p3940 N85-34419

PRESSURIZING
Behavior of pressurized tubes of candidate alloys in a simulated low-Btu environment
[DE85-003403] 09 p1298 N85-18141

PRESTON TUBES
U PITOT TUBES
U SPEED INDICATORS

PRESTRAINING
U PRESTRESSING

PRESTRESSING
Measurement of the preloading of bolted joints by the ultrasonic method
[CETIM-1-SH-38-6] 04 p0558 N85-13556
Multiaxial yield behavior of 1100 aluminum following various magnitudes of prestrain
[DE84-013904] 05 p0617 N85-13949
Durability and behavior of prestressed concrete beams. Posttensioned concrete beam investigation, supplemental laboratory tests of beams exposed from 1961 to 1982
[AD-A148821] 09 p1304 N85-18191
Vibration and buckling of rotating, pretwisted, preconed beams including Coriolis effects
[NASA-TM-87004] 15 p2577 N85-25860
In-service supervision of a prestressed concrete pressure vessel
[OEFZS-4308] 20 p3470 N85-31584
Monotonous stress-strain properties of structural steel subjected to nonstationary repetitive pre-loading 23 p3904 N85-34185
Corrosion fatigue strength and crack growth in prestrained 0.16% C carbon steel 23 p3905 N85-34192

PRETESTS
U TESTS

PRETREATMENT
NT PRESTRESSING
Influence of pretreatment, environment and strain rate on stress corrosion cracking of the aluminum alloy 7075-T6
[VTH-LR-433] 16 p2752 N85-26985

PRETWISTING
U PRESTRESSING
U TWISTING

PREVENTION
NT ACCIDENT PREVENTION
NT CORROSION PREVENTION
NT FIRE PREVENTION
NT ICE PREVENTION
Jet lag prevention: Physiological mechanisms and pharmacological therapy
[AD-A145444] 02 p0235 N85-11529
Tight Ribbon Arm Protection (TRAP) for aircrewman ejection
[AD-A150464] 13 p2143 N85-23303

PRIMARY BATTERIES
NT ALKALINE BATTERIES
NT NICKEL ZINC BATTERIES
NT SODIUM SULFUR BATTERIES
NT THERMAL BATTERIES
Electrochemistry and storage 05 p0609 N85-13869
Electrochemistry and storage panel report 05 p0611 N85-13903
Safety characteristics of non-lithium battery systems
[AD-A155733] 22 p3806 N85-33574

PRIMARY COSMIC RAYS
NT SOLAR COSMIC RAYS
Anomalon search — heavy cosmic ray interactions
[NOTA-INTERNA-825] 02 p0305 N85-11970
Radiobiological studies on egg systems exposed to heavy nuclei of cosmic galactic radiation — insects 05 p0690 N85-14440
Preliminary results of advanced Biostack experiments with plant seeds and spores — cosmic ray effects 05 p0691 N85-14441
The radiobiological advanced Biostack experiment on Spacelab 1 05 p0691 N85-14442
Isotopic composition of primary cosmic rays H-Fe for ISEE-C
[NASA-CR-175266] 05 p0746 N85-14783
UCB cosmic ray experiment 09 p1417 N85-18941
The inner granulometric density of the tracks in nuclear emulsions and its application to determine the chemical spectrum of primary cosmic ray nuclidi
[OG-4.3-9] 22 p3879 N85-34034

Observations of ultraheavy cosmic ray particles at 10 GV cutoff rigidity
[OG-4.4-2] 22 p3879 N85-34035
Primary cosmic ray spectrum in the 10 to the 12th power - 10 to the 16th power eV energy range from the NUSEX experiment
[OG-5.1-5] 22 p3881 N85-34047
Study of composition of cosmic rays with energy .7 E 3 Ee
[OG-5.1-7] 22 p3881 N85-34049
On the possibility of the determining the average mass composition near 10 to the 14th power eV through the solar magnetic field
[OG-5.1-9] 22 p3882 N85-34051
A new method to determine the chemical composition of the cosmic rays beyond 10 to the 15th power eV
[OG-5.1-11] 22 p3882 N85-34052
Cosmic ray composition between 10 to the 15th power - 10 to the 17th power eV obtained by air shower experiments
[OG-5.1-12] 22 p3882 N85-34053
Fluctuations of development maximum depth and nuclear composition of primary cosmic radiation
[OG-5.1-13] 22 p3882 N85-34054
EAS spectrum in the primary energy region above 10 to the 15th power eV by the Akeno and Yakutsk array data
[OG-5.1-16] 22 p3882 N85-34057
Implication of EAS data for the study of primary cosmic rays above 10 to the 5th power GeV
[OG-5.2-7] 22 p3883 N85-34064
High-energy multiple muons and heavy primary cosmic-rays
[OG-5.2-9] 22 p3883 N85-34065
Composition of primary cosmic rays near the knee
[OG-5.2-10] 22 p3884 N85-34066
EAS Cerenkov measurements of the composition of the cosmic ray flux around 10 to the 16th power eV
[OG-5.2-11] 22 p3884 N85-34067
Electron and muon parameters of EAS and the composition of primary cosmic rays in 10(15) to approximately 10(16) eV
[OG-5.2-12] 22 p3884 N85-34068
Variations in the propagation of UH-nuclei
[OG-7.1-1] 23 p4012 N85-34863
Secondary to primary ratio and the continuous acceleration
[OG-8.3-4] 23 p4022 N85-34923
The response of ionization chambers to relativistic heavy nuclei
[OG-9.1-13] 23 p4024 N85-34936
Empirical model for the Earth's cosmic ray shadow at 400 KM: Prohibited cosmic ray access
[SH-6.1-14] 23 p4046 N85-35087
Cosmogenic-nuclide production by primary cosmic-ray protons
[SH-7.1-6] 23 p4047 N85-35098
The neutron moderated detector and groundbased cosmic ray modulation studies
[SH-9.1-13] 23 p4052 N85-35126
Measurement of low energy cosmic rays aboard Spacelab-1
[SH-10.1-6] 23 p4053 N85-35137
Heavy cosmic ray measurement aboard Spacelab-1
[SH-10.1-7] 23 p4053 N85-35138
Energy spectra of proton and nuclei of primary cosmic rays in energy region 10 TeV/particle
[HE-3.1-10] 24 p4178 N85-35006
Size distributions of air showers accompanied with high energy gamma ray bundles observed at Mt. Chacaltaya
[HE-3.3-9] 24 p4181 N85-35027
Multidimensional analysis of data obtained in experiments with X-ray emulsion chambers and extensive air showers
[HE-3.6-2] 24 p4184 N85-35051
LPM effect and primary energy estimations
[HE-3.6-4] 24 p4185 N85-35053
The lateral distributions of charged particles of energy greater than 0.3 E sub crit in electron-photon cascades in lead and air
[HE-3.6-10] 24 p4185 N85-35057
Result of Monte-Carlo simulation of electron-photon cascades in lead and layers of lead-scintillator
[HE-3.6-11] 24 p4185 N85-35058
Intensities of high-energy cosmic rays at Mount Kanbala
[HE-3.7-5] 24 p4186 N85-35064
Ultra high energy events in ECHOS series and primary energy spectrum
[HE-3.7-9] 24 p4186 N85-35066
Study of the energy spectrum of primary cosmic rays: EAS size fluctuations at a fixed primary energy
[HE-4.4-14] 24 p4194 N85-36020
Thickness of the particle swarm in cosmic ray air showers
[HE-4.7-14] 24 p4200 N85-36064
Relevance of multiple muons detected underground to the mass composition of primary cosmic rays
[HE-5.1-4] 24 p4201 N85-36069
Multimuons events and primary composition
[HE-5.1-5] 24 p4201 N85-36070
Muon groups and primary compoeition at 10 to the 13th power to 10 to the 15th power eV
[HE-5.1-12] 24 p4201 N85-36074
Primary chemical composition from simultaneous recording of muons induced cascades and accompanying muon group underground
[HE-5.1-13] 24 p4201 N85-36075
Multiple muons in MACRO
[HE-5.2-1] 24 p4202 N85-36079
Search for tachyons associated with extensive air showers in the ground level cosmic radiation
[HE-6.2-13] 24 p4212 N85-36149
Observation of genetic relation among new phenomena Geminion, Chiron and mini-Centauro
[HE-6.2-16] 24 p4212 N85-36152
Muon and neutrino fluxes
[HE-6.2-18] 24 p4213 N85-36154

PRIMATES
NT BABOONS
NT HUMAN BEINGS
NT MONKEYS
Primate experiments on SLS-1
15 p2687 N85-26592
A brief description of the two primate experiments to be carried out on SL-4 15 p2687 N85-26597
Morphological study of primate hypothalamus and hypophysis after experiment with antiorthostatic hypokinesia 19 p3325 N85-30603
Changes in nephron and juxtaglomerular system of primate kidneys under the effect of antiorthostatic hypokinesia 19 p3326 N85-30605

PRIMERS
Development of acceptance criteria for batches of silane primer for external tank thermal protection system bonding applications
[NASA-CR-171436] 15 p2518 N85-25523
Development of acceptance criteria for batches of silane primer for external tank thermal protection system bonding applications
[NASA-CR-175850] 16 p2754 N85-26995

PRIMERS (COATINGS)
Development of acceptance criteria for batches of silane primer for external tank thermal protection system bonding applications
[NASA-CR-171266] 04 p0478 N85-13043
Polarization in chemically doped hydrogen-rich glasses
[DE84-017486] 06 p0771 N85-14936
Evaluation of properties of varnishes, exterior stains and exterior primers
[PB84-243948] 06 p0772 N85-14940
An electrochemical study of the corrosion behavior of primer coated 2219-T87 aluminum
[NASA-TP-2459] 13 p2021 N85-22662
Development of acceptance criteria for batches of silane primer for external tank thermal protection system bonding applications
[NASA-CR-171426] 14 p2259 N85-23996
Adhesive evaluation of LARC-TPI and a water-soluble version of LARC-TPI
[NASA-TM-86428] 19 p3248 N85-30136
Results of tests of weathered K5NA closeout material in the MSFC Hot Gas Facility
[NASA-CR-170893] 24 p4073 N85-35239

PRIMITIVE EARTH ATMOSPHERE
Greenhouse effect in Earth's primordial atmosphere
16 p2607 N85-27310
The composition of the primitive atmosphere and the synthesis of organic compounds on the early Earth
21 p3717 N85-33065
The problem of the Earth's CO2 content and the iron core 21 p3718 N85-33069

PRIMITIVE EQUATIONS
Numerical studies of frontal dynamics
15 p2596 N85-26014
A split explicit model for short-term numerical weather prediction 16 p2831 N85-27460
A factored implicit scheme for numerical weather prediction with small factorization error
18 p3141 N85-29447
A comparison of the bounded derivative and the normal mode initialization methods using real data
18 p3144 N85-29463
An algorithm for the generation of primitive polynomials
[FUB-17-1984] 22 p3831 N85-33730

PRINCIPAL COMPONENTS ANALYSIS
Homogeneous macroclimatic zones of the lake states
[PB84-215821] 04 p0540 N85-13436
The use of principal components analysis techniques Nimbus-7 coastal zone color scanner data to define mesoscale ocean features through a warm humid atmosphere
[AD-A148567] 08 p1176 N85-17416
Martian fretted terrain morphometry interpreted using principal components analysis 13 p2192 N85-23597
Determining mineral types and abundances from reflectance measurements 13 p2196 N85-23622

PRINTED CIRCUITS
NT LARGE SCALE INTEGRATION
Extractor for spring-lock pin connectors
[AD-D011235] 01 p0043 N85-10280
A generalized solution to a class of printed circuit antennas
[AD-A145626] 02 p0191 N85-11278
Depot level problems in the testing of printed circuit boards
[AD-P003932] 02 p0247 N85-11612
Swiss firm improves method for soldering printed circuits 03 p0341 N85-12193
Computerized circuit designs: Realization of masks to manufacture microwave circuits
[CNES-NT-107] 04 p0496 N85-13168
Polyimide-glass multilayer printed wiring boards
[DE84-015092] 05 p0631 N85-14046
Characteristics of circular-polarized printed radiators in planar phased antenna array 06 p0790 N85-15049
Diagnostic apparatus for radar pulse repetition frequency control circuit card
[AD-D011364] 07 p0937 N85-15938
MMIC devices for active phased array antennas
[NASA-CR-174281] 07 p0938 N85-15943
Evaluation of test equipment for the detection of contamination on electronic circuits — spacecraft electronics
[ESA-STM-234] 08 p1159 N85-17316
Mechanical locking between multi-layer printed wiring board conductors and through-hole plating
[AD-D011477] 10 p1481 N85-19352
CAD/CAM systems for printed circuit design, manufacture 11 p1619 N85-20188
Printed circuit balun with a dipole antenna
[AD-D011534] 12 p1833 N85-21496
Gain enhancement methods for printed circuit antennas
[AD-A150090] 12 p1835 N85-21517
The state of the art in printed wiring board inspection
[AD-A149871] 12 p1862 N85-21679
A generalized solution to a class of printed circuit antennas 13 p2062 N85-22862
Applications, specifications of Robotron CAD-CAM work stations 15 p2537 N85-25661
New designs from electronics R and D center
15 p2538 N85-25666
Design and swept-frequency measurement of printed circuit board log-periodic dipole arrays
[R-NIAS-23] 15 p2539 N85-25671
Ink jet printing of silver metallization for photovoltaics
[NASA-CR-175798] 15 p2586 N85-25943
Printed wiring board circuit isolator tool
[AD-D011638] 17 p2968 N85-28333
Drag soldering process control
[DE85-010853] 20 p3433 N85-31301
Digital integrated circuits 21 p3669 N85-32787
A comparison and analysis of Vintr's global routing algorithm with the Lee routing algorithm in two-layer printed circuit boards
[AD-A155600] 21 p3673 N85-32816
Heat sinking for printed circuitry
[DE85-011585] 22 p3783 N85-33440
Hermetic chip carrier compliant soldering pads
[AD-D011722] 23 p3938 N85-34410

PRINTERS
NT PRINTERS (DATA PROCESSING)
Program DISAS: A computer program to obtain hard-copy plots of an image displayed on a vector graphics device in a local-area-network
[AD-A153643] 18 p3162 N85-29586
Flexible satellite communications systems simulator, phase 3
[AD-A155647] 21 p3577 N85-32247

PRINTERS (DATA PROCESSING)
East Europe report: Science and technology
[JPRS-ESA-84-030] 01 p0101 N85-10670
Two programs for the HP9836C computer to acquire frequency or voltage data from a source
[AD-A146832] 06 p0654 N85-15430
Computer equipment at 1984 Leipzig Spring Fair
09 p1378 N85-18662
Microprocessor AirborneData Acquisition and Replay (MADAR) system
[AD-A151728] 20 p3514 N85-31843
Dual optical mechanical position tracker
[AD-D011739] 22 p3844 N85-33811

PRINTING
NT LITHOGRAPHY
NT PHOTOLITHOGRAPHY
Optical recording of information on paper by CO2 and YAG-lasers 02 p0261 N85-11710
The electronic typesetting program programmer's manual
[AD-A147500] 07 p1025 N85-16508
Screen printed interdigitated back contact solar cell
[NASA-CASE-LEW-13414-1] 11 p1671 N85-20530
Applications of lasers in manufacturing 14 p2308 N85-24279
Ink jet printing of silver metallization for photovoltaics
[NASA-CR-175798] 15 p2586 N85-25943
A microcomputer-based program for printing check plots of integrated circuits specified in Caltech intermediate form
[AD-A151715] 15 p2629 N85-26205
T sub EX font tables
[DE85-011394] 19 p3339 N85-30687
Ink jet printing of silver metallization for photovoltaics
[NASA-CR-176019] 19 p3343 N85-30720
Ink jet printing of silver metallization for photovoltaics
[NASA-CR-176054] 22 p3805 N85-33569
Development of metallization process: FSA project, cells and module formation research area
[NASA-CR-176136] 23 p3945 N85-34447
PRISMATIC BARS
Study on a prismatic dye vat — laser systems
[CERT-2/6124-04-RO] 16 p2791 N85-27217
PRISMS
NT PRISMATIC BARS
Extending magnitude standards to faint stars with a sub-beam prism 07 p0965 N85-16124
Sub-beam prism used at the Bosecha Schmidt telescope 07 p0965 N85-16125
Stellar photographic photometry using a double wedge technique with a focal reducer system 07 p0966 N85-16133
Spectrophotometry of cool stars from objective prism spectra 07 p0966 N85-16134
Interpreting geothermal anomalies by special points method 07 p0982 N85-16238
High resolution diffraction grating
[AD-D011541] 12 p1933 N85-22141
Reflex attachment for line alignment in spectral diffraction devices 13 p2044 N85-22794
Three-mirror open resonator for millimeter wave band 13 p2077 N85-22972
Determination of parameters of elastically strained mirror facets of rapidly rotating prisms 14 p2282 N85-24137
Operation of Prisma flexible manufacturing system 15 p2524 N85-25564
Method and apparatus for generating a structured light beam array
[AD-D011590] 15 p2652 N85-26357
PRIVACY
Federal Telecommunications Privacy Act of 1984
[H-REPT-98-815] 03 p0441 N85-12807
PRIVATE AIRCRAFT
U GENERAL AVIATION AIRCRAFT
PROBABILITY
U PROBABILITY THEORY
PROBABILITY DENSITY FUNCTIONS
NT NORMAL DENSITY FUNCTIONS
NT PEARSON DISTRIBUTIONS
NT RAYLEIGH DISTRIBUTION
NT WEIBULL DENSITY FUNCTIONS
Total positivity. A review
[AD-A145205] 01 p0114 N85-10771
Efficient methods for mechanical and structural reliability analysis and design 02 p0205 N85-11355
Nonparametric maximum penalized likelihood estimation of a density from arbitrarily right-censored observations
[AD-A145569] 02 p0251 N85-11644
Algebraic functions of H-functions with specific dependency structure
[AD-A145598] 02 p0252 N85-11647
Likelihood estimation for generalized mixed exponential distributions
[AD-A145675] 02 p0252 N85-11651
Prediction of wave height of wind-generated seas in finite water depth
[AD-A145996] 03 p0396 N85-12539
Probability distribution density of normalized radar range 04 p0485 N85-13098
Multivariate spline methods in surface fitting 07 p0965 N85-16257
Some scientific subroutines in LISP
[AD-A147889] 07 p1026 N85-16515
A coaxial probe for measuring the current density profile of intense electron beams
[AD-D011407] 08 p1164 N85-17347
Flame propagation and stabilization studies using Rayleigh scattering and laser Doppler velocimetry
[AD-A148802] 09 p1290 N85-18102
Turbulent premixed flame study
[DE85-003220] 09 p1292 N85-18112
On the probability density of signal-to-noise ratio in an improved adaptive detector, part 1
[AD-A148856] 10 p1550 N85-19772
A stochastic-mechanical approach to acoustic pulse propagation in the deep ocean sound channel
[AD-A149598] 12 p1928 N85-22110
On filter binary processes
[AD-A150328] 13 p2083 N85-22890
Invariance of probability characteristics of detector to shape of optical pulse signals 13 p2090 N85-23048
Construction of efficient algorithms for the estimation of multivariate probability densities
[AD-A151509] 15 p2640 N85-26285
A non-parametric probability density estimator and some applications
[AD-A151853] 15 p2641 N85-26287
Measurement of damping of graphite expoxy materials
[NASA-CR-175793] 16 p2743 N85-26925
A data based algorithm for choosing the window width when estimating the integral of f2(x)
[AD-A152093] 16 p2847 N85-27553
An inequality and its application to the truncated distributions 17 p3020 N85-28673
Robust tests of mean vector in symmetrical multivariate distributions
[AD-A153116] 17 p3020 N85-28674
Conditional modelling in turbulent shear flows 20 p3424 N85-31250
The microstructure approach to conserved scalar pdf models 20 p3424 N85-31251
Assessment of superlayer contribution to the conserved scalar PDF in a hydrogen turbulent jet diffusion flame 20 p3425 N85-31255
Efficiency of discrimination in some invariant signal transformations 22 p3776 N85-33399
A new approach to evaluate gamma-ray measurements
[OG-9.5-11] 23 p4031 N85-34988
Relaxation phenomena and stability of probability densities
[AD-A155923] 24 p4143 N85-35682
PROBABILITY DISTRIBUTION FUNCTIONS
On probability forecasts for temperature 01 p0084 N85-10565
Probability distribution of leadtime demand
[AD-A144952] 01 p0113 N85-10766
An iterative procedure for obtaining I-projections onto the intersection of convex sets
[AD-A145402] 02 p0251 N85-11639
Weighted distributions arising out of methods of ascertainment
[AD-A145615] 02 p0252 N85-11648
The estimation of persistance statistics from cumulative probabilities of wave height
[NMI-R183] 03 p0397 N85-12534
Probability distribution density of normalized radar range 04 p0485 N85-13098
The undetected error probability for shortened hamming codes
[NASA-CR-174175] 04 p0555 N85-13535
Interval mathematics reports
[REPT-84/1] 04 p0556 N85-13536
Risk analysis without Monte Carlo methods 04 p0556 N85-13537
Stochastic cell model for hadronic multiparticle distributions
[DE84-016480] 04 p0562 N85-13576
Spline methods for approximating quantile functions and generating random samples
[NASA-TP-2369] 07 p1035 N85-16565
Pari-mutuel as a system of aggregation of information
[AD-A147210] 07 p1035 N85-16570
An analysis of robust and efficient priors associated with a finite Bayesian model for compliance testing
[AD-A148497] 08 p1213 N85-17835
Recent results on characterization of probability distributions: A unified approach through extensions of Deny's theorem
[AD-A147631] 08 p1214 N85-17847
Calculation of cumulative distributions and detection probabilities in communications and optics
[AD-A147761] 08 p1215 N85-17850
Analysis of characteristics of digital discriminators for phase-shift keyed signals 13 p2070 N85-22930
Informative geometry of probability spaces
[AD-A150510] 13 p2153 N85-23371
Approximating posterior distributions of system reliability derived from component test data
[AD-A152057] 15 p2572 N85-25857
On the probability density of signal-to-noise ratio in an improved detector
[AD-A152529] 17 p2952 N85-28232
A collection of probability distributions
[AD-A153128] 17 p3025 N85-29704
A numerical investigation of the overlap distribution among pure states in the spin glass phase
[PREPRINT-414] 18 p3172 N85-29659
Tables for distributions of quadratic forms
[AD-A154064] 19 p3347 N85-30745
Methodology for evaluating P sub nu distributions: Results to date
[DE85-007286] 20 p3530 N85-31958
Characterizations of generalized hyperexponential distributions
[AD-A155855] 24 p4142 N85-35680
PROBABILITY THEORY
Sensitivity analysis of limit state functions for probability-based plastic design 01 p0059 N85-10388
Estimation of the threshold in fatigue crack initiation models: A Bayesian approach
[AD-A144847] 01 p0062 N85-10410
Setting hurricane conditions of readiness with high confidence
[AD-A144785] 01 p0085 N85-10570
Some weak and strong laws of large numbers for d(0,1) - valued random variables
[AD-A144845] 01 p0111 N85-10754
Construction of approximate confidence intervals for probability-of-kill via the bootstrap
[AD-A144761] 01 p0113 N85-10764
Joint probability of selected cloud and visibility thresholds around Koblenz, Germany
[AD-A145294] 02 p0231 N85-11506
A fast, compact assignment algorithm
[NRIMS-TWISK-331] 02 p0250 N85-11632
An introduction to multilinear formula score theory
[AD-A145696] 02 p0254 N85-11667
Locally optimal subset selection rules based on ranks under joint type 2 censoring
[AD-A146179] 03 p0412 N85-12632
On choosing between two probabilistic choice sub-models in a dynamic multitask environment 05 p0711 N85-14563
On the Edgeworth expansion for the sum of a function of uniform spacings
[CWI-MS-R8404] 05 p0719 N85-14619
Asymptotic distributions of estimators for posterior probabilities in a classification model with both continuous and discrete variables
[CWI-MS-R8409] 05 p0722 N85-14637
Invariant measures and the equicontinuous structure relation 1
[CWI-PM-R8403] 05 p0723 N85-14645
Invariant measures and the equicontinuous structure relation 2: The relative case
[CWI-PM-R8404] 05 p0723 N85-14646
How many Earth-approaching asteroids are there?
[NASA-CR-174209] 06 p0890 N85-15650
Analysis of subpixel registration 07 p0986 N85-16267
Experiments in forecasting atmospheric marine horizontal visibility using model output statistics with conditional probabilities of discretized parameters
[AD-A147574] 07 p1008 N85-16404
The symmetry group and exponents of operator stable probability measures
[AD-A147187] 07 p1035 N85-16568
Ambiguity and uncertainty in probabilistic inference
[AD-A147378] 07 p1035 N85-16572
Belief structures
[AD-A147526] 07 p1036 N85-16575
The effect of assumptions about cost element probability distributions on operating and support cost risk analysis
[AD-A147553] 07 p1036 N85-16576
Development of a mixed scanning interactive system for decision support
[AD-A146895] 07 p1051 N85-16670
A technique for rapid determination of probability of detection in pulse Doppler radars
[AD-D011428] 08 p1154 N85-17288
Two-dimensional modeling for lineal and areal probabilities of weather conditions
[AD-A147970] 08 p1188 N85-17486
Large deviations for processes with independent increments
[AD-A147293] 08 p1210 N85-17610
Probable cause: A decision making framework
[AD-A147642] 08 p1210 N85-17614
On the probability generating functional for point processes
[AD-A147692] 08 p1210 N85-17615
A theorem on the optimal allocation of effort
[AD-A148028] 08 p1211 N85-17623

Empirical Bayes rules for selecting good binomial populations
[AD-A147614] 08 p1214 N85-17646
Recent results on characterization of probability distributions: A unified approach through extensions of Deny's theorem
[AD-A147631] 08 p1214 N85-17647
Calculation of cumulative distributions and detection probabilities in communications and optics
[AD-A147781] 08 p1215 N85-17650
Probabilistic analysis of algorithms for NP-Complete problems
[AD-A148207] 08 p1215 N85-17653
Prematurely terminated sequential tests for MIL-STD 781C
[AD-A148417] 08 p1216 N85-17657
Exact simultaneous confidence intervals for pairwise comparisons of three normal means
[AD-A148751] 09 p1375 N85-18845
Bounding the stochastic performance of continuum structure functions 2
[AD-A149458] 10 p1548 N85-19762
Characteristic functional of a probability measure absolutely continuous with respect to a Gaussian radon measure
[AD-A149462] 10 p1548 N85-19763
On large matchings and cycles in sparse random graphs
[AD-A149194] 10 p1550 N85-19778
Estimation of variance of the regression estimator
[AD-A149407] 10 p1551 N85-19780
Identification of dynamic systems, theory and formulation
[NASA-RP-1136] 10 p1551 N85-19784
The study of certain aspects of probability with applications in communications theory
[AD-A149920] 12 p1829 N85-21476
Predicting a future response using rank predictive probabilities
[MATHEMATICS-RESEARCH-166] 12 p1923 N85-22077
Proportional odds models for survival data and estimates using ranks
[MATHEMATICS-RESEARCH-172] 12 p1923 N85-22080
A replication and extension of the inducement of the availability heuristic
[AD-A149755] 12 p1923 N85-22083
Systems vulnerability and lethality in the development phase
[AD-A149737] 12 p1924 N85-22089
Stable measures and processes in statistical physics
[AD-A149592] 12 p1925 N85-22098
Reliability of structural brittle materials 12 p1948 N85-22222
A statistical approach to vendor selection
[AD-A149781] 12 p1950 N85-22249
Rejection of anomalous observations when determining spacecraft trajectories 13 p1979 N85-22421
A Monte Carlo sampling plan for estimating network reliability
[AD-A150511] 13 p2065 N85-22898
Error probability during optimal noncoherent reception of binary signals in multibeam channel 13 p2069 N85-22922
Probability of detection of pulsed signals employing zero-gating interference suppression 13 p2085 N85-23021
Noise tolerance of diversity reception in frequency-adaptive digital transmission systems 13 p2098 N85-23024
SIGPI: A user's manual for the fast computation of the probabilistic performance of a complex system
[DE85-005447] 13 p2148 N85-23336
Why do noninvertible estimated moving averages occur?
[AD-A150388] 13 p2153 N85-23368
Tracer diffusion in an ordered alloy: Application of the path probability and Monte Carlo methods
[DE85-002766] 14 p2257 N85-23996
Monthly and Seasonal Weather Outlook for mid-December 1984 mid-January 1985, volume 38, number 24, 14 December 1984 14 p2379 N85-24887
A simple and efficient algorithm to compute tail probabilities from transforms
[AD-A150928] 14 p2409 N85-24849
Properties of systems which lead to efficient computation of reliability
[AD-A151033] 14 p2409 N85-24853
Algorithms and approximations for queueing systems
[CWI-TRACT-6] 14 p2410 N85-24850
Probabilistic analysis of combinatorial algorithms: An annotated bibliography
[CWI-OS-R8411] 14 p2411 N85-24864
Boundary crossing probabilities and statistical applications
[AD-A151027] 14 p2411 N85-24889
Inference and state estimation for stochastic point processes
[AD-A151216] 15 p2640 N85-26281
A non-parametric probability density estimator and some applications
[AD-A151853] 15 p2641 N85-26287
Lectures on probability and statistics
[DE85-007079] 15 p2641 N85-26291
The evolutive state: A new definition of system state to include sequencing of events 16 p2696 N85-26843
A mathematical model for calculating detection probability of a diffusion target
[AD-A152026] 16 p2854 N85-27601
An evaluation of discretized conditional probability and linear regression threshold techniques in model output statistics forecasting of visibility over the north Atlantic Ocean
[AD-A151955] 16 p2857 N85-27619
Probabilistic algorithms in group theory
[AD-A152253] 16 p2859 N85-27630
Refinements in the computation of collision probabilities
[DE85-006118] 16 p2864 N85-27663
Probabilistic structural analysis theory development 17 p2912 N85-27955
Probabilistic finite element development 17 p2913 N85-27956
Probabilistic structural analysis of SSME turbopump blades: Probabilistic geometry effects 17 p2913 N85-27958
Alternative theories of inference in expert systems for image analysis
[AD-A153649] 18 p3170 N85-29646
Accepting error to make less error
[AD-A153949] 18 p3171 N85-29651
Nonparametric renewal function estimation
[AD-A153474] 18 p3173 N85-29672
Nonparametric estimation of the probability of ruin
[AD-A153523] 18 p3174 N85-29674
Probabilistic analysis of combinational circuits with random delays 19 p3257 N85-30192
A comparison of four Monte Carlo methods for estimating the probability OF S=T connectedness
[AD-A154264] 19 p3348 N85-30749
Exponential order statistic models of software reliability growth
[NASA-CR-3909] 20 p3515 N85-31852
Monte Carlo: In the beginning and some great expectations
[DE85-010789] 20 p3518 N85-31872
Reliability of void detection in structural ceramics using scanning laser acoustic microscopy
[NASA-TM-87035] 21 p3597 N85-32337
Decomposing the joint distribution of several linear combinations of uniform spacings
[AD-A155056] 21 p3677 N85-32845
Analysis of unreplicated factorials allowing for possibly faulty observations
[AD-A154813] 21 p3678 N85-32848
Antistarshapedness, dispersiveness and mixtures
[AD-A155563] 21 p3678 N85-32849
Probabilistic analysis of automatic control systems for detection systems 22 p3765 N85-33335
SMACS: A system of computer programs for probabilistic seismic analysis of structures and subsystems. Volume 1: User's manual
[DE85-011653] 22 p3830 N85-33724
A formulation and analysis of combat games
[NASA-TP-2487] 22 p3835 N85-33745
The application of models to the assessment of fire hazard from consumer products
[NBSIR-85-3219] 23 p3925 N85-34325
Estimating risks of lead-induced hemoglobin decrements under conditions of uncertainty: Methodology, pilot judgments and illustrative calculations
[DE85-012293] 23 p3952 N85-34493
On the statistical significance of excess events: Remarks of caution and the need for a standard method of calculation
[OG-9.5-10] 23 p4031 N85-34987
Large deviations for the maxima of some random fields
[AD-A155909] 24 p4143 N85-35681
Relaxation phenomena and stability of probability densities
[AD-A155923] 24 p4143 N85-35682

PROBES
Precision tuneable resonant microwave cavity
[NASA-CASE-LEW-13935-1] 11 p1628 N85-20248
Heat pipe cooled probe
[NASA-CASE-LAR-12588-1] 12 p1844 N85-21568

PROBLEM SOLVING
NT ASYMPTOTIC METHODS
NT ITERATIVE SOLUTION
NT THEOREM PROVING
Results of the technical exchange agreement between NASA and DuPont on the containerless drop tube solidification of NiAl3
[NASA-TM-86473] 01 p0014 N85-10087
RADC/NBS (Rome Air Development Center/National Bureau of Standards) Workshop. Moisture Measurement and Control for Semiconductor Devices, 3
[PB84-219559] 01 p0051 N85-10337
Research in Structures and Dynamics, 1984
[NASA-CP-2335] 01 p0057 N85-10377
Application of concurrent processing to structural dynamic response computations 01 p0057 N85-10380
Recursive calculation of curved finite element stiffness matrices
[CSIR-TWISK-303] 01 p0108 N85-10726
The convergence of Garlerkin approximation schemes for second-order hyperbolic equations with dissipation
[CSIR-TWISK-325] 01 p0109 N85-10736
Solution of the Boltzmann transport equations for a permeable base transistor
[AD-A144989] 01 p0112 N85-10757
Lattice dilation in metal-hydrogen systems
[BLL-M-35758-(5825.4)] 02 p0176 N85-11176
Parallel, iterative solution of sparse linear systems: Models and architectures
[NASA-CR-172457] 02 p0243 N85-11586
A representation for the functioning of devices that supports compilation of expert problem solving structures: An extended summary
[AD-P003921] 02 p0245 N85-11601
Knowledge based tools for electronic equipment maintenance
[AD-P003940] 02 p0248 N85-11620
Numerical methods for solving systems of linear equations
[INPE-3240-RPE/463] 02 p0250 N85-11633
The numerical solution of the Helmholtz equation for wave propagation problems in underwater acoustics
[NASA-CR-172454] 02 p0250 N85-11634
An algorithm for least squares projections onto the intersection of shifted, convex cones
[AD-A145426] 02 p0251 N85-11640
On some common interests among reliability, inventory and queuing
[AD-A145595] 02 p0251 N85-11646
Cognitive coordinate systems: Accounts of mental rotation and individual differences in spatial ability
[AD-A146149] 03 p0401 N85-12557
A sequential quadratic programming algorithm for solving large, sparse nonlinear programs
[AD-A145854] 03 p0407 N85-12597
Convergence of SIP (Strongly Implicit Procedure)
[AD-A145810] 03 p0410 N85-12621
Moving finite elements in 2-D
[AD-A146266] 03 p0412 N85-12637
Psychological issues in the design of expert systems
[AD-A146081] 03 p0438 N85-12792
Economic analysis handbook
[AD-A146263] 03 p0441 N85-12805
Conservation laws and the numerical solution of ODEs
[DE84-016208] 04 p0555 N85-13531
New integration techniques for chemical kinetic rate equations. 2: Accuracy comparison
[NASA-TM-86893] 05 p0598 N85-13796
On looking into the black box: Prospects and limits in the search for mental models 05 p0700 N85-14548
Use of artificial intelligence and simple mathematics to analyze a physiological model 05 p0717 N85-14587
Conservative and nonconservative schemes for the solution of the nonlinear Schroedinger equation
[CWI-NM-R8405] 05 p0720 N85-14628
Situational interactive micro/graphic simulator system for improving maintenance performance
[AD-A146677] 06 p0757 N85-14846
Method of aperture synthesis: Fundamental relations and data processing in aperture synthesis systems (review) 06 p0781 N85-14994
Phase problem in aperture synthesis systems 06 p0782 N85-15002
Limits of applicability of long wave theory in studies of oscillations of n-layer fluid 06 p0824 N85-15234
A method for solving the inverse problem of transonic cascade flow
[AD-A146739] 07 p0899 N85-15698
Effects of individual mnemonic characteristics on problem solving 07 p1010 N85-16419
Mental models and cooperative problem solving with expert systems
[AD-A147843] 07 p1021 N85-16479

Research in applied mathematics, numerical analysis, and computer science
[NASA-CR-172505] 07 p1021 N85-16480
Implementation of a constraint machine for prism - A parallel problem solver
[AD-A147844] 07 p1026 N85-16512
Lattice statistics
[AD-A146662] 07 p1029 N85-16530
Solution of finite element problems by preconditioned conjugate gradient and Lanczos methods
[AD-A146921] 07 p1029 N85-16532
Viscosity solutions of Hamilton-Jacobi equations at the boundary
[AD-A147444] 07 p1032 N85-16553
Splitting methods for the numerical solution of the incompressible Navier-Stokes equations
[AD-A147483] 07 p1032 N85-16554
Sequential and parallel matrix computations
[AD-A147871] 07 p1034 N85-16562
Development of a mixed scanning interactive system for decision support
[AD-A146895] 07 p1051 N85-16670
On the complexity of distributed decision problems
[AD-A147174] 07 p1052 N85-16674
Distributed knowledge base systems for diagnosis and information retrieval
[AD-A146890] 07 p1054 N85-16690
Vectorizable multigrid algorithms for transonic flow calculations
[NASA-CR-174326] 08 p1077 N85-16827
Hazard assessment of a hypothetical large rocket motor 08 p1117 N85-17042
Flexible manufacturing system concept features cache memory 08 p1140 N85-17186
COPES/ADS (Control Program for Engineering Synthesis) (Automated Design Synthesis) using the ADS optimization program
[AD-A148576] 08 p1206 N85-17588
A local refinement finite element method for time dependent partial differential equations
[AD-A147943] 08 p1211 N85-17620
Distributed asynchronous relaxation methods for convex network flow problems
[AD-A148027] 08 p1211 N85-17622
Probabilistic analysis of algorithms for NP-Complete problems
[AD-A148207] 08 p1215 N85-17653
Analysis of a potential hot-wire ignition problem
[DE84-017254] 09 p1301 N85-18174
Device modeling for advanced integrated circuits 09 p1314 N85-18258
An implicit, conservative, zonal-boundary scheme for Euler equation calculations
[NASA-CR-3865] 09 p1318 N85-18290
On the local behaviour of solutions of degenerate parabolic equations with measurable coefficients
[AD-A147412] 09 p1373 N85-18631
Solution of the h-equation for a single point source excitation of magnitude K
[DE84-017574] 09 p1374 N85-18638
Towards the construction of periodic solutions of pseudodifferential equations with the aid of algebraic operators 10 p1535 N85-19674
Distributing a distributed problem solving network simulator
[AD-A149065] 10 p1537 N85-19693
A program design for an adaptive, non-linear finite element solver
[AD-A148680] 10 p1539 N85-19705
Meta-level control through fault detection and diagnosis
[AD-A149064] 10 p1540 N85-19709
Qualitative process theory
[AD-A148987] 10 p1543 N85-19729
Efficient algorithm for fuzzy linear programming with multiple objectives
[AD-A149012] 10 p1544 N85-19736
A conformal mapping suitable for problems involving interaction between given geometries and known far fields
[AD-A149050] 10 p1545 N85-19744
Neumann type boundary conditions for Hamilton-Jacobi equations
[AD-A149069] 10 p1546 N85-19746
Hamilton-Jacobi equations in infinite dimensions. Part 1. Uniqueness of viscosity solutions
[AD-A149094] 10 p1548 N85-19749
Order picking in an aisle
[AD-A149553] 10 p1548 N85-19766
Construction of solutions for two-dimensional Riemann problems
[DE85-003136] 10 p1549 N85-19770
Contribution to the study of a numerical implicit method for solving the Euler equations
[ESA-TT-872] 10 p1549 N85-19771
Robust Kalman filtering and its applications
[AD-A149044] 10 p1550 N85-19775
Heuristics based on spacefilling curves for combinatorial problems in the plane
[AD-A149320] 10 p1552 N85-19788
Coordination in a distributed problem solving network
[AD-A148925] 10 p1565 N85-19672
A study of degenerate and nondegenerate critical points in three-dimensional flow fields
[DFVLR-FB-84-36] 11 p1633 N85-20268
East Europe report: Scientific affairs
[JPRS-ESA-84-006] 11 p1700 N85-20684
Polylith and environments for mathematical computation
[DE85-002967] 11 p1702 N85-20704
Solving partial differential equations on multiprocessors
[DE85-000745] 11 p1706 N85-20734
Solution of structured non-stiff ODEs
[DE85-004137] 11 p1707 N85-20741
An exact solution to the 2 point OC (Operating-Characteristic) curve determination
[AD-A148120] 11 p1708 N85-20748
The application of expert systems to corrosion problems
[AERE-M-3445] 12 p1804 N85-21316
On the accuracy of least squares methods in the presence of corner singularities
[NASA-CR-172552] 12 p1919 N85-22050
Numerical methods for tracking interfaces
[LA-9917-MS] 12 p1919 N85-22052
Satellite-to-satellite orbit determination using minimum, discrete range and range-rate data only 13 p1985 N85-22458
Sparse matrix computations
[DE85-004780] 13 p2152 N85-23362
Personal decision making: The influence of perceived locus of control and degree of rationality on information seeking strategies 13 p2167 N85-23446
Programmer/analyst workstation evaluation report
[NASA-CR-175289] 14 p2394 N85-24749
Implementation of a C1 triangular element based on the p-version of the finite element method
[AD-A150904] 14 p2404 N85-24825
The complexity of reliability computations in planar and acyclic graphs
[AD-A150759] 14 p2408 N85-24845
Maintaining solution invariants in the numerical solution of ODEs
[DE85-005918] 14 p2410 N85-24857
Solving set covering problems using heuristics with branch and bound
[AD-A151905] 15 p2638 N85-26269
Finite-difference computations of rotor loads
[NASA-TM-86682] 16 p2700 N85-26669
Method for evaluating perturbation in algorithms for solving navigational problems 16 p2718 N85-26783
LU methods for the compressible Navier-Stokes equations 16 p2781 N85-27160
Explicit construction of contractivity matrices
[TRITA-NA-8309] 16 p2852 N85-27586
Augmented weighted diamond force of the linear nodal scheme for Cartesian coordinate systems
[DE85-005631] 17 p3020 N85-29679
A program for solving first kind Fredholm integral equations by means of regularization
[CWI-NM-R8416] 17 p3022 N85-29697
A variable-complexity norm maximization problem
[AD-A153514] 18 p3169 N85-29834
Extrapolation methods for multi-dimensional quadrature of singular and regular integrand functions
[DE85-009665] 18 p3172 N85-29855
Method for computing evolution of random hydrodynamic fields on basis of adjoint equations 19 p3292 N85-30412
Expanding expertise by use of an expert system
[DE85-010759] 19 p3344 N85-30723
On spectral multigrid methods for the time-dependent Navier-Stokes equations
[NASA-CR-172613] 19 p3344 N85-30725
On MGR (Upsilon) multigrid methods
[AD-A153867] 19 p3345 N85-30733
Numerical algorithms for solving linear algebra problems
[DE85-010310] 19 p3346 N85-30738
Floating shock-fitting in transonic potential flow calculations 20 p3367 N85-31007
Direct simulation techniques for the Boltzmann equation
[DFVLR-FB-85-13] 20 p3457 N85-31470
Compressible Lagrangian hydrodynamics without Lagrangian cells
[DE85-009597] 20 p3520 N85-31891
The formal specification of an abstract machine: Design and implementation
[AD-A155167] 21 p3672 N85-32808
A comprehensive study of the AFIT (Air Force Institute of Technology) software development environment
[AD-A155450] 21 p3672 N85-32812
A new fault-tolerant algorithm for clock synchronization
[AD-A154771] 21 p3676 N85-32836
A simulation study of Sylvester's problem in three dimensions
[AD-A155266] 21 p3679 N85-32854
Solution of problem of equilibrium confinement of plasma by magnetic field in an infinite circular cylinder 21 p3692 N85-32936
Solvability of some inverse problems in laser radiation focusing 21 p3696 N85-32963
On the problem of linear programming with approximate data 21 p3698 N85-32978
Flat is not necessarily good
[DE85-012619] 22 p3830 N85-33723
Implementing linear multistep formulas for solving DAES
[DE85-012400] 22 p3834 N85-33740
DISPL1: A software package for one and two spatially dimensioned kinetics-diffusion problems
[ANL-84-56] 23 p3958 N85-34516
A model for graphics interface tool development 23 p3960 N85-34545
Analytic solutions of inverse heat conduction problems 24 p4092 N85-35367
Algorithmic approaches in sets of good answers in inverse problems
[PM/84/18] 24 p4142 N85-35677

PROCEDURES
NT CREW PROCEDURES (INFLIGHT)
NT FINITE ELEMENT METHOD
NT FINITE VOLUME METHOD
NT OPTICAL CORRECTION PROCEDURE
NT PANEL METHOD (FLUID DYNAMICS)
The removal, mechanical handling and installation procedures for declination tachometer and Itek encoder — United Kingdom Infrared Telescope
[UKIRT-17] 09 p1414 N85-18915
The mechanical procedures for the 8 channel bolometer — United Kingdom Infrared Telescope
[UKIRT-18] 09 p1414 N85-18916
In situ washing procedures for the UKIRT 3.8 meter primary mirror — United Kingdom Infrared Telescope (UKIRT)
[UKIRT-20] 09 p1414 N85-18918
Development and evaluation of a procedure for the rapid analysis of fresh concrete
[AD-A149741] 12 p1866 N85-21703
A note on validity generalization procedures
[AD-A150065] 12 p1924 N85-22085
The acquisition of procedures from text. A production-system analysis of transfer of training
[AD-A151029] 14 p2392 N85-24732
Guide for the execution of reliability tests in the laboratory — aeronautical equipment 16 p2796 N85-27237
Method for preparing Pb-(beta)-aluminum ceramic
[DE85-011665] 22 p3752 N85-33256
Method for controlling the viscosity of siloxane oils
[DE85-011566] 23 p3909 N85-34221
Method for preparing hydride configurations and reactive metal surface
[DE85-008443] 23 p3917 N85-34274
Procedure for editing the fluxgate magnetometer data of the AFGL (Air Force Geophysics Laboratory) magnetometer network
[AD-A156331] 24 p4117 N85-35523

PROCEEDINGS
U CONFERENCES

PROCESS CONTROL (INDUSTRY)
Preparation of silicon carbide fibers
[DE84-014661] 01 p0022 N85-10137
Automated apparatus for producing gradient gels
[DE84-014507] 01 p0107 N85-10716
Computer aided process planning of machined metal parts
[AD-A145629] 02 p0189 N85-11263
Application of solidification theory to rapid solidification processing
[AD-A145953] 03 p0331 N85-12136
Critical dynamics for continuous rapid solidification processing
[AD-A146071] 03 p0332 N85-12137
DNC, CNC network for robotized machining cells 04 p0491 N85-13130
Self-tuning control of offset: A unified approach
[OUEL-1539/84] 04 p0553 N85-13520
Long-range predictive control using weighting-sequence models
[OUEL-1542/84] 04 p0553 N85-13521
Investigations regarding process analysis of liquids in the 1 to 2 micrometer spectral range
[BMFT-FB-T-84-169] 05 p0614 N85-13926

Controlled directionally solidified precision casting for superalloys and steels
[BMFT-FB-T-84-180] 05 p0619 N85-13960
Self-tuning controller design and implementation
[OUEL-1535/84] 05 p0621 N85-13975
Control of microstructure during hot working of Ti-6242 06 p0797 N85-15091
Finite element simulation of forging processes 06 p0797 N85-15093
Modelling temperature changes during hot working operations 06 p0798 N85-15095
Modelling microstructural changes during hot rolling of steels 06 p0798 N85-15096
Process research of non-Cz silicon material 06 p0830 N85-15275
Advanced dendritic web growth development 06 p0831 N85-15286
Aerosol reactor for silicon processing 06 p0832 N85-15292
Control technology for integrated circuit fabrication at Micro-Circuit Engineering, Incorporated, West Palm Beach, Florida
[PB85-100717/GAR] 07 p0949 N85-16013
An analysis of the effect of process controls on productivity and weapon system costs in DoD procurement
[AD-A147496] 07 p1052 N85-16678
Approximate models in multivariable process control: An inverse Nyquist array and robust tuning regulator interpretation
[RR-261] 08 p1216 N85-17663
Control of the manufacturing process and material flow in flexible manufacturing systems
[PNR-90234] 09 p1371 N85-18615
French firm has most advanced continuous-casting machine 11 p1592 N85-20017
Chemical approach for controlling nadimide cure temperature and rate with maleimide
[NASA-CASE-LEW-13770-3] 12 p1809 N85-21350
Chemical approach for controlling nadimide cure temperature and rate with maleimide
[NASA-CASE-LEW-13770-4] 12 p1810 N85-21351
Materials refining for solar cell silicon 12 p1877 N85-21775
Manufacturing perspective in the design of bevel gearing 14 p2221 N85-23777
Electrical features of new DNC, CNC system viewed — direct numerical control 15 p2524 N85-25562
Operation of Prisma flexible manufacturing system 15 p2524 N85-25564
East Europe report: Science and technology
[JPRS-ESA-85-018] 15 p2537 N85-25658
Process control systems for largely automated manufacturing 15 p2537 N85-25659
Summaries of FY 1984 engineering research
[DE85-006273] 15 p2664 N85-26442
Multivariable statistical modelling and its application 16 p2857 N85-27617
Integration of advanced preparation with coal liquefaction
[DE85-010432] 19 p3226 N85-30012
Identification of a mathematical model 1: Goodness of fit criterion
[HSE-TRANS-11109] 19 p3341 N85-30703
Plasma arc welding, equipment, installation and process control
[DE85-006481] 19 p3373 N85-30921
Contribution to the modelling of the gas carburizing process for steels
[BLL-OA-TRANS-3205-(6196.300)] 20 p3426 N85-31263
FAUST: Introduction and overview — self tuning control
[OUEL-1568/85] 20 p3519 N85-31682
Electrically conductive doped block copolymer of polyacetylene and polyisoprene
[DE85-009500] 24 p4082 N85-35301

PROCESS HEAT
Development and test of a high COP Rankine heat pump for generation of process steam. Phase 2: Fabrication and test
[DE85-002600] 11 p1632 N85-20275
Solar process heat: Technology program
[BMFT-FB-T-84-234] 12 p1882 N85-21812
Fuel cell applications literature review
[DE85-011691] 22 p3809 N85-33592
Solar central receiver preliminary design studies: Summary and review of contract results
[DE85-011385] 22 p3809 N85-33593
Solar thermal technologies program summary
[DE85-012253] 23 p3945 N85-34449

PROCESSES
Studies of collisional and nonlinear radiative process for development of coherent UV and XUV sources
[AD-A152001] 16 p2865 N85-27670

PROCESSING
Edge detection in SAR imagery using gradient operators — synthetic aperture radar (SAR)
[AD-A149411] 13 p2054 N85-22662
Low gravity exothermic heating/cooling apparatus
[NASA-CASE-MSC-25707-1] 18 p3104 N85-29214

PROCESSORS (COMPUTERS)
U CENTRAL PROCESSING UNITS

PROCUREMENT
NT GOVERNMENT PROCUREMENT
Electronic components for space applications
[CNES-NT-109] 04 p0496 N85-13169
An analysis of the effect of process controls on productivity and weapon system costs in DoD procurement
[AD-A147496] 07 p1052 N85-16678
Technical order managers handbook: Utilization assessment
[AD-A147579] 07 p1055 N85-16694
On estimating the cost growth of weapon systems
[AD-A147297] 08 p1230 N85-17749
Microcomputers in transit: A hardware handbook
[PB85-113660] 10 p1538 N85-19700
A statistical approach to vendor selection
[AD-A149781] 12 p1950 N85-22249
Visualization of computation results. Definition of a graphics satellite computer
[ONERA-RT-2/3587-CY] 20 p3514 N85-31845
National Aeronautics and Space Administration research and development 20 p3542 N85-32042
Lopez Energy Alternatives Project
[DE85-010589] 22 p3849 N85-33837

PROCUREMENT MANAGEMENT
Five-year plan for meeting the automatic data processing and telecommunications needs of the Federal Government. Volume 2: Major information technology systems acquisition plans of Federal executive agencies, 1984-1989
[PB84-214519] 03 p0436 N85-12778
Navy program manager's guide, 1985 edition
[AD-A151925] 16 p2876 N85-27744
Documentation for the West German Federal Cabinet's space policy decision 17 p3051 N85-28686
Progress report on implementing the recommendations of the White House Science Council's Federal Laboratory Review Panel, volume 1
[PB85-185072] 24 p4184 N85-35819

PRODUCT DEVELOPMENT
NT WEAPONS DEVELOPMENT
Abrasive products study
[PB84-223635] 01 p0033 N85-10205
Manufacturing Methods and Technology (MM/T) specifications for miniature cathode ray tube
[AD-A145597] 02 p0194 N85-11298
Development and utilization of advanced methods of neutron scattering 03 p0424 N85-12710
Construction, putting into operation, and utilization of a triple axis neutron spectrometer 03 p0425 N85-12715
Software configuration management across project boundaries and in distributed development environments
[RSRE-MEMO-3704] 04 p0549 N85-13494
Value analysis — industrial competition
[CNES-NT-110] 04 p0577 N85-13684
Special Developments and Methods in High Frequency Measuring Techniques — conference
[PTB-E-24] 05 p0629 N85-14030
Present status and development tendencies in the field of high frequency measuring techniques 05 p0629 N85-14031
Development program: Nuclear magnetic resonance gyroscope (NMR-gyro). Phase 1: Development of an experimental model
[BMFT-FB-W-84-041] 05 p0639 N85-14101
Photovoltaic power supply units 05 p0662 N85-14252
Development and construction of a prototype photovoltaic energy supply unit 05 p0662 N85-14254
Siemens solar module: Status of the technique, development tendencies 05 p0662 N85-14255
Development and utilization of CdS/Cu2S 05 p0662 N85-14256
Existing measuring systems for wind energy units 05 p0669 N85-14302
Metallo-Organic Decomposition (MOD) silver metallization for photovoltaics 06 p0830 N85-15276
What do we want: Increased speed, resolution, contrast or DOE? — astronomical photography 07 p0964 N85-16115
Possibilities and impossibilities of microcomputer systems
[AD-1984-904] 07 p1028 N85-16622
USSR report: Machine tools and metalworking equipment
[JPRS-UMM-84-021] 08 p1138 N85-17166
Preliminary concepts of candidate elements for a potential European participation in a manned space station
[MBB-UR-E-749-84-O] 11 p1587 N85-19996
The servicing vehicle of Columbus
[MBB-UR-E-750-84-O] 11 p1588 N85-19997
Design and analysis of airborne scanning optical systems 11 p1623 N85-20218
Development of the sonic pump levitator
[NASA-CR-171382] 12 p1782 N85-21186
Process development for commercial production of natural rubber from Guayule
[PB85-124956] 12 p1815 N85-21388
Development of miniature laser Doppler anemometers
[KU-SFB-210/ET/3] 12 p1857 N85-21648
Development and prototype construction of photovoltaic energy supply units 12 p1878 N85-21781
Development of an amorphous silicon panel 12 p1879 N85-21788
Development of high-efficiency economic systems for photovoltaics 12 p1880 N85-21795
Development of a CdSe thin film solar cell 12 p1880 N85-21796
Development of new solar cells 12 p1880 N85-21797
Improved Y-11 general-purpose transport designated Y-12 13 p1972 N85-22385
Giotto solar array: Design, manufacture and test 13 p2006 N85-22569
The Olympus solar array development and test program 13 p2009 N85-22596
Possibility of producing monolithic composite materials based on niobium carbide 13 p2028 N85-22707
The helicopter transmission design process 14 p2221 N85-23772
Manufacturing considerations related to aircraft gearboxes 14 p2222 N85-23778
Development of nitrile rubbers and foams having a high static modulus and low creep
[BR91465] 14 p2259 N85-24001
A 320 to have combined automatic pilot, flight control system 14 p2289 N85-24186
Research on CAD/CAM support for microprocessor development surveyed 14 p2290 N85-24193
An error generator to support the trials of the ZODIAC prototype system — raster links
[PHL-1984-71] 14 p2293 N85-24216
New directions in ARGOS instrumentation at Polar Research Lab (PRL) 14 p2323 N85-24350
Development of a low cost drifting buoy 14 p2330 N85-24408
A report on the DRIFTERS program — buoys 14 p2331 N85-24413
Flying objects
[CH-634516-A5] 15 p2469 N85-25242
Airfoil wing with flap
[CH-634767-A5] 15 p2469 N85-25243
Helicopter rotor
[CH-637890-A5] 15 p2470 N85-25245
Aircraft
[CH-642598-A5] 15 p2470 N85-25246
System for radio remote control of dropping bombs
[CH-639335-A5] 15 p2491 N85-25371
Satellite structure
[CH-642922-A5] 15 p2492 N85-25373
France develops own aluminum-based composite ceramic 15 p2534 N85-25636
Development of an integrated control unit for the PDV bus concept
[BMFT-FB-T-84-300] 15 p2551 N85-25745
The development of onboard laser velocimeter at the Saint Louis Institute (France) from 1976 to 1982
[ISL-NB-402/83] 16 p2791 N85-27216
Development of a Lagrangian drifting buoy 16 p2811 N85-27338
Development of a fuselage forward section in Carbon Fiber Reinforced Plastic (CFRP) type of construction
[MBB/LFA34/CFK/PUB/008] 17 p2965 N85-27851
Development of a microprocessor controlled communication system for ships
[BMFT-FB-T-84-275] 17 p2950 N85-28216
Ceramic turbochargers: A case study of a near-term application of high-strength ceramics
[DE85-006495] 17 p2975 N85-28379
Ultrasonic flaw detector with microcomputer interpretation
[BMFT-FB-T-84-272] 17 p2977 N85-28395
Special topics in infrared interferometry — Michelson interferometer development
[NASA-TM-87472] 17 p3038 N85-28794
Further development of high voltage SIPMOS FET's to fulfill market needs
[BMFT-FB-T-84-255] 17 p3045 N85-28843
Detection of porse in hot continuously cast rounds
[BMFT-FB-T-85-007] 18 p3072 N85-29000

Component problems plague French robotics industry
18 p3085 N85-29068
Development of corrosion resistant heat exchangers for flue gas desulfurization
[BMFT-FB-T-84-281] 18 p3103 N85-29211
Aluminum pressure die casting process for the production of low porosity castings and new casting alloys
[BMFT-FB-T-84-286] 18 p3123 N85-29335
Conceptual design of a fixed-pitch wind turbine generator system rated at 400 kilowatts
[NASA-CR-174877] 18 p3127 N85-29363
Fuel cells: A bibliography
[DE85-004585] 18 p3128 N85-29371
Plastic heliostat enclosure analysis
[DE85-009112] 18 p3130 N85-29387
Lithium-alloy/iron sulfide battery design studies
[DE85-007991] 18 p3131 N85-29389
Development of a stationary carbon monoxide detector
[BMFT-FB-T-84-253] 18 p3134 N85-29413
Development of a coal-water slurry-fueled diesel engine for industrial cogeneration. Task 1.0 topical report: Thermodynamic analysis
[DE85-010455] 19 p3236 N85-30062
Advanced evacuated tube collectors
[DE85-010271] 19 p3274 N85-30302
Studies toward a manned space station: Participation of European industry in NASA space station (MSS)
[SNIAS-S/DT-Y-25-212] 20 p3418 N85-31217
The ESA field emission electric propulsion program
[ESA-STR-213] 20 p3420 N85-31229
The Silica Aerogel Detector (SAD) story — Cherenkov detector
[USIP-84-14] 20 p3459 N85-31485
Design, manufacture and testing of a medium accuracy star tracker
[REPT-TR/84-048] 20 p3459 N85-31486
Development of an active laser gyro for inertial rotation sensing in attitude/heading reference and inertial navigation systems, phase 1
[BMFT-FB-W-85-001] 20 p3460 N85-31489
The development of complex systems
20 p3539 N85-32021
Spin-offs from technical scientific infrastructures, no. 1
20 p3540 N85-32034
Spin-offs from technical commercial infrastructures, no. 2
20 p3540 N85-32035
Spin-offs from technical scientific research organizations, no. 5
20 p3540 N85-32036
On the relationship between electronics and chemistry
[DRIC-T-7480] 22 p3743 N85-33200
Automatic rotary valve actuator
[DE85-012797] 22 p3794 N85-33505
Development of an energy-absorbing passenger seat for a transport aircraft
22 p3796 N85-33515
Drag-compensated, precision-powered hinge system
22 p3796 N85-33517
Design and development of a linear thermal actuator
22 p3796 N85-33518
The design and development of a constant-speed solar array drive
22 p3796 N85-33519
The design and development of a spacecraft appendage tie down mechanism
22 p3797 N85-33522
Block 5 documentation and solar modules
[NASA-CR-176134] 22 p3805 N85-33584
Photovoltaics technical information guide
[DE85-002924] 22 p3808 N85-33585
User commands for product design and system management
[DE85-011706] 22 p3830 N85-33721
The development and evaluation of the creep and corrosion resistant alloy IN6201
[PNR-90253] 23 p3917 N85-34278
A rational approach to cam design
23 p3923 N85-34311
Cost effective single crystals: The Rolls Royce approach — gas turbine components
[PNR-90252] 23 p3985 N85-34717
New technologies at the forefront of industrial developments
24 p4061 N85-35166
Development of position sensors for microcomputer-oriented sensor systems
[BMFT-FB-T-85-021] 24 p4091 N85-35361
Development of contactless sensors for industrial and automotive applications
[BMFT-FB-T-85-031] 24 p4097 N85-35400
Monolithic photovoltaic series array for an energy coupler
[BMFT-FB-T-85-023] 24 p4113 N85-35496
Development and operation of a measuring data acquisition system for use in light airplanes
24 p4123 N85-35556

PRODUCTION
Study of catalysts and mechanisms in synthesis reactions
[DE84-015025] 04 p0470 N85-12990
Fiat, Peugeot introduce integrated robotized engine: CAD used
07 p0936 N85-15933
Technology planning for flexible manufacturing systems
08 p1139 N85-17170
An analysis of production competition and award methodology
[AD-A147775] 08 p1228 N85-17733
Impacts of robotic and flexible manufacturing technologies on manufacturing costs and employment
[AD-A150060] 12 p1860 N85-21668
Feasibility of electrolytic hydrogen production in the Pacific Northwest
[DE85-009856] 18 p3084 N85-29060
Preparation and use of very pure o-D2
[DE85-009415] 22 p3843 N85-33800

PRODUCTION COSTS
NT AIRCRAFT PRODUCTION COSTS
A buyer's guide to space infrastructure
07 p0914 N85-15784
Production rate variations cost models
[AD-A147708] 08 p1228 N85-17732
Amorphous silicon solar cells with a view to cheap production processes
12 p1879 N85-21789
A low cost approach with larger diameter silicon wafer — solar cells
13 p2006 N85-22572
Cost and schedule implications of multinational coproduction
[AD-A154358] 19 p3360 N85-30069

PRODUCTION ENGINEERING
NT PRODUCTION PLANNING
Development of powder metallurgy in various sections of USSR
01 p0019 N85-10116
USSR report: Machine tools and metalworking equipment
[JPRS-UMM-84-019] 01 p0035 N85-10214
Growth, future of Soviet robotics sector analyzed
01 p0035 N85-10217
A review of world wide development in stainless steels
02 p0177 N85-11190
Sensor technology for second, third generation industrial robots. Optical sensor applications
03 p0342 N85-12198
Activities report of the Department of Engineering
03 p0342 N85-12202
Automation of production of semiconductor power devices
03 p0346 N85-12229
Development of rapidly quenched alloys with special physical properties and of processes for their continuous production
[BMFT-FB-T-84-179] 04 p0477 N85-13039
East Europe report: Science and technology
[JPRS-ESA-84-041] 04 p0484 N85-13060
Developments in Soviet robot technology viewed
04 p0491 N85-13127
Manufacturing Sciences and Robotics Research and Development Act of 1984
[H-REPT-98-1078] 04 p0578 N85-13686
Full-scale testing, production and cost analysis data for the advanced composite stabilizer for Boeing 737 aircraft. Volume 1: Technical summary
[NASA-CR-3849] 05 p0612 N85-13912
Full-scale testing, production and cost analysis data for the advanced composite stabilizer for Boeing 737 aircraft, volume 2
[NASA-CR-166012] 05 p0613 N85-13915
USSR report: Engineering and equipment
[JPRS-UEQ-84-007] 06 p0775 N85-14954
Situational planning of production processes in a flexible automated production system
06 p0776 N85-14959
Control technology for integrated circuit fabrication at Micro-Circuit Engineering, Incorporated, West Palm Beach, Florida
[PB85-100717/GAR] 07 p0949 N85-16013
Manufacturing methods and technology project summary reports
[AD-A148209] 08 p1138 N85-17163
Control systems for robotic production lines
08 p1138 N85-17169
Coordinated research in robotics and integrated manufacturing
[AD-A148204] 08 p1168 N85-17365
Cognitive asymmetry and occupation. Computer programmers, students, and bank personnel, part 1 and part 2
[AD-A147125] 08 p1197 N85-17540
COPES/ADS (Control Program for Engineering Synthesis) (Automated Design Synthesis) using the ADS optimization program
[AD-A148578] 08 p1206 N85-17588
Production of concentrated nitric acid
[DE84-017191] 09 p1293 N85-18121
Scania, ASEA of Sweden use robots for all production phases
09 p1310 N85-18229
Status of the Li-Al/FeS battery manufacturing technology. An evaluation for the US Army, Belvoir R and D Center
[DE85-000776] 09 p1315 N85-18264
Role of engineering psychology
09 p1361 N85-18961
Control of the manufacturing process and material flow in flexible manufacturing systems
[PNR-90234] 09 p1371 N85-18815
Production method of nickel electrode
[NASA-TM-76946] 10 p1439 N85-19069
Method of producing nickel electrode
[NASA-TM-76944] 10 p1440 N85-19077
New PCB production for robotics application
11 p1617 N85-20169
Increased use of CNC in machine tool construction
11 p1617 N85-20170
Exploratory assessment of second generation robotics and sensor-based systems
[PB85-132793] 11 p1648 N85-20388
Process development for commercial production of natural rubber from Guayule
[PB85-124956] 12 p1815 N85-21388
Silicon band spraying technique for solar cells
12 p1877 N85-21779
Amorphous silicon solar cells with a view to cheap production processes
12 p1879 N85-21789
Production and characterization of amorphous silicon (a-Si:H) as base material for solar cells
12 p1879 N85-21791
Testing and optimization of the production technology of large-surface Cu2S/CdS solar generators
12 p1880 N85-21793
A 2 x 6 Back Surface Reflection (BSR) silicon solar cell
13 p2005 N85-22570
Development of very thin large area GaAs solar cells for space application
13 p2006 N85-22579
Economic mechanism of integration of science, production
13 p2167 N85-23443
Applications of lasers in manufacturing
14 p2308 N85-24279
Lasers in automobile production
14 p2309 N85-24289
Mini-Seminar on Non-Destructive Testing
[CSIR-TSD-0009/83] 14 p2316 N85-24308
Mini-Seminar on CAD/CAM
[CSIR-TSD-0007/83] 14 p2402 N85-24809
Resources for robotics research in Europe, by country
15 p2489 N85-25364
Production cells with IR 2SO robot examined
15 p2524 N85-25561
Flexible machining systems described
15 p2524 N85-25563
Operation of Prisma flexible manufacturing system
15 p2524 N85-25564
East Europe report: Science and technology
[JPRS-ESA-85-018] 15 p2537 N85-25658
Production technology of an electrolyte for Na/S batteries
[BMFT-FB-T-84-277] 15 p2550 N85-25742
Compositional control of plate steels
15 p2565 N85-25826
Welding technology and organization in steel construction
15 p2566 N85-25828
Manufacturing and producibility technology
16 p2733 N85-26866
USSR report: Engineering and equipment
[JPRS-UEQ-84-008] 16 p2760 N85-27035
Calculating reliability and productivity of cold stamping robot complex as queuing system
16 p2761 N85-27039
Uses of laser technology described
16 p2768 N85-27060
Manufacturing methods and technology CAD/CAM (Computer-Aided Design/Computer-Aided Manufacturing) related efforts (FY 1980 - 1986)
[AD-A151617] 16 p2846 N85-27547
Integral profile method for production of carbon fiber sheets
[MBB/LFA34/CFK/PUB/006] 17 p2916 N85-27975
Uses of, experiences in production of custom designed IC's
17 p2945 N85-28160
Modern equipment for manufacture of IC's in Hungary
17 p2945 N85-28161
Manufacturing information system
[AD-A152715] 17 p3011 N85-28616
USSR report: Science and technology policy
[JPRS-UST-85-008] 17 p3049 N85-28872
Automated maintenance system test program increment VI production scheduling
[AD-A153694] 18 p3196 N85-29638
The evolution of the U.S. helicopter industry
[AD-A154290] 19 p3211 N85-29813

Producibility Engineering and Planning (PEP): Program management guidelines
[AD-A153730] 19 p3379 N85-30966
Cost and schedule implications of multinational coproduction
[AD-A154358] 19 p3380 N85-30969
Automated fabrication of composite structures for helicopters
[SNIAS-851-210-104] 20 p3393 N85-31049
Production process for steel with decarburized surface adapted for single coating enameling
[BMFT-FB-T-85-022] 20 p3432 N85-31292
CEMA venture to develop FMS, robot technology 20 p3436 N85-31330
Hidden costs of robotized production systems revealed 20 p3438 N85-31332
Utilization of microwave measuring systems for the automation of composite materials manufacturing
[SNIAS-851-430-102] 22 p3742 N85-33197
Centralized surveillance of flexible workshops for the manufacturing of composite materials
[SNIAS-851-430-103] 23 p3910 N85-34227

PRODUCTION MANAGEMENT
Abrasive products study
[PB84-223635] 01 p0033 N85-10205
Automated plant, production management system 08 p1139 N85-17171
Development of AK18 alloy production technology based on electrothermic alumin 11 p1588 N85-20048
Robot production lines in operation 11 p1617 N85-20166
USSR report: Science and technology policy
[JPRS-UST-85-002] 13 p2167 N85-23442
Welding technology: Japan — Conference
[ISBN-0-85300177-4] 15 p2585 N85-25823
Some aspects of nuclear plant fabrication in Japan and the UK relating to automatic and robotic arc welding 15 p2586 N85-25834
Design-To-Cost (DTC) methodology to achieve affordable avionics 16 p2696 N85-26645
Standard series of direct-current motors for regulated electric drives 22 p3772 N85-33375

PRODUCTION METHODS
U PRODUCTION ENGINEERING

PRODUCTION PLANNING
Computer aided process planning of machined metal parts
[AD-A145628] 02 p0169 N85-11263
Automation of assembly of electrical products 03 p0346 N85-12228
Increase in the economy of design and process planning by integrated and graphic data processing, phase 2 — aircraft design
[BMFT-FB-W-84-029] 05 p0716 N85-14589
Situational planning of production processes in a flexible automated production system 06 p0776 N85-14959
Manufacturing methods and technology project summary reports
[AD-A146209] 08 p1138 N85-17163
The planning of flexible manufacturing systems
[PNR-90230] 09 p1371 N85-18613
USSR report: Science and technology policy
[JPRS-UST-85-002] 13 p2167 N85-23442
Riga Institute seeking faster introduction of new technology 14 p2208 N85-23696
Electrical features of new DNC, CNC system viewed — direct numerical control 15 p2524 N85-25562
Industrial laser use expanding in the USSR 15 p2644 N85-26310
CEMA venture to develop FMS, robot technology 20 p3438 N85-31330
Robots, Manipulators 21 p3668 N85-32766

PRODUCTIVITY
The Marine Resources Experiment Program (MAREX)
[NASA-TM-87368] 01 p0086 N85-10580
Future robotics program at San Antonio ALC (Air Logistics Center)
[AD-P004011] 03 p0309 N85-11991
Improving operational reliability and productivity of robotized technological complexes 03 p0346 N85-12227
Technologies for space station autonomy
[NASA-CR-174112] 04 p0458 N85-12906
Advances of implementing NC machine tools discussed 04 p0491 N85-13131
Recent studies of the ocean nitrogen cycle 05 p0653 N85-14193
The climate in food production in Latin America 07 p1001 N85-16359
Contractor productivity measurement
[AD-A146756] 07 p1050 N85-16666
Feasibility of measuring technical productivity improvements in Air Force Logistics Command depot-level maintenance using the Data Envelopment Analysis (DEA) and Constrained Facet Analysis (CFA) models
[AD-A147329] 07 p1052 N85-16676
An appraisal of the USAF Technology Modernization Program
[AD-A147344] 07 p1052 N85-16677
Evaluation of the effectiveness of the weighted guidelines to induce contractor's investment in cost reducing facilities equipment
[AD-A147586] 07 p1053 N85-16681
Flexible manufacturing system for the production of aircraft parts
[BLL-PNR-90237-(8019.3153)] 08 p1137 N85-17159
USSR report: Machine tools and metalworking equipment
[JPRS-UMM-84-021] 08 p1138 N85-17166
Robotics research, integration overview presented. Application objectives cited 08 p1142 N85-17201
North American vegetation patterns observed with the NOAA-7 advanced very high resolution radiometer — North America
[E85-10062] 08 p1174 N85-17400
Advances in cutting tool technology surveyed 13 p2051 N85-22840
Scientific, technical progress as factor of intensification of economy 13 p2167 N85-23444
East Europe report: Science and technology
[JPRS-ESA-85-018] 15 p2537 N85-25658
Calculating reliability and productivity of cold stamping robot complex as queuing system 16 p2761 N85-27039
New stage in robotics development 16 p2762 N85-27045
Design of computer-related workstations in relation to job functions and productivity
[AD-A151938] 16 p2844 N85-27534
Management considerations for an information center
[AD-A151774] 16 p2875 N85-27742
World iron ore reserves
[BLL-BISI-TRANS-22280-(9022.06)] 17 p2963 N85-28435
Photosynthetic acclimation of Acer saccharum
[DE85-008247] 17 p2998 N85-28536
Proceedings of the Seminar on Space Station Human Productivity
[NASA-TM-86673] 18 p3156 N85-29539
Human productivity program definition 18 p3158 N85-29556
Mockups and human productivity studies 18 p3159 N85-29570
Rockwell experience applications to Ames space station mockup habitability/productivity studies 18 p3159 N85-29572
Capital investment motivational techniques used by prime contractors on subcontractors
[AD-A153660] 18 p3198 N85-29837
Encapsulation processing and manufacturing yield analysis 21 p3611 N85-32434
Human activity and production rate of secondary nuclei 21 p3645 N85-32645
Production of liquid fuels and chemicals by microalgae
[DE85-006780] 22 p3619 N85-33658
Resource evaluation and site selection for microalgae production systems
[DE85-006807] 23 p3951 N85-34485
Electronic information management and productivity
[DE85-013362] 24 p4164 N85-35818

PRODUCTS
NT ASPHALT
NT GREASES
NT PETROLEUM PRODUCTS
NT REACTION PRODUCTS

PROFICIENCY
U ABILITIES

PROFILE METHOD (FORECASTING)
Simulation experiments on the relative accuracy of inferred atmospheric states from idealized wind and temperature profiling systems 05 p0682 N85-14386

PROFILES
Designing the profile of turbine blades using an iteration technique 09 p1305 N85-18201
Influence of normalized frequency on time-dependent aerodynamic characteristics of vane blading profiles 09 p1306 N85-18204
Study of geological media based on scattered earthquake waves 13 p2114 N85-23166

PROFILOMETERS
Flight demonstration of new NRL real-time data acquisition system and laser video waveform sampler
[AD-A145126] 01 p0053 N85-10350
Evaluation of laser profile and deflection measuring system
[FAA-PM-84-24] 02 p0201 N85-11341
Characterization of lubricated bearing surfaces operated under high loads
[NASA-TM-86964] 12 p1811 N85-21357

PROGNOZ SATELLITES
Observation of natural noise near upper hybrid resonance in terrestrial magnetosphere by Prognoz-5 satellite 06 p0822 N85-15221
The measurements of Prognoz-4, -5, -6, -7 during IMS 14 p2355 N85-24548
Magnetic field in the Earth's outer magnetosphere: Prognoz-6, -7 data 14 p2356 N85-24556
X-ray experiment on Prognoz-9 artificial Earth satellite 15 p2478 N85-25295
More on shock-wave studies with Prognoz-10 satellite 19 p3296 N85-30432
Functions of Prognoz-10: Intercosmos' station explained 19 p3296 N85-30433
Prognoz-10 Intercosmos' station launched to study shock waves 19 p3296 N85-30434

PROGRAM MANAGEMENT
U PROJECT MANAGEMENT

PROGRAM VERIFICATION (COMPUTERS)
On the formal description and derivation of temporal proof rules for program properties
[TUM-I8405] 01 p0101 N85-10675
Program flow analyzer, volume 2
[AD-A145521] 02 p0242 N85-11576
Program flow analyzer, volume 3
[AD-A145522] 02 p0242 N85-11577
Northern Telecom, Incorporated, NTI-585/565, ACOBOL/3 Release 4.1 Version H(01)
[PB84-228022] 03 p0404 N85-12574
Northern Telecom, Incorporated NTI-585/565, ACOBOL/3 Release 4.1 Version H(01) (COBOL technical report)
[PB84-228030] 03 p0404 N85-12575
Convergent Technologies, NGEN CP001, CT COBOL version 9.0
[PB84-227784] 03 p0404 N85-12578
Convergent Technologies, mega frame CTIX BASIC interpreter version 1.03
[PB84-227776] 03 p0404 N85-12579
Convergent Technologies, mega frame, CTIX FORTRAN 77 version 2.1
[PB84-227768] 03 p0404 N85-12580
Gould Incorporated, GOULD Concept 32/87, COBOL release 1.4
[PB84-227669] 04 p0548 N85-13484
Digital Equipment Corp., VAX/750, VAX COBOL version 3.0
[PB84-227651] 04 p0548 N85-13485
Digital Equipment Corp., MICRO/PDP-11, COBOL-81 version 2.2
[PB84-227644] 04 p0548 N85-13486
Prime Computer, Inc., PRIME 750, FORTRAN-77 revision 19.4
[PB84-227628] 04 p0548 N85-13487
C3, Incorporated, C50 System, C3 COBOL/75 version 2.00
[PB84-228006] 04 p0548 N85-13488
Burroughs Corporation B26-CPU, B20 COBOL, Release 4.0
[PB84-216241] 04 p0551 N85-13505
Burroughs Corporation B26-CPU, B20 COBOL Version 4.0 (COBOL technical report)
[PB84-216258] 04 p0551 N85-13506
Convergent technologies NGEN CP001, CT COBOL Version 9.0
[PB84-216266] 04 p0551 N85-13507
Convergent Technologies, Incorporated, NGEN CP001, CT COBOL Version 9.0 (COBOL technical report)
[PB84-216274] 04 p0551 N85-13508
Computer Sciences Corporation UNIVAC 1100/80, CSTS COBOL Release COB250
[PB84-216282] 04 p0551 N85-13509
Control Data Corporation CYBER 205 model 442, FORTRAN 200 (G201-25)
[PB84-216290] 04 p0551 N85-13510
C3, Incorporated NGEN CP001, COBOL Version 9.0
[PB84-216308] 04 p0552 N85-13511
United Information Services, Inc., CRAY 1-S/2000, FORTRAN CFT 1.10
[PB84-227685] 04 p0552 N85-13512
Datapoint Corporation Datapoint 6600, 8600, DOS COBOL Version 3.6
[PB84-242973] 04 p0552 N85-13513
Northern Telecom, Inc., IBM 3033 (compilation), NTI-585/565 (execution), XCOBOL, release 4.1, version H(01) (COBOL technical report)
[PB84-228048] 05 p0714 N85-14578
Experimental techniques of formal specifications for the design of tested and reliable computer programs
[ENST-84E007] 05 p0716 N85-14591
Implementation assessment of a network service. The test responder exerciser specification
[NPL-DITC-44/84] 05 p0716 N85-14594

Data general Corporation, Eclipse C150, interactive COBOL Revision 1.30 (COBOL technical report)
[PB84-227834] 06 p0849 N85-15391
Data General Corporation, Eclipse C150, interactive COBOL Revision 1.30
[PB84-227891] 06 p0849 N85-15392
IBM Corporation, IBM Series/1 4955, IBM Series/1 host COBOL Release 1.1 EDX (COBOL technical report)
[PB84-227909] 06 p0849 N85-15393
IBM Corporation, IBM Series/1 4955, IBM Series/1 host COBOL Release 1.1 EDX
[PB84-227818] 06 p0849 N85-15394
IBM Corporation, IBM Series/1 4955, IBM Series/1 host COBOL Release 1.1 RPS
[PB84-227917] 06 p0850 N85-15395
IBM Corporation, IBM Series/1 4955, IBM Series/1 host COBOL Release 1.1 RPS (COBOL technical report)
[PB84-227925] 06 p0850 N85-15396
Gould Incorporated, Gould PS-3000, Gould PS-3000 COBOL V2.0
[PB84-229160] 06 p0850 N85-15403
Gould Incorporated, Gould PS-3000, Gould PS-3000 BASIC Interpreter Version 1.00
[PB84-229186] 06 p0851 N85-15404
Digital Equipment Corporation, PDP-11/23-PLUS PDP-11 FORTRAN-77 V5.0
[PB84-227610] 06 p0851 N85-15405
Plexus Computers, Inc., Plexus P/60, Plexus FORTRAN 77 Version 1.1
[PB84-227859] 06 p0851 N85-15407
Control Data Corporation, CYBER 835, COBOL Release 5.3 Level 614
[PB84-227842] 06 p0851 N85-15408
C3, Incorporated NGEN CP001, C3 COBOL Version 9.0 (COBOL Technical Report)
[PB84-216316] 06 p0855 N85-15435
Burroughs Corporation B26-CPU, Burroughs B20 BASIC Rel. 4.0
[PB84-216324] 06 p0855 N85-15436
Convergent Technologies NGEN CP001, CT BASIC Version 9.0
[PB84-216332] 06 p0855 N85-15437
Microsoft Corporation, Sun Microsystems, Microsoft COBOL Version 2.0
[PB84-243401] 06 p0856 N85-15443
Microsoft Corporation, IBM PC XT, Microsoft COBOL, Version 2.0
[PB84-243419] 06 p0856 N85-15444
On the generation of random variables for radar simulation purposes 07 p0938 N85-15947
Finite difference calculations of buoyant convection in an enclosure. Part 2: Verification of the nonlinear algorithm
[PB85-104065/GAR] 07 p0961 N85-16069
Ada compiler validation summary report: New York University (NYU Ada/Ed) compiler, version 1.4 for VAX 11/780, using VMS 3.5
[AD-A146924] 07 p1022 N85-16483
Ada compiler validation summary report: TeleSoft (TeleSoft Ada) compiler, version 2.0a for Sun 120 Motorola M68010, using 4.2 BSD UNIX-Sun Version 1.1
[AD-A146925] 07 p1022 N85-16484
Formal verification of mathematical software
[NASA-CR-172407] 07 p1023 N85-16489
NYU Ada/Ed user's guide: Version 1.4 for VAX/VMS systems
[AD-A146758] 07 p1024 N85-16495
Software test handbook
[AD-A146844] 07 p1024 N85-16496
Functional semantics of modules
[AD-A146923] 07 p1024 N85-16500
Debug testing and confidence testing
[AD-A147104] 07 p1025 N85-16504
Ada compiler validation summary report: TeleSoft (TeleSoft Ada) compiler, version 2.0a2 for Callan Unistar 300, using System V, version 4.1a
[AD-A147115] 07 p1025 N85-16505
The production of maintainable, trustworthy, and portable software 08 p1054 N85-16744
Software testing in an Ada programming environment 08 p1065 N85-16748
Investigating version dependence in fault-tolerant software 08 p1065 N85-16749
Software test handbook: Software test guidebook, volume 2
[AD-A147289] 08 p1204 N85-17578
DDL system: Design synthesis of digital systems
[NASA-CR-170759] 09 p1366 N85-18584
JOVIAL J73 automated verification system: Implementation phase
[AD-A148732] 09 p1368 N85-18597
High level languages in protocol specification and verification
[FUB-51-1983] 09 p1370 N85-18611
Gateway testing techniques — computer system interconnection
[NPL-DITC-49/84] 09 p1372 N85-18621
Digital Equipment Corporation VAX Ada Compiler Version T0.6-2 VAX-11/785, 11/750, 11/730, using VMS, Version 4.0 and MicroVAX 1, using MicroVMS Version 1.0
[AD-A149375] 10 p1538 N85-19606
Methodology investigation software testing of multiprocessor systems
[AD-A149446] 10 p1541 N85-19714
Four Phase Systems, Incorporated, Four Phase Series 5000, COBOL 1974 version BE08.8
[PB85-108017] 10 p1541 N85-19717
Four Phase Systems, Incorporated, Mini-Frame Series 6300, COBOL Series 6000
[PB85-108025] 10 p1541 N85-19718
Micro focus DEC Rainbow 100 + compact level 2 COBOL; V2.5
[PB85-108975] 10 p1542 N85-19719
Micro focus DEC Rainbow 100 + high performance level 2 COBOL; V2.5
[PB85-108983] 10 p1542 N85-19720
DTSS, Incorporated, DPS 8/44, DTSS COBOL Release 12
[PB85-108058] 10 p1542 N85-19721
Checking microcode algebraically
[AD-A149441] 10 p1547 N85-19759
Dynamic investigations of a spherical tank structure filled with liquid using ANSYS three-dimensional fluid elements
[MBB-UR-E-737-83-O] 11 p1654 N85-20418
Ada compiler validation summary report, Dansk Datamatik Center, VAX 11 compiler version 1.1
[AD-A149340] 11 p1699 N85-20681
Micro Focus, Intel Microprocessor Development System MDS221 CIS COBOL; V4.5
[PB85-110823] 11 p1699 N85-20682
A quality control experiment in a real time multiprocessor operating system: The Mars 860 — software testing 11 p1702 N85-20707
Validation Summary Report (VSR), Ryan-McFarland Corporation, AT and T 385, RM/COBOL Version 2.0
[PB85-102093] 11 p1703 N85-20709
Burroughs Corporation, Burroughs B3955 COBOL9 Version 6.8
[PB85-103110] 11 p1703 N85-20710
Burroughs Corporation, Burroughs B3955 FORT77 Version 6.8
[PB85-110328] 11 p1703 N85-20711
Micro Focus Plessy Micro Systems 68/50 Compact Level 2 COBOL; V2.5
[PB85-108934] 11 p1703 N85-20712
Micro Focus Plessy Micro Systems 68/50 High Performance Level 2 Cobol; V2.5
[PB85-108942] 11 p1703 N85-20713
Micro Focus IBM personal computer XT Compact Level 2 COBOL; V2.5
[PB85-108918] 11 p1703 N85-20716
Micro Focus IBM personal computer XT High Performance Level 2 COBOL; V2.5
[PB85-108926] 11 p1704 N85-20717
Micro focus Fortune 32:16 compact level 2 COBOL; V2.5
[PB85-108884] 11 p1704 N85-20718
Micro focus Fortune 32:16 high performance level 2 COBOL; V2.5
[PB85-108892] 11 p1704 N85-20719
Micro Focus IBM personal computer XT CIS COBOL; V4.5
[PB85-108868] 11 p1704 N85-20720
ICL, ICL 2966 COBOL C2COB. 1321
[PB85-108876] 11 p1704 N85-20721
MICRO FOCUS Intel Microprocessor Development System MDS221 Compact Level 2 COBOL; V2.5
[PB85-108900] 11 p1704 N85-20722
Micro focus IBM personal computer XT, high performance level, 2 COBOL, IBM PC tailored; V2.6
[PB85-110815] 11 p1705 N85-20725
A Gypsy-to-Ada program compiler
[TR-39] 12 p1913 N85-22005
Towards the generation of efficient code from verified programs
[TR-40] 12 p1914 N85-22017
Ryan-McFarland Corporation, IBM PC model XT, RM/FORTRAN, version 2.0.0
[PB85-107993] 12 p1917 N85-22037
Ryan-McFarland Corporation, sun microsystem with sky fast floating point processor, RM/FORTRAN version 1.5.0
[PB85-108009] 12 p1917 N85-22038
Requirements for a database management system
[DE85-004661] 12 p1951 N85-22259
Logic analyzer survey and reviews
[BAE-881/ELO/1845] 15 p2621 N85-26151
Using a logic analyser and trigger unit to de-bug a program
[BAE-881/ELO/1487] 15 p2626 N85-26180
The systematic integration of very large scale integrated circuit computer-aided design tools into a toolkit optimized for academic applications
[AD-A151813] 16 p2945 N85-27538
NASA guidelines for assuring the adequacy and appropriateness of security safeguards in sensitive applications
[NASA-CR-175489] 17 p3007 N85-28593
Software environment for conducting interactive statistical analysis
[AD-A153378] 17 p3012 N85-28626
Debugging distributed computations in a nested atomic action system
[AD-A153617] 18 p3162 N85-29585
Ada (trademark) compiler validation summary report: ALSYS ALSYCOMP-0001
[AD-A153750] 18 p3163 N85-29582
Specification of software quality attributes. Volume 2: Software quality specification guidebook
[AD-A153989] 18 p3163 N85-29594
Specification of software quality attributes. Volume 3: Software quality evaluation guidebook
[AD-A153990] 18 p3163 N85-29595
Statistical estimation of software reliability
[AD-A154097] 19 p3335 N85-30665
Discrete-element acoustic analysis of submerged structures using doubly asymptotic approximations
[AD-A154959] 21 p3700 N85-32987
A prototype PASCAL program validation system
[NPL-DITC-57/85] 23 p3956 N85-34813
Specifying and verifying concurrent programs
[AD-A156190] 24 p4138 N85-35852

PROGRAMMED INSTRUCTION
NT COMPUTER ASSISTED INSTRUCTION
Self-paced instruction. Factors critical to implementation in Air Force technical training: A preliminary inquiry
[AD-A145098] 01 p0097 N85-10647
Factors critical to the implementation of self-paced instruction: A background review
[AD-A145143] 01 p0097 N85-10648

PROGRAMMERS
Programming effort estimation
[AD-A145839] 03 p0406 N85-12595
Approaches to structuring the software development process
[AD-A147894] 08 p1205 N85-17582
Concept paper for the development of a DOD Ada (trademark) software engineering education and training plan
[AD-A148774] 08 p1206 N85-17592
Programmer/analyst workstation evaluation report
[NASA-CR-175299] 14 p2304 N85-24749
A learning strategy approach for teaching novice computer programmers
[AD-A151523] 15 p2629 N85-26200
CLEANROOM software development: An empirical evaluation
[AD-A152924] 17 p3011 N85-29619
Data processing professionals and DP application users' perceptions and expectations of operational roles of persons working in a DP/application user interface group 24 p4165 N85-35821

PROGRAMMING (SCHEDULING)
Computer assisted flight schedule optimization
[AD-A151699] 16 p2958 N85-27623

PROGRAMMING LANGUAGES
NT ADA (PROGRAMMING LANGUAGE)
NT ASSEMBLY LANGUAGE
NT BASIC (PROGRAMMING LANGUAGE)
NT COBOL
NT FORTRAN
NT HIGH LEVEL LANGUAGES
NT LISP (PROGRAMMING LANGUAGE)
NT NATURAL LANGUAGE (COMPUTERS)
NT PASCAL (PROGRAMMING LANGUAGE)
NT PL/1
TEQUEL: The query language of SADDLE 01 p0058 N85-10382
Psychological testing on the computer
[R/PERS-618] 01 p0097 N85-10645
Activities of the MIT Laboratory for Computer Science
[AD-A145134] 01 p0100 N85-10661
PROGEN: An incremental programming environment
[NRIMS-TWISK-315] 02 p0241 N85-11568
Research on distributed languages and algorithms
[AD-A145881] 02 p0242 N85-11580
Application of the CSRL language to the design of expert diagnosis systems: The Auto-Mech experience
[AD-P003922] 02 p0245 N85-11602
Air Force Materials Laboratory plans/projects
[AD-P004010] 03 p0306 N85-11990

Convergent Technologies, mega frame, CTIX COBOL version 2.0
[PB84-227750] 03 p0404 N85-12581
DATAPLOT: Implementation tapes guide
[PB84-214063] 03 p0408 N85-12610
Technologies for space station autonomy
[NASA-CR-174112] 04 p0458 N85-12906
Control of walking: Local control and real time systems 05 p0715 N85-14583
Towards a specification of the B programming environment
[CWI-CS-R8408] 05 p0716 N85-14593
Design and analysis of an SQL (Structured Query Language) interface for a multi-backend database system
[AD-A146534] 06 p0856 N85-15447
Control system design language implementation of a gas turbine starting controller
[AD-A147896] 07 p0905 N85-15732
What a parallel programming language has to let you say
[AD-A147854] 07 p1026 N85-16513
Some scientific subroutines in LISP
[AD-A147889] 07 p1026 N85-16515
The production of maintainable, trustworthy, and portable software 08 p1064 N85-16744
Implementation of an Intel 8086 microprocessor-based realization library for the control system design language
[AD-A148506] 08 p1202 N85-17569
DDL system: Design systhesis of digital systems
[NASA-CR-170759] 09 p1366 N85-18584
FLAD user's manual: FLAD file contents
[AD-A148700] 09 p1368 N85-18594
Proposal for a small scheme implementation
[AD-A148707] 09 p1368 N85-18595
Partial evaluation as a means of language extensibility
[AD-A148730] 09 p1368 N85-18596
Multitasking kernel for the C and FORTRAN programming languages
[DE85-001799] 09 p1370 N85-18609
French firm develops 2D, 3D computer vision system 10 p1461 N85-19208
Research into self-timed VLSI circuits
[AD-A149140] 10 p1479 N85-19339
Ada (trademark) Joint Program Office objectives and progress through 1983
[AD-A149436] 10 p1541 N85-19713
SOLIDGEN: A solid finite element data generator. User's manual
[AD-A149490] 10 p1541 N85-19715
Software standards issues — space station software development 11 p1701 N85-20692
A survey of the project CIP: Computer aided, intuition-guided programming. Wide spectrum language and program transformations
[TUM-I8406] 12 p1912 N85-22000
The four forms of omega
[AD-A149694] 12 p1915 N85-22020
Principles of software engineering environment design
[AD-A150352] 13 p2147 N85-23324
LEXICON: A structured modeling system for optimization
[AD-A150536] 13 p2147 N85-23329
ROSS: An object-oriented language for constructing simulations
[AD-A150556] 13 p2147 N85-23330
Orphan detection in the Argus system
[AD-A150562] 13 p2148 N85-23331
Multidimensional digital signal processing
[AD-A150833] 14 p2292 N85-24209
GRAFIT language for simulating two-dimensional geometric entities and sketches 14 p2401 N85-24801
Automation of development of software for switching units that are implemented in the form of multiprocessor systems on a microcomputer base 14 p2401 N85-24802
An algebraic specification language and a syntax directed editor
[AD-A150884] 14 p2403 N85-24815
The enhancement of concurrent processing through functional programming languages
[AD-A150771] 14 p2404 N85-24822
CHILL: A comprehensive histogramming language
[DE85-005356] 14 p2405 N85-24830
The design and implementation of a syntax directed editor for a space constrained microcomputer
[AD-A151313] 15 p2623 N85-26163
Programming the digital computer ODRA-1204 in MOST-2 language
[NASA-TM-87462] 15 p2627 N85-26191
The development of a programming support system for rapid prototyping. Tasks 2 and 3
[AD-A151549] 15 p2629 N85-26202
Praxis language environment: Distribution package description, revision 1
[DE85-006899] 15 p2630 N85-26212
IPAD: Integrated Programs for Aerospace-vehicle Design
[NASA-CR-3690] 15 p2632 N85-26221
Graphic simulation of a machine-repairman model
[AD-A151761] 16 p2694 N85-26633
The systematic integration of very large scale integrated circuit computer-aided design tools into a toolkit optimized for academic applications
[AD-A151813] 16 p2645 N85-27538
Reliability models for dataflow computer systems
[NASA-CR-175813] 16 p2646 N85-27543
Parallel computation of multiple-scale problems
[DE85-007230] 16 p2649 N85-27563
Continued development and implementation of the Universal Network Interface Device (UNID) 2 in the Digital Engineering Laboratory Network (DELNET), volume 2
[AD-A151947] 16 p2650 N85-27570
Internation information networks for material properties: Revision 1
[DE85-007412] 16 p2650 N85-27572
AFIT GKS: A GKS implementation in the Ada programming language
[AD-A152954] 17 p3012 N85-28620
Ada validation summary report. ALS AdaVAX version 1.1 VAX-11/780 using VAX/VMS release 3.6
[AD-A153684] 18 p3162 N85-29588
Parallel computation of multiple-scale problems, revision 1
[DE85-009447] 18 p3164 N85-29598
Development and analysis of a global compaction technique of microprograms 19 p3334 N85-30654
The BLAZE language: A parallel language for scientific programming
[NASA-CR-172615] 19 p3334 N85-30656
The design, implementation and application of a table-driven syntax-directed editor
[AD-A154234] 19 p3336 N85-30670
Ada compiler validation summary report: University of Karlsruhe-GMD/German MOD VAX 11 compiler, version v1.0
[AD-A154370] 19 p3337 N85-30678
HANDTC: A FORTRAN program to calculate inner-zone terrain corrections
[DE85-011196] 19 p3340 N85-30699
Proceedings of the Argonne Workshop on Programming the Next Generation of Supercomputers
[DE85-008348] 19 p3343 N85-30718
Data communications-Oriented Production System Language (CPSL)
[DE85-011457] 20 p3440 N85-31352
The design and implementation of an object-oriented, production-rule interpreter
[AD-A154769] 21 p3671 N85-32803
Praxis release notes, version 7.3
[DE85-011862] 21 p3673 N85-32820
Evaluation and implementation of a functional microprogram generator
[AD-A155164] 21 p3674 N85-32823
Logical and physical modeling and design of scientific and statistical databases for energy research
[DE85-006081] 22 p3833 N85-33737
Graphics interaction in databases 23 p3958 N85-34534
Architecture of languages for large CAD systems development 23 p3962 N85-34557
Software maintenance relating to the input translator and z-80 realization volume of the computer systems design environment
[AD-A155849] 24 p4136 N85-35646
Benchmark evaluation of PC simscript
[AD-A156133] 24 p4138 N85-35651
Polylith: The early goals
[DE85-012534] 24 p4139 N85-35658
Artificial intelligence in Ada (trademark): Pattern-directed processing
[AD-A156230] 24 p4141 N85-35671

PROGRAMS

NT ACEE PROGRAM
NT AGRISTARS PROJECT
NT APOLLO APPLICATIONS PROGRAM
NT APOLLO PROJECT
NT BRAZILIAN SPACE PROGRAM
NT CANADIAN SPACE PROGRAM
NT DEFENSE PROGRAM
NT EARTH RESOURCES PROGRAM
NT EUROPEAN SPACE PROGRAMS
NT FRENCH SPACE PROGRAMS
NT GALILEO PROJECT
NT GLOBAL ATMOSPHERIC RESEARCH PROGRAM
NT HELIOS PROJECT
NT INDIAN SPACE PROGRAM
NT INTERNATIONAL GEOSPHERE-BIOSPHERE PROGRAM
NT JAPANESE SPACE PROGRAM
NT MACHINE-INDEPENDENT PROGRAMS
NT NASA PROGRAMS
NT PROJECT SETI
NT PROJECTS
NT SCOUT PROJECT
NT SKYLAB PROGRAM
NT SPACE PROGRAMS
NT SUPERSONIC CRUISE AIRCRAFT RESEARCH
NT SWEDISH SPACE PROGRAM
NT TIROS PROJECT
NT U.S.S.R. SPACE PROGRAM
NT UNIVERSITY PROGRAM
NT VOYAGER PROJECT
Electrochemical Energy Storage Branch
[DE85-007592] 18 p3131 N85-29391
Index of laser program publications and related reports, calendar year 1984
[DE85-011863] 23 p3936 N85-34398

PROGRESS

Scientific, technical progress as factor of intensification of economy 13 p2167 N85-23444
High-efficiency silicon solar cell research 21 p3609 N85-32417
Confinement experiments on ISX-B
[DE85-012346] 23 p3984 N85-34709

PROJECT MANAGEMENT

ACEE program rationale and implementation
[NASA-TM-84549] 02 p0133 N85-10906
Life prediction and constitutive behavior: Overview 02 p0143 N85-10973
Developing commercial users of space 02 p0154 N85-11044
Commercializing the transfer orbit stage 02 p0155 N85-11049
Research and technology
[NASA-TM-86321] 02 p0305 N85-11973
Methodology for the implementation of a domestic satellite communications network 04 p0493 N85-13148
Project resources planning and control
[NASA-TM-86339] 04 p0575 N85-13666
NASA's SESAC report on research and analysis in space and Earth sciences 04 p0579 N85-13697
The METEOSAT exploitation project, operational use of a remote sensing system 05 p0656 N85-14223
Knowledge-based communication and management support in a system development environment 05 p0717 N85-14596
The management of research institutions: A look at government laboratories
[NASA-SP-481] 07 p1050 N85-16665
National airspace review enhancement plan, revision 3
[AD-A150743] 08 p1082 N85-16852
Space station task force perspective 08 p1106 N85-16992
Air Force space technology center space technology: Emphasis 84 09 p1333 N85-18381
The R and D project selection problem with fuzzy coefficients
[INPE-3329-PRE/626] 10 p1565 N85-19871
Space Station Software Issues
[NASA-CP-2361] 11 p1700 N85-20689
Software development environment issues --- space station software development 11 p1700 N85-20691
Air Force satellite position management 12 p1787 N85-21217
Computer integration of engineering design and production: A national opportunity
[NASA-CR-175483] 12 p1820 N85-21414
Space Station technology planning 13 p1989 N85-22471
Solid fuel combustion chamber
[VTH-LR-415] 16 p2741 N85-26916
Organizing geological work tasks for 1985 outlined 16 p2806 N85-27303
The Helios missions 16 p2884 N85-27795
Managerial benefits of Helios for the European industry 16 p2887 N85-27809
Helios project support 16 p2887 N85-27812
Summer High School Apprenticeship Research Program (SHARP) of the National Aeronautics and Space Administration
[NASA-CR-175791] 17 p3046 N85-28849
Technical services at NLR
[B6581898] 17 p3049 N85-28871
Space station study
[BL-6167] 18 p3066 N85-28959
Program planning using the GMAP procedure in SAS/GRAPH software
[DE85-008356] 18 p3199 N85-29842
Thermal Energy Storage Program annual operating plan FY 1985
[DE85-008745] 19 p3307 N85-30499

The development of an institutional structure for the Future Global Satellite System for Search and Rescue
20 p3406 N85-31138
Commission for Marine Meteorology
[WMO-640] 20 p3496 N85-31735
The development of complex systems
20 p3539 N85-32021
The 2nd World Meteorological Association Regional Association (Asia), 8th session
[WMO-642] 22 p3817 N85-33643
Project management using graphics
23 p3962 N85-34560
Analyzing performance of small projects using URS and PMAS, information pamphlet
[DE85-011964] 23 p3986 N85-34718
Management of large-scale technology
23 p4057 N85-35145

PROJECT PLANNING
Ada (trademark) training curriculum. Software engineering for managers m101 teacher's exercise guide
[AD-A145094] 01 p0104 N85-10695
AGARD bulletin technical programme, 1985
[AGARD-BUL-84-2] 02 p0305 N85-11971
Project resources planning and control
[NASA-TM-86339] 04 p0575 N85-13666
INFORM system 2-year plan, FY 1984-1985
[DE84-016044] 04 p0576 N85-13674
International Geosphere/Biosphere Program: 1984
[GPO-39-222] 04 p0578 N85-13691
Preliminary concepts of candidate elements for a potential European participation in a manned space station
[MBB-UR-E-749-84-O] 11 p1587 N85-19996
Systems research on China in year 2000
12 p1820 N85-21418
Global tropospheric chemistry: A plan for action
[NASA-CR-175545] 12 p1891 N85-21865
Space Station technology planning
13 p1989 N85-22471
Space station systems technology study (add-on task). Volume 3: Technology advancement program plan
[NASA-CR-171417] 15 p2475 N85-25280
The 1985 long-range program plan
[NASA-TM-87484] 15 p2684 N85-26440
National Airspace System Plan: Facilities, equipment and associated development 16 p2704 N85-26692
Space Station Engineering and Technology Development
[NASA-CR-175806] 16 p2731 N85-26851
Organizing geological work tasks for 1985 outlined
16 p2806 N85-27303
The significance of Helios for Europe
16 p2856 N85-27808
In orbit infrastructure. Volume 1: Executive summary — European space programs
[RX011-002/84-VOL-1] 17 p2908 N85-27928
Documentation for the West German Federal Cabinet's space policy decision 17 p3051 N85-28886
In orbit infrastructure — european space programs
[SNIAS-S/DT-24-996] 18 p3064 N85-28956
Study of a medium term flexible fixed satellite service mission
[DM51/CC-IM-0185.83] 18 p3091 N85-29136
Program planning using the GMAP procedure in SAS/GRAPH software
[DE85-006956] 18 p3199 N85-29842
Electric and hybrid vehicle program: FY 1985 program plan
[DE85-006933] 18 p3201 N85-29858
Thermal Energy Storage Program annual operating plan FY 1985
[DE85-008745] 19 p3307 N85-30499
Management of large-scale technology
23 p4057 N85-35145

PROJECT SETI
DSN 34-meter antenna optics analysis for wideband SETI investigations 10 p1465 N85-19244
The search for extraterrestrial intelligence
15 p2699 N85-26609

PROJECTILE CRATERING
Ion emission from solid surfaces: Comparison of dust impact with other excitations — Giotto mission
14 p2244 N85-23912

PROJECTILE PENETRATION
U TERMINAL BALLISTICS

PROJECTILES
NT HYPERVELOCITY PROJECTILES
NT SABOT PROJECTILES
Optical pin apparatus for measuring the arrival time and velocity of shock waves and particles
[DE84-014501] 01 p0120 N85-10824
Moment induced by liquid payload during spin-up without a critical layer
[AD-A145716] 02 p0199 N85-11327
Liquid payload moment equations
[AD-A145977] 03 p0362 N85-12319
The aerodynamics of some guided projectiles
[NASA-TM-86334] 06 p0747 N85-14788
A metallographic investigation of rotating bands for 7.5 cm artillery projectiles
[FOA-C-20551-D2] 07 p0929 N85-15888
Hypothetical zero yaw drag trajectory of spinning projectiles between M = 5 and M = 10
[AD-A148899] 10 p1421 N85-18983
Electromagnetic braking of a metallic projectile in flight
[AD-A149424] 10 p1480 N85-19345
Experimental simulation of the flow inside a gun barrel
[ISL-CO-208/83] 14 p2302 N85-24252
Experimental simulation of the flows in front of and behind a projectile with and without gas slippage
[ISL-CO-232/83] 14 p2302 N85-24258
A method of calculating the aim point for an unguided projectile fired at a moving target
[BAE-BT-12717] 15 p2489 N85-25365
Dispersion sensitivity of the eight inch advanced ramjet munitions technology projectile due to wind and minor thrust errors
[AD-A152145] 16 p2727 N85-26835
Model for computing late detonations initiated in propellants by impact (XDT reactions)
[DE85-007377] 16 p2758 N85-27019
Influence of behavior laws in the explosive deformation of metal plates
[ISL-R-122/83] 16 p2760 N85-27032
A method for the evaluation of the residual energy of a metallic fragment after perforation of a thin target
[ISL-R-113/83] 16 p2794 N85-27233
Using synchro-ballistic cameras to determine the velocity and spin rate of high-velocity projectiles
[DE85-010829] 19 p3367 N85-30884
Design and fabrication of projectiles for round bore railguns
[DE85-011871] 20 p3398 N85-31078
Preliminary considerations for the gasdynamic precompression of solid molecular hydrogen
[DE85-013256] 22 p3784 N85-33445
A 1984 environmental summary: Sandia National Laboratories Tonopah Test Range, Tonopah, Nevada
[DE85-011145] 22 p3812 N85-33612
OMEGA: Optoelectronic measurement of the incidence angle of a projectile
[ISL-CO-223/84] 23 p3974 N85-34634

PROJECTIVE GEOMETRY
NT MERCATOR PROJECTION
Choice of cartographic projection for space system data bank used in studying natural resources
02 p0165 N85-11119
The Gauss-Krueger projection of the Earth ellipsoid with direct calculation of elliptic integrals through Landen transformations
[SER-C-296] 11 p1666 N85-20495
Surfaces with canonical hyperplane sections
[CWI-TRACT-1] 14 p2410 N85-24858
Analysis of spectral operators in one-dimensional domains
[NASA-CR-172573] 15 p2633 N85-26228

PROJECTORS
Air combat visual simulation using a head slaved projector
[AD-P004327] 09 p1270 N85-17981

PROJECTS
NT AGRISTARS PROJECT
NT APOLLO PROJECT
NT GALILEO PROJECT
NT HELIOS PROJECT
NT PROJECT SETI
NT SCOUT PROJECT
NT TIROS PROJECT
NT VOYAGER PROJECT
Project manager's handbook for special projects
[AD-A147913] 07 p1053 N85-16883

PROMINENCES
NT SOLAR PROMINENCES

PROMOTION
NASA photography index
[NASA-TM-87457] 15 p2665 N85-26445

PRONE POSITION
Effect of body position and immobilization on intensity of spatial illusions in weightlessness
22 p3821 N85-33672

PROOFS
U PROVING

PROP-FAN TECHNOLOGY
Large-scale Advanced Propfan (LAP) performance, acoustic and weight estimation, January, 1984
[NASA-CR-174782] 13 p1969 N85-22368
Large-scale Advanced Propfan (LAP) program
[NASA-TM-87067] 19 p3220 N85-29964

PROPAGATION
Study of delamination cracking under static and cyclic loads of carbon-epoxy composite materials
[REPT-42-727/F] 03 p0327 N85-12102
Cosmic ray propagation in the local superbubble
[NASA-TM-85030] 03 p0449 N85-12655
ATA gas propagation: 1 foot tank experiment
[DE84-016395] 04 p0561 N85-13575
Experiments on ETA comparing wire-conditioned and non-wire-conditioned beam propagation
[DE85-004451] 11 p1725 N85-20848
Exponential anisotropy of solar cosmic rays
[SH-3.2-1] 23 p4002 N85-34817
Energetic solar particle events
[SH-3.2-2] 23 p4003 N85-34818
Channeled propagation of solar particles
[SH-3.2-3] 23 p4003 N85-34819
The local characteristic function of interplanetary particle propagation
[SH-3.2-8] 23 p4003 N85-34823

PROPAGATION (EXTENSION)
NT CRACK PROPAGATION
NT FLAME PROPAGATION

PROPAGATION MODES
Turbofan noise generation. Volume 2: Computer programs
[NASA-CR-167952] 02 p0275 N85-11791
Love and Rayleigh waves in irregular ground
04 p0523 N85-13348
Experimental determination of propagation rate of ELF signals employed by Omega radio navigation system for phase measurements 06 p0793 N85-15066
Transformation of mode composition of circular optical waveguide 07 p0950 N85-16023
Basic experiments in plasma physics (TPL)
15 p2655 N85-26379
Optical multiplexing on monomode fibers
[ENST-83E016] 20 p3533 N85-31982
Adjustment of radiation wavelength of multimode InP-GaInAsP injection heterolasers
21 p3688 N85-32913
The use of optical fibers in pulsed laser holography
[ISL-CO-226/84] 23 p3936 N85-34395
Advanced detectors and signal processing
[NASA-CR-176193] 24 p4068 N85-35343

PROPAGATION VELOCITY
Nondestructive evaluation of residual stress in low-carbon steel, introduction 04 p0512 N85-13265
Experimental determination of propagation rate of ELF signals employed by Omega radio navigation system for phase measurements 06 p0793 N85-15066
Velocity stack and slant stack inversion methods
09 p1351 N85-18497
Double reference pulsed phase locked loop (DRP-2L-2)
[NASA-CASE-LAR-13310-1] 12 p1824 N85-21441
Possibility of retrieving dynamics of reflected wave method records beneath low-velocity zone
14 p2348 N85-24503
Angular dependence of the Rayleigh-surface wave velocity in polycrystalline metals with small anisotropy
[AERE-R-11595] 15 p2509 N85-25476
Polynomial approaches for the characteristic velocity and flame temperature as a function of mixing compounding and pressure for the systems PMMA/O2, PMMA/air, PE/O2, PE/air, PS/O2 and PS/air
[VTH-LR-421] 17 p2924 N85-28024
Proceedings of the 1980 Workshop of the International Association of Seismology and Physics of the Earth's Interior on the Seismic Modeling of Laterally Varying Structures: Contributions based on data from the 1978 Saudi Arabian refraction profile
[GS-CIRC-937] 17 p2989 N85-28476
Preliminary interpretation of Saudi Arabian seismic refraction data 17 p2989 N85-28477
A preliminary examination of the 1978 refraction profiles in Saudi Arabia 17 p2990 N85-28482
The rifted margin of Saudi Arabia
17 p2990 N85-28483
On the propagation speed in relativistic quantum mechanics
[CWI-AM-R8410] 17 p3046 N85-28848
Lower bounds of propagation velocity of steady ionizing waves in field of strong electromagnetic wave
21 p3692 N85-32940
Amplification of electromagnetic wave by electron stream with negative velocity differences
21 p3692 N85-32941
The recovery of the cosmic ray flux from maximum solar modulation at IMP-8 (1 AU) and at Pioneer (R 30 AU)
[SH-4.7-7] 23 p4041 N85-35052

PROPAGATORS
U PROPAGATION

PROPANE
Catalytic conversion of C3-C4 paraffins to gasoline
[DE85-004181] 10 p1458 N85-19157

Laser schlieren, shock tube studies of high temperature hydrocarbon pyrolysis rates
[DE85-003314] 11 p1636 N85-20303
Optical waveguide sensor for methane gas
[AD-D011691] 19 p3273 N85-30294
Investigation of the flame speeds of propane/methanol gas mixtures
[DE85-012817] 23 p3912 N85-34239

PROPARGYL GROUPS
Thermoset-thermoplastic aromatic polyamide containing N-propargyl groups
[NASA-CASE-LAR-12723-1] 11 p1610 N85-20123

PROPELLANT ADDITIVES
NT PROPELLANT BINDERS
NT SOLID ROCKET BINDERS
Transition to detonation from rapid-compression (ramp-waves) generated in a burning porous bed
[AD-P004345] 10 p1455 N85-19169
Workshop report: Catalysis of Burn Rate of Energetic Binder propellants 13 p2001 N85-22545
Mechanism of burning rate enhancement by ferric oxide 13 p2002 N85-22546
Propellant plasticizer
[AD-D011501] 20 p3434 N85-31306

PROPELLANT BINDERS
NT SOLID ROCKET BINDERS
Measurement of shock and induced reaction in rocket propellants by nanosecond infrared radiometry and photography
[DE84-013209] 04 p0462 N85-13070
Combustion properties of fuel-rich magnesium propellants with HTPB as binder
[FOA-C-20555-D1] 07 p0935 N85-15924
Workshop report: Catalysis of Burn Rate of Energetic Binder propellants 13 p2001 N85-22545
Effects of HMX addition on the combustion of energetic binders 13 p2004 N85-22560

PROPELLANT CHEMISTRY
The crystal and molecular structure of a new propellant compound: Triaminoguanidium Azide Nitrate (TAZN) 13 p2002 N85-22551

PROPELLANT COMBUSTION
NT SOLID PROPELLANT COMBUSTION
NT SOLID PROPELLANT IGNITION
HMX combustion modification
[AD-A145071] 01 p0024 N85-10149
Combustion properties of fuel-rich magnesium propellants with HTPB as binder
[FOA-C-20555-D1] 07 p0935 N85-15924
Transient combustion: An important consideration in deflagration-to-detonation transition 08 p1116 N85-17037
Twenty-first JANNAF Combustion Meeting, volume 1
[AD-A150981] 13 p1998 N85-22526
Status of boron combustion research 13 p1998 N85-22528
Development of a three-phase combustion code for modeling liquid rocket engines 13 p2003 N85-22554
Atomization data requirements for rocket combustor modeling 13 p2003 N85-22555
Effects of HMX addition on the combustion of energetic binders 13 p2004 N85-22560
Study on the combustion of nitramine propulsion powder up to 1500 MPa and comparison of the performance with that of classical propulsion powders
[ISL-CO-203/83] 14 p2264 N85-24025

PROPELLANT EVAPORATION
An experimental study of spray thruster
[REPT-613] 12 p1845 N85-21578

PROPELLANT EXPLOSIONS
Hazard Studies for Solid Propellant Rocket Motors
[AGARD-CP-367] 08 p1114 N85-17025
Response of propellants to high dynamic stresses: The uses of gun launch techniques 08 p1116 N85-17035
Modelling the thermal explosion phenomenon in solid propellants: The case of fixed and variable temperatures 08 p1117 N85-17044

PROPELLANT GRAINS
Portable slotting device
[AD-D011213] 01 p0033 N85-10206
A model for grain misalignment in cylindrical port motors
[AD-A144858] 01 p0034 N85-10210
Closed vessel combustion of stick propellant
[AD-A147802] 08 p1135 N85-17154
A thermal-mechanical model of deflagration-to-detonation in granular energetic materials
[AD-P004346] 10 p1455 N85-19170
Curvilinear solid propellant grain
[AD-D011457] 10 p1458 N85-19183
Experimental high pressure equation of state of a very fast burning gun propellant
[DE85-001749] 10 p1458 N85-19184
Status of boron combustion research 13 p1998 N85-22528
Analysis of combustion oscillations in heterogeneous systems
[AD-A151999] 16 p2745 N85-26942
Fiber reinforcement of gun propellant
[AD-A152296] 16 p2757 N85-27014

PROPELLANT PROPERTIES
NT PROPELLANT SENSITIVITY
NT PROPELLANT STORABILITY

PROPELLANT SENSITIVITY
Sensitivity tests for solid propellants in Germany 08 p1115 N85-17028
Sensitiveness and explosiveness assessment at Perme Waltham Abbey 08 p1115 N85-17029
Study of the transition from deflagration to detonation of previously fragmented propellants 08 p1115 N85-17032
Effect of variable solid phase thermal properties on propellant combustion 13 p2002 N85-22547

PROPELLANT SPRAYS
An experimental study of spray thruster
[REPT-613] 12 p1845 N85-21578

PROPELLANT STORABILITY
Propellant plasticizer
[AD-D011501] 20 p3434 N85-31306

PROPELLANT STORAGE
Space station task force perspective 08 p1106 N85-16992
Earth-to-orbit propellant transportation overview 08 p1106 N85-17002
Active cooling requirements for propellant storage 08 p1108 N85-17004

PROPELLANT TANKS
An experimental study of jet impingement on a circular cylinder
[AD-A145583] 02 p0198 N85-11326
Ion thruster system (8-cm) cyclic endurance test
[NASA-CR-174745] 04 p0463 N85-12937
Propellant tank resupply system
[AD-D011288] 05 p0603 N85-13648
Fluid slosh dynamics of surface tension tanks in three axis stabilized spacecraft
[MBB-UR-E-739-84-O] 11 p1634 N85-20291
Dynamic investigations of a spherical tank structure filled with liquid using ANSYS three-dimensional fluid elements
[MBB-UR-E-737-83-O] 11 p1654 N85-20418

PROPELLANT TESTS
Review of USAF treatment of solid propellant rocket motor hazards 08 p1114 N85-17027
NATO AC/310 activities report on NATO STANAG 4170 and Allied Ordnance Publication 7 (Manual of Tests for Qualification of Explosive Materials for Military Use)
[AD-P004341] 10 p1454 N85-19165
Compatibility experiments of facilities, materials, and propellants for electrothermal thrusters
[NASA-TM-86956] 12 p1795 N85-21260
Characterization standards for solid propellant rocket motors
[AD-A150250] 13 p2013 N85-22627
Dissected motors-propellants motor number STM-012. Phase 15: Surveillance report, stage 1
[AD-A156066] 24 p4071 N85-35226

PROPELLANT TRANSFER
External tank GH2 vent arm 08 p1102 N85-16969
Propellant transfer: Attached depot 08 p1106 N85-17005
Propellant transfer: Tethered depot 08 p1106 N85-17006
OTV fluid mangement systems 08 p1106 N85-17007
Space Transportation System (STS) propellant scavenging system study. Volume 1: Technical report
[NASA-CR-171846-VOL-1] 11 p1589 N85-20000
Space Transportation System (STS) propellant scavenging system study. Volume 2: Supporting research and technology report
[NASA-CR-171846-VOL-2] 11 p1589 N85-20001
Space Transportatioln System (STS) propellant scavenging system study. Volume 3: Cost and work breakdown structure-dictionary
[NASA-CR-171850-VOL-3] 11 p1590 N85-20002
An investigation of space shuttle main engine shutdown chugging instability 12 p1946 N85-22221

PROPELLANTS
NT CASE BONDED PROPELLANTS
NT COMPOSITE PROPELLANTS
NT CRYOGENIC ROCKET PROPELLANTS
NT DOUBLE BASE PROPELLANTS
NT DOUBLE BASE ROCKET PROPELLANTS
NT GASEOUS ROCKET PROPELLANTS
NT GUN PROPELLANTS
NT HIGH ENERGY PROPELLANTS
NT HTPB PROPELLANTS
NT HYPERGOLIC ROCKET PROPELLANTS
NT LIQUID ROCKET PROPELLANTS
NT MONOPROPELLANTS
NT NITRAMINE PROPELLANTS
NT PLASTIC PROPELLANTS
NT RDX
NT ROCKET PROPELLANTS
NT SLURRY PROPELLANTS
NT SOLID PROPELLANTS
NT SOLID ROCKET PROPELLANTS
NT STORABLE PROPELLANTS
NT TATB
An optical and mass spectrometric study of the aluminum-oxygen flame
[AD-A147434] 07 p0923 N85-15849
Closed vessel combustion of stick propellant
[AD-A147802] 08 p1135 N85-17154
A thermal-mechanical model of deflagration-to-detonation in granular energetic materials
[AD-P004346] 10 p1455 N85-19170
Measurements of distributed combustion 13 p2001 N85-22542
Design of a Mobile Combustion Diagnostic Fixture (MCDF)
[AD-A151814] 16 p2745 N85-26941
Closed-bomb combustion of Hivelite-based, Very High Burn Rate (VHBR) propellant
[AD-A155740] 21 p3571 N85-32212

PROPELLER BLADES
Profile design for wings and propellers
[NASA-TM-77785] 10 p1419 N85-18953
Noise constraints effecting optimal propeller designs
[NASA-TM-86967] 11 p1575 N85-19923
Determination of aerodynamic and propulsion parameters of general aviation aircraft using steady state flight test data 13 p1971 N85-22377
Interaction of a turbulent vortex with a lifting surface 15 p2464 N85-25214
Low-speed wind-tunnel tests of an advanced eight-bladed propeller
[NASA-TM-86364] 19 p3214 N85-29926
Large-scale Advanced Propfan (LAP) program
[NASA-TM-87067] 19 p3220 N85-29964
Effects of propeller rotation direction on airplane interior noise levels
[NASA-TP-2444] 19 p3350 N85-30767
Impulsive noise due to transonic blade-vortex interactions 20 p3523 N85-31913
Two-plane balance and slip-ring design 22 p3799 N85-33536
Optimally designed propellers constrained by noise 24 p4065 N85-35196

PROPELLER DRIVE
NT HELICOPTER PROPELLER DRIVE

PROPELLER EFFICIENCY
Welcome to the Saclay Propeller Testing Center
[NASA-TM-77648] 14 p2225 N85-23799
Large-scale Advanced Propfan (LAP) program
[NASA-TM-87067] 19 p3220 N85-29964
Optimally designed propellers constrained by noise 24 p4065 N85-35196

PROPELLER FANS
Large-scale Advanced Propfan (LAP) performance, acoustic and weight estimation, January, 1984
[NASA-CR-174782] 13 p1969 N85-22368
Wind tunnel results of advanced high speed propellers in the takeoff, climb and landing operating regimes
[NASA-TM-87054] 19 p3213 N85-29925

PROPELLER SLIPSTREAMS
Studies on the interference of wings and propeller slipstreams
[NASA-CR-175753] 15 p2483 N85-25210

PROPELLERS
NT PROPELLER FANS
NT VARIABLE PITCH PROPELLERS
Analysis of noise measured from a propeller in a wake
[NASA-TP-2358] 02 p0274 N85-11788
Screw expander for light duty diesel engines 04 p0508 N85-13242
Evaluation of the Langley 4- by 7-meter tunnel for propeller noise measurements
[NASA-TM-85721] 04 p0558 N85-13553
Contribution of the study of light aircraft propeller noise
[ESA-TT-865] 09 p1376 N85-16687
Propeller propulsion system integration: State of technology survey
[NASA-CR-3882] 12 p1771 N85-21119
Towards a renewal of the propeller in aeronautics
[NASA-TM-77803] 12 p1779 N85-21169
Further comparison of wind tunnel and airplane acoustic data for advanced design high speed propeller models
[NASA-TM-86935] 12 p1927 N85-22108
Method for the prediction of the installation aerodynamics of a propfan at subsonic speeds
[NASA-CR-3887] 13 p1969 N85-22369
Wind tunnel acoustic study of a propeller installed behind an airplane empennage: Data report
[NASA-CR-177335] 13 p2154 N85-23377

Wind tunnel results of advanced high speed propellers in the takeoff, climb and landing operating regimes
[NASA-TM-87054] 19 p3213 N85-29925
An experimental investigation of propfan installations on an upswept supercritical wing at transonic Mach numbers
[NASA-CR-172605] 20 p3388 N85-31013
Wingtip vortex propeller
[NASA-CASE-LAR-13019-1] 24 p4085 N85-35194

PROPHYLAXIS
A double blind comparative trial of powdered ginger root, hyoscine hydrobromide, and cinnarizine in the prophylaxis of motion sickness induced by cross coupled stimulation
11 p1695 N85-20657

PROPORTIONAL COUNTERS
In-beam tests of an air-core superconducting-solenoid particle spectrometer
[DE85-004029] 12 p1853 N85-21625
Wide-ranging radiation dose monitor
[DE85-011596] 22 p3787 N85-33463
Search for magnetic monopoles using proportional counters filled with helium gas
[HE-6.1-1] 24 p4209 N85-36127
Magnetic monopole search by 130 m(2)sr He gas proportional counter
[HE-6.1-2] 24 p4209 N85-36128
Limits on monopole fluxes from KFG experiment
[HE-6.1-8] 24 p4209 N85-36132
Results from the UCSD magnetic monopole search
[HE-6.1-12] 24 p4210 N85-36137
Results on nucleon life-time from the Kolar gold field experiment
[HE-6.2-3] 24 p4211 N85-36139
Data acquisition system for phase-2 KGF proton decay experiment
[HE-6.2-4] 24 p4211 N85-36140

PROPORTIONAL LIMIT
The effects of pin elasticity, clearance, and friction on the stresses in a pin-loaded orthotropic plate
[NASA-CR-175816] 16 p2743 N85-26927
Prediction of lifetime for ceramic materials in the elastic and viscoelastic region by fracture mechanical methods
[ESA-TT-825] 20 p3434 N85-31305

PROPRIOCEPTION
Estimating number, time and length; a baseline study
05 p0695 N85-14473

PROPRIOCEPTORS
Gravity perception and cardiac function in the spider
15 p2006 N85-26058

PROPULSION
NT ASCENT PROPULSION SYSTEMS
NT AUXILIARY PROPULSION
NT CHEMICAL PROPULSION
NT DESCENT PROPULSION SYSTEMS
NT ELECTRIC PROPULSION
NT ELECTROMAGNETIC PROPULSION
NT ELECTROSTATIC PROPULSION
NT HYBRID PROPULSION
NT ION PROPULSION
NT JET PROPULSION
NT LOW THRUST PROPULSION
NT MARINE PROPULSION
NT MASS DRIVERS (PAYLOAD DELIVERY)
NT NUCLEAR ELECTRIC PROPULSION
NT PLASMA PROPULSION
NT SOLAR PROPULSION
NT SPACECRAFT PROPULSION
Energy efficient engine. Volume 1: Component development and integration program
[NASA-CR-173084] 02 p0146 N85-10992
Report of the Department of Aerospace Engineering
03 p0307 N85-11977
Thrust characterization of very high burning rate propellants
[AD-A145891] 03 p0340 N85-12186
Research and technology, 1984: Marshall Space Flight Center
[NASA-TM-86476] 04 p0590 N85-13765
Embedment system for ultrahigh-burning rate propellants of solid propulsion subsystems
[AD-D011257] 06 p0773 N85-14942
Air Force space technology center space technology: Emphasis 84
09 p1333 N85-18381
Characterization standards for solid propellant rocket motors
[AD-A150250] 13 p2013 N85-22627
Future directions in aeropropulsion technology
[NASA-TM-87010] 14 p2207 N85-23685
AFRPL (Air Force Rocket Propulsion Laboratory) technical objective document FY 85
[AD-A151368] 15 p2495 N85-25369
Heat transfer in aeropropulsion systems
[NASA-TM-87066] 20 p3453 N85-31444
R and D programmes at the National Aeronautical Laboratory
[AR-22] 20 p3539 N85-32022
Clarke Stations and mercurian mass-drivers: Energy for large-scale transportation systems
[DE85-009607] 21 p3560 N85-32145
Three-Dimensional Techniques Applied to Internal Flows in Propulsion Systems
[AGARD-LS-140] 21 p3586 N85-32293
Status of advanced orbital transfer propulsion
[NASA-TM-87069] 24 p4071 N85-35225

PROPULSION SYSTEM CONFIGURATIONS
NT ASCENT PROPULSION SYSTEMS
NT DESCENT PROPULSION SYSTEMS
Investigation of a pulsed electrothermal thruster system
[NASA-CR-174768] 02 p0169 N85-11132
Continuing issues (FY 1983) concerning military use of the space transportation system
[AD-A146091] 03 p0323 N85-12080
The preliminary checkout, evaluation and calibration of a 3-component force measurement system for calibrating propulsion simulators for wind tunnel models
[NASA-CR-174113] 04 p0458 N85-12903
STOL simulation requirements for development of integrated flight/propulsion control systems
05 p0701 N85-14489
Parametric estimates of propulsion system maintenance manhours
[AD-A147120] 07 p0894 N85-15662
Installed nacelle drag-improvement tests of an M = 0.8 turboprop transport configuration
[NASA-TM-84302] 07 p0902 N85-15716
Ramjets with supersonic combustion
07 p0918 N85-15817
Propulsion and power systems perspective
08 p1098 N85-16938
Orbital Maneuvering system design evolution
08 p1098 N85-16943
OTV Propulsion Issues
[NASA-CP-2347] 08 p1106 N85-16989
Analysis and optimization of small Space Shuttle propulsion platforms
[DFVLR-FB-84-28] 10 p1431 N85-19023
The 1984 JANNAF Propulsion Systems Hazards Subcommittee Meeting, volume 1
[AD-A148885] 10 p1454 N85-19162
Propeller propulsion system integration: State of technology survey
[NASA-CR-3882] 12 p1771 N85-21119
Towards a renewal of the propeller in aeronautics
[NASA-TM-77803] 12 p1779 N85-21169
Fiscal year 1986 technical objective document
[AD-A151039] 14 p2432 N85-25000
Mathematical modeling of the AEDC (Arnold Engineering Development Center) propulsion wind tunnel (16T)
[AD-A151293] 15 p2475 N85-25275
Manrating orbital transfer vehicle propulsion
[NASA-TM-87019] 15 p2494 N85-25385
Future fundamental combustion research for aeropropulsion systems
[NASA-TM-87049] 17 p2898 N85-27870
The STOL and maneuver technology program integrated control system development 17 p2905 N85-27910
The Department of Defense statement on the Science and Technology Program by Colonel Donald I. Carter, USAF Acting Deputy Under Secretary of Defense for Research and Advanced Technology before the Subcommittee on Research and Development of the Committee on Armed Services of the United States House of Representatives, 98th Congress, first session
[AD-A152467] 17 p3048 N85-28850
Advanced beamed-energy and field propulsion concepts
[NASA-CR-176106] 22 p3741 N85-33186
Presentation of the acoustic and aerodynamic results of the Aladin 2 concept qualification testing
[NASA-TM-77883] 24 p4080 N85-35161

PROPULSION SYSTEM PERFORMANCE
Energy efficient engine component development and integration program
[NASA-CR-168496] 02 p0146 N85-10989
Investigation of a pulsed electrothermal thruster system
[NASA-CR-174768] 02 p0169 N85-11132
Nonlinear system identification methodology development based on F-4S flight test data analysis
[AD-A146289] 03 p0318 N85-12053
Continuing issues (FY 1983) concerning military use of the space transportation system
[AD-A146091] 03 p0323 N85-12080
LOX/LH2 propulsion system for launch vehicle upper stage, test results
[NASA-TM-77727] 03 p0324 N85-12089
Study on control of ion engine system
[EL-847] 07 p0916 N85-15800
An update of the Canada/USA augmentor-wing project 08 p1070 N85-16781
Space Shuttle Technical Conference, part 2
[NASA-CP-2342-PT-2] 08 p1098 N85-16937
NASA OAST perspective 08 p1106 N85-16990
Aerojet advanced engine concept
08 p1107 N85-16998
Advanced OTV engines and issues
08 p1108 N85-17000
The Altitude Wind Tunnel (AWT): A unique facility for propulsion system and adverse weather testing
[NASA-TM-86921] 09 p1283 N85-18067
Analysis and optimization of small Space Shuttle propulsion platforms
[DFVLR-FB-84-28] 10 p1431 N85-19023
Propeller propulsion system integration: State of technology survey
[NASA-CR-3882] 12 p1771 N85-21119
Optimization of guidance and control using function minimization and NAVSTAR/GPS
[AD-A149956] 12 p1775 N85-21141
Determination of aerodynamic and propulsion parameters of general aviation aircraft using steady state flight test data 13 p1971 N85-22377
Missions and vehicle concepts for modern, propelled, lighter-than-air vehicles
[NASA-TM-87461] 15 p2457 N85-25170
Performance and surge limits of a TF30-P-3 turbofan engine/axisymmetric mixed-compression inlet propulsion system at Mach 2.5
[NASA-TP-2461] 15 p2472 N85-25281
Mathematical modeling of the AEDC (Arnold Engineering Development Center) propulsion wind tunnel (16T)
[AD-A151293] 15 p2475 N85-25275
Error reduction program — combustor performance evaluation codes
[NASA-CR-174776] 16 p2852 N85-27584
Test devices for aeronautical research and technology
[NASA-TM-77651] 17 p2905 N85-27914
An evaluation of oxygen-hydrogen propulsion systems for the Space Station
[NASA-TM-87058] 18 p3067 N85-28971
Energy efficient engine integrated core/low spool test hardware design report
[NASA-CR-168137] 19 p3218 N85-29956
Performance improvements of a highly integrated digital electronic control system for an F-15 airplane
[NASA-TM-86748] 21 p3556 N85-32120

PROPULSIVE EFFICIENCY
NT PROPELLER EFFICIENCY
The preliminary checkout, evaluation and calibration of a 3-component force measurement system for calibrating propulsion simulators for wind tunnel models
[NASA-CR-174113] 04 p0458 N85-12903
Propulsive efficiency of vibrating wing in supersonic flow 05 p0724 N85-14656
Design study of technology requirements for high performance single-propeller-driven business airplanes
[NASA-CR-3863] 07 p0886 N85-15692
Missions and vehicle concepts for modern, propelled, lighter-than-air vehicles
[NASA-TM-87461] 15 p2457 N85-25170
Manrating orbital transfer vehicle propulsion
[NASA-TM-87019] 15 p2494 N85-25385
Propulsion efficiency of vibrating bodies in subsonic gas stream 17 p2942 N85-28159

PROPYL COMPOUNDS
Thermolysis of 4-methyl-4-(1-propenyl)malonyl peroxide: Mechanistic limits to chemiluminescence efficiency
[AD-A151567] 15 p2505 N85-25452

PROPYLENE
Field test results of experimental EPDM (Ethylene Propylene Diene Monomer) and PUF (Polyurethane Foam) roofing
[AD-A147697] 08 p1132 N85-17133
Stabilized unsaturated polyesters
[NASA-CASE-NPO-18103-1] 18 p3078 N85-29043

PROSPECTING
U EXPLORATION

PROSTAGLANDINS
The effect of naproxen on acute mountain sickness and vascular responses to hypoxia
[AD-A145144] 01 p0095 N85-10635

PROSTHETIC DEVICES
A comparative study of alternative controls and displays for by the severely physically handicapped
05 p0709 N85-14549
Metallic aid and technique in fitting voice prosthesis
[AD-D011358] 07 p1014 N85-18442

PROTEASE
Acid phosphatase and protease activities in immobilized rat skeletal muscles
[NASA-CR-174340] 08 p1192 N85-17509

PROTECTION
NT ACCELERATION PROTECTION
NT CIRCUIT PROTECTION
NT CORROSION PREVENTION

NT ENVIRONMENT PROTECTION
NT METEOROID PROTECTION
NT RADIATION PROTECTION
NT RADIATION SHIELDING
NT THERMAL PROTECTION
Impact tests of adjusters for the HBU-12 lap belt
[AD-A148021] 08 p1080 N85-16843
Power quality and protection of electric distribution systems with small, dispersed generation devices
[DE85-000990] 09 p1344 N85-18453
Improved ceramic anodes for corrosion protection
[AD-A149492] 10 p1452 N85-19149
Hurricane storm surge research
[GPO-40-048] 12 p1893 N85-21880
EOS (electrical overstress) protection for VLSI (Very Large Scale Integration) devices
[AD-A150333] 13 p2084 N85-22891
Fire pit tests of blue flight coverall program
[AD-A151664] 15 p2620 N85-26149
Fast shutter apparatus
[DE85-006501] 23 p3928 N85-34943
PROTECTIVE CLOTHING
NT HELMETS
NT PRESSURE SUITS
NT SPACE SUITS
The experimental mod 3 firefighters' aluminized crash-rescue, fire-proximity hood
[AD-A144993] 01 p0098 N85-10955
Resistance of Navy shipboard outerwear garments and fire-resistant fabrics to extreme heat
[AD-A145414] 02 p0226 N85-11546
Anthropometric cockpit compatibility assessment of US Army aircraft for large and small personnel wearing A cold weather, armored vest, chemical defense protective clothing configuration
[AD-A145472] 02 p0236 N85-11547
Acceptance-testing procedures for air-line supplied-air suits
[DE84-016960] 05 p0712 N85-14569
Windblast leg protector assembly
[AD-D011376] 07 p0899 N85-15700
Flame-resistant materials for use in pyrotechnic safety clothing
[AD-A146867] 07 p0931 N85-15901
The effect of modified spectacles on the field of view of the helmet display unit of the integrated helmet and display sighting system
[AD-A146893] 09 p1281 N85-18055
A systems analysis of alternative concepts for aircrew cold weather clothing
[AD-A146805] 09 p1365 N85-18580
Heat stress and personal protective equipment
[DE85-003552] 10 p1532 N85-19652
The application of anthropometric survey data to aircrew clothing sizing
[AD-A150545] 13 p2143 N85-23304
Fire pit tests of blue flight coverall program
[AD-A151664] 15 p2620 N85-26149
Investigation of the requirement for auxiliary heating of Canadian forces personnel
[AD-A151950] 16 p2841 N85-27522
The design of working systems on ergonomic principles. The importance of clothes and protective equipment in the design of the workplace
[HSE-TRANS-10665] 19 p3332 N85-30639
PROTECTIVE COATINGS
NT ANODIC COATINGS
NT CERAMIC COATINGS
NT PRIMERS (COATINGS)
NT REFRACTORY COATINGS
Single-drop impact damage prediction for low density, coated ceramic materials --- rain erosion
01 p0081 N85-10402
Surface protection overview 02 p0144 N85-10978
Energy efficient engine high pressure turbine ceramic shroud support technology report
[NASA-CR-168036] 02 p0147 N85-10998
Development and performance of CVD-coatings on cutting tools 02 p0178 N85-11193
The development of CVD oxide coatings for the protection of metal surfaces --- chemical vapor deposition (CVD)
03 p0332 N85-12142
New coatings for high temperature materials protection
[AERE-R-11367] 03 p0339 N85-12180
Protective coverings for fiber reinforced epoxy composites
[PB84-231059] 04 p0480 N85-13063
A review of metallic surface treatments for corrosion mitigation
[AD-A146701] 06 p0769 N85-14918
Arc-evaporated carbon films: Optical properties and electron mean free paths
[DE85-001246] 06 p0867 N85-15510
Mechanical aspects of high temperature coatings
07 p0908 N85-15749
Qualitative and quantitative compositional analysis of shale derived by gas chromatography and combined gas Chromatography/Mass spectrometry. Executive summary
[AD-A148369] 07 p0924 N85-15851
Process for preparation of crosslinked poly(tri-n-butyltin) methacrylate with simultaneous particle size reduction
[AD-D011313] 07 p0932 N85-15905
Effect of iron on the performance of IN 625 weld deposits
[BR91456] 08 p1169 N85-17376
Experimental and analytical study of ceramic-coated turbine-tip shroud seals for small turbine engines
[NASA-TM-86861] 09 p1281 N85-18057
Cavitation erosion resistant coatings for pumps
[PB85-120210/GAR] 09 p1300 N85-18167
Antifriction nickel-phosphorous coatings on aluminum alloy products 09 p1309 N85-18221
Low power microprocessor based measurements system for determining the integrity of coatings on buried pipelines
[ERS-E.380] 09 p1324 N85-18323
Effects of MAR-M247 substrate (modified) composition on coating oxidation coating/substrate interdiffusion --- protective coatings for hot section components of gas turbine engines
[NASA-CR-174851] 10 p1440 N85-19073
Process for preparing essentially colorless polyimide film containing phenoxy-linked diamines
[NASA-CASE-LAR-13353-1] 11 p1611 N85-20128
Oxidation protection coatings for polymers
[NASA-CASE-LEW-14072-1] 11 p1611 N85-20129
A study of intumescent reaction mechanisms
[AD-A149605] 12 p1812 N85-21365
Formation of alumina layers on iron-base alloys
[BLL-T8418/BG/LRS/LRST737/84] 13 p2020 N85-22657
Properties of welded joints in argon arc welding of titanium alloy using a protective coating
13 p2032 N85-22733
Use of optical techniques in studies of wear rates of anodized aluminum and polymer coatings on aluminum
14 p2259 N85-23997
Development of acceptance criteria for batches of silane primer for external tank thermal protection system bonding applications
[NASA-CR-171428] 14 p2259 N85-23998
Dimensions of smooth mating parts with protective coatings 14 p2260 N85-24124
Self-substaining low-Z coatings for impurity control. Part 1: General considerations
[DE85-000427] 14 p2425 N85-24956
Development of coating for protection of backside of seam in welding of titanium alloys
15 p2500 N85-25421
Mechanical properties of TiN deposits obtained by PVD and TiN, TiC, TiC -+ TiN obtained by CVD
[BLL-RISLEY-TR-5097-(9091.9F)]
15 p2508 N85-25471
Detonation flame spraying extends life of automotive parts 15 p2513 N85-25507
Modified aluminosilicide coating for heat-resistant nickel alloys 15 p2514 N85-25509
Titanium diffusion method prevents metal corrosion
15 p2514 N85-25510
Inhibiting titanium corrosion in hot nitrogen nitrate solutions using sulfate ions 15 p2514 N85-25511
Protective coatings for aircraft structures: A review
[VTH-LR-413] 16 p2706 N85-26704
Effects of surface chemistry on hot corrosion life
[NASA-CR-174915] 16 p2708 N85-26711
Material technology 16 p2734 N85-26870
Characteristics of polyacrylic acid-complexed zinc phosphate conversion films deposited on metal surfaces
[DE85-004057] 16 p2750 N85-26974
Testing of materials and coatings for jet engine components under simulated operational conditions
[B8580073] 17 p2899 N85-27873
Properties of chromate coatings formed on electrolytic zinc substrates
[BLL-BISI-TRANS-22349-(9022.06)]
17 p2926 N85-28052
New process for production of bimetal with corrosion-resistant cladding layer
[BLL-BISI-TRANS-22371-(9022.06)]
17 p2927 N85-28056
Erosion of corrosion-resistant surface treatments on alloy steels
[DE85-008446] 17 p2932 N85-28100
New air-curing lacquer systems with high solids content
[BMFT-FB-T-85-005] 17 p2936 N85-28124
Technology development for thin-film-trace humidity sensors
[BMFT-FB-T-84-268] 17 p2969 N85-28338
Proper quality of anticorrosion work no matter how bad the atmospheric conditions
[BLL-BISI-TRANS-22060-(9022.06)]
17 p2975 N85-28383
Corrosion resistant coating
[NASA-CASE-NPO-15928-1] 18 p3073 N85-29005
Long-Term Materials Test Program
[DE85-003248] 18 p3077 N85-29034
Ceramic coatings for heat engine materials: Status and future needs
[DE85-006759] 18 p3080 N85-29053
Ceramic coatings for heat engine materials
[DE85-005236] 18 p3080 N85-29054
Spray applicator for spraying coatings and other fluids in space
[NASA-CASE-MSC-18852-1] 18 p3115 N85-29283
Physical-mechanical characteristics and wear resistance of coatings applied by microarc oxidation
19 p3242 N85-30104
Effect of prolonged high temperature on durability of coated high-temperature nickel alloys
19 p3243 N85-30105
Atomized magnetism-aluminum protective coatings
19 p3244 N85-30116
Ion beam sputter-deposited thin film coatings for protection of spacecraft polymers in low Earth orbit
[NASA-TM-87051] 19 p3248 N85-30137
Mechanical protection of DLC films on fused silica slides
[NASA-TM-87058] 19 p3248 N85-30138
Realization by vapor deposition of turbine blades covered with a silicon nitride layer
20 p3395 N85-31061
Protection products for the conductors of high voltage overhead lines
[BLL-OA-TRANS-3219-(6196.300)]
20 p3429 N85-31269
New corrosion protection concept for very high voltage line towers
[BLL-OA-TRANS-2691-(6196.300)]
20 p3429 N85-31270
Inhibited anticorrosion protection of automotive steel strip in the NLMK
[BLL-M-36250-(5828.4)] 20 p3430 N85-31274
Metallographic preparation of materials with various coatings
[BLL-DRIC-TRANS-7522-(3623.66)]
20 p3433 N85-31299
Silicon nitride protective coatings for silvered glass mirrors
[DE85-011637] 20 p3433 N85-31300
A study of adherent oxide scales
[AD-A155554] 21 p3567 N85-32188
Development of wide band recording materials
[AD-A154961] 21 p3589 N85-32309
Encapsulation materials research
21 p3608 N85-32407
Rationale in the selection of corrosion protective coating systems 22 p3750 N85-33242
Protective systems and maintenance policies for marine environments 22 p3750 N85-33245
Towards the development of technological processes for the preparation of cadmium plated steel articles
[BLL-M-36315-(5828.4)] 23 p3913 N85-34248
Diamondlike carbon protective coatings for IR materials
[NASA-TM-87063] 23 p3973 N85-34631
Wear-resistant coatings for tools intended for cold working
[BLL-RISLEY-TR-5040-(9091.9F)]
24 p4081 N85-35293
Space shuttle SRB TPS protective paint test and evaluation in NASA Hot Gas Facility and AEDC Tunnel C
[NASA-CR-170664] 24 p4081 N85-35294
PROTECTORS
Windblast leg protector assembly
[AD-D011376] 07 p0899 N85-15700
Flow through very porous screens
[NASA-TP-2436] 11 p1631 N85-20270
Windblast arm protector assembly
[AD-D011512] 12 p1909 N85-21984
Optoelectronic safety system for robotized technological complex 13 p2046 N85-22805
Results of tests of MTA-2 TPS on the SRB hold-down bolt blast container
[NASA-CR-170691] 24 p4070 N85-35224
PROTEIN METABOLISM
NT LIPID METABOLISM
Skeletal muscle metabolism in hypokinetic rats
[NASA-CR-174059] 02 p0233 N85-11520
Blood amino acids of cosmonauts before and after 211-day spaceflight 12 p1900 N85-21933
Calcium and calmodulin localization in gravitropically-responding plant organs
15 p2606 N85-26061

Role of glucocorticoids in the response to unloading of muscle protein and amino acid metabolism
15 p2609 N85-26077

PROTEIN SYNTHESIS
Skeletal muscle metabolism in hypokinetic rats
[NASA-CR-174059] 02 p0233 N85-11520
Nitrogen control of photosynthetic protein synthesis
[DE85-009513] 11 p1690 N85-20823

PROTEINS
NT ADENOSINE DIPHOSPHATE
NT ADENOSINE TRIPHOSPHATE
NT ADENOSINES
NT ASPARTATES
NT FIBRIN
NT GLOBULINS
NT GLUTATHIONE
NT LIPOPROTEINS
NT OXIDASE
NT OXYHEMOGLOBIN
NT PEPTIDES
NT POLYPEPTIDES
Nuclear Magnetic Resonance of Polymeric Materials
[AD-A145078] 01 p0032 N85-10192
NMR (Nuclear Magnetic Resonance) of solid biopolymers
[AD-P003912] 01 p0032 N85-10198
Static and quasielastic neutron scattering for the investigation of structure, dynamics and transport properties of lipid layers and lipid/protein compounds
03 p0432 N85-12753
Biochemistry and pathogenic hypotheses of organophosphorus-induced delayed neurotoxicity
[AD-P004028] 06 p0844 N85-15360
Plasmodium of myxomycete as research object in gravitational biology 15 p2483 N85-25327
Isolation of hybridomas for golgi-associated proteins and a plant calmodulin 15 p2615 N85-26103
Progress, goals in biotechnology summarized
17 p2945 N85-28182
Towards a statistical analysis of genetic sequences data with particular reference to protein sequences
[AD-A153605] 18 p3152 N85-29615
A computerized system for spot detection and analysis of two-dimensional electrophoresis images
23 p3958 N85-34531
Muscle protein and glycogen responses to recovery from hypogravity and unloading by tail-cast suspension
[NASA-CR-176181] 24 p4128 N85-35691

PROTOCOL (COMPUTERS)
Proceedings of the 5th LAN-Transport Workshop
[PB84-232667] 01 p0107 N85-10715
Specification of a transport protocol for computer communications. Volume 1: Overview and Services. Volume 2: Class 2 protocol. Volume 3: Class 4 protocol
[PB84-222650] 06 p0848 N85-15360
Specification of a transport protocol for computer communications. Volume 4: Service specifications. Volume 5: Guidance for the implementor. Volume 6: Guidance for implementation selection
[PB84-222668] 06 p0848 N85-15385
Specification of a transport protocol for computer communications. Volume 7: Testing OSI protocols, a compendium of papers. Volume 8: User's guide to the testing system for implementations of the ICST transport protocol. Volume 9: A test suite for implementations of the ICST transport protocol. Volume 10: Specification of a remote scenario interpreter for implementations of the ICST transport protocol
[PB84-222676] 06 p0848 N85-15386
Stuttgart Interconnection Network Project from PIX to NICS
[NASA-TM-77602] 06 p0870 N85-15528
Some experiences of testing protocol implementations — open systems interconnection
[NPL-DITC-48/84] 06 p1204 N85-17574
Interim protocol for the automated analysis of semivolatile organic compounds by Gas Chromatography/Fourier Transfer Infrared (GC/FT-IR) spectrometry
[PB85-115186] 11 p1595 N85-20035
Multicomputer communication system
[NASA-CASE-NPO-15433-1] 12 p1822 N85-21428
Evaluation of Ada (trademark) as a communications programming language. Volume 2: Communications protocols application
[AD-A152315] 16 p2848 N85-27560
Evaluation of Ada (trademark) as a communications programming language. Volume 3: Trusted software application
[AD-A152316] 16 p2848 N85-27561
A study of topologies and protocols for fiber optic local area network
[NASA-CR-175771] 16 p2864 N85-27669
A secure high-speed transaction protocol
[CWI-CS-R8417] 17 p3009 N85-29805
Performance measurement of OSI (Open System Interconnection) class 4 transport implementations
[PB85-177657] 18 p3161 N85-29582
Implementation assessment of the OSI network service. The test definition language
[NPL-DITC-52/84] 20 p3514 N85-31849
Satellite links in the ISO architecture: Models and performance evaluation
[ENST-84E017] 22 p3756 N85-33284
Petcom: A software instrument for the analysis of Petri networks, oriented towards communication protocols
[FUB-50-1983] 22 p3756 N85-33286

PROTON BEAMS
Accelerator technology program
[DE84-015052] 01 p0118 N85-10806
LAMPF transition-region mechanical fabrication
[DE84-017078] 04 p0562 N85-13577
Tune shifts for coasting beams crossing at small angles
[DE84-017174] 04 p0562 N85-13579
Performing (p vector, Jc)n), (d vector, n) and (n vector, n) measurements with a rotating magnet beam swinger
[DE84-017003] 04 p0562 N85-13582
Accelerator Technology Program
[DE84-017083] 04 p0563 N85-13586
A proton laser accelerator by means of the inverse free electron laser mechanism
[DE85-000231] 06 p0813 N85-15163
Measurement of proton autoneutralization potential
[DE85-001752] 06 p0865 N85-15501
Study in spurious sensitivity of electronics in space
[AD-A148386] 08 p1158 N85-17305
Hydrodynamic response of a radiating Al plasma excited by a proton beam
[AD-A148904] 10 p1558 N85-19824
Review of polarized proton beam techniques and a report on the workshop on polarized beams
[DE85-004390] 12 p1930 N85-22127
Distortion functions
[DE85-007511] 16 p2862 N85-27655
Slow extraction of LAMPF 2
[DE85-010744] 19 p3356 N85-30805
Transverse emittance of a 2.0-MeV RFQ beam with high brightness
[DE85-012718] 22 p3837 N85-33758
Nuclear physics in the 10 to 300 MeV energy range using a pulsed white neutron source
[DE85-003713] 22 p3839 N85-33775
Acceleration of polarized H(-) in the BNL 200 MeV linac
[DE85-011836] 22 p3840 N85-33777
Commissioning the polarized beam in the AGS
[DE85-010058] 22 p3841 N85-33788
On gamma and neutrino radiation from Cyg X-3
[OG-2.1-7] 22 p3863 N85-33924
Injection of energetic particles following the gamma-ray flares on June 7, 1980, as observed on Helios 1
[SH-1.3-9] 23 p3993 N85-34756
Major facility overhauls at LAMPF
[DE85-012724] 24 p4158 N85-35765
Los Alamos high-current proton storage ring
[DE85-012664] 24 p4158 N85-35779
Hadrone registration in emulsion chamber with carbon block
[HE-3.7-3] 24 p4186 N85-35982
Intensities of high-energy cosmic rays at Mount Kanbala
[HE-3.7-5] 24 p4186 N85-35984
Muon and neutrino fluxes
[HE-6.2-18] 24 p4213 N85-36154
Acoustic detection of air shower cores
[HE-7.1-4] 24 p4213 N85-36158

PROTON BELTS
Boundary of modulation diffusion and stochastic instability of high energy protons in inner radiation belt
15 p2482 N85-25316

PROTON DENSITY (CONCENTRATION)
NT MAGNETOSPHERIC PROTON DENSITY
On the P1 data from GMS-SEM
12 p1894 N85-21690
Properties of the reflected beams from the Earth's bow shock: A simple model
[IFSI-84-14] 20 p3549 N85-32088
Fluctuations of development maximum depth and nuclear composition of primary cosmic radiation
[OG-5.1-13] 22 p3862 N85-34054

PROTON ENERGY
A compact time-of-flight energy analyzer of high resolution — for Tokamaks
[REPT-84-154] 09 p1324 N85-18318
An operational test of a time-of-flight analyzer at the ASDEX Tokamak
[REPT-84-155] 09 p1324 N85-18319
Protons with energies above 30 KeV in Earth's radiation belt at low altitudes during magnetically quiet time close to geomagnetic equator 13 p1980 N85-22423
Properties of the reflected beams from the Earth's bow shock: A simple model
[IFSI-84-14] 20 p3549 N85-32088
Solar modulation and interplanetary gradients of the galactic electron flux, 1977 - 1984
[PAPER-SH-4.7-4] 21 p3716 N85-33059

PROTON FLUX DENSITY
An atlas of polar cap energetic particle observations. Volume 2: NOAA-6, 8 July 1979 to 10 May 1983
[PB85-109072] 12 p1891 N85-21666
Boundary of modulation diffusion and stochastic instability of high energy protons in inner radiation belt
15 p2482 N85-25316
Search for proton decay
[DE85-008283] 19 p3353 N85-30786
Study of proton and neutron activation of metal samples in low Earth orbit
[NASA-CR-171596] 21 p3558 N85-32130
Latitude variation of recurrent fluxes in the outer solar system
[SH-4.1-13] 21 p3715 N85-33054
Further observations of protons resulting from the decay of neutrons ejected by solar flares
[SH-1.4-2] 23 p3994 N85-34763
Latitude variation of recurrent fluxes in the outer solar system
[SH-4.1-13] 23 p4006 N85-34836

PROTON IRRADIATION
Investigation of the degradation of GaAs photovoltaic cells by proton and electron irradiation
13 p2008 N85-22587
Isotropic proton irradiation of GaAs solar cells
13 p2012 N85-22622
NMR imaging and spectroscopy of the mammalian central nervous system after heavy ion radiation
[DE85-004508] 14 p2366 N85-24696
Study of proton and neutron activation of metal samples in low Earth orbit
[NASA-CR-171596] 21 p3558 N85-32130

PROTON PRECIPITATION
Precipitation of protons with E sub p approximately 1 MeV near plasmopause 02 p0181 N85-11093
Electron and proton precipitation in magnetic substorms — auroral substorms
14 p2360 N85-24585

PROTON RESONANCE
Slow extraction of LAMPF 2
[DE85-010744] 19 p3356 N85-30805

PROTON SCATTERING
Stochastic cell model for hadronic multiparticle distributions
[DE84-016480] 04 p0562 N85-13578
Perturbative treatment of quasi-resonant proton neutralization at alkali-halide surfaces
[AD-A154143] 19 p3356 N85-30806
The propagation of solar flare particles in a turbulent coronal loop
[SH-1.1-3] 23 p3989 N85-34730
The neutron moderated detector and groundbased cosmic ray modulation studies
[SH-9.1-13] 23 p4052 N85-35128
Observation of nuclei with energies 8-30 MeV per nucleon in the Earth's magnetosphere at the altitudes 350 KM
[SH-10.1-5] 23 p4053 N85-35136
Some nuclear data needs in astrophysics
[DE85-012916] 24 p4168 N85-35842

PROTON TELESCOPES
U PARTICLE TELESCOPES

PROTON-PROTON REACTIONS
Spin physics at BNL
[DE85-006768] 20 p3529 N85-31955
Exotic events of p bar p-collider: Excited quark or excited color boson?
21 p3691 N85-32930
Secondary antiproton production in relativistic plasmas
[OG-6.1-4] 22 p3869 N85-34095
Small air showers and collider physics
[HE-4.1-9] 24 p4187 N85-35975
A standard source for high energy neutrino astronomy
[HE-5.3-15] 24 p4206 N85-36109
Relationship of sea level muon charge ratio to primary composition including nuclear target effects
[HE-5.4-10] 24 p4208 N85-36121

PROTONS
NT SOLAR PROTONS
Study of proton and neutron activation of metal samples in low Earth orbit
[NASA-CR-171183] 01 p0025 N85-10164
NMR (Nuclear Magnetic Resonance) of solid biopolymers
[AD-P003912] 01 p0032 N85-10198
Proton pumping in purple membrane, appendix 1
[DE84-014601] 01 p0118 N85-10811
Energy deposition in microvolumes of silicon from high energy proton reactions
[AD-A144713] 01 p0123 N85-10845

The search for proton decay: Introduction
[DE84-014349] 01 p0131 N85-10904

Bremsstrahlung from nuclear scattering at low energy near a resonance
[DE84-014852] 04 p0561 N85-13572

A proton laser accelerator by means of the inverse free electron laser mechanism
[DE85-000231] 06 p0813 N85-15163

Bunch coalescing in the main ring to form intense proton and antiproton bunches without RF counterphasing
[DE85-001364] 09 p1362 N85-18692

Stopping powers of solids for low-energy protons
[DE85-001123] 09 p1362 N85-18693

Solar radio bursts, proton events and geomagnetic activity
[AD-A149018] 10 p1571 N85-19906

Proton NMR and susceptibility measurements in TiCoH/sub x
[DE85-003309] 12 p1807 N85-21336

Effects of focusing on HRS focal-plane polarimeter measurements
[DE85-004627] 13 p2160 N85-23406

The keV electrons and 80 keV protons in the vicinity of the high latitude magnetosphere and at the bow shock 14 p2355 N85-24554

NMR imaging and spectroscopy of the mammalian central nervous system after heavy ion radiation
[DE85-004509] 14 p2386 N85-24696

Radio frequency quadrupole and alternating phase focusing methods used in proton linear accelerator technology in the USSR
[AD-A150830] 14 p2418 N85-24916

Radiation effects induced in pin photodiodes by 40- and 65-MeV protons
[NASA-CR-175676] 14 p2426 N85-24960

Spectral characteristics of protons at low and high altitudes during geomagnetic storm of 29 July 1977 16 p2719 N85-26786

Measurements of fluxes of high-energy protons and electrons by 2 oppositely oriented spectrometers aboard Cosmos-368 artificial Earth satellite 16 p2722 N85-26800

East Europe report: Science and technology
[JPRS-ESA-85-017] 17 p2945 N85-28177

Proton induced X-ray emission method, its application in analytics 17 p2945 N85-28178

Experiments with light ions at CERN super proton synchrotron
[DE85-007625] 17 p3031 N85-28744

Cluster production and entropy
[DE85-007626] 17 p3032 N85-28752

One- and two-electron transfer processes in ion-surface scattering
[AD-A154208] 19 p3353 N85-30782

Search for proton decay
[DE85-008283] 19 p3353 N85-30786

Perturbative treatment of quasi-resonant proton neutralization at alkali-halide surfaces
[AD-A154143] 19 p3356 N85-30806

Proton ring trapping in a magnetic mirror 20 p3534 N85-31980

Sulfate-reducing bacteria: Microbiology and physiology 21 p3659 N85-32732

Solar modulation and interplanetary gradients of the galactic electron flux, 1977 - 1984
[PAPER-SH-4.7-4] 21 p3716 N85-33059

K(-) hydrogen bound and continuum states in momentum space
[DE85-010429] 22 p3841 N85-33789

Absolute rigidity spectrum of protons and helium nuclei above 10 GV/c
[OG-4.1-1] 22 p3875 N85-34007

Results of a search for deuterium at 25-50 GC/c using a magnetic spectrometer
[OG-4.2-4] 22 p3878 N85-34024

Parametrized energy spectrum of cosmic-ray protons with kinetic energies down to 1 GeV
[OG-4.2-11] 22 p3878 N85-34025

Primary cosmic ray spectrum in the 10 to the 12th power - 10 to the 16th power eV energy range from the NUSEX experiment
[OG-5.1-5] 22 p3881 N85-34047

Composition of primary cosmic rays at energies 10(15) to approximately 10(16) eV
[OG-5.2-4] 22 p3883 N85-34061

Electron and muon parameters of EAS and the composition of primary cosmic rays in 10(15) to approximately 10(16) eV
[OG-5.2-12] 22 p3884 N85-34068

Anisotropy of cosmic rays above 10(14) eV
[OG-5.4-11] 22 p3887 N85-34086

A model for the proton spectrum and cosmic ray anisotropy
[OG-5.4-12] 22 p3887 N85-34089

Interpretation of cosmic-ray anisotropy below 10(14) eV
[OG-5.4-13] 22 p3887 N85-34090

Two classes of solar energetic particle events associated with impulsive and long duration soft X-ray flares
[SH-1.2-12] 23 p3992 N85-34747

Solar flare gamma-ray line spectroscopy
[SH-2.1-14] 23 p3999 N85-34795

The central engine of quasars and AGNs: A relativistic proton radiative shock
[OG-8.1-7] 23 p4018 N85-34897

Pulsars as cosmic ray particle accelerators: Proton orbits
[OG-8.2-21] 23 p4021 N85-34917

Pulsars as cosmic ray accelerators: Energy development of protons
[OG-8.2-22] 23 p4021 N85-34918

Detection of 10 (1) GeV cosmic neutrinos with a space station
[OG-9.4-10] 23 p4030 N85-34977

Solar modulation and interplanetary gradients of the galactic electrons flux, 1977 - 1984
[SH-4.7-4] 23 p4040 N85-35049

Proton albedo spectrum observation in low latitude region at Hyderabad, India
[SH-6.1-8] 23 p4045 N85-35082

Calculation of heavy-ion tracks in liquid water
[DE85-012101] 24 p4149 N85-35725

Studies of relativistic heavy ion collisions
[DE85-014686] 24 p4152 N85-35745

Proton-air and proton-proton cross sections from air shower data
[HE-1.1-1] 24 p4170 N85-35849

Proton-air inelastic cross section at S(1/2) = 30 TeV
[HE-1.1-2] 24 p4170 N85-35850

Determination of the cross section of the proton, pion and neutron inelastic interaction with lead and carbon nuclei at 0.5 - 5.0 TeV energies (PION experiment)
[HE-1.1-5] 24 p4170 N85-35853

P(P bar)P elastic scattering and cosmic ray data
[HE-1.1-6] 24 p4170 N85-35854

The method for the study of the inelastic cross-section for high energy protons by means of shower arrays with the large calorimetric area
[HE-1.1-11] 24 p4171 N85-35858

A test of the Feynman scaling in the fragmentation region
[HE-1.2-9] 24 p4172 N85-35867

Nucleon-nucleus interactions from JACEE 24 p4173 N85-35869

Determination of primary energy in nucleus-nucleus collisions and the high P(sub)T tail of alpha-particles 24 p4173 N85-35875

Ringlike inelastic events in cosmic rays and accelerators 24 p4175 N85-35887

On the halo events observed by Mount Fuji and Mount Kanbala Emulsion Chamber Experiments
[HE-3.4-9] 24 p4182 N85-35937

Particle interactions at energies over 1000 TeV inferred from gamma-families observed at Mount Fuji
[HE-3.5-1] 24 p4183 N85-35940

Giant mini-clusters as possible origin of halo phenomena observed in super-families
[HE-3.5-4] 24 p4183 N85-35943

The electromagnetic component of albedo from superhigh energy cascades in dense media
[HE-3.5-11] 24 p4184 N85-35948

Peculiarities of gamma-quanta distribution at 20 TeV energy
[HE-3.7-10] 24 p4186 N85-35967

Electrons, muons and hadrons in extensive air showers and how do they depend on nuclear interaction model, part 2 24 p4187 N85-35969

Analysis of the hadron component in E.A.S. 24 p4187 N85-35971

Small air showers and collider physics
[HE-4.1-9] 24 p4187 N85-35975

Dependence of the average spatial and energy characteristics of the hadron-lepton cascade on the strong interaction parameters at superhigh energies 24 p4188 N85-35977

Preliminary results on underground muon bundles observed in the Frejus proton-decay detector
[HE-5.1-1] 24 p4200 N85-36067

Neutrino astronomy and the atmospheric background
[HE-5.3-17] 24 p4207 N85-36111

Multiple muons of conventional and exotic origin in DUMAND
[HE-5.4-4] 24 p4207 N85-36117

An experiment to detect gut monopoles
[HE-6.1-7] 24 p4210 N85-36133

Data acquisition system for phase-2 KGF proton decay experiment
[HE-6.2-4] 24 p4211 N85-36140

PROTOPLANETS
Tidal disruption and the origin of the Moon 04 p0586 N85-13739

A numerical investigation of planetesimal collision trajectories with a Moon accumulating in Earth orbit 04 p0586 N85-13740

Origin of the Moon 04 p0587 N85-13745

Geochemical evidence for the formation of the Moon by impact induced fission of the proto-Earth 04 p0587 N85-13747

Lunar origin: role of giant impacts 04 p0587 N85-13749

Models of angular momentum input to a circumterrestrial swarm from encounters with heliocentric planetesimals 04 p0587 N85-13750

Capture of planetesimals into a circumterrestrial swarm 04 p0588 N85-13751

The lunar angular momentum problem 04 p0588 N85-13752

A circumterrestrial compositional filter 04 p0588 N85-13753

Mechanical models of close approaches and collisions of large protoplanets 04 p0588 N85-13756

Lunar origin: Role of giant impacts 13 p2179 N85-23519

A circum-terrestrial compositional filter 13 p2179 N85-23520

Models of angular momentum input to a circum-terrestrial swarm from encounters with heliocentric planetesimals 13 p2179 N85-23521

Capture of planetesimals into a circumterrestrial swarm 13 p2179 N85-23522

Orbital resonances and planetary accretion in the solar nebula 13 p2179 N85-23523

Accumulation of the terrestrial planets 13 p2179 N85-23524

Evolution of grains in a turbulent solar nebula 13 p2179 N85-23525

The Formation of preplanetary disks from the collapse of rotating molecular cloud cores 13 p2180 N85-23526

The formation of the terrestrial planets from lunar sized planetesimals 15 p2678 N85-26533

Statistical theory of planet growth 15 p2678 N85-26534

Asteroid compositional rings: Clues to the compositions of primordial planetesimals in the middle solar system 15 p2678 N85-26537

Implications for the Earth of the early dynamical environment 21 p3719 N85-33079

Late-stage planetesimals: How big? 22 p3852 N85-33857

An impact-induced terrestrial atmosphere and iron-water reactions during accretion of the Earth 22 p3854 N85-33864

Study of the parameters affecting the collapse of a rotating protostellar cloud 24 p4168 N85-35837

PROTOPLASTS
Plant cell cultures in biological space experiments 05 p0690 N85-14434

Daylily as a system to study effects of space flight on plant development 15 p2607 N85-26068

PROTOSTARS
NT T TAURI STARS
Star Formation Workshop
[ROE-CR-13] 03 p0441 N85-12809

Compact infrared sources: Protostars before IRAS 03 p0442 N85-12812

Open cluster formation — stellar evolution 03 p0442 N85-12815

Numerical models of the spectral appearance of protostellar envelopes 03 p0442 N85-12816

Spherical accretion onto a protostellar core 03 p0442 N85-12817

Future theoretical needs in studies of star formation 03 p0444 N85-12829

Dynamic thermal episodes in the protosolar nebula: Development of models from observations on CAI's 06 p0687 N85-15633

The relevance of QUASAT to the star formation problem 07 p1058 N85-16718

PROTOTYPES
SAGA: A project to automate the management of software production systems
[NASA-CR-174017] 01 p0103 N85-10685

Performance of a large area flash chamber prototype
[NOTA-INTERNA-807] 02 p0201 N85-11338

Use of prototyping for man-machine interface requirements definition on the AWDS (Automated Weather Distribution System) program
[AD-A146033] 03 p0396 N85-12526

Preliminary evaluation of RCA C83036E prototype photomultiplier
[DE84-016894] 04 p0496 N85-13165

Prototype concept design for US Army type 3A Air Traffic Control Tower (ATCT)
[AD-A148840] 09 p1284 N85-19070
A preliminary assessment of environmental noise from large Wind Energy Conversion Systems (WECS) based on experiences from Swedish prototypes
[FFA-TN-1984-48] 09 p1379 N85-19668
Improved Y-11 general-purpose transport designated Y-12
13 p1972 N85-22385
High reliability mechanical-hydraulic converter
14 p2268 N85-24055
Automated, robotized forge-press systems viewed
14 p2284 N85-24153
Solid state compressor
[AD-A150790] 14 p2311 N85-24302
The development of a programming support system for rapid prototyping. Tasks 2 and 3
[AD-A151549] 15 p2629 N85-26202
The design and implementation of an object-oriented, production-rule interpreter
[AD-A154769] 21 p3671 N85-32803
Prototyping with data dictionaries for requirements analysis
[AD-A156309] 24 p4139 N85-35654

PROTOZOA
Late Quaternary deep-water paleoceanography of the eastern equatorial Indian Ocean: Evidence from Bethnic foraminifers, carbonate dissolution, and stable isotopes
08 p1182 N85-17446

PROVING
NT THEOREM PROVING
Crewstation design and validation
06 p0752 N85-14822
Verification of a model of the Eastern Scheldt
[RAND/R-3106-NETH] 09 p1354 N85-18518
Perspective on demonstrations of compliance for high-level waste disposal
[DE85-000989] 09 p1383 N85-18698
Prime Computer, Incorporated, PRIME 750, BASICV revision 19.4
[PB85-108074] 11 p1699 N85-20683
Micro focus Cifer 2887 high performance level 2 COBOL; V2.5
[PB85-108959] 11 p1703 N85-20714
Micro focus Cifer 2887 compact level 2 COBOL; V2.5
[PB85-108967] 11 p1703 N85-20715
A note on validity generalization procedures
[AD-A150085] 12 p1924 N85-22085
Validation summary report, Burroughs Corporation, B20 FORTRAN release 4.0
[PB84-227792] 13 p2145 N85-23316
Get Away Special (GAS) thermal design summary
[X-732 83-8] 15 p2475 N85-25278
Peer Review of a Formal Verification/Design Proof Methodology
[NASA-CP-2377] 17 p3010 N85-29609
Ada validation summary report. ALS AdaVAX version 1.1 VAX-11/780 using VAX/VMS release 3.6
[AD-A153684] 18 p3162 N85-29588
Ada (trademark) compiler validation summary report. Honeywell Information systems GCOS6 Ada version 1.1
[AD-A153746] 18 p3162 N85-29590
Ada compiler validation summary report, University of Karlsruhe-GMD/German MOD Siemens - BS 2000 version 7.30
[AD-A153747] 18 p3163 N85-29591
Ada (trademark) compiler validation summary report: ALSYS ALSYCOMP-0001
[AD-A153760] 18 p3163 N85-29592
A variable-complexity norm maximization problem
[AD-A153514] 18 p3169 N85-29634
Instrument Systems Analysis and Verification Facility (ISAVF) users guide
[NASA-TM-86226] 19 p3223 N85-29982

PROVISIONING
Food acquisition: Food ingredients, raw materials and supply
14 p2393 N85-24737

PROXIMITY
Focal plane array optical proximity sensor
[NASA-CASE-NPO-15155-1] 12 p1932 N85-22139
Design of an optical proximity sensor using multiple cones of light for measuring surface shape --- application to a robot manipulator
[AD-A150050] 12 p1934 N85-22152

PROXIMITY EFFECT (ELECTRICITY)
Outlook for realization of proximity effect and Josephson direct current in helium-2
13 p2074 N85-22966

PSEUDOMONAS
Structural-functional changes in bacterial cells under spaceflight conditions
16 p2724 N85-26812
Genetics in methylotrophic bacteria
[DE85-011460] 19 p3327 N85-30615

PSEUDOPOTENTIALS
Pseudopotentials and total energy calculations: Applications to crystal stability, vibrational properties, phase transformations, and surface structures
[DE85-007657] 18 p3194 N85-29810

PSEUDORANDOM SEQUENCES
Precise bearing support dithering
[AD-D011470] 10 p1493 N85-19428
Efficient parallel pseudo-random number generation
[AD-A152235] 16 p2855 N85-27606
An algorithm for the generation of primitive polynomials
[FUB-17-1984] 22 p3831 N85-33730

PSYCHOACOUSTICS
Aircraft noise effects: An interdisciplinary study of the effect of aircraft noise on man. Part 2: Appendix
[NASA-TM-75818] 10 p1527 N85-19630
Several specific and nonspecific responses of the human and animal body to ship noise
[NASA-TM-77483] 15 p2615 N85-26116

PSYCHOLINGUISTICS
Speech analysis system for assessing pilots' working fitness
22 p3819 N85-33661

PSYCHOLOGICAL EFFECTS
NT ILLUSIONS
NT JET LAG
Psychological states (mood, affect or emotion) experienced by JASDF pilots through flying duties. 3: Flying conditions causing pilots psychological disturbance
01 p0090 N85-10606
The relationship between emotional tension scale and psychological uneasiness of JASDF pilots in flying situations
01 p0090 N85-10608
Influence of activation of ASFB-2 on human emotional status
08 p1194 N85-17522
Aircraft noise effects: An interdisciplinary study of the effects of aircraft noise on man. Part 1: Basic report
[NASA-TM-75819] 10 p1526 N85-19629
Aircraft noise effects: An interdisciplinary study of the effect of aircraft noise on man. Part 2: Appendix
[NASA-TM-75818] 10 p1527 N85-19630
Aircraft noise effects: An inter-disciplinary study of the effect of aircraft noise on man. Part 3: Supplementary analyses of the social-scientific portion of the study on aircraft noise conducted by the DFG
[NASA-TM-75802] 10 p1527 N85-19631
Observations of physiological and psychological effects of terrain following flight based on in-flight test experience
10 p1532 N85-19657
Psychological aspects of phenomenon of spatial synchronization of EEG potential
11 p1691 N85-20632
Effect of prolonged hunger during experimental hikes
11 p1692 N85-20637
Simulator sickness: Reaction to a transformed perceptual world. 6: Preliminary site surveys
11 p1694 N85-20653
Some individual differences in human response to infrasound
[UTIAS-282] 12 p1905 N85-21960
Sleep deprivation and exercise tolerance
[AD-A150628] 13 p2142 N85-23297
Mechanizing of handling operations in drop forging with hammers and presses (conducted ergonomical examinations)
[BMFT-FB-HA-84-051] 17 p3002 N85-28581
Investigation of biochemical and psychological parameters of air traffic controllers in prestart state before beginning to work
19 p3325 N85-30599
Problems of aviation and space medicine and psychology discussed at 14th Gagarin lectures
23 p3954 N85-34509

PSYCHOLOGICAL FACTORS
The effects of feedback and predictability of human judgment
[AD-A145744] 02 p0237 N85-11542
Psychological issues in online adaptive task allocation
05 p0704 N85-14516
Job and family stress as predictors of pilot health, job satisfaction and performance
[AD-A142176] 07 p1018 N85-18484
A study of the relationship between user attitudes and the success of the MAJCOM and AFRCE work information management system
[AD-A146956] 07 p1051 N85-19671
An investigation of the relationship between stressful life events and psychological, behavioral and physiological outcomes
[AD-A147754] 08 p1197 N85-17541
Probable cause: A decision making framework
[AD-A147842] 08 p1210 N85-17614
A theory of preference reversals
[AD-A147952] 08 p1218 N85-17681
Captain development training at US Air
09 p1275 N85-19012
Management training for cockpit crews at Piedmont
flight 09 p1276 N85-19013
Determination of functional mobility of human nervous system with the PNN-3 instrument
10 p1525 N85-19618
Research opportunities in human behavior and performance
[NASA-CR-175473] 10 p1529 N85-19640
Task influences in the analytic-intuitive approach to decision making
[AD-A149870] 12 p1950 N85-22250
Psychological and physiological basis of stereophonic effect
15 p2526 N85-25574
Psychological issues relevant to astronaut selection for long-duration space flight: A review of the literature
[AD-A154051] 19 p3330 N85-30627
Living aloft: Human requirements for extended spaceflight
[NASA-SP-483] 21 p3666 N85-32772

PSYCHOLOGICAL INDEXES
U PSYCHOLOGICAL TESTS

PSYCHOLOGICAL TESTS
Psychological testing on the computer
[R/PERS-618] 01 p0097 N85-10645
Conjunctive and disjunctive item response functions
[AD-A147815] 07 p1033 N85-18561
Cognitive asymmetry and occupation. Computer programmers, students, and bank personnel, part 1 and part 2
[AD-A147125] 08 p1197 N85-17540
Improved estimation procedures for item response functions
[AD-A147677] 08 p1215 N85-17648
Restructuring of the process of visual recognition as perception conditions alter
10 p1526 N85-19624
The effect of set size on color recognition
[AD-A150958] 14 p2391 N85-24726
Construction of a job-oriented test for the selection of air traffic controllers
[DFVLR-FB-84-51] 17 p3002 N85-28556
Equipercentile test equating: The effects of presmoothing and postsmoothing on the magnitude of sample-dependent errors
[AD-A154110] 19 p3347 N85-30746

PSYCHOLOGY
NT COGNITIVE PSYCHOLOGY
NT PSYCHOACOUSTICS
NT PSYCHOPHYSICS
Toward a computational neuropsychology of high-level vision
[AD-A145711] 02 p0236 N85-11540
European Scientific Notes, Number 38-9
[AD-A145663] 02 p0306 N85-11975
Evaluation of the National Library of Medicine's programs in the medical behavior sciences. Coverage of the Medical Behavioral Sciences (MBS) literature in monographic databases, study 5
[PB84-230531] 03 p0439 N85-12797
Evaluation of the National Library of Medicine's programs in the medical behavior sciences. Online searchers' reactions to database and vendor capabilities in the Medical Behavioral Sciences (MBS), study 4
[PB84-230523] 03 p0439 N85-12798
Evaluation of the National Library of Medicine's programs in the medical behavior sciences. Quality of indexing: The development and testing of a methodology comparing databases covering the Medical Behavioral Sciences (MBS) literature, study 3
[PB84-230515] 03 p0439 N85-12799
Evaluation of the National Library of Medicine's programs in the medical behavior sciences. Test retrievals in five major databases covering the Medical Behavioral Sciences (MBS) literature, study 2
[PB84-230507] 03 p0440 N85-12800
Evaluation of the National Library of Medicine's programs in the medical behavior sciences. Coverage, overlaps and gaps in bibliographic databases dealing with the Medical Behavioral Sciences (MBS) literature, study 1
[PB84-230499] 03 p0440 N85-12801
Evaluation of the National Library of Medicine's program in the medical behavior sciences. An analysis of the National Library of Medicine's (NLM) handling of Medical Behavioral Sciences (MBS) literature: Some research tests of methods for evaluating bibliographic databases, executive summary
[PB84-230481] 03 p0440 N85-12802
USSR report: Life sciences. Biomedical and behavioral sciences
[JPRS-UBB-84-015] 07 p1010 N85-18418
Ambiguity and uncertainty in probabilistic inference
[AD-A147378] 07 p1035 N85-18572
ONR (Office of Naval Research) Far East Scientific Bulletin, volume 9, number 3, July to September 1984
[AD-A147282] 08 p1202 N85-17930

Psychobiology and food perception
14 p2394 N85-24745
Review of the psychological issues relating to the effectiveness of structured programming
[AD-A154593] 21 p3665 N85-32766
The priming effect in task design research
[AD-A154589] 21 p3679 N85-32852
PSYCHOMETRICS
An investigation of the effect of correlated abilities on observed test characteristics
[AD-A144869] 01 p0113 N85-10765
Revised Uniform Summary of Surface Weather Observations (RUSSWO). Spangdahlem AB, Germany, parts A-F
[AD-A147166] 07 p1006 N85-16392
Improvement of workload estimation techniques in piloting tasks
[NASA-CR-174374] 10 p1531 N85-19646
Human cognition and intelligence: Towards an integrated theoretical perspective
[CSIR-SR-PERS-360] 13 p2143 N85-23300
Psychometric evaluation of head injury among fliers referred to the AF School of Aerospace Medicine
[AD-A151479] 15 p2617 N85-28129
Conceptualizing in assembly tasks
[AD-A155564] 21 p3665 N85-32770
PSYCHOMOTOR PERFORMANCE
Measuring workload differences between short-term memory and long-term memory scenarios in a simulated flight environment 05 p0703 N85-14513
Fitts' law? A test of the relationship between information load and movement precision 05 p0705 N85-14523
A production system model of capturing reactive moving targets 05 p0705 N85-14524
The representation of action plans in long term memory 05 p0709 N85-14545
Speech-action interrelationships in operational work
07 p1010 N85-16418
Random pattern tracking acceleration tolerance tester
[AD-D011404] 07 p1017 N85-16459
Determination of functional mobility of human nervous system with the PNN-3 instrument
10 p1525 N85-19618
Restructuring of the process of visual recognition as perception conditions alter 10 p1526 N85-19624
Multiple resources and brain laterality
[AD-A148912] 10 p1530 N85-19643
Performance Evaluation Tests for Environmental Research (PETER) evaluation of 112 measures
[AD-A152317] 17 p2999 N85-28543
Biofeedback and performance: An update
[AD-A153226] 17 p3001 N85-28553
The effects of prolonged feeding meal, ready-to-eat (MRE) operational rations
[AD-A154763] 21 p3666 N85-32773
Performance of rolling ball and isometric joystick on a 2-D target alignment task
[RSRE-MEMO-3695] 22 p3826 N85-33699
PSYCHOPHYSICS
NT PSYCHOACOUSTICS
Electrophysiological correlates of Vernier acuity in human visual cortex
[AD-A146533] 05 p0646 N85-15371
Vision algorithms and psychophysics
[AD-A151886] 15 p2620 N85-28142
PSYCHOPHYSIOLOGY
NT WORKLOADS (PSYCHOPHYSIOLOGY)
Effects of individual mnemonic characteristics on problem solving 07 p1010 N85-16419
Functional inter-hemisphere asymmetry in recognition of visual stimuli of various classes
08 p1193 N85-17517
Encephalographic correlates of autogenous change in human functional state 08 p1193 N85-17518
Influence of activation of ASFS-2 on human emotional status 08 p1194 N85-17522
Simulator sickness: Sensorimotor disturbances induced in flight simulators
[AD-P004334] 09 p1271 N85-17988
Success in learning occupation of chemical production technician as function of certain personality traits and development of psychophysiological functions
09 p1362 N85-18568
USSR report: Life sciences. Biomedical and behavioral sciences
[JPRS-UBB-85-011] 10 p1525 N85-19616
Electrosleep therapy advanced at medical institute
10 p1526 N85-19623
Methods of monitoring mental work efficiency, emotional activity 10 p1526 N85-19627
Role of mental work in human tolerance in total-body vibration 12 p1901 N85-21940
Psychophysiological studies. 1: Performance and physiological response in learning, short-term memory and discrimination tasks
[AD-A151018] 14 p2392 N85-24731
Psychophysiological nature of aircraft fear
19 p3323 N85-30587
USSR report: Space Biology and Aerospace Medicine, volume 19, no. 2, March - April 1985
[JPRS-USB-85-004] 22 p3820 N85-33667
Psychophysiological distinctions of organization and regulation of daily cyclograms of crew activities during long-term spacecraft 22 p3821 N85-33669
Operator's functional comfort zone when controlling moving object 22 p3821 N85-33670
PTM (MODULATION)
U PULSE TIME MODULATION
PUBLIC HEALTH
Health and environmental effects document for photovoltaic energy systems, 1983
[DE84-017179] 04 p0532 N85-13399
USSR report: Life sciences. Biomedical and behavioral sciences
[JPRS-UBB-84-015] 07 p1010 N85-16416
Mercury health effects update: Health issue assessment
[PB85-123925] 10 p1528 N85-19639
Hygienic standardization of electromagnetic fields of radar systems 14 p2387 N85-24703
Biological and human health effects of extremely low frequency electromagnetic fields. Post-1977 literature review
[AD-A152731] 17 p2999 N85-28539
Geothermal hydrogen and health in Rotorua, New Zealand
[DE85-901283] 19 p3301 N85-30467
Hydrodynamics and sanitation
[CT-579] 20 p3487 N85-31672
PUBLIC LAW
NT LEGAL LIABILITY
NT LIABILITIES
Civil law enforcement missions
06 p0751 N85-14812
The need for a dedicated public service helicopter design 06 p0753 N85-14828
PUBLIC RELATIONS
Community relations activities at Department of Defense sites
[AD-P004150] 09 p1349 N85-18486
NASA photography index
[NASA-TM-87457] 15 p2685 N85-26445
Origin, processing, and dissemination of scientific news, with examples from 20 research institutes
[JUEL-1940] 17 p3050 N85-28882
PUBLICATIONS
U DOCUMENTS
PUERTO RICO
Meteor wind results from Atlanta, USA, and Ramey, Puerto Rico 11 p1662 N85-20474
PULLEYS
Feasibility demonstration of a novel, flat-belt, continuously variable transmission or automotive and electric-hybrid vehicle application
[NASA-CR-174430] 10 p1569 N85-19894
PULMONARY CIRCULATION
Oxygen delivery during exercise: Limitations to maximum flow 05 p0688 N85-14424
Pulmonary blood flow and oxygenation of arterial blood in a healthy subject upon 7 days hypokinesia
07 p1014 N85-16439
Human lung fluid content during 7-day head-down tilt
12 p1902 N85-21941
Spirolit-2 instrument used to test pulmonary ventilation
12 p1903 N85-21950
Effect of 120-day antiorthostatic bedrest on gas exchange and pulmonary circulation in man
19 p3323 N85-30589
PULMONARY FUNCTIONS
Interaction between lung mechanics and gas exchange by low volume high frequency pulmonary ventilation in patients with respiratory failure
[AD-A146604] 06 p0846 N85-15372
Human lung fluid content during 7-day head-down tilt
12 p1902 N85-21941
PULMONARY LESIONS
Deposition in the human lung during respiration of small particles suspended in the air
[BLL-RISLEY-TR-5021-(9091.9F)]
03 p0400 N85-12549
PULSARS
Observations of the pulsating hydrogen: Deficient star BD+13 deg 3224, during 1980 - 1981
01 p0128 N85-10882
A search for low luminosity pulsars and its implications for the pulsar luminosity functions
02 p0296 N85-11919
Measurement of pulsar parallax by Very Long Baseline Interferometry 03 p0444 N85-12830
The parallax of pulsar 0950+08 and the local free electron density 06 p0679 N85-15584
The X-ray structure of the Crab Nebula
11 p1741 N85-20948
Search for millisecond rotational periods in some low-mass X-ray binaries observed by EXOSAT
11 p1741 N85-20949
The X-ray structure of the Crab Nebula
11 p1742 N85-20954
Recent results on the Crab Pulsar X-ray light curve
11 p1742 N85-20955
EXOSAT observations of the 35d intensity variations of Her X-1 — X ray binary source
11 p1742 N85-20956
Pulse phase spectroscopy of Her X-1 with EXOSAT — X ray binary source 11 p1743 N85-20957
Simultaneous EXOSAT and optical observations of the pulsing X-ray binary H2252-035 / AO Psc
11 p1743 N85-20958
The axisymmetric pulsar magnetosphere
12 p1955 N85-22279
Nonlinear waves in the magnetosphere of pulsars
12 p1955 N85-22281
About static and dynamic solutions of the aligned rotator model — pulsar magnetospheres
12 p1958 N85-22306
An analytic model for hydromagnetospheres — stellar winds; pulsars; cosmic jets 12 p1959 N85-22313
The luminosity distribution of pulsars
12 p1959 N85-22317
Discriminant analysis of pulsar groups in the diagram P versus P 12 p1960 N85-22319
Pulsars and interstellar medium
12 p1960 N85-22320
Optical pulsar in the Large Magellanic Cloud remnant 0540-69.3
[DE85-006707] 16 p2683 N85-27788
The radiation of the Vela pulsar
20 p3548 N85-32080
A model of pulsed radiation from the Crab pulsar
20 p3548 N85-32081
Comments on RS-17 X-ray telescope
22 p3731 N85-33132
On gamma and neutrino radiation from Cyg X-3
[OG-2.1-7] 22 p3863 N85-33924
500 TeV gamma rays from Hercules X-1
[OG-2.2-7] 22 p3865 N85-33933
A model for the UHE gamma-rays from Hercules X-1
[OG-2.2-8] 22 p3865 N85-33934
High-resolution spectroscopic observation of Vela X-1 in the hard X-ray energy range
[OG-2.2-10] 22 p3865 N85-33936
Experimental results on gamma-ray sources at E sub 0 = 10(13) - 10(14) eV
[OG-2.2-12] 22 p3865 N85-33937
Very high energy gamma rays from the Crab Nebula
[OG-2.3-3] 22 p3866 N85-33940
Microburst of TeV gamma rays from the Crab pulsar
[OG-2.3-4] 22 p3866 N85-33941
Secondary periodicities of microbursts of TeV gamma rays from the Crab pulsar
[OG-2.3-5] 22 p3866 N85-33942
Detection of gamma-ray lines from the direction of the Crab Nebula 22 p3866 N85-33943
Observation of hard X-rays from the Crab pulsar and A0535+26
[OG-2.3-7] 22 p3866 N85-33944
Gamma rays of 0.3 to 30 MeV from PSR 0531+21
[OG-2.3-8] 22 p3866 N85-33945
The 1000 GeV gamma ray emission from radio pulsars 22 p3867 N85-33946
Pulsed emission of TeV gamma rays from Vela pulsar
22 p3867 N85-33947
The 1000 GeV gamma rays from ms pulsars
[OG-2.3-12] 22 p3867 N85-33948
A search in the COS-B data base for correlated time variability in regions containing objects of interest
[OG-2.5-9] 22 p3869 N85-33964
The 4U 0115+63: Another energetic gamma ray binary pulsar
[OG-2.6-11] 22 p3870 N85-33973
On some problems of gamma-astronomy
[OG-2.7-15] 22 p3873 N85-33988
Cosmic rays in the 10(16) to 10(19) eV range from pulsars
[OG-5.4-3] 22 p3886 N85-34080
Scaling from Jupiter to pulsars and the acceleration of cosmic ray particles by pulsars, 3
[OG-8.2-3] 23 p4019 N85-34904
On magnetic pair production above fast pulsar polar caps
[OG-8.2-13] 23 p4020 N85-34909
Pulsars as cosmic ray particle accelerators: Proton orbits
[OG-8.2-21] 23 p4021 N85-34917
Pulsars as cosmic ray accelerators: Energy development of protons
[OG-8.2-22] 23 p4021 N85-34918

Pulsars as cosmic ray particle accelerators: Dynamics of electrons
[OG-6.2-23] 23 p4021 N85-34919
High energy radiation from neutron stars
[DE85-014353] 24 p4169 N85-35843
PULSATING FLOW
U UNSTEADY FLOW
PULSE AMPLITUDE
Beam pulse length determination by spectral analysis
[CSIR-NAC-83-05] 01 p0116 N85-10793
Slowly rotating pulsed radiation source
02 p0256 N85-11678
Gain instabilities in photomultipliers: How accurate are photon counting measurements?
08 p1251 N85-17903
Reception of signal with unknown amplitude and duration submerged in white noise 13 p2084 N85-23016
The latitudinal variation of geomagnetic pulsation amplitude and phase 14 p2370 N85-24646
An amplitude correlation and differencing method for the monitoring of flaws in repeat ultrasonic inspections
[AERE-R-11416] 15 p2571 N85-25854
Acoustooptic pulse-echo transducer system
[NASA-CR-175919] 17 p2951 N85-28224
Inherent angular tracking error in an amplitude comparison monopulse radar
[AD-A154212] 19 p3255 N85-30185
A modified Fresnel scattering model for the parameterization of Fresnel returns, part 2.3A
21 p3618 N85-32483
Behaviors of stress waves in a conical bar
23 p3904 N85-34182
Cosmic ray north-south anisotropy 1961 - 1983
[SH-4.2-6] 23 p4007 N85-34844
Study of the shower maximum depth by the method of detection of the EAS Cerenkov light pulse shape
[HE-4.4-15] 24 p4194 N85-36021
Analysis of Cerenkov pulses recorded simultaneously at two sites
[HE-4.4-16] 24 p4194 N85-36022
Microprocessor-based single particle calibration of scintillation counter
[HE-4.6-13] 24 p4196 N85-36049
Samarkand complex setup for investigation of cosmic ray variation in the energy range of 7 10 (9) - 10 (15) eV
[HE-4.6-14] 24 p4196 N85-36050
The structure of the shower disk observed at Mt. Norikura
[HE-4.7-1] 24 p4196 N85-36052
PULSE AMPLITUDE MODULATION
Investigation of characteristics of phased antenna array considering interaction between radiators and properties of power divider 06 p0790 N85-15051
PULSE CHARGING
Model that predicts pulse charged gas switching breakdown phenomena
[DE85-013119] 22 p3761 N85-33313
PULSE CODE MODULATION
Switched Capacitor (SC) filter and design centering of integrated circuits, part 1
[BMFT-FB-T-84-190-PT-1] 05 p0633 N85-14062
Pulse code modulation telemetry: Properties of various binary modulation types
[AD-A147214] 07 p0913 N85-15780
One-dimensional processing for adaptive image restoration
[AD-A148314] 10 p1557 N85-19815
A method and apparatus for operating on companded PCM voice data
[NASA-CASE-KSC-11285-1] 18 p3089 N85-29120
PULSE COMMUNICATION
A microcomputer aided measurement equipment for monitoring performance in digital radio relay systems
[FUB-4-1984] 01 p0101 N85-10666
Timing performance of phase-locked loops in optical pulse position modulation communication systems
[AD-A145403] 02 p0190 N85-11271
Designer on Aeroflot automated COMMO system development 08 p1067 N85-16765
Shuttle S-band communications technical concepts
08 p1099 N85-16948
Propagation Influences on Digital Transmission Systems: Problems and Solutions
[AGARD-CP-363] 10 p1469 N85-19269
Limits of the propagation medium with respect to digital signal transmission 10 p1469 N85-19270
Digital data communications over microwave radio channels 10 p1469 N85-19272
EHF air-to-air communications
10 p1469 N85-19273
Equatorial transionospheric propagation conditions affecting digital communications
10 p1470 N85-19275
Measurements of propagation at 900 MHz in an urban zone for establishing a digital radiomobile system
10 p1472 N85-19288
Theoretical study of a dynamic simulator of selective fading for digital, wireless beam microwave links
10 p1473 N85-19294
Integrated support of tactical operations by satellite communications 11 p1709 N85-20754
The study of certain aspects of probability with applications in communications theory
[AD-A149820] 12 p1829 N85-21476
Digital channel efficiency model
[AD-A150084] 12 p1829 N85-21479
Use of electronic coding-frequency meters to measure parameters of pulsed radio signals
13 p2076 N85-22984
Secure digital speech communication
[AD-D011572] 14 p2293 N85-24215
The performance of a new adaptive filter for digital communications
[AD-A151690] 15 p2543 N85-25702
Rational pulse-shaping filters for almost MSK-like modulation
[AD-A153065] 17 p2949 N85-28208
Measured noise performance of a new method of frequency hopping
[AD-A152679] 17 p2953 N85-28234
A method and apparatus for operating on companded PCM voice data
[NASA-CASE-KSC-11285-1] 18 p3089 N85-29120
Design of a jamming simulator for a binary communication system
[AD-A154617] 21 p3573 N85-32221
Optimum predistortion of digital signals for transmission over parallel channels 22 p3776 N85-33397
New directional couplers for multimode circular waveguides applied to intense pulsed microwave systems
[DE85-011753] 23 p3926 N85-34330
Joint services electronics program
[AD-A154748] 23 p3927 N85-34336
Necessary bandwidth and spectral properties of digital modulation
[PB85-185367] 24 p4068 N85-35340
PULSE COMPRESSION
Binary pulse compression techniques for MST radars
08 p1184 N85-17464
Rational pulse-shaping filters for almost MSK-like modulation
[AD-A153065] 17 p2949 N85-28208
An approach to digital level compression using the zero-crossing points of programme signals
[NHK-LABS-NOTE-308] 18 p3090 N85-29123
Huffman-coded pulse compression waveforms
[AD-A155322] 21 p3576 N85-32243
Repetitive pulse accelerator technology for light ion inertial confinement fusion
[DE85-012030] 23 p3982 N85-34693
PULSE DOPPLER RADAR
NT EARTH RESOURCES SHUTTLE IMAGING RADAR
NT MONOPULSE RADAR
Adaptive mutual interference suppression method
[AD-D011268] 05 p0626 N85-14024
Test signal generator for coherent air-to-ground radars
[AD-D011278] 05 p0626 N85-14025
Gain restoration after Doppler filtering
[AD-D011425] 08 p1154 N85-17287
A technique for rapid determination of probability of detection in pulse Doppler radars
[AD-D011426] 08 p1154 N85-17288
Development of the F-20 nose radome
[AD-P004374] 12 p1827 N85-21468
PULSE DURATION
Notes on NAC report NAC-83-05: Beam Pulse Length Determination by Spectral Analysis
[CSIR-NAC-83-06] 01 p0119 N85-10816
Estimating algorithmic error of digital recursive filters
12 p1839 N85-21543
Square-pulse generator 13 p2075 N85-22959
Use of electronic coding-frequency meters to measure parameters of pulsed radio signals
13 p2076 N85-22984
Flash radiography 14 p2317 N85-24316
Instrument for measuring dispersional distortions in optical fibers and cables 15 p2530 N85-25595
A sampling phasemeter design for pulsed continuous wave signals
[AD-A155237] 21 p3581 N85-32264
A modified Fresnel scattering model for the parameterization of Fresnel returns, part 2.3A
21 p3618 N85-32483
Establishment of steady-state power level in pulse-periodic excimer laser 21 p3685 N85-32896
Voyager 0.2-lbf thruster valve assembly short pulse test report
[NASA-CR-176121] 22 p3741 N85-33185
Method of designing digital band-pass filters with pulse response of finite duration 22 p3775 N85-33395
The 1000 GeV gamma ray emission from radio pulsars 22 p3867 N85-33946
The longitudinal thickness of air-shower fronts
[OG-9.5-1] 23 p4030 N85-34978
Sub-luminal pulses from cosmic ray air showers
[HE-4.7-13] 24 p4200 N85-36063
PULSE DURATION MODULATION
Formation of radio signals with low out-of-band radiation 07 p0950 N85-16018
Miniature high performance pulsed modulator apparatus
[AD-D011427] 08 p1158 N85-17310
PULSE FREQUENCY MODULATION
Method and means for providing frequency agile operation of MTI (Moving Target Indicator) radar
[AD-D011561] 12 p1823 N85-21436
Applicability of log-normal model to probabilistic description of quasi-pulse interference
13 p2084 N85-23014
PULSE GENERATORS
Resistance and inductance calculations for helical flux compression generators
[DE84-015088] 02 p0195 N85-11306
Optimization of ultrashort pulse generation mode of YAG laser 02 p0262 N85-11713
Power MOS fast switching techniques
[DE84-015046] 05 p0732 N85-14707
High-speed power devices with field control
06 p0794 N85-15073
Repetitive pulse generation with inductive energy storage: A new technology for defense
[DE84-017090] 06 p0805 N85-15122
Technical data on new engineering products
10 p1460 N85-19201
Investigation of the output parameters of the pulsed neutron generator NGI-5
[DE85-001823] 11 p1725 N85-20849
Power circuit utilizing self-excited Hall effect switch means
[AD-D011505] 12 p1832 N85-21496
Square-pulse generator 13 p2075 N85-22959
Accuracy of approximation of Bayes estimates in presence of noninformative parameters
13 p2084 N85-23015
Optically triggered transferred-electron device microwave burst and single pulse generators
[AD-D011614] 16 p2778 N85-27141
Generalization of the Child-Langmuir relation for 1-dimensional time-dependent diodes
[DE85-007366] 16 p2779 N85-27152
Sub-optimal control of nonlinear flexible space structures 20 p3414 N85-31190
Coordinated research program in pulsed power physics
[AD-A154629] 21 p3679 N85-32858
Operational window for a plasma erosion opening switch used for voltage multiplication on pulsed power generators
[AD-A155482] 21 p3707 N85-33020
Capacitance measuring device
[DE85-011643] 22 p3787 N85-33480
Series-counterpulse repetitive-pulse inductive storage circuit
[DE85-006438] 23 p3928 N85-34342
Photoconductive pulse power switches: A review
[DE85-014125] 24 p4091 N85-35360
Quality assurance considerations for the implementation of a pulsed power R and D project
[DE85-012357] 24 p4148 N85-35720
Beam intensity increases at the intense pulsed neutron source accelerator
[DE85-012377] 24 p4155 N85-35764
Power flow evaluations for HERMES 3
[DE85-013116] 24 p4156 N85-35769
PULSE HEATING
Optical monitoring of photo-acoustic pulse propagation in silicon wafers
[AD-A151333] 15 p2651 N85-28352
PULSE HEIGHT
U PULSE AMPLITUDE
PULSE MODULATION
NT PULSE AMPLITUDE MODULATION
NT PULSE CODE MODULATION
NT PULSE DURATION MODULATION
NT PULSE FREQUENCY MODULATION
NT PULSE POSITION MODULATION
NT PULSE TIME MODULATION
Spectrally matched modulation of radiation of injection laser in traveling-wave amplifier below 2 GHz
02 p0262 N85-11712
Study of lower ionosphere by pulse cross-modulation method 10 p1500 N85-19467
Autostochastic behavior of solid state ring laser with low frequency periodic loss modulation
11 p1717 N85-20805

Synthesis of digital nonrecursive band-elimination filters for moving-target selectors 12 p1640 N85-21545
Pulsewidth modulated speed control of brushless dc motors
[AD-A151986] 16 p2778 N85-27148
Effect of powerful pulsed low-energy ion streams on GaAs 21 p3682 N85-32977
Self Q-modulation and generation of short pulses in distributed-feedback lasers 21 p3687 N85-32907
Cosmic ray modulatin and merged interaction regions
[SH-4.1-11] 23 p4005 N85-34834
Propagation of the phase of solar modulation
[SH-4.1-12] 23 p4005 N85-34835
The 1973-1984 solar modulation of cosmic ray nuclei
[SH-4.1-16] 23 p4006 N85-34838
Cosmic ray modulation in a random anisotropic magnetic field
[SH-4.1-20] 23 p4006 N85-34839
Evidence for regions of negligible cosmic-ray modulation in the inner heliosphere (10 AU)
[SH-4.1-21] 23 p4006 N85-34840
Drift and observations in cosmic-ray modulation, 1
[SH-4.2-4] 23 p4007 N85-34842
Drift and observations in cosmic-ray modulation, 2
[SH-4.2-5] 23 p4007 N85-34843
Variations of the cosmic ray general component in Antarctica
[SH-4.4-17] 23 p4035 N85-35013

PULSE POSITION MODULATION
Timing performance of phase-locked loops in optical pulse position modulation communication systems
[AD-A145403] 02 p0190 N85-11271
Formation of radio signals with low out-of-band radiation 07 p0950 N85-16018
Detection and symbol synchronization for multiple-bit per photon optical communications 10 p1483 N85-19228
Phase locked loop synchronization for direct detection optical PPM communication systems
[NASA-CR-176026] 19 p3254 N85-30178

PULSE RADAR
NT EARTH RESOURCES SHUTTLE IMAGING RADAR
NT MONOPULSE RADAR
NT PULSE DOPPLER RADAR
Measurement of snow cover thickness by radar sounding 03 p0344 N85-12216
Reference oscillator stability effect on clutter cancellation in a radar system 07 p0938 N85-15946
Binary pulse compression techniques for MST radars 06 p1184 N85-17484
Partial reflection spaced antenna wind measurements 06 p1185 N85-17467
Multiple channel adaptive filtering using a fast orthogonalization network: An application to efficient pulsed Doppler radar processing
[AD-A147929] 08 p1211 N85-17619
Pulse heterodyne equipment for measurements of range and velocity of moving targets-pulse radar
[ESA-TT-845] 09 p1312 N85-18246
Low sidelobe phased array antenna system
[AD-D011558] 12 p1823 N85-21435
Method and means for providing frequency agile operation of MTI (Moving Target Indicator) radar
[AD-D011581] 12 p1823 N85-21436
Summator of radio pulse signals 12 p1839 N85-21539
Interference suppressor for radar MTI
[AD-D011606] 16 p2769 N85-27066
Poseidon altimeter: Study of the hyperfrequency section and specifications of the prototype components
[CNES-84/DRT/TIT/HY/T/145] 20 p3419 N85-31219
Solid state altimeter model: Simulation description; analysis of first results (narrow band filters, weighting) — satellite-borne instruments
[CNES-DRT/TIT/RL-160-T] 20 p3419 N85-31220
Millimetre wave pulse technology — satellite mapping
[ESA-CR(P)-2004] 20 p3478 N85-31611
Huffman-coded pulse compression waveforms
[AD-A155322] 21 p3576 N85-32243
Observations of frontal zone structures with a VHF Doppler radar and radiosondes, part 1.2A 21 p3616 N85-32469
Characteristics of digital range finder with stroboscopic discretization 22 p3762 N85-33319
Detection of signals from coherent pulsed radars with random variation in parameters of sounding signals from pulse to pulse against background of worst-case Gaussian noise 22 p3763 N85-33324
Signal space models for antenna arrays
[AD-A156063] 24 p4087 N85-35335

PULSE RATE
NT PULSE REPETITION RATE
Contribution to the study and realization of the CARTHAGE multiservice local network
[ENST-84E008] 05 p0716 N85-14595
Semiconductor submicrosecond power commutator switches 06 p0795 N85-15081
A study of mode-locked argon ion-dye laser systems 16 p2769 N85-27205

PULSE RECORDERS
U COUNTERS

PULSE REPETITION RATE
Multipurpose 5-MeV linear induction accelerator
[DE84-014523] 02 p0278 N85-11508
Adaptive mutual interference suppression method
[AD-D011268] 05 p0628 N85-14024
Pulse transformer package for impedance matching a laser diode to a transmission line
[AD-D011499] 12 p1855 N85-21632
Repetitive energy transfers from an inductive energy store 13 p2062 N85-22881
Square-pulse generator 13 p2075 N85-22959

PULSE TIME MODULATION
NT PULSE DURATION MODULATION
NT PULSE POSITION MODULATION
Mg 2 emission of Pop. 2 long-period Cepheids 11 p1754 N85-21032

PULSE WIDTH
U PULSE DURATION

PULSE WIDTH MODULATION
U PULSE DURATION MODULATION

PULSED JET ENGINES
Investigation of a pulsed electrothermal thruster system
[NASA-CR-174766] 02 p0169 N85-11132

PULSED LASERS
NT Q SWITCHED LASERS
NT ULTRASHORT PULSED LASERS
NT ULTRAVIOLET LASERS
High repetition rate nitrogen ion laser 02 p0201 N85-11340
Diagnostics of ionization in air produced by infrared radiation from A pulse CO2 laser
[AD-A145376] 02 p0201 N85-11342
Time variability of directionality properties of pulsed EB-EDL (Electron Beam-Electric Discharge Laser) N2-CO2 lasers
[AD-A145546] 02 p0202 N85-11344
Studies of laser melting and rapid solidification using amorphous silicon
[DE84-014737] 02 p0202 N85-11345
Using two-beam interference method for measuring wavelength of tunable pulse lasers 02 p0272 N85-11772
Pulsed neodymium glass laser system for investigating nonlinear optical phenomena in gases 03 p0348 N85-12241
Laser balancing system for high material removal rates
[NASA-CR-174731] 03 p0365 N85-12341
Simulation of the interaction of single-pulsed optical lasers with targets in a vacuum
[DE84-016476] 05 p0640 N85-14107
Pulsed electric discharge laser technology. Electron beam window foil material
[AD-A146420] 06 p0813 N85-15162
Time-resolved studies of ultrarapid solidification of highly undercooled molten silicon formed by pulsed laser irradiation
[DE84-016664] 06 p0813 N85-15164
Self-generated magnetic fields and thermal flux inhibition
[AD-A147405] 07 p0971 N85-16166
Intense excitation source of blue-green laser
[AD-A147450] 07 p0971 N85-16166
Pulsed electric discharge laser technology. Electron beam window foil material
[AD-A147486] 07 p0972 N85-16171
Simulation of repetitively-pulsed laser irradiation of graphite-epoxy composite
[AD-A148698] 09 p1325 N85-18329
Electron-hole plasma formation in semiconductors due to the absorption of pulsed CO2 laser light
[DE85-001559] 09 p1392 N85-18757
Determination of vapor phase content when metals are struck by laser radiation pulses of various densities 10 p1445 N85-19106
Temperature variation of laser mirror stability criteria 10 p1445 N85-19108
Excitation modes and parameters of stress waves in metal exposed to single laser pulses 10 p1446 N85-19109
Picosecond laser pulse interactions with metallic and semiconductor surfaces
[AD-A149112] 10 p1490 N85-19405
Pulsed excimer laser processing for cost-effective solar cells
[NASA-CR-174429] 10 p1509 N85-19517
A method for determining in situ the absorption coefficient of particulate media using pulsed laser technique
[AD-D011548] 12 p1799 N85-21281
Mathematical modeling of two-frequency laser sounding of scattering media 13 p2089 N85-23045
Time-resolved ellipsometry and reflectivity measurements of the optical properties of silicon during pulsed excimer laser irradiation
[DE85-005091] 13 p2096 N85-23079
Activation of Si-N modes in silicon by pulsed laser annealing
[DE85-009988] 13 p2097 N85-23082
Time resolved X-ray studies during pulsed laser irradiation of Ge
[DE85-005283] 13 p2097 N85-23083
Time-resolved reflectivity measurement of extrinsic silicon during pulsed laser irradiation
[AD-A150350] 13 p2159 N85-23403
Laser Welding, Cutting and Surface Treatment 14 p2308 N85-24278
The measurement of laser beam parameters 14 p2308 N85-24283
Laser welding in the manufacture of heart pacemakers 14 p2308 N85-24288
Excimer laser annealing to fabricate low cost solar cells
[NASA-CR-175702] 14 p2351 N85-24529
Elementary processes of electronically excited particles. Part 5: Deactivation of CHF (A1a' (O, V'2, O) after excitation by a pulsed dye laser
[MPIS-13/1984] 14 p2420 N85-24930
An experimental technique for the study of velocity profiles in a laminar jet using a pulsed nitrogen laser
[AD-A151496] 15 p2556 N85-25771
Laser induced damage of zinc sulphide
[BAE-BT-13363] 15 p2562 N85-25803
Electric discharge excitation and energy source integration
[AD-A151502] 15 p2562 N85-25806
Characteristics of laser emission discharge created by pulsed CO2-laser 15 p2643 N85-26305
Theoretical investigation of lasing in 4.3 micron region in CO2 laser 15 p2643 N85-26306
Optical monitoring of photo-acoustic pulse propagation in silicon wafers
[AD-A151333] 15 p2651 N85-26352
Raman studies of surface temperature in laser-heated semiconductors
[AD-A151377] 15 p2659 N85-26412
Optogalvanic measurement of even parity Rydberg levels in krypton gas
[AD-A152113] 16 p2745 N85-26943
A study of mode-locked argon ion-dye laser systems 16 p2769 N85-27205
Surface modification of solids
[DE85-007543] 16 p2871 N85-27715
Quantum statistical theory of vibrational dynamics in a laser-driven admolecule-surface system
[AD-A152022] 16 p2872 N85-27719
X-ray crystallography of steel U8 after pulsed laser hardening
[BLL-BISI-22444-(9022.06)] 17 p2925 N85-28036
Obtaining amorphous coatings of FeW and Fe-Cr-P-B alloys using laser sputtering
[BLL-BISI-22493-(9022.06)] 17 p2927 N85-28057
Laser machining and some applications
[NHK-LABS-NOTE-307] 18 p3112 N85-29266
Quantum model of dephasing-enhanced laser desorption: Master equation approach
[AD-A153769] 18 p3112 N85-29269
The application of laser resonance saturation to the development of efficient short wavelength lasers
[AD-A153951] 18 p3113 N85-29270
A simple power meter for high energy pulsed lasers
[AD-D011661] 18 p3113 N85-29271
Definition of requirements for injection locking of pulsed UV lasers
[DE85-010126] 18 p3113 N85-29275
Dye laser traveling wave amplifier
[NASA-CR-175989] 19 p3275 N85-30308
Enhanced thermal coupling by a repetitively pulsed laser
[AD-A154435] 19 p3276 N85-30317
Spectral evolution of the pulse of a dual frequency dye laser
[CNES-83/168/T/CT/DRT/TIT/10] 20 p3461 N85-31497
Detection of excited states by laser-induced fluorescence
[AD-A155558] 21 p3592 N85-32328
Pulsed excimer laser processing for cost-effective solar cells 21 p3611 N85-32432
Excimer-laser generator of powerful UV picosecond pulses synchronized with picosecond pulses in visible and IR bands 21 p3686 N85-32903

Powerful XeCl excimer electric discharge laser with good temporal stability and fast response time
21 p3688 N85-32911
The moving thermoacoustic array: A theoretical feasibility study
[AD-A154510] 21 p3699 N85-32980
Sliding discharge in CO2 and excimer lasers
22 p3773 N85-33379
Pulsed lasers for filming color holographic film images
22 p3781 N85-33426
Metal vapor lasers and their applications
[ISL-CO-218/84] 22 p3791 N85-33488
The use of optical fibers in pulsed laser holography
[ISL-CO-226/84] 23 p3936 N85-34395
Theoretical and experimental analyses of the performance of two-color laser ranging systems
[NASA-CR-176159] 23 p3936 N85-34397
Ranging system which compares an object reflected component of a light beam to a reference component of the light beam
[NASA-CASE-NPO-15865-1] 23 p3973 N85-34629
Survey of mixing in metal/insulator systems
[DE85-011936] 23 p3985 N85-34714
ATA upgrade to 150 MeV
[DE85-013174] 24 p4098 N85-35404

PULSED RADIATION
NT ELECTROMAGNETIC PULSES
NT SYSTEM GENERATED ELECTROMAGNETIC PULSES
Slowly rotating pulsed radiation source
02 p0256 N85-11678
Transient optical nutation in CO2 laser
02 p0261 N85-11709
Efficiency of photoelectric conversion of short radiation pulses
03 p0348 N85-12240
Diffraction by the time-of-flight technique at pulsed neutron sources
[DE84-015839] 03 p0418 N85-12674
Developments of optical fast-gated imaging systems
[DE84-016170] 04 p0502 N85-13204
Pulsed irradiation of optimized, MBE grown, AlGaAs/GaAs radiation hardened photodiodes
[DE84-014984] 04 p0569 N85-13631
Pulsed photothermal radiometry for remote sensing of spectroscopic and physical properties of thin film
[AD-A149080] 10 p1435 N85-19041
Behavior degradation due to 1100-RAD pulsed radiation exposure (5.8:1 neutron/gamma ratio)
[AD-A149284] 11 p1689 N85-20621
Invariance of probability characteristics of detector to shape of optical pulse signals 13 p2090 N85-23048
Flash radiography 14 p2317 N85-24316
Calorimeter for measuring high-energy optical pulses
[PB85-160695] 15 p2561 N85-25799
Variations in intensity of secondary cosmic radiation observed on 10-11 August 1981
16 p2721 N85-26796
Technique for measuring surface diffusion by laser-beam-localized surface photochemistry
[DE85-007885] 16 p3113 N85-29273
A model of pulsed radiation from the Crab pulsar
20 p3548 N85-32081
Generation of single nanosecond high-contrast radiation pules (lambda=10.6 micrometers)
21 p3684 N85-32886
Laser radiation propagation in inertialess nonlinear medium 21 p3686 N85-32896
Optimal complex nonlinear processing of continuous and pulsed signals 22 p3763 N85-33323
Scientific Opportunities with Advanced Facilities for Neutron Scattering
[DE85-012113] 22 p3839 N85-33770
Observation of hard X-rays from the Crab pulsar and A0535+26
[OG-2.3-7] 22 p3866 N85-33944
Gamma rays of 0.3 to 30 MeV from PSR 0531+21
[OG-2.3-8] 22 p3866 N85-33945
The 1000 GeV gamma ray emission from radio pulsars 22 p3857 N85-33946
Pulsed emission of TeV gamma rays from Vela pulsar
22 p3857 N85-33947
Instrumentation for sensing moisture content of material using a transient thermal pulse
[NASA-CASE-NPO-15493-2] 23 p3933 N85-34373
Cosmic ray modulatin and merged interaction regions
[SH-4.1-11] 23 p4005 N85-34634
Study of the shower maximum depth by the method of detection of the EAS Cerenkov light pulse shape
[HE-4.4-15] 24 p4194 N85-36021
Analysis of Cerenkov pulses recorded simultaneously at two sites
[HE-4.4-16] 24 p4194 N85-36022
The experimental cascade curves of EAS at E sub 0 10(17) eV obtained by the method of detection of Cherenkov pulse shape
[HE-4.4-18] 24 p4194 N85-36024

PULSES
NT ELECTRIC PULSES
NT ELECTROMAGNETIC PULSES
NT GEOMAGNETIC PULSATIONS
NT PICOSECOND PULSES
NT PRESSURE PULSES
NT SYSTEM GENERATED ELECTROMAGNETIC PULSES
Regenerators of binary pulses for optical communication systems 04 p0485 N85-13099
Westinghouse programs in pulsed homopolar power supplies 05 p0806 N85-13652
Analysis of spin echo signals in multi-pulse experiment
06 p0792 N85-15065
Degenerate four-wave mixing lineshapes in sodium vapor under pulsed excitation
[AD-A148211] 08 p1222 N85-17698
Battery response to pulse loads: A mathematical model
[DE85-001149] 09 p1316 N85-18277
Study of the pulsations of the ZZ Ceti stars
09 p1414 N85-18923
A 10/sup 11/W high current pulse electron beam accelerator described 11 p1620 N85-20200
A stochastic-mechanical approach to acoustic pulse propagation in the deep ocean sound channel
[AD-A149598] 12 p1928 N85-22110
Surface forward scattering and reflection
[AD-A150115] 12 p1928 N85-22112
Strong iron accelerating by collisionless magnetosonic shock wave propagating perpendicular to a magnetic field
[IPPJ-709] 12 p1935 N85-22161
Domain of applicability of asymptotic description of radio pulse fields near critical frequency
13 p2073 N85-22949
Optimization of number of pulses in detection of fluctuating optical signals 13 p2081 N85-22993
Probability of detection of pulsed signals employing zero-gating interference suppression
13 p2085 N85-23021
Railgun conductor heating from multiple current pulses
[DE85-005333] 14 p2265 N85-24031
Pseudo bipolar nickel-cadmium batteries used as filter elements to pulsed current loads
[AD-A151192] 15 p2547 N85-25717
Studies in electron phenomena in MOS structures: The pulsed C-V method 15 p2659 N85-26407
Investigation of electron attachment and dissociation rates in C2F6/CH4 electric gas discharges
[AD-A151796] 16 p2662 N85-27649
Investigation on the application of the pulsed eddy current method of non-destructive testing using controlled signals (CS-technique)
[BLL-BISI-TRANS-22249-(9022.06)]
16 p3119 N85-29303
Design and testing of a pulsed current transformer
[AD-A154228] 19 p3259 N85-30208
Arctic acoustic tomography MIZEX 84
[AD-A154426] 19 p3320 N85-30560
Ultrasonic flowmetering with reflected pulses
[PB85-179865] 20 p3460 N85-31482
Amplitude stabilization of pulse signals
22 p3762 N85-33320
Comparative characteristics of optical multiposition pulse signals with intersymbol distortion
22 p3764 N85-33329
On gamma and neutrino radiation from Cyg X-3
[OG-2.1-7] 22 p3863 N85-33924
Multiple-stage integrating accelerometer
[DE85-006505] 23 p3935 N85-34368
Electronic imaging system and technique
[DE85-005740] 23 p3935 N85-34369
EML pulse ionization chamber systems for (222)Rn measurements
[DE85-012320] 23 p3970 N85-34610

PULTRUSION
Pultrusion process for fabrication of tethers (preliminary concepts) 11 p1646 N85-20371

PULVERIZING
U GRINDING (COMMINUTION)

PUMP IMPELLERS
Investigation of the HPFTP first stage impeller crack
[NASA-CR-171281] 07 p0977 N85-16208
Two-phase flow in centrifugal pumps
[BLL-CE-TRANS-8085-(9022.09)]
15 p2605 N85-26053
Optimum geometry of interblade passages in impellers of thermomolecular vacuum pump
16 p2764 N85-27058

PUMPS
NT CENTRIFUGAL PUMPS
NT FUEL PUMPS
NT ION PUMPS
NT JET PUMPS
NT MOLECULAR PUMPS
NT TURBINE PUMPS
NT VACUUM PUMPS
NT WINDPOWERED PUMPS
Photovoltaic pump systems 05 p0684 N85-14269
A study of wear characteristics due to pressure for hydraulic fixed displacement vane pumps
[AD-A148023] 06 p0814 N85-15169
Cavitation erosion resistant coatings for pumps
[PB85-120210/GAR] 09 p1300 N85-18167
Operational performance of the photovoltaic-powered grain mill and water pump at Tangaye, Burkina Faso (formerly Upper Volta)
[NASA-TM-86970] 13 p2128 N85-23243
Flat magnetohydrodynamic induction pump
17 p2939 N85-28145
Dependence of characteristics of centrifugal magnetohydrodynamic conduction pump on electrical conductance of end walls. Part 1: Experiment
17 p2939 N85-28146
Reciprocating magnetic refrigerator employing tandem porous matrices within a reciprocating displacer
[NASA-CASE-NPO-16257-1] 18 p3085 N85-29082
Fluidic angular velocity sensor
[NASA-CASE-NPO-16479-1-CU]
18 p3104 N85-29219
Remotely operable peristaltic pump
[NASA-CASE-MFS-28059-1] 18 p3116 N85-29288
Physiochemically controlled accur jet array system
[AD-D011658] 19 p3308 N85-30505
An analysis of the effects of active solar energy system control sensor degradation on system performance
[DE84-013023] 22 p3804 N85-33562
Combined cold compressor/ejector helium refrigerator
[DE85-006408] 23 p3925 N85-34326
Experimental lithium system
[DE85-013252] 24 p4084 N85-35382

PUNCHES
Experience with introduction of Finish perforation of precision parts for optical instruments
16 p2761 N85-27038

PURGING
Evacuate and backfill apparatus and method
[DE85-008018] 23 p3936 N85-34411

PURIFICATION
NT AIR PURIFICATION
Opportunities for space bioprocessing
02 p0150 N85-11018
Purification of biomaterials by phase partitioning
02 p0154 N85-11043
Evaluation of survival straws (pocket purifier)
[AD-A146240] 03 p0328 N85-12114
Development of a preprototype times wastewater recovery subsystem
[NASA-CR-171815] 03 p0388 N85-12480
Addendum: Development of a preprototype times wastewater recovery subsystem
[NASA-CR-171816] 03 p0388 N85-12481
Development of a preprototype times wastewater recovery subsystem: Appendices
[NASA-CR-171817] 03 p0388 N85-12482
Process for clarification of water
[DE85-007864] 17 p2923 N85-28023
Feasibility of melt casting strontium fluoride to produce high-density heat sources
[DE85-009429] 18 p3130 N85-29381
Plutonium metal preparation and purification at Los Alamos, 1984
[DE85-010732] 19 p3239 N85-30085
Flow cytometry of human embryonic kidney cells: A light scattering approach 20 p3503 N85-31778
New and revised methods of purifying mercuric iodide
[DE85-011684] 22 p3749 N85-33237
Method for removing oxide contamination from silicon carbide powders
[DE85-011648] 23 p3919 N85-34287

PURIFIERS
U PURIFICATION

PURITY
Chemistry Institute's advances in making extra-pure aluminum 10 p1443 N85-19093
Carbothermic production of silicon solar cells using high-purity starting materials 12 p1877 N85-21777
Low defect, high purity crystalline layers grown by selective deposition
[NASA-CASE-NPO-15813-1] 19 p3373 N85-30922
JPL in-house fluidized-bed reactor research
21 p3609 N85-32414
High-purity silicon crystal growth
21 p3612 N85-32444
Monosilane and disilane, 1984 report
[DE85-008776] 22 p3752 N85-33262
Method for preparing high purity vanadium
[DE85-008412] 23 p3913 N85-34242
An X-ray diffraction study of titanium oxidation
[NASA-CR-176283] 23 p3915 N85-34264

PURPOSES
Broadening the debate 07 p0914 N85-15785
PURSUIT TRACKING
Effects of repetitive, small-spot, incoherent light flashes on pursuit tracking performance
[AD-A144848] 01 p0095 N85-10837
Space interception guidance with uncertain factors 13 p2042 N85-22781
Simple-motion pursuit-evasion differential games in the plane
[CSIR-TWISK-336] 14 p2412 N85-24874
Stochastic pursuit-evasion differential games in the plane
[CSIR-TWISK-343] 14 p2412 N85-24875
Pursuit tracking performance and flash disruption: The effects of training the non-dominant eye on target reacquisition
[AD-A153404] 17 p2999 N85-28541
PUSHBROOM SENSOR MODES
Imaging Science Panel. Multispectral Imaging Science Working Group joint meeting with Information Science Panel: Introduction 02 p0213 N85-11406
Application of pushbroom altimetry from space using large space antennas 14 p2230 N85-23817
INPE's line imaging camera: Preliminary results
[INPE-3476-PRE/719] 16 p2767 N85-27194
Investigations of the accuracy of the Digital Photogrammetry System (DPS), a rigorous three-dimensional compilation process for pushbroom imagery
[MBB-UA-753/83-O] 16 p2874 N85-27734
PWM (MODULATION)
U PULSE DURATION MODULATION
PYCNOMETERS
Pycnometer shaker
[PB85-174985] 20 p3460 N85-31491
PYLONS
Nacelle/pylon/wing integration on a transport model with a natural laminar flow nacelle
[NASA-TP-2430] 19 p3213 N85-29924
PYRAMIDS
Halfspace representations of extrusions, solids of revolution and pyramids
[DE84-015005] 01 p0104 N85-10700
Beamwidth control in pyramidal horns
[R-NIAS-27] 13 p2053 N85-22853
PYRANOMETERS
United States participation in International Energy Agency Task IX, Subtask (C): Pyranometry. 1984 participation
[DE85-009615] 18 p3110 N85-29256
PYRAZINES
NT AZINES
NT METHYLENE BLUE
PYRENEES MOUNTAINS (EUROPE)
Deep structure beneath the Pyrenees 04 p0524 N85-13351
Deep structure and seismicity in the Catalonia-Pyrenees region 04 p0524 N85-13352
Measurement of water equivalent of mountain snow cover — ARGOS system 14 p2327 N85-24366
PYRENES
Study of the kinetics of hydrogenation using aged catalysts
[DE85-010427] 19 p3230 N85-30025
PYREX (TRADEMARK)
U BOROSILICATE GLASS
PYRIDINES
Development of new and improved polymer matrix resin systems, phase 1
[NASA-CR-166595] 01 p0017 N85-10104
Chemically modified electrodes and related solution chemistry
[DE84-017110] 05 p0614 N85-13924
Electrochemistry and electrochemical methodology in molten salts
[AD-A149613] 12 p1799 N85-21284
The effect of Xe underlayers on the surface enhanced Raman scattering of pyridine on cold silver
[AD-A150109] 12 p1801 N85-21294
Evaluation of the PSP resin as a precursor of carbon
[ONERA-RT-11/1784-M] 16 p2744 N85-26932
New polymers for composites: A summary of research on polyetynylpyridines
[NASA-CR-175886] 17 p2933 N85-28106
PYRIMIDINES
NT MITOCHONDRIA
PYRITES
Improved solid-state laser sources, volume 2
[DE85-000759] 09 p1325 N85-18330
PYROELECTRICITY
Development of a polymer pressure gage with temperature compensation 03 p0365 N85-12340
Recording of acoustic wave in gaseous medium with thin-film pyroelectric transducers 15 p2525 N85-25571
Applications of piezoelectric and pyroelectric thin films: Opportunities for Langmuir-Blodgett technology
[AD-A149230] 15 p2559 N85-26406
Piezoelectric and pyroelectric polymers 16 p2758 N85-27006
PYROGRAPHALLOY
U COMPOSITE MATERIALS
U PYROLYTIC GRAPHITE
U REFRACTORY MATERIALS
PYROHELIOMETERS
Active Cavity Radiometer (ACR) 23 p3901 N85-34163
PYROLYSIS
HMX combustion modification
[AD-A145071] 01 p0024 N85-10149
The pyrolysis toxic gas analysis of aircraft interior materials
[AD-A146285] 03 p0328 N85-12115
Boron-nitrogen polymers. 1: Mechanistic studies of borazine pyrolyses
[AD-A146470] 06 p0771 N85-14933
Laser-assisted solar cell metallization processing
[NASA-CR-174213] 08 p0813 N85-15160
JPL in-house fluidized-bed reactor research 06 p0832 N85-15291
Aerosol reactor for silicon processing 06 p0832 N85-15292
Mechanism of soot formation
[AD-A146817] 07 p0922 N85-15841
Silazane precursors to silicon nitride
[AD-A146791] 07 p0931 N85-15899
Disclinations in carbon-carbon composites
[AD-A148290] 08 p1119 N85-17052
Laser schlieren, shock tube studies of high temperature hydrocarbon pyrolysis rates
[DE85-003314] 11 p1636 N85-20303
Synthesis, static and reactive characterization of supported organometallics
[DE85-004285] 12 p1808 N85-21340
Low cost, sprayed CuInSe2 solar cell research
[DE85-003467] 12 p1881 N85-21799
Methods/materials matrix of ultimate disposal techniques for spilled hazardous materials
[PB85-116653] 12 p1885 N85-21839
Shock tube study of the fuel structure effects on the chemical kinetic mechanisms responsible for soot formation, part 2
[NASA-CR-174860] 15 p2504 N85-25444
Thermolysis of 4-methyl-4-(1-propenyl)malonyl peroxide: Mechanistic limits to chemiluminescence efficiency
[AD-A151567] 15 p2505 N85-25452
Studies of the combustion of model fuels with low hydrogen content (pyrolysis of polycyclic aromatics-detection of soot precursors)
[DE85-005422] 15 p2521 N85-25541
Evaluation of the PSP resin as a precursor of carbon
[ONERA-RT-11/1784-M] 16 p2744 N85-26932
Preparation of silicon carbide-silicon nitride fibers by the pyrolysis of polycarbosilazane precursors
[NASA-TM-86505] 17 p2933 N85-28107
Sol-gel processing of lead zirconate titanate films
[ATR-85(8343)-2] 18 p3073 N85-29010
Structure-property relationships in polymeric matrix materials
[AD-A153929] 18 p3080 N85-29050
Combustion characterization of coals for industrial applications
[DE85-010673] 19 p3228 N85-30014
Supercritical solvent extraction of lignite to form carbonaceous chars
[DE85-010159] 19 p3229 N85-30019
Spray pyrolysis as a synthetic tool
[AD-A153891] 19 p3234 N85-30047
Comparison of isothermal kerogen decomposition results using reactors with different heat-up rates
[DE85-008563] 19 p3237 N85-30068
Processable and stable conductive polymers
[AD-D011684] 19 p3249 N85-30143
Flash pyrolysis of biomass with reactive and non-reactive gases
[DE85-010962] 19 p3306 N85-30496
Fuel-rich catalytic combustion: A soot-free technique for in situ hydrogen-like enrichment
[NASA-TP-2496] 20 p3423 N85-31244
Polyesters: A review of the literature on products of combustion and toxicity
[NBSIR-85-3139] 20 p3433 N85-31298
A fluidized-bed reactor for silane pyrolysis 21 p3609 N85-32413
Modeling of the silane FBR system 21 p3609 N85-32415
Silicon production in an aerosol reactor 21 p3609 N85-32416
Thermal reactions of aromatics with CaO
[DE85-010688] 22 p3742 N85-33193
Oxygen analyzer
[DE85-006002] 23 p3935 N85-34392
PYROLYTIC GRAPHITE
X-ray polarization in highly oriented pyrolytic graphite
[DE84-015573] 05 p0613 N85-13917
PYROLYTIC MATERIALS
NT PYROLYTIC GRAPHITE
Non-oxide ceramics: A new class of engineering materials 02 p0179 N85-11199
PYROMETALLURGY
Temperature, velocity, and species mapping in an induction plasma
[DE85-004005] 15 p2512 N85-25499
PYROMETERS
NT THERMOCOUPLE PYROMETERS
Dynamic gas temperature measurement system 02 p0141 N85-10958
Seven-wavelength pyrometer for determining surface temperature of ablation materials
[NASA-TM-77832] 14 p2305 N85-24268
Investigation of non-intrusive radiometers for entrained gasifier temperature measurement, revision 3
[DE85-011795] 23 p3934 N85-34385
PYROMETRY
U TEMPERATURE MEASUREMENT
PYROPHORIC MATERIALS
Pyrophoric alkylaluminum compounds in decoy flares
[FOA-C-20562-E4] 18 p3078 N85-29039
Review of zirconium-zircaloy pyrophoricity
[DE85-011169] 23 p3916 N85-34270
PYROTECHNICS
Effect of oxide coated thickness on thermal ignition of titanium-based pyrotechnics
[DE84-013081] 04 p0481 N85-13065
Laser for determining the ignition conditions of a pyrotechnic mixture
[FOA-C-20542-D1] 04 p0506 N85-13230
Flame-resistant materials for use in pyrotechnic safety clothing
[AD-A146857] 07 p0931 N85-15901
Modelling the thermal explosion phenomenon in solid propellants: The case of fixed and variable temperatures 08 p1117 N85-17044
CVD boron on calcium chromate powder
[DE85-000214] 09 p1299 N85-18158
Study of bridgewire size and pyrotechnic density relationships on all-fire levels
[DE84-016946] 09 p1302 N85-18177
NATO AC/310 activities report on NATO STANAG 4170 and Allied Ordnance Publication 7 (Manual of Tests for Qualification of Explosive Materials for Military Use)
[AD-P004341] 10 p1454 N85-19165
Measurement of the expansion velocity of an aerosol cloud during pyrotechnical dispersion
[ISL-R-125/83] 14 p2303 N85-24262
Surveillance program for the dissection and analysis of explosive and pyrotechnic components
[DE85-006105] 16 p2757 N85-27016
Short Wavelength Chemical Laser (SWCL) Workshop
[AD-A151959] 16 p2790 N85-27211
Evaluation of pyrotechnic fire suppression system for six pyrotechnic compositions
[AD-A152995] 17 p2937 N85-28130
Fully redundant mechanical release actuator
[NASA-CASE-LAR-13198-1] 18 p3116 N85-29257
Ariane launcher system. Pyrotechnics subsystem: Definition of chains and pyrotechnic components
[CNES-84/CT/DRT/SST/SE/242(1)] 20 p3396 N85-31081
PYROXENES
NT ENSTATITE
Minor elements in relict olivine grains of deep-sea spheres: Match with Mg-rich olivines from C2 meteorites 06 p0683 N85-15610
PYROXYLIN
U CELLULOSE NITRATE
PYRRHOTITE
NT TROILITE
PYRROLES
NT CARBAZOLES
NT TRYPTOPHAN
Chemical derivatization of an array of three gold microelectrodes with polypyrrole: Fabrication of a molecule-based transistor
[AD-A146221] 03 p0359 N85-12304
Potential dependence of electrical conductivity and chemical charge storage of poly(pyrrole) films on electrodes
[AD-A146513] 08 p1122 N85-17075
Polymer blends for use in photoelectrochemical cells for conversion of solar energy to electricity
[DE85-011602] 22 p3752 N85-33258
P3V AIRCRAFT
U P-3 AIRCRAFT
P78-2 SATELLITE
U SCATHA SATELLITE

Q

Q DEVICES
Confinement and heating of high beta plasmas with emphasis on compact toroids
[DE85-011459] 24 p4155 N85-35761
Q FACTORS
Comparative descriptions of software quality measures
[GMD-STUDIES-81] 01 p0102 N85-10676
Influence of scattering on Q in the lithosphere
[AD-A149318] 10 p1515 N85-19563
Piezoelectric filter with low-Q inductances
[illegible] 13 p2070 N85-22932
Q SWITCHED LASERS
Efficiency of photoelectric conversion of short radiation pulses 03 p0348 N85-12240
Determination of the drag of free flying particles in supersonic flow with a pulsed laser 12 p1773 N85-21129
Investigation of plasma processes in electronic transition lasers
[AD-A149682] 12 p1834 N85-21506
Low jitter trigger for an excimer laser
[DE85-005732] 13 p2097 N85-23080
Development of a theoretical model to describe the interaction between electric discharge and supersonic flow of a pulsed CO laser
[DFVLR-FB-84-45] 14 p2310 N85-24301
Q VALUES
Study of proton and neutron activation of metal samples in low Earth orbit
[NASA-CR-171596] 21 p3558 N85-32130
QCD
U QUANTUM CHROMODYNAMICS
QSO (RADIO SOURCES)
U QUASARS
QUADRATIC EQUATIONS
Quadratic spaces over discrete Hodge algebras 16 p2853 N85-27593
An overview of latest model reduction and control methods of large flexible space structures 20 p3414 N85-31191
Frequency domain control design of large space structures: A practical approach 20 p3415 N85-31192
A new problem in mathematical physics associated with the problem of coherent phase transformation 21 p3698 N85-32976
QUADRATIC PROGRAMMING
A research program in active control/aeroelasticity in the JIAFS at NASA Langley Research Center
[NASA-CR-174052] 02 p0148 N85-11001
A sequential quadratic programming algorithm for solving large, sparse nonlinear programs
[AD-A145854] 03 p0407 N85-12597
A dual quadratic programming algorithm
[AD-A147237] 07 p1031 N85-16547
Automatic control design procedures for restructurable aircraft control
[NASA-CR-172489] 12 p1760 N85-21173
User's guide for NPSOL (Version 2.1): A FORTRAN package for quadratic programming
[AD-A150078] 12 p1918 N85-22028
A decomposition procedure for convex quadratic programs
[AD-A151732] 16 p2854 N85-27595
A quadratic programming algorithm
[AD-A153476] 18 p3168 N85-29631
Model building and practical aspects of nonlinear programming
[AD-A155720] 22 p3829 N85-33711
QUADRATURE APPROXIMATION
U QUADRATURES
QUADRATURES
Oscillatory integrals by Hermite interpolatory rules
[CSIR-TWISK-301] 01 p0108 N85-10725
A lumped mass finite element method with quadrature for a nonlinear parabolic problem
[CTH-MATH-1984-22] 05 p0719 N85-14615
Calculation of cumulative distributions and detection probabilities in communications and optics
[AD-A147781] 06 p1215 N85-17650
A note on the use of polynomial transformations in evaluating singular integrals
[MATHEMATICS-RESEARCH-165] 12 p1920 N85-22053
The implementation of the Tanh transformations in the evaluation of singular integrals
[MATHEMATICS-RESEARCH-171] 12 p1920 N85-22054
Extrapolation methods for multi-dimensional quadrature of singular and regular integrand functions
[DE85-009665] 18 p3172 N85-29655
QUADRUPOLE LENSES
U MAGNETIC LENSES
QUADRUPOLE NETWORKS
RFQ modeling computer program
[DE85-012665] 24 p4140 N85-35681
QUADRUPOLES
Theory of nuclear magnetic relaxation
[AD-P003911] 01 p0032 N85-10197
Linac quadrupole connections
[DE84-014694] 01 p0118 N85-10810
Calculated parameters for the initial part of an accelerator with high-frequency quadrupole focusing
[RAE-TRANS-2122] 07 p1040 N85-16600
Crossing point conditions, quadrupole gradients and drift space lengths
[DE85-003223] 11 p1721 N85-20825
Ion quadrupole effects in spectral line broadening
[DE85-001504] 11 p1730 N85-20879
A computer controlled mass spectrometer system for investigating the decomposition of non-metallic materials under atmospheric conditions 12 p1948 N85-22237
Radio frequency quadrupole and alternating phase focusing methods used in proton linear accelerator technology in the USSR
[AD-A150930] 14 p2418 N85-24916
Moments in particle-in-cell simulations
[DE85-010792] 19 p3356 N85-30603
Mechanical considerations in cw linacs
[DE85-010728] 19 p3363 N85-30850
Proposed use of the radio-frequency quadrupole structure to funnel high-current ion beams
[DE85-010746] 19 p3364 N85-30857
Fabrication and test of modified quadrupole mass spectrometer
[AD-A155186] 21 p3590 N85-32312
Electron trajectories in a combined wiggler and alternating gradient quadrupole field
[DE85-010727] 22 p3842 N85-33794
QUALIFICATIONS
Certification of advanced systems 06 p0783 N85-14829
NATO AC/310 activities report on NATO STANAG 4170 and Allied Ordnance Publication 7 (Manual of Tests for Qualification of Explosive Materials for Military Use)
[AD-P004341] 10 p1454 N85-19165
IHE material qualification tests description and criteria
[DE85-004649] 13 p2040 N85-22770
Qualification of the T2 wind tunnel in cryogenic operation. B: Flow fluctuations, particle detection and qualification
[NASA-TM-77782] 14 p2227 N85-23606
Qualification needs for advanced integrated aircraft
[NASA-TM-86731] 22 p3729 N85-33119
QUALITATIVE ANALYSIS
Qualitative process theory
[AD-A146967] 10 p1543 N85-19729
Qualitative analysis of sign-bit processing
[AD-A154776] 21 p3671 N85-32904
Direct determination of metals in organic matrices by Inductively Coupled Plasma-Atomic Emission Spectrometry (ICP-AES)
[DE85-012015] 23 p3911 N85-34233
QUALITY
NT AIR QUALITY
NT ENVIRONMENTAL QUALITY
NT RIDING QUALITY
NT WATER QUALITY
Quality assurance for environmental analytical chemistry, 1983
[DE84-016045] 09 p1349 N85-18489
Characteristics of quality data
[DE85-001203] 10 p1566 N85-19689
Studies in quality improvement 2. An analysis for unreplicated fractional factorials
[AD-A153539] 18 p3169 N85-29640
The interpretation of flying qualities requirements for flight control system design
[NASA-CR-177942] 22 p3730 N85-33125
Acoustic scaling: The development of improved instrumentation
[BBC-RD-1985/7] 24 p4145 N85-35694
QUALITY CONTROL
Measurement assurance programs. Part 1: General introduction
[PB84-217988] 01 p0051 N85-10339
ICAM (Integrated Computer Aided Manufacturing) conceptual design for computer-integrated manufacturing. Volume 4, part 6: Task d. Quality assurance/quality control/technical requirement/tasks, quality assurance modeling and analysis, quality assurance program management standard recommendations (ISP)
[AD-A144891] 01 p0058 N85-10372
Comparative descriptions of software quality measures
[GMD-STUDIES-81] 01 p0102 N85-10676
Avionics integrity program (Avip). Volume 3: Program cost assessment - environmental stress screening and diagnostic techniques
[AD-A145844] 02 p0139 N85-10942
Avionics integrity program (Avip). Volume 1: Procurement phase issues: Design, manufacturing, and integration
[AD-A145861] 02 p0139 N85-10943
Advanced manufacturing development of a composite empennage component for L-1011 aircraft
[NASA-CR-165885] 02 p0170 N85-11141
A method for evaluating the contamination of steel in relation to the solidification curve
[BLL-M-35735-(5828.4)] 02 p0175 N85-11171
Investigation of the application of the marginal tension technique to test electronic devices, phase 3
[ESD-11-301] 02 p0208 N85-11380
Editorial urges improved aviation repair work quality 03 p0310 N85-12004
Development of a rapid test method for asphalt concrete content determination in hot-mix paving mixtures
[PB84-218692] 03 p0342 N85-12204
Prediction of weld defects using welding condition data
[VTT-RR-264] 03 p0370 N85-12359
Automating software design metrics
[AD-A145869] 03 p0407 N85-12588
Designing optimal AOQL sampling plans a computerized approach
[AD-A146298] 03 p0413 N85-12609
Test report no. 17.208: Statistics of the basic characteristics of carbon-epoxy composites
[DGT-23.426/A] 04 p0488 N85-12979
Quality assurance of composite materials, test report no. 45-649/F 04 p0489 N85-12981
Quality organization — quality control
[CNES-NT-106] 04 p0511 N85-13257
The ESA product assurance specification system: Explanatory note 04 p0511 N85-13259
Toward a non-bureaucratic approach to quality assurance in data processing
[DE84-007484] 04 p0550 N85-13497
Vandenberg space shuttle launch complex
[S-HRG-98-1075] 05 p0601 N85-13833
Statement of Edward C. Aldridge, Jr., Under Secretary of the Air Force, Department of the Air Force, accompanied by Lieutenant General Robert W. Bazley, Inspector General and Brigadier General Donald J. Kutyna, Director of Space Systems and Command, Control and Communications, Deputy Chief of Staff, Research, Development and Acquisition 05 p0601 N85-13834
Statement of Honorable James M. Beggs, Administrator, National Aeronautics and Space Administration 05 p0601 N85-13835
Quality assurance in the Antares Laser Fusion Construction Project
[DE84-015493] 05 p0640 N85-14104
Laboratory investigations 05 p0668 N85-14281
The effects of task structure on time-sharing efficiency and resource allocation optimality 05 p0711 N85-14562
Acceptance-testing procedures for air-line supplied-air suits
[DE84-016980] 05 p0712 N85-14569
Fabrication and quality assurance processes for superhybrid composite fan blades
[NASA-TM-83354] 06 p0783 N85-14882
Quality control of integrated circuits by parametric identification methods 06 p0796 N85-15065
Laser-guided measuring system for precisioning device 06 p0816 N85-15179
The effects of software quality control and baseline management on the acquisition of computer programs
[AD-A147051] 07 p1024 N85-16502
A survey and evaluation of software quality assurance
[AD-A147552] 07 p1026 N85-16510
An analysis of the effect of process controls on productivity and weapon system costs in DoD procurement
[AD-A147496] 07 p1052 N85-16678
A study of Air Force Quality Circle program effectiveness as viewed through facilitator's perceptions
[AD-A147833] 08 p1170 N85-17377
Improvements under way at Gorky airport 09 p1278 N85-18040
Quality control in soil compaction by behaviours of exciter
[AD-P004295] 09 p1408 N85-18872
Thematic Mapper: Design through flight evaluation
[E85-10079] 10 p1504 N85-19492
Robotics at Savannah River site: Activity report
[DE85-003957] 11 p1648 N85-20383
A quality control experiment in a real time multiprocessor operating system: The Mars 860 — software testing 11 p1702 N85-20707
An exact solution to the 2 point OC (Operating-Characteristic) curve determination
[AD-A148120] 11 p1708 N85-20746
Quality of scientific and engineering data
[DE85-000294] 11 p1739 N85-20936

Transportation
[JPRS-UTR-85-004] 12 p1769 N85-21105
Aviation repair plant directors on quality control measures 12 p1769 N85-21106
Development and evaluation of a procedure for the rapid analysis of fresh concrete
[AD-A149741] 12 p1866 N85-21703
A statistical approach to vendor selection
[AD-A149781] 12 p1950 N85-22249
Characterization standards for solid propellant rocket motors
[AD-A150250] 13 p2013 N85-22627
Measurement of internal thermal resistance for quality control of semiconductor devices 13 p2074 N85-22953
Ultrasonic non-destructive testing technique 14 p2316 N85-24313
Practical surface methods 14 p2316 N85-24314
Administration chief on air traffic control improvements 15 p2460 N85-25193
Quality control of radioelectronic apparatus components on basis of external characteristics in frequency domain 15 p2529 N85-25590
Detection and location of partial discharges in transformer windings using electrical methods 15 p2551 N85-25750
Welding technology and organisation in steel construction 15 p2566 N85-25828
Nondestructive tests of ceramic components for aircraft turbines 16 p2709 N85-26718
Cost prediction model for various payloads and instruments for the Space Shuttle Orbiter
[NASA-CR-175781] 16 p2729 N85-26842
A framework for software development
[AD-A152067] 16 p2847 N85-27551
Lidar ER2 (ozone). Crystal characterization for harmonic conversion — laser systems
[CERT-2/6129-00] 16 p2872 N85-27717
Examination of steels by chemical analysis for quality assurance
[BLL-BISI-TRANS-22068-(9022.06)] 17 p2929 N85-28074
Proper quality of anticorrosion work no matter how bad the atmospheric conditions
[BLL-BISI-TRANS-22060-(9022.06)] 17 p2975 N85-28383
Statistical models used in analyzing the quality of welded tubes
[BLL-BISI-TRANS-22232-(9022.06)] 17 p2976 N85-28384
Principal quality assurance measures in the manufacture of HF-welded high-pressure linepipe
[BLL-BISI-TRANS-21690-(9022.06)] 17 p2976 N85-28389
Integrating quality assurance and research and development
[DE85-007974] 17 p2976 N85-28392
Initial imperfection surveys on conical shells at Hoechst AG
[VTH-LR-407] 17 p2981 N85-28429
Quality assurance for RESOLVE (Research on Operations-Limiting Visual Extinction). A visibility study in the California desert
[AD-A152383] 17 p2992 N85-28494
Effects of inspection errors on curtailed Dorfman-type procedures
[AD-A152376] 17 p3024 N85-28699
Statistical effects of imperfect inspection sampling. Part 2: Double sampling, link sampling and grading
[AD-A152377] 17 p3024 N85-28700
Impurity control and vacuum pumping system design and analysis for next-generation Tokamaks
[DE85-009291] 17 p3041 N85-28815
Principles of quality assurance of chemical measurements
[PB85-177947] 18 p3072 N85-28997
Practical real-time quality control of antimisting kerosene
[DE/FAA/CT-85/1] 18 p3083 N85-29072
Specification of software quality attributes, volume 1
[AD-A153988] 18 p3163 N85-29593
Specification of software quality attributes. Volume 2: Software quality specification guidebook
[AD-A153989] 18 p3163 N85-29594
Specification of software quality attributes. Volume 3: Software quality evaluation guidebook
[AD-A153990] 18 p3163 N85-29595
Studies in quality improvement 2. An analysis for unreplicated fractional factorials
[AD-A153539] 18 p3189 N85-29640
Generic data entry quality assurance tool
[DE85-006359] 18 p3200 N85-29652
Improvements in safety testing of lithium cells 20 p3444 N85-31379
Design evaluation of high reliability lithium batteries 20 p3444 N85-31380
Philosophy of nondestructive control in aeronautics quality control. Knowledge of and improvements to nondestructive test safety
[SNIAS-851-551-101] 20 p3465 N85-31522
NASA/GSFC TOPEX gravity model operations group 20 p3492 N85-31709
Quality analysis 21 p3668 N85-32785
An automated quality assurance surveillance plan for ADP (Automated Data Processing) operations under the Navy's commercial activities program
[AD-A154767] 21 p3671 N85-32802
Current requirements for the design and maintenance against corrosion of UK military aircraft 22 p3750 N85-33244
EML pulse ionization chamber systems for (222)Rn measurements
[DE85-012320] 23 p3970 N85-34810
Quality assurance considerations for the implementation of a pulsed power R and D project
[DE85-012357] 24 p4148 N85-35720
Aeronautical Systems Division Manufacturing/Quality assurance orientation
[AD-A156128] 24 p4164 N85-35817

QUALITY FACTORS
U Q FACTORS

QUANTILES
Spline methods for approximating quantile functions and generating random samples
[NASA-TP-2389] 07 p1035 N85-16565
A kernel type estimator of a quantile function from right-censored data
[AD-A148753] 09 p1374 N85-18635
Scrawl plots, and letter and blotter strips
[DE85-001409] 11 p1707 N85-20739
Comments on estimating quantiles for Gaussian functionals by simulation
[AD-A154302] 19 p3348 N85-30750
On the confidence limits for Weibull reliability and quantiles: The case of maximum likelihood estimation from small size censored samples
[REPT-84-RR-345] 20 p3521 N85-31696

QUANTITATIVE ANALYSIS
Determination of halogens and sulfur in organic compounds and polymers by combustion-ion chromatography
[DE84-016186] 05 p0614 N85-13921
A study of the chemical interaction of gases with activated carbon
[AD-A147342] 07 p0923 N85-15846
Impact of aircraft emissions on air quality in the vicinity of airports. Volume 4. Nitrogen dioxide and hydrocarbons
[AD-A148253] 08 p1180 N85-17436
Background detection and correction in multicomponent analysis
[AD-A148251] 08 p1212 N85-17628
Multicomponent calibration and quantitation methods
[AD-A148252] 08 p1212 N85-17629
Quantitative determination of compound classes in jet turbine fuels by high performance liquid Chromatography/Differential refractive index detection: Part 2
[AD-A148298] 11 p1613 N85-20144
Interlaminar fracture toughness in resin matrix composites
[AD-A150565] 13 p2015 N85-22640
Trace metal determinations in nickel-plating baths by polarographic methods
[DE85-007064] 15 p2511 N85-25488
Procedure for certifying quantity of volatile organic compounds emitted by paint, ink and other coatings
[PB85-159044] 15 p2520 N85-25537
Quantitative analysis of defects in silicon-characterization of UCP, HAMCO, and microcrystalline material
[NASA-CR-175986] 16 p3079 N85-29046
Rapid rate-kinetic turbidometric assay for quantitation of antiviral complement-fixing antibodies
[AD-A153644] 18 p3152 N85-29516
Application of the reference intensity method to coal analysis
[DE85-009528] 19 p3228 N85-30015
Quantitative passive technique for assay of near-surface tritium in materials
[DE85-010861] 19 p3360 N85-30833
Rapid estimation of concentration of aromatic classes in middistillate fuels by high-performance liquid chromatography
[NASA-TP-2495] 20 p3434 N85-31307
Quantitative analysis in megageomorphology 21 p3603 N85-32376
Quantitative analysis of geomorphic processes using satellite image data at different scales 21 p3604 N85-32380
Quantitative geomorphologic studies from spaceborne platforms 21 p3604 N85-32381
Quantitative determination of mineral composition by powder X-ray diffraction
[DE85-011654] 22 p3760 N85-33901
Quantitative analysis of flare accelerated electrons through their hard X-ray and microwave radiation
[SH-1.2-7] 23 p3991 N85-34742

QUANTITY
U AMOUNT

QUANTIZATION
U MEASUREMENT

QUANTIZER
U COUNTERS

QUANTUM CHEMISTRY
Application of quantum chemistry of atmospheric chemistry
[AD-A147035] 07 p0922 N85-15843
Applications of molecular dynamics to the study of shock-induced chemistry
[AD-A148017] 08 p1121 N85-17068
Quantum Monte Carlo for molecules
[AD-A148159] 08 p1227 N85-17727
Atomic, Molecular and Solid-State Theory, and Computational Quantum Chemistry, part 1
[DE85-009401] 20 p3526 N85-31929

QUANTUM CHROMODYNAMICS
NT INSTANTONS
Research program in theoretical high-energy physics
[DE84-013717] 01 p0119 N85-10817
Gauge Theory on a Lattice, 1984: Proceedings
[DE84-014858] 02 p0291 N85-11892
Particle physics
[DE84-013834] 05 p0727 N85-14673
Very high energy probes of the quark-gluon plasma
[DE84-016992] 09 p1392 N85-18763
Cosmic axions
[DE85-001330] 09 p1418 N85-18944
Stochastic methods for the description of multiparticle production
[DE84-009981] 10 p1556 N85-19810
Experimental and theoretical high energy physics
[DE85-000844] 11 p1726 N85-20858
Axions in astrophysics and cosmology
[DE85-002720] 11 p1763 N85-21094
Jet topologies in hadron-hadron collisions
[DE85-001328] 12 p1929 N85-22119
Research in theoretical nuclear physics
[DE85-004349] 12 p1932 N85-22137
Resonances in photon-photon scattering
[DE85-004607] 14 p2419 N85-24928
Lattice Monte Carlo calculations of finite temperature QCD
[DE85-004035] 14 p2431 N85-24992
Space station as quark matter factory
[DE85-004606] 15 p2685 N85-26585
Discrete foundation for physics and experience
[DE85-008172] 16 p2872 N85-27720
Configuration space Faddeev calculations
[DE85-005813] 16 p2872 N85-27721
Photon structure function: Theory
[DE85-006064] 17 p3031 N85-28745
Measuring structure functions at SSC energies
[DE85-007515] 17 p3031 N85-28746
Experimental studies of diffractive phenomena
[DE85-006812] 17 p3031 N85-28749
Elementary particle theory
[DE85-006803] 17 p3034 N85-28771
Heavy quark production processes in QCD
[DE85-007240] 17 p3036 N85-28779
Some comments on SSC physics
[DE85-008444] 18 p3179 N85-29712
A comprehensive study of psi meson production
[DE85-008094] 18 p3180 N85-29718
Soliton matter as a model of dense nuclear matter
[DE85-009937] 19 p3359 N85-30825
Monte Carlo sampling strategies for lattice gauge calculations
[DE85-010756] 19 p3377 N85-30948
Toward the question of multi-quark configurations in nuclei 21 p3691 N85-32929
Spatial parity violation in elastic neutron-nuclei interaction channel 21 p3691 N85-32932
Quark structure of nuclei
[DE85-010781] 22 p3842 N85-33795
Duality of two-point functions for confined non-relativistic quark-antiquark systems
[DE85-012334] 23 p3971 N85-34618
Very high energy probes of the quark-gluon plasma 24 p4147 N85-35706
High energy physics at Tufts University
[DOE/ER-40085/7] 24 p4152 N85-35744
QCD-motivated description of very high energy particle interactions
[HE-1.2-2] 24 p4171 N85-35861

A cosmic ray super high energy multicore family event. 2: Structure and fragmentation characteristics of the jets
[HE-3.4-2] 24 p4181 N85-35931
QCD analysis of neutrino charged current structure function F2 in deep inelastic scattering
[HE-5.3-23] 24 p4207 N85-36114

QUANTUM COUNTERS
Noise tolerance of digital demodulator for complex signal system employing binary quantization
13 p2070 N85-22929
Lateral distribution on charged particles in EAS
[HE-4.3-15] 24 p4192 N85-36009

QUANTUM EFFICIENCY
Preliminary evaluation of RCA C83036E prototype photomultiplier
[DE84-016894] 04 p0496 N85-13165
Mercuric iodide photodetectors for scintillation spectroscopy
[DE85-001437] 10 p1437 N85-19056
Advanced high-efficiency concentrator cell
[DE85-000525] 14 p2351 N85-24533
A quantitative image evaluation study of a concurrent photon amplification treated emulsion
[AD-A151831] 15 p2560 N85-25796
Photon-counting image sensors for the ultraviolet
[NASA-CR-176062] 20 p3458 N85-31478

QUANTUM ELECTRODYNAMICS
Linear conformal gravitation 02 p0265 N85-11735
ASP: A new PEP experiment to measure single photons
[DE84-015732] 04 p0560 N85-13563
Implications of the chiral anomaly for quantum Hall effect devices
[NUB-2662] 05 p0629 N85-14029
Topics in high resolution spectroscopy of stored ions
[DE85-002093] 08 p0861 N85-15470
A superconducting quantum current standard
[NPL-QU-67] 08 p1224 N85-17710
Quantum noise effects in single-mode injection lasers
[FUB-11-1984] 09 p1327 N85-18338
Elementary particle theory
[DE85-006803] 17 p3034 N85-26771
The standard model and beyond
[DE85-010239] 19 p3362 N85-30847
Evaluation of parameters for particles acceleration by the zero-point field of quantum electrodynamics
[OG-8.2-16] 23 p4020 N85-34912

QUANTUM ELECTRONICS
Research activities of the Illinois University Coordinated Science Laboratory
[AD-A145589] 03 p0449 N85-12856
Electronics research at the University of Texas at Austin
[AD-A146900] 07 p0947 N85-15998
Solid state research
[NASA-CR-174285] 07 p1048 N85-16656
Quantum noise and excess noise in optical homodyne and heterodyne receivers
[AD-A148298] 08 p1157 N85-17303
Solid state research
[AD-A147840] 08 p1225 N85-17714
Annual report on electronics research at the University of Texas at Austin
[AD-A150836] 14 p2415 N85-24901
Joint services electronics program
[AD-A154348] 19 p3375 N85-30939
Solid state research
[AD-A154783] 21 p3709 N85-33025
Conference of quantum-radiooptics section
22 p3773 N85-33360
Joint services electronics program
[AD-A154748] 23 p3927 N85-34336

QUANTUM MECHANICS
NT QUANTUM ELECTRODYNAMICS
Quantum characteristics of kinetic fracturing of solids
02 p0265 N85-11732
The identification of the scientific community's choice criteria in the history of scientific research: The case of quantum mechanics
[NOTA-INTERNA-797] 02 p0291 N85-11893
Theory of non-linear index of refraction of compound semiconductors
[DE84-013660] 04 p0569 N85-13628
Refractive index of ternary and quaternary compound semiconductors below the fundamental absorption edge: Linear and nonlinear effects
[DE84-012325] 05 p0640 N85-14105
Semiconductor superlattice photodetectors
[NASA-CR-174347] 09 p1397 N85-18791
Reduction of the wavepacket: How long does it take?
[DE84-016776] 09 p1400 N85-18815
Asymmetrical harmonic oscillator and fine-structure constant
[FUB-8-1984] 09 p1401 N85-18816
Accidental degeneracies, hidden supersymmetries, and spectrum-generating superalgebras
[DE85-003547] 11 p1738 N85-20930
Macroscopic quantum tunnelling in a current biased Josephson junction
[DE85-004603] 13 p2164 N85-23424
Parton dynamics in hadronic processes
[DE85-006072] 14 p2418 N85-24922
Soliton energetics in extended Peierls-Hubbard models: A quantum Monte Carlo study
[DE85-005409] 14 p2429 N85-24981
Identification and properties of molecular systems of potential use in solar-pumped lasers
[NASA-CR-175804] 16 p2769 N85-27207
Shallow impurity cluster states in n-type semiconductors
[INPE-3495-PRE/732] 16 p2669 N85-27699
Discrete foundation for physics and experience
[DE85-008172] 16 p2672 N85-27720
Configuration space Faddeev calculations
[DE85-005813] 16 p2672 N85-27721
Multi-particle quantum mechanics obeying fractional statistics
[DE85-007830] 16 p2673 N85-27723
Memory function for cyclotron resonance of two-dimensional electron systems
[AD-A152632] 17 p3029 N85-28731
Nonrelativistic theory of heavy-ion collisions
[DE85-007538] 17 p3031 N85-28747
The strategy for time dependent quantum mechanical calculations using a Gaussian wave packet representation of the wave function
[AD-A152709] 17 p3046 N85-28845
On the propagation speed in relativistic quantum mechanics
[CWI-AM-R8410] 17 p3046 N85-28848
Adiabatic approach in the theory of polyatomic photodissociation: Application to C2N2
[DE85-006515] 18 p3071 N85-28996
Constructing a bit string universe
[DE85-006317] 18 p3197 N85-29829
Quantum effects in linear collider scaling laws
[DE85-009648] 19 p3363 N85-30851
Measurement problem in PROGRAM UNIVERSE
[DE85-006179] 19 p3376 N85-30959
Physical concepts in the development of constitutive equations 20 p3457 N85-31537
Atomic, Molecular and Solid-State Theory, and Computational Quantum Chemistry, part 1
[DE85-009401] 20 p3528 N85-31929
Lattice theory for nonspecialists, lecture notes
[NIKHEF-H/84-11] 20 p3539 N85-32019
Earth Albedo and the orbit of LAGEOS
[NASA-TM-86210] 21 p3558 N85-32131
Theoretical studies of structure and stability of hydrates of atmospheric sulfur species 21 p3650 N85-32684

QUANTUM NUMBERS
Proposal for the systematic naming of mesons and baryons
[DE85-006453] 17 p3035 N85-28773
Constructing a bit string universe
[DE85-006317] 18 p3197 N85-29829
Measurement problem in PROGRAM UNIVERSE
[DE85-006179] 19 p3376 N85-30959

QUANTUM STATISTICS
A measurement of the intensity of the cosmic background radiation at 3.9 cm
13 p2206 N85-23681
Boson degrees of freedom in Fermion many-body systems
[DE85-006997] 16 p2663 N85-27660
Spin-polarized quantum systems
[DE85-006914] 16 p2664 N85-27667

QUANTUM THEORY
Interactions in localization
[NOTA-INTERNA-615] 02 p0279 N85-11816
Toward unification of elementary particle physics and cosmology in 10-dimensions
[DE84-013950] 05 p0727 N85-14674
Stability questions for gravity in 4 and higher dimensions 05 p0734 N85-14718
Theory and applications of two-photon quantum optics
[AD-A147382] 07 p1044 N85-16631
Two-photon coherent state light - Its generation and potential applications
[AD-A146245] 08 p1186 N85-17356
Hydrodynamic flow structures in quantum field theory
[DE84-015513] 09 p1401 N85-18817
Quasiparticle aggregation in the Fractional Quantum Hall Effect
[DE85-001574] 10 p1565 N85-19668
Ultraviolet divergences and supersymmetric theories
[DE85-001849] 11 p1729 N85-20875
Stable measures and processes in statistical physics
[AD-A149592] 12 p1928 N85-22096
Study of 1/f noise in solids
[AD-A151069] 14 p2428 N85-24972
Eigenvalue approximation methods for quantum lattice Hamiltonians 16 p2656 N85-27627
Quantum statistical theory of vibrational dynamics in a laser-driven admolecule-surface system
[AD-A152022] 16 p2672 N85-27719
The enhancement of molecular fluorescence and photochemistry by small metal particles
[AD-A152740] 17 p2919 N85-27094
Quantum model of dephasing-enhanced laser desorption: Master equation approach
[AD-A153769] 18 p3112 N85-29269
Research in the theory of condensed matter and elementary particles
[DE85-010447] 20 p3531 N85-31988
Bergson and the unification of the sciences
[DE85-009961] 20 p3538 N85-32018
Activities report of the Department of Astrophysics
20 p3546 N85-32084

QUANTUM WELLS
Strained-layer superlattices and strain-induced light holes
[DE85-003675] 14 p2431 N85-24990
Optical properties of heterostructures and superlattices
[AD-A156243] 24 p4182 N85-35802

QUARKS
Quark models of hadronic interactions
[DE84-013787] 04 p0561 N85-13570
Measurements of the A-dependence of deep-inelastic electron scattering from nuclei
[DE84-013865] 05 p0728 N85-14678
Very high energy probes of the quark-gluon plasma
[DE84-016992] 09 p1392 N85-18783
Thin end of the wedge
[DE84-016439] 09 p1401 N85-18818
Research in theoretical nuclear physics
[DE85-004349] 12 p1932 N85-22137
Standard model and beyond
[DE85-004269] 14 p2418 N85-24919
Eleven lectures on the physics of the quark-gluon plasma
[DE85-004321] 15 p2662 N85-26431
Overview of the physics issues at the SSC
[DE85-007074] 16 p2659 N85-27634
Heavy quark production processes in QCD
[DE85-007240] 17 p3036 N85-28779
Experimental methods of heavy quark detection
[DE85-006316] 17 p3036 N85-28781
Measurements of heavy quark and lepton lifetimes
[DE85-006321] 18 p3181 N85-29724
Soliton matter as a model of dense nuclear matter
[DE85-006937] 19 p3359 N85-30825
Deep-inelastic lepton scattering by nuclei: The pion-exchange model
[DE85-010498] 19 p3359 N85-30826
The standard model and beyond
[DE85-010239] 19 p3362 N85-30847
Systematics of quark mass matrices in the Standard Electroweak Model
[USIP-85-05] 20 p3532 N85-31972
Toward the question of multi-quark configurations in nuclei 21 p3691 N85-32929
Exotic events of p bar p-collider: Excited quark or excited color boson? 21 p3691 N85-32930
Heavy quarks and CP: Moriond 1985
[DE85-010553] 22 p3841 N85-33790
Quark structure of nuclei
[DE85-010781] 22 p3842 N85-33795
Detectors for relativistic nuclear collisions (report from the Fixed-Target Hadron Group)
24 p4148 N85-35701
Very high energy probes of the quark-gluon plasma
24 p4147 N85-35708
Propagation of cosmic rays through the atmosphere in the quark-gluon strings model 24 p4173 N85-35873
The phi-meson and Chiral-mass-meson production in heavy-ion collisions as potential probes of quark-gluon-plasma and Chiral symmetry transitions
24 p4175 N85-35884
Heavy flavours production in quark-gluon plasma formed in high energy nuclear reactions
24 p4175 N85-35888
A cosmic ray super high energy multicore family event. 2: Structure and fragmentation characteristics of the jets
[HE-3.4-2] 24 p4181 N85-35931
On mini-cluster observed by Chacaltaya emulsion chamber experiment
[HE-3.6-12] 24 p4185 N85-35959
The maximum depth of shower with E sub 0 larger than 10(17) eV on average characteristics of EAS different components 24 p4186 N85-35961

Calculation of intensity of high energy muon groups observed deep underground
[HE-5.4-13] 24 p4208 N85-36123
High energy cosmic ray signature of quark nuggets
[HE-6.2-11] 24 p4212 N85-36147
Progress report on a new search for free e/3 quarks in the cores of 10(15) - 10(16) eV air showers
[HE-6.2-15] 24 p4212 N85-36151
Tien-Shan effect and charmed particles
[HE-6.2-17] 24 p4212 N85-36153

QUARRIES
U MINES (EXCAVATIONS)

QUARTZ
New ages of radiolarian chert from the Rampart district, east-central Alaska 04 p0516 N85-13293
Metamorphic petrology of the Table Mountain area, Circle quadrangle, Alaska 04 p0516 N85-13295
Low noise multiple crystal-controlled oscillator
[AD-D011401] 07 p0948 N85-16010
Oscillator development
[AD-A149690] 12 p1834 N85-21509
Normal coordinate monolithic crystal filter
[AD-D011498] 12 p1941 N85-22188
Stress compensation crystal device
[AD-D011497] 12 p1941 N85-22189
Method of fabricating acceleration resistant crystal resonators and acceleration resistant crystal resonators so formed
[AD-D011630] 16 p2778 N85-27145
Acceleration sensitivity reduction method
[AD-D011631] 16 p2778 N85-27146
Research and development of subsurface acoustic wave devices for sensor applications
[AD-A152197] 16 p2861 N85-27642
A new precision time and frequency source for stationary PTTI applications 17 p2963 N85-28297
New features of different frequency generating systems due to the use of electrodeless rigidly mounted VBA quartz crystal resonator 18 p3108 N85-29231
Limiting processes laser CVD
[DE85-008846] 18 p3114 N85-29276
Physical and chemical changes to rock near electrically heated boreholes at Spent Fuel Test-Climax
[DE85-010834] 19 p3302 N85-30472
Dating Archean zircon by ion microprobe: New light on an old problem 21 p3722 N85-33004
Thermal reactions of aromatics with CaO
[DE85-010888] 22 p3742 N85-33193

QUARTZ CRYSTALS
Method of heating quartz resonators
[AD-D011454] 10 p1481 N85-19347
Quartz filter transceiver 12 p1838 N85-21536
Cylindrical crystal resonator
[AD-D011575] 14 p2428 N85-24974
Cut angles for quartz crystal resonators
[AD-D011652] 17 p2951 N85-28220
Acceleration insensitive oscillator
[AD-D011621] 17 p2953 N85-28236
Crystal resonator/oscillator test facility and test results 17 p2967 N85-28322
Power generation efficiency of piezoelectric crystals 20 p3537 N85-32008
JPL in-house fluidized-bed reactor research 21 p3609 N85-32414
Data analysis for lidar and quartz crystal microbalance systems
[NASA-CR-172601] 21 p3615 N85-32464

QUASARS
Measurement of pulsar parallax by Very Long Baseline Interferometry 03 p0444 N85-12830
Far-infrared photometry of compact extragalactic sources: OJ 187 and BL Lac
[NASA-TM-86022] 04 p0560 N85-13701
The 3a-F emulsion and the quasar redshift cut-off 07 p0964 N85-16112
X-ray and UV Emission from Active Galactic Nuclei — conference
[MPE-184] 08 p1236 N85-17790
Low excitation absorptions in the spectrum of the quasar PKS 1327-206 due to the galaxy MCG 03-34-085 08 p1237 N85-17801
X-ray surveys of quasars with the Einstein observatory 08 p1238 N85-17807
One to eight month X-ray light curves for active extragalactic objects 08 p1239 N85-17817
The high energy X-ray spectrum of 3C 273 — quasar 08 p1240 N85-17818
The X-ray properties of high-redshift, optically selected QSOs 08 p1240 N85-17821
On the broadband energy spectra of quasars and BL Lac objects 08 p1240 N85-17825
A universal spectrum for AGNs and QSOs — Active Galactic Nuclei (AGN) 08 p1241 N85-17826
Shock acceleration in active galactic nuclei and quasars 08 p1241 N85-17828
Collimated winds from active galactic nuclei 08 p1241 N85-17832
Active galactic nuclei and their cosmological evolution 08 p1243 N85-17842
An objective prism quasar survey with the Schmidt telescope on Calar Alto (Spain) 08 p1243 N85-17845
Broad emission features in active galactic nuclei 11 p1746 N85-20979
The UV spectra of intermediate redshift quasars 11 p1746 N85-20980
Multifrequency observations of BL LAC objects and violently variable quasars 11 p1746 N85-20981
Consequences of hot gas in the broad line region of active galactic nuclei
[NASA-TM-86176] 11 p1763 N85-21090
The ultraviolet excess of quasars 3: The highly polarized quasars PKS 0736+017 and PKS 1510-089
[NASA-CR-175576] 12 p1953 N85-22268
University of Cambridge Institute of Astronomy report of activities 13 p2170 N85-23464
A new luminosity component in 3C48
[NASA-CR-175840] 17 p3052 N85-28894
Evolution of the luminosity function of extragalactic objects
[NASA-CR-175977] 18 p3201 N85-29860
Milliarcsecond morphology of the twin quasar 0957 + 56A,B: The view through a gravitational lens 20 p3544 N85-32054
The ultraviolet spectra of intermediate redshift quasars 20 p3544 N85-32056
Activities report of the Institute of Astronomy 20 p3545 N85-32059
Cosmic gamma rays from quasars
[OG-2.7-10] 22 p3672 N85-33983
Limits on the Doppler factor in relativistic jets by means of gamma-ray observations
[OG-2.7-12] 22 p3672 N85-33985
The central engine of quasars and AGNs: A relativistic proton radiative shock
[OG-8.1-7] 23 p4018 N85-34897

QUASAT
QUASAT: A VLBI observatory in space — conferences
[ESA-SP-213] 07 p1056 N85-16700
The galaxy scene and QUASAT — VLBI satellite 07 p1056 N85-16703
The QUASAT mission: An overview 07 p1056 N85-16704
QUASAT: Technical aspects of the proposed mission — VLBI satellite 07 p1057 N85-16706
A study on the imaging potential of QUASAT — spaceborne VLBI 07 p1057 N85-16707
Correlator and data processing requirements for QUASAT 07 p1057 N85-16709
QUASAT, gravitational lenses, and studies of the interstellar, intracluster and intergalactic medium 07 p1058 N85-16715
The relevance of QUASAT to the star formation problem 07 p1058 N85-16718
Water masers and distance measurements: The impact of QUASAT 07 p1059 N85-16721
A short note on the high precision navigation of QUASAT 07 p1059 N85-16722
QUASAT: An orbiting very long baseline interferometer program using large space antenna systems 14 p2230 N85-23822
Antenna Technology for QUASAT application — radio antenna for very long base interferometry missions 14 p2231 N85-23826

QUASI-PARTICLES
U ELEMENTARY EXCITATIONS

QUASI-STELLAR RADIO SOURCES
U QUASARS

QUASILINEARITY
U NONLINEARITY

QUATERNARY ALLOYS
Zero-flux planes and flux reversals in multicomponent diffusion
[DE84-015212] 05 p0618 N85-13950

QUATERNIONS
Application of quaternions to problems of solid body dynamics in the atmosphere 15 p2481 N85-25313
Use of quaternions in flight mechanics
[AD-A152616] 17 p2899 N85-27875

QUENCHING (ATOMIC PHYSICS)
Electronically excited atomic and molecular oxygen
[AD-A147732] 08 p1121 N85-17064
X-ray emission in heavy ion collisions
[DE85-006350] 14 p2419 N85-24927
Elementary processes of electronically excited particles. Part 5: Deactivation of CHF (A1a' (O, V'2, O) after excitation by a pulsed dye laser
[MPIS-13/1984] 14 p2420 N85-24930
Lifetime and quenching measurements of C2H emission produced by vacuum ultraviolet photolysis of C2H2
[DE85-010760] 19 p3278 N85-30330

QUENCHING (COOLING)
Strain hardening and strain aging in Fe-Al-Mn alloys 02 p0178 N85-11198
Laminar flame propagation/quench for a parallel-wall duct
[DE84-009773] 04 p0470 N85-12993
Formation of superconductive Al(GeSi) alloys by low temperature laser quenching methods
[DE84-016867] 04 p0474 N85-13021
Study of residual stresses introduced into TA6ZrD (685) cylinders by quenching
[BLL-PNR-90240-(8019.3153)] 07 p0925 N85-15859
Study of residual stresses introduced into TA6ZrD (685) cylinders by quenching — compressor disk alloy
[PNR-90240] 09 p1341 N85-18435
Initial aging phenomena in copper-chromium alloys
[NASA-TM-77790] 10 p1439 N85-19070
Phase transformations in vanadium alloys of titanium during quenching and tempering 11 p1602 N85-20073
Quenching effects on iron site partitioning in the Apollo 17 orange glass composition 13 p2184 N85-23553
Experimental methods for quenching structures in lunar-analog silicate melts: Variations as a function of quench media and composition 13 p2184 N85-23554
Thermomechanical softening treatment for bearing and tool steels
[BLL-BISI-TRANS-22432-(9022.06)] 17 p2925 N85-28035
The state of martensite after quenching in a magnetic field
[BLL-BISI-TRANS-22297-(9022.06)] 17 p2926 N85-28051
Computer studies of the quench behavior of an SSC model dipole
[DE85-010633] 19 p3360 N85-30829
Structural transformation of a 9% Cr - 2%Mo steel (type Z10CDNbV 09-02) for use in steam generators for fast neutron reactors
[BLL-CE-TRANS-7943-(9022.09)] 20 p3430 N85-31271
Application of the unloading compliance methods in fracture toughness measurements of a quenched and tempered steel
[BLL-CE-TRANS-7953-(9022.09)] 20 p3465 N85-31523

QUERY LANGUAGES
A methodology for supporting views in relational databases 03 p0437 N85-12783
Interpretation of natural language database queries using optimization methods 05 p0735 N85-14723
Tree Query Language Flat (TQLF) specifications
[PB84-217116] 06 p0855 N85-15436
Relational Query Language Flat (RQLF) specifications
[PB84-217405] 06 p0855 N85-15439
Network Query Language Flat (NQLF) specifications
[PB84-217538] 06 p0855 N85-15440
Design and analysis of an SQL (Structured Query Language) interface for a multi-backend database system
[AD-A146534] 06 p0856 N85-15447
Design of a pictorial program reference language
[AD-A149323] 10 p1540 N85-19711

QUEUEING THEORY
Development of a production order release methodology
[AD-A145213] 01 p0124 N85-10852
On some common interests among reliability, inventory and queuing
[AD-A145595] 02 p0251 N85-11648
Optimal control of waiting time in a M/G/1 queue
[INPE-2767-PRE/340] 02 p0255 N85-11671
Applications of functional analytic and Martingale methods
[AD-A145555] 02 p0255 N85-11672
On a program for solution of BCMP queueing network model
[NAL-TR-813] 03 p0405 N85-12585
The application of queueing theory to communications networks: A review
[AD-A146680] 04 p0492 N85-13140
One queue or two pushdown stores take square time on a one-head tape unit
[CWI-CS-R8406] 05 p0717 N85-14601
Relaxation times for queueing systems
[CWI-OS-R8407] 05 p0719 N85-14618
DYNA-SIM: A nonstationary queuing simulation with application to the automated test equipment problem
[AD-A146364] 06 p0857 N85-15450
Omni transforms: Applications to renewal theory
[AD-A146939] 07 p1029 N85-16534

A single server queue with mixed types of interruptions
[AD-A148538] 08 p1213 N85-17837
Inequalities for the M/G/infinity queue and related shot noise processes
[AD-A149015] 10 p1545 N85-19737
The omni-transform in single-channel queues
[AD-A151019] 14 p2409 N85-24852
Algorithms and approximations for queueing systems
[CWI-TRACT-8] 14 p2410 N85-24859
Weak convergence of a sequence of queueing and storage processes to a singular diffusion
[AD-A150655] 14 p2411 N85-24866
A note on equivalent random theory
[CWI-OS-R8410] 14 p2412 N85-24872
Constructing unifying frameworks for the study of distributed system and algorithms
[AD-A151287] 15 p2637 N85-26261
Calculating reliability and productivity of cold stamping robot complex as queuing system 16 p2761 N85-27039
Replication methods for abstract data types
[AD-A153648] 18 p3162 N85-29587
Computer Performance Modeling Tool (CPMT)
[AD-A154436] 19 p3338 N85-30682
The architectural requirements and integration analysis of a database server for office automation
[AD-A155517] 21 p3674 N85-32825

QUINOLINE
Catalytic hydrotreatment studies with model compounds
[DE85-010187] 19 p3236 N85-30064

R

RABBITS
Influence of limboreticular complex on some reactions of rabbits 19 p3326 N85-30607

RACES
The 1981 transatlantic boat race contribution for marine meteorological measurements 14 p2324 N85-24361
NASA initiatives with historically black colleges and universities
[NASA-EP-210] 19 p3379 N85-30960

RACKS (FRAMES)
Preventing explosive propagation in racks or containers of tactical missiles
[AD-P004342] 10 p1455 N85-19166
Low-profile fastener
[AD-D011667] 19 p3280 N85-30343

RACON BEACONS
U RADAR BEACONS

RADAR
NT COHERENT RADAR
NT CONTINUOUS WAVE RADAR
NT DOPPLER RADAR
NT EARTH RESOURCES SHUTTLE IMAGING RADAR
NT IMAGING RADAR
NT INCOHERENT SCATTER RADAR
NT LANDING RADAR
NT METEOROLOGICAL RADAR
NT MONOPULSE RADAR
NT MOVING TARGET INDICATORS
NT MULTISPECTRAL RADAR
NT MULTISTATIC RADAR
NT OPTICAL RADAR
NT OVER-THE-HORIZON RADAR
NT PULSE DOPPLER RADAR
NT PULSE RADAR
NT RADAR MEASUREMENT
NT RANGE AND RANGE RATE TRACKING
NT SATELLITE-BORNE RADAR
NT SEARCH RADAR
NT SECONDARY RADAR
NT SIDE-LOOKING RADAR
NT SPACE BASED RADAR
NT SURVEILLANCE RADAR
NT SYNTHETIC APERTURE RADAR
NT TRACKING RADAR
Clutter generator for use in radar evaluation
[AD-D011234] 01 p0039 N85-10245
Programmable digital band integrators for the radar high-speed data acquisition system 05 p0624 N85-13994
SAR maritime missions 06 p0751 N85-14813
Radar frequency selection strategies
[AD-A147493] 07 p0941 N85-15967
LPI-radar for helicopter obstacle warning 08 p1074 N85-16810
In situ orbital debris experiment concepts 12 p1784 N85-21198
The ambiguity function and the Wigner distribution
[AD-A150095] 12 p1829 N85-21482
Remote sensing of directional wave spectra using the surface contour radar
[NASA-TM-84440] 14 p2347 N85-24510
Hygienic standardization of electromagnetic fields of radar systems 14 p2387 N85-24703
Hardware test program for evaluation of baseline range-range rate sensor concept
[NASA-CR-175794] 16 p2787 N85-27193
An analysis of the economic impact of the AN/APS-134 FLAR (Forward Looking Airborne Radar) retrofit on Coast Guard HC-130 aircraft
[AD-A152619] 17 p2949 N85-28204
Survivable ground base sensor
[AD-D011647] 17 p2950 N85-28213
The HURRA high resolution experimental radar system sampling unit
[FOA-C-30376-E1] 18 p3091 N85-29133
Optical techniques for signal distribution and control in advanced radar and communication systems 18 p3188 N85-29773
Orthogonalizer for inphase and quadrature digital data
[AD-D011679] 19 p3254 N85-30174
A single chip VLSI architecture for radar signal processing 19 p3257 N85-30195
The use of the glistening surface concept in rough surface scattering
[AD-A154922] 21 p3575 N85-32234
Power density and threshold control strategies for radar track initiation
[AD-A155357] 22 p3756 N85-33282
A planar version of a 4.0 gigahertz reactively steered adaptive array
[AD-A156029] 24 p4087 N85-35330

RADAR ALTIMETERS
U RADIO ALTIMETERS

RADAR ANTENNAS
Turnaround control for mechanically scanned radar antennas
[AD-D011238] 01 p0039 N85-10248
Structural aspects of SAR antenna for Japanese Earth Resources Satellite 1 05 p0626 N85-14007
Technology for the ERS-1 SAR antenna 05 p0626 N85-14008
CASA technological effort in the field of antennas — satellite radar antennas 05 p0626 N85-14010
Place of aperture synthesis in general theory of antennas (review) 06 p0781 N85-14993
Resolution and accuracy of radar measurements 06 p0789 N85-15044
Broadband pillbox antennas
[AD-A146569] 06 p0799 N85-15104
Fast switching driver for inductive load, such as a phase shifter
[AD-D011368] 08 p1143 N85-17207
Conformal phased array antenna pattern corrector
[AD-D011489] 10 p1468 N85-19266
Low sidelobe phased array antenna system
[AD-D011558] 12 p1823 N85-21435
Development of the F-20 nose radome
[AD-P004374] 12 p1827 N85-21468
Adaptive control of airborne radar antennas 13 p2080 N85-22989
Performance analysis of the DSN baseband assembly (Bba) Real-Time Combiner (RTC)
[NASA-CR-175877] 17 p2947 N85-28193
Inherent angular tracking error in an amplitude comparison monopulse radar
[AD-A154212] 19 p3255 N85-30185
Accuracy of velocity and power determination by the Doppler method 21 p3620 N85-32493
Improvement of vertical velocity measurements, part 3.4B 21 p3620 N85-32494
Mesospheric measurements of irregularity patchae using a 3-antenna interferometer, part 3.6B 21 p3621 N85-32498
Summary of progress at the Poker Flat Observatory in Alaska 21 p3628 N85-32539
A note on the proposed UK VHF radar 21 p3629 N85-32545
Signal space models for antenna arrays
[AD-A156063] 24 p4087 N85-35335

RADAR APPROACH CONTROL
Planned office and facility consolidations: To improve system effectiveness and efficiency, FY 1985-87
[AD-A150441] 13 p1970 N85-22376
Investigation of imaging and flight guidance concepts for rotorcraft zero visibility approach and landing
[NASA-CR-166571] 17 p2894 N85-27843

RADAR ASTRONOMY
A review of radar observations of Saturn's rings 15 p2670 N85-26474
Saturn's rings resolved by the VLA — Very Larg Array (VLA) 15 p2670 N85-26476
Mars: Seasonally variable radar reflectivity 15 p2683 N85-26570

RADAR ATTENUATION
Using measured variance of skywave radar sea-echo power spectra to estimate ionospheric Doppler broadening of mean spectra
[PB84-214071] 03 p0369 N85-12544

RADAR BEACONS
Development and flight test of a helicopter compact, portable, precision landing system concept 08 p1076 N85-16821
Development and flight test of a helicopter, X-band, portable precision landing system concept
[NASA-TM-86710] 16 p2710 N85-26721

RADAR BEAMS
Radar echo enhancement using surface reflections
[AD-A146970] 07 p0939 N85-15955
Use of alternative solvents for low-temperature LPE growth of CdTe films
[AD-A149418] 10 p1562 N85-19653

RADAR CROSS SECTIONS
Simultaneous ocean cross-section and rainfall measurements from space with a nadir-pointing radar
[NASA-TM-86167] 07 p0967 N85-16273
Numerical methods for analyzing electromagnetic scattering
[NASA-CR-175507] 12 p1823 N85-21438
Research efforts in support of resonance extraction studies. Volume 1: Improvement and validation of TWFD (Thin-Wire Frequency-Domain): A thin-wire frequency-domain scattering code
[AD-A150298] 13 p2054 N85-22984
High frequency estimation of 2-dimensional cavity scattering
[AD-A151697] 15 p2542 N85-25696
Scattering center analysis for radar cross section modification 16 p2769 N85-27065
An empirical self-protection chaff model
[AD-A151928] 16 p2773 N85-27115
Radiation and scattering of spiral antennas
[AD-A151929] 16 p2773 N85-27116
Radar target identification through electromagnetic scattering studies
[AD-A154596] 21 p3573 N85-32220
The use of the glistening surface concept in rough surface scattering
[AD-A154922] 21 p3575 N85-32234
Head-on scattering of a tubular cylinder of finite length for radar target identification purposes
[AD-A155608] 21 p3577 N85-32246
Normal modes in an overmoded circular waveguide coated with lossy material
[NASA-CR-176186] 24 p4085 N85-35320

RADAR DATA
Preliminary assessment of very short term forecasting of rain from single radar data 01 p0076 N85-10523
Adaptive preprocessing system
[AD-D011327] 07 p0937 N85-15935
On the generation of random variables for radar simulation purposes 07 p0938 N85-15947
An adaptive Fast Fourier Transform weighting technique to increase small target sensitivity
[AD-D011434] 08 p1154 N85-17286
Programmable realtime interface between a block floating point processor and memory
[AD-D011431] 08 p1203 N85-17571
Rain volume estimation over areas using satellite and radar data
[NASA-CR-174434] 10 p1518 N85-19568
Digital coherent detector
[AD-D011560] 12 p1833 N85-21501
Visualization of radar altimetry data for Venus 13 p1982 N85-22437
Forth system for coherent-scatter radar data acquisition and processing
[NASA-CR-176055] 20 p3494 N85-31720
Hardware schemes for fast Fourier transform, part 7.4A 21 p3626 N85-32526
Criteria and algorithms for spectrum parameterization of MST radar signals 21 p3626 N85-32527

RADAR DETECTION
Optimization of moving-target selection radar devices for nonGaussian signals for stationary targets 06 p0789 N85-15043
Radar frequency selection strategies
[AD-A147493] 07 p0941 N85-15967
Intrinsic polarization basis of radar target observed by system employing diversity reception 07 p0949 N85-16015
NORAD's PARCS small satellite tests (1976 and 1978) 12 p1783 N85-21191
Use of ground radar to detect reentering debris 12 p1784 N85-21200
Survivable ground base sensor
[AD-D011647] 17 p2950 N85-28213

Convective storm downdraft outflows detected by NASA/MSFC's Airborne 10.6 micron pulsed Doppler Lidar System
[NASA-CR-3696] 17 p2905 N85-29511
Detection of signals from coherent pulsed radars with random variation in parameters of sounding signals from pulse to pulse against background of worst-case Gaussian noise 22 p3763 N85-33324

RADAR DIRECTION FINDERS
U RADIO DIRECTION FINDERS

RADAR DISPLAYS
U RADARSCOPES

RADAR ECHOES
NT CLUTTER
NT LUNAR RADAR ECHOES
NT VENUS RADAR ECHOES
A scheme for the delineation and extrapolation of thunderstorms from GOES satellite data 01 p0078 N85-10507
Simulation of information extraction from radar altimeter return echoes --- ERS-1 (ESA satellite) 03 p0383 N85-12452
Using measured variance of skywave radar sea-echo power spectra to estimate ionospheric Doppler broadening of mean spectra
[PB84-214071] 03 p0399 N85-12544
Radar echo enhancement using surface reflections
[AD-A146970] 07 p0939 N85-15955
Design of an analog spectrum analyzer for probing experiments
[AD-A147384] 07 p0941 N85-15963
Test plan for the forest-echo experiment
[DE84-017175] 09 p1343 N85-18447
Digital coherent detector
[AD-D011580] 12 p1833 N85-21501
Preliminary results of associating cloud-to-ground lightning with surface convergence and radar reflectivity at Kennedy Space Center in 1983
[NASA-CR-175543] 12 p1897 N85-21910
Mars radar catalog 13 p2198 N85-23636
Experimental study of anisotropy of scattering of radar signals by clouds and precipitation 14 p2340 N85-24473
High frequency estimation of 2-dimensional cavity scattering
[AD-A151697] 15 p2542 N85-25896
The use of radar in determining precipitation processes in the BEWMEX area 16 p2831 N85-27455
Statistical comparison of radar echoes of convective precipitation between the northern Alps and its foreland
[DFVLR-FB-86-07] 17 p2950 N85-28215
Morphology of the scattering targets: Fresnel and turbulent mechanisms, part 2.1A 21 p3616 N85-32481
Signal statistics of the radar echoes: Angle-of-arrival statistics, part 2.2A 21 p3616 N85-32482
A modified Fresnel scattering model for the parameterization of Fresnel returns, part 2.3A 21 p3616 N85-32483
Observations of mesospheric turbulence by rocket probe and VHF radar, part 2.4A 21 p3619 N85-32484
Interpretation of radar returns from the mesosphere, part 2.5A 21 p3619 N85-32485
Radar echoes at 2.66 and 40.92 MHz from the mesosphere, part 2.6A 21 p3619 N85-32486
Anisotropy of the permittivity field inferred from aspect-sensitive radar echoes 21 p3620 N85-32492
Interferometer applications of VHF radars, part 3.6A 21 p3621 N85-32497
Most desirable terrain, e.g., flat vs valley location, part 5.1B 21 p3624 N85-32513
Interpolation problems in meteor radar analysis, part 7.8A 21 p3626 N85-32526
The effects of subrefractive layers and elevated ducts on airborne radar and ESM (Electronic Surveillance Measures)
[AD-A155524] 21 p3637 N85-32592

RADAR EQUIPMENT
NT PLAN POSITION INDICATORS
NT RADAR ANTENNAS
NT RADAR BEACONS
NT RADAR FILTERS
NT RADAR RECEIVERS
NT RADAR REFLECTORS
NT RADAR TRANSMITTERS
NT RADARSCOPES
NT RETROREFLECTORS
Radar, target and ranging
[AD-A145407] 02 p0190 N85-11272
Training capabilities test of Electronics Equipment Maintenance Trainer (EEMT): Findings and conclusions
[AD-A146075] 03 p0359 N85-12302
Diagnostic apparatus for radar pulse repetition frequency control circuit card
[AD-D011364] 07 p0937 N85-15938
Tracking servo compensator with rate aiding
[AD-D011372] 07 p0942 N85-15971
Propagation and scattering considerations for the 0.2-3.0 GHz frequency range for a space-based radar
[AD-A148504] 08 p1153 N85-17262
Measurement procedures for the radar spectrum engineering criteria
[PB85-119022/GAR] 09 p1313 N85-18254
The ambiguity function of random binary-phase-coded waveforms
[AD-A148906] 10 p1466 N85-19249
NORAD's PARCS small satellite tests (1976 and 1978) 12 p1783 N85-21191
Trajectory measurements for take-off and landing tests and other short-range applications, volume 16
[AGARD-AG-160-VOL-16] 15 p2561 N85-25801
High-power solid-state rf source for accelerator cavities
[DE85-012672] 22 p3761 N85-33309
Radar wind profilers in the Colorado network
[PB85-185466] 22 p3817 N85-33647

RADAR FILTERS
Gain restoration after Doppler filtering
[AD-D011425] 08 p1154 N85-17267

RADAR GEOLOGY
Volcanism and rift formation in Beta Regio, Venus: New radar results 13 p2176 N85-23507
Classification of circular features on Venus 13 p2177 N85-23511
Shuttle imaging radar-A (SIR-A) data analysis --- geology of the Ozark Plateau of southern Missouri, land use in western Illinois, and vegetation types at Koonamore Station, Australia
[NASA-CR-175785] 16 p2809 N85-27324
Planning for VRM: Radar and sonar studies of volcanic terrains on Earth, Venus and Mars 22 p3857 N85-33864

RADAR IMAGERY
A system for meteorological satellite, radar, conventional data and model analysis 01 p0062 N85-10551
Systematic data interpretation of remote sensing in the reception of hydrocarbons, volume 1
[E85-10008] 02 p0215 N85-11421
Production of optically correlated SEASAT-A (SEA satellite) SAR (Synthetic Aperture Radar) imagery at DREO (Defence Research Establishment Ottawa)
[AD-A145970] 03 p0355 N85-12281
Aspects and applications of SAR (Synthetic Aperture Radar) imagery for mensuration
[AD-A146301] 03 p0356 N85-12290
Multispectral (X and C band) crop classification with synthetic aperture radar (SAR-580) optical data 05 p0657 N85-14217
The SPOT data bank system 05 p0659 N85-14236
The SIR-B science investigations plan
[NASA-CR-174282] 08 p1143 N85-17208
The SIR-B science investigations plan: Introduction 08 p1143 N85-17209
Southern ocean sea-ice morphology and kinematics 08 p1144 N85-17217
SIR-B analysis of the Precambrian shield of Sudan and Egypt: Penetration studies and subsurface mapping 08 p1145 N85-17219
Quantitative use of multiincidence-angle SAR for geologic mapping 08 p1145 N85-17220
Geologic mapping of Indonesian rain forest with analysis of multiple SIR-B incidence angles 08 p1145 N85-17221
Evaluation of SIR-B data for identifying rainfall event occurrence and intensity 08 p1145 N85-17223
Microwave and optical remote sensing of forest vegetation 08 p1146 N85-17228
Evaluation of SIR-B imagery for geologic and geomorphic mapping, hydrology, and oceanography in Australia 08 p1146 N85-17229
The use of digital spaceborne SAR data for the delineation of surface features indicative of malaria vector breeding habitats 08 p1146 N85-17230
Interlobate comparison of glacial-depositional style as evidenced by small-relief glacial landscape features in Illinois, Indiana, and Ohio, utilizing SIR-B 08 p1146 N85-17231
SAR internal wave signature experiment 08 p1149 N85-17253
Information extraction and transmission techniques for spaceborne synthetic aperture radar images
[NASA-CR-174341] 08 p1150 N85-17256
SEASAT 3 and 4
[AD-A148343] 08 p1152 N85-17274
Second order Bragg scattering in a SAR
[AD-A148395] 08 p1152 N85-17275
Extraction of structural information from radar signals
[FOA-C-30370-E1] 08 p1155 N85-17292
The use of synthetic aperture radar imagery to detect hazards to navigation
[AD-A149324] 10 p1422 N85-18971
Analysis of data acquired by synthetic aperture radar and LANDSAT Multispectral Scanner over Kershaw County, South Carolina, during the summer season
[E85-10071] 10 p1503 N85-19485
Earth resources research using the Shuttle Imaging Radar system 11 p1713 N85-20779
Research in image understanding as applied to 3-D tomographic imaging with near optical resolution
[AD-A150098] 12 p1829 N85-21483
The imaging of internal waves by the SEASAT-A synthetic aperture radar
[AD-A149606] 12 p1875 N85-21761
The imaging of internal waves by the SEASAT-A synthetic aperture radar
[ARE(PORTLAND)TN-720/84] 13 p2054 N85-22660
Edge detection in SAR imagery using gradient operators --- synthetic aperture radar (SAR)
[AD-A149411] 13 p2054 N85-22662
Surfaces of asteroids and cometary nuclei 13 p2176 N85-23503
Volcanism and rift formation in Beta Regio, Venus: New radar results 13 p2176 N85-23507
Venus surface composition from radio/radar measurements 13 p2177 N85-23509
Classification of circular features on Venus 13 p2177 N85-23511
Correction and geological analysis of lunar 3.8 cm radar data 13 p2198 N85-23634
Landform identification on radar images 13 p2198 N85-23635
Mars radar catalog 13 p2198 N85-23636
Radar and the detection of liquid water on Mars 13 p2199 N85-23638
Intra-eruption geologic map from an x-band radar image during the May 18, 1980 eruption of Mount St. Helens, Washington 13 p2199 N85-23639
Radar observations of fissure-fed basaltic lava flows, Craters of the Moon, Idaho 13 p2199 N85-23640
Late Tertiary and Quaternary river systems of the eastern Sahara as mapped on shuttle radar and LANDSAT images 13 p2199 N85-23641
Remote sensing of directional wave spectra using the surface contour radar
[NASA-TM-84440] 14 p2347 N85-24510
Synthetic aperture radar data processing 14 p2396 N85-24780
Increasing the accuracy of processing radar pictures by excluding systematic point coordinate error component 15 p2488 N85-25356
Analysis of the Gran Desierto, Pinacte Region, Sonora, Mexico, via shuttle imaging radar
[NASA-CR-175711] 15 p2582 N85-25927
Contamination of the fetch-limited directional wave spectrum by waves emanating from an embayment
[NASA-TM-84441] 15 p2604 N85-26048
Radar return from vegetation covered terrains
[INPE-3470-PRE/713] 16 p2770 N85-27093
Synthetic aperture side-looking radar image adjustment 16 p2806 N85-27304
Investigation of imaging and flight guidance concepts for rotorcraft zero visibility approach and landing
[NASA-CR-166571] 17 p2894 N85-27843
Evaluation of Defense Mapping Agency level 1 second edition digital data for training simulator applications
[AD-A152444] 17 p2983 N85-28437
Application of artificial intelligence (AI) to radar image understanding
[AD-A152519] 17 p3017 N85-28654
Further study of digital matching of dissimilar images
[AD-A153112] 17 p3019 N85-28672
The multiple processor machine for image processing, volume 5
[ESA-CR(P)-1976-VOL-5] 18 p3164 N85-29603
Geological analyses of the surface of Venus and Mars from lander spacecraft images and orbital radar observations 19 p3384 N85-30993
Using ship wake patterns to evaluate SAR (Synthetic Aperture Radar) ocean wave imaging mechanisms. Joint US-Canadian Ocean Wave Investigation Project
[AD-A154633] 21 p3573 N85-32223
Use of spaceborne imaging radar in regional geomorphic studies 21 p3603 N85-32377
The Boot Lake MF imaging radar 21 p3628 N85-32537
Basic properties and interpretation of synthesized radar images of sea waves with long synthatization time 22 p3773 N85-33384
An experimental study of dielectric rod antennas for millimeter-wave imaging applications
[AD-A155832] 24 p4086 N85-35328
Surface cyclogenesis as indicated by satellite imagery
[PB85-191815] 24 p4124 N85-35566

Optical synthetic aperture techniques
[AD-A156151] 24 p4154 N85-35752
RADAR MAPS
NT RADAR IMAGERY
Progress in planetary raderclinometry
13 p2198 N85-23630
Mercury radar altimetry: A preliminary analysis
13 p2198 N85-23631
Millimetre wave pulse technology — satellite mapping
[ESA-CR(P)-2004] 20 p3478 N85-31611
Geology and geomorphology of the Roraima group, southeastern Venezuela 24 p4115 N85-35511
RADAR MEASUREMENT
Thermosonde and UHF radar measurements of C2 sub n at Westford, Massachusetts - July 1981
[AD-A145398] 02 p0190 N85-11270
Measurement of snow cover thickness by radar sounding 03 p0344 N85-12216
Rain volume estimation over areas using satellite and radar data 05 p0686 N85-14406
Resolution and accuracy of radar measurements
08 p0789 N85-15044
Statistical analysis of visual wave observations and gage/radar measurements
[AD-A146358] 06 p0796 N85-15100
Lidar measurements of structural characteristics of atmospheric turbulence 06 p0824 N85-15229
Development of radar to measure sea ice merits prize nomination 06 p0826 N85-15244
Intermediate results of radar backscatter measurements from summer sea ice
[AD-A147212] 07 p0940 N85-15960
Design of an analog spectrum analyzer for probing experiments
[AD-A147384] 07 p0941 N85-15963
Simultaneous ocean cross-section and rainfall measurements from space with a nadir-pointing radar
[NASA-TM-86167] 07 p0967 N85-16273
MWR, Meteor Wind Radars 08 p1184 N85-17462
The MST radar technique 08 p1185 N85-17466
Partial reflection spaced antenna wind measurements
08 p1185 N85-17467
Airborne lidar measurements of El Chichon stratospheric aerosols, October 1982 to November 1982
[NASA-RP-1136] 10 p1514 N85-19550
Radar calibration using direct measurement equipment and oblique photometry
[AD-D011530] 12 p1822 N85-21433
Experimental test of the three subaperture method for estimating target elevation angle
[AD-A149687] 12 p1851 N85-21614
Progress in planetary raderclinometry
13 p2198 N85-23630
Mercury radar altimetry: A preliminary analysis
13 p2198 N85-23631
Mapping and geological analysis of Mercury and Venus radar ranging data 13 p2198 N85-23633
Landform identification on radar images
13 p2198 N85-23635
Intermediate results of the NORDSEE experiment
[AD-A151363] 15 p2542 N85-25693
Radar turbulence estimates. Effects of wind shear and reflectivity factor gradients
[AD-A151676] 15 p2599 N85-26023
Radar measurement of thickness of drifting ocean ice employing cepstral signal processing
15 p2644 N85-26313
Progress in radar meteorology
16 p3148 N85-29486
Use of radar with frequency modulation for studying atmospheric boundary layer 19 p3296 N85-30437
Geological analyses of the surface of Venus and Mars from lander spacecraft images and orbital radar observations 19 p3384 N85-30993
Comparison of wind and turbulence measurements from Doppler lidar and instrumented aircraft
[NASA-CR-171535] 20 p3495 N85-31729
Middle Atmosphere Program. Handbook for MAP. Volume 14: URSI/SCOSTEP Workshop on Technical Aspects of MST Radar
[NASA-CR-176085] 21 p3615 N85-32466
Gravity waves from the stratosphere to the mesosphere, part 1.3B 21 p3616 N85-32471
General circulation of the middle atmosphere, part 1.4B 21 p3617 N85-32474
Performance of the Colorado wind-profiling network, part 1.5A 21 p3617 N85-32475
Vertical transport in the atmosphere: Measurement capabilities and requirements of VHF radars, part 1.6A
21 p3617 N85-32476
Comparison of tropopause altitude determination by the Platteville Radar, Sunset Radar and the NWS Rawinsonde 21 p3617 N85-32477
Synoptic-scale dynamics with vertical velocity, part 1.8A 21 p3617 N85-32478
Practical use of a tropopause height determination algorithm on an MST radar data set, part 1.8B
21 p3618 N85-32479
Usefulness of multifrequency MST radar measurements, part 2.6B 21 p3619 N85-32487
Use of the VAD technique and measurements of momentum flux in the stratosphere at Aercibo, part 4.3A
21 p3622 N85-32505
RADAR NAVIGATION
Guidance and navigation programs and plans
06 p0751 N85-14809
National airspace review: Airport radar service area operational confirmation report
[DOT/FAA/AT-84/2] 07 p0901 N85-15707
Interplanetary navigation 14 p2396 N85-24781
Autofocus motion compensation for synthetic aperture radar and its compatibility with strapdown inertial navigation sensors on highly maneuverable aircraft
[AD-A151940] 16 p2704 N85-26693
RADAR NETWORKS
A multipurpose weather radar network
01 p0077 N85-10510
Operational precipitation observation system using digitized radar and rain gages 01 p0082 N85-10549
The French weather radar network: A status report
01 p0082 N85-10550
Project COST 72 (The European weather radar project) today 01 p0084 N85-10561
SIR-B coverage 08 p1143 N85-17211
Design and realization of a multiradar tracking system for air traffic control
[ENST-84E010] 09 p1279 N85-18044
The global meteor observation system (GLOBMET)
11 p1658 N85-20432
Middle Atmosphere Program. Handbook for MAP. Volume 14: URSI/SCOSTEP Workshop on Technical Aspects of MST Radar
[NASA-CR-176085] 21 p3615 N85-32466
Meteorological and aeronomical requirements for MST radar networks (keynote paper), part 1
21 p3615 N85-32467
Performance of the Colorado wind-profiling network, part 1.5A 21 p3617 N85-32475
Comparison of tropopause altitude determination by the Platteville Radar, Sunset Radar and the NWS Rawinsonde 21 p3617 N85-32477
RADAR OBSERVATION
U RADAR TRACKING
RADAR PHOTOGRAPHY
Metric evaluation of SAR-580 optical images for cartographic purposes 05 p0659 N85-14231
Geological analyses of the surface of Venus and Mars from lander spacecraft images and orbital radar observations 19 p3384 N85-30993
RADAR RANGE
Radar, target and ranging
[AD-A145407] 02 p0190 N85-11272
Probability distribution density of normalized radar range 04 p0486 N85-13096
SIR-B coverage 08 p1143 N85-17211
Pulse heterodyne equipment for measurements of range and velocity of moving targets-pulse radar
[ESA-TT-845] 09 p1312 N85-18246
RADAR RECEIVERS
Fast envelope detector with bias compensation
[AD-D011228] 01 p0038 N85-10243
Test and evaluation of a coherent 35 gigahertz radar repeater
[AD-A145714] 02 p0191 N85-11280
NAVSTAR GPS (Global Positioning System) marine receiver performance analysis
[AD-A146414] 06 p0753 N85-14831
Bistatic coherent radar receiving system
[AD-D011447] 10 p1466 N85-19252
Multiple loop sidelobe canceller
[AD-D011533] 12 p1823 N85-21434
Digital coherent detector
[AD-D011560] 12 p1833 N85-21501
Summator of radio pulse signals
12 p1839 N85-21539
Methods of digital correction for channels of multichannel radar receivers 13 p2082 N85-23005
Cryogenically-cooled, low-noise microwave receivers: Present status and future needs
14 p2298 N85-24226
The HURRA, a high resolution experimental radar system broadband receiver
[FOA-C-30375-E1] 18 p3091 N85-29132
A multi-channel radar receiver
[AD-A156058] 24 p4087 N85-35333
RADAR RECEPTION
Intrinsic polarization basis of radar target observed by system employing diversity reception
07 p0949 N85-16015
Survivable ground base sensor
[AD-D011647] 17 p2950 N85-28213
Criteria for site selection and frequency allocation (keynote paper), part 5 21 p3623 N85-32511
Sidelobe reduction of Barker codes, part 7.1C
21 p3625 N85-32522
RADAR REFLECTIONS
U RADAR ECHOES
RADAR REFLECTORS
A scheme for the delineation and extrapolation of thunderstorms from GOES satellite data
01 p0076 N85-10507
CASA activities in antenna technology — satellite antennas 05 p0627 N85-14015
Data appendix: F-number = 1.0 EMR with a flexible back electrode
[NASA-CR-172477] 07 p0946 N85-15994
RADAR RESOLUTION
Resolution and accuracy of radar measurements
06 p0789 N85-15044
Limitation of VLBI angular resolution
07 p1057 N85-16710
Landform identification on radar images
13 p2198 N85-23635
RADAR SCANNING
Turnaround control for mechanically scanned radar antennas
[AD-D011238] 01 p0039 N85-10246
Mathematical model of discriminator for signals with fluctuations and thermal noise 13 p2072 N85-22943
The development and application of volume scan and cell tracking capabilities for the analysis of convective cloud systems 16 p2930 N85-27451
RADAR SCATTERING
The use of dual polarisation radar for observing and predicting convective activity 01 p0077 N85-10512
Anglo-German millimeter wave backscatter measurements on snow, environmental data report
[REPT-7-84] 04 p0492 N85-13136
Scattering models in the microwave regime
[NASA-CR-174001] 04 p0525 N85-13361
A comparison between active and passive sensing of soil moisture from vegetated terrains
04 p0526 N85-13364
Simultaneous ocean cross-section and rainfall measurements from space with a nadir-pointing radar
[NASA-TM-86167] 07 p0967 N85-16273
Evaluation of the L-band scattering characteristics of volcanic terrain in aid of lithologic identification, assessment of SIR-B calibration, and development of planetary geomorphic analogs 08 p1146 N85-17232
Extraction of structural information from radar signals
[FOA-C-30370-E1] 08 p1155 N85-17292
Incoherent scatter radar studies of the mesosphere
08 p1184 N85-17463
The MST radar technique 08 p1185 N85-17466
Oceanographic and meteorological research based on the data products of SEASAT
[E85-10091] 12 p1874 N85-21753
Intermediate results of the NORDSEE experiment
[AD-A151363] 15 p2542 N85-25693
Radiation and scattering of spiral antennas
[AD-A151929] 16 p2773 N85-27116
Modeling the backscattering and transmission properties of vegetation canopies
[E85-10099] 16 p2809 N85-27320
An analysis of physical optics models for rough surface scattering
[AD-A154980] 21 p3575 N85-32235
A modified Fresnel scattering model for the parameterization of Fresnel returns, part 2.3A
21 p3618 N85-32483
Observations of mesospheric turbulence by rocket probe and VHF radar, part 2.4A 21 p3619 N85-32484
Interpretation of radar returns from the mesosphere, part 2.3A 21 p3619 N85-32485
Radar echoes at 2.66 and 40.92 MHz from the mesosphere, part 2.6A 21 p3619 N85-32486
RADAR SIGNATURES
Autoregressive modeling and the classification of land clutter — radar signatures
[ENST-C-84003] 03 p0356 N85-12292
Quantitative use of multiincidence-angle SAR for geologic mapping 08 p1145 N85-17220
Geologic mapping of Indonesian rain forest with analysis of multiple SIR-B incidence angles
08 p1145 N85-17221
An electronically controlled array for simulation of passive target/background signatures at millimeter wavelengths
[AD-D011456] 10 p1468 N85-19263
Hardware test program for evaluation of baseline range/range rate sensor concept
[NASA-CR-175910] 17 p2947 N85-28194
The use of the glistening surface concept in rough surface scattering
[AD-A154822] 21 p3575 N85-32234

Automated cell detection as a mesocyclone precursor tool
[AD-A154952] 21 p3635 N85-32577
Hardware test program for evaluation of baseline range-range rate sensor concept
[NASA-CR-176143] 23 p3933 N85-34377
RADAR TARGETS
Joint services electronics program
[AD-A145085] 01 p0042 N85-10276
Estimation of target positioning using planar arrays
[RSRE-MEMO-3675] 02 p0189 N85-11266
Intrinsic polarization basis of radar target observed by system employing diversity reception
07 p0949 N85-16015
Shuttle ku-band communications/radar technical concepts 08 p1099 N85-16949
An adaptive Fast Fourier Transform weighting technique to increase small target sensitivity
[AD-D011424] 08 p1154 N85-17286
Loop radiating elements
[AD-D011409] 08 p1158 N85-17308
Multi-bistatic radar for short range surveillance
[BAE-BT-10603] 15 p2539 N85-25673
Hardware test program for evaluation of baseline range/range rate sensor concept
[NASA-CR-175910] 17 p2947 N85-28194
Digital methods of the optimum processing of radar signals
[AD-A152469] 17 p2948 N85-28202
Inherent angular tracking error in an amplitude comparison monopulse radar
[AD-A154212] 19 p3255 N85-30185
Radar target identification through electromagnetic scattering studies
[AD-A154596] 21 p3573 N85-32220
Head-on scattering of a tubular cylinder of finite length for radar target identification purposes
[AD-A155608] 21 p3577 N85-32246
Broadside scattering of a tubular cylinder for evaluation of target identification
[AD-A155739] 21 p3577 N85-32248
Morphology of the scattering targets: Fresnel and turbulent mechanisms, part 2.1A
21 p3618 N85-32481
USSR report: Electronics and electrical engineering
[JPRS-UEE-84-015] 22 p3762 N85-33314
Method of static measurements of absolute scattering matrix of radar targets 22 p3762 N85-33316
Selectivity of weight compensator of passive interference to unknown velocities of detectable targets
22 p3762 N85-33317
Potential coordinate estimate accuracy estimation accuracy by multiposition radar systems
22 p3763 N85-33322
RADAR TRACKING
Estimation of target positioning using planar arrays
[RSRE-MEMO-3675] 02 p0189 N85-11266
Modelling of altimeter tracking over topographical surfaces — satellite antennas 03 p0363 N85-12450
A feasibility study on the use of wind profilers to support Space Shuttle launches
[NASA-CR-3881] 04 p0536 N85-13423
Tracking servo compensator with rate aiding
[AD-D011372] 07 p0942 N85-15971
Shuttle ku-band communications/radar technical concepts 08 p1099 N85-16949
Hybrid state estimation approach to multiobject tracking for airborne surveillance radars
[AD-A148459] 08 p1153 N85-17279
Methodology improvement program for the second generation mise distance radar (MIDI 2)
[AD-A148467] 08 p1153 N85-17281
Design and realization of a multiradar tracking system for air traffic control
[ENST-84E010] 09 p1279 N85-18044
Investigations relating to the simultaneous use of Combined Optical Adaptive Techniques (COAT) and angle-tracking
[ESA-TT-844] 09 p1365 N85-18712
Multi target tracking by dynamic scene analysis
[AD-A148822] 10 p1466 N85-19250
MTI system simulation and clutter output statistics
[AD-A149193] 10 p1467 N85-19255
Fundamental limits to synchronization and tracking
[AD-A149823] 12 p1833 N85-21504
Synthesis of optimum algorithms for secondary processing 13 p2090 N85-22992
High time-resolution studies of the auroral ionosphere
[AD-A150945] 14 p2409 N85-24850
Estimation of maneuvering targets
15 p2636 N85-26253
An empirical self-protection chaff model
[AD-A151928] 16 p2773 N85-27115
Ziv-Zakai bound applied to an amplitude-comparison monopulse radar
[AD-A151937] 16 p2773 N85-27118
A short range, high accuracy radar ranging system
[AD-A152195] 16 p2774 N85-27122
A constant altitude flight survey method for mapping atmospheric ambient pressure and systematic radar errors
[NASA-TM-86733] 19 p3217 N85-29951
Docking simulation analysis of range data requirements for the orbital maneuvering vehicle
[NASA-TM-86510] 20 p3407 N85-31143
RADAR TRANSMISSION
Pulse transmission through frozen silt
[AD-A147108] 07 p0940 N85-15958
Factorized algorithms for combined spatial and temporal processing of radar signals 13 p2091 N85-22997
A review of tropospheric refraction effects on Earth-to-satellite systems 16 p3107 N85-29235
Criteria and algorithms for spectrum parameterization of MST radar signals 21 p3626 N85-32527
Feasibility study of radar-transmitting materials
[AD-A155639] 24 p4087 N85-35329
RADAR TRANSMITTERS
Architecture for a demonstration radar-communication link
[AD-A147635] 08 p1150 N85-17260
Digital controller for the Wave Propagation Laboratory's VHF and UHF wind-profiling radars
[PB85-112142] 11 p1626 N85-20238
The Chinese remainder theorem and multi-PRF radars
[AD-A141375] 13 p2054 N85-22858
Summary of session on optimum transmitter and antenna configuration for MST radar, part 6
21 p3624 N85-32514
Increase of antenna area instead of transmitter power, part 6.3A 21 p3624 N85-32517
RADARSCOPES
NT PLAN POSITION INDICATORS
Visual attention to radar displays
05 p0704 N85-14514
RADIAL DISTRIBUTION
Transport experiments in the Texas experimental Tokamak 09 p1389 N85-18741
Numerical simulation of the effects of radially injected barium plasma in the ionosphere
[NASA-CR-175638] 14 p2354 N85-24542
On the radial structure of planetary rings
15 p2675 N85-26512
Inherent magnetic field error measurements in ELMO Bumpy Torus
[DE85-005855] 16 p2667 N85-27685
Testing and optimizing MST coaxial collinear arrays, part 6.4A 21 p3625 N85-32518
The galactic gamma-ray distribution and the radial cosmic ray gradient
[OG-3.1-4] 22 p3873 N85-33992
Radial distribution of cosmic ray intensity in the galaxy from gamma-ray data
[OG-3.1-5] 22 p3873 N85-33993
Constraints on the galactic distribution of cosmic rays from the COS-B gamma-ray data
[OG-3.1-6] 22 p3873 N85-33994
Breakdown of intrinsic ambipolarity for the radial diffusion due to a rotating RF field 23 p3977 N85-34660
Transports studies of ECH and ICRH-heated bumpy torus plasma in NBT-1M 23 p3978 N85-34662
Analytic and numerical calculations of the ambipolar electric field in a stellarator 23 p3978 N85-34665
Radial and latitudinal gradients of anomalous oxygen during 1977 - 1985
[SH-4.6-4] 23 p4039 N85-35042
The cosmic ray interplanetary radial gradient from 1972 - 1985
[SH-4.7-1] 23 p4040 N85-35046
A note on some statistical properties of rise time parameters used in muon arrival time measurements
[HE-4.7-12] 24 p4199 N85-36062
RADIAL DRAINAGE PATTERNS
U DRAINAGE PATTERNS
RADIAL FLOW
Turbine test report, addendum
[DE84-015130] 02 p0205 N85-11353
Stability of circular cylindrical shell with piecewise constant thickness subjected to radial pressure
06 p0779 N85-14962
The modelling of latitudinal gradients in the solar wind in the outer solar system 12 p1947 N85-22231
Coupling between velocity oscillations and solid propellant combustion
[AD-A151081] 14 p2247 N85-23927
RADIAL VELOCITY
South African Astronomical Observatory Circulars, no. 7
[SAAOC-7] 01 p0127 N85-10875
Simultaneous photometry and radial velocities of dwarf cepheids and Delta Scuti stars
01 p0128 N85-10878
A wide latitude CO survey of molecular clouds in the northern Milky Way 06 p0877 N85-15574
High precision measurement of stellar radial velocity variations 08 p1250 N85-17866
Atmospheric limitations in stellar seismology: Should one measure radial velocity or brightness fluctuations?
08 p1251 N85-17869
A spectroscopic study of LMC X-4
[NASA-CR-174414] 10 p1571 N85-19905
1983 observations of the eclipsing nucleus of the bipolar planetary nebula NGC 2346 11 p1747 N85-20997
Multi-year and possibly periodic variations in the UV spectrum of 56 Pegasi 11 p1756 N85-21046
Three short-period binaries seen at high-dispersion UX ARI, IOTA TRI and HA5110 11 p1756 N85-21047
Precise measurements of radial velocities of emission lines in the far-ultraviolet spectra of late-type stars
11 p1758 N85-21062
Experimental determination of optimum ratio of runner blade height at exit to runner blade height at entrance of radial inward-flow microturbines
13 p2049 N85-22627
The effects of image motion on the I-nu diagram
14 p2443 N85-25076
The ultraviolet spectra of intermediate redshift quasars
20 p3544 N85-32056
The distribution and dynamics of planetary nebulae in M32 and the Andromeda Galaxy
20 p3546 N85-32068
Use of the VAD technique and measurements of momentum flux in the stratosphere at Aercibo, part 4.3A
21 p3622 N85-32505
Coding schemes for improving MST radar performance, part 7.1A 21 p3625 N85-32520
RADIANCE
ISCCP Cloud Algorithm Intercomparison Workshop
01 p0073 N85-10485
Spectroradiometric calibration of the Thematic Mapper and Multispectral Scanner system
[E85-10026] 02 p0218 N85-11439
Report of the Third Session of the International Working Group on Data Management for the International Satellite Cloud Climatology Project (ISCCP)
[WCP-82] 02 p0231 N85-11504
Theoretical elements of photometry
[BLL-RISLEY-TR-5022-(9091.9F)]
02 p0279 N85-11821
Effects of atmospheric water vapor and clouds on NOAA (National Oceanic and Atmospheric Administration) AVHRR (Advanced Very High Resolution Radiometer) satellite data
[AD-A145425] 02 p0280 N85-11824
LANDSAT instruments characterization
[E85-10032] 04 p0524 N85-13356
Flux reconstruction and calibration
09 p1412 N85-18904
PMP-1: A coordinated study of the behavior of the middle atmosphere in winter 11 p1654 N85-20421
PMP-1 report: The fourth winter of PMP-1, 1981 - 1982: A winter with several interesting features
11 p1657 N85-20441
Prelaunch absolute radiometric calibration of the reflective bands on the LANDSAT-4 protoflight Thematic Mapper 11 p1689 N85-20515
Relative radiometric calibration of LANDSAT TM reflective bands 12 p1869 N85-21725
Evaluation of the radiometric integrity of LANDSAT 4 Thematic Mapper band 6 data 12 p1869 N85-21726
Thermal band characterization of the LANDSAT-4 Thematic Mapper 12 p1869 N85-21727
MTF analysis of LANDSAT-4 Thematic Mapper
12 p1871 N85-21737
GMS operational calibration procedure and status
12 p1895 N85-21893
Analysis of selective chopper radiometer data
[NASA-CR-175157] 12 p1895 N85-21894
Remote sensing of coastal wetlands biomass using Thematic Mapper wavebands — Lewes, Delaware
13 p2119 N85-23106
The relationship between marine aerosol particles and satellite-detected radiance 13 p2131 N85-23263
Sea surface temperatures from VAS MSI data
[NASA-CR-175706] 14 p2382 N85-24689
Radiative forcing of the southwest summer monsoon (a satellite perspective) 15 p2593 N85-25981
Diagnosis of vertical motions from VAS retrievals during a convective outbreak
[NASA-CR-171569] 19 p3316 N85-30554
A transportable, machine oriented library of european sky and terrain radiance distributions with contemporary radiometric and meteorological profiles
[AD-A155254] 21 p3637 N85-32500
Diurnal variations of cosmic ray geomagnetic cut-off threshold rigidities
[SH-8.1-21] 23 p4046 N85-35092

RADIANT COOLING
Selective radiative cooling with MgO and/or LiF layers
[DE85-011595] 19 p3262 N85-30226
RADIANT ENERGY
U RADIATION
RADIANT FLUX DENSITY
NT ELECTRON FLUX DENSITY
NT ILLUMINANCE
NT IRRADIANCE
NT LUMINANCE
NT LUMINOUS INTENSITY
NT NEUTRON FLUX DENSITY
NT PARTICLE FLUX DENSITY
NT PROTON FLUX DENSITY
NT RADIANCE
NT SOLAR CONSTANT
NT SOLAR FLUX DENSITY
Self-modulation of injection laser emission intensity due to external optical feedback 02 p0261 N85-11706
Einstein solid state spectrometer observation of the peculiar red dwarf Wolf 630 AB
[NASA-TM-83947] 03 p0447 N85-12843
Software used with the flux mapper at the solar parabolic dish test site
[NASA-CR-174106] 04 p0528 N85-13376
Device for measuring average power of laser radiation 06 p0786 N85-15026
Birkeland currents correlated with dc-electric fields observed during the CENTAUR BBX rocket experiments
[DRI-6-84] 06 p0834 N85-15311
NGC 2024: Multi-wavelength infrared and radio observations 08 p1246 N85-17865
New lighting technologies, their status and impacts on power densities
[DE85-000712] 09 p1315 N85-18266
Temperature variation of laser mirror stability criteria 10 p1445 N85-19108
Thermionic converter for space reactor described 11 p1621 N85-20208
EXOSAT observations of the galactic bulge X-ray source GX17+2 — X ray binary star 11 p1742 N85-20951
Performance estimate of a reflecting light pipe for infrared detectors
[AD-A141269] 13 p2158 N85-23396
Radiative forcing of the southwest summer monsoon (a satellite perspective) 15 p2593 N85-25981
Amplification of scattered induced radiation flux in high-gain laser rods 15 p2644 N85-26309
Screening ceramic materials for intense radiant heat applications
[DE85-006989] 16 p2756 N85-27006
Microwave responses of the western North Atlantic
[NASA-CR-175868] 17 p2946 N85-28191
Symposium on Luminescent Radiation Receivers and Converters 19 p3295 N85-30430
Plasma arc welding, equipment, installation and process control
[DE85-008481] 19 p3373 N85-30921
Existence of smooth solutions in problems of electromagnetic radiation focusing 21 p3697 N85-32972
Gamma-ray line intensities for depleted uranium
[DE85-012874] 22 p3843 N85-33804
Search for excess showers from Crab Nebula
[OG-2.3-2] 22 p3866 N85-33939
The 1000 GeV gamma ray emission from radio pulsars 22 p3867 N85-33948
Cosmic gamma rays from quasars
[OG-2.7-10] 22 p3872 N85-33983
Energy spectrum of extragalactic gamma-ray sources
[OG-2.7-13] 22 p3872 N85-33986
Local interstellar medium and gamma-ray astronomy
[OG-3.1-1] 22 p3873 N85-33989
The galactic gamma-ray distribution and the radial cosmic ray gradient
[OG-3.1-4] 22 p3873 N85-33992
Radial distribution of cosmic ray intensity in the galaxy from gamma-ray data
[OG-3.1-5] 22 p3873 N85-33993
Constraints on the galactic distribution of cosmic rays from the COS-B gamma-ray data
[OG-3.1-6] 22 p3873 N85-33994
Local electron spectrum above 100 MeV derived from gamma-ray emissivity spectra
[OG-3.1-7] 22 p3874 N85-33995
Relevance of cosmic gamma rays to the mass of gas in the galaxy
[OG-3.1-8] 22 p3874 N85-33996
COS-B gamma-ray sources and interstellar gas
[OG-3.1-9] 22 p3874 N85-33997
Excess gamma rays from the Loop I supernova remnant
[OG-3.1-10] 22 p3874 N85-33998
Long term variability of the cosmic ray intensity
[OG-3.1-11] 22 p3874 N85-33999
Spectrum of the gamma-ray diffuse component observed from HEAO-1
[OG-3.1-12] 22 p3874 N85-34000
Galactic antiprotons of 0.2-2 GeV energy
[OG-6.1-11] 22 p3886 N85-34101
the role of shock waves in modulation of galactic cosmic rays
[SH-4.1-7] 23 p4005 N85-34831
Cumulative effect of Forbush decreases in the heliospheric modulation during the present solar cycle
[SH-4.1-10] 23 p4005 N85-34833
Cosmic ray modulatin and merged interaction regions
[SH-4.1-11] 23 p4005 N85-34834
Propagation of the phase of solar modulation
[SH-4.1-12] 23 p4006 N85-34835
Longitudinal distribution of cosmic rays in the heliosphere
[SH-4.1-14] 23 p4006 N85-34837
The 1973-1984 solar modulation of cosmic ray nuclei
[SH-4.1-16] 23 p4006 N85-34838
Evidence for regions of negligible cosmic-ray modulation in the inner heliosphere (10 AU)
[SH-4.1-21] 23 p4006 N85-34840
Notes on drift theory
[SH-4.2-3] 23 p4006 N85-34841
Drift and observations in cosmic-ray modulation, 2
[SH-4.2-5] 23 p4007 N85-34843
Propagation and nucleosynthesis of ultraheavy cosmic rays
[OG-7.1-5] 23 p4013 N85-34857
High resolution Cherenkov detectors for cosmic ray isotope experiment
[OG-9.1-4] 23 p4023 N85-34930
The final COS-B database now publicly available
[OG-9.3-8] 23 p4028 N85-34963
The final COS-B database: In-flight calibration of instrumental parameters
[OG-9.3-9] 23 p4028 N85-34964
An observatory to study 10 (10) to 10 (17) by EV gamma rays
[OG-9.4-6] 23 p4029 N85-34973
Mini and super mini arrays for the study of highest energy cosmic rays
[OG-9.4-9] 23 p4029 N85-34976
Cosmic ray biannual variation
[SH-4.4-15] 23 p4034 N85-35011
Cosmic ray power spectral variations. 3: Solar rotation periodicities
[SH-4.4-16] 23 p4034 N85-35012
The difference in the energy spectra of galactic cosmic rays at the minima of the 19th and 20th solar activity cycles
[SH-4.4-18] 23 p4035 N85-35014
Cosmic ray variations with the period close to 27 days and their connection with solar activity longitudinal distribution
[SH-4.4-19] 23 p4035 N85-35015
Azimuthal and meridional asymmetries of the solar wind and quasiperiodic variations of intensity of Galactic Cosmic Rays (GCR)
[SH-4.4-20] 23 p4035 N85-35016
Dynamics of two-year cosmic ray variations inferred from the data of spacecraft and stratospheric measurements and from the neutron monitor data in 1958-1981
[SH-4.4-21] 23 p4035 N85-35017
Long-term modulation of galactic cosmic rays in high-energy region
[SH-4.4-22] 23 p4035 N85-35018
Diurnal effect in cosmic rays at middle latitudes according to stratospheric measurements
[SH-4.5-8] 23 p4036 N85-35026
Diurnal variation of galactic cosmic ray intensity on quiet days
[SH-4.5-11] 23 p4037 N85-35029
Diurnal variations from muon data at Takayama underground station
[SH-4.5-13] 23 p4037 N85-35030
Long term changes in cosmic ray diurnal variations observed by ion chambers in Hong Kong and Japan
[SH-4.5-14] 23 p4037 N85-35031
Cosmic ray density gradient and its dependence on the north-south asymmetry in solar activity
[SH-4.5-17] 23 p4038 N85-35034
Diagnostic of electromagnetic conditions in space using cosmic rays
[SH-4.5-19] 23 p4038 N85-35036
Solar cycle variations of the anomalous cosmic ray component
[SH-4.6-2] 23 p4039 N85-35040
Temporal variations of the anomalous oxygen component, 1977 - 1984
[SH-4.6-3] 23 p4039 N85-35041
Radial and latitudinal gradients of anomalous oxygen during 1977 - 1985
[SH-4.6-4] 23 p4039 N85-35042
The cosmic ray interplanetary radial gradient from 1972 - 1985
[SH-4.7-1] 23 p4040 N85-35046
When did the average cosmic ray flux increase?
[SH-7.1-4] 23 p4047 N85-35097
The structure of Herbig-Haro object 43 and Orion dark cloud extinction
[NASA-TM-87503] 24 p4166 N85-35831
Measurement of interaction cross section of cosmic ray Fe nuclei (E4 GeV/N) with Al target
[HE-1.1-7] 24 p4170 N85-35855
RADIANT HEATING
New concepts for measuring flame spread properties
[NBSIR-84-2943] 03 p0327 N85-12104
Ceramic/ceramic seals by microwave heating
[DE84-007486] 04 p0479 N85-13050
Summary of the origin of nonradiative heating/momentum in hot stars 08 p1236 N85-17788
Spontaneous ignition of organic solids by radiant heating 09 p1289 N85-18096
The thermal calculation of opaque heat screens
[BLL-M-36273-(5828.4)] 20 p3450 N85-31421
The Konstantinov effect and absorption of sound in inhomogeneous media 21 p3660 N85-32661
Characterization of the optical and thermal properties of matter by photothermal techniques
[DE85-012807] 24 p4076 N85-35260
Development of advanced high-temperature heat flux sensors. Phase 2: Verification testing
[NASA-CR-174973] 24 p4096 N85-35391
RADIANT INTENSITY
U RADIANT FLUX DENSITY
RADIATION
Photothermal degradation of encapsulants 06 p0830 N85-15270
Most desirable terrain, e.g., flat vs valley location, part 5.1B 21 p3624 N85-32513
Longitudinal distribution of cosmic rays in the heliosphere
[SH-4.1-14] 23 p4006 N85-34837
The identification of gamma ray induced EAS
[HE-4.5-1] 24 p4195 N85-36029
RADIATION ABSORPTION
NT ATMOSPHERIC ATTENUATION
NT ELECTROMAGNETIC ABSORPTION
NT GAMMA RAY ABSORPTION
NT INFRARED ABSORPTION
NT MOLECULAR ABSORPTION
NT MULTIPHOTON ABSORPTION
NT PHOTOABSORPTION
NT ULTRAVIOLET ABSORPTION
NT X RAY ABSORPTION
Specific absorption rate in a sitting rhesus model at 225, 1290, and 5950 MHz for E, H, and K polarizations
[AD-A145435] 02 p0234 N85-11524
Aharonov-Bohm effect in absorption of electromagnetic wave 06 p0786 N85-15022
Acoustoelectric interaction in double-layer semiconductors 06 p0786 N85-15023
Spectral estimators of absorbed photosynthetically active radiation in corn canopies
[E85-10041] 07 p0983 N85-18242
Calculation of Si(Li) X-ray detector efficiencies
[DE85-002732] 10 p1469 N85-19400
Techniques for measuring intercepted and absorbed PAR in corn canopies
[E85-10081] 10 p1505 N85-19485
Latitudinal dependence of the energy input into the mesosphere by high energy electrons 11 p1664 N85-20489
Numerical investigation of propagation of radiation pulse at xxx 11 p1718 N85-20809
Surface physics and crystallography
[DE85-003128] 11 p1735 N85-20910
A method for determining in situ the absorption coefficient of particulate media using pulsed laser technique
[AD-D011548] 12 p1799 N85-21281
Control of electronic, magnetic and optical properties of doped polyacetylene conductors
[AD-A150117] 12 p1814 N85-21375
Correctness of reflection characteristics of radio absorbent materials 13 p2081 N85-22995
A plasma initiation-flow chamber to study CW laser beamed energy absorption in light gases
[AD-A151225] 15 p2562 N85-25806
Nuclear radiation induced absorption in optical materials
[DE85-007128] 15 p2649 N85-26336
Gyrotron traveling-wave device including quarter wavelength anti-reflective dielectric layer to enhance microwave absorption
[AD-D011690] 19 p3271 N85-30285

Influence of surface films of petroleum products on conditions for absorption of solar radiation by upper water layer 19 p3289 N85-30396
Detection of excited states by laser-induced fluorescence
[AD-A155558] 21 p3592 N85-32326
Absorption and scattering properties of aerosols of aggregated particles in the infrared spectral region
[AD-A155475] 21 p3637 N85-32591
Luminescence and absorption of indium-activated potassium-borate glasses subjected to high-power excitation 21 p3661 N85-32668
Absorption of laser radiation in substance with absorption coefficient depending linearly upon temperature 21 p3694 N85-32953
A practical guide to ionization chamber dosimetry at the AFRRI reactor
[AD-A155185] 21 p3703 N85-33003
An approach of reducing the background induced by neutrons
[OG-9.3-5] 23 p4027 N85-34960
Linear absorption and scattering of laser beams
[AD-A156167] 24 p4096 N85-35401
Some nuclear data needs in astrophysics
[DE85-012016] 24 p4166 N85-35842

RADIATION BELTS
NT INNER RADIATION BELT
NT OUTER RADIATION BELT
NT PROTON BELTS
Equatorial energetic distributions of ions of terrestrial radiation belt as function of solar corona temperature response 02 p0160 N85-11097
Earth's radiation belts
[AD-A147927] 07 p0996 N85-16339
Effects of the solar-terrestrial environment on satellite operations
[DE85-002413] 11 p1590 N85-20003
Longitude and pitch-angle distributions of streams of high-energy electrons under Earth's radiation belts 13 p1978 N85-22415
Protons with energies above 30 KeV in Earth's radiation belt at low altitudes during magnetically quiet time close to geomagnetic equator 13 p1980 N85-22423
SAMBO-GEOS: Substorm trapped particle particle boundary movements, particle precipitation and acceleration 14 p2361 N85-24589
Experimental check of ion transport mechanism in Earth's radiation belt with exposure to nonsteady-state electric fields 15 p2480 N85-25308
Substorms in energetic radiation belt particles according to data from Meteor artificial Earth satellite 16 p2719 N85-26788
Cosmic-ray transport in the galactic magnetosphere
[OG-7.2-17] 23 p4016 N85-34884

RADIATION CHEMISTRY
NT PHOTODECOMPOSITION
NT PHOTODISSOCIATION
NT PHOTOLYSIS
Magnetic resonance studies of transient radicals and radical ions
[DE84-011669] 03 p0328 N85-12116
USSR report: Chemistry
[JPRS-UCH-84-012] 06 p0761 N85-14865
Local phase transformation in alloys during charged-particle irradiation
[DE85-005012] 14 p2258 N85-23990
Measurements of radiation-induced segregation and diffusion in ion irradiated alloy using implanted manganese
[AERE-R-11526] 14 p2258 N85-23994

RADIATION COUNTERS
NT CERENKOV COUNTERS
NT NEUTRON COUNTERS
NT NEUTRON SPECTROMETERS
NT PARTICLE TELESCOPES
NT PROPORTIONAL COUNTERS
NT QUANTUM COUNTERS
NT SCINTILLATION COUNTERS
NT SPARK CHAMBERS
A system for monitoring radon and its decay products in the atmosphere
[INPE-3085-PRE/494] 03 p0391 N85-12502
Isotopic composition of primary cosmic rays H-Fe for ISEE-C
[NASA-CR-175266] 05 p0746 N85-14783
Comparison measurements on optical particle counters
[BLL-DOUNREAY-TR-934-(9091.9F)] 07 p0991 N85-16082
New preamplifier for particle detectors
[DE85-004115] 12 p1836 N85-21524
On the P1 data from GMS-SEM 12 p1894 N85-21890
Photon detection with cooled avalanche photodiodes: Theory and preliminary experimental results 16 p2770 N85-27096
Evaluation of a high pressure proportional counter for the detection of radioactive noble gases
[AD-A154436] 19 p3272 N85-30292
Photon-counting image sensors for the ultraviolet
[NASA-CR-176062] 20 p3458 N85-31478
Journal of Research of the National Bureau of Standards, volume 90, number 1, January - February 1985
[PB85-179063] 20 p3522 N85-31908
Plastic scintillator detectors for the study of transfer and breakup reactions at intermediate energies
[DE85-009945] 20 p3528 N85-31945
An absolute calibration of the solid state detectors in the narrow band neutrino beam at CERN
[NIKHEF-H/84-10] 20 p3536 N85-32017
Solar Ultraviolet Spectral Irradiance Monitor (SUSIM) 23 p3901 N85-34160
The response of ionization chambers to relativistic heavy nuclei
[OG-9.1-13] 23 p4024 N85-34939
Comparisons of monthly mean cosmic ray counting rates observes from worldwide network of neutron monitors
[SH-9.1-7] 23 p4051 N85-35122
Working group on penetrating probes at fixed target facilities 24 p4146 N85-35703
Microprocessor-based single particle calibration of scintillation counter
[HE-4.6-13] 24 p4196 N85-36049
The thickness of the shower disc as observed in showers produced by primaries above 10 (19)eV
[HE-4.7-6] 24 p4199 N85-36057
Search for anomalons using plastic nuclear track detectors
[HE-6.2-12] 24 p4212 N85-36148

RADIATION DAMAGE
NT LASER DAMAGE
Microwave susceptibility experiments
[DE84-016188] 02 p0192 N85-11281
Review: Role of refractory metal alloys in fusion reactor applications
[AERE-R-11317] 03 p0422 N85-12695
Investigation of internal fields and motions, radiation damages and recovery processes using beta and gamma active probe nuclei 03 p0427 N85-12726
Spectroscopic investigations on neutron induced impurity atoms and radiation defects 03 p0430 N85-12742
A study of defects in neutron transmutation doped silicon: Gallium by hall effect analysis
[AD-A146047] 03 p0433 N85-12758
Preliminary results of advanced Biostack experiments with plant seeds and spores — cosmic ray effects 05 p0691 N85-14441
Chemical protection against ionizing radiation
[AD-A147822] 07 p1016 N85-16457
Electron-irradiated effects in metals
[DE84-016869] 09 p1297 N85-18147
Facilities for studing radiation damage in nonmetals during irradiation
[DE85-000590] 10 p1554 N85-19801
Lithium counterdoped silicon solar cell
[NASA-CASE-LEW-14177-1] 11 p1672 N85-20535
Technological process effect on the carrier lifetime degradation of silicon solar cell base layer irradiated by 1 MeV electrons (boron doping case) 13 p2007 N85-22585
The effects of lithium counterdoping on radiation damage and annealing in n(+)p silicon solar cells 13 p2007 N85-22586
Investigation of the degradation of GaAs photovoltaic cells by proton and electron irradiation 13 p2008 N85-22587
In-orbit laser regeneration of the radiation damaged solar arrays 13 p2008 N85-22588
Analysis of optimum front cover thickness for lightweight solar arrays 13 p2010 N85-22606
Annealing of radiation damage in boron and gallium doped silicon solar cells 13 p2012 N85-22624
Some observations of heated gallium arsenide heteroface solar cells
[NASA-TM-86386] 14 p2246 N85-23925
Laser annealing of ion implanted HgCdTe
[AD-A150875] 14 p2427 N85-24966
ELF (Extremely Low Frequency) communications system ecological monitoring program: Measurements of ELF electromagnetic fields for site selection and characterization, 1983
[AD-A153120] 17 p2949 N85-28209
Radiation damage and repair in cells and cell components. Part 2: Physical radiations and biological significance
[DE85-006934] 18 p3152 N85-29518
Radiation damage and repair in cells and cell component, part 1
[DE85-006667] 18 p3152 N85-29519
Thin layered interference mirrors to reduce radiation damage
[DE85-009763] 18 p3185 N85-29756
Summary of recent studies on AlGaAs/GaAs radiation hardened photodiodes
[DE85-009501] 18 p3194 N85-29812
Electron spin resonance study of interface states induced by electron injection in metal-oxide-semiconductor devices
[DE85-009502] 18 p3195 N85-29817
Collected epidemiological studies of the late effects of internal radium in man, and mechanistic investigations of those effects, part 2
[DE85-011174] 19 p3331 N85-30636
Reduction of radiation damage in solar cells — spacecraft power supplies
[ESA-CR(P)-2005] 20 p3485 N85-31659
Nuclear responses in INTOR plasma stabilization elements
[DE85-010489] 20 p3535 N85-31995
Effects of laser radiation on surfaces and coatings
[DE85-010475] 22 p3790 N85-33484
Ultraviolet radiation-damage absorption peak in solid deuterium-tritium, revision 1
[DE85-012969] 22 p3844 N85-33806
Effects of space radiation on advanced semiconductor devices. Part 3: Further cosmic ray simulation studies of single event upsets and latch-up in CMOS memories
[AERE-G-3368-PT-3] 22 p3848 N85-33833
The 1983 international intercomparison of nuclear accident dosimetry systems at Oak Ridge National Laboratory
[DE85-011303] 23 p3934 N85-34382

RADIATION DETECTORS
NT DOSIMETERS
NT SILICON RADIATION DETECTORS
NT THRESHOLD DETECTORS (DOSIMETERS)
Thick film radiation detector
[AD-D011211] 01 p0048 N85-10318
Report on solar neutrino experiments
[DE84-014567] 01 p0131 N85-10899
Sensitivity improvement of a two-mode gravitational radiation detector through the use of a transducer not perfectly tuned to the antenna
[NOTA-INTERNA-812] 02 p0192 N85-11285
High-bandwidth multichannel fiber optic system for measuring gamma rays
[DE84-014526] 04 p0564 N85-13596
100 MHz fiber optic single transient gamma ray detection system
[DE84-016818] 05 p0729 N85-14686
Sensor-atmosphere-target simulation. Computer program SENSAT
[DFVLR-FB-84-32] 08 p1176 N85-17419
P-I-N CdTe gamma-ray detectors by Liquid Phase Epitaxy (LPE)
[DE84-012276] 09 p1323 N85-18315
Linear, position-sensitive X-ray detector used for real-time calculations of small-angle scattering parameters with submillisecond resolution
[DE85-002530] 10 p1489 N85-19401
New preamplifier for particle detectors
[DE85-004115] 12 p1836 N85-21524
Dielectric detector device for registering heavy cosmic radiation particles 13 p2045 N85-22799
Magnetic monopoles
[DE85-008176] 17 p3027 N85-28719
Experiments and detectors for high energy heavy ion colliders
[DE85-007927] 17 p3031 N85-28748
Polymer Research at Synchrotron Radiation Sources: Symposium Proceedings
[DE85-008458] 18 p3061 N85-29062
The possibility of observing solar neutron events in the lower atmosphere
[NOTA-INTERNA-837] 18 p3209 N85-29908
Improved fluid flow meter for measuring the rate of fluid flow in a conduit
[NASA-CASE-MFS-29030-1] 19 p3271 N85-30286
Double photon excitation of high-Rydberg atoms as a long-lived submillimeter detector
[NASA-CASE-NPO-16372-1] 19 p3352 N85-30779
The SLC program
[DE85-011433] 19 p3357 N85-30813
Bismuth germanate scintillators: Applications in nuclear safeguards and health physics
[DE85-010730] 19 p3365 N85-30865
Annual environmental monitoring report, January-December 1984
[DE85-011689] 20 p3486 N85-31665
On the design of a global detection system for airborne radioactivity
[CM-68] 20 p3487 N85-31670
Detection of solar neutrons by ground based neutron monitors
[IFSI-84-11] 20 p3547 N85-32076

Detector problems at the SSC
[DE85-010217] 21 p3703 N85-33007
Research in extreme ultraviolet and far ultraviolet astronomy
[NASA-CR-176068] 21 p3716 N85-33060
Batteryless magneto-driven portable radiac
[DE85-011622] 22 p3780 N85-33300
Beta response of selected instruments
[DE85-013278] 22 p3788 N85-33469
Advanced instrumentation for Positron Emission Tomography
[DE85-011147] 22 p3840 N85-33779
Detection of gamma-ray lines from the direction of the Crab Nebula 22 p3966 N85-33943
Relative abundances of elements (20 or = Z or = 28) at energies up to 70 GeV/amu using relativistic rise in ion chambers
[OG-4.1-7] 22 p3876 N85-34013
CYLTRAN calculations of electron effects on XD detectors
[LA-10264-MS] 23 p3969 N85-34601
Improved method for the stabilization of NaI-photomultiplier gamma detectors against thermal and other drift
[DE85-011830] 23 p3970 N85-34613
Cross sections for the production of fragments with Z greater than or equal to 8 by fragmentation of Z greater than or equal to 9 and less than or equal to 26 nuclei
[OG-7.2-22] 23 p4016 N85-34689
The development of a high energy cosmic ray detector for Spacelab-2
[OG-9.1-8] 23 p4023 N85-34934
Cherenkov-dE/dx-range measurements on cosmic ray iron group nuclei
[OG-9.1-12] 23 p4024 N85-34937
The response of ionization chambers to relativistic heavy nuclei
[OG-9.1-13] 23 p4024 N85-34939
A balloon-borne imaging gamma-ray telescope
[OG-9.2-2] 23 p4024 N85-34941
The Figaro experiment for the observation of time marked sources in the low energy gamma-ray range
[OG-9.2-11] 23 p4026 N85-34950
A position sensitive phoswich hard X-ray detector system
[OG-9.3-12] 23 p4028 N85-34967
The Buckland Park air shower array
[OG-9.4-4] 23 p4029 N85-34971
An EAS experiment at mountain altitude for the detection of gamma-ray sources
[OG-9.4-5] 23 p4029 N85-34972
Detection of 10 (1) GeV cosmic neutrinos with a space station
[OG-9.4-10] 23 p4030 N85-34977
Shower disc sampling and the angular resolution of gamma-ray shower detectors
[OG-9.5-2] 23 p4030 N85-34980
Angular resolution of air-shower array-telescopes
[OG-9.5-6] 23 p4030 N85-34983
Astrophysical applications of high angular resolution array-telescopes
[OG-9.5-7] 23 p4031 N85-34984
Results of ultra-low level 71ge counting for application in the Gallex-solar neutrino experiment at the Gran Sasso Underground Physics Laboratory
[SH-8.1-2] 23 p4049 N85-35108
Detector calibration of the Indian cosmic ray experiment (ICNS) in Space-Shuttle Spacelab-13
[SH-9.1-2] 23 p4050 N85-35117
High resolution beam profile monitors in the SLC
[DE85-013375] 24 p4157 N85-35774
The structure of EAS at E 0.1 EeV
[HE-4.4-2] 24 p4193 N85-36012
Expected rates with mini-arrays for air showers
[HE-4.7-8] 24 p4199 N85-36059
A note on some statistical properties of rise time parameters used in muon arrival time measurements
[HE-4.7-12] 24 p4199 N85-36062
Multimuons events and primary composition
[HE-5.1-5] 24 p4201 N85-36070

RADIATION DISTRIBUTION
NT ANTENNA RADIATION PATTERNS
NT DIFFRACTION PATTERNS
NT RAINBOWS
NT SIDELOBES
Direction dependent radiation behavior in the classification of multispectral aircraft remote sensing data
[SER-C-290] 01 p0063 N85-10419
Measurements of polarization characteristics of radiation field of on-board aircraft antennas
03 p0346 N85-12230
Simple formula to estimate carbon dioxide gas effect in radiation balance of underlying surface
06 p0823 N85-15226
Theoretical studies relating to the interaction of radiation with matter: Atomic collision processes occurring in the presence of radiation fields
[AD-A146854] 07 p1040 N85-16602
Effect of scattering on instabilities in line-driven stellar winds 08 p1235 N85-17784
Radiative amplification of acoustic waves in hot stars
08 p1235 N85-17786
Evaluation of parameters of a signal (selected pages)
[AD-A146831] 09 p1312 N85-18243
Atmospheric diffusion in hilly region on middle reaches of the Chang Jiang 11 p1620 N85-20196
MSG-7: Atmospheric penetration of solar radiation in the range of Schumann-Runge bands
11 p1657 N85-20443
Radiation safety of crew and passengers of air transportation in civil aviation. Provisional standards
[NASA-TM-77610] 11 p1692 N85-20638
USSR report: Physics and mathematics
[JPRS-UPM-85-001] 11 p1715 N85-20786
Problem of frequency space variation of sonic field in stratified media 11 p1715 N85-20787
Generation of sound by a vortex point in a steady flow of slightly compressible fluid 11 p1715 N85-20789
Stellar ultraviolet flux distributions in the 912-1200 A wavelength range 11 p1762 N85-21081
Numerical methods for analyzing electromagnetic scattering
[NASA-CR-175507] 12 p1823 N85-21438
The physical interactions of radiofrequency radiation fields and biological systems 16 p2775 N85-27129
Fiber optics in high dose radiation fields
[DE85-006849] 18 p3185 N85-29755
Cavityless optical bistability in systems of two-level atoms 18 p3186 N85-29764
Measurement of RF fields associated with ISM equipment as it relates to aeronautical services
[FAA-ES-84-2] 19 p3254 N85-30180
Measurement of radiated emissions from industrial heating device equipment as it relates to aeronautical services
[FAA-ES-85-2] 19 p3255 N85-30181
Research in particles and fields
[NASA-CR-176069] 21 p3724 N85-33103
Supernova explosion in dense clouds in the galaxy and the COS-B gamma-ray sources
[OG-2.5-3] 22 p3869 N85-33960
Galactic distribution of interstellar Al-26
[OG-3.2-3] 22 p3874 N85-34002
Longitudinal distribution of cosmic rays in the heliosphere
[SH-4.1-14] 23 p4006 N85-34837
Notes on drift theory
[SH-4.2-3] 23 p4006 N85-34841
The model-independence of cosmic ray source determinations
[OG-7.2-1] 23 p4014 N85-34873
A kinetic model for predicting oxidative degradation rates in combined radiation-thermal environments
[TI85-002629] 24 p4100 N85-35414
Multiplicity distributions in interaction models used for cascade simulations
[HE-1.2-5] 24 p4172 N85-35863
Angular distribution and multiplicity of backward hadrons in hFe interactions at 0.5-5.0 TeV energies (PION Experiment)
[HE-1.2-6] 24 p4172 N85-35866
Measurement of the local density spectrum
24 p4189 N85-35884

RADIATION DOSAGE
Radiofrequency and microwave radiation
[AD-A145492] 02 p0191 N85-11274
Thermoregulatory consequences of long-term microwave exposure at controlled ambient temperatures
[PB84-236603] 05 p0697 N85-14484
Characterizing X-ray machines
[AD-A146532] 06 p0862 N85-15481
A total dose characterization of five commercial analog multiplexers
[AD-A146986] 07 p0946 N85-15997
Computer subroutines for estimation of human exposure to radiation in low Earth orbit
[NASA-TM-86324] 08 p1199 N85-17550
Approaches to radiation guidelines for space travel
[DE85-001248] 09 p1363 N85-18576
Robotics at Savannah River site: Activity report
[DE85-003657] 11 p1648 N85-20383
Models and parameters for environmental radiological assessments
[DE81-027154] 11 p1678 N85-20573
Behavior degradation due to 1100-RAD pulsed radiation exposure (5.8:1 neutron/gamma ratio)
[AD-A149284] 11 p1689 N85-20621
Radiation exposure and performance of multiple burn LEO-GEO orbit transfer trajectories
[NASA-TM-86946] 12 p1788 N85-21228
Biological effects on radiofrequency radiation
[PB85-120848] 12 p1900 N85-21930
Distribution of radium and plutonium in human bone
[DE85-005025] 13 p2142 N85-23296
Space radiation studies for the reporting period, June 1983 - July 1984
[NASA-CR-171411] 15 p2685 N85-26583
Thermal consequences of localized SAR from RFR exposure 16 p2775 N85-27130
The medical results of human exposures to radio frequency radiation 16 p2776 N85-27133
Radio Frequency Radiation (RFR) measurements in operational settings 16 p2777 N85-27136
Energy and Technology Review
[DE85-004358] 17 p3049 N85-28868
Dosimeasurements with thermoluminescence dosimeters at a Febetron 701, 600 kV in room 022 of the Interuniversity Reactor Institute (IRI)
[IRI-190-84-02] 18 p3111 N85-29282
Radiation damage and repair in cells and cell components. Part 2: Physical radiations and biological significance
[DE85-008934] 18 p3152 N85-29518
Comparison of calculations and measurements of the off-axis radiation dose (SI) in liquid nitrogen as a function of radiation length
[AD-A153676] 18 p3178 N85-29704
Measurement of radiated emissions from industrial heating device equipment as it relates to aeronautical services
[FAA-ES-85-2] 19 p3255 N85-30181
Environmental monitoring at Argonne National Laboratory
[DE85-010613] 19 p3309 N85-30516
Effects of long-term low-level radiofrequency radiation exposure on rats. Volume 8: Evaluation of longevity, cause of death, and histopathological findings
[AD-A154283] 19 p3327 N85-30610
Research on the experimental verification of dosimetry calculations
[DE85-011292] 19 p3331 N85-30637
Additional muon calculations for the SLC positron source
[DE85-011212] 19 p3383 N85-30655
The DNA metabolism and poly-(ADP-ribose) synthesis in lymphocytes of persons exposed to low doses of ionizing radiation
[OEFZS-4307] 20 p3507 N85-31800
Dosimetry and limit values for internal contamination with radionuclides: From (International Commission on Radioactive Protection) ICRP-2 to ICRP-30
[IRI-190-84-03] 20 p3507 N85-31804
Sulfur activation at the Little Boy-Comet Critical Assembly: A replica of the Hiroshima bomb
[DE85-010261] 20 p3527 N85-31938
A practical guide to ionization chamber dosimetry at the AFRRI reactor
[AD-A155185] 21 p3703 N85-33003
Empirical correlation of residual gamma radiation resulting from operation of the Health Physics Research Reactor
[DE85-012075] 21 p3704 N85-33008
Wide-ranging radiation dose monitor
[DE85-011596] 22 p3787 N85-33463
Current internal-dosimetry practices at US Department of Energy facilities
[DE85-011718] 22 p3787 N85-33466
Error evaluation in measurements with thermoluminescent dosimeters
[ISS-T-84/6] 22 p3788 N85-33471
The 1984 effluent and environmental monitoring report for the Bettis Atomic Power Laboratory
[DE85-011533] 22 p3810 N85-33602
Control technology for radioactive emissions to the atmosphere at US Department of Energy facilities: The Los Alamos Meson Physics Facility
[DE85-011402] 22 p3811 N85-33609
Airborne cloud tracking measurements during the Three Mile Island nuclear station accident, Middletown, Pennsylvania. Date of survey: March - June 1979
[DE85-012080] 22 p3816 N85-33636
Global environmental transport models for tritium
[DE85-011437] 22 p3816 N85-33639
Investigation of some aspects of amino acid metabolism in man during brief exposure to antiorthostatic hypokinesia combined with ultraviolet radiation
22 p3822 N85-33678
Long-term exposure of (238) PuO2 to a terrestrial environment, volume 3
[DE85-011696] 22 p3840 N85-33781
Microdosimetric spectra measurements of JANUS neutrons
[DE85-012106] 22 p3843 N85-33801

Marine Sample Exploitation Project: Estimates regarding the sensitivity and technology for the detection of nuclear explosion debris in the marine environment
[DE85-013176] 23 p3947 N85-34462

Circuit approaches to increasing SRAM performance in total dose environments
[DE85-009441] 23 p3966 N85-34588

A kinetic model for predicting oxidative degradation rates in combined radiation-thermal environments
[TI85-002629] 24 p4100 N85-35414

Wholebody radiation counting system
[AD-A155842] 24 p4131 N85-35807

Tritium hazard via the ingestion pathway
[DE85-012897] 24 p4133 N85-35818

Calibration of a high-level photon irradiation
[DE85-013044] 24 p4151 N85-35738

Recent advances in remote handling at LAMPF
[DE85-012725] 24 p4157 N85-35775

Total integrated dose testing of solid-state scientific CD4011, CD4013, and CD4060 devices by irradiation with CO-60 gamma rays
[NASA-CR-176196] 24 p4161 N85-35795

RADIATION EFFECTS
NT LASER DAMAGE
NT RADIATION DAMAGE
NT RADIATION INJURIES
NT RADIOLYSIS

Radiation effects on structural materials
[DE84-014771] 01 p0029 N85-10178

Energy deposition in microvolumes of silicon from high energy proton reactions
[AD-A144713] 01 p0123 N85-10945

Cosmic ray effects on microelectronics. Part 3: Propagation of cosmic rays in the atmosphere
[AD-A145026] 01 p0131 N85-10902

Diagnostics of ionization in air produced by infrared radiation from A pulse CO2 laser
[AD-A145376] 02 p0201 N85-11342

The effect of temperature on the radiation induced losses of large diameter GPS (Germanium phosphosilicate) and GBS core optical fibers
[AD-A145409] 02 p0280 N85-11823

Internal friction, microstructure and radiation effects
[DE84-013905] 02 p0298 N85-11880

Breakdown of porous metals by laser radiation
03 p0349 N85-12249

Determination of bound water in biological tissue and energy dissipated in bound water by low level microwaves
[AD-A143101] 03 p0399 N85-12547

Evaluation of ferritic alloy Fe-2 1/4Cr-1Mo after neutron irradiation: Irradiation creep and swelling
[DE84-014647] 04 p0474 N85-13022

Radiation effects in amorphous metallic alloys
[DE84-014302] 04 p0475 N85-13025

Measuring transient radiation effects in optical fibers
[DE84-015044] 04 p0565 N85-13598

Gamma-induced leakage in junction field-effect transistors
[DE84-014990] 04 p0570 N85-13634

Effects of the solar and extraterrestrial environments on space power systems 05 p0610 N85-13898

Environmental interactions working group report
05 p0611 N85-13908

Effects of irradiation fluence and creep on fracture toughness of 347/348 stainless steel
[DE84-016091] 05 p0618 N85-13953

Plant responses to solar UV-B radiation
05 p0690 N85-14436

Spacelab 1 experiment: Microorganisms in space hard environment 05 p0891 N85-14443

Transient attenuation in optical fibers
[DE84-016487] 05 p0729 N85-14687

Synergisms in surface erosion, session summary
06 p0864 N85-15493

Synergism in materials erosion due to multispecies impact 06 p0864 N85-15494

Irradiation creep induced anisotropy in a/2110 dislocation populations
[DE84-016623] 06 p0868 N85-15520

A total dose characterization of five commercial analog multiplexers
[AD-A146866] 07 p0946 N85-15997

USSR report: Life sciences. Biomedical and behavioral sciences
[JPRS-UBB-84-015] 07 p1010 N85-16416

USSR report: Life sciences. Biomedical and behavioral sciences
[JPRS-UBB-84-027] 07 p1012 N85-16426

Effect of microwave radiation on local blood circulation and oxygenation of brain tissue
07 p1012 N85-16431

Chemical protection against ionizing radiation
[AD-A147822] 07 p1016 N85-16457

Effects of high energy radiation on the mechanical properties of epoxy-graphite fiber reinforced composites
[NASA-CR-174314] 08 p1118 N85-17047

Something in the air at Windscale --- radioactive contaminants from the Sellafield nuclear Complex for reprocessing and storing irradiated fuel
[BLL-RISLEY-TR-4998-(9091.9F)]
08 p1179 N85-17429

Effect of ultraviolet radiation on transparent polymer films as determined using in situ FTIR-RA spectroscopy. Volume 2: Photophysics of poly(vinylidene fluoride) films
[DE84-013040] 09 p1299 N85-18159

Transient response of a small-signal microwave GaAs FET to X-rays
[DE85-000066] 09 p1315 N85-18265

Effect of neutron irradiation on the high temperature operation of injection laser diodes
[DE85-000068] 09 p1326 N85-18333

Effect of modulated ultrahigh frequency field on behavior and hormone level in female rats under emotional stress
09 p1361 N85-18562

Methodical approaches to determination of sanitation protective zone dimensions around TV centers and TV retransmitters 09 p1361 N85-18563

Functional and structural changes in human erythrocyte surface after irradiation by UV waves of various wavelengths. Report 1: Expression of ABO and Rhesus system antigen 09 p1361 N85-18564

Radiation response of optical fibers in a nuclear reactor
[DE84-017221] 09 p1385 N85-18710

Radiation effects in Strain-Layer Superlattice (SLS) structures
[DE85-001713] 09 p1396 N85-18799

Comparison of ionizing radiation and hot electron effects in MOS structures
[DE84-016766] 09 p1400 N85-18809

Isolated systems in general relativity
09 p1400 N85-18813

Lithography radiation effects study
[AD-A149552] 10 p1468 N85-19260

Genetic effects of microwave exposure on mammalian cells in vitro. Volume 2, Appendix A: Cytogenetics and growth kinetics data, 850 MHz
[AD-A148866] 10 p1522 N85-19599

Genetic effects of microwave exposure on mammalian cells in vitro. Volume 2, Appendix B: Cytogenetics and growth kinetics data, 1.2 GHz
[AD-A148867] 10 p1522 N85-19600

Genetic effects of microwave exposure on mammalian cells in vitro, volume 2
[AD-A149347] 10 p1523 N85-19603

Effects of the solar-terrestrial environment on satellite operations
[DE85-002413] 11 p1590 N85-20003

Metals and Ceramics Division Materials Science Program
[DE85-003795] 11 p1592 N85-20012

Conductivity changes in neutron-irradiated commercial copper alloys at approximately 450(O)C
[DE85-003007] 11 p1606 N85-20100

Design and use of nonstandard tensile specimens for irradiated materials testing
[DE85-001071] 11 p1652 N85-20406

Behavior degradation due to 1100-RAD pulsed radiation exposure (5.8:1 neutron/gamma ratio)
[AD-A149284] 11 p1689 N85-20821

Radiation safety of crew and passengers of air transportation in civil aviation. Provisional standards
[NASA-TM-77610] 11 p1692 N85-20838

Effects of neutron irradiation on the fracture properties of HT-9 weld
[DE85-001068] 12 p1807 N85-21339

Effect of ultraviolet radiation on transparent polymer films as determined using in situ FTIR-RA spectroscopy. Volume 1: Photodegradation of transparent polymer films
[DE84-013039] 12 p1814 N85-21377

Performance assessment of Class 1E pressure transmitters subjected to environmental stresses
[DE85-001623] 12 p1854 N85-21626

Research and technology activities at Ames Research Center's Biomedical Research Division
[NASA-TM-86692] 12 p1899 N85-21925

Biological effects on radiofrequency radiation
[PB85-120848] 12 p1900 N85-21930

Irradiation effects on fuels for space reactors
[DE84-016460] 12 p1931 N85-22134

Solar array dynamical simulation for illumination and temperature variation 13 p2011 N85-22611

Breakdown of thin plates by radiation
13 p2028 N85-22709

Effect of alternative aging and accident simulations on polymer properties
[DE85-002642] 13 p2037 N85-22762

Radiation-dominated snowmelt on Mars
13 p2191 N85-23592

NASA space materials research
14 p2232 N85-23831

Effect of elevated-temperature neutron irradiation or fracture toughness of ceramics
[DE85-000652] 14 p2261 N85-24010

Radiological safety aspects of industrial radiography
14 p2316 N85-24312

NMR imaging and spectroscopy of the mammalian central nervous system after heavy ion radiation
[DE85-004509] 14 p2386 N85-24686

Photoreactivation and other ultraviolet/visible light effects on DNA in human skin
[DE85-005135] 14 p2390 N85-24719

Use of irradiated foods 14 p2393 N85-24740

Influences of thermal spikes in ion beam mixing
[DE85-006130] 14 p2419 N85-24924

Radiation effects induced in pin photodiodes by 40- and 85-MeV protons
[NASA-CR-175678] 14 p2426 N85-24960

Spectroscopic analysis of radiation-generated changes in tensile properties of a polyetherimide film
[NASA-TP-2429] 15 p2502 N85-25435

Effects of ion bombardment on the morphology of lead films
[DE85-007232] 15 p2511 N85-25494

Effects of long-term low-level radiofrequency radiation exposure on rats. Volume 7: Metabolism, growth and development
[AD-A150829] 15 p2615 N85-26112

Nuclear radiation induced absorption in optical materials
[DE85-007126] 15 p2649 N85-26336

Radiation effects on structural materials
[DE85-007032] 15 p2649 N85-26338

Physics effects of accidental submersion of space power reactors in water
[DE85-005020] 15 p2650 N85-26344

Assessment of present and future large-scale semiconductor detector systems
[DE85-006606] 15 p2662 N85-26430

USSR report: Space
[JPRS-USP-85-004] 16 p2717 N85-26772

Satellite research on solar flares
16 p2717 N85-26776

Swelling behavior of titanium-modified AISI 316 alloys
[DE85-007470] 16 p2752 N85-26982

The Impact of Proposed Radio Frequency Radiation Standards on Military Operations
[AGARD-LS-138] 16 p2775 N85-27128

The physical interactions of radiofrequency radiation fields and biological systems 16 p2775 N85-27129

The biological effects of radiofrequency radiation
16 p2775 N85-27131

The medical results of human exposures to radio frequency radiation 16 p2776 N85-27133

In situ HVEM studies of electron beam-driven composition changes in thin film alloys: Displacement-rate gradient effects
[DE85-007992] 17 p2931 N85-28092

Biological and human health effects of extremely low frequency electromagnetic fields. Post-1977 literature review
[AD-A152731] 17 p2999 N85-28539

Fiber optics in high dose radiation fields
[DE85-008649] 18 p3185 N85-29755

Effects of gamma-ray irradiation on dislocations in sodium nitrate single crystals
[DE85-008291] 18 p3195 N85-29818

Activities report in energy technology
[OEFZS-4302] 18 p3199 N85-29846

Alloy development for irradiation performance
[DE85-010454] 19 p3240 N85-30091

Method of reducing impurity and anti-site defects in semiconductor crystal materials, and device and apparatus respectively produced from and utilizing same
[AD-D011696] 19 p3260 N85-30216

Effects of long-term low-level radiofrequency radiation exposure on rats. Volume 8: Evaluation of longevity, cause of death, and histopathological findings
[AD-A154283] 19 p3327 N85-30610

Repair of DNA treated with lambda-irradiation and chemical carcinogens
[DE85-010298] 19 p3327 N85-30616

Radiation interactions for tomography
[DE85-006961] 19 p3355 N85-30799

Interaction of slow electrons with high-pressure gases (quasi-liquids): Synthesis of our knowledge on slow electron-molecule interactions
[DE85-010061] 19 p3355 N85-30800

NBS (National Bureau of Standards) reactor: Summary of activities Jul. 1983 through Jun. 1984
[PB85-184836] 20 p3522 N85-31907

Sulfur activation at the Little Boy-Comet Critical Assembly: A replica of the Hiroshima bomb
[DE85-010261] 20 p3527 N85-31938
Polymer-water interaction studies
21 p3609 N85-32411
Nuclear thermal transmittance in the atmosphere using LOWTRAN-6 computer code
[AD-A154669] 21 p3630 N85-32553
USSR report: Life sciences. Biomedical and behavioral sciences
[JPRS-UBB-85-020] 21 p3683 N85-32752
USAFSAM review and analysis of radiofrequency radiation bioeffects literature
[AD-A155113] 21 p3684 N85-32760
Empirical correlation of residual gamma radiation resulting from operation of the Health Physics Research Reactor
[DE85-012075] 21 p3704 N85-33008
Tritium-helium effects in metals
[DE85-011507] 22 p3749 N85-33235
Effects of laser radiation on surfaces and coatings
[DE85-010475] 22 p3790 N85-33484
Hit-size effectiveness theory applied to high doses of low LET radiation for pink mutations in Tradescantia
[DE85-011835] 22 p3819 N85-33657
USSR report: Life sciences. Biomedical and behavioral sciences
[JPRS-UBB-85-018] 22 p3819 N85-33660
Investigation of some aspects of amino acid metabolism in man during brief exposure to antiorthostatic hypokinesia combined with ultraviolet radiation
22 p3822 N85-33678
Use of gamma radiation as a form of preservation of sweet potatoes
[DE85-011998] 22 p3841 N85-33787
Analysis of transient radiation upset in a 16K SRAM
[DE85-009442] 23 p3965 N85-34586
System expectations for Pioneer 1 foil implosion experiments
[DE85-014129] 24 p4091 N85-35359
A kinetic model for predicting oxidative degradation rates in combined radiation-thermal environments
[TI85-002629] 24 p4100 N85-35414
Biophysical research in space — radiation effects
24 p4130 N85-35603
Total integrated dose testing of solid-state scientific CD4011, CD4013, and CD4060 devices by irradiation with CO-60 gamma rays
[NASA-CR-176196] 24 p4161 N85-35795
Electron irradiation of N type cadmium telluride
[AD-A155117] 24 p4161 N85-35801

RADIATION EMISSION
U RADIATION

RADIATION EXPOSURE
U RADIATION DOSAGE

RADIATION FIELDS
U RADIATION DISTRIBUTION

RADIATION HARDENING
Pulsed irradiation of optimized, MBE grown, AlGaAs/GaAs radiation hardened photodiodes
[DE84-014984] 04 p0569 N85-13631
Radiation hardened ion-implanted GaAs field effect transistor and method for making the same specification
[AD-D011264] 05 p0731 N85-14697
Analytic models for radiation induced loss in optical fibers 2: A physical model
[AD-A147442] 07 p1044 N85-16632
The planned expansion of microelectronics capability at Sandia National Laboratory
[TI85-004326] 09 p1314 N85-18260
Corrosion behavior of Al4 aluminum alloy hardened by CO2 laser radiation 15 p2514 N85-25512
Radiation hardening for VLSI applications
[DE85-005493] 16 p2760 N85-27155
Summary of recent studies on AlGaAs/GaAs radiation hardened photodiodes
[DE85-009501] 18 p3194 N85-29812
A comparison of the radiation hardness of various VLSI technologies for defense applications
[DE85-006973] 19 p3263 N85-30236
Electron lithography STAR design guidelines. Part 2: The design of a STAR for space applications
[NASA-CR-170766] 20 p3513 N85-31841
Radiation-hardened polymeric films
[DE85-011636] 22 p3752 N85-33259
Circuit approaches to increasing SRAM performance in total dose environments
[DE85-009441] 23 p3966 N85-34588

RADIATION HAZARDS
Radiofrequency and microwave radiation
[AD-A145492] 02 p0191 N85-11274
Improved robotic equipment for radiological emergencies
[DE84-017637] 04 p0509 N85-13249
Space Nuclear Safety Program
[DE84-016973] 05 p0728 N85-14679
Assessment of radiation dosages obtained by intake of radioactive fallout contaminated food
[VTT-292] 07 p1017 N85-16460
Thermal radiation hazards from Liquified Petroleum Gas (LPG) fireballs
[VTT-304] 09 p1293 N85-18122
Approaches to radiation guidelines for space travel
[DE85-001248] 09 p1383 N85-18576
China report: Science and technology
[JPRS-CST-84-039] 11 p1621 N85-20206
Radiation safety of crew and passengers of air transportation in civil aviation. Provisional standards
[NASA-TM-77610] 11 p1692 N85-20638
The medical results of human exposures to radio frequency radiation
[AD-A149718] 12 p1905 N85-21962
The impact of Proposed Radio Frequency Radiation Standards on Military Operations
[AGARD-LS-138] 16 p2775 N85-27128
The biological effects of radiofrequency radiation
16 p2775 N85-27131
The cumulative effects of long term exposure to low levels of radiofrequency radiation (RFR)
16 p2776 N85-27132
Review of epidemiological studies of human exposures to radiofrequency radiation 16 p2776 N85-27134
Hazards of VLF electromagnetic fields
16 p2776 N85-27136
Development and application of new radiofrequency radiation safety standards 16 p2777 N85-27137
The 10 MWe solar thermal central receiver pilot plant: Beam safety tests and analyses
[SAND-83-8035] 16 p2818 N85-27379
Use of environmental health-risk analysis for managing toxic substances
[DE85-008984] 18 p3160 N85-29574
Collected epidemiological studies of the late effects of internal radium in man, and mechanistic investigations of those effects, part 2
[DE85-011174] 19 p3331 N85-30636
MELCOR Accident Consequence Code System (MACCS)
[DE85-009712] 19 p3339 N85-30689
Bulk and thermal properties of the functional Tuffaceous Beds in holes USW G-1, UE-25 no. 1, and USW G-2, Yucca Mountain, Nevada
[DE85-011181] 19 p3365 N85-30866
The DNA metabolism and poly-(ADP-ribose) synthesis in lymphocytes of persons exposed to low doses of ionizing radiation
[OEFZS-4307] 20 p3507 N85-31800
ARAC status report, 1985
[DE85-012835] 22 p3810 N85-33603
Practical consequences of the assessment of different energy health risks
[DE85-004536] 22 p3825 N85-33696
Corrosion resistant storage container for radioactive material
[DE85-011666] 22 p3838 N85-33765
MATADOR (Methods for the Analysis of Transport And Deposition Of Radionuclides) code description and user's manual
[TI85-901402] 23 p3966 N85-34592
Biophysical research in space — radiation effects
24 p4130 N85-35603
Computer code calculations of the TMI-2 accident: Initial and boundary conditions
[DE85-012613] 24 p4140 N85-35666

RADIATION HEATING
U RADIANT HEATING

RADIATION INJURIES
Radiofrequency and microwave radiation
[AD-A145492] 02 p0191 N85-11274
Thermoregulatory consequences of long-term microwave exposure at controlled ambient temperatures
[PB84-236803] 05 p0697 N85-14484
The medical results of human exposures to radio frequency radiation
[AD-A149718] 12 p1905 N85-21962
Mouse oocyte killing by neutrons: Target considerations
[DE85-011362] 19 p3328 N85-30624
The 1983 international intercomparison of nuclear accident dosimetry systems at Oak Ridge National Laboratory
[DE85-011303] 23 p3934 N85-34382

RADIATION INTENSITY
U RADIANT FLUX DENSITY

RADIATION LAWS
NT KIRCHHOFF LAW OF RADIATION
NT STOKES LAW OF RADIATION

RADIATION MEASUREMENT
Radiation measuring system using transistor flux sensors
[AD-D011239] 01 p0050 N85-10328
Combustion system for radiation investigations
02 p0145 N85-10666
Energy-active zones in north Atlantic as manifestation of interannual variability of radiation balance
02 p0164 N85-11108
Analysis of radiocobalt in environmental samples
[DRIC-T-7334] 03 p0387 N85-12477
Isotopes in day to day life
[IAEA/PI/A.6E-84-00924] 03 p0417 N85-12866
High-bandwidth multichannel fiber optic system for measuring gamma rays
[DE84-014526] 04 p0564 N85-13596
Device for measuring average power of laser radiation
06 p0766 N85-15026
Microprocessors in geophysical instruments discussed
06 p1142 N85-17199
Radio Frequency Radiation (RFR) measurements in operational settings
[AD-A149717] 12 p1826 N85-21471
Operational experience with ion concentration sensors in orientation systems 13 p1980 N85-22422
Two-dimensional signal processing and storage and theory and applications of electromagnetic measurements
[AD-A150560] 13 p2065 N85-22899
Comprehensive, integrated, remote sensing at DOE sites
[DE85-004867] 13 p2126 N85-23240
Determining atmosphere moisture content from differences in two-frequency microwave radiation measurements 14 p2341 N85-24474
Space radiation monitor observations from Salyut-4 orbital station 15 p2482 N85-25317
The gamma thermometer: A new type of fixed internal instrumentation developed by EDF
[BLL-CE-TRANS-8080-(9022.09)]
15 p2560 N85-25791
Solar wind and cosmic rain 15 p2644 N85-26312
Space radiation studies for the reporting period, June 1983 - July 1984
[NASA-CR-171411] 15 p2685 N85-26583
Space radiation studies — Spacelab 2 Payload
[NASA-CR-171410] 15 p2685 N85-26584
Measurement and interpretation of electron angle at MABE beam stop
[DE85-008583] 17 p3032 N85-28755
Dosimeasurements with thermoluminescence dosimeters at a Febetron 701, 600 kV in room 022 of the Interuniversity Reactor Institute (IRI)
[IRI-190-84-02] 18 p3111 N85-29282
Safety report, 1982 18 p3184 N85-29746
Design consideration for the X-ray Cerenkov experiment
[AD-A153636] 18 p3189 N85-29777
Measurement of RF fields associated with ISM equipment as it relates to aeronautical services
[FAA-ES-84-2] 19 p3254 N85-30180
Measurement of radiated emissions from industrial heating device equipment as it relates to aeronautical services
[FAA-ES-85-2] 19 p3255 N85-30181
Annual environmental monitoring report, January-December 1984
[DE85-011689] 20 p3486 N85-31865
Results from Astron orbiting telescope
22 p3732 N85-33134
Wide-ranging radiation dose monitor
[DE85-011598] 22 p3787 N85-33483
Environmental surveillance at Los Alamos during 1984
[DE85-011886] 22 p3811 N85-33605
The 1984 environmental monitoring report, Sandia National Laboratories, Albuquerque, New Mexico
[DE85-011175] 22 p3811 N85-33607
The 1984 environmental monitoring program report for Idaho National Engineering Laboratory site
[DE85-011209] 22 p3812 N85-33611
Airborne cloud tracking measurements during the Three Mile Island nuclear station accident, Middletown, Pennsylvania. Date of survey: March - June 1979
[DE85-012060] 22 p3816 N85-33638
Neutron flux, spectrum and dose equivalent measurements for a 4500-W(th) 238 PuO2 general purpose heat source
[DE85-011361] 22 p3841 N85-33786
The 1983 international intercomparison of nuclear accident dosimetry systems at Oak Ridge National Laboratory
[DE85-011303] 23 p3934 N85-34382
EML pulse ionization chamber systems for (222)Rn measurements
[DE85-012320] 23 p3970 N85-34610
Measurement and interpretation of electron angle at MABE beam stop
[DE85-011918] 23 p3983 N85-34698

Solar Coronal and photospheric abundances from solar energetic particle measurements
[SH-2.1-5] 23 p3998 N85-34786
Radiation measurements on magnesium flames
[BLL-CE-TRANS-8110-(9022.00)] 24 p4075 N85-35254
Study of hadron bundles observed in Chacaltaya two-story emulsion chamber
[HE-3.3-4] 24 p4180 N85-35922

RADIATION MEASURING INSTRUMENTS
NT ACTINOMETERS
NT BOLOMETERS
NT CERENKOV COUNTERS
NT DOSIMETERS
NT ELECTROPHOTOMETERS
NT ELECTROSTATIC PROBES
NT FABRY-PEROT SPECTROMETERS
NT FLIR DETECTORS
NT HODOSCOPES
NT INFRARED DETECTORS
NT INFRARED INSTRUMENTS
NT INFRARED RADIOMETERS
NT INFRARED SCANNERS
NT INFRARED SPECTROMETERS
NT INFRARED SPECTROPHOTOMETERS
NT MICROWAVE RADIOMETERS
NT NEUTRON COUNTERS
NT NEUTRON SPECTROMETERS
NT PARTICLE TELESCOPES
NT PASSIVE L-BAND RADIOMETERS
NT PHOTOMETERS
NT PROPORTIONAL COUNTERS
NT PYRANOMETERS
NT QUANTUM COUNTERS
NT RADIATION COUNTERS
NT RADIATION DETECTORS
NT RADIOMETERS
NT RIOMETERS
NT SCINTILLATION COUNTERS
NT SILICON RADIATION DETECTORS
NT SOLAR SPECTROMETERS
NT SPARK CHAMBERS
NT SPECTROHELIOGRAPHS
NT SPECTROPHOTOMETERS
NT SPECTRORADIOMETERS
NT THRESHOLD DETECTORS (DOSIMETERS)
NT ULTRAVIOLET SPECTROMETERS
NT ULTRAVIOLET SPECTROPHOTOMETERS
Software used with the flux mapper at the solar parabolic dish test site
[NASA-CR-174108] 04 p0528 N85-13376
Device for measuring average power of laser radiation
06 p0786 N85-15026
Operational problems with radiation survey meters: The university and accelerator
[DE84-015703] 06 p0811 N85-15151
Year-to-year variability of components of Earth's radiation budget according to satellite measurement data 16 p2725 N85-26821
Results from radiation monitoring equipment experiment on STS-8
[AD-A153241] 17 p3055 N85-28911
Results from radiation monitoring equipment experiments on STS-41C, 41D, 41G and 51A
[AD-A154676] 21 p3560 N85-32142
Wide-ranging radiation dose monitor
[DE85-011596] 22 p3787 N85-33463
Beta response of selected instruments
[DE85-013278] 22 p3788 N85-33469
EAS Cerenkov measurements of the composition of the cosmic ray flux around 10 to the 16th power eV
[OG-5.2-11] 22 p3884 N85-34057
Search for solar neutrons using NM-64 equipment
[SH-1.4-5] 23 p3995 N85-34765
Wholebody radiation counting system
[AD-A155842] 24 p4131 N85-35607
Monopole, astrophysics and cosmic ray observatory at Gran Sasso
[HE-6.1-4] 24 p4209 N85-36130
Monopole search below the Parker limit with the MACRO detector at Gran Sasso
[HE-6.1-5] 24 p4209 N85-36131
Upper limit on magnetic monopole flux from Baksan experiment
[HE-6.1-11] 24 p4210 N85-36136

RADIATION MEDICINE
U NUCLEAR MEDICINE

RADIATION METERS
U RADIATION MEASURING INSTRUMENTS

RADIATION NOISE
U ELECTROMAGNETIC NOISE

RADIATION PRESSURE
NT ILLUMINANCE
NT LUMINANCE
NT LUMINOUS INTENSITY
NT SOUND PRESSURE
Orbit perturbation — satellites
05 p0598 N85-13810
X-ray bursts: Observation versus theory
[NASA-CR-174415] 10 p1573 N85-19916
Dynamics of neutral small particles — in the solar system 15 p2676 N85-26521
Numerical integration through force discontinuities: Solar radiation pressure 16 p2805 N85-27296
Effect of solar eclipses on the LAGEOS semimajor axis 20 p3491 N85-31699
Effect of diffusely-reflected sunlight on the orbit of LAGEOS 20 p3491 N85-31700

RADIATION PROTECTION
NT RADIATION SHIELDING
Method for forming electromagnetic-wave-screening composite 07 p0936 N85-15930
Radiation safety of crew and passengers of air transportation in civil aviation. Provisional standards
[NASA-TM-77610] 11 p1662 N85-20638
Charge-to-mass dispersion methods for abrasion-ablation fragmentation models
[NASA-TM-86340] 11 p1726 N85-20857
Radio Frequency Radiation (RFR) measurements in operational settings
[AD-A149717] 12 p1828 N85-21471
China report: Science and technology
[JPRS-CST-85-013] 15 p2536 N85-25852
Report of the 11th Regional IRPA Congress on Recent Developments and New Trends in Radiation Protection
[IRI-190-83-13] 18 p3160 N85-29575
Working safely with ionizing radiation sources at the Interuniversity Reactor Institute (IRI) (meant for the introduction of new collaborators)
[IRI-190-84-01] 18 p3160 N85-29576
Safety system with microcomputer
[OEFZS-4294] 18 p3166 N85-29618
Radioprotective efficacy of ATP and adenosine with exposure to high energy protons
19 p3325 N85-30602
Study of a novel shielding principle for protection against intense gamma-ray beams
[AD-A154374] 19 p3357 N85-30808
East Europe report: Science and technology
[JPRS-ESA-85-023] 21 p3572 N85-32217
ARAC status report, 1985
[DE85-012835] 22 p3810 N85-33603
Design considerations for personnel access penetrations for the superconducting super collider
[DE85-013027] 24 p4182 N85-35807

RADIATION RESISTANCE
U RADIATION TOLERANCE

RADIATION SHIELDING
Computer subroutines for estimation of human exposure to radiation in low Earth orbit
[NASA-TM-86324] 08 p1199 N85-17550
Study of a novel shielding principle for protection against intense gamma-ray beams
[AD-A154374] 19 p3357 N85-30808
Additional muon calculations for the SLC positron source
[DE85-011212] 19 p3363 N85-30855
Solid-state track recorder neutron dosimetry in the Three-Mile Island Unit-2 reactor cavity
[DE85-011360] 20 p3531 N85-31966
Simulating the effects of plasma disruption with a 1 MA current pulse in a coaxial test fixture
[DE85-010491] 20 p3535 N85-31996
Key issues of fusion nuclear technology development (FINESSE)
[DE85-012599] 22 p3845 N85-33817
Container for radioactive materials
[DE85-005757] 23 p3972 N85-34626
A comparison of calculated and measured background noise rates in hard X-ray telescopes at balloon altitude
[OG-9.3-7] 23 p4028 N85-34962
Applicability of 100kWe-class of space reactor power systems to NASA manned space station missions
[NASA-CR-174696] 24 p4149 N85-35728

RADIATION SOURCES
NT MONOCHROMATORS
NT NEUTRON SOURCES
NT POINT SOURCES
Imploding plasma radiation sources: Basic concepts
[AD-A145542] 02 p0284 N85-11856
Developments of optical fast-gated imaging systems
[DE84-016170] 04 p0502 N85-13204
Method of aperture synthesis: Fundamental relations and data processing in aperture synthesis systems (review) 06 p0781 N85-14994
Developments and applications of laser fluorescence spectroscopy for studies of particle behaviours in fusion plasmas 09 p1389 N85-16735
Design and analysis of airborne scanning optical systems 11 p1623 N85-20218
Major facilities for materials research and related disciplines
[PB85-108850] 11 p1739 N85-20634
Intense, broadband, pulsed I-R source at the National Synchrotron Light Source
[DE84-010542] 12 p1935 N85-22154
Possibility of mapping active tectonic structures from mercury gas aureoles over sea surface
13 p2113 N85-23162
Supersonic flow around weak radiation sources
17 p2942 N85-28162
Polymer Research at Synchrotron Radiation Sources: Symposium Proceedings
[DE85-008468] 18 p3081 N85-29062
Plasma radiation sources. Quasi-adiabatic theory and numerical modeling in the electro-diffusive approximation
[AD-A154375] 19 p3370 N85-30906
Radiative-collision generation of sound in gases subjected to single-pulse optical excitation
21 p3689 N85-32920
Correlation of intensities of different scattering channels 21 p3694 N85-32952
Magnetically insulated diode for generating pulsed neutron and gamma ray emissions
[DE85-011658] 22 p3760 N85-33306
Unthermalized plasma in bursts sources
[OG-1.1-5] 22 p3861 N85-33907
Optical monitoring of gamma-ray source fields
[OG-1.1-7] 22 p3861 N85-33908
Search for optical bursts from the gamma ray burst source GBS 0526-66
[OG-1.1-8] 22 p3861 N85-33909
Search for infrared counterparts of gamma-ray bursters
[OG-1.1-9] 22 p3861 N85-33910
A second catalog of gamma ray bursts: 1978 - 1980 localizations from the interplanetary network
[OG-1.2-1] 22 p3861 N85-33912
Gamma ray burst size-frequency distributions: Spectral selection effects
[OG-1.2-3] 22 p3862 N85-33913
An internally consistent gamma ray burst time history phenomenology
[OG-1.2-6] 22 p3862 N85-33916
Relationships between log N-log S and celestial distribution of gamma-ray bursts
[OG-1.2-10] 22 p3862 N85-33918
Search for gamma rays of energy 10(15) eV from Cygnus X-3
[OG-2.1-1] 22 p3862 N85-33919
Observation of an excess of cosmic ray muons of energies 2 TeV from the direction of Cygnus X-3
[OG-2.1-3] 22 p3863 N85-33920
Muon content of gamma ray induced EAS from Cygnus X-3
[OG-2.1-4] 22 p3863 N85-33921
Gamma rays of energy or = 10(15) eV from Cyg X-3
[OG-2.1-5] 22 p3863 N85-33922
Experimental results on gamma-ray sources at E sub 0 = 10(13) - 10(14) eV
[OG-2.2-12] 22 p3865 N85-33937
Observation of hard X-rays from the Crab pulsar and A0535+26
[OG-2.3-7] 22 p3866 N85-33944
Periodic gamma-ray emissions from Geminga at or = 10(12) eV
[OG-2.4-2] 22 p3867 N85-33949
Search for periodicities near 59 s in the COS-B gamma-ray data of 2CG195+04 (Geminga)
[OG-2.4-3] 22 p3867 N85-33950
On the 1983 observations of the gamma-ray source 2CG195+4
[OG-2.4-5] 22 p3868 N85-33952
Observations on TeV gamma rays from Geminga and PSR 0950+08
[OG-2.4-6] 22 p3868 N85-33953
Spectral evolution of gamma-rays from adiabatically expanding sources in dense clouds
[OG-2.5-2] 22 p3869 N85-33959
Supernova explosion in dense clouds in the galaxy and the COS-B gamma-ray sources
[OG-2.5-3] 22 p3869 N85-33960
Galactic gamma-ray sources, SNOBs, and giant H2 regions
[OG-2.5-4] 22 p3869 N85-33961
Observations of potential ultra high energy gamma-ray sources above 10(15) eV
[OG-2.6-9] 22 p3870 N85-33971
COS-B gamma-ray sources and interstellar gas
[OG-3.1-9] 22 p3874 N85-33997
Implications of new measurements of O-16 + p + C-12,13, N-14,15 for the abundances of C, N isotopes at the cosmic ray source
[OG-4.3-2] 22 p3878 N85-34027
Type 3 solar radio bursts and 3HE-rich events
[SH-2.2-3] 23 p4000 N85-34798

Germanium and lead: Significant differences between meteoritic and photospheric abundances?
[OG-7.1-2] 23 p4012 N85-34864
Implications of source abundances of ultraheavy cosmic rays
[OG-7.1-4] 23 p4013 N85-34866
Propagation and nucleosynthesis of ultraheavy cosmic rays
[OG-7.1-5] 23 p4013 N85-34867
A model for the origin of high-energy cosmic rays
[OG-8.1-8] 23 p4018 N85-34898
Approximate supernova remnant dynamics with cosmic ray production
[OG-8.1-12] 23 p4019 N85-34901
Scaling from Jupiter to pulsars and the acceleration of cosmic ray particles by pulsars, 3
[OG-8.2-3] 23 p4019 N85-34904
Cooling high intensity atomic hydrogen beams to liquid helium temperatures
[DE85-012515] 24 p4148 N85-35718
Calibration of a high-level photon irradiation
[DE85-013044] 24 p4151 N85-35738

RADIATION SPECTRA
NT ABSORPTION SPECTRA
NT BALMER SERIES
NT D LINES
NT ELECTROMAGNETIC SPECTRA
NT ELECTRONIC SPECTRA
NT EMISSION SPECTRA
NT FRAUNHOFER LINES
NT GAMMA RAY SPECTRA
NT H ALPHA LINE
NT H LINES
NT INFRARED SPECTRA
NT K LINES
NT LINE SPECTRA
NT LYMAN SPECTRA
NT MICROWAVE SPECTRA
NT RADIO SPECTRA
NT RAMAN SPECTRA
NT RYDBERG SERIES
NT SOLAR SPECTRA
NT STELLAR SPECTRA
NT UBV SPECTRA
NT ULTRAVIOLET SPECTRA
NT VIBRATIONAL SPECTRA
NT VISIBLE SPECTRUM
NT X RAY SPECTRA
New measurements of the spectrum of the cosmic microwave background
[DE84-016055] 05 p0748 N85-14785
Investigation of dynamics of radiation spectrum of injection lasers by infrared impulse Fourier spectroscopy
13 p2090 N85-23047
The 10 MWe solar thermal central receiver pilot plant: Beam safety tests and analyses
[SAND-83-8035] 16 p2818 N85-27379
Summary of the discussion of the theory of radiative processes
[DE85-007812] 19 p3371 N85-30914
Correlation of intensities of different scattering channels 21 p3694 N85-32952
Solid state radiative heat pump
[DE85-011605] 22 p3760 N85-33303
Implicit Monte Carlo methods and non-equilibrium Marshak wave radiative transport
[DE85-010711] 22 p3835 N85-33743
Detection of gamma-ray lines from the direction of the Crab Nebula 22 p3866 N85-33943
HEAO 3 upper limits to the expected 1634 KeV line from SS 433
[OG-2.4-9] 22 p3868 N85-33954
High-resolution spectrum of Cygnus X-1
[OG-2.4-12] 22 p3868 N85-33956
Spectrum of the gamma-ray diffuse component observed from HEAO-1
[OG-3.1-12] 22 p3874 N85-34000
Reestimation of the production spectra of cosmic ray secondary positrons and electrons in the ISM
[OG-8.2-8] 22 p3889 N85-34107
Nucleosynthesis in the terrestrial and solar atmospheres
[SH-2.2-2] 23 p4000 N85-34797
Penetration of solar protons into the Earth's magnetosphere on November 22, 1977
[SH-8.1-15] 23 p4046 N85-35088
Standard value for the radiation length in air
[HE-4.4-4] 24 p4193 N85-36013
Lateral-angular and temporal characteristics of EAS optical radiation
[HE-4.4-19] 24 p4194 N85-36025

RADIATION THERAPY
Biology and Medicine Division
[DE85-010838] 19 p3327 N85-30813

RADIATION TOLERANCE
Visible wavelength interferometer for high speed electron density diagnostics
[AD-A145886] 02 p0277 N85-11803
The relationship between radiation sensitivity and redox equilibria — glass processing variables
[AD-A147216] 07 p0932 N85-15906
Lithium counterdoped silicon solar cell
[NASA-CASE-LEW-14177-1] 11 p1672 N85-20535
Hygienic standardization of electromagnetic fields of radar systems 14 p2387 N85-24703
Mouse oocyte killing by neutrons: Target considerations
[DE85-011362] 19 p3328 N85-30824
Additional muon calculations for the SLC positron source
[DE85-011212] 19 p3363 N85-30855

RADIATION TRANSPORT
SANDYL radiation transport code at the Naval Research Laboratory
[AD-A144890] 01 p0117 N85-10799
Radiation transport in the Earth atmosphere
04 p0522 N85-13341
Generation of radiation transport geometry from computer-generated design data — monte carlo solution of the neutron transport equation
[DE84-017380] 09 p1370 N85-18606
Imaging through a multiple scattering medium
[DE85-002051] 10 p1557 N85-19821
Introduction to combinatorial geometry
[DE85-003266] 13 p2152 N85-23364
Intercomparison of Radiation Codes in Climate Models (ICRCCM)
[DE85-007251] 16 p2835 N85-27457
Nonlinear DSA difference schemes for radiative transfer applications
[DE85-005729] 16 p2856 N85-27611
Generation and transfer of polarized radiation in the solar atmosphere: Physical mechanisms and magnetic-field diagnostics 18 p3206 N85-29890
Additional muon calculations for the SLC positron source
[DE85-011212] 19 p3363 N85-30855
A new slab geometry radiation transport differencing scheme
[DE85-006681] 19 p3366 N85-30874
Radiation transport
[DE85-010333] 21 p3703 N85-33005
Global environmental transport models for tritium
[DE85-011437] 22 p3816 N85-33639
Monte Carlo and discrete ordinates calculations of 14-MeV neturons streaming through a stainless-steel duct (L/D = 4.6): Comparison with experiment
[DE85-011423] 22 p3840 N85-33776
Long-term exposure of (238) PuO2 to a terrestrial environment, volume 3
[DE85-011896] 22 p3840 N85-33781
Halo of NGC 4631 and models of cosmic-ray transport
[OG-6.2-3] 22 p3869 N85-34103
Coupled electron-photon transport calculations using the method of discrete ordinates
[DE85-009444] 23 p3967 N85-34597
Monte Carlo techniques for analyzing deep penetration problems
[DE85-011426] 23 p3968 N85-34598
Numerical descriptions of cosmic-ray transport
[SH-4.1-3] 23 p4004 N85-34829
Numerical and analytic descriptions of cosmic-ray transport
[SH-4.1-4] 23 p4005 N85-34830
Numerical studies of high current beam compression in heavy ion fusion
[DE85-011874] 24 p4158 N85-35783

RADIATIVE HEAT TRANSFER
Predicted heat transfer loss in the expansion cylinder of a 2 cylinder reciprocating engine
[AD-A144831] 01 p0055 N85-10368
Finite element analysis of thermoelasticity problems
02 p0208 N85-11369
Resistance of Navy shipboard outerwear garments and fire-resistant fabrics to extreme heat
[AD-A145414] 02 p0236 N85-11548
The radiative hydrodynamics of flare loops heated by impulsive bursts of energetic electrons
05 p0745 N85-14781
Methods for heat transfer and temperature field analysis of the insulated diesel
[NASA-CR-174783] 07 p1056 N85-16699
Simultaneous determination of radiation and convection heat transfer 08 p1194 N85-17523
Three-dimensional analysis of heat transfer and gas flow in a radiant furnace
[DE84-011732] 11 p1633 N85-20284
Radiation heat transfer within an open-cycle MHD generator channel — mathematical models
[NLR-TR-83068-U] 14 p2304 N85-24267
Performance analysis of radiation cooled dc transmission lines for high power space systems
[NASA-TM-87040] 17 p2951 N85-28222
Performance analysis of mixed passive solar heating systems
[DE85-009624] 21 p3613 N85-32455
An analytical and numerical model of radiation heat transfer in direct injection-type diesel combustion
24 p4082 N85-35368

RADIATIVE LIFETIME
Studies of the chemistry of vibrationally and electronically excited species in planetary upper atmospheres
[NASA-CR-174134] 03 p0449 N85-12851
Absolute transition probabilities of lines in the spectra of astrophysical atoms, molecules, and ions
[NASA-CR-174141] 04 p0580 N85-13705
Lifetime and quenching measurements of C2H emission produced by vacuum ultraviolet photolysis of C2H2
[DE85-010789] 19 p3278 N85-30330
Search for proton decay
[DE85-008283] 19 p3353 N85-30786

RADIATIVE RECOMBINATION
Recombination and ionization in a nitrogen plasma
[AD-A155426] 22 p3845 N85-33813

RADIATIVE TRANSFER
NT RADIATIVE HEAT TRANSFER
Spectroradiometric calibration of the Thematic Mapper and Multispectral Scanner system
[E85-10026] 02 p0218 N85-11439
Effects of atmospheric water vapor and clouds on NOAA (National Oceanic and Atmospheric Administration) AVHRR (Advanced Very High Resolution Radiometer) satellite data
[AD-A145425] 02 p0280 N85-11824
Scattering models in the microwave regime
[NASA-CR-174001] 04 p0525 N85-13361
Scattering from randomly oriented scatterers of arbitrary shape in the low-frequency limit with application to vegetation 04 p0525 N85-13362
Non-LTE considerations in spectral diagnostics of thermal transport and implosion experiments
[DE84-015167] 05 p0730 N85-14669
Studies of radiative transfer in planetary atmospheres
[NASA-CR-174194] 05 p0745 N85-14778
Infrared emission and atomic transitions
[AD-A147840] 07 p1041 N85-16607
Radiation parameterization programs for use in general circulation models
[AD-A148015] 08 p1188 N85-17488
Evidence for non-radiative activity in hot stars
08 p1231 N85-17756
Summary of the origin of nonradiative heating/momentum in hot stars
08 p1236 N85-17769
Hydrodynamic response of a radiating Al plasma excited by a proton beam
[AD-A148904] 10 p1558 N85-19824
MAP in India 11 p1655 N85-20424
Aerosol multiple-scanning code, ASCAT
[LA-10048-MS] 12 p1823 N85-21440
Evaluation of the radiometric integrity of LANDSAT 4 Thematic Mapper band 6 data 12 p1869 N85-21726
Spectroradiometric calibration of the Thematic Mapper and Multispectral Scanner system
[E85-10094] 12 p1874 N85-21756
Atlas of reflectance patterns for uniform earth and cloud surfaces (NIMBUS-7ERB-81 days)
[PB85-116392] 12 p1891 N85-21870
Mean free path lenght of photons with broken cloud cover 14 p2338 N85-24455
A numerical simulation of the formation of solar prominences 14 p2448 N85-25112
Technical development to improve satellite sounding over radiatively complex terrain
[NASA-CR-175746] 15 p2583 N85-25929
Radiative forcing of the southwest summer monsoon (a satellite perspective) 15 p2583 N85-25931
An Earth longwave radiation climate model
[NASA-CR-175749] 15 p2594 N85-25984
Microwave model prediction and verifications for vegetated terrain
[E85-10102] 16 p2809 N85-27322
Nonlinear DSA difference schemes for radiative transfer applications
[DE85-005729] 16 p2856 N85-27611
Solar radiance models for determination of ERBE scanner filter factor
[NASA-CR-172565] 17 p2985 N85-29513
Effect of polarized radiative transfer on the Hanle magnetic field determination in prominences: Analysis of hydrogen H alpha line observations at Pic-du-Midi
18 p3207 N85-29894
A new slab geometry radiation transport differencing scheme
[DE85-006681] 19 p3366 N85-30874

The suppression of convective wavebreaking by radiative transfer processes, part 1.3C
21 p3616 N85-32472

RADICALS
NT FREE RADICALS
NT HYDROXYL RADICALS
NT VINYL RADICAL
Magnetic resonance studies of transient radicals and radical ions
[DE84-011600] 03 p0328 N85-12116
Study of catalysts and mechanisms in synthesis reactions
[DE84-015025] 04 p0470 N85-12990
Study of combustion and flame processes initiated by laser-induced multiple-photon absorption
[DE84-017095] 04 p0471 N85-12998
Combustion kinetics of metal oxide and halide radicals
[AD-A148521] 08 p1122 N85-17078
Improved lithium-intercalation cathode material
[AD-A149310] 10 p1435 N85-19043
Stable polymeric carbon radicals. Part 2: Attempts at the preparation of polyradicals of the triphenylmethyl type linked by P-phenylene units
[NASA-TM-77799] 10 p1450 N85-19134
Toxicity, mutagenesis and aging due to endogenous oxygen radicals
[AD-A150121] 12 p1900 N85-21928
Ideal gas thermodynamic properties for the phenyl, phenoxy, and o-biphenyl radicals
[NASA-TM-83800] 12 p1943 N85-22204
Combustion kinetics of metal oxide and halide radicals
[AD-A150924] 14 p2251 N85-23952
Modeling the role of radicals in the ignition of and flame propagation in hydrogen-air and methane-air mixtures
16 p2744 N85-26935
A measurement of the vibrational band strength for the upsilon sub 3 band of the HO2 radical
[NASA-CR-175858] 16 p2744 N85-26936
Cometary atmospheres: Modeling the spatial distribution of observed neutral radicals
[NASA-CR-175852] 16 p2862 N85-27781
The electronic spectra of phthalocyanine radical anions and cations
[AD-A152328] 17 p2916 N85-27986
Measurement of Franck-Condon factors for the v'=0 progression in the B-X system of PO
[AD-A152734] 17 p2919 N85-27993
Cometary atmospheres: Modeling the spatial distribution of observed neutral radicals
[NASA-CR-175862] 17 p3064 N85-28904
Spray pyrolysis as a synthetic tool
[AD-A153691] 19 p3234 N85-30047
Nested dissection on a mesh-connected processor array
[AD-A154088] 19 p3342 N85-30711
Chromophores with auxochrome-like function
[NASA-TM-77849] 20 p3421 N85-31233
Measurements of the fragmentation of (40)Ar, (28)Si and (12)C in CH2C and H targets between 300 and 1500 MeV/nuc at the Bevalac
[OG-7.2-19] 23 p4016 N85-34886

RADII
NT LARMOR RADIUS
Experimental determination of the critical cavity radius in Fe-10% Cr for ion irradiation
[DE84-016570] 04 p0571 N85-13646
Lessons from the globular cluster NGC 5466
05 p0739 N85-14749
Galactic orbits of globular clusters
05 p0739 N85-14750
On the quadratic mean radius of a polynomial in Cz
[AD-A149189] 10 p1546 N85-19751
Ohmic potential drop and gas bubble radius distribution in alkaline water electrolysis 17 p2924 N85-28025
Single-dish high sensitivity determination of solar limb emission at 22 and 44 GHz
[INPE-3545-PRE/758] 19 p3365 N85-30999
Automatic sphericity interferometer for testing lens radii
[AD-A155736] 22 p3786 N85-33457

RADIO ALTIMETERS
ERS-1 radar altimeter data products — conferences
[ESA-SP-221] 03 p0379 N85-12419
The ERS-1 radar altimeter: An overview
03 p0379 N85-12421
The ERS-1 radar altimeter instrument
03 p0379 N85-12422
Wind speed determination from radar altimeters
03 p0380 N85-12424
Ocean wave parameters extraction using satellite short-pulse radar altimeters 03 p0380 N85-12425
The use of altimeter data for sea state forecasting
03 p0380 N85-12426
The impact of satellite altimeter data on wave research 03 p0380 N85-12427
Cryospheric data products available through satellite altimetry 03 p0380 N85-12428
Special difficulties of retrieving surface elevation over continental ice — satellite radar altimetry
03 p0380 N85-12429
Requirements and special problems of land altimetry — satellite altimetry 03 p0380 N85-12430
Determination of geoid undulations and ocean heights from ERS-1 radar altimetry data
03 p0381 N85-12432
Factors affecting the archiving, processing and dissemination of ERS-1 altimeter data
03 p0381 N85-12435
ERS-1 altimeter ground segment relations to other sensors and programs 03 p0381 N85-12436
Impact of ERS-1 observations on wave forecasting in the North Sea 03 p0381 N85-12437
Extraction of wave period from altimeter data
03 p0382 N85-12439
Sea ice characteristics derived from airborne altimetry
03 p0382 N85-12440
Radar altimetry over sea ice 03 p0382 N85-12441
Eddy detection in the Norwegian, Greenland, and Barents Seas with a radar altimeter
03 p0382 N85-12442
SEASAT altimeter data over the Mediterranean: Implications for ERS-1 03 p0382 N85-12443
Satellite altimetry for sea-surfacing topography determination and geoid improvement
03 p0382 N85-12444
The Precise Range and Range Rate Equipment (PRARE) and its possible support to the radar altimeter measurement for ERS-1 03 p0382 N85-12445
Determination of the altimetric geoid and gravity anomalies in the North Sea: Implications for a solution of the general circulation problem using ERS-1 data
03 p0382 N85-12446
Satellite altimetric measurements of lake levels
03 p0383 N85-12447
Ice sheets as invariant surfaces for radar altimeter calibration and orbit determination
03 p0383 N85-12449
Modelling of altimeter tracking over topographical surfaces — satellite antennas 03 p0383 N85-12450
ERS-1 radar altimeter system performance evaluation and calibration 03 p0383 N85-12451
Simulation of information extraction from radar altimeter return echoes — ERS-1 (ESA satellite)
03 p0383 N85-12452
The altimeter as a support to the scatterometer in the representation of winds and derived wave fields in coastal waters and enclosed seas: A research at its onset
03 p0383 N85-12453
The POSEIDON altimeter description
03 p0383 N85-12454
Standardization of data formats for radar altimeter data 03 p0384 N85-12455
Calibration and validation areas — satellite altimeters
03 p0384 N85-12456
Lessons from the SEASAT and GEOS-3 altimeters data projects 03 p0384 N85-12457
Components of the time variation of sea surface height from SEASAT altimeter data 05 p0658 N85-14227
A brief investigation into the validity of SEASAT radar altimeter data acquired over land
[AD-A146560] 06 p0827 N85-15254
Visualization of radar altimetry data for Venus
13 p1982 N85-22437
Application of pushbroom altimetry from space using large space antennas 14 p2230 N85-23817
Altitude of auroral scattering observed along auroral electrojets 14 p2339 N85-24485
On geoid heights and flexure of the lithosphere at seamounts
[AD-A151220] 15 p2604 N85-26050
Poseidon altimeter: Study of the hyperfrequency section and specifications of the prototype components
[CNES-84/DRT/TIT/HY/T/145]
20 p3419 N85-31219
Solid state altimeter model: Simulation description; analysis of first results (narrow band filters, weighting) — satellite-borne instruments
[CNES-DRT/TIT/RL-160-T] 20 p3419 N85-31220

RADIO ANTENNAS
NT MICROWAVE ANTENNAS
NT SPACETENNAS
An error analysis for the use of presently available lunar radio flux data in broadbeam antenna-system measurements
[PB84-218361] 01 p0016 N85-10097
HF broadband whip antenna evaluation
[AD-A149527] 10 p1467 N85-19256
Propagation influences on the performance of a reduced bandwidth quadrature phase shift keyed digital radio system 10 p1470 N85-19274
An electronically-steerable active receiving array for h.f.
[BBC-RD-1985/2] 12 p1822 N85-21430
Antenna Technology for QUASAT application — radio antenna for very long base interferometry missions
14 p2231 N85-23626
A description of the 64-meter antenna elevation drive gears and their strange wear 16 p2771 N85-27107
Repair of the DSS-14 pedestal concrete
16 p2772 N85-27108
On the possibilities of large-scale radio and fiber optics detectors in cosmic rays
[HE-4.6-2] 24 p4196 N85-36039

RADIO ASTRONOMY
Activities report of the Radio Laboratory
[REPT-S-153] 02 p0192 N85-11288
The mapping of the Sun at 8 mm wavelength and tracking of the active regions in the period 23 May - 5 June 1983
[REPT-S-149] 02 p0297 N85-11924
Documentation for the machine-readable version of A Catalogue of Extragalactic Radio Source Identifications (Veron-Cetty and Veron 1983)
[NASA-TM-87373] 03 p0405 N85-12587
Measurement of pulsar parallax by Very Long Baseline Interferometry 03 p0444 N85-12830
Aperture synthesis for radioastronomy
06 p0781 N85-14992
Modern radioastronomical aperture synthesis systems (review) 06 p0782 N85-14997
Approximating true radioluminance distribution from observations on aperture synthesis systems
06 p0783 N85-15003
Synthesis of radio image on RATAN-600 radiotelescope 06 p0783 N85-15004
QUASAT: A VLBI observatory in space — conference
[ESA-SP-213] 07 p1056 N85-16700
Some prospects of space VLBI
07 p1056 N85-16705
QUASAT: Technical aspects of the proposed mission — VLBI satellite 07 p1057 N85-16706
The compact radio emission regions in active galactic nuclei — QUASAT VLBI mission
07 p1058 N85-16713
Very Long Base Interferometry (VLBI) in space and X-ray observations of compact sources in active galactic nuclei 07 p1058 N85-16716
Opportunities for high angular and temporal resolutions of galactic objects at radio frequencies — QUASAT
07 p1059 N85-16723
A 150 micron heterodyne spectrometer for airborne astronomy 08 p1249 N85-17887
Tunable heterodyne receiver from 100 micron to 1,000 micron for airborne observations
08 p1249 N85-17888
A new generation of sub mm telescopes, made of carbon fiber reinforced plastic 08 p1250 N85-17890
Spectroscopic observations of selected stellar systems
[NASA-CR-174288] 08 p1255 N85-17915
FRG radiotelescope made of carbon fiber-reinforced plastic 09 p1309 N85-18226
Observations of comets: Radio and otherwise — conference
[TB-64] 11 p1762 N85-21066
USSR report: Space
[JPRS-USP-85-001] 13 p1977 N85-22403
All-Union conference of radio astronomers
13 p1977 N85-22406
Studies of galactic HI in 21-centimeter absorption
13 p2170 N85-23466
Venus surface composition from radio/radar measurements 13 p2177 N85-23509
Saturn's rings resolved by the VLA — Very Larg Array (VLA) 15 p2670 N85-26476
Voyager planetary radio astronomy: Grain and particle impacts shot noise in Saturn's ring plane
15 p2673 N85-26498
Radio observations of comet P/Crommelin
[INPE-3480-PRE/723] 16 p2861 N85-27777
Calibration methods in millimeter-wave radioastronomy
[INPE-3481-PRE/724] 16 p2861 N85-27778
The Helios radio astronomy experiment
16 p2886 N85-27803
Activity and magnetic fields on stars from radio observations
[NASA-CR-175966] 18 p3202 N85-29861
Single-dish high sensitivity determination of solar limb emission at 22 and 44 GHz
[INPE-3545-PRE/758] 19 p3365 N85-30999
Laboratory evaluation and application of microwave absorption properties under simulated conditions for planetary atmospheres
[NASA-CR-176078] 22 p3851 N85-33847

RADIO ATTENUATION
NT MANDELSTAM REPRESENTATION

Propagation measurements for land-mobile satellite systems at 1541 MHz
[CRC-TN-723] 09 p1310 N85-18232
UHF communications through forested propagation channels 10 p1470 N85-19280
Results of simultaneous measurements of absorption and polarization of radio waves reflected from ionosphere 16 p2807 N85-27313

RADIO AURORAS
Relation between polarization of artificial low frequency radiation and parameters of auroral ionosphere 06 p0785 N85-15016

RADIO BEACONS
Improved legislated emergency locating transmitters and emergency position indicating radio beacons
[NASA-CASE-GSC-12892-1] 11 p1624 N85-20226
Development of ARGOS platforms for tracking of basking sharks, Cetorhinus maximus 14 p2326 N85-24378
The sinking of the Les Mutuelles du Mans trimaran 14 p2327 N85-24384
Trajectory measurements for take-off and landing tests and other short-range applications, volume 16
[AGARD-AG-160-VOL-16] 15 p2561 N85-25801
The COSPAS-SARSAT system 20 p3401 N85-31101
The 121.5 MHz ELT: Past, present and future — Emergency Locator Transmitter (ELT) 20 p3401 N85-31105
The 406 MHz ELT/EPIRBs — Emergency Locator Transmitters/Emergency Position Indicating Radio Beacons (ELT/EPIRB) 20 p3402 N85-31106
Soviet Emergency Locator Transmitter/Emergency Position Indicating Radio Beacon (ELT/EPIRBs) at 121.5 and 406 MHz 20 p3402 N85-31107
The CCIR satellite EPIRB coordinated trials programme — Emergency Position Indicating Radio Beacon (EPIRB); International Radio Consultative Committee (CCIR) 20 p3402 N85-31111
The International Radio Consultative Committee (CCIR) recommended satellite Emergency Position Indicating Radio Beacon (EPIRB) system operating through geostationary satellites at 1.6 GHz 20 p3402 N85-31112
A 406 MHz ELT processor for geostationary satellites — Emergency Locator Transmitter (ELT) 20 p3403 N85-31114
Navigation data for Emergency Position Indicating Radio Beacons (EPIRBs) 20 p3403 N85-31115
Free-float Emergency Position Indicating Radio Beacons (EPIRBs) and release mechanism on board Norwegian ships. Main specifications and user experience 20 p3404 N85-31120
Experiments of a LORAN-C aided recovery system and a proposal of its application to rescue system 20 p3404 N85-31121
A special antenna for SARSAT EPIRBs providing circular polarization and hemispheric coverage for reliable transmission to satellites — Emergency Position Indicating Radio Beacon (EPIRB) 20 p3404 N85-31122
SARSAT 406 MHz system technical evaluation 20 p3404 N85-31124

RADIO BROADCASTING
U BROADCASTING

RADIO BURSTS
NT SOLAR RADIO BURSTS
NT TYPE 3 BURSTS
NT TYPE 4 BURSTS
Electron-cyclotron maser emission during solar and stellar flares
[NASA-CR-175883] 17 p3054 N85-28907

RADIO COMMUNICATION
NT CODE DIVISION MULTIPLE ACCESS
NT RADIO RELAY SYSTEMS
NT RADIO TELEMETRY
NT TELEPHONY
NT TIME DIVISION MULTIPLE ACCESS
Resistance to HF jamming interference in mobile radio networks by an adaptive, distributed reconfiguration technique
[AD-A145117] 01 p0038 N85-10238
Gaussian Wide Sense Stationary Uncorrelated Scattering (GWSSUS) channel simulation program to be used for mobile radio systems
[FUB-40-1983] 01 p0041 N85-10265
Planning guide for the review of telecommunications systems for frequency availability and electromagnetic compatibility
[PB84-210238] 01 p0041 N85-10268
Digital radio link: Comparison of the resistance of two different 4-phase modulation forms to multipath propagation
[FOA-C-30362-E] 02 p0193 N85-11291
Ministry wants better commo facilities for agroaviation 03 p0310 N85-12003
Operational requirements versus technological capabilities 06 p1072 N85-16798
Real-time estimation of amplitude and group delay distortion in a PSK line-of-sight communications channel 09 p1311 N85-18237
Calculation of the area covered by mobile radio systems using geographic data stored in a computer
[FUB-43-1983] 09 p1312 N85-18247
Adaptive signal processing for radio communications 10 p1473 N85-19295
Spectrum resource assessment of the Aeronautical Mobile Service between 400 MHz and 17.7 GHz
[PB85-125995] 11 p1626 N85-20241
Radioelectronics and space exploration 12 p1838 N85-21533
Satellite communications and amateur radio 12 p1838 N85-21534
INMARSAT marine satellite organization 13 p1965 N85-22456
Firefighters' communication transceiver test plan
[NASA-CR-171419] 13 p2053 N85-22954
A comparison of metropolitan and non-metropolitan employment characteristics: Indications of the size of non-metropolitan mobile communication services user classes
[NASA-CR-175648] 13 p2053 N85-22955
Use of Bigaussian approximation to describe fading in scattering communications channel 13 p2084 N85-23017
Tropospheric scatter communication system having angle diversity
[AD-D011448] 14 p2291 N85-24200
Trade-off between land vehicle antenna cost and gain for satellite mobile communications
[NASA-CR-175732] 15 p2540 N85-25681
Survey of narrow band vocoder technology
[AD-A151919] 16 p2773 N85-27114
Mobile television radio link
[AD-A152381] 17 p2948 N85-28201
Tone calibrated digital radio communication system
[NASA-CASE-NPO-16414-1-CU] 18 p3089 N85-29121
The determination of daily usage or occupancy in the land-mobile band 138-174 MHz at Montreal
[CRC-1383] 19 p3253 N85-30167
Performance interface document for the S-band diplexer for space users of NASA networks
[NASA-TM-86224] 23 p3900 N85-34155

RADIO DIRECTION FINDERS
Direction finder set, radio
[AD-A140958] 12 p1775 N85-21142
Experimental test of the three subaperture method for estimating target elevation angle
[AD-A149687] 12 p1851 N85-21614
Natural electromagnetic radiation in seismically active regions 13 p2111 N85-23152
Comprehensive radio direction finder with electronically stabilized radiation pattern 22 p3782 N85-33318

RADIO ECHOES
Analysis of spin echo signals in multi-pulse experiment 06 p0792 N85-15065
Measurements of partial reflections at 3.18 MHz using the CW radar technique 11 p1659 N85-20457

RADIO ELECTRONICS
USSR report: Electronics and electrical engineering
[JPRS-UEE-85-002] 13 p2096 N85-22907
Quality control of radioelectronic apparatus components on basis of external characteristics in frequency domain 15 p2529 N85-25500
Center for Electronics and Electrical Engineering technical progress bulletin covering center programs, July-September with 1985 CEEE events calendar
[PB85-191393] 24 p4091 N85-35363

RADIO EMISSION
NT CN EMISSION
NT HYDROXYL EMISSION
NT RADIO BURSTS
NT SOLAR RADIO BURSTS
NT SOLAR RADIO EMISSION
NT TYPE 3 BURSTS
NT TYPE 4 BURSTS
FCC (Federal Communication Commission) methods of measurement of radio noise emissions from computing devices
[PB84-243591] 06 p0849 N85-15387
The compact radio emission regions in active galactic nuclei — QUASAT VLBI mission 07 p1058 N85-16713
Observations of nonthermal radio emission from early-type stars 08 p1232 N85-17758
Nonthermal radio emission and the HR diagram 08 p1232 N85-17763
Synchrotron emission from chaotic stellar winds 08 p1234 N85-17774
Radio emission from RS CVn binary systems 09 p1417 N85-18809
Analysis of Jovian low frequency radio emissions
[NASA-CR-174449] 10 p1571 N85-19909
Determining vector of radiointerferometer base from observations of natural radio emission with narrow spectrum 13 p2112 N85-23158
Direct evidence for solar wind control of Jupiter's hectometer-wavelength radio emission
[NASA-TM-86073] 16 p2883 N85-27790
Sea surface radio emission at wavelengths 0.86 and 1.3 cm near Brewster angle 19 p3293 N85-30418
The radiation of the Vela pulsar 20 p3548 N85-32080
Analysis of Jovian decametric data: Study of radio emission mechanisms
[NASA-CR-176057] 22 p3851 N85-33846
Observations of potential ultra high energy gamma-ray sources above 10(15) eV
[OG-2.6-9] 22 p3870 N85-33971
The 4U 0115+63: Another energetic gamma ray binary pulsar
[OG-2.6-11] 22 p3870 N85-33973
Evidence for a dynamical halo around the edge-on galaxy NGC 4631
[OG-6.2-1] 22 p3889 N85-34102
The final COS-B database now publicly available
[OG-9.3-6] 23 p4028 N85-34963
Sporadic radio emission connected with a definite manifestation of solar activity in the near Earth space
[SH-10.1-8] 23 p4053 N85-35139
Near Earth space sporadic radio emission bursts occurring during sunrise
[SH-10.1-9] 23 p4054 N85-35140
On the possibilities of large-scale radio and fiber optics detectors in cosmic rays
[HE-4.6-2] 24 p4196 N85-36039
On the production mechanism of radio-pulses from large extensive air showers
[HE-4.6-4] 24 p4196 N85-36041

RADIO EQUIPMENT
NT IONOSONDES
NT RADIO ANTENNAS
NT RADIO BEACONS
NT RADIO FILTERS
NT RADIO RECEIVERS
NT RADIO TELESCOPES
NT RADIO TRANSMITTERS
NT RADIOSONDES
NT RADIOTELEPHONES
NT RAWINSONDES
NT RECEPTION DIVERSITY
NT SPACECRAFT ANTENNAS
NT SUPERHETERODYNE RECEIVERS
NT TRANSMITTER RECEIVERS
NT TRANSPONDERS
NT VERY HIGH FREQUENCY RADIO EQUIPMENT
Shipboard and satellite-aided communications equipment in exhibition 06 p0819 N85-15203
Telecommunications equipment at 1984 Leipzig Spring Fair 08 p1140 N85-17179
Signal Hill solar-powered repeater report and recommendations
[DE85-000487] 09 p1316 N85-18273
Technical data on new engineering products 10 p1460 N85-19201
Application of the HARDMAN methodology to the single channel ground-airborne radio system (SINCGARS)
[NASA-CR-175486] 10 p1467 N85-19259
LOS microwave channel simulation: A survey of models, realizations and new concepts 10 p1472 N85-19291
Satellite communications and amateur radio 12 p1838 N85-21534
Algorithm for statistical simulation of electromagnetic compatibility characteristics of high-frequency transmission channels in radioelectronic facilities 12 p1842 N85-21560
Machine analysis of resonance characteristics of plate-type radio electronic equipment constructions 13 p2085 N85-23018
Results of comparison of long-wave radiation fluxes measured by Soviet and Japanese actinometric radiosounds 14 p2333 N85-24427
Application of space methods in geodesy 16 p2724 N85-26817
An analysis of the materiel fielding plan for the SINCGARS (Single Channel Ground and Airborne Radio System) radio
[AD-A155101] 21 p3576 N85-32236

RADIO FILTERS
Quartz filter transceiver 12 p1838 N85-21536
Theory of optimum M-filtration of signals against background of correlated interference 13 p2089 N85-22927
Combined processing method and matched filter for discrete composite frequency phase-shift keyed signal 13 p2070 N85-22931

Programmable filter with fanned interdigital surface acoustic wave transducer 13 p2063 N85-23008

RADIO FREQUENCIES
NT C BAND
NT EXTREMELY HIGH FREQUENCIES
NT EXTREMELY LOW RADIO FREQUENCIES
NT HIGH FREQUENCIES
NT LOW FREQUENCIES
NT MICROWAVE FREQUENCIES
NT SUPERHIGH FREQUENCIES
NT ULTRAHIGH FREQUENCIES
NT VERY HIGH FREQUENCIES
NT VERY LOW FREQUENCIES

Resistance to HF jamming interference in mobile radio networks by an adaptive, distributed reconfiguration technique
[AD-A145117] 01 p0038 N85-10238

Clutter generator for use in radar evaluation
[AD-D011234] 01 p0039 N85-10245

Transverse field interaction multibeam amplifier
[AD-D011241] 01 p0043 N85-10262

Radiofrequency and microwave radiation
[AD-A145492] 02 p0191 N85-11274

Use of a first-harmonic RF system in the NSLS booster
[DE84-016432] 02 p0277 N85-11806

The dc SQUID as a tuned radiofrequency amplifier
[DE85-000701] 06 p0805 N85-15123

A nonlocal expression for the ponderomotive potential
[IPPJ-899] 06 p0864 N85-15487

Polarization of radio molecular lines and mapping of magnetic field direction 06 p0878 N85-15581

Transmission line biased coherent array of Josephson oscillators
[AD-D011323] 07 p0944 N85-15979

RF laser array driver apparatus
[AD-D011375] 07 p0969 N85-16155

Optical RF downconverter
[AD-D011396] 07 p1042 N85-16616

Opportunities for high angular and temporal resolutions of galactic objects at radio frequencies — QUASAT 07 p1059 N85-16723

Dual mode radio frequency-infrared frequency system
[AD-D011402] 08 p1081 N85-16850

RF fiber optic link
[AD-A148679] 08 p1155 N85-17290

Slow wave antenna coupling to ion Bernstein waves for plasma heating in ICRF
[AD-B089084L] 09 p1386 N85-18717

LOS microwave channel simulation: A survey of models, realizations and new concepts 10 p1472 N85-19291

A review of transmission and channel evaluation techniques for digital communication systems 10 p1474 N85-19301

Narrowband spread spectrum systems 10 p1475 N85-19307

Genetic effects of microwave exposure on mammalian cells in vitro. Volume 2, Appendix A: Cytogenetics and growth kinetics data, 850 MHz
[AD-A148885] 10 p1522 N85-19599

Genetic effects of microwave exposure on mammalian cells in vitro, volume 2
[AD-A149347] 10 p1523 N85-19603

Precision tunable resonant microwave cavity
[NASA-CASE-LEW-13935-1] 11 p1628 N85-20248

Automated TEM (Transverse electromagnetic) cell calibration system
[PB85-134377] 11 p1638 N85-20319

Look at energy compression as an assist for high power RF production
[DE85-001568] 11 p1725 N85-20851

Biological effects on radiofrequency radiation
[PB85-120848] 12 p1900 N85-21930

Horizontal deflection TS-257 13 p2069 N85-22926

Combined processing method and matched filter for discrete composite frequency phase-shift keyed signal 13 p2070 N85-22931

Space-based antenna measurement system concepts for space station operation 14 p2236 N85-23860

Radio frequency quadrupole and alternating phase focusing methods used in proton linear accelerator technology in the USSR
[AD-A150830] 14 p2418 N85-24016

High field RF superconductivity: To pulse or not to pulse
[DE85-004381] 14 p2429 N85-24977

Quality control of radioelectronic apparatus components on basis of external characteristics in frequency domain 15 p2529 N85-25590

Land mobile satellite transmission measurements at 869 MHz: Selected results from the dedicated stratospheric balloon experiment of November 12 and 13, 1984
[NASA-CR-175734] 15 p2541 N85-25685

Annual Review, April 1983 - March 1984
[ISSN-0547-1567] 15 p2654 N85-26369

Radio frequency containment 15 p2654 N85-26375

Switching mixer
[AD-D011602] 16 p2777 N85-27139

Tone calibrated digital radio communication system
[NASA-CASE-NPO-16414-1-CU] 16 p3089 N85-29121

Performance of an RF beam monitor on the NBS-Los Alamos racetrack microtron
[DE85-010725] 19 p3262 N85-30232

Los Alamos Free-Electron Laser (FEL) RF system
[DE85-010719] 19 p3278 N85-30329

Mechanical considerations in cw linacs
[DE85-010728] 19 p3363 N85-30850

Proposed use of the radio-frequency quadrupole structure to funnel high-current ion beams
[DE85-010746] 19 p3364 N85-30857

Automated testing of developmental satellite communications systems and subsystems
[NASA-TM-87070] 20 p3440 N85-31348

Report of near field group
[DE85-010538] 20 p3527 N85-31940

VLF (Very low frequency) workshop held at San Diego California, 24-25 January 1985
[AD-A154652] 21 p3573 N85-32224

Microwave SAW (Surface Acoustic Wave) monochromator
[AD-D011718] 21 p3590 N85-32311

Radio-frequency radiation of storm clouds 21 p3602 N85-32939

Analysis of solution of Bloch's equations in time domain 22 p3771 N85-33371

Rf program for LAMPF 2
[DE85-012693] 22 p3837 N85-33760

Iris tilting and RF steering in the SLAC Linac
[DE85-011704] 22 p3841 N85-33783

Role of ECRH in potential formation for tandem mirrors
[DE85-011859] 22 p3848 N85-33834

Radio observations of four anticenter 2CG gamma-ray sources
[OG-2.5-10] 22 p3869 N85-33965

Breakdown of intrinsic ambipolarity for the radial diffusion due to a rotating RF field 23 p3977 N85-34660

Synthesis of ultrafine ceramic and metallic powders in a thermal argon rf plasma
[DE85-009634] 23 p3993 N85-34696

Sporadic radio emission connected with a definite manifestation of solar activity in the near Earth space
[SH-10.1-8] 23 p4053 N85-35139

Near Earth space sporadic radio emission busts occurring during sunrise
[SH-10.1-9] 23 p4054 N85-35140

Analyzer, flight line
[AD-A155777] 24 p4067 N85-35207

RF stabilization of interchange-ballooning modes
[DE85-012080] 24 p4090 N85-35353

Robinson instability and beam loading
[DE85-013301] 24 p4151 N85-35737

A new study on the emission of EM waves from large EAS
[HE-4.6-5] 24 p4197 N85-36042

Radio wave emitted by an extensive air showers in 10KHz to 1MHz region
[HE-4.6-15] 24 p4198 N85-36051

RADIO FREQUENCY DISCHARGE
Investigation of RF excited CW CO2 waveguide lasers
[NASA-CR-174106] 04 p0505 N85-13221

Microwave discharge in a supersonic flow for the excitation of a gas dynamic CO laser
[ESA-TT-833] 09 p1326 N85-18337

The effects of surface waves on RF discharge pumped lasers
[AD-A149689] 12 p1856 N85-21843

Statistical study of Saturnian electrostatic discharges observed by the Voyager Planetary Radio Astronomy experiment 15 p2673 N85-26500

An Earth-based attempt to detect Saturn Electrostatic Discharge (SED) at 21 centimeters 15 p2674 N85-26501

Fokker-Planck calculation of hot electron formation in the thermal barrier region of tandem mirror Gamma-10
[IPPJ-726] 23 p3979 N85-34659

RADIO FREQUENCY HEATING
High frequency plasma generator for ion thrusters
[NASA-CR-174772] 08 p1114 N85-17023

Analytical and numerical modeling of gyrotrons
[AD-A148100] 08 p1157 N85-17300

Proceedings on US-Japan Workshop on Tokamak Diagnostics by X-ray, VUV and Optical Radiations
[IPPJ-703] 09 p1386 N85-18719

X-rays spectroscopy on the PLT and TFTR Tokamaks 09 p1386 N85-18720

Electronics Engineering Department: EE technical review
[DE85-004360] 11 p1629 N85-20259

Computer simulation of equipment and processes involved in high-frequency heating of dielectrics 12 p1841 N85-21555

Observations of bulk electron heating due to return current in a tokamak discharge started up by lower hybrid waves
[IPPJ-708] 12 p1937 N85-22172

The design of megawatt gyrotrons
[DE85-007892] 17 p3032 N85-28754

Electron-cyclotron maser emission during solar and stellar flares
[NASA-CR-175883] 17 p3054 N85-28907

Measurement of radiated emissions from industrial heating device equipment as it relates to aeronautical services
[FAA-ES-85-2] 19 p3255 N85-30181

Activities of the RF Section 23 p3975 N85-34646

RF induced radial diffusion in tandem mirrors 23 p3976 N85-34649

Model of azimuthal non-uniformities induced by RF heating in RFC-XXM 23 p3977 N85-34658

RADIO FREQUENCY INTERFERENCE
NT ATMOSPHERICS
NT DAWN CHORUS
NT ELECTROMAGNETIC NOISE
NT HISS
NT IONOSPHERIC NOISE
NT SHOT NOISE
NT THERMAL NOISE
NT WHISTLERS
NT WHITE NOISE

Interference experiment with the Sirio-OTS satellites
[FUB-17-1983] 01 p0040 N85-10254

Revision of signal and interference space-time processing algorithms for implementation by microprocessors 04 p0487 N85-13105

Distribution of atmospheric radio interference 06 p0792 N85-15063

Asymptotically optimal ranking algorithms for quasi-determinate signal detection 06 p0792 N85-15064

Synoptic observations of the radio noise background in the frequency range 150-180 kHz to provide design data for the low frequency communications designer
[AD-A147438] 07 p0941 N85-15965

Measurement of signal separation between radio service and air navigation service
[IRT-TB-8-40/82] 08 p1063 N85-16860

Interference immunity of fiber-optic communication lines with spectral multiplexing of channels 13 p2069 N85-22924

Probability of detection of pulsed signals employing zero-gating interference suppression 13 p2085 N85-23021

Analysis of interference caused by interfering radio signals in communications systems with frequency seperation of telephone channels and frequency modulation 13 p2086 N85-23025

Approximate rules for signal detection against background of Gaussian correlated interference 13 p2086 N85-23027

Noise immunity of information transmission system with pseudorandom frequency switching under worst-case interference conditions 13 p2086 N85-23029

FH/MFSK performance in multitone jamming
[NASA-CR-175667] 14 p2290 N85-24197

The distortion of AM broadcast antenna patterns as caused by nearby towers and highrise buildings
[CRC-1379] 15 p2538 N85-25666

Interference suppressor for radar MTI
[AD-D011606] 16 p2769 N85-27086

Predicting the effects of non-Gaussian interference in HF (High-Frequency) broadcasting. Part 1: A methodology for an analytic approach
[PB85-171544] 18 p3092 N85-29140

Measurement of RF fields associated with ISM equipment as it relates to aeronautical services
[FAA-ES-84-2] 19 p3254 N85-30180

Adaptive signal detection and other topics in real time signal processing
[AD-A154139] 19 p3255 N85-30184

Phase synchronizing large antenna arrays using the spatial correlation properties of radar clutter 20 p3439 N85-31344

Most desirable terrain, e.g., flat vs valley location, part 5.1B 21 p3624 N85-32513

Design of a freestanding noise measurement and recording system to predict the intensity and location of electromagnetic radiation from earthquakes
[AD-A155070] 21 p3632 N85-32563

Radio-frequency radiation of storm clouds 21 p3602 N85-32939

Adaptive antenna arrays for satellite communications: Design and testing
[NASA-CR-176162] 23 p3926 N85-34329

Television interference at the Maglarp (Sweden) wind turbine 24 p4111 N85-35480
Television interference measurement at Kalkugnen (Sweden) test windmill 24 p4111 N85-35481
RADIO FREQUENCY ION THRUSTOR ENGINES
U RIT ENGINES
RADIO FREQUENCY NOISE
U ELECTROMAGNETIC NOISE
RADIO FREQUENCY RADIATION
U RADIO WAVES
RADIO GALAXIES
Observations of 15 radio galaxies from Bologna survey using RATAN-600 radio telescope 02 p0162 N85-11097
The IRAS galaxy 0421+040P06: An active spiral (?) galaxy with extended radio lobes [NASA-CR-174208] 06 p0871 N85-15536
The environment of active galactic nuclei 07 p1057 N85-16712
The compact radio emission regions in active galactic nuclei — QUASAT VLBI mission 07 p1058 N85-16713
X-ray emission from Centaurus A — Vela 5B; radio galaxy 08 p1239 N85-17813
Collimated winds from active galactic nuclei 08 p1241 N85-17832
X-ray emission from Centaurus A [DE85-002030] 09 p1417 N85-18843
Determination of physical parameters of jets in radio galaxies 12 p1958 N85-22304
Magnetohydrodynamic (MHD) turbulence in radio galaxies 12 p1958 N85-22305
Morphology and energetics of narrow angle tail radio sources 14 p2455 N85-25164
RADIO INTERFERENCE
U RADIO FREQUENCY INTERFERENCE
RADIO INTERFEROMETERS
Apparatus of short baseline centrimetric wave radiointerferometer with cable communication lines for astrophysical research 06 p0782 N85-15001
Characteristics of lateral-scan interferometer 06 p0783 N85-15006
Primary data processing in very long baseline radiointerferometer 06 p0783 N85-15008
The wide-range space radio interferometer 07 p1058 N85-16717
Determining vector of radiointerferometer base from observations of natural radio emission with narrow spectrum 13 p2112 N85-23158
Accurate baseline determination by radio interferometry on NAVSTAR GPS satellite transmissions [AD-A150661] 14 p2291 N85-24202
Interferometer applications of VHF radars, part 3.6A 21 p3621 N85-32497
RADIO METEOROLOGY
Atmospheric channel performance measurements at 10 to 100 GHz [PB84-211325] 01 p0042 N85-10271
Neutral atmosphere properties determining D-region electron densities 11 p1658 N85-20451
Prospective investigations with DFVLR radar of possible relevance in the assessment of radio interference due to scattering from precipitations — meteorological radar [DFVLR-FB-84-42] 12 p1830 N85-21485
Additional possibilities of radiometeor azimuthal method for measuring wind velocity in lower thermosphere 19 p3296 N85-30438
Meteorological and aeronomical requirements for MST radar networks (keynote paper), part 1 21 p3615 N85-32467
Troposphere-stratosphere exchange, part 1.1A 21 p3615 N85-32468
Observations of frontal zone structures with a VHF Doppler radar and radiosondes, part 1.2A 21 p3616 N85-32469
Gravity waves from the stratosphere to the mesosphere, part 1.3B 21 p3616 N85-32471
General circulation of the middle atmosphere, part 1.4B 21 p3617 N85-32474
Performance of the Colorado wind-profiling network, part 1.5A 21 p3617 N85-32475
Vertical transport in the atmosphere: Measurement capabilities and requirements of VHF radars, part 1.6A 21 p3617 N85-32476
Comparison of tropopause altitude determination by the Platteville Radar, Sunset Radar and the NWS Rawinsonde 21 p3617 N85-32477
Synoptic-scale dynamics with vertical velocity, part 1.8A 21 p3617 N85-32478
Sample interchange of MST radar data from the Urbana radar 21 p3627 N85-32531
MST radar data management 21 p3627 N85-32532
Data base for the Colorado profiling network 21 p3627 N85-32533
Further developments of EISCAT as an MST radar 21 p3627 N85-32534
Status of the Jicamarca radar 21 p3627 N85-32535
Recent results at the Sunset radar 21 p3627 N85-32536
The Boot Lake MF imaging radar 21 p3628 N85-32537
MENTOR: Adding an outlying receiver to an ST radar for meteor-wind measurement 21 p3628 N85-32538
Summary of progress at the Poker Flat Observatory in Alaska 21 p3628 N85-32539
Urbana radar systems: Possibilities and limitations 21 p3628 N85-32540
The Sondrestrom radar: Progress and proposed upgrades for ST work 21 p3628 N85-32541
Progress and plans for the Colorado Wind Profiler Network 21 p3628 N85-32542
The MU radar now partly in operation 21 p3628 N85-32543
Network ST radar and related measurements at Pennsylvania State University 21 p3629 N85-32544
A note on the proposed UK VHF radar 21 p3629 N85-32545
The Adelaide VHF radar: Capabilities and future plans 21 p3629 N85-32546
The Proust radar 21 p3629 N85-32547
Millstone Hill radar: Capabilities for S/T observations 21 p3629 N85-32548
The Ponape ST radar 21 p3629 N85-32549
Measurements of vertical velocity over flat terrain by ST radar and other related uses of the radar data set 21 p3630 N85-32550
RADIO METEORS
Additional possibilities of radiometeor azimuthal method for measuring wind velocity in lower thermosphere 19 p3296 N85-30438
RADIO NAVIGATION
NT LORAN
NT LORAN C
NT TACAN
NT VHF OMNIRANGE NAVIGATION
Experimental determination of propagation rate of ELF signals employed by Omega radio navigation system for phase measurements 06 p0793 N85-15066
Measurement of signal separation between radio service and air navigation service [IRT-TB-B-40/82] 08 p1083 N85-16860
INMARSAT marine satellite organization 13 p1985 N85-22456
Navigation: Accounting for copy 16 p2695 N85-26641
Allowance for differences in ellipsoids and geodetic control coordinate systems in determining ship's position using radio navigation systems 19 p3292 N85-30413
Use of Omega radio navigation system in geophysical work in Antarctica 19 p3296 N85-30448
Evaluation of radio navigation systems and their configuration with respect to minimum cost [ESA-TT-847] 20 p3392 N85-31043
RADIO OBSERVATION
Activity and magnetic fields on stars from radio observations [NASA-CR-175966] 18 p3202 N85-29861
RADIO OCCULTATION
Two-level model for formation of night ionosphere of Venus from radio occulation experiments 02 p0162 N85-11100
Radio scintillations observed during atmospheric occultations of Voyager: Internal gravity waves at Titan and magnetic field orientations at Jupiter and Saturn [NASA-CR-175554] 12 p1961 N85-22327
Occultations of stars and radio sources by comets: Predictions and observing prospects 14 p2437 N85-25034
Laboratory evaluation and application of microwave absorption properties under simulated conditions for planetary atmospheres [NASA-CR-176078] 22 p3851 N85-33847
RADIO PHYSICS
Decimetric-wave aperture synthesis system at Scientific Research Institute of Radiophysics 06 p0782 N85-15000
Study of lower ionosphere by pulse cross-modulation method 10 p1500 N85-19467
Millimeter-wave range masers: A review 13 p2089 N85-23042
RADIO PROBING
Experimental results of study of artificial perturbation region in upper and lower ionosphere disturbance by the method of vertical probing 06 p0784 N85-15011
Relation between polarization of artificial low frequency radiation and parameters of auroral ionosphere 06 p0785 N85-15016
Distortions of radio pulse during reflection from maximum region of ionospheric layer 06 p0792 N85-15061
Partial reflection D-region electron densities 06 p1184 N85-17461
Method and apparatus for calibrating the ionosphere and application to surveillance of geophysical events [NASA-CASE-NPO-15430-1] 12 p1887 N85-21846
RADIO PROPAGATION
U RADIO TRANSMISSION
RADIO RANGES
U RADIO BEACONS
RADIO RECEIVERS
NT SUPERHETERODYNE RECEIVERS
NT TRANSMITTER RECEIVERS
Digital radio receivers and problems of analog-to-digital conversion of narrow-band signals 04 p0486 N85-13101
Testing of a field portable GPS (Global Positioning System) geodetic receiver [AD-A148336] 08 p1092 N85-16859
Synthesis of optimum receiver and processor for signal packet of radio pulses 12 p1839 N85-21541
Receiver optimization for detection in doubly spread communication channels [AD-A151226] 15 p2541 N85-25689
The R-809 radio set [AD-A152370] 17 p2948 N85-28200
UHF IRIG G distribution system 17 p2985 N85-28308
Adaptive signal detection and other topics in real time signal processing [AD-A154139] 19 p3255 N85-30184
The NAVSTAR Global Positioning System (GPS) receiver development program, phase 1 [BMFT-FB-W-85-002] 20 p3399 N85-31065
Study of a low rate spread spectrum receiver [ENST-83E015] 20 p3441 N85-31354
New VLBI technology developments 20 p3491 N85-31702
Optimality criterion for high-frequency channel in receivers of discrete radio signals 22 p3776 N85-33401
Synthesis of system with nonideal components for optimal processing of radio signal 22 p3777 N85-33405
Developmental trends in radio receiver design 22 p3777 N85-33407
Waves in Space Plasmas (WISP) 23 p3901 N85-34164
RADIO RECEPTION
Energy correlation between natural extra-low-frequency noises at various frequencies 06 p0784 N85-15010
Evaluation of parameters of a signal (selected pages) [AD-A148631] 09 p1312 N85-18243
Ionosphere effects may replace some communications satellites 15 p2484 N85-25337
The distortion of AM broadcast antenna patterns as caused by nearby towers and highrise buildings [CRC-1379] 15 p2538 N85-25668
Receiver optimization for detection in doubly spread communication channels [AD-A151226] 15 p2541 N85-25689
Adaptive signal detection and other topics in real time signal processing [AD-A154139] 19 p3255 N85-30184
RADIO REFLECTION
U RADIO ECHOES
RADIO RELAY SYSTEMS
NT CODE DIVISION MULTIPLE ACCESS
NT TIME DIVISION MULTIPLE ACCESS
A microcomputer aided measurement equipment for monitoring performance in digital radio relay systems [FUB-4-1984] 01 p0101 N85-10668
Equipment for multiplexing multichannel radio-relay lines of communication [AD-A148402] 08 p1153 N85-17276
The impact of propagation effects on the design of high capacity digital microwave links in the 18 GHz frequency band 10 p1470 N85-19278
Wideband line-of-sight channel measurements and simulation: Application to digital radio links 10 p1471 N85-19283
Optimum path selection in automated radio relay link design 13 p2073 N85-22947
Automation of servicibility of radio-relay station equipment 15 p2527 N85-25582
System of light protection of antenna-mast structures of radio-relay lines 15 p2527 N85-25583
RADIO SCATTERING
Partial reflection D-region electron densities 06 p1184 N85-17461
D1 LF wind measurements in the 90 to 100 km height range 06 p1185 N85-17468
UHF communications through forested propagation channels 10 p1470 N85-19280

Correctness of reflection characteristics of radio absorbent materials 13 p2081 N85-22995
Ionosphere effects may replace some communications satellites 15 p2484 N85-25337
Radio wave scattering and intermittency of turbulence in the atmosphere 19 p3266 N85-30392
Radio wave scattering and turbulence intermittence in atmosphere 19 p3296 N85-30446
Theoretical investigation of single-frequency 8-element localizer signal scattering for critical area determination [FAA-PM-85-4] 20 p3391 N85-31037

RADIO SIGNAL ATTENUATION
U RADIO ATTENUATION

RADIO SIGNAL PROPAGATION
U RADIO TRANSMISSION

RADIO SIGNALS
Peculiarities of microprocessor implementation of algorithms for processing radio signals and noise in large antenna arrays 06 p0792 N85-15059
Formation of radio signals with low out-of-band radiation 07 p0950 N85-16018
Structure of frequency modulated and phase-shift keyed signals reflected from ionosphere at near-critical frequencies 07 p0952 N85-16035
Arctic marine acoustics [AD-A147482] 07 p1039 N85-16584
Digital coherent detector [AD-D011560] 12 p1833 N85-21501
Summator of radio pulse signals 12 p1839 N85-21539
The use of a high-speed 12-bit A/D converter for digital sampling of communication signal carriers [AD-A150578] 13 p2056 N85-22872
Space-time response characteristics of acoustooptic filter for compression of linearly frequency-modulated signal 13 p2071 N85-22937
Domain of applicability of asymptotic description of radio pulse fields near critical frequency 13 p2073 N85-22949
Reception noise immunity of multiposition signals 13 p2085 N85-23023
Analysis of interference caused by interfering radio signals in communications systems with frequency separation of telephone channels and frequency modulation 13 p2086 N85-23025
Investigation of influence of communications link and synchronization error on noise tolerence of group transmission of binary information based on orthogonal Walsh function 13 p2086 N85-23026
Approximate rules for signal detection against background of Gaussian correlated interference 13 p2086 N85-23027
Use of importance sampling to investigate signal detection systems by simulated method 13 p2086 N85-23028
Synthesis of system with nonideal components for optimal processing of radio signal 22 p3777 N85-33405
Radio signals from very large showers [HE-4.8-3] 24 p4196 N85-36040

RADIO SOURCES (ASTRONOMY)
NT CASSIOPEIA A
NT EXTRAGALACTIC RADIO SOURCES
NT PULSARS
NT QUASARS
NT RADIO GALAXIES
NT RADIO STARS
The catalogue of the discrete sources in the declination range from -13 deg to -2 deg [NASA-TM-77594] 01 p0129 N85-10887
Submilliarcsecond VLBI using compact close pairs of radio sources: Error analysis 05 p0622 N85-13981
Cross-shaped aperture synthesis system 06 p0782 N85-14999
Apparatus of short baseline centimetric wave radiointerferometer with cable communication lines for astrophysical research 06 p0782 N85-15001
Software for Crimea-Pushchino radiointerferometer 06 p0783 N85-15007
The IRAS galaxy 0421+040P06: An active spiral (?) galaxy with extended radio lobes [NASA-CR-174208] 06 p0871 N85-15536
Cosmology 07 p1056 N85-16701
The QUASAT mission: An overview 07 p1056 N85-16704
QUASAT: Technical aspects of the proposed mission — VLBI satellite 07 p1057 N85-16706
A study on the imaging potential of QUASAT — spaceborne VLBI 07 p1057 N85-16707
Ultraviolet and X-ray observations of active galactic nuclei: Constraints on models of the broad emission line region 11 p1744 N85-20966
A new radio emission at 3 kHz in the outer heliosphere 12 p1959 N85-22312
Absolute measurements of radiation intensity from Cassiopeia-A, Cygnus-A and crab nebula in 60-100 cm band 13 p2078 N85-22978
Comments on RS-17 X-ray telescope 22 p3731 N85-33132
Radio observations of four anticenter 2CG gamma-ray sources [OG-2.5-10] 22 p3869 N85-33965
A search for sources of ultra high energy gamma rays at air shower energies with Ooty EAS array [OG-2.6-8] 22 p3870 N85-33970
Search for the gamma-ray fluxes with energies above 10915) eV from various objects [OG-2.6-14] 22 p3871 N85-33975
CEN A observation at MeV-energies [OG-2.7-7] 22 p3871 N85-33980
The extent of the local hi halo [NASA-CR-176115] 23 p3987 N85-34724
Burst and Transient Source Experiment (BATSE) for the Gamma Ray Observatory (GRO) [OG-9.2-14] 23 p4026 N85-34953
Capabilities of the GRO/BATSE for monitoring of discrete sources [OG-9.2-16] 23 p4026 N85-34955

RADIO SPECTRA
NT MICROWAVE SPECTRA
Energy parameters of optical radiation space research systems 06 p0791 N85-15058
Radio Seyferts and the forbidden line region 08 p1236 N85-17793
The relationship between radio structures and stellar dynamics of nearby elliptical galaxies 08 p1236 N85-17794
VLBI observations of compact double radio sources 09 p1417 N85-18940
National Telecommunications and Information Administration authorization [GPO-38-660] 16 p2879 N85-27766
Microwave SAW (Surface Acoustic Wave) monochromator [AD-D011718] 21 p3590 N85-32311
Controllable companding in low-frequency FM radio communication systems 22 p3776 N85-33402

RADIO STARS
NT PULSARS
The 1000 GeV gamma rays from ms pulsars [OG-2.3-12] 22 p3867 N85-33948

RADIO TELEMETRY
Radio telemetry formula applications. A practical users guide [AD-A146247] 03 p0356 N85-12288
Meteorological Sounding System (MSS) standard operating procedures [AD-A149513] 10 p1519 N85-19578
Tracking pelagic dolphins by satellite 14 p2324 N85-24384
Polar bear telemetry results from the Nimbus-6 system 14 p2325 N85-24365
The ARGOS communications performance trials 14 p2326 N85-24376
Telemetered meteorological and engineering data from a deep sea moored body in the Long Term Upper Ocean Study (LOTUS) 14 p2329 N85-24402
The Data Acquisition Control and Telemetry (DACT) system — meteorological buoys 14 p2332 N85-24419
System for radio remote control of dropping bombs [CH-639335-A5] 15 p2491 N85-25371

RADIO TELESCOPES
Test measurements of the 100 m telescope at lambda = 7 mm [TR-18] 01 p0129 N85-10690
The Belikt experiment 02 p0159 N85-11079
Observations of 15 radio galaxies from Bologna survey using RATAN-600 radio telescope 02 p0162 N85-11097
The UK and Netherlands millimetre-wave telescope — Netherlands (NL) 05 p0625 N85-14003
Aperture synthesis (review) 06 p0781 N85-14995
Cross-shaped aperture synthesis system 06 p0782 N85-14999
Synthesis of radio image on RATAN-600 radiotelescope 06 p0783 N85-15004
Attempts to contruct two-dimensional image of Sun from observations made with RATAN-600 radiotelescope by relay race method 06 p0783 N85-15005
Research in geodesy based upon radio interferometric observations of extragalactic radio sources [AD-A147581] 07 p0988 N85-16280
FRG radiotelescope made of carbon fiber-reinforced plastic 09 p1309 N85-18226
Error in compensating phase fluctuations of wave field by means of adaptive reflectors with continuous or compound surface 13 p2060 N85-22988
QUASAT: An orbiting very long baseline interferometer program using large space antenna systems 14 p2230 N85-23822
Angular error of position of RATAN-600 screens during radial displacement 15 p2476 N85-25286
An Earth-based attempt to detect Saturn Electrostatic Discharge (SED) at 21 centimeters 15 p2674 N85-26501
Radio telescope with 256 antennas built in Siberia 22 p3732 N85-33136

RADIO TRACKING
NT WILDLIFE RADIOLOCATION
Data Collection and Platform Location by Satellite: ARGOS Users' Conference 14 p2325 N85-24366
The ARGOS contribution to the First GARP Global Experiment (FGGE) study of drifting buoys 14 p2325 N85-24371
The ARGOS system aboard research vehicles: 1981 experiment aboard the Le Suroit oceanographic vessel and the outlook [CNEXO/DFT/OPNAV/82-05] 14 p2327 N85-24382
Miscellaneous ARGOS maritime applications — yacht races 14 p2327 N85-24383
Synthesis of adaptive filters for tracking radio systems 22 p3763 N85-33325

RADIO TRANSMISSION
NT IONOSPHERIC PROPAGATION
NT MANDELSTAM REPRESENTATION
NT MICROWAVE ATTENUATION
NT MICROWAVE TRANSMISSION
NT MULTIPATH TRANSMISSION
NT SHORT WAVE RADIO TRANSMISSION
NT SINGLE SIDEBAND TRANSMISSION
NT SPREAD SPECTRUM TRANSMISSION
NT TRANSEQUATORIAL PROPAGATION
Digital radio link: Wave propagation measurements using narrow band technique [FOA-C-30364-E2] 04 p0494 N85-13152
Simulation of a transmission circuit composed of slightly nonlinear elements. Computation of the intermodulation on signals composed of N carriers [CNES-NT-105] 04 p0496 N85-13167
USSR report: Electronics and electrical engineering [JPRS-UEE-84-018] 07 p0949 N85-16014
Artificial ionospheric disturbances caused by powerful radio waves [AD-A148077] 08 p1186 N85-17473
UHF radiowave propagation through forests [AD-A149518] 10 p1467 N85-19256
Propagation Influences on Digital Transmission Systems: Problems and Solutions [AGARD-CP-363] 10 p1469 N85-19269
Limits of the propagation medium with respect to digital signal transmission 10 p1469 N85-19270
Propagation of wide bandwidth signals in a tropospheric ducting system 10 p1469 N85-19271
Propagation effects on the Doppler frequency shift of satellite transmissions 10 p1470 N85-19276
UHF communications through forested propagation channels 10 p1470 N85-19280
A comparison between predicted and measured propagation loss in the VHF/UHF range in rugged terrain 10 p1471 N85-19285
Measurements of propagation at 900 MHz in an urban zone for establishing a digital radiomobile system 10 p1472 N85-19288
A review of transmission and channel evaluation techniques for digital communication systems 10 p1474 N85-19301
A microprocessor controlled parallel model with FDPSK 10 p1475 N85-19304
Synopsis of mid-latitude radio wave absorption in Europe 11 p1659 N85-20454
L.F. RADIO-DATA: Specification of BBC phase-modulated transmissions on long-wave [BBC-RD-1984/19] 12 p1822 N85-21431
Disturbances in structure of lower ionosphere at terminators based on results of winde-band LW sounding 14 p2339 N85-24467
Land mobile satellite transmission measurements at 869 MHz: Selected results from the dedicated stratospheric balloon experiment of November 12 and 13, 1984 [NASA-CR-175734] 15 p2541 N85-25685
Meteorological conditions affecting electromagnetic propagation on the Arabian Peninsula [AD-A152019] 15 p2544 N85-25708
Active and passive remote sensing of ice [AD-A151741] 16 p2815 N85-27369
A transport theory of millimeter wave propagation in woods and forests [AD-A151883] 17 p2947 N85-28186
Effects of hydrometeors on electromagnetic wave propagation [AD-A155379] 22 p3759 N85-33297
Variation in radiowave propagation conditions in corona during solar activity cycle 22 p3763 N85-33327

RADIO TRANSMITTERS
NT IONOSONDES
NT RADIO BEACONS
NT RADIOSONDES
NT RADIOTELEPHONES
NT RAWINSONDES
NT TRANSMITTER RECEIVERS
Development and testing of a 20-kW X-band transmitter with high phase stability 05 p0623 N85-13985
Estimation of requirements for acceptable noise radiation level of communication transmitters 07 p0949 N85-16017
A reflectometer unit for a 500 kW HF balanced screened feeder
[BBC-RD-1984/13] 10 p1477 N85-19322
Adaptive regulation of transmitter radiation power in radio lines during delays of control signals 12 p1841 N85-21551
Equipment for the ARGOS system from Eidsvoll Electronics A.S. 14 p2239 N85-23985
The development of Platform Transmitter Terminal (PTT) and its application for drifting buoys 14 p2323 N85-24353
A new versatile ARGOS PTT for oceanographic applications — Platform Transmit Terminal (PTT) 14 p2331 N85-24417
Foreshortened short-wave scattering on artificial ionospheric inhomogeneities 14 p2340 N85-24466
Studies into location accuracy — ARGOS system 16 p2811 N85-27334
The R-609 radio set
[AD-A152370] 17 p2948 N85-28200
UHF IRIG G distribution system 17 p2965 N85-28306
Tone calibrated digital radio communication system
[NASA-CASE-NPO-16414-1-CU] 18 p3089 N85-29121
Waves in Space Plasmas (WISP) 23 p3901 N85-34164

RADIO WAVE REFRACTION
Theory of radio wave propagation over the ocean 02 p0259 N85-11696
Field coherence function in layerwise nonhomogeneous troposphere 06 p0784 N85-15012
QUASAT, gravitational lenses, and studies of the interstellar, intracluster and intergalactic medium 07 p1058 N85-16715
Propagation effects on the Doppler frequency shift of satellite transmissions 10 p1470 N85-19276
Possibility of determining atmospheric weather parameters by radio and radiooptical measurements of refraction of cosmic sources 13 p2110 N85-23146
Saudi Arabian refraction profile: Crustal structure of the Red Sea-Arabian Shield transition 17 p2990 N85-28484
Beam diffusion in linear ionospheric layer 21 p3695 N85-32958

RADIO WAVES
NT CENTIMETER WAVES
NT CN EMISSION
NT DECAMETRIC WAVES
NT DECIMETER WAVES
NT EXTRATERRESTRIAL RADIO WAVES
NT GALACTIC RADIO WAVES
NT HYDROXYL EMISSION
NT IONOSPHERIC NOISE
NT LONG WAVE RADIATION
NT MICROWAVE EMISSION
NT MICROWAVES
NT MILLIMETER WAVES
NT RADIO BURSTS
NT RADIO EMISSION
NT SHORT WAVE RADIATION
NT SKY WAVES
NT SOLAR RADIO BURSTS
NT SOLAR RADIO EMISSION
NT SUBMILLIMETER WAVES
NT TYPE 3 BURSTS
NT TYPE 4 BURSTS
NT WHISTLERS
Planning guide for the review of telecommunications systems for frequency availability and electromagnetic compatibility
[PB84-210238] 01 p0041 N85-10298
Formation of radio images by scanning around circle 02 p0264 N85-11727
Scattering of radio waves on magnitized meteor trail 03 p0344 N85-12221
The investigation of short wave signal structure in the vicinity of the caustic by means of a high-directed antenna
[PR-194] 03 p0354 N85-12277
Artificial defocusing lens in ionosphere 05 p0724 N85-14654
Influence of Faraday effect in ionosphere on nonmutuality of meteor radio channel 07 p0952 N85-16037
Artificial ionospheric disturbances caused by powerful radio waves
[AD-A148077] 08 p1186 N85-17473
Polarization angles of linearly polarized antennas and radio waves in satellite communications
[PB85-131613] 11 p1626 N85-20240
Winter anomaly 1982/83 in comparison with earlier winters (1980-82) 11 p1660 N85-20481
Solar terrestrial influences on the D region as shown by the level of atmospheric radio noise 11 p1664 N85-20488
Radio Frequency Radiation (RFR) measurements in operational settings
[AD-A149717] 12 p1826 N85-21471
The medical results of human exposures to radio frequency radiation
[AD-A149716] 12 p1905 N85-21962
Calculation of amplitude-phase characteristics of signal scattered obliquely on meteor trail 13 p2073 N85-22948
Noninductive current drive in Tokamaks
[DE85-005427] 14 p2424 N85-24951
Ionosphere effects may replace some communications satellites 15 p2484 N85-25337
The Impact of Proposed Radio Frequency Radiation Standards on Military Operations
[AGARD-LS-138] 16 p2775 N85-27128
The physical interactions of radiofrequency radiation fields and biological systems 16 p2775 N85-27129
The biological effects of radiofrequency radiation 16 p2775 N85-27131
The cumulative effects of long term exposure to low levels of radiofrequency radiation (RFR) 16 p2776 N85-27132
Review of epidemiological studies of human exposures to radiofrequency radiation 16 p2776 N85-27134
Hazards of VLF electromagnetic fields 16 p2776 N85-27136
Radio Frequency Radiation (RFR) measurements in operational settings 16 p2777 N85-27138
Scintillation using NNSS satellites
[AD-A152804] 17 p2949 N85-28207
A review of ionospheric effects on Earth-space propagation 18 p3106 N85-29233
Ionospheric limitations to time transfer by satellite 18 p3107 N85-29234
A review of tropospheric refraction effects on Earth-to-satellite systems 18 p3107 N85-29235
Meteorological and aeronomical requirements for MST radar networks (keynote paper), part 1 21 p3615 N85-32467
Morphology of the scattering targets: Fresnel and turbulent mechanisms, part 2.1A 21 p3618 N85-32481
Relationship of spaced antenna and Doppler techniques for velocity measurements (keynote paper), part 3 21 p3619 N85-32488
Radio telescope with 256 antennas built in Siberia 22 p3732 N85-33136
Onion-shell model for cosmic ray electrons and radio synchrotron emission in supernova remnants
[OG-8.1-10] 23 p4018 N85-34900

RADIOACTIVE AGE DETERMINATION
Automation of radiometric measurements in nuclear oceanology 14 p2337 N85-24452
Paleoenvironmental investigations at seed cave (Windust cave H-45FR46), Franklin County, Washington
[AD-A154777] 21 p3635 N85-32576
Dating Archean zircon by ion microprobe: New light on an old problem 21 p3722 N85-33094

RADIOACTIVE CONTAMINANTS
Something in the air at Windscale — radioactive contaminants from the Sellafield nuclear Complex for reprocessing and storing irradiated fuel
[BLL-RISLEY-TR-4998-(9091.9F)] 08 p1179 N85-17429
Stabilization of contaminated soils by in situ vitrification
[AD-P004144] 09 p1348 N85-18480
EPA (Environmental Protection Agency) research program guide, FY-1985, October 1, 1984 - September 30, 1985
[PB85-181881] 20 p3457 N85-31676
ARAC status report, 1985
[DE85-012835] 22 p3610 N85-33603
Control technology for radioactive emissions to the atmosphere at US Department of Energy facilities: The Los Alamos Meson Physics Facility
[DE85-011402] 22 p3611 N85-33609
Estimation of Sr90 and Cs137 activity introduced and accumulation in the Po basin until 1963
[CISE-2515] 22 p3613 N85-33617
MATADOR (Methods for the Analysis of Transport And Deposition Of Radionuclides) code description and user's manual
[TI85-901402] 23 p3966 N85-34592

RADIOACTIVE DATING
U RADIOACTIVE AGE DETERMINATION

RADIOACTIVE DECAY
NT ALPHA DECAY
NT NEUTRON EMISSION
Recent heavy particle decay in a matter dominated universe
[NASA-CR-175501] 11 p1764 N85-21095
Study of 1/f noise in solids
[AD-A151099] 14 p2428 N85-24072
Neutrino measurements on the Moon
[DE85-007700] 16 p2884 N85-27791
Theoretical basis for the determination of the concentration of radon decay products in air from the activity of a particulate air sample
[IRI-190-83-07] 17 p3035 N85-28774
Model computations of radon, and radon decay product, concentrations in an open system; the Hewlett-Packard 41C program RNSS, version 02
[IRI-190-83-12] 17 p3035 N85-28775
Theoretical studies of high energy phenomenon: Analysis of models of CP and T violation
[DE85-007455] 17 p3036 N85-28782
Selected topics from J/psi decays
[DE85-010537] 18 p3183 N85-29736
Early study of muons and muon decay
[NOTA-INTERNA-835] 18 p3184 N85-29742
Topics in intermediate vector boson physics
[NOTA-INTERNA-841] 18 p3184 N85-29743
AGS broad band neutrino beam
[DE85-010954] 19 p3366 N85-30875
Summary of the discussion of the theory of radiative processes
[DE85-007812] 19 p3371 N85-30914
Current experiments in elementary particle physics, revision 1-85
[DE85-011513] 20 p3529 N85-31950
Effects of CP violation in SU(2) sub L x SU(2) sub R x U(1) electroweak models
[DE85-010801] 20 p3531 N85-31965
Phenomenology of the standard and nonstandard Higgs particles
[USIP-85-03] 20 p3532 N85-31971
Tritium-helium effects in metals
[DE85-011507] 22 p3749 N85-33235
Electron capture decay of cosmic rays: A model of the inhomogeneous interstellar medium
[OG-7.1-10] 23 p4014 N85-34871
Preliminary results on underground muon bundles observed in the Frejus proton-decay detector
[HE-5.1-1] 24 p4200 N85-36067
Muon and neutrino results from KGF experiment at a depth of 7000 hg/square cm
[HE-5.1-2] 24 p4200 N85-36068
Relevance of multiple muons detected underground to the mass composition of primary cosmic rays
[HE-5.1-4] 24 p4201 N85-36069
On muon energy spectrum in muon groups underground
[HE-5.1-14] 24 p4201 N85-36076

RADIOACTIVE ELEMENTS
U RADIOACTIVE ISOTOPES

RADIOACTIVE ISOTOPES
NT AMERICIUM
NT AMERICIUM ISOTOPES
NT AMERICIUM 241
NT BERYLLIUM 7
NT BERYLLIUM 9
NT BERYLLIUM 10
NT CALIFORNIUM ISOTOPES
NT CARBON 14
NT CERIUM 144
NT CESIUM 134
NT CESIUM 137
NT COBALT 60
NT CURIUM
NT CURIUM 244
NT IRON 59
NT KRYPTON 85
NT PLUTONIUM
NT PLUTONIUM ISOTOPES
NT PLUTONIUM 238
NT PLUTONIUM 239
NT POTASSIUM 40
NT STRONTIUM 90
NT TRANSURANIUM ELEMENTS
NT TRITIUM

Radiotracer studies of the dispersion of solid pollutants in marine and estuarial environment: Measurement of diffusion coefficients and the phenomenon of dispersion by currents
[BLL-DRIC-TRANS-7104-(3623.66)] 02 p0224 N85-11468
Analysis of radiocobalt in environmental samples
[DRIC-T-7334] 03 p0367 N85-12477
Isotopes in day to day life
[IAEA/PI/A.6E-84-00924] 03 p0417 N85-12668
Hydrologic characteristics of the Mediterranean and Black Sea 07 p0981 N85-16228
Comparing computing formulae for estimating concentration ratios
[DE84-008644] 09 p1349 N85-18490
TRAN-STAT: Statistics for environmental studies
[DE85-000829] 10 p1513 N85-19547
Multiple element neutron-activation analysis of atmospheric aerosols with X-ray and gamma-spectrometric recording of radionuclides formed 13 p2013 N85-22631
Program RNTHR/2: An HP-41 C program for the calculation of RaA, RaB, and RaC concentrations in air based on three measurements of an air-dust sample
[IRI-190-83-10] 18 p3134 N85-29412
Colloidal particle transport with simultaneous birth, growth and capture
[DE85-010388] 19 p3235 N85-30055
Evaluation of a high pressure proportional counter for the detection of radioactive noble gases
[AD-A154436] 19 p3272 N85-30292
Environmental monitoring at Argonne National Laboratory
[DE85-010613] 19 p3309 N85-30516
Radioluminescent lighting for Alaskan runway lighting and marking
[DE85-010405] 19 p3368 N85-30867
Dosimetry and limit values for internal contamination with radionuclides: From (International Commission on Radioactive Protection) ICRP-2 to ICRP-30
[IRI-190-84-03] 20 p3507 N85-31604
Source-term considerations for a potential radioactive-waste repository located in unsaturated tuff
[DE85-010090] 20 p3529 N85-31953
Current internal-dosimetry practices at US Department of Energy facilities
[DE85-011716] 22 p3787 N85-33466
Environmental surveillance at Los Alamos during 1984
[DE85-011696] 22 p3811 N85-33605
The 1984 environmental monitoring program report for Idaho National Engineering Laboratory site
[DE85-011209] 22 p3812 N85-33611
Measurement of radionuclides in waste packages
[DE85-011674] 22 p3836 N85-33766
MATADOR (Methods for the Analysis of Transport And Deposition Of Radionuclides) code description and user's manual
[TI85-901402] 23 p3966 N85-34592
Development of the osmium-191 yields iridium-191m radionuclide generator
[DE85-011185] 23 p3970 N85-34611
Current status of the Os-191 yields Ir-191m generator
[DE85-006306] 23 p3971 N85-34614
Elemental technetium as a cosmic-ray clock
[CG-7.1-9] 23 p4013 N85-34870
Bevalac calibration of the SOFIE range and hodoscope detectors
[CG-9.1-7] 23 p4023 N85-34933
High precise measurements of cosmogenic radiocarbon abundance by complex of scintillation equipments
[SH-7.1-14] 23 p4048 N85-35105
Wholebody radiation counting system
[AD-A155842] 24 p4131 N85-35807
Tritium hazard via the ingestion pathway
[DE85-012897] 24 p4133 N85-35818

RADIOACTIVE MATERIALS

Development of an automated miniature Charpy test method
[DE85-003011] 11 p1652 N85-20405
Examination of the feasibility for demonstration and use of radioluminescent lights for Alaskan remote runway lighting
[DE85-002503] 12 p1782 N85-21185
High altitude sampling program: Radioactivity in the stratosphere
[DE85-006824] 14 p2374 N85-24676
Scanning electron microscope facility for examination of radioactive materials
[DE85-006127] 17 p2999 N85-28335
Corrosion performance of metals and alloys in a tuff geochemical environment
[DE85-009449] 18 p3077 N85-29033
Concretization of high level radioactive source in marine sediment
[AD-D011703] 19 p3249 N85-30146
Petrologic and geochemical characterization of the Topopah Spring Member of the Paintbrush Tuff: Outcrop samples used in waste package experiments
[DE85-010449] 19 p3302 N85-30470
Container for radioactive materials
[DE85-006757] 23 p3972 N85-34626
Radiation safety problems in handling highly active tritium targets
[DE85-014258] 24 p4151 N85-35742

RADIOACTIVE NUCLIDES

U RADIOACTIVE ISOTOPES

RADIOACTIVE WASTES

Americium thermodynamic data for the EQ3/6 database
[DE84-017085] 04 p0573 N85-13656
HS and E environmental sciences
[DE84-016183] 05 p0672 N85-14314
Crystalline rocks of the northeastern United States
[DE84-013674] 05 p0677 N85-14347
Integrated data base program: A status report
[DE84-013604] 05 p0795 N85-14727
Conceptual design report for a remotely operated cask handling system, revision 1
[DE85-000348] 08 p1169 N85-17371
Preliminary post-emplacement safety analysis of the subseabed disposal of high-level nuclear waste
[DE84-011162] 08 p1221 N85-17692
Ground-water level data and preliminary potentiometric-surface maps, Yucca Mountain and vicinity, Nye County, Nevada
[DE85-001771] 09 p1343 N85-18448
Field implementation of geophysical diffraction tomography
[DE84-017594] 09 p1343 N85-18449
Stabilization of contaminated soils by in situ vitrification
[AD-P004144] 09 p1348 N85-18480
Consideration of future climatic changes in three geologic settings
[DE85-001704] 09 p1357 N85-18537
Measurements of sediment temperatures, conductivity and heat flow in the North Atlantic and their relevance to radioactive waste disposal
[IOS-172] 09 p1359 N85-18551
An assessment of biological processes close to the sea bed in a slope region and its significance to the assessment of sea-bed disposal of radioactive waste
[IOS-165] 09 p1360 N85-18554
Rockwell Hanford operations defense waste and byproducts management
[DE85-000553] 09 p1362 N85-18684
Nevada nuclear waste storage investigations preliminary repository concepts report
[DE85-002132] 09 p1383 N85-18696
Planning for greater-confinement disposal
[DE85-002143] 09 p1383 N85-18697
Perspective on demonstrations of compliance for high-level waste disposal
[DE85-000969] 09 p1383 N85-18698
Commission operation. National Low-Level Radioactive Waste Management Program
[DOE/LLW-33T] 09 p1383 N85-18699
Intrusion of radioactive industrially polluted water from North Sea into central Baltic Sea 10 p1498 N85-19454
China report: Science and technology
[JPRS-CST-84-025] 11 p1620 N85-20197
Index to published geologic maps in the region around the potential Yucca Mountain nuclear waste repository site, southern Nye County, Nevada
[DE85-000290] 11 p1669 N85-20518
Models and parameters for environmental radiological assessments
[DE81-027154] 11 p1678 N85-20573
Consolidation around a point heat source
[PB85-116549] 11 p1682 N85-20601
Man/machine interface for a nuclear cask remote handling control station: System design requirements
[DE85-000258] 11 p1697 N85-20667
WESF (173)Ce gamma ray sources
[DE85-000676] 11 p1727 N85-20659
Effect of host-rock dissolution and precipitation on permeability in a nuclear waste repository in tuff
[DE85-000675] 11 p1727 N85-20660
Radioactive waste isolation in salt: Peer review of the D'Appolonia report on schematic designs for penetration seals for a repository in the Permian Basin, Texas
[DE85-000693] 11 p1727 N85-20661
Field lysimeter facility for evaluating the performance of commercial solidified low-level waste
[DE85-003886] 11 p1727 N85-20663
High-level waste processing and disposal
[DE85-003584] 11 p1728 N85-20665
Shallow land burial technology: Humid
[DE85-004432] 12 p1932 N85-22136
Research and development related to the Nevada nuclear waste storage investigations
[DE85-002303] 12 p1932 N85-22138
Application of far-field models to the disposal of nuclear waste in geologic formations
[DE85-005489] 14 p2420 N85-24932
Physical-chemical model for the mechanism of glass corrosion with particular consideration of simulated radioactive waste glasses
[DE85-007713] 17 p2935 N85-28121
Corrosion performance of metals and alloys in a tuff geochemical environment
[DE85-009449] 18 p3077 N85-29033
Shales and other argillaceous strata in the United States
[DE85-010453] 18 p3125 N85-29353
Region-to-area screening methodology for the Crystalline Repository Project
[DE85-009892] 18 p3125 N85-29354
Implications about in situ stress at Yucca Mountain
[DE85-006068] 18 p3126 N85-29356
Radionuclide mobility in the shallow portion of an active high-temperature geothermal system
[DE85-010293] 18 p3182 N85-29729
Hydrolysis, formation and ionization constants at 25(0)C, and at high temperature-high ionic strength
[DE85-010645] 19 p3236 N85-30061
Mixtures experiment where the amount of the mixture is a factor under study
[DE85-010974] 19 p3250 N85-30153
High level radioactive waste vitrification process equipment component testing
[DE85-011143] 19 p3273 N85-30296
Development of HWVP melter/turntable components for canyon-remote maintenance and replacement
[DE85-010908] 19 p3273 N85-30298
Three-dimensional finite element impact analysis of a nuclear waste truck cask
[DE85-010653] 19 p3288 N85-30369
Reference data source documentation for performance assessment studies, Basalt Waste Isolation Project, Hanford Site, Washington
[DE85-010543] 19 p3301 N85-30468
Preliminary evaluation of alterant geophysical tomography in welded tuff
[DE85-010826] 19 p3302 N85-30469
Radioactive liquid wastes discharged to ground in the 200 areas during 1984
[DE85-010819] 19 p3310 N85-30517
TMI-2 technical information and examination program
[DE85-010614] 19 p3359 N85-30627
Qualitative comparison of fusion reactor materials for waste handling and disposal
[DE85-010473] 19 p3360 N85-30630
Radioactivity in gaseous waste discharged from the separations facilities during 1984
[DE85-011373] 19 p3360 N85-30631
Source Term Experiments Project (STEP): Aerosol characterization system
[DE85-010248] 19 p3361 N85-30639
Occurrence of uranium in ground water in the vicinity of the US Department of Energy Feed Materials Production Center, Fernald, Ohio
[DE85-010340] 19 p3364 N85-30662
Bulk and thermal properties of the functional Tuffaceous Beds in holes USW G-1, UE-25 no. 1, and USW G-2, Yucca Mountain, Nevada
[DE85-011181] 19 p3365 N85-30666
Dispersal From Deep Ocean Sources: Physical and Related Scientific Processes
[DE85-010420] 20 p3497 N85-31740
Development of processes for the inclusion of radioactive waste in glass-metal compounds and ceramic materials
[BLL-CE-TRANS-8014-(9022.06)] 20 p3526 N85-31931
Geologic and hydrologic characterization and evaluation of the basin and range province relative to the disposal of high-level radioactive waste. Part 1: Introduction and guidelines
[GS-CIRC-904-A] 20 p3526 N85-31932
Geologic and hydrologic characterization and evaluation of the basin and range province relative to the disposal of high-level radioactive waste. Part 2: Geologic and hydrologic characterization
[GS-CIRC-904-B] 20 p3526 N85-31933
Geologic and hydrologic characterization and evaluation of the basin and range province relative to the disposal of high-level radioactive waste. Part 3: Geologic and hydrologic evaluation
[GS-CIRC-904-A] 20 p3526 N85-31934
Source-term considerations for a potential radioactive-waste repository located in unsaturated tuff
[DE85-010090] 20 p3529 N85-31953
East Europe report: Science and technology
[JPRS-ESA-85-021] 21 p3568 N85-32190

Centrifugal castings of stainless steel spiked with radioactive tracers
[DE85-012003] 22 p3748 N85-33234
ARAC status report, 1985
[DE85-012835] 22 p3810 N85-33603
Technology of off-gas treatment for liquid-fed ceramic melters
[DE85-012467] 22 p3812 N85-33610
Corrosion resistant storage container for radioactive material
[DE85-011666] 22 p3838 N85-33765
Measurement of radionuclides in waste packages
[DE85-011674] 22 p3838 N85-33766
Design analysis for a repository in crystalline rock
[DE85-011802] 22 p3839 N85-33771
Office of Civilian Radioactive Waste Management
[DE85-012585] 22 p3839 N85-33774
Polyethylene solidification of low-level wastes
[DE85-012568] 22 p3843 N85-33799
Method for extracting lanthanides and actinides from acid solutions by modification of Purex solvent
[DE85-005763] 23 p3909 N85-34220
Research at the Institute of Oceanographic Sciences related to the possible disposal of radioactive waste on or beneath the seafloor
[IOS-204] 23 p3973 N85-34626
Simulated effects of increased recharge on the ground-water flow system of Yucca Mountain and vicinity, Nevada-California
[DE85-012985] 24 p4108 N85-35469

RADIOACTIVITY
A dispersion model for airborne particulates inside a building
[DE84-014961] 02 p0225 N85-11473
Evaluation of arctic test of improved tritium radioluminescent lighting
[AD-A148215] 08 p1089 N85-16884
Atmospheric science and power production
[DE84-005177] 09 p1354 N85-16521
Light your runways and taxiways without electricity
[DE85-000269] 11 p1586 N85-19991
Radiative ion beams: Hot stellar reactions in the laboratory
[DE85-001570] 11 p1722 N85-20833
High altitude sampling program: Radioactivity in the stratosphere
[DE85-005924] 14 p2374 N85-24676
A remote-operated manipulator vehicle
[HSE-TRANS-11133] 19 p3281 N85-30349
Nuclear data needs for fusion energy development
[DE85-010445] 20 p3536 N85-32000
The 1984 effluent and environmental monitoring report for the Bettis Atomic Power Laboratory
[DE85-011533] 22 p3810 N85-33602
The 1984 environmental monitoring report, Sandia National Laboratories, Albuquerque, New Mexico
[DE85-011175] 22 p3811 N85-33607

RADIOBIOLOGY
Radiobiological studies on egg systems exposed to heavy nuclei of cosmic galactic radiation — insects
05 p0690 N85-14440
Preliminary results of advanced Biostack experiments with plant seeds and spores — cosmic ray effects
05 p0691 N85-14441
The radiobiological advanced Biostack experiment on Spacelab 1
05 p0691 N85-14442
USSR report: Life sciences. Biomedical and behavioral sciences
[JPRS-UBB-84-015] 07 p1010 N85-16416
European scientific notes. Volume 38, number 11
[AD-A148228] 08 p1230 N85-17745
Radiation physics, biophysics, and radiation biology
[DE84-014885] 09 p1360 N85-18557
Effect of modulated ultrahigh frequency field on behavior and hormone level in female rats under emotional stress
09 p1361 N85-18562
Radiation damage and repair in cells and cell components. Part 2: Physical radiations and biological significance
[DE85-006934] 18 p3152 N85-29518
Biology and Medicine Division
[DE85-010838] 19 p3327 N85-30613
Collected epidemiological studies of the late effects of internal radium in man, and mechanistic investigations of those effects, part 2
[DE85-011174] 19 p3331 N85-30636
Biostack experiments on STS-flights and the impact for man in space
20 p3510 N85-31821
A practical guide to ionization chamber dosimetry at the AFRRI reactor
[AD-A155185] 21 p3703 N85-33003
Biophysical research in space — radiation effects
24 p4130 N85-35803

RADIOCHEMICAL SEPARATION
Effects of primary recoil energy on the production rate of mobile defects during elevated temperature irradiation
[DE85-006218] 15 p2511 N85-25489

RADIOCHEMISTRY
NT RADIOCHEMICAL SEPARATION
Assessment of Techniques for Measuring Tropospheric H sub x O sub y
[NASA-CP-2332] 05 p0675 N85-14336
Hydrologic characteristics of the Mediterranean and Black Sea
07 p0981 N85-16228
Robotics in the radiochemical laboratory
[DE85-002824] 10 p1494 N85-19433
Activities in nuclear physics and high energy physics
11 p1728 N85-20866
Proposed solar neutrino experiment using (81)Br(nu,e(-e)) (81)Kr
[DE85-004802] 15 p2584 N85-26579
Proceedings of the Fifth International Conference on Nuclear Methods in Environmental and Energy Research
[DE84-017348] 19 p3310 N85-30521

RADIOGENIC MATERIALS
Late Paleozoic and early Mesozoic radiolarians in the Circle quadrangle, east-central Alaska
04 p0517 N85-13297
The relation between the age of the subconducting slab and the recycling of sediments into the mantle
21 p3717 N85-33063

RADIOGRAPHY
NT AUTORADIOGRAPHY
NT COMPUTER AIDED TOMOGRAPHY
NT NEUTRON RADIOGRAPHY
NT TOMOGRAPHY
Technical activities 1983, Office of Nondestructive Evaluation
[PB84-217074] 03 p0370 N85-12360
Flash radiography as a quantitative tool
[DE84-016465] 04 p0503 N85-13211
Development of a dynamic radiographic capability using high-speed video
[DE84-016477] 04 p0511 N85-13256
High-speed videography for optical and X-ray imaging
[DE84-012661] 04 p0564 N85-13595
Flywheel-powered X-ray generator
05 p0605 N85-13861
Collimation techniques for dense object flash radiography
[DE84-016461] 05 p0647 N85-14152
Characterizing X-ray machines
[AD-A146532] 06 p0862 N85-15481
X-radiography of slices of the Allende Meteorite
06 p0865 N85-15622
Metallic aid and technique in fitting voice prosthesis
[AD-D011356] 07 p1014 N85-16442
Improved radiographic viewing system
[AD-A147587] 07 p1016 N85-16456
Ultrasonic measurements, X-ray photographs and image processing
[BLL-RISLEY-TR-4586-(9091.9F)] 07 p1037 N85-16583
Proceedings of the 14th Army Science Conference. Volume 1: Principal Authors A through H
[AD-A149200] 10 p1573 N85-19920
China report: Science and technology
[JPRS-CST-84-025] 11 p1620 N85-20197
Radiographic inspection of butt welds described
11 p1620 N85-20198
Radiographic detectability limits for seeded voids in sintered silicon carbide and silicon nitride
[NASA-TM-86945] 12 p1861 N85-21674
A new NDE (Non-Destructive Evaluation) capability for thin-shelled structures
[AD-A149625] 12 p1862 N85-21678
In-situ burning rate determination using flash radiography
13 p2002 N85-22550
Mini-Seminar on Non-Destructive Testing
[CSIR-TSD-0009/83] 14 p2316 N85-24308
Basic principles of industrial radiography
14 p2316 N85-24310
Standing of industrial radiography in South Africa
14 p2316 N85-24311
Radiological safety aspects of industrial radiography
14 p2316 N85-24312
Flash radiography
14 p2317 N85-24316
New developments in industrial radiography
14 p2317 N85-24317
Axial topography from digitized real time radiography
[DE85-006767] 18 p3091 N85-29130
Visual simulation of radiographs
[DE85-010213] 18 p3110 N85-29255
Image processing: Mathematics, engineering or art
[DE85-007666] 18 p3154 N85-29527
Poisson formula for radon transformation and numerical image reconstruction algorithm
21 p3697 N85-32973

RADIOISOTOPE BATTERIES
Space nuclear safety program
[DE84-015074] 04 p0463 N85-12939
Space nuclear safety program
[DE84-015064] 04 p0463 N85-12940
General-purpose heat source development: Safety test program. Postimpact evaluation, design iteration test 2
[DE84-015978] 04 p0564 N85-13592
Technical support services for space and terrestrial systems programs
[DE84-009031] 05 p0597 N85-13606
Radioisotope space power programs
05 p0609 N85-13887
Development of advanced thermoelectric materials
[NASA-CR-175684] 14 p2351 N85-24532
LPCVD tungsten deposition on Si-Ge alloy
[DE85-005588] 16 p2750 N85-26970

RADIOLOGY
FLACS: A new sensitometer for measurement of extreme low intensity reciprocity in a controlled environment — X-ray films
07 p0963 N85-16104
Radiation physics, biophysics, and radiation biology
[DE84-014885] 09 p1360 N85-18557
China report: Science and technology
[JPRS-CST-85-013] 15 p2536 N85-25652

RADIOLYSIS
Magnetic resonance studies of transient radicals and radical ions
[DE84-011669] 03 p0328 N85-12116
Production of stable embryo particles in dense ion tracks of alpha particle emissions in the atmosphere
21 p3644 N85-32638

RADIOMETERS
NT INFRARED DETECTORS
NT INFRARED RADIOMETERS
NT INFRARED SCANNERS
NT MICROWAVE RADIOMETERS
NT PASSIVE L-BAND RADIOMETERS
NT SPECTRORADIOMETERS
A sphere-scanning radiometer for rapid directional measurements of sky and ground radiance: The PARABOLA field instrument
[NASA-TM-86171] 03 p0363 N85-12329
Self-study manual on optical radiation measurements. Part 1: Concepts. Chapter 11: Linearity considerations and calibrations
[PB84-218346] 03 p0421 N85-12690
Fidelity of satellite soundings
05 p0682 N85-14383
NBS (National Bureau of Standards) switching radiometers
[PB84-235894] 07 p0968 N85-16147
The radiation temperature of a cloud of particles
[FOA-C-30367-E4] 08 p1190 N85-17497
Photodiodes for astronomical stellar radiometry
08 p1252 N85-17908
Measurement of shock induced reaction in rocket propellants by nanosecond infrared radiometry and photography
[AD-P004349] 10 p1456 N85-19173
Liquid fuel spray processes in high-pressure gas flow
[NASA-TM-86944] 12 p1844 N85-21570
Microprocessor-controlled rotating shadowband radiometer
[DE85-003633] 12 p1854 N85-21630
Monolithic short wave infrared (SWIR) detector array
[NASA-CR-175264] 12 p1874 N85-21759
Analysis of selective chopper radiometer data
[NASA-CR-175157] 12 p1895 N85-21894
Application of field X-ray: Radiometric analysis in exploratory geology and means for its improvement
13 p2115 N85-23176
Automation of radiometric measurements in nuclear oceanology
14 p2337 N85-24452
Solar gravity modes from ACRIM-SWM irradiance data
14 p2443 N85-25071
Lidar and radiometer observations of thunderstorm tops
15 p2595 N85-25894
High-frequency microwave observations of convective precipitation
15 p2598 N85-26000
Galileo
15 p2668 N85-26601
Comparative study of the digital analysis of areas of the Earth's surface prepared for planting using different classification algorithms
[INPE-3359-PRE/637] 18 p2846 N85-27545
Radiometer integrated into a communication terminal
[AD-A151746] 17 p2947 N85-28195
Water vapor radiometry research and development phase
[NASA-CR-175887] 17 p2995 N85-28512
Offset reflector with horn feed array, used as an experimental sensor for radiometric measurements
[ESA-TT-830] 20 p3443 N85-31389
View-limiting shrouds for insolation radiometers
[NASA-CR-176041] 20 p3458 N85-31476
Ocean circulation studies 20 p3492 N85-31712

Calibration and use of clutter data for simulation
[AD-A154793] 21 p3574 N85-32229
Enhancing precision of remote temperature sensing data from satellites under cloudy atmospheric conditions
22 p3734 N85-33148
Determination of altitude of cloud cover top from Meteor satellite data 22 p3734 N85-33150
Active Cavity Radiometer (ACR)
23 p3901 N85-34163
Investigation of non-intrusive radiometers for entrained gasifier temperature measurement, revision 3
[DE85-011795] 23 p3934 N85-34385
Analyzer, flight line
[AD-A155777] 24 p4067 N85-35207
Development of advanced high-temperature heat flux sensors. Phase 2: Verification testing
[NASA-CR-174973] 24 p4096 N85-35391
Aeromagnetic and radiometric signatures of a possible porphyry system in the western Tushar Mountains, Utah
24 p4103 N85-35437

RADIOMETRIC CORRECTION
Characterizing the scientific potential of satellite sensors
[E85-10091] 05 p0654 N85-14200
Characterizing the scientific potential of satellite sensors — San Francisco, California
[E85-10044] 07 p0983 N85-16244
Characterizing the scientific potential of satellite sensors — San Francisco, California
[E85-10053] 07 p0984 N85-16249
Study of spectral/radiometric characteristics of the Thematic Mapper for land use applications
[E85-10057] 07 p0987 N85-16268
Study of spectral/radiometric characteristics of the Thematic Mapper for land use applications
[E85-10075] 10 p1504 N85-19489
Radiometric accuracy assessment of LANDSAT 4 Multispectral Scanner data 11 p1666 N85-20498
Radiometric calibration and geocoded precision processing of LANDSAT-4 Multispectral Scanner products by the Canada Centre for Remote Sensing
11 p1667 N85-20501
Radiometric calibration and processing procedure for reflective bands on LANDSAT-4 protoflight Thematic Mapper 11 p1668 N85-20510
A preliminary assessment of LANDSAT-4 Thematic Mapper data — Windsor, Ontario and Medicine Hat areas, Canada 12 p1869 N85-21728
Preliminary evaluation of the radiometric calibration of LANDSAT-4 Thematic Mapper data by the Canada Centre for Remote Sensing 12 p1870 N85-21729
In-progress absolute radiometric inflight calibration of the LANDSAT-4 sensors — New Mexico
12 p1870 N85-21733
LANDSAT-4 Thematic Mapper calibration and atmospheric correction 12 p1870 N85-21734
Scan angle and detector effects in Thematic Mapper radiometry — Iowa and Arkansas
12 p1871 N85-21735
Analysis and evaluation of the LANDSAT-4 MSS and TM sensors and ground data processing systems: Early results 13 p2117 N85-23189
LANDSAT-4/5 image data quality analysis
[E85-10105] 24 p4107 N85-35483

RADIOMETRIC RECTIFICATION
U RADIOMETRIC CORRECTION

RADIOMETRIC RESOLUTION
Study on spectral/radiometric characteristics of the Thematic Mapper for land use applications
[E85-10021] 02 p0218 N85-11434
LANDSAT instruments characterization
[E85-10032] 04 p0624 N85-13356
LANDSAT instruments characterization
[E85-10028] 05 p0654 N85-14197
LANDSAT instruments characterization
[E85-10030] 05 p0654 N85-14198
Radiation data and standards for Tokamak diagnostics
09 p1380 N85-18742
Study of spectral/radiometric characteristics of the Thematic Mapper for land use applications
[E85-10075] 10 p1504 N85-19489
Summary of MSS characterization investigations
11 p1666 N85-20497
Radiometric accuracy assessment of LANDSAT 4 Multispectral Scanner data 11 p1666 N85-20498
Investigation of radiometric properties of LANDSAT-4 MSS — California, North Carolina, South Carolina, and New England 11 p1666 N85-20500
Impact of LANDSAT MSS sensor differences on change detection analysis — New Mexico, San Francisco, CA, New Hampshire, and Connecticut
11 p1667 N85-20506
Prelaunch absolute radiometric calibration of the reflective bands on the LANDSAT-4 protoflight Thematic Mapper 11 p1669 N85-20515
Characterization of radiometric calibration of LANDSAT-4 reflective bands 11 p1669 N85-20516
LANDSAT-4 Science Characterization Early Results. Volume 3, part 2: Thematic Mapper (TM)
[E85-10069] 12 p1869 N85-21724
Relative radiometric calibration of LANDSAT TM reflective bands 12 p1869 N85-21725
Evaluation of the radiometric integrity of LANDSAT 4 Thematic Mapper band 6 data 12 p1869 N85-21726
Thermal band characterization of the LANDSAT-4 Thematic Mapper 12 p1869 N85-21727
A preliminary analysis of LANDSAT-4 Thematic Mapper radiometric performance 12 p1870 N85-21730
Evaluation of the radiometric quality of the TM data using clustering, linear transformations and multispectral distance measures — Illinois 12 p1870 N85-21731
Intraband radiometric performance of the LANDSAT 4 Thematic Mapper — Washington, DC, Arkansas, Massachusetts, Virginia, and Arizona
12 p1871 N85-21738
A preliminary evaluation of LANDSAT-4 Thematic Mapper data for their geometric and radiometric accuracies 12 p1871 N85-21739
The use of linear feature detection to investigate Thematic Mapper data performance and processing
12 p1872 N85-21740
Assessment of Thematic Mapper band-to-band registration by the block correlation method
12 p1872 N85-21743
LANDSAT 4 band 6 data evaluation
[E85-10093] 12 p1874 N85-21755
Spectroradiometric calibration of the Thematic Mapper and Multispectral Scanner system
[E85-10094] 12 p1874 N85-21756
VISSR infrared calibration by means of calculated radiances 12 p1894 N85-21869
Impact of Thematic Mapper sensor characteristics on classification accuracy — suburban Washington, D.C., Maryland, and the Chesapeake Bay
13 p2117 N85-23188
Assessing LANDSAT TM and MSS data for detecting submerged plant communities 13 p2120 N85-23203
The use of Thematic Mapper data for land cover discrimination: Preliminary results from the UK SATMaP programme 13 p2121 N85-23207
The 13 November 1984 occultation of BD +06 deg 0471 by (1) Ceres
[NASA-CR-176106] 23 p3987 N85-34725
Study of spectral/radiometric characteristics of the Thematic Mapper for land use applications
[E85-10106] 24 p4107 N85-35484

RADIONUCLIDES
U RADIOACTIVE ISOTOPES

RADIOPROTECTIVE AGENTS
U ANTIRADIATION DRUGS

RADIOSENSITIVITY
U RADIATION TOLERANCE

RADIOSONDES
NT IONOSONDES
NT RAWINSONDES
Three-dimensional mesoscale analysis of aerial soundings 01 p0074 N85-10493
Thermosonde and UHF radar measurements of C2 sub n at Westford, Massachusetts - July 1981
[AD-A145398] 02 p0190 N85-11270
Measurements on the diffusion of hydrogen chloride in the waste gas plume of incineration ships in the North Sea. Part 1: Methodology, instrumentation and presentation of data
[GKSS-84-E-23-PT-1] 05 p0672 N85-14319
C2 sub n (optical) studies in the free atmosphere based on rawinsonde data
[AD-A147307] 07 p0997 N85-16332
Comparative investigation of three commercial radiosonde systems
[KNMI-TR-53] 07 p1009 N85-16409
Wind-weighting for sounding rockets with a telemetry system
[NASA-TP-2436] 12 p1792 N85-21246
Nowcasting applications of VAS
15 p2597 N85-26003
Role of jet streaks and boundary layer processes in organizing a pre-convective environment
15 p2597 N85-26006
Lightweight aerological radiosonde MARZ
16 p2807 N85-27309
Ship-to-ship propagation: Maritime data analyses
[AD-A155484] 21 p3592 N85-32325
Observations of frontal zone structures with a VHF Doppler radar and radiosondes, part 1.2A
21 p3616 N85-32469
A modified Fresnel scattering model for the parameterization of Fresnel returns, part 2.3A
21 p3618 N85-32483
Gravity-wave spectra in the atmosphere observed by MST radar, part 4.2B 21 p3622 N85-32502
Meteorological data from the OPTOMA (Ocean Prediction Through Observations, Modeling and Analysis) program OPTOMA 2, leg D2. 30 Jun. - 10 Jul. 1984
[AD-A156134] 24 p4123 N85-35580

RADIOTELEPHONES
Estimation of requirements for acceptable noise radiation level of communication transmitters
07 p0949 N85-16017
Controllable companding in low-frequency FM radio communication systems 22 p3776 N85-33402

RADIOTHERAPY
U RADIATION THERAPY

RADIUM
Distribution of radium and plutonium in human bone
[DE85-005025] 13 p2142 N85-23296

RADIUS
U RADII

RADOME MATERIALS
Proceedings of the 17th Symposium on Electromagnetic Windows, part 1
[AD-A149185] 10 p1466 N85-19253
Proceedings of the Symposium on Electromagnetic Windows (17th) held at Georgia Inst. of Technology, Engineering Experiment Station, Atlanta, Georgia on 25-27 July 1984. Part 2
[AD-A149125] 12 p1824 N85-21444
Design and calibration of a 35GHz dielectrometer
[AD-P004363] 12 p1826 N85-21457
Pressureless sintered silicon nitride as a promising candidate for radome materials
[AD-P004367] 12 p1826 N85-21461
LL-100: A new polybutadiene (resin system for radome applications)
[AD-P004368] 12 p1826 N85-21462
Broadband thermoplastic radomes
[AD-P004369] 12 p1827 N85-21463
Development of a high temperature single impact rain erosion test capability
[AD-P004371] 12 p1827 N85-21465
Laminated thermoplastic radome
[AD-D011664] 18 p3079 N85-29045

RADOMES
Tolerance synthesis of multilayer radome walls
07 p0953 N85-16041
Electromagnetic analysis of radomes by the moment method
[AD-P004351] 12 p1824 N85-21445
A computer analysis of the RF performance of a ground-mounted, air-supported radome
[AD-P004352] 12 p1824 N85-21446
Comparison of spherical wave ray tracing and exact boundary value solutions for spherical radomes
[AD-P004353] 12 p1824 N85-21447
Generalized radome BSE (radome boresight error) characterization using superposition techniques
[AD-P004354] 12 p1825 N85-21448
A subaperture approach to the calculation of flashlobes introduced by airborne radomes
[AD-P004355] 12 p1825 N85-21449
Near-field effects on radome boresight errors
[AD-P004356] 12 p1825 N85-21450
Dual band radome wall design
[AD-P004357] 12 p1825 N85-21451
Study of laminated dielectric behavior at microwave and millimeter-wave frequencies
[AD-P004358] 12 p1825 N85-21452
Image lobe analysis for large radomes
[AD-P004359] 12 p1825 N85-21453
Supersonic Tactical Missile (STM) radome development
[AD-P004360] 12 p1825 N85-21454
A millimeter wave apparatus for free-space measurement of dielectric constants at high temperature
[AD-P004361] 12 p1826 N85-21455
Automated radome testing
[AD-P004362] 12 p1826 N85-21456
Hot radome boresight error measurements
[AD-P004364] 12 p1826 N85-21458
A broadband kevlar radome for shipboard
[AD-P004365] 12 p1826 N85-21459
Fiber reinforced fused silica for hypersonic radome applications
[AD-P004366] 12 p1826 N85-21460
LL-100: A new polybutadiene (resin system for radome applications)
[AD-P004368] 12 p1826 N85-21462
Broadband thermoplastic radomes
[AD-P004369] 12 p1827 N85-21463
Infrared material optical damage by rain
[AD-P004372] 12 p1827 N85-21466
A radome for air traffic control SSR radar systems
[AD-P004373] 12 p1827 N85-21467
Development of the F-20 nose radome
[AD-P004374] 12 p1827 N85-21468

Nose and inlet duct radomes for the firebolt aerial target
[AD-P004375] 12 p1827 N85-21469
Laminated thermoplastic radome
[AD-D011664] 18 p3079 N85-29045
RADON
NT RADON ISOTOPES
A system for monitoring radon and its decay products in the atmosphere
[INPE-3085-PRE/494] 03 p0391 N85-12502
Characteristic functional of a probability measure absolutely continuous with respect to a Gaussian radon measure
[AD-A149482] 10 p1548 N85-19763
Radon concentration inversion in the troposphere: Still unexplained
[INPE-3360-PRE/638] 16 p2826 N85-27431
Atmospheric radon measurements in the Antarctic Peninsula: A preliminary report
[INPE-3398-PRE/667] 16 p2827 N85-27436
Program RNTHR/2: An HP-41 C program for the calculation of RaA, RaB, and RaC concentrations in air based on three measurements of an air-dust sample
[IRI-190-83-10] 18 p3134 N85-29412
Production of stable embryo particles in dense ion tracks of alpha particle emissions in the atmosphere
21 p3644 N85-32638
Study of the formation of particles from natural hydrocarbons released by vegetation
21 p3644 N85-32640
Aircraft investigations of the distribution of aerosols in the lower troposphere 21 p3647 N85-32669
Poisson formula for radon transformation and numerical image reconstruction algorithm
21 p3697 N85-32973
EML pulse ionization chamber systems for (222)Rn measurements
[DE85-012320] 23 p3970 N85-34610
Groundwater radon studies for earthquake precursors in southern California
[PB85-196871] 24 p4118 N85-35529
RADON ISOTOPES
Theoretical basis for the determination of the concentration of radon decay products in air from the activity of a particulate air sample
[IRI-190-83-07] 17 p3035 N85-28774
Model computations of radon, and radon decay product, concentrations in an open system; the Hewlett-Packard 41C program RNSS, version 02
[IRI-190-83-12] 17 p3035 N85-28775
Temporal variations of Rn222 concentrations in Black Sea coastal zone 19 p3293 N85-30417
Some considerations about the natural atmospheric radioactive aerosol 21 p3647 N85-32662
RAFTS
NT LIFE RAFTS
RAIL TRANSPORTATION
Railroad safety program, volume 1
[NASA-CR-174333] 09 p1403 N85-18830
High-speed intercity rail passenger service
[GPO-35-866] 10 p1570 N85-19697
USSR report: Transportation
[JPRS-UTR-85-005] 14 p2207 N85-23688
USSR report: Transportation
[JPRS-UTR-84-008] 14 p2208 N85-23694
USSR report: Transportation
[JPRS-UTR-85-009] 15 p2460 N85-25189
USSR report: Transportation
[JPRS-UTR-84-017] 15 p2461 N85-25196
USSR report: Transportation
[JPRS-UTR-84-014] 15 p2467 N85-25229
Industry review: Locomotive dynamic characterization test-analysis
[NASA-CR-171467] 19 p3362 N85-30661
Fuel cell applications literature review
[DE85-011691] 22 p3809 N85-33592
RAILGUN ACCELERATORS
Resistance and inductance calculations for helical flux compression generators
[DE84-015088] 02 p0195 N85-11306
Preliminary analysis of space mission applications for electromagnetic launchers
[NASA-CR-174067] 03 p0321 N85-12071
Magnetic and photoconductive repetitive rail-gun opening switches
[DE84-017080] 04 p0496 N85-13183
Investigation of electromagnetic launcher behavior for impact fusion
[DE84-017401] 04 p0563 N85-13586
Distributed energy store railguns experiment and analysis 09 p1313 N85-18256
Materials physics
[DE84-017103] 09 p1377 N85-18658
Rail accelerator technology and applications
[NASA-TM-86947] 12 p1794 N85-21258
Arc-driven rail gun research
[NASA-CR-174816] 12 p1859 N85-21662
Plasma mass and effective inductance in a small railgun
[MRL-R-947] 12 p1936 N85-22162
H-division materials physics progress
[DE85-004990] 13 p2165 N85-23430
Railgun conductor heating from multiple current pulses
[DE85-005333] 14 p2265 N85-24031
Spectroscopic studies of a railgun muzzle flash
[MRL-R-952] 16 p2728 N85-26837
Metal armatures for railguns
[AD-A152129] 16 p2728 N85-26838
Examination of a method for predicting the properties of railgun plasmas
[AR-004-322] 17 p3039 N85-28799
Numerical studies of ablation and ionization of railgun materials
[DE85-010741] 19 p3223 N85-29963
Design and fabrication of projectiles for round bore railguns
[DE85-011671] 20 p3366 N85-31078
Plasma mass and effective inductance in a small railgun
[AD-A154644] 21 p3589 N85-32304
A method of accurizing rail guns
[LA-10028-MS] 22 p3737 N85-33166
Use of the computer programs PARA 80 to study results from firing the railgun ERGS-1M
[MRL-R-900] 22 p3738 N85-33167
Generation of round bores in composite structure railguns
[DE85-011672] 22 p3793 N85-33501
RAILROADS
U RAIL TRANSPORTATION
RAIN
NT ACID RAIN
Layered sloping mesoscale structures and rainbands in atmospheric frontal regions and their relation to symmetric instability 01 p0075 N85-10497
Test results from RAINSAT 01 p0076 N85-10508
The use of dual polarisation radar for observing and predicting convective activity 01 p0077 N85-10512
Preliminary assessment of very short term forecasting of rain from single radar data 01 p0078 N85-10523
Operational precipitation observation system using digitized radar and rain gages 01 p0082 N85-10549
FRONTIERS: Progress with a system for nowcasting rain — Forecasting Rain Optimized using New Techniques of Interactively Enhanced Radar and Satellite (FRONTIERS) 01 p0082 N85-10552
Northern Hemisphere atlas of 1-minute rainfall rates
[AD-A145411] 02 p0231 N85-11506
Southern Hemisphere atlas of 1-minute rainfall rates
[AD-A145421] 02 p0231 N85-11509
Modeling rain polarization effects to millimeter wave frequencies
[PB84-231042] 03 p0357 N85-12296
An interactive technique for satellite-improved rainfall monitoring 05 p0656 N85-14224
Diagnostics of rainfall anomalies in the nordeste during the global weather experiment 05 p0665 N85-14405
Rain volume estimation over areas using satellite and radar data 05 p0666 N85-14406
Probable maximum flood estimation - Eastern United States
[AD-A146536] 08 p0839 N85-15324
The influence of sample collection and methods of analysis on chemical concentrations measured in rainwater
[KNMI-TR-85] 07 p0924 N85-15853
Simultaneous ocean cross-section and rainfall measurements from space with a nadir-pointing radar
[NASA-TM-86167] 07 p0957 N85-16273
Anticoiling technology: Theories of surface coiling and performance of anticoiling surface coatings
[NASA-CR-174274] 07 p0991 N85-16296
Resolution enhancement of multichannel microwave imagery from the Nimbus-7 SMMR for maritime rainfall analysis
[NASA-CR-174367] 10 p1462 N85-19221
Nationwide urban runoff program. Relationship of urban runoff to land use and groundwater resources
[PB85-114662] 10 p1506 N85-19505
Cyclone diagnostics — rainfall estimation, backscatter, and lidar
[NASA-CR-171337] 10 p1518 N85-19567
Rain volume estimation over areas using satellite and radar data
[NASA-CR-174434] 10 p1518 N85-19568
Modeling interception of rainfall by forests and the role of interception in the water balance
[DE85-002822] 12 p1884 N85-21825
OSCAR experiment high-density network data report
[DE85-004907] 12 p1884 N85-21826
Modeling of radiothermal radiation of rain by Monte-Carlo method 14 p2341 N85-24478
Rain rate determinations from electronic weight measurements: Instrument description and data reduction techniques
[AD-A150765] 14 p2378 N85-24661
Observation of precipitating clouds by a vertically pointing radar at Morino in the Iburi District, Hokkaido, Japan 15 p2582 N85-25922
Hurricane structure and dynamics from stereoscopic and infrared satellite observations and radar data
15 p2594 N85-25988
Estimation of convective rainfall from visible and infrared satellite data 15 p2596 N85-25989
Computers in the determination of rainfall depth-duration-frequencies in Natal
15 p2627 N85-26188
EHF attenuation derived from emission temperatures in light rain
[AD-A151166] 16 p2772 N85-27110
On the 1983 drought in northeast Brazil
[INPE-3412-PRE/676] 16 p2834 N85-27476
An appraisal of the duration of the recent drought in northeast Brazil and a forecast for 1985
[INPE-3477-PRE/720] 16 p2834 N85-27478
Statistical comparison of radar echoes of convective precipitation between the northern Alps and its foreland
[DFVLR-FB-85-07] 17 p2950 N85-28215
Laminated thermoplastic radome
[AD-D011664] 18 p3079 N85-29045
Some further aspects of the influence of raindrop-size distributions on millimeter-wave propagation
[PB85-168334] 18 p3092 N85-29136
Surface hydrologic characteristics of proposed repository locations in the Palo Duro Basin of the Texas Panhandle
[DE85-010530] 18 p3126 N85-29355
Influence of land-surface roughness on atmospheric circulation and rainfall: A sensitivity study with a GCM
18 p3146 N85-29479
Synthetic rainfall and its use in hydrologic modeling
19 p3314 N85-30542
On the dynamical climatology of the Amazon Basin and associated rain producing mechanisms
[INPE-3531-RPE/477] 19 p3315 N85-30552
Rain volume estimation over areas using satellite and radar data
[NASA-CR-178050] 21 p3634 N85-32570
The distribution of giant salt nuclei inside and outside cloud ova the basin of Xin and Jiang
21 p3650 N85-32681
Tunisian climate seen through a Markov process
[CT-585] 23 p3960 N85-34482
Elemental tracers of source regions of contaminants in precipitation
[DE85-012858] 24 p4113 N85-35499
The kinematic structure of cold frontal rainbands
24 p4119 N85-35531
RAIN EROSION
Single-drop impact damage prediction for low density, coated ceramic materials — rain erosion
01 p0061 N85-10402
Proceedings of the 17th Symposium on Electromagnetic Windows, part 1
[AD-A149186] 10 p1486 N85-19253
Development of a high temperature single impact rain erosion test capability
[AD-P004371] 12 p1827 N85-21465
Infrared material optical damage by rain
[AD-P004372] 12 p1827 N85-21466
RAIN FORESTS
Eddy correlation measurements of energy partition for Amazonian forest
[INPE-3195-PRE/559] 06 p0827 N85-15252
Relationship between forest clearing and biophysical factors in tropical environments: Implications for the design of a forest change monitoring approach — Costa Rica
[E85-10051] 07 p0983 N85-16247
Geologic mapping of Indonesian rain forest with analysis of multiple SIR-B incidence angles
08 p1145 N85-17221
Information for space radar designers: Required dynamic range vs resolution and antenna calibration using the Amazon rain forest 08 p1147 N85-17239
The micrometeorology of an Amazonian rainforest
[INPE-3515-PRE/740] 19 p3315 N85-30551
Formation of particles in the air of the humid tropical forests 21 p3644 N85-32639
RAIN GAGES
Operational precipitation observation system using digitized radar and rain gages 01 p0082 N85-10549
The pluviometric recording stations in the 11 GHz radio link at Invidatella Monte S. Pancrazio — Italy
[FUB-6-1983] 01 p0086 N85-10575
Rain rate meter
[AD-D011381] 07 p0999 N85-16342

Precipitation gage network operations for wintertime research in the Central Sierra Nevada
[PB85-115020] 10 p1520 N85-19582
On the wind error of the Finnish raingauge
[REPT-37] 12 p1893 N85-21883

RAINBOWS
Classical rainbow scattering of alkali ions on metal surfaces. Application to the investigation of unknown surface structures
[MPIS-10/1984] 11 p1726 N85-20854

RAINMAKING
SCPP (Sierra Cooperative Pilot Project) Forecasting Support 16 p2837 N85-27483

RAINSTORMS
NT THUNDERSTORMS
Generation of deep convective clouds along mesoscale storm outflow boundaries 01 p0074 N85-10490
Rain bands and symmetric instability 01 p0075 N85-10496
NESDIS operational precipitation estimation techniques 01 p0076 N85-10505
Experiment on nowcasting of heavy rainfall and severe storms in central China in 1979-1981 01 p0081 N85-10545
Convection modeling and application to severe storms 15 p2595 N85-25991

RAMAN EFFECT
U RAMAN SPECTRA

RAMAN LASERS
Manual for Raman cells
[NASA-TM-77756] 01 p0052 N85-10342
Laser Raman techniques for studying flows and flames 11 p1576 N85-19929
Raman studies of laser damaged single and multi-layer optical coatings
[DE85-009431] 17 p2971 N85-28351

RAMAN SCATTERING
U RAMAN SPECTRA

RAMAN SPECTRA
Method and apparatus for determining pressure-induced frequency-shifts in shock-compressed materials
[DE84-014313] 01 p0024 N85-10151
Raman scattering from metastable GaSb(1-x) Ge(2x) alloys
[AD-A145897] 03 p0327 N85-12108
Folded acoustic and quantized optic phonons in semiconductor superlattices
[AD-A145935] 03 p0433 N85-12756
Structural properties of amorphous metals by Raman scattering
[DE84-016947] 04 p0475 N85-13027
Raman study of neutron irradiated GaAs
[DE84-016056] 05 p0731 N85-14702
In situ analysis of corrosive and passive surfaces by laser-excited Raman spectroscopy — lead, galvanized iron, and asbestos-cement pipes
[PB84-229756] 06 p0767 N85-14904
Electronics research at the University of Texas at Austin
[AD-A146900] 07 p0947 N85-15998
Rayleigh and Raman scattering for density in a swirling flow combustor 08 p1120 N85-17060
Raman sidescattering in laser-produced plasmas
[AD-A148905] 10 p1556 N85-19613
Nonlinear saturation of stimulated Raman scattering in collisional homogeneous plasma
[DE85-002814] 10 p1559 N85-19631
Nonlinear saturation of stimulated Raman scattering in homogeneous plasma
[DE85-003120] 10 p1560 N85-19637
Laser Raman techniques for studying flows and flames 11 p1576 N85-19929
Photon scattering and interaction analysis of interfacial corrosion and catalysis
[DE85-002534] 11 p1608 N85-20114
Application of Raman, TEM and other ion based techniques to oxidation problems
[AERE-R-11447] 11 p1610 N85-20121
Time resolved Raman studies of laser induced damage in TiO2 optical coatings
[DE85-003166] 11 p1640 N85-20332
The effect of Xe underlayers on the surface enhanced Raman scattering of pyridine on cold silver
[AD-A150109] 12 p1801 N85-21294
In situ monitoring of electrochemical reactions by surface enhanced Raman scattering
[PB85-149789] 12 p1803 N85-21312
Mathematical modeling of two-frequency laser sounding of scattering media 13 p2089 N85-23045
Resonant coherent anti-Stokes Raman scattering
[ESA-TT-876] 15 p2507 N85-25466
Raman scattering of light in epitaxial films of solid phosphide-gallium arsenide solutions 15 p2643 N85-26301
Raman studies of surface temperature in laser-heated semiconductors
[AD-A151377] 15 p2659 N85-26412
Fiber optic Raman thermometer for Space Shuttle main engine preburner profiling 16 p2739 N85-26904
Single-pulse Raman and photoacoustic spectroscopy studies of Triaminotrinitrobenzene (TATB) and related compounds
[DE85-010072] 18 p3084 N85-29078
An introductory view of Raman-Nath type equations
[PREPRINT-422] 18 p3172 N85-29664
High temperature Raman studies of phase transitions in thin film dielectrics
[DE85-010073] 19 p3263 N85-30234
Application of the Diffusion Raman Anti-Stokes Coherent (DRASC) method to a SNECMA combustion chamber
[YKC-3066/84] 20 p3425 N85-31260
Caviton collapse of SRS by SBS
[DE85-009605] 20 p3535 N85-31999
Temperature measurements on small droplets 21 p3653 N85-32699
Influence on bi-phonon states on Raman scattering of light in molecular crystals 21 p3660 N85-32865
Generation and amplification of radiation during stimulated Raman scattering in crystals 21 p3681 N85-32869
Participation of singlet oxygen in photodestruction of air-saturated solutions of coumarin dyes 21 p3685 N85-32891
Raman scattering studies in solids
[AD-A155528] 21 p3710 N85-33032
Measurement of velocity and concentration in free jets
[ISL-CO-215/84] 22 p3785 N85-33451
Time-resolved spectroscopic studies of detonating heterogeneous explosives
[DE85-009760] 23 p3921 N85-34297
Electronic structure and lattice dynamics of dimensionally constrained and disordered solids
[AD-A155927] 24 p4161 N85-35797

RAMAN SPECTROSCOPY
Investigation of the CARS spectrum of carbon monoxide at high pressure and temperature
[AD-A144816] 01 p0024 N85-10146
Kinetics of simple inner- and outer-sphere electrochemical reactions at rotating silver electrodes as examined using surface-enhanced Raman spectroscopy
[AD-A145606] 02 p0172 N85-11154
Raman and fluorescence spectroscopy in a methane-nitrous oxide laminar flame
[AD-A146092] 03 p0328 N85-12111
A study of structural phase transitions using light scattering techniques
[AD-A147261] 07 p1048 N85-16654
Gas temperature measurements in sooting, laminar diffusion flames
[AD-A148801] 09 p1319 N85-18294
New phases and chemical reactions in solid CO under pressure
[DE85-002033] 09 p1377 N85-18655
Laser Raman techniques for studying flows and flames 11 p1576 N85-19929
Velocity and volumetric measurement in free jets 11 p1576 N85-19931
Fundamental study of catalysts using laser Raman, infrared, auger electron spectroscopy and low energy electron diffraction
[DE85-001813] 11 p1595 N85-20033
Observation of standing spinwaves in thin Fe-films by means of Raman spectroscopy
[DE85-003036] 11 p1735 N85-20913
The effect of Xe underlayers on the surface enhanced Raman scattering of pyridine on cold silver
[AD-A150109] 12 p1801 N85-21294
Laser diagnostic analyses of sooting flames
[AD-A150478] 13 p2017 N85-22649
Raman structural studies of the nickel electrode
[NASA-CR-175619] 13 p2162 N85-23414
Picosecond lidar techniques in laboratory and field diagnostics
[AD-A150755] 14 p2309 N85-24294
Linewidth and bandwidth measurements of the q-branch of h2 using CW coherent anti-Stokes Raman spectroscopy
[AD-A151868] 15 p2506 N85-25456
Resonant coherent anti-Stokes Raman scattering
[ESA-TT-876] 15 p2507 N85-25466
Raman studies of laser damaged single and multi-layer optical coatings
[DE85-009431] 17 p2971 N85-28351
Studies of optical-beam phase-conjugation by nonlinear refraction
[AD-A152866] 17 p3037 N85-28788
Recent advances in optical measurement methods in physics and chemistry
[DE85-006695] 17 p3037 N85-28792
Properties of defects in Hg(1-x)Cd(x)Te
[AD-A153243] 17 p3044 N85-28835
Resonant CARS detection of OH radicals
[AD-A153842] 18 p3071 N85-28995
Single-pulse Raman and photoacoustic spectroscopy studies of Triaminotrinitrobenzene (TATB) and related compounds
[DE85-010072] 18 p3084 N85-29078
A basic study to assess the potential usefulness of resonance Raman spectroscopy as a means of rapidly detecting and identifying bacteria and other microorganisms
[AD-A153549] 18 p3152 N85-29513
The development of new techniques in laser spectroscopy 19 p3233 N85-30041
Participation of singlet oxygen in photodestruction of air-saturated solutions of coumarin dyes 21 p3685 N85-32891
The possibilities of remote analysis of atmospheric gases based on Raman scattering spectroscopy 21 p3685 N85-32892
Ionization detection of stimulated Raman spectra
[DE85-010672] 22 p3746 N85-33218

RAMJET ENGINES
NT SUPERSONIC COMBUSTION RAMJET ENGINES
An experimental investigation of combustion pressure oscillations in solid fuel ramjets
[AD-A144870] 01 p0024 N85-10147
Pressure oscillations in liquid-fueled ramjet engines 05 p0598 N85-13797
Combined cycle ramjet engine
[AD-D011247] 06 p0780 N85-14859
Ramjet and Ramrocket Propulsion Systems for Missiles
[AGARD-LS-136] 07 p0917 N85-15809
Ramjet and Ramrocket Propulsion Systems for Missiles: Introduction and overview 07 p0917 N85-15810
Ramjet air induction system design for tactical missile application 07 p0918 N85-15811
Some aspects of engine and airframe integration for Ramjet and Ramrocket powered missiles 07 p0918 N85-15812
Integral boost, heat protection, port covers and transition 07 p0918 N85-15813
Liquid-fueled Ramjet engines 07 p0918 N85-15814
Special problems of Ramjet with solid fuel 07 p0918 N85-15815
Combustion dynamics in rockets
[AD-A148478] 08 p1114 N85-17024
Analysis of sudden expansion flow in a two-dimensional duct with and without side-wall injection using the k-epsilon turbulence model 09 p1317 N85-18262
Window on science visit to the USA, 21 March - 22 April, 1984 — ramjets and solid propellant rocketry
[VTH-LR-426] 11 p1592 N85-20011
Study of HTPB-based SOFRAM fuels
[FOA-C-20563-D3] 11 p1614 N85-20150
Twenty-first JANNAF Combustion Meeting, volume 1
[AD-A150981] 13 p1998 N85-22526
Nonlinear interactions between vortices and acoustic waves in a rocket combustion chamber 13 p1999 N85-22533
Selection of air intake parameters for supersonic-flow operation 13 p2051 N85-22837
Mixing, chemical reaction and flow field development in ducted rockets
[DE85-004083] 14 p2247 N85-23928
Fiscal year 1986 technical objective document
[AD-A151039] 14 p2432 N85-25000
Gasdynamic evaluation of choking cascade turns
[AD-A151654] 15 p2557 N85-25776
Dispersion sensitivity of the eight inch advanced ramjet munitions technology projectile due to wind and minor thrust errors
[AD-A152145] 16 p2727 N85-26835
Solid fuel combustion chamber research in the Netherlands
[VTH-LR-444] 16 p2742 N85-26920
An experimental investigation of fuel regression rate control in solid fuel ramjets
[AD-A154251] 19 p3227 N85-30008
A model of hypersonic two-dimensional oblique detonation wave ramjet
[UTIAS-TN-257] 23 p3897 N85-34139

RAMJET MISSILES
Fuel-rich solid propellant boron combustion
[AD-A148522] 08 p1136 N85-17157

RAMP FUNCTIONS
Precision linear ramp function generator
[DE85-011647] 22 p3760 N85-33304
The collected data for ramp function tests on a NACA 23012 aerofoil. Volume 1: Description and pressure data
[GU-AERO-8413-VOL-1] 23 p3894 N85-34123

RANDOM ACCESS
Applications of functional analytic and Martingale methods
[AD-A145556] 02 p0255 N85-11672
RANDOM ACCESS MEMORY
Parallel update of minimum spanning trees in logarithmic time
[AD-A150497] 13 p2151 N85-23357
Parallel time O(log N) acceptance of deterministic CFLs
[AD-A152255] 16 p2845 N85-27539
The design of an adaptive predictive coder using a single-chip digital signal processor
[AD-A152461] 17 p2952 N85-28291
Random access memory technologies
[AD-A153069] 17 p3008 N85-28597
Microcomputer controlled image processor
[AD-D011734] 22 p3833 N85-33735
Effects of space radiation on advanced semiconductor devices. Part 3: Further cosmic ray simulation studies of single event upsets and latch-up in CMOS memories
[AERE-G-3368-PT-3] 22 p3848 N85-33833
RANDOM DISTRIBUTIONS
U STATISTICAL DISTRIBUTIONS
RANDOM ERRORS
Spectral noise density and random errors of pulse frequency characteristic meters
03 p0346 N85-12231
Accepting error to make less error
[AD-A153949] 18 p3171 N85-29851
RANDOM LOADS
NT GUST LOADS
Fractographic observation and estimation of crack growth curve of aluminum alloy under ramdom flight simulation loading
[NAL-TR-824] 06 p0768 N85-14913
Stability of viscoelastic constructions subjected to steady random compressing loads 11 p1720 N85-20819
First passage times for combinations of random loads
[AD-A153275] 17 p2960 N85-28423
Safety and reliability of steel structural materials under random service impact loads 23 p3906 N85-34197
RANDOM NOISE
NT RANDOM SIGNALS
Noise analysis of the Coarse Optical Power Spectrum Estimator (COPSE) data acquisition system
[AD-A145918] 03 p0419 N85-12577
On estimating the phase of periodic waveform in additive Gaussian noise, part 2 05 p0622 N85-13982
Treatment and expression of measurement uncertainties 05 p0630 N85-14042
Variability of short-term eddy-correlation estimates of mass exchange
[DE84-007271] 05 p0677 N85-14349
Phase of aperture synthesis in general theory of antennas (review) 06 p0781 N85-14993
The coding capacity of mismatched Gaussian channels
[AD-A149463] 10 p1551 N85-19782
Interference immunity of binary systems with second-order phase-difference modulation in various reception modes 13 p2072 N85-22944
Synthesis of quasi-optimum two-level signal discriminator with level changing at unknown point 13 p2083 N85-23010
Use of Bigaussian approximation to describe fading in scattering communications channel 13 p2084 N85-23017
Bayesian estimation of one dimensional discrete markov random fields
[AD-A151503] 15 p2640 N85-26284
Measurement of damping of graphite epoxy materials
[NASA-CR-175793] 16 p2743 N85-26925
Robust detection of fading narrow-band signals in non-Gaussian noise
[AD-A152262] 16 p2774 N85-27124
On the probability density of signal-to-noise ratio in an improved detector
[AD-A152529] 17 p2952 N85-28232
Global positioning system carrier phase: Description and use
[PB85-174126] 19 p3216 N85-29946
Modulation using four phase levels. Theoretical study of the degradation caused by a spurious phase modulation
[CNES-83/219/CT/DRT/TIT/TR] 20 p3441 N85-31360
Deterministic and random phase noise of oscillators — synthetic aperture radar
[ESA-TT-848] 20 p3449 N85-31415
Detection of signals from coherent pulsed radars with random variation in parameters of sounding signals from pulse to pulse against background of worst-case Gaussian noise 22 p3783 N85-33324
A new description of combined trellis coding with asymmetric modulation
[NASA-CR-176197] 24 p4086 N85-35323
RANDOM NUMBERS
On the generation of random variables for radar simulation purposes 07 p0938 N85-15947
Regenerative structure of Markov chains simulated via common random numbers
[AD-A149092] 10 p1550 N85-19777
Efficient parallel pseudo-random number generation
[AD-A152235] 16 p2855 N85-27608
Probabilistic algorithms in group theory
[AD-A152253] 16 p2859 N85-27630
Monte Carlo learning-biasing experiment with intelligent random numbers
[DE85-010713] 22 p3834 N85-33742
A quickly tested Pascal random number generator for microcomputers
[AD-A156059] 24 p4136 N85-35633
RANDOM PROCESSES
NT RANDOM WALK
Dynamics of symmetry breaking: Phase coherence in finite and random systems
[NOTA-INTERNA-613] 02 p0253 N85-11658
Random processes and magnetohydrodynamic turbulence 02 p0271 N85-11767
The growth and composition of supercritical branching populations on general type spaces
[CTH-MATH-1984-18] 05 p0721 N85-14631
Distribution of atmospheric radio interference 06 p0792 N85-15003
A note on the prediction error for small time lags into the future
[AD-A148221] 08 p1215 N85-17654
Asymptotic analysis of Markovian access control computer communication networks 09 p1372 N85-18619
Regenerative structure of Markov chains simulated via common random numbers
[AD-A149092] 10 p1550 N85-19777
Models of discontinuous random fields 13 p2079 N85-22963
On failure modeling, revised
[AD-A151411] 15 p2637 N85-26263
Anderson localization for large disorder or low energy
[PREPRINT-426] 16 p3176 N85-29662
Statistical methods for efficient design of community surveys of response to noise: Random coefficients regression models
[NASA-CR-177933] 21 p3666 N85-32979
RANDOM SAMPLING
Spline methods for approximating quantile functions and generating random samples
[NASA-TP-2369] 07 p1035 N85-16565
Small-sample properties of kernel density estimators from randomly right-censored data
[AD-A148752] 09 p1374 N85-18634
Nonparametric estimation of the probability of ruin
[AD-A153523] 18 p3174 N85-29674
A new approach to evaluate gamma-ray measurements
[OG-9.5-11] 23 p4031 N85-34968
RANDOM SIGNALS
Accuracy of random signal spectral parameter estimation against interference background in acousticoptical spectrum analyzers 13 p2090 N85-23052
Adaptive detection of noise signal according to Neumann-Pearson criterion 15 p2527 N85-25580
Optimal complex nonlinear processing of continuous and pulsed signals 22 p3763 N85-33323
RANDOM VARIABLES
Some weak and strong laws of large numbers for d(0,1) - valued random variables
[AD-A144845] 01 p0111 N85-10754
What is principal components analysis? 02 p0211 N85-11389
The information in the minor principal components 02 p0211 N85-11391
Algebraic functions of H-functions with specific dependency structure
[AD-A145698] 02 p0252 N85-11647
Maximum likelihood estimation of the survival functions of N stochastically ordered random variables
[AD-A145429] 02 p0254 N85-11662
Distributions of extreme values of sequences of autocorrelated random variables
[PB84-240746] 06 p0858 N85-15456
Rivista Tecnica Selenia, volume 9, number 1 07 p0938 N85-15945
On the generation of random variables for radar simulation purposes 07 p0938 N85-15947
On a random difference equation for matrices and a characterization of the gamma distribution
[AD-A146658] 07 p1029 N85-16529
Conditionally heteroscedastic autoregressions
[AD-A147166] 07 p1035 N85-16567
Generalized additive models
[AD-A147454] 07 p1036 N85-16573
Belief structures
[AD-A147526] 07 p1036 N85-16575
Recent results on characterization of probability distributions: A unified approach through extensions of Deny's theorem
[AD-A147831] 08 p1214 N85-17647
Calculation of cumulative distributions and detection probabilities in communications and optics
[AD-A147781] 08 p1215 N85-17650
Modelling and residual analysis of nonlinear auto-regressive time series in exponential variables
[AD-A149047] 10 p1550 N85-19776
The asymptotic behavior of the likelihood ratio statistic for testing a shift in mean in a sequence of independent normal variates
[AD-A149329] 10 p1550 N85-19779
Maximum matchings in a class of random graphs
[AD-A149663] 12 p1920 N85-22060
Statistics for the maximum of several positive random variables with application to networking
[AD-A150005] 12 p1922 N85-22069
Convergence rates in the strong law for bounded mixing sequences
[CWI-MS-R8412] 12 p1922 N85-22076
Skewed stable variables and processes
[AD-A150549] 13 p2153 N85-23372
A bilaterally deterministic rho-mixing stationary random sequence
[AD-A152856] 17 p3019 N85-28666
Central limit theorems in the area of large deviations for some dependent random variables
[AD-A153125] 17 p3043 N85-28931
A random layer model for reflection from ocean bottom sediments
[AD-A155019] 21 p3700 N85-32968
RANDOM VIBRATION
Non-Gaussian approach for parametric random vibration of non-linear structures 01 p0060 N85-10395
Stochastic motor blade dynamics
[AD-A148312] 03 p0318 N85-12054
Random vibrations of aircraft engine blades 06 p0777 N85-14987
The Shock and Vibration Digest, volume 16, no. 9
[AD-A146779] 07 p0976 N85-16200
Techniques for nonlinear random vibration problems 07 p0977 N85-16201
Investigation of dynamic noise affecting geodynamics information in a tethered subsatellite
[NASA-CR-174292] 08 p1174 N85-17405
Stresses in situ generating by bulldozers
[AD-P004270] 09 p1405 N85-18848
Centrifuge tests to provide closure bounds for switches subjected to random vibration
[DE85-002009] 10 p1482 N85-19357
Random vibration of nonlinear, parametrically excited systems 19 p3282 N85-30351
RANDOM WALK
Monte Carlo lattice models for adsorbed polymer conformation
[NASA-TP-2453] 14 p2426 N85-24961
Laser gyroscope random walk determination using a fast filtering technique 16 p2596 N85-26647
A trivariate version of Levy's equivalence
[AD-A153167] 17 p3025 N85-28705
The role of long term lamp fluctuations in the random walk of frequency behavior of the rubidium frequency standard: A case study
[AD-A155338] 21 p3590 N85-32314
Implicit Monte Carlo methods and non-equilibrium Marshak wave radiative transport
[DE85-010711] 22 p3835 N85-33743
Monte Carlo techniques for analyzing deep penetration problems
[DE85-011428] 23 p3958 N85-34598
RANGE
Directory of range data conversion and processing systems
[AD-A148996] 10 p1427 N85-19001
RANGE (EXTREMES)
NT FREQUENCY RANGES
NT PROPORTIONAL LIMIT
NT ROCHE LIMIT
Assessment of satellite power flux-density limits in the 2025-2300 MHz frequency range, part 2
[PB85-101244] 11 p1625 N85-20236
An empirical comparison of the accuracy of univariate and multivariate corrections for range restriction
[AD-A153071] 17 p3019 N85-28670
EOQ (Economic Order Quantity) range model
[AD-A153709] 19 p3379 N85-30965

Evaluation: Close-range photogrammetry for slope inventory and monitoring
[PB85-192755] 24 p4108 N85-35470

RANGE AND RANGE RATE TRACKING
Tracking requirements for precise ERS-1 orbit determination 03 p0380 N85-12431
The Precise Range and Range Rate Equipment (PRARE) and its possible support to the radar altimeter measurement for ERS-1 03 p0382 N85-12445
Measurements in satellite orbit tracing 05 p0598 N85-13812
Satellite-to-satellite orbit determination using minimum, discrete range and range-rate data only 13 p1985 N85-22458
Hardware test program for evaluation of baseline range-range rate sensor concept
[NASA-CR-175794] 16 p2787 N85-27193
Optimal relative data weights 16 p2805 N85-27296

RANGE CONTROL
U TRAJECTORY CONTROL

RANGE FINDERS
NT LASER RANGE FINDERS
NT OPTICAL RANGE FINDERS
USSR report: Electronics and electrical engineering
[JPRS-UEE-84-015] 22 p3762 N85-33314
Characteristics of digital range finder with stroboscopic discretization 22 p3762 N85-33319
Ranging system which compares an object reflected component of a light beam to a reference component of the light beam
[NASA-CASE-NPO-15865-1] 23 p3973 N85-34629

RANGE INDICATORS
U RANGE FINDERS

RANGE MEASUREMENT
U RANGEFINDING

RANGEFINDING
NT SOUND RANGING
Pulse heterodyne equipment for measurements of range and velocity of moving targets-pulse radar
[ESA-TT-845] 09 p1312 N85-18246
Three-dimensional sensing and interpretation
[AD-A150800] 14 p2311 N85-24304
A multi-element ultrasonic ranging array
[AD-A150806] 14 p2416 N85-24906
A short range, high accuracy radar ranging system
[AD-A152195] 16 p2774 N85-27122
Balanced system for ranging and synchronization between satellite pairs
[AD-D011697] 19 p3224 N85-29992
Hardware test program for evaluation of baseline range-range rate sensor concept
[NASA-CR-176143] 23 p3933 N85-34377

RANGELANDS
The application of remote sensing to resource management and environmental quality programs in Kansas
[E85-10023] 02 p0218 N85-11436
An integrated remote sensing approach for identifying ecological range sites — parker mountain
[E85-10050] 07 p0983 N85-16248

RANGES (FACILITIES)
NT TEST RANGES
Global coordinate system
[AD-A153878] 19 p3299 N85-30454

RANGING
U RANGEFINDING

RANK TESTS
Inference for censored matched pairs using signed ranks
[MATHEMATICS-RESEARCH-162] 12 p1923 N85-22076
Simplifications and approximations for linear rank statistics with censored data
[MATHEMATICS-RESEARCH-161] 12 p1923 N85-22079

RANKINE CYCLE
Modeling of a second-generation solar-driven Rankine air conditioner
[DE84-015132] 01 p0036 N85-10223
Overview of waste heat utilization systems
[NASA-TM-86901] 04 p0578 N85-13892
Dynamic power systems for power generation 05 p0609 N85-13892
Dynamic conversion working group summary 05 p0611 N85-13904
Phase 1-A development Idnematic Sterling/Rankine commercial gas-fired heat pump research program
[PB85-100931/GAR] 07 p0936 N85-15926
Development and demonstration of a Stirling/Rankine heat activated heat pump. Phase 3B: Engine technology development testing
[DE85-004388] 10 p1486 N85-19383
Development and test of a high COP Rankine heat pump for generation of process steam. Phase 2: Fabrication and test
[DE85-002600] 11 p1632 N85-20275
Leak detectors for organic Rankine cycle power plants: On-line and manual methods
[DE85-002792] 12 p1852 N85-21617
Direct-contact condensers for solar pond power production
[DE84-004510] 12 p1876 N85-21771
Some solar dish/heat engine design considerations
[DE85-003479] 12 p1881 N85-21802
Development of an Organic Rankine-Cycle power module for a small community solar thermal power experiment
[NASA-CR-175650] 14 p2350 N85-24523
Test results of an organic Rankine-cycle power module for a small community solar thermal power experiment
[NASA-CR-175606] 14 p2350 N85-24524
Analysis of alkali liquid metal Rankine space power systems
[DE85-005089] 16 p2741 N85-26917
Technology for industrial waste heat recovery by organic Rankine cycle systems
[DE85-006719] 18 p3102 N85-29206
Comparative evaluation of three alternative power cycles for waste heat recovery from the exhaust of adiabatic diesel engines
[NASA-TM-86953] 20 p3542 N85-32043

RANKINE-HUGONIOT RELATION
Local stability analysis for a planar shock wave
[NASA-TP-2367] 04 p0452 N85-12864
Fast and optimal solution to the Rankine-Hugoniot problem
[NASA-TM-86214] 19 p3344 N85-30724

RANKING
Asymptotically optimal ranking algorithms for quasi-determinate signal detection 06 p0792 N85-15064
A computer package for ranking, selection and multiple comparisons with the best
[AD-A147617] 08 p1204 N85-17579
Analysis of a visual performance experiment
[DE85-000710] 10 p1530 N85-19645
Predicting a future response using rank predictive probabilities
[MATHEMATICS-RESEARCH-166] 12 p1923 N85-22077
Proportional odds models for survival data and estimates using ranks
[MATHEMATICS-RESEARCH-172] 12 p1923 N85-22080
Use of ranks to fit a linear model to cross-sectional data with an application to biological rhythms
[MATHEMATICS-RESEARCH-169] 12 p1923 N85-22081
Spaceborne power systems preference analyses. Volume 1: Summary
[NASA-CR-175644] 14 p2349 N85-24517
Spaceborne power systems preference analyses. Volume 2: Decision analysis
[NASA-CR-175645] 14 p2349 N85-24518
Streamlined Test Reporting And Planning (STRAP): Computerized human factors questionnaire
[AD-A150611] 14 p2395 N85-24751
A short bibliography of recent developments in selection and ranking procedures
[AD-A155648] 21 p3679 N85-32656

RAPCON (CONTROL)
U RADAR APPROACH CONTROL

RAPID BALLISTICS IDENTIFICATION
Short-time spectroscopic measurement of the temperature of solids
[ISL-CO-202/84] 20 p3459 N85-31486
Flash X-ray diffraction
[ISL-CO-227/84] 23 p3936 N85-34396

RAPID EYE MOVEMENT STATE
Sleep and wake physiology in weightlessness 20 p3510 N85-31819

RAPID QUENCHING (METALLURGY)
Rapid solidification of steels: Model and commercial alloys 02 p0176 N85-11184
Development of rapidly quenched alloys with special physical properties and of processes for their continuous production
[BMFT-FB-T-84-179] 04 p0477 N85-13039
Rapid solidification processing and powder metallurgy of Al alloys
[AD-A146427] 08 p1130 N85-17120
Rapidly solidified NiAl and FeAl
[NASA-TM-86941] 11 p1597 N85-20042
Rapid solidification processing of magnesium alloys
[AD-A150270] 13 p2022 N85-22668
Time-resolved studies of rapid solidification in highly undercooled molten silicon
[DE85-004857] 13 p2036 N85-22765
Metallurgical characterization of aluminum powder consolidation
[AD-A151990] 15 p2510 N85-25484
Investigation of the pitting potential of rapidly solidified aluminum-lithium alloys
[VTH-LR-434] 16 p2752 N85-26986

RARE EARTH ALLOYS
NT NEODYMIUM ALLOYS
Critical evaluation of binary rare Earth diagrams
[DE84-014880] 04 p0470 N85-12991
Critical evaluation of binary rare earth phase diagrams
[DE84-015057] 05 p0614 N85-13922

RARE EARTH COMPOUNDS
NT CERIUM COMPOUNDS
NT CERIUM OXIDES
NT ERBIUM COMPOUNDS
NT EUROPIUM COMPOUNDS
NT LUTETIUM COMPOUNDS
NT NEODYMIUM COMPOUNDS
NT SAMARIUM COMPOUNDS
Magnetism of the rare earth compounds — intermetallic compounds 03 p0424 N85-12707
Growth and magnetic investigations of single crystals of intermetallic compounds of rare earths and uranium — magnetic properties 03 p0425 N85-12712
Microstructure and mechanical properties of rare-earthe-microalloyed high-speed tool steel
[BLL-BISI-TRANS-22043-(9022.06)] 17 p2928 N85-28064
Thin film phase transition materials development program
[AD-A154260] 19 p3259 N85-30209
Contact properties of rare-earth silicides and germanides on Si and Ge 19 p3374 N85-30931
Changes in lattice cell parameter of film intermetallic compounds RT2
[BLL-M-35674-(5828.4)] 23 p3915 N85-34261

RARE EARTH ELEMENTS
NT CERIUM
NT CERIUM 144
NT ERBIUM
NT GADOLINIUM
NT HOLMIUM
NT LANTHANUM
NT LUTETIUM
NT NEODYMIUM
NT NEODYMIUM ISOTOPES
NT PRASEODYMIUM
NT SAMARIUM
NT SCANDIUM
NT SCANDIUM ISOTOPES
NT YTTERBIUM
NT YTTRIUM
The marine geochemistry of the rare earth elements
[AD-A145132] 01 p0068 N85-10598
The influence of rare Earth elements on the temper embrittlement behaviour and mechanical properties of a low alloy steel 02 p0180 N85-11210
The chemistry of rare earth elements in the solar nebula 06 p0869 N85-15843
ESR (Electroslag Refining) technology in Australia: Laboratory research and industrial development
[AD-A147776] 08 p1129 N85-17114
Microscopic analysis of angular momentum projected HFB-states in terms of interacting bosons
[DE85-007629] 16 p2863 N85-27661
The influence of melting practice and of microalloying, with rare earth metals and with boron, on the quality of low-carbon steel
[BLL-BISI-22467-(9022.06)] 17 p2925 N85-28036
The corrosion resistance of chromium-nickel steel containing rare-earth metals
[BLL-BISI-TRANS-22477-(9022.06)] 17 p2925 N85-28041
Inoculation of non-metallic inclusions in steel 17GS
[BLL-BISI-TRANS-22431-(9022.06)] 17 p2925 N85-28042
Systematic view of transition intensities in the spectra of actinides and lanthanides in condensed phases
[DE85-010272] 19 p3354 N85-30789
Influence of gamma-phase on magnetic properties and structure of KhK15YuB alloy during strain-aging
[BLL-M-36281-(5828.4)] 20 p3431 N85-31280
Method for extracting lanthanides and actinides from acid solutions by modification of Purex solvent
[DE85-005763] 23 p3909 N85-34220

RARE GAS-HALIDE LASERS
NT KRYPTON FLUORIDE LASERS
NT XENON CHLORIDE LASERS
NT XENON FLUORIDE LASERS
KrCl lasers for fusion
[DE84-012210] 01 p0122 N85-10835
Investigation of plasma processes in electronic transition lasers
[AD-A155598] 21 p3593 N85-32327

RARE GASES
NT ARGON
NT ARGON ISOTOPES
NT HELIUM
NT HELIUM ATOMS
NT HELIUM ISOTOPES
NT KRYPTON
NT LIQUID HELIUM
NT LIQUID HELIUM 2
NT NEON
NT NEON ISOTOPES
NT RADON
NT RADON ISOTOPES
NT XENON
NT XENON ISOTOPES
NT XENON 129
The Boltzmann equation: Global existence for a rare gas in an infinite vacuum
[PREPRINT-78] 01 p0124 N85-10851
EXAFS and Moessbauer study of small metal clusters isolated in rare-gas solids
[DE84-015976] 04 p0470 N85-12994
The low-energy secondary cosmic ray flux: Detectors in iron meteorites 06 p0687 N85-15635
Where is the Earth's missing xenon?
06 p0688 N85-15641
Monte Carlo simulation of electron thermalization in rare gases
[NAL-TR-834T] 09 p1375 N85-18643
The behaviour of detonation waves in single phase heterogeneous systems
[AD-A149625] 12 p1846 N85-21581
Experimental study of steam condensation on water in countercurrent flow in presence of inert gases
[DE84-013028] 12 p1881 N85-21800
Effect of moisture in inert gases on density of seam metal and on mechanical characteristics of welded joints of aluminum and aluminum alloys
13 p2034 N85-22744
Evaluation of a high pressure proportional counter for the detection of radioactive noble gases
[AD-A154436] 19 p3272 N85-30292
Energy transfer and excimer formation in rare gas solids 19 p3374 N85-30930
Noble gases and the early history of the Earth: Inappropriate paradigms and assumptions inhibit research and communication 21 p3719 N85-33075
A review of noble gas geochemistry in relation to early Earth history 21 p3720 N85-33081
Terrestrial Planets: Comparative Planetology
[NASA-CR-176093] 22 p3851 N85-33849
Noble gases in meteorites and terrestrial planets
22 p3851 N85-33850
Relationships between chondritic meteorites and planets 22 p3851 N85-33851
Noble gas patterns in the atmospheres of Mars and Earth: A comparison via the SNC meteorites
22 p3852 N85-33853
Impact processes and their implications for planetary formation and early evolution 22 p3853 N85-33860
Heaterless ignition of inert gas ion thruster hollow cathodes
[NASA-TM-87066] 23 p3903 N85-34177
Gas shielding apparatus
[DE85-005992] 23 p3939 N85-34416
The 3HE in solar non-relativistic electron events
[SH-2.2-5] 23 p4000 N85-34800
Fluidized bed desulfurization
[NASA-CASE-NPO-15924-1] 24 p4075 N85-35253
Groundwater radon studies for earthquake precursors in southern California
[PB85-196871] 24 p4116 N85-35529
RAREFACTION
Construction of solutions for two-dimensional Riemann problems
[DE85-003136] 10 p1549 N85-19770
RAREFACTION WAVES
U ELASTIC WAVES
RAREFIED GAS DYNAMICS
Research activities of the Illinois University Coordinated Science Laboratory
[AD-A145589] 03 p0449 N85-12858
Study of stresses on surface of flat barrier immersed in under expanded jet of rarefied gas
16 p2765 N85-27061
The highly underexpanded exhaust plume from nozzles with boundary layers
[DFVLR-FB-85-10] 20 p3421 N85-31230
Unsteady transonic heat transfer in a transient facility
[NASA-CR-176145] 23 p3930 N85-34354
RAREFIED GASES
NT COSMIC GASES
NT INTERSTELLAR GAS
NT NEUTRAL GASES
Aerodynamic and thermal characteristics of stellate bodies in hypersonic flow of rarefied gas at angle of attack 06 p0778 N85-14974
Experimental investigation of heat transfer to bluff cylinders and cones in hypersonic rarefied gas flow
11 p1620 N85-20195
Nonequilibrium air radiation (Nequair) program: User's manual
[NASA-TM-86707] 19 p3353 N85-30780
RASERS
U MASERS
RATE METERS
U MEASURING INSTRUMENTS
RATES (PER TIME)
NT ACCELERATION (PHYSICS)
NT ACOUSTIC VELOCITY
NT AIRSPEED
NT ANGULAR ACCELERATION
NT ANGULAR VELOCITY
NT ARRHYTHMIA
NT BIT ERROR RATE
NT BURNING RATE
NT COLLISION PARAMETERS
NT COLLISION RATES
NT CRITICAL VELOCITY
NT CURRENT DENSITY
NT DECAY RATES
NT DECELERATION
NT DRIFT RATE
NT ELECTRON ACCELERATION
NT ELECTRON FLUX DENSITY
NT EVAPORATION RATE
NT EXHAUST VELOCITY
NT FLOW VELOCITY
NT FLUX (RATE)
NT FLUX DENSITY
NT GROUND SPEED
NT GROUP VELOCITY
NT HEART RATE
NT HEAT FLUX
NT HIGH ACCELERATION
NT HIGH GRAVITY ENVIRONMENTS
NT HIGH SPEED
NT HYPERSONIC SPEED
NT ILLUMINANCE
NT IMPACT ACCELERATION
NT ION PRODUCTION RATES
NT IRRADIANCE
NT LIGHT SPEED
NT LOADING RATE
NT LOW SPEED
NT LUMINANCE
NT LUMINOUS INTENSITY
NT MAGNETIC FLUX
NT MASS FLOW RATE
NT NEUTRON FLUX DENSITY
NT ORBITAL VELOCITY
NT PARTICLE ACCELERATION
NT PARTICLE FLUX DENSITY
NT PHASE VELOCITY
NT PHOTON DENSITY
NT PHYSIOLOGICAL ACCELERATION
NT PLASMA ACCELERATION
NT PROPAGATION VELOCITY
NT PROTON FLUX DENSITY
NT PULSE RATE
NT PULSE REPETITION RATE
NT RADIAL VELOCITY
NT RADIANCE
NT RADIANT FLUX DENSITY
NT RECOMBINATION COEFFICIENT
NT RELATIVISTIC VELOCITY
NT RESPIRATORY RATE
NT ROTOR SPEED
NT SIGNAL FADING RATE
NT SOLAR CONSTANT
NT SOLAR FLUX
NT SOLAR FLUX DENSITY
NT SOLAR VELOCITY
NT SOLAR WIND VELOCITY
NT SOUND INTENSITY
NT SPIN REDUCTION
NT STRAIN RATE
NT SUBSONIC SPEED
NT SUPERSONIC SPEEDS
NT TIP SPEED
NT TRANSONIC SPEED
NT TRANSVERSE ACCELERATION
NT WIND VELOCITY
Electron energy loss rates in N-2, O-2 and air
[AD-A145158] 01 p0072 N85-10476
Robust rate control system designs for a submersible
[AD-A144792] 01 p0111 N85-10753
Some of the features of movement of gas through a layer of free-flowing substance
[BLL-M-35732-(5828.4)] 02 p0196 N85-11312
Northern Hemisphere atlas of 1-minute rainfall rates
[AD-A145411] 02 p0231 N85-11508
Southern Hemisphere atlas of 1-minute rainfall rates
[AD-A145421] 02 p0231 N85-11509
Specific absorption rate in a sitting rhesus model at 225, 1290, and 5950 MHz for E, H, and K polarizations
[AD-A145435] 02 p0234 N85-11524
Ballpark reliability estimation techniques
[AD-A145971] 03 p0369 N85-12357
Analyses to develop models to project failure rates and repair costs of electronic modules and subassemblies
[AD-A146509] 06 p0816 N85-15180
Rain rate meter
[AD-D011361] 07 p0990 N85-16342
Snow characterization measurements from SNOW-TWO/Smoke Week 6
[AD-A147423] 07 p1008 N85-16402
An evaluation of flashtube signal characteristics
[AD-A149589] 10 p1423 N85-18974
Influence of extension rate on strength and deformation characteristics of titanium alloys over a broad temperature range 10 p1446 N85-19121
Development of a polysilicon process based on chemical vapor deposition of dichlorosilane in an advanced Siemen's reactor
[NASA-CR-174445] 11 p1672 N85-20532
Application of dimensional analysis to the problem of solar wind-magnetosphere energy coupling
[DE85-002414] 11 p1674 N85-20551
Influence of uncompensated solution resistance upon the evaluation of rate constants for rapid electrochemical reactions
[AD-A150657] 14 p2250 N85-23942
Use of optical techniques in studies of wear rates of anodized aluminum and polymer coatings on aluminum
14 p2259 N85-23997
Computer controlled acquistion of corrosion rate data from multiple sensors
[PB85-157378] 15 p2524 N85-25539
Removal of longitudinal internal flash from electrically welded tubes
[BLL-BISI-TRANS-22380-(9022.06)]
17 p2936 N85-28136
Inequalities for distributions with increasing failure rate
[AD-A152812] 17 p2978 N85-28390
Low-rate discharge of various electrochemical batteries for use with oceanographic instruments
[AD-A153985] 18 p3095 N85-29159
Method of characterizing critical timing paths and analyzing timing related failure modes in very large scale integrated circuits
[AD-D011731] 22 p3759 N85-33298
Limits to the burster repetition rate as deduced from the 2nd catalog of the interplanetary network
[OG-1.2-5] 22 p3862 N85-33915
Cyg X-3: Not seen in high-energy gamma rays by COS-B
[OG-2.2-2] 22 p3864 N85-33929
Constraints on cosmic-ray observation of Cygnus X-3
[OG-2.2-3] 22 p3864 N85-33930
Hercules X-1: Pulsed gamma-rays detected above 150 GeV
[OG-2.2-9] 22 p3865 N85-33935
Time-resolved spectroscopic studies of detonating heterogeneous explosives
[DE85-009760] 23 p3921 N85-34297
Dual-chamber plasma deposition of A-Si:H solar cells at high rates using disilane
[DE85-011628] 23 p3948 N85-34451
Analysis of transient radiation upset in a 16K SRAM
[DE85-009442] 23 p3965 N85-34586
Ranging system which compares an object reflected component of a light beam to a reference component of the light beam
[NASA-CASE-NPO-15865-1] 23 p3973 N85-34629
Injection of energetic particles following the gamma-ray flares on June 7, 1980, as observed on Helios 1
[SH-1.3-9] 23 p3998 N85-34758
Angular resolution of air-shower array-telescopes
[OG-9.5-6] 23 p4030 N85-34983
The angular resolution of air shower gamma ray telescopes
[OG-9.5-14] 23 p4031 N85-34990
Recording system for the solar neutron monitoring at Mt. Norikura
[SH-9.1-8] 23 p4051 N85-35123
Burst size distributions in the digitized data of the ion chambers t Mt. Norikura and sea level stations
[SH-9.1-9] 23 p4051 N85-35124
Sensitivity of single and multiple cosmic ray neutrons to the surrounding medium in a lead-free monitor
[SH-9.1-10] 23 p4051 N85-35125
The neutron moderated detector and groundbased cosmic ray modulation studies
[SH-9.1-13] 23 p4052 N85-35128

A suggested standardized format for cosmic ray ground-level event data
[SH-8.1-15] 23 p4052 N85-35130
The application of bispectral analyses to aeroelastic phenomena 24 p4060 N85-35157
The structure of the shower disk observed at Mt. Norikura
[HE-4.7-1] 24 p4198 N85-36052
Methods for roof-top mini-arrays
[HE-4.7-7] 24 p4199 N85-36058
Fast scintillation counter preamplifier for the observation of Linsley effect
[HE-4.7-9] 24 p4199 N85-36060
RATINGS
The effect of beta adrenergic blockade on ratings of perceived exertion
[AD-A148053] 08 p1195 N85-17530
Streamlined Test Reporting And Planning (STRAP): Computerized human factors questionnaire
[AD-A150911] 14 p2395 N85-24751
RATIONS
NT SPACE RATIONS
Nutritional criteria for military rations and effects of prolonged feeding on acceptability
14 p2394 N85-24742
The effects of prolonged feeding meal, ready-to-eat (MRE) operational rations
[AD-A154763] 21 p3688 N85-32773
RATIOS
NT ASPECT RATIO
NT COMPRESSION RATIO
NT DIMENSIONLESS NUMBERS
NT FUEL-AIR RATIO
NT GRASHOF NUMBER
NT HIGH ASPECT RATIO
NT HIGH REYNOLDS NUMBER
NT INDEXES (RATIOS)
NT LIFT DRAG RATIO
NT LOW ASPECT RATIO
NT LOW REYNOLDS NUMBER
NT MACH NUMBER
NT MASS RATIOS
NT MASS TO LIGHT RATIOS
NT MODULAR RATIOS
NT NUSSELT NUMBER
NT POISSON RATIO
NT PRANDTL NUMBER
NT PRESSURE RATIO
NT RAYLEIGH NUMBER
NT REYNOLDS NUMBER
NT RICHARDSON NUMBER
NT SCALE (RATIO)
NT SIGNAL TO NOISE RATIOS
NT SIMILARITY NUMBERS
NT STRESS RATIO
NT STROUHAL NUMBER
NT VOID RATIO
The effect of occupational exposure and the body weight to height ratio on exhaled methylene chloride breath concentration in females at one, eighteen and sixty-six hours post exposure 14 p2388 N85-24708
Fuzzy hierarchical analysis
[DE85-008149] 17 p3021 N85-28685
Explanation of the secondary to primary ratio within the continuous Fermi accelerator model
[OG-8.3-2] 23 p4021 N85-34921
Propagation of injected cosmic rays under distributed reacceleration
[OG-8.3-3] 23 p4021 N85-34922
RATS
Hemopoiesis in rats submitted to weightlessness
01 p0091 N85-10613
General resistance of organism of rats under hypokinesia 05 p0694 N85-14462
An atropinized heat-stressed rat model: Dose response effects and pharmacokinetics
[AD-A146851] 07 p1011 N85-18423
Acute oral toxicity (LD50) of 4-nitrophenyl monochloromethyl (Phenyl) phosphinate (TA009) in male rats
[AD-A148337] 08 p1192 N85-17513
Results of sanitary-microbiological studies aboard Cosmos-1129 biosatellites 12 p1903 N85-21952
Rat tissue opioid peptide content during long-term hypokinesia 12 p1904 N85-21964
Effect of long-term repeated exposure to high-intensity stationary magnetic field on adrenomedullary activity
12 p1904 N85-21965
Chemical characterization and toxicologic evaluation of airborne mixtures. Inhalation toxicology of diesel fuel obscurant aerosol in Sprague-Dawley rats. Phase 3. Subchronic exposures
[AD-A150100] 12 p1905 N85-21966
Brain mechanisms underlying individual differences in reaction to stress: An animal model
[AD-A150195] 13 p2143 N85-23301
Structural development and gravity
15 p2608 N85-26071
The salutary effect of dietary calcium on bone mass in a rat model of simulated weightlessness
15 p2608 N85-26073
Role of glucocorticoids in the response to unloading of muscle protein and amino acid metabolism
15 p2609 N85-26077
Constant fiber number during skeletal muscle atrophy and modified arachidonate metabolism during hypertrophy 15 p2609 N85-26078
Blood pressure responses and mineral ocorticoid levels in the suspended rat model for weightlessness
15 p2609 N85-26079
Differential effect of denervation on free radical scavenging enzymes in slow and fast muscle of rat
[NASA-CR-175719] 15 p2614 N85-26110
Effects of long-term low-level radiofrequency radiation exposure on rats. Volume 7: Metabolism, growth and development
[AD-A150829] 15 p2615 N85-26112
Preliminary assessment of climatic change during late Wisconsin time, southwest Great Basin and vicinity, Arizona, California and Nevada
[DE85-006343] 16 p2636 N85-27486
Does a 50-cycle alternating field have central nervous effects?
[BLL-CE-TRANS-8083-(9022.09)] 16 p2639 N85-27507
Experiments in microwave exposure in the rat: Body temperature, serum chemistry and the use of chemical restraint
[PB85-156834] 16 p2640 N85-27512
Rat bone tissue after flight aboard Cosmos-1129 biosatellite 19 p3324 N85-30593
Effect of periodic accelerations on physiochemical properties and Ca2+ reactivity of actomyosin in white rat myocardium and skeletal muscles
19 p3324 N85-30594
Rat blood serum and liver carbohydrates and lipids in recovery period after 15-day hypokinesia
19 p3326 N85-30606
Effects of long-term low-level radiofrequency radiation exposure on rats. Volume 8: Evaluation of longevity, cause of death, and histopathological findings
[AD-A154283] 19 p3327 N85-30610
Changes in the impedance and bioelectrical activity of the cerebral cortex of rats under the action of anaesthetic drugs
[HSE-TRANS-10371] 19 p3327 N85-30617
Effects of coating rectangular microscopic electrophoresis chamber with methylcellulose
20 p3498 N85-31748
Changes in pentose and glucuronate pathway dehydrogenases in rat brains following single or multiple hypothermic episodes 20 p3505 N85-31790
General description of experiment dealing with rat ontogenesis aboard Cosmos-1514 biosatellite
22 p3822 N85-33679
Rat plasma hormone levels following flight aboard Cosmos-1129 biosatellite 22 p3823 N85-33681
The 1984 biotic studies of Yucca Mountain, Nevada test site, Nye County, Nevada
[DE85-011715] 23 p3951 N85-34487
Rat skeletal muscles with simulation of physiological effects of weightlessness (morphological study)
23 p3953 N85-34502
Lipogenesis in rat liver after flight aboard Cosmos-1129 biosatellite 23 p3954 N85-34508
Response of amino acids in hindlimb muscles to recovery from hypogravity and unloading by tail-cast suspension
[NASA-CR-176183] 24 p4128 N85-35589
Response of rat hindlimb muscles to 12 hours recovery from tail-cast suspension
[NASA-CR-176182] 24 p4128 N85-35590
RAWINSONDES
An evaluation and comparison of vertical profile data from the VISSR Atmospheric Sounder (VAS)
[NASA-TP-2425] 07 p1000 N85-16351
The effect of the arbitrary level assignment of satellite cloud motion wind vectors on wind analyses in the pre-thunderstorm environment
[NASA-TM-86186] 10 p1517 N85-19565
Upper-air data collection during CAPTEX
[DE85-006300] 16 p2627 N85-27438
Trends in the Southern Hemisphere
16 p3144 N85-29466
Processing methods of rawinsonde measurements at the descent by parachute
[KNMI-WR-84-7] 18 p3149 N85-29498
Comparison of tropopause altitude determination by the Platteville Radar, Sunset Radar and the NWS Rawinsonde 21 p3617 N85-32477
A modified Fresnel scattering model for the parameterization of Fresnel returns, part 2.3A
21 p3618 N85-32483
RAY ACOUSTICS
U GEOMETRICAL ACOUSTICS
RAY OPTICS
U GEOMETRICAL OPTICS
RAY TRACING
Nonlinear propagation in a depth-dependent ocean
[AD-A145079] 01 p0116 N85-10791
Concentrator optical characterization using computer mathematical modelling and point source testing
[NASA-CR-174109] 04 p0528 N85-13375
Ocean acoustics
[AD-A147062] 07 p1038 N85-18591
Simulation of bent crystal spectrometers
[DE85-002042] 09 p1385 N85-18709
Three dimensional ray tracing of the Jovian magnetosphere in the low frequency range
[NASA-CR-175462] 10 p1571 N85-19909
Electromagnetic analysis of radomes by the moment method
[AD-P004351] 12 p1824 N85-21445
Comparison of spherical wave ray tracing and exact boundary value solutions for spherical radomes
[AD-P004353] 12 p1824 N85-21447
A subaperture approach to the calculation of flashlobes introduced by airborne radomes
[AD-P004355] 12 p1825 N85-21449
Image lobe analysis for large radomes
[AD-P004359] 12 p1825 N85-21453
Surface forward scattering and reflection
[AD-A150115] 12 p1928 N85-22112
A fast ray tracing routine for laterally inhomogeneous media
[AD-A150984] 14 p2421 N85-24938
High frequency estimation of 2-dimensional cavity scattering
[AD-A151697] 15 p2542 N85-25696
LIGHT: A ray tracing code to simulate light collection in scintillation spectrometers and light pipes
[DE85-007213] 16 p2665 N85-27673
Saudi Arabian refraction profile: Crustal structure of the Red Sea-Arabian Shield transition
17 p2990 N85-29484
Saudi Arabian refraction profile: A preliminary interpretation for the Red Sea-Arabian Shield transition
17 p2991 N85-29485
A preliminary analysis of the Saudi Arabian deep seismic sounding data 17 p2991 N85-29489
The addition of advanced scene rendering techniques to a general purpose graphics package
[AD-A153323] 17 p3012 N85-29625
Ray tracing general sweep defined objects
[REPT-84-36] 17 p3014 N85-29636
Circular-beam ray tracing on a microcomputer
[DE85-010754] 19 p3336 N85-30685
View-limiting shrouds for insolation radiometers
[NASA-CR-176041] 20 p3458 N85-31476
A theoretical and empirical analysis of coherent ray-tracing 23 p3957 N85-34524
A simple but systematic CSG system
23 p3963 N85-34569
A ray trace program for line-of-sight microwave communication links
[AD-A156168] 24 p4087 N85-35336
RAYLEIGH DISTRIBUTION
Spline-based Rayleigh-Ritz methods for the approximation of the natural modes of vibration for flexible beams with tip bodies
[NASA-CR-172566] 13 p2102 N85-23100
An application of the Rayleigh distribution to contract cost data
[AD-A151551] 15 p2664 N85-26441
Bivariate Rayleigh distribution: Formulas and curves, for correlation computing using the distribution function
[FOA-C-30360-E2] 20 p3521 N85-31901
1000 GeV gamma rays from Cygnus X-3: An update
[OG-2.1-8] 22 p3863 N85-33925
A new approach to evaluate gamma-ray measurements
[OG-9.5-11] 23 p4031 N85-34968
A new statistic for the analysis of circular data in gamma-ray astronomy
[OG-9.5-13] 23 p4031 N85-34969
RAYLEIGH NUMBER
Natural convection in square partitioned enclosures
[AD-A153707] 18 p3197 N85-29626
RAYLEIGH SCATTERING
Extinction by dielectric particles at optical and infrared wavelengths
[AD-A146305] 03 p0413 N85-12640
Ionospheric turbulence: Interchange instabilities and chaotic fluid behavior
[AD-A147810] 07 p0998 N85-16337

Rayleigh and Raman scattering for density in a swirling flow combustor 08 p1120 N85-17060
Flame propagation and stabilization studies using Rayleigh scattering and laser Doppler velocimetry [AD-A148602] 09 p1290 N85-18102
Fourier densitometry: A new optical method for measuring density fluctuations by Rayleigh scattering — turbulent jets 11 p1576 N85-19932
LANDSAT-4 Thematic Mapper calibration and atmospheric correction 12 p1870 N85-21734
A measurement of the intensity of the cosmic background radiation at 9.9 cm 13 p2206 N85-23681
Experimental determination of the mixing frequency parameter for coalescence/dispersion modeling of turbulent combustion [DE85-011466] 19 p3270 N85-30280
Rayleigh scattering for density measurements in premixed flames: One point, time series data 20 p3424 N85-31253

RAYLEIGH WAVES
Rayleigh-Taylor instability in compressible media [AD-A145491] 02 p0198 N85-11322
Measurement of areal mass variation in Rayleigh-Taylor unstable targets [AD-A145541] 02 p0198 N85-11325
Research in quantitative NDE techniques [AD-A145090] 03 p0369 N85-12358
Love and Rayleigh waves in irregular ground 04 p0523 N85-13348
Deep structure beneath the Pyrenees 04 p0524 N85-13351
Lightweight, broadband Rayleigh wave transducer [AD-D011345] 07 p1037 N85-16584
Influence of Bragg reflecting lattice groove depth modulation on Rayleigh wave reflection coefficient 10 p1499 N85-19458
Texture independent determination of residual stress in polycrystalline aggregates using Rayleigh waves [AERE-R-11483] 12 p1943 N85-22203
Angular dependence of the Rayleigh-surface wave velocity in polycrystalline metals with small anisotropy [AERE-R-11595] 15 p2508 N85-25476
On Rayleigh waves and Rayleigh wave extension of surface micro-cracks 15 p2572 N85-25980
Inversion of Rayleigh wave group velocities from high-explosive tests [AD-A152172] 16 p2783 N85-27175
Elastic wave gyrometer [REPT-26/4924/HF] 20 p3459 N85-31484
Development of ultrasonic modeling techniques for the study of crustal inhomogeneities [AD-A155206] 21 p3632 N85-32585

RAYS
Solar neutrino: Flux, cosmic rays and the 11 year solar cycle [SH-8.1-7] 23 p4049 N85-35112

RC CIRCUITS
The design of high order active RC-filters [DRIC-T-7147] 07 p0945 N85-15987
Development of thin film hybrid IC active filter for video band use [NHK-LABS-NOTE-312] 18 p3094 N85-29153

RC NETWORKS
U RC CIRCUITS

RDX
The influence of inert particulate material on the properties of RDX/polyethylene wax compositions [MRL-R-929] 03 p0336 N85-12159
Critical analysis of nitramine decomposition data. Preliminary comments on autoacceleration and autoinhibition in HMX and RDX decomposition [AD-A146570] 06 p0774 N85-14946
Microstructural origins of hot spots in RDX explosive and a reference inert material [AD-A146685] 06 p0774 N85-14947
Molecular dynamics in nitramines and modified nitramines [AD-A148515] 08 p1220 N85-17686
The chemistry of RDX and HMX cluster ions 13 p2004 N85-22561
Combustion-deflagration-detonation transition in a confined spherical powder [ISL-R-108/84] 22 p3747 N85-33223

REACTION BONDING
Quantum characteristics of kinetic fracturing of solids 02 p0265 N85-11732
Kinetics of reaction of metals and non-metals during diffusion welding 11 p1602 N85-20076
Radiographic detectability limits for seeded voids in sintered silicon carbide and silicon nitride [NASA-TM-86945] 12 p1861 N85-21674
Sintered silicon carbide molded body and method for its production [NASA-TM-77646] 14 p2259 N85-23999
Research and developmental study on MIS thin film solar cells of amorphous hydrogenated silicon, part 2 [BMFT-FB-T-84-290] 17 p2968 N85-28467

REACTION JETS
U JET FLOW
U JET THRUST

REACTION KINETICS
Comparison of numerical techniques for integration of stiff ordinary differential equations arising in combustion chemistry [NASA-TP-2372] 01 p0011 N85-10065
CREKID: A computer code for transient, gas-phase combustion of kinetics [NASA-TM-83806] 01 p0011 N85-10068
DYNKIN: A computer program for the description of detailed gas reactions in interaction with gas dynamics [AD-B085364] 01 p0046 N85-10296
Second All-Union Seminar on Hydromechanics and Heat and Mass Exchange in Weightlessness, summaries of reports [NASA-TM-77590] 01 p0047 N85-10305
Laser spectroscopy and gas-phase chemistry in CVD [DE84-014959] 02 p0173 N85-11158
The oxidation of transition-metal ions by molecular oxygen [BLL-M-29593-(5828.4)] 02 p0175 N85-11172
Impact cratering: The process and its effects on planetary evolution — and silicate-carbonate reactions on Venus [NASA-CR-174018] 02 p0228 N85-11488
Study of singlet oxygen-pentavalent phosphorus reactions [AD-A145896] 03 p0327 N85-12107
Mechanochemical reactions of polymethyl methacrylate and polystyrene at high pressure [DRIC-T-7307] 03 p0337 N85-12165
Kinetics of fatigue factor of AT3 titanium alloys in air, distilled water and 3.5% aqueous NaCl solution 03 p0350 N85-12255
Organic aerosol formation: OH(hydroxyl radical) versus ozone oxidation pathways [PB84-219860] 03 p0388 N85-12484
Reaction mechanisms in the formation of intercalation complexes, and properties of intercalated molecules 03 p0431 N85-12745
Low energy ion-molecule reaction dynamics and chemionization kinetics [DE84-015861] 04 p0559 N85-13562
New integration techniques for chemical kinetic rate equations. 2: Accuracy comparison [NASA-TM-86893] 05 p0596 N85-13798
Space charge, interfacial kinetics, and electrical response of condensed matter [AD-A146364] 06 p0765 N85-14893
Chemical kinetics and Earth's atmosphere 06 p0822 N85-15218
Integrating chemical kinetic rate equations by selective use of stiff and nonstiff methods [NASA-TM-86923] 07 p0904 N85-15726
Reactions of butadiyne. 1: The reaction with hydrogen atoms [NASA-TM-77805] 07 p0921 N85-15834
Interaction between chromium oxide and carbon [BLL-M-36002-(5828.4)] 07 p0926 N85-15867
Solid-phase sintering of tantalum carbide [BLL-M-36013-(5828.4)] 07 p0926 N85-15872
Kinetics of interaction between carbon and iron oxides of metallized materials in solid phase [BLL-M-36023-(5828.4)] 07 p0926 N85-15873
Photochemistry and kinetics of the O*2-HI system [AD-A147433] 07 p0971 N85-16167
Catalytic ignition and combustion of lean mixtures [AD-A148101] 08 p1121 N85-17067
Combustion in high speed air flows [AD-A148371] 08 p1122 N85-17070
Combustion kinetics of metal oxide and halide radicals [AD-A148521] 08 p1122 N85-17076
The construction and behaviour of ultramicroelectrodes: Investigations of novel electrochemical systems [AD-A148658] 08 p1123 N85-17079
Electrochemical features of the ferric sulfate leaching of CuFeS2/C aggregates [AD-A148661] 08 p1123 N85-17081
Study of reaction kinetics and development of elastic properties in network polymerization systems by the impulse technique [AD-A148187] 08 p1133 N85-17141
The kinetics of electron transfer reactions in and at films of electroactive polymers [AD-A148597] 08 p1134 N85-17149
High pressure physics research focusing on composite materials 08 p1140 N85-17185
Study in molecular lasers [AD-A148246] 08 p1166 N85-17357
Proceedings of the AFOSR/AFRPL Rocket Propulsion Research Meeting: Abstracts and Agenda [AD-A148818] 09 p1288 N85-18085
Metal-support interactions: Their effects upon adsorption, electronics, and activity/selectivity properties of cobalt in hydrogenation [DE85-003316] 09 p1292 N85-18113
Theoretical studies of the ignition and combustion of silane-hydrogen-air mixtures [NASA-CR-3876] 10 p1433 N85-19032
An infrared study of the hydrogenation of carbon dioxide on supported rhodium catalysts [AD-A149477] 10 p1436 N85-19049
Mechanisms and reaction dynamics related to methane combustion [PB85-129690] 10 p1438 N85-19065
Kinetics of saturation of porous titanium with low melting point metals 10 p1448 N85-19114
Kinetics of oxidation of titanium alloy upon heating to 1000 deg C 10 p1448 N85-19122
Thermodynamics of the reactive flow model [DE85-004405] 10 p1565 N85-19870
Dynamical studies of molecular systems [DE85-003053] 11 p1594 N85-20028
A study of interdiffusion in beta + gamma/gamma + gamma prime Ni-Cr-Al [NASA-CR-174852] 11 p1597 N85-20041
USSR report: Materials science and metallurgy [JPRS-UMS-84-005] 11 p1597 N85-20044
Direct measurement of the temperature dependence of the velocity of the reaction of deuterium atoms with vibration-excited hydrogen molecules [MPIS-12/1984] 11 p1726 N85-20858
A comparison of the efficiency of numerical methods for integrating chemical kinetic rate equations [NASA-TM-83590] 12 p1778 N85-21162
Study of the kinetics of hydrogenation using aged catalysts [DE85-004373] 12 p1802 N85-21302
Kinetics of nitric oxide formation in laminar and turbulent methane combustion [PB85-149698] 12 p1804 N85-21313
A study of intumescent reaction mechanisms [AD-A149805] 12 p1812 N85-21365
Optically pumped iodine monofluoride laser [AD-D011555] 12 p1855 N85-21637
Chemical kinetics and photochemical data for use in stratospheric modeling. Evaluation number 6 [NASA-CR-175564] 12 p1888 N85-21849
State-selected ion-molecule reaction dynamics [AD-A150068] 12 p1928 N85-22115
Theoretical nuclear physics [DE85-003468] 12 p1932 N85-22135
Ignition of mixtures of SiH sub 4, CH sub 4, O sub 2, and Ar or N sub 2 behind reflected shock waves [NASA-TP-2415] 13 p1974 N85-22395
Gasification of boron oxide drops and boron slurry agglomerates in combustion gases 13 p1999 N85-22529
Combustion kinetics of metal atoms and metallic radicals over wide temperature ranges 13 p1999 N85-22530
Combustion of zirconium carbide 13 p1999 N85-22532
Chemical kinetics of gas phase decomposition products of nitramine propellants 13 p2003 N85-22558
Kinetics of mechanism of the thermal decomposition of dimethylnitramine and dimethylnitrosamine 13 p2004 N85-22559
The chemistry of RDX and HMX cluster ions 13 p2004 N85-22561
Comprehensive mechanisms for combustion chemistry: An experimental and numerical study with emphasis on applied sensitivity analysis [DE85-000173] 13 p2018 N85-22656
Estimating degree of development of physical-chemical interaction among components in Al-B fiber composite material 13 p2027 N85-22705
Segregation of silicon in silumin-carbon fiber composites 13 p2028 N85-22706
Specifics of kinetics of polymorphous conversion upon heating of low carbon steels 13 p2030 N85-22721
Thermodynamic and kinetic studies of pulsed laser annealing from transient conductivity measurements [DE85-003677] 13 p2096 N85-23078
Influence of uncompensated solution resistance upon the evaluation of rate constants for rapid electrochemical reactions [AD-A150657] 14 p2250 N85-23942
Fundamental study of three dimensional two phase flow in combustion systems [AD-A150739] 14 p2250 N85-23945
Evaluation of unimolecular rate constants for some outer-sphere electrochemical reactions [AD-A150758] 14 p2250 N85-23946
Combustion kinetics of metal oxide and halide radicals [AD-A150924] 14 p2251 N85-23952

International Conference on Coordination Chemistry (23rd) held at Boulder, Colorado on 29 July - 3 August, 1984
[AD-A150980] 14 p2252 N85-23956
Block-implicit multigrid solution of Navier-Stokes equations in primitive variables
[DE85-004071] 14 p2301 N85-24250
Electricity production from coal through molten-carbonate fuel cells
[TI85-006072] 14 p2351 N85-24534
Extraction of ions from solutions at atmospheric pressure, mass spectrometric analysis of bioorganic substances 14 p2367 N85-24706
Theoretical studies of kinetic mechanisms of negative ion formation in plasmas
[AD-A150820] 14 p2423 N85-24946
Thermodynamic calculations and the chemical vapour deposition of hard materials 14 p2431 N85-24991
Detonations of solid explosives
[AD-A152012] 15 p2521 N85-25540
Kinetic studies following state selective laser excitations
[DE85-007173] 15 p2564 N85-25816
Dynamics of recrystallization and redistribution of impurities in semiconductors subjected to millisecond laser pulses 15 p2643 N85-26302
The overall reaction concept in premixed, laminar, steady-state flames. 2: Initial temperatures and pressures
[AD-A152132] 16 p2746 N85-26944
Transitional metal activation and functionalization of C-H bonds
[DE85-006816] 16 p2746 N85-26949
Evaluation of chemical reaction mechanisms for photochemical smog. Part 2: Quantitative evaluation of the mechanisms, revised
[PB85-166060] 16 p2822 N85-27408
The spectroscopy and reaction kinetics of coordinated unsaturated metal carbonyls
[AD-A153079] 17 p2920 N85-28003
Elementary reactions of importance in oxidation, combustion ignition and flame inhibitions
[AD-A153139] 17 p2921 N85-28004
Kinetics of hydrolysis and products of hydrolysis and photolysis of tetryl
[AD-A153144] 17 p2921 N85-28005
Study of self-propagating condensed phase reactions TiB(2) synthesis
[AD-A153198] 17 p2921 N85-28006
Kinetics of the formation of a complex alloyed boride coating on iron and its properties
[BLL-BIS-TRANS-22303-(8022.06)] 17 p2930 N85-28084
Rotational relaxation studies of hydrogen fluoride
[AD-A152711] 17 p3029 N85-28734
Rapid growth of potassium dihydrogen phosphate crystals
[DE85-007261] 17 p3045 N85-28839
Light scattering and spectroscopic studies of polymerization processes
[AD-A153407] 18 p3069 N85-28984
Chemical transformation modules for Eulerian acid deposition models. Volume 1: The gas-phase chemistry
[PB85-173714] 18 p3072 N85-29001
Spatial correlations in the decay from an unstable state in the Malthus Verhulst model --- laser cavities
[NOTA-INTERNA-632] 18 p3114 N85-29280
Kinetics and intensity of photochemical processes in the atmosphere
[BPT-10/84] 18 p3134 N85-29411
Study of the chemical mechanism in lubrication
[DE85-010768] 19 p3226 N85-30013
Determination of the association constant for pertechnetic acid
[DE85-010224] 19 p3235 N85-30057
Variational transition state theory
[DE85-010685] 19 p3235 N85-30059
Burn rates of explosives at high pressures
[DE85-010606] 19 p3251 N85-30159
On the low temperature chemistry preceding end gas autoignition
[DE85-010471] 19 p3252 N85-30162
Flow field effects on nucleation in a reacting mixing layer
[ARL/AERO-R-165] 19 p3263 N85-30237
Experimental determination of the mixing frequency parameter for coalescence/dispersion modeling of turbulent combustion
[DE85-011468] 19 p3270 N85-30280
Production of gallium atoms by excimer laser photolysis of trimethyl gallium
[DE85-010742] 19 p3276 N85-30331
Instrumentation for particle-beams research using excited merging beams
[AD-A154155] 19 p3356 N85-30807
Carbon reduction of mixtures of MnO(2) and Fe(2)O(3)
[BLL-M-36280-(5828.4)] 20 p3422 N85-31241
Computer-controlled carburizing
[BLL-OA-TRANS-3204-(6196.300)] 20 p3429 N85-31268
Mechanistic and kinetic studies of the elementary processes in catalytic combustion of methane
[PB85-186306] 20 p3435 N85-31314
Theoretical modelling of the electro-chemistry in a corrosion fatigue crack. Part 2: Mathematical aspects of associated unsteady reaction equations
[NPL-DMA(A)-100-PT-2] 20 p3465 N85-31529
Self-heating to ignition measurements and computation of critical size for solar energy collector materials
[PB85-183374] 20 p3485 N85-31663
Modeling of chemical transformations of SO(x) and NO(x) in the polluted atmosphere: An overview of approaches and current status
[PB85-173169] 20 p3487 N85-31677
Fusion reactions at low energy
[DE85-010561] 20 p3526 N85-31944
Design of micelles as dephosphorylating agents
[AD-A155589] 21 p3564 N85-32166
Imbedded thermocouples as a solid propellant combustion probe
[AD-A155630] 21 p3564 N85-32167
Introduction of structural variations into oxide polymers and their effect on sintering and crystallization
[AD-A155597] 21 p3570 N85-32206
Multilayer capacitor dielectrics produced from metallo-organic precursors
[AD-A154592] 21 p3580 N85-32254
Experimental studies of the kinetics of deposition nucleation on an ice nucleant used in weather modification 21 p3636 N85-32596
The measured rate of condensation nucleation to droplets using the techniques of chemical kinetics 21 p3652 N85-32694
Resonant energy transfer during strong excitation 21 p3689 N85-32922
Jet flows: Modelling and experiments 22 p3744 N85-33206
Nonequilibrium chemistry in an isothermal turbulent flow 22 p3745 N85-33211
Static high pressure study of nitric oxide chemistry: Proposed mechanism for nitric oxide detonation
[DE85-010795] 22 p3746 N85-33220
Theoretical aspects of corrosion and practical implications for aircraft and related systems 22 p3749 N85-33240
Development of a chemical kinetic mechanism for the US EPA (Environmental Protection Agency) regional oxidant model
[PB85-186858] 22 p3813 N85-33618
Modeling of auto exhaust smog chamber data for EKMA development
[PB85-186492] 22 p3813 N85-33619
KIVA computer program for multidimensional chemically reactive fluid flows with fuel sprays
[DE85-012730] 22 p3830 N85-33722
An impact-induced terrestrial atmosphere and iron-water reactions during accretion of the Earth 22 p3854 N85-33864
Separation of gas mixtures by supported complexes
[DE85-011996] 23 p3912 N85-34236
Effects of hot deformation on the kinetics of the pearlite transformation in eutectoid steel
[BLL-M-35844-(5828.4)] 23 p3913 N85-34250
Metal alkoxides: Models for metal oxides. Alkoxide ligands in early transition metal organometallic chemistry
[DE85-011366] 23 p3916 N85-34269
Thermally induced chemical migration: A natural analog approach
[DE85-012308] 23 p3949 N85-34474
Application of evaluated fission-product delayed-neutron precursor data in reactor kinetics calculations
[DE85-012726] 23 p3972 N85-34624
Survey of mixing in metal/insulator systems
[DE85-011938] 23 p3985 N85-34714
FTIR studies of hydrocarbon synthesis on Pd/ZSM5 catalysts
[DE85-012430] 24 p4071 N85-35230
Basic research on pulse-combustion phenomena
[PB85-200228] 24 p4077 N85-35265
A study of the chemistry of alkali metals in the upper atmosphere
[AD-A156349] 24 p4117 N85-35524

REACTION PRODUCTS
Study of singlet oxygen-pentavalent phosphorus reactions
[AD-A145896] 03 p0327 N85-12107
Determination of Toluene's degradation products under simulated atmospheric conditions 05 p0674 N85-14331
Identification and properties of molecular systems of potential use in solar-pumped lasers
[NASA-CR-175804] 16 p2789 N85-27207
Current regulatory and licensing status for byproduct sources, facilities and applications
[DE85-010987] 22 p3842 N85-33798

REACTION RATE
U REACTION KINETICS

REACTION TIME
Pattern reversal visual evoked potentials and reaction time
[CSIR-SR-PERS-354] 01 p0097 N85-10844
Workload demand and CNS depressant stressor effects on spatial orientation information processing
[AD-A145211] 01 p0098 N85-10851
Fitts' law? A test of the relationship between information load and movement precision 05 p0705 N85-14523
A production system model of capturing reactive moving targets 05 p0705 N85-14524
A control model: Interpretation of Fitts' law 05 p0706 N85-14526
The effects of task structure on time-sharing efficiency and resource allocation optimality 05 p0711 N85-14562
Choice reaction time and color: An annotated bibliography
[AD-A149722] 12 p1908 N85-21979
Fast times at high temperatures
[DE85-003306] 12 p1943 N85-22205
The effect of set size on color recognition
[AD-A150958] 14 p2391 N85-24726
Eye movement in response to single and multiple targets
[AD-A151115] 15 p2617 N85-26126
Shape with and without redundant colour as coding mechanism for simulated radar displays in a time-extended simple vigilance task
[AD-A151683] 16 p2844 N85-27533
The effect of set size on time to recall color coded information
[AD-A155013] 21 p3665 N85-32767
Transformation of spectrum of phase-code keyed signal for scanning in time 22 p3765 N85-33336

REACTION WHEELS
Magnetically suspended reaction wheel assembly 05 p0607 N85-13670
Magnetic suspension options for spacecraft inertia-wheel applications 05 p0607 N85-13671
Reaction wheels for kinetic energy storage 05 p0607 N85-13674
Emitted vibration measurement device and method
[NASA-CASE-MFS-25981-1] 11 p1635 N85-20299

REACTIVITY
Alloying effects of reactive elements in ferritic stainless steels 02 p0178 N85-11196
Reactivity of ion implanted silicon carbide
[DE85-001543] 09 p1399 N85-18802
Ligand structural influences upon electrochemical reactivity: Organic substituent effects upon Carboxylatopentaamminecobalt(3) reductions at mercury and gold electrodes
[AD-A150885] 14 p2250 N85-23944
Mechanism of the catalytic gasification and reactivity of graphite
[DE85-009932] 19 p3229 N85-30020
Microscopic control of semiconductor surface oxidation
[AD-A154799] 21 p3709 N85-33026
Experimental studies of chemical reactivity during shock initiation of hexanitrostilbene
[DE85-011726] 22 p3754 N85-33270
Method for preparing hydride configurations and reactive metal surface
[DE85-006443] 23 p3917 N85-34274

REACTOR CHEMISTRY
U RADIOCHEMISTRY

REACTOR CORES
Multigrid iteration solution procedure for solving three-dimensional sets of coupled equations
[DE84-016515] 04 p0555 N85-13532
Expected behavior of plutonium in the IFR fuel cycle
[DE85-008225] 18 p3161 N85-29725
TFCX shielding optimization
[DE85-010503] 19 p3359 N85-30626
Superconducting toroidal field coil current densities for the TFCX
[DE85-010265] 20 p3530 N85-31959
MATADOR (Methods for the Analysis of Transport And Deposition Of Radionuclides) code description and user's manual
[TI85-901402] 23 p3966 N85-34592
Liquid uranium alloy-helium fission reactor
[DE85-006511] 23 p3970 N85-34607

DEPTH-CHARGE static and time-dependent perturbation/sensitivity system for nuclear reactor core analysis, revision 1
[DE85-013103] 24 p4139 N85-35859
Neutronic calculations for a new high flux reactor
[DE85-011551] 24 p4150 N85-35734
Thermal hydraulic features of the TMI accident
[DE85-014569] 24 p4152 N85-35747
REACTOR DESIGN
Instrumentation and controls evaluation for space nuclear power systems
[DE85-000983] 09 p1383 N85-18695
Magnetic divertor design for the compact reversed-field pinch reactor
[DE85-002031] 09 p1391 N85-18753
Optimization of pressure vessels with standard intercepting spheres
[INPE-3276-PRE/600] 11 p1651 N85-20397
Space nuclear-power reactor design based on combined neutronic and thermal-fluid analyses
[DE85-002433] 11 p1727 N85-20864
Tritium catalyzed deuterium Tokamaks
[DE85-004825] 12 p1936 N85-22166
Self-substaining low-Z coatings for impurity control. Part 1: General considerations
[DE85-000427] 14 p2425 N85-24956
New directions in Tokamak reactors
[DE85-002548] 15 p2657 N85-26396
Methods of first wall structural analysis with applications to the long pulse commercial Tokamak reactor design
[DE85-004915] 15 p2657 N85-26397
Swelling behavior of titanium-modified AISI 316 alloys
[DE85-007470] 16 p2752 N85-26982
Ballooning beta limits of dee and bean shaped Tokamaks
[IPPJ-713] 16 p2866 N85-27676
TOKASTAR: A Tokamak stellarator hybrid with possible bean-shaped operation
[IPPJ-716] 16 p2866 N85-27680
Fusion-power-core design of a Compact Reversed-Field Pinch Reactor (CRFPR)
[DE85-007710] 16 p2866 N85-27692
Tokamak fusion core experiment maintenance study
[DE85-008040] 17 p3040 N85-28613
Preliminary proposal for a beryllium technology program for fusion applications
[DE85-009815] 18 p3183 N85-29737
Recent progress in stellarator reactor conceptual design
[DE85-009592] 18 p3189 N85-29780
Feasibility study of a fission-suppressed Tokamak fusion breeder
[DE85-009099] 18 p3190 N85-29786
Test cell modeling and optimization for FPD-2
[DE85-010836] 19 p3358 N85-30821
Advances in ICF power reactor design
[DE85-010930] 19 p3361 N85-30841
Poloidal variations in toroidal fusion reactor wall power loadings
[DE85-009505] 19 p3362 N85-30848
Tritium system design for the mirror reactors FPD-1, FPD-2 and FPD-3
[DE85-010490] 19 p3363 N85-30852
New concept for pumping the edge plasma
[DE85-010180] 19 p3371 N85-30909
Steady-state spheromak reactor studies
[DE85-009585] 19 p3372 N85-30916
Flow characteristics of the Cascade granular blanket
[DE85-010932] 20 p3420 N85-31227
Modeling and optimization of a test-cell upgrade for MFTF-B operating in the high neutron wall loading mode
[DE85-009697] 20 p3529 N85-31948
Simulating the effects of plasma disruption with a 1 MA current pulse in a coaxial test fixture
[DE85-010491] 20 p3535 N85-31996
Oxidation of formaldehyde solutions used for the preservation of reverse osmosis membranes
[PB85-185585] 22 p3742 N85-33194
Fusion Power Demonstration (FPD) maintenance and disassembly considerations
[DE85-011413] 22 p3846 N85-33820
Blanket optimization studies for Cascade
[DE85-010002] 22 p3846 N85-33824
REACTOR FUELS
U NUCLEAR FUELS
REACTOR MATERIALS
Heat exchanger
[DE84-014299] 01 p0047 N85-10309
Improved multiaxial creep-rupture strength criterion
[DE84-014273] 01 p0082 N85-10413
Method and apparatus for determining the content and distribution of a thermal neutron absorbing material in an object
[DE84-014319] 01 p0117 N85-10801
Materials studies for magnetic fusion energy applications at low temperatures, 7
[DE84-013497] 01 p0122 N85-10837
Stress corrosion of pressure vessel steel A533-B in high temperature water
[BLL-RISLEY-TR-4600-(9091.9F)] 03 p0330 N85-12125
Review: Role of refractory metal alloys in fusion reactor applications
[AERE-R-11317] 03 p0422 N85-12695
A physical interpretation of the structure and electron-optical data for spinel (MgAl2O4)
[AERE-R-11278] 03 p0434 N85-12767
Blanket materials for fusion reactors: Comparisons of thermochemical performance
[DE84-016240] 04 p0568 N85-13622
Proceedings of Workshop on Synergistic Effects in Surface Phenomena Related to Plasma-Wall Interactions
[IPPJ-AM-35] 06 p0864 N85-15488
Effects of monolayer coverages on substrate sputtering yields 06 p0865 N85-15496
Synergestic sputtering properties of binary alloys 06 p0865 N85-15497
Elevated temperature creep behavior of inconel alloy 625
[DE84-015836] 09 p1297 N85-18144
Synergistic sputtering properties of binary alloys
[DE84-017493] 09 p1297 N85-18148
Magnetic fusion energy plasma interactive and high heat flux components. Volume 2: Technical assessment of the critical issues and problem areas in high heat flux materials and component development
[DE85-001155] 09 p1393 N85-18764
Magnetic fusion energy plasma interactive and high heat flux components. Volume 3: Strategy for international collaborations in the areas of plasma materials interactions and high heat flux materials and components development
[DE85-001145] 10 p1559 N85-19829
Leakage-flow-induced vibration of a tube-in-tube slip joint
[DE84-007301] 11 p1652 N85-20408
Ordered carbon metal alloys for extraterrestrial power systems
[AD-A150681] 14 p2255 N85-23977
Application of new welding technology in the fabrication of nuclear power plant 15 p2568 N85-25829
New directions in Tokamak reactors
[DE85-002548] 15 p2657 N85-26396
Differential between crack and pseudo-crack indications by means of objective magnetic flux leakage testing
[BLL-BISI-TRANS-22033-(9022.06)] 17 p2978 N85-28386
Sodium concrete reaction: Structural considerations
[DE85-009031] 18 p3081 N85-29063
Behavior of reinforced concrete at elevated temperatures
[DE85-009032] 18 p3123 N85-29332
Expected behavior of plutonium in the IFR fuel cycle
[DE85-008225] 18 p3181 N85-29725
Preliminary proposal for a beryllium technology program for fusion applications
[DE85-009815] 18 p3183 N85-29737
Load-carrying capabilities of refractory alloys for space reactor power applications
[DE85-010566] 19 p3240 N85-30067
Alloy development for irradiation performance
[DE85-010454] 19 p3240 N85-30091
Qualitative comparison of fusion reactor materials for waste handling and disposal
[DE85-010473] 19 p3360 N85-30830
Source Term Experiments Project (STEP): Aerosol characterization system
[DE85-010248] 19 p3361 N85-30839
Current state of development and expected performance of copper-lithium alloys as an impurity control system in fusion applications
[DE85-009673] 19 p3372 N85-30917
Nuclear data needs for fusion energy development
[DE85-010445] 20 p3536 N85-32000
Tritium-helium effects in metals
[DE85-011507] 22 p3749 N85-33235
Reactor pressure vessel steels ASME SA533B and SA508 C 1.2
[VTT-340] 22 p3794 N85-33507
Monte Carlo and discrete ordinates calculations of 14-MeV neturons streaming through a stainless-steel duct (L/D = 4.6): Comparison with experiment
[DE85-011423] 22 p3840 N85-33778
Stress corrosion cracking susceptibility of types 316NG and 316 stainless steel in an impurity environment
[TI85-006864] 23 p3917 N85-34277
Effect of stainless steel weld overlay cladding on the structural integrity of flawed steel plates in bending, series 1
[TI85-010349] 23 p3939 N85-34418
The dynamic strain ageing of A533B class 1 nuclear pressure vessel steel
[AERE-R-11485] 24 p4078 N85-35274
Analysis of reactor material experiments investigating oxide fuel crust stability and heat transfer in jet impingement flow
[DE85-012097] 24 p4151 N85-35739
REACTOR PHYSICS
The reactor dynamic code RETRANS: Structure and users guide
[OEFZS-4257] 07 p1041 N85-16614
Refinements in the computation of collision probabilities
[DE85-006118] 16 p2564 N85-27663
Radiation transport
[DE85-010333] 21 p3703 N85-33005
REACTOR SAFETY
A pilot study of future research on seismic hazards in Sweden
[FOA-C-20544-T1] 02 p0229 N85-11498
Space nuclear safety program
[DE84-015983] 04 p0564 N85-13591
Acoustic transducers for fast reactor instrumentation
[BLL-RISLEY-TR-4979-(9091.9F)] 07 p0961 N85-16091
Austrian contributions to fuel rod failure models shown at the International Standard Problem (ISP)-14
[OEFZS-4276] 07 p1041 N85-16613
Instrumentation and controls evaluation for space nuclear power systems
[DE85-000983] 09 p1383 N85-18695
Safety program considerations for space nuclear reactor systems
[DE85-003295] 10 p1556 N85-19606
Thermal stress-dependent dilation of concrete
[DE84-014668] 11 p1653 N85-20412
Parallel processing experiences on the Denelcor HEP computer
[DE85-000653] 11 p1702 N85-20703
Hydrogen flame acceleration and transition to detonation
[DE85-000611] 12 p1802 N85-21299
Proceedings of the 1984 DOE Nuclear Reactor and Facility Safety Conference, volume 1
[DE84-012130] 12 p1931 N85-22132
Proceedings of the DOE Nuclear Reactor and Facility Safety Conference, volume 2
[DE84-012694] 12 p1931 N85-22133
Steel containment buckling
[DE85-003744] 13 p2103 N85-23111
Physics effects of accidental submersion of space power reactors in water
[DE85-000020] 15 p2650 N85-26344
Sodium concrete reaction: Structural considerations
[DE85-009031] 18 p3081 N85-29063
Behavior of reinforced concrete at elevated temperatures
[DE85-009032] 18 p3123 N85-29332
Safety report, 1982 18 p3184 N85-29746
Flow visualization study of inverted annular flow of post dryout heat transfer region
[DE85-010482] 19 p3269 N85-30275
Liquid metal reactor programs: Safeguards and program assurance
[DE85-010821] 19 p3331 N85-30635
Graphic display development program, volume 1
[DE85-011076] 19 p3335 N85-30649
MELCOR Accident Consequence Code System (MACCS)
[DE85-009712] 19 p3339 N85-30689
Simulation and operation of the EBR-2 automatic control rod drive system
[DE85-010262] 19 p3360 N85-30832
Source Term Experiments Project (STEP): Aerosol characterization system
[DE85-010248] 19 p3361 N85-30839
Advances in ICF power reactor design
[DE85-010930] 19 p3361 N85-30841
A review of the SIMMER-2 analyses of liquid-metal-cooled fast breeder reactor core-disruptive accident fuel escape
[DE85-010803] 19 p3366 N85-30876
In-service supervision of a pressurized concrete pressure vessel
[OEFZS-4308] 20 p3470 N85-31584
Two-phase flow visualization in a transparent, atmospheric pressure, boiling water loop
[DE84-016857] 21 p3588 N85-32288
Tritium technology review
[DE85-010604] 21 p3703 N85-33006
MATADOR (Methods for the Analysis of Transport And Deposition Of Radionuclides) code description and user's manual
[TI85-901402] 23 p3966 N85-34592

Transient three-phase three-component systems. Part 1: Formulation of the system of differential equations
[DE85-013267] 24 p4095 N85-35384
REACTOR STARTUP TESTS
Instrumentation and controls evaluation for space nuclear power systems
[DE85-000963] 09 p1383 N85-18695
One-dimensional hybrid code for FRM dynamics
[DE85-010687] 19 p3361 N85-30840
REACTOR TECHNOLOGY
Means of varying conditions in the expanded boundary divertor without affecting energy confinement
[DE84-013840] 01 p0122 N85-10836
Hydrogen absorption on (110) tungsten planes at 30 K: An atom-probe field-ion microscope study
[DE84-015659] 04 p0560 N85-13565
Thermal contact conductance measurements on Doublet 3 armor tile trephite
[DE84-013654] 05 p0613 N85-13916
East Europe report: Science and technology
[JPRS-ESA-84-043] 08 p1142 N85-17198
USSR report: Engineering and equipment
[JPRS-UEQ-85-003] 13 p2042 N85-22782
Winding insulation in electromagnetic systems for Tokamak reactor plants 13 p2067 N85-23035
Glossary of fusion energy
[DE84-017180] 14 p2425 N85-24958
Comparison study of toroidal-field diverters for a compact reversed-field pinch reactor
[DE85-009591] 18 p3189 N85-29781
Liquid metal reactor programs: Safeguards and program assurance
[DE85-010621] 19 p3331 N85-30635
Touch-off: A method to determine the position of an object by means of a sensor-driven robot
[DE85-011178] 19 p3339 N85-30691
US blanket technology programs
[DE85-010505] 19 p3358 N85-30817
One-dimensional hybrid code for FRM dynamics
[DE85-010687] 19 p3361 N85-30840
REACTORS
Thermodynamical characteristics of heat storage reactors using metal hydrides
[NAL-TR-822] 06 p0669 N85-15524
READ-ONLY MEMORY DEVICES
Fast envelope detector with bias compensation
[AD-D011226] 01 p0038 N85-10243
Programmable digital temperature controller apparatus
[AD-D011221] 01 p0049 N85-10319
Fault tolerant computing research
[AD-A145840] 02 p0244 N85-11690
Logic elements for systems with variable structure 07 p0955 N85-16054
A method and apparatus for operating on companded PCM voice data
[NASA-CASE-KSC-11285-1] 18 p3089 N85-29120
Microcomputer controlled image processor
[AD-D011734] 22 p3833 N85-33735
Maintenance port system
[AD-D011724] 23 p3967 N85-34594
READERS
Comparative review of single-line and multiline optical character readers used in mail processing
[PB84-234624] 04 p0548 N85-13489
Optical mark reader
[AD-D011462] 10 p1557 N85-19818
Direct reading fast microwave interferometer for EBT
[DE85-000183] 11 p1636 N85-20306
READING
Comprehension of instructions for operating devices
[AD-A145263] 01 p0098 N85-10653
Investigation into the use of the TV magnifier in the Netherlands
[HSE-TRANS-11142] 20 p3533 N85-31966
READING MACHINES
U READERS
READJUSTMENT
U ADJUSTING
READOUT
A concept for a hadron calorimeter with photodiode readout
[MPI-PAE/EXP-E1-130] 01 p0050 N85-10332
Improvements in photodiode readout for small CsI (Tl) crystals
[MPI-PAE/EXP-E1-131] 01 p0051 N85-10333
Fine grained hodoscopes based on scintillating optical fibers
[DE84-014849] 01 p0120 N85-10825
Characterization of electronic streak tubes including one with internal CCD readout
[DE84-016823] 05 p0639 N85-14096
CCDs: Their cause and cure 08 p1252 N85-17905
The ARGOS VHF direct readout mini-station and CML-80-MP data collection Platform Transmitter Terminals (PTTs) 14 p2238 N85-23873
ARGOS VHF direct readout mini-station 14 p2239 N85-23886
System for automatic recording of vibration parameters 14 p2282 N85-24135
Direct readout and dissemination of results using ARGOS keypad terminals 14 p2326 N85-24390
Digital tachometer 22 p3779 N85-33416
The read-out system of spatial distribution of thermoluminescence in meteorites
[SH-9.1-16] 23 p4052 N85-35131
Spatial distribution read-out system for thermoluminescence sheets
[HE-7.1-7] 24 p4213 N85-36161
REAGENTS
A robotic system for preparing reagent and dilution vials
[DE85-006262] 16 p2793 N85-27231
Basic research in novel inorganic reagents and fluorocarbon chemistry
[AD-A155340] 21 p3584 N85-32165
REAL NUMBERS
NT INTEGERS
Computable real analysis
[AD-A149079] 10 p1546 N85-19747
REAL TIME OPERATION
Real time sensing and control of out-of-plane distortion due to line heating by laser
[AD-A144773] 01 p0027 N85-10169
Clutter generator for use in radar evaluation
[AD-D011234] 01 p0039 N85-10245
The French weather radar network: A status report 01 p0082 N85-10550
Hardware for a real-time multiprocessor simulator
[NASA-TM-83805] 01 p0099 N85-10859
Ada (trademark) training curriculum. Real-time concepts 1303 teacher's guide
[AD-A145093] 01 p0104 N85-10894
Chemoviscoelty modeling for thermosetting resins - I
[NASA-CR-172443] 03 p0326 N85-12096
Wideband integrated voice/data technology
[AD-A146054] 03 p0355 N85-12283
Recent examples of mesoscale numerical forecasts of severe weather events along the east coast
[NASA-TM-86172] 03 p0395 N85-12523
Experimenting with the Rolm Ada language workshop for specifying and designing 03 p0408 N85-12607
A unified method for evaluating real-time computer controllers: A case study --- aircraft control
[NASA-CR-174168] 04 p0547 N85-13478
Real-time planning by an intelligent robot
[DE84-016869] 04 p0553 N85-13519
The facilities of the Calculation Center and Real Time Room for satellite positioning 05 p0599 N85-13819
Information flow in event-driven large-scale systems
[DE84-014167] 05 p0735 N85-14728
The Western Aeronautical Test Range of NASA Ames Research Center
[NASA-TM-85924] 07 p0909 N85-15756
Some characteristics of automotive gasolines and their performance in a light aircraft engine
[FAA-CT-84-12] 07 p0934 N85-15919
Real-time analysis of space characteristics of microwave electromagnetic pulse fields by means of controllable layer structures 07 p0955 N85-16052
ILIR task of digital recoil travel measurement system
[AD-A147102] 07 p0987 N85-16140
Decentralized control of scheduling in distributed systems
[AD-A147446] 07 p1022 N85-16487
JPL Robotics Laboratory computer vision software library
[NASA-CR-174272] 07 p1023 N85-16491
Ada training curriculum. Real-time systems in Ada 1401 teacher's guide, volume 1
[AD-A146782] 07 p1024 N85-16496
Ada training curriculum. Real-time systems in Ada 1401 teacher's guide, volume 2
[AD-A146783] 07 p1024 N85-16497
The effect on software design of testing by symbolic execution 08 p1065 N85-16750
Reliable software design for avionics and space applications 08 p1065 N85-16751
Real-time estimation of amplitude and group delay distortion in a PSK line-of-sight communications channel
[AD-A147735] 08 p1151 N85-17266
A commentray on the utilization of real-time channel evaluation systems in HF spectrum management
[AD-A148616] 08 p1154 N85-17289
Programmable realtime interface between a block floating point processor and memory
[AD-D011431] 08 p1203 N85-17571
Operating system for a real-time multiprocessor propulsion system simulator. User's manual
[NASA-TP-2426] 08 p1207 N85-17596
Nonlinear real-time optical signal processing
[AD-A148293] 08 p1222 N85-17699
Improved real-time ultra-high resolution image projection display using laser-addressed liquid crystal light valve
[AD-D011414] 08 p1223 N85-17705
Decentralized control of scheduling in distributed systems
[AD-A147668] 08 p1226 N85-17731
Real-time estimation of amplitude and group delay distortion in a PSK line-of-sight communications channel 09 p1311 N85-18237
Development and operation of a real-time data acquisition system for the NASA-LaRC differential absorption lidar
[NASA-CR-174384] 09 p1366 N85-18583
Directory of range data conversion and processing systems
[AD-A148996] 10 p1427 N85-19001
An H.F. simulator for use with real time channel evaluation systems 10 p1473 N85-19293
Distributed data processing design methodology
[AD-A148868] 10 p1537 N85-19692
Distributing a distributed problem solving network simulator
[AD-A149065] 10 p1537 N85-19693
The feasibility of a multiprocessor architecture for real-time contour surface display generation
[AD-A149427] 10 p1538 N85-19697
RELTIM: A library of routines used in real time machine control applications
[PB85-116507] 10 p1542 N85-19725
Effect of water vapor and water droplets on the RAM-1 (Real-Time Aerosol Monitor): Preliminary results
[PB85-109429] 11 p1637 N85-20313
Real time algorithms for robotic control of teleoperators
[DE85-001137] 11 p1647 N85-20380
A quality control experiment in a real time multiprocessor operating system: The Mara 860 --- software testing 11 p1702 N85-20707
Interface specifications for SCR (Software Cost Reduction) (A-7E) extended computer module, revised
[AD-A149948] 12 p1915 N85-22024
System for automatic recording of vibration parameters 14 p2282 N85-24135
The ARGOS communications performance trials 14 p2326 N85-24376
Structurization of programs for real-time microprocessor arrays 15 p2529 N85-25592
Real-time enhancement of a climatology or forecast of ocean thermal structure using observed ocean temperatures
[AD-A151118] 15 p2604 N85-26049
An extension of a microcomputer based system for analysis of line drawing quantization schemes
[AD-A152006] 15 p2624 N85-26171
Principles of organizing a real-time control system 15 p2625 N85-26177
High-capacity real-time computer system for processing hydrophysical data 15 p2625 N85-26178
Efficient implementation of real-time programs under the VAX/VMS operating system
[NASA-TM-86354] 15 p2627 N85-26193
Graphic simulation of a machine-repairman model
[AD-A151761] 16 p2694 N85-26633
Maintaining consistency and accommodating network repair in a self-regenerative distributed database management system (a discussion of the means and cost) 16 p2698 N85-26656
Design and specification of a local area network architecture for use in real-time flight simulation
[AD-A152242] 16 p2716 N85-26762
Implementation of a real-time, interactive, continuous speech recognition system
[AD-A151936] 16 p2773 N85-27117
Data processing on the rotor test stand at DFVLR in Brunswick: Microprogrammable interfaces and array processor as key components in a PDP 11 real time data acquisition and processing system
[DFVLR-MITT-85-03] 17 p2906 N85-27921
Performance analysis of the DSN baseband assembly (Bba) Real-Time Combiner (RTC)
[NASA-CR-175877] 17 p2947 N85-28193
The design of an adaptive predictive coder using a single-chip digital signal processor
[AD-A152461] 17 p2952 N85-28231
Real-Time Multiprocessor Programming Language (RTMPL) user's manual
[NASA-TP-2422] 17 p3010 N85-28610
Optimal design and use of retry in fault tolerant real-time computer systems
[NASA-CR-175920] 17 p3015 N85-28643
Synchronization and fault-masking in redundant real-time systems
[NASA-TM-87478] 17 p3015 N85-28644
A real-time executive for multiple-computer clusters
[AD-A152961] 17 p3015 N85-28646

Axial topography from digitized real time radiography
[DE85-006767] 18 p3091 N85-29130
HERMIES-1: A mobile robot for navigation and manipulation experiments
[DE85-006852] 18 p3118 N85-29301
The use of VLSI technology for the real-time generation of graphics displays: A proposal
[AD-A153766] 18 p3160 N85-29578
EDS operator and control software
[DE85-010470] 19 p3340 N85-30698
Implementation of a serial communication process for a fault tolerant, real time, multitransputer operating system
[AD-A154237] 19 p3343 N85-30714
A distributed real-time operating system
[NIKHEF-H/84-8] 20 p3518 N85-31876
Work in Amsterdam on local intelligence — artificial intelligence
[NIKHEF-H/84-9] 20 p3518 N85-31877
Interactive on-line conferences
[AD-A154723] 21 p3574 N85-32227
Hardware schemes for fast Fourier transform, part 7.4A 21 p3626 N85-32526
Real-time contour surface display generation
[AD-A155232] 21 p3666 N85-32780
Software for interactive on-line conference
[AD-A154742] 21 p3670 N85-32801
A real time index of geomagnetic background noise for the MAD (Magnetic Anomaly Detection) frequency band
[AD-A155717] 22 p3814 N85-33627
Modeling and measurement of fault-tolerant multiprocessors
[NASA-CR-3920] 22 p3833 N85-33732
Linear filters as a method of real-time prediction of geomagnetic activity
[DE85-010760] 22 p3860 N85-33899
Animengine: An engineering animation system
23 p3959 N85-34535
Real-time multiparameter pulse processing with decision tables
[DE85-011683] 23 p3966 N85-34589
Space Missions for Automation and Robotics Technologies (SMART) Program
[NASA-TM-86820] 24 p4066 N85-35210
Holoswitch
[AD-A155841] 24 p4096 N85-35392
Optimize computer throughput using array processors
[AD-A155843] 24 p4135 N85-35628

REAL VARIABLES
NT ABEL FUNCTION
NT ASYMPTOTES
NT ASYMPTOTIC SERIES
NT BESSEL FUNCTIONS
NT BETHE-SALPETER EQUATION
NT BIHARMONIC EQUATIONS
NT BLASIUS EQUATION
NT BOREL SETS
NT BURGER EQUATION
NT CALCULUS OF VARIATIONS
NT CHANDRASEKHAR EQUATION
NT COLLINEARITY
NT COMPOSITE FUNCTIONS
NT COPLANARITY
NT DELTA FUNCTION
NT DIFFERENTIAL EQUATIONS
NT EINSTEIN EQUATIONS
NT ELLIPTIC DIFFERENTIAL EQUATIONS
NT EULER-CAUCHY EQUATIONS
NT EXISTENCE THEOREMS
NT EXTREMUM VALUES
NT FALKNER-SKAN EQUATION
NT FOKKER-PLANCK EQUATION
NT FOURIER SERIES
NT GAUSS EQUATION
NT GREEN'S FUNCTIONS
NT HELMHOLTZ VORTICITY EQUATION
NT HYPERBOLIC DIFFERENTIAL EQUATIONS
NT HYPERBOLIC FUNCTIONS
NT INTEGRAL CALCULUS
NT J INTEGRAL
NT JACOBI MATRIX METHOD
NT KERNEL FUNCTIONS
NT LAME WAVE EQUATIONS
NT LIAPUNOV FUNCTIONS
NT LIMITS (MATHEMATICS)
NT LINEAR EQUATIONS
NT LINEAR EVOLUTION EQUATIONS
NT LIOUVILLE EQUATIONS
NT LIPSCHITZ CONDITION
NT MAXIMA
NT MEASURE AND INTEGRATION
NT MONGE-AMPERE EQUATION
NT NEUMANN PROBLEM
NT NONLINEAR EQUATIONS
NT NONLINEAR EVOLUTION EQUATIONS
NT NUMERICAL DIFFERENTIATION
NT NUMERICAL INTEGRATION
NT PADE APPROXIMATION
NT PARABOLIC DIFFERENTIAL EQUATIONS
NT PARTIAL DIFFERENTIAL EQUATIONS
NT PERIODIC FUNCTIONS
NT POISSON EQUATION
NT POWER SERIES
NT QUADRATIC EQUATIONS
NT RUNGE-KUTTA METHOD
NT SERIES (MATHEMATICS)
NT STURM-LIOUVILLE THEORY
NT TANGENTS
NT TAYLOR SERIES
NT VECTOR ANALYSIS
NT VLASOV EQUATIONS
NT VORTICITY
NT WEIGHTING FUNCTIONS
Schubert varieties are arithmetically Cohen-Macaulay
16 p2553 N85-27592
SIGMA - A stochastic-integration global minimization algorithm
[AD-A154878] 21 p3671 N85-32806

REARWARD FACING STEPS
U BACKWARD FACING STEPS

REATTACHED FLOW
Experiments on the structure of turbulent reattaching flow 05 p0635 N85-14074
Heat transfer and fluid mechanics measurements in the turbulent reattaching flow behind a backward-facing step
15 p2553 N85-25753
An experimental study of compressible turbulent reattaching free shear layers 16 p2781 N85-27161

REATTACHMENT
U ATTACHMENT

REB
U RELATIVISTIC ELECTRON BEAMS

REBREATHING
Cardiac output measured by mass spectroscopy
05 p0692 N85-14449
Cardiac output measurement with soluble gases
05 p0692 N85-14450

RECEIVERS
NT LINEAR RECEIVERS
NT LOGARITHMIC RECEIVERS
NT RADAR RECEIVERS
NT RADIO RECEIVERS
NT RADIOTELEPHONES
NT SUPERHETERODYNE RECEIVERS
NT TELEVISION RECEIVERS
The development of an optoelectronic assembly applied to computer systems
[AD-A145028] 01 p0120 N85-10821
Experimental and theoretical study of a solar thermochemical receiver module
[NASA-CR-174107] 04 p0528 N85-13374
Natural interference phenomena affecting spaceborne receivers
[NASA-CR-174256] 07 p0916 N85-15796
Hardwire missile receiver coupler
[AD-D011350] 07 p0937 N85-15936
Spaceborne receivers: Basic principles
[NASA-CR-174260] 07 p0948 N85-15960
Lightweight, broadband Rayleigh wave transducer
[AD-D011345] 07 p1037 N85-16884
Using the control system design environment in the design of a data link receiver unit for the Coast Guard HH-65A helicopter
[AD-A148624] 08 p1088 N85-16880
TDRSS S-shuttle unique receiver equipment
08 p1100 N85-16951
A variable length and sensor spacing thermistor array
[AD-D011416] 08 p1113 N85-17017
The susceptibility of aeronautical navigational aids to interference from adjacent-band broadcast transmissions
[BBC-RD-1984/12] 09 p1311 N85-18234
Coherent receiver phase and amplitude alignment circuit
[AD-D011487] 10 p1488 N85-19295
SSPS-CRS advanced sodium receiver: Construction experience report
[DE85-000825] 10 p1511 N85-19533
Direction finder set, radio
[AD-A149058] 12 p1775 N85-21142
Solid particle receiver experiments: Velocity measurements
[DE85-000257] 12 p1853 N85-21823
Method of measuring sea surface water temperature with a satellite including wideband passive synthetic-aperture multichannel receiver
[NASA-CASE-NPO-15851-1] 12 p1889 N85-21723
Programmable filter with fanned interdigital surface acoustic wave transducer 13 p2083 N85-23008
Invariance of probability characteristics of detector to shape of optical pulse signals 13 p2090 N85-23048
Microwave blackbodies for spaceborne receivers
[NASA-CR-175647] 13 p2094 N85-23068
Optoacoustic receiver with semiconductor-type radiator and photodetector 14 p2274 N85-24086
Photon detection with cooled avalanche photodiodes: Theory and preliminary experimental results
16 p2770 N85-27098
Real-time position determinations using the GPS TI4100/GEOSTAR receiver
[AD-A152561] 17 p2894 N85-27845
Thermal performance and design of a solid particle cavity receiver
[DE85-010830] 19 p3274 N85-30300
Symposium on Luminescent Radiation Receivers and Converters 19 p3295 N85-30430
Arctic acoustic tomography MIZEX 84
[AD-A154426] 19 p3320 N85-30580
Sensitivity of compressive receivers
[FOA-C-30385-E4] 22 p3756 N85-33288
Comparative characteristics of optical multiposition pulse signals with intersymbol distortion
22 p3764 N85-33329
Binary signal detection in acousto-optic receivers
22 p3782 N85-33430

RECEIVING SYSTEMS
U RECEIVERS

RECEPTACLES (CONTAINERS)
U CONTAINERS

RECEPTION DIVERSITY
Analysis of space diversity techniques for EHF (Extremely High Frequency) satellite downlinks
[AD-A151900] 15 p2544 N85-25705
Polarization diversity addition to the 10 centimeter Doppler weather radar
[AD-A150062] 24 p4087 N85-35334

RECEPTORS (PHYSIOLOGY)
NT CHEMORECEPTORS
NT GRAVIRECEPTORS
NT MECHANORECEPTORS
NT PHOTORECEPTORS
NT PROPRIOCEPTORS
Dynamics of morphological changes in articulation nervous system under hypokinetic conditions as a model of a spaceflight factor 01 p0092 N85-10821

RECESSION
Results of variable enthalpy tests of CPR-488 TIP panels in MSFC Hot Gas Facility
[NASA-CR-170889] 24 p4072 N85-35237

RECHARGING
Sixth DOE Electrochemical Contractor's Review. Extended abstracts
[DE84-013679] 16 p2779 N85-27151
Geosynchronous performance of a lithium-titanium disulfide battery 20 p3444 N85-31377
Deep reconditioning of batteries during DSCS 3 flight operations 20 p3446 N85-31397

RECIPROCATING ENGINES
U PISTON ENGINES

RECIPROCATION
Reciprocating magnetic refrigerator employing tandem porous matrices within a reciprocating displacer
[NASA-CASE-NPO-16257-1] 18 p3065 N85-29082

RECIPROCITY THEOREM
FLACS: A new sensitometer for measurement of extreme low intensity reciprocity in a controlled environment — X-ray films 07 p0963 N85-16104

RECIRCULATION
U CIRCULATION

RECIRCULATIVE FLUID FLOW
Characteristics of a turbulent plane offset jet
02 p0196 N85-11310
Momentum and heat transfers in a complex, but well-defined turbulent fluid flow
[DE85-002857] 10 p1486 N85-19381
An experimental investigation of confined, multiple, turbulent jet mixing with recirculation — flow distribution in combustors with injection plates
15 p2555 N85-25784
Confined turbulent swirling recirculating flow predictions
[NASA-CR-174917] 16 p2709 N85-26716
An experimental investigation of confined, multiple, turbulent jet mixing with recirculation
20 p3451 N85-31428
A multilevel-multigrid method for recirculating flows
21 p3583 N85-32271
Modeling of turbulent recirculating combusting flows
22 p3745 N85-33212

RECLAMATION
NT GAS RECOVERY
NT MATERIALS RECOVERY
NT NUCLEAR FUEL REPROCESSING
NT WATER RECLAMATION
Proceedings of the Environmental Systems Symposium (13th) held at Bethesda, Md., 20-22 March 1984
[AD-A148194] 09 p1348 N85-18471

Remedial action of hazardous waste US Army Corps of Engineers, Anniston, Alabama
[AD-P004141] 09 p1347 N85-18477
Practical application of earth resistivity methods in phase 2 of the installation restoration program
[AD-P004148] 09 p1348 N85-18484
Community relations activities at Department of Defense sites
[AD-P004150] 09 p1349 N85-18486
Protocol for aquifer cleanup decision making at military installations
[AD-P004151] 09 p1349 N85-18487
Technology for industrial waste heat recovery by organic Rankine cycle systems
[DE85-006719] 18 p3102 N85-29206
Orphans of the Valley: Abandoned surface mines in the Tennessee Valley. Volume 2: Maps
[DE85-901249] 19 p3301 N85-30465

RECOGNITION
NT CHARACTER RECOGNITION
NT PATTERN RECOGNITION
NT SPEECH RECOGNITION
NT TARGET RECOGNITION
NT TIMBER IDENTIFICATION
Eyelid motion sequences predictive of decision errors
[AD-A145702] 02 p0235 N85-11531
Modeling holographic recognition system by using number-theory convolution transformation
02 p0272 N85-11774
The effect of set size on color recognition
[AD-A150958] 14 p2391 N85-24726

RECOIL IONS
Dynamics and mechanisms of catalytic processes and hot chemistry
[DE85-002699] 09 p1292 N85-18114

RECOMBINATION COEFFICIENT
Ionic reactions of atmospheric importance
[AD-A147354] 07 p0997 N85-16333
Photoconductive pulse power switches: A review
[DE85-014125] 24 p4091 N85-35380

RECOMBINATION REACTIONS
NT ATOMIC RECOMBINATION
NT ELECTRON RECOMBINATION
NT ELECTRON-ION RECOMBINATION
NT HYDROGEN RECOMBINATIONS
NT ION RECOMBINATION
NT OXYGEN RECOMBINATION
NT RADIATIVE RECOMBINATION
Novel transport and recombination processes in semiconductors
[AD-A145869] 03 p0433 N85-12757
Estimate of nuclear-pumped X-ray laser mechanism
06 p0748 N85-14795
Barriers to achieving high efficiency
06 p0829 N85-15264
Study in molecular lasers
[AD-A146246] 08 p1166 N85-17357
Effect of inner subshell ionization for emission lines of OIV ion
09 p1366 N85-18729
Radiation effects in Strained-Layer Superlattice (SLS) structures
[DE85-001713] 09 p1398 N85-18790
Surface and allied studies in silicon solar cells
[NASA-CR-175488] 10 p1508 N85-19516
Development of high efficiency solar cells on silicon web
[NASA-CR-174435] 10 p1509 N85-19521
Electron production, electron attachment, and charge recombination process in high pressure gas discharges
[AD-A149535] 10 p1554 N85-19799
Surface and allied studies in silicon solar cells
[NASA-CR-174447] 11 p1671 N85-20531
Heavy doping effects in high efficiency silicon solar cells
[NASA-CR-175779] 16 p2818 N85-27383
Role and fate of ozone in the atmosphere
16 p2824 N85-27421
Experimental approaches to the measurement of dielectronic recombination
[DE85-006927] 17 p3030 N85-28743
Carrier loss in dispersive transport in amorphous semiconductors
[DE85-009122] 18 p3194 N85-29811
Recombination phenomena in high efficiency silicon solar cells 20 p3479 N85-31618
High efficiency solar cell processing
20 p3482 N85-31640
Measuring bulk recombination rates and boundary recombination velocities 21 p3609 N85-32419
Silicon surface passivation by silicon nitride deposition
21 p3610 N85-32423
Inter-zone auger recombination in GaSb laser structures 21 p3662 N85-32675

RECOMMENDATIONS
Fire protection review revisit no. 2, Argonne National Laboratory, Argonne, Illinois
[DE85-013245] 22 p3755 N85-33276
Current internal-dosimetry practices at US Department of Energy facilities
[DE85-011718] 22 p3787 N85-33466
Recommendations for content revision and alternate delivery modes for the Human Engineering Guide to Equipment Design (HEGED)
[AD-A155761] 24 p4134 N85-35624

RECOMPRESSION
U COMPRESSING

RECONNAISSANCE
NT AERIAL RECONNAISSANCE
NT PHOTORECONNAISSANCE
NT SPECTRAL RECONNAISSANCE
Satellite reconnaissance
[AD-B085034] 01 p0015 N85-10094
Marine helicopter missions 06 p0751 N85-14811
Modern signal processing and reconnaissance — conferences
[FOA-C-30374-E1] 07 p0942 N85-15975
Geothermal assessment of part of the east shore area, Davis and Weber Counties, Utah
[DE84-016817] 09 p1342 N85-18446

RECONNAISSANCE AIRCRAFT
NT MIRAGE AIRCRAFT
NT MIRAGE 3 AIRCRAFT
NT U-2 AIRCRAFT
Airworthiness and flight characteristics test of the RC-12D Guardrail V
[AD-A148046] 08 p1084 N85-16884
Electronic reconnaissance aircraft of the Soviet Union Navy
[AD-A154706] 21 p3551 N85-32091

RECONNAISSANCE SPACECRAFT
A method for determining mesoscale dynamic topography
[AD-D011412] 08 p1191 N85-17506
Target observability for satellite-based sensors
[AD-A156139] 24 p4089 N85-35217

RECONSTRUCTION
NT WAVE FRONT RECONSTRUCTION
Tomographic reconstruction of axially symmetric objects from a single radiograph
[DE84-016783] 04 p0585 N85-13599
Surface reconstruction preserving discontinuities
[AD-A146741] 07 p1026 N85-16526
Flux reconstruction and calibration
09 p1412 N85-18904
Reconstruction of past atmospheric CO/sub 2/ contents from the chemistry of the contemporary ocean: An evaluation
[DE85-008426] 18 p3133 N85-29401

RECORDERS
A limbus-sensing eye movement recorder
[AD-A144772] 01 p0049 N85-10323

RECORDING
NT DATA RECORDING
NT DATA SMOOTHING
NT MAGNETIC RECORDING
NT PHOTOGRAPHIC RECORDING
Low altitude high speed flight simulation using video disc technology
[AD-P004312] 09 p1288 N85-17966
Device for controlling operation of lithicon cathode-ray memory tube 12 p1639 N85-21542
Three-dimensional ballistocardiography in microgravity
20 p3510 N85-31616
Development of wide band recording materials
[AD-A154961] 21 p3589 N85-32309
Design of a freestanding noise measurement and recording system to predict the intensity and location of electromagnetic radiation from earthquakes
[AD-A155070] 21 p3632 N85-32563

RECORDING INSTRUMENTS
NT BATHYTHERMOGRAPHS
NT FLIGHT LOAD RECORDERS
NT OSCILLOGRAPHS
NT PLOTTERS
NT SEISMOGRAPHS
NT WEATHER DATA RECORDERS
Single viewpoint self calibration: A contribution to field calibration of recording chambers
[SER-C-289] 01 p0049 N85-10320
Acoustic scaling: The development of improved instrumentation
[BBC-RD-1985/7] 24 p4145 N85-35694

RECORDS
NT VIDEO DISKS
Primer on the registration of technical information in industry 03 p0438 N85-12786
Chronology of KSC and KSC related events for 1983
[NASA-TM-87435] 12 p1963 N85-22339
Records Disposal: A guidebook for laboratory offices
[AD-A156064] 24 p4165 N85-35823

RECOVERABLE LAUNCH VEHICLES
Winged first stages of space transport appliances
[TUM-RT-TB-84/3] 02 p0167 N85-11125

RECOVERABLE SPACECRAFT
NT APOLLO SPACECRAFT
NT CHALLENGER (ORBITER)
NT COLUMBIA (ORBITER)
NT DISCOVERY (ORBITER)
NT ENTERPRISE (ORBITER)
NT REUSABLE SPACECRAFT
NT SPACE SHUTTLES

RECOVERY
Calibration loading of a strain-gauged diverless helicopter weapon recovery system
[AD-A151486] 15 p2471 N85-25253

RECOVERY PARACHUTES
Structural and mechanical design challenges of space shuttle solid rocket boosters separation and recovery subsystems 08 p1095 N85-16917
B-52B/DTV (Drop Test Vehicle) flight test results: Drop test missions
[NASA-CR-171530] 19 p3215 N85-29934

RECOVERY VEHICLES
Calibration loading of a strain-gauged diverless helicopter weapon recovery system
[AD-A151486] 15 p2471 N85-25253

RECREATION
Combinations of remote sensing data with a digital map data base — regional planning 05 p0660 N85-14240

RECRYSTALLIZATION
Fundamental studies of structure property relationship in transformation toughened ceramics
[DE84-015344] 01 p0033 N85-10204
Time resolved calorimetry of 30 nm Te-films during laser annealing
[AD-A145047] 01 p0052 N85-10346
Electrolytic lapping technique for vanadium
[DE84-014710] 02 p0183 N85-11227
Structural recrystallization in titanium
03 p0351 N85-12258
Material problems for high-temperature, high-power space energy-conversion systems
[AD-A145940] 03 p0385 N85-12466
Amorphous materials and recrystallization
[DE85-001873] 09 p1398 N85-18801
Si-on-insulator formation using a line-source electron beam
[DE85-003449] 11 p1737 N85-20925
Enhanced diffusion from interstitial trapping during solid-phase-epitaxial growth of silicon alloys
[DE85-001285] 12 p1941 N85-22193
Dynamics of recrystallization and redistribution of impurities in semiconductors subjected to millisecond laser pulses 15 p2643 N85-26302
Thin films properties of sputtered niobium silicide on SiO2, Si3N4 and on n+ poly-Si
[AD-A152378] 17 p2952 N85-28228
Influence of recrystallization and solution on the tenacity of the 7010 and 7475 alloys. Oligocyclic fatigue of the 7010 alloy
[ONERA-RT-19/5069-M] 20 p3432 N85-31289
System for electro-optical ceramic recrystallization
21 p3682 N85-32872
Crystallization of Polyetheretherketone (PEEK) in carbon fiber composites
[AD-A156316] 24 p4075 N85-35252

RECTANGLES
An experimental investigation of an underexpanded rectangular jet ejector
[AD-A149856] 12 p1779 N85-21170
Theoretical prediction of stationary positions in the rectangular chamber during asymmetric electroosmotic flow 20 p3499 N85-31750
Acoustical absorption coefficient in a diffuse field of a plane, rectangular material of finite dimensions placed on an infinite perfectly reflecting surface
[NRC/CNR-TT-2113] 23 p3968 N85-34599

RECTANGULAR BEAMS
Quantification of Saint-Venant's principle for a general prismatic member 04 p0467 N85-12972
Improved beam theory for anisotropic materials
04 p0468 N85-12973
Basic studies of multiple free and confined jets
[AD-A149556] 10 p1485 N85-19374

RECTANGULAR COORDINATES
U CARTESIAN COORDINATES

RECTANGULAR DRAINAGE
U DRAINAGE PATTERNS

RECTANGULAR PANELS
Nonlinear dynamic analysis of sandwich panels
01 p0060 N85-10394
Noise transmission loss of a rectangular plate in an infinite baffle
[NASA-TP-2398] 12 p1927 N85-22109

RECTANGULAR PLANFORMS
NT RECTANGULAR PANELS
NT RECTANGULAR PLATES
NT RECTANGULAR WINGS
Aerodynamic improvements by discrete wing tip jets
[AD-A146981] 10 p1421 N85-18964
Basic studies of multiple free and confined jets
[AD-A149556] 10 p1485 N85-19374
An investigation of compressible flows over open cavities including sheer layer thickness effects
[AD-A150066] 12 p1847 N85-21588
RECTANGULAR PLATES
Bulletin of the Faculty of Engineering, Hokkaido University, no. 123
[ISSN-0385-602-X] 04 p0482 N85-13075
Analysis based on Reissner theory for rectangular plates with all edges built-in 04 p0483 N85-13081
A buckling analysis for rectangular orthotropic plates with centrally located cutouts
[NASA-TM-86263] 04 p0513 N85-13288
Biaxial buckling of specially orthotropic, symmetric composite rectangular plates
[AD-A152958] 17 p2979 N85-28417
RECTANGULAR WAVEGUIDES
Multielement bend discontinuities in oversize rectangular waveguides
[PR-200] 03 p0354 N85-12275
Design and construction of a mode converter from rectangular TE 10 to circular TE 11
[REPT-84-158] 05 p0633 N85-14084
Scattering of H10-mode wave by narrow conducting plate inside rectangular waveguide 06 p0788 N85-15038
Magnetostatic-wave propagation in a finite YIG-Loaded rectangular waveguide
[AD-A150332] 13 p2055 N85-22865
Calculation of the propagation constant in a rectangular waveguide containing an inhomogeneous longitudinally magnetized plasma
[DE85-012072] 21 p3577 N85-32250
RECTANGULAR WINGS
On the flow processes in sharply inclined and stalled airfoils in parallel movement and rotation
[NASA-TM-77509] 10 p1419 N85-18952
Transonic pressure distributions on a two-dimensional 0012 and supercritical MBB-A3 profile oscillating in heave and pitch 15 p2457 N85-25173
Gust load alleviation of a cantilevered rectangular elastic wing. Wind tunnel experiment and analysis
[NAK-TR-86] 18 p3063 N85-29950
RECTENNAS
Technology for satellite power conversion
[NASA-CR-174335] 09 p1343 N85-18451
RECTIFICATION
NT GEOMETRIC RECTIFICATION (IMAGERY)
RECTIFIER ANTENNAS
U RECTENNAS
RECTIFIERS
NT AVALANCHE DIODES
NT GERMANIUM DIODES
NT SILICON CONTROLLED RECTIFIERS
NT THYRATRONS
NT THYRISTORS
Planar doped barrier semiconductor device
[AD-D011591] 20 p3537 N85-32010
T/R switch design for short-range measurements, part 6.1A 21 p3624 N85-32515
RECTUM
Weight loss, rectal temperature and heart rates following the 1984 Boston Marathon
[AD-A155984] 24 p4132 N85-35612
RECUPERATORS
U REGENERATORS
RECURSION FORMULAS
U RECURSIVE FUNCTIONS
RECURSIVE FUNCTIONS
Recursive algorithms for adaptive arrays based on estimates
[REPT-5-84] 01 p0107 N85-10718
Nonlinear regression with emphasis on spline methods
[AD-A146192] 03 p0412 N85-12633
A study of the recursion yn+1=yn+tau yn aup m
[CWI-NM-R8403] 05 p0723 N85-14648
Derivation of recursive digital filters by the step-invariant and the ramp-invariant transformations
[AD-A146500] 06 p0857 N85-15452
A note on using the integrated form of ARIMA forecasts
[AD-A146965] 07 p1030 N85-16536
Recursive moment formulas for regenerative simulation
[AD-A150112] 12 p1922 N85-22070
A general simulation program for robot manipulator arm dynamics
[AD-A152121] 16 p2793 N85-27230
Applied Kalman filtering: An overview 17 p2985 N85-28313
Kalman filter modeling 18 p3107 N85-29237
Determinal representations of polynomials satisfying linear Ordinary Differential Equations (ODEs) or linear recurrence relations
[PREPRINT-417] 18 p3172 N85-29660
An introductory view of Raman-Nath type equations
[PREPRINT-422] 18 p3172 N85-29664
The Hamiltonian structure of a complex version of the Burgers hierarchy
[PREPRINT-423] 18 p3173 N85-29665
Exact invariants in resonance form for time-dependent potentials
[DE85-010733] 19 p3348 N85-30739
Fast moving average recursive least mean square fit
[DE85-010036] 19 p3348 N85-30752
Recursive nonlinear filtering through complete linearization
[AD-A155029] 21 p3677 N85-32844
Reliability prediction of the series system with spares subject to Weibull failure 24 p4100 N85-35413
Recursive partitioning estimation 24 p4141 N85-35670
RECYCLING
COST 50 - materials for gas turbines, part 1 and 2 3UK9
[NPL-DMA(A)-74] 05 p0617 N85-13943
The microstructural characteristics of revert superalloys — for turbine blades 05 p0617 N85-13945
Adaptation of remelting procedures for the use of recycled metal in nickel-base superalloy castings
[PNR-90232] 09 p1297 N85-18149
Treatment of wastewater (red water) resulting from TNT (trinitrotoluene) purification
[AD-P004146] 09 p1348 N85-18482
Control of surface composition and hydrogen recycling by plasma conditioning
[DE85-001859] 11 p1731 N85-20889
Exploration of new methods to produce efficient sources of coherent near millimeter wave radiation
[AD-A150094] 12 p1829 N85-21481
Hydrolysis of plastic wastes with the aim of recovering and reprocessing the starting components (recycling)
[BMFT-FB-T-84-250] 12 p1885 N85-21828
The controlled ecological life support system 15 p2966 N85-26603
Recycling agent selection and tentative specification
[AD-A153529] 18 p3070 N85-28968
Current concepts and future directions of CELSS 18 p3155 N85-29532
Survey of CELSS concepts and preliminary research in Japan 18 p3155 N85-29533
Development of processes for the inclusion of radioactive waste in glass-metal compounds and ceramic materials
[BLL-CE-TRANS-8014-(9022.09)] 20 p3526 N85-31931
Neutral pumping rates for a next step tokamak ignition device
[DE85-012780] 24 p4157 N85-35776
RED BLOOD CELLS
U ERYTHROCYTES
RED DWARF STARS
Solar flares and laboratory experiments on magnetic reconnection in current sheaths 02 p0162 N85-11099
Einstein solid state spectrometer observation of the peculiar red dwarf Wolf 630 AB
[NASA-TM-83947] 03 p0447 N85-12843
Evidence for a solar companion star
[DE85-002060] 10 p1571 N85-19907
RED GIANT STARS
NT CARBON STARS
Balloon observations 01 p0014 N85-10086
Spectroscopic data for globular cluster giants. 1: Stars of the red giant tip 01 p0128 N85-10865
Combined ultraviolet studies of astronomical sources
[NASA-CR-174361] 09 p1413 N85-18910
Mass distribution and evolutionary scheme for central stars of planetary nebulae 11 p1751 N85-21012
Energy and Technology Review
[DE85-011767] 21 p3716 N85-33061
RED SEA
A tectonic model of an incipient spreading center and its margins: The Northern Red Sea and the Dead Sea rift 13 p2140 N85-23286
Saudi Arabian refraction profile: Crustal structure of the Red Sea-Arabian Shield transition 17 p2990 N85-28484
Saudi Arabian refraction profile: A preliminary interpretation for the Red Sea-Arabian Shield transition 17 p2991 N85-28485
A traveltime interpretation of the 1978 seismic refraction profile in the Kingdom of Saudi Arabia 17 p2991 N85-28486
Explanation of Russian models: Saudi Arabian seismic refraction profile 17 p2991 N85-28487
Interpretation of the data of USGS seismic refraction profile across the Arabian Shield in western Saudi Arabia 17 p2991 N85-28488
One-dimensional velocity-depth functions determined for the Arabian Shield and the southwestern Red Sea: A comparison of models 17 p2992 N85-28490
A comparison of crustal sections: Arabian Shield to the Red Sea 17 p2992 N85-28491
RED SHIFT
The 3a-F emulsion and the quasar redshift cut-off 07 p0964 N85-16112
The X-ray properties of high-redshift, optically selected QSOs 08 p1240 N85-17821
The UV spectra of intermediate redshift quasars 11 p1746 N85-20980
Evolution of the luminosity function of extragalactic objects
[NASA-CR-175977] 18 p3201 N85-29860
Formation of galaxies
[DE85-009537] 18 p3202 N85-29863
Color evolution in high redshift galaxies 20 p3544 N85-32055
The ultraviolet spectra of intermediate redshift quasars 20 p3544 N85-32056
Some evidence for large gravitational redshift in Seyfert galaxy NGC 4151
[OG-2.7-11] 22 p3872 N85-33984
Ultrahigh energy gamma rays: Carriers of cosmological information
[OG-2.7-14] 22 p3872 N85-33987
REDOX CELLS
Cycling performance of the iron-chromium redox energy storage system
[NASA-TM-87034] 16 p2819 N85-27387
Evaluation of developmental membranes for the mixed reactant iron-chromium redox system
[NASA-TM-87074] 23 p3944 N85-34443
Development of electrodes for the NASA iron/chromium
[NASA-CR-174724] 24 p4109 N85-35471
REDUCED GRAVITY
Second Symposium on Space Industrialization — space commercialization
[NASA-CP-2313] 02 p0149 N85-11011
Potential utilization of glass experiments in space 02 p0151 N85-11020
Preparation of large-particle-size monodisperse latexes in space: The STS-3, STS-4, and STS-7 mission results 02 p0151 N85-11021
Low-gravity solidification of cast iron and space technology applications 02 p0151 N85-11022
Producing gallium arsenide crystals in space 02 p0151 N85-11023
Microgravity containerless processing in long drop tubes 02 p0153 N85-11037
Purification of biomaterials by phase partitioning 02 p0154 N85-11043
Design and implementation of a low-gravity solidification experiment package for the F-104 02 p0156 N85-11053
Gravitational effects on premixed particle cloud flames 02 p0171 N85-11144
Transport phenomena in the boundary layer during solution solidification under microgravity. Ice growth from a water-salt solution
[BMFT-FB-W-84-031] 03 p0329 N85-12121
NBS (National Bureau of Standards): Materials measurements
[NASA-CR-174038] 03 p0332 N85-12143
Large-diameter astromast development
[NASA-CR-171201] 03 p0342 N85-12200
Intraocular fluid dynamics in microgravity 05 p0693 N85-14455
Bone structure and microgravity 05 p0694 N85-14463
Loss of bone substance in consequence of amputation as a model for the adaptation to microgravity 05 p0694 N85-14464
Caloric stimulation of the vestibular system in microgravity 05 p0695 N85-14469
Speculations on the formation of metallic meteorite phases 06 p0869 N85-15648
SPAR X technical report for experiment 76-22 directional solidification of magnetic composites
[NASA-CR-171271] 07 p0927 N85-15880
Commerce lab: Mission analysis and payload integration study
[NASA-CR-174381] 10 p1426 N85-18993
Investigation of surface tension phenomena using the KC-135 aircraft
[NASA-TM-82508] 10 p1426 N85-18995

Modular plant culture systems for life support functions
[NASA-CR-171653] 12 p1899 N85-21924
Investigation of foam flotation and phase partitioning techniques 12 p1945 N85-22216
Material research in microgravity
[NASA-TM-77629] 14 p2228 N85-23611
Thermoregulatory and vestibular systems in the rat 15 p2610 N85-26062
Microgravity: A new tool for basic and applied research in space
[EP-212] 16 p2716 N85-26767
Free-surface phenomena under low- and zero-gravity conditions
[NASA-CR-175885] 17 p2907 N85-27922
Fluid surface behavior in low gravity. Center discretionary fund no. 83-21
[NASA-TP-2486] 17 p2957 N85-28260
ESA presents plans for European manned space station 18 p3085 N85-29087
Spray applicator for spraying coatings and other fluids in space
[NASA-CASE-MSC-18852-1] 18 p3115 N85-29283
Crystallization of aluminum-based alloys in weightlessness 19 p3242 N85-30101
Concept development evaluation for John Deere/UA STS middeck experiment location
[NASA-CR-171541] 20 p3397 N85-31071
Microgravity silicon zoning investigation
[NASA-CR-171531] 20 p3397 N85-31073
On the measurement of material damping in a simulated space environment 20 p3411 N85-31169
Kidney cell electrophoresis
[NASA-CR-171699] 20 p3498 N85-31745
Kidney cell electrophoresis, continuing task 20 p3498 N85-31747
Effects of coating rectangular microscopic electrophoresis chamber with methylcellulose 20 p3498 N85-31748
Asymmetric electroosmotic flow and mobility measurements at nonstationary positions in the rectangular chamber 20 p3499 N85-31749
Evaluation of results of cell electrophoresis experiments on space shuttle STS-3 including pre-flight and post-flight laboratory experiments 20 p3502 N85-31772
Free zone electrophoresis simulation of static column electrophoresis in microgravity on shuttle flight STS-3 20 p3502 N85-31773
Microgravity electrophoresis: A study of the factors that affect free-fluid separation 20 p3502 N85-31774
Properties of electrophoretic fractions of human embryonic kidney cells separated on space shuttle flight STS-8 20 p3503 N85-31776
Evaluation of Results of Space Experiments in Physiology and Medicine and Informal Briefings by the F-16 Medical Working Group 20 p3506 N85-31806
Some results of the European vestibular experiments in the Spacelab-1 mission 20 p3506 N85-31809
Three-dimensional ballistocardiography in microgravity 20 p3510 N85-31818
Study of requirements for and method of multidimensional acoustic imaging — spaceborne experiments
[ESA-CR(P)-2020] 20 p3525 N85-31924
Research study for gel precursors as glass and ceramic starting materials for space processing applications research
[NASA-CR-176113] 22 p3751 N85-33250
NASA Developmental Biology Workshop: A summary
[NASA-TM-86756] 24 p4126 N85-35578
Effects of microgravity and hypergravity on invertebrate development 24 p4126 N85-35579

REDUCED ORDER FILTERS
Synthesis of digital nonrecursive band-elimination filters for moving-target selectors 12 p1840 N85-21545

REDUCTION
Life and reliability modeling of bevel gear reductions
[NASA-TM-87006] 16 p2793 N85-27227

REDUCTION (CHEMISTRY)
NT DEOXIDIZING
NT HYDROGENATION
Surface environmental effects in electrochemical kinetics: Outer-sphere chromium (3) reductions at mercury, gallium, lead, and thallium surfaces
[AD-A146607] 02 p0172 N85-11155
The concept of doping of conducting polymers. The role of reduction potentials
[AD-A146480] 02 p0186 N85-11243
Electrocatalysis of fuel cell reactions: Investigation of alternate electrolytes
[NASA-CR-174783] 02 p0222 N85-11455
Intramolecular electron transfer at metal surfaces. 4: Dependence of tunneling probability upon donor-acceptor separation distance
[AD-A145811] 02 p0267 N85-11876
Stability of several substituted ferrites in a reducing atmosphere
[AD-A146106] 03 p0328 N85-12112
Preparation of low-silicon vanadium metal
[DE84-014818] 04 p0476 N85-13031
Effect of water on hydrogen permeability — Stirling engines
[NASA-TM-86604] 06 p0761 N85-14864
Electrochemical behaviour of TiCl4 solutions in low melting point organic media
[BLL-OA-TRANS-3174-(6196.3)] 06 p0764 N85-14886
Electrolytic deposition of chromium from aqueous chromium solutions containing foreign anions
[BLL-MINTEK-TR-1170-(5810.5759)] 06 p0764 N85-14889
Interaction between chromium oxide and carbon
[BLL-M-36002-(5828.4)] 07 p0926 N85-15867
Kinetics of interaction between carbon and iron oxides of metallized materials in solid phase
[BLL-M-36023-(5828.4)] 07 p0926 N85-15873
Denitrification-efficiencies of alternate carbon sources
[AD-A148029] 08 p1119 N85-17050
Photoelectrochemical reduction of carbon dioxide
[PB85-129054] 11 p1596 N85-20036
Synthesis, static and reactive characterization of supported organometallics
[DE85-004265] 12 p1808 N85-21340
Polymeric electrolytes for ambient temperature lithium batteries
[DE85-001032] 12 p1835 N85-21518
Americium metal preparation on the multigram scale
[DE85-003735] 13 p2024 N85-22683
Temperature, velocity, and species mapping in an induction plasma
[DE85-004005] 15 p2512 N85-25499
Bifunctional oxygen electrodes
[DE85-006871] 17 p2955 N85-28248
Super hydrides
[AD-A153499] 18 p3070 N85-28996
Plutonium metal preparation and purification at Los Alamos, 1964
[DE85-010732] 19 p3239 N85-30085
Carbon reduction of mixtures of MnO(2) and Fe(2)O(3)
[BLL-M-36260-(5828.4)] 20 p3422 N85-31241
Electrochemical reduction of titanium in dimethyl sulphoxide
[BLL-OA-TRANS-3225-(6196.300)] 20 p3429 N85-31267
An analysis of the feasibility of producing silicon for solar cells by a dichlorosilane/fluidized-bed reactor process
[NASA-CR-176036] 20 p3478 N85-31614
Possible roles of manganese redox chemistry in the sulfur cycle 21 p3659 N85-32731
Phototrophic bacteria and their role in the biogeochemical sulfur cycle 21 p3660 N85-32735
Sulfur reduction in sediments of marine and evaporite environments 21 p3661 N85-32742
Cyanobacterial mats: Microanalysis of community metabolism 21 p3661 N85-32743
Microanalysis of dissolved iron and phosphate in pore waters of hypersaline sediment 21 p3661 N85-32744
Electron photoejection in carbanions
[DE85-011748] 23 p3912 N85-34237
Method for preparing high purity vanadium
[DE85-006412] 23 p3913 N85-34242

REDUCTION (MATHEMATICS)
U OPTIMIZATION

REDUNDANCY
Image signals encoding techniques oriented towards the reduction of perceptive redundance
[FUB-23-1983] 01 p0040 N85-10256
A human visual system investigation applicable to image contour coding
[FUB-36-1983] 01 p0095 N85-10840
Optimization of movements of manipulators with kinematic redundancy 04 p0488 N85-13112
Performance enhancements under dual-task conditions 05 p0707 N85-14537
Optimal query processing in distributed data base management systems with data redundancy 05 p0734 N85-14722
Analytical redundancy management mechanization and flight data analysis for the F-8 digital fly-by-wire aircraft flight control sensors
[NASA-CR-170396] 06 p0757 N85-14844
Evolution of shuttle avionics redundancy management/fault tolerance 08 p1090 N85-16890
Shuttle avionics software development trials: Tribulations and successes, the backup flight system 08 p1091 N85-16892
SSME digital control design characteristics 08 p1091 N85-16893
Voice data processing in packet switching modes
[FUB-44-1983] 09 p1312 N85-18248
Analytically redundant output feedback scheme for reduction of structural loads of a flexible transport aircraft
[TT-8303] 12 p1777 N85-21154
Low thrust bipropellant engine/redundant seat valve assembly
[AD-A150293] 13 p2013 N85-22628
A theoretical basis for the analysis of redundant software subject to coincident errors
[NASA-TM-86369] 13 p2145 N85-23317
The kinematic control of redundant manipulators 15 p2566 N85-25836
Some flight test results with redundant digital flight control systems 16 p2712 N85-26739
A modular dissimilar redundant computer designed for high integrity control 16 p2714 N85-26751
A modular dissimilar redundant computer designed for high integrity control 17 p2904 N85-27904
Synchronization and fault-masking in redundant real-time systems
[NASA-TM-87478] 17 p3015 N85-28644
Replication methods for abstract data types
[AD-A153648] 18 p3162 N85-29587
Hexagonal uniformly redundant arrays for coded-aperture imaging
[OG-9.2-1] 21 p3714 N85-33048
Intelligent redundant actuation system requirements and preliminary system design
[NASA-CR-177366] 23 p3896 N85-34136
Hexagonal uniformly redundant arrays for coded-aperture imaging
[OG-9.2-1] 23 p4024 N85-34940

REDUNDANCY ENCODING
Redundancy of codes for detection and correction of unidirectional errors 12 p1842 N85-21557
Adaptation of bit error rate by coding — spacecraft transmissions
[ESA-CR(P)-1970] 15 p2545 N85-25711

REDUNDANT COMPONENTS
Synchronization and fault-masking in redundant real-time systems
[NASA-TM-87478] 17 p3015 N85-28644
Intelligent redundant actuation system requirements and preliminary system design
[NASA-CR-177366] 23 p3896 N85-34136

REDUNDANT STRUCTURES
U REDUNDANT COMPONENTS

REEFS
Diagenesis of niagaran (middle silurian) pinnacle reefs, northwest Michigan 09 p1352 N85-18508
Organogenic structures (submerged reefs) in Silhetian limestone of west Bengal basin 10 p1500 N85-19464

REENTRY
NT HYPERSONIC REENTRY
NT SPACECRAFT REENTRY
NT UNCONTROLLED REENTRY (SPACECRAFT)
Terminal control of gliding in atmosphere 06 p0777 N85-14968
Use of ground radar to detect reentering debris 12 p1784 N85-21200

REENTRY BODIES
U REENTRY VEHICLES

REENTRY EFFECTS
Orbiter entry aerothermodynamics 08 p1104 N85-16978
Correlation of predicted and measured sonic boom characteristics from the reentry of STS-1 orbiter
[NASA-TP-2475] 18 p3177 N85-29694

REENTRY GLIDERS
U LIFTING REENTRY VEHICLES

REENTRY GUIDANCE
Terminal control of gliding in atmosphere 06 p0777 N85-14968
Descent guidance and mission planning for space shuttle 08 p1092 N85-16902
Space shuttle handling qualities 08 p1092 N85-16904

REENTRY SHIELDING
Thermal design of the space shuttle external tank 08 p1103 N85-16977

REENTRY TRAJECTORIES
Natural atmospheric reentry — satellite orbit decay 05 p0600 N85-13829

REENTRY VEHICLES
NT APOLLO SPACECRAFT
NT CHALLENGER (ORBITER)
NT COLUMBIA (ORBITER)
NT DISCOVERY (ORBITER)
NT ENTERPRISE (ORBITER)
NT LIFTING REENTRY VEHICLES
NT REUSABLE SPACECRAFT
Numerical analysis of the 3-dimensional inviscid hypersonic flow around capsule-type bodies by the alternate directional implicit method
[NAL-TR-799] 01 p0002 N85-10012

Minimax optimal control in the reentry of a space glider 02 p0167 N85-11124
Navier-Stokes solution of 3-dimensional hypersonic afterbody flowfields over capsule-type vehicles [NAL-TR-819] 03 p0311 N85-12010
Terminal control of gliding in atmosphere 06 p0777 N85-14968
Evaluation of inviscid/boundary layer and paraboilzed Navier-Stokes solutions for design of reentry vehicles [DE84-014329] 10 p1428 N85-19006
One method of solving the problem of unsteady heat exchange of a body and its ablation 22 p3733 N85-33146
Thermal protection systems for reentry vehicles [CNES-NT-113] 23 p3900 N85-34157

REFERENCE ATMOSPHERES
Model of atmospheric ozone for middle latitudes 02 p0161 N85-11091
Experience with proposed improvements of the International Reference Ionosphere (IRI) [PB84-235670] 05 p0678 N85-14353
Processing methods of rawinsonde measurements at the descent by parachute [KNMI-WR-84-7] 18 p3149 N85-29496

REFERENCE STARS
Desired characteristics of catalogs for cometary astrometry 14 p2436 N85-25030
Obtaining accurate comet positions despite some inaccurate catalog stars 14 p2437 N85-25032
One aspect of determination of direction of space survey base from photographs of planetary surface and star sky 15 p2487 N85-25352

REFERENCE SYSTEMS
Geology and geomorphology of the southern central Blue Ridge: An indexed bibliography [PB84-225119] 01 p0072 N85-10480
Catalogue of earthquakes for the territory of Czechoslovakia for the period 1957 - 1980 [REPT-555] 03 p0376 N85-12396
Use and value of a geodetic reference system [PB84-216167] 03 p0379 N85-12418

REFERENCES (STANDARDS)
U STANDARDS

REFILLING
Propellant tank resupply system [AD-D011268] 05 p0603 N85-13848

REFINING
NT ELECTROSLAG REFINING
Preparation of low-silicon vanadium metal [DE84-014818] 04 p0476 N85-13031
Distribution of oxygen between metal and basic slags [BLL-M-35832-(5828.4)] 05 p0616 N85-13935
Grain refining and microstructural modification during solidification [AD-A147705] 08 p1128 N85-17111
Improved silicon grinding method and apparatus [NASA-CASE-NPO-16338-1-CU] 12 p1819 N85-21407
Materials refining for solar cell silicon 12 p1877 N85-21775
Lead shortage hastens need for improved storage batteries 15 p2461 N85-25195
Jet fuel property changes and their effect on producibility and cost in the U.S., Canada, and Europe [NASA-CR-174840] 16 p2757 N85-27012
Experimental studies of glass refining [NASA-CR-176130] 22 p3751 N85-33248

REFLECTANCE
NT SPECTRAL REFLECTANCE
Biophysical and spectral modeling for crop identification and assessment [E85-10006] 02 p0215 N85-11419
A sphere-scanning radiometer for rapid directional measurements of sky and ground radiance: The PARABOLA field instrument [NASA-TM-86171] 03 p0383 N85-12329
Anglo-German millimeter wave backscatter measurements on snow, environmental data report [REPT-7-84] 04 p0492 N85-13136
Improvement of the accuracy of reflection factor measurements by a computer 05 p0629 N85-14033
Transformation of energy spread of laser pumping via phase conjugation 05 p0725 N85-14661
Nitriding of titanium and its alloys by N2, NH3 or mixtures of N2 + H2 in a dc arc plasma at low pressures (or = to torr) [NASA-TM-83803] 06 p0814 N85-15166
Asteroid-meteorite connection: Regolith effects implied by lunar reflectance spectra 08 p0988 N85-15840
Reflection theorems for some anisotropic media 07 p0953 N85-16038
Determination of parameters of doped thin semiconductor layers from plasmatic minimum of reflection coefficient for infrared radiation 07 p0954 N85-16047
Changes in spectral properties of detached leaves [E85-10042] 07 p0983 N85-16243
The extension of an invertible coniferous forest canopy reflectance model using SIR-B and LANDSAT data 08 p1149 N85-17246
Optical frequency domain reflectometry 08 p1222 N85-17895
Reflectivity measurements of laser gyro mirrors [ESA-TT-851] 09 p1386 N85-18714
Laser rupture of composite materials 10 p1444 N85-19102
Influence of Bragg reflecting lattice groove depth modulation on Rayleigh wave reflection coefficient 10 p1499 N85-19458
Preliminary evaluation of the airborne imaging spectrometer for vegetation analysis [NASA-CR-174440] 10 p1505 N85-19496
Nonlinear saturation of stimulated Raman scattering in homogeneous plasma [DE85-003120] 10 p1560 N85-19837
Radiometric calibration and processing procedure for reflective bands on LANDSAT-4 protoflight Thematic Mapper 11 p1668 N85-20510
Wide-angle flat field telescope [NASA-CASE-GSC-12825-1] 11 p1728 N85-20868
The Jovian Stratosphere in the ultraviolet 11 p1760 N85-21069
LSS 2016: A double-lined spectroscopic binary central star with an extremely large reflection effect [NASA-CR-175503] 11 p1782 N85-21082
In-progress absolute radiometric inflight calibration of the LANDSAT-4 sensors — New Mexico 12 p1870 N85-21733
Investigations of vegetation and soils information contained in LANDSAT Thematic Mapper and Multispectral Scanner data [E85-10082] 12 p1873 N85-21747
Atlas of relectance patterns for uniform earth and cloud surfaces (NIMBUS-7ERB-61 days) [PB85-116362] 12 p1891 N85-21870
A study of low-level laser retinal damage [AD-A150048] 12 p1905 N85-21965
Correctness of reflection characteristics of radio absorbent materials 13 p2081 N85-22995
Zero-crossings on lines of curvature [AD-A150171] 13 p2150 N85-23345
Time-resolved reflectivity measurement of extrinsic silicon during pulsed laser irradiation [AD-A150350] 13 p2159 N85-23403
Surface units on Venus derived from Pioneer-Venus altimetry, roughness, and reflectivity measurements 13 p2177 N85-23510
Unsupervised classification of global radar units on Venus 13 p2198 N85-23632
Scheme for measuring specular reflection coefficient at 10.6 microns wavelength with zigzag-path cell and integrating sphere 14 p2275 N85-24097
Quantitative roughness analysis of treated surfaces with higher-class finish by methods of X-ray reflectometry 14 p2282 N85-24136
Determining characteristics of optical radiation reflectors based on results of remote sensing 15 p2488 N85-25358
Measured performance of a broadband matching section for peripherally fed helical antennas [R-NIAS-25] 15 p2539 N85-25670
Stimulated Brillouin scattering reflectivity in the presence of various aberrators [AD-A151750] 15 p2563 N85-25812
Radar turbulence estimates. Effects of wind shear and reflectivity factor gradients [AD-A151676] 15 p2599 N85-26023
Experimental and theoretical study of the infrared reflectance of thin oxide films on metals [DE85-005799] 15 p2653 N85-26366
Mars: Seasonally variable radar reflectivity 15 p2663 N85-26570
Heliocentric sail problem with variable gravity field reduction 16 p2724 N85-26816
Effects of temperature on remotely sensed mafic mineral absorption features 16 p2809 N85-27323
Technique for measuring the effective source reflection coefficient of 2-resistor power splitters [DE85-009964] 17 p2956 N85-28256
Light scattering by leaf layers with application to canopy reflectance modeling: The Scattering by Arbitrarily Inclined Leaves (SAIL) model [NLR-MP-84011-U] 17 p3038 N85-28796
Diffusely reflecting paints including polytetrafluoroethylene and method of manufacture [NASA-CASE-GSC-12883-1] 18 p3079 N85-29044
Novel analytical approaches to coal beneficiation [DE85-010437] 19 p3229 N85-30021
Separation of Drude and band-to-band spectra in polyvalent metals [DE85-010247] 19 p3240 N85-30093
Spectral reflectances of natural targets for use in remote sensing studies [NASA-RP-1139] 19 p3299 N85-30450
Preliminary investigations concerning a 90 GHz radiometer satellite experiment [ESA-TT-860] 20 p3420 N85-31225
Usefulness of multifrequency MST radar measurements, part 2.6B 21 p3619 N85-32467
Thunderstorm phenomena and weather radar scanning strategies [DOT/FAA/PM-85/14] 21 p3634 N85-32573
A random layer model for reflection from ocean bottom sediments [AD-A155019] 21 p3700 N85-32988
Enhancing precision of remote temperature sensing data from satellites under cloudy atmospheric conditions 22 p3734 N85-33148
Fiber optic moisture sensor [DE85-011651] 22 p3787 N85-33462
Empirical model for the Earth's cosmic ray shadow at 400 KM: Prohibited cosmic ray access [SH-6.1-14] 23 p4046 N85-35087

REFLECTED RADIATION
U REFLECTED WAVES

REFLECTED RAYS
U REFLECTED WAVES

REFLECTED WAVES
Distortions of radio pulse during reflection from maximum region of ionospheric layer 06 p0792 N85-15061
Mathematical modeling of wave fields by superimposition of boundary waves in reflected earthquake waves method 10 p1501 N85-19476
Intensity fluctuations of focused laser beam during reflection in turbulent atmosphere 13 p2078 N85-22975
Reflected wave travel-time curves in stratified media with vertically heterogeneous layers and slightly sloping curved boundaries 13 p2114 N85-23167
Correcting depth line on nonlongitudinal seismic profile 13 p2117 N85-23184
Geological information content of reflected wave record form 14 p2345 N85-24502
Possibility of retrieving dynamics of reflected wave method records beneath low-velocity zone 14 p2346 N85-24503
Mean intensity of wave reflected by wavefront reversing mirror in turbulent medium 22 p3782 N85-33432

REFLECTING TELESCOPES
Observations of four Beta Cephei stars in NGC6231 01 p0128 N85-10677
Error in compensating phase fluctuations of wave field by means of adaptive reflectors with continuous or compound surface 13 p2080 N85-22988
Precision antenna reflector structures 14 p2232 N85-23834
The astrometry programme at Mt. John Observatory 14 p2436 N85-25026
Activities report of the Institute of Astronomy 20 p3545 N85-32059

REFLECTION
NT INFRARED REFLECTION
NT MACH REFLECTION
NT OPTICAL REFLECTION
NT RETROREFLECTION
NT SIGNAL REFLECTION
NT SPECULAR REFLECTION
NT WAVE REFLECTION
Bragg reflection of surface electroacoustic shear waves 04 p0485 N85-13096
Reflection of volume waves in multilayer structures 04 p0485 N85-13097
Coupling of multidirectional diffusions by reflection [CTH-MATH-1984-20] 05 p0719 N85-14613
Radar echo enhancement using surface reflections [AD-A148970] 07 p0939 N85-15955
Filter reflection image guide oscillator and solid state line scanning device [AD-D011440] 10 p1479 N85-19336
Measurement of the configuration of a concave surface by the interference of reflected light [NASA-TM-77796] 11 p1728 N85-20867
Influence of individual reflections on the precision of parameter estimates in least squares refinement [DE85-000830] 11 p1735 N85-20909
Effect of ultraviolet radiation on transparent polymer films as determined using in situ FTIR-RA spectroscopy. Volume 1: Photodegradation of transparent polymer films [DE84-013039] 12 p1814 N85-21377
Near-field effects on radome boresight errors [AD-P004356] 12 p1825 N85-21450
Image lobe analysis for large radomes [AD-P004359] 12 p1825 N85-21453
Wide angle phased array dome lens antenna with a reflection/transmission switch [AD-D011562] 12 p1833 N85-21502

Analysis and computations of microwave-atmospheric interactions
[AD-A149066] 12 p1689 N85-21654
Calculation of ionospheric profiles by inverting VLF/LF reflection data. 2: Anisotropic propagation
[AD-A150105] 12 p1890 N85-21659
Multiple reflection theory for microwave measurement of solid propellant burning rates
13 p2002 N85-22549
Using color to separate reflection components
[AD-A150999] 14 p2405 N85-24628
Characterization of thin films and layered structures using X-ray absorption and reflection at grazing incidence
[DE85-006560] 15 p2662 N85-26429
Use of Goudrian model in studying laws of reflection in vegetation-soil system in optical range. 2: Influence of illumination conditions on spectral brightness coefficients 16 p2726 N85-26627
Energy reflection coefficient for H+ ions at energies between 10 and 80 keV
[DE85-007547] 16 p2883 N85-27682
LIGHT: A ray tracing code to simulate light collection in scintillation spectrometers and light pipes
[DE85-007213] 16 p2885 N85-27673
Selective radiative cooling with MgO and/or LiF layers
[DE85-011595] 19 p3262 N85-30228
Lidar techniques for search and rescue
[DE85-009596] 19 p3278 N85-30327
Attenuated total reflection method for obtaining optical constants of powders
[AD-A154094] 19 p3367 N85-30681
Effect of diffusely-reflected sunlight on the orbit of LAGEOS 20 p3491 N85-31700
Propagation and reflection of a finite amplitude ultrasonic beam including harmonic content: A numeric model
20 p3523 N85-31914
Experimental method for measuring positronium reflection from surfaces
[DE85-010949] 20 p3531 N85-31967
Improved Nominal Operating Cell Temperature (NOCT) test procedure 21 p3612 N85-32449
Mirror reflection of charged particles from +amorphous and polycrystalline surfaces 21 p3690 N85-32927
Dielectric mirror with ferromagnetic substrate
21 p3696 N85-32966
Calculating solar highlight and shadeless areas for scanning photographs from space and optimizing lighting conditions 22 p3736 N85-33160
Surface wave modes of a multilayered medium backed by a perfectly conducting ground plane: Computation of propagation constants
[DE85-011454] 22 p3829 N85-33715
Ranging system which compares an object reflected component of a light beam to a reference component of the light beam
[NASA-CASE-NPO-15865-1] 23 p3973 N85-34629
Radiation measurements on magnesium flames
[BLL-CE-TRANS-5110-(9022.09)]
24 p4075 N85-35254
Literature search for new physical methods for biological aerosol detection
[AD-A155883] 24 p4128 N85-35592

REFLECTION COEFFICIENT
U REFLECTANCE

REFLECTIVITY
U REFLECTANCE

REFLECTOMETERS
NT MICROWAVE REFLECTOMETERS
Influence of geometric conditions on the indicatrix of reflection of the perfect reflecting diffuser
[PTB-OPT-16] 03 p0420 N85-12686
Fundamentals and applications of the six port measuring technique --- reflectometer 05 p0630 N85-14039
A reflectometer unit for a 500 kW HF balanced screened feeder
[BBC-RD-1984/13] 10 p1477 N85-18322
Optical reflectometer for multimode fiber lightpipes
13 p2075 N85-22961
Quantitative roughness analysis of treated surfaces with higher-class finish by methods of X-ray reflectometry
14 p2282 N85-24136

REFLECTOR SATELLITES
U PASSIVE SATELLITES

REFLECTORS
NT FRESNEL REFLECTORS
NT PARABOLIC REFLECTORS
NT PARABOLOID MIRRORS
NT RADAR REFLECTORS
NT RETROREFLECTORS
NT SOLAR COLLECTORS
NT SOLAR REFLECTORS
NT WIGGLER MAGNETS
Research on large, highly accurate, inflatable reflectors
[AD-A145080] 01 p0016 N85-10099
Effect of an underlayer of cadmium telluride on the reflection-reducing properties of zinc sulfide on mercury cadmium telluride
[AD-A148195] 03 p0414 N85-12649
Development of a measuring procedure for the automatic evaluation of the flatness of reflective surfaces
[BMFT-FB-T-84-168] 03 p0421 N85-12668
Dual band, low sidelobe, high efficiency mirror antenna
[AD-D011329] 07 p0944 N85-15980
Optimization of piezoceramic optical deflector
11 p1719 N85-20813
Intensity fluctuations of focused laser beam during reflection in turbulent atmosphere
13 p2078 N85-22975
Error in compensating phase fluctuations of wave field by means of adaptive reflectors with continuous or compound surface 13 p2080 N85-22986
Innovative research in the design and operation of large telescopes for space: Aspects of giant telescopes in space
[NASA-CR-175626] 13 p2170 N85-23462
Cable-catenary large antenna concept
14 p2231 N85-23829
Precision space structures 14 p2232 N85-23833
Application of modern Aperture Integration (AI) and Geometrical Theory of Diffraction (GTD) techniques for analysis of large reflector antennas
14 p2234 N85-23851
Feed system design considerations for large space antenna systems. Part 1: Multiple apertures with non-overlapping feeds 14 p2234 N85-23852
Diffraction analysis of mesh deployable reflector antennas 14 p2235 N85-23854
Utilization of space station by the large deployment reflector 14 p2235 N85-23857
Large Deployable Reflector (LDR) requirements for space station accommodations
14 p2236 N85-23858
Angular error of position of RATAN-600 screens during radial displacement 15 p2476 N85-25286
Null generation using discs on a reflector
[AD-A151897] 15 p2544 N85-25703
Defocusing losses in a log periodic-fed reflector
[AD-A151616] 15 p2547 N85-25722
The weighting function for scintillation on a folded path
[AD-A152658] 17 p2949 N85-28206
Echo-response from crack-like two-dimensional reflectors in focused ultrasonic fields
17 p3027 N85-28724
Submillimeter local oscillators for spaceborne heterodyne applications
[NASA-RP-1147] 19 p3226 N85-30005
Measurements of folded path optical scintillation using a corner cube, a cat's eye and a flat mirror reflector
[AD-A154044] 19 p3367 N85-30879
Method of constructing folding umbrella-type antenna
22 p3774 N85-33386
Hoop/column antenna deployment mechanism overview 22 p3796 N85-33514
Optical receivers using rough reflectors
[NASA-CR-176200] 24 p4154 N85-35750

REFLEXES
NT VESTIBULAR NYSTAGMUS
Biological investigations of adaptive networks. Neuronal control of conditioned responding
[AD-A150959] 14 p2365 N85-24695
Test and evaluation of the 2.4-micron photorefractor ocular screening system
[NASA-TM-86492] 15 p2615 N85-26115

REFRACTED RADIATION
U REFRACTED WAVES

REFRACTED RAYS
U REFRACTED WAVES

REFRACTED WAVES
Structure of temperature field based on observations of refraction from high meteorological mast
06 p0619 N85-15199
Influence of refraction effects on informativeness of bistatic acoustical atmospheric sounding systems
06 p0625 N85-15237
Interpreting refracted waves method data on basis of automated determination of seismic drift
14 p2343 N85-24486
Saudi Arabian refraction profile: A preliminary interpretation for the Red Sea-Arabian Shield transition
17 p2991 N85-28485
A traveltime interpretation of the 1978 seismic refraction profile in the Kingdom of Saudi Arabia
17 p2991 N85-28486
Explanation of Russian models: Saudi Arabian seismic refraction profile 17 p2991 N85-28487
Interpretation of the data of USGS seismic refraction profile across the Arabian Shield in western Saudi Arabia 17 p2991 N85-28488
A preliminary analysis of the Saudi Arabian deep seismic sounding data 17 p2991 N85-28489
One-dimensional velocity-depth functions determined for the Arabian Shield and the southwestern Red Sea: A comparison of models 17 p2992 N85-28490
A theoretical study of electron capture in ion-ion and ion-atom collisions
[DE85-011154] 19 p3382 N85-30842

REFRACTING TELESCOPES
Saturn rings: Divisions, gaps and ringlets from ground-based telescopes 15 p2672 N85-26485
Stokes parameters modulator for birefringent filters
18 p3205 N85-29884

REFRACTION
NT ATMOSPHERIC REFRACTION
NT BIREFRINGENCE
NT RADIO WAVE REFRACTION
Hole shots along refraction profile R4/78 recorded at the temporary seismic station near Stary Plzenec (west Bohemia)
[REPT-549] 03 p0375 N85-12392
Design and testing of a refractive laser beam homogenizer
[AD-A146997] 07 p0970 N85-16162
Acoustic energy exchange in sheared mean flows — solid rocket motors 13 p1999 N85-22534
Reflected wave travel-time curves in stratified media with vertically heterogeneous layers and slightly sloping curved boundaries 13 p2114 N85-23167
Test and evaluation of the 2.4-micron photorefractor ocular screening system
[NASA-TM-86492] 15 p2615 N85-26115
Inversion of Rayleigh wave group velocities from high-explosive tests
[AD-A152172] 16 p2783 N85-27175
Astrometric method advances Astronomy, geodesy
16 p2908 N85-27306
High precision materials characterization in the near millimeter wave-length range
[AD-A153267] 17 p2968 N85-28331
Journal of Research of the National Bureau of Standards, volume 90, number 1, January - February 1985
[PB85-179063] 20 p3522 N85-31908
The effects of subrefractive layers and elevated ducts on airborne radar and ESM (Electronic Surveillance Measures)
[AD-A155524] 21 p3637 N85-32592
Refraction of narrow probing light beam in multilayer optical fiber 22 p3764 N85-33330
Crustal structure in southern California from array data
24 p4115 N85-35512

REFRACTIVE INDEX
U REFRACTIVITY

REFRACTIVITY
Compound class quantitation of JP-5 jet fuels by high performance liquid chromatography-differential refractive index detection
[AD-A145754] 03 p0340 N85-12165
Refractive index of ternary and quaternary compound semiconductors below the fundamental absorption edge: Linear and nonlinear effects
[DE84-012325] 05 p0640 N85-14105
C2 sub n (optical) studies in the free atmosphere based on rawinsonde data
[AD-A147307] 07 p0997 N85-16332
Thermosonde C2N measurements in Hawaii--August 1982
[AD-A148016] 08 p1189 N85-17489
Quantitative determination of compound classes in jet turbine fuels by high performance liquid Chromatography/Differential refractive index detection: Part 2
[AD-A149298] 11 p1613 N85-20144
Optical guiding in a free electron laser
[DE85-003141] 11 p1639 N85-20327
Photorefractor ocular screening system
[NASA-CASE-MFS-26011-1SB]
11 p1692 N85-20639
Imaging apparatus for transverse electrode electro-optic tunable filter
[AD-D011524] 12 p1832 N85-21497
Multifunctional elements for integrated optics
13 p2068 N85-22918
Dispersion characteristics of small-mode gradient optical fibers 13 p2082 N85-23004
Possibility of determining atmospheric weather parameters by radio and radiooptical measurements of refraction of cosmic sources 13 p2110 N85-23146
Nonuniform interference coatings with thickness-dependent refractive index
14 p2281 N85-24131
Scattering properties of a moving dielectric object
[AD-A151974] 15 p2544 N85-25706

Sound propagation through directional internal wave fields
[AD-A151166] 15 p2646 N85-26321
Design of a variable-focal-length optical system
[NASA-CR-175710] 15 p2651 N85-26349
Impurity studies
[DE85-006235] 15 p2661 N85-26423
The problem of atmospheric turbulence
[NASA-CR-175783] 16 p2832 N85-27464
LIGHT: A ray tracing code to simulate light collection in scintillation spectrometers and light pipes
[DE85-007213] 16 p2865 N85-27673
Proceedings of the 1980 Workshop of the International Association of Seismology and Physics of the Earth's Interior on the Seismic Modeling of Laterally Varying Structures: Contributions based on data from the 1978 Saudi Arabian refraction profile
[GS-CIRC-937] 17 p2989 N85-28476
A crustal section for the Arabian Shield and adjacent Red Sea margin derived from first-arrival data
17 p2990 N85-28480
A seismic refraction profile across the Arabian Shield
17 p2990 N85-28481
A preliminary examination of the 1978 refraction profiles in Saudi Arabia
17 p2990 N85-28482
An assessment of atmospheric refractivity in the northern marginal ice zone
[AD-A152346] 17 p2992 N85-28493
Optical waveguide characterization using grating couplers
[AD-A153063] 17 p3037 N85-28789
Optical modulators and bistable devices using molecular gases
18 p3186 N85-29761
An experimental nonlinear optical waveguide device
18 p3186 N85-29762
Design consideration for the X-ray Cerenkov experiment
[AD-A153636] 18 p3189 N85-29777
Radio wave scattering and intermittency of turbulence in the atmosphere
19 p3286 N85-30392
Radio wave scattering and turbulence intermittence in atmosphere
19 p3298 N85-30446
Haze over eastern North America. Part 1: Haze properties
[PB85-181857] 19 p3311 N85-30526
A comparison of electronic heterodyne moire deflectometry and electronic heterodyne holographic interferometry for flow measurements
[NASA-TM-87071] 21 p3588 N85-32302
Some recent developments in the interpretation of MST radar returns from clear air (keynote paper), part 2
21 p3618 N85-32480
Morphology of the scattering targets: Fresnel and turbulent mechanisms, part 2.1A
21 p3618 N85-32481
A modified Fresnel scattering model for the parameterization of Fresnel returns, part 2.3A
21 p3618 N85-32483
Observations of mesospheric turbulence by rocket probe and VHF radar, part 2.4A
21 p3619 N85-32484
Interpretation of radar returns from the mesosphere, part 2.3A
21 p3619 N85-32485
Usefulness of multifrequency MST radar measurements, part 2.6B
21 p3619 N85-32487
Variation of the submicron aerosol structure
21 p3647 N85-32661
Beam diffusion in linear ionospheric layer
21 p3695 N85-32958
Transmission of light by disperse medium of densely packed optically soft particles
21 p3697 N85-32969
Refraction of narrow probing light beam in multilayer optical fiber
22 p3764 N85-33330
Temperature sensitivity of fiber-optic transmission line
22 p3764 N85-33331
Refractive indices and thermo-optic coefficients of nonlinear crystals isomorphic to KH2PO4
[DE85-012966] 22 p3847 N85-33831
The use of a laser Doppler velocimeter in a standard flammability tube
[NASA-CR-174980] 24 p4096 N85-35389

REFRACTORY COATINGS
Corrosion study on zirconium refractory coatings. 1: Oxidation of zirconium nitride coatings by oxygen
[BLL-RISLEY-TR-5044-(9001.9F)]
07 p0925 N85-15857
Thermal barrier coating system
[NASA-CASE-LEW-13324-2] 12 p1796 N85-21266

REFRACTORY MATERIALS
NT CHROMIUM
NT CHROMIUM ISOTOPES
NT IRIDIUM
NT MOLYBDENUM
NT MOLYBDENUM ALLOYS
NT NIOBIUM
NT NIOBIUM ALLOYS
NT OSMIUM
NT OSMIUM ISOTOPES
NT REFRACTORY METAL ALLOYS
NT REFRACTORY METALS
NT RENE 95
NT RHENIUM
NT RHENIUM ALLOYS
NT TANTALUM
NT TANTALUM ALLOYS
NT TUNGSTEN
NT TUNGSTEN ALLOYS
USSR report: Materials science and metallurgy, no. 93
[JPRS-84810] 01 p0018 N85-10110
Silicon nitride powder
[NASA-TM-77731] 01 p0022 N85-10132
Milling of Si3N4 with Si3N4 hardware
[NASA-TM-86864] 01 p0031 N85-10191
Resistance of Navy shipboard outerwear garments and fire-resistant fabrics to extreme heat
[AD-A145414] 02 p0236 N85-11546
New coatings for high temperature materials protection
[AERE-R-11387] 03 p0339 N85-12180
Improved apparatus and techniques for high temperature and pressure deformation of crystalline materials
[DE84-016049] 04 p0569 N85-13629
Modelling of deformation and fracture in high-temperature structural materials
[DE84-016906] 06 p0818 N85-15191
A program to develop thermite reactions to produce refractory borides and carbides
[AD-A149972] 10 p1434 N85-19037
Nonlinear analysis for high-temperature multilayered fiber composite structures — turbine blades
[NASA-TM-83754] 12 p1797 N85-21273
Viscoplastic constitutive relationships with dependence on thermomechanical history
[NASA-CR-174836] 12 p1864 N85-21891
Experimental study of enthalpy of quasimonocrystal of graphite and carbon glass in temperature range of 2690-3818 deg K
13 p2036 N85-22751
Optimizing hot workability and controlling microstructures in difficult to process high strength and high temperature materials
[AD-D011586] 15 p2510 N85-25482
Refractory inclusions in the Ornans C30 chondrite
15 p2680 N85-26553
Method of fabricating material for the electrodes of gas discharge devices
[DE85-007452] 16 p2780 N85-27157
High temperature fracture mechanics of silicon nitride
[BMFT-FB-T-84-285] 17 p2961 N85-28433
Convoluted nozzle design for the RL10 derivative 2B engine
[NASA-CR-174953] 19 p3220 N85-29965
Thermo-mechanical and thermal behavior of high-temperature structural materials
[AD-A154154] 19 p3286 N85-30251
Thermodynamics of high temperature materials
[AD-A154269] 19 p3378 N85-30958
Short term determination of the creep properties of high temperature materials
[CRIF-MT-160] 20 p3432 N85-31288
Welding methods for high melting metals
22 p3794 N85-33508
Thermal protection systems for reentry vehicles
[CNES-NT-113] 23 p3900 N85-34157

REFRACTORY METAL ALLOYS
NT MOLYBDENUM ALLOYS
NT NIOBIUM ALLOYS
NT RHENIUM ALLOYS
NT TANTALUM ALLOYS
NT TUNGSTEN ALLOYS
Superpure materials research planned
03 p0353 N85-12270
Review: Role of refractory metal alloys in fusion reactor applications
[AERE-R-11317] 03 p0422 N85-12695
Effect of stress concentration fatigue resistance of refractory nickel alloys under asymmetrical multicycle loading, communication 1
11 p1604 N85-20086
Obtaining amorphous coatings of FeW and Fe-Cr-P-B alloys using laser sputtering
[BLL-BISI-22493-(9022.09)] 17 p2927 N85-28057
Load-carrying capabilities of refractory alloys for space reactor power applications
[DE85-010566] 19 p3240 N85-30057

REFRACTORY METALS
NT CHROMIUM
NT CHROMIUM ISOTOPES
NT IRIDIUM
NT MOLYBDENUM
NT NIOBIUM
NT OSMIUM
NT OSMIUM ISOTOPES
NT RHENIUM
NT TANTALUM
NT TUNGSTEN
Material problems for high-temperature, high-power space energy-conversion systems
[AD-A145940] 03 p0385 N85-12466
Electronic transport processes in refractory metal silicides
[AD-A146495] 06 p0861 N85-15468
Method for making alloy additions to base metals having higher melting points
[AD-D011403] 07 p0928 N85-15884
Studies of silicon-refractory metal interfaces: Photoemission study of interface formation and compound nucleation
[AD-A150075] 12 p1800 N85-21293
Update of thermal conductivity and electrical resistivity of electrolytic iron, tungsten and stainless steel
[PB85-115814] 12 p1803 N85-21311
An investigation of the irradiation swelling mechanisms in refractory metals at high temperatures
[AD-A154149] 19 p3238 N85-30079
Thermodynamics of high temperature materials
[AD-A154269] 19 p3378 N85-30958

REFRACTORY PERIOD
Relaxation lens in inhomogeneous binary mixture
21 p3695 N85-32957

REFRASIL (TRADEMARK)
U FIBERS
U SILICON DIOXIDE

REFRIGERANTS
Investigation of an ejector heat pump by analytical methods
[DE84-016675] 04 p0500 N85-13189
DOE/ORNL electric systems program overview
[DE85-003334] 10 p1459 N85-19197
Optimization of a ground coupled heat pump
[DE85-000273] 10 p1486 N85-19380
Determination of properties of zeolite/refrigerant combinations for solar refrigeration systems
[DE85-012009] 23 p3945 N85-34448

REFRIGERATING
Hybrid system for producing and storing ice
[DE84-017474] 09 p1304 N85-18195
Magnetic refrigeration and heat pumping design options
[DE85-003405] 13 p2092 N85-23064
Evaluation study of mechanical refrigeration systems for application to space missions — infrared astronomy
[SNIAS-1029ACA/LL/V] 22 p3755 N85-33277
Heat-mass flow enhancement system for a metal hydride assembly
[DE85-010098] 22 p3783 N85-33441
Refrigerated dynamic seal to 6.9 MPa (1000 psi)
[NASA-TM-87108] 23 p3930 N85-34356

REFRIGERATING MACHINERY
NT REFRIGERATORS
Magentically actuated compressor
[NASA-CASE-GSC-12799-1] 12 p1818 N85-21404
Testing and further development of a solar absorption cooling plant
[BMFT-FB-T-84-264] 15 p2586 N85-25954

REFRIGERATORS
Selection of regenerator geometry for magnetic refrigerator applications
[DE84-012637] 11 p1616 N85-20160
Gas-fired duplex free-piston Stirling refrigerator
12 p1819 N85-21413
Reciprocating magnetic refrigerator employing tandem porous matrices within a reciprocating displacer
[NASA-CASE-NPO-16257-1] 18 p3085 N85-29082
Ten degree Kelvin hydride refrigerator
[NASA-CASE-NPO-16393-1-CU]
18 p3085 N85-29084
Welding of steel-aluminum cooling panels for the holds of refrigerator vessels
19 p3246 N85-30129
Intrinsically irreversible acoustic heat engines
[DE85-007672] 19 p3270 N85-30278
Combined cold compressor/ejector helium refrigerator
[DE85-006408] 23 p3925 N85-34326

REFUELING
NT AIR TO AIR REFUELING
Orbit of Salyut-7 station boosted
02 p0157 N85-11067
Salyut-7 crew in orbit 150 days
02 p0157 N85-11068
Propellant tank resupply system
[AD-D011288] 05 p0603 N85-13848
Propellant transfer: Tethered depot
08 p1108 N85-17006
Safety recommendation(s), A-84-103
[REPT-3009B/101B] 14 p2216 N85-23745
Inspection evaluation and repair of the flawed feedwater nozzle of the 50 MWe Dodewaard GKN boiling water reactor
[ISBN-90-353-0017-3] 17 p2977 N85-28394

NASA space station automation: AI-based technology review. Executive summary
[NASA-CR-176096] 21 p3558 N85-32135
REGENERATION (ENGINEERING)
Recursive moment formulas for regenerative simulation
[AD-A150112] 12 p1922 N85-22070
In-orbit laser regeneration of the radiation damaged solar arrays 13 p2008 N85-22588
Regenerative stochastic Petri nets
[AD-A150343] 13 p2151 N85-23355
Regenerative simulation of non-Markovian stochastic systems
[AD-A150944] 13 p2153 N85-23367
Space shuttle revitalization system 18 p3157 N85-29548
Composite desiccant structure
[DE85-006400] 23 p3910 N85-34226
REGENERATION (PHYSIOLOGY)
Problems associated with the utilization of algae in bioregenerative life support systems
[NASA-CR-166615] 07 p1019 N85-16469
Feasibility of producing a range of food products from a limited range of undifferentiated major food components
[NASA-CR-177329] 07 p1020 N85-16473
Current concepts and future directions of CELSS 18 p3155 N85-29532
Survey of CELSS concepts and preliminary research in Japan 18 p3155 N85-29533
Advanced regenerative environmental control and life support systems: Air and water regeneration 18 p3155 N85-29535
Atmosphere behavior in gas-closed mouse-algal systems: An experimental and modelling study 18 p3155 N85-29536
Dynamic considerations for control of closed life support systems 18 p3155 N85-29537
CELSS transportation analysis 18 p3156 N85-29538
Composition and dynamics of bacteriocenosis associated with algae in human life-support systems 22 p3823 N85-33684
Experimental validation of allowable concentrations of sodium and potassium in recycled drinking water 22 p3823 N85-33685
REGENERATIVE CYCLES
U REGENERATION (ENGINEERING)
REGENERATIVE FUEL CELLS
Regenerative fuel cell energy storage system for a low Earth orbit space station
[NASA-CR-174802] 04 p0527 N85-13371
Electrochemistry and storage panel report 05 p0611 N85-13903
Investigation of bromine complexed hydrogen/bromine regenerative fuel cells for portable electric power
[AD-A146401] 06 p0833 N85-15300
Engineering model system study for a regenerative fuel cell: Study report
[NASA-CR-174801] 07 p0991 N85-16292
Develop and test fuel cell powered on-site integrated total energy systems. Phase 3: Full-scale power plant development
[NASA-CR-168338] 19 p3304 N85-30483
Regenerative fuel cell systems for space station 20 p3443 N85-31372
System level electrochemical principles 20 p3443 N85-31375
REGENERATORS
NT THERMOSIPHONS
Preliminary mechanical redesign of an existing gas-turbine engine to incorporate a high-efficiency, low-pressure-ratio, highly regenerative cycle for marine applications
[AD-A144806] 01 p0011 N85-10070
Selecting the proper ceramic material for a regenerator experiencing large temperature gradients
[AD-A144796] 01 p0032 N85-10199
Regenerators of binary pulses for optical communication systems 04 p0485 N85-13099
Selection of regenerator geometry for magnetic refrigerator applications
[DE84-012637] 11 p1616 N85-20160
REGGE POLES
Is the inelastic charge-exchange contribution constant at the large X and superhigh energies? Caut 01Kuchin, I. A. 24 p4173 N85-35871
REGIONAL PLANNING
NT URBAN PLANNING
Combinations of remote sensing data with a digital map data base — regional planning 05 p0860 N85-14240
Climate Conference for Latin America and the Caribbean
[WMO-632] 07 p1000 N85-16352
Climate applications: General 07 p1001 N85-16355
The challenge of food production: The importance of climate 07 p1001 N85-16361
The management of atmospheric resources in food production 07 p1002 N85-16362
Requirements for training in climate-related subjects 07 p1004 N85-16378
Applied climatology — regional planning 18 p3147 N85-29486
REGIONS
NT AMAZON REGION (SOUTH AMERICA)
NT ANTARCTIC REGIONS
NT ARCTIC REGIONS
NT AURORAL ZONES
NT BRILLOUIN ZONES
NT CENTRAL ATLANTIC REGION (US)
NT D REGION
NT E REGION
NT EQUATORIAL REGIONS
NT F REGION
NT FRESNEL REGION
NT HABITATS
NT INTERTROPICAL CONVERGENT ZONES
NT M REGION
NT NEW ENGLAND (US)
NT NULL ZONES
NT PACIFIC NORTHWEST (US)
NT POLAR REGIONS
NT REMOTE REGIONS
NT ROSS ICE SHELF
NT SOUTHERN CALIFORNIA
NT SUBARCTIC REGIONS
NT TEMPERATE REGIONS
NT TROPICAL REGIONS
Simple mesoscale models for operational use in regions of topographic and thermal forcing: Development and evaluation
[AD-A146667] 06 p0839 N85-15325
Modeling longitudinal motions of thermal O+ and H+ ions in magnetic field tube convective through daytime polar cusp 15 p2481 N85-25314
Annual cycle. Part 2: The annual variation of precipitation over the United States and Canada
[PB85-147684] 15 p2600 N85-26027
Discovery in earthquake forecasting and seismic zoning recorded 19 p3295 N85-30425
A new approach to linear quadtrees 23 p3961 N85-34550
An analysis and algorithm for filling propagation 23 p3961 N85-34551
REGISTERS (COMPUTERS)
Siemens introduces fast computer with pipeline architecture 11 p1618 N85-20178
Interprocess communication
[AD-A156337] 24 p4088 N85-35337
REGOLITH
Physical and mechanical properties of lunar soil as function of specifics of relief and processes in vicinity of operation of Lunokhod-2 02 p0161 N85-11090
Megaregolith thickness, heat flow, and the bulk composition of the Moon 04 p0583 N85-13723
Grainsize evolution and differential comminution in an experimental regolith 06 p0888 N85-15838
Asteroid-meteorite connection: Regolith effects implied by lunar reflectance spectra 06 p0888 N85-15840
Progress on Experimental Impact studies 13 p2181 N85-23534
Multispectral analysis of the Kasei Valle-Lanae Planum region of Mars 13 p2193 N85-23607
Investigation of the daytime lunar atmosphere
[NASA-CR-175836] 14 p2440 N85-25057
Earth's primordial differentiation, and its after-effects 21 p3722 N85-33092
Interpretation of photometric measurements of airless bodies 22 p3855 N85-33871
REGRESSION (STATISTICS)
U REGRESSION ANALYSIS
REGRESSION ANALYSIS
NT REGRESSION COEFFICIENTS
The effects of seven alloying elements on the microstructure and stress-rupture behavior of nickle-base superalloys
[NASA-TM-83791] 01 p0027 N85-10166
Statistical tropical cyclone forecasting techniques for the Southern Hemisphere
[AD-A144752] 01 p0085 N85-10569
A combined logistic regression and Zionts-Wallenius methodology for multiple criteria linear programming
[TWISK-314] 01 p0102 N85-10679
Location of several outliers in multiple regression data using elemental data
[CSIR-TWISK-300] 01 p0108 N85-10724
The information in the minor principal components
[CSIR-TWISK-320] 01 p0109 N85-10735
Statistical analysis of 11-year and 80-year solar cycles 02 p0161 N85-11095
Life distribution properties of devices subject to deterioration
[AD-A145554] 02 p0206 N85-11358
Description of a data matrix structure and model diagnosis by means of row and column Euclidean maps 02 p0211 N85-11392
Limit theory for the sample covariance and correlation functions of moving averages
[AD-A145488] 02 p0251 N85-11642
Auto-regressive moving average spectral estimation using modified and least squares modified Yule-Walker estimates
[AD-A145516] 02 p0254 N85-11663
An asymptotic theory for logistic regression when some predictors are measured with error
[AD-A145673] 02 p0254 N85-11666
Least squares estimation of conditionally heteroscedastic autoregressions
[AD-A145994] 03 p0411 N85-12626
An introduction to fuzzy regression analysis with a ballistic application
[AD-A146093] 03 p0411 N85-12629
Nonlinear regression with emphasis on spline methods
[AD-A146192] 03 p0412 N85-12633
Users manual for BRGLM: Interactive general linear model regression, version 3
[DE84-017386] 04 p0550 N85-13501
Least squares spline regression with block-diagonal variance matrices
[NPL-DITC-40/84] 04 p0554 N85-13523
Development of structured regression hypotheses/interactive descriptive geometry through five dimensions
[INT-324] 04 p0554 N85-13524
Parametric estimates of propulsion system maintenance manhours
[AD-A147120] 07 p0694 N85-15662
Exploring the use of structural models to improve remote sensing agricultural estimates 07 p0985 N85-16259
Calibration or inverse regression: Which is appropriate for crop surveys using LANDSAT data? 07 p0985 N85-16260
Experiments in forecasting atmospheric marine horizontal visibility using model output statistics with conditional probabilities of discretized parameters
[AD-A147574] 07 p1008 N85-16404
Some scientific subroutines in LISP
[AD-A147869] 07 p1026 N85-16515
Estimation for a semimartingale regression model using the method of sieves
[AD-A146809] 07 p1028 N85-16527
Conditional regression models for transient state survival analysis
[AD-A147872] 07 p1034 N85-16563
Generalized additive models
[AD-A147454] 07 p1036 N85-16573
Infinite order autoregressive representations of multivariate stationary stochastic processes
[AD-A147863] 07 p1036 N85-16580
Completely monotone regression estimates of software failure rates
[NASA-CR-174319] 08 p1204 N85-17575
The EM algorithm for censored data
[AD-A148136] 08 p1212 N85-17626
A power transformation exponential regression model for censored failure time data
[AD-A148377] 08 p1212 N85-17632
Multivariable Autoregressive Moving Average (ARMA) models: A time approach to antenna processing
[ENST-84E015] 09 p1313 N85-18252
Estimation of variance of the regression estimator
[AD-A149407] 10 p1551 N85-19780
The likelihood displacement: A unifying principle for influence measures
[AD-A149456] 10 p1551 N85-19783
Statistical analysis of autoregressive spectral estimates for noise corrupted autoregressive series
[AD-A149543] 11 p1708 N85-20747
A note on some simple influence diagnostics in accelerated life testing
[AD-A149593] 12 p1862 N85-21677
Analysis of selective chopper radiometer data
[NASA-CR-175157] 12 p1895 N85-21894
Ordinary and proper location M-estimates for ARMA models, revised
[AD-A149705] 12 p1920 N85-22081
Inference for censored matched pairs using signed ranks
[MATHEMATICS-RESEARCH-162] 12 p1923 N85-22078
Proportional odds models for survival data and estimates using ranks
[MATHEMATICS-RESEARCH-172] 12 p1923 N85-22080
Pulsars and interstellar medium 12 p1960 N85-22320

Expansion of functions describing planetary surface and gravity field 13 p1978 N85-22410
Approaches and algorithms for robust signal processing 13 p2062 N85-22878
Ozone Correlative Measurements Workshop [NASA-CP-2362] 13 p2105 N85-23112
Measurement requirements for the detection of ozone trends 13 p2105 N85-23115
Consistency of smoothing with running linear fits [AD-A150232] 13 p2150 N85-23349
A model for large sparse contingency tables [AD-A150320] 13 p2151 N85-23350
A note about the strong convergence of the nonparametric estimation of a regression function [AD-A150325] 13 p2151 N85-23353
Determining optimum service conditions for concentrator mirrors by methods of mathematically planned experiment 14 p2274 N85-24090
Classification and multiple regression through projection pursuit [AD-A150797] 14 p2411 N85-24867
Thermal traction contact performance evaluation under fully flooded and starved conditions [NASA-CR-168173] 15 p2588 N85-25848
Statistical analysis techniques for small sample sizes [NASA-CR-171872] 15 p2639 N85-26279
Statistical regularization methods in problem of navigational determination of space vehicle orbits 16 p2719 N85-26784
Multiple regression analysis of photographic image of soil properties 16 p2726 N85-26825
An interactive computer package for use with simulation models which performs multidimensional sensitivity analysis by employing the techniques of response surface methodology [AD-A151956] 16 p2846 N85-27548
Some new estimation methods for weighted regression when there are possible outliers [AD-A152104] 16 p2854 N85-27602
Locally-weighted-regression scatter-plot smoothing (LOWESS): A graphical exploratory data analysis technique [AD-A152239] 16 p2855 N85-27609
An evaluation of discretized conditional probability and linear regression threshold techniques in model output statistics forecasting of visibility over the north Atlantic Ocean [AD-A151955] 16 p2857 N85-27619
Local likelihood estimation [DE85-007236] 16 p2857 N85-27620
Surveillance report. Stage 1: Dissected motors-propellants motor number 0012199, phase 15 [AD-A153206] 17 p2916 N85-27973
MM2 LRSLA testing stage 3 propellant [AD-A152540] 17 p2937 N85-28128
The measurement of linear frequency drift in oscillators 17 p2966 N85-28316
Robust regression through robust covariances [AD-A153301] 17 p3020 N85-28677
Fuzzy hierarchical analysis [DE85-008149] 17 p3021 N85-28685
A multiple regression technique for detecting outliers [REPT-84-33] 17 p3025 N85-28706
Fixed width interval estimation in linear regression [AD-A153633] 18 p3174 N85-29875
An experimental investigation of fuel regression rate control in solid fuel ramjets [AD-A154251] 19 p3227 N85-30006
Regression diagnostics in practice: Experiences from modelling jet engine costs [AD-A154199] 19 p3347 N85-30748
Using regression analysis for determining air data sensor errors by means of an inertial navigation system [ESA-TT-886] 20 p3392 N85-31041
A multiple linear regression analysis of hot corrosion attack on a series of nickel base turbine alloys [NASA-TM-87020] 20 p3431 N85-31284
Regression metamodel summarization of model behavior [FEW-120] 20 p3522 N85-31902
On the interpretation of variables — simulation and regression models [FEW-136] 20 p3522 N85-31903
Statistical methods for efficient design of community surveys of response to noise: Random coefficients regression models [NASA-CR-177933] 21 p3698 N85-32979
Kalman filter time series analysis of gamma-ray data from NaI(T1) detectors for the ND6620 computer [AD-A154995] 21 p3705 N85-33014
Regression analysis of aircraft and ground measurement data on vegetation cover 22 p3735 N85-33158
Direct regression analysis of remote sensing data (using example of grass cover) 22 p3736 N85-33157
Development of NATOPS performance software for the SH-3D and SH-3H helicopters [AD-A156140] 24 p4065 N85-35192

REGRESSION COEFFICIENTS
A two-dimensional smoothing spline and a regression problem [AD-A149824] 12 p1921 N85-22067
Statistical methods for efficient design of community surveys of response to noise: Random coefficients regression models [NASA-CR-177933] 21 p3698 N85-32979

REGULARITY
Regularity of the free boundary for the porous medium equation [AD-A147299] 08 p1210 N85-17611

REGULATION
U CONTROL

REGULATIONS
Polychlorinated biphenyls (PCBs) in transit system electrical equipment [PB84-222207] 01 p0045 N85-10291
Major institutional arrangements affecting ground water in New York state [PB84-202506] 01 p0065 N85-10429
Airliner cabin air quality [S-REPT-98-466] 03 p0402 N85-12560
Commercial Space Launch Act [GPO-99-613] 04 p0578 N85-13690
The application of emissions trading to DoD installations [AD-P004136] 09 p1346 N85-18472
Strategies for preparing and submitting a part B application for a DoD facility [AD-P004139] 09 p1347 N85-18475
Perspective on demonstrations of compliance for high-level waste disposal [DE85-000989] 09 p1393 N85-18806
Airport bird hazards associated with solid waste disposal facilities [AD-P004197] 11 p1581 N85-19964
The FAA grant-in-aid assurances: FAR part 139, and airport hazards [AD-P004200] 11 p1583 N85-19976
Interim protocol for the automated analysis of semivolatile organic compounds by Gas Chromatography/Fourier Transfer Infrared (GC/FT-IR) spectrometry [PB85-115186] 11 p1585 N85-20035
Ultralight aircraft technology and public safety [GPO-36-948] 12 p1773 N85-21131
Do new aircraft need new technologies and certification rules? 14 p2224 N85-23795
Civil air code International flights section explained 15 p2460 N85-25194
Protecting the nation's groundwater from contamination, volume 1 [PB85-154201] 15 p2580 N85-25865
Protecting the nation's groundwater from contamination, volume 2 [PB85-154219] 15 p2580 N85-25866
White paper on new international satellite systems [PB85-162501] 16 p2775 N85-27127
Gordon Research Conference on Composites [AD-A152688] 17 p2917 N85-27979
FAA regulation of 9-seat and under passenger aircraft [GPO-42-703] 20 p3391 N85-31032
Current regulatory and licensing status for byproduct sources, facilities and applications [DE85-010967] 22 p3642 N85-33796

REGULATORS
NT AUTOMATIC FREQUENCY CONTROL
NT CURRENT REGULATORS
NT FLOW REGULATORS
NT FREQUENCY CONTROL
NT PRESSURE REGULATORS
NT SPEED REGULATORS
NT THERMOSTATS
NT VOLTAGE REGULATORS
Adaptive regulation of transmitter radiation power in radio lines during delays of control signals 12 p1841 N85-21551
Construction of high speed guaranteed regulators 14 p2270 N85-24063
Modal synthesis of multidimensional PI-regulators for objects with inertial sections 14 p2270 N85-24064
Some problems in improving reliability and accuracy of regulators with hydraulic amplifiers in main channel of power turbine 14 p2271 N85-24071
Some new results on the discrete-time Riccati Equation and their use in the design of optimal regulators and observer-estimators [AD-A151934] 16 p2854 N85-27587

REHEATING
U HEATING

REIGNITION
U IGNITION

REINFORCED MATERIALS
U COMPOSITE MATERIALS

REINFORCED PLASTICS
NT GLASS FIBER REINFORCED PLASTICS
Impressions from a study tour in Finland concerning fiber reinforced plastics, June 1984 [FOA-C-20552-D2(E4,F9)] 07 p0921 N85-15831
Theoretical and experimental study of crack resistance and macrocrack growth rate in organic fiber reinforced plastic under pure shear condition 11 p1586 N85-20053
Outlook for polymer composite materials 15 p2497 N85-25403
New material, process spins off from Volvo LCP 2000 program 15 p2536 N85-25848

REINFORCED PLATES
Impact fracture mechanism of polymer plates containing a heavy inner material 23 p3906 N85-34215

REINFORCED SHELLS
Normal mode method of solving problem forced oscillations of rib-reinforced shell of revolution in liquid 02 p0273 N85-11781
Finite element procedures applicable to nonlinear analysis of reinforced concrete shell structures [AD-A146798] 07 p0976 N85-16209
Testing of wound materials for strength with loading in the reinforcement plane 13 p2027 N85-22701
Strength computation of thin walled shell by discreet-continuous model 14 p2288 N85-24181
Natural vibrations of reinforced spherical shells 17 p2943 N85-28185
Method of solving problems of statics for multilayer shells of revolution 17 p2943 N85-28187

REINFORCEMENT (STRUCTURES)
Development of advanced constitutive model for reinforced concrete [AD-A146050] 01 p0062 N85-10411
Improved reinforcement metal 03 p0353 N85-12271
Dynamic shear failure of shallow-buried flat-roofed reinforced concrete structures subjected to blast loading [AD-A145974] 03 p0379 N85-12378
Refined modeling of reinforced concrete columns of seismic analysis [PB84-234384] 04 p0484 N85-13089
Measuring the corrosion rate of reinforcing steel in concrete [PB84-244532] 06 p0770 N85-14925
Response of earth-covered slabs in clay and sand backfills [AD-A149298] 11 p1615 N85-20157
An approach for user controlled reinforced concrete design optimization 15 p2627 N85-26167
Effects of humidity cycles on the corrosion of galvanised reinforcements in carbonated and uncarbonated mortars [BLL-CE-TRANS-8039-(8022.09)] 20 p3430 N85-31272
Membrane reinforcement in concrete shells: Design versus nonlinear behavior 24 p4084 N85-35312
User's guide: A computer program for strength analysis of non-hydraulic concrete structural elements. Report 2. Strength design of reinforced concrete column sections (PCAUC) [AD-A156393] 24 p4102 N85-35429

REINFORCING FIBERS
NT BORON FIBERS
NT CARBON FIBERS
High performance fibers for structurally reliable metal and ceramic composites — advanced gas turbine engine materials [NASA-TM-86878] 03 p0325 N85-12095
Impressions from a study tour in Finland concerning fiber reinforced plastics, June 1984 [FOA-C-20552-D2(E4,F9)] 07 p0921 N85-15831
Quantitative estimate of compatibility of fiber composite material components 10 p1444 N85-19089
Evaluation of features of reinforcing fibers by testing bundles 11 p1599 N85-20089
Preparation of silicon carbide-silicon nitride fibers by the pyrolysis of polycarbosilazane precursors [NASA-TM-86505] 17 p2933 N85-28107
Lightweight piston [NASA-CASE-LAR-13150-1] 18 p3066 N85-29875
Effect of matrix composition on steel fiber reinforced concrete properties 19 p3230 N85-30026
Features of the interaction between fibers and matrix in production of aluminum-boron composite material 19 p3244 N85-30117
Matrix fracture in fiber-reinforced ceramics [AD-A154704] 21 p3569 N85-32197
Improved process for the preparation of fiber-reinforced ceramic composites by chemical vapor deposition [DE85-011584] 22 p3752 N85-33255
Substitution of asbestos by aramid fibers and fiber blends in industrial textiles and composites with organic binders [BMFT-FB-T-85-006] 23 p3920 N85-34294

REINFORCING MATERIALS
Related studies to cathodic protection of reinforced concrete structures
[PB84-218114] 03 p0333 N85-12145
Reinforcement of molybdenum disilicide with nematic crystals of aluminum oxide 03 p0353 N85-12269
Improved reinforcement metal 03 p0353 N85-12271
Ultrasonic analysis of spherical composite test specimens
[DE85-001591] 07 p0976 N85-16197
Mechanism of strengthening plastics with rubbers 13 p2014 N85-22636
Particulate and whisker toughened alumina composites
[DE85-005239] 16 p2743 N85-26930
Anticorrosion protection of reinforcing steel in prestressed gypsum and anhydrite concrete
[BLL-BISI-TRANS-22079-(6022.06)] 17 p2926 N85-28044
Behavior of reinforced concrete at elevated temperatures
[DE85-009032] 18 p3123 N85-29332
Durability of reinforced hard-alloy draw plates
[BLL-M-36278-(5828.4)] 20 p3465 N85-31526

REISSNER THEORY
Modeling the stress field in laminated composite plates near discontinuities
[PB84-219237] 03 p0327 N85-12103
Bulletin of the Faculty of Engineering, Hokkaido University, no. 123
[ISSN-0385-602-X] 04 p0482 N85-13075
Analysis based on Reissner theory for rectangular plates with all edges built-in 04 p0483 N85-13081
Interaction of part-through cracks in a flat plate
[NASA-CR-175588] 12 p1864 N85-21692

REJECTION
Choice of criteria for rejection of insulating components in high-voltage surge equipment 06 p0785 N85-15021

RELATIONSHIPS
Compressive strength-maturity relationships of mortar containing fly ash
[AD-A148705] 09 p1339 N85-18423

RELATIVISTIC EFFECTS
An alternative to relativistic beaming in AGN — Active Galactic Nuclei (AGN) 08 p1242 N85-17833
Viking radio science data analysis and synthesis
[NASA-CR-175631] 13 p2171 N85-23471
Activities report of the Department of Astrophysics 20 p3546 N85-32084
A derivation of relativistic effects in satellite tracking
[AD-A154620] 21 p3558 N85-32132

RELATIVISTIC ELECTRON BEAMS
NRL (Naval Research Laboratory) FEL (Free Electron Laser) program
[AD-A145057] 01 p0052 N85-10347
Cerenkov radiation in the neighborhood of the emission threshold, revised
[AD-A145458] 02 p0284 N85-11855
Time-resolved tomographic images of a relativistic electron beam
[DE84-015021] 04 p0585 N85-13597
Explosive emission cathode plasmas in intensive relativistic electron beam diodes
[AD-A147917] 07 p1046 N85-16642
SIMM1: A linearized particle code
[AD-A149827] 08 p1221 N85-17689
IREB (Intense Relativistic Electron Beam) converter to ac pulses
[AD-D011479] 10 p1554 N85-19600
Directivity of Bremsstrahlung radiation from relativistic beams and the Gamma-Rays from solar flares
[NASA-CR-174433] 10 p1572 N85-19913
Novel probe for determining the size and position of a relativistic electron beam
[DE85-001044] 11 p1723 N85-20836
Theoretical study of collective ion acceleration in the Luce diode
[AD-A150107] 12 p1929 N85-22116
Collective acceleration of ions using high current relativistic electron beams
[DE85-004860] 13 p2157 N85-23393
Explosive emission cathode plasmas in intense relativistic electron beam diodes
[AD-A150869] 14 p2417 N85-24912
Principle and design of a medium-enhanced free-electron laser 15 p2561 N85-25802
Beam trapping in high current cyclic accelerators with strong focusing fields
[AD-A151392] 15 p2648 N85-26331
Microwave emission from relativistic electron beams
[AD-A151472] 15 p2648 N85-26333
Bursts of relativistic electrons in magnetopause and in outer radiation belt 16 p2722 N85-26801
Comparison of calculations and measurements of the off-axis radiation dose (Si) in liquid nitrogen as a function of radiation length
[AD-A153676] 18 p3178 N85-29704
Millimeter wave generation by relativistic electron beams
[AD-A153990] 18 p3179 N85-29706
Gyrotron traveling-wave device including quarter wavelength anti-reflective dielectric layer to enhance microwave absorption
[AD-D011690] 19 p3271 N85-30285
Profile of a relativistic electron beam propagated through a linear wiggler and an axial guide field
[AD-A154403] 19 p3353 N85-30783
Quasioptical gyroklystron
[AD-D011688] 19 p3356 N85-30801
Further studies of X-ray structure of the Perseus cluster
[OG-2.5-12] 22 p3870 N85-33967
Injection of energetic particles following the gamma-ray flares on June 7, 1980, as observed on Helios 1
[SH-1.3-9] 23 p3993 N85-34756
Ultrarelativistic electrons and solar flare gamma-radiation
[SH-1.3-11] 23 p3993 N85-34757

RELATIVISTIC PARTICLES
NT RELATIVISTIC ELECTRON BEAMS
A covariant derivation of the ponderomotive force
[AD-A145054] 01 p0121 N85-10830
Physics of nonmagnetic relativistic thermal plasmas 09 p1386 N85-18715
Pulsations of cosmic ray intensities before increasing flux of relativistic particles from solar flares 15 p2477 N85-25292
Contributions to the 19th International Cosmic Ray Conference
[NASA-CR-176049] 20 p3543 N85-32044
Classical emission of relativistic charged particles during axial channeling 21 p3681 N85-32871
Relativistic electron in curved magnetic fields
[OG-6.2-11] 22 p3890 N85-34110
Simulation studies on stability of hot electron plasma 23 p3978 N85-34684
Multiple inner shell vacancies in laser-irradiated Au plasma 23 p3981 N85-34687
Neutron-induced 2.2 MeV background in gamma ray telescopes
[OG-9.3-6] 23 p4027 N85-34961
A bi-directional charged particle telescope to observe flux, energy spectrum and angular distribution of relativistic and non-relativistic particles
[SH-9.1-4] 23 p4050 N85-35119
Proceedings of the Workshop on Detectors for Relativistic Nuclear Collisions
[LBL-16225] 24 p4146 N85-35700
Report of working group on detectors for hadrons and event parameters at colliders 24 p4146 N85-35705
A simulation of ultra-relativistic nucleus-nucleus collisions 24 p4146 N85-35707
A holographic streamer chamber for relativistic nucleus-nucleus collision experiments 24 p4147 N85-35710
Fractional charge resolution in music 24 p4147 N85-35712
Hadron thermodynamics in relativistic nuclear collisions
[HE-1.1-8] 24 p4171 N85-35856
Structure of air shower disc near the core
[HE-4.7-2] 24 p4198 N85-36053
High energy cosmic ray signature of quark nuggets
[HE-6.2-11] 24 p4212 N85-36147
Search for anomalons using plastic nuclear track detectors
[HE-6.2-12] 24 p4212 N85-36148

RELATIVISTIC PLASMAS
The environment of active galactic nuclei 07 p1057 N85-16712
Physical processes in relativistic plasmas — active galactic nuclei 08 p1240 N85-17824
Power law X- and gamma-ray emission from relativistic thermal plasmas 08 p1241 N85-17829
Centrifugally driven magnetohydrodynamic (MHD) winds and the nonthermal emission regions in Active Galactic Nuclei (AGN) 08 p1242 N85-17835
Physics of nonmagnetic relativistic thermal plasmas 09 p1386 N85-18715
On the spectrum of longitudinal waves in the hot degenerate plasma 12 p1955 N85-22280
Electron-positron pair equilibrium in strongly magnetized plasmas 12 p1957 N85-22296
Electron-positron pairs in a mildly relativistic plasma in active galactic nuclei 12 p1957 N85-22297
Spacecraft-environment interaction: The environmental plasma aspect 13 p1990 N85-22479
High energy beam experiment 15 p2654 N85-26376
Limits on the Doppler factor in relativistic jets by means of gamma-ray observations
[OG-2.7-12] 22 p3872 N85-33985
Secondary antiproton production in relativistic plasmas
[OG-6.1-4] 22 p3888 N85-34095
Multiple inner shell vacancies in laser-irradiated Au plasma 23 p3981 N85-34687
Monte Carlo calculations of relativistic solar proton propagation in interplanetary space
[SH-3.2-11] 23 p4004 N85-34826
Self-similar time dependent shock structures
[OG-8.1-4] 23 p4017 N85-34894
Detectors for relativistic nuclear collisions (report from the Fixed-Target Hadron Group) 24 p4146 N85-35701

RELATIVISTIC THEORY
NT MANDELSTAM REPRESENTATION
Topics in black-hole physics: Geometric constraints on noncollapsing, gravitating systems, and tidal distortions of a Schwarzschild black hole 05 p0742 N85-14769
The determination of the post-Newtonian parameters in gravitational theory using laser ranging to the Lageos satellite 09 p1414 N85-18924
Viking radio science data analysis and synthesis
[NASA-CR-175631] 13 p2171 N85-23471

RELATIVISTIC VELOCITY
Testing theories of superluminal motion — QUASAT 07 p1058 N85-16714
On the propagation speed in relativistic quantum mechanics
[CWI-AM-R8410] 17 p3046 N85-28848
Spectra of solar proton ground level events using neutron monitor and neutron moderated detector recordings
[SH-1.3-14] 23 p3994 N85-34759

RELATIVITY
Contributions to the error analysis in the relativity gyroscope experiment 05 p0636 N85-14095
The period of orbit as a test of the general theory of relativity 05 p0742 N85-14772
Isolated systems in general relativity 09 p1400 N85-18813
Drag-free satellite simulator
[REPT-615] 12 p1789 N85-21229
Suspension torques on a gimballed electrostatically supported gyroscope and requirements on the gyroscope and spacecraft for the relativity gyroscope experiment 12 p1851 N85-21608
Conserved quantities and radiative aspects of asymptotically anti-de Sitter space-times 12 p1958 N85-22303
Solutions of field equations in General Relativity with spinor connection 15 p2663 N85-26438
An improved servo-controlled inertial clock for laboratory tests of general relativity 19 p3378 N85-30955
The dimensional reduction transition
[DE85-003948] 19 p3383 N85-30990
Bergson and the unification of the sciences
[DE85-009861] 20 p3538 N85-32018

RELAXATION
NMR (Nuclear Magnetic Resonance) of solid biopolymers
[AD-P003912] 01 p0032 N85-10198

RELAXATION (MECHANICS)
NT SPIN-LATTICE RELAXATION
NT STRESS RELAXATION
Effect of the Basset term on particle relaxation behind normal shock waves
[AD-A145446] 02 p0198 N85-11320
Influence of translational and hyperfine relaxation on energy characteristics of oxygen-iodine laser 02 p0261 N85-11707
Relaxation of plasma rotation in a Tokamak in the presence of extraneous forces and corrugation of the magnetic field
[DE84-015628] 02 p0284 N85-11854
Internal friction, microstructure and radiation effects
[DE84-013905] 02 p0288 N85-11880
Parameters of structural relaxation and mechanical properties of amorphous alloys 03 p0349 N85-12246
Structure and properties of grain boundaries
[DE84-014368] 04 p0570 N85-13636
Transport and relaxation processes in supercritical fluids
[DE84-006591] 05 p0731 N85-14698
Structural relaxation and isoconfigurational flow of a metallic glass near equilibrium
[AD-A147888] 07 p0933 N85-15015
On the relaxation of a turbulent boundary layer after an encounter with a forward facing step 08 p1071 N85-16789
Electrical resistivity and structural changes upon relaxation and crystallization of (Mo/sub 0.6/Ru/sub 0.4)sub 100-x/B/sub x/ metallic glasses
[DE84-017281] 09 p1299 N85-18160

Reduction of the wavepacket: How long does it take?
[DE84-016778] 09 p1400 N85-18615
On relaxation of transonic flows around zero-lift airfoils and convergence of self-correcting wing tunnels
11 p1622 N85-20214
Mini-modal testing of wind turbines using novel excitation
[DE85-000666] 11 p1654 N85-20417
Energy spectrum of processes of structural relaxation of amorphous alloy FeCo70Si15B10
13 p2035 N85-22750
Numerical simulation of inverters with I2L elements including effects of high doping level
13 p2088 N85-23039
Relaxation properties and fatigue fracture resistance of austenitic spring steel
[BLL-BISI-TRANS-22300-(9022.06)]
17 p2978 N85-28406
Recent advances in d-c relaxation techniques for the measurement of kinetics of fast electrode reactions
[DE85-005029] 22 p3745 N85-33216

RELAXATION (PHYSIOLOGY)
Catecholamine excretion and subjective ratings of tension during autogenic training and mental stress
[REPT-172] 05 p0697 N85-14483
Responses of skeletal muscle to unloading, a review
[NASA-CR-176177] 24 p4128 N85-35594
Relaxation techniques
[AD-A156248] 24 p4133 N85-35621

RELAXATION METHOD (MATHEMATICS)
Relaxation times for queueing systems
[CWI-OS-R8407] 05 p0719 N85-14618
Theoretical contributions to transonic flow analysis for transport aircraft
[BMFT-FB-W-84-036] 06 p1076 N85-16838
Distributed asynchronous relaxation methods for convex network flow problems
[AD-A148027] 06 p1211 N85-17822
Investigation of three-dimensional mesh generation with precise controls
[AD-A148759] 09 p1374 N85-18636
To the theory of approximation of experimental curves by smooth functions
[PREPRINT-438] 18 p3173 N85-29671
A parallelized point successive over-relaxation method on a multiple instruction multiple data stream computer
[AD-A154377] 19 p3337 N85-30679
Optimization of a numerical method to calculate elliptic flows
[ESA-TT-889] 20 p3457 N85-31472
Relaxation phenomena and stability of probability densities
[AD-A155923] 24 p4143 N85-35682

RELAXATION TIME
Kinetics of short-range ordering in metallic glasses: Analysis of the crossover effect
[DE84-015524] 02 p0187 N85-11251
Influence of translational and hyperfine relaxation on energy characteristics of oxygen-iodine laser
02 p0261 N85-11707
Numerical experiments and theoretical analysis of the flow of an elastic liquid of the Maxwell-Oldroyd type in the presence of geometrical singularities
[WTHD-164] 08 p1163 N85-17340
NMR imaging and spectroscopy of the mammalian central nervous system after heavy ion radiation
[DE85-004500] 14 p2366 N85-24696
Infrared nonlinear processes in semiconductors
[AD-A150966] 14 p2427 N85-24968
A statistical approach to relaxation in glassy materials
[AD-A151295] 15 p2518 N85-25524
Rotational relaxation studies of hydrogen fluoride
[AD-A152711] 17 p3029 N85-28734

RELEASING
Dynamic compression and volatile release of carbonates
[NASA-CR-174076] 03 p0391 N85-12504
Theoretical thermodynamics of mixtures at high pressures
13 p2183 N85-23550
Fully redundant mechanical release actuator
[NASA-CASE-LAR-13198-1] 18 p3116 N85-29267
Slide release mechanism — for space shuttle orbiter/external tank connection device
[NASA-CASE-MSC-20080-1] 19 p3279 N85-30834
Free-float Emergency Position Indicating Radio Beacons (EPIRBs) and release mechanism on board Norwegian ships. Main specifications and user experience
20 p3404 N85-31120

RELIABILITY
NT AIRCRAFT RELIABILITY
NT CIRCUIT RELIABILITY
NT COMPONENT RELIABILITY
NT STRUCTURAL RELIABILITY
Free-piston Stirling engine development
[PB84-237767] 01 p0056 N85-10369
Ada (trademark) training curriculum. Software engineering for managers m101 teacher's exercise guide
[AD-A145094] 01 p0104 N85-10695
An integral inequality with applications to order statistics
[AD-A145081] 01 p0113 N85-10770
Total positivity. A review
[AD-A145205] 01 p0114 N85-10771
Avionics integrity program (Awip). Volume 3: Program cost assessment - environmental stress screening and diagnostic techniques
[AD-A145844] 02 p0139 N85-10942
Simulation study of a new inverse-pinch high Coulomb transfer switch
[NASA-CR-172420] 02 p0194 N85-11294
Efficient methods for mechanical and structural reliability analysis and design 02 p0205 N85-11355
Computing the reliability of k out of n systems
[AD-A145505] 02 p0206 N85-11357
Proposal for a semiautomatic program testing system
[INPE-3262-TDL/178] 02 p0240 N85-11561
On some common interests among reliability, inventory and queuing
[AD-A145595] 02 p0251 N85-11648
Editorial urges improved aviation repair work quality
03 p0310 N85-12004
Improving operational reliability and productivity of robotized technological complexes
03 p0346 N85-12227
The 30 GHz solid state amplifier for low cost low data rate ground terminals
[NASA-CR-174796] 03 p0358 N85-12300
The Lindstrom-Madden method for series systems with repeated components
[AD-A146265] 03 p0412 N85-12636
Determination sample sizes for diversified reliability test programs
[DE84-015003] 04 p0511 N85-13255
Human reliability data bank: Feasibility study
[DE84-015215] 04 p0546 N85-13476
Test experience on an ultrareliable computer communication network
[NASA-TM-85915] 04 p0552 N85-13514
Potential of flywheels for spacecraft energy storage
05 p0809 N85-13890
Analyses to develop models to project failure rates and repair costs of electronic modules and subassemblies
[AD-A146509] 06 p0816 N85-15180
More than you want to know about maximum likelihood estimation
[NASA-TM-85905] 07 p0909 N85-15752
The theory of optimal confidence limits for systems reliability with counterexamples for results on optimal confidence limits for series systems
[AD-A147236] 07 p1031 N85-16546
EDP computer tapes described
08 p1142 N85-17203
On modeling the performance and reliability of multi-mode computer systems
[AD-A148444] 08 p1208 N85-17599
An analysis of robust and efficient priors associated with a finite Bayesian model for compliance testing
[AD-A148497] 08 p1213 N85-17635
NBS (National Bureau of Standards) solar collector durability-reliability test program
[PB85-113603/GAR] 09 p1346 N85-18469
SPADE: Series-parallel directed acyclic graph evaluator
[AD-A148458] 09 p1368 N85-18592
Beyond fault trees to fault graphs
[DE84-017022] 09 p1370 N85-18608
An ultra reliable computer communication network: The dispersed sensor processing mesh
09 p1372 N85-18620
Sky coverage, confusion, completeness and reliability
09 p1412 N85-18906
Integrated Technology Rotor/Flight Research Rotor (ITR/FRR) concept definition
[NASA-CR-166445] 10 p1423 N85-18979
Integrated Technology Rotor/Flight Research Rotor (ITR/FRR) concept definition study
[NASA-CR-166444] 10 p1424 N85-18981
Reliability of adhesive bonds under severe environments. Report of the Committee on Reliability of Adhesive Bonds in Severe Environments
[AD-A149010] 10 p1451 N85-19140
Reliability studies of ceramic capacitors
[AD-A149128] 10 p1479 N85-19338
Design of explosive logic elements
[DE84-009811] 11 p1614 N85-20148
Reliability of DNC system examined
11 p1617 N85-20171
New CNC systems described
11 p1617 N85-20172
A summary and assessment of historical reliability and maintainability data for solar hot water and space conditioning systems
[DE84-004521] 12 p1876 N85-21770
AFOS (Automation of Field Operations and Services)-ERA forecast verification, September 1984
[PB85-137578] 12 p1897 N85-21912
Reliability of structural brittle materials
12 p1946 N85-22222
Effects of assuming independent component failure times, if they are actually dependent, in a series system
[AD-A150582] 13 p2101 N85-23092
Parallel test method for LSI (Large Scale Integration) microprocessors
[AD-A150237] 13 p2144 N85-23310
Contribution of instrumentation and control software to system reliability
[DE85-004693] 13 p2149 N85-23340
Electric and hybrid vehicle demonstration project
[DE85-003939] 13 p2169 N85-23455
Special power train requirements for the next generation of rotary-wing aircraft 14 p2220 N85-23769
Fine filtration: An attractive route towards lower helicopter operating costs 14 p2221 N85-23774
Estimate of fatigue stability of gas-turbine engine compressor vanes in probabilistic aspect
14 p2287 N85-24169
Cold electronics: An overview
14 p2297 N85-24221
Some recent developments in systems reliability
[AD-A150661] 14 p2317 N85-24318
Supplement to evaluation of satellite derived estimates of solar radiation
[E85-10066] 14 p2346 N85-24506
Evaluation of satellite derived estimates of solar radiation
[E85-10067] 14 p2346 N85-24507
Properties of systems which lead to efficient computation of reliability
[AD-A151033] 14 p2409 N85-24853
Convolution of the IFRA (Increasing Failure Rate Average) scaled-mins class
[AD-A151070] 14 p2411 N85-24870
Shuttle fleet operations: A simulation analysis
[AD-A151383] 15 p2491 N85-25370
Sizing capability of automated ultrasonic time-of-flight diffraction in thick section steel and aspects of reliable inspection in practice
[AERE-R-11548] 15 p2571 N85-25855
Care 3 model overview and user's guide, first revision
[NASA-TM-86404] 15 p2627 N85-26192
On failure modeling, revised
[AD-A151411] 15 p2637 N85-26263
Statistical aspects of reliability, maintainability and availability
[AD-A151228] 15 p2640 N85-26282
The evolutive state: A new definition of system state to include sequencing of events
16 p2696 N85-26643
Avionics integrity issues presented during NAECON (National Aerospace and Electronics Convention) 1984
[AD-A151923] 16 p2707 N85-26707
Technical evaluation report on the Flight Mechanics Symposium on Active Control Systems: Review, Evaluation and Projections
[AGARD-AR-220] 16 p2711 N85-26730
Active control technology: Past, present, future
16 p2711 N85-26731
Initial quality of advanced joining concepts
[AD-A152241] 16 p2759 N85-27027
Research on products obtained by powder metallurgy
16 p2768 N85-27081
Life and reliability modeling of bevel gear reductions
[NASA-TM-87008] 16 p2793 N85-27227
Photovoltaic cell reliability research: Investigation of accelerated stress factors and failure-degradation mechanisms in terrestrial solar cells
[NASA-CR-175815] 16 p2819 N85-27388
VLSI (Very large scale integrated circuits) device reliability models
[AD-A153266] 17 p2954 N85-28345
Test and evaluation plan for the Centralized Storm Information System 17 p2994 N85-28508
Reliability report for communication networks
[AD-A153764] 18 p3090 N85-29127
Silicide conductors reliability research
[AD-A153768] 18 p3095 N85-29157
Small central receiver Brayton cycle study
[DE85-006662] 18 p3128 N85-29369
Guidance on planning and implementing computer system reliability
[PB85-177996] 18 p3161 N85-29581
Specification of software quality attributes. Volume 3: Software quality evaluation guidebook
[AD-A153990] 18 p3163 N85-29585

Ultrareliable, fault-tolerant control systems: A conceptual description
[NASA-TM-86017] 19 p3221 N85-29972
A Lotus 1-2-3 based system reliability program
[DE85-010533] 19 p3340 N85-30701
Results of analysis on the design variable cells 20 p3445 N85-31388
Exponential order statistic models of software reliability growth
[NASA-CR-3909] 20 p3515 N85-31852
Globally-asynchronous locally-synchronous systems
[AD-A154624] 21 p3573 N85-32222
The optimality of lower confidence limits for the reliability of series systems obtained by the method of key test results or other related techniques
[AD-A154860] 21 p3597 N85-32338
Reliability physics 21 p3606 N85-32402
Advanced module development overview 21 p3612 N85-32445
Thin-film reliability and engineering overview 21 p3612 N85-32450
Los Alamos optical materials reliability, maintainability, and exposure testing program
[DE85-011894] 21 p3613 N85-32456
Further developments of EISCAT as an MST radar 21 p3627 N85-32534
Survival function of hypo-exponential distributions
[AD-A155516] 21 p3672 N85-32814
Ice fog as an electro-optical obscurant
[AD-A155059] 21 p3705 N85-33015
Methods of reliability design of semiconductor power devices 22 p3770 N85-33365
Photovoltaics technical information guide
[DE85-002924] 22 p3806 N85-33585
CARE 3 MENU maintenance manual
[NASA-CR-172009] 22 p3828 N85-33708
Analytical ultrasonics for structural materials
[TIB5-006132] 23 p3966 N85-34600
Development of an NBS (National Bureau of Standards) polymer gage for dynamic soil stress measurement
[PB85-208494] 24 p4118 N85-35526

RELIABILITY ANALYSIS
On discrete failure models
[AD-A145579] 02 p0206 N85-11359
Reliability considerations for the total strain range version of strainrange partitioning
[NASA-CR-174757] 02 p0209 N85-11380
Research in data management and system reliability
[AD-A145496] 03 p0436 N85-12773
Climate of the Northern Hemisphere, 1851 - 1900 compared to contemporary climate
[DE84-016368] 04 p0539 N85-13426
Analysis of the impact of error detection on computer performance
[NASA-CR-174167] 04 p0547 N85-13477
Impact of NDE unreliability on pressure vessel fracture predictions
[DE84-015586] 05 p0647 N85-14151
Predicting changes in reliability characteristics of gas turbine engines during operation 06 p0776 N85-14964
Reliability analysis of local area networks, intermediate report
[BLL-WH-610-(8091.9F)] 07 p1027 N85-16520
Completely monotone regression estimates of software failure rates
[NASA-CR-174319] 08 p1204 N85-17575
Improved models for increasing wind penetration, economics and operating reliability
[NASA-CR-175536] 11 p1674 N85-20545
Reliability analysis of automatic systems
[VTT-301] 12 p1883 N85-21682
An experiment in software reliability
[NASA-CR-172553] 14 p2403 N85-24813
Approximating posterior distributions of system reliability derived from component test data
[AD-A152057] 15 p2572 N85-25857
Cost prediction model for various payloads and instruments for the Space Shuttle Orbiter
[NASA-CR-175781] 16 p2729 N85-26842
Calculating reliability and productivity of cold stamping robot complex as queuing system 16 p2761 N85-27039
Determining availability characteristics of DSN data systems using discrepancy report data 16 p2772 N85-27109
Fatigue criterion to system design, life and reliability
[NASA-TM-87017] 16 p2793 N85-27226
Extreme evaluation of reliability indices for components of metallurgical equipment
[BLL-M-36070-(5628.4)] 16 p2796 N85-27234
An abstract specification language for Markov reliability models
[NASA-TM-86423] 16 p2857 N85-27616
Performance evaluation of fiber-optic converters 17 p2941 N85-28154
Engineering significance of fatigue thresholds and short fatigue cracks for structural design
[NLR-MP-84001-U] 17 p2961 N85-28430
There is no I/O like no I/O
[DE85-009115] 17 p3014 N85-28634
Statistical estimation of software reliability
[AD-A154097] 19 p3335 N85-30665
Weibull distribution based on maximum likelihood with interval inspection data
[NASA-TM-86515] 21 p3678 N85-32847
Reliability prediction of the series system with spares subject to Weibull failure 24 p4100 N85-35413

RELIABILITY CONTROL
U QUALITY CONTROL
U RELIABILITY ENGINEERING

RELIABILITY ENGINEERING
Component reliability and assembling technologies
[CNES-NT-108] 04 p0511 N85-13258
Design and test requirements for development of today's engines 07 p0906 N85-15737
Nondestructive inspection: Improved capabilities of technicians
[AD-A147366] 07 p0975 N85-16196
Ultrasonic transducers, performance variability, design, and manufacturing procedures
[AD-A146575] 08 p1158 N85-17306
A unified model for performance and reliability of Fault-Tolerant/Multi-Mode systems
[AD-A146789] 08 p1206 N85-17601
Material flow in the manufacturing system: Fault-diagnosis systems as support for the maintenance of highly automated manufacturing systems
[PNR-90238] 09 p1371 N85-18618
AIRLAB: A laboratory for flight-crucial-electronics system research 13 p1968 N85-22382
Introduction to methods of evaluating the operational reliability of complex systems: Application to satellite control ground support 14 p2397 N85-24771
Guide for the execution of reliability tests in the laboratory — aeronautical equipment 16 p2796 N85-27237
Characterization of solderless minimrapping connections
[CNES-NT-112] 16 p2796 N85-27238
Lightweight piston
[NASA-CASE-LAR-13150-1] 18 p3066 N85-29875
Note for a research feasibility project: High reliability design in the aeronautical field
[REPT-84-RR-350] 20 p3387 N85-31005
Statistical pooling method of fatigue data for reliability design 23 p3906 N85-34198

RELIC RADIATION
Search for the radiative decay of a cosmic relic particle with IUE
[PREPRINT-410] 04 p0580 N85-13707

RELIEF MAPS
Combinations of remote sensing data with a digital map data base — regional planning 05 p0660 N85-14240
Expansion of functions describing planetary surface and gravity field 13 p1978 N85-22410
Visualization of radar altimetry data for Venus 13 p1982 N85-22437
Mars planimetric mapping 13 p2203 N85-23666
Voyager cartography 13 p2203 N85-23668

RELIEVING
NT STRESS RELIEVING
Theory of diaphragm light modulators with electrical input signal 13 p2082 N85-23002

RELOCATION
An inexpensive radar-responding relocation device for drifting oceanographic instruments
[AD-A152170] 16 p2836 N85-27505
Predictors of transfer adjustment: A longitudinal study
[AD-A152462] 17 p3000 N85-28548

REMAGNETIZATION
U MAGNETIZATION

REMELTING
U MELTING

REMOTE CONTROL
Controlling rotation of elastic manipulator link 04 p0488 N85-13113
The human role in space. Volume 3: Generalizations on human roles in space
[NASA-CR-171225] 04 p0546 N85-13475
Application of robotics in remote fuel fabrication operations
[DE84-011481] 05 p0646 N85-14144
Review of teleoperator research 05 p0703 N85-14511
Visual systems for remotely controlled vehicles 05 p0703 N85-14512
Closing the design loop on HIMAT (highly maneuverable aircraft technology)
[NASA-TM-85923] 06 p0754 N85-14836
National airspace system configuration management interface control document. Maintenance processor subsystem to remote monitoring subsystems and remote monitoring subsystem concentrators
[NAS-MD-790] 07 p0900 N85-15705
Determining grasp points using photometric stereo and the PRISM binocular stereo system
[AD-A147782] 08 p1222 N85-17697
The influence of modern control techniques on the gas industry
[ERS-E.395] 09 p1325 N85-18326
The optimal control and design of a flexible manipulator arm 09 p1327 N85-18340
Robotics in the radiochemical laboratory
[DE85-002824] 10 p1494 N85-19433
A remotely controlled orbiting retriever 12 p1786 N85-21212
A concept for a mobile remote manipulator system 14 p2236 N85-23659
System for radio remote control of dropping bombs
[CH-639335-A5] 15 p2491 N85-25371
Optimal open loop and nonlinear feedback control for remote orbital capture
[AD-A151967] 16 p2732 N85-26859
Scanning electron microscope facility for examination of radioactive materials
[DE85-008127] 17 p2969 N85-28335
Retinally stabilized differential resolution television display
[NASA-CASE-NPO-15432-1] 18 p3089 N85-29117
Digital control of diode laser for atmospheric spectroscopy
[NASA-CASE-NPO-16000-1] 18 p3112 N85-29264
Remotely operable peristaltic pump
[NASA-CASE-MFS-28059-1] 18 p3116 N85-29286
High level radioactive waste vitrification process equipment component testing
[DE85-011143] 19 p3273 N85-30296
Development of HWVP melter/turntable components for canyon-remote maintenance and replacement
[DE85-010308] 19 p3273 N85-30298
Remote medical diagnosis 21 p3663 N85-32753
Space robot simulator vehicle
[NASA-CR-176133] 22 p3739 N85-33176
Remote temperature-set-point controller
[DE85-011614] 22 p3787 N85-33459
Telepresence work system concepts 22 p3797 N85-33525
Dual arm master controller development 22 p3797 N85-33526

REMOTE HANDLING
Advancement of remote systems technology: Past perspectives and future plans
[DE84-016710] 04 p0509 N85-13250
Conceptual design report for a remotely operated cask handling system, revision 1
[DE85-000348] 06 p1169 N85-17371
Advancement of remote technology: Past perspectives and future plans
[DE85-000934] 09 p1327 N85-18342
Advanced remotely maintainable force-reflecting servomanipulator concept
[DE85-001902] 09 p1328 N85-18345
Man/machine interface for a nuclear cask remote handling control station: System design requirements
[DE85-000256] 11 p1697 N85-20657
Tokamak fusion core experiment maintenance study
[DE85-008040] 17 p3040 N85-28813
Precision manipulator heating and cooling apparatus for use in UHV systems with sample transfer capability
[NASA-CASE-LAR-13040-1] 18 p3116 N85-29286
HERMIES-1: A mobile robot for navigation and manipulation experiments
[DE85-006852] 18 p3118 N85-29301
High level radioactive waste vitrification process equipment component testing
[DE85-011143] 19 p3273 N85-30296
Development of HWVP melter/turntable components for canyon-remote maintenance and replacement
[DE85-010308] 19 p3273 N85-30298
Manipulators in teleoperation
[DE85-010583] 20 p3512 N85-31833
NASA space station automation: AI-based technology review. Executive summary
[NASA-CR-176096] 21 p3558 N85-32135
Latch assembly
[DE85-011660] 22 p3792 N85-33492
Portable cutting apparatus
[DE85-011635] 22 p3792 N85-33496
Future of robots in nuclear plants and processes
[DE85-011505] 22 p3793 N85-33500
Telepresence work system concepts 22 p3797 N85-33525
Dual arm master controller development 22 p3797 N85-33526

Recent advances in remote handling at LAMPF
[DE85-012725] 24 p4157 N85-35775
REMOTE MANIPULATOR SYSTEM
Six degrees of freedom control with each hand?
05 p0700 N85-14492
The space shuttle orbiter remote manipulator positioning mechanism 08 p1102 N85-16963
An overview of the space remote manipulator system
08 p1102 N85-16964
Simulation 09 p1277 N85-18024
A concept for a mobile remote manipulator system
14 p2236 N85-23859
Touch-off: A method to determine the position of an object by means of a sensor-driven robot
[DE85-011178] 19 p3339 N85-30691
Telepresence work system concepts
22 p3797 N85-33525
REMOTE REGIONS
NT ANTARCTIC REGIONS
NT ARCTIC REGIONS
Project manager's handbook for special projects
[AD-A147913] 07 p1053 N85-16683
REMOTE SENSING
Satellite reconnaissance
[AD-B085034] 01 p0015 N85-10094
Direction dependent radiation behavior in the classification of multispectral aircraft remote sensing data
[SER-C-290] 01 p0063 N85-10419
Remote sensing of atmospheric particulates: Technological innovation and physical limitations in applications to short-range weather prediction
[NSF ATM-82-09684] 01 p0077 N85-10511
A lightning detection system in Sweden
01 p0078 N85-10519
The Marine Resources Experiment Program (MAREX)
[NASA-TM-87368] 01 p0086 N85-10580
Second Symposium on Space Industrialization — space commercialization
[NASA-CP-2313] 02 p0149 N85-11011
Land remote sensing commercialization: A status report 02 p0151 N85-11024
The future of satellite remote sensing: A worldwide assessment and prediction 02 p0151 N85-11025
Industrial use of land observation satellite systems
02 p0151 N85-11026
Space America's commercial space program
02 p0152 N85-11027
LANDSAT data and interactive computer mapping
02 p0152 N85-11028
Agribusiness and space: No limits to growth
02 p0152 N85-11029
Space research benefits national economy
02 p0163 N85-11107
Some statistical characteristics of atmospheric optical thickness in visible spectral range
02 p0164 N85-11109
Predicting optical image displacement velocity in survey of Earth's surface 02 p0165 N85-11116
Technological approach to automation of specialized processing of survey data 02 p0165 N85-11118
Activities report of the Radio Laboratory
[REPT-S-153] 02 p0192 N85-11288
Reducing spectral dimension of remotely sensed data using principal components analysis and a Peano scanning 02 p0212 N85-11399
The feasibility of satellite remote sensing as a technique for evaluating coal mine surface features
02 p0213 N85-11401
Relationships between grass canopy characteristics and LANDSAT Thematic Mapper bands
02 p0213 N85-11402
Active remote sensing of ocean parameters, an engineering study 02 p0213 N85-11403
Multispectral Imaging Science Working Group for Hydrologic Science: Executive summary
02 p0214 N85-11414
Fundamental remote sensing science research program. Part 1: Status report of the mathematical pattern recognition and image analysis project
[E85-10004] 02 p0215 N85-11417
A preliminary study of the feasibility of detecting the floating macrophytes by means of digital processing of MSS/LANDSAT data
[E85-10005] 02 p0215 N85-11418
Hypothesis on the origin of lineaments in the LANDSAT and SLAR images of precambrian soil in the low Contas River Valley (southern Bahia)
[E85-10007] 02 p0215 N85-11420
Utilization of LANDSAT orbital imagery in the soil survey processes at Rio Grande do Norte state
[E85-10009] 02 p0216 N85-11422
Remote sensing as a mineral prospecting technique
[E85-10010] 02 p0216 N85-11423
Development and testing of a rural credit supervision system at the level of counties and rural properties utilizing remote sensing techniqes
[E85-10018] 02 p0217 N85-11431
The application of remote sensing to resource management and environmental quality programs in Kansas
[E85-10023] 02 p0218 N85-11436
Shuttle Experimental Radar for Geological Exploration (SERGE) project: Field work relating to the Shuttle Experimental Radar A (SIR-A) in Brazil (phase 2)
[NASA-CR-174033] 02 p0219 N85-11444
Applications of remote sensing techniques to oceanography and sea ice
[FOA-B-80004-M7] 02 p0220 N85-11448
Atmospheres of Uranus and Neptune
02 p0296 N85-11929
East Europe report: Scientific affairs, no. 791
[JPRS-84624] 03 p0341 N85-12195
Satellite, airborne remote sensing development outlined 03 p0342 N85-12199
East Europe report: Science and technology
[JPRS-ESA-84-038] 03 p0343 N85-12210
Achievements in development of space meteorology
03 p0343 N85-12212
Remote sensing for landforms and soils in the arid southwest United States 03 p0378 N85-12410
ERS-1 radar altimeter data products — conference
[ESA-SP-221] 03 p0379 N85-12419
The NASA/JPL pilot ocean data system
03 p0381 N85-12433
International banking of satellite and in-situ wave data by the Marine Information and Advisory Services (MIAS)
03 p0381 N85-12434
Satellite altimetric measurements of lake levels
03 p0383 N85-12447
Report of the Division of Atmospheric Physics, 1980-1983 03 p0391 N85-12501
Millimeter-wave propagation and remote sensing of the atmosphere
[AD-A146339] 03 p0393 N85-12512
Ice-soil mixtures: Visual and near-infrared remote sensing techniques
[NASA-CR-174087] 04 p0525 N85-13358
A comparison between active and passive sensing of soil moisture from vegetated terrains
04 p0526 N85-13364
A feasibility study on the use of wind profilers to support Space Shuttle launches
[NASA-CR-3861] 04 p0538 N85-13423
Some principles of plant resources evaluation using remotely sensed data 04 p0543 N85-13480
The 1984 ASEE-NASA summer faculty fellowship program (aeronautics and research)
[NASA-TM-87393] 04 p0575 N85-13664
Basic investigation concerning the applicability of multispectral radiation data from microwave radiometry measurements to geoscientific objectives of remote sensing
[ESA-TT-846] 05 p0628 N85-14027
Development of a capacitive sensor system for high temperature application
[BMFT-FB-HA-84-027] 05 p0648 N85-14147
Air-sea heat exchange, an element of the water cycle
05 p0653 N85-14195
Contributions to remote sensing: Applications of thermal infrared
[COMMUN-34/1984] 05 p0654 N85-14196
Land Remote-Sensing Commercialization Act
[S-REPT-98-458] 05 p0654 N85-14201
EARSeL/ESA Symposium on Integrative Approaches in Remote Sensing
[ESA-SP-214] 05 p0655 N85-14202
The Interactive Planetary Image Processing System (IPIPS): A major facility for research and teaching in remote sensing 05 p0655 N85-14203
Digital comparison and correlation techniques of remote sensing images with differing spatial resolutions
05 p0655 N85-14204
The integrated use of digital cartographic data and remotely sensed imagery 05 p0655 N85-14206
Methodological research in connection with the handling of LANDSAT satellite data for archaeology
05 p0655 N85-14207
Methods for correlating geological, geochemical and geophysical data with satellite imagery in central Ireland
05 p0655 N85-14208
International cooperation in remote sensing applications 05 p0656 N85-14209
A comparison of TIROS-N series satellite data and LANDSAT data over Scotland 05 p0656 N85-14210
The Finnish approach to microwave remote sensing of snow 05 p0656 N85-14212
The areal pattern of latent and sensible heat fluxes: The combination of soil physics and remotely sensed data 05 p0656 N85-14213
Forest cover monitoring by remote sensing in Great Britain 05 p0656 N85-14214
Remote sensing of plant stress and diseases
05 p0657 N85-14216
Study of the improvement in analyzing passive microwave remote sensing data by integrated use of ground data 05 p0658 N85-14226
Remote sensing data in support of conventional data
05 p0659 N85-14232
A geoinformation expert system for synergetic use of map and image data 05 p0659 N85-14233
A methodology for an integrated spatial data model and its application to image classification
05 p0659 N85-14234
The SPOT data bank system
05 p0659 N85-14236
Evaluation of SPOT simulation data of the S GEOS campaign of the EEC by data of the test sites Freiburg and Staubing (West Germany) 05 p0659 N85-14237
Perspectives of remote sensing at the end of the decade 05 p0659 N85-14238
Combining Heat Capacity Mapping Mission (HCMM) LANDSAT and thematic map information into a unique high precision merged multichannel system — climatology 05 p0660 N85-14239
Combinations of remote sensing data with a digital map data base — regional planning 05 p0660 N85-14240
Application of high frequency 2-D digital filtering to remote sensing image processing
05 p0660 N85-14242
A multiple approach in remote sensing for structural and lithological mapping by use Modular Optoelectronic Multispectral Scanner (MOMS)/LANDSAT/Heat Capacity Mapping Mission (HCMM) data
05 p0660 N85-14244
Inventory and monitoring of national park landscapes — remote sensing 05 p0660 N85-14245
The role of expert systems in remote sensing
05 p0661 N85-14246
Electronic satellite imaging system MOMS-ESA
[BMFT-FB-W-84-033] 05 p0661 N85-14248
A diagnostic approach to obtaining planetary boundary layer winds using satellite-derived thermal data
05 p0674 N85-14330
Global Scale Atmospheric Processes Research Program Review
[NASA-CP-2344] 05 p0679 N85-14360
An investigation of the marine boundary layer during cold air outbreak 05 p0680 N85-14368
Rain volume estimation over areas using satellite and radar data 05 p0686 N85-14406
Development of a van-portable remote-sensing laser system for selective detection of natural gas leaks
[PB85-101939/GAR] 06 p0811 N85-15156
Development of radar to measure sea ice merits prize nomination 06 p0826 N85-15244
A geographic information system for resource managers based on multi-level remote sensing data
[E85-10047] 06 p0827 N85-15249
Effective use of remote sensing products in litigation
[E85-10048] 06 p0827 N85-15250
Upper Atmosphere Research Satellite (UARS) trade analysis
[NASA-CR-175269] 07 p0912 N85-15774
Intermediate results of radar backscatter measurements from summer sea ice
[AD-A147212] 07 p0940 N85-15960
Power transfer from natural emitters to collection apertures at microwave wavelengths
[NASA-CR-174275] 07 p0945 N85-15969
Stereo Electro-optical Tracking System (SETS)
[NASA-CR-172471] 07 p0962 N85-16068
Enhancement of multispectral scanner images by digital filtering
[ESA-TT-824] 07 p0969 N85-16284
Remote sensing of atmospheric gases with CO2 lasers. Continuation and conclusion of spectroscopic investigations
[BMFT-FB-W-84-030] 07 p0989 N85-16285
Remote sensing of the high latitude ionosphere
[AD-A147881] 07 p1008 N85-16405
Use of SIR-B multiincidence-angle imagery to study iceberg detectability and offshore ocean feature extraction 08 p1145 N85-17225
Geological, structural, and geomorphological analyses from SIR-B 08 p1145 N85-17226
Microwave and optical remote sensing of forest vegetation 08 p1146 N85-17228
Evaluation of SIR-B imagery for geologic and geomorphic mapping, hydrology, and oceanography in Australia 08 p1146 N85-17229
The use of digital spaceborne SAR data for the delineation of surface features indicative of malaria vector breeding habitats 08 p1146 N85-17230

Interlobate comparison of glacial-depositional style as evidenced by small-relief glacial landscape features in Illinois, Indiana, and Ohio, utilizing SIR-B
08 p1146 N85-17231

Evaluation of the L-band scattering characteristics of volcanic terrain in aid of lithologic identification, assessment of SIR-B calibration, and development of planetary geomorphic analogs 08 p1146 N85-17232

The investigation of selected oceanographic applications of spaceborne synthetic-aperture radar
08 p1146 N85-17233

Investigation of SIR-B images for lithologic mapping
08 p1148 N85-17241

Remote sensing of soil moisture
08 p1149 N85-17252

Spaceborne microwave radiometers: Background and technology requirements
[LD-R-257] 08 p1165 N85-17350

Papers of the 15th International Society for Photogrammetry and Remote Sensing (ISPRS) Congress — conferences
[TRITA-FMI-9] 08 p1175 N85-17406

Advanced technology for hydrographic mapping
[FOA-C-30371-E1] 08 p1176 N85-17418

Development of an airborne measuring system for remote sensing of Earth surface and atmosphere, spectroscopic investigations
[BMFT-FB-W-84-029] 08 p1176 N85-17420

X rays from the aurora
[AD-A148629] 08 p1186 N85-17477

Low power microprocessor based measurements system for determining the integrity of coatings on buried pipelines
[ERS-E.380] 09 p1324 N85-18323

Development and operation of a real-time data acquisition system for the NASA-LaRC differential absorption lidar
[NASA-CR-174384] 09 p1366 N85-18583

Technical evaluation report on the 46th Symposium of the Avionics Panel on Space System Applications to Tactical Operations
[AGARD-AR-203] 10 p1425 N85-18988

Pulsed photothermal radiometry for remote sensing of spectroscopic and physical properties of thin film
[AD-A149080] 10 p1435 N85-19041

Resolution enhancement of multichannel microwave imagery from the Nimbus-7 SMMR for maritime rainfall analysis
[NASA-CR-174367] 10 p1462 N85-19221

CNES, INPA do joint remote-sensing research
10 p1477 N85-19321

Brazilian Remote Sensing Shuttle Experiment (BRESEX): Characteristics and future utilization on satellites
[INPE-3313-PRE/620] 10 p1487 N85-19365

The BRESEX multispectral camera: Preliminary characteristics
[INPE-3357-PRE/635] 10 p1487 N85-19366

Earth resources: A continuing bibliography with indexes
[NASA-SP-7041(44)] 10 p1503 N85-19484

Brazilian remote sensing receiving, recording and processing ground systems in the 1980's
[E85-10079] 10 p1504 N85-19493

Preliminary evaluation of the airborne imaging spectrometer for vegetation analysis
[NASA-CR-174440] 10 p1505 N85-19496

SIR-A imagery in geologic studies of the Sierra Madre Oriental, northeastern Mexico. Part 1 (Regional stratigraphy): The use of morphostratigraphic units in remote sensing mapping
[NASA-CR-175457] 10 p1505 N85-19497

Remote sensing activities in Latin America
[INPE-3297-PRE/612] 10 p1506 N85-19501

The sharing of remote sensing techniques in Brazilian geographic research
[INPE-3307-PRE/617] 10 p1506 N85-19502

Nautical charting with remotely sensed imagery, volume 1
[AD-A149361] 10 p1506 N85-19503

Nautical charting with remotely sensed imagery. Volume 2: Case studies
[AD-A149362] 10 p1506 N85-19504

The use of image registration technique in Brasilia's urban growth monitoring
[INPE-3302-PRE/614] 10 p1509 N85-19696

Remote sensing technology now playing practical roles 11 p1619 N85-20190

Airborne remote sensing CCD imaging system
11 p1623 N85-20220

Earth observations and the polar platform
[NOAA-TR-NESDIS-18] 11 p1669 N85-20517

Influence of the atmosphere on remotely sensed reflection from vegetation surfaces
[DE85-000858] 11 p1670 N85-20521

Space System Applications to Tactical Operations
[AGARD-CP-344] 11 p1709 N85-20751

Defense Meteorological Satellite Program (DMSP)
11 p1711 N85-20766

The spot operational remote sensing satellite system: Current status and perspectives
11 p1713 N85-20776

The ESA remote sensing satellite system (ERS-1)
11 p1713 N85-20777

Preserve the sense of Earth from space — achieves of remote sensing data
[PB85-124121] 11 p1740 N85-20942

In situ orbital debris experiment concepts
12 p1784 N85-21198

Passive microwave remote sensing for sea ice research
[NASA-CR-175570] 12 p1874 N85-21758

Workshop on Remote Sensing/Lineament Applications for Energy Extraction
[DE84-009291] 12 p1875 N85-21763

Method and apparatus for calibrating the ionosphere and application to surveillance of geophysical events
[NASA-CASE-NPO-15430-1] 12 p1887 N85-21846

USSR report: Space
[JPRS-USP-85-001] 13 p1977 N85-22403

Remote sensing used for study of forest resources
13 p1983 N85-22440

China report: Science and technology
[JPRS-CST-85-005] 13 p2052 N85-22843

Geological remote sensing develops rapidly, finds broad applications 13 p2052 N85-22848

Radiosodar system for remote synchronous measurements of wind speed, temperature and its fluctuations 13 p2110 N85-23145

Remote Sensing of Snow and Evapotranspiration
[NASA-CP-2363] 13 p2123 N85-23223

NASA's land remote sensing plans for the 1990's
13 p2124 N85-23224

General report of the researches of snowpack properties, snowmelt runoff and evapotranspiration in Japan 13 p2124 N85-23225

Snowmelt-runoff model utilizing remotely-sensed data
13 p2124 N85-23226

Microwave radiometer observations of snowpack properties and comparison of U.S. Japanese results — Hokkaido, Japan and Vermont and North Dakota test sites 13 p2125 N85-23230

Estimation of regional evapotranspiration using remotely sensed land surface temperature. Part 1: Measurement of evapotranspiration at the Environmental Research Center and determination of Priestley-Taylor parameter
13 p2125 N85-23233

Estimation of regional evapotranspiration using remotely sensed land surface temperature. Part 2: Application of equilibrium evaporation model to estimate evapotranspiration by remote sensing technique — Japan
13 p2125 N85-23234

Characteristic vector analysis of inflection ratio spectra: New technique for analysis of ocean color data
[NASA-TP-2428] 13 p2126 N85-23237

Feature extraction assessment study
[AD-A150189] 13 p2126 N85-23239

Comprehensive, integrated, remote sensing at DOE sites
[DE85-004867] 13 p2126 N85-23240

Accomplishments of Institute of Cartography summarized 13 p2166 N85-23495

Zeolites on Mars: Prospects for remote sensing
13 p2195 N85-23615

Analysis of SMIRR data for volcanic and sedimentary terrains of the trans-Pecos region, Texas
13 p2197 N85-23626

Orbiting multi-beam microwave radiometer for soil moisture remote sensing 14 p2230 N85-23818

Low-frequency microwave radiometer for N-ROSS
14 p2230 N85-23819

Large space antenna technology applied to radar-imaging, rain-rate measurements, and ocean wind sensing 14 p2230 N85-23820

Advanced 2-frequency ocean sensing radar using high resolution antenna beams 14 p2230 N85-23821

The use of the ARGOS system for the study of the drift of Antarctic icebergs 14 p2240 N85-23890

China report: Science and technology
[JPRS-CST-84-012] 14 p2283 N85-24140

Remote sensing: New tool for China's geologists
14 p2283 N85-24141

Geometric error analysis for shuttle imaging spectrometer experiment
[NASA-CR-175665] 14 p2305 N85-24269

Remote sensing of directional wave spectra using the surface contour radar
[NASA-TM-84440] 14 p2347 N85-24510

Evaluation of carrying capacity and landscape damage in northern Kenya by multistage remote sensing
[DFVLR-FB-84-47] 14 p2347 N85-24514

Determination of ionospheric electron density profiles from satellite UV (ultraviolet) emission measurements
[AD-A150734] 14 p2373 N85-24667

Scientific experiments. Preprocessing of scientific data — spaceborne experiments
14 p2398 N85-24779

USSR report: Space
[JPRS-USP-85-003] 15 p2476 N85-25284

Optimization of system for observing Northern Hemisphere atmospheric pressure field
15 p2485 N85-25338

Use of space information in petroleum- and gas-prospecting work (example of Southern Mangyshlak)
15 p2485 N85-25341

Evaluating identifiability in remote sensing problems
15 p2486 N85-25347

Determining characteristics of optical radiation reflectors based on results of remote sensing
15 p2488 N85-25358

Details on spot remote sensing satellite propulsion unit 15 p2535 N85-25640

Analysis of suspended sediment distributions in the surface waters of Delaware Bay using remote sensing of optical properties 15 p2582 N85-25926

Survey of remote sensing techniques for wave measurement
[NASA-TM-84429] 15 p2583 N85-25928

SAM 2 measurements of the polar stratospheric aerosol, volume 5
[NASA-RP-1140] 15 p2590 N85-25970

Shuttle imaging radar-B (SIR-B) data analysis for identifying rainfall event occurrence and intensity
[NASA-CR-175712] 15 p2594 N85-25986

Potential climatic effects on the Greenland ice sheet
15 p2603 N85-26044

Connection between time- and frequency-domain three-dimensional inverse problems for the Schroedinger equation
[DE85-005814] 15 p2639 N85-26274

Tenth Conference of Working Group of Socialist Countries on Remote Sensing of Earth under Intercosmos Program 16 p2725 N85-26820

One approach to remote sensing of total ozone content 16 p2725 N85-26822

Scheme for atmospheric thermal sensing from satellites with enhanced vertical resolution
16 p2726 N85-26823

Multiple regression analysis of photographic image of soil properties 16 p2726 N85-26825

Contribution to space program reviewed
16 p2727 N85-26834

Radar return from vegetation covered terrains
[INPE-3470-PRE/713] 16 p2770 N85-27093

The Bresex multispectral camera: Preliminary characteristics
[INPE-3424-PRE/687] 16 p2787 N85-27195

China's integrated circuit production
16 p2806 N85-27302

Study of the urban evolution of Brasilia with the use of LANDSAT data
[E85-10101] 16 p2809 N85-27321

Simultaneous Earth observations from 2 satellites
[NASA-TM-86204] 16 p2810 N85-27325

System of interpretation of remote sensing data when hydrocarbons are present, volume 2
[INPE-3087-TDL/162-VOL-2] 16 p2810 N85-27326

SELPER (Latin American Society of Remote Sensory Specialists)
[INPE-3315-PRE/622] 16 p2810 N85-27328

Function of remote sensing in Brazil
[INPE-3314-PRE/621] 16 p2810 N85-27329

The relevance of remote sensing to Brazil
[INPE-3421-PRE/686] 16 p2811 N85-27332

Utilization of remote sensing data in the evaluation of air pollution characteristics in the south coast/Southeast Desert Air Basin
[PB85-162063] 16 p2822 N85-27407

In-situ stratospheric ozone measurements: Recent results and their implications 16 p2824 N85-27419

SAM II measurements of the polar stratospheric aerosol. Volume 6: April to October 1981
[NASA-RP-1141] 16 p2825 N85-27422

Ground-based remote sensing of atmospheric pollution 16 p2832 N85-27462

Atmospheric frontal zone studies
[NASA-CR-175293] 16 p2833 N85-27469

Experience of the Institute of Space Research with the use of remote sensing in urban planning studies
[INPE-3159-PRE/533] 16 p2880 N85-27770

Remote sensing of the plasma with time delay measurements (coronal sounding)
16 p2886 N85-27804

Solar activity monitoring satellite (SAMSAT): Impact on space environment services
[PB85-165066] 16 p2888 N85-27818

Test devices for aeronautical research and technology
[NASA-TM-77651] 17 p2905 N85-27914
Earth observation modeling based on layer scattering matrices
[NLR-MP-84015-U] 17 p2964 N85-28440
Developments in remote sensing
[B6580069] 17 p2964 N85-28441
Convective storm downdraft outflows detected by NASA/MSFC's Airborne 10.6 micron pulsed Doppler Lidar System
[NASA-CR-3898] 17 p2965 N85-28511
Light scattering by leaf layers with application to canopy reflectance modeling: The Scattering by Arbitrarily Inclined Leaves (SAIL) model
[NLR-MP-84011-U] 17 p3038 N85-28796
Experimental philosophy leading to a small scale digital data base of the conterminous United States for designing experiments with remotely sensed data
[NASA-TM-85009] 17 p3049 N85-28877
German contributions to the cartography of Antarctica by means of photogrammetry and remote sensing
18 p3124 N85-29342
Looking down looking forward: Earth observation, sciences and applications, a perspective
[ESA-SP-1073] 18 p3149 N85-29497
Arctic mixed layer dynamics
[AD-A153582] 18 p3150 N85-29505
ERS economic impace study
[ESA-CR(P)-1979] 18 p3199 N85-29847
Technology assessment of high pulse energy CO(2) lasers for remote sensing from satellites
[NASA-TM-86415] 19 p3275 N85-30309
Space methods for geological research
19 p3295 N85-30429
Spectral reflectances of natural targets for use in remote sensing studies
[NASA-RP-1139] 19 p3299 N85-30450
Nimbus 7 Coastal Zone Color Scanner (CZCS). Level 2 data product users' guide
[NASA-TM-86202] 19 p3299 N85-30452
Nimbus 7 Coastal Zone Color Scanner (CZCS). Level 1 data product users' guide
[NASA-TM-86203] 19 p3299 N85-30453
Active and passive remote sensing of ice
[AD-A154406] 19 p3300 N85-30459
Geologic interpretation of remote sensing data for the Martian volcano Ascraeus Mons
19 p3384 N85-30992
Microwave hydrology: A trilogy
[NASA-CR-176042] 20 p3477 N85-31603
Influence of spatial variability of hydraulic characteristics of soils on surface parameters obtained from remote sensing data in infrared and microwaves
[NASA-TM-77902] 20 p3477 N85-31604
Remote Sensing Technology: Symposium Proceedings
[DE85-010212] 20 p3477 N85-31606
Millimetre wave pulse technology — satellite mapping
[ESA-CR(P)-2004] 20 p3478 N85-31611
Tropical Ocean and Global Atmosphere (TOGA) heat exchange project: A summary report
[NASA-CR-176038] 20 p3496 N85-31738
A new global geomorphology?
21 p3601 N85-32358
Geomorphological similarity and uniqueness
21 p3601 N85-32361
Regional landform thresholds
21 p3601 N85-32362
Mega-geomorphology and neotectonics
21 p3602 N85-32366
Andrean examples of mega-geomorphology themes
21 p3602 N85-32367
Space imagery and some geomorphological problems of the Guiana Shield, South America
21 p3602 N85-32368
Deep sea mega-geomorphology: Progress and problems
21 p3602 N85-32369
Use of the synoptic view: Examples from Earth and other planets
21 p3602 N85-32371
Geomorphic analyses from space imagery
21 p3603 N85-32374
Use of spaceborne imaging radar in regional geomorphic studies
21 p3603 N85-32377
Techniques, problems and uses of mega-geomorphological mapping
21 p3604 N85-32378
Global geomorphology: Report of Working Group Number 1
21 p3604 N85-32382
Process thresholds: Raport of Working Group Number 3
21 p3604 N85-32384
Biogeochemical cycling and remote sensing
21 p3659 N85-32733
Remote medical diagnosis 21 p3663 N85-32753
Participation of singlet oxygen in photodestruction of air-saturated solutions of coumarin dyes
21 p3685 N85-32891
The possibilities of remote analysis of atmospheric gases based on Raman scattering spectroscopy
21 p3685 N85-32892
Cosmonauts participate in multilevel remote sensing experiment 22 p3731 N85-33130
Spacecraft-aided research discussed at geology Congress 22 p3734 N85-33147
Enhancing precision of remote temperature sensing data from satellites under cloudy atmospheric conditions
22 p3734 N85-33148
Impact of fluctuations in optical properties of atmosphere on the ratio of spectral brightness from remote sensing of agricultural land 22 p3734 N85-33149
Determination of altitude of cloud cover top from Meteor satellite data 22 p3734 N85-33150
Landscape interpretation capabilities using space photographs of regions of a multistage platform mantle structure 22 p3734 N85-33151
Interpretation of multiband photographs made during Telefoto-80 experiment for the purpose of discriminating agricultural crops 22 p3735 N85-33152
Using remote photographs in prospecting for hydrocarbons on the Kerch Peninsula
22 p3735 N85-33154
Cataloging the spectral brightness coefficients of the forested region of the European territory of the USSR
22 p3735 N85-33155
Regression analysis of aircraft and ground measurement data on vegetation cover 22 p3735 N85-33156
Direct regression analysis of remote sensing data (using example of grass cover) 22 p3736 N85-33157
Optical-fiber/microprocessor-based remote velocity sensor
[DE85-010071] 22 p3788 N85-33470
Fracture detection and characterization for geothermal reservoir definition
[DE85-006877] 22 p3815 N85-33630
Potential spin-offs of the carbon dioxide observational platform system (CO-OPS) for remote sensing opportunities
[NASA-TP-2510] 23 p3899 N85-34149
The scientific and technical issues in integrating remotely sensed imagery with geocoded data bases
23 p3900 N85-34547
Selection of segment similarity measures for hierarchical picture segmentation 23 p3900 N85-34548
The International Cometary Explorer (ICE)wallsheet teacher's guide
[NASA-TM-87498] 23 p3988 N85-34727
Microwave properties of a quiet sea
[NASA-CR-176199] 24 p4085 N85-35322
Processing of LANDSAT imagery to map surface mineral alteration on the Alaska Peninsula, Alaska
24 p4106 N85-35455
The development of assessment techniques program
24 p4106 N85-35457
Remote sensing of hydrologic transport processes using spot simulation data
[DE85-012412] 24 p4108 N85-35467
Kinematic analysis of Hurricane Frederick (1979) using satellite, aircraft and rawinsonde data
[NASA-CR-176167] 24 p4119 N85-35533
Sea surface and remotely sensed temperatures off Cape Mendocino, California
[NASA-TM-86712] 24 p4125 N85-35573

REMOTE SENSORS

Flight demonstration of new NRL real-time data acquisition system and laser video waveform sampler
[AD-A145126] 01 p0053 N85-10350
Middle infrared spectral studies of geologic materials in their natural state using photothermal beam deflection spectroscopy
[AD-A144894] 01 p0120 N85-10820
Earth Resources, A Continuing Bibliography with Indexes
[NASA-SP-7041(43)] 03 p0378 N85-12411
Thematic Mapper. Volume 1: Calibration report flight model, LANDSAT 5
[E85-10059] 07 p0987 N85-16270
Thematic Mapper. Volume 2: Flight model preshipment review
[E85-10060] 07 p0987 N85-16271
On-board processing for linescan sensors in miniature unmanned aircraft
[RAE-TM-SPACE-327] 08 p1085 N85-16870
Development of the GASCOPACT (R) pipe and cable tracer
[ERS-E.340] 09 p1324 N85-18320
GASCOPACT: A new approach to pipe and cable location
[ERS-E.363] 09 p1325 N85-18324
Nautical charting with remotely sensed imagery, volume 1
[AD-A149361] 10 p1508 N85-19503
An evaluation of wind measurements by four Doppler sodars
[PB85-115301] 10 p1520 N85-19586
Spectral characterization of the LANDAT-4 MSS sensors 11 p1666 N85-20499
LANDSAT-4 Science Characterization Early Results. Volume 2, part 1: Thematic Mapper (TM)
[E85-10068] 11 p1668 N85-20508
An overview of LANDSAT-4 and the Thematic Mapper
11 p1668 N85-20509
Remote self-contained undersea monitor
[AD-D011520] 12 p1849 N85-21599
Method of and apparatus for measuring temperature and pressure — atmospheric sounding
[NASA-CASE-GSC-12558-1] 12 p1856 N85-21639
Spatial resolution estimation of LANDSAT-4 Thematic Mapper data 12 p1872 N85-21741
Digital processing of mesoscale analysis and space sensor data
[NASA-CR-171429] 13 p2146 N85-23319
The remote detection of polynuclear aromatic hydrocarbons using laser-induced fluorescence
[AD-A152294] 16 p2757 N85-27013
Active and passive remote sensing of ice
[AD-A151741] 16 p2815 N85-27369
A transduction path method of solid state sensor analysis and investigation
[AD-A152123] 16 p2870 N85-27707
Development of an EM-Based lifeform detector
[AD-A153504] 18 p3151 N85-29512
Chemometric analysis of multisensor arrays
[AD-A153805] 18 p3174 N85-29680
A laser slope gauge and a spar buoy wave gauge: Tools for the validation of microwave remote sensors
[AD-A154038] 19 p3272 N85-30290
Touch-off: A method to determine the position of an object by means of a sensor-driven robot
[DE85-011178] 19 p3339 N85-30691
System enhancements of Mesoscale Analysis and Space Sensor (MASS) computer system
[NASA-CR-171483] 19 p3342 N85-30708
Spectroradiometric calibration of the Thematic Mapper and Multispectral Scanner system
[E85-10104] 20 p3476 N85-31601
Characteristics and sources of E-region ionization in the continuous aurora
[AD-A155018] 21 p3632 N85-32562
Target observability for satellite-based sensors
[AD-A156139] 24 p4089 N85-35217

REMOTELY PILOTED VEHICLES

Characterization of atmospheric conditions along transmission paths from a remotely piloted vehicle
[AD-A145527] 02 p0232 N85-11511
Visual systems for remotely controlled vehicles
05 p0703 N85-14512
Technology development for unmanned untethered submersible vehicle systems
[AD-A148784] 09 p1304 N85-18180
Operational effectiveness of a Multiple Aquila Control System (MACS)
[NASA-CR-174436] 10 p1427 N85-19000
Operation and maintenance requirements of the Army Remotely Piloted Vehicle (RPV)
[NASA-CR-175714] 14 p2216 N85-23755
Remote control of an impact demonstration vehicle
[NASA-TM-85925] 14 p2225 N85-23797
The PINGUIN B3: A remotely piloted vehicle for mine identification and disposal
[MBB-UM-1/84-O] 18 p2874 N85-27735
British super-shuttle 18 p3087 N85-29104
A remote-operated manipulator vehicle
[HSE-TRANS-11133] 19 p3281 N85-30349
A survey of the turbulence in the marine surface layer for the operation of low-Reynolds number aircraft
[AD-A154133] 19 p3316 N85-30558
Flight test experience and controlled impact of a large, four-engine, remotely piloted airplane
[NASA-TM-86736] 22 p3730 N85-33123

REMOVAL

Heliport snow and ice control methods and guidelines
[DOT/FAA/PM-84/22] 01 p0012 N85-10073
Digital Terrain Elevation Data (DTED) anomaly removal through the use of an interactive Fourier frequency filtering process
[AD-A145433] 02 p0219 N85-11445
Laser paint removal
[AD-P004009] 03 p0308 N85-11969
Alternatives for runway rubber removal from porous friction surfaces
[DOT/FAA/PM-84/28] 05 p0597 N85-13803
A method of making the gas-electric removal of highly dispersed particles more effective
[BLL-M-36030-(5828.4)] 06 p0765 N85-14890
The mechanical procedures for the 8 channel bolometer — United Kingdom Infrared Telescope
[UKIRT-18] 09 p1414 N85-19016

The removal, mechanical handling and installation procedures for the RA Itek encoder
[UKIRT-21] 09 p1414 N85-19919
Removal of heavy metals by artificial wetlands
[PB85-116127] 10 p1513 N85-19548
Improved techniques for removal of sediments contaminated with hazardous materials
[PB85-116093] 11 p1579 N85-20580
Hydrogen embrittlement of cadmium-plated ultra-high strength steels in paint strippers
[ARL/MAT-R-117] 12 p1806 N85-21328
Hazardous air pollutants: Dry-deposition phenomena
[PB85-136279] 12 p1867 N85-21843
The behaviour of nitride inclusions in nickel-base alloys
[BLL-BISI-TRANS-22396-(9022.06)] 17 p2927 N85-28058
A comparative evaluation of the effects of acid precipitation, natural acid production and harvesting on cation removal from forests
[DE85-010821] 19 p3309 N85-30511
Method for removing chlorine compounds from hydrocarbon mixtures
[DE85-011606] 22 p3742 N85-33191

REMS
U RAPID EYE MOVEMENT STATE

RENAL FUNCTION
The behavior of renal-regulating hormones during hypogravic stress
[NASA-CR-171877] 15 p2616 N85-26123
Mathematical modeling of fluid-electrolyte alterations during weightlessness
[NASA-CR-171881] 15 p2617 N85-26125
Fluid-electrolyte metabolism and renal function in cosmonauts following 185-day spaceflight 23 p3952 N85-34495

RENDEZVOUS
NT ORBITAL RENDEZVOUS
NT SPACE RENDEZVOUS

RENDEZVOUS GUIDANCE
Automatic assembly of space stations 20 p3409 N85-31153

RENDEZVOUS SPACECRAFT
Rendezvous with Saturn's rings 15 p2579 N85-26543

RENE 95
Comparison between the properties of conventional wrought and powder metallurgical alloys for turbine disc applications 07 p0906 N85-15739

REORIENTATION
U RETRAINING

REPAIRING
U MAINTENANCE

REPEATERS
Test and evaluation of a coherent 35 gigahertz radar repeater
[AD-A145714] 02 p0191 N85-11290
Signal Hill solar-powered repeater report and recommendations
[DE85-000487] 09 p1316 N85-18273
Preliminary investigation of the performance of repeater technology for satellite sound broadcasting
[SSP/017/82] 18 p3092 N85-29137

REPETITION
A high-repetition rate, inductively stabilized, long-pulse excimer laser
[DE84-016827] 04 p0508 N85-13229
An evaluation of flashtube signal characteristics
[AD-A146569] 10 p1423 N85-18974
Limits to the burster repetition rate as deduced from the 2nd catalog of the interplanetary network
[OG-1.2-5] 22 p3862 N85-33915
Vector calculation of particle code 23 p3961 N85-34688

REPLACING
The effect of replacing molybdenum with vanadium on the corrosion resistant properties of stainless steels 02 p0178 N85-11197
Life distribution properties of devices subject to deterioration
[AD-A145554] 02 p0206 N85-11358
The replacement of precious metal thick film inks using conductive polymer technology. Phase 1: Feasibility study
[AD-A147814] 07 p0933 N85-15913
On maximizing the expected lifetime of replaceable systems
[AD-A150003] 12 p1852 N85-21680
The role of mock-ups in the development of Orbital Replaceable Units (ORU) 18 p3160 N85-29573
F-111 automatic test equipment replacement program 20 p3437 N85-31322
Negative flexural behavior of precast composite slabs with steel joint 23 p3904 N85-34183

REPLENISHMENT
Computer simulation of multiple stability regions in an internally cooled superconducting conductor and of helium replenishment in a bath-cooled conductor
[DE85-002112] 09 p1399 N85-18805
A replenishment phase study for the NAVSTAR global positioning system
[AD-A152030] 16 p2704 N85-26695
Renewable energy research and development outlook, volume 1
[DE85-011577] 20 p3540 N85-32033
Feasibility of applications of Competition Decision Assist Package (CDAP) to spare parts
[AD-A154716] 21 p3712 N85-33036

REPLICAS
Application of extraction replicas and analytical electron microscopy to precipitate phase studies
[DE85-001253] 06 p0769 N85-14919

REPORTS
NT CONGRESSIONAL REPORTS
NT PRESIDENTIAL REPORTS
Research and technology highlights of the Lewis Research Center
[NASA-TM-86899] 08 p1261 N85-17928
Research and technology, Lyndon B. Johnson Space Center
[NASA-TM-58263] 08 p1262 N85-17929
West Europe report: Science and technology
[JPRS-WST-85-003] 09 p1309 N85-18224
USSR report: Life sciences. Biomedical and behavioral sciences
[JPRS-UBB-85-011] 10 p1525 N85-19616
USSR report: Physics and mathematics
[JPRS-UPM-85-001] 11 p1715 N85-20786
Research in surface sciences, disordered materials, and solidification and growth
[PB85-132140] 11 p1737 N85-20927
Transportation
[JPRS-UTR-85-004] 12 p1769 N85-21105
Activities of the Jet Propulsion Laboratory, 1 January - 31 December 1983
[NASA-CR-175555] 13 p2167 N85-23447
Investigations carried out under the Director's Discretionary Fund
[NASA-CR-175676] 14 p2432 N85-24999
USSR report: Transportation
[JPRS-UTR-84-025] 17 p2894 N85-27841
Experimental plasma research: Plasma summaries
[DE85-008116] 17 p3039 N85-28805
Analytical Chemistry Division
[DE85-010585] 18 p3068 N85-28974
National Archives and Records Service (NARS) twenty year preservation plan
[PB85-177640] 18 p3200 N85-29654
High-efficiency silicon solar cell research 21 p3609 N85-32417
National Center for Atmospheric Research
[PB85-191237] 22 p3846 N85-33835
NBS (National Bureau of Standards) library serial holdings, 1985
[PB85-191946] 22 p3849 N85-33839
Confinement experiments on ISX-B
[DE85-012346] 23 p3964 N85-34709

REPRESENTATIONS
A representation for the functioning of devices that supports compilation of expert problem solving structures: An extended summary
[AD-P003921] 02 p0245 N85-11601

REPRODUCTION (BIOLOGY)
Pollutant body burdens and reproduction in Platichthys stellatus from San Francisco Bay
[DE85-010407] 19 p3308 N85-30509
Vertebrate development in space: Gravity is a drag (and has been for eons and eons) 24 p4126 N85-35580

REPRODUCTION (COPYING)
Photocopiers: Do they pose a health hazard?
[P83-1E] 02 p0234 N85-11527
An investigation into the fidelity of reproduction of UKST original objective prism plates on to film — United Kingdom Schmidt Telescope (UKST) 07 p0965 N85-16123

REPTILES
NT TURTLES

REPUBLIC AIRCRAFT
NT A-10 AIRCRAFT

REPUBLIC MILITARY AIRCRAFT
U MILITARY AIRCRAFT

REPUBLIC OF CHINA
U TAIWAN

REPUBLIC OF SOUTH AFRICA
The SANCOR estuaries programme, 1982-1986
[ISBN-0-7988-2662-2] 01 p0068 N85-10454
The SANCOR programme on coastal processes, April 1982 - March 1986
[REPT-68] 01 p0069 N85-10455
Estuaries of the Cape. Part 2: Synopses of available information on individual systems. Report 12: Buffels (WES) (CSW 1), Elsies (CSW 2), Sir Lowry's Pass (CSW8), Steenbras (CSW 9), and Buffels (OOS) (CSW 11)
[CSIR-RR-411-PT-2] 01 p0066 N85-10581
Estuaries of the Cape. Part 2: Synopses of available information on individual systems. Report no. 14: Sand (CSW 4)
[CSIR-RR-413-PT-2] 01 p0086 N85-10583
Estuaries of the Cape. Part 2: Synopses of available information on individual systems. Report no. 15: Zeekoe (CSW 5)
[CSIR-RR-414-PT-2] 01 p0087 N85-10584
Estuaries of the Cape. Part 2: Synopses of available information on individual systems. Report no. 16: Eerste (CSW 6)
[CSIR-RR-415-PT-2] 01 p0087 N85-10585

REPULSION
U FORCE

REQUIREMENTS
Information requirements analysis: An application
[AD-A144896] 01 p0125 N85-10658
DOD related software technology requirements, practices, and prospects for the future
[AD-A145493] 02 p0242 N85-11575
Design of a scientific information collation and dissemination system, volumes 1 thru 3
[AD-A146002] 03 p0438 N85-12791
Operational requirements - system concepts 06 p0752 N85-14823
Man-machine interface requirements - advanced technology 06 p0753 N85-14825
View of future requirements for engine cyclic durability by analysis and testing 07 p0908 N85-15751
Estimating wartime support resource requirements. Statistical and related policy issues
[AD-A147923] 07 p1053 N85-16685
Overview od STS ground operations/orbiter turnaround STS-1 through STS-7 08 p1096 N85-16926
Safety requirements for wiring systems and connectors for photovoltaic systems
[NASA-CR-174431] 10 p1477 N85-19324
Distributed data processing design methodology
[AD-A148868] 10 p1537 N85-19692
A proposed integration among organizational information requirements, media richness and structural design
[AD-A149317] 10 p1567 N85-19881
Requirements formulation subtask 1.A of the Major Item System Mapping (MISM) project
[DE85-000976] 11 p1740 N85-20940
GSFC specification electronic data processing magnetic recording tape
[NASA-TM-80599] 12 p1851 N85-21609
1985 Resident research associateships: Postdoctoral and senior research awards
[NASA-TM-87458] 12 p1963 N85-22338
Safety with industrial manufacturing lasers 14 p2308 N85-24281
Procedures for use in compiling requirements specifications for computerized library systems
[CSTI-76] 15 p2665 N85-26446
Design and implementation of the digital engineering laboratory distributed database management system
[AD-A151694] 15 p2665 N85-26450
Technical overview structural dynamics 16 p2736 N85-26883
USAF damage tolerant design handbook: Guidelines for the analysis and design of damage tolerant aircraft structures, revision B
[AD-A153161] 17 p2896 N85-27858
Steel Tubes
[BLL-BISI-TRANS-22064-(9022.06)] 17 p2973 N85-28369
Functional and performance requirements of the next NOAA-Kasas City computer system 17 p2994 N85-28510
A systematic determination of skill and simulator requirements for airline transport pilot certification
[AD-A154136] 19 p3330 N85-30530
Proceedings of the Workshop on Detectors for Relativistic Nuclear Collisions
[LBL-18225] 24 p4146 N85-35700

RESCUE OPERATIONS
SAR maritime missions 06 p0751 N85-14813
HH-60D night hawk helicopter 06 p0752 N85-14817
Avionics system design for requirements for the United States Coast Guard HH-65A Dolphin 06 p0753 N85-14827
Shipboard and satellite-aided communications equipment in exhibition 08 p0819 N85-15203
Experimental satellite system for determining coordinates of maritime distress 09 p1308 N85-18216

The sinking of the Les Mutuelles du Mans trimaran
14 p2327 N85-24384
The SARSAT program 14 p2327 N85-24385
The ARGOS contribution to the demonstration of the effectiveness of a satellite-based search and rescue system 14 p2330 N85-24404
The SARSAT/COSPAS system for assisting satellite based search and rescue 14 p2396 N85-24776
Microcomputer application of aerospace asset surface search planning
[AD-A151833] 15 p2467 N85-25227
International conference on COSPAS-SARSAT system
15 p2484 N85-25336
Lidar techniques for search and rescue
[DE85-009586] 19 p3278 N85-30327
Satellite aided search and rescue. Experimental results and operational prospects — conference
[ISBN-2-85428-120-9] 20 p3400 N85-31088
The international organization of maritime search and rescue 20 p3400 N85-31089
Search and rescue services for international civil aviation 20 p3400 N85-31090
INMARSAT: An overview 20 p3400 N85-31091
COSPAS/SARSAT: An overview
20 p3400 N85-31092
Maritime search and rescue cooperation and planning
20 p3400 N85-31093
Search and rescue at sea in the USSR
20 p3400 N85-31094
The contribution of an operational SAR satellite system to the UK SAR organisation — search and rescue (SAR)
20 p3400 N85-31095
Search and rescue of aircraft in distress in France. Organization, means 20 p3401 N85-31096
Specific aspects of maritime search and rescue in French metropolitan and overseas territories: Expected benefits from a detection and location of distress system by satellites 20 p3401 N85-31097
Search and rescue in Canada
20 p3401 N85-31098
The national Search and Rescue (SAR) needs and organization in Norway 20 p3401 N85-31099
Possible use of the COSPAS/SARSAT system within the Swedish mountain rescue organization
20 p3401 N85-31100
The COSPAS-SARSAT system
20 p3401 N85-31101
The COSPAS-SARSAT space segment: Present status and evolution 20 p3401 N85-31102
Rescue satellite COSPAS 20 p3401 N85-31103
The 121.5 MHz ELT: Past, present and future — Emergency Locator Transmitter (ELT)
20 p3401 N85-31105
The 406 MHz ELT/EPIRBs — Emergency Locator Transmitters/Emergency Position Indicating Radio Beacons (ELT/EPIRB) 20 p3402 N85-31106
Soviet Emergency Locator Transmitter/Emergency Position Indicating Radio Beacon (ELT/EPIRBs) at 121.5 and 406 MHz 20 p3402 N85-31107
Ground segment of COSPAS system
20 p3402 N85-31108
Existing and potential INMARSAT capabilities for the Future Global Maritime Distress and Safety System
20 p3402 N85-31110
The International Radio Consultative Committee (CCIR) recommended satellite Emergency Position Indicating Radio Beacon (EPIRB) system operating through geostationary satellites at 1.6 GHz
20 p3402 N85-31112
A 406 MHz geostationary satellite SARSAT experiment 20 p3403 N85-31113
Evolution of 406 MHz Search and Rescue (SAR) processor 20 p3403 N85-31116
Free-float Emergency Position Indicating Radio Beacons (EPIRBs) and release mechanism on board Norwegian ships. Main specifications and user experience
20 p3404 N85-31120
Experiments of a LORAN-C aided recovery system and a proposal of its application to rescue system
20 p3404 N85-31121
SARSAT 406 MHz system technical evaluation
20 p3404 N85-31124
The COSPAS system tests. Technical results
20 p3404 N85-31125
Use of 121.5/243.0 MHz COSPAS-SARSAT data by North American SAR agencies — search and rescue (SAR)
20 p3405 N85-31127
The COSPAS/SARSAT demonstration and evaluation. Results of the first year in the United States
20 p3405 N85-31128
COSPAS-SARSAT demonstration and evaluation results in Canada 20 p3405 N85-31129
COSPAS-SARSAT demonstration and evaluation phase: COSPAS tests in the USSR and their results
20 p3405 N85-31130
The SARSAT-COSPAS demonstration in France
20 p3405 N85-31131
UK experience with COSPAS-SARSAT and INMARSAT distress systems 20 p3406 N85-31132
The COSPAS-SARSAT system evaluation in Norway
20 p3406 N85-31133
INMARSAT distress and safety communication
20 p3406 N85-31134
Maritime mobile satellite techniques as an integral part of the Future Global Maritime Distress and Safety System (FGMDSS): The position of the Federal Republic of Germany 20 p3406 N85-31136
Future prospects for a combined INMARSAT polar communication and search and rescue satellite system
20 p3406 N85-31137
The development of an institutional structure for the Future Global Satellite System for Search and Rescue
20 p3406 N85-31138
Aircraft accident report: World Airways Inc., Flight 30H, McDonnell Douglas DC-10-30CF, N113WA, Boston-Logan International Airport, Boston, Massachusetts, January 23, 1982
[PB85-910406] 22 p3726 N85-33114
RESEARCH
NT DYNAMIC PROGRAMMING
NT LINEAR PROGRAMMING
NT LOW DENSITY RESEARCH
NT MARKET RESEARCH
NT MATHEMATICAL PROGRAMMING
NT NONLINEAR PROGRAMMING
NT NUCLEAR RESEARCH
NT QUADRATIC PROGRAMMING
South African Antarctic research report to SCAR, no. 24, 1982. 1: Record of activities: April 1981 - September 1982. 2: Planned activities: October 1982 - September 1983. 3: Recent publications: 1981/1982
[CSIR-SR-SCAR-24] 01 p0063 N85-10417
National Science Foundation, fiscal year 1983, volume 1
[PB84-212315] 01 p0124 N85-10653
Publications of the National Bureau of Standards, 1983 catalog
[PB84-218031] 01 p0126 N85-10669
Artificial intelligence applications to maintenance
[AD-P003914] 02 p0244 N85-11594
Navy programs on ion implantation for materials modification
[AD-P003952] 02 p0266 N85-11858
Characteristics of systems engineering in aviation science research
[AD-A145602] 02 p0292 N85-11899
Computer equipment for research in statistics
[AD-A145755] 03 p0406 N85-12591
Priorities for a national program of continental drilling for scientific purposes 04 p0534 N85-13418
The 1984 NASA/ASEE summer faculty fellowship program
[NASA-TM-87392] 04 p0574 N85-13662
Activities at the Lunar and Planetary Institute
[NASA-CR-174069] 04 p0579 N85-13694
Activities at the Lunar and Planetary Institute, introduction 04 p0579 N85-13695
Resident research associateships. Postdoctoral and senior research awards
[NASA-TM-87399] 05 p0734 N85-14717
Research into topics in transonic flow theory
[AD-A148526] 08 p1078 N85-16837
Beam propagation studies at NRL (Naval Research Laboratory) July 1983 to June 1984, volume 2
[AD-A148199] 08 p1152 N85-17270
Use of iterative linear and nonlinear algebraic methods for solving large stiff systems of ODEs
[AD-A148616] 08 p1213 N85-17838
Research in stochastic processes
[AD-A148622] 08 p1215 N85-17860
Resident research associateships. Postdoctoral and senior research awards: Opportunities for research at the Jet Propulsion Laboratory
[NASA-CR-174343] 09 p1418 N85-18945
Keyword thesaurus: A list of terms and codes to identify areas of interest for research and other types of sponsored programs (revised October 1984)
[PB85-136893] 10 p1588 N85-19880
China report: Science and technology
[JPRS-CST-84-026] 11 p1619 N85-20189
China report: Science and technology
[JPRS-CST-84-025] 11 p1620 N85-20197
Thermophysical properties of matter
11 p1620 N85-20199
China report: Science and technology
[JPRS-CST-85-008] 12 p1820 N85-21418
Report on the Second Annual Review Meeting of the National Acid Precipitation Assessment Program. Research to assist decisionmaking: Summary
[DE85-009009] 12 p1884 N85-21820
Bibliography of Lewis Research Center technical publications announced in 1983
[NASA-TM-83693] 12 p1951 N85-22258
University of Cambridge Institute of Astronomy report of activities 13 p2170 N85-23484
O. F. Mossotti and the physics of molecules
[NOTA-INTERNA-822] 14 p2420 N85-24931
Discovery refutation and verification refutation: The proposals of Von Neumann and Wiener in the development of 20th century physics
[NOTA-INTERNA-840] 14 p2431 N85-24993
The conservation and utilization of scientific research documents: Practical aspects and organization
[NOTA-INTERNA-834] 14 p2433 N85-25006
AFRPL (Air Force Rocket Propulsion Laboratory) technical objective document FY 85
[AD-A151368] 15 p2495 N85-25369
China report: Science and technology
[JPRS-CST-85-011] 15 p2551 N85-25748
Physics, Computer Science and Mathematics Div.
[DE85-006868] 15 p2642 N85-26236
Theoretical studies of Elmo Bumpy Torus
[DE85-007202] 15 p2658 N85-26402
Summaries of FY 1984 engineering research
[DE85-006273] 15 p2664 N85-26442
The search for extraterrestrial intelligence
15 p2669 N85-26609
Recent Naval Postgraduate School publications
[AD-A151723] 16 p2975 N85-27740
Magnetic monopoles
[DE85-008176] 17 p3027 N85-28719
Laboratory research: A question of when, not if
[AD-A153296] 17 p3048 N85-28867
Catalog of research projects at Lawrence Berkeley Laboratory, 1985
[DE85-006679] 17 p3049 N85-28869
Silicide conductors reliability research
[AD-A153766] 18 p3095 N85-29157
Photovoltaic Systems Development Project: An activity summary
[DE85-009994] 18 p3129 N85-29379
Proceedings of the 14th European Solid State Device Research Conference Including Solid State Device Technology, ESSDERC 84
[AD-A153409] 18 p3193 N85-29804
Space station automation study. Volume 1: Executive summary. Autonomous systems and assembly
[NASA-CR-171514] 19 p3226 N85-30002
High-efficiency silicon solar cell research
21 p3609 N85-32417
Activities report of the Aeronomy Department
[G-774-1984] 21 p3633 N85-32599
Air force technical objective document, Aerospace Medical Division, Fiscal Year 1986
[AD-A155195] 21 p3664 N85-32762
Air Force Office of Scientific Research (AFOSR). Technical report summaries: First quarter (CY)
[AD-A154757] 21 p3713 N85-33041
Investigation of DBMS (Data Base Management Systems) for use in a research environment
[AD-A154982] 21 p3713 N85-33042
The flow of scientific and technical information in the US Army Research Laboratories
[AD-A155050] 21 p3713 N85-33043
Energy efficient transport technology: Program summary and bibliography
[NASA-RP-1135] 22 p3729 N85-33116
National Center for Atmospheric Research
[PB85-191237] 22 p3848 N85-33835
RESEARCH AIRCRAFT
NT B-70 AIRCRAFT
NT ROTOR SYSTEMS RESEARCH AIRCRAFT
NT U-2 AIRCRAFT
NT X-15 AIRCRAFT
A preliminary flight evaluation of the peripheral vision display using the NT-33A aircraft
[AD-A145123] 01 p0010 N85-10060
YO-3A acoustics research aircraft systems manual
[NASA-TM-85968] 01 p0012 N85-10074
Role of research aircraft in technology development
[NASA-TM-85913] 02 p0137 N85-10932
First stage of equipping a Do 28 as a research aircraft for icing, and first research results
[ESA-TT-855] 11 p1584 N85-19662
ADAPS (Airborne Data Acquisition and Processing System) operation and maintenance manual
[AD-A149297] 11 p1585 N85-19663
Miniature electrooptical air flow sensor
[NASA-CASE-LAR-13065-1] 11 p1635 N85-20295
Civil avionics flight testing with the RAE(B) BAC1-11
13 p1967 N85-22354
Multivariable control law design for the X-29 aircraft
[AD-A151828] 15 p2472 N85-25259
X-29 digital flight control system design
17 p2901 N85-27869

The flight control system for the Experimental Aircraft Programme (EAP) demonstration aircraft
17 p2904 N85-27908
West Europe report: Science and technology
[JPRS-WST-85-020] 20 p3436 N85-31333
MBB demonstrates new research aircraft ATTAS
20 p3438 N85-31334

RESEARCH AND DEVELOPMENT

Aeronautics Technology Possibilities for 2000: Report of a workshop
[NASA-CR-174018] 01 p0001 N85-10001
East Europe report: Science and technology
[JPRS-ESA-84-029] 01 p0115 N85-10783
Lagging development of biotechnology described
01 p0115 N85-10787
Canada report to COSPAR 01 p0131 N85-10906
Space commercialization: Analysis of R and D investments with long time horizons
02 p0155 N85-11052
Development of space instrumentation of Intercosmos member countries 02 p0163 N85-11106
The need for improvements in weapon system maintenance: What can AI (Artificial Intelligence) contribute?
[AD-P003913] 02 p0244 N85-11593
Research and development requirements for ion implantation
[AD-P003951] 02 p0286 N85-11867
The status of synthetic fuels and cost-shared energy R and D facilities
[GPO-38-903] 03 p0339 N85-12182
Project resources planning and control
[NASA-TM-86339] 04 p0575 N85-13656
Research report 1979-1982. Part 2: Projects
[ISBN-3-7983-0980-4] 04 p0575 N85-13657
The characteristics of generation and the rate of distribution for science and technology information in our country (China)
[AD-A141037] 04 p0575 N85-13671
The Uniform Science and Technology Research and Development Utilization Act
[GPO-38-327] 04 p0577 N85-13885
Uniform Science and Technology Research and Development Utilization Act
[H-REPT-98-983-PT-1] 04 p0577 N85-13886
International comparative study of systems for the government advancement of research and development
[NASA-TM-77589] 04 p0578 N85-13889
The 15 photovoltaic pilot projects of the European Communities 05 p0663 N85-14283
The management of research institutions: A look at government laboratories
[NASA-SP-481] 07 p1050 N85-16685
Organizations and information processing: A field study of research and development units within the United States Air Force Systems Command
[AD-A147381] 07 p1054 N85-16691
Research and technology, 1984 report
[NASA-TM-83096] 07 p1061 N85-16730
Technology developments for laminar boundary layer control on subsonic transport aircraft
08 p1071 N85-16787
Blade technology program for large wind turbines, phase 1
[BMFT-FB-T-84-217] 08 p1179 N85-17426
Aeroacoustics at the DFVLR Brunswick Research Center: A survey on recent and current activities
[DFVLR-MITT-84-14] 08 p1219 N85-17677
Autonomy in the industrial R and D lab
[AD-A148075] 08 p1228 N85-17736
Outlook for expanding the Federal research in progress system
[AD-A148354] 08 p1229 N85-17737
Research and technology highlights of the Lewis Research Center
[NASA-TM-86899] 08 p1261 N85-17928
Research and technology, Lyndon B. Johnson Space Center
[NASA-TM-58263] 08 p1262 N85-17929
Innovation in British industry (notably the aircraft industry) and its value: Collected papers
[BAE-KRS-N-GEN-286] 09 p1283 N85-17933
Emerging role of the national laboratory in the development and transfer of materials technology
[DE85-001252] 09 p1288 N85-18086
Activities report in aerospace in West Germany
[ISSN-0070-3966] 09 p1418 N85-18947
Worldwide report: Telecommunications policy, research and development
[JPRS-TTP-85-002] 10 p1475 N85-19309
The R and D project selection problem with fuzzy coefficients
[INPE-3329-PRE/626] 10 p1565 N85-19871
Characteristics of quality data
[DE85-001203] 10 p1568 N85-19889
Calendar of selected aeronautical and space meetings
[AGARD-CAL-84/2] 10 p1573 N85-19917
Activities in French aerospace
11 p1587 N85-19995
French research minister on policy, technology transfer 11 p1618 N85-20182
China report: Science and technology
[JPRS-CST-84-039] 11 p1621 N85-20206
Research in environmental biology reviewed
11 p1622 N85-20211
Oversight review of the five-year outlook report on science and technology
[GPO-41-058] 12 p1949 N85-22243
An agenda for a study of government science policy
[GPO-40-860] 12 p1949 N85-22245
President's private sector survey on cost control, report on research and development
[PB84-173269] 12 p1951 N85-22253
1985 Resident research associateships: Postdoctoral and senior research awards
[NASA-TM-87458] 12 p1983 N85-22338
Research and technology: Fiscal year 1984 report
[NASA-TM-85231] 12 p1984 N85-22340
China report: Science and technology
[JPRS-CST-84-030] 13 p2041 N85-22777
Physicists' role in new technological development discussed 13 p2166 N85-23436
Activities in flight mechanics and flight control
[ISSN-0720-7808] 14 p2227 N85-23803
Applications of ultrasonic technology
14 p2263 N85-24144
Thirty-three years of research with shock tubes in the Franco-German Research Institute, Saint Louis (France)
[ISL-CO-226/83] 14 p2302 N85-24257
Summaries of FY 1984 research in high energy physics
[DE85-005641] 14 p2420 N85-24934
Accomplishments of science by the year 2000
14 p2432 N85-24996
Investigations carried out under the Director's Discretionary Fund
[NASA-CR-175676] 14 p2432 N85-24999
Research and technology
[NASA-TM-86662] 14 p2456 N85-25166
Air Force Office of Scientific Research (AFOSR): Technical report summaries. Fourth quarter (CY)
[AD-A150860] 14 p2456 N85-25167
Resources for robotics research in Europe, by country
15 p2489 N85-25364
Outlook for polymer composite materials
15 p2497 N85-25403
Research, development of composite materials described 15 p2497 N85-25404
France officially proposes development of Ariane 5 to ESA 15 p2532 N85-25613
Academic science and engineering: R and D funds, fiscal year 1982 (detailed statistical tables)
[PB85-154763] 15 p2664 N85-26443
AGARD bulletin: Meetings, publications, membership
[AGARD-BUL-85-1] 15 p2686 N85-26589
Flight testing and development of the F/A-18A digital flight control system 16 p2713 N85-26743
East Europe report: Science and technology
[JPRS-ESA-84-032] 16 p2727 N85-26833
Research and development. Technical and scientific reports 1984 16 p2873 N85-27724
NBS (National Bureau of Standards) research reports
[PB85-127421] 16 p2879 N85-27764
Activities in aerospace 17 p2891 N85-27821
Test devices for aeronautical research and technology
[NASA-TM-77651] 17 p2905 N85-27914
Gordon Research Conference on Composites
[AD-A152688] 17 p2917 N85-27979
Integrating quality assurance and research and development
[DE85-007974] 17 p2976 N85-28392
Experimental plasma research: Plasma summaries
[DE85-008116] 17 p3039 N85-28805
The Department of Defense statement on the Science and Technology Program by Colonel Donald I. Carter, USAF Acting Deputy Under Secretary of Defense for Research and Advanced Technology before the Subcommittee on Research and Development of the Committee on Armed Services of the United States House of Representatives, 99th Congress, first session
[AD-A152467] 17 p3046 N85-28850
Multicriteria decision analysis as an aid to strategic planning of energy research and development
[REPT-84-02] 17 p3049 N85-28870
Bibliography of Lewis Research Center technical publications announced in 1984
[NASA-TM-87012] 17 p3049 N85-28876
Multi-ducted inlet combustor research and development
[AD-A153753] 18 p3063 N85-28946
Space station study
[BL-6167] 18 p3066 N85-28959
West Europe report: Science and technology
[JPRS-WST-84-022] 18 p3085 N85-29066
Results of Italian research in high power lasers
18 p3086 N85-29097
Rifa of Sweden conducts research in 3-5 materials
18 p3088 N85-29107
SERI photovoltaic advanced research and development project: FY 1984 accomplishments
[DE85-002939] 18 p3128 N85-29366
Electrochemical Energy Storage Branch
[DE85-007592] 18 p3131 N85-29391
Activities at the Lunar and Planetary Institute
[NASA-CR-175914] 18 p3201 N85-29859
Alloy development for irradiation performance
[DE85-010454] 19 p3240 N85-30091
Present and future directions of atomic physics research with multiply-charged ions at Brookhaven National Laboratory
[DE85-010960] 19 p3354 N85-30788
Strained-layer-superlattice optoelectronic devices
[DE85-009148] 19 p3377 N85-30953
The economics of private sector R and D decisionmaking in aeronautics
[NASA-CR-176007] 19 p3379 N85-30962
National Aeronautics and Space Administration
19 p3382 N85-30980
Note for a research feasibility project: High reliability design in the aeronautical field
[REPT-84-RR-350] 20 p3387 N85-31005
Space research at NLR 20 p3397 N85-31075
NASA Space controls research and technology program 20 p3406 N85-31149
Reciprocating Brayton cycle motor
[REPT-84-RR-336] 20 p3462 N85-31507
The Department of Defense report on the technology base and support of university research
[AD-A154309] 20 p3540 N85-32030
Renewable energy research and development outlook, volume 1
[DE85-011577] 20 p3540 N85-32033
Spin-offs from technical scientific infrastructures, no. 1
20 p3540 N85-32034
Spin-offs from technical scientific research organizations, no. 5 20 p3540 N85-32036
A comprehensive study of the AFIT (Air Force Institute of Technology) software development environment
[AD-A155450] 21 p3672 N85-32812
Management of Corrosion
[AGARD-LS-141] 22 p3749 N85-33238
Photovoltaics technical information guide
[DE85-002924] 22 p3808 N85-33585
Transfer of battery technology developed by the US Department of Energy
[DE85-009868] 22 p3808 N85-33588
Electron photoejection in carbanions
[DE85-011747] 23 p3911 N85-34230
Development of flight mechanics research in Brunswick 24 p4061 N85-35166
Piezoelectric transducers, state of research
24 p4089 N85-35345
Development and evaluation of sulfonated polysulfone membranes for the zinc-ferricyanide battery
[DE85-009104] 24 p4090 N85-35357
United States Army welding research and development topical and coordination meeting
[AD-A155834] 24 p4099 N85-35409
Quality assurance considerations for the implementation of a pulsed power R and D project
[DE85-012357] 24 p4148 N85-35720
The 1986 National Aeronautics and Space Administration authorization
[GPO-47-635] 24 p4166 N85-35829

RESEARCH FACILITIES

Mathmatics and Computer Science Division activities
[DE84-014842] 01 p0104 N85-10701
Ocean energy systems at the Johns Hopkins University Applied Physics Laboratory
[PB84-225705] 03 p0387 N85-12474
Investigation of special facilities for a spallation neutron source 03 p0427 N85-12724
Hydrogen technology evaluation center at Brookhaven National Laboratory
[DE84-014099] 04 p0470 N85-12966
Instrumentation at national facilities for synchrotron radiation topography
[DE84-016256] 04 p0564 N85-13583
Summary and analysis of hearing on improving the research infrastructure at US universities and colleges
[GPO-38-854] 04 p0574 N85-13660
Improving the research infrastructure at US universities and colleges
[GPO-35-290] 04 p0574 N85-13661
NASA-Ames vertical gun 04 p0579 N85-13686

Upper Atmosphere Research Satellite (UARS) trade analysis
[NASA-CR-175269] 07 p0912 N85-15774
Electronics research at the University of Texas at Austin
[AD-A146800] 07 p0947 N85-15968
The management of research institutions: A look at government laboratories
[NASA-SP-481] 07 p1050 N85-16865
Hybrid data processing research facility
[AD-A148092] 08 p1202 N85-17567
Research and technology highlights of the Lewis Research Center
[NASA-TM-86899] 08 p1261 N85-17928
Research and technology, Lyndon B. Johnson Space Center
[NASA-TM-58263] 08 p1262 N85-17929
The Prandtl Hergesell project of a national research establishment for aeronautics
[ESA-TT-835] 09 p1272 N85-17993
The planned expansion of microelectronics capability at Sandia National Laboratory
[TI85-004328] 09 p1314 N85-18260
Air Force space technology center space technology: Emphasis 84
Decade of the Varlov Kupola 09 p1333 N85-18381
10 p1497 N85-19448
Rocky Flats Wind Energy Research Center FY 1983 report
[DE85-004500] 10 p1511 N85-19535
Personal desktop computing in a research and development laboratory
[DE85-002765] 11 p1705 N85-20728
Research in surface sciences, disordered materials, and solidification and growth
[PB85-132140] 11 p1737 N85-20927
Major facilities for materials research and related disciplines
[PB85-106850] 11 p1739 N85-20934
Task and future of the Large Institutes of Technology (LIT)
[B8474720] 11 p1741 N85-20945
Computing Division two-year operational plan, FY 1984 - 1985
[LA-9978-MS] 12 p1913 N85-22006
1985 Resident research associateships: Postdoctoral and senior research awards
[NASA-TM-87458] 12 p1983 N85-22338
Activities of the Jet Propulsion Laboratory, 1 January - 31 December 1983
[NASA-CR-175555] 13 p2167 N85-23447
JESS facility modification and environmental/power plans
[NASA-CR-175685] 14 p2227 N85-23807
French robotics research at Grenoble labs
15 p2523 N85-25555
Soviet Institute director on GDR-USSR welding technology 15 p2536 N85-25562
Geophysical Fluid Dynamics Laboratory activities, FY84, plans, FY85
[PB85-147601] 15 p2558 N85-25783
Basic studies. 1: Basic experiments in plasma physics 15 p2655 N85-26378
High beta pinch plasma (STP-3(M))
15 p2655 N85-26380
Ignition of metals in high pressure oxygen
16 p2735 N85-26874
A summary of the Naval Postgraduate School research program
[AD-A151721] 16 p2875 N85-27736
Nucleon-nucleon program at TRIUMF
[DE85-900430] 17 p3032 N85-28756
Origin, processing, and dissemination of scientific news, with examples from 20 research institutes
[JUEL-1940] 17 p3050 N85-28862
Selected university laboratory needs in support of national security
[AD-A153511] 18 p3197 N85-29833
Metrology and Oceanology Institutes' underwater acoustics R and D 19 p3289 N85-30304
The SLC program
[DE85-011439] 19 p3357 N85-30813
Additional muon calculations for the SLC positron source
[DE85-011212] 19 p3363 N85-30855
High efficiency solar cell research for space applications 20 p3480 N85-31824
Fixed-target physics at Fermilab
[DE85-010141] 20 p3528 N85-31942
R and D activities of the Computer Centre
20 p3540 N85-32029
The flow of scientific and technical information in the US Army Research Laboratories
[AD-A155050] 21 p3713 N85-33043
Current internal-dosimetry practices at US Department of Energy facilities
[DE85-011718] 22 p3787 N85-33466
Langley aeronautics and space test highlights, 1984
[NASA-TM-87585] 23 p4057 N85-35151
United States Army welding research and development topical and coordination meeting
[AD-A155834] 24 p4099 N85-35409

RESEARCH MANAGEMENT

Exploratory investigation of the need for and feasibility of a Lower Atmosphere Research Satellite (LARS) program
[NASA-CR-171181] 01 p0015 N85-10091
Research study: Studies in atmospheric processes from Space Platforms
[NASA-CR-171176] 01 p0072 N85-10473
Numerical algorithms and parallel tasking
[AD-A145090] 01 p0104 N85-10693
Fusion and its future in Illinois
[DE84-014686] 01 p0122 N85-10833
Publications of the National Bureau of Standards, 1983 catalog
[PB84-218031] 01 p0126 N85-10869
Conceptual design and evaluation of selected Space Station concepts, volume 1
[NASA-TM-87383] 02 p0168 N85-11129
Proceedings of the Ion Implantation for Army Needs Workshop
[AD-A145474] 02 p0266 N85-11663
Navy programs on ion implantation for materials modification
[AD-P003952] 02 p0266 N85-11666
Characteristics of systems engineering in aviation science research
[AD-A145602] 02 p0292 N85-11899
Research and technology
[NASA-TM-86321] 02 p0305 N85-11973
Air Force Materials Laboratory plans/projects
[AD-P004010] 03 p0306 N85-11990
Scientific communications and national security
[GPO-36-093] 04 p0492 N85-13136
International coordination in scientific research
04 p0519 N85-13311
Five year research plan, 1984-1988. Photovoltaics: Electricity from sunlight
[DE84-013009] 04 p0528 N85-13377
R and D project selection with nonnumerical returns
[INPE-2760-PRE/395] 04 p0575 N85-13665
International comparative study of systems for the government advancement of research and development
[NASA-TM-77589] 04 p0578 N85-13669
NASA's SESAC report on research and analysis in space and Earth sciences 04 p0579 N85-13697
Activities of the Coastal Research Center
[PB84-231323] 05 p0672 N85-14320
A summary of the foundation research program
[AD-A146524] 06 p0891 N85-15656
Integrated technology wing study (oral presentation)
[NASA-CR-168497] 07 p0902 N85-15718
Evaluation of the musculoskeletal diseases program
[PB84-230648] 07 p1017 N85-16461
Organizations and information processing: A field study of research and development units within the United States Air Force Systems Command
[AD-A147361] 07 p1054 N85-16691
UK, FRG, France: R and D in sensors, related fields
08 p1142 N85-17197
On the validation of computer science theories
[AD-A148637] 08 p1203 N85-17572
Autonomy in the industrial R and D lab
[AD-A149075] 08 p1226 N85-17736
Outlook for expanding the Federal research in progress system
[AD-A148354] 08 p1229 N85-17737
An overview of the research program at the visual technology research simulator
[AD-P004321] 09 p1269 N85-17975
Emerging role of the national laboratory in the development and transfer of materials technology
[DE85-001252] 09 p1286 N85-18086
Evaluation of the Fundamental Research on Explosives (FRE) program
[DE85-001537] 09 p1301 N85-18172
European Scientific Notes, volume 38, number 12
[AD-A148713] 09 p1418 N85-18948
Biomechanical studies of impact acceleration research
[AD-A149077] 10 p1522 N85-19601
National solar-terrestrial research program, part 1. Solar-terrestrial research for the 1990's, part 2
[AD-A149542] 11 p1681 N85-20591
Needs, opportunities, and options for large scale systems research
[DE85-002684] 11 p1709 N85-20750
Task and future of the Large Institutes of Technology (LIT)
[B8474720] 11 p1741 N85-20945
Systems research on China in year 2000
12 p1820 N85-21418
Global tropospheric chemistry: A plan for action
[NASA-CR-175545] 12 p1891 N85-21865
1985 Resident research associateships: Postdoctoral and senior research awards
[NASA-TM-87458] 12 p1983 N85-22338
Research in the optical sciences
[AD-A150196] 13 p2159 N85-23401
Activities of the Jet Propulsion Laboratory, 1 January - 31 December 1983
[NASA-CR-175555] 13 p2167 N85-23447
Authorizing appropriations to the National Aeronautics and Space Administration for fiscal year 1986
[H-REPT-99-32] 13 p2168 N85-23452
Investigations carried out under the Director's Discretionary Fund
[NASA-CR-175676] 14 p2432 N85-24909
Wind energy systems: Program summary for fiscal year, 1983
[DE85-002927] 17 p2965 N85-28451
Nucleon-nucleon program at TRIUMF
[DE85-900430] 17 p3032 N85-28756
Air Force technical objective document FY 86
[AD-A152730] 17 p3047 N85-28855
Science and Technology in the Soviet Union
[AD-A152826] 17 p3047 N85-28856
The outlook for Soviet advanced technologies
[AD-P004564] 17 p3048 N85-28859
Social and political problems in Soviet basic research
[AD-P004565] 17 p3048 N85-28860
Close encounters with S/T (science and technology) in the Soviet Union
[AD-P004570] 17 p3048 N85-28864
R/D contracts in the Soviet Union
[AD-P004580] 17 p3048 N85-28865
Laboratory research: A question of when, not if
[AD-A153296] 17 p3048 N85-28867
Research on structural analysis at the DFVLR, Brunswick 18 p3120 N85-29314
The evolution of the U.S. helicopter industry
[AD-A154290] 19 p3211 N85-29913
EPA (Environmental Protection Agency) research program guide, FY-1985, October 1, 1984 - September 30, 1985
[PB85-181881] 20 p3487 N85-31676
Commission for Marine Meteorology
[WMO-640] 20 p3496 N85-31735
Human factors engineering contracts in Sweden: An overview
[FOA-C-56043-H2] 20 p3513 N85-31836
The Department of Defense report on the technology base and support of university research
[AD-A154309] 20 p3540 N85-32030
The Human Resource Management Information Network (HRMIN): A cost comparison in accordance with Office of Management and Budget (OMB) Circular no. A-76, 5 April 1979
[AD-A154563] 21 p3713 N85-33039
Investigation of DBMS (Data Base Management Systems) for use in a research environment
[AD-A154862] 21 p3713 N85-33042
Research report program of the US Army in Europe
24 p4061 N85-35167
DoD Value Engineering conference report. Value Engineering (VE): A tool that benefits line management. Part 3, Workshop A: VE in the program office
[AD-A156069] 24 p4163 N85-35812

RESEARCH PROJECTS

The application of remote sensing to resource management and environmental quality programs in Kansas
[E85-10023] 02 p0218 N85-11436
Determination sample sizes for diversified reliability test programs
[DE84-015003] 04 p0511 N85-13255
High-Beta plasma theory
[DE84-016471] 04 p0568 N85-13619
Research report 1979-1982. Part 2: Projects
[ISBN-3-7983-0980-4] 04 p0575 N85-13667
International comparative study of systems for the government advancement of research and development
[NASA-TM-77589] 04 p0578 N85-13669
Lightning research: A user's lament
07 p0999 N85-16348
An overview of the research program at the visual technology research simulator
[AD-P004321] 09 p1269 N85-17975
Evaluation of the Fundamental Research on Explosives (FRE) program
[DE85-001537] 09 p1301 N85-18172
European Scientific Notes. Volume 39, number 1
[AD-A149498] 10 p1566 N85-19866
Space Station Spartan study
[NASA-TM-86215] 16 p2731 N85-26852

Summary of research for the Inertial Confinement Fusion Program at Los Alamos National Laboratory
[DE85-010330] 19 p3361 N85-30636

RESEARCH VEHICLES
NT UNDERWATER RESEARCH LABORATORIES
Machine Mechanics Institute builds walking vehicle
04 p0543 N85-13455
The transpacific experimental sailing by YASEIGO 3
14 p2327 N85-24380
Test plan for acceptance, verification and performance testing of the Bedford Lucas Chloride Electric Van. Part 1: Acceptance and verification testing at EG and G Automotive Research. Part 2: INEL performance testing, revision 1
[DE85-005157] 17 p3051 N85-29868
Preliminary results of an ALVIN dive program on active hydrothermal vents at the southern Juan de Fuca Ridge
24 p4106 N85-35454

RESERVES
International strategic minerals inventory. Summary report: Manganese
[GS-CIRC-930-A] 02 p0219 N85-11442
Geology and resources of the Tar Sand Triangle, southeastern Utah
[DE84-012017] 05 p0677 N85-14346
World iron ore reserves
[BLL-BISI-TRANS-22280-(9022.06)]
17 p2983 N85-28435
AUTSKED: An addendum
[DE85-010410] 22 p3829 N85-33712
Preliminary SPR thermal model description and results for WH-11 and BM-4
[DE85-013171] 23 p3931 N85-34360

RESERVOIRS
Identification and parameter estimation of phosphate balance models in drinking water reservoirs
[PUBL-313] 06 p1181 N85-17439
Electrical resistivity technique to assess the integrity of geomembrane liners
[PB85-122414/GAR] 09 p1325 N85-18327
Results from geopressured-geothermal subsidence studies
[DE84-016279] 09 p1354 N85-18520
Laboratory investigation of formation damage of an artificial fracture at simulated geothermal conditions
[DE85-010301] 18 p3102 N85-29201
Modeling water resources systems for water quality
[AD-A154268] 19 p3300 N85-30457
Hydrodynamic solutions for the diffusion of components in confined media 20 p3456 N85-31464
Empirical methods for predicting eutrophication in impoundments. Report 3. Phase 2. Model refinements
[AD-A155483] 21 p3614 N85-32462
Carbon and sulfur cycling through geologic time
21 p3658 N85-32720
Fracture detection and characterization for geothermal reservoir definition
[DE85-006877] 22 p3815 N85-33630
Comprehensive fracture diagnostics experiement. Part 2: Comparison of seven fracture azimuth measurements
[DE85-011707] 23 p3948 N85-34470
Studies in thermo-hydro-chemical transport in porous and fractured media
[DE85-012555] 23 p3949 N85-34473
National program for inspection of non-federal dams. Woodward reservoir dam (VT 00209), Connecticut River Basin, Plymouth, Vermont. Phase 1 inspection report
[AD-A156256] 24 p4144 N85-35693

RESIDENTIAL ENERGY
Microcomputer control of a residential photovoltaic power conditioning system
[DE84-013667] 04 p0547 N85-13480
Correlations of solar irradiance and daylight illuminance for building energy analysis
[DE85-001736] 06 p0839 N85-15326
Microcomputer control of a residential photovoltaic power conditioning system
[DE84-014774] 07 p1022 N85-16488
An assessment of ground-coil heat-pump technology
[DE85-002567] 10 p1486 N85-19382
Solar collection
[DE85-000060] 10 p1512 N85-19540
Solar-gas systems impact analysis study
[PB85-129086] 11 p1616 N85-20163
Latent heat storage technology and application workshop. Summary report: Session 6
[DE85-001097] 12 p1862 N85-21808
A multifunction wall system for application with solar heating and ground cooling
[DE85-006792] 16 p2820 N85-27395
Solid desiccant dehumidification systems for residential applications
[PB85-198469] 22 p3755 N85-33279
Advanced heat pump research and development
[DE85-000540] 23 p3932 N85-34372
Design and construction of an advanced power conditioning subsystem for small photovoltaic applications
[DE85-013940] 24 p4113 N85-35495

RESIDUAL STRENGTH
The three-dimensional J-integral. An investigation into its use for post-yield fracture safety assessment
[WTHD-167] 20 p3472 N85-31578

RESIDUAL STRESS
Nondestructive evaluation of residual stress in low-carbon steel
[NASA-CR-174157] 04 p0512 N85-13264
Nondestructive evaluation of residual stress in low-carbon steel, introduction 04 p0512 N85-13265
Flexible matrix composite laminated disk/ring flywheel
05 p0606 N85-13866
The fourth LBF colloquium
[ISSN-0721-5320] 05 p0648 N85-14163
Fatigue life improvement due to mechanically induced compressive residual stresses 05 p0650 N85-14175
Influence of residual stresses resulting from manufacturing on the fatigue strength of welded joints
05 p0650 N85-14177
Influence of the shape and distribution of inclusions of the fatigue strength of bearing steels in rotary bending
[BLL-PNR-90243-(8019.3153)]
06 p0768 N85-14912
Stress studies in EFG 06 p0831 N85-15285
Silicon-sheet surface studies
06 p0831 N85-15287
Study of residual stresses introduced into TA6ZrD (685) cylinders by quenching
[BLL-PNR-90240-(8019.3153)]
07 p0925 N85-15859
Residual stresses at small diffusion welds
[DE84-014962] 07 p0974 N85-16189
Nondestructive measurement of bulk residual stresses
[AD-A147063] 07 p0978 N85-16211
In-situ stress determination in soil and rock using the acoustic emission method
[AD-A147459] 07 p0979 N85-16215
A finite element analysis of viscoelastic materials with varying time scales 09 p1330 N85-18355
Study of residual stresses introduced into TA6ZrD (685) cylinders by quenching --- compressor disk alloy
[PNR-90240] 09 p1341 N85-18435
Calculating residual stresses in composite materials
10 p1443 N85-19095
Evaluation of residual stress in laminated metallic composites 11 p1598 N85-20052
Residual stress after laser processing
11 p1600 N85-20065
Evaluation of machining damage in brittle materials
[DE85-001794] 11 p1612 N85-20136
The measurement of residual stresses using ultrasonics
[AERE-R-11415] 12 p1868 N85-21722
Texture independent determination of residual stress in polycrystalline aggregates using Rayleigh waves
[AERE-R-11483] 12 p1943 N85-22203
Brittle fracture resistance of electron beam-welded joints in titanium Alpha alloys 15 p2500 N85-25419
On residual stresses and stress intensity factors in composite materials 15 p2572 N85-25859
Evaluation of the blind hole drilling method for the measurement of residual stress
[AD-A151459] 15 p2579 N85-25905
A study of the time dependence in fracture processes relating to service prediction of adhesive joints and advanced composites
[AD-A152064] 15 p2579 N85-25910
Advanced life analysis methods. Volume 6: User's manual for LUGRO computer program to predict crack growth in attachment lugs
[AD-A151235] 15 p2628 N85-26195
Mechanical properties of high performance carbon fibers 16 p2742 N85-26922
Study of oscillations of composite cylindrical shells using a dynamic stiffness technique 16 p2766 N85-27066
Stressed-strained state of tubular shells under uniformly distributed pressure 16 p2766 N85-27067
On residual stress in an elastic body
16 p2798 N85-27248
Principles of wave formation along web of H-beams
[BLL-M-36041-(5828.4)] 16 p2798 N85-27253
An X-ray study of residual stresses in narrow groove TIG weldments
[DE85-006485] 16 p2802 N85-27274
Local heat treatment of welded joints of pipes and rotary vessels 17 p2924 N85-28028
X-ray diffraction study of changes in stress-strain distributions during fatigue of a 2-phase alloy
[AD-A152367] 17 p2930 N85-28087
An X-ray diffraction study of the residual stress-strain distribution in shot-peened 2-phase brass
[AD-A152418] 17 p2930 N85-28088
Local heat treatment of welded joints of pipes and rotary vessels
[BLL-BISI-TRANS-22197-(9022.06)]
17 p2972 N85-28354
Cyclic torsion of a circular cylinder and its residual stress distribution
[AD-A153347] 17 p2980 N85-28424
Residual stress distributions in (plastically) surface deformed two-phase materials 19 p3283 N85-30356
Effect of nonuniform size on internal stresses in a rapid, simple shear flow of granular materials. Part 1: Two grain sizes
[AD-A154045] 19 p3285 N85-30372
Fundamental studies related to failure of adhesively bonded structures
[AD-A154072] 19 p3285 N85-30374
Measurement and analysis of critical crack tip processes during fatigue crack growth
[NASA-CR-172597] 21 p3598 N85-32342
Stress concentration in the elastoplastic state and residual stress after unloading
[AD-A155628] 21 p3600 N85-32356
Effects of residual stresses and distortion on the nickel 200 and stainless steel 304 weldments
[DE85-011868] 22 p3748 N85-33233
Stresses and deformations in cross-ply composite tubes subjected to a uniform temperature change: Elasticity and Approximate Solutions
[NASA-CR-176147] 22 p3800 N85-33545
X-ray residual stress analysis on the coarse grain of copper and its application to the brazed copper
23 p3907 N85-34202
Study on the correlation between grinding conditions and residual stresses in ground surface of steel by the X-ray method 23 p3907 N85-34203
Multiaxial stress analysis taking account of penetration depth of X-rays. A solution by means of polynomial approximation 23 p3907 N85-34204
Influence of cyclic thermal loading on internal stress in casted epoxy resin 23 p3908 N85-34211
Development of a mathematical model for predicting the percentage fatigue life increase resulting from shot peened components
[AD-A155774] 24 p4101 N85-35425

RESIDUES
Analysis of Nonvolatile Residue (NVR) from spacecraft systems
[NASA-TM-86184] 08 p1113 N85-17019
Transformation of polar ice sublimate residue into Martian circumpolar sand 13 p2189 N85-23580

RESILIENCE
Experimental AC (Asphalt Concrete) overlays of PCC pavement
[PB84-216171] 03 p0342 N85-12203
New deformable secondary aluminum alloys
13 p2026 N85-22694

RESIN MATRIX COMPOSITES
NT GRAPHITE-EPOXY COMPOSITES
Tough Composite Materials
[NASA-CP-2334] 04 p0463 N85-12941
Characterizing delamination resistance of toughened resin composites 04 p0464 N85-12943
Composite materials characterization and development at AFWAL 04 p0464 N85-12944
Effects of constituent properties on compression failure mechanisms 04 p0464 N85-12946
The effect of matrix and fiber properties on impact resistance 04 p0464 N85-12947
Fundamental studies of composite toughness
04 p0464 N85-12948
Development of a heterogeneous laminating resin
04 p0465 N85-12956
System for rapid repair of damaged airfield runways
[AD-D011325] 07 p0909 N85-15754
The use of microdielectrometry in monitoring the cure of resins and composites
[AD-A148619] 08 p1119 N85-17055
Fatigue-creep interaction in + or - 45 deg carbon-resin composites --- aircraft construction materials
[ONERA-RT/40/7086/M] 11 p1594 N85-20027
Interlaminar fracture toughness in resin matrix composites
[AD-A150565] 13 p2015 N85-22640
NASA/aircraft industry standard specification for graphite fiber toughened thermoset resin composite material
[NASA-RP-1142] 16 p2742 N85-26923
Characterization-curing-property studies of HBRF 55A resin formulations
[NASA-CR-175836] 16 p2753 N85-26989
High performance mixed bisimide resins and composites based thereon
[NASA-CASE-ARC-11538-1-SB]
19 p3231 N85-30033
Transversely reinforced piezoelectric composites
[AD-D011676] 19 p3260 N85-30214

Development of an impact- and solvent-resistant thermoplastic composite matrix, phase 3
[NASA-CR-172568] 20 p3422 N85-31239
Effect of strain rate on the initial failure of notched GRP laminates 23 p3908 N85-34214

RESINS
NT ACRYLIC RESINS
NT ALKYD RESINS
NT EPOXY RESINS
NT ION EXCHANGE RESINS
NT KEVLAR (TRADEMARK)
NT NYLON (TRADEMARK)
NT PHENOLIC RESINS
NT POLYAMIDE RESINS
NT POLYESTER RESINS
NT POLYETHER RESINS
NT POLYIMIDE RESINS
NT POLYMETHYL METHACRYLATE
NT POLYURETHANE RESINS
NT SILICONE RESINS
NT SYNTHETIC RESINS
NT THERMOPLASTIC FILMS
NT THERMOPLASTIC RESINS
NT THERMOSETTING RESINS
NT VINYL COPOLYMERS
Development of new and improved polymer matrix resin systems, phase 1
[NASA-CR-166595] 01 p0017 N85-10104
Quasi-steady analysis of aircraft panel flammability
[AD-A145461] 02 p0138 N85-10038
Moisture absorbing anti-arcing coating and method for applying same
[AD-D011310] 07 p0932 N85-15904
Development of a heterogeneous laminating resin system
[NASA-CR-172459] 09 p1288 N85-18089
Synthesis and thermomechanical properties of new AT-Phenylene R systems
[AD-A149961] 12 p1813 N85-21372
Characterization and optimization of polyethylene resins and gas pipe
[PB85-118511] 12 p1815 N85-21382
High performance mixed bisimide resins and composites based thereon
[NASA-CASE-ARC-11538-1-SB] 19 p3231 N85-30033

RESISTANCE
Influence of tire on resistance and steering forces of tires
[AD-P004306] 09 p1410 N85-18883
Basic study on the turning resistance of track
[AD-P004307] 09 p1410 N85-18884
Theoretical and experimental study of crack resistance and macrocrack growth rate in organic fiber reinforced plastic under pure shear condition 11 p1598 N85-20053
Flow through very porous screens
[NASA-TP-2436] 11 p1631 N85-20270

RESISTANCE COEFFICIENTS
U RESISTANCE

RESISTANCE HEATING
Reducing electric power losses in discharge chamber of induction plasmatron 12 p1841 N85-21553
Instrumentation for sensing moisture content of material using a transient thermal pulse
[NASA-CASE-NPO-15493-2] 23 p3933 N85-34373
High Temperature Heating System (HTHS)
[PB85-188340] 24 p4084 N85-35316

RESISTANCE THERMOMETERS
Platinum thin film resistors as accurate and stable temperature sensors
[NASA-TM-77728] 01 p0049 N85-10322
High temperature static strain sensor development program 02 p0141 N85-10959
Effects of temperature on the response time of thermocouples and resistance thermometers
[DE84-016855] 06 p0811 N85-15154
Response time correlations for platinum resistance thermometers in flowing fluids
[NASA-CR-172523] 12 p1850 N85-21606
MFTF sensor verification computer program
[DE85-004452] 12 p1916 N85-22029

RESISTIVITY
U ELECTRICAL RESISTIVITY

RESISTOJET ENGINES
Compatibility experiments of facilities, materials, and propellants for electrothermal thrusters
[NASA-TM-86956] 12 p1795 N85-21260
Space station propulsion: The advanced development program at Lewis
[NASA-TM-86999] 15 p2494 N85-25386
An evaluation of oxygen-hydrogen propulsion systems for the Space Station
[NASA-TM-87059] 18 p3067 N85-28971

RESISTOJETS
U RESISTOJET ENGINES

RESISTORS
NT POTENTIOMETERS (RESISTORS)
NT THERMISTORS
Platinum thin film resistors as accurate and stable temperature sensors
[NASA-TM-77728] 01 p0049 N85-10322
High sheet resistance, arsenic implanted polycrystalline silicon for integrated circuit resistors
[DE85-004355] 13 p2065 N85-22902
Stability of highly nonlinear oxide-zinc resistors under continuous voltage of industrial frequency 13 p2087 N85-23030
Derated application of parts for (Electronic Systems Division) systems development. Revision
[AD-A153299] 17 p2955 N85-28246
Technique for measuring the effective source reflection coefficient of 2-resistor power splitters
[DE85-009984] 17 p2956 N85-28256
Morphology of GaAs/sub 1-x/P/sub x/ superlattices grown by MOCVD and chloride VPE
[DE85-002944] 17 p3045 N85-28842
Low noise polycrystalline semiconductor resistors by hydrogen passivation
[AD-D011721] 23 p3927 N85-34338

RESOLUTION
NT ANGULAR RESOLUTION
NT HIGH RESOLUTION
NT IMAGE RESOLUTION
NT RADAR RESOLUTION
NT RADIOMETRIC RESOLUTION
NT SPATIAL RESOLUTION
NT SPECTRAL RESOLUTION
NT TEMPORAL RESOLUTION
Characteristics of lateral-scan interferometer 06 p0783 N85-15006
An operator method for computing the asymptotics of a collision resolution interval
[AD-A146837] 07 p1028 N85-16528
SODERN Visualization System (SVS) for flight simulation
[AD-P004320] 09 p1269 N85-17974
Study of resolution of deep MT soundings by means of physical model 13 p2112 N85-23155
Rayleigh criteria resolution of optical correlations
[AD-A151711] 15 p2652 N85-26359
Improvements in the energy resolution and high-count-rate performance of bismuth germanate
[DE85-010763] 19 p3240 N85-30092
Resolution at its current limit: Applications of the Berkeley ARM
[DE85-009959] 19 p3274 N85-30301
Optical image of bounded objects 21 p3697 N85-32968
Single-point diamond crushing of Zerodur with in-situ polishing and metrology on a diamond turning machine
[DE85-012918] 24 p4083 N85-35305
LANDSAT-4/5 image data quality analysis
[E85-10105] 24 p4107 N85-35483

RESOLVERS
Angular measurement system
[NASA-CASE-MFS-25825-1] 11 p1635 N85-20298

RESOLVING POWER
U RESOLUTION

RESONANCE
NT BARYON RESONANCE
NT CYCLOTRON RESONANCE
NT ELECTRON PARAMAGNETIC RESONANCE
NT FERROMAGNETIC RESONANCE
NT MAGNETIC RESONANCE
NT MAGNETOSONIC RESONANCE
NT MICROWAVE RESONANCE
NT NUCLEAR MAGNETIC RESONANCE
NT OPTICAL RESONANCE
NT PLASMA RESONANCE
NT PROTON RESONANCE
NT RESONANT VIBRATION
NT SPIN RESONANCE
Semiclassical theory of resonances
[REPT-67] 01 p0114 N85-10777
Rapid nonresonant rotation of a spacecraft in nominally periodic orbits in limited 3 body problem 02 p0160 N85-11083
Vibrational power transmission of an idealised gearbox
[ISVR-TR-124] 02 p0204 N85-11346
Selective observation of elastic-body resonances via their ringing in transient acoustic scattering
[AD-A145666] 03 p0416 N85-12656
Resonance model of Pc3 in subtropical regions — geomagnetism 04 p0520 N85-13323
Bremsstrahlung from nuclear scattering at low energy near a resonance
[DE84-014652] 04 p0561 N85-13572
Experimental on-stream elimination of resonant whirl in a large centrifugal compressor 05 p0642 N85-14121
Multiphoton ionization of benzene in solution
[DE85-000693] 06 p0766 N85-14899
Resonant scattering of acoustic waves by elastic spherical shell in fluid 06 p0778 N85-14972
Laser ablation studies using RIS
[DE85-001118] 09 p1326 N85-18336
Experimental investigations of driven Alfven wave resonances in a Tokamak plasma using carbon dioxide laser interferometry
[DE85-001049] 09 p1392 N85-18758
A picosecond population modulation study of near interband resonances in semiconductors 09 p1396 N85-18787
Resonant activation of a Josephson junction
[DE85-000702] 10 p1563 N85-19857
Precision tunable resonant microwave cavity
[NASA-CASE-LEW-13935-1] 11 p1626 N85-20248
Gain enhancement methods for printed circuit antennas
[AD-A150090] 12 p1835 N85-21517
Dipole active surface vibrational resonances on clean and hydrogen covered Ni(110)
[AD-A150546] 13 p2163 N85-23420
Stability of the Galilean satellites in deep orbital resonance 13 p2172 N85-23477
Studies of planetary rings 13 p2174 N85-23486
Orbital resonances and planetary accretion in the solar nebula 13 p2179 N85-23523
Theoretical aspects of the nucleon-nucleon workshop
[DE85-003740] 14 p2420 N85-24933
The resonant count diagram and solar g mode oscillations 14 p2445 N85-25086
Vapor sensing by means of a ZnO-on-Si surface acoustic wave resonator
[DE85-003250] 15 p2646 N85-26324
Pyrotechnic shock simulation using the controlled response of a resonating bar fixture
[DE85-006537] 16 p2784 N85-27181
Distortion functions
[DE85-007511] 16 p2862 N85-27855
Resonance ionization mass spectrometry of carbon
[DE85-009040] 17 p2923 N85-28018
Transverse electron resonance accelerator
[DE85-008269] 17 p3032 N85-28758
On the origin of streamwise vortices in a turbulent boundary layer
[AD-A153651] 18 p3100 N85-29188
The application of laser resonance saturation to the development of efficient short wavelength lasers
[AD-A153951] 18 p3113 N85-29270
Stochastic resonance in the Landau-Ginzburg equation
[PREPRINT-430] 18 p3175 N85-29685
Arrangement for damping the resonance in a laser diode
[NASA-CASE-NPO-15980-1] 19 p3274 N85-30305
Shifts and widths of hydrogenic ion lines
[DE85-011375] 19 p3277 N85-30323
An algorithm for the influence numbers in the expansion of the lumped gravitational potential coefficients in the presence of resonant inclination variation
[AD-A154229] 19 p3338 N85-30869
Exact invariants in resonance form for time-dependent potentials
[DE85-010733] 19 p3346 N85-30739
Spontaneous emission by two atoms with different resonance frequencies near a metal surface
[AD-A154115] 19 p3353 N85-30781
Resonant-transfer-and-excitation for highly charged ions (16 or = Z or = 23) in collisions with helium
[DE85-010550] 19 p3359 N85-30823
Fundamentals of radio optical theory of resonant and directional quasi-optical devices 22 p3780 N85-33420
Photoionization of alkali and alkaline earth atoms: Na and Mg
[DE85-011812] 22 p3837 N85-33755
Accelerator vibration issues
[DE85-010766] 22 p3842 N85-33791
Role of ECRH in potential formation for tandem mirrors
[DE85-011859] 22 p3848 N85-33834
Calculating the interatomic pair potential allowing for resonance interaction in titanium, nickel and vanadium
[BLL-M-35843-(5828.4)] 23 p3913 N85-34249
Capture in the 1.15-keV iron resonance
[DE85-011913] 23 p3970 N85-34612
Some aspects of internal gravity waves in a multi-layered moving stratified flow 24 p4092 N85-35369
Width of nonlinear difference resonances
[DE85-013026] 24 p4148 N85-35719
Exit channels of autoionization resonances in atoms
[DE85-012299] 24 p4149 N85-35726
Resonance localization in tokamaks excited with ICRF waves
[DE85-014559] 24 p4160 N85-35791

RESONANCE FLUORESCENCE
Development of novel lamps for study of enhanced production of resonance by low-density mercury discharges
[DE84-016889] 05 p0632 N85-14053
Degenerate four-wave mixing lineshapes in sodium vapor under pulsed excitation
[AD-A148211] 08 p1222 N85-17698
The enhancement of molecular fluorescence and photochemistry by small metal particles
[AD-A152740] 17 p2919 N85-27994

RESONANCE LINES
Narrow absorption components in Be star winds 08 p1232 N85-17760
An episodic red-wing structure of SiIV, lambda 1394A, in gamma Cas 11 p1750 N85-21009
Variability of ultraviolet emission lines in the carbon star TX Psc 11 p1753 N85-21027
Atmospheric properties of RU Lupi derived from high- and low-resolution IUE spectra 11 p1754 N85-21031
Betageuse at maximum luminosity 11 p1758 N85-21061

RESONANCE PROBES
NT CYCLOTRON RESONANCE DEVICES
Proposal for continuation of research on megawatt gyrotrons for the period January 1, 1985 through December 31, 1986
[DE85-009662] 18 p3110 N85-29360
The heavy ion composition in 3HE-rich solar flares
[SH-2.2-7] 23 p4000 N85-34802

RESONANCE RADIATION
U RESONANCE FLUORESCENCE

RESONANCE SCATTERING
Observation of pure resonance and threshold effects in electron impact experiments in high intensity laser fields
[AD-A150725] 14 p2309 N85-24293
Resonances in photon-photon scattering
[DE85-004607] 14 p2419 N85-24928
Influence on bi-phonon states on Raman scattering of light in molecular crystals 21 p3690 N85-32665
Circumstellar shells of late-type stars: A study at millimeter and infrared wavelengths 24 p4167 N85-35836

RESONANT CAVITIES
U CAVITY RESONATORS

RESONANT FREQUENCIES
Resonant frequencies and mode shapes for single and double cylindrical shells
[AD-A144778] 01 p0062 N85-10408
Hardware and software selection for experimental modal analysis 02 p0206 N85-11373
NATFREQ users manual: A FORTRAN 4 program for computing natural frequencies, mode shapes and drag coefficients for taut strumming cables with attached masses and spring-mass combinations
[AD-A146058] 03 p0407 N85-12600
Analysis of piezoelectric disks and cylinders using finite element method
[AD-A146323] 03 p0414 N85-12650
The use of an optical data acquisition system for bladed disk vibration analysis
[NASA-TM-86691] 06 p0617 N85-15184
Electromagnetic resonances of cylinders and aircraft model with resistive wires
[NASA-CR-174203] 06 p0638 N85-15319
Evaluation of resonant modes in isolated dielectric resonators using a surface integral equation formulation
[PB85-110831] 12 p1837 N85-21528
Compensation of acoustic wave devices
[AD-D011562] 15 p2646 N85-28322
Approximate solution of the problem of fluid oscillations in cavities of revolution 16 p2764 N85-27056
Acoustic oscillations of rods and plates 17 p2944 N85-28170
Methods to recover the narrow Dicke sub-Doppler feature in evacuated wall-coated cells without restrictions on cell size 18 p3105 N85-29225
Diode laser 87Rb optical pumping in an evacuated wall-coated cell 18 p3105 N85-29226
Coherently pumped two-frequency laser-type devices
[AD-A154085] 19 p3275 N85-30311
Self-tuning adaptive-controller using online frequency identification 20 p3417 N85-31205
Adaptive filtering for large space structures: A closed-form solution 20 p3417 N85-31206
Experimental and theoretical investigations of open resonators — precipitation measurement
[DFVLR-FB-85-12] 20 p3449 N85-31414
Substructure coupling in the frequency domain
[NASA-CR-176140] 22 p3800 N85-33543
Rotor blade test apparatus
[AD-D011725] 23 p3934 N85-34381

RESONANT VIBRATION
Experimental investigation of vibroimpact of two cantilever beams 09 p1336 N85-16399
Acoustic agglomeration methods and apparatus
[NASA-CASE-NPO-15466-1] 12 p1827 N85-22104
Turbine blade friction damping study 16 p2736 N85-26886
Solar array flight experiment
[NASA-TM-86506] 17 p2909 N85-27935
Acoustic resonances in cylinder bundles oscillating in a compressible fluid
[DE85-004066] 24 p4145 N85-35699

RESONATORS
NT CAVITY RESONATORS
NT HELMHOLTZ RESONATORS
NT MULTIMODE RESONATORS
NT OPTICAL RESONATORS
Acoustic resonator and method of making same
[DE84-014655] 01 p0116 N85-10792
Sensitivity improvement of a two-mode gravitational radiation detector through the use of a transducer not perfectly tuned to the antenna
[NOTA-INTERNA-812] 02 p0192 N85-11285
Biaxial-crystal laser with waveguide resonator 02 p0262 N85-11717
Forced oscillations theory for resonant extended interaction electron devices
[PR-206] 03 p0358 N85-12298
Analyses of energy extraction efficiency of unstable resonators
[AD-A146391] 06 p0613 N85-15161
Reverse wave suppression in unstable ring resonator
[AD-A146825] 07 p0939 N85-15952
Low noise multiple crystal-controlled oscillator
[AD-D011401] 07 p0948 N85-16010
Microwave resonator using lateral excitation
[AD-D011374] 07 p1039 N85-16596
Status of RF superconductivity at Argonne National Laboratory
[DE85-002145] 09 p1312 N85-18245
Method of heating quartz resonators
[AD-D011454] 10 p1481 N85-19347
KMSF X-ray laser experiments, task no. 2
[DE85-000291] 11 p1640 N85-20335
Oscillator development
[AD-A149699] 12 p1834 N85-21509
Evaluation of resonant modes in isolated dielectric resonators using a surface integral equation formulation
[PB85-110831] 12 p1837 N85-21528
Stress compensation crystal device
[AD-D011497] 12 p1941 N85-22189
Three-mirror open resonator for millimeter wave band 13 p2077 N85-22972
Effect of space-charge field on output characteristics of O-type oscillators with distributed interaction 13 p2089 N85-23043
Dielectric resonator
[AD-D011573] 14 p2299 N85-24233
Cylindrical crystal resonator
[AD-D011575] 14 p2428 N85-24974
Suppression of vibration effects on piezoelectric crystal resonators
[AD-D011625] 16 p2778 N85-27142
Acceleration-resistant crystal resonator
[AD-D011627] 16 p2778 N85-27144
Method of fabricating acceleration resistant crystal resonators and acceleration resistant crystal resonators so formed
[AD-D011630] 16 p2778 N85-27145
Acceleration sensitivity reduction method
[AD-D011631] 16 p2778 N85-27146
Cut angles for quartz crystal resonators
[AD-D011652] 17 p2951 N85-28220
High performances from a new design of crystal oscillator 17 p2966 N85-28318
Design of SC cut 10 MHZ H.Q. crystals with G. sensitivity better than 2.10(-10)/G 17 p2966 N85-28319
Crystal resonator/oscillator test facility and test results 17 p2967 N85-28322
The superconducting cavity stability ruby maser oscillator 17 p2967 N85-28324
New features of different frequency generating systems due to the use of electrodeless rigidly mounted VBA quartz crystal resonator 18 p3106 N85-29231
Passivation on high Q acoustic strain sensor for accelerometer
[AD-A153565] 18 p3177 N85-29695
Dielectric resonator stabilized microstrip oscillator
[AD-D011708] 19 p3261 N85-30219
Dielectric resonator oscillators with digital temperature compensation
[AD-D011715] 19 p3261 N85-30221
Miniature two-mode filters 22 p3775 N85-33394
Fundamentals of radio optical theory of resonant and directional quasi-optical devices 22 p3780 N85-33420

RESOURCE ALLOCATION
The effects of task structure on time-sharing efficiency and resource allocation optimality 05 p0711 N85-14562
Control and modeling of a CELSS (Controlled Ecological Life Support System)
[NASA-CR-177324] 07 p1020 N85-16472
The international environment UNISPACE '82 and the ITU: A relationship between orbit-spectrum resource allocation and orbital debris 12 p1787 N85-21215
Metal waste in machine tool industry examined 14 p2283 N85-24147
Glossary of landscape and vegetation ecology for Alaska
[PB85-153831] 16 p2816 N85-27372
Selected university laboratory needs in support of national security
[AD-A153511] 18 p3197 N85-29633
Routing algorithms and stochastic analysis for large communications networks
[AD-A154654] 21 p3573 N85-32225
Resource allocation in cerebral specialization of function: Behavioral and electrophysiological studies
[AD-A155092] 21 p3664 N85-32759

RESOURCES
NT AQUIFERS
NT COAL
NT CRUDE OIL
NT EARTH RESOURCES
NT EXTRATERRESTRIAL RESOURCES
NT FORESTS
NT FOSSIL FUELS
NT GEOTHERMAL RESOURCES
NT GEYSERS
NT GLACIERS
NT ICEBERGS
NT LAND ICE
NT LIGNITE
NT MARINE RESOURCES
NT OIL FIELDS
NT RAIN FORESTS
NT SPRINGS (WATER)
NT TAR SANDS
NT THERMAL RESOURCES
NT UNDERWATER RESOURCES
NT WATER RESOURCES
Arctic and offshore research
[DE85-001995] 22 p3818 N85-33653
Expert systems research in regional resource evaluation: Experiences in the application of microcomputer technologies 24 p4105 N85-35450
Applications of the mineral resources data system and the international strategic minerals inventory in mineral-resource assessments by region and commodity 24 p4105 N85-35451

RESOURCES MANAGEMENT
NT FOREST MANAGEMENT
NT LAND MANAGEMENT
Estuaries of the Cape. Part 2: Synposes of available information on individual systems. Report no. 19: Groot (WES) (CMS 23) and Sout (CMS 22)
[CSIR-RR-418] 01 p0087 N85-10588
Cartography 02 p0214 N85-11412
Multispectral Imaging Science Working Group for Hydrologic Science: Executive summary 02 p0214 N85-11414
ONR (Office of Naval Research) Far east Scientific Bulletin, Volume 9, Number 2, April - June 1984
[AD-A145881] 02 p0305 N85-11974
A methodology for comparing the variable costs of the continuous and periodic review models
[AD-A146351] 03 p0436 N85-12776
Assessing erosion on US cropland: Land management and physical features
[PB84-219252] 04 p0526 N85-13366
Project resources planning and control
[NASA-TM-86339] 04 p0575 N85-13666
Remote sensing data in support of conventional data 05 p0659 N85-14232
A geographic information system for resource managers based on multi-level remote sensing data
[E85-10047] 06 p0827 N85-15249
Climate Conference for Latin America and the Caribbean
[WMO-632] 07 p1000 N85-16352
The management of atmospheric resources in food production 07 p1002 N85-16362
Evaluation of the climatic resources of Cuba applied to agricultural work 07 p1004 N85-16360
Managing recoverable aircraft components in the PPB and related processes: Executive summary
[AD-A146806] 07 p1050 N85-16667

Feasibility of measuring technical productivity improvements in Air Force Logistics Command depot-level maintenance using the Data Envelopment Analysis (DEA) and Constrained Facet Analysis (CFA) models
[AD-A147329] 07 p1052 N85-16676
Estimating wartime support resource requirements. Statistical and related policy issues
[AD-A147923] 07 p1053 N85-16685
Cockpit resource management training 09 p1276 N85-18023
Compatible goals: Defense and environmental protection
[AD-P004137] 09 p1347 N85-18473
An integrated GIS/remote sensing data base in North Cache soil conservation district, Utah: A pilot project for the Utah Department of Agriculture's RIMS (Resource Inventory and Monitoring System)
[E85-10073] 10 p1504 N85-19487
The evolution from data processing to information resource management
[AD-A149429] 10 p1567 N85-19678
Remote sensing technology now playing practical roles 11 p1619 N85-20190
Proceedings of the 1st Glacier Bay Science Symposium
[PB85-115913] 11 p1682 N85-20599
Remote sensing research for agricultural applications — San Joaquin County, California and Snake River Plain and Twin Falls area, Idaho
[E85-10090] 12 p1873 N85-21752
Building a functional, integrated GIS/remote sensing resource analysis and planning system — Utah
[E85-10092] 12 p1874 N85-21754
Review of computer mapping and display techniques applicable to regional analysis
[DE85-003545] 12 p1875 N85-21764
A formal method for specifying computer resources in an implementation independent manner
[AD-A149955] 12 p1918 N85-22043
Technologies to sustain tropical forest resources
[TI85-001085] 13 p2126 N85-23241
Metal waste in machine tool industry examined 14 p2283 N85-24147
Geometric error analysis for shuttle imaging spectrometer experiment
[NASA-CR-175665] 14 p2305 N85-24269
Managing recoverable aircraft components in the PPB (Planning, Programming and Budgeting) and related processes. Technical volume
[AD-A152014] 15 p2457 N85-25169
Navy geothermal plan
[AD-A152478] 17 p2985 N85-28450
Assessment of computer resource management plan for division support weapon system
[AD-A154142] 19 p3342 N85-30712
Resource management for the tagged token dataflow architecture
[AD-A154773] 21 p3667 N85-32779
Solar energy meteorological research and training program: Region 4
[DE85-011783] 22 p3816 N85-33640
Some recent deposit modeling efforts 24 p4106 N85-35453
Mineral resources programs 24 p4106 N85-35456
Federal Mineral Land Information System 24 p4106 N85-35459
USGS coastal research, studies and maps: A source of information for coastal decision making
[USGS-CIRC-883] 24 p4108 N85-35465

RESPIRATION
NT HIGH ALTITUDE BREATHING
NT PRESSURE BREATHING
Carbon cycle: Terrestrial interactions 05 p0652 N85-14187
Control technology for fiber reinforced plastics industry at AMF Hatteras Yachts, New Bern Division, New Bern, North Carolina
[PB85-109015] 10 p1480 N85-19198
Mercury health effects update: Health issue assessment
[PB85-123925] 10 p1526 N85-19639
USSR report: Space Biology and Aerospace Medicine, volume 18, no. 6, November - December 1984
[JPRS-USB-85-002] 12 p1900 N85-21931
Main component method used to study variations of cardiovascular parameters 12 p1901 N85-21939
Chemical characterization and toxicologic evaluation of airborne mixtures. Inhalation toxicology of diesel fuel obscurant aerosol in Sprague-Dawley rats. Phase 3. Subchronic exposures
[AD-A150100] 12 p1905 N85-21966
Hazards in welding due to oxygen changes in the workplace atmosphere
[BLL-WI-TRANS-684-(8312.57)] 16 p2792 N85-27224
Development of an EM-Based lifeform detector
[AD-A153504] 18 p3151 N85-29512
Changes in the impedance and bioelectrical activity of the cerebral cortex of rats under the action of anaesthetic drugs
[HSE-TRANS-10371] 19 p3327 N85-30617
Typological characteristics of hemodynamic states of healthy subjects in orthostatic position 22 p3821 N85-33673
Effect of short-term antiorthostatic hypokinesia on dynamics of cardiorespiratory parameters during graded physical exercise 22 p3822 N85-33677
An analysis of aerobic capacity in a large United States population
[AD-A156200] 24 p4132 N85-35614

RESPIRATORS
Respiratory protection for children 3 - 6 years of age
[FOA-C-40197-C2] 02 p0238 N85-11550

RESPIRATORY DISEASES
NT ASTHMA
NT INFLUENZA
Interaction between lung mechanics and gas exchange by low volume high frequency pulmonary ventilation in patients with respiratory failure
[AD-A146604] 06 p0846 N85-15372

RESPIRATORY PHYSIOLOGY
Effect of maximum physical load on oxygen-transport properties of blood 01 p0093 N85-10627
Interaction between lung mechanics and gas exchange by low volume high frequency pulmonary ventilation in patients with respiratory failure
[AD-A146604] 06 p0846 N85-15372
Short-term human respiratory effects of nitrogen dioxide: Determination of quantitative dose-response profiles. Phase 2: Exposure of asthmatic volunteers to 4 PPM NO2
[PB85-104368/GAR] 07 p1017 N85-16462
Dynamics of external respiration and gas metabolism under combined effect of hypoxia and hypercapnia 08 p1193 N85-17519
Hyperbaric physiology (status and prospects) 08 p1194 N85-17521

RESPIRATORY RATE
Factors determining effectiveness of voluntary decrease in ventilation during muscular work using instrumented feedback 08 p1193 N85-17520
Scattering of electromagnetic waves by human body and its applications 09 p1383 N85-18572
External respiration, gas exchange and energy expenditures of man in weightlessness 12 p1900 N85-21932

RESPIRATORY SYSTEM
NT BRONCHI
NT DIAPHRAGM (ANATOMY)
NT LUNGS
Deposition in the human lung during respiration of small particles suspended in the air
[BLL-RISLEY-TR-5021-(9091.9F)] 03 p0400 N85-12549
Respiratory chain of alkalophilic bacteria
[DE84-012558] 09 p1380 N85-18556
Air quality criteria for ozone and other photochemical oxidants. External review draft, volume 4
[PB85-126068] 12 p1886 N85-21838
Human lung fluid content during 7-day head-down tilt 12 p1902 N85-21941
Spiroilt-2 instrument used to test pulmonary ventilation 12 p1903 N85-21950
Principal patterns of functional changes of human respiratory system in adaptation to high pressure 14 p2387 N85-24704
Cardiorespiratory function and work performance during adaptation to industrial labor in midalpine conditions 22 p3820 N85-33665

RESPONDERS
U TRANSPONDERS

RESPONSE TIME (COMPUTERS)
On a program for solution of BCMP queueing network model
[NAL-TR-813] 03 p0405 N85-12585
Development of graphical time response using the OPTSYSX program
[AD-A152221] 16 p2648 N85-27557
Using percent-done program indicators to enhance user interface 23 p3960 N85-34548

RESPONSES
NT DYNAMIC RESPONSE
NT GALVANIC SKIN RESPONSE
NT HEMODYNAMIC RESPONSES
NT MODAL RESPONSE
NT PHYSIOLOGICAL RESPONSES
NT TRANSIENT RESPONSE
Conjunctive and disjunctive item response functions
[AD-A147815] 07 p1033 N85-16561
Models for mixture experiments when the response depends on the total amount
[DE85-000370] 09 p1374 N85-18637
The response of explosive systems to thermal stimuli: A state-of-the-art assessment
[DE85-000919] 11 p1614 N85-20148
Temperature responses of composite panels
[AD-A150053] 12 p1796 N85-21277
Use of the ORACLE DEMS in determining the response of complex scientific instrumentation
[DE85-001742] 12 p1853 N85-21621
Optimized response functions for 2-dimensional observations of solar oscillations 14 p2443 N85-25075
Airsickness control using biofeedback to self-regulate psychophysiological responses
[AD-A151167] 15 p2617 N85-26128
An interactive computer package for use with simulation models which performs multidimensional sensitivity analysis by employing the techniques of response surface methodology
[AD-A151956] 16 p2846 N85-27548
Controller requirements for uncoupled aircraft motion, volume 2
[AD-A153300] 17 p2900 N85-27879
Optical fiber magnetic field sensor with nanosecond response time
[DE85-008409] 18 p3110 N85-29259
Interaction of opiate and phencyclidine derivatives with the acetylcholine receptor
[AD-A155119] 21 p3664 N85-32761
The effect of set size on time to recall color coded information
[AD-A155013] 21 p3665 N85-32767
Models for multidimensional tests and hierarchically structured training materials
[AD-A155231] 21 p3665 N85-32768
Powerful XeCl excimer electric discharge laser with good temporal stability and fast response time 21 p3668 N85-32911
Relaxation phenomena and stability of probability densities
[AD-A155923] 24 p4143 N85-35662

REST
NT BED REST

RESTORATION
Restoration of multichannel microwave radiometric images
[NASA-CR-174115] 04 p0554 N85-13527
State-of-the-art of aquifer restoration. Volume 1: Sections 1 through 8
[PB85-181071] 20 p3478 N85-31612
State-of-the-art of aquifer restoration. Volume 2: Appendices A through G
[PB85-181089] 20 p3478 N85-31613

RESTRAINTS
U CONSTRAINTS

RESTRICTIONS
U CONSTRICTIONS

RESUSCITATION
Liposome-encapsulated hemoglobin for emergency resuscitation
[AD-A146794] 07 p1015 N85-16446

RETAINING
Studies on seismic earth pressure of cohesive backfill 09 p1303 N85-18186

RETARDANTS
NT FLAME RETARDANTS

RETARDERS (DEVICES)
Sensitivity of single and multiple cosmic ray neutrons to the surrounding medium in a lead-free monitor
[SH-9.1-10] 23 p4051 N85-35125

RETARDING
Suppression of vibration effects on piezoelectric crystal resonators
[AD-D011625] 16 p2778 N85-27142
Dual species ion implantation of ternary compounds based on In-Ga-As
[AD-D011617] 16 p2869 N85-27698

RETARDING ION MASS SPECTROMETERS
U MASS SPECTROMETERS

RETENTION (PSYCHOLOGY)
Problems of psychological support of automated organization control systems 09 p1362 N85-18570
Oral discussion, group-to-individual transfer and achievement in cooperative learning groups
[AD-A153209] 17 p3001 N85-28552

RETICLES
Derivation of model topography 18 p3141 N85-29449

RETINA
A study of low-level laser retinal damage
[AD-A150046] 12 p1905 N85-21965
Mammalian tissue sensitivity to long-term exposure to high-intensity stationary magnetic fields 22 p3823 N85-33666

RETINAL ADAPTATION
NT DARK ADAPTATION
NT LIGHT ADAPTATION
Predictive model of electron beam induced flashblindness
[AD-A155260] 21 p3664 N85-32763
RETINAL IMAGES
Retinal information mapping system
[AD-D011531] 12 p1849 N85-21601
Retinally stabilized differential resolution television display
[NASA-CASE-NPO-15432-1] 18 p3089 N85-29117
RETIREMENT FOR CAUSE
Exploratory development of advanced surface flaw detection methods
[AD-A148757] 09 p1261 N85-18060
RETRACTABLE EQUIPMENT
Electronic module insertion and retraction mechanism
[AD-D011309] 07 p0947 N85-16002
Blanket integrated cushioning of foldable and retractable solar arrays 13 p2011 N85-22612
Concept for controlled fold by fold deployment and retraction of flexible, foldable solar generators 13 p2011 N85-22613
Growth capabilities of European retractable solar arrays 13 p2012 N85-22625
Selection of effective arrangement of heavy undercarriage systems for use with concrete runways 14 p2265 N85-24158
Retractable Rigid Solar Generator (GSR)
[SNIAS-851-440-101] 20 p3484 N85-31654
RETRACTABLE LANDING GEAR
U LANDING GEAR
U RETRACTABLE EQUIPMENT
RETRAINING
Data processing professionals and DP application users' perceptions and expectations of operational roles of persons working in a DP/application user interface group 24 p4165 N85-35821
RETRIEVAL
NT DATA RETRIEVAL
NT INFORMATION RETRIEVAL
NT PAYLOAD RETRIEVAL (STS)
The ARGOS contribution to the successful dredging of a deep moored current meter 14 p2327 N85-24361
RETROFITTING
NT ACOUSTIC RETROFITTING
Natural gas the new locomotive fuel
[DE84-901824] 09 p1302 N85-18179
Computer-generated display system guidelines. Volume 1: Display design
[DE85-000879] 11 p1701 N85-20699
RETROREFLECTION
Transparent electrode for optical switch
[DE85-011618] 22 p3761 N85-33310
RETROREFLECTORS
Retroreflective armbands: Influences of wearing mode, aging and other factors on the visibility distance
[IZF-1984-28] 14 p2422 N85-24942
RETURN BEAM VIDICONS
NT THERMICONS
Preliminary study for an IR-vidicon for the 8 to 14 micron range, phase 1
[BMFT-FB-W-84-025] 05 p0633 N85-14057
REUSABLE HEAT SHIELDING
Results of tests of advanced flexible insulation vortex and flow environments in the North American Aerodynamics Laboratory lowspeed wind tunnel using 0.0405-scale Space Shuttle Orbiter model 16-0 (test OA-309)
[NASA-CR-167692] 01 p0015 N85-10096
Verification tests of durable TPS concepts
[NASA-TM-86313] 03 p0323 N85-12085
The challenging scales of the bird: Shuttle tile structural integrity 08 p1095 N85-16919
Study of outgassing and decomposition of space shuttle heat protection tiles, fillers and adhesive
[NASA-CR-175565] 12 p1791 N85-21242
Electron beam charging of Space Shuttle thermal protection system tiles 13 p1990 N85-22478
Thermal protection systems for reentry vehicles
[CNES-NT-113] 23 p3900 N85-34157
Experimental aerodynamic heating to simulated space shuttle tiles in laminar and turbulent boundary layers with variable flow angles at a nominal Mach number of 7
[NASA-TP-2307] 23 p3929 N85-34351
REUSABLE LAUNCH VEHICLES
Future launching systems, 3rd prospective phase
[SNIAS-S/DT/Y-25-063] 11 p1589 N85-19999
REUSABLE ROCKET ENGINES
Methane heat transfer investigation
[NASA-CR-171190] 03 p0362 N85-12318
The aerodynamic challenges of SRB recovery 08 p1093 N85-16908
Aerojet advanced engine concept 08 p1107 N85-16999
Studies on rocket engines for future European launchers
[SEP-TPRL/K-19572/84] 15 p2495 N85-25393
Structural integrity and Durability of Reusable Space Propulsion Systems
[NASA-CP-2361] 17 p2910 N85-27941
REUSABLE SPACECRAFT
NT CHALLENGER (ORBITER)
NT COLUMBIA (ORBITER)
NT DISCOVERY (ORBITER)
NT ENTERPRISE (ORBITER)
NT SPACE SHUTTLES
Winged first stages of space transport appliances
[TUM-RT-TB-84/3] 02 p0167 N85-11125
Ground man-machine interfaces for orbiter checkout 06 p1091 N85-16897
Drives and benefits overview 06 p1107 N85-16998
Advanced research and technology programs for advanced high-pressure oxygen-hydrogen rocket propulsion
[NASA-TM-86969] 12 p1789 N85-21231
British super-shuttle 18 p3087 N85-29104
REUSE
Reusable software
[AD-A146575] 06 p0654 N85-15427
Reusable software: A concept for cost reduction 16 p2697 N85-26655
REVENUE
Financing considerations and Federal budget impacts 07 p0915 N85-15792
REVERBERATION
Total area of diffusion elements in a reverberation chamber and measured degree of sound absorption
[NRC/CNR-TT-2110] 03 p0415 N85-12653
Reverberation effects on directionality and response of stationary monopole and dipole sources in a wind tunnel
[NASA-TM-87063] 20 p3453 N85-31443
Toward the theory of acoustic scattering on uneven free surface 21 p3680 N85-32662
REVERSE FIELD PINCH
NT CYLINDRICAL PLASMAS
Physics of reversed-field pinch profile sustainment
[DE84-014024] 04 p0565 N85-13602
Theoretical studies of Field-Reversed Configurations (FRC) and experimental study of the FRC during translation
[DE84-016467] 04 p0566 N85-13603
Oscillating field current drive for reversed field pinch discharges
[DE84-015090] 04 p0567 N85-13610
Transport experiments in the Texas experimental Tokamak 09 p1389 N85-18741
Design and construction details of the FRX-C/T device: A compact toroid plasma translation experiment
[DE85-001527] 09 p1390 N85-18749
Magnetic divertor design for the compact reversed-field pinch reactor
[DE85-002031] 09 p1391 N85-18753
Role of multiple helicity nonlinear interaction of tearing modes in dynamo and anomalous thermal transport in the Reversed Pitch Field
[DE85-002176] 10 p1560 N85-19639
FRC translation dynamics and plasma confinement properties in FRX-C/T
[DE85-002386] 10 p1560 N85-19642
Magnetic fluctuations, field reversal maintenance, and anomalous thermal transport in the reversed field pinch
[DE85-003604] 11 p1732 N85-20892
High beta pinch plasma (STP-3(M)) 15 p2655 N85-26380
High beta pinch plasma (STP-L) 15 p2655 N85-26381
Asymmetric flux generation and its relaxation in reversed field pinch
[IPPJ-712] 15 p2656 N85-26387
Internal field probing of translating FRCs
[DE85-003732] 15 p2657 N85-26394
Poloidal rotation of magnetic fluctuations in reversed field pinch plasma
[IPPJ-715] 16 p2666 N85-27677
Fusion-power-core design of a Compact Reversed-Field Pinch Reactor (CRFPR)
[DE85-007710] 16 p2668 N85-27692
Two-dimensional TBR calculations for conceptual compact reversed-field pinch reactor blanket
[DE85-007636] 17 p3040 N85-28812
Reversed field pinch dynamics and transport studies
[DE85-007553] 18 p3189 N85-29778
Comparison study of toroidal-field divertors for a compact reversed-field pinch reactor
[DE85-009591] 18 p3189 N85-29781
One-dimensional hybrid code for FRM dynamics
[DE85-010687] 19 p3361 N85-30840
Radiation-cooled helicity-injecting reversed field pinch formed with relativistic electrons
[IPPJ-721] 19 p3370 N85-30901
Proposed FRX-D experiment
[DE85-012766] 24 p4158 N85-35778
REVERSE OSMOSIS
Operating experiences of reverse osmosis plants treating Rand Water Board (RWB) water: Pitfalls and problems 01 p0023 N85-10142
Reverse osmosis treatment to control inorganic and volatile organic contamination
[PB84-223528] 01 p0071 N85-10470
Ultrafiltration as pretreatment for the preparation of drinking water by reverse osmosis onboard ships
[PML-1984-32] 01 p0098 N85-10654
Feasibility study for small group water desalination equipment
[AD-A155106] 21 p3563 N85-32164
Oxidation of formaldehyde solutions used for the preservation of reverse osmosis membranes
[PB85-165585] 22 p3742 N85-33194
REVERSE TIME
U REACTION TIME
REVERSED FLOW
Characteristics of a turbulent plane offset jet 02 p0196 N85-11310
Dilution jet configurations in a reverse flow combustor
[NASA-CR-174888] 13 p1974 N85-22392
Determination of boundary line between reverse jet and surrounding stream 13 p2043 N85-22789
Small gas turbine combustor study: Fuel injector performance in a transpiration-cooled liner
[NASA-TM-86969] 15 p2473 N85-25264
REVERSING
Mean intensity of wave reflected by wavefront reversing mirror in turbulent medium 22 p3782 N85-33432
Latitudinal gradients of cosmic rays and the polarity reversal of the heliospheric magnetic field: A preliminary evaluation
[SH-4.2-16] 23 p4008 N85-34853
A new drawing technique for nylon 6 by reversible plasticization with iodine
[AD-A156272] 24 p4162 N85-35803
REVIEWING
A review of some aspects of robust inference for time series
[AD-A149706] 12 p1923 N85-22082
REVISIONS
Preliminary mechanical redesign of an existing gas-turbine engine to incorporate a high-efficiency, low-pressure-ratio, highly regenerative cycle for marine applications
[AD-A144808] 01 p0011 N85-10070
United States Air force aircraft modification process: A system dynamics analysis
[AD-A146954] 07 p0893 N85-15659
Reanalysis of continuous dynamic systems with continuous modifications 09 p1337 N85-18411
Testing of scanner-assisted revision of the topographic map 1:25,000 (TK 25) 16 p2814 N85-27359
Automatic engraving of map frames in the revision of the TK 25, 1:25,000 topographical map 16 p2814 N85-27362
A concept for map updating using digital image processing methods 16 p2815 N85-27364
Structural dynamics modification of generalized beams using a local eigenvalue modification procedure 19 p3282 N85-30353
Modification of the grain size of sputtered copper with additions of oxygen, krypton, silver, or yttrium
[DE85-010975] 21 p3567 N85-32189
Progress and plans for the Colorado Wind Profiler Network 21 p3628 N85-32542
AUTSKED: An addendum
[DE85-010410] 22 p3829 N85-33712
REVOLUTION (MOTION)
U REVOLVING
REVOLVING
Variable loading of elastic-plastic shells of revolution 06 p0779 N85-14981
REYNOLDS EQUATION
A local dynamical interpretation method of numerical weather forecasting 01 p0080 N85-10536
Applications of Canuto's method to Rayleigh-Taylor-initiated turbulence
[DE85-010635] 18 p3102 N85-29202
Turbulent mixing and combustion 22 p3744 N85-33207
REYNOLDS LAW
U REYNOLDS EQUATION
REYNOLDS NUMBER
NT HIGH REYNOLDS NUMBER
NT LOW REYNOLDS NUMBER
A review and analysis of boundary layer transition data for turbine application
[NASA-TM-86880] 01 p0047 N85-10306

Laminar flow heat exchangers. Viscosity induced non-uniform flow
[AD-A144777] 01 p0047 N85-10307
Development of the code NSFOIL for analyzing high Reynolds number transonic flow around an airfoil
[NAL-TR-816] 06 p0749 N85-14801
High Marangoni number convection in a square cavity
[NASA-CR-174283] 07 p0959 N85-18078
Pneumatic turbulators: A device for drag reduction at Reynolds numbers below 5 million
08 p1071 N85-18791
A visual study of a delta wing in steady and unsteady motion
[AD-P004158] 09 p1264 N85-17943
Skin friction measurements for 2 relatively thick airfoil sections at high Reynolds number
[AD-A150021] 12 p1772 N85-21125
Application of large eddy interaction model to channel flow
[NASA-TM-86691] 12 p1844 N85-21572
Surface-slip equations for multicomponent nonequilibrium air flow
[NASA-TM-85820] 12 p1845 N85-21573
Cryogenic wind tunnels: A selected annotated bibliography
[NASA-TM-86346] 13 p1976 N85-22401
The structure of separated flow regions occurring near the leading edge of airfoils, including transition
[NASA-CR-175670] 14 p2209 N85-23703
Flat magnetohydrodynamic induction pump
17 p2939 N85-28145
Instability at the interface between two shearing fluids in a channel
[AD-A153532] 18 p3099 N85-29185
Experimental investigations of the unsteady turbulent friction behavior with pressure impulses in a circular pipe
[IWAWI-MITT-102] 18 p3103 N85-29210
High Reynolds number tests of a NASA SC(3)-0712(B) airfoil in the Langley 0.3-meter transonic cryogenic tunnel
[NASA-TM-86371] 19 p3213 N85-29826
Pressure distribution from high Reynolds number tests of a NASA SC(3)-0712(B) airfoil in the Langley 0.3-meter transonic cryogenic tunnel
[NASA-TM-86370] 19 p3213 N85-29827
Low-speed tests of a high-aspect-ratio, supercritical-wing transport model equipped with a high-lift flap system in the Langley 4- by 7-meter and Ames 12-foot pressure tunnels
[NASA-TP-2097] 20 p3368 N85-31010
Transition in a disturbed environment
20 p3452 N85-31436
Heat transfer in aeropropulsion systems
[NASA-TM-87066] 20 p3453 N85-31444
Development of a new laser Doppler velocimeter for the Ames High Reynolds Channel No. 2
[NASA-TM-86772] 20 p3458 N85-31477
A numerical study of Taylor-Vortex flow
[AD-A154787] 21 p3584 N85-32277
Numerical solutions of turbulent models for flow over a flat plate with angle of attack
[DE85-010360] 21 p3585 N85-32286
The aerodynamic characteristics of a GU25-5(11)8 aerofoil for low Reynolds numbers
[GU-AERO-8410] 23 p3894 N85-34121

REYNOLDS STRESS
A study of Reynolds-stress closure model
[NASA-CR-174342] 08 p1161 N85-17324
Analysis of sudden expansion flow in a two-dimensional duct with and without side-wall injection using the k-epsilon turbulence model 09 p1317 N85-18282
On the influence of turbulent motions on non-radial oscillations 14 p2444 N85-25063
Computational models of the viscous sublayer and limiting behavior of turbulence near a wall
[AD-A151198] 15 p2556 N85-25767
Turbulent wake of a submerged flat plate
[AD-A153776] 18 p3100 N85-29190
A study of the second and third order closure models of turbulence for prediction of separated shear flows
[NASA-CR-176127] 23 p3929 N85-34353

RF-8 AIRCRAFT
U F-8 AIRCRAFT

RF-4 AIRCRAFT
Peripheral vision horizon display testing in RF-4C aircraft 01 p0009 N85-10064

RH-2 HELICOPTER
U UH-1 HELICOPTER

RHENIUM
Compatibility experiments of facilities, materials, and propellants for electrothermal thrusters
[NASA-TM-86958] 12 p1795 N85-21260

RHENIUM ALLOYS
Solution softening in molybdenum-rhenium alloys
[DE85-006708] 16 p2750 N85-28972

RHEOENCEPHALOGRAPHY
Effect of 120-day antiorthostatic bedrest on gas exchange and pulmonary circulation in man
19 p3323 N85-30569

RHEOLOGY
The rheology of icy satellites
[NASA-CR-174024] 02 p0302 N85-11959
Elastomers and other organic composites
[AD-A147624] 08 p1131 N85-17131
The stress-strain-time graph of rheological soils and its application
[AD-P004266] 09 p1407 N85-18663
A new rheological model for concrete structural analysis
[DE84-014743] 11 p1653 N85-20413
Rheology of dissemination
[AD-A150006] 12 p1813 N85-21373
Thermal and thermoelastic effects in rolling/sliding contacts
[AD-A150435] 13 p2165 N85-23429
Sulfur volcanoes on Io? 13 p2173 N85-23479
Geomorphic classification of lava flows on Io
13 p2173 N85-23480
Emplacement of long lava flows on Mauna Loa (Hawaii) and Alba (Mars) 13 p2186 N85-23583
Field measurements of the 1983 Royal Gardens lava flows, Kilauea Volcano, and 1984 Mauna Loa lava flows, Hawaii 13 p2186 N85-23585
Surface structures of Hawaiian lavas
13 p2186 N85-23586
Submarine volcanic eruptions and potential analogs for Venus 13 p2187 N85-23673
Creep of ice: Further studies
13 p2201 N85-23655
Theoretical and experimental studies of the mechanics of viscoelastic liquids
[AD-A153505] 18 p3070 N85-28987
Characteristics of charge transfer in the dispersed phase of electrorheological suspensions
[RAE-TRANS-2125] 19 p3233 N85-30040
Synthesis and characterization of copolyimides with varying flexibilizing groups
[NASA-TM-86416] 20 p3433 N85-31296
Intraplate crustal deformation due to continental collisions 20 p3490 N85-31693
Finite element methods for viscoelastic flow
[AD-A154877] 22 p3783 N85-33437
Vascular mechanisms of adaptation to antiorthostatic position 22 p3822 N85-33675
Cerebral hemodynamics and ventricular function in -15 deg antiorthostatic position 22 p3822 N85-33676
A solid-state framework for terrestrial upper mantles
22 p3856 N85-33878

RHEOMETERS
An investigation of the suitability of using a Steiglaff-McKelvey high shear rate melt rheometer for the measurement of low viscosity polymer solutions
[AD-A146275] 03 p0338 N85-12174
Natural electrical activity of human sympathetic nerve fibers, recorded from body surface
07 p1013 N85-16433

RHODIUM
Characterization of CO binding sites on Rh(111) and Rh(331) surfaces by XPS and LEED (Low Energy Electron Diffraction): Comparison to EELS (Electron Energy Loss Spectroscopy) results
[AD-A148331] 10 p1435 N85-19044
An infrared study of isotopic exchange during methanation over supported rhodium catalysts; an inverse spillover effect
[AD-A148390] 10 p1435 N85-19046
An infrared study of the hydrogenation of carbon dioxide on supported rhodium catalysts
[AD-A148477] 10 p1436 N85-19049
An infrared study of the oxidation of carbon monoxide over supported rhodium catalysts
[AD-A148478] 10 p1436 N85-19050
Optical second harmonic generation for surface studies
[DE85-000870] 11 p1640 N85-20333
An infrared study of the dissociation of carbon dioxide over supported rhodium catalysts
[AD-A149813] 12 p1800 N85-21291
Advanced thin film thermocouples
[NASA-CR-175541] 12 p1850 N85-21607
Transition metal catalyzed transformations of unsaturated molecules
[DE85-009531] 18 p3080 N85-29055

RHODIUM COMPOUNDS
Anomalous magnetism of CeRh3B2 under pressure
[DE85-003069] 13 p2164 N85-23425
Magnitude and range of the RKKy interaction in SmRh4B4
[DE85-012284] 23 p3965 N85-34712

RHOMBIC ANTENNAS
Surface wave excitation study
[DE85-005301] 13 p2058 N85-22875

RHYTHM (BIOLOGY)
NT CIRCADIAN RHYTHMS
Mathematical Models of the Circadian Sleep-Wake Cycle
[AD-A145712] 02 p0235 N85-11532
Timing in dry seeds 05 p0690 N85-14437
The physiology of ultradian rhythms and their role in affecting disease resistance
[AD-A148842] 09 p1363 N85-18575
Effect of stationary magnetic field on bleeding time
12 p1904 N85-21956
Use of ranks to fit a linear model to cross-sectional data with an application to biological rhythms
[MATHEMATICS-RESEARCH-169] 12 p1923 N85-22081

RIBBONS
Silicon-sheet surface studies
06 p0831 N85-15287
Ribbon growing method and apparatus
[NASA-CASE-NPO-16306-1-CU] 19 p3375 N85-30934

RIBONUCLEIC ACIDS
Phylogenic distribution of the large 5S rRNA from Halococcus morrhuae
[NASA-CR-174019] 02 p0234 N85-11523
Development of a new class of chemical and biological ultrasensors: Ribonuclease contamination and control
[NASA-CR-175466] 11 p1635 N85-20296
Insights into the phylogenetic positions of photosynthetic bacteria obtained from 5S rRNA and 16S rRNA sequence data 21 p3658 N85-32719

RIBOSE
Molecular toxicology of chromatin: The role of Poly(ADP-Ribose) in gene control
[AD-A154415] 19 p3327 N85-30611
The DNA metabolism and poly-(ADP-ribose) synthesis in lymphocytes of persons exposed to low doses of ionizing radiation
[OEFZS-4307] 20 p3507 N85-31800
Insights into the phylogenetic positions of photosynthetic bacteria obtained from 5S rRNA and 16S rRNA sequence data 21 p3658 N85-32719

RIBS (SUPPORTS)
Heat transfer and pressure drop in blade cooling channels with turbulence promoters
[NASA-CR-3837] 03 p0361 N85-12315
The residual strength of cracked specimens representing a section of the mirage into wing main spar
[ARL/STRUC-R-406] 12 p1865 N85-21699
Research in the field of rib stiffened shell stability
16 p2766 N85-27068

RICCATI EQUATION
Numerical algorithms and software for matrix Riccati equations
[AD-A150148] 13 p2150 N85-23344
Some new results on the discrete-time Riccati Equation and their use in the design of optimal regulators and observer-estimators
[AD-A151934] 16 p2864 N85-27597

RICE
Remote sensing of rice fields and sea pollution by SIR-B 08 p1145 N85-17222

RICHARDSON NUMBER
On the classification and nonlinear solution of one type of stratified shear flow
[AD-A148632] 09 p1319 N85-18295
Three-dimensional baroclinic instability of a Hadley cell for small Richardson number
[NASA-TP-2450] 11 p1667 N85-20805
Modeling of shear flow in a stratified fluid
14 p2340 N85-24459

RICHARDSON-DUSHMAN EQUATION
U TEMPERATURE EFFECTS
U THERMIONIC EMISSION

RIDGES
New data on structure of Shirshov Ridge (Bering Sea)
10 p1498 N85-19456

RIDING QUALITY
Design of a digital ride quality augmentation system for commuter aircraft
[NASA-CR-172419] 01 p0006 N85-10037
Design of a digital ride quality augmentation system for commuter aircraft
[AD-A148233] 08 p1088 N85-16879
Ride comfort of off-road vehicles
[AD-P004279] 09 p1406 N85-18655
Further development in ride quality assessment
[AD-P004280] 09 p1406 N85-18656
Comparison of measured and simulated ride comfort for an agricultural tractor and influence of travel speed and tyre-inflation pressure on dynamic response
[AD-P004281] 09 p1407 N85-18657

Seakeeping and vibration tests of the Coast Guard 110 foot surface effect ship SEA BIRD class (WSES)
[AD-A154150] 19 p3252 N85-30166
RIEMANN INTEGRAL
U MEASURE AND INTEGRATION
RIEMANN MANIFOLD
Unrestricted convergence for generalized Poisson integrals
[CTH-MATH-1984-13] 04 p0556 N85-13540
A geometric approach to high resolution TVD schemes
[NASA-CR-172484] 06 p0857 N85-15449
Riemann foliations on simply connected varieties 11 p1699 N85-20677
Nonlinear sigma-models and integration methods
[DE85-004447] 12 p1922 N85-22071
On meromorphic functions continuous on the Stollow boundary 15 p2633 N85-26232
Conditions for the possibility of conformal sewing
[ST-AASF-IMD-58] 16 p2858 N85-27625
Admissible convergence of Poisson integrals in symmetric spaces
[CTH-MATH-1985-04] 22 p3836 N85-33750
RIEMANN PROBLEM
U CAUCHY PROBLEM
RIEMANN SPACE
U RIEMANN MANIFOLD
RIEMANN SPHERE
U RIEMANN MANIFOLD
RIFT VALLEYS
U VALLEYS
RIFTS
U GEOLOGICAL FAULTS
RIGGING
Behavior of the lean methane-air flame at zero-gravity
[NASA-CR-175586] 12 p1799 N85-21283
A novel type of stayed tower for wind turbines
[ISD-295] 15 p2587 N85-25952
Actuator rigging test set electromagnetic interference test (CE03)
[AD-A155819] 24 p4066 N85-35327
RIGID BODIES
U RIGID STRUCTURES
RIGID MOUNTING
New features of different frequency generating systems due to the use of electrodeless rigidly mounted VBA quartz crystal resonator 18 p3106 N85-29231
RIGID ROTOR HELICOPTERS
Application of Floquet theory to helicopter blade flapping stability
[AD-A154460] 19 p3218 N85-29952
RIGID ROTORS
The analysis on the dynamic performance of a single lug
[AD-P004289] 09 p1408 N85-18866
RIGID ROTORS (PLASMA PHYSICS)
NT PLASMA PHYSICS
RIGID STRUCTURES
NT RIGID ROTORS
NT RIGID WINGS
A rigid body mechanism in structural dynamics 02 p0206 N85-11361
Measurement of the inertial constants of a rigid or flexible structure of arbitrary shape through a vibration test
[NASA-TM-77567] 02 p0209 N85-11381
Elimination of uncontrollable rigid body mode, appendix C 05 p0803 N85-13842
Composite repair of aircraft structures 08 p1120 N85-17059
Least favorable response of inelastic structures 09 p1336 N85-18398
Planar dynamics of a uniform beam with rigid bodies affixed to the ends
[NASA-CR-175566] 12 p1864 N85-21693
Computer aided engineering applied to the design and verification of the generic Advanced Rigid Array (ARA) — solar array 13 p2008 N85-22593
Development and qualification of the electrical part of the Advanced Rigid Array (ARA) — solar array 13 p2008 N85-22594
Rigid Solar Generator (GSR) solar arrays 13 p2009 N85-22596
Retractable Rigid Solar Generator (GSR) 13 p2009 N85-22597
Generic design and verification of an Advanced Rigid Array (ARA) — solar array 13 p2012 N85-22621
Sound emission by particle beam passing through hole in rigid shield 15 p2525 N85-25570
Experience with free bodies 15 p2576 N85-25887
An improved torsional method for determining the fracture toughness of stiff materials and of adhesive joints
[AD-A152001] 16 p2800 N85-27267
The stability and dynamics of elastic structures and fluid flows
[AD-A154188] 19 p3268 N85-30252
Space station dynamic modeling, disturbance accommodation, and adaptive control 20 p3409 N85-31154
Retractable Rigid Solar Generator (GSR)
[SNIAS-851-440-101] 20 p3484 N85-31654
Rigid Solar Generator (GSR) solar arrays
[SNIAS-851-440-102] 20 p3484 N85-31655
Joint design for improved fatigue life of diffusion-bonded box-stiffened panels
[NASA-TP-2480] 22 p3799 N85-33537
The dynamics of articulated rigid bodies for purposes of animation 23 p3965 N85-34579
Identification and control of structures in space
[NASA-CR-176175] 24 p4089 N85-35214
RIGID WINGS
Theoretical study of non-linear unsteady aerodynamics of a non-rigid lifting body
[AD-P004169] 09 p1266 N85-17954
The aerodynamic characteristics of a GU25-5(11)8 aerofoil for low Reynolds numbers
[GU-AERO-8410] 23 p3894 N85-34121
RIGIDITY
Rigid zeolite containing polyurethane foams
[DE85-006406] 23 p3919 N85-34286
Effects of solar magnetic field on cosmic rays
[SH-4.2-12] 23 p4006 N85-34850
The expected cosmic ray density and stream distributions at the heliolatitudinal asymmetry of solar wind
[SH-4.2-14] 23 p4006 N85-34852
The dependence of solar modulation on the sign of the cosmic ray particle charge
[SH-4.2-23] 23 p4009 N85-34860
Observation of nuclei with energies 8-30 MeV per nucleon in the Earth's magnetosphere at the altitudes 350 KM
[SH-10.1-5] 23 p4053 N85-35196
RILLS
U VALLEYS
RIMS
Chondrule rims and interchondrule matrix in UOC 06 p0882 N85-15804
RING CURRENTS
Relations between the particle precipitation events in mid-latitudes, the ring current intensity and the polarity of the interplanetary magnetic field 04 p0519 N85-13316
Earth's radiation belts
[AD-A147927] 07 p0998 N85-16339
Correlation of ring current and ionospheric gap in morning and evening hours 14 p2339 N85-24466
Ring current dynamics and plasma sheet sources — magnetic storms 14 p2359 N85-24577
The temporal evolution of a small auroral substorm as viewed from high altitudes with Dynamics Explorer 1
[NASA-CR-176064] 20 p3493 N85-31718
RING LASERS
Experimental properties of an inhomogeneously broadened He-Xe unstable ring laser
[AD-A144824] 01 p0052 N85-10344
Autostochastic behavior of solid state ring laser with low frequency periodic loss modulation 11 p1717 N85-20905
Status of and outlook for producing means of transmitting units of plane angle, angular velocity and acceleration with ring lasers 13 p2074 N85-22955
Measurements of laser gyro errors as a function of the beam path
[DFVLR-FB-85-02] 17 p2969 N85-28336
Fiber optic gyroscope with alternating output signal
[AD-D011669] 19 p3271 N85-30284
Influence of mirror anisotropy and Brewster window orientation on radiation characteristics of ring lasers 21 p3684 N85-32669
Possibility of measurement of small displacements by ring laser 21 p3687 N85-32904
RING STRUCTURES
Seismotectonic nature of some annular photoanomalies registered by remote methods 02 p0164 N85-11110
Large-scale bubble structure of the interstellar medium (ISM) and properties of the Local Spiral Arm (LSA) 06 p0879 N85-15588
Method for introducing fluorine into an aromatic ring
[AD-D011397] 08 p1120 N85-17061
Two-dimensional shock response of a mass on energy-absorbing shock mounts 09 p1334 N85-18389
The structure and dynamics of ringed galaxies 09 p1415 N85-18926
Solar system studies with the IUE: 1982 - 1984 11 p1744 N85-20964
Torso sizing ring construction for hard space suit
[NASA-CASE-ARC-11616-1] 12 p1910 N85-21987
Observations of high resistance on slip-rings employing Ag/MoS2/Cu brushes — solar array drives
[ESA-ESTL-70] 18 p3123 N85-29333
A rotating electrical transfer device 22 p3798 N85-33529
Two-plane balance and slip-ring design 22 p3799 N85-33536
SRB attach ring phenolic TPS fishtail seal evaluation tests
[NASA-CR-170887] 24 p4098 N85-35407
RINGS
Flexible matrix composite laminated disk/ring flywheel 05 p0606 N85-13866
Acceleration of an electron ring in a modified betatron with transverse pressure
[AD-A148626] 08 p1221 N85-17688
RINGS (MATHEMATICS)
Polynomial and power series FGS-rings have trivial coefficient rings
[TWISK-326] 01 p0109 N85-10737
On Bezout domains, elementary divisor rings, and pole assignability
[CSIR-TWISK-330] 01 p0110 N85-10740
On localization of injective modules
[CSIR-TWISK-342] 14 p2413 N85-24878
Quadratic spaces over discrete Hodge algebras 16 p2853 N85-27593
On the turning lozange of constant side whose vertices alternate between two fixed circles of a ring
[AD-A154803] 21 p3677 N85-32840
RIO GRANDE (NORTH AMERICA)
Rio Grande rift: Problems and perspectives
[DE84-015492] 04 p0534 N85-13417
Water resources data for Colorado, water year 1983. Volume 1: Missouri River Basin, Arkansas River Basin and Rio Grande Basin
[PB85-123859] 11 p1671 N85-20528
Evaluation of geothermal potential of Rio Grande rift and Basin and Range province, New Mexico
[DE85-001380] 19 p3301 N85-30466
RIOMETERS
Autumn and winter anomalies in ionospheric absorption as measured by riometers 11 p1660 N85-20460
RIPPLES
Ripple ring basins on Ganymede and Callisto 13 p2183 N85-23547
Water wave propagation over uneven bottoms
[AD-A151450] 15 p2556 N85-25769
Neoclassical diffusion including ellipticity in a heliotron-like configuration 23 p3978 N85-34667
RISK
Differences in health risks by aircraft model among US Navy pilots
[AD-A146147] 03 p0401 N85-12556
Interval mathematics reports
[REPT-84/1] 04 p0556 N85-13536
Risk analysis without Monte Carlo methods 04 p0556 N85-13537
Conditional regression models for transient state survival analysis
[AD-A147872] 07 p1034 N85-16563
Ambiguity and uncertainty in probabilistic inference
[AD-A147378] 07 p1035 N85-16572
A theory of preference reversals
[AD-A147952] 08 p1216 N85-17661
Application of the isoenergy principle and the A weighting to evaluate lesion risks due to noise in a military environment
[ISL-CO-231/83] 14 p2390 N85-24720
LFMR definition study
[AD-A153691] 18 p3090 N85-29126
The human role in space (THURIS) 18 p3158 N85-29557
Procedure for estimating orbital debris risks
[NASA-TP-2507] 22 p3738 N85-33169
Description of a test site for large-scale heavy gas dispersion and combustion experiments
[DE85-004987] 23 p3911 N85-34231
The application of models to the assessment of fire hazard from consumer products
[NBSIR-85-3219] 23 p3925 N85-34325
Fire service emergency management handbook
[AD-A155780] 24 p4084 N85-35313
Calculation of trajectories of detached wind turbine blades and prediction of site risk levels associated with failures of HAWT's 24 p4110 N85-35475
The physical and empirical basis for a specific clear-air turbulence risk index
[NASA-CR-178522] 24 p4120 N85-35540
Risk analysis and sensitivity: Antithesis or synthesis
[86562444] 24 p4144 N85-35687
RIT ENGINES
Analysis of beam interaction of the electrical thruster RIT 10 (particle emission) with surfaces
[ESA-TT-826] 20 p3421 N85-31231
RITZ AVERAGING METHOD
Comparison of free component mode synthesis technique using MSC/NASTRAN
[DE84-014451] 04 p0514 N85-13278

Spline-based Rayleigh-Ritz methods for the approximation of the natural modes of vibration for flexible beams with tip bodies
[NASA-CR-172568] 13 p2102 N85-23100
A study of internal and distributed damping for vibrating turbomachine blades
[NASA-CR-175901] 17 p2698 N85-27868

RIVER BASINS
NT MISSOURI RIVER BASIN (US)
Systematic data interpretation of remote sensing in the reception of hydrocarbons, volume 1
[E85-10008] 02 p0215 N85-11421
Evaluation of criteria for selecting the spectral attributes of digital LANDSAT MSS imagery for discriminating lithological units in the lower Curaca River Valley, Bahia — Brazil
[E85-10036] 03 p0379 N85-12415
Late quarterly glaciolacustrine and vegetational history of the Copper River Basin, south-central Alaska
03 p0391 N85-12499
Report of the field work performed in the Basins of the Quebra Oseo and Tanque Petro Rivers in the Cates Altas quadrangle, Minas Gerais
[INPE-3268-NTE/225] 04 p0525 N85-13359
Deforestation, floodplain dynamics, and carbon biogeochemistry in the Amazon Basin
08 p1144 N85-17216
Comparison of land cover information from LANDSAT Multispectral Scanner (MSS) and airborne Thematic Mapper simulator (TMS) data for hydrologic applications — Clinton River Basin, Michigan
13 p2122 N85-23211
General report of the researches of snowpack properties, snowmelt runoff and evapotranspiration in Japan 13 p2124 N85-23225
Snowmelt-runoff model utilizing remotely-sensed data
13 p2124 N85-23226
Snowmelt runoff model in Japan
13 p2124 N85-23227
Application of Martinec-Rango model to river basin in Japan 13 p2124 N85-23228
Distribution of snow and maximum snow water equivalent obtained by LANDSAT data and degree day method 13 p2124 N85-23229
The geology of East Butte, a rhyolitic volcanic dome on the Eastern Snake River Plain, Idaho
13 p2187 N85-23570
Automatic hydrological data collection facility using ARGOS 14 p2324 N85-24363
The ARGOS system and hydrology: The use of Platform Terminal Transmitter (PTT) with built-in memory and direct reception by the Seine basin hydrology service
14 p2328 N85-24389
Study of Volga river delta using space photosurvey materials 15 p2485 N85-25340
Estimation of Sr90 and Cs137 activity introduced and accumulation in the Po basin until 1983
[CISE-2515] 22 p3813 N85-33617

RIVERS
NT COLORADO RIVER (NORTH AMERICA)
NT MISSISSIPPI RIVER (US)
NT RIO GRANDE (NORTH AMERICA)
The SANCOR estuaries programme, 1982-1986
[ISBN-0-7988-2662-2] 01 p0068 N85-10454
Estuaries of the Cape. Part 2: Synopses of available information on individual systems. Report 12: Buffels (WES) (CSW 1), Elsies (CSW 2), Sir Lowry's Pass (CSW8), Steenbras (CSW 9), and Buffels (OOS) (CSW 11)
[CSIR-RR-411-PT-2] 01 p0068 N85-10581
Estuaries of the Cape. Part 2: Synopses of available information on individual systems. Report no. 14: Sand (CSW 4)
[CSIR-RR-413-PT-2] 01 p0066 N85-10583
Estuaries of the Cape. Part 2: Synopses of available information on individual systems. Report no. 15: Zeekoe (CSW 5)
[CSIR-RR-414-PT-2] 01 p0067 N85-10584
Estuaries of the Cape. Part 2: Synopses of available information on individual systems. Report no. 16: Bot/Kleinmond system (CSW 13)
[CSIR-RR-417-PT-2] 01 p0067 N85-10587
Spatial relationships in stream flow residuals
02 p0212 N85-11397
Petrology of deep crustal xenoliths from the eastern Snake River Plain, Idaho 02 p0226 N85-11477
Geothermal assessment of the lower Bear River drainage and northern East Shore ground-water areas, Box Elder County, Utah
[DE84-017358] 04 p0526 N85-13368
Carbon cycle: Terrestrial interactions
05 p0652 N85-14187
Image-to-image correspondence: Linear structure matching 07 p0966 N85-16266
Forecasting water temperature decline and freeze-up in rivers
[AD-A147068] 07 p0987 N85-16274
Verification of a model of the Eastern Scheldt
[RAND/R-3106-NETH] 09 p1354 N85-18518
Freeze-up, breakup and data of maximum ice thickness for the Saint Lawrence River, 1971 - 1978
[PB85-119451] 10 p1507 N85-19509
Examples of environment services: Hydrological and pollution measurements in the Po River (Italy)
[CISE-2299] 11 p1679 N85-20578
A comparison of terrestrial saltation flux in the laboratory and the field 13 p2189 N85-23582
The ARGOS system and hydrology. Results obtained by ORSTROM and benefits of a degree of standardization 14 p2239 N85-23681
Applications of Kalman filtering and recursive least-squares in river flow modelling
15 p2636 N85-26254
Modeling water resources systems for water quality
[AD-A154286] 19 p3300 N85-30457
Sand dispersion from an ephemeral river delta on the wave-dominated central California coast
[AD-A154352] 19 p3300 N85-30458
Microwave hydrology: A trilogy
[NASA-CR-176042] 20 p3477 N85-31603
Depositional systems and coal occurrence in the Fort Union Formation (Paleocene), Powder River Basin, Wyoming and Montana 24 p4114 N85-35505
Bibliography on tidal hydraulics. Report 2. Supplement 9: Supplementary material compiled from June 1980 - June 1983. Tidal flows in rivers and harbors
[AD-A155990] 24 p4125 N85-35574

RIVETED JOINTS
Defect detection threshold in riveted joints, test report no.44-833/F — in aircraft 04 p0511 N85-13280
The influence of fastener flexibility on load transfer and fatigue life predictions for multirow bolted and riveted joints — aircraft structures
[LBF-FB-172/84] 07 p0979 N85-16219
The application of BRILES rivets for mechanical jointing of Aramid Reinforced Aluminum Laminate (ARALL)
[VTH-LR-387] 16 p2802 N85-27279
Mechanical jointing in Aramid fiber composites: An experimental study
[VTH-LR-371] 16 p2802 N85-27280

RIVETING
The application of BRILES rivets for mechanical jointing of Aramid Reinforced Aluminum Laminate (ARALL)
[VTH-LR-387] 16 p2802 N85-27279
Utilization of an automated riveting system in aircraft construction
[MBB-UT-11/84-O] 16 p2875 N85-27736

RIVETS
Future robotics program at San Antonio ALC (Air Logistics Center)
[AD-P004011] 03 p0309 N85-11991
The application of BRILES rivets for mechanical jointing of Aramid Reinforced Aluminum Laminate (ARALL)
[VTH-LR-387] 16 p2802 N85-27279

RL-10 ENGINES
Convoluted nozzle design for the RL10 derivative 2B engine
[NASA-CR-174953] 19 p3220 N85-29965

RNA
U RIBONUCLEIC ACIDS

ROADS
NT HIGHWAYS
Pavement friction measurements on nontangent sections of roadways, vol. 1
[PB84-219732] 01 p0036 N85-10227
A study of bituminous pavements to determine a correlation between pavement structure designs and tripping of asphalt cement
[PB84-217751] 01 p0037 N85-10231
Automatic land vehicle navigation using road map data
[DE84-017178] 09 p1278 N85-18043
Microwave methods for paving
[DE85-004194] 14 p2285 N85-24032
A greedy algorithm for the transhipment along a single road problem
[AD-A152343] 17 p3025 N85-28709
Review of rigid pavement design for vehicular parking areas
[AD-A154284] 19 p3222 N85-29975
Design and implementation of an interactive route editor 23 p3982 N85-34559

ROASTING
Sintered silicon nitride workpiece
[NASA-TM-77600] 01 p0021 N85-10129

ROBOTICS
Terrain navigation concepts for autonomous vehicles
[AD-A144994] 01 p0005 N85-10031
USSR report: Machine tools and metalworking equipment
[JPRS-UMM-84-019] 01 p0035 N85-10214
Growth, future of Soviet robotics sector analyzed
01 p0035 N85-10217
Publications of Center for Manufacturing Engineering (of the National Bureau of Standards), 1978-1983
[PB84-224526] 01 p0036 N85-10228
East Europe report: Science and technology
[JPRS-ESA-84-030] 01 p0101 N85-10670
Robotics investment decision model user's manual
[AD-A145487] 02 p0204 N85-11347
European Scientific Notes, Number 38-9
[AD-A145883] 02 p0306 N85-11975
Current successful robotics applications by the Automatix Company
[AD-P003998] 03 p0307 N85-11979
Air Force Materials Laboratory plans/projects
[AD-P004010] 03 p0308 N85-11990
Future robotics program at San Antonio ALC (Air Logistics Center)
[AD-P004011] 03 p0309 N85-11991
Robotics in nondestructive inspection at Sacramento Air Logistics Center
[AD-P004012] 03 p0309 N85-11992
Supply center processes
[AD-P004014] 03 p0309 N85-11993
Potential application of robotics and state-of-the art end effectors at Letterkenny Army Depot
[AD-P004015] 03 p0309 N85-11994
Field applications for robotic material handling
[AD-P004016] 03 p0309 N85-11995
West Europe report: Science and technology, no. 166
[JPRS-84845] 03 p0341 N85-12190
French firms develop artificial intelligence robot
03 p0341 N85-12192
East Europe report: Scientific affairs, no. 791
[JPRS-84624] 03 p0341 N85-12195
Sensor technology for second, third generation industrial robots. Optical sensor applications
03 p0342 N85-12198
Test-bed for programmable automation research. Phase 1
[AD-A145872] 03 p0409 N85-12814
USSR report: Machine tools and metalworking equipment
[JPRS-UMM-84-020] 04 p0491 N85-13126
Developments in Soviet robot technology viewed
04 p0491 N85-13127
DNC, CNC network for robotized machining cells
04 p0491 N85-13130
Development of robot technology in Shanghai surveyed 04 p0492 N85-13134
Machine Mechanics Institute builds walking vehicle
04 p0543 N85-13455
Evaluation of automated decisionmaking methodologies and development of an integrated robotic system simulation
[NASA-CR-172401] 04 p0552 N85-13516
Manufacturing Sciences and Robotics Research and Development Act of 1984
[H-REPT-98-1078] 04 p0576 N85-13686
Instantaneous kinematics and joint displacement analysis of fully-parallel robotic devices
05 p0641 N85-14113
Application of robotics in remote fuel fabrication operations
[DE84-011481] 05 p0646 N85-14144
Robotic technology: An assessment and forecast
[AD-A146672] 06 p0815 N85-15171
NC programming, machine tool information
06 p0816 N85-15178
Fiat, Peugeot introduce integrated robotized engine: CAD used 07 p0936 N85-15933
Improvement of electromechanical systems by utilization of microelectronic technology 07 p0955 N85-16053
Computer science research in Europe
[AD-A146905] 07 p1022 N85-16462
JPL Robotics Laboratory computer vision software library
[NASA-CR-174272] 07 p1023 N85-16491
USSR report: Machine tools and metalworking equipment
[JPRS-UMM-84-021] 08 p1138 N85-17168
Control systems for robotic production lines
08 p1138 N85-17169
USSR report: Machine tools and metalworking equipment
[JPRS-UMM-85-001] 08 p1139 N85-17172
Design features, applications of new robots
08 p1139 N85-17174
East Europe report: Science and technology
[JPRS-ESA-84-046] 08 p1139 N85-17176
Man-machine communication research for robotics reported 08 p1139 N85-17177
Robotics application in construction industry assessed
08 p1139 N85-17178
East Europe report: Science and technology
[JPRS-ESA-84-047] 08 p1140 N85-17183
Researchers on third generation robotics development
08 p1140 N85-17184

Flexible manufacturing system concept features cache memory
08 p1140 N85-17186
East Europe report: Science and technology
[JPRS-ESA-84-043] 08 p1142 N85-17196
Chemical, material electronics studies established
08 p1142 N85-17200
Robotics research, integration overview presented. Application objectives cited
08 p1142 N85-17201
Coordinated research in robotics and integrated manufacturing
[AD-A148204] 08 p1168 N85-17365
Conceptual design report for a remotely operated cask handling system, revision 1
[DE85-000348] 08 p1169 N85-17371
Cognitive asymmetry and occupation. Computer programmers, students, and bank personnel, part 1 and part 2
[AD-A147125] 08 p1197 N85-17540
Recognition of complex 3-dimensional objects using 3-dimensional moment invariants
[AD-A148119] 08 p1212 N85-17625
Investigation on experimental techniques to detect, locate and quantify gear noise in helicopter transmissions
[NASA-CR-3847] 08 p1217 N85-17667
Advancement of remote technology: Past perspectives and future plans
[DE85-000934] 09 p1327 N85-18342
Optical data processing for missile guidance
[AD-A149346] 10 p1422 N85-19072
Researchers, projects at French intelligent machine center
10 p1460 N85-19207
French firm develops 2D, 3D computer vision system
10 p1461 N85-19208
USSR report: Machine tools and metalworking equipment
[JPRS-UMM-85-003] 10 p1461 N85-19211
Dean of Kiev State University on impact of robots
10 p1461 N85-19213
Robotized blanks loader for new forge press
10 p1461 N85-19216
Flexible applications robot used in Moscow training course
10 p1462 N85-19217
Control system of complex CNC machining cell
10 p1462 N85-19218
On motion planning with uncertainty: Revised
[AD-A149521] 10 p1492 N85-19421
Contact insertion and wire lay robotic end effector apparatus
[AD-D011451] 10 p1492 N85-19424
New developments in robotics: The Robots 8 Conference and Exposition
[DE85-000263] 10 p1493 N85-19429
Robotics in the radiochemical laboratory
[DE85-002824] 10 p1494 N85-19433
Optical implementation of the synthetic discriminant function
[AD-A149582] 10 p1557 N85-19617
Novel concept in design of ASEA's new assembly robot
11 p1592 N85-20016
East Europe report: Science and technology
[JPRS-ESA-85-009] 11 p1616 N85-20165
New PCB production for robotics application
11 p1617 N85-20169
Overview of leading-edge research at French CNRS lab
11 p1618 N85-20179
French panel makes specific proposals for robotics research. Current state of French robotics
11 p1618 N85-20180
Real time algorithms for robotic control of teleoperators
[DE85-001137] 11 p1647 N85-20380
Robotics at Savannah River site: Activity report
[DE85-003657] 11 p1648 N85-20383
Advanced industrial robot control systems
[PB85-110773] 11 p1648 N85-20385
Advanced industrial robot control systems
[PB85-110781] 11 p1648 N85-20386
Dynamic world modeling for an intelligent mobile robot using a rotating ultra-sonic ranging device
[AD-A149979] 12 p1775 N85-21143
Impacts of robotic and flexible manufacturing technologies on manufacturing costs and employment
[AD-A150080] 12 p1860 N85-21668
Mechanical properties for the grasp of a robotic hand
[AD-A150082] 12 p1860 N85-21669
A formal method for specifying computer resources in an implementation independent manner
[AD-A149955] 12 p1918 N85-22043
Design of an optical proximity sensor using multiple cones of light for measuring surface shape — application to a robot manipulator
[AD-A150060] 12 p1934 N85-22152
Sensor control of robot arc welding
12 p1948 N85-22233
Advancing automation and robotics technology for the Space Station and for the US economy. Volume 1: Executive overview
[NASA-TM-87566-VOL-1] 13 p1966 N85-22460
Advancing automation and robotics technology for the Space Station and for the US economy, volume 2
[NASA-TM-87566-VOL-2] 13 p1967 N85-22461
Reliability of robotized welding apparatus
13 p2034 N85-22741
Optoelectronic safety system for robotized technological complex
13 p2046 N85-22905
Optimum design of electrical motors for multilink manipulators and automated manufacturing systems
13 p2062 N85-22880
Motion planning with six degrees of freedom
[AD-A150312] 13 p2165 N85-23432
Classification of holding jigs for objects of robotized assembly
14 p2266 N85-24039
USSR report: Machine tools and metalworking equipment
[JPRS-UMM-85-004] 14 p2284 N85-24152
Automated, robotized forge-press systems viewed
14 p2284 N85-24153
Robots for application in forge-press operation
14 p2284 N85-24154
Modular design, versatility of robots viewed
14 p2284 N85-24155
Integrated control system for FMS components
14 p2285 N85-24156
Robotized system for treating gear wheels
14 p2285 N85-24162
Investigation of transport operations of ergatic robot
14 p2286 N85-24166
East Europe report: Science and technology
[JPRS-ESA-85-015] 14 p2289 N85-24189
Plans, developments in robotics
14 p2289 N85-24191
3D (Three-Dimensional) sensor for adaptive suspension vehicle
[AD-A150921] 14 p2311 N85-24305
Our future in the cosmos: Computers
14 p2432 N85-24997
West Europe report: Science and technology
[JPRS-WST-85-014] 15 p2489 N85-25362
Resources for robotics research in Europe, by country
15 p2489 N85-25364
Study of experimental robotized system for arc welding based on Universal-15 manipulator
15 p2500 N85-25423
West Europe report: Science and technology
[JPRS-WST-84-012] 15 p2523 N85-25552
French robotics research at Grenoble labs
15 p2523 N85-25555
French firm develops new kind of CTD camera for robots
15 p2523 N85-25556
China report: Science and technology
[JPRS-CST-85-009] 15 p2530 N85-25586
Development of robots, robotics discussed
15 p2530 N85-25589
West Europe report: Science and technology
[JPRS-WST-84-027] 15 p2532 N85-25612
A preliminary investigation into the intelligibility of Microspeech-2, a speech synthesiser
[BAE-BT-12284] 15 p2539 N85-25675
Robotic arc welding
15 p2566 N85-25830
Automation and robotics in welding
15 p2566 N85-25831
Some aspects of nuclear plant fabrication in Japan and the UK relating to automatic and robotic arc welding
15 p2566 N85-25834
The kinematic control of redundant manipulators
15 p2566 N85-25836
Development of robots and application to industrial processes
[NASA-CR-175754] 15 p2567 N85-25840
East Europe report: Science and technology
[JPRS-ESA-84-032] 16 p2727 N85-26833
Optimal open loop and nonlinear feedback control for remote orbital capture
[AD-A151967] 16 p2732 N85-26859
Method of selecting robotized system design for pressing process
16 p2761 N85-27040
Experience of sheet stamping robotic complexes
16 p2761 N85-27041
USSR report: Machine tools and metalworking equipment
[JPRS-UMM-84-010] 16 p2767 N85-27071
New robotized, vertical broaching machine featured
16 p2767 N85-27074
Guidelines for optimization of robotized machining cells
16 p2767 N85-27076
A robotic system for preparing reagent and dilution vials
[DE85-008262] 16 p2793 N85-27231
Automation and robotics for the National Space Program
[NASA-CR-175881] 17 p2909 N85-27936
Engineering robot actions in a computer integrated manufacturing environment
[CWI-CS-R8415] 17 p2938 N85-28139
USSR report: Machine tools and metalworking equipment
[JPRS-UMM-84-014] 17 p2946 N85-28168
Applications of robots in machine tool industry reviewed
17 p2946 N85-28169
Robotic safety systems and methods: Savannah River site
[DE85-006261] 17 p2974 N85-28375
West Europe report: Science and technology
[JPRS-WST-84-022] 18 p3085 N85-29066
Component problems plague French robotics industry
18 p3085 N85-29068
Multinational program to develop intelligent robots
18 p3086 N85-29094
Analysis of remote operating systems for space-based servicing operations, volume 1
[NASA-CR-171885] 19 p3225 N85-29993
Analysis of remote operating systems for space-based servicing operations. Volume 2: Study results
[NASA-CR-171886] 19 p3225 N85-29994
Space station automation study-satellite servicing. Volume 1: Executive summary
[NASA-CR-171512] 19 p3226 N85-29999
Space station automation study-satellite servicing, volume 2
[NASA-CR-171513] 19 p3226 N85-30000
Some examples of the application of automatically guided vehicle systems
[HSE-TRANS-11134] 19 p3281 N85-30348
Touch-off: A method to determine the position of an object by means of a sensor-driven robot
[DE85-011178] 19 p3339 N85-30691
Acoustic imaging systems (for robotic object acquisition)
[AD-A154043] 19 p3351 N85-30772
Space optics
[CNES-84/105/T/CT/DRT/TIT/10]
20 p3533 N85-31985
NASA space station automation: AI-based technology review
[NASA-CR-176094] 21 p3558 N85-32134
NASA space station automation: AI-based technology review. Executive summary
[NASA-CR-176006] 21 p3558 N85-32135
East Europe report: Science and technology
[JPRS-ESA-85-021] 21 p3568 N85-32190
East Europe report: Science and technology
[JPRS-ESA-85-023] 21 p3572 N85-32217
Importance of automation, robotization in economy
21 p3572 N85-32219
Ultrasonic position reference systems for an autonomous sentry robot and a robot manipulator arm
[AD-A155481] 21 p3598 N85-32336
Space station automation and robotics study. Operator-systems interface
[NASA-CR-176095] 22 p3738 N85-33172
Testimony of Robert A. Frosch before the Subcommittee on HUD and Independent Agencies of the Senate Committee on Appropriations
[NASA-TM-87496] 22 p3738 N85-33173
Statement of Aaron Cohen, Director, Research and Engineering, Johnson Space Center and Chairman, Space Station Advanced Technology Advisory Committee, National Aeronautics and Space Administration, before the Subcommittee on Science, Technology, and Space, Committee on Commerce, Science, and Transportation, United States Senate
[NASA-TM-87497] 22 p3739 N85-33174
Space station automation study: Autonomous systems and assembly, volume 2
[NASA-CR-176092] 22 p3739 N85-33175
Study and realization of a command system adapted to space robotics
[SNIAS-851-440-106] 22 p3740 N85-33183
Robotic order picking
[AD-D011737] 22 p3792 N85-33493
Machine intelligence for robotics applications
[DE85-011430] 22 p3793 N85-33503
A strategy planner for NASA robotics applications
[NASA-CR-175319] 22 p3834 N85-33738
Space Missions for Automation and Robotics Technologies (SMART) Program
[NASA-TM-86820] 24 p4068 N85-35210
Investment justification of robotic technology in aerospace manufacturing. User's manual
[AD-A156193] 24 p4090 N85-35410
TRICCS: A proposed teleoperator/robot integrated command and control system for space applications
[NASA-TM-87577] 24 p4136 N85-35637

ROBOTS

Optical seam tracking of robotic arc welding
[VTT-272] 01 p0055 N85-10368

Methods, applications of image processing
01 p0115 N85-10785

DoD Robotics Application Workshop Proceedings
[AD-A145867] 03 p0307 N85-11978

Current successful robotics applications by the Automatix Company
[AD-P003996] 03 p0307 N85-11979

Air force, robotic painting
[AD-P004006] 03 p0308 N85-11986

East Europe report: Science and technology
[JPRS-ESA-84-038] 03 p0343 N85-12210

Development, production, application of robots assessed
03 p0343 N85-12211

Industrial robots and transmanipulations: Important link in setup of automated production lines
03 p0345 N85-12222

Modular electromechanical industrial robots
03 p0345 N85-12223

International exhibition: Industrial Robots, 1982
03 p0345 N85-12224

Robotization of electric welding processes
03 p0345 N85-12225

Robotization of technological processes in high-frequency heating and welding
03 p0345 N85-12226

Improving operational reliability and productivity of robotized technological complexes
03 p0346 N85-12227

Test-bed for programmable automation research. Phase 1
[AD-A145872] 03 p0409 N85-12614

East Europe report: Science and technology
[JPRS-ESA-84-041] 04 p0484 N85-13090

Use of robotics in heavy machinery, equipment construction industry 04 p0485 N85-13093

Robotics technology application assessed, statistics
04 p0485 N85-13094

Mathematical modeling of assembly processes involving use of sensitized robots 04 p0488 N85-13111

Optimization of movements of manipulators with kinematic redundancy 04 p0488 N85-13112

Soviet robot exhibition reviewed
04 p0491 N85-13128

Development, new application of Soviet robots
04 p0491 N85-13129

China report: Science and technology
[JPRS-CST-84-003] 04 p0491 N85-13132

Development of robot technology in Shanghai surveyed 04 p0492 N85-13134

Improved robotic equipment for radiological emergencies
[DE84-017637] 04 p0509 N85-13249

Design of a flexible machining system
[CETIM-1-3E-140] 04 p0510 N85-13252

Real-time planning by an intelligent robot
[DE84-016669] 04 p0553 N85-13519

The acquisition, processing, and use of tactile sensor data in robot control 05 p0641 N85-14114

Robotic technology: An assessment and forecast
[AD-A146672] 06 p0815 N85-15171

East Europe report: Science and technology
[JPRS-ESA-84-045] 06 p0815 N85-15175

New concepts for industrial robots outlined
06 p0815 N85-15176

Translational control of a graphically simulated robot arm by kinematic rate equations that overcome elbow joint singularity
[NASA-TP-2376] 06 p0856 N85-15446

NyKINM, a further development of KINM 22 — simulation of a robot attack on an aircraft
[FOA-C-20559-D8(E3)] 07 p0903 N85-15720

Precise control of flexible manipulators
[NASA-CR-174210] 07 p0973 N85-16178

Vision by man and machine: How the brain processes visual information may be suggested by studies in computer vision (and vice versa)
[AD-A147890] 07 p1017 N85-16458

New applications for robot loaders, unloaders
08 p1139 N85-17175

General assessment of GDR microelectronics industry, applications 08 p1142 N85-17202

The combinatorics of local constraints in model-based recognition and localization
[AD-A148338] 08 p1230 N85-17746

Dutch institutes do research in tactile visual robot sensors 09 p1310 N85-18228

Scania, ASEA of Sweden use robots for all production phases 09 p1310 N85-18229

The optimal control and design of a flexible manipulator arm 09 p1327 N85-18340

Parallel algorithms for robot dynamics
[DE84-016563] 09 p1369 N85-18605

Strategy planning by an intelligent machine
[DE84-016609] 09 p1372 N85-18624

Double pinch-push contact insertion end-effector
[AD-D011485] 10 p1459 N85-19196

Armenia markets new drive motors for machine tools
10 p1461 N85-19212

Production turret lathe retrofitted with robot
10 p1461 N85-19214

Specifications, applications of gantry robots viewed
10 p1461 N85-19215

Planning of minimum-time trajectories for robot arms
[AD-A148956] 10 p1492 N85-19418

Simplified grasping and manipulation with dextrous robot hands
[AD-A148962] 10 p1492 N85-19419

Fourth International Conference on Robot Vision and Sensory Controls
[AD-A149524] 10 p1492 N85-19422

Contact insertion and wire lay robotic end effector apparatus
[AD-D011451] 10 p1492 N85-19424

New developments in robotics: The Robots 8 Conference and Exposition
[DE85-000263] 10 p1493 N85-19429

Robotic safety
[DE85-002314] 10 p1493 N85-19431

Robotics in the radiochemical laboratory
[DE85-002824] 10 p1494 N85-19433

Monitoring the execution of plans in SIPE (System for Interactive Planning and Execution) monitoring
[AD-A149138] 10 p1544 N85-19731

Novel concept in design of ASEA's new assembly robot 11 p1592 N85-20016

East Europe report: Science and technology
[JPRS-ESA-85-009] 11 p1616 N85-20165

Robot production lines in operation
11 p1617 N85-20166

Increased use of CNC in machine tool construction
11 p1617 N85-20170

Robotics at Savannah River site: Activity report
[DE85-003657] 11 p1648 N85-20383

Exploratory assessment of second generation robotics and sensor-based systems
[PB85-132793] 11 p1648 N85-20388

Man/machine interface for a nuclear cask remote handling control station: System design requirements
[DE85-000256] 11 p1697 N85-20667

Navigation for an intelligent mobile robot
[AD-A150051] 12 p1775 N85-21144

A functional vehicle for autonomous mobile robot research
[AD-A150052] 12 p1860 N85-21666

Dynamic visual servo control of robots: An adaptive image-based approach
[AD-A150057] 12 p1860 N85-21667

Impacts of robotic and flexible manufacturing technologies on manufacturing costs and employment
[AD-A150060] 12 p1860 N85-21668

Mechanical properties for the grasp of a robotic hand
[AD-A150062] 12 p1860 N85-21669

Oversight review of the five-year outlook report on science and technology
[GPO-41-058] 12 p1949 N85-22243

Cyclic industrial robots with mechanical energy storing devices: Multipositional system with one or several degrees of freedom 13 p2045 N85-22803

Hydraulic brakes for industrial robots
13 p2046 N85-22806

Cyclic industrial robots with mechanical energy storing devices: Principles of drive design
13 p2046 N85-22807

Assembly robot control algorithms
13 p2046 N85-22808

Optimum design and automated dynamic analysis of flexible mechanisms
[AD-A150152] 13 p2099 N85-23066

USSR report: Machine tools and metalworking equipment
[JPRS-UMM-85-006] 14 p2283 N85-24146

New CNC turning centers described
14 p2284 N85-24148

Minister B. V. Balmont on status of automation drive
14 p2284 N85-24151

Auxiliary units for Robots 14 p2285 N85-24161

Robotized system for treating gear wheels
14 p2285 N85-24162

Investigation of transport operations of angelic robot
14 p2286 N85-24166

Robotic deburring. Part 2: Evaluation of cutters and noncompliant tooling
[DE85-006182] 14 p2311 N85-24306

Production cells with IR 2SO robot examined
15 p2524 N85-25561

Development of robots, robotics discussed
15 p2530 N85-25599

Robot use in FRG increases but sensor technology lags 15 p2531 N85-25605

West Europe report: Science and technology
[JPRS-WST-84-009] 15 p2535 N85-25639

French consulting firm develops own robotics
15 p2535 N85-25642

Italy invents robot to compete with Asea, Hitachi
15 p2535 N85-25643

Italy's Fiat uses Sweden's Asea seeing robot
15 p2536 N85-25650

Applicability of modular versus universal robots discussed 15 p2536 N85-25664

Sonars with high noise and clutter rejection for use with adaptive robots
[AD-A151875] 15 p2543 N85-25701

Manipulation and simulation of general robots using the zero-position description 15 p2567 N85-25838

Artificial intelligence based control of a sensor-driven machine
[DE85-006972] 15 p2633 N85-26227

Structural design and kinematic configuration of two-armed robots 16 p2761 N85-27037

Calculating reliability and productivity of cold stamping robot complex as queuing system
16 p2761 N85-27039

Automatic manipulators for forging rollers
16 p2762 N85-27042

Updating model RPD-1.25 industrial robot
16 p2762 N85-27043

Industrial robots and automatic manipulators for forging and pressing operations at Second International Exhibition 16 p2762 N85-27044

New stage in robotics development
16 p2762 N85-27045

Control of motion of manipulator robots on basis of first-order kinematic algorithms
16 p2762 N85-27047

Robotic thermal battery pellet fabrication
[DE85-007755] 16 p2779 N85-27154

Creating a Mobile Autonomous Robot Research System (MARRS)
[AD-A151983] 16 p2793 N85-27229

A general simulation program for robot manipulator arm dynamics
[AD-A152121] 16 p2793 N85-27230

Kinematic rate control of simulated robot hand at or near wrist singularity
[NASA-TP-2440] 16 p2851 N85-27575

Positioning of a robotic manipulator through the use of visual feedback
[AD-A151933] 16 p2851 N85-27577

Robots, automatic devices inside VW's Wolfsburg plant 17 p2948 N85-28186

Future directions of robotics, automation in Italy
17 p2948 N85-28187

Component problems plague French robotics industry
18 p3085 N85-29088

Multinational program to develop intelligent robots
18 p3088 N85-29094

HERMIES-1: A mobile robot for navigation and manipulation experiments
[DE85-008652] 18 p3118 N85-29301

Short and long-term robot feedback
[PB85-180735] 19 p3281 N85-30047

A remote-operated manipulator vehicle
[HSE-TRANS-11133] 19 p3281 N85-30349

Acoustic imaging systems (for robotic object acquisition)
[AD-A154043] 19 p3351 N85-30772

CEMA venture to develop FMS, robot technology
20 p3436 N85-31330

CEMA cooperation in development of robotics, FMS viewed 20 p3436 N85-31331

Hidden costs of robotized production systems revealed 20 p3436 N85-31332

West Europe report: Science and technology
[JPRS-WST-85-020] 20 p3438 N85-31333

Robot, laser tridimensional cutting technology detailed
20 p3438 N85-31335

An analysis of multi-fingered hands
20 p3462 N85-31504

Philosophy of nondestructive control in aeronautics quality control. Knowledge of and improvements to nondestructive test safety
[SNIAS-851-551-101] 20 p3465 N85-31522

Discovery regarding visual neuron adaptation applicable to robot use 20 p3504 N85-31786

Manipulators in teleoperation
[DE85-010563] 20 p3512 N85-31839

Coordinate transformations and programming for small revolute coordinate robots
[RR-273] 20 p3519 N85-31881

Ultrasonic position reference systems for an autonomous sentry robot and a robot manipulator arm
[AD-A155481] 21 p3596 N85-32336

East Europe report: Science and technology. Selections on CSSR computer technology
[JPRS-ESA-84-017] 21 p3666 N85-32781
Robots, Manipulators 21 p3668 N85-32786
Space station automation and robotics study. Operator-systems interface
[NASA-CR-176095] 22 p3738 N85-33172
Space robot simulator vehicle
[NASA-CR-176133] 22 p3739 N85-33176
Study and realization of a command system adapted to space robotics
[SNIAS-851-440-106] 22 p3740 N85-33183
Latch assembly
[DE85-011660] 22 p3792 N85-33492
Future of robots in nuclear plants and processes
[DE85-011505] 22 p3793 N85-33500
Research on distributed artificial intelligence
[AD-A155356] 22 p3833 N85-33733
Multi-robot assembly of IC's 23 p3984 N85-34577
Robot environment expert system
[NASA-CR-3915] 23 p3987 N85-34593
The compliance of end effector force sensors for robot manipulator control 24 p4096 N85-35406
Testbed for sensory control of intelligent machines
[DE85-012355] 24 p4099 N85-35412

ROBUSTNESS (MATHEMATICS)
Location of several outliers in multiple regression data using elemental data
[CSIR-TWISK-300] 01 p0108 N85-10724
Robust rate control system designs for a submersible
[AD-A144792] 01 p0111 N85-10753
Influential observations in time series
[AD-A144719] 01 p0112 N85-10763
The numerical range: A tool for robust stability studies — multivariable feedback systems
[RR-255] 02 p0253 N85-11660
On the relationship between Lehtomaki's robustness test and an inverse Nyquist based test
[OUEL-1526/84] 03 p0409 N85-12616
An H-infinity-minimax approach to the design of robust control systems
[OUEL-1537/84] 05 p0717 N85-14600
Utilization of numerical optimization techniques in the design of robust multi-input, multi-output control systems
[AD-A148289] 08 p1212 N85-17630
An analysis of robust and efficient priors associated with a finite Bayesian model for compliance testing
[AD-A148497] 08 p1213 N85-17635
The performance of variable sampling plans when the normal distribution is truncated
[AD-A147717] 08 p1215 N85-17649
Approximate models in multivariable process control: An inverse Nyquist array and robust tuning regulator interpretation
[RR-261] 08 p1216 N85-17663
Methods of computer-aided analysis of non-Gaussian noise and application to robust adaptive detection, part 2
[AD-A148879] 10 p1539 N85-19704
Robust Kalman filtering and its applications
[AD-A149044] 10 p1550 N85-19775
Robustness of discrete-time dynamical systems: Application to the multivariable digital control of combat aircraft
[ONERA-NT-1984-2] 11 p1585 N85-19966
Automatic control design procedures for restructurable aircraft control
[NASA-CR-172489] 12 p1780 N85-21173
A review of some aspects of robust inference for time series
[AD-A149706] 12 p1923 N85-22082
Asymptotics for configural estimators
[AD-A150106] 12 p1924 N85-22087
Approaches and algorithms for robust signal processing 13 p2062 N85-22878
Bootstrapping the Kalman filter
[AD-A150509] 13 p2153 N85-23370
A research program in active control/aeroelasticity
[NASA-CR-175674] 14 p2218 N85-23752
Estimation of optimum scores for partition detectors using stochastic approximation techniques 14 p2411 N85-24865
Compensator development and examination of performance and robustness
[NASA-CR-175703] 15 p2540 N85-25678
Robust detection of fading narrow-band signals in non-Gaussian noise
[AD-A152262] 16 p2774 N85-27124
Robust regression through robust covariances
[AD-A153301] 17 p3020 N85-29677
On the stability of collocated controllers in the presence or uncertain nonlinearities and other perils 20 p3416 N85-31201
Robust adaptive control 20 p3417 N85-31207
Feedforward-feedback control logic for robust target-tracking 20 p3436 N85-31317
Extensions of the small-mu test for robust stability — control stability
[OUEL-1573/85-REV] 20 p3519 N85-31884
Decentralized stabilization by high gain feedback
[BU-115] 24 p4144 N85-35689

ROCHE LIMIT
The Moon's orbit history and inferences on its origin 04 p0585 N85-13735
Formation of the prelunar accretion disk 04 p0588 N85-13755
Mechanical models of close approaches and collisions of large protoplanets 04 p0588 N85-13756

ROCK INTRUSIONS
NT BATHOLITHS
Rio Grande rift: Problems and perspectives
[DE84-015492] 04 p0534 N85-13417
High-resolution microseismicity study of possible magmatic intrusion in the Long Valley Caldera
[DE85-001078] 11 p1661 N85-20593
Nd-isotopic evidence for the origin of the Sudbury complex by meteoritic impact 15 p2680 N85-26554
Three-dimensional gravity ideal body studies in rough terrain
[DE85-014097] 24 p4118 N85-35525

ROCK MECHANICS
Remote sensing as a mineral prospecting technique
[E85-10010] 02 p0216 N85-11423
Seismology in rockburst research
[REPT-551] 03 p0375 N85-12394
Summaries of physical research in the geosciences
[DE85-001862] 06 p0818 N85-15194
Some specifics of methods for mass detailed studies of rock heat conductivity 10 p1502 N85-19477
Rock mechanics: Issues and research needs in the disposal of wastes in hydraulic fractures
[DE85-001369] 10 p1556 N85-19609
Improved model for fluid-driven cracks in jointed rock
[DE85-006963] 18 p3125 N85-29349
Thermal-cycle testing of the G-tunnel heated block
[DE85-006408] 18 p3126 N85-29359
Measurement and calculation of the mechanical response of a highly fractured rock
[DE85-006421] 18 p3127 N85-29362
Comparison and evaluation of field and numerical results from the Site A heater test at Avery Island
[DE85-010625] 19 p3268 N85-30269
Geologic and hydrologic characterization and evaluation of the basin and range province relative to the disposal of high-level radioactive waste. Part 2: Geologic and hydrologic characterization
[GS-CIRC-904-B] 20 p3526 N85-31933
Geologic and hydrologic characterization and evaluation of the basin and range province relative to the disposal of high-level radioactive waste. Part 3: Geologic and hydrologic evaluation
[GS-CIRC-904-A] 20 p3526 N85-31934
Precambrian evolution and the rock record 21 p3656 N85-32711
Calibrator for displacement gages used in the rock mechanics laboratory
[DE85-013257] 24 p4096 N85-35393
Seismic stratigraphic analysis of the Mississippi Fan 24 p4115 N85-35507
Crustal structure in southern California from array data 24 p4115 N85-35512

ROCKET BOOSTERS
U BOOSTER ROCKET ENGINES

ROCKET CHAMBERS
U THRUST CHAMBERS

ROCKET ENGINE CASES
The effect of 2 strength reducing techniques on the ultimate tensile strength of AISI 4130 steel: Rocket motor case venting
[AD-A145526] 02 p0169 N85-11134
Integral boost, heat protection, port covers and transition 07 p0918 N85-15813
Solid rocket booster retrieval operations 08 p1096 N85-16928
A study on a medium-sized rocket with Burnout frame
[NAL-TR-821] 09 p1287 N85-18082
Integrated insulation wall assembly — for a solid rocket motor case
[AD-D011553] 12 p1784 N85-21257
Characterization standards for solid propellant rocket motors
[AD-A150250] 13 p2013 N85-22627
Verification of the SRB motor case pin retainer band tips
[NASA-CR-170882] 24 p4070 N85-35220

ROCKET ENGINE CONTROL
Shuttle avionics software trials, tribulations and success 08 p1090 N85-16891
Man-machine interface and control of the shuttle digital flight system 08 p1091 N85-16894
Space shuttle main engine hardware simulation 08 p1091 N85-16895

ROCKET ENGINE DESIGN
Ramjet air induction system design for tactical missile application 07 p0918 N85-15811
Design and analysis report for the RL10-2B breadboard low thrust engine
[NASA-CR-174857] 10 p1430 N85-19020
Studies on rocket engines for future European launchers
[SEP-TPRL/K-19572/84] 15 p2495 N85-25393

ROCKET ENGINES
NT ARC JET ENGINES
NT BOOSTER ROCKET ENGINES
NT DUCTED ROCKET ENGINES
NT ELECTROSTATIC ENGINES
NT ELECTROTHERMAL ENGINES
NT HYDRAZINE ENGINES
NT HYDROGEN OXYGEN ENGINES
NT ION ENGINES
NT LIQUID PROPELLANT ROCKET ENGINES
NT MERCURY ION ENGINES
NT MICROROCKET ENGINES
NT ORBIT MANEUVERING ENGINE (SPACE SHUTTLE)
NT RESISTOJET ENGINES
NT REUSABLE ROCKET ENGINES
NT RIT ENGINES
NT RL-10 ENGINES
NT SOLID PROPELLANT ROCKET ENGINES
NT SPACE SHUTTLE MAIN ENGINE
NT TURBOROCKET ENGINES
NT UPPER STAGE ROCKET ENGINES
Characterization of 8-cm engineering model thruster
[NASA-CR-174673] 02 p0169 N85-11131
Ramjet and Ramrocket Propulsion Systems for Missiles
[AGARD-LS-136] 07 p0917 N85-15809
Ramjet and Ramrocket Propulsion Systems for Missiles: Introduction and overview 07 p0917 N85-15810
Some aspects of engine and airframe integration for Ramjet and Ramrocket powered missiles 07 p0918 N85-15812
Drives and benefits overview 08 p1107 N85-16998
Advanced OTV engines and issues 08 p1108 N85-17000
Advanced OTV engine concepts 08 p1108 N85-17001
Proceedings of the AFOSR/AFRPL Rocket Propulsion Research Meeting: Abstracts and Agenda
[AD-A148818] 09 p1288 N85-18085
One rocket multiple satellite launch technology
[AD-A149228] 10 p1427 N85-19002
Design and analysis report for the RL10-2B breadboard low thrust engine
[NASA-CR-174857] 10 p1430 N85-19020
A diffuser heat transfer code
[AD-A149270] 10 p1430 N85-19022
Ring-cusp ion thruster with shell anode
[NASA-CASE-LEW-13861-1] 12 p1794 N85-21256
An experimental study of spray thruster
[REPT-613] 12 p1845 N85-21578
Twenty-first JANNAF Combustion Meeting, volume 1
[AD-A150981] 13 p1996 N85-22526
Minimizing plume contamination production in bipropellant thrusters 13 p2003 N85-22557
West Europe report: Science and technology
[JPRS-WST-84-027] 15 p2532 N85-25612
France officially proposes development of Ariane 5 to ESA 15 p2532 N85-25613
SEP of France to make Ariane HM-60 cryogenic engine 15 p2532 N85-25614
Ion sensor signal fluctuations during operation of spacecraft reaction engines 16 p2724 N85-29615
Liquid rocket combustor computer code development 16 p2740 N85-29910
Model for computing late detonations initiated in propellants by impact (XDT reactions)
[DE85-007377] 16 p2758 N85-27019
A theoretical study of two stage thrust augmenting ejectors
[ARL/AERO-R-166] 19 p3218 N85-29954
Solar rocket component study
[AD-A154186] 19 p3227 N85-30007
Modeling the exhaust of the pulsed plasma thruster
[AD-A155344] 21 p3707 N85-33018
Voyager 0.2-lbf thruster valve assembly short pulse test report
[NASA-CR-176121] 22 p3741 N85-33185
SRB attach ring phenolic TPS fishtail seal evaluation tests
[NASA-CR-170887] 24 p4096 N85-35407

ROCKET EXHAUST
Description and use of the single-color transmissometer plume diagnostic code A32CODE
[AD-A146181] 03 p0325 N85-12090

High altitude chemically reacting gas particle mixtures. Volume 1: A theoretical analysis and development of the numerical solution — rocket nozzle and orbital plume flow fields
[NASA-CR-171826] 07 p0916 N85-15801
High altitude chemically reacting gas particle mixtures. Volume 2: Program manual for RAMP2 — rocket nozzle and orbital plume flow fields
[NASA-CR-171827] 07 p0916 N85-15802
High altitude chemically reacting gas particle mixtures. Volume 3: Computer code user's and applications manual — rocket nozzle and orbital plume flow fields
[NASA-CR-171828] 07 p0917 N85-15803
Proceedings of the AFOSR/AFRPL Rocket Propulsion Research Meeting: Abstracts and Agenda
[AD-A146818] 09 p1288 N85-18085
Particle size, number, composition and velocity from solid rocket motors 12 p1785 N85-21201
Minimizing plume contamination production in bipropellant thrusters 13 p2003 N85-22557
Technical manual: Description and operation Slaved Tracking System
[DE85-004607] 13 p2094 N85-23070
Surface pressure produced by Space Transportation System flight 41B
[AD-A150793] 14 p2242 N85-23901
The highly underexpanded exhaust plume from nozzles with boundary layers
[DFVLR-FB-85-10] 20 p3421 N85-31230

ROCKET LAUNCHERS
Lightweight composite launcher pod
[AD-D011236] 01 p0015 N85-10092

ROCKET LAUNCHING
NT ORBITAL LAUNCHING
Rocket observations 01 p0014 N85-10084
Launch summary for 1978 - 1982 — sounding rockets, space probes, and satellites
[NASA-TM-87375] 04 p0461 N85-12924
Rocket body charge neutralization processes in ARAKS experiment (data from two launches) 13 p1980 N85-22426
Ariane space general director on satellite launcher market 18 p3087 N85-29103

ROCKET LININGS
Alternate nozzle ablative materials program
[NASA-CR-175658] 14 p2246 N85-23924

ROCKET MOTOR CASES
U ROCKET ENGINE CASES

ROCKET NOZZLES
A computer program for the performance analysis of scarfed nozzles
[AD-A147370] 07 p0905 N85-15730
Carbon/carbon rocket motor exit cone reinforcement
[AD-D011360] 07 p0916 N85-15799
High altitude chemically reacting gas particle mixtures. Volume 1: A theoretical analysis and development of the numerical solution — rocket nozzle and orbital plume flow fields
[NASA-CR-171826] 07 p0916 N85-15801
High altitude chemically reacting gas particle mixtures. Volume 2: Program manual for RAMP2 — rocket nozzle and orbital plume flow fields
[NASA-CR-171827] 07 p0916 N85-15802
High altitude chemically reacting gas particle mixtures. Volume 3: Computer code user's and applications manual — rocket nozzle and orbital plume flow fields
[NASA-CR-171828] 07 p0917 N85-15803
Thermophysical property testing using transient techniques
[AD-A147085] 07 p1049 N85-16664
Characterization standards for solid propellant rocket motors
[AD-A150250] 13 p2013 N85-22627
Alternate nozzle ablative materials program
[NASA-CR-175658] 14 p2246 N85-23924
An experimental study of clustered, two-dimensional rocket nozzles
[AD-A151889] 15 p2495 N85-25390
Effective specific impulse of secondary flow injected into a rocket nozzle
[NAL-TR-848T] 18 p3067 N85-28970
Thrust vectoring apparatus for maneuvering missile in flight
[AD-D011693] 19 p3226 N85-30004
Recession of graphitic nozzles in rocket motors 21 p3580 N85-32144

ROCKET PLANES
NT X-15 AIRCRAFT

ROCKET PROPELLANT TANKS
U PROPELLANT TANKS

ROCKET PROPELLANTS
NT CRYOGENIC ROCKET PROPELLANTS
NT DOUBLE BASE ROCKET PROPELLANTS
NT GASEOUS ROCKET PROPELLANTS
NT HYPERGOLIC ROCKET PROPELLANTS
NT LIQUID ROCKET PROPELLANTS
NT MONOPROPELLANTS
NT NITRAMINE PROPELLANTS
NT SLURRY PROPELLANTS
NT SOLID ROCKET PROPELLANTS
NT TATB
Measurement of shock and induced reaction in rocket propellants by nanosecond infrared radiometry and photography
[DE84-013209] 04 p0482 N85-13070
The 1984 JANNAF Propulsion Systems Hazards Subcommittee Meeting, volume 1
[AD-A148865] 10 p1454 N85-19162
Twenty-first JANNAF Combustion Meeting, volume 1
[AD-A150981] 13 p1998 N85-22526
Mixing, chemical reaction and flow field development in ducted rockets
[DE85-004083] 14 p2247 N85-23928
Model for computing late detonations initiated in propellants by impact (XDT reactions)
[DE85-007377] 16 p2758 N85-27019

ROCKET PROPELLED SLEDS
Nondestructive deceleration of a rocket sled — target penetration tests
[FOA-C-20549-D3] 07 p0912 N85-15771

ROCKET SONDES
U SOUNDING ROCKETS

ROCKET SOUNDING
Lyman alpha coronagraph research sounding rocket program
[NASA-CR-174378] 09 p1354 N85-18517
Rocket observations of the ionosphere during the eclipse of 26 February 1979
[NASA-CR-175513] 12 p1888 N85-21850
Experiment for measuring electric fields within the sounding rocket project Energy Budget
[BMFT-FB-W-84-048] 12 p1891 N85-21866
Characteristics of the electrodynamics of auroral arcs as inferred from rocket and ground-base observations during IMS 14 p2363 N85-24601
Observations of the MF-HF plasma wave emissions in active auroras by the sounding rocket experiments at Syowa station 14 p2366 N85-24620
Experimental research on ionospheric disturbance caused by cumulative barium vapor injection 16 p2719 N85-26787
Observations of airglow O2(1-Sigma) atmospheric band at 8645 A and the rotational temperature at 23 deg S
[INPE-3378-PRE/653] 16 p2826 N85-27435
Rocket measurements of mesospheric ionization irregularities
[NASA-CR-176056] 20 p3484 N85-31721

ROCKET TEST FACILITIES
Making sure: A brief outline and history of ESA's test and checkout services
[ESA-BR-22] 09 p1286 N85-18077

ROCKET THRUST
Experiments on residual thrust and prediction for upper-stage solid propellant rockets
[NAL-TR-800] 03 p0324 N85-12087
Orbital maneuvers with finite thrust. Volume 1: Mathematical formulation, numerical methods, catalog concept
[ESA-CR(P)-1910-VOL-1] 06 p0758 N85-14848
Orbit maneuvers with finite thrust. Volume 2: Reference manual, part 1
[ESA-CR(P)-1910-VOL-2-PT-1] 06 p0758 N85-14849
Orbit maneuvers with finite thrust. Volume 3: User's guide, part 2
[ESA-CR(P)-1910-VOL-3-PT-2] 06 p0758 N85-14850
Orbit maneuvers with finite thrust. Volume 3: Reference catalog, parts 1 and 2
[ESA-CR(P)-1910-VOL-3-PT-1/2] 06 p0758 N85-14851
Gyrodynamic fixture for measuring thrust force components
[AD-D011258] 06 p0760 N85-14860
Qualification of an electrothermal hydrazine thruster with a vacuum thrust of 0.5 to 2.0 N
[BMFT-FB-W-84-043] 07 p0917 N85-15808
Advanced OTV engines and issues 08 p1106 N85-17000
Ion sensor signal fluctuations during operation of spacecraft reaction engines 16 p2724 N85-26815
Heaterless ignition of inert gas ion thruster hollow cathodes
[NASA-TM-87086] 23 p3903 N85-34177

ROCKET VEHICLES
NT ARIANE LAUNCH VEHICLE
NT ATLAS CENTAUR LAUNCH VEHICLE
NT CENTAUR LAUNCH VEHICLE
NT MULTISTAGE ROCKET VEHICLES
NT SOUNDING ROCKETS
NT TITAN CENTAUR LAUNCH VEHICLE
NT VEGA LAUNCH VEHICLE

ROCKET-BORNE INSTRUMENTS
Launch summary for 1978 - 1982 — sounding rockets, space probes, and satellites
[NASA-TM-87375] 04 p0461 N85-12924
The multi-anode microchannel array detector system: Current status and future prospects 11 p1761 N85-21080
Stellar ultraviolet flux distributions in the 912-1200 A wavelength range 11 p1762 N85-21081
An improved rocket-borne electric field meter for the middle atmosphere
[NASA-CR-175510] 12 p1886 N85-21851
A rocket-borne X-ray observation of SN1006 with the imaging gas scintillation proportional counter 14 p2435 N85-25014

ROCKS
NT ANORTHOSITE
NT BALTIC SHIELD (EUROPE)
NT BASALT
NT BEDROCK
NT BRECCIA
NT COAL
NT ECLOGITE
NT GNEISS
NT GRANITE
NT IGNEOUS ROCKS
NT LIGNITE
NT LIMESTONE
NT LUNAR ROCKS
NT PERIDOTITE
NT REGOLITH
NT SANDSTONES
NT SCHIST
NT SEDIMENTARY ROCKS
NT SHALES
Compilation of elemental concentration data for NBS (National Bureau of Standards) biological, geological and environmental standard reference materials, 1982
[PB84-218338] 01 p0025 N85-10158
Middle infrared spectral studies of geologic materials in their natural state using photothermal beam deflection spectroscopy
[AD-A144894] 01 p0120 N85-10820
A paleomagnetic study of the Prince William terrane and Nixon Fork terrane, Alaska 02 p0226 N85-11478
Magnetic characteristics of some volcanic rocks of the west Carpathians
[REPT-557] 03 p0376 N85-12400
Electric properties of neovolcanic rocks of central and east Slovakia
[REPT-558] 03 p0376 N85-12401
Reconnaissance geology of the northern part of the Unalaklaet quadrangle 04 p0516 N85-13291
Stratigraphy, petrology, and structure of the Pingston terrane, Mount Hayes C-5 and C-6 quadrangles, eastern Alaska Range, Alaska 04 p0517 N85-13301
Paleomagnetic latitude of paleocene volcanic rocks of the Cantwell Formation, central Alaska 04 p0517 N85-13302
Paleogene volcanic rocks of the Matanuska Valley area and the displacement history of the Castle Mountain fault 04 p0518 N85-13303
Progress in lead/uranium zircon studies of lower paleozoic rocks of the southern Alexander terrane 04 p0518 N85-13304
The northern coast plutonic-metamorphic complex, southeastern Alaska and northwestern British Columbia 04 p0518 N85-13305
Cretaceous plutonic rocks, Mitkof and Kupreanof Islands, Petersburg quadrangle, southeastern Alaska 04 p0518 N85-13306
Late oligocene gabbro near Ketchikan, southeastern Alaska 04 p0518 N85-13307
Petrology and petrogenesis of Batholitic rocks, San Jacinto Mountains, southern California 05 p0673 N85-14322
Sedimentation, structure and tectonics of the Umpqua group (paleocene to early eocene), southwestern Oregon 05 p0678 N85-14354
Geochemical data for rock samples from the Petersburg and parts of the Port Alexander and Sumdum quadrangles, southeastern Alaska (documentation)
[PB84-234434] 08 p0836 N85-15318
In-situ stress determination in soil and rock using the acoustic emission method
[AD-A147459] 07 p0979 N85-16215
Geology of the Batopilas mining district, Chihuahua, Mexico, volumes 1 and 2 09 p1351 N85-18498
Quaternary stratigraphy of the lower Iowa and Cedar River Valleys, southeast Iowa 09 p1352 N85-18504
Part 1. Stratigraphy, structure and petrology of the Peterborough 1.5-minute quadrangle, New Hampshire and part 2. Graphite textural and isotropic variations in plutonic rocks, south-central New Hampshire 09 p1353 N85-18511

Study of the physical properties of crystalline rocks in the southeast Voronezh anteclise
[NASA-TM-77823] 10 p1514 N86-19551
China report: Science and technology
[JPRS-CST-84-025] 11 p1620 N85-20197
Micro-deformation of quartz under dynamic action and its applications 11 p1620 N85-20201
Piezoelectric stress transducer used for measurements of explosions in hard rock 11 p1636 N85-20316
Effect of host-rock dissolution and precipitation on permeability in a nuclear waste repository in tuff
[DE85-000675] 11 p1727 N85-20860
Effects of fracture roughness on fluid flow through a single deformable fracture
[DE85-004593] 13 p2092 N85-23062
Geomagnetic field dynamics 13 p2116 N85-23182
Assessment of computer based geologic mapping of rock units in the LANDSAT-4 scene of northern Death Valley, California 13 p2119 N85-23195
Geological information content of reflected wave record form 14 p2345 N85-24502
Location of continental Permian volcanites of central Asia and its tectonic interpretation 14 p2346 N85-24505
The impact ejection of living organisms into space 15 p2682 N85-26566
In-situ rock melting applied to lunar base construction and for exploration drilling and coring on the moon
[DE85-006716] 16 p2717 N85-26770
Analysis of mesofissuring on space photographs: New technique for study of petroleum and gas deposits 16 p2726 N85-26828
In situ Tuff water migration/heater experiment
[DE85-010415] 18 p3101 N85-29200
Laboratory investigation of formation damage of an artificial fracture at simulated geothermal conditions
[DE85-010301] 18 p3102 N85-29201
Improved model for fluid-driven cracks in jointed rock
[DE85-008983] 18 p3125 N85-29349
Interim rock mass properties and conditions for analyses of a repository in crystalline rock
[DE85-010700] 18 p3125 N85-29352
Implications about in situ stress at Yucca Mountain
[DE85-008008] 18 p3126 N85-29356
Measurement and calculation of the mechanical response of a highly fractured rock
[DE85-008421] 18 p3127 N85-29362
Hot Dry Rock Geothermal Energy Developement Program
[DE85-010570] 19 p3268 N85-30264
Ultramicroscopic study of structure of phosphorites from Sea of Japan floor 19 p3290 N85-30400
Microstructural analysis of Pacific Ocean and Indian Ocean ultrabasites 19 p3291 N85-30405
Analysis of the elastic and strength properties of Yucca Mountain tuff, Nevada
[DE85-006975] 19 p3300 N85-30460
Preliminary evaluation of alterant geophysical tomography in welded tuff
[DE85-010626] 19 p3302 N85-30469
Structural and tectonic history of the Golconda allochton, southern Toiyabe Range, Nevada 19 p3312 N85-30529
Stratigraphic analysis of Pennsylvania rocks using hierarchy of transgressive-regressive units 19 p3312 N85-30531
Geometry, velocity structure and penetration depths of descending slabs in the western Pacific 19 p3319 N85-30574
Geothermal COMPAX drill hit development
[DE85-011353] 20 p3469 N85-31556
Source-term considerations for a potential radioactive-waste repository located in unsaturated tuff
[DE85-010090] 20 p3529 N85-31953
Hydrothermal alteration in the 3.5 b.y. old Onverwacht Group of South Africa 21 p3718 N85-33071
The 3.5 b.y. old Onverwacht Group: A remnant of ancient oceanic crust 21 p3718 N85-33073
The Aravalli sequence of Rajasthan, India: A Precambrian continental margin? 21 p3720 N85-33084
Deep-burial diagenesis in carbonates
[DE85-011224] 22 p3802 N85-33554
Discontinuous deformation analysis
[DE85-011208] 22 p3814 N85-33629
Subcritical fracture propagation in rocks: An examination using the methods of fracture mechanics and non-destructive testing 24 p4116 N85-35516
Underwater measurements of muon intensity
[HE-5.1-16] 24 p4202 N85-36078
Results of low energy background measurements with the Liquid Scintillation Detector (LSD) of the Mont Blanc Laboratory
[HE-5.3-5] 24 p4205 N85-36099
The research program of the Liquid Scintillation Detector (LSD) in the Mont Blanc Laboratory
[HE-5.3-6] 24 p4205 N85-36100

ROCKY MOUNTAINS (NORTH AMERICA)
On the nowcasting of mountain-generated thunderstorm systems 01 p0074 N85-10489
Measurements of the surface energy budget in the southern Gobi Desert of China, and in the Rocky Mountains of Colorado
[NASA-CR-175506] 12 p1668 N85-21647

RODENTS
NT GUINEA PIGS
NT MICE
NT RABBITS
NT RATS

RODS
NT CONTROL RODS
Physical-chemical properties of articulated rodlike polymers
[AD-A145549] 02 p0186 N85-11244
Post buckling behavior of a circular rod constrained within a circular cylinder 02 p0207 N85-11365
Nonlinear waves in a rod. Results for incompressible elastic materials
[AD-A147485] 07 p0979 N85-16216
Acoustic oscillations of rods and plates 17 p2944 N85-26170
Torsion-tension coupling in rods 18 p3120 N85-29315
Stress-intensity factors for circumferential surface cracks in pipes and rods under tension and bending loads
[NASA-TM-87594] 24 p4101 N85-35424

ROENTGEN SATELLITE
U ROSAT MISSION

ROGALLO WINGS
U FLEXIBLE WINGS
U FOLDING STRUCTURES

ROLL
Mean and random errors of visual roll rate perception from central and peripheral visual displays 05 p0704 N85-14519
Accuracy of system step response roll magnitude estimation from central and peripheral visual displays and simulator cockpit motion 05 p0705 N85-14522
Models for the effects of G-seat cuing on roll-axis tracking performance 05 p0707 N85-14532
Theory of wing rock 09 p1282 N85-18064
Forces on undriven, angled wheels
[AD-P004303] 09 p1409 N85-18880
Some effects of display format variables on the perception of aircraft spatial orientation 10 p1534 N85-19666
Perception of roll rate from an artificial horizon and peripheral displays
[VTH-LR-403] 17 p3002 N85-28557
In-flight evaluation of pure time delays in pitch and roll
[NASA-TM-86744] 21 p3556 N85-32123

ROLL CONTROL
U LATERAL CONTROL

ROLL FORMING
Microstructural design in low alloy steels 02 p0176 N85-11179
The influence of aluminum on the qualities of low and medium carbon steel
[BLL-M-35754-(5828.4)] 03 p0330 N85-12123
Defining effect of hardening on mean yield strength in deformation zone
[BLL-M-35934-(5828.4)] 05 p0647 N85-14154
Development of surface cracks in AMg6 alloy under low-cycle loading conditions 10 p1442 N85-19069
Hot rolling of ceramics by the use of self propagating synthesis
[AD-D011486] 10 p1453 N85-19154
Method for continuously casting
[AD-D011481] 10 p1459 N85-19195
Division boundary in Al-B composite material with boron in contact with solid and liquid aluminum 13 p2027 N85-22704
Ultrasonic SH wave velocity in textured aluminum plates
[AERE-R-11516] 15 p2509 N85-25475
Superplasticity in a thermo-mechanically processed Aluminum-10.2%Mg-0.52%Mn alloy
[AD-A152016] 15 p2510 N85-25485
Development of high strength ship hull steel for high heat input welding — controlled rolling and accelerated cooling 15 p2585 N85-25827
Automatic manipulators for forging rollers 16 p2762 N85-27042
Principles of wave formation along web of H-beams
[BLL-M-36041-(5828.4)] 16 p2766 N85-27253
High tensile strength, punchable, hot rolled strips with good plasticity
[BMFT-FB-T-84-256] 18 p3078 N85-29040
Rolling contact fatigue testing of thermomechanically processed M-50 steel
[AD-A153640] 18 p3122 N85-29327
The character of observed porosity and its possible effects on rolling contact fatigue life of M-50 steel
[AD-A155930] 24 p4079 N85-35279
Effect of prior warm rolling on the retained austenite content and hardening response of VIM-VAR (vacuum-induction melted-vacuum-arc remelted) AISI M-50 steel
[AD-A156145] 24 p4079 N85-35281

ROLLER BEARINGS
Performance evaluation of automotive wheel bearing greases
[AD-A145948] 03 p0337 N85-12166
Effect of two inner-ring oil-flow distribution schemes on the operating characteristics of a 35 millimeter bore ball bearing to 2.5 million DN
[NASA-TP-2404] 04 p0507 N85-13233
Influence of shot-peening methods on surface quality and service life of bearings 06 p0776 N85-14960
Grease versus oil lubrication of wheel bearings in Army equipment
[AD-A147546] 07 p0973 N85-16184
Lubrication and performance of high-speed rolling-element bearings
[NASA-TM-86958] 12 p1859 N85-21658
Load capacity of cages of roller bearings for planet wheels 14 p2221 N85-23775
The characteristics of surface roughness important to gear and rolling bearing problems 14 p2222 N85-23782
Effect of speed and press fit on fatigue life of roller-bearing inner-race contact
[NASA-TP-2496] 20 p3463 N85-31511
The use of ultrasound to monitor incipient failure of rolling element bearings 23 p3924 N85-34317
Elastohydrodynamic lubrication calculations used as a tool to study scuffing
[NASA-TM-87097] 23 p3938 N85-34408
Design and lubrication of high-speed rolling-element bearings
[NASA-TM-87107] 23 p3938 N85-34409
Planetary-gear-support bearing test rig design
[NASA-CR-174927] 24 p4064 N85-35186

ROLLERS
Roller crosshead analysis 04 p0507 N85-13238
Stability of rigid motions and rollers in bicomponent flows of immiscible liquids
[AD-A147302] 07 p0960 N85-16081
No-slump Roller-Compacted Concrete (RCC) for use in mass concrete construction
[AD-A148564] 08 p1138 N85-17164
A rotating electrical transfer device 22 p3798 N85-33529

ROLLING CONTACT LOADS
Numerical analysis of some problems related to the mechanics of pneumatic tires: Finite deformation/rolling contact of a viscoelastic cylinder and finite deformation of cord-reinforced rubber composites 01 p0060 N85-10397
The characteristics of surface roughness important to gear and rolling bearing problems 14 p2222 N85-23782
Evaluation of the blind hole drilling method for the measurement of residual stress
[AD-A151459] 15 p2579 N85-25905
Temperature and surface damage under lubricated sliding-rolling contacts 19 p3280 N85-30336
Effect of speed and press fit on fatigue life of roller-bearing inner-race contact
[NASA-TP-2496] 20 p3463 N85-31511
Rolling, slip and traction measurements on low modulus materials
[NASA-CR-174909] 22 p3791 N85-33491
The properties of thin-section, four-point-contact ball bearings in space 22 p3797 N85-33521

ROLLING MOMENTS
The generation of rolling moments with the superconducting solenoid model
[NASA-CR-172520] 09 p1283 N85-18068
Operational and developmental experience with the F/A-18A digital flight control system 16 p2713 N85-26742
Experimental and theoretical determination of the wing-induced lateral wind on the tail surfaces in oscillating rolling motion. Part 1: Application of the Mobile Oscillating Derivatives (MOD) on an experimental part
[IFD-1/84-PT-1] 18 p3061 N85-28939

ROLLUP SOLAR ARRAYS
U SOLAR ARRAYS

ROOFS
Field test results of experimental EPDM (Ethylene Propylene Diene Monomer) and PUF (Polyurethane Foam) roofing
[AD-A147697] 08 p1132 N85-17133

Photovoltaic roofing tile systems
12 p1678 N85-21783
Evaluating wind flow around buildings on heliport placement
[FAA-PM-84-25] 12 p1693 N85-21881
ROOM TEMPERATURE
Visible and ultraviolet lasers based on excimer transitions in the homonuclear halogens
[AD-D011311] 07 p0971 N85-16163
Temperature: Curvature relationships for unsymmetric graphite-epoxy laminates
[VPI-E-85-08] 16 p2743 N85-26926
Effects of temperature on remotely sensed mafic mineral absorption features 16 p2809 N85-27323
A study of Ga(.47)In(.53)As and Al(.48)In(.52)As for very high frequency device applications
[AD-A151995] 16 p2870 N85-27706
Strength and failure analysis of composite laminates with holes at room and elevated temperatures
[AD-A153263] 17 p2917 N85-27981
ROOMS
NT CLEAN ROOMS
Penetration of short duration airblast into protective structures 09 p1336 N85-18404
Acoustic scaling: A re-evaluation of the acoustic model of Manchester Studio 7
[BBC-RD-1984/18] 12 p1622 N85-21432
ROOT-MEAN-SQUARE ERRORS
An objective error measure for the comparison of calculated and measured transient response histories
09 p1395 N85-18595
Clock characterization tutorial
17 p2965 N85-28311
Satellite measurements of atmospheric aerosols
[AD-A153807] 19 p3316 N85-30556
1000 GeV gamma rays from Cygnus X-3: An update
[OG-2.1-8] 22 p3663 N85-33825
Comparative analysis of operational forecasts versus actual weather conditions in airline flight planning, volume 3
[NASA-CR-167864] 24 p4120 N85-35536
Study of the time-differentiated particle flux density at various distances from EAS axis
[HE-4.7-15] 24 p4200 N85-36065
ROOTS OF EQUATIONS
On edge detection
[AD-A148573] 08 p1223 N85-17703
Zero-crossings on lines of curvature
[AD-A150171] 13 p2150 N85-23345
Convergence of Newton's method for a single real equation
[NASA-TP-2489] 17 p3017 N85-28656
Finding the roots of the transcendental equations in problems in determining the thermal conductivity of spheres with heterogeneous boundary conditions
[BLL-M-35876-(5828.4)] 23 p3929 N85-34347
ROSAT MISSION
The ROSAT all-sky survey in X-rays
08 p1243 N85-17843
The ROSAT XUV wide field camera
08 p1243 N85-17844
On the unique capabilities of the Hubble space telescope for studies of ROSAT deep-survey X-ray sources
08 p1243 N85-17846
X-ray satellite
[NASA-TM-77682] 20 p3407 N85-31145
The design, development, testing, fabrication, calibration and integration of a High Resolution Imager (HRI) for the Roentgen Satellite (ROSAT)
[NASA-CR-175302] 22 p3741 N85-33184
ROSS ICE SHELF
Microbial ecology of extreme environments: Antarctic yeasts and growth in substrate-limited habitats
[NASA-CR-175810] 16 p2839 N85-27509
Aerosol formation by wave action over Ross Sea, Antarctica 21 p3651 N85-32066
ROSSBY REGIMES
Spectral modeling of a potential vorticity equation for a barotropic flow on a beta-plane
[CWI-AM-R8409] 08 p1186 N85-17478
Combined effects of baroclinic and barotropic instability in a nonlinear low order model
[DM-41] 09 p1358 N85-18544
Evolution of set of Rossby waves toward anisotropic equilibrium state 13 p2109 N85-23141
Stability of Rossby waves within framework of three-component analysis 13 p2109 N85-23142
Study of the functions of similarity of the planetary boundary layer. Part 1: Theory
[INPE-3129-PRE/520-PT-1] 16 p2826 N85-27426
The effect of the Benthic Boundary Layer on the physics of intense mesoscale eddies
[AD-A153193] 17 p2958 N85-28270
Finite amplitude stability of a Rossby wave in a channel 19 p3314 N85-30543
ROSSBY WAVES
U PLANETARY WAVES
ROTARY DRIVES
U MECHANICAL DRIVES
ROTARY ENGINES
Evaluation of heat engine for hybrid vehicle application
[NASA-CR-174163] 04 p0506 N85-13245
Stratified charge rotary aircraft engine technology enablement program
[NASA-CR-174812] 12 p1778 N85-21163
Installation, maintenance and operating manual for the Lucas-type fuel injection system of the 3 B rotary engine
[NASA-TM-77872] 15 p2568 N85-25846
ROTARY GYROSCOPES
Fiber optic gyroscope with alternating output signal
[AD-D011689] 19 p3271 N85-30284
ROTARY STABILITY
NT GYROSCOPIC STABILITY
Structural response of a rotating bladed disk to rotor whirl
[NASA-CR-175605] 13 p1973 N85-22391
Rotational motion of a satellite
13 p1981 N85-22428
Damping seals for turbomachinery
16 p2738 N85-26894
Housing flexibility effects on rotor stability
16 p2738 N85-26896
Influence of materials creep on rotor dynamics
[DE85-008545] 17 p2981 N85-28426
Application of Floquet theory to helicopter blade flapping stability
[AD-A154460] 19 p3218 N85-29952
Recent developments in rotary-balance testing of fighter aircraft configurations at NASA Ames Research Center
[NASA-TM-86714] 21 p3551 N85-32090
ROTARY WING AIRCRAFT
NT BO-105 HELICOPTER
NT CH-47 HELICOPTER
NT HELICOPTERS
NT MILITARY HELICOPTERS
NT P-531 HELICOPTER
NT RIGID ROTOR HELICOPTERS
NT ROTOR SYSTEMS RESEARCH AIRCRAFT
NT TILT ROTOR AIRCRAFT
NT UH-1 HELICOPTER
NT UH-60A HELICOPTER
Rotary-wing aircraft noise measurements: Analysis of variations and proposed measurement standard
[AD-A146207] 03 p0416 N85-12682
Mission-oriented requirements for updating MIL-H-8501. Volume 1: STI proposed structure — military rotorcraft
[NASA-CR-177331-VOL-1] 08 p1066 N85-16877
Mission-oriented requirements for updating MIL-H-8501. Volume 2: STI background and rationale — military rotorcraft
[NASA-CR-177331-VOL-2] 08 p1066 N85-16878
A methodology for the determination of rotary wing aircraft vulnerabilities in air-to-air combat simulation
[AD-A148984] 10 p1424 N85-18984
Special power train requirements for the next generation of rotary-wing aircraft 14 p2220 N85-23769
Rotorcraft digital advanced avionics system (RODAAS) functional description
[NASA-CR-166611] 15 p2468 N85-25237
Rotorcraft research testing in the National Full-Scale Aerodynamics Complex at NASA Ames Research Center
[NASA-TM-86687] 17 p2896 N85-27854
Analysis of rotorcraft crash dynamics for development of improved crashworthiness design criteria
[FAA-CT-85-11] 20 p3391 N85-31031
Fixed gain and adaptive techniques for rotorcraft vibration control
[NASA-CR-177344] 22 p3728 N85-33111
ROTARY WINGS
NT BEARINGLESS ROTORS
NT LIFTING ROTORS
NT RIGID ROTORS
NT TILTING ROTORS
NT TIP DRIVEN ROTORS
Helicopter rotor blade design for minimum vibration
[NASA-CR-3625] 01 p0006 N85-10032
DFVLR rotorcraft: Construction and engineering
[NASA-TM-77740] 01 p0006 N85-10035
Data input, processing and presentation — helicopter rotor balance measurement
[NASA-TM-77739] 01 p0125 N85-10856
Transonic flow analysis for rotors. Part 1: Three-dimensional quasi-steady, full-potential calculation
[NASA-TP-2375-PT-1] 02 p0134 N85-10914
Lifting surface theory for a helicopter rotor in forward flight
[NASA-TM-86315] 02 p0134 N85-10916
Extended aeroelastic analysis for helicopter rotors with prescribed hub motion and blade appended pendulum vibration absorbers
[NASA-CR-172455] 03 p0315 N85-12036
Stochastic motor blade dynamics
[AD-A146312] 03 p0318 N85-12054
Estimation of helicopter performance using a program based on blade element analysis
[AD-A146341] 03 p0318 N85-12055
Detection, classification, and extraction of helicopter-radiated noise
[AD-A145993] 03 p0416 N85-12661
Initial feasibility ground test of a proposed photogrammetric system for measuring the shapes of ice accretions on helicopter rotor blades during forward flight
[NASA-TM-87391] 04 p0455 N85-12887
An experimental investigation of the parallel blade-vortex interaction
[NASA-TM-86005] 05 p0592 N85-13777
Study to eliminate ground resonance using active controls
[NASA-CR-166609] 07 p0902 N85-15715
Helicopter active control with rotor blades relaxation
08 p1075 N85-16619
Integrated technology rotor/flight research rotor concept definition study
[NASA-CR-166446] 10 p1424 N85-18980
Experimental study of main rotor tip geometry and tail rotor interactions in hover. Volume 1. Text and figures
[NASA-CR-177336-VOL-1] 13 p1965 N85-22344
Experimental study of main rotor tip geometry and tail rotor interactions in hover. Volume 2: Run log and tabulated data
[NASA-CR-177336-VOL-2] 13 p1965 N85-22345
Study for prediction of rotor/wake/fuselage interference, part 1
[NASA-CR-177340-VOL-1] 13 p1965 N85-22346
Study for prediction of rotor/wake/fuselage interference. Part 2: Program users guide
[NASA-CR-177340-VOL-2] 13 p1966 N85-22347
Simple theoretical models for composite rotor blades
[NASA-CR-175820] 13 p1971 N85-22382
Computations of two-dimensional airfoil-vortex interactions — helicopter rotor flowfields
[NASA-CR-3865] 14 p2210 N85-23709
Unsteady analysis of rotor blade tip flow
[NASA-CR-3868] 15 p2482 N85-25202
Interaction of a turbulent vortex with a lifting surface
15 p2484 N85-25214
Helicopter rotor
[CH-637890-A5] 15 p2470 N85-25245
Rotor blade flap-lag stability and response in forward flight in turbulent flows 16 p2705 N85-26698
Helicopter Aeromechanics
[AGARD-LS-139] 18 p3057 N85-28913
Rotorcraft noise 18 p3057 N85-28916
Recent developments in the dynamics of advanced rotor systems 18 p3057 N85-28917
Application of Floquet theory to helicopter blade flapping stability
[AD-A154460] 19 p3218 N85-29952
Design of helicopter rotor blades for optimum dynamic characteristics
[NASA-CR-176076] 20 p3393 N85-31044
Impulsive noise due to transonic blade-vortex interactions 20 p3523 N85-31913
Tip vortex computer code SRATIP. User's guide
[NASA-CR-172603] 21 p3551 N85-32093
A three-dimensional viscous flow analysis for the helicopter tip vortex generation problem
[NASA-CR-3906] 23 p3893 N85-34114
An evaluation of three helicopter rotor sections
[NASA-TM-86719] 23 p3893 N85-34115
The effects of parameter variation on helicopter performance
[AD-A156027] 24 p4064 N85-35189
ROTATING
U ROTATION
ROTATING BODIES
NT BEARINGLESS ROTORS
NT COMPRESSOR ROTORS
NT FLYWHEELS
NT HELICOPTER TAIL ROTORS
NT IMPELLERS
NT LIFTING ROTORS
NT LUNAR ROTATION
NT PUMP IMPELLERS
NT RIGID ROTORS
NT ROTARY WINGS
NT ROTATING CYLINDERS
NT ROTATING DISKS
NT ROTATING SPHERES
NT ROTORS
NT TAIL ROTORS

NT TILTING ROTORS
NT TIP DRIVEN ROTORS
NT TURBINE WHEELS
Slowly rotating pulsed radiation source
02 p0256 N85-11678
Advanced high-power transfer through rotary interfaces
05 p0607 N85-13875
Lateral fluid forces acting on a whirling centrifugal impeller in vaneless and vaned diffuser
05 p0643 N85-14123
Design of two-mirror scanner with axes of rotation not in plane of mirrors
06 p0777 N85-14969
Hypothetical zero yaw drag trajectory of spinning projectiles between M = 5 and M = 10
[AD-A148899] 10 p1421 N85-18963
Flight dynamics of axisymmetrical rotating bodies in air medium
13 p2043 N85-22791
Axisymmetrical oscillations of shell systems subjected to impulse loads
13 p2047 N85-22814
Optimum rotation of solid body with 1 axis of symmetry
16 p2718 N85-26781
Nonlinear equations for dynamics of pretwisted beams undergoing small strains and large rotations
[NASA-TP-2470] 16 p2799 N85-27258
Dynamic stability of a spinning tube conveying a flowing fluid
[DE85-007583] 18 p3102 N85-29207
Speckle interferometry applied to asteroids and other solar system objects
[NASA-CR-175976] 19 p3384 N85-30995
A rotating electrical transfer device
22 p3798 N85-33529

ROTATING CYLINDERS
A study of the critical layer in a rotating liquid payload
[AD-A146094] 03 p0362 N85-12321
The use of horizontal clinostats in studies of plant statocyte development
05 p0690 N85-14435
Turbulent flow around circular cylinder uniformly rotating in infinite incompressible fluid
14 p2277 N85-24109
Stability of steady rotation of a cylinder filled with a stratified viscous incompressible fluid
14 p2278 N85-24112
Flow around rotating and nonmoving circular cylinder near flat screen. Report 1: Aerodynamic forces in cylinder
16 p2765 N85-27059
The Mises yield condition for thin rotationally symmetric shells
[BLL-BISI-TRANS-22047-(9022.05)]
17 p2978 N85-28409
Non-backdriveable free wheeling coupling
[NASA-CASE-MSC-20475-1] 18 p3116 N85-29290

ROTATING DISKS
Analysis of turbomachine blades: A review
02 p0206 N85-11374
Corrosion of a zinc rotating disk in one molar hydrochloric acid
[DE84-015874] 04 p0474 N85-13015
Development of a mass transfer machine for gas/liquid operations in the absence of gravity
[BMFT-FB-W-84-027] 05 p0637 N85-14091
CFM 56-2. Oligocyclic fatigue of the turbofan disk: Dimensioning and tests for verification and improvements
07 p0906 N85-15750
Possibilities for a more accurate life prediction of components — gas turbine disks
07 p0976 N85-16198
Some problems of optimum journal design for disk-drum rotors under antisymmetric loading
14 p2286 N85-24167
Abrasive cutting-off wheel
15 p2568 N85-25843
A rational approach to cam design
23 p3923 N85-34311

ROTATING ENVIRONMENTS
Internal gravity waves in real atmosphere
06 p0825 N85-15236
Small scale structure and the Spiner model for active galactic nuclei
12 p1959 N85-22316

ROTATING FLUIDS
NT ROTATING LIQUIDS
Linear long-wave stability of cylindrical steady laminar flame in rotating medium
02 p0268 N85-11752
Fluid motion in a rotating and nutating container
[AD-A146175] 03 p0362 N85-12322
Corotating interaction regions in stellar winds: Particle acceleration and non-thermal radio emission in hot stars
08 p1234 N85-17773
Winds from rotating, magnetic, hot stars
08 p1234 N85-17775
Turbulent jet flow in a channel with a circulation region
09 p1305 N85-18215
Regions of propagation of short-wave perturbations in spherical layer of rotating fluid
13 p2107 N85-23130
Turbulent flow around circular cylinder uniformly rotating in infinite incompressible fluid
14 p2277 N85-24109
Solution of Onsager's equation for a rotating compressible fluid in a multiply-connected domain
[DE85-007046] 16 p2784 N85-27178
Boundary layer and parabolic flows
[DFVLR-FB-84-46] 17 p2960 N85-28285

ROTATING GENERATORS
NT AC GENERATORS
NT DYNAMOMETERS
NT HOMOPOLAR GENERATORS
NT TURBOGENERATORS
Assessing expired fatigue life in large turbine shafts
[DE84-016676] 09 p1340 N85-18427
A device for generating motive force through the expansion of a non-elastic dense fluid
[NASA-TM-77664] 20 p3454 N85-31446
A small-scale self-excited rotor electrostatic generator
[AD-A155264] 21 p3581 N85-32265

ROTATING LIQUIDS
A study of the critical layer in a rotating liquid payload
[AD-A146094] 03 p0362 N85-12321
Double and inverse Taylor-Hogg vortices in a stratified ocean
13 p2106 N85-23137
Very high speed lap with positive lift effect
[AD-D011710] 19 p3280 N85-30344
Very high speed lap with negative lift effect
[AD-D011711] 19 p3281 N85-30345

ROTATING MIRRORS
Dual band, low sidelobe, high efficiency mirror antenna
[AD-D011329] 07 p0944 N85-15980
Determination of parameters of elastically strained mirror facets of rapidly rotating prisms
14 p2282 N85-24137

ROTATING PLASMAS
Fluctuation spectrum for linear gyroviscous MHD
[IPP-6/237] 01 p0121 N85-10828
Pressure-gradient-driven Tokamak resistive MHD instability in the banana-plateau collisionality regime
[DE85-004568] 12 p1937 N85-22171
About static and dynamic solutions of the aligned rotator model — pulsar magnetosphere
12 p1958 N85-22306

ROTATING SHAFTS
NT SHAFTS (MACHINE ELEMENTS)
NT TURBOSHAFTS
Identification of dynamic coefficients of annular turbulent seals
05 p0644 N85-14133
Analysis of experimental shaft seal data for high-performance turbomachines, as for Space Shuttle main engines
[NASA-TM-86928] 12 p1844 N85-21589
Study of fatigue strength of shafts with segmented channels
14 p2282 N85-24138
An analytical investigation of dynamic coupling in nonlinear, geared rotor systems
16 p2792 N85-27218
Variable force, eddy-current or magnetic damper
[NASA-CASE-LEW-13717-1] 19 p3279 N85-30333

ROTATING SPHERES
Some important problems in unsteady boundary layers including separation. 2: Unsteady boundary layers close to the stagnation region of slender bodies
[AD-A146964] 07 p0958 N85-16060
Sedimentation of two arbitrarily oriented spheroids in a viscous fluid
[AD-A147303] 07 p0960 N85-16062
Finite element analysis of nonlinear oscillations and flutter of shells of revolution
[AD-A149071] 10 p1496 N85-19440
The effect of power law body forces on a thermally-driven flow between concentric rotating spheres
[NASA-TM-87596] 24 p4093 N85-35374

ROTATING STALLS
Subsynchronous vibrations in a high pressure centrifugal compressor: A case history
05 p0642 N85-14118
A theory of post-stall transients in multistage axial compression systems
[NASA-CR-3678] 12 p1771 N85-21117

ROTATING VEHICLES
U ROTATING BODIES

ROTATION
NT EARTH ROTATION
NT MOLECULAR ROTATION
NT MUON SPIN ROTATION
NT PLANETARY ROTATION
NT SATELLITE ROTATION
NT SOLAR ROTATION
NT STELLAR ROTATION
The NBS tri-directional test facility
[PB84-217482] 01 p0051 N85-10334
A short-term forecast model for thunderstorm rotation
01 p0081 N85-10542
Environmentally independent fiber optic rotation sensor
[AD-D011219] 01 p0119 N85-10818
Experimental observation of neoclassical currents
[DE84-015113] 01 p0122 N85-10834
Relaxation of plasma rotation in a Tokamak in the presence of extraneous forces and corrugation of the magnetic field
[DE84-015628] 02 p0284 N85-11854
Dynamics of the Uranian rings
02 p0302 N85-11956
Fluid motion in a rotating and nutating container
[AD-A146175] 03 p0362 N85-12322
Controlling rotation of elastic manipulator link
04 p0488 N85-13113
Rotation of a tenuous plasma with a high toroidal velocity in a Tokamak
[DE84-012990] 04 p0567 N85-13615
Experimental on-stream elimination of resonant whirl in a large centrifugal compressor
05 p0642 N85-14121
Hydraulic forces on a centrifugal impeller undergoing synchronous whirl
05 p0643 N85-14124
Two-dimensional unsteady analysis of fluid forces on a whirling centrifugal impeller in a volute
05 p0643 N85-14126
Controllable rotation of system of two solid bodies with elastic elements
06 p0780 N85-14988
A free electron laser with a rotating quadrupole wiggler
[AD-A149052] 10 p1489 N85-19404
Theory of oriented nucleation with asymmetric single elements. 2: Effects of rotational diffusion
[IFTR-32/1984] 12 p1939 N85-22179
Study of energy versus misorientation for grain boundaries in gold by crystallite rotation method. 1: 001 twist boundaries
[DE85-004598] 12 p1943 N85-22201
Absolute stability of unsteady movement of axisymmetrical rotating flight vehicle
13 p2044 N85-22793
The unsteady boundary layer on an elliptic cylinder following the impulsive onset of translational and rotational motion — dynamic stall
14 p2209 N85-23699
Linearization of digital derived rate algorithm for use in linear stability analysis
[NASA-TM-87000] 14 p2243 N85-23904
Precise mounting of instruments in universal suspension with skewed axes
14 p2273 N85-24083
Polar motions measurement study
[AD-A150690] 14 p2372 N85-24664
On the boundary behaviour of a rotation automorphic function with finite spherical Dirichlet integral
15 p2634 N85-26238
High beta pinch plasma (STP-L)
15 p2655 N85-26381
Damping seals for turbomachinery
16 p2738 N85-26894
Poloidal rotation of magnetic fluctuations in reversed field pinch plasma
[IPPJ-715] 16 p2866 N85-27677
Use of quaternions in flight mechanics
[AD-A152616] 17 p2899 N85-27875
Influence of materials creep on rotor dynamics
[DE85-008545] 17 p2981 N85-28426
Efficient parallel solution of linear systems with hyperbolic rotations
[AD-A152355] 17 p3018 N85-28661
Experimental and theoretical investigation of microwave and millimeter wave radiation from hollow, rotating electron beams
[AD-A153827] 18 p3179 N85-29706
Load-induced rotordynamic instabilities in turbomachinery
19 p3280 N85-30340
Analysis and modeling of variations in length of day
19 p3349 N85-30761
Development of the Cascade inertial-confinement-fusion reactor
[DE85-010933] 19 p3357 N85-30812
Viscous flows in rotating pipes with internal cavities and related vortex breakdowns
[NASA-TM-86761] 20 p3454 N85-31447
Development of an active laser gyro for inertial rotation sensing in attitude/heading reference and inertial navigation systems, phase 1
[BMFT-FB-W-85-001] 20 p3460 N85-31489
A model of pulsed radiation from the Crab pulsar
20 p3548 N85-32081
Aerodynamic characteristics of the standard dynamics model in coning motion at Mach 0.6
[NASA-TM-86717] 21 p3552 N85-32094
Automatic rotary valve actuator
[DE85-012797] 22 p3794 N85-33505
Development of a microorifice uniform deposit cascade impactor
[DE85-006765] 22 p3812 N85-33614
Breakdown of intrinsic ambipolarity for the radial diffusion due to a rotating RF field
23 p3977 N85-34660

Measurement of low energy cosmic rays aboard Spacelab-1
[SH-10.1-6] 23 p4053 N85-35137
Heavy cosmic ray measurement aboard Spacelab-1
[SH-10.1-7] 23 p4053 N85-35138
Optimally designed propellers constrained by noise 24 p4065 N85-35196

ROTATIONAL FLOW
U FLUID FLOW
U VORTICES

ROTONS
Scaling violation in the fragmentation region of inclusive nucleon spektrum 24 p4173 N85-35874

ROTOR AERODYNAMICS
Some considerations on Aeroelastic instabilities caused by coupling between propeller-type rotor and its supporting structure
[NAL-TR-804] 01 p0003 N85-10013
Data input, processing and presentation — helicopter rotor balance measurement
[NASA-TM-77739] 01 p0125 N85-10656
Lifting surface theory for a helicopter rotor in forward flight
[NASA-TM-86315] 02 p0134 N85-10916
Extended aeroelastic analysis for helicopter rotors with prescribed hub motion and blade appended pendulum vibration absorbers
[NASA-CR-172455] 03 p0315 N85-12038
Rotordynamic Instability Problems in High-Performance Turbomachinery
[NASA-CP-2338] 05 p0642 N85-14116
Analysis for leakage and rotordynamic coefficients of surface roughened tapered annular gas seals 05 p0644 N85-14135
Effects of fluid inertia and turbulence on force coefficients for squeeze film dampers 05 p0645 N85-14137
The UH-1H helicopter icing flight test program: An overview
[NASA-TM-86925] 07 p0900 N85-15702
Clearance flow-generated transverse forces at the rotors of thermal turbomachines
[NASA-TM-77292] 07 p0973 N85-16180
Synthesized airfoil data method for prediction of dynamic stall and unsteady airloads
[NASA-CR-3672] 09 p1274 N85-18005
Integrated technology rotor/flight research rotor hub concept definition
[NASA-CR-166447] 09 p1280 N85-18051
Theory versus experiment for the rotordynamic coefficients of annular gas seals. Part 2: Constant clearance and convergent-tapered geometry
[NASA-CR-174413] 10 p1491 N85-19416
Theory versus experiment for the rotordynamic coefficients of annular gas seals. Part 1: Test facility and apparatus
[NASA-CR-174409] 10 p1491 N85-19417
A study for calculating rotor loads using free vortex concept 11 p1620 N85-20194
Analytical and flight investigation of the influence of rotor and other high-order dynamics on helicopter flight-control system bandwidth
[NASA-TM-86696] 12 p1780 N85-21174
Computer analysis of wind turbine blade dynamic loads
[DE85-000530] 12 p1867 N85-21714
Research Reports: 1984 NASA/ASEE Summer Faculty Fellowship Program
[NASA-CR-171317] 12 p1944 N85-22210
Study for prediction of rotor/wake/fuselage interference, part 1
[NASA-CR-177340-VOL-1] 13 p1965 N85-22346
Study for prediction of rotor/wake/fuselage interference. Part 2: Program users guide
[NASA-CR-177340-VOL-2] 13 p1966 N85-22347
Flight dynamics of axisymmetrical rotating bodies in air medium 13 p2043 N85-22791
Recent developments in the dynamics of advanced rotor systems
[NASA-TM-86669] 14 p2317 N85-24320
Finite-difference computations of rotor loads
[NASA-TM-86682] 16 p2700 N85-26680
Vibration characteristics of the HPOTP (High Pressure Oxygen Turbopump) of the SSME (Space Shuttle Main Engine) 16 p2738 N85-26695
Housing flexibility effects on rotor stability 16 p2738 N85-26696
Operating characteristics of a 0.87 kW-hr flywheel energy storage module
[NASA-TM-87038] 17 p2974 N85-28371
Helicopter Aeromechanics
[AGARD-LS-139] 18 p3057 N85-28913
A survey of recent development in helicopter aerodynamics 18 p3057 N85-28915
Rotorcraft noise 18 p3057 N85-28916
Recent developments in the dynamics of advanced rotor systems 18 p3057 N85-28917
Vibration control of rotor shaft
[NASA-TM-87053] 18 p3117 N85-29292

ROTOR BLADES
Turbofan noise generation. Volume 2: Computer programs
[NASA-CR-167952] 02 p0275 N85-11791

ROTOR BLADES (TURBOMACHINERY)
Thermal fatigue of gas turbine engine blades made of material based on silicon nitride and silicon carbide 01 p0019 N85-10115
Variable geometry Darrieus wind machine
[PB84-207281] 01 p0068 N85-10453
Coolant passage heat transfer with rotation 02 p0143 N85-10988
Structural analysis 02 p0143 N85-10989
Incompressible lifting-surface aerodynamics for a rotor-stator combination
[NASA-TM-83767] 03 p0316 N85-12039
Evaluation of the unsteady effects for a class of wind turbines 05 p0592 N85-13772
In-flight evalution of LCF life consumption of critical rotor components subjected to high transient thermal stress 07 p0906 N85-15734
Helicopter model rotor-blade vortex interaction impulsive noise: Scalability and parametric variations
[NASA-TM-86007] 08 p1077 N85-16826
Blade technology program for large wind turbines, phase 1
[BMFT-FB-T-84-217] 08 p1179 N85-17426
A feasibility study of free-tip rotor application as a passive cyclic control device 09 p1279 N85-18046
Integrated technology rotor/flight research rotor hub concept definition
[NASA-CR-166447] 09 p1280 N85-18051
Influence of normalized frequency on time-dependent aerodynamic characteristics of vane blading profiles 09 p1306 N85-18204
Influence of secondary flow rate on dynamic stresses in turbine rotor blades 09 p1306 N85-18205
One-piece HPTR blade squealer tip
[AD-D011452] 10 p1425 N85-18989
High pressure turbine rotor two-piece blade retainer
[AD-D011498] 12 p1858 N85-21653
Cooled turbine blade tip closure
[AD-D011525] 12 p1858 N85-21654
Structural response of a rotating bladed disk to rotor whirl
[NASA-CR-175605] 13 p1973 N85-22391
Experimental determination of optimum ratio of runner blade height at exit to runner blade height at entrance of radial inward-flow microturbines 13 p2049 N85-22827
An experimental investigation of the chopping of helicopter main rotor tip vortices by the tail rotor
[NASA-CR-177338] 13 p2154 N85-23376
Calculation of three-dimensional, viscous flow through turbomachinery blade passages by parabolic marching
[NASA-TM-86984] 14 p2211 N85-23711
Vibration and buckling of rotating, prestressed, preconed beams including Coriolis effects
[NASA-TM-87004] 15 p2577 N85-25863
Development of a rotor wake-vortex model, volume 1
[NASA-CR-174849] 16 p2699 N85-26668
Aerodynamic detuning analysis of an unstalled supersonic turbofan cascade
[NASA-TM-87001] 16 p2700 N85-26670
Ice shapes and the resulting drag increase for a NACA 0012 airfoil
[NASA-TM-83556] 17 p2894 N85-27839
A survey of recent development in helicopter aerodynamics 18 p3057 N85-28915
Rotor blade test apparatus
[AD-D011725] 23 p3934 N85-34361
Reflection plane tests of a wind turbine blade tip section with aileron
[NASA-TM-87018] 23 p3945 N85-34444

ROTOR DISKS
U TURBINE WHEELS

ROTOR HUBS
U HUBS
U ROTORS

ROTOR SPEED
Shutdown characteristics of the Mod-O wind turbine with aileron controls
[NASA-TM-86918] 07 p0992 N85-16209
Experimental study of main rotor tip geometry and tail rotor interactions in hover. Volume 1. Text and figures
[NASA-CR-177336-VOL-1] 13 p1965 N85-22344
Development of a rotor wake-vortex model, volume 1
[NASA-CR-174849] 16 p2699 N85-26668
Improved turbopump dynamics
[NASA-TM-86514] 20 p3462 N85-31509
A comparison of experimental and theoretical results for rotordynamic coefficients of four annular gas seals
[NASA-CR-176086] 21 p3596 N85-32332

ROTOR SYSTEMS RESEARCH AIRCRAFT
Rotor systems research aircraft airplane configuration flight-test results
[NASA-TM-85911] 01 p0006 N85-10034
Numerical analysis of the first static calibration of the RSRA helicopter active-isolator rotor balance system
[NASA-TM-85975] 08 p1083 N85-16883
Fuselage upwash effects on RSRA rotor systems
[NASA-CR-177349] 20 p3388 N85-31015
Estimation of dynamic rotor loads for the rotor systems research aircraft: Methodology development and validation
[NASA-CR-177362] 20 p3393 N85-31045
Flight testing the fixed-wing configuration of the Rotor Systems Research Aircraft (RSRA)
[NASA-TM-86782] 23 p3896 N85-34135

ROTORCRAFT
U ROTARY WING AIRCRAFT

ROTORCRAFT AIRCRAFT
Effects of side-stick controllers on rotorcraft handling qualities for terrain flight
[NASA-TM-88688] 15 p2473 N85-25267

ROTORS
NT BEARINGLESS ROTORS
NT COMPRESSOR ROTORS
NT FLYWHEELS
NT HELICOPTER TAIL ROTORS
NT IMPELLERS
NT LIFTING ROTORS
NT PUMP IMPELLERS
NT RIGID ROTORS
NT ROTARY WINGS
NT TAIL ROTORS
NT TILTING ROTORS
NT TIP DRIVEN ROTORS
NT TURBINE WHEELS
Some considerations on Aeroelastic instabilities caused by coupling between propeller-type rotor and its supporting structure
[NAL-TR-804] 01 p0003 N85-10013
A mathematical simulation model of the CH-47B helicopter, volume 1
[NASA-TM-84351-VOL-1] 01 p0006 N85-10033
Singular asymptotic expansions in nonlinear rotordynamics
[NASA-CR-174012] 01 p0017 N85-10100
Rotordynamic analysis of the SSME turbopumps using reduced models
[NASA-CR-171170] 01 p0054 N85-10355
Aileron controls for wind turbine applications
[NASA-TM-86867] 02 p0222 N85-11458
Laser balancing system for high material removal rates
[NASA-CR-174731] 03 p0365 N85-12341
European development experience on energy storage wheels for space 05 p0605 N85-13858
Summary results of the DOE flywheel development effort 05 p0606 N85-13865
General Electric composite ring-disk flywheel: Recent and potential developments 05 p0606 N85-13867
Flywheel containment and safety considerations 05 p0606 N85-13869
Control of rotordynamic instability in a typical gas turbine's power system 05 p0642 N85-14120
Hydrodynamic impeller stiffness, damping, and inertia in the rotordynamics of centrifugal flow pumps 05 p0643 N85-14125
Preliminary investigation of labyrinth packing pressure drops at onset of swirl-induced rotor instability 05 p0644 N85-14132
Design of electromagnetic bearing for vibration control of flexible transmission shaft 05 p0645 N85-14136
Squeeze-film dampers for turbomachinery stabilization 05 p0645 N85-14138
Damping capacity of a sealed squeeze film bearing 05 p0645 N85-14139
Dynamic stiffness characteristics of high eccentricity ratio bearings and seals by perturbation testing 05 p0645 N85-14141
Measurement data acquisition and processing system for wind rotor measurements in the wind channel of Bremen University 05 p0668 N85-14298
Device for measuring relative axial expansion of turbine rotor employing space-vector tracking method 06 p0778 N85-14962
Two-rotor alternators with superconductor field winding 06 p0795 N85-15082
The use of an optical data acquisition system for bladed disk vibration analysis
[NASA-TM-86891] 06 p0817 N85-15184
Superconducting rotor dynamics
[AD-A147176] 07 p0947 N85-16000

Development of a Navier-Stokes rotor and stator analysis
[AD-A146967] 07 p0958 N85-16070
Theoretical and experimental study of hydro-elastic instability on the line of shafting of a rotating machine
[BLL-DOUNREAY-TR-937-(9091.9F)] 07 p0972 N85-16174
Experimental investigation of the oscillation behaviour of a liquid-filled rotor with centrifugal motion
[BLL-DOUNREAY-TR-936-(9091.9F)] 08 p1160 N85-17317
Eigenvalues of rotating machinery 08 p1167 N85-17361
Prediction accuracy of the torques for rotary tillage by an analog tool
[AD-P004298] 09 p1408 N85-18865
Integrated Technology Rotor/Flight Research Rotor (ITR/FRR) concept definition
[NASA-CR-168443] 10 p1423 N85-18978
Integrated Technology Rotor/Flight Research Rotor (ITR/FRR) concept definition
[NASA-CR-168445] 10 p1423 N85-18979
Singular asymptotic expansions in nonlinear rotordynamics 12 p1845 N85-22218
Oscillations of gas turbine installation rotors under operating conditions 14 p2272 N85-24077
Stability of steady modes of motion by axis of rotating wheel in nonlinear bearings 14 p2279 N85-24117
Stability of permanent rotation modes of asymmetric heavy solid body 14 p2279 N85-24118
Thermal deformation of flexible rotors in friction bearings 14 p2280 N85-24123
Superconducting gyroscope research
[NASA-CR-171406] 15 p2560 N85-25795
Rotordynamics 16 p2737 N85-26688
Effects of bearing deadbands on bearing loads and rotor stability 16 p2737 N85-26689
Rotor response for transient unbalance changes in a nonlinear simulation 16 p2737 N85-26692
Damping seals for turbomachinery 16 p2738 N85-26694
Vibration characteristics of the HPOTP (High Pressure Oxygen Turbopump) of the SSME (Space Shuttle Main Engine) 16 p2738 N85-26695
Reusable rocket engine turbopump condition monitoring 16 p2740 N85-26907
An analytical investigation of dynamic coupling in nonlinear, geared rotor systems 16 p2792 N85-27218
Vibrations of rotors connected through couplings with backlash 17 p2940 N85-29147
Influence of materials creep on rotor dynamics
[DE85-006545] 17 p2961 N85-29426
Damping seal for turbomachinery
[NASA-CASE-MFS-25842-2] 19 p3280 N85-30041
Effect of ground and/or ceiling planes on thrust of rotors in hover
[NASA-TM-86754] 20 p3368 N85-31014
Estimation of dynamic rotor loads for the rotor systems research aircraft: Methodology development and validation
[NASA-CR-177362] 20 p3393 N85-31045
A theoretical model for the study of nonlinear dynamics of magnetic bearings 20 p3462 N85-31505
R and D activities of the Structural Sciences Division 20 p3539 N85-32026
A panel method study of vortex sheets with special emphasis on sheets of axisymmetric geometry
[NASA-CR-177365] 21 p3552 N85-32095
A phase-locked frequency multiplier for the signal averaging of the vibration of the Wessex helicopter input spiral bevel pinion
[AD-A154914] 21 p3555 N85-32113
Proposal for modifications to the Wessex helicopter main rotor gearbox vibration monitoring program
[AD-A155106] 21 p3555 N85-32117

ROUGHNESS
NT SEA ROUGHNESS
NT SURFACE ROUGHNESS
Comparison of predicted and measured friction for a tilt-pad thrust bearing with crown and roughness under hydrodynamic and mixed lubrication
[AD-A145752] 09 p0371 N85-12371
Hydraulic drag of rod with artificial microroughness in longitudinal flow 14 p2278 N85-24111
Predicting microfracture in ceramics via a microcontract model
[DE85-005854] 18 p3081 N85-29060
Mechanical properties of plasma arc cut steel 23 p3905 N85-34188

ROUND TRIP TRAJECTORIES
Mars exploration, Venus swingby and conjunction class mission modes, time period 2000 to 2045
[NASA-TM-86477] 02 p0303 N85-11961

ROUTES
Asynchronous distributed flow control algorithms
[AD-A148452] 08 p1206 N85-17600
Local search in routing problems with time windows
[CWI-OS-R8409] 12 p1922 N85-22075
Routing algorithms and stochastic analysis for large communications networks
[AD-A154864] 21 p3573 N85-32225

ROVING VEHICLES
NT LUNOKHOD LUNAR ROVING VEHICLES
An autonomous roving vehicle for the planet Mars: A summary of over 15 years of research
[RPI-TR-MP-83] 07 p0973 N85-16179
Mathematical model for rollout of planet roving vehicle from landing craft 15 p2484 N85-25334
Mars landing sites 22 p3859 N85-33883

RPV
U REMOTELY PILOTED VEHICLES

RUBBER
NT CHLOROPRENE RESINS
NT ELASTOMERS
NT LATEX
NT SILICONE RUBBER
NT SYNTHETIC RUBBERS
NT VULCANIZED ELASTOMERS
Diblock copolymers of polystyrene/1,2 polybutadiene and polystyrene/polybutene-1: Molecular structure, morphology and mechanical properties
[AD-A144660] 01 p0033 N85-10201
Guide to the selection of rubbers
[AMTE(N)-TM-84301] 03 p0336 N85-12164
Modified epoxy composites 04 p0466 N85-12957
Alternatives for runway rubber removal from porous friction surfaces
[DOT/FAA/PM-84/26] 05 p0597 N85-13803
Low frequency electrical properties of selected dielectrics
[DE84-016220] 05 p0832 N85-14052
Rubber-modified epoxies. 1: Cure, transitions, and morphology
[AD-A147377] 07 p0932 N85-15906
Rubber-modified epoxies. Part 2: Morphology, transitions, and mechanical properties
[AD-A147962] 08 p1132 N85-17137
Runway rubber removal specification development field evaluation procedures development
[FAA-PM-84-27] 12 p1781 N85-21179
Rubber modified epoxy adhesive
[AD-D011527] 12 p1810 N85-21354
Process development for commercial production of natural rubber from Guayule
[PB85-124956] 12 p1815 N85-21368
Finger materials for air cushion vehicles. Volume 2: Base fabrics for finger materials
[AD-A149701] 12 p1819 N85-21408
Mechanism of strengthening plastics with rubbers 13 p2014 N85-22636

RUBBER COATINGS
Design, manufacture, and testing of compliant coatings for reduction of turbulent drag
[AD-A145510] 02 p0196 N85-11323
Anticorrosion protection of reinforcing steel in prestressed gypsum and anhydrite concrete
[BLL-BISI-TRANS-22079-(9022.06)] 17 p2926 N85-29044
Description of an holographic interferometry nondestructive test installation: Application to bond tests
[SNIAS-851-430-101] 20 p3464 N85-31521

RUBIDIUM
NT RUBIDIUM ISOTOPES
Calorimetric investigation into the possibility of a charge density wave ground state in alkali metals
[DE85-002005] 09 p1397 N85-18795
Lifetime and reliability of rubidium discharge lamps for use in atomic frequency standards
[AD-A150787] 14 p2417 N85-24915
Physics element design aspects for a tactical rubidium frequency standard 17 p2967 N85-29321
On-orbit frequency stability analysis of the GPS NAVSTAR-1 quartz clock and the NAVSTARs-6 and -8 rubidium clocks 18 p3105 N85-29227
A miniature tactical Rb frequency standard 18 p3106 N85-29229
The Rubidium-Crystal Oscillator Hybrid Development Program 18 p3106 N85-29230
The system design of a rubidium maser frequency standard 18 p3106 N85-29232
The role of long term lamp fluctuations in the random walk of frequency behavior of the rubidium frequency standard: A case study
[AD-A155338] 21 p3590 N85-32314

RUBIDIUM ISOTOPES
Diode laser 87Rb optical pumping in an evacuated wall-coated cell 18 p3105 N85-29226

RUBY
The Faraday effect in ruby and corundum in strong magnetic fields 21 p3697 N85-32967

RUBY LASERS
Neutral beam interactions with materials
[AD-A145636] 02 p0285 N85-11857
Coherent amplification of ultrasonic pulses in activated crystals 05 p0724 N85-14653
High-speed, eight-frame electro-optic camera with multipulsed ruby laser illuminator
[DE85-001748] 09 p1323 N85-18314
Effect of transparent coatings on generation of laser-induced shock waves in metals 13 p2028 N85-22711
Ruby wavefront-conjugation laser for obtaining high temperature plasma 13 p2044 N85-22795
System for lower hybrid current startup 15 p2654 N85-26373
Visibility and vertical structure measurements in southern Germany
[AD-A154714] 21 p3635 N85-32574
Operation of solid state lasers exposed to electron beam 21 p3685 N85-32995
Instrument to synchronize Thomson scattering diagnostic measurements with MHD activity in a Tokamak
[DE85-012082] 23 p3984 N85-34708

RUDDERS
NT AERIAL RUDDERS
Flight-service program for advanced composite rudders on transport aircraft
[NASA-CR-174537] 19 p3217 N85-29950

RULES
NT INSTRUMENT FLIGHT RULES
NT VISUAL FLIGHT RULES
Safety with industrial manufacturing lasers 14 p2308 N85-24281

RUN TIME (COMPUTERS)
Relative performance of micro and mainframe computers
[AD-A149281] 10 p1538 N85-19695
Exploiting multiprocessors: Issues and options
[DE85-003144] 13 p2145 N85-23313
Trends in computational capabilities for fluid dynamics 15 p2457 N85-25172
Efficient implementation of real-time programs under the VAX/VMS operating system
[NASA-TM-86354] 15 p2627 N85-26193
The completion time of a job on multi-mode systems
[AD-A154113] 19 p3336 N85-30686
Experiments and improvements of the ordinary differential equation solvers DEPAC on the CRAY computer
[DE85-013260] 22 p3831 N85-33726

RUNGE-KUTTA METHOD
Computation of the nonequilibrium flow in a gasdynamic laser
[AD-A141022] 04 p0505 N85-13224
Art of programming programmable microcalculators. Part 12: Solution of differential equations 07 p0953 N85-16043
Fixed vs. variable order Runge-Kutta
[DE85-001320] 09 p1374 N85-18639
Solution of structured non-stiff ODEs
[DE85-004137] 11 p1707 N85-20741
Electromagnetic rail launcher as a circuit element
[AD-A150067] 12 p1835 N85-21516
The performance of a type-insensitive Runge-Kutta code on a personal computer
[TUM-I8410] 12 p1919 N85-22048
Runge-Kutta formula with cheap error estimate
[DE85-005674] 13 p2152 N85-23363
On the algebraic equations in implicit Runge-Kutta methods
[CWI-NM-R8413] 17 p3022 N85-28696
Compressible two-phase flow instabilities simulated with a hybrid Lagrange-Euler pseudospectral method
[DE85-009904] 23 p3931 N85-34361

RUNNING
The energy cost of women walking and running in shoes and boots
[AD-A151022] 14 p2389 N85-24716
Weight loss, rectal temperature and heart rates following the 1984 Boston Marathon
[AD-A155664] 24 p4132 N85-35812

RUNOFFS
U DRAINAGE

RUNWAY ALIGNMENT
Closely spaced independent parallel runway simulation
[DOT/FAA/CT-84/45] 04 p0457 N85-12902

RUNWAY CONDITIONS
Aircraft accident report: Flying Tigers, Inc., Flight 2468, McDonell Douglas DC8-63, N797FT, Chambers Field, Naval Air Station, Norfolk, Virginia, October 25, 1983
[PB84-910408] 02 p0136 N85-10625

Closely spaced independent parallel runway simulation
[DOT/FAA/CT-84/45] 04 p0457 N85-12002
To take off and to land safely, Hoechst 1676 for ice and snow free runways 05 p0595 N85-13791
A model for forecasting runway surface temperature and verification with subjective forecasts
[TR-28] 10 p1518 N85-19569
Aircraft accident report: World Airways Inc., Flight 30H, McDonnell Douglas DC-10-30CF, N113WA, Boston-Logan International Airport, Boston, Massachusetts, January 23, 1982
[PB85-910406] 22 p3728 N85-33114
RUNWAY LIGHTS
Flares and photoflash items
[AD-A145442] 02 p0187 N85-11253
Evaluation of arctic test of improved tritium radioluminescent lighting
[DE84-014887] 05 p0597 N85-13805
Wind-powered electric generation runway lighting system demonstration project
[DE84-014982] 05 p0670 N85-14311
Light your runways and taxiways without electricity
[DE85-000269] 11 p1586 N85-19991
Examination of the feasibility for demonstration and use of radioluminescent lights for Alaskan remote runway lighting
[DE85-002503] 12 p1782 N85-21185
Radioluminescent lighting for rural Alaskan runway lighting and marking
[DE85-007022] 16 p2716 N85-26764
Acceptability testing of radioluminescent lights for VFR-night air taxi operations
[DE85-007303] 16 p2716 N85-26765
Radioluminescent lighting for Alaskan runway lighting and marking
[DE85-010405] 19 p3368 N85-30887
RUNWAYS
Materials for emergency repair of runways
[AD-A146139] 03 p0320 N85-12068
Development of a pavement maintenance management system. Volume 9: Development of airfield pavement performance prediction models
[AD-A146150] 03 p0321 N85-12069
Alternatives for runway rubber removal from porous friction surfaces
[DOT/FAA/PM-84/28] 05 p0597 N85-13803
Prefabricated panels for rapidly runway repair and expedient airfield surfacing
[AD-D011277] 05 p0597 N85-13804
System for rapid repair of damaged airfield runways
[AD-D011325] 07 p0909 N85-15754
Development of a preliminary ALRS stabilized material pavement analysis system (SPAS)
[AD-A147116] 07 p0910 N85-15760
International projects, other work of Aeroproyekt Institute 08 p1068 N85-16767
Aeroproyekt develops improved runway surfacing 08 p1068 N85-16770
New runway enables IL-76 flights to Tenkeli in far north 12 p1769 N85-21108
Runway rubber removal specification development field evaluation procedures development
[FAA-PM-84-27] 12 p1781 N85-21179
Field validation of statistically-based acceptance plan for bituminous airport pavements. Volume 1: Correlation analysis of Marshall properties of laboratory-compacted specimens
[FAA-PM-84-12-VOL-1] 12 p1781 N85-21180
Field validation of statistically-based acceptance plan for bituminous airport pavements. Volume 2: Statistical analysis of Marshall properties of plant-produced bituminous materials
[FAA-PM-84-12-VOL-2] 12 p1781 N85-21181
Field validation of statistically-based acceptance plan for bituminous airport pavements. Volume 3: Statistical analysis of 3 methods for determining maximum specific gravity of bituminous concrete mixtures
[FAA-PM-84-12-VOL-3] 12 p1781 N85-21182
Field validation of statistically-based acceptance plan for bituminous airport pavements. Volume 4: Computer simulation of multiple acceptance criteria
[FAA-PM-84-12-VOL-4] 12 p1782 N85-21183
Field validation of statistically-based acceptance plan for bituminous airport pavements. Volume 5: Summary of validation studies
[FAA-PM-84-12-VOL-5] 12 p1782 N85-21184
Probabilistic computer model of optimal runway turnoffs
[NASA-CR-172549] 16 p2715 N85-26760
Study of acceptance criteria for joint densities in bituminous airport pavements
[FAA-PM-85-5] 16 p2715 N85-26761
OWEMA report: A project study concerning the possibilities and the desirability of a east-west runway for Maastricht Airport (Netherlands) as a Euro-regional air freight center
[B8476490] 18 p3064 N85-28855
Review of rigid pavement design for vehicular parking areas
[AD-A154284] 19 p3222 N85-29975
Expedient runway surfacing with post tensioning system for expeditionary airfields
[AD-D011677] 19 p3222 N85-29976
Guidelines for the evaluation of visual approach slope indicators
[ARL/SYS-R-32] 23 p3896 N85-34132
RUPTURING
Toughness in high speed steels and hard metals 02 p0178 N85-11181
Laser rupture of composite materials 10 p1444 N85-19102
Preliminary review of statistical treatment of S-glass/epoxy stress rupture data
[AD-A149810] 12 p1797 N85-21275
Limiting values of stress state index after rupture of metals
[BLL-BISI-TRANS-22293-(9022.06)] 17 p2978 N85-28407
A continuous damage model based on stepwise-stress creep rupture tests
[NASA-CR-174941] 21 p3597 N85-32341
RURAL AREAS
Examination of the feasibility for demonstration and use of radioluminescent lights for Alaskan remote runway lighting
[DE85-002503] 12 p1782 N85-21185
A comparison of metropolitan and non-metropolitan employment characteristics: Indications of the size of non-metropolitan mobile communication services user classes
[NASA-CR-175848] 13 p2053 N85-22855
Trace element concentrations in atmospheric aerosol over Hungary 21 p3646 N85-32652
Motor glider measurements during the Urban Atmosphere Energy Budget Experiment (EESA 1) 24 p4122 N85-35553
RURAL LAND USE
Development and testing of a rural credit supervision system at the level of counties and rural properties utilizing remote sensing techniques
[E85-10018] 02 p0217 N85-11431
A field control methodology of remotely sensed data for statistical purposes: An example of SPOT simulated data in eastern Belgium — land use statistics 05 p0660 N85-14241
The challenge of food production: The importance of climate 07 p1001 N85-16361
RUSTING
Continuous measurement of zircaloy corrosion in air with an ultrasonic corrosion monitor
[DE85-003683] 12 p1807 N85-21337
Forming of coating protection system: Mechanism of paint-coating anti-corrosion protection of steel
[BLL-BISI-TRANS-22061-(9022.06)] 17 p2925 N85-28039
RUTHENIUM
Laser studies of chemical dynamics at the gas-solid interface
[DE84-017590] 11 p1736 N85-20920
Technology of off-gas treatment for liquid-fed ceramic melters
[DE85-012467] 22 p3812 N85-33610
RUTHENIUM ALLOYS
Electrical resistivity and structural changes upon relaxation and crystallization of (Mo/sub 0.6/Ru/sub 0.4)sub 100-x/B/sub x/ metallic glasses
[DE84-017261] 09 p1290 N85-18160
RUTHENIUM COMPOUNDS
Transition metal carbene complexes
[AD-A144879] 01 p0028 N85-10173
Chemically modified electrodes and related solution chemistry
[DE84-017110] 05 p0614 N85-13924
RUTILE
Mechanisms of impurity diffusion in rutile
[DE84-014741] 06 p0766 N85-14902
RYDBERG SERIES
Physico-chemical investigation of some areas of fundamental significance to biophysics
[DE84-018385] 04 p0471 N85-12999
Infrared emission and atomic transitions
[AD-A147840] 07 p1041 N85-16607
Nonlinear optical studies of rydberg atoms using degenerate four-wave mixing
[AD-A148827] 07 p1043 N85-16623
Collision-induced dipole moments
[AD-A147662] 08 p1121 N85-17063
Basic studies of atomic dynamics
[DE84-015661] 09 p1380 N85-18675
Alignment of high Ryberg states in hydrogen
[DE85-000582] 09 p1380 N85-18677
Photoelectron studies of autoionizing Rydberg states in HCl
[DE85-011813] 21 p3702 N85-33001

S

S BAND
U SUPERHIGH FREQUENCIES
U ULTRAHIGH FREQUENCIES
S GLASS
Passive Orbital Disconnect Strut (PODS 3) structural test program
[NASA-CR-177325] 08 p1113 N85-17020
Preliminary review of statistical treatment of S-glass/epoxy stress rupture data
[AD-A149810] 12 p1797 N85-21275
S MATRIX THEORY
Semiclassical theory of resonances
[REPT-57] 01 p0114 N85-10777
The S-matrix and acoustic signal structure in simple and compound waveguides
[PP-583] 03 p0415 N85-12852
Scattering matrix of antenna array with Joule losses in radiators 06 p0791 N85-15053
Theory of resonant light scattering from a rough surface 09 p1383 N85-18701
Shielded enclosures for experimental studies of shielding topology
[AD-A149292] 11 p1624 N85-20227
S-matrix theory of nuclear forces
[DE85-007633] 18 p3179 N85-29710
Method of static measurements of absolute scattering matrix of radar targets 22 p3782 N85-33316
Interrelations for the elements of the scattering matrix 22 p3855 N85-33972
Duality of two-point functions for confined non-relativistic quark-antiquark systems
[DE85-012334] 23 p3971 N85-34818
S STARS
NT CARBON STARS
NT GIANT STARS
NT RED GIANT STARS
S WAVES
Response and characteristics of structures subjected to S-H waves 01 p0080 N85-10396
Bragg reflection of surface electroacoustic shear waves 04 p0485 N85-13096
Propagation of acoustic shear waves through active periodic structure 04 p0490 N85-13125
Characterization of stressed metals using acoustic shear waves 05 p0648 N85-14159
Optical method of measuring velocity of shear waves 06 p0787 N85-15029
Modeling of real UT transducer field/flaw interactions
[DE85-000341] 09 p1329 N85-18351
Experimental high pressure equation of state of a very fast burning gun propellant
[DE85-001749] 10 p1458 N85-19184
Effects of magnetic shear on lower hybrid waves in the suprauroral region
[AD-A151980] 15 p2656 N85-26392
Radar echoes at 2.66 and 40.92 MHz from the mesosphere, part 2.6A 21 p3619 N85-32486
On the cosmic ray diffusion in a violent interstellar medium
[OG-7.2-14] 23 p4015 N85-34681
Scale separation closure and Alfven wave turbulence
[DE85-013124] 24 p4095 N85-35385
S-A-W DEVICES
U SURFACE ACOUSTIC WAVE DEVICES
S-N DIAGRAMS
Fatigue behavior of HY-130 steel weldments containing fabrication discontinuities
[AD-A153630] 18 p3122 N85-29326
Controlled indentation flaws for the construction of toughness and fatigue master maps
[PB85-179067] 20 p3473 N85-31562
SABOT PROJECTILES
Stress in axially symmetrical heavy metal projectiles during discharge — numerical simulation
[ISL-CO-219/83] 14 p2321 N85-24345
Metal armatures for railguns
[AD-A152129] 16 p2728 N85-26838
SACCADIC EYE MOVEMENTS
Application of the system identification technique to goal-directed saccades
[AD-A150132] 12 p1906 N85-21987
SACCHARIDES
U CARBOHYDRATES

SACRAMENTO VALLEY (CA)
Investigation of several aspects of LANDSAT 4/5 data quality
[E85-10036] 04 p0525 N85-13357

SADDLE POINTS
NT SADDLE POINTS (GAME THEORY)
Existence, uniqueness and stability conditions for general finite element methods in linear elasticity
09 p1332 N85-18372
Analysis of the convergence of mixed finite element methods
[HTKK-MAT-A227] 16 p2866 N85-27613

SADDLE POINTS (GAME THEORY)
General saddlepoint approximations with applications to l-statistics
[AD-A150073] 12 p1924 N85-22066

SAFETY
NT AEROSPACE SAFETY
NT AIRCRAFT SAFETY
NT FLIGHT SAFETY
NT INDUSTRIAL SAFETY
NT REACTOR SAFETY
Manual for Raman cells
[NASA-TM-77756] 01 p0052 N85-10342
A dispersion model for airborne particulates inside a building
[DE84-014961] 02 p0225 N85-11473
Photocopiers: Do they pose a health hazard?
[PB3-1E] 02 p0234 N85-11527
The IMX double direct process
[AD-A146250] 03 p0340 N85-12188
Activities report in technology
[ISBN-951-38-1996-1] 04 p0577 N85-13681
Flywheel containment and safety considerations
05 p0806 N85-13869
The detection and assessment of defects in automatic ultrasonic inspection
[BLL-RISLEY-TR-4597-(8091.9F)] 05 p0847 N85-14150
Computer science and technology: Overview of computer security certification and accreditation
[PB84-217619] 06 p0848 N85-15384
Flame-resistant materials for use in pyrotechnic safety clothing
[AD-A146857] 07 p0931 N85-15901
Safety evaluation of an electronic totalizer containing a Li/(CF)x cell
[AD-A147306] 07 p0993 N85-16305
Aims and requirements of NATO group AC/310
08 p1114 N85-17026
Sensitivity tests for solid propellants in Germany
08 p1115 N85-17028
Sensitiveness and explosiveness assessment at Perme Waltham Abbey
08 p1115 N85-17029
Penguin warhead safety tests
08 p1115 N85-17031
The vulnerability of cast double base rocket motors to thermomechanical attack
08 p1115 N85-17033
Tolerance endpoint for evaluating the effects of heat stress in dogs
[AD-A148104] 08 p1192 N85-17511
A study on a medium-sized rocket with Burnout frame
[NAL-TR-821] 09 p1287 N85-18082
Railroad safety program, volume 1
[NASA-CR-174333] 09 p1403 N85-18830
Preventing explosive propagation in racks or containers of tactical missiles
[AD-P004342] 10 p1455 N85-19166
Safety aspects of prepackaged liquid propellant stages for strategic missiles
[AD-P004350] 10 p1456 N85-19174
A review of hazard assessment procedures for liquid gun propellants
[AD-A149470] 10 p1457 N85-19182
Ultralight aircraft technology and public safety
[GPO-36-948] 12 p1773 N85-21131
General-purpose heat source development: Safety test program. Postimpact evaluation, design iteration test 4
[LA-10217-SR] 12 p1930 N85-22128
US Army human Engineering Laboratory Communications Survey: A Pilot Study (HELCOMS-PS)
[AD-A151434] 15 p2521 N85-25544
Pavement-marking materials: New York's experience
[PB85-153294] 15 p2523 N85-25558
Some aspects of how to design cost-effective flight control systems
16 p2695 N85-28639
The certification of airborne complex digital systems
16 p2714 N85-28754
A review of safety practices and safety training for the explosives field
[AD-A152295] 16 p2759 N85-27028
Space Station crew safety alternatives study. Volume 5: Space Station safety plan
[NASA-CR-3858] 17 p2908 N85-27930
Space Station crew safety alternatives study. Volume 4: Appendices
[NASA-CR-3857] 18 p3065 N85-28958
Space station crew safety: Human factors interaction model
18 p3156 N85-29540
Space station crew safety alternatives study, third quarter briefing
18 p3156 N85-29541
Experimental program to determine maximum temperatures for dry storage of spent fuel
[DE85-010307] 19 p3236 N85-30060
Working with flammable solvents, thinners, paints and adhesives
[HSE-TRANS-11066] 19 p3250 N85-30154
SAFEORD: Safety of explosive ordnance databank
[AD-A154058] 19 p3380 N85-30972
The CCIR satellite EPIRB coordinated trials programme --- Emergency Position Indicating Radio Beacon (EPIRB); International Radio Consultative Committee (CCIR)
20 p3402 N85-31111
The International Radio Consultative Committee (CCIR) recommended satellite Emergency Position Indicating Radio Beacon (EPIRB) system operating through geostationary satellites at 1.6 GHz
20 p3402 N85-31112
Improvements in safety testing of lithium cells
20 p3444 N85-31379
Safety of Li-SOCl2 cells
20 p3444 N85-31383
Basic cryogenics and materials. Phase 1
[NASA-CR-177932] 21 p3572 N85-32215
Safety characteristics of non-lithium battery systems
[AD-A155733] 22 p3806 N85-33574
Experimental lithium system
[DE85-013252] 24 p4094 N85-35382

SAFETY DEVICES
NT ARRESTING GEAR
NT EJECTION SEATS
NT HELMETS
NT SEAT BELTS
NT SPACE SUITS
Safing and arming mechanism
[AD-D011281] 05 p0821 N85-13969
Flow of nitrogen-presurized Halon 1301 in fire extinguishing systems
[NASA-CR-174271] 07 p0900 N85-15701
Powered articulated headrest system
[AD-D011353] 07 p0901 N85-15710
S-3A ballast block final design and engineering tests
[AD-A147685] 08 p1080 N85-16842
SPH-4 US Army flight helmet performance, 1972 - 1983
[AD-A148674] 08 p1201 N85-17562
Optoelectronic safety system for robotized technological complex
13 p2046 N85-22805
Retroreflective armbands: Influences of wearing mode, aging and other factors on the visibility distance
[IZF-1984-28] 14 p2422 N85-24942
Parachute extraction device for ultralight gliders
[CH-643499-A5] 16 p2699 N85-26663
Torso restraint system
[AD-D011609] 16 p2702 N85-26684
Robotic safety systems and methods: Savannah River site
[DE85-008261] 17 p2974 N85-28375
Investigation, development, and certification of a burst disk for cryogenic fuel tanks
[GCP-3/MT-CM-21-2546] 18 p3067 N85-28972
Development of a stationary carbon monoxide detector
[BMFT-FB-T-84-253] 18 p3134 N85-29413
The design of working systems on ergonomic principles. The importance of clothes and protective equipment in the design of the workplace
[HSE-TRANS-10865] 19 p3332 N85-30639
Free-float Emergency Position Indicating Radio Beacons (EPIRBs) and release mechanism on board Norwegian ships. Main specifications and user experience
20 p3404 N85-31120
Fast shutter apparatus
[DE85-006501] 23 p3928 N85-34343

SAFETY FACTORS
Aircraft chocks
[AD-A145135] 01 p0012 N85-10077
System engineering and integration contract for implementation of the National Airspace System plan, volume 1, sections 1.0-4.0, 6.0
[AD-A145763] 03 p0317 N85-12048
Test methods for cable cars
[CETIM-1-5K-45-1] 04 p0515 N85-13282
Vandenberg space shuttle launch complex
[S-HRG-98-1075] 05 p0601 N85-13833
Statement of Edward C. Aldridge, Jr., Under Secretary of the Air Force, Department of the Air Force, accompanied by Lieutenant General Robert W. Bazley, Inspector General and Brigadier General Donald J. Kutyna, Director of Space Systems and Command, Control and Communications, Deputy Chief of Staff, Research, Development and Acquisition
05 p0601 N85-13834
Statement of Honorable James M. Beggs, Administrator, National Aeronautics and Space Administration
05 p0601 N85-13835
Space Nuclear Safety Program
[DE84-016973] 05 p0728 N85-14879
Electric and hybrid vehicle demonstration project
[DE84-014622] 06 p0871 N85-15535
Safety requirements for wiring systems and connectors for photovoltaic systems
[NASA-CR-174431] 10 p1477 N85-19324
Design of explosive logic elements
[DE84-009611] 11 p1614 N85-20146
Six-inch HYGE vertical impact facility
[AD-A150665] 14 p2228 N85-23809
Ultrasonic non-destructive testing technique
14 p2316 N85-24313
Evaluation of adequacy pf JP54 protection level for large electric machines
15 p2528 N85-25588
Development and application of new radiofrequency radiation safety standards
16 p2777 N85-27137
Space station crew safety alternatives study, volume 1
[NASA-CR-3854] 19 p3223 N85-29965
Organic air pollutants during manufacturing and handling of PVC floor tiles
[FOA-E-40018] 20 p3487 N85-31669
Space Station crew safety alternatives study. Volume 2: Threat development
[NASA-CR-3855] 21 p3558 N85-32133
Safety and reliability of steel structural materials under random service impact loads
23 p3906 N85-34197
General-purpose heat source development: Safety test program. Postimpact evaluation, design iteration test
[LA-10034-SR] 23 p3969 N85-34606

SAFETY MANAGEMENT
Safety requirements for wiring systems and connectors for photovoltaic systems
[NASA-CR-174211] 06 p0803 N85-15110
The aviation safety reporting system
09 p1276 N85-18021
The development of fire evaluation system for detention and correctional occupancies
[NBSIR-84-2976] 10 p1459 N85-19192
Safety program considerations for space nuclear reactor systems
[DE85-003295] 10 p1556 N85-19606
Airport bird hazards associated with solid waste disposal facilities
[AD-P004197] 11 p1581 N85-19964
Successful control of gulls and other birds at a sanitary landfill
[AD-P004198] 11 p1582 N85-19965
Effectiveness of an overhead wire barrier system in reducing gull use at the BFI Jedburg sanitary landfill, Berkeley and Dorchester counties, South Carolina
[AD-P004200] 11 p1582 N85-19967
Control technology for integrated circuit fabrication at Honeywell Optoelectronics Division, Richardson, Texas
[PB85-109023] 11 p1616 N85-20162
Radiation safety of crew and passengers of air transportation in civil aviation. Provisional standards
[NASA-TM-77610] 11 p1692 N85-20638
Aerospace Safety Advisory Panel
[NASA-TM-87428] 12 p1774 N85-21135
Geosynchronous satellite collision avoidance
12 p1784 N85-21197
General-purpose heat source development: Safety test program. Postimpact evaluation, design iteration test 5
[LA-10232-SR] 12 p1931 N85-22129
Radiological safety aspects of industrial radiography
14 p2316 N85-24312
Dosimeasurements with thermoluminescence dosimeters at a Febetron 701, 600 kV in room 022 of the Interuniversity Reactor Institute (IRI)
[IRI-190-84-02] 18 p3111 N85-29262
Ambient air contamination: Characterization and detection techniques
18 p3157 N85-29546
Report of the 11th Regional IRPA Congress on Recent Developments and New Trends in Radiation Protection
[IRI-190-83-13] 18 p3160 N85-29575
Working safely with ionizing radiation sources at the Interuniversity Reactor Institute (IRI) (meant for the introduction of new collaborators)
[IRI-190-84-01] 18 p3160 N85-29576
Safety system with microcomputer
[OEFZS-4294] 18 p3166 N85-29618
Safety report, 1982
18 p3184 N85-29746
Space station crew safety alternatives study, volume 1
[NASA-CR-3854] 19 p3223 N85-29965

Description of a test site for large-scale heavy gas dispersion and combustion experiments
[DE85-004987] 23 p3911 N85-34231
SAGE SATELLITE
Utilization of SAGE aerosol profiles in the analysis of Mauna Loa stratospheric lidar data
[NASA-CR-174196] 05 p0675 N85-14332
Development of algorithms for using satellite meteorological data sets to study global transport of stratospheric aerosols and ozone
[NASA-CR-172540] 15 p2591 N85-25974
SAHARA DESERT (AFRICA)
Late Tertiary and Quaternary river systems of the eastern Sahara as mapped on shuttle radar and LANDSAT images 13 p2199 N85-23641
Sahara Desert dust transport to the south 21 p3648 N85-32666
SAILPLANES
U GLIDERS
SAILS
NT SOLAR SAILS
The Satellite sail 11 p1647 N85-20376
La Recherche Aerospatiale Bimonthly Bulletin, Number 1984-4, 221/July-August
[ESA-TT-884] 16 p2695 N85-26637
Clarke Stations and mercurian mass-drivers: Energy for large-scale transportation systems
[DE85-009607] 21 p3560 N85-32145
SAINT VENANT FLEXURE PROBLEM
U SAINT VENANT PRINCIPLE
SAINT VENANT PRINCIPLE
Quantification of Saint-Venant's principle for a general prismatic member 04 p0467 N85-12972
SALINITY
The gulf stream deflection and meander energetics experiment. Current meter and bottom pressure gauge data report for the September, 1981 to April, 1982 mooring period
[AD-A144977] 01 p0088 N85-10595
Site-specific research conducted in support of the Salton Sea Solar Pond Project, FY 1982 report
[NASA-CR-174182] 05 p0666 N85-14280
Solar pond overview 05 p0667 N85-14287
Solar pond fluid dynamics and heat transfer 05 p0667 N85-14288
Summary of salt gradient solar pond research 05 p0667 N85-14292
Hydrographic data collected in 1982 and 1983 for EPOCS (Equatorial Pacific Ocean Climate Studies)
[PB85-110799] 12 p1876 N85-21765
Geographic variation in the relationships of temperature, salinity or sigma sub t versus plant nutrient concentrations in the world ocean — silicic acid, nitrate, and phosphate concentration
[NASA-CR-175821] 13 p2140 N85-23287
Frontal nature of Cromwell Current 14 p2336 N85-24445
Representation of temperature and salinity fields using statistically orthogonal functions (in example of polymode data) 14 p2337 N85-24449
Nationwide Urban Runoff Project, Champaign, Illinois: The biological impact of urban runoff on the Saline Branch Drainage Ditch and Boneyard Creek
[PB85-150274] 14 p2348 N85-24515
An experimental study of brine upward migration in thin sea ice 15 p2582 N85-25923
Characteristics of snow cover on sea ice and formation of snow ice II 15 p2582 N85-25924
Characteristics of fast sea ice collected near Barrow, Alaska 15 p2582 N85-25925
North Atlantic Deep Water Formation
[NASA-CP-2367] 15 p2601 N85-26028
Review of North Atlantic source waters 15 p2601 N85-26029
Temporal and spatial scales of Labrador Sea water formation 15 p2601 N85-26031
Chemical signatures associated with the freshening of Northern Atlantic waters between 1972 and 1981 15 p2601 N85-26032
North Atlantic Deep Water and the world ocean 15 p2602 N85-26033
Ocean circulation and meteorology off the Georgia coast. Part 1: Real-time telemetry system for data collection
[PB85-155935] 15 p2605 N85-26052
The effects of sea water and concentrated salt solutions on the fatigue of nylon 6,6 fibers 17 p2979 N85-28416
Chemical, biological, and physical measurements from the subtropical western North Atlantic Ocean. Summer 1982, USNS Lynch, cruise 710-82
[AD-A153823] 18 p3201 N85-29857
Microbiology of solar salt ponds 21 p3658 N85-32724
The role of sulfur in osmoregulation and salinity tolerance in cyanobacteria, algae, and plants 21 p3660 N85-32736
Sulfur reduction in sediments of marine and evaporite environments 21 p3661 N85-32742
Microanalysis of dissolved iron and phosphate in pore waters of hypersaline sediment 21 p3661 N85-32744
Salinity driven oceanographic upwelling
[DE85-011664] 22 p3818 N85-33652
SALT BATHS
Development of low-melting fused salts 8: Formation of molybdenum film from molten ammonium formate bath
[BLL-OA-TRANS-3195-(6196.300)] 20 p3429 N85-31264
SALT BEDS
Landform evaluation through integrated remote sensing methods. A case study in parts of Haryana, India 05 p0657 N85-14221
Radioactive waste isolation in salt: Peer review of the Office of Nuclear Waste Isolation's report on the organic geochemistry of deep groundwaters from the Palo Duro Basin, Texas
[DE85-001439] 10 p1556 N85-19811
Radioactive waste isolation in salt: Peer review of the D'Appolonia report on schematic designs for penetration seals for a repository in the Permian Basin, Texas
[DE85-000693] 11 p1727 N85-20861
Comparison and evaluation of field and numerical results from the Site A heater test at Avery Island
[DE85-010625] 19 p3268 N85-30269
Microbiology of solar salt ponds 21 p3658 N85-32724
WIPP horizon in situ permeability measurements
[DE85-012667] 22 p3802 N85-33557
Preliminary SPR thermal model description and results for WH-11 and BM-4
[DE85-013171] 23 p3931 N85-34360
SALT FLATS
U FLATS (LANDFORMS)
SALT SPRAY TESTS
Influence of 3% NaCl solution on rate of accumulation of damage and residual strength of aluminum-boron composite 13 p2027 N85-22699
SALTON SEA (CA)
Site-specific research conducted in support of the Salton Sea Solar Pond Project, FY 1982 report
[NASA-CR-174182] 05 p0666 N85-14280
Laboratory investigations 05 p0666 N85-14281
Analytical models 05 p0666 N85-14282
Material selection consideration for solar ponds 05 p0666 N85-14284
Salton Sea solar pond power plant design study and regional applicability 05 p0667 N85-14290
SALTS
Airfoil deposition model 02 p0144 N85-10979
New data on presence of ores in salt dome structures of Dnieper-Donets Basin 07 p0981 N85-16234
Measurements of giant salt nuclei from inland in east China 21 p3648 N85-32668
The distribution of giant salt nuclei inside and outside cloud over the basin of Xin and Jiang 21 p3650 N85-32681
Experimental characterization and stability of salt- and nonsalt-containing grouts and mortars (BCT-1F- and BCT-1FF-related)
[DE85-012339] 22 p3753 N85-33263
SALYUT SPACE STATION
Vitamin metabolism in cosmonauts following short-term flights 01 p0091 N85-10615
USSR report: Space
[JPRS-USP-84-005] 02 p0156 N85-11060
Features of new solar panels on Salyut-7 02 p0157 N85-11062
Tass reports launch of Progress-22 02 p0157 N85-11063
Progress-22 docks with Salyut-7 02 p0157 N85-11064
Cosmonauts complete 4th month aboard Salyut-7 02 p0157 N85-11065
Geophysical experiments, photography aboard Salyut-7 02 p0157 N85-11066
Orbit of Salyut-7 station boosted 02 p0157 N85-11067
Salyut-7 crew in orbit 150 days 02 p0157 N85-11068
Commentary on cosmonauts geological mapping, photography 02 p0158 N85-11069
Tass reports launch of Soyuz T-12 02 p0158 N85-11070
Tass reports medical, materials studies aboard Salyut-7 02 p0158 N85-11071
Commentary on Salyut-7 electrophoresis, plugging mortar experiments 02 p0158 N85-11072
Tass reports experiments during visiting crew's third day 02 p0158 N85-11073
Commentary on derivation of biological materials, cosmonaut adaptation 02 p0158 N85-11074
Tass reports astrophysical, atmospheric studies on Salyut-7 02 p0158 N85-11075
EVA of cosmonauts Savitskaya and Dzhanibekov 02 p0158 N85-11076
Commentary on hand tool used in cosmonaut EVA 02 p0159 N85-11077
Further details in welding, spray-coating tool 02 p0159 N85-11078
Lyakhov and Aleksandrov on 150-day flight 13 p1977 N85-22405
Comments on Salyut-7 150-day flight 13 p1977 N85-22406
Remote sensing used for study of forest resources 13 p1983 N85-22440
USSR report: Space
[JPRS-USP-85-004] 16 p2717 N85-26772
Tass reports program for Salyut-7 fully completed 16 p2717 N85-26773
Cosmonaut Savitskaya says many women in cosmonaut training 16 p2717 N85-26774
Cosmonauts' postural reactions after long-term missions aboard Salyut-6 orbital station 19 p3323 N85-30585
Cosmonauts' cardiovascular system function during long-term orbital flights aboard Salyut-6 station 22 p3733 N85-33141
Vatra television complex for Salyut orbital space station 22 p3783 N85-33321
SAMARIUM
The growth of metastable peritectic compounds
[NASA-CR-171289] 07 p0920 N85-15824
SAMARIUM COMPOUNDS
Magnitude and range of the RKKy interaction in SmRh4B4
[DE85-012284] 23 p3985 N85-34712
SAMPLED DATA
U DATA SAMPLING
SAMPLED DATA SYSTEMS
U DATA SAMPLING
SAMPLERS
Precision digital sampler
[AD-D011285] 06 p0809 N85-15143
Sampling device
[AD-D011256] 06 p0814 N85-15166
New stage in robotics development 16 p2762 N85-27045
Acid rain: Towards automated monitoring 16 p2829 N85-27444
Microstore: The Stanford analog memory unit
[DE85-005534] 18 p3095 N85-29160
Liquid sampling system
[DE85-011673] 19 p3265 N85-30248
Soil extraction kit
[AD-D011736] 22 p3742 N85-33190
SAMPLES
Study of proton and neutron activation of metal samples in low Earth orbit
[NASA-CR-171183] 01 p0026 N85-10164
Statistical analysis techniques for small sample sizes
[NASA-CR-171672] 15 p2639 N85-26279
A gel-halo sample pellet: The best of both worlds? Stubby zones without a constricted sample gate 20 p3502 N85-31770
Efficiency tests of samplers for microbiological aerosols, a review
[FOA-C-40199-B1] 20 p3504 N85-31783
Optimization of sampling in statistical physics experiments 21 p3698 N85-32975
SAMPLING
NT AIR SAMPLING
NT CORE SAMPLING
NT DATA SAMPLING
NT PARTICULATE SAMPLING
NT RANDOM SAMPLING
Designing optimal AOQL sampling plans a computerized approach
[AD-A146288] 03 p0413 N85-12639
The growth and composition of supercritical branching populations on general type spaces
[CTH-MATH-1984-18] 05 p0721 N85-14831
The influence of sample collection and methods of analysis on chemical concentrations measured in rainwater
[KNMI-TR-55] 07 p0924 N85-15853
A complete characterization of triply balanced matrices with applications to survey sampling
[AD-A147083] 07 p1031 N85-16542
Bayesian estimation of undetected errors
[AD-A147198] 07 p1031 N85-16545
Developing double sampling plans for attributes to meet sample size criteria
[AD-A148144] 08 p1205 N85-17587

A numerical analysis of sampling plans based on prior distribution and costs
[AD-A147718] 08 p1210 N85-17616
The performance of variable sampling plans when the normal distribution is truncated
[AD-A147717] 08 p1215 N85-17649
Antisampling for estimation: An overview
[AD-A148545] 08 p1216 N85-17659
Applying an innovative approach to field investigations at a remedial action site
[AD-P004145] 09 p1348 N85-18481
Location of volatile buried wastes by field portable instrumentation
[AD-P004147] 09 p1348 N85-18483
Sampling errors. They may deprive the analytical results of any meaning
[BLL-MINTEK-TR-1109-(5810.5759)] 09 p1373 N85-18625
Simple approximate variances for b-letter values. A sampling enquiry: Supplement
[DE85-001410] 09 p1376 N85-18647
An optically coupled sampling system with 4 GHz bandwith
[AD-A148057] 09 p1384 N85-18702
Ground-based snow and ice crystal observation system used in Sierra Nevada winter orographic storms
[PB85-115343] 10 p1520 N85-19584
W.E. Johnson's Sufficientness postulate
[AD-A149014] 10 p1550 N85-19774
Estimation of variance of the regression estimator
[AD-A149407] 10 p1551 N85-19760
Asymptotic distributions of the sample mean, autocovariances and autocorrelations of long-memory time series
[AD-A149409] 10 p1551 N85-19781
A computer system for generating single and double sampling plans for attributes data
[AD-A149548] 11 p1701 N85-20698
Inference for censored matched pairs using signed ranks
[MATHEMATICS-RESEARCH-162] 12 p1923 N85-22078
Simplifications and approximations for linear rank statistics with censored data
[MATHEMATICS-RESEARCH-161] 12 p1923 N85-22079
The use of a high-speed 12-bit A/D converter for digital sampling of communication signal carriers
[AD-A150578] 13 p2056 N85-22872
A Monte Carlo sampling plan for estimating network reliability
[AD-A150511] 13 p2085 N85-22696
Use of importance sampling to investigate signal detection systems by simulated method 13 p2086 N85-23028
Tutorial discussion of electronic sampling systems for recording wide-bandwidth transient signals
[DE85-006577] 15 p2549 N85-25735
Multivariable statistical modelling and its application 16 p2857 N85-27617
Statistical effects of imperfect inspection sampling. Part 2: Double sampling, link sampling and grading
[AD-A152377] 17 p3024 N85-28700
Estimating random integrals from noisy observations: Sampling designs and their performance
[AD-A152926] 17 p3025 N85-28702
Moisture content and gas sampling device
[NASA-CASE-MSC-18666-1] 18 p3103 N85-29213
Effect of some estimators on a large sample approximation to the non-null distribution of the pearson chi-square statistic
[AD-A153515] 18 p3173 N85-29673
Liquid sampling system
[DE85-011673] 19 p3285 N85-30248
A comparison of four Monte Carlo methods for estimating the probability OF S=T connectedness
[AD-A154264] 19 p3348 N85-30749
A critique of Deming's discussion of acceptance sampling procedures
[AD-A154305] 19 p3348 N85-30751
Low-discrepancy point sets in transport codes
[DE85-010786] 19 p3348 N85-30755
Intermittency, conditional sampling and turbulent combustion 20 p3424 N85-31249
Organic air pollutants during manufacturing and handling of PVC floor tiles
[FOA-E-40016] 20 p3487 N85-31689
Optimization of sampling in statistical physics experiments 21 p3696 N85-32975
The 1984 environmental monitoring program report for Idaho National Engineering Laboratory site
[DE85-011209] 22 p3812 N85-33611
Marine Sample Exploitation Project: Estimates regarding the sensitivity and technology for the detection of nuclear explosion debris in the marine environment
[DE85-013176] 23 p3947 N85-34462
Ultrasonic inspection of carbon fiber reinforced plastic by means of sample-recognition methods
[NASA-TM-77896] 24 p4074 N85-35245

SAMPLING DEVICES
U SAMPLERS

SAN ANDREAS FAULT
Geodynamics Branch research program
[NASA-TM-86223] 20 p3489 N85-31688
First epoch measurements by Mark III VLBI of the San Andreas Fault experiment baseline 20 p3490 N85-31691
Geophysical interpretation of satellite laser ranging measurements 20 p3490 N85-31692
Carbon fiber strainmeter studies in southern California
[PB85-196889] 24 p4118 N85-35526

SAN ANDREAS FAULT EXPERIMENT
Geodynamics Branch research program
[NASA-TM-86223] 20 p3489 N85-31688
First epoch measurements by Mark III VLBI of the San Andreas Fault experiment baseline 20 p3490 N85-31691
Geophysical interpretation of satellite laser ranging measurements 20 p3490 N85-31692

SAN FRANCISCO (CA)
Characterizing the scientific potential of satellite sensors — San Francisco, California
[E85-10044] 07 p0983 N85-16244
Characterizing the scientific potential of satellite sensors — San Francisco, California
[E85-10053] 07 p0984 N85-16249
Impact of LANDSAT MSS sensor differences on change detection analysis — New Mexico, San Francisco, CA, New Hampshire, and Connecticut 11 p1667 N85-20506

SAN FRANCISCO BAY (CA)
Field studies of run-up generated by wind waves on dissipative beaches
[AD-A148793] 09 p1359 N85-18548
Pollutant body burdens and reproduction in Platichthys stellatus from San Francisco Bay
[DE85-010407] 19 p3308 N85-30509

SAND DUNES
U DUNES

SANDS
NT TAR SANDS
Submarine sand ridges: Geology and development, New Jersey, USA 02 p0227 N85-11482
Application of SIR-B data for groundwater exploration in the Arabian shield and sand-drift monitoring in the AN Nafud and Al Jafurah fringe areas, Kingdom of Saudi Arabia 08 p1144 N85-17214
A wind-tunnel study of the saltation of heterogeneous (size, density) sands 08 p1182 N85-17449
Influence of grain size distribution on the undrained dynamic properties of saturated sand
[PB85-102362/GAR] 09 p1305 N85-18197
The rolling resistance and sinkage of towed dual wheel combination in sand
[AD-P004261] 09 p1404 N85-18837
Performance prediction of pneumatic tyres on sand
[AD-P004262] 09 p1404 N85-18838
Prediction of in-sand tire and wheeled vehicle drawbar performance
[AD-P004265] 09 p1404 N85-18841
Compaction of sand using ordinary off-road vehicles
[AD-P004297] 09 p1409 N85-18874
Transformation of polar ice sublimate residue into Martian circumpolar sand 13 p2189 N85-23580
A comparison of terrestrial saltation flux in the laboratory and the field 13 p2189 N85-23582
Potential bedforms on Venus: Wind tunnel simulations 13 p2189 N85-23583
Experimentally determined distribution of stress around a horizontally loaded model pile in dense sand
[CE-43] 16 p2796 N85-27239
Western gas sands
[DE85-001985] 18 p3126 N85-29360
Sand dispersion from an ephemeral river delta on the wave-dominated central California coast
[AD-A154352] 19 p3300 N85-30458
Propagation of sound in a layered laboratory model
[AD-A155141] 21 p3700 N85-32969
Steamflood pilots in the O'Connell Ranch field and the T-4 Ranch field
[DE85-001363] 24 p4108 N85-35468
Simplified procedures for the evaluation of settlements in sands due to earthquake shaking
[PB85-197887] 24 p4118 N85-35527

SANDSTONES
Paleoenvironmental interpretation of the upper cretaceous Point Lookout sandstone: Implications for shoreline progradation and basin tectonic history, San Juan basin, New Mexico 02 p0227 N85-11486
Sedimentary petrology and provenance of the upper Jackforth Sandstone (Morrowan) Quachita Mountains, Arkansas, USA 08 p1182 N85-17447
Lithologic and environmental atlas of Berea Sandstone (Mississippian) in the Appalachian Basin
[PB85-129039] 11 p1682 N85-20600
Subsurface petroleum geology of Santa Rosa sandstone (Triassic), northeast New Mexico
[TI85-901364] 19 p3313 N85-30538
Crosswell acoustic surveying in gas sands: Travel-time pattern recognition, seismic Q and channel waves
[DE85-010777] 19 p3352 N85-30778
Measurement and analysis of two-phase flow through low permeability media, task 3
[PB85-188373] 20 p3435 N85-31313
Steamflood pilots in the O'Connell Ranch field and the T-4 Ranch field
[DE85-901363] 24 p4108 N85-35468

SANDWICH CONSTRUCTION
U SANDWICH STRUCTURES

SANDWICH STRUCTURES
Development of new and improved polymer matrix resin systems, phase 1
[NASA-CR-166595] 01 p0017 N85-10104
Nonlinear dynamic analysis of sandwich panels 01 p0060 N85-10394
Simulation of vibration processes in damped structures with allowance for temperature-frequency characteristics of vibration absorbing materials 02 p0257 N85-11660
Numerical simulations of compliant material response to turbulent flow, revision 1
[AD-A145801] 03 p0372 N85-12373
Composite repair of aircraft structures 08 p1120 N85-17059
Mechanical locking between multi-layer printed wiring board conductors and through-hole plating
[AD-D011477] 10 p1481 N85-19352
OTEC (Ocean Thermal Energy Conversion) Cold Water Pipe At-Sea Test Program. Phase 2: Suspended pipe test
[PB85-119931] 10 p1512 N85-19542
Aircraft safety improvement 15 p2688 N85-26502
Stability of anisotropic cylindrical sandwich shells 16 p2766 N85-27065
Method of solving problems of statics for multilayer shells of revolution 17 p2943 N85-28167

SANITATION
Design concept definition study for an improved shuttle waste collection subsystem
[NASA-CR-171634] 08 p1196 N85-17548
Hydrodynamics and sanitation
[CT-579] 20 p3487 N85-31672

SAPPHIRE
Factors affecting SOS (Silicon-On-Sapphire) yield and reliability
[AD-A150004] 12 p1835 N85-21515
The Valence- and conduction-band structure of the sapphire (1102) surface
[AD-A150001] 12 p1940 N85-22184
Incident beam polarization for laser Doppler velocimetry employing a sapphire cylindrical window
[NASA-TM-87064] 17 p3037 N85-28786
Producing titanium-sapphire items by solid-phase bonding through aluminum gasket 19 p3246 N85-30127
Size and shape dependence of CO adsorption sites on sapphire supported Fe microcrystals
[NASA-CR-176171] 24 p4160 N85-35794

SARCOMA
U CANCER

SARSAT
Terrestrial locating — of buoys from space 05 p0599 N85-13816
The Search And Rescue Satellite Aided Tracking (SARSAT) experiment. Presentation of CNES processing for the SARGOS project: Context and orbit processing 05 p0600 N85-13830
Experimental satellite system for determining coordinates of maritime distress 09 p1306 N85-18216
The SARSAT program 14 p2327 N85-24385
The SARSAT/COSPAS system for assisting satellite based search and rescue 14 p2396 N85-24776
COSPAS-SARSAT satellite orbit predictor, volume 5
[NASA-TM-85015-VOL-5] 14 p2439 N85-25052
International conference on COSPAS-SARSAT system 15 p2484 N85-25336
Satellite aided search and rescue. Experimental results and operational prospects — conference
[ISBN-2-85428-120-9] 20 p3400 N85-31068
COSPAS/SARSAT: An overview 20 p3400 N85-31092
Possible use of the COSPAS/SARSAT system within the Swedish mountain rescue organization 20 p3401 N85-31100
The COSPAS-SARSAT system 20 p3401 N85-31101

The COSPAS-SARSAT space segment: Present status and evolution 20 p3401 N85-31102
Canadian Astronautics Limited's SARSAT ground stations 20 p3401 N85-31104
The 406 MHz ELT/EPIRBs — Emergency Locator Transmitters/Emergency Position Indicating Radio Beacons (ELT/EPIRB) 20 p3402 N85-31106
Soviet Emergency Locator Transmitter/Emergency Position Indicating Radio Beacon (ELT/EPIRBs) at 121.5 and 406 MHz 20 p3402 N85-31107
Ground segment of COSPAS system 20 p3402 N85-31108
The COSPAS/SARSAT local user terminal in Tromso, Norway. Special considerations and experience with high latitude location (69 deg, 43 min N) 20 p3402 N85-31109
A 406 MHz geostationary satellite SARSAT experiment 20 p3403 N85-31113
Evolution of 406 MHz Search and Rescue (SAR) processor 20 p3403 N85-31116
A micro/PDP-11 system for 406 MHz COSPAS/SARSAT processing 20 p3403 N85-31117
Search and rescue satellite (SARSAT) error analysis of the 406 MHz system 20 p3403 N85-31118
A special antenna for SARSAT EPIRBs providing circular polarization and hemispheric coverage for reliable transmission to satellites — Emergency Position Indicating Radio Beacon (EPIRB) 20 p3404 N85-31122
Fault tolerant multiprocessor SARSAT-COSPAS 406 MHz local user terminal 20 p3404 N85-31123
SARSAT 406 MHz system technical evaluation 20 p3404 N85-31124
SARSAT 121.5/243 MHz technical evaluation 20 p3405 N85-31126
Use of 121.5/243.0 MHz COSPAS-SARSAT data by North American SAR agencies — search and rescue (SAR) 20 p3405 N85-31127
The COSPAS/SARSAT demonstration and evaluation. Results of the first year in the United States 20 p3405 N85-31128
COSPAS-SARSAT demonstration and evaluation results in Canada 20 p3405 N85-31129
COSPAS-SARSAT demonstration and evaluation phase: COSPAS tests in the USSR and their results 20 p3405 N85-31130
The SARSAT-COSPAS demonstration in France 20 p3405 N85-31131
UK experience with COSPAS-SARSAT and INMARSAT distress systems 20 p3406 N85-31132
The COSPAS-SARSAT system evaluation in Norway 20 p3406 N85-31133
JANUS: An autonomous platform optimized for SARSAT type missions 20 p3406 N85-31135
United States-Soviet satellite accord: SARSAT/Cospas search-and-rescue program
[GPO-41-113] 20 p3541 N85-32040
LOCAT: A data retrieval program
[AD-A156004] 24 p4165 N85-35822

SAS-D
U IUE

SATAN (SENSOR)
U TERRAIN ANALYSIS

SATELLITE ANTENNAS
Workshop on Mechanical Technology for Antennas — conferences; satellite antennas
[ESA-SP-225] 05 p0625 N85-13999
Antenna mechanical technologies within ESA 05 p0625 N85-14000
High performance deployable antenna structures 05 p0625 N85-14001
Offset unfurlable antenna concepts 05 p0625 N85-14002
Distortional measurement of antennas under space simulation conditions by means of holography 05 p0625 N85-14005
Electrical consequences of mechanical antenna characteristics 05 p0625 N85-14006
Structural aspects of SAR antenna for Japanese Earth Resources Satellite 1 05 p0626 N85-14007
Technology for the ERS-1 SAR antenna 05 p0626 N85-14008
Mechanical/thermal design of a polarization sensitive reflector — communication satellites 05 p0626 N85-14009
CASA technological effort in the field of antennas — satellite radar antennas 05 p0626 N85-14010
BAe antenna hardware technology for current satellite projects 05 p0626 N85-14011
Technology and performances of structural thermal mechanical equipment used for antenna of TV.SAT-TDF 1 program 05 p0626 N85-14012
The dimensional stability of advanced composite antenna reflectors: Analytical and test evaluation — satellite antennas 05 p0626 N85-14014
CASA activities in antenna technology — satellite antennas 05 p0627 N85-14015
Structural design and thermal stability of TELE-X antenna tower 05 p0627 N85-14016
Analytical thermal formulations for antenna dishes — satellite antennas 05 p0627 N85-14017
In-orbit performance of INTELSAT V communications antennae deployment systems 05 p0627 N85-14018
Study of structure control dynamic interaction for radio frequency antenna control systems — satellite antennas 05 p0627 N85-14020
Hemispherical antenna pointing mechanism — satellite antennas 05 p0627 N85-14021
ARABSAT spacecraft: Rx and Tx antenna mechanisms 05 p0628 N85-14022
Configuration study for a 30 GHz monolithic receive array, volume 2
[NASA-CR-174697-VOL-2] 09 p1311 N85-16240
Operational fitness of box truss antennas in response to dynamic slewing
[NASA-CR-172470] 10 p1429 N85-19012
Polarization angles of linearly polarized antennas and radio waves in satellite communications
[PB85-131613] 11 p1626 N85-20240
The Ferranti Tactical SHF SATCOM station (MANSAT) 11 p1710 N85-20759
Large Space Antenna Systems Technology, 1984
[NASA-CP-2368-PT-1] 14 p2229 N85-23813
NASA mobile satellite program 14 p2229 N85-23814
Alternatives for satellite sound broadcast systems at HF and VHF 14 p2229 N85-23815
Development concerns for satellite-based air traffic control surveillance systems 14 p2230 N85-23816
Application of pushbroom altimetry from space using large space antennas 14 p2230 N85-23817
Orbiting multi-beam microwave radiometer for soil moisture remote sensing 14 p2230 N85-23818
Space-based antenna measurement system concepts for space station operation 14 p2236 N85-23860
Satellite reception of reentry vehicle telemetry
[AD-A151851] 15 p2492 N85-25372
Thin Route Project 15 p2587 N85-26598
Communications 15 p2587 N85-26600
Earth station antenna sidelobe characteristics
[PB85-164966] 16 p2780 N85-27159
Ionospheric effects on antenna impedance
[BMFT-FB-W-84-052] 17 p2950 N85-28217
Nonlinear plasma reactions on the antenna impedance of high transmission power satellites
[BMFT-FB-W-84-053] 18 p3192 N85-29799
High reflective surfaces for millimeter RF waves, phase A — satellite antenna reflectors
[HRS-FR-01] 20 p3442 N85-31366

SATELLITE ATMOSPHERES
NT LUNAR ATMOSPHERE
Composition, structure and evolution of Uranian and Neptunian satellites 02 p0300 N85-11944
Satellite masses in the Uranus and Neptune systems
[PSI-CONTRIB-198] 02 p0301 N85-11947
Seasonal variations in Triton's atmospheric mass and composition 02 p0301 N85-11948
Do the satellites of Uranus control its magnetosphere? 02 p0301 N85-11952
Outer satellite atmospheres: Their nature and planetary interactions
[NASA-CR-174146] 04 p0589 N85-13759
Extended atmospheres of outer planet satellites and comets
[NASA-CR-174398] 09 p1416 N85-18933
A modeling analysis program for the JPL Table Mountain Io sodium cloud data
[NASA-CR-175493] 11 p1681 N85-20589
Radio scintillations observed during atmospheric occultations of Voyager: Internal gravity waves at Titan and magnetic field orientations at Jupiter and Saturn
[NASA-CR-175554] 12 p1981 N85-22327
Extended atmospheres of outer planet satellites and comets
[NASA-CR-175673] 14 p2440 N85-25058
A modeling analysis program for the JPL table mountain Io sodium cloud
[NASA-CR-176851] 16 p2833 N85-27468
Volatiles in the outer solar system. 1: Thermodynamics of clathrate hydrates. 2: Ethane ocean on Titan. 3: Evolution of primordial Titan atmosphere 19 p3382 N85-30984
Quasi non-intrusive sampling and analysis of gases associated with the boundary layer on the tethered satellite and similar supersonic and hypersonic research vehicles
[NASA-CR-176075] 20 p3407 N85-31140
Extended atmospheres of outer planet satellites and comets
[NASA-CR-176137] 22 p3851 N85-33848

SATELLITE ATTITUDE CONTROL
In-orbit experiments on IRAS for application to the ISO satellite
[FOK-TR-R-84-057] 03 p0322 N85-12078
Overview of Autonomous Payload Control Experiment 04 p0459 N85-12911
Satellite attitude determination 05 p0599 N85-13814
Stationkeeping strategies for geostationary satellites 05 p0600 N85-13825
Magnetically suspended flywheel system study 05 p0607 N85-13873
Reaction wheels for kinetic energy storage 05 p0607 N85-13874
Study of structure control dynamic interaction for radio frequency antenna control systems — satellite antennas 05 p0627 N85-14020
Qualification of a hydrazine gas generator system with electrothermal/catalytic gas generator
[BMFT-FB-W-84-040] 06 p1110 N85-17018
Satellite description 09 p1412 N85-18900
Application Number 3: Using tethers for attitude control 11 p1646 N85-20373
Application of model following control and estimation techniques to attitude control of maneuvering spacecraft. Part 2: Simulation software description
[NLR-TR-82116-U-PT-2] 12 p1793 N85-21254
Minimizing plume contamination production in bipropellant thrusters 13 p2003 N85-22557
Modeling needed for the design and definition of spacecraft attitude and orbit control systems 14 p2397 N85-24766
Spaceborne automatic data processing 14 p2397 N85-24769
Details on spot remote sensing satellite propulsion unit 15 p2535 N85-25640
Optimum parameters of aerogyrocopic satellite orientation system 16 p2718 N85-26762
Maximizing the semi-major axis for a freely coning solar sailcraft
[AD-A153175] 17 p2909 N85-27938
Application of model following control and estimation techniques to attitude control of maneuvering spacecraft. Part 1: Theory and simulation results
[NLR-TR-82116-U-PT-1] 18 p3065 N85-28957
The attitude control model tests for the Infrared Astronomical Satellite (IRAS)
[E8580071] 18 p3067 N85-28967
Research on an expert system for database operation of simulation-emulation math models. Volume 1, Phase 1: Results
[NASA-CR-176087] 21 p3669 N85-32792
Research on an expert system for database operation of simulation-emulation math models. Volume 2, Phase 1: Results
[NASA-CR-176088] 21 p3669 N85-32793

SATELLITE ATTITUDE DISTURBANCE
U ATTITUDE STABILITY
U SPACECRAFT STABILITY

SATELLITE CAPTURE
U SPACECRAFT RECOVERY

SATELLITE COMMUNICATION
U SPACECRAFT COMMUNICATION

SATELLITE CONFIGURATIONS
Shuttle tethered satellite system program overview 11 p1642 N85-20342
TSS Satellite overview 11 p1642 N85-20343
Satellite module design 11 p1642 N85-20344
Multimission advanced configurations study — telecommunication satellites
[MATRA-DM.51/CC/FL/0151.83] 12 p1790 N85-21237
A study of spacecraft technology and design concepts, volume 1
[NASA-CR-172579-VOL-1] 16 p2730 N85-26844
A study of spacecraft technology and design concepts. Volume 2: Appendices
[NASA-CR-172579-VOL-2] 16 p2730 N85-26845
Spacecraft configuration study for second generation mobile satellite system
[NASA-CR-175774] 16 p2730 N85-26849
Study of a medium term flexible fixed satellite service mission
[DM51/CC-IM-0185.83] 18 p3091 N85-29136

SATELLITE CONTROL
NT SATELLITE ATTITUDE CONTROL
The application of microprocessors in the command and control of satellites by the MECB stations
[INPE-3282-RPE/466] 02 p0239 N85-11553
Telemetry (TM)/telecommand (TC) processor study
[ESA-CR(P)-1915] 03 p0323 N85-12081
Inertial storage for satellites 05 p0605 N85-13859
Air Force space technology center space technology: Emphasis 84 09 p1333 N85-18381
Effects of the solar-terrestrial environment on satellite operations
[DE85-002413] 11 p1580 N85-20003
Definition of ground test for Large Space Structure (LSS) control verification
[NASA-TM-86495] 12 p1792 N85-21249

Space Mathematics for the Preparation and Development of satellite Exploitation
[ISBN-2-85428-115-2] 14 p2395 N85-24753
Introduction to methods of evaluating the operational reliability of complex systems: Application to satellite control ground support 14 p2397 N85-24771
Orbital positioning and stationkeeping of geostationary satellites 14 p2397 N85-24772
The steering of GPS time 17 p2984 N85-28301
Timing of spacecraft data: Time accuracy requirements and timing facilities of the European Space Agency (ESA) 17 p2984 N85-28307
A study of the ESA-NAVSAT control segment
[ESA-CR(P)-2000] 20 p3398 N85-31079
Advanced (unfloated) gyros for satellite control
[ESA-CR(P)-2010] 20 p3419 N85-31222

SATELLITE DEFENSE
U SPACECRAFT DEFENSE

SATELLITE DESIGN
The ESA remote sensing satellite system (ERS-1) 03 p0379 N85-12420
Conceptual ideas for a second generation METEOSAT system 05 p0858 N85-14228
QUASAT: Technical aspects of the proposed mission — VLBI satellite 07 p1067 N85-16706
UK Skynet 4 communications satellites 11 p1710 N85-20757
Drag-free satellite simulator
[REPT-615] 12 p1789 N85-21229
Multimission advanced configurations study — telecommunication satellites
[MATRA-DM.51/CC/FL/0151.83] 12 p1790 N85-21237
Satellite structure
[CH-642922-A5] 15 p2462 N85-25373
Shuttle-tethered satellite system definition study. Volume 1: Executive study
[NASA-CR-171474] 17 p2907 N85-27924
IRAS: Space technology from the Netherlands
[B8561841] 17 p2908 N85-27929
JANUS: An autonomous platform optimized for SARSAT type missions 20 p3406 N85-31135
Evolution of spacecraft design methods as a function of environmental and geometrical constraints
[ESA-CR(P)-2012] 20 p3418 N85-31216
Second-generation mobile satellite system. A conceptual design and trade-off study
[NASA-CR-176195] 24 p4066 N85-35325

SATELLITE DOPPLER POSITIONING
Diagnosis and therapy of geodetic satellite networks of Doppler type — error analysis
[SER-C-293] 01 p0015 N85-10090
Data Collection and Platform Location by Satellite: ARGOS Users' Conference 14 p2237 N85-23869
The ARGOS system status report after 2 years operation 14 p2237 N85-23870
Data Collection and Platform Location by Satellite: ARGOS Users' Conference 14 p2239 N85-23883
The ARGOS system status report 14 p2239 N85-23884
Some experience from ARGOS stations in the open sea 14 p2240 N85-23891
Proceedings of the ARGOS Users Conference on Data Collection and Location by Satellite 14 p2322 N85-24348
Improvements brought about to the system since 1978 and statements on future development 14 p2323 N85-24349
New directions in ARGOS instrumentation at Polar Research Lab (PRL) 14 p2323 N85-24350
The Edmonton data collection platform processing and locating facility 14 p2323 N85-24352
The development of Platform Transmitter Terminal (PTT) and its application for drifting buoys 14 p2323 N85-24353
US programs using the ARGOS data collection and platform location system 14 p2323 N85-24355
Data Collection and Platform Location by Satellite: ARGOS Users' Conference 14 p2325 N85-24366
The ARGOS system main characteristics — satellite based localization 14 p2325 N85-24367
The ARGOS system after 3 years operation 14 p2325 N85-24368
Location and data collection for long stratospheric balloon flights 14 p2326 N85-24377
The ARGOS contribution to the successful dredging of a deep moored current meter 14 p2327 N85-24381
The ARGOS system aboard research vehicles: 1981 experiment aboard the Le Suroit oceanographic vessel and the outlook
[CNEXO/DFT/OPNAV/82-05] 14 p2327 N85-24382
The SARSAT program 14 p2327 N85-24385
Data Collection and Platform Location by Satellite: ARGOS users' Conference 14 p2328 N85-24391
US programs using the ARGOS data collection and platform location system 14 p2329 N85-24401
Data Collection and Platform Location by Satellite: ARGOS Users' Conference 14 p2330 N85-24409
US program using the ARGOS data collection and platform location system 14 p2330 N85-24410
Moored buoy stationkeeping and location system 14 p2331 N85-24416
The ARGOS program — satellite based localization 14 p2397 N85-24775
The SARSAT/COSPAS system for assisting satellite based search and rescue 14 p2398 N85-24776
The TRANSIT and Global Positioning System (GPS) systems. Precision navigation and localization 14 p2398 N85-24777
DORIS: Prediction in Doppler measurement — satellite onboard measurement
[CNES-CT/DTI/MS/AE/170] 16 p2729 N85-26843
Data Collection and Platform Location by Satellite: ARGOS Users' Conference 16 p2811 N85-27333
Studies into location accuracy — ARGOS system 16 p2811 N85-27334
Positioning accuracy of the ARGOS system in operational use 16 p2811 N85-27335
Checking on the position of navigation marker buoys by the ARGOS system 16 p2813 N85-27354
Location and data collection satellite system ARGOS. User's guide — satellite based localization 16 p2816 N85-27371
Influence of coherent mesoscale structures on satellite-based Doppler lidar wind measurements
[NASA-CR-175853] 16 p2833 N85-27467
COSPAS/SARSAT: An overview 20 p3400 N85-31092
The contribution of an operational SAR satellite system to the UK SAR organisation — search and rescue (SAR) 20 p3400 N85-31095
Specific aspects of maritime search and rescue in French metropolitan and overseas territories: Expected benefits from a detection and location of distress system by satellites 20 p3401 N85-31097
The COSPAS-SARSAT system 20 p3401 N85-31101
The COSPAS-SARSAT space segment: Present status and evolution 20 p3401 N85-31102
Canadian Astronautics Limited's SARSAT ground stations 20 p3401 N85-31104
A 406 MHz ELT processor for geostationary satellites — Emergency Locator Transmitter (ELT) 20 p3403 N85-31114
Fault tolerant multiprocessor SARSAT-COSPAS 406 MHz local user terminal 20 p3404 N85-31123
SARSAT 406 MHz system technical evaluation 20 p3404 N85-31124
The COSPAS system tests. Technical results 20 p3404 N85-31125
SARSAT 121.5/243 MHz technical evaluation 20 p3405 N85-31126
The COSPAS/SARSAT demonstration and evaluation. Results of the first year in the United States 20 p3405 N85-31128
COSPAS-SARSAT demonstration and evaluation results in Canada 20 p3405 N85-31129
The SARSAT-COSPAS demonstration in France 20 p3405 N85-31131
UK experience with COSPAS-SARSAT and INMARSAT distress systems 20 p3406 N85-31132
Interplanetary plasma turbulence and the Doppler detection of a gravitational background radiation
[IFSI-85-1] 20 p3546 N85-32066

SATELLITE DRAG
Drag-free satellite simulator
[REPT-615] 12 p1789 N85-21229
Optical best arc RMS test results 16 p2804 N85-27290
Consummative expressions for satellite drag perturbations in a spherically symmetrical atmosphere
[AD-A154230] 19 p3222 N85-29981

SATELLITE GROUND SUPPORT
The current formal status of the ERS-1 ground segment 03 p0380 N85-12423
ERS-1 altimeter ground segment relations to other sensors and programs 03 p0381 N85-12436
The 2 GHz network and the network operations center — satellite tracking 05 p0599 N85-13617
The facilities of the Calculation Center and Real Time Room for satellite positioning 05 p0599 N85-13619
The satellite maneuvers determination department 05 p0599 N85-13620
The operational orbit tracking center 05 p0599 N85-13621
Development of the TT and C station equipment at INPE
[INPE-3327-PRE/625] 10 p1427 N85-18999
Introduction to methods of evaluating the operational reliability of complex systems: Application to satellite control ground support 14 p2397 N85-24771
A study of the ESA-NAVSAT control segment
[ESA-CR(P)-2000] 20 p3398 N85-31079

SATELLITE GROUND TRACKS
Altimetry, orbits and tides
[E85-10066] 08 p1174 N85-17404
Scientific requirements for ozone measurements 13 p2105 N85-23113
Comparison of gravity field solution techniques 16 p2805 N85-27295

SATELLITE GUIDANCE
The facilities of the Calculation Center and Real Time Room for satellite positioning 05 p0599 N85-13619
Satellite positioning — in geosynchronous orbit 05 p0600 N85-13623

SATELLITE IMAGERY
ISCCP Cloud Algorithm Intercomparison Workshop 01 p0073 N85-10485
A system for meteorological satellite, radar, conventional data and model analysis 01 p0082 N85-10551
The future of satellite remote sensing: A worldwide assessment and prediction 02 p0151 N85-11025
LANDSAT data and interactive computer mapping 02 p0152 N85-11028
Seismotectonic nature of some annular photoanomalies registered by remote methods 02 p0164 N85-11110
Predicting fracturing zones in Caspian depression subsalt deposits on basis of space information and geological-geophysical data 02 p0164 N85-11111
Method for interpreting soil cover of flowed fields using spectral brightnesses measured from space photographs 02 p0164 N85-11112
Space observation of latitudinal changes in vegetation cover 02 p0164 N85-11113
Choice of cartographic projection for space system data bank used in studying natural resources 02 p0165 N85-11119
The application of principal components analysis to LANDSAT MSS data 02 p0212 N85-11398
The Multispectral Imaging Science Working Group. Volume 1: Executive summary
[E85-10001] 02 p0213 N85-11404
The Multispectral Imaging Science Working Group. Volume 2: Working group reports
[E85-10002] 02 p0213 N85-11405
Workshop on the Use of Future Multispectral Imaging Capabilities for Lithologic Mapping: Workshop summary 02 p0214 N85-11413
Utilization of LANDSAT orbital imagery in the soil survey processes at Rio Grande do Norte state
[E85-10009] 02 p0216 N85-11422
Spectroradiometric calibration of the Thematic Mapper and Multispectral Scanner system
[E85-10026] 02 p0218 N85-11439
Production of optically correlated SEASAT-A (SEA satellite) SAR (Synthetic Aperture Radar) imagery at DREO (Defence Research Establishment Ottawa)
[AD-A145970] 03 p0355 N85-12281
Specification and preliminary design of the CARTA system for satellite cartography
[E85-10035] 03 p0378 N85-12414
Evaluation of criteria for selecting the spectral attributes of digital LANDSAT MSS imagery for discriminating lithological units in the lower Curaca River Valley, Bahia — Brazil
[E85-10036] 03 p0379 N85-12415
The United States Geological Survey in Alaska: Accomplishments during 1981
[USGS-CIRC-868] 04 p0515 N85-13283
Summary of LANDSAT quadrangle studies in Alaska 04 p0515 N85-13284
Investigations of severe/tornadic thunderstorm development and evolution based on satellite and AVE/SESAME/VAS data
[NASA-CR-174154] 04 p0538 N85-13424
Noise removal in multichannel images
[NASA-CR-174116] 04 p0554 N85-13526
Mars polar volatiles: Topographic and geologic setting
[NASA-CR-174089] 04 p0581 N85-13708
Air-sea heat exchange, an element of the water cycle 05 p0653 N85-14195
LANDSAT instruments characterization
[E85-10028] 05 p0654 N85-14197
LANDSAT instruments characterization
[E85-10029] 05 p0654 N85-14198
Classification of vegetation communities in the Battle Mountain SE quadrangle, Nevada with MSS digital data
[E85-10043] 06 p0826 N85-15246
Experiences with digital processing of images at INPE
[E85-10045] 06 p0826 N85-15247
An integrated LANDSAT/ancillary data classification of desert rangeland
[E85-10046] 06 p0826 N85-15248
A geographic information system for resource managers based on multi-level remote sensing data
[E85-10047] 06 p0827 N85-15249

Multi crop area estimation in Idaho using EDITOR
[E85-10054] 08 p0827 N85-15251
Characterizing the scientific potential of satellite sensors — San Francisco, California
[E85-10044] 07 p0983 N85-16244
Characterizing the scientific potential of satellite sensors — San Francisco, California
[E85-10053] 07 p0984 N85-16249
LANDSAT-4 Thematic Mapper Modulation Transfer Function (MFT) evaluation — California and New Mexico
[E85-10055] 07 p0984 N85-16250
Proceedings of the Second Annual Symposium on Mathematical Pattern Recognition and Image Analysis Program
[E85-10056] 07 p0984 N85-16251
Exploring the use of structural models to improve remote sensing agricultural estimates 07 p0985 N85-16259
Calibration or inverse regression: Which is appropriate for crop surveys using LANDSAT data?
07 p0985 N85-16260
Rectification of single and multiple frames of satellite scanner imagery using points and edges as control
07 p0986 N85-16263
The influence of the number of ground control points on the scene-to-map registration accuracy — Kansas, Louisiana, Mississipp, and Missouri
07 p0986 N85-16264
Southern ocean sea-ice morphology and kinematics
08 p1144 N85-17217
Optical wave propagation and imaging in the atmosphere 08 p1222 N85-17694
SIRTF: The next step 08 p1250 N85-17891
Resolution enhancement of multichannel microwave imagery from the Nimbus-7 SMMR for maritime rainfall analysis
[NASA-CR-174367] 10 p1482 N85-19221
Assessment of LANDSAT for rangeland mapping, Rush Valley, Utah
[E85-10072] 10 p1503 N85-19486
Anaysis of the quality of image data required by the LANDSAT-4 Thematic Mapper and Multispectral Scanner — agricultural and forest cover types in California
[E85-10074] 10 p1504 N85-19488
Thematic Mapper: Design through flight evaluation
[E85-10078] 10 p1504 N85-19492
The sharing of remote sensing techniques in Brazilian geographic research
[INPE-3307-PRE/617] 10 p1506 N85-19502
Satellite support to the Sierra Cooperative Pilot Project: 1979/80 and 1980/81
[PB85-115079] 10 p1520 N85-19583
LANDSAT-4 Science Characterization Early Results. Volume 1: Multispectral Scanner (MSS)
[E85-10067] 11 p1666 N85-20496
Summary of MSS characterization investigations
11 p1666 N85-20497
Radiometric accuracy assessment of LANDSAT 4 Multispectral Scanner data 11 p1666 N85-20498
Investigation of radiometric properties of LANDSAT-4 MSS — California, North Carolina, South Carolina, and New England 11 p1666 N85-20500
Radiometric calibration and geocoded precision processing of LANDSAT-4 Multispectral Scanner products by the Canada Centre for Remote Sensing
11 p1667 N85-20501
Geodetic accuracy of LANDSAT 4 Multispectral Scanner and Thematic Mapper data — Washington, DC, California, Alabama, South Dakota, and Illinois
11 p1667 N85-20504
Geometric accuracy assessment of LANDSAT-4 Multispectral Scanner (MSS) data
11 p1667 N85-20505
LS-4 MSS geometric correction: Methods and results
11 p1668 N85-20507
LANDSAT-4 Science Characterization Early Results. Volume 2, part 1: Thematic Mapper (TM)
[E85-10068] 11 p1668 N85-20508
TM digital image products for applications
11 p1668 N85-20512
Canadian plans for Thematic Mapper data
11 p1668 N85-20513
Development of satellite data presentation for environmental forecasting 11 p1712 N85-20770
Practical applications of satellite-derived meteorological and oceanographic data in Naval operations
11 p1712 N85-20771
LANDSAT-4 Science Characterization Early Results. Volume 3, part 2: Thematic Mapper (TM)
[E85-10069] 12 p1869 N85-21724
A preliminary assessment of LANDSAT-4 Thematic Mapper data — Windsor, Ontario and Medicine Hat areas, Canada 12 p1869 N85-21726
Evaluation of the radiometric quality of the TM data using clustering, linear transformations and multispectral distance measures — Illinois 12 p1870 N85-21731
TM geometric performance: Line to Line Displacement Analysis (LLDA) — New Mexico
12 p1870 N85-21732
In-progress absolute radiometric inflight calibration of the LANDSAT-4 sensors — New Mexico
12 p1870 N85-21733
Scan angle and detector effects in Thematic Mapper radiometry — Iowa and Arkansas
12 p1871 N85-21735
Thematic Mapper spectral dimensionality and data structure 12 p1871 N85-21736
Intraband radiometric performance of the LANDSAT 4 Thematic Mapper — Washington, DC, Arkansas, Massachusetts, Virginia, and Arizona
12 p1871 N85-21738
Tests of low-frequency geometric distortions in LANDSAT 4 images 12 p1872 N85-21744
Investigation of TM band-to-band registration using the JSC registration processor 12 p1872 N85-21745
Meteorological Satellite Center Technical Note No. 10, 1984
[MSC-TN-10] 12 p1894 N85-21884
On the relative motion of typhoons: In the case of Typhoon 8305 and Typhoons 6306 and 8307
12 p1894 N85-21885
Accuracy of typhoon center determined by GMS imagery 12 p1894 N85-21887
The development of image processing of NOAA AVHRR data and its application to sea surface temperature
12 p1895 N85-21901
A supplement study on the subsynoptic cloud system off the south coast of Japan 12 p1895 N85-21902
Nation said to rank high with 15 satellites
13 p2041 N85-22778
LANDSAT-4 Science Characterization Early Results. Volume 4: Applications — agriculture, soils land use, geology, hydrology, wetlands, water quality, biomass identification, and snow mapping
[E85-10070] 13 p2117 N85-23186
Overview of TM applications research reports
13 p2117 N85-23187
Characterization of LANDSAT-4 TM and MSS image quality for the interpretation of California's agricultural resources — Central Valley 13 p2118 N85-23190
Preliminary evaluation of Thematic Mapper image data quality 13 p2118 N85-23194
A concept for the processing and display of Thematic Mapper data 13 p2119 N85-23196
Quick look analysis of TM data of the Washington, District of Columbia, area 13 p2119 N85-23197
A preliminary comparison of the information content of data from the LANDSAT 4 Thematic Mapper and Multispectral Scanner — Arkansas
13 p2119 N85-23199
Thematic Mapper data quality and performance assessment in renewable resources/agriculture/remote sensing 13 p2120 N85-23201
Preliminary evaluation of TM for soils information
13 p2121 N85-23206
Comparison of MSS and TM data for landcover classification in the Chesapeake Bay area: A preliminary report — Taylor's Island, Maryland
13 p2121 N85-23210
An investigation of several aspects of LANDSAT-5 data quality — Palmer County, Shelby, mt; White sands, NM; Great Salt Lake, UT; San Matted Bridge and Sacramento, California
[E85-10096] 13 p2122 N85-23214
Distribution of snow and maximum snow water equivalent obtained by LANDSAT data and degree day method 13 p2124 N85-23229
Analysis of NIMBUS-7 SMMR data — Hokkaido, Japan snow cover 13 p2125 N85-23232
The relationship between marine aerosol particles and satellite-detected radiance 13 p2131 N85-23263
Analysis of the inflow layer and air-sea interactions in Hurricane Frederic (1979)
[NASA-CR-175616] 13 p2137 N85-23271
Use of space photographic information to map plant cover 15 p2468 N85-25359
Identification of structure of soil-vegetation cover using aerial and space photographs 16 p2725 N85-26826
Contribution to space program reviewed
16 p2727 N85-26834
China's integrated circuit production
16 p2808 N85-27302
CNPq/INPE LANDSAT system: Report of activities from October 1, 1983 to September 30, 1984 — Brazil
[E85-10097] 16 p2808 N85-27318
Noise correction on LANDSAT images using a spline-like algorithm
[E85-10098] 16 p2808 N85-27319
The relevance of remote sensing to Brazil
[INPE-3421-PRE/686] 16 p2811 N85-27332
Experience of the Institute of Space Research with the use of remote sensing in urban planning studies
[INPE-3159-PRE/533] 16 p2880 N85-27770
Information relative to cartography and geodesy. Series 2: Translations, number 42, volume 1
[ISSN-0469-4244] 18 p3123 N85-29338
Two satellite image maps of Central Europe
18 p3123 N85-29339
Digital image mapping of Antarctica using NOAA-7 AVHRR imagery 18 p3124 N85-29340
Satellite measurements of atmospheric aerosols
[AD-A153807] 19 p3316 N85-30566
Microwave hydrology: A trilogy
[NASA-CR-176042] 20 p3477 N85-31603
Regional landform thresholds
21 p3601 N85-32362
Geomorphology, tectonics, and exploration
21 p3601 N85-32365
Quantitative analysis of geomorphic processes using satellite image data at different scales
21 p3604 N85-32380
Use of space photographs for analysis of structural and dynamic conditions of formation of ancient phlogopite and apatite deposits 22 p3735 N85-33153
Physico-geographical regionalization of Caspian lowland based on space survey materials
22 p3736 N85-33162
Repetition of dense cloud cover above Indian Ocean from generalized satellite data 22 p3737 N85-33165

SATELLITE INSTRUMENTS
NT MULTISPECTRAL LINEAR ARRAYS
Optical analysis of the star-tracker telescope for Gravity Probe
[NASA-TM-86474] 01 p0129 N85-10086
An overview of Multispectral Electro-Optical Stereo Scanner (MEOSS) mission 04 p0458 N85-12908
Research relative to the development of a cryogenic microwave cavity gradiometer for orbital use
[NASA-CR-174249] 07 p0982 N85-16095
Thematic Mapper. Volume 1: Calibration report flight model, LANDSAT 5
[E85-10059] 07 p0987 N85-16270
Thematic Mapper. Volume 2: Flight model preshipment review
[E85-10060] 07 p0987 N85-16271
Solar Corona Explorer: A mission for the physical diagnosis of the solar corona
[NASA-TM-87416] 10 p1572 N85-19912
Instrumentation for Application Number 1: Mass spectrometric analysis of the boundary layer associated with the tethered satellite 11 p1646 N85-20372
Development of Faraday cup onboard MS-T5 for solar wind measurements
[REPT-616] 12 p1794 N85-21255
Development and testing of a spacecraft surface potential monitor 13 p2007 N85-22582
Kovtunenko comments on Vega flight plan, instrumentation 15 p2482 N85-25318
French and West German equipment for Vega Project
16 p2722 N85-26805
Comparison of ERS-1 scatterometer Monte Carlo performance simulations using a weighted nonlinear least squares and a maximum likelihood estimation method
20 p3420 N85-31224
SAR swath widening technique — satellite radar
[BL-6198] 20 p3441 N85-31358
Six mechanisms used on the SSM/I radiometer
22 p3798 N85-33534

SATELLITE LAUNCHING
U SPACECRAFT LAUNCHING

SATELLITE LIFETIME
Satellite observations 01 p0013 N85-10083
Natural atmospheric reentry — satellite orbit decay
05 p0800 N85-13829
Natural reentry of satellites 14 p2397 N85-24774

SATELLITE MANEUVERS
U SPACECRAFT MANEUVERS

SATELLITE NAVIGATION SYSTEMS
Diagnosis and therapy of geodetic satellite networks of Doppler type — error analysis
[SER-C-293] 01 p0015 N85-10090
Satellite navigation
[S-HRG-98-856] 08 p1082 N85-16851
The Global Positioning System (GPS): Program status update 11 p1710 N85-20781
Program INNAVSAT: Global Positioning System (GPS): Test and demonstration program
[BMFT-FB-W-84-047] 12 p1775 N85-21145
Global positioning system: A modification to the baseline satellite constellation for improved geometric performance
[AD-A151692] 15 p2469 N85-25239
GPS navigation experiment using high precision GPS timing receivers 17 p2963 N85-29299
A review of tropospheric refraction effects on Earth-to-satellite systems 18 p3107 N85-29295

Using GPS and VLBI technology to maintain 14 digit synchronization 18 p3109 N85-29250
Allowance for differences in ellipsoids and geodetic control coordinate systems in determining ship's position using radio navigation systems 19 p3292 N85-30413
A study of the ESA-NAVSAT control segment [ESA-CR(P)-2000] 20 p3398 N85-31079
The NAVSTAR Global Positioning System (GPS) receiver development program, phase 1 [BMFT-FB-W-85-002] 20 p3399 N85-31085

SATELLITE NETWORKS
Simple methods in very short-range forecasting based on data from a mesoscale network of automatic stations (ANETZ) and from satellite (Meteosat) and radar — Swiss Alps 01 p0062 N85-10548
SLIM TDMA ANIK B pilot project [CRC-REPT-1368] 03 p0354 N85-12278
The NASA/JPL pilot ocean data system 03 p0361 N85-12433
Ongoing activities in the field of communication at DFVLR 04 p0459 N85-12913
APOLLO system requirements specification — electronic document delivery [ESA-SP-1068] 04 p0494 N85-13150
The motion of the Earth by Doppler observing campaign (MEDOC) 05 p0601 N85-13831
Demand for satellite-provided domestic communications services up to the year 2000 [NASA-TM-86894] 06 p0798 N85-15099
Shipboard and satellite-aided communications equipment in exhibition 06 p0819 N85-15203
Satellite broadcasting: The performance of C-MAC in a hardware simulation of a DBS transmission chain [BBC-RD-1984/9] 08 p1143 N85-17206
Experimental satellite system for determining coordinates of maritime distress 09 p1308 N85-18216
China's future domestic satellite communications systems 10 p1476 N85-19312
The Global Positioning System (GPS): Program status update 11 p1710 N85-20761
GPS system field testing 11 p1711 N85-20762
Coverage and buildup of the Navstar constellation 11 p1711 N85-20764
Tactical applications of GPS user equipment 11 p1711 N85-20765
Combat capable space systems for tactical support 11 p1713 N85-20775
Assessment of effectiveness of signal-code constructions in time division-multi-access satellite systems 13 p2066 N85-22908
Satellite bridges in communications networks 13 p2067 N85-22910
Onboard demand scheduling of a multibeam SS/TDMA satellite with integrated circuit and packet switching 14 p2229 N85-23812
The ARGOS system status report after 2 years operation 14 p2237 N85-23870
System performance, data distribution and technical files — ARGOS project 14 p2237 N85-23871
Applications of ARGOS data collection systems in Arctic regions 14 p2238 N85-23875
The ARGOS system and hydrology. Results obtained by ORSTROM and benefits of a degree of standardization 14 p2239 N85-23881
The ARGOS system status report 14 p2239 N85-23884
Operational experiences with the ARGOS system in oceanography and oil spill emergency planning. Future plans for the use of the ARGOS system as a component in offshore data collection system 14 p2239 N85-23887
The experience of the Swedish Meteorological and Hydrological Institute (SMHI) with the ARGOS system [PM-U1/81] 14 p2240 N85-23892
Applications of ARGOS data collection system for automatic meteorological observatories in Arctic regions 14 p2240 N85-23893
Automatic weather stations in Antarctica 14 p2324 N85-24360
Automatic hydrological data collection facility using ARGOS 14 p2324 N85-24363
The ARGOS system after 3 years operation 14 p2325 N85-24368
The ARGOS contribution to the First GARP Global Experiment (FGGE) study of drifting buoys 14 p2325 N85-24371
The ARGOS communications performance trials 14 p2326 N85-24376
Miscellaneous ARGOS maritime applications — yacht races 14 p2327 N85-24383
The SARSAT program 14 p2327 N85-24385
Measurement of water equivalent of mountain snow cover — ARGOS system 14 p2327 N85-24386
Hydrology and climatic conditions in Greenland 14 p2327 N85-24387
The ARGOS system and hydrology: The use of Platform Terminal Transmitter (PTT) with built-in memory and direct reception by the Seine basin hydrology service 14 p2328 N85-24389
Direct readout and dissemination of results using ARGOS keypad terminals 14 p2328 N85-24390
Service ARGOS technical report and improvement 14 p2328 N85-24395
Antarctic automatic weather stations 14 p2329 N85-24397
Collecting meteorological reports with the ARGOS system 14 p2329 N85-24398
Telemetered meteorological and engineering data from a deep sea moored body in the Long Term Upper Ocean Study (LOTUS) 14 p2329 N85-24402
The ARGOS contribution to the demonstration of the effectiveness of a satellite-based search and rescue system 14 p2330 N85-24404
Drifting buoy development and future programs — Japanese ARGOS program 14 p2330 N85-24406
Data transmission using ARGOS keypad platform transmitter terminals (PTT) 14 p2330 N85-24407
Applications of ARGOS measurements in equatorial Pacific Ocean-atmosphere interaction studies 14 p2331 N85-24414
Overview of data processing at AES local user terminals — Canadian Atmospheric Environment Service (AES) 14 p2331 N85-24418
The SARSAT/COSPAS system for assisting satellite based search and rescue 14 p2398 N85-24776
Methods for cloud cover estimation 14 p2444 N85-25081
White paper on new international satellite systems [PB85-162501] 16 p2775 N85-27127
Routine wave and meteorological measurements in offshore areas using ARGOS data surveillance 16 p2812 N85-27344
Present stage of utilization of the ARGOS system by the ORSTOM hydrological service for hydrometric data collection 16 p2813 N85-27348
The ARGOS system in Brazil — hydrology 16 p2813 N85-27349
A seismic ARGOS data collection platform 16 p2813 N85-27350
An operational buoy network collecting meteorological data 16 p2813 N85-27351
Operational experiences with the ARGOS system in Greenland 16 p2813 N85-27353
Personal mobile communications by satellite [REPT-15-4572] 18 p3091 N85-29135
Study of a medium term flexible fixed satellite service mission [DM51/CC-IM-0185.83] 18 p3091 N85-29136
Time transfer techniques: Historical overview, current practices and future capabilities 18 p3108 N85-29245
Satellite aided search and rescue. Experimental results and operational prospects — conference [ISBN-2-85428-120-9] 20 p3400 N85-31088
INMARSAT: An overview 20 p3400 N85-31091
COSPAS/SARSAT: An overview 20 p3400 N85-31092
The contribution of an operational SAR satellite system to the UK SAR organisation — search and rescue (SAR) 20 p3400 N85-31095
The COSPAS-SARSAT system 20 p3401 N85-31101
The COSPAS-SARSAT space segment: Present status and evolution 20 p3401 N85-31102
The CCIR satellite EPIRB coordinated trials programme — Emergency Position Indicating Radio Beacon (EPIRB); International Radio Consultative Committee (CCIR) 20 p3402 N85-31111
Navigation data for Emergency Position Indicating Radio Beacons (EPIRBs) 20 p3403 N85-31115
INMARSAT distress and safety communication 20 p3406 N85-31134
The development of an institutional structure for the Future Global Satellite System for Search and Rescue 20 p3406 N85-31138
Remote medical diagnosis 21 p3663 N85-32753
International prototype network in Dubna experimental satellite communications system 22 p3773 N85-33383
Pluribus satellite IMP (Interface Message Processors) development mobile access terminal network [AD-A155754] 24 p4069 N85-35216
Second-generation mobile satellite system. A conceptual design and trade-off study [NASA-CR-176195] 24 p4086 N85-35325

SATELLITE OBSERVATION
Exploratory investigation of the need for and feasibility of a Lower Atmosphere Research Satellite (LARS) program [NASA-CR-171181] 01 p0015 N85-10091
Satellite reconnaissance [AD-B065034] 01 p0015 N85-10094
The Marine Resources Experiment Program (MAREX) [NASA-TM-87368] 01 p0066 N85-10580
Industrial use of land observation satellite systems 02 p0151 N85-11026
A proof-of-principle getaway special free-flying satellite demonstration 02 p0155 N85-11051
The feasibility of satellite remote sensing as a technique for evaluating coal mine surface features 02 p0213 N85-11401
A prospectus for Thematic Mapper research in the Earth sciences [E85-10003] 02 p0215 N85-11416
A report on the training course at Fortaleza (Ceara) [E85-10013] 02 p0216 N85-11426
Achievements in development of space meteorology 03 p0343 N85-12212
Earth Resources, A Continuing Bibliography with Indexes [NASA-SP-7041(43)] 03 p0378 N85-12411
The structures and the role of an international agency for the control of satellites [NASA-TM-76765] 03 p0441 N85-12606
Space observations of solar flares 04 p0519 N85-13313
Weather research program report; FY 1983 [PB84-236694] 04 p0541 N85-13440
A diagnostic approach to obtaining planetary boundary layer winds using satellite-derived thermal data 05 p0674 N85-14330
Spectral general circulation model development 05 p0679 N85-14363
Applications of sequential estimation to numerical weather prediction 05 p0681 N85-14374
Investigation of satellite measurements in the presence of clouds, forcing influences on clouds and feedback to the large scale following convection 05 p0682 N85-14381
The use of available potential energy to evaluate two GLAS FGGE data sets 05 p0682 N85-14387
Energy diagnostics and impact studies of FGGE global data sets and GLAS GCM simulations 05 p0683 N85-14390
Numerical prediction of the president's day cyclone 05 p0684 N85-14399
Rain volume estimation over areas using satellite and radar data 05 p0686 N85-14406
Mixed layers and satellite retrievals 05 p0686 N85-14411
Autoregressive spectral estimation for two dimensional time series 07 p0965 N85-16258
Remote sensing of the high latitude ionosphere [AD-A147881] 07 p1008 N85-16405
Testing of a field portable GPS (Global Positioning System) geodetic receiver [AD-A148336] 08 p1082 N85-16859
North American vegetation patterns observed with the NOAA-7 advanced very high resolution radiometer — North America [E85-10062] 08 p1174 N85-17400
Solitons and SEASAT [AD-A148396] 08 p1176 N85-17414
Satellite stratospheric aerosol measurement validation [NASA-TM-86003] 08 p1187 N85-17479
Earth resources: A continuing bibliography with indexes [NASA-SP-7041(44)] 10 p1503 N85-19484
Remote sensing activities in Latin America [INPE-3297-PRE/612] 10 p1506 N85-19501
The effect of the arbitrary level assignment of satellite cloud motion wind vectors on wind analyses in the pre-thunderstorm environment [NASA-TM-86186] 10 p1517 N85-19565
Rain volume estimation over areas using satellite and radar data [NASA-CR-174434] 10 p1518 N85-19568
Cut-off lows and their influence on the weather in Switzerland [REPT-45] 10 p1519 N85-19574
Preserve the sense of Earth from space — achieves of remote sensing data [PB85-124121] 11 p1740 N85-20942
Evaluating accuracy in determining position of Earth's center of mass and elements of orientation of geodetic coordinate system 13 p1983 N85-22441
New method of reconstructing conditions of recent differentiation of oil and gas in the Amudarya Basin (based on results of interpretation of space photographs) 13 p1984 N85-22446

MAGSAT anomaly field data of the crustal properties of Australia
[E85-10100] 13 p2122 N85-23215
A method for estimating soil moisture availability
[NASA-CR-175606] 13 p2126 N85-23238
Development concerns for satellite-based air traffic control surveillance systems 14 p2230 N85-23816
Supplement to evaluation of satellite derived estimates of solar radiation
[E85-10066] 14 p2346 N85-24506
Evaluation of satellite derived estimates of solar radiation
[E85-10067] 14 p2346 N85-24507
Variational mesoscale satellite data assimilation and initialization
[NASA-CR-175704] 14 p2378 N85-24680
Scientific experiments. Preprocessing of scientific data — spaceborne experiments
14 p2398 N85-24779
Methods for cloud cover estimation
14 p2444 N85-25061
Space radiation monitor observations from Salyut-4 orbital station 15 p2482 N85-25317
Preliminary processing of laser ranging data from LAGEOS artificial Earth satellite during short merit program observation period 15 p2488 N85-25355
A FORTRAN program for deep space sensor analysis
[AD-A151700] 15 p2489 N85-25366
Mesoscale Atmospheric Processes Research Program Science Review
[NASA-TM-87465] 15 p2594 N85-25987
Hurricane structure and dynamics from stereoscopic and infrared satellite observations and radar data
15 p2594 N85-25988
Monitoring tropical cyclone growth using GOES VISSR/VAS and Nimbus-7 TOMS data
15 p2595 N85-25989
Utilization of satellite data in mesoscale modeling of severe weather 15 p2597 N85-26007
Three-dimensional/perspective display techniques for meteorological data sets 15 p2599 N85-26018
Long-term observations of Cyg X-3 with Vela 5B
[DE85-005556] 15 p2686 N85-26586
Year-to-year variability of components of Earth's radiation budget according to satellite measurement data 16 p2725 N85-26821
Gravity model development software status
16 p2804 N85-27289
Atmospheric frontal zone studies
[NASA-CR-175293] 16 p2833 N85-27469
Solar activity monitoring satellite (SAMSAT): Impact on space environment services
[PB85-165066] 16 p2886 N85-27818
Research Review, 1983
[NASA-TM-86219] 18 p3139 N85-29433
Utilization of satellite data and regional scale numerical models in short range weather forecasting
[NASA-CR-175980] 19 p3314 N85-30545
Diagnosis of vertical motions from VAS retrievals during a convective outbreak
[NASA-CR-171569] 19 p3316 N85-30554
Precipitation estimation using collocated GOES satellite and surface data
[AD-A154248] 19 p3317 N85-30559
Improving the geological interpretation of magnetic and gravity satellite anomalies
[E85-10103] 20 p3473 N85-31585
Geologic analysis of averaged magnetic satellite anomalies 20 p3474 N85-31586
Statistical magnetic anomalies from satellite measurements for geologic analysis
20 p3474 N85-31589
Binning of satellite magnetic anomalies
20 p3474 N85-31590
Continental and oceanic magnetic anomalies: Enhancement through GRM 20 p3476 N85-31598
Results of the MIZEX preliminary campaign: 29 June to 19 July 1983 — Marginal Ice Zone Experiment (MIZEX), satellite observation
[CNES-84/142/T/CT/DRT/TIT/RL]
20 p3478 N85-31609
Structure of the distant geotail: ISEE-3 observations
20 p3488 N85-31678
Geophysical interpretation of satellite laser ranging measurements 20 p3490 N85-31692
New optical satellite data 20 p3492 N85-31705
NASA/GSFC TOPEX gravity model operations group
20 p3492 N85-31709
Ocean circulation studies 20 p3492 N85-31712
Ocean tidal parameters from LAGEOS
20 p3493 N85-31716
Tropical Ocean and Global Atmosphere (TOGA) heat exchange project: A summary report
[NASA-CR-176038] 20 p3496 N85-31738
Space optics
[CNES-84/105/T/CT/DRT/TIT/10]
20 p3533 N85-31985
Radio counterparts of galactic gamma-ray sources
20 p3549 N85-32085
Doppler satellite data characteristics
[AD-A154868] 21 p3575 N85-32231
Use of the synoptic view: Examples from Earth and other planets 21 p3602 N85-32371
Rain volume estimation over areas using satellite and radar data
[NASA-CR-176050] 21 p3634 N85-32570
Parameter estimation in communication system tracking satellite observations
[AD-A155137] 21 p3636 N85-32582
Large-scale sea surface temperature variability from satellite and shipboard measurements
[NASA-CR-176123] 22 p3818 N85-33651
Method and apparatus for Delta Kappa synthetic aperture radar measurement of ocean current
[NASA-CASE-NPO-15704-1] 23 p3925 N85-34327
Target observability for satellite-based sensors
[AD-A156139] 24 p4089 N85-35217
Remote sensing of hydrologic transport processes using spot simulation data
[DE85-012412] 24 p4108 N85-35467
Two-dimensional quasineutral description of particles and fields above discrete auroral arcs
[NASA-CR-176170] 24 p4116 N85-35517
Mean cloudiness over the global tropics from satellite observations
[AD-A156188] 24 p4123 N85-35561

SATELLITE ORBIT CALCULATION
U ORBIT CALCULATION

SATELLITE ORBITS
NT GEOSYNCHRONOUS ORBITS
NT PARKING ORBITS
NT POLAR ORBITS
NT STATIONARY ORBITS
Geopotential harmonics of order 15 and 30, from analysis of the orbit of satellite 1971-108
[RAE-TR-84008] 02 p0165 N85-11121
Satellite motion: Lectures and exercises on space mechanics
[ISBN-2-85428-114-4] 05 p0598 N85-13807
Keplerian and perturbed motion — satellite motion
05 p0598 N85-13808
Orbit extrapolation — satellite orbits
05 p0598 N85-13811
Measurements in satellite orbit tracing
05 p0598 N85-13812
Satellite orbit determination 05 p0598 N85-13813
The satellite maneuvers determination department
05 p0599 N85-13820
The operational orbit tracking center
05 p0599 N85-13821
Helioeynchronism and phasing. Application to the SPOT orbit 05 p0600 N85-13826
Choice of orbit for scientific satellites: SIGMA, the submillimeter telescope — Ariane-borne gamma imagery satellite (SIGMA) 05 p0600 N85-13828
The Search And Rescue Satellite Aided Tracking (SARSAT) experiment. Presentation of CNES processing for the SARGOS project: Context and orbit processing
05 p0600 N85-13830
Spatial mechanics formulas and exercises
05 p0601 N85-13832
Individual geopotential coefficients of order 15 and 30, from resonant satellite orbits
[AD-A146687] 06 p0828 N85-15256
Thermal and cryogenic design study for space infrared telescope facility (SIRTF)
[NASA-CR-166613] 07 p0915 N85-15793
Individual geopotential coefficients of order 15 and 30, from resonant satellite orbits
[RAE-TR-84021] 08 p1105 N85-16985
Altimetry, orbits and tides
[E85-10066] 08 p1174 N85-17404
Theory of the orbital motion of an artificial Earth Satellite
[NAL-TR-807] 09 p1285 N85-18075
The determination of the post-Newtonian parameters in gravitational theory using laser ranging to the Lageos satellite 09 p1414 N85-18924
A modeling analysis program for the JPL table mountain lo sodium cloud data
[NASA-CR-175474] 10 p1572 N85-19910
Tactical military communications by satellite relay at high latitudes 11 p1709 N85-20756
Proposed preliminary design criteria model environment for the 1990's 12 p1784 N85-21194
Transmission and orbital constraints in space-related programs: Briefing summary 12 p1787 N85-21216
Air Force satellite position management
12 p1787 N85-21217
Engineering calculations for communications satellite systems planning
[NASA-CR-175552] 12 p1789 N85-21233
Nontraditional method for determining unperturbed orbits of unknown space objects using incomplete optical observational data 13 p1979 N85-22417
Satellite oscillations in elliptical orbit
13 p1981 N85-22429
Satellite-to-satellite orbit determination using minimum, discrete range and range-rate data only
13 p1985 N85-22458
Method for determining the number of correlative measurements required to validate the SBUV/2 ozone retrievals 13 p2105 N85-23114
Small solar system bodies 13 p2175 N85-23499
Motion of satellite with total dynamic symmetry around rotating aspherical Earth 14 p2287 N85-24174
Space Mathematics for the Preparation and Development of satellite Exploitation
[ISBN-2-85428-115-2] 14 p2395 N85-24753
Orbit perturbation. Extrapolation of perturbed orbits
14 p2396 N85-24763
Orbit reconstitution — satellite orbits
14 p2396 N85-24765
COSPAS-SARSAT satellite orbit predictor, volume 5
[NASA-TM-85015-VOL-5] 14 p2439 N85-25052
Global positioning system: A modification to the baseline satellite constellation for improved geometric performance
[AD-A151692] 15 p2469 N85-25239
Some numerical estimates of perturbation of orbital elements of artificial Earth satellite with total dynamic symmetry about rotating aspherical Earth
15 p2478 N85-25294
Use of atmospheric models in predicting artificial Earth satellite motion 15 p2478 N85-25296
Using velocity vector in determining Keplerian orbit of geodectic satellite 15 p2478 N85-25297
Minimax problem of estimating trajectory parameters in continuous formulation 15 p2479 N85-25301
Construction of conditionally periodic solutions of problem of reciprocating motion of axially symmetric satellite of triaxial planet 15 p2480 N85-25304
List of recent Soviet space launches
15 p2489 N85-25361
Statistical regularization methods in problem of navigational determination of space vehicle orbits
16 p2719 N85-26784
Satellite physical and orbital characteristics
16 p2904 N85-27287
Radial orbit error spectrum for Topex
16 p2905 N85-27292
Analytical generation of satellite orbits at the RAE (Royal Aircraft Establishment)
[AD-A152665] 17 p3053 N85-28901
An introduction to satellite orbits
[RAE-TM-SPACE-344] 20 p3387 N85-31076
Update on the evolution of the LAGEOS orbit
20 p3491 N85-31698
Error spectrum of Goddard satellite models for the gravity field 20 p3491 N85-31704
New optical satellite data 20 p3492 N85-31705
Optical best arc RMS test results
20 p3492 N85-31706
Spacecraft-aided research discussed at geology Congress 22 p3734 N85-33147

SATELLITE ORIENTATION
Attitude measurements and determination
14 p2397 N85-24767
Consummative expressions for satellite drag perturbations in a spherically symmetrical atmosphere
[AD-A154230] 19 p3222 N85-29981
Doppler satellite data characteristics
[AD-A154868] 21 p3575 N85-32231

SATELLITE PERTURBATION
Periodic oscillation of gyrostat-satellite about its center of mass in an elliptical orbit 02 p0159 N85-11080
Keplerian and perturbed motion — satellite motion
05 p0598 N85-13808
Orbit perturbation — satellites
05 p0598 N85-13810
Perturbations in geostationary orbit
05 p0600 N85-13824
Spatial mechanics formulas and exercises
05 p0601 N85-13832
Theory of the orbital motion of an artificial Earth Satellite
[NAL-TR-807] 09 p1285 N85-18075
Approximate perturbing part of geopotential by polynomials of stipulated form 13 p1984 N85-22448
Orbit perturbation. Extrapolation of perturbed orbits
14 p2396 N85-24763
Some numerical estimates of perturbation of orbital elements of artificial Earth satellite with total dynamic symmetry about rotating aspherical Earth
15 p2478 N85-25294

Application of perturbation theory to problem in orbital theory 15 p2537 N85-25656
Accuracy in predicting orbital motion of artificial Earth satellite 16 p2720 N85-26793
Satellite selection criteria 16 p2804 N85-27288
The study of the physics of cometary nuclei [NASA-CR-175917] 17 p3054 N85-28905
Consummative expressions for satellite drag perturbations in a spherically symmetrical atmosphere [AD-A154230] 19 p3222 N85-29981
Investigation of dynamic noise affecting geodynamics information in a tethered subsatellite [NASA-CR-176031] 20 p3476 N85-31602
Spaceborne gradiometer error analysis 20 p3492 N85-31707

SATELLITE RENDEZVOUS
U ORBITAL RENDEZVOUS

SATELLITE ROTATION
Rapid nonresonant rotation of a spacecraft in nominally periodic orbits in limited 3 body problem 02 p0160 N85-11063
Magnetic spin reduction system for free spinning objects [NASA-CASE-MFS-25986-1] 02 p0166 N85-11122
Development of Faraday cup onboard MS-T5 for solar wind measurements [REPT-616] 12 p1794 N85-21255
Non-contacting electromagnetic de-spin system for Earth orbiting satellites 12 p1946 N85-22225
Motion of symmetrical satellite with flexible viscoelastic rods about center of mass in circular orbit 13 p1979 N85-22420
Rotational motion of a satellite 13 p1981 N85-22428
Electric field effects on ion currents in satellite wakes 13 p1991 N85-22485
Patterns of fracture and tidal stresses due to nonsynchronous rotation: Implications for fracturing on Europa 13 p2173 N85-23483
Resonant rotations of satellite in polar orbit in magnetic and gravitational fields 15 p2479 N85-25302
The investigation of tethered satellite system dynamics [NASA-CR-171433] 15 p2492 N85-25375
Investigation of dynamic noise affecting geodynamics information in a tethered subsatellite [NASA-CR-176031] 20 p3476 N85-31602

SATELLITE SOUNDING
The past, present, and anticipated future contributions of geosynchronous satellites to short range prediction 01 p0076 N85-10503
Use of satellite soundings and imagery for nowcasting and very-short-range forecasting 01 p0076 N85-10504
Variation of fast charged particles in event of 22 November 1977 based on Cosmos-900 satellite data 02 p0161 N85-11092
International banking of satellite and in-situ wave data by the Marine Information and Advisory Services (MIAS) 03 p0381 N85-12434
Water vapor profile retrievals from the HIRS/MSU satellite sounder 05 p0681 N85-14378
Applications of TOMS ozone data and clustering techniques in satellite soundings 05 p0681 N85-14379
Fidelity of satellite soundings 05 p0682 N85-14383
Actual altitudes of radioacoustic sounding in decimeter wavelength band 06 p0826 N85-15243
Convective scale weather analysis and forecasting [NASA-CR-174185] 06 p0836 N85-15320
Environmental satellites 14 p2328 N85-24392
VLF wave-particle interaction experiments by EXOS-B/Siple station transmissions 14 p2366 N85-24622
Advances in magnetospheric plasma diagnosis by active experiments — IMS satellites 14 p2371 N85-24654
Technical development to improve satellite sounding over radiatively complex terrain [NASA-CR-175746] 15 p2583 N85-25929
Substorms in energetic radiation belt particles according to data from Meteor artificial Earth satellite 16 p2719 N85-26788
Determining effective rate of plasma heating in outer equatorial ionosphere using data from ISIS-1 and ISIS-2 satellites 16 p2721 N85-26797
The validation of sea surface temperatures determined from AVHRR data using in situ data recovered via system ARGOS 16 p2812 N85-27342
Assessment of VAS soundings in the analysis of a preconvective environment [NASA-TM-86205] 16 p2825 N85-27427
Remote sensing of the plasma with time delay measurements (coronal sounding) 16 p2866 N85-27804
Applications of fuzzy set theory to satellite soundings 18 p3141 N85-29445
Applications of some artificial intelligence methods to satellite soundings 18 p3141 N85-29446
Utilization of satellite data and regional scale numerical models in short range weather forecasting [NASA-CR-175980] 19 p3314 N85-30545
Observations of low energy magnetospheric plasma outside the plasmasphere [KGI-PREPRINT-075] 20 p3536 N85-32004

SATELLITE SURFACES
The rheology of icy satellites [NASA-CR-174024] 02 p0302 N85-11959
The violet absorber on Io: Disulfur monoxide derivatives 13 p2173 N85-23482
Polar cap formation on Ganymede 13 p2174 N85-23486
Interaction of the magnetospheric ions with the surfaces of the icy satellites of Saturn 13 p2174 N85-23491
Plasma production by meteoroid impact 13 p2174 N85-23492
Ripple ring basins on Ganymede and Callisto 13 p2183 N85-23547
Permafrost and subsurface ice in the solar system 13 p2191 N85-23594
Planetary analogs in Antarctica: Icy satellites 13 p2193 N85-23605
The geomorphology of Rhea 13 p2193 N85-23606
Io: Precise comparison of Voyager spectral curves with laboratory measurements 13 p2196 N85-23619
Photometric analysis of Jupiter-illuminated images of Io 13 p2196 N85-23620
Spectral units on Europa and Ganymede 13 p2196 N85-23621
Fault offsets and lateral crustal movement on Europa 13 p2201 N85-23656
Lineaments on Ganymede: New evidence for late tectonic activity 13 p2202 N85-23658
Global tectonics on Ganymede 13 p2202 N85-23659
Tectonics of the Galileo Regio on Ganymede 13 p2202 N85-23660
Importance of the tectonic motions on Ganymede 13 p2202 N85-23661
Tectonics of the Valhalla structure on Callisto 13 p2202 N85-23662
The Galilean Satellite Geological Mapping Program, 1984 13 p2203 N85-23664
Geology of the Ganymede quadrangle Jg7 13 p2203 N85-23665
Voyager cartography 13 p2203 N85-23668
Jupiter/Voyager data analysis [NASA-CR-175723] 15 p2579 N85-26545

SATELLITE TELEVISION
Technology and performances of structural thermal mechanical equipment used for antenna of TV.SAT-TDF 1 program 05 p0626 N85-14012
Activities of Istituto Elettrotecnico Nazionale Galileo Ferraris 18 p3199 N85-29845

SATELLITE TEMPERATURE
Space environment simulation to test satellite thermal control coatings, volume 1 [CERT-4128-VOL-1] 08 p1109 N85-17012
Space environment simulation to test satellite thermal control coatings. Volume 2: Annex 1 [ESA-CR(P)-1870-VOL-2] 08 p1109 N85-17013
Space environment simulation to test satellite thermal control coatings. Volume 2: Annexes 2, 3, 4 [ESA-CR(P)-1870-VOL-3] 08 p1109 N85-17014
On the improvement of satellite temperature retrievals by means of boundary layer models 18 p3140 N85-29443

SATELLITE TRACKING
Tracking requirements for precise ERS-1 orbit determination 03 p0350 N85-12431
Measurements in satellite orbit tracing 05 p0598 N85-13812
The 2 GHz network and the network operations center — satellite tracking 05 p0599 N85-13817
The operational orbit tracking center 05 p0599 N85-13821
Development of the TT and C station equipment at INPE [INPE-3327-PRE/625] 10 p1427 N85-18999
Orbital Debris [NASA-CP-2360] 12 p1783 N85-21188
NORAD operational system 12 p1783 N85-21189
History of satellite break-ups in space 12 p1783 N85-21190
Geosynchronous satellite collision avoidance 12 p1784 N85-21197
China report: Science and technology [JPRS-CST-85-005] 13 p2052 N85-22843
Development, prospect of satellite dynamics discussed 13 p2052 N85-22847
Proceedings of the ARGOS Users Conference on Data Collection and Location by Satellite 14 p2322 N85-24348
One thousand days in the brine — platform transmitter terminals 14 p2324 N85-24359
Tracking pelagic dolphins by satellite 14 p2324 N85-24364
Polar bear telemetry results from the Nimbus-6 system 14 p2325 N85-24365
Data Collection and Platform Location by Satellite: ARGOS users' Conference 14 p2326 N85-24391
US programs using the ARGOS data collection and platform location system 14 p2329 N85-24401
Tracking whale migrations with the ARGOS satellite system 14 p2330 N85-24403
Data Collection and Platform Location by Satellite: ARGOS Users' Conference 14 p2330 N85-24409
US program using the ARGOS data collection and platform location system 14 p2330 N85-24410
Arabian gulf circulation — pollution monitoring 14 p2331 N85-24412
Drifting buoys on the Labrador shelf 14 p2331 N85-24415
Some methods of computing platform transmitter terminal location estimates — ARGOS system; whale tracking 14 p2332 N85-24420
The ARGOS system used for tracking gray whales 14 p2332 N85-24421
The MEDOC 2: Experimental Doppler measurement of Earth kinematics 14 p2399 N85-24786
Data Collection and Platform Location by Satellite: ARGOS Users' Conference 16 p2811 N85-27333
Long term drifting float for measuring mean oceanic circulation using ARGOS system 16 p2811 N85-27339
Results of an initial trial of a satellite telemetering buoy measuring near surface current 16 p2812 N85-27345
The ARGOS system used for tracking gray whales 16 p2812 N85-27347
A new precision time and frequency source for stationary PTTI applications 17 p2963 N85-28297
CPS navigation experiment using high precision GPS timing receivers 17 p2963 N85-28299
International time transfer and portable clock evaluation using GPS timing receivers: Preliminary results 17 p2964 N85-28303
Maintenance of time and frequency in the Jet Propulsion Laboratory's Deep Space Network using the Global Positioning System 18 p3109 N85-29249
Fault tolerant multiprocessor SARSAT-COSPAS 406 MHz local user terminal 20 p3404 N85-31123
Optical best arc RMS test results 20 p3492 N85-31706
United States-Soviet satellite accord: SARSAT/Cospas search-and-rescue program [GPO-41-113] 20 p3541 N85-32040
Interplanetary plasma turbulence and the Doppler detection of a gravitational background radiation [IFSI-85-1] 20 p3546 N85-32066
A derivation of relativistic effects in satellite tracking [AD-A154620] 21 p3558 N85-32132

SATELLITE TRANSMISSION
Ongoing activities in the field of communication at DFVLR 04 p0459 N85-12913
Television transmission in frequency modulation 04 p0493 N85-13146
A transmission analysis for the use of 2-4 PSK modulation in satellite broadcasting [ESA-STM-231] 04 p0494 N85-13151
Satellite broadcasting: The performance of C-MAC in a hardware simulation of a DBS transmission chain [BBC-RD-1984/9] 08 p1143 N85-17206
Study of factors affecting an HF/VHF direct broadcasting satellite service [PB85-120869/GAR] 09 p1313 N85-18255
Equatorial transionospheric propagation conditions affecting digital communications 10 p1470 N85-19275
Propagation effects on the Doppler frequency shift of satellite transmissions 10 p1470 N85-19276
A technical solution to fadings in tactical satellite digital transmissions 10 p1473 N85-19297
China's domestic satellite communications 10 p1476 N85-19313
Satellite-computer interface 10 p1476 N85-19318
Development of a 20 GHz modulator for the payload of a satellite for propagation and transmission experiments, including the required converters of the test equipment [BMFT-FB-W-84-044] 11 p1590 N85-20004
The Ferranti Tactical SHF SATCOM station (MANSAT) 11 p1710 N85-20759
Tactical satellite terminals for land and airborne C3 applications 11 p1710 N85-20760
Coverage and buildup of the Navstar constellation 11 p1711 N85-20764

Tactical applications of GPS user equipment
11 p1711 N85-20765
Brussels Satellite Convention
[S-EXEC-REPT-98-52] 12 p1790 N85-21234
Assessment of effectiveness of signal-code constructions in time division-multi-access satellite systems 13 p2066 N85-22908
Satellite bridges in communications networks
13 p2067 N85-22910
Development of TV systems for spacecraft
15 p2484 N85-25392
Propagation considerations in land mobile satellite transmission
[NASA-CR-175733] 15 p2540 N85-25684
SESC (Space Environment Services Center) satellite broadcasting 10-year plan
[PB85-163541] 16 p2775 N85-27126
Station for in-orbit testing of satellites
[MBB-UR-708/84-O] 16 p2874 N85-27733
Time synchronization experiments with APPLE
17 p2967 N85-28323
Preliminary investigation of the performance of repeater technology for satellite sound broadcasting
[SSP/017/82] 18 p3092 N85-29137
Nonlinear plasma reactions on the antenna impedance of high transmission power satellites
[BMFT-FB-W-84-053] 18 p3192 N85-29799
Radiometry: A useful prediction tool — atmospheric attenuation
[ESA-SP-1071] 20 p3399 N85-31084
Modulation using four phase levels. Theoretical study of the degradation caused by a spurious phase modulation
[CNES-83/219/CT/DRT/TIT/TR]
20 p3441 N85-31360
Study of a limited band signal transmission chain
[CNES-CT/DRT/TIT/TR-83/221]
20 p3442 N85-31361
Adaptive antenna arrays for satellite communications: Design and testing
[NASA-CR-176162] 23 p3926 N85-34329

SATELLITE-BORNE INSTRUMENTS

Periodic oscillation of gyrostat-satellite about its center of mass in an elliptical orbit 02 p0159 N85-11060
The ESA remote sensing satellite system (ERS-1)
03 p0379 N85-12420
The ERS-1 radar altimeter: An overview
03 p0379 N85-12421
The ERS-1 radar altimeter instrument
03 p0379 N85-12422
Wind speed determination from radar altimeters
03 p0380 N85-12424
Ocean wave parameters extraction using satellite short-pulse radar altimeters 03 p0380 N85-12425
The use of altimeter data for sea state forecasting
03 p0380 N85-12426
The impact of satellite altimeter data on wave research 03 p0380 N85-12427
Cryospheric data products available through satellite altimetry 03 p0380 N85-12428
Special difficulties of retrieving surface elevation over continental ice — satellite radar altimetry
03 p0380 N85-12429
Requirements and special problems of land altimetry — satellite altimetry 03 p0380 N85-12430
ERS-1 altimeter ground segment relations to other sensors and programs 03 p0381 N85-12436
Satellite altimetry for sea-surfacing topography determination and geoid improvement
03 p0382 N85-12444
Satellite altimetric measurements of lake levels
03 p0383 N85-12447
Modelling of altimeter tracking over topographical surfaces — satellite antennas 03 p0383 N85-12450
ERS-1 radar altimeter system performance evaluation and calibration 03 p0383 N85-12451
The POSEIDON altimeter description
03 p0383 N85-12454
Standardization of data formats for radar altimeter data 03 p0384 N85-12455
Calibration and validation areas — satellite altimeters
03 p0384 N85-12456
Feasibility study of a satellite-borne 90 GHz radiometer 04 p0459 N85-12914
Launch summary for 1978 - 1982 — sounding rockets, space probes, and satellites
[NASA-TM-87375] 04 p0461 N85-12924
Conceptual ideas for a second generation METEOSAT system 05 p0658 N85-14228
Spaceborne microwave radiometers: Background and technology requirements
[LD-R-267] 08 p1165 N85-17350
Development of a 20 GHz modulator for the payload of a satellite for propagation and transmission experiments, including the required converters of the test equipment
[BMFT-FB-W-84-044] 11 p1590 N85-20004
MAP-related activities in the United States
11 p1655 N85-20427
UK Skynet 4 communications satellites
11 p1710 N85-20757
The multi-anode microchannel array detector system: Current status and future prospects
11 p1761 N85-21060
Method of measuring sea surface water temperature with a satellite including wideband passive synthetic-aperture multichannel receiver
[NASA-CASE-NPO-15651-1] 12 p1869 N85-21723
Spatial resolution estimation of LANDSAT-4 Thematic Mapper data 12 p1872 N85-21741
On the P1 data from GMS-SEM
12 p1894 N85-21890
Dielectric detector device for registering heavy cosmic radiation particles 13 p2045 N85-22709
Scientific requirements for ozone measurements
13 p2105 N85-23113
Results of the Langmuir-probe experiment on board Intercosmos-18 — ionosphere-magnetosphere interaction 14 p2382 N85-24596
Optic's institute's development of equipment for comet probe 15 p2484 N85-25333
Development of algorithms for using satellite meteorological data sets to study global transport of stratospheric aerosols and ozone
[NASA-CR-172540] 15 p2591 N85-25974
Satellite detection of severe thunderstorms
15 p2596 N85-25996
Severe storm detection with passive 37 GHz observations 15 p2596 N85-25997
Soil moisture and evapotranspiration estimates based on satellite data 15 p2596 N85-25998
Estimation of convective rainfall from visible and infrared satellite data 15 p2596 N85-25999
Mesoscale analysis and modeling group
15 p2596 N85-26001
Carbon foil secondary electron emission during ion passage through the 40 to 500 keV energy field
[MPE-190] 18 p3184 N85-29747
Some design considerations for a satellite-borne magnetograph 18 p3204 N85-29879
Poseidon altimeter: Study of the hyperfrequency section and specifications of the prototype components
[CNES-84/DRT/TIT/HY/T/145]
20 p3419 N85-31219
Solid state altimeter model: Simulation description; analysis of first results (narrow band filters, weighting) — satellite-borne instruments
[CNES-DRT/TIT/RL-160-T] 20 p3419 N85-31220
Preliminary investigations concerning a 90 GHz radiometer satellite experiment
[ESA-TT-860] 20 p3420 N85-31225
Spacecraft-aided research discussed at geology Congress 22 p3734 N85-33147
SONTRAC: A solar neutron track chamber detector
[SH-9.1-12] 23 p4052 N85-35127
Measurement of low energy cosmic rays aboard Spacelab-1
[SH-10.1-6] 23 p4053 N85-35137

SATELLITE-BORNE PHOTOGRAPHY

Use of satellite soundings and imagery for nowcasting and very-short-range forecasting
01 p0076 N85-10504
Method for interpreting soil cover of flowed fields using spectral brightnesses measured from space photographs
02 p0164 N85-11112
Economic evaluation of space survey materials use in land improvement engineering field work
02 p0165 N85-11115
Methods for determining atmospheric optical parameters using results of space survey of Earth's surface
02 p0165 N85-11117
Methods for correlating geological, geochemical and geophysical data with satellite imagery in central Ireland
05 p0655 N85-14206
Use of photographs of meteorologic satellites in synoptic analysis
[SESIT-5] 05 p0679 N85-14357
Evaluating accuracy in orientation of topographic photograph and satellite-centered direction from star photograph 13 p1983 N85-22442
New method of reconstructing conditions of recent differentiation of oil and gas in the Amudarya Basin (based on results of interpretation of space photographs)
13 p1984 N85-22446
One aspect of determination of direction of space survey base from photographs of planetary surface and star sky
15 p2487 N85-25352
Minimizing influence of Earth's curvature in projective rectification of space photographs into photoplans and photomaps 16 p2727 N85-26829
First results of oceanography utilization of infrared high resolution picture transmission images
[KNMI-TR-59] 18 p3151 N85-29511
Spacecraft-aided research discussed at geology Congress 22 p3734 N85-33147
Landscape interpretation capabilities using space photographs of regions of a multistage platform mantle structure 22 p3734 N85-33151
Surface cyclogenesis as indicated by satellite imagery
[PB85-191815] 24 p4124 N85-35566

SATELLITE-BORNE RADAR

Terrestrial locating — of buoys from space
05 p0599 N85-13816
Earth resources research using the Shuttle Imaging Radar system 11 p1713 N85-20779
Synthetic aperture radar data processing — satellite-borne radar
[CNES-198-T-CT/DRT/TIT/RL]
20 p3442 N85-31363
Digital signal processing for spaceborne synthetic aperture radar
[FOA-C-30381-E1] 20 p3442 N85-31364

SATELLITES

NT AERONAUTICAL SATELLITES
NT AEROS SATELLITE
NT ALOUETTE 2 SATELLITE
NT ANIK SATELLITES
NT ARABSAT
NT ARTIFICIAL SATELLITES
NT ASTRONOMICAL SATELLITES
NT ATS
NT BIOSATELLITES
NT CALLISTO
NT CHARON
NT COMMUNICATION SATELLITES
NT COMMUNICATIONS TECHNOLOGY SATELLITE
NT COS-B SATELLITE
NT COSMOS SATELLITES
NT COSMOS 936 SATELLITE
NT COSMOS 1129 SATELLITE
NT COSPAS
NT DEIMOS
NT DMSP SATELLITES
NT DYNAMICS EXPLORER 1 SATELLITE
NT ENCELADUS
NT EOSS
NT ERS-1 (ESA SATELLITE)
NT EUROPA
NT EUROPEAN COMMUNICATIONS SATELLITE
NT EXOSAT SATELLITE
NT EXPLORER SATELLITES
NT EXPLORER 10 SATELLITE
NT EXPLORER 43 SATELLITE
NT EXPLORER 46 SATELLITE
NT EXPLORER 50 SATELLITE
NT EXPLORER 51 SATELLITE
NT EXTREME ULTRAVIOLET EXPLORER SATELLITE
NT FAR UV SPECTROSCOPIC EXPLORER
NT GALILEAN SATELLITES
NT GANYMEDE
NT GEODETIC SATELLITES
NT GEOPHYSICAL SATELLITES
NT GEOS SATELLITES (ESA)
NT GEOS 1 SATELLITE
NT GEOS 2 SATELLITE
NT GEOS 3 SATELLITE
NT GOES SATELLITES
NT GOES 5
NT GRAVITY GRADIENT SATELLITES
NT HEAO 1
NT HEAO 2
NT HEAO 3
NT HELIOS SATELLITES
NT HELIOS 1
NT HELIOS 2
NT HEOS B SATELLITE
NT HUBBLE SPACE TELESCOPE
NT IMP
NT INFRARED ASTRONOMY SATELLITE
NT INTELSAT SATELLITES
NT INTERCOSMOS SATELLITES
NT INTERNATIONAL SUN EARTH EXPLORER 1
NT INTERNATIONAL SUN EARTH EXPLORER 2
NT INTERNATIONAL SUN EARTH EXPLORER 3
NT INTERNATIONAL SUN EARTH EXPLORERS
NT IO
NT ISIS SATELLITES
NT IUE
NT JUPITER SATELLITES
NT L-SAT
NT LAGEOS (SATELLITE)
NT LANDSAT SATELLITES
NT LANDSAT 1
NT LANDSAT 4
NT LANDSAT 5
NT LONG DURATION EXPOSURE FACILITY
NT LUNAR SATELLITES
NT MAGSAT SATELLITES
NT MARISAT SATELLITES

NT MARITIME SATELLITES
NT METEOROLOGICAL SATELLITES
NT METEOSAT SATELLITE
NT MIRANDA SATELLITE
NT MOON
NT MULTISPECTRAL RESOURCE SAMPLER
NT NATURAL SATELLITES
NT NAVIGATION SATELLITES
NT NAVSTAR SATELLITES
NT NIMBUS SATELLITES
NT NIMBUS 5 SATELLITE
NT NIMBUS 7 SATELLITE
NT NOAA SATELLITES
NT NOAA 6 SATELLITE
NT NOAA 7 SATELLITE
NT NOAA 8 SATELLITE
NT OAO 3
NT OGO
NT ORBITAL SPACE STATIONS
NT OTS (ESA)
NT PASSIVE SATELLITES
NT PROGNOZ SATELLITES
NT QUASAT
NT ROSAT MISSION
NT SAGE SATELLITE
NT SARSAT
NT SATURN SATELLITES
NT SCATHA SATELLITE
NT SCIENTIFIC SATELLITES
NT SEASAT SATELLITES
NT SEASAT 1
NT SIRIO SATELLITE
NT SIRS B SATELLITE
NT SKYNET SATELLITES
NT SOLAR MESOSPHERE EXPLORER
NT SOLAR POWER SATELLITES
NT SPACE INFRARED TELESCOPE FACILITY
NT SPARTAN SATELLITES
NT SPOT (FRENCH SATELLITE)
NT STORMSAT SATELLITE
NT SYMPHONIE SATELLITES
NT SYNCHRONOUS SATELLITES
NT TDR SATELLITES
NT TETHERED SATELLITES
NT TIROS N SERIES SATELLITES
NT TIROS SATELLITES
NT TITAN
NT TRANSIT SATELLITES
NT TRITON
NT UK SATELLITES
NT VELA SATELLITES
NT VENERA SATELLITES
NT VENERA 11 SATELLITE
On-orbit support of DARPA-301 payload
[AD-A146897] 07 p0911 N85-15767
The BRESEX multispectral camera: Preliminary characteristics
[INPE-3367-PRE/635] 10 p1487 N85-19386
Modeling 12 p1787 N85-21221
West Europe report: Science and technology
[JPRS-WST-85-013] 14 p2269 N85-24183
Ariane space general director on satellite launcher market 18 p3067 N85-29103
Images of the Earth's aurora and geocorona from the Dynamics Explorer Mission
[NASA-CR-175983] 18 p3136 N85-29423
Fuel cell applications literature review
[DE85-011891] 22 p3809 N85-33592

SATURATED HYDROCARBONS
U ALKANES

SATURATION
Response of saturated porous nonlinear materials to dynamic loadings
[AD-A148528] 06 p1173 N85-17394
A comprehensive strategy for saturation decompression with nitrogen-oxygen
[AD-A151800] 16 p2841 N85-27520
Saturation effect in multilevel lasing media
21 p3686 N85-32901

SATURATION (CHEMISTRY)
Influence of grain size distribution on the undrained dynamic properties of saturated sand
[PB85-102382/GAR] 09 p1305 N85-18197
Kinetics of saturation of porous titanium with low melting point metals 10 p1446 N85-19114
Mechanism of heterogeneous deposition ice nucleation near water-saturation 21 p3638 N85-32597

SATURN (PLANET)
Charged particle erosion of icy satellites: Coronal atmospheres and surface redistribution
03 p0448 N85-12845
Detection of the J-10 manifold of the pure rotational band of phosphine on Saturn 05 p1245 N85-17855
Investigations of planetary ring phenomena
13 p2174 N85-23487
Studies of planetary rings 13 p2174 N85-23488
Dynamical studies of Saturn's rings
13 p2174 N85-23489
Meteoroidal impacts, plasma, fine structure of ringlets and spokes on Saturn's ring B 13 p2174 N85-23490
Interaction of the magnetospheric ions with the surfaces of the icy satellites of Saturn 13 p2174 N85-23491
Plasma production by meteoroid impact
13 p2174 N85-23492
Origin and evolution of the Saturn system
13 p2175 N85-23493
Saturn electrostatic discharges
15 p2673 N85-26499
Statistical study of Saturnian electrostatic discharges observed by the Voyager Planetary Radio Astronomy experiment 15 p2673 N85-26500
An Earth-based attempt to detect Saturn Electrostatic Discharge (SED) at 21 centimeters
15 p2674 N85-26501
Electrons and cosmic ray produced protons in Saturn's inner magnetosphere
[NASA-TM-87469] 15 p2679 N85-26546
Extended atmospheres of outer planet satellites and comets
[NASA-CR-176137] 22 p3851 N85-33848

SATURN ATMOSPHERE
Exploration of the solar system by airborne astronomy
08 p1244 N85-17851
Near infrared modeling of the equatorial regions of Jupiter and Saturn 09 p1415 N85-18930
Dynamics of charged small particles — Jupiter, Saturn magnetospheres 15 p2676 N85-26522
Possible period of Jovian activity and possibility of seasons 16 p2723 N85-26810

SATURN RINGS
A review of radar observations of Saturn's rings
15 p2670 N85-26474
Microwave emission from Saturn's rings
15 p2670 N85-26475
Saturn's rings resolved by the VLA — Very Larg Array (VLA) 15 p2670 N85-26476
Apparent thichness of Saturn's rings from the observations of the ring plane crossing
15 p2671 N85-26477
Azimuthal variations in Saturn's A ring
15 p2671 N85-26478
A model containing blobs for the A ring of Saturn
15 p2671 N85-26479
Saturn's E-ring in the red spectral region
15 p2671 N85-26480
Saturn's E ring 15 p2671 N85-26481
Summary of optical groundbased E ring observations at the University of Arizona 15 p2671 N85-26482
Photometric study of the Saturn E ring
15 p2671 N85-26483
The Saturn ring particles from optical reflectance polarimetry 15 p2671 N85-26484
Saturn rings: Divisions, gaps and ringlets from ground-based telescopes 15 p2672 N85-26485
Physical properties of Saturn's rings
15 p2672 N85-26493
Structure and dynamics of Saturn's rings as seen by the Voyager stellar occultation 15 p2673 N85-26494
The C ring of Saturn: A high resolution view of some of its structure 15 p2673 N85-26495
The eccentric ringlet at 1.29 R sub S — Saturn radius (RS) 15 p2673 N85-26496
Voyager UVS observations of stellar occultations by the rings of Saturn — ultraviolet spectrometer (UVS)
15 p2673 N85-26497
Voyager planetary radio astronomy: Grain and particle impacts shot noise in Saturn's ring plane
15 p2673 N85-26498
Saturn electrostatic discharges
15 p2673 N85-26499
Solved und unsolved problems in planetary ring dynamics 15 p2674 N85-26502
Resonance identifications in Saturn's rings
15 p2674 N85-26504
A simple model of Saturn's rings revisited
15 p2674 N85-26506
Viscosity in Saturn's rings 15 p2674 N85-26507
Physical and geological nature of Saturn's larger ring particles 15 p2674 N85-26509
Effects of shepherd conjunctions on Saturn's F-ring
15 p2675 N85-26511
Orbital elements of Saturn's F ring and its shepherding satellites 15 p2675 N85-26515
Dense but collisionless orbiting rings — Saturn rings
15 p2675 N85-26517
Instabilities and the fine structure of Saturn's rings
15 p2676 N85-26520
The formation of spokes in Saturn's rings
15 p2676 N85-26524
On the role of mother-planet magnetic field in spiral structure explanation of formation of spokes — Saturn rings 15 p2676 N85-26525
On planetary rings as sources and sinks of magnetospheric plasmas 15 p2677 N85-26526
The E-ring of Saturn 15 p2677 N85-26527
Macrostructure and microphysics of Saturn's E-ring
15 p2677 N85-26528
Multivalued electrostatic potentials; chance or necessity for the charge of solid particles near Saturn?
15 p2677 N85-26529
A priority of space exploration: Observation of Saturn's rings from a Saturn orbiter 15 p2679 N85-26542
Rendezvous with Saturn's rings
15 p2679 N85-26543

SATURN SATELLITES
NT ENCELADUS
NT TITAN
Voyager cartography 13 p2203 N85-23668
The control networks of the satellites of Jupiter and Saturn 13 p2204 N85-23671
Orbital elements of Saturn's F ring and its shepherding satellites 15 p2675 N85-26515
Jupiter/Voyager data analysis
[NASA-CR-175723] 15 p2679 N85-26545

SAUDI ARABIA
Meteorological conditions affecting electromagnetic propagation on the Arabian Peninsula
[AD-A152019] 15 p2544 N85-25708
Saudi Arabian refraction profile: Crustal structure of the Red Sea-Arabian Shield transition
17 p2990 N85-28484
Saudi Arabian refraction profile: A preliminary interpretation for the Red Sea-Arabian Shield transition
17 p2991 N85-28485
A traveltime interpretation of the 1978 seismic refraction profile in the Kingdom of Saudi Arabia
17 p2991 N85-28486
Explanation of Russian models: Saudi Arabian seismic refraction profile 17 p2991 N85-28487
Interpretation of the data of USGS seismic refraction profile across the Arabian Shield in western Saudi Arabia 17 p2991 N85-28488
A preliminary analysis of the Saudi Arabian deep seismic sounding data 17 p2991 N85-28489
One-dimensional velocity-depth functions determined for the Arabian Shield and the southwestern Red Sea: A comparison of models 17 p2992 N85-28490
A comparison of crustal sections: Arabian Shield to the Red Sea 17 p2992 N85-28491

SAVANNAHS
U GRASSLANDS

SAWS
Ingot slicing machine and method
[NASA-CASE-NPO-15483-1] 12 p1857 N85-21650

SAWTOOTH WAVEFORMS
A simulation of weather in 3D space
[AD-A155221] 21 p3636 N85-32586

SCALAR MAGNETIC CHARGE
U MAGNETIC CHARGE DENSITY

SCALARS
Renormalization theory in four dimensional scalar fields
[NOTA-INTERNA-824] 02 p0292 N85-11895
Second order modeling of scalar turbulent flows
03 p0360 N85-12311
Accuracy of the finite analytic method for scalar transport calculations
[DE85-001474] 09 p1320 N85-18300
Nonlinear sigma-models and integration methods
[DE85-004447] 12 p1922 N85-22071
Did bosonic sneutrino stars ever exist
[PREPRINT-421] 18 p3202 N85-29867
On the convergence of difference approximations to scalar conservation laws
[NASA-CR-172814] 19 p3344 N85-30728
Intermittency, conditional sampling and turbulent combustion 20 p3424 N85-31249
Conditional modelling in turbulent shear flows
20 p3424 N85-31250
The microstructure approach to conserved scalar pdf models 20 p3424 N85-31251
Recent measurements in turbulent jet flames at Sandia Combustion Research Facility 20 p3424 N85-31254
Assessment of superlayer contribution to the conserved scalar PDF in a hydrogen turbulent jet diffusion flame
20 p3425 N85-31255
Experimental and theoretical investigations of open resonators — precipitation measurement
[DFVLR-FB-85-12] 20 p3449 N85-31414
Vortex dynamics simulation of conserved scalar dissipation 22 p3745 N85-33210
Scalar/Vector potential formulation for compressible viscous unsteady flows
[NASA-CR-3921] 23 p3893 N85-34113
Three-dimensional gravity ideal body studies in rough terrain
[DE85-014097] 24 p4118 N85-35525

SCALE
Model robust response surface designs: Scaling 2-level factorials
[AD-A147494] 07 p1033 N85-16556
SCALE (CORROSION)
Study of the reactive-element effect in oxidation of Fe-Cr alloys using transverse section analytical electron microscopy
[DE84-016237] 04 p0571 N85-13641
Elevated temperature erosion corrosion of 9Cr1Mo steel
[DE85-008445] 18 p3074 N85-29016
Corrosion Research Center of the University of Minnesota
[DE85-009418] 18 p3075 N85-29022
Corrosion-erosion rates/mechanisms of 9Cr1Mo steel
[DE85-008508] 18 p3076 N85-29029
The effect of temperature on the corrosion-erosion of 9Cr1Mo steel
[DE85-008507] 18 p3076 N85-29030
Optimization of MCr Al coating compositions for marine gas turbines
[BR91159] 20 p3394 N85-31056
A study of adherent oxide scales
[AD-A155554] 21 p3567 N85-32188
The preparation of TEM specimens showing oxide scales in transverse cross-section
[AERE-R-11579] 24 p4078 N85-36276
SCALE (RATIO)
Color and grey scale in sonar displays
05 p0710 N85-14552
Mars radar catalog 13 p2198 N85-23636
Design of a physical model of the cochlea. Displacement sensor for small amplitudes in a highly viscous liquid
[STN-6] 20 p3507 N85-31802
The problem of scale in planetary geomorphology
21 p3603 N85-32375
Quantitative analysis of geomorphic processes using satellite image data at different scales
21 p3604 N85-32380
Scaling violation in the fragmentation region of inclusive nucleon spektrum 24 p4173 N85-36874
SCALE EFFECT
Investigations into the effects of scale and compressibility on lift and drag in the RAE 5m pressurized low-speed wind tunnel 08 p1068 N85-16773
Investigations into the effects of scale and compressibility on lift and drag in the RAE 5m pressurised low-speed wind tunnel
[RAE-TM-AERO-2006] 13 p1969 N85-22372
The Shock and Vibration Digest, volume 17, no. 2
[AD-A153129] 17 p2977 N85-28400
Recent progress in the dynamic plastic behaviour of structures, part 4 17 p2978 N85-28402
Least-squares approximation to minimum chi-square estimators of location and scale parameters and their effect on the Pearson chi-square test
[AD-A153534] 18 p3169 N85-29638
Hard X-ray measurements of the hot electron rings in Nagoya BUMPY TORUS (NBT-1M)
[IPPJ-720] 19 p3370 N85-30899
Scale separation closure and Alfven wave turbulence
[DE85-013124] 24 p4095 N85-35385
SCALE MODELS
Model study of the interaction of a blast wave with the superstructure of ships. Part 5: Application of optical measurement methods to the study of blast interaction
[PML-1984-12-PT-5] 01 p0057 N85-10375
Singular perturbations, coherency and aggregation of dynamic systems
[DE84-014166] 01 p0114 N85-10772
Review of requirements and status of simulation and scaling of transonic, viscous flows
[AD-A146357] 06 p0808 N85-15137
Discrete modifications to continuous dynamic structural systems 09 p1337 N85-18410
Analysis of ground pressure distribution beneath tracked model with respect to external loading
[AD-P004275] 09 p1406 N85-18851
Acoustic scaling: A re-evaluation of the acoustic model of Manchester Studio 7
[BBC-RD-1984/18] 12 p1822 N85-21432
A new model for thin plates with rapidly varying thickness. Part 3: Comparison of different scalings
[AD-A149748] 12 p1868 N85-21704
Impact studies of a 1/3-scale model of an air cushion vehicle
[NASA-TM-86360] 14 p2218 N85-23757
An evaluation of proposed acoustic treatments for the NASA LaRC 4 x 7 meter wind tunnel
[NASA-CR-172577] 15 p2646 N85-26319
Plasma heating 15 p2654 N85-26372
Wind-tunnel evaluation of a 21-percent-scale powered model of a prototype advanced scout helicopter
[NASA-TP-2420] 18 p3058 N85-28923
Design of a physical model of the cochlea. Displacement sensor for small amplitudes in a highly viscous liquid
[STN-6] 20 p3507 N85-31802
Reverification of the Chesapeake Bay model
[AD-A155486] 21 p3655 N85-32706
SCALERS
Construction of solutions for two-dimensional Riemann problems
[DE85-003136] 10 p1549 N85-19770
SCALING
Universal binding energy relations in metallic adhesion
[NASA-TM-86889] 03 p0331 N85-12132
SCALING LAWS
Thermal fluid-structure interaction: A few scaling considerations — nuclear reactors
[GKSS-84-E-18] 01 p0048 N85-10314
K-shell yield scaling law for conventional PRS loads
[AD-A145155] 01 p0121 N85-10831
Factor analysis applied to a silane coupling agent on E-glass fiber system
[AD-A145687] 02 p0187 N85-11249
Similarity considerations in 1-component 2-phase flow
[DE84-016370] 04 p0499 N85-13184
Theoretical studies of Field-Reversed Configurations (FRC) and experimental study of the FRC during translation
[DE84-016467] 04 p0566 N85-13603
A nonlocal expression for the ponderomotive potential
[IPPJ-699] 06 p0864 N85-15487
Wavelength scaling of laser plasma coupling
[DE84-014537] 06 p0866 N85-15505
On existence and uniqueness of solutions of Hamilton-Jacobi equations
[AD-A147597] 07 p1033 N85-16560
Hazard assessment of a hypothetical large rocket motor 08 p1117 N85-17042
The scaling of coronal models from one star to another 08 p1233 N85-17771
FRC translation dynamics and plasma confinement properties in FRX-C/T
[DE85-002386] 10 p1560 N85-19842
Magnetic fluctuations, field reversal maintenance, and anomalous thermal transport in the reversed field pinch
[DE85-003804] 11 p1732 N85-20692
Impact crater scaling laws 13 p2181 N85-23532
Los Alamos Science, Number 11, Summer-Fall, 1984
[DE85-004634] 14 p2419 N85-24926
Experimental investigation of annular air curtain domes
[UTIAS-288] 15 p2521 N85-25543
Theoretical studies of Elmo Bumpy Torus
[DE85-007202] 15 p2658 N85-26402
Restrike particle beam experiments on a dense plasma focus. Opening switch research on a dense plasma focus
[AD-A152991] 17 p3039 N85-28802
Quantum effects in linear collider scaling laws
[DE85-009846] 19 p3363 N85-30851
Computer programs for smoothing and scaling airfoil coordinates
[NASA-TM-84666] 20 p3388 N85-31011
TNT equivalency of EAK explosive
[AD-A155737] 21 p3571 N85-32211
Soil extraction kit
[AD-D011736] 22 p3742 N85-33190
Magnetic field generation in the cores of terrestrial bodies 22 p3859 N85-33894
Scaling parameters of flashover
[NBS-GCR-85-497] 23 p3911 N85-34229
Scaling differences between large interplate and intraplate earthquakes
[NASA-CR-176149] 23 p3948 N85-34467
Confinement experiments on ISX-B
[DE85-012346] 23 p3964 N85-34709
Model robust response surface designs: Scaling two-level factorials
[AD-A156218] 24 p4143 N85-35688
Scaling violation in hadron-nucleus interaction
[HE-3.2-8] 24 p4179 N85-35916
Particle interactions at energies over 1000 TeV inferred from gamma-families observed at Mount Fuji
[HE-3.5-1] 24 p4183 N85-35940
Multidimensional analysis of data obtained in experiments with X-ray emulsion chambers and extensive air showers
[HE-3.6-2] 24 p4184 N85-35951
Hadrons registration in emulsion chamber with carbon block
[HE-3.7-3] 24 p4186 N85-35962
Intensities of high-energy cosmic rays at Mount Kanbala
[HE-3.7-5] 24 p4188 N85-35964
Simulation of EAS properties on the basis of high energy interaction model deduced from the accelerator data
24 p4187 N85-35973
SCANDINAVIA
Ground magnetic observations of high-latitude Pi2 pulsations: Scandinavian magnetometer array results
14 p2370 N85-24649
SCANDIUM
NT SCANDIUM ISOTOPES
Effect of ScAl3 phase dispersion on hardening of alloy Al-6.3 percent Mg-0.21 percent Sc
19 p3241 N85-30096
Possible causes of modification and strengthening of aluminum by scandium 19 p3241 N85-30099
The isotopic composition of cosmic ray calcium
[OG-4.3-5] 22 p3879 N85-34030
SCANDIUM ISOTOPES
Mechanisms of impurity diffusion in rutile
[DE84-014741] 06 p0766 N85-14902
SCANDIUM 46
U SCANDIUM ISOTOPES
SCANNERS
NT COASTAL ZONE COLOR SCANNER
NT HORIZON SCANNERS
NT INFRARED SCANNERS
NT MULTISPECTRAL BAND SCANNERS
NT OPTICAL SCANNERS
NT ULTRASONIC SCANNERS
A scanning alarm electronic processor
[AD-D011419] 08 p1158 N85-17309
Filter reflection image guide oscillator and solid state line scanning device
[AD-D011440] 10 p1479 N85-19336
Defense Mapping Agency (DMA) raster-to-Vector benchmark testing
[AD-A154152] 19 p3338 N85-30683
Six mechanisms used on the SSM/1 radiometer
22 p3796 N85-33534
Method and apparatus for measuring areas of photoelectric cells and photoelectric cell performance parameters
[DE85-011629] 22 p3810 N85-33599
Cylindrical lens-array antenna for wideband electronic scanning
[AD-A156085] 24 p4090 N85-35350
SCANNING
NT CONICAL SCANNING
NT FREQUENCY SCANNING
NT RADAR SCANNING
Characteristics of polarization grids made of parallel metal strips during hemispherical scanning
06 p0792 N85-15062
Filter reflection image guide oscillator and solid state line scanning device
[AD-D011440] 10 p1479 N85-19336
New high resolution scanning ion microprobe and focused ion beam applications
[AD-A149982] 12 p1852 N85-21616
NDE methods for green ceramics
[DE85-004019] 13 p2038 N85-22766
Factors affecting dwell times on digital displaying
[NASA-TM-86406] 14 p2390 N85-24722
A new NASTRAN capability for data reduction
15 p2574 N85-25874
Eye movement in response to single and multiple targets
[AD-A151115] 15 p2617 N85-26128
An error-dependent model of instrument-scanning behavior in commercial airline pilots
[NASA-CR-3908] 21 p3665 N85-32765
Intermolecular explosives
[DE85-009809] 23 p3921 N85-34296
LANDSAT-4/5 image data quality analysis
[E85-10105] 24 p4107 N85-35483
SCANNING DEVICES
U SCANNERS
SCANNING LASER ACOUSTIC MICROSCOPE (SLAM)
U ACOUSTIC MICROSCOPES
SCAR PROGRAM
U SUPERSONIC CRUISE AIRCRAFT RESEARCH
SCARFING
Detection of pores in hot continuously cast rounds
[BMFT-FB-T-85-007] 18 p3072 N85-29000
SCARPS
U ESCARPMENTS
SCARS (GEOLOGY)
U EROSION
SCATHA SATELLITE
SCATHA (spacecraft charging at high altitudes) plasma interaction experiment: SC-3 high energy particle spectrometer; SC-8 energetic ion composition experiment
[AD-A146728] 12 p1793 N85-21252
Aerospace spacecraft-charging guidelines document
13 p1994 N85-22501
Automatic charge control system for satellites
13 p1995 N85-22508
Results of the SCATHA ion composition experiment during the IMS 14 p2359 N85-24580

SCATTER PROPAGATION
Research on acoustical and optical scattering, optics of bubbles, diffraction catastrophes, laser generation of sound, and shock induced cavitation
[AD-A146703] 06 p0880 N85-15466
Limits of the propagation medium with respect to digital signal transmission 10 p1469 N85-19270
Tropospheric scatter communication system having angle diversity
[AD-D011446] 14 p2291 N85-24200
A transport theory of millimeter wave propagation in woods and forests
[AD-A151883] 17 p2947 N85-28196
Implications of cross section errors for cosmic ray propagation
[OG-7.2-3] 23 p4014 N85-34875
Alfven wave scattering and the secondary to primary ratio
[OG-7.2-9] 23 p4015 N85-34878
Interstellar turbulence, random density variations, and scintillation measurements
[OG-7.2-13] 23 p4015 N85-34880
Relativistic transport theory for cosmic-rays
[OG-8.3-8] 23 p4022 N85-34926
An experiment to measure the energy spectrum of cosmic ray antiprotons from 100 to 1000 MeV
[OG-9.1-3] 23 p4022 N85-34929
Linear absorption and scattering of laser beams
[AD-A156167] 24 p4098 N85-35401

SCATTERERS
U SCATTERING

SCATTERING
NT ACOUSTIC SCATTERING
NT ATMOSPHERIC SCATTERING
NT BACKSCATTERING
NT COHERENT SCATTERING
NT COMPTON EFFECT
NT ELASTIC SCATTERING
NT ELECTROMAGNETIC SCATTERING
NT ELECTRON SCATTERING
NT FORWARD SCATTERING
NT HALOS
NT INCOHERENT SCATTERING
NT INELASTIC SCATTERING
NT INVERSE SCATTERING
NT ION SCATTERING
NT LIGHT SCATTERING
NT MICROWAVE SCATTERING
NT MIE SCATTERING
NT NEUTRON SCATTERING
NT NUCLEAR SCATTERING
NT NUCLEON-NUCLEON SCATTERING
NT PROTON SCATTERING
NT RADAR SCATTERING
NT RAMAN SPECTRA
NT RAYLEIGH SCATTERING
NT RESONANCE SCATTERING
NT REVERBERATION
NT THOMSON SCATTERING
NT TROPOSPHERIC SCATTERING
NT WAVE SCATTERING
NT X RAY SCATTERING
Spline-Galerkin solution of integral equations for 3-body scattering above break-up
[TWISK-327] 01 p0109 N85-10738
A finite element projection method for the solution of particle transport problems with anisotropic scattering
[AD-A145382] 02 p0250 N85-11637
Total area of diffusion elements in a reverberation chamber and measured degree of sound absorption
[NRC/CNR-TT-2110] 03 p0415 N85-12653
Scattering from multi-scale surface — Infrared lasers
[RSRE-MEMO-3656] 04 p0505 N85-13222
Laboratory studies of atomic collision processes of importance in planetary atmospheres
[NASA-CR-174142] 04 p0589 N85-13758
Transient currents of ideally conducting body of revolution with transient diffraction
06 p0785 N85-15019
Structural studies of amorphous Mo-Ge alloys using synchrotron radiation
[DE85-002061] 08 p1131 N85-17125
Effects of heterogeneities on the propagation, scattering and attenuation of seismic waves and the characterization of seismic source
[AD-A148284] 08 p1186 N85-17478
Optical wave propagation and imaging in the atmosphere 08 p1222 N85-17694
Effect of scattering on instabilities in line-driven stellar winds 08 p1235 N85-17764
DSN 34-meter antenna optics analysis for wideband SETI investigations 10 p1465 N85-19244
Influence of scattering on Q in the lithosphere
[AD-A149318] 10 p1515 N85-19563
Quantum mechanical and semiclassical approaches to molecular dynamics
[DE85-003458] 10 p1555 N85-19803
Imaging through a multiple scattering medium
[DE85-002051] 10 p1557 N85-19821
Dynamical studies of molecular systems
[DE85-009053] 11 p1594 N85-20028
Electron acceleration by laser fields in a gas
[DE85-000575] 11 p1639 N85-20323
Self-Optimized Sector (SOS) model of self-consistent energy loss and scattering for an electron beam propagating in air
[DE85-003161] 11 p1722 N85-20631
An iteration method for complex scattering problems
[AD-A150038] 12 p1934 N85-22151
High energy facilities advanced projects: Intrabeam scattering for a beam of gold ions
[DE85-000687] 12 p1941 N85-22192
Paramagnetic scattering from Ni
[DE85-004207] 12 p1942 N85-22198
Mathematical modeling of two-frequency laser sounding of scattering media 13 p2089 N85-23045
Improvement in magnetic field properties of vanadium-gallium superconductors by enhancement of spin-orbit scattering
[DE85-002893] 13 p2164 N85-23422
Receiver optimization for detection in doubly spread communication channels
[AD-A151226] 15 p2541 N85-25689
Space shuttle molecular and wake vacuum measurements
[NASA-TM-86509] 19 p3222 N85-29978
Microwave bandstop filter
[AD-D011716] 19 p3261 N85-30222
Measurement problem in PROGRAM UNIVERSE
[DE85-008179] 19 p3378 N85-30959
Guided-mode launching in a slab waveguide by way of diffraction at the edge of a conducting screen residing on one surface of the slab
[AD-A154886] 21 p3575 N85-32232
Interpretation of photometric measurements of airless bodies 22 p3855 N85-33871
Monte Carlo techniques for analyzing deep penetration problems
[DE85-011426] 23 p3968 N85-34598
Fokker-Planck calculation of hot electron formation in the thermal barrier region of tandem mirror Gamma-10
[IPPJ-726] 23 p3979 N85-34669
Stochastic particle acceleration in solar flares
[SH-1.1-4] 23 p3989 N85-34731
Exponential anisotropy of solar cosmic rays
[SH-3.2-1] 23 p4002 N85-34817
Energetic solar particle events
[SH-3.2-2] 23 p4003 N85-34818
Channeled propagation of solar particles
[SH-3.2-3] 23 p4003 N85-34819
The local characteristic function of interplanetary particle propagation
[SH-3.2-8] 23 p4003 N85-34823
Spatial distribution of cosmic rays in magnetic cycles of the Sun
[SH-4.2-20] 23 p4009 N85-34857
SONTRAC: A solar neutron track chamber detector
[SH-9.1-12] 23 p4052 N85-35127
The HEAO-2 Guest Investigator Program: Non-linear growth of instabilities in line-driven stellar winds
[NASA-CR-176168] 24 p4168 N85-35840
Scattering and stopping of hadrons in nuclear matter
24 p4174 N85-35882
The hump in the Cerenkov lateral distribution of gamma ray showers
[HE-4.5-9] 24 p4195 N85-36032
Search for tachyons associated with extensive air showers in the ground level cosmic radiation
[HE-6.2-13] 24 p4212 N85-36149

SCATTERING AMPLITUDE
Scattering of plane wave on cylindrical shell in low-frequency region 02 p0256 N85-11677
Nonlinear saturation of stimulated Raman scattering in homogeneous plasma
[DE85-003120] 10 p1560 N85-19837
Calculation of amplitude-phase characteristics of signal scattered obliquely on meteor trail
13 p2073 N85-22948
Measurement and analysis of critical crack tip processes during fatigue crack growth
[NASA-CR-172597] 21 p3598 N85-32342

SCATTERING COEFFICIENTS
Relation between atmospheric scattering and backscattering coefficient
[ESA-TT-837] 05 p0677 N85-14350
Evaluation of machining damage in brittle materials
[DE85-001794] 11 p1612 N85-20136
A method for determining in situ the absorption coefficient of particulate media using pulsed laser technique
[AD-D011548] 12 p1799 N85-21281
Test of lidar inversion algorithm sensitivity to atmospheric backscatter and extinction parameters, revision A
[AD-A152062] 16 p2865 N85-27671
Light scattering by leaf layers with application to canopy reflectance modeling: The Scattering by Arbitrarily Inclined Leaves (SAIL) model
[NLR-MP-84011-U] 17 p3038 N85-28796
Active and passive remote sensing of ice
[AD-A154406] 19 p3300 N85-30459
Variability of rural aerosols under stable weather conditions 21 p3647 N85-32663

SCATTERING CROSS SECTIONS
Study of structure of nuclei with neutrons and nuclear data measurements for MFE
[DE84-015128] 01 p0117 N85-10802
Measurement of magnetic sublevel differential scattering cross sections for potassium and mercury
[MPIS-10/1983] 01 p0119 N85-10815
Influence of strut cross-section on strut radiation of reflector antennas
[FI-455-TBR-39] 03 p0357 N85-12295
Acoustic scattering cross sections for truly composite wind-wave surfaces. Scattering without bubbles
[AD-A145672] 03 p0415 N85-12655
Fast neutron capture with a white neutron source
[DE84-016799] 04 p0562 N85-13580
Energy transfer in atom-molecule scattering experiments in the 1eV region with SF6-Ar, CF4-Ne and Xe-CO2 systems as examples
[REPT-11/1983] 04 p0563 N85-13588
Investigation on K (4 2P3/2) Hg interaction at collision energies from 0.5 to 5.7 eV
[MPIS-15/1983] 04 p0563 N85-13589
Rotational inelastic scattering of He-atoms at HF-, HCl-, CF4-, SF6-, C2H6- and C2F6-molecules
[MPIS-9/1984] 04 p0564 N85-13590
Measurement of scattering cross sections of liquid and solid hydrogen deuterium and deuterium hydride for thermal neutrons
[DE84-014814] 05 p0727 N85-14671
Scattering experiments on interactions of excited atoms: Differential cross sections of the system Na (3P)+K(4S)
[MPIS-8/1984] 05 p0728 N85-14677
Measurements of the A-dependance of deep-inelastic electron scattering from nuclei
[DE84-013965] 05 p0728 N85-14678
Pion inelastic scattering to the first three excited states of Lithium-6
[AD-A147560] 07 p1041 N85-16606
Theoretical cross sections for inner-shell vacancy production by high-energy electrons
[DE84-007346] 11 p1721 N85-20627
Theoretical study of near-threshold electron-molecule scattering
[DE85-004530] 12 p1930 N85-22126
Particle shape characterization
[AD-A151981] 15 p2544 N85-25707
Theory of electron-impact atomic ionization cross sections
[AD-A151763] 16 p2861 N85-27648
Electromagnetic transmission through a slot in a perfectly conducting plane
[AD-A153224] 17 p2949 N85-28210
Application of forward scattering renormalization to scattering in turbid media
[AD-A153232] 17 p2959 N85-28271
A study of excitations during collisionally-induced electron detachment of negative ions
[AD-A152879] 17 p3030 N85-28739
New experimental results in two photon physics
[NIKHEF-H/84-16] 17 p3035 N85-28776
Theory of high energy collision processes
[DE85-010183] 19 p3362 N85-30846
AGS broad band neutrino beam
[DE85-010954] 19 p3366 N85-30875
Study of proton and neutron activation of metal samples in low Earth orbit
[NASA-CR-171596] 21 p3558 N85-32130
The use of the glistening surface concept in rough surface scattering
[AD-A154922] 21 p3575 N85-32234
An analysis of physical optics models for rough surface scattering
[AD-A154960] 21 p3575 N85-32235
Head-on scattering of a tubular cylinder of finite length for radar target identification purposes
[AD-A155608] 21 p3577 N85-32246
Radar echoes at 2.66 and 40.92 MHz from the mesosphere, part 2.6A 21 p3619 N85-32486

Implicit Monte Carlo methods and non-equilibrium Marshak wave radiative transport
[DE85-010711] 22 p3835 N85-33743
Implications of cross section errors for cosmic ray propagation
[OG-7.2-3] 23 p4014 N85-34875
On the importance of interstellar helium for the propagation of heavy cosmic rays
[OG-7.2-11] 23 p4015 N85-34879
Proton-air and proton-proton cross sections from air shower data
[HE-1.1-1] 24 p4170 N85-35849
Proton-air inelastic cross section at S(1/2) = 30 TeV
[HE-1.1-2] 24 p4170 N85-35850
Hadron cross sections at ultra high energies and unitarity bounds on diffraction dissociation
[HE-1.1-3] 24 p4170 N85-35851
On total cross sections and slopes at superhigh energies
[HE-1.1-4] 24 p4170 N85-35852
Determination of the cross section of the proton, pion and neutron inelastic interaction with lead and carbon nuclei at 0.5 - 5.0 TeV energies (PION experiment)
[HE-1.1-5] 24 p4170 N85-35853
P(P bar)P elastic scattering and cosmic ray data
[HE-1.1-6] 24 p4170 N85-35854
Measurement of interaction cross section of cosmic ray Fe nuclei (E4 GeV/N) with Al target
[HE-1.1-7] 24 p4170 N85-35855
Hadron thermodynamics in relativistic nuclear collisions
[HE-1.1-8] 24 p4171 N85-35856
The method for the study of the inelastic cross-section for high energy protons by means of shower arrays with the large calorimetric area
[HE-1.1-11] 24 p4171 N85-35858
QCD-motivated description of very high energy particle interactions
[HE-1.2-2] 24 p4171 N85-35861
Is the inelastic charge-exchange contribution constant at the large X and superhigh energies? Qaut 01Kuchin, I. A. 24 p4173 N85-35871
General consequences of the violated Feynman scaling 24 p4173 N85-35872
Intensities of high-energy cosmic rays at Mount Kanbala
[HE-3.7-5] 24 p4186 N85-35964

SCATTERING FUNCTIONS
Scattering theory by Enss' method for operator valued matrices: Dirac operator in an electric field
[REPT-64] 01 p0045 N85-10290
Calculation of the scattering function of rotating molecules with emphasis on the tunnel spectra of absorbed molecules 03 p0427 N85-12725
Scattering of waves by axisymmetrical edge 13 p2080 N85-22987
Numerical solution of a first kind Fredholm integral equation arising in electron-atom scattering
[CWI-NM-R8414] 14 p2414 N85-24897
Multiple scattering of electromagnetic waves in discrete random media
[AD-A151766] 16 p2772 N85-27112
Characteristics of optical information-measurement channels with utilization of scattering effects 22 p3781 N85-33429

SCATTERING MATRIX
U S MATRIX THEORY

SCATTEROMETERS
The altimeter as a support to the scatterometer in the representation of winds and derived wave fields in coastal waters and enclosed seas: A research at its onset 03 p0383 N85-12453
Studies of coastal mesoscale winds using SIR-B 08 p1147 N85-17238
Information for space radar designers: Required dynamic range vs resolution and antenna calibration using the Amazon rain forest 08 p1147 N85-17239
Science opportunities using the NASA scatterometer on N-ROSS
[NASA-CR-175639] 13 p2123 N85-23222
The impact of scatterometer data on limited-area model predictions of the QE 2 storm 18 p3139 N85-29436
Utilization of the SEASAT scatterometer winds for ocean mixed layer modeling
[AD-A153748] 18 p3150 N85-29508
Comparison of ERS-1 scatterometer Monte Carlo performance simulations using a weighted nonlinear least squares and a maximum likelihood estimation method 20 p3420 N85-31224
Results of the MIZEX preliminary campaign: 29 June to 19 July 1983 — Marginal Ice Zone Experiment (MIZEX), satellite observation
[CNES-84/142/T/CT/DRT/TIT/RL] 20 p3478 N85-31609
AMI calibration study. Volume 1: SAR calibration. Volume 2: Ground Targets. Volume 3: Scatterometer calibration — Active Microwave Instrument (AMI) ERS-1
[C2248/4/4-VOL-1] 23 p3936 N85-34394

SCAVENGING
Earth-to-orbit propellant transportation overview 08 p1108 N85-17002
Space Transportation System (STS) propellant scavenging system study. Volume 1: Technical report
[NASA-CR-171848-VOL-1] 11 p1589 N85-20000
Space Transportation System (STS) propellant scavenging system study. Volume 2: Supporting research and technology report
[NASA-CR-171849-VOL-2] 11 p1589 N85-20001
Space Transportation System (STS) propellant scavenging system study. Volume 3: Cost and work breakdown structure-dictionary
[NASA-CR-171850-VOL-3] 11 p1590 N85-20002

SCENE ANALYSIS
Analysis of accretion and deletion at boundaries in dynamic scenes
[AD-A145944] 03 p0419 N85-12678
Texture classification using autoregressive filtering 07 p0984 N85-16254
Multi target tracking by dynamic scene analysis
[AD-A148922] 10 p1466 N85-19250
A method for reduction of ambiguity in segmentation of images
[INPE-3394-TDL/186] 11 p1697 N85-20664
Preliminary study of information extraction of LANDSAT TM data for a suburban/regional test site 13 p2121 N85-23208
Validation of the ERBE scanner scene identification methodology: Analysis with Nimbus-7 ERB data
[NASA-CR-172596] 16 p2832 N85-27466
Scene analysis using recursive frequency domain correlation with energy normalization
[AD-A151777] 16 p2854 N85-27596
An image compression survey and algorithm switching based on scene activity
[NASA-TP-2458] 22 p3727 N85-33106

SCF
U SELF CONSISTENT FIELDS

SCHEDULES
NT COUNTDOWN
List of recent Soviet space launches 02 p0165 N85-11120
AGARD bulletin technical programme, 1985
[AGARD-BUL-84-2] 02 p0305 N85-11971
Space telescope cost, schedule, and performance review, 1984
[GPO-39-085] 04 p0579 N85-13698
Overview od STS ground operations/orbiter turnaround STS-1 through STS-7 08 p1096 N85-16926
Calendar of selected aeronautical and space meetings
[AGARD-CAL-84/2] 10 p1573 N85-19917
Space Transportation System. Space shuttle payload flight assignments
[NASA-TM-87492] 19 p3224 N85-29989
Space Transportation System. Space shuttle payload flight assignments
[NASA-TM-87491] 19 p3224 N85-29990

SCHEDULING
NT PREDICTION ANALYSIS TECHNIQUES
Constraint-based scheduling in an intelligent logistics support system: An artificial intelligence approach
[AD-A145613] 02 p0293 N85-11900
Decentralized control of scheduling in distributed systems
[AD-A147446] 07 p1022 N85-16487
Transmission scheduling to reduce convex delay costs in packet networks
[AD-A148451] 08 p1153 N85-17278
Order picking in an aisle
[AD-A149553] 10 p1548 N85-19766
On maximizing the expected lifetime of replaceable systems
[AD-A150003] 12 p1862 N85-21680
State dependent priority rules for scheduling
[AD-A149972] 12 p1924 N85-22090
Onboard demand scheduling of a multibeam SS/TDMA satellite with integrated circuit and packet switching 14 p2229 N85-23812
Information technology applications in voluntary sector transport operations. SP1: Objectives and programme of work
[TT-8501] 15 p2667 N85-26457
Large scale electricity production scheduling via nonlinear optimization
[REPT-84-07] 17 p3017 N85-28655
Automated maintenance system test program increment VI production scheduling
[AD-A153694] 18 p3198 N85-29836
Cost and schedule implications of multinational coproduction
[AD-A154358] 19 p3380 N85-30989
Simulation studies of time-control procedures for the advanced air traffic control system
[NASA-TP-2493] 21 p3553 N85-32101
Aviation system delays
[S-HRG-98-1241] 21 p3553 N85-32102
Deficit irrigation feasibility study and demonstration project
[DE85-011531] 22 p3802 N85-33555

SCHEMATICS
U CIRCUIT DIAGRAMS

SCHIFF BASES
U IMINES

SCHIST
Metamorphic petrology of the Table Mountain area, Circle quadrangle, Alaska 04 p0516 N85-13295

SCHLIEREN PHOTOGRAPHY
Experimental investigation of a pulse combustor: Flow visualization by Schlieren photography
[DE85-002662] 11 p1636 N85-20004

SCHMIDT CAMERAS
Some aspects of photography with a small Schmidt camera — astronomical photography 07 p0964 N85-16116
The UK Schmidt telescope and the facilities in Edinburgh 07 p0965 N85-16121
Astronomers' problems with the calibration of Schmidt plates 07 p0965 N85-16128
Cometary astrometry with Schmidt cameras 14 p2435 N85-25020
Astrometry at La Silla 14 p2436 N85-25025

SCHMIDT TELESCOPES
What do we want: Increased speed, resolution, contrast or DQE? — astronomical photography 07 p0964 N85-16115
The UK Schmidt telescope and the facilities in Edinburgh 07 p0965 N85-16121
An investigation into the fidelity of reproduction of UKST original objective prism plates on to film — United Kingdom Schmidt Telescope (UKST) 07 p0965 N85-16123
Sub-beam prism used at the Bosscha Schmidt telescope 07 p0965 N85-16125
The Malin effect in stellar photography 07 p0966 N85-16131
An objective prism quasar survey with the Schmidt telescope on Calar Alto (Spain) 08 p1243 N85-17845

SCHOOLS
Computer Literacy Act of 1983, part 2
[H-REPT-98-752-PT-2] 04 p0578 N85-13687
Recent naval Postgraduate School publications
[AD-A151723] 16 p2875 N85-27740

SCHOTTKY BARRIER DIODES
U SCHOTTKY DIODES

SCHOTTKY DIODES
Coplanar Schottky variable phase shifter
[AD-A146304] 03 p0359 N85-12305
Effect of barrier height on friction behavior of the semiconductors silicon and gallium arsenide in contact with pure metals
[NASA-TP-2405] 04 p0478 N85-13044
Planning of hybrid integrated circuits for microwave-band oscillators 04 p0490 N85-13124
Imaging polarimeter-interferometer arrays for Tokamak measurements
[DE84-015916] 05 p0730 N85-14693
Amorphous metallic layers in Si metallization systems 06 p0830 N85-15277
Photoluminescent and electroluminescent properties of Cd sub 0.95 Mn sub 0.05 Se electrodes
[AD-A146775] 07 p0946 N85-15995
Buried junction enhanced Schottky barrier device
[AD-D011399] 07 p1044 N85-16535
Electronics component R and D, production capability reviewed 08 p1140 N85-17161
Low capacitance e-beam fabricated beam-lead Schottky barrier diodes
[AD-A150238] 13 p2083 N85-22998
Fabrication and I-V characterization of AlGaAs/GaAs MODFETs with P-type surface layers grown by molecular beam epitaxy
[AD-A151695] 15 p2660 N85-26415
Completely consumed carbide: A new process for dielectric isolation
[AD-A152379] 17 p2918 N85-27967
Research and developmental study on MIS thin film solar cells of amorphous hydrogenated silicon, part 2
[BMFT-FB-T-84-290] 17 p2988 N85-28467
Heterojunction Schottky gate MESFET with lower channel ridge barrier
[AD-D011673] 19 p3258 N85-30199
Schottky theory of three component plasmas
[AD-A154461] 19 p3371 N85-30907
Contact properties of rare-earth silicides and germanides on Si and Ge 19 p3374 N85-30931

Numerical simulation of nonisothermal transient processes in GaAs diode structures
22 p3767 N85-33350
SCHOTTKY EFFECT
U WORK FUNCTIONS
SCHROEDINGER EQUATION
Semiclassical theory of resonances
[REPT-67] 01 p0114 N85-10777
Reduction of nonlinear problems to Schroedinger or heat equations: Formation of Kepler orbits, singular solutions for hydrodynamical equations
[REPT-72] 01 p0129 N85-10882
Difference schemes for equations of Schrodinger type
[AD-A145812] 03 p0410 N85-12622
Conservative and nonconservative schemes for the solution of the nonlinear Schroedinger equation
[CWI-NM-R8405] 05 p0720 N85-14628
Multidimensional inverse scattering for first order systems
[AD-A148711] 08 p1214 N85-17642
Connection between time- and frequency-domain three-dimensional inverse problems for the Schroedinger equation
[DE85-005914] 15 p2639 N85-26274
Computer modeling of vibrational energy levels of potential laser candidates (diatomic molecules)
[AD-A151765] 16 p2790 N85-27209
Anderson localization for large disorder or low energy
[PREPRINT-426] 18 p3176 N85-29692
Attractors for the Kuramoto-Sivashinsky equations
[DE85-009831] 20 p3520 N85-31892
K(-) hydrogen bound and continuum states in momentum space
[DE85-010429] 22 p3841 N85-33789
SCHUMANN-RUNGE BANDS
MSG-7: Atmospheric penetration of solar radiation in the range of Schumann-Runge bands
11 p1657 N85-20443
Determination of band oscillator strengths of atmospheric molecules from high resolution vacuum ultraviolet cross section measurements
[NASA-CR-176150] 22 p3814 N85-33624
SCHWARTZ INEQUALITY
Some ideas for decomposing the domain of elliptic partial differential equations in the Schwarz process
[DE85-011844] 22 p3834 N85-33739
SCHWARZSCHILD METRIC
A derivation of relativistic effects in satellite tracking
[AD-A154620] 21 p3558 N85-32132
SCIATIC REGION
Differential effect of denervation on free radical scavenging enzymes in slow and fast muscle of rat
[NASA-CR-175719] 15 p2614 N85-26110
Changes in the cholinergic system of rat sciatic nerve and skeletal muscle following suspension induced disuse
[NASA-CR-175718] 15 p2615 N85-26111
SCIENCE
Emergency Mathematics and Science Education Act
[GPO-29-561] 03 p0435 N85-12770
European Scientific Notes, volume 38, number 12
[AD-A148713] 09 p1418 N85-18946
China report: Science and technology
[JPRS-CST-84-037] 10 p1424 N85-18982
West Europe report: Science and technology
[JPRS-WST-85-006] 11 p1592 N85-20013
The Impact of Science on Society
[NASA-SP-482] 14 p2431 N85-24894
The legacy of science 14 p2432 N85-24895
East European report: Science and technology
[JPRS-ESA-85-010] 15 p2524 N85-25560
Characteristics of recent science/engineering graduates, 1982: Detailed statistical tables
[PB85-149060] 15 p2663 N85-26437
Academic science and engineering: Graduate enrollment and support, fall 1982 (detailed statistical tables)
[PB85-154730] 15 p2664 N85-26438
Academic science and engineering: R and D funds, fiscal year 1982 (detailed statistical tables)
[PB85-154763] 15 p2664 N85-26443
SCIENTIFIC SATELLITES
NT ASTRONOMICAL SATELLITES
NT ATS
NT EXOSAT SATELLITE
NT MAGSAT SATELLITES
NT UK SATELLITES
Space Research in Japan. National report
01 p0013 N85-10082
Satellite observations 01 p0013 N85-10083
The galaxy scene and QUASAT — VLBI satellite
07 p1056 N85-16703
The QUASAT mission: An overview
07 p1056 N85-16704
Solar Corona Explorer: A mission for the physical diagnosis of the solar corona
[NASA-TM-87416] 10 p1572 N85-19912
Drag-free satellite simulator
[REPT-615] 12 p1789 N85-21229
S3-3 ONR-118 data analysis
[AD-A149725] 12 p1869 N85-21855
Assessment study of liquid content measurement methods applicable to space missions — Infrared Space Observatory
[TU-HH-TRI-ESA-84-2] 17 p2938 N85-28135
SCIENTISTS
Synthesis and characterization of advanced materials
[PB84-215326] 01 p0025 N85-10156
A bibliography of planetary geology and geophysics principal investigators and their associates, 1983 - 1984
[NASA-TM-87361] 01 p0127 N85-10874
The identification of the scientific community's choice criteria in the history of scientific research: The case of quantum mechanics
[NOTA-INTERNA-797] 02 p0291 N85-11893
Fiber optics development, prospects assessed
03 p0343 N85-12214
Scientific communications and national security
[GPO-38-093] 04 p0492 N85-13138
Fr. Angelo Secchi, a pioneer in the study of solar-terrestrial relationships 04 p0519 N85-13312
The 1984 NASA/ASEE summer faculty fellowship program
[NASA-TM-87392] 04 p0574 N85-13662
Training guide for scientific and engineering trainees 1984
[AD-A147963] 09 p1198 N85-17542
Fundamentals of computer programming for engineers
[AD-A147964] 08 p1205 N85-17583
Middle Atmosphere Program. Handbook for MAP, volume 6
[NASA-CR-175480] 11 p1656 N85-20436
China report: Science and technology
[JPRS-CST-85-003] 13 p2166 N85-23433
Physicists' role in new technological development discussed 13 p2166 N85-23436
Some historical and other notes about the Mertens conjecture and its recent disproof
[CWI-NM-R8415] 14 p2414 N85-24898
O. F. Mossotti and the physics of molecules
[NOTA-INTERNA-822] 14 p2420 N85-24931
Discovery refutation and verification refutation: The proposals of Von Neumann and Wiener in the development of 20th century physics
[NOTA-INTERNA-840] 14 p2431 N85-24993
Institute's contribution to Soviet welding technology noted 16 p2767 N85-27072
Span graphics display utilities handbook, first edition
[NASA-TM-86500] 16 p2849 N85-27567
Harold Hazen and the theory and design of servomechanism
[RR-270] 22 p3794 N85-33506
SCINTILLATION
Scattering from multi-scale surface — infrared lasers
[RSRE-MEMO-3856] 04 p0505 N85-13222
Ionospheric scintillation: A brief review
04 p0522 N85-13337
Observations of plasma bubbles and their zonal drift using polarimeters
[INPE-3219-PRE/572] 05 p0729 N85-14688
Unsteady pressure measurements on a biconvex airfoil in a transonic oscillating cascade
[NASA-TM-86914] 07 p0898 N85-15689
Optical wave propagation and imaging in the atmosphere 08 p1222 N85-17694
Description of amplitude scintillations on a 11 GHz slant path in terms of forward scattering from turbulent layers
[FI-455-TBR-76] 11 p1625 N85-20232
Remote sensing of irregularities in the equatorial ionosphere using the radio scintillation technique
16 p2808 N85-27317
Scintillation using NNSS satellites
[AD-A152804] 17 p2949 N85-28207
Measurements of folded path optical scintillation using a corner cube, a cat's eye and a flat mirror reflector
[AD-A154044] 19 p3367 N85-30679
Equitorial scintillations: Advances since ISEA-6
[AD-A154962] 21 p3631 N85-32559
EAS spectrum in the primary energy region above 10 to the 15th power eV by the Akeno and Yakutsk array data
[OG-5.1-16] 22 p3882 N85-34057
Methods and software for cosmic ray scintillation studies
[SH-9.1-17] 23 p4052 N85-35132
Air fluorescence detection of large air showers below the horizon
[HE-4.6-6] 24 p4197 N85-36043
SCINTILLATION COUNTERS
Improvements in photodiode readout for small CsI (T1) crystals
[MPI-PAE/EXP-E1-131] 01 p0051 N85-10333
Fine grained hodoscopes based on scintillating optical fibers
[DE84-014849] 01 p0120 N85-10625
Recent progress in BGO development for high resolution calorimetry
[MPI-PAE/EXP-E1-129] 01 p0124 N85-10648
Study for a large area underground detector made with organic scintillators for searching for magnetic monopoles
[NOTA-INTERNA-814] 02 p0201 N85-11339
Advances in room-temperature solid-state gamma-ray spectrometry
[DE84-015944] 04 p0469 N85-12987
Simulation of optical configurations and signal processing methods in Anger-type neutron-position scintillation detector
[DE84-012095] 04 p0503 N85-13210
Scintillator-fiber charged particle track-imaging detector
[NASA-CR-174160] 04 p0559 N85-13560
Mercuric iodide photodetectors for scintillation spectroscopy
[DE85-001437] 10 p1437 N85-19056
The effect of the choice or response matrix on unfolded bonner sphere spectra
[AD-A150462] 13 p2159 N85-23404
Assessment of present and future large-scale semiconductor detector systems
[DE85-006606] 15 p2682 N85-26430
LIGHT: A ray tracing code to simulate light collection in scintillation spectrometers and light pipes
[DE85-007213] 16 p2865 N85-27673
A possible digital circuit able to recognize magnetic monopoles crossing a thick scintillator counter
[NOTA-INTERNA-826] 18 p3097 N85-29173
Study for a large area acrylic scintillator detector — magnetic monopoles
[NOTA-INTERNA-827] 18 p3097 N85-29174
Measurement of the attenuation length of an acrylic scintillator — magnetic monopoles
[NOTA-INTERNA-828] 18 p3097 N85-29175
Experimental performance of a digital circuit able to recognize magnetic monopole events
[NOTA-INTERNA-838] 18 p3097 N85-29176
New concept for a wall detector for alpha particles
[DE85-009037] 18 p3183 N85-29740
Improvements in the energy resolution and high-count-rate performance of bismuth germanate
[DE85-010763] 19 p3240 N85-30092
Bismuth germenate scintillators: Applications in nuclear safeguards and health physics
[DE85-010730] 19 p3365 N85-30665
Plastic scintillator detectors for the study of transfer and breakup reactions at intermediate energies
[DE85-009945] 20 p3528 N85-31945
Search for neutrino oscillations at the Brookhaven AGS
[DE85-009766] 20 p3530 N85-31957
Intercomparison of the calculated absolute efficiency values between true coaxial and true closed-end coaxial Ge (Li) and NaI detectors
[REPT-5-1984] 20 p3532 N85-31976
Reduction of reabsorption effects in scintillators by employing solutes with large Stokes shifts
[DE85-011645] 22 p3838 N85-33767
Observation of hard X-rays from the Crab pulsar and A0535+26
[OG-2.3-7] 22 p3866 N85-33944
Specificity of (71)Ga(p,n) (71)Ge at 35 MeV for Gamow-Teller strength
[DE85-011837] 23 p3971 N85-34615
A balloon-borne imaging gamma-ray telescope
[OG-9.2-2] 23 p4024 N85-34941
Gamma-ray burst spectroscopy capabilities of the BATSE/GRO experiment
[OG-9.2-15] 23 p4026 N85-34954
A position sensitive phoswich hard X-ray detector system
[OG-9.3-12] 23 p4026 N85-34967
The Buckland Park air shower array
[OG-9.4-4] 23 p4029 N85-34971
A new array for the study of ultra high energy gamma-ray sources
[OG-9.4-7] 23 p4029 N85-34974
Akeno 20 km (2) air shower array (Akeno Branch)
[OG-9.4-8] 23 p4029 N85-34975
The longitudinal thickness of air-shower fronts
[OG-9.5-1] 23 p4030 N85-34978
Shower disc sampling and the angular resolution of gamma-ray shower detectors
[OG-9.5-2] 23 p4030 N85-34980

Angular resolution of air-shower array-telescopes
[OG-9.5-6] 23 p4030 N85-34983
Astrophysical applications of high angular resolution array-telescopes
[OG-9.5-7] 23 p4031 N85-34984
The angular resolution of air shower gamma ray telescopes
[OG-9.5-14] 23 p4031 N85-34990
Study of cosmic ray scintillations from 5-minute data of the scintillations telescope Izmiran and world-wide network stations
[SH-5.1-18] 23 p4043 N85-35071
High precise measurements of cosmogenic radiocarbon abundance by complex of scintillation equipments
[SH-7.1-14] 23 p4048 N85-35105
Plastic scintillators in coincidence for the study of multi-particle production of sea level cosmic rays in dense medium
[SH-9.1-11] 23 p4052 N85-35126
Wholebody radiation counting system
[AD-A155842] 24 p4131 N85-35607
A lead glass tubing drift calorimeter
24 p4147 N85-35711
The response of a scintillation counter below an emulsion chamber to heavy nucleus interactions in the chamber
24 p4175 N85-35889
Result of Monte-Carlo simulation of electron-photon cascades in lead and layers of lead-scintillator
[HE-3.6-11] 24 p4185 N85-35958
Application of photodiodes to the detection of electromagnetic bursts 24 p4189 N85-35988
Study of muons near shower cores at sea level using the E594 neutrino detector 24 p4191 N85-36000
Average features of the muon component of EAS or = 10(17) eV
[HE-4.3-10] 24 p4191 N85-36004
Transition effect of air shower particles in plastic scintillators
[HE-4.4-9] 24 p4193 N85-36017
A new study on the emission of EM waves from large EAS
[HE-4.6-5] 24 p4197 N85-36042
Fast scintillation counter system and performance
[HE-4.6-10] 24 p4197 N85-36047
Performance of a local electron density trigger to select extensive air showers at sea level
[HE-4.6-11] 24 p4198 N85-36048
Microprocessor-based single particle calibration of scintillation counter
[HE-4.6-13] 24 p4198 N85-36049
Samarkand complex setup for investigation of cosmic ray variation in the energy range of 7 10 (9) - 10 (15) eV
[HE-4.6-14] 24 p4198 N85-36050
The structure of the shower disk observed at Mt. Norikura
[HE-4.7-1] 24 p4198 N85-36052
Arrival time distributions of electrons in air showers with primary energies above 10 (18)eV observed at 900m above sea level
[HE-4.7-5] 24 p4199 N85-36056
Methods for roof-top mini-arrays
[HE-4.7-7] 24 p4199 N85-36058
Fast scintillation counter preamplifier for the observation of Linsley effect
[HE-4.7-9] 24 p4199 N85-36060
A mini-array for large air showers
[HE-4.7-10] 24 p4199 N85-36061
Sub-luminal pulses from cosmic ray air showers
[HE-4.7-13] 24 p4200 N85-36063
Thickness of the particle swarm in cosmic ray air showers
[HE-4.7-14] 24 p4200 N85-36064
Study of the time-differentiated particle flux density at various distances from EAS axis
[HE-4.7-15] 24 p4200 N85-36065
On method of muon spectrum measurements by the scintillation detectors of a large thickness T4t sub o
[HE-5.2-18] 24 p4204 N85-36094
Results of low energy background measurements with the Liquid Scintillation Detector (LSD) of the Mont Blanc Laboratory
[HE-5.3-5] 24 p4205 N85-36099
The research program of the Liquid Scintillation Detector (LSD) in the Mont Blanc Laboratory
[HE-5.3-6] 24 p4205 N85-36100
Search for stellar collapse with the MACRO detector at Gran Sasso
[HE-5.3-11] 24 p4206 N85-36105
The homestake surface-underground scintillations: Description
[HE-6.1-9] 24 p4210 N85-36135
A search for heavy long lived particles in high energy cosmic rays
[HE-6.2-7] 24 p4211 N85-36143
Delayed particles in EAS at Akeno
[HE-6.2-8] 24 p4211 N85-36144
Energetic delayed hadrons in large air showers observed at 5200m above sea level
[HE-6.2-9] 24 p4211 N85-36145
Search for long-lived massive particles in extensive air showers
[HE-6.2-10] 24 p4212 N85-36146
Search for tachyons associated with extensive air showers in the ground level cosmic radiation
[HE-6.2-13] 24 p4212 N85-36149
Progress report on a new search for free e/3 quarks in the cores of 10(15) - 10(16) eV air showers
[HE-6.2-15] 24 p4212 N85-36151
Exploring results of the possibility on detecting cosmic ray particles by acoustic way
[HE-7.1-3] 24 p4213 N85-36157

SCINTILLATORS
U SCINTILLATION COUNTERS

SCINTILLOMETERS
U SCINTILLATION COUNTERS

SCOOPS
Ramjets with supersonic combustion
07 p0918 N85-15817

SCORING
An introduction to multilinear formula score theory
[AD-A145696] 02 p0254 N85-11667
Efficient scores, variance decompositions and Monte Carlo swindles
[AD-A146673] 08 p0858 N85-15458
A 2 x 6 Back Surface Reflection (BSR) silicon solar cell 13 p2005 N85-22570

SCOUT HELICOPTER
U P-531 HELICOPTER

SCOUT PROJECT
User's operating procedures. Volume 1: Scout project information programs
[NASA-CR-177948] 23 p3956 N85-34518
User's operating procedures. Volume 1: Scout project financial analysis program
[NASA-CR-177949] 23 p3956 N85-34519

SCPC TRANSMISSION
U SINGLE CHANNEL PER CARRIER TRANSMISSION

SCR (RECTIFIERS)
U SILICON CONTROLLED RECTIFIERS

SCRAMBLING (COMMUNICATION)
The average power density spectra of additive scrambler signals and their versions in AMI code
[FUB-27-1983] 01 p0040 N85-10258
Digital scrambling for shuttle communication links: Do drawbacks outweigh advantages?
08 p1101 N85-16956

SCRAMJET ENGINES
U SUPERSONIC COMBUSTION RAMJET ENGINES

SCRAMJETS
U SUPERSONIC COMBUSTION RAMJET ENGINES

SCRAP
Spectral characteristics of grinding sparks used for identification of scrap metals
[PB85-198570] 24 p4080 N85-35290
Deposition of nickel-cobalt alloys by controlled-potential electrolysis
[PB85-198562] 24 p4081 N85-35291

SCREEN EFFECT
Method for forming electromagnetic-wave-screening composite 07 p0936 N85-15930

SCREENS
Diffraction of electromagnetic wave by screen of arbitrary shape 02 p0273 N85-11778
Flow through very porous inclined screens
[NASA-TM-86979] 15 p2555 N85-25761
The thermal calculation of opaque heat screens
[BLL-M-36273-(5826.4)] 20 p3450 N85-31421
Development of metallization process: FSA project, cells and module formation research area
[NASA-CR-176136] 23 p3945 N85-34447

SCREW DISLOCATIONS
Fracture toughness of materials
[DE85-004306] 12 p1667 N85-21713
Determination of edge and screw dislocation density in single crystals of high-purity iron
[DE85-010237] 20 p3537 N85-32012

SCREWS
Alignment and assembly tool for very large diameter cylinders
[NASA-CASE-MFS-28001-1] 18 p3116 N85-29289
Failure analysis of fractured capscrews in centrifugal coolant compressor
[DE85-010029] 19 p3287 N85-30364

SCRIBING
U SCORING

SCRUBBERS
Operating and maintenance guidelines for the kinergetics (trade name) environmental control system. Carbon dioxide scrubber model DH-10 and heat exchanger model CCU-01
[AD-A148107] 08 p1200 N85-17557
Nebulization reflux concentrator
[NASA-CASE-LAR-13254-1] 11 p1615 N85-20154
Control of acid deposition precursors through dry scrubbing
[DE85-010281] 19 p3235 N85-30056
Evaluation of the Santee limestone for use in flue-gas desulfurization systems
[DE85-901277] 19 p3249 N85-30148
Technology of off-gas treatment for liquid-fed ceramic melters
[DE85-012467] 22 p3812 N85-33610
A study of the control of particulate emissions from turbine engine test cells 24 p4067 N85-35205

SCRUBBING
U WASHING

SCRUBS (BOTANY)
U BRUSH (BOTANY)

SDV
U SHUTTLE DERIVED VEHICLES

SEA BREEZE
Sea breeze-induced mesoscale systems and severe weather
[NASA-CR-174317] 08 p1187 N85-17480
Sea breeze-induced mesoscale systems and severe weather 15 p2598 N85-26012
Air flow of the western coastal boundary of South Africa and its influence on the ocean 18 p2831 N85-27459

SEA ICE
NT ICE FLOES
NT ICEBERGS
NT PRESSURE ICE
Sea ice data buoys in the Weddell Sea
[AD-A144953] 01 p0088 N85-10594
Investigation of ice dynamics in the marginal ice zone
[AD-A145110] 01 p0088 N85-10597
Drift characteristics of northeastern Bering Sea ice during 1982
[PB84-213982] 01 p0089 N85-10604
Active microwave measurements of sea ice under fall conditions: The RADARSAT/FIREX fall experiment — in the Canadian Arctic
[E85-10019] 02 p0217 N85-11432
Applications of remote sensing techniques to oceanography and sea ice
[FOA-B-60004-M7] 02 p0220 N85-11448
Handbook for sea ice analysis and forecasting
[AD-A145286] 02 p0233 N85-11516
MIZEX. A program for mesoscale air-ice-ocean interaction experiments in arctic marginal ice zones. III: Modeling the marginal ice zone
[AD-A145351] 02 p0233 N85-11517
Sea ice characteristics derived from airborne altimetry
03 p0382 N85-12440
Radar altimetry over sea ice 03 p0382 N85-12441
Physical oceanography report. Helicopter-based STD data from MIZEX 83 (Marginal ice zone experiment)
[AD-A145848] 03 p0398 N85-12538
Eastern-Western Arctic Sea ice analysis 1983
[AD-A146133] 03 p0398 N85-12541
A comparison between active and passive sensing of soil moisture from vegetated terrains
04 p0526 N85-13364
Dynamics of coupled ice-ocean system in the marginal ice zone: Study of the mesoscale processes and of constitutive equations for sea ice
[NASA-CR-174171] 04 p0542 N85-13448
Arctic ice island and sea ice movements and mechanical properties
[DE84-016323] 04 p0542 N85-13450
Development of radar to measure sea ice merits prize nomination 06 p0826 N85-15244
Intermediate results of radar backscatter measurements from summer sea ice
[AD-A147212] 07 p0940 N85-15960
Ice dynamics
[AD-A147376] 07 p0988 N85-16278
Investigation of the ice dynamics in the marginal ice zone
[AD-A146729] 07 p1009 N85-16411
Southern ocean sea-ice morphology and kinematics
08 p1144 N85-17217
MIZEX. A program for mesoscale Air-Ice-Ocean interaction experiments in arctic marginal ice zones. 4: Initial results and analysis from MIZEX 83
[AD-A148255] 08 p1173 N85-17399
Shore ice ride-up and pile-up features. Part 2. Alaska's Beaufort Sea coast, 1983 - 1984
[AD-A148428] 08 p1190 N85-17501
SAI (Science Applications, Inc.) Interim Scattering Model/Ice (SISM/ICE)
[AD-A148596] 08 p1213 N85-17636
Crystalline structure of urea ice sheets used in modeling experiments in the CRREL test basin
[AD-A148434] 08 p1226 N85-17722

Data report on variations in the composition of sea ice during MIZEX/East'83 with the Nimbus-7 SMMR
[NASA-TM-86170] 09 p1342 N85-18443
Atlas of the Beaufort Sea
[AD-A149545] 11 p1689 N85-20619
Report of the International Ice Patrol Services in the North Atlantic Ocean, season of 1982
[AD-A149595] 12 p1698 N85-21917
Drifting ice as mechanical factor in purifying and polluting hydrosphere 13 p2108 N85-23132
Digital processing of passive Ka-band microwave images for sea-ice classification
[AD-A150866] 14 p2347 N85-24511
Low Temperature Science. Series A: Physical Sciences
[ISSN-0439-3538] 15 p2581 N85-25917
An experimental study of brine upward migration in thin sea ice 15 p2582 N85-25923
Characteristics of snow cover on sea ice and formation of snow ice II 15 p2582 N85-25924
Characteristics of fast sea ice collected near Barrow, Alaska 15 p2582 N85-25925
Oceanographic variations in recent decades and their impact on the fertility of the Iceland Sea 15 p2602 N85-26034
Glacial-to-interglacial changes in NADW fluxes? 15 p2602 N85-26037
Numerical simulation of North Atlantic Sea ice variability, 1951 - 1980 15 p2603 N85-26040
Sea ice, climate and Fram Strait 15 p2603 N85-26042
Greenland ice sheet mass balance 15 p2603 N85-26043
Potential climatic effects on the Greenland ice sheet 15 p2603 N85-26044
Active and passive remote sensing of ice
[AD-A151741] 16 p2815 N85-27369
An assessment of atmospheric refractivity in the northern marginal ice zone
[AD-A152346] 17 p2992 N85-29493
Regional meteorology of the Bering Sea during MIZEX-West, February and March 1983
[PB85-173699] 18 p3150 N85-29503
Arctic mixed layer dynamics
[AD-A153582] 18 p3150 N85-29505
MIZEX, 1984, NASA CV-990 flight report
[NASA-TM-86216] 19 p3299 N85-30451
Arctic acoustic tomography MIZEX 84
[AD-A154426] 19 p3320 N85-30580
Numerical modeling of sea ice dynamics and ice thickness characteristics
[AD-A154600] 21 p3654 N85-32700
Arctic and offshore research
[DE85-001695] 22 p3818 N85-33653
The NORDA/FNOC (Naval Ocean Research and Development Activity's/Fleet Numerical Oceanography Center) Polar Ice Prediction System (PIPS)-Arctic: A technical description
[AD-A156332] 24 p4126 N85-35577

SEA LEVEL

Sea-level in the world ocean. Part 5: The North-East Pacific and Arctic Oceans, a catalogue of measurements
[CSIR-T/SEA-8303-5] 01 p0067 N85-10589
Sea-level in the world ocean. Part 6: The South Atlantic and South Pacific Oceans, a catalogue of measurements
[CSIR-T/SEA-8303-6] 01 p0067 N85-10590
Sea-level in the world ocean. Part 7: The Indian Ocean, a catalogue of measurements
[CSIR-T/SEA-8303-7] 01 p0067 N85-10591
Determination of geoid undulations and ocean heights from ERS-1 radar altimetry data 03 p0361 N85-12432
Parameterizing extreme still water levels and waves in design level studies
[IOS-183] 03 p0398 N85-12542
An alternative to reduction of surface pressure to sea level
[NASA-CR-174174] 04 p0538 N85-13422
The Midway Atoll coral cap: Meteoric diagenesis, amplitude of sea-level fluctuation and dolomitization 09 p1351 N85-18499
The wobble of the Earth and the low frequency dynamics of the ocean 09 p1358 N85-18546
Hemodynamics responses to upright tilt at sea level and high altitude
[AD-A148848] 10 p1527 N85-19634
Calculation of level surface in problems of large-scale ocean circulation 13 p2108 N85-23136
Global paleoclimatic data base for 6000 years BP
[DE85-006828] 15 p2600 N85-26024
The sea level response to weather along the coast of southern Africa 16 p2829 N85-27446
Trends in the Southern Hemisphere 18 p3144 N85-29486
Stratigraphic analysis of Pennsylvania rocks using hierarchy of transgressive-regressive units 19 p3312 N85-30531
The worldwide distribution of the seasonal cycle of mean sea level
[IOS-190] 20 p3497 N85-31743
Composition of primary cosmic rays near the bend from a study of hadrons in air showers at sea level
[OG-5.2-2] 22 p3883 N85-34059
The composition of cosmic rays near the Bend (10 to the 15th power eV) from a study of muons in air showers at sea level
[OG-5.2-3] 22 p3883 N85-34060
Plastic scintillators in coincidence for the study of multi-particle production of sea level cosmic rays in dense medium
[SH-9.1-11] 23 p4052 N85-35126
The neutron moderated detector and groundbased cosmic ray modulation studies
[SH-9.1-13] 23 p4052 N85-35128
Strong earthquakes, novae and cosmic ray environment
[SH-10.1-3] 23 p4053 N85-35135
Particle distributions in approximately 10(14) 10(16) eV air shower cores at sea level 24 p4189 N85-35990
Comparison of simulation results with sea-level experimental data on 10(14) - 10(16) air shower cores 24 p4190 N85-35993
Particle distributions in approximately 10(13) - 10(16) eV air shower cores at mountain altitude and comparison with Monte Carlo simulations
[HE-4.2-18] 24 p4190 N85-35994
Energy spectrum of cascades generated by muons in Baksan underground scintillation telescope
[HE-5.1-15] 24 p4202 N85-36077
Range fluctuations of high energy muons passing through matter
[HE-5.2-19] 24 p4204 N85-36095

SEA OF JAPAN

Ultramicroscopic study of structure of phosphorites from Sea of Japan floor 19 p3290 N85-30400

SEA ROUGHNESS

The spatial evolution of t he directional wave spectrum in the Southern Ocean: Its relation to extreme waves in Agulhas Current 08 p1144 N85-17213
Rip in White Sea 19 p3290 N85-30401

SEA STATES

The use of altimeter data for sea state forecasting 03 p0360 N85-12426
Evaluation of wave energy resources on the French Atlantic seaboard 14 p2325 N85-24369

SEA SURFACE TEMPERATURE

Heat sources in the tropics and large scale flow anomalies associated with precipitation anomalies in northeast Brazil
[INPE-3211-TDL/175] 04 p0538 N85-13421
Study of the improvement in analyzing passive microwave remote sensing data by integrated use of ground data 05 p0658 N85-14226
Energy active areas of ocean 06 p0820 N85-15204
Droughts and floods in South America due to the 1982-83 El Nino-southern oscillation episode
[INPE-3408-PRE/677] 09 p1357 N85-18535
Planetary scale circulation anomalies associated with droughts over northeast Brazil
[INPE-3351-PRE/630] 10 p1518 N85-19570
Method of measuring sea surface water temperature with a satellite including wideband passive synthetic-aperture multichannel receiver
[NASA-CASE-NPO-15851-1] 12 p1699 N85-21723
The development of image processing of NOAA AVHRR data and its application to sea surface temperature 12 p1895 N85-21891
Low-frequency microwave radiometer for N-ROSS 14 p2230 N85-23819
Proposed use of system ARGOS with data buoys for calibration of thermal infrared imagery of North British waters for sea surface temperature maps 14 p2240 N85-23889
Applications of ARGOS measurements in equatorial Pacific Ocean-atmosphere interaction studies 14 p2331 N85-24414
Sea surface temperatures from VAS MSI data
[NASA-CR-175706] 14 p2382 N85-24689
China's integrated circuit production 16 p2806 N85-27302
The validation of sea surface temperatures determined from AVHRR data using in situ data recovered via system ARGOS 16 p2812 N85-27342
Observations of surface water temperature in the Netherlands since 1860: Statistics
[KNMI-WR-84-3] 17 p2997 N85-28531
Observations of surface water temperature in the Netherlands since 1860: Tables for light vessels
[KNMI-WR-84-4] 17 p2998 N85-28532
Observations of surface water temperature in the Netherlands since 1860: Series from KNMI-RWS
[KNMI-WR-84-5] 17 p2998 N85-28533
Mechanistic experiments to determine the origin of Southern Hemisphere stationary waves 18 p3143 N85-29461
Atmospheric planetary wave response to external forcing
[NASA-CR-176000] 19 p3315 N85-30548
Tropical Ocean and Global Atmosphere (TOGA) heat exchange project: A summary report
[NASA-CR-176038] 20 p3496 N85-31736
Sea surface and remotely sensed temperatures off Cape Mendocino, California
[NASA-TM-86712] 24 p4125 N85-35573

SEA TRUTH

Study of the improvement in analyzing passive microwave remote sensing data by integrated use of ground data 05 p0658 N85-14226
An assessment of the potential role of multispectral imagery in bathymetric charting
[AD-A152460] 17 p2984 N85-28438

SEA WATER

Evaluation of hollow fiber ultrafiltration as a pretreatment for reverse osmosis desalination of seawater
[PB84-212406] 01 p0026 N85-10160
Biofouling and corrosion studies at the Seacoast Test Facility in Hawaii
[DE84-014643] 01 p0029 N85-10180
Sea water rope batteries
[AD-A144775] 01 p0042 N85-10275
The development of a diode laser Doppler velocimeter for boundary layer measurements under ice: A feasibility investigation
[AD-A145076] 01 p0053 N85-10348
Variations with time of the carbon dioxide partial pressure in central and south Atlantic surface waters
[AD-A145825] 03 p0398 N85-12537
A simple, low cost potentiostat for corrosion studies
[NPL-DMA(A)-47] 04 p0502 N85-13203
Hydrologic characteristics of the Mediterranean and Black Sea 07 p0981 N85-16228
Propagation of electromagnetic fields along the sea/sea-bed interface
[AD-A149523] 10 p1467 N85-19257
Possible role of ocean biota in global carbon balance — phytoplankton production 13 p2107 N85-23129
Mathematical-cartographic model for study of distribution of hydrochemical elements in sea water (using dissolved oxygen in the Pacific Ocean as an example) 13 p2109 N85-23138
Geographic variation in the relationships of temperature, salinity or sigma sub t versus plant nutrient concentrations in the world ocean — silicic acid, nitrate, and phosphate concentration
[NASA-CR-175621] 13 p2140 N85-23287
Luminescence in the ocean
[AD-B089136L] 13 p2140 N85-23288
Variability in constant-load-amplitude fatigue crack growth rates in marine environments
[AD-A150786] 14 p2255 N85-23975
Resistance of optical coatings to alkali solutions and sea water 14 p2281 N85-24129
Some approximations of geophysical hydrodynamics 14 p2336 N85-24448
Representation of temperature and salinity fields using statistically orthogonal functions (in example of polymode data) 14 p2337 N85-24449
Real-time enhancement of a climatology or forecast of ocean thermal structure using observed ocean temperatures
[AD-A151118] 15 p2604 N85-26049
Fatigue of synthetic fibers for marine rope applications
[MIT-R84-2] 17 p2979 N85-28414
The effects of sea water and concentrated salt solutions on the fatigue of nylon 6,6 fibers 17 p2979 N85-28416
Resistance to corrosion fatigue in aluminum alloy 1561 in sea water 19 p3243 N85-30108
Concretization of high level radioactive source in marine sediment
[AD-D011703] 19 p3249 N85-30146
Geochemistry of manganese in ocean 19 p3291 N85-30406
Sea water photoluminescence 19 p3292 N85-30415
Environmental background measurement program
[AD-A153860] 19 p3319 N85-30577
Theoretical modelling of the electro-chemistry in a corrosion fatigue crack. Part 2: Mathematical aspects of associated unsteady reaction equations
[NPL-DMA(A)-100-PT-2] 20 p3485 N85-31529
A microprocessor-controlled, multichannel fluorimeter for analysis of sea water
[AD-A154966] 21 p3590 N85-32310

Granulometric study of the acidity and sulfate excess in marine aerosols 21 p0652 N85-32691
Determination of organobromide compounds in water by gas chromatography-negative ion chemical ionisation mass spectrometry
[DRIC-T-7411] 22 p3743 N85-33199
A manual of methods for the continuous flow determination of ammonia, nitrate-nitrite, phosphate and silicate in seawater
[IOS-177] 23 p3913 N85-34243
Microwave properties of a quiet sea
[NASA-CR-176159] 24 p4065 N85-35322
Underwater measurements of muon intensity
[HE-5.1-16] 24 p4202 N85-36078
Background light measurements at the DUMAND site
[HE-5.2-7] 24 p4203 N85-36084
Measurements of light background at large depth in the ocean
[HE-5.2-8] 24 p4203 N85-36085
Analytical calculation of muon intensities under deep sea-water
[HE-5.2-16] 24 p4204 N85-36092
Modular detector for deep underwater registration of muons and muon groups
[HE-5.4-15] 24 p4208 N85-36125

SEALANTS
U SEALERS

SEALERS
Sealing ceramic material in low melting point glass
[NASA-TM-77599] 01 p0031 N85-10190
Encapsulation materials and processing 06 p0830 N85-15269
Effect of sealants of the sound absorption coefficients of acoustical friable insulating materials
[AD-A146541] 06 p1218 N85-17674
Interactions between F-111 fuselage fuel tank sealants. Part 2: Variation in performance properties of polysulfides after contact with polyester degradation products
[AD-A149777] 12 p1812 N85-21368
Fuel cell separator plate with bellows-type sealing flanges
[DE85-005991] 23 p3947 N85-34459

SEALING
NT SELF SEALING
Low leakage turbine shaft seals for advanced combined cycle systems
[AD-A149372] 10 p1492 N85-19420
Radioactive waste isolation in salt: Peer review of the D'Appolonia report on schematic designs for penetration seals for a repository in the Permian Basin, Texas
[DE85-000683] 11 p1727 N85-20861
Preventing the formation of an anomalous structure in chemically sealed low carbon steel
[BLL-BISI-TRANS-22373-(9022.06)] 17 p2930 N85-28085
Sodium nitrate containing mixture for producing ceramic-glass-ceramic seal by microwave heating
[DE85-011610] 22 p3751 N85-33254
Experimental characterization and stability of salt- and nonsalt-containing grouts and mortars (BCT-1F- and BCT-1FF-related)
[DE85-012339] 22 p3753 N85-33263

SEALS (ANIMALS)
Motivation for satellite tracking of southern elephant seals Mirounga leonina at sea 16 p2812 N85-27348

SEALS (STOPPERS)
NT GASKETS
NT GLANDS (SEALS)
NT HERMETIC SEALS
NT LABYRINTH SEALS
NT O RING SEALS
NT PACKINGS (SEALS)
NT PLUGS
Collapsable seal member
[DE84-014300] 01 p0055 N85-10357
High-temperature erosion of plasma-sprayed, yttria-stabilized zirconia in a simulated turbine environment
[NASA-TP-2406] 04 p0478 N85-13045
Identification of dynamic coefficients of annular turbulent seals 05 p0644 N85-14133
Analysis and testing for rotordynamic coefficients of turbulent annular seals with different, directionally homogeneous surface-roughness treatment for rotor and stator elements 05 p0644 N85-14134
Analysis for leakage and rotordynamic coefficients of surface roughened tapered annular gas seals 05 p0644 N85-14135
Dynamic stiffness characteristics of high eccentricity ratio bearings and seals by perturbation testing 05 p0645 N85-14141
Analysis of physical-chemical processes governing SSME internal fluid flows
[NASA-CR-174245] 06 p0760 N85-14882
High temperature ultra-high vacuum infrared window seal
[AD-D011333] 07 p0929 N85-15890
Cryogenic glass-to-metal seal
[AD-D011370] 07 p0933 N85-15911
Space shuttle elevon seal panel mechanism 08 p1101 N85-16961
Computational fluid mechanics utilizing the variational principle of modeling damping seals
[NASA-CR-174332] 08 p1161 N85-17325
Sealing assembly
[AD-D011463] 10 p1452 N85-19151
Experimental study of ceramic coated tip seals for turbojet engines
[NASA-TM-86939] 10 p1483 N85-19363
Ribbon burner simulation of T-700 turbine shroud for ceramic lined seals research
[NASA-TM-86940] 10 p1483 N85-19364
Theory versus experiment for the rotordynamic coefficients of annular gas seals. Part 2: Constant clearance and convergent-tapered geometry
[NASA-CR-174413] 10 p1491 N85-19416
Theory versus experiment for the rotordynamic coefficients of annular gas seals. Part 1: Test facility and apparatus
[NASA-CR-174409] 10 p1491 N85-19417
Low leakage turbine shaft seals for advanced combined cycle systems
[AD-A149372] 10 p1492 N85-19420
Variable friction secondary seal for face seals
[NASA-CASE-LEW-14170-1] 11 p1647 N85-20377
Finger materials for air cushion vehicles. Volume 2: Base fabrics for finger materials
[AD-A149701] 12 p1819 N85-21406
Sliding seal materials for adiabatic engines
[NASA-CR-174893] 13 p2037 N85-22757
Experimental stiffness of tapered bore seals
[NASA-TM-86978] 15 p2568 N85-25847
Damping seal verification setup 16 p2738 N85-26893
Damping seals for turbomachinery 16 p2738 N85-26894
Spacer structure
[AD-D011641] 17 p2897 N85-27866
Damping seal for turbomachinery
[NASA-CASE-MFS-25842-2] 19 p3280 N85-30341
SSME seal test program: Test results for hole-pattern damper seals
[NASA-CR-171595] 20 p3395 N85-31059
A comparison of experimental and theoretical results for rotordynamic coefficients of four annular gas seals
[NASA-CR-176066] 21 p3596 N85-32332
Tape casting as an approach to an all-ceramic turbine shroud seal
[NASA-TM-87078] 21 p3596 N85-32333
Mechanical connection for a tubular assembly
[DE85-011500] 22 p3792 N85-33497
Refrigerated dynamic seal to 6.9 MPa (1000 psi)
[NASA-TM-87108] 23 p3930 N85-34356
Oxidizing seal for a turbine tip gas path
[NASA-CASE-LEW-14053-1] 23 p3937 N85-34402
Thermal stress analysis of a new turbine shroud seal concept
[NASA-TM-87062] 23 p3938 N85-34406
SRB attach ring phenolic TPS fishtail seal evaluation tests
[NASA-CR-170687] 24 p4098 N85-35407

SEAMOUNTS
On geoid heights and flexure of the lithosphere at seamounts
[AD-A151220] 15 p2604 N85-26050

SEAMS (JOINTS)
Optical seam tracking of robotic arc welding
[VTT-272] 01 p0055 N85-10368
Softening of metal near seam during welding of heat-resistant nickel alloys 13 p2035 N85-22747
Increasing seam formation stability in electron beam welding of very thick titanium alloys 15 p2500 N85-25420
Development of coating for protection of backside of seam in welding of titanium alloys 15 p2500 N85-25421
Study of acceptance criteria for joint densities in bituminous airport pavements
[FAA-PM-85-5] 16 p2715 N85-26761

SEAPLANES
The effect of changes in the angle of incidence in the event of a richochet at a float step
[RAE-TRANS-2120] 07 p0902 N85-15712

SEARCH AND RESCUE SATELLITE
U SARSAT

SEARCH FOR EXTRATERRESTRIAL INTELLIGENCE
U PROJECT SETI

SEARCH PROFILES
Guide to human factors information sources
[AD-A149102] 10 p1531 N85-19649
Local search in routing problems with time windows
[CWI-OS-R8409] 12 p1922 N85-22075
Evaluation of the vocabulary switching systems
[PB85-127157] 12 p1951 N85-22260
Document retrieval from a relational database management system: An investigation of multiple-line query formulation using SEQUEL 15 p2665 N85-26447
Retrieval performance in a full text journal article database 16 p2577 N85-27747
Individual differences in online search behavior: The effect of learning styles and cognitive abilities on process and outcome 20 p3541 N85-32037

SEARCH RADAR
NT OVER-THE-HORIZON RADAR
Terrestrial locating — of buoys from space 05 p0599 N85-13816

SEARCHING
NT SEARCH PROFILES
Optimizing search with positive information feedback
[CSIR-TWISK-313] 01 p0125 N85-10855
Some attributes of online search intermediaries that relate to search outcome 05 p0734 N85-14721
Shipboard and satellite-aided communications equipment in exhibition 06 p0819 N85-15203
Experimental satellite system for determining coordinates of maritime distress 09 p1306 N85-18216
Online database search strategies and thesaural relationship models 09 p1402 N85-18822
The ARGOS contribution to the successful dredging of a deep moored current meter 14 p2327 N85-24381
The SARSAT program 14 p2327 N85-24385
The ARGOS contribution to the demonstration of the effectiveness of a satellite-based search and rescue system 14 p2330 N85-24404
The SARSAT/COSPAS system for assisting satellite based search and rescue 14 p2398 N85-24776
Microcomputer application of aerospace asset surface search planning
[AD-A151833] 15 p2467 N85-25227
Visual search strategy predictions: The use of aspect ratio as a cue
[BAE-BT-12565] 15 p2619 N85-26136
Forward library searching of previously-quantitated peaks, using a scan list created from a quantitation list by a novel FORTRAN program for the INCOS data system
[PB85-165835] 16 p2845 N85-27541
Satellite aided search and rescue. Experimental results and operational prospects — conference
[ISBN-2-85428-120-9] 20 p3400 N85-31088
The international organization of maritime search and rescue 20 p3400 N85-31089
Search and rescue services for international civil aviation 20 p3400 N85-31090
COSPAS/SARSAT: An overview 20 p3400 N85-31092
Maritime search and rescue cooperation and planning 20 p3400 N85-31093
Search and rescue at sea in the USSR 20 p3400 N85-31094
The contribution of an operational SAR satellite system to the UK SAR organisation — search and rescue (SAR) 20 p3400 N85-31095
Search and rescue of aircraft in distress in France. Organization, means 20 p3401 N85-31096
Specific aspects of maritime search and rescue in French metropolitan and overseas territories: Expected benefits from a detection and location of distress system by satellites 20 p3401 N85-31097
Search and rescue in Canada 20 p3401 N85-31098
The national Search and Rescue (SAR) needs and organization in Norway 20 p3401 N85-31099
The COSPAS-SARSAT system 20 p3401 N85-31101
The COSPAS-SARSAT space segment: Present status and evolution 20 p3401 N85-31102
Rescue satellite COSPAS 20 p3401 N85-31103
The 121.5 MHz ELT: Past, present and future — Emergency Locator Transmitter (ELT) 20 p3401 N85-31105
The 406 MHz ELT/EPIRBs — Emergency Locator Transmitters/Emergency Position Indicating Radio Beacons (ELT/EPIRB) 20 p3402 N85-31106
Soviet Emergency Locator Transmitter/Emergency Position Indicating Radio Beacon (ELT/EPIRBs) at 121.5 and 406 MHz 20 p3402 N85-31107
Ground segment of COSPAS system 20 p3402 N85-31108
Existing and potential INMARSAT capabilities for the Future Global Maritime Distress and Safety System 20 p3402 N85-31110

The International Radio Consultative Committee (CCIR) recommended satellite Emergency Position Indicating Radio Beacon (EPIRB) system operating through geostationary satellites at 1.6 GHz
20 p3402 N85-31112
A 406 MHz geostationary satellite SARSAT experiment
20 p3403 N85-31113
Evolution of 406 MHz Search and Rescue (SAR) processor
20 p3403 N85-31116
Free-float Emergency Position Indicating Radio Beacons (EPIRBs) and release mechanism on board Norwegian ships. Main specifications and user experience
20 p3404 N85-31120
Experiments of a LORAN-C aided recovery system and a proposal of its application to rescue system
20 p3404 N85-31121
SARSAT 406 MHz system technical evaluation
20 p3404 N85-31124
The COSPAS system tests. Technical results
20 p3404 N85-31125
Use of 121.5/243.0 MHz COSPAS-SARSAT data by North American SAR agencies — search and rescue (SAR)
20 p3405 N85-31127
The COSPAS/SARSAT demonstration and evaluation. Results of the first year in the United States
20 p3405 N85-31128
COSPAS-SARSAT demonstration and evaluation results in Canada
20 p3405 N85-31129
COSPAS-SARSAT demonstration and evaluation phase: COSPAS tests in the USSR and their results
20 p3405 N85-31130
The SARSAT-COSPAS demonstration in France
20 p3405 N85-31131
UK experience with COSPAS-SARSAT and INMARSAT distress systems
20 p3406 N85-31132
The COSPAS-SARSAT system evaluation in Norway
20 p3406 N85-31133
INMARSAT distress and safety communication
20 p3406 N85-31134
Maritime mobile satellite techniques as an integral part of the Future Global Maritime Distress and Safety System (FGMDSS): The position of the Federal Republic of Germany
20 p3406 N85-31136
Future prospects for a combined INMARSAT polar communication and search and rescue satellite system
20 p3406 N85-31137
The development of an institutional structure for the Future Global Satellite System for Search and Rescue
20 p3406 N85-31138

SEAS
NT ARABIAN SEA
NT BALTIC SEA
NT BARENTS SEA
NT BEAUFORT SEA (NORTH AMERICA)
NT BERING SEA
NT BLACK SEA
NT CARIBBEAN SEA
NT CASPIAN SEA
NT MEDITERRANEAN SEA
NT NORTH SEA
NT RED SEA
NT SALTON SEA (CA)
NT SEA OF JAPAN
Prediction of wave height of wind-generated seas in finite water depth
[AD-A145996] 03 p0398 N85-12539
Multivariate analyses of sedimentological data at two early Bronze age sites, Bab edh-Dhra and Numeira, southeast Dead Sea Graben, Jordan
05 p0674 N85-14326
Behavior of mode frequency characteristics in shallow sea with variation of P-wave veocity in bottom sediment layer and sonic velocity profile in water layer
10 p1496 N85-19457
Preliminary results of study of space-time variability of shallow sea on steady acoustical path
10 p1499 N85-19459
Studies of the development of cyclones over Southern China coastal areas and adjacent seas
[AD-A150108] 12 p1896 N85-21901
Preliminary results of the oceanographic cruise of USCGC NORTHWIND to the Greenland Sea
[AD-A149802] 12 p1898 N85-21919
Maritime search and rescue cooperation and planning
20 p3400 N85-31093
SEASAT altimetry for surface height of inland seas
20 p3493 N85-31714
Aerosol formation by wave action over Ross Sea, Antartica
21 p3651 N85-32688
Marine Sample Exploitation Project: Estimates regarding the sensitivity and technology for the detection of nuclear explosion debris in the marine environment
[DE85-013176] 23 p3947 N85-34462

SEASAT SATELLITES
NT SEASAT 1
Lithospheric structure in the Pacific geoid
[NASA-CR-174155] 04 p0526 N85-13365
Components of the time variation of sea surface height from SEASAT altimeter data
05 p0658 N85-14227
SAR internal wave signature experiment
08 p1149 N85-17253
SEASAT 3 and 4
[AD-A148343] 08 p1152 N85-17274
Solitons and SEASAT
[AD-A148396] 08 p1176 N85-17414
Along-track deflection of the vertical from SEASAT: GEBCO (General Bathymetric Chart of the Oceans) overlays
[PB85-129641] 12 p1876 N85-21767
Advanced 2-frequency ocean sensing radar using high resolution antenna beams
14 p2230 N85-23821
SEASAT report
[AD-A151283] 15 p2583 N85-25931
Utilization of the SEASAT scatterometer winds for ocean mixed layer modeling
[AD-A153748] 18 p3150 N85-29506
Global mean sea surface based upon a combination of the GEOS-3 and SEASAT altimeter data
20 p3492 N85-31710
SEASAT altimetry for surface height of inland seas
20 p3493 N85-31714

SEASAT 1
Production of optically correlated SEASAT-A (SEA satellite) SAR (Synthetic Aperture Radar) imagery at DREO (Defence Research Establishment Ottawa)
[AD-A145970] 03 p0355 N85-12281
Intercomparison of GEOS 3/SEASAT wave data and wave model data
03 p0381 N85-12438
SEASAT altimeter data over the Mediterranean: Implications for ERS-1
03 p0382 N85-12443
Lessons from the SEASAT and GEOS-3 altimeters data projects
03 p0384 N85-12457
A brief investigation into the validity of SEASAT radar altimeter data acquired over land
[AD-A146560] 06 p0827 N85-15254
The imaging of internal waves by the SEASAT-A synthetic aperture radar
[ARE(PORTLAND)TN-720/84]
13 p2054 N85-22860

SEASONAL VARIATIONS
U ANNUAL VARIATIONS

SEASONS
NT SUMMER
NT WINTER
Predictor model for seasonal variations in skid resistance, volume 1
[PB84-226612] 01 p0036 N85-10229
Seasonal variations in Triton's atmospheric mass and composition
02 p0301 N85-11948
Spring changeover of the middle atmosphere circulation compared with rocket wind data up to 80 km
11 p1661 N85-20466
Annual cycle. Part 1: The annual variation of surface temperatures over the United States and Canada
[PB85-147676] 15 p2600 N85-26026
The worldwide distribution of the seasonal cycle of mean sea level
[IOS-190] 20 p3497 N85-31743

SEAT BELTS
Impact tests of adjusters for the HBU-12 lap belt
[AD-A148021] 08 p1060 N85-16843
Impact tests of automatic lap belt configurations
[AD-A148034] 08 p1061 N85-16844
Improving inflight negative Gz restraint for aircrewmen
[AD-A151909] 16 p2703 N85-26688

SEATS
NT EJECTION SEATS
Low thrust bipropellant engine/redundant seat valve assembly
[AD-A150293] 13 p2013 N85-22628
Thermal response of aircraft cabin ceiling materials during a post-crash, external fuel-spill, fire scenario
[PB85-145847] 14 p2220 N85-23764
Seat experiments for the full-scale transport aircraft controlled impact demonstration
[AD-A155024] 21 p3553 N85-32106
Development of an energy-absorbing passenger seat for a transport aircraft
22 p3796 N85-33515
Design and testing of an energy-absorbing crewseat for the F/FB-111 aircraft, volume 1
[NASA-CR-3916] 23 p3896 N85-34133
Design and testing of an energy-absorbing crewseat for the F/FB-111 aircraft. Volume 3: Data from crew module testing
[NASA-CR-3918] 23 p3896 N85-34134

SECONDARY BATTERIES
U STORAGE BATTERIES

SECONDARY COSMIC RAYS
Variations in intensity of secondary cosmic radiation observed on 10-11 August 1981
16 p2721 N85-26796
Early study of muons and muon decay
[NOTA-INTERNA-835] 18 p3184 N85-29742
The isotopic composition of cosmic ray chlorine
[OG-4.3-3] 22 p3878 N85-34028
Propagation and secondary production of low energy antiprotons in the atmosphere
[OG-6.1-3] 22 p3887 N85-34094
Secondary antiproton production in relativistic plasmas
[OG-6.1-4] 22 p3888 N85-34095
Observed antiprotons and energy dependent confinement of cosmic rays: A conflict?
[OG-6.1-7] 22 p3888 N85-34096
Reestimation of the production spectra of cosmic ray secondary positrons and electrons in the ISM
[OG-6.2-6] 22 p3889 N85-34107
The effects of newly measured cross sections in hydrogen on the production of secondary nuclei during the propagation of cosmic rays through interstellar H
[OG-7.2-2] 23 p4014 N85-34874
Cosmic ray secondary nuclei and the structure of the galaxy
[OG-7.2-4] 23 p4014 N85-34876
Alfven wave scattering and the secondary to primary ratio
[OG-7.2-9] 23 p4015 N85-34878
Influence of the source distribution on the age distribution of galactic cosmic rays
[OG-8.3-1] 23 p4021 N85-34920
Explanation of the secondary to primary ratio within the continuous Fermi accelerator model
[OG-8.3-2] 23 p4021 N85-34921
Secondary to primary ratio and the continuous acceleration
[OG-8.3-4] 23 p4022 N85-34923
The multiplicity and the spectra of secondaries correlated with the leading particle energy
[HE-3.2-11] 24 p4179 N85-35919
Characteristics of anomalously high multiplicity cosmic ray interactions
[HE-3.3-1] 24 p4180 N85-35920
Peculiarities of gamma-quanta distribution at 20 TeV energy
[HE-3.7-10] 24 p4186 N85-35967

SECONDARY EMISSION
Textured carbon surfaces on copper
[NASA-CASE-LEW-14130-1] 11 p1615 N85-20156
Correlated 2 electron effects in collisions of multiply charged Au ions with He
[DE85-003064] 11 p1723 N85-20837
Coincidence studies of secondary electron emission in light ion-atom collisions
[DE85-002373] 11 p1725 N85-20852
Calculation of secondary-electron escape currents from inclined-spacecraft surfaces in a magnetic field
13 p1992 N85-22491
Self-consistent simulation of plasma interactions with secondary-emitting insulators
13 p1993 N85-22492
Electron yields from spacecraft materials
13 p1996 N85-22512
Measurement of charged secondary particle emission under ion and neutral impact — Giotto mission
14 p2243 N85-23906
Measurements of integral yields of charged secondary particles using neutral beams simulating a cometary fly-by — Giotto mission
14 p2244 N85-23908
Simulations of satellite-plasma interaction, including electron space charges — Giotto mission
14 p2245 N85-23916
Electron stimulated desorption and the role of secondary electrons
[AD-A150974] 14 p2252 N85-23955
Convoy electron production by heavy ions in solids
[DE85-005256] 15 p2660 N85-26418
Multivalued electrostatic potentials; chance or necessity for the charge of solid particles near Saturn?
15 p2677 N85-26529
Wide-angle optics with strong magnetic fields for efficient generation of secondary-particle beams
[DE85-007727] 18 p3179 N85-29713
Carbon foil secondary electron emission during ion passage through the 40 to 500 keV energy field
[MPE-190] 18 p3184 N85-29747
Characteristics of slow particles emitted in the charged current interactions of neutrinos with emulsion nuclei
[HE-5.3-22] 24 p4207 N85-36113
Underground measurements on secondary cosmic rays
[HE-5.4-1] 24 p4207 N85-36116
Analysis of the electron component of EAS at observational level 700 g x cm(-2) with a scale breaking interaction model and gammaisation hypothesis
[HE-5.4-8] 24 p4208 N85-36119

SECONDARY FLOW
Turbulent boundary layers with secondary flow
[NASA-TM-77494] 04 p0498 N85-13176

Computation of flow and heat transfer in flow around a 180 deg bend
[AD-A148065] 08 p1162 N85-17330
Secondary flow in cascades
[AD-A148415] 08 p1162 N85-17333
Basic consideration of the lifting capability of stoppable rotors
[AD-A150650] 14 p2219 N85-23759
Effective specific impulse of secondary flow injected into a rocket nozzle
[NAL-TR-846T] 18 p3067 N85-28970
Experiments on the influence of active walls on the initial amplitudes and growths of instability waves
[AD-A154630] 21 p3583 N85-32275

SECONDARY RADAR
Synthesis of optimum algorithms for secondary processing 13 p2080 N85-22992
Developments in the area of air traffic control systems and the relation with meteorology
[NLR-MP-84029-U] 17 p2995 N85-27848

SECONDARY WAVES
U S WAVES

SECRETIONS
NT ADRENOCORTICOTROPIN (ACTH)
NT HORMONES
NT HYDROXYCORTICOSTEROID
NT INSULIN
NT PROSTAGLANDINS
NT SWEAT
Biliganic function of white rat liver 01 p0093 N85-10824

SECULAR PERTURBATION
U LONG TERM EFFECTS

SECULAR VARIATIONS
Geomagnetic secular variation: A jerk in 1970 04 p0521 N85-13329
Comparisons of secular variation in two-dipole and spherical harmonic models with observatory data in Eurasia, 1965-1975 04 p0521 N85-13330
Geomagnetic secular variation at Ebro Observatory during the past 70 years 04 p0521 N85-13331
Insolation changes on Pluto caused by orbital element variations
[AERONOMICA-ACTA-A-290-1984] 20 p3546 N85-32070
Cosmic ray secular variations in terrestrial records and aurorae
[SH-7.1-3] 23 p4047 N85-35096

SECURITY
NT COMPUTER INFORMATION SECURITY
Scientific communications and national security
[GPO-36-093] 04 p0492 N85-13138
Semiannual report to Congress on the effectiveness of the civil aviation security program
[AD-A149522] 10 p1421 N85-18967
Brussels Satellite Convention
[S-EXEC-REPT-98-82] 12 p1790 N85-21234
Literature survey of underground construction methods for application to hardened facilities
[AD-A155212] 21 p3599 N85-32351

SEDIMENT TRANSPORT
Dynamic response of electromagnetic current meters
[PB84-229731] 06 p0842 N85-15344
Analysis of suspended sediment distributions in the surface waters of Delaware Bay using remote sensing of optical properties 15 p2582 N85-25926
Modern sedimentation in the northern Barents Sea: Input, dispersal and deposition of suspended sediments from glacial meltwater
[AD-A152520] 17 p2997 N85-28530
Use of a two-dimensional flow model to quantify aquatic habitat
[AD-A154287] 19 p3268 N85-30253
Sand dispersion from an ephemeral river delta on the wave-dominated central California coast
[AD-A154362] 19 p3300 N85-30458
New estimating procedures for surface runoff, sediment yield, and contaminant transport in Los Alamos County, New Mexico
[DE85-011890] 21 p3606 N85-32393

SEDIMENTARY ROCKS
NT COAL
NT LIGNITE
NT LIMESTONE
NT PEAT
NT SANDSTONES
NT SHALES
Franciscan and related rocks of southern Humboldt County, northern California coast ranges: Analysis of structure, tectonics, sedimentary petrology, paleogeography, depositional history, and thermal maturity 03 p0390 N85-12495
Post-Sonoman conodont biofacies of the Triassic of northwestern Nevada 03 p0390 N85-12497
The Kanayut Conglomerate in the westernmost Brooks Range, Alaska 04 p0516 N85-13289
Reconnaissance geology of the northern part of the Unalakleet quadrangle 04 p0516 N85-13291
Newly recognized sedimentary environments in the Shellkof Formation, Alaska 04 p0516 N85-13292
New ages of radiolarian chert from the Rampart district, east-central Alaska 04 p0516 N85-13293
Concordant bands of augen gneiss within metasedimentary rocks in the Big Delta C-2 quadrangle, east-central Alaska 04 p0516 N85-13294
Lacustrine and eolian deposits of Wisconsin age at Riverside Bluff in the upper Tanana River valley, Alaska 04 p0517 N85-13299
Archean sedimentation and tectonics in southern Africa
[NASA-CR-174156] 04 p0533 N85-13408
The Georges Bank monitoring program 1983: Analysis of trace metals in bottom sediments
[CIRC-915] 05 p0688 N85-14423
Normal-fault and fold development in sedimentary rocks above a pre-existing basement normal fault 13 p2131 N85-23250
Evaluating structure-forming role of late Paleozoic and Mesozoic-Cenozoic tectonic movements in Baltic Sea region 14 p2337 N85-24450
Carbon isotope geochemistry and geobiology 21 p3657 N85-32718
Archean sedimentary systems and crustal evolution 21 p3720 N85-33082
Organic solvent alteration of hydraulic properties of sedimentary rocks of low permeability: A review
[DE85-012537] 22 p3815 N85-33835
Marine phosphorite deposits model for exploration, with emphasis on deposits in the US Atlantic coastal plain 24 p4104 N85-35439
Seismic stratigraphic analysis of the Mississippi Fan 24 p4115 N85-35507
Geology and geomorphology of the Roraima group, southeastern Venezuela 24 p4115 N85-35511

SEDIMENTS
NT SANDS
NT TAR SANDS
Chemistry of fuel deposits and sediments and their precursors
[NASA-CR-174778] 01 p0034 N85-10209
Erosion and sedimentation chronology of three watersheds in Maryland
[PB84-207356] 01 p0071 N85-10467
Late quaternary glacial cycles in the Bahamian deep basins and in the adjacent Atlantic Ocean 02 p0226 N85-11476
Paleohydrology and geomorphology of selected reaches of the upper Wabash Valley, Indiana 02 p0226 N85-11481
Paleoenvironmental interpretation of the upper cretaceous Point Lookout sandstone: Implications for shoreline progradation and basin tectonic history, San Juan basin, New Mexico 02 p0227 N85-11486
Stratigraphy, sedimentology and tectonic significance of the Upper Cretaceous Virginian Ridge formation, Method Basin, Washington: Implications for tectonic history of the North Cascades 03 p0390 N85-12494
Late quarterly glaciolacustrine and vegetational history of the Copper River Basin, south-central Alaska 03 p0391 N85-12499
Glacial-lake deposits in the Mount Harper area, Yukon-Tanana Upland 04 p0517 N85-13300
Constraints on lunar origin: Evidence preserved in Precambrian stromatolites 04 p0564 N85-13731
Multivariate analyses of sedimentological data at two early Bronze age sites, Bab edh-Dhra and Numeira, southeast Dead Sea Graben, Jordan 05 p0674 N85-14328
Sedimentation, structure and tectonics of the Umpqua group (paleocene to early eocene), southwestern Oregon 05 p0678 N85-14364
The Georges Bank monitoring program 1983: Analysis of trace metals in bottom sediments
[CIRC-915] 05 p0688 N85-14423
Storage stability of jet fuels
[AD-A146360] 06 p0773 N85-14943
Manganese in recent sediments of Ukrainian SSR Black Sea shelf 06 p0819 N85-15200
Uraninability of ferromanganese nodules 06 p0819 N85-15202
Some methodological aspects of study of layer associations in continents and oceans 06 p0820 N85-15205
Platinum group nuggets in deep sea sediments 06 p0863 N85-15611
Pulse transmission through frozen silt
[AD-A147108] 07 p0940 N85-15958
Ocean acoustics
[AD-A147082] 07 p1038 N85-16591
Soil formation on tertiary landsurfaces of the New Jersey coastal plain 08 p1181 N85-17441
Preliminary post-emplacement safety analysis of the subseabed disposal of high-level nuclear waste
[DE84-011162] 08 p1221 N85-17592
The pleistocene geology of Vilas County, Wisconsin 09 p1353 N85-18509
Quaternary stratigraphy, geochronology and carbon isotope geology of alluvial deposits in the Texas panhandle 09 p1353 N85-18514
Measurements of sediment temperatures, conductivity and heat flow in the North Atlantic and their relevance to radioactive waste disposal
[IOS-172] 09 p1359 N85-19551
Evolution of sedimentation basins in Earth's history 10 p1497 N85-19451
Behavior of mode frequency characteristics in shallow sea with variation of P-wave veocity in bottom sediment layer and sonic velocity profile in water layer 10 p1498 N85-19457
Aluminum in biogenic cycle and forms of its occurence in ocean 10 p1499 N85-19463
SIR-A imagery in geologic studies of the Sierra Madre Oriental, northeastern Mexico. Part 1 (Regional stratigraphy): The use of morphostratigraphic units in remote sensing mapping
[NASA-CR-175457] 10 p1505 N85-19497
U, Th, K content, heat production and thermal conductivity of Sao Paulo, Brazil continental shelf sediments: A reconnaissance work
[INPE-3401-PRE/670] 10 p1515 N85-19558
Improved techniques for removal of sediments contaminated with hazardous materials
[PB85-116093] 11 p1679 N85-20580
Special features of computations of vertical distribution of concentration of suspended sediments under marine conditions 13 p2106 N85-23125
Determining adsorption of surface-active substances by sea bottom deposits 13 p2107 N85-23128
Review of problems in lithology 13 p2113 N85-23160
A first evaluation of LANDSAT TM data to monitor suspended sediments in lakes — Lake Chicot, Arkansas 13 p2120 N85-23204
Electromagnetic field of currents and its use to estimate total conductivity of sedimentary deposits in Western Black Sea 14 p2334 N85-24434
Absolute movement of Pacific Ocean plate based on paleoclimatic and paleomagnetic data and trajectory of hot spots during last 120 million years 14 p2334 N85-24435
Evaluating structure-forming role of late Paleozoic and Mesozoic-Cenozoic tectonic movements in Baltic Sea region 14 p2337 N85-24450
Modern sedimentation in the northern Barents Sea: Input, dispersal and deposition of suspended sediments from glacial meltwater
[AD-A152520] 17 p2997 N85-28530
Numerical benchmark study for the finite element computer code NEPTUNE
[DE85-008400] 17 p3013 N85-28630
Structure of Reykjanes Ridge rift zone and Icelandic thermal anomaly 19 p3299 N85-30395
Natural gas anomaly in bottom waters of South China Sea 19 p3290 N85-30399
Sand dispersion from an ephemeral river delta on the wave-dominated central California coast
[AD-A154352] 19 p3300 N85-30458
Physiochemically controlled scour jet array system
[AD-D011688] 19 p3308 N85-30605
Offshore oceanographic and environmental monitoring services for the Strategic Petroleum Reserve, volume 3
[DE85-009907] 20 p3497 N85-31741
Sulfur diagenesis in marine sediments 21 p3658 N85-32721
Sulfur cycling in freshwater sediments 21 p3658 N85-32726
Sulfur and carbon cycling in organic-rich marine sediments 21 p3659 N85-32729
Sulfur reduction in sediments of marine and evaporite environments 21 p3661 N85-32742
Microanalysis of dissolved iron and phosphate in pore waters of hypersaline sediment 21 p3661 N85-32744
A random layer model for reflection from ocean bottom sediments
[AD-A155019] 21 p3700 N85-32988
Archean sedimentary systems and crustal evolution 21 p3720 N85-33082
Subduction zone tectonic studies to develop concepts for the occurrence of sediment subduction
[DE85-011794] 22 p3815 N85-33832
Bedrock geology of the Brattleboro Quadrangle, Vermont-New Hampshire
[DE85-011027] 22 p3815 N85-33834
Origin of sedimentary humic acids, potential carriers of ore-forming elements 24 p4104 N85-35443

Depositional systems and coal occurrence in the Fort Union Formation (Paleocene), Powder River Basin, Wyoming and Montana 24 p4114 N85-35505
Bibliography on tidal hydraulics. Report 2. Supplement 6: Supplementary material compiled from June 1980 - June 1983. Tidal flows in rivers and harbors
[AD-A155990] 24 p4125 N85-35574
SEEBECK COEFFICIENT
U SEEBECK EFFECT
SEEBECK EFFECT
Anomalous electronic transport in boron carbides
[DE84-015620] 06 p0868 N85-15518
SEEDING (INOCULATION)
U INOCULATION
SEEDS
Timing in dry seeds 05 p0690 N85-14437
Attempts to localize and identify the gravity-sensing device of plant seedlings 15 p2607 N85-26064
Effect of seeds of heavy charged particles of galactic cosmic radiation 23 p3954 N85-34505
SEEKERS
U HOMING DEVICES
SEGMENTS
Integrating non-semantic knowledge into image segmentation processes
[AD-A149571] 12 p1851 N85-21612
Twisting of segmental shafts 14 p2279 N85-24119
Study of fatigue strength of shafts with segmented channels 14 p2282 N85-24138
Computations for segmented radial bearings 14 p2288 N85-24180
Selection of segment similarity measures for hierarchical picture segmentation 23 p3960 N85-34548
SEGREGATION
U SEPARATION
SEISMIC ENERGY
Horizontal-strain observations in the Shumagin Island and Yakataga seismic gaps, Alaska 04 p0515 N85-13287
Deployment of a regional array in Norway
[AD-A147032] 07 p0997 N85-16330
Interrelationship of earthquake magnitude and lithospheric-asthenospheric thermodynamic parameters in seismically active zones 13 p2116 N85-23163
Relationship between seismic status of Earth and relative position of bodies in sun-earth-moon system 14 p2345 N85-24499
Study of earthquake preparation processes from distribution of weak tremor epicenters 14 p2345 N85-24501
Development of ultrasonic modeling techniques for the study of crustal inhomogeneities
[AD-A155206] 21 p3632 N85-32565
SMACS: A system of computer programs for probabilistic seismic analysis of structures and subsystems. Volume 1: User's manual
[DE85-011653] 22 p3830 N85-33724
SEISMIC WAVES
NT LOVE WAVES
NT MICROSEISMS
NT RAYLEIGH WAVES
Response and characteristics of structures subjected to S-H waves 01 p0060 N85-10396
Specific phenomena associated with the propagation of seismic waves in central Europe
[REPT-548] 03 p0375 N85-12391
Hole shots along refraction profile R4/78 recorded at the temporary seismic station near Stary Plzenec (west Bohemia)
[REPT-549] 03 p0375 N85-12392
In situ experiment on shear waves generation and determination of elastic properties of soils
[REPT-550] 03 p0375 N85-12393
Finite-difference synthetic seismograms for SH waves
[AD-A146834] 03 p0392 N85-12508
Coupling of airborne sound into the Earth
[AD-A146231] 03 p0416 N85-12663
Characteristics of a recent Columbian earthquake, December 12, 1979 04 p0523 N85-13347
Possible effects of interaction of electric seismic fields with the ionosphere 06 p0823 N85-15228
Nonlinear wave propagation study
[AD-A147011] 07 p0996 N85-16329
Short period guided waves over oceanic and continental paths
[AD-A147053] 07 p0997 N85-16331
The Shock and Vibration Digest, volume 16, no. 11
[AD-A148466] 08 p1171 N85-17362
On seismic waves 08 p1171 N85-17363
Seismic performance of low-rise light-framed wood buildings 08 p1171 N85-17384
Effects of heterogeneities on the propagation, scattering and attenuation of seismic waves and the characterization of seismic source
[AD-A148284] 08 p1186 N85-17476
Studies on seismic earth pressure of cohesive backfill 09 p1303 N85-18186
Earthquake-modeling experiment using unique press 10 p1500 N85-19469
Mathematical modeling of wave fields by superimposition of boundary waves in reflected earthquake waves method 10 p1501 N85-19476
Influence of scattering on Q in the lithosphere
[AD-A149318] 10 p1515 N85-19563
An analysis of short-to-medium-range seismic attenuation tests using a multilayered viscoelastic seismic propagation model
[AD-A149771] 12 p1889 N85-21856
Twenty-five sound propagation tests on the continental shelf between Long Island, New York and Cape Canaveral, Florida
[AD-A149869] 12 p1928 N85-22111
Two-and-one-half dimensional in-plane wave propagation
[AD-A150467] 13 p2055 N85-22867
Determining degree of partial melting of asthenosphere from seismic data 13 p2107 N85-23127
More precise curve of dependence between density and velocity of longitudinal waves in consolidated crust and top of mantle in oceanic structures 13 p2110 N85-23143
Nature of seismic images with amplitude and time fluctuations of recorded oscillations 13 p2112 N85-23156
Magmatism in continent-ocean transition zone (development of ideas of A. N. Zavaritskiy) 13 p2113 N85-23161
Boundary velocities of longitudinal seismic waves and lateral inhomogeneities of upper ocean mantle 13 p2113 N85-23165
Seismic waves and dispersion relations 13 p2116 N85-23181
Interrelationship of earthquake magnitude and lithospheric-asthenospheric thermodynamic parameters in seismically active zones 13 p2116 N85-23163
Correcting depth line on nonlongitudinal seismic profile 13 p2117 N85-23184
Attenuation of seismic waves at regional distances
[AD-A150198] 13 p2132 N85-23267
Influence scattering and Q in the lithosphere
[AD-A150930] 14 p2293 N85-24213
Seismic analysis of rotating mechanical systems
[PB85-149599] 14 p2311 N85-24307
Interpreting refracted waves method data on basis of automated determination of seismic drift 14 p2343 N85-24486
Determining geometrical divergence using seismic observation data 14 p2343 N85-24489
New methods for interpreting seismic time fields in media with variable velocities 14 p2343 N85-24490
Possibility of retrieving dynamics of reflected wave method records beneath low-velocity zone 14 p2346 N85-24503
Results of studies of wave field internal structure in prediction of geological cross section 14 p2346 N85-24504
Regional seismic wave propagation
[AD-A150801] 14 p2373 N85-24671
Asymptotic construction of a procedure for plane-wave synthesis and migration
[AD-A150969] 14 p2374 N85-24672
Seafloor seismic measurements in the southern Bering
[DE85-004908] 14 p2374 N85-24675
On coupling factors of explosion 15 p2551 N85-25747
Connection between time- and frequency-domain three-dimensional inverse problems for the Schroedinger equation
[DE85-005914] 15 p2639 N85-26274
The Shock and Vibration Digest, volume 17, no. 2
[AD-A153129] 17 p2977 N85-29400
The effects of seismic waves 17 p2978 N85-29401
Proceedings of the 1980 Workshop of the International Association of Seismology and Physics of the Earth's Interior on the Seismic Modeling of Laterally Varying Structures: Contributions based on data from the 1978 Saudi Arabian refraction profile
[GS-CIRC-937] 17 p2989 N85-29478
Two-dimensional inverse kinematic problem: Application to the Saudi Arabian refraction profile 17 p2990 N85-29478
Crustal structure of the Red Sea-Arabian Shield transition 17 p2990 N85-29479
A seismic refraction profile across the Arabian Shield 17 p2990 N85-29481
The rifted margin of Saudi Arabia 17 p2990 N85-29483
Surface wavesseismic yields as measured by the Regional Seismic Test Network
[DE85-010532] 18 p3137 N85-29425
Wave-theoretical approach to seismic modeling problems (WELMOD)
[BMFT-FB-T-84-258] 18 p3137 N85-29429
Discovery in earthquake forecasting and seismic zoning recorded 19 p3295 N85-30426
Well-posedness of one-way wave equations and absorbing boundary conditions
[NASA-CR-172619] 19 p3345 N85-30727
Crosswell acoustic surveying in gas sands: Travel-time pattern recognition, seismic Q and channel waves
[DE85-010777] 19 p3352 N85-30778
Effects of contact area of an interface on acoustic wave transmission characteristics
[DE85-009935] 20 p3524 N85-31920
Robust detection and classification of regional seismic signals using a two mode/two stage cascaded adaptive arma (CAARMA) model
[AD-A154710] 21 p3630 N85-32554
The Norwegian seismic array (NORSAR)
[AD-A154751] 21 p3631 N85-32555
Experimental and analytic characterization of nonlinear seismic attenuation
[AD-A154760] 21 p3631 N85-32556
Design of a freestanding noise measurement and recording system to predict the intensity and location of electromagnetic radiation from earthquakes
[AD-A155070] 21 p3632 N85-32563
Qualitative analysis of sign-bit processing
[AD-A154776] 21 p3671 N85-32804
Attenuation properties of the Petatlan region, Mexico, and a local magnitude scale for microearthquakes in this area 24 p4116 N85-35513
Applications of the Kirchoff-Helmholtz integral to problems in body wave seismology 24 p4116 N85-35515
Workshop Proceedings: Interpretation of Seismic Wave Propagation in Laterally Heterogeneous Structures
[BMR-258] 24 p4118 N85-35530
SEISMOGRAMS
Finite-difference synthetic seismograms for SH waves
[AD-A145834] 03 p0392 N85-12508
SEISMOGRAPHS
Standardization of amplitude characteristics of galvanometric seismographs in the KAPG network
[REPT-552] 03 p0375 N85-12395
SVKD and SVKM-3 seismographs with a low-sensitivity channel
[REPT-553] 03 p0376 N85-12396
Short-period seismograph SVSN-6
[REPT-554] 03 p0376 N85-12397
Microseism level, time variations at Turkmen seismic stations studied 07 p0981 N85-16231
Deployment of a regional array in Norway
[AD-A147032] 07 p0997 N85-16330
Seismic performance of low-rise light-framed wood buildings 08 p1171 N85-17384
Use of mobile surface station for synchronous satellite measurements in seismological research 13 p1984 N85-22447
A seismic ARGOS data collection platform 16 p2613 N85-27350
SEISMOLOGY
NT HELIOSEISMOLOGY
Microseismic monitoring of Chocolate Bayou, Texas: The Pleasant Bayou no. 2 geopressured/geothermal energy test well program
[DE84-014825] 01 p0072 N85-10477
Seismotectonic nature of some annular photoanomalies registered by remote methods 02 p0164 N85-11110
A comparison of seismic properties of young and mature oceanic crust 02 p0226 N85-11479
Seismology 1983: Nuclear test ban verification, earthquake and Earth resource investigation
[FOA-C-20537-T1] 02 p0229 N85-11495
A pilot study of future research on seismic hazards in Sweden
[FOA-C-20544-T1] 02 p0229 N85-11496
Archiving and exchange of a computerized marine seismic database: The ROSE (Rivera Ocean Seismic Experiment) data archive system
[AD-A145658] 02 p0294 N85-11908
Geophysical Works during 1981, volume 29, no. 547-566 03 p0375 N85-12389
In situ experiment on shear waves generation and determination of elastic properties of soils
[REPT-550] 03 p0375 N85-12393
Seismology in rockburst research
[REPT-551] 03 p0375 N85-12394
Coupling of airborne sound into the Earth
[AD-A146231] 03 p0416 N85-12663
Seismic studies in southern Alaska 04 p0515 N85-13286

Scientific contributions in commemoration of Ebro Observatory's 75th anniversary — conference
[ISBN-84-00-05360-X] 04 p0518 N85-13308
Seismology today 04 p0523 N85-13348
A review of seismicity in peninsular Spain 04 p0523 N85-13349
Deep structure beneath the Pyrenees 04 p0524 N85-13351
Earthquake catalog for northern New Mexico
[DE84-016984] 04 p0534 N85-13416
Archiving and exchange of a computerized marine seismic database: The ROSE data archive system
[DE84-901483] 04 p0576 N85-13677
Documentation of earthquake algorithms
[PB84-235324] 05 p0677 N85-14351
Evaluation of the RSTN (Regional Seismic Test Network) network and further improvement to automatic association
[AD-A146395] 06 p0835 N85-15312
Microseism level, time variations at Turkmen seismic stations studied 07 p0981 N85-16231
General model of earthquakes and the place of warnings in it 07 p0981 N85-16232
Research activities of the Norwegian seismic array (NORSAR)
[AD-A146778] 07 p0996 N85-16326
Deployment of a regional array in Norway
[AD-A147032] 07 p0997 N85-16330
Short period guided waves over oceanic and continental paths
[AD-A147053] 07 p0997 N85-16331
Seismicity of southern Sweden
[FOA-C-20543-T1] 07 p0998 N85-16340
Research of inverse methods to describe the structure of the earth and ocean bottom
[AD-A147082] 07 p1030 N85-16541
An efficient numerical solution technique for wave propagation in horizontally stratified ocean environments
[AD-A148537] 08 p1190 N85-17502
Detailed oceanic crustal modeling
[AD-A148589] 08 p1191 N85-17507
Atmospheric limitations in stellar seismology: Should one measure radial velocity or brightness fluctuations?
08 p1251 N85-17899
Technology reports of the Yamaguchi University, volume 3, no. 3
[ISSN-0386-3433] 09 p1302 N85-18182
Earth Sciences Division report, 1983
[DE85-001036] 09 p1341 N85-18436
Field implementation of geophysical diffraction tomography
[DE84-017594] 09 p1343 N85-18449
Velocity stack and slant stack inversion methods 09 p1351 N85-18497
Nonlinear seismology 10 p1503 N85-19482
Statistical study of anthropogenic seismic noise with IVK-7 computer system 10 p1503 N85-19483
High-resolution microseismicity study of possible magmatic intrusion in the Long Valley Caldera
[DE85-001078] 11 p1681 N85-20593
Resolution of 2-dimensional seismologic problems by a finite element approximation. Application to the Love wave propagation through the Atlantic border of the Iberic Peninsula 11 p1681 N85-20594
Resolution of 2-dimensional seismologic problems by a finite element approximation. Application to the Love wave propagation through the Atlantic border of the Iberic Peninsula. Appendix: Graphs of results — Lagrange coordinates 11 p1681 N85-20595
Seismic observation of infrasonic signals
[AD-A149574] 12 p1889 N85-21853
Use of mobile surface station for synchronous satellite measurements in seismological research 13 p1984 N85-22447
Geophysical laser interferometer with 12.5 meter base 13 p2089 N85-23046
Crustal and upper mantle density model of Owen fault zone 13 p2110 N85-23144
Observation of long-period oscillations of Earth 13 p2110 N85-23149
Natural electromagnetic radiation in seismically active regions 13 p2111 N85-23152
Determination of density of the crust and upper mantle from deep seismic sounding and gravimetry, 2 13 p2111 N85-23153
Geomagnetic precursors of intensive earthquakes in the 1-0.-2 Hz frequency range of geomagnetic pulsations 13 p2116 N85-23176
Correcting depth line on nonlongitudinal seismic profile 13 p2117 N85-23184
Method for processing broad-profile data 13 p2117 N85-23185
Attenuation of seismic waves at regional distances
[AD-A150198] 13 p2132 N85-23267
Seismic analysis of rotating mechanical systems
[PB85-149599] 14 p2311 N85-24307
USSR report: Earth sciences
[JPRS-UES-85-004] 14 p2332 N85-24424
Evaluating structure-forming role of late Paleozoic and Mesozoic-Cenozoic tectonic movements in Baltic Sea region 14 p2337 N85-24450
Interpreting refracted waves method data on basis of automated determination of seismic drift 14 p2343 N85-24486
Electromagnetic fields migration method 14 p2343 N85-24487
New methods for interpreting seismic time fields in media with variable velocities 14 p2343 N85-24490
Asymptotic construction of a procedure for plane-wave synthesis and migration
[AD-A150969] 14 p2374 N85-24672
Seafloor seismic measurements in the southern Bering
[DE85-004908] 14 p2374 N85-24675
A fast ray tracing routine for laterally inhomogeneous media
[AD-A150984] 14 p2421 N85-24938
China report: Science and technology
[JPRS-CST-85-011] 15 p2551 N85-25746
On coupling factors of explosion 15 p2551 N85-25747
Frequency dependence of Q in the mantle underlying the shield areas of eurasia
[AD-A151367] 15 p2592 N85-25978
GEMINI: A computer program for two and three dimensional linear static and seismic structural analysis, CDC 7600 version
[DE85-007496] 15 p2631 N85-26218
A seismic ARGOS data collection platform 16 p2813 N85-27350
Response of a wind turbine blade to seismic and turbulent wind excitations 16 p2817 N85-27375
Symposium on Atmospheric Sciences in South Africa
[CSIR-S-331] 16 p2829 N85-27442
Born inversion with a stratified reference velocity
[AD-A149222] 16 p2853 N85-27594
The Shock and Vibration Digest, volume 17, no. 2
[AD-A153129] 17 p2977 N85-28400
The effects of seismic waves 17 p2978 N85-28401
Australian seismological report, 1980
[REPT-252] 17 p2989 N85-28473
Proceedings of the 1980 Workshop of the International Association of Seismology and Physics of the Earth's Interior on the Seismic Modeling of Laterally Varying Structures: Contributions based on data from the 1978 Saudi Arabian refraction profile
[GS-CIRC-837] 17 p2989 N85-28476
Preliminary interpretation of Saudi Arabian seismic refraction data 17 p2989 N85-28477
Two-dimensional inverse kinematic problem: Application to the Saudi Arabian refraction profile 17 p2990 N85-28478
Crustal structure of the Red Sea-Arabian Shield transition 17 p2990 N85-28479
A crustal section for the Arabian Shield and adjacent Red Sea margin derived from first-arrival data 17 p2990 N85-28480
A seismic refraction profile across the Arabian Shield 17 p2990 N85-28481
A preliminary examination of the 1978 refraction profiles in Saudi Arabia 17 p2990 N85-28482
The rifted margin of Saudi Arabia 17 p2990 N85-28483
Saudi Arabian refraction profile: Crustal structure of the Red Sea-Arabian Shield transition 17 p2990 N85-28484
Saudi Arabian refraction profile: A preliminary interpretation for the Red Sea-Arabian Shield transition 17 p2991 N85-28485
A traveltime interpretation of the 1978 seismic refraction profile in the Kingdom of Saudi Arabia 17 p2991 N85-28486
Explanation of Russian models: Saudi Arabian seismic refraction profile 17 p2991 N85-28487
Interpretation of the data of USGS seismic refraction profile across the Arabian Shield in western Saudi Arabia 17 p2991 N85-28488
A preliminary analysis of the Saudi Arabian deep seismic sounding data 17 p2991 N85-28489
One-dimensional velocity-depth functions determined for the Arabian Shield and the southwestern Red Sea: A comparison of models 17 p2992 N85-28490
Revised draft: Southeastern regional geologic characterization report
[DE85-006295] 18 p3125 N85-29351
Surface waveseismic yields as measured by the Regional Seismic Test Network
[DE85-010532] 18 p3137 N85-29425
Seismic analysis of liquid-filled tanks with an eccentric core barrel
[DE85-010249] 19 p3289 N85-30272
Analysis of seismic sloshing of reactor tanks considering submerged components and seismic isolation
[DE85-010499] 19 p3289 N85-30273
Tectonic structure features of some deep faults in Atlantic and Pacific Oceans (according to deep seismic sounding-reflected waves method data) 19 p3295 N85-30428
Deployment of a regional array in Norway
[AD-A154120] 19 p3313 N85-30536
Seismic discrimination
[AD-A154167] 20 p3494 N85-31722
The Norwegian seismic array (NORSAR)
[AD-A154751] 21 p3631 N85-32555
Tectonic stability and expected ground motion at Yucca Mountain
[DE85-012004] 22 p3814 N85-33629
SMACS: A system of computer programs for probabilistic seismic analysis of structures and subsystems. Volume 1: User's manual
[DE85-011853] 22 p3830 N85-33724
Geophysical-geological studies of possible extensions of the New Madrid fault zone
[TI85-901341] 23 p3949 N85-34475
Strong earthquakes, novae and cosmic ray environment
[SH-10.1-3] 23 p4053 N85-35135
Seismic stratigraphic analysis of the Mississippi Fan 24 p4115 N85-35507
Attenuation properties of the Petatlan region, Mexico, and a local magnitude scale for microearthquakes in this area 24 p4116 N85-35513
Applications of the Kirchoff-Helmholtz integral to problems in body wave seismology 24 p4116 N85-35515

SEISMOMETERS
U SEISMOGRAPHS

SELECTION
NT PERSONNEL SELECTION
NT PILOT SELECTION
NT SITE SELECTION
Guide to the selection of rubbers
[AMTE(N)-TM-84301] 03 p0336 N85-12164
R and D project selection with nonnumerical returns
[INPE-2760-PRE/335] 04 p0575 N85-13665
On choosing between two probabilistic choice sub-models in a dynamic multitask environment 05 p0711 N85-14583
A theoretical method for selecting space craft and space suit atmospheres
[AD-A148219] 08 p1200 N85-17559
A computer package for ranking, selection and multiple comparisons with the best
[AD-A147617] 08 p1204 N85-17579
The R and D project selection problem with fuzzy coefficients
[INPE-3329-PRE/626] 10 p1565 N85-19871
Selection criteria for a CAD/CM system 14 p2402 N85-24810
Selection criteria and computer aided design (CAD) systems
[NLR-MP-84037-U] 14 p2406 N85-24834
Method of selecting robotized system design for pressing process 16 p2761 N85-27040
Satellite selection criteria 16 p2804 N85-27288
A short bibliography of recent developments in selection and ranking procedures
[AD-A155648] 21 p3679 N85-32656
Robotic order picking
[AD-D011737] 22 p3792 N85-33483
Knowledge engineering application in image processing 23 p3965 N85-34583

SELECTIVE DISSEMINATION OF INFORMATION
Environmental geologic atlas of the North Carolina coastal zone: Dare, Hyde, Tyrrell and Washington Counties
[PB84-222975] 01 p0066 N85-10439
International strategic minerals inventory. Summary report: Manganese
[GS-CIRC-930-A] 02 p0219 N85-11442
Ocean services user needs assessment. Volume 1: Survey results, conclusions and recommendations
[NASA-CR-174104] 04 p0541 N85-13445
Nuclear criticality information system: Database examples
[DE84-014482] 04 p0576 N85-13678
Organization of scientific, technical information services 17 p3049 N85-28873
The U.S. Geological Survey in Alaska: Accomplishments during 1982
[US-GEOL-SURV-CIRC-939] 20 p3493 N85-31719
Source header list, supplement 3
[AD-A158100] 24 p4165 N85-35824
Source hierarchy list. Volume 2: I through Z
[AD-A158301] 24 p4165 N85-35826

SELECTIVE FADING
Digital radio link: Wave propagation measurements using narrow band technique
[FOA-C-30364-E2] 04 p0494 N85-13152
Digital data communications over microwave radio channels 10 p1469 N85-19272
Theoretical study of a dynamic simulator of selective fading for digital, wireless beam microwave links 10 p1473 N85-19294

SELECTIVE SURFACES
Selective coatings for solar-to-thermal energy converters 14 p2260 N85-24127
High-altitude testing of selective optical coatings for solar radiators and collectors 17 p2939 N85-28143
Selective coatings for solar heat converters 17 p2939 N85-28144
Thickness-insensitive selective surface paint
[DE85-010598] 19 p3250 N85-30150

SELECTIVITY
Color-selective coating for viewfinder in optical instruments 14 p2276 N85-24008
Correlation of zeolite ZSM-5 acid strength with catalytic activity and selectivity
[DE85-005415] 17 p2922 N85-28013
High-altitude testing of selective optical coatings for solar radiators and collectors 17 p2939 N85-28143
Selective coatings for solar heat converters 17 p2939 N85-28144
Waveguide dielectric millimeter band filter with enhanced selectivity 22 p3760 N85-33421

SELECTORS
High-frequency input device for superheterodyne radio receiver with wideband preselector 12 p1839 N85-21540
Gyrator frequency selectors with bandwidth independent of input signal level 13 p2063 N85-23009

SELENIDES
NT CADMIUM SELENIDES
NT COPPER SELENIDES
NT ZINC SELENIDES
Thio and seleno compounds of the transition metals with the d (o) configuration
[BLL-MINTEK-TR-1177-(5810.5759)] 07 p0925 N85-15663
Positron measurements in 2H-TaSe2 crystals
[DE85-010607] 20 p3529 N85-31949

SELENIUM
Environmental surveillance at Los Alamos during 1984
[DE85-011686] 22 p3611 N85-33605

SELENIUM ALLOYS
Philips tested new materials for optical data storage 15 p2532 N85-25620

SELENIUM COMPOUNDS
NT CADMIUM SELENIDES
NT COPPER SELENIDES
NT SELENIDES
NT ZINC SELENIDES
Effect of light pulses on film of chalcogenide vitreous semiconductors 02 p0258 N85-11667

SELENOGRAPHY
Analysis of systematic errors in systems of selenodetic coordinates 13 p1962 N85-22435

SELENOLOGY
NT LUNAR CORE
Activities at the Lunar and Planetary Institute
[NASA-CR-174069] 04 p0579 N85-13694
Activities at the Lunar and Planetary Institute. Introduction 04 p0579 N85-13695
Volatile elements in and on lunar volcanic glasses: What do they tell us about lunar genesis? 04 p0584 N85-13728
The origin of the Moon 04 p0588 N85-13754
A unified lunar control network 13 p2203 N85-23669
Surface exploration geophysics applied to the Moon
[DE85-006714] 16 p2884 N85-27793

SELF ADAPTIVE CONTROL SYSTEMS
Self-tuning control of offset: A unified approach
[OUEL-1539/84] 04 p0553 N85-13520
Error correction coding for a self-adaptive modem: Theoretical and experimental results 10 p1474 N85-19303
Adaptive control of airborne radar antennas 13 p2080 N85-22689
Technical evaluation report on the Flight Mechanics Symposium on Active Control Systems: Review, Evaluation and Projections
[AGARD-AR-220] 16 p2711 N85-26730
High gain adaptive control of decentralized systems
[DE85-010040] 19 p3339 N85-30898
FAUST: Introduction and overview --- self tuning control
[OUEL-1568/85] 20 p3519 N85-31882
Multivariable model-following self-tuning control with offset rejection
[OUEL-1572/85] 20 p3519 N85-31883

SELF ALIGNMENT
Simulation of gyrocompassing alignment and calibration of strapdown inertial navigation system in a swaying vehicle
[DFVLR-MITT-84-20] 17 p2895 N85-27850
Self-aligned GaAs FET with low 1/F noise
[AD-D011687] 19 p3260 N85-30215
Space station dynamic modeling, disturbance accommodation, and adaptive control 20 p3409 N85-31154

SELF CONSISTENT FIELDS
Field consistency and the finite element analysis of multifield structural problems 18 p3120 N85-29316
A method to estimate the self-consistency effects on electronic structure calculations
[INPE-3536-PRE/752] 19 p3375 N85-30936

SELF DEPLOYING SPACE STATIONS
U SELF ERECTING DEVICES
U SPACE STATIONS

SELF DIFFUSION (SOLID STATE)
Mossbauer spectroscopic investigations of the diffusion and correlation of lattice defects (complementary to neutron spectroscopic investigations) 03 p0429 N85-12736
Comparisons between computed and observed grain boundary structures and properties in metals
[DE85-002596] 10 p1442 N85-19085

SELF ERECTING DEVICES
Hoop/column antenna deployment mechanism overview 22 p3796 N85-33514

SELF EXCITATION
Internal hysteresis experienced on a high pressure syn gas compressor 05 p0642 N85-14122
Theoretical approach to labyrinth seal forces - cross-coupled stiffness of a straight-through labyrinth seal 05 p0643 N85-14127
Experimental investigation of lateral forces induced by flow through model labyrinth glands 05 p0643 N85-14128
Buildup of oscillations in two-mode gyrotron 06 p0786 N85-15037
Clearance flow-generated transverse forces at the rotors of thermal turbomachines
[NASA-TM-77292] 07 p0973 N85-16180
Leakage-flow-induced vibration of a tube-in-tube slip joint
[DE84-007301] 11 p1652 N85-20406
Turbine blade-tip clearance excitation forces
[NASA-CR-171534] 19 p3220 N85-29983
Random vibration of nonlinear, parametrically excited systems 19 p3262 N85-30351

SELF FOCUSING
Brillouin scattering in underdense UV laser-produced plasmas
[DE84-015184] 04 p0567 N85-13614

SELF INDUCED VIBRATION
NT SUBSONIC FLUTTER
NT SUPERSONIC FLUTTER
NT TRANSONIC FLUTTER
Stability of turbine runners in sliding bearings under external circulation forces 14 p2272 N85-24074

SELF LUBRICATING MATERIALS
Mechanical modification of friction surfaces of aluminum alloys by friction transfer 19 p3241 N85-30097

SELF LUBRICATION
Observations of high resistance on slip-rings employing Ag/MoS2/Cu brushes --- solar array drives
[ESA-ESTL-70] 18 p3123 N85-29333

SELF ORGANIZING SYSTEMS
A self-organizing database system: A different approach to query optimization 05 p0735 N85-14725

SELF OSCILLATION
Parametric study of autooscillation upon flow of supersonic jet into cylindrical cavity 16 p2765 N85-27060

SELF PROPAGATION
Hot rolling of ceramics by the use of self propagating synthesis
[AD-D011486] 10 p1453 N85-19154

SELF REGULATING
U AUTOMATIC CONTROL

SELF SEALING
Experimental stiffness of tapered bore seals
[NASA-TM-86978] 15 p2568 N85-25847
Refrigerated dynamic seal to 6.9 MPa (1000 psi)
[NASA-TM-87108] 23 p3890 N85-34356

SELF SUBTRACTION HOLOGRAPHY
U HOLOGRAPHIC SUBTRACTION

SELSYNS (TRADEMARK)
U SERVOMOTORS

SEMANTICS
Model theory for infinitely deep languages
[ISSN-0355-0087] 01 p0101 N85-10674
On update semantics and relational views
[AD-A145822] 02 p0294 N85-11907
Research in knowledge representation for natural language understanding
[AD-A145807] 03 p0409 N85-12813
Knowledge representation and natural-language semantics
[AD-A146025] 03 p0409 N85-12815
Crew communication as a factor in aviation accidents 05 p0710 N85-14555
Functional semantics of modules
[AD-A146923] 07 p1024 N85-16500
Speech analysis by parametric methods: A survey
[ENST-84C004] 09 p1313 N85-18251
JOVIAL J73 automated verification system: Implementation phase
[AD-A148732] 09 p1368 N85-18597
Precedency control and other semantic integrity issues in a workbench database 13 p2123 N85-23220
The identification of semantics for the file/database problem domain and their use in a template-based software environment 14 p2401 N85-24803
Functional analysis of programs
[AD-A150742] 14 p2404 N85-24819
Semantic networks and neural nets
[AD-A150750] 14 p2407 N85-24840
Research in knowledge representation for natural language understanding
[AD-A152260] 16 p2851 N85-27579
Towards a uniform topological treatment of streams and functions on streams
[CWI-CS-R8422] 17 p3014 N85-29839
Survey of Ada (Trademark)-based PDLs (Program Design Language)
[AD-A154402] 19 p3338 N85-30880
Design and implementation of an intelligence database
[AD-A154095] 19 p3361 N85-30973
The formal specification of an abstract machine: Design and implementation
[AD-A155167] 21 p3672 N85-32806
Research on distributed artificial intelligence
[AD-A155356] 22 p3833 N85-33733

SEMICONDUCTING FILMS
Studies of hydrogenated amorphous silicon
[DE84-013038] 01 p0067 N85-10443
Effect of liquid phase composition on thickness of epitaxial Ga sub (1-x) Al sub x As films 02 p0257 N85-11663
Determining composition in surface region of semiconductor crystals by method of sudden changes in X-ray photoelectric effect 02 p0267 N85-11746
Some investigations of molecular beam epitaxial growth of 3-5 semiconductor films via Monte-Carlo computer simulations, carrier tunneling and spectroscopic ellipsometry
[AD-A149465] 10 p1583 N85-19854
Method for the preparation of epitaxial films of mercury cadmium telluride
[AD-D011532] 12 p1938 N85-22175
Process for the epitaxial deposition of III-V compounds utilizing a continuous in-situ hydrogen chloride etch
[AD-D011557] 12 p1939 N85-22177
Non-linear optical techniques for visible and UV lasers and thin film deposition
[AD-A150469] 13 p2096 N85-23077
Investigation of a Si and related semiconductors as materials for photovoltaic conversion
[DE85-002932] 18 p3096 N85-29163
Glow discharge deposition at high rates using diflane
[DE85-010236] 19 p3263 N85-30235
Microwave-enhanced thin-film deposition 21 p3611 N85-32431

SEMICONDUCTOR DEVICES
NT AVALANCHE DIODES
NT BIPOLAR TRANSISTORS
NT CHARGE COUPLED DEVICES
NT CHARGE INJECTION DEVICES
NT CHARGE TRANSFER DEVICES
NT CMOS
NT FIELD EFFECT TRANSISTORS
NT GALLIUM ARSENIDE LASERS
NT GERMANIUM DIODES
NT HETEROJUNCTION DEVICES
NT JFET
NT JUNCTION DIODES
NT JUNCTION TRANSISTORS
NT LIGHT EMITTING DIODES
NT METAL OXIDE SEMICONDUCTORS
NT MIM (SEMICONDUCTORS)
NT MIM DIODES
NT MIS (SEMICONDUCTORS)
NT PHOTODIODES
NT PHOTOTRANSISTORS
NT PHOTOVOLTAIC CELLS
NT SCHOTTKY DIODES
NT SEMICONDUCTOR LASERS
NT SILICON CONTROLLED RECTIFIERS

NT SILICON TRANSISTORS
NT THERMISTORS
NT THYRISTORS
NT TRANSISTOR AMPLIFIERS
NT TRANSISTORS
NT VARACTOR DIODES
NT VARISTORS
Center for Electronics and Electrical Engineering Technical Bulletin covering center programs with 1984 CEEE events calendar
[PB84-222785] 01 p0045 N85-10292
Center for Electronics and Electrical Engineering Technical Bulletin covering center programs with 1984 CEEE events calendar
[PB84-223684] 01 p0045 N85-10293
Center for Electronics and Electrical Engineering Technical Bulletin covering center programs
[PB84-219716] 01 p0045 N85-10295
Radiation measuring system using transistor flux sensors
[AD-D011239] 01 p0050 N85-10328
RADC/NBS (Rome Air Development Center/National Bureau of Standards) Workshop. Moisture Measurement and Control for Semiconductor Devices, 3
[PB84-219559] 01 p0051 N85-10337
Reversible change in parameters of GaAs-based surface-barrier metal-semiconductor diodes induced by hydrogen absorption-desorption
02 p0258 N85-11690
Method of splitting for solution of problems in semiconductor physics 02 p0265 N85-11736
Proceedings of the Ion Implantation for Army Needs Workshop
[AD-A145474] 02 p0296 N85-11983
Automation of production of semiconductor power devices 03 p0348 N85-12229
Research activities of the Illinois University Coordinated Science Laboratory
[AD-A145589] 03 p0449 N85-12856
Comprehensive silicon solar cell computer modeling
[NASA-CR-174151] 04 p0530 N85-13386
Semiconductor high-voltage power devices: State of art and outlook 06 p0794 N85-15074
New methods of fast switching of high power by means of semiconductor devices 06 p0794 N85-15075
Integrated power devices with three-dimensional connection for automation systems
06 p0794 N85-15077
Development of technology of silicon single-crystal production semiconductor power devices: State of art outlook 06 p0795 N85-15078
Current-voltage characteristics of semiconductor power devices operating at high current densities
06 p0795 N85-15079
Theoretical investigation of device aspects of semiconductor superlattices
[AD-A146641] 06 p0867 N85-15509
Mobility and trapping time measurements in HgI2
[DE84-015954] 06 p0869 N85-15522
Charge domain filters for enhanced monolithic signal processing
[AD-A147428] 07 p0941 N85-15984
An asymptotic analysis of a transient p-n junction model
[AD-A147270] 07 p0947 N85-16004
The constant current strain gauge bridge
[ARL/STRUC-TM-385] 07 p0962 N85-16097
Superlattice ultrasonic wave generator
[AD-D011363] 07 p1038 N85-16585
Two carrier dual injector apparatus
[AD-D011357] 07 p1047 N85-16646
Characterization of III-V compound semiconductor device materials
[AD-A148203] 08 p1226 N85-17719
Gallium arsenide/AlGaAs multilayer structures with special doping profiles for microwave and optoelectronic devices
[BMFT-FB-T-84-207] 08 p1227 N85-17725
East Europe report: Science and technology
[JPRS-ESA-85-005] 09 p1377 N85-18659
Semiconductors at Leipzig Spring Fair
09 p1377 N85-18660
Semiconductor superlattice photodetectors
[NASA-CR-174347] 09 p1397 N85-18791
Asymptotic representation of solutions of the basic semiconductor device equations
[AD-A149040] 10 p1545 N85-19741
A new very high voltage semiconductor switch
[NASA-TM-86957] 11 p1627 N85-20246
Method and apparatus for measuring minority carrier lifetime in a direct band-gap semiconductor
[NASA-CASE-NPO-16337-1-1] 11 p1628 N85-20251
Measurement of the configuration of a concave surface by the interference of reflected light
[NASA-TM-77796] 11 p1728 N85-20867
Low stress semiconductor-insulator interface for cryogenic device applications
[NASA-CASE-NPO-16394-1] 11 p1734 N85-20906
Inelastic tunnel diodes
[NASA-CASE-LEW-13833-1] 12 p1832 N85-21492
Method for the fabrication of dielectric isolated junction field effect transistor and PNP transistor
[AD-D011500] 12 p1832 N85-21494
Process for the epitaxial deposition of III-V compounds utilizing a continuous in-situ hydrogen chloride etch
[AD-D011557] 12 p1939 N85-22177
Investigation of device and electronic interactions in GaAs device processing
[AD-A149747] 12 p1940 N85-22182
Electrical performance of semiconductor devices at cryogenic temperatures 12 p1948 N85-22239
Drift fields and boundary conditions at grain boundaries in bipolar P/N junction silicon devices
13 p2062 N85-22879
Electrical overstress protection of submicron devices
[AD-A150334] 13 p2064 N85-22892
Measurement of internal thermal resistance for quality control of semiconductor devices
13 p2074 N85-22953
Requirements placed on information processing equipment
[BLL-CE-TRANS-7983-(9022.09)] 13 p2144 N85-23307
Solar cells based on polycrystalline silicon with isothermal potential barriers along grain boundaries
14 p2275 N85-24091
Proceedings of the Cold Electronics Workshop
[NASA-CR-175662] 14 p2297 N85-24220
Cold electronics: An overview
14 p2297 N85-24221
Acoustic emission of semiconductor devices
15 p2529 N85-25593
Developments in microelectronics: Past and future
15 p2530 N85-25597
Future prospects of China's microwave semiconductor technology 15 p2530 N85-25598
China report: Science and technology
[JPRS-CST-85-013] 15 p2536 N85-25652
Heavy doping effects in high efficiency silicon solar cells
[NASA-CR-175661] 15 p2586 N85-25940
Solution of coupled system of PDE by the transistorized multigrid method
[DE85-006377] 15 p2639 N85-26278
Charge isolation in a spatial light modulator
[AD-D011581] 15 p2652 N85-26356
Assessment of present and future large-scale semiconductor detector systems
[DE85-006606] 15 p2662 N85-26430
Space power plants 16 p2724 N85-26813
Cryostat and electronic development associated with multi-detector spectrometer systems
[DE85-007824] 16 p2788 N85-27200
Shallow impurity cluster states in n-type semiconductors
[INPE-3495-PRE/732] 16 p2869 N85-27699
Investigation of superlattice device structures
[NASA-CR-3903] 16 p3094 N85-29152
Optical fiber magnetic field sensor with nanosecond response time
[DE85-008409] 16 p3110 N85-29259
A stored data acquisition system: Update
[DE85-010534] 16 p3166 N85-29616
Optically nonlinear and bistable behaviour of direct gap semiconductors 16 p3166 N85-29759
The potential of semiconductors for optical integrated circuits 16 p3167 N85-29768
Electron spin resonance study of interface states induced by electron injection in metal-oxide-semiconductor devices
[DE85-009502] 16 p3195 N85-29617
Low defect, high purity crystalline layers grown by selective deposition
[NASA-CASE-NPO-15813-1] 16 p3373 N85-30922
Theoretical investigation of material characteristics of semiconductor superlattices
[AD-A154126] 19 p3375 N85-30936
Planar doped barrier semiconductor device
[AD-D011591] 20 p3537 N85-32010
Microwave semiconductor research: Materials, devices and circuits and gallium arsenide ballistic electron transistors
[AD-A154698] 21 p3709 N85-33024
A second order difference scheme for transient semiconductor device simulation
[AD-A154824] 21 p3709 N85-33027
A review of the physics and response models for burnout of semiconductor devices
[AD-A155031] 21 p3709 N85-33028
Modulation doped GaAs/Al(x)Ga(1-x)As layered structures with applications to field effect transistors
[AD-A155360] 22 p3759 N85-33296
Thermoelectric generator and method for the fabrication thereof
[DE85-011650] 22 p3760 N85-33302
Solid state radiative heat pump
[DE85-011605] 22 p3760 N85-33303
Electron beam enhanced surface modification for making highly resolved structures
[DE85-011609] 22 p3760 N85-33305
TEMO and TEB thermoelectronic devices
22 p3770 N85-33415
Transient two-dimensional simulation of SEU in a CMOS SRAM cell
[DE85-008419] 22 p3860 N85-34111
Joint services electronics program
[AD-A154748] 23 p3927 N85-34336
Applications of CdTe to nuclear medicine
[DE85-011877] 23 p3952 N85-34492
Analysis of transient radiation upset in a 16K SRAM
[DE85-009442] 23 p3965 N85-34586
Circuit approaches to increasing SRAM performance in total dose environments
[DE85-009441] 23 p3966 N85-34588
Error-correcting codes for computer memories
24 p4136 N85-35636
Electron irradiation of N type cadmium telluride
[AD-A156117] 24 p4161 N85-35801
Optical properties of heterostructures and superlattices
[AD-A156243] 24 p4162 N85-35802
SEMICONDUCTOR DIODES
NT AVALANCHE DIODES
NT GERMANIUM DIODES
NT GUNN DIODES
NT JUNCTION DIODES
NT LIGHT EMITTING DIODES
NT PHOTODIODES
NT SCHOTTKY DIODES
NT TUNNEL DIODES
NT VARACTOR DIODES
The behavior of Pb(1-x)Sn(x)Te semiconductor laser diodes in a magnetic field
[AD-A145431] 02 p0287 N85-11872
Heatsink requirements for coherent operation of high-power semiconductor laser arrays
[AD-A146184] 03 p0366 N85-12348
Lifetime of excess charge carriers in weakly doped epitaxial GaAs layers 04 p0487 N85-13108
Strained-layer superlattice emitter and detector structures using modulation-doped active regions
[DE85-000084] 06 p0867 N85-15511
AlAs/GaAs superlattice barrier unipolar diode structure
[DE85-001904] 11 p1736 N85-20921
Pulse transformer package for impedance matching a laser diode to a transmission line
[AD-D011409] 12 p1855 N85-21632
SEM (Scanning Electron Microscope) investigation of silicon diodes using the electron beam induced current method
[AD-A150358] 13 p2064 N85-22894
Monolithic planar doped barrier limiter
[AD-D011578] 15 p2548 N85-25723
Controlled-linewidth laser source
[AD-D011981] 19 p3274 N85-30306
SEMICONDUCTOR INSULATOR SEMICONDUCTORS
U SIS (SEMICONDUCTORS)
SEMICONDUCTOR JUNCTIONS
NT P-I-N JUNCTIONS
NT P-N JUNCTIONS
NT P-N-P JUNCTIONS
NT P-N-P-N JUNCTIONS
NT SILICON JUNCTIONS
Multijunction cells for concentrators: Technology prospects
[NASA-CR-174259] 07 p0991 N85-16295
Advanced high-efficiency concentrator cells
[DE84-013020] 09 p1344 N85-18459
Screen printed interdigitated back contact solar cell
[NASA-CASE-LEW-13414-1] 11 p1671 N85-20530
Drift fields and boundary conditions at grain boundaries in bipolar P/N junction silicon devices
13 p2062 N85-22879
Flat-plate solar array project process development area: Process research of non-CZ silicon material
[NASA-CR-175777] 16 p2818 N85-27382
A second order difference scheme for transient semiconductor device simulation
[AD-A154824] 21 p3709 N85-33027
Flat-plate solar array project process development area process research of non-CZ silicon material
[NASA-CR-176117] 23 p3945 N85-34445

Rapid annealing of temperature-compensated, precision voltage references following fast-neutron irradiation
[DE85-009621] 23 p3970 N85-34609
HgCdTe surface and defect study program
[AD-A156079] 24 p4161 N85-35799

SEMICONDUCTOR LASERS
NT GALLIUM ARSENIDE LASERS
Synchronously pumped mode-locked semiconductor platelet laser
[AD-D011214] 01 p0051 N85-10340
Tunable CW semiconductor platelet laser
[AD-D011215] 01 p0052 N85-10341
High frequency phase-noise in semiconductor lasers
[FUB-20-1983] 01 p0053 N85-10353
Biaxial-crystal laser with waveguide resonator
02 p0262 N85-11717
Theoretical analysis of physical processes of lasing medium degradation in semiconductor lasers
02 p0269 N85-11759
The behavior of Pb(1-x)Sn(x)Te semiconductor laser diodes in a magnetic field
[AD-A145431] 02 p0287 N85-11872
Diffusion barrier for long wavelength laser diodes
[AD-D011390] 07 p0970 N85-16157
Phased locked array laser systems
[AD-D011317] 07 p0971 N85-16164
Optical computer studies at UK's Heriot-Watt University 09 p1309 N85-18227
Effect of neutron irradiation on the high temperature operation of injection laser diodes
[DE85-000066] 09 p1326 N85-18333
Quantum noise effects in single-mode injection lasers
[FUB-11-1984] 09 p1327 N85-18336
Effect of impurities on absorption in semiconductors and lasing of semiconductor lasers 11 p1716 N85-20797
Pulse transformer package for impedance matching a laser diode to a transmission line
[AD-D011499] 12 p1855 N85-21632
Mode control and wavelength tuning in open ended Michelson interferometric semiconductor laser
13 p2095 N85-23073
Wavelength dependent, tunable, optical time delay system for electrical signals
[AD-D011584] 15 p2548 N85-25725
Possible uses of tunable diode lasers in infrared spectroscopy
[ESA-TT-869] 15 p2564 N85-25818
The construction and study of improved Al(x)Ga(1-x)As-GaAs heterostructure devices
[AD-A153264] 17 p2954 N85-28244
Injection laser structure design
[AD-A153210] 17 p2971 N85-28345
Diode laser 87Rb optical pumping in an evacuated wall-coated cell 18 p3105 N85-29226
1.5 micrometer GaInAsP high pulsed power diode lasers
[AD-A153568] 18 p3193 N85-29805
Controlled-linewidth laser source
[AD-D011661] 19 p3274 N85-30306
Sensitive detection of tunable diode laser absorption by polarization rotation
[DE85-009621] 19 p3277 N85-30322
Optical properties of heterostructures and superlattices
[AD-A156243] 24 p4162 N85-35802

SEMICONDUCTOR PLASMAS
Demonstration of feasibility of depositing semiconductor layers using microwave enhanced plasma techniques
[NASA-CR-174392] 13 p2163 N85-23421
Some dynamic electronic properties of semiconductor surfaces and interfaces 20 p3537 N85-32007

SEMICONDUCTORS (MATERIALS)
NT ACCEPTOR MATERIALS
NT AMORPHOUS SEMICONDUCTORS
NT CHARGE TRANSFER DEVICES
NT CMOS
NT DONOR MATERIALS
NT METAL OXIDE SEMICONDUCTORS
NT MIM (SEMICONDUCTORS)
NT MIS (SEMICONDUCTORS)
NT N-TYPE SEMICONDUCTORS
NT ORGANIC SEMICONDUCTORS
NT P-TYPE SEMICONDUCTORS
NT PHOTOCONDUCTORS
NT SUPERLATTICES
Center for Electronics and Electrical Engineering Technical Bulletin covering center programs with 1984 CEEE events calendar
[PB84-222785] 01 p0045 N85-10292
Preparation and properties of single crystals of hydrogen bis(phthalocyaninato) neodymium(3)
[AD-A144933] 01 p0123 N85-10846
Solidification and crystal growth of solid solution semiconducting alloys 02 p0155 N85-11046
Experiments with phase transitions at very high pressure
[NASA-CR-174029] 02 p0172 N85-11148
Complex formation and temperature stability of electrophysical properties of GaAs semiinsulating single crystals 02 p0258 N85-11689
Formation of lattice defects by nitrogen laser exposure in A2B6 semiconductors with wide forbidden band
02 p0258 N85-11692
USSR report: Physics and mathematics
[JPRS-UPM-84-004] 02 p0266 N85-11737
Nonlinear absorption of laser radiation in InP and in GaAs 02 p0266 N85-11740
Photocurrent oscillations in Bi12GeO20 metal-semiconductor-metal structures
02 p0266 N85-11741
Capacitive reactance of compensated semiconductors with deep centers under conditions of transmission of exclusion and double injection currents
02 p0266 N85-11742
Magnetoabsorption of weak light wave in presence of intense light wave in semiconductor with narrow forbidden band 02 p0267 N85-11743
Mechanisms of laser annealing of semiconductors
02 p0267 N85-11744
Instability in semiconductors exposed to ionizing radiation 02 p0267 N85-11747
Injection lasers based on AlGaAsSb/GaSb and InGaAsSb/GaSb heterostructures
02 p0270 N85-11761
Characteristics of ion implanters for fabrication of electronic devices
[AD-P003949] 02 p0286 N85-11865
Current controlled LPE (Liquid Phase Epitaxy) growth of semiconductors
[AD-A145536] 02 p0287 N85-11875
Nonlinear electromagnetic waves in ferromagnetic conducting media 03 p0346 N85-12232
Producing semiconductor materials by superfast cooling of melt 03 p0354 N85-12274
Center for Electronic and Electrical Engineering Technical Progress Bulletin, January - March 1983, no. 2
[PB84-231224] 03 p0360 N85-12308
Inelastic neutron scattering on crystals for the clarification of structure and semiconductor properties
03 p0425 N85-12714
Measurement of state and dynamic solid state properties in nonmetals using excited probe nuclei on the Erlanger 12 MeV tandem accelerator 03 p0428 N85-12730
Neutron irradiation of semiconductors --- lattice defects, electron irradiation 03 p0428 N85-12732
Studies of grown-in defects versus growth parameters in 3-4 compound semiconductors
[AD-A145864] 03 p0433 N85-12755
Research activities of the Illinois University Coordinated Science Laboratory
[AD-A145589] 03 p0449 N85-12856
Effect of barrier height on friction behavior of the semiconductors silicon and gallium arsenide in contact with pure metals
[NASA-TP-2405] 04 p0478 N85-13044
Nonthermal mechanism for laser annealing of semiconductors and formation of super structure
04 p0487 N85-13109
Investigation of effect of photocurrent amplification in meta-dielectric-semiconductor structures based on silicon 04 p0488 N85-13110
Physics and design of advanced infrared bolometers and photoconductors
[DE84-016863] 04 p0503 N85-13213
Silicon for solar cells
[DE84-004503] 04 p0529 N85-13381
Materials characterization using ion, electron, and photon probes
[DE84-004518] 04 p0560 N85-13568
Theory of non-linear index of refraction of compound semiconductors
[DE84-013660] 04 p0569 N85-13626
Single crystal semiconductor multilayers for electrically active optical interference filters
[DE84-015614] 04 p0571 N85-13640
Refractive index of ternary and quaternary compound semiconductors below the fundamental absorption edge: Linear and nonlinear effects
[DE84-012325] 05 p0640 N85-14105
USSR report: Physics and mathematics
[JPRS-UPM-84-007] 05 p0723 N85-14651
LPE (Liquid phase epitaxy) semiconductor material transfer method
[AD-D011250] 05 p0731 N85-14696
InAsSb strained-layer superlattices (SLSs) for long wavelength detector applications
[DE84-016111] 05 p0732 N85-14706
Acoustoelectric interaction in double-layer semiconductors 06 p0786 N85-15023
Computer investigation of effects of high injection in transistor large integrated circuit structures
06 p0793 N85-15068
Trends in development of bipolar power transistors
06 p0793 N85-15072
Investigation of structural and electrical properties of low-angle silicon sheet 06 p0831 N85-15288
Characterization of surface electronic properties of semi-insulating InP
[AD-A146553] 06 p0866 N85-15507
The growth and properties of semiconductor strained-layer superlattices
[DE84-012979] 06 p0868 N85-15515
Float zone experiments in space
[NASA-CR-171284] 07 p0911 N85-15766
Determination of moments of initial estimate during linear approximation of distribution of ejected impurity
07 p0954 N85-16045
Determination of parameters of doped thin semiconductor layers from plasmatic minimum of reflection coefficient for infrared radiation
07 p0954 N85-16047
Superlattice ultrasonic wave generator
[AD-D011363] 07 p1038 N85-16585
Ion microscopy of metals and semiconductors
[AD-A147118] 07 p1043 N85-16626
Ion implantation and laser processing of III-V compound semiconductors with applications to the fabrication of microwave devices
[AD-A146846] 07 p1047 N85-16651
Laser annealing of ion implanted semiconductors
[AD-A146979] 07 p1047 N85-16652
Method of preparing single crystalline cubic silicon carbide layers
[AD-D011305] 07 p1048 N85-16653
Clusters of defects in semiconductors
[AD-A147426] 07 p1048 N85-16655
Electron distribution function and mobility in 3-5 compounds for high and low fields
[AD-A147447] 07 p1048 N85-16658
X-ray and backscattering analysis of ion implantation phenomena in GaAs and related compounds
[AD-A147449] 07 p1048 N85-16659
Transport properties and distribution functions in 3-5 semiconductors
[AD-A147525] 07 p1049 N85-16660
Electronics component R and D, production capability reviewed 08 p1140 N85-17181
French research on gallium arsenide devices
08 p1141 N85-17196
General assessment of GDR microelectronics industry, applications 08 p1142 N85-17202
Life cycle cost model for very high speed integrated circuits
[AD-A147796] 08 p1157 N85-17298
Formation of a limiting composition in the preparation of ternary 3-5 semiconductors by the VPE (Vapor Phase Epitaxy) Hydride technique
[AD-A147639] 08 p1225 N85-17713
Electronic structure of semiconductor interfaces
[AD-A147663] 08 p1225 N85-17715
Characterization of III-V compound semiconductor device materials
[AD-A148203] 08 p1226 N85-17719
Ion implantation in 3-5 compound semiconductors
[AD-A148462] 08 p1226 N85-17723
Device modeling for advanced integrated circuits
09 p1314 N85-18258
Nondestructive characterization of semiconductor surfaces and interfaces 09 p1329 N85-18349
Electron-hole plasma formation in semiconductors due to the absorption of pulsed CO2 laser light
[DE85-001559] 09 p1392 N85-18757
A picosecond population modulation study of near interband resonances in semiconductors
09 p1396 N85-18787
Ion-implantation doping of strained-layer superlattices
[DE85-001903] 09 p1400 N85-18811
Siemens' CAD system designs VLSI circuits
10 p1461 N85-19209
Picosecond laser pulse interactions with metallic and semiconductor surfaces
[AD-A149112] 10 p1490 N85-19405
Silicon film solar cell process
[NASA-CR-174446] 10 p1508 N85-19514
Metal-nonmetal transitions in N-doped many-valley Si and Ge
[INPE-3358-PRE/636] 10 p1562 N85-19848
Quaternary narrow-band semiconductors (HgTe)x (InSb)1-x for far-infrared detectors
[AD-A149350] 10 p1562 N85-19852
Applications of the Heavy-Ion Rutherford Backscattering Spectrometry (HIRBS) to the analysis of contact structures on GaAs and Ge
[DE85-000671] 10 p1564 N85-19861

Solar fuel synthesis based on colloidal and particulate semiconductors
[PB85-129104] 11 p1614 N85-20152
Method for increasing linearity of load cell
11 p1623 N85-20221
Optically bistable devices using semiconductor materials
[AD-A149551] 11 p1628 N85-20253
USSR report: Physics and mathematics
[JPRS-UPM-85-001] 11 p1715 N85-20786
Effect of impurities on absorption in semiconductors and lasing of semiconductor lasers 11 p1716 N85-20797
Laser-plasma interactions for the deposition and etching of semiconductor materials
[DE85-000458] 11 p1731 N85-20885
Determination of the mobility profile in GaAs-MESFETs
[NASA-TM-77818] 11 p1734 N85-20905
Subnanosecond time-resolved emission study of Cu2O and GaAs
[DE85-002070] 11 p1735 N85-20912
Preliminary studies on the low-cost preparation of chalcogenide semiconductors from solution depositions
[DE85-000638] 11 p1736 N85-20918
Impurity complexes in pure elemental semiconductors
11 p1736 N85-20919
Research in surface sciences, disordered materials, and solidification and growth
[PB85-132140] 11 p1737 N85-20927
GaAs and 3-5 compound solar cells status and prospects for use in space
[NASA-TM-86960] 12 p1795 N85-21261
Transmissive Dewar cooling chamber for optically pumped semiconductor ring lasers
[AD-D011550] 12 p1855 N85-21636
Process for the epitaxial deposition of III-V compounds utilizing a continuous in-situ hydrogen chloride etch
[AD-D011557] 12 p1939 N85-22177
Total immersion crystal growth
[NASA-CASE-NPO-15800-2] 12 p1939 N85-22178
Semiconductor materials for high frequency solid state sources
[AD-A150020] 12 p1940 N85-22186
Germanium resistance thermometer calibration at superfluid helium temperatures
12 p1947 N85-22228
Clustering and ordering in 3-5 alloys
[AD-A150604] 13 p2022 N85-22870
Noise characteristics of sulfur-doped silicon diodes
13 p2073 N85-22952
Numerical simulation of inverters with I2L elements including effects of high doping level
13 p2088 N85-23039
Electronic transport in hydrogenated amorphous silicon films
[DE85-002901] 13 p2164 N85-23426
Proceedings of the Cold Electronics Workshop
[NASA-CR-175682] 14 p2297 N85-24220
Cold electronics: An overview
14 p2297 N85-24221
Recent developments in semiconductor research
14 p2297 N85-24222
AlN insulator for 3-5 MIS applications
[AD-A150674] 14 p2426 N85-24962
Electrical and thermal transport property studies of high-temperature thermoelectric materials
[AD-A150900] 14 p2427 N85-24967
Infrared nonlinear processes in semiconductors
[AD-A150966] 14 p2427 N85-24968
Theory and calculations of the electronic structure of solids having directional bonding
[AD-A151082] 14 p2428 N85-24971
Strained-layer superlattices and strain-induced light holes
[DE85-003675] 14 p2431 N85-24990
Future directions in computers
15 p2625 N85-26183
USSR report: Physics and mathematics
[JPRS-UPM-85-003] 15 p2642 N85-26300
Pressure-dependence of TlS(2) and TlSe(2) bandstructures
[AD-A151200] 15 p2659 N85-26410
ONR (Office of Naval Research) Far East Scientific Bulletin, Volume 9, Number 4, October-December 1984
[AD-A151274] 15 p2665 N85-26448
The impact of VLSI on guidance and control system design 16 p2697 N85-26654
Periodic cluster simulation of a disordered impurity system
[INPE-3453-PRE/705] 16 p2858 N85-27626
On some physical impurity properties of doped-indirect gap semiconductors at low and intermediate concentrations
[INPE-3452-PRE/704] 16 p2869 N85-27701
Density of impurity states associated to inversion layers
[INPE-3406-PRE/675] 16 p2869 N85-27702
Optimum convection conditions for Czochralski growth of semiconductors
[INPE-3395-PRE/665] 16 p2870 N85-27703
Impurity bands associated with MOS inversion layers
[INPE-3483-PRE/726] 16 p2870 N85-27704
On the choice of coordinates for semiconductor simulation
[AD-A152214] 16 p2870 N85-27706
Heat pipe and method of making same
[AD-D011654] 17 p2959 N85-28273
Laser measurement techniques: Laser spectroscopy in semiconductors
[DE85-007887] 17 p2971 N85-28350
Optical waveguide characterization using grating couplers
[AD-A153063] 17 p3037 N85-28789
Morphology of GaAs/sub 1-x/P/sub x/ superlattices grown by MOCVD and chloride VPE
[DE85-002944] 17 p3045 N85-28842
Research on electrochemical photovoltaic cells
[DE85-008775] 18 p3131 N85-29362
The potential of semiconductors for optical integrated circuits 18 p3187 N85-29768
Process for the epitaxial deposition of 3-5 compounds utilizing a binary alloy as the metallic source
[AD-D011663] 18 p3193 N85-29801
Growth mechanism and properties of the thermal and anodic oxides of the 3-5 compound semiconductors
[AD-A153408] 18 p3193 N85-29803
Processable and stable conductive polymers
[AD-D011684] 19 p3249 N85-30143
Electron irradiation of light emitting diodes
[AD-A154441] 19 p3260 N85-30213
Method of reducing impurity and antisite defects in semiconductor crystal materials, and device and apparatus respectively produced from and utilizing same
[AD-D011698] 19 p3260 N85-30216
Method for producing high quality germanium-germanium nitride interfaces for germanium semiconductors and device produced thereby
[AD-D011702] 19 p3260 N85-30218
Method for determining the point of zero zeta potential of semiconductor
[NASA-CASE-LAR-12893-1] 19 p3373 N85-30923
Fluorescence quenching by metal semiconductor and insulator surfaces 19 p3374 N85-30929
Method for growing low defect, high purity crystalline layers
[NASA-CASE-NPO-15813-2] 19 p3374 N85-30933
Crystal growth of device quality GaAs in space
[NASA-CR-176024] 19 p3375 N85-30935
Theoretical investigation of material characteristics of semiconductor superlattices
[AD-A154126] 19 p3375 N85-30936
Chemistry and physics of silicon-based amorphous semiconductors
[DE85-001931] 19 p3377 N85-30949
Strained-layer-superlattice optoelectronic devices
[DE85-009148] 19 p3377 N85-30953
Predamage threshold electron emission from insulator and semiconductor surfaces
[DE85-006968] 19 p3377 N85-30954
Leading-edge microelectronics research at Sweden's Chalmers 20 p3438 N85-31337
Swedish program for sensor research, development
20 p3438 N85-31338
Center for Electronics and Electrical Engineering technical progress bulletin covering center programs, April-June 1984 with 1984 CEEE (Center for Electronics and Electrical Engineering) events calendar, issue 7
[PB85-187540] 20 p3450 N85-31419
Interface chemistry of Hg(1-x)Cd(x)Te
[AD-A154878] 21 p3563 N85-32161
Z-contrast imaging and electron channeling analysis of dopants in semiconductors
[DE85-011410] 21 p3582 N85-32269
On the dependence of the convergence of Gummel's algorithm on the regularity of the solution
[AD-A154628] 21 p3675 N85-32632
Influence on bi-phonon states on Raman scattering of light in molecular crystals 21 p3680 N85-32865
Influence of coherent light beams on free carriers in semiconductors 21 p3681 N85-32867
Quasi-steady-state melting mode during combined laser irradiation of semiconductor materials
21 p3682 N85-32874
Photo-acoustic effect in finite-dimensional semiconductors 21 p3682 N85-32876
Effect of powerful pulsed low-energy ion streams on GaAs 21 p3682 N85-32877
A second order difference scheme for transient semiconductor device simulation
[AD-A154824] 21 p3709 N85-33027
Raman scattering studies in solids
[AD-A155526] 21 p3710 N85-33032
Electronic phenomena near semiconductor grain boundaries
[DE85-011543] 21 p3711 N85-33035
Consortium program for the study of boron-rich borides
[DE85-011378] 22 p3762 N85-33260
In-situ observations of the development of heavy-ion damage in semiconductors
[DE85-010269] 22 p3781 N85-33307
Photovoltaics technical information guide
[DE85-002924] 22 p3808 N85-33585
Electronic structure and lattice dynamics of dimensionally constrained and disordered solids
[AD-A155627] 24 p4161 N85-35797
Investigations of the molecular beam epitaxial growth and characteristics of external excitation induced non-equilibrium phases of immiscible 3-5 compound semiconductors
[AD-A156325] 24 p4162 N85-35804

SEMIMETALS
U METALLOIDS

SENDERS
U TRANSMITTERS

SENSE ORGANS
NT CHEMORECEPTORS
NT COCHLEA
NT EAR
NT EYE (ANATOMY)
NT GRAVIRECEPTORS
NT LABYRINTH
NT MECHANORECEPTORS
NT OCULOMOTOR NERVES
NT OTOLITH ORGANS
NT PHOTORECEPTORS
NT PROPRIOCEPTORS
NT RETINA
NT VESTIBULES

SENSES
U SENSORY PERCEPTION

SENSIBILITY
U SENSITIVITY

SENSING
U DETECTION

SENSITIVITY
NT IMPACT RESISTANCE
NT LIGHT ADAPTATION
NT NOTCH SENSITIVITY
NT PHOTOSENSITIVITY
NT PHOTOTROPISM
NT PROPELLANT SENSITIVITY
NT RADIATION TOLERANCE
NT SENSITOMETRY
NT SPECTRAL SENSITIVITY
Design sensitivity analysis of an antisymmetric angle-ply laminate
[CSIR-TWISK-318] 01 p0021 N85-10128
Motion sensor evaluation using simulation
[DE84-014869] 01 p0050 N85-10331
Sensitivity analysis of limit state functions for probability-based plastic design
01 p0059 N85-10368
Sensitivity analysis in generalized rational approximation with restricted denominator
[CSIR-TWISK-319] 01 p0109 N85-10734
Definition of acceptable levels of mismatch for equivalent systems of augmented CTOL (Conventional Take-Off and Landing) aircraft
[AD-A145619] 02 p0149 N85-11007
Unified approach to sensitivity and uncertainty analysis
[DE84-014049] 02 p0255 N85-11669
New uses for sensitivity analysis: How different movement tasks affect limb model parameter sensitivity
05 p0706 N85-14529
Sensitivity analysis of discrete structural systems: A survey
[NASA-TM-86333] 06 p0817 N85-15186
Human reactions to transient electric currents, volume 12
[PB84-231463] 06 p0848 N85-15374
Optical fibers with reduced pressure sensitivity to high frequency acoustic field
[AD-D011306] 07 p1043 N85-16827
An adaptive Fast Fourier Transform weighting technique to increase small target sensitivity
[AD-D011424] 08 p1154 N85-17286
CP DDT detonators. Part 1: Design sensitivity study
[DE84-017256] 09 p1302 N85-18180
Treatment of general boundary conditions and point-wise state variable constraints in optimum design for static and dynamic response
09 p1330 N85-18358

Issues in sensitivity and statistical analysis of large-scale, computer-based models
[PB86-116317/GAR] 09 p1376 N85-18650
Dual adaptive control based upon sensitivity functions
[NASA-CR-169331] 10 p1543 N85-19727
Radiographic detectability limits for seeded voids in sintered silicon carbide and silicon nitride
[NASA-TM-86945] 12 p1661 N85-21674
Structural sensitivity analysis: Methods, applications and needs
[NASA-TM-85827] 12 p1665 N85-21695
Investigation of adaptive distinctions of mechanism of controlled glycemia in Macaca rheesus monkeys
12 p1902 N85-21946
A user's guide to sensitivity testing on computer models at Los Alamos National Laboratory
[LA-10104-M] 12 p1914 N85-22018
Comprehensive mechanisms for combustion chemistry: An experimental and numerical study with emphasis on applied sensitivity analysis
[DE85-000173] 13 p2018 N85-22656
Visual simulation requirements for aircraft aspect recognition at real world distances
[AD-A151040] 14 p2228 N85-23810
Measurement of sensitivity of shadowgraphic instruments with spherical autocollimating mirror
14 p2274 N85-24067
Thresholds of optical breakdown in alkali-halide crystals under pulses from CO2-laser 14 p2282 N85-24134
Effect of axisymmetric vibration modes on sensitivity and directivity characteristics of piezoceramic sphere — hydrophones 15 p2525 N85-25589
Acceleration-resistant crystal resonator
[AD-D011627] 16 p2778 N85-27144
Acceleration sensitivity reduction method
[AD-D011631] 16 p2778 N85-27146
Earth station antenna sidelobe characteristics
[PB85-164986] 16 p2780 N85-27159
An interactive computer package for use with simulation models which performs multidimensional sensitivity analysis by employing the techniques of response surface methodology
[AD-A151956] 16 p2848 N85-27548
Design of SC cut 10 MHZ H.Q. crystals with G. sensitivity better than 2.10(-10)/G 17 p2966 N85-28319
Mass spectrometry technology at the Jet Propulsion Laboratory (JPL) 18 p3157 N85-29552
Surface acoustic wave devices as chemical vapor microsensors
[AD-A153752] 18 p3177 N85-29696
Fiber optic gyroscope with alternating output signal
[AD-D011669] 19 p3271 N85-30284
New concepts in free electron lasers
20 p3460 N85-31493
Test evaluation of the Honeywell GG1111 Single-Degree-of-Freedom (SDF) strapdown gyroscope
[AD-A154768] 21 p3589 N85-32307
Visibility and vertical structure measurements in southern Germany
[AD-A154714] 21 p3635 N85-32574
Rhodium-103 and Indium-115 inelastic scattering reactions for fission neutron dosimetry
21 p3703 N85-33004
Sensitivity and performance characterization of DINGU
[DE85-010750] 22 p3754 N85-33289
Sensitivity of compressive receivers
[FOA-C-30385-E4] 22 p3756 N85-33288
Determination of sensitivity functions for discrete dynamic systems from results of function modeling on digital computer 22 p3769 N85-33359
Design of inductive shift transducers
22 p3771 N85-33368
Selecting step sizes in sensitivity analysis by finite differences
[NASA-TM-86362] 22 p3799 N85-33536
Experimental test for interpreting the increase in sensibility of doped CR-39
[OG-4.4-11] 22 p3860 N85-34042
A multi-touch three dimensional touch-sensitive tablet (executive summary) 23 p3961 N85-34553
The final COS-B database: In-flight calibration of instrumental parameters
[OG-9.3-9] 23 p4028 N85-34964
Friction, impact, and electrostatic discharge sensitivities of energetic materials
[DE85-013321] 24 p4093 N85-35309
Assessment of metal heating technologies for ferrous forging: A pilot study of the form value of natural gas
[PB85-204364] 24 p4094 N85-35314
Reliability prediction of the series system with spares subject to Weibull failure 24 p4100 N85-35413
Risk analysis and sensitivity: Antithesis or synthesis
[B8562444] 24 p4144 N85-35687
Measurement of uranium enrichment for gaseous uranium at low pressure
[DE85-012697] 24 p4150 N85-35733

SENSITIZING
Investigation and optimization of fuel production using dye-based transition metal complexes as charge-transfer intermediates
[PB85-161941] 14 p2264 N85-24029
Stereotype traits can be processed automatically
[AD-A150947] 14 p2391 N85-24725
SENSITOMETRY
Astronomical photography 1984 — conferences
[ROE-OR-14] 07 p0962 N85-16102
Recalibration of the KPNO spot sensitometers — Kitt Peak National Observatory 07 p0963 N85-16103
FLACS: A new sensitometer for measurement of extreme low intensity reciprocity in a controlled environment — X-ray films 07 p0963 N85-16104
SENSIT.FOR: A program for sensitometric reduction
07 p0963 N85-16105
A spectrosensitometer with an absolute calibration
07 p0963 N85-16106
Effects of tasks on responses of human skin mechanoreceptors 11 p1691 N85-20635
SENSORIMOTOR PERFORMANCE
NT PSYCHOMOTOR PERFORMANCE
Medication interference with space research: An example from a mass-discrimination experiment on Spacelab 1 05 p0695 N85-14472
Estimating number, time and length; a baseline study
05 p0695 N85-14473
Effect of modulated ultrahigh frequency field on behavior and hormone level in female rats under emotional stress
09 p1361 N85-18562
Topography of human brain electric potentials and dominance 11 p1691 N85-20633
Psychological components in the development and prevention of air sickness 11 p1695 N85-20659
Role of mental work in human tolerance in total-body vibration 12 p1901 N85-21940
A portable battery for objective, non-obstrusive measures of human performance
[NASA-CR-171868] 15 p2586 N85-25942
Measurement and modification of sensory system EEG (electroencephalographic) characteristics during visual-motor performance
[AD-A151901] 15 p2618 N85-26133
M-BLASER: A device to study pursuit tracking in the rhesus monkey
[AD-A152965] 17 p2998 N85-28534
Psychophysiological nature of aircraft fuel
19 p3323 N85-30587
Effect of triphthasine and elenium on changes in evoked bioelectrical activity of the brain exposed to stationary magnetic field 19 p3325 N85-30601
SENSORS
Non-intrusive speed sensor — space shuttle main engine turbopumps
[NASA-CR-171204] 03 p0364 N85-12331
Variability of short-term eddy-correlation estimates of mass exchange
[DE84-007271] 05 p0677 N85-14349
Dutch institutes do research in tactile visual robot sensors 09 p1310 N85-18228
An ultra reliable computer communication network: The dispersed sensor processing mesh
09 p1372 N85-18620
Infrared horizon sensor modeling for attitude determination and control: Analysis and mission experience
[NASA-TM-86181] 10 p1429 N85-19016
NORAD operational system 12 p1783 N85-21189
New atmospheric sensor analysis study
[NASA-CR-171426] 13 p2094 N85-23069
Technical Digest: Symposium on Optical Fiber measurements, 1984
[PB85-114700] 13 p2160 N85-23407
A FORTRAN program for deep space sensor analysis
[AD-A151700] 15 p2489 N85-25366
New sensor for industrial metrology developed
15 p2538 N85-25665
Low-resolution target classification from a staring infrared sensor
[AD-A151690] 15 p2652 N85-26358
Hardware test program for evaluation of baseline range/range rate sensor concept
[NASA-CR-175910] 17 p2947 N85-28194
Trace water sensor
[NASA-CASE-NPO-15722-1] 18 p3103 N85-29212
Experiments in structural dynamics and control using a grid 20 p3410 N85-31165
The experimental computer control of a two-dimensional hyperbolic system 20 p3411 N85-31166
Optimal sensor locations for structural identification
20 p3417 N85-31209
Electrochemical methane sensor
[DE85-011663] 22 p3757 N85-33464
Optical-fiber/microprocessor-based remote velocity sensor
[DE85-010071] 22 p3788 N85-33470
Electronic temperature equalizer
[PB85-181485] 22 p3789 N85-33475
Durability of oxygen sensors
[PB85-183093] 22 p3789 N85-33477
Atmospheric nitrogen oxides: Their detection and chemistry
[PB85-193910] 24 p4114 N85-35502
SENSORY DEPRIVATION
G-Induced Loss of Consciousness (GLC)
20 p3510 N85-31823
SENSORY DISCRIMINATION
NT TACTILE DISCRIMINATION
NT VISUAL DISCRIMINATION
Reflection of lateration of sound stimuli in evoked potentials of human brain 04 p0544 N85-13463
SENSORY FEEDBACK
What is being done to control motion sickness?
15 p2687 N85-26599
SENSORY PERCEPTION
NT AUDITORY PERCEPTION
NT CONSCIOUSNESS
NT PROPRIOCEPTION
NT SPACE PERCEPTION
NT TACTILE DISCRIMINATION
NT TOUCH
NT VERTICAL PERCEPTION
NT VISUAL DISCRIMINATION
NT VISUAL PERCEPTION
Reflection of lateration of sound stimuli in evoked potentials of human brain 04 p0544 N85-13463
Susceptability to kinetoses and the amplitude perceived from sensory illusions 11 p1694 N85-20651
Psychophysiological nature of aircraft feel
19 p3323 N85-30587
Reinterpretation of otolith input as a primary factor in space motion sickness 20 p3509 N85-31812
Dissociation of autonomic and sensory vestibular reactions 23 p3953 N85-34501
Testbed for sensory control of intelligent machines
[DE85-012355] 24 p4099 N85-35412
A review of motion sickness with special reference to simulator sickness
[AD-A155975] 24 p4131 N85-35611
Thirst and fluid intake following graded hypohydration levels in humans
[AD-A156201] 24 p4132 N85-35615
SENSORY STIMULATION
USSR report: Life Sciences: Biomedical and behavioral sciences
[JPRS-UBB-84-026] 04 p0543 N85-13457
Central regulation of sensory flow in human visual system 07 p1013 N85-16435
SENTENCES
NT WORDS (LANGUAGE)
SEO (INDIAN SPACECRAFT)
U INDIAN SPACECRAFT
SEPARATED FLOW
NT BOUNDARY LAYER SEPARATION
Oil flow patterns of separated flow on a hemispherical cylinder at incidence
[DFVLR-FB-84-20] 01 p0048 N85-10313
The structure of the vorticity field in turbulent channel flow. Part 2: Study of ensemble-averaged fields
[NASA-TM-86657] 03 p0361 N85-12317
Laminar and turbulent boundary layers in a plane of symmetry
[AD-A146261] 03 p0362 N85-12323
Laser anemometer study of separated flow on wing profiles
[ISL-CO-214/83] 04 p0453 N85-12872
Simulation of separated transonic airfoil flow by finite-difference viscous-inviscid interaction
05 p0591 N85-13768
Experiments on the structure of turbulent reattaching flow 05 p0635 N85-14074
Investigation of phase separation models in RELAP 4/MOD 6
[OEFZS-4286] 05 p0638 N85-14093
Flight test results on stall characteristics of a large jet transport
[NAL-TR-817] 06 p0754 N85-14835
A collection of flow visualization techniques used in the Aerodynamic Research Branch
[NASA-TM-85966] 06 p0806 N85-15135
A scanning laser velocimeter for turbulence research
[NASA-CR-172493] 07 p0997 N85-15886
The structure of dilute combusting sprays
[NASA-CR-174838] 07 p0905 N85-15728
Turbulent bubbles behind airfoils and wings at high angle of attack 08 p1069 N85-16779
Application of the vortex-lattice concept to flows with smooth-surface separation 08 p1160 N85-17320

Proceedings of the workshop on unsteady separated flow held at the United States Air Force Academy on August 10-11, 1983
[AD-A148249] 09 p1263 N85-17937
Potential applications of forced unsteady flows
[AD-P004155] 09 p1264 N85-17940
A visual study of a delta wing in steady and unsteady motion
[AD-P004158] 09 p1264 N85-17943
Comparative visualization of accelerating flow around various bodies, starting from rest
[AD-P004159] 09 p1264 N85-17944
Numerical solution of the Navier-Stokes equations for unsteady separated flows
[AD-P004161] 09 p1265 N85-17946
Some structural features of unsteady separating turbulent shear flows
[AD-P004164] 09 p1265 N85-17949
Unsteady separated flow: Forced and common vorticity about oscillating airfoils
[AD-P004167] 09 p1265 N85-17952
Unsteady separated flows: Generation and use by insects
[AD-P004168] 09 p1266 N85-17953
Experiments on controlled, unsteady, separated turbulent boundary layers
[AD-P004172] 09 p1266 N85-17957
Flow separation induced by periodic aerodynamic interference
[AD-P004174] 09 p1266 N85-17959
On the flow processes in sharply inclined and stalled airfoils in parallel movement and rotation
[NASA-TM-77509] 10 p1419 N85-18952
Vacuum chamber pressure effects on thrust measurements of low Reynolds number nozzles
[NASA-TM-86955] 12 p1794 N85-21259
Theoretical and empirical studies of the basic structure of turbulent shear flows, including separated flows and effects of wall curvature
[AD-A149657] 12 p1848 N85-21580
Annular groove in compressor casing as device for control of air stream 13 p2050 N85-22832
Transonic merging separated flows
[AD-A150667] 14 p2213 N85-23724
Investigation of the turbulent separated flow behind a spoiler
[ISL-CO-240/83] 14 p2213 N85-23726
Calculation of an unsteady transonic flow with shock waves and separation in Laval nozzles
[MPIS-14/1984] 14 p2213 N85-23728
Stability of vortex structures during separation flow past array of wings 14 p2278 N85-24110
Contribution to the theory of stationary separation areas
[NASA-TM-77825] 14 p2300 N85-24244
Calculation of unsteady transonic separated flows by viscous-inviscid interaction 15 p2458 N85-25178
Heat transfer and fluid mechanics measurements in the turbulent reattaching flow behind a backward-facing step 15 p2553 N85-25753
An exploratory investigation of sharp fin-induced shock wave/turbulent boundary layer interactions at high shock strengths
[AD-A151571] 15 p2556 N85-25772
Problems and opportunities with three-dimensional boundary layers — aircraft, missile, and ship components 15 p2559 N85-25789
The role of computational fluid dynamics in aeronautical engineering 16 p2694 N85-26629
Numerical analysis of flow non-uniformity in the hot gas manifold of the Space Shuttle main engine 16 p2738 N85-26899
Structural stability and bifurcation in conical flow fields
[VTH-LR-424] 16 p2803 N85-27292
Method of calculating separation flow of subsonic gas stream around wings 17 p2942 N85-28161
Proceedings of the 9th US Air Force and the Federal Republic of Germany Data Exchange Agreement Meeting, Viscous and Interacting Flow Field Effects
[AD-A153020] 17 p2958 N85-28256
Characteristics of a confined jet thrust vector control nozzle
[AD-A153087] 17 p2958 N85-28268
A three-dimensional turbulent separated flow and related measurements
[NASA-CR-175913] 18 p3096 N85-29161
Additional flow field studies of the GA(W)-1 airfoil with 30-percent chord Fowler flap including slot-gap variations and cove shape modifications
[NASA-CR-3667] 19 p3212 N85-29919
High Re separated flow solutions using the Navier-Stokes and approximate equations
[AD-A152252] 20 p3454 N85-31451
Two-dimensional separation in an incompressible fluid — boundary layer separation
[ONERA-RTS-16/3232-RY-060-R] 20 p3456 N85-31459
Experimental investigations on airfoils with different geometries in the domain of high angles of attack-flow separation
[NASA-TM-77892] 22 p3728 N85-33110
Modelling of unsteady, incompressible separation on an aerofoil using an inviscid flow algorithm
[GU-AERO-8412] 23 p3894 N85-34122
A study of the second and third order closure models of turbulence for prediction of separated shear flows
[NASA-CR-176127] 23 p3929 N85-34353
Block-implicit calculations of three-dimensional laminar flow in strongly curved ducts
[DE85-003047] 23 p3931 N85-34363

SEPARATION
Ge abundances in the lunar mantle and implications for the origin of the Moon 04 p0582 N85-13721
Investigation of structure-permeability relationships of silicone polymer membranes
[PB85-148476] 11 p1596 N85-20038
Investigation of foam flotation and phase partitioning techniques 12 p1945 N85-22216
Grain boundary composition and intergranular fracture of steels. Volume 1: Detection of grain boundary segregation in steels
[DE85-006850] 15 p2682 N85-26428
Dual optical mechanical position tracker
[AD-D011739] 22 p3844 N85-33811
Separation of gas mixtures by supported complexes
[DE85-011996] 23 p3912 N85-34236
Separation of uranium from technetium in recovery of spent nuclear fuel
[DE85-006499] 23 p3972 N85-34827

SEPARATORS
NT AIR FILTERS
NT DRYING APPARATUS
NT DUST COLLECTORS
NT ELECTROSTATIC PRECIPITATORS
NT EVAPORATORS
NT FLUID FILTERS
NT PRECIPITATORS
NT SIEVES
NT STILLS
Purification of biomaterials by phase partitioning 02 p0154 N85-11043
Separation of metal species by supported liquid membranes
[DE84-014536] 04 p0470 N85-12292
Development of a mass transfer machine for gas/liquid operations in the absence of gravity
[BMFT-FB-W-84-027] 05 p0637 N85-14091
Phosphoric acid electric utility fuel cell technology development
[NASA-CR-174215] 08 p0805 N85-15124
Design and development of a sealed 100-Ah nickel-hydrogen battery
[DE84-016935] 08 p0805 N85-15128
Electric utility acid fuel cell stack technology advancement
[NASA-CR-174804] 08 p1178 N85-17422
Diffusion separation of reacting gas mixtures 11 p1718 N85-20810
Improved silicon grinding method and apparatus
[NASA-CASE-NPO-16336-1-CU] 12 p1819 N85-21407
Supported liquid membrane battery separators
[DE85-001031] 12 p1836 N85-21519
Research on separators for alkaline zinc batteries
[DE85-003062] 12 p1836 N85-21523
Magnetic field in main gap of separator 12 p1843 N85-21563
Development of molten carbonate fuel cell power plant technology
[DE84-016839] 14 p2352 N85-24536
Alkaline battery containing a separator of a cross-linked copolymer of vinyl alcohol and unsaturated carboxylic acid
[NASA-CASE-LEW-13102-1] 18 p3093 N85-29144
Aluminum-air power cell: The M3-3 experiment
[DE85-008878] 18 p3096 N85-29168
Development of a lithium secondary battery separator 20 p3444 N85-31378
RCA's planned test program to compare the performance and life of NiCd cells containing Pellon 2536 in contrast with Pellon 2505 separator material 20 p3445 N85-31385
Free zone electrophoresis simulation of static column electrophoresis in microgravity on shuttle flight STS-3 20 p3502 N85-31773
Microgravity electrophoresis: A study of the factors that affect free-fluid separation 20 p3502 N85-31774
Properties of electrophoretic fractions of human embryonic kidney cells separated on space shuttle flight STS-8 20 p3503 N85-31776
Vapor-liquid phase separator studies
[NASA-CR-166546] 21 p3583 N85-32272
Drying of pulverized material with heated condensible vapor
[DE85-011656] 22 p3783 N85-33438
Development of a prototype energy meter
[PB85-196430] 22 p3789 N85-33476
Molten carbonate fuel cell separator
[DE85-011615] 22 p3806 N85-33577
Fuel cell separator plate with bellows-type sealing flanges
[DE85-005991] 23 p3947 N85-34459
Cationic exchange membrane for the zinc-ferricyanide battery
[DE85-013152] 24 p4112 N85-35489

SEQUENCING
Comprehension of instructions for operating devices
[AD-A145283] 01 p0098 N85-10653
Modular detonator device
[AD-D011232] 03 p0340 N85-12184
Sequence of effects in the crack initiation and crack propagation phase 05 p0649 N85-14188
Steps towards parsing of query sequences to a database
[AD-A148769] 08 p1208 N85-17590
Low-resolution target classification from a staring infrared sensor
[AD-A151690] 15 p2652 N85-26358
The evolutive state: A new definition of system state to include sequencing of events 16 p2696 N85-26643
Bandpass filter formed by serial gratings operating in a wood's anomaly region
[AD-D011660] 18 p3093 N85-29148
Towards a statistical analysis of genetic sequences data with particular reference to protein sequences
[AD-A153606] 18 p3152 N85-29515
Study of a low rate spread spectrum receiver
[ENST-83E015] 20 p3441 N85-31354
Construction of complementary code sequence sets, part 7.1D 21 p3625 N85-32523

SEQUENTIAL ANALYSIS
Model for non-linear crack growth prediction, taking load sequence (LOSEQ) effects into consideration
[BLL-RAE-TRANS-2114-(5207)] 02 p0208 N85-11371
Nonlinear processing of optical pulse signals 07 p0951 N85-16026
Local dependence and point processes of exceedances in stationary sequences
[AD-A147959] 07 p1035 N85-16578
Sequential data processing for photogrammetric acquisition of digital elevation models 08 p1178 N85-17413
Sequential minimization for sum of squares of unknown functions
[DE85-004162] 11 p1707 N85-20738
Automatic pickup of trajectory by method of sequential analysis taking into account deviation of radar markers from center of strobe 12 p1836 N85-21535
Boundary crossing probabilities and statistical applications
[AD-A151027] 14 p2411 N85-24989
A software simulation study of a sequential decoder using the Fano algorithm 16 p2771 N85-27100
Sequential regularizsion solution of the inverse heat conduction problem
[DE85-010657] 23 p3931 N85-34362

SEQUENTIAL COMPUTERS
Construction of complementary code sequence sets, part 7.1D 21 p3625 N85-32523

SEQUENTIAL CONTROL
Sequential syndrome decoding of convolutional codes 05 p0824 N85-13992
Asymptotically optimum multialternative sequential procedures for discernment of processes minimizing average length of observations 13 p2064 N85-23012
Principles of organizing a real-time control system 15 p2625 N85-26177
A comparison of methods of least squares adjustment of traverses
[AD-A153612] 18 p3170 N85-29645

SERIES (MATHEMATICS)
NT ASYMPTOTIC SERIES
NT FOURIER SERIES
NT PADE APPROXIMATION
NT POWER SERIES
NT TAYLOR SERIES
The Lindstrom-Maddan method for series systems with repeated components
[AD-A145265] 03 p0412 N85-12636

Local dependence and point processes of exceedances in stationary sequences
[AD-A147659] 07 p1036 N85-16578
On the spans of polynomials and the spans of a Laguerre-Polya-Schur sequence of polynomials
[AD-A149364] 10 p1547 N85-19754
Effects of assuming independent component failure times, if they are actually dependent, in a series system
[AD-A150582] 13 p2101 N85-23092
An integral representation of the generalized Euler-Mascheroni constants
[NASA-TP-2456] 13 p2144 N85-23305
Squares of Gegenbauer polynomials and Milin type inequalities
[CWI-PM-R8412] 14 p2410 N85-24862
Disproof of the Mertens conjecture
[CWI-NM-R8412] 14 p2414 N85-24896
On the exceedance point process for a stationary sequence
[AD-A152827] 17 p3018 N85-29865
The optimality of lower confidence limits for the reliability of series systems obtained by the method of key test results or other related techniques
[AD-A154880] 21 p3597 N85-32338
Method of estimating convergence of Haar coefficients in message compression problems
22 p3769 N85-33358

SERIES EXPANSION
Model diagnosis in two-way tables by means of row and column Euclidean maps
[CSIR-TWISK-307] 01 p0108 N85-10730
Upwind compact finite difference schemes
[CSIR-TWISK-334] 01 p0110 N85-10742
Scattering by a parabolic cylinder: A uniform asymptotic expansion
[AD-A145686] 02 p0252 N85-11652
On the Edgeworth expansion for the sum of a function of uniform spacings
[CWI-MS-R8404] 05 p0719 N85-14619
A propagator expansion method for solving linearized plasma kinetic equations with collisions
[AD-A147524] 07 p1045 N85-16640
First derivatives of flow quantities behind two-dimensional, nonuniform supersonic flow over a convex corner
[NASA-TM-86272] 08 p1077 N85-16828
A series expansion study of the Navier-Stokes equations
[DFVLR-FB-84-34] 09 p1321 N85-18306
A convergent series expansion for hyperbolic systems of conservation laws
[NASA-CR-172557] 12 p1910 N85-21990
Transient analysis of loaded thin-wire antennas and transmission lines 13 p2053 N85-22852
Asymptotic expansions of the distribution of test statistics associated with several two parameter exponential distributions
[AD-A151906] 15 p2641 N85-26289
Asymptotic expansion of Jacobi polynomials
[REPT-84-35] 17 p3021 N85-29689
Uniform asymptotic expansions of integrals
[CWI-AM-R8412] 17 p3022 N85-29694
Evaluation of densities and distributions via hermite and generalized laguerre series employing high-order expansion coefficients determined recursively via moments or cumulants
[AD-A153950] 18 p3175 N85-29882
Asymptotic expansions for finite element eigenvalues and finite element solution 19 p3345 N85-30730

SERPENTINE
The mineralogy of global magnetic anomalies
[E85-10061] 07 p0987 N85-16272

SERUMS
The role of vitamin D in the bone changes associated with simulated weightlessness 15 p2608 N85-26072
Experiments in microwave exposure in the rat: Body temperature, serum chemistry and the use of chemical restraint
[PB85-156834] 16 p2840 N85-27512
Rat blood serum and liver carbohydrates and lipids in recovery period after 15-day hypokinesia
19 p3326 N85-30606

SERVICE LIFE
Retardation analytical model to extend service life
[NASA-CR-171177] 01 p0057 N85-10376
Avionics integrity program (Avip). Volume 4: Force management. Economic life considerations
[AD-A145592] 02 p0138 N85-10941
Equivalent damage: A critical assessment
02 p0140 N85-10952
On discrete failure models
[AD-A145579] 02 p0206 N85-11359
Performance of improved lead acid batteries for electric vehicles
[DE84-015845] 04 p0495 N85-13160
A high-repetition rate, inductively stabilized, long-pulse excimer laser
[DE84-016827] 04 p0506 N85-13229
Perspectives on energy storage wheels for space station application 05 p0605 N85-13860
Influence of shot-peening methods on surface quality and service life of bearings 06 p0776 N85-14960
Predicting changes in reliability characteristics of gas turbine engines during operation
06 p0776 N85-14964
Longevity of thin-walled engine parts subjected to transient stresses under creep conditions
06 p0777 N85-14966
Performance on advanced lead-acid batteries for load-leveling applications
[DE84-015817] 08 p0805 N85-15125
Impact of temperature on cycle life of globe ISOA EV-3000 lead-acid batteries
[DE84-015840] 08 p0805 N85-15126
Predicting electrochemical breakdown in terrestrial photovoltaic modules 08 p0830 N85-15273
Structural flight load measurement demonstration of structural integrity 07 p0895 N85-15670
CF-5 vertical stabilizer flight load survey
07 p0895 N85-15673
US Army helicopter operational flight loads
07 p0895 N85-15675
Helicopter data acquisition in WHL
07 p0896 N85-15676
Prematurely terminated sequential tests for MIL-STD 781C
[AD-A148417] 08 p1216 N85-17657
Determination of blade service life under irregular loading conditions 09 p1309 N85-18222
A kernel type estimator of a quantile function from right-censored data
[AD-A148753] 09 p1374 N85-18635
Measurement techniques for evaluating solar reflector materials
[DE85-002194] 10 p1510 N85-19531
Seven-year thermal-vacuum real-life test of a solar array drive mechanism manufactured by Marconi Space and Defence Systems (Model No. 002)
[ESA-ESTL-62] 11 p1616 N85-20161
Rep rated long life capacitor development: Phase 1 and 2
[DE85-000719] 11 p1629 N85-20256
Tailored airfoils for vertical axis wind turbines
[DE85-004628] 12 p1772 N85-21128
Finger materials for air cushion vehicles. Volume 2: Base fabrics for finger materials
[AD-A149701] 12 p1819 N85-21408
Supported liquid membrane battery separators
[DE85-001031] 12 p1836 N85-21519
On maximizing the expected lifetime of replaceable systems
[AD-A150003] 12 p1882 N85-21660
Approach for service life extension of explosive devices for aircraft escape systems
[NASA-TM-86323] 13 p1971 N85-22381
Survival testing of silicon solar modules
13 p2009 N85-22602
Development of molten carbonate fuel cell power plant technology
[DE84-016839] 14 p2352 N85-24536
Long-life high performance fuel cell program
[NASA-CR-174874] 15 p2494 N85-25384
NASA welding assessment program
[NASA-CR-175863] 15 p2568 N85-25845
Thrust chamber life prediction
16 p2733 N85-26665
Fatigue criterion to system design, life and reliability
[NASA-TM-87017] 16 p2793 N85-27228
Bifunctional oxygen electrodes
[DE85-006871] 17 p2955 N85-28248
DOE/Sandia point-focus concentrator program, draft
[DE85-006209] 17 p3036 N85-28793
Additional experiments relative to the shelf life of Li(Si)/FeS2 thermal batteries
[DE85-008482] 18 p3095 N85-29162
Nickel-cadmium cell design variable program data analysis
[NASA-TM-86198] 19 p3258 N85-30203
Life cycle test results of a bipolar nickel hydrogen battery
[NASA-TM-87046] 19 p3304 N85-30480
Free-piston Stirling engine/linear alternator 1000-hour endurance test
[NASA-CR-174771] 19 p3304 N85-30481
Design evaluation of high reliability lithium batteries
20 p3444 N85-31380
RAY-O-VAC BR2325 lithium carbon monofluoride cell performance 20 p3444 N85-31382
AUSSAT battery life test program
20 p3446 N85-31395
Design principles for nickel-hydrogen cells and batteries
[NASA-TM-87037] 20 p3483 N85-31646
High temperature electronics technology: Life test report
[AD-A154881] 21 p3580 N85-32257
Los Alamos optical materials reliability, maintainability, and exposure testing program
[DE85-011894] 21 p3613 N85-32456
Performance improvements from surfacing in aero engine components
[PNR-90257] 23 p3897 N85-34142

SERVICES
NT MEDICAL SERVICES
NT METEOROLOGICAL SERVICES
Demand for satellite-provided domestic communications services up to the year 2000
[NASA-TM-86894] 06 p0798 N85-15099
A comparison of metropolitan and non-metropolitan employment characteristics: Indications of the size of non-metropolitan mobile communication services user classes
[NASA-CR-175848] 13 p2053 N85-22855
Food service management 14 p2393 N85-24736

SERVOCONTROL
Active dispersion control for a Doppler broadened laser
[AD-D011570] 14 p2310 N85-24297
Control of motion of manipulator robots on basis of first-order kinematic algorithms
16 p2762 N85-27047
An improved servo-controlled inertial clock for laboratory tests of general relativity 19 p3378 N85-30955

SERVOMECHANISMS
NT SERVOMOTORS
Experimental study with parameter variations on a hydraulic positioning servo with computer implemented observer
[FOA-C-20545-E3] 02 p0256 N85-11673
Tracking servo compensator with rate aiding
[AD-D011372] 07 p0942 N85-15871
Improvement of electromechanical systems by utilization of microelectronic technology 07 p0955 N85-16053
Mirror actuator control system
[AD-D011383] 07 p1042 N85-16619
Control and electronic subsystems for the advanced servomanipulator
[DE85-001900] 09 p1327 N85-18343
Dual arm master controller concept
[DE85-001901] 09 p1327 N85-18344
Advanced remotely maintainable force-reflecting servomanipulator concept
[DE85-001902] 09 p1328 N85-18345
Servo operated anti-G suit pressurization system
[AD-D011466] 10 p1531 N85-19651
Flutter taming: A new tool for the aeroelastic designer
[AD-A150834] 14 p2226 N85-23602
New equipment complex Kaskad 2 for automatic control 14 p2266 N85-24042
Italy's Fiat uses Sweden's Asea seeing robot
15 p2536 N85-25650
Control of motion of manipulator robots on basis of first-order kinematic algorithms
16 p2762 N85-27047
Proceedings of the Workshop on Identification and Control of Flexible Space Structures, volume 1
[NASA-CR-176051] 20 p3406 N85-31148
A study on the control of third generation spacecraft
20 p3415 N85-31196
Harold Hazen and the theory and design of servomechanism
[RR-270] 22 p3794 N85-33506
Application of traction drives as servo mechanisms
22 p3797 N85-33520
Dual arm master controller development
22 p3797 N85-33526

SERVOMOTORS
Design and test of a four channel motor for electromechanical flight control actuation
[NASA-CR-171838] 08 p1156 N85-17294
Analysis and design of hydraulic servo systems within the scope of the improvement of a fatigue testing installation of the Royal Dutch Army
[LEOK-TR-1984-09] 14 p2265 N85-24033
Novel drives for machine tools
14 p2268 N85-24053
Robot use in FRG increases but sensor technology lags 15 p2531 N85-25605
Basic development of one-chip control circuitry for commutatorless dc motors
[BMFT-FB-T-84-305] 18 p3098 N85-29178
Computer simulation of a cruise missile using brushless dc motor fin control
[AD-A155935] 24 p4089 N85-35349

SERVOS
U SERVOMOTORS

SERVOSTABILITY CONTROL
U SERVOCONTROL
SES
U SURFACE EFFECT SHIPS
SET THEORY
NT BOREL SETS
NT EQUIVALENCE
NT THRESHOLD LOGIC
Set-theoretic problems of null completion in relational databases
[AD-A145045] 01 p0125 N85-10861
An iterative procedure for obtaining I-projections onto the intersection of convex sets
[AD-A145402] 02 p0251 N85-11639
Constrained optimization using iterated partial Kuhn-Tucker vectors
[AD-A145476] 02 p0251 N85-11641
An investigation into fuzzy clustering and classification
[AD-A145571] 02 p0251 N85-11645
Advanced Ada (trademark)
[AD-A146257] 03 p0407 N85-12602
Locally optimal subset selection rules based on ranks under joint type 2 censoring
[AD-A146179] 03 p0412 N85-12632
Stable monotone variational inequalities
[AD-A147123] 07 p1031 N85-16544
Condenser capacities and removable sets in W1p1
10 p1536 N85-19682
Relative-entropy minimization with uncertain constraints--theory and application to spectrum analysis
[AD-A149192] 10 p1546 N85-19752
Some facets of the tri-index assignment polytope
[AD-A149195] 10 p1547 N85-19753
Connected simple systems and the Conley index of isolated invariant sets
[AD-A149383] 10 p1552 N85-19789
Some data manipulation requirements for the exploratory analysis of large data sets
[DE85-002541] 10 p1568 N85-19887
Maximum matchings in a class of random graphs
[AD-A149863] 12 p1920 N85-22060
Optimal designs for comparisons between two sets of treatments
[AD-A150821] 13 p2152 N85-23360
Topology and Order Structures, part 2
[MCT-169-PT-2] 14 p2413 N85-24879
When is a GO-space JO(2)? 14 p2414 N85-24880
Solving the minimal least squares problem subject to bounds on the variables
[TRITA-NA-8215] 16 p2852 N85-27580
Schubert varieties are arithmetically Cohen-Macaulay
16 p2853 N85-27582
A note on integral operators
[REPT-83-26] 17 p3021 N85-29686
Applications of fuzzy set theory to satellite soundings
18 p3141 N85-29445
Applications of some artificial intelligence methods to satellite soundings 18 p3141 N85-29446
Ada developments
[REPT-84-29] 18 p3164 N85-29604
Hybrid uncertainty theory
[DE85-008357] 18 p3167 N85-29622
A variable-complexity norm maximization problem
[AD-A153514] 18 p3169 N85-29634
On approximating a set-valued function locally
[AD-A153540] 18 p3170 N85-29641
Construction of complementary code sequence sets, part 7.1D 21 p3625 N85-32523
SETI
U PROJECT SETI
SETTING
Setting hurricane conditions of readiness with high confidence
[AD-A144785] 01 p0085 N85-10570
SEVERE STORMS OBSERVING SATELLITE
U STORMSAT SATELLITE
SEWAGE
NT SOLID WASTES
SEWERS
Hydrodynamics and sanitation
[CT-579] 20 p3487 N85-31672
SEWING
Re-designing a mechanism for higher speed: A case history from textile machinery 23 p3923 N85-34310
SEX FACTOR
Physiological differences between men and women in exercise-heat tolerance and heat acclimation
[AD-A152048] 15 p2618 N85-26135
SEYFERT GALAXIES
X-ray observations of the Seyfert 1 galaxies AKN120 and MCG8-11-11
[NASA-TM-80663] 03 p0446 N85-12839
The X-ray spectrum and time variability of narrow emission line galaxies
[NASA-TM-83859] 03 p0446 N85-12842
The IRAS galaxy 0421+040P06: An active spiral (?) galaxy with extended radio lobes
[NASA-CR-174208] 06 p0871 N85-15536
X-ray and UV Emission from Active Galactic Nuclei — conference
[MPE-184] 08 p1236 N85-17790
Radio Seyferts and the forbidden line region
08 p1236 N85-17793
A new estimate of the local luminosity function of Seyfert 1 nuclei 08 p1237 N85-17796
Continuous transition from star burst galaxies to Seyfert galaxies 08 p1237 N85-17798
Spatially resolved optical spectroscopy of the radio jet of the X-ray galaxy NGC 2110 08 p1238 N85-17804
EXOSAT observations of active galactic nuclei
08 p1238 N85-17809
The X-ray spectra of NGC 4151 — Seyfert galaxy
08 p1239 N85-17815
An inverse Compton model of the X-ray emission in Seyfert galaxies 08 p1241 N85-17827
Theoretical studies of emission line variability in type 1 Seyfert galaxies 08 p1242 N85-17839
Active galactic nuclei and their cosmological evolution
08 p1243 N85-17842
Ultraviolet and X-ray observations of active galactic nuclei: Constraints on models of the broad emission line region 11 p1744 N85-20966
Broad emission features in active galactic nuclei
11 p1746 N85-20979
Fluorescent excitation of Fe 2, Mn 2, Ti 2, N 1 lines by V 4, N 5, O 6: Emission lines in the spectra of symbiotic stars and Seyfert galaxies 11 p1746 N85-20984
A model for the variable continuum of the Seyfert 1 galaxy NGC 5548 11 p1747 N85-20985
X-ray emission from active galactic nuclei
[NASA-TM-86175] 11 p1763 N85-21066
IRAS observations of Seyfert galaxies
[NASA-CR-175557] 12 p1953 N85-22267
IRAS observations of active galaxies
[NASA-CR-175720] 15 p2666 N85-26463
The ultraviolet spectra of intermediate redshift quasars
20 p3544 N85-32056
Interactions of galaxies and their nuclear activity
20 p3545 N85-32060
Balloon observations of hard X-rays from NGC 4151 and an X-ray transient source
[OG-2.7-6] 22 p3871 N85-33979
Gamma-radiation with E gamma 5 MeV detected from Seyfert galaxy 3C120 and region with 1° = 190 deg and b° = 20 deg
[OG-2.8-8] 22 p3871 N85-33981
Some evidence for large gravitational redshift in Seyfert galaxy NGC 4151
[OG-2.7-11] 22 p3872 N85-33984
SFERICS
U ATMOSPHERICS
SGEMP
U SYSTEM GENERATED ELECTROMAGNETIC PULSES
SHADOWGRAPH PHOTOGRAPHY
NT SCHLIEREN PHOTOGRAPHY
Measurement of sensitivity of shadowgraphic instruments with spherical autocollimating mirror
14 p2274 N85-24087
Optical system for measuring shadowgraph data
[AD-D011642] 17 p3036 N85-28784
SHADOWGRAPHS
U SHADOWGRAPH PHOTOGRAPHY
SHADOWS
NT PENUMBRAS
Numerical simulation of static and dynamic shadow patterns using an atomistic description of crack initiation and propagation
[DE85-003226] 12 p1867 N85-21715
Poisson and multinomial shadowing processes
[AD-A151600] 15 p2640 N85-26286
On the possibility of the determining the average mass composition near 10 to the 14th power eV through the solar magnetic field
[OG-5.1-9] 22 p3882 N85-34051
Shadow volumes for non-planar polygons
23 p3965 N85-34580
Empirical model for the Earth's cosmic ray shadow at 400 KM: Prohibited cosmic ray access
[SH-6.1-14] 23 p4046 N85-35067
SHAFTS (MACHINE ELEMENTS)
NT TURBOSHAFTS
Stability of hollow shafts under torsion
06 p0780 N85-14986
Improvement of the corrosion resistance of turbine engine bearings
[AD-A147430] 07 p0905 N85-15731
Theoretical and experimental study of hydro-elastic instability on the line of shafting of a rotating machine
[BLL-DOUNREAY-TR-937-(9091.9F)]
07 p0972 N85-16174
Measurement and evaluation of the loading of shafts by torsional vibrations 07 p0980 N85-16222
Assessment of the operating characteristics of the SSME LOX turbopump pump-end bearing
[NASA-CR-171287] 09 p1167 N85-17362
Effect of coupled torsional-flexural vibration of a geared shaft system on the dynamic tooth load
09 p1338 N85-18415
Assessing expired fatigue life in large turbine shafts
[DE84-016676] 09 p1340 N85-18427
Low leakage turbine shaft seals for advanced combined cycle systems
[AD-A149372] 10 p1492 N85-19420
Angular measurement system
[NASA-CASE-MFS-25825-1] 11 p1835 N85-20298
Influence of axial shaft load on operation of magnetoelastic torque transducer
14 p2270 N85-24065
Twisting of segmental shafts
14 p2279 N85-24119
Some problems of optimum journal design for disk-drum rotors under antisymmetric loading
14 p2286 N85-24167
SHAFT: Interactive shaft design program
[DE85-007333] 15 p2568 N85-25850
Electric motors with elastically mounted rotors
16 p2763 N85-27048
Monitoring of turbo-machines by shaft vibration measurement
[BLL-CE-TRANS-7900-(9022.09)]
16 p2799 N85-27255
Quasi-steady vibrations of a rotating shaft grazing an obstacle: Spiral vibration
[BLL-CE-TRANS-7962-(9022.09)]
16 p2799 N85-27256
Calculation of friction at spherical bearing journals in turbomachines 17 p2940 N85-28150
Determination of wear intensity and resource of crankshafts and cylinder liners of ZIL-130 and ZMZ-53 engines
[BLL-BISI-TRANS-21393-(9022.06)]
17 p2972 N85-28355
Method for driving two-phase turbines with enhanced efficiency
[NASA-CASE-NPO-15037-2] 18 p3115 N85-29282
Non-backdriveable free wheeling coupling
[NASA-CASE-MSC-20475-1] 18 p3116 N85-29290
Vibration control of rotor shaft
[NASA-TM-87053] 18 p3117 N85-29292
SHAKERS
Pycnometer shaker
[PB85-174985] 20 p3460 N85-31491
Measurement of damping of graphite epoxy materials
[NASA-CR-176073] 21 p3596 N85-32334
SHAKING
NT DITHERS
Mechanical stress regulation of plant growth and development 15 p2610 N85-26087
SHALE OIL
Mechanisms of syncrude-synfuel degradation
[DE84-015206] 01 p0034 N85-10212
Lubricity of well-characterized jet and broad-cut fuels by ball-on-cylinder machine
[NASA-TM-83607] 03 p0339 N85-12183
Oil-shale exploration expansion urged
07 p0994 N85-16317
Data base of all known, published data on trace elements in oil shale and its products
[DE85-003399] 18 p3126 N85-29357
Aspects of high-resolution gas chromatography as applied to the analysis of hydrocarbon fuels and other complex organic mixtures. Volume 1
[AD-A156154] 24 p4076 N85-35257
SHALES
Workshop on Remote Sensing/Lineament Applications for Energy Extraction
[DE84-009291] 12 p1875 N85-21763
Shales and other argillaceous strata in the United States
[DE85-010453] 18 p3125 N85-29353
SHALLOW SHELLS
Buckling and postbuckling behavior of shallow shells
18 p3120 N85-29317
SHALLOW WATER
An analytical model of periodic waves in shallow water
[AD-A147501] 07 p0960 N85-16065
An analytical model of periodic waves in shallow water
[AD-A147502] 07 p0960 N85-16066
The investigation of selected oceanographic applications of spaceborne synthetic-aperture radar
08 p1146 N85-17233
Weakly-reflective boundary conditions for two-dimensional shallow water flow problems
[PUBL-322] 08 p1163 N85-17341

Evaluation of time integrators for the shallow water equations
[CWI-NM-R8406] 11 p1634 N85-20292
Modifications to a propagation model for the combinded refraction-diffraction of stokes waves; shallow water, large angle and breaking wave effects
[AD-A151428] 15 p2556 N85-25768
The theoretical response of a vertical line array to wind-generated noise in shallow water
[AD-A151730] 16 p2860 N85-27838
Rip In White Sea 19 p3290 N85-30401
Propagation of sound in a layered laboratory model
[AD-A155141] 21 p3700 N85-32980

SHANKS
U JOINTS (JUNCTIONS)

SHANNON INFORMATION THEORY
U INFORMATION THEORY

SHAPE CONTROL
Constellations 11 p1643 N85-20352
Control Of Flexible Structures (COFS) flight experiment background and description 14 p2236 N85-23864
The effect of sensor and actuator errors on static shape control for large space structures
[NASA-TM-86446] 19 p3225 N85-29998
Multivariable control of a soft coupled space station 20 p3408 N85-31151
Stiffness control of large space structures 20 p3414 N85-31189
Sub-optimal control of nonlinear flexible space structures 20 p3414 N85-31190

SHAPE MEMORY ALLOYS
NT NITINOL ALLOYS
Effect of form memory in alloys based on Cu-Al systems 11 p1604 N85-20068
The effect of prior parent phase cold work on martensite transformation in Cu-Zn-Al shape memory alloys
[AD-A155140] 21 p3566 N85-32163
Comparison of the response of shape memory alloy actuators using air-cooling and water-cooling
[AD-A155216] 21 p3567 N85-32165
Shape memory effect in uranium-niobium alloys below room temperature
[DE85-012984] 23 p3916 N85-34268

SHAPED CHARGES
Making high explosive bodies for shaped charges by casting or pressing. Shaped charge research at Research Institute of National Defence (FOA) in 1972 - 1983, part 1
[FOA-C-20554-D4-PT-1] 07 p0935 N85-15823
Generation of detonation waves of given spatial and temporal characteristics
[ISL-R-103/83] 16 p2758 N85-27021
SCAP: A Shaped Charge Analysis Program. User's manual for SCAP 1.0
[DE85-011182] 20 p3515 N85-31854

SHAPES
NT CONVEXITY
NT ELLIPTICITY
NT FLATNESS
NT LINE SHAPE
An error analysis for the use of presently available lunar radio flux data in broadbeam antenna-system measurements
[PB84-218361] 01 p0016 N85-10097
Resonant frequencies and mode shapes for single and double cylindrical shells
[AD-A144778] 01 p0062 N85-10408
Optimization of the die entrance shape for polymeric extrusion
[DE85-001588] 06 p0772 N85-14937
Effects of body shape on the aerodynamics of a body of revolution at Mach numbers from 1.6 to 4.6
[NASA-TM-86345] 07 p0893 N85-15657
Free-surface boundary layer and the origin of bow vortices
[AD-A147427] 07 p0960 N85-16063
Experimental investigation of a turbulent incompressible boundary layer on a curved wall 11 p1577 N85-19936
Semianalytic modeling of aerodynamic shapes
[NASA-TP-2413] 12 p1771 N85-21120
A stochastic-mechanical approach to acoustic pulse propagation in the deep ocean sound channel
[AD-A149598] 12 p1926 N85-22110
A description of the Langley wireframe geometry standard (LaWGS) format
[NASA-TM-85767] 13 p1971 N85-22380
Shape optimization for minimal stress concentration 13 p2101 N85-23093
Surfaces of asteroids and cometary nuclei 13 p2176 N85-23503
Some problems of optimum journal design for disk-drum rotors under antisymmetric loading 14 p2286 N85-24167
Effect of form and clearance of a piston launched in a tube on the boundary layer and the heat transfer
[ISL-CO-216/83] 14 p2302 N85-24255
Scattering properties of a moving dielectric object
[AD-A151974] 15 p2544 N85-25706
An IKBS approach to image understanding
[AD-A151992] 16 p2854 N85-27599
Fluid surface behavior in low gravity. Center discretionary fund no. 83-21
[NASA-TP-2486] 17 p2957 N85-28260
Shape preserving spline interpolation 17 p3003 N85-28564
The construction of curves and surfaces using numerical optimization techniques 17 p3003 N85-28565
Free-form design in solid modelling 17 p3004 N85-28569
Triangular Bernstein-Bezier patches, a survey and new results 17 p3005 N85-28577
Um models and beta-splines 17 p3005 N85-28580
A new technique for system-to-system transfer of surface data 17 p3007 N85-28589
Texture perception and shape from texture
[AD-A154278] 19 p3336 N85-30672
Spectrum of the gamma-ray diffuse component observed from HEAO-1
[OG-3.1-12] 22 p3874 N85-34000
Spectral shape variation of interstellar electrons at high energies
[OG-6.2-7] 22 p3889 N85-34106
Block-implicit calculations of three-dimensional laminar flow in strongly curved ducts
[DE85-003047] 23 p3931 N85-34363
A user-friendly computer-aided construction of boundaries 23 p3962 N85-34564
Non-rigid body motion 23 p3964 N85-34576

SHARKS
Development of ARGOS platforms for tracking of basking sharks. Cetorhinus maximus 14 p2326 N85-24378

SHATTERING
U FRAGMENTATION

SHEAR
Shear deformation plate continua of large double-layered space structures 01 p0059 N85-10391

SHEAR CREEP
The effects of radial yarns, 3-dimensionally reinforced carbon-carbon composite
[AD-A144751] 01 p0022 N85-10134

SHEAR DISTURBANCES
U S WAVES

SHEAR FATIGUE
U SHEAR STRESS

SHEAR FLOW
A perturbation solution for rigid dumbbell suspensions in steady shear flow
[AD-A144876] 01 p0111 N85-10755
Study of the structure of turbulent shear flows at supersonic speeds and high Reynolds number
[NASA-CR-174144] 04 p0452 N85-12865
Progress in the development of a two-fluid model of turbulence for near-wall flows, part 1
[CFD/84/7-PT-1] 04 p0501 N85-13196
Turbulent shear fields for dispersion of aqueous drops in organic liquids and application to gel-sphere processes
[DE84-016562] 06 p0809 N85-15141
Study of low-frequency sound with point source in stream with shear 06 p0825 N85-15239
Some structural features of unsteady separating turbulent shear flows
[AD-P004164] 09 p1285 N85-17949
Single integral constitutive equations for viscoelastic fluids
[AD-A149410] 10 p1547 N85-19758
A three-dimensional spectral algorithm for simulations of transition and turbulence
[NASA-CR-172561] 12 p1845 N85-21575
Theoretical and empirical studies of the basic structure of turbulent shear flows, including separated flows and effects of wall curvature
[AD-A149657] 12 p1846 N85-21580
Acoustic energy exchange in sheared mean flows -- solid rocket motors 13 p1999 N85-22534
Modeling of shear flow in a stratified fluid 14 p2340 N85-24469
Three-dimensional boundary layers and shear flows activities at ONERA/CERT 15 p2558 N85-25785
An experimental study of the noise generated by vaporous cavitation in turbulent shear flows produced by confined orifice plates 15 p2645 N85-26316
Studies of structure and modeling in turbulent shear flows
[AD-A151807] 16 p2782 N85-27170
Practical real-time quality control of antimisting kerosene
[DE/FAA/CT-85/1] 18 p3083 N85-29072
Transverse vorticity measurements using an array of four hot-wire probes
[FSFL-R-85-006] 18 p3099 N85-29184
Effect of nonuniform size on internal stresses in a rapid, simple shear flow of granular materials. Part 1: Two grain sizes
[AD-A154045] 19 p3285 N85-30372
Effect of nonuniform size on internal stresses in a rapid, simple shear flow of granular materials. Part 2: Multiple grain sizes
[AD-A154046] 19 p3285 N85-30373
Intermittency, conditional sampling and turbulent combustion 20 p3424 N85-31249
Conditional modelling in turbulent shear flows 20 p3424 N85-31250
Turbulent reacting flows 20 p3451 N85-31427
Wall effect on lateral migration of spherical particles in a linear shear flow 20 p3452 N85-31432
Moist barotropic instability in the tropics 20 p3489 N85-31683
On the solution for the sound field in a semi-infinite uniform duct with sheared mean flow 20 p3523 N85-31912
Techniques for the study of gravity waves and turbulence (keynote paper), part 4 21 p3621 N85-32499
Second order modelling in non-constant density flows 22 p3744 N85-33206
Turbulent mixing and combustion 22 p3744 N85-33207
Modeling of turbulent recirculating combusting flows 22 p3745 N85-33212
Turbulence modelling for the prediction of turbulent jets: Wakes and plumes
[CFD/84/5] 22 p3784 N85-33447
A study of the second and third order closure models of turbulence for prediction of separated shear flows
[NASA-CR-176127] 23 p3929 N85-34353

SHEAR LAYERS
The aerodynamics of bluff bodies in turbulent shear layers 05 p0593 N85-13780
Amiet shear layer correction with an additional temperature gradient considered: Nomograms for the correction of noise signatures from open jet wind tunnel tests
[DFVLR-MITT-84-11] 05 p0726 N85-14669
Aero-optics experimental techniques
[AD-A146755] 07 p0957 N85-16067
Modelling circulation control by blowing -- airfoils 08 p1069 N85-16778
A free shear layer prediction of the turbulent wake of a flat plate towed below a free surface
[AD-A148699] 09 p1319 N85-18293
On the interaction of a sound pulse with the shear layer of an axisymmetric jet. Part 3: Nonlinear effects
[NASA-CR-172512] 09 p1378 N85-18663
Effects of a periodic disturbance on structure and mixing in turbulent shear layers and wakes
[AD-A149278] 10 p1484 N85-19370
An investigation of compressible flows over open cavities including shear layer thickness effects
[AD-A150088] 12 p1847 N85-21588
Variations in resistivity of upper crustal layer 13 p2113 N85-23164
Interactions of unstable shear layers with leading edges and associated pressure fields 14 p2299 N85-24236
An experimental study of compressible turbulent reattaching free shear layers 16 p2781 N85-27161
Transverse vorticity measurements using an array of four hot-wire probes
[FSFL-R-85-006] 18 p3099 N85-29184
Transient combustion dynamics
[AD-A154430] 19 p3235 N85-30052
Effect of vertical shear on regional-scale trajectories in near-frontal conditions
[DE85-007554] 19 p3317 N85-30561
Turbulent solutions of equations of fluid motion 20 p3453 N85-31441
Amiet shear layer correction with an additional temperature gradient considered: Nomograms for the correction of noise signatures from open jet wind tunnel tests
[ESA-TT-897] 20 p3525 N85-31926
Comments on two matters related to turbulent combustion 22 p3743 N85-33204

SHEAR PROPERTIES
NT SHEAR STRENGTH
Butene oxidation by molybdenum crystalographic shear compounds
[DE84-013910] 05 p0614 N85-13923
Strain rate effects and temperature history effects for three different tempers of 4340 VAR steel
[AD-A146372] 06 p0768 N85-14915

Disclinations in carbon-carbon composites
[AD-A148290] 08 p1119 N85-17052
Natural unsteadiness of a separation bubble behind a backward-facing step
[AD-P004176] 09 p1267 N85-17981
A free shear layer prediction of the turbulent wake of a flat plate towed below a free surface
[AD-A148699] 09 p1319 N85-18283
Verification and application of the Iosipescu shear test method
[NASA-CR-174346] 09 p1333 N85-18376
Determination of shear coefficient of a general beam cross section by finite element method
09 p1338 N85-18413
Antiplane cracks in solid propellants
[AD-P004344] 10 p1455 N85-19168
Journal of Research of the National Bureau of Standards, volume 89, number 2, March - April 1984
[PB85-115426] 12 p1926 N85-22103
In-plane shear properties of graphite Fibre/Epoxy composites for aerospace applications: Evaluation of test methods by the decision analysis technique
[AD-A151599] 15 p2503 N85-25440
Effects of magnetic shear on lower hybrid waves in the suprauroral region
[AD-A151980] 15 p2856 N85-26392
Studies of structure and modeling in turbulent shear flows
[AD-A151807] 16 p2782 N85-27170
Coherent structure reflective turbulent viscous flow modeling
[AD-A153086] 17 p2958 N85-28267
Analytical shear buckling investigation of curved composite panels
[AD-A153138] 17 p2980 N85-28421
Structural characteristics of high temperature composites
[NASA-CR-175998] 19 p3232 N85-30037
On design of off-axis specimens
[AD-A154328] 19 p3286 N85-30379
Shear-stress distribution and shear stiffness in the case represented by a non-homogeneous cross-section, of any shape, but composed of an orthotropic material, when subjected to a shear force
[DRIC-T-7430] 20 p3469 N85-31554
Modeling granular explosive detonations with shear band concepts
[DE85-011823] 22 p3754 N85-33271
Pressure-shear loading of PBX-9404
[DE85-009982] 23 p3921 N85-34296

SHEAR STRAIN
Deformation measurements of composite multi-span beam shear specimens by Moire interferometry
[NASA-CR-3844] 02 p0169 N85-11135
Effective moduli of elasticity of unidirectional fibrous composite
02 p0265 N85-11733
Simple higher-order theory for laminated composite plates
[NASA-CR-174421] 10 p1496 N85-19445
Elastic equilibrium of composite shells with finite shear rigidity
17 p2942 N85-28163
Shear-stress distribution and shear stiffness in the case represented by a non-homogeneous cross-section, of any shape, but composed of an orthotropic material, when subjected to a shear force
[DRIC-T-7430] 20 p3469 N85-31554

SHEAR STRENGTH
Dynamic shear failure of shallow-buried flat-roofed reinforced concrete structures subjected to blast loading
[AD-A145974] 03 p0373 N85-12378
The chemical nature of the fiber/resin interface in composite materials
04 p0465 N85-12953
Composite property dependence on the fiber, matrix, and the interphase
04 p0465 N85-12954
Exploratory study of shear strength of joints for precast segmental bridges
[PB84-235449] 05 p0651 N85-14182
Mechanical property data 7050-t736511 alloy
[AD-A147365] 07 p0928 N85-15882
Imide modified epoxy matrix resins
[NASA-CR-174695] 07 p0930 N85-15892
Laboratory investigation on adhesives for Naval facilities construction
[AD-A147453] 07 p0932 N85-15909
Graphite/PMR polyimide composites with improved toughness
[NASA-TM-87061] 21 p3561 N85-32148
Pressure-shear loading of PBX-9404
[DE85-009982] 23 p3921 N85-34296

SHEAR STRESS
NT TORSIONAL STRESS
Development of a floating element wall shear transducer
[AD-A144794] 01 p0049 N85-10324
Three programs for evaluating bending moments, deflections and shear forces in simply-supported uniform bridge decks under South African NA loading: NAB, NAD and NAS. NITRR manual P13
[ISBN-0-7988-2283-X] 01 p0102 N85-10881
Mechanochemical reactions of elastomers with metals
[AD-A145657] 02 p0186 N85-11246
The structure of the vorticity field in turbulent channel flow. Part 2: Study of ensemble-averaged fields
[NASA-TM-86657] 03 p0361 N85-12317
Composite materials characterization and development at AFWAL
04 p0484 N85-12944
Studies of the wall shear stress in a turbulent pulsating pipe flow
[AD-A146772] 07 p0957 N85-16068
Effects of high energy radiation on the mechanical properties of epoxy-graphite fiber reinforced composites
[NASA-CR-174314] 08 p1116 N85-17047
A study of Reynolds-stress closure model
[NASA-CR-174342] 08 p1161 N85-17324
Development of a floating element wall shear transducer
[AD-A148450] 08 p1164 N85-17346
Crack problems for bonded nonhomogeneous materials under antiplane shear loading
[NASA-CR-172532] 10 p1495 N85-19438
Theoretical and experimental study of crack resistance and macrocrack growth rate in organic fiber reinforced plastic under pure shear condition
11 p1598 N85-20053
Influence of external electric field on structural-mechanical properties of powdered materials
13 p2013 N85-22630
Longitudinal splitting in unidirectional composites, analysis and experiments
[NASA-CR-3861] 13 p2015 N85-22639
Study of stresses on surface of flat barrier immersed in under expanded jet of rarefied gas
16 p2765 N85-27061
Recent progress in the dynamic plastic behaviour of structures, part 4
17 p2978 N85-28402
Investigations of the material factors in the adiabatic shearing of steels
[AD-A153084] 17 p2979 N85-28418
Surface shear stress characteristics in turbulent flows
19 p3211 N85-29914
Granular Flow Project
[DE85-010015] 19 p3270 N85-30279
The initiation and growth of adiabatic shear bands
[AD-A154459] 19 p3287 N85-30382
Shear-stress distribution and shear stiffness in the case represented by a non-homogeneous cross-section, of any shape, but composed of an orthotropic material, when subjected to a shear force
[DRIC-T-7430] 20 p3469 N85-31554
A refinement of the transverse shear deformation theory for multilayered anisotropic plates
[STN-5] 20 p3471 N85-31571
A cracked orthotropic sheet stiffened by a semi-infinite orthotropic sheet
[NASA-TP-2455] 21 p3597 N85-32339
Pressure-shear loading of PBX-9404
[DE85-009982] 23 p3921 N85-34296
Stress analysis of axisymmetric sandwich shells of variable thickness
24 p4101 N85-35419

SHEAR WAVES
U S WAVES

SHEARING
The shearing contribution in transformation toughening of brittle materials
[AD-A154656] 21 p3588 N85-32195

SHEARING STRESS
U SHEAR STRESS

SHEATHS
NT ION SHEATHS
NT PLASMA SHEATHS
Subcable test facility
[DE85-002103] 09 p1315 N85-18269

SHEEP
The 1984 environmental monitoring program report for Idaho National Engineering Laboratory site
[DE85-011209] 22 p3812 N85-33611

SHEET METAL
U METAL SHEETS

SHELL ANODES
Ring-cusp ion thruster with shell anode
[NASA-CASE-LEW-13881-1] 12 p1794 N85-21256

SHELL STABILITY
Variable loading of elastic-plastic shells of revolution
06 p0779 N85-14961
Stability of circular cylindrical shell with piecewise constant thickness subjected to radial pressure
06 p0779 N85-14962
Analysis of shell type structures subjected to time dependent mechanical and thermal loading
[NASA-CR-175747] 15 p2577 N85-25866
Dynamic creep buckling: Analysis of shell structures subjected to time-dependent mechanical and thermal loading
17 p2913 N85-27959
Elastic equilibrium of composite shells with finite shear rigidity
17 p2942 N85-28163
Stability of cylindrical shells with variable thickness under external pressure
17 p2943 N85-28164
Initial imperfection surveys on conical shells at Hoechst AG
[VTH-LR-407] 17 p2981 N85-28429
Stress analysis of axisymmetric sandwich shells of variable thickness
24 p4101 N85-35419

SHELL THEORY
Numerical modeling of complex interaction of shell of revolution and its filler with allowance for friction
06 p0779 N85-14960
A review of imperfection sensitivity of stiffened shells
[AD-A147311] 07 p0978 N85-16213
On a general nonlinear theory of plates and shells: Formulation and applications
08 p1172 N85-17387
The principle of virtual work and associated variational principles
[ESA-TT-873] 09 p1340 N85-18428
Shell-model Lanczos-method studies of the Gamow-Teller strength function in astrophysics
[DE85-004205] 11 p1763 N85-21093
Vacancy-rearrangement theory in the first Magnus approximation
[DE85-004435] 12 p1930 N85-22123
The nonlinear analysis of thick composite plates using a cubic spline function
[AD-A152115] 16 p2801 N85-27268
An analysis for axially compressed orthotropic shells with a multimode imperfection representation
[VTH-LR-422] 16 p2803 N85-27281
Dynamic creep buckling: Analysis of shell structures subjected to time-dependent mechanical and thermal loading
17 p2913 N85-27959
Elastic equilibrium of composite shells with finite shear rigidity
17 p2942 N85-28163
Method of solving problems of statics for multilayer shells of revolution
17 p2943 N85-28167

SHELLS (STRUCTURAL FORMS)
NT ANISOTROPIC SHELLS
NT CIRCULAR SHELLS
NT CONICAL SHELLS
NT CORRUGATED SHELLS
NT CYLINDRICAL SHELLS
NT ELASTIC SHELLS
NT FLUID FILLED SHELLS
NT LIQUID FILLED SHELLS
NT METAL SHELLS
NT ORTHOTROPIC SHELLS
NT RADOMES
NT REINFORCED SHELLS
NT SHALLOW SHELLS
NT SPHERICAL CAPS
NT SPHERICAL SHELLS
NT THIN WALLED SHELLS
NT TOROIDAL SHELLS
Heat exchanger
[DE84-014290] 01 p0047 N85-10309
Internal heat transfer and pressure drop measurements in a variously baffled shell and tube heat exchanger
03 p0360 N85-12310
Complex frequency analysis of damped thin-walled beams with open cross sections
03 p0371 N85-12386
Finite element procedures applicable to nonlinear analysis of reinforced concrete shell structures
[AD-A146706] 07 p0978 N85-16209
A review of imperfection sensitivity of stiffened shells
[AD-A147311] 07 p0978 N85-16213
Coriolis effects on the vibrations of rotating beams, plates and shells
09 p1331 N85-18368
Fluidelastic instability in shell and tube heat exchangers: A framework for a prediction method
[DE84-006518] 10 p1496 N85-19444
A solution method for nonlinear dynamic analysis of shell structures
[AD-A149648] 12 p1868 N85-21708
Nonlinear analysis of layered composite plates and shells
[PB85-127181] 12 p1868 N85-21719
Geometrically nonlinear analysis of laminated elastic structures
[NASA-CR-175809] 12 p1868 N85-21720
USSR report: Engineering and equipment
[JPRS-UEQ-85-003] 13 p2042 N85-22782
Stability of three-layer glass-reinforced plastic shells of rotation
13 p2047 N85-22813
Axisymmetrical oscillations of shell systems subjected to impulse loads
13 p2047 N85-22814
Reaction of piezoceramic shell to concentrated forces
14 p2279 N85-24115

Stressed-strained state of tubular shells under uniformly distributed pressure
16 p2766 N85-27067
Research in the field of rib stiffened shell stability
16 p2766 N85-27068
Dynamic response of shells and plates subjected to variable magnitude traveling loads
16 p2798 N85-27250
The statistical analysis of initial imperfection measurements — shell profiles
[VTH-LR-442] 18 p2857 N85-27622
Propagation of non-axisymmetric elastic waves through shell with filler under radial load at one end
17 p2943 N85-28169
The Mises yield condition for thin rotationally symmetric shells
[BLL-BISI-TRANS-22047-(9022.06)]
17 p2978 N85-28409
Computer-aided thermohydraulic design of TEMA type E shell and tube heat exchangers for use in low pressure, liquid-to-liquid, single phase applications
[AD-A153779] 18 p3100 N85-29191
An investigation into the comparisons of the underwater shock effects on a stiffened flat plate to the predictive nature of a computer model
[AD-A155812] 21 p3600 N85-32355
Membrane reinforcement in concrete shells: Design versus nonlinear behavior
24 p4084 N85-35312
Response of a BWR Mark 2 containment vessel head to loads beyond the design basis
[DE85-010524] 24 p4103 N85-35432

SHELTERS
NT LUNAR SHELTERS
A comparison of lightning and nuclear electromagnetic pulse response of tactical shelters
07 p1000 N85-16350
Field testing of a lightweight relocatable structure in a temperate environment
[AD-A155171] 21 p3599 N85-32350
SHELTER: Description of a program code — indoor climate
[FOA-C-59002-H1] 22 p3755 N85-33278

SHIELDING
NT ELECTROMAGNETIC SHIELDING
NT ELECTROSTATIC SHIELDING
NT HEAT SHIELDING
NT MAGNETIC SHIELDING
NT RADIATION SHIELDING
NT REENTRY SHIELDING
NT REUSABLE HEAT SHIELDING
NT SPACECRAFT SHIELDING
EMP injection on conduit entries, type Brattberg — electromagnetic pulse (EMP) injection
[FOA-E-30001-A3] 02 p0193 N85-11290
Experimental study of aerodynamic shielding of turbojet engine air intake against exhaust gases
09 p1307 N85-18210
Explosion-proof properties and hydraulic resistance of fire-barrier elements based on knitted metallic screens
11 p1601 N85-20067
Shielded enclosures for experimental studies of shielding topology
[AD-A149292] 11 p1624 N85-20227
TFCK shielding optimization
[DE85-010503] 19 p3359 N85-30826
MFTF-(alpha) + T shield design
[DE85-010496] 20 p3529 N85-31948
Rhodium-103 and indium-115 inelastic scattering reactions for fission neutron dosimetry
21 p3703 N85-33004
Calculation of external magnetic field of a shielded transformer
22 p3771 N85-33373
Magnetic field and equivalent circuit of induction motors with shielded poles
22 p3772 N85-33378
Removable cleanable antireflection shield
[AD-D011735] 22 p3844 N85-33810
Gas shielding apparatus
[DE85-005992] 23 p3939 N85-34416
Coupled electron-photon transport calculations using the method of discrete ordinates
[DE85-009444] 23 p3967 N85-34597
Monte Carlo techniques for analyzing deep penetration problems
[DE85-011426] 23 p3968 N85-34598
Design considerations for personnel access penetrations for the superconducting super collider
[DE85-013027] 24 p4162 N85-35807

SHIELDS (GEOLOGY)
U BEDROCK

SHIFT REGISTERS
A two-cycle shift register with error detection
[AD-A150768] 14 p2400 N85-24791

SHIP HULLS
Design proposals for torsional buckling of stiffeners
[AD-A144783] 01 p0062 N85-10409
Numerical simulations of compliant material response to turbulent flow, revision 1
[AD-A145801] 03 p0372 N85-12373
Direct energy minimization approach to whipping analysis of pressure hulls
09 p1335 N85-18393
Remote self-contained undersea monitor
[AD-D011520] 12 p1849 N85-21599
Corrosion problems in the Canadian maritime forces
[AD-A151694] 15 p2509 N85-25481
Development of high strength ship hull steel for high heat input welding — controlled rolling and accelerated cooling
15 p2565 N85-25627
Seakeeping and vibration tests of the Coast Guard 110 foot surface effect ship SEA BIRD class (WSES)
[AD-A154150] 19 p3252 N85-30166
Fatigue characterization of fabricated ship details for design
[SSC-316] 19 p3285 N85-30371
Design of transversely stiffenand FRP panels under compressive load — fiber reinforced plastic (FRP) ships
[AMTE(S)-R-84104] 23 p3940 N85-34424

SHIP TO SHORE COMMUNICATION
Shipboard and satellite-aided communications equipment in exhibition
06 p0819 N85-15203
Development of a microprocessor controlled communication system for ships
[BMFT-FB-T-84-275] 17 p2950 N85-28216
Navigation data for Emergency Position Indicating Radio Beacons (EPIRBs)
20 p3403 N85-31115

SHIPS
NT AIRCRAFT CARRIERS
NT SUBMARINES
NT SURFACE EFFECT SHIPS
NT TANKER SHIPS
Model study of the interaction of a blast wave with the superstructure of ships. Part 5: Application of optical measurement methods to the study of blast interaction
[PML-1984-12-PT-5] 01 p0057 N85-10375
The climate of Denmark. Summaries of observations from light vessels. 3: Sea temperature
[ISBN-87-7478-215-0] 01 p0073 N85-10481
Experiences with a high-blockage model tested in the NASA Ames 12-foot pressure wind tunnel
03 p0315 N85-12032
Theoretical and experimental modal analysis of a rotor test rig — shipboard equipment
[AMTE(N)-TM-83079] 03 p0371 N85-12370
Solar power supplies for ships
05 p0665 N85-14274
Simulation evaluation of two VTOL control/display systems in IMC approach and shipboard landing
[NASA-TM-85996] 06 p0756 N85-14841
Copper-nickel sheathing study, phase 2. Two-year service performance of test panels on the ARCO TEXAS
[PB84-242411] 06 p0775 N85-14952
Marnera weather log, volume 28, no. 3, July-August-September 1984
[PB85-107266] 06 p0840 N85-15334
Free-surface boundary layer and the origin of bow vortices
[AD-A147427] 07 p0960 N85-16063
Installation options for the NAVSTAR global positioning system in surface ships
[AD-A148190] 08 p1082 N85-16856
Using the control system design environment in the design of a data link receiver unit for the Coast Guard HH-65A helicopter
[AD-A148624] 08 p1088 N85-16880
Solid rocket booster retrieval operations
08 p1096 N85-16928
Improvements in linked-spar motion-compensated lifting system
[AD-D011413] 08 p1138 N85-17165
SEASAT 3 and 4
[AD-A148343] 08 p1152 N85-17274
Second order Bragg scattering in a SAR
[AD-A148395] 08 p1152 N85-17275
Speed governor for diesel engine
09 p1307 N85-18214
Use of braking stages for control of turbine speed
09 p1308 N85-18215
Reflections on trends in dynamics: The Navy's perspective
09 p1334 N85-18382
The Shock and Vibration Bulletin 54. Part 2: Ship shock, shock and blast and ground shock
[AD-A148132] 09 p1334 N85-18388
Two-dimensional shock response of a mass on energy-absorbing shock mounts
09 p1334 N85-18389
Shipboard shock response of the model structure DSM: Experimental results versus responses predicted by eight participants
09 p1335 N85-18392
High-strength composite materials for aircraft, body armor
11 p1599 N85-20057
International list of selected, supplementary and auxiliary ships — WMO
[WMO-47-ED-84] 11 p1687 N85-20609
A broadband kevlar radome for shipboard
[AD-P004365] 12 p1826 N85-21459
INMARSAT marine satellite organization
13 p1965 N85-22456
Uses of composite materials
13 p2027 N85-22698
USSR report: Transportation
[JPRS-UTR-85-005] 14 p2207 N85-23668
USSR report: Engineering and equipment
[JPRS-UEQ-84-001] 14 p2265 N85-24034
Investigation of errors of acoustic goniometer information-measurement systems on rocking base
14 p2283 N85-24139
Pluribus Satellite IMP (Interface Message Provision) development mobile access terminal network
[AD-A151312] 15 p2542 N85-25692
Several specific and nonspecific responses of the human and animal body to ship noise
[NASA-TM-77483] 15 p2615 N85-26116
Special features of the one-sided automatic welding of structures of Al-Mg alloys
16 p2792 N85-27222
An inexpensive radar-responding relocation device for drifting oceanographic instruments
[AD-A152170] 16 p2836 N85-27505
The PINGUIN B3: A remotely piloted vehicle for mine identification and disposal
[MBB-UM-1/84-O] 16 p2874 N85-27735
USSR report: Engineering and equipment
[JPRS-UEQ-85-004] 17 p2939 N85-28142
Operation guiding light-scientific program and field plan. The pilot field experiment for NORDA project chemical dynamics in ocean frontal areas
[AD-A153765] 18 p3150 N85-29507
Fatigue characterization of fabricated ship details for design
[SSC-318] 19 p3285 N85-30371
Soviet Emergency Locator Transmitter/Emergency Position Indicating Radio Beacon (ELT/EPIRBs) at 121.5 and 406 MHz
20 p3402 N85-31107
Existing and potential INMARSAT capabilities for the Future Global Maritime Distress and Safety System
20 p3402 N85-31110
The CCIR satellite EPIRB coordinated trials programme — Emergency Position Indicating Radio Beacon (EPIRB); International Radio Consultative Committee (CCIR)
20 p3402 N85-31111
The International Radio Consultative Committee (CCIR) recommended satellite Emergency Position Indicating Radio Beacon (EPIRB) system operating through geostationary satellites at 1.6 GHz
20 p3402 N85-31112
Free-float Emergency Position Indicating Radio Beacons (EPIRBs) and release mechanism on board Norwegian ships. Main specifications and user experience
20 p3404 N85-31120
Experiments of a LORAN-C aided recovery system and a proposal of its application to rescue system
20 p3404 N85-31121
LORAN-C harbor and harbor entrance survey: Charleston, South Carolina
[AD-A154875] 21 p3554 N85-32106
Fuel cell applications literature review
[DE85-011691] 22 p3809 N85-33592
A life-saving device for ships
[NASA-TM-77670] 23 p3895 N85-34129

SHIVERING
NT DITHERS

SHOCK (PHYSIOLOGY)
Fatal hemorrhagic shock and acetate solutions
[AD-A146754] 07 p1014 N85-16444
Hazards of VLF electromagnetic fields
16 p2776 N85-27136

SHOCK ABSORBERS
Simulation of vibration processes in damped structures with allowance for temperature-frequency characteristics of vibration absorbing materials
02 p0257 N85-11680
Multiple rate shock isolator damping valve
[AD-D011429] 08 p1168 N85-17368
Optimum design for nonlinear shock mounts for transient inputs
09 p1334 N85-18390
Missile launcher integral shock isolation and running gear system
[AD-D011490] 11 p1589 N85-19998
Development of an energy-absorbing passenger seat for a transport aircraft
22 p3796 N85-33515

SHOCK DIFFUSERS
U DIFFUSERS
U SHOCK WAVE ATTENUATION

SHOCK DISCONTINUITY
Characteristics of steady-state hypersonic flow about blunted bodies with discontinuities in generators
17 p2941 N85-28155

SHOCK FRONTS
Optical pin apparatus for measuring the arrival time and velocity of shock waves and particles
[DE84-014501] 01 p0120 N85-10824
A neutral gas jet in a low velocity shock front at the boundary of the Draco Nebula 08 p0878 N85-15576
Shock acceleration in active galactic nuclei and quasars 08 p1241 N85-17826
Influence of shock wave front on nature of luminescence of recombining laser plasma 11 p1719 N85-20818
The 2-D simulations of the NRL (Naval Research Laboratory) laser experiment
[AD-A154915] 21 p3592 N85-32321
Energetic ion acceleration at collisionless shocks
[SH-1.5-3] 23 p3996 N85-34772
On reflecting boundary behind the Earth's orbit at propagation of fast particles from solar flares
[SH-3.2-13] 23 p4004 N85-34827
The nucleosynthesis of deterium and helium-3
[OG-8.2-18] 23 p4020 N85-34914
Nuclear reactions in shock wave front during supernova events
[OG-8.2-19] 23 p4021 N85-34915
Propagation of injected cosmic rays under distributed reacceleration
[OG-8.3-3] 23 p4021 N85-34922
Properties of 10 (18)-10 (19)eV EAS at far core distance
[HE-4.7-3] 24 p4198 N85-36054
A note on some statistical properties of rise time parameters used in muon arrival time measurements
[HE-4.7-12] 24 p4199 N85-36062

SHOCK HEATING
Measurement of shock and induced reaction in rocket propellants by nanosecond infrared radiometry and photography
[DE84-013209] 04 p0482 N85-13070
Physical conditions in low-luminosity active galactic nuclei 05 p0742 N85-14771
Shuttle system ascent aerodynamic and plume heating 06 p1103 N85-16975
Centrifugally driven magnetohydrodynamic (MHD) winds and the nonthermal emission regions in Active Galactic Nuclei (AGN) 08 p1242 N85-17835
Measurement of shock induced reaction in rocket propellants by nanosecond infrared radiometry and photography
[AD-P004349] 10 p1456 N85-19173
Study of structural changes of dual-phase titanium alloy during shock wave loading 15 p2498 N85-25408

SHOCK LAYERS
Aerothermal tests of a 12.5 percent cone at Mach 6.7 for various Reynolds numbers, angles of attack and nose shapes — conducted in Langley 8-foot high temperature tunnel
[NASA-TP-2345] 08 p1161 N85-17322

SHOCK LOADS
NT BLAST LOADS
Method and apparatus for determining pressure-induced frequency-shifts in shock-compressed materials
[DE84-014313] 01 p0024 N85-10151
The Shock and Vibration Digest, volume 16, no. 8
[AD-A145653] 02 p0208 N85-11372
Constitutive features of solids at shock-wave loading rates
[DE84-015715] 03 p0362 N85-12325
Optimum replacement of a system subject to shocks
[AD-A145811] 03 p0372 N85-12374
Computer molecular dynamics of 2-D water (ice) structures under shock
[AD-A145816] 03 p0372 N85-12375
Shock-induced CO2 loss from CaCO3: Implications for early planetary atmospheres
[NASA-CR-174197] 05 p0745 N85-14777
Shock response analysis by personal computer using the extended IFT algorithm 09 p1335 N85-18397
Models for shock damage to marine structural materials 09 p1336 N85-18400
A study of the effect of mass loading on the shock environment 09 p1336 N85-18401
Assessment of seismic survivability 09 p1336 N85-18402
Ground shock effect on soil field inclusions 09 p1336 N85-18403
Shock propagation in the exhaust gas handling system of the proposed large altitude rocket cell: Methods and preliminary analysis
[DE85-003055] 11 p1591 N85-20010
Evaluation of air and ground launched cruise missile navigational element containers
[AD-A149654] 12 p1774 N85-21138
Comparison of shock-induced displacements with displacements produced by a centrifuge acceleration
[DE85-000467] 12 p1852 N85-21618
Sound velocity of carbon at high pressures
[DE85-002016] 12 p1928 N85-22113
Molecular dynamics studies of energy transfer processes in crystal systems
[AD-A150161] 13 p2163 N85-23416
Dynamic shock studies of PZT 95/5 ferroelectric ceramic
[DE85-006137] 14 p2261 N85-24015
Preliminary considerations for the gasdynamic precompression of solid molecular hydrogen
[DE85-013256] 22 p3784 N85-33445

SHOCK RESISTANCE
NT IMPACT RESISTANCE
The Shock and Vibration Digest, volume 16, no. 11
[AD-A148466] 08 p1171 N85-17382
The Shock and Vibration Bulletin 54. Part 2: Ship shock, shock and blast and ground shock
[AD-A148132] 09 p1334 N85-18388
Shipboard shock response of the model structure DSM: Experimental results versus responses predicted by eight participants 09 p1335 N85-18392
Prediction of the resistance of structural materials to cavitation erosion
[BLL-DRIC-TRANS-7435-(3623.66)]
13 p2020 N85-22659
Dispersed-metal-toughened alumina
[NASA-CR-174687] 13 p2037 N85-22758
Design of SC cut 10 MHZ H.Q. crystals with G. sensitivity better than 2.10(-10)/G 17 p2966 N85-28319

SHOCK SIMULATORS
The Shock and Vibration Digest, volume 16, no. 11
[AD-A148466] 08 p1171 N85-17382

SHOCK SPECTRA
The Shock and Vibration Digest, volume 16, no. 11
[AD-A148466] 08 p1171 N85-17382
Alternative shock characterizations for consistent shock test specifications 09 p1335 N85-18396
Least favorable response of inelastic structures 09 p1336 N85-18398
Recovery of pyroshock data from distorted acceleration records
[NASA-TP-2494] 20 p3407 N85-31141
Short-time spectroscopic measurement of the temperature of solids
[ISL-CO-202/84] 20 p3459 N85-31486

SHOCK TESTS
Vibration, acoustic, and shock design and test criteria for components on the Solid Rocket Boosters (SRB), Lightweight External Tank (LWT), and Space Shuttle Main Engines (SSME)
[NASA-RP-1127] 01 p0061 N85-10405
Particle velocity experiments in anorthosite and gabbro
[NASA-CR-174158] 04 p0533 N85-13407
Shock testing of a nitrogen tank (Cryo diffusion type 220 VLR) on the middle weight shock stand
[NASA-TM-77747] 06 p0617 N85-15183
Sensitivity tests for solid propellants in Germany 06 p1115 N85-17028
Evaluation of air and ground launched cruise missile navigational element containers
[AD-A149654] 12 p1774 N85-21138

SHOCK TUBES
Particle entrainment in a compressible vortex
[ISL-CO-230/83] 04 p0500 N85-13192
A Van Leer shock capturing algorithm for the Euler equations
[AD-A148761] 08 p1163 N85-17335
Pseudo-stationary oblique-shock-wave reflections in a polyatomic gas, sulfur hexafluoride
[UTIAS-TN-253] 12 p1845 N85-21577
Turbulence measurements in shock induced flows 13 p2091 N85-23065
Collaborative shock tube studies of benzene pyrolysis
[DE85-006347] 14 p2253 N85-23962
Experimental simulation of the flow inside a gun barrel
[ISL-CO-208/83] 14 p2302 N85-24252
Thirty-three years of research with shock tubes in the Franco-German Research Institute, Saint Louis (France)
[ISL-CO-226/83] 14 p2302 N85-24257
Experimental simulation of the flows in front of and behind a projectile with and without gas slippage
[ISL-CO-232/83] 14 p2302 N85-24258
Compression waves in front of and behind a piston launched in a shock tube
[ISL-R-101/83] 14 p2303 N85-24260
Simulation of interior ballistics flows in a shock tube
[ISL-CO-222/83] 16 p2784 N85-27183
Investigation of heat transfer to a turbine blade cascade using a shock tube
[AD-A153090] 17 p2898 N85-27871
Characteristics of steady-state hypersonic flow about blunted bodies with discontinuities in generators 17 p2941 N85-28155
Impact starting of plane nozzles with wide divergence angle 17 p2941 N85-28156
Experimental observation of transition behavior on a flat plate 20 p3452 N85-31437
Environmental airblast around large shock tubes
[DE85-010854] 20 p3463 N85-31512
Shock tube measurements of growth constants in the branched-chain ethane-carbon monoxide-oxygen system
[NASA-TM-87068] 21 p3562 N85-32256
A variable node finite element method applied to the gas dynamics equations
[AD-A155211] 21 p3584 N85-32281
Velocity and transient measurements in a shock tube using a hot-wire anemometer
[AD-A154694] 21 p3589 N85-32305
Experimental simulation of in-bore flows using a high pressure shock tube
[ISL-CO-217/84] 22 p3785 N85-33452

SHOCK WAVE ATTENUATION
Supersonic flow with feeding of energy
[NASA-TM-77912] 24 p4081 N85-35163
Attenuation properties of the Petatlan region, Mexico, and a local magnitude scale for microearthquakes in this area 24 p4116 N85-35513

SHOCK WAVE CONTROL
Selection of air intake parameters for supersonic-flow operation 13 p2051 N85-22837

SHOCK WAVE GENERATORS
NT SHOCK TUBES
Flow-induced vibrations of a circular cylinder due to turbulent internal flows
[DE85-002766] 13 p2103 N85-23110
Shock compression of liquid helium to 56 GPa (560) kbar 13 p2184 N85-23551
Generation of detonation waves of given spatial and temporal characteristics
[ISL-R-103/83] 16 p2758 N85-27021

SHOCK WAVE INTERACTION
Experimental study of Mach reflection of weak shock waves 02 p0260 N85-11703
Geometric characteristics of turbulent boundary layer separation upon action with direct shock wave in conical flows 02 p0269 N85-11755
Shock/turbulent boundary layer interaction and its control 06 p1071 N85-16792
Oblique shock wave-turbulent boundary layer interaction on a porous wall with suction 08 p1072 N85-16794
Active and passive shock/boundary layer interaction control on supercritical airfoils 08 p1072 N85-16795
Transonic shock interaction with a tangentially-injected turbulent boundary layer 08 p1072 N85-16796
Velocity measurements in a 3D shock wave laminar boundary layer interaction. Part 1: Low speed 2D LDV measurements
[AD-A149533] 10 p1485 N85-19373
Influence of shock wave front on nature of luminescence of recombining laser plasma 11 p1719 N85-20818
The behaviour of detonation waves in single phase heterogeneous systems
[AD-A149825] 12 p1846 N85-21581
Study of geological media based on scattered earthquake waves 13 p2114 N85-23168
Application possibilities of laser Doppler anemometry in the investigation of the transonic interaction between shock wave and boundary layer
[ISL-R-131/83] 14 p2304 N85-24265
An exploratory investigation of sharp fin-induced shock wave/turbulent boundary layer interactions at high shock strengths
[AD-A151571] 15 p2558 N85-25772
Viscous effects on blast wave flowfields
[AD-A152013] 15 p2558 N85-25779
A curved test section for research on transonic shock wave-boundary layer interaction
[VTH-LR-414] 16 p2701 N85-26682
Numerical solution of transonic normal shock wave-boundary layer interaction using the Bohning-Zierop model — wind tunnel flow
[VTH-LR-416] 16 p2701 N85-26683
Theoretical investigation of three-dimensional shock wave turbulent boundary layer interactions. Part 3
[AD-A152251] 16 p2783 N85-27177
An experimental investigation of the interaction between a shock wave and a turbulent boundary layer on a convex wall
[VTH-LR-428] 16 p2785 N85-27187
Underwater shock-induced responses of stiffened flat plates: An investigation into the predictive capabilities of the USA-STAGS code
[AD-A154245] 19 p3286 N85-30377
The application of laser anemometry to the study of transonic shock boundary-layer interactions
[ISL-CO-204/84] 20 p3396 N85-31067
Shock waves in adjacent engine inlets
[ISL-R-104/84] 20 p3396 N85-31068

SHOCK WAVE LUMINESCENCE
A program of ground-based astronomy to complement einstein observations
[AD-A151111] 15 p2668 N85-26486

SHOCK WAVE PROFILES
Deceleration of a supersonic flow behind a curved shock wave with isentropic precompression
[NASA-TM-77920] 24 p4061 N85-35164
Ground motion measurements for the QUESO nuclear event
[DE85-014806] 24 p4151 N85-35743

SHOCK WAVE PROPAGATION
Self-similar expansion of dense matter due to heat transfer by nonlinear conduction
[MPQ-81] 01 p0046 N85-10297
Plastic deformation and microstructural transformations of metals under shock waves 02 p0272 N85-11775
An experimental investigation of the parallel blade-vortex interaction
[NASA-TM-86005] 05 p0592 N85-13777
Research on acoustical and optical scattering, optics of bubbles, diffraction catastrophes, laser generation of sound, and shock induced cavitation
[AD-A146703] 06 p0860 N85-15466
Strong iron accelerating by collisionless magnetosonic shock wave propagating perpendicular to a magnetic field
[IPPJ-709] 12 p1935 N85-22161
Interplanetary shock waves during April and May of 1981 13 p1982 N85-22434
Molecular spectroscopy from the Kuiper Airborne Observatory
[NASA-CR-175748] 16 p2662 N85-27763
Impact starting of plane nozzles with wide divergence angle 17 p2941 N85-28156
Supersonic flow around blunt wedge 17 p2942 N85-28158
Proceedings of the 1980 Workshop of the International Association of Seismology and Physics of the Earth's Interior on the Seismic Modeling of Laterally Varying Structures: Contributions based on data from the 1976 Saudi Arabian refraction profile
[GS-CIRC-937] 17 p2969 N85-28476
Preliminary interpretation of Saudi Arabian seismic refraction data 17 p2969 N85-28477
Two-dimensional inverse kinematic problem: Application to the Saudi Arabian refraction profile 17 p2990 N85-28478
Crustal structure of the Red Sea-Arabian Shield transition 17 p2990 N85-28479
A seismic refraction profile across the Arabian Shield 17 p2990 N85-28481
A preliminary examination of the 1978 refraction profiles in Saudi Arabia 17 p2990 N85-28482
The rifted margin of Saudi Arabia 17 p2990 N85-28483
Solar wind observations associated with a slow forward shock wave at 0.31 AU
[MPAE-W-79-84-46] 17 p3055 N85-28909
Wave-theoretical approach to seismic modeling problems (WELMOD)
[BMFT-FB-T-84-258] 18 p3137 N85-29429
Shock waves in adjacent engine inlets
[ISL-R-104/84] 20 p3396 N85-31068
Weak shock waves propagating in fluid-gas mixtures
[AD-A154759] 21 p3584 N85-32278
Resonant ion acceleration by oblique magnetosonic shock wave in a collisionless plasma
[IPPJ-735] 23 p3975 N85-34843
Workshop report on Simulation Techniques for Shock Wave Phenomena and Characteristics of Plasmas in Inertial Confinement Fusion
[IPPJ-725] 23 p3979 N85-34670
Simulation of instability of cylindrically converging shock waves 23 p3980 N85-34679
Stability of ion distribution in strong ion shock structure 23 p3980 N85-34681
First-order shock acceleration in solar flares
[SH-1.1-5] 23 p3999 N85-34732
On reflecting boundary behind the Earth's orbit at propagation of fast particles from solar flares
[SH-3.2-13] 23 p4004 N85-34827
The intensity recovery of Forbush-type decreases as a function of heliocentric distance and its relationship to the 11-year variation
[SH-4.1-9] 23 p4005 N85-34832
On the cosmic ray diffusion in a violent interstellar medium
[OG-7.2-14] 23 p4015 N85-34881
The central engine of quasars and AGNs: A relativistic proton radiative shock
[OG-8.1-7] 23 p4018 N85-34897
Propagation of cosmic rays and new evidence for distributed acceleration
[OG-8.3-5] 23 p4022 N85-34924
Ground motion measurements for the QUESO nuclear event
[DE85-014806] 24 p4151 N85-35743

SHOCK WAVES
NT DETONATION WAVES
NT NORMAL SHOCK WAVES
NT OBLIQUE SHOCK WAVES
NT SONIC BOOMS
Observations from varying the lift and drag inputs to a noise prediction method for supersonic helical tip speed propellers
[NASA-TM-83797] 01 p0115 N85-10788
Optical pin apparatus for measuring the arrival time and velocity of shock waves and particles
[DE84-014501] 01 p0120 N85-10824
Weak shocks and steady waves in a nonlinear elastic rod or granular material
[AD-A145715] 02 p0209 N85-11383
Experimental study of Mach reflection of weak shock waves 02 p0260 N85-11703
Using fiber-optics light guides in diagnosing intense shock waves 02 p0272 N85-11773
Problems in theory of diffusion under shock wave 02 p0272 N85-11776
Review of simulation of quasiparallel collisionless shocks
[DE84-015489] 02 p0304 N85-11957
Numerical studies of unsteady transonic flow over an oscillating airfoil
[NASA-TM-86011] 03 p0361 N85-12316
Constitutive features of solids at shock-wave loading rates
[DE84-015715] 03 p0362 N85-12325
Magnetohydrodynamic and gasdynamic theories for planetary bow waves
[NASA-CR-174132] 03 p0448 N85-12850
Local stability analysis for a planar shock wave
[NASA-TP-2367] 04 p0452 N85-12864
Seismic studies in southern Alaska 04 p0515 N85-13286
Experimental investigation of shock-cell noise reduction for dual-stream nozzles in simulated flight
[NASA-CR-3846] 04 p0557 N85-13549
Lunar origin from impact on the Earth 04 p0588 N85-13757
Pressure oscillations in liquid-fueled ramjet engines 05 p0596 N85-13797
Experimental investigation and analysis of oscillations of thin-walled spherical shell during pulse loading 05 p0725 N85-14662
Multiple steady states for characteristic initial value problems
[NASA-CR-172486] 06 p0749 N85-14800
A model of the soft X-ray background as a blast wave viewed from inside 06 p0879 N85-15586
Waves and instabilities in collisionless shocks
[AD-A146689] 06 p0881 N85-15597
A comparative study of the nonuniqueness problem of the potential equation
[NASA-TP-2385] 07 p0896 N85-15694
Numerical reconstruction of part of an actual blast-wave flow field to agree with available experimental data
[UTIAS-TN-251] 07 p0956 N85-16061
Bulk cavitation caused by a plane shock wave
[AD-A147031] 07 p0958 N85-16072
On the asymptotic analysis of travelling shocks and phase boundaries in elastic bars
[AD-A147239] 07 p0959 N85-16076
Nonlinear waves in a rod. Results for incompressible elastic materials
[AD-A147485] 07 p0979 N85-16216
Shock/turbulent boundary layer interaction and its control 08 p1071 N85-16792
Active and passive shock/boundary layer interaction control on supercritical airfoils 08 p1072 N85-16795
Transonic shock interaction with a tangentially-injected turbulent boundary layer 08 p1072 N85-16796
Shock waves in transonic flows at moderate Reynolds Number 08 p1076 N85-16823
The NYU inverse swept wing code
[NASA-CR-3662] 08 p1077 N85-16830
Analysis of Deflagration to Shock to Detonation Transition (DSDT) in porous energetic solid propellants 08 p1115 N85-17030
Numerical simulation of the shock detonation transition 08 p1116 N85-17039
Shock and impact response of solid rocket propellants: Experimental and theoretical 08 p1116 N85-17040
A numerical study of several supersonic flows 09 p1272 N85-17995
The Shock and Vibration Bulletin 54. Part 1: Welcome, keynote address, invited papers MIL-STD-810D, MIL-STD-810D panel session
[AD-A148131] 09 p1333 N85-18377
Keynote address 09 p1333 N85-18378
Analysis of Shock to Detonation Transition (SDT) of porous high energy propellant from ramp-wave compression loading
[AD-A149333] 10 p1457 N85-19180
A shock wave capability for the improved Two-Dimensional Kinetics (TDK) computer program
[NASA-CR-171302] 10 p1483 N85-19360
Velocity measurements in a 3D shock wave laminar boundary layer interaction. Part 1: Low speed 2D LDV measurements
[AD-A149533] 10 p1485 N85-19373
Construction of solutions for two-dimensional Riemann problems
[DE85-003136] 10 p1549 N85-19770
Research study of space plasma boundary processes
[NASA-CR-174351] 10 p1558 N85-19823
Micro-deformation of quartz under dynamic action and its applications 11 p1620 N85-20201
On detached shock wave of sphere moving with transonic velocities 11 p1622 N85-20215
Magnetic and structural properties of shock-synthesized zinc ferrite
[DE85-000469] 11 p1736 N85-20915
Wavecode constitutive models: Nonhomogeneous mixtures
[DE85-000836] 12 p1798 N85-21278
Pseudo-stationary oblique-shock-wave reflections in a polyatomic gas, sulfur hexafluoride
[UTIAS-TN-253] 12 p1845 N85-21577
Front tracking and two dimensional Riemann problems: A conference report
[DE85-002209] 12 p1847 N85-21589
Biological effects of blast and impact waves
[FOA-C-52006-H4-D7] 12 p1906 N85-21968
Adaptive meshes in the 2DL code
[LA-9938-MS] 12 p1914 N85-22011
Recovering pointwise values of discontinuous data within spectral accuracy
[NASA-CR-172535] 12 p1919 N85-22049
Self-similar modified shock structures — cosmic rays 12 p1956 N85-22290
Aerodynamic heating rate distributions induced by trailing edge controls on hypersonic aircraft configurations at Mach 8
[NASA-TM-87453] 13 p1969 N85-22370
Ignition of mixtures of SiH sub 4, CH sub 4, O sub 2, and Ar or N sub 2 behind reflected shock waves
[NASA-TP-2415] 13 p1974 N85-22395
Effect of transparent coatings on generation of laser-induced shock waves in metals 13 p2028 N85-22711
Space and time distribtuion of aftershocks 13 p2112 N85-23157
Study of geological media based on scattered earthquake waves 13 p2114 N85-23168
Physics of the inner heliosphere: Mechanisms, models and observational signatures
[NASA-CR-175632] 13 p2205 N85-23677
Wave motion of three-component medium under load moving on plane boundary 14 p2277 N85-24105
Compression waves in front of and behind a piston launched in a shock tube
[ISL-R-101/83] 14 p2303 N85-24260
Diagram of nonstationary rejoining of magnetic force lines 14 p2344 N85-24492
Electric field and plasma observations near the magnetopause and bow shock during a rapid compression 14 p2355 N85-24553
The keV electrons and 80 keV protons in the vicinity of the high latitude magnetosphere and at the bow shock 14 p2355 N85-24554
The downshift of electron plasma oscillations in the electron foreshock region
[NASA-CR-175633] 14 p2423 N85-24945
Numerical studies of unsteady transonic flow over oscillating airfoil 15 p2458 N85-25174
Magnetohydrodynamics of Earth's bow shock 15 p2481 N85-25311
Vapor explosions in superheated liquids and fundamental studies of the physics of detonation
[AD-A151362] 15 p2504 N85-25447
Measurement of material properties to Mbar pressures using time-resolved shock wave techniques
[DE85-007319] 15 p2558 N85-25780
An experimental investigation into the dynamic response of a stiffened flat plate loaded impulsively by an underwater shockwave
[AD-A151321] 15 p2578 N85-25909
Investigation to optimize the passive shock wave/boundary layer control for supercritical airfoil drag reduction
[NASA-CR-175788] 16 p2599 N85-26665
Evaluation of an algorithm for the solution of the time-dependent Euler equations
[AD-A151993] 16 p2854 N85-27600
Analyses of orderly structures in jets and the relationship with emitted noise
[ISL-R-117/83] 16 p2861 N85-27646

The soft X-ray background as a supernova blast wave viewed from inside: Solar abundance models
[NASA-CR-175767] 16 p2887 N85-27813
Characteristics of steady-state hypersonic flow about blunted bodies with discontinuities in generators
17 p2941 N85-28155
Formation of a fine structure during shock wave welding
[BLL-BISI-TRANS-22401-(9022.06)] 17 p2973 N85-28368
Australian seismological report, 1980
[REPT-252] 17 p2989 N85-28473
The shock desensitization of PBX-9404 and composition B-3
[DE85-009604] 18 p3084 N85-29077
Shock capturing
[NASA-CR-172592] 18 p3168 N85-29827
Shocks in the solar wind between 1 and 8.5 AU: Voyager 1 observations
[NASA-CR-175911] 18 p3209 N85-29905
A numerical solution of a nonisothermal wall using the two-dimensional Navier-Stokes equations
[AD-A154467] 19 p3266 N85-30257
Highly accurate shock flow calculations with moving grids and mesh refinements, revision 1
[DE85-010929] 19 p3267 N85-30260
Strain-path modeling for geo-materials
[AD-A154378] 19 p3286 N85-30380
More on shock-wave studies with Prognoz-10 satellite
19 p3296 N85-30432
Functions of Prognoz-10: Intercosmos' station explained
19 p3296 N85-30433
Prognoz-10 Intercosmos' station launched to study shock waves
19 p3296 N85-30434
A multiphase continuum model to describe dynamic loading effects in nonlinear porous media
[DE85-010102] 19 p3301 N85-30463
Fast and optimal solution to the Rankine-Hugoniot problem
[NASA-TM-86214] 19 p3344 N85-30724
Floating shock-fitting in transonic potential flow calculations
20 p3367 N85-31007
Interaction between an interplanetary shock and the Earth's magnetosphere on 27 August 1978: ISEE-1 electric field and ISEE-2 plasma observations
[IFSI-84-15] 20 p3548 N85-32078
Properties of the reflected beams from the Earth's bow shock: A simple model
[IFSI-84-14] 20 p3549 N85-32088
Development of a temperature-compensated hot-film anemometer system for boundary-layer transition detection on high-performance aircraft
[NASA-TM-86732] 22 p3730 N85-33121
Static high pressure study of nitric oxide chemistry: Proposed mechanism for nitric oxide detonation
[DE85-010795] 22 p3746 N85-33220
Experimental studies of chemical reactivity during shock initiation of hexanitrostilbene
[DE85-011726] 22 p3754 N85-33270
Modeling granular explosive detonations with shear band concepts
[DE85-011823] 22 p3754 N85-33271
Two-dimensional simulation of instability growth due to shocks
[DE85-011869] 22 p3784 N85-33442
Gradient scaling for nonuniform meshes
[DE85-009625] 22 p3784 N85-33443
Detonation in tungsten-loaded HMX
[DE85-009606] 23 p3922 N85-34299
Three-dimensional hydrodynamic hot-spot model
[DE85-009587] 23 p3922 N85-34301
Shock and release equation of state of calcite
[DE85-013151] 23 p3942 N85-34432
Cubic interpolated pseudo-particle method (CIP) for solving hyperbolic-type equation
23 p3979 N85-34673
Moving finite element method for ICF target implosion
23 p3980 N85-34675
Numerical calculations on shock loaded materials
23 p3980 N85-34676
Simulation of instability of cylindrically converging shock waves
23 p3980 N85-34679
Stochastic particle acceleration in solar flares
[SH-1.1-4] 23 p3989 N85-34731
Prompt acceleration of ions by oblique turbulent shocks in solar flares
[SH-1.1-6] 23 p3989 N85-34733
Shock and statistical acceleration of energetic particles in the interplanetary medium
[SH-1.5-1] 23 p3996 N85-34771
Energetic ion acceleration at collisionless shocks
[SH-1.5-3] 23 p3996 N85-34772
Pitch angle distributions of 35-1000 keV protons at quasi-perpendicular interplanetary shocks
[SH-1.5-6] 23 p3996 N85-34775
Spatial dependence of the local diffusion coefficient measured upstream of the November 12, 1978 interplanetary traveling shock
[SH-1.5-12] 23 p3996 N85-34776
Latitude dependence of co-rotating shock acceleration
[SH-1.5-14] 23 p3997 N85-34777
Cosmic ray acceleration by stellar wind. Simulation for heliosphere
[SH-1.5-17] 23 p3997 N85-34780
the role of shock waves in modulation of galactic cosmic rays
[SH-4.1-7] 23 p4005 N85-34831
Cosmic ray secondary nuclei and the structure of the galaxy
[OG-7.2-4] 23 p4014 N85-34876
On the cosmic ray diffusion in a violent interstellar medium
[OG-7.2-14] 23 p4015 N85-34881
The cosmic-ray shock structure problem for relativistic shocks
[OG-8.1-1] 23 p4017 N85-34891
Instabilities in decelerating supersonic flows with applications to cosmic ray shocks
[OG-8.1-2] 23 p4017 N85-34892
Time-dependent nonlinear cosmic ray shocks confirming abstract
[OG-8.1-3] 23 p4017 N85-34893
Selfsimilar time dependent shock structures
[OG-8.1-4] 23 p4017 N85-34894
A cosmic ray driven instability
[OG-8.1-5] 23 p4018 N85-34895
Relativistic cosmic ray spectra in the full non-linear theory of shock acceleration
[OG-8.1-6] 23 p4018 N85-34896
The central engine of quasars and AGNs: A relativistic proton radiative shock
[OG-8.1-7] 23 p4018 N85-34897
A model for the origin of high-energy cosmic rays
[OG-8.1-8] 23 p4018 N85-34898
Acceleration of cosmic rays in supernova-remnants
[OG-8.1-9] 23 p4018 N85-34899
Efficiency of regular acceleration of particles by a shock wave at different injection regimes
[OG-8.1-13] 23 p4019 N85-34902
A numerical study of diffusive shock acceleration of cosmic rays in supernova shocks
[OG-8.2-2] 23 p4019 N85-34903
Nuclear reactions in shock wave front during supernova events
[OG-8.2-19] 23 p4021 N85-34915
The theoretical and experimental investigation of cosmic ray Forbush-effects
[SH-5.1-20] 23 p4044 N85-35072
Finite analytic solutions of supersonic flows in two-dimensional non-symmetrical channels
24 p4059 N85-35154
Unsteady flow in a supersonic cascade with two in-passage shocks
[NASA-CR-3925] 24 p4060 N85-35158
Numerical studies of 2-dimensional flows
[NASA-CR-3930] 24 p4060 N85-35160
Computation of three-dimensional shock wave and boundary-layer interactions
[NASA-TM-86780] 24 p4093 N85-35372

SHOES
The energy cost of women walking and running in shoes and boots
[AD-A151022] 14 p2389 N85-24716

SHOOTING STAR AIRCRAFT
U T-33 AIRCRAFT

SHOPS
Development of a production order release methodology
[AD-A145213] 01 p0124 N85-10652

SHORELINES
Progress in developing tidal electric power plants reported
07 p0994 N85-16314
Shore ice ride-up and pile-up features. Part 2. Alaska's Beaufort Sea coast, 1983 - 1984
[AD-A148428] 08 p1190 N85-17501
Establishment of hydrographic shore control by Doppler satellite techniques
[AD-A150709] 14 p2347 N85-24512
Sand dispersion from an ephemeral river delta on the wave-dominated central California coast
[AD-A154352] 19 p3300 N85-30458

SHORT CIRCUIT CURRENTS
New high-efficiency silicon solar cells
[NASA-CR-175643] 13 p2128 N85-23244
Process Research on Polycrystalline Silicon Material (PROPSM)
[NASA-CR-175761] 15 p2587 N85-25951
Measurement of electrical parameters and current components in the bulk of silicon solar cells
20 p3481 N85-31635

SHORT CIRCUITS
Diagnosis of insulation defects in 1000+ V distribution networks with insulated neutral
07 p0954 N85-16044
Surface and allied studies in silicon solar cells
[NASA-CR-174447] 11 p1671 N85-20531
Nickel-cadmium battery cell reversal from resistive network effects
[AD-A149628] 12 p1834 N85-21505
Study of the degradation of short-circuit current and the open-circuit tension of spatial solar cells as a function of the fluency of 1MeV electrons
[INPE-3356-PRE/634] 16 p2887 N85-27814
Failure modes experienced on spacecraft NiCd batteries
20 p3445 N85-31386
Nickel-cadmium battery cell reversal from resistive network effects
20 p3446 N85-31392
Thin-film reliability and engineering overview
21 p3612 N85-32450

SHORT HAUL AIRCRAFT
NT A-310 AIRCRAFT
NT A-320 AIRCRAFT
NT CESSNA 402B AIRCRAFT
NT EUROPEAN AIRBUS

SHORT TAKEOFF AIRCRAFT
NT A-310 AIRCRAFT
NT A-320 AIRCRAFT
NT ALADIN 2 AIRCRAFT
NT EUROPEAN AIRBUS
STOL simulation requirements for development of integrated flight/propulsion control systems
05 p0701 N85-14489
Circulation control: A bibliography of DTNSRDC research and selected outside references: Update
[AD-A146966] 07 p0893 N85-15861
Low-speed wind tunnel tests of the NAL fan-jet STOL research aircraft model with ground simulation by tangential blowing
[NAL-TR-828] 10 p1423 N85-18976
The use of pressure sensing taps on the aircraft wing as sensor for flight control systems
16 p2886 N85-26960
The STOL and maneuver technology program integrated control system
16 p2715 N85-26757
Analysis of control system from a viewpoint of desired pole placement and desired degree of robustness
[AD-A152627] 17 p2899 N85-27876
The STOL and maneuver technology program integrated control system development
17 p2905 N85-27910
Discussion of the paper, Some Aspects of Propulsion for the Augmenter-Wing Concept, by D. C. Whitley
[NASA-TM-77884] 22 p3727 N85-33108
Presentation of the acoustic and aerodynamic results of the Aladin 2 concept qualification testing
[NASA-TM-77883] 24 p4060 N85-35161

SHORT WAVE RADIATION
NT CENTIMETER WAVES
NT DECIMETER WAVES
NT MICROWAVE EMISSION
NT MICROWAVES
NT MILLIMETER WAVES
NT SUBMILLIMETER WAVES
SWIR and visible atomic emission from laser-produced oxygen and nitrogen plasmas
[AD-A147528] 07 p1045 N85-16841
Two-stage free electron laser research
[AD-A148951] 10 p1469 N85-19402
Explanation of the normal winter anomaly from the seasonal variation of short wave absorption
11 p1660 N85-20463
Year-to-year variability of components of Earth's radiation budget according to satellite measurement data
16 p2725 N85-26821
Short Wavelength Chemical Laser (SWCL) Workshop
[AD-A151959] 16 p2790 N85-27211
Solar radiance models for determination of ERBE scanner filter factor
[NASA-CR-172595] 17 p2966 N85-28513
Global geoid and gravity anomaly predictions using the collocation and point mass technique
[AD-A154517] 21 p3605 N85-32387
Developmental trends in radio receiver design
22 p3777 N85-33407

SHORT WAVE RADIO TRANSMISSION
Theory of radio wave propagation over the ocean
02 p0259 N85-11699
The investigation of short wave signal structure in the vicinity of the caustic by means of a high-directed antenna
[PR-194] 03 p0354 N85-12277
Experimental results of study of artificial perturbation region in upper and lower ionosphere disturbance by the method of vertical probing
08 p0784 N85-15011
A reflectometer unit for a 500 kW HF balanced screened feeder
[BBC-RD-1984/13] 10 p1477 N85-19322

Measurements and predictions of HF ground wave radio propagation over irregular, inhomogeneous terrain
[PB85-110666] 12 p1830 N85-21487
Influence of tropical F region in ionosphere on propagation of short radio waves
16 p2721 N85-26798

SHORTENING
U REDUCTION

SHOT NOISE
Inequalities for the M/G/Infinity queue and related shot noise processes
[AD-A149015] 10 p1545 N85-19737
Voyager planetary radio astronomy: Grain and particle impacts shot noise in Saturn's ring plane
15 p2673 N85-26498

SHOT PEENING
Influence of shot-peening methods on surface quality and service life of bearings 06 p0776 N85-14960
Residual stress distributions in (plastically) surface deformed two-phase materials 19 p3283 N85-30356
Development of a mathematical model for predicting the percentage fatigue life increase resulting from shot peened components
[AD-A155774] 24 p4101 N85-35425

SHOULDERS
Shoulder and hip joint for hard space suits and the like
[NASA-CASE-ARC-11543-1] 12 p1910 N85-21986
The position and mobility of the shoulder, spinal column and pelvis in seated subjects
[AD-A153751] 18 p3153 N85-29524

SHOWERS
Fast electromagnetic (EM) shower simulation
[NOTA-INTERNA-831] 18 p3175 N85-29683

SHRAPNEL
Holographic assembly for measuring velocity fields of supersonic ballistic splinters at a large distance
[ISL-CO-203/84] 20 p3459 N85-31467

SHRINKAGE
Method for calculating linear shrinkage and expansion of metals and alloys
[BLL-M-35747-(5828.4)] 02 p0175 N85-11173
On shrinkage and molecular extension
[AD-A149100] 10 p1451 N85-19144
Microshrink, tensile properties, and the detection of microshrink
[AD-A155875] 24 p4079 N85-35278

SHROUDED BODIES
U SHROUDS

SHROUDED TURBINES
Ribbon burner simulation of T-700 turbine shroud for ceramic lined seals research
[NASA-TM-86940] 10 p1483 N85-19364
Shroud segments for unshrouded blade turbines
[PNR-90260] 23 p3897 N85-34143
Thermal stress analysis of a new turbine shroud seal concept
[NASA-TM-87062] 23 p3936 N85-34406

SHROUDS
Energy efficient engine high pressure turbine ceramic shroud support technology report
[NASA-CR-168036] 02 p0147 N85-10996
An experimental investigation of two-dimensional thrust augmenting ejectors, part 2
[NASA-CR-174110] 04 p0456 N85-12895
Experimental and analytical study of ceramic-coated turbine-tip shroud seals for small turbine engines
[NASA-TM-86861] 09 p1281 N85-18057
View-limiting shrouds for insolation radiometers
[NASA-CR-176041] 20 p3458 N85-31476
Shroud segments for unshrouded blade turbines
[PNR-90260] 23 p3897 N85-34143

SHUNTS
U BYPASSES
U CIRCUITS

SHUTDOWNS
Shutdown characteristics of the Mod-O wind turbine with aileron controls
[NASA-TM-86918] 07 p0992 N85-16299
Analytical model for predicting emergency shutdown of a two-bladed horizontal axis wind turbine
[NASA-TM-83472] 19 p3303 N85-30476

SHUTTLE BOOSTERS
U SPACE SHUTTLE BOOSTERS

SHUTTLE DERIVED VEHICLES
Assessment of candidate-expendable launch vehicles for large payloads
[NASA-CR-175540] 14 p2237 N85-23887
East Europe report: Science and technology
[JPRS-ESA-84-016] 15 p2533 N85-25824
Flight tests of experimental shuttle craft described
15 p2533 N85-25825

SHUTTLE IMAGING RADAR
The SIR-B science investigations plan
[NASA-CR-174282] 08 p1143 N85-17208
The SIR-B science investigations plan: Introduction
08 p1143 N85-17209
Experiment description 08 p1143 N85-17210
SIR-B coverage 08 p1143 N85-17211
The interpretation of SIR-B imagery of surface waves and other oceanographic features using in-situ, meteorological satellite, and infrared satellite data
08 p1143 N85-17212
The spatial evolution of the directional wave spectrum in the Southern Ocean: Its relation to extreme waves in Agulhas Current 08 p1144 N85-17213
Application of SIR-B data for groundwater exploration in the Arabian shield and sand-drift monitoring in the AN Nafud and Al Jafurah fringe areas, Kingdom of Saudi Arabia 08 p1144 N85-17214
Tectonic, volcanic, and climatic geomorphology study of the Sierras Pampeanas Andes, northwestern Argentina 08 p1144 N85-17215
Deforestation, floodplain dynamics, and carbon biogeochemistry in the Amazon Basin
08 p1144 N85-17216
Southern ocean sea-ice morphology and kinematics
08 p1144 N85-17217
New Zealand SIR-B science investigations
08 p1144 N85-17218
SIR-B analysis of the Precambrian shield of Sudan and Egypt: Penetration studies and subsurface mapping
08 p1145 N85-17219
Quantitative use of multiincidence-angle SAR for geologic mapping 08 p1145 N85-17220
Geologic mapping of Indonesian rain forest with analysis of multiple SIR-B incidence angles
08 p1145 N85-17221
Remote sensing of rice fields and sea pollution by SIR-B 08 p1145 N85-17222
Evaluation of SIR-B data for identifying rainfall event occurrence and intensity 08 p1145 N85-17223
SIR-B interferometric topography
08 p1145 N85-17224
Use of SIR-B multiincidence-angle imagery to study iceberg detectability and offshore ocean feature extraction 08 p1145 N85-17225
Geological, structural, and geomorphological analyses from SIR-B 08 p1145 N85-17226
Amplitude calibration experiment for SIR-B
08 p1146 N85-17227
Microwave and optical remote sensing of forest vegetation 08 p1146 N85-17228
Evaluation of SIR-B imagery for geologic and geomorphic mapping, hydrology, and oceanography in Australia 08 p1146 N85-17229
Interlobate comparison of glacial-depositional style as evidenced by small-relief glacial landscape features in Illinois, Indiana, and Ohio, utilizing SIR-B
08 p1146 N85-17231
Evaluation of the L-band scattering characteristics of volcanic terrain in aid of lithologic identification, assessment of SIR-B calibration, and development of planetary geomorphic analogs 08 p1146 N85-17232
The investigation of selected oceanographic applications of spaceborne synthetic-aperture radar
08 p1146 N85-17233
SIR-B cartography and stereo topographic mapping
08 p1147 N85-17234
Monitoring of the tidal dynamics of the Dutch Waddensea by SIR-B 08 p1147 N85-17235
Structural investigation of the Canadian Shield by orbital radar and LANDSAT 08 p1147 N85-17236
Structural investigation of the Grenville Province by radar and other imaging and nonimaging sensors
08 p1147 N85-17237
Information for space radar designers: Required dynamic range vs resolution and antenna calibration using the Amazon rain forest 08 p1147 N85-17239
Development and evaluation of techniques for using combined microwave and optical image data for vegetation studies 08 p1148 N85-17240
Investigation of SIR-B images for lithologic mapping
08 p1148 N85-17241
Australian Multiexperimental Assessment of SIR-B (AMAS) 08 p1148 N85-17243
Application and calibration of the subsurface mapping capability of SIR-B in desert regions
08 p1148 N85-17244
German Radar Observation Shuttle Experiment (ROSE) 08 p1148 N85-17245
The extension of an invertible coniferous forest canopy reflectance model using SIR-B and LANDSAT data
08 p1149 N85-17246
An investigation of ionospheric irregularity effects on SIR-B image processing and information extraction
08 p1149 N85-17247
Analysis of SIR-B radar illumination of geometry for depth of penetration and surface feature and vegetation detection, Nevada and California
08 p1149 N85-17248
Delineation of major geologic structures in Turkey using SIR-B data 08 p1149 N85-17249
Evaluation of the radar response to land surfaces and volumes: Examination of theoretical models, target statistics, and applications 08 p1149 N85-17250
Ground truth for SIR-B images obtained by SIR system 8 impulse radar 08 p1149 N85-17251
Remote sensing of soil moisture
08 p1149 N85-17252
SAR internal wave signature experiment
08 p1149 N85-17253
Data user's manual 08 p1150 N85-17254
SIR-A imagery in geologic studies of the Sierra Madre Oriental, northeastern Mexico. Part 1 (Regional stratigraphy): The use of morphostratigraphic units in remote sensing mapping
[NASA-CR-175457] 10 p1505 N85-19497
Earth resources research using the Shuttle Imaging Radar system 11 p1713 N85-20779
Analysis of the Gran Desierto, Pinacte Region, Sonora, Mexico, via shuttle imaging radar
[NASA-CR-175711] 15 p2582 N85-25927
Shuttle imaging radar-B (SIR-B) data analysis for identifying rainfall event occurrence and intensity
[NASA-CR-175712] 15 p2594 N85-25986
Shuttle imaging radar-A (SIR-A) data analysis — geology of the Ozark Plateau of southern Missouri, land use in western Illinois, and vegetation types at Koonamore Station, Australia
[NASA-CR-175785] 16 p2809 N85-27324
Design of a shuttle-borne SAR for the DFVLR's planning study
[ERYS-019/84] 20 p3419 N85-31218

SHUTTLE ORBITERS
U SPACE SHUTTLE ORBITERS

SIALON
Oxidation resistance of silicon ceramics
[NASA-TM-77429] 07 p0931 N85-15898

SIBERIA
Deep structure of terrestrial crust and upper mantle in southeastern Siberia and Far East according geological-geophysical data 06 p0821 N85-15212
Deep structure of Western Siberia
07 p0961 N85-16235
The dynamics of ionospheric D region over East Siberia 11 p1662 N85-20477
Snow cover in the Siberian forest-steppe
[NASA-TM-77914] 23 p3943 N85-34435

SICKNESSES
NT ALTITUDE SICKNESS
NT DECOMPRESSION SICKNESS
Morbidity and mortality associated with exposure to Otto Fuel II in the U.S. Navy 1966-1979
[AD-A148726] 09 p1363 N85-18574

SID (IONOSPHERIC DISTURBANCES)
U SUDDEN IONOSPHERIC DISTURBANCES

SIDE-LOOKING RADAR
NT RADAR IMAGERY
Intra-eruption geologic map from an x-band radar image during the May 18, 1980 eruption of Mount St. Helens, Washington 13 p2199 N85-23639
Synthetic aperture side-looking radar image adjustment 16 p2806 N85-27304
Developments in remote sensing
[B8580069] 17 p2984 N85-28441

SIDEBANDS
The spectral distribution of field components for a sinusoidal power modulated monofrequency optical carrier source
[FI-44-TBR-84] 04 p0565 N85-13601
Wideband phase keyers 12 p1839 N85-21544

SIDELOBE REDUCTION
Influence of strut cross-section on strut radiation of reflector antennas
[FI-455-TBR-39] 03 p0357 N85-12295
Configuration study for a 30 GHz monolithic receive array, volume 2
[NASA-CR-174697-VOL-2] 09 p1311 N85-18240
Criteria for site selection and frequency allocation (keynote paper), part 5 21 p3623 N85-32511
Sidelobe reduction of Barker codes, part 7.1C
21 p3625 N85-32522

SIDELOBES
Reflector antenna having sidelobe suppression elements
[AD-D011227] 01 p0039 N85-10244
The 20 GHz proof-of-concept test model results for a multiple scan beam dual reflector antenna
[NASA-CR-174268] 07 p0938 N85-15844
Array sidelobes, error tolerance, gain, and beamwidth
[AD-A147004] 07 p0940 N85-15858
Multiple loop sidelobe canceller
[AD-D011533] 12 p1823 N85-21434
Low sidelobe phased array antenna system
[AD-D011558] 12 p1823 N85-21435

Accuracy of velocity and power determination by the Doppler method 21 p3620 N85-32493
Reducing grating lobes due to subarray amplitude tapering
[AD-D011723] 23 p3927 N85-34339

SIDEREAL TIME
The sidereal anisotropy of cosmic rays around 3 x 10 (15) eV observed at a middle north latitude
[OG-5.3-6] 22 p3884 N85-34072
Cosmic ray intensity variations at primary rigidities near 1900 GV
[OG-5.3-0] 22 p3885 N85-34075
Cosmic ray sidereal diurnal variation of galactic origin observed by neutron monitors
[SH-4.4-2] 23 p4033 N85-35000
Sidereal anisotropies in the median rigidity range 60-600GV in 1976-1983
[SH-4.4-3] 23 p4033 N85-35001
Sidereal variations deep underground in Tasmania
[SH-4.4-4] 23 p4033 N85-35002
The effect of the interplanetary magnetic field on sidereal variations observed at medium depth underground detectors
[SH-4.4-5] 23 p4033 N85-35003
The sidereal semi-diurnal variation observed at high zenith angles at Mawson, 1968-1984, and the polarity of the solar main field
[SH-4.4-6] 23 p4033 N85-35004
Corrected sidereal anisotropy for underground muons
[SH-4.4-7] 23 p4033 N85-35005
Sidereal anisotropy of cosmic rays
[SH-4.4-8] 23 p4034 N85-35006

SIDERITE METEORITES
U IRON METEORITES

SIDERITES
Origin of mesosiderites as a natural consequence of planet formation 15 p2683 N85-26574

SIDES
Effect of upstream sidewall boundary layer removal on an airfoil test — conducted in Langley 0.3-m transonic cryogenic tunnel 03 p0313 N85-12019

SIDESLIP
Wind tunnel calibration of a hemispherical head angle of attack and angle of sideslip indicator
[FFA-TN-1984-11] 02 p0135 N85-10923
Supermaneuverability
[AD-P004153] 09 p1283 N85-17938
Aerodynamic characteristics of the standard dynamics model in coning motion at Mach 0.6
[NASA-TM-86717] 21 p3552 N85-32094

SIDEWINDER MISSILES
Air force, robotic painting
[AD-P004006] 03 p0308 N85-11986

SIERRA NEVADA MOUNTAINS (CA)
Precipitation gage network operations for wintertime research in the Central Sierra Nevada
[PB85-115020] 10 p1520 N85-19582
Ground-based snow and ice crystal observation system used in Sierra Nevada winter orographic storms
[PB85-115343] 10 p1520 N85-19584

SIEVES
Estimation for a semimartingale regression model using the method of sieves
[AD-A146809] 07 p1026 N85-16527
Rigid zeolite containing polyurethane foams
[DE85-006406] 23 p3919 N85-34256
Molecular and macromolecular sieving by asymmetric ultrafiltration membranes
[PB85-157766] 24 p4077 N85-35266

SIGHT
U VISUAL PERCEPTION

SIGNAL ANALYSIS
NT CEPSTRAL ANALYSIS
Autoregressive nonsteady methods for the analysis and synthesis of the human voice
[FUB-3-1984] 01 p0041 N85-10266
On maximum entropy signal analysis
[AD-A144374] 03 p0410 N85-12618
Automatic correction of static characteristics of measurement channel of digital oscillograph 06 p0795 N85-15063
Interactive Signal Analysis Software (ISAS). User's manual
[AD-A146999] 07 p1022 N85-16485
Use of the analytic signal in ultrasonic imaging
[DE84-016843] 07 p1039 N85-16586
Initialization of Thompson-Pisarenko's algorithm — sinusoidal signal parameter estimation
[FUB-46-1983] 09 p1375 N85-18641
Performance of time-position discriminator of composite signal 13 p2072 N85-22941
Synthesis of quasi-optimum two-level signal discriminator with level changing at unknown point 13 p2083 N85-23010
Accuracy of approximation of Bayes estimates in presence of noninformative parameters 13 p2084 N85-23015
Signal analysis techniques for incipient failure detection in turbomachinery 16 p2736 N85-26884
Algorithms for determining the relative complexity of dynamic signals
[BLL-M-36111-(5828.4)] 16 p2851 N85-27574
Synthesis of adaptive filters for tracking radio systems 22 p3763 N85-33325

SIGNAL ANALYZERS
Noise analysis of the Coarse Optical Power Spectrum Estimator (COPSE) data acquisition system
[AD-A145918] 03 p0419 N85-12677
China report: Science and technology
[JPRS-CST-84-001] 04 p0557 N85-13545
Present status, future prospects of domestic acoustical instruments 04 p0557 N85-13548
The adaptive spectrum analyser 05 p0622 N85-13978
Design of an analog spectrum analyzer for probing experiments
[AD-A147364] 07 p0941 N85-15983
The Statistical Loop Analyzer (SLA) 08 p1100 N85-16955
Development of a modified time delay spectrometry technique for underwater acoustic measurements in a multipath environment
[AD-A152111] 16 p2860 N85-27639
A portable pulse analyzer for nuclear geophysics using a Sinclair-TK microcomputer
[INPE-3278-PRE/601] 16 p2864 N85-27666
Measurement of permittivity and permeability of microwave materials
[AD-D011656] 18 p3176 N85-29688
Hierarchical beamforming with application to a large aperture array system 20 p3439 N85-31345
Transmitter spectrum analyzer 22 p3774 N85-33389

SIGNAL DETECTION
NT CORRELATION DETECTION
Detection and coding techniques of contours in image signals
[FUB-8-1983] 01 p0039 N85-10251
Rules for post-detector detection of weak signals in non-Gaussian noise of unknown power 03 p0344 N85-12218
Optoacoustic spectroscopy
[AD-A145995] 03 p0419 N85-12679
A model for the effectiveness of aircraft alerting and warning systems 05 p0702 N85-14506
Selection of parameters for image decomposition by television system for recognition of group of point sources 06 p0785 N85-15018
Asymptotically optimal ranking algorithms for quasi-determinate signal detection 06 p0792 N85-15064
Human engineer's guide to auditory displays. Volume 2: Elements of signal reception and resolution affecting auditory displays
[AD-A146513] 08 p0959 N85-15462
Potential effectiveness of spatial processing in detecting signals against background of interfering reflections 07 p0952 N85-16032
A technique for rapid determination of probability of detection in pulse Doppler radars
[AD-D011426] 08 p1154 N85-17288
Quantum noise and excess noise in optical homodyne and heterodyne receivers
[AD-A148296] 08 p1157 N85-17303
Experimental satellite system for determining coordinates of maritime distress 09 p1308 N85-18216
Methods of computer-aided analysis of non-Gaussian noise and application to robust adaptive detection, part 2
[AD-A148879] 10 p1539 N85-19704
Digital coherent detector
[AD-D011560] 12 p1833 N85-21501
Method and apparatus for detecting acoustic emissions from metal matrix wire
[AD-D011556] 12 p1927 N85-22107
Theory of optimum M-filtration of signals against background of correlated interference 13 p2069 N85-22927
Effect of variance of photoreceiver frequency characteristics on characteristics of measuring instruments 13 p2076 N85-22965
Asymptotically optimum multialternative sequential procedures for discernment of processes minimizing average length of observations 13 p2084 N85-23012
Extraction of signals from background interference with unknown parameters in quantized sample 13 p2084 N85-23013
Reception of signal with unknown amplitude and duration submerged in white noise 13 p2084 N85-23016
Synthesis of quasi-optimum algorithms for signal recognition against background of correlated noise employing discrete spectral transformations 13 p2085 N85-23020
Probability of detection of pulsed signals employing zero-gating interference suppression 13 p2085 N85-23021
Approximate rules for signal detection against background of Gaussian correlated interference 13 p2086 N85-23027
Use of importance sampling to investigate signal detection systems by simulated method 13 p2086 N85-23028
Transition detection using surface pressure noise 14 p2212 N85-23722
Investigations of the experimental detection of boundary layer transitions 14 p2213 N85-23723
Adaptive detection of noise signal according to Neumann-Pearson criterion 15 p2527 N85-25580
Statistical techniques for signal processing
[AD-A151231] 15 p2541 N85-25660
Nonparametric detection of narrowband signals
[AD-A151280] 15 p2542 N85-25691
Bit error rate of coherent M-ary PSK 16 p2770 N85-27098
Robust detection of fading narrow-band signals in non-Gaussian noise
[AD-A152262] 16 p2774 N85-27124
Phase-lock fiber optic interferometer
[AD-D011603] 16 p2786 N85-27191
Microwave responses of the western North Atlantic
[NASA-CR-175886] 17 p2946 N85-28191
Research on signal detection and block truncation coding for image compression
[AD-A153444] 19 p3168 N85-29628
Adaptive signal detection and other topics in real time signal processing
[AD-A154139] 19 p3255 N85-30184
Fiber optic gyroscope with alternating output signal
[AD-D011689] 19 p3271 N85-30294
Robust detection and classification of regional seismic signals using a two mode/two stage cascaded adaptive arma (CAARMA) model
[AD-A154710] 21 p3630 N85-32554
Selectivity of weight compensator of passive interference to unknown velocities of detectable targets 22 p3762 N85-33317
Detection of signals from coherent pulsed radars with random variation in parameters of sounding signals from pulse to pulse against background of worst-case Gaussian noise 22 p3763 N85-33324
Efficiency of discrimination in some invariant signal transformations 22 p3776 N85-33399
Optimality criterion for high-frequency channel in receivers of discrete radio signals 22 p3776 N85-33401
Binary signal detection in acoustooptic receivers 22 p3782 N85-33430
Manual and computer-aided sequential diagnostic inference
[AD-A156229] 24 p4133 N85-35820

SIGNAL DETECTORS
Minimization of anomalous errors in measuring systems employing search and testing devices 03 p0344 N85-12219
A miniature urethane molded acoustic transducer
[AD-A146459] 06 p0804 N85-15114
Lightweight, broadband Rayleigh wave transducer
[AD-D011345] 07 p1037 N85-16584
Detection of angular modulated electromagnetic signals
[AD-D011563] 12 p1823 N85-21437
Digital detector of harmonic signals 12 p1840 N85-21549
Method and apparatus for detecting acoustic emissions from metal matrix wire
[AD-D011556] 12 p1927 N85-22107
Efficiency of multitarget signal detection by digital radar data processing devices 13 p2080 N85-22991
Short-range radiotechnical point sensor 13 p2081 N85-22998
Synthesis of quasi-optimum two-level signal discriminator with level changing at unknown point 13 p2083 N85-23010
Statistical techniques for signal processing
[AD-A151231] 15 p2541 N85-25660
Research and development of subsurface acoustic wave devices for sensor applications
[AD-A152197] 16 p2861 N85-27642
Calibration and use of clutter data for simulation
[AD-A154793] 21 p3574 N85-32229
Advanced detectors and signal processing
[NASA-CR-176193] 24 p4088 N85-35343

SIGNAL DISCRIMINATORS
U SIGNAL DETECTORS
SIGNAL DISTORTION
The average power density spectra of additive scrambler signals and their versions in AMI code
[FUB-27-1983] 01 p0040 N85-10258
Electrical consequences of mechanical antenna characteristics 05 p0625 N85-14006
Distortions of radio pulse during reflection from maximum region of ionospheric layer 06 p0792 N85-15061
Real-time estimation of amplitude and group delay distortion in a PSK line-of-sight communications channel 09 p1311 N85-18237
Digital data communications over microwave radio channels 10 p1469 N85-19272
Some propagation experimental results on protection techniques for line-of-sight digital systems 10 p1472 N85-19286
Ionospheric distortions of digital signals with wideband modulation 13 p2072 N85-22945
Simple detonation meter 13 p2077 N85-22971
Nature of seismic images with amplitude and time fluctuations of recorded oscillations 13 p2112 N85-23156
The effects of seeing on noise 14 p2443 N85-25077
Specifics of laser sounding of atmosphere along horizontal and slightly slanting paths over water surface 19 p3297 N85-30441
Recovery of pyroshock data from distorted acceleration records
[NASA-TP-2494] 20 p3407 N85-31141
Solid state altimeter model: Simulation description; analysis of first results (narrow band filters, weighting) — satellite-borne instruments
[CNES-DRT/TIT/RL-160-T] 20 p3419 N85-31220
Compression of spread spectrum signals on an excessively dispersive channel
[AD-A155184] 21 p3576 N85-32240
An image compression survey and algorithm switching based on scene activity
[NASA-TP-2458] 22 p3727 N85-33106
Optimum predistortion of digital signals for transmission over parallel channels 22 p3776 N85-33397
Study of nonlinear distortion in microwave amplifiers using Schottky gate field effect transistors 22 p3780 N85-33423
SIGNAL ENCODING
Improvement of the narrowband linear predictive coder. Part 2: Synthesis improvements
[AD-A146031] 01 p0038 N85-10237
Detection and coding techniques of contours in image signals
[FUB-8-1983] 01 p0039 N85-10251
Image signals encoding techniques oriented towards the reduction of perceptive redundance
[FUB-23-1983] 01 p0040 N85-10256
The average power density spectra of additive scrambler signals and their versions in AMI code
[FUB-27-1983] 01 p0040 N85-10258
Voice phonetic coding and decoding processes
[FUB-29-1983] 01 p0040 N85-10259
A human visual system investigation applicable to image contour coding
[FUB-36-1983] 01 p0095 N85-10640
Improved digital baseband transmission by application of maximum likelihood decoding to an 8-level signal generated by convolution and block coding
[FI-44-TBR-93] 07 p0942 N85-15973
A public key cryptographic algorithm based on a generalization of the knapsack problem
[FUB-7-1984] 09 p1313 N85-18250
Tally cell circuit
[AD-D011492] 11 p1629 N85-20254
Fundamental limits to synchronization and tracking
[AD-A149623] 12 p1833 N85-21504
Secure digital speech communication
[AD-D011572] 14 p2293 N85-24215
Synchronizing heavily encoded data in bad weather 16 p2770 N85-27099
Symbol stream combining in a convolutionally coded system 16 p2771 N85-27101
Combined trellis coding with asymmetric MPSK modulation: An MSAT-X report
[NASA-CR-176039] 20 p3440 N85-31347
Study of a low rate spread spectrum receiver
[ENST-83E015] 20 p3441 N85-31354
Coding schemes for improving MST radar performance, part 7.1A 21 p3625 N85-32520
SIGNAL FADEOUT
U SIGNAL FADING
SIGNAL FADING
NT SELECTIVE FADING
Propagation measurements for land-mobile satellite services in the 800 MHz band
[CRC-TN-724] 09 p1310 N85-18231
A technical solution to fadings in tactical satellite digital transmissions 10 p1473 N85-19297
Fast data and voice transmission for mobile services with high immunity against multipath and co-channel interference 10 p1475 N85-19306
Effective millimeter wave transmission under severe multipath conditions 10 p1475 N85-19308
Optimal threshold and weight sorting of elevation angle readings under conditions of fadeouts of a directed signal 12 p1840 N85-21547
Robust detection of fading narrow-band signals in non-Gaussian noise
[AD-A152262] 16 p2774 N85-27124
Radiometry: A useful prediction tool — atmospheric attenuation
[ESA-SP-1071] 20 p3399 N85-31084
SIGNAL FADING RATE
Moving random surfaces and correlation analysis
[CRC-1384] 19 p3253 N85-30168
SIGNAL GENERATORS
NT FREQUENCY SYNTHESIZERS
NT FUNCTION GENERATORS
China report: Science and technology
[JPRS-CST-84-001] 04 p0557 N85-13545
Present status, future prospects of domestic acoustical instruments 04 p0557 N85-13548
Test signal generator for coherent air-to-ground radars
[AD-D011278] 05 p0628 N85-14025
Formation of radio signals with low out-of-band radiation 07 p0950 N85-16018
Application of K176-series microcircuits 13 p2077 N85-22973
Computing convolution of multifrequency signal employing truncated fast Fourier transform algorithms 13 p2085 N85-23019
Dielectric resonator
[AD-D011573] 14 p2299 N85-24233
Rotor blade test apparatus
[AD-D011725] 23 p3934 N85-34381
SIGNAL MEASUREMENT
Digital radio link: Wave propagation measurements using narrow band technique
[FOA-C-30364-E2] 04 p0494 N85-13152
Noncontact photo-thermal probe-beam deflection measurement of thermal diffusivity in an confined hot gas
[AD-A147481] 07 p0971 N85-16170
A sampling phasemeter design for pulsed continuous wave signals
[AD-A155237] 21 p3581 N85-32284
Visibility and vertical structure measurements in southern Germany
[AD-A154714] 21 p3635 N85-32574
SIGNAL MIXING
Error probability during optimal noncoherent reception of binary signals in multibeam channel 13 p2069 N85-22922
SIGNAL PROCESSING
Fast envelope detector with bias compensation
[AD-D011226] 01 p0038 N85-10243
Center for Electronics and Electrical Engineering Technical Bulletin covering center programs with 1984 CEEE events calendar
[PB84-222785] 01 p0045 N85-10292
Center for Electronics and Electrical Engineering Technical Bulletin covering center programs
[PB84-219716] 01 p0045 N85-10295
Guided-wave optic devices for integrated optic information processing
[AD-A145695] 02 p0280 N85-11827
Aspects and applications of SAR (Synthetic Aperture Radar) imagery for mensuration
[AD-A146301] 03 p0356 N85-12290
Center for Electronic and Electrical Engineering Technical Progress Bulletin, January - March 1983, no. 2
[PB84-231224] 03 p0360 N85-12308
Electronic bandwidth compression module
[AD-A145843] 03 p0366 N85-12343
Simulation of information extraction from radar altimeter return echoes — ERS-1 (ESA satellite) 03 p0383 N85-12452
Signal processing algorithms
[AD-A145748] 03 p0406 N85-12590
Extinction by dielectric particles at optical and infrared wavelengths
[AD-A146305] 03 p0413 N85-12640
Research on materials and components for opto-electronic signal processing
[AD-A145808] 03 p0433 N85-12754
Research activities of the Illinois University Coordinated Science Laboratory
[AD-A145589] 03 p0449 N85-12856
USSR report: Electronics and electrical engineering
[JPRS-UEE-84-010] 04 p0485 N85-13095
Bragg reflection of surface electroacoustic shear waves 04 p0485 N85-13096
Interference immunity of digital equipment for coherent processing of wideband signals 04 p0486 N85-13100
Digital radio receivers and problems of analog-to-digital conversion of narrow-band signals 04 p0486 N85-13101
Architecture of adaptive space-frequency-time signal processing system 04 p0486 N85-13103
Microprocessor implementation of algorithms of nonlinear filtration 04 p0486 N85-13104
Revision of signal and interference space-time processing algorithms for implementation by microprocessors 04 p0487 N85-13105
Efficiency of computer system digital processing of signals 04 p0487 N85-13106
Carrier acquisition and tracking by a COSTAS loop with automatic frequency control
[ESA-TT-836] 04 p0493 N85-13149
On estimating the phase of periodic waveform in additive Gaussian noise, part 2 05 p0622 N85-13982
Parametric models for signal processing: Autoregressive (AR), Moving Average (MA) and mixed autoregressive with moving average (ARMA)
[ENST-84D001] 05 p0628 N85-14026
Study and realization of a Doppler system with pulsed, directional, multiport (128) emission and sequential signal treatment — ultrasonic echography, blood flow
[ENST-84E008] 05 p0639 N85-14102
Detailed performance calculations: Portland State Group, appendix F 05 p0676 N85-14343
Fast algorithms and specialized architectures 05 p0714 N85-14579
Fly's eye sensor nonlinear signal processing
[AD-D011290] 05 p0729 N85-14684
Place of aperture synthesis in general theory of antennas (review) 06 p0781 N85-14993
Primary data processing in very long baseline radiointerferometer 06 p0783 N85-15008
Device for frequency stabilization of microwave oscillators 06 p0788 N85-15033
USSR report: Electronics and electrical engineering
[JPRS-UEE-84-011] 06 p0789 N85-15042
Synthesis of systems for coherent weighted signal processing against background of correlated interference 06 p0790 N85-15045
Teletrack: A special effect
[BBC-RD-1984/10] 06 p0796 N85-15097
Wavelength coded image transmission and holographic optical elements
[AD-A146490] 06 p0810 N85-15147
Actual altitudes of radioacoustic sounding in decimeter wavelength band 06 p0826 N85-15243
Development of radar to measure sea ice merits prize nomination 06 p0826 N85-15244
Evaluation of the RSTN (Regional Seismic Test Network) network and further improvement to automatic association
[AD-A146395] 06 p0835 N85-15312
Adaptive MTI (Moving Target Indicator) system
[AD-D011361] 07 p0937 N85-15937
Two-dimensional signal processing and storage and theory and applications of electromagnetic measurements. Supplemental appendix
[AD-A146846] 07 p0939 N85-15953
Studies in statistical signal processing
[AD-A147130] 07 p0940 N85-15959
Charge domain filters for enhanced monolithic signal processing
[AD-A147428] 07 p0941 N85-15964
New technology high efficiency and high stability color motion video compression system
[AD-A147523] 07 p0941 N85-15968
Parallel processor configuration for adaptive antenna arrays
[AD-D011347] 07 p0942 N85-15970
Modern signal processing and reconnaissance — conferences
[FOA-C-30374-E1] 07 p0942 N85-15975
Electronics research at the University of Texas at Austin
[AD-A146900] 07 p0947 N85-15998
USSR report: Electronics and electrical engineering
[JPRS-UEE-84-018] 07 p0949 N85-16014
Digital signal demodulators with single-sideband 07 p0950 N85-16019
USSR report: Electronics and electrical engineering
[JPRS-UEE-84-017] 07 p0951 N85-16025
Nonlinear processing of optical pulse signals 07 p0951 N85-16026
Analysis of effectiveness of partial optimization of spatial processing systems 07 p0952 N85-16031
Potential effectiveness of spatial processing in detecting signals against background of interfering reflections 07 p0952 N85-16032
Digital thermometer with linearizer on slide wire 07 p0954 N85-16049

Improvement of electromechanical systems by utilization of microelectronic technology 07 p0955 N85-16053
White-light optical information processing and holography
[AD-A146938] 07 p0967 N85-16138
Interactive Signal Analysis Software (ISAS). User's manual
[AD-A146999] 07 p1022 N85-16485
Electro-optical target detection
[AD-D011366] 07 p1042 N85-16617
Solid state research
[NASA-CR-174285] 07 p1048 N85-16656
NSWC-NADC interactive communication links for AN/UYS-1 loadtape creation and retrieval
[AD-A148418] 08 p1153 N85-17277
An adaptive Fast Fourier Transform weighting technique to increase small target sensitivity
[AD-D011424] 08 p1154 N85-17286
A technique for rapid determination of probability of detection in pulse Doppler radars
[AD-D011426] 08 p1154 N85-17288
Extraction of structural information from radar signals
[FOA-C-30370-E1] 08 p1155 N85-17292
A scanning alarm electronic processor
[AD-D011419] 08 p1158 N85-17309
Data acquisition channel apparatus
[AD-D011428] 08 p1159 N85-17311
Electromagnetic inspection of wire ropes using sensor arrays
[AD-A148317] 08 p1170 N85-17379
Lidar studies of temperature and density using Rayleigh scattering 08 p1184 N85-17459
Programmable realtime interface between a block floating point processor and memory
[AD-D011431] 08 p1203 N85-17571
Multidimensional digital signal processing
[AD-A148055] 08 p1205 N85-17585
Multiple channel adaptive filtering using a fast orthogonalization network: An application to efficient pulsed Doppler radar processing
[AD-A147929] 08 p1211 N85-17619
Robust linear filtering for multivariable stationary time series, part 3
[AD-A148169] 08 p1212 N85-17627
Calculation of cumulative distributions and detection probabilities in communications and optics
[AD-A147761] 08 p1215 N85-17650
Research in stochastic processes
[AD-A148622] 08 p1216 N85-17660
Nonlinear real-time optical signal processing
[AD-A148293] 08 p1222 N85-17699
Matrix-matrix multiplication using an electrooptical systolic-engagement array processing architecture
[AD-D011410] 08 p1223 N85-17704
Subjective evaluation of the effect of noise and interference on frequency modulated NTSC television signals
[CRC-1367] 09 p1310 N85-18230
Multivariable Autoregressive Moving Average (ARMA) models: A time approach to antenna processing
[ENST-84E015] 09 p1313 N85-18252
Signal Hill solar-powered repeater report and recommendations
[DE85-000487] 09 p1316 N85-18273
Neurocognitive pattern analysis of an auditory and visual numeric motor control task. Part 1: Development of methods
[AD-A148809] 09 p1364 N85-18578
Survey of VLF-OMEGA transmissions received during summer at Antarctic peninsula
[INPE-3399-PRE/666] 10 p1462 N85-19223
Performance of the DSA's subcarrier demodulation digital loop 10 p1465 N85-19242
The ambiguity function of random binary-phase-coded waveforms
[AD-A148906] 10 p1466 N85-19249
An object-oriented signal processing environment: The knowledge-based signal processing package
[AD-A148963] 10 p1466 N85-19251
Adaptive signal processing for radio communications 10 p1473 N85-19295
Time and space domain filtering for improved HF communication 10 p1473 N85-19298
Overview of RADC adaptive antenna developments for communications 10 p1474 N85-19299
Asynchronous transmission with strong spectral spread 10 p1474 N85-19300
Effective millimeter wave transmission under severe multipath conditions 10 p1475 N85-19306
On the probability density of signal-to-noise ratio in an improved adaptive detector, part 1
[AD-A148856] 10 p1550 N85-19772
Elimination of sensor artifacts from infrared data
[AD-A149048] 10 p1556 N85-19814
Optical implementation of the synthetic discriminant function
[AD-A149562] 10 p1557 N85-19817
Signal processing and range spreading in the FM-CW radar
[PB85-108256] 11 p1626 N85-20239
Processing circuit with asymmetry corrector and convolutional encoder for digital data
[NASA-CASE-MSC-20187-1] 11 p1628 N85-20249
Optical eigenvector
[AD-A149550] 11 p1729 N85-20871
Direction finder set, radio
[AD-A149958] 12 p1775 N85-21142
Detection of angular modulated electromagnetic signals
[AD-D011563] 12 p1823 N85-21437
Digital coherent detector
[AD-D011560] 12 p1833 N85-21501
Tubes and transistors in audio amplifiers 12 p1837 N85-21532
Summator of radio pulse signals 12 p1839 N85-21539
Synthesis of optimum receiver and processor for signal packet of radio pulses 12 p1839 N85-21541
Multichannel digital processing of wideband signals 12 p1840 N85-21548
Optimal discrete filtration of intricate phase-keyed signals 12 p1840 N85-21550
Retinal information mapping system
[AD-D011531] 12 p1849 N85-21601
Application of homomorphic signal processing to stress wave factor analysis
[NAS 1.26:174871] 12 p1861 N85-21673
Seismic observation of infrasonic signals
[AD-A149574] 12 p1869 N85-21853
Electrical characterization of analog microprocessors
[AD-A149629] 12 p1911 N85-21995
Instrumentation award
[AD-A150081] 12 p1912 N85-21999
Topics in optical materials and device research, 3: Volume 1
[AD-A149726] 12 p1933 N85-22145
Switchable zero order diffraction gratings as light valves
[AD-A150129] 12 p1934 N85-22153
The future of lightwave technology
[PB85-109759] 12 p1935 N85-22155
Approaches and algorithms for robust signal processing 13 p2062 N85-22878
Acousto-optically addressed Fourier transform matched filters
[AD-A150296] 13 p2063 N85-22889
Two-dimensional signal processing and storage and theory and applications of electromagnetic measurements
[AD-A150590] 13 p2065 N85-22899
USSR report: Electronics and electrical engineering
[JPRS-UEE-85-002] 13 p2066 N85-22907
Assessment of effectiveness of signal-code constructions in time division-multi-access satellite systems 13 p2066 N85-22908
Processing of signals in experiments with scattering of short radio pulses by conducting sphere 13 p2068 N85-22917
Dispersion of phase-shift keyed systems with fixed number of blocks 13 p2070 N85-22928
Noise tolerance of digital demodulator for complex signal system employing binary quantization 13 p2070 N85-22929
Combined processing method and matched filter for discrete composite frequency phase-shift keyed signal 13 p2070 N85-22931
Space-time response characteristics of acoustooptic filter for compression of linearly frequency-modulated signal 13 p2071 N85-22937
Dynamics of adaptive signal corrector 13 p2071 N85-22940
Spectra of incidental interference resulting from nonlinear conversion of signals from transmitters 13 p2073 N85-22950
Models of discontinous random fields 13 p2079 N85-22963
Synthesis of optimum single-channel discrete signals and filters 13 p2080 N85-22990
Synthesis of optimum algorithms for secondary processing 13 p2080 N85-22992
Factorized algorithms for combined spatial and temporal processing of radar signals 13 p2081 N85-22997
Electrothermal transducer with short time constant 13 p2088 N85-23040
Acoustooptic demodulation of frequency-modulated signals 13 p2090 N85-23050
Optical processing in radon space
[AD-A150289] 13 p2159 N85-23402
Condition monitoring of helicopter gearboxes using automatic vibration analysis techniques 14 p2223 N85-23790
Six-inch HYGE vertical impact facility
[AD-A150665] 14 p2226 N85-23809
Multidimensional digital signal processing
[AD-A150833] 14 p2292 N85-24209
Advanced detectors and signal processing for bubble memories
[NASA-CR-172534] 14 p2297 N85-24219
Design, fabrication and testing of a multibeam forming network
[NASA-CR-175695] 14 p2298 N85-24228
Picosecond lidar techniques in laboratory and field diagnostics
[AD-A150755] 14 p2309 N85-24294
Annual report on electronics research at the University of Texas at Austin
[AD-A150836] 14 p2415 N85-24901
USSR report: Electronics and electrical engineering
[JPRS-UEE-85-005] 15 p2524 N85-25565
Space processing of acoustic signals in plane-parallel waveguide — antenna arrays 15 p2525 N85-25572
Converters of sum/difference of codes to frequency 15 p2526 N85-25578
Analysis of spectral characteristics of multilevel digital computing synthesis 15 p2527 N85-25579
MHB4046 phase-lock circuit 15 p2533 N85-25629
Additional PLL designs 15 p2534 N85-25632
Receiver optimization for detection in doubly spread communication channels
[AD-A151228] 15 p2541 N85-25689
Statistical techniques for signal processing
[AD-A151231] 15 p2541 N85-25690
Nonparametric detection of narrowband signals
[AD-A151280] 15 p2542 N85-25691
Processing speech for analysis using optical Fourier techniques
[AD-A151898] 15 p2544 N85-25704
Conversion of algorithms to custom integrated circuit devices
[AD-A151288] 15 p2547 N85-25720
Wavelength dependent, tunable, optical time delay system for electrical signals
[AD-D011584] 15 p2548 N85-25725
Parallel programmable charge domain device
[AD-D011599] 15 p2549 N85-25733
Radar measurement of thickness of drifting ocean ice employing cepstral signal processing 15 p2644 N85-26313
Ultrasonic characterization of porosity: Theory
[DE85-005922] 15 p2648 N85-26325
Mode dependent, optical time delay system for electrical signals
[AD-D011596] 15 p2653 N85-26363
Three new fiber-optic components
[DE85-006289] 15 p2653 N85-26364
The impact of VLSI on guidance and control system design 16 p2697 N85-26654
Synchronizing heavily encoded data in bad weather 16 p2770 N85-27099
Symbol stream combining in a convolutionally coded system 16 p2771 N85-27101
High-speed digital baseband mixer 16 p2771 N85-27103
Signal processing for the analysis of transient electromagnetic data
[DE85-007244] 16 p2774 N85-27125
The origin of brain potentials associated with selective visual attention
[AD-A152291] 16 p2840 N85-27511
Algorithms for determining the relative complexity of dynamic signals
[BLL-M-98111-(5828.4)] 16 p2851 N85-27574
Topics in time delay estimation
[AD-A152231] 16 p2855 N85-27607
Performance analysis of the DSN baseband assembly (Bba) Real-Time Combiner (RTC)
[NASA-CR-175878] 17 p2946 N85-28190
Digital methods of the optimum processing of radar signals
[AD-A152469] 17 p2948 N85-28202
Pipelined programmable charge domain device
[AD-D011598] 17 p2951 N85-28225
Research on superconductive signal-processing devices
[AD-A152703] 17 p2953 N85-28235
A plan for the development of inertial reconstruction of initial state clock (IRIS) 17 p2966 N85-28317
Studies of optical-beam phase-conjugation by nonlinear refraction
[AD-A152865] 17 p3037 N85-28788
An approach to digital level compression using the zero-crossing points of programme signals
[NHK-LABS-NOTE-308] 18 p3090 N85-29123

Theoretical investigations of the propagation and interactions of surface waves
[AD-A153548] 18 p3165 N85-29753
Digital Optical Circuit Technology
[AGARD-CP-362] 18 p3165 N85-29757
Prospects for parallel nonlinear optical signal processing using GaAs etalons and ZnS interference filters
18 p3167 N85-29765
Multiport optical detectors 18 p3167 N85-29769
Optical techniques for signal distribution and control in advanced radar and communication systems
18 p3168 N85-29773
A study of reflex optoelectronic switching matrices and their derivatives
[CRC-TN-720] 19 p3253 N85-30169
Orthogonalizer for inphase and quadrature digital data
[AD-D011679] 19 p3254 N85-30174
Control and regulation of generalized linear systems
19 p3257 N85-30193
A single chip VLSI architecture for radar signal processing 19 p3257 N85-30195
Linear time-invariant, space-variant filters and the WKB approximation with applications to underwater acoustic signal processing
[AD-A154250] 19 p3352 N85-30775
A 406 MHz ELT processor for geostationary satellites — Emergency Locator Transmitter (ELT)
20 p3403 N85-31114
Adaptive identification and control of structural dynamics systems using recursive lattice filters
[NASA-TP-2371] 20 p3407 N85-31142
Swedish program for sensor research, development
20 p3438 N85-31338
Scattering models in signal processing
20 p3439 N85-31339
Fast eigenvector methods for digital signal processing
20 p3439 N85-31341
Hierarchical beamforming with application to a large aperture array system 20 p3439 N85-31345
Combined trellis coding with asymmetric MPSK modulation: An MSAT-X report
[NASA-CR-176039] 20 p3440 N85-31347
Synthetic aperture radar data processing — satellite-borne radar
[CNES-196-T-CT/DRT/TIT/RL]
20 p3442 N85-31363
Digital signal processing for spaceborne synthetic aperture radar
[FOA-C-30361-E1] 20 p3442 N85-31364
Center for Electronics and Electrical Engineering technical progress bulletin covering center programs, April-June 1984 with 1984 CEEE (Center for Electronics and Electrical Engineering) events calendar, issue 7
[PB85-187540] 20 p3450 N85-31419
Forth system for coherent-scatter radar data acquisition and processing
[NASA-CR-176055] 20 p3494 N85-31720
An overview of nonlinear systems identification
[RR-271] 20 p3520 N85-31894
Spectral methods for the estimation of acoustic intensity, energy density, and surface velocity using a multimicrophone probe 20 p3524 N85-31916
Particle sizing from forward scattered light at two angles using a Variable-Focal-Length optical system
[AD-A154164] 20 p3533 N85-31980
Electronics Division research and development
[DE85-011867] 20 p3540 N85-32032
A phase-locked frequency multiplier for the signal averaging of the vibration of the Wessex helicopter input spiral bevel pinion
[AD-A154914] 21 p3555 N85-32113
Calibration and use of clutter data for simulation
[AD-A154793] 21 p3574 N85-32229
Compression of spread spectrum signals on an excessively dispersive channel
[AD-A155184] 21 p3576 N85-32240
A high-speed digital signal processor for atmospheric radar, part 7.3A 21 p3626 N85-32525
Qualitative analysis of sign-bit processing
[AD-A154776] 21 p3671 N85-32804
Bayesian vs MAP multiple model adaptive estimation for field of view expansion in tracking airborne targets
[AD-A155466] 21 p3679 N85-32855
Solid state research
[AD-A154783] 21 p3709 N85-33025
USSR report: Electronics and electrical engineering
[JPRS-UEE-84-015] 22 p3762 N85-33314
Signal processing in quasi-holographic system as an inverse problem 22 p3762 N85-33315
Method of static measurements of absolute scattering matrix of radar targets 22 p3762 N85-33316
Characteristics of digital range finder with stroboscopic discretization 22 p3762 N85-33319
Amplitude stabilization of pulse signals
22 p3762 N85-33320
Potential coordinate estimate accuracy estimation accuracy by multiposition radar systems
22 p3763 N85-33322
Optimal complex nonlinear processing of continuous and pulsed signals 22 p3763 N85-33323
Variation in radiowave propagation conditions in corona during solar activity cycle 22 p3763 N85-33327
Adaptive synthesis of antennas with separation of signals by direction of arrival 22 p3764 N85-33328
Probabilistic analysis of automatic control systems for detection systems 22 p3765 N85-33335
Transformation of spectrum of phase-code keyed signal for scanning in time 22 p3765 N85-33338
Synthesis of optimum receiver and processor for interfering radio pulse signals 22 p3769 N85-33361
Design of digital bandpass filters with finite memory
22 p3775 N85-33392
Method of designing digital band-pass filters with pulse response of finite duration 22 p3775 N85-33395
Generalization of discrete Fourier transform for interpolation in time domain 22 p3775 N85-33396
Generalization of discrete Fourier transformation for interpolation in time domain 22 p3776 N85-33400
Controllable companding in low-frequency FM radio communication systems 22 p3776 N85-33402
Synthesis of system with nonideal components for optimal processing of radio signal
22 p3777 N85-33405
General design principles of high speed frequency synthesizers based on phase synchronization systems
22 p3779 N85-33417
Methods for the optical processing of signals
[DRIC-T-7439] 22 p3844 N85-33809
The improved display of 625-line television pictures: Adaptive interpolation
[BBC-RD-1985/5] 23 p3925 N85-34328
A general purpose image processing package
23 p3961 N85-34549
Nonlinear digital phase-locked loops with application to Loran-C receivers 24 p4063 N85-35178
Advanced detectors and signal processing
[NASA-CR-176193] 24 p4068 N85-35343
Aspects of input signal design for order and parameter estimation in linear dynamical systems
[ER-83/05] 24 p4091 N85-35362
SIG: A general-purpose signal processing program. User's manual: Revision 1
[DE85-013035] 24 p4140 N85-35662

SIGNAL RECEPTION
NT SYMBOLS
NT TELEVISION RECEPTION
Reflector antenna having sidelobe suppression elements
[AD-D011227] 01 p0039 N85-10244
Detection, classification, and extraction of helicopter-radiated noise
[AD-A145993] 03 p0416 N85-12661
Analysis of threshold effects during estimation of arrival time of optical signals 07 p0951 N85-16030
Structure of frequency modulated and phase-shift keyed signals reflected from ionosphere at near-critical frequencies 07 p0952 N85-16035
DSN 34-meter antenna optics analysis for wideband SETI investigations 10 p1465 N85-19244
Base communications issues for the 1980s
[AD-A149764] 12 p1828 N85-21474
Optimal threshold and weight sorting of elevation angle readings under conditions of fadeouts of a directed signal 12 p1840 N85-21547
Error probability during optimal noncoherent reception of binary signals in multibeam channel
13 p2069 N85-22922
Regular synthesis of pairs of phase-keyed binary minimax signals 13 p2069 N85-22923
Interference immunity of binary systems with second-order phase-difference modulation in various reception modes 13 p2072 N85-22944
Reception of signal with unknown amplitude and duration submerged in white noise 13 p2064 N85-23016
Reception noise immunity of multiposition signals
13 p2065 N85-23023
Measurement results from a balloon experiment simulating land mobile satellite transmissions
[NASA-CR-175740] 15 p2540 N85-25683
Global positioning system carrier phase: Description and use
[PB85-174126] 19 p3216 N85-29946
Specifics of laser sounding of atmosphere along horizontal and slightly slanting paths over water surface
19 p3297 N85-30441
Study of the interferences of 2 GHz radio beams with a DORIS system — precise low orbit determination system (DORIS)
[CNES-CT/DRT/TIT/RL-84/140-T]
20 p3442 N85-31362

SIGNAL REFLECTION
Potential effectiveness of spatial processing in detecting signals against background of interfering reflections
07 p0952 N85-16032
Velocity inversion using a stratified reference
[AD-A150082] 12 p1689 N85-21858
Parameters of amplitude-modulated signal upon reflections 13 p2076 N85-22986
Axial focusing of signal from distant point radiator reflected twice in deep paraboloid
13 p2078 N85-22979
Digital RF delay line for ECM (electronic countermeasure) look-through
[AD-A152120] 16 p2774 N85-27120
Kirchhoff modeling via wave equation datuming
[AD-A152399] 17 p3028 N85-28727
Small-scale structure of ionospheric F-region
19 p3297 N85-30440
A random layer model for reflection from ocean bottom sediments
[AD-A155019] 21 p3700 N85-32988
Theoretical and experimental analyses of the performance of two-color laser ranging systems
[NASA-CR-176159] 23 p3936 N85-34397

SIGNAL TO NOISE RATIOS
A limbus-sensing eye movement recorder
[AD-A144772] 01 p0049 N85-10323
The development of a diode laser Doppler velocimeter for boundary layer measurements under ice: A feasibility investigation
[AD-A145076] 01 p0053 N85-10348
A Monte Carlo comparison of the recovery of winds near upwind and downwind from the SASS-1 model function by means of the sum of squares algorithm and a maximum likelihood estimator
[NASA-CR-3839] 01 p0064 N85-10421
Radio telemetry formula applications. A practical users guide
[AD-A146247] 03 p0356 N85-12288
Algorithm for astronomical, extended source, signal-to-noise radio calculations
[NASA-TP-2396] 03 p0445 N85-12833
Algorithm for astronomical, point source, signal to noise ratio calculations
[NASA-TP-2397] 03 p0445 N85-12834
Television transmission in frequency modulation
04 p0493 N85-13146
Thermal shock as a carbide grade development tool
[DE84-016939] 04 p0509 N85-13251
Synthesis of systems for coherent weighted signal processing against background of correlated interference 06 p0790 N85-15045
Efficiency in integral active antennas
06 p0792 N85-15060
A noise-suppressing digital frequency meter
06 p0796 N85-15084
Reference oscillator stability effect on clutter cancellation in a radar system 07 p0938 N85-15946
Improved digital baseband transmission by application of maximum likelihood decoding to an 8-level signal generated by convolution and block coding
[FI-44-TBR-93] 07 p0942 N85-15973
Some applications of signal-to-noise in photographic stellar photometry 07 p0966 N85-16132
Electro-optical target detection
[AD-D011366] 07 p1042 N85-16617
Measurement of signal separation between radio service and air navigation service
[IRT-TB-B-40/82] 08 p1063 N85-16860
Configuration study for a 30 GHz monolithic receive array, volume 2
[NASA-CR-174697-VOL-2] 09 p1311 N85-18240
Further results on rate 1/N convolutional code constructions with minimum required SNR criterion
10 p1464 N85-19235
Performance of the DSA's subcarrier demodulation digital loop 10 p1465 N85-19242
On the probability density of signal-to-noise ratio in an improved adaptive detector, part 1
[AD-A148656] 10 p1550 N85-19772
The noise of laser diodes with modulated injection current
[FI-465-TBR-23] 11 p1625 N85-20233
Detection of angular modulated electromagnetic signals
[AD-D011563] 12 p1823 N85-21437
Fundamental limits to synchronization and tracking
[AD-A149623] 12 p1833 N85-21504
Optimal threshold and weight sorting of elevation angle readings under conditions of fadeouts of a directed signal 12 p1840 N85-21547
Shuttle flight test of an advanced gamma-ray detection system
[AD-A150316] 13 p1988 N85-22469
Moving target detection 13 p2067 N85-22915

Theory of optimum M-filtration of signals against background of correlated interference
13 p2069 N85-22927
Performance of time-position discriminator of composite signal 13 p2072 N85-22941
Effect of variance of photoreceiver frequency characteristics on characteristics of measuring instruments 13 p2076 N85-22965
Accuracy of approximation of Bayes estimates in presence of noninformative parameters
13 p2084 N85-23015
Reception of signal with unknown amplitude and duration submerged in white noise 13 p2084 N85-23016
Synthesis of quasi-optimum algorithms for signal recognition against background of correlated noise employing discrete spectral transformations
13 p2085 N85-23020
Noise tolerance of diversity reception in frequency-adaptive digital transmission systems
13 p2086 N85-23024
Algorithms for reconstruction of partially known, band limited Fourier transform pairs from noisy data
[AD-A150194] 13 p2150 N85-23347
An examination of signal-to-noise enhancement at the Edzell CDAA (Circular Disposed Antenna Array)
[AD-A150708] 14 p2291 N85-24204
Frequency selective signals-to-noise enhancer/limiter apparatus
[AD-D011583] 15 p2548 N85-25724
Performance of charge-injection-device infrared detector arrays at low and moderate backgrounds
[NASA-TM-86667] 15 p2560 N85-25793
On the probability density of signal-to-noise ratio in an improved detector
[AD-A152529] 17 p2952 N85-28232
Experimental performance of a frequency measurement circuit
[AD-A152951] 17 p2953 N85-28239
Improved high performance television receiver
[PB85-170751] 18 p3092 N85-29139
Modulation using four phase levels. Theoretical study of the degradation caused by a spurious phase modulation
[CNES-83/219/CT/DRT/TIT/TR]
20 p3441 N85-31360
Sidelobe reduction of Barker codes, part 7.1C
21 p3625 N85-32522
Qualitative analysis of sign-bit processing
[AD-A154778] 21 p3671 N85-32604
Sensitivity of compressive receivers
[FOA-C-30385-E4] 22 p3756 N85-33288
Adaptive corrector operating in frequency domain
22 p3765 N85-33337
Estimate of signal-to-interference energy ratio in discrete-data transmission 22 p3776 N85-33398
A new array for the study of ultra high energy gamma-ray sources
[OG-9.4-7] 23 p4029 N85-34974
Astrophysical applications of high angular resolution array-telescopes
[OG-9.5-7] 23 p4031 N85-34984
Search for acoustic signals from high energy cascades
[HE-7.1-1] 24 p4213 N85-36155
Acoustic detection of air shower cores
[HE-7.1-4] 24 p4213 N85-36158

SIGNAL TRANSMISSION
NT CODE DIVISION MULTIPLE ACCESS
NT DATA TRANSMISSION
NT FREQUENCY DIVISION MULTIPLE ACCESS
NT IONOSPHERIC PROPAGATION
NT MANDELSTAM REPRESENTATION
NT MICROWAVE ATTENUATION
NT MICROWAVE TRANSMISSION
NT MULTIPATH TRANSMISSION
NT MULTIPLE ACCESS
NT PCM TELEMETRY
NT RADAR TRANSMISSION
NT RADIO TELEMETRY
NT RADIO TRANSMISSION
NT SATELLITE TRANSMISSION
NT SHORT WAVE RADIO TRANSMISSION
NT SINGLE CHANNEL PER CARRIER TRANSMISSION
NT SINGLE SIDEBAND TRANSMISSION
NT TELEMETRY
NT TELEVISION TRANSMISSION
NT TRANSEQUATORIAL PROPAGATION
An optically isolated amplifier
[CSIR-SR-ELEK-257] 01 p0049 N85-10321
Development of a microcomputer coupled atmospheric and oceanic boundary layer prediction model
[AD-A146334] 03 p0397 N85-12530
Detailed performance calculations: Georgia Institute of Technology Group, appendix E
05 p0676 N85-14342
Hardwire missile receiver coupler
[AD-D011350] 07 p0937 N85-15936
Improved digital baseband transmission by application of maximum likelihood decoding to an 8-level signal generated by convolution and block coding
[FI-44-TBR-93] 07 p0942 N85-15973
NTT (Nippon Telegraph and Telephone Public Corporation) develops new optical fiber
10 p1478 N85-19311
Effect of interfacial characteristics of metal clad polymeric substrates on electrical high frequency interconnection performance
[NASA-TM-86948] 11 p1624 N85-20223
Signal propagation delay, wire length distribution and the efficiency of VLSI circuits
[CWI-CS-R8412] 11 p1630 N85-20266
Circuit topology, signal propagation delay and the efficiency of VLSI circuits
[CWI-CS-R8414] 11 p1630 N85-20267
The use of a high-speed 12-bit A/D converter for digital sampling of communication signal carriers
[AD-A150578] 13 p2056 N85-22872
Analysis and design of linear microwave transistor amplifiers 13 p2088 N85-23036
Frequency selection for dispersion signal in satellite communication lines 15 p2528 N85-25584
Signal flow model for sequential logic built from combinational logic elements and its implementation in Prolog
[DE85-005792] 15 p2549 N85-25734
Measurements of VHF/UHF radio propagation in a maritime temperate climate
[CRC-1380] 18 p3069 N85-29119
The determination of daily usage or occupancy in the land-mobile band 138-174 MHz at Montreal
[CRC-1383] 19 p3253 N85-30167
Combined trellis coding with asymmetric MPSK modulation: An MSAT-X report
[NASA-CR-176039] 20 p3440 N85-31347
Center for Electronics and Electrical Engineering technical progress bulletin covering center programs, April-June 1984 with 1984 CEEE (Center for Electronics and Electrical Engineering) events calendar, issue 7
[PB85-187540] 20 p3450 N85-31419
Testing and optimizing MST coaxial collinear arrays, part 6.4A 21 p3625 N85-32518
Criteria and algorithms for spectrum parameterization of MST radar signals 21 p3626 N85-32527
Transformation of spectrum of phase-code keyed signal for scanning in time 22 p3765 N85-33338
Digital matched filter 22 p3765 N85-33339
Optimum predistortion of digital signals for transmission over parallel channels 22 p3776 N85-33397
Photothyristor optrons and optron microcircuits, part 1
22 p3781 N85-33424
Characteristics of optical information-measurement channels with utilization of scattering effects
22 p3781 N85-33429
Signal space models for antenna arrays
[AD-A156063] 24 p4087 N85-35335

SIGNALS
Digital sound: Programme-modulated noise levels in sound signals subjected to a number of digital companding processes
[BBC-RD-1984/11] 09 p1310 N85-18233
Evaluation of parameters of a signal (selected pages)
[AD-A148831] 09 p1312 N85-18243

SIGNATURE ANALYSIS
Description of the Dutch-Danish (DUDA) scanner — thermal signatures
[AD-B084893] 01 p0121 N85-10826
Basic principles, methodology, and applications of remote sensing in agriculture
[E85-10016] 02 p0217 N85-11429
The monitoring of machines
[CETIM-15-J-041] 04 p0510 N85-13253
Solar physics applications of computer graphics and image processing 18 p3208 N85-29903
Hardware test program for evaluation of baseline range-range rate sensor concept
[NASA-CR-176143] 23 p3933 N85-34377

SIGNATURES
NT MAGNETIC SIGNATURES
NT RADAR SIGNATURES
NT SPECTRAL SIGNATURES
Joint services electronics program
[AD-A145085] 01 p0042 N85-10276
Digital signatures: An update
[NPL-DITC-51/84] 09 p1367 N85-18589
Real-time automated detection of mesocyclones and tornado vortex signatures
[AD-A154998] 21 p3635 N85-32578

SIGNS (SYMBOLS)
U SYMBOLS

SIGNS AND SYMPTOMS
The effects of prolonged feeding meal, ready-to-eat (MRE) operational rations
[AD-A154763] 21 p3666 N85-32773
Labyrinthine and extralabyrinthine mechanisms of development of motion sickness in weightlessness
22 p3821 N85-33668
A review of motion sickness with special reference to simulator sickness
[AD-A155975] 24 p4131 N85-35611

SIKORSKY AIRCRAFT
NT UH-60A HELICOPTER

SILANES
NT CHLOROSILANES
Chemical vapor deposition of amorphous silicon films produced by using higher order silanes
[DE84-004519] 01 p0123 N85-10847
The silane interphase of composites: Effects of process conditions on gamma-aminopropyltriethoxysilane
[AD-A145578] 02 p0171 N85-11143
Laser spectroscopy and gas-phase chemistry in CVD
[DE84-014959] 02 p0173 N85-11158
Factor analysis applied to a silane coupling agent on E-glass fiber system
[AD-A145687] 02 p0187 N85-11249
Structure of silane coupling agents adsorbed on silicon powder
[AD-A145803] 03 p0327 N85-12105
Development of acceptance criteria for batches of silane primer for external tank thermal protection system bonding applications
[NASA-CR-171266] 04 p0478 N85-13043
Development of a polysilicon process based on chemical vapor deposition of dichlorosilane in an advanced Siemen's reactor
[NASA-CR-174148] 04 p0483 N85-13083
Electrical properties of 10-50 nm TEOS (Tetraethoxysilane) LPCVD (Low Pressure Chemical Vapor Deposition) films
[AD-A146416] 06 p0803 N85-15111
Electrochemical production of silicon
06 p0832 N85-15290
Theoretical studies of the ignition and combustion of silane-hydrogen-air mixtures
[NASA-CR-3876] 10 p1433 N85-19032
Development of a polysilicon process based on chemical vapor deposition of dichlorosilane in an advanced Siemen's reactor
[NASA-CR-174445] 11 p1672 N85-20532
Process for producing tris s(n-methylamino) methylsilane
[NASA-CASE-MFS-25721-1] 12 p1799 N85-21280
Ignition of mixtures of SiH sub 4, CH sub 4, O sub 2, and Ar or N sub 2 behind reflected shock waves
[NASA-TP-2415] 13 p1974 N85-22395
Development of acceptance criteria for batches of silane primer for external tank thermal protection system bonding applications
[NASA-CR-171428] 14 p2259 N85-23998
Development of acceptance criteria for batches of silane primer for external tank thermal protection system bonding applications
[NASA-CR-171436] 15 p2518 N85-25523
Development of acceptance criteria for batches of silane primer for external tank thermal protection system bonding applications
[NASA-CR-175850] 16 p2754 N85-26995
Self-developing polysilane deep-UV resists: Photochemistry, photophysics and submicron lithography
[DE85-007608] 19 p3237 N85-30057
A fluidized-bed reactor for silane pyrolysis
21 p3609 N85-32413
Modeling of the silane FBR system
21 p3609 N85-32415
Silicon production in an aerosol reactor
21 p3609 N85-32416
Monosilane and disilane, 1984 report
[DE85-008776] 22 p3752 N85-33282
1985 Amorphous Silicon Review Meeting
[DE85-008794] 22 p3807 N85-33582
Dual-chamber plasma deposition of A-Si:H solar cells at high rates using disilane
[DE85-011626] 23 p3946 N85-34451

SILENCERS
Exhaust systems for passenger vehicles: Test procedure for resistance to internal corrosion of silencers
[BLL-BISI-TRANS-22360-(9022.09)]
17 p2973 N85-28361

SILICA
U SILICON DIOXIDE

SILICA GEL
Structure and chemistry of sol-gel derived transparent silica aerogel
[DE85-009902] 20 p3434 N85-31309

The Silica Aerogel Detector (SAD) story — Cherenkov detector
[USIP-84-14] 20 p3459 N85-31465

SILICA GLASS
Optical contacting for gravity probe star tracker
[NASA-TM-86475] 01 p0120 N85-10819
Emissivity enhancement of fused silica for space applications — solar cells 13 p2011 N85-22615
Downdraw extrusion of ULE(TM) glass
[AD-A153783] 18 p3079 N85-29048

SILICATES
NT ALUMINUM SILICATES
NT BERYL
NT ENSTATITE
NT FELDSPARS
NT GARNETS
NT PYROXENES
NT SODIUM SILICATES
NT YTTRIUM-ALUMINUM GARNET
NT YTTRIUM-IRON GARNET
NT ZEOLITES
Impact cratering: The process and its effects on planetary evolution — and silicate-carbonate reactions on Venus
[NASA-CR-174016] 02 p0228 N85-11488
The effect of temperature on the radiation induced losses of large diameter GPS (Germanium phosphosilicate) and GBS core optical fibers
[AD-A145409] 02 p0260 N85-11823
The problem of iron partition between Earth and Moon during simultaneous formation as a double planet system 04 p0687 N85-13744
Dynamic crystallization of silicate melts
[NASA-CR-174103] 05 p0743 N85-14774
Calculation of energy of atomization in silicate tetrahedron Si4(4-)
[BLL-M-36000-(5828.4)] 07 p1040 N85-16599
A circum-terrestrial compositional filter 13 p2179 N85-23620
Quenching effects on iron site partitioning in the Apollo 17 orange glass composition 13 p2184 N85-23553
Experimental methods for quenching structures in lunar-analog silicate melts: Variations as a function of quench media and composition 13 p2184 N85-23554
Mechanical properties of lunar materials under anhydrous, hard vacuum conditions: Applications of lunar glass structural components
[DE85-006662] 16 p2901 N85-27271
Influence of eutectic silicate inclusions on micro-processes during deformation and fracture of 12GS steel
[BLL-BISI-TRANS-22296-(9022.09)] 17 p2929 N85-28073
Model for the growth of fractal silica polymers
[DE85-007864] 17 p2935 N85-28115
Chemical constraints on the evolution of Archean continental crust 21 p3722 N85-33093
Dating Archean zircon by ion microprobe: New light on an old problem 21 p3722 N85-33094
Thermodynamic data for mineral technology
[PB85-184391] 22 p3803 N85-33560
Volatile loss following very large impacts 22 p3653 N85-33662

SILICIDES
NT DISILICIDES
Electronic transport processes in refractory metal silicides
[AD-A148495] 06 p0661 N85-15468
Preparation and electronic properties of MoS(2) and WS(2) single crystals grown in the presence of cobalt
[AD-A146508] 06 p0666 N85-15506
Improving operational properties of titanium alloys by diffusion siliciding 11 p1602 N85-20075
Thin films properties of sputtered niobium silicide on SiO2, SiN4 and on n+ poly-Si
[AD-A152378] 17 p2952 N85-26226
Silicide conductors reliability research
[AD-A153768] 18 p3095 N85-29157
Contact properties of rare-earth silicides and germanides on Si and Ge 19 p3374 N85-30931
Flux-line lattice anisotropy in V3Si: Observation and interpretation
[DE85-011935] 23 p3965 N85-34713

SILICON
NT SILICON ISOTOPES
Center for Electronics and Electrical Engineering Technical Bulletin covering center programs
[PB84-218056] 01 p0045 N85-10296
Process Research of Polycrystalline Silicon Material (PROPSM)
[NASA-CR-173838] 01 p0067 N85-10446
Energy deposition in microvolumes of silicon from high energy proton reactions
[AD-A144713] 01 p0123 N85-10845
Studies of laser melting and rapid solidification using amorphous silicon
[DE84-014737] 02 p0202 N85-11345
Silicon sheet with molecular beam epitaxy for high efficiency solar cells
[NASA-CR-174022] 02 p0222 N85-11459
Hydrogen passivation of electrically active defects in crystalline silicon solar cells
[DE84-004590] 02 p0223 N85-11461
Large-area sheet task advanced dendritic web growth development
[NASA-CR-174021] 02 p0223 N85-11463
Research on crystalline silicon solar cells
[DE84-114591] 02 p0223 N85-11465
Optimized conditions for the formation of buried insulating layers in Si by high dose implantation of oxygen
[DE84-015369] 02 p0288 N85-11882
Structure of silane coupling agents adsorbed on silicon powder
[AD-A145803] 03 p0327 N85-12105
NBS (National Bureau of Standards): Materials measurements
[NASA-CR-174036] 03 p0332 N85-12143
Application of a silicon compiler to VLSI (Very Large Scale Integrated circuits) design of digital pipelined multipliers
[AD-A146328] 03 p0403 N85-12569
A study of defects in neutron transmutation doped silicon: Gallium by hall effect analysis
[AD-A146047] 03 p0433 N85-12758
Thermodynamics and phase equilibria in the vanadium-silicon system
[AD-A145870] 03 p0435 N85-12769
Preparation of low-silicon vanadium metal
[DE84-014818] 04 p0476 N85-13031
Effect of barrier height on friction behavior of the semiconductors silicon and gallium arsenide in contact with pure metals
[NASA-TP-2405] 04 p0478 N85-13044
Photoconductivity and emission from the impurity excited states in silicon
[DE84-015563] 04 p0479 N85-13052
Investigation of effect of photocurrent amplification in meta-dielectric-semiconductor structures based on silicon 04 p0488 N85-13110
NMOS test chip for a course in semiconductor parameter measurements
[PB84-216506] 04 p0497 N85-13174
Silicon for solar cells
[DE84-004503] 04 p0529 N85-13361
CO-2-silica geothermometer for low temperature geothermal resource assessment, with application to resources in the Safford Basin, Arizona
[DE84-013958] 04 p0534 N85-13411
On the origins of structural defects in BF2(+)-implanted and rapid thermally annealed silicon: Conditions for defect free regrowth
[DE84-016060] 04 p0572 N85-13650
Trends in space photovoltaic technology 05 p0609 N85-13866
Testing of production of silicon-titanium-magnesium alloying composition
[BLL-M-35904-(5828.4)] 05 p0616 N85-13937
Process research of polycrystalline silicon material (PROPSM)
[NASA-CR-174130] 05 p0619 N85-13962
Solar generators made of amorphous silicon 05 p0662 N85-14257
Material models and device structures for GaAs solar cells
[DE85-000501] 05 p0665 N85-14275
GaAs material properties and models 05 p0665 N85-14277
Electron channeling and EBIC studies of polycrystalline silicon sheets
[DE84-004515] 05 p0670 N85-14309
EPR linewidth studies of unpaired electrons at the Si-SiO2
[DE84-016727] 05 p0733 N85-14712
New methods of fast switching of high power by means of semiconductor devices 06 p0794 N85-15075
Development of technology of silicon single-crystal production semiconductor power devices: State of art outlook 06 p0795 N85-15078
Time-resolved studies of ultrarapid solidification of highly undercooled molten silicon formed by pulsed laser irradiation
[DE84-016684] 06 p0813 N85-15164
Development of high-efficiency solar cells on silicon web
[NASA-CR-174212] 06 p0828 N85-15259
Process research of non-Cz silicon material 06 p0830 N85-15275
Process Research On Polycrystalline Silicon Material (PROPSM) 06 p0830 N85-15276
Amorphous metallic layers in Si metallization systems 06 p0830 N85-15277
Silicon-sheet surface studies 06 p0831 N85-15287
Investigation of structural and electrical properties of low-angle silicon sheet 06 p0831 N85-15288
Semicrystalline casting process development and verification 06 p0832 N85-15289
Electrochemical production of silicon 06 p0832 N85-15290
Aerosol reactor for silicon processing 06 p0832 N85-15292
Proceedings of the 22nd Project Integration Meeting
[DE85-000334] 06 p0833 N85-15302
Advances and opportunities in the amorphous silicon research field
[DE84-004526] 06 p0833 N85-15304
Recent developments in photovoltaics
[DE84-004528] 06 p0833 N85-15305
Specialized silicon compilers for language recognition
[AD-A146526] 06 p0853 N85-15425
Charge trapping in low temperature MOS (Metal-Oxide-Silicon) oxides
[AD-A146450] 06 p0860 N85-15467
Evidence for pairing of implanted nitrogen in silicon
[DE84-015622] 06 p0868 N85-15517
Microbiological method for the desiliconization of high-silica bauxites
[BLL-MINTEK-TR-1168-(5810.5759)] 07 p0925 N85-15864
Silicon superlattices. 2: Si-Ge heterostructures and MOS systems
[NASA-CR-174287] 08 p1224 N85-17711
Advanced NMR characterization of zeolite catalysts
[DE85-000458] 09 p1291 N85-18104
Calculations of high-current characteristics of silicon diodes at microwave frequencies
[AD-A147406] 09 p1314 N85-18261
Theory of silicon superlattices: Band structure and mobility enhancement 09 p1396 N85-18789
Influence of the amorphous-crystalline interface morphology on dislocation nucleation in pre-amorphized silicon
[DE85-002068] 09 p1398 N85-18800
Ion beam processes in Si
[DE85-001254] 09 p1399 N85-18808
Single crystal silicon as a low-temperature structural material
[DE84-017469] 09 p1400 N85-18810
The Si/SiO2 intrinsic states and interface charges. Chapter 1: Origin, properties, models, impact
[HMI-B-413] 09 p1400 N85-18812
Calculation of Si(Li) X-ray detector efficiencies
[DE85-002732] 10 p1489 N85-19400
Picosecond laser pulse interactions with metallic and semiconductor surfaces
[AD-A149112] 10 p1490 N85-19405
Stress studies in EFG
[NASA-CR-174441] 10 p1508 N85-19515
Surface and allied studies in silicon solar cells
[NASA-CR-175468] 10 p1508 N85-19516
Investigation of welded interconnection of large area wraparound contacted silicon solar cells
[NASA-CR-174436] 10 p1509 N85-19519
Stress-strain analysis of silicon ribbon
[NASA-CR-175459] 10 p1510 N85-19525
US Amorphous Silicon Research Project
[DE85-000536] 10 p1511 N85-19536
Metal-nonmetal transitions in N-doped many-valley Si and Ge
[INPE-3358-PRE/836] 10 p1562 N85-19648
Microstrain analysis in bent single crystal silicon by double crystal X-ray topography technique
[DE85-000422] 10 p1584 N85-19663
Development of AK18 alloy production technology based on electrothermic silumin 11 p1598 N85-20048
Effect of silicon and titanium properties on N88Co9Mb5Ti steel 11 p1601 N85-20069
Optical second harmonic generation for surface studies
[DE85-000670] 11 p1640 N85-20393
Development of a polysilicon process based on chemical vapor deposition of dichlorosilane in an advanced Siemen's reactor
[NASA-CR-174445] 11 p1672 N85-20532
Research on the basic understanding of high efficiency in silicon solar cells
[DE85-000607] 11 p1672 N85-20537
Electronic structure of silicon superlattices
[NASA-CR-175539] 11 p1736 N85-20916
An episodic red-wing structure of SiIV, lambda 1394A, in gamma Cas 11 p1750 N85-21009
Carbon, silicon, and oxygen in the white dwarf star GD 40 11 p1752 N85-21017

The abundances of the elements -carbon to silicon- in Nova Corona Austrina 1981 11 p1753 N85-21024
Preparation of crystal growth experiments in Spacelab: Si (FSLP), CdTe (D1), ZnS (D1)
[BMFT-FB-W-84-045] 12 p1788 N85-21227
Slip casting and nitridation of silicon powder
[NASA-TM-77609] 12 p1818 N85-21406
Improved silicon grinding method and apparatus
[NASA-CASE-NPO-16336-1-CU] 12 p1819 N85-21407
Factors affecting SOS (Silicon-On-Sapphire) yield and reliability
[AD-A150004] 12 p1835 N85-21515
Crystallization methods for solar cell silicon 12 p1877 N85-21774
Materials refining for solar cell silicon 12 p1877 N85-21775
Flat-plate silicon for solar cells 12 p1877 N85-21776
Silicon band spraying technique for solar cells 12 p1877 N85-21777
Development of silicon nitride materials for the casting of solar cell silicon 12 p1878 N85-21779
Development of new process technologies for solar cells with high efficiency starting from purified silicon 12 p1878 N85-21785
Investigation of the optical properties of solar elements 12 p1879 N85-21786
Pin solar cells made of amorphous silicon 12 p1879 N85-21787
Development of an amorphous silicon panel 12 p1879 N85-21788
Amorphous silicon solar cells with a view to cheap production processes 12 p1879 N85-21789
Plasmachemical evaporation and doping of amorphous silicon 12 p1879 N85-21790
Gallium arsenide arrays versus silicon arrays for space application 13 p2006 N85-22574
Availability of AlGaAs/GaAs solar cells in space 13 p2006 N85-22576
Technological process effect on the carrier lifetime degradation of silicon solar cell base layer irradiated by 1 MeV electrons (boron doping case) 13 p2007 N85-22585
The effects of lithium counterdoping on radiation damage and annealing in n(+)p silicon solar cells 13 p2007 N85-22586
Study of processes of modification of Al-Si alloys 13 p2026 N85-22695
Segregation of silicon in alumin-carbon fiber composites 13 p2026 N85-22706
Time-resolved studies of rapid solidification in highly undercooled molten silicon
[DE85-004857] 13 p2038 N85-22765
Drift fields and boundary conditions at grain boundaries in bipolar P/N junction silicon devices 13 p2062 N85-22879
SEM (Scanning Electron Microscope) investigation of silicon diodes using the electron beam induced current method
[AD-A150356] 13 p2064 N85-22894
High sheet resistance, arsenic implanted polycrystalline silicon for integrated circuit resistors
[DE85-004355] 13 p2065 N85-22902
Noise characteristics of sulfur-doped silicon diodes 13 p2073 N85-22952
Thermodynamic and kinetic studies of pulsed laser annealing from transient conductivity measurements
[DE85-003677] 13 p2096 N85-23078
Time-resolved ellipsometry and reflectivity measurements of the optical properties of silicon during pulsed excimer laser irradiation
[DE85-006091] 13 p2096 N85-23079
Time-resolved reflectivity measurement of extrinsic silicon during pulsed laser irradiation
[AD-A150350] 13 p2159 N85-23403
Transport properties of silica thermally grown on silicon
[AD-A150304] 13 p2163 N85-23418
Demonstration of feasibility of depositing semiconductor layers using microwave enhanced plasma techniques
[NASA-CR-174392] 13 p2163 N85-23421
Electronic transport in hydrogenated amorphous silicon films
[DE85-002901] 13 p2164 N85-23426
Influence of substrate heating and thermal annealing on the surface crystallinity in single Si crystals implanted with high doses of (16)O
[DE85-006264] 13 p2164 N85-23428
Charge transfer, polarization and relaxation effects in the Auger lineshapes of Si
[AD-A150938] 14 p2252 N85-23954
Dependence of parameters of silicon photovoltaic cells on temperature and light intensity 14 p2275 N85-24094
Characterization of terrestrial solar cells for space applications: Electrical characteristics of thin Westinghouse dendritic web cells as a function of solar intensity, temperature, and incidence angle
[NASA-CR-175642] 14 p2349 N85-24518
Silicon-sheet and thin-film cell and module technology potential: Issue study
[NASA-CR-175654] 14 p2349 N85-24520
Solid/melt interface studies of high-speed silicon sheet growth
[NASA-CR-175698] 14 p2350 N85-24525
Laser-assisted solar cell metallization processing
[NASA-CR-175688] 14 p2350 N85-24528
Excimer laser annealing to fabricate low cost solar cells
[NASA-CR-175702] 14 p2351 N85-24529
Stress and efficiency studies
[NASA-CR-175688] 14 p2351 N85-24531
High resolution Z-contrast imaging and lattice location analysis of dopants in ion-implanted silicon
[DE85-005261] 14 p2429 N85-24980
Dopant incorporation in silicon during nonequilibrium solidification: Comparison of 2 processes
[DE85-005568] 14 p2430 N85-24988
Ion beam mixing of marker layers in Al and Si
[DE85-008227] 15 p2511 N85-25490
Reduced-chromium stainless steel substitutes containing silicon and aluminum
[PB85-160786] 15 p2513 N85-25502
Heavy doping effects in high efficiency silicon solar cells
[NASA-CR-175667] 15 p2585 N85-25937
Investigation of silicon surface passivation by silicon nitride film deposition
[NASA-CR-175693] 15 p2585 N85-25938
Heavy doping effects in high efficiency silicon solar cells
[NASA-CR-175681] 15 p2586 N85-25940
Vapor sensing by means of a ZnO-on-Si surface acoustic wave resonator
[DE85-003250] 15 p2646 N85-26324
Raman studies of surface temperature in laser-heated semiconductors
[AD-A151377] 15 p2659 N85-26412
Chemical vapor deposition of amorphous semiconductor films
[DE85-002917] 15 p2661 N85-26421
Thin-film polycrystalline silicon research
[DE85-002908] 15 p2663 N85-26434
An advanced solid state pressure transducer for high reliability SSME application 16 p2739 N85-26905
Effect of nickel addition on the thermal, magnetic and magnetomechanical properties of Fe(80)B(15)Si(5)
[AD-A152281] 16 p2749 N85-26967
Flat-plate solar array project process development area: Process research of non-CZ silicon material
[NASA-CR-175777] 16 p2816 N85-27362
Heavy doping effects in high efficiency silicon solar cells
[NASA-CR-175779] 16 p2818 N85-27383
Electronic density of states for the double donor system Si:P, As
[INPE-3447-PRE/700] 16 p2869 N85-27700
Influence of manganese and heat treatment on structure and properties of Fe-0.1 percent-C-14 percent Cr-based steels
[BLL-BISI-TRANS-22299-(9022.06)] 17 p2928 N85-28071
Fracture mechanics analysis of cold drawn Si-Cr valve steel
[BLL-BISI-TRANS-22216-(9022.06)] 17 p2978 N85-28405
Comprehensive silicon solar cell computer modeling
[NASA-CR-175959] 17 p2997 N85-28461
Research and developmental study on MIS thin film solar cells of amorphous hydrogenated silicon, part 2
[BMFT-FB-T-84-290] 17 p2998 N85-28467
The effect of ion-bombardment-induced atomic mixing on depth-profiling of interfaces
[AD-A153199] 17 p3044 N85-28834
Quantitative analysis of defects in silicon-characterization of UCP, HAMCO, and microcrystalline material
[NASA-CR-175998] 18 p3079 N85-29046
Semicrystalline casting process development and verification
[DE85-007695] 18 p3081 N85-29056
Silicide conductors reliability research
[AD-A153768] 18 p3095 N85-29157
Investigation of a Si and related semiconductors as materials for photovoltaic conversion
[DE85-002932] 18 p3096 N85-29163
Evaluation of VLSI technology -- space applications
[CD.6501702] 18 p3096 N85-29177
Mechanically-stacked multijunction solar cells
[DE85-010369] 18 p3129 N85-29377
Electronic states in silicon and on its interfaces
[AD-A153664] 18 p3193 N85-29807
Oxygen-nitrogen interactions in ion-implanted silicon
[DE85-010091] 18 p3195 N85-29819
Research pressure instrumentation for NASA space shuttle main engine
[NASA-CR-176014] 19 p3227 N85-30006
Action of plasma and explosion products on silumins 19 p3242 N85-30100
Influence of type of processing of AK4 alloy on its surface state and strength of bonding of plasma coatings 19 p3242 N85-30103
Glow discharge deposition at high rates using diglane
[DE85-010236] 19 p3263 N85-30235
Increased voltage photovoltaic cell
[NASA-CASE-NPO-16155-1] 19 p3303 N85-30475
Current status of silicon materials research for photovoltaic applications
[DE85-008799] 19 p3304 N85-30482
Research on the basic understanding of high efficiency in silicon solar cells
[DE85-006774] 19 p3305 N85-30487
Ribbon growing method and apparatus
[NASA-CASE-NPO-16308-1-CU] 19 p3375 N85-30934
Chemistry and physics of silicon-based amorphous semiconductors
[DE85-001931] 19 p3377 N85-30949
Leading-edge microelectronics research at Sweden's Chalmers 20 p3436 N85-31337
An analysis of the feasibility of producing silicon for solar cells by a dichlorosilane/fluidized-bed reactor process
[NASA-CR-176036] 20 p3476 N85-31614
Historical perspective of barriers to achieving high-efficiency silicon solar cells 20 p3479 N85-31616
Aspects of silicon bulk lifetimes 20 p3479 N85-31617
Silicon solar cell efficiency improvement: Status and outlook 20 p3479 N85-31619
Some practical considerations for economical back contact formation on high efficiency solar cells 20 p3479 N85-31620
Silicon MINP solar cells 20 p3480 N85-31623
New adatom model for Si(11) 7X7 and Si(111)Ge 5X5 reconstructed surfaces 20 p3480 N85-31625
Compositional analysis of silicon 20 p3480 N85-31626
Surface passivation and junction formation using low energy hydrogen implants 20 p3480 N85-31628
Chemical structure of interfaces 20 p3480 N85-31629
Structural defects in crystalline silicon 20 p3481 N85-31630
Oxygen and carbon impurities and related defects in silicon 20 p3481 N85-31631
Current understanding of point defects and diffusion processes in silicon 20 p3481 N85-31632
Electrical and structural characterization of web dendrite crystals 20 p3481 N85-31633
EBIC characterization and hydrogen passivation in silicon sheet 20 p3481 N85-31634
Current status of one- and two-dimensional numerical models: Successes and limitations 20 p3482 N85-31636
Application of closed-form solutions to a mesh point field in silicon solar cells 20 p3482 N85-31637
Phenomena simulation for heavy doping and surface recombination velocity 20 p3482 N85-31638
High efficiency large area polysilicon solar cells 20 p3482 N85-31639
High efficiency solar cell processing 20 p3482 N85-31640
Process and design considerations for high-efficiency solar cells 20 p3482 N85-31641
Processing technology for high efficiency silicon solar cells 20 p3483 N85-31642
Recent improvements in materials for thin GaAs and multibandgap solar cells
[DE85-009800] 20 p3484 N85-31651
Gallium arsenide arrays versus silicon arrays for space application
[SNIAS-851-440-104] 20 p3485 N85-31657
Infrared absorption of oxygen complexes in electron-irradiated silicon
[FOA-C-30379-E1,E2,E3,E4] 20 p3539 N85-32015
High temperature electronics technology: Life test report
[AD-A154881] 21 p3580 N85-32257
Electrical properties of bulk grown nitrogen doped silicon
[AD-A155471] 21 p3581 N85-32266
Thermoelectric properties of beta-boron and some boron compounds
[DE85-011978] 21 p3582 N85-32270

High-frequency furnace
[DE85-011210] 21 p3586 N85-32291
Predicting photothermal field performance
21 p3608 N85-32404
Interfacial bonding stability 21 p3608 N85-32409
Silicon refinement by chemical vapor transport
21 p3609 N85-32412
JPL in-house fluidized-bed reactor research
21 p3609 N85-32414
Silicon production in an aerosol reactor
21 p3609 N85-32416
Physics of heavily doped silicon and solar-cell parameter measurement 21 p3609 N85-32418
Measuring bulk recombination rates and boundary recombination velocities 21 p3609 N85-32419
Studies of oxygen- and carbon-related defects in high-efficiency silicon solar cells
21 p3609 N85-32420
Comprehensive silicon solar-cell computer modeling
21 p3609 N85-32421
Sensitivity analysis of high-efficiency silicon solar-cell design parameters 21 p3610 N85-32422
Silicon surface passivation by silicon nitride deposition
21 p3610 N85-32423
Important loss mechanisms in high-efficiency solar cells 21 p3610 N85-32424
Development of high-efficiency solar cells on silicon web 21 p3610 N85-32425
Simultaneous junction formation
21 p3610 N85-32426
Amorphous metallic films in silicon metallization systems 21 p3610 N85-32427
Silicon dendritic web growth 21 p3611 N85-32435
Temperature-stress modeling
21 p3611 N85-32436
Silicon ribbon stress-strain activities
21 p3611 N85-32437
Analysis of stress-strain relationships in silicon ribbon
21 p3611 N85-32438
Stress and buckling analysis 21 p3611 N85-32439
Stress and efficiency studies in EFG
21 p3611 N85-32440
Silicon sheet surface studies
21 p3611 N85-32441
Analysis of inclined growth of silicon sheet
21 p3612 N85-32442
Edge-defined film-fed growth of thin silicon sheets
21 p3612 N85-32443
High-purity silicon crystal growth
21 p3612 N85-32444
Thin-film reliability and engineering overview
21 p3612 N85-32450
Defect formation in amorphous hydrated silicon subjected to laser radiation 21 p3682 N85-32873
Influence of background electrically neutral argon admixture on mechanical strength of silicon crystals
21 p3683 N85-32878
Microscopic control of semiconductor surface oxidation
[AD-A154799] 21 p3709 N85-33026
A theory of exciton photoluminescence for two types of neutral acceptors in silicon. A study of the systems Si:(B, In), Si:(Al), (Si), Si:(Ga, In), Si:(B, Al), Si:(B, Ga), and Si:(Al, GA)
[AD-A155452] 21 p3710 N85-33031
Cryogenic laser calorimetry for impurity analysis
[NASA-CR-176102] 22 p3743 N85-33201
Solid-melt interface studies of high-speed silicon sheet growth
[NASA-CR-176112] 22 p3751 N85-33249
Stress and efficiency studies in EFG
[NASA-CR-176125] 22 p3751 N85-33251
In-situ observations of the development of heavy-ion damage in semiconductors
[DE85-010289] 22 p3761 N85-33307
Method and apparatus for casting conductive and semi-conductive materials
[DE85-011655] 22 p3792 N85-33494
Development of high-efficiency solar cells on silicon web
[NASA-CR-176101] 22 p3805 N85-33566
Ultrasonic seam welding on thin silicon solar cells
[NASA-CR-176116] 22 p3805 N85-33570
Use of low energy hydrogen ion implants in high efficiency crystalline silicon solar cells
[NASA-CR-176109] 22 p3806 N85-33571
Investigation of the microstructure and photovoltaic properties of semicrystalline silicon
22 p3806 N85-33573
1985 Amorphous Silicon Review Meeting
[DE85-006794] 22 p3807 N85-33582
Low-cost high-performance silicon concentrator cells
[DE85-006875] 22 p3807 N85-33584
Striation free doped silicon
[AD-A155730] 22 p3847 N85-33827
Apparatus and method for the horizontal, crucible-free growth of silicon sheet crystals
[DE85-011568] 22 p3847 N85-33829
A new analysis of cosmic ray isotopes at 3 GeV/n from HEAO3-C2 data
[OG-4.3-6] 22 p3879 N85-34031
Enthalpies of formation of liquid Fe-Ce-Si and Fe-Ce-Al three-component alloys
[BLL-M-36296-(5828.4)] 23 p3913 N85-34247
Dual-chamber plasma deposition of A-Si:H solar cells at high rates using disilane
[DE85-011828] 23 p3946 N85-34451
Formation of amorphous silicon by light ion damage
[DE85-012605] 23 p3972 N85-34623
Silicon to iron abundances in solar cosmic rays and in the sun
[SH-2.1-6] 23 p3998 N85-34787
The mean ionic charge of silicon in 3HE-rich solar flares
[SH-2.2-8] 23 p4000 N85-34803
A silicon surface barrier telescope for solar particles identification
[SH-9.1-3] 23 p4050 N85-35118
Oxidation resistant slurry coating for carbon-based materials
[NASA-CASE-LEW-13923-1] 24 p4077 N85-35267
Dangling bonds and sub-gap optical absorption in silicon
[DE85-011752] 24 p4082 N85-35302
Advanced detectors and signal processing
[NASA-CR-176193] 24 p4088 N85-35343
Photoconductive pulse power switches: A review
[DE85-014125] 24 p4091 N85-35360
Cryogenic laser calorimetry for impurity analysis
[NASA-CR-176179] 24 p4097 N85-35395
Electronic structure and lattice dynamics of dimensionally constrained and disordered solids
[AD-A155927] 24 p4161 N85-35797

SILICON ALLOYS

Alloying specially low carbon silicon-bearing steel with nitrogen
[BLL-M-35707-(5828.4)] 02 p0175 N85-11170
Optical properties of composite materials
[AD-A146768] 07 p0920 N85-15826
Fluctuation phenomena studies in chemically sensitive field effect transistor. Part 1: Corrosion of aluminum
[AD-A148240] 08 p1129 N85-17118
Radiation-induced compositional redistribution and local phase transformation in irradiated alloys
[DE85-000080] 10 p1441 N85-19082
Structure-phase state and properties of high-durability VAL8 alloy 11 p1597 N85-20046
Enhanced diffusion from interstitial trapping during solid-phase-epitaxial growth of silicon alloys
[DE85-001285] 12 p1941 N85-22193
The structural and electronic properties of amorphous silicon based alloy materials
[DE85-002909] 15 p2660 N85-26419
Compensation of dangling bonds in A-Si, Ge:H alloys
[DE85-002905] 15 p2662 N85-26433
LPCVD tungsten deposition on Si-Ge alloy
[DE85-005588] 16 p2750 N85-26970
Experimental and theoretical study of fatigue crack initiation in metals 19 p3283 N85-30357
Development of improved thermoelectric materials for space nuclear power systems
[DE85-013079] 22 p3844 N85-33807
Studies of the crystallization process of aluminum-silicon alloys using a high temperature microscope
[NASA-TM-77869] 24 p4078 N85-35272

SILICON CARBIDES

Treating silicon carbide sinter by heating in nitrogen
[NASA-TM-77601] 01 p0021 N85-10130
Silicon nitride sintered body
[NASA-TM-77602] 01 p0021 N85-10131
Preparation of silicon carbide fibers
[DE84-014661] 01 p0022 N85-10137
Powder containing 2H-type silicon carbide produced by reacting silicon dioxide and carbon powder in nitrogen atmosphere in the presence of aluminum
[NASA-TM-77597] 01 p0027 N85-10167
Critical conditions for the growth of SiC, Si3N4, and SiO2
[DE84-014824] 01 p0030 N85-10185
Silicon carbide ceramic production
[NASA-TM-77598] 01 p0035 N85-10220
Injection molding of silicon carbide capable of being sintered without pressure
[NASA-TM-77736] 01 p0035 N85-10221
Sintering behavior of ultrafine silicon carbide powders obtained by vapor phase reaction
[NASA-TM-77422] 03 p0336 N85-12161
Bending strength studies on hot-pressed silicon carbide
[NASA-TM-77512] 03 p0371 N85-12369
Development and fabrication of refractory bodies for gas turbine engines
[BMFT-FB-T-84-180] 04 p0457 N85-12899
Preparation of sinter-active silicon carbide powders
[BMFT-FB-T-84-189] 04 p0469 N85-12982
Electrokinetic potential and stability of SIC suspensions in electrolyte solutions
[NASA-TM-77492] 04 p0469 N85-12984
Reactive sintering of SIC 04 p0473 N85-13010
High temperature corrosion of ceramics
[DE84-017084] 05 p0620 N85-13967
Creep of chemically vapor deposited SiC fibers
[NASA-TM-86897] 06 p0763 N85-14878
Fatigue behavior of continuous fiber silicon-carbide-aluminum composites
[NASA-TM-86332] 06 p0763 N85-14879
Fundamental tribological properties of ceramics
[NASA-TM-86915] 07 p0930 N85-15893
Oxidation resistance of silicon ceramics
[NASA-TM-77429] 07 p0931 N85-15898
Development and production of improved silicon carbide powder for pressureless sintering and hot pressing
[BMFT-FB-T-84-211] 07 p0934 N85-15917
Gas cooled fuel cell systems technology development
[NASA-CR-174732] 07 p0991 N85-16291
Method of preparing single crystalline cubic silicon carbide layers
[AD-D011305] 07 p1048 N85-16653
Fabrication of SiC whiskers and composites
[DE85-002038] 09 p1289 N85-18091
Fabrication of ceramic-ceramic composites by chemical vapor deposition
[DE85-000981] 09 p1298 N85-18155
Reactivity of ion implanted silicon carbide
[DE85-001543] 09 p1399 N85-18802
Amorphization of ceramics by ion beams
[DE85-000936] 10 p1453 N85-19156
Fundamental studies of growth, doping and transformation in beta silicon carbide
[AD-A149339] 10 p1562 N85-19851
Tensile testing of SiC whiskers
[DE85-003712] 11 p1593 N85-20025
High temperature corrosion of ceramics
[DE85-002179] 11 p1612 N85-20139
West Europe report: Science and technology
[JPRS-WST-85-006] 11 p1618 N85-20183
SEP of France manufactures its first silicon carbide fibers 11 p1618 N85-20184
NDE for heat engine ceramics
[NASA-TM-86949] 11 p1649 N85-20389
Slit-ring test for evaluating fracture in tubular cross sections
[DE85-003550] 11 p1654 N85-20416
Parametric evaluation of ball milling of SiC in water
[NASA-TM-86974] 12 p1811 N85-21356
Radiographic detectability limits for seeded voids in sintered silicon carbide and silicon nitride
[NASA-TM-86945] 12 p1861 N85-21674
Silicon carbide-silicon nitride fibers: Preparation and characterization of polycarbosilazane precursors
12 p1945 N85-22214
Particulate toughened silicon carbide
[DE85-004797] 13 p2016 N85-22643
The effect of notch acuity on the fracture toughness of silicon carbide/aluminum metal matrix composites
[AD-A150970] 14 p2248 N85-23936
Localized corrosion currents from graphite/aluminum and welded SiC/Al metal matrix composites
[AD-A150988] 14 p2256 N85-23980
Sintered silicon carbide molded body and method for its production
[NASA-TM-77646] 14 p2259 N85-23999
Environmental effects on the tensile strength of chemically vapor deposited silicon carbide fibers
[NASA-TM-86981] 14 p2259 N85-24000
A novel polymeric organosilazane precursor to Si3N4/SiC ceramics
[AD-A150748] 14 p2260 N85-24003
Thermodynamic calculations and the chemical vapour deposition of hard materials 14 p2431 N85-24991
Effect of fatigue and thermal loads on silicon carbide fiber reinforced glass matrix composites
[DE85-006069] 15 p2503 N85-25441
Fabrication of fiber reinforced ceramic composites by chemical vapor infiltration
[DE85-007565] 15 p2520 N85-25536
Fundamental studies of growth, doping and transformation in beta silicon carbide
[AD-A152047] 15 p2660 N85-26418
Particulate and whisker toughened alumina composites
[DE85-005239] 16 p2743 N85-26930
Reaction-bonded and fiber-reinforced SiC static and dynamic gas turbine components
[BMFT-FB-T-84-302] 17 p2899 N85-27874

Completely consumed carbide: A new process for dielectric isolation
[AD-A152379] 17 p2918 N85-27967
Titanium metal-matrix composites
[AD-D011643] 17 p2930 N85-28066
Preparation of silicon carbide-silicon nitride fibers by the pyrolysis of polycarbosilazane precursors
[NASA-TM-86505] 17 p2933 N85-28107
Development of high temperature resistant noncorrodible silicon carbide components for gas turbine applications, follow-up report
[BMFT-FB-T-85-016] 17 p2936 N85-28126
Limiting processes laser CVD
[DE85-008646] 18 p3114 N85-29279
Burner rig corrosion of SiC at 1000 deg C
[NASA-TM-87061] 19 p3227 N85-30011
Mechanism of strength degradation for hot corrosion of alpha-SiC
[NASA-TM-87052] 19 p3248 N85-30135
Development of the Cascade inertial-confinement-fusion reactor
[DE85-010933] 19 p3357 N85-30812
Reliability of void detection in structural ceramics using scanning laser acoustic microscopy
[NASA-TM-87035] 21 p3597 N85-32337
Dispersion toughened ceramic composites and method for making same
[DE85-011601] 22 p3751 N85-33252
Woven heat exchanger
[DE85-011633] 22 p3783 N85-33439
Rotating bending fatigue strength of silicon carbide and alumina-fiber reinforced aluminum
23 p3907 N85-34208
Mechanical properties of SiC fiber-reinforced reaction-bonded Si3N4 composites
[NASA-TM-87085] 23 p3909 N85-34223
Method for removing oxide contamination from silicon carbide powders
[DE85-011648] 23 p3919 N85-34287
Oxidation resistant slurry coating for carbon-based materials
[NASA-CASE-LEW-13923-1] 24 p4077 N85-35267

SILICON COMPOUNDS
NT ALUMINUM SILICATES
NT BERYL
NT CHLOROSILANES
NT DISILICIDES
NT ENSTATITE
NT FELDSPARS
NT GARNETS
NT ORGANIC SILICON COMPOUNDS
NT PYROXENES
NT QUARTZ
NT SILANES
NT SILICATES
NT SILICIDES
NT SILICON CARBIDES
NT SILICON DIOXIDE
NT SILICON NITRIDES
NT SILICON OXIDES
NT SODIUM SILICATES
NT YTTRIUM-ALUMINUM GARNET
NT YTTRIUM-IRON GARNET
NT ZEOLITES
Two silicon phthalocyanines and a silicon naphthalocyanine: Synthesis, electrochemistry and electrogenerated chemiluminescence
[AD-A144760] 01 p0023 N85-10145
A silicon phthalocyanine and a silicon naphthalocyanine: Synthesis, electrochemistry, and electrogenerated chemiluminescence
[AD-A146441] 06 p0765 N85-14895
Electronic and redox properties of stacked-ring silicon phthalocyanines from molecular orbital theory
[AD-A147161] 07 p0922 N85-15844
Effects of primary recoil energy on the production rate of mobile defects during elevated temperature irradiation
[DE85-006218] 15 p2511 N85-25489
Chemical structure of interfaces
20 p3480 N85-31629
A fluidized-bed reactor for silane pyrolysis
21 p3609 N85-32413
Advanced module development overview
21 p3612 N85-32445
An enhanced photoresponse at dislocation subgrain boundaries revealed by X-ray topography of polysilicon solar cells
22 p3806 N85-33572
Calculation of mixed depth for some metal-Si systems
[DE85-011907] 23 p3971 N85-34616
Center for Electronics and Electrical Engineering technical progress bulletin covering center programs, July-September with 1985 CEEE events calendar
[PB85-191393] 24 p4091 N85-35363
Circumstellar shells of late-type stars: A study at millimeter and infrared wavelengths
24 p4167 N85-35836

SILICON CONTROLLED RECTIFIERS
Isolated load switching with surge suppression
[AD-D011218] 01 p0042 N85-10274
Random access memory technologies
[AD-A153089] 17 p3006 N85-28597

SILICON DIOXIDE
NT QUARTZ
The rheology of icy satellites
[NASA-CR-174024] 02 p0302 N85-11959
The development of CVD oxide coatings for the protection of metal surfaces — chemical vapor deposition (CVD)
03 p0332 N85-12142
Transient attenuation in optical fibers
[DE84-016487] 05 p0729 N85-14687
Oxide charge characteristics of low temperature MOS (Metal-Oxide-Silicon) oxide films
[AD-A146447] 06 p0803 N85-15113
Metal atom diffusion in amorphous silica and at the silica surface
[DE84-017351] 09 p1380 N85-18674
The Si/SiO2 intrinsic states and interface charges. Chapter 1: Origin, properties, models, impact
[HMI-B-413] 09 p1400 N85-18812
Fiber reinforced fused silica for hypersonic radome applications
[AD-P004366] 12 p1826 N85-21460
Transport properties of silica thermally grown on silicon
[AD-A150304] 13 p2163 N85-23418
A silicic shield volcano in Bolivia
13 p2187 N85-23572
Dendritic growth from amorphous matrix
[DE85-007630] 16 p2871 N85-27712
Influence of eutectic silicate inclusions on micro-processes during deformation and fracture of 12GS steel
[BLL-BISI-TRANS-22296-(9022.06)]
17 p2929 N85-28073
Analysis of time dependent dielectric failures
[AD-A153200] 17 p2954 N85-28243
Silica problem in the design of geothermal power plants
[DE85-008245] 17 p2986 N85-28453
Mechanical protection of DLC films on fused silica slides
[NASA-TM-87056] 19 p3248 N85-30138
Nitridation of SiO2 for surface passivation
20 p3480 N85-31627
Process for improving the quality of epitaxial silicon films grown on insulating substrates
[AD-D011730] 22 p3847 N85-33828
Uranium, thorium isotopic analyses and uranium-series ages of calcite and opal and stable isotopic compositions of calcite from drill cores UE25a no. 1, USR G-2 and USW G-3/GU-3, Yucca Mountain, Nevada
[DE85-013039] 23 p3948 N85-34471
Characterization of catalysts with metal-support effects and of the species adsorbed on their surfaces
[DE85-012254] 24 p4096 N85-35394

SILICON FILMS
Studies of hydrogenated amorphous silicon
[DE84-013036] 01 p0067 N85-10443
Chemical vapor deposition of amorphous silicon films produced by using higher order silanes
[DE84-004519] 01 p0123 N85-10847
Effect of heat treatment on phase composition and crystal structure of thin WSi2 films on silicon substrates
03 p0350 N85-12253
Material models and device structures for GaAs solar cells, introduction
05 p0665 N85-14276
Evaluation of the ion implantation process for production of solar cells from silicon sheet materials
06 p0831 N85-15281
Ion cluster beam deposition research
06 p0831 N85-15283
Miniworkshop on effects of stress and strain in high-speed-growth silicon ribbons
06 p0831 N85-15284
Stress studies in EFG
06 p0831 N85-15285
Research on submicrometer structures
[AD-A146578] 06 p0867 N85-15508
Density of states and recombination in amorphous silicon (a-Si:H)
[BMFT-FB-T-84-216] 08 p1135 N85-17151
French research on gallium arsenide devices
08 p1141 N85-17196
Silicon film solar cell process
[NASA-CR-174446] 10 p1508 N85-19514
Infrared modulation of photoluminescence in glow discharge amorphous silicon
[DE85-016993] 11 p1737 N85-20922
Ingot slicing machine and method
[NASA-CASE-NPO-15483-1] 12 p1857 N85-21650
Technology of thin silicon foils for the fabrication of monolithic integrated sensors
[BMFT-FB-T-84-209] 12 p1943 N85-22202
Investigation of silicon surface passivation by silicon nitride film deposition
[NASA-CR-175693] 15 p2585 N85-25938
Diagnostics of a glow discharge used to produce hydrogenated amorphous silicon films
[DE85-002914] 15 p2661 N85-26420
In plane stress analysis
[NASA-CR-175775] 16 p2799 N85-27259
Photovoltaic cell reliability research: Investigation of accelerated stress factors and failure-degradation mechanisms in terrestrial solar cells
[NASA-CR-175815] 16 p2819 N85-27388
Investigation of superlattice device structures
[NASA-CR-3903] 18 p3094 N85-29152
Superconducting electronic film structures
[AD-A154196] 19 p3259 N85-30207
Electrohydrodynamic process for the production of large area polycrystalline silicon sheet
[DE85-008781] 19 p3261 N85-30225
High-efficiency cell concepts on low-cost silicon sheets
20 p3479 N85-31621
The development and evaluation of point defect models for the growth of passive films on single crystal, polycrystalline, and amorphous metal surfaces
[AD-A154685] 21 p3709 N85-33023
Process for improving the quality of epitaxial silicon films grown on insulating substrates
[AD-D011730] 22 p3847 N85-33828

SILICON ISOTOPES
Measurements of the fragmentation of (40)Ar, (28)Si and (12)C in CH2C and H targets between 300 and 1500 MeV/nuc at the Bevalac
[OG-7.2-19] 23 p4016 N85-34886

SILICON JUNCTIONS
Solar cells based on polycrystalline silicon with isothermal potential barriers along grain boundaries
14 p2275 N85-24091
The future of crystalline silicon technology in the US Department of Energy program
21 p3607 N85-32399
Advanced module development overview
21 p3612 N85-32445

SILICON NITRIDES
Sintered silicon nitride workpiece
[NASA-TM-77000] 01 p0021 N85-10129
Silicon nitride powder
[NASA-TM-77731] 01 p0022 N85-10132
Critical conditions for the growth of SiC, Si3N4, and SiO2
[DE84-014824] 01 p0030 N85-10185
Fabrication and characterization of Si3N4 ceramics without additives by high pressure hot pressing
[NASA-TM-77724] 01 p0031 N85-10189
Milling of Si3N4 with Si3N4 hardware
[NASA-TM-86864] 01 p0031 N85-10191
Silicon nitride joining
[AD-A145868] 02 p0187 N85-11248
Development and fabrication of refractory bodies for gas turbine engines
[BMFT-FB-T-84-180] 04 p0457 N85-12899
Study of the pore structure of ceramics prepared by the slip casting method
[NASA-TM-77495] 04 p0478 N85-13048
High temperature corrosion of ceramics
[DE84-017084] 05 p0620 N85-13967
Investigation of silicon surface passivation by silicon nitride deposition
06 p0829 N85-15266
Development and production of improved alpha-phase silicon nitride powders for hot pressing and sintering
[BMFT-FB-T-84-206] 07 p0921 N85-15830
Oxidation resistance of silicon ceramics
[NASA-TM-77429] 07 p0931 N85-15898
Silazane precursors to silicon nitride
[AD-A146791] 07 p0931 N85-15899
Fluctuation phenomena studies in chemically sensitive field effect transistors. Part 2: Corrosion of silicon oxynitride
[AD-A148227] 08 p1157 N85-17302
Tensile test of pressureless-sintered silicon nitride at elevated temperature
[NASA-TM-77777] 08 p1172 N85-17390
Factors influencing the ball milling of Si3N4 in water
[NASA-TM-86932] 10 p1460 N85-19136
Evaluation of machining damage in brittle materials
[DE85-001794] 11 p1612 N85-20136
High temperature corrosion of ceramics
[DE85-002179] 11 p1612 N85-20139
NDE for heat engine ceramics
[NASA-TM-86949] 11 p1649 N85-20369
Oxidation and hot corrosion of hot-pressed Si3N4 at 1000 deg C
[NASA-TM-86977] 12 p1811 N85-21358
Pressureless sintered silicon nitride as a promising candidate for radome materials
[AD-P004367] 12 p1826 N85-21461

Radiographic detectability limits for seeded voids in sintered silicon carbide and silicon nitride
[NASA-TM-86945] 12 p1861 N85-21674
Development of silicon nitride materials for the casting of solar cell silicon 12 p1878 N85-21779
Optimization of silicon-nitride-inversion layer solar cells 12 p1878 N85-21784
Silicon carbide-silicon nitride fibers: Preparation and characterization of polycarbosilazane precursors 12 p1945 N85-22214
Degassification of silicon nitride powders of various origins 13 p2030 N85-22718
Ammonia formation caused by the presence of water in the wet grinding of silicon nitride powder
[NASA-TM-77746] 14 p2249 N85-23937
A novel polymeric organosilazane precursor to Si3N4/SiC ceramics
[AD-A150748] 14 p2260 N85-24003
Sintering phenomena of non-oxide silicon compounds
[DE85-006876] 15 p2520 N85-25535
Fabrication of fiber reinforced ceramic composites by chemical vapor infiltration
[DE85-007585] 15 p2520 N85-25536
Flat conducts R and D in ceramic parts for diesel engine 15 p2534 N85-25637
Sweden invents new ceramic for more durable cutting tools 15 p2536 N85-25645
Investigation of silicon surface passivation by silicon nitride film deposition
[NASA-CR-175693] 15 p2585 N85-25938
Preparation of silicon carbide-silicon nitride fibers by the pyrolysis of polycarbosilazane precursors
[NASA-TM-86505] 17 p2933 N85-28107
Development of high temperature resistant, noncorrosible, non-metallic ceramic materials, especially silicon nitride in gas turbine application
[BMFT-FB-T-85-015] 17 p2938 N85-28125
High temperature fracture mechanics of silicon nitride
[BMFT-FB-T-84-265] 17 p2981 N85-28433
Preparation of sinteractive silicon nitride powders
[BMFT-FB-T-84-303] 18 p3062 N85-29066
High-temperature oxidation of reaction-roasted silicon nitride with various additives 19 p3244 N85-30114
Method for producing high quality germanium-germanium nitride interfaces for germanium semiconductors and device produced thereby
[AD-D011702] 19 p3260 N85-30218
Vibrational properties of disordered solids: Far infrared studies
[DE85-010400] 19 p3377 N85-30951
Realization by vapor deposition of turbine blades covered with a silicon nitride layer 20 p3395 N85-31061
Silicon nitride protective coatings for silvered glass mirrors
[DE85-011637] 20 p3433 N85-31300
Reliability of void detection in structural ceramics using scanning laser acoustic microscopy
[NASA-TM-87035] 21 p3597 N85-32337
Silicon surface passivation by silicon nitride deposition 21 p3610 N85-32423
Mechanical properties of SiC fiber-reinforced reaction-bonded Si3N4 composites
[NASA-TM-87035] 23 p3909 N85-34223
Reliability of two sintered silicon nitride materials
[NASA-TM-87092] 23 p3919 N85-34284
Method for measuring surface activity of silicon nitride powder
[NASA-TM-77908] 24 p4073 N85-35242

SILICON OXIDES
NT QUARTZ
NT SILICON DIOXIDE
Critical conditions for the growth of SiC, Si3N4, and SiO2
[DE84-014824] 01 p0030 N85-10185
Phase transformations of AlPO4 with SiO2 structures 03 p0425 N85-12713
High temperature corrosion of ceramics
[DE84-017084] 05 p0620 N85-13957
The atomic structure of Si-SiO2 interfaces suggesting a ledge mechanism of silicon oxidation
[DE84-016057] 05 p0731 N85-14703
EPR linewidth studies of unpaired electrons at the Si-SiO2
[DE84-016727] 05 p0733 N85-14712
Density and thermal expansion measurements of several mixed oxide glasses in the acid and liquid regions
[DE85-006134] 14 p2261 N85-24014
Impurity bands associated with MOS inversion layers
[INPE-3483-PRE/726] 16 p2870 N85-27704

SILICON POLYMERS
NT METHYL POLYSILOXANE
NT SILICONE RESINS
NT SILICONES
NT SILOXANES
Thin polymer film collectors as a contribution to the solar industry
[DE84-015299] 04 p0529 N85-13383
French research on gallium arsenide devices 08 p1141 N85-17196
Investigation of structure-permeability relationships of silicone polymer membranes
[PB85-148476] 11 p1596 N85-20038
EOS (electrical overstress) protection for VLSI (Very Large Scale Integration) devices
[AD-A150333] 13 p2084 N85-22891
A novel polymeric organosilazane precursor to Si3N4/SiC ceramics
[AD-A150748] 14 p2260 N85-24003
Preparation of silicon carbide-silicon nitride fibers by the pyrolysis of polycarbosilazane precursors
[NASA-TM-86505] 17 p2933 N85-28107
EVA-glass interface bond stability 21 p3606 N85-32406
Interfacial bonding stability 21 p3606 N85-32409
Topics in electrochemical degradation of photovoltaic modules 21 p3606 N85-32410
Polymer-water interaction studies 21 p3609 N85-32411

SILICON RADIATION DETECTORS
The Silica Aerogel Detector (SAD) story — Cherenkov detector
[USIP-84-14] 20 p3459 N85-31485

SILICON SOLAR CELLS
U SOLAR CELLS

SILICON TRANSISTORS
The construction and study of improved Al(x)Ga(1-x)As-GaAs heterostructure devices
[AD-A153264] 17 p2954 N85-28244
KT3127A, KT3128A transistors 22 p3779 N85-33414

SILICONE RESINS
Thermal conductivity and interface resistance of particle-filled silicone resin
[DE84-011681] 04 p0479 N85-13056

SILICONE RUBBER
General studies on composite materials. Evaluation of auxiliary products of national origin
[SNIAS-2500/DCI-PR/84] 03 p0326 N85-12101
Simple EOS for the silicone rubber Sylgard 184
[DE85-001394] 12 p1814 N85-21376
Oil resistant silicone elastomers
[AD-131523] 16 p2753 N85-26967

SILICONES
NT METHYL POLYSILOXANE
NT SILOXANES
Development of a polysilicon process based on chemical vapor deposition of dichlorosilane in an advanced Siemen's reactor
[NASA-CR-174148] 04 p0483 N85-13083
Vacuum ultraviolet electronic properties of liquids
[DE85-000305] 10 p1563 N85-19858
Model for the growth of fractal silica polymers
[DE85-007684] 17 p2935 N85-28115

SILICONIZING
Studies of the crystallization process of aluminum-silicon alloys using a high temperature microscope
[NASA-TM-77869] 24 p4078 N85-35272

SILOS (MISSILE STORAGE)
U MISSILE SILOS

SILOXANES
Neutron scattering on polysiloxanes 03 p0432 N85-12751
Properties of ultra-violet cured poly(dimethylsiloxane)-urea acrylates
[AD-A148570] 08 p1134 N85-17146
Poly(dimethylsiloxane)-polyurethane elastomers: Synthesis and properties of segmented copolymers and related zwitterionomers
[AD-A148571] 08 p1134 N85-17147
High performance size exclusion chromatography (IX) bulk and component analysis of silanol groups in polydimethylsiloxanes: Process development endeavor
[DE85-006653] 15 p2506 N85-25458
Formulation/cure technology for ultrahigh molecular weight silphenylene-siloxane polymers
[NASA-TP-2476] 16 p2753 N85-26990
Thermally stable elastomers: Review of silarylene-siloxane polymers and polysilmethylenes
[AD-A152323] 17 p2934 N85-28111
Self-developing polysilane deep-UV resists: Photochemistry, photophysics and submicron lithography
[DE85-007606] 19 p3237 N85-30067
Method for controlling the viscosity of siloxane oils
[DE85-011586] 23 p3909 N85-34221

SILTS
U SEDIMENTS

SILVER
Relationships between electronic structure and stability of metallic glasses
[AD-A145141] 01 p0028 N85-10176
Kinetics of simple inner- and outer-sphere electrochemical reactions at rotating silver electrodes as examined using surface-enhanced Raman spectroscopy
[AD-A145606] 02 p0172 N85-11154
EXAFS and Moessbauer study of small metal clusters isolated in rare-gas solids
[DE84-015976] 04 p0470 N85-12994
Behaviour of lead-silver anodes in zinc electrodeposition from sulphuric acid baths
[BLL-MINTEK-TR-1160-(5810.5759)] 06 p0764 N85-14887
Effects of silver and group 2 fluorides addition to plasma sprayed chromium carbide high temperature solid lubricant for foil gas bearing to 650 deg C
[NASA-TM-86895] 06 p0770 N85-14928
Metallo-Organic Decomposition (MOD) silver metallization for photovoltaics 06 p0830 N85-15278
Ion cluster beam deposition research 06 p0831 N85-15283
Electronic structure, chemical bonding, and superconductivity of silver films on germanium
[AD-A147720] 08 p1128 N85-17112
Silver metallogeny in Earth's Pacific Ocean segment 10 p1498 N85-19455
The role of silver in self-lubricating coatings for use at extreme temperatures
[NASA-TM-86943] 11 p1611 N85-20127
The effect of Xe underlayers on the surface enhanced Raman scattering of pyridine on cold silver
[AD-A150109] 12 p1801 N85-21294
EXAFS of monolayers on silver electrodes: SSRL proposal number 717M
[AD-A150623] 13 p2018 N85-22652
Ink jet printing of silver metallization for photovoltaics
[NASA-CR-175798] 15 p2586 N85-25943
MOD silver metallization for photovoltaics
[NASA-CR-175773] 16 p2818 N85-27381
The loss of material from the cathode of metal arcs
[NASA-TM-77845] 17 p2918 N85-27985
Silvered polymer reflectors
[DE85-006782] 18 p3130 N85-29384
Modification of the grain size of sputtered copper with additions of oxygen, krypton, silver, or yttrium
[DE85-010975] 21 p3567 N85-32189
MOD silver metallization for photovoltaics 21 p3610 N85-32428
Ice nucleation of single water droplet by silver iodide: A laboratory observation 21 p3643 N85-32630
Monte Carlo studies of H2O layers adsorbed on a model basal face of AgI 21 p3643 N85-32633
Method of bonding silver to glass and mirrors produced according to this method
[DE85-011642] 22 p3792 N85-33495
Ink jet printing of silver metallization for photovoltaics
[NASA-CR-176054] 22 p3805 N85-33569
Environmental surveillance at Los Alamos during 1984
[DE85-011886] 22 p3811 N85-33605
Polarisation insensitive achromatic cube beamsplitter — binocular microscopes
[NPL-MOM-72] 23 p3973 N85-34630
Noise in silver beta alumina ceramics
[AD-A156135] 24 p4082 N85-35297
New silver resource map of the United States: Potential for increased domestic silver production 24 p4105 N85-35445

SILVER ALLOYS
Alloy supercooling on Salyut-7 11 p1604 N85-20083
Application of solidification theory to rapid solidification processing
[AD-A151251] 15 p2509 N85-25480
Study of the kinetics and thermodynamics of hydrogen in Pd-based alloys
[DE85-007341] 16 p2750 N85-26969
Age hardening and atomic structure of an aluminum-6 at. % silver alloy
[DE85-009977] 18 p3077 N85-29031
The precipitation mechanism in a metallic solid solution crystal: Case of the aluminum-copper and aluminum-silver systems
[DE85-009981] 18 p3077 N85-29032
Studies of the crystallization process of aluminum-silicon alloys using a high temperature microscope
[NASA-TM-77869] 24 p4078 N85-35272

SILVER CHLORIDES
Determination of low chloride values in Rocky Flats scrub alloy solutions and other complex matrices
[DE85-011506] 23 p3911 N85-34234

SILVER COMPOUNDS
NT SILVER CHLORIDES
NT SILVER HALIDES
NT SILVER IODIDES

SILVER HALIDES
NT SILVER CHLORIDES
NT SILVER IODIDES

Infrared presensitization photography
[AD-A146968] 07 p0967 N85-16139
Infrared presensitization photography
16 p2786 N85-27189
SILVER HYDROGEN BATTERIES
Analysis and testing of the thermal properties of space battery cells, phase B, draft
[ESA-CR(P)-1971] 15 p2550 N85-25741
SILVER IODIDES
Inactivation of silver iodide by atmospheric nucleation inhibitors 21 p3638 N85-32599
Ice nucleation by silver iodine particles with nearly critical sizes 21 p3638 N85-32600
Photoinduced active sites on ice nucleating aerosol of silver iodide 21 p3639 N85-32601
SIMICOR (IMAGE CORRELATOR)
U IMAGE CORRELATORS
SIMILARITIES
U ANALOGIES
SIMILARITY NUMBERS
Study of the functions of similarity of the planetary boundary layer. Part 2: Results
[INPE-3130-PRE/521-VOL-2] 16 p2826 N85-27429
Application of field similitude theory to calculation of stripline heating 22 p3780 N85-33419
Selection of segment similarity measures for hierarchical picture segmentation 23 p3960 N85-34548
SIMILARITY THEOREM
Similarity criteria of spectra of pressure pulsations of turbulent boundary layer near wall
02 p0256 N85-11679
Study of the functions of similarity of the planetary boundary layer. Part 1: Theory
[INPE-3129-PRE/520-PT-1] 16 p2826 N85-27428
Parameterization of surface fluxes in the VVR Fourth Order GCM 18 p3142 N85-29454
SIMPLEX METHOD
New labeling procedures for the basis graph in generalized networks
[AD-A146217] 03 p0407 N85-12601
The stable evaluation of multivariate b-splines
[AD-A147386] 07 p1032 N85-16551
An iterative scheme for linear complementarity problems
[AD-A147464] 07 p1032 N85-16555
Minimal cost flow in processing networks: A primal approach
[CWI-TRACT-4] 14 p2432 N85-25001
A greedy algorithm for the transhipment along a single road problem
[AD-A152343] 17 p3025 N85-28709
On the step size in Karmarkar's algorithm
[AD-A154040] 19 p3395 N85-30861
A practical approach to Karmarkar's algorithm
[AD-A155714] 21 p3673 N85-32818
SIMULATED ALTITUDE
U ALTITUDE SIMULATION
SIMULATION
NT ALTITUDE SIMULATION
NT ANALOG SIMULATION
NT ATMOSPHERIC ENTRY SIMULATION
NT COMPUTER SYSTEMS SIMULATION
NT COMPUTERIZED SIMULATION
NT CONTROL SIMULATION
NT DIGITAL SIMULATION
NT ENVIRONMENT SIMULATION
NT EXHAUST FLOW SIMULATION
NT FLIGHT SIMULATION
NT LANDING SIMULATION
NT MOTION SIMULATION
NT SOLAR SIMULATION
NT SPACE ENVIRONMENT SIMULATION
NT SYSTEMS SIMULATION
NT THERMAL SIMULATION
NT WEIGHTLESSNESS SIMULATION
Simulation of contact surface erosion for impact problems 01 p0060 N85-10396
Simulation uses of the exponential distribution
[AD-A144940] 01 p0112 N85-10756
Simulation of vibration processes in damped structures with allowance for temperature-frequency characteristics of vibration absorbing materials
02 p0257 N85-11680
The structure of the vorticity field in turbulent channel flow. Part 2: Study of ensemble-averaged fields
[NASA-TM-86657] 03 p0361 N85-12317
Surge transient simulation in turbo-jet engine
05 p0596 N85-13796
Possibilities of increasing the simulation quality of multiaxial test stands — vehicle testing
05 p0649 N85-14189
Massively parallel processor 05 p0680 N85-14366
NOAA/NASA joint simulation of AMTS and HIRS
05 p0682 N85-14384
ECMWF/NMC/GLAS joint simulation study
05 p0682 N85-14385
Simulation evaluation of two VTOL control/display systems in IMC approach and shipboard landing
[NASA-TM-85986] 06 p0756 N85-14841
Review of requirements and status of simulation and scaling of transonic, viscous flows
[AD-A146357] 06 p0808 N85-15137
Region 1 birkeland currents from a global MHD simulation of the magnetosphere
[AD-A147435] 07 p0997 N85-16335
Matrix display simulation
[AD-D011371] 07 p1055 N85-16695
Automatic software for controlling cryogenic systems
08 p1097 N85-16932
Small-sample properties of kernel density estimators from randomly right-censored data
[AD-A148752] 09 p1374 N85-18634
A tracked vehicle test plant for the simulation of dynamic operation
[AD-P004305] 09 p1410 N85-18882
Simulation of the ion-beam-driven drift instability in a magnetic trap, 1
[AD-A149451] 10 p1452 N85-19147
An electronically controlled array for simulation of passive target/background signatures at millimeter wavelengths
[AD-D011456] 10 p1468 N85-19263
LOS microwave channel simulation: A survey of models, realizations and new concepts 10 p1472 N85-19291
Simulation of the ion-beam-driven drift instability in a magnetic trap, 2
[AD-A149452] 10 p1554 N85-19798
Compensator development and examination of performance and robustness
[NASA-CR-175470] 11 p1827 N85-20244
Radiative ion beams: Hot stellar reactions in the laboratory
[DE85-001570] 11 p1722 N85-20833
Algorithm for statistical simulation of electromagnetic compatibility characteristics of high-frequency transmission channels in radioelectronic facilities
12 p1842 N85-21560
NOAA-AISC user's guide for implementing CERES wheat model for large area yield estimation
[E85-10085] 12 p1873 N85-21750
Estimating solar radiation for plant simulation models
[E85-10089] 12 p1873 N85-21751
Recursive moment formulas for regenerative simulation
[AD-A150112] 12 p1922 N85-22070
Air combat simulation: Methods, models, trends
13 p1987 N85-22359
Microwave blackbodies for spaceborne receivers
[NASA-CR-175647] 13 p2094 N85-23068
Markov method for simulating non-Gaussian wind speed time series
[DE85-003450] 13 p2139 N85-23284
Calculating boundary layer on profile with laminar and turbulent flow zone 14 p2288 N85-24177
Synthetic aperture radar simulation study
[AD-A151000] 14 p2293 N85-24214
Investigation of a failure detection/identification system for a tactical aircraft navigation system
[AD-A151846] 15 p2469 N85-25240
Shuttle communications and tracking systems modeling and TDRSS link simulations studies
[NASA-CR-171861] 15 p2491 N85-25369
Compensator development and examination of performance and robustness
[NASA-CR-175703] 15 p2540 N85-25678
Numerical experiments of jet streak ageostrophic circulations using pseudo-geostrophic initialization and perspectives 15 p2500 N85-25969
Aerosol deposition along the respiratory tract at zero gravity: A theoretical study
[DE85-006703] 15 p2619 N85-26136
Evaluating computer-communication networks with simulation techniques
[AD-A151852] 15 p2632 N85-26222
Solution of coupled system of PDE by the transistorized multigrid method
[DE85-006377] 15 p2639 N85-26276
Flight testing and development of the F/A-18A digital flight control system 16 p2713 N85-26743
Development of a persistent chemical agent simulation system
[NASA-CR-175780] 16 p2745 N85-26937
Development of a Persistent Chemical Agent Simulator System (PCASS)
[NASA-CR-175776] 16 p2745 N85-26938
Pyrotechnic shock simulation using the controlled response of a resonating bar fixture
[DE85-006537] 16 p2784 N85-27181
In plane stress analysis
[NASA-CR-175775] 16 p2799 N85-27259
The selection of the starting field: General versus tailored model 16 p2805 N85-27294
Comparison of gravity field solution techniques
16 p2805 N85-27296
Kinetic theory and simulation of multi-species plasmas in Tokamaks excited with ICRF microwaves
[DE85-008119] 16 p2868 N85-27691
The evolution of ACS for helicopters: Conceptual simulation studies to preliminary design
17 p2902 N85-27890
Physical-chemical model for the mechanism of glass corrosion with particular consideration of simulated radioactive waste glasses
[DE85-007713] 17 p2935 N85-28121
Conformational and mechanical properties at high strain rates
[AD-A153401] 17 p2969 N85-28272
Study of a simulated test for assessing the machinability of steels
[BLL-BISI-TRANS-22344-(9022.06)] 17 p2972 N85-28357
Mathematical modeling and simulation of climate and climatic change
[DE85-008974] 17 p2997 N85-28526
Robust regression through robust covariances
[AD-A153301] 17 p3020 N85-28677
An experimental investigation of the angular scattering and backscattering behaviors of the simulated clouds of the outer planets
[NASA-CR-175909] 17 p3052 N85-28896
Multi-ducted inlet combustor research and development
[AD-A153753] 18 p3063 N85-28948
Diffusion of gases in porous solids: Simulation and measurements
[DE85-006870] 18 p3101 N85-29196
Methods for simulating gas phase SO2 oxidation in atmospheric models
[PB85-173110] 18 p3135 N85-29418
Forecast impact simulation studies
18 p3139 N85-29435
Preliminary results from numerical experiments on the summer 1980 heat wave and drought
18 p3140 N85-29438
A numerical study of the Pacific polar low
[AD-A153777] 18 p3149 N85-29495
Simulation for human factors research. A central question: Fidelity 18 p3159 N85-29568
Limit theorems for the method of replication
[AD-A153541] 18 p3170 N85-29642
Fault detection and accommodation testing on an F100 engine in an F-15 airplane
[NASA-TM-86735] 19 p3219 N85-29962
Decay of a coherent scalar disturbance in a turbulent flow
[NASA-TM-86700] 19 p3264 N85-30244
Highly accurate shock flow calculations with moving grids and mesh refinements, revision 1
[DE85-010929] 19 p3267 N85-30260
Numerical simulation of chemical and physical properties of cumulus clouds
[DE85-009744] 19 p3317 N85-30564
One-dimensional model hindcasts of warm anomalies in the North Pacific Ocean
[AD-A154128] 19 p3320 N85-30579
Evaluation of curve-smoothing techniques
[HSE-TRANS-11108] 19 p3349 N85-30759
Double layer formation due to contact of different temperature plasmas
[IPPJ-722] 19 p3370 N85-30900
Monte Carlo simulations of fermion systems: The determinant method
[DE85-010706] 19 p3378 N85-30947
Venus thermospheric circulation
[PB85-180420] 19 p3384 N85-30997
A study of the application of differential techniques to the global positioning system for a helicopter precision approach
[NASA-CR-177326] 20 p3391 N85-31035
Vortex simulation of v-shaped flame
20 p3425 N85-31259
Simulation and analysis of airborne antenna radiation patterns 20 p3439 N85-31342
Coal slurry ignition in a diesel engine simulator
[DE85-010987] 20 p3463 N85-31513
Pressure chamber simulation of 450-meter dive
20 p3505 N85-31788
Diving simulation experiment with pressure chambers
20 p3508 N85-31793
A systems analysis of the erythropoietic responses to weightlessness. Volume 1: Mathematical model simulations of the erythropoietic response to weightlessness
[NASA-CR-171890] 20 p3506 N85-31794
Simulation model of acoustic emission due to microscopic fracture in metals
[BLL-BISI-TRANS-22367-(9022.06)] 20 p3523 N85-31909

Impulsive noise due to transonic blade-vortex interactions 20 p3523 N85-31913
Simulating the effects of plasma disruption with a 1 MA current pulse in a coaxial test fixture
[DE85-010491] 20 p3535 N85-31998
Caviton collapse of SRS by SBS
[DE85-009605] 20 p3535 N85-31999
Two-phase flow visualization in a transparent, atmospheric pressure, boiling water loop
[DE84-016857] 21 p3586 N85-32288
The 2-D simulations of the NRL (Naval Research Laboratory) laser experiment
[AD-A154915] 21 p3592 N85-32321
A simulation of weather in 3D space
[AD-A155221] 21 p3636 N85-32586
Numerical modeling of sea ice dynamics and ice thickness characteristics
[AD-A154600] 21 p3654 N85-32700
On the dependence of the convergence of Gummel's algorithm on the regularity of the solution
[AD-A154628] 21 p3675 N85-32832
The priming effect in task design research
[AD-A154589] 21 p3679 N85-32852
A simulation study of Sylvester's problem in three dimensions
[AD-A155266] 21 p3679 N85-32854
Intracardiac hemodynamics and human heart function in simulated weightlessness 22 p3733 N85-33140
Synthesis of optimum receiver and processor for interfering radio pulse signals 22 p3769 N85-33361
New formulation for linear accelerator design
[DE85-011171] 22 p3842 N85-33792
Laboratory evaluation and application of microwave absorption properties under simulated conditions for planetary atmospheres
[NASA-CR-176078] 22 p3851 N85-33847
Late-stage planetesimals: How big?
22 p3852 N85-33857
A simulation of high energy cosmic ray propagation 2
[OG-5.4-2] 22 p3865 N85-34079
Effect of interference on the performance of a minimum TCAS 2
[FAA-PM-84-33] 23 p3895 N85-34131
The 1983 international intercomparison of nuclear accident dosimetry systems at Oak Ridge National Laboratory
[DE85-011303] 23 p3934 N85-34382
Image synthesis: Optical identity or pictorial communication? 23 p3963 N85-34585
Simulation studies on stability of hot electron plasma
23 p3978 N85-34664
Numerical simulation in astrophysics: Smoothed particle methods 23 p3979 N85-34674
Simulation of instability of cylindrically converging shock waves 23 p3980 N85-34679
A position sensitive phoswich hard X-ray detector system
[OG-9.3-12] 23 p4028 N85-34967
Simulated effects of increased recharge on the ground-water flow system of Yucca Mountain and vicinity, Nevada-California
[DE85-012985] 24 p4108 N85-35469
Application of pulsed power in the simulation of severe natural lightning
[DE85-012986] 24 p4124 N85-35564
Simulation of high +Gz onset in the dynamic environment simulator
[AD-A155963] 24 p4131 N85-35610
Constrained stiffness matrix adjustment using mode data
[AD-A155988] 24 p4143 N85-35685
A simulation of ultra-relativistic nucleus-nucleus collisions 24 p4146 N85-35707
Detector requirements for intensity interferometry measurements 24 p4147 N85-35709
A lead glass tubing drift calorimeter
24 p4147 N85-35711
Pulsed-neutron-source models for the astrophysical s-process
[DE85-012927] 24 p4151 N85-35740
Numerical studies of high current beam compression in heavy ion fusion
[DE85-011874] 24 p4158 N85-35783
Multiplicity distributions in interaction models used for cascade simulations
[HE-1.2-5] 24 p4172 N85-35863
Some remarks about simulation of cosmic ray phenomena with use of nuclear interaction models based on the current SPS proton-antiproton data
[HE-1.2-6] 24 p4172 N85-35864
Relation between gamma-ray family and EAS core: Monte-Carlo simulation of EAS core
[HE-3.6-7] 24 p4185 N85-35958
The lateral distributions of charged particles of energy greater than 0.3 E sub crit in electron-photon cascades in lead and air
[HE-3.6-10] 24 p4185 N85-35957
Result of Monte-Carlo simulation of electron-photon cascades in lead and layers of lead-scintillator
[HE-3.6-11] 24 p4185 N85-35958
A study of gamma-families generated in nucleon-nucleus (NA) and pion-nucleus (pi A) interactions
[HE-3.7-2] 24 p4186 N85-35961
Hadrons registration in emulsion chamber with carbon block
[HE-3.7-3] 24 p4186 N85-35962
New analysis of nuclear interaction observed by Mt. Kanbara emulsion chamber experiment
[HE-3.7-4] 24 p4186 N85-35963
Intensities of high-energy cosmic rays at Mount Kanbala
[HE-3.7-5] 24 p4186 N85-35964
Structured events in Pamir carbon X-ray chambers
[HE-3.7-7] 24 p4186 N85-35965
Ultra high energy events in ECHOS series and primary energy spectrum
[HE-3.7-9] 24 p4186 N85-35966
Peculiarities of gamma-quanta distribution at 20 TeV energy
[HE-3.7-10] 24 p4186 N85-35967
Analysis of equi-intensity curves and NU distribution of EAS 24 p4187 N85-35970
Electrons, muons and hadrons in extensive air showers and how do they depend on nuclear interaction model, part 1 24 p4187 N85-35972
Simulation of EAS properties on the basis of high energy interaction model deduced from the accelerator data
24 p4187 N85-35973
New aspects in nucleon-nucleus collisions and EAS properties around 10(6) GeV 24 p4187 N85-35974
Small air showers and collider physics
[HE-4.1-9] 24 p4187 N85-35975
High energy hadrons in extensive air showers
24 p4187 N85-35976
Hadronic components of EAS by rigorous saddle point method in the energy range between 10(5) and 10(8) GeV 24 p4188 N85-35978
About increase of the large transvers momentum processes fraction in hA interactions at energies 5.10(14) - 10(16) eV according to the data on E.A.S. hadrons
24 p4188 N85-35979
Phenomenology of soft hadron interactions and the relevant EAS data 24 p4188 N85-35980
Theoretical study of EAS hadronic structure
24 p4189 N85-35991
Comparison of simulation results with sea-level experimental data on 10(14) - 10(16) air shower cores
24 p4190 N85-35993
Particle distributions in approximately 10(13) - 10(16) eV air shower cores at mountain altitude and comparison with Monte Carlo simulations
[HE-4.2-18] 24 p4190 N85-35994
The longitudinal development of muons in cosmic ray air showers at energies 10(15) - 10(17) eV
[HE-4.3-12] 24 p4192 N85-36006
Topological aspects of age parameter
[HE-4.3-13] 24 p4192 N85-36007
Monte Carlo simulation of EAS generated by 10(14) - 10(16) eV protons
[HE-4.3-14] 24 p4192 N85-36008
Hybrid TLC-pair meter for the Sphinx Project
[HE-5.2-10] 24 p4203 N85-36086

SIMULATOR TRAINING
U TRAINING SIMULATORS

SIMULATORS
NT COCKPIT SIMULATORS
NT CONTROL SIMULATION
NT ENVIRONMENT SIMULATORS
NT FLIGHT SIMULATORS
NT MOTION SIMULATORS
NT SHOCK SIMULATORS
NT SOLAR SIMULATORS
NT SPACE SIMULATORS
NT SPACECRAFT CABIN SIMULATORS
NT TARGET SIMULATORS
NT TRAINING SIMULATORS
NT VIBRATION SIMULATORS
Clutter generator for use in radar evaluation
[AD-D011234] 01 p0039 N85-10245
Effects of repetitive, small-spot, incoherent light flashes on pursuit tracking performance
[AD-A144848] 01 p0095 N85-10637
Hardware for a real-time multiprocessor simulator
[NASA-TM-83805] 01 p0099 N85-10659
Test signal generator for coherent air-to-ground radars
[AD-D011278] 05 p0626 N85-14025
POPCORN: A supervisory control simulation for workload and performance research
05 p0704 N85-14515
A simulator for studying helicopter weapons systems
08 p1075 N85-16616
Novel applications of the NASA/GSFC Viterbi decoder hardware simulator 08 p1101 N85-16957
Operating system for a real-time multiprocessor propulsion system simulator. User's manual
[NASA-TP-2426] 08 p1207 N85-17596
An electronically controlled array for simulation of passive target/background signatures at millimeter wavelengths
[AD-D011456] 10 p1468 N85-19263
An H.F. simulator for use with real time channel evaluation systems 10 p1473 N85-19293
Theoretical study of a dynamic simulator of selective fading for digital, wireless beam microwave links
10 p1473 N85-19294
Drag-free satellite simulator
[REPT-615] 12 p1789 N85-21229
Rotorcraft digital advanced avionics system (Rodasa)
15 p2668 N85-26608
The gust simulation apparatus of the 3m x 3m low speed wind tunnel of the DFVLR in Goettingen, West Germany
[DFVLR-FB-85-04] 17 p2906 N85-27920
SAPIENS Memo 8: Electromagnetic properties of the EMP simulator SAPIENS
[FOA-C-30382-A3] 20 p3442 N85-31365
PHOENICS 84: A multi-dimensional multi-phase general-purpose computer simulator for fluid flow, heat transfer and combustion: 36 lecture panels
[CFD/84/18] 20 p3457 N85-31488
Construction of University of Missouri, Rolla's full scale cloud simulation chamber and applied research
[AD-A154682] 21 p3557 N85-32126
Design of a jamming simulator for a binary communication system
[AD-A154617] 21 p3573 N85-32221
Flexible satellite communications systems simulator, phase 3
[AD-A155647] 21 p3577 N85-32247
Reference-cell calibration activities
21 p3613 N85-32453
Gust simulation for flight mechanical wind tunnel tests
24 p4062 N85-35172
A review of motion sickness with special reference to simulator sickness
[AD-A155975] 24 p4131 N85-35611

SIMULTANEOUS EQUATIONS
Method and apparatus for self-calibration and phasing of array antenna
[NASA-CASE-NPO-15920-1] 12 p1832 N85-21493
MATRIX: A program that shows how row and column orderings affect matrix fill-in
[DE85-007522] 15 p2630 N85-26213

SIMULTANEOUS IMAGE CORRELATOR
U IMAGE CORRELATORS

SINE WAVES
The ML (Maximum Likelihood) method for frequency estimation of real sinusoids in noise
[AD-A146053] 03 p0411 N85-12628
Effect of a thermal gradient applied to a sinusoidal surface profile
[DE84-015649] 03 p0434 N85-12765
Characteristic impedance of a porous center during transmission of quasi-static sinusoidal vibrations
[ISSN-0208-5658] 05 p0647 N85-14155
Initialization of Thompson-Pisarenko's algorithm — sinusoidal signal parameter estimation
[FUB-46-1983] 09 p1375 N85-18641
Modulated sinusoidal currents in management of vibration sickness 10 p1524 N85-19612
Microwave SAW (Surface Acoustic Wave) monochromator
[AD-D011718] 21 p3590 N85-32311

SINGLE CHANNEL PER CARRIER TRANSMISSION
Analog voice processing for FM transmission in a telephone channel
[INPE-2798-PRE/359] 03 p0354 N85-12279

SINGLE CRYSTALS
Morphological changes of gamma prime precipitates in nickel-base superalloy single crystals
[NASA-TM-83696] 01 p0026 N85-10165
Process Research of Polycrystalline Silicon Material (PROPSM)
[NASA-CR-173838] 01 p0067 N85-10446
Preparation and properties of single crystals of hydrogen bis(phthalocyaninato) neodymium(3)
[AD-A144933] 01 p0123 N85-10646
Life prediction and constitutive models for anisotropic materials 02 p0144 N85-10976
Trivalent ion exchange in beta alumina
[AD-A145373] 02 p0172 N85-11151
Surface chemistry of palladium
[DE84-014572] 02 p0173 N85-11163
The transient oxidation of single crystal NiAl+Zr
[NASA-CR-174756] 02 p0182 N85-11221

The effect of tantalum and carbon on the structure/properties of a single crystal nickel-base superalloy
[NASA-CR-174779] 02 p0182 N85-11223
Preparation and properties of evaporated CdTe films compared with single crystal CdTe
[DE85-000502] 02 p0222 N85-11452
Complex formation and temperature stability of electrophysical properties of GaAs semiinsulating single crystals 02 p0258 N85-11689
Focusing beam of 1-GeV protons with volumetric capture to the mode of channeling by bent single crystal 02 p0266 N85-11750
Splitting of surface polariton spectrum by holographic grating 02 p0272 N85-11771
Biaxial constitutive equation development for single crystals
[NASA-CR-174056] 02 p0288 N85-11862
Plastic strain localization in superalloy single crystals
[AD-A145705] 02 p0288 N85-11878
The effect of orientation on fatigue growth in a nickel-based single crystal superalloy
[PNR-90207] 03 p0332 N85-12141
Diffusion of Fe-55 in Fe-2O-3 single crystals
[AERE-R-11286] 03 p0333 N85-12147
Growth and magnetic investigations of single crystals of intermetallic compounds of rare earths and uranium — magnetic properties 03 p0425 N85-12712
Quasielastic neutron scattering on single crystals of solid ionic conductor 03 p0426 N85-12719
Construction of a neutron single crystal diffractometer 03 p0427 N85-12723
Spectroscopic investigations on neutron induced impurity atoms and radiation defects 03 p0430 N85-12742
Neutron scattering on macromolecular solid state materials, solutions and melts 03 p0431 N85-12747
Kohn anomaly in metastable fcc lanthanum at low temperatures
[DE84-015459] 04 p0569 N85-13628
Magnetic susceptibility, electrical resistivity, and specific heat of single crystal LaFe-4P-12
[DE84-009979] 04 p0570 N85-13633
Single crystal semiconductor multilayers for electrically active optical interference filters
[DE84-015614] 04 p0571 N85-13640
Development of high responsitivity Ge:Ga photoconductors
[DE84-016902] 04 p0571 N85-13643
Luminescent properties of graded cadmium sulfoselenide electrodes prepared from cadmium sulfide substrates
[AD-A146710] 06 p0766 N85-14898
Development of technology of silicon single-crystal production semiconductor power devices: State of art outlook 06 p0795 N85-15078
Analysis of optical and electrical performance of a TCP-coated solar cell 06 p0832 N85-15293
Preparation and electronic properties of MoS(2) and WS(2) single crystals grown in the presence of cobalt
[AD-A146506] 06 p0866 N85-15506
Low noise multiple crystal-controlled oscillator
[AD-D011401] 07 p0948 N85-16010
Crystal growth and characterization of BaMgF4
[AD-A146805] 07 p1047 N85-16650
The fundamentals of dislocation transport of hydrogen in bcc iron
[AD-A146143] 08 p1129 N85-17117
Process development for the production of technically high quality monocrystalline diamond grits
[BMFT-FB-T-84-204] 08 p1136 N85-17166
Automatic Monoellipsoidal Mirror Furnace Facility (AMMFF), volume 1 — spaceborne crystal growth
[AMF-RP.100-DS-015-VOL-1] 09 p1285 N85-18073
Improved solid-state laser sources, volume 2
[DE85-000750] 09 p1325 N85-18330
The growth of large diameter single crystals by vertical solidification of the melt
[AD-A148756] 09 p1397 N85-18792
Single crystal silicon as a low-temperature structural material
[DE84-017469] 09 p1400 N85-18810
Characterization of CO binding sites on Rh(111) and Rh(331) surfaces by XPS and LEED (Low Energy Electron Diffraction): Comparison to EELS (Electron Energy Loss Spectroscopy) results
[AD-A149331] 10 p1435 N85-19044
Low cycle fatigue of MAR-M 200 single crystals at 760 and 870 deg C
[NASA-TM-86933] 10 p1440 N85-19074
Magnetic excitation in CuMn spin glass alloy
[DE85-002564] 10 p1453 N85-19159
Method for synthesizing indium phosphide
[AD-D011475] 10 p1583 N85-19855
Microstrain analysis in bent single crystal silicon by double crystal X-ray topography technique
[DE85-000422] 10 p1584 N85-19863
Studies of the kinetics and mechanisms of ammonia synthesis and hydrodesulfurization on metal single crystal surfaces
[DE85-001650] 11 p1595 N85-20030
Phonon-impurity relaxation and acoustic wave absorption in yttrium-aluminum garnet crystals with impurities 11 p1715 N85-20790
Electron-oscillatory spectra of yttrium-erbium-aluminum garnet of crystals and their role in laser pumping 11 p1715 N85-20791
Low stress semiconductor-insulator interface for cryogenic device applications
[NASA-CASE-NPO-16394-1] 11 p1734 N85-20906
Diamondlike flakes
[NASA-CASE-LEW-13837-2] 12 p1796 N85-21267
Fracture toughness of materials
[DE85-004306] 12 p1867 N85-21713
Total immersion crystal growth
[NASA-CASE-NPO-15800-2] 12 p1939 N85-22178
Orientation and temperature dependence of some mechanical properties of the single-crystal nickel-base superalloy Rene N4. 3: Tension-compression anisotropy
[NASA-TM-86982] 13 p2021 N85-22660
Basis and pyramidal slipping in single crystals of alpha-alloy Ti-Al-Sn 13 p2032 N85-22730
Fracture mechanics evaluation of GaAs
[NASA-CR-175857] 13 p2102 N85-23101
Influence of substrate heating and thermal annealing on the surface crystallinity in single Si crystals implanted with high doses of (16)O
[DE85-005264] 13 p2164 N85-23428
The cyclic stress-strain behavior of nickel-base superalloy poly- and single crystals 14 p2254 N85-23969
Effect of elevated-temperature neutron irradiation on fracture toughness of ceramics
[DE85-000652] 14 p2261 N85-24010
A two-cycle shift register with error detection
[AD-A150768] 14 p2400 N85-24791
Ferroelectric tungsten bronze bulk crystals and epitaxial thin films for electro-optic device applications
[AD-A151044] 14 p2427 N85-24970
Surface acoustic wave structure and volume waves 15 p2525 N85-25568
Materials for advanced rocket engine turbopump turbine blades 16 p2734 N85-26872
High-pressure hydrogen testing of single crystal superalloys for advanced rocket engine turbopump turbine blades 16 p2735 N85-26875
Secondary ion mass spectrometry studies of solids and surfaces
[AD-A151744] 16 p2745 N85-26939
Effects of wear on structure-sensitive magnetic properties of ceramic ferrite in contact with magnetic tape
[NASA-TM-87007] 16 p2753 N85-26991
Acceleration-resistant crystal resonator
[AD-D011627] 16 p2776 N85-27144
Studies of strain rate effects in the deformation of solids by means of stress pulses and ultrasonic methods
[DE85-009463] 18 p3122 N85-29329
Study of the equilibrium vacancy ensemble in aluminum using 1D- and 2D-angular correlation of annihilation radiation
[DE85-008957] 18 p3194 N85-29813
Effects of gamma-ray irradiation on dislocations in sodium nitrate single crystals
[DE85-008291] 18 p3195 N85-29818
Laser Schlieren crystal monitor
[NASA-CASE-MFS-28080-1] 19 p3374 N85-30932
Crystal growth of device quality GaAs in space
[NASA-CR-176024] 19 p3375 N85-30935
Low-temperature positron lifetime and Doppler-broadening measurements for single-crystal nickel oxide containing cation vacancies
[DE85-010238] 19 p3376 N85-30944
Debye temperature and static displacements in LuH sub x single crystals from energy dispersive X-ray diffraction
[DE85-010961] 19 p3376 N85-30946
Reduction of the trapping of positrons in dislocated single crystals of iron when charged with hydrogen
[DE85-010235] 19 p3377 N85-30950
Microgravity silicon zoning investigation
[NASA-CR-171531] 20 p3397 N85-31073
Photoeffects of semiconductor electrolyte interfaces
[AD-A154163] 20 p3449 N85-31411
Constitutive modeling of superalloy single crystals and directionally solidified materials 20 p3466 N85-31535
Compositional analysis of silicon 20 p3480 N85-31626
Positron measurements in 2H-TaSe2 crystals
[DE85-010507] 20 p3529 N85-31949
Temperature field around a spherical, cylindrical, and needle-shaped crystal, growing in a pre-cooled melt
[NASA-TM-77689] 20 p3537 N85-32011
Determination of edge and screw dislocation density in single crystals of high-purity iron
[DE85-010237] 20 p3537 N85-32012
The measurement of strain fields by X-ray topographic contour mapping
[AD-A154870] 21 p3589 N85-32348
A fluidized-bed reactor for silane pyrolysis 21 p3609 N85-32413
Basic ice nucleation mechanisms on mono and microcrystals and ice forming nuclei. Theoretical analysis and experimental results achieved in the laboratory over the past ten years: Review paper 21 p3642 N85-32629
Spectral-luminescence characteristics and induced emission of Nd-3(+) ion in Gd(2-x)Nd(x)(WO4)3 crystals 21 p3698 N85-32912
The development and evaluation of point defect models for the growth of passive films on single crystal, polycrystalline, and amorphous metal surfaces
[AD-A154685] 21 p3709 N85-33023
Microstructure-mechanical property relationships in the transformation-toughened ceramics
[DE85-011946] 22 p3752 N85-33261
Infrared studies of the influence of alkali metals on the C-O bond in chemisorbed carbon monoxide
[DE85-005306] 23 p3911 N85-34232
Cost effective single crystals: The Rolls Royce approach — gas turbine components
[PNR-90262] 23 p3966 N85-34717
Wholebody radiation counting system
[AD-A155842] 24 p4131 N85-35607

SINGLE SIDEBAND MODULATION
U SINGLE SIDEBAND TRANSMISSION

SINGLE SIDEBAND TRANSMISSION
Digital signal demodulators with single-sideband 07 p0950 N85-16019
Use of the analytic signal in ultrasonic imaging
[DE84-016843] 07 p1039 N85-16698
Study of phase radiogeodetic systems with phase-locked loops 13 p2115 N85-23172

SINGULAR INTEGRAL EQUATIONS
Sinc method of solution of singular integral equations
[AD-A146155] 03 p0411 N85-12631
A note on the use of polynomial transformations in evaluating singular integrals
[MATHEMATICS-RESEARCH-165] 12 p1920 N85-22053
Calculating dominant (quasi-t) mode group velocity in shielded microstrip line 22 p3780 N85-33422

SINGULARITY (MATHEMATICS)
Implementation of the supersonic triplet singularity into the USTORE computer code
[CSIR-NIAST-83/47] 01 p0001 N85-10006
Stable and chaotic dynamical systems and their singularities in the complex time plan
[DE84-011780] 01 p0035 N85-10222
Classical free-streamline flow over a polygonal obstacle
[NASA-CR-172448] 01 p0048 N85-10301
Applications of integral equations with strong singularities in fracture mechanics 03 p0371 N85-12367
Removal of singularities in Tresca and Mohr-Coulomb yield functions
[OUEL-1528/84] 03 p0413 N85-12642
Singularity model for the analysis of wall interference in closed wind tunnels according to the wall pressure signature method (blockage and lift)
[FW-FO-1612] 04 p0453 N85-12874
Computation of the nonequilibrium flow in a gasdynamic laser
[AD-A141022] 04 p0505 N85-13224
Flow calculation on a thin wing, with specific attention to separation point at the trailing edge
[FTW-FO-1721] 05 p0584 N85-13787
Translational control of a graphically simulated robot arm by kinematic rate equations that overcome elbow joint singularity
[NASA-TP-2376] 06 p0856 N85-15448
Numerical experiments and theoretical analysis of the flow of an elastic liquid of the Maxwell-Oldroyd type in the presence of geometrical singularities
[WTHD-164] 08 p1163 N85-17340
Topological triviality of versal unfoldings of complete intersections 11 p1699 N85-20878
On the accuracy of least squares methods in the presence of corner singularities
[NASA-CR-172552] 12 p1919 N85-22050
Transient analysis of loaded thin-wire antennas and transmission lines 13 p2053 N85-22852

Structural stability and bifurcation in conical flow fields
[VTH-LR-424] 16 p2803 N85-27282

SINKS
NT HEAT SINKS
Three dimensional global modeling of atmospheric CO2 05 p0652 N85-14189
The nitrogen cycle: Atmosphere interactions 05 p0653 N85-14191
Evolution of set of Rossby waves toward anisotropic equilibrium state 13 p2109 N85-23141
Flow past a flat plat with a vortex/sink combination
[JAAA-TR-58] 16 p2464 N85-25215
On planetary rings as sources and sinks of magnetospheric plasmas 15 p2677 N85-26526
Tribological sinks: Money down the drain
[DE85-010019] 17 p2974 N85-28376

SINKS (GEOLOGY)
U STRUCTURAL BASINS

SINTERED ALUMINUM POWDER
Engineering property comparisons of PM and IM aluminum alloy forgings
[AD-B088146L] 08 p1173 N85-17396

SINTERING
Sintered silicon nitride workpiece
[NASA-TM-77600] 01 p0021 N85-10129
Treating silicon carbide sinter by heating in nitrogen
[NASA-TM-77601] 01 p0021 N85-10130
Silicon nitride sintered body
[NASA-TM-77602] 01 p0021 N85-10131
Silicon carbide ceramic production
[NASA-TM-77598] 01 p0035 N85-10220
Injection molding of silicon carbide capable of being sintered without pressure
[NASA-TM-77736] 01 p0035 N85-10221
Erosion of sintered WC-Co alloys 02 p0179 N85-11201
An investigation of the role of sintering in gas-solid interactions
[DE84-015481] 02 p0288 N85-11884
Ceramic powder for sintering materials
[NASA-TM-77434] 03 p0336 N85-12160
Sintering behavior of ultrafine silicon carbide powders obtained by vapor phase reaction
[NASA-TM-77422] 03 p0336 N85-12161
Ceramic microstructure development
[AD-A145753] 03 p0337 N85-12166
Preparation of sinter-active silicon carbide powders
[BMFT-FB-T-84-189] 04 p0469 N85-12982
Reactive sintering of SiC 04 p0473 N85-13010
Tests and modeling for sintering theory
[DE84-015110] 04 p0473 N85-13012
Fatigue behavior of sintered steels and measurement criteria for sintered prefabricated parts 05 p0650 N85-14174
Development and production of improved alpha-phase silicon nitride powders for hot pressing and sintering
[BMFT-FB-T-84-208] 07 p0921 N85-15830
Influence of size grading of sintering ore on the sintering process
[BLL-M-36004-(5828.4)] 07 p0924 N85-15854
Procedure for investigating high-temperature properties of iron-ore materials
[BLL-M-36020-(5828.4)] 07 p0926 N85-15868
The determination of vertical sintering speed of sinter charges
[BLL-M-36033-(5828.4)] 07 p0926 N85-15869
Solid-phase sintering of tantalum carbide
[BLL-M-36013-(5828.4)] 07 p0926 N85-15872
Fatigue strength of different sintered steels and design criteria for porous material (PM) parts
[LBF-FB-170/84] 07 p0928 N85-15886
Development and production of improved silicon carbide powder for pressureless sintering and hot pressing
[BMFT-FB-T-84-211] 07 p0934 N85-15917
Tensile test of pressureless-sintered silicon nitride at elevated temperature
[NASA-TM-77777] 08 p1172 N85-17390
Consolidation of thermites by pressing and sintering
[DE84-016943] 09 p1297 N85-18146
Sub-eutectic densification and second phase formation in Al2O3 - CaO
[DE85-002066] 09 p1398 N85-18796
Optimization of production of composite diamond-containing materials using titanium carbide-steel alloys 10 p1446 N85-19113
Kinetics of saturation of porous titanium with low melting point metals 10 p1446 N85-19114
Behavior and specifics of fracture of porous fiber materials in extension 10 p1447 N85-19118
Densification of submicron YSZ (Yttria-Stabilized Zirconia) powders with alumina and borate additives
[AD-A149520] 10 p1452 N85-19150
Positive electrodes of nickel-cadmium batteries
[NASA-TM-77808] 10 p1478 N85-19330
Structure and properties of copper-titanium-aluminum composites obtained by thermoreactive sintering 11 p1600 N85-20081
Laser processing of ceramics
[DE85-001184] 11 p1612 N85-20135
High-temperature, solid oxide electrolyte fuel cell power generation system
[DE85-002978] 11 p1675 N85-20552
Slip casting and nitridation of silicon powder
[NASA-TM-77809] 12 p1818 N85-21406
Pressureless sintered silicon nitride as a promising candidate for radome materials
[AD-P004367] 12 p1826 N85-21461
Development of a sintered shim
[DE85-006183] 13 p2025 N85-22685
Densification and deformation in the presence of a liquid phase
[DE85-005101] 13 p2038 N85-22763
Sintered silicon carbide molded body and method for its production
[NASA-TM-77646] 14 p2259 N85-23999
Influence of oxygen traces on the properties of tungsten heavy metals
[BLL-RARDE-TR-1177-(7291.7965)] 15 p2508 N85-25470
Comparative sinterability of combustion synthesized and commercial titanium carbides
[DE85-006255] 15 p2512 N85-25498
Sintering phenomena of non-oxide silicon compounds
[DE85-006676] 15 p2520 N85-25535
Flat conducts R and D in ceramic parts for diesel engine 15 p2534 N85-25637
Production of shaped parts of NITINOL alloys by solid-state sintering
[AD-A152089] 16 p2749 N85-26966
Test and modeling for sintering theory
[DE85-007761] 16 p2755 N85-27004
Impact of optical inhomogeneity in sintered interface between glasses on laser emission characteristics 16 p2763 N85-27053
Reaction-bonded and fiber-reinforced SiC static and dynamic gas turbine components
[BMFT-FB-T-84-302] 17 p2899 N85-27874
Powder-metallurgy alloys and steels
[BLL-BISI-TRANS-22239-(9022.08)] 17 p2926 N85-28050
Sintering and properties of metal-ceramic alloys of the Kovar type
[BLL-BISI-TRANS-21822-(9022.06)] 17 p2927 N85-28060
Process for making electrodes for discharge tubes
[DE85-008898] 17 p2955 N85-28247
Electrodes for flash discharge lamps
[DE85-008897] 17 p2955 N85-28250
Effects of processing chemistry on electrical properties of high field ZnO varistors
[DE85-007688] 17 p2956 N85-28254
Sintering reactions, structure and properties of a cobalt free nonconventional hard material
[DE85-007704] 18 p3076 N85-29025
French, UK, Swedish research in powder metallurgy, HIP 18 p3088 N85-29109
Powder metallurgy forged gear development
[NASA-TM-87483] 18 p3117 N85-29295
Joining of sintered composite TiC-steel materials by welding
[BLL-M-36253-(5828.4)] 20 p3461 N85-31502
Introduction of structural variations into oxide polymers and their effect on sintering and crystallization
[AD-A155597] 21 p3570 N85-32206
Sintering studies project
[AD-A154750] 21 p3572 N85-32216
Hot isostatically pressed Sm(2)(TM)17 magnets
[AD-A155479] 21 p3582 N85-32267
Reliability of void detection in structural ceramics using scanning laser acoustic microscopy
[NASA-TM-87035] 21 p3597 N85-32337
Influence of particle arrangement on sintering
[AD-A155337] 21 p3599 N85-32352
Ultra-trace analysis of sinter tantalum with SIMS
[BLL-RARDE-TR-1220-(7291.7965)] 23 p3913 N85-34245
Reliability of two sintered silicon nitride materials
[NASA-TM-87092] 23 p3919 N85-34284

SINUSOIDS
U SINE WAVES

SIPHONS
A siphon flow model for Evershed motion — sunspot regions 14 p2453 N85-25147

SIR-A
U SHUTTLE IMAGING RADAR

SIR-B
U SHUTTLE IMAGING RADAR

SIRIO SATELLITE
Interference experiment with the Sirio-OTS satellites
[FUB-17-1983] 01 p0040 N85-10254
Attenuation experimental data bank in the COST 205 project. Structure and management of the final supports
[FUB-5-1983] 01 p0126 N85-10865

SIRS B SATELLITE
SIR-B cartography and stereo topographic mapping 08 p1147 N85-17234
Monitoring of the tidal dynamics of the Dutch Waddensea by SIR-B 08 p1147 N85-17235
Studies of coastal mesoscale winds using SIR-B 08 p1147 N85-17238

SIS (SEMICONDUCTORS)
AlAs/GaAs superlattice barrier unipolar diode structure
[DE85-001904] 11 p1736 N85-20921

SITE SELECTION
A pilot study of future research on seismic hazards in Sweden
[FOA-C-20544-T1] 02 p0229 N85-11496
Calibration and validation areas — satellite altimeters 03 p0384 N85-12456
Carbon monoxide study, Anchorage, Alaska, November 22, 1982 to February 11, 1983
[PB84-236595] 05 p0673 N85-14321
Potential affiliate stations to work with the EVN — European VLBI Network; QUASAT 07 p1057 N85-16708
Ground-water level data and preliminary potentiometric-surface maps, Yucca Mountain and vicinity, Nye County, Nevada
[DE85-001771] 09 p1343 N85-18448
Preliminary survey of wind generation in Washington: Site studies and selected wind speed data
[DE85-000058] 09 p1345 N85-18462
Assessment of wave power available at key United Kingdom sites
[IOS-166] 09 p1346 N85-18466
Planning for greater-confinement disposal
[DE85-002143] 09 p1383 N85-18697
Airport site selection and design
[AD-P004193] 11 p1581 N85-19959
Index to published geologic maps in the region around the potential Yucca Mountain nuclear waste repository site, southern Nye County, Nevada
[DE85-000260] 11 p1669 N85-20518
Shallow magma targets in the western US
[DE85-003274] 12 p1881 N85-21803
Optimum path selection in automated radio relay link design 13 p2073 N85-22947
Selection of promising sites for magma energy experiments
[DE85-006832] 16 p2820 N85-27393
Parabolic dish test site: History and operating experience
[NASA-CR-175892] 17 p2985 N85-28447
Conceptual hydrologic model of flow in the unsaturated zone, Yucca Mountain, Nevada
[DE85-008346] 18 p3125 N85-29350
Region-to-area screening methodology for the Crystalline Repository Project
[DE85-009892] 18 p3125 N85-29354
Reference data source documentation for performance assessment studies, Basalt Waste Isolation Project, Hanford Site, Washington
[DE85-010543] 19 p3301 N85-30468
Design of the National Trends Network for monitoring the chemistry of atmospheric precipitation
[GS-CIRC-964] 20 p3486 N85-31664
Detection of solar neutrons by ground based neutron monitors
[IFSI-84-11] 20 p3547 N85-32076
Criteria for site selection and frequency allocation (keynote paper), part 5 21 p3623 N85-32511
Frequency and site selection criteria for MST radars, part 5.1A 21 p3624 N85-32512
Fusion facility siting considerations
[DE85-012694] 22 p3843 N85-33605
Mars landing sites 22 p3859 N85-33893
Reports from the German Meteorological Service. No. 166: The optimal spectral density of climatological station networks
[ISBN-3-88148-214-8] 23 p3950 N85-34478
Resource evaluation and site selection for microalgae production systems
[DE85-006807] 23 p3951 N85-34485
The 1984 biotic studies of Yucca Mountain, Nevada test site, Nye County, Nevada
[DE85-011715] 23 p3951 N85-34487
Simulated effects of increased recharge on the ground-water flow system of Yucca Mountain and vicinity, Nevada-California
[DE85-012985] 24 p4108 N85-35469
Siting of large scale wind turbines in Denmark 24 p4111 N85-35483
Special questions of siting wind turbine arrays and networks — West Germany 24 p4111 N85-35484

Environmental aspects of the Netherlands wind farm project 24 p4111 N85-35485
Visual impact of GROWIAN and resulting recommendations for siting of large wind energy converters 24 p4112 N85-35486

SITES
NT LANDING SITES
NT LAUNCHING PADS
NT LAUNCHING SITES
Community relations activities at Department of Defense sites
[AD-P004150] 09 p1349 N85-18486
Adsorption site, adsorption energy and normal vibration frequency of H/Ni(100) via total energy calculations
[AD-A150555] 13 p2156 N85-23388
Literature survey of underground construction methods for application to hardened facilities
[AD-A155212] 21 p3599 N85-32351

SITTING POSITION
Effect of body position and immobilization on intensity of spatial illusions in weightlessness 22 p3821 N85-33672

SIZE (DIMENSIONS)
NT GRAIN SIZE
Size specific total particulate emission factors for mobile sources
[PB84-226853] 01 p0071 N85-10471
The smallest sizes of diffuse interstellar clouds 06 p0878 N85-15578
Space nuclear-power reactor design based on combined neutronic and thermal-fluid analyses
[DE85-002433] 11 p1727 N85-20864
Torso sizing ring construction for hard space suit
[NASA-CASE-ARC-11616-1] 12 p1910 N85-21987
A Gimbal sizing analysis for an IPACS rotating assembly
[NASA-CR-172524] 16 p2741 N85-26913
Grain structure identification by ultrasound frequency averaging and deconvolution
[AD-A154332] 19 p3352 N85-30777
The effect of set size on time to recall color coded information
[AD-A155013] 21 p3665 N85-32767
An exploratory study of the effect of screen size and resolution on the legibility of graphics in automated job performance aids
[AD-A155989] 24 p4136 N85-35632

SIZE DETERMINATION
NT PRECIPITATION PARTICLE MEASUREMENT
The size of the lunar core 04 p0581 N85-13713
Programming and application of numerical controlled measuring machines (NCMES)
[BMFT-FB-T-84-153] 05 p0717 N85-14599
Size dependence of chondrule textural types 06 p0882 N85-15606
Computer sizing of fighter aircraft
[NASA-TM-86351] 08 p1067 N85-16759
Research study of droplet sizing technology leading to the development of an advanced droplet sizing system
[NASA-CR-174839] 12 p1950 N85-21604
Recent trends in particle size analysis techniques
[NASA-TM-77735] 13 p2017 N85-22645

SIZE DISTRIBUTION
NT PARTICLE SIZE DISTRIBUTION
Experimental study of the spray characteristics of a research airblast atomizer
[NASA-TM-86911] 07 p0904 N85-15727
Measurement of drop-size distributions with the aid of a scattered light particle size counting analyser
[BLL-TRANS-WH-620-(9091.9F)] 09 p1317 N85-18278
Application of scattered light particle size counting analysis to the determination of wide drop size distributions
[BLL-TRANS-WH-619-(9091.9F)] 09 p1317 N85-18279
Asteroid collisional evolution studies 13 p2176 N85-23501
Evolution of stratospheric aerosol size distribution from ground-based radiometric measurements: A study of El Chichon aerosol
[DE85-007555] 18 p2827 N85-27439
Elemental analysis of aerosols in Transvaal urban and power-producing areas using time and size-resolved samples 16 p2829 N85-27443
The dynamical behavior of the age-size-distribution of a cell population
[CWI-AM-R8414] 17 p2998 N85-28536
Ice fog as an electro-optical obscurant
[AD-A155059] 21 p3705 N85-33015
Burst size distributions in the digitized data of the ion chambers t Mt. Norikura and sea level stations
[SH-9.1-9] 23 p4061 N85-35124
Atmospheric neutrinos observed in underground detectors
[HE-5.3-8] 24 p4205 N85-36102

SIZE SEPARATION
Improved silicon grinding method and apparatus
[NASA-CASE-NPO-16336-1-CU] 12 p1810 N85-21407
Acoustic particle separation
[NASA-CASE-NPO-155559-1] 19 p3350 N85-30765
Size and DNA distributions of electrophoretically separated cultured human kidney cells 20 p3500 N85-31759

SIZING (SEPARATION)
U SIZE SEPARATION

SIZING (SHAPING)
Application of finite element method to the sizing of mechanical parts — helicopter design
[SNIAS-851-210-105] 20 p3463 N85-31515
Preliminary sizing and performance of aircraft
[NASA-TM-86357] 21 p3554 N85-32111

SIZING (SURFACE TREATMENT)
The application of anthropometric survey data to aircrew clothing sizing
[AD-A150545] 13 p2143 N85-23304

SKELETON
U MUSCULOSKELETAL SYSTEM

SKEWNESS
Transformation of heterogeneous surface waves by skewed streams 02 p0259 N85-11697
Compensation of skew passband of a SAW filter using predistortion 12 p1821 N85-21422
Skewed stable variables and processes
[AD-A150549] 13 p2153 N85-23372

SKID LANDINGS
Aircraft accident report: World Airways Inc., Flight 30H, McDonnell Douglas DC-10-30CF, N113WA, Boston-Logan International Airport, Boston, Massachusetts, January 23, 1982
[PB85-910406] 22 p3728 N85-33114

SKIDDING
Predictor model for seasonal variations in skid resistance, volume 1
[PB84-226812] 01 p0036 N85-10229
Predictor model for seasonal variations in skid resistance. Volume 2: Comprehensive report
[PB84-226820] 01 p0037 N85-10230
Skid resistance of bituminous surfaces in Ohio
[PB84-234491] 04 p0484 N85-13066
Evaluation of Epoxo 300-C nonskid coating for use on bridge decks
[PB85-108843] 12 p1819 N85-21412
Skid steering of wheeled and tracked vehicles: Analysis with Coulomb friction assumptions
[AD-A149826] 12 p1860 N85-21684

SKILLS
U ABILITIES

SKIN (ANATOMY)
NT EPITHELIUM
In vivo dermal absorption method and system for laboratory animals
[AD-D011231] 01 p0094 N85-10635
Natural electrical activity of human sympathetic nerve fibers, recorded from body surface 07 p1013 N85-18433
Technique for measuring body circumferences and skinfold thicknesses
[AD-A148166] 08 p1195 N85-17532
Specifics of human thermal regulatory reactions upon exposure to coriolis acceleration 10 p1525 N85-19617
Evaluation of a field expedient technique for sweat sample collection
[AD-A151916] 16 p2841 N85-27521
Carcinogenesis of nitrated toluenes and benzenes skin and lung tumor assays in mice
[AD-A155723] 22 p3818 N85-33655

SKIN (STRUCTURAL MEMBER)
Zero adhesion system
[AD-D011237] 01 p0015 N85-10093
Low power laminar aircraft structures 04 p0451 N85-12857
Aircraft skin penetrator and agent applicator. Volume 2: Test and evaluation
[AD-A151609] 15 p2466 N85-25225
Development of a field repair technique for mini-sandwich Kevlar/epoxy aircraft skin
[AD-A151989] 15 p2503 N85-25439
Friction and wear behavior of aluminum and composite I-beam stiffened airplane skins
[NASA-TM-86418] 17 p2895 N85-27852
Laminated thermoplastic radome
[AD-D011664] 18 p3079 N85-29045
Impact dynamics research on composite transport structures
[NASA-TM-86391] 19 p3284 N85-30367
A normal incidence X-ray telescope sounding rocket payload
[NASA-CR-176169] 24 p4153 N85-35749

SKIN FRICTION
NT AERODYNAMIC DRAG
NT FRICTION DRAG
NT VISCOUS DRAG
Turbulent boundary layers over rough surfaces hypersonic flow
[AD-A145040] 01 p0003 N85-10016
Full scale experiments into the use of large eddy breakup devices for drag reduction on aircraft 08 p1071 N85-16790
A two-axis, self-nulling skin friction balance
[NASA-CASE-LAR-13294-1] 12 p1851 N85-21610
Surface shear stress characteristics in turbulent flows 19 p3211 N85-29914
The effects of microbubbles on turbulent boundary layer skin friction 20 p3451 N85-31425
Numerical solutions of turbulent models for flow over a flat plate with angle of attack
[DE85-010380] 21 p3585 N85-32286
A three-dimensional turbulent boundary layer undergoing transverse strain and streamwise pressure gradient
[NASA-TM-86768] 23 p3930 N85-34358

SKIN TEMPERATURE (BIOLOGY)
Specifics of human thermal regulatory reactions upon exposure to coriolis acceleration 10 p1525 N85-19617
Circadian rhythm of human body temperature during spaceflights 12 p1901 N85-21934

SKIN TEMPERATURE (NON-BIOLOGICAL)
Turbine heat transfer 02 p0142 N85-10964

SKIRTS
Water impact laboratory and flight test results for the space shuttle solid rocket booster aft skirt 09 p1335 N85-18364
Finger materials for air cushion vehicles. Volume 2: Base fabrics for finger materials
[AD-A149701] 12 p1819 N85-21408
Results of tests on a specimen of the SRB aft skirt heat shield curtain in the MSFC LRLF
[NASA-CR-170883] 24 p4070 N85-35221
SRB TPS closeout materials characterization
[NASA-CR-170885] 24 p4070 N85-35222
Study of NSI and related cable performance during tests performed in the NASA Hot Gas Facility
[NASA-CR-170886] 24 p4101 N85-35423

SKIS
Determination of parameters of cupped aircraft landing ski 06 p0775 N85-14956

SKULL
SSMIR (Solid State Memory Instrumentation Recorder): A new approach to acquiring data during an aircraft seat/sled ejection sequence
[AD-A154780] 21 p3589 N85-32306

SKY
NT NIGHT SKY
HEAO-1 diffuse soft X-ray sky maps 06 p0877 N85-15570
A FORTRAN program for deep space sensor analysis
[AD-A151700] 15 p2489 N85-25366
Issue of sky conditions
[DE85-010590] 19 p3317 N85-30562
Correlation analysis of 1 to 30 MeV celestial gamma rays 20 p3549 N85-32083
A transportable, machine oriented library of european sky and terrain radiance distributions with contemporary radiometric and meteorological profiles
[AD-A155254] 21 p3637 N85-32590

SKY BRIGHTNESS
NBS (National Bureau of Standards) daylight availability database
[PB84-245745] 07 p1054 N85-15668
The IRAS mission 09 p1412 N85-18901
Flux reconstruction and calibration 09 p1412 N85-18904
Analysis of processing 09 p1412 N85-18905
Investigating statistical characteristics of atmospheric background brightness and star background density in equatorial region of celestial sphere 15 p2478 N85-25298
Issue of sky conditions
[DE85-010590] 19 p3317 N85-30562

SKY RADIATION
NT AIRGLOW
NT GEOCORONAL EMISSIONS
NT NIGHTGLOW
NT TWILIGHT GLOW
Thermal characterization of photovoltaic modules in natural environments 06 p0832 N85-15298
Improved Nominal Operating Cell Temperature (NOCT) test procedure 21 p3612 N85-32449

SKY WAVES
NT WHISTLERS
Skywave radar detectability of volcanic aerosols
[AD-A151448] 15 p2542 N85-25894

SKYLAB PROGRAM
The evolution of civilian in-space infrastructure, i.e., space station concepts in the United States
07 p0914 N85-15788
Material research in microgravity
[NASA-TM-77626] 14 p2228 N85-23811
Primate experiments on SLS-1
15 p2687 N85-26592

SKYLAB 3
Relative abundances of sub-iron to iron nuclei in low energy (50-250 MeV/N) cosmic rays as observed in the Skylab experiment
[OG-4.1-4] 22 p3878 N85-34010

SKYLAB 4
Hypervelocity impacts on Skylab 4/Apollo windows
12 p1785 N85-21202
Hypervelocity impact investigations and meteoroid shielding experience related to Apollo and Skylab
12 p1785 N85-21206

SKYNET SATELLITES
UK Skynet 4 communications satellites
11 p1710 N85-20757

SL 3
U SKYLAB 3

SL 4
U SKYLAB 4

SLABS
Microwave measurement of the complex dielectric tensor of anisotropic slab materials
[DE84-017050] 04 p0493 N85-13144
A remote source system for measuring relative positron annihilation line widths in individual slab cylindrical samples
[AERE-R-10549] 12 p1938 N85-22173
Guided-mode launching in a slab waveguide by way of diffraction at the edge of a conducting screen residing on one surface of the slab
[AD-A154886] 21 p3575 N85-32232
Multiple collision solutions for time-dependent neutron transport in slabs of finite thickness
[OEFZS-4312] 22 p3838 N85-33762
Negative flexural behavior of precase composite slabs with steel joint
23 p3904 N85-34183

SLAGS
The electrochemical deoxidation of molten oxide substances
[BLL-M-35982-(5828.4)] 05 p0614 N85-13920
Distribution of oxygen between metal and basic slags
[BLL-M-35932-(5828.4)] 05 p0616 N85-13935
Calculation of energy of atomization in silicate tetrahedron Si4(4-)
[BLL-M-36000-(5828.4)] 07 p1040 N85-16599
The development of titanium production in the USSR
[BLL-OA-TRANS-3226-(6196.3)]
23 p3913 N85-34244

SLANT
U SLOPES

SLANT PERCEPTION
U SPACE PERCEPTION

SLASHES
U CLEARINGS (OPENINGS)

SLEDS
NT ROCKET PROPELLED SLEDS
Design and testing of an energy-absorbing crewseat for the F/FB-111 aircraft. Volume 2: Data from seat testing
[NASA-CR-3917] 24 p4064 N85-35184

SLEEP
The effect of sleep loss on the human visual event-related potential
[AD-A145364] 02 p0234 N85-11526
Effect of physical work and sleep loss on recovery sleep
[AD-A146082] 03 p0401 N85-12554
Sleep physiology in weightlessness (experiment 1ES 030) — Spacelab
05 p0695 N85-14474
Computerized sleep staging by detecting eye and hand movement, delta EEG activity and EMG, using portable solid state technique — spaceborne experiments
05 p0695 N85-14475
Laboratory note: Effect on sleep latency of pre-sleep AEP (Auditory Evoked Potential) procedures
[AD-A147620] 08 p1194 N85-17527
Electrosleep therapy advanced at medical institute
10 p1526 N85-19623
Homeostasis in primates in the hyperdynamic environment — circadian timekeeping and effects of lower body positive pressure on sleep
15 p2610 N85-26085
Sleep and wake physiology in weightlessness
20 p3510 N85-31819

SLEEP DEPRIVATION
The effect of sleep loss on the human visual event-related potential
[AD-A145364] 02 p0234 N85-11526
Cognitive performance during successive sustained physical work episodes
[AD-A148061] 08 p1200 N85-17556
Effects of partial deprivation of slow-wave sleep on sleep-wakefulness cycles
10 p1524 N85-19613
Sleep deprivation and exercise tolerance
[AD-A150180] 13 p2142 N85-23295
Sleep deprivation and exercise tolerance
[AD-A150566] 13 p2142 N85-23296
Sleep deprivation and exercise tolerance
[AD-A150626] 13 p2142 N85-23297
Sleep deprivation and performance: Older age performance and limited sleep period use
[AD-A153102] 17 p2999 N85-26540
Human performance in continuous/sustained operations and the demands of extended work/rest schedules. An annotated bibliography
[AD-A155619] 21 p3666 N85-32771

SLEEVES
Manifold insulated with knitted impregnated sleeve
[AD-D011270] 06 p0614 N85-15167
Windblast arm protector assembly
[AD-D011512] 12 p1909 N85-21964
Direct transient analysis of a fuze assembly by axisymmetric solid elements
15 p2576 N85-25890

SLENDER BODIES
NT SLENDER CONES
Comparison of uniform perturbation solutions and numerical solutions for some potential flows past slender bodies
[NASA-CR-172485] 06 p0749 N85-14799
Transonic flow of elastic medium past slender solid body
06 p0778 N85-14976
Some important problems in unsteady boundary layers including separation. 2: Unsteady boundary layers close to the stagnation region of slender bodies
[AD-A146964] 07 p0958 N85-16069
Generation of a pair of symmetric eddies behind a slender axisymmetric body with pitch angle
[ISL-R-121/83] 11 p1577 N85-19934
An experimental and analytical study of the aerodynamic interference effects between two Sears-Haack bodies at Mach 2.7
[NASA-TM-85729] 16 p2700 N85-26673

SLENDER CONES
Experimental investigations of prismatic cylinders in flow with harmonic pulsations
[KU-SFB-210/E/4] 16 p2785 N85-27186

SLENDER WINGS
Transonic wing and far field test data on a high aspect ratio transport wing for three dimensional computational method evaluation
01 p0004 N85-10021
Flutter parametric studies of cantilevered twin-engine transport type wing with and without winglet. Volume 2: Transonic and density effect investigations
[NASA-CR-172410-VOL-2] 04 p0513 N85-13270
A calculation of slender delta wing with leading-edge separation by quasi-vortex-lattice method
12 p1821 N85-21423
Numerical simulation of transonic flutter of a high-aspect ratio transport wing
16 p2694 N85-26630
Aerodynamic performance of a wing in ground effect using the PANAIR program
[AD-A153303] 17 p2892 N85-27832
Low-speed tests of a high-aspect-ratio, supercritical-wing transport model equipped with a high-lift flap system in the Langley 4- by 7-meter and Ames 12-foot pressure tunnels
[NASA-TP-2097] 20 p3368 N85-31010

SLEWING
Operational fitness of box truss antennas in response to dynamic slewing
[NASA-CR-172470] 10 p1429 N85-19012
Time-optimal bang-bang slew of rigidized SCOLE configuration
20 p3410 N85-31164

SLICING
The read-out system of spatial distribution of thermoluminescence in meteorites
[SH-9.1-16] 23 p4052 N85-35131

SLICKS
U OIL SLICKS

SLIDES
U CHUTES

SLIDES (MICROSCOPY)
The Fibrin slide assay for detecting urokinase activity in human fetal kidney cells
20 p3502 N85-31766

SLIDING
Control of tractors on sloping ground
[AD-P004292] 09 p1408 N85-18869
Sealing assembly
[AD-D011463] 10 p1452 N85-19151
Interaction among inhomogeneities and inclusions
[AD-A153114] 17 p2979 N85-28419
The effect of stress and hot corrosion on nickel-base superalloys
[AD-A154722] 21 p3566 N85-32181

SLIDING FRICTION
An experimental investigation and numerical simulation of the thermomechanical phenomena in compressor rotor tip rubbing
03 p0367 N85-12352
Effect of barrier height on friction behavior of the semiconductors silicon and gallium arsenide in contact with pure metals
[NASA-TP-2405] 04 p0478 N85-13044
Effect of asperity interactions on scuffing
[AD-A146544] 06 p0614 N85-15170
Computational methods for nonlinear dynamics problems in solid and structural mechanics
[AD-A148352] 08 p1172 N85-17392
Analytical and experimental investigation of rubbing interaction in labyrinth seals for a liquid hydrogen fuel pump — space shuttle main engine
[NASA-CR-174657] 09 p1287 N85-18084
Sliding seal materials for adiabatic engines
[NASA-CR-174893] 13 p2097 N85-22757
Significant parameters of the behavior and of the surface damage of the lubricated Hertzian contact: An application to gears
14 p2222 N85-23783
Wear reduction by lubricants in confined contacts
14 p2223 N85-23786
Sliding interfaces with contact-impact in large scale Lagrangian computations
[DE85-006451] 15 p2639 N85-26277
Mechanical interactions of rough surfaces
[DE85-005653] 18 p3118 N85-29299
Granular Flow Project
[DE85-010015] 19 p3270 N85-30279
Kinetic friction coefficient of ice
[AD-A155035] 21 p3680 N85-32859
Rolling, slip and traction measurements on low modulus materials
[NASA-CR-174909] 22 p3791 N85-33491
Anti wear property of two phasic metal composite
23 p3906 N85-34199

SLIP BANDS
U EDGE DISLOCATIONS

SLIP CASTING
Study of the pore structure of ceramics prepared by the slip casting method
[NASA-TM-77495] 04 p0478 N85-13048
Nitinol devices, phase 2, integration of slip ring system and tracking mechanism with memory drive
[BMFT-FB-W-84-032] 05 p0619 N85-13959
Slip casting and nitridation of silicon powder
[NASA-TM-77809] 12 p1818 N85-21406

SLIPSTREAMS
NT PROPELLER SLIPSTREAMS
Turbulent jet flow in a channel with a circulation region
09 p1308 N85-18218
An experimental investigation of propfan installations on an upswept supercritical wing at transonic Mach numbers
[NASA-CR-172605] 20 p3388 N85-31013

SLITS
The effect of grazing flow on the impedance of the Helmholtz resonator
05 p0635 N85-14078

SLOPES
NT GLIDE PATHS
Terrain analysis procedural guide for surface configuration
[AD-A145637] 02 p0219 N85-11446
Occurrences of the polar slant E condition (SEC) at Narssarssuaq, Godhavn, Thule 1982
03 p0393 N85-12514
Relationship between forest clearing and biophysical factors in tropical environments: Implications for the design of a forest change monitoring approach — Costa Rica
[E85-10051] 07 p0983 N85-16247
Study of the motion of agricultural vehicles on steep grass-covered slopes
[AD-P004290] 09 p1408 N85-18867
Some stability and control problems with trailed farm tankers on slopes
[AD-P004291] 09 p1408 N85-18868
Control of tractors on sloping ground
[AD-P004292] 09 p1408 N85-18869
Analysis of slope stability, Wilmington to Lindenkohl Canyons, US mid-Atlantic margin
[DE84-012278] 12 p1899 N85-21921
Relationship between brightness spectrum of photographic image and spectrum of rises on a water surface with waves
13 p2115 N85-23171
A statistical treatment of the regional slope characteristics of Venus and Earth
13 p2178 N85-23517
Lithologic and structural control on slope morphology in the Valles Marineris
13 p2201 N85-23651
Guidelines for the evaluation of visual approach slope indicators
[ARL/SYS-R-32] 23 p3896 N85-34132

Evaluation: Close-range photogrammetry for slope inventory and monitoring
[PB85-192755] 24 p4106 N85-35470
Turbulent structure of stably stratified nocturnal slope flows
[AD-A155845] 24 p4123 N85-35559

SLOSHING
U LIQUID SLOSHING

SLOT ANTENNAS
Experimental measurements of the ion cyclotron antennas' coupling and RF characteristics
[DE85-011569] 23 p3982 N85-34694
Characteristic modes for slots in a ground plane TE case
[AD-A155757] 24 p4086 N85-35326

SLOTS
Portable slotting device
[AD-D011213] 01 p0033 N85-10206
Electromagnetic transmission through a slot in a perfectly conducting plane
[AD-A153224] 17 p2949 N85-28210
A multiplying slot array
[AD-A155570] 21 p3576 N85-32245
Induction motors with minimum waste of magnetic iron
22 p3772 N85-33377
Dual optical mechanical position tracker
[AD-D011739] 22 p3844 N85-33811

SLOTTED ANTENNAS
U SLOT ANTENNAS

SLOTTED WIND TUNNELS
Interference from slotted walls
03 p0314 N85-12028
An interference assessment approach for a three-dimensional slotted tunnel with sparse wall pressure data
03 p0314 N85-12030
A local slot boundary condition for transonic flow calculations in slotted-wall test sections of wind tunnels
[FFA-TN-1984-34] 04 p0453 N85-12879
Investigation for the improvement of the transonic tunnel working section of the Emmen Federal Aircraft Works (Switzerland)
[FW-FO-1681] 04 p0458 N85-12904
Flow quality of NAL 2-dimensional transonic wind tunnel. Part 2: Extensive and systematic pressure fluctuations study in the settling chamber, test section and second throat of the NAL 2-D transonic wind tunnel
[NAL-TR-836-PT2] 09 p1283 N85-18066
Finite difference computation of the flow around airfoils in two-dimensional transonic slotted wall wind tunnel
11 p1623 N85-20216
Wind tunnel wall interference
[AD-A151212] 15 p2474 N85-25273

SLOW NEUTRONS
U THERMAL NEUTRONS

SLUDGE
Remedial action of hazardous waste US Army Corps of Engineers, Anniston, Alabama
[AD-P004141] 09 p1347 N85-18477

SLURRIES
Additives for heat engine coal slurry fuels
[DE84-016434] 05 p0621 N85-13971
Gasification of boron oxide drops and boron slurry agglomerates in combustion gases
13 p1999 N85-22529
Catalyst and reactor development for a liquid phase Fischer-Tropsch process
[DE85-005894] 17 p2922 N85-28014
Transport characteristics of slurries in pipelines: Flow regimes and pressure drop
[DE85-009453] 18 p3101 N85-29198
Development of a coal-water slurry-fueled diesel engine for industrial cogeneration. Task 1.0 topical report: Thermodynamic analysis
[DE85-010455] 19 p3236 N85-30062
Very high speed lap with positive lift effect
[AD-D011710] 19 p3280 N85-30344
Very high speed lap with negative lift effect
[AD-D011711] 19 p3281 N85-30345
Effect of nonuniform size on internal stresses in a rapid, simple shear flow of granular materials. Part 1: Two grain sizes
[AD-A154015] 19 p3285 N85-30372
Coal slurry ignition in a diesel engine simulator
[DE85-010987] 20 p3463 N85-31513
Superheated fuel injection for combustion of liquid-solid slurries
[DE85-011624] 22 p3753 N85-33286
Drying of pulverized material with heated condensible vapor
[DE85-011656] 22 p3783 N85-33436
Method of preparing thin porous sheets of ceramic material
[DE85-008399] 24 p4082 N85-35300

SLURRY PROPELLANTS
Status of boron combustion research
[AD-A154762] 21 p3563 N85-32160

SMALL PERTURBATION FLOW
Robust calculation of three-dimensional transonic potential flow based on the nonlinear gas multigrid method and a mixed incomplete lower upper decomposition/strongly implicit procedure (ILU/SIP) algorithm
[NLR-MP-84003-U] 12 p1848 N85-21593
Extension of the small perturbations method in three-dimensional transonic, unsteady flow to the case of real wings
[ONERA-NT-17/3064-RY-070-R]
20 p3389 N85-31017

SMELTING
New ferrous metallurgy technology
01 p0019 N85-10114
Sweden develops new rapid solidification process
15 p2531 N85-25610
Assessment of metal heating technologies for ferrous forging: A pilot study of the form value of natural gas
[PB85-204394] 24 p4084 N85-35314

SMOG
Impact of alcohol fuels on urban air pollution: Methanol photochemistry study
[DE84-012950] 04 p0531 N85-13397
Evaluation of chemical reaction mechanisms for photochemical smog. Part 2: Quantitative evaluation of the mechanisms, revised
[PB85-166080] 16 p2822 N85-27408
Effect of traffic and meteorology on air pollution
16 p2830 N85-27452
Development of a chemical kinetic mechanism for the US EPA (Environmental Protection Agency) regional oxidant model
[PB85-185858] 22 p3813 N85-33618
Modeling of auto exhaust smog chamber data for EKMA development
[PB85-186492] 22 p3813 N85-33619
Atmospheric reaction products from hazardous air pollutant degradation
[PB85-185841] 22 p3813 N85-33620
Studies in photochemical smog chemistry. 1: Atmospheric chemistry of toulene. 2: Analysis of chemical reaction mechanisms for photochemical smog
24 p4113 N85-35497

SMOKE
The perceptual quality of smoke screens: An analysis of the Oldebroek 2 trials, May 1981
[IZF-1984-20] 01 p0095 N85-10641
The prediction of observer responses from photometric data on smoke screens; an analysis of the Oldebroek 2 trials, May 1981
[IZF-1984-21] 01 p0095 N85-10642
Analytical fuel property effects: Small combustors, phase 2
[NASA-CR-174848] 10 p1456 N85-19175
Continuous laminar smoke generator
[NASA-CASE-LAR-13014-1] 12 p1781 N85-21178
Ionic mechanisms of soot formation in flames
[AD-A150119] 12 p1801 N85-21297
Time and space variability of turbulent concentration fluctuations
[AD-A149963] 12 p1806 N85-21606
Effects of interactive transport and scavenging of smoke on the calculated temperature change resulting from large amounts of smoke
[DE85-006450] 14 p2378 N85-24684
Advanced smoke meter development survey and analysis
[NASA-CR-168287] 15 p2560 N85-25792
Evaluation of pyrotechnic fire suppression system for six pyrotechnic compositions
[AD-A152995] 17 p2937 N85-28130

SMOKE ABATEMENT
Laboratory simulation of smoke reduction from aircraft engine test cell exhaust using a fluidized bed filter
[AD-A149600] 08 p1089 N85-16585
Numerical simulations of the effect of floor and ceiling venting on fire and smoke spread in aircraft cabins
[PB85-178333] 19 p3216 N85-29939

SMOKE DETECTORS
Test results from a comparative evaluation of a condensation nuclei fire detector
[NASA-CR-3974] 12 p1882 N85-21675
Evaluation of pyrotechnic fire suppression system for six pyrotechnic compositions
[AD-A152995] 17 p2937 N85-28130

SMOKE TRAILS
Numerical simulations of the effect of floor and ceiling venting on fire and smoke spread in aircraft cabins
[PB85-178333] 19 p3216 N85-29939

SMOOTHING
NT DATA SMOOTHING
Improved carrier tracking by smoothing estimators
05 p0623 N85-13069
Recovering pointwise values of discontinuous data within spectral accuracy
[NASA-CR-172535] 12 p1919 N85-22049
Consistency of smoothing with running linear fits
[AD-A150232] 13 p2150 N85-23349
Kalman filtering and exponential smoothing in economics
15 p2635 N85-26248
Uniformly high-order accurate non-oscillatory schemes, 1
[NASA-CR-175768] 16 p2853 N85-27589
The essence of inversity
[CSIR-TWISK-321] 16 p2858 N85-27626
To the theory of approximation of experimental curves by smooth functions
[PREPRINT-438] 16 p3173 N85-29871
Computer programs for smoothing and scaling airfoil coordinates
[NASA-TM-84666] 20 p3388 N85-31011
A residuals approach to filtering, smoothing and identification for static distributed systems
20 p3418 N85-31213

SNAKING
U LATERAL OSCILLATION

SNAP
SNAP (Space Nuclear Auxiliary Power) reactor overview
[AD-A146831] 07 p1041 N85-16812

SNATCHING
U SPACECRAFT RECOVERY

SNOW
Heliport snow and ice control methods and guidelines
[DOT/FAA/PM-84/22] 01 p0012 N85-10073
Some mesoscale weather effects and the very short-range forecasting impact of variable snow cover
01 p0075 N85-10409
Fractals: From snow flakes to galactic clusters
[NOTA-INTERNA-796] 02 p0296 N85-11918
Anglo-German millimeter wave backscatter measurements on snow, environmental data report
[REPT-7-84] 04 p0492 N85-13136
The Finnish approach to microwave remote sensing of snow
05 p0656 N85-14212
Snow characterization measurements from SNOW-TWO/Smoke Week 8
[AD-A147423] 07 p1008 N85-16402
Climate at CRREL (Cold Regions Research and Engineering Laboratory) Hanover, New Hampshire
[AD-A148400] 08 p1189 N85-17495
Regional and seasonal variations in snow-cover density in the USSR
[AD-A148429] 08 p1189 N85-17496
Atlas of snow and ice resources
10 p1497 N85-19449
Ground-based snow and ice crystal observation system used in Sierra Nevada winter orographic storms
[PB85-115943] 10 p1520 N85-19584
Snow reflectance from Thematic Mapper
13 p2120 N85-23205
Remote Sensing of Snow and Evapotranspiration
[NASA-CP-2363] 13 p2123 N85-23223
General report of the researches of snowpack properties, snowmelt runoff and evapotranspiration in Japan
13 p2124 N85-23225
Snowmelt-runoff model utilizing remotely-sensed data
13 p2124 N85-23226
Snowmelt runoff model in Japan
13 p2124 N85-23227
Studies on physical properties of snow based on multi channel microwave radiometer
13 p2125 N85-23231
Radiation-dominated snowmelt on Mars
13 p2191 N85-23592
An equation of profile of snow drift density during snowfall
15 p2581 N85-25919
Measuring methods of atmospheric electric elements at the Earth's surface during snowfall and investigation of these relationships
15 p2581 N85-25920
Case studies of snow clouds by means of snow crystal sondes
15 p2581 N85-25921
A survey of major east coast snowstorms, 1960-1983. Part 2. Summary of surface and upperlevel characteristics
[NASA-TM-86195] 16 p2833 N85-27471
A survey of major east coast snowstorms, 1960-1983. Part 2: Case studies of eighteen storms
[NASA-TM-86196] 16 p2833 N85-27472
Snow Scale/Rate meter
[AD-D011648] 17 p2904 N85-28505
The capture of ice nucleating and non ice-nucleating aerosols by ice phase precipitation
21 p3641 N85-32620
Ice-forming efficiency of the soluble and insoluble portions of dust contained in snow
21 p3643 N85-32631

Scavenging of submicron aerosol particles by snow crystals: Theory and experiments
21 p3648 N85-32867
Elemental tracers of source regions of contaminants in precipitation
[DE85-012856] 24 p4113 N85-35499

SNOW COVER
Measurement of snow cover thickness by radar sounding 03 p0344 N85-12216
Scattering from snow backgrounds at 35, 98, and 140 GHz
[AD-A145798] 03 p0355 N85-12280
A comparison between active and passive sensing of soil moisture from vegetated terrains
04 p0526 N85-13364
Synoptical observations of snow depths at Dutch meteorological stations, 1956 - 1977
[KNMI-TR-61] 07 p1008 N85-16407
Microwave emissions from snow
[ESS-10085] 08 p1174 N85-17403
Application of Martinec-Rango model to river basin in Japan 13 p2124 N85-23228
Distribution of snow and maximum snow water equivalent obtained by LANDSAT data and degree day method 13 p2124 N85-23229
Microwave radiometer observations of snowpack properties and comparison of U.S. Japanese results — Hokkaido, Japan and Vermont and North Dakota test sites 13 p2125 N85-23230
Analysis of NIMBUS-7 SMMR data — Hokkaido, Japan snow cover 13 p2125 N85-23232
Estimation of regional evapotranspiration using remotely sensed land surface temperature. Part 2: Application of equilibrium evaporation model to estimate evapotranspiration by remote sensing technique — Japan 13 p2125 N85-23234
Measurement of water equivalent of mountain snow cover — ARGOS system 14 p2327 N85-24366
Low Temperature Science. Series A: Physical Sciences
[ISSN-0439-3538] 15 p2581 N85-25917
The temperature fluctuation in stable stratification above snow cover 15 p2581 N85-25918
Characteristics of snow cover on sea ice and formation of snow ice II 15 p2582 N85-25924
Atmospheric frontal zone studies
[NASA-CR-175299] 16 p2833 N85-27469
Precipitation and snow cover data, 1977
[ISBN-951-697-215-2] 17 p2995 N85-28514
Permafrost, seasonally frozen ground, snow cover and vegetation in the USSR
[AD-A153628] 18 p3124 N85-29346
Snow cover in the Siberian forest-steppe
[NASA-TM-77914] 23 p3943 N85-34435
Comparisons of the North Polar Cap of Mars and the Earth's Northern Hemisphere snow cover
[NASA-TM-86191] 23 p3969 N85-34728

SNOWPLOW EFFECT
U PLASMA DYNAMICS

SNOWSTORMS
East coast snowstorm survey
15 p2596 N85-25013
A survey of major east coast snowstorms, 1960-1983. Part 2. Summary of surface and upperlevel characteristics
[NASA-TM-86195] 16 p2833 N85-27471
A survey of major east coast snowstorms, 1960-1983. Part 2: Case studies of eighteen storms
[NASA-TM-86196] 16 p2833 N85-27472
Circulation analysis of two snowstorms during the SNOW-TWO program
[AD-A155225] 21 p3637 N85-32567

SOBOLEV SPACE
Loeb Sobolev spaces with applications to variational integrals and differential equations
[CTH-MATH-1984-19] 04 p0556 N85-13544
A non-hypoelliptic Dirichlet problem from stochastics
10 p1537 N85-19567
On the accuracy of least squares methods in the presence of corner singularities
[NASA-CR-172552] 12 p1919 N85-22050
Some properties of Loeb-Sobolev spaces
[CTH-MATH-1985-01] 22 p3835 N85-33748

SOCIAL FACTORS
Some aspects of matching nowcasting and Very-Short-Range Forecasting (VSRF) products with the need of a multilingual community of a mountainous country — Swiss Alps 01 p0084 N85-10566
The identification of the scientific community's choice criteria in the history of scientific research: The case of quantum mechanics
[NOTA-INTERNA-797] 02 p0291 N85-11893
Area handbook series. Honduras: A country study
[AD-A146510] 06 p0827 N85-15253
Socio-economic impact of climate — Mexico
07 p1003 N85-16372
Climate and fisheries: A Peruvian case study
07 p1003 N85-16373
Job and family stress as predictors of pilot health, job satisfaction and performance
[AD-A142176] 07 p1018 N85-16484
Aeronautical Engineering: A continuing bibliography with indexes, supplement 185
[NASA-SP-7037(185)] 13 p1985 N85-22342
Disturbance to the population due to flight operations at landing fields. Questionnaire on community reaction to non-commercial and sporting aviation
[NASA-TM-78531] 14 p2353 N85-24537
The effects of controversy and concurrence seeking on effective decision making
[AD-A153370] 17 p3002 N85-29555
Social and political problems in Soviet basic research
[AD-P004565] 17 p3048 N85-29860
Symbolic and interactional perspectives on leadership: An integrative framework
[AD-A155247] 21 p3665 N85-32769

SOCIOLOGY
NT SOCIAL FACTORS
National Science Foundation grants and awards for fiscal year 1983, volume 2
[PB84-212323] 01 p0125 N85-10654
An open-ended future: In defense of a new humanism
[NASA-TM-77613] 12 p1944 N85-22209
The Impact of Science on Society
[NASA-SP-482] 14 p2431 N85-24994
Accomplishments of science by the year 2000
14 p2432 N85-24996
Our future in the cosmos: Space
14 p2432 N85-24998
Science and Technology in the Soviet Union
[AD-A152828] 17 p3047 N85-28856
Space ventures and society long-term perspectives
[NASA-CR-176012] 19 p3379 N85-30963

SODAR
An operational forecasting system for stratus and fog with sodar 01 p0081 N85-10539
An evaluation of wind measurements by four Doppler sodars
[PB85-115301] 10 p1520 N85-19586
Radiosodar system for remote synchronous measurements of wind speed, temperature and its fluctuations 13 p2110 N85-23145
Verification of Doppler sodar measurements — atmospheric boundary layer
[KNMI-WR-85-2] 22 p3617 N85-33645

SODIUM
NT LIQUID SODIUM
NT SODIUM ISOTOPES
NT SODIUM VAPOR
Trivalent ion exchange in beta alumina
[AD-A145373] 02 p0172 N85-11151
Scattering experiments on interactions of excited atoms: Differential cross sections of the system Na (3P)+K(4S)
[MPIS-8/1984] 05 p0728 N85-14677
A high-resolution study of local interstellar sodium
06 p0875 N85-15556
Forces on neutral atoms due to electromagnetic fields
[AD-A146984] 07 p1040 N85-16603
Collision-induced dipole moments
[AD-A147662] 08 p1121 N85-17063
SSPS-CRS advanced sodium receiver: Construction experience report
[DE85-000825] 10 p1511 N85-19533
First sodium nightglow results for Natal
[INPE-3397-PRE/666] 10 p1515 N85-19560
A modeling analysis program for the JPL table mountain lo sodium cloud data
[NASA-CR-175474] 10 p1572 N85-19910
Study of processes of modification of Al-Si alloys
13 p2026 N85-22695
Sodium and lithium corrosion in molybedenum heat pipes
[DE85-005561] 16 p2784 N85-27179
A modeling analysis program for the JPL table mountain lo sodium cloud
[NASA-CR-175851] 16 p2833 N85-27468
Sodium concrete reaction: Structural considerations
[DE85-009031] 18 p3081 N85-29063
Intrinsically irreversible acoustic heat engines
[DE85-007672] 19 p3270 N85-30276
Intercomparison of the calculated absolute efficiency values between true coaxial and true closed-end coaxial Ge (Li) and NaI detectors
[REPT-5-1984] 20 p3532 N85-31976
The diurnal variation of the neutral sodium species in the upper atmosphere: A model study
[AD-A154988] 21 p3631 N85-32561
Physical and chemical aerosol characteristics in extremely clean air masses at Cape Grim, Tasmania
21 p3646 N85-32655
Photoionization of alkali and alkaline earth atoms: Na and Mg
[DE85-011812] 22 p3837 N85-33755
Effect of temperature and ionic impurities at very low concentrations on stress corrosion cracking of Type 304 stainless steel
[TI85-003048] 24 p4079 N85-35283
Development and evaluation of sulfonated polysulfone membranes for the zinc-ferricyanide battery
[DE85-009104] 24 p4090 N85-35357
A study of the chemistry of alkali metals in the upper atmosphere
[AD-A156349] 24 p4117 N85-35524
Noise in sodium beta alumina crystals
[AD-A156025] 24 p4161 N85-35798
A new drawing technique for nylon 6 by reversible plasticization with iodine
[AD-A156272] 24 p4162 N85-35803

SODIUM ALLOYS
Thermodynamic properties of liquid Li-Pb, Na-Pb and K-Pb alloys: Similarities and Differences
[DE85-004074] 18 p3197 N85-29830

SODIUM CHLORIDES
Effect of fluid and salt supplements to food allowance on endurance of head-to-pelvis accelerations following 7-day dry immersion and under ordinary motor activity conditions 01 p0092 N85-10618
Salt action on concrete
[AD-A147812] 07 p0933 N85-15912
Application of electrochemical engineering methods and theory to solving corrosion and adhesion problems with organic coatings
[AD-A147799] 08 p1129 N85-17115
Thermodynamic properties of aqueous NaCl from 273 to 823 K with estimates for higher temperatures
[DE85-000392] 09 p1292 N85-18116
Mechanisms of heat and mass transfer across a double-diffusive interface
[PB85-148468] 12 p1848 N85-21594
Resistance of hydrogenated alpha-titanium alloys to corrosion-fatigue fracture 15 p2499 N85-25413
The use of moments of momentum to account for crystal habits
[NASA-CR-3907] 20 p3421 N85-31232
Experimental investigation of radiative-acoustic effects in the water by the thermodynamical conditions of Dumand
[HE-7.1-2] 24 p4213 N85-36156

SODIUM COMPOUNDS
NT SODIUM CHLORIDES
NT SODIUM IODIDES
NT SODIUM NITRATES
NT SODIUM SILICATES
NT SODIUM SULFATES
Synthesis and properties of Hexachloromolybdates(5) and related species
[AD-A139599] 07 p0924 N85-15852
Ames Laboratory measurements of alkali levels in the Curtiss-Wright PFBC gas stream
[DE85-011357] 22 p3745 N85-33214

SODIUM IODIDES
Measurement of nuclear lines with a dual Ge(Li) telescope aboard a stratospheric balloon
[INPE-3360-TDL/165] 11 p1762 N85-21083
Improved method for the stabilization of NaI-photomultiplier gamma detectors against thermal and other drift
[DE85-011630] 23 p3970 N85-34613

SODIUM ISOTOPES
Cosmogenic Na-22 and Al-26 in Luna-24 lunar drill core soil samples 13 p1981 N85-22427

SODIUM NITRATES
Effects of gamma-ray irradiation on dislocations in sodium nitrate single crystals
[DE85-008291] 18 p3195 N85-29818
Sodium nitrate containing mixture for producing ceramic-glass-ceramic seal by microwave heating
[DE85-011610] 22 p3751 N85-33254

SODIUM SILICATES
EXAFS studies of sodium silicate glasses containing dissolved actinides
[DE84-015835] 04 p0479 N85-13051

SODIUM SULFATES
Interactions between corrosion and creep of uncoated and coated superalloys in sulfate melts
04 p0477 N85-13038

SODIUM SULFUR BATTERIES
Physico-chemical investigations on the electronic partial conductivity of molten electrolytes, especially of the eutectic mixture LiCl-KCl
[BMFT-FB-T-84-205] 05 p0633 N85-14063
BBC of Switzerland develops electric car
08 p1141 N85-17192
Prospects for advanced storage battery technologies
[DE84-015706] 09 p1345 N85-18484

Production technology of an electrolyte for Na/S batteries
[BMFT-FB-T-84-277] 15 p2550 N85-25742
Degradation phenomena in solid electrolytes
[DE85-007066] 15 p2587 N85-25949
Sixth DOE Electrochemical Contractor's Review. Extended abstracts
[DE84-013679] 16 p2779 N85-27151
Transfer of battery technology developed by the US Department of Energy
[DE85-009868] 22 p3808 N85-33586
SODIUM VAPOR
Degenerate four-wave mixing lineshapes in sodium vapor under pulsed excitation
[AD-A148211] 08 p1222 N85-17698
Astronomy and sodium lighting
[RAND/N-2069-RC] 09 p1413 N85-18914
A modeling analysis program for the JPL Table Mountain Io sodium cloud data
[NASA-CR-175493] 11 p1681 N85-20589
Instrumentation for particle-beams research using excited merging beams
[AD-A154155] 19 p3356 N85-30807
SOFT LANDING SPACECRAFT
NT APOLLO SPACECRAFT
SOFTENING
Response of ferritic steels to nonsteady loading at elevated temperatures
[DE84-014280] 04 p0513 N85-13272
Non equilibrium ionization in the local hot bubble
06 p0679 N85-15587
Softening of metal near seam during welding of heat-resistant nickel alloys 13 p2035 N85-22747
Solution softening in molybdenum-rhenium alloys
[DE85-006706] 16 p2750 N85-26972
Thermomechanical softening treatment for bearing and tool steels
[BLL-BISI-TRANS-22432-(9022.06)]
17 p2925 N85-28035
SOFTNESS
Strength and aging behaviour of soft soldered joints
[BLL-T6385/BG/WH600/84] 07 p0925 N85-15862
SOFTWARE (COMPUTERS)
U COMPUTER PROGRAMS
U COMPUTER SYSTEMS PROGRAMS
SOFTWARE ENGINEERING
NT ASSEMBLER ROUTINES
NT COMPUTER PROGRAMMING
NT LANGUAGE PROGRAMMING
NT LOGIC PROGRAMMING
NT MICROPROGRAMMING
NT MULTIPROGRAMMING
NT PARALLEL PROGRAMMING
NT SYMBOLIC PROGRAMMING
Potential use of dialogue with computers in biomedical research 01 p0091 N85-10614
Comparative descriptions of software quality measures
[GMD-STUDIES-81] 01 p0102 N85-10676
SAGA: A project to automate the management of software production systems
[NASA-CR-174017] 01 p0103 N85-10685
Ada (trademark) training curriculum. Software engineering for managers m101 teacher's exercise guide
[AD-A145094] 01 p0104 N85-10695
Mathmatics and Computer Science Division activities
[DE84-014842] 01 p0104 N85-10701
Establishing a Software Engineering Technology (SET)
[PB84-212141] 01 p0105 N85-10702
Microcomputers in Hungary 01 p0115 N85-10786
Software engineering environments for mission critical applications: STARS alternative programmatic approaches
[AD-A145285] 02 p0241 N85-11571
Program flow analyzer, volume 1
[AD-A145320] 02 p0241 N85-11572
Description of the software acquisition process (SWAP) model
[AD-A145413] 02 p0241 N85-11573
DOD related software technology requirements, practices, and prospects for the future
[AD-A145493] 02 p0242 N85-11575
Program flow analyzer, volume 3
[AD-A145522] 02 p0242 N85-11577
Concurrent processing and the decomposition of problems
[DE84-015285] 02 p0242 N85-11581
A representation for the functioning of devices that supports compilation of expert problem solving structures: An extended summary
[AD-P003921] 02 p0245 N85-11601
Artificial intelligence applications to automatic test equipment
[AD-P003936] 02 p0247 N85-11616
Programming effort estimation
[AD-A145839] 03 p0406 N85-12595
Automating software design metrics
[AD-A145869] 03 p0407 N85-12596
Configuration management for mission-critical software: The Los Alamos solution
[DE84-015515] 03 p0408 N85-12606
Information Center handbook
[PB84-211341] 03 p0439 N85-12795
Software configuration management across project boundaries and in distributed development environments
[RSRE-MEMO-3704] 04 p0549 N85-13494
Documentation for DIGLIB: Device independent graphics library
[DE84-017365] 04 p0550 N85-13500
Burroughs Corporation B26-CPU, B20 COBOL Version 4.0 (COBOL technical report)
[PB84-216258] 04 p0551 N85-13508
Convergent Technologies, Incorporated, NGEN CP001, CT COBOL Version 9.0 (COBOL technical report)
[PB84-216274] 04 p0551 N85-13508
Research in computer science
[NASA-CR-174088] 05 p0713 N85-14572
Technical Workshop: Advanced Helicopter Cockpit Design
[NASA-CP-2351] 06 p0750 N85-14806
Reusable software
[AD-A146575] 06 p0854 N85-15427
Trends in development of software for computer-aided analysis of large-scale integrated circuits
07 p0955 N85-16055
JPL Robotics Laboratory computer vision software library
[NASA-CR-174272] 07 p1023 N85-16491
Software test handbook
[AD-A146844] 07 p1024 N85-16498
Functional semantics of modules
[AD-A146923] 07 p1024 N85-16500
On the structure of information in software
[AD-A147580] 07 p1026 N85-16511
Ultrasound instrumentation for the 7 inch Mach seven tunnel
[NASA-CR-174277] 07 p1038 N85-16588
Built-in-test for first line testing
08 p1064 N85-16739
Functional built-in-test in a pipelined image processor
08 p1064 N85-16740
The production of maintainable, trustworthy, and portable software 08 p1064 N85-16744
Documentation and separate test program development is most important for test/maintenance
08 p1065 N85-16745
Effective life cycle software support: A study in discipline and versatility 08 p1065 N85-16746
Experience in using on-aircraft software for testing integrated systems 08 p1065 N85-16747
Software testing in an Ada programming environment
08 p1065 N85-16748
Cryogenic propellant management: Integration of design, performance and operational requirements
08 p1098 N85-16939
Fast arithmetic for microcomputers
08 p1140 N85-17180
Researchers on third generation robotics development
08 p1140 N85-17184
ES devices at fair 08 p1141 N85-17187
East Europe report: Science and technology
[JPRS-ESA-84-043] 08 p1142 N85-17198
Plasma and magnetospheric research
[NASA-CR-171293] 08 p1183 N85-17451
VICOM technical description
[REPT-611-0012-REV-A] 08 p1202 N85-17563
Software test handbook: Software test guidebook, volume 2
[AD-A147289] 08 p1204 N85-17578
Concept paper for the development of a DOD Ada (trademark) software engineering education and training plan
[AD-A148774] 08 p1206 N85-17592
Study of application of space telescope science operations software for SIRTF use
[NASA-CR-177337] 09 p1287 N85-18060
Development and operation of a real-time data acquisition system for the NASA-LaRC differential absorption lidar
[NASA-CR-174384] 09 p1366 N85-18583
Concepts and tools for the software life cycle
10 p1484 N85-19236
A program design for an adaptive, non-linear finite element solver
[AD-A148880] 10 p1539 N85-19705
Selected NBSNET software
[PB85-109148] 10 p1542 N85-19723
French work toward flexible software workshops
11 p1592 N85-20015
Space Station Software Issues
[NASA-CP-2361] 11 p1700 N85-20689
Software management issues — space station software development 11 p1700 N85-20690
Software development environment issues — space station software development 11 p1700 N85-20691
Software standards issues — space station software development 11 p1701 N85-20692
Information systems issues 11 p1701 N85-20693
Shuttle software production facility
11 p1701 N85-20694
Software technology within NASA
11 p1701 N85-20695
Communications software for Olympics Micromation Computer System
[PB85-109510] 11 p1704 N85-20723
AFOS (Automation of Field Operations and Service) surface observation decoding
[PB85-137586] 12 p1898 N85-21913
A survey of the project CIP: Computer aided, intuition-guided programming, Wide spectrum language and program transformations
[TUM-I8406] 12 p1912 N85-22000
Earth radiation budget experiment software development
[NASA-CR-172567] 12 p1912 N85-22002
DOS 21: PCDOS 2.0 support subroutine package for the IBM personal computer
[LA-10142-MS] 12 p1914 N85-22012
Microcomputers in transit: A software handbook
[PB85-136414] 12 p1918 N85-22042
A formal method for specifying computer resources in an implementation independent manner
[AD-A149855] 12 p1918 N85-22043
Validation summary report, Burroughs Corporation, B20 FORTRAN release 4.0
[PB84-227792] 13 p2145 N85-23316
Principles of software engineering environment design
[AD-A150362] 13 p2147 N85-23324
Measurement of SIFT operating system overhead
[NASA-TM-86322] 13 p2149 N85-23337
Investigation of doubly-fed machine in variable speed application
[DE85-004378] 14 p2299 N85-24234
Ultraviolet Spectrometer and Polarimeter (UVSP) software development and hardware tests for the solar maximum mission
[NASA-CR-175279] 14 p2305 N85-24271
The identification of semantics for the file/database problem domain and their use in a template-based software environment 14 p2401 N85-24803
An experiment in software reliability
[NASA-CR-172553] 14 p2403 N85-24813
An algebraic specification language and a syntax directed editor
[AD-A150664] 14 p2403 N85-24815
Computers and the consulting engineer
15 p2626 N85-26184
A learning strategy approach for teaching novice computer programmers
[AD-A151523] 15 p2628 N85-26200
Extension of the software development workbench to include microcomputer workstations
[AD-A151903] 15 p2630 N85-26207
Prade language environment: Distribution package description, revision 1
[DE85-006899] 15 p2630 N85-26212
IPAD: Integrated Programs for Aerospace-vehicle Design
[NASA-CR-3890] 15 p2632 N85-26221
Mathematical software for hyperbolic equations and two point boundary value problems
[AD-A151982] 15 p2638 N85-26270
Space radiation studies — Spacelab 2 Payload
[NASA-CR-171410] 15 p2685 N85-26584
Active control technology: Past, present, future
16 p2711 N85-26731
East Europe report: Science and technology
[JPRS-ESA-84-032] 16 p2727 N85-26833
A robotic system for preparing reagent and dilution vials
[DE85-008262] 16 p2793 N85-27231
Fujian forges ahead in electronic production
16 p2808 N85-27301
Symbiosis between postgraduate training and research projects: A successful experience
[INPE-3216-PRE/569] 16 p2810 N85-27330
A framework for software development
[AD-A152067] 16 p2847 N85-27551
Diagnosis: Using automatic test equipment and an artificial intelligence expert system
[AD-A151918] 16 p2851 N85-27576
Software for reflectivity calculations of X-ray mirrors, revision 1
[DE85-008842] 16 p2867 N85-27688
COSMIC Software Catalog, 1985 edition
[NASA-CR-174070] 17 p3010 N85-28608

Peer Review of a Formal Verification/Design Proof Methodology
[NASA-CP-2377] 17 p3010 N85-28609
Automatic distribution of programs in MASCOT and Ada (trademark) environments: A feasibility study
[AD-A152665] 17 p3010 N85-28614
Implementation of a general finite element code on an IBM PC compatible microcomputer
[AD-A152681] 17 p3011 N85-28615
A test methodology for an automated and interactive software development environment
[AD-A152857] 17 p3011 N85-28618
CLEANROOM software development: An empirical evaluation
[AD-A152924] 17 p3011 N85-28619
CAMAC 486 module: 68000 based GPIB interface module
[DE85-009367] 17 p3014 N85-28635
Micro-CAE mechanical engineering software development at Lawrence Livermore National Laboratory and participating universities and technology transfer
[DE85-008660] 18 p3163 N85-29597
Annotated bibliography of recent papers on software engineering environments
[PB85-191365] 18 p3165 N85-29607
Statistical estimation of software reliability
[AD-A154097] 19 p3335 N85-30665
Implementation of a proposed system for automated microcode generation
[AD-A154235] 19 p3336 N85-30671
Guide on logical database design
[PB85-177970] 19 p3361 N85-30976
PIPE-1000: An implementation of piping on an HP-1000 minicomputer
[PB85-191955] 20 p3514 N85-31847
Evaluative report on the Institute for Computer Sciences and Technology, National Bureau of Standards, fiscal year 1984
[PB85-176097] 20 p3514 N85-31848
Implementation assessment of the OSI network service. The test definition language
[NPL-DITC-52/84] 20 p3514 N85-31849
Integrated software engineering system (SIGL)
[DT/GL/7254/Z462/G-C./MJ] 20 p3516 N85-31863
Study of the applicability of higher order languages for on-board satellite software production
[ESA-CR(P)-2024] 20 p3516 N85-31864
Determining functional requirements for NASA Goddard's command management system software design using expert systems 20 p3539 N85-32020
The effect of communication-language designs on software specifications
[AD-A155173] 21 p3672 N85-32809
A comprehensive study of the AFIT (Air Force Institute of Technology) software development environment
[AD-A155450] 21 p3672 N85-32812
Experiments and improvements of the ordinary differential equation solvers DEPAC on the CRAY computer
[DE85-013260] 22 p3831 N85-33726
Software for mechanism design 23 p3925 N85-34324
A prototype PASCAL program validation system
[NPL-DITC-57/85] 23 p3956 N85-34513
The parser generator as a general purpose tool
[NASA-CR-177955] 23 p3957 N85-34521
Calculation of the diffusion of light by aerosols: Description of the MIELOR software and results obtained
[REPT-80] 24 p4137 N85-35638
CRAYCDC
[NASA-CR-177374] 24 p4137 N85-35639
CDCCRAY
[NASA-CR-177375] 24 p4137 N85-35640
Study of fault tolerant software technology for dynamic systems
[NASA-CR-172618] 24 p4137 N85-35642
Attacking software crisis: A macro approach
[AD-A155845] 24 p4138 N85-35645
Prototyping with data dictionaries for requirements analysis
[AD-A156303] 24 p4139 N85-35654
Toolpack
[DE85-013135] 24 p4140 N85-35665

SOFTWARE TOOLS

Remote data processing system software in Hungary 01 p0101 N85-10673
FSTC (Federal Software Testing Center) software tool catalog
[PB84-212158] 01 p0105 N85-10703
Study on spectral/radiometric characteristics of the Thematic Mapper for land use applications
[E85-10021] 02 p0216 N85-11434
Proposal for a semiautomatic program testing system
[INPE-3282-TDL/178] 02 p0240 N85-11561
Program flow analyzer, volume 1
[AD-A145320] 02 p0241 N85-11572
Program flow analyzer, volume 2
[AD-A145521] 02 p0242 N85-11576
Program flow analyzer, volume 3
[AD-A145522] 02 p0242 N85-11577
Software for Crimea-Pushchino radiointerferometer 06 p0783 N85-15007
Some experiences of testing protocol implementations --- open systems interconnection
[NPL-DITC-48/84] 08 p1204 N85-17574
Multidimensional digital signal processing
[AD-A148055] 08 p1205 N85-17585
Solutions to structural dynamics problems 09 p1334 N85-18384
Identification of emerging designer needs and high payoff CAE tools
[DE85-000755] 09 p1369 N85-18599
High level languages in protocol specification and verification
[FUB-51-1983] 09 p1370 N85-18611
Concepts and tools for the software life cycle 10 p1464 N85-19236
A low-cost, general purpose image processing system
[INPE-3292-PRE/607] 10 p1537 N85-19690
FORTRAN 66 analyser: User's manual
[PB85-111748] 10 p1542 N85-19724
Microcomputers and the electrical engineer
[AD-A150499] 13 p2147 N85-23325
The HORNE reasoning system, revision
[AD-A150983] 14 p2405 N85-24827
CaD systems for electronic component design reviewed 15 p2537 N85-25660
Symposium on Computers in Civil Engineering 1983
[CSIR-S-298] 15 p2626 N85-26182
Programme development: A state of the art 15 p2626 N85-26185
Extension of the software development workbench to include microcomputer workstations
[AD-A151903] 15 p2630 N85-26207
VAX-based graphics mail system
[DE85-007231] 15 p2630 N85-26214
Development of computer aided database design and maintenance tools
[AD-A151782] 16 p2845 N85-27537
Further development of an Interactive Control Engineering Computer Analysis Package (ICECAP) for discrete and continuous systems
[AD-A151783] 16 p2846 N85-27546
The interactive generation of specifications for an onboard software series (GISELE) 17 p2904 N85-27906
COSMIC Software Catalog, 1985 edition
[NASA-CR-174070] 17 p3010 N85-28608
ZOG-Vinson technology demonstration project. Volume 2: System description
[AD-A153871] 19 p3333 N85-30645
Production verification of the acoustic emission weld monitor
[AD-A154168] 20 p3464 N85-31519
Integrated software engineering system (SIGL)
[DT/GL/7254/Z462/G-C./MJ] 20 p3516 N85-31863
Integrated Support Software System (ISSS)
[AD-A155715] 22 p3829 N85-33710
The parser generator as a general purpose tool
[NASA-CR-177955] 23 p3957 N85-34521
Developing graphical tools with minimal GKS 23 p3964 N85-34573
Study of fault tolerant software technology for dynamic systems
[NASA-CR-172618] 24 p4137 N85-35642
Attacking software crisis: A macro approach
[AD-A155848] 24 p4138 N85-35645
Error message recording and reporting in the SLC control system
[DE85-013057] 24 p4140 N85-35664

SOIL EROSION

Erosion and sedimentation chronology of three watersheds in Maryland
[PB84-207356] 01 p0071 N85-10467
Assessing erosion on US cropland: Land management and physical features
[PB84-219252] 04 p0526 N85-13366
Mineral aerosols and source identification 21 p3646 N85-32654

SOIL MAPPING

Method for interpreting soil cover of flowed fields using spectral brightnesses measured from space photographs 02 p0164 N85-11112
Utilization of LANDSAT orbital imagery in the soil survey processes at Rio Grande do Norte state
[E85-10009] 02 p0216 N85-11422
Remote sensing for landforms and soils in the arid southwest United States 03 p0378 N85-12410
The use of Thematic Mapper data for land cover survey 05 p0657 N85-14220
Evaluation of SIR-B imagery for geologic and geomorphic mapping, hydrology, and oceanography in Australia 08 p1146 N85-17229
Preliminary evaluation of TM for soils information 13 p2121 N85-23206
Variability of coefficients of spectral brightness of soils 15 p2486 N85-25346
Identification of structure of soil-vegetation cover using aerial and space photographs 16 p2726 N85-26826
Airphoto interpretation of vegetation and landforms for soil mapping 17 p2983 N85-28436
Space imagery and some geomorphological problems of the Guiana Shield, South America 21 p3602 N85-32368

SOIL MECHANICS

Multispectral passive microwave correlations with an antecedent precipitation index using the Nimbus 7 SMMR
[AD-A145419] 02 p0200 N85-11334
In situ experiment on shear waves generation and determination of elastic properties of soils
[REPT-550] 03 p0375 N85-12393
Development of a preliminary ALRS stabilized material pavement analysis system (SPAS)
[AD-A147116] 07 p0910 N85-15760
Computer program for determining induced stresses and consolidation settlements (CSETT)
[AD-A146730] 07 p1023 N85-16493
Technology reports of the Yamaguchi University, volume 3, no. 3
[ISSN-0386-9433] 09 p1302 N85-18182
Studies on seismic earth pressure of cohesive backfill 09 p1303 N85-18186
Creep deformation of compacted decomposed granite soils 09 p1303 N85-18187
Influence of grain size distribution on the undrained dynamic properties of saturated sand
[PB85-102382/GAR] 09 p1305 N85-18197
Approximation of difference in water table positions by horizontal stratum in studies of their influence on gravity 10 p1502 N85-19478
Analysis of slope stability, Wilmington to Lindenkohl Canyons, US mid-Atlantic margin
[DE84-012278] 12 p1899 N85-21921
Engineering geology of selected areas, US army engineer division, lower Mississippi valley. The American bottom area, MO-IL. Volume 1
[AD-A154258] 19 p3299 N85-30455
Influence of spatial variability of hydraulic characteristics of soils on surface parameters obtained from remote sensing data in infrared and microwaves
[NASA-TM-77902] 20 p3477 N85-31604

SOIL MOISTURE

Multispectral passive microwave correlations with an antecedent precipitation index using the Nimbus 7 SMMR
[AD-A145419] 02 p0200 N85-11334
Surface soil moisture measurements of the White Sands, New Mexico
[NOAA-TM-NESDIS-7] 02 p0219 N85-11441
Scattering models in the microwave regime
[NASA-CR-174001] 04 p0525 N85-13361
A comparison between active and passive sensing of soil moisture from vegetated terrains 04 p0526 N85-13364
New Zealand SIR-B science investigations 08 p1144 N85-17218
Evaluation of the radar response to land surfaces and volumes: Examination of theoretical models, target statistics, and applications 08 p1149 N85-17250
Ground truth for SIR-B images obtained by SIR system 8 impulse radar 08 p1149 N85-17251
Remote sensing of soil moisture 08 p1149 N85-17252
The effects of soil moisture on bistatic clutter power
[AD-A147636] 08 p1150 N85-17261
The influence of soil moisture distribution on the severe-storm environment of the southern Great Plains: A numerical study of the SESAME 4 case 09 p1357 N85-18534
Investigations of vegetation and soils information contained in LANDSAT Thematic Mapper and Multispectral Scanner data
[E85-10082] 12 p1873 N85-21747
Estimation of regional evapotranspiration using remotely sensed land surface temperature. Part 1: Measurement of evapotranspiration at the Environmental Research Center and determination of Priestley-Taylor parameter 13 p2125 N85-23233
Microwave remote sensing of soil moisture 13 p2125 N85-23235

Testing an energy balance model for estimating actual evapotranspiration using remotely sensed data — Hannover, West Germany barley and wheat fields
13 p2125 N85-23236
A method for estimating soil moisture availability
[NASA-CR-175606] 13 p2126 N85-23238
Orbiting multi-beam microwave radiometer for soil moisture remote sensing 14 p2230 N85-23618
Development of the microwave antenna range of the national antenna test facility at Paardefontein
[R-NIAS-21] 15 p2539 N85-25689
Soil moisture and evapotranspiration estimates based on satellite data 15 p2596 N85-25698
Aerospace technology determines forest-fire danger
19 p3295 N85-30427
Thermomigration in porous media. Study of the development of a drying zone 20 p3456 N85-31462
Influence of spatial variability of hydraulic characteristics of soils on surface parameters obtained from remote sensing data in infrared and microwaves
[NASA-TM-77902] 20 p3477 N85-31604

SOIL SCIENCE

Utilization of LANDSAT orbital imagery in the soil survey processes at Rio Grande do Norte state
[E85-10009] 02 p0216 N85-11422
International strategic minerals inventory. Summary report: Manganese
[GS-CIRC-930-A] 02 p0219 N85-11442
Applying an innovative approach to field investigations at a remedial action site
[AD-P004145] 09 p1348 N85-18481
Growth of soil bacteria in presence of Martian soil analog, carbon dioxide and hydrogen peroxide
09 p1361 N85-18560
Glossary of the soil sciences
[PB85-133452] 12 p1952 N85-22283
Microbial ecology of extreme environments: Antarctic yeasts and growth in substrate-limited habitats
[NASA-CR-175810] 16 p2639 N85-27509
Mathematical model of the nitrogen cycle in a nonsaturated area of cultivated soil
20 p3478 N85-31610
Mineral aerosols and source identification
21 p3648 N85-32654
The 1984 environmental monitoring program report for Idaho National Engineering Laboratory site
[DE85-011209] 22 p3812 N85-33611

SOILS

NT ALLUVIUM
NT DIRT
NT LUNAR SOIL
NT PERMAFROST
NT SANDS
NT TAR SANDS

Response and characteristics of structures subjected to S-H waves 01 p0060 N85-10396
The use of fixed-bed adsorber models to predict the fluxes of toxic substances in groundwaters and soil environments
[PB84-202563] 01 p0071 N85-10468
Remote sensing for landforms and soils in the arid southwest United States 03 p0378 N85-12410
Ice-soil mixtures: Visual and near-infrared remote sensing techniques
[NASA-CR-174087] 04 p0525 N85-13358
Thermal properties of soils and soils testing
[DE84-015312] 04 p0525 N85-13360
Effects of acid rain on plant microbial associations in California
[PB84-242122] 04 p0532 N85-13404
The areal pattern of latent and sensible heat fluxes: The combination of soil physics and remotely sensed data 05 p0656 N85-14213
Development of a preliminary ALRS stabilized material pavement analysis system (SPAS)
[AD-A147116] 07 p0910 N85-15760
In-situ stress determination in soil and rock using the acoustic emission method
[AD-A147459] 07 p0979 N85-16215
An integrated remote sensing approach for identifying ecological range sites — parker mountain
[E85-10050] 07 p0983 N85-16246
Relationship between forest clearing and biophysical factors in tropical environments: Implications for the design of a forest change monitoring approach — Costa Rica
[E85-10051] 07 p0983 N85-16247
Fate and disposition of trichloroethylene in surface soils
[AD-A147918] 07 p0995 N85-16321
Computer program to compute soil thermal conductivity from transient temperature measurements
[PB85-100550] 07 p0998 N85-16341
Computer program for determining induced stresses and consolidation settlements (CSETT)
[AD-A146730] 07 p1023 N85-16493
Interactions of hydrazine and of hydrazine derivatives with soil constituents and with soils
[AD-A148475] 08 p1122 N85-17074
Response of saturated porous nonlinear materials to dynamic loadings
[AD-A148528] 08 p1173 N85-17394
Soil formation on tertiary landsurfaces of the New Jersey coastal plain 08 p1181 N85-17441
Chronologic and climatic control on soil development, northern Bighorn Basin, Wyoming and Montana
08 p1181 N85-17443
Ground shock effect on soil field inclusions
09 p1336 N85-18403
Incineration of explosives contaminated soils
[AD-P004142] 09 p1347 N85-18478
Stabilization of contaminated soils by in situ vitrification
[AD-P004144] 09 p1348 N85-18480
Applying an innovative approach to field investigations at a remedial action site
[AD-P004145] 09 p1348 N85-18481
Location of volatile buried wastes by field portable instrumentation
[AD-P004147] 09 p1348 N85-18483
Community relations activities at Department of Defense sites
[AD-P004150] 09 p1349 N85-18486
Protocol for aquifer cleanup decision making at military installations
[AD-P004151] 09 p1349 N85-18487
Results from geopressured-geothermal subsidence studies
[DE84-016279] 09 p1354 N85-18520
Modelling of off-road tyres and soil for improved traction
[AD-P004258] 09 p1404 N85-18834
Development of a soil-wheel interaction model
[AD-P004259] 09 p1404 N85-18835
Soil compliance influence on tyre performance
[AD-P004260] 09 p1404 N85-18836
Effects of slip on energy distribution between tyre and soil
[AD-P004263] 09 p1404 N85-18839
Traction forces of drive tyre on the compacted soil
[AD-P004264] 09 p1404 N85-18840
A rig for testing the soft soil performance of track systems
[AD-P004272] 09 p1405 N85-18848
The dependence of soil bearing capacity and drawbar pull on the spacing between track
[AD-P004273] 09 p1406 N85-18849
The dynamic interaction between track and soil
[AD-P004274] 09 p1406 N85-18850
Effect of hitch positions on the performance of track-grouser systems
[AD-P004277] 09 p1406 N85-18853
The research of driving wheel with movable lugs of the paddy field floating tractor
[AD-P004283] 09 p1407 N85-18860
Mobility of the small combine (track type) on soft ground-relationship between the position of the center of gravity and the mobility
[AD-P004285] 09 p1407 N85-18862
The stress-strain-time graph of rheological soils and its application
[AD-P004286] 09 p1407 N85-18863
Behaviour of soil under a lugged wheel
[AD-P004287] 09 p1407 N85-18864
Prediction accuracy of the torques for rotary tillage by an analog tool
[AD-P004288] 09 p1408 N85-18865
The analysis on the dynamic performance of a single lug
[AD-P004289] 09 p1408 N85-18866
Pressure tests in soil below tires of agricultural vehicles
[AD-P004294] 09 p1408 N85-18871
Quality control in soil compaction by behaviours of exciter
[AD-P004295] 09 p1408 N85-18872
Smoother terrain-machine
[AD-P004296] 09 p1409 N85-18873
A simple prediction model for soil compaction under various wheel loads and geometries as an aid to vehicle design
[AD-P004298] 09 p1409 N85-18875
Flotation tires and subsurface compaction
[AD-P004299] 09 p1409 N85-18876
Tractor power selection with compaction constraints
[AD-P004300] 09 p1409 N85-18877
Composition and method for cleaning embedded soil from surfaces having low gloss coatings
[AD-D011465] 10 p1459 N85-19194
An assessment of ground-coil heat-pump technology
[DE85-002567] 10 p1486 N85-19382
Consolidation around a point heat source
[PB85-116549] 11 p1662 N85-20601
Field lysimeter facility for evaluating the performance of commercial solidified low-level waste
[DE85-003886] 11 p1727 N85-20883
Thematic Mapper spectral dimensionality and data structure 12 p1871 N85-21736
Remote sensing research for agricultural applications — San Joaquin County, California and Snake River Plain and Twin Falls area, Idaho
[E85-10090] 12 p1873 N85-21752
Glossary of the soil sciences
[PB85-133452] 12 p1952 N85-22283
Characterization of LANDSAT-4 TM and MSS image quality for the interpretation of California's agricultural resources — Central Valley 13 p2116 N85-23190
Preliminary comparisons of the information content and utility of TM versus MSS data 13 p2120 N85-23202
Calculations of microwave brightness temperature of rough soil surfaces: Bare field
[NASA-TM-86200] 13 p2123 N85-23221
Areas with forest soils sensitive to acidic deposition under alternative damage hypotheses
[DE85-005257] 13 p2130 N85-23257
Chemical weathering of soils from the dry valleys of Antarctica: A terrestrial analog of Martian weathering processes 13 p2197 N85-23626
Determination of electromagnetic properties of mesh material using advanced radiometer techniques
14 p2235 N85-23655
Innovation in earthquake and natural hazards research: Determining soil liquefaction potential
[PB85-149573] 14 p2374 N85-24678
Impact of soil moisture in organizing a severe storm outbreak 15 p2597 N85-25009
Multiple regression analysis of photographic image of soil properties 16 p2726 N85-26825
Use of Goudrian model in studying laws of reflection in vegetation-soil system in optical range. 2: Influence of illumination conditions on spectral brightness coefficients 16 p2726 N85-26827
Interactive effects of acid rain and gaseous air pollutants on natural terrestrial vegetation
[DE85-005255] 18 p2821 N85-27401
Ultrasonic dispersion of soils for routine particle size analysis: Recommended procedures
[DE85-006530] 18 p2961 N85-27643
Effect of the agressive action of soil on metallic pipelines. New possibilities for the passive and active corrosion protection
[BLL-BISI-TRANS-21630-(9022.06)] 17 p2928 N85-28070
Constitutive modeling for blast-induced wave propagation
[AD-A153576] 18 p3099 N85-29187
Survival of microorganisms and bacterial predation in nature
[AD-A153574] 18 p3152 N85-29514
Soil temperature extrema recovery rates after precipitation cooling 20 p3491 N85-31607
Numerical modeling of subsurface communication
[DE85-012818] 21 p3577 N85-32249
Mineral aerosols and source identification
21 p3648 N85-32654
Biogeochemical cycling and remote sensing
21 p3659 N85-32733
Soil extraction kit
[AD-D011736] 22 p3742 N85-33190
WIPP horizon in situ permeability measurements
[DE85-012687] 22 p3802 N85-33557
Geologic, technical, and economic sensitivity analysis in support of the GRI (Gas Research Institute) tight gas reservoirs project area
[PB85-192276] 22 p3802 N85-33559
Environmental surveillance at Los Alamos during 1984
[DE85-011888] 22 p3811 N85-33605
Global environmental transport models for tritium
[DE85-011437] 22 p3816 N85-33639
Arctic and offshore research
[DE85-001995] 22 p3818 N85-33653
Development of solid thorium-232 reference materials
[DE85-011453] 22 p3841 N85-33785
Effects of acid rain on forest nutrient status
[DE85-012486] 23 p3947 N85-34483
Multi-solute subsurface transfer modeling for energy solid wastes: Highlights FY 1984
[DE85-012788] 23 p3966 N85-34581
Mineral deposit models: Theory and practice
24 p4105 N85-35448
Development of an NBS (National Bureau of Standards) polymer gage for dynamic soil stress measurement
[PB85-208494] 24 p4118 N85-35526
The measurement of nitrogen oxide (NO, NO2) exchange over plant/soil surfaces
[CSIRO-DAR-TP-8] 24 p4127 N85-35587

SOL-GEL PROCESSES
Structural evolution during the gel to glass conversion
[DE84-014954] 06 p0772 N85-14939
Sol-gel-derived AR coatings for solar receivers
[DE85-000192] 11 p1673 N85-20541

SOLAR ACTIVITY
NT FACULAE
NT SOLAR FLARES
NT SOLAR PROMINENCES
NT SOLAR STORMS
NT SPICULES
NT STELLAR FLARES
NT SUNSPOTS
Research study: Studies in atmospheric processes from Space Platforms
[NASA-CR-171176] 01 p0072 N85-10473
The mapping of the Sun at 8 mm wavelength and tracking of the active regions in the period 23 May - 5 June 1983
[REPT-S-149] 02 p0297 N85-11924
Variability of Neptune 02 p0299 N85-11938
The soft X-ray diffuse background: Implications for the nature of the local interstellar medium
06 p0876 N85-15566
Solar-geophysical data number 478, June 1984. Part 1 (prompt reports): Data for May 1984, Apr. 1984, and late data
[PB84-243153] 06 p0890 N85-15653
Solar-geophysical data number 478, June 1984. Part 2 (comprehensive reports): Data for December 1983 and miscellanea
[PB84-243161] 06 p0890 N85-15654
User's guide for the Nimbus 7 ERB Solar Analysis Tape (ESAT)
[NASA-TM-86143] 10 p1572 N85-19914
Explanation of the normal winter anomaly from the seasonal variation of short wave absorption
11 p1660 N85-20463
Aeronomical aspects of mesospheric photodissociation: Processes resulting from the solar H Lyman alpha line
[AERONOMICA-ACTA-A-285-1984]
11 p1680 N85-20587
National solar-terrestrial research program, part 1. Solar-terrestrial research for the 1980's, part 2
[AD-A149542] 11 p1681 N85-20591
Solar-Geophysical Data. Part 1: (Prompt reports)
[PB85-112068] 11 p1766 N85-21100
Plasma and nuclear processes in solar matter
12 p1954 N85-22277
Solar-geophysical data number 479, July 1984. Part 1: (Prompt reports). Data for June 1984, May 1984 and later data
[NASA-CR-175542] 12 p1962 N85-22333
NIMBUS-7 SBUV (Solar Backscatter Ultraviolet) observations of solar UV spectral irradiance variations caused by solar rotation and active-region evolution for the period November 7, 1978 - November 1, 1980
[NASA-CR-175544] 12 p1962 N85-22334
Solar-geophysical data number 483, November 1984. Part 1: (Prompt reports). Data for October 1984, September 1984 and late data
[PB85-147692] 12 p1962 N85-22335
Solar-geophysical data number 483, November 1984. Part 2: (Comprehensive reports). Data for May 1984, December 1981 and miscellenea
[PB85-147700] 12 p1962 N85-22336
Auroral-polar cap environment and its impact on spacecraft plasma interactions 13 p1991 N85-22484
Solar Seismology From Space. A conference at Snowmass, Colorado
[NASA-CR-175651] 14 p2441 N85-25060
Overview of solar seismology: Oscillations as probes of internal structure and dynamics in the Sun
14 p2441 N85-25061
The magneto-optical filter, working principles and recent progress 14 p2442 N85-25066
Observed spatial properties of the solar eigenfunctions and the implications for the existence of resolved multiplets 14 p2443 N85-25074
The hydromagnetics of the Sun — conference
[ESA-SP-220] 14 p2445 N85-25091
Nonlinear dynamos — solar activity
14 p2447 N85-25106
A consideration of the solar cycle in the light of the behavior of the large active regions
14 p2452 N85-25140
Observations concerning energy balance in solar magnetic regions 14 p2452 N85-25145
About sudden disappearances and reappearances — solar activity 14 p2454 N85-25157
Solar magnetohydrodynamics: Symposium review
14 p2455 N85-25162
Modeling 22-year solar activity cycle within framework of dynamo theory with allowance for primary field
15 p2477 N85-25288
Sixteenth Lunar and Planetary Science Conference. Press abstracts
[NASA-CR-175692] 15 p2660 N85-26548
Bern solar data for January-December 1984
[REPT-51] 15 p2665 N85-26581
Periodicity of variations in galactic cosmic ray fluxes and solar activity parameters near 20th cycle minimum
16 p2720 N85-26791
Dependence of equatorial F-region plasma bubble rise velocity and dynamo electric field on solar cycle
[INPE-3430-PRE/606] 16 p2826 N85-27434
Very large array observations of coronal loops and related observations of solar type stars
[AD-A152027] 16 p2868 N85-27817
Solar activity monitoring satellite (SAMSAT): Impact on space environment services
[PB85-165066] 16 p2868 N85-27818
Solar-Geophysical Data Number 484, December 1984. Part 1 (prompt reports): Data for November 1984, October 1984 and late data
[NASA-CR-175829] 16 p2868 N85-27819
Inferred flows of electric currents in solar active regions 16 p3206 N85-29899
Evidence for submergencew of magnetic flux in a growing active region 16 p3206 N85-29902
Solar-geophysical data no. 485, January 1985. Part 1 (prompt reports): Data for December 1984, November 1984 and late data
[PB85-181360] 20 p3548 N85-32079
Doppler satellite data characteristics
[AD-A154668] 21 p3575 N85-32231
Variation in radiowave propagation conditions in corona during solar activity cycle 22 p3763 N85-33327
Comparisons of the North Polar Cap of Mars and the Earth's Northern Hemisphere snow cover
[NASA-TM-86191] 23 p3989 N85-34728
Precision measurements of solar energetic particle elemental composition
[SH-2.1-4] 23 p3998 N85-34785
Energetic solar particle events
[SH-3.2-2] 23 p4003 N85-34818
A study of periodicities and recurrences in solar activity and cosmic ray modulation
[SH-4.4-14] 23 p4034 N85-35010
Variations of the cosmic ray general component in Antarctica
[SH-4.4-17] 23 p4035 N85-35013
The difference in the energy spectra of galactic cosmic rays at the minima of the 19th and 20th solar activity cycles
[SH-4.4-18] 23 p4035 N85-35014
Cosmic ray variations with the period close to 27 days and their connection with solar activity longitudinal distribution
[SH-4.4-19] 23 p4035 N85-35015
Long-term modulation of galactic cosmic rays in high-energy region
[SH-4.4-22] 23 p4035 N85-35018
Diurnal anisotropy during solar activity cycle twenty and diffusion-convection model
[SH-4.5-7] 23 p4036 N85-35025
Diurnal variations from muon data at Takeyama underground station
[SH-4.5-13] 23 p4037 N85-35030
The modulation features of the long-period cosmic ray variations in connection with the sign change of the general magnetic field of the Sun
[SH-4.5-15] 23 p4037 N85-35032
Cosmic ray density gradient and its dependence on the north-south asymmetry in solar activity
[SH-4.5-17] 23 p4038 N85-35034
Anomalous increase of solar anisotropy above 150GV in 1961-1983
[SH-4.5-18] 23 p4038 N85-35035
Change of cosmic ray anisotropy with solar activity
[SH-4.5-20] 23 p4038 N85-35037
The large scale dynamics of the outer heliosphere and the long-term modulation of galactic cosmic rays
[SH-4.7-3] 23 p4040 N85-35048
Galactic cosmic ray radial gradients and the anomalous He component near maximum solar modulation and to radii beyond 34 AU from the Sun
[SH-4.7-5] 23 p4040 N85-35050
The recovery of the cosmic ray flux from maximum solar modulation at IMP-8 (1 AU) and at Pioneer (R 30 AU)
[SH-4.7-7] 23 p4041 N85-35052
The solar wind effect on cosmic rays and solar activity
[SH-5.1-13] 23 p4043 N85-35066
Solar activity beyond the disk and variations of the cosmic ray gradient
[SH-5.1-23] 23 p4044 N85-35075
Cosmic rays 10Be biennal data and their relationship to aurorae and sunspots
[SH-7.1-1] 23 p4047 N85-35094

SOLAR ACTIVITY EFFECTS
Theoretical study of electron concentration in Venusian atmosphere as function of zenith angle of sun and solar activity in areas of photochemical equilibrium
02 p0163 N85-11104
Scientific contributions in commemoration of Ebro Observatory's 75th anniversary — conference
[ISBN-84-00-05380-X] 04 p0518 N85-13308
Local geomagnetic characteristics of solar activity (Dourbes 1960-1978) 04 p0521 N85-13326
The response of mid-latitude total electron content to solar activity 04 p0522 N85-13336
Solar wind dynamics at small distances from the sun
06 p0823 N85-15227
Solar flare and IMF sector structure effects in the lower ionosphere 11 p1664 N85-20486
The influence of the local solar wind structures on the propagation of low energy particles
12 p1959 N85-22314
Interplanetary shock waves during April and May of 1981 13 p1982 N85-22434
The effects of seeing on noise
14 p2443 N85-25077
The effects of a nearly 100% duty cycle in observations of solar oscillations 14 p2443 N85-25078
Methods for cloud cover estimation
14 p2444 N85-25081
Variability of the structure of the granulation over the solar activity cycle 14 p2447 N85-25100
Nonlinear time-evolution of kink-unstable magnetic flux tubes in the convection zone of the Sun
14 p2447 N85-25105
The first effect of the amplitude of a solar cycle
14 p2452 N85-25143
Variability of the quiet photospheric network
14 p2452 N85-25144
About sudden disappearances and reappearances — solar activity 14 p2454 N85-25157
Multistep orbital correction algorithms for an Earth satellite using low thrust engine
15 p2479 N85-25303
Space-time features of solar cosmic ray penetration into high latitude regions of Earth's magnetosphere based on Intercosmos-19 satellite data 15 p2481 N85-25310
Bursts of relativistic electrons in magnetopause and in outer radiation belt 16 p2722 N85-26801
Some properties of flare-not-associated Forbush decreases
[IFSI-84-13] 20 p3548 N85-32077
Solar radio fluxes as indices of solar activity
[AERONOMICA-ACTA-A-282-1984]
21 p3722 N85-33095
Solar variability observed through changes in solar figure and mean diameter
[DE85-012857] 22 p3860 N85-33900
Search for solar neutrons using NM-64 equipment
[SH-1.4-5] 23 p3995 N85-34765
A search for solar neutrons on a long duration balloon flight
[SH-1.4-6] 23 p3995 N85-34766
On the retention of high-energy protons and nuclei with charges Z or equal to 2 in large solar flares after the process of their acceleration
[SH-2.1-8] 23 p3998 N85-34789
Nucleosynthesis in the terrestrial and solar atmospheres
[SH-2.2-2] 23 p4000 N85-34797
Type 3 solar radio bursts and 3HE-rich events
[SH-2.2-3] 23 p4000 N85-34798
Anomalous low level of cosmic ray intensity decreases observed during 1980
[SH-5.1-15] 23 p4043 N85-35068
When did the average cosmic ray flux increase?
[SH-7.1-4] 23 p4047 N85-35097
Cosmic-ray exposure records and origins of meteorites
[SH-7.1-7] 23 p4047 N85-35099

SOLAR ARRAYS
NT SOLAR BLANKETS
Space know-how, twenty years' space experience
04 p0461 N85-12926
Autonomous momentum management for space station
[NASA-CR-174085] 04 p0462 N85-12931
Autonomous momentum management for space station, exhibit A
[NASA-CR-171256] 04 p0462 N85-12933
FSA field test
[NASA-CR-174114] 04 p0528 N85-13373
Study program for encapsulation materials interface for Flat-plate Solar Array (FSA) project
[NASA-CR-174152] 04 p0530 N85-13385
Trends in space photovoltaic technology
05 p0609 N85-13688
Photovoltaic working group report
05 p0611 N85-13902

A historical overview of the electrical power systems in the US manned and some US unmanned spacecraft
[NASA-CR-174806] 05 p0612 N85-13910
Circuit transients due to negative bias arcs on a high-voltage solar array in low Earth orbit
[NASA-TP-2407] 06 p0760 N85-14858
Safety requirements for wiring systems and connectors for photovoltaic systems
[NASA-CR-174211] 06 p0803 N85-15110
Proceedings of the 23rd Project Integration Meeting
[NASA-CR-174186] 06 p0829 N85-15260
Barriers to achieving high efficiency
06 p0829 N85-15264
Encapsulation design analysis
06 p0829 N85-15266
Polymer-metal interface bond stability
06 p0830 N85-15272
Module flammability research
06 p0830 N85-15274
Performance loss with shorted cells
06 p0832 N85-15294
Investigation of accelerated stress factors and failure/degradation mechanisms
06 p0832 N85-15295
Annual energy spectrum for tracking arrays
06 p0832 N85-15297
Summary of photovoltaic performance models
06 p0832 N85-15298
Proceedings of the 22nd Project Integration Meeting
[DE85-000334] 06 p0833 N85-15302
Demonstration of transparent solar array module design
[NASA-CR-174257] 07 p0992 N85-18302
Manned space station solar array study
[ESA-CR(P)-1941] 09 p1267 N85-18081
Analysis of inverter models and harmonic propagation. Part 1: A physical simulator for large solar cell arrays
[DE85-002312] 09 p1315 N85-18271
Efficient structures for geosynchronous spacecraft solar arrays
[NASA-CR-174448] 10 p1428 N85-19004
Safety requirements for wiring systems and connectors for photovoltaic systems
[NASA-CR-174431] 10 p1477 N85-19324
Analysis of inverter models and harmonic propagation. Part 2: Harmonic propagation
[DE85-000198] 10 p1482 N85-19356
MOD silver metallization for photovoltaics
[NASA-CR-175460] 10 p1510 N85-19526
Seven-year thermal-vacuum real-life test of a solar array drive mechanism manufactured by Marconi Space and Defence Systems (Model No. 002)
[ESA-ESTL-62] 11 p1616 N85-20161
Report of the Electrodynamic Interactions Panel
11 p1645 N85-20363
Control of large collector arrays: The SSPS experience
[DE85-001461] 11 p1675 N85-20553
NASA welding assessment program
[NASA-CR-175512] 12 p1859 N85-21661
Solar powered actuator with continuously variable auxiliary power control
[NASA-CASE-MFS-25637-1] 12 p1876 N85-21769
User's manual for the University of Houston individual heliostat layout and performance code
[DE85-004643] 12 p1882 N85-21808
Interactions between large space power systems and low-Earth-orbit plasmas 13 p1992 N85-22490
The PIX-2 experiment: An overview
13 p1993 N85-22494
Plasma interaction experiment 2 (PIX 2): Laboratory and flight results 13 p1993 N85-22496
Discharges on a negatively biased solar cell array in a charged-particle environment 13 p1994 N85-22499
Space test program of high-voltage solar array-space plasma interactions 13 p1997 N85-22519
Photovoltaic Generators in Space — conference
[ESA-SP-210] 13 p2005 N85-22565
Thin and ultrathin silicon solar cells for space use
13 p2005 N85-22567
Space solar cells: Adjusting to new demands
13 p2005 N85-22568
Bifacial light sensitive space solar cell
13 p2006 N85-22573
Gallium arsenide arrays versus silicon arrays for space application 13 p2006 N85-22574
Availability of AlGaAs/GaAs solar cells in space
13 p2006 N85-22576
Comparative study of GaAs solar cell potentialities for space applications 13 p2006 N85-22577
Investigation of high output gallium arsenide solar cells 13 p2006 N85-22578
Development of very thin large area GaAs solar cells for space application 13 p2006 N85-22579
GaAs and 3-5 compound solar cells status and prospects for use in space 13 p2007 N85-22580
Development and testing of a spacecraft surface potential monitor 13 p2007 N85-22582
Electrostatic discharge testing on a carbon fiber solar panel structure 13 p2007 N85-22584
In-orbit laser regeneration of the radiation damaged solar arrays 13 p2008 N85-22588
Giotto solar array: Design, manufacture and test
13 p2008 N85-22589
The DFS-Kopernikus solar generator electrical design
13 p2008 N85-22590
The DFS-Kopernikus solar generator
13 p2008 N85-22591
Electrical design of the Intelsat 6 solar generator
13 p2008 N85-22592
Computer aided engineering applied to the design and verification of the generic Advanced Rigid Array (ARA) — solar array 13 p2008 N85-22593
Development and qualification of the electrical part of the Advanced Rigid Array (ARA) — solar array
13 p2008 N85-22594
SPOT solar array 13 p2009 N85-22595
Rigid Solar Generator (GSR) solar arrays
13 p2009 N85-22596
Retractable Rigid Solar Generator (GSR)
13 p2009 N85-22597
Derivation of the Olympus solar array requirements
13 p2009 N85-22598
The Olympus solar array development and test program 13 p2009 N85-22599
The performance of the Olympus power subsystem with its solar array 13 p2009 N85-22601
Survival testing of silicon solar modules
13 p2009 N85-22602
Analysis of optimum front cover thickness for lightweight solar arrays 13 p2010 N85-22606
Problems with electrical interference between solar generators and shunt type regulators
13 p2010 N85-22607
Development of Halley's Comet explorer PLANET-A solar array 13 p2010 N85-22608
Concentrator technologies evaluation for large solar arrays and their application for space stations/platforms
13 p2010 N85-22609
Space Station solar array 13 p2010 N85-22610
Solar array dynamical simulation for illumination and temperature variation 13 p2011 N85-22611
Aspects of low cost module technology — spacecraft solar arrays 13 p2011 N85-22614
Deployment analysis of the Olympus Astromast and comparison with test measurements — solar arrays
13 p2011 N85-22616
NASA photovoltaic research and technology development program for space applications
13 p2011 N85-22617
Study of concentration for space photovoltaic generators 13 p2011 N85-22618
Developments in deployable masts to support flexible solar arrays 13 p2012 N85-22620
Generic design and verification of an Advanced Rigid Array (ARA) — solar array 13 p2012 N85-22621
Growth capabilities of European retractable solar arrays 13 p2012 N85-22625
MSFC data analysis of the SAFE/DAE experiment
14 p2233 N85-23843
Langley Research Center photogrammetric measurements of solar array dynamics: Preliminary results 14 p2233 N85-23844
Solar Array Experiment (SAE) flight experience
14 p2236 N85-23861
Intermediate load modules for test and evaluation
[NASA-CR-175697] 14 p2350 N85-24526
Selection of optimal control program for solar cell panels of Earth satellites 15 p2464 N85-25335
NASA welding assessment program
[NASA-CR-175682] 15 p2566 N85-25844
Module performance and failure analysis area: Flat-plate solar array project
[NASA-CR-175689] 15 p2585 N85-25936
Proposed energy systems for the Brazilian data collection satellite
[INPE-3393-PRE/684] 16 p2731 N85-26856
MOD silver metallization for photovoltaics
[NASA-CR-175773] 16 p2818 N85-27361
Design and development of a linear Fresnel lens air-cooled photovoltaic module and a stand-alone photovoltaic collector array
[DE85-006854] 16 p2819 N85-27391
Relative potentials of concentrating and two-axis tracking flat-plate photovoltaic arrays for central-station applications
[NASA-CR-175869] 17 p2985 N85-28446
Observations of high resistance on slip-rings employing Ag/MoS2/Cu brushes — solar array drives
[ESA-ESTL-70] 18 p3123 N85-29333
Measurements of vector fields with diode array
18 p3204 N85-29660
Using PVFORM, a systems performance model, to determine optimum mounting configurations for flat-plate photovoltaic modules
[DE85-011191] 19 p3306 N85-30485
Multi-kW solar arrays for Earth orbit applications
[NASA-CR-171538] 20 p3406 N85-31139
A dual spin space station design
20 p3408 N85-31152
Frequency domain control design of large space structures: A practical approach
20 p3415 N85-31192
A concept for the intrinsic dielectric strength of electrical insulation materials
[NASA-CR-176040] 20 p3448 N85-31410
Proceedings of the Flat-Plate Solar Array Project Research Forum on High-Efficiency Crystalline Silicon Solar Cells
[NASA-CR-176047] 20 p3478 N85-31615
Activities report of the European Space Tribology Laboratory
[ESA-ESTL-66] 20 p3484 N85-31653
Retractable Rigid Solar Generator (GSR)
[SNIAS-851-440-101] 20 p3484 N85-31654
The SPOT solar array
[SNIAS-851-440-103] 20 p3485 N85-31656
Gallium arsenide arrays versus silicon arrays for space application
[SNIAS-851-440-104] 20 p3485 N85-31657
Study of concentration for space photovoltaic generators
[SNIAS-851-440-105] 20 p3485 N85-31658
Forced convection on solar collector arrays
[DE85-010361] 21 p3585 N85-32287
Proceedings of the 24th Project Integration Meeting
[NASA-CR-176058] 21 p3607 N85-32394
High-efficiency module and array research
21 p3607 N85-32397
Flat-plate module efficiency versus cost tradeoffs
21 p3607 N85-32398
Block V module program 21 p3607 N85-32401
Reliability physics 21 p3608 N85-32402
MOD silver metallization for photovoltaics
21 p3610 N85-32428
The design and development of a constant-speed solar array drive 22 p3796 N85-33519
Features of the solar array drive mechanism for the space telescope 22 p3798 N85-33532
Structural dynamics model and response of the deployable reference configuration space station
[NASA-TM-86386] 22 p3799 N85-33539
Surface voltage gradient role in high voltage solar array-plasma interaction: Center Director's discretionary fund
[NASA-TM-86516] 22 p3805 N85-33567
Photovoltaics technical information guide
[DE85-002924] 22 p3808 N85-33585
Solar maximum: Solar array degradation
[NASA-TM-86194] 23 p3903 N85-34175

SOLAR ATMOSPHERE

Physics of the inner heliosphere 1-10R sub O plasma diagnostics and models
[NASA-CR-174010] 02 p0304 N85-11964
Vector magnetic field analysis of Lorentz forces acting in the solar atmosphere
[AD-A145941] 03 p0449 N85-12852
Kinematics of B and A stars 05 p0741 N85-14766
The radiative hydrodynamics of flare loops heated by impulsive bursts of energetic electrons
05 p0745 N85-14781
Heating in the solar mantle 08 p1233 N85-17769
The calculation of theoretical chromospheric models and the interpretation of solar spectra from rockets and spacecraft
[NASA-CR-174289] 08 p1259 N85-17922
Plasma and nuclear processes in solar matter
12 p1954 N85-22277
Equilibrium model of thin magnetic flux tubes — solar atmosphere 12 p1958 N85-22310
Ultraviolet spectral diagnostics of solar flares and heating events 13 p2205 N85-23675
The hydromagnetics of the Sun — conference
[ESA-SP-220] 14 p2445 N85-25091
Magnetoconvection: The interaction of convection and small scale magnetic fields — photosphere
14 p2448 N85-25096
Coronal structures 14 p2448 N85-25110
Waves in inhomogeneous media — magnetohydrodynamic waves; solar atmosphere
14 p2449 N85-25116
Science with the Solar Optical Telescope (SOT)
14 p2449 N85-25120
A model for the dynamics of the deep photosphere
14 p2450 N85-25129
Linear models of acoustic waves in sunspot umbrae
14 p2450 N85-25130

Dynamo action of magnetostrophic waves — solar atmosphere 14 p2451 N85-25136
Cyclic flows in the solar convection zone due to the dynamo reaction 14 p2451 N85-25137
Effects of atmospheric stratification on dissipative acoustic and Alfven waves — solar atmosphere 14 p2453 N85-25149
Solar magnetohydrodynamics: Symposium review 14 p2455 N85-25162
Measurements of Solar Vector Magnetic Fields [NASA-CP-2374] 18 p3203 N85-29869
The vector structure of active magnetic fields 18 p3203 N85-29870
On the numerical computation of nonlinear force-free magnetic fields 18 p3203 N85-29871
Modeling solar magnetic structures 18 p3203 N85-29872
Generation and transfer of polarized radiation in the solar atmosphere: Physical mechanisms and magnetic-field diagnostics 18 p3206 N85-29890
Contribution functions for Zeeman-split lines, and line formation in photospheric faculae 18 p3207 N85-29893
Solar photospheric and coronal abundances from solar energetic particle measurements [NASA-CR-176029] 20 p3547 N85-32079
Solar convection [AD-A155214] 21 p3723 N85-33098
Temporal evolution of an energetic electron population in an inhomogeneous medium: Application to solar hard X-ray bursts [SH-1.2-6] 23 p3991 N85-34741
Ultrarelativistic electrons and solar flare gamma-radiation [SH-1.3-11] 23 p3993 N85-34757
Precision measurements of solar energetic particle elemental composition [SH-2.1-4] 23 p3998 N85-34785
Solar Coronal and photospheric abundances from solar energetic particle measurements [SH-2.1-5] 23 p3998 N85-34786
Nucleosynthesis in the terrestrial and solar atmospheres [SH-2.2-2] 23 p4000 N85-34797
Dynamics of the penetration boundaries of solar protons during a strong magnetic storm [SH-6.1-16] 23 p4046 N85-35089
Neutrino production from the solar atmosphere [SH-9.1-9] 23 p4050 N85-35114

SOLAR AUXILIARY POWER UNITS
Features of new solar panels on Salyut-7 02 p0157 N85-11062

SOLAR AZIMUTH
U AZIMUTH
U SOLAR POSITION

SOLAR BLANKETS
Development of a foldline concept for automatic refolding of a flexible blanket (folding analysis) — spaceborne solar generators [ESA-CR(P)-1933] 06 p1179 N85-17428
Design and qualification testing of the Olympus solar array blanket 13 p2009 N85-22600
Blanket integrated cushioning of foldable and retractable solar arrays 13 p2011 N85-22612
Concept for controlled fold by fold deployment and retraction of flexible, foldable solar generators 13 p2011 N85-22613
The Olympus solar array structure and mechanisms 13 p2012 N85-22623
Solar array flight experiment [NASA-TM-86506] 17 p2909 N85-27935
STACBEAM 2 [NASA-CR-176126] 23 p3944 N85-34442

SOLAR CELLS
NT HOMOJUNCTIONS
NT VERTICAL JUNCTION SOLAR CELLS
MOD silver metallization for photovoltaics [NASA-CR-174011] 01 p0026 N85-10163
Development of copper sulfide/cadmium sulfide thin-film solar cells [DE84-004513] 01 p0044 N85-10287
Process Research of Polycrystalline Silicon Material (PROPSM) [NASA-CR-173838] 01 p0067 N85-10446
Liquid cooled, linear focus solar cell receiver [DE84-014446] 01 p0067 N85-10448
The effect of plasma on solar cell array arc characteristics [NASA-TM-88887] 02 p0169 N85-11133
Preparation and properties of evaporated CdTe films compared with single crystal CdTe [DE85-000502] 02 p0222 N85-11452
Research on gallium arsenide diffused junction solar cells [NASA-CR-174057] 02 p0222 N85-11457
Silicon sheet with molecular beam epitaxy for high efficiency solar cells [NASA-CR-174022] 02 p0222 N85-11459
Hydrogen passivation of electrically active defects in crystalline silicon solar cells [DE84-004590] 02 p0223 N85-11461
Research directions and progress in the SERI advanced high efficiency concept program [DE84-004592] 02 p0223 N85-11462
DOE/SERI polycrystalline thin-film photovoltaic research [DE84-004518] 02 p0223 N85-11464
Research on crystalline silicon solar cells [DE84-114591] 02 p0223 N85-11465
Thin film (Al, Ga)As heterojunction solar cells 02 p0258 N85-11691
Cascaded solar photovoltaic cells based on InP-GaInPAs and InP-CdS heterostructures 02 p0268 N85-11749
Development of the production technology of Cu2S/CdS solar generators [BMFT-FB-T-84-137] 03 p0366 N85-12469
Five year research plan, 1984-1988. Photovoltaics: Electricity from sunlight [DE84-013009] 04 p0526 N85-13377
Evaluation of some photovoltaic concentrator solar cell-heat sink coupling materials [DE84-016027] 04 p0529 N85-13378
Silicon for solar cells [DE84-004503] 04 p0529 N85-13381
Comprehensive silicon solar cell computer modeling [NASA-CR-174151] 04 p0530 N85-13386
National Photovoltaics Program Annual Review Meeting, abstracts [DE84-013003] 04 p0530 N85-13390
Trends in space photovoltaic technology 05 p0609 N85-13668
Glow discharge amorphous silicon tin alloys [DE84-013001] 05 p0618 N85-13952
Process research of polycrystalline silicon material (PROPSM) [NASA-CR-174130] 05 p0619 N85-13962
Siemens solar module: Status of the technique, development tendencies 05 p0662 N85-14255
Development and utilization of CdS/Cu2S 05 p0662 N85-14256
Telephoning with light and sun — glass fibers, solar cells 05 p0663 N85-14264
Mains-connected photovoltaic system for a house 05 p0664 N85-14267
Material models and device structures for GaAs solar cells [DE85-000501] 05 p0665 N85-14275
Material models and device structures for GaAs solar cells, introduction 05 p0665 N85-14276
GaAs material properties and models 05 p0665 N85-14277
Anti-reflection coatings materials and models 05 p0665 N85-14278
Comparison of SCAPID/GaAs to experiment 05 p0665 N85-14279
Solar cell coverslide extraction method and apparatus [AD-D011275] 05 p0669 N85-14306
Safety requirements for wiring systems and connectors for photovoltaic systems [NASA-CR-174211] 06 p0803 N85-15110
Development of high-efficiency solar cells on silicon web [NASA-CR-174212] 06 p0826 N85-15259
High-efficiency silicon solar cell research 06 p0829 N85-15261
High-efficiency solar-cell design modeling 06 p0829 N85-15262
Efficiency estimation and sensitivity modeling 06 p0829 N85-15263
MBE growth for high-efficiency silicon solar cells 06 p0829 N85-15265
Investigation of silicon surface passivation by silicon nitride deposition 06 p0829 N85-15266
Development and analysis of silicon solar cells near 20% efficiency 06 p0829 N85-15267
Encapsulation design analysis 06 p0829 N85-15268
Encapsulation materials and processing 06 p0830 N85-15269
Photothermal degradation of encapsulants 06 p0830 N85-15270
Polymer-polymer interface bond stability 06 p0830 N85-15271
Polymer-metal interface bond stability 06 p0830 N85-15272
Predicting electrochemical breakdown in terrestrial photovoltaic modules 06 p0830 N85-15273
Module flammability research 06 p0830 N85-15274
Process research of non-Cz silicon material 06 p0830 N85-15275
Process Research On Polycrystalline Silicon Material (PROPSM) 06 p0830 N85-15276
Evaluation of the ion implantation process for production of solar cells from silicon sheet materials 06 p0831 N85-15281
Laser-assisted solar-cell metallization processing 06 p0831 N85-15282
Miniworkshop on effects of stress and strain in high-speed-growth silicon ribbons 06 p0831 N85-15284
Stress studies in EFG 06 p0831 N85-15285
Advanced dendritic web growth development 06 p0831 N85-15286
Silicon-sheet surface studies 06 p0831 N85-15287
Investigation of structural and electrical properties of low-angle silicon sheet 06 p0831 N85-15288
Semicrystalline casting process development and verification 06 p0832 N85-15289
Electrochemical production of silicon 06 p0832 N85-15290
Analysis of optical and electrical performance of a TCP-coated solar cell 06 p0832 N85-15293
Performance loss with shorted cells 06 p0832 N85-15294
Investigation of accelerated stress factors and failure/degradation mechanisms 06 p0832 N85-15295
Summary of photovoltaic performance models 06 p0832 N85-15296
Proceedings of the 22nd Project Integration Meeting [DE85-000334] 06 p0833 N85-15302
Advances and opportunities in the amorphous silicon research field [DE84-004526] 06 p0833 N85-15304
Recent developments in photovoltaics [DE84-004528] 06 p0833 N85-15305
Results of the 1984 NASA/JPL balloon flight solar cell calibration program [NASA-CR-174270] 07 p0991 N85-16294
Multijunction cells for concentrators: Technology prospects [NASA-CR-174259] 07 p0991 N85-16295
Automated assembly of Gallium Arsenide and 50-micron thick silicon solar cell modules [NASA-CR-174331] 08 p1168 N85-17364
Compilation of Sandia papers contributed to the 17th IEEE Photovoltaic Specialists Conference [DE84-017456] 09 p1315 N85-18267
Analysis of inverter models and harmonic propagation. Part 1: A physical simulator for large solar cell arrays [DE85-002312] 09 p1315 N85-18271
Signal Hill solar-powered repeater report and recommendations [DE85-000487] 09 p1316 N85-18273
Advanced high-efficiency concentrator cells [DE84-013020] 09 p1344 N85-18459
Analysis of inverter models and harmonic propagation. Part 2: Harmonic propagation [DE85-000198] 10 p1482 N85-19356
Intermediate load modules for test and evaluation: Flat-Plate Solar Array Project [NASA-CR-174450] 10 p1508 N85-19512
Silicon film solar cell process [NASA-CR-174446] 10 p1508 N85-19514
Surface and allied studies in silicon solar cells [NASA-CR-175468] 10 p1508 N85-19516
Pulsed excimer laser processing for cost-effective solar cells [NASA-CR-174429] 10 p1509 N85-19517
Mod silver metallization for photovoltaics [NASA-CR-174444] 10 p1509 N85-19518
Investigation of welded interconnection of large area wraparound contacted silicon solar cells [NASA-CR-174438] 10 p1509 N85-19519
Pulsed excimer laser processing for cost-effective solar cells [NASA-CR-175465] 10 p1509 N85-19520
Development of high efficiency solar cells on silicon web [NASA-CR-174435] 10 p1509 N85-19521
Stress studies in EFG [NASA-CR-175464] 10 p1509 N85-19522
Process Research on Polycrystalline Silicon Material (PROPSM) [NASA-CR-175461] 10 p1509 N85-19523
Investigation of accelerated stress factors and failure/degradation mechanisms in terrestrial solar cells [NASA-CR-175469] 10 p1510 N85-19524
Stress-strain analysis of silicon ribbon [NASA-CR-175459] 10 p1510 N85-19525
Mask aligner for solar cell fabrication [AD-D011450] 10 p1510 N85-19529

US Amorphous Silicon Research Project
[DE85-000536] 10 p1511 N85-19536
Overview of photovoltaic concentrator technology
[DE84-016790] 10 p1512 N85-19539
Solar collection
[DE85-000060] 10 p1512 N85-19540
Stress studies in EFG
[NASA-CR-175488] 10 p1563 N85-19856
Screen printed interdigitated back contact solar cell
[NASA-CASE-LEW-13414-1] 11 p1671 N85-20530
Surface and allied studies in silicon solar cells
[NASA-CR-174447] 11 p1671 N85-20531
Lithium counterdoped silicon solar cell
[NASA-CASE-LEW-14177-1] 11 p1672 N85-20535
Research on the basic understanding of high efficiency in silicon solar cells
[DE85-000507] 11 p1672 N85-20537
Excimer laser annealing to fabricate low cost solar cells
[NASA-CR-174394] 11 p1673 N85-20538
Fabrication of monocrystalline GaAs solar cells utilizing NaCl sacrificial substrates
[DE84-013016] 11 p1673 N85-20544
Phase 2 fabrication and construction of the Sky Harbor Airport, solar photovoltaic concentrator project
[DE85-000019] 11 p1676 N85-20561
The temperature of a glass-encapsulated solar cell estimated from ambient air temperature and global radiation
[GKSS-84-E-36] 11 p1676 N85-20563
GaAs and 3-5 compound solar cells status and prospects for use in space
[NASA-TM-86960] 12 p1795 N85-21261
International Congress Centrum Berlin report on photovoltaics 12 p1877 N85-21773
Crystallization methods for solar cell silicon
12 p1877 N85-21774
Materials refining for solar cell silicon
12 p1877 N85-21775
Flat-plate silicon for solar cells
12 p1877 N85-21776
Carbothermic production of silicon solar cells using high-purity starting materials 12 p1877 N85-21777
Silicon band spraying technique for solar cells
12 p1877 N85-21778
Development of silicon nitride materials for the casting of solar cell silicon 12 p1878 N85-21779
Photovoltaic solar components
12 p1878 N85-21782
Optimization of silicon-nitride-inversion layer solar cells
12 p1878 N85-21784
Development of new process technologies for solar cells with high efficiency starting from purified silicon
12 p1878 N85-21785
Investigation of the optical properties of solar elements 12 p1879 N85-21786
Pin solar cells made of amorphous silicon
12 p1879 N85-21787
Development of an amorphous silicon panel
12 p1879 N85-21788
Amorphous silicon solar cells with a view to cheap production processes 12 p1879 N85-21789
Production and characterization of amorphous silicon (a-Si:H) as base material for solar cells
12 p1879 N85-21791
Thin-film solar cells from sputtered and vapor-deposited amorphous silicon 12 p1879 N85-21792
Physical-chemical investigations of copper sulfides for use in CdS/Cu2S solar cells 12 p1880 N85-21794
Development of high-efficiency economic systems for photovoltaics 12 p1880 N85-21795
Development of a CdSe thin film solar cell
12 p1880 N85-21796
Development of new solar cells
12 p1880 N85-21797
An investigation of arc discharging on negatively biased dielectric conductor samples in a plasma
13 p1994 N85-22498
Discharges on a negatively biased solar cell array in a charged-particle environment 13 p1994 N85-22499
Photovoltaic Generators in Space — conference
[ESA-SP-210] 13 p2005 N85-22565
History and future views on solar cells of Japanese scientific satellites 13 p2005 N85-22566
Thin and ultrathin silicon solar cells for space use
13 p2005 N85-22567
Space solar cells: Adjusting to new demands
13 p2005 N85-22568
The high voltage silicon cell: A comparative analysis
13 p2005 N85-22569
A 2 x 6 Back Surface Reflection (BSR) silicon solar cell 13 p2005 N85-22570
Experiences with implanted Back Surface Field (BSF) solar cells 13 p2005 N85-22571
A low cost approach with larger diameter silicon wafer — solar cells 13 p2006 N85-22572
Bifacial light sensitive space solar cell
13 p2006 N85-22573
Gallium arsenide arrays versus silicon arrays for space application 13 p2006 N85-22574
Space qualified AlGaAs/GaAs solar cells
13 p2006 N85-22575
Availability of AlGaAs/GaAs solar cells in space
13 p2006 N85-22576
Development of very thin large area GaAs solar cells for space application 13 p2006 N85-22579
GaAlAs-GaAs solar cell development: Prospective for space applications under concentration
13 p2007 N85-22581
Phenomenology of discharges in space: Application to a solar generator — SPOT satellite
13 p2007 N85-22583
Technological process effect on the carrier lifetime degradation of silicon solar cell base layer irradiated by 1 MeV electrons (boron doping case)
13 p2007 N85-22585
The effects of lithium counterdoping on radiation damage and annealing in n(+)p silicon solar cells
13 p2007 N85-22586
Investigation of the degradation of GaAs photovoltaic cells by proton and electron irradiation
13 p2008 N85-22587
The DFS-Kopernikus solar generator electrical design
13 p2008 N85-22590
The DFS-Kopernikus solar generator
13 p2008 N85-22591
Electrical design of the Intelsat 6 solar generator
13 p2008 N85-22592
Development and qualification of the electrical part of the Advanced Rigid Array (ARA) — solar array
13 p2008 N85-22594
Survival testing of silicon solar modules
13 p2009 N85-22602
Calibration of solar cells outside the atmosphere
13 p2009 N85-22603
Inverse behavior of silicon photovoltaic cells
13 p2010 N85-22604
Nonlinearity and spectral mismatch problems of solar cells 13 p2010 N85-22605
Emissivity enhancement of fused silica for space applications — solar cells 13 p2011 N85-22615
NASA photovoltaic research and technology development program for space applications
13 p2011 N85-22617
Improved modeling of the open circuit voltage of solar cells 13 p2011 N85-22619
Isotropic proton irradiation of GaAs solar cells
13 p2012 N85-22622
Annealing of radiation damage in boron and gallium doped silicon solar cells 13 p2012 N85-22624
Fracture mechanics evaluation of GaAs
[NASA-CR-175657] 13 p2102 N85-23101
New high-efficiency silicon solar cells
[NASA-CR-175643] 13 p2128 N85-23244
Demonstration of feasibility of depositing semiconductor layers using microwave enhanced plasma technique
[NASA-CR-174392] 13 p2163 N85-23421
Some observations of heated gallium arsenide heteroface solar cells
[NASA-TM-86368] 14 p2246 N85-23925
Solar cells based on polycrystalline silicon with isothermal potential barriers along grain boundaries
14 p2275 N85-24091
Solar cells with distributed parameters: Current-voltage characteristics under uniform and nonuniform illumination 14 p2275 N85-24093
Characterization of terrestrial solar cells for space applications: Electrical characteristics of thin Westinghouse dendritic web cells as a function of solar intensity, temperature, and incidence angle
[NASA-CR-175642] 14 p2340 N85-24516
Silicon-sheet and thin-film cell and module technology potential: Issue study
[NASA-CR-175654] 14 p2349 N85-24520
Intermediate load modules for test and evaluation
[NASA-CR-175697] 14 p2350 N85-24526
Modelling of photodegradation in solar cell modules of substrate and superstrate design made with ethylene-vinyl acetate as pottant material
[NASA-CR-175690] 14 p2350 N85-24527
Laser-assisted solar cell metallization processing
[NASA-CR-175686] 14 p2350 N85-24528
Excimer laser annealing to fabricate low cost solar cells
[NASA-CR-175702] 14 p2351 N85-24529
Pulsed excimer laser processing for cost-effective solar cells
[NASA-CR-175700] 14 p2351 N85-24530
Advanced high-efficiency concentrator cell
[DE85-000525] 14 p2351 N85-24533
NASA welding assessment program
[NASA-CR-175682] 15 p2568 N85-25844
NASA welding assessment program
[NASA-CR-175683] 15 p2568 N85-25845
Electrical research on solar cells and photovoltaic materials
[NASA-CR-175699] 15 p2585 N85-25935
Module performance and failure analysis area: Flat-plate solar array project
[NASA-CR-175689] 15 p2585 N85-25936
Heavy doping effects in high efficiency silicon solar cells
[NASA-CR-175687] 15 p2585 N85-25937
Investigation of silicon surface passivation by silicon nitride film deposition
[NASA-CR-175693] 15 p2585 N85-25938
Development of high-efficiency solar cells on silicon web
[NASA-CR-175707] 15 p2585 N85-25939
A study of the stability of cadmium sulfide/copper sulfide and cadmium sulfide copper-indium-diselenide solar cells
[DE85-002902] 15 p2587 N85-25947
Thin film cadmium telluride and zinc phosphide solar cells
[DE85-002904] 15 p2587 N85-25950
Process Research on Polycrystalline Silicon Material (PROPSM)
[NASA-CR-175761] 15 p2587 N85-25951
The structural and electronic properties of amorphous silicon based alloy materials
[DE85-002909] 15 p2660 N85-26419
Chemical vapor deposition of amorphous semiconductor films
[DE85-002917] 15 p2661 N85-26421
Proposed energy systems for the Brazilian data collection satellite
[INPE-3393-PRE/864] 16 p2731 N85-26856
Analysis of orbit transfer vehicles for GPS Block 3 satellites
[AD-A152021] 16 p2732 N85-26860
Solar elements with distributed parameters
16 p2760 N85-27036
Heavy doping effects in high efficiency silicon solar cells
[NASA-CR-175779] 16 p2818 N85-27383
Documentation and solar cell modules
[NASA-CR-175769] 16 p2818 N85-27384
Photovoltaic cell reliability research: Investigation of accelerated stress factors and failure-degradation mechanisms in terrestrial solar cells
[NASA-CR-175815] 16 p2819 N85-27388
Maintenance of photovoltaic power systems
[AD-A152299] 16 p2819 N85-27390
Polycrystalline semiconductor heterojunction modelling (CdS/CuInSe(sub)2)
[DE85-002913] 16 p2871 N85-27713
Study of the degradation of short-circuit current and the open-circuit tension of spatial solar cells as a function of the fluency of 1MeV electrons
[INPE-3356-PRE/834] 16 p2887 N85-27814
Electrical research on solar cells and photovoltaic materials
[NASA-CR-175897] 17 p2986 N85-28452
Comprehensive silicon solar cell computer modeling
[NASA-CR-175959] 17 p2987 N85-28461
Report on high intensity solar cells
[DE85-006396] 17 p2987 N85-28462
Terrestrial photovoltaic power systems with sunlight concentration
[DE85-006398] 17 p2987 N85-28464
Research and developmental study on MIS thin film solar cells of amorphous hydrogenated silicon, part 2
[BMFT-FB-T-84-290] 17 p2988 N85-28467
Zn3P2 as an improved semiconductor for photovoltaic solar cells
[DE85-006772] 18 p3097 N85-29171
SERI photovoltaic advanced research and development project: FY 1984 accomplishments
[DE85-002939] 18 p3128 N85-29368
Post-deposition heat treatments of CdS/CuInSe2 solar cells
[DE85-002943] 18 p3128 N85-29373
Mechanically-stacked multijunction solar cells
[DE85-010389] 18 p3129 N85-29377
Research on electrochemical photovoltaic cells
[DE85-006775] 18 p3131 N85-29392
Current status of silicon materials research for photovoltaic applications
[DE85-008799] 19 p3304 N85-30482
Cadmium sulfide/copper ternary heterojunction cell research
[DE85-006778] 19 p3305 N85-30486
Research on the basic understanding of high efficiency in silicon solar cells
[DE85-006774] 19 p3305 N85-30487
Optical effects of thin film adhesives in multijunction solar cells
[DE85-010120] 19 p3305 N85-30488

High-efficiency, low-cost, passively-cooled PV concentrator module
[DE85-010013] 19 p3305 N85-30490
Design and operation of epitaxial reactor
[DE85-011099] 19 p3306 N85-30491
Block 5 documentation and solar modules
[NASA-CR-176009] 19 p3306 N85-30494
Using PVFORM, a systems performance model, to determine optimum mounting configurations for flat-plate photovoltaic modules
[DE85-011191] 19 p3306 N85-30495
Ink jet printing of silver metallization for photovoltaics
[NASA-CR-176019] 19 p3343 N85-30720
A concept for the intrinsic dielectric strength of electrical insulation materials
[NASA-CR-176040] 20 p3448 N85-31410
An analysis of the feasibility of producing silicon for solar cells by a dichlorosilane/fluidized-bed reactor process
[NASA-CR-176036] 20 p3478 N85-31614
Proceedings of the Flat-Plate Solar Array Project Research Forum on High-Efficiency Crystalline Silicon Solar Cells
[NASA-CR-176047] 20 p3478 N85-31615
Historical perspective of barriers to achieving high-efficiency silicon solar cells
20 p3479 N85-31616
Aspects of silicon bulk lifetimes
20 p3479 N85-31617
Recombination phenomena in high efficiency silicon solar cells 20 p3479 N85-31618
Silicon solar cell efficiency improvement: Status and outlook 20 p3479 N85-31619
Some practical considerations for economical back contact formation on high efficiency solar cells
20 p3479 N85-31620
High-efficiency cell concepts on low-cost silicon sheets 20 p3479 N85-31621
High lifetime solar cell processing and design
20 p3480 N85-31622
Silicon MINP solar cells 20 p3480 N85-31623
High efficiency solar cell research for space applications 20 p3480 N85-31624
Compositional analysis of silicon
20 p3480 N85-31626
Surface passivation and junction formation using low energy hydrogen implants 20 p3480 N85-31628
Measurement of electrical parameters and current components in the bulk of silicon solar cells
20 p3481 N85-31635
Current status of one- and two-dimensional numerical models: Successes and limitations
20 p3482 N85-31636
Application of closed-form solutions to a mesh point field in silicon solar cells 20 p3482 N85-31637
Phenomena simulation for heavy doping and surface recombination velocity 20 p3482 N85-31638
High efficiency large area polysilicon solar cells
20 p3482 N85-31639
High efficiency solar cell processing
20 p3482 N85-31640
Process and design considerations for high-efficiency solar cells 20 p3482 N85-31641
Processing technology for high efficiency silicon solar cells 20 p3483 N85-31642
Texture etching of (100) silicon for solar cells
20 p3483 N85-31643
User handbook for block 5 silicon solar cell modules
[NASA-CR-176043] 20 p3483 N85-31644
Recent improvements in materials for thin GaAs and multibandgap solar cells
[DE85-006800] 20 p3484 N85-31651
Gallium arsenide arrays versus silicon arrays for space application
[SNAS-551-440-104] 20 p3485 N85-31657
Reduction of radiation damage in solar cells — spacecraft power supplies
[ESA-CR(P)-2005] 20 p3485 N85-31659
Photovoltaic solar devices
[BMFT-FB-T-84-288] 20 p3485 N85-31660
High-efficiency crystalline silicon technology development 21 p3607 N85-32395
Summary of the high-efficiency crystalline solar cell research forum 21 p3607 N85-32396
High-efficiency module and array research
21 p3607 N85-32397
The future of crystalline silicon technology in the US Department of Energy program
21 p3607 N85-32399
Predicting photothermal field performance
21 p3608 N85-32404
Polymerizable ultraviolet stabilizers
21 p3608 N85-32406
Encapsulation materials research
21 p3608 N85-32407
Topics in electrochemical degradation of photovoltaic modules 21 p3608 N85-32410
Polymer-water interaction studies
21 p3609 N85-32411
Silicon refinement by chemical vapor transport
21 p3609 N85-32412
High-efficiency silicon solar cell research
21 p3609 N85-32417
Physics of heavily doped silicon and solar-cell parameter measurement 21 p3609 N85-32418
Measuring bulk recombination rates and boundary recombination velocities 21 p3609 N85-32419
Studies of oxygen- and carbon-related defects in high-efficiency silicon solar cells
21 p3609 N85-32420
Comprehensive silicon solar-cell computer modeling
21 p3609 N85-32421
Sensitivity analysis of high-efficiency silicon solar-cell design parameters 21 p3610 N85-32422
Silicon surface passivation by silicon nitride deposition
21 p3610 N85-32423
Important loss mechanisms in high-efficiency solar cells 21 p3610 N85-32424
Development of high-efficiency solar cells on silicon web 21 p3610 N85-32425
Simultaneous junction formation
21 p3610 N85-32426
Laser-assisted solar-cell metallization processing
21 p3610 N85-32429
A non-noble front metallization process
21 p3611 N85-32430
Pulsed excimer laser processing for cost-effective solar cells 21 p3611 N85-32432
Excimer laser annealing for fabrication of low-cost solar cells 21 p3611 N85-32433
High-purity silicon crystal growth
21 p3612 N85-32444
Advanced module development overview
21 p3612 N85-32445
Status of high-efficiency module design and fabrication 21 p3612 N85-32446
Photovoltaic module spread-of-flame testing
21 p3612 N85-32448
Improved Nominal Operating Cell Temperature (NOCT) test procedure 21 p3612 N85-32449
Thin-film reliability and engineering overview
21 p3612 N85-32450
Accelerated stress factors and failure/degradation mechanisms in terrestrial solar cells
21 p3613 N85-32451
Failure analysis of thin-film amorphous-silicon solar-cell modules 21 p3613 N85-32452
Reference-cell calibration activities
21 p3613 N85-32453
Solid-melt interface studies of high-speed silicon sheet growth
[NASA-CR-176112] 22 p3751 N85-33249
Block 5 documentation and solar modules
[NASA-CR-176134] 22 p3805 N85-33564
Laser-assisted solar cell metallization processing
[NASA-CR-176124] 22 p3805 N85-33565
Diffusion welding of Cassegrainian concentrator cell stack assemblies
[NASA-CR-176104] 22 p3805 N85-33566
Development of high-efficiency solar cells on silicon web
[NASA-CR-176101] 22 p3805 N85-33568
Ultrasonic seam welding on thin silicon solar cells
[NASA-CR-176116] 22 p3805 N85-33570
Use of low energy hydrogen ion implants in high efficiency crystalline silicon solar cells
[NASA-CR-176109] 22 p3806 N85-33571
An enhanced photoresponse at dislocation subgrain boundaries revealed by X-ray topography of polysilicon solar cells 22 p3806 N85-33572
Photovoltaic energy systems
[DE85-011630] 22 p3807 N85-33581
1985 Amorphous Silicon Review Meeting
[DE85-008794] 22 p3807 N85-33582
Low-cost high-performance silicon concentrator cells
[DE85-008875] 22 p3807 N85-33584
Photovoltaics technical information guide
[DE85-002924] 22 p3808 N85-33585
Solar maximum: Solar array degradation
[NASA-TM-86194] 23 p3903 N85-34175
Flat-plate solar array project process development area process research of non-CZ silicon material
[NASA-CR-176117] 23 p3945 N85-34445
Investigation of test methods, material properties, and processes for solar cell encapsulants
[NASA-CR-176132] 23 p3945 N85-34446
Development of metallization process: FSA project, cells and module formation research area
[NASA-CR-176136] 23 p3945 N85-34447
Dual-chamber plasma deposition of A-Si:H solar cells at high rates using disilane
[DE85-011828] 23 p3946 N85-34451
Practical aspects of photovoltaic technology, applications and cost (revised)
[NASA-CR-174963] 24 p4110 N85-35472
Photovoltaics technology program summary
[DE85-013096] 24 p4112 N85-35493
Design and construction of an advanced power conditioning subsystem for small photovoltaic applications
[DE85-013940] 24 p4113 N85-35495

SOLAR COLLECTORS
NT SOLAR REFLECTORS
Modeling of a second-generation solar-driven Rankine air conditioner
[DE84-015132] 01 p0036 N85-10223
Technical Review of the Solid Particle Receiver Program
[DE84-015181] 01 p0068 N85-10451
Test methods and standards development for active solar heating and cooling systems
[PB84-217447] 03 p0343 N85-12209
Superpure materials research planned
03 p0353 N85-12270
Fluorescent dyes for luminescent solar concentrators
[BMFT-FB-T-84-164] 04 p0480 N85-13061
Concentrator optical characterization using computer mathematical modelling and point source testing
[NASA-CR-174109] 04 p0528 N85-13375
Software used with the flux mapper at the solar parabolic dish test site
[NASA-CR-174108] 04 p0528 N85-13376
Thin polymer film collectors as a contribution to the solar industry
[DE84-015299] 04 p0529 N85-13383
Solar pond overview 05 p0667 N85-14287
Proceedings of the 22nd Project Integration Meeting
[DE85-000334] 06 p0833 N85-15302
Multijunction cells for concentrators: Technology prospects
[NASA-CR-174259] 07 p0991 N85-16295
Antisoiling technology: Theories of surface soiling and performance of antisoiling surface coatings
[NASA-CR-174274] 07 p0991 N85-16296
Performance and cost of energy transport and storage systems for dish applications using reversible chemical reactions
[NASA-CR-174263] 07 p0992 N85-16298
Solar energy conversion based on the principle of fluorescent collectors. Installation of a test collector to deliver several Watts power
[BMFT-FB-T-84-192] 07 p0993 N85-16306
Solar energy conversion based on the principle of fluorescent collectors
[BMFT-FB-T-84-193] 07 p0994 N85-16309
Compilation of Sandia papers contributed to the 17th IEEE Photovoltaic Specialists Conference
[DE84-017456] 09 p1315 N85-18267
NBS (National Bureau of Standards) solar collector durability-reliability test program
[PB85-113603/GAR] 09 p1348 N85-18469
Overview of photovoltaic concentrator technology
[DE84-016790] 10 p1512 N85-19539
Development of mass-producible line-focus tracking concentrating solar collectors. Category 2: Trackers
[DE85-002673] 10 p1512 N85-19543
Photosynthesis of ammonia
[DE85-001482] 11 p1585 N85-20029
Flame spread on combustible solar collector glazing materials
[DE85-002586] 11 p1585 N85-20032
Innovative solar thermal dish technology development
[DE85-002767] 11 p1673 N85-20539
Solar thermal technology
[DE84-013029] 11 p1673 N85-20540
Sol-gel-derived AR coatings for solar receivers
[DE85-000192] 11 p1673 N85-20541
Advanced glazings research
[DE85-000539] 11 p1674 N85-20549
Control of large collector arrays: The SSPS experience
[DE85-001461] 11 p1675 N85-20553
Performance of solar thermal systems with liquid metal MHD conversion
[DE85-002758] 11 p1675 N85-20555
Evaluation of infrared reflectance as a technique for measuring absorber materials degradation
[DE85-002171] 11 p1729 N85-20674
An investigation of aerowindows for solar receivers
[DE84-010931] 12 p1877 N85-21772
Performance evaluation of an active solar cooling system utilizing low cost plastic collectors and an evaporatively-cooled absorption chiller
[DE84-010813] 12 p1880 N85-21798
NBS solar collector durability/reliability test program
[DE85-003489] 12 p1881 N85-21801
Some solar dish/heat engine design considerations
[DE85-003479] 12 p1881 N85-21802

User's manual for the University of Houston individual heliostat layout and performance code
[DE85-004643] 12 p1882 N85-21808
Solar process heat: Technology program
[BMFT-FB-T-84-234] 12 p1882 N85-21812
Power from the Sun: Light at night
[PB85-124097] 12 p1883 N85-21814
Ecological observations at the site of the 10 MWe solar thermal power system (1978-1984)
[DE85-004572] 12 p1885 N85-21827
ROSA: A computer model for optical power ratio calculations
[DE85-005174] 13 p2129 N85-23251
Use of heat pipes for heat collection and transmission in solar plants 14 p2265 N85-24037
Selective coatings for solar-to-thermal energy converters 14 p2280 N85-24127
Silicon-sheet and thin-film cell and module technology potential: Issue study
[NASA-CR-175654] 14 p2349 N85-24520
Development and testing of Parabolic Dish Concentrator No. 1
[NASA-CR-175651] 14 p2350 N85-24522
Advanced high-efficiency concentrator cell
[DE85-000525] 14 p2351 N85-24533
An evaluation of thermal storage for liquid-metal, solar thermal receivers
[DE85-002929] 16 p2820 N85-27394
High-altitude testing of selective optical coatings for solar radiators and collectors 17 p2939 N85-28143
Selective coatings for solar heat converters 17 p2939 N85-28144
Relative potentials of concentrating and two-axis tracking flat-plate photovoltaic arrays for central-station applications
[NASA-CR-175689] 17 p2985 N85-28446
Parabolic dish test site: History and operating experience
[NASA-CR-175692] 17 p2985 N85-28447
A program for the calculation of paraboloidal-dish solar thermal power plant performance
[NASA-CR-175874] 17 p2985 N85-28449
Development of mass-producible line-focus tracking concentrating solar collectors. Category 2: Control systems
[DE85-007873] 17 p2987 N85-28459
Shenandoah parabolic dish solar collector
[DE85-008326] 17 p2987 N85-28460
DOE/Sandia point-focus concentrator program, draft
[DE85-006209] 17 p3038 N85-28793
United States participation in International Energy Agency Task IX, Subtask (C): Pyranometry, 1984 participation
[DE85-009615] 18 p3110 N85-29256
Absorber coatings degradation
[DE85-008628] 18 p3128 N85-29367
Airport solar photovoltaic concentrator phase 3
[DE85-006773] 18 p3128 N85-29370
Progress in solar thermal distributed receiver technology
[DE85-008086] 18 p3128 N85-29372
Foamglass solar window collector
[DE85-009197] 18 p3129 N85-29374
Liquid metal thermoelectric converter (LMTEC) for solar applications
[DE85-008405] 18 p3129 N85-29376
Silvered polymer reflectors
[DE85-008782] 18 p3130 N85-29384
Solar Thermal Research Program
[DE85-000514] 18 p3131 N85-29386
10 MWe Solar Thermal Central Receiver Pilot Plant total capital costs
[DE85-009113] 18 p3131 N85-29390
Thermal performance testing and mathematically modeling of integral collector storage solar hot water systems
[PB85-186906] 18 p3132 N85-29398
Design and operation of solar thermal heat transfer systems
[DE85-009837] 19 p3267 N85-30263
Receiver loss study of optimized solar central receiver systems as a function of receiver thermal loss per unit area
[DE85-010831] 19 p3268 N85-30265
Thermal performance and design of a solid particle cavity receiver
[DE85-010830] 19 p3274 N85-30300
Advanced evacuated tube collectors
[DE85-010271] 19 p3274 N85-30302
High-efficiency, low-cost, passively-cooled PV concentrator module
[DE85-010013] 19 p3305 N85-30490
Calibration of relevant measuring sensors
[DE85-009820] 19 p3306 N85-30492
Proceedings of the Distributed Receiver Solar Thermal Technology Conference
[DE85-010551] 19 p3306 N85-30493
A model for the economic assessment of solar power plants
[DE85-009355] 19 p3381 N85-30977
Solar dynamic systems 20 p3443 N85-31374
View-limiting shrouds for insolation radiometers
[NASA-CR-176041] 20 p3458 N85-31476
Control system for parabolic dish concentrator No. 1
[NASA-CR-176045] 20 p3463 N85-31510
Nomographs for estimating the levelized cost of energy from flat-plate and concentrator photovoltaic systems
[NASA-CR-176048] 20 p3483 N85-31645
Photovoltaic concentrator research status
[DE85-010119] 20 p3483 N85-31647
Self-heating to ignition measurements and computation of critical size for solar energy collector materials
[PB85-183374] 20 p3486 N85-31663
An investigation into the fluidization and heat transfer of low density particles in a fluidized bed with applications
[AD-A155259] 21 p3584 N85-32282
Forced convection on solar collector arrays
[DE85-010361] 21 p3585 N85-32287
Advanced module development overview 21 p3612 N85-32445
Status of high-efficiency module design and fabrication 21 p3612 N85-32446
Module Hipot and ground continuity test results 21 p3612 N85-32447
Photovoltaic module spread-of-flame testing 21 p3612 N85-32448
Improved Nominal Operating Cell Temperature (NOCT) test procedure 21 p3612 N85-32449
Thin-film reliability and engineering overview 21 p3612 N85-32450
Department of Energy gear drive unit final prototype testing and design evaluation
[DE85-003296] 22 p3793 N85-33499
An analysis of the effects of active solar energy system control sensor degradation on system performance
[DE84-013023] 22 p3804 N85-33562
Theory of cellwise optimization for solar central receiver system
[DE85-012586] 22 p3807 N85-33579
Solar central receiver preliminary design studies: Summary and review of contract results
[DE85-011385] 22 p3809 N85-33593
Study of alternative system conversions for the Solar One pilot plant
[DE85-010026] 22 p3809 N85-33594
Long-term goals for solar thermal technology
[DE85-013032] 22 p3809 N85-33597
Optical analysis of parabolic dish concentrators for solar dynamic power systems in space
[NASA-TM-87080] 23 p3903 N85-34176
Vapor phase heat transport concepts
[DE85-009550] 23 p3931 N85-34366
Solar thermal technologies program summary
[DE85-012253] 23 p3945 N85-34449
Solar heat pump
[DE85-011323] 23 p3946 N85-34453
Solar energy education: Renewable energy activities for chemistry and physics
[DE85-010371] 23 p3946 N85-34455
Solar pond technology for Navy applications
[AD-A155877] 24 p4112 N85-35488

SOLAR CONSTANT
Spectroradiometric calibration of the Thematic Mapper and Multispectral Scanner system
[E85-10094] 12 p1874 N85-21756
Global solar oscillations in irradiance and velocity: A comparison 14 p2446 N85-25094

SOLAR CONVERTERS
U SOLAR GENERATORS

SOLAR COOLING
Solar heating and cooling R and D program coordination support
[DE84-013479] 01 p0088 N85-10449
Turbine test report, addendum
[DE84-015130] 02 p0205 N85-11353
Test methods and standards development for active solar heating and cooling systems
[PB84-217447] 03 p0343 N85-12209
Passive solar/Earth sheltered office/dormitory cooling season thermal performance
[DE84-016662] 05 p0869 N85-14308
Performance of the SERI parallel-passage dehumidifier
[DE85-000509] 11 p1672 N85-20536
High performance solar desiccant cooling system: Performance evaluation and research recommendations
[DE85-000508] 11 p1676 N85-20559
A summary and assessment of historical reliability and maintainability data for solar hot water and space conditioning systems
[DE84-004521] 12 p1876 N85-21770
Development of a single-family absorption chiller for use in a solar heating and cooling system, phase 3, volume 2
[DE85-003218] 13 p2130 N85-23253
Testing and further development of a solar absorption cooling plant
[BMFT-FB-T-84-264] 15 p2588 N85-25964
Operation of a low temperature absorption chiller at rating point and at reduced evaporator temperature
[DE85-006308] 16 p2760 N85-27030
Experiments on sorption characteristics of solid desiccant materials for solar desiccant cooling systems
[DE85-000542] 17 p2923 N85-28019
Proceedings of the Distributed Receiver Solar Thermal Technology Conference
[DE85-010551] 19 p3306 N85-30493
Comparative evaluation of ground-coupled heat pumps that use solar energy
[DE85-010950] 20 p3484 N85-31649
Evaporatively cooled chiller for solar air conditioning systems design and field test
[DE84-014154] 20 p3484 N85-31652
Solid desiccant dehumidification systems for residential applications
[PB85-198489] 22 p3755 N85-33279
Advances in open-cycle solid desiccant cooling
[DE85-008797] 22 p3808 N85-33590

SOLAR CORONA
NT CORONAL HOLES
NT CORONAL LOOPS
Studies of solar flares and coronal loops
[AD-A145009] 01 p0130 N85-10808
Study of the solar corona using radio and space observations
[NASA-CR-174034] 02 p0304 N85-11963
Physics of the inner heliosphere 1-10R sub O plasma diagnostics and models
[NASA-CR-174010] 02 p0304 N85-11964
Active regions — and the Solar Maximum Mission
[NASA-CR-170628] 02 p0304 N85-11965
Vector magnetic field analysis of Lorentz forces acting in the solar atmosphere
[AD-A145941] 03 p0449 N85-12852
Magnetic helicity in the solar corona 05 p0745 N85-14780
Structure and evolution of the large scale solar and heliospheric magnetic fields 05 p0746 N85-14782
Distribution of the K-corona over the polar regions of the solar disk: 1966-1983
[PB84-230077] 06 p0835 N85-15317
Meteoritic constraints on processes in the solar nebula 06 p0867 N85-15630
Chemical evolution of the solar nebula: A new model 06 p0867 N85-15631
Homogeneous condensation of gaseous mixtures of Si, Fe, O, N, and C in relative cosmic abundance and implications for astronomical condensation 06 p0867 N85-15632
Dynamic thermal episodes in the protosolar nebula: Development of models from observations on CAI's 06 p0867 N85-15633
The chemistry of rare earth elements in the solar nebula 06 p0869 N85-15643
Differentiated meteorites and the components of chondrites
[NASA-CR-174201] 06 p0890 N85-15649
Polar rain: Solar coronal electrons in the Earth's magnetosphere
[NASA-TM-86150] 07 p1060 N85-16726
Evidence for non-radiative activity in hot stars 08 p1231 N85-17756
Heating in the solar mantle 08 p1233 N85-17769
Coronal and chromospheric physics — Sun, sunspots, and solar limb
[NASA-CR-174290] 08 p1259 N85-17821
Solar Corona Explorer: A mission for the physical diagnosis of the solar corona
[NASA-TM-87416] 10 p1572 N85-19912
Global aspects of stream evolution in the solar wind
[DE85-002207] 11 p1766 N85-21101
Activation of solar flares 12 p1954 N85-22276
Thermal stability of static coronal loops: Part 1: Effects of boundary conditions
[NASA-CR-175495] 12 p1961 N85-22330
A normal incidence, high resolution X-ray telescope for solar coronal observations
[NASA-CR-175622] 13 p2169 N85-23461
Orbital resonances and planetary accretion in the solar nebula 13 p2179 N85-23523
Evolution of grains in a turbulent solar nebula 13 p2179 N85-23525

Research on the early history of the solar system
13 p2180 N85-23527
Physics of the inner heliosphere: Mechanisms, models and observational signatures
[NASA-CR-175632] 13 p2205 N85-23677
The hydromagnetics of the Sun — conferences
[ESA-SP-220] 14 p2445 N85-25091
Coronal structures 14 p2448 N85-25110
The Fe XIII 10747 A and Fe XIV 5303 A coronal emission lines polarization 14 p2448 N85-25111
Mechanisms of magnetic heating of the solar corona 14 p2448 N85-25113
Observational constraints on heating processes — solar corona 14 p2449 N85-25115
Axisymmetric magnetofluidstatic (MFS) equilibria of solar coronal loops: An integral equation approach 14 p2449 N85-25116
Coronal heating by turbulent phase mixed MHD waves — solar corona 14 p2453 N85-25148
The possible role of electrical currents in coronal phenomena 14 p2453 N85-25151
Coronal structures observed at metric wavelengths with the Nancay radioheliograph 14 p2453 N85-25152
Empirical model of the solar corona using solar-cycle related parameters 14 p2453 N85-25153
Harmonic analysis of the solar magnetic field 14 p2454 N85-25154
About sudden disappearances and reappearances — solar activity 14 p2454 N85-25157
Solar maximum mission results on the energetics of the impulsive phase of solar flares 14 p2454 N85-25159
Solar magnetohydrodynamics: Symposium review 14 p2455 N85-25162
Analysis of short-period changes in intensity of hard X-radiation of solar flares registered aboard Venera-13 and Venera-14 spacecraft 16 p2723 N85-26806
Remote sensing of the plasma with time delay measurements (coronal sounding) 16 p2866 N85-27804
The Faraday rotation experiment — solar corona 16 p2866 N85-27805
Very large array observations of coronal loops and related observations of solar type stars
[AD-A152027] 16 p2868 N85-27817
The solar coronal X-ray spectrum 5.5-12 A
[AD-A152334] 17 p3054 N85-28908
Application of the MHD energy principle to magnetostatic atmospheres
[NASA-CR-175967] 18 p3136 N85-29420
Measurements of Solar Vector Magnetic Fields
[NASA-CP-2374] 18 p3203 N85-29869
Magnetic and thermodynamic structure of the solar corona during sunspot minimum 18 p3203 N85-29873
Current evolution in a numerical emerging-magnetic-flux model 18 p3204 N85-29875
Turbulence and wave particle interactions in solar-terrestrial plasmas
[NASA-CR-175970] 18 p3209 N85-29906
Effects of coronal disturbances on the ionization state of the solar wind
[NASA-CR-175997] 19 p3385 N85-31000
Solar photospheric and coronal abundances from solar energetic particle measurements
[NASA-CR-176029] 20 p3547 N85-32073
Contributions to the 19th International Cosmic Ray Conference
[NASA-CR-176060] 21 p3714 N85-33044
Solar coronal and photospheric abundances from solar energetic particle measurements
[PAPER-SH-2.1-5] 21 p3715 N85-33053
Latitude variation of recurrent fluxes in the outer solar system
[SH-4.1-13] 21 p3715 N85-33054
A study of the cyclical variations of coronal holes and their relation to open magnetic fields
[AD-A155251] 21 p3723 N85-33099
Variation in radiowave propagation conditions in corona during solar activity cycle 22 p3763 N85-33327
Relationships between chondritic meteorites and planets 22 p3851 N85-33851
Nebular volatile fractionations associated with chondrule formation 22 p3852 N85-33855
The distribution of compositional classes in the asteroid belt: A cosmochemical fingerprint?
22 p3852 N85-33856
Soft X-Ray Telescope (SXRT)
23 p3900 N85-34159
White Light Coronograph (WLC) and Ultra-Violet Coronal Spectrometer (UVCS) 23 p3901 N85-34161
Prompt acceleration of ions by oblique turbulent shocks in solar flares
[SH-1.1-6] 23 p3989 N85-34733
Study of photon emission by electron capture during solar nuclei acceleration. 3: Photon production evaluations
[SH-1.1-10] 23 p3990 N85-34737
Spectral and spatial properties of solar microflares
[SH-1.2-4] 23 p3991 N85-34740
Two classes of solar energetic particle events associated with impulsive and long duration soft X-ray flares
[SH-1.2-12] 23 p3992 N85-34747
The starting conditions for an optically small solar gamma ray flare
[SH-1.3-2] 23 p3993 N85-34751
Energetic protons from a disappearing solar filament
[SH-1.3-7] 23 p3993 N85-34754
Solar Coronal and photospheric abundances from solar energetic particle measurements
[SH-2.1-5] 23 p3998 N85-34786
Diffusion in the chromosphere and the composition of the solar corona and energetic particles
[SH-2.1-9] 23 p3999 N85-34790
Anomalous abundances of solar energetic particles and coronal gas: Coulomb effects and First Ionization Potential (FIP) ordering
[SH-2.1-10] 23 p3999 N85-34791
Coronal propagation of solar flare particles observed by satellite
[SH-3.1-2] 23 p4001 N85-34807
Coronal propagation of flare associated electrons and protons
[SH-3.1-3] 23 p4001 N85-34808
Peculiarities of propagation of charged particles in solar corona
[SH-3.1-6] 23 p4001 N85-34810
The propagation of solar energetic particles in magnetic channels
[SH-3.2-4] 23 p4003 N85-34820
The flare origin of Forbush decreases not associated with solar flares on the visible hemisphere of the Sun
[SH-5.1-4] 23 p4041 N85-35058
The 4He1H ratios in the chemical compositions of solar flare particles and the primordial solar nebula
[SH-7.1-12] 23 p4048 N85-35104

SOLAR CORPUSCULAR RADIATION
NT SOLAR ELECTRONS
NT SOLAR NEUTRINOS
NT SOLAR PROTONS
Plasma and nuclear processes in solar matter
12 p1954 N85-22277
Solar-geophysical data number 483, November 1984. Part 2: (Comprehensive reports). Data for May 1984, December 1981 and miscellanea
[PB85-147700] 12 p1962 N85-22336
Cyclic changes in barometric coefficient of cosmic ray neutron component 15 p2478 N85-25293
Nineteenth International Cosmic Ray Conference. SH sessions, volume 4
[NASA-CP-2376-VOL-4] 23 p3989 N85-34729
Nineteenth International Cosmic Ray Conference. SH sessions, volume 5
[NASA-CP-2376-VOL-5] 23 p4031 N85-34991

SOLAR COSMIC RAYS
Variation of fast charged particles in event of 22 November 1977 based on Cosmos-900 satellite data
02 p0161 N85-11092
Solar cosmic ray produced neon in lunar soils and their implication for gas-rich meteorite studies
06 p0887 N85-15636
Solar-Geophysical Data. Part 1: (Prompt reports)
[PB85-112068] 11 p1766 N85-21100
Correlated fluctuations of charged particle fluxes and magnetic field according to data from Intercosmos-10 satellite 16 p2722 N85-26802
Solar coronal and photospheric abundances from solar energetic particle measurements
[PAPER-SH-2.1-5] 21 p3715 N85-33053
Differential measurement of cosmic-ray gradient with respect to interplanetary current sheet
[PAPER-SH-4.2-9] 21 p3715 N85-33055
Changes in the energy spectrum of anomalous oxygen and helium during 1977 - 1985
[PAPER-SH-4.6-1] 21 p3715 N85-33056
Solar cycle variations of the anomalous cosmic ray component
[PAPER-SH-4.6-2] 21 p3715 N85-33057
Radial and latitudinal gradients of anomalous oxygen during 1977 - 1985
[PAPER-SH-4.6-4] 21 p3716 N85-33058
Solar modulation and interplanetary gradients of the galactic electron flux, 1977 - 1984
[PAPER-SH-4.7-4] 21 p3716 N85-33059
Source energy spectra from demodulation of solar particle data by interplanetary and coronal transport
[SH-1.3-13] 23 p3994 N85-34758
Ground increase of cosmic ray intensity on February 16, 1984
[SH-1.3-15] 23 p3994 N85-34760
The SCR flare of 16 February 1984 as recorded by the Sayan spectrograph
[SH-1.3-17] 23 p3994 N85-34761
Time extended production of neutrons during a solar flare
[SH-1.4-1] 23 p3994 N85-34762
Further obeservations of protons resulting from the decay of neutrons ejected by solar flares
[SH-1.4-2] 23 p3994 N85-34763
Suggestions for improving the efficiency of ground-based neutron monitors for detecting solar neutrons
[SH-1.4-3] 23 p3995 N85-34764
Precision measurements of solar energetic particle elemental composition
[SH-2.1-4] 23 p3998 N85-34785
Solar Coronal and photospheric abundances from solar energetic particle measurements
[SH-2.1-5] 23 p3998 N85-34786
Silicon to iron abundances in solar cosmic rays and in the sun
[SH-2.1-6] 23 p3998 N85-34787
Variations in elemental composition of several MEV/nucleon ions observed in interplanetary space
[SH-2.1-7] 23 p3998 N85-34788
The mean ionic charges of N, Ne, MG, SI and S in solar energetic particle events
[SH-2.1-11] 23 p3999 N85-34792
Nucleosynthesis in the terrestrial and solar atmospheres
[SH-2.2-2] 23 p4000 N85-34797
Solar source regions of 3HE-rich particle events
[SH-2.2-4] 23 p4000 N85-34799
The 3HE in solar non-relativistic electron events
[SH-2.2-5] 23 p4000 N85-34800
Elemental abundance differences between nuclei accleated in CIR shocks and solar flares
[SH-2.2-6] 23 p4000 N85-34801
The heavy ion composition in 3HE-rich solar flares
[SH-2.2-7] 23 p4000 N85-34802
The mean ionic charge of silicon in 3HE-rich solar flares
[SH-2.2-8] 23 p4000 N85-34803
On the connection between the 3HE-enrichment and spectral index of solar energetic particles
[SH-2.2-9] 23 p4001 N85-34804
The plasma mechanism for preferential acceleration of heavy ions
[SH-2.2-10] 23 p4001 N85-34805
Observations of solar energetic particles at a synchronous orbit
[SH-3.1-1] 23 p4001 N85-34806
Coronal propagation of solar flare particles observed by satellite
[SH-3.1-2] 23 p4001 N85-34807
Coronal propagation of flare associated electrons and protons
[SH-3.1-3] 23 p4001 N85-34808
Geometry of the diffusive propagation region in the August 14, 1982 solar electron event
[SH-3.1-5] 23 p4001 N85-34809
Some characteristics of the solar flare event of February 16, 1984
[SH-3.1-7] 23 p4001 N85-34811
Constraints of solar flare particle transport models from anisotropy observations at Voyager 1
[SH-3.1-8] 23 p4002 N85-34812
Determination of the pitch-angle distribution and transverse anisotropy of interplanetary particles
[SH-3.1-11] 23 p4002 N85-34815
Pitch angle distributions of solar energetic particles and the local scattering properties of the interplanetary magnetic field
[SH-3.1-13] 23 p4002 N85-34816
Exponential anisotropy of solar cosmic rays
[SH-3.2-1] 23 p4002 N85-34817
Energetic solar particle events
[SH-3.2-2] 23 p4003 N85-34818
Channeled propagation of solar particles
[SH-3.2-3] 23 p4003 N85-34819
The propagation of solar energetic particles in magnetic channels
[SH-3.2-4] 23 p4003 N85-34820
Radial transport of approximately 1 MeV/nucleon ions during the 22 November 1977 solar particle event
[SH-3.2-5] 23 p4003 N85-34821
Energetic solar particle fluxes out to 3 AU during the 7 May 1978 flare event
[SH-3.2-6] 23 p4003 N85-34822
The local characteristic function of interplanetary particle propagation
[SH-3.2-8] 23 p4003 N85-34823

Investigation of cosmic ray propagation in interplanetary space
[SH-3.2-9] 23 p4004 N85-34824
Diffusion-convection function of cosmic rays
[SH-3.2-10] 23 p4004 N85-34825
On reflecting boundary behind the Earth's orbit at propagation of fast particles from solar flares
[SH-3.2-13] 23 p4004 N85-34827
Propagation of the phase of solar modulation
[SH-4.1-12] 23 p4005 N85-34835
North-south asymmetry in activity on the Sun and cosmic ray density gradients
[SH-4.2-7] 23 p4007 N85-34845
Gradients and anisotropies of high energy cosmic rays in the outer heliosphere
[SH-4.3-7] 23 p4032 N85-34992
IMF-sense-dependent cosmic ray anisotropy produced from diffusion-convection in heliosphere
[SH-4.3-9] 23 p4032 N85-34994
Influence of the neutral sheet on the Swinson's type north-south anisotropy of cosmic rays
[SH-4.3-10] 23 p4032 N85-34995
Characteristics of cosmic ray pole-equator anisotropy derived from spherical harmonic analysis of neutron monitor data
[SH-4.3-12] 23 p4032 N85-34996
First zonal harmonic component of cosmic ray neutron intensity
[SH-4.3-13] 23 p4032 N85-34997
Cosmic ray intensity distribution perpendicular to solar equatorial plane at 1 A.U. during 1978-83
[SH-4.3-14] 23 p4032 N85-34998
The corotating variation of the north-south anisotropy of cosmic rays
[SH-4.3-15] 23 p4033 N85-34999
Sidereal anisotropy of cosmic rays
[SH-4.4-8] 23 p4034 N85-35006
Cosmic ray intensity variations observed at Matsushiro (220 M.W.E. in depth)
[SH-4.4-9] 23 p4034 N85-35007
Long-term modulation of cosmic rays during solar cycle 21
[SH-4.4-10] 23 p4034 N85-35008
Role of solar flare index in long term modulation of cosmic ray intensity
[SH-4.4-12] 23 p4034 N85-35009
Azimuthal and meridional asymmetries of the solar wind and quasiperiodic variations of intensity of Galactic Cosmic Rays (GCR)
[SH-4.4-20] 23 p4035 N85-35016
Dynamics of two-year cosmic ray variations inferred from the data of spacecraft and stratospheric measurements and from the neutron monitor data in 1959-1981
[SH-4.4-21] 23 p4035 N85-35017
Solar tri-diurnal variation of cosmic rays in a wide range of rigidity
[SH-4.5-3] 23 p4036 N85-35021
Upper cut-off rigidity for corotation anisotropy during solar activity cycles 20 and 21
[SH-4.5-4] 23 p4036 N85-35022
Twenty-two-year cycle of the upper limiting rigidity of Daily waves
[SH-4.5-5] 23 p4036 N85-35023
Solar wind velocity and daily variation of cosmic rays
[SH-4.5-6] 23 p4036 N85-35024
Time and energy dependence of the cosmic ray gradient in the outer heliosphere
[SH-4.7-2] 23 p4040 N85-35047
Frequency spectra of short-period variations of cosmic ray
[SH-5.1-17] 23 p4043 N85-35070
Penetration of solar protons into the Earth's magnetosphere on November 22, 1977
[SH-6.1-15] 23 p4046 N85-35088
Dynamics of the penetration boundaries of solar protons during a strong magnetic storm
[SH-6.1-16] 23 p4046 N85-35089
Solar cosmic ray bursts and solar neutrino fluxes
[SH-8.1-10] 23 p4050 N85-35115
A silicon surface barrier telescope for solar particles identification
[SH-9.1-3] 23 p4050 N85-35118
Strong earthquakes, novae and cosmic ray environment
[SH-10.1-3] 23 p4053 N85-35135

SOLAR CYCLES
NT SUNSPOT CYCLE
Statistical analysis of 11-year and 80-year solar cycles
02 p0161 N85-11095
Statistical properties of geomagnetic pulsations at the Observatory of Fuerstenfeldbruck determined with the aid of pulsation indices. Part 2: Periodicity in the occurrence of pulsations
[REPT-556] 03 p0376 N85-12389
Middle Atmosphere Program. Handbook for MAP, volume 8
[NASA-CR-175478] 11 p1657 N85-20445
Report on the Workshop on Intercomparison of Solar UV Irradiance Measurements and Related Instrument Calibration 11 p1658 N85-20448
Nonlinear time-evolution of kink-unstable magnetic flux tubes in the convection zone of the Sun
14 p2447 N85-25105
Solar and stellar magnetic cycles: Unity and multiplicity 14 p2448 N85-25109
A consideration of the solar cycle in the light of the behavior of the large active regions
14 p2452 N85-25140
Solar cycle variation of ephemeral active regions
14 p2452 N85-25142
The first effect of the amplitude of a solar cycle
14 p2452 N85-25143
Empirical model of the solar corona using solar-cycle related parameters 14 p2453 N85-25153
About sudden disappearances and reappearances — solar activity 14 p2454 N85-25157
Modeling 22-year solar activity cycle within framework of dynamo theory with allowance for primary field
15 p2477 N85-25288
Cyclic changes in barometric coefficient of cosmic ray neutron component 15 p2478 N85-25293
Contributions to the 19th International Cosmic Ray Conference
[NASA-CR-176060] 21 p3714 N85-33044
Solar cycle variations of the anomalous cosmic ray component
[PAPER-SH-4.6-2] 21 p3715 N85-33057
Radial and latitudinal gradients of anomalous oxygen during 1977 - 1985
[PAPER-SH-4.6-4] 21 p3716 N85-33058
Solar modulation and interplanetary gradients of the galactic electron flux, 1977 - 1984
[PAPER-SH-4.7-4] 21 p3716 N85-33059
Solar cycle variation of ephemeral regions
[AD-A154967] 21 p3723 N85-33097
A study of the cyclical variations of coronal holes and their relation to open magnetic fields
[AD-A155251] 21 p3723 N85-33099
Variation in radiowave propagation conditions in corona during solar activity cycle 22 p3763 N85-33327
Elemental abundances in corotating events
[SH-1.5-15] 23 p3997 N85-34778
Solar and interplanetary particles at 2 to 4 MEV during solar cycles 21, solar cycle variations of event sizes, and compositions
[SH-1.5-16] 23 p3997 N85-34779
Cumulative effect of Forbush decreases in the heliospheric modulation during the present solar cycle
[SH-4.1-10] 23 p4005 N85-34833
Cosmic ray north-south anisotropy 1961 - 1983
[SH-4.2-6] 23 p4007 N85-34844
The expected cosmic ray density and stream distributions at the heliolatitudinal asymmetry of solar wind
[SH-4.2-14] 23 p4008 N85-34852
The effect of the neutral sheet structure of the interplanetary magnetic field on cosmic ray distribution in space
[SH-4.2-18] 23 p4008 N85-34855
Spatial distribution of cosmic rays in magnetic cycles of the Sun
[SH-4.2-20] 23 p4009 N85-34857
11- and 22-year variations of the cosmic ray density and of the solar wind speed
[SH-4.2-21] 23 p4009 N85-34858
Difference between even and odd 11-year cycles in cosmic ray intensity
[SH-4.2-22] 23 p4009 N85-34859
An update on the correlation between the cosmic radiation intensity and the geomagnetic AA index
[SH-4.2-24] 23 p4009 N85-34861
Gradients and anisotropies of high energy cosmic rays in the outer heliosphere
[SH-4.3-7] 23 p4032 N85-34992
Long-term modulation of cosmic rays during solar cycle 21
[SH-4.4-10] 23 p4034 N85-35008
Cosmic ray biannual variation
[SH-4.4-15] 23 p4034 N85-35011
The difference in the energy spectra of galactic cosmic rays at the minima of the 19th and 20th solar activity cycles
[SH-4.4-18] 23 p4035 N85-35014
Cosmic ray variations with the period close to 27 days and their connection with solar activity longitudinal distribution
[SH-4.4-19] 23 p4035 N85-35015
Diurnal anisotropy during solar activity cycle twenty and diffusion-convection model
[SH-4.5-7] 23 p4036 N85-35025
Diurnal variations from muon data at Takeyama underground station
[SH-4.5-13] 23 p4037 N85-35030
Solar cycle variations of the anomalous cosmic ray component
[SH-4.6-2] 23 p4039 N85-35040
Time and energy dependence of the cosmic ray gradient in the outer heliosphere
[SH-4.7-2] 23 p4040 N85-35047
Dimensions of the solar wind cavity and of the region of interplanetary cosmic ray modulation
[SH-4.7-11] 23 p4041 N85-35055
The solar wind effect on cosmic rays and solar activity
[SH-5.1-13] 23 p4043 N85-35068
On the solar cycle variation in the barometer coefficients of high latitude neutron monitors
[SH-6.1-2] 23 p4044 N85-35077
Cosmic ray secular variations in terrestrial records and aurorae
[SH-7.1-3] 23 p4047 N85-35096
When did the average cosmic ray flux increase?
[SH-7.1-4] 23 p4047 N85-35097
Solar neutrino: Flux, cosmic rays and the 11 year solar cycle
[SH-8.1-7] 23 p4049 N85-35112
Solar cosmic ray bursts and solar neutrino fluxes
[SH-8.1-10] 23 p4050 N85-35115
The influences of the galactic cosmic ray on the atmospheric ozone
[SH-10.1-1] 23 p4053 N85-35133

SOLAR DIAMETER
Solar variability observed through changes in solar figure and mean diameter
[DE85-012857] 22 p3860 N85-33900

SOLAR DISK
U SUN

SOLAR DYNAMICS
U HELIOSEISMOLOGY

SOLAR ECLIPSES
Extreme limb profiles of the Sun at far infrared and submillimeter wavelengths 06 p1244 N85-17852
Rocket observations of the ionosphere during the eclipse of 26 February 1979
[NASA-CR-175513] 12 p1886 N85-21850
Effect of solar eclipses on the LAGEOS semimajor axis 20 p3491 N85-31699

SOLAR ELECTRONS
Solar He-3-rich events and non-relativistic electron events: A new association
[NASA-TM-86179] 06 p0890 N85-15852
Polar rain: Solar coronal electrons in the Earth's magnetosphere
[NASA-TM-86150] 07 p1060 N85-18726
The 3HE in solar non-relativistic electron events
[SH-2.2-5] 23 p4000 N85-34800

SOLAR ENERGY
Solar heating and cooling R and D program coordination support
[DE84-013479] 01 p0068 N85-10449
National solar-terrestrial research program
[PB84-216183] 01 p0072 N85-10479
USSR report: Space
[JPRS-USP-84-005] 02 p0156 N85-11060
Features of new solar panels on Salyut-7
02 p0157 N85-11062
Modular photovoltaic array field
[SAND-83-7028] 02 p0222 N85-11454
FSA field test
[NASA-CR-174114] 04 p0528 N85-13373
Experimental and theoretical study of a solar thermochemical receiver module
[NASA-CR-174107] 04 p0528 N85-13374
Joint Indo-German program on solar energy: Parabolic dish program, step 1
[BMFT-FB-T-84-175] 05 p0870 N85-14312
Encapsulation materials and processing
06 p0890 N85-15289
Polymer-polymer interface bond stability
06 p0890 N85-15271
Polymer-metal interface bond stability
06 p0890 N85-15272
Correlations of solar irradiance and daylight illuminance for building energy analysis
[DE85-001736] 06 p0899 N85-15328
National Bureau of Standards passive solar test facility: Instrumentation and site handbook
[PB85-100451/GAR] 07 p0968 N85-16148
Multijunction cells for concentrators: Technology prospects
[NASA-CR-174259] 07 p0991 N85-16295
Evaluation of the measured energy performance of four solar systems
[AD-A147912] 07 p0993 N85-16306
Conference on Singlet Molecular Oxygen (COSMO 84), program and abstracts
[AD-A147281] 07 p1040 N85-16605

Thermal design requirements of a 50-kW zinc/redox flow battery for solar electrical energy storage
[DE84-017088] 09 p1345 N85-18463
Hydrogen from solar energy
[DE85-001914] 10 p1437 N85-19055
Solar thermochemical process interface study
[NASA-CR-174442] 10 p1510 N85-19527
Overview of photovoltaic concentrator technology
[DE84-016780] 10 p1512 N85-19539
Solar collection
[DE85-000060] 10 p1512 N85-19540
Vertical solar louver project
[DE84-017335] 11 p1676 N85-20558
A summary and assessment of historical reliability and maintainability data for solar hot water and space conditioning systems
[DE84-004521] 12 p1876 N85-21770
Large-size fine-granular graphite for solar techniques
12 p1878 N85-21780
Performance evaluation of an active solar cooling system utilizing low cost plastic collectors and an evaporatively-cooled absorption chiller
[DE84-010613] 12 p1880 N85-21798
Latent heat storage technology and application workshop. Summary report: Session 6
[DE85-001097] 12 p1882 N85-21806
Evaluation of etringite and related compounds for use in solar energy storage
[DE85-003249] 12 p1882 N85-21809
Multi-year plan for Experimental Systems Research: Passive and hybrid solar energy program
[DE85-004696] 12 p1882 N85-21810
Phase change thermal energy storage and the model building codes
[PB85-111201] 12 p1883 N85-21813
Power from the Sun: Light at night
[PB85-124097] 12 p1883 N85-21814
Multiyear plan for experimental systems research passive and hybrid solar energy program
[PB85-146868] 12 p1883 N85-21815
Evaluation of etringite and related compounds for use in solar energy storage
[PB85-146876] 12 p1883 N85-21816
Ecological observations at the site of the 10 MWe solar thermal power system (1978-1984)
[DE85-004572] 12 p1885 N85-21827
ROSA: A computer model for optical power ratio calculations
[DE85-005174] 13 p2129 N85-23251
A review of development and application of heat pump technology
[CSIR-RR-585] 14 p2300 N85-24241
A bibliography of reports of the Sandia solar thermal distributed receiver systems project
[SAND-84-0313] 16 p2617 N85-27378
A multifunction wall system for application with solar heating and ground cooling
[DE85-006792] 16 p2820 N85-27395
United States participation in International Energy Agency Task IX, Subtask (C): Pyranometry. 1984 participation
[DE85-009615] 18 p3110 N85-29258
Solar pond research at the Los Alamos National Laboratory
[DE85-008631] 18 p3128 N85-29366
Salt-gradient solar ponds
[DE85-006626] 18 p3129 N85-29380
SERI Solar Energy Storage Program: FY 1984
[DE85-002936] 18 p3130 N85-29385
Solar Thermal Research Program
[DE85-000514] 18 p3131 N85-29388
Materials research for passive solar systems: Solid-state phase-change materials
[DE85-006779] 18 p3132 N85-29395
Investigation of the transferability of measures of passive solar energy utilization in the USA to the Federal Republic of Germany
[BMFT-FB-T-84-284] 18 p3132 N85-29396
Electrochromic and thermochromic materials for solar energy applications with emphasis on niobium and vanadium oxides
[DE85-010830] 19 p3249 N85-30147
Thickness-insensitive selective surface paint
[DE85-010568] 19 p3250 N85-30150
Thermal performance and design of a solid particle cavity receiver
[DE85-010830] 19 p3274 N85-30300
Proceedings of the Distributed Receiver Solar Thermal Technology Conference
[DE85-010551] 19 p3306 N85-30483
Renewable technologies program summaries
[DE85-001509] 19 p3307 N85-30500
Recombination phenomena in high efficiency silicon solar cells 20 p3479 N85-31618
High efficiency solar cell processing
20 p3482 N85-31640
Comparative evaluation of ground-coupled heat pumps that use solar energy
[DE85-010950] 20 p3484 N85-31649
Recent improvements in materials for thin GaAs and multibandgap solar cells
[DE85-008600] 20 p3484 N85-31651
Self-heating to ignition measurements and computation of critical size for solar energy collector materials
[PB85-163374] 20 p3485 N85-31663
Proceedings of the 24th Project Integration Meeting
[NASA-CR-176058] 21 p3807 N85-32394
Reliability physics 21 p3808 N85-32402
Failure testing of active solar energy system components
[DE84-013024] 22 p3804 N85-33561
An analysis of the effects of active solar energy system control sensor degradation on system performance
[DE84-013023] 22 p3804 N85-33562
Solar central receiver preliminary design studies: Summary and review of contract results
[DE85-011365] 22 p3809 N85-33593
Study of alternative system conversions for the Solar One pilot plant
[DE85-010026] 22 p3809 N85-33594
Optical analysis of parabolic dish concentrators for solar dynamic power systems in space
[NASA-TM-87060] 23 p3903 N85-34176
Solar thermal technologies program summary
[DE85-012253] 23 p3945 N85-34449
Solar energy education. Renewable energy: A background text
[DE85-010365] 23 p3946 N85-34452
Solar energy education: Renewable energy activities for chemistry and physics
[DE85-010371] 23 p3946 N85-34455
Anomalous abundances of solar energetic particles and coronal gas: Coulomb effects and First Ionization Potential (FIP) ordering
[SH-2.1-10] 23 p3999 N85-34791

SOLAR ENERGY ABSORBERS
Progress on solar absorber selective paint research
[DE84-015536] 04 p0480 N85-13059
Development of a single-family absorption chiller for use in a solar heating and cooling system, phase 3, volume 2
[DE85-003218] 13 p2130 N85-23253
Selective coatings for solar heat converters
17 p2939 N85-28144
Absorber coatings degradation
[DE85-008628] 18 p3128 N85-29367
Solar rocket component study
[AD-A154186] 19 p3227 N85-30007
Electrochromic and thermochromic materials for solar energy applications with emphasis on niobium and vanadium oxides
[DE85-010830] 19 p3249 N85-30147
Thickness-insensitive selective surface paint
[DE85-010568] 19 p3250 N85-30150
Solar dynamic systems 20 p3443 N85-31374

SOLAR ENERGY CONVERSION
NT SOLAR TOTAL ENERGY SYSTEMS
Solar-pumped lasers: A review
02 p0261 N85-11711
Compact welding apparatus with solar power supply
03 p0352 N85-12263
Control and performance of a photovoltaic-thermal energy system 03 p0387 N85-12475
Trends in concentrator, receiver, and storage development for terrestrial applications
05 p0609 N85-13891
The liquid droplet radiator - an ultralightweight heat rejection system for efficient energy conversion in space
05 p0610 N85-13900
Photovoltaic working group report
05 p0811 N85-13902
Stimulation of technologies towards photovoltaic energy conversion 05 p0861 N85-14251
Fundamentals of solar energy conversion based on fluorescence collectors 05 p0862 N85-14258
Utilization of solar energy for the production of hydrogen 05 p0863 N85-14262
Solar energy supplied mobile water purification unit
05 p0864 N85-14270
Material models and device structures for GaAs solar cells
[DE85-000501] 05 p0865 N85-14275
Site-specific research conducted in support of the Salton Sea Solar Pond Project, FY 1982 report
[NASA-CR-174182] 05 p0866 N85-14280
The spectrophotometric method of determining the transmission of solar energy in salt gradient solar ponds
05 p0866 N85-14283
Material selection consideration for solar ponds
05 p0866 N85-14284
Solar pond fluid dynamics and heat transfer
05 p0867 N85-14286
Summary of salt gradient solar pond research
05 p0867 N85-14292
Proceedings of the 23rd Project Integration Meeting
[NASA-CR-174186] 06 p0829 N85-15260
Advances and opportunities in the amorphous silicon research field
[DE84-004526] 06 p0833 N85-15304
Evaluation of the measured energy performance of four solar systems
[AD-A147912] 07 p0993 N85-16306
Solar energy conversion based on the principle of fluorescent collectors. Installation of a test collector to deliver several Watts power
[BMFT-FB-T-84-192] 07 p0993 N85-16308
Solar energy conversion based on the principle of fluorescent collectors
[BMFT-FB-T-84-193] 07 p0994 N85-16309
Heliostat tested 07 p0994 N85-16318
Lunar nuclear power feasibility study
[NASA-CR-171831] 07 p1041 N85-16611
Development of high efficiency solar cells on silicon web
[NASA-CR-174435] 10 p1509 N85-19521
US Amorphous Silicon Research Project
[DE85-000536] 10 p1511 N85-19536
The 35 kilowatt peak power photovoltaic system
[DE85-000189] 10 p1511 N85-19537
Study of low energy density photovoltaic applications under varying rate structures
[DE85-000185] 10 p1511 N85-19538
Solar-gas systems impact analysis study
[PB85-129088] 11 p1616 N85-20163
Solar thermal technology
[DE84-013029] 11 p1673 N85-20540
Energy transfer and photochemistry in biomimetic solar conversion
[PB85-129112] 11 p1677 N85-20566
Photosynthetic water splitting
[DE85-002460] 11 p1690 N85-20627
Solar-assisted hydrogen generation by photoelectrocatalysis
[PB85-149706] 12 p1804 N85-21314
Solar energy converter using surface plasma waves
[NASA-CASE-LEW-13827-1] 12 p1876 N85-21768
Research on microemulsions for storage and conversion of solar energy
[DE85-000181] 12 p1882 N85-21807
A theoretical analysis of solar-driven natural convection energy conversion systems
[DE84-004431] 13 p2128 N85-23245
USSR report: Engineering and equipment
[JPRS-UEQ-84-001] 14 p2265 N85-24034
Drop of coolant temperature in individual components of solar heating system 14 p2265 N85-24035
Power plants of modular construction with quasi-paraboloidal concentrators of solar energy
14 p2266 N85-24038
Selective coatings for solar-to-thermal energy converters 14 p2280 N85-24127
Silicon-sheet and thin-film cell and module technology potential: Issue study
[NASA-CR-175654] 14 p2349 N85-24520
Development and testing of Parabolic Dish Concentrator No. 1
[NASA-CR-175651] 14 p2350 N85-24522
Development of an Organic Rankine-Cycle power module for a small community solar thermal power experiment
[NASA-CR-175650] 14 p2350 N85-24523
Bioenergy, solar biotech research in France, Europe
15 p2536 N85-25648
Eight DOE Solar Photochemistry Research Conference: Proceedings
[DE85-005094] 15 p2587 N85-25948
Space power plants 16 p2724 N85-26813
Solar elements with distributed parameters
16 p2760 N85-27036
A bibliography of reports of the Sandia solar thermal distributed receiver systems project
[SAND-84-0313] 16 p2617 N85-27378
Alternative heat sources for heat pumps
[DE85-007610] 17 p2959 N85-28275
Activity and accomplishments of dish/Stirling electric power system development
[NASA-CR-175841] 17 p2985 N85-28445
Parabolic dish test site: History and operating experience
[NASA-CR-175892] 17 p2985 N85-28447
A program for the calculation of paraboloidal-dish solar thermal power plant performance
[NASA-CR-175874] 17 p2985 N85-28449
Airport solar photovoltaic concentrator phase 3
[DE85-006773] 18 p3128 N85-29370
Foamglass solar window collector
[DE85-009197] 18 p3129 N85-29374

Liquid metal thermoelectric converter (LMTEC) for solar applications
[DE85-008405] 18 p3129 N85-29376
Thermal performance testing and mathematically modeling of integral collector storage solar hot water systems
[PB85-186906] 18 p3132 N85-29396
Advanced evacuated tube collectors
[DE85-010271] 19 p3274 N85-30302
Proceedings of the Distributed Receiver Solar Thermal Technology Conference
[DE85-010551] 19 p3306 N85-30493
Control system for parabolic dish concentrator No. 1
[NASA-CR-176045] 20 p3463 N85-31510
Proceedings of the Flat-Plate Solar Array Project Research Forum on High-Efficiency Crystalline Silicon Solar Cells
[NASA-CR-176047] 20 p3478 N85-31615
Silicon solar cell efficiency improvement: Status and outlook 20 p3479 N85-31619
Nomographs for estimating the levelized cost of energy from flat-plate and concentrator photovoltaic systems
[NASA-CR-176048] 20 p3483 N85-31645
Proceedings of the 24th Project Integration Meeting
[NASA-CR-176058] 21 p3607 N85-32394
Summary of the high-efficiency crystalline solar cell research forum 21 p3607 N85-32396
Silicon refinement by chemical vapor transport 21 p3609 N85-32412
Performance analysis of mixed passive solar heating systems
[DE85-009624] 21 p3613 N85-32455
Prospects for a new kind of synthesis: Assembly of molecular components to achieve functions
[AD-A155023] 21 p3702 N85-32997
Polymer blends for use in photoelectrochemical cells for conversion of solar energy to electricity
[DE85-011602] 22 p3752 N85-33258
Long-term goals for solar thermal technology
[DE85-013032] 22 p3809 N85-33597
Electron photoejection in carbenions
[DE85-011747] 23 p3911 N85-34230
Electron photoejection in carbenions
[DE85-011748] 23 p3912 N85-34237
Practical aspects of photovoltaic technology, applications and cost (revised)
[NASA-CR-174983] 24 p4110 N85-35472

SOLAR FACULAE
U FACULAE

SOLAR FLARES
Studies of solar flares and coronal loops
[AD-A145009] 01 p0130 N85-10696
Solar-geophysical data number 477, May 1984. Part 2: (Comprehensive reports). Data for November 1983, July 1981 and miscellanea. Explanation of data reports issued as number 474 (supplement) February 1984
[PB84-225036] 01 p0131 N85-10900
Solar-geophysical data number 477, May 1984. Part 1: (Prompt reports). Data for April 1984, March 1984 and late data. Explanation of data reports issued as number 474 (supplement) February 1984
[PB84-225028] 01 p0131 N85-10901
Variation of fast charged particles in event of 22 November 1977 based on Cosmos-900 satellite data 02 p0161 N85-11092
Solar flares and laboratory experiments on magnetic reconnection in current sheaths 02 p0162 N85-11099
Energetic electrons in impulsive solar flares 02 p0303 N85-11962
Study of the solar corona using radio and space observations
[NASA-CR-174034] 02 p0304 N85-11963
Active regions — and the Solar Maximum Mission
[NASA-CR-170628] 02 p0304 N85-11965
Vector magnetic field analysis of Lorentz forces acting in the solar atmosphere
[AD-A145941] 03 p0449 N85-12852
Space observations of solar flares 04 p0519 N85-13313
Particle acceleration in two-ribbon flares — solar flares 04 p0519 N85-13314
The radiative hydrodynamics of flare loops heated by impulsive bursts of energetic electrons 05 p0745 N85-14781
Repulsive force of magnetic clouds during solar flares and magnetospheric substorms 06 p0824 N85-15233
Solar He-3-rich events and non-relativistic electron events: A new association
[NASA-TM-86179] 06 p0890 N85-15652
Temporal and spectral characteristics of solar flare hard X-ray emission
[NASA-TM-86187] 08 p1259 N85-17923
Energy release in solar flares
[NASA-CR-174302] 08 p1259 N85-17924
Directivity of Bremsstrahlung radiation from relativistic beams and the Gamma-Rays from solar flares
[NASA-CR-174433] 10 p1572 N85-19913
Physical aspects of the prediction of solar flares
[NASA-CR-175487] 10 p1572 N85-19915
Effects of the solar-terrestrial environment on satellite operations
[DE85-002413] 11 p1590 N85-20003
Solar-Geophysical Data. Part 1: (Prompt reports)
[PB85-112068] 11 p1766 N85-21100
Activation of solar flares 12 p1954 N85-22276
Neutron and gamma-ray signatures for particle acceleration in solar flares 12 p1954 N85-22278
Forced recognition by nonlinear MHD waves and sequential triggering of solar flares 12 p1956 N85-22291
Signatures of the coalescence instability in solar flares 12 p1956 N85-22293
Solar-geophysical data. Part 2: (Comprehensive reports)
[PB85-112076] 12 p1962 N85-22332
Solar-geophysical data number 479, July 1984. Part 1: (Prompt reports). Data for June 1984, May 1984 and later data
[NASA-CR-175542] 12 p1962 N85-22333
Ultraviolet spectral diagnostics of solar flares and heating events 13 p2205 N85-23675
Solar-geophysical data number 479, August 1981. Part 2: (Comprehensive reports), data for January 1984 and August 1981 and miscellanea. Explanation of data reports issued as number 474 (supplement) February 1984
[NASA-CR-175607] 13 p2205 N85-23679
Diagram of nonstationary rejoining of magnetic force lines 14 p2344 N85-24492
X-ray polarimetry: The measurement of the polarization of solar flare X-rays and the design of a Compton polarimeter 14 p2441 N85-25059
Prominences, two-ribbon flares and coronal transients 14 p2454 N85-25158
Solar maximum mission results on the energetics of the impulsive phase of solar flares 14 p2454 N85-25159
A study of the morphology of solar flares as observed by the hard X-ray imaging spectrometer — Solar Maximum Mission 14 p2454 N85-25160
High resolution hard X-ray spectra of solar and cosmic sources 14 p2455 N85-25163
Pulsations of cosmic ray intensities before increasing flux of relativistic particles from solar flares 15 p2477 N85-25292
Evidence in meteorites for an active early Sun 15 p2660 N85-26550
Satellite research on solar flares 16 p2717 N85-26776
Analysis of short-period changes in intensity of hard X-radiation of solar flares registered aboard Venera-13 and Venera-14 spacecraft 16 p2723 N85-26806
Solar-Geophysical Data Number 484, December 1984. Part 2 (comprehensive reports): Data for June 1984, January 1982 and Miscellanea
[NASA-CR-175826] 16 p2888 N85-27820
Electron-cyclotron maser emission during solar and stellar flares
[NASA-CR-175883] 17 p3054 N85-28907
Turbulence and wave particle interactions in solar-terrestrial plasmas
[NASA-CR-175970] 18 p3209 N85-29906
The influence of the heliospheric current sheet and angular separation on flare accelerated solar wind
[NASA-CR-175982] 18 p3209 N85-29907
The possibility of observing solar neutron events in the lower atmosphere
[NOTA-INTERNA-537] 18 p3209 N85-29908
Effects of coronal disturbances on the ionization state of the solar wind
[NASA-CR-175997] 19 p3385 N85-31000
Solar photospheric and coronal abundances from solar energetic particle measurements
[NASA-CR-176029] 20 p3547 N85-32073
Detection of solar neutrons by ground based neutron monitors
[IFSI-84-11] 20 p3547 N85-32076
Some properties of flare-not-associated Forbush decreases
[IFSI-84-13] 20 p3548 N85-32077
Contributions to the 19th International Cosmic Ray Conference
[NASA-CR-176060] 21 p3714 N85-33044
Precision measurements of solar energetic particle elemental composition
[PAPER-SH-2.1-4] 21 p3715 N85-33052
Solar coronal and photospheric abundances from solar energetic particle measurements
[PAPER-SH-2.1-5] 21 p3715 N85-33053
Soft X-ray polychromator for the Solar Maximum Mission
[NASA-CR-175297] 21 p3723 N85-33096
Heating of the deep chromosphere during solar flares
[AD-A155256] 21 p3723 N85-33100
Search for the north-south asymmetry in solar activity
[AD-A155525] 21 p3724 N85-33102
Radio telescope with 256 antennas built in Siberia 22 p3732 N85-33136
High Resolution Telescope and Spectrograph (HRTS) 23 p3901 N85-34162
Nineteenth International Cosmic Ray Conference. SH sessions, volume 4
[NASA-CP-2376-VOL-4] 23 p3989 N85-34729
The propagation of solar flare particles in a turbulent coronal loop
[SH-1.1-3] 23 p3989 N85-34730
Stochastic particle acceleration in solar flares
[SH-1.1-4] 23 p3989 N85-34731
First-order shock acceleration in solar flares
[SH-1.1-5] 23 p3989 N85-34732
Prompt acceleration of ions by oblique turbulent shocks in solar flares
[SH-1.1-6] 23 p3989 N85-34733
Fast drift kilometric radio bursts and solar proton events
[SH-1.1-7] 23 p3990 N85-34734
Study of photon emission by electron capture during solar nuclei acceleration. 2: Delimitation of conditions for charge transfert establishment
[SH-1.1-9] 23 p3990 N85-34736
Study of photon emission by electron capture during solar nuclei acceleration. 3: Photon production evaluations
[SH-1.1-10] 23 p3990 N85-34737
Study of non-thermal photon production under different scenarios in solar flares. 1: Scenarios and formulations
[SH-1.2-2] 23 p3991 N85-34738
Study of non-thermal photon production under different scenarios in solar flares. 2: The Compton inverse and Bremsstrahlung models and fittings
[SH-1.2-3] 23 p3991 N85-34739
Spectral and spatial properties of solar microflares
[SH-1.2-4] 23 p3991 N85-34740
Temporal evolution of an energetic electron population in an inhomogeneous medium: Application to solar hard X-ray bursts
[SH-1.2-6] 23 p3991 N85-34741
Quantitative analysis of flare accelerated electrons through their hard X-ray and microwave radiation
[SH-1.2-7] 23 p3991 N85-34742
An extended superhot solar flare X-ray source
[SH-1.2-8] 23 p3991 N85-34743
Observations of solar flare photon energy spectra from 20 keV to 7 MeV
[SH-1.2-9] 23 p3992 N85-34744
Ion energy storage for post-flare loops
[SH-1.2-10] 23 p3992 N85-34745
Two types of electron events in solar flares
[SH-1.2-11] 23 p3992 N85-34746
Two classes of solar energetic particle events associated with impulsive and long duration soft X-ray flares
[SH-1.2-12] 23 p3992 N85-34747
A dominant role for protons at the onset of solar flares
[SH-1.2-13] 23 p3992 N85-34748
The energy spectra of solar flare electrons
[SH-1.2-14] 23 p3992 N85-34749
Onset of solar flares as predicted by two-dimensional MHD-models of quiescent prominences
[SH-1.3-1] 23 p3992 N85-34750
The starting conditions for an optically small solar gamma ray flare
[SH-1.3-2] 23 p3993 N85-34751
On the detectability of key-MeV solar protons through their nonthermal Lyman-alpha emission
[SH-1.3-5] 23 p3993 N85-34752
Observations of solar flare gamma-rays and protons
[SH-1.3-6] 23 p3993 N85-34753
Energetic protons from a disappearing solar filament
[SH-1.3-7] 23 p3993 N85-34754
Helios 1 energetic particle observations of the solar gamma ray flare events of 7, 21 June 1980 and 3 June 1982
[SH-1.3-8] 23 p3993 N85-34755
Injection of energetic particles following the gamma-ray flares on June 7, 1980, as observed on Helios 1
[SH-1.3-9] 23 p3993 N85-34756
Ultrarelativistic electrons and solar flare gamma-radiation
[SH-1.3-11] 23 p3993 N85-34757
Source energy spectra from demodulation of solar particle data by interplanetary and coronal transport
[SH-1.3-13] 23 p3994 N85-34758
Spectra of solar proton ground level events using neutron monitor and neutron moderated detector recordings
[SH-1.3-14] 23 p3994 N85-34759

Ground increase of cosmic ray intensity on February 16, 1984
[SH-1.3-15] 23 p3994 N85-34760
The SCR flare of 16 February 1984 as recorded by the Sayan spectrograph
[SH-1.3-17] 23 p3994 N85-34761
Time extended production of neutrons during a solar flare
[SH-1.4-1] 23 p3994 N85-34762
Further observations of protons resulting from the decay of neutrons ejected by solar flares
[SH-1.4-2] 23 p3994 N85-34763
Suggestions for improving the efficiency of ground-based neutron monitors for detecting solar neutrons
[SH-1.4-3] 23 p3995 N85-34764
Search for solar neutrons using NM-64 equipment
[SH-1.4-5] 23 p3995 N85-34765
A search for solar neutrons at a long duration balloon flight
[SH-1.4-6] 23 p3995 N85-34766
Neutral pion production in solar flares
[SH-1.4-7] 23 p3995 N85-34767
High energy neutron and gamma-radiation generated during the solar flares
[SH-1.4-8] 23 p3995 N85-34768
On the angular and energy distribution of solar neutrons generated in P-P reactions
[SH-1.4-9] 23 p3995 N85-34769
Possible detection of flare-generated positrons by Helios 1 on 3 Jun 1982
[SH-1.4-10] 23 p3996 N85-34770
Elemental abundances in corotating events
[SH-1.5-15] 23 p3997 N85-34778
Solar and interplanetary particles at 2 to 4 MEV during solar cycles 21, solar cycle variations of event sizes, and compositions
[SH-1.5-16] 23 p3997 N85-34779
Observation of the fluxes of nuclei with energies 10-20 MEV per nucleon during the solar flare of April 26, 1984
[SH-2.1-1] 23 p3998 N85-34783
Energetic particle observations of the solar-gamma ray/neutron flare events of 3 Jun 1982 and 21 June 1980 isotopic and chemical composition
[SH-2.1-3] 23 p3998 N85-34784
Precision measurements of solar energetic particle elemental composition
[SH-2.1-4] 23 p3998 N85-34785
On the retention of high-energy protons and nuclei with charges Z or equal to 2 in large solar flares after the process of their acceleration
[SH-2.1-8] 23 p3998 N85-34789
The mean ionic charges of N, Ne, MG, SI and S in solar energetic particle events
[SH-2.1-11] 23 p3999 N85-34792
Abundances from solar-flare gamma-ray line spectroscopy
[SH-2.1-13] 23 p3999 N85-34794
Solar flare gamma-ray line spectroscopy
[SH-2.1-14] 23 p3999 N85-34795
Isotopic oversbundances and the energetic particle model of solar flares
[SH-2.2-1] 23 p4000 N85-34796
Solar source regions of 3HE-rich particle events
[SH-2.2-4] 23 p4000 N85-34799
Elemental abundance differences between nuclei accleraled in CIR shocks and solar flares
[SH-2.2-6] 23 p4000 N85-34801
The heavy ion composition in 3HE-rich solar flares
[SH-2.2-7] 23 p4000 N85-34802
The mean ionic charge of silicon in 3HE-rich solar flares
[SH-2.2-8] 23 p4000 N85-34803
Coronal propagation of solar flare particles observed by satellite
[SH-3.1-2] 23 p4001 N85-34807
Coronal propagation of flare associated electrons and protons
[SH-3.1-3] 23 p4001 N85-34808
Geometry of the diffusive propagation region in the August 14, 1982 solar electron event
[SH-3.1-5] 23 p4001 N85-34809
Peculiarities of propagation of charged particles in solar corona
[SH-3.1-6] 23 p4001 N85-34810
Some characteristics of the solar flare event of February 16, 1984
[SH-3.1-7] 23 p4001 N85-34811
Constraints of solar flare particle transport models from anisotropy observations at Voyager 1
[SH-3.1-8] 23 p4002 N85-34812
Exponential anisotropy of solar cosmic rays
[SH-3.2-1] 23 p4002 N85-34817
The propagation of solar energetic particles in magnetic channels
[SH-3.2-4] 23 p4003 N85-34820
Radial transport of approximately 1 MeV/nucleon ions during the 22 November 1977 solar particle event
[SH-3.2-5] 23 p4003 N85-34821
Energetic solar particle fluxes out to 3 AU during the 7 May 1978 flare event
[SH-3.2-6] 23 p4003 N85-34822
The local characteristic function of interplanetary particle propagation
[SH-3.2-8] 23 p4003 N85-34823
On reflecting boundary behind the Earth's orbit at propagation of fast particles from solar flares
[SH-3.2-13] 23 p4004 N85-34827
Cumulative effect of Forbush decreases in the heliospheric modulation during the present solar cycle
[SH-4.1-10] 23 p4005 N85-34833
North-south asymmetry in activity on the Sun and cosmic ray density gradients
[SH-4.2-7] 23 p4007 N85-34845
Role of solar flare index in long term modulation of cosmic ray intensity
[SH-4.4-12] 23 p4034 N85-35009
Drift and Forbush decreases
[SH-5.1-2] 23 p4041 N85-35056
The flare origin of Forbush decreases not associated with solar flares on the visible hemisphere of the Sun
[SH-5.1-4] 23 p4041 N85-35058
Longitudinal dependence of the interplanetary perturbation produced by energetic type 4 solar flares and of the associated cosmic ray modulation
[SH-5.1-5] 23 p4042 N85-35059
Spectral analysis of the Forbush decrease of 13 July 1982
[SH-5.1-7] 23 p4042 N85-35061
Study of dominating parameters of high speed solar plasma streams in relation to cosmic ray and geomagnetic storms
[SH-5.1-11] 23 p4042 N85-35064
Anomalous low level of cosmic ray intensity decreases observed during 1980
[SH-5.1-15] 23 p4043 N85-35068
Peculiarities of Galactic Cosmic Ray (GCR) anisotropy variation in connection with the recurrent and sporadic Forbush effects
[SH-5.1-21] 23 p4044 N85-35073
Cosmic ray modulation by high-speed solar wind fluxes
[SH-5.1-22] 23 p4044 N85-35074
Penetration of solar protons into the Earth's magnetosphere on November 22, 1977
[SH-6.1-15] 23 p4046 N85-35088
Solar modulation of cosmic ray intensity and solar flare events inferred from (14)C contents in dated tree rings
[SH-7.1-2] 23 p4047 N85-35095
The 4He1H ratios in the chemical compositions of solar flare particles and the primordial solar nebula
[SH-7.1-12] 23 p4048 N85-35104
Solar neutrinos, solar flares, solar activity cycle and the proton decay
[SH-8.1-8] 23 p4049 N85-35113
Solar cosmic ray bursts and solar neutrino fluxes
[SH-8.1-10] 23 p4050 N85-35115
SONTRAC: A solar neutron track chamber detector
[SH-9.1-12] 23 p4052 N85-35127
A suggested standardized format for cosmic ray ground-level event data
[SH-9.1-15] 23 p4052 N85-35130
Sporadic radio emission connected with a definite manifestation of solar activity in the near Earth space
[SH-10.1-8] 23 p4053 N85-35139
Near Earth space sporadic radio emission busts occurring during sunrise
[SH-10.1-9] 23 p4054 N85-35140
Preliminary results of the Cerenkov EAS flashes the Crimean Astrophysical Observatory
[HE-4.4-17] 24 p4194 N85-36023
High-energy neutrinos from a lunar observatory
[HE-5.3-21] 24 p4207 N85-36112

SOLAR FLUX
Theoretical development of Monte Carlo codes for modeling cumulus cloud fields
[NASA-CR-174063] 02 p0230 N85-11500
Trends in ozone and temperature structure: Comparison of theory and measurements
[DE84-016201] 04 p0539 N85-13426
Detailed performance calculations: Goddard Group, appendix D 05 p0676 N85-14341
MAP/GLOBUS campaign 1983 11 p1658 N85-20447
Response of Earth's atmosphere to increases in solar flux and implications for loss of water from Venus 13 p2178 N85-23518
Convective collapse and overstable oscillations in solar flux tubes 14 p2452 N85-25138
Forecast verification of the 10.7 centimeter solar flux and the Ap daily geomagnetic activity indices
[AD-A152959] 17 p2993 N85-28499
Thermal performance and design of a solid particle cavity receiver
[DE85-010830] 19 p3274 N85-30300
Solar modulation and interplanetary gradients of the galactic electron flux, 1977 - 1984
[PAPER-SH-4.7-4] 21 p3716 N85-33059
The polar caps and the climatic evolution of Mars 22 p3854 N85-33866
Results of ultra-low level 71ge counting for application in the Gallex-solar neutrino experiment at the Gran Sasso Underground Physics Laboratory
[SH-8.1-2] 23 p4049 N85-35108
Correlation between solar neutrino flux and other solar phenomena 23 p4049 N85-35109
A possible mechanism to cause the quasi-biennial variability on the solar neutrino flux
[SH-8.1-5] 23 p4049 N85-35110
The conjecture concerning time variations in the solar neutrino flux
[SH-8.1-6] 23 p4049 N85-35111
Solar neutrino: Flux, cosmic rays and the 11 year solar cycle
[SH-8.1-7] 23 p4049 N85-35112
Solar cosmic ray bursts and solar neutrino fluxes
[SH-8.1-10] 23 p4050 N85-35115

SOLAR FLUX DENSITY
NT SOLAR CONSTANT
Variation of fast charged particles in event of 22 November 1977 based on Cosmos-900 satellite data 02 p0161 N85-11092
Preliminary investigation into using the sun as a source for G/T (Gain to System Noise Temperature) measurements
[PB85-128148] 12 p1952 N85-22265
Peculiarities of propagation of charged particles in solar corona
[SH-3.1-6] 23 p4001 N85-34810
Energetic solar particle fluxes out to 3 AU during the 7 May 1978 flare event
[SH-3.2-6] 23 p4003 N85-34822

SOLAR FURNACES
Superpure materials research planned 03 p0353 N85-12270
Preparation of crystal growth experiments in Spacelab: Si (FSLP), CdTe (D1), ZnS (D1)
[BMFT-FB-W-84-045] 12 p1788 N85-21227
High temperature solar electrothermal processing 2. Zinc from zinc oxide
[AD-A154747] 21 p3562 N85-32159
Decomposition of sulfuric acid using solar thermal energy
[DE85-012288] 21 p3564 N85-32170

SOLAR GENERATORS
NT HOMOJUNCTIONS
NT SOLAR AUXILIARY POWER UNITS
NT SOLAR CELLS
NT VERTICAL JUNCTION SOLAR CELLS
Information package on photovoltaics 05 p0661 N85-14250
Photovoltaic power supply units 05 p0662 N85-14252
Global radiation in West Germany — solar generators 05 p0662 N85-14253
Development and construction of a prototype photovoltaic energy supply unit 05 p0662 N85-14254
Siemens solar module: Status of the technique, development tendencies 05 p0662 N85-14255
Solar generators made of amorphous silicon 05 p0662 N85-14257
Biaxial tracking solar generator 05 p0663 N85-14259
Photovoltaic 100 kWp pilot plant on the Greek island Kythnos 05 p0664 N85-14266
Mains-connected photovoltaic system for a house 05 p0664 N85-14267
Project Pellworm: Solar electric energy supply for a health center 05 p0664 N85-14268
Realized field tests — solar generators 05 p0664 N85-14271
Considerations on the dimensioning of photovoltaic supply systems in the low power range 05 p0665 N85-14273
Solar power supplies for ships 05 p0665 N85-14274
A system simulator for the solar generator of artificial satellites
[INPE-3320-TDL/180] 11 p1672 N85-20534
Development and prototype construction of photovoltaic energy supply units 12 p1878 N85-21781
Photovoltaic solar components 12 p1878 N85-21782
Testing and optimization of the production technology of large-surface Cu2S/CdS solar generators 12 p1880 N85-21793

Ecological observations at the site of the 10 MWe solar thermal power system (1978-1984)
[DE85-004572] 12 p1885 N85-21827
Comprehensive evaluation of cost effectiveness of solar electric power plants 14 p2265 N85-24036
Use of heat pipes for heat collection and transmission in solar plants 14 p2265 N85-24037
Power plants of modular construction with quasi-paraboloidal concentrators of solar energy 14 p2266 N85-24038
Parabolic dish test site: History and operating experience
[NASA-CR-175892] 17 p2985 N85-28447
Plastic heliostat enclosure analysis
[DE85-009112] 18 p3130 N85-29387
Thermochemical energy transport using a hydrogen rich working fluid
[AD-D011696] 19 p3233 N85-30042
Calibration of relevant measuring sensors
[DE85-009820] 19 p3306 N85-30492
Advanced module development overview 21 p3612 N85-32445
Module Hipot and ground continuity test results 21 p3612 N85-32447
Thin-film reliability and engineering overview 21 p3612 N85-32450

SOLAR GRANULATION
Variability of the structure of the granulation over the solar activity cycle 14 p2447 N85-25100
Amplification and maintenance of thin magnetic flux tubes by compressible convection — solar magnetism 14 p2447 N85-25104
Stellar granulation 14 p2451 N85-25132
The flux rope models checked by some observations — solar activity 14 p2452 N85-25139
Activities report of the Institute of Astronomy and Astrophysics 17 p3052 N85-28691
Activities report of the Institute of Astronomy and Astrophysics 17 p3052 N85-28692

SOLAR GRAVITATION
Detection of solar gravity mode oscillations 14 p2442 N85-25070
Solar gravity modes from ACRIM-SWM irradiance data 14 p2443 N85-25071
Heliocentric sail problem with variable gravity field reduction 16 p2724 N85-26816

SOLAR HEATING
Solar heating and cooling R and D program coordination support
[DE84-013479] 01 p0068 N85-10449
Test methods and standards development for active solar heating and cooling systems
[PB84-217447] 03 p0343 N85-12209
Superpure materials research planned 03 p0353 N85-12270
A refined computer program for the transient simulation of ground coupled heat pump systems
[DE84-014098] 05 p0637 N85-14068
Passive solar/Earth sheltered office/dormitory cooling season thermal performance
[DE84-016662] 05 p0669 N85-14308
Development of design and economic parameters for passive solar systems
[AD-A147181] 07 p0993 N85-16303
Heat-transfer enhancement in natural convection enclosure flow
[DE84-013048] 09 p1319 N85-18297
Actual versus design performance of solar systems in the National Solar Data Network
[DE85-001190] 09 p1344 N85-18456
Thermal performance testing of passive solar components in NBS (National Bureau of Standards) calorimeter
[PB85-119345/GAR] 09 p1346 N85-18470
Solar collection
[DE85-000060] 10 p1512 N85-19540
A summary and assessment of historical reliability and maintainability data for solar hot water and space conditioning systems
[DE84-004521] 12 p1876 N85-21770
Multiyear plan for experimental systems research passive and hybrid solar energy program
[PB85-146868] 12 p1883 N85-21815
Overview of latent storage for passive solar applications
[DE85-005354] 13 p2129 N85-23249
Development of a single-family absorption chiller for use in a solar heating and cooling system, phase 3, volume 2
[DE85-003218] 13 p2130 N85-23253
Drop of coolant temperature in individual components of solar heating system 14 p2265 N85-24035
Comprehensive evaluation of cost effectiveness of solar electric power plants 14 p2265 N85-24036
Scaling blackbody laser to high powers
[NASA-TM-86395] 14 p2309 N85-24292
Mechanisms of magnetic heating of the solar corona 14 p2448 N85-25113
Heating of coronal loops by tearing turbulence 14 p2448 N85-25114
Observational constraints on heating processes — solar corona 14 p2449 N85-25115
Coronal heating by turbulent phase mixed MHD waves — solar corona 14 p2453 N85-25148
Solar maximum mission results on the energetics of the impulsive phase of solar flares 14 p2454 N85-25159
Solar houses, Freiburg
[BMFT-FB-T-84-249] 15 p2588 N85-25953
A multifunction wall system for application with solar heating and ground cooling
[DE85-006792] 16 p2820 N85-27395
Development of mass-producible line-focus tracking concentrating solar collectors. Category 2: Control systems
[DE85-007873] 17 p2987 N85-28459
Foamglass solar window collector
[DE85-009197] 18 p3129 N85-29374
Solar energy for highway uses
[DE84-015653] 18 p3130 N85-29382
Establishment of a methodology for predicting lifetimes in active solar systems
[DE85-008629] 18 p3130 N85-29383
Investigation of the transferability of measures of passive solar energy utilization in the USA to the Federal Republic of Germany
[BMFT-FB-T-84-284] 18 p3132 N85-29396
Solar rocket component study
[AD-A154186] 19 p3227 N85-30007
Comparative evaluation of ground-coupled heat pumps that use solar energy
[DE85-010950] 20 p3484 N85-31849
Geodynamics Branch research program
[NASA-TM-86223] 20 p3489 N85-31888
Soil temperature extrema recovery rates after precipitation cooling 20 p3491 N85-31897
Performance analysis of mixed passive solar heating systems
[DE85-009624] 21 p3613 N85-32455
Laser sealed evacuated window glazings
[DE85-000512] 22 p3754 N85-33273
Failure testing of active solar energy system components
[DE84-013024] 22 p3804 N85-33561
An analysis of the effects of active solar energy system control sensor degradation on system performance
[DE84-013023] 22 p3804 N85-33562
Lopez Energy Alternatives Project
[DE85-010589] 22 p3849 N85-33837
Solar heat pump
[DE85-011323] 23 p3946 N85-34453
Solar system fault detection
[DE85-005967] 23 p3946 N85-34458
Solar pond technology for Navy applications
[AD-A155877] 24 p4112 N85-35488

SOLAR HOUSES
Thermal performance testing of passive solar components in NBS (National Bureau of Standards) calorimeter
[PB85-119345/GAR] 09 p1346 N85-18470
Solar house, Freiburg
[BMFT-FB-T-84-249] 15 p2588 N85-25953
A multifunction wall system for application with solar heating and ground cooling
[DE85-006792] 16 p2820 N85-27395
Investigation of the transferability of measures of passive solar energy utilization in the USA to the Federal Republic of Germany
[BMFT-FB-T-84-284] 18 p3132 N85-29396

SOLAR INSTRUMENTS
NT SPECTROHELIOGRAPHS
Attempts to contruct two-dimensional image of Sun from observations made with RATAN-600 radiotelescope by relay race method 06 p0783 N85-15005
The scanning heliometer 14 p2451 N85-25134

SOLAR LASERS
U SOLAR-PUMPED LASERS

SOLAR LIMB
Extreme limb profiles of the Sun at far infrared and submillimeter wavelengths 08 p1244 N85-17852
Coronal and chromospheric physics — Sun, sunspots, and solar limb
[NASA-CR-174290] 08 p1259 N85-17921
Observed spatial properties of the solar eigenfunctions and the implications for the existence of resolved multiplets 14 p2443 N85-25074
Single-dish high sensitivity determination of solar limb emission at 22 and 44 GHz
[INPE-3545-PRE/758] 19 p3385 N85-30999
An extended superhot solar flare X-ray source
[SH-1.2-6] 23 p3991 N85-34743
Ultrarelativistic electrons and solar flare gamma-radiation
[SH-1.3-11] 23 p3993 N85-34757
Search for solar neutrons using NM-64 equipment
[SH-1.4-5] 23 p3995 N85-34766

SOLAR MAGNETIC FIELD
Structure and evolution of the large scale solar and heliospheric magnetic fields
[NASA-CR-175268] 01 p0130 N85-10897
Solar-geophysical data number 477, May 1984. Part 1: (Prompt reports). Data for April 1984, March 1984 and late data. Explanation of data reports issued as number 474 (supplement) February 1984
[PB84-225028] 01 p0131 N85-10901
Solar flares and laboratory experiments on magnetic reconnection in current sheaths 02 p0162 N85-11099
Study of the solar corona using radio and space observations
[NASA-CR-174034] 02 p0304 N85-11983
Active regions — and the Solar Maximum Mission
[NASA-CR-170628] 02 p0304 N85-11985
Magnetohydrodynamic and gasdynamic theories for planetary bow waves
[NASA-CR-174132] 03 p0448 N85-12850
Structure and evolution of the large scale solar and heliospheric magnetic fields 05 p0748 N85-14782
Energy release in solar flares
[NASA-CR-174302] 08 p1259 N85-17934
Solar-Geophysical Data. Part 1: (Prompt reports)
[PB85-112068] 11 p1766 N85-21100
Magnetospheres in the solar system 12 p1954 N85-22274
Activation of solar flares 12 p1954 N85-22276
What would a dynamo theorist like to know about the dynamics of the solar convection zone? 14 p2441 N85-25062
The magneto-optical filter, working principles and recent progress 14 p2442 N85-25068
Numerical simulations of convectively excited gravity waves 14 p2444 N85-25082
The hydromagnetics of the Sun — conference
[ESA-SP-220] 14 p2445 N85-25091
Magnetoconvection: The interaction of convection and small scale magnetic fields — photosphere 14 p2446 N85-25098
Magnetic buoyancy instabilities in the convective overshoot zone — Sun 14 p2447 N85-25101
On the structure of magnetic fields in the solar convection zone 14 p2447 N85-25103
Amplification and maintenance of thin magnetic flux tubes by compressible convection — solar magnetism 14 p2447 N85-25104
Nonlinear time-evolution of kink-unstable magnetic flux tubes in the convection zone of the Sun 14 p2447 N85-25105
The Fe XIII 10747 A and Fe XIV 5303 A coronal emission lines polarization 14 p2448 N85-25111
Magnetic instabilities — solar magnetism 14 p2449 N85-25117
The role of differential rotation in magnetic energy storage — coronal loops 14 p2449 N85-25119
Observational aspects of sunspot oscillations 14 p2451 N85-25131
Convective collapse and overstable oscillations in solar flux tubes 14 p2452 N85-25138
The first effect of the amplitude of a solar cycle 14 p2452 N85-25143
Observations concerning energy balance in solar magnetic regions 14 p2452 N85-25145
A study of the material motion into an eruptive prominence — solar prominence 14 p2453 N85-25146
A siphon flow model for Evershed motion — sunspot regions 14 p2453 N85-25147
On running penumbral waves 14 p2453 N85-25150
Harmonic analysis of the solar magnetic field 14 p2454 N85-25154
Magnetic instabilities in solar filaments: Models of twisting motions and ejecta 14 p2454 N85-25156
Magnetic field structures of hard X-ray flares observed by HINOTORI spacecraft — solar flares 14 p2455 N85-25161
Solar magnetohydrodynamics: Symposium review 14 p2455 N85-25162
Elementary sunspot energy model 15 p2476 N85-25287
Modeling 22-year solar activity cycle within framework of dynamo theory with allowance for primary field 15 p2477 N85-25288
The Faraday rotation experiment — solar corona 16 p2696 N85-27805
Measurements of Solar Vector Magnetic Fields
[NASA-CP-2374] 18 p3203 N85-29669

On the numerical computation of nonlinear force-free magnetic fields 18 p3203 N85-29671
Modeling solar magnetic structures 18 p3203 N85-29672
Magnetic and thermodynamic structure of the solar corona during sunspot minimum 18 p3203 N85-29673
Theoretical approach to evolution of solar magnetic field 18 p3204 N85-29674
Current evolution in a numerical emerging-magnetic-flux model 18 p3204 N85-29675
The global structure of magnetic fields which support quiescent prominences 18 p3204 N85-29676
Trends in measurement of solar vector magnetic fields using the Zeeman effect 18 p3204 N85-29677
The solar vector magnetograph of the Okayama Astrophysical Observatory 18 p3205 N85-29682
Vector magnetic field observations with the Haleakala polarimeter 18 p3205 N85-29683
The San Fernando Observatory video Stokes polarimeter 18 p3205 N85-29685
The new solar magnetograph for the Canary Islands Observatory THEMIS 18 p3205 N85-29686
The vector magnetograph of the Sayan Solar Observatory 18 p3206 N85-29687
Multichannel birefringent filter 18 p3206 N85-29688
Diagnostics of vector magnetic fields 18 p3206 N85-29689
Generation and transfer of polarized radiation in the solar atmosphere: Physical mechanisms and magnetic-field diagnostics 18 p3206 N85-29690
Dynamic models of flux tubes in the interpretation of polarization measurements 18 p3206 N85-29691
Least squares inversion of Stokes profiles in the presence of velocity gradients 18 p3207 N85-29692
Effect of polarized radiative transfer on the Hanle magnetic field determination in prominences: Analysis of hydrogen H alpha line observations at Pic-du-Midi 18 p3207 N85-29694
The effect of line damping, magneto-optics and parasitic light on the derivation of sunspot vector magnetic fields 18 p3207 N85-29695
The inference of vector magnetic fields from polarization measurements with limited spectral resolution 18 p3207 N85-29696
Solar monochromatic images in magneto-sensitive spectral lines and maps of vector magnetic fields 18 p3207 N85-29697
Magnetic field-vector measurements in quiescent prominences via the Hanle effect: Analysis of prominences observed at Pic-du-Midi and at Sacramento Peak 18 p3208 N85-29698
Turbulence and wave particle interactions in solar-terrestrial plasmas [NASA-CR-175970] 18 p3209 N85-29906
Magnetic probing of the solar interior [NASA-CR-176025] 19 p3385 N85-30998
Solar-geophysical data no. 485, January 1985. Part 1 (prompt reports): Data for December 1984, November 1984 and late data [PB85-181360] 20 p3548 N85-32079
Differential measurement of cosmic-ray gradient with respect to interplanetary current sheet [PAPER-SH-4.2-9] 21 p3715 N85-33055
A study of the cyclical variations of coronal holes and their relation to open magnetic fields [AD-A155251] 21 p3723 N85-33099
Simultaneous Solar Maximum Mission and Very Large Array (VLA) observations of solar active regions [NASA-CR-176090] 22 p3859 N85-33897
On the possibility of the determining the average mass composition near 10 to the 14th power eV through the solar magnetic field [OG-5.1-9] 22 p3862 N85-34051
Ultrarelativistic electrons and solar flare gamma-radiation [SH-1.3-11] 23 p3993 N85-34757
Peculiarities of propagation of charged particles in solar corona [SH-3.1-6] 23 p4001 N85-34810
Some characteristics of the solar flare event of February 16, 1984 [SH-3.1-7] 23 p4001 N85-34811
Low energy proton bidirectional anisotropies and their relation to transient interplanetary magnetic structures: ISEE-3 observations [SH-3.1-9] 23 p4002 N85-34813
The role of shock waves in modulation of galactic cosmic rays [SH-4.1-7] 23 p4005 N85-34831
Cosmic ray intensity and the tilt of the neutral sheet [SH-4.2-6] 23 p4007 N85-34846
Differential measurement of cosmic-ray gradient with respect to interplanetary current sheet [SH-4.2-9] 23 p4007 N85-34847
Spatial variation of cosmic rays near the heliospheric current sheet [SH-4.2-10] 23 p4007 N85-34848
Effects of a wavy neutral sheet on cosmic ray anisotropies [SH-4.2-11] 23 p4008 N85-34849
Effects of solar magnetic field on cosmic rays [SH-4.2-12] 23 p4008 N85-34850
Determination of galactic cosmic ray latitudinal gradient using Earth based detectors [SH-4.2-13] 23 p4008 N85-34851
The expected cosmic ray density and stream distributions at the heliolatitudinal asymmetry of solar wind [SH-4.2-14] 23 p4008 N85-34852
Latitudinal gradients of cosmic rays and the polarity reversal of the heliospheric magnetic field: A preliminary evaluation [SH-4.2-16] 23 p4008 N85-34853
The influence of nonstationarity of the solar activity and general solar field on modulation of cosmic rays [SH-4.2-17] 23 p4008 N85-34854
On the influence of the heliomagnetospheric periphery on the galactic cosmic rays [SH-4.2-19] 23 p4009 N85-34856
Spatial distribution of cosmic rays in magnetic cycles of the Sun [SH-4.2-20] 23 p4009 N85-34857
An update on the correlation between the cosmic radiation intensity and the geomagnetic AA index [SH-4.2-24] 23 p4009 N85-34861
Astrophysical applications of high angular resolution array-telescopes [OG-9.5-7] 23 p4031 N85-34984
Gradients and anisotropies of high energy cosmic rays in the outer heliosphere [SH-4.3-7] 23 p4032 N85-34992
Cosmic ray sidereal diurnal variation of galactic origin observed by neutron monitors [SH-4.4-2] 23 p4033 N85-35000
Long-term modulation of galactic cosmic rays in high-energy region [SH-4.4-22] 23 p4035 N85-35018
Diurnal variation of galactic cosmic ray intensity on quiet days [SH-4.5-11] 23 p4037 N85-35029
Long term changes in cosmic ray diurnal variations observed by ion chambers in Hong Kong and Japan [SH-4.5-14] 23 p4037 N85-35031
The modulation features of the long-period cosmic ray variations in connection with the sign change of the general magnetic field of the Sun [SH-4.5-15] 23 p4037 N85-35032
Cosmic ray density gradient and its dependence on the north-south asymmetry in solar activity [SH-4.5-17] 23 p4038 N85-35034
Anomalous increase of solar anisotropy above 150GV in 1981-1983 [SH-4.5-18] 23 p4038 N85-35035
Changes in the energy spectrum of anomalous oxygen and helium during 1977-1985 [SH-4.6-1] 23 p4039 N85-35039
Radial and latitudinal gradients of anomalous oxygen during 1977 - 1985 [SH-4.6-4] 23 p4039 N85-35042
The cosmic ray interplanetary radial gradient from 1972 - 1985 [SH-4.7-1] 23 p4040 N85-35046
The large scale dynamics of the outer heliosphere and the long-term modulation of galactic cosmic rays [SH-4.7-3] 23 p4040 N85-35048

SOLAR MAXIMUM MISSION
Energetic electrons in impulsive solar flares 02 p0303 N85-11962
Active regions — and the Solar Maximum Mission [NASA-CR-170628] 02 p0304 N85-11965
Statement of Frank Cepollina, Solar Maximum Repair Mission Project Manager, Goddard Space Flight Center 04 p0461 N85-12930
Space observations of solar flares 04 p0519 N85-13313
Research and technology: Fiscal year 1984 report [NASA-TM-85231] 12 p1964 N85-22340
Ultraviolet spectral diagnostics of solar flares and heating events 13 p2206 N85-23675
Ultraviolet Spectrometer and Polarimeter (UVSP) software development and hardware tests for the solar maximum mission [NASA-CR-175279] 14 p2305 N85-24271
Solar gravity modes from ACRIM-SWM irradiance data 14 p2443 N85-25071
Observations of low-degree modes from the solar maximum mission (extended abstract) 14 p2443 N85-25072
Solar maximum mission results on the energetics of the impulsive phase of solar flares 14 p2454 N85-25159
A study of the morphology of solar flares as observed by the hard X-ray imaging spectrometer — Solar Maximum Mission 14 p2454 N85-25160
Examination of returned solar-max surfaces for impacting orbital debris and meteoroids 15 p2681 N85-26580
Soft X-ray polychromator for the Solar Maximum Mission [NASA-CR-175297] 21 p3723 N85-33096
Solar maximum: Solar array degradation [NASA-TM-86194] 23 p3903 N85-34175
Monte Carlo calibration of the SMM gamma ray spectrometer for high energy gamma rays and neutrons [SH-9.1-6] 23 p4051 N85-35121
The 1986 National Aeronautics and Space Administration authorization [GPO-47-635] 24 p4166 N85-35829

SOLAR MESOSPHERE EXPLORER
Flight experience of Solar Mesosphere Explorer's two nickel-cadmium batteries 20 p3446 N85-31396

SOLAR NEBULA
U SOLAR CORONA

SOLAR NEUTRINOS
Report on solar neutrino experiments [DE84-014567] 01 p0131 N85-10899
Solar neutrinos: Prospects for detection and implications [DE84-015522] 02 p0304 N85-11966
Solar neutrino spectroscopy [DE84-015518] 02 p0304 N85-11968
Chlorine and bromine solar neutrino experiments [DE84-015720] 02 p0304 N85-11969
Molybdenum solar neutrino experiment [DE85-003747] 14 p2445 N85-25090
Proposed solar neutrino experiment using (81)Br(nu,e(-e)) (81)Kr [DE85-004802] 15 p2684 N85-26579
Weak interactions of quarks and leptons: Experimental status [DE85-008171] 18 p3181 N85-29723
Specificity of (71)Ga(p,n) (71)Ge at 35 MeV for Gamow-Teller strength [DE85-011837] 23 p3971 N85-34615
Nineteenth International Cosmic Ray Conference. SH sessions, volume 5 [NASA-CP-2376-VOL-5] 23 p4031 N85-34991
Results of ultra-low level 71ge counting for application in the Gallex-solar neutrino experiment at the Gran Sasso Underground Physics Laboratory [SH-8.1-2] 23 p4049 N85-35108
Correlation between solar neutrino flux and other solar phenomena 23 p4049 N85-35109
A possible mechanism to cause the quasi-biennial variability on the solar neutrino flux [SH-8.1-5] 23 p4049 N85-35110
The conjecture concerning time variations in the solar neutrino flux [SH-8.1-6] 23 p4049 N85-35111
Solar neutrino: Flux, cosmic rays and the 11 year solar cycle [SH-8.1-7] 23 p4049 N85-35112
Solar neutrinos, solar flares, solar activity cycle and the proton decay [SH-8.1-8] 23 p4049 N85-35113
The research program of the Liquid Scintillation Detector (LSD) in the Mont Blanc Laboratory [HE-5.3-6] 24 p4205 N85-36100
High energy neutrino astronomy with MACRO [HE-5.3-12] 24 p4206 N85-36106

SOLAR NOISE
U SOLAR RADIO EMISSION

SOLAR OBSERVATORIES
The Ebro Observatory and international scientific organizations 04 p0518 N85-13309
Use of Ebro Observatory data at Word Data Center A for Solar-Terrestrial Physics 04 p0518 N85-13310
Fr. Angelo Secchi, a pioneer in the study of solar-terrestrial relationships 04 p0519 N85-13312
A normal incidence, high resolution X-ray telescope for solar coronal observations [NASA-CR-175622] 13 p2169 N85-23461
Solar oscillations from two widely separated stations 14 p2446 N85-25093
Science with the Solar and Heliospheric Observatory (SOHO) 14 p2449 N85-25121
Bern solar data for January-December 1984 [REPT-51] 15 p2685 N85-26581
Very large array observations of coronal loops and related observations of solar type stars [AD-A152027] 16 p2868 N85-27817
The vector magnetograph of the Sayan Solar Observatory 18 p3206 N85-29687
Solar cycle variation of ephemeral regions [AD-A154967] 21 p3723 N85-33097
Solar adaptive optics [AD-A155434] 21 p3724 N85-33101

Radio telescope with 256 antennas built in Siberia
22 p3732 N85-33136
Coordinated study of solar-terrestrial payloads on space station
[NASA-CR-176160] 23 p3900 N85-34158
Soft X-Ray Telescope (SXRT)
23 p3900 N85-34159
Solar Ultraviolet Spectral Irradiance Monitor (SUSIM)
23 p3901 N85-34160
White Light Coronograph (WLC) and Ultra-Violet Coronal Spectrometer (UVCS)
23 p3901 N85-34161
High Resolution Telescope and Spectrograph (HRTS)
23 p3901 N85-34162
Active Cavity Radiometer (ACR)
23 p3901 N85-34163
Waves in Space Plasmas (WISP)
23 p3901 N85-34164
Space Experiments with Particle Accelerators (SEPAC)
23 p3901 N85-34165
Theoretical and Experimental Beam Plasma Physics (TEBPP)
23 p3901 N85-34166
Recoverable Plasma Diagnostics Package (RPDP)
23 p3902 N85-34167
Electrodynamic tether
23 p3902 N85-34168
Imaging Spectrometric Observatory (ISO)
23 p3902 N85-34169
Atmospheric Emission Photometric Imaging (AEPI)
23 p3902 N85-34170
Magnetospheric multiprobes: MMP/CHEMSAT
23 p3902 N85-34171
Wide Angle Michelson Doppler Imaging Interferometer (WAMDII)
23 p3902 N85-34172
Vehicle Charging And Potential (VCAP)
23 p3902 N85-34173
Initial placement of STO instruments
23 p3902 N85-34174
Development of observational and instrumental techniques in hard X-ray and medium energy gamma-ray astronomy
[NASA-CR-176172] 24 p4168 N85-35841

SOLAR OPTICAL TELESCOPE
Solar optical telescope primary mirror controller
[NASA-CR-174416] 10 p1570 N85-19903
Science with the Solar Optical Telescope (SOT)
14 p2449 N85-25120

SOLAR ORBITS
NT PERIHELIONS
Some considerations on elliptic heliocentric orbits
[INPE-3217-PRE/570] 02 p0297 N85-11928
Heliosynchronism and phasing. Application to the SPOT orbit
05 p0800 N85-13826
Thermal and cryogenic design study for space infrared telescope facility (SIRTF)
[NASA-CR-166613] 07 p0915 N85-15793
Models of angular momentum input to a circum-terrestrial swarm from encounters with heliocentric planetesimals
13 p2179 N85-23521
Analysis of motions of Jupiter's great red spot and white ovals
15 p2670 N85-26472
Heliocentric sail problem with variable gravity field reduction
16 p2724 N85-26816
A comprehensive investigation of the dynamics of micron and submicron lunar ejecta in heliocentric space
19 p3384 N85-30994
Development of observational and instrumental techniques in hard X-ray and medium energy gamma-ray astronomy
[NASA-CR-176172] 24 p4168 N85-35841

SOLAR OSCILLATIONS
Effects of core mixing on solar oscillation frequencies
[DE84-015540] 03 p0449 N85-12853
Nonlocal and nonlinear effects on solar oscillations
09 p1416 N85-18934
Constraints of observations of solar oscillations on solar models with mixing by turbulent diffusion
[DE85-003741] 13 p2205 N85-23678
Solar Seismology From Space. A conference at Snowmass, Colorado
[NASA-CR-175661] 14 p2441 N85-25060
Overview of solar seismology: Oscillations as probes of internal structure and dynamics in the Sun
14 p2441 N85-25061
Solar inverse theory
14 p2441 N85-25063
Rotational inversion from global solar oscillations
14 p2442 N85-25064
Sensitivity of inferred subphotospheric velocity field to mode selection, analysis technique and noise
14 p2442 N85-25065
The magneto-optical filter, working principles and recent progress
14 p2442 N85-25066
Evaluation of a magneto-optical filter and a Fabry-Perot interferometer for the measurement of solar velocity fields from space
14 p2442 N85-25067
The Fourier tachometer 2: An instrument for measuring global solar velocity fields
14 p2442 N85-25068
Observations of intermediate-degree solar oscillations
14 p2442 N85-25069
Detection of solar gravity mode oscillations
14 p2442 N85-25070
Solar gravity modes from ACRIM-SWM irradiance data
14 p2443 N85-25071
Observations of low-degree modes from the solar maximum mission (extended abstract)
14 p2443 N85-25072
Implications of observed frequencies of solar P modes
14 p2443 N85-25073
Observed spatial properties of the solar eigenfunctions and the implications for the existence of resolved multiplets
14 p2443 N85-25074
Optimized response functions for 2-dimensional observations of solar oscillations
14 p2443 N85-25075
The effects of image motion on the l-nu diagram
14 p2443 N85-25076
The effects of seeing on noise
14 p2443 N85-25077
The effects of a nearly 100% duty cycle in observations of solar oscillations
14 p2443 N85-25078
Analysis and interpretation of synthetic time strings of oscillation data
14 p2444 N85-25079
Methods for cloud cover estimation
14 p2444 N85-25081
On the influence of turbulent motions on non-radial oscillations
14 p2444 N85-25083
The stability of the low-degree 5-minute solar oscillations
14 p2444 N85-25084
An excitation mechanism for solar 5-minute oscillation of intermediate and high degree
14 p2444 N85-25085
The resonant count diagram and solar g mode oscillations
14 p2445 N85-25086
Fine structure of solar acoustic oscillations due to rotation
14 p2445 N85-25087
The sensitivity of solar eigenfrequencies to the treatment of the equation of state
14 p2445 N85-25089
Solar oscillations
14 p2445 N85-25092
Solar oscillations from two widely separated stations
14 p2446 N85-25093
Global solar oscillations in irradiance and velocity: A comparison
14 p2446 N85-25094
Oscillatory convection in sunspots
14 p2448 N85-25099
The intern. rotation of the Sun inferred from the rotational splitting of acoustic and gravity mode multiplets
14 p2449 N85-25122
Ten years observations of long-period oscillations of the Sun
14 p2450 N85-25123
The response of the line KI 7699 to the solar oscillations
14 p2450 N85-25124
Conditions of the small oscillations excitation in the different solar models with the mixed core
14 p2450 N85-25126
Linear models of acoustic waves in sunspot umbrae
14 p2450 N85-25130
Observational aspects of sunspot oscillations
14 p2451 N85-25131
The scanning heliometer
14 p2451 N85-25134
The problem of atmospheric turbulence
[NASA-CR-175783] 16 p2832 N85-27464
Activities report of the Institute of Astronomy and Astrophysics
17 p3052 N85-28891
Activities report of the Institute of Astronomy and Astrophysics
17 p3052 N85-28892
Solar variability observed through changes in solar figure and mean diameter
[DE85-012857] 22 p3860 N85-33900

SOLAR PHYSICS
National solar-terrestrial research program
[PB84-216183] 01 p0072 N85-10479
Research and technology, 1984: Marshall Space Flight Center
[NASA-TM-86476] 04 p0590 N85-13765
Heating in the solar mantle
08 p1233 N85-17769
Energy release in solar flares
[NASA-CR-174302] 08 p1259 N85-17924
Solar-geophysical data number 476, April 1984. Part 1: (Prompt reports). Data for March 1984, February 1984 and late data
[PB84-215060] 09 p1416 N85-18936
Solar-geophysical data number 476, April 1984. Part 2: (Comprehensive reports). Data for October 1983, June 1981 and miscellanea
[PB84-215076] 09 p1417 N85-18937
Solar Corona Explorer: A mission for the physical diagnosis of the solar corona
[NASA-TM-87416] 10 p1572 N85-19912
Solar Seismology From Space. A conference at Snowmass, Colorado
[NASA-CR-175661] 14 p2441 N85-25060
Magnetic instabilities --- solar magnetism
14 p2449 N85-25117
Science with the Solar Optical Telescope (SOT)
14 p2449 N85-25120
Science with the Solar and Heliospheric Observatory (SOHO)
14 p2449 N85-25121
Solar-Geophysical Data Number 484, December 1984. Part 2 (comprehensive reports): Data for June 1984, January 1982 and Miscellanea
[NASA-CR-175826] 16 p2888 N85-27820
Diagnostics of vector magnetic fields
18 p3206 N85-29889
Evidence for submergence of magnetic flux in a growing active region
18 p3206 N85-29902
Solar physics applications of computer graphics and image processing
18 p3206 N85-29903
Activities report of the Laboratory of Stellar and Planetary Physics
[G-127] 20 p3544 N85-32052
Solar-geophysical data no. 485, January 1985. Part 1 (prompt reports): Data for December 1984, November 1984 and late data
[PB85-181360] 20 p3548 N85-32079
Activities report of the Aeronomy Department
[G-774-1984] 21 p3633 N85-32569

SOLAR PLANETARY INTERACTIONS
NT SOLAR TERRESTRIAL INTERACTIONS
Response of Earth's atmosphere to increases in solar flux and implications for loss of water from Venus
13 p2178 N85-23518
Development of a global 3-D magnetohydrodynamic computational model for solar wind/cometary and planetary studies
[NASA-CR-175724] 15 p2684 N85-26577

SOLAR PLASMA (RADIATION)
U SOLAR WIND

SOLAR PONDS (HEAT STORAGE)
Site-specific research conducted in support of the Salton Sea Solar Pond Project, FY 1982 report
[NASA-CR-174182] 05 p0666 N85-14280
Laboratory investigations
05 p0666 N85-14281
Analytical models
05 p0666 N85-14282
The spectrophotometric method of determining the transmission of solar energy in salt gradient solar ponds
05 p0666 N85-14283
Material selection consideration for solar ponds
05 p0666 N85-14284
A summary description of a computer program concept for the design and simulation of solar pond electric power generation systems
05 p0666 N85-14285
Salt-gradient solar ponds: Summary of US Department of Energy sponsored research
[NASA-CR-174183] 05 p0667 N85-14286
Solar pond overview
05 p0667 N85-14287
Solar pond fluid dynamics and heat transfer
05 p0667 N85-14288
Review of SERI solar pond work
05 p0667 N85-14289
Salton Sea solar pond power plant design study and regional applicability
05 p0667 N85-14290
Solar pond research at Argonne National Laboratory
05 p0667 N85-14291
Summary of salt gradient solar pond research
05 p0667 N85-14292
Doubly diffusive linear stability with nonconstant gradients
[DE84-013008] 05 p0670 N85-14310
Heat and mass exchange in a partially stratified fluid
[DE85-000528] 10 p1488 N85-19384
Direct-contact condensers for solar pond power production
[DE84-004510] 12 p1876 N85-21771
Solar pond technology for Navy applications
[AD-A155877] 24 p4112 N85-35486
Energy from low temperature differences
[DE85-008617] 24 p4112 N85-35492

SOLAR POSITION
Theoretical study of electron concentration in Venusian atmosphere as function of zenith angle of sun and solar activity in areas of photochemical equilibrium
02 p0163 N85-11104
Integration of multispectral data obtained at different view angles for vegetation analysis
05 p0657 N85-14218
Dark matter near the sun: Simulated star counts and the Oort limit
06 p0880 N85-15582
Simultaneous Earth observations from 2 satellites
[NASA-TM-86204] 16 p2810 N85-27325
Terrain illumination conditions when taking scanning photographs from space
22 p3736 N85-33159
Cosmic ray intensity distribution perpendicular to solar equatorial plane at 1 A.U. during 1978-83
[SH-4.3-14] 23 p4032 N85-34996

SOLAR POWER GENERATION
U SOLAR GENERATORS

SOLAR POWER SATELLITES
Argon ion pollution of the magnetosphere
13 p1998 N85-22523

SOLAR POWER SOURCES
U SOLAR GENERATORS
SOLAR POWERED AIRCRAFT
Mission analysis of solar powered aircraft
[NASA-CR-172583] 20 p3397 N85-31072
SOLAR PROBES
NT HELIOS 1
NT HELIOS 2
SOLAR PROMINENCES
Solar-geophysical data. Part 2: (Comprehensive reports)
[PB85-112076] 12 p1962 N85-22332
A numerical simulation of the formation of solar prominences 14 p2448 N85-25112
A study of the material motion into an eruptive prominence — solar prominence 14 p2453 N85-25146
Energy balance in resistive instabilities — solar prominences 14 p2454 N85-25155
Magnetic instabilities in solar filaments: Models of twisting motions and ejecta 14 p2454 N85-25156
Prominences, two-ribbon flares and coronal transients 14 p2454 N85-25158
The global structure of magnetic fields which support quiescent prominences 18 p3204 N85-29876
Magnetic field-vector measurements in quiescent prominences via the Hanle effect: Analysis of prominences observed at Pic-du-Midi and at Sacramento Peak 18 p3208 N85-29898
Onset of solar flares as predicted by two-dimensional MHD-models of quiescent prominences
[SH-1.3-1] 23 p3992 N85-34750
SOLAR PROPULSION
Proceedings of the AFOSR/AFRPL Rocket Propulsion Research Meeting: Abstracts and Agenda
[AD-A146818] 09 p1286 N85-18085
Solar rocket component study
[AD-A154186] 19 p3227 N85-30007
Mission analysis of solar powered aircraft
[NASA-CR-172583] 20 p3397 N85-31072
SOLAR PROTONS
Entry of solar energetic protons into the distant plasma sheet dependence on distance from the neutral sheet 14 p2357 N85-24567
Magnetosonic waves and their relationship with energetic protons 14 p2368 N85-24635
Latitude variation of recurrent fluxes in the outer solar system
[SH-4.1-13] 21 p3715 N85-33054
The propagation of solar flare particles in a turbulent coronal loop
[SH-1.1-3] 23 p3989 N85-34730
Stochastic particle acceleration in solar flares
[SH-1.1-4] 23 p3989 N85-34731
Fast drift kilometric radio bursts and solar proton events
[SH-1.1-7] 23 p3990 N85-34734
Spectral and spatial properties of solar microflares
[SH-1.2-4] 23 p3991 N85-34740
Ion energy storage for post-flare loops
[SH-1.2-10] 23 p3992 N85-34745
A dominant role for protons at the onset of solar flares
[SH-1.2-13] 23 p3992 N85-34748
The starting conditions for an optically small solar gamma ray flare
[SH-1.3-2] 23 p3993 N85-34751
On the detectability of key-MeV solar protons through their nonthermal Lyman-alpha emission
[SH-1.3-5] 23 p3993 N85-34752
Observations of solar flare gamma-rays and protons
[SH-1.3-6] 23 p3993 N85-34753
Energetic protons from a disappearing solar filament
[SH-1.3-7] 23 p3993 N85-34754
Spectra of solar proton ground level events using neutron monitor and neutron moderated detector recordings
[SH-1.3-14] 23 p3994 N85-34759
On the retention of high-energy protons and nuclei with charges Z or equal to 2 in large solar flares after the process of their acceleration
[SH-2.1-8] 23 p3998 N85-34789
Observations of solar energetic particles at a synchronous orbit
[SH-3.1-1] 23 p4001 N85-34806
Coronal propagation of flare associated electrons and protons
[SH-3.1-3] 23 p4001 N85-34808
Constraints of solar flare particle transport models from anisotropy observations at Voyager 1
[SH-3.1-8] 23 p4002 N85-34812
Low energy proton bidirectional anisotropies and their relation to transient interplanetary magnetic structures: ISEE-3 observations
[SH-3.1-9] 23 p4002 N85-34813
Determination of the pitch-angle distribution and transverse anisotropy of interplanetary particles
[SH-3.1-11] 23 p4002 N85-34815
Channeled propagation of solar particles
[SH-3.2-3] 23 p4003 N85-34819
Energetic solar particle fluxes out to 3 AU during the 7 May 1978 flare event
[SH-3.2-6] 23 p4003 N85-34822
Monte Carlo calculations of relativistic solar proton propagation in interplanetary space
[SH-3.2-11] 23 p4004 N85-34826
Latitude variation of recurrent fluxes in the outer solar system
[SH-4.1-13] 23 p4006 N85-34836
Penetration of solar protons into the Earth's magnetosphere on November 22, 1977
[SH-6.1-15] 23 p4046 N85-35088
Dynamics of the penetration boundaries of solar protons during a strong magnetic storm
[SH-6.1-16] 23 p4046 N85-35089
The influence of the Earth's magnetosphere on the high-energy solar protons
[SH-6.1-22] 23 p4046 N85-35093
Solar neutrinos, solar flares, solar activity cycle and the proton decay
[SH-8.1-8] 23 p4049 N85-35113
SOLAR RADIATION
NT CIRCUMSOLAR RADIATION
NT SOLAR CORPUSCULAR RADIATION
NT SOLAR COSMIC RAYS
NT SOLAR ELECTRONS
NT SOLAR NEUTRINOS
NT SOLAR PROTONS
NT SOLAR RADIO BURSTS
NT SOLAR RADIO EMISSION
NT SOLAR WIND
NT SOLAR X-RAYS
NT SUNLIGHT
NT TYPE 3 BURSTS
NT TYPE 4 BURSTS
Workshop on the Use of Future Multispectral Imaging Capabilities for Lithologic Mapping: Workshop summary 02 p0214 N85-11413
Solar radiation in the ozone layer 04 p0522 N85-13342
Distribution of total solar radiation in Spain 04 p0523 N85-13344
Global radiation in West Germany — solar generators 05 p0662 N85-14253
Plant responses to solar UV-B radiation 05 p0690 N85-14436
Natural interference phenomena affecting spaceborne receivers
[NASA-CR-174256] 07 p0916 N85-15798
Deciduous forest radiation regimes: Effects of forest structure, phenology and Earth-Sun geometry upon their spatial, temporal and spectral variability
[AD-A146804] 07 p0996 N85-16327
NBS (National Bureau of Standards) daylight availability database
[PB84-245745] 07 p1054 N85-16686
Radiation parameterization programs for use in general circulation models
[AD-A148015] 08 p1186 N85-17486
Climate at CRREL (Cold Regions Research and Engineering Laboratory) Hanover, New Hampshire
[AD-A148400] 08 p1189 N85-17495
Weather data for simplified energy calculation methods. Volume 1. Eastern United States: TRY data
[DE85-000493] 09 p1358 N85-18541
Middle Atmosphere Program. Handbook for MAP, volume 7
[NASA-CR-175479] 11 p1656 N85-20437
MSG-7: Atmospheric penetration of solar radiation in the range of Schumann-Runge bands 11 p1657 N85-20443
Middle Atmosphere Program. Handbook for MAP, volume 8
[NASA-CR-175478] 11 p1657 N85-20445
MSG-7: Molecular absorption processes related to the penetration of ultraviolet solar radiation into the middle atmosphere 11 p1658 N85-20449
Ionospheric absorption on 1539 kHz in relation to solar ionizing radiation 11 p1659 N85-20455
Influence of the atmosphere on remotely sensed reflection from vegetation surfaces
[DE85-000658] 11 p1670 N85-20521
Short duration winter-time performances of different passive solar systems
[DE85-000850] 11 p1675 N85-20557
National solar-terrestrial research program, part 1. Solar-terrestrial research for the 1980's, part 2
[AD-A149542] 11 p1681 N85-20591
Microprocessor-controlled rotating shadowband radiometer
[DE85-000833] 12 p1854 N85-21630
Estimating solar radiation for plant simulation models
[E85-10089] 12 p1873 N85-21751
Multi-year plan for Experimental Systems Research: Passive and hybrid solar energy program
[DE85-004698] 12 p1882 N85-21810
NIMBUS-7 SBUV (Solar Backscatter Ultraviolet) observations of solar UV spectral irradiance variations caused by solar rotation and active-region evolution for the period November 7, 1978 - November 1, 1980
[NASA-CR-175544] 12 p1962 N85-22334
Study of integral and spectral direct solar radiation over Atlantic 14 p2341 N85-24475
Supplement to evaluation of satellite derived estimates of solar radiation
[E85-10086] 14 p2346 N85-24506
Evaluation of satellite derived estimates of solar radiation
[E85-10087] 14 p2346 N85-24507
ILUM code: Solar and lunar flux calculations for multi-cloud layered atmospheres
[DE85-005578] 15 p2600 N85-26025
Numerical integration through force discontinuities: Solar radiation pressure 16 p2805 N85-27296
Intercomparison of Radiation Codes in Climate Models (ICRCCM)
[DE85-007251] 16 p2835 N85-27487
Results from the Helios galactic and solar cosmic ray experiment (E7) 16 p2886 N85-27807
Solar radiance models for determination of ERBE scanner filter factor
[NASA-CR-172595] 17 p2995 N85-28513
Preliminary GCM results with a new radiation parameterization 18 p3145 N85-29474
Pacific Northwest solar radiation data
[DE85-009773] 18 p3149 N85-29496
Radiation damage and repair in cells and cell components. Part 2: Physical radiations and biological significance
[DE85-008934] 18 p3152 N85-29518
The possibility of observing solar neutron events in the lower atmosphere
[NOTA-INTERNA-837] 18 p3209 N85-29908
Thermal performance and design of a solid particle cavity receiver
[DE85-010830] 19 p3274 N85-30300
Influence of surface films of petroleum products on conditions for absorption of solar radiation by upper water layer 19 p3289 N85-30396
Stable density stratification solar pond
[NASA-CASE-NPO-15419-2] 19 p3303 N85-30474
View-limiting shrouds for insolation radiometers
[NASA-CR-176041] 20 p3458 N85-31476
Detection of solar neutrons by ground based neutron monitors
[IFSI-84-11] 20 p3547 N85-32076
Clarke Stations and mercurian mass-drivers: Energy for large-scale transportation systems
[DE85-009607] 21 p3580 N85-32145
Calculating solar highlight and shadeless areas for scanning photographs from space and optimizing lighting conditions 22 p3736 N85-33160
Solar energy meteorological research and training program: Region 4
[DE85-011783] 22 p3816 N85-33640
Three dimensional calculation of flux of low energy atmospheric neutrinos
[SH-8.1-11] 23 p4050 N85-35116
Monte Carlo calibration of the SMM gamma ray spectrometer for high energy gamma rays and neutrons
[SH-9.1-6] 23 p4051 N85-35121
Recording system for the solar neutron monitoring at Mt. Norikura
[SH-9.1-8] 23 p4051 N85-35123
Using the information of cosmic rays to predict influenza epidemic
[SH-10.1-2] 23 p4053 N85-35134
Space Station Polar Platform: Integrating research and operational missions
[PB85-195279] 24 p4069 N85-35218
SOLAR RADIO BURSTS
NT TYPE 3 BURSTS
NT TYPE 4 BURSTS
Solar-geophysical data number 477, May 1984. Part 2: (Comprehensive reports). Data for November 1983, July 1981 and miscellanea. Explanation of data reports issued as number 474 (supplement) February 1984
[PB84-225036] 01 p0131 N85-10900
Solar-geophysical data number 478, June 1984. Part 2 (comprehensive reports): Data for December 1983 and miscellanea
[PB84-243161] 06 p0690 N85-15654
Solar-geophysical data number 476, April 1984. Part 2: (Comprehensive reports). Data for October 1983, June 1981 and miscellanea
[PB84-215078] 09 p1417 N85-18837

Solar radio bursts, proton events and geomagnetic activity
[AD-A149018] 10 p1571 N85-19906
Solar-geophysical data. Part 2: (Comprehensive reports)
[PB85-112076] 12 p1962 N85-22332
Solar-geophysical data number 483, November 1984. Part 2: (Comprehensive reports). Data for May 1984, December 1981 and miscellanea
[PB85-147700] 12 p1962 N85-22336
Solar-geophysical data number 479, August 1981. Part 2: (Comprehensive reports), data for January 1984 and August 1981 and miscellanea. Explanation of data reports issued as number 474 (supplement) February 1984
[NASA-CR-175607] 13 p2205 N85-23679
Coronal structures observed at metric wavelengths with the Nancay radiohelligraph 14 p2453 N85-25152
The Helice radio astronomy experiment 16 p2886 N85-27803
Microwaves and hard X-rays ultrafast time structures at the impulsive phase of solar bursts
[INPE-3478-PRE/721] 16 p2888 N85-27816
Quenching of the beam-plasma instability by 3-D spectra of large scale density fluctuations
[NASA-CR-175969] 19 p3369 N85-30897
Fast drift kilometric radio bursts and solar proton events
[SH-1.1-7] 23 p3990 N85-34734
Temporal evolution of an energetic electron population in an inhomogeneous medium: Application to solar hard X-ray bursts
[SH-1.2-6] 23 p3991 N85-34741
Two types of electron events in solar flares
[SH-1.2-11] 23 p3992 N85-34746
A dominant role for protons at the onset of solar flares
[SH-1.2-13] 23 p3992 N85-34748
Ground increase of cosmic ray intensity on February 16, 1984
[SH-1.3-15] 23 p3994 N85-34760
Type 3 solar radio bursts and 3HE-rich events
[SH-2.2-3] 23 p4000 N85-34798
The 3HE in solar non-relativistic electron events
[SH-2.2-5] 23 p4000 N85-34800

SOLAR RADIO EMISSION
NT SOLAR RADIO BURSTS
NT TYPE 3 BURSTS
NT TYPE 4 BURSTS
Solar-geophysical data number 477, May 1984. Part 1: (Prompt reports). Data for April 1984, March 1984 and late data. Explanation of data reports issued as number 474 (supplement) February 1984
[PB84-225028] 01 p0131 N85-10901
Attempts to contruct two-dimensional image of Sun from observations made with RATAN-600 radiotelescope by relay race method 06 p0783 N85-15005
Solar-geophysical data number 478, June 1984. Part 1 (prompt reports): Data for May 1984, Apr. 1984, and late data
[PB84-243153] 06 p0890 N85-15653
Solar-geophysical data number 476, April 1984. Part 1: (Prompt reports). Data for March 1984, February 1984 and late data
[PB84-215060] 09 p1416 N85-18936
Solar-Geophysical Data. Part 1: (Prompt reports)
[PB85-112068] 11 p1766 N85-21100
Preliminary investigation into using the sun as a source for G/T (Gain to System Noise Temperature) measurements
[PB85-126146] 12 p1952 N85-22285
A new radio emission at 3 kHz in the outer heliosphere 12 p1959 N85-22312
Solar-geophysical data number 479, July 1984. Part 1: (Prompt reports). Data for June 1984, May 1984 and later data
[NASA-CR-175542] 12 p1962 N85-22333
Solar-geophysical data number 483. November 1984. Part 1: (Prompt reports). Data for October 1984, September 1984 and late data
[PB85-147692] 12 p1962 N85-22335
A synchrotron/inverse Compton interpretation of a solar burst producing fast pulses at lambda 3 mm and hard X-rays 16 p2887 N85-27815
Turbulence and wave particle interactions in solar-terrestrial plasmas
[NASA-CR-175970] 18 p3209 N85-29906
Single-dish high sensitivity determination of solar limb emission at 22 and 44 GHz
[INPE-3545-PRE/758] 19 p3385 N85-30999
Solar-geophysical data no. 485, January 1985. Part 1 (prompt reports): Data for December 1984, November 1984 and late data
[PB85-181360] 20 p3548 N85-32079
Solar radio fluxes as indices of solar activity
[AERONOMICA-ACTA-A-282-1984] 21 p3722 N85-33096

SOLAR RADIO WAVES
U SOLAR RADIO EMISSION

SOLAR RECEIVERS
U SOLAR COLLECTORS

SOLAR REFLECTORS
Joint Indo-German program on solar energy: Parabolic dish program, step 1
[BMFT-FB-T-84-175] 05 p0670 N85-14312
Measurement techniques for evaluating solar reflector materials
[DE85-002194] 10 p1510 N85-19531
Measurement techniques for evaluating solar reflector materials
[PB85-119469] 10 p1512 N85-19541
Accelerated aging of aluminized acrylic solar mirror materials
[DE85-002683] 11 p1812 N85-20138
Electrical research on solar cells and photovoltaic materials
[NASA-CR-175699] 15 p2585 N85-25935
MOD silver metallization for photovoltaics
[NASA-CR-175773] 16 p2818 N85-27381
Silvered polymer reflectors
[DE85-008782] 18 p3130 N85-29384
Plastic heliostat enclosure analysis
[DE85-009112] 18 p3130 N85-29387
MOD silver metallization for photovoltaics 21 p3610 N85-32428
Theory of cellwise optimization for solar central receiver system
[DE85-012586] 22 p3807 N85-33579

SOLAR ROTATION
NIMBUS-7 SBUV (Solar Backscatter Ultraviolet) observations of solar UV spectral irradiance variations caused by solar rotation and active-region evolution for the period November 7, 1978 - November 1, 1980
[NASA-CR-175544] 12 p1962 N85-22334
Solar Seismology From Space. A conference at Snowmass, Colorado
[NASA-CR-175661] 14 p2441 N85-25060
Rotational inversion from global solar oscillations 14 p2442 N85-25064
Analysis and interpretation of synthetic time strings of oscillation data 14 p2444 N85-25079
Fine structure of solar acoustic oscillations due to rotation 14 p2445 N85-25087
On the determination of the solar rotation and indications of the solar differential rotation from an analysis of solar integrated light 14 p2446 N85-25096
Models of solar differential rotation 14 p2446 N85-25097
The solar dynamo and the complex Lorenz equations 14 p2447 N85-25107
The role of differential rotation in magnetic energy storage — coronal loops 14 p2449 N85-25119
The intern. rotation of the Sun inferred from the rotational splitting of acoustic and gravity mode multiplets 14 p2449 N85-25122
Did the young Sun rotate at 100 km/s 14 p2451 N85-25133
Dynamo action of magnetostrophic waves — solar atmosphere 14 p2451 N85-25136
Cyclic flows in the solar convection zone due to the dynamo reaction 14 p2451 N85-25137
Stream dynamics between 1 AU and 2 AU: A detailed comparison of observations and theory
[NASA-TM-86086] 15 p2684 N85-26578
The corotating variation of the north-south anisotropy of cosmic rays
[SH-4.3-15] 23 p4033 N85-34899
Cosmic ray power spectral variations. 3: Solar rotation periodicities
[SH-4.4-16] 23 p4034 N85-35012
Study of spectral exponent on quiet and disturbed days
[SH-4.5-10] 23 p4037 N85-35028

SOLAR SAILS
Heliocentric sail problem with variable gravity field reduction 16 p2724 N85-26816
Maximizing the semi-major axis for a freely coning solar sailcraft
[AD-A153175] 17 p2909 N85-27938

SOLAR SEA POWER PLANTS
Temperature sensors for OTEC applications
[DE85-009807] 18 p3110 N85-29254

SOLAR SEISMOLOGY
U HELIOSEISMOLOGY

SOLAR SELECTIVE COATINGS
U SELECTIVE SURFACES

SOLAR SENSORS
Biaxial tracking solar generator 05 p0663 N85-14259
Integration of an Apple 2 Plus computer into an existing dual axis sun tracker system
[AD-A150778] 14 p2404 N85-24823

SOLAR SIMULATION
Isotropic proton irradiation of GaAs solar cells 13 p2012 N85-22622

SOLAR SIMULATORS
Analysis of inverter models and harmonic propagation. Part 1: A physical simulator for large solar cell arrays
[DE85-002312] 09 p1315 N85-18271

SOLAR SPECTRA
Chlorine and bromine solar neutrino experiments
[DE84-015720] 02 p0304 N85-11969
The Fourier tachometer 2: An instrument for measuring global solar velocity fields 14 p2442 N85-25058
Observations of intermediate-degree solar oscillations 14 p2442 N85-25059
Solar oscillations from two widely separated stations 14 p2446 N85-25093
On the determination of the solar rotation and indications of the solar differential rotation from an analysis of solar integrated light 14 p2446 N85-25096
The Fe XIII 10747 A and Fe XIV 5303 A coronal emission lines polarization 14 p2448 N85-25111
Ten years observations of long-period oscillations of the Sun 14 p2450 N85-25123
The response of the line KI 7699 to the solar oscillations 14 p2450 N85-25124
Activities report of the Institute of Astronomy and Astrophysics 17 p3052 N85-28892
The solar coronal X-ray spectrum 5.5-12 A
[AD-A152334] 17 p3054 N85-28906
Simple solar spectral model for direct and diffuse irradiance on horizontal and tilted planes at the Earth's surface for cloudless atmospheres
[DE85-002933] 18 p3137 N85-29424
Multichannel birefringent filter 18 p3206 N85-29888
Diagnostics of vector magnetic fields 18 p3206 N85-29889
Acetonitrile in the Earth's atmosphere: An upper limit deduced from infrared solar spectra
[AERONOMICA-ACTA-A-295-1985] 22 p3813 N85-33623
Application of nonlinear least squares methods to the analysis of solar spectra
[NASA-CR-176122] 22 p3816 N85-33637
Source energy spectra from demodulation of solar particle data by interplanetary and coronal transport
[SH-1.3-13] 23 p3994 N85-34758
Spectra of solar proton ground level events using neutron monitor and neutron moderated detector recordings
[SH-1.3-14] 23 p3994 N85-34759

SOLAR SPECTROMETERS
Middle Atmosphere Program. Handbook for MAP, volume 8
[NASA-CR-175478] 11 p1657 N85-20445
Report on the Workshop on Intercomparison of Solar UV Irradiance Measurements and Related Instrument Calibration 11 p1658 N85-20448
White Light Coronograph (WLC) and Ultra-Violet Coronal Spectrometer (UVCS) 23 p3901 N85-34161
The Jovian electron spectrum: 1978-1984
[SH-1.5-19] 23 p3998 N85-34782

SOLAR STORMS
Interplanetary radio storms. 2: Emission levels and solar wind speed in the range 0.05-0.8 AU
[NASA-TM-84946] 04 p0589 N85-13761
Dynamics of the penetration boundaries of solar protons during a strong magnetic storm
[SH-6.1-16] 23 p4046 N85-35089

SOLAR STREAMS
U SOLAR CORPUSCULAR RADIATION

SOLAR SYSTEM
NT HALLEY'S COMET
Cosmic ray propagation in the local superbubble
[NASA-TM-85030] 03 p0449 N85-12855
Bulk composition of the Moon in the context of models for condensation in the solar nebula 04 p0583 N85-13725
The abundance of deuterium in the outer solar system from ground-based measurements of monodeuterated methane 07 p1060 N85-16725
Airborne Astronomy Symposium. A symposium commemorating the tenth anniversary of operations of the Kuiper Airborne Observatory
[NASA-CP-2353] 08 p1244 N85-17848
Exploring the solar system with stellar occultations 08 p1245 N85-17857
Research and technology, Lyndon B. Johnson Space Center
[NASA-TM-58263] 08 p1262 N85-17929
Future of Ultraviolet Astronomy Based on Six Years of IUE Research
[NASA-CP-2349] 11 p1743 N85-20961
Solar system studies with the IUE: 1982 - 1984 11 p1744 N85-20964

Space research and the new approach to the mechanics of fluid media in cosmos 12 p1953 N85-22271
Magnetospheres in the solar system 12 p1954 N85-22274
Planetary geology in the 1980s [NASA-SP-467] 13 p2169 N85-23457
Viking radio science data analysis and synthesis [NASA-CR-175831] 13 p2171 N85-23471
On the origin of Triton and Pluto 13 p2175 N85-23497
Small solar system bodies 13 p2175 N85-23499
Asteroid collisional evolution studies 13 p2176 N85-23501
Impacts in ice: Commissions of solar system crater population 13 p2181 N85-23538
The solar system: Improving knowledge of the system 14 p2398 N85-24782
Formation of the solar system 15 p2677 N85-26532
Statistical theory of planet growth 15 p2678 N85-26534
The propagation of ultraheavy cosmic rays 15 p2685 N85-26582
European space science horizon 2000 [ESA-SP-1070] 16 p2717 N85-26771
The micrometeorite experiment on Helios — inner solar system 16 p2885 N85-27797
The fast individualists in the solar system: Cosmic rays 16 p2886 N85-27806
The study of the physics of cometary nuclei [NASA-CR-175917] 17 p3054 N85-28805
Gas chromatography: Possible application of advanced instrumentation developed for solar system exploration to space station cabin atmospheres 18 p3157 N85-29551
Volatiles in the outer solar system. 1: Thermodynamics of clathrate hydrates. 2: Ethane ocean on Titan. 3: Evolution of primordial Titan atmosphere 19 p3382 N85-30964
Space research in the United Kingdom: An assessment [AD-A155334] 21 p3712 N85-33038
Program for observations of Halley's comet 22 p3732 N85-33139
Relationships between chondritic meteorites and planets 22 p3851 N85-33851
Nebular volatile fractionations associated with chondrule formation 22 p3852 N85-33855
What determines the location of satellites and planets? 22 p3853 N85-33858
Volatiles on satellites of the outer solar system 22 p3854 N85-33868
Implications of source abundances of ultraheavy cosmic rays [OG-7.1-4] 23 p4013 N85-34866
The nature and origin of outer solar system asteroids from reflectance spectrophotometry 24 p4168 N85-35838

SOLAR TEMPERATURE
Solar cycle variations of sunspot temperatures 14 p2452 N85-25141

SOLAR TERRESTRIAL INTERACTIONS
National solar-terrestrial research program [PB84-216163] 01 p0072 N85-10479
Equatorial energetic distributions of ions of terrestrial radiation belt as function of solar corona temperature response 02 p0160 N85-11067
Fr. Angelo Secchi, a pioneer in the study of solar-terrestrial relationships 04 p0519 N85-13312
Relations between the particle precipitation events in mid-latitudes, the ring current intensity and the polarity of the interplanetary magnetic field 04 p0519 N85-13316
Daily magnetic variations at Ebro, Spain 04 p0520 N85-13325
Helium and hydrogen of the local interstellar mdium observed in the vicinity of the Sun 06 p0673 N85-15540
Middle Atmosphere Program. Handbook for MAP, volume 10 [NASA-CR-175477] 11 p1658 N85-20450
Solar terrestrial influences on the D region as shown by the level of atmospheric radio noise 11 p1664 N85-20488
Geomagnetic disturbances caused by internal atmospheric dynamics 11 p1665 N85-20491
Interplanetary shock waves during April and May of 1981 13 p1962 N85-22434
World ocean level oscillations and their relationship to change in inflow of continental waters 13 p2108 N85-23133
Achievements of the International Magnetospheric Study (IMS) — conference [ESA-SP-217] 14 p2354 N85-24544
The application of dimensional analysis to the problem of solar wind-magnetosphere energy coupling 14 p2357 N85-24564
Coupling of the solar wind to measures of magnetic activity 14 p2357 N85-24565
The GEOS-2 electric field observations at times of solar wind discontinuities 14 p2360 N85-24584
Solar wind control of electric fields and currents in the magnetosphere and ionosphere 14 p2364 N85-24608
Solar wind control of magnetospheric convection 14 p2365 N85-24615
Solar wind and cosmic rain 15 p2644 N85-26312
Coupling of the solar wind to measures of magnetic activity [DE85-002415] 15 p2685 N85-26580
Geophysical responses of dynamics of solar wind transition region 16 p2721 N85-26795
Some features of the interplanetary medium during Forbush decreases [NOTA-INTERNA-836] 18 p3202 N85-29866
Turbulence and wave particle interactions in solar-terrestrial plasmas [NASA-CR-175970] 18 p3209 N85-29906
Magnetospheric response to solar wind variations [DE85-010762] 20 p3547 N85-32074
Interaction between an interplanetary shock and the Earth's magnetosphere on 27 August 1978: ISEE-1 electric field and ISEE-2 plasma observations [IFSI-84-15] 20 p3548 N85-32078
Effect of ions on cloud formation and its role in solar terrestrial relationship 21 p3653 N85-32697
Solar energy meteorological research and training program: Region 4 [DE85-011783] 22 p3816 N85-33640
Space Station Polar Platform: Integrating research and operational missions [PB85-195279] 24 p4069 N85-35218

SOLAR THERMAL ELECTRIC POWER PLANTS
Development of an Organic Rankine-Cycle power module for a small community solar thermal power experiment [NASA-CR-175650] 14 p2350 N85-24523
Test results of an organic Rankine-cycle power module for a small community solar thermal power experiment [NASA-CR-175696] 14 p2350 N85-24524
An evaluation of thermal storage for liquid-metal, solar thermal receivers [DE85-002920] 16 p2820 N85-27394
Solar Thermal Research Program [DE85-000514] 18 p3131 N85-29388
Long-term goals for solar thermal technology [DE85-013032] 22 p3809 N85-33597

SOLAR TOTAL ENERGY SYSTEMS
Shenandoah parabolic dish solar collector [DE85-006326] 17 p2987 N85-28460

SOLAR VELOCITY
What would a dynamo theorist like to know about the dynamics of the solar convection zone? 14 p2441 N85-25062
The magneto-optical filter, working principles and recent progress 14 p2442 N85-25066

SOLAR WIND
Structure and evolution of the large scale solar and heliospheric magnetic fields [NASA-CR-175268] 01 p0130 N85-10897
Magnetospheric structures: Uranus and Neptune 02 p0301 N85-11949
The solar wind at 20-30 AU 02 p0301 N85-11950
Physics of the inner heliosphere 1-10R sub O plasma diagnostics and models [NASA-CR-174010] 02 p0304 N85-11964
Magnetohydrodynamic and gasdynamic theories for planetary bow waves [NASA-CR-174132] 03 p0448 N85-12850
Magnetohydrodynamic and gasdynamic theories for planetary bow waves [NASA-CR-174135] 04 p0589 N85-13760
Interplanetary radio storms. 2: Emission levels and solar wind speed in the range 0.05-0.8 AU [NASA-TM-84946] 04 p0589 N85-13761
Helium and hydrogen of the local interstellar mdium observed in the vicinity of the Sun 06 p0673 N85-15540
Changes of LISM characteristics in the heliospheric interface 06 p0673 N85-15542
Broadening of the interplanetary helium cone structure due to elastic collisions of LISM helium atoms with solar wind ions 06 p0673 N85-15543
Solar wind and cosmic ray irradiation of grains and ices - application to erosion and synthesis of organic compounds in the solar system 06 p0686 N85-15637
Polar rain: Solar coronal electrons in the Earth's magnetosphere [NASA-TM-86150] 07 p1060 N85-16726
Spicules and surges [AD-A146785] 07 p1081 N85-16727
Corotating interaction regions in stellar winds: Particle acceleration and non-thermal radio emission in hot stars 08 p1234 N85-17773
Lyman alpha coronagraph research sounding rocket program [NASA-CR-174376] 09 p1354 N85-18517
Data analysis of electron measurements of the plasma experiment aboard the HELIOS probes [MPE-185] 09 p1418 N85-18935
Recent investigations at INPE in magnetospheric physics and geomagnetism [INPE-3280-PRE/603] 10 p1514 N85-19555
Research study of space plasma boundary processes [NASA-CR-174351] 10 p1558 N85-19823
Effects of the solar-terrestrial environment on satellite operations [DE85-002413] 11 p1590 N85-20003
Geomagnetic disturbances caused by internal atmospheric dynamics 11 p1665 N85-20491
Application of dimensional analysis to the problem of solar wind-magnetosphere energy coupling [DE85-002414] 11 p1674 N85-20551
Global aspects of stream evolution in the solar wind [DE85-002207] 11 p1766 N85-21101
Discovery of the solar wind 12 p1954 N85-22272
Velocity distributions of solar wind ions and electrons 12 p1954 N85-22273
The influence of the local solar wind structures on the propagation of low energy particles 12 p1959 N85-22314
The international VEGA 'Venus-Halley' (1984-1986 experiment: Description and scientific objectives [NASA-TM-77536] 12 p1960 N85-22324
Development of a Global 3-D magnetohydrodynamic computational model for solar wind-cometary and planetary studies [NASA-CR-175490] 12 p1962 N85-22331
Solar-geophysical data number 483, November 1984. Part 2: (Comprehensive reports). Data for May 1984, December 1981 and miscellanea [PB85-147700] 12 p1962 N85-22336
Plans for Interbol satellite experiment 13 p1977 N85-22407
Correlation of interplanetary medium parameters in transition region of high-velocity solar wind streams 13 p1978 N85-22412
Polar plasmas as observed by Dynamics Explorers 1 and 2 13 p1991 N85-22483
Physics of the inner heliosphere: Mechanisms, models and observational signatures [NASA-CR-175632] 13 p2205 N85-23677
Ultraviolet Spectrometer and Polarimeter (UVSP) software development and hardware tests for the solar maximum mission [NASA-CR-175279] 14 p2305 N85-24271
The application of dimensional analysis to the problem of solar wind-magnetosphere energy coupling 14 p2357 N85-24564
Coupling of the solar wind to measures of magnetic activity 14 p2357 N85-24565
Particle sources, transport, storage and precipitation — magnetosphere 14 p2359 N85-24576
The GEOS-2 electric field observations at times of solar wind discontinuities 14 p2360 N85-24584
Solar wind control of electric fields and currents in the magnetosphere and ionosphere 14 p2364 N85-24608
Solar wind control of magnetospheric convection 14 p2365 N85-24615
Implications of the global appearance of Pi2 and Pc 3 bursts 14 p2371 N85-24652
Active Magnetospheric Particle Tracing Explorers (AMPTE) [AD-A151072] 14 p2374 N85-24674
The downshift of electron plasma oscillations in the electron foreshock region [NASA-CR-175633] 14 p2423 N85-24945
The first effect of the amplitude of a solar cycle 14 p2452 N85-25143
Solar wind and cosmic rain 15 p2644 N85-26312
Development of a global 3-D magnetohydrodynamic computational model for solar wind/cometary and planetary studies [NASA-CR-175724] 15 p2684 N85-26577
Stream dynamics between 1 AU and 2 AU: A detailed comparison of observations and theory [NASA-TM-86086] 15 p2684 N85-26578
Coupling of the solar wind to measures of magnetic activity [DE85-002415] 15 p2685 N85-26580
Instability of solar wind near streamlined bodies 16 p2720 N85-26794
Geophysical responses of dynamics of solar wind transition region 16 p2721 N85-26795

Electric field and energy transfer by magnetopause reconnection
[INPE-3448-PRE/701] 16 p2826 N85-27432
An interplanetary magnetic field ensemble at 1 AU
[NASA-TM-86209] 16 p2862 N85-27784
Direct evidence for solar wind control of Jupiter's hectometer-wavelength radio emission
[NASA-TM-86073] 16 p2863 N85-27790
Ten years solar wind experiments on Helios 1 and Helios 2 16 p2885 N85-27798
Plasma waves in the solar wind: Ten years of Helios observations 16 p2885 N85-27801
Supersonic flow around weak radiation sources 17 p2942 N85-28162
Solar wind observations associated with a slow forward shock wave at 0.31 AU
[MPAE-W-79-84-46] 17 p3055 N85-28809
Shocks in the solar wind between 1 and 8.5 AU: Voyager 1 observations
[NASA-CR-175911] 18 p3209 N85-29905
The influence of the heliospheric current sheet and angular separation on flare accelerated solar wind
[NASA-CR-175962] 18 p3209 N85-29907
More on shock-wave studies with Prognoz-10 satellite 19 p3296 N85-30432
Functions of Prognoz-10: Intercosmos' station explained 19 p3296 N85-30433
Prognoz-10 intercosmos' station launched to study shock waves 19 p3296 N85-30434
Effects of coronal disturbances on the ionization state of the solar wind
[NASA-CR-175997] 19 p3385 N85-31000
Solar-wind magnetosphere energy input functions
[NASA-CR-176021] 19 p3385 N85-31001
Solar photospheric and coronal abundances from solar energetic particle measurements
[NASA-CR-176029] 20 p3547 N85-32073
Magnetospheric response to solar wind variations
[DE85-010762] 20 p3547 N85-32074
Soft X-ray polychromator for the Solar Maximum Mission
[NASA-CR-175297] 21 p3723 N85-33096
Yakutsk institute's cosmic ray research facility 22 p3732 N85-33135
Spectral measurements of magnetic energy and magnetic helicity between 0.29 and 0.97 AU
[IFSI-85-2] 22 p3850 N85-33844
Magnetotails of the terrestrial planets: A comparative study 22 p3856 N85-33875
Simultaneous Solar Maximum Mission and Very Large Array (VLA) observations of solar active regions
[NASA-CR-176090] 22 p3859 N85-33897
Statistical analyses in the study of solar wind-magnetosphere coupling
[DE85-009596] 22 p3859 N85-33898
White Light Coronograph (WLC) and Ultra-Violet Coronal Spectrometer (UVCS) 23 p3901 N85-34161
Shock and statistical acceleration of energetic particles in the interplanetary medium
[SH-1.5-1] 23 p3996 N85-34771
Pitch angle distributions of 35-1000 keV protons at quasi-perpendicular interplanetary shocks
[SH-1.5-8] 23 p3996 N85-34775
Elemental abundances in corotating events
[SH-1.5-15] 23 p3997 N85-34778
Cosmic ray acceleration by stellar wind. Simulation for heliosphere
[SH-1.5-17] 23 p3997 N85-34780
Low energy proton bidirectional anisotropies and their relation to transient interplanetary magnetic structures: ISEE-3 observations
[SH-3.1-9] 23 p4002 N85-34813
The propagation of solar energetic particles in magnetic channels
[SH-3.2-4] 23 p4003 N85-34820
Effects of a wavy neutral sheet on cosmic ray anisotropies
[SH-4.2-11] 23 p4008 N85-34849
On the influence of the heliomagnetospheric periphery on the galactic cosmic rays
[SH-4.2-19] 23 p4009 N85-34856
An update on the correlation between the cosmic radiation intensity and the geomagnetic AA index
[SH-4.2-24] 23 p4000 N85-34861
Gradients and anisotropies of high energy cosmic rays in the outer heliosphere
[SH-4.3-7] 23 p4032 N85-34992
The corotating variation of the north-south anisotropy of cosmic rays
[SH-4.3-15] 23 p4033 N85-34999
A study of periodicities and recurrences in solar activity and cosmic ray modulation
[SH-4.4-14] 23 p4034 N85-35010
Azimuthal and meridional asymmetries of the solar wind and quasiperiodic variations of intensity of Galactic Cosmic Rays (GCR)
[SH-4.4-20] 23 p4035 N85-35016
Diagnostic of electromagnetic conditions in space using cosmic rays
[SH-4.5-19] 23 p4038 N85-35036
Observation of pick-up ions in the solar wind: Evidence for the source of the anomalous cosmic ray component?
[SH-4.6-5] 23 p4039 N85-35043
On the anomalous component
[SH-4.6-6] 23 p4039 N85-35044
The large-scale modulation of cosmic rays in mid-1982: Its dependence on heliospheric longitude and radius
[SH-4.7-9] 23 p4041 N85-35053
Dimensions of the solar wind cavity and of the region of interplanetary cosmic ray modulation
[SH-4.7-11] 23 p4041 N85-35055
Galactic cosmic ray currents and magnetic field irregularity degree in high-speed solar wind streams
[SH-5.1-9] 23 p4042 N85-35063
Influence of magnetic clouds on cosmic ray intensity variations
[SH-5.1-12] 23 p4042 N85-35065
Peculiarities of Galactic Cosmic Ray (GCR) anisotropy variation in connection with the recurrent and sporadic Forbush effects
[SH-5.1-21] 23 p4044 N85-35073
Cosmic ray modulation by high-speed solar wind fluxes
[SH-5.1-22] 23 p4044 N85-35074
Coupling functions for lead and lead-free neutron monitors from the latitudinal measurements performed in 1982 in the research station Academician Kurchatov
[SH-6.1-1] 23 p4044 N85-35076
Cosmic rays 108e biennal data and their relationship to aurorae and sunspots
[SH-7.1-1] 23 p4047 N85-35094
Parallel fast-forward shock within 1 AU: Helios-1 and 2 observations
[MPAE-W-79-84-27] 24 p4189 N85-35847

SOLAR WIND VELOCITY
Solar wind dynamics at small distances from the sun 06 p0823 N85-15227
Kinematics of nearby gas and stars 06 p0880 N85-15591
Correlation of interplanetary medium parameters in transition region of high-velocity solar wind streams 13 p1978 N85-22412
Linear filters as a method of real-time prediction of geomagnetic activity
[DE85-010760] 22 p3880 N85-33899
Determination of the pitch-angle distribution and transverse anisotropy of interplanetary particles
[SH-3.1-11] 23 p4002 N85-34815
Evidence for regions of negligible cosmic-ray modulation in the inner heliosphere (10 AU)
[SH-4.1-21] 23 p4006 N85-34840
Determination of galactic cosmic ray latitudinal gradient using Earth based detectors
[SH-4.2-13] 23 p4006 N85-34851
The expected cosmic ray density and stream distributions at the heliolatitudinal asymmetry of solar wind
[SH-4.2-14] 23 p4008 N85-34852
Latitudinal gradients of cosmic rays and the polarity reversal of the heliospheric magnetic field: A preliminary evaluation
[SH-4.2-16] 23 p4008 N85-34853
The effect of the neutral sheet structure of the interplanetary magnetic field on cosmic ray distribution in space
[SH-4.2-18] 23 p4008 N85-34855
11- and 22-year variations of the cosmic ray density and of the solar wind speed
[SH-4.2-21] 23 p4009 N85-34858
The corotating variation of the north-south anisotropy of cosmic rays
[SH-4.3-15] 23 p4033 N85-34999
Long-term modulation of galactic cosmic rays in high-energy region
[SH-4.4-22] 23 p4035 N85-35018
Solar wind velocity and daily variation of cosmic rays
[SH-4.5-6] 23 p4036 N85-35024
The cosmic ray interplanetary radial gradient from 1972 - 1985
[SH-4.7-1] 23 p4040 N85-35048
The recovery of the cosmic ray flux from maximum solar modulation at IMP-8 (1 AU) and at Pioneer (R 30 AU)
[SH-4.7-7] 23 p4041 N85-35052
The large-scale modulation of cosmic rays in mid-1982: Its dependence on heliospheric longitude and radius
[SH-4.7-9] 23 p4041 N85-35053
Nonstationary modulation of galactic cosmic rays in a nonlinear model
[SH-4.7-10] 23 p4041 N85-35054
Study of dominating parameters of high speed solar plasma streams in relation to cosmic ray and geomagnetic storms
[SH-5.1-11] 23 p4042 N85-35064
The solar wind effect on cosmic rays and solar activity
[SH-5.1-13] 23 p4043 N85-35066

SOLAR X-RAYS
Studies of solar flares and coronal loops
[AD-A145009] 01 p0130 N85-10898
Particle acceleration in two-ribbon flares --- solar flares 04 p0519 N85-13314
Temporal and spectral characteristics of solar flare hard X-ray emission
[NASA-TM-86187] 06 p1259 N85-17923
Solar-geophysical data. Part 2: (Comprehensive reports)
[PB85-112076] 12 p1962 N85-22332
Solar-geophysical data number 483, November 1984. Part 2: (Comprehensive reports). Data for May 1984, December 1981 and miscellanea
[PB85-147700] 12 p1962 N85-22336
Solar and stellar coronal plasmas
[NASA-CR-175623] 13 p2205 N85-23676
Solar-geophysical data number 479, August 1981. Part 2: (Comprehensive reports), data for January 1984 and August 1981 and miscellanea. Explanation of data reports issued as number 474 (supplement) February 1984
[NASA-CR-175807] 13 p2205 N85-23679
A study of the morphology of solar flares as observed by the hard X-ray imaging spectrometer --- Solar Maximum Mission 14 p2454 N85-25160
Magnetic field structures of hard X-ray flares observed by HINOTORI spacecraft --- solar flares 14 p2455 N85-25161
Microwaves and hard X-rays ultrafast time structures at the impulsive phase of solar bursts
[INPE-3478-PRE/721] 16 p2888 N85-27816
The solar coronal X-ray spectrum 5.5-12 A
[AD-A152334] 17 p3054 N85-28808
A study of the cyclical variations of coronal holes and their relation to open magnetic fields
[AD-A155251] 21 p3723 N85-33099
Study of non-thermal photon production under different scenarios in solar flares. 1: Scenarios and formulations
[SH-1.2-2] 23 p3991 N85-34736
Study of non-thermal photon production under different scenarios in solar flares. 2: The Compton inverse and Bremsstrahlung models and fittings
[SH-1.2-3] 23 p3991 N85-34739
Spectral and spatial properties of solar microflares
[SH-1.2-4] 23 p3991 N85-34740
Temporal evolution of an energetic electron population in an inhomogeneous medium: Application to solar hard X-ray bursts
[SH-1.2-6] 23 p3991 N85-34741
Quantitative analysis of flare accelerated electrons through their hard X-ray and microwave radiation
[SH-1.2-7] 23 p3991 N85-34742
Two types of electron events in solar flares
[SH-1.2-11] 23 p3992 N85-34746
Two classes of solar energetic particle events associated with impulsive and long duration soft X-ray flares
[SH-1.2-12] 23 p3992 N85-34747
A dominant role for protons at the onset of solar flares
[SH-1.2-13] 23 p3992 N85-34748
Photometric and spectroscopic gamma-ray observations of solar transient phenomena using long duration balloons
[SH-9.1-5] 23 p4051 N85-35120

SOLAR-PUMPED LASERS
Theoretical studies of solar-pumped lasers
[NASA-CR-175801] 16 p2769 N85-27206

SOLDERED JOINTS
The metallurgical processes during the soft soldering of copper and copper alloys and the strength characteristics of soldered joints
[BLL-T6366/BG/WH803/84] 06 p0767 N85-14908
Strength and aging behaviour of soft soldered joints
[BLL-T6365/BG/WH800/84] 07 p0925 N85-15862
Investigation of the creep behaviour of soft soldered joints with solder L-SnAg5 at ambient temperature
[BLL-T6363/BG/WH798/84] 07 p0926 N85-15865
NASA welding assessment program
[NASA-CR-175512] 12 p1859 N85-21661
Aging of gold thick-film solder joints
[DE85-009847] 18 p3077 N85-29037
Drag soldering process control
[DE85-010853] 20 p3433 N85-31301

SOLDERING
Swiss firm improves method for soldering printed circuits 03 p0341 N85-12163
Laser spot welding in the electronics industry 14 p2308 N85-24287

Printed wiring board circuit isolator tool
[AD-D011638] 17 p2968 N85-26333
Method for ultrasonic bonding to soft microelectronic substrates
[NASA-CASE-NPO-16087-1] 18 p3094 N85-29151
Drag soldering process control
[DE85-010853] 20 p9433 N85-31301
Hermetic chip carrier compliant soldering pads
[AD-D011722] 23 p3936 N85-34410

SOLDERS
Special soft solder TK-3 (L-SnCu 3 - DIN 1707)
[BLL-T6384/BG/WH790/84(9022.48)] 06 p0767 N85-14907

SOLENOID VALVES
Locking of Automotive Products hydraulic selector valves
[BAE-EXPER/NOTE-459] 15 p2567 N85-25839

SOLENOIDS
Optimum dimensions of power solenoids for magnetic suspension 04 p0489 N85-13118
The generation of rolling moments with the superconducting solenoid model
[NASA-CR-172520] 09 p1283 N85-18068
Virtual cathode oscillator study
[AD-A149268] 10 p1480 N85-19342
In-beam tests of an air-core superconducting-solenoid particle spectrometer
[DE85-004029] 12 p1853 N85-21825
Stability and vibrations of internal windings of high-current superconducting solenoid magnets
[AD-A151465] 15 p2656 N85-26390
Effect of superconducting solenoid model cores on spanwise iron magnet roll control
[NASA-TM-86378] 17 p2905 N85-27915
Optimum dimensions of power solenoids for magnetic suspension
[NASA-TM-77864] 17 p3026 N85-28716
Rotor blade test apparatus
[AD-D011725] 23 p3934 N85-34381
Theoretical and computational research on the focused transport of intense charged particle beams
[DE85-012980] 23 p3972 N85-34621

SOLID ARGON
U SOLIDIFIED GASES

SOLID ELECTROLYTES
Trivalent ion exchange in beta alumina
[AD-A145373] 02 p0172 N85-11151
Study of application of organic semiconductors to electronic components
[BMFT-FB-T-84-142] 02 p0289 N85-11890
Solid electrolytes for medium temperature steam electrolysis
[DE84-014364] 04 p0463 N85-12938
Development and testing of thin film cells for high temperature water vapor electrolysis
[BMFT-FB-T-84-146] 04 p0471 N85-13001
Polyphosphazene solid electrolytes
[AD-A147008] 07 p0931 N85-15902
Ionic and molecular transport in beta- and beta''-alumina
[DE85-000984] 09 p1380 N85-18680
A two photoelectrode solid-state photoelectrochemical cell
[AD-A148982] 10 p1434 N85-19038
High-temperature, solid oxide electrolyte fuel cell power generation system
[DE85-002978] 11 p1675 N85-20552
Solid electrolytes: Mechanisms for achieving optimal conductivity
[AD-A150116] 12 p1801 N85-21296
Production technology of an electrolyte for Na/S batteries
[BMFT-FB-T-84-277] 15 p2550 N85-25742
Degradation phenomena in solid electrolytes
[DE85-007066] 15 p2587 N85-25949
F-cell: The Aspen fuel cell model
[DE85-001975] 18 p3131 N85-29393
Polyethylene imine-metal salt solid electrolyte
[AD-D011678] 19 p3305 N85-30485
Defect interactions at high concentrations in solid oxide electrolytes
[DE85-011824] 22 p3807 N85-33560

SOLID LUBRICANTS
Experimental test program for evaluation of solid lubricant coating as applied to compliant foil gas bearings to 315 deg C
[NASA-CR-174837] 07 p0930 N85-15895
The role of silver in self-lubricating coatings for use at extreme temperatures
[NASA-TM-86943] 11 p1611 N85-20127
Wear reduction by lubricants in confined contacts 14 p2223 N85-23786
Effect of counterface material type and its topography on the tribological properties of polyimide composites
[NASA-TM-87035] 16 p2754 N85-26993
Tooth wear in worm gears in vacuum 16 p2766 N85-27070
Molybdenum disulphide lubrication: A continuation survey, 1981 - 1983
[REPT-84-549] 18 p3082 N85-29065
Friction and wear of solid-lubricated contact in gas turbine engine bearings
[AD-A155042] 21 p3596 N85-32335
Advances in sputtered and ion plated solid film lubrication 22 p3797 N85-33524

SOLID MECHANICS
Proceedings of the 9th Biennial Army Symposium on Solid Mechanics. Advances in Solid Mechanics for Design and Analysis
[AD-A150042] 12 p1867 N85-21710
USSR report: Physics and mathematics
[JPRS-UPM-85-004] 21 p3660 N85-32860

SOLID PHASES
Re-evaluation of phase separation in Ti-Zr-Be metallic glasses
[DE84-015603] 03 p0338 N85-12176
A study of tetrataenite 06 p0865 N85-15623
Speculations on the formation of metallic meteorite phases 06 p0869 N85-15648
Influence of temperatures of reactants on nature of product of solid-phase reactions
[BLL-M-36019-(5828.4)] 07 p0921 N85-15832
The formation of isolated phase precipitates during the decomposition of high-coercive force Fe-Cr-Co alloys
[BLL-M-36028-(5828.4)] 07 p0924 N85-15855
Kinetics of interaction between carbon and iron oxides of metallized materials in solid phase
[BLL-M-36023-(5828.4)] 07 p0926 N85-15873
Electron-diffraction structural examination of amorphous iron-tin alloys 11 p1604 N85-20084
Investigation of vanadium solid solution and zeta phase regions of vanadium-carbon system
[DE85-002678] 11 p1605 N85-20092
Effect of variable solid phase thermal properties on propellant combustion 13 p2002 N85-22547
Phase separation in polyurethanes: A deuterium NMR study
[AD-A151515] 15 p2505 N85-25451
Detonations of solid explosives
[AD-A152012] 15 p2521 N85-25540
X-ray diffraction study of changes in stress-strain distributions during fatigue of a 2-phase alloy
[AD-A152367] 17 p2930 N85-28087
Solid phase reactions among manganese, potassium perchlorate and barium chromate
[HSE-TRANS-11166] 19 p3237 N85-30071
Fundamental studies of beta phase decomposition modes in titanium alloys
[AD-A154122] 19 p3238 N85-30078

SOLID PROPELLANT COMBUSTION
NT SOLID PROPELLANT IGNITION
An experimental investigation of combustion pressure oscillations in solid fuel ramjets
[AD-A144870] 01 p0024 N85-10147
Critical analysis of nitramine decomposition data. Preliminary comments on autoacceleration and autoinhibition in HMX and RDX decomposition
[AD-A146570] 06 p0774 N85-14946
Analysis of Deflagration to Shock to Detonation Transition (DSDT) in porous energetic solid propellants 08 p1115 N85-17030
Fuel-rich solid propellant boron combustion
[AD-A148522] 08 p1136 N85-17157
Molecular dynamics in nitramines and modified nitramines
[AD-A148515] 08 p1220 N85-17686
Recovery of damaged solid propellants by interrupting burning and crack-propagation processes
[AD-P004343] 10 p1455 N85-19167
Effects of perforation L/D ratio and slotting on stick propellant combustion
[AD-A148854] 10 p1456 N85-19177
Solid propellant combustion diagnostics and automated data retrieval from holograms 13 p1998 N85-22527
Combustion of zirconium carbide 13 p1999 N85-22532
Coupling between velocity oscillations and solid propellant combustion 13 p2000 N85-22536
Mechanism of burning rate enhancement by ferric oxide 13 p2002 N85-22546
Effect of variable solid phase thermal properties on propellant combustion 13 p2002 N85-22547
Mutiple reflection theory for microwave measurement of solid propellant burning rates 13 p2002 N85-22549
In-situ burning rate determination using flash radiography 13 p2002 N85-22550
Molecular dynamics of propellant gases, part 2 13 p2002 N85-22552
Application of atomic fluorescence to measurement of combustion temperature in solid propellants
[AD-A150733] 14 p2263 N85-24021
Components of the combustion gases of propellant charge powders after reaction in the high pressure bomb in the pressure range up to 1000 MPa. Part 1: Nitroglycerine powder GB Pa 125
[ISL-CO-217/83-PT-1] 14 p2264 N85-24027
Solid fuel combustion chamber
[VTH-LR-415] 16 p2741 N85-26918
Solid fuel combustion chamber
[VTH-LR-438] 16 p2741 N85-26919
Solid fuel combustion chamber research in the Netherlands
[VTH-LR-444] 16 p2742 N85-26920
The development of a computational model for a two-dimensional turbulent flow. Part 1: Mathematical background — solid fuel combustion
[VTH-LR-436-PT-1] 16 p2785 N85-27188
Holographic investigation of solid propellant combustion in a two-dimensional motor
[AD-A153546] 18 p3070 N85-29089
Imbedded thermocouples as a solid propellant combustion probe
[AD-A155630] 21 p3564 N85-32167
Closed-bomb combustion of Hivelite-based, Very High Burn Rate (VHBR) propellant
[AD-A155740] 21 p3571 N85-32212

SOLID PROPELLANT IGNITION
The vulnerability of cast double base rocket motors to thermomechanical attack 08 p1115 N85-17033
Response of propellants to high dynamic stresses: The uses of gun launch techniques 08 p1116 N85-17035
Some aspects of the micromechanics of hot spot formation in energetic materials 08 p1116 N85-17036
A two-step bomb to determine the inflammability of propellant charge powders
[ISL-CO-211/83] 14 p2264 N85-24026
Investigation of the choking effect of an inert granular bed on an ignition gas jet charged with particles
[ISL-CO-235/83] 14 p2264 N85-24028
Status of boron combustion research
[AD-A154762] 21 p3563 N85-32160

SOLID PROPELLANT ROCKET ENGINES
A model for grain misalignment in cylindrical port motors
[AD-A144856] 01 p0034 N85-10210
One-dimensional two-phase constant lag flow in combustion chamber of solid propellant rocket motors
[AD-A145679] 02 p0173 N85-11157
Experiments on residual thrust and prediction for upper-stage solid propellant rockets
[NAL-TR-800] 03 p0324 N85-12087
Carbon/carbon rocket motor exit cone reinforcement
[AD-D011360] 07 p0916 N85-15799
Solid propellant Ramrockets 07 p0918 N85-15816
The space shuttle launch vehicle aerodynamic verification challenges 08 p1093 N85-16907
The aerodynamic challenges of SRB recovery 08 p1093 N85-16908
External tank processing from barge to pad 08 p1096 N85-16927
Solid rocket booster retrieval operations 08 p1096 N85-16928
Solid rocket motor certification to meet space shuttle requirements from challenge to achievement 08 p1098 N85-16941
The solid rocket booster auxiliary power unit: Meeting the challenge 08 p1099 N85-16946
Hazard Studies for Solid Propellant Rocket Motors
[AGARD-CP-367] 08 p1114 N85-17025
Review of USAF treatment of solid propellant rocket motor hazards 08 p1114 N85-17027
The vulnerability of cast double base rocket motors to thermomechanical attack 08 p1115 N85-17033
Hazard assessment of a hypothetical large rocket motor 08 p1117 N85-17042
Water impact laboratory and flight test results for the space shuttle solid rocket booster aft skirt 09 p1335 N85-18394
Report on AGARD Meeting: Hazards Studies for Solid Propellant Rocket Motors
[AD-P004340] 10 p1454 N85-19164
Window on science visit to the USA, 21 March - 22 April, 1984 — ramjets and solid propellant rocketry
[VTH-LR-426] 11 p1592 N85-20011
Space Shuttle booster thrust imbalance analysis
[NASA-TM-86493] 12 p1791 N85-21241
Integrated insulation wall assembly — for a solid rocket motor case
[AD-D011553] 12 p1794 N85-21257
Plasticizer system for propellant compositions
[AD-D011502] 12 p1816 N85-21390

Plasticizer system for propellant compositions
[AD-D011508] 12 p1816 N85-21391
Plasticizer system for propellant compositions
[AD-D011516] 12 p1817 N85-21394
Plasticizer system for propellant compositions
[AD-D011517] 12 p1817 N85-21395
SRM filament wound case resin characterization studies 12 p1944 N85-22212
Investigation of the effects of NaOH dopant level on the physical and mechanical properties of carbon/phenolic composite material 12 p1945 N85-22213
Nonlinear interactions between vortices and acoustic waves in a rocket combustion chamber 13 p1999 N85-22533
Acoustic energy exchange in sheared mean flows — solid rocket motors 13 p1999 N85-22534
Investigations of reactive and non reactive acoustic boundary layers in porous walled ducts 13 p2000 N85-22535
Comparisons of solid propellant with instability predictions and motor firing experience 13 p2001 N85-22541
Internal fluid mechanism of solid propellant rocket motors 13 p2001 N85-22544
Characterization standards for solid propellant rocket motors
[AD-A150250] 13 p2013 N85-22627
Alternate nozzle ablative materials program
[NASA-CR-175658] 14 p2246 N85-23924
Ignition, separation of boosters, stages in Ariane 3 14 p2289 N85-24185
A fundamental study of liquid phase particle breakup. Revision
[AD-A150791] 14 p2301 N85-24249
AFRPL (Air Force Rocket Propulsion Laboratory) technical objective document FY 85
[AD-A151368] 15 p2495 N85-25389
Analysis of combustion oscillations in heterogeneous systems
[AD-A151999] 16 p2745 N85-26942
Surveillance report. Stage 1: Dissected motors-propellants motor number 0012199, phase 15
[AD-A153206] 17 p2916 N85-27973
MM2 LRSLA testing stage 3 propellant
[AD-A152540] 17 p2937 N85-28128
Recession of graphitic nozzles in rocket motors 21 p3560 N85-32144
Verification of the SRB motor case pin retainer band tips
[NASA-CR-170882] 24 p4070 N85-35220
Results of tests on a specimen of the SRB aft skirt heat shield curtain in the MSFC LRLF
[NASA-CR-170883] 24 p4070 N85-35221
Dissected motors-propellants motor number STM-012. Phase 15: Surveillance report, stage 1
[AD-A156088] 24 p4071 N85-35226
Results of tests of K5NA and a revised formulation of EPDM/cork patch material in MSFC Hot Gas Facility
[NASA-CR-170890] 24 p4073 N85-35238
Evaluation of SRB phenolic TPS material made by an alternate vendor
[NASA-CR-170894] 24 p4073 N85-35240
Space shuttle SRB TPS protective paint test and evaluation in NASA Hot Gas Facility and AEDC Tunnel C
[NASA-CR-170884] 24 p4081 N85-35294
Results of tests of Insta-Foam Thermal Protection System (TPS) material for protection of equipment inside the SRB aft skirt
[NASA-CR-170892] 24 p4081 N85-35295

SOLID PROPELLANTS
NT CASE BONDED PROPELLANTS
NT COMPOSITE PROPELLANTS
NT DOUBLE BASE ROCKET PROPELLANTS
NT HTPB PROPELLANTS
NT NITRAMINE PROPELLANTS
NT PLASTIC PROPELLANTS
NT SOLID ROCKET PROPELLANTS
Catalyzed low burning rate propellants for upper-stage solid rocket motor
[NAL-TR-805] 03 p0339 N85-12181
Special problems of Ramjet with solid fuel 07 p0918 N85-15815
Combustion properties of fuel-rich magnesium propellants with HTPB as binder
[FOA-C-20555-D1] 07 p0935 N85-15924
Sensitivity tests for solid propellants in Germany 08 p1115 N85-17026
Modelling the thermal explosion phenomenon in solid propellants: The case of fixed and variable temperatures 08 p1117 N85-17044
Analysis of deflagration to detonation transition in high-energy solid propellants
[AD-A148302] 08 p1135 N85-17156
Investigation of the pressure-and velocity-coupled responses of solid propellants using impedance tube method 09 p1300 N85-18168
Antiplane cracks in solid propellants
[AD-P004344] 10 p1455 N85-19168
A summary of the mechanism of delayed detonation
[AD-P004347] 10 p1455 N85-19171
Curvilinear solid propellant grain
[AD-D011457] 10 p1458 N85-19183
Application of fluorescence to measurement of surface temperature in solid propellants 13 p2002 N85-22548
The crystal and molecular structure of a new propellant compound: Triaminoguanidium Azide Nitrate (TAZN) 13 p2002 N85-22551
Non-steady combustion of composite solid propellants
[AD-A150827] 14 p2250 N85-23947
A two-step bomb to determine the inflammability of propellant charge powders
[ISL-CO-211/83] 14 p2264 N85-24026
Components of the combustion gases of propellant charge powders after reaction in the high pressure bomb in the pressure range up to 1000 MPa. Part 1: Nitroglycerine powder GB Pa 125
[ISL-CO-217/83-PT-1] 14 p2264 N85-24027
Technical instructions for a control operating system of the gas flow installation for the solid fuel combustion chamber
[VTH-LR-410] 18 p3118 N85-29302
Closed-bomb combustion of Hivelite-based, Very High Burn Rate (VHBR) propellant
[AD-A155740] 21 p3571 N85-32212

SOLID ROCKET BINDERS
Study of HTPB-based SOFRAM fuels
[FOA-C-20563-D3] 11 p1614 N85-20150
Amine salts as bonding agents
[AD-D011543] 12 p1817 N85-21396

SOLID ROCKET PROPELLANTS
NT DOUBLE BASE ROCKET PROPELLANTS
NT HTPB PROPELLANTS
A model for grain misalignment in cylindrical port motors
[AD-A144856] 01 p0034 N85-10210
Combined cycle ramjet engine
[AD-D011247] 06 p0760 N85-14859
An optical and mass spectrometric study of the aluminum-oxygen flame
[AD-A147434] 07 p0923 N85-15849
Thermophysical property testing using transient techniques
[AD-A147085] 07 p1049 N85-16864
Combustion dynamics in rockets
[AD-A148478] 08 p1114 N85-17024
Hazard Studies for Solid Propellant Rocket Motors
[AGARD-CP-367] 08 p1114 N85-17025
Aims and requirements of NATO group AC/310 08 p1114 N85-17026
Review of USAF treatment of solid propellant rocket motor hazards 08 p1114 N85-17027
Analysis of Deflagration to Shock to Detonation Transition (DSDT) in porous energetic solid propellants 08 p1115 N85-17030
Some aspects of the micromechanics of hot spot formation in energetic materials 08 p1116 N85-17036
Shock and impact response of solid rocket propellants: Experimental and theoretical 08 p1116 N85-17040
Ballistic/detonic transition of propellants 08 p1117 N85-17041
The heat sensitivity of solid propellants 08 p1117 N85-17043
The pressure deflagration limit of solid rocket propellants 08 p1117 N85-17046
Fuel-rich solid propellant boron combustion
[AD-A148522] 08 p1136 N85-17157
Recovery of damaged solid propellants by interrupting burning and crack-propagation processes
[AD-P004343] 10 p1455 N85-19167
Transition to detonation from rapid-compression (ramp-waves) generated in a burning porous bed
[AD-P004345] 10 p1455 N85-19169
Measurement of shock induced reaction in rocket propellants by nanosecond infrared radiometry and photography
[AD-P004349] 10 p1456 N85-19173
Analysis of Shock to Detonation Transition (SDT) of porous high energy propellant from ramp-wave compression loading
[AD-A149333] 10 p1457 N85-19180
Azido nitramino ether containing solid propellants
[AD-D011511] 12 p1816 N85-21392
Plasticizer system for propellant compositions
[AD-D011514] 12 p1817 N85-21393
Investigation of the characteristics of the velocity-coupled response functions of solid propellants 13 p2001 N85-22540
Comparisons of solid propellant with instability predictions and motor firing experience 13 p2001 N85-22541
Distributed combustion: A mechanism of acoustic suppression 13 p2001 N85-22543
Chemical kinetics of gas phase decomposition products of nitramine propellants 13 p2003 N85-22558
An apparatus for sizing particulate matter in solid rocket motors
[AD-A151282] 15 p2495 N85-25388
Analysis of combustion oscillations in heterogeneous systems
[AD-A151999] 16 p2745 N85-26942
Analysis of deflagration to detonation transition in high-energy solid propellants 16 p2757 N85-27010
Surveillance report. Stage 1: Dissected motors-propellants motor number 0012199, phase 15
[AD-A153206] 17 p2916 N85-27973
Holographic investigation of solid propellant combustion in a two-dimensional motor
[AD-A153546] 18 p3070 N85-29089
Propellant plasticizer
[AD-D011501] 20 p3434 N85-31306

SOLID ROTATION
U ROTATING BODIES

SOLID SOLUTIONS
Determining composition in surface region of semiconductor crystals by method of sudden changes in X-ray photoelectric effect 02 p0267 N85-11746
Producing semiconductor materials by superfast cooling of melt 03 p0354 N85-12274
Investigation of the isothermal precipitation behavior of nickel-base alloys using electrochemical phase extraction
[JUEL-1903] 05 p0619 N85-13958
Defective nature of the crystalline lattice of nickel ferrite-based solid solutions
[BLL-TRANS-WH-595-(9091.9F)] 10 p1439 N85-19068
Solution growth facility, phase A design study, executive summary — EURECA
[RPT/SGF/00014/TER] 11 p1591 N85-20006
Investigation of vanadium solid solution and zeta phase regions of vanadium-carbon system
[DE85-002678] 11 p1605 N85-20092
Solid sorbent air sampler
[NASA-CASE-MSC-20653-1] 11 p1636 N85-20301
Dissolution of solid solutions in absence of internal mass transfer
[BLL-M-36092-(5828.4)] 16 p2748 N85-26959
The precipitation mechanism in a metallic solid solution crystal: Case of the aluminum-copper and aluminum-silver systems
[DE85-009981] 18 p3077 N85-29032
Solids mixing in a three phase fluidized bed containing spherically shaped-porous solid particles
[PB85-187961] 22 p3785 N85-33453
Cluster variation study of coherent ordering in FCC and BCC solid solutions
[AD-A156039] 24 p4079 N85-35280

SOLID STATE
Synthesis and characterization of advanced materials
[PB84-215326] 01 p0025 N85-10155
Report on research results in solid state nuclear physics, 1960-1962
[JUEL-SPEZ-250] 03 p0422 N85-12696
Investigations on low-dimensional solid state substances — solitons 03 p0426 N85-12720
Investigation of solid state problems using the hyperfine interaction between static and dynamic internal fields with short live excited probe nuclei 03 p0428 N85-12729
Solid state investigations with nuclear physics methods 03 p0428 N85-12731
Utilization of a tandem accelerator for the investigation of solid state properties by means of heavy ions 03 p0429 N85-12733
Fast ions as probes in solid state research 03 p0430 N85-12740
X-ray and neutron scattering and X-ray spectroscopy for the study of defects in solid state materials 03 p0430 N85-12741
Neutron scattering on macromolecular solid state materials, solutions and melts 03 p0431 N85-12747
Neutron scattering for the investigation of solid state materials, utilization in chemical structures 03 p0432 N85-12752
Nonthermal mechanism for laser annealing of semiconductors and formation of super structure 04 p0487 N85-13109
Solid state research
[AD-A147840] 08 p1225 N85-17714
Synthesis chemistry of ceramics by solid-state combustion processes in micro-gravity
[DE85-009595] 18 p3081 N85-29081

Solid State Division report on its mission-oriented basic research
[DE85-008766] 19 p3376 N85-30941
SSMIR (Solid State Memory Instrumentation Recorder): A new approach to acquiring data during an aircraft seat/sled ejection sequence
[AD-A154780] 21 p3589 N85-32308
A solid-state framework for terrestrial upper mantles 22 p3956 N85-33878
Solid state high power amplifier for driving the SLC injector klystron
[DE85-013063] 24 p4090 N85-35356
State-of-the-art of solid-state motor controllers
[TIS5-009674] 24 p4162 N85-35808
Ionic crystals
[DE85-009462] 24 p4163 N85-35809

SOLID STATE DEVICES
NT AVALANCHE DIODES
NT BIPOLAR TRANSISTORS
NT CHARGE COUPLED DEVICES
NT CHARGE INJECTION DEVICES
NT CHARGE TRANSFER DEVICES
NT CMOS
NT FIELD EFFECT TRANSISTORS
NT GALLIUM ARSENIDE LASERS
NT GERMANIUM DIODES
NT HETEROJUNCTION DEVICES
NT HOMOJUNCTIONS
NT JFET
NT JUNCTION DIODES
NT JUNCTION TRANSISTORS
NT LIGHT EMITTING DIODES
NT METAL OXIDE SEMICONDUCTORS
NT MIM (SEMICONDUCTORS)
NT MIM DIODES
NT MIS (SEMICONDUCTORS)
NT MULTISPECTRAL LINEAR ARRAYS
NT PHOTODIODES
NT PHOTOTRANSISTORS
NT PHOTOVOLTAIC CELLS
NT RUBY LASERS
NT SCHOTTKY DIODES
NT SEMICONDUCTOR DEVICES
NT SEMICONDUCTOR LASERS
NT SILICON CONTROLLED RECTIFIERS
NT SILICON TRANSISTORS
NT SIS (SEMICONDUCTORS)
NT SOLID STATE LASERS
NT THERMISTORS
NT THYRISTORS
NT TRANSISTOR AMPLIFIERS
NT TRANSISTORS
NT VARACTOR DIODES
NT VARISTORS
NT YAG LASERS

Workshop on the Use of Future Multispectral Imaging Capabilities for Lithologic Mapping: Workshop summary 02 p0214 N85-11413
USSR report: Electronics and electrical engineering
[JPRS-UEE-84-014] 03 p0344 N85-12215
The 30 GHz solid state amplifier for low cost low data rate ground terminals
[NASA-CR-174795] 03 p0358 N85-12300
High-speed videography for optical and X-ray imaging
[DE84-012981] 04 p0564 N85-13595
High or low-side solid state relay with current limiting and operational testing
[AD-D011260] 05 p0631 N85-14046
Electronics research at the University of Texas at Austin
[AD-A146000] 07 p0947 N85-15998
Basic research in electronic (JSEP): Joint Services Electronics Program
[AD-A147891] 07 p0948 N85-16007
Solid state research
[NASA-CR-174285] 07 p1048 N85-16856
Photometry with Multi-Anode Microchannel Arrays (MAMAs) and Charge Injection Devices (CIDs)
08 p1252 N85-17909
Filter reflection image guide oscillator and solid state line scanning device
[AD-D011440] 10 p1479 N85-19336
Optical mark reader
[AD-D011462] 10 p1557 N85-19818
A new very high voltage semiconductor switch
[NASA-TM-86957] 11 p1627 N85-20246
Solar energy converter using surface plasma waves
[NASA-CASE-LEW-13827-1] 12 p1876 N85-21768
Semiconductor materials for high frequency solid state sources
[AD-A150020] 12 p1940 N85-22186
Research in the optical sciences
[AD-A150198] 13 p2159 N85-23401
Further developments of CCD line array telecine
[BBC-RD-1985/3] 14 p2293 N85-24217
Basic research in electronics (JSEP)
[AD-A151002] 14 p2296 N85-24230
Annual report on electronics research at the University of Texas at Austin
[AD-A150836] 14 p2415 N85-24901
Development of solid state infrared emitters for gas detection applications
[PB85-148450] 15 p2561 N85-25800
NASA welding assessment program
[NASA-CR-175683] 15 p2568 N85-25845
An advanced solid state pressure transducer for high reliability SSME application 16 p2739 N85-28905
Technology development for thin-film-trace humidity sensors
[BMFT-FB-T-84-268] 17 p2969 N85-28336
Proceedings of the 14th European Solid State Device Research Conference Including Solid State Device Technology, ESSDERC 84
[AD-A153409] 18 p3193 N85-29804
Joint services electronics program
[AD-A154348] 19 p3375 N85-30939
An absolute calibration of the solid state detectors in the narrow band neutrino beam at CERN
[NIKHEF-H/84-10] 20 p3536 N85-32017
Experiments on the influence of active walls on the initial amplitudes and growths of instability waves
[AD-A154630] 21 p3583 N85-32275
Solid state research
[AD-A154783] 21 p3709 N85-33025
TEMO and TEB thermoelectronic devices 22 p3779 N85-33415

SOLID STATE LASERS
NT GALLIUM ARSENIDE LASERS
NT RUBY LASERS
NT YAG LASERS

Peripheral vision displays: The future 01 p0009 N85-10058
Solar-pumped lasers: A review 02 p0261 N85-11711
Optimization of ultrashort pulse generation mode of YAG laser 02 p0262 N85-11713
Improved solid-state laser sources, volume 2
[DE85-000759] 09 p1325 N85-18330
Modern solid state laser materials
[DE85-003665] 10 p1490 N85-19410
Potential of high-average-power solid state lasers
[DE85-003684] 11 p1639 N85-20329
Autostochastic behavior of solid state ring laser with low frequency periodic loss modulation 11 p1717 N85-20805
Advanced crystalline laser materials
[DE85-003142] 12 p1857 N85-21647
Low jitter trigger for an excimer laser
[DE85-005732] 13 p2097 N85-23060
Research progress on laser crystals in China 13 p2166 N85-23440
Submillimeter-band solid state distributed feedback laser 15 p2644 N85-26307
Spectroscopic investigation of materials for tunable infrared lasers
[AD-A154124] 19 p3272 N85-30291
Pulsed lasers for filming color holographic film images 22 p3781 N85-33426
Trivalent cerium doped crystals as tunable laser systems: Two bad apples
[DE85-008168] 22 p3790 N85-33482

SOLID STATE PHYSICS
USSR report: Physics and mathematics
[JPRS-UPM-84-006] 02 p0256 N85-11676
Research in the theory of condensed matter and elementary particles
[DE85-010447] 20 p3531 N85-31968

SOLID SURFACES
NT CRYSTAL SURFACES

Simulation of contact surface erosion for impact problems 01 p0060 N85-10398
Electron spin polarization effects in low energy electron diffraction, ion neutralization and metastable atom deexcitation at solid surfaces
[DE84-016550] 04 p0572 N85-13849
Macrocyclic poly(tertiary) phosphines for the attachment of metals to surfaces of photodevices
[DE84-015552] 05 p0617 N85-13946
Ion emission from solid surfaces: Comparison of dust impact with other excitations -- Giotto mission 14 p2244 N85-23912
Investigation to optimize the passive shock wave/boundary layer control for supercritical airfoil drag reduction
[NASA-CR-175788] 16 p2699 N85-26665
Theory of laser-stimulated surface process. 2: A generalized-master-equation approach to energy transfer between an IR laser, an aspecties and phonons
[AD-A153083] 17 p2970 N85-28344
Statistical mechanics of adsorption and wetting
[DE85-010093] 19 p3269 N85-30271
Effects of laser radiation on surfaces and coatings
[DE85-010475] 22 p3790 N85-33484
Unsteady transonic heat transfer in a transient facility
[NASA-CR-176145] 23 p3930 N85-34354
System maintenance manual for master modeling of aerodynamic surfaces by three-dimensional explicit representation
[NASA-CR-178224] 23 p3956 N85-34517
The dynamics of articulated rigid bodies for purposes of animation 23 p3965 N85-34579

SOLID SUSPENSIONS
Transport properties of multiphase systems
[DE84-015560] 02 p0173 N85-11159
Characteristics of charge transfer in the dispersed phase of electrorheological suspensions
[RAE-TRANS-2125] 19 p3233 N85-30040

SOLID WASTES
Immobilization of toxic waste by embedding it in bitumen
[OEFZS-4277] 07 p0995 N85-16322
FAA policy regarding solid waste disposal facilities
[AD-P004196] 11 p1581 N85-19963
Airport bird hazards associated with solid waste disposal facilities
[AD-P004197] 11 p1581 N85-19964
Field lysimeter facility for evaluating the performance of commercial solidified low-level waste
[DE85-003686] 11 p1727 N85-20663
Large-scale commercial combustion systems for producing energy from municipal solid waste
[DE85-007097] 15 p2587 N85-25946
Measurement of radionuclides in waste packages
[DE85-011674] 22 p3838 N85-33766
Multi-solute subsurface transfer modeling for energy solid wastes: Highlights FY 1984
[DE85-012788] 23 p3966 N85-34591

SOLID-SOLID INTERFACES
Simulation of contact surface erosion for impact problems 01 p0060 N85-10398
Evaluation of interfacial stresses from the amplitude of reflected ultrasonic signal
[DE84-015472] 02 p0276 N85-11798
Electronic structure of semiconductor interfaces
[AD-A147663] 08 p1225 N85-17715
The Si/SiO2 intrinsic states and interface charges. Chapter 1: Origin, properties, models, impact
[HMI-B-413] 09 p1400 N85-18612
Study of metal oxide semiconductor structures by capacitive transient spectroscopy
[ENST-84E011] 11 p1737 N85-20926
Segregation of silicon in silumin-carbon fiber composites 13 p2028 N85-22706
Sliding interfaces with contact-impact in large scale Lagrangian computations
[DE85-006451] 15 p2639 N85-26277

SOLIDIFICATION
NT MELT SPINNING

Low-gravity solidification of cast iron and space technology applications 02 p0151 N85-11022
Directional solidification of flake and nodular cast iron during KC-135 low-g maneuvers 02 p0154 N85-11040
Containerless drop tube solidification and grain refinement of NiAl3 02 p0154 N85-11042
Solidification and crystal growth of solid solution semiconducting alloys 02 p0155 N85-11046
Design and implementation of a low-gravity solidification experiment package for the F-104 02 p0156 N85-11053
A method for evaluating the contamination of steel in relation to the solidification curve
[BLL-M-35735-(5826.4)] 02 p0175 N85-11171
Rapid solidification processing and the control of structure/property relationships 02 p0176 N85-11178
Rapid solidification of steels: Model and commercial alloys 02 p0176 N85-11184
The structure of rapidly solidified nickel-base alloys 02 p0181 N85-11215
Biform resolidification and amorphous phases in a laser and electron beam processed tantalum-iridium alloy
[DE84-013334] 02 p0184 N85-11234
Studies of laser melting and rapid solidification using amorphous silicon
[DE84-014737] 02 p0202 N85-11345
European Scientific Notes, Number 38-9
[AD-A145883] 02 p0306 N85-11975
Weld metal solidification cracking in a carbon-manganese steel 03 p0330 N85-12126
Application of solidification theory to rapid solidification processing
[AD-A145953] 03 p0331 N85-12136
Critical dynamics for continuous rapid solidification processing
[AD-A146071] 03 p0332 N85-12137

NBS (National Bureau of Standards): Materials measurements
[NASA-CR-174038] 03 p0332 N85-12143
Microstructure of ceramics fabricated by unidirectional solidification
[NASA-TM-77423] 03 p0336 N85-12157
The Al-Be system: The effects of RSP on structure and phase relating
[DE84-015604] 04 p0474 N85-13019
Solidification and aging behavior of types 308 and 308CRE stainless steel welds
[DE84-016552] 04 p0476 N85-13029
Inclusion formation during solidification of steels with improved machinability
[BMFT-FB-T-84-160] 05 p0619 N85-13957
Application of solidification theory to rapid solidification processing
[AD-A146619] 06 p0769 N85-14917
Microstructure of rapidly quenched type 308 stainless steel weld filler metal and its implications on rapid solidification processes
[DE85-000930] 06 p0769 N85-14920
Time-resolved studies of ultrarapid solidification of highly undercooled molten silicon formed by pulsed laser irradiation
[DE84-016664] 06 p0813 N85-15164
Experimental and theoretical study of the formation of the 2AB, 3AB, and 9A meteorite chemical groups from the parent liquid 06 p0886 N85-15628
Investigations concerning the magmatic iron meteorites: Static vs. dynamic experiments 06 p0886 N85-15629
The growth of metastable peritectic compounds
[NASA-CR-171289] 07 p0920 N85-15824
The growth of metastable peritectic compounds
[NASA-CR-171290] 07 p0920 N85-15825
Investigation of granules of molybdenum-base alloys obtained with pulsed discharges
[BLL-M-36012-(5828.4)] 07 p0926 N85-15871
SPAR X technical report for experiment 76-22 directional solidification of magnetic composites
[NASA-CR-171271] 07 p0927 N85-15880
Analysis of the heating process of a body in a melt
[BLL-M-36014-(5828.4)] 07 p0956 N85-16057
Grain refining and microstructural modification during solidification
[AD-A147705] 08 p1126 N85-17111
Rapid solidification processing and powder metallurgy of Al alloys
[AD-A146427] 08 p1130 N85-17120
The growth of large diameter single crystals by vertical solidification of the melt
[AD-A148756] 09 p1397 N85-18792
The feasibility of low-G grey solidification of nodular iron in the F-104 experimental furnace package
[NASA-TM-82527] 10 p1426 N85-18998
Research on rapidly solidified alloys
[AD-A149380] 10 p1441 N85-19060
1984 model of binary alloy solidification
[DE85-002497] 11 p1608 N85-20110
Hot melt adhesive attachment pad
[NASA-CASE-LAR-12894-1] 11 p1610 N85-20125
Laser processing of ceramics
[DE85-001184] 11 p1612 N85-20135
Research in surface sciences, disordered materials, and solidification and growth
[PB85-132140] 11 p1737 N85-20927
Experimental determination of systems suitable for study as monotectic binary metallic alloy solidification models 12 p1948 N85-22235
Rapid solidification processing of magnesium alloys
[AD-A150270] 13 p2022 N85-22668
Time-resolved studies of rapid solidification in highly undercooled molten silicon
[DE85-004857] 13 p2038 N85-22765
Dopant incorporation in silicon during nonequilibrium solidification: Comparison of 2 processes
[DE85-005568] 14 p2430 N85-24988
Microstructural characteristics during the controlled solidification of a binary system
[DE85-005200] 15 p2507 N85-25461
Application of solidification theory to rapid solidification processing
[AD-A151251] 15 p2509 N85-25480
Metallurgical characterization of aluminum powder consolidation
[AD-A151990] 15 p2510 N85-25484
Sweden develops new rapid solidification process 15 p2531 N85-25610
Microstructures and properties of rapidly solidified alloys
[NASA-CR-172377] 16 p2748 N85-26961
Rapid solidification of candidate ferritic steels
[DE85-006596] 16 p2750 N85-26971
Use of principle of local equilibrium for assessing diffusional supersaturation during solidification of alloys
[BLL-BISI-TRANS-22467-(9022.06)] 17 p2929 N85-28077
Investigation for low-cost permanent magnets
[AD-A154387] 19 p3260 N85-30212
Consolidated fuel reprocessing program
[DE85-006750] 19 p3366 N85-30671
Linking R and D to problems experienced in solids processing
[AD-A154238] 19 p3360 N85-30968
Concept development evaluation for John Deere/UA STS middeck experiment location
[NASA-CR-171541] 20 p3397 N85-31071
Directional solidification of an eutectic Bi-MnBi alloy
[BLL-M-36270-(5828.4)] 20 p3430 N85-31275
MPS solidification model. Analysis and calculation of macrosegregation in a casting ingot
[NASA-CR-171589] 21 p3568 N85-32178
Polyethylene solidification of low-level wastes
[DE85-012568] 22 p3843 N85-33799
Approximate determination of the extent of the solid-liquid zone
[BLL-M-35829-(5828.4)] 23 p3914 N85-34251
Microstructures in rapidly solidified Ni-Mo alloys
[NASA-TM-87100] 23 p3915 N85-34266
Method for making a low density polyethylene waste form for safe disposal of low level radioactive material
[DE85-006401] 23 p3920 N85-34292

SOLIDIFIED GASES
Understanding the high pressure properties of molecular solids and molecular surfaces deposited on hetrogeneous substrates
[NASA-CR-174262] 07 p1047 N85-16649

SOLIDS
NT SOLIDIFIED GASES
NT THREE DIMENSIONAL BODIES
Synthesis and characterization of advanced materials
[PB84-215326] 01 p0025 N85-10156
13C and 1H NMR (Nuclear Magnetic Resonance) studies of solid polyolefines
[AD-P003909] 01 p0032 N85-10195
NMR (Nuclear Magnetic Resonance) of solid biopolymers
[AD-P003912] 01 p0032 N85-10198
Halfspace representations of extrusions, solids of revolution and pyramids
[DE84-015005] 01 p0104 N85-10700
Finite element analysis of thermoelasticity problems 02 p0208 N85-11369
Mechanism of brittle heat fracture of inhomogeneous solids by high temperature gas jets 02 p0265 N85-11731
Nonlinear acoustics
[AD-A145580] 02 p0276 N85-11796
Constitutive features of solids at shock-wave loading rates
[DE84-015715] 03 p0362 N85-12325
On the co-variant formulation of the law of motion of passive particles in a field of turbulence
[REPT-584] 03 p0377 N85-12407
EXAFS and Moessbauer study of small metal clusters isolated in rare-gas solids
[DE84-015978] 04 p0470 N85-12994
Diffusion of gases in porous solids: Simulation and measurements
[DE84-016292] 04 p0500 N85-13191
High resolution photoacoustic and photothermal imaging 05 p0723 N85-14849
Laser excitation of coupled surface electromagnetic and acoustic waves and of static structures in solids 05 p0723 N85-14852
Measurement of scattering cross sections of liquid and solid hydrogen deuterium and deuterium hydride for thermal neutrons
[DE84-014814] 05 p0727 N85-14671
The concept of solid solvent as processing aid
[AD-A146556] 06 p0771 N85-14934
Transonic flow of elastic medium past slender solid body 06 p0776 N85-14976
Controllable rotation of system of two solid bodies with elastic elements 06 p0780 N85-14988
Motion of heavy symmetric body with flexible bars about stationary point 06 p0780 N85-14989
Theory of harmonic generation of finite amplitude ultrasonic waves in solids of hexagonal symmetry
[AD-A146636] 06 p0880 N85-15465
Optics of solids (surface related) and effect of surface roughness on MOS
[AD-A146883] 07 p0946 N85-15996
A virial equation of state option for the TIGER computer program
[AD-A147490] 07 p1025 N85-16507
Structure of solids surfaces in wear situations
[AD-A148480] 08 p1188 N85-17366
NMR study on rotational fluctuation in solid hydrogen and deuterium 09 p1289 N85-18093
Spontaneous ignition of organic solids by radiant heating 09 p1289 N85-18096
Measurement and control of electrostatic charges on solids in a gaseous suspension
[DE85-001450] 09 p1291 N85-18105
USSR report: Engineering and equipment
[JPRS-UEQ-85-001] 09 p1305 N85-18200
Electromagnetic processing of materials
[AD-A148604] 09 p1311 N85-18241
Stopping powers of solids for low-energy protons
[DE85-001123] 09 p1362 N85-18693
Transport relaxation processes in supercritical fluids
[DE85-002076] 09 p1386 N85-18798
Microscopic determinations of lattice and electronic structures of solids
[DE84-017323] 09 p1399 N85-18806
Theta pinch discharges for solids vaporization and elemental chemical analysis
[DE85-002966] 11 p1733 N85-20699
Explorations into thermodynamics analogies and critical points in reference to gas-solid transport
[DE85-000616] 11 p1736 N85-20829
Photoacoustic effect and its applications 12 p1820 N85-21421
Moving nonlocal crack: Anti-plane shear case
[AD-A149996] 12 p1866 N85-21709
A study of the compatibility of an existing CFD package with a broader class of material constitutions 12 p1945 N85-22219
Division boundary in Al-B composite material with boron in contact with solid and liquid aluminum 13 p2027 N85-22704
USSR report: Engineering and equipment
[JPRS-UEQ-85-003] 13 p2042 N85-22782
Some problems in optimally designing shells of revolution 14 p2278 N85-24114
X-ray emission in heavy ion collisions
[DE85-006350] 14 p2419 N85-24927
Theory and calculations of the electronic structure of solids having directional bonding
[AD-A151062] 14 p2428 N85-24971
Energy trapping, release, and transport in three-dimensional energetic solids and molecular crystals: Theory of defects and impurities
[AD-A151071] 14 p2428 N85-24973
Chaotic dynamics of instabilities in solids
[DE85-004909] 14 p2429 N85-24978
X-ray spectroscopy of solids under pressure
[DE85-006699] 15 p2507 N85-25465
Summary of recent investigations of the mechanical properties of polycrystalline solids
[DE85-006776] 15 p2511 N85-25492
Optical monitoring of photo-acoustic pulse propagation in silicon wafers
[AD-A151333] 15 p2651 N85-26352
Secondary ion mass spectrometry studies of solids and surfaces
[AD-A151744] 16 p2745 N85-26939
Bound and free moisture studies of solid materials by FTNMR
[DE85-003227] 16 p2747 N85-26952
Numerical resolution calculation for elastic-plastic impact problems
[AD-A152292] 16 p2801 N85-27270
Transverse periodic boundary conditions in molecular dynamics with uniaxial strain shock waves
[DE85-008497] 16 p2863 N85-27656
Experiments on sorption characteristics of solid desiccant materials for solar desiccant cooling systems
[DE85-000542] 17 p2923 N85-29019
Free-form design in solid modelling 17 p3004 N85-29589
Boundary to constructive solid geometry mappings: A focus on 2-D issues 17 p3004 N85-29570
A unified representation scheme for solid geometric objects using B-splines (extended abstract) 17 p3006 N85-29585
Diffusion of gases in porous solids: Simulation and measurements
[DE85-008870] 18 p3101 N85-29196
Studies of strain rate effects in the deformation of solids by means of stress pulses and ultrasonic methods
[DE85-009463] 18 p3122 N85-29329
Resolution at its current limit: Applications of the Berkeley ARM
[DE85-009959] 19 p3274 N85-30301
Energy transfer and excimer formation in rare gas solids 19 p3374 N85-30930
Vibrational properties of disordered solids: Far infrared studies
[DE85-010400] 19 p3377 N85-30951
Linking R and D to problems experienced in solids processing
[AD-A154238] 19 p3360 N85-30968

Constitutive modeling of superalloy single crystals and directionally solidified materials
20 p3466 N85-31535
The interactions of composition and stress in crystalline solids
[PB85-179075] 20 p3473 N85-31583
Source characterization of point-like and distributed sources of acoustic emission 20 p3523 N85-31910
X-ray spectroscopy of solids under pressure
[DE85-011486] 22 p3745 N85-33213
Preliminary considerations for the gasdynamic precompression of solid molecular hydrogen
[DE85-013256] 22 p3784 N85-33445
SANCHO: A finite element computer program for the quasistatic, large deformation, inelastic response of two-dimensional solids
[DE85-011456] 22 p3829 N85-33714
Experimental technique for measuring the isentrope of hydrogen to several megabars
[DE85-014332] 24 p4095 N85-35366
Analysis of the nonlinear equations describing the elastic, thermal, and electromagnetic behavior of solids: Existence of solutions of semi-inverse problems
24 p4100 N85-35415

SOLIDS FLOW
Granular Flow Project
[DE85-010015] 19 p3270 N85-30279
Effect of nonuniform size on internal stresses in a rapid, simple shear flow of granular materials. Part 2: Multiple grain sizes
[AD-A154046] 19 p3285 N85-30373

SOLIDUS
Studies on copper alloys containing chromium on the copper side phase diagram
[NASA-TM-77752] 07 p0927 N85-15876

SOLITARY WAVES
Statistical Plasma Physics. Proceedings of the Workshop of the US-Japan Joint Institute for Fusion Theory Program
[IPPJ-699] 02 p0282 N85-11C32
Stochastic property of K-dV solitons perturbed by random forces — Korteweg-Devries equation
02 p0283 N85-11843
Chaotic behavior induced by solitons in perturbed integrable systems 02 p0283 N85-11844
Investigations on low-dimensional solid state substances — solitons 03 p0426 N85-12720
Solitons and SEASAT
[AD-A148396] 08 p1176 N85-17414
Mathematical physics approaches to lightning discharge problems
[NASA-TM-86349] 08 p1187 N85-17482
Determination of gravity wave envelope solitons on surface of stratified fluid interacting with wind
14 p2334 N85-24433
Propagation of sound in matter
[AD-A151052] 14 p2416 N85-24908
Soliton energetics in extended Peierls-Hubbard models: A quantum Monte Carlo study
[DE85-005409] 14 p2429 N85-24981
Wave propagation in density stratified fluids
16 p2781 N85-27162
Coherent state description of non-topological solitons and momentum projection
[DE85-007814] 17 p3033 N85-28761
Pattern selection and instability in nonlinear wave equation: An aspect of soliton and chaos
[DE85-009578] 18 p3101 N85-29197
Electromagnetic solitary waves in magnetized plasmas
[DE85-010084] 18 p3190 N85-29788
Theory of soliton waves
[AD-A154784] 21 p3676 N85-32837

SOLITONS
U SOLITARY WAVES

SOLSTICES
Seasonal variations in Triton's atmospheric mass and composition 02 p0301 N85-11948

SOLUBILITY
Effect of toluene on the solubility of biohazardous volatile synthetic organic compounds
[AD-A145188] 01 p0018 N85-10109
An investigation of the solubility and diffusivity of chromium in gallium arsenide
[AD-A144849] 01 p0024 N85-10148
The determination of soluble and insoluble boron in steel by emission spectrometry using an inductively coupled plasma and a scanning monochromator
02 p0180 N85-11211
The behaviour of unstable surfaces: A literature review
[CFD/84/6] 02 p0199 N85-11329
Americium thermodynamic data for the EQ3/6 database
[DE84-017085] 04 p0573 N85-13656
Bicomponent flow problems in rheological fluid mechanics 05 p0635 N85-14073
Transport and relaxation processes in supercritical fluids
[DE84-006591] 05 p0731 N85-14696
Reciprocal solubility of phases in multi-component systems
[BLL-M-36003-(5626.4)] 07 p0926 N85-15870
Studies on copper alloys containing chromium on the copper side phase diagram
[NASA-TM-77752] 07 p0927 N85-15876
SPAR X technical report for experiment 76-22 directional solidification of magnetic composites
[NASA-CR-171271] 07 p0927 N85-15880
Properties of miscible polymer blends
[AD-A147090] 07 p0931 N85-15903
Transport and relaxation processes in supercritical fluids
[DE85-002079] 09 p1398 N85-18797
Transport relaxation processes in supercritical fluids
[DE85-002076] 09 p1398 N85-18798
Vapor pressure studies of the solubilization of hydrocarbons by surfactant micelles
[DE85-004316] 12 p1803 N85-21306
Alloy development, processing and characterization of devitrified titanium base microcrystalline alloys
[AD-A140609] 12 p1806 N85-21327
Application of solidification theory to rapid solidification processing
[AD-A151251] 15 p2509 N85-25480
Method for growth of crystals by pressure reduction of supercritical or subcritical solution
[NASA-CASE-NPO-15772-1] 18 p3192 N85-29800
Microstructures and mechanical properties of microalloyed medium carbon steels
19 p3238 N85-30074
Adhesive evaluation of LARC-TPI and a water-soluble version of LARC-TPI
[NASA-TM-86428] 19 p3248 N85-30136
Advanced fuel cell development
[DE85-009662] 19 p3306 N85-30497
Transport and relaxation processes in supercritical fluids
[DE85-010554] 19 p3358 N85-30816
Development of an impact- and solvent-resistant thermoplastic composite matrix, phase 3
[NASA-CR-172566] 20 p3422 N85-31239
Bubble dynamics in polymer solutions undergoing shear
[AD-A154575] 21 p3566 N85-32193
Measurements of the critical supersaturation of 0.029 to 0.095 micron radius particles at Washington, District of Columbia 21 p3649 N85-32676
Stability of two-dimensional immiscible flow to viscous fingering
[DE85-011403] 23 p3931 N85-34364

SOLUTES
Interaction of solutes with stretched polymers
[AD-A154662] 21 p3589 N85-32196

SOLUTION
Electrochemistry of polymer films not immersed in solution: Electron transfer on an ion budget
[AD-A152989] 17 p2920 N85-27998

SOLUTIONS
NT AQUEOUS SOLUTIONS
NT GAS MIXTURES
NT NUCLEAR EMULSIONS
NT PHOTOGRAPHIC EMULSIONS
NT SOLID SOLUTIONS
Dynamics of polymers in solution and melts
[AD-P003907] 01 p0032 N85-10193
NMR (Nuclear Magnetic Resonance) and macromolecular migration in a melt or in concentrated solutions
[AD-P003908] 01 p0032 N85-10194
A perturbation solution for rigid dumbbell suspensions in steady shear flow
[AD-A144876] 01 p0111 N85-10755
Factor analysis applied to a silane coupling agent on E-glass fiber system
[AD-A145687] 02 p0187 N85-11249
Thermomechanical cracking in layered media from moving friction load
[AD-A146022] 03 p0373 N85-12379
Homomonotone games and monocore solutions, revised
[AD-A146216] 03 p0413 N85-12645
Neutron scattering on macromolecular solid state materials, solutions and melts 03 p0431 N85-12747
Fatal hemorrhagic shock and acetate solutions
[AD-A146754] 07 p1014 N85-16444
On existence and uniqueness of solutions of Hamilton-Jacobi equations
[AD-A147597] 07 p1033 N85-16560
Periodic solutions of prescribed energy for a class of Hamiltonian systems
[AD-A149487] 10 p1548 N85-19764
Rheology of dissemination
[AD-A150006] 12 p1813 N85-21373
A method of calculating periodic solutions of second order dynamical systems
[AD-A149634] 12 p1920 N85-22058
Influence of uncompensated solution resistance upon the evaluation of rate constants for rapid electrochemical reactions
[AD-A150857] 14 p2250 N85-23942
E-beam-induced fluorescence of excimers in cryogenic solutions
[DE85-010703] 19 p3278 N85-30328
Discovery of a nonpropagating hydrodynamic soliton
[AD-A155569] 21 p3562 N85-32268
SPLINES. Their equivalence to collocation
[AD-A155250] 21 p3632 N85-32566

SOLVATION
Solvent effects upon electrochemical kinetics: Influences of interfacial solvation and solvent relaxation dynamics
[AD-A145624] 02 p0173 N85-11156
Supersonic molecular jet study of the liquid state
[AD-A147416] 09 p1379 N85-18671

SOLVENT EXTRACTION
ECUT, Energy Conversion and Utilization Technologies program: Isothermal separation processes update
[NASA-CR-175463] 10 p1433 N85-19033
ECUT, Energy Conversion and Utilization Technologies program: Technical and economic assessment of processes for the production of butanol and acetone. Phase 2: Analysis of research advances
[NASA-CR-175471] 10 p1434 N85-19034
Guest molecules in coal
[DE85-010435] 19 p3228 N85-30016
Supercritical solvent extraction of lignite to form carbonaceous chars
[DE85-010159] 19 p3229 N85-30019
Novel analytical approaches to coal beneficiation
[DE85-010437] 19 p3229 N85-30021
The mobile phase in coals: Its nature and modes of release
[DE85-011696] 19 p3230 N85-30026
TRU decontamination of high-level PUREX waste by solvent extraction using a mixed octyl(phenyl)-N,N-dibutyl-carbamoyl methylphosphine oxide/TBP/NPH (TRUEX) solvent
[DE85-010251] 19 p3235 N85-30054
Consolidated fuel reprocessing program
[DE85-010591] 19 p3358 N85-30818
Consolidated fuel reprocessing program
[DE85-008750] 19 p3368 N85-30871
Method for extracting lanthanides and actinides from acid solutions by modification of Purex solvent
[DE85-005763] 23 p3909 N85-34220
Separation of uranium from technetium in recovery of spent nuclear fuel
[DE85-006499] 23 p3972 N85-34627

SOLVENTS
NT TETRAHYDROFURAN
Solvent effects upon electrochemical kinetics: Influences of interfacial solvation and solvent relaxation dynamics
[AD-A145624] 02 p0173 N85-11156
The concept of solid solvent as processing aid
[AD-A146556] 06 p0771 N85-14934
Aspects of solvent toxicity in mixtures
[AD-P004036] 06 p0845 N85-15366
Voltammetry and coulometry with immersed thin layer electrodes. Part 1: Model for effects of solution resistivity in linear sweep voltammetry
[AD-A148655] 08 p1159 N85-17313
Nebulization reflux concentrator
[NASA-CASE-LAR-13254-1] 11 p1615 N85-20154
Process for producing tris s(n-methylamino) methylsilane
[NASA-CASE-MFS-25721-1] 12 p1799 N85-21280
Electrochemistry and electrochemical methodology in molten salts
[AD-A149613] 12 p1799 N85-21284
Research to explore the feasibility of sulfolanes as electrolytic solvents for rechargeable lithium batteries
[DE85-004345] 12 p1837 N85-21525
Noncontinuum solvent effects upon the intrinsic free-energy barrier for electron-transfer reactions
[AD-A150662] 14 p2250 N85-23943
Investigation of the structure and dynamics of electrolytes in solvents used for primary and secondary Li-batteries
[AD-A153099] 17 p2954 N85-28240
Method for growth of crystals by pressure reduction of supercritical or subcritical solution
[NASA-CASE-NPO-15772-1] 18 p3192 N85-29800
Electrochemical studies in liquid crystals
[AD-A154317] 19 p3234 N85-30050

Comparison of TT-F-1098 solvent-thinned block fillers with water-thinnable block fillers
[AD-A154207] 19 p3249 N85-30142
Working with flammable solvents, thinners, paints and adhesives
[HSE-TRANS-11086] 19 p3250 N85-30154
Soil extraction kit
[AD-D011736] 22 p3742 N85-33190
Rechargeable lithium-organic electrolyte battery having overcharge protection and method of providing overcharge protection for a lithium-organic electrolyte battery
[AD-D011738] 22 p3806 N85-33575
Organic solvent alteration of hydraulic properties of sedimentary rocks of low permeability: A review
[DE85-012537] 22 p3815 N85-33635
Production of butanol by fermentation in the presence of cocultures of clostridium
[NASA-CASE-NPO-16203-1] 24 p4071 N85-35227

SOMMERFELD WAVES
Image theory for a vertical electric dipole above a wire grid with square cells
[REPT-S-150] 02 p0192 N85-11286
General image theory for the Sommerfeld problem
[REPT-S-154] 02 p0193 N85-11289

SONAR
Detection, classification, and extraction of helicopter-radiated noise
[AD-A145993] 03 p0416 N85-12661
Color and grey scale in sonar displays
05 p0710 N85-14552
Research on nondestructive testing
[AD-A148375] 06 p1171 N85-17380
Technology development for unmanned untethered submersible vehicle systems
[AD-A148794] 09 p1304 N85-18190
Sonars with high noise and clutter rejection for use with adaptive robots
[AD-A151875] 15 p2543 N85-25701
An overview of stochastic signal modeling
[AD-A152144] 16 p2855 N85-27605
HERMIES-1: A mobile robot for navigation and manipulation experiments
[DE85-006852] 18 p3118 N85-29301
Effect of background/foreground color coding on detection in acoustic data displays
[AD-A154105] 19 p3352 N85-30774
The moving thermoacoustic array: A theoretical feasibility study
[AD-A154510] 21 p3699 N85-32960
Planning for VRM: Radar and sonar studies of volcanic terrains on Earth, Venus and Mars
22 p3857 N85-33684
Magnetic search system
[PB85-185108] 23 p3949 N85-34477

SONDES
NT IONOSONDES
NT RADIOSONDES
NT RAWINSONDES
Error analysis of wind determined using a VLF Omega sonde
[WSRL-0361-TM] 06 p0838 N85-15321
Cut-off lows and their influence on the weather in Switzerland
[REPT-45] 10 p1519 N85-19574

SONIC BOOMS
Correlation of predicted and measured sonic boom characteristics from the reentry of STS-1 orbiter
[NASA-TP-2475] 18 p3177 N85-29694

SONIC FLOW
U TRANSONIC FLOW

SONIC SPEED
U ACOUSTIC VELOCITY

SONOHOLOGRAPHY
U ACOUSTICAL HOLOGRAPHY

SOOT
Hot-gas cleanup for molten carbonate fuel cells-dechlorination and soot formation
[DE84-003072] 01 p0068 N85-10450
Analysis and characterization of organic carbon compounds in atmospheric particulate matter
[PB84-232636] 08 p0786 N85-14903
Mechanism of soot formation
[AD-A148617] 07 p0922 N85-15841
Investigation of fuel additive effects on sooting flames
[AD-A149154] 10 p1457 N85-19179
Ionic mechanisms of soot formation in flames
[AD-A150119] 12 p1801 N85-21297
Ideal gas thermodynamic properties for the phenyl, phenoxy, and o-biphenyl radicals
[NASA-TM-83900] 12 p1943 N85-22204
Laser diagnostic analyses of sooting flames
[AD-A150478] 13 p2017 N85-22649
A standard aircraft diffusion flame: Spectral characteristics and a feasibility study for developing an alternate calibration source for aircraft optical fire detection systems
[AD-A150231] 13 p2039 N85-22768
Effects of interactive transport and scavenging of smoke on the calculated temperature change resulting from large amounts of smoke
[DE85-006450] 14 p2378 N85-24684
Shock tube study of the fuel structure effects on the chemical kinetic mechanisms responsible for soot formation, part 2
[NASA-CR-174880] 15 p2504 N85-25444
Studies of the combustion of model fuels with low hydrogen content (pyrolysis of polycyclic aromatics-detection of soot precursors)
[DE85-005422] 15 p2521 N85-25541
An investigation into the soot production processes in a gas turbine engine
[AD-A152710] 17 p2919 N85-27992
Fuel-rich catalytic combustion: A soot-free technique for in situ hydrogen-like enrichment
[NASA-TP-2498] 20 p3423 N85-31244
An analytical and numerical model of radiation heat transfer in direct injection-type diesel combustion
24 p4092 N85-35368

SORBENTS
NT ABSORBENTS
NT ADSORBENTS
Solid sorbent air sampler
[NASA-CASE-MSC-20653-1] 11 p1698 N85-20301
Low pressure storage of methane on interlayered clays for potential vehicular applications
[DE85-006949] 18 p2758 N85-27017

SORPTION
NT ADSORPTION
NT CHEMISORPTION
Development of novel lamps for study of enhanced production of resonance by low-density mercury discharges
[DE84-016689] 05 p0632 N85-14053
Synergistic effects related to surface composition, session summary 06 p0865 N85-15495
Functional and structural changes in human erythrocyte surface after irradiation by UV waves of various wavelenghts. Report 2: Adsorption of alcyan blue by external premembranous components
09 p1361 N85-18565
Drifting ice as mechanical factor in purifying and polluting hydrosphere 13 p2108 N85-23132
Evidence that resorption of bone by rat peritonal macrophages occurs in an acidic environment
15 p2612 N85-26098
Experiments on sorption characteristics of solid desiccant materials for solar desiccant cooling systems
[DE85-000542] 17 p2923 N85-28019
Permeation of mixed penetrants through glassy polymer membranes
[AD-A155605] 21 p3570 N85-32207
Biodegradation of jet fuel by aquatic microbial communities
[PB85-191971] 24 p4084 N85-35311

SORTING
U CLASSIFYING

SOT
U SOLAR OPTICAL TELESCOPE

SOUND
U ACOUSTICS

SOUND ABSORPTION
U SOUND TRANSMISSION

SOUND AMPLIFICATION
Study of optical sound generation and amplification
[AD-A147359] 07 p1039 N85-16592

SOUND BARRIER
U ACOUSTIC VELOCITY

SOUND DETECTORS
U SOUND TRANSDUCERS

SOUND FIELDS
Element methods for calculation of sound fields
[RUB-IFM-MITT-41] 05 p0726 N85-14665
Analysis of the surface load and radiated sound of a vibrating airfoil with application to the experiment of Brooks
[NASA-CR-3884] 07 p1038 N85-16590
Optical fibers with reduced pressure sensitivity to high frequency acoustic field
[AD-D011306] 07 p1043 N85-16627
An efficient numerical solution technique for wave propagation in horizontally stratified ocean environments
[AD-A148537] 08 p1190 N85-17502
Behavior of mode frequency characteristics in shallow sea with variation of P-wave vecoity in bottom sediment layer and sonic velocity profile in water layer
10 p1498 N85-19457
USSR report: Physics and mathematics
[JPRS-UPM-85-001] 11 p1715 N85-20786
Problem of frequency space variation of sonic field in stratified media 11 p1715 N85-20787
The effects of internal waves on acoustic normal modes
[AD-A150235] 13 p2155 N85-23379
An overview of stochastic signal modeling
[AD-A152144] 16 p2855 N85-27605
The theoretical response of a vertical line array to wind-generated noise in shallow water
[AD-A151730] 16 p2860 N85-27638
Geoacoustic models: Washington state continental margin
[AD-A153781] 18 p3177 N85-29689
On the solution for the sound field in a semi-infinite uniform duct with sheared mean flow
20 p3523 N85-31912
Development of computer programs using the method of images to predict the sound field in a wedge overlaying a fast fluid and comparison with laboratory experiments
[AD-A154580] 21 p3670 N85-32787
The Konstantinov effect and absorption of sound in inhomogeneous media 21 p3680 N85-32881
The sound field of a moving laser-induced acoustic array (theory)
[AD-A154553] 21 p3699 N85-32961

SOUND GENERATORS
Generation of sound by a vortex point in a steady flow of slightly compressible fluid 11 p1715 N85-20789
Acoustic agglomeration methods and apparatus
[NASA-CASE-NPO-15466-1] 12 p1927 N85-22104
An electro-optic spatial light modulator for thermoelastic generation of programmably focused ultrasound
[AD-A152066] 15 p2646 N85-26323
Radiative-collision generation of sound in gases subjected to single-pulse optical excitation
21 p3689 N85-32920

SOUND HOLOGRAPHY
U ACOUSTICAL HOLOGRAPHY

SOUND INTENSITY
Average sound intensity decrease rule in irregular hydroacoustical waveguide 10 p1499 N85-19461
Research on the effect of noise at different times of day: Models, methods and findings
[NASA-CR-3868] 13 p2154 N85-23375
High-frequency acoustic variability in the arctic
[AD-A150560] 13 p2155 N85-23383
Contribution of tonal components to the overall loudness, annoyance and noisiness of noise: Relation between single tones and noise spectral shape
[NASA-CR-3892] 15 p2645 N85-26317
Acoustic propagation in a thermally stratified atmosphere
[NASA-CR-175787] 16 p2860 N85-27636
The Shock and Vibration Digest, volume 17, no. 1
[AD-A151051] 17 p2977 N85-28397
Sound intensity measurement
17 p2977 N85-28398
A study of interior noise levels, noise sources and transmission paths in light aircraft
[NASA-CR-172152] 19 p3360 N85-30766
Spectral methods for the estimation of acoustic intensity, energy density, and surface velocity using a multimicrophone probe 20 p3524 N85-31918

SOUND LOCALIZATION
Foreshortened short-wave scattering on artificial ionospheric inhomogeneities 14 p2340 N85-24488

SOUND MEASUREMENT
U ACOUSTIC MEASUREMENT

SOUND PERCEPTION
U AUDITORY PERCEPTION

SOUND PRESSURE
The acoustic pressure in a wedge-shaped water layer overlying a fast fluid bottom
[AD-A145517] 02 p0276 N85-11795
Determination of the pressure sensitivity of 1 inch condenser microphones
[PTB-AK-28] 05 p0633 N85-14056
An improved source model for aircraft interior noise studies
[NASA-CR-172517] 08 p1217 N85-17668
Effects of vane/blade ratio and spacing on fan noise, volume 1
[NASA-CR-174864] 10 p1553 N85-19791
Influence of pressure on speed of sound in single-phase region of stratifying mixtures 11 p1715 N85-20788
Wind tunnel acoustic study of a propeller installed behind an airplane empennage: Data report
[NASA-CR-177335] 13 p2154 N85-23377
Localization of sources of equivalent noise in fast cold jets, excited and nonexcited
[ISL-CO-201/83] 14 p2418 N85-24910
Wave description of sound propagation through stratified moving atmosphere 15 p2525 N85-25567

SOUND PROPAGATION
Nonlinear propagation in a depth-dependent ocean
[AD-A145079] 01 p0116 N85-10791

The acoustic pressure in a wedge-shaped water layer overlying a fast fluid bottom
[AD-A145517] 02 p0276 N85-11795
USSR report: Life Sciences: Biomedical and behavioral sciences
[JPRS-UBB-84-026] 04 p0543 N85-13457
Amiet shear layer correction with an additional temperature gradient considered: Nomograms for the correction of noise signatures from open jet wind tunnel tests
[DFVLR-MITT-84-11] 05 p0726 N85-14669
Long-distance propagation of infrasound in atmosphere near Earth's surface 06 p0825 N85-15238
Study of optical sound generation and amplification
[AD-A147359] 07 p1039 N85-16592
The Shock and Vibration Digest, volume 16, no. 10
[AD-A147568] 09 p1331 N85-18361
Sound transmission in ducts 09 p1331 N85-18362
Twenty-five sound propagation tests on the continental shelf between Long Island, New York and Cape Canaveral, Florida
[AD-A149869] 12 p1928 N85-22111
Intensity vectors of sound scattering by a spherical shell
[AD-A147847] 13 p2103 N85-23107
Noise measurement flight test: Data/Analyses, hughes 500 D/E helicopter
[AD-A148110] 14 p2219 N85-23758
Fundamental studies of structure borne noise for advanced turboprop applications
[NASA-CR-176737] 15 p2646 N85-26320
Sound propagation through directional internal wave fields
[AD-A151166] 15 p2646 N85-26321
The Shock and Vibration Digest, volume 17, no. 1
[AD-A151051] 17 p2977 N85-28397
Sound intensity measurement 17 p2977 N85-28398
Numerical evaluation of low frequency sound propagation in layered media
[AD-A152690] 17 p3028 N85-28728
Squid detection of acoustomagnetic effects 19 p3373 N85-30924
Amiet shear layer correction with an additional temperature gradient considered: Nomograms for the correction of noise signatures from open jet wind tunnel tests
[ESA-TT-897] 20 p3525 N85-31926

SOUND RANGING
High-frequency acoustic variability in the arctic
[AD-A150550] 13 p2155 N85-23363
Sonars with high noise and clutter rejection for use with adaptive robots
[AD-A151875] 15 p2543 N85-25701

SOUND TRANSDUCERS
NT ELECTROACOUSTIC TRANSDUCERS
NT HYDROPHONES
NT LOUDSPEAKERS
NT MICROPHONES
Acoustic imaging in a water filled metallic pipe — monitoring heat exchangers in nuclear power reactors
[DE84-016051] 09 p1378 N85-18665
Analysis and optimization of parameters of fanned surface acoustic wave transducers 13 p2070 N85-22934
A literature review of EMATs, with stress calculations for simple EMAT geometries
[AERE-R-11415] 15 p2642 N85-26295
Acoustooptic pulse-echo transducer system
[NASA-CR-175919] 17 p2951 N85-28224
The Shock and Vibration Digest, volume 17, no. 1
[AD-A151051] 17 p2977 N85-28397
Sound intensity measurement 17 p2977 N85-28398

SOUND TRANSMISSION
Low-frequency sound absorption measurements in air
[NASA-RP-1128] 02 p0275 N85-11789
Shear-layer correction after Amiet under consideration of additional temperature gradient. Working diagrams for correction of signals
[NASA-TM-77741] 03 p0415 N85-12654
Simple prediction of convergence zone propagation in waters around australia
[AD-A145986] 03 p0416 N85-12659
Coupling of airborne sound into the Earth
[AD-A146231] 03 p0416 N85-12663
A transmission analysis for the use of 2-4 PSK modulation in satellite broadcasting
[ESA-STM-231] 04 p0494 N85-13151
Current and current shear effects in the parabolic approximation for underwater sound channels
[AD-A147833] 07 p1039 N85-16597
Estimate of sound absorption due to magnetoelastic interactions
[AD-A148216] 08 p1218 N85-17671
The susceptibility of aeronautical navigational aids to interference from adjacent-band broadcast transmissions
[BBC-RD-1984/12] 09 p1311 N85-18234
Linear and nonlinear ultrasonic interaction on liquid-solid boundaries
[AD-A148979] 10 p1553 N85-19793
Arctic acoustic propagation model with ice scattering
[AD-A149430] 10 p1553 N85-19795
Simple detonation meter 13 p2077 N85-22971
Ice statistics and acoustic scattering in the Arctic basin
[AD-A150141] 13 p2140 N85-23289
Propagation of sound in matter
[AD-A151013] 14 p2416 N85-24907
Propagation of sound in matter
[AD-A151052] 14 p2416 N85-24908
The theoretical response of a vertical line array to wind-generated noise in shallow water
[AD-A151730] 16 p2660 N85-27638
Development of a modified time delay spectrometry technique for underwater acoustic measurements in a multipath environment
[AD-A152111] 16 p2660 N85-27639
Mobile television radio link
[AD-A152381] 17 p2948 N85-28201
Sound intensity measurement 17 p2977 N85-28398
Numerical evaluation of low frequency sound propagation in layered media
[AD-A152690] 17 p3028 N85-28728
Preliminary investigation of the performance of repeater technology for satellite sound broadcasting
[SSP/017/82] 18 p3092 N85-29137
Study of sound attenuation in sediments
[AD-A153690] 18 p3177 N85-29697
Measured acoustic properties of variable and low density bulk absorbers
[NASA-TM-87065] 19 p3351 N85-30770
Airborne sound transmission loss characteristics of wood-frame construction
[AD-A154174] 20 p3524 N85-31919
Development of computer programs using the method of images to predict the sound field in a wedge overlaying a fast fluid and comparison with laboratory experiments
[AD-A154580] 21 p3670 N85-32797
The Konstantinov effect and absorption of sound in inhomogeneous media 21 p3680 N85-32861
Propagation of sound in a layered laboratory model
[AD-A155141] 21 p3700 N85-32969

SOUND VELOCITY
U ACOUSTIC VELOCITY

SOUND WAVES
NT AERODYNAMIC NOISE
NT AIRCRAFT NOISE
NT ELECTROACOUSTIC WAVES
NT ENGINE NOISE
NT ION ACOUSTIC WAVES
NT JET AIRCRAFT NOISE
NT LAMB WAVES
NT NOISE (SOUND)
NT SONIC BOOMS
NT THERMAL NOISE
Human response to vibroacoustic environments of space vehicles
[NASA-TM-86316] 01 p0116 N85-10789
Acoustic resonator and method of making same
[DE84-014655] 01 p0116 N85-10792
Characteristics of light diffraction by two acoustic waves, one with complex frequency composition 03 p0348 N85-12243
Research in quantitative NDE techniques
[AD-A145990] 03 p0369 N85-12358
Shear-layer correction after Amiet under consideration of additional temperature gradient. Working diagrams for correction of signals
[NASA-TM-77741] 03 p0415 N85-12654
Coupling of airborne sound into the Earth
[AD-A146231] 03 p0416 N85-12663
Optoacoustic spectroscopy
[AD-A145995] 03 p0419 N85-12679
USSR report: Electronics and electrical engineering
[JPRS-UEE-84-010] 04 p0485 N85-13095
Reflection of volume waves in multilayer structures 04 p0485 N85-13097
Vibroacoustic control diagnostics of selected machines based on research on the slide bearing of an automobile engine and the alternator
[ISSN-0208-5658] 05 p0641 N85-14112
Resonant scattering of acoustic waves by elastic spherical shell in fluid 06 p0778 N85-14972
Acoustoelectric interaction in double-layer semiconductors 06 p0786 N85-15023
An extension of the Born inversion method to a depth dependent reference profile
[AD-A146469] 06 p0859 N85-15461
Theory of harmonic generation of finite amplitude ultrasonic waves in solids of hexagonal symmetry
[AD-A146636] 06 p0860 N85-15465
Research on acoustical and optical scattering, optics of bubbles, diffraction catastrophes, laser generation of sound, and shock induced cavitation
[AD-A146703] 06 p0860 N85-15466
On the long range propagation of sound over irregular terrain
[NASA-CR-3862] 07 p1036 N85-16589
Acoustic radiation from single and double ribbed circular cylindrical shells
[AD-A148771] 08 p1219 N85-17676
Radiative amplification of acoustic waves in hot stars 08 p1235 N85-17786
Computation of noise radiation from a free jet perpendicular to its axis via laser anemometry measurements
[ESA-TT-870] 09 p1379 N85-18869
Preliminary results of study of space-time variability of shallow sea on steady acoustical path 10 p1499 N85-19459
USSR report: Physics and mathematics
[JPRS-UPM-85-001] 11 p1715 N85-20786
Problem of frequency space variation of sonic field in stratified media 11 p1715 N85-20787
Phonon-impurity relaxation and acoustic wave absorption in yttrium-aluminum garnet crystals with impurities 11 p1715 N85-20790
Acoustic agglomeration methods and apparatus
[NASA-CASE-NPO-15466-1] 12 p1927 N85-22104
A stochastic-mechanical approach to acoustic pulse propagation in the deep ocean sound channel
[AD-A149598] 12 p1928 N85-22110
Nonlinear interactions between vortices and acoustic waves in a rocket combustion chamber 13 p1999 N85-22533
Generation of longitudinal acoustic waves by modulated helicon waves — nonlinear steady state waves in metals 13 p2090 N85-23049
Intensity vectors of sound scattering by a spherical shell
[AD-A147847] 13 p2103 N85-23107
Numerical results of acoustic radiation, transmission and reflection of steel plate in water
[AMTE(N)-TM-84037] 13 p2155 N85-23378
Properties of materials using acoustic waves
[AD-A150465] 13 p2155 N85-23382
Coupling between velocity oscillations and solid propellant combustion
[AD-A151081] 14 p2247 N85-23927
Generation and development of small-amplitude disturbances in a laminar boundary layer in the presence of an acoustic field
[NASA-TM-77826] 14 p2299 N85-24237
Acoustic radiation from bilaminar plates 14 p2415 N85-24903
Linear models of acoustic waves in sunspot umbrae 14 p2450 N85-25130
Effects of atmospheric stratification on dissipative acoustic and Alfven waves — solar atmosphere 14 p2453 N85-25149
Recording of acoustic wave in gaseous medium with thin-film pyroelectric transducers 15 p2525 N85-25571
Recent progress in the development and application of the parabolic equation
[AD-A151475] 15 p2637 N85-26265
Long range downwind propagation of low-frequency sound
[NASA-TM-86409] 15 p2645 N85-26318
Optical monitoring of photo-acoustic pulse propagation in silicon wafers
[AD-A151333] 15 p2651 N85-26352
An experimental investigation of two-dimensional flame-vortex interactions 16 p2744 N85-28934
Acoustic propagation in a thermally stratified atmosphere
[NASA-CR-175787] 16 p2660 N85-27636
The theoretical response of a vertical line array to wind-generated noise in shallow water
[AD-A151730] 16 p2660 N85-27638
Research and development of subsurface acoustic wave devices for sensor applications
[AD-A152197] 16 p2661 N85-27642
Chemical-acoustic interactions in combustion systems
[AD-A153857] 19 p3233 N85-30046
The acoustic mode in numerical calculations of subsonic combustion
[DE85-010788] 19 p3237 N85-30066
Dual differential interferometer
[NASA-CASE-LAR-12966-1] 19 p3271 N85-30282
Metrology and Oceanology Institutes' underwater acoustics R and D 19 p3289 N85-30394
Propagation of acoustic pulse in atmospheric waveguide 19 p3297 N85-30443

Acoustic particle separation
[NASA-CASE-NPO-155559-1] 19 p3350 N85-30765
Linear time-invariant, space-variant filters and the WKB approximation with applications to underwater acoustic signal processing
[AD-A154250] 19 p3352 N85-30775
Squid detection of acoustomagnetic effects 19 p3373 N85-30924
Optical beam deflection detection of thermal waves in opaque solids 19 p3374 N85-30927
Mean and large-scale turbulence characteristics of the noise-producing region of an acoustically excited round jet 20 p3523 N85-31911
Effects of contact area of an interface on acoustic wave transmission characteristics
[DE85-009935] 20 p3524 N85-31920
Qualitative analysis of sign-bit processing
[AD-A154776] 21 p3671 N85-32804
New approximations and findings of theory of nonlinear acoustic beams 21 p3680 N85-32883
Reflection of acoustic beam from inhomogeneous boundary 21 p3680 N85-32884
Acoustic wave scattering by round cylindrical shell reinforced with stringers 21 p3688 N85-32916
Radiative-collision generation of sound in gases subjected to single-pulse optical excitation 21 p3689 N85-32920
Iteration solution for a submerged force-driven finite cylinder
[AD-A154587] 21 p3699 N85-32982
Acoustic radiation from concentric shells containing an inner fluid
[AD-A155476] 21 p3700 N85-32991
Asymmetry of diffraction orders with light diffraction at surface acoustic wave 22 p3782 N85-33431
A comparison of multipath arrival structures observed in the presence of a surface duct with predictions obtained using classical ray techniques and the parabolic equation method
[AD-A156024] 24 p4145 N85-35606
Search for acoustic signals from high energy cascades
[HE-7.1-1] 24 p4213 N85-36155
Experimental investigation of radiative-acoustic effects in the water by the thermodynamical conditions of Dumand
[HE-7.1-2] 24 p4213 N85-36156
Acoustic detection of air shower corse
[HE-7.1-4] 24 p4213 N85-36158

SOUNDERS
U SOUNDING

SOUNDING
NT ACOUSTIC SOUNDING
NT ATMOSPHERIC SOUNDING
NT BALLOON SOUNDING
NT ECHO SOUNDING
NT IONOSPHERIC SOUNDING
NT MICROWAVE SOUNDING
NT ROCKET SOUNDING
NT SATELLITE SOUNDING
On the Apollo subsatellite evidence for a lunar core 04 p0581 N85-13714
NOAA/NASA joint simulation of AMTS and HIRS 05 p0682 N85-14384
ECMWF/NMC/GLAS joint simulation study 05 p0682 N85-14385
Remote sounding of fields in feed radiators of multi-element antenna system with allowance for interaction with sounding device 08 p0790 N85-15047
Khibiny experiment described 07 p0981 N85-16230
Preliminary results of the oceanographic cruise of USCGC NORTHWIND to the Greenland Sea
[AD-A149802] 12 p1696 N85-21919
Mathematical modeling of two-frequency laser sounding of scattering media 13 p2069 N85-23045
Induction excitation of deep conducting zones 13 p2111 N85-23154
Study of resolution of deep MT soundings by means of physical model 13 p2112 N85-23155
Primary processing of experimental magnetovariation sounding data using spline functions 13 p2115 N85-23175
Disturbances in structure of lower ionosphere at terminators based on results of winde-band LW sounding 14 p2339 N85-24457
Interpretation of directional magnetotelluric soundings by analytical continuation method 14 p2343 N85-24488
High-frequency microwave observations of convective precipitation 15 p2586 N85-26000
Accuracy in determining velocity of fluid movement by Doppler method 19 p3293 N85-30419
Variability of air humidity profiles over ocean determined by lidar sounding 19 p3296 N85-30436
The transient electromagnetic depth sounding technique applied to hydrocarbons and geothermal exploration
[MITT-42] 23 p3949 N85-34476

SOUNDING ROCKETS
Space Research in Japan. National report 01 p0013 N85-10082
Rocket observations 01 p0014 N85-10084
Launch summary for 1978 - 1982 — sounding rockets, space probes, and satellites
[NASA-TM-87375] 04 p0461 N85-12924
Ultrasoft X-ray background observations of the local interstellar medium 06 p0677 N85-15571
Data analysis techniques for vehicle attitudinal, positional and experimental measurements
[AD-A147752] 08 p1188 N85-17484
A study on a medium-sized rocket with Burnout frame
[NAL-TR-821] 09 p1287 N85-18082
Research in extreme ultraviolet and far ultraviolet astronomy
[NASA-CR-174432] 10 p1570 N85-19902
Sounding rocket program Aeronomie. The payload M-I in the project MAP-WINE
[BMFT-FB-W-84-046] 12 p1790 N85-21238
Radar echoes at 2.66 and 40.92 MHz from the mesosphere, part 2.6A 21 p3619 N85-32486
Research in extreme ultraviolet and far ultraviolet astronomy
[NASA-CR-176068] 21 p3716 N85-33060
A normal incidence X-ray telescope sounding rocket payload
[NASA-CR-176169] 24 p4153 N85-35749

SOUTH AFRICA
U REPUBLIC OF SOUTH AFRICA

SOUTH AMERICA
Climate Conference for Latin America and the Caribbean
[WMO-632] 07 p1000 N85-16352
Review of climate problems in Latin America and the Caribbean 07 p1001 N85-16354
Climate and climate data. Report on the workshop held in Brasilia (Argentina) from 11-15 April 1983 07 p1001 N85-16357
The climate in food production in Latin America 07 p1001 N85-16359
The ocean and the dynamics of the tropical atmosphere; its possible predictability 07 p1002 N85-16366
Climatological information and water resources 07 p1002 N85-16367
Energy and climate: Problems in Latin America 07 p1003 N85-16375
Education and training for the climate related activities in Latin America and the Caribbean 07 p1004 N85-16379
Droughts and floods in South America due to the 1982-83 El Nino-southern oscillation episode
[INPE-3408-PRE/677] 09 p1357 N85-18535
Some aspects of atmospheric circulation near South America and interactions with the Antarctic regions
[INPE-3306-PRE/618] 10 p1515 N85-19561
Meridional penetration of frontal systems in South America and its relation to organized convection in the Amazon
[INPE-3407-PRE/676] 10 p1518 N85-19572
El Nino, the capricious child 13 p2106 N85-23121
MAGSAT scalar anomaly map of South America 20 p3473 N85-31586
MAGSAT satellite magnetic anomaly map over South America 20 p3474 N85-31587

SOUTH CAROLINA
Multispectral remote sensing of inland wetlands in South Carolina: Selecting the appropriate sensor
[DE84-013951] 05 p0681 N85-14247
Analysis of data acquired by synthetic aperture radar and LANDSAT Multispectral Scanner over Kershaw County, South Carolina, during the summer season
[E85-10071] 10 p1503 N85-19465
Investigation of radiometric properties of LANDSAT-4 MSS — California, North Carolina, South Carolina, and New England 11 p1686 N85-20500

SOUTH DAKOTA
Image variance and spatial structure in remotely sensed scenes — South Dakota, California, Missouri, Kentucky, Louisiana, Tennessee, District of Columbia, and Oregon 07 p0986 N85-16265
Geodetic accuracy of LANDSAT 4 Multispectral Scanner and Thematic Mapper data — Washington, DC, California, Alabama, South Dakota, and Illinois 11 p1687 N85-20504

SOUTH WEST AFRICA
U NAMIBIA

SOUTHERN CALIFORNIA
Petrology and petrogenesis of Batholitic rocks, San Jacinto Mountains, southern California 05 p0673 N85-14322
Visibility monitoring in the southern California desert for the Department of Defense: Research on operations-limiting visual extinction, RESOLVE protocol
[AD-A146617] 06 p0835 N85-15315
Preliminary assessment of climatic change during late Wisconsin time, southwest Great Basin and vicinity, Arizona, California and Nevada
[DE85-008343] 16 p2936 N85-27488

SOUTHERN HEMISPHERE
NT ANTARCTIC REGIONS
NT ROSS ICE SHELF
Statistical tropical cyclone forecasting techniques for the Southern Hemisphere
[AD-A144752] 01 p0065 N85-10589
Analysis of diabatic heating during FGGE 05 p0683 N85-14393
Structure and energetics of medium-scale atmospheric waves in the southern hemisphere summer 05 p0685 N85-14403
An analysis of the seasonal variations in the water vapor transport fields over the Southern Hemisphere 09 p1356 N85-18531
A new NASA/MSFC mission analysis global cloud cover data base
[NASA-TP-2448] 12 p1693 N85-21878
The ARGOS contribution to the First GARP Global Experiment (FGGE) study of drifting buoys 14 p2325 N85-24371
Observation of polar aurora from the Salyut-6 space station during the great geomagnetic storm of 11-13 Apr. 1981 15 p2477 N85-25291
The South Pacific convergence zone and energy balance of the southern hemisphere 15 p2593 N85-25960
Motivation for satellite tracking of southern elephant seals Mirounga leonina at sea 16 p2812 N85-27348
X-ray intensification at balloon altitudes of the South Atlantic magnetic anomaly in association with geomagnetic activity
[INPE-3469-PRE/712] 16 p2827 N85-27437
Mechanistic experiments to determine the origin of Southern Hemisphere stationary waves 18 p3143 N85-29481
Quasi stationary states in the Southern Hemisphere 18 p3144 N85-29465
Trends in the Southern Hemisphere 18 p3144 N85-29466
Structure and energetics of medium-scale atmospheric waves in the Southern Hemisphere 20 p3489 N85-31685

SOUTHERN SKY
Dark cloud and globule distribution for galactic longitudes 230 to 360 degrees 06 p0878 N85-15575
Documentation for the machine-readable version of the Cape Photographic Durchmusterung (CPD)
[NASA-TM-87442] 14 p2439 N85-25050

SOVIET SATELLITES
NT COSMOS SATELLITES
NT COSMOS 936 SATELLITE
NT COSMOS 1129 SATELLITE
NT INTERCOSMOS SATELLITES
NT PROGNOZ SATELLITES
NT VENERA SATELLITES
NT VENERA 11 SATELLITE

SOVIET SPACECRAFT
NT LUNIK LUNAR PROBES
NT SALYUT SPACE STATION
NT SOYUZ SPACECRAFT
Cloud cover sampling capability of various satellite combinations for ISCCP 01 p0073 N85-10484
French, Soviets decide to launch Sigma space telescope 03 p0341 N85-12191
The Venus Balloon Project 10 p1465 N85-19243
List of recent Soviet space launches 13 p1965 N85-22457
List of recent Soviet space launches 15 p2489 N85-25361
East Europe report: Science and technology
[JPRS-ESA-84-016] 15 p2533 N85-25624
Flight tests of experimental shuttle craft described 15 p2533 N85-25625
Substorms in energetic radiation belt particles according to data from Meteor artificial Earth satellite 16 p2719 N85-26788

SOVIET UNION
U U.S.S.R.

SOYBEANS
Variation in spectral response of soybeans with respect to illumination, view, and canopy geometry
[E85-10040] 07 p0982 N85-16241
Shortwave infrared detection of vegetation
[E85-10084] 08 p1174 N85-17402
Effect of elevated atmospheric CO2 on plant communities
[DE85-001810] 11 p1678 N85-20576

Mechanical stress regulation of plant growth and development 15 p2610 N85-28087
Modeling the backscattering and transmission properties of vegetation canopies [E85-10099] 16 p2809 N85-27320

SOYUZ SPACECRAFT
Vitamin metabolism in cosmonauts following short-term flights 01 p0091 N85-10615
Tass reports medical, materials studies aboard Salyut-7 02 p0158 N85-11071
The space flight of the Soviet-Indian crew [NASA-TM-77615] 12 p1788 N85-21226
Feoktistov says manned lunar, Mars flights lack justification 13 p1985 N85-22452

SPACE ADAPTATION SYNDROME
Physiological considerations of artificial gravity 11 p1645 N85-20366
Prediction of the space adaptation syndrome 11 p1693 N85-20648
Space adaptation syndrome: Incidence and operational implications for the space transportation system program 11 p1695 N85-20655
Shuttle operational test and scientific investigations 14 p2294 N85-24748

SPACE BASED RADAR
Development concerns for satellite-based air traffic control surveillance systems 14 p2230 N85-23816
Measurement of ocean surface currents from space with multi-frequency microwave radars 15 p2539 N85-25872
Primary propulsion of electrothermal, ion and chemical systems for space-based radar orbit transfer [NASA-TM-87043] 17 p2916 N85-27972

SPACE BASES
NT SPACE COLONIES
Aerojet advanced engine concept 08 p1107 N85-16699
Opening up the future in space with nuclear power [DE85-002411] 11 p1727 N85-20862

SPACE BIOLOGY
U EXOBIOLOGY

SPACE CAPSULES
Numerical analysis of the 3-dimensional inviscid hypersonic flow around capsule-type bodies by the alternate directional implicit method [NAL-TR-799] 01 p0002 N85-10012

SPACE CHARGE
Method of splitting for solution of problems in semiconductor physics 02 p0265 N85-11736
Intense non-relativistic cesium ion beam [DE84-012575] 04 p0560 N85-13566
In-line beam current monitor [DE84-014054] 04 p0560 N85-13567
Space charge, interfacial kinetics, and electrical response of condensed matter [AD-A146364] 06 p0765 N85-14693
Low frequency noise in oscillator with limited space-charge accumulation 06 p0766 N85-15024
Measurement of proton autoneutralization potential [DE85-001752] 06 p0865 N85-15501
Close-spaced high temperature Knudsen flow [AD-A148477] 08 p1178 N85-17424
Force balance limiting current for charged particle beams [DE84-016976] 09 p1361 N85-18685
Calculations pertaining to the design of a prebuncher for a 150-MeV electron linear accelerator 3. Comparisons with experimental data [DE85-002866] 11 p1724 N85-20844
Statistical phenomena in particle beams [DE85-001050] 12 p1929 N85-22118
Simulation of space charge effects in particle accelerators [DE85-001828] 12 p1929 N85-22120
High energy facilities advanced projects: Intrabeam scattering for a beam of gold ions [DE85-000887] 12 p1941 N85-22192
Discharge pulse phenomenology 13 p1995 N85-22500
Effect of space-charge field on output characteristics of O-type oscillators with distributed interaction 13 p2089 N85-23043
Measuring methods of atmospheric electric elements at the Earth's surface during snowfall and investigation of these relationships 15 p2581 N85-25920
Optically triggered transferred-electron device microwave burst and single pulse generators [AD-D011614] 16 p2778 N85-27141
The design of megawatt gyrotrons [DE85-007692] 17 p3032 N85-28754
Numerical solutions of the potential distribution within the vacuum region of the FEATRON [AD-A159663] 18 p3178 N85-29705
A collective interaction klystron specification [AD-D011704] 19 p3255 N85-30186
Quenching of the beam-plasma instability by 3-D spectra of large scale density fluctuations [NASA-CR-175969] 19 p3369 N85-30697
Development of power system measurements [PB85-182582] 20 p3450 N85-31420
Preliminary investigation of dispersion of pollutants in model building wake flows using bipolar space charge [IC-AERO-84-04] 20 p3487 N85-31671
Electron photoejection in carbenions [DE85-011747] 23 p3911 N85-34230
Repetitive pulse accelerator technology for light ion inertial confinement fusion [DE85-012030] 23 p3982 N85-34693
Numerical studies of high current beam compression in heavy ion fusion [DE85-011674] 24 p4158 N85-35783
Relation between field energy and RMS emittance in intense particle beams [DE85-012655] 24 p4159 N85-35784

SPACE COLONIES
Feoktistov discusses need for space colonization 13 p1985 N85-22454
Our future in the cosmos: Space 14 p2432 N85-24998
Controlled Ecological Life Support Systems (CELSS) 15 p2668 N85-26604
Historical perspective on the Moon base: The British perspective [DE85-005905] 17 p2907 N85-27925

SPACE COMMERCIALIZATION
Second Symposium on Space Industrialization — space commercialization [NASA-CP-2313] 02 p0149 N85-11011
Non-US approaches to space commercialization 02 p0150 N85-11012
Legal considerations and cooperative opportunities for space commercial activities 02 p0150 N85-11013
Financial issues for commercial space ventures: Paying for the dreams 02 p0150 N85-11014
Space industrialization: A national perspective 02 p0150 N85-11015
Land remote sensing commercialization: A status report 02 p0151 N85-11024
Space America's commercial space program 02 p0152 N85-11027
Fluids Experiment Apparatus (FEA) 02 p0155 N85-11048
Commercializing the transfer orbit stage 02 p0155 N85-11049
Space commercialization: Analysis of R and D investments with long time horizons 02 p0155 N85-11052
Advances in electrophoretic separations 02 p0156 N85-11054
Opportunities for commercial organizations 02 p0156 N85-11055
Doing business in space: How to get there from here 02 p0156 N85-11057
Initiatives to promote space commercialization [GPO-37-551] 02 p0158 N85-11058
Statement of Hon. James M. Beggs, Administrator, NASA, Washington, DC 02 p0156 N85-11059
International cooperation and competition in space [GPO-38-001] 02 p0295 N85-11911
International cooperation and competition in space. Introduction 02 p0295 N85-11912
Statement of Kenneth S. Pedersen, Director, International Affairs Division, National Aeronautics and Space Administration 02 p0295 N85-11913
Commercial Space Launch Act [GPO-39-613] 04 p0578 N85-13690
Land Remote-Sensing Commercialization Act [S-REPT-98-458] 05 p0654 N85-14201
Civilian space stations and the US future in space [OTA-STI-241] 07 p0914 N85-15781
Issues and findings 07 p0914 N85-15782
Space infrastructure 07 p0914 N85-15783
Toward a goal-oriented civilian space program 07 p0914 N85-15786
Commerce Lab: Mission analysis and payload integration study [NASA-CR-171272] 08 p1104 N85-16981
International cooperation and competition in civilian space activities [OTA-ISC-240] 08 p1231 N85-17750
Commerce lab: Mission analysis and payload integration study [NASA-CR-174381] 10 p1426 N85-18993
West Europe report: Science and technology [JPRS-WST-85-004] 10 p1460 N85-19204
Commercial space: Europe should have independent strategy 10 p1460 N85-19205
Status of the National Space Transportation System 11 p1712 N85-20772
Commercial space launches [S-REPT-98-656] 12 p1788 N85-21225
The Ariane launch vehicle is the key of the Europeans to the space market 17 p2908 N85-27931
International space research perspectives of commercialization for German industry [NASA-TM-77657] 19 p3222 N85-29979
Commerce Lab: Mission analysis payload integration study. Appendix A: Data bases [NASA-CR-176016] 19 p3224 N85-29988
Insurance and the commercialization of space [S-PRT-99-16] 20 p3397 N85-31074
Study to encourage and facilitate industrial investment and involvement in space [NASA-CR-176152] 23 p3898 N85-34147

SPACE COMMUNICATION
NT INTERPLANETARY COMMUNICATION
NT SPACECRAFT COMMUNICATION
JPL highlights, 1983 [NASA-CR-175558] 12 p1951 N85-22256
Interkosmos program of space communication development 15 p2528 N85-25585
Meteorological factors in Earth-Satellite propagation [NASA-CR-175764] 16 p2769 N85-27089
The Telecommunications and Data Acquisition Report [NASA-CR-175842] 16 p2770 N85-27094
Synchronizing heavily encoded data in bad weather 16 p2770 N85-27099
A review of tropospheric refraction effects on Earth-to-satellite systems 18 p3107 N85-29235
Interpolation problems in meteor radar analysis, part 7.6A 21 p3626 N85-32528

SPACE COOLING (BUILDINGS)
Thermal energy storage [DE85-001492] 09 p1344 N85-18454
Experimental testing of cooling by low pressure adsorption in a zeolite [DE85-007509] 16 p2716 N85-26763
Onset of freezing in residential air-to-air heat exchangers [DE85-009960] 19 p3267 N85-30259
Advanced heat pump research and development [DE85-009540] 23 p3932 N85-34372

SPACE DEBRIS
Orbital Debris [NASA-CP-2360] 12 p1783 N85-21188
NORAD operational system 12 p1783 N85-21189
History of satellite break-ups in space 12 p1783 N85-21190
NORAD's PARCS small satellite tests (1976 and 1978) 12 p1783 N85-21191
Manmade orbital debris studies at NASA Langley 12 p1783 N85-21192
NASA/JSC orbital debris study: Debris model 12 p1783 N85-21193
Proposed preliminary design criteria model environment for the 1990's 12 p1784 N85-21194
Assessment of satellite collision hazards by simulated sampling in space 12 p1784 N85-21195
A model for the evolution of on-orbit manmade debris environment 12 p1784 N85-21196
Geosynchronous satellite collision avoidance 12 p1784 N85-21197
In situ orbital debris experiment concepts 12 p1784 N85-21198
Preliminary design of an Earth-based debris detection system using current technology and existing installations 12 p1784 N85-21199
Use of ground radar to detect reentering debris 12 p1784 N85-21200
Particle size, number, composition and velocity from solid rocket motors 12 p1785 N85-21201
Hypervelocity impacts on Skylab 4/Apollo windows 12 p1785 N85-21202
Survey of probable micrometer-sized Earth-orbital debris fragments in the NASA-JSC cosmic dust sample collection 12 p1785 N85-21203
Impacts on Explorer 46 from an Earth orbiting population 12 p1785 N85-21204
In-situ detection of micron-sized dust particles in near-Earth space 12 p1785 N85-21205
Hypervelocity impact investigations and meteoroid shielding experience related to Apollo and Skylab 12 p1785 N85-21206
Space debris protection for a reusable orbital transfer vehicle 12 p1786 N85-21208
Parametric analysis: SOC meteoroid and debris protection 12 p1786 N85-21209
Space heat rejection radiators: Meteoroid/debris considera?on 12 p1786 N85-21210
A remotely controlled orbiting retriever 12 p1786 N85-21212
The international environment UNISPACE '82 and the ITU: A relationship between orbit-spectrum resource allocation and orbital debris 12 p1787 N85-21215
Orbital debris policy issues: Battelle involvement and some personal observations 12 p1787 N85-21218

Considerations for policy on man-made debris propagation control 12 p1787 N85-21219
Environment definition, large particles 12 p1787 N85-21220
Modeling 12 p1787 N85-21221
Measurements 12 p1787 N85-21222
Environment definition, small particles, diameter less than or equal to 1 MM 12 p1788 N85-21223
Spacecraft hazard and shielding requirements 12 p1788 N85-21224
Debris impact on Earth-orbiting spacecraft 12 p1948 N85-22234
Analysis of space station operations in the space debris environment
[AD-A151872] 15 p2493 N85-25380
What we know about Mars (but otherwise wouldn't) if it is the shergottite parent body 15 p2582 N85-26585
Procedure for estimating orbital debris risks
[NASA-TP-2507] 22 p3738 N85-33189

SPACE DENSITY
Probe of the nearby interstellar medium by the vacant line of sight to Beta CMa 06 p0874 N85-15551
Local interstellar extinction with an emphasis on uvby beta results 06 p0875 N85-15559
The dependence of interstellar element depletions on mean space density 11 p1749 N85-20998
X-ray gauge measures areal density variations as small as 0.1%
[DE85-003774] 12 p1854 N85-21629
Investigating statistical characteristics of atmospheric background brightness and star background density in equatorial region of celestial sphere 15 p2478 N85-25298

SPACE DIVERSITY
U RECEPTION DIVERSITY

SPACE ENVIRONMENT
U AEROSPACE ENVIRONMENTS

SPACE ENVIRONMENT SIMULATION
NT WEIGHTLESSNESS SIMULATION
Distortional measurement of antennas under space simulation conditions by means of holography 05 p0625 N85-14005
Spontaneous motility of goldfish in absence of terrestrial zeitgebers: Space flight simulation in a mine 05 p0689 N85-14432
Electrostatic wave observation during a space simulation Beam-Plasma-Discharge (BPD)
[NASA-CR-174288] 07 p1045 N85-16639
Space environment simulation to test satellite thermal control coatings, volume 1
[CERT-4128-VOL-1] 08 p1109 N85-17012
Space environment simulation to test satellite thermal control coatings. Volume 2: Annex 1
[ESA-CR(P)-1870-VOL-2] 08 p1109 N85-17013
Space environment simulation to test satellite thermal control coatings. Volume 2: Annexes 2, 3, 4
[ESA-CR(P)-1870-VOL-3] 08 p1109 N85-17014
Giotto solar array: Design, manufacture and test 13 p2008 N85-22589
Survival testing of silicon solar modules 13 p2009 N85-22602
Measurements of integral yields of charged secondary particles using neutral beams simulating a cometary fly-by — Giotto mission 14 p2244 N85-23908
ESABASE extension to spacecraft charging analysis. Phase 1: NASCAP software (VAX version)
[ESA-CR(P)-1968] 15 p2493 N85-26381
Human productivity experience and undersea habitat design 18 p3159 N85-29563
Experiences with neutral buoyance testing mockups 18 p3159 N85-29571
Space-flight simulations of calcium metabolism using a mathematical model of calcium regulation
[NASA-CR-171883] 19 p3328 N85-30821
Measurement of material damping in a simulated space environment 20 p3397 N85-31070
European Space Tribology Laboratory: Facilities, services, capabilities
[ESA-BR-12] 20 p3308 N85-31080
The use of perfluoroether lubricants in unprotected space environments 22 p3797 N85-33523
Effects of space radiation on advanced semiconductor devices. Part 3: Further cosmic ray simulation studies of single event upsets and latch-up in CMOS memories
[AERE-G-3368-PT-3] 22 p3848 N85-33833
DMSK: A practical 2400-bps receiver for the mobile satellite service: An MSAT-X Report
[NASA-CR-176194] 24 p4086 N85-35324

SPACE ENVIRONMENTAL LUBRICATION
U SPACECRAFT LUBRICATION

SPACE ERECTABLE STRUCTURES
Conceptual design and evaluation of selected Space Station concepts: Executive summary
[NASA-TM-87382] 02 p0167 N85-11128
Conceptual design and evaluation of selected Space Station concepts, volume 1
[NASA-TM-87383] 02 p0168 N85-11129
Conceptual design and evaluation of selected Space Station concepts, volume 2
[NASA-TM-87384] 02 p0168 N85-11130
Definition of technology development missions for early space stations: Large space structures
[NASA-CR-171209] 03 p0323 N85-12084
Large-diameter astromast development
[NASA-CR-171201] 03 p0342 N85-12200
Large spaceborne antenna reflectors using inflatable space rigidized structures 05 p0625 N85-14004
Development of a foldline concept for automatic refolding of a flexible blanket (folding analysis) — spaceborne solar generators
[ESA-CR(P)-1933] 06 p1179 N85-17428
Ground test article for deployable space structure systems
[NASA-CR-171301] 10 p1429 N85-19011
Variable geometry truss concept
[REPT-814] 12 p1865 N85-21697
New concepts in deployable beam structures 14 p2232 N85-23832
Space Station structures 14 p2232 N85-23835
Verification for large space structures 14 p2232 N85-23836
MSFC data analysis of the SAFE/DAE experiment 14 p2233 N85-23843
Langley Research Center photogrammetric measurements of solar array dynamics: Preliminary results 14 p2233 N85-23844
Diffraction analysis of mesh deployable reflector antennas 14 p2235 N85-23854
Assembly Concept for Construction of Erectible Space Structure (ACCESS) neutral buoyancy testing results 14 p2236 N85-23862
Definition of technology development missions for early space stations: Large space structures
[NASA-CR-171446] 15 p2476 N85-25261
Construction in space 15 p2484 N85-25328
Construction in space
[NASA-TM-77630] 15 p2492 N85-25374
Deployable controllable geometry truss beam
[NASA-TM-86366] 17 p2909 N85-27934
Solar array flight experiment
[NASA-TM-86506] 17 p2909 N85-27935
Application of the ADAMS program to deployable space truss structures
[NASA-CR-177927] 19 p3284 N85-30366

SPACE EXPLORATION
NT VIKING MARS PROGRAM
International cooperation and competition in space
[GPO-38-001] 02 p0295 N85-11911
Statement of Kenneth S. Pedersen, Director, International Affairs Division, National Aeronautics and Space Administration 02 p0295 N85-11913
Statement of Otho E. Eskin, Director, Office of Advanced Technology, Department of State 02 p0295 N85-11914
Statement of John H. McElroy, Assistant Administrator for Environmental Satellite, Data and Information Services, National Oceanic and Atmospheric Administration 02 p0295 N85-11915
International cooperation and competition in civilian space activities, summary, appendix 1 02 p0295 N85-11916
Space research and the new approach to the mechanics of fluid media in cosmos
[TRITA-EPP-84-04] 03 p0447 N85-12844
Mission science value-cost savings from the Advanced Imaging Communication System (AICS)
[NASA-CR-174170] 04 p0458 N85-12905
Interstellar mission 04 p0458 N85-12916
NASA's SESAC report on research and analysis in space and Earth sciences 04 p0579 N85-13697
Man in Space: National Historic Landmark Theme Study
[PB85-107233/GAR] 07 p0911 N85-15768
Title 2: National Commission on Space (Public Law 98-361) 07 p0915 N85-15791
Reliable software design for avionics and space applications 08 p1065 N85-16751
Spanish language equivalents for a glossary of terms used in the field of space exploration
[NASA-TM-87403] 08 p1229 N85-17739
Opening up the future in space with nuclear power
[DE85-002411] 11 p1727 N85-20662
A new look at the planets — space probes
[AERONOMICA-ACTA-37-1984] 11 p1765 N85-21096
JPL highlights
[NASA-CR-175517] 11 p1767 N85-21102
JPL highlights, 1983
[NASA-CR-175558] 12 p1951 N85-22258
Planetary cartography in the next decade (1984 - 1994)
[NASA-SP-475] 12 p1960 N85-22323
Activities of the Jet Propulsion Laboratory, 1 January - 31 December 1983
[NASA-CR-175555] 13 p2167 N85-23447
Planetary geology in the 1980s
[NASA-SP-467] 13 p2169 N85-23467
Our future in the cosmos: Space 14 p2432 N85-24998
Cometary Astrometry
[NASA-CR-175660] 14 p2435 N85-25015
MBB/Erno's views, future plans in aerospace activities 15 p2531 N85-25609
Analysis of the Gran Desierto, Pinacte Region, Sonora, Mexico, via shuttle imaging radar
[NASA-CR-175711] 15 p2582 N85-25827
The 1985 long-range program plan
[NASA-TM-87464] 15 p2664 N85-26440
Sixteenth Lunar and Planetary Science Conference. Press abstracts
[NASA-CR-175692] 15 p2680 N85-26548
USSR report: Space
[JPRS-USP-85-004] 16 p2717 N85-26772
Forecasts on long-range development of space programs 16 p2727 N85-26830
US said to seek military advantage in space 16 p2727 N85-26831
East Europe report: Science and technology
[JPRS-ESA-85-019] 16 p2767 N85-27077
International cooperation in space exploration 16 p2768 N85-27079
East-West cooperation in outer space
[S-HRG-98-1084] 16 p2879 N85-27767
New ESA director on space station, military space 18 p3068 N85-28962
DFVLR study recommends European independence in space systems 18 p3068 N85-29111
Swedish space program includes research satellites 18 p3068 N85-29113
Gas chromatography: Possible application of advanced instrumentation developed for solar system exploration to space station cabin atmospheres 18 p3157 N85-29551
The human role in space (THURIS) 18 p3158 N85-29557
Space ventures and society long-term perspectives
[NASA-CR-176012] 19 p3379 N85-30963
Geophysical interpretation of Venus gravity data
[NASA-CR-176063] 20 p3547 N85-32071
Far travelers: The exploring machines
[NASA-SP-480] 22 p3731 N85-33126
A spacefaring people: Perspectives on early spaceflight
[NASA-SP-4405] 23 p4056 N85-35142
Space science and exploration: A historical perspective 23 p4056 N85-35143
The next assignment: The state of the literature on space 23 p4057 N85-35146
The idea of space exploration 23 p4057 N85-35150

SPACE FLIGHT
NT HYPERSONIC REENTRY
NT INTERPLANETARY FLIGHT
NT INTERSTELLAR TRAVEL
NT LONG DURATION SPACE FLIGHT
NT MANNED SPACE FLIGHT
NT SPACE SHUTTLE MISSION 31-C
NT SPACE SHUTTLE MISSION 41-B
NT SPACE SHUTTLE MISSION 41-C
NT SPACE SHUTTLE MISSION 41-G
NT SPACE SHUTTLE MISSION 51-A
NT SPACE SHUTTLE MISSION 51-C
NT SPACE SHUTTLE MISSIONS
NT SPACECRAFT REENTRY
NT VIKING MARS PROGRAM
Vitamin metabolism in cosmonauts following short-term flights 01 p0091 N85-10615
Development of space instrumentation of Intercosmos member countries 02 p0163 N85-11106
Research and technology
[NASA-TM-86321] 02 p0305 N85-11973
The human role in space. Volume 1: Executive summary
[NASA-CR-171223] 04 p0546 N85-13473
BDLI memorandum on the future of space flight in the Federal Republic of Germany
[NASA-TM-77624] 07 p0911 N85-15765
Space motion sickness monitoring experiment: Spacelab 1 11 p1805 N85-20654
Parameters of carbohydrate metabolism and blood serum enzyme activity after short-term spaceflights 12 p1903 N85-21951
Second Soviet-French Symposium on Space Cytology 14 p2388 N85-24899

Food service and nutritional needs
14 p2394 N85-24744
NASA Space Biology Program: 9th Annual Symposium
[NASA-CP-2336] 15 p2605 N85-26054
Effects of weightlessness of Aurelia Ephyra differentiation and statolith synthesis
15 p2605 N85-26056
A detailed analysis of the erythropoietic control system in the human, squirrel, monkey, rat and mouse
[NASA-CR-171879] 15 p2614 N85-26107
Aerosol deposition along the respiratory tract at zero gravity: A theoretical study
[DE85-006703] 15 p2619 N85-26136
Crystal growth from the vapor in low gravity environments
[DE85-009620] 16 p3195 N85-29816
Flow cytometry for health monitoring in space
[DE85-009572] 19 p3329 N85-30625
Maximum likelihood estimation with emphasis on aircraft flight data 20 p3417 N85-31208
Microorganisms in space flight
23 p3951 N85-34490

SPACE FLIGHT FEEDING
Feasibility of producing a range of food products from a limited range of undifferentiated major food components
[NASA-CR-177329] 07 p1020 N85-16473
Characterization of heat transfer in nutrient materials — space flight feeding
[NASA-CR-171841] 08 p1199 N85-17551
Self-charging metering and dispensing device for fluids
[NASA-CASE-MSC-20275-1] 12 p1848 N85-21595
Food Service and Nutrition for the Space Station
[NASA-CP-2370] 14 p2393 N85-24733
The context for food service and nutrition in the space station 14 p2393 N85-24734
Food service and nutritional needs
14 p2394 N85-24744
Psychobiology and food perception
14 p2394 N85-24745

SPACE FLIGHT STRESS
Distinctions of SPF rats used in experiments aboard biosatellites 07 p1012 N85-16427
Research opportunities in human behavior and performance
[NASA-CR-175473] 10 p1529 N85-19640
Physiological considerations of artificial gravity
11 p1643 N85-20351
Description, validation, and modification of the Guyton model for space-flight applications. Part A. Guyton model of circulatory, fluid and electrolyte control. Part B. Modification of the Guyton model for circulatory, fluid and electrolyte control
[NASA-CR-171876] 15 p2616 N85-26122
Mathematical modeling of fluid-electrolyte alterations during weightlessness
[NASA-CR-171881] 15 p2617 N85-26125
Cardiovascular effects of weightlessness
15 p2606 N85-26607
Psychological issues relevant to astronaut selection for long-duration space flight: A review of the literature
[AD-A154051] 19 p3330 N85-30627
An integrated analysis of the physiological effects of space flight: Executive summary
[NASA-CR-171892] 20 p3506 N85-31796
Mission operations requirements document for D-1 Experiment 102, Vestibular Experiments in Spacelab
[NASA-TM-87405] 21 p3557 N85-32129
Spacelab 1 hematology experiment (INS103): Influence of space flight on erythrokinetics in man
[NASA-TM-58268] 22 p3824 N85-33493

SPACE FLIGHT TRAINING
Cosmonaut Savitskaya says many women in cosmonaut training 16 p2717 N85-25774

SPACE GLIDERS
U LIFTING REENTRY VEHICLES

SPACE GLOSSARIES
Spanish language equivalents for a glossary of terms used in the field of space exploration
[NASA-TM-87403] 08 p1229 N85-17739
Space Transportation System and associated payloads: Glossary, acronyms, and abbreviations
[NASA-RP-1059-REV] 10 p1428 N85-19007
Tenth Conference of Working Group of Socialist Countries on Remote Sensing of Earth under Intercosmos Program 16 p2725 N85-26820

SPACE HABITATS
Overview: Human factors issues in space station architecture 18 p3158 N85-29558

SPACE HEATING (BUILDINGS)
Project Pellworm: Solar electric energy supply for a health center 05 p0664 N85-14268
Review of SERI solar pond work
05 p0667 N85-14289
Passive solar/Earth sheltered office/dormitory cooling season thermal performance
[DE84-016662] 05 p0669 N85-14308
Hangar heating and energy conservation manual
[AD-A147893] 07 p0910 N85-15782
FORTRAN 77 computer program for test procedure calculations of vented heaters
[PB85-109627/GAR] 09 p1305 N85-18198
Thermal energy storage
[DE85-001492] 09 p1344 N85-18454
Actual versus design performance of solar systems in the National Solar Data Network
[DE85-001190] 09 p1344 N85-18455
Optimization of design and control strategies for geothermal space heating systems
[DE85-000496] 09 p1344 N85-18458
Research on heat-exchanger corrosion
[PB85-126316] 11 p1616 N85-20164
A summary and assessment of historical reliability and maintainability data for solar hot water and space conditioning systems
[DE84-004521] 12 p1876 N85-21770
Overview of latent storage for passive solar applications
[DE85-005354] 13 p2129 N85-23249
A review of development and application of heat pump technology
[CSIR-RR-585] 14 p2300 N85-24241
Solar house, Freiburg
[BMFT-FB-T-84-249] 15 p2588 N85-25953
Foamglass solar window collector
[DE85-009197] 18 p3129 N85-29374
Solar energy for highway uses
[DE84-015653] 18 p3130 N85-29382
Onset of freezing in residential air-to-air heat exchangers
[DE85-009660] 19 p3267 N85-30259
Comparative evaluation of ground-coupled heat pumps that use solar energy
[DE85-010950] 20 p3484 N85-31649
Pagosa Springs geothermal project
[DE85-011308] 22 p3607 N85-33583

SPACE INDUSTRIALIZATION
NT SPACE MANUFACTURING
NT SPACE PROCESSING
Second Symposium on Space Industrialization — space commercialization
[NASA-CP-2313] 02 p0149 N85-11011
Space Industrialization: A national perspective
02 p0150 N85-11015
Industrial use of land observation satellite systems
02 p0151 N85-11026
Space America's commercial space program
02 p0152 N85-11027
Role of Space Station: The how of space industrialization 02 p0153 N85-11036
Commercial space services 02 p0153 N85-11039
Developing commercial users of space
02 p0154 N85-11044
FRG opinion on Spacelab benefits, space station participation 15 p2532 N85-25618
Space ventures and society long-term perspectives
[NASA-CR-176012] 19 p3379 N85-30983

SPACE INFRARED TELESCOPE FACILITY
Study of application of space telescope science operations software for SIRTF use
[NASA-CR-177337] 09 p1287 N85-18080
Performance of charge-injection-device infrared detector arrays at low and moderate backgrounds
[NASA-TM-86667] 15 p2580 N85-25793

SPACE LABORATORIES
NT MANNED ORBITAL LABORATORIES
NT MANNED ORBITAL RESEARCH LABORATORIES
NT SPACELAB
Commerce Lab: Mission analysis and payload integration study
[NASA-CR-171272] 08 p1104 N85-16981
Botany facility, phase A study. Part 1: Executive summary — EURECA
[BF-DOC-10-VOL-1] 08 p1110 N85-17015
Commerce lab: Mission analysis and payload integration study
[NASA-CR-174381] 10 p1426 N85-18993
Documentation for the West German Federal Cabinet's space policy decision 17 p3051 N85-28885
Life sciences flight experiments program mission science requirements document. The first life sciences dedicated Spacelab mission, part 1
[NASA-TM-87494] 21 p3559 N85-32137

SPACE LAW
Outer space law: A problem of astronautics
[NASA-TM-77760] 07 p1055 N85-16697
Militarization of space activity in United States
15 p2488 N85-25360

SPACE LOGISTICS
Impact of lunar and planetary missions on the space station: Preliminary STS logistics report
[NASA-CR-171837] 09 p1285 N85-18072
In orbit infrastructure. Volume 1: Executive summary — European space programs
[RX011-002/84-VOL-1] 17 p2908 N85-27928
In orbit infrastructure — european space programs
[SNIAS-S/DT-24-996] 18 p3064 N85-28956

SPACE MAINTENANCE
In-orbit laser regeneration of the radiation damaged solar arrays 13 p2006 N85-22586
A concept for a mobile remote manipulator system
14 p2236 N85-23959
In orbit infrastructure. Volume 1: Executive summary — European space programs
[RX011-002/84-VOL-1] 17 p2908 N85-27928
In orbit infrastructure — european space programs
[SNIAS-S/DT-24-996] 18 p3064 N85-28956
Maintenance of long life space systems, volume 1
[MATRA-0316/DX60-VOL-1] 18 p3066 N85-28964
Maintenance of long life space systems, volume 2
[MATRA-0350/DX60-VOL-2] 18 p3066 N85-28965
DFVLR official on areas of US-FRG Space Station cooperation 18 p3066 N85-29091
Space station automation study-satellite servicing. Volume 1: Executive summary
[NASA-CR-171512] 19 p3226 N85-29999
Telepresence work system concepts
22 p3797 N85-33525
A strategy planner for NASA robotics applications
[NASA-CR-175319] 22 p3834 N85-33736

SPACE MANUFACTURING
Non-US approaches to space commercialization
02 p0150 N85-11012
Developing commercial users of space
02 p0154 N85-11044
Statement of Hon. James M. Beggs, Administrator, NASA, Washington, DC 02 p0158 N85-11059
Cosmonauts report on space welding at conference
15 p2484 N85-25329
An analysis of alternate hydrogen sources for lunar manufacture
[DE85-007234] 16 p2684 N85-27792
Low gravity exothermic heating/cooling apparatus
[NASA-CASE-MSC-25707-1] 18 p3104 N85-29214
International space research perspectives of commercialization for German industry
[NASA-TM-77657] 19 p3222 N85-29979
Kidney cell electrophoresis
[NASA-CR-171889] 20 p3498 N85-31745
Prospective uses for diffusion welding in vacuum
22 p3733 N85-33145
Space station automation study. Automation requirements derived from space manufacturing concepts. Volume 1: Executive summary
[NASA-CR-176099] 22 p3736 N85-33170
Space Station automation study. Automation requirements derived from space manufacturing concepts. Volume 2: Technical report
[NASA-CR-176100] 22 p3738 N85-33171
Investment justification of robotic technology in aerospace manufacturing. User's manual
[AD-A156193] 24 p4099 N85-35410

SPACE MECHANICS
NT ASTRODYNAMICS
NT CELESTIAL MECHANICS
NT KEPLER LAWS
NT MINIMUM VARIANCE ORBIT DETERMINATION
NT ORBITAL MECHANICS
Space Mathematics for the Preparation and Development of satellite Exploitation
[ISBN-2-85428-115-2] 14 p2395 N85-24753
The computing facilities of the Toulouse Space Center
14 p2397 N85-24770
Reference systems — in space mechanics
14 p2399 N85-24784

SPACE MISSIONS
NT ASTEROID MISSIONS
NT GIOTTO MISSION
NT SOLAR MAXIMUM MISSION
Space research benefits national economy
02 p0163 N85-11107
Preliminary analysis of space mission applications for electromagnetic launchers
[NASA-CR-174067] 03 p0321 N85-12071
Definition of technology development missions for early space stations: Large space structures
[NASA-CR-171209] 03 p0323 N85-12084
On-orbit support of DARPA-301 payload
[AD-A146897] 07 p0911 N85-15767
The investigation of tethered satellite system dynamics
[NASA-CR-171278] 07 p0912 N85-15772

SNAP (Space Nuclear Auxiliary Power) reactor overview
[AD-A146831] 07 p1041 N85-16612
An optimization method for the preliminary design of interplanetary aerobraking missions
08 p1076 N85-16822
Impact of lunar and planetary missions on the space station
[NASA-CR-171832] 08 p1106 N85-16968
Space Station needs, attributes, and architectural option study
[NASA-CR-174316] 08 p1109 N85-17011
The SIR-B science investigations plan
[NASA-CR-174282] 08 p1143 N85-17208
Impact of lunar and planetary missions on the space station: Preliminary STS logistics report
[NASA-CR-171837] 09 p1285 N85-18072
Data Requirement (DR) MA-03: Payload missions integration — Spacelab payloads
[NASA-CR-171331] 10 p1428 N85-19009
Reed-Solomon code synchronization revisited
10 p1464 N85-19234
Solar Corona Explorer: A mission for the physical diagnosis of the solar corona
[NASA-TM-87416] 10 p1572 N85-19912
Tethered satellite system project overview
11 p1642 N85-20341
Summary presentation of the Science Applications Panel 11 p1644 N85-20355
Summary presentation of the Electrodynamics Interactions Panel 11 p1644 N85-20356
Summary presentation of the Transportation Panel
11 p1644 N85-20357
Summary presentation of the technology and test panel 11 p1644 N85-20360
Results of Space Shuttle flight 41-D
[GPO-39-481] 12 p1791 N85-21243
D-1 report: The first German spacelab mission
[NASA-TM-77637] 13 p1977 N85-22402
Ignition, separation of boosters, stages in Ariane 3
14 p2280 N85-24185
Rendezvous with Saturn's rings
15 p2579 N85-26543
European space science horizon 2000
[ESA-SP-1070] 16 p2717 N85-26771
A SLAM II simulation model for analyzing space station mission processing requirements
[NASA-CR-175664] 16 p2731 N85-26853
Life sciences flight experiments program mission science requirements document. The first life sciences dedicated Spacelab mission, part 1
[NASA-TM-87494] 21 p3559 N85-32137
Space Missions for Automation and Robotics Technologies (SMART) Program
[NASA-TM-86820] 24 p4068 N85-35210

SPACE NAVIGATION
NT INTERPLANETARY NAVIGATION
Planning of navigation measurements using TD criterion for determination of movement of spacecraft by method of least squares 02 p0159 N85-11081
Autonomous navigation of USAF spacecraft
03 p0321 N85-12074
Time comparison with GPS technique and first results with the DFVLR C/A code receiver
[DFVLR-MITT-84-05] 05 p0595 N85-13794
Errors of analog of inertial coordinate systems modeled in astronavigation system 07 p0951 N85-16026
A short note on the high precision navigation of QUASAT 07 p1059 N85-16722
Technical evaluation report on the 46th Symposium of the Avionics Panel on Space System Applications to Tactical Operations
[AGARD-AR-203] 10 p1425 N85-18988
JPL highlights, 1983
[NASA-CR-175558] 12 p1951 N85-22258
The TRANSIT and Global Positioning System (GPS) systems. Precision navigation and localization
14 p2398 N85-24777
Perturbations of Kalman filtering process
15 p2480 N85-25305
Autonomous state determination for an Earth orbiting satellite using horizon and star sensors
[AD-A151827] 15 p2493 N85-25379
Method for evaluating perturbation in algorithms for solving navigational problems 16 p2718 N85-26783
Statistical regularization methods in problem of navigational determination of space vehicle orbits
16 p2719 N85-26784

SPACE OBSERVATIONS (FROM EARTH)
Preliminary design of an Earth-based debris detection system using current technology and existing installations 12 p1784 N85-21199
Use of ground radar to detect reentering debris
12 p1784 N85-21200
Solar Seismology From Space. A conference at Snowmass, Colorado
[NASA-CR-175661] 14 p2441 N85-25060
Planetary Rings. Colloquium 75 — conferences
[ISBN-2-85428-100-4] 15 p2670 N85-26473
Future observations of planetary rings from ground-based observatories and Earth-orbiting satellites
15 p2678 N85-26540
Dust emission of Comet Halley at large heliocentric distances 15 p2681 N85-26558
Activity and magnetic fields on stars from radio observations
[NASA-CR-175966] 18 p3202 N85-29861
Star formation in NGC 7538: Multi-wavelength observations and issues 20 p3545 N85-32063

SPACE PERCEPTION
Theory underlying the peripheral vision horizon device
01 p0008 N85-10048
Cognitive coordinate systems: Accounts of mental rotation and individual differences in spatial ability
[AD-A146149] 03 p0401 N85-12557
Lighting for remote viewing systems
[DE85-001898] 11 p1729 N85-20873
Texture perception and shape from texture
[AD-A154278] 19 p3336 N85-30672

SPACE PHOTOGRAPHY
U SPACEBORNE PHOTOGRAPHY

SPACE PLASMAS
NT SOLAR WIND
NT STELLAR WINDS
Convection of plasma in polar ionosphere, comparison of measurements from Cosmos-184 with model dependent on interplanetary magnetic field vector
02 p0160 N85-11086
The solar wind at 20-30 AU 02 p0301 N85-11950
Impedance measurements on a VLF multi-turn loop antenna in a space plasma simulation chamber
[AD-A145104] 04 p0492 N85-13141
Plasma flow in the near and distant geomagnetic tail
[DE84-014029] 04 p0534 N85-13415
The radiative hydrodynamics of flare loops heated by impulsive bursts of energetic electrons
05 p0745 N85-14781
A warm magnetoactive plasma in a large volume of space 06 p0878 N85-15579
Research study of space plasma boundary processes
[NASA-CR-174351] 10 p1558 N85-19823
Science Applications, part 1 11 p1643 N85-20348
Hydromagnetic precursors of interplanetary plasma burst 13 p1978 N85-22414
One-dimensional model of auroral magnetic force with longitudinal current and cyclotron heating of ions
13 p1980 N85-22424
Interplanetary shock waves during April and May of 1981 13 p1982 N85-22434
Spacecraft-environment interaction: The environmental plasma aspect 13 p1990 N85-22479
Direct measurements of severe spacecraft charging in auroral ionosphere 13 p1991 N85-22480
Polar plasmas as observed by Dynamics Explorers 1 and 2 13 p1991 N85-22483
Auroral-polar cap environment and its impact on spacecraft plasma interactions 13 p1991 N85-22484
Three-dimensional calculation of shuttle charging in polar orbit 13 p1992 N85-22486
Interactions between large space power systems and low-Earth-orbit plasmas 13 p1992 N85-22490
Self-consistent simulation of plasma interactions with secondary-emitting insulators 13 p1993 N85-22492
Surface interactions and high-voltage current collection 13 p1993 N85-22493
The PIX-2 experiment: An overview
13 p1993 N85-22494
Plasma interaction experiment 2 (PIX 2): Laboratory and flight results 13 p1993 N85-22495
Ram-wake effects on plasma current collection of the PIX 2 Langmuir probe 13 p1993 N85-22496
NASCAP simulation of PIX 2 experiments
13 p1993 N85-22497
An investigation of arc discharging on negatively biased dielectric conductor samples in a plasma
13 p1994 N85-22498
Space test program of high-voltage solar array-space plasma interactions 13 p1997 N85-22519
Preliminary investigation of the electrodynamics of a conducting tether 13 p1997 N85-22521
Excitation of low-frequency resonance waves by moving conductor in space plasma 13 p2067 N85-22912
Spacecraft environment during the Giotto-Halley encounter: A summary 14 p2248 N85-23921
Observations of auroras and related plasma phenomena by the Kyokko and Jikken satellite in IMS — EXOS-A and B satellite 14 p2354 N85-24547
Response of magnetospheric substorm activity to changes in the interplanetary magnetized plasma
14 p2357 N85-24563
Measuring electrical field fluctuations by Langmuir Double Probe Method 16 p2720 N85-26789
Geophysical responses of dynamics of solar wind transition region 16 p2721 N85-26795
Determining effective rate of plasma heating in outer equatorial ionosphere using data from ISIS-1 and ISIS-2 satellites 16 p2721 N85-26797
Observations of low energy magnetospheric plasma outside the plasmasphere
[KGI-PREPRINT-075] 20 p3536 N85-32004
Surface voltage gradient role in high voltage solar array-plasma interaction: Center Director's discretionary fund
[NASA-TM-86516] 22 p3805 N85-33567

SPACE PLATFORMS
NT EURECA (ESA)
NT SYNCHRONOUS PLATFORMS
Research study: Studies in atmospheric processes from Space Platforms
[NASA-CR-171176] 01 p0072 N85-10473
Modular experimental platform for science and applications 02 p0152 N85-11031
Selected tether applications in space: An analysis of five selected concepts
[NASA-CR-171222] 04 p0480 N85-12921
Autonomous momentum management for space station
[NASA-CR-174065] 04 p0482 N85-12931
Autonomous momentum management for space station, exhibit A
[NASA-CR-171256] 04 p0482 N85-12933
Tethers open new space options
11 p1642 N85-20340
Earth observations and the polar platform
[NOAA-TR-NESDIS-18] 11 p1689 N85-20517
Space Station
[NASA-EP-211] 12 p1793 N85-21251
Space Technology Experiments Platform (STEP) status: An in-space test facility 14 p2236 N85-23863
Utilization of the polar platform of NASA's Space Station Program for operational Earth observations
[PB85-152502] 14 p2240 N85-23895
MBB/Erno's views, future plans in aerospace activities
15 p2531 N85-25609
Study on the extension of experiment resources in the MAUS project
[BMFT-FB-W-84-051] 15 p2650 N85-26343
Artificial intelligence in space platforms
[AD-A152078] 16 p2851 N85-27578
Comparative study on data system architectures — spacecraft data processing
[ESA-CR(P)-2015] 21 p3675 N85-32828
Initial placement of STO instruments
23 p3902 N85-34174

SPACE POWER REACTORS
NT SPACE POWER UNIT REACTORS
Emerging space nuclear power needs
05 p0606 N85-13682
Technology status of thermionic fuel elements for space nuclear power 05 p0610 N85-13693
Advanced concepts liquid droplet radiator
05 p0610 N85-13699
The liquid droplet radiator - an ultralightweight heat rejection system for efficient energy conversion in space
05 p0610 N85-13900
Lunar nuclear power feasibility study
[NASA-CR-171831] 07 p1041 N85-16611
Interagency program on space nuclear power: Directory of participants in the SP-100 program
[DE85-026339] 08 p1221 N85-17691
Instrumentation and controls evaluation for space nuclear power systems
[DE85-000983] 09 p1383 N85-18695
Safety program considerations for space nuclear reactor systems
[DE85-003295] 10 p1556 N85-19808
Thermionic converter for space reactor described
11 p1621 N85-20208
Opening up the future in space with nuclear power
[DE85-002411] 11 p1727 N85-20862
Space nuclear-power reactor design based on combined neutronic and thermal-fluid analyses
[DE85-002433] 11 p1727 N85-20864
Irradiation effects on fuels for space reactors
[DE84-016460] 12 p1931 N85-22134
Ordered carbon metal alloys for extraterrestrial power systems
[AD-A150881] 14 p2255 N85-23977
Physics effects of accidental submersion of space power reactors in water
[DE85-005020] 15 p2650 N85-26344
Space reactor ground tests, assessment of facility needs
[DE85-006814] 15 p2650 N85-26345

Analysis of alkali liquid metal Rankine space power systems
[DE85-005089] 16 p2741 N85-26917
Load-carrying capabilities of refractory alloys for space reactor power applications
[DE85-010566] 19 p3240 N85-30087
Development of improved thermoelectric materials for space nuclear power systems
[DE85-013079] 22 p3844 N85-33807
SP-100 Thermionic Technology Program
[DE85-012311] 23 p3972 N85-34625
Strategic defense initiative
[DE85-012778] 24 p4150 N85-35735

SPACE POWER UNIT REACTORS
Overview of the 1985 NASA Lewis Research Center SP-100 free-piston Stirling engine activities
[NASA-TM-87028] 16 p2680 N85-27769

SPACE PROBES
NT GALILEO PROBE
NT GALILEO SPACECRAFT
NT GIOTTO MISSION
NT HELIOS 1
NT HELIOS 2
NT JUPITER PROBES
NT LUNIK LUNAR PROBES
NT MARINER 5 SPACE PROBE
NT MARINER 9 SPACE PROBE
NT MARS PROBES
NT PIONEER SPACE PROBES
NT PIONEER 10 SPACE PROBE
NT PIONEER 11 SPACE PROBE
NT VENERA SATELLITES
NT VENERA 11 SATELLITE
NT VENUS PROBES
NT VIKING MARS PROGRAM
NT VIKING SPACECRAFT
Launch summary for 1978 - 1982 — sounding rockets, space probes, and satellites
[NASA-TM-87375] 04 p0461 N85-12924
A priority of space exploration: Observation of Saturn's rings from a Saturn orbiter 15 p2679 N85-26542
Rendezvous with Saturn's rings 15 p2679 N85-26543
Magnetospheric multiprobes: MMP/CHEMSAT 23 p3902 N85-34171
Precision measurements of solar energetic particle elemental composition
[SH-2.1-4] 23 p3998 N85-34785

SPACE PROCESSING
Second Symposium on Space Industrialization — space commercialization
[NASA-CP-2313] 02 p0149 N85-11011
Financial issues for commercial space ventures: Paying for the dreams 02 p0150 N85-11014
Opportunities for space bioprocessing 02 p0150 N85-11018
Potential utilization of glass experiments in space 02 p0151 N85-11020
Preparation of large-particle-size monodisperse latexes in space: The STS-3, STS-4, and STS-7 mission results 02 p0151 N85-11021
Producing gallium arsenide crystals in space 02 p0151 N85-11023
Microgravity containerless processing in long drop tubes 02 p0153 N85-11037
Opportunities for commercial organizations 02 p0156 N85-11055
NBS (National Bureau of Standards): Materials measurements
[NASA-CR-174038] 03 p0332 N85-12143
Bioprocessing in space 05 p0690 N85-14436
Bioprocessing in space 05 p0690 N85-14439
Commerce lab: Mission analysis and payload integration study
[NASA-CR-174381] 10 p1426 N85-18993
The feasibility of low-G grey solidification of nodular iron in the F-104 experimental furnace package
[NASA-TM-82527] 10 p1426 N85-18996
Alloy supercooling on Salyut-7 11 p1604 N85-20083
Development of the sonic pump levitator
[NASA-CR-171362] 12 p1782 N85-21186
Monodisperse Latex Reactor (MLR): A materials processing space shuttle mid-deck payload
[NASA-TM-86467] 12 p1782 N85-21187
Material research in microgravity
[NASA-TM-77626] 14 p2228 N85-23811
Microgravity: A new tool for basic and applied research in space
[EP-212] 16 p2716 N85-26767
Crystallization of aluminum-based alloys in weightlessness 19 p3242 N85-30101
Concept development evaluation for John Deere/UA STS middeck experiment location
[NASA-CR-171541] 20 p3397 N85-31071
Microgravity silicon zoning investigation
[NASA-CR-171531] 20 p3397 N85-31073
German payloads for EURECA 1
[BMFT-FB-W-85-003] 20 p3419 N85-31223
Kidney cell electrophoresis
[NASA-CR-171869] 20 p3498 N85-31745
Task description for the 1983 catalog of tasks for the materials processing in space program 20 p3498 N85-31746
Asymmetric electroosmotic flow and mobility measurements at nonstationary positions in the rectangular chamber 20 p3499 N85-31749
Theoretical prediction of stationary positions in the rectangular chamber during asymmetric electroosmotic flow 20 p3499 N85-31750
A computer program for determining the electrophoretic mobility of cells in a rectangular chamber during asymmetric electroosmotic flow 20 p3499 N85-31751
Evaluation of results of cell electrophoresis experiments on space shuttle STS-3 including pre-flight and post-flight laboratory experiments 20 p3502 N85-31772
Free zone electrophoresis simulation of static column electrophoresis in microgravity on shuttle flight STS-3 20 p3502 N85-31773
Microgravity electrophoresis: A study of the factors that affect free-fluid separation 20 p3502 N85-31774
Pre-flight report on cultured human embryonic kidney cell handling and cell electrophoresis. Prepared prior to continuous-flow electrophoretic separation experiments aboard space shuttle flight STS-8 20 p3503 N85-31775
Properties of electrophoretic fractions of human embryonic kidney cells separated on space shuttle flight STS-8 20 p3503 N85-31776
Study of requirements for and method of multidimensional acoustic imaging — spaceborne experiments
[ESA-CR(P)-2020] 20 p3525 N85-31924
The EURECA solution growth facility conceptual design study. Executive summary
[ESA-CR(P)-2007] 20 p3538 N85-32016

SPACE PROCESSING APPLICATIONS ROCKET
Technological experiments on high-altitude rockets 16 p2725 N85-26818

SPACE PROGRAMS
NT BRAZILIAN SPACE PROGRAM
NT CANADIAN SPACE PROGRAM
NT EUROPEAN SPACE PROGRAMS
NT FRENCH SPACE PROGRAMS
NT INDIAN SPACE PROGRAM
NT JAPANESE SPACE PROGRAM
NT SWEDISH SPACE PROGRAM
NT U.S.S.R. SPACE PROGRAM
Space America's commercial space program 02 p0152 N85-11027
Fokker wants to start new Netherlands space program 03 p0310 N85-11999
Space Nuclear Safety Program
[DE84-016973] 05 p0728 N85-14679
A buyer's guide to space infrastructure 07 p0914 N85-15784
Broadening the debate 07 p0914 N85-15785
Toward a goal-oriented civilian space program 07 p0914 N85-15786
Results of principal NASA studies on space station uses and functional requirements 07 p0914 N85-15787
Title 2: National Commission on Space (Public Law 98-361) 07 p0915 N85-15791
China report: Science and technology
[JPRS-CST-84-039] 11 p1621 N85-20206
PRC journal discusses 'Star Wars' space program 11 p1621 N85-20207
Space Shuttle aerothermodynamic data report, phase C
[NASA-CR-171858] 14 p2241 N85-23897
NASA photography index
[NASA-TM-87457] 15 p2685 N85-26445
East Europe report: Science and technology
[JPRS-ESA-84-032] 16 p2727 N85-26833
Contribution to space program reviewed 16 p2727 N85-26834
Department of Housing and Urban Development-independent agencies appropriations for 1986. Part 6: National Aeronautics and Space Administration
[GPO-47-235] 16 p2879 N85-27766
A spacefaring people: Perspectives on early spaceflight
[NASA-SP-4405] 23 p4056 N85-35142
Space science and exploration: A historical perspective 23 p4056 N85-35143
The next assignment: The state of the literature on space 23 p4057 N85-35146
Opportunities for policy historians: The evolution of the US civilian space program 23 p4057 N85-35147
Space-age Europe, 1957-1980 23 p4057 N85-35148
Space activities in the Soviet Union, Japan, and the People's Republic of China 23 p4057 N85-35149

SPACE RADIATION
U EXTRATERRESTRIAL RADIATION

SPACE RADIATORS
U SPACECRAFT RADIATORS

SPACE RATIONS
Research on zero-gravity botany apparatus 16 p2723 N85-26811

SPACE RENDEZVOUS
NT ORBITAL RENDEZVOUS
Progress-22 docks with Salyut-7 02 p0157 N85-11064
Transportation applications, part 2 11 p1643 N85-20350
Evaluation of OMV ranging and docking systems 12 p1947 N85-22230
National Space Transportation Systems Program mission report
[NASA-TM-87455] 14 p2242 N85-23900
Automatic rendezvous and docking systems functional and performance requirements
[NASA-CR-171866] 15 p2492 N85-25378
Hardware test program for evaluation of baseline range-range rate sensor concept
[NASA-CR-176143] 23 p3933 N85-34377

SPACE SCIENCES
U AEROSPACE SCIENCES

SPACE SHUTTLE ASCENT STAGE
Shuttle navigation status 08 p1092 N85-16901
Debris control design achievements of the booster separation motors 08 p1098 N85-16942
Shuttle system ascent aerodynamic and plume heating 08 p1103 N85-16975
Shuttle/Centaur upper stage capability 11 p1712 N85-20773

SPACE SHUTTLE BOOSTERS
Vibration, acoustic, and shock design and test criteria for components on the Solid Rocket Boosters (SRB), Lightweight External Tank (LWT), and Space Shuttle Main Engines (SSME)
[NASA-RP-1127] 01 p0061 N85-10405
The solid rocket booster auxiliary power unit: Meeting the challenge 08 p1099 N85-16948
Space Shuttle booster thrust imbalance analysis
[NASA-TM-86493] 12 p1791 N85-21241
B-52B/DTV (Drop Test Vehicle) flight test results: Drop test missions
[NASA-CR-171530] 19 p3215 N85-29934
SRB TPS closeout materials characterization
[NASA-CR-170885] 24 p4070 N85-35222
SRB thermal protection systems materials test results in an arc-heated nitrogen environment
[NASA-CR-170661] 24 p4072 N85-35236
Study of NSI and related cable performance during tests performed in the NASA Hot Gas Facility
[NASA-CR-170686] 24 p4101 N85-35423

SPACE SHUTTLE MAIN ENGINE
Rotordynamic analysis of the SSME turbopumps using reduced models
[NASA-CR-171170] 01 p0054 N85-10355
Retardation analytical model to extend service life
[NASA-CR-171177] 01 p0057 N85-10376
Vibration, acoustic, and shock design and test criteria for components on the Solid Rocket Boosters (SRB), Lightweight External Tank (LWT), and Space Shuttle Main Engines (SSME)
[NASA-RP-1127] 01 p0061 N85-10405
An electrochemical study of hydrogen uptake and elimination by bare and gold-plated waspaloy
[NASA-TM-86479] 02 p0182 N85-11222
Non-intrusive speed sensor — space shuttle main engine turbopumps
[NASA-CR-171204] 03 p0364 N85-12331
Analysis of physical-chemical processes governing SSME internal fluid flows
[NASA-CR-171247] 04 p0451 N85-12859
Turbine blade damping study, introduction 04 p0456 N85-12891
Prediction of force coefficients for labyrinth seals 05 p0644 N85-14130
Identification of dynamic coefficients of annular turbulent seals 05 p0644 N85-14133
Analysis of physical-chemical processes governing SSME internal fluid flows
[NASA-CR-174245] 06 p0760 N85-14862
Shuttle avionics software trials, tribulations and success 08 p1090 N85-16891
Man-machine interface and control of the shuttle digital flight system 08 p1091 N85-16894
Space shuttle main engine hardware simulation 08 p1091 N85-16895

SSME lifetime prediction and verification, integrating environments, structures, materials: The challenge
08 p1095 N85-16918
Space shuttle flight readiness firing dress rehearsal for STS-1
08 p1097 N85-16929
Cryogenic propellant management: Integration of design, performance and operational requirements
08 p1098 N85-16939
Space shuttle main engine: Interactive design challenges
08 p1098 N85-16940
Debris control design achievements of the booster separation motors
08 p1098 N85-16942
Computational fluid mechanics utilizing the variational principle of modeling damping seals
[NASA-CR-174332] 08 p1161 N85-17325
Assessment of the operating characteristics of the SSME LOX turbopump pump-end bearing
[NASA-CR-171287] 08 p1167 N85-17362
Analytical and experimental investigation of rubbing interaction in labyrinth seals for a liquid hydrogen fuel pump — space shuttle main engine
[NASA-CR-174657] 09 p1287 N85-18084
The analysis by the lumped parameter method of slade platform friction dampers used in the high pressure fuel turbopump on the space shuttle main engine
09 p1338 N85-18417
SSME thrust chamber simulation using Navier-Stokes equations
[NASA-CR-171349] 10 p1430 N85-19017
Thrust chamber performance using Navier-Stokes solution — space shuttle main engine viscous nozzle calculation
[NASA-CR-171346] 10 p1430 N85-19019
Preliminary analysis of selected gas dynamic problems — space shuttle main engine main combustion transients and IUS nozzle flow
[NASA-CR-171343] 10 p1483 N85-19361
Calculation of flow about posts and powerhead model — space shuttle main engine
[NASA-CR-171344] 10 p1483 N85-19362
STS-1 Pogo analysis
[NASA-TM-87433] 11 p1591 N85-20007
Using a data base management system for modelling SSME test history data
12 p1944 N85-22211
An investigation of space shuttle main engine shutdown chugging instability
12 p1946 N85-22221
Sensor control of robot arc welding
12 p1948 N85-22233
Evaluation of PHOENICS as a design analysis tool for SSME
12 p1949 N85-22240
Nonlinear rotordynamics analysis
[NASA-CR-171425] 13 p1968 N85-22364
High-pressure rocket engine turnaround duct computational fluid dynamics analysis
13 p2003 N85-22556
HPFTP flow diverter analysis
[NASA-CR-171424] 13 p2091 N85-23057
Cyclic structural analyses of anisotropic turbine blades for reusable space propulsion systems — same fuel turbopump
[NASA-TM-86990] 14 p2320 N85-24339
Flow induced vibration of the SSME LOX posts
[NASA-CR-175808] 15 p2495 N85-25391
Study of high performance alloy electroforming
[NASA-CR-175741] 15 p2508 N85-25473
Advanced High Pressure O2/H2 Technology
[NASA-CP-2372] 16 p2733 N85-26862
Thrust chamber life prediction
16 p2733 N85-26865
Manufacturing and producibility technology
16 p2733 N85-26866
Ceramics for advanced O2/H2 application
16 p2734 N85-26868
Vacuum plasma coatings for turbine blades
16 p2734 N85-26869
Material technology
16 p2734 N85-26870
Design overview of fiber-reinforced superalloy composites for the Space Shuttle main engine
16 p2734 N85-26871
Development of hydrogen resistant alloys
16 p2735 N85-26873
Development of new materials for turbopump bearings
16 p2735 N85-26877
Bearings working group
16 p2735 N85-26878
Advanced rocket engine cryogenic turbopump bearing thermal model
16 p2735 N85-26879
Hybrid bearings for LH2 and LO2 turbopumps
16 p2736 N85-26880
Powder metallurgy bearings for advanced rocket engines
16 p2736 N85-26881
Rolling contact fatigue life of chromium ion plated 440C bearing steel
16 p2736 N85-26882
Technical overview structural dynamics
16 p2736 N85-26883
Signal analysis techniques for incipient failure detection in turbomachinery
16 p2736 N85-26884
Flow dynamic environment data base development for the SSME
16 p2736 N85-26885
Turbine blade friction damping study
16 p2736 N85-26886
Preliminary results on passive eddy current damper technology for SSME turbomachinery
16 p2737 N85-26890
Rotor response for transient unbalance changes in a nonlinear simulation
16 p2737 N85-26892
Damping seal verification setup
16 p2738 N85-26893
Damping seals for turbomachinery
16 p2738 N85-26894
Vibration characteristics of the HPOTP (High Pressure Oxygen Turbopump) of the SSME (Space Shuttle Main Engine)
16 p2738 N85-26895
Fluid and gas dynamics
16 p2738 N85-26897
Experimental evaluation of an advanced Space Shuttle main engine hot-gas manifold design concept
16 p2738 N85-26898
Redistribution of the inlet temperature profile through the SSME fuel turbine
16 p2739 N85-26901
Analytical study of flow phenomena in SSME turnaround duct geometries
16 p2739 N85-26902
Instrumentation technology overview
16 p2739 N85-26903
Fiber optic Raman thermometer for Space Shuttle main engine preburner profiling
16 p2739 N85-26904
An advanced solid state pressure transducer for high reliability SSME application
16 p2739 N85-26905
Nonintrusive shaft speed sensor
16 p2740 N85-26908
Flow-induced vibration of the SSME LOX posts: Additional issues
[DE85-007339] 16 p2741 N85-26916
Structural integrity and Durability of Reusable Space Propulsion Systems
[NASA-CP-2381] 17 p2910 N85-27941
Overview of aerothermodynamic loads definition study
17 p2910 N85-27942
SSME fuel preburner two-dimensional analysis
17 p2911 N85-27943
SSME turbopump turbine computations
17 p2911 N85-27944
Simulation of multistage turbine flows
17 p2911 N85-27945
New facility to study unsteady wake effects on turbine airfoil heat transfer
17 p2911 N85-27948
Calculation of viscous compressible flows in small gas turbines
17 p2912 N85-27950
Flow-induced vibration of SSME main injector liquid-oxygen posts
17 p2912 N85-27951
Overview of structural response: Probabilistic structural analysis
17 p2912 N85-27952
Composite loads spectra for select space propulsion structural components
17 p2912 N85-27953
Probabilistic structural analysis of SSME turbopump blades: Probabilistic geometry effects
17 p2913 N85-27958
Structural tailoring of SSME blades (vanes)
17 p2913 N85-27960
Cyclic structural analyses of SSME turbine blades
17 p2914 N85-27963
Effects of high mean stress on high-cycle fatigue behavior of PWA 1480
17 p2914 N85-27964
Constitutive cyclic deformation behavior in single-crystal and directionally solidified SSME high-pressure fuel turbopump airfoil materials
17 p2914 N85-27965
Thin-film sensors for space propulsion technology
17 p2915 N85-27968
Optical strain measurement system development
17 p2915 N85-27969
Heat flux sensor calibrator
17 p2915 N85-27970
Feasibility of mapping velocity flow fields in SSME powerhead by laser anemometry techniques
17 p2915 N85-27971
Analysis of physical-chemical processes governing SSME internal fluid flows
[NASA-CR-175893] 17 p2957 N85-28261
Research pressure instrumentation for NASA space shuttle main engine
[NASA-CR-176014] 19 p3227 N85-30006
SSME seal test program: Test results for hole-pattern damper seals
[NASA-CR-171595] 20 p3366 N85-31059
SRB thermal protection systems materials test results in an arc-heated nitrogen environment
[NASA-CR-170881] 24 p4072 N85-35236

SPACE SHUTTLE MISSION 31-C
Modular Optoelektronischer Multispektraler Scanner (MOMS), interpretation and evaluation of the MOMS image Arica, West Coast of South America — STS-7 flight
05 p0657 N85-14222

SPACE SHUTTLE MISSION 41-B
National Space Transportation Systems Program mission report
[NASA-TM-87454] 14 p2242 N85-23899
Results from radiation monitoring equipment experiment on STS-11
[AD-A152531] 17 p2908 N85-27932

SPACE SHUTTLE MISSION 41-C
National Space Transportation Systems Program mission report
[NASA-TM-87455] 14 p2242 N85-23900

SPACE SHUTTLE MISSION 41-G
Atmospheric environment for Space Shuttle (STS-41G) launch
[NASA-TM-86486] 07 p0995 N85-16320

SPACE SHUTTLE MISSION 51-A
Atmospheric environment for Space Shuttle (STS-51A) launch
[NASA-TM-86497] 12 p1892 N85-21875

SPACE SHUTTLE MISSION 51-C
Atmospheric environment for space shuttle (STS-51C) launch
[NASA-TM-86508] 19 p3315 N85-30547

SPACE SHUTTLE MISSIONS
NT SPACE SHUTTLE MISSION 31-C
NT SPACE SHUTTLE MISSION 41-B
NT SPACE SHUTTLE MISSION 41-C
NT SPACE SHUTTLE MISSION 41-G
NT SPACE SHUTTLE MISSION 51-A
NT SPACE SHUTTLE MISSION 51-C
Atmospheric environment for Space Shuttle (STS-41D) launch
[NASA-TM-86494] 05 p0679 N85-14358

SPACE SHUTTLE ORBITAL FLIGHT TEST 1
U SPACE TRANSPORTATION SYSTEM 1 FLIGHT

SPACE SHUTTLE ORBITAL FLIGHT TEST 3
U SPACE TRANSPORTATION SYSTEM 3 FLIGHT

SPACE SHUTTLE ORBITAL FLIGHT TEST 4
U SPACE TRANSPORTATION SYSTEM 4 FLIGHT

SPACE SHUTTLE ORBITAL FLIGHT TESTS
U SPACE TRANSPORTATION SYSTEM FLIGHTS

SPACE SHUTTLE ORBITAL FLIGHT 7
U SPACE SHUTTLE MISSION 31-C

SPACE SHUTTLE ORBITAL FLIGHTS
U SPACE TRANSPORTATION SYSTEM FLIGHTS

SPACE SHUTTLE ORBITER 099
U CHALLENGER (ORBITER)

SPACE SHUTTLE ORBITER 101
U ENTERPRISE (ORBITER)

SPACE SHUTTLE ORBITER 102
U COLUMBIA (ORBITER)

SPACE SHUTTLE ORBITER 103
U DISCOVERY (ORBITER)

SPACE SHUTTLE ORBITERS
NT CHALLENGER (ORBITER)
NT COLUMBIA (ORBITER)
NT DISCOVERY (ORBITER)
NT ENTERPRISE (ORBITER)
Structural analysis of the Space Shuttle Orbiter
01 p0081 N85-10401
Space Shuttle Orbiter trimmed center-of-gravity extension study. Volume 8: Effects of configuration modifications on the aerodynamic characteristics of the 140 A/B Orbiter at a Mach number of 5.97
[NASA-TM-72661-VOL-8] 04 p0452 N85-12957
Selected tether applications in space: An analysis of five selected concepts
[NASA-CR-171222] 04 p0460 N85-12921
Columbia: The first 5 flights entry heating data series. Volume 1: An overview
[NASA-CR-171820] 07 p0913 N85-15777
Effect of aerodynamic and angle-of-attack uncertainties on the May 1979 entry flight control system of the Space Shuttle from Mach 8 to 1.5
[NASA-TP-2365] 07 p0913 N85-15778
Space Shuttle Technical Conference, part 1
[NASA-CP-2342-PT-1] 08 p1090 N85-16889
Evolution of shuttle avionics redundancy management/fault tolerance
08 p1090 N85-16890
Shuttle avionics software trials, tribulations and success
08 p1090 N85-16891
Shuttle avionics software development trials: Tribulations and successes, the backup flight system
08 p1091 N85-16892
SSME digital control design characteristics
08 p1091 N85-16893
Development and implementation of the verification process for the shuttle avionics system
08 p1091 N85-16896
Ground man-machine interfaces for orbiter checkout
08 p1091 N85-16897
Integration of ground and on-board system for terminal count
08 p1092 N85-16898
Integrated design checkout of shuttle payload avionics interfaces
08 p1092 N85-16899

Descent guidance and mission planning for space shuttle 08 p1092 N85-16902
Some effects of digital sampling on orbiter flight control system operation 08 p1092 N85-16903
Space shuttle handling qualities 08 p1092 N85-16904
The development and application of aerodynamic uncertainties: And flight test verification for the space shuttle orbiter 08 p1093 N85-16910
Aerodynamic challenges of ALT 08 p1094 N85-16911
The orbiter air data system 08 p1094 N85-16912
Orbiter structural design and verification 08 p1094 N85-16915
The challenging scales of the bird: Shuttle tile structural integrity 08 p1095 N85-16919
Challenges in the development of the orbiter atmosphere revitalization subsystem 08 p1095 N85-16920
Challenges in the development of the orbiter active thermal control subsystem 08 p1096 N85-16923
Other challenges in the development of the orbiter environmental control hardware 08 p1096 N85-16924
Challenges in the development of the orbiter radiator system 08 p1096 N85-16925
Debris control design achievements of the booster separation motors 08 p1098 N85-16942
Orbital Maneuvering system design evolution 08 p1098 N85-16943
Design evolution of the orbiter reaction control subsystem 08 p1099 N85-16944
Space shuttle orbiter auxiliary power unit development challenges 08 p1099 N85-16945
Space shuttle electrical power generation and reactant supply system 08 p1099 N85-16947
Shuttle S-band communications technical concepts 08 p1099 N85-16948
Shuttle ku-band communications/radar technical concepts 08 p1099 N85-16949
Shuttle payload S-band communications system 08 p1100 N85-16950
TDRSS S-shuttle unique receiver equipment 08 p1100 N85-16951
The Statistical Loop Analyzer (SLA) 08 p1100 N85-16955
Digital scrambling for shuttle communication links: Do drawbacks outweigh advantages? 08 p1101 N85-16956
Electronics systems test laboratory testing of shuttle communications systems 08 p1101 N85-16958
Orbiter wheel and tire certification 08 p1101 N85-16959
Orbiter processing facility: Access platforms Kennedy Space Center, Florida, from challenge to achievement 08 p1102 N85-16968
Payload transportation at KSC 08 p1103 N85-16970
STS payload ground handling mechanism at John F. Kennedy Space Center 08 p1103 N85-16971
The orbiter mate/demate device 08 p1103 N85-16972
In-flight testing of the space shuttle orbiter thermal control system 08 p1103 N85-16974
Thermal design of the space shuttle external tank 08 p1103 N85-16977
Orbiter entry aerothermodynamics 08 p1104 N85-16978
Orbiter thermal protection system 08 p1104 N85-16979
Shuttle on-orbit contamination and environmental effects 08 p1104 N85-16980
Design concept definition study for an improved shuttle waste collection subsystem [NASA-CR-171834] 08 p1198 N85-17546
Improved orbiter waste collection system study [NASA-CR-171830] 08 p1199 N85-17548
Improved orbiter waste collection system study, appendix D [NASA-CR-171833] 08 p1199 N85-17549
Waste collection subsystem study [NASA-CR-171836] 08 p1199 N85-17552
Space Shuttle Orbiter waste collection system conceptual study [NASA-CR-171844] 08 p1199 N85-17553
Space Shuttle Orbiter trimmed center-of-gravity extension study. Volume 9: Effects of configuration modifications on the aerodynamic characteristics of the 140 A/B Orbiter at Mach numbers of 1.5, 2.0, and 2.5 — wind tunnel tests [NASA-TM-72861-VOL-9] 10 p1420 N85-18956
Space Shuttle orbiter trimmed center-of-gravity extension study [NASA-TP-2264] 10 p1428 N85-19003
Study of several factors affecting crew escape trajectories from the Space Shuttle Orbiter at low-subsonic speeds [NASA-TM-86303] 10 p1428 N85-19008
STS-1 Pogo analysis [NASA-TM-87433] 11 p1591 N85-20007
Shuttle tethered satellite system program overview 11 p1642 N85-20342
Results of Space Shuttle flight 41-D [GPO-39-461] 12 p1791 N85-21243
Aerospace Safety Advisory Panel [NASA-TM-87426] 13 p1970 N85-22373
Results of a M = 5.3 heat transfer test of the integrated vehicle using phase-change paint techniques on the 0.0175-scale model 56-OTS in the NASA/Ames Research Center 3.5-foot hypersonic wind tunnel [NASA-CR-167695] 13 p1988 N85-22468
Wakes and differential charging of large bodies in low Earth orbit 13 p1992 N85-22488
Active control technology experience with the Space Shuttle in the landing regime 17 p2903 N85-27900
Shuttle-tethered satellite system definition study. Volume 1: Executive study [NASA-CR-171474] 17 p2907 N85-27924
Numerical computation of space shuttle orbiter flow field [NASA-CR-175912] 18 p3058 N85-28921
Modeling and analysis of pinhole occulter experiment: Initial study phase [NASA-CR-175978] 19 p3272 N85-30287
Use of a hyperbolic grid generation scheme in simulating supersonic viscous flow about three-dimensional winged configuration [NASA-TM-85344] 23 p3893 N85-34116

SPACE SHUTTLE PAYLOADS
NT ATMOSPHERIC GENERAL CIRCULATION EXPERIMENT
NT EARTH RADIATION BUDGET EXPERIMENT
NT OSS-1 PAYLOAD
NT PLASMA INTERACTION EXPERIMENT
NT SPACEBORNE EXPERIMENTS
NT SPACELAB
NT X RAY ASTROPHYSICS FACILITY

Space Research in Japan. National report 01 p0013 N85-10082
SEPAC (space experiments with particle accelerators) 01 p0014 N85-10085
Small Payload Flight Systems (SPFS) 02 p0152 N85-11030
European retrievable carrier (Eureca) and evolutionary space carrier for microgravity, Earth observation and technology demonstration 02 p0152 N85-11032
Project Explorer 02 p0154 N85-11041
Fluids Experiment Apparatus (FEA) 02 p0155 N85-11048
External tank aft cargo carrier 02 p0155 N85-11050
Proceedings of a Workshop on the Applications of Tethers in Space, Volume 1 [NASA-CR-171196] 03 p0322 N85-12076
Proceedings of a Workshop on Applications of Tethers in Space, Volume 2 [NASA-CR-171197] 03 p0322 N85-12077
Continuing issues (FY 1983) concerning military use of the space transportation system [AD-A146091] 03 p0323 N85-12080
The calibration of photographic and spectroscopic films: A densitometric analysis of IIaO film flown aboard the Space Shuttle 3 [NASA-CR-174278] 07 p0962 N85-16101
Lunar nuclear power feasibility study [NASA-CR-171831] 07 p1041 N85-16611
Integrated design checkout of shuttle payload avionics interfaces 08 p1092 N85-16899
Shuttle payload S-band communications system 08 p1100 N85-16950
Payload transportation at KSC 08 p1103 N85-16970
STS payload ground handling mechanism at John F. Kennedy Space Center 08 p1103 N85-16971
Computer aided processing using laser measurements 08 p1103 N85-16973
Shuttle on-orbit contamination and environmental effects 08 p1104 N85-16980
Commerce Lab: Mission analysis and payload integration study [NASA-CR-171272] 08 p1104 N85-16981
Shuttle/Centaur project perspective 08 p1106 N85-16991
Commerce lab: Mission analysis and payload integration study [NASA-CR-174381] 10 p1426 N85-18993
A preliminary study of a cryogenic equivalence principle experiment on Shuttle [NASA-CR-171300] 10 p1426 N85-18994
Commercial space: Europe should have independent strategy 10 p1460 N85-19205
British aerospace studies HOTOL satellite launcher 10 p1460 N85-19206
Brazilian Remote Sensing Shuttle Experiment (BRESEX): Characteristics and future utilization on satellites [INPE-3313-PRE/620] 10 p1487 N85-19385
The BRESEX multispectral camera: Preliminary characteristics [INPE-3357-PRE/635] 10 p1487 N85-19386
Space Transportation System (STS) propellant scavenging system study. Volume 1: Technical report [NASA-CR-171848-VOL-1] 11 p1589 N85-20000
Tether fundamentals 11 p1643 N85-20345
Science Applications, part 1 11 p1643 N85-20346
Status of the National Space Transportation System 11 p1712 N85-20772
Monodisperse Latex Reactor (MLR): A materials processing space shuttle mid-deck payload [NASA-TM-86487] 12 p1782 N85-21187
Satellite services and orbital retrieval 12 p1786 N85-21211
Results of Space Shuttle flight 41-D [GPO-39-461] 12 p1791 N85-21243
Report on final recommendations for IMPS engineering-science payload [NASA-CR-175659] 13 p1988 N85-22484
Suprathermal plasma observed on STS-3 Mission by plasma diagnostics package 13 p1989 N85-22472
Electron and ion density depletions measured in the STS-3 orbiter wake 13 p1989 N85-22474
Shuttle electrical environment 13 p1990 N85-22475
Interactions measurement payload for Shuttle 13 p1997 N85-22518
Electrostatic forming and testing of polymer films on a 16-foot diameter test fixture [NASA-TM-86328] 13 p2063 N85-22885
QUASAT: An orbiting very long baseline interferometer program using large space antenna systems 14 p2230 N85-23822
LDR system concepts and technology 14 p2231 N85-23823
Development of the 15-meter hoop-column antenna system 14 p2231 N85-23825
Box truss development and its application 14 p2231 N85-23826
Cable-catenary large antenna concept 14 p2231 N85-23829
Large Space Antenna Systems Technology, 1984 [NASA-CP-2368-PT-2] 14 p2233 N85-23840
Shuttle payload bay dynamic environments: Summary and conclusion report for STS flights 1-5 and 9 [NASA-CR-175856] 14 p2241 N85-23896
Geometric error analysis for shuttle imaging spectrometer experiment [NASA-CR-175865] 14 p2305 N85-24269
X-ray polarimetry: The measurement of the polarization of solar flare X-rays and the design of a Compton polarimeter 14 p2441 N85-25059
Study on the extension of experiment resources in the MAUS project [BMFT-FB-W-84-051] 15 p2650 N85-28343
Space radiation studies for the reporting period, June 1983 - July 1984 [NASA-CR-171411] 15 p2685 N85-26583
Microgravity: A new tool for basic and applied research in space [EP-212] 16 p2716 N85-26767
Orbiter middeck/payload standard interfaces control document [NASA-TM-87473] 16 p2729 N85-26840
Space Transportation System. Space shuttle payload flight assignments [NASA-TM-87492] 19 p3224 N85-29989
Space Transportation System. Space shuttle payload flight assignments [NASA-TM-87491] 19 p3224 N85-29990
On the accuracy of modelling the dynamics of large space structures 19 p3225 N85-29995
Evaluation of results of cell electrophoresis experiments on space shuttle STS-3 including pre-flight and post-flight laboratory experiments 20 p3502 N85-31772
Free zone electrophoresis simulation of static column electrophoresis in microgravity on shuttle flight STS-3 20 p3502 N85-31773
Microgravity electrophoresis: A study of the factors that affect free-fluid separation 20 p3502 N85-31774
Properties of electrophoretic fractions of human embryonic kidney cells separated on space shuttle flight STS-8 20 p3503 N85-31776
Appendange deployment mechanism for the Hubble Space Telescope program 22 p3798 N85-33533

SPACE SHUTTLE UPPER STAGES
Commercializing the transfer orbit stage
02 p0155 N85-11049

SPACE SHUTTLES
Active control technology experience with the Space Shuttle in the landing regime
[NASA-TM-85910] 01 p0012 N85-10071
Results of tests of advanced flexible insulation vortex and flow environments in the North American Aerodynamics Laboratory lowspeed wind tunnel using 0.0405-scale Space Shuttle Orbiter model 16-0 (test OA-309)
[NASA-CR-167692] 01 p0015 N85-10096
Vibration, acoustic, and shock design and test criteria for components on the Solid Rocket Boosters (SRB), Lightweight External Tank (LWT), and Space Shuttle Main Engines (SSME)
[NASA-RP-1127] 01 p0061 N85-10405
Space Shuttle Environmental Effects: The First 5 Flights
[NASA-CR-171612] 01 p0069 N85-10457
Toxicological evaluation of Columbia spacecraft
01 p0094 N85-10631
The evolution of small payload carrier systems
02 p0153 N85-11038
An experimental study of jet impingement on a circular cylinder
[AD-A145583] 02 p0196 N85-11326
Shuttle Experimental Radar for Geological Exploration (SERGE) project: Field work relating to the Shuttle Experimental Radar A (SIR-A) in Brazil (phase 2)
[NASA-CR-174033] 02 p0219 N85-11444
International cooperation and competition in space
[GPO-38-001] 02 p0295 N85-11911
International cooperation and competition in space. Introduction
02 p0295 N85-11912
STS natural environment analysis
[NASA-CR-171221] 03 p0322 N85-12079
Charging of the DMSP F-2 spacecraft in the aurora on 10 January 1983
[AD-A146303] 03 p0324 N85-12086
Development of computational fluid dynamics at NASA Ames Research Center
[NASA-TM-86021] 04 p0452 N85-12866
Launching systems
[CNES-NT-111] 04 p0460 N85-12917
Off-flow study of a Space Shuttle orbiter tip-fin controller
[NASA-TM-86276] 04 p0460 N85-12920
Review of Space Shuttle requirements, operations, and future plans
[GPO-39-101] 04 p0461 N85-12927
Statement of Frank Capolino, Solar Maximum Repair Mission Project Manager, Goddard Space Flight Center
04 p0461 N85-12930
A feasibility study on the use of wind profilers to support Space Shuttle launches
[NASA-CR-3661] 04 p0538 N85-13423
Vandenberg space shuttle launch complex
[S-HRG-98-1075] 05 p0601 N85-13633
Statement of Edward C. Aldridge, Jr., Under Secretary of the Air Force, Department of the Air Force, accompanied by Lieutenant General Robert W. Bazley, Inspector General and Brigadier General Donald J. Kutyna, Director of Space Systems and Command, Control and Communications, Deputy Chief of Staff, Research, Development and Acquisition
05 p0601 N85-13634
Statement of Honorable James M. Beggs, Administrator, National Aeronautics and Space Administration
05 p0601 N85-13635
A distributed expert system for Space Shuttle flight control
05 p0602 N85-13636
Six degrees of freedom control with each hand?
05 p0700 N85-14492
Searching for impact craters using space shuttle photography
06 p0869 N85-15645
Issues and findings
07 p0914 N85-15782
Space infrastructure
07 p0914 N85-15783
A buyer's guide to space infrastructure
07 p0914 N85-15784
Reduction method for thermal analysis of complex aerospace structures
[NASA-TP-2373] 07 p0957 N85-16066
Space Shuttle Technical Conference, part 1
[NASA-CP-2342-PT-1] 08 p1090 N85-16889
Automation of checkout for the shuttle operations era
08 p1092 N85-16900
Shuttle navigation status
08 p1092 N85-16901
Low-speed longitudinal orbiter qualities
08 p1092 N85-16905
The space shuttle ascent vehicle aerodynamic challenges configuration design and data base development
08 p1093 N85-16906
The space shuttle launch vehicle aerodynamic verification challenges
08 p1093 N85-16907
The aerodynamic challenges of SRB recovery
08 p1093 N85-16908
The aerodynamic challenges of the design and development of the space shuttle orbiter
08 p1093 N85-16909
Shuttle structural dynamics characteristics: The analysis and verification
08 p1094 N85-16913
Structural load challenges during space shuttle development
08 p1094 N85-16914
Orbiter structural design and verification
08 p1094 N85-16915
Space shuttle external tank performance improvements: The challenge
08 p1094 N85-16916
Structural and mechanical design challenges of space shuttle solid rocket boosters separation and recovery subsystems
08 p1095 N85-16917
SSME lifetime prediction and verification, integrating environments, structures, materials: The challenge
08 p1095 N85-16918
Challenges of developing an electro-optical system for measuring man's operational envelope
08 p1095 N85-16921
Challenges in the development of the shuttle extravehicular mobility unit
08 p1095 N85-16922
Transition to the space shuttle operations era
08 p1097 N85-16930
Launch processing system concept to reality
08 p1097 N85-16931
Automatic software for controlling cryogenic systems
08 p1097 N85-16932
Mathematical models for space shuttle ground systems
08 p1097 N85-16933
Managing computer-controlled operations
08 p1097 N85-16934
Support systems design and analysis
08 p1097 N85-16935
History, design and performance of the space shuttle hazardous gas detection system
08 p1098 N85-16936
Space Shuttle Technical Conference, part 2
[NASA-CP-2342-PT-2] 08 p1098 N85-16937
Propulsion and power systems perspective
08 p1098 N85-16938
Cryogenic propellant management: Integration of design, performance and operational requirements
08 p1098 N85-16939
Solid rocket motor certification to meet space shuttle requirements from challenge to achievement
08 p1098 N85-16941
The space shuttle program from challenge to achievement: Space exploration rolling on tires
08 p1101 N85-16960
Space shuttle elevon seal panel mechanism
08 p1101 N85-16961
Space shuttle wheels and brakes
08 p1101 N85-16962
The space shuttle orbiter remote manipulator positioning mechanism
08 p1102 N85-16963
An overview of the space remote manipulator system
08 p1102 N85-16964
Space shuttle rudder/speedbrake actuation subsystem
08 p1102 N85-16965
Development of the space shuttle body flap actuation subsystem
08 p1102 N85-16966
Mechanical features of the shuttle rotating service structure
08 p1102 N85-16967
External tank GH2 vent arm
08 p1102 N85-16969
Computer aided processing using laser measurements
08 p1103 N85-16973
Thermal design of the space shuttle solid rocket booster
08 p1103 N85-16976
Impact of activation optimization on the Vandenberg Ground Support System using Q-GERT analysis
[AD-A148448] 08 p1105 N85-16986
The design of an ion-neutral mass spectrometer to be used in the Shuttle environment
[AD-A148093] 08 p1114 N85-17022
Natural environment analysis
[NASA-CR-174330] 08 p1160 N85-17433
Prototype wash water renovation system integration with government-furnished wash fixture
[NASA-CR-171829] 08 p1198 N85-17547
Chronology of KSC and KSC related events for 1983
[NASA-TM-87400] 08 p1261 N85-17927
Water impact laboratory and flight test results for the space shuttle solid rocket booster aft skirt
09 p1335 N85-18394
Natural environment analysis
[NASA-CR-171333] 10 p1428 N85-19010
Analysis and optimization of small Space Shuttle propulsion platforms
[DFVLR-FB-84-28] 10 p1431 N85-19023
Shuttle S-band high gain switched beam breadboard antennas
[NASA-CR-171852] 10 p1478 N85-19327
Tethers open new space options
11 p1642 N85-20340
Tethered satellite system project overview
11 p1642 N85-20341
Summary presentation of the Transportation Panel
11 p1644 N85-20357
The Satellite sail
11 p1647 N85-20376
Preflight and postflight motion sickness testing of the Spacelab 1 crew
11 p1694 N85-20652
Space motion sickness monitoring experiment: Spacelab 1
11 p1695 N85-20654
Shuttle software production facility
11 p1701 N85-20694
Shuttle/Centaur upper stage capability
11 p1712 N85-20773
Earth resources research using the Shuttle Imaging Radar system
11 p1713 N85-20779
Aerospace Safety Advisory Panel
[NASA-TM-87428] 12 p1774 N85-21135
Space debris protection for a reusable orbital transfer vehicle
12 p1786 N85-21206
Space heat rejection radiators: Meteoroid/debris consideration
12 p1786 N85-21210
A remotely controlled orbiting retriever
12 p1786 N85-21212
Environment definition, small particles, diameter less than or equal to 1 MM
12 p1788 N85-21223
Feasibility of producing commodities and electricity for space shuttle operations at Vandenberg Air Force Base
[DCN-84-203-001-80-21] 12 p1789 N85-21230
Advanced research and technology programs for advanced high-pressure oxygen-hydrogen rocket propulsion
[NASA-TM-86969] 12 p1789 N85-21231
Study of outgassing and decomposition of space shuttle heat protection tiles, fillers and adhesive
[NASA-CR-175585] 12 p1791 N85-21242
Impacts of Space Shuttle thermal protection system tile on F-15 aircraft vertical tile
[NASA-TM-85904] 12 p1792 N85-21245
Space Shuttle interactive meteorological data system study
[NASA-CR-171418] 12 p1892 N85-21876
Research Reports: 1984 NASA/ASEE Summer Faculty Fellowship Program
[NASA-CR-171317] 12 p1944 N85-22210
Characterization of material surfaces exposed to atomic oxygen on space shuttle missions
12 p1946 N85-22220
Ground and flight testing for aircraft guidance and control
[AGARD-AG-282] 13 p1966 N85-22350
Feoktistov argues against U.S. space shuttle design concept
13 p1985 N85-22453
Selected tether applications in space: Phase 2. Executive summary
[NASA-CR-171421] 13 p1987 N85-22462
Selected tether applications in space: Phase 2
[NASA-CR-171422] 13 p1987 N85-22463
Vibroacoustic study of the NASA Goddard Space Flight Center OSS-1 payload
[NASA-CR-175320] 13 p1988 N85-22465
Results of aeroheating DFI and ET design-data test on a 0.0175-scale model 60-OTS conducted in the Von Karman Gas Dynamics Facility (VKF) 40' supersonic and the 50' hypersonic wind tunnels A and C
[NASA-CR-167693] 13 p1988 N85-22466
Spacecraft Environmental Interactions Technology, 1983
[NASA-CP-2359] 13 p1989 N85-22470
Space Station technology planning
13 p1989 N85-22471
Vehicle charging on STS-3 Mission
13 p1989 N85-22473
Measured electron contribution to Shuttle plasma environment: Abbreviated update
13 p1990 N85-22476
Laboratory studies of Kapton degradation in an oxygen ion beam
13 p1990 N85-22477
Electron beam charging of Space Shuttle thermal protection system tiles
13 p1990 N85-22478
Interactions measurement payload for Shuttle
13 p1997 N85-22518
Preliminary investigation of the electrodynamics of a conducting tether
13 p1997 N85-22521
Astronaut hazard during free-flight polar EVA
13 p1997 N85-22522
Research opportunities in human behavior and performance
[NASA-CR-3868] 13 p2142 N85-23299
Large space antenna technology applied to radar-imaging, rain-rate measurements, and ocean wind sensing
14 p2230 N85-23620
Shuttle attached antenna Flight Experiment Definition Study (FEDS)
14 p2237 N85-23665

Electro-science requirements for shuttle-attached antenna flight experiments 14 p2237 N85-23866
Space Shuttle aerothermodynamic data report, phase C
[NASA-CR-171858] 14 p2241 N85-23897
Surface pressure produced by Space Transportation System flight 41B
[AD-A150793] 14 p2242 N85-23901
Alternate nozzle ablative materials program
[NASA-CR-175658] 14 p2246 N85-23924
Shuttle operational test and scientific investigations 14 p2394 N85-24748
Shuttle communications and tracking systems modeling and TDRSS link simulations studies
[NASA-CR-171661] 15 p2491 N85-25369
Shuttle fleet operations: A simulation analysis
[AD-A151383] 15 p2491 N85-25370
Costs, payload of Ariane, US Space Shuttle compared 15 p2530 N85-25601
Formulation and implementation of nonstationary adaptive estimation algorithm with applications to air-data reconstruction
[NASA-TM-86727] 16 p2706 N85-26699
Active control technology experience with the Space Shuttle in the landing regime 16 p2713 N85-26747
Space Shuttle program communication and tracking systems interface analysis
[NASA-CR-171662] 16 p2729 N85-26841
Cost prediction model for various payloads and instruments for the Space Shuttle Orbiter
[NASA-CR-175761] 16 p2729 N85-26842
Consultative Committee for Space Data Systems. Panel 1: Support
[NASA-CR-175786] 16 p2769 N85-27090
The Bressx multispectral camera: Preliminary characteristics
[INPE-3424-PRE/687] 16 p2787 N85-27195
Shuttle-tethered satellite system definition study extension
[NASA-CR-171473] 17 p2907 N85-27923
Results from radiation monitoring equipment experiment on STS-11
[AD-A152331] 17 p2908 N85-27932
Mathematical modeling and control of a large space structure as applied to a shuttle-antenna configuration
[AD-A153269] 17 p2910 N85-27939
Analysis of heat-transfer measurements from 2 AEDC wind tunnels on the Shuttle external tank
[NASA-CR-171470] 17 p2957 N85-28263
Heating parameter estimation using coaxial thermocouple gages in wind tunnel test articles
[AD-A153039] 17 p2966 N85-28328
Space insurance firms view shuttle, Ariane reliability 18 p3086 N85-29090
British super-shuttle 18 p3087 N85-29104
Astronautical conference hears details on Hermes minishuttle 18 p3088 N85-29112
Internal contamination issues 18 p3156 N85-29543
Space shuttle revitalization system 18 p3157 N85-29548
Publications of the Jet Propulsion Laboratory 1983
[NASA-CR-175979] 18 p3199 N85-29648
Space shuttle molecular and wake vacuum measurements
[NASA-TM-86609] 19 p3222 N85-29978
Hemispherical latching apparatus
[NASA-CASE-MFS-25837-1] 19 p3224 N85-29991
Study of Kapton under simulated shuttle environment
[NASA-CR-176003] 19 p3225 N85-29997
Slide release mechanism — for space shuttle orbiter/external tank connection device
[NASA-CASE-MSC-20060-1] 19 p3279 N85-30334
Insurance and the commercialization of space
[S-PRT-99-16] 20 p3397 N85-31074
Vibration/libration interaction dynamics during the orbiter based deployment of flexible members 20 p3411 N85-31171
Civilian Space Stations and the US future in Space
[OTA-STI-242] 20 p3418 N85-31215
Three-dimensional ballistocardiography in microgravity 20 p3510 N85-31618
Biostack experiments on STS-flights and the impact for man in space 20 p3510 N85-31621
Pricing options for the space shuttle. Special study 21 p3559 N85-32136
The space shuttle glow
[AD-A154937] 21 p3559 N85-32139
Spacelab 1 hematology experiment (INS103): Influence of space flight on erythrokinetics in man
[NASA-TM-58268] 22 p3824 N85-33693
Results of a study to build a gamma-ray telescope in an external tank
[OG-9.3-3] 23 p4027 N85-34958
Space Missions for Automation and Robotics Technologies (SMART) Program
[NASA-TM-86820] 24 p4066 N85-35210
Results of tests of the SRB aft skirt heat shield curtain in the MSFC Hot Gas Facility
[NASA-CR-170888] 24 p4070 N85-35223
Evaluation of SRB phenolic TPS material made by an alternate vendor
[NASA-CR-170894] 24 p4073 N85-35240
Space shuttle SRB TPS protective paint test and evaluation in NASA Hot Gas Facility and AEDC Tunnel C
[NASA-CR-170884] 24 p4081 N85-35294
Results of tests of Insta-Foam Thermal Protection System (TPS) material for protection of equipment inside the SRB aft skirt
[NASA-CR-170892] 24 p4081 N85-35295
The 1986 National Aeronautics and Space Administration authorization
[GPO-47-635] 24 p4166 N85-35829

SPACE SIMULATORS
Functional capacities of elderly subjects exposed to simulated spaceflight factors 01 p0091 N85-10617

SPACE STATIONS
NT LONG DURATION EXPOSURE FACILITY
NT ORBITAL SPACE STATIONS
NT ORBITING LUNAR STATIONS
NT SALYUT SPACE STATION
NT SKYLAB 3
NT SKYLAB 4
Communications protocols for a fault tolerant, integrated local area network for Space Station applications
[NASA-TM-86304] 01 p0106 N85-10711
Human response to vibroacoustic environments of space vehicles
[NASA-TM-86316] 01 p0116 N85-10789
Office of Technology Assessment 01 p0127 N85-10672
Workshop on Automated Space Station 01 p0127 N85-10673
Second Symposium on Space Industrialization — space commercialization
[NASA-CP-2313] 02 p0149 N85-11011
The computer-communication link for the innovative use of Space Station 02 p0150 N85-11016
Role of Space Station: The how of space industrialization 02 p0153 N85-11036
Commercial space services 02 p0153 N85-11039
Features and uses of progress cargo ships 02 p0157 N85-11061
Conceptual design and evaluation of selected Space Station concepts: Executive summary
[NASA-TM-87382] 02 p0167 N85-11128
Conceptual design and evaluation of selected Space Station concepts, volume 1
[NASA-TM-87383] 02 p0168 N85-11129
Conceptual design and evaluation of selected Space Station concepts, volume 2
[NASA-TM-87384] 02 p0168 N85-11130
An evaluation of grease type ball bearing lubricants operating in various environments
[NASA-TM-86480] 02 p0185 N85-11239
SMP: A solid modeling program
[NASA-CR-172473] 02 p0241 N85-11570
International cooperation and competition in space
[GPO-38-001] 02 p0295 N85-11911
Statement of Kenneth S. Pedersen, Director, International Affairs Division, National Aeronautics and Space Administration 02 p0295 N85-11913
Civilian space stations and the US future in space: Summary
[OTA-STI-242] 03 p0323 N85-12063
Power subsystem automation study
[NASA-CR-171213] 03 p0358 N85-12299
Technologies for space station autonomy
[NASA-CR-174112] 04 p0458 N85-12906
Selected tether applications in space: An analysis of five selected concepts
[NASA-CR-171222] 04 p0460 N85-12921
Definition of technology development missions for early Space Station satellite servicing. Volume 2: Technical
[NASA-CR-171229] 04 p0461 N85-12923
Autonomous momentum management for space station, exhibit A
[NASA-CR-171256] 04 p0462 N85-12933
Regenerative fuel cell energy storage system for a low Earth orbit space station
[NASA-CR-174802] 04 p0527 N85-13371
Research and technology, 1984: Marshall Space Flight Center
[NASA-TM-86476] 04 p0590 N85-13765
Comparative energy storage assessment item 05 p0605 N85-13858
Perspectives on energy storage wheels for space station application 05 p0605 N85-13860
Space Power
[NASA-CP-2352] 05 p0606 N85-13880
Space station power system 05 p0606 N85-13881
Power for commercial space applications 05 p0606 N85-13884
Thermal management technology status 05 p0610 N85-13895
Civilian space stations and the US future in space
[OTA-STI-241] 07 p0914 N85-15781
Issues and findings 07 p0914 N85-15782
Space infrastructure 07 p0914 N85-15783
A buyer's guide to space infrastructure 07 p0914 N85-15784
Broadening the debate 07 p0914 N85-15785
Toward a goal-oriented civilian space program 07 p0914 N85-15786
Results of principal NASA studies on space station uses and functional requirements 07 p0914 N85-15787
The evolution of civilian in-space infrastructure, i.e., space station concepts in the United States 07 p0914 N85-15788
International involvement in a civilian space station program 07 p0915 N85-15789
Synopsis of the OTA Workshop on Cost Containment of Civilian Infrastructure (Civilian Space Station) Elements 07 p0915 N85-15790
Financing considerations and Federal budget impacts 07 p0915 N85-15792
Space Station truss structures and construction considerations
[NASA-TM-86336] 07 p0916 N85-15796
Impact of lunar and planetary missions on the space station
[NASA-CR-171832] 08 p1106 N85-16988
NASA OAST perspective 08 p1106 N85-16990
Space station task force perspective 08 p1106 N85-16992
Earth-to-orbit propellant transportation overview 08 p1108 N85-17002
Passive storage technologies 08 p1108 N85-17003
Active cooling requirements for propellant storage 08 p1108 N85-17004
Propellant transfer: Attached depot 08 p1108 N85-17005
Space Station needs, attributes, and architectural option study
[NASA-CR-174316] 08 p1109 N85-17011
FRG study looks at participation in ESA, US space station 08 p1141 N85-17191
Characterization of heat transfer in nutrient materials — space flight feeding
[NASA-CR-171841] 08 p1199 N85-17551
Summary of activities of Aeronautics and Space Engineering Board
[NASA-CR-174294] 08 p1228 N85-17729
Impact of lunar and planetary missions on the space station: Preliminary STS logistics report
[NASA-CR-171837] 09 p1285 N85-18072
Space Station engineering and technology development
[NASA-CR-174383] 09 p1287 N85-18079
Commercial space: Europe should have independent strategy 10 p1460 N85-19205
West Europe report: Science and technology
[JPRS-WST-85-008] 11 p1617 N85-20174
FRG's DFVLR ready for participation in space station 11 p1618 N85-20176
Applications of Tethers in Space, volume 1
[NASA-CP-2364] 11 p1642 N85-20339
Transportation applications, part 2 11 p1643 N85-20350
Summary presentation of the Transportation Panel 11 p1644 N85-20357
Summary presentation to the Artificial Gravity Panel 11 p1644 N85-20358
Report of the Artificial Gravity Panel 11 p1645 N85-20365
Physiological considerations of artificial gravity 11 p1645 N85-20366
Some aspects of attitude stability of tethered space stations 11 p1646 N85-20369
Charge-to-mass dispersion methods for abrasion-ablation fragmentation models
[NASA-TM-86340] 11 p1726 N85-20857
Environment definition, small particles, diameter less than or equal to 1 MM 12 p1788 N85-21223
Advanced research and technology programs for advanced high-pressure oxygen-hydrogen rocket propulsion
[NASA-TM-86969] 12 p1789 N85-21231
Space Station
[NASA-EP-211] 12 p1793 N85-21251
Aerospace Safety Advisory Panel
[NASA-TM-87426] 13 p1970 N85-22373

Feoktistov argues against U.S. space shuttle design concept 13 p1985 N85-22453
Space station systems technology study (add-on task). Volume 1: Executive summary
[NASA-CR-171415] 13 p1986 N85-22459
Advancing automation and robotics technology for the Space Station and for the US economy. Volume 1: Executive overview
[NASA-TM-87566-VOL-1] 13 p1986 N85-22460
Advancing automation and robotics technology for the Space Station and for the US economy, volume 2
[NASA-TM-87566-VOL-2] 13 p1987 N85-22461
Selected tether applications in space: Phase 2. Executive summary
[NASA-CR-171421] 13 p1987 N85-22462
Selected tether applications in space: Phase 2
[NASA-CR-171422] 13 p1987 N85-22463
Space Station technology planning 13 p1989 N85-22471
Space test program of high-voltage solar array-space plasma interactions 13 p1997 N85-22519
Research opportunities in human behavior and performance
[NASA-CR-3866] 13 p2142 N85-23299
Large Space Antenna Systems Technology, 1984
[NASA-CP-2368-PT-2] 14 p2233 N85-23840
Determination of electromagnetic properties of mesh material using advanced radiometer techniques 14 p2235 N85-23855
The space station as a construction base for large space structures 14 p2235 N85-23856
Utilization of space station by the large deployment reflector 14 p2235 N85-23857
Large Deployable Reflector (LDR) requirements for space station accommodations 14 p2236 N85-23858
Utilization of the polar platform of NASA's Space Station Program for operational Earth observations
[PB85-152502] 14 p2240 N85-23895
The context for food service and nutrition in the space station 14 p2393 N85-24734
NASA plans for a space station 14 p2393 N85-24735
Food service management 14 p2393 N85-24736
Alternative food preservation techniques, new technology in food preparation and appropriateness of food supply for the permanently manned space station 14 p2393 N85-24739
Nutritional criteria for military rations and effects of prolonged feeding on acceptability 14 p2394 N85-24742
Food service and nutritional needs 14 p2394 N85-24744
Packaging's contribution for the effectiveness of the space station's food service operation 14 p2394 N85-24746
Packaging for food service 14 p2394 N85-24747
Space station systems technology study (add-on task). Volume 2: Trade study and technology selection
[NASA-CR-171416] 15 p2475 N85-25279
Space station systems technology study (add-on task). Volume 3: Technology advancement program plan
[NASA-CR-171417] 15 p2475 N85-25280
Definition of technology development missions for early space stations: Large space structures
[NASA-CR-171446] 15 p2476 N85-25281
Construction in space
[NASA-TM-77630] 15 p2492 N85-25374
Long-life high performance fuel cell program
[NASA-CR-174874] 15 p2494 N85-25384
Space station propulsion: The advanced development program at Lewis
[NASA-TM-86999] 15 p2494 N85-25386
West Europe report: Science and technology
[JPRS-WST-84-008] 15 p2531 N85-25606
European views differ on space station concept 15 p2531 N85-25608
West Europe report: Science and technology
[JPRS-WST-84-026] 15 p2532 N85-25617
FRG opinion on Spacelab benefits, space station participation 15 p2532 N85-25618
West Europe report: Science and technology
[JPRS-WST-84-010] 15 p2535 N85-25644
A brief description of the two primate experiments to be carried out on SL-4 15 p2687 N85-26597
The NASA Space Station program plans
[NASA-TM-87474] 16 p2730 N85-26846
Spacestation: The next logical step
[NASA-EP-213] 16 p2730 N85-26847
Space Station Engineering and Technology Development
[NASA-CR-175806] 16 p2731 N85-26851
Space Station Spartan study
[NASA-TM-86215] 16 p2731 N85-26852
A SLAM II simulation model for analyzing space station mission processing requirements
[NASA-CR-175864] 16 p2731 N85-26853
Tethered nuclear power for the Space Station
[NASA-TM-87023] 16 p2740 N85-26912
Space Station crew safety alternatives study. Volume 5: Space Station safety plan
[NASA-CR-3858] 17 p2908 N85-27930
Automation and robotics for the National Space Program
[NASA-CR-175881] 17 p2909 N85-27936
Performance analysis of radiation cooled dc transmission lines for high power space systems
[NASA-TM-87040] 17 p2951 N85-28222
Documentation for the West German Federal Cabinet's space policy decision 17 p3051 N85-28886
Space Station crew safety alternatives study. Volume 4: Appendices
[NASA-CR-3857] 18 p3065 N85-28958
An evaluation of oxygen-hydrogen propulsion systems for the Space Station
[NASA-TM-87059] 18 p3067 N85-28971
West Europe report: Science and technology
[JPRS-WST-84-022] 18 p3085 N85-29086
West Europe report: Science and technology
[JPRS-WST-84-031] 18 p3086 N85-29089
DFVLR official on areas of US-FRG Space Station cooperation 18 p3086 N85-29091
FRG weighs ESA participation, budget issues 18 p3086 N85-29110
DFVLR study recommends European independence in space systems 18 p3086 N85-29111
Proceedings of the Seminar on Space Station Human Productivity
[NASA-TM-86673] 18 p3156 N85-29539
Space station crew safety: Human factors interaction model 18 p3156 N85-29540
Space station crew safety alternatives study, third quarter briefing 18 p3156 N85-29541
Statement of contamination problem 18 p3156 N85-29542
Internal contamination issues 18 p3156 N85-29543
Materials and processes control for space applications 18 p3156 N85-29544
Some problems associated with trace contaminant removal systems for spacecabins 18 p3158 N85-29554
Contamination control for increased crew productivity 18 p3158 N85-29555
Human productivity program definition 18 p3158 N85-29556
Overview: Human factors issues in space station architecture 18 p3158 N85-29558
A preliminary human factors planning and design outline of parameters related to space station windows and CCTV monitoring 18 p3158 N85-29559
Human factors issues in space station architecture 18 p3158 N85-29560
Man-machine tradeoff study 18 p3158 N85-29561
Some ideas and questions regarding space station design for human use 18 p3158 N85-29562
Human productivity experience and undersea habitat design 18 p3159 N85-29563
Considerations for space station interior architecture 18 p3159 N85-29564
Human factors in space station architecture: The ECLSS module concept 18 p3159 N85-29565
Habitability sleep accommodations 18 p3159 N85-29566
Customer and mission influence on space station architecture 18 p3159 N85-29567
Space station models, mockups and simulators 18 p3159 N85-29569
Mockups and human productivity studies 18 p3159 N85-29570
Experiences with neutral buoyance testing mockups 18 p3159 N85-29571
Rockwell experience applications to Amee space station mockup habitability/productivity studies 18 p3159 N85-29572
The role of mock-ups in the development of Orbital Replaceable Units (ORU) 18 p3160 N85-29573
International space research perspectives of commercialization for German industry
[NASA-TM-77657] 19 p3222 N85-29979
Space station crew safety alternatives study. Volume 3: Safety impact of human factors
[NASA-CR-3856] 19 p3223 N85-29984
Space station crew safety alternatives study, volume 1
[NASA-CR-3854] 19 p3223 N85-29985
Space station automation study. Volume 2: Technical report. Autonomous systems and assembly
[NASA-CR-171515] 19 p3226 N85-30001
Space station automation study. Volume 1: Executive summary. Autonomous systems and assembly
[NASA-CR-171514] 19 p3226 N85-30002
Flow cytometry for health monitoring in space
[DE85-009572] 19 p3329 N85-30625
Department of Housing and Urban Development-Independent Agencies Appropriation Bill, 1986
[H-REPT-99-212] 19 p3382 N85-30979
Space Station reference configuration description
[NASA-TM-87493] 20 p3408 N85-31146
Space Station man-machine automation trade-off analysis
[NASA-CR-176048] 20 p3408 N85-31147
Automatic assembly of space stations 20 p3409 N85-31153
Space station dynamic modeling, disturbance accommodation, and adaptive control 20 p3409 N85-31154
Space station configuration and flight dynamics identification 20 p3410 N85-31162
Design of multivariable controllers using the Integrated Analysis Capability (IAC) 20 p3412 N85-31172
Attitude control tradeoff study between the use of a flexible beam and a tether configuration for the connection of two bodies in orbit 20 p3412 N85-31174
Space station parametric models 20 p3413 N85-31180
Civilian Space Stations and the US future in Space
[OTA-STI-242] 20 p3418 N85-31215
The 1984 Goddard Space Flight Center Battery Workshop
[NASA-CP-2382] 20 p3443 N85-31371
Regenerative fuel cell systems for space station 20 p3443 N85-31372
Space Station crew safety alternatives study. Volume 2: Threat development
[NASA-CR-3855] 21 p3558 N85-32133
NASA space station automation: AI-based technology review
[NASA-CR-176094] 21 p3558 N85-32134
Automation study for space station subsystems and mission ground support
[NASA-CR-176097] 21 p3559 N85-32136
Space station ECLSS integration analysis: Simplified General Cluster Systems Model, ECLS System Assessment Program enhancements
[NASA-CR-176089] 21 p3670 N85-32796
A survey of structural material issues for a space station
[NASA-TM-86385] 22 p3738 N85-33168
Space station automation study. Automation requirements derived from space manufacturing concepts. Volume 1: Executive summary
[NASA-CR-176099] 22 p3738 N85-33170
Space Station automation study. Automation requirements derived from space manufacturing concepts. Volume 2: Technical report
[NASA-CR-176100] 22 p3738 N85-33171
Space station automation and robotics study. Operator-systems interface
[NASA-CR-176095] 22 p3738 N85-33172
Testimony of Robert A. Froach before the Subcommittee on HUD and Independent Agencies of the Senate Committee on Appropriations
[NASA-TM-87496] 22 p3738 N85-33173
Statement of Aaron Cohen, Director, Research and Engineering, Johnson Space Center and Chairman, Space Station Advanced Technology Advisory Committee, National Aeronautics and Space Administration, before the Subcommittee on Science, Technology, and Space, Committee on Commerce, Science, and Transportation, United States Senate
[NASA-TM-87497] 22 p3739 N85-33174
Space station automation study: Autonomous systems and assembly, volume 2
[NASA-CR-176092] 22 p3739 N85-33175
Deployable-erectable trade study for space station truss structures
[NASA-TM-87573] 22 p3740 N85-33181
The space station polar platform: NOAA systems considerations and requirements
[NOAA-TR-NESDIS-22] 22 p3740 N85-33182
Structural dynamics model and response of the deployable reference configuration space station
[NASA-TM-86386] 22 p3799 N85-33539
Study to encourage and facilitate industrial investment and involvement in space
[NASA-CR-176152] 23 p3898 N85-34147
Space station rotational equations of motion
[NASA-TP-2511] 23 p3899 N85-34148
Space Station Engineering and Technology Development: Proceedings of the Panel on In-Space Engineering Research and Technology Development
[NASA-CR-176110] 23 p3899 N85-34153

The role of tethers on space station
[NASA-TM-86519] 23 p3900 N85-34154
Coordinated study of solar-terrestrial payloads on space station
[NASA-CR-176180] 23 p3900 N85-34158
Soft X-Ray Telescope (SXRT)
23 p3900 N85-34159
Solar Ultraviolet Spectral Irradience Monitor (SUSIM)
23 p3901 N85-34160
White Light Coronograph (WLC) and Ultra-Violet Coronal Spectrometer (UVCS)
23 p3901 N85-34161
High Resolution Telescope and Spectrograph (HRTS)
23 p3901 N85-34162
Active Cavity Radiometer (ACR)
23 p3901 N85-34163
Waves in Space Plasmas (WISP)
23 p3901 N85-34164
Space Experiments with Particle Accelerators (SEPAC)
23 p3901 N85-34165
Theoretical and Experimental Beam Plasma Physics (TEBPP)
23 p3901 N85-34166
Recoverable Plasma Diagnostics Package (RPDP)
23 p3902 N85-34167
Electrodynamic tether
23 p3902 N85-34168
Imaging Spectrometric Observatory (ISO)
23 p3902 N85-34169
Atmospheric Emission Photometric Imaging (AEPI)
23 p3902 N85-34170
Magnetospheric multiprobes: MMP/CHEMSAT
23 p3902 N85-34171
Wide Angle Michelson Doppler Imaging Interferometer (WAMDII)
23 p3902 N85-34172
Vehicle Charging And Potential (VCAP)
23 p3902 N85-34173
Initial placement of STO instruments
23 p3902 N85-34174
Optical analysis of parabolic dish concentrators for solar dynamic power systems in space
[NASA-TM-87060] 23 p3903 N85-34176
Detection of 10 (1) GeV cosmic neutrinos with a space station
[OG-8.4-10] 23 p4030 N85-34977
Technology for large space systems: A bibliography with indexes
[NASA-SP-7046(12)] 24 p4068 N85-35209
Space Missions for Automation and Robotics Technologies (SMART) Program
[NASA-TM-86820] 24 p4068 N85-35210
Space Station Polar Platform: Integrating research and operational missions
[PB85-195279] 24 p4069 N85-35218
The 1986 National Aeronautics and Space Administration authorization
[GPO-47-635] 24 p4166 N85-35829

SPACE STORAGE
Earth-to-orbit propellant transportation overview
06 p1108 N85-17002
Hemispherical latching apparatus
[NASA-CASE-MFS-25837-1] 19 p3224 N85-29991

SPACE SUITS
Flame resistant fibrous materials development
[NASA-CR-167817] 07 p0920 N85-15827
Challenges in the development of the shuttle extravehicular mobility unit 06 p1096 N85-16922
A theoretical method for selecting space craft and space suit atmospheres
[AD-A148219] 06 p1200 N85-17559
Elbow and knee joint for hard space suits and the like
[NASA-CASE-ARC-11610-1] 11 p1697 N85-20666
Shoulder and hip joint for hard space suits and the like
[NASA-CASE-ARC-11543-1] 12 p1910 N85-21966
Torso sizing ring construction for hard space suit
[NASA-CASE-ARC-11616-1] 12 p1910 N85-21967

SPACE SURVEILLANCE (GROUND BASED)
NORAD operational system 12 p1783 N85-21189

SPACE SURVEILLANCE (SPACEBORNE)
NORAD operational system 12 p1783 N85-21189
Computing parameters characterizing possibility of planets falling in star camera field of view during space survey 15 p2457 N85-25351

SPACE SYSTEMS ENGINEERING
U AEROSPACE ENGINEERING

SPACE TECHNOLOGY EXPERIMENTS
Space Technology Experiments Platform (STEP) status: An in-space test facility 14 p2236 N85-23663

SPACE TELESCOPE
U HUBBLE SPACE TELESCOPE

SPACE TOOLS
EVA of cosmonauts Savitskaya and Dzhanibekov
02 p0158 N85-11076
Commentary on hand tool used in cosmonaut EVA
02 p0159 N85-11077
Further details in welding, spray-coating tool
02 p0159 N85-11078
Electric Welding Institute's space-technology test results 03 p0352 N85-12267
Special tools used by cosmonauts in EVA
22 p3731 N85-33129

SPACE TRANSPORTATION
NT CHALLENGER (ORBITER)
NT COLUMBIA (ORBITER)
NT DISCOVERY (ORBITER)
NT ENTERPRISE (ORBITER)
NT SPACE SHUTTLE BOOSTERS
NT SPACE SHUTTLE MISSION 31-C
NT SPACE SHUTTLE MISSION 41-B
NT SPACE SHUTTLE MISSION 41-C
NT SPACE SHUTTLE MISSION 41-G
NT SPACE SHUTTLE MISSION 51-A
NT SPACE SHUTTLE MISSION 51-C
NT SPACE SHUTTLE MISSIONS
NT SPACE SHUTTLE ORBITERS
NT SPACE TRANSPORTATION SYSTEM
Conestoga 2: A low cost commercial space transport system 02 p0153 N85-11033
Winged first stages of space transport appliances
[TUM-RT-TB-84/3] 02 p0167 N85-11125
Possibilities and limits of electromagnetic acceleration in space applications
[ILR-MITT-136] 02 p0193 N85-11292
Verification tests of durable TPS concepts
[NASA-TM-86313] 03 p0323 N85-12085
Space infrastructure 07 p0914 N85-15783
Applications of Tethers in Space, volume 1
[NASA-CP-2364] 11 p1642 N85-20339
Transportation applications, part 1
11 p1643 N85-20340
Report of the Transportation Panel
11 p1645 N85-20364
Optimization of guidance and control using function minimization and NAVSTAR/GPS
[AD-A149058] 12 p1775 N85-21141
Shuttle fleet operations: A simulation analysis
[AD-A151383] 15 p2491 N85-25370

SPACE TRANSPORTATION SYSTEM
NT CHALLENGER (ORBITER)
NT COLUMBIA (ORBITER)
NT DISCOVERY (ORBITER)
NT ENTERPRISE (ORBITER)
NT SPACE SHUTTLE BOOSTERS
NT SPACE SHUTTLE MISSION 31-C
NT SPACE SHUTTLE MISSION 41-B
NT SPACE SHUTTLE MISSION 41-C
NT SPACE SHUTTLE MISSION 41-G
NT SPACE SHUTTLE MISSION 51-A
NT SPACE SHUTTLE MISSION 51-C
NT SPACE SHUTTLE MISSIONS
NT SPACE SHUTTLE ORBITERS
NT SPACE TRANSPORTATION SYSTEM FLIGHTS
National Aeronautics and Space Administration
01 p0127 N85-10871
Legal considerations and cooperative opportunities for space commercial activities 02 p0150 N85-11013
External tank aft cargo carrier
02 p0155 N85-11050
Continuing issues (FY 1983) concerning military use of the space transportation system
[AD-A146091] 03 p0323 N85-12080
Selected tether applications in space: An analysis of five selected concepts
[NASA-CR-171222] 04 p0460 N85-12921
Resident research associateships. Postdoctoral and senior research awards
[NASA-TM-87399] 05 p0734 N85-14717
The aerodynamic challenges of SRB recovery
06 p1093 N85-16906
Space Transportation System and associated payloads: Glossary, acronyms, and abbreviations
[NASA-RP-1059-REV] 10 p1428 N85-19007
Space Transportation System (STS) propellant scavenging system study. Volume 1: Technical report
[NASA-CR-171848-VOL-1] 11 p1589 N85-20000
Space Transportation System (STS) propellant scavenging system study. Volume 2: Supporting research and technology report
[NASA-CR-171849-VOL-2] 11 p1589 N85-20001
Space Transportatioin System (STS) propellant scavenging system study. Volume 3: Cost and work breakdown structure-dictionary
[NASA-CR-171850-VOL-3] 11 p1590 N85-20002
Applications of Tethers in Space, volume 2
[NASA-CP-2365] 11 p1644 N85-20361
Status of the National Space Transportation System
11 p1712 N85-20772
Space Shuttle interactive meteorological data system study
[NASA-CR-171418] 12 p1892 N85-21876
Aerospace Safety Advisory Panel
[NASA-TM-87426] 13 p1970 N85-22373
NASA R and T aerospace plane vehicles: Progress and plans
[NASA-TM-86429] 15 p2491 N85-25366
Costs, payload of Ariane, US Space Shuttle compared
15 p2530 N85-25601
Telescope in lunar orbit 15 p2552 N85-25566

SPACE TRANSPORTATION SYSTEM FLIGHTS
NT SPACE TRANSPORTATION SYSTEM 1 FLIGHT
NT SPACE TRANSPORTATION SYSTEM 3 FLIGHT
NT SPACE TRANSPORTATION SYSTEM 4 FLIGHT
Ground man-machine interfaces for orbiter checkout
06 p1091 N85-16897
Overview od STS ground operations/orbiter turnaround STS-1 through STS-7 06 p1096 N85-16926
STS atmospheric luminosities
[NASA-CR-175514] 12 p1791 N85-21240
Results of Space Shuttle flight 41-D
[GPO-39-481] 12 p1791 N85-21243
Shuttle payload bay dynamic environments: Summary and conclusion report for STS flights 1-5 and 9
[NASA-CR-175656] 14 p2241 N85-23896
National Space Transportation Systems Program mission report
[NASA-TM-87456] 14 p2241 N85-23898
National Space Transportation Systems Program mission report
[NASA-TM-87454] 14 p2242 N85-23899
Surface pressure produced by Space Transportation System flight 41B
[AD-A150793] 14 p2242 N85-23901
Recommendations and calculations concerning physical characteristics of the EEVT apparatus
20 p3502 N85-31769
Clarke Stations and mercurian mass-drivers: Energy for large-scale transportation systems
[DE85-009607] 21 p3560 N85-32145

SPACE TRANSPORTATION SYSTEM 1 FLIGHT
STS-1 Pogo analysis
[NASA-TM-87433] 11 p1591 N85-20007

SPACE TRANSPORTATION SYSTEM 3 FLIGHT
Get Away Special (GAS) thermal design summary
[X-732-83-8] 15 p2475 N85-25278

SPACE TRANSPORTATION SYSTEM 4 FLIGHT
Shuttle electrical environment
13 p1990 N85-22475

SPACE TRANSPORTATION SYSTEM 11 FLIGHT
Results of Space Shuttle Flight 41-C
[GPO-36-092] 04 p0461 N85-12926
Statement of Captain Robert L. Crippen, USN, Commander of Space Shuttle Flight 41-C; Francis R. Scobee, pilot; Doctor George D. Nelson, Mission Specialist; Terry J. Hart, Mission Specialist; and Doctor James D. Van Hoften, Mission Specialist; accompanied by Frank Capolino, Solar Maximum Repair Mission Project Manager, Goddard Space Flight Center
04 p0461 N85-12929
Statement of Frank Capolino, Solar Maximum Repair Mission Project Manager, Goddard Space Flight Center
04 p0461 N85-12930

SPACE VEHICLE CHECKOUT PROGRAM
Integrated design checkout of shuttle payload avionics interfaces 06 p1092 N85-16899
Automation of checkout for the shuttle operations era
06 p1092 N85-16900

SPACE VEHICLE CONTROL
U SPACECRAFT CONTROL

SPACE VEHICLES
U SPACECRAFT

SPACE WEAPONS
NT LASER WEAPONS
PRC journal discusses 'Star Wars' space program
11 p1621 N85-20207
Combat capable space systems for tactical support
11 p1713 N85-20775
High energy lasers: A primer on directed energy weapons for space use
[AD-A151279] 15 p2562 N85-25807
US said to seek military advantage in space
16 p2727 N85-26831
Military journal on US intelligence satellites
16 p2727 N85-26832
Strategic defense initiative
[DE85-012778] 24 p4150 N85-35735

SPACE-TIME CONTINUUM
U RELATIVITY

SPACE-TIME FUNCTIONS
Gravitational vacuum 02 p0265 N85-11734
Change in relationship of biopotentials of brain zones for various levels of working capacity
07 p1013 N85-16438
Algorithm for space-time analysis of data on geomagnetic field
[NASA-TM-77804] 08 p1209 N85-17609
Conserved quantities and radiative aspects of asymptotically anti-de Sitter space-times
12 p1958 N85-22303

A practical system for collecting reliable data on the space-time behavior of people
[AD-A151174] 15 p2619 N85-26140
Comment on quantum effects on 4-dimensional space-time symmetries
[DE85-007780] 16 p2872 N85-27722
Characteristics of optical information-measurement channels with utilization of scattering effects
22 p3781 N85-33429

SPACE-TIME METRIC
U SPACE-TIME FUNCTIONS

SPACEBORNE ASTRONOMY
Algorithm for astronomical, extended source, signal-to-noise radio calculations
[NASA-TP-2396] 03 p0445 N85-12833
Algorithm for astronomical, point source, signal to noise ratio calculations
[NASA-TP-2397] 03 p0445 N85-12834
Space research and the new approach to the mechanics of fluid media in cosmos
[TRITA-EPP-84-04] 03 p0447 N85-12844
X-ray and ultraviolet observations of BL Lacertae objects 05 p0741 N85-14767
Future studies of the local interstellar medium with Space Telescope and Columbus 06 p0880 N85-15593
Observations of local ISM emission with the Berkeley EUV/FUV shuttle telescope 06 p0880 N85-15594
QUASAT: A VLBI observatory in space — conferences
[ESA-SP-213] 07 p1056 N85-16700
The galaxy scene and QUASAT — VLBI satellite
07 p1056 N85-16703
The QUASAT mission: An overview
07 p1056 N85-16704
Some prospects of space VLBI
07 p1056 N85-16705
QUASAT: Technical aspects of the proposed mission — VLBI satellite 07 p1057 N85-16706
A study on the imaging potential of QUASAT — spaceborne VLBI 07 p1057 N85-16707
Correlator and data processing requirements for QUASAT 07 p1057 N85-16709
Processing system for space VLBI
07 p1057 N85-16711
Testing theories of superluminal motion — QUASAT
07 p1058 N85-16714
QUASAT, gravitational lenses, and studies of the interstellar, intracluster and intergalactic medium
07 p1058 N85-16715
Very Long Base Interferometry (VLBI) in space and X-ray observations of compact sources in active galactic nuclei 07 p1058 N85-16716
The wide-range space radio interferometer
07 p1058 N85-16717
The relevance of QUASAT to the star formation problem 07 p1058 N85-16718
Galactic OH and H2O masers — QUASAT project
07 p1058 N85-16719
Water masers and distance measurements: The impact of QUASAT 07 p1059 N85-16721
A short note on the high precision navigation of QUASAT 07 p1059 N85-16722
Opportunities for high angular and temporal resolutions of galactic objects at radio frequencies — QUASAT
07 p1059 N85-16723
Characteristics of X-ray spectra from galactic and extragalactic X-ray sources 08 p1239 N85-17811
The ROSAT all-sky survey in X-rays
08 p1243 N85-17843
A new look at the planets — space probes
[AERONOMICA-ACTA-37-1984]
11 p1765 N85-21096
X-ray experiment on Prognoz-9 artificial Earth satellite
15 p2478 N85-25295
Planetary Rings. Colloquium 75 — conferences
[ISBN-2-85428-100-4] 15 p2670 N85-26473
Future observations of planetary rings from ground-based observatories and Earth-orbiting satellites
15 p2676 N85-26540
A priority of space exploration: Observation of Saturn's rings from a Saturn orbiter 15 p2679 N85-26542
European space science horizon 2000
[ESA-SP-1070] 16 p2717 N85-26771
IRAS: Space technology from the Netherlands
[B8561841] 17 p2908 N85-27929
Assessment study of liquid content measurement methods applicable to space missions — Infrared Space Observatory
[TU-HH-TRI-ESA-84-2] 17 p2938 N85-28135
Spacelab 2
[NASA-EP-217] 19 p3222 N85-29977
Mapping with QUASAT (quasar satellite) using short observation times
[AD-A155155] 21 p3559 N85-32141
Comments on RS-17 X-ray telescope
22 p3731 N85-33132
Results from Astron orbiting telescope
22 p3732 N85-33134
Mosaic Infrared Sensor for Space Astronomy (MIRSSA)
[NASA-CR-176154] 22 p3786 N85-33456

SPACEBORNE EXPERIMENTS
NT ATMOSPHERIC GENERAL CIRCULATION EXPERIMENT
NT EARTH RADIATION BUDGET EXPERIMENT
NT PLASMA INTERACTION EXPERIMENT
Effect of spaceflight factors on rat bone marrow cells
01 p0092 N85-10820
European retrievable carrier (Eureca) and evolutionary space carrier for microgravity, Earth observation and technology demonstration 02 p0152 N85-11032
The evolution of small payload carrier systems
02 p0153 N85-11038
Fluids Experiment Apparatus (FEA)
02 p0155 N85-11048
Commentary on Salyut-7 electrophoresis, plugging mortar experiments 02 p0156 N85-11072
Tass reports experiments during visiting crew's third day 02 p0158 N85-11073
Commentary on derivation of biological materials, cosmonaut adaptation 02 p0158 N85-11074
Tass reports astrophysical, atmospheric studies on Salyut-7 02 p0158 N85-11075
EVA of cosmonauts Savitskaya and Dzhanibekov
02 p0158 N85-11076
Further details in welding, spray-coating tool
02 p0159 N85-11078
Use of gravitational stabilization in performance of experiments 02 p0160 N85-11084
Research and technology, 1984: Marshall Space Flight Center
[NASA-TM-86476] 04 p0580 N85-13765
Life Sciences Research in Space — conference
[ESA-SP-212] 05 p0689 N85-14425
Bioprocessing in space 05 p0690 N85-14439
Medication interference with space research: An example from a mass-discrimination experiment on Spacelab 1 05 p0695 N85-14472
Computerized sleep staging by detecting eye and hand movement, delta EEG activity and EMG, using portable solid state technique — spaceborne experiments
05 p0695 N85-14475
Overview of German microgravity activities in the field of life science 05 p0696 N85-14476
Space station: New frontier for life sciences in space
05 p0696 N85-14477
Controlled ecological life support system higher plant flight experiments
[NASA-CR-177323] 07 p1020 N85-16471
Botany facility, phase A study. Part 1: Executive summary — EURECA
[BF-DOC-10-VOL-1] 08 p1110 N85-17015
Spaceborne distributed SAR antenna
[NASA-CR-171835] 08 p1150 N85-17259
A method for determining mesoscale dynamic topography
[AD-D011412] 08 p1191 N85-17506
Automatic Monoellipsoidal Mirror Furnace Facility (AMMFF), volume 1 — spaceborne crystal growth
[AMF-RP.100-DS-015-VOL-1] 09 p1295 N85-18073
Development of a 20 GHz modulator for the payload of a satellite for propagation and transmission experiments, including the required converters of the test equipment
[BMFT-FB-W-84-044] 11 p1580 N85-20004
Solution growth facility, phase A design study, executive summary — EURECA
[RPT/SGF/00014/TER] 11 p1591 N85-20006
Alloy supercooling on Salyut-7
11 p1604 N85-20083
Fluid slosh dynamics of surface tension tanks in three axis stabilized spacecraft
[MBB-UR-E-739-84-O] 11 p1634 N85-20291
The space flight of the Soviet-Indian crew
[NASA-TM-77615] 12 p1758 N85-21226
Lyakhov and Aleksandrov on 150-day flight
13 p1977 N85-22405
Comments on Salyut-7 150-day flight
13 p1977 N85-22406
Langley Research Center photogrammetric measurements of solar array dynamics: Preliminary results 14 p2233 N85-23844
Space Technology Experiments Platform (STEP) status: An in-space test facility 14 p2236 N85-23863
Shuttle attached antenna Flight Experiment Definition Study (FEDS) 14 p2237 N85-23865
Electro-science requirements for shuttle-attached antenna flight experiments 14 p2237 N85-23866
National Space Transportation Systems Program mission report
[NASA-TM-87455] 14 p2242 N85-23900
Scientific experiments. Preprocessing of scientific data — spaceborne experiments
14 p2398 N85-24779
Holography in space 15 p2476 N85-25285
Second Soviet-French Symposium on Space Technology 15 p2483 N85-25326
Cosmonauts report on space welding at conference
15 p2484 N85-25329
Paton comments on results of space welding tests
15 p2484 N85-25330
Space brain research in China reported
15 p2537 N85-25657
Importance of gravity for plant growth and behavior
15 p2606 N85-26070
Study on the extension of experiment resources in the MAUS project
[BMFT-FB-W-84-051] 15 p2650 N85-26343
Sixteenth Lunar and Planetary Science Conference. Press abstracts
[NASA-CR-175892] 15 p2660 N85-26548
NASA Ames Summer High School Apprenticeship Research Program
[NASA-TM-86006] 15 p2686 N85-26590
Academician Zuyev notes plans for lasers on spacecraft for atmospheric research 16 p2717 N85-26775
Satellite research on solar flares
16 p2717 N85-26776
Botany facility phase A study. Core payload number 6 EURECA carrier, volume 1
[ESA-CR(P)-1978-VOL-1] 17 p2906 N85-27918
Botany facility phase A study. Core payload number 6 for EURECA carrier, volume 2
[BF-TD-DRD-03-VOL-2] 17 p2906 N85-27919
Long life feasibility study for the shuttle infrared telescope facility
[NASA-CR-3722] 17 p3052 N85-28893
Gas chromatography: Possible application of advanced instrumentation developed for solar system exploration to space station cabin atmospheres
18 p3157 N85-29551
Spacelab 2
[NASA-EP-217] 19 p3222 N85-29977
Space shuttle molecular and wake vacuum measurements
[NASA-TM-86509] 19 p3222 N85-29978
Dynamic response of a flexible space beam
[NASA-TM-86441] 19 p3285 N85-30368
Shuttle Molecular Gun: Smog. Potential experiment for the electrodynamic Tethered Satellite System (TSS) mission
[IFSI-84-17] 20 p3419 N85-31221
Recommendations and calculations concerning physical characteristics of the EEVT apparatus
20 p3502 N85-31769
Experience of science astronaut on the Spacelab-1 mission 20 p3508 N85-31807
Mass-discrimination during prolonged weightlessness
20 p3509 N85-31814
Study of requirements for and method of multidimensional acoustic imaging — spaceborne experiments
[ESA-CR(P)-2020] 20 p3525 N85-31924
Energy spectra of elements with 18 less than or equal to Z less than or equal to 28 between 10 and 300 GeV/amu 20 p3543 N85-32045
Elemental abundances of cosmic rays with Z33 as measured on HEAO-3 20 p3543 N85-32046
Study of proton and neutron activation of metal samples in low Earth orbit
[NASA-CR-171596] 21 p3658 N85-32130
USSR Space Life Sciences Digest
[NASA-CR-3922] 21 p3658 N85-32709
Salyut-7 cosmonauts work with RS-17 and GSPS X-ray telescopes 22 p3731 N85-33131
Results and prospects of physiological research during spaceflights 22 p3732 N85-33139
Effect of substrate moisture on growth and structure of corn leaf 22 p3824 N85-33992
The development of a high energy cosmic ray detector for Spacelab-2
[OG-8.1-8] 23 p4023 N85-34934
The heavy ions in space experiment
[OG-8.1-10] 23 p4023 N85-34936
NASA Developmental Biology Workshop: A summary
[NASA-TM-86758] 24 p4126 N85-35578

SPACEBORNE PHOTOGRAPHY
NT SATELLITE-BORNE PHOTOGRAPHY
Tass reports experiments during visiting crew's third day 02 p0158 N85-11073
The possibility of detection and measurement of cloud structure in the atmosphere of Uranus
02 p0299 N85-11937
Metric camera experiment: Spacelab 1 mission
05 p0658 N85-14229
The photogrammetric camera experiment on Spacelab 1 05 p0658 N85-14230

Searching for impact craters using space shuttle photography 06 p0889 N85-15545
Lyakhov and Aleksandrov on 150-day flight 13 p1977 N85-22405
Experience in automated interpretation of aerospace photographs 13 p1983 N85-22444
Geoindication method for interpreting aerial and space photographs: Status and prospects 13 p1984 N85-22445
Experience in combined special mapping using space information 13 p1984 N85-22449
Study of Volga river delta using space photosurvey materials 15 p2485 N85-25340
Use of space information in petroleum- and gas-prospecting work (example of Southern Mangyshlak) 15 p2485 N85-25341
Example of joint use of data from surface studies and space photographs in investigating dynamics of zone of North Zeravshan seismogenic faults 15 p2485 N85-25342
Relative geological information yield from small-scale multizonal space images (example of Fergana depression and its mountainous margins) 15 p2485 N85-25343
Identifying land use structures of multizonal aerospace photographs using digital data processing 15 p2486 N85-25348
Experience in automation of data processing in interpretation and defining of linear elements from space photographs 15 p2486 N85-25349
Computing parameters characterizing possibility of planets falling in star camera field of view during space survey 15 p2487 N85-25351
Glow of ionospheric F-layer in Line 630 nm determined from photographs taken aboard Salyut-6 orbital station: Interpretation of results 16 p2721 N85-26799
SVIT complex for analysis of space photography 16 p2725 N85-26819
Tenth Conference of Working Group of Socialist Countries on Remote Sensing of Earth under Intercosmos Program 16 p2725 N85-26820
Study and mapping of anthropogenic effect on environment in different regions of USSR on basis of space photographs 16 p2726 N85-26824
Multiple regression analysis of photographic image of soil properties 16 p2726 N85-26825
Analysis of mesofissuring on space photographs: New technique for study of petroleum and gas deposits 16 p2726 N85-26828
Space photographs confirm 40-year-old hydrodynamics discovery 19 p3289 N85-30393
Large format camera photographs: A new tool for understanding arid environments 21 p3604 N85-32379
Terrain illumination conditions when taking scanning photographs from space 22 p3736 N85-33150
Calculating solar highlight and shadeless areas for scanning photographs from space and optimizing lighting conditions 22 p3736 N85-33160
Discrimination of linear contour elements of space photographs based on visual perception model 22 p3736 N85-33161
Mapping of dynamics of deltas by space photography 22 p3737 N85-33163
Comprehensive mapping of arid territories of Arizona using space photography 22 p3737 N85-33164

SPACEBORNE TELESCOPES
NT HUBBLE SPACE TELESCOPE
NT SOLAR OPTICAL TELESCOPE
NT SPACE INFRARED TELESCOPE FACILITY
Optical contacting for gravity probe star tracker [NASA-TM-86475] 01 p0120 N85-10619
Optical analysis of the star-tracker telescope for Gravity Probe [NASA-TM-86474] 01 p0129 N85-10688
The Bellkt experiment 02 p0159 N85-11079
West Europe report: Science and technology, no. 166 [JPRS-84845] 03 p0341 N85-12190
French, Soviets decide to launch Sigma space telescope 03 p0341 N85-12191
Choice of orbit for scientific satellites: SIGMA, the submillimeter telescope — Ariane-borne gamma imagery satellite (SIGMA) 05 p0600 N85-13828
Pointing and control system design study for the space infrared telescope facility (SIRTF) [NASA-CR-166612] 07 p0915 N85-15795
SIRTF: The next step [NASA-TM-86683] 07 p1059 N85-16724
SIRTF: The next step 08 p1250 N85-17691
Satellite description 09 p1412 N85-18900
Sixteenth Lunar and Planetary Science Conference. Press abstracts [NASA-CR-175602] 15 p2680 N85-26548
Dell-Null tester for spaceborne applications [AD-A151772] 16 p2881 N85-27779
Long life feasibility study for the shuttle infrared telescope facility [NASA-CR-3722] 17 p3052 N85-28893
The Extended Range X-Ray Telescope center director's discretionary fund report [NASA-TM-86507] 19 p3382 N85-30983
Astron telescope stabilization system 22 p3732 N85-33133
Results from Astron orbiting telescope 22 p3732 N85-33134
Astron X-ray experiment 22 p3732 N85-33137

SPACECRAFT
Space Shuttle Orbiter trimmed center-of-gravity extension study. Volume 8: Effects of configuration modifications on the aerodynamic characteristics of the 140 A/B Orbiter at a Mach number of 5.97 [NASA-TM-72661-VOL-8] 04 p0452 N85-12867
An optimization method for the preliminary design of interplanetary aerobraking missions 08 p1076 N85-16822
On the frontier: Flight research at Dryden 1946-1981 [NASA-SP-4303] 09 p1263 N85-17934
Clarke Stations and mercurian mass-drivers: Energy for large-scale transportation systems [DE85-009607] 21 p3560 N85-32145
Fuel cell applications literature review [DE85-011891] 22 p3809 N85-33592

SPACECRAFT ANTENNAS
Large spaceborne antenna reflectors using inflatable space rigidized structures 05 p0625 N85-14004
Elastic dispersion effects on dynamics and control of large modular antennas — spacecraft antennas 05 p0627 N85-14019
Interleaved array antenna technology development [NASA-CR-171845] 10 p1477 N85-19328
Precision antenna reflector structures 14 p2232 N85-23834
An optimization study to minimize surface distortions of a hoop-column antenna 14 p2232 N85-23837
Structural dynamics analysis 14 p2233 N85-23838
AFWAL space control technology program 14 p2233 N85-23839
Large antenna control methods: Current status and future trends 14 p2234 N85-23845
Application of modern Aperture Integration (AI) and Geometrical Theory of Diffraction (GTD) techniques for analysis of large reflector antennas 14 p2234 N85-23851
Feed system design considerations for large space antenna systems. Part 1: Multiple apertures with non-overlapping feeds 14 p2234 N85-23852
The space station as a construction base for large space structures 14 p2235 N85-23856
Compensator development and examination of performance and robustness [NASA-CR-175703] 15 p2540 N85-25678
Bonded stripline power splitter for ERS-1 [RML-009-84-124] 15 p2550 N85-25740
Application of the ADAMS program to deployable space truss structures [NASA-CR-177927] 19 p3284 N85-30366
Proceedings of the Workshop on Identification and Control of Flexible Space Structures, volume 1 [NASA-CR-176051] 20 p3408 N85-31148
AFWAL control technology programs 20 p3408 N85-31150
Design and evaluation of control systems for large communications satellites 20 p3409 N85-31157
Control of large antennas based on electromagnetic performance criteria 20 p3409 N85-31158
Vibration control experiment design for the 15-m hoop/column antenna 20 p3409 N85-31159
A hardware demonstration of distributed control for a flexible offset-feed antenna 20 p3410 N85-31160
Time-optimal bang-bang slew of rigidized SCOLE configuration 20 p3410 N85-31164
The experimental computer control of a two-dimensional hyperbolic system 20 p3411 N85-31166
Approximation of optimal infinite dimensional compensators for flexible structures 20 p3413 N85-31181
Control of a flexible space antenna: A finite dimensional perspective based on distributed parameter theory 20 p3413 N85-31182
Box truss analysis and technology development. Task 1: Mesh analysis and control [NASA-CR-172570] 23 p3900 N85-34156

SPACECRAFT CABIN ATMOSPHERES
Toxicological evaluation of Columbia spacecraft 01 p0094 N85-10631
Human response to vibroacoustic environments of space vehicles [NASA-TM-86316] 01 p0116 N85-10789
Solid sorbent air sampler [NASA-CASE-MSC-20653-1] 11 p1636 N85-20301
Proceedings of the Seminar on Space Station Human Productivity [NASA-TM-86673] 18 p3156 N85-29539
Internal contamination issues 18 p3156 N85-29543
Extended mission life support systems 18 p3157 N85-29547
Gas chromatography: Possible application of advanced instrumentation developed for solar system exploration to space station cabin atmospheres 18 p3157 N85-29551

SPACECRAFT CABIN SIMULATORS
Space station models, mockups and simulators 18 p3159 N85-29569

SPACECRAFT CABINS
Challenges in the development of the orbiter atmosphere revitalization subsystem 08 p1095 N85-16920
Habitability sleep accommodations 18 p3159 N85-29566

SPACECRAFT CHARGING
SEPAC (space experiments with particle accelerators) 01 p0014 N85-10085
Charging of the DMSP F-2 spacecraft in the aurora on 10 January 1983 [AD-A146303] 03 p0324 N85-12066
Effects of the solar and extraterrestrial environments on space power systems 05 p0610 N85-13898
Rocket body charge neutralization processes in ARAKS experiment (data from two launches) 13 p1960 N85-22426
Spacecraft Environmental Interactions Technology, 1983 [NASA-CP-2359] 13 p1969 N85-22470
Vehicle charging on STS-3 Mission 13 p1969 N85-22473
Electron and ion density depletions measured in the STS-3 orbiter wake 13 p1969 N85-22474
Shuttle electrical environment 13 p1990 N85-22475
Measured electron contribution to Shuttle plasma environment: Abbreviated update 13 p1990 N85-22476
Laboratory studies of Kapton degradation in an oxygen ion beam 13 p1990 N85-22477
Electron beam charging of Space Shuttle thermal protection system tiles 13 p1990 N85-22478
Charging of DMSP/F6 spacecraft in aurora on 10 January 1983 13 p1991 N85-22481
Average and worst-case specifications of precipitating auroral electron environment 13 p1991 N85-22482
Auroral-polar cap environment and its impact on spacecraft plasma interactions 13 p1991 N85-22484
Electric field effects on ion currents in satellite wakes 13 p1991 N85-22485
Three-dimensional calculation of shuttle charging in polar orbit 13 p1992 N85-22486
Polar orbit electrostatic charging of objects in shuttle wake 13 p1992 N85-22487
Wakes and differential charging of large bodies in low Earth orbit 13 p1992 N85-22488
Sheath ionization model of beam emissions from large spacecraft 13 p1992 N85-22489
Interactions between large space power systems and low-Earth-orbit plasmas 13 p1992 N85-22490
Calculation of secondary-electron escape currents from inclined-spacecraft surfaces in a magnetic field 13 p1992 N85-22491
Self-consistent simulation of plasma interactions with secondary-emitting insulators 13 p1993 N85-22492
Surface interactions and high-voltage current collection 13 p1993 N85-22493
The PIX-2 experiment: An overview 13 p1993 N85-22494
Plasma interaction experiment 2 (PIX 2): Laboratory and flight results 13 p1993 N85-22495
Design guidelines for assessing and controlling spacecraft charging effects 13 p1994 N85-22500
Aerospace spacecraft-charging guidelines document 13 p1994 N85-22501
EMI characteristics of a potential control system 13 p1994 N85-22502
Anomalously high potentials observed on ISEE 13 p1994 N85-22503
Characteristics of EMI generated by negative metal-positive dielectric voltage stresses due to spacecraft charging 13 p1995 N85-22505
Laboratory studies of spacecraft response to transient discharge pulses 13 p1995 N85-22506
Development of a continuous broad-energy-spectrum electron source 13 p1995 N85-22507
Automatic charge control system for satellites 13 p1995 N85-22508
Discharge pulse phenomenology 13 p1995 N85-22509

Discharge characteristics of dielectric materials examined in mono-, dual-, and spectral energy electron charging environments 13 p1995 N85-22510
Electron yields from spacecraft materials 13 p1996 N85-22512
Electrical conduction in polymer dielectrics 13 p1996 N85-22514
Spacecraft environmental interactions: A joint Air Force and NASA research and technology program 13 p1997 N85-22517
Interactions measurement payload for Shuttle 13 p1997 N85-22518
Astronaut hazard during free-flight polar EVA 13 p1997 N85-22522
Development and testing of a spacecraft surface potential monitor 13 p2007 N85-22582
Phenomenology of discharges in space: Application to a solar generator — SPOT satellite 13 p2007 N85-22583
Electrostatic discharge testing on a carbon fiber solar panel structure 13 p2007 N85-22584
Measurement of charged secondary particle emission under ion and neutral impact — Giotto mission 14 p2243 N85-23906
Giotto residual ionization 14 p2244 N85-23909
Experimental investigations on ion emission with dust impact on solid surfaces — Giotto spacecraft 14 p2244 N85-23911
Ion emission from solid surfaces: Comparison of dust impact with other excitations — Giotto mission 14 p2244 N85-23912
Electrostatic charging of the Giotto spacecraft due to neutral gas impact 14 p2244 N85-23913
Giotto plasmasheath and wake charging near Halley's Comet: Revised parameters 14 p2245 N85-23915
Simulations of satellite-plasma interaction, including electron space charges — Giotto mission 14 p2245 N85-23916
Anticipated impact plasma problems for the COPERNIC-RPA experiment in the cometary environment — Giotto mission 14 p2245 N85-23917
Plasma environment effects on the Giotto Ion Mass Spectrometer 14 p2245 N85-23919
Electric potential of satellite in electron emitting experiments in initial stage of electron beam injection in steady-state mode 15 p2480 N85-25309
ESABASE extension to spacecraft charging analysis. Phase 1: NASCAP software (VAX version)
[ESA-CR(P)-1968] 15 p2493 N85-25381
Preliminary documentation for the polar code
[AD-A154125] 19 p3336 N85-30667
Surface voltage gradient role in high voltage solar array-plasma interaction: Center Director's discretionary fund
[NASA-TM-86516] 22 p3805 N85-33567

SPACECRAFT COMMUNICATION

Communications protocols for a fault tolerant, integrated local area network for Space Station applications
[NASA-TM-86304] 01 p0106 N85-10711
The real world: The user 02 p0150 N85-11017
Pluribus satellite IMP (Interface Message Provision) development mobile access terminal network
[AD-A145348] 02 p0190 N85-11269
Timing performance of phase-locked loops in optical pulse position modulation communication systems
[AD-A145403] 02 p0190 N85-11271
Telemetry (TM)/telecommand (TC) processor study
[ESA-CR(P)-1915] 03 p0323 N85-12081
The Telecommunications and Data Acquisition Report
[NASA-CR-174149] 05 p0822 N85-13960
Problems of development of space communication 06 p0793 N85-15087
Demand for satellite-provided domestic communications services up to the year 2000
[NASA-TM-86894] 06 p0798 N85-15099
Spacecraft system study: A study to define the impact of laser communication systems on their host spacecraft
[NASA-CR-175272] 07 p0970 N85-16159
Shuttle ku-band communications/radar technical concepts 08 p1099 N85-16949
Shuttle payload S-band communications system 08 p1100 N85-16950
The Communications link analysis and simulation system (CLASS) 08 p1100 N85-16952
The Statistical Loop Analyzer (SLA) 08 p1100 N85-16955
Digital scrambling for shuttle communication links: Do drawbacks outweigh advantages? 08 p1101 N85-16956
Novel applications of the NASA/GSFC Viterbi decoder hardware simulator 08 p1101 N85-16957
Electronics systems test laboratory testing of shuttle communications systems 08 p1101 N85-16958
Coding for reliable satellite communications
[NASA-CR-174315] 08 p1150 N85-17257
Pluribus satellite IMP development mobile access terminal network
[AD-A147875] 08 p1151 N85-17264
A modified Monte-Carlo technique for the simulation of satellite communication systems
[AD-A148689] 08 p1214 N85-17641
Research and technology highlights of the Lewis Research Center
[NASA-TM-86899] 08 p1261 N85-17928
Experimental satellite system for determining coordinates of maritime distress 09 p1306 N85-18216
Technical evaluation report on the 46th Symposium of the Avionics Panel on Space System Applications to Tactical Operations
[AGARD-AR-203] 10 p1425 N85-18988
Description of amplitude scintillations on a 11 GHz slant path in terms of forward scattering from turbulent layers
[FI-455-TBR-76] 11 p1625 N85-20232
Polarization angles of linearly polarized antennas and radio waves in satellite communications
[PB85-131613] 11 p1626 N85-20240
Reed-Solomon decoder — applicable to Galileo Project requirements
[NASA-CASE-NPO-15982-1] 11 p1699 N85-20680
Tactical operations and space applications 11 p1709 N85-20752
Integrated support of tactical operations by satellite communications 11 p1709 N85-20754
EHF MILSATCOM systems for tactical users 11 p1709 N85-20755
Combat capable space systems for tactical support 11 p1713 N85-20775
Transmission and orbital constraints in space-related programs: Briefing summary 12 p1787 N85-21216
Ionospheric distortions of digital signals with wideband modulation 13 p2072 N85-22945
Space-based antenna measurement system concepts for space station operation 14 p2236 N85-23660
The transpacific experimental sailing by YASEIGO 3 14 p2327 N85-24360
Shuttle communications and tracking systems modeling and TDRSS link simulations studies
[NASA-CR-171861] 15 p2491 N85-25369
Pluribus Satellite IMP (Interface Message Provision) development mobile access terminal network
[AD-A151201] 15 p2541 N85-25688
Pluribus Satellite IMP (Interface Message Provision) development mobile access terminal network
[AD-A151312] 15 p2542 N85-25692
Analysis of space diversity techniques for EHF (Extremely High Frequency) satellite downlinks
[AD-A151900] 15 p2544 N85-25705
Adaptation of bit error rate by coding — spacecraft transmissions
[ESA-CR(P)-1970] 15 p2545 N85-25711
Space Shuttle program communication and tracking systems interface analysis
[NASA-CR-171862] 16 p2729 N85-26841
Consultative Committee for Space Data Systems. Panel 1: Support
[NASA-CR-175786] 16 p2769 N85-27090
SESC (Space Environment Services Center) satellite broadcasting 10-year plan
[PB85-163541] 16 p2775 N85-27126
Water vapor radiometry research and development phase
[NASA-CR-175887] 17 p2995 N85-28512
Optical techniques for signal distribution and control in advanced radar and communication systems 18 p3188 N85-29773
Serial Minimum Shift Keying (SMSK) follow-on study — spacecraft communication
[ESA-CR(P)-2026] 20 p3399 N85-31083
Control of flexible structures 20 p3410 N85-31161
Automated testing of developmental satellite communications systems and subsystems
[NASA-TM-87070] 20 p3440 N85-31348
Study of the interferences of 2 GHz radio beams with a DORIS system — precise low orbit determination system (DORIS)
[CNES-CT/DRT/TIT/RL-84/140-T] 20 p3442 N85-31362
Phase-locked loops for optical homodyne detection, volume 1 — spaceborne receivers
[ESA-CR(P)-2029-VOL-1] 20 p3442 N85-31367
Thirty GHz low noise GaAs FET amplifiers — satellite-ground communication
[CD.5500686] 20 p3449 N85-31413
A comparison of millimeter wave, direct detect and heterodyne laser intersatellite links
[AD-A151984] 20 p3461 N85-31496
Intersatellite optical links: The point ahead angle
[CNES-83/DRT/TIT/TR/150] 20 p3533 N85-31984
Automation study for space station subsystems and mission ground support
[NASA-CR-176097] 21 p3559 N85-32138
A model for predicting propagation-related DSCS (Defense Communications Engineering Center) margin requirements
[AD-A155355] 22 p3756 N85-33281
Satellite links in the ISO architecture: Models and performance evaluation
[ENST-84E017] 22 p3756 N85-33284
Variation in radiowave propagation conditions in corona during solar activity cycle 22 p3763 N85-33327
On the principle of uniformity of satellite communications systems 22 p3773 N85-33362
Second-generation mobile satellite system. A conceptual design and trade-off study
[NASA-CR-176195] 24 p4086 N85-35325

SPACECRAFT COMPONENTS

NT SPACECRAFT CABINS
NT SPACECRAFT MODULES

Damping synthesis for a spacecraft using substructure and component data
[CRC-1365] 03 p0323 N85-12082
Advanced high-power transfer through rotary interfaces 05 p0807 N85-13875
Procedures for testing and evaluating spacecraft-type heat pipes
[AD-A146671] 06 p0809 N85-15139
On-orbit support of DARPA-301 payload
[AD-A146897] 07 p0911 N85-15767
A total dose characterization of five commercial analog multiplexers
[AD-A146886] 07 p0946 N85-15997
Analysis of Nonvolatile Residue (NVR) from spacecraft systems
[NASA-TM-86184] 08 p1113 N85-17019
Study in spurious sensitivity of electronics in space
[AD-A148386] 08 p1158 N85-17305
The wear of small polyacetal and polymide gears in vacuum — spacecraft gears
[ESA-ESTL-058] 08 p1189 N85-17374
Environment definition, large particles 12 p1787 N85-21220
NASA welding assessment program
[NASA-CR-175512] 12 p1859 N85-21661
Two-phase fluid thermal transport for spacecraft
[AD-A151316] 15 p2493 N85-25378
The GIW handbook for data compilation of irradiation tested electronic components, volume 3
[HMI-B-353-VOL-3] 17 p2956 N85-28258
Evaluation of VLSI technology — space applications
[CD.6501702] 18 p3096 N85-29177
The role of mock-ups in the development of Orbital Replaceable Units (ORU) 18 p3160 N85-29573
Results from radiation monitoring equipment experiments on STS-41C, 41D, 41G and 51A
[AD-A154678] 21 p3560 N85-32142
Background equatorial astronomical measurements focal plane assembly (refurbished HI STAR SOUTH)
[AD-A155215] 21 p3590 N85-32313

SPACECRAFT CONFIGURATIONS

NT SATELLITE CONFIGURATIONS

Space Shuttle wind tunnel testing program
[NASA-RP-1125] 02 p0167 N85-11127
Conceptual design and evaluation of selected Space Station concepts: Executive summary
[NASA-TM-87382] 02 p0167 N85-11128
Shuttle structural dynamics characteristics: The analysis and verification 08 p1094 N85-16913
Structural load challenges during space shuttle development 08 p1094 N85-16914
Vehicle/engine integration — orbit transfer vehicles 08 p1109 N85-17008
Satellite description 09 p1412 N85-18900
Constellations 11 p1643 N85-20352
Summary presentation of the Constellations Panel 11 p1644 N85-20359
Report of the Constellations Panel 11 p1645 N85-20368
Some aspects of attitude stability of tethered space stations 11 p1648 N85-20369
The ARIANE family 11 p1712 N85-20774
Model control of structural systems
[AD-A149734] 12 p1790 N85-21235
On-orbit systems identification of flexible spacecraft Technol., 1984, Pt. 2 p 465-481 14 p2233 N85-23841
Space Technology Experiments Platform (STEP) status: An in-space test facility 14 p2236 N85-23663
Numerical experiments on flexible spacecraft with the aid of the Dynamic Control and Analysis Package (DCAP)
[ESA-STM-229] 15 p2493 N85-25382
Incorporating control into the optimal structural design of large flexible space structures
[AD-A152858] 17 p2909 N85-27937

Space Station reference configuration description
[NASA-TM-87493] 20 p3408 N85-31146
Parametric stiffness control of flexible structures
20 p3414 N85-31187
A study on the control of third generation spacecraft
20 p3415 N85-31196
Nickel-hydrogen spacecraft module configurations study
20 p3447 N85-31401
The space station polar platform: NOAA systems considerations and requirements
[NOAA-TR-NESDIS-22] 22 p3740 N85-33182
Advanced beamed-energy and field propulsion concepts
[NASA-CR-176108] 22 p3741 N85-33186
Spacecraft (Mobile Satellite) configuration design study
[NASA-CR-176153] 23 p3899 N85-34152

SPACECRAFT CONSTRUCTION MATERIALS
Constituent property - composite property relationships in thermoset matrices 04 p0465 N85-12950
Space Station truss structures and construction considerations
[NASA-TM-86336] 07 p0916 N85-15796
SSME lifetime prediction and verification, integrating environments, structures, materials: The challenge
08 p1095 N85-16918
Oxidation protection coatings for polymers
[NASA-CASE-LEW-14072-1] 11 p1611 N85-20129
NASA space materials research
14 p2232 N85-23831
Materials and processes control for space applications
18 p3156 N85-29544
Ion beam sputter-deposited thin film coatings for protection of spacecraft polymers in low Earth orbit
[NASA-TM-87051] 19 p3248 N85-30137
R and D activities of the Structural Sciences Division
20 p3539 N85-32026
A survey of structural material issues for a space station
[NASA-TM-86385] 22 p3738 N85-33168

SPACECRAFT CONTAMINATION
Shuttle on-orbit contamination and environmental effects 08 p1104 N85-16980
Space environment simulation to test satellite thermal control coatings, volume 1
[CERT-4128-VOL-1] 08 p1109 N85-17012
Space environment simulation to test satellite thermal control coatings. Volume 2: Annex 1
[ESA-CR(P)-1870-VOL-2] 08 p1109 N85-17013
Space environment simulation to test satellite thermal control coatings. Volume 2: Annexes 2, 3, 4
[ESA-CR(P)-1870-VOL-3] 08 p1109 N85-17014
Analysis of Nonvolatile Residue (NVR) from spacecraft systems
[NASA-TM-86164] 08 p1113 N85-17019
Minimizing plume contamination production in bipropellant thrusters 13 p2003 N85-22557
Measurement of the nighttime infrared luminosity of Spacelab 1 in the H- and K-bands
[NASA-TM-85972] 14 p2434 N85-25011
Proceedings of the Seminar on Space Station Human Productivity
[NASA-TM-86673] 18 p3156 N85-29539
Statement of contamination problem
18 p3156 N85-29542
Internal contamination issues
18 p3156 N85-29543
Materials and processes control for space applications
18 p3156 N85-29544
Space station trace contaminant control
18 p3157 N85-29550
Mass spectrometry technology at the Jet Propulsion Laboratory (JPL) 18 p3157 N85-29552
Atmosphere monitoring requirements
18 p3158 N85-29553
Some problems associated with trace contaminant removal systems for spacecabins
18 p3158 N85-29554
Contamination control for increased crew productivity
18 p3158 N85-29555
Human productivity program definition
18 p3158 N85-29556
Space shuttle molecular and wake vacuum measurements
[NASA-TM-86509] 19 p3222 N85-29978
Particulate contamination control in clean rooms by particle fallout (PFO) measurements
[ESA-PSS-01-204-ISSUE-1] 20 p3487 N85-31673

SPACECRAFT CONTROL
NT SATELLITE ATTITUDE CONTROL
NT SATELLITE CONTROL
Use of gravitational stabilization in performance of experiments 02 p0160 N85-11064
A user's guide to the Flexible Spacecraft Dynamics and Control Program
[NASA-TM-87389] 03 p0405 N85-12586
Propellant tank resupply system
[AD-D011288] 05 p0603 N85-13848
Torque command steering law for double-gimbaled control moment gyros applied to rotor energy storage
05 p0608 N85-13879
Disturbance propagation in structural networks; control of large space structures 06 p0759 N85-14856
Active nutation control of spacecraft using a magnetic bearing momentum wheel with Vernier gimballing capability
[NAL-TR-8201] 06 p0759 N85-14857
SSME digital control design characteristics
08 p1091 N85-16893
Development and implementation of the verification process for the shuttle avionics system
08 p1091 N85-16896
Summary presentation of the Constellations Panel
11 p1644 N85-20359
The Satellite sail 11 p1647 N85-20376
Attitude data consistence check of rocket payloads
[BMFT-FB-W-84-049] 12 p1790 N85-21239
Stability analysis of flexible spacecraft with PID controller
[CRC-1372] 12 p1792 N85-21247
Radioelectronics and space exploration
12 p1838 N85-21533
Station keeping of geostationary satellites by electric propulsion
[NASA-TM-77820] 14 p2320 N85-24337
Identification and control of structures in space
[NASA-CR-175790] 16 p2731 N85-26850
Artificial intelligence in space platforms
[AD-A152078] 16 p2851 N85-27578
In orbit infrastructure
[DM-51/CC-FL-044-83] 18 p3066 N85-28966
Standard Generic approach for Spacecraft Autonomy and Automation, phase 2 (SGASA-2). Volume 1: Executive summary
[ESA053-1-VOL-1] 18 p3167 N85-29623
Standard Generic Approach for Spacecraft Autonomy and Automation, phase 2 (SGASA-2). Volume 2: Technical report
[ESA053-1-VOL-2] 18 p3167 N85-29624
Standard Generic Approach for Spacecraft Autonomy and Automation, phase 2 (SGASA-2). Volume 3: Appendices
[ESA053-1-VOL-3] 18 p3167 N85-29625
Proceedings of the Workshop on Identification and Control of Flexible Space Structures, volume 1
[NASA-CR-176051] 20 p3408 N85-31148
Control of flexible structures 20 p3410 N85-31161
Design of multivariable controllers using the Integrated Analysis Capability (IAC) 20 p3412 N85-31172
A structural dynamics approach to the simulation of spacecraft control/structure interaction
20 p3412 N85-31173
Proceedings of the Workshop on Identification and Control of Flexible Space Structures, volume 3
[NASA-CR-176053] 20 p3415 N85-31195
A study on the control of third generation spacecraft
20 p3415 N85-31196
Matrix transfer function design for flexible structures: An application 20 p3416 N85-31199
Robust control design for large space structures
20 p3416 N85-31200
On the stability of collocated controllers in the presence or uncertain nonlinearities and other perils
20 p3416 N85-31201
Research and development activities in unified control-structure modeling and design
[NASA-CR-176111] 22 p3740 N85-33180
Space station rotational equations of motion
[NASA-TP-2511] 23 p3899 N85-34148
Hardware math for the 6502 microprocessor
[NASA-TM-86517] 23 p3955 N85-34511
Identification and control of structures in space
[NASA-CR-176175] 24 p4069 N85-35214
TRICCS: A proposed teleoperator/robot integrated command and control system for space applications
[NASA-TM-87577] 24 p4136 N85-35637
Enhancement of the flexible spacecraft dynamics program for open spacecraft
[NASA-CR-175309] 24 p4137 N85-35641

SPACECRAFT DEFENSE
Combat capable space systems for tactical support
11 p1713 N85-20775
Transmission and reflection of laser beams propagating through aerosol clouds in space
[LA-9996-MS] 12 p1856 N85-21638

SPACECRAFT DESIGN
NT SATELLITE DESIGN
Vibration, acoustic, and shock design and test criteria for components on the Solid Rocket Boosters (SRB), Lightweight External Tank (LWT), and Space Shuttle Main Engines (SSME)
[NASA-RP-1127] 01 p0061 N85-10405
Modular experimental platform for science and applications 02 p0152 N85-11031
External tank aft cargo carrier
02 p0155 N85-11050
Space Shuttle wind tunnel testing program
[NASA-RP-1125] 02 p0167 N85-11127
SMP: A solid modeling program
[NASA-CR-172473] 02 p0241 N85-11570
General Electric composite ring-disk flywheel: Recent and potential developments 05 p0606 N85-13867
Space power management and distribution status and trends 05 p0610 N85-13896
Analytical modeling of spacecraft power systems
05 p0610 N85-13897
Effects of the solar and extraterrestrial environments on space power systems 05 p0610 N85-13898
Aerodynamic characteristics of some lifting reentry concepts applicable to transatmospheric vehicle design studies
[NASA-TM-86331] 06 p0747 N85-14787
Pointing and control system design study for the space infrared telescope facility (SIRTF)
[NASA-CR-166612] 07 p0915 N85-15795
Space Shuttle Technical Conference, part 1
[NASA-CP-2342-PT-1] 08 p1090 N85-16889
Shuttle structural dynamics characteristics: The analysis and verification 08 p1094 N85-16913
Structural load challenges during space shuttle development 08 p1094 N85-16914
Orbiter structural design and verification
08 p1094 N85-16915
Space shuttle external tank performance improvements: The challenge 08 p1094 N85-16916
Structural and mechanical design challenges of space shuttle solid rocket boosters separation and recovery subsystems 08 p1095 N85-16917
SSME lifetime prediction and verification, integrating environments, structures, materials: The challenge
08 p1095 N85-16918
Orbiter processing facility: Access platforms Kennedy Space Center, Florida, from challenge to achievement
08 p1102 N85-16968
External tank GH2 vent arm 08 p1102 N85-16969
In-flight testing of the space shuttle orbiter thermal control system 08 p1103 N85-16974
Impact of lunar and planetary missions on the space station
[NASA-CR-171832] 08 p1106 N85-16988
OTV fluid mangement systems
08 p1108 N85-17007
Orbital transfer vehicle propulsion issues
08 p1109 N85-17009
Space based OTV servicing 08 p1109 N85-17010
Space Station needs, attributes, and architectural option study
[NASA-CR-174316] 08 p1109 N85-17011
Waste collection subsystem study
[NASA-CR-171836] 08 p1199 N85-17552
Space Shuttle Orbiter waste collection system conceptual study
[NASA-CR-171844] 08 p1199 N85-17553
Vibration analysis of a multipurpose platform
[NAL-TR-803] 09 p1286 N85-18078
Efficient structures for geosynchronous spacecraft solar arrays
[NASA-CR-174448] 10 p1428 N85-19004
Constellations 11 p1643 N85-20352
Study proposal for the possible use of ISS as an aerodynamic facility for aerospace applications
11 p1646 N85-20374
Space heat rejection radiators: Meteoroid/debris consideration 12 p1786 N85-21210
Space Station
[NASA-EP-211] 12 p1793 N85-21251
Design study of an integrated aerobraking orbital transfer vehicle
[NASA-TM-58264] 12 p1795 N85-21282
Deployable folded antenna apparatus
[AD-D011503] 12 p1832 N85-21495
Debris impact on Earth-orbiting spacecraft
12 p1948 N85-22234
Feoktistov recalls period leading to Gagarin spaceflight 13 p1985 N85-22451
Feoktistov argues against U.S. space shuttle design concept 13 p1985 N85-22453
Feoktistov discusses need for space colonization
13 p1985 N85-22454
Report on final recommendations for IMPS engineering-science payload
[NASA-CR-175659] 13 p1988 N85-22464
Design guidelines for assessing and controlling spacecraft charging effects 13 p1994 N85-22500
Uses of composite materials
13 p2027 N85-22698
Precision space structures 14 p2232 N85-23833

Thermal design of the Giotto spacecraft
14 p2245 N85-23920
Progress of computational fluid dynamics in the world
16 p2691 N85-26812
A study of spacecraft technology and design concepts, volume 1
[NASA-CR-172579-VOL-1] 16 p2730 N85-26844
A study of spacecraft technology and design concepts. Volume 2: Appendices
[NASA-CR-172579-VOL-2] 16 p2730 N85-26845
The NASA Space Station program plans
[NASA-TM-87474] 16 p2730 N85-26846
Spacestation: The next logical step
[NASA-EP-213] 16 p2730 N85-26847
Space Station Spartan study
[NASA-TM-86215] 16 p2731 N85-26852
In orbit infrastructure
[DM-51/CC-FL-044-83] 18 p3086 N85-28986
Astronautical conference hears details on Hermes minishuttle
18 p3088 N85-29112
Proceedings of the Seminar on Space Station Human Productivity
[NASA-TM-86673] 18 p3156 N85-29539
Human factors issues in space station architecture
18 p3158 N85-29560
Considerations for space station interior architecture
18 p3159 N85-29564
Human factors in space station architecture: The ECLSS module concept
18 p3159 N85-29565
Habitability sleep accommodations
18 p3159 N85-29566
Customer and mission influence on space station architecture
18 p3159 N85-29567
Mockups and human productivity studies
18 p3159 N85-29570
Rockwell experience applications to Ames space station mockup habitability/productivity studies
18 p3159 N85-29572
Standard Generic approach for Spacecraft Autonomy and Automation, phase 2 (SGASA-2). Volume 1: Executive summary
[ESA053-1-VOL-1] 18 p3167 N85-29623
Standard Generic Approach for Spacecraft Autonomy and Automation, phase 2 (SGASA-2). Volume 2: Technical report
[ESA053-1-VOL-2] 18 p3167 N85-29624
Standard Generic Approach for Spacecraft Autonomy and Automation, phase 2 (SGASA-2). Volume 3: Appendices
[ESA053-1-VOL-3] 18 p3167 N85-29625
Space station automation study. Volume 2: Technical report. Autonomous systems and assembly
[NASA-CR-171515] 19 p3226 N85-30001
Spacecraft, straight-tube evaporator design
[AD-A154462] 19 p3226 N85-30003
A dual spin space station design
20 p3408 N85-31152
Control of a flexible space antenna: A finite dimensional perspective based on distributed parameter theory
20 p3413 N85-31162
An integrated control and minimum mass structural optimization algorithm for large space structures
20 p3413 N85-31163
ISAAC (Integrated Structural Analysis and Control) via continuum modeling and distributed frequency domain design techniques
20 p3414 N85-31165
Studies toward a manned space station: Participation of European industry in NASA space station (MSS)
[SNIAS-S/DT-Y-25-212] 20 p3418 N85-31217
AUSSAT battery life test program
20 p3446 N85-31395
Research and development activities in unified control-structure modeling and design
[NASA-CR-176111] 22 p3740 N85-33180
Study and realization of a command system adapted to space robotics
[SNIAS-851-440-106] 22 p3740 N85-33183
Evaluation study of mechanical refrigeration systems for application to space missions — infrared astronomy
[SNIAS-1029ACA/LL/V] 22 p3755 N85-33277

SPACECRAFT DOCKING

Tass reports medical, materials studies aboard Salyut-7
02 p0158 N85-11071
Transportation applications, part 2
11 p1643 N85-20350
Evaluation of OMV ranging and docking systems
12 p1947 N85-22230
Swedish equipment for automatic docking in space
15 p2489 N85-25383
Automatic rendezvous and docking systems functional and performance requirements
[NASA-CR-171866] 15 p2492 N85-25376
Astronautical conference hears details on Hermes minishuttle
18 p3088 N85-29112
Docking simulation analysis of range data requirements for the orbital maneuvering vehicle
[NASA-TM-86510] 20 p3407 N85-31143
Space station dynamic modeling, disturbance accommodation, and adaptive control
20 p3409 N85-31154
A modular docking mechanism for in-orbit assembly and spacecraft servicing
22 p3796 N85-33516
Hardware test program for evaluation of baseline range-range rate sensor concept
[NASA-CR-176143] 23 p3933 N85-34377

SPACECRAFT ELECTRONIC EQUIPMENT

Evaluation of test equipment for the detection of contamination on electronic circuits — spacecraft electronics
[ESA-STM-234] 08 p1159 N85-17316

SPACECRAFT ENVIRONMENTS

Toxicological evaluation of Columbia spacecraft
01 p0094 N85-10631
Human response to vibroacoustic environments of space vehicles
[NASA-TM-86316] 01 p0116 N85-10789
Conceptual design and evaluation of selected Space Station concepts, volume 2
[NASA-TM-87384] 02 p0168 N85-11130
An evaluation of grease type ball bearing lubricants operating in various environments
[NASA-TM-86460] 02 p0185 N85-11230
Thermal management technology status
05 p0610 N85-13895
A buyer's guide to space infrastructure
07 p0914 N85-15784
Challenges in the development of the orbiter atmosphere revitalization subsystem
08 p1095 N85-16920
Challenges of developing an electro-optical system for measuring man's operational envelope
08 p1095 N85-16921
Other challenges in the development of the orbiter environmental control hardware
08 p1096 N85-16924
Characterization of heat transfer in nutrient materials — space flight feeding
[NASA-CR-171841] 08 p1139 N85-17551
Physiological considerations of artificial gravity
11 p1643 N85-20351
Aerospace Medicine and Biology: A continuing bibliography with indexes, supplement 267, January 1985
[NASA-SP-7011(267)] 12 p1904 N85-21959
Vibroacoustic study of the NASA Goddard Space Flight Center OSS-1 payload
[NASA-CR-175320] 13 p1988 N85-22465
BLSS: A contribution to future life support
18 p3155 N85-29534
CELSS transportation analysis
18 p3156 N85-29536
Some problems associated with trace contaminant removal systems for spacecabins
18 p3158 N85-29554
Contamination control for increased crew productivity
18 p3158 N85-29555
Human productivity program definition
18 p3158 N85-29556
Some ideas and questions regarding space station design for human use
18 p3158 N85-29562
Publications of the NASA CELSS (Controlled Ecological Life Support Systems) program
[NASA-CR-3911] 19 p3326 N85-30808
Electrophoretic mobilities of erythrocytes in various buffers
20 p3500 N85-31756
Results of Space Experiments in Physiology and Medicine and Informal Briefings by the F-16 Medical Working Group
[AGARD-CP-377] 20 p3507 N85-31805
Some results of the European vestibular experiments in the Spacelab-1 mission
20 p3508 N85-31809
Automation study for space station subsystems and mission ground support
[NASA-CR-176097] 21 p3689 N85-32136
Hydroponics developments for spaceship garden
21 p3693 N85-32754
Mathematical analysis of heart rhythm assessment of distinctive features in adaptation to spaceflight conditions
22 p3733 N85-33142
USSR report: Space Biology and Aerospace Medicine, vol. 19, no. 3, May - June 1985
[JPRS-USB-85-005] 23 p3952 N85-34494

SPACECRAFT EQUIPMENT

NT SPACECRAFT ELECTRONIC EQUIPMENT
Optical contacting for gravity probe star tracker
[NASA-TM-86475] 01 p0120 N85-10819
Definition of technology development missions for early Space Station satellite servicing. Volume 1: Executive summary
[NASA-CR-171228] 04 p0480 N85-12922
Magnetic suspension options for spacecraft inertia-wheel applications
05 p0607 N85-13871
Developments in space power components for power management and distribution
05 p0608 N85-13877
Power transfer from natural emitters to collection aperture at microwave wavelengths
[NASA-CR-174275] 07 p0945 N85-15989
Spaceborne receivers: Basic principles
[NASA-CR-174269] 07 p0948 N85-15990
The Statistical Loop Analyzer (SLA)
08 p1100 N85-16955
Waste collection subsystem study
[NASA-CR-171838] 08 p1199 N85-17552
Space Shuttle Orbiter waste collection system conceptual study
[NASA-CR-171844] 08 p1199 N85-17553
Transient vibration test criteria for spacecraft hardware — galileo spacecraft
09 p1338 N85-19418
High-voltage, high-power, solid-state remote power controllers for aerospace applications
[NASA-TP-2437] 12 p1795 N85-21263
Automated extraction of absorption bands from reflectance special
13 p2197 N85-23624
Earth Resources: A continuing bibliography with indexes, issue 45
[NASA-SP-7041(45)] 18 p3123 N85-29336

SPACECRAFT GUIDANCE

NT SATELLITE GUIDANCE
Analysis and simulation of an inertial system (Strapdown) for auxiliary attitude determination by adaptive drift estimation
[INPE-3257-TDL/177] 04 p0454 N85-12682

SPACECRAFT INSTRUMENTS

NT MULTISPECTRAL LINEAR ARRAYS
NT SATELLITE INSTRUMENTS
NT SPACECRAFT POSITION INDICATORS
Natural interference phenomena affecting spaceborne receivers
[NASA-CR-174256] 07 p0916 N85-15798
Reduction of signal modulation caused by polarization in visible optical scanning systems
[AD-D011389] 07 p1042 N85-16620
The design of an ion-neutral mass spectrometer to be used in the Shuttle environment
[AD-A148093] 08 p1114 N85-17022
Multiplex gas chromatography for use in space craft
[NASA-TM-86668] 09 p1290 N85-18097
In-situ detection of micron-sized dust particles in near-Earth space
12 p1785 N85-21205
Microwave blackbodies for spaceborne receivers
[NASA-CR-175647] 13 p2094 N85-23088
Optical system
[NASA-CASE-NPO-15801-1] 13 p2158 N85-23396
Plasma environment effects on the Giotto Ion Mass Spectrometer
14 p2245 N85-23919
Cosmic X-ray physics
[NASA-CR-175906] 17 p3055 N85-28910
Fully redundant mechanical release actuator
[NASA-CASE-LAR-13198-1] 18 p3116 N85-29287
Space optics
[CNES-84/105/T/CT/DRT/TIT/10]
20 p3533 N85-31985

SPACECRAFT LANDING

NT HORIZONTAL SPACECRAFT LANDING
NT MARS LANDING
NT PLANETARY LANDING
Active control technology experience with the Space Shuttle in the landing regime
[NASA-TM-86910] 01 p0012 N85-10071
STS natural environment analysis
[NASA-CR-171221] 03 p0322 N85-12079
Space shuttle handling qualities
08 p1092 N85-16904
Low-speed longitudinal orbiter qualities
08 p1092 N85-16905
Space shuttle main engine: Interactive design challenges
08 p1096 N85-16940
Feoktistov recalls period leading to Gagarin spaceflight
13 p1985 N85-23451
Small solar system bodies
13 p2175 N85-23499
Astronautical conference hears details on Hermes minishuttle
18 p3088 N85-29112

SPACECRAFT LAUNCHING

Tass reports launch of Progress-22
02 p0157 N85-11063
Sweden's Kiruna may be future launch site for satellites
03 p0310 N85-12000
View of Ariane countdown procedures, Kourou launch facilities
03 p0310 N85-12001
STS natural environment analysis
[NASA-CR-171221] 03 p0322 N85-12079
Launching systems
[CNES-NT-111] 04 p0460 N85-12917
Launch summary for 1978 - 1982 — sounding rockets, space probes, and satellites
[NASA-TM-87375] 04 p0461 N85-12924

Commercial Space Launch Act
[GPO-39-613] 04 p0578 N85-13690
Relationships between Ariane trajectories and satellite orbits 05 p0599 N85-13815
The launch window of a geostationary satellite 05 p0600 N85-13822
Atmospheric environment for Space Shuttle (STS-41D) launch
[NASA-TM-86484] 05 p0679 N85-14358
The space shuttle launch vehicle aerodynamic verification challenges 08 p1093 N85-16007
Structural load challenges during space shuttle development 08 p1094 N85-16014
Space shuttle flight readiness firing dress rehearsal for STS-1 08 p1097 N85-16929
Launch processing system concept to reality 08 p1097 N85-16931
Managing computer-controlled operations 08 p1097 N85-16934
Support systems design and analysis 08 p1097 N85-16935
History, design and performance of the space shuttle hazardous gas detection system 08 p1098 N85-16936
Natural environment analysis
[NASA-CR-171333] 10 p1426 N85-19010
British aerospace studies HOTOL satellite launcher 10 p1460 N85-19206
Environmental effects of space activities 11 p1678 N85-20577
Atmospheric environment for Space Shuttle (STS-51A) launch
[NASA-TM-86497] 12 p1892 N85-21875
Increase in hydrogen emission of upper atmosphere following launches of space vehicles 13 p1981 N85-22431
Feoktistov argues against U.S. space shuttle design concept 13 p1985 N85-22453
List of recent Soviet space launches 13 p1985 N85-22457
China report: Science and technology
[JPRS-CST-84-030] 13 p2041 N85-22777
Surface pressure produced by Space Transportation System flight 41B
[AD-A150793] 14 p2242 N85-23901
West Europe report: Science and technology
[JPRS-WST-85-013] 14 p2289 N85-24183
Ignition, separation of boosters, stages in Ariane 3 14 p2289 N85-24185
Orbital positioning and station-keeping of geostationary satellites 14 p2397 N85-24772
List of recent Soviet space launches 15 p2489 N85-25361
Calendar of Ariane launches 1984 - 1987 15 p2523 N85-25554
Structure of SYLDA double launch system for Ariane 17 p2946 N85-28185
Ariane space general director on satellite launcher market 18 p3087 N85-29103
Evolution of spacecraft design methods as a function of environmental and geometrical constraints
[ESA-CR(P)-2012] 20 p3418 N85-31216
Pricing options for the space shuttle. Special study 21 p3559 N85-32138
The development of staging mechanisms for the Japanese satellite launcher Mu-3SII 22 p3798 N85-33528

SPACECRAFT LUBRICATION
The European Space Tribology Laboratory (ESTL) activities report
[ESA-ESTL-61] 05 p0646 N85-14146
The performance of Fomblin Z25 oil in ball bearings operating in vacuum — spacecraft lubricant
[ESA-ESTL-056] 08 p1134 N85-17150
Observations of high resistance on slip-rings employing Ag/MoS2/Cu brushes — solar array drives
[ESA-ESTL-70] 18 p3123 N85-29333
European Space Tribology Laboratory: Facilities, services, capabilities
[ESA-BR-12] 20 p3398 N85-31060

SPACECRAFT MAINTENANCE
Satellite servicing: A business opportunity? 02 p0156 N85-11056
Space based OTV servicing 08 p1109 N85-17010
Maintenance of long life space systems, volume 1
[MATRA-0316/DX80-VOL-1] 18 p3066 N85-29864
Maintenance of long life space systems, volume 2
[MATRA-0350/DX80-VOL-2] 18 p3066 N85-29865
Experiences with neutral buoyance testing mockups 18 p3159 N85-29571
The role of mock-ups in the development of Orbital Replaceable Units (ORU) 18 p3160 N85-29573
Technology requirements to be addressed by the NASA Lewis Research Center Cryogenic Fluid Management Facility program
[NASA-TM-87048] 19 p3224 N85-29987
A modular docking mechanism for in-orbit assembly and spacecraft servicing 22 p3796 N85-33516

SPACECRAFT MANEUVERS
NT ORBITAL MANEUVERS
Optimal nonlinear feedback control of spacecraft attitude maneuvers 02 p0167 N85-11126
The satellite maneuvers determination department 05 p0599 N85-13820
Application of model following control and estimation techniques to attitude control of maneuvering spacecraft. Part 1: Theory and simulation results
[NLR-TR-82116-U-PT-1] 18 p3065 N85-28957
Characteristic elastic systems of time-limited optimal maneuvers 20 p3413 N85-31184
Study and realization of a command system adapted to space robotics
[SNIAS-851-440-106] 22 p3740 N85-33183
Identification and control of structures in space
[NASA-CR-176175] 24 p4069 N85-35214

SPACECRAFT MODELS
Satellite orbit determination 05 p0598 N85-13813
Satellite attitude determination 05 p0599 N85-13814
Perturbations in geostationary orbit 05 p0600 N85-13824
A model of plasma cloud expansion generated by a dust particle impact — Giotto mission 14 p2245 N85-23914
The attitude control model tests for the Infrared Astronomical Satellite (IRAS)
[B8580071] 18 p3067 N85-28967
Space station models, mockups and simulators 18 p3159 N85-29569
Experiences with neutral buoyance testing mockups 18 p3159 N85-29571
The role of mock-ups in the development of Orbital Replaceable Units (ORU) 18 p3160 N85-29573

SPACECRAFT MODULES
Modular experimental platform for science and applications 02 p0152 N85-11031
Mass analysis of neutral particles and ions released during electrical breakdowns on spacecraft surfaces
[NASA-CR-175585] 12 p1793 N85-21250
Space Station structures 14 p2232 N85-23835

SPACECRAFT MOTION
Planning of navigation measurements using TD criterion for determination of movement of spacecraft by method of least squares 02 p0159 N85-11061
Use of gravitational stabilization in performance of experiments 02 p0160 N85-11084
Control of lateral conjectory motion of spacecraft in atmosphere 02 p0160 N85-11085
A user's guide to the Flexible Spacecraft Dynamics and Control Program
[NASA-TM-87369] 03 p0405 N85-12586
Positions of relative equilibrium of satellite-gyrostat 16 p2718 N85-26777
Optimum parameters of aerogyroscopic satellite orientation system 16 p2718 N85-26782

SPACECRAFT ORBITAL ASSEMBLY
U ORBITAL ASSEMBLY

SPACECRAFT ORBITS
NT GEOSYNCHRONOUS ORBITS
NT INTERPLANETARY TRANSFER ORBITS
NT PARKING ORBITS
NT POLAR ORBITS
NT SATELLITE ORBITS
NT STATIONARY ORBITS
NT TRANSFER ORBITS
Rapid nonresonant rotation of a spacecraft in nominally periodic orbits in limited 3 body problem 02 p0160 N85-11083
Mars exploration, Venus swingby and conjunction class mission modes, time period 2000 to 2045
[NASA-TM-86477] 02 p0303 N85-11961
Planning for the on-orbit servicing of military spacecraft
[AD-A148447] 08 p1104 N85-16983
Summary presentation of the Constellations Panel 11 p1644 N85-20359
Assessment of satellite collision hazards by simulated sampling in space 12 p1784 N85-21195
Models of angular momentum input to a circum-terrestrial swarm from encounters with heliocentric planetesimals 13 p2179 N85-23521
Orbital resonances and planetary accretion in the solar nebula 13 p2179 N85-23523
NASA welding assessment program
[NASA-CR-175682] 15 p2568 N85-25844
Telescope in lunar orbit 15 p2682 N85-26568
Life cycle test results of a bipolar nickel hydrogen battery 20 p3448 N85-31406

SPACECRAFT PERFORMANCE
Spacecraft system study: A study to define the impact of laser communication systems on their host spacecraft
[NASA-CR-175272] 07 p0970 N85-16159

SPACECRAFT POSITION INDICATORS
Operational experience with ion concentration sensors in orientation systems 13 p1960 N85-22422

SPACECRAFT POWER SUPPLIES
Space power distribution system technology. Volume 3: Test facility design
[NASA-CR-171230] 04 p0483 N85-12936
Space nuclear safety program
[DE84-015983] 04 p0564 N85-13591
General-purpose heat source development: Safety test program. Postimpact evaluation, design iteration test 2
[DE84-015978] 04 p0564 N85-13592
Technical support services for space and terrestrial systems programs
[DE84-009031] 05 p0597 N85-13806
Merits of flywheels for spacecraft energy storage 05 p0605 N85-13857
Inertial storage for satellites 05 p0605 N85-13859
Magnetically suspended flywheel system study 05 p0607 N85-13873
Reaction wheels for kinetic energy storage 05 p0607 N85-13874
Motor/generator and electronic control considerations for energy storage flywheels 05 p0608 N85-13878
Torque command steering law for double-gimbaled control moment gyros applied to rotor energy storage 05 p0608 N85-13879
Space Power
[NASA-CP-2352] 05 p0608 N85-13880
Space station power system 05 p0608 N85-13881
Space power for communication satellites beyond 1995 05 p0608 N85-13883
Power for commercial space applications 05 p0608 N85-13884
Missions/planning panel 05 p0609 N85-13886
Radioisotope space power programs 05 p0609 N85-13887
Electrochemistry and storage 05 p0609 N85-13889
Potential of flywheels for spacecraft energy storage 05 p0609 N85-13890
Trends in concentrator, receiver, and storage development for terrestrial applications 05 p0609 N85-13891
Dynamic power systems for power generation 05 p0609 N85-13892
Technology status of thermionic fuel elements for space nuclear power 05 p0610 N85-13893
Space power management and distribution status and trends 05 p0610 N85-13896
Analytical modeling of spacecraft power systems 05 p0610 N85-13897
Effects of the solar and extraterrestrial environments on space power systems 05 p0610 N85-13898
Advanced concepts liquid droplet radiator 05 p0610 N85-13899
The liquid droplet radiator - an ultralightweight heat rejection system for efficient energy conversion in space 05 p0610 N85-13900
Electrodynamic tethers. 1: Power generator in LEO. 2: Thrust for propulsion and power storage 05 p0611 N85-13901
Photovoltaic working group report 05 p0611 N85-13902
Electrochemistry and storage panel report 05 p0611 N85-13903
Dynamic conversion working group summary 05 p0611 N85-13904
Thermoelectric and thermionic conversion technology 05 p0611 N85-13905
Heat rejection working group synopsis 05 p0611 N85-13906
Electrical system technology Working Group (WG) report 05 p0611 N85-13907
Environmental interactions working group report 05 p0611 N85-13908
Advanced and nontraditional concepts working group report 05 p0612 N85-13909
Engineering model system study for a regenerative fuel cell: Study report
[NASA-CR-174801] 07 p0991 N85-16292
Results of the 1984 NASA/JPL balloon flight solar cell calibration program
[NASA-CR-174270] 07 p0991 N85-16294
Space shuttle orbiter auxiliary power unit development challenges 08 p1099 N85-16945
The solid rocket booster auxiliary power unit: Meeting the challenge 08 p1099 N85-16946
Space shuttle electrical power generation and reactant supply system 08 p1099 N85-16947
Air Force space technology center space technology: Emphasis 84 09 p1333 N85-18361
Technology for satellite power conversion
[NASA-CR-174335] 09 p1343 N85-18451
Opening up the future in space with nuclear power
[DE85-002411] 11 p1727 N85-20662

GaAs and 3-5 compound solar cells status and prospects for use in space
[NASA-TM-86960] 12 p1795 N85-21261
General-purpose heat source development: Safety test program. Postimpact evaluation, design iteration test 4
[LA-10217-SR] 12 p1930 N85-22128
General-purpose heat source development: Safety test program. Postimpact evaluation, design iteration test 5
[LA-10232-SR] 12 p1931 N85-22129
General-purpose heat source development: Safety test program. Postimpact evaluation, design iteration test 1
[LA-9880-SR] 12 p1931 N85-22131
Interactions between large space power systems and low-Earth-orbit plasmas 13 p1992 N85-22490
Photovoltaic Generators in Space — conferences
[ESA-SP-210] 13 p2005 N85-22565
History and future views on solar cells of Japanese scientific satellites 13 p2005 N85-22566
Thin and ultrathin silicon solar cells for space use 13 p2005 N85-22567
Space solar cells: Adjusting to new demands 13 p2005 N85-22568
Bifacial light sensitive space solar cell 13 p2006 N85-22573
Space qualified AlGaAs/GaAs solar cells 13 p2006 N85-22575
Availability of AlGaAs/GaAs solar cells in space 13 p2006 N85-22576
Comparative study of GaAs solar cell potentialities for space applications 13 p2006 N85-22577
Investigation of high output gallium arsenide solar cells 13 p2006 N85-22578
Development of very thin large area GaAs solar cells for space application 13 p2006 N85-22579
GaAs and 3-5 compound solar cells status and prospects for use in space 13 p2007 N85-22580
GaAlAs-GaAs solar cell development: Prospective for space applications under concentration 13 p2007 N85-22581
Phenomenology of discharges in space: Application to a solar generator — SPOT satellite 13 p2007 N85-22583
In-orbit laser regeneration of the radiation damaged solar arrays 13 p2008 N85-22588
The DFS-Kopernikus solar generator electrical design 13 p2008 N85-22590
The DFS-Kopernikus solar generator 13 p2008 N85-22591
Electrical design of the Intelsat 6 solar generator 13 p2008 N85-22592
Computer aided engineering applied to the design and verification of the generic Advanced Rigid Array (ARA) — solar array 13 p2008 N85-22593
Development and qualification of the electrical part of the Advanced Rigid Array (ARA) — solar array 13 p2008 N85-22594
SPOT solar array 13 p2009 N85-22595
Rigid Solar Generator (GSR) solar arrays 13 p2009 N85-22596
Retractable Rigid Solar Generator (GSR) 13 p2009 N85-22597
Derivation of the Olympus solar array requirements 13 p2009 N85-22598
The Olympus solar array development and test program 13 p2009 N85-22599
Design and qualification testing of the Olympus solar array blanket 13 p2009 N85-22600
The performance of the Olympus power subsystem with its solar array 13 p2009 N85-22601
Analysis of optimum front cover thickness for lightweight solar arrays 13 p2010 N85-22606
Development of Halley's Comet explorer PLANET-A solar array 13 p2010 N85-22608
Concentrator technologies evaluation for large solar arrays and their application for space stations/platforms 13 p2010 N85-22609
Space Station solar array 13 p2010 N85-22610
Solar array dynamical simulation for illumination and temperature variation 13 p2011 N85-22611
Blanket integrated cushioning of foldable and retractable solar arrays 13 p2011 N85-22612
Concept for controlled fold by fold deployment and retraction of flexible, foldable solar generators 13 p2011 N85-22613
Aspects of low cost module technology — spacecraft solar arrays 13 p2011 N85-22614
Emissivity enhancement of fused silica for space applications — solar cells 13 p2011 N85-22615
NASA photovoltaic research and technology development program for space applications 13 p2011 N85-22617
Study of concentration for space photovoltaic generators 13 p2011 N85-22618
Developments in deployable masts to support flexible solar arrays 13 p2012 N85-22620
Generic design and verification of an Advanced Rigid Array (ARA) — solar array 13 p2012 N85-22621
Growth capabilities of European retractable solar arrays 13 p2012 N85-22625
High output photovoltaic conversion: The quadrispectral project — spacecraft power supplies 13 p2012 N85-22626
Characterization of terrestrial solar cells for space applications: Electrical characteristics of thin Westinghouse dendritic web cells as a function of solar intensity, temperature, and incidence angle
[NASA-CR-175642] 14 p2349 N85-24516
Spaceborne power systems preference analyses. Volume 1: Summary
[NASA-CR-175644] 14 p2349 N85-24517
Spaceborne power systems preference analyses. Volume 2: Decision analysis
[NASA-CR-175645] 14 p2349 N85-24518
Long-life high performance fuel cell program
[NASA-CR-174874] 15 p2494 N85-25384
Long-term exposure of pressed plutonium oxide heat sources to aquatic environments
[DE85-007385] 15 p2495 N85-25392
Analysis and testing of the thermal properties of space battery cells, phase B, draft
[ESA-CR(P)-1971] 15 p2550 N85-25741
Proposed energy systems for the Brazilian data collection satellite
[INPE-3393-PRE/664] 16 p2731 N85-26856
Tethered nuclear power for the Space Station
[NASA-TM-87023] 16 p2740 N85-26912
Performance analysis of radiation cooled dc transmission lines for high power space systems
[NASA-TM-87040] 17 p2951 N85-28222
Multi-kW solar arrays for Earth orbit applications
[NASA-CR-171538] 20 p3406 N85-31139
The 1984 Goddard Space Flight Center Battery Workshop
[NASA-CP-2382] 20 p3443 N85-31371
Multikilowatt hydrogen-nickel oxide battery system 20 p3443 N85-31373
Solar dynamic systems 20 p3443 N85-31374
System level electrochemical principles 20 p3443 N85-31375
Advances in rechargeable lithium molybdenum disulfide batteries 20 p3444 N85-31376
Geosynchronous performance of a lithium-titanium disulfide battery 20 p3444 N85-31377
RCA's planned test program to compare the performance and life of NiCd cells containing Pellon 2536 in contrast with Pellon 2505 separator material 20 p3445 N85-31385
Failure modes experienced on spacecraft NiCd batteries 20 p3445 N85-31386
Nickel cadmium cell design variable program data analysis 20 p3445 N85-31387
Results of analysis on the design variable cells 20 p3445 N85-31388
Fundamental algorithms of the Goddard battery model 20 p3445 N85-31389
AUSSAT battery life test program 20 p3446 N85-31395
Flight experience of Solar Mesosphere Explorer's two nickel-cadmium batteries 20 p3446 N85-31396
Deep reconditioning of batteries during DSCS 3 flight operations 20 p3446 N85-31397
Design principles for nickel hydrogen cells and batteries 20 p3447 N85-31398
Improved specific energy Ni-H2 cell 20 p3447 N85-31399
Bipolar nickel-hydrogen battery design 20 p3447 N85-31400
Nickel-hydrogen spacecraft module configurations study 20 p3447 N85-31401
Nickel hydrogen bipolar battery electrode design 20 p3447 N85-31402
Nickel-cadmium cell life test 20 p3447 N85-31403
Accelerated and real-time geosynchronous life cycling test performance of nickel-hydrogen batteries 20 p3448 N85-31405
Life cycle test results of a bipolar nickel hydrogen battery 20 p3448 N85-31406
Nickel-hydrogen cell test program summary 20 p3448 N85-31407
The failure mechanism of a nickel electrode in a nickel-hydrogen cell 20 p3448 N85-31408
An industry and government survey: A nickel-hydrogen testing data base 20 p3448 N85-31409
High efficiency solar cell research for space applications 20 p3480 N85-31624
Design principles for nickel-hydrogen cells and batteries
[NASA-TM-87037] 20 p3483 N85-31646
Retractable Rigid Solar Generator (GSR)
[SNIAS-851-440-101] 20 p3484 N85-31654
Rigid Solar Generator (GSR) solar arrays
[SNIAS-851-440-102] 20 p3484 N85-31655
The SPOT solar array
[SNIAS-851-440-103] 20 p3485 N85-31658
Study of concentration for space photovoltaic generators
[SNIAS-851-440-105] 20 p3485 N85-31659
Reduction of radiation damage in solar cells — spacecraft power supplies
[ESA-CR(P)-2005] 20 p3485 N85-31659
Automation study for space station subsystems and mission ground support
[NASA-CR-176097] 21 p3559 N85-32136
Solar maximum: Solar array degradation
[NASA-TM-86194] 23 p3903 N85-34175
Optical analysis of parabolic dish concentrators for solar dynamic power systems in space
[NASA-TM-87060] 23 p3903 N85-34176
STACBEAM 2
[NASA-CR-176126] 23 p3944 N85-34442
General-purpose heat source development: Safety test program. Postimpact evaluation, design iteration test
[LA-10034-SR] 23 p3999 N85-34606
Development and characterization of carbon-bonded carbon fiber insulation for radioisotope space power systems
[DE85-013365] 24 p4062 N85-35299

SPACECRAFT PRELAUNCH TESTS
U SPACE VEHICLE CHECKOUT PROGRAM

SPACECRAFT PROPULSION
NT ELECTROMAGNETIC PROPULSION
NT ELECTROSTATIC PROPULSION
NT ION PROPULSION
NT MASS DRIVERS (PAYLOAD DELIVERY)
NT PLASMA PROPULSION
NT SOLAR PROPULSION
Mars exploration, Venus swingby and conjunction class mission modes, time period 2000 to 2045
[NASA-TM-86477] 02 p0303 N85-11961
LOX/LH2 propulsion system for launch vehicle upper stage, test results
[NASA-TM-77727] 03 p0324 N85-12069
Interstellar mission 04 p0459 N85-12916
Propellant tank resupply system
[AD-D011288] 05 p0603 N85-13848
Electrodynamic tethers. 1: Power generator in LEO. 2: Thrust for propulsion and power storage 05 p0611 N85-13901
A historical overview of the electrical power systems in the US manned and some US unmanned spacecraft
[NASA-CR-174806] 05 p0612 N85-13910
OTV propulsion tecnology programmatic overview 08 p1107 N85-16997
Drives and benefits overview 08 p1107 N85-16998
Advanced OTV engine concepts 08 p1108 N85-17001
Vehicle/engine integration — orbit transfer vehicles 08 p1109 N85-17008
Orbital transfer vehicle propulsion issues 08 p1109 N85-17009
Design study of an integrated aerobraking orbital transfer vehicle
[NASA-TM-58264] 12 p1795 N85-21262
Characterization of terrestrial solar cells for space applications: Electrical characteristics of thin Westinghouse dendritic web cells as a function of solar intensity, temperature, and incidence angle
[NASA-CR-175642] 14 p2349 N85-24516
Fiscal year 1986 technical objective document
[AD-A151039] 14 p2432 N85-25000
Space station propulsion: The advanced development program at Lewis
[NASA-TM-86999] 15 p2494 N85-25386
West Europe report: Science and technology
[JPRS-WST-84-009] 15 p2535 N85-25639
Details on spot remote sensing satellite propulsion unit 15 p2535 N85-25640
Advanced energy storage systems
[AD-A152244] 16 p2741 N85-26915
Structural Integrity and Durability of Reusable Space Propulsion Systems
[NASA-CP-2381] 17 p2910 N85-27941
Composite loads spectra for select space propulsion structural components: Probabilistic load model development 17 p2912 N85-27954
Probabilistic structural analysis theory development 17 p2912 N85-27955
Probabilistic finite element development 17 p2913 N85-27956
Thin-film sensors for space propulsion technology 17 p2915 N85-27968
Experimental research on electrical propulsion
[NASA-TM-77876] 18 p3067 N85-28969

SPACECRAFT RADIATORS
Advanced concepts liquid droplet radiator
05 p0610 N85-13899
The liquid droplet radiator - an ultralightweight heat rejection system for efficient energy conversion in space
05 p0610 N85-13900
Heat rejection working group synopsis
05 p0611 N85-13906
Preliminary evaluation of a liquid belt radiator for space applications
[NASA-CR-174807] 07 p0917 N85-15804
Space heat rejection radiators: Meteoroid/debris consideration 12 p1766 N85-21210
Advanced radiator concepts
[NASA-TM-87008] 14 p2300 N85-24245
Automation study for space station subsystems and mission ground support
[NASA-CR-176097] 21 p3559 N85-32136
SPACECRAFT RECOVERY
Magnetic spin reduction system for free spinning objects
[NASA-CASE-MFS-25966-1] 02 p0166 N85-11122
Structural and mechanical design challenges of space shuttle solid rocket boosters separation and recovery subsystems 08 p1095 N85-16917
SPACECRAFT REENTRY
NT UNCONTROLLED REENTRY (SPACECRAFT)
Effect of aerodynamic and angle-of-attack uncertainties on the May 1979 entry flight control system of the Space Shuttle from Mach 8 to 1.5
[NASA-TP-2365] 07 p0913 N85-15778
Transportation applications, part 2
11 p1643 N85-20350
Predictions of cardiovascular responses during STS reentry using mathematical models
[NASA-CR-171671] 15 p2616 N85-26119
SPACECRAFT RENDEZVOUS
U SPACE RENDEZVOUS
SPACECRAFT SENSORS
U SPACECRAFT INSTRUMENTS
SPACECRAFT SHIELDING
The challenging scales of the bird: Shuttle tile structural integrity 08 p1095 N85-16919
Hypervelocity impact investigations and meteoroid shielding experience related to Apollo and Skylab
12 p1785 N85-21206
Solid particle environment and protection for the Galileo Orbiter 12 p1786 N85-21207
Space debris protection for a reusable orbital transfer vehicle 12 p1786 N85-21208
Parametric analysis: SOC meteoroid and debris protection 12 p1786 N85-21209
Spacecraft hazard and shielding requirements
12 p1788 N85-21224
Mechanical fastener
[NASA-CASE-LAR-12738-2] 19 p3279 N85-30335
SPACECRAFT STABILITY
In-orbit experiments on IRAS for application to the ISO satellite
[FOK-TR-R-84-057] 03 p0322 N85-12078
Summary presentation of the Constellations Panel
11 p1644 N85-20359
Application Number 3: Using tethers for attitude control 11 p1646 N85-20373
Rotational motion of a satellite
13 p1981 N85-22428
Stability of periodic satellite motions relative to center of mass in circular orbit 16 p2718 N85-26780
Dynamics and control of tethers in elliptical orbits
20 p3399 N85-31067
SPACECRAFT STRUCTURES
Small Payload Flight Systems (SPFS)
02 p0152 N85-11030
Measurement of the inertial constants of a rigid or flexible structure of arbitrary shape through a vibration test
[NASA-TM-77557] 02 p0209 N85-11381
Spacecraft structural acoustic studies: Development of structural acoustic design guides
[ESA-CR(P)-1916] 05 p0604 N85-13849
Influence of thermal cycling on the behavior of CFRP material for space structures 05 p0626 N85-14013
Space Shuttle Technical Conference, part 2
[NASA-CP-2342-PT-2] 08 p1096 N85-16937
Thermoviscoelastic analysis of dimensionally stable fiber composite space structures
[AD-A149275] 11 p1593 N85-20021
ACOSS 17 (Active Control of Space Structures)
[AD-A150007] 12 p1793 N85-21253
Elastomer toughened polyimide adhesives — bonding metal and composite material structures for aircraft and spacecraft
[NASA-CASE-LAR-12775-2] 12 p1809 N85-21349
Experimental investigations on ion emission with dust impact on solid surfaces — Giotto spacecraft
14 p2244 N85-23911
Analysis of elastoplastic grids under conditions of variable loads
[REPT-16/1984] 16 p2797 N85-27242
Structure of SYLDA double launch system for Ariane
17 p2948 N85-28185
Finite element thermal-structural analysis of cable-stiffened space structures
[AD-A153822] 18 p3066 N85-28963
R and D activities of the Structural Sciences Division
20 p3539 N85-32026
Effects of environment on spacecraft materials
22 p3733 N85-33144
Research and development activities in unified control-structure modeling and design
[NASA-CR-176111] 22 p3740 N85-33160
SPACECRAFT SURVIVABILITY
A study of spacecraft technology and design concepts. Volume 2: Appendices
[NASA-CR-172579-VOL-2] 16 p2730 N85-26845
SPACECRAFT TELEVISION
NT SATELLITE TELEVISION
Development of TV systems for spacecraft
15 p2484 N85-25332
Optic's institute's development of equipment for comet probe 15 p2484 N85-25333
USSR report: Electronics and electrical engineering
[JPRS-UEE-84-015] 22 p3762 N85-33314
Vatra television complex for Salyut orbital space station
22 p3763 N85-33321
SPACECRAFT TRACKING
NT SATELLITE TRACKING
Ocean services user needs assessment. Volume 1: Survey results, conclusions and recommendations
[NASA-CR-174104] 04 p0541 N85-13445
The Western Aeronautical Test Range of NASA Ames Research Center
[NASA-TM-85924] 07 p0909 N85-15756
The Statistical Loop Analyzer (SLA)
08 p1100 N85-16955
The Telecommunications and Data Acquisition Report
[NASA-CR-174366] 10 p1462 N85-19224
Space interception guidance with uncertain factors
13 p2042 N85-22781
Shuttle communications and tracking systems modeling and TDRSS link simulations studies
[NASA-CR-171861] 15 p2491 N85-25369
Space Shuttle program communication and tracking systems interface analysis
[NASA-CR-171862] 16 p2729 N85-26841
Water vapor radiometry research and development phase
[NASA-CR-175867] 17 p2995 N85-28512
Optical receivers using rough reflectors
[NASA-CR-176200] 24 p4154 N85-35750
SPACECRAFT TRAJECTORIES
NT EARTH-VENUS TRAJECTORIES
NT INTERPLANETARY TRAJECTORIES
Mars exploration, Venus swingby and conjunction class mission modes, time period 2000 to 2045
[NASA-TM-86477] 02 p0303 N85-11961
Satellite orbit determination 05 p0596 N85-13813
Relationships between Ariane trajectories and satellite orbits 05 p0599 N85-13815
Optimal multiple-impulse nonlinear orbital rendezvous
08 p1105 N85-16984
Rejection of anomalous observations when determining spacecraft trajectories 13 p1979 N85-22421
Approximate analytic method of calculating trajectories of movement of a flight vehicle in the atmosphere
14 p2279 N85-24121
Optimal space trajectories 14 p2396 N85-24756
SPACECREWS
Thresholds of perception of whole body linear oscillation: Modification by spaceflight 05 p0694 N85-14467
The adaptation of vestibulo-spinal reflexes as a function of spaceflight and their relationship to space motion sickness 05 p0694 N85-14468
Challenges of developing an electro-optical system for measuring man's operational envelope
08 p1095 N85-16921
Results from radiation monitoring equipment experiment on STS-11
[AD-A152531] 17 p2908 N85-27932
Space Station crew safety alternatives study. Volume 4: Appendices
[NASA-CR-3857] 18 p3065 N85-28958
Proceedings of the Seminar on Space Station Human Productivity
[NASA-TM-86573] 18 p3156 N85-29539
Space station crew safety: Human factors interaction model 18 p3156 N85-29540
Space station crew safety alternatives study, third quarter briefing 18 p3156 N85-29541
Internal contamination issues
18 p3156 N85-29543
Human productivity program definition
18 p3158 N85-29556
The human role in space (THURIS)
18 p3158 N85-29557
Flow cytometry for health monitoring in space
[DE85-009572] 19 p3329 N85-30625
Psychological issues relevant to astronaut selection for long-duration space flight: A review of the literature
[AD-A154051] 19 p3330 N85-30627
Experience of science astronaut on the Spacelab-1 mission 20 p3506 N85-31807
Living aloft: Human requirements for extended spaceflight
[NASA-SP-483] 21 p3666 N85-32772
Psychophysiological distinctions of organization and regulation of daily cyclograms of crew activities during long-term spacecraft 22 p3821 N85-33669
Results of microbiological studies conducted during operation of Salyut-6 orbital station
22 p3823 N85-33682
SPACELAB
Study of proton and neutron activation of metal samples in low Earth orbit
[NASA-CR-171183] 01 p0026 N85-10164
PDSS/IMC CIS user's guide
[NASA-CR-171179] 01 p0102 N85-10682
Fokker wants to start new Netherlands space program
03 p0310 N85-11999
Improving the Spacelab mass memory unit tape layout with a simulation model
[NASA-TM-86483] 05 p0713 N85-14571
Space infrastructure 07 p0914 N85-15783
FRG's DFVLR ready for participation in space station
11 p1618 N85-20176
Preflight and postflight motion sickness testing of the Spacelab 1 crew 11 p1694 N85-20652
Space motion sickness monitoring experiment: Spacelab 1 11 p1695 N85-20654
D-1 report: The first German spacelab mission
[NASA-TM-77637] 13 p1977 N85-22402
National Space Transportation Systems Program mission report
[NASA-TM-87456] 14 p2241 N85-23898
NASA plans for a space station
14 p2393 N85-24735
Measurement of the nighttime infrared luminosity of Spacelab 1 in the H- and K-bands
[NASA-TM-85972] 14 p2434 N85-25011
European views differ on space station concept
15 p2531 N85-25606
MBB/Erno's views, future plans in aerospace activities
15 p2531 N85-25609
West Europe report: Science and technology
[JPRS-WST-84-026] 15 p2532 N85-25617
FRG opinion on Spacelab benefits, space station participation 15 p2532 N85-25618
Infrared telescope
[NASA-CR-171392] 15 p2668 N85-26465
Primate experiments on SLS-1
15 p2687 N85-26592
A brief description of the two primate experiments to be carried out on SL-4 15 p2687 N85-26597
ESA presents plans for European manned space station 18 p3065 N85-29087
Spacelab 2
[NASA-EP-217] 19 p3222 N85-29977
International space research perspectives of commercialization for German industry
[NASA-TM-77657] 19 p3222 N85-29979
Commerce Lab: Mission analysis payload integration study. Appendix A: Data bases
[NASA-CR-176016] 19 p3224 N85-29988
Experience of science astronaut on the Spacelab-1 mission 20 p3508 N85-31807
The European vestibular experiments of the Spacelab-1 mission 20 p3508 N85-31808
Some results of the European vestibular experiments in the Spacelab-1 mission 20 p3508 N85-31809
Sleep and wake physiology in weightlessness
20 p3510 N85-31819
Mission operations requirements document for D-1 Experiment 102, Vestibular Experiments in Spacelab
[NASA-TM-87495] 21 p3557 N85-32129
Spacelab 1 hematology experiment (INS103): Influence of space flight on erythrokinetics in man
[NASA-TM-58268] 22 p3824 N85-33693
The 1986 National Aeronautics and Space Administration authorization
[GPO-47-635] 24 p4166 N85-35829
SPACELAB PAYLOADS
NT ATMOSPHERIC GENERAL CIRCULATION EXPERIMENT
NT POINTING CONTROL SYSTEMS

The design, fabrication and delivery of a spacelab neutral buoyancy Instrument Pointing System (IPS) mockup — underwater training simulator
[NASA-CR-171233] 04 p0462 N85-12934
Metric camera experiment: Spacelab 1 mission
05 p0658 N85-14229
The photogrammetric camera experiment on Spacelab 1 05 p0658 N85-14230
Spacelab mission D1 Frog statolith experiment STATEX: Hardware family and experiment operational sequence
05 p0689 N85-14426
An automatic device for amphibian egg fertilization in space: Technical aspects and biological requirements
05 p0689 N85-14427
Experiment 1ES031 on Spacelab 1: Are cells sensitive to gravity? — lymphocyte proliferation
05 p0689 N85-14428
Further cell biology experiments with Physarum polycephalum for a reflight of Biorack
05 p0689 N85-14429
Preliminary results of advanced Biostack experiments with plant seeds and spores — cosmic ray effects
05 p0691 N85-14441
The radiobiological advanced Biostack experiment on Spacelab 1 05 p0691 N85-14442
Spacelab 1 experiment: Microorganisms in space hard environment 05 p0691 N85-14443
Three-dimensional ballistocardiography in weightlessness (experiment 1ES 028) — Spacelab
05 p0691 N85-14447
Miniature personal physiological tape recorder (experiment 1ES 30) — Spacelab
05 p0692 N85-14448
The European vestibular experiments in the Spacelab 1 mission 05 p0694 N85-14466
Thresholds of perception of whole body linear oscillation: Modification by spaceflight 05 p0694 N85-14467
The adaptation of vestibulo-spinal reflexes as a function of spaceflight and their relationship to space motion sickness 05 p0694 N85-14468
Caloric stimulation of the vestibular system in microgravity 05 p0695 N85-14469
Sleep physiology in weightlessness (experiment 1ES 030) — Spacelab 05 p0695 N85-14474
Data Requirement (DR) MA-03: Payload missions integration — Spacelab payloads
[NASA-CR-171331] 10 p1428 N85-19009
Middle atmosphere NO and NO2 observed by means of the Spacelab one grille spectrometer
[AERONOMICA-ACTA-A-293-1984]
11 p1680 N85-20568
Future ultraviolet experiments, including FUSE/COLUMBUS 11 p1744 N85-20069
Infrared telescope
[NASA-CR-171392] 15 p2668 N85-26485
Space radiation studies — Spacelab 2 Payload
[NASA-CR-171410] 15 p2685 N85-26584
Long life feasibility study for the shuttle infrared telescope facility
[NASA-CR-3722] 17 p3052 N85-28893
Spacelab 2
[NASA-EP-217] 19 p3222 N85-29977
Commerce Lab: Mission analysis payload integration study. Appendix A: Data bases
[NASA-CR-176016] 19 p3224 N85-29988
Hemispherical latching apparatus
[NASA-CASE-MFS-25837-1] 19 p3224 N85-29991
Gas analysis techniques for human physiological measurements in space — Spacelab
[A/6537] 20 p3507 N85-31803
Activities report of the Aeronomy Department
[G-774-1984] 21 p3633 N85-32589
Detector calibration of the Indian cosmic ray experiment (IONS) in Space-Shuttle Spacelab-13
[SH-9.1-2] 23 p4050 N85-35117

SPACELAB UV-OPTICAL TELESCOPE FACILITY
U STARLAB

SPACERS
Spacer structure
[AD-D011641] 17 p2897 N85-27866

SPACETENNAS
Relationship of spaced antenna and Doppler techniques for velocity measurements (keynote paper), part 3
21 p3619 N85-32488
A simple model for testing the effects of gravity-wave-produced vertical oscillations of scattering irregularities on spaced-antenna, horizontal drift measurements 21 p3619 N85-32489
Potential advantages of the spaced antenna method for operational wind profiling, part 3.1B
21 p3620 N85-32490
Criteria for optimum spacing of spaced antenna, part 3.2A 2. p3620 N85-32491
Accuracy of velocity and power determination by the Doppler method 21 p3620 N85-32493
Interferometer applications of VHF radars, part 3.5A
21 p3621 N85-32497

SPACING
NT AIRCRAFT APPROACH SPACING
The dependence of soil bearing capacity and drawbar pull on the spacing between track
[AD-P004273] 09 p1406 N85-16849
Effects of vane/blade ratio and spacing on fan noise, volume 1
[NASA-CR-174664] 10 p1553 N85-19791
Effects of vane/blade ratio and spacing on fan noise. Volume 2: Data supplement
[NASA-CR-174665] 10 p1553 N85-19792
Variation in the spacing of dislocations in subgrain boundaries with creep strain in Type 304 stainless steel
[DE85-006184] 15 p2511 N85-25493
A heuristic solution to the spacing problem: Maximizing the minimum Euclidean distance among N points in a convex region
[AD-A152116] 16 p2855 N85-27603
Decomposing the joint distribution of several linear combinations of uniform spacings
[AD-A155056] 21 p3677 N85-32845

SPAIN
Scientific contributions in commemoration of Ebro Observatory's 75th anniversary — conference
[ISBN-84-00-05360-X] 04 p0518 N85-13308
Distribution of total solar radiation in Spain
04 p0523 N85-13344
A review of seismicity in peninsular Spain
04 p0523 N85-13349
Structure of the crust and upper mantle of the Iberian continental platform 04 p0523 N85-13350
Deep structure and seismicity in the Catalonia-Pyrenees region 04 p0524 N85-13352
Space research in Spain 06 p1231 N85-17751
A statistical analysis of ice nuclei concentrations at urban and rural sites in Valladolid, Spain
21 p3640 N85-32614

SPALLATION
Investigation of special facilities for a spallation neutron source 03 p0427 N85-12724
Solar cosmic ray produced neon in lunar soils and their implication for gas-rich meteorite studies
06 p0867 N85-15636
Salt action on concrete
[AD-A147812] 07 p0933 N85-15912
Research directed advanced high temperature coating system beyond current state-of-the art systems
[AD-A150696] 14 p2255 N85-23974
Scientific Opportunities with Advanced Facilities for Neutron Scattering
[DE85-012113] 22 p3839 N85-33770
Calculation of improved spallation cross sections
[OG-7.2-23] 23 p4017 N85-34880
Spallogenic origin of nuclei in meteorites
[SH-7.1-10] 23 p4048 N85-35102
Los Alamos high-current proton storage ring
[DE85-012664] 24 p4158 N85-35779

SPALLING
Impact and collisional processes in the solar system
[NASA-CR-174297] 06 p1255 N85-17914
Impact and collisional processes in the solar system
13 p2180 N85-23530
High temperature corrosion of ceramics
[DE85-013481] 24 p4083 N85-35303

SPANWISE BLOWING
NT BLOWING
Low-speed stability and control wind-tunnel investigations of effects of spanwise blowing on fighter flight characteristics at high angles of attack — Langely 12-ft low-speed tunnel and 30- by 60-ft tunnel
[NASA-TP-2431] 14 p2210 N85-23708

SPAR (ROCKET)
U SPACE PROCESSING APPLICATIONS ROCKET

SPARE PARTS
DYNA-SIM: A nonstationary queuing simulation with application to the automated test equipment problem
[AD-A146384] 06 p0857 N85-15450
Managing recoverable aircraft components in the PPB and related processes: Executive summary
[AD-A146606] 07 p1050 N85-16657
A simulation model for Air Launched Cruise Missile engine management
[AD-A147018] 07 p1051 N85-16672
The Air Force can improve its forecasts of aircraft spare parts requirements
[AD-A147911] 07 p1053 N85-16682
Estimating wartime support resource requirements. Statistical and related policy issues
[AD-A147923] 07 p1053 N85-16685
Excessive Air Force inventories result from duplicative spare parts requirements
[AD-A147777] 08 p1228 N85-17734
Automated parts storage and retrieval system positioning device and method
[AD-D011494] 11 p1647 N85-20379
On maximizing the expected lifetime of replaceable systems
[AD-A150003] 12 p1882 N85-21680
Managing recoverable aircraft components in the PPB (Planning, Programming and Budgeting) and related processes. Technical volume
[AD-A152014] 15 p2457 N85-25169
Feasibility of applications of Competition Decision Assist Package (CDAP) to spare parts
[AD-A154716] 21 p3712 N85-33096
Reliability prediction of the series system with spares subject to Weibull failure 24 p4100 N85-35413
DoD Value Engineering conference report. Value Engineering (VE): A tool that benefits line management. Part 4, Workshop B: VE on spare parts
[AD-A156070] 24 p4183 N85-35813

SPARK CHAMBERS
Relation between gamma-ray family and EAS core: Monte-Carlo simulation of EAS core
[HE-3.6-7] 24 p4185 N85-35855
The Nagoya cosmic-ray muon spectrometer 3, part 2: Track detector
[HE-5.2-3] 24 p4202 N85-36081

SPARK DISCHARGES
U ELECTRIC SPARKS

SPARK GAPS
Spark column plasma dynamics model (a first principles model for laser triggered spark gaps)
[AD-A147954] 08 p1186 N85-17354
Low jitter trigger for an excimer laser
[DE85-005732] 13 p2097 N85-23060
Spark gap electrode erosion
[AD-A152802] 17 p2953 N85-28237
Statistical distribution of breakdown voltages in rep-rate spark gaps
[DE85-012813] 24 p4090 N85-35354

SPARK IGNITION
Measurement and analysis of spark ignition engine pressure data to determine heat release profiles
[AD-A144770] 01 p0065 N85-10363
Analysis and simulation of the I C engine Otto cycle using the second law of thermodynamics
02 p0291 N85-11891
FRG ceramic engine components (PET)
08 p1141 N85-17193
Radiation/catalytic augmented combustion
[AD-A148758] 09 p1290 N85-18101
Research and development of alcohol fuel usage in spark ignited engines 09 p1301 N85-18175
Photochemical ignition studies. 1: Laser ignition of flowing premixed gases
[AD-A153048] 17 p2920 N85-29002
Ignition characterization of LOX/hydrocarbon propellants
[NASA-CR-171884] 18 p3083 N85-29070
Ignition characterization of LOX/hydrocarbon propellants
[NASA-CR-171882] 18 p3083 N85-29071
On the low temperature chemistry preceding end gas autoignition
[DE85-010471] 19 p3252 N85-30182
Experimental study of engine knock
[DE85-009851] 22 p3754 N85-33268
Multiparameter conditionally sampled laser velocimetry measurements during flame propagation in a spark ignition engine
[DE85-009850] 22 p3793 N85-33502

SPARK MACHINING
A new theory aiming to define the mechanism of material removal in electroerosion
[NASA-TM-77875] 18 p3176 N85-29689

SPARK SHADOWGRAPH PHOTOGRAPHY
U SHADOWGRAPH PHOTOGRAPHY

SPARKS
NT ELECTRIC SPARKS
Spectral characteristics of grinding sparks used for identification of scrap metals
[PB85-199570] 24 p4080 N85-35290

SPARTAN SATELLITES
Space Station Spartan study
[NASA-TM-86215] 18 p2731 N85-28852

SPATIAL DEPENDENCIES
The spatial dependence of the Jovian auroral emissions 11 p1759 N85-21088
Spatial dependence of the local diffusion coefficient measured upstream of the November 12, 1978 interplanetary traveling shock
[SH-1.5-12] 23 p3996 N85-34776

SPATIAL DISTRIBUTION
NT STAR DISTRIBUTION
Strain distribution in a type 316/16-6-2 stainless steel weldment during cyclic loading
[DE84-015844] 02 p0210 N85-11384

Dynamics of growth of surface periodic structures when intense light acts on condensed media
02 p0266 N85-11748
The number and distribution of molecular clouds in the inner galaxy
03 p0442 N85-12811
Formation of subsurface Al2O3 layers in aluminum by oxygen ion implantation
[DE84-015599] 04 p0474 N85-13020
On the scale of distances of the galaxy
05 p0737 N85-14735
Local interstellar extinction with an emphasis on uvby beta results
06 p0875 N85-15559
The asteroidal source region of ordinary chondrites
06 p0881 N85-15600
Potential effectiveness of spatial processing in detecting signals against background of interfering reflections
07 p0952 N85-16032
Determination of moments of initial estimate during linear approximation of distribution of ejected impurity
07 p0954 N85-16045
Estimating location parameters in a mixture
07 p0984 N85-16252
Spatial estimation from remotely sensed data via empirical Bayes models
07 p0985 N85-16256
Neutral-current x-distributions
[DE84-016522] 09 p1382 N85-18691
Spatial distribution of auroras and its relationship to geological structure of Norilsk region
10 p1497 N85-19447
Modeling thermal plasma material processing experiments
[DE85-001551] 10 p1560 N85-19638
Mesoscale studies of flow regimes and fluxes of particulate matter in coastal waters
[DE85-003825] 11 p1689 N85-20620
Psychological aspects of phenomenon of spatial synchronization of EEG potential
11 p1691 N85-20632
Short-wavelength observations of HH-2H and HH-24A
11 p1747 N85-20990
Cometary atmospheres: Modeling the spatial distribution of observed neutral radicals
[NASA-CR-175491] 11 p1765 N85-21097
MTF analysis of LANDSAT-4 Thematic Mapper
12 p1871 N85-21737
Technical support for creating an artificial intelligence system for feature extraction and experimental design
[NASA-CR-175286] 12 p1916 N85-22044
Space and time distribution of aftershocks
13 p2112 N85-23157
Motion planning with six degrees of freedom
[AD-A150312] 13 p2165 N85-23432
Distribution and properties of large symmetric knobs on Mars
13 p2192 N85-23598
An analytical and numerical study of the interaction of rarefaction waves with area changes in ducts. Part 2: Area enlargements
[UTIAS-273] 14 p2300 N85-24242
Location of continental Permian volcanites of central Asia and its tectonic interpretation
14 p2346 N85-24505
The dawn-dusk asymmetry of particles near the neutral sheet of geomagnetotail
14 p2358 N85-24574
IMS advances in studies of field-aligned currents and their related electrodynamics
14 p2359 N85-24576
The relationship between auroral electrojet and visual aurora
14 p2363 N85-24602
Spatial characteristics of ULF pulsations and their modification by the ionosphere: IMS results
14 p2364 N85-24612
High time-resolution studies of the auroral ionosphere
[AD-A150945] 14 p2409 N85-24850
Charge isolation in a spatial light modulator
[AD-D011581] 15 p2652 N85-26356
Saturn's E ring
15 p2671 N85-26481
Multiple scattering of electromagnetic waves in discrete random media
[AD-A151786] 16 p2772 N85-27112
Study of spatial distribution of auroras
16 p2808 N85-27315
Spatial and temporal visual masking and visibility
[AD-A151998] 16 p2842 N85-27524
Spatial light modulator having a capacitively coupled photoconductor
[AD-D011646] 17 p3037 N85-28790
Cometary atmospheres: Modeling the spatial distribution of observed neutral radicals
[NASA-CR-175862] 17 p3054 N85-28904
Spatial correlations in the decay from an unstable state in the Malthus Verhulst model — laser cavities
[NOTA-INTERNA-832] 18 p3114 N85-29280
Areal coverage of storm precipitation
[NASA-CR-176013] 19 p3315 N85-30550
Influence of particle arrangement on sintering
[AD-A155337] 21 p3509 N85-32352
Interferometer applications of VHF radars, part 3.6A
21 p3621 N85-32497
Aircraft investigations of the distribution of aerosols in the lower troposphere
21 p3647 N85-32659
The distribution of giant salt nuclei inside and outside cloud over the basin of Xin and Jiang
21 p3650 N85-32681
Resource allocation in cerebral specialization of function: Behavioral and electrophysiological studies
[AD-A155092] 21 p3664 N85-32759
Interrelationships among the terrestrial planets
22 p3853 N85-33859
Constraints on the galactic distribution of cosmic rays from the COS-B gamma-ray data
[OG-3.1-6] 22 p3873 N85-33994
SMM detection of interstellar Al-26 gamma radiation
[OG-3.2-1] 22 p3874 N85-34001
The expected cosmic ray density and stream distributions at the heliolatitudinal asymmetry of solar wind
[SH-4.2-14] 23 p4006 N85-34852
Spatial distribution of cosmic rays in magnetic cycles of the Sun
[SH-4.2-20] 23 p4009 N85-34857
Influence of the source distribution on the age distribution of galactic cosmic rays
[OG-8.3-1] 23 p4021 N85-34920
Explanation of the secondary to primary ratio within the continuous Fermi accelerator model
[OG-8.3-2] 23 p4021 N85-34921
The modulation features of the long-period cosmic ray variations in connection with the sign change of the general magnetic field of the Sun
[SH-4.5-15] 23 p4037 N85-35032
On the anomalous component
[SH-4.8-6] 23 p4039 N85-35044
The read-out system of spatial distribution of thermoluminescence in meteorites
[SH-9.1-16] 23 p4052 N85-35131
Noise-sustained structure, intermittency and the Ginzburg-Landau equation
[DE85-009626] 24 p4094 N85-35379
Use of a minimum-ellipse criterion in the study of ion-beam extraction systems
[DE85-012670] 24 p4148 N85-35721
Tekhra-Takaro complex intended for the investigations of EAS spatial characteristics near axis
24 p4190 N85-35995
Hybrid TLC-pair meter for the Sphinx Project
[HE-5.2-10] 24 p4203 N85-36066
Spatial distribution read-out system for thermoluminescence sheets
[HE-7.1-7] 24 p4213 N85-36161

SPATIAL FILTERING
Effect of hydrogen on formation of energy spectrum of multiply charged and copper ions
02 p0263 N85-11720
Analysis of effectiveness of partial optimization of spatial processing systems
07 p0952 N85-16031
Time and space domain filtering for improved HF communication
10 p1473 N85-19298
Overview of RADC adaptive antenna developments for communications
10 p1474 N85-19299
Method of multivariant intraclass pattern recognition
[AD-D011548] 12 p1818 N85-21405
Acoustooptic cell as space-frequency filter
13 p2090 N85-23051
Analysis and interpretation of synthetic time strings of oscillation data
14 p2444 N85-25079
Jinc-trap resonator
[AD-D011650] 17 p2970 N85-28339
Theoretical principles of vertical subsampling of color difference signals at half the sampling rate — television
[FI-447-TBR-18] 23 p3926 N85-34332

SPATIAL ISOTROPY
U ISOTROPY
U SPATIAL DISTRIBUTION

SPATIAL ORIENTATION
U ATTITUDE (INCLINATION)

SPATIAL RESOLUTION
Geographic science: Executive summary
02 p0214 N85-11406
Geographic science
02 p0214 N85-11409
Geomorphology
02 p0214 N85-11411
Fundamental remote sensing science research program. Part 1: Status report of the mathematical pattern recognition and image analysis project
[E85-10004] 02 p0215 N85-11417
Remote sensing as a mineral prospecting technique
[E85-10010] 02 p0216 N85-11423
Water resources by orbital remote sensing: Examples of applications
[E85-10015] 02 p0217 N85-11428
Vertical coherence along a macroray path in an inhomogeneous anisotropic ocean
[AD-A145992] 03 p0416 N85-12660
Fundamental limitations in antenna resolution by maximum entropy methods
[DE84-017052] 04 p0483 N85-13145
Simulation of optical configurations and signal processing methods in Anger-type neutron-position scintillation detector
[DE84-012095] 04 p0503 N85-13210
Positron ring system using Anger-type detectors
[DE84-016788] 04 p0503 N85-13212
Investigation of several aspects of LANDSAT 4/5 data quality
[E85-10038] 04 p0525 N85-13357
Tomographic reconstruction of axially symmetric objects from a single radiograph
[DE84-016783] 04 p0565 N85-13599
Digital comparison and correlation techniques of remote sensing images with differing spatial resolutions
05 p0655 N85-14204
A vertically resolved planetary boundary layer
05 p0660 N85-14367
Research relative to high spatial resolution passive microwave sounding systems
05 p0681 N85-14380
Diurnal variation harmonics and spatial change in cosmic ray flux
06 p0824 N85-15230
Classification of vegetation communities in the Battle Mountain SE quadrangle, Nevada with MSS digital data
[E85-10043] 06 p0826 N85-15246
Multi crop area estimation in Idaho using EDITOR
[E85-10054] 06 p0827 N85-15251
Rectification of single and multiple frames of satellite scanner imagery using points and edges as control
07 p0966 N85-16263
The influence of the number of ground control points on the scene-to-map registration accuracy — Kansas, Louisiana, Mississipp, and Missouri
07 p0966 N85-16264
Image variance and spatial structure in remotely sensed scenes — South Dakota, California, Missouri, Kentucky, Louisiana, Tennessee, District of Columbia, and Oregon
07 p0966 N85-16265
Analysis of subpixel registration
07 p0966 N85-16267
Use of the analytic signal in ultrasonic imaging
[DE84-016843] 07 p1039 N85-16598
Millimeter wave antenna technology
[AD-A148694] 08 p1155 N85-17291
Resolution enhancement of multichannel microwave imagery from the Nimbus-7 SMMR for maritime rainfall analysis
[NASA-CR-174367] 10 p1462 N85-19221
X-ray holography of biological specimens
[DE85-002437] 10 p1489 N85-19396
Electronic displays: Their strengths and weaknesses for advanced high performance aircraft
10 p1533 N85-19664
LANDSAT scene-to-scene registration accuracy assessment
11 p1667 N85-20502
Geodetic accuracy of LANDSAT 4 Multispectral Scanner and Thematic Mapper data — Washington, DC, California, Alabama, South Dakota, and Illinois
11 p1667 N85-20504
Geometric accuracy assessment of LANDSAT-4 Multispectral Scanner (MSS) data
11 p1667 N85-20505
Wide-angle flat field telescope
[NASA-CASE-GSC-12825-1] 11 p1728 N85-20868
Scan angle and detector effects in Thematic Mapper radiometry — Iowa and Arkansas
12 p1871 N85-21735
The use of linear feature detection to investigate Thematic Mapper data performance and processing
12 p1872 N85-21740
Development of high resolution imaging detectors for X-ray astronomy
[NASA-CR-175505] 12 p1953 N85-22266
High-resolution SIT TV tube for subnanosecond image shuttering
[DE85-005189] 13 p2095 N85-23072
Impact of Thematic Mapper sensor characteristics on classification accuracy — suburban Washington, D.C., Maryland, and the Chesapeake Bay
13 p2117 N85-23188
Quick look analysis of TM data of the Washington, District of Columbia, area
13 p2119 N85-23197
Preliminary comparisons of the information content and utility of TM versus MSS data
13 p2120 N85-23202
Assessing LANDSAT TM and MSS data for detecting submerged plant communities
13 p2120 N85-23203
The use of Thematic Mapper data for land cover discrimination: Preliminary results from the UK SATMAP programme
13 p2121 N85-23207
Preliminary study of information extraction of LANDSAT TM data for a suburban/regional test site
13 p2121 N85-23208

Comparison of land cover information from LANDSAT Multispectral Scanner (MSS) and airborne Thematic Mapper simulator (TMS) data for hydrologic applications — Clinton River Basin, Michigan
13 p2122 N85-23211
Surface units on Venus derived from Pioneer-Venus altimetry, roughness, and reflectivity measurements
13 p2177 N85-23510
High time-resolution studies of the auroral ionosphere
[AD-A150945] 14 p2409 N85-24850
Spatial resolution of small particles in silane discharge
[AD-A150953] 14 p2423 N85-24948
Observed spatial properties of the solar eigenfunctions and the implications for the existence of resolved multiplets
14 p2443 N85-25074
Looking at more than three dimensions
[DE85-007764] 17 p3009 N85-26800
Image processing: Mathematics, engineering or art
[DE85-007666] 18 p3154 N85-29527
Measurements of vector fields with diode array
18 p3204 N85-29880
Three-dimensional photochemical machining with lasers
[AD-A154711] 21 p3591 N85-32320
Selective population of N = 3 OVIII level during expansion of laser plasma in helium
21 p3688 N85-32914
Hexagonal uniformly redundant arrays for coded-aperture imaging
[OG-9.2-1] 21 p3714 N85-33048
Research in extreme ultraviolet and far ultraviolet astronomy
[NASA-CR-176068] 21 p3716 N85-33060
Advanced instrumentation for Positron Emission Tomography
[DE85-011147] 22 p3840 N85-33779
Adaptive rezoner in a two-dimensional Lagrangian hydrodynamic code
[DE85-010109] 24 p4094 N85-35381
Proportional drift tubes for large area muon detectors
[HE-5.2-11] 24 p4203 N85-36087

SPECIFIC GRAVITY
U DENSITY (MASS/VOLUME)

SPECIFIC HEAT
Accurate measurement of heat capacity by differential scanning calorimetry 04 p0468 N85-12975
Magnetic susceptibility, electrical resistivity, and specific heat of single crystal LaFe-4P-12
[DE84-009979] 04 p0570 N85-13633
The isochoric heat capacity of fluid substances in the critical region. Pre-examinations for a Spacelab experiment
[BMFT-FB-W-84-034] 05 p0723 N85-14650
Thermophysical property testing using transient techniques
[AD-A147085] 07 p1049 N85-16664
Theoretical interpretation of thermal arrest data from differential thermal analysis measurements
12 p1949 N85-22241
Effect of variable solid phase thermal properties on propellant combustion 13 p2002 N85-22547
Characterization-curing-property studies of HBRF 55A resin formulations
[NASA-CR-175836] 16 p2753 N85-26989
Debye temperature and static displacements in LuH sub x single crystals from energy dispersive X-ray diffraction
[DE85-010961] 19 p3376 N85-30946
Basic cryogenics and materials. Phase 1
[NASA-CR-177932] 21 p3572 N85-32215
Dynamics of the melting of chromium-manganese alloys in molten steel
[BLL-M-35850-(5828.4)] 23 p3914 N85-34252
Experimental investigation of radiative-acoustic effects in the water by the thermodynamical conditions of Dumand
[HE-7.1-2] 24 p4213 N85-36156

SPECIFIC IMPULSE
Ion thruster project
[NASA-TM-77728] 07 p0917 N85-15805

SPECIFICATIONS
NT AIRCRAFT SPECIFICATIONS
NT EQUIPMENT SPECIFICATIONS
NT FUNCTIONAL DESIGN SPECIFICATIONS
Tendencies in the development of utilization protocols, seminar report — communication networks
[FUB-11-1983] 01 p0039 N85-10252
Requirements and specifications for cartographic video discs
[AD-A144006] 01 p0049 N85-10325
Logical database processor interface specifications
[PB84-216456] 01 p0105 N85-10705
Investigation of current setting procedures for sector magnets
[CSIR-NAC-83-03] 01 p0117 N85-10795
Manufacturing Methods and Technology (MM/T) specifications for miniature cathode ray tube
[AD-A145597] 02 p0194 N85-11298
APOLLO system requirements specification — electronic document delivery
[ESA-SP-1068] 04 p0494 N85-13150
Improved robotic equipment for radiological emergencies
[DE84-017837] 04 p0509 N85-13249
Quality organization — quality control
[CNES-NT-106] 04 p0511 N85-13257
The ESA product assurance specification system: Explanatory note 04 p0511 N85-13259
Physical database processor preliminary interface specifications
[PB84-217561] 04 p0548 N85-13483
Experimental techniques of formal specifications for the design of tested and reliable computer programs
[ENST-84E007] 05 p0716 N85-14591
Towards a specification of the B programming environment
[CWI-CS-R8408] 05 p0716 N85-14593
Priority rewrite systems — computer programming
[CWI-CS-R8407] 05 p0720 N85-14621
A buyer's guide to space infrastructure
07 p0914 N85-15784
Reliability analysis of local area networks, intermediate report
[BLL-WH-610-(9091.9F)] 07 p1027 N85-16520
Mission-oriented requirements for updating MIL-H-8501. Volume 1: STI proposed structure — military rotorcraft
[NASA-CR-177331-VOL-1] 08 p1088 N85-16877
Mission-oriented requirements for updating MIL-H-8501. Volume 2: STI background and rationale — military rotorcraft
[NASA-CR-177331-VOL-2] 08 p1088 N85-16878
Using the control system design environment in the design of a data link receiver unit for the Coast Guard HH-65A helicopter
[AD-A148624] 08 p1088 N85-16880
Preliminary design criteria and certification test specifications for blast resistant windows
09 p1337 N85-18405
Laser-Electron-Gamma-Source (LEGS)
[DE85-003204] 11 p1638 N85-20322
Object-oriented algebraic specification: Proposal for a notation and 12 examples
[CWI-CS-R8411] 11 p1707 N85-20744
WESF (173)Cs gamma ray sources
[DE85-000676] 11 p1727 N85-20859
GSFC specification electronic data processing magnetic recording tape
[NASA-TM-80599] 12 p1851 N85-21609
Requirements for a database management system
[DE85-004661] 12 p1951 N85-22259
Spacecraft environmental interactions: A joint Air Force and NASA research and technology program
13 p1997 N85-22517
Computer aided draughting in a civil engineering consulting practice 15 p2627 N85-26189
Space reactor ground tests, assessment of facility needs
[DE85-006814] 15 p2650 N85-26345
A description of the process of elaborating man-machine dialog in an aircraft equipped with cathode tubes: Rules and specifications of piloted simulation methods
16 p2696 N85-26658
Water brake convertor: A simple device to convert mechanical energy into heat energy
[DE85-006021] 16 p2716 N85-26766
Orbiter middeck/payload standard interfaces control document
[NASA-TM-87473] 16 p2729 N85-26840
Standards and specifications for geodetic control networks
[PB85-166479] 16 p2916 N85-27374
Avionics data base
[AD-A152415] 17 p2897 N85-27863
The interactive generation of specifications for an onboard software series (GISELE)
17 p2904 N85-27906
Steel Tubes
[BLL-BISI-TRANS-22064-(9022.06)]
17 p2973 N85-29369
Electric Peugeot to have new nickel-iron batteries
18 p3086 N85-29096
Specification of surface roughness over oceans in the GLAS Fourth Order GCM 18 p3142 N85-29455
Atmosphere monitoring requirements
18 p3158 N85-29553
Specification of software quality attributes, volume 1
[AD-A153998] 18 p3163 N85-29580
Specification of software quality attributes. Volume 2: Software quality specification guidebook
[AD-A153999] 18 p3163 N85-29594
Advanced fuel cell development
[DE85-009662] 19 p3306 N85-30497
Maintenance training simulators prime item development specification. Model specification and handbook
[AD-A154108] 19 p3330 N85-30628
Combined function lattices for a 6 GeV synchrotron light source
[DE85-010959] 19 p3367 N85-30885
Standard procedures to be used in specifying basic properties of plastics and polymers
[NPL-DMA(A)-99] 20 p3433 N85-31295
Ultrasonic flowmetering with reflected pulses
[PB85-179985] 20 p3460 N85-31492
The Proust radar 21 p3629 N85-32547
An automated quality assurance surveillance plan for ADP (Automated Data Processing) operations under the Navy's commercial activities program
[AD-A154767] 21 p3671 N85-32902
Portable database driven control system for SPEAR
[DE85-010465] 22 p3830 N85-33720
Stellarator approach to fusion plasma confinement
[DE85-011420] 23 p3984 N85-34704
Specifying and verifying concurrent programs
[AD-A156190] 24 p4138 N85-35862
SLC arc transport system: Magnet design and construction
[DE85-014269] 24 p4159 N85-35789

SPECIMEN GEOMETRY
Influence of test method and material stiffness on the damage produced by low velocity impacts on carbon-epoxy composites No. 45.387/1
[REPT-45.387/1] 03 p0326 N85-12100
Instrumented impact testing machine with reduced specimen oscillation effects
[VTT-290] 04 p0504 N85-13218
Applicability of fatigue strength data obtained from small separately cast specimens on large cast components
05 p0651 N85-14178
Stress intensity factor in a tapered specimen
[NASA-CR-175589] 13 p2102 N85-23099
Fatigue strength of alpha-titanium alloys under cophasal action of variable normal and tangential stresses
15 p2498 N85-25407
A cracked orthotropic sheet stiffened by a semi-infinite orthotropic sheet
[NASA-TP-2455] 21 p3597 N85-32339
Results of an interlaboratory fatigue test program conducted on alloy 800H at room and elevated temperatures
[NASA-CR-174940] 21 p3597 N85-32340

SPECIMENS
X-ray holography of biological specimens
[DE85-002437] 10 p1489 N85-19398
Development of an automated miniature Charpy test method
[DE85-003011] 11 p1652 N85-20405
The preparation of TEM specimens showing oxide scales in transverse cross-section
[AERE-R-11579] 24 p4078 N85-35278

SPECKLE PATTERNS
Laser speckle technique for burner liner strain measurements 02 p0142 N85-10960
Scattering from multi-scale surface — infrared lasers
[RSRE-MEMO-3656] 04 p0505 N85-13222
Measurement of high temperature strain by the laser-speckle strain gauge
[NASA-TM-77751] 07 p0977 N85-16207
Automatic analysis of speckle photographs by microcomputer
[NPL-DITC-47/84] 09 p1322 N85-18308
Image processing instrumentation for speckle interferometry and imaging
[AD-A149308] 11 p1782 N85-21084
Investigations of high resolution imaging through the Earth's atmosphere using speckle interferometry
[AD-A150880] 14 p2439 N85-25053

SPECTRA
NT ABSORPTION SPECTRA
NT ATOMIC SPECTRA
NT BALMER SERIES
NT CONTINUOUS SPECTRA
NT D LINES
NT ELECTROMAGNETIC SPECTRA
NT ELECTRONIC SPECTRA
NT EMISSION SPECTRA
NT ENERGY SPECTRA
NT FRAUNHOFER LINES
NT GAMMA RAY SPECTRA
NT H ALPHA LINE
NT H LINES
NT INFRARED SPECTRA
NT K LINES
NT LINE SPECTRA
NT LYMAN SPECTRA
NT MASS SPECTRA
NT MICROWAVE SPECTRA

NT MOLECULAR SPECTRA
NT NEUTRON SPECTRA
NT NOISE SPECTRA
NT OXYGEN SPECTRA
NT PHOTOLUMINESCENT BANDS
NT PLASMA SPECTRA
NT POWER SPECTRA
NT RADIATION SPECTRA
NT RADIO SPECTRA
NT RAMAN SPECTRA
NT RYDBERG SERIES
NT SCHUMANN-RUNGE BANDS
NT SHOCK SPECTRA
NT SOLAR SPECTRA
NT SPECTRAL BANDS
NT STELLAR SPECTRA
NT UBV SPECTRA
NT ULTRAVIOLET SPECTRA
NT VIBRATIONAL SPECTRA
NT VISIBLE SPECTRUM
NT X RAY SPECTRA

13C and 1H NMR (Nuclear Magnetic Resonance) studies of solid polyolefines
[AD-P003909] 01 p0032 N85-10195

The spatial evolution of t he directional wave spectrum in the Southern Ocean: Its relation to extreme waves in Agulhas Current 08 p1144 N85-17213

Measurement procedures for the radar spectrum engineering criteria
[PB85-119022/GAR] 09 p1313 N85-18254

Surface forward scattering and reflection
[AD-A150115] 12 p1628 N85-22112

Wave directional spectra via ARGOS
16 p2812 N85-27343

One mechanism for generation of wave disturbances in spectra of turbulent flows near ocean surface
19 p3289 N85-30397

Atmospheric planetary wave response to external forcing
[NASA-CR-176000] 19 p3315 N85-30548

A global low order spectral model designed for climate sensitivity studies
[NASA-CR-175999] 19 p3315 N85-30549

Some studies in filtering of atmospheric turbulence
[AD-A154042] 19 p3316 N85-30557

Verification of theoretically computed spectra for a point rotating in a vertical plane
[DE85-011957] 20 p3520 N85-31893

Criteria and algorithms for spectrum parameterization of MST radar signals 21 p3626 N85-32527

Paleoenvironmental investigations at seed cave (Windust cave H-45FR46), Franklin County, Washington
[AD-A154777] 21 p3635 N85-32576

Device for frequency modulation of a laser output spectrum
[DE85-011634] 22 p3790 N85-33479

The 1000 GeV gamma rays from me pulsars
[OG-2.3-12] 22 p3667 N85-33948

Absolute rigidity spectrum of protons and helium nuclei above 10 GV/c
[OG-4.1-1] 22 p3675 N85-34007

Spectral and spatial properties of solar microflares
[SH-1.2-4] 23 p3991 N85-34740

Relativistic cosmic ray spectra in the full non-linear theory of shock acceleration
[OG-8.1-6] 23 p4018 N85-34896

Master Fit users' guide, version 1.0
[DE85-014199] 24 p4140 N85-35667

SPECTRAL ABSORPTION
U ABSORPTION SPECTRA

SPECTRAL ANALYSIS
U SPECTRUM ANALYSIS

SPECTRAL BANDS
NT ABSORPTION SPECTRA
NT FRAUNHOFER LINES
NT PHOTOLUMINESCENT BANDS
NT SCHUMANN-RUNGE BANDS

Noise jammer discrimination by noise spectral bandwidth
[AD-D011224] 01 p0038 N85-10242

Biophysical and spectral modeling for crop identification and assessment
[E85-10006] 02 p0215 N85-11419

Evaluation of criteria for selecting the spectral attributes of digital LANDSAT MSS imagery for discriminating lithological units in the lower Curaca River Valley, Bahia — Brazil
[E85-10036] 03 p0379 N85-12415

LANDSAT instruments characterization
[E85-10032] 04 p0524 N85-13356

Detection of the J-10 manifold of the pure rotational band of phosphine on Saturn 08 p1245 N85-17855

Study of spectral/radiometric characteristics of the Thematic Mapper for land use applications
[E85-10075] 10 p1504 N85-19489

Prelaunch absolute radiometric calibration of the reflective bands on the LANDSAT-4 protoflight Thematic Mapper 11 p1669 N85-20515

Relative radiometric calibration of LANDSAT TM reflective bands 12 p1869 N85-21725

Evaluation of the radiometric integrity of LANDSAT 4 Thematic Mapper band 6 data 12 p1869 N85-21726

Thermal band characterization of the LANDSAT-4 Thematic Mapper 12 p1869 N85-21727

A preliminary analysis of LANDSAT-4 Thematic Mapper radiometric performance 12 p1870 N85-21730

A preliminary evaluation of LANDSAT-4 Thematic Mapper data for their geometric and radiometric accuracies 12 p1871 N85-21739

Assessment of Thematic Mapper band-to-band registration by the block correlation method
12 p1872 N85-21743

LANDSAT 4 band 6 data evaluation
[E85-10093] 12 p1874 N85-21755

LANDSAT 4 investigations of Thematic Mapper and Multispectral Scanner applications — Drum Mountains, Utah and Tonopath, Nevada
[E85-10095] 12 p1874 N85-21757

Semiconductor materials for high frequency solid state sources
[AD-A150020] 12 p1940 N85-22186

Snow reflectance from Thematic Mapper
13 p2120 N85-23205

Relative accuracy assessment of LANDSAT-4 MSS and TM data for level 1 land cover inventory — Washington, D.C.
13 p2122 N85-23212

Reassignment of the iron (3) absorption bands in the spectra of Mars 13 p2195 N85-23614

Determination of mineral type, abundance, and grain size with remotely obtained reflectance spectra
13 p2196 N85-23623

Reduction of reabsorption effects in scintillators by employing solutes with large Stokes shifts
[DE85-011645] 22 p3838 N85-33767

SPECTRAL EMISSION
Luminous points and breakdown in structure of GaAs transistors 02 p0257 N85-11684

Spectral distribution of radiation in n junctions of GaAs during avalanche breakdown 02 p0258 N85-11688

Scattering models in the microwave regime
[NASA-CR-174001] 04 p0525 N85-13361

A comparison between active and passive sensing of soil moisture from vegetated terrains
04 p0526 N85-13364

Voyager EUV and FUV observations
06 p0875 N85-15554

The unidentified emission features: A study of the Orion Bar and planetary nebulae 08 p1246 N85-17862

Long term variability of the IO torus
11 p1760 N85-21070

Interference immunity of fiber-optic communication lines with spectral multiplexing of channels
13 p2069 N85-22924

Study of integral and spectral direct solar radiation over Atlantic 14 p2341 N85-24475

The use of the spectral matrix in analyzing the propagation characteristics of electromagnetic emissions — magnetosphere 14 p2371 N85-24658

Magnetospheric wave characteristics derived from cross-spectral analysis 14 p2371 N85-24659

Optical radiation emissions from selected sources. Part 2: High intensity discharge lamps
[PB85-149136] 15 p2523 N85-25551

Free electron lasers for the EUV spectral region
[DE85-006804] 15 p2563 N85-25815

Spectroscopic studies of a railgun muzzle flash
[MRL-R-952] 16 p2728 N85-26837

X-ray emission and the winds of cataclysmic variables
[DE85-007663] 17 p3053 N85-28902

Carbon foil secondary electron emission during ion passage through the 40 to 500 keV energy field
[MPE-190] 18 p3184 N85-29747

Recent results of the Los Alamos free-electron laser oscillator experiment
[DE85-010736] 19 p3277 N85-30324

Star formation in NGC 7538: Multi-wavelength observations and issues 20 p3545 N85-32063

Impact of fluctuations in optical properties of atmosphere on the ratio of spectral brightness from remote sensing of agricultural land 22 p3734 N85-33149

Cataloging the spectral brightness coefficients of the forested region of the European territory of the USSR
22 p3735 N85-33155

Direct regression analysis of remote sensing data (using example of grass cover) 22 p3736 N85-33157

A comparison of LANDSAT thematic mapper, multispectral scanner and airborne sensors for mapping the distribution of alteration minerals: Examples from the southwestern United States 24 p4106 N85-35452

Observations of far-infrared transitions between excited states of OH
[NASA-TM-86722] 24 p4167 N85-35833

SPECTRAL ENERGY DISTRIBUTION
Measures of distance between speech signals in the frequency domain — speech recognition
[FUB-5-1984] 01 p0041 N85-10267

Spectral distribution of radiation in n junctions of GaAs during avalanche breakdown 02 p0258 N85-11688

Global aspects of stream evolution in the solar wind
[DE85-002207] 11 p1766 N85-21101

Jet topologies in hadron-hadron collisions
[DE85-001328] 12 p1929 N85-22119

Maximum entropy spectral analysis
[LEOK-TR-1984-06] 14 p2299 N85-24235

A program of ground-based astronomy to complement einstein observations
[AD-A151111] 15 p2668 N85-26486

Recent results of the Los Alamos free-electron laser oscillator experiment
[DE85-010736] 19 p3277 N85-30324

Comparison of simulation with experiment in an RFQ
[DE85-010770] 19 p3349 N85-30757

Requirements for attaining Treanor's distribution of vibrational energy among CO2 levels in CW gasdynamic laser flows
[STN-3] 20 p3461 N85-31499

Some rigorous results concerning spectral theory for ideal MHD
[DE85-013427] 24 p4156 N85-35770

The structure of the shower disk observed at Mt. Norikura
[HE-4.7-1] 24 p4198 N85-36052

Structure of air shower disc near the core
[HE-4.7-2] 24 p4198 N85-36053

A mini-array for large air showers
[HE-4.7-10] 24 p4199 N85-36061

A note on some statistical properties of rise time parameters used in muon arrival time measurements
[HE-4.7-12] 24 p4199 N85-36062

SPECTRAL LINE WIDTH
The X-ray spectrum and time variability of narrow emission line galaxies
[NASA-TM-83859] 03 p0446 N85-12842

Spectral frequency of eigenvalues in optimal problems of stability of cylindrical shells of variable thickness
13 p2047 N85-22815

SPECTRAL LINES
U LINE SPECTRA

SPECTRAL METHODS
Auto-regressive moving average spectral estimation using modified and least squares modified Yule-Walker estimates
[AD-A145516] 02 p0254 N85-11663

Study of CW injection laser with a dispersive external cavity 02 p0270 N85-11760

A pseudospectral Legendre method for hyperbolic equations with an improved stability condition
[NASA-CR-172475] 03 p0410 N85-12617

Effective use of remote sensing products in litigation
[E85-10048] 06 p0827 N85-15250

On the instability of a 3-dimensional attachment line boundary layer: Weakly nonlinear theory and a numerical approach
[NASA-CR-172504] 07 p0957 N85-16063

Autoregressive spectral estimation for two dimensional time series 07 p0965 N85-16258

Data-driven choice of a spectrum estimate: Extending the applicability of cross-validation methods
[DE85-001411] 10 p1437 N85-19058

Spectral methods in time for parabolic problems
[NASA-CR-172539] 11 p1706 N85-20730

Complex symmetric matrices with strongly stable iterates
[NASA-CR-172542] 11 p1706 N85-20731

Simulation of estimating periodicity of seasonally stationary time series
[DE85-003517] 11 p1706 N85-20748

Recovering pointwise values of discontinuous data within spectral accuracy
[NASA-CR-172535] 12 p1919 N85-22049

Synthesis of quasi-optimum algorithms for signal recognition against background of correlated noise employing discrete spectral transformations
13 p2085 N85-23020

Automated extraction of absorption bands from reflectance special 13 p2197 N85-23624

Spectral methods for modeling supersonic chemically reacting flow fields
[NASA-CR-172578] 14 p2300 N85-24240

Analysis of spectral operators in one-dimensional domains
[NASA-CR-172573] 15 p2633 N85-26228

Kolmogorov and scalar spectral regimes in numerical turbulence
[NASA-TM-86699] 17 p2957 N85-28264

On spectral multigrid methods for the time-dependent Navier-Stokes equations
[NASA-CR-172613] 19 p3344 N85-30725
Spectral methods for limited area models 20 p3488 N85-31679
Spectral Theory of Sturm-Liouville Differential Operators: Proceedings of the 1984 Workshop
[DE85-009693] 20 p3520 N85-31890
A review of spectral methods
[NASA-CR-172502] 23 p3929 N85-34350
Study of spectral/radiometric characteristics of the Thematic Mapper for land use applications
[E85-10106] 24 p4107 N85-35464

SPECTRAL NOISE
U WHITE NOISE

SPECTRAL RECONNAISSANCE
Earth resources: A continuing bibliography with indexes
[NASA-SP-7041(44)] 10 p1503 N85-19484
The spot operational remote sensing satellite system: Current status and perspectives 11 p1713 N85-20776
Feature extraction assessment study
[AD-A150189] 13 p2126 N85-23239

SPECTRAL REFLECTANCE
Flight demonstration of new NRL real-time data acquisition system and laser video waveform sampler
[AD-A145126] 01 p0053 N85-10350
Relationships between grass canopy characteristics and LANDSAT Thematic Mapper bands 02 p0213 N85-11402
Botanical sciences team 02 p0214 N85-11407
A comparison between active and passive sensing of soil moisture from vegetated terrains 04 p0526 N85-13364
Spectral reflectance studies on the orientale region of the Moon 06 p0888 N85-15639
Variation in spectral response of soybeans with respect to illumination, view, and canopy geometry
[E85-10040] 07 p0962 N85-16241
Spectral estimators of absorbed photosynthetically active radiation in corn canopies
[E85-10041] 07 p0963 N85-16242
Growth/reflectance model interface for wheat and corresponding model
[E85-10058] 07 p0967 N85-16269
North American vegetation patterns observed with the NOAA-7 advanced very high resolution radiometer — North America
[E85-10062] 08 p1174 N85-17400
Analysis of terrestrial conditions and dynamics
[E85-10063] 08 p1174 N85-17401
Growth and reflectance characteristics of winter wheat canopies
[E85-10080] 10 p1505 N85-19494
Evaluation of infrared reflectance as a technique for measuring absorber materials degradation
[PB85-108488] 11 p1677 N85-20567
Evaluation of infrared reflectance as a technique for measuring absorber materials degradation
[DE85-002171] 11 p1729 N85-20674
Snow reflectance from Thematic Mapper 13 p2120 N85-23205
Multispectral analysis of the Kasei Vallis-Lunae Planum region of Mars 13 p2193 N85-23607
Geologic interpretation of remote sensing data for the Martian volcano, Ascraeus Mons 13 p2194 N85-23608
The search for igneous materials at the Viking landing sites 13 p2194 N85-23609
Basalts of Mars: Constraints on volatile evolution 13 p2194 N85-23610
Zeolites on Mars: Prospects for remote sensing 13 p2195 N85-23615
Remote sensing analyses of localized lunar dark mantle deposits 13 p2195 N85-23616
Spectral reflectance studies of the Orientale basin 13 p2195 N85-23617
Io: Precise comparison of Voyager spectral curves with laboratory measurements 13 p2196 N85-23619
Spectral units on Europa and Ganymede 13 p2196 N85-23621
Determining mineral types and abundances from reflectance measurements 13 p2196 N85-23622
Determination of mineral type, abundance, and grain size with remotely obtained reflectance spectra 13 p2196 N85-23623
Automated extraction of absorption bands from reflectance special 13 p2197 N85-23624
Quantitative analyses of planetary reflectance spectra 13 p2197 N85-23625
Variability of coefficients of spectral brightness of soils 15 p2486 N85-25348
Asteroid amphitrite: Surface composition and prospects for the possible Galileo flyby 15 p2680 N85-26549
Spectral reflectances of natural targets for use in remote sensing studies
[NASA-RP-1139] 19 p3299 N85-30450
Optical effects of thin film adhesives in multijunction solar cells
[DE85-010120] 19 p3305 N85-30488
Regression analysis of aircraft and ground measurement data on vegetation cover 22 p3735 N85-33158
Processing of LANDSAT imagery to map surface mineral alteration on the Alaska Peninsula, Alaska 24 p4106 N85-35455

SPECTRAL RESOLUTION
Reducing spectral dimension of remotely sensed data using principal components analysis and a Peano scanning 02 p0212 N85-11399
Cartography 02 p0214 N85-11412
Fundamental remote sensing science research program. Part 1: Status report of the mathematical pattern recognition and image analysis project
[E85-10004] 02 p0215 N85-11417
Remote sensing as a mineral prospecting technique
[E85-10010] 02 p0216 N85-11423
Water resources by orbital remote sensing: Examples of applications
[E85-10015] 02 p0217 N85-11428
NOAA/NASA joint simulation of AMTS and HIRS 05 p0662 N85-14384
The low-resolution spectra 09 p1413 N85-18907
LANDSAT-4 Science Characterization Early Results. Volume 2, part 1: Thematic Mapper (TM)
[E85-10068] 11 p1668 N85-20508
Spectral characterization of the LANDSAT Thematic Mapper sensors 11 p1669 N85-20514
Atmospheric properties of RU Lupi derived from high- and low-resolution IUE spectra 11 p1754 N85-21031
LANDSAT-4 Science Characterization Early Results. Volume 3, part 2: Thematic Mapper (TM)
[E85-10069] 12 p1869 N85-21724
Thematic Mapper spectral dimensionality and data structure 12 p1871 N85-21736
An analysis of the data obtained by a simultaneous observation of GMS and GMS-2: A study of the difference between the brightness temperatures by GMS and those by GMS-2 12 p1894 N85-21888
Impact of Thematic Mapper sensor characteristics on classification accuracy — suburban Washington, D.C., Maryland, and the Chesapeake Bay 13 p2117 N85-23186
Quick look analysis of TM data of the Washington, District of Columbia, area 13 p2119 N85-23197
Preliminary comparisons of the information content and utility of TM versus MSS data 13 p2120 N85-23202
Assessing LANDSAT TM and MSS data for detecting submerged plant communities 13 p2120 N85-23203
The use of Thematic Mapper data for land cover discrimination: Preliminary results from the UK SATMaP programme 13 p2121 N85-23207
Preliminary study of information extraction of LANDSAT TM data for a suburban/regional test site 13 p2121 N85-23208
Comparison of land cover information from LANDSAT Multispectral Scanner (MSS) and airborne Thematic Mapper simulator (TMS) data for hydrologic applications — Clinton River Basin, Michigan 13 p2122 N85-23211
Automated extraction of absorption bands from reflectance special 13 p2197 N85-23624
Measurements of vector fields with diode array 18 p3204 N85-29880
Mass resolution optimization in a large isotopic composition experiment
[OG-9.1-9] 23 p4023 N85-34935

SPECTRAL SENSITIVITY
SVKD and SVKM-3 seismographs with a low-sensitivity channel
[REPT-553] 03 p0376 N85-12396
SENSIT.FOR: A program for sensitometric reduction 07 p0963 N85-16105
A spectrosensitometer with an absolute calibration 07 p0963 N85-16106
The most effective astronomical photographic emulsions for recording of faint and low-contrast objects 07 p0963 N85-16110
Thematic Mapper. Volume 1: Calibration report flight model, LANDSAT 5
[E85-10059] 07 p0967 N85-16270
Color measurement and discrimination
[NASA-CR-3824] 09 p1365 N85-18579
Spectral characterization of the LANDAT-4 MSS sensors 11 p1668 N85-20499
Investigation of the optical properties of solar elements 12 p1879 N85-21788
LANDSAT-4 Science Characterization Early Results. Volume 4: Applications — agriculture, soils land use, geology, hydrology, wetlands, water quality, biomass identification, and snow mapping
[E85-10070] 13 p2117 N85-23186
A first evaluation of LANDSAT TM data to monitor suspended sediments in lakes — Lake Chicot, Arkansas 13 p2120 N85-23204
Preliminary evaluation of TM for soils information 13 p2121 N85-23206
Comparison of MSS and TM data for landcover classification in the Chesapeake Bay area: A preliminary report — Taylor's Island, Maryland 13 p2121 N85-23210
A global low order spectral model designed for climate sensitivity studies
[NASA-CR-175999] 19 p3315 N85-30549
Paired ion chamber constants for fission gamma-neutron fields
[AD-A155089] 21 p3702 N85-32999

SPECTRAL SIGNATURES
Description of the Dutch-Danish (DUDA) scanner — thermal signatures
[AD-B084893] 01 p0121 N85-10826
Basic principles, methodology, and applications of remote sensing in agriculture
[E85-10016] 02 p0217 N85-11429
Assessment of computer techniques for processing digital LANDSAT MSS data for lithological discrimination of Serra do Ramalho, State of Bahia
[E85-10033] 03 p0378 N85-12412
Ice-soil mixtures: Visual and near-infrared remote sensing techniques
[NASA-CR-174087] 04 p0525 N85-13358
An electronically controlled array for simulation of passive target/background signatures at millimeter wavelengths
[AD-D011458] 10 p1468 N85-19283
Analysis of data acquired by synthetic aperture radar and LANDSAT Multispectral Scanner over Kershaw County, South Carolina, during the summer season
[E85-10071] 10 p1503 N85-19485
Radiometric calibration and processing procedure for reflective bands on LANDSAT-4 protoflight Thematic Mapper 11 p1668 N85-20510
Improved continuum definition in high-background IUE images 11 p1761 N85-21078
Investigations of vegetation and soils information contained in LANDSAT Thematic Mapper and Multispectral Scanner data
[E85-10082] 12 p1873 N85-21747
Remote sensing research for agricultural applications — San Joaquin County, California and Snake River Plain and Twin Falls area, Idaho
[E85-10090] 12 p1873 N85-21752
Overview of TM applications research reports 13 p2117 N85-23187
A concept for the processing and display of Thematic Mapper data 13 p2119 N85-23196
Early results of investigations of LANDSAT 4 Thematic Mapper and Multispectral Scanner applications — Washington, D.C. 13 p2119 N85-23200
Experimental methods for quenching structures in lunar-analog silicate melts: Variations as a function of quench media and composition 13 p2184 N85-23554
Optical 3-D signature device for detecting chemical agents
[AD-D011689] 19 p3272 N85-30293
Physico-geographical regionalization of Caspian lowland based on space survey materials 22 p3736 N85-33162

SPECTRAL THEORY
On a spectral theory of the excitation mechanism of galactic spirals 12 p1955 N85-22284
Simple solar spectral model for direct and diffuse irradiance on horizontal and tilted planes at the Earth's surface for cloudless atmospheres
[DE85-002933] 18 p3137 N85-29424
Approximate inverse spectral transform for the Korteweg-de Vries equation
[PREPRINT-411] 18 p3172 N85-29658
Some rigorous results concerning spectral theory for ideal MHD
[DE85-013427] 24 p4156 N85-35770

SPECTROGRAMS
Tests of the automatic recognition of words spoken by different voices based on collected groups of modal binary spectrograms
[ISSN-0208-5658] 05 p0622 N85-13977
Analysis of spacecraft data
[NASA-CR-171587] 21 p3689 N85-32789
Spacecraft-aided research discussed at geology Congress 22 p3734 N85-33147

SPECTROGRAPHS
Future studies of the local interstellar medium with Space Telescope and Columbus 06 p0880 N85-15593
Spectroscopic instrumentation for Tokamak diagnostics 09 p1366 N85-18732
The multi-anode microchannel array detector system: Current status and future prospects 11 p1761 N85-21080
The solar vector magnetograph of the Okayama Astrophysical Observatory 16 p3205 N85-29882
The new solar magnetograph for the Canary Islands Observatory THEMIS 16 p3205 N85-29886
A new study of muons in air showers by NBU air shower array 24 p4190 N85-35997

SPECTROHELIOGRAPHS
The evaluation of a deformable diffraction grating for a stigmatic EUV spectroheliometer [NASA-CR-174246] 07 p1042 N85-16621
The calculation of theoretical chromospheric models and the interpretation of solar spectra from rockets and spacecraft [NASA-CR-174289] 06 p1259 N85-17922
Coronal structures observed at metric wavelengths with the Nancay radioheliograph 14 p2453 N85-25152
The San Fernando Observatory video Stokes polarimeter 16 p3205 N85-29885
The new solar magnetograph for the Canary Islands Observatory THEMIS 16 p3205 N85-29886
High Resolution Telescope and Spectrograph (HRTS) 23 p3901 N85-34162

SPECTROHELIOSCOPES
U SPECTROHELIOGRAPHS

SPECTROMETERS
NT FABRY-PEROT SPECTROMETERS
NT GAMMA RAY SPECTROMETERS
NT INFRARED SPECTROMETERS
NT LASER SPECTROMETERS
NT MASS SPECTROMETERS
NT MICROWAVE SPECTROMETERS
NT NEUTRON SPECTROMETERS
NT SOLAR SPECTROMETERS
NT SPECTROHELIOGRAPHS
NT TIME OF FLIGHT SPECTROMETERS
NT ULTRAVIOLET SPECTROMETERS
A high resolution spectroscopic study of the oxygen molecule [NASA-CR-174061] 02 p0172 N85-11150
Imaging Science Panel. Multispectral Imaging Science Working Group joint meeting with Information Science Panel: Introduction 02 p0213 N85-11406
Multiple object spectroscopy: The MX spectrometer design 02 p0296 N85-11920
Simultaneous measuring absorption spectrometer [BMFT-FB-T-84-132] 03 p0365 N85-12339
Einstein solid state spectrometer observation of the peculiar red dwarf Wolf 630 AB [NASA-TM-83947] 03 p0447 N85-12843
Advances in room-temperature solid-state gamma-ray spectrometry [DE84-015944] 04 p0469 N85-12967
Study of instrument design options for the Columbus spectroscopy mission [NASA-CR-174072] 04 p0502 N85-13205
LANDSAT instruments characterization [E85-10028] 05 p0654 N85-14197
Clinical measurements using fiber optics and optrodes [DE84-015043] 05 p0696 N85-14481
Measurements of X-ray spectra from laser produced plasma 06 p0748 N85-14794
Comparison measurements on optical particle counters [BLL-DOUNREAY-TR-934-(9091.9F)] 07 p0961 N85-16092
A 150 micron heterodyne spectrometer for airborne astronomy 08 p1249 N85-17867
Tunable heterodyne receiver from 100 micron to 1,000 micron for airborne observations 08 p1249 N85-17868
SIRTF: The next step 08 p1250 N85-17891
Simulation of bent crystal spectrometers [DE85-002042] 09 p1365 N85-18709
Improved performance for large area triple layer microchannel plate detector for a neutral spectrometer in Doublet III [DE85-001719] 10 p1488 N85-19395
Application of layered synthetic microstructures to high temperature plasma diagnostics [DE85-002035] 10 p1559 N85-19828
Research in extreme ultraviolet and far ultraviolet astronomy [NASA-CR-174432] 10 p1570 N85-19902
Investigation of the output parameters of the pulsed neutron generator NGI-5 [DE85-001823] 11 p1725 N85-20849
Design, construction and initial evaluation of an absolute, time-integrating/time-resolving spectrometer for the diagnostics of pulsed, high temperature plasma X-ray sources in the 100-10,000 eV region [DE85-003528] 11 p1732 N85-20896
SCATHA (spacecraft charging at high altitudes) plasma interaction experiment: SC-3 high energy particle spectrometer; SC-8 energetic ion composition experiment [AD-A149728] 12 p1793 N85-21252
Use of the ORACLE DEMS in determining the response of complex scientific instrumentation [DE85-001742] 12 p1853 N85-21621
Inelastic scattering in condensed matter with high intensity Moessbauer radiation [DE85-003531] 12 p1854 N85-21627
High resolution diffraction grating [AD-D011541] 12 p1933 N85-22141
Protons with energies above 30 KeV in Earth's radiation belt at low altitudes during magnetically quiet time close to geomagnetic equator 13 p1960 N85-22423
Rocket body charge neutralization processes in ARAKS experiment (data from two launches) 13 p1960 N85-22426
Reflex attachment for line alignment in spectral diffraction devices 13 p2044 N85-22794
Possibility of mapping active tectonic structures from mercury gas aureoles over sea surface 13 p2113 N85-23162
Effects of focusing on HRS focal-plane polarimeter measurements [DE85-004627] 13 p2160 N85-23406
Comparison of flame photometer data with total particle volume calculated from laser spectrometer particle count data [AD-A151008] 14 p2252 N85-23958
Geometric error analysis for shuttle imaging spectrometer experiment [NASA-CR-175665] 14 p2305 N85-24269
Mossbauer spectrometry: Testing of a new computer based system and its application to a study of an aluminum-iron-cerium alloy [AD-A151826] 15 p2510 N85-25483
Mirror accessory for line straightening in diffraction spectrometers 16 p2764 N85-27054
New focal plane detector system for the broad range spectrometer [DE85-005370] 16 p2788 N85-27201
Cryostat and electronic development associated with multi-detector spectrometer systems [DE85-007624] 16 p2788 N85-27203
Acousto-optical spectrometers at Itapetinga Radio Observatory [INPE-3479-PRE/722] 16 p2881 N85-27776
Results from a Bragg curve spectrometer [DE85-007870] 18 p3176 N85-29681
Squid detection of acoustomagnetic effects 19 p3373 N85-30924
A Cerenkov-delta E-Cerenkov detector for high energy cosmic ray isotopes and an accelerator study of Ar-40 and Fe-56 fragmentation [NASA-CR-176028] 20 p3549 N85-32086
A microprocessor-controlled, multichannel fluorimeter for analysis of sea water [AD-A154986] 21 p3590 N85-32310
Research in extreme ultraviolet and far ultraviolet astronomy [NASA-CR-176068] 21 p3716 N85-33060
Program for observations of Halley's comet 22 p3732 N85-33138
Direct regression analysis of remote sensing data (using example of grass cover) 22 p3736 N85-33157
High-resolution spectrum of Cygnus X-1 [OG-2.4-12] 22 p3868 N85-33956
Absolute rigidity spectrum of protons and helium nuclei above 10 GV/c [OG-4.1-1] 22 p3875 N85-34007
Results of a search for deuterium at 25-50 GC/c using a magnetic spectrometer [OG-4.2-4] 22 p3878 N85-34024
Galactic antiprotons of 0.2-2 GeV energy [OG-6.1-11] 22 p3888 N85-34101
Imaging Spectrometric Observatory (ISO) 23 p3902 N85-34169
Investigation of non-intrusive radiometers for entrained gasifier temperature measurement, revision 3 [DE85-011795] 23 p3934 N85-34385
Measurements of Fe and Ar fragmentation cross sections [OG-7.2-20] 23 p4016 N85-34887
Investigation of cosmic rays in very short time scales [HE-4.6-7] 24 p4197 N85-36044
A facility for investigation of multiple hadrons at cosmic-ray energies [HE-4.6-8] 24 p4197 N85-36045
Fast scintillation counter system and performance [HE-4.6-10] 24 p4197 N85-36047

SPECTROMETRY
U SPECTROMETERS

SPECTROPHOTOMETERS
NT INFRARED SPECTROPHOTOMETERS
NT ULTRAVIOLET SPECTROPHOTOMETERS
Five-minute P modes detected in Doppler shift measurement on Alpha Centauri 08 p1250 N85-17895
Compatibility, contamination and IR microspectrophotometry [DE85-010809] 19 p3273 N85-30297

SPECTROPHOTOMETRY
NT STELLAR SPECTROPHOTOMETRY
Spectrophotometric studies of iodine complexes in an aluminum chloride - butylpyridinium chloride ionic liquid [AD-A145074] 01 p0024 N85-10150
Physical properties of the satellites of Neptune 02 p0300 N85-11945
Interactions of hydrazine and of hydrazine derivatives with soil constituents and with soils [AD-A148475] 08 p1122 N85-17074
Spectral characteristics of dust in planetary nebulae 08 p1247 N85-17873
Aromatics determination in middle distillate petroleum fractions by spectrophotometric titration [PNR-90239] 09 p1293 N85-18123
Observations of cataclysmic variable star winds 11 p1755 N85-21041
The essence of binary star coalescence: A coordinated ground-based photometric and IUE ultraviolet study of FK Comae 11 p1756 N85-21044
Microstructure of Venus cloud layer based on spectrophotometric data from Venera-11 spacecraft 13 p1982 N85-22436
Determining adsorption of surface-active substances by sea bottom deposits 13 p2107 N85-23128
Photometric study of Pluto near perihelion. Part 2: Refinement of rotation period: Color indices 15 p2483 N85-25325
Infrared observations of the Uranian rings 15 p2672 N85-26488
Stellar occultations by Uranus rings on 15 August 1980 and 22 April 1982 15 p2672 N85-26489
Fourier transform infrared spectrophotometric analysis of resin mix stoichiometry, revision 1 [DE85-007272] 16 p2747 N85-26951
Lightcurve CCD spectrophotometry of Pluto 20 p3545 N85-32057
Transparency of water 9n 186 - 500 nm region 21 p3690 N85-32923
The nature and origin of outer solar system asteroids from reflectance spectrophotometry 24 p4168 N85-35838

SPECTROPOLARIMETERS
U POLARIMETERS

SPECTRORADIOMETERS
A comparison of LANDSAT thematic mapper, multispectral scanner and airborne sensors for mapping the distribution of alteration minerals: Examples from the southwestern United States 24 p4106 N85-35452

SPECTROSCOPES
U SPECTROMETERS

SPECTROSCOPIC ANALYSIS
NT FLAME SPECTROSCOPY
Development of a rapid test method for asphalt concrete content determination in hot-mix paving mixtures [PB84-218692] 03 p0342 N85-12204
Methodology for the collection and analysis of trace metals in atmospheric precipitation [CM-67] 09 p1350 N85-18491
Beam-foil spectroscopy of highly ionized aluminum atoms 09 p1390 N85-18746
Synchrotron X-ray fluorescence and extended X-ray absorption fine structure analysis [DE85-003606] 10 p1438 N85-19063
Spectroscopic study of sources and control of impurities in TMX-U: Revision 1 [DE85-004423] 12 p1937 N85-22170
Multiple element neutron-activation analysis of atmospheric aerosols with X-ray and gamma-spectrometric recording of radionuclides formed 13 p2013 N85-22631
Spectroscopic study of gas pollutants in atmosphere over large cities: A review 14 p2341 N85-24478
Spectroscopic analysis of radiation-generated changes in tensile properties of a polyetherimide film [NASA-TP-2429] 15 p2502 N85-25435
Chemical spectroscopy [DE85-009594] 18 p3191 N85-29790
Initial results from the Caltech/DSRI balloon-borne isotope experiment [OG-4.3-8] 21 p3714 N85-33046
Dating Archean zircon by ion microprobe: New light on an old problem 21 p3722 N85-33094

Precision measurements of solar energetic particle elemental composition
[SH-2.1-4] 23 p3998 N85-34785
SPECTROSCOPIC TELESCOPES
Dall-Null tester for spaceborne applications
[AD-A151772] 16 p2881 N85-27779
Stokes parameters modulator for birefringent filters 18 p3205 N85-29684
The new solar magnetograph for the Canary Islands Observatory THEMIS 18 p3205 N85-29686
The vector magnetograph of the Sayan Solar Observatory 18 p3206 N85-29687
A Cerenkov-delta E-Cerenkov detector for high energy cosmic ray isotopes and an accelerator study of Ar-40 and Fe-56 fragmentation
[NASA-CR-176028] 20 p3549 N85-32086
A balloon-borne imaging gamma-ray telescope
[OG-9.2-2] 21 p3714 N85-33049
Balloon-borne video cassette recorders for digital data storage
[OG-9.3-11] 21 p3715 N85-33050
SPECTROSCOPY
NT ABSORPTION SPECTROSCOPY
NT ASTRONOMICAL SPECTROSCOPY
NT AUGER SPECTROSCOPY
NT AURORAL SPECTROSCOPY
NT ELECTRON SPECTROSCOPY
NT FLAME SPECTROSCOPY
NT HOLOGRAPHIC SPECTROSCOPY
NT INFRARED SPECTROSCOPY
NT LASER SPECTROSCOPY
NT MAGNETIC SPECTROSCOPY
NT MASS SPECTROSCOPY
NT MOLECULAR SPECTROSCOPY
NT NUCLEAR RADIATION SPECTROSCOPY
NT OPTICAL EMISSION SPECTROSCOPY
NT OPTOGALVANIC SPECTROSCOPY
NT PHOTOACOUSTIC SPECTROSCOPY
NT PHOTOELECTRON SPECTROSCOPY
NT RAMAN SPECTROSCOPY
NT SPECTROPHOTOMETRY
NT SPECTROSCOPIC ANALYSIS
NT STELLAR SPECTROPHOTOMETRY
NT ULTRASONIC SPECTROSCOPY
NT ULTRAVIOLET SPECTROSCOPY
NT X RAY SPECTROSCOPY
Application of positron annihilation in materials science
[DE84-014733] 02 p0288 N85-11883
Spectroscopic investigations on neutron induced impurity atoms and radiation defects 03 p0430 N85-12742
The present state of the International Star Cluster Photometry Programme 05 p0737 N85-14741
Topics in high resolution spectroscopy of stored ions
[DE85-002093] 06 p0861 N85-15470
A study of structural phase transitions using light scattering techniques
[AD-A147261] 07 p1048 N85-16654
Electrochemical interfaces and electrode processes
[AD-A147414] 09 p1290 N85-18098
Supercritical fluid chromatography/supersonic jet spectroscopy
[DE85-003310] 09 p1292 N85-18115
Beam probe spectroscopic technique for ion temperature and magnetic field measurements 09 p1369 N85-18738
Pulsed photothermal radiometry for remote sensing of spectroscopic and physical properties of thin film
[AD-A149060] 10 p1435 N85-19041
Interim protocol for the automated analysis of semivolatile organic compounds by Gas Chromatography/Fourier Transfer Infrared (GC/FT-IR) spectrometry
[PB85-115186] 11 p1595 N85-20035
KMSF X-ray laser experiments, task no. 2
[DE85-000291] 11 p1640 N85-20335
Coronal spectroscopy in laser plasmas
[DE85-002617] 11 p1730 N85-20880
Research in the optical sciences
[AD-A150196] 13 p2159 N85-23401
Collaborative shock tube studies of benzene pyrolysis
[DE85-006347] 14 p2253 N85-23982
Synthesis and properties of elevated temperature P/M aluminum alloys
[AD-A151031] 14 p2256 N85-23981
Characterization of atomic defects and their aggregates using positron annihilation spectroscopy
[DE85-008206] 14 p2418 N85-24918
Spectroscopy of quasimolecular X-rays with H-like decelerated ions
[DE85-006585] 15 p2649 N85-26397
Proposed solar neutrino experiment using (81)Br(nu,e(-e)) (81)Kr
[DE85-004802] 15 p2684 N85-26579
Spectroscopic investigation of materials for frequency agile laser systems
[AD-A151731] 16 p2790 N85-27208
Nuclear spectroscopic studies
[DE85-006894] 16 p2862 N85-27652
Positron annihilation studies of vacancy formation in tungsten, chromium, and niobium
[DE85-006837] 16 p2871 N85-27710
An investigation of molecular structure of copolymers using positron annihilation spectroscopy
[NASA-TM-86431] 17 p2916 N85-27977
The spectroscopy and reaction kinetics of coordinated unsaturated metal carbonyls
[AD-A153079] 17 p2920 N85-28003
East Europe report: Science and technology
[JPRS-ESA-85-017] 17 p2945 N85-28177
PAS determination of the vacancy formation enthalpy in tungsten
[DE85-010283] 19 p3240 N85-30086
Atomic data for controlled fusion research. Volume 4: Spectroscopic data for iron
[DE85-009658] 19 p3354 N85-30787
Calculation of molecular constants potential energy curves and Franck-Condon factors for lead oxide
[AD-A154521] 21 p3562 N85-32158
Multidimensional luminescence measurements
[AD-A154950] 21 p3563 N85-32162
Basic research in novel inorganic reagents and fluorocarbon chemistry
[AD-A155340] 21 p3564 N85-32165
Aerosol analysis and emission spectrometry with free jets
[DE85-010576] 21 p3564 N85-32168
Electrochemistry of Hexanitroazobenzene (HNAB)
[DE85-010807] 21 p3565 N85-32171
Multi-channel electric aerosol spectrometer 21 p3642 N85-32623
USSR report: Physics and mathematics
[JPRS-UPM-85-004] 21 p3680 N85-32860
Cataloging the spectral brightness coefficients of the forested region of the European territory of the USSR 22 p3735 N85-33155
Supercritical fluid chromatography/supersonic jet spectroscopy
[DE85-007005] 22 p3746 N85-33221
1985 Amorphous Silicon Review Meeting
[DE85-006794] 22 p3807 N85-33582
High-resolution spectroscopic observation of Vela X-1 in the hard X-ray energy range
[OG-2.2-10] 22 p3865 N85-33936
Direct determination of metals in organic matrices by Inductively Coupled Plasma-Atomic Emission Spectrometry (ICP-AES)
[DE85-012015] 23 p3911 N85-34233
Time-resolved spectroscopic studies of detonating heterogeneous explosives
[DE85-009760] 23 p3921 N85-34297
Apparatus and method for the spectrochemical analysis of liquids using the laser spark
[DE85-005749] 23 p3935 N85-34367
Solar flare gamma-ray line spectroscopy
[SH-2.1-14] 23 p3999 N85-34795
Results of ultra-low level 71ge counting for application in the Gallex-solar neutrino experiment at the Gran Sasso Underground Physics Laboratory
[SH-8.1-2] 23 p4049 N85-35108
The read-out system of spatial distribution of thermoluminescence in meteorites
[SH-9.1-16] 23 p4052 N85-35131
Literature search for new physical methods for biological aerosol detection
[AD-A155863] 24 p4128 N85-35592
High-resolution spectroscopy and dynamics of multiphoton processes in atoms and molecules
[AD-A155862] 24 p4147 N85-35714
SPECTRUM ANALYSIS
NT CEPSTRAL ANALYSIS
NT FLAME SPECTROSCOPY
NT MAXIMUM ENTROPY METHOD
Noise on NAC report NAC-83-05: Beam Pulse Length Determination by Spectral Analysis
[CSIR-NAC-83-06] 01 p0119 N85-10816
Giacobini-Zinner comet: Polarimetric and physical observations
[NASA-TM-77771] 01 p0130 N85-10894
Laser on copper and gold vapors with space diversity media 02 p0270 N85-11762
Splitting of surface polariton spectrum by holographic grating 02 p0272 N85-11771
Optical constant determination of thin polymer films in the infrared
[AD-A145669] 02 p0287 N85-11877
Uranus and Neptune
[NASA-CP-2330] 02 p0298 N85-11927
Evaluation of moduli and thicknesses of pavement systems by spectral-analysis-of-surface-waves method
[PB84-219112] 03 p0342 N85-12205
Simultaneous measuring absorption spectrometer
[BMFT-FB-T-84-132] 03 p0365 N85-12339
Signal processing algorithms
[AD-A145748] 03 p0406 N85-12390
Meteorological analysis for clusters of wind turbines
[DE84-013164] 04 p0539 N85-13425
LANDSAT instruments characterization
[E85-10029] 05 p0654 N85-14196
Measurement-technical investigations of wind energy units in the short-time range — spectrum analysis 05 p0668 N85-14294
Resonant scattering of acoustic waves by elastic spherical shell in fluid 06 p0778 N85-14972
Spectrum of geomagnetic field variations in the range of periods between 1 and 10 years 06 p0821 N85-15215
Asteroid-meteorite connection: Regolith effects implied by lunar reflectance spectra 06 p0868 N85-15840
Laser spectroscopy of alkali atom-tetrahaloethylene reactions
[AD-A147431] 07 p0923 N85-15848
Design of an analog spectrum analyzer for probing experiments
[AD-A147384] 07 p0941 N85-15963
Power spectrum analysis of astronomical photographs digitised with small apertures 07 p0965 N85-16127
Bragg cell spectrum analyzer specification
[AD-D011320] 07 p1044 N85-16629
Data analysis techniques for vehicle attitudinal, positional and experimental measurements
[AD-A147752] 08 p1188 N85-17484
Shock response analysis by personal computer using the extended IFT algorithm 09 p1335 N85-18397
Initialization of Thompson-Pisarenko's algorithm — sinusoidal signal parameter estimation
[FUB-48-1983] 09 p1375 N85-18641
Confinement of low-energy electrons near metallic surfaces for plasmon generation
[DE85-001119] 09 p1381 N85-18668
Radiation data and standards for Tokamak diagnostics 09 p1390 N85-18742
Relative-entropy minimization with uncertain constraints--theory and application to spectrum analysis
[AD-A149192] 10 p1546 N85-19752
White dwarf stars at ultraviolet wavelengths 11 p1744 N85-20971
Analysis of white dwarf Lyman alpha profiles 11 p1752 N85-21018
Ultraviolet observations of Population 2 Cepheids 11 p1754 N85-21034
LSS 2018: A double-lined spectroscopic binary central star with an extremely large reflection effect
[NASA-CR-175503] 11 p1762 N85-21082
Pseudospectral calculations of two-dimensional transonic flow (Task 1). Numerical investigation of VTOL aerodynamics (Task 2)
[AD-A150123] 12 p1772 N85-21126
Effects of scatterer spacing statistics on ultrasonic backscatter signal spectra
[DE85-003259] 12 p1928 N85-22114
Research in particles and fields
[NASA-CR-175472] 12 p1963 N85-22337
Spectra of incidental interference resulting from nonlinear conversion of signals from transmitters 13 p2073 N85-22950
Efficiency of multitarget signal detection by digital radar data processing devices 13 p2080 N85-22991
Accuracy of random signal spectral parameter estimation against interference background in acoustooptical spectrum analyzers 13 p2090 N85-23052
Determining vector of radiointerferometer base from observations of natural radio emission with narrow spectrum 13 p2112 N85-23158
Relationship between brightness spectrum of photographic image and spectrum of rises on a water surface with waves 13 p2115 N85-23171
Sulfur oxygen processes on Io 13 p2173 N85-23481
Photometric analysis of Jupiter-illuminated images of Io 13 p2196 N85-23820
Maximum entropy spectral analysis
[LEOK-TR-1984-08] 14 p2299 N85-24235
Dynamic spectra of mean monthly values of geomagnetic field elements based on spectral-time analysis data 14 p2344 N85-24496
Remote sensing of directional wave spectra using the surface contour radar
[NASA-TM-84440] 14 p2347 N85-24510
A structural classification of geomagnetic pulsations 14 p2371 N85-24657

The use of the spectral matrix in analyzing the propagation characteristics of electromagnetic emissions — magnetosphere 14 p2371 N85-24658
Magnetospheric wave characteristics derived from cross-spectral analysis 14 p2371 N85-24659
Observations of intermediate-degree solar oscillations 14 p2442 N85-25069
Spectral analysis of diurnal nonuniformity of Earth's rotation 15 p2477 N85-25269
Analysis of spectral characteristics of multilevel digital computing synthesis 15 p2527 N85-25579
Possible uses of tunable diode lasers in infrared spectroscopy
[ESA-TT-869] 15 p2564 N85-25818
A calorimetric approach for measuring emittance and normal spectral absorptance at elevated temperatures
[AD-A151292] 15 p2651 N85-26351
User manual for IMAGER: The DREO (Defence Research Establishment Ottawa) image processing system
[AD-A151754] 15 p2653 N85-26362
Saturn's E-ring in the red spectral region 15 p2671 N85-26480
Asteroid amphibia: Surface composition and prospects for the possible Galileo flyby 15 p2680 N85-26549
Spectral characteristics of protons at low and high altitudes during geomagnetic storm of 29 July 1977 16 p2719 N85-26786
Multiple regression analysis of photographic image of soil properties 16 p2726 N85-26825
Spectroscopic studies of a railgun muzzle flash
[MRL-R-952] 16 p2728 N85-26937
A phase modulation evaluation procedure for an ARGOS type signal 16 p2811 N85-27396
Development of a modified time delay spectrometry technique for underwater acoustic measurements in a multipath environment
[AD-A152111] 16 p2860 N85-27639
Variability of short term eddy-correlation estimates of mass exchange
[PB85-172641] 18 p3138 N85-29431
Solar monochromatic images in magneto-sensitive spectral lines and maps of vector magnetic fields 16 p3207 N85-29697
Separation of Drude and ba.nd-to-band spectra in polyvalent metals
[DE85-010247] 19 p3240 N85-30093
Explosibility of ammonium nitrate
[HSE-TRANS-11111] 19 p3252 N85-30164
Sea water photoluminescence 19 p3292 N85-30415
Comparison of 8 to 12 micrometer and 3 to 5 micrometer CVF transmissometer data with LOWTRAN calculations
[AD-A154216] 19 p3350 N85-30763
Analysis of ferrates and ferrites of three transition metals using Mossebauer effects
[BLL-CE-TRANS-8019-(0022.00)] 20 p3430 N85-31273
Spectral evolution of the pulse of a dual frequency dye laser
[CNES-83/168/T/CT/DRT/TIT/10] 20 p3461 N85-31497
Lightcurve CCD spectrophotometry of Pluto 20 p3545 N85-32057
High resolution evidence for the Garrett-Munk spectrum of stratospheric gravity waves 21 p3622 N85-32503
A relationship between cloud droplet size and CCN critical supersaturation 21 p3649 N85-32677
In-cavity laser IR spectrum analyzer for investigating non-steady-state processes 21 p3685 N85-32894
Spectral-luminescence characteristics and induced emission of Nd-3(+) ion in Gd(2-x)Nd(x)(WO4)3 crystals 21 p3688 N85-32912
Doppler spectrometer for measuring narrow photochemical gaps in inhomogeneously broadened spectra 21 p3689 N85-32921
A balloon-borne imaging gamma-ray telescope
[OG-6.2-2] 21 p3714 N85-33049
Transmitter spectrum analyzer 22 p3774 N85-33389
Binary signal detection in acoustooptic receivers 22 p3782 N85-33430
Acetonitrile in the Earth's atmosphere: An upper limit deduced from infrared solar spectra
[AERONOMICA-ACTA-A-295-1985] 22 p3813 N85-33623
Spectra and positions of galactic gamma-ray sources
[OG-2.5-7] 22 p3869 N85-33963
The universal spectrum of AGNs and QSOs
[OG-2.7-9] 22 p3872 N85-33982
Spectral shape variation of interstellar electrons at high energies
[OG-6.2-7] 22 p3889 N85-34106
On the cosmic ray diffusion in a violent interstellar medium
[OG-7.2-14] 23 p4015 N85-34881
Study of spectral exponent on quiet and disturbed days
[SH-4.5-10] 23 p4037 N85-35028
Spectral analysis of the Forbush decrease of 13 July 1982
[SH-5.1-7] 23 p4042 N85-35061
Proton albedo spectrum observation in low latitude region at Hyderabad, India
[SH-6.1-8] 23 p4045 N85-35082
The application of bispectral analyses to aeroelastic phenomena 24 p4080 N85-35157
The spectrum of cosmic ray muons obtained with 100-ton scintillation detector underground and the analysis of recent experimental data
[HE-5.1-6] 24 p4201 N85-36071

SPECULAR REFLECTION
TM digital image products for applications 11 p1668 N85-20512
Diffraction-limited imaging of space objects 2
[AD-A149344] 11 p1728 N85-20870
Research in image understanding as applied to 3-D tomographic imaging with near optical resolution
[AD-A150098] 12 p1829 N85-21483
Surface forward scattering and reflection
[AD-A150115] 12 p1928 N85-22112
Scheme for measuring specular reflection coefficient at 10.6 microns wavelength with zigzag-path cell and integrating sphere 14 p2275 N85-24097
Aspects of SAR image segmentation
[AD-A154965] 21 p3575 N85-32236
Signal space models for antenna arrays
[AD-A156063] 24 p4087 N85-35335

SPEECH
NT CONVERSATION
NT PHONEMES
NT PHONETICS
NT TALKING
NT WORDS (LANGUAGE)
Status report on speech research. A report on the status and progress of studies on the nature of speech, instrumentation for its investigation, and practical applications
[AD-A145585] 02 p0191 N85-11277
Rech-1 speech synthesizer for man-machine dialog 04 p0543 N85-13456
A comparative study of alternative controls and displays for by the severely physically handicapped 05 p0709 N85-14549
Fast algorithms and specialized architectures 05 p0714 N85-14579
Speech-action interrelationships in operational work 07 p1010 N85-16418
Low-bit rate speech encoders based on Line-Spectrum Frequencies (LSF)
[AD-A150518] 13 p2056 N85-22871
Comparative architectures for a multiple function speech processor
[AD-A150673] 14 p2292 N85-24211
A preliminary investigation into the intelligibility of Microspeech-2, a speech synthesiser
[BAE-BT-12284] 15 p2539 N85-25675
Speech understanding research
[AD-A155482] 21 p3700 N85-32990

SPEECH DISCRIMINATION
U SPEECH RECOGNITION

SPEECH RECOGNITION
A review of selected studies of computerized speech recognition conducted at the Naval Postgraduate School
[AD-A144841] 01 p0037 N85-10235
Classification methods for Italian vowels — speech recognition
[FUB-61-1982] 01 p0039 N85-10248
Description of a semiannual selection procedure of vowel parts of the voice signal using a PDP 11/34 computer
[FUB-4-1983] 01 p0039 N85-10250
Determination of vowel zones in speech — speech recognition
[FUB-16-1983] 01 p0040 N85-10253
Vowel phoneme identification in speech
[FUB-26-1983] 01 p0040 N85-10257
Voice phonetic coding and decoding processes
[FUB-29-1983] 01 p0040 N85-10259
Comparative analysis of the clustering of the LPC coefficients in phoneme recognition
[FUB-39-1983] 01 p0041 N85-10264
Autoregressive nonsteady methods for the analysis and synthesis of the human voice
[FUB-3-1984] 01 p0041 N85-10266
Measures of distance between speech signals in the frequency domain — speech recognition
[FUB-5-1984] 01 p0041 N85-10267
Royal Signals and Radar Establishment speech database recordings 1983: Part 2: Recordings made for automatic speech recognition assessment and research
[RSRE-84008-PT-2] 02 p0190 N85-11267
Identification as a function of familiarity for known voices talking over an unprocessed channel and an LPC (Linear Predictive Coding) voice processor
[AD-A145545] 02 p0191 N85-11278
Implications of artificial intelligence for a user defined technical information system
[AD-P003938] 02 p0248 N85-11618
Wideband integrated voice/data technology
[AD-A146054] 03 p0355 N85-12283
Rech-1 speech synthesizer for man-machine dialog 04 p0543 N85-13456
Tests of the automatic recognition of words spoken by different voices based on collected groups of model binary spectrograms
[ISSN-0208-5658] 05 p0822 N85-13977
VOTAN V5000 speech recognition system performance test report
[AD-A146726] 07 p0939 N85-15950
Literature review of voice recognition and generation technology for Army helicopter applications
[AD-A146878] 07 p0939 N85-15954
Compository speech output (KOSA) with a very large scale integration speech synthesis chip
[FI-13-TBR-18] 07 p0942 N85-15974
Man-machine communication research for robotics reported 08 p1139 N85-17177
Automatic speech recognition in severe environments
[AD-A148481] 08 p1153 N85-17280
A voice-actuated wind tunnel model leak checking system
[NASA-TM-86359] 09 p1263 N85-17936
Speech analysis by parametric methods: A survey
[ENST-84C004] 09 p1313 N85-18251
Overview of leading-edge research at French CNRS lab 11 p1618 N85-20179
Automatic speech recognition in severe environments
[PB85-121697] 12 p1830 N85-21480
Research in continuous speech recognition
[AD-A150474] 13 p2055 N85-22868
Preliminary assessment of the Heuristics H2000 speechlink - speech recognition device — voice data input for Apple 2 computer
[BAE-BT-12276] 15 p2539 N85-25674
A preliminary investigation into the intelligibility of Microspeech-2, a speech synthesiser
[BAE-BT-12284] 15 p2539 N85-25675
A review of speech systems
[BAE-BT-12285] 15 p2539 N85-25676
An introductory study of automatic speech recognition systems
[BAE-BT-12286] 15 p2539 N85-25677
Automation of the process of speech signal segmentation in an analogic-numeric system
[REPT-5/1984] 16 p2768 N85-27062
Implementation of a real-time, interactive, continuous speech recognition system
[AD-A151936] 16 p2773 N85-27117
Evaluating syntactic constraints to speech recognition in a fighter aircraft environment
[AD-A152117] 16 p2773 N85-27119
Wideband integrated voice/data technology
[AD-A152329] 17 p2947 N85-28197
A study of error rates in voice recognition
[AD-A153282] 17 p2949 N85-28211
Study to determine potential flight applications and human factors design guidelines for voice recognition and synthesis systems
[NASA-CR-172590] 20 p3440 N85-31349
A classification vocoder: A very low rate speech transmission by vector quantization of the spectrum
[ENST-84D003] 20 p3441 N85-31350
Speech analysis system for assessing pilots' working fitness 22 p3819 N85-33661

SPEECHES
U LECTURES

SPEED
U VELOCITY

SPEED CONTROL
Use of braking stages for control of turbine speed 09 p1308 N85-18215
Feasibility demonstration of a novel, flat-belt, continuously variable transmission or automotive and electric-hybrid vehicle application
[NASA-CR-174430] 10 p1569 N85-19694
Cost comparison of small gas turbines versus electric motors in a variable load industrial application
[PB85-149783] 12 p1837 N85-21530
Pulsewidth modulated speed control of brushless dc motors
[AD-A151966] 16 p2778 N85-27148
Experimental investigation of a variable speed constant frequency electric generating system from a utility perspective
[NASA-CR-174950] 21 p3579 N85-32251

SPEED INDICATORS
NT ANEMOMETERS
NT HOT-FILM ANEMOMETERS
NT HOT-WIRE ANEMOMETERS
NT LASER ANEMOMETERS
NT TACHOMETERS
Airspeed sensing pressure valve system
[AD-D011472] 10 p1425 N85-18987
Miniature electrooptical air flow sensor
[NASA-CASE-LAR-13065-1] 11 p1635 N85-20295
Metrological support for remote transport vehicle speedometers 13 p2076 N85-22963
Digital tachometer 22 p3779 N85-33416
Development of contactless sensors for industrial and automative applications
[BMFT-FB-T-85-031] 24 p4097 N85-35400
SPEED REGULATION
U SPEED CONTROL
SPEED REGULATORS
Speed governor for diesel engine 09 p1307 N85-18214
Investigation of doubly-fed machine in variable speed application
[DE85-004378] 14 p2299 N85-24234
SPEEDOMETERS
U SPEED INDICATORS
SPENT FUELS
Integrated data base program: A status report
[DE84-013604] 05 p0735 N85-14727
Corrosion performance of metals and alloys in a tuff geochemical environment
[DE85-009449] 18 p3077 N85-29033
Binary phase diagram determinations
[DE85-010856] 19 p3235 N85-30058
Experimental program to determine maximum temperatures for dry storage of spent fuel
[DE85-010307] 19 p3236 N85-30060
Physical and chemical changes to rock near electrically heated boreholes at Spent Fuel Test-Climax
[DE85-010834] 19 p3302 N85-30472
Consolidated fuel reprocessing program
[DE85-010591] 19 p3358 N85-30818
Source Term Experiments Project (STEP): Aerosol characterization system
[DE85-010248] 19 p3361 N85-30839
Consolidated fuel reprocessing program
[DE85-008750] 19 p3368 N85-30871
Office of Civilian Radioactive Waste Management
[DE85-012565] 22 p3639 N85-33774
Analytical methods in the purex process
[BLL-DOUNREAY-TR-952(9091.9F)] 24 p4149 N85-35727
SPERMATOCYTES
U GAMETOCYTES
SPERMATOGENESIS
Mammalian tissue sensitivity to long-term exposure to high-intensity stationary magnetic fields 22 p3823 N85-33686
SPHERES
NT CELESTIAL SPHERE
NT CONCENTRIC SPHERES
NT FALLING SPHERES
NT POINCARE SPHERES
NT ROTATING SPHERES
Elastic fields under a spherical indenter
[AD-A146519] 06 p0817 N85-15188
The resistance and mobility functions of two equal spheres in low Reynolds number flow
[AD-A147301] 07 p0959 N85-16080
Temperature prediction in mechanical components, an analytical approach 09 p1327 N85-18339
On detached shock wave of sphere moving with transonic velocities 11 p1622 N85-20215
Optimization of pressure vessels with standard intercepting spheres
[INPE-3276-PRE/600] 11 p1651 N85-20397
Scheme for measuring specular reflection coefficient at 10.6 microns wavelength with zigzag-path cell and integrating sphere 14 p2275 N85-24097
A counterpart of Faxen's formula in potential flow
[REPT-84-09] 17 p2950 N85-28279
Multiple equilibria of the barotropic vorticity equation on a sphere 18 p3146 N85-29475
Method of measuring spherical aberration and apparatus therefor
[AD-D011706] 19 p3367 N85-30882
Solid-state resistance welding cylinders and spheres
[DE85-010084] 20 p3489 N85-31555
SPLINES. Their equivalence to collocation
[AD-A155250] 21 p3632 N85-32568
Combustion-deflagration-detonation transition in a confined spherical powder
[ISL-R-109/84] 22 p3747 N85-33223
Thermal transport measurements of UV laser irradiated spherical targets
[DE85-011038] 23 p3931 N85-34365
Improved flow cytometer measurement of binding assays
[DE85-006407] 23 p3935 N85-34390
SPHERICAL CAPS
Estimation of the depth of a spherical cap in an hydraulic drawing test for some simple conditions of loss of stability
[REPT-4/1984] 16 p2748 N85-26956
SPHERICAL COORDINATES
Comparison of the multigrid and ICCG methods in solving the diffusion equation
[DE84-014409] 02 p0253 N85-11657
Convection schemes for use with curvilinear coordinate systems: A survey
[AD-A147093] 07 p1031 N85-16543
Solution of direct magnetometric problem on spherical Earth 13 p2116 N85-23179
Global coordinate system
[AD-A153878] 19 p3299 N85-30454
Evaluation of coordinate measuring machines
[DE85-011712] 22 p3788 N85-33467
Algorithm for calculation of strain state from measurements of node coordinates of arbitrary curvilinear grid
[BLL-M-36304-(5828.4)] 23 p3940 N85-34422
SPHERICAL HARMONICS
Advantages and limitations of spherical harmonic analyses of geomagnetic data 04 p0519 N85-13318
Geomagnetic secular variation: A jerk in 1970 04 p0521 N85-13329
Comparisons of secular variation in two-dipole and spherical harmonic models with observatory data in Eurasia, 1965-1975 04 p0521 N85-13330
Algorithm for space-time analysis of data on geomagnetic field
[NASA-TM-77804] 08 p1209 N85-17609
Non-radiative energy from differential rotation in hot stars 08 p1234 N85-17778
Isolated systems in general relativity 09 p1400 N85-18813
Time dependent interaction of internal pressure wave with system of two spherical shells 13 p2046 N85-22809
Venus gravity: Global field results 13 p2177 N85-23512
Potential models — Earth gravity 14 p2396 N85-24784
Error spectrum of Goddard satellite models for the gravity field 20 p3491 N85-31704
Characteristics of cosmic ray pole-equator anisotropy derived from spherical harmonic analysis of neutron monitor data
[SH-4.3-12] 23 p4032 N85-34996
Sidereal anisotropy of cosmic rays
[SH-4.4-6] 23 p4034 N85-35006
SPHERICAL PLASMAS
Ion velocity distributions from spherical 1054 nm and 351 nm laser plasmas
[DE85-002816] 10 p1559 N85-19833
Magnetohydrodynamic equilibrium and stability of spheromak with spheroidal plasma-vacuum interface
[IPPJ-732] 23 p3974 N85-34640
SPHERICAL SHELLS
NT SPHERICAL CAPS
Experimental investigation and analysis of oscillations of thin-walled spherical shell during pulse loading 05 p0725 N85-14662
Resonant scattering of acoustic waves by elastic spherical shell in fluid 06 p0778 N85-14972
Tests of the load-bearing and deformation behaviour of reinforced concrete spherical shells under point loading
[BLL-RISLEY-TR-4550-9091.9F)] 06 p0816 N85-15182
Ultrasonic analysis of spherical composite test specimens
[DE85-001591] 07 p0976 N85-16197
Finite element analysis of nonlinear oscillations and flutter of shells of revolution
[AD-A149071] 10 p1496 N85-19440
Radiographic inspection of butt welds described 11 p1620 N85-20198
Time dependent interaction of internal pressure wave with system of two spherical shells 13 p2046 N85-22809
Nonlinear behavior and stability of thin spherical shells subjected to non-axisymmetrical loading 13 p2048 N85-22821
Intensity vectors of sound scattering by a spherical shell
[AD-A147847] 13 p2103 N85-23107
Effect of axisymmetric vibration modes on sensitivity and directivity characteristics of piezoceramic sphere — hydrophones 15 p2525 N85-25569
Natural vibrations of reinforced spherical shells 17 p2943 N85-28165
Finite elastic deformations of cylindrical and spherical shells under pressure
[OUEL-1549/84] 20 p3470 N85-31559
A mixed pseudospectral/finite difference method for a thermally driven fluid in a nonuniform gravitational field
[NASA-TM-87581] 22 p3783 N85-33436
The effect of power law body forces on a thermally-driven flow between concentric rotating spheres
[NASA-TM-87596] 24 p4093 N85-35374
SPHERICAL WAVES
Design criteria for limited scan antennas at digital microwave line of sight links 10 p1471 N85-19284
Comparison of spherical wave ray tracing and exact boundary value solutions for spherical radomes
[AD-P004353] 12 p1824 N85-21447
Sphericity gauge for wavefront of laser radiation 14 p2275 N85-24096
SPHEROIDS
NT OBLATE SPHEROIDS
Sedimentation of two arbitrarily oriented spheroids in a viscous fluid
[AD-A147303] 07 p0960 N85-16082
Milling of spherical zones in parts 14 p2266 N85-24041
Spheroidal functions: Properties and tabulation. Application to antenna synthesis 14 p2396 N85-24758
Wall effect on lateral migration of spherical particles in a linear shear flow 20 p3452 N85-31432
SPHEROMAKS
Compact toroid development, activity plan for spheromaks
[DE84-016736] 04 p0567 N85-13817
Proceedings of the US-Japan Theory Workshop on 3-D MHD Studies
[DE84-012019] 04 p0568 N85-13820
Magnetohydrodynamic stability of spheromak plasma in toroidal flux conserver with rectangular cross section
[IPPJ-716] 16 p2966 N85-27678
Steady-state spheromak reactor studies
[DE85-009585] 19 p3372 N85-30916
Los Alamos Spheromak Program
[DE85-010748] 20 p3398 N85-31077
Confinement and heating of high beta plasma with emphasis on compact toroids. Compact toroid research
[DE85-011463] 22 p3846 N85-33621
SPHERULES
Neutron activation analysis of stoney spherules from a marine sediment sample 06 p0863 N85-15608
Oxygen isotopes in deep sea spherules 06 p0863 N85-15609
Peculiar spherules from Antarctica and their origin 06 p0863 N85-15612
Fractionation of siderophiles in cosmic spherules and its implications 06 p0864 N85-15613
Survey of probable micrometer-sized Earth-orbital debris fragments in the NASA-JSC cosmic dust sample collection 12 p1785 N85-21203
SPICULES
Spicules and surges
[AD-A146785] 07 p1061 N85-16727
SPIDERS
Gravity perception and cardiac function in the spider 15 p2606 N85-26058
SPIKE ANTENNAS
U MONOPOLE ANTENNAS
SPILLING
Penetration of the atmosphere by flammable mixtures as a result of spillage of LNG on the ground 06 p1179 N85-17432
Methods/materials matrix of ultimate disposal techniques for spilled hazardous materials
[PB85-116853] 12 p1865 N85-21833
Hydrocarbon pool and vapor fire data analysis
[DE85-005857] 15 p2523 N85-25550
Facility for large-scale hazardous gas testing
[DE85-011852] 21 p3584 N85-32169
Description of a test site for large-scale heavy gas dispersion and combustion experiments
[DE85-004987] 23 p3911 N85-34231
Evaluation of source strength and dispersion model predications with data from large nitrogen tetroxide field experiments
[DE85-011855] 23 p3947 N85-34485
MATADOR (Methods for the Analysis of Transport And Deposition Of Radionuclides) code description and user's manual
[TI85-901402] 23 p3986 N85-34592
SPIN
NT ELECTRON CAPTURE
NT ELECTRON SPIN
NT METAL SPINNING
NT NUCLEAR SPIN
NT PARTICLE SPIN
NT SPIN-ORBIT INTERACTIONS
NT SPIN-SPIN COUPLING

Theory of nuclear magnetic relaxation
[AD-P003911] 01 p0032 N85-10197
Analysis of spin echo signals in multi-pulse experiment
06 p0792 N85-15065
A method for estimating the rolling moment due to spin rate for arbitrary planform wings
[NASA-TM-86365] 10 p1425 N85-18990
Thermal traction contact performance evaluation under fully flooded and starved conditions
[NASA-CR-168173] 15 p2568 N85-25848
Spin distributions in heavy ion fusion at and below the Coulomb barrier
[DE85-007817] 17 p3031 N85-28751
Magnetic impurities in superconductors
[DE85-008372] 18 p3196 N85-29825
Neutron scattering study of the heavy fermion system UBe-13
[DE85-010955] 19 p3358 N85-30804

SPIN DYNAMICS
Moment induced by liquid payload during spin-up without a critical layer
[AD-A145716] 02 p0199 N85-11327
Liquid payload moment equations
[AD-A145977] 03 p0362 N85-12319
Application of quantum chemistry of atmospheric chemistry
[AD-A147035] 07 p0922 N85-15843
Theoretical issues involving traps for neutral spin-polarized atoms
[AD-A148035] 08 p1220 N85-17682
Magnetic excitation in CuMn spin glass alloy
[DE85-002564] 10 p1453 N85-19159
Liquid moment on a filled coning cylinder during spin-up: Ad hoc model
[AD-A150290] 13 p2092 N85-23060
Observation of a novel low-lying excited state in zinc complexes
[AD-A150188] 13 p2156 N85-23365
Polar motions measurement study
[AD-A150690] 14 p2372 N85-24664
Theoretical and experimental studies of stabilized metastable helium
[AD-A150706] 14 p2417 N85-24913
Flight investigation of stall, spin and recovery characteristics of a low-wing, single-engine, T-tail light airplane
[NASA-TP-2427] 15 p2470 N85-25248
Use of quaternions in flight mechanics
[AD-A152616] 17 p2899 N85-27875
Lattice actions improved by block-spin renormalisation group and maximally symmetric lattices
[DE85-007416] 17 p3045 N85-28841
Modifications to SOLA-VOF for flow dynamics in spinning cylinders
[AD-A154093] 19 p3265 N85-30250
NMR investigation of crystalline electric field effect on spin-spin relaxation in (Y(1-x)RE(x))Rh4B4
[DE85-010512] 19 p3357 N85-30814
Electron-atom collision studies using optically state selected beams
[DE85-010848] 19 p3368 N85-30888
Spin physics at BNL
[DE85-009766] 20 p3529 N85-31955
Dual towline spin-recovery device
[NASA-CASE-LAR-13076-1] 24 p4066 N85-35200
Studies of the solar mesosphere explorer: Dynamics and horizon sensor performance. Part A: Spin axis precession and atmospheric drag. Part B: Clouds
[NASA-CR-175308] 24 p4089 N85-35213
The NORDA/FNOC (Naval Ocean Research and Development Activity's/Fleet Numerical Oceanography Center) Polar Ice Prediction System (PIPS)-Arctic: A technical description
[AD-A156332] 24 p4126 N85-35577

SPIN EXCHANGE
Polarized internal target apparatus
[DE85-011611] 19 p3354 N85-30793
Electron-atom collision studies using optically state selected beams
[DE85-010848] 19 p3368 N85-30888

SPIN FORMING
U METAL SPINNING

SPIN GLASS
Magnetic excitation in CuMn spin glass alloy
[DE85-002564] 10 p1453 N85-19159
Microstructural and electronic characteristics of metallic spin glasses
[AD-A149959] 12 p1813 N85-21371
Coexistence of antiferromagnetism and spin-glass ordering in the Ising system FeO 55MgO 45Cl2
[DE85-004164] 12 p1942 N85-22197
A numerical investigation of the overlap distribution among pure states in the spin glass phase
[PREPRINT-414] 18 p3172 N85-29659

SPIN REDUCTION
Magnetic spin reduction system for free spinning objects
[NASA-CASE-MFS-25966-1] 02 p0166 N85-11122

SPIN RESONANCE
Dangling bonds and sub-gap optical absorption in silicon
[DE85-011752] 24 p4082 N85-35302

SPIN STABILIZATION
Use of gravitational stabilization in performance of experiments 02 p0160 N85-11084
Hypothetical zero yaw drag trajectory of spinning projectiles between M = 5 and M = 10
[AD-A148899] 10 p1421 N85-18983
Non-contacting electromagnetic de-spin system for Earth orbiting satellites 12 p1946 N85-22225

SPIN WAVES
U MAGNONS

SPIN-LATTICE RELAXATION
Nuclear Magnetic Resonance of Polymeric Materials
[AD-A145078] 01 p0032 N85-10192
13C and 1H NMR (Nuclear Magnetic Resonance) studies of solid polyolefines
[AD-P003909] 01 p0032 N85-10195
Paramagnetic impurity effects in NMR determinations of hydrogen diffusion and electronic structure in metal hydrides. Cerium in YH-2 and LaH-2.25
[DE84-014127] 04 p0472 N85-13005
Anisotropy and relaxation effects of Co2+ ions in LiTi ferrite
[AD-A146550] 06 p0861 N85-15469
Proton NMR and susceptibility measurements in TiCoH/sub x
[DE85-003309] 12 p1807 N85-21336
NMR investigation of crystalline electric field effect on spin-spin relaxation in (Y(1-x)RE(x))Rh4B4
[DE85-010512] 19 p3357 N85-30814

SPIN-ORBIT INTERACTIONS
NT ELECTRON CAPTURE
Magnetic alignment theory and the interpretation of polarization 06 p0880 N85-15590
Inter-zone auger recombination in GaSb laser structures 21 p3682 N85-32875

SPIN-SPIN COUPLING
Novel transport and recombination processes in semiconductors
[AD-A145869] 03 p0433 N85-12757
Vacancy-rearrangement theory in the first Magnus approximation
[DE85-004435] 12 p1930 N85-22123
Finite-perturbation intermediate neglect of differential overlap molecular orbital calculations of nuclear magnetic resonance spin-spin coupling constants for polycyclic aromatic hydrocarbons and aromatic nitrogen heterocyclics
[NASA-TM-87466] 20 p3525 N85-31927

SPINAL CORD
NT SPINE
The position and mobility of the shoulder, spinal column and pelvis in seated subjects
[AD-A153751] 18 p3153 N85-29524

SPINE
An investigation of spinal injury potential from the use of the ACES 2 ejection seat by lower weight female pilots
[AD-A148449] 08 p1196 N85-17537
The clinical and radiological assessment of cervical injury, Annex A 12 p1907 N85-21976

SPINEL
A physical interpretation of the structure and electron-optical data for spinel (MgAl2O4)
[AERE-R-11278] 03 p0434 N85-12767
Anisotropy and relaxation effects of Co2+ ions in LiTi ferrite
[AD-A146550] 06 p0861 N85-15469
Defective nature of the crystalline lattice of nickel ferrite-based solid solutions
[BLL-TRANS-WH-595-(9091.9F)]
10 p1439 N85-19068
Magnetic and structural properties of shock-synthesized zinc ferrite
[DE85-000469] 11 p1736 N85-20915
Oxygen evolution on NiCo2O4 electrodes
17 p2924 N85-28026
Integrated current collector and catalyst support
[DE85-011616] 22 p3761 N85-33311

SPINNING (METALLURGY)
U METAL SPINNING

SPINOR GROUPS
Solutions of field equations in General Relativity with spinor connection 15 p2663 N85-26436

SPIRAL ANTENNAS
Design and measured performance of a broadband Archimedes spiral antenna
[R-NIAS-22] 14 p2290 N85-24194
Radiation and scattering of spiral antennas
[AD-A151929] 16 p2773 N85-27116

SPIRAL GALAXIES
NT BARRED GALAXIES
NT MILKY WAY GALAXY
Molecules in external galaxies
03 p0444 N85-12828
The galactic distribution of open clusters of different ages and the angular velocity of the spiral structure
05 p0737 N85-14737
Excitation of spiral patterns in responsible density wave theory 05 p0740 N85-14764
The correlation between excitation parameter and nebular luminosity for galactic HII regions with application to regions of star formation in M33
05 p0743 N85-14773
The IRAS galaxy 0421+040P08: An active spiral (?) galaxy with extended radio lobes
[NASA-CR-174208] 06 p0871 N85-15536
Large-scale bubble structure of the interstellar medium (ISM) and properties of the Local Spiral Arm (LSA)
06 p0879 N85-15588
A comparison of some photometric parameters of active and normal spiral galaxies 08 p1238 N85-17806
Dust reradiation from NGC 6946
08 p1248 N85-17880
The structure and dynamics of ringed galaxies
09 p1415 N85-18926
On the morphology of spiral modes --- disk galaxies
12 p1955 N85-22283
On a spectral theory of the excitation mechanism of galactic spirals 12 p1955 N85-22284
Drift-accretion theory of the spiral structure of galaxies
12 p1957 N85-22298
Some constraints on magnetic fields in galactic spiral arms 12 p1957 N85-22300
The hydrodynamic effects of nuclear active galaxy winds on host galaxies 20 p3545 N85-32082
The galactic gamma-ray distribution and the radial cosmic ray gradient
[OG-3.1-4] 22 p3873 N85-33992
Halo of NGC 4631 and models of cosmic-ray transport
[OG-6.2-3] 22 p3889 N85-34103

SPIRAL WRAPPING
Generated spiral bevel gears: Optimal machine-tool settings and tooth contact analysis
[NASA-TM-87075] 23 p3937 N85-34405

SPLEEN
Distinctions of rat lymphatic organ reactions to acute stress factor during hypokinesia
19 p3324 N85-30596

SPLINE FUNCTIONS
Spline-Galerkin solution of integral equations for 3-body scattering above break-up
[TWISK-327] 01 p0109 N85-10738
Approximation methods for inverse problems involving the vibration of beams with tip bodies
[NASA-CR-172468] 02 p0209 N85-11379
Nonlinear regression with emphasis on spline methods
[AD-A146192] 03 p0412 N85-12633
Application of summability methods to Jackson theorems for splines
[AD-A146256] 03 p0412 N85-12635
Least squares spline regression with block-diagonal variance matrices
[NPL-DITC-40/84] 04 p0554 N85-13523
Multivariate spline methods in surface fitting
07 p0965 N85-16257
A counterexample to a result of Strang and Fix concerning controlled approximation
[AD-A147360] 07 p1032 N85-16550
The stable evaluation of multivariate b-splines
[AD-A147386] 07 p1032 N85-16551
Spline methods for approximating quantile functions and generating random samples
[NASA-TP-2369] 07 p1035 N85-16565
Some qualitative properties of bivariate Euler-Frobenius polynomials
[AD-A149408] 10 p1547 N85-19755
Scattered data interpolation using thin plate splines with tension
[AD-A149603] 12 p1866 N85-21705
A two-dimensional smoothing spline and a regression problem
[AD-A149624] 12 p1921 N85-22067
Spline-based Rayleigh-Ritz methods for the approximation of the natural modes of vibration for flexible beams with tip bodies
[NASA-CR-172566] 13 p2102 N85-23100
Primary processing of experimental magnetovariation sounding data using spline functions
13 p2115 N85-23175
Spline techniques for magnetic fields
[DE85-004919] 14 p2415 N85-24902
The nonlinear analysis of thick composite plates using a cubic spline function 16 p2798 N85-27252

Noise correction on LANDSAT images using a spline-like algorithm
[E85-10098] 16 p2808 N85-27319
An interpolation method with the possibility of first derivative correction
[INPE-3352-PRE/631] 16 p2853 N85-27590
Surface interpolation using weighted splines
[INPE-3387-PRE/658] 16 p2853 N85-27591
Shape preserving spline interpolation 17 p3003 N85-28564
Multivariate spline algorithms for CAGD 17 p3003 N85-28566
Examination of the circle spline routine 17 p3004 N85-28573
Convex interpolating splines of arbitrary degree 17 p3004 N85-28574
A natural bias approach to cardinal spline curves 17 p3004 N85-28575
An intuitive approach to geometric continuity for parametric curves and surfaces (extended abstract) 17 p3005 N85-28579
Um models and beta-splines 17 p3005 N85-28580
Computer programs for smoothing and scaling airfoil coordinates
[NASA-TM-84666] 20 p3388 N85-31011
Combined state and parameter estimation for a static model of the Maypole (Hoop-Column) antenna suface 20 p3417 N85-31210
SPLINES. Their equivalence to collocation
[AD-A155250] 21 p3632 N85-32566
An intuitive approach to geometric continuity for parametric curves and surfaces 23 p3963 N85-34571
Smoothing surface data by spline functions
[AD-A156629] 24 p4142 N85-35678

SPLINES
Control of rotordynamic instability in a typical gas turbine's power system 05 p0642 N85-14120
Controlled approximation and a characterization of the local approximation order
[AD-A149095] 10 p1546 N85-19750
The definition and computation of a metric on plane curves. The meaning of a face on a geometric model 17 p3004 N85-28571
Spline curves, wire frames and B-value 17 p3006 N85-28587
A robust estimator of location using an adaptive spline model
[AD-A153662] 18 p3174 N85-29676
SPLINES. Their equivalence to collocation
[AD-A155250] 21 p3632 N85-32566

SPLITS (GEOLOGY)
U GEOLOGICAL FAULTS

SPLITTING
Splitting methods for the numerical solution of the incompressible Navier-Stokes equations
[AD-A147463] 07 p1032 N85-16554
Photosynthetic water splitting
[DE85-002460] 11 p1680 N85-20627
Alternative anodic reactions in water splitting
[DE85-004159] 12 p1802 N85-21300
Longitudinal splitting in unidirectional composites, analysis and experiments
[NASA-CR-3881] 13 p2015 N85-22939
Analysis and interpretation of synthetic time strings of oscillation data 14 p2444 N85-25079
Fracture mechanics analysis of cold drawn SI-Cr valve steel
[BLL-BISI-TRANS-22216-(9022.06)] 17 p2978 N85-28405
Study of solute segregation at interfaces using Auger electron spectroscopy
[DE85-005709] 20 p3423 N85-31247

SPOILERS
Investigations on the dynamic loading of wind energy converters with vertical axis and problems of control during starting and overload conditions
[BMFT-FB-T-84-155] 03 p0386 N85-12472
An experimental study of airfoil-spoiler aerodynamics
[NASA-CR-177328] 06 p0748 N85-14796
Repair of composites 08 p1120 N85-17056
Investigation of the turbulent separated flow behind a spoiler
[ISL-CO-240/83] 14 p2213 N85-23726
Calculation of unsteady transonic separated flows by viscous-inviscid interaction 15 p2458 N85-25178
Study of boundary layer separation on a supercritical profile with a spoiler by means of a laser Doppler velocimeter
[ISL-CO-225/84] 23 p3895 N85-34128

SPOKES
The formation of spokes in Saturn's rings 15 p2676 N85-26524
On the role of mother-planet magnetic field in spiral structure explanation of formation of spokes — Saturn rings 15 p2676 N85-26525

SPONTANEOUS COMBUSTION
The reaction of oxygen-nitrogen mixtures with granular activated carbons below the spontaneous ignition temperature
[AD-A149041] 10 p1434 N85-19039
On the low temperature chemistry preceding end gas autoignition
[DE85-010471] 19 p3252 N85-30162

SPONTANEOUS EMISSION
Spontaneous emission by two atoms with different resonance frequencies near a metal surface
[AD-A154115] 19 p3353 N85-30781

SPORADIC E LAYER
Observations and prognosis of HF wave propagation via the sporadic E layer
[UIO-SR-84-04] 03 p0356 N85-12294

SPOT (FRENCH SATELLITE)
Attenuation experimental data bank in the COST 205 project. Structure and management of the final supports
[FUB-5-1963] 01 p0126 N85-10865
Helioeynchronism and phasing. Application to the SPOT orbit 05 p0600 N85-13826
The SPOT data bank system 05 p0659 N85-14236
Evaluation of SPOT simulation data of the S GEOS campaign of the EEC by data of the test sites Freiburg and Staubing (West Germany) 05 p0659 N85-14237
A field control methodology of remotely sensed data for statistical purposes: An example of SPOT simulated data in eastern Belgium — land use statistics 05 p0660 N85-14241
CNES, INRA do joint remote-sensing research 10 p1477 N85-19321
The spot operational remote sensing satellite system: Current status and perspectives 11 p1713 N85-20776
SPOT solar array 13 p2009 N85-22595
Mission analysis and orbit control of the helioeynchronous satellite SPOT 14 p2397 N85-24773
Details on spot remote sensing satellite propulsion unit 15 p2535 N85-25640
DORIS: Prediction in Doppler measurement — satellite onboard measurement
[CNES-CT/DTI/MS/AE/170] 16 p2729 N85-26843
The SPOT solar array
[SNIAS-851-440-103] 20 p3485 N85-31856

SPOT WELDS
Robotization of electric welding processes 03 p0345 N85-12225
Variations in the structure and in the composition of austenitic and carbon steel in spot welds
[BLL-BISI-TRANS-21765-(9022.06)] 18 p3073 N85-29007

SPRAY CHARACTERISTICS
Development of holographic particle field data reduction by Fourier analysis
[AD-A148684] 08 p1165 N85-17348
Description of a technique to measure spray distribution in an air stream
[AD-A149780] 12 p1771 N85-21122

SPRAY NOZZLES
Experimental study of the spray characteristics of a research airblast atomizer
[NASA-TM-86911] 07 p0904 N85-15727
An experimental study of spray thruster
[REPT-613] 12 p1845 N85-21578

SPRAYED COATINGS
Air force plasma spray at SA-ALC (San Antonio Air Logistics Center)
[AD-P004004] 03 p0308 N85-11984
An investigation of enhanced capability thermal barrier coating systems for diesel engine components
[NASA-CR-174820] 09 p1298 N85-18154
Infrared-thermal wave scanner for NDE of naval thermal spray coatings
[DE85-002237] 11 p1650 N85-20391
Low cost, sprayed CuInSe2 solar cell research
[DE85-003467] 12 p1881 N85-21799
System for NDH of thermal spray coating bonds
[DE85-007483] 15 p2572 N85-25858
Rocket thrust chamber thermal barrier coatings 16 p2734 N85-26867
Vacuum plasma coatings for turbine blades 16 p2734 N85-26869
Erosion of corrosion-resistant surface treatments on alloy steels
[DE85-008446] 17 p2932 N85-28100
Spray applicator for spraying coatings and other fluids in space
[NASA-CASE-MSC-18852-1] 18 p3115 N85-29283

SPRAYED PROTECTIVE COATINGS
U PROTECTIVE COATINGS
U SPRAYED COATINGS

SPRAYERS
The structure of dilute combusting sprays
[NASA-CR-174838] 07 p0905 N85-15728
Improved sprayer for AN-2 cropdusting work 08 p1068 N85-16769
Development of holographic particle field data reduction by Fourier analysis
[AD-A148684] 08 p1165 N85-17348
Swirling turbulent spray group combustion 09 p1289 N85-18095
Research study of droplet sizing technology leading to the development of an advanced droplet sizing system
[NASA-CR-174839] 12 p1860 N85-21604
Size and velocity distributions of particles and droplets in spray combustion systems
[AD-A150355] 13 p2017 N85-22648
Spray applicator for spraying coatings and other fluids in space
[NASA-CASE-MSC-18852-1] 18 p3115 N85-29283
Spray pyrolysis as a synthetic tool
[AD-A153891] 19 p3234 N85-30047

SPRAYING
NT ARC SPRAYING
NT CROP DUSTING
NT FLAME SPRAYING
NT METAL SPRAYING
NT PLASMA SPRAYING
Silicon band spraying technique for solar cells 12 p1877 N85-21778
MATADOR (Methods for the Analysis of Transport And Deposition Of Radionuclides) code description and user's manual
[TI85-901402] 23 p3966 N85-34592

SPRAYING APPARATUS
U SPRAYERS

SPRAYS
U SPRAYERS

SPREAD F
Kinetic Rayleigh-Taylor instability theory in the ionosphere near equator 13 p2067 N85-22911
Equatorial F-region irregularity latitudinal extension and dynamo electric field
[INPE-3494-PRE/731] 16 p2826 N85-27433

SPREAD SPECTRUM TRANSMISSION
Resistance to HF jamming interference in mobile radio networks by an adaptive, distributed reconfiguration technique
[AD-A145117] 01 p0038 N85-10238
Digital correlator speed improvement by multiplexing
[AD-A145207] 01 p0100 N85-10662
Spread-spectrum communications
[AD-A146135] 03 p0355 N85-12295
Distributed reservation-based code division multiple access
[AD-A147007] 07 p0940 N85-15957
Optimum jamming effects on frequency-hopping M-ary FSK (Frequency-Shift Keying) systems under certain ECCM (Electronic counter-countermeasures) receiver design strategies
[AD-A147768] 08 p1151 N85-17267
AWQPSK: An optimum modulation technique for spread spectrum communication 09 p1311 N85-18235
Fast synchronization model for UHF spread-spectrum communication system 10 p1473 N85-19296
Asynchronous transmission with strong spectral spread 10 p1474 N85-19300
Narrowband spread spectrum systems 10 p1475 N85-19307
Research on adaptive antenna techniques 6
[AD-A149341] 11 p1624 N85-20228
Tactical satellite terminals for land and airborne C3 applications 11 p1710 N85-20760
Detection of angular modulated electromagnetic signals
[AD-D011563] 12 p1823 N85-21437
Spread spectrum mobile radio communications
[AD-A149936] 12 p1829 N85-21477
The performance of a new adaptive filter for digital communications
[AD-A151690] 15 p2543 N85-25702
Measured noise performance of a new method of frequency hopping
[AD-A152679] 17 p2953 N85-28234
Study of a low rate spread spectrum receiver
[ENST-83E015] 20 p3441 N85-31354
Compression of spread spectrum signals on an excessively dispersive channel
[AD-A155184] 21 p3576 N85-32240

SPREADING
Spreading upon compacting of fiber composite materials with porous metal matrix 10 p1443 N85-19096

SPRINGS (ELASTIC)
A gyro sensor block suspension
[AD-D011411] 08 p1154 N85-17284
Elastic compliance of imperfect interfaces: Review and relationship to ultrasonic scattering
[DE85-003068] 11 p1652 N85-20404
Pneumatic clamping device
[AD-D011544] 12 p1858 N85-21656
SPRING: Helical spring design software for microcomputers
[DE85-006200] 15 p2631 N85-26217
Investigation of fatigue strength of spring steel after high-temperature thermomechanical working (HTMW) by helical drawing
[BLL-M-38274-(5826.4)] 20 p3465 N85-31525
SPRINGS (WATER)
Hydrogeochemical investigation of thermal springs in the Black Canyon-Hoover Dam area, Nevada and Arizona
[PB84-202472] 01 p0064 N85-10426
Investigation of mineral and thermomineral springs in the Eifel Mountains regarding thermal indications
[BMFT-FB-T-84-019] 02 p0220 N85-11451
Geothermal assessment of part of the east shore area, Davis and Weber Counties, Utah
[DE84-016817] 09 p1342 N85-18446
Evaluation of low-temperature geothermal potential in Utah and Goshen Valleys and adjacent areas, Utah. Part 2: Water temperature and chemistry
[DE85-009344] 23 p3943 N85-34436
SPUR (REACTORS)
U SPACE POWER UNIT REACTORS
SPUTTERING
NT MAGNETRON SPUTTERING
Sputtering of gold irradiated with thermal neutrons
03 p0429 N85-12738
Effects of monolayer coverages on substrate sputtering yields
[DE84-016312] 04 p0476 N85-13033
Ion contrasting chamber for discrimination of grains and textures
[BMFT-FB-T-84-151] 04 p0477 N85-13036
Effects of monolayer coverages on substrate sputtering yields
06 p0865 N85-15496
Synergestic sputtering properties of binary alloys
06 p0865 N85-15497
Optical properties of composite materials
[AD-A146768] 07 p0920 N85-15826
Rivista Tecnica Selenia, volume 9, number 1
07 p0938 N85-15945
Sputtering in thin film technology for optics — laser systems
07 p0938 N85-15948
Structural studies of amorphous Mo-Ge alloys using synchrotron radiation
[DE85-002061] 08 p1131 N85-17125
Synergistic sputtering properties of binary alloys
[DE84-017493] 09 p1297 N85-18148
Application of NbN films to the development of very high field superconducting magnets
[DE85-002729] 10 p1565 N85-19867
Oxidation protection coatings for polymers
[NASA-CASE-LEW-14072-1] 11 p1611 N85-20129
Textured carbon surfaces on copper
[NASA-CASE-LEW-14130-1] 11 p1615 N85-20156
Diamondlike flakes
[NASA-CASE-LEW-13637-2] 12 p1796 N85-21267
Sputter-induced compositional modifications in a Ni-Au alloy
[DE85-002771] 12 p1807 N85-21333
Use of markets to elucidate reacting sputtering processes
[DE85-005723] 13 p2018 N85-22655
Synthesis and characterization of superconducting electronic materials
[AD-A151112] 15 p2659 N85-26409
Measurement of NSLS distributed diode sputter ion pump characteristics
[DE85-006550] 16 p2760 N85-27031
Obtaining amorphous coatings of FeW and Fe-Cr-P-B alloys using laser sputtering
[BLL-BISI-22493-(8022.06)] 17 p2927 N85-28057
Self-sustaining coatings for fusion applications: Copper lithium alloys
[DE85-009740] 18 p3190 N85-29783
Ion beam sputter-deposited thin film coatings for protection of spacecraft polymers in low Earth orbit
[NASA-TM-87051] 19 p3248 N85-30137
Surface effects on sputtered atoms and their angular and energy dependence
[DE85-010508] 19 p3354 N85-30790
Current state of development and expected performance of copper-lithium alloys as an impurity control system in fusion applications
[DE85-009673] 19 p3372 N85-30917
Analysis of beam interaction of the electrical thruster RIT 10 (particle emission) with surfaces
[ESA-TT-828] 20 p3421 N85-31231
Modification of the grain size of sputtered copper with additions of oxygen, krypton, silver, or yttrium
[DE85-010975] 21 p3587 N85-32189
Advances in sputtered and ion plated solid film lubrication
22 p3797 N85-33524
Liquid crystal light valve structures
[NASA-CASE-MSC-20036-1] 22 p3847 N85-33826
Low-energy sputterings with the Monte Carlo Program ACAT
[IPPJ-AM-40] 23 p3982 N85-34690
SPUTTERING GAGES
Thin-film sensors for space propulsion technology
17 p2915 N85-27968
SQUALLS
Short period forecasts in West Africa using Meteosat data
01 p0079 N85-10526
SQUARE WAVES
Square-pulse generator
13 p2075 N85-22959
SQUEEZE FILMS
Effects of fluid inertia and turbulence on force coefficients for squeeze film dampers
05 p0645 N85-14137
Squeeze-film dampers for turbomachinery stabilization
05 p0645 N85-14138
Damping capacity of a sealed squeeze film bearing
05 p0645 N85-14139
Dual clearance squeeze film damper
[NASA-CASE-LEW-13509-1] 22 p3791 N85-33490
SQUEEZING
U COMPRESSING
SQUID (DETECTORS)
The dc SQUID as a tuned radiofrequency amplifier
[DE85-000701] 06 p0805 N85-15123
Ultrasensitive measuring devices
[DE85-000672] 12 p1853 N85-21622
Superconducting gyroscope research
[NASA-CR-171406] 15 p2560 N85-25795
ST VENANT FLEXURE PROBLEM
U SAINT VENANT PRINCIPLE
STABILITY
NT ACOUSTIC INSTABILITY
NT AERODYNAMIC STABILITY
NT AIRCRAFT STABILITY
NT ATTITUDE STABILITY
NT BAROCLINIC INSTABILITY
NT BOUNDARY LAYER STABILITY
NT COMBUSTION STABILITY
NT CONTROL STABILITY
NT DIMENSIONAL STABILITY
NT DIRECTIONAL STABILITY
NT DYNAMIC STABILITY
NT FLAME STABILITY
NT FLOW STABILITY
NT FREQUENCY STABILITY
NT GOERTLER INSTABILITY
NT GYROSCOPIC STABILITY
NT LATERAL STABILITY
NT LONGITUDINAL STABILITY
NT LOW SPEED STABILITY
NT MAGNETOHYDRODYNAMIC STABILITY
NT MAGNETOSPHERIC INSTABILITY
NT MOTION STABILITY
NT ROTARY STABILITY
NT SHELL STABILITY
NT SPACECRAFT STABILITY
NT STATIC STABILITY
NT STORAGE STABILITY
NT STRUCTURAL STABILITY
NT SURFACE STABILITY
NT SYSTEMS STABILITY
NT THERMAL STABILITY
Effect of combined pressure and temperature distortion orientation on high-bypass-ratio turbofan engine stability
[NASA-TM-83771] 01 p0011 N85-10067
Standards for commercially emerging technologies: A preliminary cost-benefit assessment for the Optical Digital data disk (OD3) technology for mass data storage applications
[PB84-223593] 01 p0101 N85-10669
Legendre-Tau approximation for functional differential equations. Part 3: Eigenvalue approximations and uniform stability
[NASA-CR-172447] 01 p0110 N85-10744
Development and flight evaluation of an augmented stability active controls concept: Executive summary
[NASA-CR-166009] 02 p0149 N85-11006
Inorganic composites for space applications
02 p0155 N85-11047
Nonlinear oscillations of 2 body system relative to center of mass in elliptical orbit
02 p0159 N85-11082
Rayleigh-Taylor instability in compressible media
[AD-A145491] 02 p0198 N85-11322
Qualitative results for distributed systems with discrete damping and stiffness with application to control
[AD-A145525] 02 p0209 N85-11382
Relationships between electronic structure and stability of metallic glasses
[AD-A145506] 02 p0287 N85-11874
A simple electronic apparatus for determining the oxidation stability of lubricants and other organic compounds
[AD-A146080] 03 p0338 N85-12172
A comparison of methods for predicting ductile crack growth instability
[AERE-R-11199] 03 p0374 N85-12367
A pseudospectral Legendre method for hyperbolic equations with an improved stability condition
[NASA-CR-172475] 03 p0410 N85-12617
Liquid hydrocarbon fuels from syngas
[DE84-015942] 04 p0482 N85-13069
Stable isotope studies
[DE84-016752] 04 p0562 N85-13583
Development and testing of a 20-kW X-band transmitter with high phase stability
05 p0623 N85-13965
Calibration of noise power transfer standards, measurement uncertainties and long term stability
05 p0630 N85-14035
Rotordynamic Instability Problems in High-Performance Turbomachinery
[NASA-CP-2338] 05 p0642 N85-14116
Full load testing in the platform module prior to tow-out: A case history of subsynchronous instability
05 p0642 N85-14117
Internal hysteresis experienced on a high pressure syn gas compressor
05 p0642 N85-14122
Squeeze-film dampers for turbomachinery stabilization
05 p0645 N85-14138
Normal mode initialization
05 p0680 N85-14372
Stability questions for gravity in 4 and higher dimensions
05 p0734 N85-14716
Polymer-metal interface bond stability
06 p0830 N85-15272
ATA probe beam experiment
[DE84-016017] 06 p0862 N85-15477
Theoretical and experimental study of hydro-elastic instability on the line of shafting of a rotating machine
[BLL-DOUNREAY-TR-937-(9091.9F)]
07 p0972 N85-16174
The pressure deflagration limit of solid rocket propellants
08 p1117 N85-17048
New instabilities in line driven winds
08 p1235 N85-17785
Gain instabilities in photomultipliers: How accurate are photon counting measurements?
08 p1251 N85-17903
Stability of amorphous metals on semiconductor substrates
[DE84-017256] 09 p1295 N85-18134
Computer simulation of multiple stability regions in an internally cooled superconducting conductor and of helium replenishment in a bath-cooled conductor
[DE85-002112] 09 p1399 N85-18805
Stability indicators for front end loaders
[AD-P004293] 09 p1408 N85-18870
Study on controllability and stability of high speed tracked vehicles
[AD-P004302] 09 p1409 N85-18879
Integrated Technology Rotor/Flight Research Rotor (ITR/FRR) concept definition
[NASA-CR-166443] 10 p1423 N85-18978
Integrated Technology Rotor/Flight Research Rotor (ITR/FRR) concept definition
[NASA-CR-166445] 10 p1423 N85-18979
Simulation of the ion-beam-driven drift instability in a magnetic trap, 1
[AD-A149451] 10 p1452 N85-19147
Fluidelastic instability in shell and tube heat exchangers: A framework for a prediction method
[DE84-006518] 10 p1496 N85-19444
Simulation of the ion-beam-driven drift instability in a magnetic trap, 2
[AD-A149452] 10 p1554 N85-19796
Research in nonlinear problems of energy: Informal technical report
[DE85-001529] 11 p1595 N85-20031
Stability evaluation of sulfur dioxide nitric oxide and carbon monoxide gases in cylinders
11 p1648 N85-20387
Complex symmetric matrices with strongly stable iterates
[NASA-CR-172542] 11 p1706 N85-20731
Stability of superconducting composites in a magnetic field
[DE85-002731] 11 p1734 N85-20907
Field validation of statistically-based acceptance plan for bituminous airport pavements. Volume 2: Statistical analysis of Marshall properties of plant-produced bituminous materials
[FAA-PM-84-12-VOL-2] 12 p1781 N85-21181

Field validation of statistically-based acceptance plan for bituminous airport pavements. Volume 4: Computer simulation of multiple acceptance criteria
[FAA-PM-84-12-VOL-4] 12 p1782 N85-21183
Stability of organic audit materials and results of source test analysis audits
[PB85-116184] 12 p1885 N85-21832
Analysis of slope stability, Wilmington to Lindenkohl Canyons, US mid-Atlantic margin
[DE84-012278] 12 p1899 N85-21921
Suppression of tilting instability of a compact torus by energetic particle beams
[IPPJ-705] 12 p1935 N85-22157
Stability of cylindrical shells with one-way constraints
13 p2048 N85-22820
Nonlinear behavior and stability of thin spherical shells subjected to non-axisymmetrical loading
13 p2048 N85-22821
Effect of compliability of hot walls in liquid-propellant engine on low frequency instability
13 p2049 N85-22824
Stability of highly nonlinear oxide-zinc resistors under continuous voltage of industrial frequency
13 p2087 N85-23030
Electrodynamic stability of composite liquid-metal contacts 13 p2087 N85-23031
Stability of turbine runners in sliding bearings under external circulation forces 14 p2272 N85-24074
Stability of vortex structures during separation flow past array of wings 14 p2276 N85-24110
Stability of steady rotation of a cylinder filled with a stratified viscous incompressible fluid
14 p2276 N85-24112
Increasing seam formation stability in electron beam welding of very thick titanium alloys
15 p2500 N85-25420
A study of the stability of cadmium sulfide/copper sulfide and cadmium sulfide copper-indium-diselenide solar cells
[DE85-002902] 15 p2567 N85-25947
Uniqueness and stability in nonlinear elasticity and viscoelasticity
[AD-A151470] 15 p2637 N85-26284
Effects of finite current channel width on the current convective instability
[AD-A151414] 15 p2656 N85-26389
Estimation of the depth of a spherical cap in an hydraulic drawing test for some simple conditions of loss of stability
[REPT-4/1984] 16 p2748 N85-26956
Models of long-period superstructure
[DE85-007659] 16 p2751 N85-26981
A closed loop analysis of POGO instability
[AD-A153121] 17 p2937 N85-28132
Fluid surface behavior in low gravity. Center discretionary fund no. 83-21
[NASA-TP-2486] 17 p2957 N85-28260
Instabilities and chaotic behavior of active and passive laser systems
[AD-A153366] 17 p2971 N85-28346
How a swing behaves
[DE85-008290] 17 p3027 N85-28720
Stability in dynamical systems
[DE85-006696] 17 p3034 N85-28766
Morphological stability and fluid dynamics of vapor crystal growth
[NASA-CR-175879] 17 p3042 N85-28822
Morphological stability and fluid dynamics of vapor crystal growth
[NASA-CR-175880] 17 p3042 N85-28823
Study of the chemical mechanism in lubrication
[DE85-010766] 19 p3228 N85-30013
Optical stability, atmospheric transparency and aerosol absorption 19 p3297 N85-30442
High gain adaptive control of decentralized systems
[DE85-010040] 19 p3339 N85-30688
High gain adaptive control of decentralized systems
[DE85-001566] 19 p3343 N85-30717
Frequency domain control design of large space structures: A practical approach
20 p3415 N85-31192
A control concept for large flexible spacecraft using order reduction techniques 20 p3415 N85-31193
Influence of error of determination of moire isotach orders on the stability of their approximation
[BLL-M-36277-(5828.4)] 20 p3450 N85-31423
Bypass transition to turbulence and research Desiderata 20 p3453 N85-31442
Slow tearing modes: Transitions to instability
20 p3534 N85-31989
Notes on atmospheric stability, turbulence, and its measurements
[AD-A155230] 21 p3637 N85-32588
Two-dimensional simulation of instability growth due to shocks
[DE85-011869] 22 p3784 N85-33442
Tectonic stability and expected ground motion at Yucca Mountain
[DE85-012004] 22 p3814 N85-33629
Saturation of a longitudinal instability due to nonlinearity of the wake field
[DE85-012514] 22 p3837 N85-33761
Compressible two-phase flow instabilities simulated with a hybrid Lagrange-Euler pseudospectral method
[DE85-009904] 23 p3931 N85-34361
Stability of two-dimensional immiscible flow to viscous fingering
[DE85-011403] 23 p3931 N85-34364
Simulation studies on stability of hot electron plasma
23 p3978 N85-34664
Workshop report on Simulation Techniques for Shock Wave Phenomena and Characteristics of Plasmas in Inertial Confinement Fusion
[IPPJ-725] 23 p3979 N85-34670
Instabilities in decelerating supersonic flows with applications to cosmic ray shocks
[OG-6.1-2] 23 p4017 N85-34892
Parametric stability of analytical close-range photogrammetry 24 p4107 N85-35461
Relaxation phenomena and stability of probability densities
[AD-A155923] 24 p4143 N85-35682
Analysis of reactor material experiments investigating oxide fuel crust stability and heat transfer in jet impingement flow
[DE85-012097] 24 p4151 N85-35739

STABILITY AUGMENTATION
Integrated Application of Active Controls (IAAC) technology to an advanced subsonic transport project. ACT/Control/Guidance System study, volume 1
[NASA-CR-165963-VOL-1] 08 p0754 N85-14837
Integrated Application of Active Controls (IAAC) technology to an advanced subsonic transport project. ACT/Control/Guidance System study. Volume 2: Appendices
[NASA-CR-165963-VOL-2] 08 p0754 N85-14838
Leading edge flap system for aircraft control augmentation
[NASA-CASE-LAR-12787-2] 11 p1585 N85-19985
A perspective on supersugmented flight control advantages and problems 16 p2712 N85-26733
Demonstration of relaxed stability on a commercial transport 16 p2713 N85-26745
Multivariable control of a soft coupled space station
20 p3408 N85-31151

STABILITY DERIVATIVES
NT PITCHING MOMENTS
NT ROLLING MOMENTS
NT YAWING MOMENTS
The development of a dynamic model of a generalised combat aircraft with forward wings for the identification of stability and control characteristics
[CAR-84-33] 09 p1280 N85-18050

STABILITY TESTS
NT FLIGHT STABILITY TESTS
NT WIND TUNNEL STABILITY TESTS
Local stability analysis for a planar shock wave
[NASA-TP-2367] 04 p0452 N85-12984
MSFC data analysis of the SAFE/DAE experiment
14 p2233 N85-23843
Langley Research Center photogrammetric measurements of solar array dynamics: Preliminary results 14 p2233 N85-23844
Environmental stability of intercalated graphite fibers
[NASA-TM-87025] 16 p2753 N85-26992
Recent developments in rotary-balance testing of fighter aircraft configurations at NASA Ames Research Center
[NASA-TM-86714] 21 p3551 N85-32090

STABILIZATION
NT SPIN STABILIZATION
NT THREE AXIS STABILIZATION
A high-repetition rate, inductively stabilized, long-pulse excimer laser
[DE84-016827] 04 p0506 N85-13229
Experimental research on electric propulsion. Note 7: Analysis of the performance of an arc-jet driven by means of hydrogen and nitrogen
[NASA-TM-77473] 08 p0760 N85-14861
Beam propagation study: Stabilization of the resistive hose instability in intense electron beams
[AD-A148071] 08 p1220 N85-17684
Stability analysis of flexible spacecraft with PID controller
[CRC-1372] 12 p1792 N85-21247
Stabilization of steady motion of mechanical systems
14 p2260 N85-24122
Mechanical stabilization of austenite against epsilon martensite and its effect on deformation behavior in high manganese steels
[DE85-007654] 17 p2932 N85-28097
Stabilizing force feedback in bio-actuated control systems
[AD-D011634] 17 p3002 N85-28560
Stability of high energy particle plasmas to MHD-like modes
[DE85-007879] 17 p3039 N85-28803
The Stambda/4 post coupler for drift-tube linacs
[DE85-010753] 20 p3531 N85-31962
Optical output stabilization method for direct current arc lamps
[AD-A154987] 21 p3705 N85-33013
Astron telescope stabilization system
22 p3732 N85-33133
Amplitude stabilization of pulse signals
22 p3762 N85-33320
Optimization of design parameters for alternating current stabilizer based on magnetic suspension
22 p3772 N85-33374
Electron photoejection in carbanions
[DE85-011747] 23 p3911 N85-34230
The balancing of complex linkage mechanisms
23 p3924 N85-34313
Method and apparatus for transfer function simulator for testing complex systems
[NASA-CASE-NPO-15806-1] 23 p3926 N85-34333
Improved method for the stabilization of NaI-photomultiplier gamma detectors against thermal and other drift
[DE85-011830] 23 p3970 N85-34613
Design of dynamic compensators of prescribed pattern
[BU-109] 24 p4142 N85-35674
Spreading the control complexity in decentralized control of interconnected systems
[BU-117] 24 p4144 N85-35688
Decentralized stabilization by high gain feedback
[BU-115] 24 p4144 N85-35689

STABILIZED PLATFORMS
Some notes on a tangent plane oriented heading reference --- stabilized platforms
[RAE-TM-IEE-144] 02 p0136 N85-10928
Evaluation of nose, roof, and mast mounted sensor platforms for piloting and sighting, integrated in future combat helicopters 08 p1074 N85-16806
A concept for a mobile remote manipulator system
14 p2236 N85-23859
Estimates of errors of a gyroscope stabilized platform
16 p2763 N85-27050

STABILIZERS (AGENTS)
Micromolecular modeling 21 p3606 N85-32405
Polymerizable ultraviolet stabilizers
21 p3606 N85-32406

STABILIZERS (FLUID DYNAMICS)
NT HORIZONTAL TAIL SURFACES
Advanced composite stabilizer for Boeing 737 aircraft
[NASA-CR-166451] 02 p0137 N85-10934
Advanced manufacturing development of a composite empennage component for L-1011 aircraft
[NASA-CR-165885] 02 p0170 N85-11141
Full-scale testing, production and cost analysis data for the advanced composite stabilizer for Boeing 737 aircraft. Volume 1: Technical summary
[NASA-CR-3649] 05 p0612 N85-13912
Design, ancillary testing, analysis and fabrication data for the advanced composite stabilizer for Boeing 737 aircraft. Volume 1: Technical summary
[NASA-CR-3648] 05 p0612 N85-13913
Design, ancillary testing, analysis and fabrication data for the advanced composite stabilizer for Boeing 737 aircraft, volume 2
[NASA-CR-166011] 05 p0612 N85-13914
Full-scale testing, production and cost analysis data for the advanced composite stabilizer for Boeing 737 aircraft, volume 2
[NASA-CR-166012] 05 p0613 N85-13915
CF-5 vertical stabilizer flight load survey
07 p0895 N85-15873
TUTOR (CL-41A) tail flight load survey
07 p0896 N85-15875
Flutter clearance of the Schweizer 1-36 deep-stall sailplane
[NASA-TM-85917] 22 p3729 N85-33118
A towed instrument vehicle for deep ocean sampling
[AD-A156322] 24 p4125 N85-35576

STABLE OSCILLATIONS
Buildup of oscillations in two-mode gyrotron
06 p0788 N85-15037
Magnetically-localizable, polymerized lipid vesicles and method of disrupting same
[AD-D011666] 19 p3249 N85-30144
Oscillatory solutions of the Peaceman-Rachford alternating direction implicit method and a comparison of methods for the solution of the two dimensional heat diffusion equation
[AD-A154870] 21 p3675 N85-32833

STACKING FAULTS
U CRYSTAL DEFECTS
STACKS
Gas cooled fuel cell systems technology development
[NASA-CR-174732] 07 p0991 N85-16291
Develop and test fuel cell powered on-site integrated total energy systems. Phase 3: Full-scale power plant development
[NASA-CR-174887] 15 p2586 N85-25941
STAGE SEPARATION
Debris control design achievements of the booster separation motors 08 p1096 N85-16942
A theoretical study of two stage thrust augmenting ejectors
[ARL/AERO-R-166] 19 p3218 N85-29954
The development of staging mechanisms for the Japanese satellite launcher Mu-3SII 22 p3798 N85-33528
STAGING (ROCKETS)
U STAGE SEPARATION
STAGNATION FLOW
Physics on aircraft wakes
[NASA-CR-174105] 04 p0453 N85-12871
Laminar jet issuing into stagnant surroundings — PHOENICS code
[PDR/CFDU-IC/15] 04 p0501 N85-13200
Some important problems in unsteady boundary layers including separation. 2: Unsteady boundary layers close to the stagnation region of slender bodies
[AD-A146964] 07 p0958 N85-16089
Stagnation zone impaction on a simple terrain feature in stable flow 13 p2130 N85-23255
STAGNATION POINT
Preliminary results of a study of the relationship between free stream turbulence and stagnation region heat transfer
[NASA-TM-86664] 02 p0197 N85-11317
Influence of turbulence on erosion by a particle-laden fluid jet
[DE84-014365] 09 p1320 N85-16301
The influence of jet-grid turbulence on heat transfer from the stagnation region of a cylinder in crossflow
[NASA-TM-87011] 15 p2554 N85-25760
Conical stagnation points in the flow around an external corner — delta wings
[VTH-LR-396] 16 p2701 N85-26680
Preliminary results of a study of the relationship between free-stream turbulence and stagnation region heat transfer 20 p3452 N85-31435
Two-dimensional separation in an incompressible fluid — boundary layer separation
[ONERA-RTS-16/3282-RY-080-R] 20 p3456 N85-31459
STAGNATION PRESSURE
Basic studies of multiple free and confined jets
[AD-A149556] 10 p1485 N85-19374
STAGNATION REGION
U STAGNATION POINT
STAINING
Processing of LANDSAT imagery to map surface mineral alteration on the Alaska Peninsula, Alaska 24 p4106 N85-35455
STAINLESS STEELS
NT AUSTENITIC STAINLESS STEELS
NT FERRITIC STAINLESS STEELS
NT MARTENSITIC STAINLESS STEELS
New ferrous metallurgy technology 01 p0019 N85-10114
The oxidation behaviour of a 20 percent Cr/25 percent Ni/Nb stabilized stainless steel in carbon dioxide at high temperatures and its improvement by cerium and yttrium
[AERE-R-11228] 01 p0029 N85-10182
Minor element effects on gas tungsten arc weld penetration
[PB84-222579] 01 p0056 N85-10370
International Conference on Recent Developments in Specialty Steels and Hard Materials. Conference abstracts
[CSIR-S-256] 02 p0176 N85-11177
A review of world wide development in stainless steels 02 p0177 N85-11190
Metalurgy of a 12 percent chromium stainless steel 02 p0178 N85-11195
The effect of replacing molybdenum with vanadium on the corrosion resistant properties of stainless steels 02 p0178 N85-11197
The influence of metallurgical aspects on the pitting corrosion behaviour of high alloy stainless steels 02 p0179 N85-11202
Detection of hydrogen assisted crack growth
[DE84-015920] 02 p0183 N85-11226
Detection of hydrogen assisted crack growth by measurement of modulus changes and acoustic emission
[DE84-015752] 02 p0184 N85-11236
Strain distribution in a type 316/16-8-2 stainless steel weldment during cyclic loading
[DE84-015644] 02 p0210 N85-11384
Diffusion of Cr-51 tracer in Cr-2O-3 and the growth of Cr-2O-3 films
[AERE-R-11314] 03 p0333 N85-12146
A study of precipitation and boron distribution in 20 Cr 25Ni base stainless steels
[AERE-M-3353] 03 p0334 N85-12154
New coatings for high temperature materials protection
[AERE-R-11387] 03 p0339 N85-12160
Subgrains, dislocations and the elevated-temperature strength of type 304 stainless steel
[DE84-001233] 04 p0473 N85-13014
Localized corrosion and stress corrosion cracking behavior of stainless steel weldments
[DE84-016095] 04 p0474 N85-13017
Erosion of multiphase materials
[DE84-015816] 04 p0474 N85-13018
Solidification and aging behavior of types 308 and 308CRE stainless steel welds
[DE84-016552] 04 p0476 N85-13029
Ultrasonic and metallurgical examination of a cracked type 304 stainless steel BWR pipe weldment
[TI84-014968] 04 p0511 N85-13254
Tensile properties and swelling of 20%-cold-worked Type 316 stainless steel irradiated in HFIR
[DE84-014060] 05 p0617 N85-13948
Effects of irradiation fluence and creep on fracture toughness of 347/348 stainless steel
[DE84-016091] 05 p0618 N85-13953
Current and potential transients during localized corrosion of stainless steel
[DE84-014100] 05 p0618 N85-13954
Swelling behavior of titanium-modified AISI 316 alloys
[DE84-013940] 05 p0618 N85-13956
Application of extraction replicas and analytical electron microscopy to precipitate phase studies
[DE85-001253] 06 p0769 N85-14919
Microstructure of rapidly quenched type 308 stainless steel weld filler metal and its implications on rapid solidification processes
[DE85-000930] 06 p0769 N85-14920
Modeling microstructural changes during hot rolling of steels 06 p0798 N85-15096
SANS and TEM studies of carbide precipitation and creep damage in type 304 stainless steel
[DE85-000933] 09 p1296 N85-16139
Stochastic models of pitting corrosion of stainless steels. Part 1: Modelling of the initiation and growth of pits at constant potential
[AERE-R-11146-PT-1] 09 p1298 N85-16151
Picking of stainless steels: A review
[PB85-111979] 10 p1442 N85-19087
Effect of implantation species on the tribological response of stainless steel surfaces
[DE85-003530] 10 p1493 N85-19432
Patterns in the occurrence of the brittle topologically close-packed phases: Al
[DE85-000592] 11 p1607 N85-20106
Chemical cleaning of 304 and 304-L stainless steel surfaces by the nitradd passivation process
[DE85-003714] 11 p1615 N85-20158
Research on heat-exchanger corrosion
[PB85-126316] 11 p1616 N85-20164
Transverse microstructure of an oxide scale formed on a 20 % Cr/25 % Ni niobium stabilized stainless steel
[AERE-R-11034] 12 p1804 N85-21315
Nondestructive testing of stainless steel to improve quality and output efficiency of the processing of ingot and continuous casting
[BMFT-FB-T-84-240] 12 p1808 N85-21345
Local electrochemistry of pitting corrosion in stainless steels
[DE85-005207] 13 p2023 N85-22673
Development of a sintered shim
[DE85-006183] 13 p2025 N85-22685
Use of ferrofluids in machining of metals 13 p2045 N85-22802
Fatigue life, crack initiation, and propagation of 304 stainless steel with non-proportional axial/torsional strain-paths 13 p2101 N85-23094
Studies of the initiation of pitting corrosion on stainless steels
[AERE-M-3400] 14 p2254 N85-23967
Exploratory corrosion tests on alloys in molten salts at 900(0)C
[DE85-000511] 14 p2257 N85-23983
Improvement by cerium and yttrium ion implantation of oxidation behaviour of stabilised stainless steel in carbon dioxide
[AERE-R-11523] 14 p2259 N85-23996
The design and construction of a flow channel and rig for corrosion studies
[AERE-M-3455] 15 p2508 N85-25474
Variation in the spacing of dislocations in subgrain boundaries with creep strain in Type 304 stainless steel
[DE85-006184] 15 p2511 N85-25483
Ignition of metals in high pressure oxygen 16 p2795 N85-26874
Creep-fatigue interaction of notched 304 stainless steel bars 16 p2796 N85-27249
Thermomechanical treatment aimed at the protection of type 316 stainless steel from IGC and IGSCC
[BLL-BISI-TRANS-22498-(9022.06)] 17 p2925 N85-28040
Effect of texture in steel on the susceptibility of hydrogen embrittlement
[BLL-BISI-TRANS-22026-(9022.06)] 17 p2926 N85-28048
Metallurgical means of preventing the corrosion of metal
[BLL-BISI-TRANS-22320-(9022.06)] 17 p2929 N85-28062
Properties of nitrogen containing stainless alloy designed for high resistance to pitting
[DE85-008282] 17 p2931 N85-28095
Experimental and theoretical studies on transport processes in laser welding
[DE84-009572] 17 p2975 N85-28378
Surface degradation of ductile metal in elevated temperature gas-particle streams
[DE85-008428] 18 p3074 N85-29017
Establishment of a methodology for predicting lifetimes in active solar systems
[DE85-009629] 18 p3130 N85-29383
Performance characteristics of gravity-assisted potassium heat pipes
[DE85-010717] 19 p3287 N85-30367
Consolidated fuel reprocessing program
[DE85-008750] 19 p3366 N85-30871
Solid-state resistance welding cylinders and spheres
[DE85-010064] 20 p3469 N85-31555
Machining-induced deformation in stepped specimens of PH 13-8 Mo, 18 nickel maraging steel grade 200T1 and grain-refined HP 9-4-20
[NASA-CR-172450] 21 p3565 N85-32177
Film condensation of steam on externally finned horizontal tubes
[AD-A155642] 21 p3585 N85-32285
Thermodynamic properties of alloys in the Fe-Ti system
[NPL-DMA(A)-96] 22 p3748 N85-33229
Effects of residual stresses and distortion on the nickel 200 and stainless steel 304 weldments
[DE85-011568] 22 p3748 N85-33233
Centrifugal castings of stainless steel spiked with radioactive tracers
[DE85-012003] 22 p3748 N85-33234
Tritium-helium effects in metals
[DE85-011507] 22 p3749 N85-33235
Mechanical properties of plasma arc cut steel 23 p3905 N85-34186
Approximate determination of the extent of the solid-liquid zone
[BLL-M-35829-(5828.4)] 23 p3914 N85-34251
Influence of particle erosion on the microstructural changes in metals and alloys
[TI85-901384] 23 p3917 N85-34276
Stress corrosion cracking susceptibility of types 316NG and 316 stainless steel in an impurity environment
[TI85-006884] 23 p3917 N85-34277
Effect of stainless steel weld overlay cladding on the structural integrity of flawed steel plates in bending, series 1
[TI85-010349] 23 p3939 N85-34416
Analytical ultrasonics for structural materials
[TI85-006132] 23 p3968 N85-34600
Shield design for next-generation, low-neutron-fluence, superconducting tokamaks
[DE85-011409] 23 p3982 N85-34695
Electrochemical method for investigation of the susceptibility of corrosion-resistant steels to intercrystalline corrosion
[BLL-CE-TRANS-8062-(9022.09)] 24 p4077 N85-35269
Effect of temperature and ionic impurities at very low concentrations on stress corrosion cracking of Type 304 stainless steel
[TI85-003048] 24 p4079 N85-35283
X-ray fluorescence analysis of 304L stainless steel
[DE85-013254] 24 p4080 N85-35288
Spectral characteristics of grinding sparks used for identification of scrap metals
[PB85-198570] 24 p4080 N85-35290
Analysis of reactor material experiments investigating oxide fuel crust stability and heat transfer in jet impingement flow
[DE85-012097] 24 p4151 N85-35739

STALLING
Preliminary airworthiness evaluation of the Rutan Aircraft Factory (RAF), Inc. LONG-EZ airplane with external sight
[AD-A145381] 02 p0138 N85-10937
STAMPING
Summaries of press automation conference presented
08 p1139 N85-17173
Calculating reliability and productivity of cold stamping robot complex as queuing system
16 p2761 N85-27039
Experience of sheet stamping robotic complexes
16 p2761 N85-27041
New method for determining stampability of sheet materials
[BLL-BISI-22486-(9022.06)] 17 p2972 N85-28360
STANDARD ATMOSPHERES
U REFERENCE ATMOSPHERES
STANDARD DEVIATION
Battery control and fault detection method
[AD-D011384] 07 p0993 N85-16307
Determination of the laws governing the changes in the standard deviations of the distribution of pollution based on observations of the atmospheric turbulence spectrum and the possibility of simulating it in the laboratory
[BLL-TR-T6373/BG/MRS14883/84]
08 p1179 N85-17431
Positioning accuracy of the ARGOS system in operational use 16 p2811 N85-27335
Derivation of model topography
18 p3141 N85-29449
On the statistical significance of excess events: Remarks of caution and the need for a standard method of calculation
[OG-9.5-10] 23 p4031 N85-34987
Large deviations for the maxima of some random fields
[AD-A155909] 24 p4143 N85-35681
STANDARDIZATION
Increased joint avionics standardization could result in major economies and operational benefits
[AD-A145730] 02 p0139 N85-10945
Standardized efficiency terms: Comparison of some Stirling engine performance figures
[DE84-015407] 02 p0205 N85-11352
SLC nomenclature for beamline components
[DE84-014776] 02 p0279 N85-11816
Standardization of amplitude characteristics of galvanometric seismographs in the KAPG network
[REPT-552] 03 p0375 N85-12395
Standardization of data formats for radar altimeter data 03 p0384 N85-12455
Standardization of flammability tests for hydraulic fluids
[AD-A146468] 06 p0771 N85-14932
Proceedings of the National Bureau of Standards and National Security Agency Workshop on Standardization Issues for Optical Data Disk (OD3) Technology
[PB84-217765] 06 p0848 N85-15383
A standard operating system interface for microcomputer software development
[AD-A146584] 06 p0854 N85-15428
Methodology for evaluating related databases and a computerized algorithm for merging their output
09 p1401 N85-18821
Report on AGARD Meeting: Hazards Studies for Solid Propellant Rocket Motors
[AD-P004340] 10 p1454 N85-19164
Update of thermal conductivity and electrical resistivity of electrolytic iron, tungsten and stainless steel
[PB85-115814] 12 p1803 N85-21311
The ARGOS system and hydrology. Results obtained by ORSTROM and benefits of a degree of standardization 14 p2239 N85-23881
An analysis of data dictionaries and their role in information resource management
[AD-A152134] 16 p2774 N85-27121
NBS physical measurement services
[NBSIR-84-2875] 16 p2859 N85-27639
DOD manual for standard data elements, part 1
[AD-A152201] 16 p2878 N85-27754
High temperature position sensors based on monolithic GaAs Hall IC
[BMFT-FB-T-84-266] 17 p2969 N85-28337
Standard procedures to be used in specifying basic properties of plastics and polymers
[NPL-DMA(A)-99] 20 p3433 N85-31295
Standard series of direct-current motors for regulated electric drives 22 p3772 N85-33375
Development of NATOPS (Naval Air Training and Operating Procedure Standardization) performance software for the H-46D helicopter
[AD-A156089] 24 p4064 N85-35190
Necessary bandwidth and spectral properties of digital modulation
[PB85-185387] 24 p4088 N85-35340
Redefining the scratch standards
[PB85-194736] 24 p4154 N85-35755
STANDARDS
NT FREQUENCY STANDARDS
NT REFERENCE ATMOSPHERES
Compilation of elemental concentration data for NBS (National Bureau of Standards) biological, geological and environmental standard reference materials, 1982
[PB84-218338] 01 p0025 N85-10158
Force standard machines of the National Institutes for Metrology, vol. 2
[PTB-ME-62-VOL-2] 01 p0036 N85-10224
A coaxial noise standard for the 1 GHz to 12.4 GHz frequency range
[PB84-217884] 01 p0042 N85-10272
Requirements and specifications for cartographic video discs
[AD-A144906] 01 p0049 N85-10325
Measurement assurance programs. Part 2: Development and implementation
[PB84-217876] 01 p0051 N85-10338
Measurement assurance programs. Part 1: General introduction
[PB84-217868] 01 p0051 N85-10339
Demonstrating air quality improvements: A review of alternatives
[DE84-014274] 01 p0070 N85-10482
Standards for commercially emerging technologies: A preliminary cost-benefit assessment for the Optical Digital data disk (OD3) technology for mass data storage applications
[PB84-223593] 01 p0101 N85-10669
Analysis of three database system architectures using benchmarks
[PB84-217512] 01 p0105 N85-10706
Automated Data Systems (ADS) documentation standards
[AD-A144867] 01 p0125 N85-10857
Improving technical documents
[AD-B084855] 01 p0126 N85-10866
South African Astronomical Observatory Circulars, no. 7
[SAAOC-7] 01 p0127 N85-10875
Local photometric standards for CaII emission stars
01 p0128 N85-10883
Test methods and standards development for active solar heating and cooling systems
[PB84-217447] 03 p0343 N85-12209
Evolution of the NWC (Naval Weapons Center) thermal standard. Part 5: Thermal standard development and applications
[AD-A146173] 03 p0364 N85-12334
Review of the NAAQS (National Ambient Air Quality Standards) for carbon monoxide: Reassessment of scientific and technical information
[PB84-231315] 03 p0388 N85-12485
Ways to improve management of Federal funded computerized models
[LCD-75-111] 03 p0435 N85-12771
Present practice for the recording of the Earth magnetic field — geophysical observatories
04 p0519 N85-13317
VOC emissions from volatile organic liquid storage tanks: Background information for proposed standards
[PB84-237320] 04 p0532 N85-13403
Special Developments and Methods in High Frequency Measuring Techniques — conferences
[PTB-E-24] 05 p0629 N85-14030
Admittance measurement with twin-T devices in the frequency range between 1 and 300 MHz
05 p0629 N85-14032
Realization of noise power in the microwave range by thermal noise standards 05 p0629 N85-14034
Calibration of noise power transfer standards, measurement uncertainties and long term stability
05 p0630 N85-14035
Voltage dependence of the relative AC-DC transfer difference for HF voltage-transfer standards
05 p0630 N85-14038
A group delay standard for the MHz frequency range
05 p0630 N85-14040
The detection and assessment of defects in automatic ultrasonic inspection
[BLL-RISLEY-TR-4597-(9091.9F)]
05 p0847 N85-14150
Experimentation and measurement
[PB84-233659] 06 p0812 N85-15157
NAAQS (National Ambient Air Quality Standards) Exposure Model (NEM) applied to carbon monoxide
[PB84-242551] 06 p0834 N85-15310
Standard SHEF (Standard Hydrometeorologic Exchange Format) decoder Version 1.1
[PB85-106508/GAR] 06 p0840 N85-15332
Proceedings of the National Bureau of Standards and National Security Agency Workshop on Standardization Issues for Optical Data Disk (OD3) Technology
[PB84-217765] 06 p0848 N85-15383
Prime Computer, Inc., PRIME 750, COBOL-74 Revision 19.3.2
[PB84-227826] 06 p0851 N85-15409
NBS (National Bureau of Standards) and WR62 and WR90 reference noise standards
[PB84-235704] 07 p0942 N85-15977
Estimation of requirements for acceptable noise radiation level of communication transmitters
07 p0949 N85-16017
What should DOE do to help establish voluntary consensus standards for measuring and rating the performance of PV modules?
[NASA-CR-174265] 07 p0992 N85-16297
A superconducting quantum current standard
[NPL-QU-67] 08 p1224 N85-17710
Defect tolerance in pipeline girth welds
[ERS-E.353] 09 p1329 N85-18347
Impact of 810D on dynamic test laboratories
09 p1334 N85-18386
Evaluation of the particulate levels occurring under 1.0/1.2 g/mi nitrogen oxide standards for light duty diesel vehicles and light duty diesel trucks
[PB85-115939/GAR] 09 p1350 N85-18494
Perspective on demonstrations of compliance for high-level waste disposal
[DE85-000989] 09 p1383 N85-18688
Radiation data and standards for Tokamak diagnostics
09 p1390 N85-18742
Proceedings of Colloquium/Workshop on Composite Materials and Structures, Standardization, Qualification, Certification held at washington, D.C. on 8-10 May 1984
[AD-A149039] 10 p1432 N85-19029
Historical cost curves for hydrogen masers and cesium beam frequency and timing standards
10 p1465 N85-19245
Health standards for general vibration
10 p1523 N85-19607
Abstract and index collection
[PB85-119501] 10 p1569 N85-19892
FAA policy regarding solid waste disposal facilities
[AD-P004196] 11 p1581 N85-19983
Magnetic measurements, calibrations, and standards: Report on a survey
[PB85-127827] 11 p1636 N85-20317
Radiation safety of crew and passengers of air transportation in civil aviation. Provisional standards
[NASA-TM-77610] 11 p1692 N85-20836
Prime Computer, Incorporated, PRIME 750, BASICV revision 19.4
[PB85-108074] 11 p1699 N85-20883
Software standards issues — space station software development 11 p1701 N85-20892
Micro focus Cifer 2687 high performance level 2 COBOL; V2.5
[PB85-108959] 11 p1703 N85-20714
Micro focus Cifer 2687 compact level 2 COBOL; V2.5
[PB85-108967] 11 p1703 N85-20715
Metrology for Electronic Technology: A bibliography of NBS (National Bureau of Standards)
[PB85-112895] 12 p1830 N85-21436
Stability of organic audit materials and results of source test analysis audits
[PB85-116184] 12 p1885 N85-21832
Air quality criteria for ozone and other photochemical oxidants. External review draft, volume 2
[PB85-126043] 12 p1886 N85-21836
Air quality criteria for ozone and other photochemical oxidants, external review draft, volume 3
[PB85-126050] 12 p1886 N85-21837
Head/neck injury: Post mortem procedures, Annex B
12 p1907 N85-21977
Journal of Research of the National Bureau of Standards, volume 89, number 2, March - April 1984
[PB85-115426] 12 p1926 N85-22103
A description of the Langley wireframe geometry standard (LaWGS) format
[NASA-TM-85767] 13 p1971 N85-22380
Characterization standards for solid propellant rocket motors
[AD-A150250] 13 p2013 N85-22627
Digital standards conversion: Interpolation theory and aperture synthesis
[BBC-RD-1984/20] 13 p2053 N85-22857
Critical current measurements on an NbTi superconducting wire standard reference material
[PB85-116594] 13 p2086 N85-22906
Validation summary report, Burroughs Corporation, B20 FORTRAN release 4.0
[PB84-227792] 13 p2145 N85-23316
Do new aircraft need new technologies and certification rules? 14 p2224 N85-23795

Establishment and maintenance of certification standards for helicopter and turboprop power transmission systems 14 p2224 N85-25796
Safety with industrial manufacturing lasers 14 p2306 N85-24281
Guidelines for development structured FORTRAN programs [NASA-TM-86407] 14 p2402 N85-24808
Titanium alloys, products, standards listed 15 p2533 N85-25620
New sensor for industrial metrology developed 15 p2536 N85-25665
Standards in process: Foundation and profiles of ISDN (Integrated Services Digital Network) and OSI (Open Systems Interconnection) studies [PB85-165041/GAR] 15 p2545 N85-25712
Compositional control of plate steels 15 p2565 N85-25626
Papers from the Symposium on Emissions: The Value of Incentives and Guidelines for Control [S-336] 15 p2590 N85-25967
Management of vacuum leak-detection processes, standards and calibration [DE86-006705] 16 p2786 N85-27202
Standards and specifications for geodetic control networks [PB85-168478] 16 p2816 N85-27374
Review of national emission standards for mercury [PB85-153906] 16 p2822 N85-27406
Mapping principles for the standards interface for computer aided design [PB85-177905] 16 p2849 N85-27566
NBS physical measurement services [NBSIR-84-2875] 16 p2859 N85-27633
DoD manual for standard data elements, part 2 [AD-A152202] 16 p2878 N85-27755
DoD manual for standard data elements, part 3 [AD-A152203] 16 p2878 N85-27756
NBS (National Bureau of Standards) research reports [PB85-127421] 16 p2879 N85-27764
Development of new circuit symbols for binary logic elements [MBB-Z-38/85-O] 17 p3014 N85-29840
State Weights and Measures Laboratories: Program handbook [PB85-183356] 18 p3111 N85-29283
Development of guidelines for setting physiological and hygienic standards for noise levels in aerospace medicine 19 p3323 N85-30584
A systematic determination of skill and simulator requirements for airline transport pilot certification [AD-A154135] 19 p3330 N85-30630
Liquid metal reactor programs: Safeguards and program assurance [DE85-010621] 19 p3331 N85-30635
Standards Committee activities of the National Bureau of Standards: 1984 highlights [PB85-183382] 19 p3350 N85-30764
Auto fuel efficiency standards, part 2 [GPO-41-169] 20 p3435 N85-31309
The 1982 National Measurement Requirements Survey [NMRC-83-01-SUMM] 20 p3436 N85-31321
Journal of Research of the National Bureau of Standards, volume 90, number 1, January - February 1985 [PB85-179083] 20 p3522 N85-31906
Improved coordinate measuring machine calibration and control [DE85-012053] 21 p3590 N85-32315
Digital matched filter 22 p3765 N85-33339
Modeling of auto exhaust smog chamber data for EKMA development [PB85-195492] 22 p3813 N85-33619
Development of solid thorium-232 reference materials [DE85-011453] 22 p3841 N85-33785
Recommendations for the design and equipping of engineering metrology laboratories [NPL-MOM-22] 23 p3898 N85-34145
Redefining the scratch standards [PB85-194736] 24 p4154 N85-35755

STANDING WAVES

Tides and tidal currents of the inland waters of Western Washington [PB84-237379] 06 p0842 N85-15348
Standing wave pattern of HF radio waves in the ionospheric reflection region. Part 1: General formulas [UIO-SR-84-05-PT-1] 09 p1313 N85-18253
Observation of standing spinwaves in thin Fe-films by means of Raman spectroscopy [DE85-003036] 11 p1735 N85-20913
Nonrelativistic Kapitza-Dirac scattering [AD-A150622] 13 p2159 N85-23405
Magnetic pulsations recorded in northern Scandinavia during the IMS; a study of Pc 4-5 events 14 p2370 N85-24647
Nonrelativistic Kapitza-Dirac scattering [AD-A150649] 14 p2417 N85-24911

STANDS

U SUPPORTS

STANNIDES

NT NIOBIUM STANNIDES

STAPHYLOCOCCUS

Structural-functional changes in bacterial cells under spaceflight conditions 16 p2724 N85-26812

STAR CLUSTERS

NT PRAESEPE STAR CLUSTERS
NT VIRGO GALACTIC CLUSTER
Observations of four Beta Cephei stars in NGC6231 01 p0126 N85-10877
Search for white dwarf companions of cool stars with peculiar element abundances [NASA-CR-174030] 02 p0297 N85-11923
Studies of extragalactic RR Lyrae stars 03 p0444 N85-12831
An infrared study of the bi-polar outflow region GGD 12-15 [NASA-TM-86655] 03 p0445 N85-12835
Fifth Conference on Star Clusters and Associations and Their Relation to the Evolution of the Galaxy [PUBL-56] 05 p0736 N85-14732
Structural properties of open star clusters and their relation to the galaxy 05 p0736 N85-14733
Open star clusters and the evolution of the galactic disk 05 p0736 N85-14734
The galactic distribution of open clusters of different ages and the angular velocity of the spiral structure 05 p0737 N85-14737
On collective effects in the rotation of stars in clusters and associations 05 p0737 N85-14739
A search for possible members of open clusters among known Ap stars 05 p0737 N85-14740
The present state of the International Star Cluster Photometry Programme 05 p0737 N85-14741
The Lund catalogue of open cluster parameters 05 p0738 N85-14742
Collective processes and formation of star clusters 05 p0738 N85-14743
The distribution of dust in the region of the Rosette Nebula and MON OB2 association 05 p0739 N85-14753
Proper motions and kinematical properties of Orion trapezium type stellar systems 05 p0739 N85-14755
On the most probable number of flare stars in the Pleiades field 05 p0739 N85-14756
Hyades moving group 05 p0740 N85-14757
The influence of stellar luminosity and temperature calibration on the determination of the initial mass function 05 p0740 N85-14760
High sensitivity, high angular resolution far-infrared photometry from the KAO 08 p1246 N85-17867
International Ultraviolet Explorer observations of amorphous hot galaxies [NASA-CR-174354] 10 p1571 N85-19904
Ultraviolet studies of the young populous cluster NGC 2100 in the LMC 11 p1748 N85-20995
Processes and problems in secondary star formation [DE85-003623] 12 p1960 N85-22322
A study of W Serpentis binaries: SX Cassiopeiae, RX Cassiopeiae, and W Serpentis 20 p3544 N85-32053
Far-infrared observations of young clusters embedded in the R Coronae Australinae and RHO Ophiuchi dark clouds [NASA-TM-86661] 24 p4167 N85-35834

STAR DISTRIBUTION

Lessons from the globular cluster NGC 5466 05 p0739 N85-14749
Galactic orbits of globular clusters 05 p0739 N85-14750
The fragmentation of molecular clouds and the IMF 05 p0740 N85-14759
Automated star counts in nebulous areas 07 p0967 N85-16137
International Ultraviolet Explorer observations of amorphous hot galaxies [NASA-CR-174354] 10 p1571 N85-19904
Discriminant analysis of pulsar groups in the diagram P versus P 12 p1960 N85-22319
Processes and problems in secondary star formation [DE85-003623] 12 p1960 N85-22322
The color excesses of classical cepheids and the structure of our galaxy 13 p2169 N85-23459
The structure and angular momentum content of dark clouds 14 p2439 N85-25054
A star camera aspect system suitable for use in balloon experiments [OG-9.3-10] 23 p4028 N85-34965

STAR FIELDS

U STAR DISTRIBUTION

STAR TRACKERS

NT CCD STAR TRACKER
Optical contacting for gravity probe star tracker [NASA-TM-86475] 01 p0120 N85-10819
Optical analysis of the star-tracker telescope for Gravity Probe [NASA-TM-86474] 01 p0129 N85-10888
The de Tiffini star pointer characterization and conclusions on the 1982 transmediterranean flight [CESR-83-1070] 02 p0139 N85-10946
Optimization of orientation in navigation by two heavenly bodies 07 p0951 N85-16027
The UKIRT centre section structural investigation — United Kingdom Infrared Telescope (UKIRT) [UKIRT-22] 09 p1414 N85-16920
Integration of an Apple 2 Plus computer into an existing dual axis sun tracker system [AD-A150778] 14 p2404 N85-24623
Autonomous state determination for an Earth orbiting satellite using horizon and star sensors [AD-A151827] 15 p2493 N85-25379
Charge Injection Device (CID) used as a photodector: Implementation and performance. Application to light source tracking (stars, lasers) [CNES-83/CT/DRT/TIT/OE/146] 20 p3533 N85-31983

STAR TRACKING

U STAR TRACKERS

STARCHES

Synthesis and characterization of novel polymers from non-petroleum sources for use in enhanced oil recovery [DE85-010922] 19 p3250 N85-30151

STARFIGHTER AIRCRAFT

U F-104 AIRCRAFT

STARK EFFECT

Stark broadening of H(-) resonances in large electric fields [DE84-016974] 04 p0496 N85-13164
The adsorption of acrylonitrile at a gold electrode: An EMIRS measurement of the electrochemical stark effect [AD-A148664] 08 p1123 N85-17082
X-ray line broadening of a diagnostic in laser produced plasma [DE85-001179] 10 p1580 N85-19841

STARLAB

Future ultraviolet experiments, including FUSE/COLUMBUS 11 p1744 N85-20989

STARLIFTER AIRCRAFT

U C-141 AIRCRAFT

STARS

NT A STARS
NT B STARS
NT BINARY STARS
NT BLACK HOLES (ASTRONOMY)
NT BLUE STARS
NT CARBON STARS
NT CATACLYSMIC VARIABLES
NT CEPHEID VARIABLES
NT COMPANION STARS
NT COOL STARS
NT DWARF NOVAE
NT DWARF STARS
NT EARLY STARS
NT ECLIPSING BINARY STARS
NT FLARE STARS
NT GIANT STARS
NT HERBIG-HARO OBJECTS
NT HERCULES NOVA
NT HOT STARS
NT INFRARED STARS
NT LATE STARS
NT M STARS
NT MAGNETIC STARS
NT MAIN SEQUENCE STARS
NT METALLIC STARS
NT NEUTRON STARS
NT NOVAE
NT O STARS
NT PECULIAR STARS
NT PRAESEPE STAR CLUSTERS
NT PRE-MAIN SEQUENCE STARS
NT PROTOSTARS
NT PULSARS
NT RADIO STARS
NT RED DWARF STARS
NT RED GIANT STARS
NT REFERENCE STARS
NT STELLAR GRAVITATION
NT SUBDWARF STARS
NT SUBGIANT STARS
NT SUN
NT SUPERGIANT STARS
NT SUPERMASSIVE STARS
NT SUPERNOVAE
NT SYMBIOTIC STARS
NT T TAURI STARS
NT VARIABLE STARS
NT WHITE DWARF STARS

NT WOLF-RAYET STARS
NT X RAY BINARIES
NT ZETA AURIGAE STAR
UBV photometry of E region standard stars of intermediate brightness 01 p0128 N85-10879
Observations of the pulsating hydrogen: Deficient star BD+13 deg 3224, during 1980 - 1981 01 p0128 N85-10882
Local photometric standards for CeII emission stars 01 p0128 N85-10883
Documentation for the machine-readable version of the ANS Ultraviolet Photometry Catalogue of Point Sources (Wesselius et al 1982) [NASA-TM-87379] 03 p0406 N85-12589
Studies of extragalactic RR Lyrae stars 03 p0444 N85-12831
Documentation for the machine-readable version of the MK classification extension catalogue Morris-Kennedy (1983) [NASA-TM-87372] 04 p0549 N85-13491
Documentation for the machine-readable version of the Perth 75: A Catalogue of Positions of 2589 FK4 and FK4S Stars (Nikoloff and Hog 1982) [NASA-TM-87376] 04 p0549 N85-13492
Documentation for the machine-readable version of the AGK3 Star Catalogue of Positions and Proper Motions North of -2 deg .5 declination (Dieckvoss and Collaborators 1975) [NASA-TM-87378] 04 p0549 N85-13493
Collective processes and formation of star clusters 05 p0738 N85-14743
Iron core collapse models of Type 2 supernovae [DE84-013909] 05 p0743 N85-14775
Local interstellar extinction with an emphasis on uvby beta results 06 p0875 N85-15559
Do the arching HI filaments show in local reddening data? 06 p0876 N85-15561
Radio and UV observations of high latitude HI 06 p0879 N85-15583
Narrow absorption components in Be star winds 08 p1232 N85-17760
Ultraviolet spectral morphology of O-type stellar winds 08 p1232 N85-17762
Airborne Astronomy Symposium. A symposium commemorating the tenth anniversary of operations of the Kuiper Airborne Observatory [NASA-CP-2353] 08 p1244 N85-17848
History of photometric precision 08 p1250 N85-17893
Photometric precision needed for planetary detection 08 p1250 N85-17894
Five-minute P modes detected in Doppler shift measurement on Alpha Centauri 08 p1250 N85-17895
Atmospheric limitations in stellar seismology: Should one measure radial velocity or brightness fluctuations? 08 p1251 N85-17899
The atmospheric extinction problem 08 p1251 N85-17901
Reduction to outside the atmosphere and statistical tests used in Geneva photometry 08 p1251 N85-17902
A CCD system for photometry of direct and spectroscopic images 08 p1252 N85-17904
Elemental abundances of mercury-manganese stars and the population 2 type star HD 109995 [NASA-CR-174298] 08 p1255 N85-17913
A comparative study of dust and young stars in three small galaxies 09 p1415 N85-18928
IUE observations of blue horizontal branch globular clusters and UV-bright stars 11 p1748 N85-20992
The UV extinction laws in two very young clusters, NGC 6530 in the galaxy and NGC 2100 in the LMC 11 p1748 N85-20994
The central star of NGC 40 11 p1751 N85-21013
Chromospheric emission lines in high-resolution LWR spectra (220 - 3000 alpha) of gamma CRU (M3 3) and alpha ORI (M2 Iab) 11 p1758 N85-21058
Active late-type stars and the applicability of coronal loop models 11 p1758 N85-21059
Co-rotating interaction regions in stellar winds 11 p1758 N85-21060
IUE low-dispersion reference atlas 11 p1760 N85-21073
IUE observations of faint standard stars for calibration of the space telescope 11 p1761 N85-21076
A survey of Mg II h and k emission in near-solar type stars [NASA-CR-175572] 12 p1953 N85-22289
University of Cambridge Institute of Astronomy report of activities 13 p2170 N85-23484
Activities report of the Institute for Astronomy and Astrophysics [MITT-5] 14 p2434 N85-25012
Documentation for the machine-readable version of the Cape Photographic Durchmusterung (CPD) [NASA-TM-87442] 14 p2439 N85-25060
Very large array observations of coronal loops and related observations of solar type stars [AD-A152027] 16 p2888 N85-27817
Activities report of the Institute of Astronomy 20 p3545 N85-32059
Star formation in NGC 7538: Multi-wavelength observations and issues 20 p3545 N85-32063
Basic formulae for the computation of the deflection of the vertical from astronomical star observations [AD-A154912] 21 p3605 N85-32390
Neutrino-antineutrino annihilation around collapsing star [OG-1.1-10] 22 p3861 N85-33911
Search for gamma rays of energy 10(15) eV from Cygnus X-3 [OG-2.1-1] 22 p3862 N85-33919
Observation of an excess of cosmic ray muons of energies 2 TeV from the direction of Cygnus X-3 [OG-2.1-3] 22 p3863 N85-33920
Muon content of gamma ray induced EAS from Cygnus X-3 [OG-2.1-4] 22 p3863 N85-33921
Gamma rays of energy or = 10(15) eV from Cyg X-3 [OG-2.1-5] 22 p3863 N85-33922
The capability of the existing network of installations for detecting the antineutrino burst from collapsing stars [HE-5.3-13] 24 p4206 N85-36107
STARTERS
NT ENGINE STARTERS
STARTING
Control system design language implementation of a gas turbine starting controller [AD-A147896] 07 p0905 N85-15732
Comparative visualization of accelerating flow around various bodies, starting from rest [AD-P004159] 09 p1264 N85-17944
Engine wear and cold startability of methanol fueled engines. [DE85-001206] 11 p1647 N85-20381
STATE EQUATIONS
U EQUATIONS OF STATE
STATE ESTIMATION
Hybrid state estimation approach to multiobject tracking for airborne surveillance radars [AD-A148459] 08 p1153 N85-17279
STATE VECTORS
Optimum design for nonlinear shock mounts for transient inputs 09 p1334 N85-18390
High level languages in protocol specification and verification [FUB-51-1983] 09 p1370 N85-18611
Computer program TRAMP: Inclusion of state space facilities and the analysis of non-linear elements [BAE-BT-12643] 15 p2626 N85-26181
Fundamental equivalence of generalized state space systems [MATHEMATICS-RESEARCH-182] 15 p2642 N85-26293
Adaptive filtering for large space structures: A closed-form solution 20 p3417 N85-31206
STATIC AERODYNAMIC CHARACTERISTICS
The aerodynamics of bluff bodies in turbulent shear layers 05 p0593 N85-13780
Experimental techniques and instrumentation for bluff body aerodynamics 05 p0593 N85-13781
Automatic correction of static characteristics of measurement channel of digital oscillograph 08 p0795 N85-15083
Static longitudinal stability and control characteristics of the Fokker F27 Friendship calculated by simple handbook methods [VTH-LR-394] 16 p2711 N85-26726
STATIC CHARACTERISTICS
NT STATIC AERODYNAMIC CHARACTERISTICS
Structural analysis of the Space Shuttle Orbiter 01 p0081 N85-10401
Static and dynamic characteristics of materials with beam-microstructure 03 p0370 N85-12361
Sensitivity analysis of discrete structural systems: A survey [NASA-TM-86333] 06 p0817 N85-15186
Treatment of general boundary conditions and point-wise state variable constraints in optimum design for static and dynamic response 09 p1330 N85-18358
Electrothermal transducer with short time constant 13 p2086 N85-23040
Method of static measurements of absolute scattering matrix of radar targets 22 p3762 N85-33316
STATIC DEFORMATION
NIKE3D: An implicit, finite-deformation, finite element code for analyzing the static and dynamic response of three-dimensional solids, revision 1 [DE84-017161] 04 p0514 N85-13277
Consolidation theory with consideration of frame plasticity [REPT-9/1984] 16 p2796 N85-27240
Liquid-metal transducers for strain measurement during in-pile materials testing 17 p2945 N85-28176
The static aeroelasticity of a composite wing 18 p3121 N85-29321
Mechanical properties of aligned short carbon fiber reinforced PES and PI laminates [ESA-TT-896] 20 p3422 N85-31240
STATIC ELECTRICITY
International Aerospace and Ground Conference on Lightning and Static Electricity. 1984 technical papers. Supplement [NASA-CP-2356] 07 p0999 N85-16343
STATIC FIRING
Qualification of an electrothermal hydrazine thruster with a vacuum thrust of 0.5 to 2.0 N [BMFT-FB-W-84-043] 07 p0917 N85-15808
Space shuttle flight readiness firing dress rehearsal for STS-1 08 p1097 N85-16929
STATIC LOADS
Strength of welded joints in VT23 alloy upon repeated static loading 01 p0020 N85-10120
Interactive buckling of thin-walled structural components under static and dynamic loads 01 p0059 N85-10302
Study of delamination cracking under static and cyclic loads of carbon-epoxy composite materials [REPT-42-727/F] 03 p0327 N85-12102
Free-edge failures of composite laminates 04 p0467 N85-12971
Characterization of fiber optic cables under large tensile loads [DE84-016816] 05 p0651 N85-14180
Stability of hollow shafts under torsion 06 p0780 N85-14986
Tests of the load-bearing and deformation behaviour of reinforced concrete spherical shells under point loading [BLL-RISLEY-TR-4550-9091.9F)] 06 p0816 N85-15182
Preliminary report on tests of tensile specimens with a part-through surface notch for a filament wound graphite/epoxy material [NASA-CR-172545] 10 p1431 N85-19026
Sensitivity of titanium alloys to stress concentration during repeated static loads 11 p1802 N85-20074
Elastic compliance of imperfect interfaces: Review and relationship to ultrasonic scattering [DE85-003068] 11 p1852 N85-20404
Yield joint condition for three-dimensional I-beams [ILR-MITT-137] 12 p1867 N85-21716
Some problems in optimally designing shells of revolution 14 p2278 N85-24114
Investigation to optimize the passive shock wave/boundary layer control for supercritical airfoil drag reduction [NASA-CR-175788] 16 p2599 N85-26665
Forced structural response using component mode synthesis [DE85-008479] 19 p3287 N85-30383
Static and cyclic behavior of semi-rigid steel beam-column connections [PB85-194363] 24 p4103 N85-35433
STATIC PRESSURE
NT HYDROSTATIC PRESSURE
Effect of combined pressure and temperature distortion orientation on high-bypass-ratio turbofan engine stability [NASA-TM-83771] 01 p0011 N85-10067
High temperature static strain sensor development program 02 p0141 N85-10959
Effects of inlet distortion on a static pressure probe mounted on the engine hub in an F-15 airplane [NASA-TP-2411] 13 p1974 N85-22394
Transition detection using surface pressure holes 14 p2212 N85-23722
Measurement of turbofan-turbojet thrust from tailpipe static pressure [AD-A154036] 19 p3220 N85-29957
On the evaluation of boundary layer measurements on boattailed bodies of revolution in axisymmetric compressible subsonic flow [ESA-TT-863] 20 p3457 N85-31471
Static high pressure study of nitric oxide chemistry: Proposed mechanism for nitric oxide detonation [DE85-010795] 22 p3746 N85-33220
Explosive containment study [DE85-011719] 22 p3753 N85-33267
STATIC STABILITY
NT DIMENSIONAL STABILITY
NT SHELL STABILITY
NT STRUCTURAL STABILITY

Integrated Application of Active Controls (IAAC) technology to an advanced subsonic transport project-longitudinal handling qualities study of a relaxed-stability airplane
[NASA-CR-3660] 02 p0148 N85-11005
Generation and evolution of diabatic planetary waves in continuously stratified atmosphere with Ekman dissipation 09 p1354 N85-18515
Approximate neutral point of a subsonic canard aircraft
[NASA-TM-86094] 15 p2462 N85-25205
Numerical experiments of jet streak ageostrophic circulations using pseudo-geostrophic initialization and perspectives 15 p2590 N85-25969
Realisation of relaxed static stability on a commercial transport 16 p2713 N85-26748
Demonstration of relaxed static stability on a commercial transport 17 p2903 N85-27896
Realisation of relaxed static stability on a commercial transport 17 p2903 N85-27899

STATIC TESTS
NT STATIC FIRING
Initial sailplane project: The RP-1 04 p0468 N85-12976
Static jet noise test results of four 0.35 scale-model QCGAT mixer nozzles
[NASA-TM-86871] 04 p0558 N85-13551
Measuring methods to determine the static and dynamic behavior of wind energy converters 05 p0668 N85-14297
Static internal performance of single-expansion-ramp nozzles with various combinations of internal geometric parameters
[NASA-TM-86270] 06 p0749 N85-14797
Using a data base management system for modelling SSME test history data 12 p1944 N85-22211
Modifications to the nozzle test chamber to extend nozzle static-test capability
[NASA-TM-86368] 15 p2464 N85-25216
Static investigation of several yaw vectoring concepts on nonaxisymmetric nozzles
[NASA-TP-2432] 16 p3058 N85-28924
Static and cyclic behavior of semi-rigid steel beam-column connections
[PB85-194363] 24 p4103 N85-35433

STATICS
NT ELECTROSTATICS
NT HYDROSTATICS
Numerical solution of one-dimensional nonlinear problems of statics for elastic beams and shells under rigid constraints 17 p2943 N85-28166
Method of solving problems of statics for multilayer shells of revolution 17 p2943 N85-28167
Scattering by distributions of small thin particles 19 p3253 N85-30172

STATIONARY ORBITS
Non-stable motions and instability in stellar associations 05 p0739 N85-14754
Construction and functioning of extended orbital systems 16 p2724 N85-26814
Geostationary orbit capacity study
[REPT-44-3558] 18 p3091 N85-29134

STATIONKEEPING
Stationkeeping strategies for geostationary satellites 05 p0600 N85-13825
The investigation of tethered satellite system dynamics
[NASA-CR-171278] 07 p0912 N85-15772
Station keeping of geostationary satellites by electric propulsion
[NASA-TM-77820] 14 p2320 N85-24337
Moored buoy stationkeeping and location system 14 p2331 N85-24416
Orbital positioning and stationkeeping of geostationary satellites 14 p2397 N85-24772
Artificial intelligence in space platforms
[AD-A152078] 16 p2851 N85-27578

STATIONS
NT AUTOMATIC WEATHER STATIONS
NT CREW STATIONS
NT CREW WORKSTATIONS
NT EARTH TERMINALS
NT EOSS
NT GLOBAL TRACKING NETWORK
NT GROUND STATIONS
NT HYDROELECTRIC POWER STATIONS
NT LONG DURATION EXPOSURE FACILITY
NT ORBITAL SPACE STATIONS
NT ORBITING LUNAR STATIONS
NT PAYLOAD STATIONS
NT POLYSTATION DOPPLER TRACKING SYSTEM
NT SALYUT SPACE STATION
NT SPACE STATIONS
NT TRACKING STATIONS
NT WEATHER STATIONS
NT WORKSTATIONS
Sector suite man-machine functional capabilities and performance requirements
[AD-A148881] 10 p1531 N85-19647
Use of mobile surface station for synchronous satellite measurements in seismological research 13 p1984 N85-22447
Applications, specifications of Robotron CAD-CAM work stations 15 p2537 N85-25661
Deployment of a regional array in Norway
[AD-A154120] 19 p3313 N85-30536

STATISTICAL ANALYSIS
NT AMPLITUDE DISTRIBUTION ANALYSIS
NT ANALYSIS OF VARIANCE
NT BIVARIATE ANALYSIS
NT CORRELATION COEFFICIENTS
NT COVARIANCE
NT DISCRIMINANT ANALYSIS (STATISTICS)
NT FACTOR ANALYSIS
NT GOODNESS OF FIT
NT KOLMOGOROFF-SMIRNOFF TEST
NT LIKELIHOOD RATIO
NT MAXWELL-BOLTZMANN DENSITY FUNCTION
NT MULTIVARIATE STATISTICAL ANALYSIS
NT NONPARAMETRIC STATISTICS
NT NORMAL DENSITY FUNCTIONS
NT ORTHOGONALITY
NT PEARSON DISTRIBUTIONS
NT POISSON DENSITY FUNCTIONS
NT PROBABILITY DENSITY FUNCTIONS
NT PROBABILITY DISTRIBUTION FUNCTIONS
NT QUANTILES
NT RANK TESTS
NT RAYLEIGH DISTRIBUTION
NT REGRESSION ANALYSIS
NT REGRESSION COEFFICIENTS
NT SEQUENTIAL ANALYSIS
NT STANDARD DEVIATION
NT STATISTICAL CORRELATION
NT STATISTICAL DECISION THEORY
NT STATISTICAL TESTS
NT VARIANCE (STATISTICS)
NT WEIBULL DENSITY FUNCTIONS
Equation of state study for polar fluids
[PB84-222801] 01 p0025 N85-10157
Measurement assurance programs. Part 2: Development and implementation
[PB84-217876] 01 p0051 N85-10338
Simulation uses of the exponential distribution
[AD-A144940] 01 p0112 N85-10756
Harmonizable, Cramer, and Karhunen classes of processes
[AD-A144984] 01 p0113 N85-10767
An integral inequality with applications to order statistics
[AD-A145081] 01 p0113 N85-10770
Optimizing search with positive information feedback
[CSIR-TWISK-313] 01 p0125 N85-10855
Some statistical characteristics of atmospheric optical thickness in visible spectral range 02 p0164 N85-11109
A study of environmental characterization of conventional and advanced aluminum alloys for selection and design. Phase 2: The breaking load test method
[NASA-CR-172387-PHASE-2] 02 p0182 N85-11219
Seminar on Principal Components Analysis in the Atmospheric and Earth Sciences
[CSIR-S-334] 02 p0211 N85-11388
What is principal components analysis? 02 p0211 N85-11389
Principal components: A review 02 p0211 N85-11390
Application of correspondence analysis to meteorological data 02 p0211 N85-11393
A principal component analysis of eastern Transvaal seasonal rainfall, 1950 to 1981 02 p0212 N85-11395
The application of principal component analysis in a study of rainfall 02 p0212 N85-11396
Spatial relationships in stream flow residuals 02 p0212 N85-11397
The application of principal components analysis to LANDSAT MSS data 02 p0212 N85-11398
Northern Hemisphere atlas of 1-minute rainfall rates
[AD-A145411] 02 p0231 N85-11508
Weighted distributions arising out of methods of ascertainment
[AD-A145615] 02 p0252 N85-11648
Fluctuations in parameters of light beam along path with reflection in turbulent atmosphere 02 p0263 N85-11722
Spread-spectrum communications
[AD-A146135] 03 p0355 N85-12285
Statistical properties of geomagnetic pulsations at the Observatory of Fuerstenfeldbruck determined with the aid of pulsation indices. Part 2: Periodicity in the occurrence of pulsations
[REPT-556] 03 p0376 N85-12399
GASP cloud- and particle-encounter statistics and their application to LFC aircraft studies. Volume 2: Appendixes
[NASA-TM-85835-VOL-2] 03 p0395 N85-12522
Statistical analysis of some traveling salesman algorithms
[AD-A145786] 03 p0410 N85-12620
A building blocks approach to statistical databases 03 p0437 N85-12782
Test report no. 17.208: Statistics of the basic characteristics of carbon-epoxy composites
[DGT-23.426/A] 04 p0488 N85-12979
Analysis of frequency-selective integrated circuits in system of normal coordinates 04 p0489 N85-13119
Thermal shock as a carbide grade development tool
[DE84-016939] 04 p0509 N85-13251
Design and implementation of a modular program system for statistical analyses
[IKE-4-114] 04 p0551 N85-13503
Satellite orbit determination 05 p0596 N85-13813
Synthesis of load-time histories resulting from statistical analysis 05 p0650 N85-14171
Some techniques in image processing 05 p0721 N85-14629
Approximating the percentage points of Greenwood's statistic with Cornish-Fisher expansions
[CWI-MS-R8405] 05 p0721 N85-14634
Methodology for economic evaluation of process technologies in the early research and development stages
[DE84-015863] 05 p0736 N85-14731
Statistics from the operation of the low-level wind shear alert system (LLWAS) during the Joint Airport Weather Studies (JAWS) Project
[DOT/FAA/PM-84/32] 06 p0750 N85-14804
Annual review of aircraft accident data: US general aviation, calendar year, 1981
[PB84-230960] 06 p0750 N85-14805
Statistical analysis of visual wave observations and gage/radar measurements
[AD-A146358] 06 p0798 N85-15100
Information-theoretic properties of languages and their grammars
[AD-A146688] 06 p0799 N85-15106
Frequency and motion of western North Pacific tropical cyclones
[PB85-106466/GAR] 06 p0839 N85-15331
Statistical filtering as method for detecting transcrustal acoustic anomalies 07 p0982 N85-16237
An evaluation and comparison of vertical profile data from the VISSR Atmospheric Sounder (VAS)
[NASA-TP-2425] 07 p1000 N85-16351
Lattice statistics
[AD-A146862] 07 p1029 N85-16530
A complete characterization of triply balanced matrices with applications to survey sampling
[AD-A147083] 07 p1031 N85-16542
Model robust response surface designs: Scaling 2-level factorials
[AD-A147494] 07 p1033 N85-16556
On the power functions of test statistics in order restricted inference
[AD-A147126] 07 p1035 N85-16566
FAA (Federal Aviation Administration) statistical handbook of aviation, calendar year 1983
[AD-A148171] 08 p1067 N85-16760
An analysis of robust and efficient priors associated with a finite Bayesian model for compliance testing
[AD-A148497] 08 p1213 N85-17635
Antisampling for estimation: An overview
[AD-A148545] 08 p1216 N85-17659
A statistical evaluation of the limitations of single-channel intermediate-band photoelectric stellar photometry 08 p1251 N85-17900
An objective error measure for the comparison of calculated and measured transient response histories 09 p1335 N85-18395
Field studies of run-up generated by wind waves on dissipative beaches
[AD-A148793] 09 p1359 N85-18548
Computing environments for data analysis. Part 1. Introduction
[AD-A148577] 09 p1373 N85-18632
Computing environments for data analysis. Part 2. Hardware
[AD-A148678] 09 p1374 N85-18633
Estimating the scale parameter of an exponential distribution from a sample of time-censored r-th order statistics
[AD-A148060] 09 p1375 N85-18644

Simple approximate variances for b-letter values. A sampling enquiry: Supplement
[DE85-001410] 09 p1378 N85-18647
Issues in sensitivity and statistical analysis of large-scale, computer-based models
[PB85-116317/GAR] 09 p1376 N85-19850
Evaluation of the birdstrike threat to the F-15 present fleet, rapid deployment force, and dual role fighter transparencies
[AD-A148954] 10 p1421 N85-19966
Factors influencing the ball milling of Si3N4 in water
[NASA-TM-86932] 10 p1450 N85-19136
The ambiguity function of random binary-phase-coded waveforms
[AD-A148906] 10 p1466 N85-19249
TRAN-STAT: Statistics for environmental studies
[DE85-000829] 10 p1513 N85-19547
Frozen precipitation and concurrent weather: A case study for Munchan-Riem, West Germany
[AD-A149227] 10 p1519 N85-19577
Robust Kalman filtering and its applications
[AD-A149044] 10 p1550 N85-19775
Worldwide birdstrike statistics of Lufthansa German Airlines
[AD-P004183] 11 p1579 N85-19945
Microscopic identification of feathers in order to improve birdstrike statistics
[AD-P004187] 11 p1579 N85-19950
Statistical theory of fragmentation processes
[DE85-002206] 11 p1653 N85-20414
National Performance Audit Program ambient air audits of analytical proficiency
[PB85-136204] 11 p1680 N85-20586
User's guide for the computer program response factor (REFAC)
[PB85-136600] 11 p1705 N85-20726
Checking the shape of discrete distributions
[DE85-000177] 11 p1706 N85-20733
An exact solution to the 2 point OC (Operating-Characteristic) curve determination
[AD-A148120] 11 p1708 N85-20746
An IUE high-resolution atlas of O-type spectra
11 p1760 N85-21074
General aviation activity and avionics survey
[AD-A149572] 12 p1769 N85-21103
Field validation of statistically-based acceptance plan for bituminous airport pavements. Volume 1: Correlation analysis of Marshall properties of laboratory-compacted specimens
[FAA-PM-84-12-VOL-1] 12 p1781 N85-21180
Field validation of statistically-based acceptance plan for bituminous airport pavements. Volume 2: Statistical analysis of Marshall properties of plant-produced bituminous materials
[FAA-PM-84-12-VOL-2] 12 p1781 N85-21181
Field validation of statistically-based acceptance plan for bituminous airport pavements. Volume 3: Statistical analysis of 3 methods for determining maximum specific gravity of bituminous concrete mixtures
[FAA-PM-84-12-VOL-3] 12 p1781 N85-21182
Field validation of statistically-based acceptance plan for bituminous airport pavements. Volume 4: Computer simulation of multiple acceptance criteria
[FAA-PM-84-12-VOL-4] 12 p1782 N85-21183
Field validation of statistically-based acceptance plan for bituminous airport pavements. Volume 5: Summary of validation studies
[FAA-PM-84-12-VOL-5] 12 p1782 N85-21184
Preliminary review of statistical treatment of S-glass/epoxy stress rupture data
[AD-A149810] 12 p1797 N85-21275
Algorithm for statistical simulation of electromagnetic compatibility characteristics of high-frequency transmission channels in radioelectronic facilities
12 p1842 N85-21560
Statistics of french Armee de l'air ejections 1970 - 1980
12 p1906 N85-21971
List of head/neck injury on ejection in the German Armed Forces from 1972-1981
12 p1906 N85-21972
General saddlepoint approximations with applications to l-statistics
[AD-A150073] 12 p1924 N85-22086
Surface forward scattering and reflection
[AD-A150115] 12 p1928 N85-22112
Statistical phenomena in particle beams
[DE85-001060] 12 p1929 N85-22118
A statistical approach to vendor selection
[AD-A149781] 12 p1950 N85-22249
Motion of symmetrical satellite with flexible viscoelastic rods about center of mass in circular orbit
13 p1979 N85-22420
Ice statistics and acoustic scattering in the Arctic basin
[AD-A150141] 13 p2140 N85-23289
Microcomputer: Controlled statistics analyzer
[BLL-CE-TRANS-7971-(9022.09)]
13 p2144 N85-23306
Bootstrapping the Kalman filter
[AD-A150509] 13 p2153 N85-23370
Informative geometry of probability spaces
[AD-A150510] 13 p2153 N85-23371
Unsupervised classification of global radar units on Venus
13 p2196 N85-23632
Estimate of fatigue stability of gas-turbine engine compressor vanes in probabilistic aspect
14 p2287 N85-24169
Statistical/Trend analysis of the marine atmospheric boundary layer model
[AD-A151053] 14 p2374 N85-24673
Circulation statistics based on FGGE (First GARP Global Experiment) level 3-B analyses produced by GFDL (Geophysics Fluid Dynamics Laboratory)
[PB85-149318] 14 p2379 N85-24688
Boundary crossing probabilities and statistical applications
[AD-A151027] 14 p2411 N85-24869
Shuttle fleet operations: A simulation analysis
[AD-A151383] 15 p2491 N85-25370
Statistical techniques for signal processing
[AD-A151231] 15 p2541 N85-25690
Nonparametric detection of narrowband signals
[AD-A151280] 15 p2542 N85-25691
Statistical analysis of partial discharge inception in high voltage
15 p2546 N85-25715
Recent VAS imaging/sounding research
15 p2597 N85-26004
Interactive graphical data analysis
[DE85-005946] 15 p2631 N85-26215
Higher order residual analysis for nonlinear time series with autoregressive correlation structures
[AD-A149232] 15 p2636 N85-26257
Intermediate term forecasting techniques for management
[AD-A151370] 15 p2637 N85-26262
Statistical comparison of pooled nitrogen washout data of various altitude decompression response groups
[NASA-TM-58265] 15 p2639 N85-26278
Statistical analysis techniques for small sample sizes
[NASA-CR-171872] 15 p2639 N85-26279
Point processes associated with extreme value theory
[AD-A151211] 15 p2640 N85-26280
Statistical aspects of reliability, maintainability and availability
[AD-A151228] 15 p2640 N85-26282
Scattered data interpolation and approximation
[DE85-007495] 15 p2641 N85-26290
Lectures on probability and statistics
[DE85-007079] 15 p2641 N85-26291
An evaluation of the performance of a new storm tracking methodology
[AD-A152234] 16 p2835 N85-27484
Circulation statistics from January and July: Simulation with the NCAR (National Center for Atmospheric Research) community climate model (CCMOB)
[PB85-165637] 16 p2837 N85-27497
Statistical study of the dynamic analysis of the workload in the A310 certification campaign
16 p2844 N85-27531
Locally-weighted-regression scatter-plot smoothing (LOWESS): A graphical exploratory data analysis technique
[AD-A152230] 16 p2855 N85-27609
Multivariable statistical modelling and its application
16 p2857 N85-27617
Mutil-particle quantum mechanics obeying fractional statistics
[DE85-007830] 16 p2873 N85-27723
Data management issues of statistical databases
[DE85-007616] 16 p2879 N85-27763
The effect of microalloying with calcium and magnesium on the plasticity of Poldi AKN 20 Ni-based alloy
[BLL-BISI-TRANS-2174-(9022.06)]
17 p2929 N85-28075
Computing environments for data analysis. Part 1: Introduction
[DE85-007919] 17 p3009 N85-28603
Computing environments for data analysis. Part 2: Hardware
[DE85-008320] 17 p3009 N85-28604
Computer program for prediction of capture maneuver probability for an on-off reaction controlled upper stage
[NASA-CR-165837] 17 p3010 N85-28611
Software environment for conducting interactive statistical analysis
[AD-A153378] 17 p3012 N85-28626
Improved statistical analysis method for prediction of maximum inlet distortion
[AD-A153767] 18 p3063 N85-28947
Statistical fracture theories for brittle materials
[AD-A153530] 18 p3121 N85-29324
Intercomparison of sea-surface temperature anomaly fields
18 p3140 N85-29440
A comparison of the bounded derivative and the normal mode initialization methods using real data
18 p3144 N85-29463
Pacific Northwest solar radiation data
[DE85-009773] 18 p3149 N85-29496
Towards a statistical analysis of genetic sequences data with particular reference to protein sequences
[AD-A153605] 18 p3152 N85-29515
Accepting error to make less error
[AD-A153949] 18 p3171 N85-29651
Extrapolation methods for multi-dimensional quadrature of singular and regular integrand functions
[DE85-009665] 18 p3172 N85-29655
Cavityless optical bistability in systems of two-level atoms
18 p3186 N85-29764
Corrosion fatigue cooperative testing program statistical analysis
[AD-A153886] 19 p3238 N85-30077
Diagnosis of vertical motions from VAS retrievals during a convective outbreak
[NASA-CR-171569] 19 p3316 N85-30584
Precipitation estimation using collocated GOES satellite and surface data
[AD-A154248] 19 p3317 N85-30559
Workshop on objective analysis: Analysis strategies for field-dependent estimation
[PB85-179901] 19 p3318 N85-30560
Troposphere-stratosphere (surface-55 km) monthly general circulation statistics for the Northern Hemisphere-four year averages
[NASA-TM-86182] 20 p3495 N85-31730
A cluster analysis method for identification of subpopulations of cells in flow cytometric list-mode arrays
20 p3503 N85-31779
A guide to the statistical analysis of the results of linear and nonlinear least-squares data fitting
[NPL-DITC-53/84] 20 p3521 N85-31895
Reliability of void detection in structural ceramics using scanning laser acoustic microscopy
[NASA-TM-87035] 21 p3597 N85-32337
Signal statistics of the radar echoes: Angle-of-arrival statistics, part 2.2A
21 p3618 N85-32482
A statistical analysis of ice nuclei concentrations at urban and rural sites in Valladolid, Spain
21 p3640 N85-32614
A statistical study of CCN concentration in subequatorial climate: The particular case of the tropical wet forest
21 p3649 N85-32673
An error-dependent model of instrument-scanning behavior in commercial airline pilots
[NASA-CR-3908] 21 p3665 N85-32765
Theory of soliton waves
[AD-A154784] 21 p3676 N85-32837
Optimization of sampling in statistical physics experiments
21 p3696 N85-32975
Enhancing precision of remote temperature sensing data from satellites under cloudy atmospheric conditions
22 p3734 N85-33148
Logical and physical modeling and design of scientific and statistical databases for energy research
[DE85-006081] 22 p3833 N85-33737
Statistical analyses in the study of solar wind-magnetosphere coupling
[DE85-006696] 22 p3859 N85-33898
Observations of the Crab Nebula at energies 4.10(11)
[OG-2.3-1] 22 p3865 N85-33938
Statistical pooling method of fatigue data for reliability design
23 p3906 N85-34198
Theoretical and experimental analyses of the performance of two-color laser ranging systems
[NASA-CR-176159] 23 p3936 N85-34397
On the statistical significance of excess events: Remarks of caution and the need for a standard method of calculation
[OG-9.5-10] 23 p4031 N85-34567
A new statistic for the analysis of circular data in gamma-ray astronomy
[OG-9.5-13] 23 p4031 N85-34569
Rigidity spectrum of Forbush decrease
[SH-5.1-6] 23 p4042 N85-35060
Methods and software for cosmic ray scintillation studies
[SH-9.1-17] 23 p4052 N85-35132
Statistical distribution of breakdown voltages in rep-rate spark gaps
[DE85-012813] 24 p4090 N85-35354
Users guide for optimum interpolation method of global data assimilation
[AD-A155929] 24 p4138 N85-35648
Risk analysis and sensitivity: Antithesis or synthesis
[B8562444] 24 p4144 N85-35687

STATISTICAL COMMUNICATION THEORY
U COMMUNICATION THEORY

STATISTICAL CORRELATION
Assessment of Thematic Mapper band-to-band registration by the block correlation method
12 p1872 N85-21743
More precise curve of dependence between density and velocity of longitudinal waves in consolidated crust and top of mantle in oceanic structures
13 p2110 N85-23143
Solar radio fluxes as indices of solar activity
[AERONOMICA-ACTA-A-282-1984]
21 p3722 N85-33095
Estimate of signal-to-interference energy ratio in discrete-data transmission 22 p3776 N85-33398
The relationship between personality and performance
24 p4129 N85-35600

STATISTICAL DECISION THEORY
Markovian control problems: Functional equations and algorithms
[MCTH-97] 01 p0107 N85-10717
Total positivity. A review
[AD-A145205] 01 p0114 N85-10771
A note on validity generalization procedures
[AD-A150065] 12 p1924 N85-22085
Generation and termination of binary decision trees for nonparametric multiclass classification
[AD-A151361] 15 p2640 N85-26263

STATISTICAL DISTRIBUTIONS
NT BRIGHTNESS DISTRIBUTION
NT PEARSON DISTRIBUTIONS
NT PROBABILITY DISTRIBUTION FUNCTIONS
NT RAYLEIGH DISTRIBUTION
A simple transport model 02 p0284 N85-11853
On the Edgeworth expansion for the sum of a function of uniform spacings
[CWI-MS-R8404] 05 p0719 N85-14619
A monotonicity property of the power function of multivariate tests
[CWI-MS-R8406] 05 p0721 N85-14635
Lower level inference control in statistical database systems
[DE84-016005] 05 p0735 N85-14729
On the most probable number of flare stars in the Pleiades field 05 p0739 N85-14756
Blood pressure levels of active pilots compared with those of air traffic controllers
[AD-A146645] 06 p0846 N85-15373
Distributions of extreme values of sequences of autocorrelated random variables
[PB84-240746] 06 p0858 N85-15456
On a random difference equation for matrices and a characterization of the gamma distribution
[AD-A146858] 07 p1029 N85-16529
The effect of assumptions about cost element probability distributions on operating and support cost risk analysis
[AD-A147553] 07 p1036 N85-16576
A numerical analysis of sampling plans based on prior distribution and costs
[AD-A147718] 08 p1210 N85-17616
Stochastic dynamic analysis of a structure with frictional joints 09 p1337 N85-18406
Morphology of keV-electrons in the Earth's magnetosphere as observed by GEOS 1
[DRI-3-84] 09 p1350 N85-18496
MTI system simulation and clutter output statistics
[AD-A149193] 10 p1467 N85-19255
Scarwl plots, and letter and blotter strips
[DE85-001409] 11 p1707 N85-20739
Tests of fit based on normalized spacings
[AD-A149740] 12 p1921 N85-22062
General saddlepoint approximations with applications to l-statistics
[AD-A150073] 12 p1924 N85-22066
Stable measures and processes in statistical physics
[AD-A149592] 12 p1926 N85-22068
Skewed stable variables and processes
[AD-A150549] 13 p2153 N85-23372
Average spacing for rings of individual multi-ring basins is 2.0(0.5)D 13 p2182 N85-23541
A note on equivalent random theory
[CWI-OS-R8410] 14 p2412 N85-24872
A statistical approach to relaxation in glassy materials
[AD-A151265] 15 p2518 N85-25524
On limiting empirical distribution function of the eigenvalues of a multivariate F matrix, revised
[AD-A151865] 15 p2641 N85-26288
On asymptotic joint distribution of the eigenvalues of the noncentral manova matrix for nonnormal populations
[AD-A151886] 15 p2642 N85-26294
Brownian motion with quadratic killing and some implications: Revision
[AD-A151323] 15 p2642 N85-26296
Multinomial form of the solution of problems of the statistics of elastic rectangular disks
[REPT-17/1984] 16 p2797 N85-27244
Inequalities for distributions with increasing failure rate
[AD-A152812] 17 p2976 N85-28390
Statistical interpretation of the ECMWF model using MOS to predict surface wind and temperature
[WSR-2] 17 p2995 N85-28515
Estimating random integrals from noisy observations: Sampling designs and their performance
[AD-A152926] 17 p3025 N85-28702
A collection of probability distributions
[AD-A153128] 17 p3025 N85-28704
Recent measurements in turbulent jet flames at Sandia Combustion Research Facility 20 p3424 N85-31254
The distribution of the number of empty cells in a generalized random allocation scheme
[AD-A154806] 21 p3677 N85-32841
Decomposing the joint distribution of several linear combinations of uniform spacings
[AD-A155056] 21 p3677 N85-32845
Antistarshapedness, dispersiveness and mixtures
[AD-A155583] 21 p3678 N85-32849
Phonetic transcription statistics: Constitution and statistical utilization
[ENST-85D001] 22 p3756 N85-33285
Search for bursts in air shower data
[OG-5.3-10] 22 p3885 N85-34076
Statistical distribution of breakdown voltages in rep-rate spark gaps
[DE85-012813] 24 p4090 N85-35354
Large deviations for the maxima of some random fields
[AD-A155909] 24 p4143 N85-35681
The model of independent particles emission in the multiparticle production theory
[HE-3.2-10] 24 p4179 N85-35918

STATISTICAL MECHANICS
Fluctuation spectrum for linear gyroviscous MHD
[IPP-6/237] 01 p0121 N85-10828
Equipartition threshold in nonlinear large Hamiltonian systems: The Fermi-Pasta-Ulam model
[NOTA-INTERNA-819] 02 p0255 N85-11670
Statistical Plasma Physics. Proceedings of the Workshop of the US-Japan Joint Institute for Fusion Theory Program
[IPPJ-689] 02 p0282 N85-11832
Large deviations for processes with independent increments
[AD-A147293] 08 p1210 N85-17610
Reduction of the wavepacket: How long does it take?
[DE84-016778] 09 p1400 N85-18615
Stable measures and processes in statistical physics
[AD-A149592] 12 p1926 N85-22098
Detonation behavior of LX-14 and PBX-9404: Theoretical aspect
[DE85-010038] 18 p3084 N85-29076
Statistical mechanics of adsorption and wetting
[DE85-010093] 19 p3269 N85-30271
Physical concepts in the development of constitutive equations 20 p3467 N85-31537
Cluster variation study of coherent ordering in FCC and BCC solid solutions
[AD-A156039] 24 p4079 N85-35280

STATISTICAL MOMENTS
U DISTRIBUTION MOMENTS

STATISTICAL PROBABILITY
U PROBABILITY THEORY

STATISTICAL TESTS
NT KOLMOGOROFF-SMIRNOFF TEST
NT RANK TESTS
Probability distribution of leadtime demand
[AD-A144952] 01 p0113 N85-10766
Neuro-linguistic programming: Eye movements as indicators of representational systems
[AD-A147541] 07 p1016 N85-16454
Prematurely terminated sequential tests for MIL-STD 781C
[AD-A148417] 08 p1216 N85-17657
Reduction to outside the atmosphere and statistical tests used in Geneva photometry 08 p1251 N85-17902
The asymptotic behavior of the likelihood ratio statistic for testing a shift in mean in a sequence of independent normal variates
[AD-A149329] 10 p1550 N85-19779
A non-parametric probability density estimator and some applications
[AD-A151853] 15 p2641 N85-26287
Asymptotic expansions of the distribution of test statistics associated with several two parameter exponential distributions
[AD-A151906] 15 p2641 N85-26289
An empirical comparison of the accuracy of univariate and multivariate corrections for range restriction
[AD-A153071] 17 p3019 N85-28670
A collection of probability distributions
[AD-A153128] 17 p3025 N85-28704
Effect of some estimators on a large sample approximation to the non-null distribution of the pearson chi-square statistic
[AD-A153515] 18 p3173 N85-29673
Detection of multivariate outliers with dispersion slippage in elliptically symmetric distributions
[AD-A153785] 18 p3174 N85-29677
Corrosion fatigue cooperative testing program statistical analysis
[AD-A153886] 19 p3238 N85-30077
Performance envelopes and optimal appropriateness measurement
[AD-A154129] 19 p3330 N85-30629
Equipercentile test equating: The effects of presmoothing and postsmoothing on the magnitude of sample-dependent errors
[AD-A154110] 19 p3347 N85-30746

STATISTICAL WEATHER FORECASTING
A short-term forecast model for thunderstorm rotation
01 p0081 N85-10542
Short-term forecasting using a REMOS approach — regime model output statistics (REMOS)
01 p0081 N85-10544
On probability forecasts for temperature
01 p0084 N85-10565
Severe weather statistics STADTS decoder (SXW) and plotter (SWY)
[PB84-213693] 01 p0086 N85-10576
Forecast of the northeastern drought by the method of periodicities: Use and abuses
[INPE-3109-PRE/506] 02 p0230 N85-11502
Statistical interpretation of NWP model output: An overview of techniques used and results achieved
[REPT-551.509.313] 02 p0231 N85-11503
Development of guidance forecasts at the Royal Netherlands Meteorological Institute (KNMI). Part 1: General information
[KNMI-TR-54-PT-1] 08 p1190 N85-17499
Development of guidance forecasts at the Royal Netherlands Meteorological Institute (KNMI). Part 2: Extreme wind speed at IJmuiden
[KNMI-TR-54-PT-2] 08 p1190 N85-17500
On the relationship between maximum surface temperature and various parameters; with reference to objective forecasting
[KNMI-TR-58] 12 p1897 N85-21905
A weather service for agriculture
16 p2830 N85-27450
On the interannual variability of the Indian monsoon and the Southern Oscillation 20 p3495 N85-31728
An evaluation of discretized conditional probability and linear regression threshold techniques in model output statistics forecasting of cloud amount and ceiling over the North Atlantic Ocean
[AD-A155100] 21 p3636 N85-32581
Tunisian climate seen through a Markov process
[CT-585] 23 p3950 N85-34482
An atmospheric boundary layer model forced by the operational ECMWV-model
[WSR-3] 24 p4120 N85-35541
Users guide for optimum interpolation method of global data assimilation
[AD-A155929] 24 p4138 N85-35648
Two methods of global data assimilation
[AD-A155981] 24 p4143 N85-35684

STATISTICS
Computer equipment for research in statistics
[AD-A145755] 03 p0406 N85-12591
On the weak limits of elementary symmetric polynomials
[CWI-MS-R8407] 05 p0719 N85-14620
Principal curves and surfaces
[AD-A148833] 09 p1375 N85-18648

STATOR BLADES
Study of controlled diffusion stator blading
[NASA-CR-167995] 09 p1261 N85-18058
Development of a rotor wake-vortex model, volume 1
[NASA-CR-174849] 16 p2699 N85-26668

STATORS
Energy efficient engine component development and integration program
[NASA-CR-170034] 02 p0148 N85-10960
Analysis for leakage and rotordynamic coefficients of surface roughened tapered annular gas seals
05 p0644 N85-14135
Development of a Navier-Stokes rotor and stator analysis
[AD-A148667] 07 p0958 N85-16070
Magnetic noise in single-machine rotating frequency converters 13 p2077 N85-22960
Transient technique for measuring heat transfer coefficients on stator airfoils in a jet engine environment
[NASA-TM-87005] 15 p2580 N85-25794
Spacer structure
[AD-D011641] 17 p2897 N85-27866
Damping seal for turbomachinery
[NASA-CASE-MFS-25842-2] 19 p3280 N85-30341
Induction motors with minimum waste of magnetic iron
22 p3772 N85-33377

Magnetic field and equivalent circuit of induction motors with shielded poles 22 p3772 N85-33378
STAYS
U GUY WIRES
STEADY FLOW
NT COUETTE FLOW
A perturbation solution for rigid dumbbell suspensions in steady shear flow
[AD-A144876] 01 p0111 N85-10755
Random processes and magnetohydrodynamic turbulence 02 p0271 N85-11767
Numerical calculation of steady turbulent flows in adverse pressure gradients
[CFD/83/9] 04 p0501 N85-13195
Bicomponent flow problems in rheological fluid mechanics 05 p0835 N85-14073
An experimental study of airfoil-spoiler aerodynamics
[NASA-CR-177326] 06 p0748 N85-14796
Dynamic response of electromagnetic current meters
[PB84-229731] 06 p0842 N85-15344
Contamination and distortion of steady flow field induced by discrete frequency in aircraft gas turbines
[AD-A147092] 07 p0958 N85-16073
Existence of slow steady flows of viscoelastic fluids with differential constitutive equations
[AD-A147240] 07 p0959 N85-16077
Steady flow model user's guide
[DE85-002001] 08 p1163 N85-17337
On the shedding of vorticity at separation
[AD-P004166] 09 p1265 N85-17951
Theoretical investigation of dynamic stall using a momentum integral method
[AD-P004170] 09 p1266 N85-17955
A turbulent closure model for the free atmosphere 09 p1351 N85-18502
Recent developments and open problems in the mathematical theory of viscoelasticity
[AD-A149043] 10 p1545 N85-19742
Generation of sound by a vortex point in a steady flow of slightly compressible fluid 11 p1715 N85-20769
The split-coefficient matrix method for supersonic three dimensional flow 12 p1821 N85-21425
Internal fluid mechanism of solid propellant rocket motors 13 p2001 N85-22544
Stabilization of steady motion of mechanical systems 14 p2280 N85-24122
An analytical and numerical study of the interaction of rarefaction waves with area changes in ducts. Part 2: Area enlargements
[UTIAS-273] 14 p2300 N85-24242
Contribution to the theory of stationary separation areas
[NASA-TM-77825] 14 p2300 N85-24244
Nonlinear problems in flight dynamics involving aerodynamic bifurcations
[NASA-TM-86706] 15 p2462 N85-25206
Pseudo-unsteady systems for steady inviscid flows
[ESA-TT-877] 15 p2558 N85-25782
Boundary layer at moving cylinder surface 16 p2765 N85-27064
Upwind-difference methods for aerodynamic problems governed by the Euler equations
[REPT-84-23] 17 p2893 N85-27834
Method of calculating separation flow of subsonic gas stream around wings 17 p2942 N85-28161
Steady, incompressible, inviscid flow through a finite collapsible tube under longitudinal tension
[REPT-84-01] 17 p2959 N85-28276
The method of residual minimization in compressible steady flows
[AD-A153924] 18 p3100 N85-29193
Numerical simulation of potential flow in transonic steady regimes 20 p3389 N85-31016
Data set 9: LANN wing. Pitching oscillation 20 p3390 N85-31030
High Re separated flow solutions using the Navier-Stokes and approximate equations
[AD-A152252] 20 p3454 N85-31451
Optimization of a numerical method to calculate elliptic flows
[ESA-TT-889] 20 p3457 N85-31472
STEADY STATE
Three degree of freedom steady state point performance program: Updated version 1
[CSIR-NIAST-83/48] 01 p0001 N85-10005
Forced vibrations of friction-damped beam structures in two dimensions
[UDR-TM-82-08] 04 p0458 N85-12892
Multiple steady states for characteristic initial value problems
[NASA-CR-172486] 06 p0749 N85-14800
Effect of steady-state temperature distortion on inlet flow to a high-bypass-ratio turbofan engine
[NASA-TM-86886] 07 p0904 N85-15725
On vortex transport in turbine channels 09 p1308 N85-18217
Identification of vibration parameters of flexible structures 09 p1331 N85-18360
Permanent magnet motors
[DE85-000860] 10 p1482 N85-19355
Initial testing of a variable-stroke Stirling engine
[NASA-TM-86875] 10 p1569 N85-19895
A simple model of electron beam initiated dielectric breakdown 13 p1995 N85-22516
Internal fluid mechanism of solid propellant rocket motors 13 p2001 N85-22544
Confidence intervals using the regenerative method for simulation output analysis
[AD-A150147] 13 p2149 N85-23343
A research program in active control/aeroelasticity
[NASA-CR-175574] 14 p2218 N85-23752
Stability of steady modes of motion by axis of rotating wheel in nonlinear bearings 14 p2279 N85-24117
Stability of permanent rotation modes of asymmetric heavy solid body 14 p2279 N85-24118
Stability of steady motions of dynamically symmetrical solid at a triangular libration point 14 p2279 N85-24120
Stabilization of steady motion of mechanical systems 14 p2280 N85-24122
Ergodicity and Steady-State-Equilibrium conditions for Markov chains
[AD-A151038] 14 p2409 N85-24854
Steady state solution of the Fokker-Planck equation combined with unidirectional quasilinear diffusion under detailed balance conditions
[DE85-004917] 14 p2425 N85-24959
Is there more than one steady state for NOx? 15 p2687 N85-26593
Rotor blade flap-lag stability and response in forward flight in turbulent flows 16 p2705 N85-26698
Numerical analysis of flow non-uniformity in the hot gas manifold of the Space Shuttle main engine 16 p2736 N85-26899
Luminescence probe studies of ionomers. I: Steady-state measurements from nafion membrane
[AD-A152475] 17 p3029 N85-28730
Limit theorems for the method of replication
[AD-A153541] 18 p3170 N85-29842
Stationary properties and switching characteristics of dispersive optical bistability in CuCl 18 p3186 N85-29763
Steady-state spheromak reactor studies
[DE85-009585] 19 p3372 N85-30916
Aspects of silicon bulk lifetimes 20 p3479 N85-31617
MPS solidification model. Analysis and calculation of macrosegregation in a casting ingot
[NASA-CR-171589] 21 p3586 N85-32178
Weak shock waves propagating in fluid-gas mixtures
[AD-A154759] 21 p3584 N85-32276
Radar echoes at 2.66 and 40.92 MHz from the mesosphere, part 2.6A 21 p3619 N85-32486
Generalized formulation of a class of explicit and implicit TVD schemes
[NASA-TM-86775] 21 p3675 N85-32830
On the dependence of the convergence of Gummel's algorithm on the regularity of the solution
[AD-A154628] 21 p3675 N85-32832
Quasi-steady-state melting mode during combined laser irradiation of semiconductor materials 21 p3682 N85-32874
Establishment of steady-state power level in pulse-periodic excimer laser 21 p3685 N85-32908
A system of magnetohydrodynamic-type equations 21 p3693 N85-32946
On one nonlinear problem of laser thermochemistry 21 p3697 N85-32971
Chemical evolution of the Earth: Equilibrium or disequilibrium process? 21 p3721 N85-33088
Soft X-ray polychromator for the Solar Maximum Mission
[NASA-CR-175297] 21 p3723 N85-33096
Scientific Opportunities with Advanced Facilities for Neutron Scattering
[DE85-012113] 22 p3839 N85-33770
Transports studies of ECH and ICRH-heated bumpy torus plasma in NBT-1M 23 p3978 N85-34662
Analytic and numerical calculations of the ambipolar electric field in a stellarator 23 p3978 N85-34665
Numerical descriptions of cosmic-ray transport
[SH-4.1-3] 23 p4004 N85-34829
The 1973-1984 solar modulation of cosmic ray nuclei
[SH-4.1-16] 23 p4006 N85-34836
Exact solutions for sporadic acceleration of cosmic rays
[OG-8.3-7] 23 p4022 N85-34925
Stochastic particle acceleration in flaring stars
[OG-8.3-9] 23 p4022 N85-34927
The geostatistical approach to the inverse problem in two-dimensional steady state groundwater modeling 24 p4107 N85-35482
STEADY STATE CREEP
Transverse vibration and buckling of a cantilevered beam with tip body under constant axial base acceleration
[NASA-CR-175567] 12 p1864 N85-21694
Steady-state reaction of three-layered cylindrical shell to effect of moving load 13 p2047 N85-22811
Short term determination of the creep properties of high temperature materials
[CRIF-MT-160] 20 p3432 N85-31286
Design and fabrication of durable owner-built wind turbine blades
[DE85-009200] 20 p3484 N85-31850
STEADY STATE FLOW
U EQUILIBRIUM FLOW
STEAM
Solid electrolytes for medium temperature steam electrolysis
[DE84-014384] 04 p0463 N85-12938
Hydrogen production employing high-temperature solid oxide cells
[DE84-014559] 06 p0768 N85-14901
Open-cycle vapor compression heat pump
[PB85-101475/GAR] 06 p0775 N85-14951
Experiment on triggered fragmentation of a molten copper droplet in water
[BLL-WH-602-(9081.9F)] 08 p1125 N85-17091
Hydrogen flame acceleration and transition to detonation
[DE85-000611] 12 p1802 N85-21299
Steam generator tube vibration tests
[DE85-003599] 12 p1867 N85-21712
Experimental study of steam condensation on water in countercurrent flow in presence of inert gases
[DE84-013028] 12 p1881 N85-21800
Dependents of velocity distribution in exit section of converging channel on shape of inlet channel in regulating valve 14 p2277 N85-24106
Response of steam-water mixtures to pressure transients
[DE85-010798] 19 p3287 N85-30282
Geothermal hydrogen and health in Rotorua, New Zealand
[DE85-901263] 19 p3301 N85-30467
Film condensation of steam on externally finned horizontal tubes
[AD-A155642] 21 p3585 N85-32285
Method for determining depth and shape of a sub-surface conductive object
[DE85-006502] 23 p3935 N85-34369
Control system for fluid heated steam generator
[DE85-005734] 23 p3939 N85-34417
Calculations on the feasibility of ultrasonic inspection of steam generator tubing in pressurized water reactors
[AERE-R-10960] 23 p3940 N85-34419
Downstream behavior of volatile fission product species
[DE85-012124] 23 p3971 N85-34817
Pressure measurements in a hydrogen combustion environment: Hydrogen-air combustion test series 1 and 2 in the FITS tank, volume 1
[TI85-009899] 24 p4076 N85-36259
Heat transfer coefficients for particles in liquid in axially rotating cans 24 p4093 N85-36370
Steamflood pilots in the O'Connell Ranch field and the T-4 Ranch field
[DE85-901363] 24 p4108 N85-36468
STEAM GENERATORS
U BOILERS
STEAM TURBINES
Advanced technology cogeneration system conceptual design study: Closed cycle gas turbines
[NASA-CR-168222] 07 p0992 N85-16300
Low leakage turbine shaft seals for advanced combined cycle systems
[AD-A149372] 10 p1482 N85-19420
Development and test of a high COP Rankine heat pump for generation of process steam. Phase 2: Fabrication and test
[DE85-002600] 11 p1832 N85-20275
Axial bearings with lever-type equalizer system 14 p2267 N85-24048
Group technology for working turbine drive wheel disks 14 p2269 N85-24061
Selection of bearing type for large steam turbines 14 p2271 N85-24069
Estimating defectiveness buildup during service in metal of welded runner in low-pressure cylinder of turbine 14 p2271 N85-24070
Some problems in improving reliability and accuracy of regulators with hydraulic amplifiers in main channel of power turbine 14 p2271 N85-24071
Stability of turbine runners in sliding bearings under external circulation forces 14 p2272 N85-24074
Causes and means of prevention of erosion of exit edges of drive vanes in final stages of K-300-240 turbine 14 p2272 N85-24076

Computer code calculations of the TMI-2 accident: Initial and boundary conditions
[DE85-012813] 24 p4140 N85-35686

STEEL STRUCTURES

Delayed fracture of high-strength steels in spherical tanks for LP gas
[BLL-RISLEY-TR-4926-(9091.9F)] 01 p0026 N85-10162

The use of vanadium in low alloy structural steels 02 p0180 N85-11207

Processes to increase the fatigue life of constructions with already initiated cracks 05 p0650 N85-14176

Mechanical properties of Shielded Metal Arc (SMA) and Submerged Arc (SA) welded joints for quenched and tempered steel StE 470.
[VTT-319] 09 p1328 N85-16346

Investigation of steel structures using ultrasonic waves
[BRS3258] 13 p2101 N85-23091

Pressure welding of corrosion-resistant steel with AMg6 aluminum 15 p2501 N85-25426

Durability of joints of 30KhGSA and 12Kh18N10T steels made by diffusion welding 15 p2501 N85-25428

Welding technology and organisation in steel construction 15 p2566 N85-25828

Effects of the phase compositions of cast low-pearlite steels micro-alloyed with vanadium and titanium of their structure and properties
[BLL-BISI-TRANS-22301-(9022.06)] 17 p2928 N85-28067

Initial imperfection surveys on conical shells at Hoechst AG
[VTH-LR-407] 17 p2981 N85-28429

Experimental and theoretical assessment of a new technique for the non-destructive evaluation of laminated panels
[AD-A155822] 21 p3562 N85-32155

Monotonous stress-strain properties of structural steel subjected to nonstationary repetitive pre-loading 23 p3904 N85-34185

Safety and reliability of steel structural materials under random service impact loads 23 p3906 N85-34197

STEELS

NT AUSTENITIC STAINLESS STEELS
NT CARBON STEELS
NT CHROMIUM STEELS
NT FERRITIC STAINLESS STEELS
NT HIGH STRENGTH STEELS
NT LOW CARBON STEELS
NT MARAGING STEELS
NT MARTENSITIC STAINLESS STEELS
NT NICKEL STEELS
NT STAINLESS STEELS

Material degradation in heavy steel plates caused by bending with a laser
[AD-A144784] 01 p0052 N85-10343

The effect of 2 strength reducing techniques on the ultimate tensile strength of AISI 4130 steel: Rocket motor case venting
[AD-A145526] 02 p0169 N85-11134

Energy-saving technological methods of obtaining controlled atmospheres
[BLL-M-35724-(5828.4)] 02 p0171 N85-11145

A method for evaluating the contamination of steel in relation to the solidification curve
[BLL-M-35735-(5828.4)] 02 p0175 N85-11171

Rapid solidification of steels: Model and commercial alloys 02 p0176 N85-11184

Design of strong, ductile, duplex low alloy steels 02 p0177 N85-11189

The adhesion of hard and wear resistant coatings 02 p0179 N85-11203

The constitution as the basis for recent and future developments of wear resistant materials 02 p0179 N85-11205

Recent developments on the role of molybdenum in irons and steels 02 p0180 N85-11206

The use of vanadium in low alloy structural steels 02 p0180 N85-11207

An investigation into the superhardening effect in molybdenum-free steel with specific reference to alloy substitution 02 p0180 N85-11209

The influence of rare Earth elements on the temper embrittlement behaviour and mechanical properties of a low alloy steel 02 p0180 N85-11210

The determination of soluble and insoluble boron in steel by emission spectrometry using an inductively coupled plasma and a scanning monochromator 02 p0180 N85-11211

The role of molybdenum as an alloy element in adhesive wear resistance 02 p0181 N85-11212

Contributions to the 7th International Acoustic Emission Symposium
[AD-A145368] 02 p0275 N85-11792

Stress corrosion of pressure vessel steel A533-B in high temperature water
[BLL-RISLEY-TR-4600-(9091.9F)] 03 p0330 N85-12125

Weld metal solidification cracking in a carbon-manganese steel 03 p0330 N85-12126

Mechanical properties of a leaded, resulfurized, rephosphorized steel in various thermo/mechanical conditions
[PB84-216464] 03 p0333 N85-12144

Related studies to cathodic protection of reinforced concrete structures
[PB84-216114] 03 p0333 N85-12145

Causes of strength reduction in welded titanium-steel joints 03 p0352 N85-12262

Evaluation of ferritic alloy Fe-2 1/4Cr-1Mo after neutron irradiation: Irradiation creep and swelling
[DE84-014647] 04 p0474 N85-13022

Corrosion resistance of nitrided low-alloy steels
[PB84-235027] 04 p0477 N85-13040

Effect of lubricant extreme-pressure additives on surface fatigue life of AISI 9310 spur gears
[NASA-TP-2406] 04 p0507 N85-13234

Response of ferritic steels to nonsteady loading at elevated temperatures
[DE84-014280] 04 p0513 N85-13272

Impact toughness of wire after cold deformation and annealing
[BLL-M-35941-(5828.4)] 05 p0615 N85-13930

Reproducibility of readings from oxygen concentration elements
[BLL-M-35920-(5828.4)] 05 p0616 N85-13941

Inclusion formation during solidification of steels with improved machinability
[BMFT-FB-T-84-160] 05 p0619 N85-13957

Fatigue behavior of sintered steels and measurement criteria for sintered prefabricated parts 05 p0650 N85-14174

Influence of the shape and distribution of inclusions of the fatigue strength of bearing steels in rotary bending
[BLL-PNR-90243-(8019.3153)] 06 p0753 N85-14912

Strain rate effects and temperature history effects for three different tempers of 4340 VAR steel
[AD-A146372] 06 p0766 N85-14915

Improvement of the ladle deoxidizing of Al-killed steel
[BMFT-FB-T-84-172] 06 p0769 N85-14923

Measuring the corrosion rate of reinforcing steel in concrete
[PB84-244532] 06 p0770 N85-14925

Effect of crack-tip region constraint on fracture in the ductile-to-brittle transition
[PB84-237395] 06 p0770 N85-14926

Effect of external magnetic field on characteristics of current-carrying steel tape 06 p0788 N85-15034

Prediction of forming limit diagrams for deep drawing 06 p0796 N85-15089

Characterizing X-ray machines
[AD-A146532] 06 p0862 N85-15481

Testing of non-alloyed and low-alloyed steels for their behaviour with respect to intercrystalline stress corrosion cracking
[BLL-RISLEY-TR-4546-(9091.9F)] 07 p0925 N85-15861

Comparison of the sensitivities of ultrasonic, radiographic and acoustic emission test methods for the examination of a thick weld
[BLL-RISLEY-TR-4547-(9091.9F)] 07 p0975 N85-16194

A hydrogen partitioning model for hydrogen assisted crack growth
[AD-A147386] 07 p0978 N85-16214

Verification of the fatigue properties of (small) wind turbines
[NLR-MP-83055-U] 07 p0994 N85-16311

Effect of microstructure and trapping on the hydrogen embrittlement susceptibility of a Ti-bearing HSLA steel
[AD-A146810] 08 p1130 N85-17122

Electrodes for repairing power engineering equipment made from creep resisting steel
[BLL-CE-TRANS-8084-(9022.09)] 08 p1167 N85-17360

Implantation of Ti + C for reduced friction and wear of steels
[DE85-001606] 09 p1295 N85-18135

Effect of temperature on the stress-relaxation response of a pressure vessel steel
[TI85-003588] 09 p1339 N85-18424

Results of an EPRG round robin test programme with DWTT specimens --- drop weight test (DWTT):pipe steels
[ERS-E.365] 09 p1341 N85-18432

New method for heat treatment of metals 10 p1446 N85-19110

Influence of laser hardening on mechanical properties of type 45 steel with various preliminary heat treatments 10 p1446 N85-19111

Optimization of production of composite diamond-containing materials using titanium carbide-steel alloys 10 p1446 N85-19113

Fracture resistance of surface layer with technological defects under cyclical loading 10 p1448 N85-19126

Influence of melting conditions on strength of transition zone between steel and composite material 10 p1450 N85-19133

The effect of filler wire and flux compositions on the microstructure and properties of microalloyed steel weld metal
[AD-A149529] 10 p1492 N85-19423

USSR report: Materials science and metallurgy
[JPRS-UMS-84-005] 11 p1597 N85-20044

Method of constructing diagram of bimetal fatigue failure 11 p1599 N85-20058

Residual stress after laser processing 11 p1600 N85-20065

Effect of silicon and titanium properties on Ni8Co9Mb5Ti steel 11 p1601 N85-20069

Distribution of hydrogen in multi-layer welded joints of alloyed steels 11 p1603 N85-20079

Hydrogen attack of steel
[DE85-002645] 11 p1608 N85-20113

Ion-beam nitriding of steels
[NASA-CASE-LEW-14104-1] 12 p1805 N85-21324

Hydrogen embrittlement of cadmium-plated ultra-high strength steels in paint strippers
[ARL/MAT-R-117] 12 p1806 N85-21326

Characterization of lubricated bearing surfaces operated under high loads
[NASA-TM-86964] 12 p1811 N85-21357

Steel castings by the electroslag casting technique
[DE85-003812] 12 p1819 N85-21409

Delayed cracking strength of experimental grades of 42 CD 4 steel in aqueous H2S surroundings
[BLL-T6419/BG/LRS/LRST738/84] 13 p2020 N85-22658

USSR report: Materials science and metallurgy
[JPRS-UMS-85-002] 13 p2025 N85-22668

Specifics of laser heat treatment of high steel tools 13 p2029 N85-22714

Comparison of dynamic-tension and constant-load strength characteristics of heat-resistant materials 13 p2030 N85-22722

Mechanical properties and brittle fracture resistance of welded multilayer elements for high pressure vessels 13 p2033 N85-22736

Structure and mechanical characteristics of heterogeneous joints produced by laser welding 13 p2034 N85-22742

New tooling for plasma cutting technology 13 p2051 N85-22842

Case depth on flanks of gears for helicopter gearboxes 14 p2222 N85-23780

The effect of water chemistry on the rates of hydrogen generation for galvanized steel corrosion at post-loca conditions
[NUREG/CR-3361] 14 p2253 N85-23063

Fracture toughness of HY-130 steel weld metals
[AD-A150841] 14 p2255 N85-23978

Laser cutting: A new tool for shipbuilding 14 p2308 N85-24285

Titanium diffusion method prevents metal corrosion 15 p2514 N85-25510

The influence of abrasive blast cleaning and corrosion inhibitors on protective paint coatings 15 p2517 N85-25522

Electrically conductive polymer concrete overlays
[DE85-006728] 15 p2522 N85-25549

Studies of ferritic filler metals for welding 9 percent nickel steel 15 p2565 N85-25825

Compositional control of plate steels 15 p2565 N85-25826

SHAFT: Interactive shaft design program
[DE85-007333] 15 p2568 N85-25850

Sizing capability of automated ultrasonic time-of-flight diffraction in thick section steel and aspects of reliable inspection in practice
[AERE-R-11548] 15 p2571 N85-25855

The effect of overload cycles on fatigue crack propagation in structural steels 15 p2577 N85-25897

Grain boundary composition and intergranular fracture of steels. Volume 1: Detection of grain boundary segregation in steels
[DE85-006850] 15 p2662 N85-26428

Rolling contact fatigue life of chromium ion plated 440C bearing steel 16 p2736 N85-26882

Determination of permissible heating rate of metal
[BLL-M-36107-(5828.4)] 16 p2748 N85-26957

Study of oscillations of composite cylindrical shells using a dynamic stiffness technique 16 p2766 N85-27066

Full statistical characteristics of microdeformation
[BLL-M-36076-(5828.4)] 16 p2798 N85-27254
An X-ray study of residual stresses in narrow groove TIG weldments
[DE85-006485] 16 p2802 N85-27274
Weldability of micro-alloy steels as reaction of structure and inclusions
[BLL-BISI-TRANS-22196-(9022.06)]
17 p2924 N85-28027
Physio-chemical mechanisms of the processes of the formation of globular inclusions in ball-bearing metal
[BLL-BISI-TRANS-22235-(9022.06)]
17 p2924 N85-28030
Forming of coating protection system: Mechanism of paint-coating anti-corrosion protection of steel
[BLL-BISI-TRANS-22081-(9022.06)]
17 p2925 N85-28033
Corrosion characteristics of some steels produced through a self-cleaning rotating electrode
[BLL-BISI-TRANS-22046-(9022.06)]
17 p2925 N85-28034
Thermomechanical softening treatment for bearing and tool steels
[BLL-BISI-TRANS-22432-(9022.06)]
17 p2925 N85-28035
X-ray crystallography of steel U8 after pulsed laser hardening
[BLL-BISI-22444-(9022.06)] 17 p2925 N85-28036
Steels with improved machinability
[BLL-BISI-22341-(9022.06)] 17 p2927 N85-28061
Textural transformations taking place during heat and mechanical treatment in triplex steels
[BLL-BISI-TRANS-22404-(9022.06)]
17 p2927 N85-28063
Microstructure and mechanical properties of rare-earths-microalloyed high-speed tool steel
[BLL-BISI-TRANS-22043-(9022.06)]
17 p2928 N85-28064
Physical properties of steels and their temperature dependence
[BLL-BISI-TRANS-22285-(9022.06)]
17 p2928 N85-28065
Study on mechanism of surface deformation induced by stress corrosion cracking
[BLL-BISI-TRANS-21896-(9022.06)]
17 p2928 N85-28066
Influence of structural state and alloy content of austenite on formation of martensitic phases in steels
[BLL-BISI-TRANS-22365-(9022.06)]
17 p2928 N85-28068
Effect of the agressive action of soil on metallic pipelines. New possibilities for the passive and active corrosion protection
[BLL-BISI-TRANS-21630-(9022.06)]
17 p2928 N85-28070
Influence of manganese and heat treatment on structure and properties of Fe-0.1 percent-C-14 percent Cr-based steels
[BLL-BISI-TRANS-22299-(9022.06)]
17 p2928 N85-28071
Part played by non-metallic inclusions during deformation and fracture of steel with different grain sizes
[BLL-BISI-TRANS-22321-(9022.06)]
17 p2928 N85-28072
Influence of eutectic silicate inclusions on micro-processes during deformation and fracture of 12GS steel
[BLL-BISI-TRANS-22296-(9022.06)]
17 p2929 N85-28073
Examination of steels by chemical analysis for quality assurance
[BLL-BISI-TRANS-22068-(9022.06)]
17 p2929 N85-28074
Influence of preliminary thermomechanical treatment on depth and hardness of nitrided layers
[BLL-BISI-TRANS-22486-(9022.06)]
17 p2929 N85-28078
Mechanical stabilization of austenite against epsilon martensite and its effect on deformation behavior in high manganese steels
[DE85-007654] 17 p2932 N85-28097
Temperature and manganese content dependences of tensile deformation in iron-high manganese binary alloys
[DE85-007656] 17 p2932 N85-28098
Hydrogen degradation of pipeline steels
[DE85-008930] 17 p2932 N85-28101
Welding of 11 458.1 steel in shielding atmospheres
[BLL-BISI-TRANS-21763-(9022.06)]
17 p2972 N85-28353
Submerged arc welding of new Czechoslovak micro-alloy steels
[BLL-BISI-TRANS-22193-(9022.06)]
17 p2972 N85-28356
Application of 4-wire submerged arc method to welding UOE pipe
[BLL-BISI-TRANS-22417-(9022.06)]
17 p2972 N85-28358
Examples of application of machinability tests
[BLL-BISI-TRANS-22346-(9022.06)]
17 p2973 N85-28363
Assessing the machinability of gearwheel steels during manufacture
[BLL-BISI-TRANS-22343-(9902.06)]
17 p2973 N85-28365
Steel Tubes
[BLL-BISI-TRANS-22064-(9022.06)]
17 p2973 N85-28369
Quality testing to the specifications of the Stahl-Eisen-Pruefblatt 1570/71 using an automatic image analysis system
[BLL-BISI-TRANS-22253-(9022.06)]
17 p2976 N85-28385
Tests of low-cycle fatigue of elected steels of class 11
[BLL-BISI-TRANS-22039-(9022.06)]
17 p2978 N85-28404
On validity of threshold values of fatigue strength of steel structures
[BLL-BISI-TRANS-22192-(9022.06)]
17 p2978 N85-28408
Investigations of the material factors in the adiabatic shearing of steels
[AD-A153084] 17 p2979 N85-28418
Critical conditions for failure in materials subjected to high rates of loading
[AD-A153135] 17 p2980 N85-28420
World iron ore reserves
[BLL-BISI-TRANS-22280-(9022.06)]
17 p2983 N85-28435
Strength versus toughness relation in Fe-high manganese alloys
[DE85-007682] 18 p3074 N85-29013
Specimen thickness effects for elastic-plastic CTOD toughness of A36 steel
[DE85-006992] 18 p3077 N85-29038
Magnetic steels with the lowest specific total losses
[BMFT-FB-T-84-263] 18 p3078 N85-29042
Behavior of reinforced concrete at elevated temperatures
[DE85-009032] 18 p3123 N85-29332
Effect of matrix composition on steel fiber reinforced concrete properties 19 p3230 N85-30028
Welding of steel-aluminum cooling panels for the holds of refrigerator vessels 19 p3246 N85-30129
Study of intermediate velocity penetration of steel spheres into deep aluminum targets
[DE85-010419] 19 p3287 N85-30365
Contribution to the modelling of the gas carburizing process for steels
[BLL-OA-TRANS-3205-(6198.300)]
20 p3428 N85-31263
Effects of humidity cycles on the corrosion of galvanised reinforcements in carbonated and uncarbonated mortars
[BLL-CE-TRANS-8039-(9022.09)]
20 p3430 N85-31272
Joining of sintered composite TiC-steel materials by welding
[BLL-M-36253-(5828.4)] 20 p3461 N85-31502
Investigation of fatigue strength of spring steel after high-temperature thermomechanical working (HTMW) by helical drawing
[BLL-M-36274-(5828.4)] 20 p3465 N85-31525
Theoretical modelling of the electro-chemistry in a corrosion fatigue crack. Part 2: Mathematical aspects of associated unsteady reaction equations
[NPL-DMA(A)-100-PT-2] 20 p3465 N85-31529
Assessment of dynamic test methods for the measurement of fracture toughness — steels
[OUEL-1561/85] 20 p3470 N85-31565
Decomposition of sulfuric acid using solar thermal energy
[DE85-012288] 21 p3564 N85-32170
Understanding and laboratory prediction of the atmospheric corrosion behavior of steels and of non-ferrous metals and alloys
[AD-A154642] 21 p3566 N85-32179
Development of improved dynamic failure models
[AD-A155586] 21 p3600 N85-32354
Rapid analysis of steels using laser-based techniques
[DE85-010747] 22 p3748 N85-33232
Management of Corrosion
[AGARD-LS-141] 22 p3749 N85-33236
Corrosion management strategies for aircraft and related systems 22 p3749 N85-33239
Induction motors with minimum waste of magnetic iron
22 p3772 N85-33377
The study of the effect of residual microimpurities on the fatigue strength of 55S2 steel
[BLL-M-36317-(5828.4)] 23 p3913 N85-34246
Special features of the fracture of ball-bearing steel close to non-metallic inclusion eutectics
[BLL-M-35809-(5828.4)] 23 p3914 N85-34258
Properties of tungsten-free steel for cutting tools
[BLL-M-35808-(5828.4)] 23 p3915 N85-34259
Chromium-base powder alloys for welding cladding layer of bimetal
[BLL-M-35778-(5828.4)] 23 p3915 N85-34260
The properties of VSt3sp inoculated steel
[BLL-M-35894-(5828.4)] 23 p3915 N85-34263
Hydrogen embrittlement testing
[DE85-007352] 23 p3916 N85-34273
Decomposition of martensite in R6M5 and R6AM5 steels after direct immersion in liquid nitrogen
[BLL-M-36305] 24 p4077 N85-35268
Tests on zirconium nitride coatings applied to SW 18 steel using the chemical vapor deposition method
24 p4078 N85-35271
The dynamic strain ageing of A533B class 1 nuclear pressure vessel steel
[AERE-R-11465] 24 p4078 N85-35274
The character of observed porosity and its possible effects on rolling contact fatigue life of M-50 steel
[AD-A155930] 24 p4079 N85-35279
Effect of prior warm rolling on the retained austenite content and hardening response of VIM-VAR (vacuum-induction melted-vacuum-arc remelted) AISI M-50 steel
[AD-A156145] 24 p4079 N85-35281

STEEP GRADIENT AIRCRAFT
U V/STOL AIRCRAFT

STEEPEST ASCENT METHOD
U STEEPEST DESCENT METHOD

STEEPEST DESCENT METHOD
Use of shanks transformation for speeding up adaptation process in antenna arrays 07 p0951 N85-16029
Some plant location problems — computer networks
[FUB-14-1984] 22 p3835 N85-33748

STEEPNESS
U SLOPES

STEERABLE ANTENNAS
Simulation of the performance of adaptively controlled Navstar antennas in battlefield scenarios
10 p1472 N85-19292
An electronically-steerable active receiving array for h.f.
[BBC-RD-1985/2] 12 p1822 N85-21430
Concepts and cost trade-offs for land vehicle antennas in satellite mobile communications
[NASA-CR-175731] 15 p2540 N85-25680
A simulation study of jammer nulling trade-offs in a reactively steered adaptive array
[AD-A153461] 18 p3090 N85-29124
A planar version of a 4.0 gigahertz reactively steered adaptive array
[AD-A156029] 24 p4087 N85-35330

STEERING
Tracking servo compensator with rate aiding
[AD-D011372] 07 p0942 N85-15971
Development of a soil-wheel interaction model
[AD-P004259] 09 p1404 N85-18835
The guidelines to design the lever turning gears in articulated vehicles
[AD-P004301] 09 p1409 N85-18878
Study on controllability and stability of high speed tracked vehicles
[AD-P004302] 09 p1409 N85-18879
Forces on undriven, angled wheels
[AD-P004303] 09 p1409 N85-18880
Influence of tire on resistance and steering forces of tires
[AD-P004306] 09 p1410 N85-18883
Basic study on the turning resistance of track
[AD-P004307] 09 p1410 N85-18884
Study on steerability of articulated tracked vehicles
[AD-P004308] 09 p1410 N85-18885
Skid steering of wheeled and tracked vehicles: Analysis with Coulomb friction assumptions
[AD-A149826] 12 p1860 N85-21664
Practicality of electronic beam steering for MST/ST radars, part 6.2A 21 p3624 N85-32516
Iris tilting and RF steering in the SLAC Linac
[DE85-011704] 22 p3841 N85-33783

STELLAR (STAR TRACKER)
U CCD STAR TRACKER

STELLAR ACTIVITY
NT FACULAE
NT SOLAR ACTIVITY
NT SOLAR FLARES
NT SOLAR PROMINENCES
NT SOLAR STORMS
NT SPICULES
NT STELLAR FLARES
NT SUNSPOTS
Non-stable motions and instability in stellar associations 05 p0739 N85-14754

Study of the pulsations of the ZZ Ceti stars
09 p1414 N85-18923
The vertical structure and stability of alpha model accretion disks
09 p1417 N85-18936
Radiative ion beams: Hot stellar reactions in the laboratory
[DE85-001570] 11 p1722 N85-20833
Solar and stellar coronal plasmas
[NASA-CR-175623] 13 p2205 N85-23676
Solar and stellar magnetic cycles: Unity and multiplicity
14 p2448 N85-25109
Stellar surface phenomena: A spectroscopic study of the RS canum venaticorum binaries
15 p2669 N85-26467
Activity and magnetic fields on stars from radio observations
[NASA-CR-175966] 16 p3202 N85-29861
Search for stellar collapse with the MACRO detector at Gran Sasso
[HE-5.3-11] 24 p4206 N85-36105

STELLAR ATMOSPHERES
NT CHROMOSPHERE
NT SOLAR ATMOSPHERE
Outer atmospheres of giant and supergiant stars
[NASA-CR-174165] 04 p0580 N85-13703
RS CV sub n binary systems
[NASA-CR-174164] 04 p0580 N85-13704
The distribution of dust in the region of the Rosette Nebula and MON OB2 association
05 p0739 N85-14753
On the content of nitrogen in atmospheres of late giants derived from molecular bands on NH in the UV spectral range
05 p0740 N85-14761
Stability of stellar disk and ratio of halo to disk masses in the galaxy
05 p0740 N85-14763
Theoretical studies of chromospheres and winds in cool stars
[NASA-CR-174204] 06 p0880 N85-15596
Homogeneous condensation of gaseous mixtures of Si, Fe, O, N, and C in relative cosmic abundance and implications for astronomical condensation
06 p0887 N85-15632
The Origin of Nonradiative Heating/Momentum in Hot Stars
[NASA-CP-2358] 08 p1231 N85-17755
Evidence for non-radiative activity in hot stars
08 p1231 N85-17758
Evidence for non-radiative activity in stars with T sub eff 10000 K
08 p1231 N85-17757
Nonthermal radio emission and the HR diagram
08 p1232 N85-17763
Departures from LTE populations versus anomalous abundances: The effects of heating
08 p1234 N85-17776
Is the ratio of observed X-ray luminosity to bolometric luminosity in early-type stars really a constant?
08 p1234 N85-17777
Magnetic effects in the heating and modification of flows in the outer stellar atmospheres with application to early type star case
08 p1235 N85-17783
Summary of the origin of nonradiative heating/momentum in hot stars
08 p1236 N85-17789
Outer atmospheres of cool stars observed with IUE
11 p1744 N85-20968
Carbon, silicon, and oxygen in the white dwarf star GD 40
11 p1752 N85-21017
The solar stellar connection in the far ultraviolet
11 p1757 N85-21055
A progress report on the analysis of long exposure SWP high resolution spectra of cool stars
11 p1758 N85-21057
Active late-type stars and the applicability of coronal loop models
11 p1758 N85-21059
Observations of Cygnus X-3 above 10(15) eV from 1979 - 1984
[OG-2.1-6] 22 p3863 N85-33923
On gamma and neutrino radiation from Cyg X-3
[OG-2.1-7] 22 p3863 N85-33924
X-ray spectra of bursting neutron stars
23 p3961 N85-34686
The HEAO-2 Guest Investigator Program: Non-linear growth of instabilities in line-driven stellar winds
[NASA-CR-176168] 24 p4168 N85-35840

STELLAR COLOR
Ultraviolet studies of the young populous cluster NGC 2100 in the LMC
11 p1748 N85-20995
The color excesses of classical cepheids and the structure of our galaxy
13 p2169 N85-23459

STELLAR COMPOSITION
Collective processes and formation of star clusters
05 p0738 N85-14743
Evolution of globular clusters
05 p0738 N85-14746
On the content of nitrogen in atmospheres of late giants derived from molecular bands on NH in the UV spectral range
05 p0740 N85-14761
Large-scale bubble structure of the interstellar medium (ISM) and properties of the Local Spiral Arm (LSA)
06 p0879 N85-15586
Magellanic cloud objects
11 p1744 N85-20965
The usual hot stars in unusual galaxies
11 p1745 N85-20975
IUE and Voyager observations of very hot O-type subdwarfs
11 p1751 N85-21010
Analysis of high-depression IUE spectra of subdwarf B stars
11 p1751 N85-21011
Ultraviolet and optical spectroscopy and polarimetry of the helium weak star HD 21699: Evidence for a magnetically controlled stellar wind
11 p1758 N85-21065
Magnetospheres and winds in the helium weak stars: Observations of C 5 in upper main sequence CP stars
11 p1759 N85-21066
IUE spectrophotometry of helium weak and silicon stars
11 p1759 N85-21067
Search for stellar collapse with the MACRO detector at Gran Sasso
[HE-5.3-11] 24 p4206 N85-36105

STELLAR CORES
Evolution of globular clusters
05 p0738 N85-14746
Brightness distribution in globular clusters derived by the narrow-slit scanning method
05 p0738 N85-14748
Lessons from the globular cluster NGC 5466
05 p0739 N85-14749
The fate of globular clusters
05 p0739 N85-14751
Solar oscillations
14 p2445 N85-25092
Mixing in the solar interior
14 p2446 N85-25095
Conditions of the small oscillations excitation in the different solar models with the mixed core
14 p2450 N85-25126

STELLAR CORONAS
NT CORONAL LOOPS
NT SOLAR CORONA
Outer atmospheres of giant and supergiant stars
[NASA-CR-174165] 04 p0580 N85-13703
A search for possible members of open clusters among known Ap stars
05 p0737 N85-14740
Stability of stellar disk and ratio of halo to disk masses in the galaxy
05 p0740 N85-14763
Evidence for non-radiative activity in stars with T sub eff 10000 K
08 p1231 N85-17757
Coronal temperatures
08 p1233 N85-17766
The scaling of coronal models from one star to another
08 p1233 N85-17771
Overheated open coronal regions
08 p1234 N85-17772
Non-radiative energy from differential rotation in hot stars
08 p1234 N85-17778
A leaky waveguide model for MHD wave driven winds from coronal holes
08 p1235 N85-17781
X-ray coronae of late type stars: Theoretical implications
11 p1742 N85-20953
Coronal effects of the winds of early-type stars
11 p1749 N85-21002
Solar and stellar coronal plasmas
[NASA-CR-175623] 13 p2205 N85-23676
A program of ground-based astronomy to complement einstein observations
[AD-A151111] 15 p2668 N85-26466
The kinematic and radial properties of normal luminous SC galaxies
20 p3545 N85-32061

STELLAR DOPPLER SHIFT
U DOPPLER EFFECT
U EXTRATERRESTRIAL RADIATION

STELLAR ENVELOPES
Numerical models of the spectral appearance of protostellar envelopes
03 p0442 N85-12816
Shapes of wind driven circumstellar shells
03 p0443 N85-12821
Theoretical studies of chromospheres and winds in cool stars
[NASA-CR-174204] 06 p0880 N85-15596
Active phenomena in the pre-main sequence star AB AUR
08 p1233 N85-17765
IUE and ESO observations of the P Cyg star AG Carinae and its ring nebula
11 p1750 N85-21006
Ultraviolet observations of circumstellar matter in Algol type binary systems
11 p1756 N85-21043
Circumstellar material in Algols and Serpentids
11 p1757 N85-21051
Ultraviolet, radio and X-ray observations of hybrid stars
11 p1759 N85-21063
Electrons and positrons from expanding supernova envelopes in dense clouds
[OG-6.2-9] 22 p3869 N85-34108

STELLAR EVOLUTION
NT STELLAR MASS ACCRETION
Variations of the H and K emission lines of singly ionized calcium in the eclipsing binary star system AR Lacertae
02 p0296 N85-11921
Solar neutrinos: Prospects for detection and implications
[DE84-015522] 02 p0304 N85-11666
Star Formation Workshop
[ROE-OR-13] 03 p0441 N85-12809
Distribution and properties of molecular clouds in the galaxy
03 p0442 N85-12810
Compact infrared sources: Protostars before IRAS
03 p0442 N85-12812
IRAS observations of galactic star formation
03 p0442 N85-12813
Far-infrared observations of some regions of star formation
03 p0442 N85-12814
Open cluster formation — stellar evolution
03 p0442 N85-12815
Numerical models of the spectral appearance of protostellar envelopes
03 p0442 N85-12816
Spherical accretion onto a protostellar core
03 p0442 N85-12817
Masers associated with regions of recent star formation
03 p0443 N85-12820
Shapes of wind driven circumstellar shells
03 p0443 N85-12821
The rotation of B-type stars and processes of star formation
03 p0443 N85-12823
The significance of comets for star formation
03 p0443 N85-12824
Star formation in interacting galaxies
03 p0444 N85-12826
Infrared mapping of galaxian centers: Star forming regions with kiloparsec scale sizes
03 p0444 N85-12827
Molecules in external galaxies
03 p0444 N85-12828
Future theoretical needs in studies of star formation
03 p0444 N85-12829
Age groups and composite diagrams for young open clusters
05 p0737 N85-14736
The behaviour of brighter binaries and yellow giants in open clusters
05 p0737 N85-14738
The present state of the International Star Cluster Photometry Programme
05 p0737 N85-14741
Binaries and evolution of globular clusters
05 p0738 N85-14744
Evolution of globular clusters
05 p0738 N85-14745
Evolution of globular clusters
05 p0738 N85-14746
Non-stable motions and instability in stellar associations
05 p0739 N85-14754
The evolution of a sparse stellar system
05 p0740 N85-14758
The fragmentation of molecular clouds and the IMF
05 p0740 N85-14759
On the content of nitrogen in atmospheres of late giants derived from molecular bands on NH in the UV spectral range
05 p0740 N85-14761
The velocity-age relation for B and A stars
05 p0740 N85-14762
Kinematics of B and A stars
05 p0741 N85-14766
The correlation between excitation parameter and nebular luminosity for galactic HII regions with application to regions of star formation in M83
05 p0743 N85-14773
The relevance of QUASAT to the star formation problem
07 p1058 N85-16718
The Origin of Nonradiative Heating/Momentum in Hot Stars
[NASA-CP-2358] 08 p1231 N85-17755
Active inner regions of isolated galaxies
08 p1237 N85-17795
On the surface density of X-ray selected BL Lacertae objects
08 p1240 N85-17822
Active galactic nuclei and their cosmological evolution
08 p1243 N85-17842
Star formation in globules
08 p1247 N85-17868
Far infrared observations of molecular clouds in the outer galaxy
08 p1247 N85-17869
Far infrared emission from galaxies
08 p1248 N85-17875
Starbursts in galaxies: Implications of molecular and far-infrared observations
08 p1248 N85-17881
Spectroscopic observations of selected stellar systems
[NASA-CR-174288] 08 p1255 N85-17915
On the progenitors of white dwarfs
[NASA-CR-174378] 09 p1413 N85-18913
Boundary conditions for the paleoenvironment: Chemical and physical processes in the pre-solar nebula — molecular clouds, interstellar matter, and abundance
[NASA-CR-174370] 10 p1570 N85-19901
Fragmentation and turbulence in collapsing gas clouds
[DE85-003745] 11 p1633 N85-20282

Future of Ultraviolet Astronomy Based on Six Years of IUE Research
[NASA-CP-2349] 11 p1743 N85-20961
Hot stars: Six years of progress 11 p1743 N85-20963
Magellanic cloud objects 11 p1744 N85-20965
Interacting binary systems 11 p1744 N85-20967
UV observations and results on pre-main sequence stars 11 p1744 N85-20970
The usual hot stars in unusual galaxies 11 p1745 N85-20975
IUE observations of blue horizontal branch globular clusters and UV-bright stars 11 p1748 N85-20992
Mass distribution and evolutionary scheme for central stars of planetary nebulae 11 p1751 N85-21012
Hydrodynamic simulations of recurrent novae 11 p1753 N85-21025
Old and new neutron stars
[DE85-002716] 11 p1762 N85-21085
The luminosity distribution of pulsars 12 p1959 N85-22317
All-Union conference of radio astronomers 13 p1977 N85-22406
Dynamics of long-period comets 13 p2176 N85-23506
The Formation of preplanetary disks from the collapse of rotating molecular cloud cores 13 p2180 N85-23526
Research on the early history of the solar system 13 p2180 N85-23527
Numerical study of a two-fluid hydrodynamical model of interstellar medium and population 1 stars 14 p2440 N85-25055
Molybdenum solar neutrino experiment
[DE85-003747] 14 p2445 N85-25090
Did the young Sun rotate at 100 km/s 14 p2451 N85-25133
Formation of the solar system 15 p2677 N85-26532
Did bosonic sneutrino stars ever exist
[PREPRINT-421] 18 p3202 N85-29867
The kinematic and radial properties of normal luminous SC galaxies 20 p3545 N85-32061
Star formation in NGC 7538: Multi-wavelength observations and issues 20 p3545 N85-32063
Search for the universal ancestors
[NASA-SP-477] 21 p3667 N85-32777
Noble gases and the early history of the Earth: Inappropriate paradigms and assumptions inhibit research and communication 21 p3719 N85-33075
Search for stellar collapse with the MACRO detector at Gran Sasso
[HE-5.3-11] 24 p4206 N85-36105

STELLAR FIELDS
U STAR DISTRIBUTION

STELLAR FLARES
NT SOLAR FLARES
Light variations of the B-type star HD 160202 08 p1232 N85-17761
X-ray activity in pre-main sequence stars 08 p1233 N85-17764
Outer atmospheres of cool stars observed with IUE 11 p1744 N85-20966
The solar stellar connection in the far ultraviolet 11 p1757 N85-21055

STELLAR GRAVITATION
Some evidence for large gravitational redshift in Seyfert galaxy NGC 4151
[OG-2.7-11] 22 p3872 N85-33984

STELLAR LUMINOSITY
The influence of stellar luminosity and temperature calibration on the determination of the initial mass function 05 p0740 N85-14760
Unidentified IRAS sources: Ultrahigh luminosity galaxies
[NASA-CR-174207] 06 p0872 N85-15537
Observations of highly-ionized interstellar iron 06 p0876 N85-15565
Some aspects of active galactic nuclei 07 p1056 N85-16702
Light variations of the B-type star HD 160202 08 p1232 N85-17761
Stellar winds: Observational evidence for a hot-cool star connection 08 p1233 N85-17766
On the role played by lines in radiatively driven stellar winds depending on the position of the stars in the HR diagram 08 p1236 N85-17787
A new estimate of the local luminosity function of Seyfert 1 nuclei 08 p1237 N85-17796
Star formation in globules 08 p1247 N85-17868
Far infrared observations of molecular clouds in the outer galaxy 08 p1247 N85-17869
SIRTF: The next step 08 p1250 N85-17891
The ground based photometric limitations to the search for light variations due to 5-minute solar-type oscillations in other stars 08 p1251 N85-17896
IUE observations of blue horizontal branch globular clusters and UV-bright stars 11 p1748 N85-20992
Ultraviolet studies of the young populous cluster NGC 2100 in the LMC 11 p1748 N85-20995
Superionized species and winds in low luminosity B and Be stars 11 p1749 N85-21003
Betegeuse at maximum luminosity 11 p1758 N85-21061
IUE low-dispersion reference atlas 11 p1760 N85-21073
An IUE high-resolution atlas of O-type spectra 11 p1760 N85-21074
IUE observations of faint standard stars for calibration of the space telescope 11 p1761 N85-21076
Dynamics of elliptical galaxies and the r sup 1/4 luminosity law 12 p1955 N85-22282
The luminosity distribution of pulsars 12 p1959 N85-22317
Formation of optical-line emitting regions in the jets of SS433 12 p1959 N85-22318
Observations concerning energy balance in solar magnetic regions 14 p2452 N85-25145
Investigating statistical characteristics of atmospheric background brightness and star background density in equatorial region of celestial sphere 15 p2478 N85-25298
The ultraviolet spectra of intermediate redshift quasars 20 p3544 N85-32056
The kinematic and radial properties of normal luminous SC galaxies 20 p3545 N85-32061

STELLAR MAGNETIC FIELDS
NT SOLAR MAGNETIC FIELD
Theory tested by means of the stars — viability of the alpha-omega dynamo model 08 p1233 N85-17770
Bipolar flows and X-ray emission from young stellar object 08 p1234 N85-17779
Magnetic effects in the heating and modification of flows in the outer stellar atmospheres with application to early type star case 08 p1235 N85-17783
Transport properties of the outer crust of magnetic neutron stars 09 p1415 N85-18927
Ultraviolet and optical spectroscopy and polarimetry of the helium weak star HD 21699: Evidence for a magnetically controlled stellar wind 11 p1759 N85-21065
The modelling of latitudinal gradients in the solar wind in the outer solar system 12 p1947 N85-22231
The axisymmetric pulsar magnetosphere 12 p1955 N85-22279
Nonlinear waves in the magnetosphere of pulsars 12 p1955 N85-22281
Thermal convection and magnetic fields in accretion disks of black holes 12 p1955 N85-22285
About static and dynamic solutions of the aligned rotator model — pulsar magnetosphere 12 p1958 N85-22306
Solar and stellar magnetic cycles: Unity and multiplicity 14 p2448 N85-25109
The generation of magnetic fields by a flow with chaotic streamlines 14 p2451 N85-25135
Activity and magnetic fields on stars from radio observations
[NASA-CR-175966] 18 p3202 N85-29861
Observations of Cygnus X-3 above 10(15) eV from 1979 - 1984
[OG-2.1-6] 22 p3863 N85-33923

STELLAR MAGNITUDE
South African Astronomical Observatory Circulars, no. 7
[SAAOC-7] 01 p0127 N85-10875
Extending magnitude standards to faint stars with a sub-beam prism 07 p0965 N85-16124
Sub-beam prism used at the Boscha Schmidt telescope 07 p0965 N85-16125
Astronomers' problems with the calibration of Schmidt plates 07 p0965 N85-16126
A statistical evaluation of the limitations of single-channel intermediate-band photoelectric stellar photometry 08 p1251 N85-17900
Documentation for the machine-readable version of the Cordoba Durchmusterung (CD)
[NASA-TM-87441] 14 p2439 N85-25049

STELLAR MASS
NT STELLAR GRAVITATION
Gravitational vacuum 02 p0265 N85-11734
The behaviour of brighter binaries and yellow giants in open clusters 05 p0737 N85-14738
On the role played by lines in radiatively driven stellar winds depending on the position of the stars in the HR diagram 08 p1236 N85-17787
Multiline transfer and the dynamics of stellar winds 08 p1236 N85-17788
Spectroscopic observations of selected stellar systems
[NASA-CR-174288] 08 p1255 N85-17915
UV observations and results on pre-main sequence stars 11 p1744 N85-20970
Mass distribution and evolutionary scheme for central stars of planetary nebulae 11 p1751 N85-21012
Three short-period binaries seen at high-dispersion UX ARI, IOTA TRI and HA5110 11 p1756 N85-21047
The Formation of preplanetary disks from the collapse of rotating molecular cloud cores 13 p2180 N85-23526
Relevance of cosmic gamma rays to the mass of gas in the galaxy
[OG-3.1-8] 22 p3874 N85-33986

STELLAR MASS ACCRETION
Spherical accretion onto a protostellar core 03 p0442 N85-12617
Age groups and composite diagrams for young open clusters 05 p0737 N85-14736
Accretion in the zeta Aurigae and 32 Cygni shock cones 11 p1754 N85-21036
Orbital resonances and planetary accretion in the solar nebula 13 p2179 N85-23523
Research on the early history of the solar system 13 p2180 N85-23527
Thermal and magnetic properties of neutron stars 16 p2980 N85-27774
X-ray spectra of bursting neutron stars 23 p3981 N85-34686

STELLAR MASS EJECTION
Solar-geophysical data number 477, May 1984. Part 2: (Comprehensive reports). Data for November 1983, July 1981 and miscellanea. Explanation of data reports issued as number 474 (supplement) February 1984
[PB84-225036] 01 p0131 N85-10900
Nonradial pulsation and mass loss in early B stars 08 p1232 N85-17759
Bipolar ejection of matter from hot stars 08 p1233 N85-17767
Nonradiative heating and enhanced mass-loss due to shear turbulence in massive hot stars 08 p1235 N85-17780
Further investigation of mass loss phenomena in hot white dwarfs and O subdwarfs 11 p1751 N85-21014
Mechanical energy release by protostars to molecular clouds 12 p1957 N85-22302

STELLAR MODELS
Variations of the H and K emission lines of singly ionized calcium in the eclipsing binary star system AR Lacertae 02 p0296 N85-11921
Thermal effects in stellar pulsations 02 p0297 N85-11925
Numerical models of the spectral appearance of protostellar envelopes 03 p0442 N85-12618
Shapes of wind driven circumstellar shells 03 p0443 N85-12621
Particle acceleration in two-ribbon flares — solar flares 04 p0519 N85-13314
Time dependent effects at the foot of the chromosphere
[NASA-CR-174143] 04 p0589 N85-13762
The fragmentation of molecular clouds and the IMF 05 p0740 N85-14759
Iron core collapse models of Type 2 supernovae
[DE84-013909] 05 p0743 N85-14775
The radiative hydrodynamics of flare loops heated by impulsive bursts of energetic electrons 05 p0745 N85-14781
Chemical evolution of the solar nebula: A new model 06 p0887 N85-15831
Dynamic thermal episodes in the protosolar nebula: Development of models from observations on CAI's 06 p0887 N85-15833
Narrow absorption components in Be star winds 08 p1232 N85-17760
Ultraviolet spectral morphology of O-type stellar winds 08 p1232 N85-17762
Active phenomena in the pre-main sequence star AB AUR 08 p1233 N85-17765
Bipolar ejection of matter from hot stars 08 p1233 N85-17767
Theory tested by means of the stars — viability of the alpha-omega dynamo model 08 p1233 N85-17770
The scaling of coronal models from one star to another 08 p1233 N85-17771
A leaky waveguide model for MHD wave driven winds from coronal holes 08 p1235 N85-17781
Transport properties of the outer crust of magnetic neutron stars 09 p1415 N85-18927
A comparative study of dust and young stars in three small galaxies 09 p1415 N85-18928
IUE observations of blue horizontal branch globular clusters and UV-bright stars 11 p1748 N85-20992
The fading of R coronae borealis 11 p1753 N85-21029
Active late-type stars and the applicability of coronal loop models 11 p1758 N85-21059

Thermal stability of static coronal loops: Part 1: Effects of boundary conditions
[NASA-CR-175495] 12 p1861 N85-22330
Theoretical and observational studies of stellar activity 13 p2171 N85-23468
Constraints of observations of solar oscillations on solar models with mixing by turbulent diffusion
[DE85-003741] 13 p2205 N85-23678
Numerical study of a two-fluid hydrodynamical model of interstellar medium and population I stars 14 p2440 N85-25055
Models of solar differential rotation 14 p2446 N85-25097
Amplification and maintenance of thin magnetic flux tubes by compressible convection — solar magnetism 14 p2447 N85-25104
The solar dynamo and the complex Lorenz equations 14 p2447 N85-25107
A numerical simulation of the formation of solar prominences 14 p2448 N85-25112
Conditions of the small oscillations excitation in the different solar models with the mixed core 14 p2450 N85-25126
Linear models of acoustic waves in sunspot umbrae 14 p2450 N85-25130
The flux rope models checked by some observations — solar activity 14 p2452 N85-25139
Empirical model of the solar corona using solar-cycle related parameters 14 p2453 N85-25153
Modeling 22-year solar activity cycle within framework of dynamo theory with allowance for primary field 15 p2477 N85-25288
Activities report of the Institute of Astronomy and Astrophysics 17 p3052 N85-28892
Self-consistent models for the X-ray emission from supernova remnants 20 p3548 N85-32082

STELLAR MOTIONS
NT STELLAR OSCILLATIONS
NT STELLAR ROTATION
Documentation for the machine-readable version of the Perth 75: A Catalogue of Positions of 2589 FK4 and FK4S Stars (Nikoloff and Hog 1982)
[NASA-TM-87376] 04 p0549 N85-13492
Documentation for the machine-readable version of the AGK3 Star Catalogue of Positions and Proper Motions North of -2 deg .5 declination (Dieckvoss and Collaborators 1975)
[NASA-TM-87378] 04 p0549 N85-13493
Evolution of globular clusters 05 p0738 N85-14745
Investigation of central parts of globular clusters, performed in Pulkovo 05 p0738 N85-14747
Non-stable motions and instability in stellar associations 05 p0739 N85-14754
Proper motions and kinematical properties of Orion trapezium type stellar systems 05 p0739 N85-14755
Hyades moving group 05 p0740 N85-14757
The evolution of a sparse stellar system 05 p0740 N85-14758
Radiative amplification of acoustic waves in hot stars 08 p1235 N85-17786
The relationship between radio structures and stellar dynamics of nearby elliptical galaxies 08 p1236 N85-17794
Documentation for the machine readable version of the Yale Catalogue of the Positions and Proper Motions of Stars between Declinations -60 deg and -70 deg (Fallon 1983)
[NASA-TM-87443] 14 p2439 N85-25051
Solar convection
[AD-A155214] 21 p3723 N85-33098

STELLAR OCCULTATION
Catalogue of observations of total occultations of stars by the Moon for the years 1972 to 1980 and of grazing occultations for the years 1963 to 1980
[BULL-192] 05 p0741 N85-14768
Exploring the solar system with stellar occultations 08 p1245 N85-17857
Occultations of stars and radio sources by comets: Predictions and observing prospects 14 p2437 N85-25034
The rings of Uranus 15 p2672 N85-26486
Stellar occultations by Uranus rings on 15 August 1980 and 22 April 1982 15 p2672 N85-26489
Rings around Neptune? 15 p2672 N85-26491
Structure and dynamics of Saturn's rings as seen by the Voyager stellar occultation 15 p2673 N85-26494
The C ring of Saturn: A high resolution view of some of its structure 15 p2673 N85-26495
The eccentric ringlet at 1.29 R sub S — Saturn radius (RS) 15 p2673 N85-26496
Voyager UVS observations of stellar occultations by the rings of Saturn — ultraviolet spectrometer (UVS) 15 p2673 N85-26497
Occultation detection of a Neptune ring segment 15 p2691 N85-26558
The 13 November 1984 occultation of BD +08 deg 0471 by (1) Ceres
[NASA-CR-176106] 23 p3987 N85-34725

STELLAR OSCILLATIONS
NT SOLAR OSCILLATIONS
The ground based photometric limitations to the search for light variations due to 5-minute solar-type oscillations in other stars 08 p1251 N85-17898
Atmospheric limitations in stellar seismology: Should one measure radial velocity or brightness fluctuations? 08 p1251 N85-17899
Energy relations on the small oscillations excitation in the stars 14 p2450 N85-25125
Quasiperiodic oscillations in bright galactic-bulge X-ray sources
[NASA-CR-176138] 23 p3987 N85-34723

STELLAR PARALLAX
Astrometric applications of the Mt. Stromlo PDS 1010A — microdensitometer 07 p0967 N85-16136

STELLAR PHYSICS
NT SOLAR PHYSICS

STELLAR RADIATION
NT STELLAR WINDS
Fast Hartmann method for problems in astronomical adaptive optics 02 p0161 N85-11094
Masers associated with regions of recent star formation 03 p0443 N85-12820
Stability of stellar disk and ratio of halo to disk masses in the galaxy 05 p0740 N85-14763
Voyager EUV and FUV observations 06 p0875 N85-15554
Natural interference phenomena affecting spaceborne receivers
[NASA-CR-174256] 07 p0916 N85-15798
Radiative amplification of acoustic waves in hot stars 08 p1235 N85-17786
Multiline transfer and the dynamics of stellar winds 08 p1236 N85-17788
A survey of fast X-ray transients using the HEAO A-1 Sky Survey experiment 09 p1411 N85-18895
Radio emission from RS CVn binary systems 09 p1417 N85-18939
Coordinated ultraviolet and visual observations of Omega Orionis 1982-1983 11 p1750 N85-21007
A survey of Mg II h and k emission in near-solar type stars
[NASA-CR-175572] 12 p1953 N85-22269
Activity and magnetic fields on stars from radio observations
[NASA-CR-175966] 18 p3202 N85-29861
The radiation of the Vela pulsar 20 p3548 N85-32080
Microburst of TeV gamma rays from the Crab pulsar
[OG-2.3-4] 22 p3866 N85-33941
Secondary periodicities of microbursts of TeV gamma rays from the Crab pulsar
[OG-2.3-5] 22 p3866 N85-33942
Gamma-ray line emission from Al-26 produced by Wolf-Rayet stars
[OG-3.2-5] 22 p3875 N85-34003
Electrons and positrons from expanding supernova envelopes in dense clouds
[OG-6.2-9] 22 p3889 N85-34108
Investigations of the cyclotron resonance effects in the X ray spectrum of the neutron star Hercules X-1
[MPE-191] 22 p3890 N85-34112
Low-excitation Herbig-Haro objects and interstellar extinction
[NASA-CR-176142] 23 p3988 N85-34726

STELLAR ROTATION
NT SOLAR ROTATION
The rotation of B-type stars and processes of star formation 03 p0443 N85-12823
On collective effects in the rotation of stars in clusters and associations 05 p0737 N85-14739
Corotating interaction regions in stellar winds: Particle acceleration and non-thermal radio emission in hot stars 08 p1234 N85-17773
Winds from rotating, magnetic, hot stars 08 p1234 N85-17775
Non-radiative energy from differential rotation in hot stars 08 p1234 N85-17778
Nonradiative heating and enhanced mass-loss due to shear turbulence in massive hot stars 08 p1235 N85-17780
Search for millisecond rotational periods in some low-mass X-ray binaries observed by EXOSAT 11 p1741 N85-20949
Rotational modulation of chromospheric emission in cool giants and hybrid stars 11 p1759 N85-21064
The structure and angular momentum content of dark clouds 14 p2439 N85-25054
Study of the parameters affecting the collapse of a rotating protostellar cloud 24 p4168 N85-35837

STELLAR SPECTRA
NT SOLAR SPECTRA
Local photometric standards for CaII emission stars 01 p0128 N85-10883
A spectroscopic survey of 113 nearby red dwarf stars 01 p0129 N85-10886
Compact infrared sources: Protostars before IRAS 03 p0442 N85-12812
Far-infrared observations of some regions of star formation 03 p0442 N85-12814
Numerical models of the spectral appearance of protostellar envelopes 03 p0442 N85-12816
Masers associated with regions of recent star formation 03 p0443 N85-12820
RS CV sub n binary systems
[NASA-CR-174164] 04 p0580 N85-13704
Observations of highly-ionized interstellar iron 06 p0876 N85-15565
Modelling the local interstellar medium as a supernova remnant in a multiphase gas 06 p0879 N85-15585
The Torun measuring system for astronomical spectra 07 p0966 N85-16130
Spectrophotometry of cool stars from objective prism spectra 07 p0966 N85-16134
Narrow absorption components in Be star winds 08 p1232 N85-17760
Coronal temperatures 08 p1233 N85-17766
Departures from LTE populations versus anomalous abundances: The effects of heating 08 p1234 N85-17776
On the role played by lines in radiatively driven stellar winds depending on the position of the stars in the HR diagram 08 p1236 N85-17787
Multiline transfer and the dynamics of stellar winds 08 p1236 N85-17788
Optical studies of X-ray selected Active Galactic Nuclei (AGN) in the direction of the Large Magellanic Cloud (LMC) 08 p1237 N85-17797
Carbon stars: There is no such thing as a dead leg 08 p1247 N85-17871
Mid-infrared spectroscopy of planetary nebulae 08 p1247 N85-17872
Image quality on the KAO 08 p1249 N85-17885
High precision measurement of stellar radial velocity variations 08 p1250 N85-17896
Experimental determination of the 1 sigma(+) state electron-dipole-moment function of carbon monoxide up to a large internuclear separation
[NASA-TM-85979] 09 p1379 N85-18670
Contributions of the X-ray astronomy group — conference
[MPE-PREPRINT-29] 11 p1742 N85-20952
X-ray coronae of late type stars: Theoretical implications 11 p1742 N85-20953
Simultaneous EXOSAT and optical observations of the pulsing X-ray binary H2252-035 / AO Psc 11 p1743 N85-20958
Spectral studies of low-mass X-ray binaries observed by EXOSAT 11 p1743 N85-20959
EXOSAT observations of 4U1705-44 — X ray binary 11 p1743 N85-20960
Further investigation of mass loss phenomena in hot white dwarfs and O subdwarfs 11 p1751 N85-21014
IUE spectrophotometry of the hot helium-rich PG1159 DO degenerates 11 p1751 N85-21015
Self-consistent recalibration of IUE determination of hot DA white dwarf effective temperatures 11 p1751 N85-21016
Carbon, silicon, and oxygen in the white dwarf star GD 40 11 p1752 N85-21017
Analysis of white dwarf Lyman alpha profiles 11 p1752 N85-21018
The outburst and long term behavior of the triple period cataclysmic variable TV Col 11 p1752 N85-21021
FP Cygni profiles in HL CMa 11 p1752 N85-21022
New results on PU VUL 11 p1753 N85-21023
The UV extinction of HR 5999 11 p1753 N85-21026
Variability of ultraviolet emission lines in the carbon star TX Psc 11 p1753 N85-21027
Temporal UV emission from the peculiar star RX Puppis 11 p1753 N85-21028
Three short-period binaries seen at high-dispersion UX ARI, IOTA TRI and HA5110 11 p1756 N85-21047
The eclipsing binary U Sagittae: Evidence for CNO processing and mass exchange in the past 11 p1757 N85-21049
A search for the spectroscopic binary companions of Polaris using IUE spectra 11 p1757 N85-21053
Co-rotating interaction regions in stellar winds 11 p1758 N85-21060
Ultraviolet, radio and X-ray observations of hybrid stars 11 p1759 N85-21063
Rotational modulation of chromospheric emission in cool giants and hybrid stars 11 p1759 N85-21064

Magnetospheres and winds in the helium weak stars: Observations of C 5 in upper main sequence CP stars
11 p1759 N85-21066
IUE low-dispersion reference atlas
11 p1760 N85-21073
An IUE high-resolution atlas of O-type spectra
11 p1760 N85-21074
Statistical classification of IUE low-despersion stellar spectra: Progress report 11 p1760 N85-21075
Stellar ultraviolet flux distributions in the 912-1200 A wavelength range 11 p1762 N85-21081
The ultraviolet excess of quasars 3: The highly polarized quasars PKS 0736+017 and PKS 1510-089
[NASA-CR-175576] 12 p1953 N85-22268
A survey of Mg II h and k emission in near-solar type stars
[NASA-CR-175572] 12 p1953 N85-22269
Plasma processes in Herbig-Haro objects
12 p1957 N85-22301
Formation of optical-line emitting regions in the jets of SS433 12 p1959 N85-22318
Solar and stellar coronal plasmas
[NASA-CR-175623] 13 p2205 N85-23676
Documentation for the machine-readable version of the Stellar Spectrophotometric Atlas, 3130 A lambda 10600 A of Gunn and Stryker (1983)
[NASA-TM-87437] 14 p2438 N85-25045
Documentation for the machine-readable version of A Library of Stellar Spectra (Jacoby, Hunter and Christian 1984)
[NASA-TM-87438] 14 p2438 N85-25046
Documentation for the machine-readable version of A Finding List for the Multiplet Tables of NSRDS-NBS 3, Sections 1-10 (Adelman, Adelman, Fischel and Warren 1984)
[NASA-TM-87440] 14 p2438 N85-25048
Did the young Sun rotate at 100 km/s
14 p2451 N85-25133
Stellar surface phenomena: A spectroscopic study of the RS canum venaticorum binaries
15 p2689 N85-26467
Activities report of the Institute of Astronomy and Astrophysics 17 p3052 N85-28892
A study of W Serpentis binaries: SX Cassiopeiae, RX Cassiopeiae, and W Serpentis 20 p3544 N85-32053
Investigations of the cyclotron resonance effects in the X ray spectrum of the neutron star Hercules X-1
[MPE-191] 22 p3890 N85-34112
The cosmic ray interplanetary radial gradient from 1972 - 1985
[SH-4.7-1] 23 p4040 N85-35046
The HEAO-2 Guest Investigator Program: Non-linear growth of instabilities in line-driven stellar winds
[NASA-CR-176166] 24 p4168 N85-35840

STELLAR SPECTROPHOTOMETRY

Local photometric standards for CaII emission stars
01 p0128 N85-10883
Photoelectric photometry of globular cluster giants
01 p0128 N85-10884
Spectroscopic data for globular cluster giants. 1: Stars of the red giant tip 01 p0128 N85-10885
Einstein solid state spectrometer observation of the peculiar red dwarf Wolf 630 AB
[NASA-TM-83947] 03 p0447 N85-12843
Astronomical photography 1984 — conferences
[ROE-OR-14] 07 p0962 N85-16102
The Malin effect in stellar photography
07 p0966 N85-16131
Some applications of signal-to-noise in photographic stellar photometry 07 p0966 N85-16132
Stellar photographic photometry using a double wedge technique with a focal reducer system
07 p0966 N85-16133
Spectrophotometry of cool stars from objective prism spectra 07 p0966 N85-16134
Summary of the origin of nonradiative heating/momentum in hot stars
08 p1236 N85-17769
A comparison of some photometric parameters of active and normal spiral galaxies 08 p1238 N85-17806
Five-minute P modes detected in Doppler shift measurement on Alpha Centauri
08 p1250 N85-17895
A statistical evaluation of the limitations of single-channel intermediate-band photoelectric stellar photometry 08 p1251 N85-17900
A CCD system for photometry of direct and spectroscopic images 08 p1252 N85-17904
Ultraviolet spectroscopy of selected astronomical sources
[NASA-CR-174379] 09 p1413 N85-13912
UKIRT spectro-photometry system — United Kingdom Infrared Telescope (UKIRT)
[UKIRT-23] 09 p1414 N85-18921
The central star of NGC 40 11 p1751 N85-21013
IUE spectrophotometry of the hot helium-rich PG1159 DO degenerates 11 p1751 N85-21015
Eclipse observations of Epsilon Aurigae
11 p1755 N85-21037
IUE spectrophotometry of helium weak and silicon stars 11 p1759 N85-21067
IUE observations of faint standard stars for calibration of the space telescope 11 p1761 N85-21078
Calibrations of wavelengths in SWP echelle spectra
11 p1761 N85-21077
Documentation for the machine-readable version of the Stellar Spectrophotometric Atlas, 3130 A lambda 10600 A of Gunn and Stryker (1983)
[NASA-TM-87437] 14 p2438 N85-25045
Activities report of the Institute of Astronomy and Astrophysics 17 p3052 N85-28891
Activities report of the Institute of Astronomy and Astrophysics 17 p3052 N85-28892
The San Fernando Observatory video Stokes polarimeter 18 p3205 N85-29885
Photometric and spectroscopic gamma-ray observations of solar transient phenomena using long duration balloons
[SH-9.1-5] 23 p4051 N85-35120

STELLAR STRUCTURE

Age groups and composite diagrams for young open clusters 05 p0737 N85-14738
The dynamical evolution of the environment of an OB association 05 p0739 N85-14752
Proper motions and kinematical properties of Orion trapezium type stellar systems 05 p0739 N85-14755
On the most probable number of flare stars in the Pleiades field 05 p0739 N85-14756
The velocity-age relation for B and A stars
05 p0740 N85-14762
The nature of the soft X-ray emitting region in the direction of the North Polar spur
06 p0877 N85-15568
HEAO-1 diffuse soft X-ray sky maps
06 p0877 N85-15570
The X-ray structure of the Crab Nebula
11 p1741 N85-20948
The X-ray structure of the Crab Nebula
11 p1742 N85-20954
Research on the early history of the solar system
13 p2180 N85-23527
Overview of solar seismology: Oscillations as probes of internal structure and dynamics in the Sun
14 p2441 N85-25061
Solar inverse theory 14 p2441 N85-25063
The hydromagnetics of the Sun — conference
[ESA-SP-220] 14 p2445 N85-25091
Coronal structures 14 p2448 N85-25110
Solar magnetohydrodynamics: Symposium review
14 p2455 N85-25162
Activities report of the Institute of Astronomy and Astrophysics 17 p3052 N85-28891
Activities report of the Laboratory of Stellar and Planetary Physics
[G-127] 20 p3544 N85-32052
The kinematic and radial properties of normal luminous SC galaxies 20 p3545 N85-32061
A possible mechanism to cause the quasi-biennial variability on the solar neutrino flux
[SH-8.1-5] 23 p4049 N85-35110

STELLAR TEMPERATURE

Thermal effects in stellar pulsations
02 p0297 N85-11925
The influence of stellar luminosity and temperature calibration on the determination of the initial mass function 05 p0740 N85-14760
The Origin of Nonradiative Heating/Momentum in Hot Stars
[NASA-CP-2358] 08 p1231 N85-17755
Coronal temperatures 08 p1233 N85-17766
Stellar winds: Observational evidence for a hot-cool star connection 08 p1233 N85-17768
Heating in the solar mantle 08 p1233 N85-17769
Overheated open coronal regions
08 p1234 N85-17772
Transport properties of the outer crust of magnetic neutron stars 09 p1415 N85-18927
The UV extinction laws in two very young clusters, NGC 6530 in the galaxy and NGC 2100 in the LMC
11 p1748 N85-20994
Ultraviolet studies of the young populous cluster NGC 2100 in the LMC 11 p1748 N85-20995
Stellar winds in the young galactic cluster NGC 6530
11 p1750 N85-21004
IUE and Voyager observations of very hot O-type subdwarfs 11 p1751 N85-21010
Self-consistent recalibration of IUE determination of hot DA white dwarf effective temperatures
11 p1751 N85-21018
Cooling of neutron stars with hyperons
[DE85-004641] 13 p2171 N85-23472

STELLAR WINDS

Helium atoms in interstellar and interplanetary media, part 3: Temperature and velocity of interstellar wind
02 p0160 N85-11068
Relation of core structure to high velocity outflow in G35.2-0.74 and other molecular clouds
03 p0443 N85-12818
Molecular hydrogen emission associated with high velocity flows. A tracer for low velocity shocks
03 p0443 N85-12819
Shapes of wind driven circumstellar shells
03 p0443 N85-12821
The dynamical evolution of the environment of an OB association 05 p0739 N85-14752
Stromgren trails of hot white dwarfs
05 p0879 N85-15589
Theoretical studies of chromospheres and winds in cool stars
[NASA-CR-174204] 06 p0880 N85-15598
Observations of nonthermal radio emission from early-type stars 08 p1232 N85-17758
Narrow absorption components in Be star winds
08 p1232 N85-17760
Ultraviolet spectral morphology of O-type stellar winds
08 p1232 N85-17762
X-ray activity in pre-main sequence stars
08 p1233 N85-17764
Stellar winds: Observational evidence for a hot-cool star connection 08 p1233 N85-17768
Corotating interaction regions in stellar winds: Particle acceleration and non-thermal radio emission in hot stars
08 p1234 N85-17773
Synchrotron emission from chaotic stellar winds
08 p1234 N85-17774
Winds from rotating, magnetic, hot stars
08 p1234 N85-17775
Is the ratio of observed X-ray luminosity to bolometric luminosity in early-type stars really a constant?
08 p1234 N85-17777
Nonradiative heating and enhanced mass-loss due to shear turbulence in massive hot stars
08 p1235 N85-17780
A leaky waveguide model for MHD wave driven winds from coronal holes 08 p1235 N85-17781
Radiatively driven winds and what they imply: A review of radiative driven instabilities and their importance in hot stars 08 p1235 N85-17782
Effect of scattering on instabilities in line-driven stellar winds 08 p1235 N85-17784
New instabilities in line driven winds
08 p1235 N85-17785
On the role played by lines in radiatively driven stellar winds depending on the position of the stars in the HR diagram 08 p1236 N85-17787
Multiline transfer and the dynamics of stellar winds
08 p1236 N85-17788
Collimated winds from active galactic nuclei
08 p1241 N85-17832
Centrifugally driven magnetohydrodynamic (MHD) winds and the nonthermal emission regions in Active Galactic Nuclei (AGN) 08 p1242 N85-17835
Duelling winds: A model for broad-line regions — galactic nuclei 08 p1242 N85-17837
Far-infrared photometry of low-mass pre-main-sequence stars with broad CO wings 08 p1246 N85-17866
Spectroscopic observations of selected stellar systems
[NASA-CR-174288] 08 p1255 N85-17915
Combined ultraviolet studies of astronomical sources
[NASA-CR-174361] 09 p1413 N85-18910
Hot stars: Six years of progress
11 p1743 N85-20963
Coronal effects of the winds of early-type stars
11 p1749 N85-21002
Superionized species and winds in low luminosity B and Be stars 11 p1749 N85-21003
Stellar winds in the young galactic cluster NGC 6530
11 p1750 N85-21004
Main sequence B stars with strong winds
11 p1750 N85-21005
FP Cygni profiles in HL CMa
11 p1752 N85-21022
Atmospheric properties of RU Lupi derived from high- and low-resolution IUE spectra
11 p1754 N85-21031
The stellar wind in the BO V-type eclipsing binary Y Cygni 11 p1755 N85-21040
Observations of cataclysmic variable star winds
11 p1755 N85-21041
Chromospheric emission lines in high-resolution LWR spectra (220 - 3000 alpha) of gamma CRU (M3 3) and alpha ORI (M2 Iab) 11 p1758 N85-21058
Co-rotating interaction regions in stellar winds
11 p1758 N85-21060
Ultraviolet, radio and X-ray observations of hybrid stars 11 p1759 N85-21063

Ultraviolet and optical spectroscopy and polarimetry of the helium weak star HD 21699: Evidence for a magnetically controlled stellar wind
11 p1759 N85-21065

Magnetospheres and winds in the helium weak stars: Observations of C 5 in upper main sequence CP stars
11 p1759 N85-21066

Old and new neutron stars
[DE85-002716] 11 p1762 N85-21085

The modelling of latitudinal gradients in the solar wind in the outer solar system
12 p1947 N85-22231

Plasma processes in Herbig-Haro objects
12 p1957 N85-22301

An analytic model for hydromagnetospheres — stellar winds; pulsars; cosmic jets
12 p1959 N85-22313

Processes and problems in secondary star formation
[DE85-003623] 12 p1960 N85-22322

Winds in cataclysmic variable stars
[DE85-006708] 15 p2689 N85-26470

X-ray emission and the winds of cataclysmic variables
[DE85-007663] 17 p3053 N85-28902

The hydrodynamic effects of nuclear active galaxy winds on host galaxies
20 p3545 N85-32062

Excess gamma-rays in the direction of the rho Ophiuchi cloud: An exotic object?
[OG-2.5-1] 22 p3688 N85-33958

Evidence for a dynamical halo around the edge-on galaxy NGC 4631
[OG-6.2-1] 22 p3689 N85-34102

Possible origin of the anomalous component of cosmic rays
[SH-4.6-7] 23 p4039 N85-35045

The HEAO-2 Guest Investigator Program: Non-linear growth of instabilities in line-driven stellar winds
[NASA-CR-176168] 24 p4168 N85-35840

STELLARATORS

Elimination of stochasticity in stellarators
02 p0282 N85-11839

Proceedings of the US-Japan Theory Workshop on 3-D MHD Studies
[DE84-012019] 04 p0588 N85-13820

Zero-current, high beta stellaration equilibria with rotational transform profile control
[DE84-016835] 04 p0588 N85-13824

Monte Carlo studies of transport in stellarators
[DE84-017633] 04 p0588 N85-13825

MHD equilibrium and stability for stellarator/torsatron configurations
[DE85-001139] 09 p1391 N85-18750

Electron cyclotron resonance heating system for the stellarator W 7-AS
[IPF-84-5] 09 p1395 N85-18779

Wave absorption and transport studies on Electron Cyclotron Resonance (ECR) heated stellarator plasmas in W 7-A
[IPF-84-9] 09 p1395 N85-18782

Fusion Energy Division
[DE85-001701] 11 p1731 N85-20864

Activities report of the Institute of Plasma Research
11 p1733 N85-20903

TOKASTAR: A Tokamak stellarator hybrid with possible bean-shaped operation
[IPPJ-718] 16 p2866 N85-27680

I. F. S. (Institute for Fusion Studies) Newsletter, Volume 4, Number 1
[DE85-007917] 17 p3040 N85-28809

Recent progress in stellarator reactor conceptual design
[DE85-009592] 18 p3189 N85-29780

Alternating current OHMIC heating in a toroidal stellerator
20 p3534 N85-31988

Cyclotron absorption of fast magnetosonic wave in stellarator
21 p3693 N85-32945

Method and apparatus for maintaining equilibrium in a helical axis stellarator
[DE85-011626] 22 p3845 N85-33815

Proceedings of the US-Japan Workshop on Transport in Open-Ended Systems
[IPPJ-727] 23 p3975 N85-34644

Analytic and numerical calculations of the ambipolar electric field in a stellarator
23 p3978 N85-34665

Behavior of helically-trapped fast ion orbits in heliotron E
23 p3978 N85-34666

Advanced Toroidal Facility (ATF)
[DE85-011567] 23 p3983 N85-34699

Stellarator approach to fusion plasma confinement
[DE85-011420] 23 p3984 N85-34704

Confinement and heating of high beta plasmas with emphasis on compact toroids
[DE85-011450] 24 p4155 N85-35761

STELLITE (TRADEMARK)

Interaction of high-cycle and low-cycle fatigue of Haynes 188 alloy at 1400 F deg
17 p2913 N85-27961

STEMS

Gravitropism in leafy dicot stems
15 p2610 N85-26066

STEP FAULTS

U GEOLOGICAL FAULTS

STEPPES

Snow cover in the Siberian forest-steppe
[NASA-TM-77914] 23 p3943 N85-34435

STEREOCHEMISTRY

Synthesis of stereoisomeric - metal complexes using phase-transfer catalysis and photochemical transforms
[AD-A145787] 03 p0331 N85-12134

A metal-catalyzed rearrangement of alkene-alkynes and the stereochemistry of metallacyclobutene ring opening
[AD-A149084] 10 p1435 N85-19042

Chemical applications of topology and group theory. 18: Polyhedral isomerizations of seven-coordinate complexes
[AD-A149461] 10 p1436 N85-19047

STEREOGRAPHY

U STEREOPHOTOGRAPHY

STEREOPHONICS

Psychological and physiological basis of stereophonic effect
15 p2526 N85-25574

STEREOPHOTOGRAPHY

An overview of Multispectral Electro-Optical Stereo Scanner (MEOSS) mission
04 p0458 N85-12908

The Monocular Electro-Optical Stereo Scanner Experiment (MEOSS)
04 p0459 N85-12910

Hierarchical data structures and algorithms for digital stereoscopical mensuration
08 p1175 N85-17410

Determining grasp points using photometric stereo and the PRISM binocular stereo system
[AD-A147782] 08 p1222 N85-17697

A generalized ordering constraint for stereo correspondence
[AD-A149182] 10 p1487 N85-19390

Processing of underwater photographs
10 p1499 N85-19462

The position and mobility of the shoulder, spinal column and pelvis in seated subjects
[AD-A153751] 18 p3153 N85-29524

Use of stereographic projection in marine geodesy
19 p3294 N85-30421

Large format camera photographs: A new tool for understanding arid environments
21 p3604 N85-32379

Progress report on a new search for free e/3 quarks in the cores of 10(15) - 10(16) eV air showers
[HE-6.2-15] 24 p4212 N85-36151

STEREOSCOPIC PHOTOGRAPHY

U STEREOPHOTOGRAPHY

STEREOSCOPY

NT STEREOPHOTOGRAPHY

SIR-B cartography and stereo topographic mapping
08 p1147 N85-17234

Automatic terrain elevation mapping and registration
08 p1148 N85-17242

Hurricane structure and dynamics from stereoscopic and infrared satellite observations and radar data
15 p2594 N85-25988

STERILIZATION EFFECTS

NT CHEMICAL EFFECTS
NT DECONTAMINATION
NT THERMAL DEGRADATION

STERNS

U AFTERBODIES

STEROIDS

NT ALDOSTERONE
NT CORTICOSTEROIDS
NT CORTISONE
NT HYDROXYCORTICOSTEROID

Modulation of the cytosolic androgen receptor in striated muscle by sex steroids
[NASA-CR-174173] 04 p0545 N85-13468

STIFF STRUCTURES

U RIGID STRUCTURES

STIFFENING

Design proposals for torsional buckling of stiffeners
[AD-A144783] 01 p0062 N85-10409

An experimental investigation into the dynamic response of a stiffened flat plate loaded impulsively by an underwater shockwave
[AD-A151321] 15 p2578 N85-25903

Finite element thermal-structural analysis of cable-stiffened space structures
[AD-A153622] 18 p3066 N85-28963

Design of transversely stiffenend FRP panels under compressive load — fiber reinforced plastic (FRP) ships
[AMTE(S)-R-84104] 23 p3940 N85-34424

STIFFNESS

Comparison of numerical techniques for integration of stiff ordinary differential equations arising in combustion chemistry
[NASA-TP-2372] 01 p0011 N85-10065

The theory of elastic modulus of fabric composites and its examination by experiments
[NAL-TR-808] 01 p0022 N85-10133

Influence of test method and material stiffness on the damage produced by low velocity impacts on carbon-epoxy composites No. 45.387/1
[REPT-45.387/1] 03 p0326 N85-12100

Interactions among system stiffness, wear and vibrations
03 p0370 N85-12364

Hydrodynamic impeller stiffness, damping, and inertia in the rotordynamics of centrifugal flow pumps
05 p0643 N85-14125

Theoretical approach to labyrinth seal forces - cross-coupled stiffness of a straight-through labyrinth seal
05 p0643 N85-14127

Experimental investigation of lateral forces induced by flow through model labyrinth glands
05 p0643 N85-14128

Dynamic stiffness characteristics of high eccentricity ratio bearings and seals by perturbation testing
05 p0645 N85-14141

A review of imperfection sensitivity of stiffened shells
[AD-A147311] 07 p0978 N85-16213

A gyro sensor block suspension
[AD-D011411] 08 p1154 N85-17284

Modelling and identification of the structural properties of an astromast
[CRC-1374] 09 p1329 N85-18352

Theory versus experiment for the rotordynamic coefficients of annular gas seals. Part 2: Constant clearance and convergent-tapered geometry
[NASA-CR-174413] 10 p1491 N85-19416

Predicting stability of full-scale composite constructions of the basis of stiffness
11 p1599 N85-20054

Elastic compliance of imperfect interfaces: Review and relationship to ultrasonic scattering
[DE85-003068] 11 p1652 N85-20404

Experimental stiffness of tapered bore seals
[NASA-TM-86978] 15 p2568 N85-25847

Effect of internal pressure on flexibility and stress intensification factors for pipe elbows analyzed by the finite element method
[AD-A151161] 15 p2578 N85-25901

Study of oscillations of composite cylindrical shells using a dynamic stiffness technique
16 p2766 N85-27066

Friction and wear behavior of aluminum and composite I-beam stiffened airplane skins
[NASA-TM-86418] 17 p2895 N85-27852

Design of helicopter rotor blades for optimum dynamic characteristics
[NASA-CR-176076] 20 p3393 N85-31044

Vibrational stabilization of flexible structures
20 p3414 N85-31188

Stiffness control of large space structures
20 p3414 N85-31189

An overview of latest model reduction and control methods of large flexible space structures
20 p3414 N85-31191

Thermomechanically induced pre- and postbuckling of general structure
20 p3467 N85-31540

Shear-stress distribution and shear stiffness in the case represented by a non-homogeneous cross-section, of any shape, but composed of an orthotropic material, when subjected to a shear force
[DRIC-T-7430] 20 p3469 N85-31554

Application of traction drives as servo mechanisms
22 p3797 N85-33520

The properties of thin-section, four-point-contact ball bearings in space
22 p3797 N85-33521

An introduction to finite elements
23 p3924 N85-34319

STIFFNESS MATRIX

Recursive calculation of curved finite element stiffness matrices
[CSIR-TWISK-303] 01 p0108 N85-10726

Parallel triangularization of substructured finite element problems
[NASA-CR-172466] 02 p0241 N85-11569

An algorithm for assembly of stiffness matrices into a compacted data structure
[AD-A146727] 07 p1023 N85-16492

Finite axisymmetric deformation of a thin shell of revolution
16 p2798 N85-27251

Parametric stiffness control of flexible structures
20 p3414 N85-31187

Automated dynamic analytical model improvement for damped structures
[NASA-CR-177945] 23 p3941 N85-34425

Constrained stiffness matrix adjustment using mode data
[AD-A155988] 24 p4143 N85-35685

STIGMATISM

Electrostatic astigmatic tubular lens
21 p3695 N85-32955

STILLS

Alcohol fuel from Ohio farms: An introduction
[TI-84-901290] 05 p0621 N85-13970

STIMULANTS
NT ATROPINE
NT NOREPINEPHRINE
STIMULATED EMISSION
NT WATER MASERS
Four-photon resonant third harmonic generation
[DE85-010070] 19 p3367 N85-30683
STIMULATED EMISSION DEVICES
NT ARGON LASERS
NT ATMOSPHERIC LASERS
NT CARBON DIOXIDE LASERS
NT CARBON LASERS
NT CARBON MONOXIDE LASERS
NT CHEMICAL LASERS
NT CONTINUOUS WAVE LASERS
NT DF LASERS
NT DYE LASERS
NT EXCIMER LASERS
NT FREE ELECTRON LASERS
NT GALLIUM ARSENIDE LASERS
NT GAS LASERS
NT GASDYNAMIC LASERS
NT GLASS LASERS
NT HCN LASERS
NT HELIUM-NEON LASERS
NT HF LASERS
NT HIGH POWER LASERS
NT HYDROGEN MASERS
NT INFRARED LASERS
NT INJECTION LASERS
NT INTERSTELLAR MASERS
NT IODINE LASERS
NT KRYPTON FLUORIDE LASERS
NT LASERS
NT MASERS
NT METAL VAPOR LASERS
NT NEODYMIUM LASERS
NT NITROGEN LASERS
NT NOVA LASER SYSTEM
NT NUCLEAR PUMPED LASERS
NT ORGANIC LASERS
NT PLASMADYNAMIC LASERS
NT PULSED LASERS
NT Q SWITCHED LASERS
NT RAMAN LASERS
NT RARE GAS-HALIDE LASERS
NT RING LASERS
NT RUBY LASERS
NT SEMICONDUCTOR LASERS
NT SOLAR-PUMPED LASERS
NT SOLID STATE LASERS
NT TEA LASERS
NT TRAVELING WAVE MASERS
NT TUNABLE LASERS
NT TWO-WAVELENGTH LASERS
NT ULTRASHORT PULSED LASERS
NT ULTRAVIOLET LASERS
NT WATER MASERS
NT WAVEGUIDE LASERS
NT X RAY LASERS
NT XENON CHLORIDE LASERS
NT XENON FLUORIDE LASERS
NT YAG LASERS
STIMULATION
NT AUDITORY STIMULI
NT SENSORY STIMULATION
Space-time characteristics of radiation of single-mode injection lasers 02 p0269 N85-11758
Effect of triphthasine and elenium on changes in evoked bioelectrical activity of the brain exposed to stationary magnetic field 19 p3325 N85-30601
STIMULI
Laboratory note: Effect on sleep latency of pre-sleep AEP (Auditory Evoked Potential) procedures
[AD-A147620] 08 p1194 N85-17527
STIRLING CYCLE
Free-piston Stirling engine development
[PB84-237767] 01 p0056 N85-10369
Liquid-piston Stirling machines
[DE84-014255] 02 p0205 N85-11351
Standardized efficiency terms: Comparison of some Stirling engine performance figures
[DE84-015407] 02 p0205 N85-11352
Stirling material technology
[NASA-TM-86886] 04 p0472 N85-13007
Linear harmonic analysis for Stirling machines and second law analysis of four important losses
[DE84-016595] 04 p0573 N85-13655
Linear harmonic analysis of Stirling engine thermodynamics
[DE84-016646] 04 p0574 N85-13657
Overview of waste heat utilization systems
[NASA-TM-86901] 04 p0578 N85-13692
Dynamic power systems for power generation 05 p0609 N85-13692
Dynamic conversion working group summary 05 p0611 N85-13904
Stirling engine development, state of the art, possible engine applications and suitability in comparison to established plants and systems
[BMFT-FB-T-84-196] 05 p0648 N85-14149
Effect of water on hydrogen permeability — Stirling engines
[NASA-TM-86904] 06 p0761 N85-14864
Phase 1-A development kinematic Sterling/Rankine commercial gas-fired heat pump research program
[PB85-100931/GAR] 07 p0936 N85-15928
Initial testing of a variable-stroke Stirling engine
[NASA-TM-86875] 10 p1589 N85-19895
Introducing engine innovations: An examination of future markets for Brayton and Stirling automotive engines
[DE84-016319] 11 p1647 N85-20382
Magentically actuated compressor
[NASA-CASE-GSC-12799-1] 12 p1818 N85-21404
Gas-fired duplex free-piston Stirling refrigerator 12 p1819 N85-21413
Some solar dish/heat engine design considerations
[DE85-003479] 12 p1881 N85-21802
Parameters of symmetric rhombic drive mechanism for single-cylinder Stirling engine 14 p2271 N85-24072
Overview of the 1985 NASA Lewis Research Center SP-100 free-piston Stirling engine activities
[NASA-TM-87028] 16 p2880 N85-27769
Activity and accomplishments of dish/Stirling electric power system development
[NASA-CR-175841] 17 p2985 N85-28445
Simplified analysis of Stirling engines and heat pumps
[DE85-008753] 17 p2996 N85-28457
Report to Congress on the Automotive Technology Development Program
[DE85-005640] 17 p3052 N85-28890
Free-piston Stirling engine/linear alternator 1000-hour endurance test
[NASA-CR-174771] 19 p3304 N85-30481
STOCHASTIC PROCESSES
NT MARKOV CHAINS
NT MARKOV PROCESSES
NT RANDOM PROCESSES
NT RANDOM WALK
Theory of nuclear magnetic relaxation
[AD-P003911] 01 p0032 N85-10197
Some weak and strong laws of large numbers for d(0,1) - valued random variables
[AD-A144845] 01 p0111 N85-10754
Simulation uses of the exponential distribution
[AD-A144940] 01 p0112 N85-10758
On the Pontryagin principle for stochastic optimal control
[TWISK-328] 01 p0112 N85-10782
Stochastic properties of a sequence of interfailure times under minimal repair and under revival
[AD-A145003] 01 p0113 N85-10769
Asynchronous discrete control of continuous processes
[AD-A145570] 02 p0189 N85-11262
Asymptotically optimal adaptive control
[AD-A145686] 02 p0249 N85-11629
Limit theory for the sample covariance and correlation functions of moving averages
[AD-A145488] 02 p0251 N85-11642
Maximum likelihood estimation of the survival functions of N stochastically ordered random variables
[AD-A145429] 02 p0254 N85-11662
On the rate of mean convergence of finite linear predictors of multivariate stationary stochastic processes
[AD-A145809] 02 p0254 N85-11664
Diffusion and intermittency in an extended one-dimensional maps 02 p0282 N85-11834
Long time correlation and stochastic diffusion in the standard map 02 p0282 N85-11835
Stochasticity and transport in Hamiltonian systems 02 p0282 N85-11836
Long-time tail in the two-wave model 02 p0282 N85-11837
Stochastic property of K-dV solitons perturbed by random forces — Korteweg-Devries equation 02 p0283 N85-11843
Stable distribution and Levy process in fractal turbulence 02 p0283 N85-11846
On-line fatigue life prediction under stochastic loading by the time series modeling 03 p0370 N85-12362
Regenerative simulation methods for local area computer networks
[AD-A146197] 03 p0409 N85-12612
Return difference feedback design for robust uncertainty tolerance in stochastic multivariable control systems
[AD-A145861] 03 p0411 N85-12624
Vertical coherence along a mecroray path in an inhomogeneous anisotropic ocean
[AD-A145992] 03 p0416 N85-12660
A stochastic model for optimizing the consumption and exploration of nonrenewable natural resources
[INPE-2770-PRE/343] 03 p0440 N85-12804
Accounting for error stochasticity in terminal homing of aircraft 04 p0469 N85-13115
Stochastic cell model for hadronic multiparticle distributions
[DE84-016480] 04 p0562 N85-13578
Stochastic does not equal ad hoc — theories of lunar origin 04 p0566 N85-13741
Evaluation of the stochastic drift of rate-integrating gyros as preparation for the analysis of laser gyro drift measurements
[ESA-TT-827] 05 p0639 N85-14090
Coupling of multidirectional diffusions by reflection
[CTH-MATH-1984-20] 05 p0719 N85-14813
An on-line parameter estimation algorithm for counting process observations
[CWI-OS-R8406] 05 p0721 N85-14832
Information flow in event-driven large-scale systems
[DE84-014167] 05 p0735 N85-14728
Studies in statistical signal processing
[AD-A147130] 07 p0940 N85-15869
The Shock and Vibration Digest, volume 16, no. 9
[AD-A146779] 07 p0976 N85-16200
Techniques for nonlinear random vibration problems 07 p0977 N85-16201
Estimation for a semimartingale regression model using the method of sieves
[AD-A146809] 07 p1028 N85-16527
Numerical methods and approximation and modelling problems in stochastic control theory
[AD-A146927] 07 p1029 N85-16533
The symmetry group and exponents of operator stable probability measures
[AD-A147167] 07 p1035 N85-16566
Limiting distributions of functionals of Markov chains
[AD-A147832] 07 p1036 N85-16577
Local dependence and point processes of exceedances in stationary sequences
[AD-A147859] 07 p1036 N85-16578
Robust prediction and interpolation for vector stationary processes, part 3
[AD-A147860] 07 p1036 N85-16579
Infinite order autoregressive representations of multivariate stationary stochastic processes
[AD-A147863] 07 p1036 N85-16580
On modeling the performance and reliability of multi-mode computer systems
[AD-A148444] 08 p1206 N85-17599
Optimal stochastic LQ control with measurements displaced in time
[OUEL-1547/84] 08 p1209 N85-17605
Large deviations for processes with independent increments
[AD-A147293] 08 p1210 N85-17610
Asymptotic methods for the analysis, estimation, and control of stochastic dynamic systems
[AD-A147758] 08 p1211 N85-17618
Extended Stochastic Petri Nets: Applications and analysis
[AD-A148439] 08 p1213 N85-17633
Bounding the stochastic performance of continuum structure functions 1
[AD-A148621] 08 p1213 N85-17640
Methods and applications of time series analysis. Part 2: Linear stochastic models
[AD-A147292] 08 p1214 N85-17645
Research in stochastic processes
[AD-A148622] 08 p1216 N85-17660
Stochastic models of pitting corrosion of stainless steels. Part 1: Modelling of the initiation and growth of pits at constant potential
[AERE-R-11146-PT-1] 09 p1298 N85-18151
Stochastic dynamic analysis of a structure with frictional joints 09 p1337 N85-18406
Modeling stochastic wind loads on vertical axis wind turbines
[DE85-001148] 09 p1340 N85-18426
SPADE: Series-parallel directed acyclic graph evaluator
[AD-A148458] 09 p1388 N85-18592
Nicolai maps and stochastic observables from a coupling constant flow
[BONN-HE-84-26] 09 p1376 N85-18653
Data-driven choice of a spectrum estimate: Extending the applicability of cross-validation methods
[DE85-001411] 10 p1437 N85-19058
UHF communications through forested propagation channels 10 p1470 N85-19280
A non-hypoelliptic Dirichlet problem from stochastics 10 p1537 N85-19687
Research in adaptive and decentralized control
[AD-A148954] 10 p1543 N85-19728

Bounding the stochastic performance of continuum structure functions 2
[AD-A149458] 10 p1548 N85-19762
Stochastic methods for the description of multiparticle production
[DE84-009981] 10 p1556 N85-19810
Stochastic runaway of dynamical systems
[IPP-6/244] 11 p1708 N85-20745
Bayesian analysis of time series 1: Householder transformation analyses
[DE85-004449] 11 p1708 N85-20749
Autostochastic behavior of solid state ring laser with low frequency periodic loss modulation
11 p1717 N85-20805
Stochastic convective-dispersive transport model for wastes disposed at the 106-mile ocean disposal site
[PB85-116176] 12 p1885 N85-21831
The effect of stochastic surface heat fluxes on the climatology of the seasonal thermocline
[AD-A149957] 12 p1889 N85-21857
Distributed asynchronous deterministic and stochastic gradient optimization algorithms: Revision
[AD-A149997] 12 p1921 N85-22068
Rates of convergence of semistochastic approximation procedures for solving stochastic optimization problems
12 p1924 N85-22088
A stochastic-mechanical approach to acoustic pulse propagation in the deep ocean sound channel
[AD-A149588] 12 p1928 N85-22110
Statistical phenomena in particle beams
[DE85-001050] 12 p1929 N85-22118
An analysis of a dynamic project cost problem
[CSIR-TWISK-336] 13 p2149 N85-23341
The design of a unified package for the solution of stochastic petri net models
[AD-A150326] 13 p2151 N85-23354
Regenerative stochastic Petri nets
[AD-A150343] 13 p2151 N85-23355
Regenerative simulation of non-Markovian stochastic systems
[AD-A150344] 13 p2153 N85-23367
Application of the maximum entropy/optimal projection control design approach for large space structures
14 p2234 N85-23849
Studies of the initiation of pitting corrosion on stainless steels
[AERE-M-3400] 14 p2254 N85-23967
Dynamic stochastic model of long-period variability of ocean surface temperature 14 p2334 N85-24437
Parameter estimation in stochastic dynamic systems
14 p2365 N85-24754
Ergodicity and Steady-State-Equilibrium conditions for Markov chains
[AD-A151038] 14 p2409 N85-24854
Estimation of optimum scores for partition detectors using stochastic approximation techniques
14 p2411 N85-24885
Stochastic pursuit-evasion differential games in the plane
[CSIR-TWISK-343] 14 p2412 N85-24875
Kinematic dynamo theory for an arbitrary mean flow
14 p2448 N85-25108
Boundary of modulation diffusion and stochastic instability of high energy protons in inner radiation belt
15 p2482 N85-25316
Theory and Applications of State Estimation. NRIMS Summer Seminar Series
[CSIR-SWISK-37] 15 p2635 N85-26244
Nonlinear estimation 15 p2635 N85-26245
The Kalman filter 15 p2635 N85-26246
Linear filtering with non-Gaussian initial conditions
15 p2635 N85-26247
Truncated nonlinear filters 15 p2635 N85-26249
Some aspects of decentralized Kalman filtering
15 p2635 N85-26250
Tracking filters 15 p2635 N85-26252
Point processes associated with extreme value theory
[AD-A151211] 15 p2640 N85-26280
Inference and state estimation for stochastic point processes
[AD-A151216] 15 p2640 N85-26281
Stochastic modeling of planetary ring systems
15 p2675 N85-26516
Graphic simulation of a machine-repairman model
[AD-A151761] 16 p2694 N85-26633
Characteristic functionals of stochastic wave processes
[REPT-14/1984] 16 p2786 N85-27084
Some new results on the discrete-time Riccati Equation and their use in the design of optimal regulators and observer-estimators
[AD-A151934] 16 p2854 N85-27597
An application of Markov chains to the problem of migration in inventory systems
[AD-A151954] 16 p2857 N85-27618
Probabilistic finite element development
17 p2913 N85-27956
On the exceedance point process for a stationary sequence
[AD-A152827] 17 p3016 N85-28665
Extension of three theorems of Fourier series on the disc to the torus
[AD-A153017] 17 p3019 N85-28669
On stochastic integral representation of stable processes with sample paths in Banach spaces
[AD-A152927] 17 p3025 N85-28703
Maximum flow in planar networks with exponentially distributed arc capacities
[AD-A153158] 17 p3026 N85-28710
I. F. S. (Institute for Fusion Studies) Newsletter, Volume 4, Number 1
[DE85-007917] 17 p3040 N85-28809
A global optimization algorithm using stochastic differential equations
[AD-A153526] 18 p3161 N85-29583
Limit behaviour for stochastic monotonicity and applications
[AD-A153814] 18 p3170 N85-29648
High performance asynchronous limited sensing algorithms for CSMA and CSMA-CD channels
[AD-A153919] 18 p3171 N85-29650
Performance evaluation of stochastic timed decision-free Petri Nets
[AD-A153987] 18 p3171 N85-29652
Numerical simulation of the transient by the unstable state in a Lotka-Volterra model
[NOTA-INTERNA-833] 18 p3175 N85-29684
Stochastic resonance in the Landau-Ginzburg equation
[PREPRINT-430] 18 p3175 N85-29685
Short and long-term robot feedback
[PB85-180735] 19 p3281 N85-30347
Use of adjoint equations in problems of evaluating state of random hydrodynamic fields
19 p3289 N85-30398
Method for computing evolution of random hydrodynamic fields on basis of adjoint equations
19 p3292 N85-30412
Expected utility, penalty functions, and duality in stochastic nonlinear programming, revised
[AD-A154034] 19 p3335 N85-30660
An overview of latest model reduction and control methods of large flexible space structures
20 p3414 N85-31191
Routing algorithms and stochastic analysis for large communications networks
[AD-A154654] 21 p3573 N85-32225
A simulation of weather in 3D space
[AD-A155221] 21 p3636 N85-32586
SIGMA - A stochastic-integration global minimization algorithm
[AD-A154878] 21 p3671 N85-32806
Relating corrosion maintenance to environmental factors 22 p3750 N85-33247
Stochastic groundwater flow modeling using the second-order method
[DE85-011250] 22 p3802 N85-33556
Modeling and measurement of fault-tolerant multiprocessors
[NASA-CR-3920] 22 p3833 N85-33732
Frame buffer algorithms for stochastic models
23 p3957 N85-34525
Specifying stochastic objects in a hierarchical graphics system 23 p3957 N85-34526
Stochastic particle acceleration in flaring stars
[OG-8.3-9] 23 p4022 N85-34927
On the statistical significance of excess events: Remarks of caution and the need for a standard method of calculation
[OG-9.5-10] 23 p4031 N85-34987

STOICHIOMETRY
Effect of oxidizing medium and heat treatment on stoichiometry of ZnSe crystal surface
03 p0353 N85-12272
Catalytic oxidation by transition metal ions in zeolites
[AD-A146828] 07 p0922 N85-15842
Homogeneous reaction involving components of different redox couples. 2: Polarographic studies of the interactions of alkali metal cations with anthracene and fluoranthene dianions in N,N-dimethylformamide and acetonitrile
[AD-A148667] 08 p1124 N85-17085
Study of self-propagating condensed phase reactions TiB(2) synthesis
[AD-A153198] 17 p2921 N85-26006
New examples of clusters, extended metal-metal bonding and interstitial derivatives
[DE85-005926] 17 p3044 N85-26837
Combustion characterization of coals for industrial applications
[DE85-010873] 19 p3228 N85-30014
Lithium cell reactions
[AD-A154429] 19 p3305 N85-30484
Survey of mixing in metal/insulator systems
[DE85-011938] 23 p3985 N85-34714
CO + H2 reaction over nitrogn-modified iron catalysts
[DE85-013791] 24 p4072 N85-35231
Size and shape dependence of CO adsorption sites on sapphire supported Fe microcrystals
[NASA-CR-176171] 24 p4160 N85-35794

STOKES FLOW
A counterpart of Faxen's formula in potential flow
[REPT-84-09] 17 p2960 N85-28279

STOKES LAW (FLUID MECHANICS)
Experiments on controlled, unsteady, separated turbulent boundary layers
[AD-P004172] 09 p1266 N85-17957

STOKES LAW OF RADIATION
Modifications to a propagation model for the combinded refraction-diffraction of stokes waves; shallow water, large angle and breaking wave effects
[AD-A151428] 15 p2556 N85-25788
Measurements of vector fields with diode array
18 p3204 N85-29680
Dynamic models of flux tubes in the interpretation of polarization measurements 18 p3206 N85-29691
Contribution functions for Zeeman-split lines, and line formation in photospheric faculae
18 p3207 N85-29693
The effect of line damping, magneto-optics and parasitic light on the derivation of sunspot vector magnetic fields
18 p3207 N85-29695

STOKES THEOREM (VECTOR CALCULUS)
Measurements of vector fields with diode array
18 p3204 N85-29680
Analysis of the new polarimeter for the Marshall Space Flight Center vector magnetograph
18 p3205 N85-29681
The solar vector magnetograph of the Okayama Astrophysical Observatory 18 p3205 N85-29682

STOL AIRCRAFT
U SHORT TAKEOFF AIRCRAFT

STONES (ROCKS)
U ROCKS

STONY METEORITES
NT ALLENDE METEORITE
NT CARBONACEOUS CHONDRITES
NT CARBONACEOUS METEORITES
NT CHONDRITES
NT PANTAR CHONDRITES
NT TEKTITES
Origin of mesosiderites as a natural consequence of planet formation 15 p2683 N85-26574

STOPCOCKS
U COCKS

STOPPING POWER
Stopping powers of solids for low-energy protons
[DE85-001123] 09 p1382 N85-18693
Slowing down of charged particles by the bound electrons in a plasma --- ion beams, nuclear fusion
[LP-209] 14 p2419 N85-24929

STORABLE PROPELLANTS
NT AIRCRAFT FUELS
Space Transportation System (STS) propellant scavenging system study. Volume 1: Technical report
[NASA-CR-171848-VOL-1] 11 p1589 N85-20000
Space Transportation System (STS) propellant scavenging system study. Volume 2: Supporting research and technology report
[NASA-CR-171849-VOL-2] 11 p1589 N85-20001
Surveillance report. Stage 1: Dissected motors-propellants motor number 0012199, phase 15
[AD-A153206] 17 p2916 N85-27973

STORAGE
Depot modernization at the Defense Logistics Agency
[AD-P004008] 03 p0306 N85-11988
Changes in spectral properties of detached leaves
[E85-10042] 07 p0983 N85-16243
Characterization and selection of polymer materials for binary munitions storage. Part 2: Characterization of LLDPE resins
[AD-A148324] 08 p1133 N85-17144

STORAGE BATTERIES
NT LEAD ACID BATTERIES
NT NICKEL CADMIUM BATTERIES
NT NICKEL HYDROGEN BATTERIES
NT NICKEL ZINC BATTERIES
NT SILVER HYDROGEN BATTERIES
NT ZINC-BROMIDE BATTERIES
NT ZINC-CHLORINE BATTERIES
Electrochemistry and storage
05 p0609 N85-13899
Electrochemistry and storage panel report
05 p0611 N85-13903
Energy storage for stationary and mobile operation as a buffer of power supply from additive energy sources
05 p0663 N85-14261

Rechargeable lithium cell
[AD-D011302] 07 p0993 N85-16304
Polymer electrolytes: An investigation of some poly (N-propyleziridine)/lithium salt compositions
[RAE-TR-84036] 08 p1131 N85-17130
BBC of Switzerland develops electric car 08 p1141 N85-17192
Status of French research in plastic batteries 15 p2530 N85-25803
Calcium/thionyl chloride battery technology
[AD-A151975] 15 p2586 N85-25845
Maintenance of photovoltaic power systems
[AD-A152299] 16 p2819 N85-27390
Regenerative fuel cell systems for space station 20 p3443 N85-31372
System level electrochemical principles 20 p3443 N85-31375
Advances in rechargeable lithium molybdenum disulfide batteries 20 p3444 N85-31376
Geosynchronous performance of a lithium-titanium disulfide battery 20 p3444 N85-31377
Rechargeable lithium-organic electrolyte battery having overcharge protection and method of providing overcharge protection for a lithium-organic electrolyte battery
[AD-D011738] 22 p3806 N85-33575
Solar heat pump
[DE85-011323] 23 p3946 N85-34453

STORAGE RINGS (PARTICLE ACCELERATORS)
The Berkeley mini-collider
[DE84-014594] 01 p0118 N85-10808
Self potentials of an electron ring in a torus for large ring displacement from the minor axis
[AD-A148088] 03 p0421 N85-12691
Positron ring system using Anger-type detectors
[DE84-016788] 04 p0503 N85-13212
A normal-incidence monochromator branch line on the FEL-undulator for experimental studies in the 5 to 30 eV region
[DE84-014379] 04 p0505 N85-13225
ASP: A new PEP experiment to measure single photons
[DE84-015732] 04 p0560 N85-13563
Tune shifts for coasting beams crossing at small angles
[DE84-017174] 04 p0562 N85-13579
Instrumentation at national facilities for synchrotron radiation topography
[DE84-016256] 04 p0564 N85-13593
Crossing point conditions, quadrupole gradients and drift space lengths
[DE85-003223] 11 p1721 N85-20825
Electron storage ring beam lifetime dependence on pressure and pumping speed
[DE85-003208] 11 p1724 N85-20845
Review of polarized proton beam techniques and a report on the workshop on polarized beams
[DE85-004390] 12 p1930 N85-22127
Intense, broadband, pulsed I-R source at the National Synchrotron Light Source
[DE84-010542] 12 p1935 N85-22154
Study of the potential usefulness of superfine holographic x-ray gratings in AXAF and astrophysics in general 12 p1945 N85-22215
Electronics Engineering Department EE Technical Review
[UCRL-50025-84-1] 13 p2063 N85-22987
Application of permanent magnets in accelerators and electron storage rings
[DE85-004981] 15 p2642 N85-26297
Energy dependence of the emittance of damping ring beams
[DE85-007060] 15 p2649 N85-26341
Measurement of NSLS distributed diode sputter ion pump characteristics
[DE85-006550] 16 p2760 N85-27031
Proceedings of the Workshop on Polarized Targets in Storage Rings
[DE85-002704] 16 p2862 N85-27653
Distortion functions
[DE85-007511] 16 p2862 N85-27655
Calculations of beam dynamics in Sandia linear electron accelerators, 1984
[DE85-010417] 18 p3180 N85-29719
Coherent X-rays and vacuum-ultraviolet radiation from storage-ring-based undulators and free electron lasers
[DE85-009968] 18 p3183 N85-29738
Experience with a high-brightness storage ring: The NSLS 750 MeV VUV ring
[DE85-010547] 18 p3190 N85-29787
Present and future directions of atomic physics research with multiply-charged ions at Brookhaven National Laboratory
[DE85-010960] 1J p3354 N85-30788
Experiments with stored heavy ions
[DE85-009976] 19 p3356 N85-30802
Guide to the Main Ring DO overpass
[DE85-011722] 20 p3531 N85-31963
Saturation of a longitudinal instability due to nonlinearity of the wake field
[DE85-012514] 22 p3837 N85-33761
Multiple-frequency electron cyclotron heating of hot electron rings in EBT-1
[DE85-011302] 23 p3963 N85-34701
Forty-five years of e(+)e(-) annihilation physics: 1956 to 2001
[DE85-013052] 24 p4149 N85-35723
Breeding new light into old machines (and new)
[DE85-013055] 24 p4155 N85-35763
Vacuum system for the Argonne 6 GeV synchrotron light source
[DE85-012286] 24 p4157 N85-35773
Los Alamos high-current proton storage ring
[DE85-012664] 24 p4158 N85-35779
Accelerator physics measurements at the damping ring
[DE85-013373] 24 p4159 N85-35785
TOSCA calculations and measurements for the SLAC SLC damping ring dipole magnet
[DE85-014366] 24 p4160 N85-35793

STORAGE STABILITY
Storage life of thermal detents
[DE84-016934] 04 p0476 N85-13030
Storage stability of jet fuels
[AD-A146360] 06 p0773 N85-14943
Microspots on spectroscopic plates — astronomical photography 07 p0964 N85-16113
Passive storage technologies 08 p1108 N85-17003
Mechanisms of heat and mass transfer across a double-diffusive interface
[PB85-148468] 12 p1848 N85-21594
Prediction of the long term stability of polyester-based recording media
[PB85-160133] 14 p2262 N85-24019
Conservation of turbines by inhibited air 14 p2268 N85-24054
Alternative food preservation techniques, new technology in food preparation and appropriateness of food supply for the permanently manned space station 14 p2393 N85-24739
Solid state hydrogen pumping and storage material
[AD-D011610] 16 p2757 N85-27011
Surveillance report. Stage 1: Dissected motors-propellants motor number 0012199, phase 15
[AD-A153206] 17 p2916 N85-27973
Additional experiments relative to the shelf life of Li(Si)/FeS2 thermal batteries
[DE85-008482] 18 p3095 N85-29162
Review of zirconium-zircaloy pyrophoricity
[DE85-011169] 23 p3916 N85-34270
Dissected motors-propellants motor number STM-012. Phase 15: Surveillance report, stage 1
[AD-A156068] 24 p4071 N85-35226

STORAGE TANKS
Insulating polymer concrete
[DE84-017239] 04 p0480 N85-13057
VOC emissions from volatile organic liquid storage tanks: Background information for proposed standards
[PB84-237320] 04 p0532 N85-13403
Shock testing of a nitrogen tank (Cryo diffusion type 220 VLR) on the middle weight shock stand
[NASA-TM-77747] 06 p0817 N85-15183
Risks in the transport and storage of liquefied natural gas. Sub-project 5-2: Investigation into building damage
[BLL-RISLEY-TR-4606-(9091.9F)] 07 p0935 N85-15926
Passive Orbital Disconnect Strut (PODS 3) structural test program
[NASA-CR-177325] 08 p1113 N85-17020
High temperature sensible heat storage options
[DE85-000534] 18 p3129 N85-29375
Mixtures experiment where the amount of the mixture is a factor under study
[DE85-010974] 19 p3250 N85-30153
Cultural data base implementation study and computer-aided scene modeling system users manual
[AD-A154232] 19 p3333 N85-30648
Oil tank electrostatic charging report
[DRIC-T-6987] 20 p3436 N85-31319
Results of variable enthalpy tests of CPR-488 TIP panels in MSFC Hot Gas Facility
[NASA-CR-170889] 24 p4072 N85-35237

STORE RELEASE
U EXTERNAL STORE SEPARATION

STORM DAMAGE
Effects of a lightning strike on a civil defense operation center
[FOA-A-30035-A3] 02 p0232 N85-11514
Hurricane Alicia, Galveston and Houston, Texas, 17-18 August 1983
[PB84-237056] 04 p0541 N85-13441
California coastal erosion and storm damage during the winter 1982 - 1983, a reconnaissance report
[PB85-121705] 10 p1521 N85-19591

STORMS
NT CYCLOGENESIS
NT CYCLONES
NT DUST STORMS
NT HURRICANES
NT IONOSPHERIC STORMS
NT MAGNETIC STORMS
NT POLAR SUBSTORMS
NT RAINSTORMS
NT SNOWSTORMS
NT SOLAR STORMS
NT STORMS (METEOROLOGY)
NT SUDDEN IONOSPHERIC DISTURBANCES
NT THUNDERSTORMS
NT TORNADOES
NT TROPICAL STORMS
NT TYPHOONS
Effect of mountain wave dynamics on orographic storms
[DE84-014713] 04 p0540 N85-13433
Probable maximum flood estimation - Eastern United States
[AD-A146538] 06 p0839 N85-15324
Behavior and characteristics of storm cold outflows 09 p1356 N85-18529
Mesoscale storm and dry period parameters from hourly precipitation data: Program documentation
[DE85-001366] 09 p1357 N85-18538
Hurricane alicia storm surge and wave data
[AD-A149668] 12 p1895 N85-21896
Mesoscale analysis and modeling group 15 p2595 N85-26001
Review of VAS demonstration 15 p2596 N85-26002
Impact of soil moisture in organizing a severe storm outbreak 15 p2597 N85-26009
Role of frontal circulations and gravity waves in initiating convective storm systems 15 p2598 N85-26010
An evaluation of the performance of a new storm tracking methodology
[AD-A152234] 16 p2835 N85-27484
Centralized Storm Information System (CSIS)
[NASA-CR-175898] 17 p2904 N85-28506
A report from the Space Science and Engineering Center, the University of Wisconsin-Madison, Madison, Wisconsin 17 p2904 N85-28507
Test and evaluation plan for the Centralized Storm Information System 17 p2904 N85-28508
CSIS test and evaluation 17 p2904 N85-28509
Functional and performance requirements of the next NOAA-Kansas City computer system 17 p2904 N85-28510
Convective storm downdraft outflows detected by NASA/MSFC's Airborne 10.6 micron pulsed Doppler Lidar System
[NASA-CR-3898] 17 p2905 N85-28511
A numerical study of the Pacific polar low
[AD-A153777] 18 p3149 N85-29495
The temporal evolution of a small auroral substorm as viewed from high altitudes with Dynamics Explorer 1
[NASA-CR-176084] 20 p3493 N85-31718
Radio-frequency radiation of storm clouds 21 p3692 N85-32939

STORMS (METEOROLOGY)
NT DUST STORMS
NT HURRICANES
NT POLAR SUBSTORMS
NT RAINSTORMS
NT SNOWSTORMS
NT THUNDERSTORMS
NT TORNADOES
NT TROPICAL STORMS
NT TYPHOONS
Energy correlation between natural extra-low-frequency noises at various frequencies 06 p0784 N85-15010
Spring program summary, 1983
[PB84-222223] 06 p0839 N85-15330
The rationale and suggested approaches for research geosynchronous satellite measurements for severe storm and mesoscale investigations
[NASA-TM-86185] 09 p1356 N85-18532
The influence of soil moisture distribution on the severe-storm environment of the southern Great Plains: A numerical study of the SESAME 4 case 09 p1357 N85-18534
Cut-off lows and their influence on the weather in Switzerland
[REPT-45] 10 p1519 N85-19574
Varying structure and intensity change characteristics of 4 Western North Pacific tropical cyclones
[AD-A149628] 12 p1895 N85-21895
Model sensitivity studies of major east coast storms 15 p2598 N85-26016

Justification and plan for participation in GALE
15 p2599 N85-28017
The seasonal cycle of storminess as measured by band-pass fluctuations
18 p3144 N85-29467
Environmental Research Laboratories publication abstracts, FY 1984
[PB85-180594] 19 p3313 N85-30540
A probabilistic forecasting model of tropical cyclone-generated storm surge for a straight coastline
19 p3314 N85-30544
Areal coverage of storm precipitation
[NASA-CR-176013] 19 p3315 N85-30550

STORMSAT SATELLITE
The rationale and suggested approaches for research geosynchronous satellite measurements for severe storm and mesoscale investigations
[NASA-TM-86185] 09 p1356 N85-16532
The effect of the arbitrary level assignment of satellite cloud motion wind vectors on wind analyses in the pre-thunderstorm environment
[NASA-TM-86186] 10 p1517 N85-19565

STOSS-AND-LEE TOPOGRAPHY
U GLACIAL DRIFT

STOWAGE (ONBOARD EQUIPMENT)
Hemispherical latching apparatus
[NASA-CASE-MFS-25837-1] 19 p3224 N85-29991

STRAIGHT WINGS
U RECTANGULAR WINGS

STRAIN AGING
U PRECIPITATION HARDENING

STRAIN DISTRIBUTION
U STRESS CONCENTRATION

STRAIN ENERGY METHODS
The effect of cross-link density on the toughening mechanism of elastomer-modified epoxies
04 p0465 N85-12951
Numerical investigation of the micromechanics of composite fracture
04 p0467 N85-12970
Toughening mechanism in elastomer-modified epoxy resins, part 2
[NASA-CR-3852] 04 p0478 N85-13046
Stress intensity factors for corner cracks at holes located near an edge
[FFA-TN-1984-20] 04 p0514 N85-13279
Residual thermal and moisture influences on the strain energy release rate analysis of edge delamination
[NASA-TM-86437] 20 p3422 N85-31238
Finite elastic deformations of cylindrical and spherical shells under pressure
[OUEL-1549/84] 20 p3470 N85-31559
Stored energy and structural failure
[OUEL-1564/85] 20 p3471 N85-31567

STRAIN FATIGUE
U FATIGUE (MATERIALS)

STRAIN GAGE ACCELEROMETERS
Navy operational loads data sources and systems
07 p0895 N85-15668

STRAIN GAGES
High temperature static strain sensor development program
02 p0141 N85-10059
Instrumentation techniques for measuring large, high rate strains with foil resistance strain gages
[AD-A146248] 03 p0364 N85-12337
Semiconductor-type transducer with universal strain gauge for measurement of low pressures
04 p0489 N85-13116
A preliminary study of using a strain-gauged balance and parameter estimation techniques for the determination of aerodynamic forces on a model in a very short duration wind tunnel
[AD-A146473] 06 p0810 N85-15145
Structural load measurements on a Northrop NF-5A
07 p0894 N85-15667
Tornado: Structural Usage Monitoring System (SUMS)
07 p0896 N85-15680
Diffusion in metals under high mechanical strain and acceleration
[JUEL-1913] 07 p0928 N85-15887
The constant current strain gauge bridge
[ARL/STRUC-TM-385] 07 p0962 N85-16097
Six-component strain gage block scale 167-6B. Part 1: Calibration, September 1983
[F+W-FO-1699] 07 p0966 N85-16143
Residual stresses at small diffusion welds
[DE84-014982] 07 p0974 N85-16189
Measurement of high temperature strain by the laser-speckle strain gauge
[NASA-TM-77751] 07 p0977 N85-16207
Recommendations for the use of Ni-Cr-base alloy extensometers for measurement of creep strain
[NPL-DMA(A)-81] 08 p1164 N85-17342
Pressure measurements in a hydrogen combustion environment: An evaluation of 3 pressure transducers
[TI85-003845] 09 p1323 N85-18312
Resistance fail strain gage technology as applied to composite materials
[NASA-CR-3872] 10 p1431 N85-19024
Thin film strain transducer --- suitable for in-flight measurement of scientific balloon strain
[NASA-CASE-WLP-10055-2] 12 p1849 N85-21598
Evaluation results of the 700 deg C Chinese strain gauges --- for gas turbine engine
[NASA-TM-86973] 12 p1850 N85-21605
MFTF sensor verification computer program
[DE85-004452] 12 p1916 N85-22029
Root stresses in conformal gears-strain gauge and photoelastic investigations
14 p2223 N85-23787
Effect of drag behind nozzle array on its force and energy characteristics
14 p2277 N85-24107
An experimental investigation into the dynamic response of a stiffened flat plate loaded impulsively by an underwater shockwave
[AD-A151321] 15 p2578 N85-25903
A strain gage manual
[AD-A151602] 16 p2787 N85-27197
Optical strain measurement system development
17 p2915 N85-27969
Liquid-metal transducers for strain measurement during in-pile materials testing
17 p2945 N85-28176
R and D activities of the Systems Engineering Division
20 p3540 N85-32027
The compliance of end effector force sensors for robot manipulator control
24 p4096 N85-35406
Carbon fiber strainmeter studies in southern California
[PB85-196689] 24 p4118 N85-35528

STRAIN HARDENING
Strain hardening and strain aging in Fe-Al-Mn alloys
02 p0178 N85-11198
High temperature low-cycle fatigue mechanisms in single crystals of nickel-based superalloy Mar-M 200
[NASA-CR-174739] 03 p0331 N85-12130
The influence of porosity on the deformation and fracture of alloys
[AD-A148766] 08 p1130 N85-17124
Ultrasonic characterization of advanced composite flywheels
[DE85-000158] 11 p1593 N85-20026
Influence of work-hardening on the Portevin-LeChatelier effect
[DE85-002505] 11 p1605 N85-20093
Structural basis for the mechanical properties of polyethlenes
[PB85-149771] 11 p1613 N85-20142
Measurement of material properties to Mbar pressures using time-resolved shock wave techniques
[DE85-007319] 15 p2558 N85-25780
Slideline verification for multilayer pressure vessels and piping analysis including strain hardening
[DE85-005816] 22 p3801 N85-33549

STRAIN MEASUREMENT
Laser speckle technique for burner liner strain measurements
02 p0142 N85-10060
Device for measuring relative axial expansion of turbine rotor employing space-vector tracking method
06 p0776 N85-14982
Advanced fatigue monitoring on service aircraft
07 p0895 N85-15671
Experiences obtained from service fatigue monitoring exercises
07 p0895 N85-15672
Residual stresses at small diffusion welds
[DE84-014982] 07 p0974 N85-16189
Recommendations for the use of Ni-Cr-base alloy extensometers for measurement of creep strain
[NPL-DMA(A)-81] 08 p1164 N85-17342
Resistance fail strain gage technology as applied to composite materials
[NASA-CR-3872] 10 p1431 N85-19024
Thin film strain transducer --- suitable for in-flight measurement of scientific balloon strain
[NASA-CASE-WLP-10055-2] 12 p1849 N85-21598
Fibre composite laminated plate analysis using a card programmable calculator (HP41C/CV)
[NIAST-83/86] 13 p2103 N85-23106
Some advances in experimentation supporting development of viscoplastic constitutive models
[NASA-CR-174855] 16 p2799 N85-27260
Liquid-metal transducers for strain measurement during in-pile materials testing
17 p2945 N85-28176
Fatigue strength of Inconel 625 plate and weldments used in the DIII-D configuration vacuum vessel
[DE85-006276] 17 p2981 N85-28427
Inhomogeneous deformation: The theory and geological application of finite strain compatibility
19 p3312 N85-30532
Some advances in experimentation supporting development of viscoplastic constitutive models
20 p3468 N85-31545
Algorithm for calculation of strain state from measurements of node coordinates of arbitrary curvilinear grid
[BLL-M-36304-(5828.4)] 23 p3940 N85-34422
Strain measurement using point recognition picture processing
[DRIC-T-7407] 24 p4101 N85-35421
1983 review of experimental stress and strain analysis
[DRIC-T-7469] 24 p4101 N85-35422

STRAIN RATE
Reliability considerations for the total strain range version of strainrange partitioning
[NASA-CR-174757] 02 p0209 N85-11380
Instrumentation techniques for measuring large, high rate strains with foil resistance strain gages
[AD-A146248] 03 p0364 N85-12337
Horizontal-strain observations in the Shumagin Island and Yakataga seismic gaps, Alaska
04 p0515 N85-13287
Strain rate effects and temperature history effects for three different tempers of 4340 VAR steel
[AD-A146372] 06 p0768 N85-14915
The role of microstructure in the modelling of plastic flow in P/M superalloys at forging temperatures and strain rate
06 p0796 N85-15090
The influence of strain rate and porosity on the deformation and fracture of titanium and nickel
[AD-A148670] 08 p1130 N85-17123
Deformation and fracture of P/M (Powder/Metallurgy) titanium alloys
[AD-A148672] 09 p1294 N85-18128
Models for shock damage to marine structural materials
09 p1336 N85-18400
Cavitation phenomenon in superplastic creep
[DE85-001716] 10 p1441 N85-19083
Behavior of fiber-reinforced composites under dynamic tension
[AD-A150619] 13 p2015 N85-22841
Effect of oxygen on mechanical properties of Nb-V alloy
[DE85-002661] 14 p2256 N85-23982
Influence of pretreatment, environment and strain rate on stress corrosion cracking of the aluminum alloy 7075-T6
[VTH-LR-433] 16 p2752 N85-26985
Conformational and mechanical properties at high strain rates
[AD-A153401] 17 p2959 N85-28272
Studies of strain rate effects in the deformation of solids by means of stress pulses and ultrasonic methods
[DE85-009453] 18 p3122 N85-29329
Short term determination of the creep properties of high temperature materials
[CRIF-MT-160] 20 p3432 N85-31288
Synthesis and characterization of copolyimides with varying flexibilizing groups
[NASA-TM-86416] 20 p3433 N85-31296
Viscoplasticity based on overstress with a differential growth law for the equilibrium stress
20 p3466 N85-31532
Fundamental investigations of failure during superplastic forming process
[AD-A154647] 21 p3568 N85-32194
Strain rate sensitivity estimation from high velocity impact data
[AD-A154703] 21 p3599 N85-32347
Influence of particle arrangement on sintering
[AD-A155337] 21 p3599 N85-32352
On high strain rate fragmentation of a closed vessel
23 p3904 N85-34167
Experimental study on time and temperature dependent behavior of crack growth in viscoelastic strip
23 p3905 N85-34193
Effect of strain rate on the initial failure of notched GRP laminates
23 p3908 N85-34214
Carbon fiber strainmeter studies in southern California
[PB85-196689] 24 p4118 N85-35528
Simulation of lattice damage due to dynamic loading
[DE85-008468] 24 p4162 N85-35808

STRAIN SOFTENING
U PLASTIC DEFORMATION

STRAITS
Internal waves in marine straits
[PREPRINT-415] 18 p3151 N85-29510

STRAKES
Flight mechanics analysis of dynamic derivatives of the Dornier variable wind tunnel model
[ESA-TT-854] 11 p1577 N85-19037

STRANGE ATTRACTORS
A case of a not-so-strange strange attractor
[CWI-AM-R8406] 08 p1214 N85-17643

STRANGENESS
A holographic streamer chamber for relativistic nucleus-nucleus collision experiments
24 p4147 N85-35710

STRAPDOWN INERTIAL GUIDANCE
Analysis and simulation of an inertial system (Strapdown) for auxiliary attitude determination by adaptive drift estimation
[INPE-3257-TDL/177] 04 p0454 N85-12882
Flight testing of Litton laser gyro strapdown system LTN-90 for general aviation
[DFVLR-MITT-84-16] 07 p0901 N85-15709
Standard Attitude Heading Reference System (SAHRS) full scale development program
08 p1073 N85-16804
A discussion of coning errors exhibited by inertial navigation systems
[RAE-TM-RAD-NAV-243] 08 p1082 N85-16854
Implementation of an inertial navigation algorithm using a limited wordlength microprocessor for a strapdown navigation computer
[BAE-BT-12792] 15 p2468 N85-25234
Navigation: Accounting for copy
16 p2695 N85-26641
Preguidance and piloting with the aid of composite inertial sensors 16 p2696 N85-26646
Autofocus motion compensation for synthetic aperture radar and its compatibility with strapdown inertial navigation sensors on highly maneuverable aircraft
[AD-A151940] 16 p2704 N85-26693
Simulation of gyrocompassing alignment and calibration of strapdown inertial navigation system in a swaying vehicle
[DFVLR-MITT-84-20] 17 p2895 N85-27850
The DREO (Defence Research Establishment Ottawa) Inertial Navigation Laboratory: Development and test capabilities
[AD-A154425] 19 p3216 N85-29945
Simulations of strapdown-system errors and error compensation methods — transport aircraft navigation
[DFVLR-MITT-84-22] 20 p3392 N85-31040
Flight testing the Litton LTN 90 laser gyro strapdown system for civil aviation
[ESA-TT-904] 20 p3392 N85-31042
Test evaluation of the Honeywell GG1111 Single-Degree-of-Freedom (SDF) strapdown gyroscope
[AD-A154768] 21 p3589 N85-32307

STRAPS
Retroreflective armbands: Influences of wearing mode, aging and other factors on the visibility distance
[IZF-1984-28] 14 p2422 N85-24942
Verification of the SRB motor case pin retainer band tips
[NASA-CR-170882] 24 p4070 N85-35220

STRATA
NT SUBSTRATES
Boundary condition effects in the energy loss spectrum of layered systems
[NOTA-INTERNA-602] 02 p0269 N85-11887
Problem of frequency space variation of sonic field in stratified media 11 p1715 N85-20787
Mechanisms of heat and mass transfer across a double-diffusive interface
[PB85-148466] 12 p1848 N85-21594
Regions of propagation of short-wave perturbations in spherical layer of rotating fluid 13 p2107 N85-23130
Radar echoes at 2.66 and 40.92 MHz from the mesosphere, part 2.6A 21 p3619 N85-32456

STRATEGIC MATERIALS
Research and development requirements for ion implantation
[AD-P003951] 02 p0286 N85-11867
Use of ion implantation to modify the corrosion behavior of metals
[AD-P003953] 02 p0288 N85-11869
Guayule research
[GPO-29-562] 04 p0477 N85-13042
The B2 aluminides as alternative materials
[NASA-TM-86937] 10 p1440 N85-19076
Preliminary SPR thermal model description and results for WH-11 and BM-4
[DE85-013171] 23 p3931 N85-34360
Applications of the mineral resources data system and the International strategic minerals inventory in mineral-resource assessments by region and commodity
24 p4105 N85-35451
Mineral resources programs 24 p4106 N85-35456
The Conterminous United States Mineral Assessment Program 24 p4106 N85-35458

STRATEGY
A strategy for the adjustment and analysis of densification networks — geodetic networks
[SER-C-295] 01 p0083 N85-10420
The effect of strategy in second order manual control on resource competition with a sternberg memory search task
[AD-A150985] 14 p2391 N85-24727
Equilibrium solutions, stabilities and dynamics of Lanchester's equations with optimization of initial force commitments
[AD-A151510] 15 p2637 N85-26266
An incremental multigrid strategy for the fluid dynamics equations
[AD-A151953] 16 p2783 N85-27172
Space Station crew safety alternatives study. Volume 4: Appendices
[NASA-CR-3857] 18 p3065 N85-28958
Strategic use of business graphics: A stakeholder approach 23 p3963 N85-34566
Arms control and The President's Strategic Defense Initiative
[AD-A156334] 24 p4068 N85-35212

STRATIFICATION
NT ATMOSPHERIC STRATIFICATION
NT INTERCALATION
Doubly diffusive linear stability with nonconstant gradients
[DE84-013008] 05 p0670 N85-14310
Heat and mass exchange in a partially stratified fluid
[DE85-000528] 10 p1486 N85-19384
Stratified charge rotary aircraft engine technology enablement program
[NASA-CR-174812] 12 p1778 N85-21163
Horizontal coherence of temperature microstructure in upper ocean layer 13 p2109 N85-23139
Wave propagation in density stratified fluids
16 p2781 N85-27162
The effect of the Benthic Boundary Layer on the physics of intense mesoscale eddies
[AD-A153193] 17 p2958 N85-28270
Arctic mixed layer dynamics
[AD-A153582] 18 p3150 N85-29505
Buoyant jet entrainment in stratified fluids
19 p3263 N85-30238
Numerical modeling of subsurface communication
[DE85-012818] 21 p3577 N85-32249
Turbulent structure of stably stratified nocturnal slope flows
[AD-A155845] 24 p4123 N85-35559
Analysis of two-parameter constant background born inversion for acoustic synthetic data
[AD-A156394] 24 p4145 N85-35698

STRATIFIED FLOW
Numerical calculations of stratified Ekman layer flow over ridges with a finite element model
[DE84-014482] 04 p0499 N85-13179
On the classification and nonlinear solution of one type of stratified shear flow
[AD-A148832] 09 p1319 N85-18295
Thermal striping downstream of a horizontal elbow under thermally stratified transient flow conditions
[DE84-014687] 09 p1320 N85-18302
Some approximations of geophysical hydrodynamics
14 p2336 N85-24448
Modeling of shear flow in a stratified fluid
14 p2340 N85-24469
Buildup of oscillation of bodies in stratified fluid
17 p2941 N85-28157
Numerical techniques for steady two-dimensional transcritical stratified flow problems, with an application to the intermediate field dynamics of ocean thermal energy conversion plants
[DE85-008347] 18 p3151 N85-29509
Natural convection experiments in a stratified liquid-saturated porous medium
[DE85-009003] 20 p3455 N85-31457
Some remarks on the constitutive equations of stratified gas-liquid flow
[EME-137] 20 p3456 N85-31466
Resolution of thermal striping issue downstream of a horizontal pipe elbow in stratified pipe flow
[DE85-006195] 21 p3586 N85-32292
Some aspects of internal gravity waves in a multi-layered moving stratified flow 24 p4092 N85-35369

STRATIFIED LAYERS
U STRATA

STRATIGRAPHY
Geothermal resources of the Laramie, Hanna, and Shirley Basins, Wyoming
[DE84-016104] 01 p0064 N85-10423
Seismic discrimination of a geothermal field: Cerro Prieto
[DE84-014581] 01 p0064 N85-10425
Erosion and sedimentation chronology of three watersheds in Maryland
[PB84-207356] 01 p0071 N85-10467
Paleoenvironmental interpretation of the upper cretaceous Point Lookout sandstone: Implications for shoreline progradation and basin tectonic history, San Juan basin, New Mexico 02 p0227 N85-11486
Stratigraphy, petrology, and tectonic setting of the Alisitos Group, Baja California, Mexico
03 p0389 N85-12488
Stratigraphy, sedimentology and tectonic significance of the Upper Cretaceous Virginian Ridge formation, Method Basin, Washington: Implications for tectonic history of the North Cascades 03 p0390 N85-12494
Geographic and stratigraphic distribution of Miocene palynomorphs in north Idaho 03 p0390 N85-12496
Late quarternary glaciolacustrine and vegetational history of the Copper River Basin, south-central Alaska
03 p0391 N85-12499
The Kansyut Conglomerate in the westernmost Brooks Range, Alaska 04 p0516 N85-13289
Newly recognized sedimentary environments in the Shelikof Formation, Alaska 04 p0516 N85-13292
Stratigraphy, petrology, and structure of the Pingston terrane, Mount Hayes C-5 and C-6 quadrangles, eastern Alaska Range, Alaska 04 p0517 N85-13301
Geothermal resource assessment for North Dakota
[DE84-016128] 04 p0526 N85-13367
Some methodological aspects of study of layer associations in continents and oceans
06 p0820 N85-15205
Geothermal assessment of a portion of the Escalante Valley, Utah
[DE84-015964] 06 p0829 N85-15257
Time series analysis programs for stratigraphic data
[AD-A146627] 06 p0854 N85-15429
Quaternary stratigraphy of the lower Iowa and Cedar River Valleys, southeast Iowa 09 p1352 N85-18504
Stratigraphy of early ordovician El Paso group of the southern Hueco Mountains, Hudspeth County, Texas
09 p1353 N85-18510
Part 1. Stratigraphy, structure and petrology of the Peterborough 1.5-minute quadrangle, New Hampshire and part 2. Graphite textural and isotropic variations in plutonic rocks, south-central New Hampshire
09 p1353 N85-18511
Structure and stratigraphy of Midterhuken Peninsula, Bellsund, West Spitsbergen 09 p1353 N85-18513
Quaternary stratigraphy, geochronology and carbon isotope geology of alluvial deposits in the Texas panhandle 09 p1353 N85-18514
SIR-A imagery in geologic studies of the Sierra Madre Oriental, northeastern Mexico. Part 1 (Regional stratigraphy): The use of morphostratigraphic units in remote sensing mapping
[NASA-CR-175457] 10 p1505 N85-19407
Study of stratigraphy of the Precambrian Soviet Baltic shield 13 p2110 N85-23148
Reflected wave travel-time curves in stratified media with vertically heterogeneous layers and slightly sloping curved boundaries 13 p2114 N85-23167
Assessment of computer based geologic mapping of rock units in the LANDSAT-4 scene of northern Death Valley, California 13 p2119 N85-23195
Dark halo craters and the thickness of grooved terrain on Ganymede 13 p2173 N85-23484
Valles Marineris basin beds: A complex story
13 p2201 N85-23652
Mars: Stratigraphy of western highlands and polar regions 13 p2201 N85-23653
Evaluating structure-forming role of late Paleozoic and Mesozoic-Cenozoic tectonic movements in Baltic Sea region 14 p2337 N85-24450
Shales and other argillaceous strata in the United States
[DE85-010453] 18 p3125 N85-29353
Stratigraphic analysis of Pennsylvania rocks using hierarchy of transgressive-regressive units
19 p3312 N85-30531
Paleoenvironmental investigations at seed cave (Windust cave H-45FR46), Franklin County, Washington
[AD-A154777] 21 p3635 N85-32576
Sulfur transformations at the hydrogen sulfide/oxygen interface in stratified waters and in cyanobacterial mats
21 p3657 N85-32715
The Aravalli sequence of Rajasthan, India: A Precambrian continental margin?
21 p3720 N85-33084
Lithology and stratigraphy of drill holes completed during 1984 in LANL use areas of Yucca Flat, Nevada Test Site, volume 6
[DE85-010895] 22 p3815 N85-33631
Bedrock geology of the Brattleboro Quadrangle, Vermont-New Hampshire
[DE85-011027] 22 p3815 N85-33634
Geology and petroleum resources of basins in western China
[DE85-013038] 23 p3948 N85-34469
Seismic stratigraphic analysis of the Mississippi Fan
24 p4115 N85-35507

STRATOCUMULUS CLOUDS
Conditions governing the formation of stratocumulus clouds over the western Atlantic during cold air outbreaks
[AD-A146780] 07 p1004 N85-16383

The physics of the marine stratocumulus-capped mixed layer 15 p2593 N85-25979

STRATOPAUSE

Coupling between the thermosphere and the stratosphere: The role of nitric oxide 11 p1662 N85-20472

STRATOSPHERE

A comparison of 2- and 3-dimensional transport within a stratospheric circulation model 02 p0227 N85-11485

Solar radiation in the ozone layer 04 p0522 N85-13342

Trends in ozone and temperature structure: Comparison of theory and measurements [DE84-016201] 04 p0539 N85-13428

Comparison of wind derived from the LIMS (Limb Infrared Monitor of the Stratosphere) satellite instrument with rocket observations [NASA-CR-174083] 04 p0541 N85-13444

Aspects of the comparison of stratospheric trace species measurements with photochemical models [DE84-017028] 05 p0672 N85-14317

Utilization of SAGE aerosol profiles in the analysis of Mauna Loa stratospheric lidar data [NASA-CR-174198] 05 p0675 N85-14332

Jet stream errors and tropospheric-stratospheric interactions in the GLAS general circulation model 05 p0683 N85-14392

Nature of short-period variations of cosmic rays in stratosphere 06 p0823 N85-15224

Study of infrared atmospheric emission [AD-A147517] 07 p0998 N85-16336

Optical studies of nitrogen oxides in the stratosphere 08 p1183 N85-17455

Satellite stratospheric aerosol measurement validation [NASA-TM-86003] 08 p1187 N85-17479

Generation and evolution of diabatic planetary waves in continuously stratified atmosphere with Ekman dissipation 09 p1354 N85-18515

Stratospheric concentration of nitric acid, ozone and carbonyl sulfide: Measurement of nitric acid absorption in the Q branch of the V4 band as a function of temperature [ESA-TT-864] 09 p1355 N85-18524

Airborne lidar measurements of El Chichon stratospheric aerosols, October 1982 to November 1982 [NASA-RP-1136] 10 p1514 N85-19550

Aerosol limb absorption — stratosphere [NASA-TM-77733] 10 p1515 N85-19562

Health assessment document for carbon tetrachloride [PB85-124196] 10 p1528 N85-19638

PMP-2: Equatorial wave dynamics 11 p1655 N85-20422

Middle Atmosphere Program. Handbook for MAP, volume 5 [NASA-CR-175481] 11 p1656 N85-20434

A catalogue of dynamic parameters describing the variability of the middle stratosphere during the northern winters 11 p1656 N85-20435

Middle Atmosphere Program. Handbook for MAP, volume 7 [NASA-CR-175479] 11 p1656 N85-20437

PMP-1 report: The fourth winter of PMP-1, 1981 - 1982: A winter with several interesting features 11 p1657 N85-20441

Workshop on Comparison of Data and Derived Dynamical Quantities During Northern Hemisphere (PMP-1) Winters 11 p1657 N85-20444

MAP/GLOBUS campaign 1983 11 p1658 N85-20447

Abnormal circulation changes in the winter stratosphere, detected through variations of D region ionospheric absorption 11 p1659 N85-20458

Midwinter disturbances in the middle atmosphere 11 p1661 N85-20465

Large scale winter time disturbances in meteor winds over central and eastern Europe 11 p1661 N85-20467

VHF radar observations in the stratosphere and mesosphere during a stratospheric warming 11 p1661 N85-20468

Changes in the ozone content over central Europe during reversals of stratospheric circulation in late winter 11 p1661 N85-20469

Aspects of planetary wave transports in the middle atmosphere 11 p1661 N85-20471

Coupling between the thermosphere and the stratosphere: The role of nitric oxide 11 p1662 N85-20472

Lidar observations of stratospheric aerosol over Mauna Loa Observatory, 1974 - 1981 [PB85-115061] 11 p1682 N85-20597

The Jovian Stratosphere in the ultraviolet 11 p1760 N85-21069

Measurement of nuclear lines with a dual Ge(Li) telescope aboard a stratospheric balloon [INPE-3360-TDL/185] 11 p1762 N85-21083

Chemical kinetics and photochemical data for use in stratospheric modeling. Evaluation number 6 [NASA-CR-175564] 12 p1888 N85-21849

Observation of cosmic ray flux variations in stratosphere 13 p1981 N85-22430

Calibration of solar cells outside the atmosphere 13 p2009 N85-22603

A theoretical study of the ozone quasi-biennial oscillation in the tropical stratosphere 13 p2132 N85-23264

One-dimensional nonstationary model of photochemical transformations of gas impurities in stratosphere 14 p2342 N85-24484

High altitude sampling program: Radioactivity in the stratosphere [DE85-005924] 14 p2374 N85-24676

The source of stratospheric NO and N2O [NASA-CR-175713] 15 p2588 N85-25956

SAM 2 measurements of the polar stratospheric aerosol, volume 5 [NASA-RP-1140] 15 p2590 N85-25970

Wave dynamics and transport in the stratosphere [NASA-CR-175789] 16 p2823 N85-27413

Stratospheric ClO: In-situ detection with a new approach 16 p2824 N85-27416

The copper vapor laser 16 p2824 N85-27417

Research and development of new instruments 16 p2824 N85-27418

Water vapor 16 p2824 N85-27420

Role and fate of ozone in the atmosphere 16 p2824 N85-27421

SAM II measurements of the polar stratospheric aerosol. Volume 6: April to October 1981 [NASA-RP-1141] 16 p2825 N85-27422

Investigation of the reaction system NOX/ClOX/HOX under tropospheric and stratospheric conditions [BPT-11/84] 18 p3137 N85-29427

Photochemical processes in the lower stratosphere (ozone layer) 18 p3148 N85-29490

Circulation and transport in the middle atmosphere: Troposphere and lower atmosphere 18 p3148 N85-29491

Development of a technique for in situ detection of stratospheric nitrogen dioxide 19 p3312 N85-30534

Short meridional scale anomalies in the lower stratosphere and upper troposphere 20 p3489 N85-31684

Troposphere-stratosphere (surface-55 km) monthly general circulation statistics for the Northern Hemisphere-four year averages [NASA-TM-86182] 20 p3495 N85-31730

Tropospheric-stratospheric exchange, part 1.1A 21 p3615 N85-32468

Gravity waves from the stratosphere to the mesosphere, part 1.3B 21 p3616 N85-32471

A numerical analysis of transient planetary waves and the vertical structure in a meso-strato-troposphere model, part 1.4A 21 p3617 N85-32473

Vertical transport in the atmosphere: Measurement capabilities and requirements of VHF radars, part 1.6A 21 p3617 N85-32476

Morphology of the scattering targets: Fresnel and turbulent mechanisms, part 2.1A 21 p3618 N85-32481

Antenna induced range smearing in MST radars 21 p3620 N85-32495

High resolution evidence for the Garrett-Munk spectrum of stratospheric gravity waves 21 p3622 N85-32503

Relationship of isolated turbulent regions to the general turbulent background, part 4.4A 21 p3623 N85-32506

Estimation of vertical diffusion from observations of Atmospheric turbulence layers, part 4.4B 21 p3623 N85-32507

Further developments of EISCAT as an MST radar 21 p3627 N85-32534

Urbana radar systems: Possibilities and limitations 21 p3628 N85-32540

Millstone Hill radar: Capabilities for S/T observations 21 p3629 N85-32548

The Ponape ST radar 21 p3629 N85-32549

Measurements of vertical velocity over flat terrain by ST radar and other related uses of the radar data set 21 p3630 N85-32550

Activities report of the Aeronomy Department [G-774-1984] 21 p3633 N85-32569

A new hypothesis for the observed vertical distribution of atmospheric aerosols 21 p3645 N85-32646

Theoretical studies of structure and stability of hydrates of atmospheric sulfur species 21 p3650 N85-32684

Ozone during sudden stratospheric warming: A three-dimensional simulation [AERONOMICA-ACTA-A-292-1984] 22 p3813 N85-33621

Voigt line profile computation of infrared lines in the stratosphere and mesosphere [AERONOMICA-ACTA-A-294-1985] 22 p3813 N85-33622

A comparison of calculated and measured background noise rates in hard X-ray telescopes at balloon altitude [OG-9.3-7] 23 p4028 N85-34962

Dynamics of two-year cosmic ray variations inferred from the data of spacecraft and stratospheric measurements and from the neutron monitor data in 1959-1981 [SH-4.4-21] 23 p4035 N85-35017

Diurnal effect in cosmic rays at middle latitudes according to stratospheric measurements [SH-4.5-8] 23 p4036 N85-35026

STRATOSPHERIC AEROSOL & GAS EXPERIMENT

U SAGE SATELLITE

STRATOTANKER AIRCRAFT

U C-135 AIRCRAFT

STRATUS CLOUDS

An operational numerical model for prediction of fog and stratus 01 p0080 N85-10537

A 1-dimensional model with a sub-grid scale condensation scheme for stratiform clouds and fog 01 p0080 N85-10538

An operational forecasting system for stratus and fog with sodar 01 p0081 N85-10539

Fog advection in the Namib 16 p2831 N85-27454

Transport and formation of summertime cloud condensation nuclei over the Arctic Ocean 21 p3651 N85-32686

STREAK CAMERAS

Fore-optics systems designed for electronic streak cameras using fiber optics [DE84-014525] 02 p0281 N85-11830

A means of extending streak camera recording into the important 1300-1600 nm wavelength regime: Parametric frequency upconversion [DE84-015666] 04 p0503 N85-13208

High-bandwidth multichannel fiber optic system for measuring gamma rays [DE84-014526] 04 p0564 N85-13586

Characterization of electronic streak tubes including one with internal CCD readout [DE84-016823] 05 p0639 N85-14098

A microchannel plate streak camera [DE84-016536] 06 p0811 N85-15153

Approaches to ultrafast neutron detectors [DE85-001206] 11 p1636 N85-20307

Photonic methods of high speed analog data recording [DE84-016723] 11 p1637 N85-20308

Neutron streak camera electron gun design [DE85-000620] 11 p1637 N85-20315

Microchannel plate streak camera [DE85-011604] 20 p3458 N85-31481

Coordinated research program in pulsed power physics [AD-A154629] 21 p3679 N85-32858

STREAK PHOTOGRAPHY

Developments of optical fast-gated imaging systems [DE84-016170] 04 p0502 N85-13204

Measuring transient radiation effects in optical fibers [DE84-015044] 04 p0565 N85-13598

Improvements in avalanche-transistor sweep circuitry for electrooptic streak cameras [DE84-016195] 06 p0811 N85-15155

Approaches to ultrafast neutron detectors [DE85-001206] 11 p1636 N85-20307

Design, construction and initial evaluation of an absolute, time-integrating/time-resolving spectrometer for the diagnostics of pulsed, high temperature plasma X-ray sources in the 100-10,000 eV region [DE85-003526] 11 p1732 N85-20896

Streak tube characterization [DE85-009874] 17 p2956 N85-28255

STREAM FUNCTIONS (FLUIDS)

Some numerical analyses of flows with separation 16 p2692 N85-26616

A stream function approach to solving the conservative Euler equations for transonic flows 24 p4059 N85-35156

STREAMLINE FLOW

U LAMINAR FLOW

STREAMLINED BODIES

NT FAIRINGS

An experimental and analytical study of the aerodynamic interference effects between two Sears-Haack bodies at Mach 2.7 [NASA-TM-85729] 16 p2700 N85-26673

Instability of solar wind near streamlined bodies 16 p2720 N85-26794

STREAMLINING

Transonic merging separated flows [AD-A150667] 14 p2213 N85-23724

STREAMS

NT GAS STREAMS

Potential for acidification of six remote ponds in the White Mountains of New Hampshire
[PB84-207349] 02 p0225 N85-11475
Post-Laramide history of North Central Wyoming
08 p1181 N85-17444
Theoretical study of collective ion acceleration in the Luce diode
[AD-A150107] 12 p1929 N85-22116
Late Tertiary and Quaternary river systems of the eastern Sahara as mapped on shuttle radar and LANDSAT images 13 p2199 N85-23641
The ionospheric O+ streams in the magnetotail between 22 RE and 6 RE 14 p2360 N85-24582
Applications of Kalman filtering and recursive least-squares in river flow modelling
15 p2636 N85-26254
Towards a uniform topological treatment of streams and functions on streams
[CWI-CS-R8422] 17 p3014 N85-28639
On the origin of streamwise vortices in a turbulent boundary layer
[AD-A153651] 18 p3100 N85-29188
Geomorphic analyses from space imagery
21 p3603 N85-32374
Hydrology
[PB85-182954] 23 p3944 N85-34440

STRENGTH
Fundamentals of microcrack nucleation mechanics
[NASA-CR-3851] 07 p0975 N85-16195

STRENGTH OF MATERIALS
U MECHANICAL PROPERTIES

STRESS (PHYSIOLOGY)
NT ACCELERATION STRESSES (PHYSIOLOGY)
NT CENTRIFUGING STRESS
Effect of short-term hypokinesia on rat opioid system reaction 01 p0093 N85-10625
The role of physical and physiological capacities and their modification on the tolerance to various stress experienced by Air Force personnel
[AD-A145779] 03 p0400 N85-12550
Endocrine responses to nonhypotensive gravitational stress: Vasopressin and aldosterone
05 p0693 N85-14459
Endocrine responses to hypotensive gravitational stress: Catecholamines, pancreatic polypeptide, and vasopressin 05 p0693 N85-14460
Blood pressure levels of active pilots compared with those of air traffic controllers
[AD-A146645] 06 p0846 N85-15373
An atropinized heat-stressed rat model: Dose response effects and pharmacokinetics
[AD-A146851] 07 p1011 N85-16423
Change in relationship of biopotentials of brain zones for various levels of working capacity
07 p1013 N85-16438
Human factors survey: C-5 pilots
[AD-A147106] 07 p1020 N85-16477
Tolerance endpoint for evaluating the effects of heat stress in dogs
[AD-A148104] 08 p1192 N85-17511
Thermoregulatory responses during exercise at graded hypohydration levels
[AD-A147733] 08 p1195 N85-17528
Advanced development of an active neuromusculature response to mechanical stress
[AD-A148436] 08 p1196 N85-17536
Study of bodily functional status and quality of controlling action of power unit operators with various intensities of labor 09 p1362 N85-18569
The physiology of ultradian rhythms and their role in affecting disease resistance
[AD-A148842] 09 p1363 N85-18575
Work physiology of operating personnel at power plants in arid regions 10 p1523 N85-19606
Effects of overall vibration and noise on operational personnel 10 p1523 N85-19608
Skeletal muscle metabolism during exercise is influenced by heat acclimation
[AD-A148845] 10 p1527 N85-19632
LBNP training of crew members on main missions aboard Salyut-6 orbital station 12 p1901 N85-21938
Main component method used to study variations of cardiovascular parameters 12 p1901 N85-21939
Distinctive morphological manifestations of acute stress reaction in adrenal cortex of hypokinetic rats
12 p1902 N85-21944
Brain mechanisms underlying individual differences in reaction to stress: An animal model
[AD-A150195] 13 p2143 N85-23301
Exercise-heat strain during hypohydration: Interaction with heat acclimation and aerobic fitness
[AD-A151023] 14 p2389 N85-24717
Mechanical stress regulation of plant growth and development 15 p2610 N85-26087
A detailed analysis of the erythropoietic control system in the human, squirrel, monkey, rat and mouse
[NASA-CR-171879] 15 p2614 N85-26107
Description, validation, and modification of the Guyton model for space-flight applications. Part A. Guyton model of circulatory, fluid and electrolyte control. Part B. Modification of the Guyton model for circulatory, fluid and electrolyte control
[NASA-CR-171876] 15 p2616 N85-26122
The behavior of renal-regulating hormones during hypogravic stress
[NASA-CR-171877] 15 p2616 N85-26123
What is being done to control motion sickness?
15 p2687 N85-26599
Plasma hormonal responses at graded hypohydration levels during exercise/heat stress
[AD-A153681] 18 p3153 N85-29523
Distinctions of rat lymphatic organ reactions to acute stress factor during hypokinesia
19 p3324 N85-30596
Phenomenon of universal rosette-forming cell stimulation by extreme stress 20 p3505 N85-31789
Anatomy of stress 20 p3505 N85-31791
Physical training and G tolerance
20 p3511 N85-31824
Status of the air traffic control system
[GPO-40-343] 21 p3554 N85-32107
Regulation of physical activity in antiorthostatic position by acting on adrenosympathetic and hypophyseo-adrenocortical systems
22 p3824 N85-33689
Thermal stress suffered by tank crews working in summer heat
[DRIC-T-7492] 22 p3826 N85-33698
Determination of individual tolerance in hyperbaric oxygen 23 p3954 N85-34507
Report of Amphibian Development Group
24 p4127 N85-35583
Weight loss, rectal temperature and heart rates following the 1984 Boston Marathon
[AD-A155984] 24 p4132 N85-35612

STRESS (PSYCHOLOGY)
The role of physical and physiological capacities and their modification on the tolerance to various stress experienced by Air Force personnel
[AD-A145779] 03 p0400 N85-12550
Catecholamine excretion and subjective ratings of tension during autogenic training and mental stress
[REPT-172] 05 p0697 N85-14483
Blood pressure levels of active pilots compared with those of air traffic controllers
[AD-A146645] 06 p0846 N85-15373
Job and family stress as predictors of pilot health, job satisfaction and performance
[AD-A142176] 07 p1018 N85-16464
Human factors survey: C-5 pilots
[AD-A147106] 07 p1020 N85-16477
An investigation of the relationship between stressful life events and psychological, behavioral and physiological outcomes
[AD-A147754] 08 p1197 N85-17541
Decision making in stressful conditions: A model based on the coping perspective
[FOA-C-55064-H3] 08 p1229 N85-17738
Effect of modulated ultrahigh frequency field on behavior and hormone level in female rats under emotional stress
09 p1361 N85-18562
Research opportunities in human behavior and performance
[NASA-CR-175473] 10 p1529 N85-19640
NASA: Model development for human factors interfacing
[NASA-CR-175584] 12 p1910 N85-21985
Psychological issues relevant to astronaut selection for long-duration space flight: A review of the literature
[AD-A154051] 19 p3330 N85-30627
Phenomenon of universal rosette-forming cell stimulation by extreme stress 20 p3505 N85-31789
Anatomy of stress 20 p3505 N85-31791
Status of the air traffic control system
[GPO-40-343] 21 p3554 N85-32107
Operator's functional comfort zone when controlling moving object 22 p3821 N85-33670
Regulation of physical activity in antiorthostatic position by acting on adrenosympathetic and hypophyseo-adrenocortical systems
22 p3824 N85-33689

STRESS ANALYSIS
NT BOUNDARY ELEMENT METHOD
NT X RAY STRESS ANALYSIS
Design proposals for torsional buckling of stiffeners
[AD-A144783] 01 p0062 N85-10409
Improved multiaxial creep-rupture strength criterion
[DE84-014273] 01 p0062 N85-10413
The 3-D inelastic analysis methods for hot section components: Brief description 02 p0143 N85-10972
Directional nature of strengthening during thermomechanical treatment
[BLL-M-35746-(5828.4)] 02 p0175 N85-11174
Environment-induced embrittlement: Effect of impurity segregation and state of stress
[DE84-015436] 02 p0184 N85-11235
Stress analysis of pin-loaded orthotropic plates using orthotropic photoelasticity 02 p0207 N85-11366
Materials properties, loads, and stress analysis, Spartan REM: Appendix A
[NASA-CR-171092] 02 p0208 N85-11375
A digital algorithm for composite laminate analysis: FORTRAN, Revised
[AD-A145833] 03 p0326 N85-12098
Sour-gas cracking in ferritic steels
[AERE-R-10908] 03 p0333 N85-12148
Evaluation of laterally loaded laminated glass units by theory and experiment
[PB84-216423] 03 p0339 N85-12179
Fatigue limit analysis involving biaxial stress components 03 p0370 N85-12363
Dispersion forces of solids under stress. Chemisorption under stress
[AD-A146171] 03 p0373 N85-12380
Stress relief cracking studies of 2 1/4Cr1Mo steel
[AERE-R-11111] 03 p0374 N85-12388
Characterization of stressed metals using acoustic shear waves 05 p0648 N85-14159
Stress studies of EFG
[NASA-CR-174078] 05 p0651 N85-14179
Encapsulation design analysis
06 p0829 N85-15266
Strain analysis of the Leoville chondrite and conditions in asteroidal interiors 06 p0885 N85-15620
A study of interply layer effects on the free-edge stress field of angleplied laminates
[NASA-TM-86924] 07 p0919 N85-15822
A theoretical view on the stress analysis of fully inflated parachute canopies
[AD-A148387] 08 p1078 N85-16835
Contact behavior, impact response and damage in graphite-epoxy laminates subjected to initial stresses
08 p1171 N85-17386
A study of constitutive relations for polycrystalline aluminum during finite dynamic plastic deformation
08 p1172 N85-17388
Determination of the elastic constants of inhomogeneous materials with X-ray diffraction
[AD-A148469] 08 p1173 N85-17393
A simple engineering treatment of center cracked tension panels in the regime of nonlinear fracture mechanics under plane stress conditions
[GKSS-84-E-38] 08 p1173 N85-17396
Thermal-stress analysis for a wood composite blade
[NASA-CR-174794] 08 p1176 N85-17421
Evaluation of laterally loaded laminated glass units by theory and experiment
[PB85-111532/GAR] 09 p1300 N85-18166
East Europe report: Science and technology
[JPRS-ESA-85-008] 10 p1460 N85-19200
Methodology for stress analysis of heavy metal plate
10 p1460 N85-19203
Statistical study of anthropogenic seismic noise with IVK-7 computer system 10 p1503 N85-19483
Stress studies in EFG
[NASA-CR-175464] 10 p1509 N85-19522
Stress studies in EFG
[NASA-CR-175488] 10 p1563 N85-19856
Comparison of methods for predicting fiber stresses in a cracked Kevlar/epoxy monolayer
[DE84-016118] 11 p1593 N85-20022
Application of hysteresis modelling to the non-destructive inspection of stress
[DE85-003081] 11 p1650 N85-20393
USSR report: Physics and mathematics
[JPRS-UPM-85-001] 11 p1715 N85-20786
Advanced stress analysis methods applicable to turbine engine structures
[NASA-CR-175573] 12 p1778 N85-21165
Finite element analysis of problems associated with life enhancement techniques
[ARL/STRUC-R-404] 12 p1862 N85-21678
Symmetric primal-dual variational formulations of coupled dynamic systems: Three-dimensional elasticity, shells, fluid-structure interaction
[ONERA-1983-91] 12 p1883 N85-21684
3-D inelastic analysis methods for hot section components (base program) — turbine blades, turbine vanes, and combustor liners
[NASA-CR-174700] 12 p1883 N85-21686
Transverse vibration and buckling of a cantilevered beam with tip body under constant axial base acceleration
[NASA-CR-175567] 12 p1884 N85-21694
On the stress analysis of bonded inserts
[ARL/STRUC-R-407] 12 p1885 N85-21698

Scattered data interpolation using thin plate splines with tension
[AD-A148603] 12 p1866 N85-21705
Texture independent determination of residual stress in polycrystalline aggregates using Rayleigh waves
[AERE-R-11483] 12 p1943 N85-22203
A study of the compatibility of an existing CFD package with a broader class of material constitutions
12 p1945 N85-22219
Root stresses in conformal gears-strain gauge and photoelastic investigations 14 p2223 N85-23787
Analysis of slabs-on-grade for a variety of loading and support conditions
[AD-A150985] 14 p2264 N85-24030
Reduction of free-edge stress concentration
[AD-A150732] 14 p2321 N85-24340
Stress in axially symmetrical heavy metal projectiles during discharge — numerical simulation
[ISL-CO-219/83] 14 p2321 N85-24345
Stress and efficiency studies
[NASA-CR-175668] 14 p2351 N85-24531
Crack growth direction in unidirectional off-axis graphite epoxy
[NASA-CR-175752] 15 p2502 N85-25433
The accuracy of approximate solutions in the analysis of fracture of composites
[NASA-CR-175736] 15 p2503 N85-25437
Reduced-chromium stainless steel substitutes containing silicon and aluminum
[PB85-160786] 15 p2513 N85-25502
Acoustic emission of semiconductor devices
15 p2529 N85-25593
Symmetric composite laminate stress analysis
15 p2575 N85-25878
Structural analysis of electronic assembly housing
[DE86-005794] 15 p2580 N85-25913
Enhanced thermal-structural analysis by integrated finite elements
[AD-A151103] 15 p2636 N85-26258
The physical effects of different stress situations on graphite/epoxy compounds 15 p2667 N85-26594
Impact of magnetic isolation on pointing system performance in the presence of structural flexibility
[NASA-CR-172481] 16 p2732 N85-26661
Determination of permissible heating rate of metal
[BLL-M-36107-(5628.4)] 16 p2748 N85-26957
In plane stress analysis
[NASA-CR-175775] 16 p2799 N85-27259
Component-specific modeling
[NASA-CR-174765] 16 p2799 N85-27261
Effects of high mean stress on high-cycle fatigue behavior of PWA 1480 17 p2914 N85-27964
First passage times for combinations of random loads
[AD-A153275] 17 p2980 N85-28423
Mechanics of composite materials, theory and application
[VTH-LR-431] 18 p3123 N85-29334
Effect of edge distance on yield initiation in a remotely loaded half-plane containing interference-fit disc of the same material
[ARL/STRUC-R-413] 19 p3285 N85-30369
Computational methods in advanced stress and durability analyses
[AD-A154119] 19 p3286 N85-30375
On design of off-axis specimens
[AD-A154328] 19 p3286 N85-30379
Strain-path modeling for geo-materials
[AD-A154378] 19 p3286 N85-30380
Effects of high mean stress on the high-cycle fatigue behavior of PWA 1480
[NASA-CR-176020] 19 p3287 N85-30388
Micromechanism of fracture for stage 1 hydrogen-induced crack growth
[DE85-010027] 19 p3288 N85-30390
The location of stress in clothing
[AD-A154423] 19 p3331 N85-30633
Effect of speed and press fit on fatigue life of roller-bearing inner-race contact
[NASA-TP-2496] 20 p3463 N85-31511
Construction of constraint equation for stresses and strains
[BLL-M-36239-(5628.4)] 20 p3465 N85-31524
Load transfer by analytical methods
[SNIAS-851-111-109] 20 p3470 N85-31561
Journal of Research of the National Bureau of Standards, volume 89, no. 6, November - December 1984
[PB85-179042] 20 p3472 N85-31580
Development and test of advanced composite components. Center Directors discretionary fund program
[NASA-TM-86512] 21 p3561 N85-32147
The shearing contribution in transformation toughening of brittle materials
[AD-A154656] 21 p3568 N85-32195
Matrix fracture in fiber-reinforced ceramics
[AD-A154704] 21 p3569 N85-32197
User's guide for computer program CGFAG, Concrete General Flexure Analysis with Graphics
[AD-A155555] 21 p3570 N85-32204
Dynamic fracture of concrete and other heterogeneous materials
[AD-A154513] 21 p3598 N85-32343
Stress and buckling analysis 21 p3611 N85-32439
Remote temperature-set-point controller
[DE85-011614] 22 p3787 N85-33459
Shear wave transducer for boreholes
[DE85-011662] 22 p3787 N85-33461
Proceedings of the Mechanisms Conference, volume 1 23 p3923 N85-34309
The use of ultrasound to monitor incipient failure of rolling element bearings 23 p3924 N85-34317
Inertial stresses and deformations in mechanisms
23 p3924 N85-34320
Thermal stress analysis of a new turbine shroud seal concept
[NASA-TM-87062] 23 p3938 N85-34406
Design of transversely stiffenend FRP panels under compressive load — fiber reinforced plastic (FRP) ships
[AMTE(S)-R-84104] 23 p3940 N85-34424
The stress pattern analysis of coarse grain titanium specimens
[PNR-90250] 23 p3942 N85-34433
Damage induced stress redistribution in composite laminates 24 p4072 N85-35235
Development of a high strength isothermally heat-treated nodular iron road wheel arm
[AD-A155755] 24 p4099 N85-35406
Stress analysis of axisymmetric sandwich shells of variable thickness 24 p4101 N85-35419
1983 review of experimental stress and strain analysis
[DRIC-T-7469] 24 p4101 N85-35422
On size effects in plane stress crack-growth resistance
[AD-A155926] 24 p4102 N85-35426
Simplified procedures for the evaluation of settlements in sands due to earthquake shaking
[PB85-197887] 24 p4118 N85-35527
Establishment of a Computer-Aided Design (CAD)-Computer-Aided Manufacturing (CAM) process for the production of cold forged gears
[AD-A155756] 24 p4137 N85-35644
The finite element-difference method
24 p4141 N85-35672

STRESS CALCULATIONS
U STRESS ANALYSIS

STRESS CONCENTRATION
Finite element modelling of buried structures
01 p0061 N85-10403
Distributions of fatigue life and fatigue strength in notched specimens of a carbon 8-harness-satin laminate
[NAL-TR-809T] 01 p0061 N85-10407
Benchmark notch test for life prediction
02 p0140 N85-10953
Effect of stress concentrations in composite structures
[NASA-CR-173976] 02 p0170 N85-11140
Strain distribution in a type 316/16-8-2 stainless steel weldment during cyclic loading
[DE84-015644] 02 p0210 N85-11384
Modeling the stress field in laminated composite plates near discontinuities
[PB84-219237] 03 p0327 N85-12103
Viscoplastic finite element analysis of rapid fracture
03 p0370 N85-12365
Flow-based analyses of metal deformation processes: An overview 06 p0796 N85-15087
Disc fatigue life predictions for gas turbine engines
07 p0907 N85-15743
Fundamentals of microcrack nucleation mechanics
[NASA-CR-3851] 07 p0975 N85-16195
Stresses in pin-loaded orthotropic plates using photoelasticity
[NASA-CR-172496] 07 p0977 N85-16204
Modeling localized stress fields in composite laminates
[AD-A148630] 08 p1120 N85-17056
Finite element calculation for a Y-joint and comparison of results with strain measurements
[BLL-RISLEY-TR-4526-(9091.9F)]
08 p1171 N85-17381
Influence of setting angle of jet cooling nozzles on temperature and stress state of a turbine wheel
09 p1306 N85-18208
The fracture mechanics of a slit crack with crack-tip dual zones 09 p1332 N85-18371
Integrated Technology Rotor/Flight Research Rotor (ITR/FRR) concept definition
[NASA-CR-168443] 10 p1423 N85-18978
Stress concentration due to axial tension of loaded nonsymmetric-shaped grooves
[AD-A149425] 10 p1496 N85-19442
Stress studies in EFG
[NASA-CR-174441] 10 p1508 N85-19515
Stress-strain analysis of silicon ribbon
[NASA-CR-175459] 10 p1510 N85-19525
Residual stress after laser processing
11 p1600 N85-20085
Sensitivity of titanium alloys to stress concentration during repeated static loads 11 p1602 N85-20074
Effect of stress concentration fatigue resistance of refractory nickel alloys under asymmetrical multicycle loading, communication 1 11 p1604 N85-20086
Local strain redistribution corrections for a simplified inelastic analysis procedure based on an elastic finite-element analysis
[NASA-TP-2421] 11 p1651 N85-20306
On local total strain redistribution using a simplified cyclic inelastic analysis based on an elastic solution
[NASA-TM-86913] 12 p1864 N85-21690
Stresses in a half-plane containing either a pressurized hole or an interference-fit disc
[ARL/STRUC-R-409] 12 p1865 N85-21700
Elastic response of a half-plane to a bonded interference-fit disc of the same material
[ARL/STRUC-R-406] 12 p1865 N85-21701
Moving nonlocal crack: Anti-plane shear case
[AD-A149996] 12 p1866 N85-21709
Fracture analysis of cracks in complete cylindrical shells
[AD-A150091] 12 p1867 N85-21711
Reliability of structural brittle materials
12 p1946 N85-22222
Shape optimization for minimal stress concentration
13 p2101 N85-23093
On Hybrid and mixed finite element methods
[NASA-CR-175551] 13 p2101 N85-23096
Elasticity solution of an adhesively bonded joint
[NASA-CR-175591] 13 p2101 N85-23097
Advanced life analysis methods. Volume 2: Crack growth analysis methods for attachment lugs
[AD-A150420] 13 p2103 N85-23109
Role of residual stresses in stress corrosion cracking in alloy 600 tubes. Part 1: Determination of throughwall residual stresses and their modification by transient heat treatment
[DE85-004648] 14 p2257 N85-23988
Reaction of piezoceramic shell to concentrated forces
14 p2279 N85-24115
Reduction of free-edge stress concentration
[AD-A150732] 14 p2321 N85-24340
Elastic-plastic analysis for cyclic loading using a linearized yield condition
[PB85-149607] 14 p2322 N85-24346
Finite element model for creep in composite masonry
[PB85-150324] 14 p2322 N85-24347
Evaluation of stress concentration coefficients in butt-welded joints with displaced edges
15 p2501 N85-25425
The effects of pin elasticity, clearance, and friction on the stresses in a pin-loaded orthotropic plate
[NASA-CR-175816] 16 p2743 N85-26927
Experimentally determined distribution of stress around a horizontally loaded model pile in dense sand
[CE-43] 16 p2796 N85-27239
In plane stress analysis
[NASA-CR-175775] 16 p2799 N85-27259
Accuracy of the calculated stress field around a craze
[DE85-005520] 16 p2801 N85-27272
An X-ray diffraction study of the residual stress-strain distribution in shot-peened 2-phase brass
[AD-A152418] 17 p2930 N85-28068
Natural vibrations of reinforced spherical shells
17 p2943 N85-28165
Cyclic torsion of a circular cylinder and its residual stress distribution
[AD-A153347] 17 p2980 N85-28424
Numerical analysis of end effects in symmetric laminated plates
[NAL-TR-850] 18 p3088 N85-28977
Strain fields for aluminum at different tooling temperatures and extrusion ratios
[DE85-008257] 18 p3075 N85-29020
Fatigue behavior of unidirectional FP-Al composites with circular holes
[AD-A153466] 18 p3121 N85-29322
Mechanics of composite materials, theory and application
[VTH-LR-431] 18 p3123 N85-29334
Effect of thermochemical processing on fatigue resistance of titanium alloys 19 p3244 N85-30112
Residual stress distributions in (plastically) surface deformed two-phase materials 19 p3283 N85-30356
Multiaxial fatigue and fracture: A literature review
[ARL/STRUC-R-410] 19 p3285 N85-30370
Effects of high mean stress on the high-cycle fatigue behavior of PWA 1480
[NASA-CR-176020] 19 p3287 N85-30388

Inhomogeneous deformation: The theory and geological application of finite strain compatibility
19 p3312 N85-30532
Integral constraints on stress energy perturbations in general relativity and applications to cosmology
19 p3363 N85-30985
Two simplified procedures for predicting cyclic material response from a strain history 20 p3467 N85-31543
A clamped rectangular plate containing a crack
[NASA-CR-177925] 20 p3469 N85-31552
Shear-stress distribution and shear stiffness in the case represented by a non-homogeneous cross-section, of any shape, but composed of an orthotropic material, when subjected to a shear force
[DRIC-T-7430] 20 p3469 N85-31554
On the variation of the stress intensity factor along the front of a surface flaw
[OUEL-1565/85] 20 p3471 N85-31568
The interactions of composition and stress in crystalline solids
[PB85-179075] 20 p3473 N85-31583
Mechanics of near tip microcracking in brittle material
[AD-A154684] 21 p3598 N85-32346
Stress concentration in the elastoplastic state and residual stress after unloading
[AD-A155628] 21 p3600 N85-32356
Stress and efficiency studies in EFG
[NASA-CR-176125] 22 p3751 N85-33251
The stress distribution in pin-loaded orthotropic plates
[NASA-CR-176146] 22 p3800 N85-33547
Fractographic analysis for nonpropagating conditions of fatigue crack at high stress ratios in mild steel
23 p3905 N85-34194
Multiaxial stress analysis taking account of penetration depth of X-rays. A solution by means of polynomial approximation 23 p3907 N85-34204
Stress distribution of fiberglass reinforced plastic beam with a delamination under three-point bending
23 p3908 N85-34210
Stresses and strains in a plate resulting from two closely-spaced interference-fit fasteners
[ARL/STRUC-TM-409] 23 p3941 N85-34429
The stress pattern analysis of coarse grain titanium specimens
[PNR-90250] 23 p3942 N85-34433
Geophysical-geological studies of possible extensions of the New Madrid fault zone
[TI85-901341] 23 p3949 N85-34475
Damage induced stress redistribution in composite laminates 24 p4072 N85-35235
Static and cyclic behavior of semi-rigid steel beam-column connections
[PB85-194363] 24 p4103 N85-35433
The finite element-difference method
24 p4141 N85-35672

STRESS CORROSION
NT STRESS CORROSION CRACKING
Influence of nitrogen on the sensitization, corrosion, mechanical, and microstructural properties of austenitic stainless steels
[DE84-015134] 01 p0029 N85-10177
A study of environmental characterization of conventional and advanced aluminum alloys for selection and design. Phase 1: Literature review
[NASA-CR-172387-PHASE-1] 02 p0181 N85-11218
Corrosion of brass in potable water service
[CETIM-100390] 04 p0477 N85-13037
In-situ stress relief of expanded alloy 600 steam generator tubing
[DE84-014560] 04 p0513 N85-13273
Stress relief of transition zones
[DE85-000234] 11 p1653 N85-20411
The effect of stress and hot corrosion on nickel-base superalloys
[AD-A154722] 21 p3566 N85-32181
Automatic capability to store and retrieve component data and to calculate structural integrity of these components
[DE85-012429] 22 p3831 N85-33728

STRESS CORROSION CRACKING
A study of environmental characterization of conventional and advanced aluminum alloys for selection and design. Phase 1: Literature review
[NASA-CR-172387-PHASE-1] 02 p0181 N85-11218
A study of environmental characterization of conventional and advanced aluminum alloys for selection and design. Phase 2: The breaking load test method
[NASA-CR-172387-PHASE-2] 02 p0182 N85-11219
Stress corrosion of pressure vessel steel A533-B in high temperature water
[BLL-RISLEY-TR-4600-(9091.9F)]
03 p0330 N85-12125
Localized corrosion and stress corrosion cracking behavior of stainless steel weldments
[DE84-016095] 04 p0474 N85-13017
Fractographic study of stress corrosion cracking of SUS 304 stainless steel in various environments
[BLL-RISLEY-TR-4586-(9091.9F)]
05 p0615 N85-13928
Influence of the mechanical and electrochemical characteristics of austenitic and austenoferritic steels on the propagation rate and morphology of stress corrosion cracking
[BLL-RISLEY-TR-4545-(9091.9F)]
06 p0767 N85-14906
Testing of non-alloyed and low-alloyed steels for their behaviour with respect to intercrystalline stress corrosion cracking
[BLL-RISLEY-TR-4548-(9091.9F)]
07 p0925 N85-15861
Stochastic models of pitting corrosion of stainless steels. Part 1: Modelling of the initiation and growth of pits at constant potential
[AERE-R-11146-PT-1] 09 p1298 N85-18151
Contributions of segregated phosphorus to the intergranular stress corrosion cracking of nickel
[DE85-003112] 11 p1606 N85-20099
Stress corrosion cracking and oxidation characteristics of boride-strengthened microcrystalline iron and nickel based alloys
[AD-A149805] 12 p1806 N85-21328
Stress corrosion cracking behavior of tungsten heavy alloys
[AD-A149843] 12 p1806 N85-21329
Role of segregated P and S in intergranular stress corrosion cracking of nickel
[DE85-004547] 13 p2024 N85-22679
Advanced life analysis methods. Volume 1: Cracking data survey and NDI (nondestructive inspection) assessment for attachment lugs
[AD-A150419] 13 p2103 N85-23108
The role of hydrogen in the stress corrosion failure of high strength Al-Zn-Mg alloys
[AD-A150891] 14 p2256 N85-23978
Role of residual stresses in stress corrosion cracking in alloy 600 tubes. Part 1: Determination of throughwall residual stresses and their modification by transient heat treatment
[DE85-004648] 14 p2257 N85-23988
Anode formation of passivating films on titanium alloy at temperatures up to 200 deg C
15 p2515 N85-25519
Microscopic study of the influence of impurities on interface bonding
[AD-A151725] 16 p2743 N85-28928
Influence of pretreatment, environment and strain rate on stress corrosion cracking of the aluminum alloy 7075-T6
[VTH-LR-433] 16 p2752 N85-28985
Corrosion characteristics of some steels produced through a self-cleaning rotating electrode
[BLL-BISI-TRANS-22046-(9022.06)]
17 p2925 N85-29034
The synergistic actions of stress corrosion cracking and corrosion fatigue
[BLL-BISI-TRANS-22334-(9022.06)]
17 p2926 N85-29045
Study on mechanism of surface deformation induced by stress corrosion cracking
[BLL-BISI-TRANS-21896-(9022.06)]
17 p2928 N85-29066
Tendency of selected low-carbon steels to corrosion cracking in nitrates
[BLL-BISI-TRANS-22262-(9022.06)]
18 p3073 N85-29006
Marine corrosion
[AD-A153843] 18 p3074 N85-29012
Publications of the Jet Propulsion Laboratory 1983
[NASA-CR-175979] 18 p3199 N85-29848
Effect of multi-functional inhibitors on the electrochemistry within corrosion crack
19 p3238 N85-30075
Resistance to corrosion fatigue in aluminum alloy 1561 in sea water 19 p3243 N85-30108
Kinetics of H-induced stress corrosion cracking. Part 1: Important features of cracking in respect of high strength steels
[BLL-BISI-TRANS-(9022.06)] 19 p3282 N85-30350
Theoretical modelling of the electro-chemistry in a corrosion fatigue crack. Part 2: Mathematical aspects of associated unsteady reaction equations
[NPL-DMA(A)-100-PT-2] 20 p3465 N85-31529
Stress corrosion of ceramic materials
[AD-A155020] 21 p3570 N85-32202
Current requirements for the design and maintenance against corrosion of UK military aircraft
22 p3750 N85-33244
Relating corrosion maintenance to environmental factors 22 p3750 N85-33247
The influence of temperature on static and dynamic SCC crack growth behavior in aluminum alloy
23 p3905 N85-34190
A fractographic study on mode 2 and mode 3 SCC crack growth in an Al-Zn-Mg alloy 23 p3905 N85-34191
Stress corrosion cracking susceptibility of types 316NG and 316 stainless steel in an impurity environment
[TI85-006884] 23 p3917 N85-34277
Effect of temperature and ionic impurities at very low concentrations on stress corrosion cracking of Type 304 stainless steel
[TI85-003048] 24 p4079 N85-35283

STRESS CYCLES
Distributions of fatigue life and fatigue strength in notched specimens of a carbon 8-harness-satin laminate
[NAL-TR-809T] 01 p0061 N85-10407
Comparison between cycle ergometers with different mechanical braking systems
[FOA-C-54058-H1] 07 p0975 N85-16193
Compaction of sand using ordinary off-road vehicles
[AD-P004297] 09 p1409 N85-18874
Two simplified procedures for predicting cyclic material response from a strain history 20 p3467 N85-31543
Simplified procedures for the evaluation of settlements in sands due to earthquake shaking
[PB85-197887] 24 p4118 N85-35527

STRESS DISTRIBUTION
U STRESS CONCENTRATION

STRESS FUNCTIONS
Recent advances in hybrid/mixed finite elements
[NASA-CR-175574] 12 p1863 N85-21687
Fillet weld stress using finite element methods
15 p2576 N85-25884

STRESS INTENSITY FACTORS
Stress-derivative control of keystoning deformation in finite element codes 01 p0058 N85-10365
Crack tip opening displacement for work hardening materials
[GKSS-84-E-26] 01 p0063 N85-10415
Stress intensity factors for a circular ring with uniform array of radial cracks of unequal depth
[AD-A145893] 03 p0372 N85-12377
Stress intensity factors for corner cracks at holes located near an edge
[FFA-TN-1984-20] 04 p0514 N85-13279
Elastodynamic stress intensity factors of an interface finite-width crack
[DE84-016908] 06 p0817 N85-15190
Experimental compliance calibration of the NASA Lewis Research Center Mode 2 fatigue specimen
[NASA-TM-86908] 07 p0977 N85-16205
Circumferential cracks in cylindrical shells
09 p1330 N85-18354
finite element analysis of bi-material systems with applications in hydraulic fracturing
09 p1332 N85-18369
The fracture mechanics of a slit crack with crack-tip dual zones 09 p1332 N85-18371
Crack problems for bonded nonhomogeneous materials under antiplane shear loading
[NASA-CR-172532] 10 p1495 N85-19438
Fracture analysis of notched composites
[NASA-CR-172583] 11 p1593 N85-20020
On the stress analysis of bonded inserts
[ARL/STRUC-R-407] 12 p1865 N85-21698
The residual strength of cracked specimens representing a section of the mirage into wing main spar
[ARL/STRUC-R-408] 12 p1865 N85-21699
Effect of phase state of TiC-NiTi powder composite materials on nature of failure and mechanical properties
13 p2027 N85-22702
Stress intensity factor in a tapered specimen
[NASA-CR-175589] 13 p2102 N85-23099
Crack propagation under constant and variable stress amplitudes: A comparison of calculations based on the Striation spacing and tests 14 p2320 N85-24336
On residual stresses and stress intensity factors in composite materials 15 p2572 N85-25859
Transition region for corner cracks at holes
[AD-A151835] 15 p2579 N85-25908
Study to optimize Cr-Mo steels to resist hydrogen and temper embrittlement
[DE85-005492] 17 p2932 N85-28096
Crack propation in unidirectional laminates by the stress intensity factors 18 p3121 N85-29320
Fracture of laminated composite materials
19 p3230 N85-30030
Kinetics of H-induced stress corrosion cracking. Part 1: Important features of cracking in respect of high strength steels
[BLL-BISI-TRANS-(9022.06)] 19 p3282 N85-30350
Fracture mechanics formulas on microcomputers
[NASA-TM-77850] 19 p3284 N85-30362
On the variation of the stress intensity factor along the front of a surface flaw
[OUEL-1565/85] 20 p3471 N85-31568

A cracked orthotropic sheet stiffened by a semi-infinite orthotropic sheet
[NASA-TP-2455] 21 p3597 N85-32339
On the methods to determine the stress intensity factors in boundary element method 23 p3905 N85-34189
Time and temperature dependence of fracture surface in soft epoxy resin 23 p3908 N85-34213
Nonlinear adhesive behavior effects in a cracked orthotropic sheet stiffened by a semi-infinite orthotropic sheet
[NASA-TM-87584] 23 p3941 N85-34426
Stress-intensity factors for circumferential surface cracks in pipes and rods under tension and bending loads
[NASA-TM-87594] 24 p4101 N85-35424

STRESS MEASUREMENT
Composite laminate optimization program suitable for microcomputers 01 p0059 N85-10389
Evaluation of interfacial stresses from the amplitude of reflected ultrasonic signal
[DE84-015472] 02 p0276 N85-11798
Back stress in dislocation creep. Part 1: Basic concepts and measuring techniques
[NASA-TM-77773] 07 p0977 N85-16206
Measurement of stress in clothing: A literature review and methods selected
[AD-A147674] 08 p1132 N85-17132
Piezoelectric stress transducer used for measurements of explosions in hard rock 11 p1638 N85-20316
The measurement of residual stresses using ultrasonics
[AERE-R-11415] 12 p1868 N85-21722
Load carrying capacity of double circular arc gears 14 p2221 N85-23776
Evaluation of the blind hole drilling method for the measurement of residual stress
[AD-A151459] 15 p2579 N85-25905
Surface shear stress characteristics in turbulent flows 19 p3211 N85-29914
Development of an NBS (National Bureau of Standards) polymer gage for dynamic soil stress measurement
[PB85-208494] 24 p4118 N85-35526

STRESS PROPAGATION
Wave propagation in heterogeneous media
[AD-A150800] 14 p2321 N85-24341
Constitutive modeling for blast-induced wave propagation
[AD-A153576] 18 p3099 N85-29187
On the variation of the stress intensity factor along the front of a surface flaw
[OUEL-1565/85] 20 p3471 N85-31568

STRESS RATIO
Fractographic analysis for nonpropagating conditions of fatigue crack at high stress ratios in mild steel 23 p3905 N85-34194

STRESS RELAXATION
Equibiaxial extension of two polymer melts: Polystyrene and low density polyethylene
[AD-A144803] 01 p0032 N85-10200
Stress relief cracking studies of 2 1/4Cr1Mo steel
[AERE-R-11111] 03 p0374 N85-12386
Free volume considerations in thermoplastic and thermosetting resins 04 p0465 N85-12952
In-situ stress relief of expanded alloy 600 steam generator tubing
[DE84-014560] 04 p0513 N85-13273
Effect of temperature on the stress-relaxation response of a pressure vessel steel
[TIB5-003588] 09 p1339 N85-18424
Stress relief of transition zones
[DE85-000234] 11 p1653 N85-20411
Rheology of dissemination
[AD-A150006] 12 p1813 N85-21373
MM2 LRSLA testing stage 3 propellant
[AD-A152540] 17 p2937 N85-28128
A state variable approach to transient creep deformation in stress reduction experiments
[DE85-009492] 18 p3122 N85-29331
Mechanics of near tip microcracking in brittle material
[AD-A154684] 21 p3598 N85-32346

STRESS RELIEVING
Stress-relieving interlayers for bituminous resurfacings
[PB85-136865] 12 p1820 N85-21415
Possible use of rapid heating for improving mechanical properties of titanium alloys 15 p2498 N85-25409
Local heat treatment of welded joints of pipes and rotary vessels 17 p2924 N85-28028
Welding of 11 458.1 steel in shielding atmospheres
[BLL-BISI-TRANS-21763-(9022.06)] 17 p2972 N85-28353

STRESS RUPTURE STRENGTH
U CREEP RUPTURE STRENGTH

STRESS TENSORS
Analysis of the nonlinear equations describing the elastic, thermal, and electromagnetic behavior of solids: Existence of solutions of semi-inverse problems 24 p4100 N85-35415

STRESS WAVES
Excitation modes and parameters of stress waves in metal exposed to single laser pulses 10 p1446 N85-19109
Piezoelectric stress transducer used for measurements of explosions in hard rock 11 p1638 N85-20316
Stress waves in an isotropic elastic plate excited by a circular transducer
[NASA-CR-3877] 11 p1650 N85-20390
Application of homomorphic signal processing to stress wave factor analysis
[NAS 1.26:174871] 12 p1861 N85-21673
Wave propagation in heterogeneous media
[AD-A150800] 14 p2321 N85-24341
Altimetry data and the elastic stress tensor of subduction zones
[NASA-CR-175796] 16 p2825 N85-27425
Interaction of large amplitude stress waves in layered elastic-plastic materials
[AD-A153519] 18 p3121 N85-29323
A study of the stress wave factor technique for the characterization of composite materials
[NASA-CR-174870] 19 p3231 N85-30035
Behaviors of stress waves in a conical bar 23 p3904 N85-34182

STRESS-STRAIN DIAGRAMS
Dependence of microplasticity of beryllium on grain size and heat treatment 03 p0353 N85-12273
The cyclic stress-strain behavior of nickel-base superalloy poly- and single crystals 14 p2254 N85-23969

STRESS-STRAIN DISTRIBUTION
U STRESS CONCENTRATION

STRESS-STRAIN RELATIONSHIPS
Benchmark notch test for life prediction 02 p0140 N85-10953
Viscoplastic finite element analysis of rapid fracture 03 p0370 N85-12385
Investigation of toughened neat resins and their relations to advanced composite mechanical properties 04 p0464 N85-12949
Strain rate effects and temperature history effects for three different tempers of 4340 VAR steel
[AD-A146372] 06 p0768 N85-14915
Strength analysis of fan-shaped wing considering temperature deformation and creep deformations 06 p0779 N85-14983
Analysis of thin-walled airframe members in geometrically nonlinear statement 06 p0780 N85-14985
Miniworkshop on effects of stress and strain in high-speed-growth silicon ribbons 06 p0831 N85-15284
A study of Reynolds-stress closure model
[NASA-CR-174342] 08 p1161 N85-17324
Deformation and fracture of P/M (Powder/Metallurgy) titanium alloys
[AD-A148672] 09 p1294 N85-18128
On solving nonlinear problems of aircraft structural mechanical design 09 p1309 N85-18223
Verification and application of the Ioslpescu shear test method
[NASA-CR-174346] 09 p1333 N85-18376
Evaluation of failure criterion for graphite/epoxy fabric laminates
[NASA-CR-172547] 10 p1431 N85-19025
Microstrain analysis in bent single crystal silicon by double crystal X-ray topography technique
[DE85-000422] 10 p1584 N85-19863
Local strain redistribution corrections for a simplified inelastic analysis procedure based on an elastic finite-element analysis
[NASA-TP-2421] 11 p1651 N85-20396
A solution method for nonlinear dynamic analysis of shell structures
[AD-A149646] 12 p1866 N85-21706
A study of the compatibility of an existing CFD package with a broader class of material constitutions 12 p1945 N85-22219
Behavior of fiber-reinforced composites under dynamic tension
[AD-A150619] 13 p2015 N85-22641
Dissipation of energy in composite material 13 p2027 N85-22703
Method of calculating strength of joint produced by cold welding of aluminum under discrete loading 13 p2034 N85-22743
Determination of stresses and deformations in linearly elastic conical shell subjected to aerodynamic loading and heating 13 p2047 N85-22812
Theoretical and experimental investigation of mechanically fastened composites
[AD-A150981] 14 p2248 N85-23935
Strength computation of thin walled shell by discreet-continuous model 14 p2288 N85-24181
A preliminary investigation into transverse fracture of unidirectional fiber composites
[AERE-R-11494] 15 p2503 N85-25438
Superplasticity in a thermo-mechanically processed Aluminum-10.2%Mg-0.52%Mn alloy
[AD-A152016] 15 p2510 N85-25485
Dependence of plasticity of VT1-00 titanium alloy on microstructure 15 p2515 N85-25516
Compressive strength of epoxy resin cubes subjected to elevated temperatures
[AD-A152018] 15 p2519 N85-25532
On thermomechanical testing in support of constitutive equation development for high temperature alloys
[NASA-CR-174879] 15 p2577 N85-25894
Fiber reinforcement of gun propellant
[AD-A152295] 16 p2757 N85-27014
Stressed-strained state of tubular shells under uniformly distributed pressure 16 p2766 N85-27067
Stressed state of multilayer thick-walled longitudinally corrugated cylinders 16 p2768 N85-27069
Cyclic structural analyses of SSME turbine blades 17 p2914 N85-27963
X-ray diffraction study of changes in stress-strain distributions during fatigue of a 2-phase alloy
[AD-A152367] 17 p2930 N85-28087
An X-ray diffraction study of the residual stress-strain distribution in shot-peened 2-phase brass
[AD-A152418] 17 p2930 N85-28088
State of stress and penetration of plastic deformation in forming
[BLL-BISI-22199-(9022.06)] 17 p2977 N85-28396
Cyclic torsion of a circular cylinder and its residual stress distribution
[AD-A153347] 17 p2980 N85-28424
Finite element thermal-structural analysis of cable-stiffened space structures
[AD-A153822] 18 p3066 N85-28983
Strain fields for aluminum at different tooling temperatures and extrusion ratios
[DE85-008257] 18 p3075 N85-29020
Transient dynamic solutions of some half space problems by the boundary element method 19 p3283 N85-30360
Effect of nonuniform size on internal stresses in a rapid, simple shear flow of granular materials. Part 1: Two grain sizes
[AD-A154045] 19 p3285 N85-30372
Strain-path modeling for geo-materials
[AD-A154378] 19 p3286 N85-30380
The initiation and growth of adiabatic shear bands
[AD-A154459] 19 p3287 N85-30382
Inhomogeneous deformation: The theory and geological application of finite strain compatibility 19 p3312 N85-30532
Residual thermal and moisture influences on the strain energy release rate analysis of edge delamination
[NASA-TM-86437] 20 p3422 N85-31238
On elastic-plastic fracture criterion 20 p3465 N85-31528
Finite element analysis of notch behavior using a state variable constitutive equation 20 p3468 N85-31548
Component-specific modeling
[NASA-CR-174925] 21 p3556 N85-32119
Effects of weak interfaces on thermostructural behavior of carbon-carbon composites
[AD-A155330] 21 p3562 N85-32154
Fundamental investigations of failure during superplastic forming process
[AD-A154647] 21 p3568 N85-32194
Hertzian contact in two and three dimensions
[NASA-TP-2473] 21 p3596 N85-32331
Analysis of stress-strain relationships in silicon ribbon 21 p3611 N85-32438
Stress and efficiency studies in EFG
[NASA-CR-176125] 22 p3751 N85-33251
Remote temperature-set-point controller
[DE85-011614] 22 p3787 N85-33459
Monotonous stress-strain properties of structural steel subjected to nonstationary repetitive pre-loading 23 p3904 N85-34185
Development and application of a unified viscoelastic constitutive model for the prediction of material response under thermomechanical loading 24 p4101 N85-35420
1983 review of experimental stress and strain analysis
[DRIC-T-7469] 24 p4101 N85-35422

STRESS-STRAIN-TIME RELATIONS
The stress-strain-time graph of rheological soils and its application
[AD-P004266] 09 p1407 N85-18863

Constitutive modeling for blast-induced wave propagation
[AD-A153576] 18 p3099 N85-29187

STRESSES
NT AXIAL STRESS
NT COMBINED STRESS
NT CRITICAL LOADING
NT RESIDUAL STRESS
NT REYNOLDS STRESS
NT SHEAR STRESS
NT TENSILE STRESS
NT THERMAL STRESSES
NT TORSIONAL STRESS
NT TRIAXIAL STRESSES
NT VIBRATIONAL STRESS

Equivalent damage: A critical assessment 02 p0140 N85-10952
Response of propellants to high dynamic stresses: The uses of gun launch techniques
[DE84-013223] 02 p0188 N85-11259
Large-area sheet task advanced dendritic web growth development
[NASA-CR-174021] 02 p0223 N85-11463
Stress intensity factors for a circular ring with uniform array of radial cracks of unequal depth
[AD-A145893] 03 p0372 N85-12377
Dispersion forces of solids under stress. Chemisorption under stress
[AD-A146171] 03 p0373 N85-12380
Bulletin of the Faculty of Engineering, Hokkaido University, no. 123
[ISSN-0385-802-X] 04 p0482 N85-13075
Estimation of dynamic stresses around the shot point by scale model experiment 04 p0482 N85-13076
Longevity of thin-walled engine parts subjected to transient stresses under creep conditions 06 p0777 N85-14966
Stresses and strains in lithosphere caused by Earth's thermoconvective oscillations 06 p0822 N85-15217
Free surface effects on the wake of a flat plate
[AD-A146968] 07 p0958 N85-16071
Computer program for determining induced stresses and consolidation settlements (CSETT)
[AD-A146730] 07 p1023 N85-16493
Response of propellants to high dynamic stresses: The uses of gun launch techniques 08 p1116 N85-17035
Modeling localized stress fields in composite laminates
[AD-A148630] 08 p1120 N85-17056
The fracture mechanics of a slit crack with crack-tip dual zones 09 p1332 N85-18371
NOAA OTEC CWP (National Oceanic and Atmospheric Administration Ocean Thermal Energy Conversion Cold Water Pipe) at-sea test. Volume 3, part 1: Tabulation of the power spectra for selected channels
[PB84-236955] 09 p1346 N85-18467
Stresses in situ generating by bulldozers
[AD-P004270] 09 p1405 N85-18848
Finite element analysis of ground deformation beneath moving track loads
[AD-P004271] 09 p1405 N85-18847
Investigation of accelerated stress factors and failure/degradation mechanisms in terrestrial solar cells
[NASA-CR-175469] 10 p1510 N85-19524
Fractographic features of titanium alloy fatigue failure under repeated static stress and high frequency vibration 11 p1601 N85-20070
Characteristics of EMI generated by negative metal-positive dielectric voltage stresses due to spacecraft charging 13 p1995 N85-22505
Load capacity of cages of roller bearings for planet wheels 14 p2221 N85-23775
On the corner singularity of a 3-D Griffith crack
[AD-A150989] 14 p2321 N85-24342
Magnetohydrodynamic considerations for the design of self-cooled liquid-metal fusion reactor blankets
[DE85-000242] 14 p2425 N85-24957
Yield stress determination from miniaturized disk bend test data
[DE85-009495] 18 p3122 N85-29330
Interim rock mass properties and conditions for analyses of a repository in crystalline rock
[DE85-010700] 18 p3125 N85-29352
Implications about in situ stress at Yucca Mountain
[DE85-008068] 18 p3126 N85-29356
Measurement and calculation of the mechanical response of a highly fractured rock
[DE85-008421] 18 p3127 N85-29362
A multiphase continuum model to describe dynamic loading effects in nonlinear porous media
[DE85-010102] 19 p3301 N85-30483
The location of stress in clothing
[AD-A154423] 19 p3331 N85-30833
Comparative analysis of laboratory and fullscale experimental data for metal flow displacements and speeds
[BLL-M-36266-(5828.4)] 20 p3430 N85-31276
Machining-induced deformation in stepped specimens of PH 13-8 Mo, 18 nickel maraging steel grade 200T1 and grain-refined HP 9-4-20
[NASA-CR-172450] 21 p3565 N85-32177
Sintering studies project
[AD-A154750] 21 p3572 N85-32216
Thin-film reliability and engineering overview 21 p3612 N85-32450
Temperature sensitivity of fiber-optic transmission line 22 p3764 N85-33331
Slideline verification for multilayer pressure vessels and piping analysis including strain hardening
[DE85-005816] 22 p3801 N85-33549
Damage induced stress redistribution in composite laminates 24 p4072 N85-35235

STRETCHING
Equibiaxial extension of two polymer melts: Polystyrene and low density polyethylene
[AD-A144893] 01 p0032 N85-10200
Finite element method calculation of a necking tension specimen including heat transfer influence
[RUB-IFM-MITT-40] 05 p0648 N85-14162
Thermal stress-dependent dilation of concrete
[DE84-014668] 11 p1653 N85-20412
Critical events in inelastic deformation of glassy polymers in adsorptive medium 13 p2014 N85-22634

STRIATION
The role of finite parallel length on the stability of barium clouds
[AD-A146972] 07 p0996 N85-16328
Application of optical and electron microscopic techniques in the fractographic determination of fatigue crack growth rates 14 p2320 N85-24334
Crack propagation under constant and variable stress amplitudes: A comparison of calculations based on the Striation spacing and tests 14 p2320 N85-24336
Striation free doped silicon
[AD-A155730] 22 p3847 N85-33827

STRINGERS
Tensile strength of composite sheets with unidirectional stringers and crack-like damage: A brief report
[NASA-TM-86310] 02 p0170 N85-11139
A cracked orthotropic sheet stiffened by a semi-infinite orthotropic sheet
[NASA-TP-2455] 21 p3597 N85-32339
Acoustic wave scattering by round cylindrical shell reinforced with stringers 21 p3688 N85-32916
Nonlinear adhesive behavior effects in a cracked orthotropic sheet stiffened by a semi-infinite orthotropic sheet
[NASA-TM-87584] 23 p3941 N85-34426

STRIP TRANSMISSION LINES
NT MICROSTRIP TRANSMISSION LINES

A generalized solution to a class of printed circuit antennas
[AD-A145626] 02 p0191 N85-11278
A coaxial cavity gunn oscillator using probe coupled microstrip
[AD-D011437] 10 p1479 N85-19334
Bonded stripline power splitter for ERS-1
[RML-009-84-124] 15 p2550 N85-25740
Research on superconductive signal-processing devices
[AD-A152703] 17 p2953 N85-28235
MMIC devices for active phased array antennas
[NASA-CR-176015] 19 p3254 N85-30177
Application of field similitude theory to calculation of stripline heating 22 p3780 N85-33419
Power flow evaluations for HERMES 3
[DE85-013116] 24 p4156 N85-35769

STROBOSCOPES
Orbit extrapolation — satellite orbits 05 p0598 N85-13811
Characteristics of digital range finder with stroboscopic discretization 22 p3762 N85-33319

STRONG INTERACTIONS (FIELD THEORY)
Experimental studies of diffractive phenomena
[DE85-006812] 17 p3031 N85-28749
Dependence of the average spatial and energy characteristics of the hadron-lepton cascade on the strong interaction parameters at superhigh energies 24 p4188 N85-35977

STRONGLY COUPLED PLASMAS
Many-body correlations in strongly-coupled plasmas 02 p0284 N85-11850
Local fields in strongly coupled plasmas
[DE84-013375] 04 p0567 N85-13611
Spatial resolution of small particles in silane discharge
[AD-A150953] 14 p2423 N85-24948
Equations of state of strongly coupled plasma mixtures
[DE85-006163] 15 p2857 N85-26393
Enhanced thermal coupling by a repetitively pulsed laser
[AD-A154435] 19 p3276 N85-30917
Activities of Rutgers - The State University Department of Mathematics
[AD-A154158] 19 p3370 N85-30804
Strong coupling effects on bound states in plasmas
[AD-A154353] 19 p3370 N85-30905
Low frequency instabilities driven by an ion temperature anisotropy
[AD-A154902] 21 p3707 N85-33016

STRONTIUM
NT STRONTIUM 90

STRONTIUM COMPOUNDS
NT STRONTIUM FLUORIDES
NT STRONTIUM TITANATES

STRONTIUM FLUORIDES
Feasibility of melt casting strontium fluoride to produce high-density heat sources
[DE85-009429] 18 p3130 N85-29381

STRONTIUM ISOTOPES
NT STRONTIUM 90

STRONTIUM TITANATES
A study of structural phase transitions using light scattering techniques
[AD-A147261] 07 p1048 N85-16854
Planar ferroelectric microcapacitors for microwave devices 13 p2067 N85-23032

STRONTIUM 90
Environmental surveillance at Los Alamos during 1984
[DE85-011886] 22 p3811 N85-33605
Estimation of Sr90 and Cs137 activity introduced and accumulation in the Po basin until 1963
[CISE-2515] 22 p3813 N85-33617

STROUHAL NUMBER
Periodic vortex shedding in the supersonic wake of a planar plate
[NASA-TM-77854] 15 p2463 N85-25207

STRUCTURAL ANALYSIS
NT DYNAMIC STRUCTURAL ANALYSIS
NT ENERGY METHODS
NT EQUILIBRIUM METHODS
NT FLUTTER ANALYSIS
NT MATRIX METHODS
NT STRAIN ENERGY METHODS

A study of bituminous pavements to determine a correlation between pavement structure designs and tripping of asphalt cement
[PB84-217751] 01 p0037 N85-10231
Broadband transverse field interaction continuous beam amplifier
[AD-D011229] 01 p0043 N85-10279
Application of concurrent processing to structural dynamic response computations 01 p0057 N85-10380
Initial experience with distributing structural calculations among computers operating in parallel 01 p0058 N85-10381
Structural analysis of the Space Shuttle Orbiter 01 p0061 N85-10401
Finite element modelling of buried structures 01 p0061 N85-10403
On the computer analysis of structures and mechanical systems 01 p0061 N85-10404
Development of advanced constitutive model for reinforced concrete
[AD-A145050] 01 p0062 N85-10411
Turbine Engine Hot Section Technology (HOST)
[NASA-TM-83022] 02 p0140 N85-10951
Nonlinear structural and life analyses of a turbine blade 02 p0141 N85-10954
Nonlinear structural and life analyses of a combustor liner 02 p0141 N85-10955
Component-specific modeling 02 p0143 N85-10971
The 3-D inelastic analysis methods for hot section components: Brief description 02 p0143 N85-10972
Constitutive model development for isotropic materials 02 p0144 N85-10975
Validation of structural analysis methods using the in-house liner cyclic rigs 02 p0146 N85-10987
Quasi-Newton algorithms for large scale nonlinear systems 02 p0208 N85-11370
Optical waveguide spatial filters
[AD-A145674] 02 p0280 N85-11825
Biaxial constitutive equation development for single crystals
[NASA-CR-174056] 02 p0286 N85-11882
Study of structure of sponge titanium varieties 03 p0350 N85-12256
Constituent properties and interrelationships 04 p0467 N85-12964

Bulletin of the Faculty of Engineering, Hokkaido University, no. 123
[ISSN-0385-602-X] 04 p0482 N85-13075

Implication structures for generalized implication matrix in ISM
04 p0483 N85-13079

Design, ancillary testing, analysis and fabrication data for the advanced composite stabilizer for Boeing 737 aircraft, volume 2
[NASA-CR-166011] 05 p0612 N85-13914

Analytical thermal formulations for antenna dishes — satellite antennas
05 p0627 N85-14017

Structure errors in system identification
05 p0700 N85-14495

USSR report: Engineering and equipment
[JPRS-UEQ-84-007] 06 p0775 N85-14954

Iterative method of calculating strength of airframe members using finite element method
06 p0775 N85-14955

Sensitivity analysis of discrete structural systems: A survey
[NASA-TM-86333] 06 p0817 N85-15186

Encapsulation design analysis
06 p0829 N85-15268

CF-5 vertical stabilizer flight load survey
07 p0895 N85-15673

Keeping up with operational loads in the French Air Force: Defining new equipment
07 p0896 N85-15681

USAF approach to airborne structural data recording: Airborne Data Acquisition Multifunction System (ADAMS)
07 p0897 N85-15683

Engine cyclic durability by analysis and material testing
07 p0907 N85-15744

Flutter control with unsteady aerodynamic models
[AD-A147858] 07 p0909 N85-15753

Reduction method for thermal analysis of complex aerospace structures
[NASA-TP-2373] 07 p0957 N85-16066

A review of imperfection sensitivity of stiffened shells
[AD-A147311] 07 p0978 N85-16213

Advances in composites technology
[NASA-TM-86353] 08 p1118 N85-17048

Composites with a periodic structure, mathematical analysis and numerical treatment
[AD-A148301] 08 p1119 N85-17053

Mechanical properties of adhesively bonded aluminum structures protected with hydration inhibitors
[AD-A148123] 08 p1133 N85-17139

Computational methods for nonlinear dynamics problems in solid and structural mechanics
[AD-A148352] 08 p1172 N85-17392

Vibration analysis of a multipurpose platform
[NAL-TR-803] 09 p1286 N85-18078

Treatment of general boundary conditions and point-wise state variable constraints in optimum design for static and dynamic response
09 p1330 N85-18358

NASA Lewis Research Center/University Graduate Research Program on Engine Structures
[NASA-TM-86916] 09 p1333 N85-18375

The Shock and Vibration Bulletin 54. Part 2: Ship shock, shock and blast and ground shock
[AD-A146132] 09 p1334 N85-18388

Assessment of seismic survivability
09 p1336 N85-18402

Penetration of short duration airblast into protective structures
09 p1336 N85-18404

A pole-free reduced-order characteristic determinant method for linear vibration analysis based on sub-structuring
09 p1338 N85-18412

Determination of shear coefficient of a general beam cross section by finite element method
09 p1338 N85-18413

Applications of the Heavy-Ion Rutherford Backscattering Spectrometry (HIRBS) to the analysis of contact structures on GaAs and Ge
[DE85-000671] 10 p1584 N85-19861

SANS studies of polymers
[DE85-002471] 11 p1612 N85-20134

A new rheological model for concrete structural analysis
[DE84-014743] 11 p1653 N85-20413

Innovative solar thermal dish technology development
[DE85-002787] 11 p1673 N85-20539

Alternative approximation concepts for space frame synthesis
[NASA-CR-172526] 12 p1776 N85-21150

Nonlinear analysis for high-temperature multilayered fiber composite structures — turbine blades
[NASA-TM-83754] 12 p1797 N85-21273

Symmetric primal-dual variational formulations of coupled dynamic systems: Three-dimensional elasticity, shells, fluid-structure interaction
[ONERA-1983-91] 12 p1863 N85-21684

3-D inelastic analysis methods for hot section components (base program) — turbine blades, turbine vanes, and combustor liners
[NASA-CR-174700] 12 p1863 N85-21686

On local total strain redistribution using a simplified cyclic inelastic analysis based on an elastic solution
[NASA-TM-86913] 12 p1864 N85-21690

Time marching numerical solution of the dynamic response of nonlinear systems
[NAF-AN-25] 12 p1865 N85-21696

A solution method for large deformation contact problems
[AD-A149842] 12 p1866 N85-21707

A solution method for nonlinear dynamic analysis of shell structures
[AD-A149846] 12 p1866 N85-21708

Geometrically nonlinear analysis of laminated elastic structures
[NASA-CR-175609] 12 p1868 N85-21720

Systems vulnerability and lethality in the development phase
[AD-A149737] 12 p1924 N85-22089

Simple theoretical models for composite rotor blades
[NASA-CR-175620] 13 p1971 N85-22382

Specifics of kinetics of polymorphous conversion upon heating of low carbon steels 13 p2030 N85-22721

Machine analysis of resonance characteristics of plate-type radio electronic equipment constructions
13 p2085 N85-23018

Operational loads measurement: A philosophy and its implementation — aircraft structures
[AD-A149445] 13 p2144 N85-23308

Raman structural studies of the nickel electrode
[NASA-CR-175619] 13 p2162 N85-23414

Meteoroidal impacts, plasma, fine structure of ringlets and spokes on Saturn's ring B 13 p2174 N85-23490

The olivine asteroids: Discovery, mineralogy, and relationship to palasites 13 p2175 N85-23500

Research on composite materials for structural design
[AD-A150802] 14 p2260 N85-24004

Unified constitutive material models for nonlinear finite-element structural analysis — gas turbine engine blades and vanes
[NASA-TM-86985] 14 p2320 N85-24338

Cyclic structural analyses of anisotropic turbine blades for reusable space propulsion systems — some fuel turbopump
[NASA-TM-86990] 14 p2320 N85-24339

Finite Element Methods in South Africa 1983 — conference
[S-332] 14 p2410 N85-24863

On the structure of the turbulent vortex
15 p2463 N85-25213

Automatic Dynamic Aircraft Modeler (ADAM), volume 1
[AD-A151410] 15 p2471 N85-25252

NASA R and T aerospace plane vehicles: Progress and plans
[NASA-TM-86429] 15 p2491 N85-25368

Definition of ground test for verification of large space structure control
[NASA-CR-171438] 15 p2492 N85-25377

Thirteenth NASTRAN Users' Colloquium
[NASA-CP-2373] 15 p2573 N85-25863

New enhancements in April 85 NASTRAN release
15 p2573 N85-25864

Improved accuracy in solid isoparametric elements using selectively reduced integration 15 p2573 N85-25865

Crack elements for COSMIC/NASTRAN
15 p2573 N85-25866

A 4-node bilinear isoparametric element in Rockwell NASTRAN 15 p2573 N85-25867

Layered composite analysis capability
15 p2573 N85-25868

NPLOT: An interactive plotting program for NASTRAN finite element models 15 p2573 N85-25869

COSMIC/NASTRAN-PATRAN interface
15 p2574 N85-25870

Two interactive graphics postprocessors for NASTRAN 15 p2574 N85-25871

An unusual application of NASTRAN contour plotting capability 15 p2574 N85-25872

CADS: A Computer Aided Design System
15 p2574 N85-25876

Learjet Model 55 wing analysis with landing loads
15 p2575 N85-25883

Fillet weld stress using finite element methods
15 p2576 N85-25884

The structural finite element model of the C-5A
15 p2576 N85-25885

Using NASTRAN to model missile inertia loads
15 p2576 N85-25886

Experience with free bodies 15 p2576 N85-25887

NASTRAN analysis comparison to shock tube tests used to simulate nuclear overpressures
15 p2576 N85-25888

Direct transient analysis of a fuze assembly by axisymmetric solid elements 15 p2576 N85-25890

Transient analysis of a magnetic heat pump
15 p2576 N85-25891

Vibration and buckling of rotating, pretwisted, preconed beams including Coriolis effects
[NASA-TM-87004] 15 p2577 N85-25893

Structures and Dynamics Division research and technology plans for FY 1985 and accomplishments for FY 1984
[NASA-TM-86417] 15 p2577 N85-25895

Elastic-workhardening SDF (Single-Degree-of-Freedom) system subjected to random blast excitations
[AD-A151866] 15 p2579 N85-25909

Structural analysis of electronic assembly housing
[DE85-005794] 15 p2580 N85-25913

GEMINI: A computer program for two and three dimensional linear static and seismic structural analysis, CDC 7600 version
[DE85-007496] 15 p2631 N85-26218

Enhanced thermal-structural analysis by integrated finite elements
[AD-A151103] 15 p2636 N85-26258

Methods of first wall structural analysis with applications to the long pulse commercial Tokamak reactor design
[DE85-004915] 15 p2657 N85-26397

ESP (External-Stores Program): A pilot computer program for determining flutter-critical external-store configurations. Volume 1: User's manual
[AD-A152268] 16 p2710 N85-26725

A study of structural concepts for ultralightweight spacecraft
[NASA-CR-175765] 16 p2730 N85-26848

Nonlinear structural analysis for fiber-reinforced superalloy turbine blades 16 p2737 N85-26867

Adaptation of continuous beams and the method of optimizing the flexibility of their elastic supports. Theorem on maximal adaptation loading, supplement
[REPT-10/1984-SUPPL] 16 p2797 N85-27241

Optimal modeling with a minimum of local distortion
[REPT-18/1984] 16 p2797 N85-27243

A computer analysis program for interfacing thermal and structural codes
[NASA-TM-87021] 16 p2800 N85-27264

USAF damage tolerant design handbook: Guidelines for the analysis and design of damage tolerant aircraft structures, revision B
[AD-A153161] 17 p2896 N85-27858

Probabilistic structural analysis theory development
17 p2912 N85-27955

Probabilistic finite element: Variational theory
17 p2913 N85-27957

Probabilistic structural analysis of SSME turbopump blades: Probabilistic geometry effects
17 p2913 N85-27958

Cyclic structural analyses of SSME turbine blades
17 p2914 N85-27963

Coherent structure reflective turbulent viscous flow modeling
[AD-A153066] 17 p2958 N85-28267

The Shock and Vibration Digest, volume 17, no. 1
[AD-A151051] 17 p2977 N85-28397

Continuum modeling of latticed structures
17 p2977 N85-28399

First passage times for combinations of random loads
[AD-A153275] 17 p2980 N85-28423

Structural analysis of terrane accretions in the eastern Brooks Range and adjacent areas in central Alaska and Canada
[DE85-006279] 17 p2993 N85-28501

Implementation of a general finite element code on an IBM PC compatible microcomputer
[AD-A152661] 17 p3011 N85-28615

Sample problems for STAGSC-1
[AD-A153142] 17 p3012 N85-28621

Finite element thermal-structural analysis of cable-stiffened space structures
[AD-A153822] 18 p3066 N85-28963

Constitutive modeling for blast-induced wave propagation
[AD-A153578] 18 p3099 N85-29187

Structural Analysis
[DFVLR-MITT-84-21] 18 p3120 N85-29313

Research on structural analysis at the DFVLR, Brunswick 18 p3120 N85-29314

Field consistency and the finite element analysis of multifield structural problems 18 p3120 N85-29316

Low-energy electron diffraction experiment and theory
[DE85-009967] 18 p3195 N85-29620

Action of plasma and explosion products on alumina
19 p3242 N85-30100

Structural analysis and cost estimate of an eight-leg space frame as a support structure for horizontal axis wind turbines
[NASA-TM-83470] 19 p3284 N85-30361

Large deflections of a cantilever beam under arbitrarily directed tip load
[NASA-TM-86442] 19 p3284 N85-30363
Underwater shock-induced responses of stiffened flat plates: An investigation into the predictive capabilities of the USA-STAGS code
[AD-A154245] 19 p3286 N85-30377
Seismic pipe support construction practices
[DE85-901315] 19 p3287 N85-30386
Three-dimensional finite element impact analysis of a nuclear waste truck cask
[DE85-010653] 19 p3288 N85-30389
Fire performance of interstitial space construction system
[NBSIR-85-3158] 20 p3436 N85-31318
Activities report of the Laboratory of Mechanics and Energetics 20 p3437 N85-31326
A numerical algorithm for endochronic plasticity and comparison with experiment 20 p3467 N85-31539
Two simplified procedures for predicting cyclic material response from a strain history 20 p3467 N85-31543
Detection of internal structure by scattered light intensity: Application to kidney cell sorting
20 p3503 N85-31777
Efficient solution methods for nonlinear finite element analysis 20 p3519 N85-31886
Iteration solution for a submerged force-driven finite cylinder
[AD-A154587] 21 p3699 N85-32982
SANCHO: A finite element computer program for the quasistatic, large deformation, inelastic response of two-dimensional solids
[DE85-011456] 22 p3829 N85-33714
Intermittent motion 23 p3925 N85-34323
Software for mechanism design
23 p3925 N85-34324
Kinematic analysis of Hurricane Frederick (1979) using satellite, aircraft and rawinsonde data
[NASA-CR-176167] 24 p4119 N85-35533
A new method of differential structural analysis of gamma-family basic parameters
[HE-3.6-3] 24 p4184 N85-35952

STRUCTURAL BASINS
NT MISSOURI RIVER BASIN (US)
NT RIVER BASINS
NT WATERSHEDS
Predicting fracturing zones in Caspian depression subsalt deposits on basis of space information and geological-geophysical data 02 p0164 N85-11111
Marine geological and geophysical investigations of the Antarctic Continental Margin, 1984
[GS-CIRC-935] 02 p0212 N85-11400
Late quaternary glacial cycles in the Bahamian deep basins and in the adjacent Atlantic Ocean
02 p0226 N85-11478
Geophysical investigations of the central part of Niger State, Nigeria 03 p0390 N85-12498
Martian impact basins: Morphology differences and tectonic provinces
[NASA-CR-174074] 03 p0448 N85-12847
Reconnaissance geology of the northern part of the Unalakleet quadrangle 04 p0516 N85-13291
Paleomagnetic latitude of paleocene volcanic rocks of the Cantwell Formation, central Alaska
04 p0517 N85-13302
CO-2-silica geothermometer for low temperature geothermal resource assessment, with application to resources in the Safford Basin, Arizona
[DE84-013958] 04 p0534 N85-13411
Directional properties of circular Maria: Interpretation in the context of a testable gravitational capture model for lunar origin 04 p0586 N85-13743
Effect of lithology and climate on the morphology of drainage basins in northwestern Colorado
[PB84-228238] 06 p0628 N85-15258
Spectral reflectance studies on the orientale region of the Moon 06 p0668 N85-15639
New data on presence of ores in salt dome structures of Dnieper-Donets Basin 07 p0981 N85-16234
Deep water mass circulation in the Western Alboran Basin: Measurements in July and September 1980 (Alboran I experiment)
[AD-A148566] 08 p1191 N85-17504
Petrography, diagenesis and depositional models of the St. Louis limestone, valmeyeran (middle Mississippian), Illinois Basin, USA 09 p1352 N85-18506
Diagenesis of niagaran (middle silurian) pinnacle reefs, northwest Michigan 09 p1352 N85-18508
Mercury 09 p1411 N85-18890
Moon 09 p1411 N85-18893
Evolution of sedimentation basins in Earth's history
10 p1497 N85-19451
Post-carboniferous tectonics in the Anadarko Basin, Oklahoma: Evidence from side-looking radar imagery
[NASA-CR-175458] 10 p1505 N85-19498
Crustal stretching and subsidence in sedimentary eastern Switzerland and permo-carboniferous basins in the continental United States
[DE85-000622] 11 p1681 N85-20592
Lithologic and environmental atlas of Berea Sandstone (Mississippian) in the Appalachian Basin
[PB85-129039] 11 p1682 N85-20600
Review of problems in lithology
13 p2113 N85-23160
Average spacing for rings of individual multi-ring basins is 2.0(0.5)D 13 p2182 N85-23541
Ring-diameter ratios for multi-ring basins average 2.0(0.5)D 13 p2182 N85-23542
Ripple ring basins on Ganymede and Callisto
13 p2183 N85-23547
Fluvial drainage basins and valley networks: Eastern Margaritifer Sinus, Mars 13 p2190 N85-23586
Spectral reflectance studies of the Orientale basin
13 p2195 N85-23617
The deep structure of lunar basins: Clues to the understanding of basin formation and modification
13 p2200 N85-23647
Valles Marineris basin beds: A complex story
13 p2201 N85-23652
Global tectonics on Ganymede
13 p2202 N85-23659
Preliminary assessment of climatic change during late Wisconsin time, southwest Great Basin and vicinity, Arizona, California and Nevada
[DE85-008343] 16 p2836 N85-27488
Tidal rectification in lateral viscous boundary layers of a semienclosed basin
[CWI-AM-R8415] 17 p2960 N85-28284
Geoacoustic models: Washington state continental margin
[AD-A153781] 18 p3177 N85-29699
Flood-runoff forecasting with HEC1F
[AD-A154286] 19 p3300 N85-30456
An objective analysis technique for extrapolating tidal fields 20 p3493 N85-31715
Great Lakes hydrometeorologic and hydraulic data needs 20 p3496 N85-31739
Lunar and Martian impact basins: Exposed records of terrestrial bombardment? 21 p3721 N85-33090
Geothermal resources of the Laramie, Hanna and Shirley Basins, Wyoming
[DE85-005005] 23 p3943 N85-34436
Hydrology
[PB85-182954] 23 p3944 N85-34440
Geology and petroleum resources of basins in western China
[DE85-013038] 23 p3948 N85-34469
Geothermal resources of the Washakie and Great Divide basins, Wyoming
[DE85-013004] 24 p4112 N85-35491
Depositional systems and coal occurrence in the Fort Union Formation (Paleocene), Powder River Basin, Wyoming and Montana 24 p4114 N85-35505
Geology: Structural history and fluvial geomorphology of the southern Death Valley Fault Zone, Inyo and San Bernardino Counties, California
24 p4114 N85-35506

STRUCTURAL BEAMS
U BEAMS (SUPPORTS)

STRUCTURAL DESIGN
NT PRESSURE VESSEL DESIGN
The Influence of Large Scale Computing on Aircraft Structural Design
[AGARD-R-706] 01 p0007 N85-10040
Initial postbuckling analysis of elastoplastic thin-shear structures 01 p0059 N85-10393
Interactive aircraft flight control and aeroelastic stabilization
[NASA-CR-174025] 02 p0148 N85-11003
Structural design guidelines for heliports
[FAA-PM-84-23] 02 p0149 N85-11010
Design of alternate launch and recovery surfaces for environmental effects
[AD-A145800] 03 p0320 N85-12066
Design, ancillary testing, analysis and fabrication data for the advanced composite stabilizer for Boeing 737 aircraft. Volume 1: Technical summary
[NASA-CR-3648] 05 p0612 N85-13913
Structural design and thermal stability of TELE-X antenna tower 05 p0627 N85-14016
The need for a dedicated public service helicopter design 06 p0753 N85-14828
Cross-shaped aperture synthesis system
06 p0782 N85-14999
Space Station truss structures and construction considerations
[NASA-TM-86338] 07 p0916 N85-15796
Design procedures for fiber composite structural components: Panels subjected to combined in-plane loads
[NASA-TM-86909] 07 p0919 N85-15823
Aeroproyekt develops improved runway surfacing
08 p1068 N85-16770
Orbiter structural design and verification
08 p1094 N85-16915
Space shuttle external tank performance improvements: The challenge 08 p1094 N85-16916
Structural and mechanical design challenges of space shuttle solid rocket boosters separation and recovery subsystems 08 p1095 N85-16917
Orbiter processing facility: Access platforms Kennedy Space Center, Florida, from challenge to achievement
08 p1102 N85-16968
Passive Orbital Disconnect Strut (PODS 3) structural test program
[NASA-CR-177325] 08 p1113 N85-17020
Finite element computation of structural design sensitivity analysis 09 p1330 N85-18383
Design oriented identification of critical points in transient response 09 p1330 N85-18357
Optimization of vibrating beams including the effects of coupled bending and torsional modes
09 p1331 N85-18364
Reflections on trends in dynamics: The Navy's perspective 09 p1334 N85-18382
Direct energy minimization approach to whipping analysis of pressure hulls 09 p1335 N85-18393
Assessment of seismic survivability
09 p1336 N85-18402
Design and construction details of the FRX-C/T device: A compact toroid plasma translation experiment
[DE85-001527] 09 p1390 N85-18749
Heat transfer and mechanical interactions in fusion nuclear systems
[DE84-016233] 09 p1392 N85-18761
Versator divertor experiment: Preliminary designs
[DE84-017159] 09 p1393 N85-18769
Sealing assembly
[AD-D011463] 10 p1452 N85-19151
Characteristics of the elevation drive suspension of the 64-meter antennas 10 p1464 N85-19240
SSPS-CRS advanced sodium receiver: Construction experience report
[DE85-000625] 10 p1511 N85-19533
Innovative solar thermal dish technology development
[DE85-002787] 11 p1673 N85-20539
Developments in deployable masts to support flexible solar arrays 13 p2012 N85-22620
Generic design and verification of an Advanced Rigid Array (ARA) — solar array 13 p2012 N85-22621
The Olympus solar array structure and mechanisms
13 p2012 N85-22623
Experimental investigation of crippling strength of Chinese aluminum alloy (LY12CZ) sections
13 p2041 N85-22779
Shape optimization for minimal stress concentration
13 p2101 N85-23093
Precision space structures 14 p2232 N85-23633
Research on composite materials for structural design
[AD-A150802] 14 p2260 N85-24004
Invariant system of technological preparation of production 14 p2268 N85-24056
Mechanical aspects of interfaces and surfaces in ceramic containing systems
[AD-A151978] 15 p2519 N85-25530
Design of shear deformable antisymmetric angle-ply laminates to maximize the fundamental frequency and frequency separation
[CSIR-TWISK-333] 15 p2577 N85-25892
Creep ratcheting simplified methods experience from structural design of elevated temperature components
[DE85-007433] 15 p2580 N85-25915
A literature review of EMATs, with stress calculations for simple EMAT geometries
[AERE-R-11415] 15 p2642 N85-26295
Structural design and kinematic configuration of two-armed robots 16 p2761 N85-27037
Design and construction of a computer controlled microthermocouple probe for the study of buoyant jets
[AD-A152224] 16 p2769 N85-27199
Numerical optimization algorithm for engineering problems using microcomputer
[AD-A152135] 16 p2847 N85-27554
The application of computer aided structural optimization to the design of aircraft components
[MBB-UT-21/84-O] 16 p2873 N85-27728
Some aspects of how to design cost-effective flight control systems
[MBB-LKE-32/S/PUB/143] 16 p2873 N85-27729
Design and construction of a CW ND:YAG laser using a single elliptical cavity and water cooled krypton arc lamp pumping
[AD-A152657] 17 p2970 N85-28340
Engineering significance of fatigue thresholds and short fatigue cracks for structural design
[NLR-MP-84001-U] 17 p2981 N85-28430

Structural design of the Sandia 34-meter vertical-axis wind turbine
[DE85-011146] 18 p3118 N85-29300
Impact dynamics research on composite transport structures
[NASA-TM-86391] 19 p3284 N85-30367
Fatigue characterization of fabricated ship details for design
[SSC-316] 19 p3295 N85-30371
Operational results for the experimental DOE/NASA Mod-OA wind turbine project
[NASA-TM-83517] 19 p3304 N85-30479
Physical dimensions of humans; values; the effect of clothing, working clothes and protective equipment on the design of work places
[HSE-TRANS-10868] 19 p3331 N85-30636
Design of aggressive superconducting TFCX magnet systems
[DE85-010003] 19 p3376 N85-30943
Fire performance of interstitial space construction system
[NBSIR-85-3158] 20 p3436 N85-31318
Structural dynamics model and response of the deployable reference configuration space station
[NASA-TM-86386] 22 p3799 N85-33539
A rational approach to cam design
23 p3923 N85-34311

STRUCTURAL DESIGN CRITERIA
Energy efficient engine combustor test hardware detailed design report
[NASA-CR-167945] 02 p0140 N85-10950
Structural analysis 02 p0143 N85-10969
Materials properties, loads, and stress analysis, Spartan REM: Appendix A
[NASA-CR-171092] 02 p0206 N85-11375
Computer models and output, Spartan REM: Appendix B
[NASA-CR-171093] 02 p0206 N85-11376
Large-diameter astromast development
[NASA-CR-171201] 03 p0342 N85-12200
DCS (Defense Communications System) network synchronization design criteria
[AD-A146251] 03 p0356 N85-12289
Design of electromagnetic bearing for vibration control of flexible transmission shaft 05 p0645 N85-14136
Technical Workshop: Advanced Helicopter Cockpit Design
[NASA-CP-2351] 06 p0750 N85-14806
Supersupermented rotorcraft program
06 p0750 N85-14807
High-efficiency silicon solar cell research
06 p0829 N85-15261
High-efficiency solar-cell design modeling
06 p0829 N85-15262
Barriers to achieving high efficiency
06 p0829 N85-15264
Evaluation of operational loads to verify structural design 07 p0896 N85-15677
Special problems of Ramjet with solid fuel
07 p0918 N85-15815
Solid propellant Ramrockets 07 p0918 N85-15816
Damping capacity of multilayer tube during torsion
[BLL-M-36011-(5828.4)] 07 p0977 N85-16202
Design criteria for small wind turbines
[NLR-MP-83054-U] 07 p0994 N85-16310
Calculated parameters for the initial part of an accelerator with high-frequency quadrupole focusing
[RAE-TRANS-2122] 07 p1040 N85-16800
The aerodynamic challenges of the design and development of the space shuttle orbiter
08 p1093 N85-16909
Structural load challenges during space shuttle development 08 p1094 N85-16914
Propulsion and power systems perspective
08 p1095 N85-16938
Space shuttle main engine: Interactive design challenges 08 p1098 N85-16940
Shipboard shock response of the model structure DSM: Experimental results versus responses predicted by eight participants 09 p1335 N85-18392
Preliminary design criteria and certification test specifications for blast resistant windows
09 p1337 N85-18405
Over the wing propeller
[NASA-CASE-LAR-13134-1] 11 p1584 N85-19980
Space Transportation System (STS) propellant scavenging system study. Volume 3: Cost and work breakdown structure-dictionary
[NASA-CR-171850-VOL-3] 11 p1590 N85-20002
Calculations pertaining to the design of a prebuncher for a 150-MeV electron linear accelerator 3. Comparisons with experimental data
[DE85-002666] 11 p1724 N85-20844
Image lobe analysis for large radomes
[AD-P004359] 12 p1825 N85-21453
Broadband thermoplastic radomes
[AD-P004369] 12 p1827 N85-21463
Study for the optimization of a transport aircraft wing for maximum fuel efficiency. Volume 1: Methodology, criteria, aeroelastic model definition and results
[NASA-CR-172551] 13 p1971 N85-22378
Verification for large space structures
14 p2232 N85-23836
An optimization study to minimize surface distortions of a hoop-column antenna 14 p2232 N85-23837
Experimental facility for studying MHD effects in liquid metal cooled blankets
[DE85-000563] 14 p2423 N85-24943
Definition of technology development missions for early space stations: Large space structures
[NASA-CR-171446] 15 p2476 N85-25281
Oxygen-hydrogen thrusters for Space Station auxiliary propulsion systems
[NASA-CR-175691] 15 p2494 N85-25383
Concepts and cost trade-offs for land vehicle antennas in satellite mobile communications
[NASA-CR-175731] 15 p2540 N85-25680
Multikilowatt hydrogen-nickel oxide battery system
[DE85-003339] 15 p2550 N85-25737
Two-phase flow in centrifugal pumps
[BLL-CE-TRANS-8065-(9022.09)]
15 p2605 N85-26053
Computers in the determination of rainfall septh-duration-frequencies in Natal
15 p2627 N85-26186
Radiation effects on structural materials
[DE85-007032] 15 p2649 N85-26338
A scanning optical microprobe for infrared detector measurement
[AD-A151748] 15 p2653 N85-26361
Synthesis study: Validation of a gust generator in the presence of a model in a wind tunnel
[ONERA-RT-16/5108-RY-051]
16 p2701 N85-26678
Bearings working group 16 p2735 N85-26678
Hybrid bearings for LH2 and LO2 turbopumps
16 p2736 N85-26680
Rotordynamics 16 p2737 N85-26688
Research in the field of rib stiffened shell stability
16 p2766 N85-27068
Deployable controllable geometry truss beam
[NASA-TM-86366] 17 p2909 N85-27934
Overview of structural response: Probabilistic structural analysis 17 p2912 N85-27952
A ten channel temperature controller
[AD-A152664] 17 p2967 N85-28326
Frangibility of obstacles at airports
[NLR-MP-84002-U] 17 p2981 N85-28431
On the accuracy of modelling the dynamics of large space structures 19 p3225 N85-29995
The dynamics and control of large flexible space structures, 8
[NASA-CR-175986] 19 p3225 N85-29996
Analysis of rotorcraft crash dynamics for development of improved crashworthiness design criteria
[FAA-CT-85-11] 20 p3391 N85-31031
SPAR improved structural-fluid dynamic analysis capability
[NASA-CR-171549] 20 p3454 N85-31449
A model parameter extraction procedure applicable to linear time-invariant dynamic systems
[NASA-CR-176120] 22 p3835 N85-33747
Design of transversely stiffened FRP panels under compressive load --- fiber reinforced plastic (FRP) ships
[AMTE(S)-R-84104] 23 p3940 N85-34424

STRUCTURAL DYNAMICS
U DYNAMIC STRUCTURAL ANALYSIS

STRUCTURAL ENGINEERING
STARS: A general-purpose finite element computer program for analysis of engineering structures
[NASA-RP-1129] 02 p0209 N85-11378
Activities report of the Department of Engineering
03 p0342 N85-12202
Underground engineering (selected articles)
[AD-A141053] 04 p0483 N85-13082
Earthquake engineering facilities and instrumentation
[PB84-231661] 04 p0504 N85-13220
Orbiter processing facility: Access platforms Kennedy Space Center, Florida, from challenge to achievement
08 p1102 N85-16968
On solving nonlinear problems of aircraft structural mechanical design 09 p1309 N85-18223
FRG firms jump into market for auto, aircraft ceramics
09 p1309 N85-18225
Reflections on trends in dynamics: The Navy's perspective 09 p1334 N85-18382
Solutions to structural dynamics problems
09 p1334 N85-18384
The Shock and Vibration Bulletin 54. Part 3: Structural dynamics, machinery dynamics and vibration problems
[AD-A148133] 09 p1337 N85-18406
System software for the finite element machine
[NASA-CR-3670] 09 p1372 N85-18622
Planning for greater-confinement disposal
[DE85-002143] 09 p1383 N85-18697
Hydrodynamic flow structures in quantum field theory
[DE84-015513] 09 p1401 N85-18817
Geometric Hamiltonian structures and perturbation theory
[DE85-002005] 11 p1707 N85-20737
Proceedings of the 9th Biennial Army Symposium on Solid Mechanics. Advances in Solid Mechanics for Design and Analysis
[AD-A150042] 12 p1867 N85-21710
Computer-Aided Structural Engineering (CASE) project. Seepage analysis of confined flow problems by the method of fragments (CFRAG)
[AD-A150015] 12 p1875 N85-21782
New concepts in deployable beam structures
14 p2232 N85-23832
Technology for large space systems: A bibliography with indexes, supplement 11
[NASA-SP-7046(11)] 15 p2475 N85-25277
Automatic Dynamic Aircraft Modeler (ADAM) for the computer program NASTRAN 15 p2574 N85-25875
Symmetric composite laminate stress analysis
15 p2575 N85-25876
Symposium on Computers in Civil Engineering 1983
[CSIR-S-298] 15 p2626 N85-26182
Programme development: A state of the art
15 p2626 N85-26185
Progress through cooperation and exchange of ideas and experiences 15 p2626 N85-26186
An approach for user controlled reinforced concrete design optimization 15 p2627 N85-26187
Computers in the determination of rainfall septh-duration-frequencies in Natal
15 p2627 N85-26188
A study of spacecraft technology and design concepts, volume 1
[NASA-CR-172579-VOL-1] 16 p2730 N85-26844
Incorporating control into the optimal structural design of large flexible space structures
[AD-A152858] 17 p2909 N85-27937
Research on structural analysis at the DFVLR, Brunswick 18 p3120 N85-29314
Cultural data base implementation study and computer-aided scene modeling system users manual
[AD-A154232] 19 p3333 N85-30846
Mechanical considerations in cw linacs
[DE85-010726] 19 p3363 N85-30850
Field testing of a lightweight relocatable structure in a temperate environment
[AD-A155171] 21 p3599 N85-32350
Proceedings of the 24th Project Integration Meeting
[NASA-CR-176058] 21 p3607 N85-32394
Designing a graphics application interface
23 p3964 N85-34574

STRUCTURAL FAILURE
Development of failure criterion for Kevlar-epoxy fabric laminates
[NASA-CR-172485] 02 p0170 N85-11138
Studies on reliability of structural systems
02 p0206 N85-11362
Formulation and solution methods for classical problems of static buckling
[CETIM-101010] 04 p0514 N85-13280
Nonlinear deformation and static linear buckling of structures under pressure
[CETIM-11-E-350] 04 p0514 N85-13281
TUTOR (CL-41A) tail flight load survey
07 p0896 N85-15678
Steel containment buckling
[DE85-003744] 13 p2103 N85-23111
Study of failure mechanism of fibrous composition materials taking into account physicochemical reactions of components 19 p3243 N85-30106
Effect of matrix plasticity on durability of fibrous composition materials 19 p3243 N85-30107
Fatigue resistance of VT3-1 titanium alloy related to surface cold working 19 p3245 N85-30120
Effect of protective method on cyclic durability and nature of failure of titanium alloy welded joints
19 p3245 N85-30122
Fatigue characterization of fabricated ship details for design
[SSC-316] 19 p3295 N85-30371
Stored energy and structural failure
[OUEL-1564/85] 20 p3471 N85-31567
Automatic capability to store and retrieve component data and to calculate structural integrity of these components
[DE85-012429] 22 p3831 N85-33726
Safety and reliability of steel structural materials under random service impact loads 23 p3908 N85-34197
Effect of strain rate on the initial failure of notched GRP laminates 23 p3908 N85-34214

Three-dimensional finite element failure model for predicting failure in fibre reinforced bolted joints
[BR94778] 23 p3940 N85-34423
STRUCTURAL FATIGUE
U FATIGUE (MATERIALS)
STRUCTURAL FOUNDATIONS
U FOUNDATIONS
STRUCTURAL MATERIALS
U CONSTRUCTION MATERIALS
STRUCTURAL MEMBERS
NT ANISOTROPIC PLATES
NT BEAMS (SUPPORTS)
NT CANTILEVER BEAMS
NT CANTILEVER PLATES
NT CIRCULAR PLATES
NT COLUMNS (SUPPORTS)
NT CURVED BEAMS
NT ELASTIC PLATES
NT FLAT PLATES
NT I BEAMS
NT LONGERONS
NT MEMBRANE STRUCTURES
NT METAL PLATES
NT ORTHOTROPIC PLATES
NT PERFORATED PLATES
NT PLATES (STRUCTURAL MEMBERS)
NT POROUS PLATES
NT RECTANGULAR BEAMS
NT REINFORCED PLATES
NT SKIN (STRUCTURAL MEMBER)
NT STRAKES
NT STRINGERS
NT STRUTS
NT TRUSSES
NT WING PANELS
Research on large, highly accurate, inflatable reflectors
[AD-A145080] 01 p0016 N85-10099
Radiation effects on structural materials
[DE84-014771] 01 p0029 N85-10178
Design proposals for torsional buckling of stiffeners
[AD-A144783] 01 p0062 N85-10409
Report of the Department of Aerospace Engineering
03 p0307 N85-11977
Analysis of thin-walled airframe members in geometrically nonlinear statement
06 p0780 N85-14985
Thermally isolated structural support link
[AD-D011349] 07 p0972 N85-16176
The Shock and Vibration Digest, volume 16, no. 10
[AD-A147588] 09 p1331 N85-18361
The Shock and Vibration Bulletin 54. Part 2: Ship shock, shock and blast and ground shock
[AD-A148132] 09 p1334 N85-18388
Models for shock damage to marine structural materials 09 p1336 N85-18400
Adjustment structure
[AD-D011461] 10 p1459 N85-19193
Viscoplastic constitutive relationships with dependence on thermomechanical history
[NASA-CR-174836] 12 p1864 N85-21691
An overview of the MIL-HDBK-5 program
[AD-A147788] 14 p2254 N85-29970
Daze fasteners
[NASA-CASE-LAR-13009-1] 18 p3116 N85-29285
Viscoplasticity based on overstress with a differential growth law for the equilibrium stress
20 p3466 N85-31532
A comparison of smooth specimen and analytical simulation technique for notched members at elevated temperatures 20 p3468 N85-31548
Poly-functional building material from fiberglass (its fabrication and properties) 23 p3908 N85-34209
A simple but systematic CSG system
23 p3963 N85-34569
Analytical ultrasonics for structural materials
[TI85-008132] 23 p3968 N85-34600
User's guide: A computer program for strength analysis of non-hydraulic concrete structural elements. Report 2. Strength design of reinforced concrete column sections (PCAUC)
[AD-A156393] 24 p4102 N85-35429
STRUCTURAL PROPERTIES (GEOLOGY)
Geothermal resources of the Laramie, Hanna, and Shirley Basins, Wyoming
[DE84-016104] 01 p0064 N85-10423
Predicting fracturing zones in Caspian depression subsalt deposits on basis of space information and geological-geophysical data 02 p0164 N85-11111
Hypothesis on the origin of lineaments in the LANDSAT and SLAR images of precambrian soil in the low Contas River Valley (southern Bahia)
[E85-10007] 02 p0215 N85-11420
Systematic data interpretation of remote sensing in the reception of hydrocarbons, volume 1
[E85-10008] 02 p0215 N85-11421
Shuttle Experimental Radar for Geological Exploration (SERGE) project: Field work relating to the Shuttle Experimental Radar A (SIR-A) in Brazil (phase 2)
[NASA-CR-174033] 02 p0219 N85-11444
Interior structure of Uranus 02 p0299 N85-11939
Mars-Earth geographical comparisons: A pictorial view
[NASA-TM-86166] 02 p0302 N85-11957
The colloidal chemistry of ceramic clays
[NASA-TM-77734] 03 p0336 N85-12163
Seismology in rockburst research
[REPT-551] 03 p0375 N85-12394
Franciscan and related rocks of southern Humbolt County, northern California coast ranges: Analysis of structure, tectonics, sedimentary petrology, paleogeography, depositional history, and thermal maturity 03 p0390 N85-12495
Geophysical investigations of the central part of Niger State, Nigeria 03 p0390 N85-12496
Multispectral and geomorphic studies of processed Voyager 2 images of Europa
[NASA-CR-174075] 03 p0448 N85-12848
Structural observations in the Circle quadrangle, Yukon-Tanana Upland, Alaska 04 p0517 N85-13296
Structure of the crust and upper mantle of the Iberian continental platform 04 p0523 N85-13350
Deep structure beneath the Pyrenees
04 p0524 N85-13351
Deep structure and seismicity in the Catalonia-Pyrenees region 04 p0524 N85-13352
Methods for correlating geological, geochemical and geophysical data with satellite imagery in central Ireland
05 p0655 N85-14208
A multiple approach in remote sensing for structural and lithological mapping by use Modular Optoelectronic Multispectral Scanner (MOMS)/LANDSAT/Heat Capacity Mapping Mission (HCMM) data
05 p0660 N85-14244
Geology and resources of the Tar Sand Triangle, southeastern Utah
[DE84-012017] 05 p0677 N85-14346
Documentation of earthquake algorithms
[PB84-235324] 05 p0677 N85-14351
Summaries of physical research in the geosciences
[DE85-001882] 06 p0818 N85-15194
Deep structure of terrestrial crust and upper mantle in southeastern Siberia and Far East according geological-geophysical data 06 p0821 N85-15212
Geological, structural, and geomorphological analyses from SIR-B 08 p1145 N85-17226
Structural investigation of the Canadian Shield by orbital radar and LANDSAT 08 p1147 N85-17236
Structural investigation of the Grenville Province by radar and other imaging and nonimaging sensors
08 p1147 N85-17237
Delineation of major geologic structures in Turkey using SIR-B data 08 p1149 N85-17249
Structure and stratigraphy of Midterhuken Peninsula, Befsund, West Spitsbergen 09 p1353 N85-18513
Vertical movements and structure formation within island systems of northeast Asia 10 p1501 N85-19471
Basic structural features and probable mechanism of formation of the Kuril Island system
10 p1501 N85-19472
Mesozoic magmatism of Mongolian-Okhotsk Belt and its possible geodynamic interpretation
10 p1502 N85-19481
Geological reasons for change in intensity of linear magnetic anomalies of the Kursk magnetic anomaly
[NASA-TM-77824] 10 p1514 N85-19552
Crustal stretching and subsidence in sedimentary eastern Switzerland and permo-carboniferous basins in the continental United States
[DE85-000622] 11 p1681 N85-20592
Workshop on Remote Sensing/Lineament Applications for Energy Extraction
[DE84-009291] 12 p1875 N85-21783
The origin and evolution of terrestrial and Martian rock labyrinths
[NASA-CR-175511] 12 p1961 N85-22326
Review of problems in lithology
13 p2113 N85-23160
Normal and anomalous geothermal fields and their relationship to hierarchy of geological bodies
13 p2113 N85-23163
Planetary geology in the 1980s
[NASA-SP-467] 13 p2169 N85-23457
Io: Generation of silicate magma by shear melting at the base of a basaltic lithosphere
13 p2172 N85-23476
Topographic evidence for shield volcanism on Io
13 p2172 N85-23478
Sulfur volcanoes on Io? 13 p2173 N85-23479
Patterns of fracture and tidal stresses due to nonsynchronous rotation: Implications for fracturing on Europa 13 p2173 N85-23483
Formation of bright terrain bands on Ganymede by unstable lithosphere extension 13 p2173 N85-23485
Progress on studies of early intense cratering
13 p2181 N85-23535
Impacts in Ice: Commissions of solar system crater population 13 p2181 N85-23538
Problems in recovering crater production functions
13 p2182 N85-23539
The nature of Martian flow ejecta craters
13 p2183 N85-23545
Distribution and properties of large symmetric knobs on Mars 13 p2192 N85-23598
Planetary analogs in Antarctica: Icy satellites
13 p2193 N85-23605
Lithologic and structural control on slope morphology in the Valles Marineris 13 p2201 N85-23651
Three-layer generic Ganymedes: Structure and evolution 13 p2202 N85-23657
Lineaments on Ganymede: New evidence for late tectonic activity 13 p2202 N85-23658
Tectonics of the Valhalla structure on Callisto
13 p2202 N85-23662
Mars geologic mapping: A review and new concepts
13 p2202 N85-23663
Geology of the Ganymede quadrangle Jg7
13 p2203 N85-23665
Structure and origin of Martian satellites
15 p2483 N85-25323
Use of space information in petroleum- and gas-prospecting work (example of Southern Mangyshlak)
15 p2485 N85-25341
Interpretation of space photolineaments
15 p2487 N85-25353
Analysis of the Gran Desierto, Pinacte Region, Sonora, Mexico, via shuttle imaging radar
[NASA-CR-175711] 15 p2582 N85-25927
Nd-isotopic evidence for the origin of the Sudbury complex by meteoritic impact 15 p2660 N85-26554
Inversion of Rayleigh wave group velocities from high-explosive tests
[AD-A152172] 16 p2783 N85-27175
System of interpretation of remote sensing data when hydrocarbons are present, volume 2
[INPE-3067-TDL/162-VOL-2] 16 p2810 N85-27326
Surface exploration geophysics applied to the Moon
[DE85-006714] 16 p2884 N85-27793
The Shock and Vibration Digest, volume 17, no. 2
[AD-A153129] 17 p2977 N85-28400
The effects of seismic waves
17 p2978 N85-28401
Yearbook of the Bureau of Mineral Resources, Geology and Physics: Geoscientific research, resource assessment, and database development, 1 Jul. 1983 to 30 Jun. 1984
[BMR-84] 17 p2989 N85-28474
Proceedings of the 1980 Workshop of the International Association of Seismology and Physics of the Earth's Interior on the Seismic Modeling of Laterally Varying Structures: Contributions based on data from the 1978 Saudi Arabian refraction profile
[GS-CIRC-937] 17 p2989 N85-28476
Preliminary interpretation of Saudi Arabian seismic refraction data 17 p2989 N85-28477
Explanation of Russian models: Saudi Arabian seismic refraction profile 17 p2991 N85-28487
Geoacoustic models: Washington state continental margin
[AD-A153781] 18 p3177 N85-29690
Transport properties of Topopah Spring tuff
[DE85-010448] 19 p3270 N85-30278
Tectonic structure features of some deep faults in Atlantic and Pacific Oceans (according to deep seismic sounding-reflected waves method data)
19 p3295 N85-30428
Physical and chemical changes to rock near electrically heated boreholes at Spent Fuel Test-Climax
[DE85-010834] 19 p3302 N85-30472
Structural and tectonic history of the Goiconda allochton, southern Tolyabe Range, Nevada
19 p3312 N85-30529
Comparative study of fracture planes computed from topography and lineaments from imagery with structures and mineralization in the magnetic belt of Washington State
[DE85-010972] 20 p3477 N85-31606
Global Mega-Geomorphology
[NASA-CP-2312] 21 p3600 N85-32357
Andrean examples of mega-geomorphology themes
21 p3602 N85-32367
Lunar and Martian impact basins: Exposed records of terrestrial bombardment? 21 p3721 N85-33090
Earth's primordial differentiation, and its after-effects
21 p3722 N85-33092
Compressional environment in the location and orientation of planetary dorsa and terrestrial earthquake fault structures 22 p3857 N85-33885

Structural development of the west-central Grant Range, Nye County, Nevada 24 p4115 N85-35508
Crustal structure in southern California from array data 24 p4115 N85-35512

STRUCTURAL RELIABILITY
Studies on reliability of structural systems 02 p0206 N85-11362
Assuring structural integrity in Army systems [NASA-CR-175492] 11 p1651 N85-20398
Adomatic characterizations of continuum structure functions [AD-A149817] 12 p1866 N85-21706
Overview of structural response: Probabilistic structural analysis 17 p2912 N85-27952
Reactor pressure vessel steels ASME SA533B and SA508 C 1.2 [VTT-340] 22 p3794 N85-33507
Safety and reliability of steel structural materials under random service impact loads 23 p3906 N85-34197
Statistical pooling method of fatigue data for reliability design 23 p3906 N85-34198

STRUCTURAL RIGIDITY
U STRUCTURAL STABILITY

STRUCTURAL STABILITY
NT SHELL STABILITY
Effects of cobalt, boron, and zirconium on the microstructure of Udimet 738 [NASA-CR-174762] 01 p0027 N85-10166
Structural stability of nickel heat resistant alloys at high temperatures 03 p0350 N85-12251
Section 1. Method of determining mode shapes and natural frequencies of the NASA unmodified test structure. Section 2. Continuous beam closed from solution to the NASA-LSS astromast torsional vibration, appendix E 05 p0603 N85-13844
The problem of protecting the structure of a packet composite of optimal thinwall elements 10 p1444 N85-19101
Methodology for stress analysis of heavy metal plate 10 p1460 N85-19203
Influence of plastic deformation on structural stability of nichrome-tungsten composite materials 11 p1599 N85-20060
Stability of viscoelastic constructions subjected to steady random compressing loads 11 p1720 N85-20819
Behavior of buried flexible cylinders under the influence of nonuniform hoop compression [PB85-116523] 12 p1868 N85-21718
MSFC data analysis of the SAFE/DAE experiment 14 p2233 N85-23843
Langley Research Center photogrammetric measurements of solar array dynamics: Preliminary results 14 p2233 N85-23844
Structural changes with one- and two-stage aging of alloys Ti-Al-Mo-Fe and Ti-Zr-V-Al-Sn 15 p2499 N85-25415
USSR report: Engineering and equipment [JPRS-UEQ-84-006] 16 p2760 N85-27035
Stability of anisotropic cylindrical sandwich shells 16 p2766 N85-27065
Research in the field of rib stiffened shell stability 16 p2766 N85-27068
Structural stability and bifurcation in conical flow fields [VTH-LR-424] 16 p2803 N85-27282
Injection laser structure design [AD-A153210] 17 p2971 N85-28345
The Shock and Vibration Digest, volume 17, no. 1 [AD-A151051] 17 p2977 N85-28397
Continuum modeling of latticed structures 17 p2977 N85-28399
The Shock and Vibration Digest, volume 17, no. 2 [AD-A153129] 17 p2977 N85-28400
Recent progress in the dynamic plastic behaviour of structures, part 4 17 p2978 N85-28402
Constitutive modeling for blast-induced wave propagation [AD-A153576] 18 p3099 N85-29187
On the accuracy of modeling the dynamics of large space structures 19 p3225 N85-29995
The dynamics and control of large flexible space structures, 8 [NASA-CR-175986] 19 p3225 N85-29996
New directions in asymptotically stable finite-dimensional adaptive control of linear distributed parameter systems 20 p3412 N85-31177
Vibrational stabilization of flexible structures 20 p3414 N85-31188
A systematic plan for the continued study of dimensional stability of metallic alloys considered for the fabrication of cryogenic wind tunnel models [NASA-CR-172449] 21 p3585 N85-32172

STRUCTURAL STRAIN
Design sensitivity analysis of an antisymmetric angle-ply laminate [CSIR-TWISK-316] 01 p0021 N85-10128
Advanced fatigue monitoring on service aircraft 07 p0895 N85-15671
Experiences obtained from service fatigue monitoring exercises 07 p0895 N85-15672
CF-5 vertical stabilizer flight load survey 07 p0895 N85-15673
Tornado: Structural Usage Monitoring System (SUMS) 07 p0896 N85-15680
Flight parameters recording for structure fatigue life monitoring 07 p0896 N85-15682
A literature survey of ground load statistics for landing gear fatigue design purposes [FFA-TN-1984-39] 09 p1260 N85-18054
Modal analysis of structural systems involving nonlinear coupling 09 p1337 N85-18409
Fatigue-creep interaction in + or - 45 deg carbon-resin composites — aircraft construction materials [ONERA-RT/40/7086/M] 11 p1594 N85-20027
Optimal modeling with a minimum of local distortion [REPT-18/1984] 16 p2797 N85-27243
Multinomial form of the solution of problems of the statistics of elastic rectangular disks [REPT-17/1984] 16 p2797 N85-27244
Recent progress in the dynamic plastic behaviour of structures, part 4 17 p2978 N85-28402
Torsion-tension coupling in rods 18 p3120 N85-29315
Stored energy and structural failure [OUEL-1564/85] 20 p3471 N85-31567

STRUCTURAL VIBRATION
NT BENDING VIBRATION
NT FLUTTER
NT LINEAR VIBRATION
NT MISSILE VIBRATION
NT SELF INDUCED VIBRATION
NT SUBSONIC FLUTTER
NT SUPERSONIC FLUTTER
NT TORSIONAL VIBRATION
NT TRANSONIC FLUTTER
A rigid body mechanism in structural dynamics 02 p0206 N85-11361
Power flow between non-conservatively coupled oscillators [ISVR-TR-125] 02 p0209 N85-11377
Simulation of vibration processes in damped structures with allowance for temperature-frequency characteristics of vibration absorbing materials 02 p0257 N85-11680
Normal mode method of solving problem forced oscillations of rib-reinforced shell of revolution in liquid 02 p0273 N85-11781
Theoretical and experimental modal analysis of a rotor test rig — shipboard equipment [AMTE(N)-TM-83079] 03 p0371 N85-12370
Comparison of free component mode synthesis techniques using MSC/NASTRAN [DE84-014451] 04 p0514 N85-13278
Response measurements for two building structures excited by noise from a large horizontal axis wind turbine generator [NASA-CR-172482] 04 p0558 N85-13552
Definition of ground test for Large Space Structure (LSS) control verification, appendix G 05 p0603 N85-13845
The Shock and Vibration Digest, volume 16, no. 11 [AD-A148486] 08 p1171 N85-17382
Modelling and identification of the structural properties of an astromast [CRC-1374] 09 p1329 N85-18352
The Shock and Vibration Bulletin 54. Part 1: Welcome, keynote address, invited papers MIL-STD-810D, MIL-STD-810D panel session [AD-A148131] 09 p1333 N85-18377
Keynote address 09 p1333 N85-18378
Least favorable response of inelastic structures 09 p1336 N85-18398
Leakage-flow induced vibrations of a chimney structure suspended in a liquid flow — nuclear reactors 09 p1339 N85-18420
Assessing expired fatigue life in large turbine shafts [DE84-016676] 09 p1340 N85-18427
Flow-induced tube vibration thresholds in heat exchangers from shellside water tests [DE84-006603] 11 p1652 N85-20407
The effect of an elastic foundation and of dissipative forces on the stability of fluid conveying pipes [TAE-563] 12 p1863 N85-21688
Planar dynamics of a uniform beam with rigid bodies affixed to the ends [NASA-CR-175586] 12 p1864 N85-21693
A quantitative comparison of active and passive damping for large space structures [UTIAS-TN-249] 13 p1998 N85-22524
Spline-based Rayleigh-Ritz methods for the approximation of the natural modes of vibration for flexible beams with tip bodies [NASA-CR-172566] 13 p2102 N85-23100
Applications of the conformal mapping method to the solution of mechanical vibrations problems 13 p2102 N85-23103
Structural dynamics analysis 14 p2233 N85-23838
MSFC data analysis of the SAFE/DAE experiment 14 p2233 N85-23843
Langley Research Center photogrammetric measurements of solar array dynamics: Preliminary results 14 p2233 N85-23844
La Recherche Aerospatiale Bimonthly Bulletin Number 1984-3, 220/May-June [ESA-TT-882] 16 p2695 N85-26636
Internal resonance in nonlinear vibrating systems [REPT-15/1984] 16 p2797 N85-27245
On the wind-induced vibrations of a mass-spring system [REPT-84-04] 17 p2981 N85-28428
Vibration/libration interaction dynamics during the orbiter based deployment of flexible members 20 p3411 N85-31171
Experimental and theoretical assessment of a new technique for the non-destructive evaluation of laminated panels [AD-A155622] 21 p3562 N85-32155
Fixed gain and adaptive techniques for rotorcraft vibration control [NASA-CR-177344] 22 p3728 N85-33111
Flutter clearance of the Schweizer 1-36 deep-stall sailplane [NASA-TM-85917] 22 p3729 N85-33118

STRUCTURAL WEIGHT
Ultralightweight oxygen container [PB84-220730] 01 p0036 N85-10226
Space shuttle external tank performance improvements: The challenge 08 p1094 N85-16916
A study of structural concepts for ultralightweight spacecraft [NASA-CR-175765] 16 p2730 N85-26848
Multi-kW solar arrays for Earth orbit applications [NASA-CR-171538] 20 p3406 N85-31139

STRUCTURES
Bounding the stochastic performance of continuum structure functions 2 [AD-A149458] 10 p1548 N85-19762

STRUTS
Stall elimination and restart enhancement device [AD-D011217] 01 p0010 N85-10082
Influence of strut cross-section on strut radiation of reflector antennas [FI-455-TBR-39] 03 p0357 N85-12295
Passive Orbital Disconnect Strut (PODS 3) structural test program [NASA-CR-177325] 08 p1113 N85-17020
Variable length strut with longitudinal compliance and locking capability [NASA-CASE-MFS-25907-1] 23 p3937 N85-34401

STS
U SPACE TRANSPORTATION SYSTEM

STS-1
U SPACE TRANSPORTATION SYSTEM 1 FLIGHT

STS-3
U SPACE TRANSPORTATION SYSTEM 3 FLIGHT

STS-4
U SPACE TRANSPORTATION SYSTEM 4 FLIGHT

STS-7
U SPACE SHUTTLE MISSION 31-C

STS-11
U SPACE SHUTTLE MISSION 41-B

STS-13
U SPACE SHUTTLE MISSION 41-C

STS-17
U SPACE SHUTTLE MISSION 41-G

STS-19
U SPACE SHUTTLE MISSION 51-A

STS-20
U SPACE SHUTTLE MISSION 51-C

STUDENTS
Project Explorer 02 p0154 N85-11041
Designing an expert system for training automotive electrical troubleshooting [AD-P003926] 02 p0246 N85-11606
Training guide for scientific and engineering trainees 1984 [AD-A147963] 08 p1198 N85-17542
Satellite communications and amateur radio 12 p1838 N85-21534
NASA Ames Summer High School Apprenticeship Research Program [NASA-TM-86006] 15 p2686 N85-26590
The impact of group processing on achievement in cooperative learning groups [AD-A153168] 17 p3001 N85-28551

Oral discussion, group-to-individual transfer and achievement in cooperative learning groups
[AD-A153209] 17 p3001 N85-28552
Summer High School Apprenticeship Research Program (SHARP) of the National Aeronautics and Space Administration
[NASA-CR-175791] 17 p3046 N85-28849
STUDIES
U INVESTIGATION
STURM-LIOUVILLE OPERATOR
U STURM-LIOUVILLE THEORY
STURM-LIOUVILLE THEORY
Spectral Theory of Sturm-Liouville Differential Operators: Proceedings of the 1984 Workshop
[DE85-009693] 20 p3520 N85-31890
STYRENES
NT POLYSTYRENE
Volatile organic emissions from adhesives with indoor applications
[DE84-015965] 05 p0620 N85-13966
Control technology for fiber reinforced plastics industry at AMF Hatteras Yachts, New Bern Division, New Bern, North Carolina
[PB85-109015] 10 p1460 N85-19196
Influence of hydrogen bonding in block copolymers and their blends 13 p2036 N85-22752
Damage development during low cycle fatigue of carbon-black loaded SBR
[DE85-006234] 15 p2519 N85-25533
Stabilized unsaturated polyesters
[NASA-CASE-NPO-16103-1] 18 p3078 N85-29043
SUBARCTIC REGIONS
Current inventory of anthropogenic carbon dioxide in the North Pacific Subarctic Gyre
[PB85-187938] 24 p4125 N85-35570
SUBASSEMBLIES
Multistage spent particle collector and a method for making same
[NASA-CASE-LEW-13914-1] 22 p3791 N85-33489
SUBCARRIER WAVES
U CARRIER WAVES
SUBCIRCUITS
U CIRCUITS
U SUBASSEMBLIES
SUBCRITICAL FLOW
Performance of two transonic airfoil wind tunnels utilizing limited ventilation 03 p0313 N85-12020
Method for growth of crystals by pressure reduction of supercritical or subcritical solution
[NASA-CASE-NPO-15772-1] 18 p3192 N85-29800
SUBDUCTION (GEOLOGY)
Oceanic plateaus, anomalous subduction, and the accretion of buoyant features at convergent margins 05 p0686 N85-14422
Kuril-Aleutian subduction 19 p3290 N85-30402
Thermal evolution of coastal California with implications for hydrocarbon maturation 24 p4115 N85-35509
A dynamic model of Venus's gravity field
[NASA-CR-176173] 24 p4169 N85-35845
SUBDWARF STARS
Observations of the O-type subdwarf eclipsing binary system LB 3459 (AA Dor) 01 p0128 N85-10881
Ultraviolet spectroscopy of selected astronomical sources
[NASA-CR-174379] 09 p1413 N85-18912
IUE and Voyager observations of very hot O-type subdwarfs 11 p1751 N85-21010
Analysis of high-depression IUE spectra of subdwarf B stars 11 p1751 N85-21011
Further investigation of mass loss phenomena in hot white dwarfs and O subdwarfs 11 p1751 N85-21014
Studies of hot B subdwarfs. Part 2: Energy distributions of three bright sdB/sdOB stars in the 950-5500 angstrom range
[NASA-CR-175854] 16 p2881 N85-27775
SUBGIANT STARS
Evidence for non-radiative activity in stars with T sub eff 10000 K 08 p1231 N85-17757
A search for white-dwarf companions of subgiant CH stars 11 p1752 N85-21019
SUBGRAVITY
U REDUCED GRAVITY
SUBJECTS
Energy data base: Subject categories and scope
[DE84-017376] 17 p3050 N85-28881
SUBLATTICES
U LATTICES (MATHEMATICS)
SUBLAYERS
U SUBSTRATES
SUBLIMATION
Synergisms in surface erosion, session summary 08 p0884 N85-15493
Synergistic effects related to surface composition, session summary 08 p0885 N85-15495
SUBLIMINAL STIMULI
Subliminal communication technology
[GPO-38-833] 05 p0822 N85-13979
SUBMARINE CABLES
Metallized synthetic cable
[AD-D011263] 05 p0628 N85-14023
SUBMARINES
The development of a method for the shock-resistant securing of large batteries in submarines 09 p1335 N85-18391
Research on ocean floor electrical surveys
[AD-A149831] 12 p1899 N85-21920
The body burden of organic vapors in artificial air trial measurements aboard a moored submarine
[AD-A149808] 12 p1910 N85-21988
Ventilation flow: Submerged 18 p3156 N85-29545
Preliminary results of an ALVIN dive program on active hydrothermal vents at the southern Juan de Fuca Ridge 24 p4106 N85-35454
SUBMERGED BODIES
NT DIVING (UNDERWATER)
NT UNDERWATER RESEARCH LABORATORIES
The low frequency behaviour of an immersed structure at a standstill in a high density fluid with free surface
[TP-1983-31] 13 p2103 N85-23105
SUBMERGING
Modernization of IDTs-6 ultrasonic installation
[BLL-M-35716-(5828.4)] 02 p0206 N85-11356
Comparison of simulation of weightlessness by Head Down Tilt (HDT) and Water Immersion (WI) 05 p0692 N85-14454
Hemodynamics and plasma arginine vasopressin during water immersion in normal man 05 p0693 N85-14458
Physics effects of accidental submersion of space power reactors in water
[DE85-005020] 15 p2650 N85-26344
SUBMERSIBLE AIRCRAFT
Robust rate control system designs for a submersible
[AD-A144792] 01 p0111 N85-10753
SUBMILLIMETER WAVES
Detection of submillimeter polarization in the Orion Nebula
[NASA-TM-86013] 04 p0579 N85-13700
Choice of orbit for scientific satellites: SIGMA, the submillimeter telescope — Ariane-borne gamma imagery satellite (SIGMA) 05 p0800 N85-13828
A new free electron laser using a relativistic beam with spiralling electron
[AD-D011318] 07 p0971 N85-16165
Far infrared and submillimeter observations of the giant planets 08 p1245 N85-17856
Far-infrared spectroscopy of interstellar gas 08 p1245 N85-17858
First results of submillimeter polarimetry 08 p1246 N85-17861
Instrumentation for submillimeter polarimetry 08 p1250 N85-17869
A new generation of sub mm telescopes, made of carbon fiber reinforced plastic 08 p1250 N85-17890
Absorption of radiation by water vapor in windows of relative transparency of 95-145 micrometer range 13 p2076 N85-22968
Submillimeter-band solid state distributed feedback laser 15 p2644 N85-26307
Submillimeter local oscillators for spaceborne heterodyne applications
[NASA-RP-1147] 19 p3226 N85-30005
Double photon excitation of high-Rydberg atoms as a long-lived submillimeter detector
[NASA-CASE-NPO-16372-1] 19 p3362 N85-30779
SUBREFLECTORS
Microwave surface resistivity of several materials at ambient temperature 10 p1463 N85-19226
Design procedure for the new 70-meter antenna subreflector positioner 10 p1463 N85-19232
Subreflector focusing techniques applied to new DSS-15 and DSS-45 34-meter antennas 10 p1464 N85-19233
Electromagnetic scattering by arbitrarily shaped reflectors: Subreflector efficiency
[AD-A149224] 15 p2541 N85-25687
SUBROUTINE LIBRARIES (COMPUTERS)
ZTL: A subroutine package for the IBM personal computer to support the Ziatech ZT1488 IEEE-488 controller
[LA-10141-MS] 12 p1913 N85-22010
TRANIO: A subroutine package for the IBM personal computer to support the transfer 6002 CAMAC crate controller
[LA-10145-MS] 12 p1914 N85-22015
Using MATHLIB on the IBM computer and sundry plotting examples with a taste of IMSL
[DE85-011395] 19 p3340 N85-30695
SUBROUTINES
Description and use of the single-color transmissometer plume diagnostic code A32CODE
[AD-A146181] 03 p0325 N85-12090
High altitude chemically reacting gas particle mixtures. Volume 2: Program manual for RAMP2 — rocket nozzle and orbital plume flow fields
[NASA-CR-171627] 07 p0916 N85-15802
On the generation of random variables for radar simulation purposes 07 p0939 N85-15947
Some scientific subroutines in LISP
[AD-A147889] 07 p1026 N85-16515
Computer center CDC libraries/NSRD (subprograms)
[AD-A148792] 08 p1206 N85-17593
Three-dimensional, direct and vectorized elliptic solvers for various boundary conditions
[AD-B088266L] 08 p1206 N85-17595
Calibration of thermocouples based on two state points of water and BS 4937; part 5, 1974 09 p1324 N85-18317
Solutions to structural dynamics problems 09 p1334 N85-18384
Modeling relationships using groups and items 09 p1367 N85-18591
Monitoring the execution of plans in SIPE (System for Interactive Planning and Execution) monitoring
[AD-A149136] 10 p1544 N85-19731
A computer system for generating single and double sampling plans for attributes data
[AD-A149548] 11 p1701 N85-20698
Standardized format for computer series
[PB85-109668] 11 p1705 N85-20724
DOS 21: PCDOS 2.0 support subroutine package for the IBM personal computer
[LA-10142-MS] 12 p1914 N85-22012
HGRAPH: A subroutine package for the IBM personal computer to support the Hercules Graphic Card
[LA-10144-MS] 12 p1914 N85-22013
ZTLCK: A subroutine package for the IBM personal computer to support the Ziatech ZT1488 real time clock
[LA-10146-MS] 12 p1914 N85-22014
Programs for dynamic loading of precompiled subroutine packages, especially for applications with the Watfiv compiler
[DFVLR-MITT-84-18] 12 p1917 N85-22035
BLAS (Basic Linear Algebra Subroutines), linear algebra modules and supercomputers
[AD-A151504] 15 p2628 N85-26199
A general purpose scatter storage subsystem and a comparison of hashing methods
[NASA-CR-175814] 16 p2845 N85-27542
Proposal for an extended set of FORTRAN Basic Linear Algebra subprograms
[DE85-007241] 16 p2848 N85-27562
A set of subroutines for masked three-dimensional plotting with rotations
[MEAH-33] 20 p3514 N85-31848
Evaluation and implementation of a functional microprogram generator
[AD-A155164] 21 p3674 N85-32823
A versatile computer package for mechanism analysis 23 p3924 N85-34314
Software for mechanism design 23 p3925 N85-34324
A quickly tested Pascal random number generator for microcomputers
[AD-A156059] 24 p4136 N85-35633
CRAYCDC
[NASA-CR-177374] 24 p4137 N85-35639
CDCCRAY
[NASA-CR-177375] 24 p4137 N85-35640
SUBSETS (MATHEMATICS)
U SET THEORY
SUBSIDENCE
Results from geopressured-geothermal subsidence studies
[DE84-016279] 09 p1354 N85-18520
Crustal stretching and subsidence in sedimentary eastern Switzerland and permo-carboniferous basins in the continental United States
[DE85-000822] 11 p1681 N85-20592
Evolution of the oceanic upper mantle and effects on sea floor subsidence geoid height and heat flow 19 p3319 N85-30575
SUBSONIC AIRCRAFT
Energy efficient engine component development and integration program
[NASA-CR-170034] 02 p0146 N85-10990
Technology developments for laminar boundary layer control on subsonic transport aircraft 08 p1071 N85-16787

SUBSONIC FLOW

PAN AIR: A computer program for predicting subsonic or supersonic linear potential flows about arbitrary configurations using a higher order panel method. Volume 3: Case manual (version 1.0)
[NASA-CR-3253] 02 p0135 N85-10022

Further development of a transonic cascade analysis
[AD-A145410] 02 p0196 N85-11319

Flow calculation on a thin wing, with specific attention to separation point at the trailing edge
[FTW-FO-1721] 05 p0594 N85-13787

PROGRAM VSAERO: A computer program for calculating the non-linear aerodynamic characteristics of arbitrary configurations: User's manual
[NASA-CR-166476] 06 p0749 N85-14602

Basic instability mechanisms in chemically reacting subsonic and supersonic flows
[AD-A148406] 08 p1122 N85-17071

Calculations for aerodynamic characteristics on a 3-D lifting body in a subsonic flow using boundary element method
[NAL-TR-835] 09 p1272 N85-17996

A locally linearized panel method for tran-/subsonic flow past an oscillating wing 11 p1622 N85-20212

Aerodynamic behavior of ventilated wind tunnel walls 13 p1968 N85-22363

Investigation of parabolic computational techniques for internal high-speed viscous flows
[NASA-CR-172555] 13 p2091 N85-23056

Approximate neutral point of a subsonic canard aircraft
[NASA-TM-86694] 15 p2462 N85-25205

Static and dynamic pressure measurements on a NACA 0012 airfoil in the Ames High Reynolds Number Facility
[NASA-TP-2485] 17 p2891 N85-27823

Propulsion efficiency of vibrating bodies in subsonic gas stream 17 p2942 N85-28159

Method of calculating separation flow of subsonic gas stream around wings 17 p2942 N85-28161

Supersonic flow around weak radiation sources 17 p2942 N85-28162

On the evaluation of boundary layer measurements on boattailed bodies of revolution in axisymmetric compressible subsonic flow
[ESA-TT-883] 20 p3457 N85-31471

A comparison of laser Doppler anemometry and probe measurements within the boundary layer of an airfoil at subsonic flow
[ISL-CO-219/84] 23 p3895 N85-34127

SUBSONIC FLUTTER

Numerical simulation of the subsonic wing-rock phenomenon 03 p0320 N85-12064

SUBSONIC SPEED

Empirical formulas for the prediction of the base pressure of missile bodies at subsonic velocities
[DFVLR-FB-84-23] 03 p0316 N85-12044

Aileron effectiveness for a subsonic transport model with a high-aspect-ratio supercritical wing
[NASA-TM-85674] 07 p0898 N85-15695

Natural unsteadiness of a separation bubble behind a backward-facing step
[AD-P004176] 09 p1267 N85-17981

A computer program for the drag prediction of subsonic, turbine powered aircraft in the en-route configuration
[VTH-LR-412] 16 p2701 N85-26881

Analysis of unsteady pressure measurements on a supercritical airfoil with a harmonically oscillating trailing edge flap at subsonic and transonic speeds
[DFVLR-FB-84-49] 17 p2893 N85-27837

Subsonic and transonic aerodynamics of a wraparound fin configuration
[AD-A153646] 18 p3059 N85-28927

Empirical formulas for the prediction of the base pressure of missile bodies at subsonic velocities
[ESA-TT-893] 20 p3399 N85-31082

SUBSONIC WIND TUNNELS

Effect of boundary layers on solid walls in three-dimensional subsonic wind tunnels 03 p0313 N85-12023

Analytical modeling of circuit aerodynamics in the new NASA Lewis wind tunnel
[NASA-TM-86912] 07 p0897 N85-15688

Six-component strain gage block scale 167-6B. Part 1: Calibration, September 1983
[F+W-FO-1699] 07 p0968 N85-16143

Aeronautical facilities catalogue. Volume 1: Wind tunnels
[NASA-RP-1132] 10 p1426 N85-18991

Wall interference estimation of the NAL's two-dimensional wind tunnel
[NAL-TR-829] 10 p1426 N85-18992

Harbin's subsonic, transonic wind tunnel detailed 14 p2263 N85-24143

SUBSTANCES

U MATERIALS

SUBSTITUTES

Use of ion implantation to modify the corrosion behavior of metals
[AD-P003953] 02 p0286 N85-11869

General studies on composite materials. Evaluation of auxiliary products of national origin
[SNIAS-2500/DCI-PR/84] 03 p0326 N85-12101

Polyimide resin characteristics, test
[DGT-24.322] 04 p0479 N85-13049

Effects of heteroatom substituents on the properties of 1,2-dioxetanes
[AD-A148727] 09 p1290 N85-18100

The B2 aluminides as alternative materials
[NASA-TM-86937] 10 p1440 N85-19076

Partial replacement of chromium in austenitic stainless steels by molybdenum, copper, and vanadium, report of investigations 1984
[PB85-116508] 12 p1809 N85-21348

Substituent effects on the electrical conductivities of the phenazine derivatives
[NASA-TM-77792] 14 p2249 N85-23938

SUBSTITUTION

U SUBSTITUTES

SUBSTRATES

Acoustic resonator and method of making same
[DE84-014655] 01 p0116 N85-10792

Cleaning procedures of laser mirror substrates
[DFVLR-MITT-84-06] 05 p0640 N85-14106

Ultrasonic girth weld evaluation for aluminum substrate of spherical Kevlar-epoxy test specimens
[DE85-001592] 06 p0816 N85-15181

Elastodynamic stress intensity factors of an interface finite-width crack
[DE84-016908] 06 p0817 N85-15190

Substrate preparation for thin film deposition: A survey
[DE84-016119] 06 p0868 N85-15514

Deposition of titanium nitride coatings by reactive evaporation and electrically activated reactive evaporation
[BLL-TRANS-5043-(9091.9F)] 07 p0925 N85-15658

Slow wave circuit with shaped dielectric substrate
[AD-D011385] 07 p0945 N85-15986

Aluminum nitride insulator for 3-5 MIS (Metal-Insulator-Semiconductor) applications
[AD-A147842] 07 p1049 N85-16662

Stability of amorphous metals on semiconductor substrates
[DE84-017256] 09 p1295 N85-18134

Effects of MAR-M247 substrate (modified) composition on coating oxidation coating/substrate interdiffusion — protective coatings for hot section components of gas turbine engines
[NASA-CR-174851] 10 p1440 N85-19073

Adsorption thermodynamics and surface transport of metal catalyst poisons
[DE85-002866] 10 p1441 N85-19084

Investigation of welded interconnection of large area wraparound contacted silicon solar cells
[NASA-CR-174438] 10 p1509 N85-19519

Low temperature deposition of nickel films
[AD-D011568] 12 p1805 N85-21319

A process to produce fine line metallic collection patterns on semiconductors devices
[NASA-CASE-NPO-16413-1] 12 p1805 N85-21325

Distributed Gunn effect devices; a numerical analysis of microstrip circuits on thin active GaAs substrates
[FOA-C-30383-E] 12 p1837 N85-21527

Influence of substrate heating and thermal annealing on the surface crystallinity in single Si crystals implanted with high doses of (16)O
[DE85-005264] 13 p2164 N85-23428

High-temperature X-ray diffraction study of coating-substrate compatibility in yttria-coated graphite
[DE85-005916] 14 p2262 N85-24016

Investigation of the MBE growth of InSb and novel quantum well structures
[AD-A151014] 14 p2427 N85-24969

NASA welding assessment program
[NASA-CR-175882] 15 p2568 N85-25844

Investigation of basic characteristics of laser heating in thermoluminescence and of laser-stimulated luminescence
[AD-A152143] 16 p2790 N85-27212

Glassy metals: New highly resistant material
[BLL-BISI-TRANS-21764-(9022.06)] 17 p2926 N85-28049

Properties of chromate coatings formed on electrolytic zinc substrates
[BLL-BISI-TRANS-22349-(9022.06)] 17 p2926 N85-28052

The structure of ion plated films in relation to coating properties
[NASA-TM-87055] 18 p3085 N85-29085

Method for ultrasonic bonding to soft microelectronic substrates
[NASA-CASE-NPO-16087-1] 18 p3084 N85-29151

Investigation of superlattice device structures
[NASA-CR-3903] 18 p3094 N85-29152

Silicide conductors reliability research
[AD-A153768] 18 p3095 N85-29157

An experimental study of the pressure in a fast bottom beneath the apex of an overlying fluid wedge
[AD-A153618] 18 p3177 N85-29696

Integrated electrooptical components using dielectric substrates 18 p3187 N85-29767

Process for the epitaxial deposition of 3-5 compounds utilizing a binary alloy as the metallic source
[AD-D011663] 18 p3193 N85-29801

Glow discharge deposition at high rates using disilane
[DE85-010236] 19 p3263 N85-30235

Increased voltage photovoltaic cell
[NASA-CASE-NPO-16155-1] 19 p3303 N85-30475

Microwave SAW (Surface Acoustic Wave) monochromator
[AD-D011718] 21 p3590 N85-32311

Thin-film reliability and engineering overview 21 p3812 N85-32450

Rationale in the selection of corrosion protective coating systems 22 p3750 N85-33242

Thermoelectric generator and method for the fabrication thereof
[DE85-011650] 22 p3760 N85-33302

Electron beam enhanced surface modification for making highly resolved structures
[DE85-011609] 22 p3760 N85-33305

Effect of substrate moisture on growth and structure of corn leaf 22 p3824 N85-33692

Liquid crystal light valve structures
[NASA-CASE-MSC-20036-1] 22 p3847 N85-33826

Thermal barrier coating system
[NASA-CASE-LEW-14057-1] 24 p4072 N85-35233

Oxidation resistant slurry coating for carbon-based materials
[NASA-CASE-LEW-13923-1] 24 p4077 N85-35267

Wear-resistant coatings for tools intended for cold working
[BLL-RISLEY-TR-5040-(9091.9F)] 24 p4081 N85-35293

Advanced detectors and signal processing
[NASA-CR-176193] 24 p4088 N85-35343

Solid neon sources for plasma and X-ray lasers
[DE85-011347] 24 p4096 N85-35402

SUBSTRUCTURES

Damping synthesis for a spacecraft using substructure and component data
[CRC-1365] 03 p0323 N85-12082

Full-scale crash-test evaluation of two load-limiting subfloors for general aviation airframes
[NASA-TP-2380] 04 p0512 N85-13267

An effective substructure technique applied to crack problems 18 p3121 N85-29319

A substructure coupling procedure applicable to general linear time-invariant dynamic systems
[NASA-CR-176144] 22 p3800 N85-33542

SUBTROPICAL REGIONS

U TEMPERATE REGIONS
U TROPICAL REGIONS

SUBURBAN AREAS

A comparison of metropolitan and non-metropolitan employment characteristics: Indications of the size of non-metropolitan mobile communication services user classes
[NASA-CR-175648] 13 p2053 N85-22855

Assessment of the role of nitrogen oxides in nonurban ozone formation
[PB85-173680] 19 p3311 N85-30524

SUCROSE

The use of moments of momentum to account for crystal habits
[NASA-CR-3907] 20 p3421 N85-31232

SUCTION

Hybrid laminar flow control study
[NASA-CR-165930] 02 p0137 N85-10933

Approximate solution of a laminar flow over a flat plate with suction and pressure gradient
[AD-A145482] 02 p0196 N85-11321

Drag reduction due to boundary-layer control by combined blowing and suction 06 p1070 N85-16785

Design studies of thick laminar flow airfoils for low speed flight employing turbulent boundary layer suction over the rear part 06 p1070 N85-16786

Turbulent drag reduction research 06 p1071 N85-16788

Active and passive shock/boundary layer interaction control on supercritical airfoils 06 p1072 N85-16795

Air intake efficiency at zero speed and lip suction — jet engines
[BAE-KRS-N-GEN-303] 09 p1272 N85-17996

Calibration of sonic valves for the laminar flow control, leading-edge flight test
[NASA-TP-2423] 14 p2210 N85-23707
SUD AVIATION AIRCRAFT
NT CONCORDE AIRCRAFT
SUDAN
SIR-B analysis of the Precambrian shield of Sudan and Egypt: Penetration studies and subsurface mapping
08 p1145 N85-17219
SUDDEN IONOSPHERIC DISTURBANCES
Solar-geophysical data number 476, April 1984. Part 1: (Prompt reports). Data for March 1984, February 1984 and late data
[PB84-215060] 09 p1416 N85-18936
Solar flare and IMF sector structure effects in the lower ionosphere 11 p1664 N85-20486
Solar-geophysical data number 483. November 1984. Part 1: (Prompt reports). Data for October 1984, September 1984 and late data
[PB85-147692] 12 p1962 N85-22335
SUDDEN STORM COMMENCEMENTS
A simulation experiment of a rapidly developed medium scale cyclone 01 p0079 N85-10530
Solar-geophysical data number 479, July 1984. Part 1: (Prompt reports). Data for June 1984, May 1984 and later data
[NASA-CR-175542] 12 p1962 N85-22333
Observations during a magnetosphere substorm triggered by a Storm Sudden Commencement (SSC): A case study 14 p2361 N85-24588
Sudden Storm Commencement (SSC) associated hydromagnetic variations at geosynchronous altitude and on the ground 14 p2369 N85-24642
SUGAR BEETS
Multi crop area estimation in Idaho using EDITOR
[E85-10054] 06 p0827 N85-15251
SUGAR CANE
Development and testing of a rural credit supervision system at the level of counties and rural properties utilizing remote sensing techniques
[E85-10018] 02 p0217 N85-11431
SUGARS
NT GALACTOSE
NT GLUCOSE
NT PENTOSE
NT RIBOSE
NT SUCROSE
Production of butanol by fermentation in the presence of cocultures of clostridium
[NASA-CASE-NPO-16203-1] 24 p4071 N85-35227
SUITS
NT PRESSURE SUITS
NT SPACE SUITS
SULFATES
NT SODIUM SULFATES
The concentration of sulfate in broken cloud layers
[DE85-000228] 11 p1678 N85-20574
Applicability of laboratory kinetics studies to the evaluation of aqueous phase atmospheric oxidation of sulfur-4
[DE85-000586] 12 p1883 N85-21819
Studies of the mechanisms and rates with which nitrogen species are incorporated into cloud water and precipitation
[PB85-144350] 12 p1898 N85-21914
Chemical weathering of soils from the dry valleys of Antarctica: A terrestrial analog of Martian weathering processes 13 p2197 N85-23628
A comparative evaluation of the effects of acid precipitation, natural acid production and harvesting of cation removal from forests
[DE85-005254] 15 p2589 N85-25961
Qualitative and quantitative examination of the performance of regional air quality models representing different modeling approaches
[DE85-010508] 19 p3310 N85-30518
Sulfates in marine aerosols over the tropical Western Pacific Ocean 21 p3651 N85-32690
Granulometric study of the acidity and sulfate excess in marine aerosols 21 p3652 N85-32691
Geology and geochemistry of sulfide and sulfate deposition 21 p3656 N85-32723
Phototrophic bacteria and their role in the biogeochemical sulfur cycle 21 p3660 N85-32735
Sulfur reduction in sediments of marine and evaporite environments 21 p3661 N85-32742
Thermodynamic data for mineral technology
[PB85-184331] 22 p3803 N85-33560
Effects of H2S on molten carbonate fuel cells. Literature review on the impact of SO2 in the oxidant supplied to molten carbonate fuel cells
[DE85-011698] 22 p3808 N85-33586
Environmental surveillance at Los Alamos during 1984
[DE85-011886] 22 p3811 N85-33605
Effects of acid rain on forest nutrient status
[DE85-012486] 23 p3947 N85-34463
Throughfall rate and chemistry studies: Whiteface Mountain
[DE85-012407] 23 p3947 N85-34464
Incorporating meteorological data into receptor analysis: RAPS (Regional Air Pollution Study) revisited
[PB85-188944] 24 p4114 N85-35503
A new drawing technique for nylon 6 by reversible plasticization with iodine
[AD-A156272] 24 p4162 N85-36603
SULFATION
Molecular orbital studies in oxidation: Sulfate formation and metal-metal oxide adhesion
[NASA-CR-176070] 21 p3565 N85-32174
Adsorption of O2, SO2, and SO3 on nickel oxide. Mechanism for sulfate formation
[NASA-CR-176072] 21 p3565 N85-32175
SULFIDATION
Behavior of pressurized tubes of candidate alloys in a simulated low-Btu environment
[DE85-003403] 09 p1296 N85-18141
SULFIDES
NT BARIUM SULFIDES
NT CADMIUM SULFIDES
NT CALCIUM SULFIDES
NT CARBON DISULFIDE
NT COPPER SULFIDES
NT DISULFIDES
NT HYDROGEN SULFIDE
NT MOLYBDENUM DISULFIDES
NT POLYSULFIDES
NT PYRITES
NT TROILITE
NT ZINC SULFIDES
Research on electroluminescence in thin film yttrium oxysulfide
[AD-A146909] 07 p1037 N85-16582
Quality testing to the specifications of the Stahl-Eisen-Pruefblatt 1570/71 using an automatic image analysis system
[BLL-BISI-TRANS-22253-(9022.06)] 17 p2978 N85-28385
Lithium-alloy/iron sulfide battery design studies
[DE85-007991] 18 p3131 N85-29389
The global sulfur cycle
[NASA-TM-87570] 21 p3656 N85-32710
Sulfur diagenesis in marine sediments 21 p3656 N85-32721
Geology and geochemistry of sulfide and sulfate deposition 21 p3658 N85-32723
Sulfate-reducing bacteria: Microbiology and physiology 21 p3659 N85-32732
Structure and physiology of Beggiatoa and Thiothrix 21 p3659 N85-32734
Enrichments for phototrophic bacteria and characterization by morphology and pigment analysis 21 p3660 N85-32736
Interactions among sulfide-oxidizing bacteria 21 p3661 N85-32741
Sulfur reduction in sediments of marine and evaporite environments 21 p3661 N85-32742
Microbial communities and microprofiles of sulfide and oxygen of alum rock sulfur springs 21 p3661 N85-32746
Microbial colonization and growth on metal sulfides and other mineral surfaces 21 p3662 N85-32747
Thermodynamic data for mineral technology
[PB85-184331] 22 p3803 N85-33560
Special features of the fracture of ball-bearing steel close to non-metallic inclusion eutectics
[BLL-M-35809-(5828.4)] 23 p3914 N85-34258
Some geophysical guides to ore in southern and southwestern Alaska 24 p4103 N85-35436
Massive sulfide deposits from the southern Juan de Fuca Ridge 24 p4105 N85-35446
SULFONATES
An investigation of chemiluminescent reactions
[AD-A148460] 08 p1122 N85-17073
Luminescence probe studies of ionomers. 2. Steady-state measurements from sulfonated polyethylene and teflon membranes
[AD-A152233] 16 p2755 N85-27000
Development and evaluation of sulfonated polysulfone membranes for the zinc-ferricyanide battery
[DE85-009104] 24 p4090 N85-35357
SULFONES
Characterization of a thermoplastic polyimidesulfone
[NASA-TM-86358] 10 p1450 N85-19135
Characterization of acetylene-terminated resin cure states
[AD-A149463] 10 p1452 N85-19148
Process for preparing solvent resistant, thermoplastic aromatic poly(imidesulfone)
[NASA-CASE-LAR-12858-2] 11 p1610 N85-20124
Research to explore the feasibility of sultolanes as electrolytic solvents for rechargeable lithium batteries
[DE85-004345] 12 p1837 N85-21525
Fracture surface analysis in composite and titanium bonding: Part 1: Titanium bonding
[NASA-CR-175750] 15 p2502 N85-25434
Polyaromatic ether-sulfone-ketones with fluoro-substituted-p-cyclophane units as cross-linking sites
[AD-D011649] 17 p2933 N85-28105
Mechanical properties of aligned short carbon fiber reinforced PES and PI laminates
[ESA-TT-898] 20 p3422 N85-31240
Synthesis and properties of arylethersulfone thermoset systems
[AD-A154811] 21 p3569 N85-32198
SULFUR
Surface segregation of sulfur during oscillatory pin-on-plate wear studies of precious metal electrical contact alloys. 1: Friction and electrical contact resistance
[DE84-006662] 02 p0195 N85-11303
Mechanical properties of a leaded, resulfurized, rephosphorized steel in various thermo/mechanical conditions
[PB84-215454] 03 p0333 N85-12144
Determination of halogens and sulfur in organic compounds and polymers by combustion-ion chromatography
[DE84-016186] 05 p0614 N85-13921
Effects of heteroatom substituents on the properties of 1,2-dioxetanes
[AD-A146727] 09 p1290 N85-18100
Non-photochemical interactions of sulfur and nitrogen compounds in acid deposition
[DE84-016141] 10 p1513 N85-19548
Implications of the presence of S2 in cometary ice 11 p1760 N85-21072
Sulfur volcanoes on Io? 13 p2173 N85-23479
Sulfur oxygen processes on Io 13 p2173 N85-23481
Diagrams of chemical and electrochemical equilibria in the presence of oxygen and sulphur
[AD-A150929] 14 p2251 N85-23953
Trends of petroleum fuels
[DE85-000116] 14 p2263 N85-24023
Systematic nomenclature of the nitrogen, oxygen and sulfur functional polycyclic aromatic hydrocarbons
[DE85-007426] 17 p2916 N85-27974
Gas phase ion-molecule chemistry of carbon, nitrogen and oxygen compounds
[AD-A152876] 17 p2919 N85-27998
Part played by non-metallic inclusions during deformation and fracture of steel with different grain sizes
[BLL-BISI-TRANS-22321-(9022.06)] 17 p2928 N85-28072
Study of the explosive combustion of drops of sulphur at high temperatures
[HSE-TRANS-11182] 19 p3252 N85-30183
Advanced fuel cell development
[DE85-009662] 19 p3306 N85-30497
Sulfur activation at the Little Boy-Comet Critical Assembly: A replica of the Hiroshima bomb
[DE85-010261] 20 p3527 N85-31936
Theoretical studies of structure and stability of hydrates of atmospheric sulfur species 21 p3650 N85-32684
Variations of particulate sulfur concentrations in a coastal atmospheric environment in connection with the change of air masses origin 21 p3652 N85-32692
The global sulfur cycle
[NASA-TM-87570] 21 p3656 N85-32710
Sulfur transformations at the hydrogen sulfide/oxygen interface in stratified waters and in cyanobacterial mats 21 p3657 N85-32715
Cytochromes and iron sulfur proteins in sulfur metabolism of phototrophic bacteria 21 p3657 N85-32718
Carbon and sulfur cycling through geologic time 21 p3658 N85-32720
Ecophysiology of phototrophic sulfur bacteria in lakes: Vertical distribution of planktonic populations 21 p3658 N85-32722
Sulfur cycling in freshwater sediments 21 p3658 N85-32726
Some thoughts on GAIA and the sulfur cycle 21 p3658 N85-32727
Sulfur and carbon cycling in organic-rich marine sediments 21 p3659 N85-32729
Possible roles of manganese redox chemistry in the sulfur cycle 21 p3659 N85-32731
Phototrophic bacteria and their role in the biogeochemical sulfur cycle 21 p3660 N85-32735
The role of sulfur in osmoregulation and salinity tolerance in cyanobacteria, algae, and plants 21 p3660 N85-32736
Sulfur cycling and metabolism of phototrophic and filamentous sulfur bacteria 21 p3660 N85-32737

Anaerobic reduction of elemental sulfur by Chromatium vinosum and Beggiatoa alba 21 p3660 N85-32739
Sulfur Cycle 21 p3662 N85-32748
Multiphoton production and detection of atoms [AD-A155561] 21 p3702 N85-33000
A new analysis of cosmic ray isotopes at 3 GeV/n from HEAO3-C2 data [OG-4.3-6] 22 p3879 N85-34031
Circumstellar shells of late-type stars: A study at millimeter and infrared wavelengths 24 p4167 N85-36836

SULFUR COMPOUNDS
NT BARIUM SULFIDES
NT CADMIUM SULFIDES
NT CALCIUM SULFIDES
NT CARBON DISULFIDE
NT COPPER SULFIDES
NT DISULFIDES
NT HYDROGEN SULFIDE
NT MOLYBDENUM DISULFIDES
NT ORGANIC SULFUR COMPOUNDS
NT POLYSULFIDES
NT PYRITES
NT SODIUM SULFATES
NT SULFATES
NT SULFIDES
NT SULFONATES
NT SULFONES
NT SULFUR DIOXIDES
NT SULFUR FLUORIDES
NT SULFUR OXIDES
NT SULFURIC ACID
NT THIAZINE (TRADEMARK)
NT THIOLS
NT TROILITE
NT ZINC SULFIDES
Environmental Research Division report: Atmospheric physics [DE85-009859] 18 p3133 N85-29404

SULFUR DIOXIDES
Estimation of the potential and probable source regions for acid precipitation [DE84-015119] 02 p0225 N85-11472
Stability evaluation of sulfur dioxide nitric oxide and carbon monoxide gases in cylinders 11 p1648 N85-20387
Effect of elevated atmospheric CO2 on plant communities [DE85-001810] 11 p1678 N85-20576
National Acid Precipitation Assessment Program. Report to the President and Congress (1983) [PB85-116713] 11 p1679 N85-20581
Continued research in mesoscale air pollution simulation modeling. Volume 5: Refinements in numerical analysis, transport, chemistry, and pollutant removal [PB85-137362] 11 p1680 N85-20585
National Performance Audit Program ambient air audits of analytical proficiency [PB85-136204] 11 p1680 N85-20586
Evaluation of complex terrain air quality simulation models [PB85-119485] 12 p1808 N85-21635
Gas phase ion-molecule chemistry of carbon, nitrogen and oxygen compounds [AD-A152876] 17 p2919 N85-27998
Absolute calibrations of SO2 and NO analyzers by photographic methods [DFVLR-MITT-86-02] 17 p2994 N85-29504
Methods for simulating gas phase SO2 oxidation in atmospheric models [PB85-173110] 18 p3135 N85-29418
Qualitative and quantitative examination of the performance of regional air quality models representing different modeling approaches [DE85-010508] 19 p3310 N85-30518
Historic emissions of sulfur and nitrogen oxides in the U.S. from 1900 to 1980. Volume 1: Results [PB85-191195] 20 p3487 N85-31674
Historic emissions of sulfur and nitrogen oxides in the U.S. from 1900 to 1980. Volume 2: Data [PB85-191203] 20 p3487 N85-31675
Modeling of chemical transformations of SO(x) and NO(x) in the polluted atmosphere: An overview of approaches and current status [PB85-173169] 20 p3487 N85-31677
Experimental studies of the formation of Aitken nuclei in the atmosphere 21 p3644 N85-32641
Effects of H2S on molten carbonate fuel cells. Literature review on the impact of SO2 in the oxidant supplied to molten carbonate fuel cells [DE85-011698] 22 p3808 N85-33586
The 1984 environmental monitoring program report for Idaho National Engineering Laboratory site [DE85-011209] 22 p3812 N85-33611
Forecasting future industrial SO2 and NC/sub x/ emissions, revised 23 p3947 N85-34461
Throughfall rate and chemistry studies: Whiteface Mountain [DE85-012407] 23 p3947 N85-34464

SULFUR FLUORIDES
Recent advances in gaseous dielectrics [DE84-014279] 02 p0195 N85-11304
Green River air quality model development: Meteorological and tracer data, July/August 1982. Field study in Brush Valley, Colorado [DE84-014975] 02 p0225 N85-11474
The use of tracers for the study of atmospheric chemical and physical transformation processes [DE84-015267] 05 p0671 N85-14313
Transport and relaxation processes in supercritical fluids [DE84-006591] 05 p0731 N85-14698
Atmospheric wind and diffusion from analysis of an SF6 release at 350 km altitude [AD-A147965] 08 p1185 N85-17471
Pseudo-stationary oblique-shock-wave reflections in a polyatomic gas, sulfur hexafluoride [UTIAS-TN-253] 12 p1845 N85-21577
Predischarge parameters of SF6-CO2 determined by laser 15 p2564 N85-25821

SULFUR OXIDES
NT SULFUR DIOXIDES
Evaluation of recent SO/sub x/ and NO/sub x/ emission inventories [DE85-002649] 11 p1677 N85-20570
Reduction of pollutant formation in combustion processes [DE85-010181] 19 p3309 N85-30512
Safety of Li-SOCl2 cells 20 p3444 N85-31383
Adsorption of O2, SO2, and SO3 on nickel oxide. Mechanism for sulfate formation [NASA-CR-176072] 21 p3565 N85-32175
Environmental surveillance at Los Alamos during 1984 [DE85-011866] 22 p3811 N85-33605

SULFURIC ACID
Laboratory evaluation of microwave absorption properties under simulated conditions for planetary atmospheres [NASA-CR-174060] 02 p0303 N85-11960
Sulfuric acid chemical heat pump program, March - November 1982 [DE84-017436] 09 p1320 N85-18304
Solar thermochemical process interface study [NASA-CR-174442] 10 p1510 N85-19527
Study of the formation of sulfuric acid aerosols [DE85-008102] 17 p2922 N85-28011
Oxygen isotopic study of the oxidation of SO2 by H2O2 in the atmosphere [DE85-004017] 17 p2968 N85-28468
Rapid estimation of concentration of aromatic classes in middlestillate fuels by high-performance liquid chromatography [NASA-TP-2495] 20 p3434 N85-31307
Decomposition of sulfuric acid using solar thermal energy [DE85-012288] 21 p3564 N85-32170
Aerobic sulfur-oxidizing bacteria: Environmental selection and diversification 21 p3656 N85-32712
Synthesis of 2,4,8,10-tetroxaspiro5,5undecane [NASA-CASE-ARC-11243-2] 22 p3741 N85-33187
Determination of the viscosity number of thermoplastics in dilute solution; polyamides (PA) [NASA-TM-77673] 24 p4081 N85-35296

SUMMARIES
NT ABSTRACTS
Beyond fault trees to fault graphs [DE84-017022] 09 p1370 N85-18608
Summaries of FY 1984 engineering research [DE85-006273] 15 p2664 N85-26442
Experimental plasma research: Plasma summaries [DE85-008116] 17 p3039 N85-28605
Photovoltaic Systems Development Project: An activity summary [DE85-009994] 18 p3129 N85-29379
Activities at the Lunar and Planetary Institute [NASA-CR-175914] 18 p3201 N85-29859
Standards Committee activities of the National Bureau of Standards: 1984 highlights [PB85-183382] 19 p3350 N85-30764
A research program to reduce the interior noise in general aviation aircraft, index and summary [NASA-CR-176176] 24 p4145 N85-35695

SUMMER
Combining radar and satellite data for the localization and identification of summer convection 01 p0077 N85-10509
Forecast impact of components of the FGGE observing system 05 p0681 N85-14373
Structure and energetics of medium-scale atmospheric waves in the southern hemisphere summer 05 p0685 N85-14403
Sea breeze-induced mesoscale systems and severe weather [NASA-CR-174317] 08 p1187 N85-17480
The 500 millibar sign frequency teleconnection charts: Summer [PB85-111359] 11 p1686 N85-20613
Sector analysis of relevant meteorological parameters for long range transport of air pollutants [NR-27] 12 p1893 N85-21682
Collection and use of lightning strike data in the western US during summer 1983 [PB85-110534] 12 p1897 N85-21907
Variation of Arctic cloud cover in summer [DE85-004507] 13 p2139 N85-23285
The BALSAMINE experiment 14 p2236 N85-23676
Radiative forcing of the southwest summer monsoon (a satellite perspective) 15 p2593 N85-25981
The use of radar in determining precipitation processes in the BEWMEX area 16 p2831 N85-27455
Evaluation of the area and severity of last night's frosts [REPT-109] 16 p2833 N85-27473
Structure and energetics of medium-scale atmospheric waves in the Southern Hemisphere 20 p3489 N85-31685
Agricultural weather report for the IJsselmeer polders in the 1984 summer season; a verification report [KNMI-TR-61] 20 p3496 N85-31737
Aircraft observations of condensation and ice nuclei at a tropical station 21 p3640 N85-32613
Transport and formation of summertime cloud condensation nuclei over the Arctic Ocean 21 p3651 N85-32666

SUMS
On an algorithm for Pythagorean sums and its connection with continued fractions [NPL-DITC-42/84] 05 p0718 N85-14603
Sequential minimization for sum of squares of unknown functions [DE85-004162] 11 p1707 N85-20738

SUN
Estimating sunspot number [NASA-TM-86471] 01 p0130 N85-10896
Report on solar neutrino experiments [DE84-014567] 01 p0131 N85-10899
The mapping of the Sun at 8 mm wavelength and tracking of the active regions in the period 23 May - 5 June 1983 [REPT-S-149] 02 p0297 N85-11924
Active regions — and the Solar Maximum Mission [NASA-CR-170628] 02 p0304 N85-11985
Chlorine and bromine solar neutrino experiments [DE84-015720] 02 p0304 N85-11989
Time dependent effects at the foot of the chromosphere [NASA-CR-174143] 04 p0589 N85-13782
Structure and evolution of the large scale solar and heliospheric magnetic fields 05 p0746 N85-14782
Distribution of the K-corona over the polar regions of the solar disk: 1965-1983 [PB84-230077] 06 p0835 N85-15317
Local Interstellar Medium. International Astronomical Union Colloquium No. 81 [NASA-CP-2345] 06 p0872 N85-15539
Helium and hydrogen of the local interstellar mdium observed in the vicinity of the Sun 06 p0873 N85-15540
Absorption line studies and the distribution of neutral gas in the local interstellar medium 06 p0873 N85-15544
Synthesis of data on the local interstellar medium 06 p0874 N85-15545
Meteoritic constraints on processes in the solar nebula 06 p0887 N85-15630
Chemical evolution of the solar nebula: A new model 06 p0887 N85-15631
Dynamic thermal episodes in the protosolar nebula: Development of models from observations on CAI's 06 p0887 N85-15633
Solar He-3-rich events and non-relativistic electron events: A new association [NASA-TM-86179] 06 p0890 N85-15652
Variation in spectral response of soybeans with respect to illumination, view, and canopy geometry [E85-10040] 07 p0962 N85-16241
Spicules and surges [AD-A146765] 07 p1061 N85-16727
Sun-aligned polar cap auroral arcs [AD-A146052] 08 p1185 N85-17472
Extreme limb profiles of the Sun at far infrared and submillimeter wavelengths 08 p1244 N85-17852
Coronal and chromospheric physics — Sun, sunspots, and solar limb [NASA-CR-174290] 08 p1259 N85-17921
Evidence for a solar companion star [DE85-002089] 10 p1571 N85-19907

User's guide for the Nimbus 7 ERB Solar Analysis Tape (ESAT)
[NASA-TM-86143] 10 p1572 N85-19914
National solar-terrestrial research program, part 1. Solar-terrestrial research for the 1980's, part 2
[AD-A149542] 11 p1681 N85-20591
Herstmonceux observations of the Sun, planets and Moon, 1957 - 1982
[BULL-193] 11 p1762 N85-21087
Plasma and nuclear processes in solar matter
12 p1954 N85-22277
Helium atoms in interstellar and interplanetary space. II: Determination of direction of interstellar gas motion relative to Sun
13 p1980 N85-22425
Relationship between seismic status of Earth and relative position of bodies in sun-earth-moon system
14 p2345 N85-24499
Ionization equilibrium and equation of state in the solar interior
14 p2445 N85-25088
The hydromagnetics of the Sun --- conference
[ESA-SP-220] 14 p2445 N85-25091
Mixing in the solar interior 14 p2446 N85-25095
Did the young Sun rotate at 100 km/s
14 p2451 N85-25133
Solar magnetohydrodynamics: Symposium review
14 p2455 N85-25162
Apparent thickness of Saturn's rings from the observations of the ring plane crossing
15 p2671 N85-26477
Formation of the solar system
15 p2677 N85-26532
Evidence in meteorites for an active early Sun
15 p2680 N85-26550
Stokes parameters modulator for birefringent filters
18 p3205 N85-29884
The San Fernando Observatory video Stokes polarimeter 18 p3205 N85-29885
The new solar magnetograph for the Canary Islands Observatory THEMIS 18 p3205 N85-29886
Multichannel birefringent filter
18 p3206 N85-29888
Solar convection
[AD-A155214] 21 p3723 N85-33096
Heating of the deep chromosphere during solar flares
[AD-A155256] 21 p3723 N85-33100
Search for the north-south asymmetry in solar activity
[AD-A155525] 21 p3724 N85-33102
Terrain illumination conditions when taking scanning photographs from space 22 p3736 N85-33159
On the possibility of the determining the average mass composition near 10 to the 14th power eV through the solar magnetic field
[OG-5.1-9] 22 p3882 N85-34051
Coordinated study of solar-terrestrial payloads on space station
[NASA-CR-176160] 23 p3900 N85-34158
Soft X-Ray Telescope (SXRT)
23 p3900 N85-34159
Solar Ultraviolet Spectral Irradiance Monitor (SUSIM)
23 p3901 N85-34160
White Light Coronograph (WLC) and Ultra-Violet Coronal Spectrometer (UVCS) 23 p3901 N85-34161
High Resolution Telescope and Spectrograph (HRTS)
23 p3901 N85-34162
Active Cavity Radiometer (ACR)
23 p3901 N85-34163
Sidereal anisotropies in the median rigidity range 60-600GV in 1978-1983
[SH-4.4-3] 23 p4033 N85-35001
The sidereal semi-diurnal variation observed at high zenith angles at Mawson, 1968-1984, and the polarity of the solar main field
[SH-4.4-6] 23 p4033 N85-35004
A study of periodicities and recurrences in solar activity and cosmic ray modulation
[SH-4.4-14] 23 p4034 N85-35010
Results of ultra-low level 71ge counting for application in the Gallex-solar neutrino experiment at the Gran Sasso Underground Physics Laboratory
[SH-8.1-2] 23 p4049 N85-35108
Correlation between solar neutrino flux and other solar phenomena 23 p4049 N85-35109
A possible mechanism to cause the quasi-biennial variability on the solar neutrino flux
[SH-8.1-5] 23 p4049 N85-35110
The conjecture concerning time variations in the solar neutrino flux
[SH-8.1-6] 23 p4049 N85-35111
Solar neutrino: Flux, cosmic rays and the 11 year solar cycle
[SH-8.1-7] 23 p4049 N85-35112
Solar neutrinos, solar flares, solar activity cycle and the proton decay
[SH-8.1-8] 23 p4049 N85-35113
Neutrino production from the solar atmosphere
[SH-8.1-9] 23 p4050 N85-35114
Solar cosmic ray bursts and solar neutrino fluxes
[SH-8.1-10] 23 p4050 N85-35115
A silicon surface barrier telescope for solar particles identification
[SH-9.1-3] 23 p4050 N85-35118
Photometric and spectroscopic gamma-ray observations of solar transient phenomena using long duration balloons
[SH-9.1-5] 23 p4051 N85-35120
Monte Carlo calibration of the SMM gamma ray spectrometer for high energy gamma rays and neutrons
[SH-9.1-6] 23 p4051 N85-35121

SUN SENSORS
U SOLAR SENSORS

SUNLIGHT
Structure of temperature field based on observations of refraction from high meteorological mast
06 p0619 N85-15199
The temperature of a glass-encapsulated solar cell estimated from ambient air temperature and global radiation
[GKSS-84-E-36] 11 p1676 N85-20563
On the determination of the solar rotation and indications of the solar differential rotation from an analysis of solar integrated light 14 p2446 N85-25096
Terrestrial photovoltaic power systems with sunlight concentration
[DE85-008398] 17 p2987 N85-28464
Solar energy for highway uses
[DE84-015653] 18 p3130 N85-29382
Electricity from sunlight: The emergence of photovoltaics, revised edition
[DE85-002920] 19 p3307 N85-30502

SUNRISE
The investigation of short wave signal structure in the vicinity of the caustic by means of a high-directed antenna
[PR-194] 03 p0354 N85-12277
Computing worldwide sunrise, sunset, moonrise, moonset and twilight times using 5 WWPs 105-3 and 105-4
[AD-A148049] 08 p1189 N85-17490

SUNSET
The investigation of short wave signal structure in the vicinity of the caustic by means of a high-directed antenna
[PR-194] 03 p0354 N85-12277
Computing worldwide sunrise, sunset, moonrise, moonset and twilight times using 5 WWPs 105-3 and 105-4
[AD-A148049] 08 p1189 N85-17490

SUNSPOT CYCLE
Estimating sunspot number
[NASA-TM-86471] 01 p0130 N85-10896
Solar cycle variations of sunspot temperatures
14 p2452 N85-25141
Dependence of equatorial F-region plasma bubble rise velocity and dynamo electric field on solar cycle
[INPE-3439-PRE/806] 16 p2826 N85-27434
Magnetic and thermodynamic structure of the solar corona during sunspot minimum
18 p3203 N85-29873
Equitorial scintillations: Advances since ISEA-6
[AD-A154962] 21 p3631 N85-32559
Difference between even and odd 11-year cycles in cosmic ray intensity
[SH-4.2-22] 23 p4009 N85-34859
An update on the correlation between the cosmic radiation intensity and the geomagnetic AA index
[SH-4.2-24] 23 p4009 N85-34861

SUNSPOTS
Estimating sunspot number
[NASA-TM-86471] 01 p0130 N85-10896
Solar-geophysical data number 477, May 1984. Part 1: (Prompt reports). Data for April 1984, March 1984 and late data. Explanation of data reports issued as number 474 (supplement) February 1984
[PB84-225028] 01 p0131 N85-10901
Coronal and chromospheric physics --- Sun, sunspots, and solar limb
[NASA-CR-174290] 08 p1259 N85-17921
Geomagnetic disturbances caused by internal atmospheric dynamics 11 p1665 N85-20491
Oscillatory convection in sunspots
14 p2446 N85-25099
Linear models of acoustic waves in sunspot umbrae
14 p2450 N85-25130
Observational aspects of sunspot oscillations
14 p2451 N85-25131
The flux rope models checked by some observations --- solar activity 14 p2452 N85-25139
Solar cycle variation of ephemeral active regions
14 p2452 N85-25142
A siphon flow model for Evershed motion --- sunspot regions 14 p2453 N85-25147
Elementary sunspot energy model
15 p2476 N85-25287
Stokes parameters modulator for birefringent filters
18 p3205 N85-29884
Least squares inversion of Stokes profiles in the presence of velocity gradients 18 p3207 N85-29892
The effect of line damping, magneto-optics and parasitic light on the derivation of sunspot vector magnetic fields
18 p3207 N85-29895
Comparisons of simultaneous vector magnetograms
18 p3208 N85-29900
Solar cycle variation of ephemeral regions
[AD-A154967] 21 p3723 N85-33097
High Resolution Telescope and Spectrograph (HRTS)
23 p3901 N85-34162
Anomalous low level of cosmic ray intensity decreases observed during 1980
[SH-5.1-15] 23 p4043 N85-35068
Cosmic rays 10Be biennial data and their relationship to aurorae and sunspots
[SH-7.1-1] 23 p4047 N85-35094
Correlation between solar neutrino flux and other solar phenomena 23 p4049 N85-35109
Solar neutrino: Flux, cosmic rays and the 11 year solar cycle
[SH-8.1-7] 23 p4049 N85-35112
Solar neutrinos, solar flares, solar activity cycle and the proton decay
[SH-8.1-8] 23 p4049 N85-35113
Using the information of cosmic rays to predict influence epidemic
[SH-10.1-2] 23 p4053 N85-35134

SUPERALLOYS
U HEAT RESISTANT ALLOYS

SUPERCHARGERS
Ceramic turbochargers: A case study of a near-term application of high-strength ceramics
[DE85-006495] 17 p2975 N85-28379
Future of ceramic turbochargers: Promises and pitfalls
[DE85-006209] 17 p2975 N85-28380

SUPERCHARGING
U SUPERCHARGERS

SUPERCOMPUTERS
NT CRAY COMPUTERS
Supercomputers and VLSI: The effect of large scale integration on computer architecture
[AD-A145408] 02 p0239 N85-11555
Gauge Theory on a Lattice, 1984: Proceedings
[DE84-014858] 02 p0291 N85-11892
Development of the NLTSS operating system
[DE84-013702] 05 p0714 N85-14576
Vector computer memory bank contention
[NASA-CR-177342] 09 p1376 N85-18649
Computational plasma physics and supercomputers
[DE85-001739] 09 p1393 N85-18766
Developments in the simulation of compressible inviscid and viscous flow on supercomputers
[NASA-TM-86674] 11 p1575 N85-19924
Bottleneckology: Evaluating supercomputers
[DE85-005574] 13 p2145 N85-23315
Very large least squares problems and supercomputers
[AD-A151270] 15 p2623 N85-26162
Supercomputers and symbolic computation
[AD-A151376] 15 p2623 N85-26166
Role of supercomputers in energy research programs
[DE85-006865] 15 p2624 N85-26172
BLAS (Basic Linear Algebra Subroutines), linear algebra modules and supercomputers
[AD-A151504] 15 p2628 N85-26199
Lattice overview
[DE85-007282] 15 p2662 N85-26427
Recent advances in supercomputers
16 p2693 N85-26825
Computational plasma physics and supercomputers, revision 1
[DE85-007228] 16 p2867 N85-27687
France's use of Cray 1, plans for national supercomputer 18 p3066 N85-29093
Proceedings of the Argonne Workshop on Programming the Next Generation of Supercomputers
[DE85-008348] 19 p3343 N85-30718
The NAS kernel benchmark program
[NASA-TM-86711] 21 p3670 N85-32795
The impact of supercomputers on experimentation: A view from a national laboratory
[NASA-TM-86822] 23 p3965 N85-34510
Vector calculation of particle code
23 p3981 N85-34688

SUPERCONDUCTING MAGNETS
Materials studies for magnetic fusion energy applications at low temperatures, 7
[DE84-013487] 01 p0122 N85-10837
Superconducting magnet for probing eddy currents in dynamic models 04 p0489 N85-13117

Two-rotor alternators with superconductor field winding 06 p0795 N85-15082
High-performance TF coil design for the Toroidal Fusion Core Experiment (TFCX)
[DE85-001127] 08 p1159 N85-17315
Design and operating experience of an ac-dc power converter for a superconducting magnetic energy storage unit
[DE84-014041] 09 p1316 N85-18275
Fracture toughness of austenitic stainless steel weld metal at 4 K
[DE84-016638] 09 p1340 N85-18425
Computer simulation of multiple stability regions in an internally cooled superconducting conductor and of helium replenishment in a bath-cooled conductor
[DE85-002112] 09 p1399 N85-18805
Experience highlights from the design and manufacture of US LCT coils
[DE84-017504] 10 p1482 N85-19354
Application of NbN films to the development of very high field superconducting magnets
[DE85-002729] 10 p1585 N85-19667
Magnetic heat pump feasibility assessment
[DE85-002806] 11 p1632 N85-20278
Development of high field Nb-Ti accelerator dipoles
[DE85-000621] 11 p1714 N85-20782
Crossing point conditions, quadrupole gradients and drift space lengths
[DE85-003223] 11 p1721 N85-20825
Stability of superconducting composites in a magnetic field
[DE85-002731] 11 p1734 N85-20907
In-beam tests of an air-core superconducting-solenoid particle spectrometer
[DE85-004029] 12 p1853 N85-21625
Superconducting magnet technology for accelerators
[DE85-004192] 12 p1926 N85-22102
Design considerations for a 100 kW CW, 140 GHz gyrotron oscillator
[DE85-005282] 13 p2066 N85-22904
High-field dipoles for future accelerators
[DE85-002315] 13 p2157 N85-23391
Special purpose materials for fusion application
[DE85-005346] 14 p2424 N85-24950
Stability and vibrations of internal windings of high-current superconducting solenoid magnets
[AD-A151465] 15 p2656 N85-26390
Effect of superconducting solenoid model cores on spanwise iron magnet roll control
[NASA-TM-86378] 17 p2905 N85-27915
Experience with operation of a large magnet system in the international fusion superconducting magnet test facility
[DE85-006286] 17 p3027 N85-28721
Handbook on superconductivity: The large-scale applications. Chapter 4
[DE85-006170] 17 p3044 N85-28838
Reciprocating magnetic refrigerator employing tandem porous matrices within a reciprocating displacer
[NASA-CASE-NPO-16257-1] 18 p3085 N85-29082
Tokamak ignition/burn experimental research device
[DE85-009999] 18 p3190 N85-29785
High harmonic rectangular gyrotron
19 p3256 N85-30189
Computer studies of the quench behavior of an SSC model dipole
[DE85-010633] 19 p3360 N85-30829
Design of aggressive superconducting TFCX magnet systems
[DE85-010003] 19 p3376 N85-30943
Cryogenics for the Superconducting Super Collider: Workshop Proceedings
[DE85-010951] 20 p3437 N85-31327
Superconducting toroidal field coil current densities for the TFCX
[DE85-010285] 20 p3530 N85-31959
140 GHz gyrotron development program
[DE85-010348] 20 p3537 N85-32013
Design improvements and cost reductions for a 5000 MWh superconducting Magnetic Energy Storage plant
[DE85-010572] 22 p3847 N85-33830
Shield design for next-generation, low-neutron-fluence, superconducting tokamaks
[DE85-011409] 23 p3982 N85-34695
A high resolution gas Cerenkov detector for the superconducting magnet facility
[OG-9.1-6] 23 p4023 N85-34932
Enhanced heat transfer computations for internally cooled cable superconductor
[DE85-011897] 24 p4095 N85-35383
Effect of Cu4Ti compound formation on the characteristics of NbTi accelerator magnet wire
[DE85-014226] 24 p4159 N85-35788

SUPERCONDUCTING POWER TRANSMISSION
Operational test results of a prototype superconducting power transmission system and their extrapolation to the performance of a large system
[DE85-006731] 16 p2779 N85-27153
SUPERCONDUCTING QUANTUM INTERFEROMETERS
U SQUID (DETECTORS)
SUPERCONDUCTIVITY
NT KONDO EFFECT
Considerations regarding the choice of beam parameters and IP configuration for the SSC
[DE84-014532] 01 p0118 N85-10603
Low temperature properties of Mo/Mi superlattices
[DE84-014729] 02 p0288 N85-11881
Mossbauer effect and contactless conductivity studies of superconducting actinides intermetallics and hydrides. Mossbauer high pressure studies
03 p0430 N85-12743
Formation of superconductive Al(GeSi) alloys by low temperature laser quenching methods
[DE84-016667] 04 p0474 N85-13021
Strong-coupling superconductivity of Mg in proximity to Ta
[DE84-015462] 04 p0569 N85-13627
Report of the reference designs study group on the superconducting super collider
[DE84-015567] 04 p0589 N85-13630
Superconducting NbTi and Pb(Cu) bandpass filters
05 p0623 N85-13986
Phase diagrams of organic superconductors
[DE84-016219] 05 p0731 N85-14699
Actinides, the narrowest bands
[DE84-016463] 05 p0733 N85-14710
ASC 1984 Applied Superconductivity Conference
[DE84-016204] 06 p0868 N85-15521
Fast granular superconducting bolometer
[AD-D011332] 07 p0961 N85-16093
Electronic structure, chemical bonding, and superconductivity of silver films on germanium
[AD-A147720] 08 p1128 N85-17112
Structure-property relationships in intercalated graphite
[AD-A147849] 08 p1219 N85-17680
A superconducting quantum current standard
[NPL-QU-67] 08 p1224 N85-17710
The generation of rolling moments with the superconducting solenoid model
[NASA-CR-172520] 09 p1283 N85-18068
Status of RF superconductivity at Argonne National Laboratory
[DE85-002145] 09 p1312 N85-18245
Operational characteristics of a 1000 MVA superconducting power transmission system
[DE85-000232] 09 p1314 N85-18263
Characterization of Nb-8 wt % Al wires by analytical electron microscopy
[DE85-002726] 10 p1442 N85-19086
Metrology for Electronic Technology: A bibliography of NBS (National Bureau of Standards)
[PB85-112895] 12 p1830 N85-21486
Rotating squid magnetometers and gradiometers
[AD-D011529] 12 p1849 N85-21600
The UFe4P12 and CeFe4P12: Non-metallic isotopes of superconducting LaFe4P12
[DE85-003724] 12 p1942 N85-22195
Critical current measurements on an NbTi superconducting wire standard reference material
[PB85-118594] 13 p2066 N85-22906
Outlook for realization of proximity effect and Josephson direct current in helium-2 13 p2074 N85-22956
Microstructural study on the processing and properties of high-field A15 superconducting materials
[DE85-004652] 13 p2164 N85-23423
Synthesis and characterization of superconducting electronic materials
[AD-A151112] 15 p2659 N85-26409
Superconducting traveling wave accelerators
[DE85-006247] 15 p2661 N85-26424
Electronic transport in Mo/Ni superlattice
[DE85-006835] 15 p2661 N85-26425
The superconducting cavity stability ruby maser oscillator 17 p2967 N85-28324
Handbook on superconductivity: The large-scale applications. Chapter 4
[DE85-006170] 17 p3044 N85-28838
Simultaneous phase and frequency control of a three-phase inductor-convertor bridge
[DE85-006197] 18 p3096 N85-29164
Some comments on SSC physics
[DE85-008444] 18 p3179 N85-29712
Magnetic impurities in superconductors
[DE85-006372] 18 p3196 N85-29825
Magnetoconductance in aluminum films, wires, and cylinders 19 p3374 N85-30928
Critical current density and microstructural state of an internal tin multifilamentary superconducting wire
[DE85-009966] 22 p3761 N85-33308
Physics Division annual review, 1 April 1983 - 31 March 1984
[ANL-84-24] 23 p3969 N85-34602
Magnitude and range of the RKKy interaction in SmRh4B4
[DE85-012284] 23 p3985 N85-34712
Design considerations for personnel access penetrations for the superconducting super collider
[DE85-013027] 24 p4162 N85-35807
SUPERCONDUCTORS
Conversion of microwave signals by superconducting films in the resistive state
[NASA-TM-77595] 01 p0123 N85-10643
Experiments with phase transitions at very high pressure
[NASA-CR-174029] 02 p0172 N85-11148
Calculation of critical temperature for Nb-Cu multilayer film superconductor
[AD-A144321] 02 p0274 N85-11786
Theory of the double critical state in type-2 superconductors
[DE84-015461] 02 p0289 N85-11896
Radiation induced defects in superconductors of type 2
03 p0429 N85-12734
ASC 1984 Applied Superconductivity Conference
[DE84-016204] 06 p0868 N85-15521
Superconducting rotor dynamics
[AD-A147176] 07 p0947 N85-16000
Forces on neutral atoms due to electromagnetic fields
[AD-A146984] 07 p1040 N85-16603
Short range order-long range order in superconducting materials
[AD-A148764] 08 p1227 N85-17724
Subcable test facility
[DE85-002103] 09 p1315 N85-18269
Thermally induced quasiparticle branch imbalance in thin film superconductors 09 p1396 N85-18786
Computer simulation of multiple stability regions in an internally cooled superconducting conductor and of helium replenishment in a bath-cooled conductor
[DE85-002112] 09 p1399 N85-18805
Report of the Technology and Test Panel
11 p1646 N85-20370
Stability of superconducting composites in a magnetic field
[DE85-002731] 11 p1734 N85-20907
Thin film technology of high-critical-temperature superconducting electronics
[AD-A150010] 12 p1940 N85-22185
Measurement of the induced moment magnetic form factor of a heavy fermion superconductor
[DE85-004165] 12 p1942 N85-22194
Survey of the state-of-the-art of miniature cryocoolers for superconductive devices
[AD-A150319] 13 p2041 N85-22774
Critical current measurements on an NbTi superconducting wire standard reference material
[PB85-118594] 13 p2066 N85-22906
Spectral evaluation of irregularity of superconducting coaxial cables 13 p2082 N85-23000
Winding insulation in electromagnetic systems for Tokamak reactor plants 13 p2087 N85-23035
Improvement in magnetic field properties of vanadium-gallium superconductors by enhancement of spin-orbit scattering
[DE85-002693] 13 p2164 N85-23422
Tunneling in magnetic superconducting systems
[AD-A150677] 14 p2426 N85-24963
High field RF superconductivity: To pulse or not to pulse
[DE85-004381] 14 p2429 N85-24977
Superconducting gyroscope research
[NASA-CR-171406] 15 p2560 N85-25795
Stability and vibrations of internal windings of high-current superconducting solenoid magnets
[AD-A151465] 15 p2656 N85-26390
Synthesis and characterization of superconducting electronic materials
[AD-A151112] 15 p2659 N85-26409
Approximate closed-form expression for the electron-scattering-induced interaction between magnetic flux lines and grain boundaries
[DE85-004699] 15 p2660 N85-26417
Research on design of cryotransformers and its prospects for the future
[AD-A152400] 17 p2952 N85-28230
Research on superconductive signal-processing devices
[AD-A152703] 17 p2953 N85-28235
Measuring structure functions at SSC energies
[DE85-007515] 17 p3031 N85-28746
Operation of HFTF to test the MIT 12 T coil
[DE85-010409] 18 p3195 N85-29821

Magnetic impurities in superconductors
[DE85-008372] 18 p3196 N85-29825
Superconducting electronic film structures
[AD-A154196] 19 p3259 N85-30207
Flux pinning and flux flow studies in superconductors using flux flow noise techniques
[DE85-010814] 19 p3376 N85-30945
Detector problems at the SSC
[DE85-010217] 21 p3703 N85-33007
Cryogenic system for the University of Washington Superconducting Booster
[DE85-010604] 22 p3754 N85-33274
Magnetic shielding with superconductors based on niobium-tin compounds 22 p3771 N85-33370
Magnitude and range of the RKKy interaction in SmRh4B4
[DE85-012284] 23 p3985 N85-34712
Flux-line lattice anisotropy in V3Si: Observation and interpretation
[DE85-011935] 23 p3985 N85-34713
Center for Electronics and Electrical Engineering technical progress bulletin covering center programs, July-September with 1985 CEEE events calendar
[PB85-191393] 24 p4091 N85-35363

SUPERCOOLING

NT CRYOGENIC COOLING
Rapid solidification processing and the control of structure/property relationships
02 p0176 N85-11178
Frazil ice formation
[AD-A147425] 07 p0988 N85-16279
Alloy supercooling on Salyut-7
11 p1604 N85-20083
The nucleation of ice crystals during the freezing of large supercooled drops 21 p3640 N85-32608

SUPERCRITICAL AIRFOILS

NT SUPERCRITICAL WINGS
Effect of upstream sidewall boundary layer removal on an airfoil test — conducted in Langley 0.3-m transonic cryogenic tunnel 03 p0313 N85-12019
Steady- and unsteady-pressure measurements on a supercritical-wing model with oscillating control surfaces at subsonic and transonic speeds
[NASA-TM-84543] 08 p1077 N85-16831
Investigation to optimize the passive shock wave/boundary layer control for supercritical airfoil drag reduction
[NASA-CR-175788] 16 p2899 N85-26665
High Reynolds number tests of a NASA SC(3)-0712(B) airfoil in the Langley 0.3-meter transonic cryogenic tunnel
[NASA-TM-86371] 19 p3213 N85-29926
Pressure distribution from high Reynolds number tests of a NASA SC(3)-0712(B) airfoil in the Langley 0.3-meter transonic cryogenic tunnel
[NASA-TM-86370] 19 p3213 N85-29927
Data set 9: LANN wing. Pitching oscillation
20 p3390 N85-31030

SUPERCRITICAL FLOW

Performance of two transonic airfoil wind tunnels utilizing limited ventilation 03 p0313 N85-12020
Joined wing transonic design and test validation
[AD-A148355] 08 p1078 N85-16834
Supercritical fluid chromatography/supersonic jet spectroscopy
[DE85-003310] 09 p1292 N85-18115
Transport and relaxation processes in supercritical fluids
[DE85-002079] 09 p1398 N85-18797
Transport relaxation processes in supercritical fluids
[DE85-002076] 09 p1398 N85-18798
Nested subcritical flows within supercritical systems
[NASA-TM-86980] 12 p1845 N85-21574
Separating polymer solutions using high pressure LCST Lower Critical Solution Temperature) phenomena
[AD-A151536] 15 p2516 N85-25526
Static and dynamic pressure measurements on a NACA 0012 airfoil in the Ames High Reynolds Number Facility
[NASA-TP-2485] 17 p2891 N85-27823
Methods for design aerodynamics of modern transport aircraft
[DFVLR-FB-85-05] 17 p2893 N85-27838
Transport and relaxation processes in supercritical fluids
[DE85-010554] 19 p3358 N85-30616

SUPERCRITICAL FLUIDS

Transport and relaxation processes in supercritical fluids
[DE84-006581] 05 p0731 N85-14698
Electrochemistry in near-critical and supercritical fluids. I. Ammonia
[AD-A146429] 06 p0765 N85-14894
Transport and relaxation processes in supercritical fluids
[DE85-002079] 09 p1398 N85-18797
Transport relaxation processes in supercritical fluids
[DE85-002076] 09 p1398 N85-18798
Method for growth of crystals by pressure reduction of supercritical or subcritical solution
[NASA-CASE-NPO-15772-1] 18 p3192 N85-29800
Micro-scale methods for characterization of supercritical fluid extraction and fractionation processes
[DE85-010968] 20 p3455 N85-31456
Supercritical fluid chromatography/supersonic jet spectroscopy
[DE85-007005] 22 p3746 N85-33221

SUPERCRITICAL PRESSURES

Transport and relaxation processes in supercritical fluids
[DE84-006591] 05 p0731 N85-14698
Comparison of analytical and experimental steadyand unsteady-pressure distributions at Mach number 0.78 for a high-aspect-ratio supercritical wing model with oscillating control surfaces
[NASA-TM-84589] 07 p0899 N85-15697
Polymer solution-supercritical fluid behavior
[AD-A154514] 21 p3568 N85-32192

SUPERCRITICAL WINGS

Transonic wing and far field test data on a high aspect ratio transport wing for three dimensional computational method evaluation 01 p0004 N85-10021
Experimental trim drag values and flow-field measurements for a wide-body transport model with conventional and supercritical wings
[NASA-TP-2071] 02 p0135 N85-10920
Aileron effectiveness for a subsonic transport model with a high-aspect-ratio supercritical wing
[NASA-TM-85674] 07 p0898 N85-15695
Comparison of analytical and experimental steadyand unsteady-pressure distributions at Mach number 0.78 for a high-aspect-ratio supercritical wing model with oscillating control surfaces
[NASA-TM-84589] 07 p0899 N85-15697
Installed nacelle drag-improvement tests of an M = 0.8 turboprop transport configuration
[NASA-TM-84302] 07 p0902 N85-15716
Active and passive shock/boundary layer interaction control on supercritical airfoils 08 p1072 N85-16795
The NYU inverse swept wing code
[NASA-CR-3662] 08 p1077 N85-16830
Transonic steady- and unsteady-pressure measurements on a high-aspect-ratio supercritical-wing model with oscillating control surfaces
[NASA-TM-81868] 09 p1273 N85-18003
Subsonic and transonic pressure measurements on a high-aspect-ratio supercritical-wing model with oscillating control surfaces
[NASA-TM-83201] 09 p1273 N85-18004
Measured unsteady transonic aerodynamic characteristics of an elastic supercritical wing with an oscillating control surface
[NASA-TM-86376] 12 p1771 N85-21116
Unsteady transonic pressure measurements on a semi-span wind-tunnel model of a transport-type supercritical wing (Lann model). Part 2: Pressure distributions (plotted) and plots of the vibration modes
[AD-A130488] 12 p1846 N85-21579
Preliminary development of an approximation procedure for supercritical wing design optimization applications
[AD-A150177] 13 p1972 N85-22383
Transonic pressure distributions on a two-dimensional 0012 and supercritical MBB-A3 profile oscillating in heave and pitch 15 p2457 N85-25173
Analysis of transonic aerodynamic characteristics for a supercritical airfoil oscillating in heave, pitch and with oscillating flap 15 p2458 N85-25175
Experience with transonic unsteady aerodynamic calculations 15 p2458 N85-25176
The development of unsteady transonic 3-D full potential code and its aeroelastic applications
15 p2460 N85-25187
Aerodynamic research in preparation for a new Dutch transport aircraft with supercritical wings
[B6580077] 17 p2893 N85-27836
Analysis of unsteady pressure measurements on a supercritical airfoil with a harmonically oscillating trailing edge flap at subsonic and transonic speeds
[DFVLR-FB-84-49] 17 p2893 N85-27837
Pressure distribution data from tests of 2.29 M (7.5 feet) span EET high-lift transport aircraft model in the Ames 12-foot pressure tunnel
[NASA-TM-84517] 19 p3211 N85-29912
Low-speed tests of a high-aspect-ratio, supercritical-wing transport model equipped with a high-lift flap system in the Langley 4- by 7-meter and Ames 12-foot pressure tunnels
[NASA-TP-2097] 20 p3388 N85-31010
Transonic calculations for a flexible supercritical wing and comparison with experiment
[NASA-TM-86439] 20 p3388 N85-31012
An experimental investigation of propfan installations on an upswept supercritical wing at transonic Mach numbers
[NASA-CR-172805] 20 p3388 N85-31013
Extension of the small perturbations method in three-dimensional transonic, unsteady flow to the case of real wings
[ONERA-NT-17/3064-RY-070-R]
20 p3389 N85-31017
Verification of calculation methods for unsteady airloads in the precipitation of transonic flutter
[NLR-MP-84016-U] 20 p3390 N85-31027
The application of laser anemometry to the study of transonic shock boundary-layer interactions
[ISL-CO-204/84] 20 p3396 N85-31067
Study of boundary layer separation on a supercritical profile with a spoiler by means of a laser Doppler velocimeter
[ISL-CO-225/84] 23 p3895 N85-34128

SUPERFLUID FLOW

U SUPERFLUIDITY

SUPERFLUIDITY

Momentum distributions in superfluid helium: Bose condensate fraction
[DE84-014676] 05 p0731 N85-14700
Thermal and cryogenic design study for space infrared telescope facility (SIRTF)
[NASA-CR-166613] 07 p0915 N85-15793
Critical velocities in He II for independently varied superfluid and normal fluid velocities
09 p1396 N85-18784
Turbulence in pure superfluid flow
09 p1397 N85-18790
Germanium resistance thermometer calibration at superfluid helium temperatures
12 p1947 N85-22228
Outlook for realization of proximity effect and Josephson direct current in helium-2 13 p2074 N85-22956
Entropy of He 2 and universality near the superfluid in He(4) 19 p3378 N85-30957

SUPERGIANT STARS

Outer atmospheres of giant and supergiant stars
[NASA-CR-174165] 04 p0580 N85-13709
Theoretical studies of chromospheres and winds in cool stars
[NASA-CR-174204] 06 p0880 N85-15596
The spectroscopic antics of S 18/SMC
11 p1750 N85-21008
Ultraviolet analysis of the peculiar F supergiant HD 112374 11 p1754 N85-21035
Egress spectra of the new eclipsing supergiant 22 Vulpeculae 11 p1755 N85-21039
Multi-year and possibly periodic variations in the UV spectrum of 56 Pegasi 11 p1756 N85-21046
IUE and optical observations of LMC X-ray binaries
11 p1757 N85-21050
MU Sagittarii and Beta Lyrae: Combined IUE/Voyager observations 11 p1757 N85-21052
A search for the spectroscopic binary companions of Polaris using IUE spectra 11 p1757 N85-21053
Betegeuse at maximum luminosity
11 p1758 N85-21061

SUPERHEATING

An investigation into the superhardening effect in molybdenum-free steel with specific reference to alloy substitution 02 p0180 N85-11209
Anomalies of aluminum structure and properties
13 p2026 N85-22683
Vapor explosions in superheated liquids and fundamental studies of the physics of detonation
[AD-A151362] 15 p2504 N85-25447
Effects of ambient pressure on the instability of a liquid boiling explosively at the superheat limit
[DE85-009478] 23 p3932 N85-34370

SUPERHETERODYNE RECEIVERS

Construction of a superheterodyne receiver for 10 micron waves to be put on a Cassegrain optics telescope for spectroscopic research on the Mars and Venus atmospheres
[MPE-183] 06 p0872 N85-15838
High-frequency input device for superheterodyne radio receiver with wideband preselector
12 p1839 N85-21540

SUPERHIGH FREQUENCIES

Development and testing of a 20-kW X-band transmitter with high phase stability 05 p0623 N85-13985
Electrical consequences of mechanical antenna characteristics 05 p0625 N85-14006
The Finnish approach to microwave remote sensing of snow 05 p0656 N85-14212
Shuttle S-band communications technical concepts
08 p1099 N85-16948
Shuttle ku-band communications/radar technical concepts 08 p1099 N85-16949
Shuttle payload S-band communications system
08 p1100 N85-16950

TDRSS S-shuttle unique receiver equipment
08 p1100 N85-16951
Shuttle S-band high gain switched beam breadboard antennas
[NASA-CR-171852] 10 p1478 N85-19327
Description of amplitude scintillations on a 11 GHz slant path in terms of forward scattering from turbulent layers
[FI-455-TBR-76] 11 p1625 N85-20232
Minimization of system vulnerability in Naval satellite communication networks 11 p1710 N85-20758
Satellite reception of reentry vehicle telemetry
[AD-A151851] 15 p2492 N85-25372
Development and flight test of a helicopter, X-band, portable precision landing system concept
[NASA-TM-86710] 16 p2710 N85-26721
Radar study of the melting layer
[ESA-CR(P)-1974] 17 p2907 N85-28527
Channel multiplexers for broadcast satellite transponders in the 12 GHz band
[NHK-LABS-NOTE-310] 16 p3090 N85-29122
The HURRA, a high resolution experimental radar system broadband receiver
[FOA-C-30375-E1] 18 p3091 N85-29132
Measurement of permittivity and permeability of microwave materials
[AD-D011656] 18 p3176 N85-29688
Design of a shuttle-borne SAR for the DFVLR's planning study
[ERYS-019/84] 20 p3419 N85-31218
Paired ion chamber constants for fission gamma-neutron fields
[AD-A155069] 21 p3702 N85-32999
On total cross sections and slopes at superhigh energies
[HE-1.1-4] 24 p4170 N85-35852

SUPERHYBRID MATERIALS
NT GRAPHITE-EPOXY COMPOSITES
Fabrication and quality assurance processes for superhybrid composite fan blades
[NASA-TM-83354] 06 p0763 N85-14882

SUPERIMPOSITION (MATHEMATICS)
U SUPERPOSITION (MATHEMATICS)

SUPERLATTICES
Low temperature properties of Mo/Mi superlattices
[DE84-014729] 02 p0288 N85-11881
Folded acoustic and quantized optic phonons in semiconductor superlattices
[AD-A145935] 03 p0433 N85-12756
Electron and hole effective masses for two-dimensional transport in strained-layer superlattices
[DE84-016222] 04 p0570 N85-13637
Single crystal semiconductor multilayers for electrically active optical interference filters
[DE84-015614] 04 p0571 N85-13640
Photoluminescence studies of Ga(As,P) strained-layer superlattices
[DE84-015709] 05 p0731 N85-14701
InAsSb strained-layer superlattices (SLSs) for long wavelength detector applications
[DE84-016111] 05 p0732 N85-14706
Theoretical investigation of device aspects of semiconductor superlattices
[AD-A146641] 06 p0667 N85-15509
Strained-layer superlattice emitter and detector structures using modulation-doped active regions
[DE85-000064] 06 p0667 N85-15511
The growth and properties of semiconductor strained-layer superlattices
[DE84-012979] 06 p0668 N85-15515
Silicon superlattices. 2: Si-Ge heterostructures and MOS systems
[NASA-CR-174287] 08 p1224 N85-17711
Ionic and molecular transport in beta- and beta"-alumina
[DE85-000984] 09 p1380 N85-18680
Theory of silicon superlattices: Band structure and mobility enhancement 09 p1396 N85-18789
Semiconductor superlattice photodetectors
[NASA-CR-174347] 09 p1397 N85-18791
Radiation effects in Strain-Layer Superlattice (SLS) structures
[DE85-001713] 09 p1398 N85-18799
Effect of hydrostatic pressure on trapping centers in strained-layer superlattice structures
[DE85-001362] 09 p1399 N85-18807
Ion-implantation doping of strained-layer superlattices
[DE85-001903] 09 p1400 N85-18811
Ion implanted lateral in 2Ga 8As/GaAs strained-layer superlattice photodector
[DE85-001365] 10 p1563 N85-19859
Ferromagnetic resonance in a Ni-Mo superlattice
[DE85-003039] 11 p1735 N85-20911
Electronic structure of silicon superlattices
[NASA-CR-175536] 11 p1736 N85-20916
AlAs/GaAs superlattice barrier unipolar diode structure
[DE85-001904] 11 p1736 N85-20921
Evaluation of implantation-disordering of (InGa)As/GaAs strained-layer superlattices
[DE85-003533] 12 p1942 N85-22200
Ion implantation disorder in strained-layer superlattices
[DE85-004466] 14 p2430 N85-24984
InGaAs/GaAs, Strained-Layer Superlattice (SLS), junction photodetectors, LED's, injection LASER's and FET's for optoelectronic IC applications
[DE85-001940] 14 p2430 N85-24986
Novel materials properties of strained-layer superlattices
[DE85-003676] 14 p2430 N85-24989
Strained-layer superlattices and strain-induced light holes
[DE85-003675] 14 p2431 N85-24990
Models of long-period superstructure
[DE85-007659] 16 p2751 N85-26981
Morphology of GaAs/sub 1-x/P/sub x/ superlattices grown by MOCVD and chloride VPE
[DE85-002944] 17 p3045 N85-28842
Theoretical investigation of material characteristics of semiconductor superlattices
[AD-A154126] 19 p3375 N85-30936
Doping superlattices in organometallic VPE InP
[AD-A155151] 21 p3710 N85-33029
Optical properties of heterostructures and superlattices
[AD-A156243] 24 p4162 N85-35802

SUPERMASSIVE STARS
Radiative ion beams: Hot stellar reactions in the laboratory
[DE85-001570] 11 p1722 N85-20833

SUPERNOVA REMNANTS
Non-local origin of a substantial portion of the soft X-ray background 06 p0677 N85-15567
Modelling the local interstellar medium as a supernova remnant in a multiphase gas 06 p0679 N85-15585
Non equilibrium ionization in the local hot bubble
06 p0679 N85-15587
X-ray spectra of supernova remnants
[NASA-TM-86169] 09 p1413 N85-18909
Combined ultraviolet studies of astronomical sources
[NASA-CR-174361] 09 p1413 N85-18910
Supernova remnants and the carbon abundance in M33 11 p1745 N85-20972
A soft X-ray survey of galactic supernova remnants with the Einstein Observatory 14 p2434 N85-25013
A rocket-borne X-ray observation of SN1006 with the imaging gas scintillation proportional counter
14 p2435 N85-25014
Interstellar Al-26 and excess Mg-26
15 p2660 N85-26551
Self-consistent models for the X-ray emission from supernova remnants 20 p3548 N85-32062
On some problems of gamma-astronomy
[OG-2.7-15] 22 p3873 N85-33988
Local interstellar medium and gamma-ray astronomy
[OG-3.1-1] 22 p3873 N85-33989
Excess gamma rays from the Loop I supernova remnant
[OG-3.1-10] 22 p3874 N85-33998
The electron spectra in the synchrotron nebula of the supernova remnant G 29.7-0.3
[OG-6.2-10] 22 p3889 N85-34109
Cosmic ray secondary nuclei and the structure of the galaxy
[OG-7.2-4] 23 p4014 N85-34878
On the cosmic ray diffusion in a violent interstellar medium
[OG-7.2-14] 23 p4015 N85-34881
Acceleration of cosmic rays in supernova-remnants
[OG-8.1-9] 23 p4018 N85-34899
Onion-shell model for cosmic ray electrons and radio synchrotron emission in supernova remnants
[OG-8.1-10] 23 p4018 N85-34900
Approximate supernova remnant dynamics with cosmic ray production
[OG-8.1-12] 23 p4019 N85-34901
Interstellar (Ne-22) as a possible source of the excess (Ne-22) in the galactic cosmic ray
[OG-8.2-12] 23 p4020 N85-34908
The origins of cosmic rays and quantum effects on gravity
[OG-8.2-15] 23 p4020 N85-34911

SUPERNOVAE
A search for low luminosity pulsars and its implications for the pulsar luminosity functions
02 p0296 N85-11919
Supernova envelope shock origin of cosmic rays: A review
[DE84-016479] 04 p0580 N85-13763
Iron core collapse models of Type 2 supernovae
[DE84-013909] 05 p0743 N85-14775
Research in nuclear astrophysics: Stellar collapse and supernovae
[DE84-015559] 05 p0743 N85-14776
Distances of local clouds from optical line observations 06 p0675 N85-15558
A model of the soft X-ray background as a blast wave viewed from inside 06 p0679 N85-15586
Processes and problems in secondary star formation
[DE85-003623] 12 p1960 N85-22322
A program of ground-based astronomy to complement einstein observations
[AD-A151111] 15 p2668 N85-26488
The soft X-ray background as a supernova blast wave viewed from inside: Solar abundance models
[NASA-CR-175767] 18 p2987 N85-27813
Spectral evolution of gamma-rays from adiabatically expanding sources in dense clouds
[OG-2.5-2] 22 p3869 N85-33959
Supernova explosion in dense clouds in the galaxy and the COS-B gamma-ray sources
[OG-2.5-3] 22 p3869 N85-33960
Diffuse galactic annihilation radiation from supernova nucleosynthesis
[OG-3.2-8] 22 p3875 N85-34004
Electrons and positrons from expanding supernova envelopes in dense clouds
[OG-6.2-9] 22 p3889 N85-34108
A very important process of nucleosynthesis in stars
[OG-7.1-11] 23 p4014 N85-34872
A numerical study of diffusive shock acceleration of cosmic rays in supernova shocks
[OG-8.2-2] 23 p4019 N85-34903
Do supernovae of type 1 paly a role in cosmic-ray production?
[OG-8.2-5] 23 p4019 N85-34905
The nucleosynthesis of deterium and helium-3
[OG-8.2-18] 23 p4020 N85-34914
Nuclear reactions in shock wave front during supernova events
[OG-8.2-19] 23 p4021 N85-34915
Propagation of injected cosmic rays under distributed reacceleration
[OG-8.3-3] 23 p4021 N85-34922
Propagation of cosmic rays and new evidence for distributed acceleration
[OG-8.3-5] 23 p4022 N85-34924

SUPEROXIDES
U INORGANIC PEROXIDES

SUPERPLASTICITY
Evaluation of the role of diffusion creep in superplastic deformation 01 p0021 N85-10127
Cavitation phenomenon in superplastic creep
[DE84-015484] 04 p0513 N85-13271
Cavitation phenomenon in superplastic creep
[DE85-001716] 10 p1441 N85-19083
Study of superplastic alloys based on Al-Zn-Ca
10 p1442 N85-19092
MBB uses superplastic forming, diffusion bonding for alloys 11 p1618 N85-20177
Dependence of superplastic flow on state of grain boundaries 13 p2025 N85-22689
Aluminum alloy ATs5K5 (5% Zn + 5% Ca) for superplastic forming 13 p2026 N85-22697
Characteristics and applications of superplastic materials for aeronautics
[MBB-BB-565/84-O] 16 p2673 N85-27727
Precision die forging of blades or gas turbines
17 p2940 N85-28148
Effects of annealing treatments on superplasticity in a thermomechanically processed Aluminum-10.2%Mg-0.52%Mn
[AD-A154414] 19 p3239 N85-30080
The effect of alloy additions on superplasticity in thermomechanically processed high magnesium aluminum-magnesium alloys
[AD-A155142] 21 p3567 N85-32184

SUPERPOSITION (MATHEMATICS)
A limit theorem for the superposition of renewal processes
[CWI-MS-R8408] 05 p0722 N85-14836
Magnetic field calculation for ideal conductors by method of equivalent currents 06 p0768 N85-15035
Mathematical modeling of wave fields by superimposition of boundary waves in reflected earthquake waves method 10 p1501 N85-19476
Normal mode calculations for fuselage type intricate structures by regarding them as systems with superposed constraints 13 p2048 N85-22817

SUPERPRESSURE BALLOONS
Location and data collection for long stratospheric balloon flights 14 p2326 N85-24377

SUPERSATURATION
Chemical engineering principles of constant temperature-constant supersaturation growth of potassium dihydrogen phosphate (KDP) crystals
[DE84-017081] 04 p0571 N85-13645

Use of principle of local equilibrium for assessing diffusional supersaturation during solidification of alloys [BLL-BISI-TRANS-22487-(9022.06)] 17 p2929 N85-28077
Experimental investigation of properties of ice-forming reagents 21 p3639 N85-32602
The effect of supersaturation, temperature and particle size on ice-nucleating ability of atmospheric aerosol 21 p3639 N85-32604
On the efficiency of the mechanism of ice particles formation in the vapor supersaturation field around a freezing droplet 21 p3639 N85-32606
Supersaturation apect A of Ice Nuclei at different locations in Europe and over the North-Atlantic 21 p3640 N85-32615
Supersaturation obtained in a condensation nucleus counter 21 p3642 N85-32624
Analysis of performance of dynamic thermal diffusion chamber 21 p3642 N85-32625
Critical supersaturations with respect to water for fast condensation-freezing ice nucleation 21 p3643 N85-32632
A simple model to investigate the activation process in waterclouds 21 p3649 N85-32675
Measurements of the critical supersaturation of 0.029 to 0.095 micron radius particles at Washington, District of Columbia 21 p3649 N85-32676
A relationship between cloud droplet size and CCN critical supersaturation 21 p3649 N85-32677
Fog activation and supersaturation 21 p3650 N85-32678

SUPERSONIC AIRCRAFT
NT B-70 AIRCRAFT
NT CONCORDE AIRCRAFT
NT F-8 AIRCRAFT
NT F-14 AIRCRAFT
NT F-15 AIRCRAFT
NT F-16 AIRCRAFT
NT F-17 AIRCRAFT
NT F-104 AIRCRAFT
NT F-106 AIRCRAFT
NT F-111 AIRCRAFT
NT JAGUAR AIRCRAFT
NT MIG AIRCRAFT
NT MIRAGE AIRCRAFT
NT MIRAGE 3 AIRCRAFT
NT RF-4 AIRCRAFT
NT SUPERSONIC TRANSPORTS
NT X-15 AIRCRAFT
An engine trade study for a supersonic STOVL fighter-attack aircraft, volume 1 [NASA-CR-166304] 02 p0133 N85-10910
F-7 supersonic day fighter viewed — Jian-7 aircraft 06 p0747 N85-14791
A-5 supersonic attack aircraft described — Qiang-5 aircraft 06 p0747 N85-14792
Details of export A-5 close-support aircraft given — Qiang-5 aircraft 06 p0748 N85-14793
Preliminary performance of a vertical-attitude takeoff and landing, supersonic cruise aircraft concept having thrust vectoring integrated into the flight control system [NASA-CR-172530] 10 p1423 N85-18977
Details of export A-5 close-support aircraft given 10 p1424 N85-18983
Some aspects of the design of a fly-by-wire flying control system for a supersonic V/STOL fighter aircraft [COLL-AERON-8413] 12 p1780 N85-21175
Study of an efficient long-range Mach 2.7 supersonic transport configuration concept [NASA-TM-86414] 21 p3554 N85-32110

SUPERSONIC AIRFOILS
Experimental and theoretical study of the longitudinal aerodynamic characteristics of delta and double-delta wings at Mach numbers of 1.60, 1.90, and 2.16 [NASA-TP-2433] 19 p3213 N85-29922
Effect of leading-edge load constraints on the design and performance of supersonic wings [NASA-TP-2446] 19 p3213 N85-29923
A theory of quasi-conical solutions of noninteger degree — flow fields on supersonic wings [UTH-LR-420] 20 p3390 N85-31024

SUPERSONIC BOUNDARY LAYERS
Development of artificially produced perturbations in supersonic boundary layer 21 p3683 N85-32879

SUPERSONIC COMBUSTION RAMJET ENGINES
Ramjets with supersonic combustion 07 p0918 N85-15817
Computational analysis of scramjet dual mode operation [NASA-CR-174250] 07 p0956 N85-16060
Langley Mach 4 scramjet test facility [NASA-TM-86277] 08 p1069 N85-16583
Investigation of parabolic computational techniques for internal high-speed viscous flows [NASA-CR-172555] 13 p2091 N85-23056

SUPERSONIC CRUISE AIRCRAFT RESEARCH
Supersonic cruise technology [NASA-SP-472] 18 p3057 N85-28912
Application of an aerodynamic analysis method including attainable thrust estimates to low speed leading-edge flap design for supersonic cruise vehicles [NASA-CR-165843] 19 p3212 N85-29918

SUPERSONIC DIFFUSERS
The role of convective perturbations in supercritical inlet oscillations 13 p2004 N85-22563

SUPERSONIC FLIGHT
Selection of air intake parameters for supersonic-flow operation 13 p2051 N85-22837
Supersonic cruise technology [NASA-SP-472] 18 p3057 N85-28912
China has developed a new version of fighter aircraft [AD-A155293] 21 p3555 N85-32118

SUPERSONIC FLOW
Implementation of the supersonic triplet singularity into the USTORE computer code [CSIR-NIAST-83/47] 01 p0001 N85-10006
PAN AIR: A computer program for predicting subsonic or supersonic linear potential flows about arbitrary configurations using a higher order panel method. Volume 3: Case manual (version 1.0) [NASA-CR-3253] 02 p0135 N85-10922
Study of the structure of turbulent shear flows at supersonic speeds and high Reynolds number [NASA-CR-174144] 04 p0452 N85-12865
Wall adaptation at Mach 1.2 — wind tunnel tests [ONERA-RTS-26/3075-AY-402] 04 p0453 N85-12873
Friction and heat exchange in laminar and turbulent boundary layers with axisymmetrical bodies exposed to heterogeneous supersonic flow 05 p0724 N85-14655
Numerical method for computing supersonic flow over wings of flight vehicles 05 p0725 N85-14659
Supersonic nonlinear potential analysis [NASA-CR-172456] 07 p0697 N85-15685
An investigation of vortex-induced aerodynamic characteristics of supersonic cruise configurations [NASA-CR-174299] 07 p0698 N85-15690
A second-order accurate parabolized Navier-Stokes algorithm for internal flows [NASA-CR-174258] 07 p0956 N85-16059
Recent advances in computational methods to solve the high-lift multi-component airfoil problem 08 p1068 N85-16774
First derivatives of flow quantities behind two-dimensional, nonuniform supersonic flow over a convex corner [NASA-TM-86272] 08 p1077 N85-16828
Basic instability mechanisms in chemically reacting subsonic and supersonic flows [AD-A148408] 08 p1122 N85-17071
A numerical study of several supersonic flows 09 p1272 N85-17995
A first-order Green's function approach to supersonic oscillatory flow: A mixed analytic and numeric treatment [NASA-CR-172207] 09 p1273 N85-18002
Microwave discharge in a supersonic flow for the excitation of a gas dynamic CO laser [ESA-TT-833] 09 p1326 N85-18337
A shock wave capability for the Improved Two-Dimensional Kinetics (TDK) computer program [NASA-CR-171302] 10 p1483 N85-19360
Comparison of two-dimensional laser and hot-wire velocimetry for a supersonic turbulent boundary layer 11 p1576 N85-19927
LOVEL-84: A LOw-VELocity aerodynamic heating code for flat plates, wedges, and cones [DE85-002604] 11 p1576 N85-19933
Characteristics of flow of oscillatory-relaxing gas in nozzles with constant cross-sections in throat region 11 p1716 N85-20794
Determination of the drag of free flying particles in supersonic flow with a pulsed laser 12 p1773 N85-21129
The split-coefficient matrix method for supersonic three dimensional flow 12 p1821 N85-21425
Investigation of parabolic computational techniques for internal high-speed viscous flows [NASA-CR-172555] 13 p2091 N85-23056
Spectral methods for modeling supersonic chemically reacting flow fields [NASA-CR-172578] 14 p2300 N85-24240
Development of a theoretical model to describe the interaction between electric discharge and supersonic flow of a pulsed CO laser [DFVLR-FB-84-45] 14 p2310 N85-24301
A semi-empirical unsteady transonic method with supersonic free stream 15 p2458 N85-25179
A computer program to calculate the supersonic flow over a solid cone in air or water [AD-A151102] 15 p2464 N85-25217
Numerical calculation of subsonic jets in crossflow with reduced numerical diffusion [NASA-TM-87003] 15 p2472 N85-25283
Characteristics of heat exchange in the region of injection into a supersonic high-temperature flow [NASA-TM-77833] 15 p2555 N85-25782
An experimental and analytical study of the aerodynamic interference effects between two Sears-Haack bodies at Mach 2.7 [NASA-TM-85729] 16 p2700 N85-26673
Measurements of the symmetric aerodynamic coefficients for flat faced cylinders in the angle of attack regime 0 to 90 deg for transonic and supersonic speeds [FFA-TN-1984-04] 16 p2700 N85-26675
Supersonic flow around blunt wedge 17 p2942 N85-28158
Experimental and theoretical study of the longitudinal aerodynamic characteristics of delta and double-delta wings at Mach numbers of 1.60, 1.90, and 2.16 [NASA-TP-2433] 19 p3213 N85-29922
Effect of leading-edge load constraints on the design and performance of supersonic wings [NASA-TP-2446] 19 p3213 N85-29923
A first-order time-domain Green's function approach to supersonic unsteady flow [NASA-CR-172208] 19 p3214 N85-29930
A theory of quasi-conical solutions of noninteger degree — flow fields on supersonic wings [UTH-LR-420] 20 p3390 N85-31024
A supersonic potential gradient method for the calculation of unsteady aerodynamic pressures on harmonically oscillating wings [DFVLR-FB-85-11] 20 p3390 N85-31026
Requirements for attaining Treanor's distribution of vibrational energy among CO2 levels in CW gasdynamic laser flows [STN-3] 20 p3461 N85-31499
Use of a hyperbolic grid generation scheme in simulating supersonic viscous flow about three-dimensional winged configuration [NASA-TM-85344] 23 p3893 N85-34116
Instabilities in decelerating supersonic flows with applications to cosmic ray shocks [OG-8.1-2] 23 p4017 N85-34892
Finite analytic solutions of supersonic flows in two-dimensional non-symmetrical channels 24 p4059 N85-35154
Unsteady flow in a supersonic cascade with two in-passage shocks [NASA-CR-3925] 24 p4060 N85-35158
Supersonic flow with feeding of energy [NASA-TM-77912] 24 p4061 N85-35163
Deceleration of a supersonic flow behind a curved shock wave with isentropic precompression [NASA-TM-77920] 24 p4061 N85-35164

SUPERSONIC FLOW INLETS
U SUPERSONIC INLETS

SUPERSONIC FLUTTER
A comparison of measured and predicted unsteady pressure on a fan blade in unstalled supersonic flutter [PNR-90223] 08 p1079 N85-16839

SUPERSONIC INLETS
An inviscid computational method for supersonic inlets [AD-A145997] 03 p0316 N85-12042
A mixed finite difference analysis of the internal and external transonic flow fields of inlets with centerbody 11 p1619 N85-20192

SUPERSONIC JET FLOW
Density distribution in supersonic jet discharged into vacuum from nozzle with bevel tip 02 p0269 N85-11757
Aeroacoustic data for high Reynolds number supersonic axisymmetric jets [NASA-TM-86296] 07 p1038 N85-16587
Supercritical fluid chromatography/supersonic jet spectroscopy [DE85-003310] 09 p1292 N85-18115
Parametric study of autooscillation upon flow of supersonic jet into cylindrical cavity 16 p2765 N85-27060

SUPERSONIC NOZZLES
Calculation of an unsteady transonic flow with shock waves and separation in Laval nozzles [MPIS-14/1984] 14 p2213 N85-23728
An experimental study of clustered, two-dimensional rocket nozzles [AD-A151889] 15 p2495 N85-25390
Impact starting of plane nozzles with wide divergance angle 17 p2941 N85-28156

SUPERSONIC SPEEDS
Observations from varying the lift and drag inputs to a noise prediction method for supersonic helical tip speed propellers [NASA-TM-83797] 01 p0115 N85-10786

Supersonic Tactical Missile (STM) radome development
[AD-P004360] 12 p1825 N85-21454
Supersonic aerodynamic characteristics of canard, tailless, and aft-tail configurations for 2 wing planforms
[NASA-TP-2434] 17 p2891 N85-27822
Supersonic cruise technology
[NASA-SP-472] 18 p3057 N85-28912
Lee-side flow over delta wings at supersonic speeds
[NASA-TP-2430] 19 p3212 N85-29921
Two approaches for the prediction of plume-induced separation
[AD-A154099] 19 p3215 N85-29935

SUPERSONIC TEST APPARATUS
Analysis of heat-transfer measurements from 2 AEDC wind tunnels on the Shuttle external tank
[NASA-CR-171470] 17 p2957 N85-28263

SUPERSONIC TRANSPORTS
NT CONCORDE AIRCRAFT
Effects of leading-edge devices on the low-speed aerodynamic characteristics of a highly-swept arrow-wing
[NASA-CR-172531] 13 p1986 N85-22365
Supersonic cruise technology
[NASA-SP-472] 18 p3057 N85-28912
Study of an efficient long-range Mach 2.7 supersonic transport configuration concept
[NASA-TM-86414] 21 p3554 N85-32110

SUPERSONIC WAKES
Wakes and differential charging of large bodies in low Earth orbit 13 p1992 N85-22488
Periodic vortex shedding in the supersonic wake of a planar plate
[NASA-TM-77854] 15 p2463 N85-25207

SUPERSONIC WIND TUNNELS
Investigation of light source and scattering medium related to vapor-screen flow visualization in a supersonic wind tunnel
[NASA-TM-86290] 06 p0610 N85-15144
The S2MA wind tunnel at the Modane-Avrieux aerodynamic test center
[ESA-TT-862] 09 p1284 N85-18071
Aeronautical facilities catalogue. Volume 1: Wind tunnels
[NASA-RP-1132] 10 p1426 N85-18901
Transonic and supersonic wind tunnel tests on control effectiveness on schematic missile configurations
[FFA-TN-1983-20] 20 p3389 N85-31020
Transonic and supersonic wind tunnel tests on control effectiveness on schematic missile configurations: Supplement
[FFA-TN-1983-20-SUPPL] 20 p3389 N85-31021
Supersonic flow with feeding of energy
[NASA-TM-77912] 24 p4061 N85-35163

SUPERSONICS
Supersonic cruise technology
[NASA-SP-472] 18 p3057 N85-28912

SUPINE POSITION
Effect of body position and immobilization on intensity of spatial illusions in weightlessness 22 p3821 N85-33672
Investigation of spectrum of human bile acids during 120-day antiorthostatic hypokinesia 22 p3821 N85-33674
Vascular mechanisms of adaptation to antiorthostatic position 22 p3822 N85-33675
Cerebral hemodynamics and ventricular function in -15 deg antiorthostatic position 22 p3822 N85-33676
Effect of short-term antiorthostatic hypokinesia on dynamics of cardiorespiratory parameters during graded physical exercise 22 p3822 N85-33677
Investigation of some aspects of amino acid metabolism in man during brief exposure to antiorthostatic hypokinesia combined with ultraviolet radiation 22 p3822 N85-33678

SUPPLEMENTS
NASA Thesaurus supplement: A 3-part cumulative supplement to the 1982 edition of the NASA Thesaurus
[NASA-SP-7051(SUPPL-2)] 03 p0437 N85-12785

SUPPLYING
Chronic fuel shortages in Volga civil aviation administration 15 p2461 N85-25198

SUPPORT SYSTEMS
NT CLOSED ECOLOGICAL SYSTEMS
NT EMERGENCY LIFE SUSTAINING SYSTEMS
NT GROUND SUPPORT SYSTEMS
NT LIFE SUPPORT SYSTEMS
Air Force Human Resources Laboratory report: Fiscal year, 1983
[AD-A145647] 02 p0238 N85-11548
Constraint-based scheduling in an intelligent logistics support system: An artificial intelligence approach
[AD-A145613] 02 p0293 N85-11900
The human role in space. Volume 2: Research analysis and technology report
[NASA-CR-171224] 04 p0548 N85-13474
UH-60A external stores support system fixed provision fairings drag determination
[AD-A147188] 07 p0902 N85-15719
Acquisition planning at the Defense Communications Agency
[AD-A146877] 07 p1051 N85-16669
Lateral support system for canister-launched missile
[AD-D011369] 08 p1106 N85-16987
Close air support mission: Development of a unitary measure of pilot performance
[AD-A149285] 11 p1697 N85-20665
JESS facility modification and environmental/power plans
[NASA-CR-175685] 14 p2227 N85-23807
The development of a programming support system for rapid prototyping. Tasks 2 and 3
[AD-A151549] 15 p2629 N85-26202
Logical design of a decision support system to forecast technology, prices and costs for the national communications system
[AD-A152330] 17 p2948 N85-28198

SUPPORTS
NT PYLONS
Small Payload Flight Systems (SPFS) 02 p0152 N85-11030
The evolution of small payload carrier systems 02 p0153 N85-11038
Heavy duty precision pan and tilt head
[AD-A146669] 04 p0509 N85-13246
Dynamic testing of NOVA laser switchyard tower
[DE84-014450] 05 p0640 N85-14103
Thermally isolated structural support link
[AD-D011349] 07 p0972 N85-16176
Flexible line support assembly
[AD-D011391] 07 p0972 N85-16177
High efficiency electron beam gun foil support
[AD-D011494] 08 p1159 N85-17312
Two-dimensional shock response of a mass on energy-absorbing shock mounts 09 p1334 N85-18369
Optimum design for nonlinear shock mounts for transient inputs 09 p1334 N85-18390
Gear case vibration isolation in a geared turbine generator 09 p1338 N85-18414
Hydrostatic bearing pad maximum load and overturning conditions for the 70-meter antenna 10 p1465 N85-19241
Precise bearing support dithered
[AD-D011470] 10 p1493 N85-19428
Remote pivot decoupler pylon: Wing/store suppression
[NASA-CASE-LAR-13173-1] 11 p1584 N85-19981
Portable pallet weighing apparatus
[NASA-CASE-GSC-12786-1] 11 p1635 N85-20294
Support structures for optical components in the Laser Demonstration Facility
[DE85-008879] 17 p2971 N85-28349
Production of thin-walled electricity welded tubes with reduced internal flash
[BLL-BISI-TRANS-22381-(9022.06)] 17 p2973 N85-28364
Buckling and bracing of cantilevers
[CE-42] 17 p2979 N85-28413
Low-profile fastener
[AD-D011667] 19 p3280 N85-30343
Seismic pipe support construction practices
[DE85-901315] 19 p3287 N85-30366
Properties of Ti-6Al-4V spun formed fuze supports
[DE85-011968] 22 p3792 N85-33496
STACBEAM 2
[NASA-CR-176126] 23 p3944 N85-34442

SUPPRESSION
U RETARDING

SUPPRESSORS
NT ECHO SUPPRESSORS
Isolated load switching with surge suppression
[AD-D011218] 01 p0042 N85-10274
Reverse wave suppression in unstable ring resonator
[AD-A146825] 07 p0939 N85-15952
Development of a 30 GHz/1 kW broadband traveling wave tube with suppression of band edge oscillations
[BMFT-FB-W-84-035] 07 p0948 N85-16011
The ac power line protection for an IEEE 587 Class B environment 07 p1000 N85-16347
Improved operation of transversely exited N2O lasers
[AD-D011488] 10 p1490 N85-19409
Measurements of distributed combustion 13 p2001 N85-22542
Distributed combustion: A mechanism of acoustic suppression 13 p2001 N85-22543
The design and operation of a simple low-speed flutter-suppression model
[AD-A151610] 15 p2474 N85-25269
Suppression of vibration effects on piezoelectric crystal resonators
[AD-D011625] 16 p2778 N85-27142

SURFACE ACOUSTIC WAVE DEVICES
Conductor structure for thick film electrical device
[AD-D011240] 01 p0043 N85-10281
Radio frequency probing apparatus for surface acoustic wave devices
[AD-D011230] 01 p0050 N85-10327
Multiple passband transducers for tone selection from a frequency comb generator
[RSRE-MEMO-3647] 02 p0194 N85-11295
Laser excitation of coupled surface electromagnetic and acoustic waves and of static structures in solids 05 p0723 N85-14652
Dutch institutes do research in tactile visual robot sensors 09 p1310 N85-18226
Compensation of skew passband of a SAW filter using predistortion 12 p1821 N85-21422
Improvement of VHF(MB) model
[AD-A150087] 12 p1829 N85-21480
SAW oscillator with digital compensation for the temperature related frequency changes
[AD-D011537] 12 p1833 N85-21500
Monolithic thin film SAW (Surface Acoustic Wave) structures
[AD-A149782] 12 p1835 N85-21511
Optimal synthesis of surface acoustic wave filters 13 p2070 N85-22933
Analysis and optimization of parameters of fanned surface acoustic wave transducers 13 p2070 N85-22934
Experimental study of high-stability oscillator with surface-acoustic-wave resonator in feedback loop 13 p2090 N85-23053
Optical processing in radon space
[AD-A150289] 13 p2159 N85-23402
Surface acoustic wave structure and volume waves 15 p2525 N85-25568
System of phase-lock automatic frequency control with acoustoelectronic convolver 15 p2526 N85-25573
Development of a Digitally Compensated SAW Oscillator (DCSO) to provide temperature stable frequency
[AD-A151907] 15 p2549 N85-25730
Compensation of acoustic wave devices
[AD-D011582] 15 p2646 N85-26322
Vapor sensing by means of a ZnO-on-Si surface acoustic wave resonator
[DE85-003250] 15 p2646 N85-26324
Research and development of subsurface acoustic wave devices for sensor applications
[AD-A152197] 16 p2861 N85-27642
Derated application of parts for (Electronic Systems Division) systems development. Revision
[AD-A153299] 17 p2955 N85-28248
Passivation on high Q acoustic strain sensor for accelerometer
[AD-A153565] 18 p3177 N85-29695
Surface acoustic wave devices as chemical vapor microsensors
[AD-A153752] 18 p3177 N85-29696
Investigation of fast reaction SAW (Surface Acoustic Wave) accelerometer
[AD-A153876] 19 p3216 N85-29943
Gas sensing with surface acoustic wave devices
[DE85-009125] 20 p3524 N85-31921
Microwave SAW (Surface Acoustic Wave) monochromator
[AD-D011718] 21 p3590 N85-32311

SURFACE COOLING
Picosecond laser pulse interactions with metallic and semiconductor surfaces
[AD-A149112] 10 p1490 N85-19405
Unsteady heat transfer due to time-dependent free stream velocity 17 p2911 N85-27947

SURFACE CRACKS
Detection of cracks in a plastics pipe joint by reflection holography
[NPL-DMA(A)-87/MOM-70] 04 p0502 N85-13202
Behavior of pressurized tubes of candidate alloys in a simulated low-Btu environment
[DE85-003403] 09 p1296 N85-18141
Development of surface cracks in AMg6 alloy under low-cycle loading conditions 10 p1442 N85-19069
Evaluation of machining damage in brittle materials
[DE85-001794] 11 p1612 N85-20136
Modifications of flight by flight load sequences to provide for good fracture surface readability 14 p2319 N85-24330
On the use of marker loads and replicas for measuring growth rates for small cracks 14 p2319 N85-24331
On Rayleigh waves and Rayleigh wave extension of surface micro-cracks 15 p2572 N85-25860
Accuracy of the calculated stress field around a craze
[DE85-005520] 16 p2801 N85-27272

Field theory analysis using the finite element method to determine the deliberation curves of three dimensional fracture mechanics specimens with a semicircular surface crack applying the electrical direct current potential method for crack depth measurement
[GKSS-84-E-53] 17 p2982 N85-28434

SURFACE DEFECTS
Exploratory development of advanced surface flaw detection methods
[AD-A148757] 09 p1281 N85-18080
Low power microprocessor based measurements system for determining the integrity of coatings on buried pipelines
[ERS-E.380] 09 p1324 N85-18323
Defect tolerance in pipeline girth welds
[ERS-E.353] 09 p1326 N85-18347
GaAlAs Sb APD optimization
[AD-A149406] 10 p1480 N85-19344
Study of metal oxide semiconductor structures by capacitive transient spectroscopy
[ENST-84E011] 11 p1737 N85-20926
Correlation of uniaxial and biaxial fracture strengths of ceramics
[DE85-003779] 14 p2261 N85-24011
Practical surface methods 14 p2316 N85-24314
Study on mechanism of surface deformation induced by stress corrosion cracking
[BLL-BISI-TRANS-21696-(9022.06)] 17 p2928 N85-28066
On the variation of the stress intensity factor along the front of a surface flaw
[OUEL-1565/85] 20 p3471 N85-31568
Surface passivation and junction formation using low energy hydrogen implants 20 p3480 N85-31628
Redefining the scratch standards
[PB85-194736] 24 p4154 N85-35755

SURFACE DIFFUSION
Surface diffusion of high temperature vapors in porous alumina
[DE84-015966] 04 p0479 N85-13053
Technique for measuring surface diffusion by laser-beam-localized surface photochemistry
[DE85-007885] 18 p3113 N85-29273
Micro-reactions of metal contacts on various types of GaAs surfaces
[AD-A153650] 18 p3193 N85-29606
The use of the glistening surface concept in rough surface scattering
[AD-A154922] 21 p3575 N85-32234
An analysis of physical optics models for rough surface scattering
[AD-A154960] 21 p3575 N85-32235
Mean flow and turbulence in complex terrain
[AD-A155138] 21 p3636 N85-32583

SURFACE DISTORTION
An optimization study to minimize surface distortions of a hoop-column antenna 14 p2232 N85-23837
Electromagnetic analysis for surface tolerance effects on large space antennas 14 p2234 N85-23850
Lidar ER2 (ozone). Crystal characterization for harmonic conversion — laser systems
[CERT-2/6129-00] 16 p2872 N85-27717
Moving random surfaces and correlation analysis
[CRC-1384] 19 p3253 N85-30168

SURFACE EFFECT SHIPS
Detection, classification, and extraction of helicopter-radiated noise
[AD-A145993] 03 p0416 N85-12661
Analysis of head motion during simulated, rough water operation of a 2200 ton surface effect ship 11 p1695 N85-20656
Seakeeping and vibration tests of the Coast Guard 110 foot surface effect ship SEA BIRD class (WSES)
[AD-A154150] 19 p3252 N85-30166

SURFACE ENERGY
Numerical simulations of fuel droplet flows using a Lagrangian triangular mesh
[AD-A146087] 03 p0362 N85-12320
The chemical nature of the fiber/resin interface in composite materials 04 p0465 N85-12953
Effects of high energy radiation on the mechanical properties of epoxy-graphite fiber reinforced composites
[NASA-CR-174314] 08 p1118 N85-17047
Measurements of the surface energy budget in the southern Gobi Desert of China, and in the Rocky Mountains of Colorado
[NASA-CR-175506] 12 p1868 N85-21847
Fluorinated polyesters
[AD-D011611] 16 p2753 N85-26966
Fracture toughness of MgCr(sub)2O(sub)4-ZrO(sub)2
[DE85-007945] 17 p2917 N85-27982
New adatom model for Si(111) 7X7 and Si(111)Ge 5X5 reconstructed surfaces 20 p3480 N85-31625
Effect of precipitation variables on the specific surface and explosion characteristics of pentaerythritol tetranitrate
[DE85-009620] 23 p3922 N85-34302

SURFACE FINISHING
Electro-spark case-hardening of contoured surfaces 01 p0035 N85-10216
Publications of Center for Manufacturing Engineering (of the National Bureau of Standards), 1978-1983
[PB84-224526] 01 p0036 N85-10228
The use of ion implantation for materials processing
[AD-A145438] 02 p0287 N85-11873
DoD Robotics Application Workshop Proceedings
[AD-A145867] 03 p0307 N85-11978
Air force, robotic painting
[AD-P004006] 03 p0308 N85-11986
The development of CVD oxide coatings for the protection of metal surfaces — chemical vapor deposition (CVD) 03 p0332 N85-12142
Surface coatings for low emittance in the thermal surveillance band
[MRL-R-937] 03 p0336 N85-12158
Laser balancing system for high material removal rates
[NASA-CR-174731] 03 p0365 N85-12341
Contamination problems during surface cleaning for thermocompression bonding
[DE84-013066] 04 p0475 N85-13023
Ion beam and laser induced surface modifications
[DE84-016569] 04 p0571 N85-13642
A review of metallic surface treatments for corrosion mitigation
[AD-A146701] 06 p0769 N85-14918
Influence of shot-peening methods on surface quality and service life of bearings 06 p0776 N85-14960
Ceramic fabrication process before firing-surface treatment of ceramic powder
[NASA-TM-77437] 08 p1131 N85-17129
Process development for the production of technically high quality monocrystalline diamond grits
[BMFT-FB-T-84-204] 08 p1138 N85-17166
Initial investigation of cryogenic wind tunnel model filler materials
[NASA-TM-86363] 09 p1283 N85-18069
Antifriction nickel-phosphorous coatings on aluminum alloy products 09 p1309 N85-18221
Survey of the finish characteristics of machined optical surfaces
[DE85-001343] 09 p1385 N85-18706
Estimate of quality of aluminum alloy surface preparation for arc welding 10 p1449 N85-19128
Textured carbon surfaces on copper
[NASA-CASE-LEW-14130-1] 11 p1615 N85-20158
Diamondlike flakes
[NASA-CASE-LEW-13837-2] 12 p1796 N85-21267
Ion-beam nitriding of steels
[NASA-CASE-LEW-14104-1] 12 p1805 N85-21324
A process to produce fine line metallic collection patterns on semiconductors devices
[NASA-CASE-NPO-16413-1] 12 p1805 N85-21325
Sputter-induced compositional modifications in a Ni-Au alloy
[DE85-002771] 12 p1807 N85-21333
New application possibilities for clad steel by reducing surface treatment expenditure and by using improved welding technology
[BMFT-FB-T-84-236] 12 p1861 N85-21672
Innovative research in the design and operation of large telescopes for space: Aspects of giant telescopes in space
[NASA-CR-175626] 13 p2170 N85-23462
New technology of finish cutting teeth in large gear blanks 14 p2267 N85-24047
Laser surface treatments 14 p2308 N85-24284
Mechanical properties of TiN deposits obtained by PVD and TiN, TiC, TiC + TiN obtained by CVD
[BLL-RISLEY-TR-5097-(9091.9F)] 15 p2508 N85-25471
Electrochemical behavior of amorphous alloys based on iron, cobalt and nickel in H3PO4 solutions alone and mixed with HF 15 p2513 N85-25505
The influence of abrasive blast cleaning and corrosion inhibitors on protective paint coatings 15 p2517 N85-25522
New material, process spins off from Volvo LCP 2000 program 15 p2536 N85-25648
Investigation of silicon surface passivation by silicon nitride film deposition
[NASA-CR-175693] 15 p2585 N85-25938
Interaction of liquid crystals with inhomogeneous surfaces
[AD-A151557] 15 p2660 N85-26413
MOD silver metallization for photovoltaics
[NASA-CR-175773] 16 p2818 N85-27381
Surface modification of solids
[DE85-007543] 16 p2871 N85-27715
Corrosion characteristics of some steels produced through a self-cleaning rotating electrode
[BLL-BISI-TRANS-22046-(9022.06)] 17 p2925 N85-28034
Properties of chromate coatings formed on electrolytic zinc substrates
[BLL-BISI-TRANS-22349-(9022.08)] 17 p2926 N85-28052
Mechanical interactions of rough surfaces
[DE85-005853] 18 p3118 N85-29299
Atomized magnetism-aluminum protective coatings 19 p3244 N85-30116
New metal coating method developed 21 p3568 N85-32191
Reliability of void detection in structural ceramics using scanning laser acoustic microscopy
[NASA-TM-87035] 21 p3597 N85-32337
MOD silver metallization for photovoltaics 21 p3610 N85-32428
Implementation of polymer impregnation as a bridge deck sealant
[PB85-185718] 22 p3753 N85-33265
Performance improvements from surfacing in aero engine components
[PNR-90257] 23 p3897 N85-34142
Towards the development of technological processes for the preparation of cadmium plated steel articles
[BLL-M-36315-(5826.4)] 23 p3913 N85-34248
Results of tests of weathered K5NA closeout material in the MSFC Hot Gas Facility
[NASA-CR-170693] 24 p4073 N85-35239
Wear-resistant coatings for tools intended for cold working
[BLL-RISLEY-TR-5040-(9091.9F)] 24 p4081 N85-35293
Size and shape dependence of CO adsorption sites on sapphire supported Fe microcrystals
[NASA-CR-176171] 24 p4160 N85-35794

SURFACE GEOMETRY
Semianalytic modeling of aerodynamic shapes
[NASA-TP-2413] 12 p1771 N85-21120
A deformation analysis of flat flexible gear and its equation of original curved surfaces
[NASA-TM-77493] 12 p1859 N85-21660

SURFACE INTERACTIONS
U SURFACE REACTIONS

SURFACE IONIZATION
Computerized study of several electrostatic, surface-ionization ion-source configurations
[DE85-001512] 11 p1721 N85-20823
Sputter-induced compositional modifications in a Ni-Au alloy
[DE85-002771] 12 p1807 N85-21333
Ion emission from solid surfaces: Comparison of dust impact with other excitations — Giotto mission 14 p2244 N85-23912
A model of plasma cloud expansion generated by a dust particle impact — Giotto mission 14 p2245 N85-23914
Fluorescence quenching by metal semiconductor and insulator surfaces 19 p3374 N85-30929

SURFACE LAYERS
NT MONOMOLECULAR FILMS
The influence of surface layers on the friction and wear behavior of materials 01 p0054 N85-10357
Non-oxide ceramics: A new class of engineering materials 02 p0179 N85-11199
Characterization of amorphous surface layers in Fe implanted with Ti and C
[DE84-014960] 02 p0289 N85-11885
Thermomechanical cracking in layered media from moving friction load
[AD-A146022] 03 p0373 N85-12379
Aeroproyekt develops improved runway surfacing 08 p1068 N85-16770
Mossebauer study of amorphous Fe(67)Co(18)B(14)Si(1)
[AERE-R-11528] 11 p1737 N85-20928
The effect of Xe underlayers on the surface enhanced Raman scattering of pyridine on cold silver
[AD-A150109] 12 p1801 N85-21294
Some unique aspects of fouling on copper as compared to titanium or nickel
[AD-A150072] 12 p1808 N85-21332
Role of passive surface films on corrosion fatigue crack initiation
[DE85-000438] 14 p2257 N85-23905
Most important geochemical barrier zones in ocean (with example of Atlantic Ocean basin) 14 p2343 N85-24491
Fracture surface analysis in composite and titanium bonding: Part 1: Titanium bonding
[NASA-CR-175750] 15 p2502 N85-25434
The theoretical response of a vertical line array to wind-generated noise in shallow water
[AD-A151730] 16 p2860 N85-27838

Investigation of reaction layer formation in high-load capacity lubricating oils
[MPA-83-01] 17 p2975 N85-28381
A survey of the turbulence in the marine surface layer for the operation of low-Reynolds number aircraft
[AD-A154133] 19 p3316 N85-30558
Surface wave modes of a multilayered medium backed by a perfectly conducting ground plane: Computation of propagation constants
[DE85-011454] 22 p3829 N85-33715
Method of precisely modifying predetermined surface layers of a workpiece by cluster ion impact therewith
[DE85-006519] 23 p3984 N85-34710

SURFACE NAVIGATION
Terrain navigation concepts for autonomous vehicles
[AD-A144994] 01 p0005 N85-10031
NAVSTAR GPS (Global Positioning System) marine receiver performance analysis
[AD-A146414] 06 p0753 N85-14831
Use of three omega radionavigation system position lines for solving problems in marine geodesy
13 p2107 N85-23131
Checking on the position of navigation marker buoys by the ARGOS system 16 p2813 N85-27354

SURFACE PRESSURE
U PRESSURE

SURFACE PROPERTIES
NT ADHESION
NT ADSORPTIVITY
NT COEFFICIENT OF FRICTION
NT INTERFACIAL TENSION
NT SKIN TEMPERATURE (NON-BIOLOGICAL)
NT SPECTRAL REFLECTANCE
NT SURFACE CRACKS
NT SURFACE DEFECTS
NT SURFACE ENERGY
NT SURFACE ROUGHNESS
NT SURFACE STABILITY
NT SURFACE TEMPERATURE
NT WALL TEMPERATURE
Test measurements of the 100 m telescope at lambda = 7 mm
[TR-18] 01 p0129 N85-10890
Dynamics of growth of surface periodic structures when intense light acts on condensed media
02 p0268 N85-11748
Design of alternate launch and recovery surfaces for environmental effects
[AD-A145800] 03 p0320 N85-12066
Polycyclic aromatic hydrocarbons on the inner surfaces of copper tubing
[AD-A145979] 03 p0337 N85-12169
Vertical coherence along a macroray path in an inhomogeneous anisotropic ocean
[AD-A145992] 03 p0416 N85-12660
HgCdTe surface and defect study program
[AD-A146343] 03 p0434 N85-12764
Effect of a thermal gradient applied to a sinusoidal surface profile
[DE84-015849] 03 p0434 N85-12765
Surface diffusion of high temperature vapors in porous alumina
[DE84-015988] 04 p0479 N85-13053
Reflection of volume waves in multilayer structures
04 p0485 N85-13097
Surface structure determination with ARPEFS
[DE84-016904] 04 p0571 N85-13644
Biosphere/atmosphere interactions
05 p0679 N85-14364
Laser excitation of coupled surface electromagnetic and acoustic waves and of static structures in solids
05 p0723 N85-14652
Characterization of surface electronic properties of semi-insulating InP
[AD-A146553] 06 p0866 N85-15507
Solid state, surface and catalytic properties of oxides
[DE85-002096] 06 p0867 N85-15512
Surface studies of Nb, its compounds, and coatings
[DE84-017353] 06 p0868 N85-15516
Test your contacts by measuring their constriction resistance
[BLL-WH-611-(9091.9F)] 07 p0944 N85-15978
Effect of five lubricants on life of AISI 9310 spur gears
[NASA-TP-2419] 07 p0982 N85-16090
Theoretical study of laser-induced surface excitations on a grating
[AD-A147655] 07 p0972 N85-16172
Antisoiling technology: Theories of surface soiling and performance of antisoiling surface coatings
[NASA-CR-174274] 07 p0991 N85-16296
Preparation and evaluation of ZnSe and ZnS sub X Se sub 1-x epitaxial layers on Ge substrates for applications in surface passivation and heterojunction devices
[AD-A147432] 07 p1048 N85-16657
Optimization of technical catalysts with the help of surface analysis
[BMFT-FB-T-84-225] 08 p1124 N85-17066
Australian Multiexperimental Assessment of SIR-B (AMAS) 08 p1148 N85-17243
Investigations of vacuum ultraviolet and soft X-ray lasers
[AD-A148277] 08 p1167 N85-17358
Structure of solids surfaces in wear situations
[AD-A146480] 08 p1168 N85-17366
Research on nondestructive testing
[AD-A146375] 08 p1171 N85-17380
Determining grasp points using photometric stereo and the PRISM binocular stereo system
[AD-A147782] 08 p1222 N85-17607
Flow separation induced by periodic aerodynamic interference
[AD-P004174] 09 p1286 N85-17959
Surface mechanical properties and wear behavior of ion implanted TiB2
[DE85-001130] 09 p1295 N85-18133
Calculating heat transfer coefficients for turbine profiles taking surface curvature and elevated flow turbulence into account 09 p1307 N85-18212
Nondestructive characterization of semiconductor surfaces and interfaces 09 p1329 N85-18349
Effective antireflection coatings of transparent polymeric materials by gas-phase surface fluorination
[DE84-013027] 09 p1385 N85-18711
Surface and allied studies in silicon solar cells
[NASA-CR-175468] 10 p1508 N85-19516
Optical second harmonic generation for surface studies
[DE85-000670] 11 p1640 N85-20333
Classical rainbow scattering of alkali ions on metal surfaces. Application to the investigation of unknown surface structures
[MPIS-10/1984] 11 p1726 N85-20854
Measurement of the configuration of a concave surface by the interference of reflected light
[NASA-TM-77796] 11 p1726 N85-20867
Surface physics instrumentation
[AD-A149304] 11 p1726 N85-20869
Surface physics and crystallography
[DE85-003128] 11 p1735 N85-20910
Laser studies of chemical dynamics at the gas-solid interface
[DE84-017590] 11 p1736 N85-20920
Runway rubber removal specification development field evaluation procedures development
[FAA-PM-84-27] 12 p1781 N85-21179
Solar-assisted hydrogen generation by photoelectrocatalysis
[PB85-149706] 12 p1804 N85-21314
Tribological properties of boron nitride synthesized by ion beam deposition
[NASA-TM-86962] 12 p1810 N85-21355
Evaluation of corrosion-erosion behavior of various ceramic materials
[AD-A149756] 12 p1812 N85-21357
Surface-slip equations for multicomponent nonequilibrium air flow
[NASA-TM-85820] 12 p1845 N85-21573
Planar dynamics of a uniform beam with rigid bodies affixed to the ends
[NASA-CR-175566] 12 p1864 N85-21683
Problem of diffraction by wavy surface: Comparison of numerical methods of solution
13 p2079 N85-22985
Method for processing broad-profile data
13 p2117 N85-23185
Dipole active surface vibrational resonances on clean and hydrogen covered Ni(110)
[AD-A150546] 13 p2163 N85-23420
Study and estimation of planet-crossing asteroid populations: Discoveries and analysis
13 p2175 N85-23498
The olivine asteroids: Discovery, mineralogy, and relationship to palasites 13 p2175 N85-23500
Surfaces of asteroids and cometary nuclei
13 p2176 N85-23503
Venus surface composition from radio/radar measurements 13 p2177 N85-23509
Surface structures of Hawaiian lavas
13 p2186 N85-23566
Significant parameters of the behavior and of the surface damage of the lubricated Hertzian contact: An application to gears 14 p2222 N85-23783
Fatigue fracture topography 14 p2318 N85-24323
Determination of temperature and degree of roughness of sea and land surfaces by microwave radiometric polarization measurements 14 p2334 N85-24432
X-ray emission in heavy ion collisions
[DE85-006350] 14 p2419 N85-24927
Monte Carlo lattice models for adsorbed polymer conformation
[NASA-TP-2453] 14 p2426 N85-24961
Residual oxygen pressure in contact gap upon diffusion welding of titanium 15 p2499 N85-25418
Surface composition, properties and thermal stability of massive and fine metallic glasses
15 p2513 N85-25506
Mechanisms of buildup and properties of aluminum coatings on heat-resistant nickel alloys
15 p2513 N85-25508
Development of high-efficiency solar cells on silicon web
[NASA-CR-175707] 15 p2585 N85-25939
Threshold electron studies of gas-surface interactions
[AD-A151271] 15 p2647 N85-26328
Diagnostics of a glow discharge used to produce hydrogenated amorphous silicon films
[DE85-002914] 15 p2661 N85-26420
Secondary ion mass spectrometry studies of solids and surfaces
[AD-A151744] 16 p2745 N85-26939
Free-surface phenomena under low- and zero-gravity conditions
[NASA-CR-175835] 16 p2782 N85-27168
Inversion of Rayleigh wave group velocities from high-explosive tests
[AD-A152172] 16 p2783 N85-27175
Surface exploration geophysics applied to the Moon
[DE85-006714] 16 p2884 N85-27793
Interaction of high-cycle and low-cycle fatigue of Haynes 188 alloy at 1400 F deg 17 p2913 N85-27961
Coadsorption studies on transition metals
[PB85-183713] 18 p3072 N85-29003
Predicting microfracture in ceramics via a microcontract model
[DE85-005654] 18 p3081 N85-29060
Studies on surface processes during friction and wear
[AD-A153509] 18 p3117 N85-29296
Surface hydrologic characteristics of proposed repository locations in the Palo Duro Basin of the Texas Panhandle
[DE85-010530] 18 p3126 N85-29355
Effect of surface stats on durability of aluminized boron fibers 19 p3244 N85-30115
Moving random surfaces and correlation analysis
[CRC-1384] 19 p3253 N85-30168
Residual stress distributions in (plastically) surface deformed two-phase materials 19 p3283 N85-30358
Solid surface characterization by contact angle measurements
[FOA-C-40209-C,B2] 20 p3459 N85-31483
Nitridation of SiO2 for surface passivation
20 p3480 N85-31627
Using ship wake patterns to evaluate SAR (Synthetic Aperture Radar) ocean wave imaging mechanisms. Joint US-Canadian Ocean Wave Investigation Project
[AD-A154633] 21 p3573 N85-32223
Toward the theory of acoustic scattering on uneven free surface 21 p3680 N85-32862
Acoustic radiation from concentric shells containing an inner fluid
[AD-A155476] 21 p3700 N85-32991
Considerations of large scale impact and the early Earth 21 p3718 N85-33070
Solar cycle variation of ephemeral regions
[AD-A154967] 21 p3723 N85-33097
Anti wear property of two phasic metal composite
23 p3906 N85-34199
Infrared studies of the influence of alkali metals on the C-C bond in chemisorbed carbon monoxide
[DE85-005306] 23 p3911 N85-34232
Method for preparing hydride configurations and reactive metal surface
[DE85-006443] 23 p3917 N85-34274
Redefining the scratch standards
[PB85-194736] 24 p4154 N85-35755
Size and shape dependence of CO adsorption sites on sapphire supported Fe microcrystals
[NASA-CR-176171] 24 p4160 N85-35794
Electronic structure and lattice dynamics of dimensionally constrained and disordered solids
[AD-A155927] 24 p4161 N85-35797

SURFACE REACTIONS
Plasma surface interactions in magnetic fusion systems
[DE84-015255] 01 p0123 N85-10842
Surface production of negative hydrogen ions
[AD-A145437] 02 p0277 N85-11801
Ceramic powder for sintering materials
[NASA-TM-77434] 03 p0336 N85-12160
One-dimensional model of thin films. Analysis of aluminum surface 03 p0350 N85-12254
Comparison of wide aperture and short residence time ion lenses
[DE84-015274] 03 p0420 N85-12685

The 6th International Summer Institute in Surface Science 1983)
[AD-A146253] 03 p0434 N85-12762
Low energy ion-molecule reaction dynamics and chemionization kinetics
[DE84-015881] 04 p0559 N85-13562
Hydrogen absorption on (110) tungsten planes at 30 K: An atom-probe field-ion microscope study
[DE84-015659] 04 p0560 N85-13565
Effects of surface interactions and mechanical properties of PBXs (plastic bonded explosives) on explosive sensitivity
[AD-A146368] 06 p0773 N85-14944
Structure of adsorbed monolayers. The surface chemical bond
[DE84-016879] 06 p0861 N85-15471
Proceedings of Workshop on Synergistic Effects in Surface Phenomena Related to Plasma-Wall Interactions
[IPPJ-AM-35] 06 p0864 N85-15488
Synergistic effects in fusion machines, session summary 06 p0864 N85-15489
Plasma surface interaction processes and possible synergisms 06 p0864 N85-15490
Synergisms in hydrogen recycling, session summary 06 p0864 N85-15491
Steady state hydrogen transport in solids 06 p0864 N85-15492
Synergisms in surface erosion, session summary 06 p0864 N85-15493
Synergism in materials erosion due to multispecies impact 06 p0864 N85-15494
Synergistic effects related to surface composition, session summary 06 p0865 N85-15495
Effects of monolayer coverages on substrate sputtering yields 06 p0865 N85-15496
Plasma-surface interactions in large tandem mirror devices, MFTF-B
[DE85-001753] 06 p0865 N85-15499
Vibrational spectroscopy of chemisorption phenomena on model catalyst surfaces
[AD-A146753] 07 p0922 N85-15840
Phase-dissipative mechanisms for laser-induced surface desorption-dissociation processes
[AD-A147961] 08 p1121 N85-17065
Estimation of the rate of electron transfers between 2 contacting polymer surfaces
[AD-A148416] 08 p1122 N85-17072
Optimization of technical catalysts with the help of surface analysis
[BMFT-FB-T-84-225] 08 p1124 N85-17086
Hydrogen trapping, diffusion, and recombination in austenitic stainless steels
[DE85-001871] 09 p1294 N85-18129
Low and moderate temperature oxidation of atomically clean nickel, chromium and Ni-Cr alloys
[DE84-017350] 09 p1295 N85-18131
Ion beam studies of hydrogen in metals
[DE84-017422] 09 p1297 N85-18145
Two-dimensional modeling of conduction-mode laser welding
[DE85-001804] 09 p1327 N85-18341
Plasma surface interaction processes and possible synergisms
[DE85-001861] 09 p1391 N85-18752
Reactivity of ion implanted silicon carbide
[DE85-001543] 09 p1399 N85-18802
Fundamental aspects on ion-beam surface modification: Defect production and migration processes
[DE85-000093] 09 p1399 N85-18804
Characterization of erosion of metallic materials under cavitation attack in a mineral oil
[NASA-TM-86934] 10 p1440 N85-19075
Composition and method for cleaning embedded soil from surfaces having low gloss coatings
[AD-D011465] 10 p1459 N85-19194
Plasma states near surface of metal irradiated by CO2 laser 11 p1719 N85-20815
Studies of silicon-refractory metal interfaces: Photoemission study of interface formation and compound nucleation
[AD-A150075] 12 p1800 N85-21293
Three-dimensional calculation of shuttle charging in polar orbit 13 p1992 N85-22486
Confinement properties of high energy density plasmas in the Wisconsin levitated octupole 13 p2161 N85-23406
Hydrogen on impurity-covered iron surfaces 14 p2254 N85-23968
Practical surface methods 14 p2316 N85-24314
Self-substaining low-Z coatings for impurity control. Part 1: General considerations
[DE85-000427] 14 p2425 N85-24956
C2H(n) fragments on metal surfaces
[AD-A151474] 15 p2505 N85-25449
Studies of metal/carbon surface chemistry
[DE85-005513] 15 p2507 N85-25463
Numerical modeling of gas dynamic phenomena during supersonic flow of viscous gas in channel with electrical flow discharge 15 p2643 N85-26304
Neutralization and excitation in low-energy ion-surface collisions
[AD-A151568] 15 p2660 N85-26414
Effects of surface chemistry on hot corrosion life
[NASA-CR-174915] 16 p2706 N85-26711
The role of surface generated radicals in catalytic combustion 17 p2898 N85-27869
Corrosion Research Center of the University of Minnesota
[DE85-009418] 18 p3075 N85-29022
Technique for measuring surface diffusion by laser-beam-localized surface photochemistry
[DE85-007865] 18 p3113 N85-29273
Micro-reactions of metal contacts on various types of GaAs surfaces
[AD-A153650] 18 p3193 N85-29606
Method for predicting the performance of cathode materials
[AD-D011665] 19 p3257 N85-30198
Perturbative treatment of quasi-resonant proton neutralization at alkali-halide surfaces
[AD-A154143] 19 p3358 N85-30806
Elementary processes in the catalytic combustion of methane (mechanism, intermediates, and controlling reactions)
[PB85-188357] 20 p3436 N85-31316
Overlap integrals for atom-metal surface interactions
[AD-A155038] 21 p3702 N85-32998
Method for measuring surface activity of silicon nitride powder
[NASA-TM-77906] 24 p4073 N85-35242
Prediction of plasticity characteristics for three-dimensional fracture specimens comparison with experiment
[AD-A156425] 24 p4102 N85-35430

SURFACE ROUGHNESS

Turbulent boundary layers over rough surfaces hypersonic flow
[AD-A145040] 01 p0003 N85-10016
Terrain analysis procedural guide for surface configuration
[AD-A145837] 02 p0219 N85-11448
The chemical nature of the fiber/resin interface in composite materials 04 p0465 N85-12953
Analysis for leakage and rotordynamic coefficients of surface roughened tapered annular gas seals 05 p0844 N85-14135
Intensification of convective heat transfer by means of artificial surface roughness 06 p0778 N85-14975
Effect of asperity interactions on scuffing
[AD-A146544] 06 p0814 N85-15170
Optics of solids (surface related) and effect of surface roughness on MOS
[AD-A146883] 07 p0946 N85-15996
Interactive digital image processing for terrain data extraction
[AD-A148580] 08 p1176 N85-17417
On the virtual wall height in open channel flow with large relative roughness 09 p1303 N85-18188
Theory of resonant light scattering from a rough surface 09 p1383 N85-18701
Comparison of measured and simulated ride comfort for an agricultural tractor and influence of travel speed and tyre-inflation pressure on dynamic response
[AD-P004281] 09 p1407 N85-18857
Characteristics of farm field profiles as sources of tractor vibration
[AD-P004282] 09 p1407 N85-18858
Scanning photoacoustic microscopy of aluminum with aluminum oxide, roughness standards and rubber
[AD-A149460] 10 p1441 N85-19081
Mechanical interactions of rough surfaces
[DE85-000814] 10 p1494 N85-19434
An experimental investigation of microstrip properties on soft substrates from 2 to 40 GHz
[NASA-TM-86961] 11 p1624 N85-20224
Wind-tunnel research on the mechanics of plumes in the atmospheric surface layer
[AD-A150019] 12 p1845 N85-21584
Electromagnetic Acoustic Transducers (EMATs) for erosion monitoring
[DE85-004634] 12 p1854 N85-21628
Surface forward scattering and reflection
[AD-A150115] 12 p1928 N85-22112
A posteriori increase of resolving power of optical system forming averaged monochromatic images 13 p2082 N85-23009
Effects of fracture roughness on fluid flow through a single deformable fracture
[DE85-004593] 13 p2092 N85-23082
Calculations of microwave brightness temperature of rough soil surfaces: Bare field
[NASA-TM-86200] 13 p2123 N85-23221
Microwave remote sensing of soil moisture 13 p2125 N85-23235
A systematic study of light scattering by irregularly shaped particles
[AD-A150192] 13 p2159 N85-23400
Unsupervised classification of global radar units on Venus 13 p2196 N85-23632
Mapping and geological analysis of Mercury and Venus radar ranging data 13 p2196 N85-23633
Mars radar catalog 13 p2196 N85-23636
Statistics of Aeolian surface of Mars 13 p2199 N85-23637
Investigation of the conditions for tripping transition with roughness elements and their influence on boundary layer development 14 p2212 N85-23720
The characteristics of surface roughness important to gear and rolling bearing problems 14 p2222 N85-23782
Quantitative roughness analysis of treated surfaces with higher-class finish by methods of X-ray reflectometry 14 p2282 N85-24136
Effect of flight sequences in complex load histories on crack front marking 14 p2318 N85-24326
Generation of marker lines on fatigue fracture surfaces 14 p2319 N85-24328
Proceedings of the 9th US Air Force and the Federal Republic of Germany Data Exchange Agreement Meeting, Viscous and Interacting Flow Field Effects
[AD-A153020] 17 p2958 N85-26266
Mechanical interactions of rough surfaces
[DE85-005663] 18 p3118 N85-29299
Specification of surface roughness over oceans in the GLAS Fourth Order GCM 18 p3142 N85-29455
Influence of land-surface roughness on atmospheric circulation and rainfall: A sensitivity study with a GCM 18 p3146 N85-29479
Measurement of mode interaction due to waveguide surface roughness
[AD-A154039] 19 p3255 N85-30183
Using ship wake patterns to evaluate SAR (Synthetic Aperture Radar) ocean wave imaging mechanisms. Joint US-Canadian Ocean Wave Investigation Project
[AD-A154633] 21 p3573 N85-32223
The use of the glistening surface concept in rough surface scattering
[AD-A154922] 21 p3575 N85-32234
An analysis of physical optics models for rough surface scattering
[AD-A154960] 21 p3575 N85-32235
Surface roughness effects in elastohydrodynamic contacts
[NASA-TP-2488] 21 p3595 N85-32329
Toward the theory of acoustic scattering on uneven free surface 21 p3680 N85-32662

SURFACE ROUGHNESS EFFECTS

Numerical forecast of pressure field by considering the mutual influence of orography, thermal nonhomogeneity and surface friction 01 p0080 N85-10534
Proposal for wall function for friction and heat transfer in the presence of roughness and mass transfer
[CFD/84/12] 04 p0501 N85-13198
Scattering from multi-scale surface — Infrared lasers
[RSRE-MEMO-3856] 04 p0505 N85-13222
Scattering of electromagnetic waves by surface with small asperities 06 p0784 N85-15013
Approach to solution of diffraction problem for waves at rough surface 06 p0784 N85-15014
Development of an artificial boundary layer for different outlet flows 14 p2212 N85-23719
Energy reflection coefficient for H+ ions at energies between 10 and 50 keV
[DE85-007547] 18 p2883 N85-27882
Comparison of findings of theories describing reflection from real surface with experiments in region of ultrasoft X-radiation 21 p3694 N85-32950

SURFACE STABILITY

The behaviour of unstable surfaces: A literature review
[CFD/84/8] 02 p0199 N85-11329
Development of a preliminary ALRS stabilized material pavement analysis system (SPAS)
[AD-A147118] 07 p0910 N85-15760
Soil compliance influence on tyre performance
[AD-P004260] 09 p1404 N85-18836
Quality control in soil compaction by behaviours of exciter
[AD-P004295] 09 p1408 N85-18872
Adsorption thermodynamics and surface transport of metal catalyst poisons
[DE85-002868] 10 p1441 N85-19084
Experiments on the influence of active walls on the initial amplitudes and growths of instability waves
[AD-A154630] 21 p3583 N85-32275
Instability and chaotic behavior in a free-surface flow
[AD-A154879] 21 p3584 N85-32279
Interfacial bonding stability 21 p3608 N85-32409

SURFACE TEMPERATURE
NT SKIN TEMPERATURE (NON-BIOLOGICAL)
NT WALL TEMPERATURE
The Martian climate: Energy balance models with CO2/H2O atmospheres
[NASA-CR-174073] 03 p0448 N85-12849
The need for integrating ground thermal measurements with thermal aircraft imagery 05 p0660 N85-14243
Satellite definition of the bio-optical and thermal variation of coastal eddies associated with the African current
[AD-A147910] 07 p0969 N85-16282
Laser-initiated combustion studies on metallic alloys in pressurized oxygen
[PB85-126114] 10 p1438 N85-19066
Analytical fuel property effects: Small combustors, phase 2
[NASA-CR-174846] 10 p1456 N85-19175
A model for forecasting runway surface temperature and verification with subjective forecasts
[TR-28] 10 p1518 N85-19589
Thermal investigation of an electrical high-current arc with porous gas-cooled anode
[NASA-TM-77789] 11 p1627 N85-20245
Applications of pulsed-laser techniques and thermographic phosphors to dynamic thermometry of rotating surfaces
[DE85-000403] 11 p1639 N85-20328
Hot radome boresight error measurements
[AD-P004364] 12 p1826 N85-21458
The effect of stochastic surface heat fluxes on the climatology of the seasonal thermocline
[AD-A149957] 12 p1869 N85-21857
Oceanic role in terrestrial climate
[DE85-004422] 12 p1896 N85-21904
On the relationship between maximum surface temperature and various parameters; with reference to objective forecasting
[KNMI-TR-58] 12 p1897 N85-21905
Application of fluorescence to measurement of surface temperature in solid propellants
13 p2002 N85-22548
Estimation of regional evapotranspiration using remotely sensed land surface temperature. Part 1: Measurement of evapotranspiration at the Environmental Research Center and determination of Priestley-Taylor parameter
13 p2125 N85-23233
Estimation of regional evapotranspiration using remotely sensed land surface temperature. Part 2: Application of equilibrium evaporation model to estimate evapotranspiration by remote sensing technique — Japan
13 p2125 N85-23234
Testing an energy balance model for estimating actual evapotranspiration using remotely sensed data — Hannover, West Germany barley and wheat fields
13 p2125 N85-23236
A method for estimating soil moisture availability
[NASA-CR-175806] 13 p2128 N85-23238
Fabrication of ceramic substrate-reinforced and free forms
[NASA-TM-86994] 14 p2247 N85-23926
Application of atomic fluorescence to measurement of combustion temperature in solid propellants
[AD-A150733] 14 p2263 N85-24021
Seven-wavelength pyrometer for determining surface temperature of ablation materials
[NASA-TM-77832] 14 p2305 N85-24268
Dynamic stochastic model of long-period variability of ocean surface temperature 14 p2334 N85-24437
Choice of optimum pairs of spectral intervals for IR-range survey of Earth's surface 15 p2486 N85-25344
Numerical simulation of boundary layer excitation by surface heating/cooling
[NASA-CR-172575] 15 p2554 N85-25756
Annual cycle. Part 1: The annual variation of surface temperatures over the United States and Canada
[PB85-147676] 15 p2600 N85-26026
Raman studies of surface temperature in laser-heated semiconductors
[AD-A151377] 15 p2659 N85-26412
Regularities in recent changes in surface air temperature and atmospheric precipitation fields
16 p2807 N85-27311
Evaluation of the area and severity of last night's frosts
[REPT-109] 16 p2833 N85-27473
Simulation of a synchronously coupled atmosphere-ocean prediction model
[AD-A152020] 16 p2835 N85-27482
A GCM study of the atmospheric response to tropical SST anomalies 18 p3146 N85-29477
Temperature and surface damage under lubricated sliding-rolling contacts 19 p3280 N85-30336
Facility for large-scale hazardous gas testing
[DE85-011652] 21 p3564 N85-32169
Surface temperature distribution along a thin liquid layer due to thermocapillary convection
[NASA-TM-87115] 23 p3930 N85-34357
SURFACE TENSION
U INTERFACIAL TENSION
SURFACE TO SURFACE MISSILES
NT CRUISE MISSILES
NT INTERCONTINENTAL BALLISTIC MISSILES
NT MINUTEMAN ICBM
NT POLARIS MISSILES
Dissected motors-propellants motor number STM-012. Phase 15: Surveillance report, stage 1
[AD-A156088] 24 p4071 N85-35226
SURFACE TREATMENT
U SURFACE FINISHING
SURFACE VEHICLES
NT AIRCRAFT CARRIERS
NT AUTOMATED GUIDEWAY TRANSIT VEHICLES
NT AUTOMATED TRANSIT VEHICLES
NT AUTOMOBILES
NT BOATS
NT ELECTRIC AUTOMOBILES
NT ELECTRIC HYBRID VEHICLES
NT ELECTRIC MOTOR VEHICLES
NT LIFEBOATS
NT LUNOKHOD LUNAR ROVING VEHICLES
NT MOTOR VEHICLES
NT ROCKET PROPELLED SLEDS
NT ROVING VEHICLES
NT SLEDS
NT SURFACE EFFECT SHIPS
NT TANK TRUCKS
NT TANKER SHIPS
NT TANKS (COMBAT VEHICLES)
NT TRACKED VEHICLES
NT TRACTORS
NT TRANSPORTER
NT TRUCKS
NT WALKING MACHINES
Terrain navigation concepts for autonomous vehicles
[AD-A144994] 01 p0005 N85-10031
Study of annoyance due to urban automobile traffic. Annex 4: A catalog of the characteristics of noise at different measuring points
[NASA-TM-77516] 03 p0367 N85-12478
Synthesis of transit practice: Diesel fuel quality and effects of fuel additives
[PB84-235686] 05 p0621 N85-13973
Vehicle anchoring system
[AD-D011292] 06 p0815 N85-15173
Automatic land vehicle navigation using road map data
[DE84-017178] 09 p1278 N85-18043
Calculation of the area covered by mobile radio systems using geographic data stored in a computer
[FUB-43-1983] 09 p1312 N85-18247
The experimental performance of an off-road vehicle utilizing a semi-active suspension — off-road motorcycles
09 p1339 N85-18421
Modelling of off-road tyres and soil for improved traction
[AD-P004258] 09 p1404 N85-18834
Development of a soil-wheel interaction model
[AD-P004259] 09 p1404 N85-18835
Soil compliance influence on tyre performance
[AD-P004260] 09 p1404 N85-18836
The rolling resistance and sinkage of towed dual wheel combination in sand
[AD-P004261] 09 p1404 N85-18837
Performance prediction of pneumatic tyres on sand
[AD-P004262] 09 p1404 N85-18838
Traction forces of drive tyre on the compacted soil
[AD-P004264] 09 p1404 N85-18840
Prediction of in-sand tire and wheeled vehicle drawbar performance
[AD-P004265] 09 p1404 N85-18841
Designing off-road vehicles with good ride behaviour
[AD-P004267] 09 p1405 N85-18843
Ride comfort of off-road vehicles
[AD-P004279] 09 p1406 N85-18855
Proceedings of the 8th International Conference on the Performance of Off-Road Vehicles and Machines, volume 2
[AD-A148835] 09 p1407 N85-18859
Study of the motion of agricultural vehicles on steep grass-covered slopes
[AD-P004290] 09 p1408 N85-18867
Pressure tests in soil below tires of agricultural vehicles
[AD-P004294] 09 p1408 N85-18871
Smoother terrain-machine
[AD-P004296] 09 p1409 N85-18873
Compaction of sand using ordinary off-road vehicles
[AD-P004297] 09 p1409 N85-18874
Flotation tires and subsurface compaction
[AD-P004299] 09 p1409 N85-18876
The guidelines to design the lever turning gears in articulated vehicles
[AD-P004301] 09 p1409 N85-18878
Influence of tire on resistance and steering forces of tires
[AD-P004306] 09 p1410 N85-18883
Planning of air cushion transport vehicles
14 p2265 N85-24160
Hybrid propulsion technologies for urban bus transit
[PB85-157469] 16 p2880 N85-27773
Evaluation of semiconductor devices for Electric and Hybrid Vehicle (EHV) ac-drive applications, volume 1
[NASA-CR-176118] 23 p3927 N85-34335
Visual position determination for autonomous vehicle navigation
[AD-A156007] 24 p4063 N85-35181
SURFACE WATER
Water resources data, Mississippi, water year 1982
[PB84-224559] 01 p0065 N85-10434
Water resources data, Florida, water year 1982. Volume 4: Northwest Florida
[PB84-223445] 01 p0066 N85-10437
Isolation, concentration and subsequent analysis by capillary gas chromatography of trace amounts of organophosphorus compounds from aqueous samples
[AD-B089301L] 12 p1803 N85-21308
A preliminary analysis of LANDSAT-4 Thematic Mapper radiometric performance 12 p1870 N85-21730
Literature review for development of the master analytical scheme for organic compounds in water
[PB85-152874] 15 p2507 N85-25468
Analysis of suspended sediment distributions in the surface waters of Delaware Bay using remote sensing of optical properties 15 p2582 N85-25926
Operation guiding light-scientific program and field plan. The pilot field experiment for NORDA project chemical dynamics in ocean frontal areas
[AD-A153765] 18 p3150 N85-29507
Microwave hydrology: A trilogy
[NASA-CR-176042] 20 p3477 N85-31603
Global environmental transport models for tritium
[DE85-011437] 22 p3816 N85-33839
Hydrology
[PB85-182954] 23 p3944 N85-34440
SURFACE WAVES
NT BAROCLINIC WAVES
NT CAPILLARY WAVES
NT ELECTROMAGNETIC SURFACE WAVES
NT GRAVITY WAVES
NT RIPPLES
NT SOMMERFELD WAVES
Transformation of heterogeneous surface waves by skewed streams 02 p0259 N85-11697
Evaluation of moduli and thicknesses of pavement systems by spectral-analysis-of-surface-waves method
[PB84-219112] 03 p0342 N85-12205
Propagation of acoustic shear waves through active periodic structure 04 p0490 N85-13125
Slow surface magnetoplasma waves in oblique magnetic field 07 p0952 N85-16034
The investigation of selected oceanographic applications of spaceborne synthetic-aperture radar
08 p1146 N85-17233
SEASAT 3 and 4
[AD-A148343] 08 p1152 N85-17274
Second order Bragg scattering in a SAR
[AD-A148395] 08 p1152 N85-17275
Evolution of nonlinear wave groups on water of slowly-varying depth
[AD-A147947] 08 p1162 N85-17329
Short range order-long range order in superconducting materials
[AD-A148764] 08 p1227 N85-17724
The effects of surface waves on RF discharge pumped lasers
[AD-A149689] 12 p1856 N85-21643
Solar energy converter using surface plasma waves
[NASA-CASE-LEW-13827-1] 12 p1876 N85-21768
Surface wave excitation study
[DE85-006301] 13 p2056 N85-22875
Results of an initial trial of a satellite telemetering buoy measuring near surface current
16 p2812 N85-27345
Surface wavesseismic yields as measured by the Regional Seismic Test Network
[DE85-010532] 18 p3137 N85-29425
Surface acoustic wave devices as chemical vapor microsensors
[AD-A153752] 18 p3177 N85-29696
Theoretical investigations of the propagation and interactions of surface waves
[AD-A153548] 18 p3185 N85-29753
Microwave bandstop filter
[AD-D011716] 19 p3261 N85-30222
Dual differential interferometer
[NASA-CASE-LAR-12966-1] 19 p3271 N85-30282

Discovery of a nonpropagating hydrodynamic soliton
[AD-A155569] 21 p3582 N85-32268
Large-time behavior of viscous surface waves
[AD-A154805] 21 p3584 N85-32278
Upward continuation of surface gravity anomalies
[AD-A154973] 21 p3631 N85-32580
Solid state research
[AD-A154783] 21 p3709 N85-33025
Asymmetry of diffraction orders with light diffraction at surface acoustic wave 22 p3782 N85-33431
Numerical experiment of elastic wave propagation by framework model
[DRIC-T-7462] 22 p3795 N85-33511
Surface wave modes of a multilayered medium backed by a perfectly conducting ground plane: Computation of propagation constants
[DE85-011454] 22 p3829 N85-33715
Heterodyne holographic interferometry for visualization of surface acoustic waves
[AD-A155405] 22 p3836 N85-33753
Second Colloquim on the Scattering of Ultrasonic Waves
[AD-A156298] 24 p4145 N85-35697

SURFACES

Surface chemistry of palladium
[DE84-014572] 02 p0173 N85-11163
Determining composition in surface region of semiconductor crystals by method of sudden changes in X-ray photoelectric effect 02 p0267 N85-11746
Incompressible lifting-surface aerodynamics for a rotor-stator combination
[NASA-TM-83767] 03 p0316 N85-12039
Choice of criteria for rejection of insulating components in high-voltage surge equipment 06 p0785 N85-15021
Free-surface boundary layer and the origin of bow vortices
[AD-A147427] 07 p0960 N85-16083
Model robust response surface designs: Scaling 2-level factorials
[AD-A147494] 07 p1033 N85-16556
A free shear layer prediction of the turbulent wake of a flat plate towed below a free surface
[AD-A148699] 09 p1319 N85-18293
Experimental investigation of a turbulent incompressible boundary layer on a curved wall 11 p1577 N85-19936
Surface physics instrumentation
[AD-A149304] 11 p1726 N85-20669
The construction of curves and surfaces using numerical optimization techniques 17 p3003 N85-28565
A survey of patch methods 17 p3003 N85-28567
Some negative results in N-sided patches 17 p3004 N85-28572
Unsteady transonic flow calculations for interfering lifting surface configurations
[NASA-TM-86432] 19 p3214 N85-29931
Experimental method for measuring positronium reflection from surfaces
[DE85-010949] 20 p3531 N85-31957
Removable cleanable antireflection shield
[AD-D011735] 22 p3844 N85-33810
Block-implicit calculations of three-dimensional laminar flow in strongly curved ducts
[DE85-003047] 23 p3931 N85-34383
Acoustical absorption coefficient in a diffuse field of a plane, rectangular material of finite dimensions placed on an infinite perfectly reflecting surface
[NRC/CNR-TT-2113] 23 p3968 N85-34599

SURFACTANTS

Vapor pressure studies of the solubilization of hydrocarbons by surfactant micelles
[DE85-004319] 12 p1803 N85-21306
Turbulent flows of surfacant solutions
[AD-B089137L] 13 p2092 N85-23058
Determining adsorption of surface-active substances by sea bottom deposits 13 p2107 N85-23128
On the question to the effect of surfactants on the spectrum of cloud drops in the process of their condensation growth 21 p3650 N85-32679

SURGERY

Applications of CdTe to nuclear medicine
[DE85-011877] 23 p3952 N85-34492

SURGES

Isolated load switching with surge suppression
[AD-D011218] 01 p0042 N85-10274
A model for the propagation of the westward traveling surge
[TRITA-EPP-84-03] 03 p0383 N85-12515
Surge transient simulation in turbo-jet engine 05 p0596 N85-13795
Surge and stall in centrifugal compressors 05 p0837 N85-14087
Circuit transients due to negative bias arcs on a high-voltage solar array in low Earth orbit
[NASA-TP-2407] 06 p0760 N85-14858
Allowable surge currents and failure mechanisms in semiconductor power devices in various modes of operation 06 p0795 N85-15080
Spicules and surges
[AD-A146785] 07 p1061 N85-16727
On one design principle of surge protector for gas turbine engine compressor 09 p1306 N85-18206
Electromagnetic pulse (EMP) interaction with electric power systems. Power Systems Technology Program
[DE85-000166] 09 p1312 N85-18244
Observation of a westward travelling surge from satellites at low, medium and high altitudes
[NASA-TM-87434] 09 p1342 N85-18442
A survey of fast X-ray transients using the HEAO A-1 Sky Survey experiment 09 p1411 N85-18895
Flashover failures from wet-wire arcing and tracking
[AD-A149055] 10 p1478 N85-19332
A theory of post-stall transients in multistage axial compression systems
[NASA-CR-3878] 12 p1771 N85-21117
Hurricane storm surge research
[GPO-40-048] 12 p1893 N85-21880
Hurricane alicia storm surge and wave data
[AD-A149668] 12 p1895 N85-21896
Surge strength of symmetric cable with monolithic polyethylene insulation of quads 13 p2082 N85-23001
Transients during the switching of SF6-insulated isolating switches
[BLL-CE-TRANS-7966-(9022.09)] 15 p2546 N85-25713
An investigation of hydraulic transients in combination free surface and pressurized flows 19 p3264 N85-30239
Resolution of thermal striping issue downstream of a horizontal pipe elbow in stratified pipe flow
[DE85-006195] 21 p3586 N85-32292
Nonlinear spectroscopy
[AD-A154706] 21 p3704 N85-33010
Exploring results of the possibility on detecting cosmic ray particles by acoustic way
[HE-7.1-3] 24 p4213 N85-36157

SURVEILLANCE

NT SPACE SURVEILLANCE (GROUND BASED)
NT SPACE SURVEILLANCE (SPACEBORNE)
Hybrid state estimation approach to multiobject tracking for airborne surveillance radars
[AD-A148459] 08 p1153 N85-17279
TCAS II: Design and validation of the high-traffic-density surveillance subsystem
[DOT/FAA/PM-84/5] 13 p1970 N85-22375
Surveillance program for the dissection and analysis of explosive and pyrotechnic components
[DE85-006105] 16 p2757 N85-27016
An automated quality assurance surveillance plan for ADP (Automated Data Processing) operations under the Navy's commercial activities program
[AD-A154767] 21 p3671 N85-32602
Power density and threshold control strategies for radar track initiation
[AD-A155357] 22 p3756 N85-33282
Evaluation of nuclear detonation location capability under high attack scenario
[AD-A155761] 24 p4149 N85-35729

SURVEILLANCE RADAR

NT MULTISTATIC RADAR
Design and realization of a multiradar tracking system for air traffic control
[ENST-84E010] 09 p1279 N85-18044
The use of small mobile radars to detect, monitor, and quantify bird movements
[AD-P004188] 11 p1580 N85-19951
On the altitudinal distribution of birds and bird strikes in the Netherlands
[AD-P004189] 11 p1580 N85-19952
Method and means for providing frequency agile operation of MTI (Moving Target Indicator) radar
[AD-D011561] 12 p1823 N85-21436
Development concerns for satellite-based air traffic control surveillance systems 14 p2230 N85-23816
Multi-bistatic radar for short range surveillance
[BAE-BT-10603] 15 p2539 N85-25673
The effects of subrefractive layers and elevated ducts on airborne radar and ESM (Electronic Surveillance Measures)
[AD-A155524] 21 p3637 N85-32592

SURVEYING

U SURVEYS

SURVEYS

NT GEODETIC SURVEYS
NT GEOLOGICAL SURVEYS
Chemical heat pump state-of-the-art survey
[DE84-013552] 01 p0048 N85-10312
A survey and evaluation of software quality assurance
[AD-A147552] 07 p1026 N85-16510
A complete characterization of triply balanced matrices with applications to survey sampling
[AD-A147083] 07 p1031 N85-16542
Manufacturing costs, equipment needs and technological opportunities among small and medium-size manufacturers
[DE85-000479] 09 p1304 N85-18193
Practical application of earth resistivity methods in phase 2 of the installation restoration program
[AD-P004148] 09 p1348 N85-18484
Benthic boundary layer, IOS observational programme: Discovery Gap measurements, March 1984 — Institute of Oceanographic Sciences (IOS)
[ISO-150] 09 p1359 N85-18552
Atlas of snow and ice resources 10 p1497 N85-19449
MAP-related activities in the United States 11 p1655 N85-20427
General aviation activity and avionics survey
[AD-A149572] 12 p1769 N85-21103
A community survey of helicopter noise annoyance conducted under controlled noise exposure conditions
[NASA-TM-86400] 13 p2154 N85-23374
Research on the effect of noise at different times of day: Models, methods and findings
[NASA-CR-3886] 13 p2154 N85-23375
Development, achievements in China's cartography work 13 p2166 N85-23434
A constant altitude flight survey method for mapping atmospheric ambient pressures and systematic radar errors
[NASA-TM-86733] 19 p3217 N85-29951

SURVIVAL

Maximum likelihood estimation of the survival functions of N stochastically ordered random variables
[AD-A145429] 02 p0254 N85-11662
Conditional regression models for transient state survival analysis
[AD-A147872] 07 p1034 N85-16563
Effects of pyridostigmine on psychomotor and visual performance
[AD-A148553] 08 p1196 N85-17539
Assessment of seismic survivability 09 p1336 N85-18402
Effect of prolonged hunger during experimental hikes 11 p1692 N85-20637
Proportional odds models for survival data and estimates using ranks
[MATHEMATICS-RESEARCH-172] 12 p1923 N85-22080
Survival of microorganisms and bacterial predation in nature
[AD-A153574] 18 p3152 N85-29514
Effects of long-term low-level radiofrequency radiation exposure on rats. Volume 6: Evaluation of longevity, cause of death, and histopathological findings
[AD-A154283] 19 p3327 N85-30610
Aviation safety (aircraft passenger survivability and cabin safety)
[GPO-99-847] 23 p3895 N85-34130

SURVIVAL EQUIPMENT

Evaluation of survival straws (pocket purifier)
[AD-A146240] 03 p0328 N85-12114

SUSCEPTIBILITY (MAGNETISM)

U MAGNETIC PERMEABILITY

SUSPENDING (HANGING)

NT MAGNETIC SUSPENSION
Test methods for cable cars
[CETIM-1-5K-45-1] 04 p0515 N85-13282
A gyro sensor block suspension
[AD-D011411] 08 p1154 N85-17284
A Lagrange-D'Alembert formulation of the equations of motion of a helicopter carrying an externally suspended load
[NASA-TM-85864] 12 p1776 N85-21149
Precise mounting of instruments in universal suspension with skewed axes 14 p2273 N85-24083
Constant fiber number during skeletal muscle atrophy and modified arachidonate metabolism during hypertrophy 15 p2609 N85-26078
Blood pressure responses and mineral ocorticoid levels in the suspended rat model for weightlessness 15 p2609 N85-26079

SUSPENSION SYSTEMS (VEHICLES)

The experimental performance of an off-road vehicle utilizing a semi-active suspension — off-road motorcyles 09 p1339 N85-18421
A theoretical investigation of an active suspension system for wheeled tractors
[AD-P004268] 09 p1405 N85-18844
Low-profile fastener
[AD-D011667] 19 p3280 N85-30343
Damping of suspension oscillations for stratospheric balloon experiments
[MPE-IR-42] 20 p3463 N85-31517

SWAGING
Development of intercalated wire and cable
[AD-A146502] 06 p0774 N85-14949
SWALLOWING
Tritium hazard via the ingestion pathway
[DE85-012897] 24 p4133 N85-35618
SWAMPS
U MARSHLANDS
SWATH WIDTH
Cartography 02 p0214 N85-11412
SAR swath widening techniques — satellite radar
[BL-6199] 20 p3441 N85-31358
SWEAT
Evaluation of a field expedient technique for sweat sample collection
[AD-A151916] 16 p2841 N85-27521
SWEAT COOLING
Advanced liner-cooling techniques for gas turbine combustors
[NASA-TM-86952] 12 p1770 N85-21115
Exercise-heat strain during hypohydration: Interaction with heat acclimation and aerobic fitness
[AD-A151023] 14 p2389 N85-24717
SWEATING
U PERSPIRATION
SWEDEN
PROMIS 600: The pilot project for the future Swedish weather service 01 p0083 N85-10580
A pilot study of future research on seismic hazards in Sweden
[FOA-C-20544-T1] 02 p0229 N85-11496
Sweden's Kiruna may be future launch site for satellites 03 p0310 N85-12000
Space research in Sweden 03 p0321 N85-12073
Seismicity of southern Sweden
[FOA-C-20543-T1] 07 p0998 N85-16340
Ground truth for SIR-B images obtained by SIR system 8 impulse radar 08 p1149 N85-17251
Finnair, LOT, SAS reps in USSR on present operations, plans 09 p1278 N85-18035
Scania, ASEA of Sweden use robots for all production phases 09 p1310 N85-18229
Overview of major Swedish institutions in polymer research 11 p1592 N85-20014
Catastrophic-flood features in Swedish Lapland as a terrestrial analog for Martian channel flows
13 p2190 N85-23587
Hydrological data collection from Swedish mountain areas 14 p2327 N85-24388
Sweden develops new rapid solidification process
15 p2531 N85-25810
Sweden invents new ceramic for more durable cutting tools 15 p2536 N85-25845
Swedish space program includes research satellites
16 p3086 N85-29113
Possible use of the COSPAS/SARSAT system within the Swedish mountain rescue organization
20 p3401 N85-31100
Human factors engineering contracts in Sweden: An overview
[FOA-C-56043-H2] 20 p3513 N85-31636
SWEDISH SPACE PROGRAM
Swedish equipment for automatic docking in space
15 p2489 N85-25383
SWEEP CIRCUITS
Improvements in avalanche-transistor sweep circuitry for electrooptic streak cameras
[DE84-016195] 06 p0811 N85-15155
SWEEP EFFECT
Design of a basic profile for a low sweep airfoil. Part 2: Experimental investigation on the DFVLR-W1 airfoil profile in the Brunswick transonic wind tunnel
[DFVLR-FB-85-01-PT-2] 17 p2892 N85-27833
SWEEP FREQUENCY
Simple sweep frequency generator
13 p2075 N85-22960
SWELLING
Evaluation of ferritic alloy Fe-2 1/4Cr-1Mo after neutron irradiation: Irradiation creep and swelling
[DE84-014647] 04 p0474 N85-13022
Tensile properties and swelling of 20%-cold-worked Type 316 stainless steel irradiated in HFIR
[DE84-014080] 05 p0617 N85-13948
Swelling behavior of titanium-modified AISI 316 alloys
[DE84-013940] 05 p0618 N85-13956
Mechanisms of elevated temperature rupture in single phase ceramics
[DE85-000697] 09 p1299 N85-18156
Swelling behavior of manganese-bearing AISI 216 steel
[DE85-005712] 15 p2512 N85-25495
The physical effects of different stress situations on graphite/epoxy compounds 15 p2667 N85-26594
Swelling behavior of titanium-modified AISI 316 alloys
[DE85-007470] 16 p2752 N85-26662
An investigation of the irradiation swelling mechanisms in refractory metals at high temperatures
[AD-A154149] 19 p3236 N85-30079
SWEPT FORWARD WINGS
The development of a dynamic model of a generalised combat aircraft with forward wings for the identification of stability and control characteristics
[CAR-84-33] 09 p1280 N85-18050
Active control of forward swept wings with divergence and flutter aeroelastic instabilities
09 p1282 N85-18063
Multivariable control law design for the X-29 aircraft
[AD-A151828] 15 p2472 N85-25259
Active control of forward swept wings with divergence and flutter aeroelastic instabilities
[AD-A151837] 15 p2474 N85-25270
Some effects of sweep direction and strakes for wings with sharp leading edges
[CA-8421] 17 p2892 N85-27826
X-29 digital flight control system design
17 p2901 N85-27889
The static aeroelasticity of a composite wing
18 p3121 N85-29321
SWEPT WINGS
NT DELTA WINGS
NT SWEPT FORWARD WINGS
NT SWEPTBACK WINGS
Experiments suitable for wind tunnel wall interference assessment/correction 03 p0313 N85-12021
Design of a basic airfoil for a slightly swept wing. Part 1: Theoretical transonic airfoil design
[DFVLR-FB-84-19-PT-1] 03 p0316 N85-12043
Experimental study on transonic flutter characteristics of sweptback wing with core composite plates having different fiber orientations
[NAL-TR-827] 06 p0756 N85-14842
Application of two and three-dimensional criteria for calculating transitions and boundary layers over swept wings 08 p1070 N85-16783
Full scale experiments into the use of large eddy breakup devices for drag reduction on aircraft
08 p1071 N85-16790
Joined wing transonic design and test validation
[AD-A146355] 08 p1078 N85-16834
Unsteady stall penetration of an oscillating swept wing
[AD-P004156] 09 p1264 N85-17941
Effects of leading-edge devices on the low-speed aerodynamic characteristics of a highly-swept arrow-wing
[NASA-CR-172531] 13 p1968 N85-22365
Calculation of vortex-flap aerodynamic characteristics
[NASA-CR-175624] 13 p1969 N85-22367
Calculation of unsteady transonic flow around a high swept wing 15 p2459 N85-25184
La Recherche Aerospatiale Bimonthly Bulletin, Number 1984-4, 221/July-August
[ESA-TT-884] 16 p2695 N85-26637
On the effect of wing taper and sweep direction on leading edge transition
[CA-8435] 17 p2892 N85-27827
Effect of leading-edge load constraints on the design and performance of supersonic wings
[NASA-TP-2446] 19 p3213 N85-29923
Selecting step sizes in sensitivity analysis by finite differences
[NASA-TM-86382] 22 p3799 N85-33538
SWEPTBACK WINGS
NT DELTA WINGS
Experience with transonic unsteady aerodynamic calculations 15 p2458 N85-25176
Some effects of sweep direction and strakes for wings with sharp leading edges
[CA-8421] 17 p2892 N85-27826
Experimental and theoretical study of the longitudinal aerodynamic characteristics of delta and double-delta wings at Mach numbers of 1.60, 1.90, and 2.16
[NASA-TP-2433] 19 p3213 N85-29922
Design of a basic airfoil for a slightly swept wing. Part 1: Theoretical transonic airfoil design
[ESA-TT-892] 20 p3394 N85-31054
SWINGBY TECHNIQUE
Mars exploration, Venus swingby and conjunction class mission modes, time period 2000 to 2045
[NASA-TM-86477] 02 p0303 N85-11961
SWIRLING
Design of swirled axisymmetric turbulent jets
05 p0724 N85-14657
Rayleigh and Raman scattering for density in a swirling flow combustor 08 p1120 N85-17060
Swirling turbulent spray group combustion
09 p1289 N85-18095
Workshop report: Swirl Enhanced Combustion
13 p2005 N85-22584
Turbulence characteristics of swirling flowfields
[NASA-CR-174918] 16 p2709 N85-26717
Flow modifying device
[NASA-CASE-LEW-13562-2] 24 p4065 N85-35195
SWIRLING WAKES
U TURBULENT WAKES
SWITCHES
NT CAPACITANCE SWITCHES
NT ELECTRIC RELAYS
NT ELECTRIC SWITCHES
NT FLUID SWITCHING ELEMENTS
NT SWITCHING CIRCUITS
NT THERMOSTATS
LED multifunction keyboard engineering study
[AD-A145199] 01 p0010 N85-10061
Simulation study of a new inverse-pinch high Coulomb transfer switch
[NASA-CR-172420] 02 p0194 N85-11294
Vacuum inductive pulsed power compression for inertial confinement fusion
[DE84-010935] 03 p0421 N85-12693
High-temperature optically activated GaAs power switching for aircraft digital electronic control
[NASA-CR-174711] 04 p0457 N85-12901
Storage life of thermal detents
[DE84-016934] 04 p0476 N85-13030
Magnetic and photoconductive repetitive rail-gun opening switches
[DE84-017060] 04 p0496 N85-13163
Integrated power devices with three-dimensional connection for automation systems
06 p0794 N85-15077
Switchable zero order diffraction gratings as light valves
[AD-A147575] 07 p1044 N85-16633
Centrifuge tests to provide closure bounds for switches subjected to random vibration
[DE85-002003] 10 p1482 N85-19357
A new very high voltage semiconductor switch
[NASA-TM-86957] 11 p1627 N85-20246
Wide angle phased array dome lens antenna with a reflection/transmission switch
[AD-D011562] 12 p1833 N85-21502
KAM-250 antenna switch 13 p2068 N85-22916
Picosecond photoconductive devices for 10 Gbit/s optoelectronic switching 18 p3167 N85-29770
Development of a resistive load for PBFA 2 rimfire gas switch simultaneity and laser triggering tests
[DE85-011080] 19 p3365 N85-30869
The plasma erosion opening switch
[AD-A154942] 21 p3580 N85-32259
Coordinated research program in pulsed power physics
[AD-A154629] 21 p3679 N85-32858
Operational window for a plasma erosion opening switch used for voltage multiplication on pulsed power generators
[AD-A155482] 21 p3707 N85-33020
Electro-optic harmonic conversion to switch a laser beam out of a cavity
[DE85-011619] 22 p3790 N85-33483
Multiple-stage integrating accelerometer
[DE85-006505] 23 p3935 N85-34388
Photoconductive pulse power switches: A review
[DE85-014125] 24 p4091 N85-35360
SWITCHING
NT MICROWAVE SWITCHING
NT PACKET SWITCHING
NT PACKET TRANSMISSION
DC switching regulated power supply for driving an inductive load
[DE84-014238] 01 p0044 N85-10285
Formation of reference signals in laser-type gas analyzers with mechanical switching of optical channels
06 p0787 N85-15027
High-speed power thyristors with excellent switching and load characteristics 06 p0793 N85-15070
NBS (National Bureau of Standards) switching radiometers
[PB84-235894] 07 p0968 N85-16147
Stereo decoder without subcarrier restoration
13 p2068 N85-22921
Energy considerations in second breakdown
[AD-A152389] 17 p2952 N85-28229
Pursuit tracking performance and flash disruption: The effects of training the non-dominant eye on target reacquisition
[AD-A153404] 17 p2999 N85-28541
Picosecond photoconductive devices for 10 Gbit/s optoelectronic switching 18 p3167 N85-29770
Experimental demonstration of an optoelectronic switch matrix for satellite-switched TDMA signals in the 0.3-4.0 GHz band
[CRC-TN-717] 19 p3253 N85-30170
Control of energy-storage dc-to-dc converters: The large-signal time-domain approach
19 p3257 N85-30196

Switchable zero order diffraction gratings as light valves
[AD-A154471] 20 p3533 N85-31981
Plasma erosion opening switch
[DE85-011384] 20 p3535 N85-31998
The plasma erosion opening switch
[AD-A154942] 21 p3580 N85-32259
Model that predicts pulse charged gas switching breakdown phenomena
[DE85-013119] 22 p3761 N85-33313

SWITCHING CIRCUITS
NT FLUID SWITCHING ELEMENTS
Isolated load switching with surge suppression
[AD-D011218] 01 p0042 N85-10274
Noise isolation system for high-speed circuits
[DE84-014229] 01 p0043 N85-10283
High or low-side solid state relay with current limiting and operational testing
[AD-D011260] 05 p0631 N85-14046
Power MOS fast switching techniques
[DE84-015046] 05 p0732 N85-14707
Trends in development of bipolar power transistors
06 p0793 N85-15072
Fast switching driver for inductive load, such as a phase shifter
[AD-D011368] 08 p1143 N85-17207
Development of photoconductive power switch technology
[DE85-001514] 09 p1315 N85-18270
Surface and allied studies in silicon solar cells
[NASA-CR-174447] 11 p1671 N85-20531
Power circuit utilizing self-excited Hall effect switch means
[AD-D011505] 12 p1832 N85-21496
Transients during the switching of SF6-insulated isolating switches
[BLL-CE-TRANS-7966-(9022.09)] 15 p2546 N85-25713
Development of a butterfly multiprocessor test bed description of butterfly components
[AD-A153692] 18 p3095 N85-29155
Stationary properties and switching characteristics of dispersive optical bistability in CuCl
18 p3186 N85-29763
Experimental demonstration of an optoelectronic switch matrix for satellite-switched TDMA signals in the 0.3-4.0 GHz band
[CRC-TN-717] 19 p3253 N85-30170
Fast transient behavior of thyristor switches
[AD-A154109] 19 p3259 N85-30206
Performance of the butterfly processor-memory interconnection in a vector environment
[DE85-007931] 19 p3261 N85-30224
T/R switch design for short-range measurements, part 6.1A 21 p3624 N85-32515
Coordinated research program in pulsed power physics
[AD-A154629] 21 p3679 N85-32858
Switching power supply
[DE85-005993] 22 p3761 N85-33312
Capacitance measuring device
[DE85-011643] 22 p3787 N85-33460
Series-counterpulse repetitive-pulse inductive storage circuit
[DE85-006436] 23 p3828 N85-34342

SWITCHING ELEMENTS
U SWITCHING CIRCUITS

SWITCHING THEORY
Onboard demand scheduling of a multibeam SS/TDMA satellite with integrated circuit and packet switching
14 p2229 N85-23612
Automation of development of software for switching units that are implemented in the form of multiprocessor systems on a microcomputer base
14 p2401 N85-24802

SWITZERLAND
Deformation mechanisms associated with mesoscopic kinkbands, Jura Mountains (Switzerland) and Chaines Subalpines (France) 03 p0389 N85-12492
West Europe report: Science and technology
[JPRS-WST-84-007] 15 p2530 N85-25600

SYMBIOSIS
From microbial communities to cells
21 p3659 N85-32728

SYMBIOTIC STARS
Fluorescent excitation of Fe 2, Mn 2, Ti 2, N 1 lines by V 4, N 5, O 6: Emission lines in the spectra of symbiotic stars and Seyfert galaxies 11 p1746 N85-20984
IUE observations of the jet emission feature in R Aquarii 11 p1747 N85-20988
Physical models for the UV continua of symbiotic stars
11 p1756 N85-21046

SYMBOLIC PROGRAMMING
Representation and refinement of visual specifications in PegaSys
[AD-A146733] 09 p1368 N85-18598
Supercomputers and symbolic computation
[AD-A151376] 15 p2623 N85-26166
Use of REDUCE 2 for symbolic programming
[INPE-3355-PRE/633] 16 p2846 N85-27544
Tenth-order expansion formulae for the orbital eccentricity function K (sub ipq)(e) obtained using a symbolic algebraic manipulation system
[AD-A153754] 18 p3170 N85-29647

SYMBOLS
Information-theoretic properties of languages and their grammars
[AD-A146868] 08 p0799 N85-15106
Symbol structure, information content and visual form: A carto-semiotic theory of map signs
09 p1342 N85-18439
FLAD user's manual: FLAD file contents
[AD-A148700] 09 p1368 N85-18594
Automatic symbolic solution of Markov chains
[AD-A150476] 13 p2153 N85-23369
Symbol stream combining in a convolutionally coded system 16 p2771 N85-27101
Development of new circuit symbols for binary logic elements
[MBB-Z-39/85-O] 17 p3014 N85-28640
Proposal for the systematic naming of mesons and baryons
[DE85-006453] 17 p3035 N85-28773

SYMMETRICAL BODIES
NT AXISYMMETRIC BODIES
NT BODIES OF REVOLUTION
NT CELESTIAL SPHERE
NT CONCENTRIC SPHERES
NT CONICAL BODIES
NT CYLINDRICAL BODIES
NT ELLIPSOIDS
NT FAIRINGS
NT FALLING SPHERES
NT PARABOLIC BODIES
NT POINCARE SPHERES
NT ROTATING CYLINDERS
NT ROTATING SPHERES
NT SLENDER CONES
NT SPHERES
NT STREAMLINED BODIES
NT TORUSES
Two lunar global asymmetries
04 p0585 N85-13734
Motion of heavy symmetric body with flexible bars about stationary point 06 p0780 N85-14989
Dynamics of solid body with ellipsoidal cavity containing magnetic fluid 14 p2279 N85-24116
Stability of steady motions of dynamically symmetrical solid at a triangular libration point
14 p2279 N85-24120
The Mises yield condition for thin rotationally symmetric shells
[BLL-BISI-TRANS-22047-(9022.06)] 17 p2978 N85-28409
Magnetic field and equivalent circuit of induction motors with shielded poles 22 p3772 N85-33378

SYMMETRY
NT BROKEN SYMMETRY
Searching for top, Higgs, and supersymmetry: The minimum invariant mass technique
[DE84-014539] 01 p0119 N85-10813
Nonlinear symmetrization of picosecond pulses in optical fibers 02 p0264 N85-11725
On the weak limits of elementary symmetric polynomials
[CWI-MS-R8407] 05 p0719 N85-14620
On the nature of the baryon asymmetry
[NASA-TM-86156] 05 p0746 N85-14784
Downwash in the plane of symmetry of an elliptically loaded wing
[NASA-TP-2414] 07 p0898 N85-15693
The symmetry group and exponents of operator stable probability measures
[AD-A147187] 07 p1035 N85-16568
A numerical approach for the vibration analysis of an axisymmetric shell structure with a nonuniform edge constraint
[AD-A149286] 11 p1651 N85-20402
Complex symmetric matrices with strongly stable iterates
[NASA-CR-172542] 11 p1706 N85-20731
Ultraviolet divergences and supersymmetric theories
[DE85-001649] 11 p1729 N85-20875
Simulating supersymmetry at the SSC
[DE85-000699] 11 p1736 N85-20917
Accidental degeneracies, hidden supersymmetries, and spectrum-generating superalgebras
[DE85-003547] 11 p1738 N85-20930
Efficient heating and confinement of ions in an axisymmetric magnetic mirror supplemented with dc electric field
[IPPJ-707] 12 p1935 N85-22160
Determining geometrical divergence using seismic observation data 14 p2343 N85-24489
Determination of symmetry of immediate surroundings in amorphous Co-P alloys 15 p2496 N85-25398
Effect of axisymmetric vibration modes on sensitivity and directivity characteristics of piezoceramic sphere — hydrophones 15 p2525 N85-25589
Antenna with outboard exciter for 3.4-13.25 GHz frequency range 15 p2528 N85-25577
Temperature: Curvature relationships for unsymmetric graphite-epoxy laminates
[VPI-E-85-06] 16 p2743 N85-26936
On residual stress in an elastic body
16 p2796 N85-27248
Chemical applications of topology and group theory. 17: An information theoretical approach to polyhedral symmetry
[AD-A152521] 17 p2919 N85-27995
Lattice actions improved by block-spin renormalisation group and maximally symmetric lattices
[DE85-007416] 17 p3045 N85-28841
Hamiltonian picture of the free electron laser and unitary symmetries
[PREPRINT-436] 18 p3114 N85-29281
Detection of multivariate outliers with dispersion slippage in elliptically symmetric distributions
[AD-A153785] 18 p3174 N85-29677
Weak interactions of quarks and leptons: Experimental status
[DE85-006171] 18 p3181 N85-29723
Distribution of density in closed-impression die forging of axisymmetrical products from metal powders
19 p3245 N85-30118
Boson-fermion symmetries in the W-Pt region
[DE85-009755] 19 p3362 N85-30845
Primordial inflation and supergravity
[DE85-009538] 19 p3383 N85-30989
Theoretical prediction of stationary positions in the rectangular chamber during asymmetric electroosmotic flow 20 p3499 N85-31750
New O(6) region near A = 130 and the interplay of triaxiality and gamma-softness in the IBA
[DE85-010957] 20 p3530 N85-31981
Remarks on nucleon-nucleon hard scattering
[NIKHEF-H/84-14] 20 p3532 N85-31979
Possibility of developing charged-particle energy analyzer based on hyperboloidal axisymmetrical lens
21 p3691 N85-32933

SYMMETRY BREAKING
U BROKEN SYMMETRY

SYMPATHETIC NERVOUS SYSTEM
Natural electrical activity of human sympathetic nerve fibers, recorded from body surface
07 p1013 N85-16433
Regulation of physical activity in antiorthostatic position by acting on adrenosympathetic and hypophyseo-adrenocortical systems
22 p3624 N85-33689

SYMPATHOMIMETICS
U ADRENERGICS

SYMPHONIE SATELLITES
Clock synchronization by the Symphonie and Laser Synchronization from Stationary Orbit (LASSO) geostationary satellites 14 p2398 N85-24778

SYMPTOMS
U SIGNS AND SYMPTOMS

SYNAPSES
Natural electrical activity of human sympathetic nerve fibers, recorded from body surface
07 p1013 N85-16433
Direct assessment of synaptic modification rules
[AD-A146376] 08 p1196 N85-17534
Effects of hypothermia on brain metabolism
11 p1692 N85-20636
A model for generalization and specification by single neurons
[AD-A150871] 14 p2391 N85-24724

SYNCHRONISM
NT BIT SYNCHRONIZATION
NT FREQUENCY SYNCHRONIZATION
DCS (Defense Communications System) network synchronization design criteria
[AD-A146251] 03 p0356 N85-12289
Adaptive mutual interference suppression method
[AD-D011268] 05 p0628 N85-14024
Experiences with nonsynchronous forced vibration in centrifugal compressors 05 p0642 N85-14119
Digital raster timing encoder-decoder
[AD-D011279] 06 p0804 N85-15120
Reed-Solomon code synchronization revisited
10 p1464 N85-19234
Fast synchronization model for UHF spread-spectrum communication system 10 p1473 N85-19296
A technical solution to fadings in tactical satellite digital transmissions 10 p1473 N85-19297

Asynchronous transmission with strong spectral spread 10 p1474 N85-19300
Design of a semi-custom integrated circuit for the SLAC SLC timing control system
[DE85-003091] 11 p1629 N85-20258
Psychological aspects of phenomenon of spatial synchronization of EEG potential 11 p1691 N85-20632
Investigation of influence of communications link and synchronization error on noise tolerence of group transmission of binary information based on orthogonal Walsh function 13 p2096 N85-23026
Location and synchronization — space-time coordinates 14 p2397 N85-24768
Constructing unifying frameworks for the study of distributed system and algorithms
[AD-A151267] 15 p2637 N85-26261
Synchronizing heavily encoded data in bad weather 16 p2770 N85-27099
Symbol stream combining in a convolutionally coded system 16 p2771 N85-27101
UHF IRIG G distribution system 17 p2965 N85-28308
Precise time transfer using MKIII VLBI technology 17 p2965 N85-28310
Time synchronization experiments with APPLE 17 p2967 N85-28323
New GOES satellite synchronized time code generation 18 p3109 N85-29247
The time and frequency comparisons via Loran-C and National TV Network in Yugoslavia 18 p3109 N85-29248
Introduction to programming multiple-processor computers
[DE85-010274] 18 p3164 N85-29599
Balanced system for ranging and synchronization between satellite pairs
[AD-D011697] 19 p3224 N85-29992
Phase locked loop synchronization for direct detection optical PPM communication systems
[NASA-CR-176026] 19 p3254 N85-30178
Development of a resistive load for PBFA 2 rimfire gas switch simultaneity and laser triggering tests
[DE85-011080] 19 p3365 N85-30869
Globally-asynchronous locally-synchronous systems
[AD-A154624] 21 p3573 N85-32222
Consensus in the presence of partial synchrony (Preliminary version)
[AD-A154705] 21 p3670 N85-32799
A new fault-tolerant algorithm for clock synchronization
[AD-A154771] 21 p3676 N85-32836

SYNCHRONIZATION
U SYNCHRONISM

SYNCHRONIZERS
Hydraulic forces on a centrifugal impeller undergoing synchronous whirl 05 p0643 N85-14124
Instrument to synchronize Thomson scattering diagnostic measurements with MHD activity in a Tokamak
[DE85-012062] 23 p3984 N85-34706

SYNCHRONOUS DETECTORS
U CORRELATORS

SYNCHRONOUS MOTORS
Operational behavior of wind energy converters. Control and dynamic and types of generators, volume 1
[BMFT-FB-T-84-154-VOL-1] 03 p0386 N85-12470
Operational behavior of wind energy converters: Control and dynamic and types of generators, volume 2
[BMFT-FB-T-84-154-VOL-2] 03 p0386 N85-12471
The performance of an alternating-current thyristor-controlled motor 15 p2546 N85-25716

SYNCHRONOUS PLATFORMS
Full load testing in the platform module prior to tow-out: A case history of subsynchronous instability 05 p0642 N85-14117
Vibration analysis of a multipurpose platform
[NAL-TR-803] 09 p1286 N85-18078
Concentrator technologies evaluation for large solar arrays and their application for space stations/platforms 13 p2010 N85-22609
JANUS: An autonomous platform optimized for SARSAT type missions 20 p3406 N85-31135
The space station polar platform: NOAA systems considerations and requirements
[NOAA-TR-NESDIS-22] 22 p3740 N85-33182

SYNCHRONOUS SATELLITES
NT AEROS SATELLITE
NT ANIK SATELLITES
NT GOES SATELLITES
NT GOES 5
NT MIRANDA SATELLITE
NT SIRIO SATELLITE
NT STORMSAT SATELLITE
The past, present, and anticipated future contributions of geosynchronous satellites to short range prediction 01 p0076 N85-10603
Charging of the DMSP F-2 spacecraft in the aurora on 10 January 1983
[AD-A146303] 03 p0324 N85-12086
The launch window of a geostationary satellite 05 p0600 N85-13822
Perturbations in geostationary orbit 05 p0600 N85-13824
Stationkeeping strategies for geostationary satellites 05 p0600 N85-13825
Debris in the geostationary orbit ring, the endless shooting gallery: The necessity for a disposal policy 12 p1786 N85-21214
Navy tactical applications guide. Volume 4. Part 1. Eastern North Pacific weather analysis and forecast applications
[AD-A150097] 12 p1896 N85-21900
In-orbit laser regeneration of the radiation damaged solar arrays 13 p2008 N85-22588
The DFS-Kopernikus solar generator electrical design 13 p2008 N85-22590
The DFS-Kopernikus solar generator 13 p2008 N85-22591
Station keeping of geostationary satellites by electric propulsion
[NASA-TM-77820] 14 p2320 N85-24337
Orbital positioning and stationkeeping of geostationary satellites 14 p2397 N85-24772
A FORTRAN program for deep space sensor analysis
[AD-A151700] 15 p2489 N85-25366
A simulation experiment on the impact of geostationary temperature retrievals in numerical models 15 p2597 N85-26005
Study of a medium term flexible fixed satellite service mission
[DM51/CC-IM-0185.83] 18 p3091 N85-29136
A 406 MHz ELT processor for geostationary satellites — Emergency Locator Transmitter (ELT) 20 p3403 N85-31114
Navigation data for Emergency Position Indicating Radio Beacons (EPIRBs) 20 p3403 N85-31115
International prototype network in Dubna experimental satellite communications system 22 p3773 N85-33383

SYNCHROPHASING
An improved source model for aircraft interior noise studies
[NASA-CR-172517] 08 p1217 N85-17668

SYNCHROTRON RADIATION
Applications of synchrotron X-ray diffraction topography to fractography
[DE84-016257] 04 p0513 N85-13274
Instrumentation at national facilities for synchrotron radiation topography
[DE84-016256] 04 p0584 N85-13593
Electron spectrometry experiments with the use of synchrotron radiation
[DE85-001286] 07 p1041 N85-16610
Structural studies of amorphous Mo-Ge alloys using synchrotron radiation
[DE85-002061] 08 p1131 N85-17125
Synchrotron emission from chaotic stellar winds 08 p1234 N85-17774
Application of tunable monochromatic synchrotron radiation to the quantitative determination of trace elements
[DE85-001271] 09 p1291 N85-18106
Radio emission from RS CVn binary systems 09 p1417 N85-18939
Synchrotron X-ray fluorescence and extended X-ray absorption fine structure analysis
[DE85-003606] 10 p1438 N85-19063
Linear, position-sensitive X-ray detector used for real-time calculations of small-angle scattering parameters with submillisecond resolution
[DE85-002530] 10 p1489 N85-19401
Surface physics and crystallography
[DE85-003126] 11 p1735 N85-20910
Major facilities for materials research and related disciplines
[PB85-106650] 11 p1739 N85-20934
Multifrequency observations of BL LAC objects and violently variable quasars 11 p1748 N85-20981
Coordinated multifrequency observations of the BL LAC objects MRK 180, MRK 421, and MRK 501 11 p1746 N85-20983
Betatron-synchrotron detrapping in a tapered wiggler free electron laser
[AD-A149666] 12 p1856 N85-21642
Resonance between betatron and synchrotron oscillations in a free electron laser: A 3-D numerical study
[AD-A150059] 12 p1857 N85-21645
Intense, broadband, pulsed I-R source at the National Synchrotron Light Source
[DE84-010542] 12 p1935 N85-22154
Angle-resolved photoemission study of AuGa2 and AuIn2 intermetallic compounds
[AD-A150000] 12 p1940 N85-22183
EXAFS of monolayers on silver electrodes: SSRL proposal number 717M
[AD-A150623] 13 p2018 N85-22652
Threshold double photoionization of argon with synchrotron radiation
[AD-A150615] 13 p2157 N85-23389
Noninductive current drive in Tokamaks
[DE85-005427] 14 p2424 N85-24951
Application of permanent magnets in accelerators and electron storage rings
[DE85-004961] 15 p2642 N85-26297
Measurement of NSLS distributed diode sputter ion pump characteristics
[DE85-006550] 16 p2760 N85-27031
A synchrotron/inverse Compton interpretation of a solar burst producing fast pulses at lambda 3 mm and hard X-rays 16 p2887 N85-27815
Polymer Research at Synchrotron Radiation Sources: Symposium Proceedings
[DE85-008468] 18 p3081 N85-29062
VUV synchrotron light as a technique for studying the interface quality and properties of thin overlayers
[DE85-009822] 19 p3262 N85-30227
Present and future directions of atomic physics research with multiply-charged ions at Brookhaven National Laboratory
[DE85-010960] 19 p3354 N85-30788
Frequent observations of extragalactic compact sources at 24 GHz 19 p3386 N85-31003
The Silica Aerogel Detector (SAD) story — Cherenkov detector
[USIP-84-14] 20 p3459 N85-31485
Permanent magnets for production and use of high energy particle beams
[DE85-009934] 20 p3522 N85-31905
Microscopic control of semiconductor surface oxidation
[AD-A154799] 21 p3709 N85-33026
Photoionization of alkali and alkaline earth atoms: Na and Mg
[DE85-011812] 22 p3837 N85-33755
Saturation of a longitudinal instability due to nonlinearity of the wake field
[DE85-012514] 22 p3837 N85-33761
On the emission region of gamma ray bursts
[OG-1.1-4] 22 p3861 N85-33906
The electron spectra in the synchrotron nebula of the supernova remnant G 29.7-0.3
[OG-6.2-10] 22 p3889 N85-34109
Onion-shell model for cosmic ray electrons and radio synchrotron emission in supernova remnants
[OG-8.1-10] 23 p4018 N85-34900
Dissociative and double photoionization cross sections of NO from threshold to 120 A
[NASA-CR-176185] 24 p4147 N85-35713
Exit channels of autoionization resonances in atoms
[DE85-012299] 24 p4149 N85-35726
Breeding new light into old machines (and new)
[DE85-013055] 24 p4155 N85-35763
Accelerator physics measurements at the damping ring
[DE85-013373] 24 p4159 N85-35765

SYNCHROTRONS
NT STORAGE RINGS (PARTICLE ACCELERATORS)
Design study of the vacuum pump of the ESRP — synchrotron radiation
[NIKHEF-MTG-21] 08 p1138 N85-17167
A study of the K-edge absorption spectra of selected vanadium compounds
[AD-A149334] 10 p1435 N85-19045
First- and second-order charged particle optics
[DE85-006310] 14 p2421 N85-24940
Future accelerator studies of high energy heavy ion collisions
[DE85-005885] 15 p2650 N85-26346
Experiments with light ions at CERN super proton synchrotron
[DE85-007625] 17 p3031 N85-28744
Alternating gradient synchrotron
[DE85-005950] 17 p3033 N85-28759
Muon spin rotation studies 17 p3042 N85-28819
3d calculations of a fixed field alternating gradient synchrotron magnet
[DE85-002742] 18 p3183 N85-29739
Experience with a high-brightness storage ring: The NSLS 750 MeV VUV ring
[DE85-010547] 18 p3190 N85-29787
Slow extraction of LAMPF 2
[DE85-010744] 19 p3356 N85-30805

Combined function lattices for a 6 GeV synchrotron light source
[DE85-010959] 19 p3367 N85-30885
Longitudinal tune control in synchrotrons
[DE85-010745] 20 p3527 N85-31937
Spin physics at BNL
[DE85-009768] 20 p3529 N85-31955
Tailored vacuum chambers for ac magnets
[DE85-010767] 21 p3591 N85-32319
High-energy Physics Institute building 3-trillion-ev accelerator 21 p3691 N85-32934
Heavy ion medical accelerator options
[DE85-011204] 22 p3841 N85-33784
Commissioning the polarized beam in the AGS
[DE85-010958] 22 p3841 N85-33786
Robinson instability and beam loading
[DE85-013301] 24 p4151 N85-35737
Vacuum system for the Argonne 6 GeV synchrotron light source
[DE85-012286] 24 p4157 N85-35773

SYNCOPE
NT BLACKOUT (PHYSIOLOGY)

SYNDROMES
U SIGNS AND SYMPTOMS

SYNOPTIC MEASUREMENT
Empirical and modeled synoptic cloud climatology of the Arctic Ocean
[NASA-CR-175628] 13 p2137 N85-23272
Diagnostics of severe convection and subsynoptic scale ageostrophic circulations
[NASA-CR-171581] 21 p3634 N85-32571

SYNOPTIC METEOROLOGY
Application of automatic pattern methods in very-short-range forecasting 01 p0078 N85-10521
Short-term forecasting using a REMOS approach — regime model output statistics (REMOS) 01 p0081 N85-10544
Investigation of summertime convection over the upper Current River valley of southeast Missouri
[PB84-222389] 01 p0086 N85-10578
The identification of rain-bearing synoptic systems through principal component analysis 02 p0212 N85-11394
The application of principal component analysis in a study of rainfall 02 p0212 N85-11396
Bibliography of climate textbooks and studies
[WCP-84] 02 p0231 N85-11505
The METEOSAT exploitation project, operational use of a remote sensing system 05 p0658 N85-14223
Use of photographs of meteorologic satellites in synoptic analysis
[SESIT-5] 05 p0679 N85-14357
The use of available potential energy to evaluate two GLAS FGGE data sets 05 p0682 N85-14387
The influence of synoptic scales on low-frequency modes of variability 05 p0687 N85-14412
Distribution of the K-corona over the polar regions of the solar disk: 1965-1983
[PB84-230077] 06 p0835 N85-15317
Synoptical observations of snow depths at Dutch meteorological stations, 1956 - 1977
[KNMI-TR-51] 07 p1008 N85-16407
Sea breeze-induced mesoscale systems and severe weather
[NASA-CR-174317] 08 p1187 N85-17480
Development of guidance forecasts at the Royal Netherlands Meteorological Institute (KNMI). Part 1: General information
[KNMI-TR-54-PT-1] 08 p1190 N85-17499
Some aspects of atmospheric circulation near South America and interactions with the Antarctic regions
[INPE-3308-PRE/616] 10 p1515 N85-19561
Oceanographic and meteorological research based on the data products of SEASAT
[E85-10091] 12 p1874 N85-21753
AFOS (Automation of Field Operations and Service) surface observation decoding
[PB85-137586] 12 p1898 N85-21913
Sea breeze-induced mesoscale systems and severe weather 15 p2598 N85-26012
Development of a graphic system: Example using the outline of synoptic charts
[INPE-3296-PRE/611] 16 p2810 N85-27327
Fog advection in the Namib 16 p2831 N85-27454
A graphic system for drawing synoptic maps by computer
[INPE-3215-PRE/568] 16 p2834 N85-27474
SINOGRAFO: A system for influencing and forecasting weather
[INPE-3349-PRE/628] 16 p2834 N85-27475
Statistical interpretation of the ECMWF model using MOS to predict surface wind and temperature
[WSR-2] 17 p2995 N85-28515
Towards a study of synoptic-scale variability of the California current system
[NASA-CR-175671] 17 p2997 N85-28529
Atmospheric cross sections for the Arctic gas and aerosol sampling program, March - April 1983
[NASA-CR-176027] 19 p3314 N85-30541
On the state of knowledge on meteorologically caused icing of aircraft in clouds
[ESA-TT-861] 20 p3496 N85-31736
Frequency and site selection criteria for MST radars, part 5.1A 21 p3624 N85-32512

SYNTAX
NT WORDS (LANGUAGE)
Model theory for infinitely deep languages
[ISSN-0355-0087] 01 p0101 N85-10674
PROGEN: An incremental programming environment
[NRIMS-TWISK-315] 02 p0241 N85-11568
Research in knowledge representation for natural language understanding
[AD-A145807] 03 p0409 N85-12613
Toward a principle-based parser
[AD-A147637] 08 p1202 N85-17565
Speech analysis by parametric methods: A survey
[ENST-84C004] 09 p1313 N85-18251
An algorithm for generating abstract syntax trees
[NASA-CR-172541] 12 p1912 N85-22003
The four forms of omega
[AD-A149694] 12 p1915 N85-22020
The design and implementation of a syntax directed editor for a space constrained microcomputer
[AD-A151313] 15 p2623 N85-26163
Evaluating syntactic constraints to speech recognition in a fighter aircraft environment
[AD-A152117] 16 p2773 N85-27119
Research in knowledge representation for natural language understanding
[AD-A152260] 16 p2851 N85-27579
The design, implementation and application of a table-driven syntax-directed editor
[AD-A154234] 19 p3336 N85-30670
Survey of Ada (Trademark)-based PDLs (Program Design Language)
[AD-A154402] 19 p3338 N85-30680
Speech understanding research
[AD-A155462] 21 p3700 N85-32990
Research on distributed artificial intelligence
[AD-A155356] 22 p3833 N85-33733

SYNTHESIS
Electrochemistry of Hexanitroazobenzene (HNAB)
[DE85-010607] 21 p3565 N85-32171

SYNTHESIS (CHEMISTRY)
A method for obtaining new cyclical imides of derivative benzimidazoles
[AD-A145042] 01 p0017 N85-10106
Method of obtaining polychalcones
[AD-A145051] 01 p0018 N85-10107
Method of obtaining polybenzimidazopyrrolones
[AD-A145140] 01 p0018 N85-10108
Synthesis of pentafluorotellurium hypofluorite
[AD-D011212] 01 p0023 N85-10139
Two silicon phthalocyanines and a silicon naphthalocyanine: Synthesis, electrochemistry and electrogenerated chemiluminescence
[AD-A144760] 01 p0023 N85-10145
Synthesis and characterization of advanced materials
[PB84-215326] 01 p0025 N85-10156
Powder containing 2H-type silicon carbide produced by reacting silicon dioxide and carbon powder in nitrogen atmosphere in the presence of aluminum
[NASA-TM-77597] 01 p0027 N85-10167
Transition metal carbene complexes
[AD-A144879] 01 p0028 N85-10173
Method for the preparation of poly(carbonyl fluoride) oligomers
[AD-D011207] 01 p0030 N85-10184
Preparation and properties of single crystals of hydrogen bis(phthalocyaninato) neodymium(3)
[AD-A144933] 01 p0123 N85-10846
Recent progress in BGO development for high resolution calorimetry
[MPI-PAE/EXP-E1-129] 01 p0124 N85-10848
A new heat-resistant polymer from dimer diamine bismaleimide. Part 1: Preparation and free radical cure of dimer diamine bismaleimide
[AD-A145684] 02 p0186 N85-11247
The 7-Amino-4,6-Dinitrobenzofuroxan, an insensitive high explosive
[AD-A145685] 02 p0186 N85-11257
Synthesis of stereoisomeric - metal complexes using phase-transfer catalysis and photochemical transforms
[AD-A145787] 03 p0331 N85-12134
Syntheses of polyhedranes and polyhedral carboranes
[AD-A146076] 03 p0340 N85-12187
Thermoplastic/melt-processable polyimides 04 p0466 N85-12961
Matrix synthesis and characterization 04 p0467 N85-12965
Study of catalysts and mechanisms in synthesis reactions
[DE84-015025] 04 p0470 N85-12990
Physics and design of advanced infrared bolometers and photoconductors
[DE84-016883] 04 p0503 N85-13213
Low temperature synthesis of polycaproamide copolymers grafted with polydimethylaminothylmethacrylate 06 p0761 N85-14868
Synthesis of reinforced composite threads based on polymer mixtures 06 p0761 N85-14869
Synthesis of antimicrobial chemical fibers and fibrous materials containing quaternary ammonium compounds and their utilization 06 p0762 N85-14872
A silicon phthalocyanine and a silicon naphthalocyanine: Synthesis, electrochemistry, and electrogenerated chemiluminescence
[AD-A146441] 06 p0765 N85-14885
Polymerization and halogen scrambling behavior of phenyl-substituted cyclotriphosphazenes
[AD-A146366] 06 p0771 N85-14930
Synthesis of film-forming electron-accepting polymers
[AD-A146430] 06 p0771 N85-14931
Solar wind and cosmic ray irradiation of grains and ices - application to erosion and synthesis of organic compounds in the solar system 06 p0888 N85-15637
Pseudo-p-1,2,2,9,9,10,10-octofluoro (2,2)-p-cyclophane bis-acid chloride
[AD-D011393] 07 p0919 N85-15818
Structural and synthetic organosilicon chemistry
[AD-A147101] 07 p0919 N85-15820
Synthesis and properties of Hexachloromolybdates(5) and related species
[AD-A139599] 07 p0924 N85-15862
Fluorinated diacrylic esters
[AD-D011328] 07 p0929 N85-15889
Polyphosphazene solid electrolytes
[AD-A147008] 07 p0931 N85-15902
Synthesis and characterization of unique liquid crystalline block copolyesters. A proposal for a polymer research center at the Atlanta University
[AD-A147280] 07 p0932 N85-15907
New synthesis of phosphazene polymers
[AD-A147567] 07 p0933 N85-15910
Elastomers and other organic composites
[AD-A147624] 08 p1131 N85-17131
Synthesis and characterization of a 1,4 Polybutadiene/Isotactic polypropylene block copolymer
[AD-A148199] 08 p1133 N85-17142
The synthesis and characterization of Poly(Oxy(2-Methyl-1,3-Phenylene) Methyl-1,3 -Phenylene) Oxyterephthaloyl)Oxy
[AD-A148269] 08 p1133 N85-17143
Properties of ultra-violet cured poly(dimethylsiloxane)-urea acrylates
[AD-A148570] 08 p1134 N85-17146
Poly(dimethylsiloxane)-polyurethane elastomers: Synthesis and properties of segmented copolymers and related zwitterionomers
[AD-A148571] 08 p1134 N85-17147
Metal-support interactions: The effect of catalyst preparation on catalytic activity
[DE84-017425] 09 p1293 N85-18118
Continuous organic electrochemical synthesis
[DE85-001400] 10 p1437 N85-19057
Stable polymeric carbon radicals. Part 2: Attempts at the preparation of polyradicals of the triphenylmethyl type linked by P-phenylene units
[NASA-TM-77799] 10 p1450 N85-19134
Method for making heterocyclic block copolymers
[AD-D011448] 10 p1451 N85-19143
Polymer electrolytes: An investigation of some poly (N-propylaziridine)/lithium salt compositions
[AD-A149444] 10 p1452 N85-19148
Method for synthesizing indium phosphide
[AD-D011475] 10 p1583 N85-19655
Studies of the kinetics and mechanisms of ammonia synthesis and hydrodesulfurization on metal single crystal surfaces
[DE85-001650] 11 p1595 N85-20030
Investigation of structure-permeability relationships of silicone polymer membranes
[PB85-148476] 11 p1596 N85-20038
Solar fuel synthesis based on colloidal and particulate semiconductors
[PB85-129104] 11 p1614 N85-20152
The synthesis, structural characterization and reactions of closo-Rhodacarborane Anions containing a formal d8 metal vertex 1,2
[AD-A149640] 12 p1799 N85-21265
Fire resistant polymers based on 1-(diorgano oxyphosphonyl)methyl-2,4- and 2,6-diamino benzenes
[NASA-CASE-ARC-11512-2] 12 p1811 N85-21362

Scale-up of vanadium trineodecanoate
[AD-A149935] 12 p1813 N85-21370
Plasticizer system for propellant compositions
[AD-D011602] 12 p1816 N85-21390
Plasticizer system for propellant compositions
[AD-D011508] 12 p1816 N85-21391
Plasticizer system for propellant compositions
[AD-D011517] 12 p1817 N85-21395
Ideal gas thermodynamic properties for the phenyl, phenoxy, and o-biphenyl radicals
[NASA-TM-83800] 12 p1943 N85-22204
Synthesis and characterization of poly(vinylidene fluoride)
[AD-A150201] 13 p2037 N85-22759
Geomagnetic field dynamics 13 p2116 N85-23182
Preparations of methoxynitrophenazines and their photoconductivities
[NASA-TM-77775] 14 p2247 N85-23929
Synthesis and properties of elevated temperature P/M aluminum alloys
[AD-A151031] 14 p2256 N85-23981
Synthesis of hydrophobic, crosslinkable resins
[AD-A150658] 14 p2260 N85-24002
Investigation of the MBE growth of InSb and novel quantum well structures
[AD-A151014] 14 p2427 N85-24989
Comparative sinterability of combustion synthesized and commercial titanium carbides
[DE85-006255] 15 p2512 N85-25498
A soluble linear Schiff-base coordination polymer containing eight-coordinate zirconium(4)
[AD-A151446] 15 p2518 N85-25527
Synthesis of phenols from metal-carbynes and diynes
[AD-A151913] 16 p2754 N85-26997
Michelle-derived catalysts for extended Schulz-Flory
[DE85-005656] 17 p2922 N85-28012
Polyaromatic ether-sulfone-keytones with fluoro-substituted-p-cyclophane units as cross-linking sites
[AD-D011649] 17 p2933 N85-28105
Preparation of silicon carbide-silicon nitride fibers by the pyrolysis of polycarbosilazane precursors
[NASA-TM-86505] 17 p2933 N85-28107
New examples of clusters, extended metal-metal bonding and interstitial derivatives
[DE85-005926] 17 p3044 N85-28837
Phenoxy resins containing pendent ethynyl groups and cured resins obtained therefrom
[NASA-CASE-LAR-13262-1] 18 p3068 N85-28973
The conversion of smaller borane fragments to larger structures. Systematics of boron hydride reactions
[AD-A153443] 18 p3070 N85-28985
New synthetic routes to boron cage compounds
[AD-A153554] 18 p3071 N85-28991
Study of synthesis gas conversion over metal oxides
[DE85-010136] 18 p3072 N85-28999
Synthesis chemistry of ceramics by solid-state combustion processes in micro-gravity
[DE85-009595] 18 p3081 N85-29061
Liquid hydrocarbon fuels from anygas
[DE85-009613] 19 p3228 N85-30017
Spray pyrolysis as a synthetic tool
[AD-A153891] 19 p3234 N85-30047
Metallophthalocyanine dimers incorporating five atom covalent bridges
[AD-A154365] 19 p3234 N85-30051
New approaches to functionalized fluorocarbons
[AD-A154206] 19 p3248 N85-30141
Synthesis and characterization of novel polymers from non-petroleum sources for use in enhanced oil recovery
[DE85-010922] 19 p3250 N85-30151
Design and chemical synthesis of iodine-containing molecules for application to solar-pumped I* lasers
[NASA-CR-176010] 19 p3275 N85-30310
Development of an impact- and solvent-resistant thermoplastic composite matrix, phase 3
[NASA-CR-172568] 20 p3422 N85-31239
Synthesis and characterization of copolyimides with varying flexibilizing groups
[NASA-TM-86416] 20 p3433 N85-31298
Propellant plasticizer
[AD-D011501] 20 p3434 N85-31306
Synthesis and properties of arylethersulfone thermoset systems
[AD-A154811] 21 p3569 N85-32198
Synthesis of energetic materials
[AD-A154887] 21 p3571 N85-32210
Origin of life 21 p3657 N85-32713
The composition of the primitive atmosphere and the synthesis of organic compounds on the early Earth
21 p3717 N85-33065
Synthesis of 2,4,8,10-tetroxaspiro5,5undecane
[NASA-CASE-ARC-11243-2] 22 p3741 N85-33187
Electrolytic synthesis of colored eta alumina film
23 p3908 N85-34201
Fire-resistant phosphorus containing polyimides and copolyimides
[NASA-CASE-ARC-11522-2] 23 p3918 N85-34260
Preparation of ethylenediamine dinitrate
[DE85-006423] 23 p3922 N85-34305
Ethylenediamine salt of 5-nitrotetrazole and preparation
[DE85-005738] 23 p3923 N85-34306
Synthesis of ultrafine ceramic and metallic powders in a thermal argon rf plasma
[DE85-009634] 23 p3983 N85-34696
FTIR studies of hydrocarbon synthesis on Pd/ZSM5 catalysts
[DE85-012430] 24 p4071 N85-35230
System for the continuous generation of phosphorous aerosols from red phosphorus-butyl rubber
[DE85-013527] 24 p4072 N85-35232
SYNTHESIZERS
Rech-1 speech synthesizer for man-machine dialog
04 p0543 N85-13456
Optimal design efforts in Shanghai described
13 p1972 N85-22366
Analysis of spectral characteristics of multilevel digital computing synthesis 15 p2527 N85-25579
A preliminary investigation into the intelligibility of Microspeech-2, a speech synthesiser
[BAE-BT-12284] 15 p2539 N85-25675
SYNTHETIC APERTURE RADAR
NT SIDE-LOOKING RADAR
Ultrasonic synthetic aperture focusing using unfocused pulse-echo transducers
[AERE-R-11230] 01 p0057 N85-10374
Production of optically correlated SEASAT-A (SEA satellite) SAR (Synthetic Aperture Radar) imagery at DREO (Defence Research Establishment Ottawa)
[AD-A145970] 03 p0355 N85-12281
Aspects and applications of SAR (Synthetic Aperture Radar) imagery for mensuration
[AD-A146301] 03 p0356 N85-12290
Structural aspects of SAR antenna for Japanese Earth Resources Satellite 1 05 p0626 N85-14007
Technology for the ERS-1 SAR antenna
05 p0626 N85-14008
Multispectral (X and C band) crop classification with synthetic aperture radar (SAR-580) optical data
05 p0657 N85-14217
Metric evaluation of SAR-580 optical images for cartographic purposes 05 p0659 N85-14231
The wide-range space radio interferometer
07 p1058 N85-16717
The use of digital spaceborne SAR data for the delineation of surface features indicative of malaria vector breeding habitats 08 p1146 N85-17230
The investigation of selected oceanographic applications of spaceborne synthetic-aperture radar
08 p1146 N85-17233
SIR-B cartography and stereo topographic mapping
08 p1147 N85-17234
Investigation of SIR-B images for lithologic mapping
08 p1148 N85-17241
Automatic terrain elevation mapping and registration
08 p1148 N85-17242
Australian Multiexperimental Assessment of SIR-B (AMAS) 08 p1148 N85-17243
German Radar Observation Shuttle Experiment (ROSE) 08 p1148 N85-17245
SAR internal wave signature experiment
08 p1149 N85-17253
Information extraction and transmission techniques for spaceborne synthetic aperture radar images
[NASA-CR-174341] 08 p1150 N85-17256
Spaceborne distributed SAR antenna
[NASA-CR-171835] 08 p1150 N85-17259
Extraction of structural information from radar signals
[FOA-C-30370-E1] 08 p1155 N85-17292
The use of synthetic aperture radar imagery to detect hazards to navigation
[AD-A149324] 10 p1422 N85-18971
Interleaved array antenna technology development
[NASA-CR-171845] 10 p1477 N85-19326
China report: Science and technology
[JPRS-CST-84-032] 11 p1621 N85-20202
Optical processor for synthetic aperture radar
11 p1621 N85-20203
Quantization study for ERS-1 wave mode
[DFVLR-FB-84-39] 11 p1625 N85-20234
A modern approach of a synthetic aperture radar processor and its technological aspects
11 p1713 N85-20778
Earth resources research using the Shuttle Imaging Radar system 11 p1713 N85-20779
JPL highlights
[NASA-CR-175517] 11 p1767 N85-21102
The imaging of internal waves by the SEASAT-A synthetic aperture radar
[AD-A149808] 12 p1875 N85-21761
The imaging of internal waves by the SEASAT-A synthetic aperture radar
[ARE(PORTLAND)TN-720/84]
13 p2054 N85-22860
Edge detection in SAR imagery using gradient operators — synthetic aperture radar (SAR)
[AD-A149411] 13 p2054 N85-22862
Synthetic aperture radar simulation study
[AD-A151000] 14 p2293 N85-24214
Synthetic aperture radar data processing
14 p2368 N85-24780
SEASAT report
[AD-A151283] 15 p2583 N85-25931
Autofocus motion compensation for synthetic aperture radar and its compatibility with strapdown inertial navigation sensors on highly maneuverable aircraft
[AD-A151940] 16 p2704 N85-26693
Application of artificial intelligence (AI) to radar image understanding
[AD-A152519] 17 p3017 N85-28654
The multiple processor machine for image processing, volume 5
[ESA-CR(P)-1976-VOL-5] 18 p3164 N85-29603
Computer simulation of the effects of a distributed array antenna on synthetic aperture radar images
[NASA-CR-171888] 19 p3254 N85-30178
Design of a shuttle-borne SAR for the DFVLR's planning study
[ERYS-019/84] 20 p3419 N85-31218
SAR swath widening techniques — satellite radar
[BL-6198] 20 p3441 N85-31358
Synthetic aperture radar data processing — satellite-borne radar
[CNES-196-T-CT/DRT/TIT/RL]
20 p3442 N85-31363
Digital signal processing for spaceborne synthetic aperture radar
[FOA-C-30361-E1] 20 p3442 N85-31364
Deterministic and random phase noise of oscillators — synthetic aperture radar
[ESA-TT-848] 20 p3449 N85-31415
Using ship wake patterns to evaluate SAR (Synthetic Aperture Radar) ocean wave imaging mechanisms. Joint US-Canadian Ocean Wave Investigation Project
[AD-A154633] 21 p3573 N85-32223
Aspects of SAR image segmentation
[AD-A154965] 21 p3575 N85-32236
Basic properties and interpretation of synthesized radar images of sea waves with long synthetization time
22 p3773 N85-33364
Method and apparatus for Delta Kappa synthetic aperture radar measurement of ocean current
[NASA-CASE-NPO-15704-1] 23 p3925 N85-34327
AMI calibration study. Volume 1: SAR calibration. Volume 2: Ground Targets. Volume 3: Scatterometer calibration — Active Microwave Instrument (AMI) ERS-1
[C2248/4/4-VOL-1] 23 p3936 N85-34394
SYNTHETIC APERTURES
Electromagnetic-acoustic-transducer e system for thick-weld inspection
[PB84-219492] 01 p0051 N85-10336
Aperture synthesis for radioastronomy
06 p0781 N85-14992
Place of aperture synthesis in general theory of antennas (review) 06 p0781 N85-14993
Method of aperture synthesis: Fundamental relations and data processing in aperture synthesis systems (review) 06 p0781 N85-14994
Aperture synthesis (review) 06 p0781 N85-14995
Modern radioastronomical aperture synthesis systems (review) 06 p0782 N85-14997
Metric-wave and decimetric-wave aperture synthesis systems (review) 06 p0782 N85-14998
Cross-shaped aperture synthesis system
06 p0782 N85-14999
Decimetric-wave aperture synthesis system at Scientific Research Institute of Radiophysics
06 p0782 N85-15000
Phase problem in aperture synthesis systems
06 p0782 N85-15002
Approximating true radioluminance distribution from observations on aperture synthesis systems
06 p0783 N85-15003
Synthesis of radio image on RATAN-600 radiotelescope 06 p0783 N85-15004
Attempts to contruct two-dimensional image of Sun from observations made with RATAN-600 radiotelescope by relay race method 06 p0783 N85-15005
Invariance of mean-square effective area of synthesized apertures 06 p0784 N85-15009
Emerging technology of synthetic aperture focusing for ultrasonic testing
[DE85-000373] 09 p1378 N85-18664
Digital standards conversion: Interpolation theory and aperture synthesis
[BBC-RD-1984/20] 13 p2053 N85-22857

Analysis and interpretation of synthetic time strings of oscillation data 14 p2444 N85-25079
Spectral information from gapped data. A comparison of technique 14 p2444 N85-25080
Synthetic aperture side-looking radar image adjustment 16 p2606 N85-27304
Advanced ultrasonic imaging of piping in Dresden and Vermont Yankee reactors
[TI85-010049] 20 p3464 N85-31520
Optical synthetic aperture techniques
[AD-A156151] 24 p4154 N85-35752

SYNTHETIC FIBERS
NT CERAMIC FIBERS
NT GLASS FIBERS
NT NYLON (TRADEMARK)
Method of obtaining polybenzimidazopyrrolones
[AD-A145140] 01 p0018 N85-10108
New type of unique frequency laser communications
[AD-A145128] 01 p0038 N85-10239
Thermoplastic-carbon fiber hybrid yarn
[NASA-CR-3849] 03 p0325 N85-12093
Metallized synthetic cable
[AD-D011263] 05 p0628 N85-14023
Properties of polycaproamide fibers modified by grafted polyacrylonitrile 06 p0761 N85-14867
Low temperature synthesis of polycaproamide copolymers grafted with polydimethylaminothylmethacrylate 06 p0761 N85-14868
Synthesis of reinforced composite threads based on polymer mixtures 06 p0761 N85-14869
Comparison of methods for predicting fiber stresses in a cracked Kevlar/epoxy monolayer
[DE84-016118] 11 p1593 N85-20022
Diamond cutters' grinders 13 p2051 N85-22841
Mechanics of polymers and composites: Research opportunities
[DE85-007052] 15 p2503 N85-25442
Fatigue of synthetic fibers for marine rope applications
[MIT-R84-2] 17 p2979 N85-28414
Fatigue behavior of synthetic fibers, yarns and ropes 17 p2979 N85-28415
The effects of sea water and concentrated salt solutions on the fatigue of nylon 6,6 fibers 17 p2979 N85-28416
Substitution of asbestos by aramid fibers and fiber blends in industrial textiles and composites with organic binders
[BMFT-FB-T-85-006] 23 p3920 N85-34294

SYNTHETIC FUELS
NT GASOHOL (FUEL)
Mechanisms of syncrude-synfuel degradation
[DE84-015206] 01 p0034 N85-10212
The status of synthetic fuels and cost-shared energy R and D facilities
[GPO-36-903] 03 p0339 N85-12182
Inertial confinement fusion: Present status and future potential
[DE84-016177] 04 p0567 N85-13616
The infrastructure for a surge in synfuels production: The potential role of the AE and C industry and of owner operators
[RAND/N-2172-SFC] 09 p1301 N85-18170
Test report for Getty Synthetic Fuels, Inc., Calumet City, Illinois
[PB85-119493] 10 p1459 N85-19191
Synthetic fuels policy
[GPO-34-227] 11 p1613 N85-20143
Trifunctional catalysts for conversion of syngas to alcohols
[DE85-004577] 13 p2040 N85-22771
Current alternative energy research and development in Illinois
[PB85-163137] 16 p2820 N85-27397
Linking R and D to problems experienced in solids processing
[AD-A154238] 19 p3380 N85-30968
Improved catalysts for liquid hydrocarbon fuels from syngas
[DE85-011062] 20 p3421 N85-31234
A comparison of two bench scale tests of fuel low temperature flow properties
[AD-A154477] 20 p3435 N85-31311
Biomass thermochemical conversion program
[DE85-011867] 21 p3572 N85-32213
Seventh Symposium on Biotechnology for Fuels and Chemicals: Program and abstracts
[DE85-011197] 22 p3742 N85-33192
Aspects of high-resolution gas chromatography as applied to the analysis of hydrocarbon fuels and other complex organic mixtures. Volume 1
[AD-A156154] 24 p4076 N85-35257

SYNTHETIC METALS
The replacement of precious metal thick film inks using conductive polymer technology
[AD-A152002] 16 p2749 N85-26965

SYNTHETIC RESINS
NT ACRYLIC RESINS
NT EPOXY RESINS
NT KEVLAR (TRADEMARK)
NT NYLON (TRADEMARK)
NT PHENOLIC RESINS
NT POLYAMIDE RESINS
NT POLYESTER RESINS
NT POLYETHER RESINS
NT POLYMETHYL METHACRYLATE
NT THERMOPLASTIC FILMS
NT THERMOPLASTIC RESINS
NT THERMOSETTING RESINS
NT VINYL COPOLYMERS
Fundamental studies of composite toughness 04 p0464 N85-12948
Polymeric liner selection for military waste impoundments
[AD-P004143] 09 p1348 N85-18479
Evaluation of the PSP resin as a precursor of carbon
[ONERA-RT-11/1784-M] 16 p2744 N85-26932
The replacement of precious metal thick film inks using conductive polymer technology
[AD-A152002] 16 p2749 N85-26965
Ambient air contamination: Characterization and detection techniques 18 p3157 N85-29548

SYNTHETIC RUBBERS
NT CHLOROPRENE RESINS
NT ELASTOMERS
NT VULCANIZED ELASTOMERS
Damage development during low cycle fatigue of carbon-black loaded SBR
[DE85-006234] 15 p2519 N85-25533
System for the continuous generation of phosphorous aerosols from red phosphorus-butyl rubber
[DE85-013527] 24 p4072 N85-35232

SYSTEM EFFECTIVENESS
Energy-saving technological methods of obtaining controlled atmospheres
[BLL-M-35724-(5828.4)] 02 p0171 N85-11145
Investigation of the gas-content of gas-liquid systems
[BLL-M-35748-(5828.4)] 02 p0171 N85-11146
NASA Redox Storage System Development Project
[NASA-TM-83677] 03 p0385 N85-12485
Holographic displacement analysis with fiber optics
[AD-A146185] 03 p0420 N85-12680
Maintenance Management Information and Control System (MMICS): Administrative boon or burden
[AD-A145762] 03 p0438 N85-12790
Advancement of remote systems technology: Past perspectives and future plans
[DE84-016710] 04 p0509 N85-13250
Effectiveness of agricultural aviation 04 p0544 N85-13460
Operation of aviation support bases 04 p0544 N85-13461
Flying qualities and control system characteristics for supersaugmented aircraft
[NASA-CR-170419] 05 p0596 N85-13800
Analytical models 05 p0666 N85-14282
Army aviation today and tomorrow 06 p0751 N85-14810
Survey relating to the implementation of cost/schedule control systems criteria within the Department of Defense and industry
[AD-A146664] 06 p0870 N85-15526
Reverse wave suppression in unstable ring resonator
[AD-A146825] 07 p0939 N85-15952
Analysis of effectiveness of partial optimization of spatial processing systems 07 p0952 N85-16031
Nondestructive tests and fracture mechanics investigations in the Component Integrity Research Programme
[BLL-RISLEY-TR-4541-(9091.9F)] 07 p0976 N85-16199
Evaluation of the measured energy performance of four solar systems
[AD-A147912] 07 p0993 N85-16306
Lunar nuclear power feasibility study
[NASA-CR-171831] 07 p1041 N85-16611
S-3A ballast block final design and engineering tests
[AD-A147685] 08 p1080 N85-16842
A study of Air Force Quality Circle program effectiveness as viewed through facilitator's perceptions
[AD-A147633] 08 p1170 N85-17377
Comparative usefulness of flue gas oxygen and carbon dioxide analysis
[BLL-TRANS-T6358/BG/WH783/84] 08 p1179 N85-17430
Strategic management for organizational effectiveness. The effect of human resource planning on retention and related issues, volume 1
[AD-A149398] 10 p1566 N85-19674
Strategic management for organizational effectiveness. The effect of human resource planning on retention and related issues, volume 2
[AD-A149399] 10 p1568 N85-19675
A computer-based gaming system for assessing recognition performance (RECOG)
[AD-A149752] 12 p1915 N85-22022
Transmission efficiency measurements and correlations with physical characteristics of the lubricant 14 p2222 N85-23781
Problems regarding the practical evaluation of efficiency of worm gears 14 p2224 N85-23793
Axial bearings with lever-type equalizer system 14 p2267 N85-24048
Analysis of team performance in a programmed environment
[NASA-CR-175834] 14 p2392 N85-24728
Combinatorial performance/cost analysis of an autonomous navigation system for aircraft 16 p2695 N85-26640
Construction and functioning of extended orbital systems 16 p2724 N85-26814
Proposal of a method for evaluating accuracy of estimated impulse response of a system 16 p2759 N85-27024
Operational test results of a prototype superconducting power transmission system and their extrapolation to the performance of a large system
[DE85-006731] 16 p2779 N85-27153

SYSTEM FAILURES
Artificial intelligence approaches to monitoring system integrity
[AD-P003930] 02 p0248 N85-11610
Ballpark reliability estimation techniques
[AD-A145971] 03 p0389 N85-12357
Material flow in the manufacturing system: Fault-diagnosis systems as support for the maintenance of highly automated manufacturing systems
[PNR-90238] 09 p1371 N85-18618
ECS (electrical overstress) protection for VLSI (Very Large Scale Integration) devices
[AD-A150333] 13 p2064 N85-22891
Parallel test method for LSI (Large Scale Integration) microprocessors
[AD-A150237] 13 p2144 N85-23310
Contribution of instrumentation and control software to system reliability
[DE85-004693] 13 p2149 N85-23340
Some critical factors that limit the effectiveness of machine intelligence technology in military systems applications
[AD-A150584] 14 p2407 N85-24838
Automation of servicibility of radio-relay station equipment 15 p2527 N85-25582
Determining availability characteristics of DSN data systems using discrepancy report data 16 p2772 N85-27109
How to handle failures in advanced flight control systems of future transport aircraft 17 p2904 N85-27905
Dynamic considerations for control of closed life support systems 18 p3155 N85-29537
Materials and processes control for space applications 18 p3156 N85-29544
Problems and solutions in analyzing partial-reflection drift data by correlation techniques 21 p3826 N85-32529
Failure testing of active solar energy system components
[DE84-013024] 22 p3804 N85-33561

SYSTEM GENERATED ELECTROMAGNETIC PULSES
Laboratory studies of spacecraft response to transient discharge pulses 13 p1995 N85-22508
Discharge pulse phenomenology 13 p1995 N85-22509
Electron yields from spacecraft materials 13 p1996 N85-22512

SYSTEM IDENTIFICATION
Time invariant memoryless nonlinear systems identification method
[FUB-9-1983] 01 p0114 N85-10773
Nonlinear system identification methodology development based on F-4S flight test data analysis
[AD-A146289] 03 p0318 N85-12053
Structure errors in system identification 05 p0700 N85-14495
The practical identification of systems with nonlinearities
[RR-264] 08 p1209 N85-17607
Identification of dynamic systems, theory and formulation
[NASA-RP-1138] 10 p1551 N85-19784
Three algorithms for parametric frequency domain system identification
[DE85-002901] 11 p1706 N85-20735

Application of the system identification technique to goal-directed saccades
[AD-A150132] 12 p1906 N85-21967
Proposal of a method for evaluating accuracy of estimated impulse response of a system
16 p2759 N85-27024
Identification of gust input and gust response characteristics from Do 28 TNT flight test data
[DFVLR-FB-84-48] 17 p2900 N85-27681
Space station configuration and flight dynamics identification 20 p3410 N85-31162
Large space structure flight experiment
20 p3410 N85-31163
Experiments in structural dynamics and control using a grid 20 p3410 N85-31165
Optimal sensor locations for structural identification
20 p3417 N85-31209
Combined state and parameter estimation for a static model of the Maypole (Hoop-Column) antenna suface
20 p3417 N85-31210
Experimental verification of identification algorithms for control of flexible structures 20 p3418 N85-31211
An Eigensystem Realization Algorithm (ERA) for modal parameter identification and model reduction
20 p3418 N85-31212
Numerical experimentation with maximum likelihood identification in static distributed systems
20 p3418 N85-31214
A system identification package for VAX and LSI 11
[OUEL-1569/85] 20 p3516 N85-31862
An overview of nonlinear systems identification
[RR-271] 20 p3520 N85-31894
On the choice of parameterization for identification
[OUEL-1554/84] 20 p3522 N85-31904
Multishaker modal testing
[NASA-CR-178139] 22 p3800 N85-33544
Lectures of a Flight Mechanics Conference — conferences
[ESA-TT-831] 24 p4061 N85-35165
The effect of instrumentation system parameters on the results of a flight mechanical system identification
24 p4061 N85-35170

SYSTEMS ANALYSIS
NT SYSTEM IDENTIFICATION
Modelling the demand for construction
[CSIR-TWISK-322] 01 p0035 N85-10218
On the computer analysis of structures and mechanical systems 01 p0061 N85-10404
Time invariant memoryless nonlinear systems identification method
[FUB-S-1983] 01 p0114 N85-10773
Information requirements analysis: An application
[AD-A144896] 01 p0125 N85-10858
Energy efficient engine. Volume 1: Component development and integration program
[NASA-CR-173084] 02 p0146 N85-10992
Computing the reliability of k out of n systems
[AD-A145505] 02 p0206 N85-11357
Aeroelastic stability analysis with interacting structural nonlinearities 02 p0207 N85-11364
A prospectus for Thematic Mapper research in the Earth sciences
[E85-10003] 02 p0215 N85-11416
Systems analysis for microcomputer acquisitions
[AD-A145447] 02 p0239 N85-11556
Diagnosis based on description of structure and function
[AD-P003919] 02 p0245 N85-11599
A representation for the functioning of devices that supports compilation of expert problem solving structures: An extended summary
[AD-P003921] 02 p0245 N85-11601
Artificial intelligence approaches to monitoring system integrity
[AD-P003930] 02 p0246 N85-11610
DELTA: An expert system for diesel electric locomotive repair
[AD-P003941] 02 p0248 N85-11621
The ACE (Automated Cable Expert) experiment: Initial evaluation of an expert system for preventive maintenance
[AD-P003943] 02 p0248 N85-11623
The application of artificial intelligence to a maintenance and diagnostic information system
[AD-P003945] 02 p0249 N85-11625
On the requirements of expert systems for fault isolation
[AD-P003947] 02 p0249 N85-11627
Gain-phase structures for linear multivariable systems
[RR-256] 02 p0256 N85-11674
Preliminary analysis of space mission applications for electromagnetic launchers
[NASA-CR-174067] 03 p0321 N85-12071
The human operator and system effectiveness
[AD-A146326] 03 p0402 N85-12563
Introduction to the subjective transfer function approach to analyzing systems
[AD-A145817] 03 p0436 N85-12774
Design of a scientific information collation and dissemination system, volumes 1 thru 3
[AD-A146002] 03 p0438 N85-12791
Development and demonstration of a vertical axis wind turbine POWERHOUSE
[DE84-901449] 04 p0527 N85-13389
Evaluation of automated decisionmaking methodologies and development of an integrated robotic system simulation
[NASA-CR-172401] 04 p0552 N85-13516
Linear harmonic analysis for Stirling machines and second law analysis of four important losses
[DE84-016595] 04 p0573 N85-13655
ECUT energy data reference series: Lightweight materials for ground transportation
[DE84-015269] 05 p0621 N85-13974
Detailed performance calculations: Goddard Group, appendix D 05 p0676 N85-14341
New uses for sensitivity analysis: How different movement tasks effect limb model parameter sensitivity
05 p0706 N85-14529
Operational requirements - system concepts
06 p0752 N85-14823
NAVSTAR GPS (Global Positioning System) marine receiver performance analysis
[AD-A146414] 06 p0753 N85-14831
The theory of optimal confidence limits for systems reliability with counterexamples for results on optimal confidence limits for series systems
[AD-A147236] 07 p1031 N85-16546
Software testing in an Ada programming environment
08 p1065 N85-16748
Impact of activation optimization on the Vandenberg Ground Support System using Q-GERT analysis
[AD-A148448] 08 p1105 N85-16986
The description of large systems
[AD-A148072] 08 p1205 N85-17586
Asymptotic methods for the analysis, estimation, and control of stochastic dynamic systems
[AD-A147758] 08 p1211 N85-17618
Representation and refinement of visual specifications in PegaSys
[AD-A148733] 09 p1368 N85-18598
Analysis and optimization of small Space Shuttle propulsion platforms
[DFVLR-FB-84-28] 10 p1431 N85-19023
A decision model for selection of microcomputers and operating systems
[AD-A149076] 10 p1536 N85-19694
Predicting the performance of distributed knowledge-based systems: A modeling approach
[AD-A149021] 10 p1545 N85-19738
TSS Satellite overview 11 p1642 N85-20343
The use of analytical models to interpret data properly
[ERS-E.341] 11 p1651 N85-20399
The use of analytical models to interpret measured data properly. 1. General background theory
11 p1651 N85-20400
Advanced concepts in systems analysis and simulation
[DE85-002728] 11 p1702 N85-20701
Needs, opportunities, and options for large scale systems research
[DE85-002664] 11 p1709 N85-20750
Reliability analysis of automatic systems
[VTT-301] 12 p1863 N85-21682
Needs, opportunities, and options for large scale systems research
[DE85-004642] 12 p1925 N85-22091
Reluctance and doubly-excited reluctance motors
[DE85-003585] 13 p2065 N85-22900
Cooling performance improvement of a horizontal ground coupled heat pump
[DE85-002470] 13 p2093 N85-23065
SIGPI: A user's manual for the fast computation of the probabilistic performance of a complex system
[DE85-005447] 13 p2148 N85-23336
Automatic symbolic solution of Markov chains
[AD-A150476] 13 p2153 N85-23369
Application of the Hardman methodology to the Single Channel Ground-Airborne Radio System (SINCGARS)
[NASA-CR-175694] 14 p2216 N85-23756
Model and controller reduction of uncertain systems using covariance equivalent realizations
14 p2243 N85-23902
Some recent developments in systems reliability
[AD-A150661] 14 p2317 N85-24318
Space Mathematics for the Preparation and Development of satellite Exploitation
[ISBN-2-85428-115-2] 14 p2395 N85-24753
Introduction to methods of evaluating the operational reliability of complex systems: Application to satellite control ground support 14 p2397 N85-24771
Identification of dynamic systems
[AGARD-AG-300-VOL-2] 15 p2470 N85-25249
Space station systems technology study (add-on task). Volume 3: Technology advancement program plan
[NASA-CR-171417] 15 p2475 N85-25280
Logic analyzer survey and reviews
[BAE-861/ELO/1645] 15 p2621 N85-26151
An extension of a microcomputer based system for analysis of line drawing quantization schemes
[AD-A152008] 15 p2624 N85-26171
Computer program TRAMP: Inclusion of state space facilities and the analysis of non-linear elements
[BAE-BT-12643] 15 p2626 N85-26181
Computer science and technology: A guide to performance evaluation of database systems
[PB85-155794] 15 p2631 N85-26219
Design of a variable-focal-length optical system
[NASA-CR-175710] 15 p2651 N85-26349
A database design for the Brazilian Air Force Flying Unit Operational Control System
[AD-A151848] 15 p2666 N85-26452
Analysis and specification of a universal data model for distributed data base systems
[AD-A151856] 15 p2666 N85-26453
The evolutive state: A new definition of system state to include sequencing of events
16 p2696 N85-26643
An evaluation of thermal storage for liquid-metal, solar thermal receivers
[DE85-002929] 16 p2820 N85-27394
Central solar heating plants with seasonal storage. Evaluation of systems concepts based on heat storage in aquifers
[DE85-006788] 16 p2820 N85-27396
An ultrasensitive and element specific photoionization detection system for environmental analysis
[AD-A153365] 17 p2966 N85-28332
System analysis of a field Army Topographic Support System
[AD-A153318] 17 p2984 N85-28439
System Analysis for the Huntsville Operation Support Center, Distributed Computer System
[NASA-CR-171506] 17 p3015 N85-28642
An examination of alternative forms of fit in contingency theory
[AD-A152602] 17 p3047 N85-28853
The concept of fit in contingency theory
[AD-A152603] 17 p3047 N85-28854
Experimental philosophy leading to a small scale digital data base of the conterminous United States for designing experiments with remotely sensed data
[NASA-TM-85009] 17 p3049 N85-28877
Guidance on planning and implementing computer system reliability
[PB85-177996] 18 p3161 N85-29581
An operational analysis of system calibration
[AD-A153556] 18 p3170 N85-29644
Alternative theories of inference in expert systems for image analysis
[AD-A153649] 18 p3170 N85-29648
Instrument Systems Analysis and Verification Facility (ISAVF) users guide
[NASA-TM-86226] 19 p3223 N85-29982
Automatic ac/dc thermal voltage converter and ac voltage calibration system
[PB85-182574] 19 p3274 N85-30304
Modeling water resources systems for water quality
[AD-A154288] 19 p3300 N85-30457
A Lotus 1-2-3 based system reliability program
[DE85-010533] 19 p3340 N85-30701
ZOG/VINSON technology demonstration project system description. Volume 1
[AD-A154211] 19 p3342 N85-30713
A systems analysis of the erythropoietic responses to weightlessness. Volume 1: Mathematical model simulations of the erythropoietic responses to weightlessness
[NASA-CR-171890] 20 p3506 N85-31794
A systems analysis of the erythropoietic responses to weightlessness. Volume 2: Description of the model of erythropoiesis regulation. Part A: Model for regulation of erythropoiesis. Part B: Detailed description of the model for regulation of erythropoiesis
[NASA-CR-171891] 20 p3506 N85-31795
A numerical study of Taylor-Vortex flow
[AD-A154787] 21 p3584 N85-32277
The optimality of lower confidence limits for the reliability of series systems obtained by the method of key test results or other related techniques
[AD-A154880] 21 p3597 N85-32336
Space station ECLSS integration analysis: Simplified General Cluster Systems Model, ECLS System Assessment Program enhancements
[NASA-CR-176089] 21 p3670 N85-32796

A comprehensive study of the AFIT (Air Force Institute of Technology) software development environment
[AD-A155450] 21 p3672 N85-32812
Survival function of hypo-exponential distributions
[AD-A155518] 21 p3672 N85-32814
Determination of sensitivity functions for discrete dynamic systems from results of function modeling on digital computer 22 p3769 N85-33359
An evaluation of a class of practical optimization techniques for structural dynamics applications
[PB85-195766] 24 p4103 N85-35434
Prototyping with data dictionaries for requirements analysis
[AD-A156303] 24 p4139 N85-35654

SYSTEMS COMPATIBILITY
Documentation for DIGLIB: Device independent graphics library
[DE84-017365] 04 p0550 N85-13500
Software for special functions
[DE85-004884] 12 p1917 N85-22033
Basic EMC (Electromagnetic Compatibility) technology advancement for C3 systems: Model revision for IEMCAP (Intrasystem Electromagnetic Compatibility Analysis Program)
[AD-A150795] 14 p2292 N85-24208
The evolutive state: A new definition of system state to include sequencing of events 16 p2696 N85-26643

SYSTEMS DESIGN
U SYSTEMS ENGINEERING

SYSTEMS ENGINEERING
NT COMPUTER SYSTEMS DESIGN
NT CONTROL SYSTEMS DESIGN
A production peripheral vision display system 01 p0010 N85-10059
A multipurpose weather radar network 01 p0077 N85-10510
Hardware implementation of a support system for the 2501 Western digital LSI, complete controller of the second level, first version of the CCITT 25 (CAP) recommendations
[FUB-60-1982] 01 p0100 N85-10666
ADS: A FORTRAN program for automated design synthesis, version 1.00
[NASA-CR-172460] 01 p0102 N85-10684
System engineering and integration contract for implementation of the National Airspace System Plan. Volume 2: Section 5.0
[AD-A145710] 02 p0137 N85-10929
Avionics Integrity Program (Avip). Volume 2: Hardware case studies
[AD-A145689] 02 p0139 N85-10944
Combustion system for radiation investigations 02 p0145 N85-10966
Software engineering environments for mission critical applications: STARS alternative programmatic approaches
[AD-A145285] 02 p0241 N85-11571
The need for improvements in weapon system maintenance: What can AI (Artificial Intelligence) contribute?
[AD-P003913] 02 p0244 N85-11593
Diagnosis via causal reasoning: Paths of interaction and the locality principle
[AD-P003920] 02 p0245 N85-11600
An expert system for representing procedural knowledge
[AD-P003923] 02 p0245 N85-11603
Optical waveguide spatial filters
[AD-A145674] 02 p0280 N85-11825
Characteristics of systems engineering in aviation science research
[AD-A145602] 02 p0292 N85-11899
Activities report of the Department of Engineering 03 p0342 N85-12202
Automation of assembly of electrical products 03 p0348 N85-12228
Interactions among system stiffness, wear and vibrations 03 p0370 N85-12364
The ERS-1 radar altimeter: An overview 03 p0379 N85-12421
Automating software design metrics
[AD-A145869] 03 p0407 N85-12598
An input translator for a computer-aided design system
[AD-A146337] 03 p0408 N85-12605
System status display information
[NASA-CR-172347] 04 p0455 N85-12889
Study of instrument design options for the Columbus spectroscopy mission
[NASA-CR-174072] 04 p0502 N85-13205
Expert systems in design and manufacture
[DE84-005522] 04 p0550 N85-13496
Dynamics and controls working group summary 05 p0604 N85-13954
Self-tuning controller design and implementation
[OUEL-1535/84] 05 p0621 N85-13975
A generalized LQG approach to self-tuning control. Part 1: Aspects of design. Part 2: Implementation and simulation
[OUEL-1536/84] 05 p0622 N85-13976
Avionics technology - system concepts 06 p0753 N85-14824
Attack helicopter (AH-1T) cockpit systems integration 06 p0753 N85-14826
Workshop on Computer Architecture
[AD-A146455] 06 p0847 N85-15378
Architecture, design, and system; performance assessment and development methodology for computer-based systems. Volume 1: Methodology description, discussion, and assessment
[AD-A146577] 06 p0847 N85-15379
Implementation of a Zilog Z-80 base realization library for the computer systems design environment
[AD-A146359] 06 p0853 N85-15423
A framework for the development of Navy computer-based systems: Combat system architecture and combat system engineering put into perspective
[AD-A146460] 06 p0856 N85-15445
United States Air force aircraft modification process: A system dynamics analysis
[AD-A146954] 07 p0893 N85-15659
The investigation of tethered satellite system dynamics
[NASA-CR-171278] 07 p0912 N85-15772
Future database machine architectures
[AD-A146786] 07 p1022 N85-16481
Software test handbook
[AD-A146844] 07 p1024 N85-16498
Program visualization: Graphics support for software development
[AD-A146867] 07 p1024 N85-16499
Technical performance measurement handbook
[AD-A147314] 07 p1052 N85-16675
Automatic briefing and mission management systems for battlefield support 08 p1073 N85-16799
Development and flight test of a helicopter compact, portable, precision landing system concept 08 p1076 N85-16821
Transition to the space shuttle operations era 08 p1097 N85-16930
Launch processing system concept to reality 08 p1097 N85-16931
Automatic software for controlling cryogenic systems 08 p1097 N85-16932
Support systems design and analysis 08 p1097 N85-16935
Orbital Manouvering system design evolution 08 p1098 N85-16943
Design evolution of the orbiter reaction control subsystem 08 p1099 N85-16944
Space shuttle orbiter auxiliary power unit development challenges 08 p1099 N85-16945
Space shuttle electrical power generation and reactant supply system 08 p1099 N85-16947
Design study of the vacuum pump of the ESRP — synchrotron radiation
[NIKHEF-MTG-21] 08 p1138 N85-17167
A cometary ion mass spectrometer
[NASA-CR-174326] 08 p1164 N85-17343
Design and fabrication of a CCD camera for use with relay optics in solar X-ray astronomy
[NASA-CR-174334] 08 p1164 N85-17344
Approaches to structuring the software development process
[AD-A147894] 08 p1205 N85-17582
Complexity, testability, and fault analysis of digital, analog and hybrid systems
[AD-A148465] 08 p1213 N85-17634
Design of mismatched Smith predictors using plant step data
[RR-263] 08 p1217 N85-17664
Open-cycle centrifugal vapor-compression heat pump
[PB85-113405/GAR] 09 p1328 N85-18348
Large electrostatic accelerators
[DE85-001120] 09 p1382 N85-18689
Stability indicators for front end loaders
[AD-P004293] 09 p1408 N85-18870
Study on steerability of articulated tracked vehicles
[AD-P004308] 09 p1410 N85-18885
Distributed data processing design methodology
[AD-A148888] 10 p1537 N85-19692
Ada in mission critical system acquisition: A guidebook
[AD-A149271] 10 p1540 N85-19710
Methodology investigation software testing of multiprocessor systems
[AD-A149446] 10 p1541 N85-19714
Improving engineering system design by formal decomposition, sensitivity analysis, and optimization
[NASA-TM-86377] 10 p1551 N85-19785
The EURECA Automatic Gradient Heating Facility (AGHF), phase A study
[ESA-CR(P)-1939] 11 p1591 N85-20005
Shuttle tethered satellite system program overview 11 p1642 N85-20342
US MILSATCOM: Present and future 11 p1709 N85-20753
Integrated control system engineering support
[AD-A149742] 12 p1780 N85-21177
China report: Science and technology
[JPRS-CST-85-008] 12 p1820 N85-21416
Systems research on China in year 2000 12 p1820 N85-21418
Needs, opportunities, and options for large scale systems research
[DE85-004642] 12 p1925 N85-22091
Derivation of the Olympus solar array requirements 13 p2009 N85-22598
Optimal allocation of components in parallel-series and series-parallel systems
[AD-A150169] 13 p2144 N85-23309
Performance evaluation of distributed systems with unbalanced flows: An analysis of the INFOPLEX data storage hierarchy
[AD-A150528] 13 p2147 N85-23328
LEXICON: A structured modeling system for optimization
[AD-A150536] 13 p2147 N85-23329
Operation and maintenance requirements of the Army Remotely Piloted Vehicle (RPV)
[NASA-CR-175714] 14 p2218 N85-23755
Application of the Hardman methodology to the Single Channel Ground-Airborne Radio System (SINCGARS)
[NASA-CR-175694] 14 p2218 N85-23756
Advanced life analysis methods. Volume 5: Executive summary and damage tolerance criteria recommendations for attachment lugs
[AD-A151017] 14 p2219 N85-23761
Model and controller reduction of uncertain systems using covariance equivalent realizations 14 p2243 N85-23902
Some recent developments in systems reliability
[AD-A150661] 14 p2317 N85-24318
Sensitivities of projected 1990 photovoltaic system costs to major system cost drivers
[NASA-CR-175699] 14 p2349 N85-24519
Some critical factors that limit the effectiveness of machine intelligence technology in military systems applications
[AD-A150684] 14 p2407 N85-24838
Response to NAS plan audit report recommendations
[FAA-ES-85-1] 15 p2468 N85-25235
Standards in process: Foundation and profiles of ISDN (Integrated Services Digital Network) and OSI (Open Systems Interconnection) studies
[PB85-165041/GAR] 15 p2545 N85-25712
A critical review of selected recent advancements in arc welding equipment and processes 15 p2566 N85-25833
Research in the design of high-performance reconfigurable systems
[NASA-CR-175705] 15 p2621 N85-26153
Design specifications for IMAGER: The DREO (Defence Research Establishment Ottawa) image processing system
[AD-A151752] 15 p2624 N85-26166
Future directions in computers 15 p2626 N85-26183
Evaluating computer-communication networks with simulation techniques
[AD-A151652] 15 p2632 N85-26222
Design and implementation of the digital engineering laboratory distributed database management system
[AD-A151694] 15 p2665 N85-26450
Design adequacy: An effectiveness factor 16 p2695 N85-26642
The evolutive state: A new definition of system state to include sequencing of events 16 p2696 N85-26643
Simulation: A tool for cost-effective systems design and live test reduction 16 p2696 N85-26657
Cost-effective missile guidance through distributed architecture and standard processes 16 p2698 N85-26662
Technical evaluation report on the Flight Mechanics Symposium on Active Control Systems: Review, Evaluation and Projections
[AGARD-AR-220] 16 p2711 N85-26730
X-29A digital flight control system design 16 p2712 N85-26736
ACT flight research experience 16 p2713 N85-26741
Operational and developmental experience with the F/A-18A digital flight control system 16 p2713 N85-26742

Flight testing and development of the F/A-18A digital flight control system 16 p2713 N85-28743
Construction and functioning of extended orbital systems 16 p2724 N85-28814
Spacecraft configuration study for second generation mobile satellite system [NASA-CR-175774] 16 p2730 N85-28849
Historical perspectives on information transmission engineering 16 p2759 N85-27023
Automated CPX support system preliminary design phase [NASA-CR-175784] 16 p2769 N85-27091
Fatigue criterion to system design, life and reliability [NASA-TM-87017] 16 p2793 N85-27226
Development of graphical time response using the OPTSYSX program [AD-A152221] 16 p2848 N85-27557
Evaluation of Ada (trademark) as a communications programming language, volume 1 [AD-A152314] 16 p2848 N85-27559
Analysis of control system from a viewpoint of desired pole placement and desired degree of robustness [AD-A152627] 17 p2899 N85-27876
The gust simulation apparatus of the 3m x 3m low speed wind tunnel of the DFVLR in Goettingen, West Germany [DFVLR-FB-85-04] 17 p2906 N85-27920
Engineering robot actions in a computer integrated manufacturing environment [CWI-CS-R8415] 17 p2938 N85-28139
Performance analysis of the DSN baseband assembly (Bba) Real-Time Combiner (RTC) [NASA-CR-175878] 17 p2946 N85-28190
NASA guidelines for assuring the adequacy and appropriateness of security safeguards in sensitive applications [NASA-CR-175489] 17 p3007 N85-28593
The touch panel system: Design and development [AD-A153014] 17 p3008 N85-28596
A test methodology for an automated and interactive software development environment [AD-A152857] 17 p3011 N85-28618
Impurity control and vacuum pumping system design and analysis for next-generation Tokamaks [DE85-009291] 17 p3041 N85-28815
Complete development and implement AFIT/ENG database management system, volume 1 [AD-A153043] 17 p3048 N85-28886
The development of information systems at NLR [B8580079] 17 p3051 N85-28884
Evaluation of a fault tolerant system for an integrated avionics sensor configuration with TSRV flight data [NASA-CR-172589] 18 p3062 N85-28941
LFMR definition study [AD-A153691] 18 p3090 N85-29126
System design of multi-layer (3-dimensional) integrated circuits [AD-A153466] 18 p3094 N85-29154
The system design of a rubidium maser frequency standard 18 p3106 N85-29232
Fuel cells: A bibliography [DE85-004565] 18 p3128 N85-29371
Development of molten carbonate fuel cell power plant, volume 1 [DE85-006743] 18 p3131 N85-29394
Materials and processes control for space applications 18 p3156 N85-29544
Guidance on planning and implementing computer system reliability [PB85-177996] 18 p3161 N85-29581
Annotated bibliography of recent papers on software engineering environments [PB85-191385] 18 p3165 N85-29607
Activities of Istituto Elettrotecnico Nazionale Galileo Ferraris 18 p3199 N85-29645
Space station automation study. Volume 2: Technical report. Autonomous systems and assembly [NASA-CR-171515] 19 p3220 N85-30001
Automatic ac/dc thermal voltage converter and ac voltage calibration system [PB85-182574] 19 p3274 N85-30304
Forced structural response using component mode synthesis [DE85-006479] 19 p3287 N85-30383
Design and implementation of an intelligence database [AD-A154095] 19 p3361 N85-30973
Proceedings of the Workshop on Identification and Control of Flexible Space Structures, volume 1 [NASA-CR-176051] 20 p3408 N85-31148
Control of flexible structures 20 p3410 N85-31161
Space station configuration and flight dynamics identification 20 p3410 N85-31162
ISAAC (Integrated Structural Analysis and Control) via continuum modeling and distributed frequency domain design techniques 20 p3414 N85-31165
New measurement solutions for low frequency systems 20 p3437 N85-31325
Study of terrestrial mobile systems for personal communications [MCS-8436] 20 p3441 N85-31357
Improved specific energy Ni-H2 cell 20 p3447 N85-31399
Evaporatively cooled chiller for solar air conditioning systems design and field test [DE84-014154] 20 p3484 N85-31652
Proceedings of the 1st Workshop for the Design of Expert System Partial Differential Equation Solvers [AD-A154192] 20 p3515 N85-31853
RESO: Expert system applied to company computer networks [ENST-84E016] 20 p3518 N85-31874
Decentralized control synthesis method for large-scale interconnected systems [DE85-000748] 20 p3518 N85-31878
The development of complex systems 20 p3539 N85-32021
R and D programmes at the National Aeronautical Laboratory [AR-22] 20 p3539 N85-32022
R and D activities of the Systems Engineering Division 20 p3540 N85-32027
Development of reduced order models for control system design using the OPTSYSX program [AD-A154552] 21 p3556 N85-32124
The documentation assistant: An intelligent system for documentation [AD-A154709] 21 p3670 N85-32800
A comprehensive study of the AFIT (Air Force Institute of Technology) software development environment [AD-A155450] 21 p3672 N85-32812
Evaluation of a software design approach: Develop a threat resolution module in Ada (trademark) [AD-A155699] 21 p3672 N85-32815
Distributed name management [AD-A154785] 21 p3712 N85-33037
System for computer-aided design of analog electronic circuits 22 p3768 N85-33353
Integrated Support Software System (ISSS) [AD-A155715] 22 p3829 N85-33710
Portable database driven control system for SPEAR [DE85-010465] 22 p3830 N85-33720
Flat is not necessarily good [DE85-012819] 22 p3830 N85-33723
Space Station Engineering and Technology Development: Proceedings of the Panel on In-Space Engineering Research and Technology Development [NASA-CR-176110] 23 p3899 N85-34153
A methodology for the design of testable custom large-scale integrated circuits [AD-A156098] 24 p4090 N85-35351
Wind turbine noise: Prediction tools and design parameter dependence 24 p4110 N85-35477
Recommendations for content revision and alternate delivery modes for the Human Engineering Guide to Equipment Design (HEGED) [AD-A155781] 24 p4134 N85-35624
An approach to determining computer security requirements for Navy systems [AD-A155750] 24 p4135 N85-35627

SYSTEMS FOR NUCLEAR AUXILIARY POWER
U SNAP

SYSTEMS INTEGRATION
PROFS: An approach to improved operational weather services — Program for Regional Observing and Forecasting Services (PROFS) 01 p0083 N85-10555
Numerical algorithms and parallel tasking [AD-A145090] 01 p0104 N85-10693
Avionics Integrity Program (Avip). Volume 2: Hardware case studies [AD-A145689] 02 p0139 N85-10944
Supercomputers and VLSI: The effect of large scale integration on computer architecture [AD-A145408] 02 p0239 N85-11555
AFHRL (Air Force Human Resources Laboratory) program for artificial intelligence applications to maintenance and training [AD-P003931] 02 p0247 N85-11611
Developments in Soviet robot technology viewed 04 p0491 N85-13127
Superaugmented rotorcraft program 06 p0750 N85-14807
HH-65A Dolphin digital integrated avionics 06 p0751 N85-14815
Integrated cockpit design for the Army helicopter improvement program 06 p0751 N85-14816
Integrated navigation systems: Where are we headed? [AD-A146425] 06 p0753 N85-14832
Setting time standards at NISTARS (Naval Integrated Storage and Retrieval System) [AD-A146371] 06 p0870 N85-15529
The design and development of an integrated core system for battlefield helicopters 06 p1074 N85-16811
Evolution toward a multi-bus architecture for Army helicopter avionic systems 06 p1074 N85-16812
Integration of sensor fusion in advanced helicopter cockpit design 06 p1074 N85-16813
Development, production and testing of central control and display unit for helicopters [BMFT-FB-W-84-039] 06 p1085 N85-16871
Integrated design checkout of shuttle payload avionics interfaces 06 p1092 N85-16899
Managing computer-controlled operations 06 p1097 N85-16934
Support systems design and analysis 06 p1097 N85-16935
Robotics research, integration overview presented. Application objectives cited 06 p1142 N85-17201
Coordinated research in robotics and integrated manufacturing [AD-A148204] 06 p1168 N85-17365
Cognitive asymmetry and occupation. Computer programmers, students, and bank personnel, part 1 and part 2 [AD-A147125] 06 p1197 N85-17540
Towards an ideal database server for office automation environments [AD-A148184] 06 p1229 N85-17742
Integrated technology rotor/flight research rotor hub concept definition [NASA-CR-166447] 09 p1290 N85-18051
Data Requirement (DR) MA-03: Payload missions integration — Spacelab payloads [NASA-CR-171331] 10 p1428 N85-19009
MATRA has Europe's largest white room for satellites 10 p1477 N85-19320
A safety evaluation of the relocation of the ACM (Air Combat Maneuver) panel in the F-14 ( )/AIP (Avionics Integration Program) [AD-A149596] 12 p1777 N85-21158
Dual band radome wall design [AD-P004357] 12 p1825 N85-21451
Integrated digital networks [AD-A150605] 13 p2056 N85-22873
Invariant system of technological preparation of production 14 p2266 N85-24056
Integrated control system for FMS components 14 p2285 N85-24156
Response to NAS plan audit report recommendations [FAA-ES-85-1] 15 p2468 N85-25235
Space station systems technology study (add-on task). Volume 3: Technology advancement program plan [NASA-CR-171417] 15 p2475 N85-25280
Standards in process: Foundation and profiles of ISDN (Integrated Services Digital Network) and OSI (Open Systems Interconnection) studies [PB85-165041/GAR] 15 p2545 N85-25712
Computerized biophysical data acquisition system for motion sickness studies [AD-A151691] 15 p2618 N85-26131
Computers and the consulting engineer 15 p2626 N85-26184
The STOL and maneuver technology program integrated control system development 17 p2905 N85-27910
An evaluation of oxygen-hydrogen propulsion systems for the Space Station [NASA-TM-87059] 18 p3067 N85-28971
Investigation of fast reaction SAW (Surface Acoustic Wave) accelerometer [AD-A153876] 19 p3216 N85-29943
Local automation model software benchmarking: Test plan [AD-A154349] 19 p3337 N85-30676
High gain adaptive control of decentralized systems [DE85-010040] 19 p3339 N85-30688
Performance improvements of a highly integrated digital electronic control system for an F-15 airplane [NASA-TM-86748] 21 p3556 N85-32120
High temperature electronics technology: Life test report [AD-A154681] 21 p3580 N85-32257
Characteristics of a numerical fluid dynamics simulator [DE85-009602] 21 p3586 N85-32290
Qualification needs for advanced integrated aircraft [NASA-TM-86731] 22 p3729 N85-33119
Digital matched filter 22 p3765 N85-33339
The integrated manual and automatic control of complex flight systems [NASA-CR-176166] 24 p4066 N85-35201
Analog, still without fear [AD-A155920] 24 p4089 N85-35348

SYSTEMS MANAGEMENT
On some common interests among reliability, inventory and queuing [AD-A145595] 02 p0251 N85-11646

Research in data management and system reliability
[AD-A145498] 03 p0436 N85-12773
Computer aided processing using laser measurements
08 p1103 N85-16973
Training guide for scientific and engineering trainees 1984
[AD-A147963] 08 p1198 N85-17542
Research and Modeling of Supervisory Control Behavior, report of a workshop
[AD-A149621] 12 p1950 N85-22248
Management aspects of software maintenance
[AD-A152035] 16 p2847 N85-27550
Management control systems and interdependencies: An empirical study
[AD-A152280] 16 p2876 N85-27746
Cost savings from multiyear contracting
[AD-A153564] 18 p3197 N85-29834
NASA Space controls research and technology program 20 p3408 N85-31149
Program Manager: The journal of the defense systems management college, volume 14, number 2, March-April 1985
[AD-A154219] 20 p3540 N85-32031
Navy information systems: Planning, policy, organization, and management
[PB85-176113] 20 p3541 N85-32038
NASA space station automation: AI-based technology review
[NASA-CR-176094] 21 p3558 N85-32134
Analysis of spacecraft data
[NASA-CR-171597] 21 p3669 N85-32790
User commands for product design and system management
[DE85-011708] 22 p3830 N85-33721

SYSTEMS SIMULATION
Optimizing search with positive information feedback
[CSIR-TWISK-313] 01 p0125 N85-10855
ERS-1 radar altimeter system performance evaluation and calibration 03 p0383 N85-12451
Simplified planar model of ground test verification structure, appendix B 05 p0603 N85-13841
Elimination of uncontrollable rigid body mode, appendix C 05 p0603 N85-13842
Evaluation of SPOT simulation data of the S GEOS campaign of the EEC by data of the test sites Freiburg and Staubing (West Germany) 05 p0659 N85-14237
A digital piloting system for the combat helicopter
08 p1074 N85-16806
A simulator for studying helicopter weapons systems
08 p1075 N85-16816
The use of simulation for the technical and economic evaluation of flexible manufacturing systems. Part 2: Results of the simulation
[PNR-90233-PT-2] 09 p1371 N85-18614
MTI system simulation and clutter output statistics
[AD-A149193] 10 p1467 N85-19255
TVENT1P user's manual, a computer code for analyzing tornado induced gas dynamic transients in flow networks
[DE85-002346] 10 p1466 N85-19379
The noise of laser diodes with modulated injection current
[FI-465-TBR-23] 11 p1625 N85-20233
The use of analytical models to interpret measured data properly. 1. General background theory
11 p1651 N85-20400
A system simulator for the solar generator of artificial satellites
[INPE-3320-TDL/160] 11 p1672 N85-20534
Solar array dynamical simulation for illumination and temperature variation 13 p2011 N85-22611
Transition fixing and simulation of high Reynolds number flow at transonic velocities 14 p2212 N85-23721
System theoretic description of physical systems
[CWI-TRACT-3] 14 p2414 N85-24894
Space station systems technology study (add-on task). Volume 3: Technology advancement program plan
[NASA-CR-171417] 15 p2475 N85-25280
Manipulation and simulation of general robots using the zero-position description 15 p2567 N85-25838
Simulation: A tool for cost-effective systems design and live test reduction 16 p2696 N85-26657
A description of the process of elaborating man-machine dialog in an aircraft equipped with cathode tubes: Roles and specifications of piloted simulation methods
16 p2698 N85-26658
A complete inference system for regular processes with silent moves
[CWI-CS-R8420] 17 p3014 N85-28838
Simulations of strapdown-system errors and error compensation methods — transport aircraft navigation
[DFVLR-MITT-84-22] 20 p3392 N85-31040
Reduced order models and simulation data in control systems design
[RR-267] 20 p3463 N85-31516
Linear system structure and cone containment for bilinear systems
[RR-268] 20 p3519 N85-31879
Design of simulation experiments
[FEW-123] 20 p3519 N85-31885
Regression metamodel summarization of model behavior
[FEW-120] 20 p3522 N85-31902
On the interpretation of variables — simulation and regression models
[FEW-136] 20 p3522 N85-31903
Performance of rolling ball and isometric joystick on a 2-D target alignment task
[RSRE-MEMO-3695] 22 p3826 N85-33699
Discrete simulation models - their role in the design, development and management of inventory control systems
[PNR-90249] 23 p3986 N85-34719

SYSTEMS STABILITY
Aeroelastic stability analysis with interacting structural nonlinearities 02 p0207 N85-11364
The dimensional stability of advanced composite antenna reflectors: Analytical and test evaluation — satellite antennas 05 p0626 N85-14014
Effects of transport delays of manual control system performance 05 p0701 N85-14498
Relaxation times for queuing systems
[CWI-OS-R8407] 05 p0719 N85-14618
The stability of an infinite elastic pipe with uniform mean flow
[AD-A146886] 08 p1161 N85-17326
Brief outline of analytic stability studies of magnetically insulated systems — bibliolographies
[DE85-000212] 09 p1393 N85-18765
Contribution to the study of perturbational stabilization
[ONERA-NT-1984-1] 11 p1714 N85-20781
Instabilities and the fine structure of Saturn's rings
15 p2676 N85-26520
Stability and feasibility of model ecosystems
[PREPRINT-431] 18 p3134 N85-29408

T

T TAURI STARS
Bipolar molecular outflows: T Tauri stars and Herbig-Haro objects 03 p0448 N85-12837
UV observations and results on pre-main sequence stars 11 p1744 N85-20970
Atmospheric properties of RU Lupi derived from high- and low-resolution IUE spectra
11 p1754 N85-21031
Mechanical energy release by protostars to molecular clouds 12 p1957 N85-22302

T-33 AIRCRAFT
A preliminary flight evaluation of the peripheral vision display using the NT-33A aircraft
[AD-A145123] 01 p0010 N85-10060

TABLES (DATA)
NT MATHEMATICAL TABLES
Water resources data, Maryland and Delaware, water year 1983
[PB84-225135] 01 p0085 N85-10431
Water resources data, California, water year 1982. Volume 4: Northern central valley basins and the Great Basin from Honey Lake Basin to Oregon state line
[PB84-225127] 01 p0085 N85-10432
Water resources data, California, water year 1982. Volume 2: Pacific slope basins from Arroyo Grande to Oregon state line except Central Valley
[PB84-224708] 01 p0085 N85-10433
Water resources data, Virginia, water year 1983
[PB84-224542] 01 p0086 N85-10435
Water resources data, Ohio, water year 1983. Volume 2: St. Lawrence River basin statewide project data
[PB84-223676] 01 p0086 N85-10436
A building blocks approach to statistical databases
03 p0437 N85-12782
Tide tables 1985, high and low water predictions, central and western Pacific Ocean and Indian Ocean
[PB84-236393] 04 p0542 N85-13451
Tide tables 1985. High and low ster predictions: Europe and West Coast of Africa including the Mediterranean Sea
[PB84-230093] 06 p0841 N85-15343
Safe decompression schedules for caisson workers
[PB85-109612/GAR] 07 p1017 N85-16483
Experimental study of main rotor tip geometry and tail rotor interactions in hover. Volume 2: Run log and tabulated data
[NASA-CR-177336-VOL-2] 13 p1965 N85-22345
A model for large sparse contingency tables
[AD-A150320] 13 p2151 N85-23350
An atlas of pure water vapor spectra from 500 to 5000/cm, volume 1
[AD-A151756] 15 p2505 N85-25454
Bern solar data for January-December 1984
[REPT-51] 15 p2695 N85-26581
Summary of Meteorological Observations, Surface (SMOS), Dallas, Texas
[AD-A150599] 16 p2835 N85-27480
Climatological data of stations in the Netherlands No. 11: Frequency tables and tables with runs according to measurements at principal climatological stations 1961-1980, sunshine stations 1956-1980, precipitation stations 1951-1980
[KNMI-150-11] 18 p3149 N85-29499
Bayesian full rank marginalization for 2-way contingency tables
[AD-A153841] 18 p3171 N85-29849
Atomic data for controlled fusion research. Volume 4: Spectroscopic data for iron
[DE85-009858] 19 p3354 N85-30787
Tables of generalized hydrogen diffusion profiles and permeating fluxes for fusion applications
[DE85-008676] 19 p3372 N85-30919
Compendium of unsteady aerodynamic measurements, addendum 1
[AGARD-R-702-ADD-1] 20 p3390 N85-31028
Phonetic transcription statistics: Constitution and statistical utilization
[ENST-85D001] 22 p3756 N85-33285

TABLETS
A multi-touch three dimensional touch-sensitive tablet (executive summary) 23 p3961 N85-34553

TABS (CONTROL SURFACES)
Aircraft rotor blade with passive tuned tab
[NASA-CASE-ARC-11444-1] 19 p3217 N85-29947

TABULATING
U TABULATION PROCESSES

TABULATION PROCESSES
(NAT)Fe(n,n'x) spectra at 65.5 MeV
[AD-A155776] 24 p4150 N85-35730

TACAN
Shuttle navigation status 06 p1092 N85-16901
Distance Measuring Equipment (DME), general
[AD-A152585] 17 p2895 N85-27846

TACHOMETERS
The removal, mechanical handling and installation procedures for declination tachometer and fisk encoder — United Kingdom Infrared Telescope
[UKIRT-17] 09 p1414 N85-18915
Two-stage gyrocompass 14 p2273 N85-24080
The Fourier tachometer 2: An instrument for measuring global solar velocity fields 14 p2442 N85-25068
Digital tachometer 22 p3779 N85-33416

TACHYONS
Results of a search for monopoles and tachyons in horizontal cosmic ray flux
[HE-6.1-3] 24 p4209 N85-36129
Search for tachyons associated with extensive air showers in the ground level cosmic radiation
[HE-6.2-13] 24 p4212 N85-36149

TACTICAL AIR NAVIGATION
U TACAN

TACTICS
Increased joint avionics standardization could result in major economies and operational benefits
[AD-A145730] 02 p0139 N85-10945
Intelligent interfaces for tactical airborne platforms
08 p0752 N85-14820
A framework for the development of Navy computer-based systems: Combat system architecture and combat system engineering put into perspective
[AD-A146460] 08 p0856 N85-15445
Human factors and training research in military organizations and systems
[AD-A146832] 07 p1020 N85-16475
Close air support mission: Development of a unitary measure of pilot performance
[AD-A149285] 11 p1697 N85-20665
Combat capable space systems for tactical support
11 p1713 N85-20775
Supersonic Tactical Missile (STM) radome development
[AD-P004360] 12 p1825 N85-21454
Equilibrium solutions, stabilities and dynamics of Lanchester's equations with optimization of initial force commitments
[AD-A151510] 15 p2637 N85-26266
Transceiver test device
[AD-D011728] 22 p3786 N85-33458

TACTILE DISCRIMINATION
Dutch institutes do research in tactile visual robot sensors 09 p1310 N85-18228
Short and long-term robot feedback
[PB85-180735] 19 p3281 N85-30347

TACTILE SENSATION
U TOUCH

TAGGING
U MARKING

TAIL ASSEMBLIES
An experimental study on the induced normal force on tail-fins due to wing-tail interference
[NAL-TR-814] 03 p0318 N85-12051
Experiences obtained from service fatigue monitoring exercises 07 p0896 N85-15572
TUTOR (CL-41A) tail flight load survey 07 p0896 N85-15578
All-composite Airbus empennage 07 p0936 N85-15931
Wind tunnel acoustic study of a propeller installed behind an airplane empennage: Data report
[NASA-CR-177335] 13 p2154 N85-23377
Description of a computer program treating transonic steady state aeroelastic effects for a canard or tail airplane
[FFA-TN-1983-23] 16 p2700 N85-26674
The influence of helicopter tail shape on drag: An aerodynamic study using a low speed wind tunnel
[AD-A156304] 24 p4062 N85-35174
TAIL MOUNTINGS
U TAIL ASSEMBLIES
TAIL PLANES
U HORIZONTAL TAIL SURFACES
TAIL ROTORS
NT HELICOPTER TAIL ROTORS
Aircraft accident report, Western Helicopters, Inc., Bell UH-1B, N87701, Valencia, California, July 23, 1982
[PB84-910414] 05 p0594 N85-13789
An experimental investigation of the chopping of helicopter main rotor tip vortices by the tail rotor
[NASA-CR-177338] 13 p2154 N85-23376
TAIL SURFACES
NT HORIZONTAL TAIL SURFACES
TAILLESS AIRCRAFT
NT F-106 AIRCRAFT
NT MIRAGE 3 AIRCRAFT
TAILORING
U DESIGN
TAILS (ASSEMBLIES)
U TAIL ASSEMBLIES
TAIWAN
Sedimentary and tectonic evolution of the western Taiwan foredeep 03 p0369 N85-12401
Crustal dynamics studies in China
[NASA-CR-176817] 13 p2132 N85-23265
TAKEOFF
Preliminary airworthiness evaluation of the Rutan Aircraft Factory (RAF), Inc. LONG-EZ airplane with external sight
[AD-A145361] 02 p0138 N85-10937
Performance capabilities of the C-5 and C-17 cargo aircraft
[AD-A145518] 02 p0138 N85-10939
Insight. Background information for multipurpose pilots: Flight phenomena 02 p0138 N85-10940
To take off and to land safely, Hoechst 1678 for ice and snow free runways 05 p0595 N85-13791
Airport activity statistics of certificated route air carriers
[AD-A148472] 08 p1081 N85-16846
Optimum performance parameters for ski-jump operations of USAF fighter aircraft
[AD-A148532] 08 p1084 N85-16867
Boundary layer transition control for takeoff and landing configurations 14 p2211 N85-23714
Trajectory measurements for take-off and landing tests and other short-range applications, volume 16
[AGARD-AG-160-VOL-16] 15 p2561 N85-25801
The use of pressure sensing tape on the aircraft wing as sensor for flight control systems 16 p2696 N85-26660
Probabilistic computer model of optimal runway turnoffs
[NASA-CR-172549] 16 p2715 N85-26760
A system for take-off and landing measurements (STALIMS)
[B6580072] 17 p2895 N85-27849
Addition of flexible body option to the TOLA computer program, part 1
[NASA-CR-132732-1] 17 p2896 N85-27855
Addition of flexible body option to the TOLA computer program. Part 2: User and programmer documentation
[NASA-CR-132732-2] 17 p2896 N85-27856
Wind tunnel results of advanced high speed propellers in the takeoff, climb and landing operating regimes
[NASA-TM-87054] 19 p3213 N85-29925
TAKEOFF RUNS
Probabilistic computer model of optimal runway turnoffs
[NASA-CR-172549] 16 p2715 N85-26760
TALKING
NT WORDS (LANGUAGE)
Post fire interview: Development and field validation of the behavioral sequence interview technique
[NBS-GCR-84-477] 04 p0454 N85-12881
TANDEM ROTOR HELICOPTERS
NT CH-47 HELICOPTER
TANDEM WING AIRCRAFT
Parametric study of a canard-configured transport using conceptual design optimization
[NASA-TP-2400] 11 p1584 N85-19979
TANGENTS
Cones of tangent cones and Clarke's tangent cone
[CSIR-TWISK-314] 01 p0108 N85-10727
TANK TRUCKS
Some stability and control problems with trailed farm tankers on slopes
[AD-P004291] 09 p1408 N85-18668
TANKER SHIPS
A crew exposure study. Phase II. Volume 2. At sea. Part A
[AD-A155233] 21 p3666 N85-32774
Further studies on liquid sloshing
[PB85-196695] 24 p4095 N85-35388
TANKS (COMBAT VEHICLES)
Assuring structural integrity in Army systems
[NASA-CR-175492] 11 p1651 N85-20398
Ground evaluation of helicopter air-to-air warfare 13 p1967 N85-22360
Improvements in tank tread assemblies
[NASA-CASE-NPO-16321-1] 18 p3117 N85-29291
Production verification of the acoustic emission weld monitor
[AD-A154168] 20 p3464 N85-31519
Thermal stress suffered by tank crews working in summer heat
[DRIC-T-7492] 22 p3826 N85-33698
TANKS (CONTAINERS)
NT CYLINDRICAL TANKS
NT EXTERNAL TANKS
NT FUEL TANKS
NT PROPELLANT TANKS
NT STORAGE TANKS
NT WING TANKS
Ultralightweight oxygen container
[PB84-220730] 01 p0036 N85-10226
The analysis of tank calibration data from several runs
[DE84-015529] 02 p0200 N85-11337
Analysis of seismic sloshing of reactor tanks considering submerged components and seismic isolation
[DE85-010499] 19 p3269 N85-30273
Elastomers used in aeronautics industry
[SNIAS-851-551-103] 20 p3434 N85-31304
TANTALUM
Strong-coupling superconductivity of Mg in proximity to Ta
[DE84-015462] 04 p0569 N85-13627
The effect of tantalum on the structure/properties of two polycrystalline nickel-base superalloys: B-1900 + Hf MAR-M247
[NASA-CR-174847] 09 p1294 N85-18127
Stability of amorphous metals on semiconductor substrates
[DE84-017256] 09 p1295 N85-18134
Wavecode constitutive models: Nonhomogeneous mixtures
[DE85-000636] 12 p1798 N85-21278
Gigantic lithium deposit discovered in France 14 p2269 N85-24184
Ultra-trace analysis of sinter tantalum with SIMS
[BLL-RARDE-TR-1220-(7291.7965)] 23 p3913 N85-34245
TANTALUM ALLOYS
Bilform resolidification and amorphous phases in a laser and electron beam processed tantalum-iridium alloy
[DE84-013334] 02 p0184 N85-11234
Effects of MAR-M247 substrate (modified) composition on coating oxidation coating/substrate interdiffusion --- protective coatings for hot section components of gas turbine engines
[NASA-CR-174851] 10 p1440 N85-19073
TANTALUM COMPOUNDS
Positron measurements in 2H-TaSe2 crystals
[DE85-010507] 20 p3529 N85-31949
TAPE RECORDERS
Miniature personal physiological tape recorder (experiment 1ES 30) --- Spacelab 05 p0692 N85-14448
Operating time meter for tape recorder 12 p1838 N85-21537
Playback amplifier with high interference immunity 13 p2077 N85-22970
Operation of autotracking system in various video playback modes 16 p2764 N85-27055
Module for interfacing microprocessors and microcomputer 22 p3774 N85-33390
TAPER
U TAPERING
TAPERED WINGS
U SWEPT WINGS
TAPERING
Parabolic tapers for overmoded waveguides
[DE84-014237] 01 p0039 N85-10247
Reducing grating lobes due to subarray amplitude tapering
[AD-D011723] 23 p3927 N85-34339
TAPES
Evaluation and prediction of long-term environmental effects of nonmetallic materials
[NASA-CR-171353] 10 p1450 N85-19137
TAR SANDS
Aviation turbine fuels from tar sands bitumen and heavy oils. Part 1: Process analysis
[AD-A151319] 15 p2521 N85-25539
Subsurface petroleum geology of Santa Rosa sandstone (Triassic), northeast New Mexico
[TI85-901364] 19 p3313 N85-30538
TARE (DATA REDUCTION)
U DATA REDUCTION
TARGET ACQUISITION
The prediction of observer responses from photometric data on smoke screens; an analysis of the Oldebroek 2 trials, May 1981
[IZF-1984-21] 01 p0095 N85-10642
Description of the Dutch-Danish (DUDA) scanner --- thermal signatures
[AD-B084893] 01 p0121 N85-10826
Army aviation today and tomorrow 06 p0751 N85-14810
Radar echo enhancement using surface reflections
[AD-A146970] 07 p0939 N85-15955
Binocular overlap in a fiber optic helmet mounted display
[AD-P004331] 09 p1270 N85-17985
Synthesis of digital nonrecursive band-elimination filters for moving-target selectors 12 p1840 N85-21545
Efficiency of multitarget signal detection by digital radar data processing devices 13 p2080 N85-22991
Operation and maintenance requirements of the Army Remotely Piloted Vehicle (RPV)
[NASA-CR-175714] 14 p2218 N85-23755
An MRTD-compatible bar pattern response model for TV and direct view sighting systems
[BAE-BT-12090] 15 p2620 N85-26146
Optimizing the specifications for an air-surface laser system 16 p2696 N85-26644
Performance of rolling ball and isometric joystick on a 2-D target alignment task
[RSRE-MEMO-3695] 22 p3826 N85-33699
TARGET PENETRATION
U TERMINAL BALLISTICS
TARGET RECOGNITION
Content, variety, and augmentation of simulated visual scenes for teaching air-to-ground attack
[AD-A145218] 01 p0013 N85-10080
Joint services electronics program
[AD-A145085] 01 p0042 N85-10276
The perceptual quality of smoke screens: An analysis of the Oldebroek 2 trials, May 1981
[IZF-1984-20] 01 p0095 N85-10641
Digital correlator speed improvement by multiplexing
[AD-A145207] 01 p0100 N85-10682
Using gross outline features in long range target identification
[FOA-C-53018-H2] 02 p0237 N85-11543
About ambiguity and Q-functions
[AD-A145293] 02 p0250 N85-11636
Design of edge detectors for reduced images
[AD-A145700] 02 p0252 N85-11653
Distributed sensor networks
[AD-A146209] 03 p0355 N85-12286
The development of new methods for solving the target identification or inverse scattering problem for time-harmonic acoustic and electromagnetic waves
[AD-A145821] 03 p0415 N85-12657
Visibility of various target-background color combinations under different chromatic ambient illuminations
[AD-A146348] 03 p0420 N85-12684
Color and grey scale in sonar displays 05 p0710 N85-14552
Optimization of moving-target selection radar devices for nonGaussian signals for stationary targets 06 p0789 N85-15043
Radar echo enhancement using surface reflections
[AD-A146970] 07 p0939 N85-15955
Target detection using microwave irradiances from natural sources: A passive, local and global surveillance system
[NASA-CR-174260] 07 p0946 N85-15991
Human factors and training research in military organizations and systems
[AD-A146832] 07 p1020 N85-16475
Multi target tracking by dynamic scene analysis
[AD-A146922] 10 p1466 N85-19250

Optical implementation of the synthetic discriminant function
[AD-A149562] 10 p1557 N85-19617
Automatic pickup of trajectory by method of sequential analysis taking into account deviation of radar markers from center of strobe 12 p1838 N85-21535
Research on ocean floor electrical surveys
[AD-A149631] 12 p1899 N85-21920
The accuracy in calculations of intervisibility with digital terrain models — digital models
[FOA-C-20557-D8(E1)] 12 p1909 N85-21983
Moving target detection 13 p2067 N85-22915
Visual simulation requirements for aircraft aspect recognition at real world distances
[AD-A151040] 14 p2228 N85-23810
Digital computer applications of Kalman filter in target tracking
[AD-A150770] 14 p2404 N85-24821
Eye movement in response to single and multiple targets
[AD-A151115] 15 p2617 N85-26126
Visual search strategy predictions: The use of aspect ratio as a cue
[BAE-BT-12565] 15 p2619 N85-26138
Poisson and multinomial shadowing processes
[AD-A151600] 15 p2640 N85-26286
An investigation into generalised matched filter techniques
[BAE-BR-12971] 15 p2651 N85-26348
Low-resolution target classification from a staring infrared sensor
[AD-A151690] 15 p2652 N85-26358
Design adequacy: An effectiveness factor
16 p2695 N85-26642
Scene analysis using recursive frequency domain correlation with energy normalization
[AD-A151777] 16 p2854 N85-27596
A mathematical model for calculating detection probability of a diffusion target
[AD-A152026] 16 p2854 N85-27601
Target discrimination using infrared techniques: Theoretical considerations
[AD-A154070] 19 p3350 N85-30762
Feedforward-feedback control logic for robust target-tracking 20 p3436 N85-31317
Radar target identification through electromagnetic scattering studies
[AD-A154596] 21 p3573 N85-32220
Broadside scattering of a tubular cylinder for evaluation of target identification
[AD-A155739] 21 p3577 N85-32248
Bayesian vs MAP multiple model adaptive estimation for field of view expansion in tracking airborne targets
[AD-A155486] 21 p3679 N85-32855
Selectivity of weight compensator of passive interference to unknown velocities of detectable targets
22 p3762 N85-33317
Hardware test program for evaluation of baseline range-range rate sensor concept
[NASA-CR-176143] 23 p3933 N85-34377

TARGET SIMULATORS
Docking simulation analysis of range data requirements for the orbital maneuvering vehicle
[NASA-TM-86510] 20 p3407 N85-31143

TARGET THICKNESS
A method for the evaluation of the residual energy of a metallic fragment after perforation of a thin target
[ISL-R-113/83] 16 p2794 N85-27233

TARGETS
NT LASER TARGETS
NT PARTICLE ACCELERATOR TARGETS
NT RADAR TARGETS
A production system model of capturing reactive moving targets 05 p0705 N85-14524
Analysis of the impact of a deformable missile model on a deformable obstruction
[BLL-RISLEY-TR-8534-(9091.9F)] 06 p0859 N85-15459
Electro-optical target detection
[AD-D011368] 07 p1042 N85-16617
The value and utility of inflight onboard simulation
[AD-A148033] 08 p1198 N85-17543
An electronically controlled array for simulation of passive target/background signatures at millimeter wavelengths
[AD-D011456] 10 p1468 N85-19263
Nose and inlet duct radomes for the firebolt aerial target
[AD-P004375] 12 p1827 N85-21469
Experimental test of the three subaperture method for estimating target elevation angle
[AD-A149667] 12 p1851 N85-21614
Shallow magma targets in the western US
[DE85-003274] 12 p1881 N85-21803
Variable fleeing device for targets in internal beams of charged particle accelerators 13 p2044 N85-22797
Microwave blackbodies for spaceborne receivers
[NASA-CR-175647] 13 p2094 N85-23068
Eye movement in response to single and multiple targets
[AD-A151115] 15 p2617 N85-26126
Angular tracking error in A phase comparison monopulse tracking radar: A critical review and extension of the phase front distortion approach
[AD-A152628] 17 p2949 N85-28205
Tracking algorithm performance analysis program (TRAPP)
[DE85-007304] 17 p3009 N85-28601
Study of intermediate velocity penetration of steel spheres into deep aluminum targets
[DE85-010419] 19 p3287 N85-30385
Spectral reflectances of natural targets for use in remote sensing studies
[NASA-RP-1139] 19 p3299 N85-30450
Polarized internal target apparatus
[DE85-011611] 19 p3354 N85-30793
Ion beam-plasma interactions
[DE85-010202] 19 p3371 N85-30913
Moving finite element method for ICF target implosion
23 p3980 N85-34675
Target observability for satellite-based sensors
[AD-A156139] 24 p4069 N85-35217

TASK COMPLEXITY
The design and use of subtasks in part training and their relationship to the whole task
05 p0711 N85-14559
On choosing between two probabilistic choice sub-models in a dynamic multitask environment
05 p0711 N85-14563
No fatigue effect on blink rate
05 p0712 N85-14564

TASKS
NT AUDITORY TASKS
NT VISUAL TASKS
Comprehension of instructions for operating devices
[AD-A145263] 01 p0098 N85-10653
Ada (trademark) training curriculum. Real-time concepts I303 teacher's guide
[AD-A145093] 01 p0104 N85-10694
Decision tree rating scales for workload estimation: Theme and variations
[NASA-CR-174062] 02 p0237 N85-11544
Models of natural intelligence in fault diagnosis tasks: Implications for training and aiding of maintenance personnel
[AD-P003927] 02 p0246 N85-11607
Helicopter pilot performance for discrete-maneuver flight tasks 05 p0702 N85-14502
Psychological issues in online adaptive task allocation
05 p0704 N85-14516
Twentieth Annual Conference on Manual Control, volume 2
[NASA-CP-2341-VOL-2] 05 p0707 N85-14535
Performance enhancements under dual-task conditions 05 p0707 N85-14537
The effects of task structure on time-sharing efficiency and resource allocation optimality
05 p0711 N85-14562
Multiple resources and display formatting: The implications of task integration in a simulated air traffic control task
[AD-A150713] 14 p2292 N85-24205
The effect of strategy in second order manual control on resource competition with a sternberg memory search task
[AD-A150985] 14 p2391 N85-24727
Shape with and without redundant colour as coding mechanism for simulated radar displays in a time-extended simple vigilance task
[AD-A151683] 16 p2844 N85-27533
Resource allocation in cerebral specialization of function: Behavioral and electrophysiological studies
[AD-A155092] 21 p3664 N85-32759
Conceptualizing in assembly tasks
[AD-A155564] 21 p3665 N85-32770

TASMANIA
Sidereal variations deep underground in Tasmania
[SH-4.4-4] 23 p4033 N85-35002

TATB
Sensitivity and performance characterization of DINGU
[DE85-010750] 22 p3754 N85-33269
Friction, impact, and electrostatic discharge sensitivities of energetic materials
[DE85-013321] 24 p4083 N85-35309

TAXIING
New airport ground traffic control system planned
03 p0310 N85-12006
A feasibility study for using low boiling point fluids to change aircraft tire deflection
[AD-A152096] 16 p2706 N85-26701

TAXONOMY
Fungi of Mt. Babia Gora. 1: Mycoflora of forests
[NASA-TM-77484] 02 p0234 N85-11522
Asteroid taxonomy from cluster analysis of Photometry
09 p1411 N85-18697
Microalgae culture collection, 1984-1985
[DE84-013035] 11 p1690 N85-20626
Microplankton species assemblages at the Scripps Pier from March to November 1983 during the 1982-1984 El Nino event
[NASA-CR-175553] 12 p1899 N85-21926
Asteroid compositional rings: Clues to the compositions of primordial planetesimals in the middle solar system
15 p2678 N85-25537
A new taxonomy for distributed computer systems based upon operating system structure
[NASA-TM-86438] 19 p3342 N85-30709

TAYLOR INSTABILITY
Large-scale bubble structure of the interstellar medium (ISM) and properties of the Local Spiral Arm (LSA)
06 p0879 N85-15588
Kinetic Rayleigh-Taylor instability theory in the ionosphere near equator 13 p2067 N85-22911
Applications of Canuto's method to Rayleigh-Taylor-initiated turbulence
[DE85-010635] 18 p3102 N85-29202

TAYLOR SERIES
Stress-derivative control of keystoning deformation in finite element codes 01 p0068 N85-10385
Model diagnosis in two-way tables by means of row and column Euclidean maps
[CSIR-TWISK-307] 01 p0108 N85-10730
Upwind compact finite difference schemes
[CSIR-TWISK-334] 01 p0110 N85-10742
Determination of nonlinear viscoelasticity parameters for polymeric and composite materials by numerical methods
[AD-A145311] 02 p0185 N85-11240
Kinematics of nearby gas and stars
06 p0560 N85-15591
First derivatives of flow quantities behind two-dimensional, nonuniform supersonic flow over a convex corner
[NASA-TM-86272] 08 p1077 N85-16826
A series expansion study of the Navier-Stokes equations
[DFVLR-FB-84-34] 09 p1321 N85-18308
Efficiency of algorithms for gas-air channel diagnostics in gas turbine engines based on gas thermodynamic parameters 13 p2048 N85-22823
An incremental multigrid strategy for the fluid dynamics equations
[AD-A151953] 16 p2763 N85-27172
On the equivalent bilinearization of nonlinear controlled delay systems
[RR-272] 20 p3519 N85-31880

TAYLOR THEOREM
U TAYLOR SERIES

TAYLOR-GOERTLER INSTABILITY
U GOERTLER INSTABILITY

TDMA
U TIME DIVISION MULTIPLE ACCESS

TDR SATELLITES
TDRSS S-shuttle unique receiver equipment
08 p1100 N85-16951
The Communications link analysis and simulation system (CLASS) 08 p1100 N85-16952
Modeling techniques used in the communications link analysis and simulation system (CLASS)
08 p1100 N85-16953
Validation of the communications link analysis and simulation system (CLASS) 08 p1100 N85-16954
Digital scrambling for shuttle communication links: Do drawbacks outweigh advantages?
08 p1101 N85-16956
SIR-B coverage 08 p1143 N85-17211

TEA LASERS
Carbon dioxide laser radar for monitoring atmospheric transmittance and atmospheric aerosol
09 p1354 N85-18516
Improved operation of transversely exited N2O lasers
[AD-D011488] 10 p1490 N85-19409
Absorption of ozone molecules in strong field of tea CO2 injection laser 11 p1718 N85-20808
Obtaining amorphous coatings of FeW and Fe-Cr-P-B alloys using laser sputtering
[BLL-BISI-22493-(9022.06)] 17 p2927 N85-28057

TEACHING
U EDUCATION

TEAMS
Model of team organization and behavior and team description method
[AD-A147540] 07 p1053 N85-16680
Team dimensions: Their identity, their measurement and their relationships
[AD-A149682] 12 p1908 N85-21978

Assessing the behavior and performance of teams in organizations: The case of air transport crews
[AD-A150356] 13 p2143 N85-23302
Analysis of team performance in a programmed environment
[NASA-CR-175834] 14 p2392 N85-24728

TEARING
Impact dynamics research on composite transport structures
[NASA-TM-86391] 19 p3284 N85-30367
On size effects in plane stress crack-growth resistance
[AD-A155926] 24 p4102 N85-35428

TEARING MODES (PLASMAS)
Proceedings of the US-Japan Theory Workshop on 3-D MHD Studies
[DE84-012019] 04 p0568 N85-13620
Role of multiple helicity nonlinear interaction of tearing modes in dynamo and anomalous thermal transport in the Reversed Pitch Field
[DE85-002176] 10 p1580 N85-19839
Forced recognition by nonlinear MHD waves and sequential triggering of solar flares
12 p1956 N85-22291
Heating of coronal loops by tearing turbulence
14 p2446 N85-25114
Energy balance in resistive instabilities — solar prominences 14 p2454 N85-25155

TECHNETIUM
Molybdenum solar neutrino experiment
[DE85-003747] 14 p2445 N85-25080
Separation of uranium from technetium in recovery of spent nuclear fuel
[DE85-006499] 23 p3972 N85-34627
Elemental technetium as a cosmic-ray clock
[OG-7.1-9] 23 p4013 N85-34870

TECHNICAL WRITING
Improving technical documents
[AD-B084855] 01 p0126 N85-10696
The characteristics of generation and the rate of distribution for science and technology information in our country (China)
[AD-A141037] 04 p0575 N85-13671
Write while you work: Painless technical writing for Sandia engineers
[DE84-010869] 04 p0577 N85-13679
European Scientific Notes. Volume 39, number 1
[AD-A149498] 10 p1566 N85-19886
The potential for advanced computerized aids for comprehensible writing of technical documents
[AD-A150501] 13 p2055 N85-22870
Coping with computer terminology
[DE85-006076] 18 p3161 N85-29579
Standard procedures to be used in specifying basic properties of plastics and polymers
[NPL-DMA(A)-99] 20 p3433 N85-31295

TECHNIQUES
U METHODOLOGY

TECHNOLOGICAL FORECASTING
NT DELPHI METHOD (FORECASTING)
NT PATTERN METHOD (FORECASTING)
NT PROFILE METHOD (FORECASTING)
The future of satellite remote sensing: A worldwide assessment and prediction 02 p0151 N85-11025
Tactical missiles technologies. Research and prospectives
[SNIAS-841-320-101] 04 p0461 N85-12925
Perspectives of remote sensing at the end of the decade 05 p0859 N85-14238
Integrated Application of Active Controls (IAAC) technology to an advanced subsonic transport project. ACT/Control/Guidance System study, volume 1
[NASA-CR-165983-VOL-1] 06 p0754 N85-14837
A modified unit commitment and generation control for utilities with large wind generation penetrations
[DE84-015362] 06 p0808 N85-15129
Robotic technology: An assessment and forecast
[AD-A146672] 06 p0815 N85-15171
The application of a technology index to aircraft turbine engine cost estimating relationships
[AD-A147701] 08 p1087 N85-16874
The aircraft engine of the future
[PNR-90226] 08 p1087 N85-16875
USSR report: Machine tools and metalworking equipment
[JPRS-UMM-84-021] 08 p1138 N85-17166
Technology planning for flexible manufacturing systems 08 p1139 N85-17170
Developments in gas metering technology
[ERS-E.348] 09 p1321 N85-18307
Long-range electronics program outlined
11 p1700 N85-20667
Software technology within NASA
11 p1701 N85-20695
Technological and economic assessment of advanced ceramic materials. Volume 1: Summary and conclusions
[PB85-113082] 12 p1815 N85-21383
Technological and economic assessment of advanced ceramic materials. Volume 6: A case study of ceramic cutting tools
[PB85-113132] 12 p1815 N85-21387
GaAlAs-GaAs solar cell development: Prospective for space applications under concentration
13 p2007 N85-22581
Growth capabilities of European retractable solar arrays 13 p2012 N85-22625
FORTRAN in the 90's
[DE85-006154] 13 p2148 N85-23332
Inferences of future operations drawn from past and present applications of drifting buoys
14 p2323 N85-24356
Accomplishments of science by the year 2000
14 p2432 N85-24996
Fiscal year 1986 technical objective document
[AD-A151039] 14 p2432 N85-25000
A decision support methodology for space technology advocacy
[AD-A151895] 15 p2476 N85-25283
Future information technology, 1984: Telecommunications
[NBS/SP-500/119] 16 p2878 N85-27762
In orbit infrastructure. Volume 1: Executive summary — European space programs
[RX011-002/84-VOL-1] 17 p2906 N85-27928
Aluminum-lithium alloys: The answer of the aluminum industry to the threat of advanced fiber-reinforced materials
[VTH-LR-406] 17 p2932 N85-28102
Logical design of a decision support system to forecast technology, prices and costs for the national communications system
[AD-A152330] 17 p2948 N85-28196
Air Force technical objective document FY 86
[AD-A152730] 17 p3047 N85-28855
In orbit infrastructure — european space programs
[SNIAS-S/DT-24-996] 18 p3064 N85-28956
Outside users payload model
[NASA-CR-176011] 19 p3223 N85-29986
Technology for increasing the uranium-235 isotopic abundance in natural uranium feed on a productive scale
[DE85-011252] 19 p3357 N85-30810
Space ventures and society long-term perspectives
[NASA-CR-176012] 19 p3379 N85-30963
Evolution of spacecraft design methods as a function of environmental and geometrical constraints
[ESA-CR(P)-2012] 20 p3418 N85-31216
Structure and functions of ultra-thin films of organic compounds
[DRIC-T-7461] 22 p3741 N85-33188
Telecommunications forecast for ITU Region 2 to the year 1995
[NASA-TM-87077] 23 p3899 N85-34150
Towards the year 2000: Developments in inspection and product assurance to be anticipated during the next 15 years — aircraft engines
[PNR-90258] 23 p3940 N85-34421

TECHNOLOGIES
NT BIOTECHNOLOGY
NT ENERGY TECHNOLOGY
NT GEOTHERMAL TECHNOLOGY
NT MARINE TECHNOLOGY
NT MILITARY TECHNOLOGY
NT REACTOR TECHNOLOGY
Primer on the registration of technical information in industry 03 p0438 N85-12766
Development of robot technology in Shanghai surveyed 04 p0492 N85-13134
China report: Science and technology
[JPRS-CST-84-042] 06 p0747 N85-14789
East Europe report: Science and technology
[JPRS-ESA-85-005] 09 p1377 N85-18659
China report: Science and technology
[JPRS-CST-84-037] 10 p1424 N85-18982
West Europe report: Science and technology
[JPRS-WST-85-005] 11 p1592 N85-20013
China report: Science and technology
[JPRS-CST-84-026] 11 p1619 N85-20189
China report: Science and technology
[JPRS-CST-85-008] 12 p1820 N85-21416
Impacts of robotic and flexible manufacturing technologies on manufacturing costs and employment
[AD-A150060] 12 p1860 N85-21668
An open-ended future: In defense of a new humanism
[NASA-TM-77613] 12 p1944 N85-22209
Oversight review of the five-year outlook report on science and technology
[GPO-41-058] 12 p1949 N85-22243
Space Technology Experiments Platform (STEP) status: An in-space test facility 14 p2236 N85-23863
USSR report: Engineering and equipment
[JPRS-UEQ-84-005] 14 p2285 N85-24157
The impact of Science on Society
[NASA-SP-482] 14 p2431 N85-24994
The legacy of science 14 p2432 N85-24995
West Europe report: Science and technology
[JPRS-WST-85-014] 15 p2489 N85-25362
East European report: Science and technology
[JPRS-ESA-85-010] 15 p2524 N85-25560
USSR report: Electronics and electrical engineering
[JPRS-UEE-85-005] 15 p2524 N85-25565
China report: Science and technology
[JPRS-CST-85-009] 15 p2530 N85-25596
West Europe report: Science and technology
[JPRS-WST-84-020] 15 p2534 N85-25633
West Europe report: Science and technology
[JPRS-WST-84-003] 15 p2534 N85-25635
China report: Science and technology
[JPRS-CST-85-010] 15 p2564 N85-25819
The development and implementation of advanced welding technology 15 p2565 N85-25824
A study of spacecraft technology and design concepts, volume 1
[NASA-CR-172579-VOL-1] 16 p2730 N85-26844
The Department of Defense statement on the Science and Technology Program by Colonel Donald I. Carter, USAF Acting Deputy Under Secretary of Defense for Research and Advanced Technology before the Subcommittee on Research and Development of the Committee on Armed Services of the United States House of Representatives, 99th Congress, first session
[AD-A152467] 17 p3046 N85-28850
The outlook for Soviet advanced technologies
[AD-P004564] 17 p3048 N85-28859
Technology and Soviet political choices
[AD-P004566] 17 p3048 N85-28861
Management of large-scale technology
23 p4057 N85-35145
EPALIT: A data management system applied to the control and retrieval of technical reports
[PB85-193066] 24 p4166 N85-35828

TECHNOLOGY ASSESSMENT
Aeronautics Technology Possibilities for 2000: Report of a workshop
[NASA-CR-174018] 01 p0001 N85-10001
Development trends and requirements of propulsion system technology for civil aircraft
01 p0011 N85-10066
Satellite reconnaissance
[AD-B085034] 01 p0015 N85-10094
Technical Review of the Solid Particle Receiver Program
[DE84-015181] 01 p0068 N85-10451
A subjective evaluation of the PROFS operational workstation based upon a real-time forecasting experiment in summer 1983 — Program for Regional Observing and Forecasting Services (PROFS) 01 p0083 N85-10556
Interactive computer display systems in nowcasting
01 p0083 N85-10557
Fusion and its future in Illinois
[DE84-014686] 01 p0122 N85-10633
Office of Technology Assessment
01 p0127 N85-10672
Foreign civil aviation competition: 1976 summary and implications
[NASA-TM-X-73907] 02 p0133 N85-10907
Role of research aircraft in technology development
[NASA-TM-85913] 02 p0137 N85-10932
The future of satellite remote sensing: A worldwide assessment and prediction 02 p0151 N85-11025
Developing commercial users of space
02 p0154 N85-11044
Advances in electrophoretic separations
02 p0156 N85-11054
Opportunities for commercial organizations
02 p0156 N85-11055
Doing business in space: How to get there from here
02 p0156 N85-11057
Space research benefits national economy
02 p0163 N85-11107
The Multispectral Imaging Science Working Group. Volume 1: Executive summary
[E85-10001] 02 p0213 N85-11404
The Multispectral Imaging Science Working Group. Volume 2: Working group reports
[E85-10002] 02 p0213 N85-11405
Information Science Panel joint meeting with Imaging Science Panel 02 p0214 N85-11415
A prospectus for Thematic Mapper research in the Earth sciences
[E85-10003] 02 p0215 N85-11416
A report on the training course at Fortaleza (Ceara)
[E85-10013] 02 p0216 N85-11426

DOD related software technology requirements, practices, and prospects for the future
[AD-A145493] 02 p0242 N85-11575
The microprocessor control of a motor-alternator
[RAE-TM-NAV-ENG-1023(L)] 02 p0244 N85-11591
Artificial intelligence applications to maintenance
[AD-P003914] 02 p0244 N85-11594
An overview of the Joint Logistics Commanders Automatic Test Equipment Panel
[AD-P003916] 02 p0244 N85-11596
Narrowband tunable dye laser with amplifier pumped by powerful nitrogen laser 02 p0262 N85-11716
Auditory information systems in military aircraft: Current configurations versus the state of the art
[AD-A145469] 02 p0275 N85-11794
Proceedings of the Ion Implantation for Army Needs Workshop
[AD-A145474] 02 p0286 N85-11863
Review of the University of Manchester Ion Implantation Conference
[AD-P003950] 02 p0286 N85-11866
Research and technology
[NASA-TM-86321] 02 p0305 N85-11973
Preliminary analysis of space mission applications for electromagnetic launchers
[NASA-CR-174067] 03 p0321 N85-12071
Civilian space stations and the US future in space: Summary
[OTA-STI-242] 03 p0323 N85-12083
Sensor technology for second, third generation industrial robots. Optical sensor applications 03 p0342 N85-12196
Improving operational reliability and productivity of robotized technological complexes 03 p0346 N85-12227
New welding equipment for mechanized welding and trends in further development 03 p0352 N85-12264
Dynamic and other secondary benefits of compressed air energy storage
[DE84-015571] 03 p0366 N85-12468
Interstellar mission 04 p0459 N85-12916
Definition of technology development missions for early Space Station satellite servicing. Volume 2: Technical
[NASA-CR-171229] 04 p0461 N85-12923
Tactical missiles technologies. Research and prospectives
[SNIAS-841-320-101] 04 p0461 N85-12925
Electroforming of nickel
[SNIAS-841-501-101] 04 p0484 N85-13085
Metal oxide semiconductors power transistors
[CNES-84/QPE/FT/190] 04 p0496 N85-13166
China report: Science and technology
[JPRS-CST-84-001] 04 p0557 N85-13545
Present status, future prospects of domestic acoustical instruments 04 p0557 N85-13548
Value analysis — industrial competition
[CNES-NT-110] 04 p0577 N85-13684
Electromechanical/electromagnetics working group summary 05 p0604 N85-13852
A summary of the 1983 Integrated Flywheel Technology Workshop 05 p0605 N85-13855
Merits of flywheels for spacecraft energy storage 05 p0605 N85-13857
Evaluating NASA technology programs in terms of private sector impacts 05 p0606 N85-13865
Missions/planning panel 05 p0609 N85-13866
Basic investigation concerning the applicability of multispectral radiation data from microwave radiometry measurements to geoscientific objectives of remote sensing
[ESA-TT-846] 05 p0628 N85-14027
Metric evaluation of SAR-580 optical images for cartographic purposes 05 p0659 N85-14231
The role of expert systems in remote sensing 05 p0661 N85-14246
Solar pond overview 05 p0667 N85-14287
Bioprocessing in space 05 p0690 N85-14439
An overview of some monoplanar missile programs
[NASA-TM-86330] 06 p0747 N85-14786
Aperture synthesis (review) 06 p0781 N85-14995
Robotic technology: An assessment and forecast
[AD-A146672] 06 p0815 N85-15171
Civilian space stations and the US future in space
[OTA-STI-241] 07 p0914 N85-15781
Toward a goal-oriented civilian space program 07 p0914 N85-15786
Comparative investigation of three commercial radiosonde systems
[KNMI-TR-53] 07 p1009 N85-16409
The application of a technology index to aircraft turbine engine cost estimating relationships
[AD-A147701] 08 p1067 N85-16874
Low lift-to-drag aero-assisted orbit transfer vehicles 08 p1107 N85-16904
Flight crew training technology: A review 09 p1275 N85-18010
West Europe report: Science and technology
[JPRS-WST-85-003] 09 p1309 N85-18224
Configuration study for a 30 GHz monolithic receive array: Technical assessment
[NASA-CR-174697] 09 p1311 N85-18238
Impact of 810D on dynamic test laboratories 09 p1334 N85-18386
State and development of the machine-tool industry in Japan. Part 2: Flexible manufacturing systems
[PNR-90236-PT-2] 09 p1371 N85-18617
NASA new technology identification and evaluation
[NASA-CR-174368] 09 p1403 N85-18832
DOE/ORNL electric systems program overview
[DE85-003334] 10 p1459 N85-19197
Overview of photovoltaic concentrator technology
[DE84-016790] 10 p1512 N85-19539
Measurement techniques for evaluating solar reflector materials
[PB85-119489] 10 p1512 N85-19541
High energy pulsed particle accelerator
[AD-A149247] 10 p1554 N85-19797
Technological and economic assessment of advanced ceramic materials. Volume 3: A case study of ceramic capacitors
[PB85-113106] 11 p1613 N85-20141
The response of explosive systems to thermal stimuli: A state-of-the-art assessment
[DE85-000919] 11 p1614 N85-20148
Institute director surveys industrial automation drive 11 p1617 N85-20167
Developments in GDR metal forming technology assessed 11 p1617 N85-20168
Thermophysical properties of matter 11 p1620 N85-20199
Progress toward free-electron lasers for applications
[DE85-002208] 11 p1639 N85-20326
Technology and test 11 p1643 N85-20353
Where are we going in tethers 11 p1644 N85-20354
Introducing engine innovations: An examination of future markets for Brayton and Stirling automotive engines
[DE84-016319] 11 p1647 N85-20382
Exploratory assessment of second generation robotics and sensor-based systems
[PB85-132793] 11 p1648 N85-20386
High performance solar desiccant cooling system: Performance evaluation and research recommendations
[DE85-000508] 11 p1676 N85-20559
Software technology within NASA 11 p1701 N85-20695
Technological and economic assessment of advanced ceramic materials. Volume 2: A case study of ceramics in heat engine applications
[PB85-113090] 12 p1815 N85-21384
Technological and economic assessment of advanced ceramic materials. Volume 5: A case study of ceramic toxic and combustible gas sensors
[PB85-113124] 12 p1815 N85-21386
High-technology ceramics in Japan
[PB85-125029] 12 p1815 N85-21389
Latent heat storage technology and application workshop. Summary report: Session 6
[DE85-001097] 12 p1882 N85-21806
Multiyear plan for experimental systems research passive and hybrid solar energy program
[PB85-146666] 12 p1883 N85-21815
1984 science and technology posture hearing with the director of the Office of Science and Technology Policy
[GPO-41-060] 12 p1949 N85-22244
The high voltage silicon cell: A comparative analysis 13 p2005 N85-22569
Gallium arsenide arrays versus silicon arrays for space application 13 p2006 N85-22574
Availability of AlGaAs/GaAs solar cells in space 13 p2006 N85-22576
Comparative study of GaAs solar cell potentialities for space applications 13 p2006 N85-22577
Survival testing of silicon solar modules 13 p2009 N85-22602
Aspects of low cost module technology — spacecraft solar arrays 13 p2011 N85-22614
Study of concentration for space photovoltaic generators 13 p2011 N85-22618
Isotropic proton irradiation of GaAs solar cells 13 p2012 N85-22622
Recent trends in particle size analysis techniques
[NASA-TM-77735] 13 p2017 N85-22645
Survey of the state-of-the-art of miniature cryocoolers for superconductive devices
[AD-A150319] 13 p2041 N85-22774
Nation said to rank high with 15 satellites 13 p2041 N85-22776
USSR report: Machine tools and metalworking equipment
[JPRS-UMM-85-005] 13 p2051 N85-22839
Technologies to sustain tropical forest resources
[TI85-901065] 13 p2126 N85-23241
Spatial acquisition algorithms and systems for intersatellite optical communication links
[AD-A150794] 14 p2292 N85-24207
The 1981 transatlantic boat race contribution for marine meteorological measurements 14 p2324 N85-24361
Miscellaneous ARGOS maritime applications — yacht races 14 p2327 N85-24383
Drifting buoy studies for weather applications 14 p2329 N85-24396
USSR report: Cybernetics, computers, and automation technology
[JPRS-UCC-85-002] 14 p2400 N85-24794
Investigation of technology needs for avoiding helicopter pilot error related accidents
[NASA-CR-3895] 15 p2465 N85-25220
European views differ on space station concept 15 p2531 N85-25606
East Europe report: Science and technology
[JPRS-ESA-85-018] 15 p2537 N85-25658
Soviet Institute director on GDR-USSR welding technology 15 p2538 N85-25662
Mathematical aspect of welding technology research discussed 15 p2538 N85-25663
Applicability of modular versus universal robots discussed 15 p2538 N85-25664
Multi-bistatic radar for short range surveillance
[BAE-BT-10803] 15 p2539 N85-25673
Welding techniques in pressure part technology 15 p2566 N85-25835
Biotechnology in Japan
[PB85-166464] 15 p2615 N85-26113
Supercomputers and symbolic computation
[AD-A151376] 15 p2623 N85-26166
USSR report: Cybernetics, computers and automation technology
[JPRS-UCC-85-003] 15 p2625 N85-26174
Protective coatings for aircraft structures: A review
[VTH-LR-413] 16 p2706 N85-26704
The state-of-the-art and future of flight control systems 16 p2712 N85-26732
Forecasts on long-range development of space programs 16 p2727 N85-26830
US said to seek military advantage in space 16 p2727 N85-26831
Instrumentation technology overview 16 p2739 N85-26903
East Europe report: Science and technology
[JPRS-ESA-85-019] 16 p2767 N85-27077
Preliminary technology utilization assessment of the robotic fruit harvester
[NASA-CR-175834] 16 p2844 N85-27532
Flight test support aircraft Advanced Technologies Testing Aircraft System (ATTAS) for the DFVLR
[MBB-FE-732/S/PUB/154] 16 p2874 N85-27730
The Helios missions 16 p2884 N85-27795
Controller requirements for uncoupled aircraft motion, volume 1
[AD-A153173] 17 p2900 N85-27878
Glassy metals: New highly resistant material
[BLL-BISI-TRANS-21764-(9022.06)] 17 p2926 N85-28049
USSR report: Science and technology policy
[JPRS-UST-85-008] 17 p3049 N85-28872
General laws of development of technology 17 p3049 N85-28875
Advanced vehicle systems assessment. Volume 1: Executive summary
[NASA-CR-175876] 17 p3051 N85-28887
West European report: Science and technology
[JPRS-WST-84-036] 18 p3066 N85-28960
Conservation and substitution technology for critical metals in bearings and related components for industrial equipment and opportunities for improved bearing performance
[PB85-176246] 18 p3082 N85-29069
West Europe report: Science and technology
[JPRS-WST-84-022] 18 p3085 N85-29086
France's use of Cray 1, plans for national supercomputer 18 p3096 N85-29093
Preliminary investigation of the performance of repeater technology for satellite sound broadcasting
[SSP/017/82] 18 p3092 N85-29137
Evaluation of VLSI technology — space applications
[CD.6501702] 18 p3096 N85-29177
New technologies to improve laboratory testing
[DE85-008151] 18 p3110 N85-29257
Small central receiver Brayton cycle study
[DE85-008582] 18 p3128 N85-29369
Progress in solar thermal distributed receiver technology
[DE85-006066] 18 p3128 N85-29372
Progress in radar meteorology 18 p3148 N85-29488

Direct digital control study
[AD-A153665] 18 p3167 N85-29821
Sub-committee on advanced technology and technology transfer
[AD-A153645] 18 p3198 N85-29836
Current activities and background of technology transfer and exchange program at Lawrence Livermore National Laboratory
[DE85-009526] 18 p3199 N85-29843
Space station automation study-satellite servicing, volume 2
[NASA-CR-171513] 19 p3226 N85-30000
New form of graphite 19 p3243 N85-30111
The Federal Wind Program at NASA Lewis Research Center
[NASA-TM-83480] 19 p3304 N85-30478
Uniform cost-estimation method for biomass production and conversion technologies
[DE85-011714] 19 p3360 N85-30970
The application of laser anemometry to the study of transonic shock boundary-layer interactions
[ISL-CO-204/84] 20 p3396 N85-31087
Specific aspects of maritime search and rescue in French metropolitan and overseas territories: Expected benefits from a detection and location of distress system by satellites 20 p3401 N85-31097
Possible use of the COSPAS/SARSAT system within the Swedish mountain rescue organization 20 p3401 N85-31100
Maritime mobile satellite techniques as an integral part of the Future Global Maritime Distress and Safety System (FGMDSS): The position of the Federal Republic of Germany 20 p3406 N85-31136
Advanced (unfloated) gyros for satellite control
[ESA-CR(P)-2010] 20 p3419 N85-31222
An overview of measurement solutions for digital systems 20 p3437 N85-31326
SAR swath widening techniques — satellite radar
[BL-6196] 20 p3441 N85-31358
A survey of unified constitutive theories 20 p3466 N85-31531
Moire interferometric measurement of relative displacements in dovetail joints
[OUEL-1563/85] 20 p3471 N85-31566
Gas hydrates
[DE85-001966] 20 p3477 N85-31607
Millimetre wave pulse technology — satellite mapping
[ESA-CR(P)-2004] 20 p3478 N85-31611
Gallium arsenide arrays versus silicon arrays for space application
[SNIAS-851-440-104] 20 p3485 N85-31657
Study of concentration for space photovoltaic generators
[SNIAS-851-440-105] 20 p3485 N85-31658
The Department of Defense report on the technology base and support of university research
[AD-A154309] 20 p3540 N85-32030
Renewable energy research and development outlook, volume 1
[DE85-011577] 20 p3540 N85-32033
GAO (General Accounting Office) assessment of DOD's Very High Speed Integrated Circuits (VHSIC) technology program
[AD-A155109] 21 p3581 N85-32261
Space station ECLSS integration analysis: Simplified General Cluster Systems Model, ECLS System Assessment Program enhancements
[NASA-CR-176069] 21 p3670 N85-32796
Detector problems at the SSC
[DE85-010217] 21 p3703 N85-33007
Advanced beamed-energy and field propulsion concepts
[NASA-CR-176108] 22 p3741 N85-33186
Military hydrology. Report 9: State-of-the-art review and annotated bibliography of dam-breach flood forecasting
[AD-A155383] 22 p3801 N85-33553
Low-head hydroelectric power demonstration project: City of Gonzales, Texas
[DE85-010403] 22 p3809 N85-33595
Photovoltaic industry progress through 1984
[DE85-013029] 22 p3809 N85-33596
The development of titanium production in the USSR
[BLL-OA-TRANS-3226-(6196.3)] 23 p3913 N85-34244
Vapor phase heat transport concepts
[DE85-009550] 23 p3931 N85-34366
SP-100 Thermionic Technology Program
[DE85-012311] 23 p3972 N85-34625
Analysis of incompressible cascade flows using state-of-the-art computer programs
[AD-A155850] 24 p4062 N85-35173
Energy Efficient Engine Program technology benefit/cost study, volume 2
[NASA-CR-174766-VOL-2] 24 p4096 N85-35196
Technology for large space systems: A bibliography with indexes
[NASA-SP-7046(12)] 24 p4068 N85-35209
State-of-the-art construction technology for deep tunnels and shafts in rock
[AD-A156362] 24 p4099 N85-35411
Practical aspects of photovoltaic technology, applications and cost (revised)
[NASA-CR-174963] 24 p4110 N85-35472
A Programmable Automatic Noise Data and Other Related parameter Acquisition system (PANDORA) — wind energy converters 24 p4111 N85-35479
Visit to test facility Stoetten (West Germany) May 9, 1984, including the Voith Wind Energy Converter (WEC) 520 turbine. The annual production of various wind energy plants in selected locations 24 p4112 N85-35487
TECHNOLOGY TRANSFER
NT AEROSPACE TECHNOLOGY TRANSFER
PROFS: An approach to improved operational weather services — Program for Regional Observing and Forecasting Services (PROFS) 01 p0083 N85-10555
Project COST 72 (The European weather radar project) today 01 p0084 N85-10561
Factors critical to the implementation of self-paced instruction: A background review
[AD-A145143] 01 p0097 N85-10648
Integrated computer-aided manufacturing (ICAM) architecture. Part 3, volume 8: Technology transfer
[AD-A144732] 01 p0103 N85-10689
Energy efficient engine. Volume 2. Appendix A: Component development and integration program
[NASA-CR-173085] 02 p0146 N85-10991
Opportunities for commercial organizations 02 p0156 N85-11055
Development of space instrumentation of Intercosmos member countries 02 p0163 N85-11106
Remote sensing applications program
[E85-10022] 02 p0218 N85-11435
Artificial Intelligence in Maintenance: Proceedings of the Joint Services Workshop
[AD-A145349] 02 p0244 N85-11592
AGARD Highlights
[AGARD-HIGHLIGHTS-84/2] 02 p0305 N85-11972
Proceedings of a Workshop on Applications of Tethers in Space, Executive Summary
[NASA-CR-171195] 03 p0322 N85-12075
Dynamics and controls working group summary 05 p0604 N85-13854
Land Remote-Sensing Commercialization Act
[S-REPT-98-458] 05 p0654 N85-14201
The availability of Japanese scientific and technical information in the United States
[GPO-35-241] 05 p0735 N85-14726
Naval surface weapons center technology transfer report (FY83)
[AD-A146501] 06 p0871 N85-15534
Propulsion and power systems perspective 08 p1098 N85-16936
Microwave radiometric studies of composition and structure 08 p1183 N85-17456
Study of application of space telescope science operations software for SIRTF use
[NASA-CR-177337] 09 p1287 N85-18060
Emerging role of the national laboratory in the development and transfer of materials technology
[DE85-001252] 09 p1288 N85-18068
West Europe report: Science and technology
[JPRS-WST-85-003] 09 p1309 N85-18224
NASA new technology identification and evaluation
[NASA-CR-174368] 09 p1403 N85-18832
West Europe report: Science and technology
[JPRS-WST-85-004] 10 p1460 N85-19204
French research minister on policy, technology transfer 11 p1618 N85-20182
China report: Science and technology
[JPRS-CST-84-040] 11 p1623 N85-20219
Oversight review of the five-year outlook report on science and technology
[GPO-41-058] 12 p1949 N85-22243
Transfer of technology
[S-REPT-98-664] 12 p1949 N85-22246
Transfer of technology
[S-HRG-98-996] 12 p1949 N85-22247
The availability of Japanese scientific and technical information in the United States
[GPO-39-478] 12 p1951 N85-22254
Technology transfer to the Middle East
[PB85-127744] 12 p1952 N85-22264
China report: Science and technology
[JPRS-CST-85-003] 13 p2186 N85-23433
West Europe report: Science and technology
[JPRS-WST-85-013] 14 p2269 N85-24183
East Europe report: Science and technology
[JPRS-ESA-85-015] 14 p2269 N85-24189
West Europe report: Science and technology
[JPRS-WST-84-007] 15 p2530 N85-25600
China report: Science and technology
[JPRS-CST-85-007] 15 p2533 N85-25621
Energy Data Base: Subject thesaurus permutated listing. Revision 6, appendix
[DE84-016963] 15 p2666 N85-26454
China report: Science and Technology
[JPRS-CST-85-012] 16 p2806 N85-27300
Bioengineering and rehabilitation: Windows of opportunity past, present and future
[NASA-EP-216] 16 p2841 N85-27516
Soviet space programs, 1976-1980 (with supplementary data through 1983). Part 3: Unmanned space activities
[S-PRT-98-235-PT-3] 16 p2879 N85-27765
The significance of Helios for Europe 16 p2866 N85-27808
West Europe report: Science and technology
[JPRS-WST-84-024] 17 p2945 N85-28183
Technology and Soviet political choices
[AD-P004566] 17 p3048 N85-28861
Close encounters with S/T (science and technology) in the Soviet Union
[AD-P004570] 17 p3048 N85-28864
Catalog of research projects at Lawrence Berkeley Laboratory, 1985
[DE85-008679] 17 p3049 N85-28869
Report to Congress on the Automotive Technology Development Program
[DE85-005640] 17 p3052 N85-28890
West European report: Science and technology
[JPRS-WST-84-036] 18 p3066 N85-28960
West Europe report: Science and technology
[JPRS-WST-84-032] 18 p3066 N85-29095
Results of Italian research in high power lasers 18 p3066 N85-29097
US restrictions on technology transfer reviewed 18 p3068 N85-29115
Photovoltaic Systems Development Project: An activity summary
[DE85-009994] 18 p3129 N85-29379
Sub-committee on advanced technology and technology transfer
[AD-A153645] 18 p3198 N85-29636
Current activities and background of technology transfer and exchange program at Lawrence Livermore National Laboratory
[DE85-009526] 18 p3199 N85-29843
U.S.-China conference on science policy
[PB85-176345] 19 p3360 N85-30971
West Europe report: Science and technology
[JPRS-WST-85-020] 20 p3438 N85-31333
Evaluative report on the Institute for Computer Sciences and Technology, National Bureau of Standards, fiscal year 1984
[PB85-176097] 20 p3514 N85-31848
Spin-offs from technical scientific infrastructures, no. 1 20 p3540 N85-32034
Spin-offs from technical commercial infrastructures, no. 2 20 p3540 N85-32035
Photovoltaics technical information guide
[DE85-002924] 22 p3806 N85-33585
Technology transfer report: Feasibility study for the use of geothermal brine in the Ashdod area, Israel
[DE85-013316] 22 p3810 N85-33598
New innovative businesses from industry. Experiences in the Netherlands in the successful transfer of technology from university to industry 22 p3849 N85-33843
Proceedings of the 14th Army Science Conference. Volume 3: Principal authors P through Z
[AD-A149202] 24 p4144 N85-35691
Electronic information management and productivity
[DE85-013362] 24 p4164 N85-35818
TECHNOLOGY UTILIZATION
PROFS: An approach to improved operational weather services — Program for Regional Observing and Forecasting Services (PROFS) 01 p0083 N85-10555
Canada report to COSPAR 01 p0131 N85-10906
Industrial use of land observation satellite systems 02 p0151 N85-11026
Agribusiness and space: No limits to growth 02 p0152 N85-11029
Economic evaluation of space survey materials use in land improvement engineering field work 02 p0165 N85-11115
A prospectus for Thematic Mapper research in the Earth sciences
[E85-10003] 02 p0215 N85-11418
A report on the training course at Fortaleza (Ceara)
[E85-10013] 02 p0216 N85-11426
Applications of remote sensing techniques to oceanography and sea ice
[FOA-B-60004-M7] 02 p0220 N85-11448
On applying AI (Artificial Intelligence) to maintenance and troubleshooting
[AD-P003915] 02 p0244 N85-11595

AI (Artificial Intelligence) approaches to troubleshooting
[AD-P003918] 02 p0245 N85-11598
Navy programs on ion implantation for materials modification
[AD-P003952] 02 p0288 N85-11868
Requirements and special problems of land altimetry — satellite altimetry 03 p0380 N85-12430
The applications of fibre optics in gas turbine engine instrumentation
[PNR-90209] 03 p0420 N85-12687
The Uniform Science and Technology Research and Development Utilization Act
[GPO-36-327] 04 p0577 N85-13685
Uniform Science and Technology Research and Development Utilization Act
[H-REPT-98-983-PT-1] 04 p0577 N85-13686
Rotating assembly working group summary 05 p0604 N85-13851
Fundamentals and applications of the six port measuring technique — reflectometer 05 p0630 N85-14039
Stirling engine development, state of the art, possible engine applications and suitability in comparison to established plants and systems
[BMFT-FB-T-84-196] 05 p0646 N85-14149
Contributions to remote sensing : Applications of thermal infrared
[COMMUN-34/1984] 05 p0654 N85-14196
Methorological research in connection with the handling of LANDSAT satellite data for archaeology 05 p0655 N85-14207
Remote sensing data in support of conventional data 05 p0659 N85-14232
ERS-1 and its potential for industrial utilization 05 p0659 N85-14235
Utilization possibilities of photovoltaics in the private sector 05 p0664 N85-14272
ASC 1984 Applied Superconductivity Conference
[DE84-016204] 06 p0868 N85-15521
Integrated technology wing study (oral presentation)
[NASA-CR-169497] 07 p0902 N85-15718
Impressions from a study tour in Finland concerning fiber reinforced plastics, June 1984
[FOA-C-20552-D2(E4,F9)] 07 p0921 N85-15831
Where to next in astronomical photography? — tabular grain emulsions 07 p0964 N85-16114
Use of minicomputers for the formation of hydrological data banks 07 p1001 N85-16358
Possibilities and impossibilities of microcomputer systems
[AD-1984-904] 07 p1028 N85-16522
Research and technology, 1984 report
[NASA-TM-83096] 07 p1061 N85-16730
Research and technology, Lyndon B. Johnson Space Center
[NASA-TM-58263] 08 p1262 N85-17929
Manufacturing costs, equipment needs and technological opportunities among small and medium-size manufacturers
[DE85-000479] 09 p1304 N85-18193
Computers and education
[GPO-28-378] 10 p1537 N85-19689
Magnetic heat pump feasibility assessment
[DE85-002806] 11 p1632 N85-20276
Tactical operations and space applications 11 p1709 N85-20752
Technological and economic assessment of advanced ceramic materials: Volume 4: A case study of integrated optic devices
[PB85-113116] 12 p1815 N85-21385
Applications of Tethers in Space
[NASA-CP-2366] 12 p1859 N85-21659
New application possibilities for clad steel by reducing surface treatment expenditure and by using improved welding technology
[BMFT-FB-T-84-236] 12 p1861 N85-21672
Latent heat storage technology and application workshop. Summary report: Session 6
[DE85-001097] 12 p1882 N85-21806
Space solar cells: Adjusting to new demands 13 p2005 N85-22566
Metal-semiconductor phase transition and its application
[DRIC-T-7149] 13 p2021 N85-22665
Role of optical disk at computing centers
[DE85-005124] 13 p2145 N85-23314
Physicists' role in new technological development discussed 13 p2166 N85-23436
Economic mechanism of integration of science, production 13 p2167 N85-23443
Technology and Economics, Inc. Technology Application Team
[NASA-CR-175830] 13 p2168 N85-23454
Riga Institute seeking faster introduction of new technology 14 p2206 N85-23696
Possible technological answers to new design requirements for power transmission systems 14 p2222 N85-23779
Piezoelectric plastics — polyvinyl fluoride
[ISL-CO-202/83] 14 p2262 N85-24017
Group technology for working turbine drive wheel disks 14 p2269 N85-24061
Remote sensing: New tool for China's geologists 14 p2283 N85-24141
Applications of ultrasonic technology 14 p2283 N85-24144
Minister B. V. Balmont on status of automation drive 14 p2284 N85-24151
Application possibilities of laser Doppler anemometry in the investigation of the transonic interaction between shock wave and boundary layer
[ISL-R-131/83] 14 p2304 N85-24265
Utilization of microchannel plates in the flash X-ray technique
[ISL-CO-228/83] 14 p2306 N85-24275
Lasers in the domains of ultrashort-time phenomena physics and ballistics
[ISL-CO-236/83] 14 p2310 N85-24299
Inferences of future operations drawn from past and present applications of drifting buoys 14 p2323 N85-24356
The 1981 transatlantic boat race contribution for marine meteorological measurements 14 p2324 N85-24361
Miscellaneous ARGOS maritime applications — yacht races 14 p2327 N85-24383
The Effect of Computers on the Generation and Use of Technical Data
[NBSIR-84-2907] 14 p2400 N85-24792
Accomplishments of science by the year 2000 14 p2432 N85-24996
Our future in the cosmos: Computers 14 p2432 N85-24997
Performance testing and system characterization. DOE hybrid test vehicle, phase 3
[NASA-CR-175668] 14 p2434 N85-25010
Roundtable on effective use of flight simulators 15 p2460 N85-25190
Holography in space 15 p2476 N85-25285
French robotics research at Grenoble labs 15 p2523 N85-25555
West Europe report: Science and technology
[JPRS-WST-84-014] 15 p2536 N85-25647
An introductory study of automatic speech recognition systems
[BAE-BT-12286] 15 p2539 N85-25677
Industrial applications of pattern recognition and image processing 15 p2622 N85-26157
Summaries of FY 1984 engineering research
[DE85-006273] 15 p2664 N85-26442
Aspects of application of ACT systems for pilot workload alleviation 16 p2712 N85-26734
Uses of laser technology described 16 p2768 N85-27080
Function of remote sensing in Brazil
[INPE-3314-PRE/621] 16 p2810 N85-27329
Status of computer aided mapping in hydrographic services 16 p2815 N85-27366
Surveying and optical tooling technologies combined to align a skewed beamline at the LAMPF accelerator
[DE85-005902] 16 p2864 N85-27664
Characteristics and applications of superplastic materials for aeronautics
[MBB-BB-585/84-O] 16 p2873 N85-27727
New materials and techniques for aircraft structures
[B8580074] 17 p2897 N85-27861
Automation and robotics for the National Space Program
[NASA-CR-175881] 17 p2909 N85-27936
Aluminum-lithium alloys: The answer of the aluminum industry to the threat of advanced fiber-reinforced materials
[VTH-LR-406] 17 p2932 N85-28102
Hot Isostatic Pressing (HIP): Techniques, applications and economical use
[JUEL-SPEZ-298] 17 p2939 N85-28141
USSR report: Engineering and equipment
[JPRS-UEQ-85-004] 17 p2939 N85-28142
Applications of robots in machine tool industry reviewed 17 p2946 N85-28189
Catalog of research projects at Lawrence Berkeley Laboratory, 1985
[DE85-006879] 17 p3049 N85-28869
General laws of development of technology 17 p3049 N85-28875
Results of Italian research in high power lasers 18 p3086 N85-29097
Some applications of aeronautical engineering in the construction of yachts
[NLR-MP-83042-U] 20 p3394 N85-31052
Existing and potential INMARSAT capabilities for the Future Global Maritime Distress and Safety System 20 p3402 N85-31110
Solar dynamic systems 20 p3443 N85-31374
The role of scientific ballooning for exploration of the magnetosphere
[TRITA-EPP-84-07] 20 p3494 N85-31724
A systematic plan for the continued study of dimensional stability of metallic alloys considered for the fabrication of cryogenic wind tunnel models
[NASA-CR-172449] 21 p3565 N85-32172
Deep sea mega-geomorphology: Progress and problems 21 p3602 N85-32369
Use of the synoptic view: Examples from Earth and other planets 21 p3602 N85-32371
Statement of Aaron Cohen, Director, Research and Engineering, Johnson Space Center and Chairman, Space Station Advanced Technology Advisory Committee, National Aeronautics and Space Administration, before the Subcommittee on Science, Technology, and Space, Committee on Commerce, Science, and Transportation, United States Senate
[NASA-TM-87497] 22 p3739 N85-33174
High powered epicyclic gears: Some recent development 23 p3924 N85-34316
Energy Efficient Engine Program technology benefit/cost study, volume 1
[NASA-CR-174766-VOL-1] 24 p4066 N85-35197
Motor glider meteorology 24 p4121 N85-35543

TECTONIC MOVEMENT
U TECTONICS

TECTONICS
Seismotectonic nature of some annular photoanomalies registered by remote methods 02 p0164 N85-11110
Hypothesis on the origin of lineaments in the LANDSAT and SLAR images of precambrian soil in the low Contas River Valley (southern Bahia)
[E85-10007] 02 p0215 N85-11420
Paleoenvironmental interpretation of the upper cretaceous Point Lookout sandstone: Implications for shoreline progradation and basin tectonic history, San Juan basin, New Mexico 02 p0227 N85-11488
Vertical crustal movements in southern California, 1974 to 1978
[GS-CIRC-905] 02 p022R N85-11491
Heat flow map of Europe: Brief summary of the geophysical implications
[REPT-562] 03 p0377 N85-12405
Stratigraphy, petrology, and tectonic setting of the Alisitos Group, Baja California, Mexico 03 p0389 N85-12488
Stratigraphy, sedimentology and tectonic significance of the Upper Cretaceous Virginian Ridge formation, Method Basin, Washington: Implications for tectonic history of the North Cascades 03 p0390 N85-12494
Franciscan and related rocks of southern Humboldt County, northern California coast ranges: Analysis of structure, tectonics, sedimentary petrology, paleogeography, depositional history, and thermal maturity 03 p0390 N85-12495
Geophysical investigations of the central part of Niger State, Nigeria 03 p0390 N85-12496
Martian impact basins: Morphology differences and tectonic provinces
[NASA-CR-174074] 03 p0448 N85-12847
Horizontal-strain observations in the Shumagin Island and Yakataga seismic gaps, Alaska 04 p0515 N85-13287
Deep structure and seismicity in the Catalonia-Pyrenees region 04 p0524 N85-13352
Archean sedimentation and tectonics in southern Africa
[NASA-CR-174156] 04 p0533 N85-13408
Models for volcanic processes in Long Valley, California: Testing by continental drilling
[DE84-014943] 04 p0534 N85-13414
Priorities for a national program of continental drilling for scientific purposes 04 p0534 N85-13418
A tectonic and metamorphic history of the north-central Klamath Mountains, California 05 p0573 N85-14323
Tectonic history of a continent: Island arc boundary, west-central Idaho 05 p0573 N85-14324
Geology, petrology, and tectonic setting of the Mafic rocks of the 1480 Ma old granite-rhyolite terrane of Missouri, USA 05 p0574 N85-14327
Sedimentation, structure and tectonics of the Umpqua group (paleocene to early eocene), southwestern Oregon 05 p0578 N85-14354
Earthquakes and tectonics of Pacific Ocean margins 06 p0820 N85-15206
Some trends in the modern Earth sciences — plate tectonics and Earth's crust 06 p0820 N85-15207
Boundary velocities of mohorovicic discontinuity and upper mantle structure of Pacific Ocean bed 06 p0821 N85-15211

General model of earthquakes and the place of warnings in it 07 p0981 N85-16232
Model of earthquake mechanism 07 p0982 N85-16236
Tectonic, volcanic, and climatic geomorphology study of the Sierras Pampeanas Andes, northwestern Argentina 08 p1144 N85-17215
Structure and stratigraphy of Midterhuken Peninsula, Bellsund, West Spitsbergen 09 p1353 N85-18513
Mercury 09 p1411 N85-18890
Venus 09 p1411 N85-18891
Earth 09 p1411 N85-18892
Utilization of mobile VLBI for geodetic measurements 10 p1466 N85-19248
Localization of destruction process 10 p1500 N85-19470
Vertical movements and structure formation within island systems of northeast Asia 10 p1501 N85-19471
Study of tectonic earthquake precursors by geodetic methods 10 p1502 N85-19479
Mesozoic magmatism of Mongolian-Okhotsk Belt and its possible geodynamic interpretation 10 p1502 N85-19481
Post-carboniferous tectonics in the Anadarko Basin, Oklahoma: Evidence from side-looking radar imagery [NASA-CR-175458] 10 p1505 N85-19498
Tectonic lineaments in the cenozoic volcanics of southern Guatemala: Evidence for a broad continental plate boundary zone [NASA-CR-175456] 10 p1505 N85-19499
Crustal stretching and subsidence in sedimentary eastern Switzerland and permo-carboniferous basins in the continental United States [DE85-000622] 11 p1681 N85-20592
Use of paleomagnetic data in tectonic analysis of oceanic structures 13 p2106 N85-23135
Review of problems in lithology 13 p2113 N85-23160
Possibility of mapping active tectonic structures from mercury gas aureoles over sea surface 13 p2113 N85-23162
Geomagnetic precursors of intensive earthquakes in the 1-0.-2 Hz frequency range of geomagnetic pulsations 13 p2116 N85-23178
A tectonic model of an incipient spreading center and its margins: The Northern Red Sea and the Dead Sea rift 13 p2140 N85-23266
Venus chasmata: A lithosphere stretching model 13 p2178 N85-23516
Terrestrial analog studies for Martian patterned ground 13 p2190 N85-23590
Terrestrial analogs for planetary wrinkle ridges 13 p2199 N85-23644
Planetary interior modeling and tectonic implications 13 p2200 N85-23649
Elysium region, Mars: Tests of lithospheric loading models for the formation of tectonic features 13 p2200 N85-23650
Kasei Valls of Mars: Dating the interplay of tectonics and geomorphology 13 p2201 N85-23654
Creep of ice: Further studies 13 p2201 N85-23655
Lineaments on Ganymede: New evidence for late tectonic activity 13 p2202 N85-23658
Global tectonics on Ganymede 13 p2202 N85-23659
Tectonics of the Galileo Regio on Ganymede 13 p2202 N85-23660
Importance of the tectonic motions on Ganymede 13 p2202 N85-23661
Tectonics of the Valhalla structure on Callisto 13 p2202 N85-23662
Evaluating structure-forming role of late Paleozoic and Mesozoic-Cenozoic tectonic movements in Baltic Sea region 14 p2337 N85-24450
Location of continental Permian volcanites of central Asia and its tectonic interpretation 14 p2346 N85-24505
Example of joint use of data from surface studies and space photographs in investigating dynamics of zone of North Zeravshan seismogenic faults 15 p2485 N85-25342
Periodic cometary showers: Real or imaginary? 15 p2660 N85-26555
Analysis of mesofissuring on space photographs: New technique for study of petroleum and gas deposits 16 p2726 N85-26828
A traveltime interpretation of the 1978 seismic refraction profile in the Kingdom of Saudi Arabia 17 p2991 N85-28486
Natural gas anomaly in bottom waters of South China Sea 19 p3290 N85-30399
Microstructural analysis of Pacific Ocean and Indian Ocean ultrabasites 19 p3291 N85-30405
Density characteristics of asthenosphere in Atlantic Ocean 19 p3294 N85-30423
Tectonic structure features of some deep faults in Atlantic and Pacific Oceans (according to deep seismic sounding-reflected waves method data) 19 p3295 N85-30428
Highly important features of regional tectonics of Earth's Arctic sector 19 p3296 N85-30449
Structural and tectonic history of the Golconda allochton, southern Tolyabe Range, Nevada 19 p3312 N85-30529
Euro-African MAGSAT anomaly-tectonic observations 20 p3475 N85-31596
Long-wavelength magnetic and gravity anomaly correlations on Africa and Europe 20 p3476 N85-31597
Continental magnetic anomaly constraints on continental reconstruction 20 p3476 N85-31599
Regional magnetic anomaly constraints on continental rifting 20 p3476 N85-31600
Geodynamics Branch research program [NASA-TM-86223] 20 p3489 N85-31688
Contemporary plate motions from LAGEOS 20 p3489 N85-31689
The global VLBI fiducial network 20 p3490 N85-31690
First epoch measurements by Mark III VLBI of the San Andreas Fault experiment baseline 20 p3490 N85-31691
Geophysical interpretation of satellite laser ranging measurements 20 p3490 N85-31692
Geologic and hydrologic characterization and evaluation of the basin and range province relative to the disposal of high-level radioactive waste. Part 3: Geologic and hydrologic evaluation [GS-CIRC-904-A] 20 p3526 N85-31934
Global Mega-Geomorphology [NASA-CP-2312] 21 p3600 N85-32357
Global geomorphology 21 p3601 N85-32359
Quantitative analysis in megageomorphology 21 p3603 N85-32376
Techniques, problems and uses of mega-geomorphological mapping 21 p3604 N85-32378
Planetary perspective. Report of Working Group Number 4 21 p3605 N85-32385
A review of tectonic aspects of the Limpopo belt and other Archean high-grade gneissic terranes 21 p3720 N85-33080
Use of space photographs for analysis of structural and dynamic conditions of formation of ancient phlogopite and apatite deposits 22 p3735 N85-33153
Crustal Dynamics Project: Catalogue of site information [NASA-TM-86218] 22 p3801 N85-33552
Tectonic stability and expected ground motion at Yucca Mountain [DE85-012004] 22 p3814 N85-33629
Subduction zone tectonic studies to develop concepts for the occurrence of sediment subduction [DE85-011794] 22 p3815 N85-33632
Impact processes and their implications for planetary formation and early evolution 22 p3853 N85-33860
Planetary surface processes: A review 22 p3855 N85-33869
A solid-state framework for terrestrial upper mantles 22 p3856 N85-33878
Crustal development in the terrestrial planets 22 p3856 N85-33879
Contrasts in evolution of Venus and Earth 22 p3857 N85-33880
Compressional environment in the location and orientation of planetary dorsa and terrestrial earthquake fault structures 22 p3857 N85-33885
Geology and petroleum resources of basins in western China [DE85-013036] 23 p3948 N85-34469
Some recent deposit modeling efforts 24 p4106 N85-35453
Seismic stratigraphic analysis of the Mississippi Fan 24 p4115 N85-35507
A dynamic model of Venus's gravity field [NASA-CR-176173] 24 p4169 N85-35845

TEETH

An experimental investigation of microstrip properties on soft substrates from 2 to 40 GHz [NASA-TM-86961] 11 p1624 N85-20224
Spectral evaluation of irregularity of superconducting coaxial cables 13 p2082 N85-23000
Method for ultrasonic bonding to soft microelectronic substrates [NASA-CASE-NPO-16087-1] 18 p3094 N85-29151
Elliptical X-ray analyzer spectrograph application to a laser-produced plasma [DE85-013790] 24 p4097 N85-35398

TEKTITES

Microtektite discovered in Beijing [NASA-TM-77765] 01 p0130 N85-10695

TELECHIRICS

U REMOTE HANDLING

TELECOMMUNICATION

NT AIRCRAFT COMMUNICATION
NT BROADCASTING
NT CODE DIVISION MULTIPLE ACCESS
NT COLOR TELEVISION
NT COMMUNICATION
NT DATA LINKS
NT DEFENSE COMMUNICATIONS SATELLITE SYSTEM
NT DEFENSE COMMUNICATIONS SYSTEM (DCS)
NT DEMAND ASSIGNMENT MULTIPLE ACCESS
NT ELECTRONIC MAIL
NT FACSIMILE COMMUNICATION
NT FREQUENCY DIVISION MULTIPLE ACCESS
NT GROUND-AIR-GROUND COMMUNICATION
NT INTERPLANETARY COMMUNICATION
NT LINE OF SIGHT COMMUNICATION
NT MULTICHANNEL COMMUNICATION
NT MULTIPLE ACCESS
NT OPTICAL COMMUNICATION
NT PCM TELEMETRY
NT PULSE COMMUNICATION
NT RADIO COMMUNICATION
NT RADIO RELAY SYSTEMS
NT RADIO TELEMETRY
NT RADIOTELEPHONES
NT SATELLITE TELEVISION
NT SELECTIVE DISSEMINATION OF INFORMATION
NT SHIP TO SHORE COMMUNICATION
NT SINGLE CHANNEL PER CARRIER TRANSMISSION
NT SPACE COMMUNICATION
NT SPACECRAFT ANTENNAS
NT SPACECRAFT COMMUNICATION
NT SPACECRAFT TELEVISION
NT TELEMETRY
NT TELEPHONY
NT TIME DIVISION MULTIPLE ACCESS
NT VIDEO COMMUNICATION
NT VOICE COMMUNICATION
NT VOICE DATA PROCESSING
NT WIDEBAND COMMUNICATION
NT WIRELESS COMMUNICATION

Tendencies in the development of utilization protocols, seminar report — communication networks [FUB-11-1983] 01 p0039 N85-10252
Availability of transmission systems in continental and intercontinental connections — telecommunication [FUB-33-1983] 01 p0040 N85-10261
Hardware implementation of a support system for the 2501 Western digital LSI, complete controller of the second level, first version of the CCITT 25 (CAP) recommendations [FUB-60-1982] 01 p0100 N85-10666
An investigation of the use, cost, perceived value and social context of telecommunications tools in two-year college libraries in the southeastern United States 02 p0293 N85-11901
DCS (Defense Communications System) network synchronization design criteria [AD-A146251] 03 p0356 N85-12289
Five-year plan for meeting the automatic data processing and telecommunications needs of the Federal Government. Volume 1: Planning strategies [PB84-214501] 03 p0436 N85-12777
Federal Telecommunications Privacy Act of 1984 [H-REPT-98-815] 03 p0441 N85-12807
Mission science value-cost savings from the Advanced Imaging Communication System (AICS) [NASA-CR-174170] 04 p0458 N85-12905
China report: Science and technology [JPRS-CST-84-003] 04 p0491 N85-13132
New telecommunications optical fiber developed 04 p0492 N85-13135
The Telecom 1 satellite telecommunication system 04 p0493 N85-13147
USSR report: Electronics and electrical engineering [JPRS-UEE-84-011] 06 p0789 N85-15042
Problems of development of space communication 06 p0793 N85-15067
US objectives generally achieved at broadcasting satellite international conference. Improvements can help in future conferences [PB84-235316] 06 p0800 N85-15109
USSR report: Electronics and electrical engineering [JPRS-UEE-84-018] 07 p0949 N85-16014
USSR report: Electronics and electrical engineering [JPRS-UEE-84-017] 07 p0951 N85-16025

Life cycle cost management master plan for the Defense Communications Agency
[AD-A146876] 07 p1050 N85-16668
Acquisition planning at the Defense Communications Agency
[AD-A146877] 07 p1051 N85-16669
On the complexity of distributed decision problems
[AD-A147174] 07 p1052 N85-16674
East Europe report: Science and technology
[JPRS-ESA-84-046] 08 p1139 N85-17176
Telecommunications equipment at 1984 Leipzig Spring Fair 08 p1140 N85-17179
Compilation of annual reports of the Navy ELF (Extremely Low Frequency) communications system ecological monitoring program. Volume 1: Tabs A-E
[AD-A146326] 08 p1152 N85-17272
Compilation of annual reports of the Navy ELF (Extremely Low Frequency) communications system ecological monitoring program (1983). Volume 2: Tabs F-J
[AD-A146327] 08 p1152 N85-17273
A modified Monte-Carlo technique for the simulation of satellite communication systems
[AD-A146880] 08 p1214 N85-17641
Calculation of cumulative distributions and detection probabilities in communications and optics
[AD-A147781] 08 p1215 N85-17650
Star on the horizon: The emergence of the direct broadcast satellite in American mass communications
[AD-A146819] 09 p1312 N85-18242
Study of factors affecting an HF/VHF direct broadcasting satellite service
[PB85-120889/GAR] 09 p1313 N85-18255
The Telecommunications and Data Acquisition Report
[NASA-CR-174366] 10 p1462 N85-19224
A system for measuring the characteristics of the ionospheric channel by digital tranamission 10 p1472 N85-19287
An H.F. simulator for use with real time channel evaluation systems 10 p1473 N85-19293
Worldwide report: Telecommunications policy, research and development
[JPRS-TTP-85-002] 10 p1475 N85-19309
NTT (Nippon Telegraph and Telephone Public Corporation) develops new optical fiber 10 p1476 N85-19311
Worldwide report: Telecommunications policy, research and development
[JPRS-TTP-85-006] 10 p1476 N85-19314
Spectrum resource assessment of the 7125-8500 MHz band
[PB85-127413] 11 p1626 N85-20242
Spectrum resource assessment of the fixed and mobile services in the 947-17,700 MHz band, phase 1
[PB85-128288] 11 p1626 N85-20243
East Europe report: Scientific affairs
[JPRS-ESA-84-006] 11 p1700 N85-20684
Communications software for Olympics Micromation Computer System
[PB85-109510] 11 p1704 N85-20723
Base communications issues for the 1980s
[AD-A149764] 12 p1828 N85-21474
Digital channel efficiency model
[AD-A150084] 12 p1829 N85-21479
Sample size and precision in communication performance measurements
[PB85-1143270] 12 p1830 N85-21486
Algorithm for statistical simulation of electromagnetic compatibility characteristics of high-frequency transmission channels in radioelectronic facilities 12 p1842 N85-21560
Computer and communications security and privacy
[GPO-39-741] 12 p1911 N85-21994
A concatenated coding scheme for error control
[NASA-CR-175504] 12 p1912 N85-22001
Oversight review of the five-year outlook report on science and technology
[GPO-41-058] 12 p1949 N85-22243
Technology transfer to the Middle East
[PB85-127744] 12 p1952 N85-22264
Integrated digital networks
[AD-A150605] 13 p2056 N85-22873
USSR report: Electronics and electrical engineering
[JPRS-UEE-85-001] 13 p2078 N85-22976
Analysis of interference caused by interfering radio signals in communications systems with frequency separation of telephone channels and frequency modulation 13 p2086 N85-23025
Further developments of CCD line array telecine
[BBC-RD-1985/3] 14 p2293 N85-24217
Interactive communication channel
[AD-D011580] 15 p2542 N85-25695
Wideband fiber optic communications link
[AD-A151704] 15 p2542 N85-25697
Standards in process: Foundation and profiles of ISDN (Integrated Services Digital Network) and OSI (Open Systems Interconnection) studies
[PB85-165041/GAR] 15 p2545 N85-25712
Future information technology, 1984 telecommunications
[PB85-165850] 15 p2624 N85-26173
Thin Route Project 15 p2667 N85-26596
Communications 15 p2667 N85-26600
The Record of Electrical and Communication Engineering Conversazione, volume 53, no. 2, November 1984
[ISSN-0385-7719] 16 p2758 N85-27022
Historical perspectives on information transmission engineering 16 p2759 N85-27023
Optical non-line-of-sight covert, secure high data communication system
[AD-D011607] 16 p2769 N85-27087
Satellite provided customer promises services, a forecast of potential domestic demand through the year 2000. Volume 4: Sensitivity analysis
[NASA-CR-174662] 16 p2769 N85-27092
Future information technology, 1984: Telecommunications
[NBS/SP-500/119] 16 p2878 N85-27762
National Telecommunications and Information Administration authorization
[GPO-38-560] 16 p2879 N85-27766
East Europe report: Science and technology
[JPRS-ESA-85-017] 17 p2945 N85-28177
Radiometer integrated into a communication terminal
[AD-A151746] 17 p2947 N85-28195
Logical design of a decision support system to forecast technology, prices and costs for the national communications system
[AD-A152330] 17 p2948 N85-28198
ELF (Extremely Low Frequency) communications system ecological monitoring program: Measurements of ELF electromagnetic fields for site selection and characterization, 1983
[AD-A153120] 17 p2949 N85-28209
Moon bounce communications to small terminals
[AD-A153297] 17 p2950 N85-28212
Discrete mathematics for communications systems
[AD-A152814] 17 p3018 N85-29064
Rome Development Center Air Force technical objective document CSI FY-86
[AD-A152476] 17 p3047 N85-28851
Study of a medium term flexible fixed satellite service mission
[DM51/CC-IM-0185.83] 18 p3091 N85-29136
Master and secondary clock in telecommunications networks 18 p3108 N85-29246
Publications of the Jet Propulsion Laboratory 1983
[NASA-CR-175979] 18 p3199 N85-29848
Implementation of a serial communication process for a fault tolerant, real time, multitransputer operating system
[AD-A154237] 19 p3343 N85-30714
Antenna pointing of large flexible telecommunications spacecraft 20 p3409 N85-31158
Basic EMC (Electromagnetic Compatibility) technology advancement for C3 systems. Volume 1B: Demodulation radio frequency interference effects in operational amplifier circuits
[AD-A154121] 20 p3440 N85-31350
Scientific report of the Department of Systems and Communications
[ENST-84D002] 20 p3441 N85-31355
An analysis of physical optics models for rough surface scattering
[AD-A154960] 21 p3575 N85-32235
Security controls in the Stockpoint Logistics Integrated Communications Environment (SPLICE)
[AD-A155536] 21 p3576 N85-32244
Parameter estimation in communication system tracking satellite observations
[AD-A155137] 21 p3636 N85-32582
A model for predicting propagation-related DSCS (Defense Communications Engineering Center) margin requirements
[AD-A155355] 22 p3756 N85-33281
USSR report: Electronics and electrical engineering
[JPRS-UEE-84-003] 22 p3773 N85-33381
Telecommunication market research processing
[ENST-83E018] 23 p3926 N85-34331
Interprocess communication
[AD-A156337] 24 p4088 N85-35337
Proceedings of the 14th Army Science Conference. Volume 3: Principal authors P through Z
[AD-A149202] 24 p4144 N85-35691

TELECONFERENCING
Software for interactive on-line conferences
[AD-A154742] 21 p3570 N85-32801

TELEGRAPH SYSTEMS
Transient processes in tuned amplifier during phase-shift keying with smooth phase variation 15 p2527 N85-25581

TELEGRAPHY
U TELEGRAPH SYSTEMS

TELEMETERS
U TELEMETRY

TELEMETRY
NT PCM TELEMETRY
NT RADIO TELEMETRY
High-data-rate wide-angle underwater acoustic telemetry system
[DE84-015696] 02 p0233 N85-11519
Signal characteristics of an underwater explosive acoustic telemetry system
[DE84-016653] 05 p0726 N85-14668
Pulse code modulation telemetry: Properties of various binary modulation types
[AD-A147214] 07 p0913 N85-15780
An autonomous roving vehicle for the planet Mars: A summary of over 15 years of research
[RPI-TR-MP-83] 07 p0973 N85-16179
A variable length and sensor spacing thermistor array
[AD-D011416] 08 p1113 N85-17017
Development of the TT and C station equipment at INPE
[INPE-3327-PRE/825] 10 p1427 N85-18999
Directory of range data conversion and processing systems
[AD-A148996] 10 p1427 N85-19001
Telemetry systems of Interkosmos satellites 11 p1617 N85-20173
An overview of the Thematic Mapper geometric correction system 11 p1668 N85-20511
Wind-weighting for sounding rockets with a telemetry system
[NASA-TP-2438] 12 p1792 N85-21246
Remote control of an impact demonstration vehicle
[NASA-TM-85925] 14 p2225 N85-23797
Hydrometric telemetry in Canada 14 p2239 N85-23882
Programming for Pioneer 12 15 p2666 N85-26606
Present stage of utilization of the ARGOS system by the ORSTOM hydrological service for hydrometric data collection 16 p2813 N85-27348
Use of a network of telemetered meteorological stations for prediction of the distribution of an atmospheric tracer 16 p2931 N85-27458
Telemetry system for the transmission of data from projectiles during the acceleration phase in the gun barrel
[ISL-CO-207/84] 22 p3739 N85-33178
Development of an adjustable buoyancy balloon tracer of atmospheric motion. Phase 1: Systems design and demonstration of feasibility
[PB85-185817] 22 p3817 N85-33648
Design, development and operation of a high simultaneous capacity digital telemetry system — turbomachine blade flutter
[PNR-90261] 23 p3899 N85-34151
Miniature infra-red data acquisition and telemetry system
[NASA-CR-177953] 24 p4096 N85-35390

TELEOPERATOR MANEUVERING SYSTEM
U TELEOPERATORS

TELEOPERATORS
Review of teleoperator research 05 p0703 N85-14511
Translational control of a graphically simulated robot arm by kinematic rate equations that overcome elbow joint singularity
[NASA-TP-2376] 06 p0858 N85-15448
Transportation applications, part 2 11 p1643 N85-20350
Real time algorithms for robotic control of teleoperators
[DE85-001137] 11 p1647 N85-20360
Investigation of dynamics of manipulator with elastic sections 13 p2048 N85-22819
Hand controllers for teleoperation. A state-of-the-art technology survey and evaluation
[NASA-CR-175890] 17 p3002 N85-28659
Analysis of remote operating systems for space-based servicing operations, volume 1
[NASA-CR-171885] 19 p3225 N85-29993
Analysis of remote operating systems for space-based servicing operations. Volume 2: Study results
[NASA-CR-171886] 19 p3225 N85-29994
Space station automation study-satellite servicing. Volume 1: Executive summary
[NASA-CR-171512] 19 p3226 N85-29999
Space station automation study-satellite servicing, volume 2
[NASA-CR-171513] 19 p3226 N85-30000

Manipulators in teleoperation
[DE85-010563] 20 p3512 N85-31833
NASA space station automation: AI-based technology review
[NASA-CR-176094] 21 p3558 N85-32134
NASA space station automation: AI-based technology review. Executive summary
[NASA-CR-176096] 21 p3558 N85-32135
Space station automation and robotics study. Operator-systems interface
[NASA-CR-176095] 22 p3736 N85-33172
Space station automation study: Autonomous systems and assembly, volume 2
[NASA-CR-176092] 22 p3739 N85-33175
Telepresence work system concepts
22 p3797 N85-33525
Dual arm master controller development
22 p3797 N85-33526
Space Missions for Automation and Robotics Technologies (SMART) Program
[NASA-TM-86820] 24 p4066 N85-35210

TELEPHONES
NT RADIOTELEPHONES
Energy supply problems for emergency telephones
05 p0663 N85-14265
A single optical fiber telephone system
[AD-D011293] 06 p0799 N85-15107
Fast data and voice transmission for mobile services with high immunity against multipath and co-channel interference 10 p1475 N85-19306

TELEPHONY
RF characteristics of the hoop column antenna for the land mobile satellite system mission
[NASA-CR-3842] 02 p0189 N85-11264
The ACE (Automated Cable Expert) experiment: Initial evaluation of an expert system for preventive maintenance
[AD-P003943] 02 p0248 N85-11623
Analog voice processing for FM transmission in a telephone channel
[INPE-2798-PRE/359] 03 p0354 N85-12279
Telephoning with light and sun — glass fibers, solar cells 05 p0663 N85-14264
Energy supply problems for emergency telephones
05 p0663 N85-14265
A single optical fiber telephone system
[AD-D011293] 06 p0799 N85-15107
Equipment for multiplexing multichannel radio-relay lines of communication
[AD-A148402] 08 p1153 N85-17276
Low voltage two wire to four wire telephone circuit converter apparatus
[AD-D011449] 10 p1468 N85-19261
Self-adaptive echo cancellation for telephony
[ENST-84E013] 20 p3441 N85-31353

TELESCOPES
NT ASTRONOMICAL TELESCOPES
NT GAMMA RAY TELESCOPES
NT HELIOMETERS
NT HUBBLE SPACE TELESCOPE
NT INFRARED TELESCOPES
NT PARTICLE TELESCOPES
NT PYROHELIOMETERS
NT RADIO TELESCOPES
NT REFLECTING TELESCOPES
NT REFRACTING TELESCOPES
NT SCHMIDT CAMERAS
NT SCHMIDT TELESCOPES
NT SOLAR OPTICAL TELESCOPE
NT SPACE INFRARED TELESCOPE FACILITY
NT SPACEBORNE TELESCOPES
NT SPECTROSCOPIC TELESCOPES
NT ULTRAVIOLET TELESCOPES
NT X RAY TELESCOPES
Direct view helmet mounted telescope
[AD-D011291] 06 p0755 N85-14839
Dual-secondary mirror Cassegrain optical system
[AD-D011273] 06 p0862 N85-15478
Helmet mounted telescope
[AD-D011355] 07 p1019 N85-16487
Evaluation of nose, roof, and mast mounted sensor platforms for piloting and sighting, integrated in future combat helicopters 08 p1074 N85-16806
On the unique capabilities of the Hubble space telescope for studies of ROSAT deep-survey X-ray sources
08 p1243 N85-17846
A CCD system for photometry of direct and spectroscopic images 08 p1252 N85-17904
Utilization of mobile VLBI for geodetic measurements
10 p1466 N85-19248
Wide-angle flat field telescope
[NASA-CASE-GSC-12825-1] 11 p1728 N85-20866
Utilization of space station by the large deployment reflector 14 p2235 N85-23857
Laser beam shaping system with reduced objective diameter 14 p2275 N85-24095
Aberration characteristics of plane-parallel compensator plate 14 p2276 N85-24100
Astrometry at La Silla 14 p2436 N85-25025
Evaluation of a magneto-optical filter and a Fabry-Perot interferometer for the measurement of solar velocity fields from space 14 p2442 N85-25067
An MRTD-compatible bar pattern response model for TV and direct view sighting systems
[BAE-BT-12090] 15 p2620 N85-26146
Stress analysis of the space telescope focal plane structure joint
[NASA-CR-175797] 16 p2803 N85-27264
Holographic corrector in objective with compound main mirror 17 p2941 N85-28153
Trends in measurement of solar vector magnetic fields using the Zeeman effect 18 p3204 N85-29877
The San Fernando Observatory video Stokes polarimeter 18 p3205 N85-29885
Multichannel birefringent filter
18 p3206 N85-29886
Grazing incidence beam expander
[DE85-010784] 19 p3368 N85-30889
Cosmic ray charge and energy spectrum measurements using a new large area Cerenkov x dE/dx telescope
[OG-4.1-5] 22 p3876 N85-34011
High Resolution Telescope and Spectrograph (HRTS)
23 p3901 N85-34162
Angular resolution of air-shower array-telescopes
[OG-9.5-6] 23 p4030 N85-34983
New Matsushiro underground cosmic ray station (220 M.W.E. in depth)
[SH-9.1-14] 23 p4052 N85-35129
Upper limit on magnetic monopole flux from Baksan experiment
[HE-6.1-11] 24 p4210 N85-36136

TELESCOPING STRUCTURES
U FOLDING STRUCTURES

TELEVISION CAMERAS
East Europe report: Science and technology
[JPRS-ESA-84-030] 01 p0101 N85-10670
Underwater television equipment described
01 p0101 N85-10672
Television camera video level control system
[NASA-CASE-MSC-18578-1] 12 p1821 N85-21427
Italy's Fiat uses Sweden's Asea seeing robot
15 p2536 N85-25650
Electronic detection and concealment of film dirt
[BBC-RD-1985/4] 15 p2538 N85-25667
The San Fernando Observatory video Stokes polarimeter 18 p3205 N85-29885
A digital contour-corrector for a high-definition TV camera
[NHK-LABS-NOTE-311] 19 p3254 N85-30179
LI461 and LI482 vidicons for two-tube color TV cameras with improved image quality 22 p3764 N85-33333
Electronic imaging system and technique
[DE85-005740] 23 p3935 N85-34393
Spatial distribution read-out system for thermoluminescence sheets
[HE-7.1-7] 24 p4213 N85-36161

TELEVISION EQUIPMENT
NT IMAGE DISSECTOR TUBES
NT TELEVISION CAMERAS
NT TELEVISION RECEIVERS
Videotex and weather services: Finnish applications
01 p0084 N85-10567
Television animation store: Recording pictures on a parallel transfer magnetic disc
[BBC-RD-1984/17] 10 p1462 N85-19220
Lighting for remote viewing systems
[DE85-001898] 11 p1729 N85-20873
Device for controlling operation of lithicon cathode-ray memory tube 12 p1839 N85-21542
Welder training/welder testing
[BLL-WI-TRANS-683-(9312.57)] 16 p2792 N85-27223

TELEVISION RECEIVERS
Correlating and adaptive digital filters
[BMFT-FB-T-84-299] 15 p2551 N85-25744
Improved high performance television receiver
[PB85-170751] 18 p3092 N85-29139
East Europe report: Science and technology. Selections on CSSR computer technology
[JPRS-ESA-84-017] 21 p3668 N85-32781

TELEVISION RECEPTION
BBC receiving terminal for the European orbital test satellite
[BBC-RD-1984/15] 08 p1142 N85-17205
Satellite broadcasting: The performance of C-MAC in a hardware simulation of a DBS transmission chain
[BBC-RD-1984/9] 08 p1143 N85-17206
Problems relevant to town incoming radio TV links
[NASA-TM-77623] 08 p1150 N85-17255
Subjective evaluation of the effect of noise and interference on frequency modulated NTSC television signals
[CRC-1367] 09 p1310 N85-18230
Horizontal deflection TS-257
13 p2069 N85-22926
Timing accuracy of LF and TV synchronization techniques 17 p2961 N85-28288
Retinally stabilized differential resolution television display
[NASA-CASE-NPO-15432-1] 18 p3089 N85-29117
GROWIAN: First observations of the environmental impact at the GROWIAN site — wind energy converter
24 p4110 N85-35476
Television interference at the Maglarp (Sweden) wind turbine 24 p4111 N85-35480
Television interference measurement at Kalkugnen (Sweden) test windmill 24 p4111 N85-35481

TELEVISION SYSTEMS
NT COLOR TELEVISION
NT SATELLITE TELEVISION
NT SPACECRAFT TELEVISION
Videotex and weather services: Finnish applications
01 p0084 N85-10567
East Europe report: Science and technology
[JPRS-ESA-84-030] 01 p0101 N85-10670
Underwater television equipment described
01 p0101 N85-10672
Selection of parameters for image decomposition by television system for recognition of group of point sources 06 p0785 N85-15018
Teletrack: A special effect
[BBC-RD-1984/10] 06 p0798 N85-15097
US objectives generally achieved at broadcasting satellite international conference. Improvements can help in future conferences
[PB84-235316] 06 p0800 N85-15109
Digital raster timing encoder-decoder
[AD-D011279] 06 p0804 N85-15120
Estimation of the impulse response of television channels from digitized waveforms
[CRC-1376] 12 p1822 N85-21429
Television animation store: Digital chroma, key and mixer units
[BBC-RD-1984/16] 12 p1824 N85-21442
Electronic generation of text for television
[BBC-RD-1984/14] 13 p2053 N85-22856
Superfine laser position control using statistically enhanced resolution in real time
[DE85-005643] 15 p2564 N85-25817
An MRTD-compatible bar pattern response model for TV and direct view sighting systems
[BAE-BT-12090] 15 p2620 N85-26146
Mobile television radio link
[AD-A152381] 17 p2948 N85-28201
Investigation into the use of the TV magnifier in the Netherlands
[HSE-TRANS-11142] 20 p3533 N85-31866
Space Experiments with Particle Accelerators (SEPAC) 23 p3901 N85-34165
Computer animation in distance teaching
23 p3965 N85-34581

TELEVISION TRANSMISSION
Television transmission in frequency modulation
04 p0493 N85-13148
Subjective evaluation of the effect of noise and interference on frequency modulated NTSC television signals
[CRC-1367] 09 p1310 N85-18230
Brussels Satellite Convention
[S-EXEC-REPT-98-52] 12 p1790 N85-21234
Estimation of the impulse response of television channels from digitized waveforms
[CRC-1376] 12 p1822 N85-21429
Digital standards conversion: Interpolation theory and aperture synthesis
[BBC-RD-1984/20] 13 p2053 N85-22857
Horizontal deflection TS-257
13 p2069 N85-22926
Development of TV systems for spacecraft
15 p2484 N85-25332
Mobile television radio link
[AD-A152381] 17 p2948 N85-28201
Timing accuracy of LF and TV synchronization techniques 17 p2961 N85-28288
Unattended TV time transfer results
17 p2964 N85-28305
Improved high performance television receiver
[PB85-170751] 18 p3092 N85-29139
The time and frequency comparisons via Loran-C and National TV Network in Yugoslavia
18 p3109 N85-29248

TELLEGEN THEORY
U GYRATORS
U NETWORK ANALYSIS
U NETWORK SYNTHESIS

TELLURIC CURRENTS
Directional analysis of wave packets of magnetotelluric field 14 p2344 N85-24495
TELLURIDES
NT CADMIUM TELLURIDES
NT INDIUM TELLURIDES
NT LEAD TELLURIDES
NT MERCURY TELLURIDES
NT TIN TELLURIDES
TELLURIUM
Time resolved calorimetry of 30 nm Te-films during laser annealing
[AD-A145047] 01 p0052 N85-10346
Optical bistability in Cd(x)Hg(1-x)Te 18 p3186 N85-29760
TELLURIUM COMPOUNDS
NT CADMIUM TELLURIDES
NT INDIUM TELLURIDES
NT LEAD TELLURIDES
NT MERCURY TELLURIDES
NT TIN TELLURIDES
Synthesis of pentafluorotellurium hypofluorite
[AD-D011212] 01 p0023 N85-10139
TEMPERATE REGIONS
The response of mid-latitude total electron content to solar activity 04 p0522 N85-13396
Monthly and seasonal climatology over the global tropics and subtropics for the decade 1973 to 1983. Volume 1: 200 mb winds
[AD-A146521] 06 p0838 N85-15322
Precipitation characteristics of a dual mesoscale convective complex
[PB84-226711] 06 p0840 N85-15337
Chemical, biological, and physical measurements from the subtropical western North Atlantic Ocean. Summer 1982, USNS Lynch, cruise 710-82
[AD-A153823] 18 p3201 N85-29857
TEMPERATURE
NT AMBIENT TEMPERATURE
NT ATMOSPHERIC TEMPERATURE
NT BODY TEMPERATURE
NT BRIGHTNESS TEMPERATURE
NT COMBUSTION TEMPERATURE
NT CRITICAL TEMPERATURE
NT CURIE TEMPERATURE
NT FLAME TEMPERATURE
NT FLASH POINT
NT GAS TEMPERATURE
NT HIGH TEMPERATURE
NT IGNITION TEMPERATURE
NT INLET TEMPERATURE
NT ION TEMPERATURE
NT IONOSPHERIC TEMPERATURE
NT LOW TEMPERATURE
NT LUNAR TEMPERATURE
NT NEEL TEMPERATURE
NT NOISE TEMPERATURE
NT OCEAN TEMPERATURE
NT OPERATING TEMPERATURE
NT PLANETARY TEMPERATURE
NT PLASMA TEMPERATURE
NT ROOM TEMPERATURE
NT SATELLITE TEMPERATURE
NT SEA SURFACE TEMPERATURE
NT SKIN TEMPERATURE (BIOLOGY)
NT SKIN TEMPERATURE (NON-BIOLOGICAL)
NT SOLAR TEMPERATURE
NT STELLAR TEMPERATURE
NT SURFACE TEMPERATURE
NT TRANSITION TEMPERATURE
NT ULTRALOW TEMPERATURES
NT WALL TEMPERATURE
NT WATER TEMPERATURE
Deuteron NMR (Nuclear Magnetic Resonance) in relation to the glass transition in polymers
[AD-P003910] 01 p0032 N85-10196
Allowable surge currents and failure mechanisms in semiconductor power devices in various modes of operation 06 p0795 N85-15060
Homogeneous condensation of gaseous mixtures of Si, Fe, O, N, and C in relative cosmic abundance and implications for astronomical condensation 06 p0887 N85-15632
Temperature variation of laser mirror stability criteria 10 p1445 N85-19108
Decaying particles do not heat up the Universe
[DE85-002191] 11 p1783 N85-21091
Temperature responses of composite panels
[AD-A150053] 12 p1798 N85-21277
Digital temperature and velocity control of mach 0.3 atmospheric pressure durability testing burner rigs in long time, unattended cyclic testing
[NASA-TM-86959] 12 p1805 N85-21321
Externally compensated crystal oscillator (ECXO) study
[AD-A150335] 13 p2064 N85-22893
Structure and properties of ion-implanted Al sub 2 O sub 3
[DE85-005374] 14 p2430 N85-24987
Adjustment of the frequency-temperature characteristics of crystal oscillators
[AD-D011588] 15 p2548 N85-25726
Monthly and seasonal weather outlook for mid-January to mid-February 1985, volume 39, number 2, January 15, 1985
[PB85-164572] 16 p2837 N85-27500
Monthly and seasonal weather outlook for February 1985, volume 39, number 3, January 30, 1985
[PB85-164424] 16 p2838 N85-27502
Urban climate and air hygiene before, during, and after the lifework of Hellmut Berg. Overview of a branch of applied meteorology 18 p3147 N85-29487
TEMPERATURE COMPENSATION
Development of a polymer pressure gage with temperature compensation 03 p0365 N85-12340
Dynamic polymer pressure transducer with temperature compensation
[AD-D011373] 07 p0967 N85-16142
Dielectric resonator oscillators with digital temperature compensation
[AD-D011715] 19 p3261 N85-30221
Development of a temperature-compensated hot-film anemometer system for boundary-layer transition detection on high-performance aircraft
[NASA-TM-86732] 22 p3730 N85-33121
TEMPERATURE CONTROL
Programmable digital temperature controller apparatus
[AD-D011221] 01 p0049 N85-10319
Thermal management technology status 05 p0610 N85-13895
Determining lamp/ballast system performance with a temperature-controlled integrating chamber
[DE84-014806] 05 p0631 N85-14049
Thermoregulatory consequences of long-term microwave exposure at controlled ambient temperatures
[PB84-236603] 05 p0697 N85-14484
Procedures for testing and evaluating spacecraft-type heat pipes
[AD-A146671] 06 p0809 N85-15139
Development of a preprototype times wastewater recovery subsystem, addendum
[NASA-CR-171823] 07 p1019 N85-16468
Space shuttle main engine: Interactive design challenges 08 p1098 N85-16940
In-flight testing of the space shuttle orbiter thermal control system 08 p1103 N85-16974
Active cooling requirements for propellant storage 08 p1108 N85-17004
Propellant transfer: Attached depot 08 p1108 N85-17005
Thermoregulatory responses during exercise at graded hypohydration levels
[AD-A147733] 08 p1195 N85-17526
Transmissive Dewar cooling chamber for optically pumped semiconductor ring lasers
[AD-D011550] 12 p1855 N85-21636
High temperature acoustic levitator
[NASA-CASE-NPO-16022-1] 12 p1927 N85-22105
Thermal design of the Glotto spacecraft 14 p2245 N85-23920
Erosion of corrosion-resistant surface treatments on alloy steels
[DE85-008446] 17 p2932 N85-28100
A ten channel temperature controller
[AD-A152664] 17 p2967 N85-28326
Microprocessor controlled temperature chassis
[DE85-008392] 17 p3009 N85-28602
Heat management system for aircraft
[AD-D011658] 18 p3061 N85-28936
Advanced thermal barrier system bond coatings for use on Ni, Co-, and Fe-base alloy substrates
[NASA-TM-87062] 20 p3431 N85-31283
Remote temperature-set-point controller
[DE85-011614] 22 p3787 N85-33459
Electronic temperature equalizer
[PB85-181485] 22 p3789 N85-33475
Feedback regulated induction heater for a flowing fluid
[DE85-006508] 23 p3939 N85-34414
TEMPERATURE DEPENDENCE
Thermal fatigue of gas turbine engine blades made of material based on silicon nitride and silicon carbide 01 p0019 N85-10115
Critical point wetting drop tower experiment 02 p0155 N85-11045
NBS (National Bureau of Standards): Materials measurements
[NASA-CR-174036] 03 p0332 N85-12143
Time-temperature dependence of the strength of commercial zirconia ceramics
[AD-A146233] 03 p0338 N85-12173
Magnetic properties of and superfine interactions in amorphous Fe-Cr-Co-Si-B alloys 03 p0349 N85-12248
Energy of stacking fault and dislocation structure of titanium alloys 03 p0351 N85-12259
Electric properties of neovolcanic rocks of central and east Slovakia
[REPT-558] 03 p0376 N85-12401
Nondestructive evaluation of residual stress in low-carbon steel, introduction 04 p0512 N85-13265
Kohn anomaly in metastable fcc lanthanum at low temperatures
[DE84-015459] 04 p0569 N85-13828
Chemical engineering principles of constant temperature-constant supersaturation growth of potassium dihydrogen phosphate (KDP) crystals
[DE84-017081] 04 p0571 N85-13845
Thermal diffusivity and conductivity of chromium-manganese alloying compositions
[BLL-M-35925-(5828.4)] 05 p0616 N85-13938
Electronic bandstructure of an incommensurate crystal
[DE84-016891] 05 p0733 N85-14714
Effects of temperature on the response time of thermocouples and resistance thermometers
[DE84-016955] 06 p0811 N85-15154
Anisotropy and microstructure of rare earth permanent magnet materials
[AD-A146549] 06 p0859 N85-15460
Structural relaxation and isoconfigurational flow of a metallic glass near equilibrium
[AD-A147868] 07 p0933 N85-15915
Nondestructive measurement of bulk residual stresses
[AD-A147063] 07 p0978 N85-16211
A hydrogen partitioning model for hydrogen assisted crack growth
[AD-A147385] 07 p0978 N85-16214
Temperature dependence of the crystal structures of Nylon 11
[AD-A147563] 07 p1049 N85-16661
The heat sensitivity of solid propellants 08 p1117 N85-17043
Low temperature properties of CeOs2 in the C14 and C15 crystallographic Laves phases
[DE85-003754] 10 p1564 N85-19866
Effects of hydrogen on magnetic properties of amorphous zirconium alloys
[DE85-003303] 11 p1607 N85-20107
Applications of pulsed-laser techniques and thermographic phosphors to dynamic thermometry of rotating surfaces
[DE85-000403] 11 p1639 N85-20328
Direct measurement of the temperature dependence of the velocity of the reaction of deuterium atoms with vibration-excited hydrogen molecules
[MPIS-12/1984] 11 p1726 N85-20856
Study of the kinetics of hydrogenation using aged catalysts
[DE85-004373] 12 p1802 N85-21302
The UFe4P12 and CaFe4P12: Non-metallic isotopes of superconducting LaFe4P12
[DE85-003724] 12 p1942 N85-22195
Combustion kinetics of metal atoms and metallic radicals over wide temperature ranges 13 p1999 N85-22530
Orientation and temperature dependence of some mechanical properties of the single-crystal nickel-base superalloy Rene N4. 3: Tension-compression anisotropy
[NASA-TM-86962] 13 p2021 N85-22680
Magnetic studies of Ni3Al(Fe) compounds
[DE85-005262] 13 p2025 N85-22686
Division boundary in Al-B composite material with boron in contact with solid and liquid aluminum 13 p2027 N85-22704
Temperature dependence of propagation of high-current electron beam through drift space 13 p2079 N85-22982
Change of electrical characteristics of radio-frequency cables under thermal effect 13 p2081 N85-22999
Photovoltaic cells of InP-CdS heterojunction type and their temperature characteristics under A-M illumination 14 p2275 N85-24092
Dependence of parameters of silicon photovoltaic cells on temperature and light intensity 14 p2275 N85-24094
Characterization of terrestrial solar cells for space applications: Electrical characteristics of thin Westinghouse dendritic web cells as a function of solar intensity, temperature, and incidence angle
[NASA-CR-175842] 14 p2349 N85-24516
Temperature variation of resistivity of certain alloys based on transition and simple metals in amorphous and crystalline states 15 p2496 N85-25399
Thermoregulatory and vestibular systems in the rat 16 p2610 N85-26082

Special features of the temperature dependence of the capillary constant in the vicinity of the critical point
[BLL-T8436/BG/LRS/LRST750/85] 16 p2659 N85-27832
Mechanical properties of polycrystalline alpa titanium
[BLL-BISI-TRANS-21923-(9022.06)] 17 p2924 N85-28029
Physical properties of steels and their temperature dependence
[BLL-BISI-TRANS-2228S-(9022.06)] 17 p2928 N85-28065
Temperature and manganese content dependences of tensile deformation in iron-high manganese binary alloys
[DE85-007656] 17 p2932 N85-28098
The temperature dependence of diffracted beam intensities in atom-surface scattering
[AD-A152762] 17 p3029 N85-28736
The effect of temperature on the corrosion-erosion of 9Cr1Mo steel
[DE85-006507] 18 p3076 N85-29030
Development and testing of the variable vertical resolution Fourth Order GCM 18 p3142 N85-29453
Improvements in the energy resolution and high-count-rate performance of bismuth germanate
[DE85-010763] 19 p3240 N85-30092
High temperature Raman studies of phase transitions in thin film dielectrics
[DE85-010973] 19 p3263 N85-30234
Fatigue-crack propagation behavior of alloy A-286
[DE85-007460] 19 p3286 N85-30391
Method for determining Wagner parameters of interaction of first and second orders
[BLL-M-36261-(5828.4)] 20 p3430 N85-31278
LEO life testing with different charge control 20 p3446 N85-31393
A survey of unified constitutive theories 20 p3466 N85-31531
Positron measurements in 2H-TaSe2 crystals
[DE85-010507] 20 p3529 N85-31949
Remarks on preparation of indandione detection reagents
[NASA-TM-77905] 21 p3560 N85-32146
Absorption of laser radiation in substance with absorption coefficient depending linearly upon temperature 21 p3694 N85-32953
The influence of temperature on static and dynamic SCC crack growth behavior in aluminum alloy 23 p3905 N85-34190
Experimental study on time and temperature dependent behavior of crack growth in viscoelastic strip 23 p3905 N85-34193
Time and temperature dependence of fracture surface in soft epoxy resin 23 p3908 N85-34213
Shape memory effect in uranium-niobium alloys below room temperature
[DE85-012984] 23 p3916 N85-34288
Study of photon emission by electron capture during solar nuclei acceleration, 1: Temperature-dependent cross section for charge changing processes
[SH-1.1-8] 23 p3990 N85-34735
Aqueous volatile weak electrolyte equilibria to 300 C
[DE85-013840] 24 p4078 N85-35261

TEMPERATURE DIFFERENCES
U TEMPERATURE GRADIENTS

TEMPERATURE DISTRIBUTION
Manual of phosphoric acid fuel cell stack three-dimensional model and computer program
[NASA-CR-174722] 01 p0067 N85-10447
Numerical forecast of pressure field by considering the mutual influence of orography, thermal nonhomogeneity and surface friction 01 p0080 N85-10534
Alpine meteorology: Translations of classic contributions by Wagner, A., Ekhart, E. and Defant, F.
[DE84-014929] 01 p0085 N85-10574
Analytical modeling of random thermal fluctuations in the NORDA high-frequency sound scattering facility
[AD-A145024] 01 p0116 N85-10790
Numerical analysis of flow and heat transfer in the VAFB LOX storage Dewar tank
[NASA-CR-171203] 02 p0197 N85-11315
Temperature structures and infrared-derived properties of the atmosphere of Uranus and Neptune 02 p0296 N85-11931
Open cycle OTEC thermal-hydraulic systems analysis and parametric studies
[DE84-013011] 04 p0530 N85-13391
Analysis of diabatic heating during FGGE 05 p0683 N85-14393
Structure of temperature field based on observations of refraction from high meteorological mast 06 p0819 N85-15199
Allowing for the temperature field in the wall thickness of checkerwork in thermal calculation
[BLL-M-36015-(5828.4)] 07 p0956 N85-16058
Influence of setting angle of jet cooling nozzles on temperature and stress state of a turbine wheel 09 p1306 N85-18208
Two-dimensional modeling of conduction-mode laser welding
[DE85-001804] 09 p1327 N85-18341
Transport properties of the outer crust of magnetic neutron stars 09 p1415 N85-18927
Stress studies in EFG
[NASA-CR-174441] 10 p1506 N85-19515
Mathematical simulation of thermal processes involved in electron-beam treatment 12 p1843 N85-21565
Dilution jet configurations in a reverse flow combustor
[NASA-CR-174686] 13 p1974 N85-22392
Effects of temperature variation among droplets in an evaporating fuel spray 13 p2004 N85-22562
Horizontal coherence of temperature microstructure in upper ocean layer 13 p2109 N85-23139
Analysis of NIMBUS-7 SMMR data --- Hokkaido, Japan snow cover 13 p2125 N85-23232
Thermal and thermoelastic effects in rolling/sliding contacts
[AD-A150436] 13 p2165 N85-23429
Qualification of the T2 wind tunnel in cryogenic operation. A: Thermal field, preliminary study of a schematic model
[NASA-TM-77781] 14 p2227 N85-23805
Religun conductor heating from multiple current pulses
[DE85-005333] 14 p2265 N85-24031
Estimating defectiveness buildup during service in metal of welded runner in low-pressure cylinder of turbine 14 p2271 N85-24070
Structure of cold film in water-air boundary layer 14 p2335 N85-24443
The photospheric temperature structure of magnetic flux tubes 14 p2447 N85-25102
Development of a temperature measurement system with application to a jet in a cross flow experiment
[NASA-CR-174898] 15 p2472 N85-25262
Hermetic sealing of nonlubricated gas seal and friction characteristics, chapter 7
[DE85-006375] 15 p2589 N85-25851
Density characteristics of asthenosphere in Atlantic Ocean 19 p3294 N85-30423
Short meridional scale anomalies in the lower stratosphere and upper troposphere 20 p3489 N85-31684
High pressure working mode of hollow cathode arc discharges
[NASA-TM-77860] 20 p3535 N85-31992
Temperature field around a spherical, cylindrical, and needle-shaped crystal, growing in a pre-cooled melt
[NASA-TM-77869] 20 p3537 N85-32011
Quasi-steady-state melting mode during combined laser irradiation of semiconductor materials 21 p3682 N85-32874
On one nonlinear problem of laser thermochemistry 21 p3697 N85-32971
Enhancing precision of remote temperature sensing data from satellites under cloudy atmospheric conditions 22 p3734 N85-33148
Surface temperature distribution along a thin liquid layer due to thermocapillary convection
[NASA-TM-87115] 23 p3930 N85-34357
Interaction of trace elements and welding parameters on GTA weld shape
[DE85-004046] 24 p4080 N85-35284
Heat transfer coefficients for particles in liquid in axially rotating cans 24 p4093 N85-35370
A two-phase flow and heat transfer model for zero gravity
[AD-A156097] 24 p4094 N85-35377
Response of a BWR Mark 2 containment vessel head to loads beyond the design basis
[DE85-010524] 24 p4103 N85-35432

TEMPERATURE EFFECTS
Interpolation formulas for viscosity of six gases: Air, nitrogen, carbon dioxide, helium, argon and oxygen
[PB84-217801] 01 p0026 N85-10161
Stability of bromine intercalated graphite fibers
[NASA-TM-88859] 01 p0031 N85-10187
13C and 1H NMR (Nuclear Magnetic Resonance) studies of solid polyolefines
[AD-P003909] 01 p0032 N85-10195
Platinum thin film resistors as accurate and stable temperature sensors
[NASA-TM-77726] 01 p0049 N85-10322
Inorganic composites for space applications 02 p0155 N85-11047
The silane interphase of composites: Effects of process conditions on gamma-aminopropyltriethoxysilane
[AD-A145578] 02 p0171 N85-11143
Thermodynamics of reactions of deoxidation of nickel melts
[BLL-M-35729-(5828.4)] 02 p0175 N85-11166
The influence of metallurgical aspects on the pitting corrosion behaviour of high alloy stainless steels 02 p0179 N85-11202
Microstructure and creep behaviour at elevated temperature of unidirectionally solidified eutectic nickel base superalloys 02 p0191 N85-11216
Stability of heated boundary layers 02 p0196 N85-11311
Complex formation and temperature stability of electrophysical properties of GaAs semiinsulating single crystals 02 p0258 N85-11669
Contributions to the 7th International Acoustic Emission Symposium
[AD-A145368] 02 p0275 N85-11792
The effect of temperature on the radiation induced losses of large diameter GPS (Germanium phosphosilicate) and GBS core optical fibers
[AD-A145409] 02 p0290 N85-11823
Long-term thermal aging of 2 graphite-polyimide composite materials
[NASA-TP-2369] 03 p0325 N85-12094
Effects of prior austenite and ferrite grain size on fracture properties of a plain carbon steel
[AD-A146276] 03 p0332 N85-12138
Effect of a thermal gradient applied to a sinusoidal surface profile
[DE84-015649] 03 p0434 N85-12765
Experimental and theoretical studies of moisture and temperature effects on the mechanical properties of graphite/epoxy laminates and neat resins 04 p0467 N85-12969
Tap noise-pressure fluctuations. Study of the acoustic behavior of hydraulic equipment in buildings as a function of the temperature
[CETIM-11-H-337] 04 p0502 N85-13201
The effect of temperature and pressure on the composition density of alkaline metals
[BLL-M-35940-(5828.4)] 05 p0616 N85-13934
Tensile properties and swelling of 20%-cold-worked Type 316 stainless steel irradiated in HFIR
[DE84-014080] 05 p0617 N85-13948
Additives for heat engine coal slurry fuels
[DE84-016434] 05 p0621 N85-13971
Site-specific research conducted in support of the Salton Sea Solar Pond Project, FY 1982 report
[NASA-CR-174182] 05 p0666 N85-14280
Strain rate effects and temperature history effects for three different tempers of 4340 VAR steel
[AD-A146372] 06 p0768 N85-14915
Impact of temperature on cycle life of globe ISOA EV-3000 lead-acid batteries
[DE84-015840] 06 p0805 N85-15126
Effects of temperature on the response time of thermocouples and resistance thermometers
[DE84-016855] 06 p0811 N85-15154
Special features of the deformation of molybdenum at high temperatures
[BLL-M-36027-(5828.4)] 07 p0924 N85-15856
Kinetics of interaction between carbon and iron oxides of metallized materials in solid phase
[BLL-M-36023-(5828.4)] 07 p0926 N85-15873
The relationship between radiation sensitivity and redox equilibria --- glass processing variables
[AD-A147216] 07 p0932 N85-15906
Effects of low temperatures on the growth and unfrozen water content of an aquatic plant
[AD-A147107] 07 p1011 N85-16424
Biochemical evaluation of bodily influence of high and low temperatures 07 p1014 N85-16441
On reversion phenomena in Cu-Zr-Cr alloys
[NASA-TM-77791] 08 p1125 N85-17092
Application of electricity to the reheating of metals prior to forming. Forging, lamination, induction
[BLL-TR-T6399/BG/MRS14903/84] 08 p1137 N85-17160
Departures from LTE populations versus anomalous abundances: The effects of heating 08 p1234 N85-17776
Effect of temperature on the stress-relaxation response of a pressure vessel steel
[TI85-003586] 09 p1339 N85-18424
Influence of temperature on wear resistance of detonation coatings of alloy powders 10 p1447 N85-19116
Study of the volumetric changes in VT23 alloy upon heating 10 p1448 N85-19123
Evaluation and prediction of long-term environmental effects of nonmetallic materials
[NASA-CR-171353] 10 p1450 N85-19137
Investigation of welded interconnection of large area wraparound contacted silicon solar cells
[NASA-CR-174436] 10 p1509 N85-19519
Heat stress and personal protective equipment
[DE85-003552] 10 p1532 N85-19652
Evaluation of residual stress in laminated metallic composites 11 p1598 N85-20052

Effect of temperature and deformation rate on hardness of copper 11 p1605 N85-20090
Non-isothermal irradiation creep of nickel alloys Inconel 706 and PE-16
[DE85-000842] 11 p1607 N85-20102
Micrographic and fractographic examination of alloys 2214 and 2024 for conditions which would cause burning of the metal on being put into solution, trial 17/175
[DGT-23.419] 11 p1609 N85-20117
The response of explosive systems to thermal stimuli: A state-of-the-art assessment
[DE85-000919] 11 p1614 N85-20148
Electrical and thermal performance during charging and discharging a Phase 1 gel cell battery
[PB85-114312] 11 p1677 N85-20585
Vapor pressure studies of the solubilization of hydrocarbons by surfactant micelles
[DE85-004319] 12 p1803 N85-21306
Performance assessment of Class 1E pressure tranamitters subjected to environmental stresses
[DE85-001623] 12 p1854 N85-21626
Evaluation of ettringite and related compounds for use in solar energy storage
[PB85-146876] 12 p1883 N85-21816
Preventive effect of acute heat factors during hypokinesia 12 p1902 N85-21945
Effects of temperature variation among droplets in an evaporating fuel spray 13 p2004 N85-22582
Solar array dynamical simulation for illumination and temperature variation 13 p2011 N85-22611
Study of effective physiological temperature
13 p2042 N85-22780
Cooling performance improvement of a horizontal ground coupled heat pump
[DE85-002470] 13 p2093 N85-23065
Thermal and thermoelastic effects in rolling/sliding contacts
[AD-A150435] 13 p2165 N85-23429
Io: Generation of silicate magma by shear melting at the base of a basaltic lithosphere
13 p2172 N85-23476
Characteristics of basaltic lava flows on Venus
13 p2177 N85-23508
Terrestrial analog studies for Martian patterned ground
13 p2190 N85-23590
Effect of elevated-temperature neutron irradiation on fracture toughness of ceramics
[DE85-000652] 14 p2261 N85-24010
Drop of coolant temperature in individual components of solar heating system 14 p2265 N85-24035
Stability of turbine runners in sliding bearings under external circulation forces 14 p2272 N85-24074
Effects of interactive transport and scavenging of smoke on the calculated temperature change resulting from large amounts of smoke
[DE85-006450] 14 p2378 N85-24684
Influences of thermal spikes in ion beam mixing
[DE85-006130] 14 p2419 N85-24924
Peltier heat of a small polaron in a magnetic semiconductor
[DE85-000470] 14 p2430 N85-24983
Effect of deep cooling on crack resistance and low-temperature hardening of aluminum alloys
15 p2496 N85-25396
Effects of primary recoil energy on the production rate of mobile defects during elevated temperature irradiation
[DE85-006218] 15 p2511 N85-25489
Ion beam mixing of marker layers in Al and Si
[DE85-006227] 15 p2511 N85-25490
Anode formation of passivating films on titanium alloy at temperatures up to 200 deg C
15 p2515 N85-25519
Compressive strength of epoxy resin chocks subjected to elevated temperatures
[AD-A152018] 15 p2519 N85-25532
Development of a Digitally Compensated SAW Oscillator (DCSO) to provide temperature stable frequency
[AD-A151907] 15 p2549 N85-25730
Modeling of midwest severe thunderstorms
15 p2596 N85-25995
Qualification of a wall gage for the SIMA wagon, adapted to the test of half models motorized by compressed air turbines — SIMA wind tunnel
[ONERA-PV-1/8068-GY] 16 p2701 N85-26677
Ca-Ga, Sr-Ga and Ba-Ga binary systems
[DE85-006454] 16 p2751 N85-26980
Screening ceramic materials for intense radiant heat applications
[DE85-006869] 16 p2756 N85-27006
Thermal consequences of localized SAR from RFR exposures 16 p2775 N85-27130
Effects of temperature on remotely sensed mafic mineral absorption features 16 p2809 N85-27323
High-thermal-gradient superalloy crystal growth
17 p2914 N85-27966
Influence of temperature in melting and casting on quality of medium-alloy steel
[BLL-BISI-TRANS-22310-(9902.06)]
17 p2938 N85-28137
Effects of level broadening on the magnetothermal oscillations in two-dimensional electron systems
[AD-A152639] 17 p3029 N85-28732
Tendency of selected low-carbon steels to corrosion cracking in nitrates
[BLL-BISI-TRANS-22282-(9022.06)]
18 p3073 N85-29006
Aging study of copper alloy 172
[DE85-009848] 18 p3075 N85-29023
Preliminary results of the Inconel 617 optimization program. Advanced gas cooled reactor materials program
[DE85-006235] 18 p3075 N85-29024
The effect of temperature on the corrosion-erosion of 9Cr1Mo steel
[DE85-006507] 18 p3076 N85-29030
Aging of gold thick-film solder joints
[DE85-009847] 18 p3077 N85-29037
The effects of extreme temperatures on thermocouples
[DE85-006850] 18 p3110 N85-29258
Electrochemical and morphological study of the effect of temperature on the restructuring and loss of capacity of alkaline battery electrodes
[DE85-006869] 18 p3129 N85-29378
Effects of thermal fluctuations on systems with small surface tension
[PREPRINT-437] 18 p3152 N85-29520
Burner rig corrosion of SiC at 1000 deg C
[NASA-TM-87061] 19 p3227 N85-30011
Diffusion welding of incompatible materials
19 p3245 N85-30121
Effect of heating temperature in a vacuum on state of surface layers of welded OT4 titanium alloy
19 p3245 N85-30123
Comparison and evaluation of field and numerical results from the Site A heater test at Avery Island
[DE85-010625] 19 p3268 N85-30269
An investigation of cementation and carbonitriding by means of ionic bombardment
[BLL-OA-TRANS-3203-(6196.300)]
20 p3429 N85-31265
A study of the effect of a mismatch in gamma and gamma prime phase lattice spacings on the high temperature strength characteristics of dispersion-hardened nickel alloys
[BLL-CE-TRANS-8048-(9022.09)]
20 p3430 N85-31279
Cells for measuring thermoelectromotive force and electrical resistance of metals in temperature range of 20-950 degrees Celsius
[BLL-M-36240-(5828.4)] 20 p3457 N85-31473
Nonlinear Constitutive Relations for High Temperature Application, 1984
[NASA-CP-2369] 20 p3465 N85-31530
Micromechanics of high temperature deformation and failure 20 p3466 N85-31534
On the use of internal state variables in thermoviscoplastic constitutive equations
20 p3466 N85-31536
Oxygen and carbon impurities and related defects in silicon 20 p3481 N85-31631
Friction and wear of solid-lubricated contact in gas turbine engine bearings
[AD-A155042] 21 p3596 N85-32335
Interfacial bonding stability 21 p3606 N85-32409
Temperature sensitivity of fiber-optic transmission line
22 p3764 N85-33331
Thermal stress suffered by tank crews working in summer heat
[DRIC-T-7492] 22 p3826 N85-33698
Design analysis for a repository in crystalline rock
[DE85-011802] 22 p3839 N85-33771
The influence of temperature on the composition density of the transition metals
[BLL-M-35896-(5826.4)] 23 p3915 N85-34282
Evaluation of source strength and dispersion model predications with data from large nitrogen tetroxide field experimenta
[DE85-011855] 23 p3947 N85-34485
Studies in thermo-hydro-chemical transport in porous and fractured media
[DE85-012555] 23 p3949 N85-34473
Thermally induced chemical migration: A natural analog approach
[DE85-012308] 23 p3949 N85-34474
Pressure measurements in a hydrogen combustion environment: Hydrogen-air combustion test series 1 and 2 in the FITS tank, volume 1
[TI85-009899] 24 p4076 N85-35259
Effect of temperature and ionic impurities at very low concentrations on stress corrosion cracking of Type 304 stainless steel
[TI85-003048] 24 p4079 N85-35283
Search for acoustic signals from high energy cascades
[HE-7.1-1] 24 p4213 N85-36155
Experimental investigation of radiative-acoustic effects in the water by the thermodynamical conditions of Dumand
[HE-7.1-2] 24 p4213 N85-36156

TEMPERATURE FIELDS
U TEMPERATURE DISTRIBUTION

TEMPERATURE GRADIENTS
NT THERMOCLINES
Selecting the proper ceramic material for a regenerator experiencing large temperature gradients
[AD-A144796] 01 p0032 N85-10199
Method for calculating linear shrinkage and expansion of metals and alloys
[BLL-M-35747-(5826.4)] 02 p0175 N85-11173
Shear-layer correction after Amiet under consideration of additional temperature gradient. Working diagrams for correction of signals
[NASA-TM-77741] 03 p0415 N85-12654
Effect of a thermal gradient applied to a sinusoidal surface profile
[DE84-015649] 03 p0434 N85-12765
Numerical modeling of the atmosphere
05 p0680 N85-14370
Amiet shear layer correction with an additional temperature gradient considered: Nomograms for the correction of noise signatures from open jet wind tunnel tests
[DFVLR-MITT-84-11] 05 p0726 N85-14869
Modelling temperature changes during hot working operations 06 p0798 N85-15095
Stresses and strains in lithosphere caused by Earth's thermoconvective oscillations 06 p0822 N85-15217
Temperature distortion generator for turboshaft engine testing
[NASA-TM-83748] 07 p0893 N85-15658
A diffuser heat transfer code
[AD-A149270] 10 p1430 N85-19022
Discovery about temperature fluctuations in turbulent air flows 10 p1500 N85-19466
The EURECA Automatic Gradient Heating Facility (AGHF), phase A study
[ESA-CR(P)-1939] 11 p1591 N85-20005
Fluid temperature and concentration gradient measurement study — for spaceborne experiments
[CISE-R/FL/1/04] 11 p1637 N85-20309
Winter anomaly of the lower ionosphere and its possible causes 11 p1660 N85-20459
Winter anomaly 1982/83 in comparison with earlier winters (1960-82) 11 p1660 N85-20461
Heat flux in Lorentzian plasma
[IPPJ-704] 12 p1935 N85-22158
Turbulence measurements in shock induced flows
13 p2091 N85-23055
Fine structure of vertical distribution of light attenuation index of sea water 13 p2109 N85-23140
Characteristics of basaltic lava flows on Venus
13 p2177 N85-23508
Estimating defectiveness buildup during service in metal of welded runner in low-pressure cylinder of turbine
14 p2271 N85-24070
Preliminary report on the results of hydrological measurements in the southern Tyrrhenian Sea, in the Messina strait and in the western Ionian sea
[PREPRINT-433] 14 p2382 N85-24693
Sea ice, climate and Fram Strait
15 p2603 N85-26042
Scheme for atmospheric thermal sensing from satellites with enhanced vertical resolution
16 p2726 N85-26823
Arctic mixed layer dynamics
[AD-A153582] 18 p3150 N85-29505
The thermal calculation of opaque heat screens
[BLL-M-36273-(5828.4)] 20 p3450 N85-31421
DHC: A diurnal heat capacity program for microcomputers
[DE85-009545] 20 p3516 N85-31859
Amiet shear layer correction with an additional temperature gradient considered: Nomograms for the correction of noise signatures from open jet wind tunnel tests
[ESA-TT-897] 20 p3525 N85-31926
A positron annihilation Doppler broadening study of niobium
[DE85-010287] 20 p3527 N85-31936
Temperature measurements on small droplets
21 p3553 N85-32699
Electronic temperature equalizer
[PB85-181485] 22 p3789 N85-33475

Approximate determination of the extent of the solid-liquid zone
[BLL-M-35829-(6828.4)] 23 p3914 N85-34251
Control system for fluid heated steam generator
[DE85-006734] 23 p3939 N85-34417
Integral representation for nonlinear heat transport 23 p3981 N85-34683
Evaluation of low-temperature geothermal potential in north-central Box Elder County, Utah
[DE85-009541] 24 p4112 N85-35490
Comparative analysis of operational forecasts versus actual weather conditions in airline flight planning, volume 4
[NASA-CR-167885] 24 p4120 N85-35537

TEMPERATURE INDICATORS
U INDICATING INSTRUMENTS
U TEMPERATURE MEASURING INSTRUMENTS

TEMPERATURE INSTRUMENTS
U TEMPERATURE MEASURING INSTRUMENTS

TEMPERATURE INVERSIONS
NT CENTRIFUGING STRESS
NT INTERFACIAL TENSION
Green River air quality model development: Meteorological and tracer data, July/August 1982. Field study in Brush Valley, Colorado
[DE84-014975] 02 p0225 N85-11474
Stresses and strains in lithosphere caused by Earth's thermoconvective oscillations 06 p0822 N85-15217
Effect of steady-state temperature distortion on inlet flow to a high-bypass-ration turbofan engine
[NASA-TM-86896] 07 p0904 N85-15725
Thermal deformation of flexible rotors in friction bearings 14 p2280 N85-24123
The temperature fluctuation in stable stratification above snow cover 15 p2581 N85-25918
Average collisional vibrational energy transfer quantities and the inversion temperature
[AD-A152674] 17 p3029 N85-28733
Reports from the German Meteorological Service. No. 167: Results of aerological soundings in the model area upper Rhine: Heat release project upper Rhine area, part 3
[ISBN-3-88148-216-4] 23 p3950 N85-34479
Analytic solutions of inverse heat conduction problems 24 p4092 N85-35367

TEMPERATURE MEASUREMENT
Effect of combined pressure and temperature distortion orientation on high-bypass-ratio turbofan engine stability
[NASA-TM-83771] 01 p0011 N85-10067
A thermodynamic surface for the critical region of ethylene
[PB84-217850] 01 p0025 N85-10159
Description of the Dutch-Danish (DUDA) scanner --- thermal signatures
[AD-B084693] 01 p0121 N85-10826
An interactive computer code for calculation of gas-phase chemical equilibrium (EQLBRM)
[NASA-CR-166337] 02 p0140 N85-10948
Dynamic gas temperature measurement system 02 p0141 N85-10958
Spectroradiometric calibration of the Thematic Mapper and Multispectral Scanner system
[E85-10026] 02 p0218 N85-11439
Large-area sheet task advanced dendritic web growth development
[NASA-CR-174021] 02 p0223 N85-11463
A temperature climatology for New York State 03 p0394 N85-12517
Evaluation of thermocouple junction temperature
[DE84-015159] 04 p0502 N85-13206
Development of a feasibility model for a thin-film precision power meter
[BMFT-FB-T-84-161] 04 p0504 N85-13217
Climate-chamber experiments to improve pilots' work conditions 04 p0543 N85-13454
Improved apparatus and techniques for high temperature and pressure deformation of crystalline materials
[DE84-016049] 04 p0589 N85-13629
Applications of TOMS ozone data and clustering techniques in satellite soundings 05 p0681 N85-14379
Fidelity of satellite soundings 05 p0682 N85-14383
Computer program to compute soil thermal conductivity from transient temperature measurements
[PB85-100550] 07 p0998 N85-16341
Revised Uniform Summary of Surface Weather Observations (RUSSWO). Spangdahlem AB, Germany, parts A-F
[AD-A147166] 07 p1006 N85-16392
Ground-based measurements of mesosphere temperatures by optical means 08 p1183 N85-17453
Application of Fabry-Perot spectrometers for measurement of upper atmosphere temperatures and winds 08 p1183 N85-17454
Lidar studies of temperature and density using Rayleigh scattering 08 p1184 N85-17459
Lidar studies of the alkali metals 08 p1184 N85-17460
Measurements of sediment temperatures, conductivity and heat flow in the North Atlantic and their relevance to radioactive waste disposal
[IOS-172] 09 p1359 N85-18551
Materials physics
[DE84-017103] 09 p1377 N85-18658
Investigation of surface tension phenomena using the KC-135 aircraft
[NASA-TM-82508] 10 p1426 N85-18995
Investigation of fuel additive effects on sooting flames
[AD-A149154] 10 p1457 N85-19179
1984 AFOSR Research Meeting on Diagnostics of Reacting Flow held at New Haven, Connecticut on 21-22 March 1984
[AD-A149023] 10 p1484 N85-19367
Problems in high temperature thermocouple thermometry
[DE85-000606] 10 p1488 N85-19397
Satellite support to the Sierra Cooperative Pilot Project: 1979/80 and 1980/81
[PB85-115079] 10 p1520 N85-19583
Fluid temperature and concentration gradient measurement study --- for spaceborne experiments
[CISE-R/FL/1/04] 11 p1637 N85-20309
The temperature of a glass-encapsulated solar cell estimated from ambient air temperature and global radiation
[GKSS-84-E-36] 11 p1676 N85-20563
Ferromagnetic resonance in a Ni-Mo superlattice
[DE85-003039] 11 p1735 N85-20911
Ionic mechanisms of soot formation in flames
[AD-A150119] 12 p1801 N85-21297
Method of and apparatus for measuring temperature and pressure --- atmospheric sounding
[NASA-CASE-GSC-12558-1] 12 p1856 N85-21639
Method of measuring sea surface water temperature with a satellite including wideband passive synthetic-aperture multichannel receiver
[NASA-CASE-NPO-15651-1] 12 p1869 N85-21723
Dilution jet configurations in a reverse flow combustor
[NASA-CR-174886] 13 p1974 N85-22392
Application of fluorescence to measurement of surface temperature in solid propellants 13 p2002 N85-22548
Radioacoustic system for remote synchronous measurements of wind speed, temperature and its fluctuations 13 p2110 N85-23145
Modulation of light energy transduction in photosynthesis
[DE85-004711] 13 p2141 N85-23292
Analysis and interpretation of observations of airglow at 297 nm in the Venus thermosphere 13 p2172 N85-23473
Qualification of the T2 wind tunnel in cryogenic operation. A: Thermal field, preliminary study of a schematic model
[NASA-TM-77781] 14 p2227 N85-23805
Application of atomic fluorescence to measurement of combustion temperature in solid propellants
[AD-A150733] 14 p2263 N85-24021
Advanced diagnostics for reacting flows
[AD-A150675] 14 p2301 N85-24246
Seven-wavelength pyrometer for determining surface temperature of ablation materials
[NASA-TM-77832] 14 p2305 N85-24266
Possible multiple atmospheric thermal modes with time scale on order of one month 14 p2333 N85-24430
Determination of temperature and degree of roughness of sea and land surfaces by microwave radiometric polarization measurements 14 p2334 N85-24432
Monthly and Seasonal Weather Outlook for mid-December 1984 mid-January 1985, volume 38, number 24, 14 December 1984 14 p2379 N85-24687
Development of a temperature measurement system with application to a jet in a cross flow experiment
[NASA-CR-174896] 15 p2472 N85-25262
System for NDH of thermal spray coating bonds
[DE85-007463] 15 p2572 N85-25858
A simulation experiment on the impact of geostationary temperature retrievals in numerical models 15 p2597 N85-26005
Utilization of satellite data in mesoscale modeling of severe weather 15 p2597 N85-26007
The validation of sea surface temperatures determined from AVHRR data using in situ data recovered via system ARGOS 16 p2812 N85-27342
Observations of airglow O2(1-Sigma) atmospheric band at 8645 A and the rotational temperature at 23 deg S
[INPE-3378-PRE/653] 16 p2826 N85-27435
High resolution spectroscopy of C13O16 in gas mixtures
[AD-A152625] 17 p2919 N85-27991
NMR manometer for measuring high pressures at liquid-helium temperatures 17 p2944 N85-28171
Apparatus for measuring velocity of sound in fluids 17 p2944 N85-28175
Observations of surface water temperature in the Netherlands since 1860: Statistics
[KNMI-WR-84-3] 17 p2997 N85-28531
Observations of surface water temperature in the Netherlands since 1860: Tables for light vessels
[KNMI-WR-84-4] 17 p2998 N85-28532
Observations of surface water temperature in the Netherlands since 1860: Series from KNMI-RWS
[KNMI-WR-84-5] 17 p2998 N85-28533
Automatic liquid-metal temperature monitoring with the use of immersed transducers
[BLL-BISI-TRANS-22427-(9022.06)] 18 p3104 N85-29215
Applications of fuzzy clustering techniques to stratified by tropopause MSU temperature retrievals 18 p3141 N85-29444
Temperature sensitive oscillator
[NASA-CASE-GSC-12958-1] 19 p3258 N85-30201
Method for thermal monitoring subcutaneous tissue
[NASA-CASE-LAR-13028-1] 19 p3328 N85-30618
Intermittency, conditional sampling and turbulent combustion 20 p3424 N85-31249
Application of the Diffusion Raman Anti-Stokes Coherent (DRASC) method to a SNECMA combustion chamber
[YKC-3086/84] 20 p3425 N85-31260
Short-time spectroscopic measurement of the temperature of solids
[ISL-CO-202/84] 20 p3459 N85-31486
DHC: A diurnal heat capacity program for microcomputers
[DE85-009545] 20 p3516 N85-31859
In-situ measurement of wall thermal performance: Data interpretation and apparatus design recommendations
[DE85-011979] 21 p3586 N85-32289
Temperature measurements on small droplets 21 p3653 N85-32699
Application of field similitude theory to calculation of stripline heating 22 p3780 N85-33419
IEA-SSPS CRS calibration report: Calibration of relevant measuring sensors
[DE85-010174] 22 p3788 N85-33468
Electronic temperature equalizer
[PB85-181485] 22 p3789 N85-33475
Measurement and correlation of jet fuel viscosities at low temperatures
[NASA-CR-174911] 23 p3921 N85-34295
Preliminary SPR thermal model description and results for WH-11 and BM-4
[DE85-013171] 23 p3931 N85-34360
Investigation of non-intrusive radiometers for entrained gasifier temperature measurement, revision 3
[DE85-011795] 23 p3934 N85-34365
Control system for fluid heated steam generator
[DE85-005734] 23 p3939 N85-34417
Measurement and interpretation of electron angle at MABE beam stop
[DE85-011918] 23 p3963 N85-34698
Electron irradiation of N type cadmium telluride
[AD-A156117] 24 p4161 N85-35801

TEMPERATURE MEASURING INSTRUMENTS
NT BATHYTHERMOGRAPHS
NT PYROMETERS
NT RESISTANCE THERMOMETERS
NT TEMPERATURE PROBES
NT THERMOCOUPLE PYROMETERS
NT THERMOMETERS
Thermosonde and UHF radar measurements of C2 sub n at Westford, Massachusetts - July 1981
[AD-A145398] 02 p0190 N85-11270
Evolution of the NWC (Naval Weapons Center) thermal standard. Part 5: Thermal standard development and applications
[AD-A146173] 03 p0364 N85-12334
External cavity diode laser sensor
[AD-D011341] 07 p0969 N85-16152
Fluid temperature and concentration gradient measurement study --- for spaceborne experiments
[CISE-R/FL/1/04] 11 p1637 N85-20309
Automatic liquid-metal temperature monitoring with the use of immersed transducers
[BLL-BISI-TRANS-22427-(9022.06)] 18 p3104 N85-29215

TEMPERATURE PROBES
Germanium resistance thermometer calibration at superfluid helium temperatures 12 p1947 N85-22228

TEMPERATURE PROFILES
Use of ground based microwave radiometers for nowcasting 01 p0078 N85-10517

CHORDS: A new temperature or sound speed profile thinning algorithm
[AD-A145484] 02 p0275 N85-11793
Water vapor profile retrievals from the HIRS/MSU satellite sounder 05 p0681 N85-14378
Diurnal and seasonal patterns of temperature and wind flow in the planetary boundary layer for ten locations in complex terrain
[PB85-106698/GAR] 06 p0840 N85-15333
An evaluation and comparison of vertical profile data from the VISSR Atmospheric Sounder (VAS)
[NASA-TP-2425] 07 p1000 N85-16351
The pressure deflagration limit of solid rocket propellants 08 p1117 N85-17046
Determination of ion temperature and rotation velocity profiles by visible, UV and X-ray spectroscopy on Doublet 3 09 p1388 N85-18734
Stress-strain analysis of silicon ribbon
[NASA-CR-175459] 10 p1510 N85-19525
Thermal investigation of an electrical high-current arc with porous gas-cooled anode
[NASA-TM-77789] 11 p1627 N85-20245
Effect of input distributions on the probabilistic fracture mechanics analysis of reactor pressure vessels
[DE85-000832] 11 p1652 N85-20403
Winter anomaly of the lower ionosphere and its possible causes 11 p1660 N85-20459
Theoretical analysis of condensation in the presence of noncondensable gases as applied to open cycle OTEC condensers
[DE84-015809] 11 p1675 N85-20556
Monthly and seasonal weather outlook for October 1984, volume 38, number 19, 29 September 1984
[PB85-113538] 11 p1687 N85-20610
Monthly and seasonal weather outlook for mid-October to mid-November 1984, volume 38, number 20, 13 October 1984
[PB85-113546] 11 p1687 N85-20611
Co-rotating interaction regions in stellar winds 11 p1758 N85-21060
Analysis of selective chopper radiometer data
[NASA-CR-175157] 12 p1895 N85-21894
Two-dimensional numerical model of sensible and latent heat transport in an irrigated field under advective conditions 13 p2131 N85-23261
Radiation-dominated snowmelt on Mars 13 p2191 N85-23592
The effect of air holes on combustor liner wall temperature profile: Experiments
[NAL-TR-840] 15 p2504 N85-25443
Real-time enhancement of a climatology or forecast of ocean thermal structure using observed ocean temperatures
[AD-A151118] 15 p2604 N85-26049
Acoustic propagation in a thermally stratified atmosphere
[NASA-CR-175787] 16 p2860 N85-27636
An investigation into the soot production processes in a gas turbine engine
[AD-A152710] 17 p2919 N85-27992
Energy deposition and its effects on the E+ capture section at Sector 20
[DE85-010984] 18 p3162 N85-29727
Imbedded thermocouples as a solid propellant combustion probe
[AD-A155630] 21 p3564 N85-32167
Application of nonlinear least squares methods to the analysis of solar spectra
[NASA-CR-176122] 22 p3816 N85-33637
Turbulent structure of stably stratified nocturnal slope flows
[AD-A155845] 24 p4123 N85-35559

TEMPERATURE SCALES
A comparison of two bench scale tests of fuel low temperature flow properties
[AD-A154477] 20 p3435 N85-31311
Self-study manual on optical radiation measurements. Part 1: Concepts. Chapter 12: Blackbodies, blackbody radiation, and temperature scales
[PB85-195303] 24 p4154 N85-35754

TEMPERATURE SENSORS
NT THERMISTORS
Platinum thin film resistors as accurate and stable temperature sensors
[NASA-TM-77728] 01 p0049 N85-10322
Fiber optic, Fabry-Perot high temperature sensor
[NASA-CR-174712] 04 p0564 N85-13594
Temperature sensors for OTEC applications
[DE85-009807] 18 p3110 N85-29254
On-line temperature sensor
[DE85-011641] 22 p3787 N85-33465
Materials and process development for microcomputer-compatible pressure, temperature, and position sensors
[BMFT-FB-T-85-024] 24 p4097 N85-35399

TEMPERING
Study to optimize Cr-Mo steels to resist hydrogen and temper embrittlement. A study of carbides formed in low alloy Cr-Mo steels
[DE84-015206] 01 p0029 N85-10179
Wear properties of rapidly solidified surfaces of a pseudo-binary Fe-TiC alloy 02 p0179 N85-11204
Effect of tempering on the strength and toughness of 2 1/4 Cr-1 Mo steel weldments
[DE85-003818] 09 p1296 N85-18140
Residual stress after laser processing 11 p1600 N85-20065
Phase transformations in vanadium alloys of titanium during quenching and tempering 11 p1602 N85-20073
Kinetics of reaction of metals and non-metals during diffusion welding 11 p1602 N85-20076
Effect of mill run and temper variations on barrier anodic film format ion on 6061 aluminum alloy
[DE85-000447] 11 p1606 N85-20112
Effect of aluminum on nature of titanium alloy failure 15 p2496 N85-25411
Powder-metallurgy alloys and steels
[BLL-BISI-TRANS-22239-(9022.06)] 17 p2926 N85-28050
The characteristic structure of weld metal of high temperature alloy X20CrMoV 121
[BLL-BISI-TRANS-21623-(9022.06)] 17 p2928 N85-28069
Study to optimize Cr-Mo steels to resist hydrogen and temper embrittlement
[DE85-005492] 17 p2932 N85-28096
Application of the unloading compliance methods in fracture toughness measurements of a quenched and tempered steel
[BLL-CE-TRANS-7953-(9022.09)] 20 p3465 N85-31523

TEMPLATES
Computer-generated latitude and longitude templates for rapid determination of geographic positions in Alaska 04 p0516 N85-13288
Mask aligner for solar cell fabrication
[AD-D011450] 10 p1510 N85-19529

TEMPORAL DISTRIBUTION
Specifics of dynamics of brain biopotentials under the influence of complex audible communicative signals 07 p1014 N85-16440
Space and time distribtuion of aftershocks 13 p2112 N85-23157
The relationship between auroral electrojet and visual aurora 14 p2363 N85-24602
Elemental analysis of aerosols in Transvaal urban and power-producing areas using time and size-resolved samples 16 p2829 N85-27443
Resource allocation in cerebral specialization of function: Behavioral and electrophysiological studies
[AD-A155092] 21 p3664 N85-32759
Temporal variations of the anomalous oxygen component, 1977 - 1984
[SH-4.6-3] 23 p4039 N85-35041

TEMPORAL RESOLUTION
Fundamental remote sensing science research program. Part 1: Status report of the mathematical pattern recognition and image analysis project
[E85-10004] 02 p0215 N85-11417
Water resources by orbital remote sensing: Examples of applications
[E85-10015] 02 p0217 N85-11428
Time-resolved spectroscopy of evanescent-wave excited fluorescence
[DE84-015213] 04 p0473 N85-13013
Time-resolved tomographic images of a relativistic electron beam
[DE84-015021] 04 p0565 N85-13597
Opportunities for high angular and temporal resolutions of galactic objects at radio frequencies --- QUASAT 07 p1059 N85-16723
LANDSAT scene-to-scene registration accuracy assessment 11 p1667 N85-20502
Geometric accuracy assessment of LANDSAT-4 Multispectral Scanner (MSS) data 11 p1667 N85-20505
Spectral methods in time for parabolic problems
[NASA-CR-172539] 11 p1706 N85-20730
Fast times at high temperatures
[DE85-003306] 12 p1943 N85-22205
Time-resolved studies of rapid solidification in highly undercooled molten silicon
[DE85-004857] 13 p2038 N85-22765
Observed spatial properties of the solar eigenfunctions and the implications for the existence of resolved multiflets 14 p2443 N85-25074
Time-resolving electron temperature diagnostic for ALCATOR C
[DE85-004916] 16 p2868 N85-27690

TENNESSEE
Image variance and spatial structure in remotely sensed scenes --- South Dakota, California, Missouri, Kentucky, Louisiana, Tennessee, District of Columbia, and Oregon 07 p0966 N85-16265

TENSILE CREEP
Morphological changes of gamma prime precipitates in nickel-base superalloy single crystals
[NASA-TM-83696] 01 p0026 N85-10165
Mechanisms of elevated temperature rupture in single phase ceramics
[DE85-000697] 09 p1299 N85-18156
Fatigue-creep interaction in + or - 45 deg carbon-resin composites --- aircraft construction materials
[ONERA-RT/40/7086/M] 11 p1594 N85-20027

TENSILE DEFORMATION
Structure and properties of titanium alloys after isothermal deformation at low speeds 03 p0351 N85-12260
Strength analysis of fan-shaped wing considering temperature deformation and creep deformations 06 p0779 N85-14983
The influence of porosity on the deformation and fracture of alloys
[AD-A146786] 08 p1130 N85-17124
Influence of work-hardening on the Portevin-LeChatelier effect
[DE85-002505] 11 p1605 N85-20093

TENSILE PROPERTIES
Tensile properties and swelling of 20%-cold-worked Type 316 stainless steel irradiated in HFIR
[DE84-014080] 05 p0617 N85-13948
Characterization of fiber optic cables under large tensile loads
[DE84-016816] 05 p0651 N85-14180
Characterization of newly developed conductive composites
[AD-A146852] 06 p0764 N85-14884
Weldability and mechanical property characterization of weld clad alloy 800H tubesheet forging
[DE85-001737] 11 p1609 N85-20116
Structural basis for the mechanical properties of polyethlenes
[PB85-149771] 11 p1613 N85-20142
Steel castings by the electroslag casting technique
[DE85-003812] 12 p1819 N85-21409
Effects of neutron irradiation at 450(0)C and 16 dpa on the properties of various commercial copper alloys
[DE85-005716] 13 p2024 N85-22684
Spectroscopic analysis of radiation-generated changes in tensile properties of a polyetherimide film
[NASA-TP-2429] 15 p2502 N85-25435
Temperature and manganese content dependences of tensile deformation in iron-high manganese binary alloys
[DE85-007656] 17 p2932 N85-28098
Preliminary results of the Inconel 617 optimization program. Advanced gas cooled reactor materials program
[DE85-006235] 18 p3075 N85-29024
Influence of recrystallization and solution on the tenacity of the 7010 and 7475 alloys. Oligocyclic fatigue of the 7010 alloy
[ONERA-RT-19/5069-M] 20 p3432 N85-31289
Numerical study of tensile fracture in plane stress
[ONERA-RT-22/7169-RY-070-R] 20 p3470 N85-31583
Effects of weak interfaces on thermostructural behavior of carbon-carbon composites
[AD-A155330] 21 p3562 N85-32154
Fracture behavior of aluminum composites reinforced with fiber 23 p3907 N85-34207
Apparatus producing constant cable tension for intermittent demand
[DE85-006434] 23 p3938 N85-34412
Effect of thermal ageing on the mechanical properties of PWR pressure vessel steels and weldments
[AERE-R-11480] 24 p4078 N85-35275
Microshrink, tensile properties, and the detection of microshrink
[AD-A155875] 24 p4079 N85-35278

TENSILE STRENGTH
The effect of 2 strength reducing techniques on the ultimate tensile strength of AISI 4130 steel: Rocket motor case venting
[AD-A145526] 02 p0169 N85-11134
Tensile strength of composite sheets with unidirectional stringers and crack-like damage: A brief report
[NASA-TM-86310] 02 p0170 N85-11139
Resistance of Navy shipboard outerwear garments and fire-resistant fabrics to extreme heat
[AD-A145414] 02 p0238 N85-11548
Effects of tin on microstructure and mechanical behavior of Inconel 718
[NASA-TM-86966] 03 p0330 N85-12129

Test report no. 17.208: Statistics of the basic characteristics of carbon-epoxy composites
[DGT-23.426/A] 04 p0468 N85-12979
Tensile properties and swelling of 20%-cold-worked Type 316 stainless steel irradiated in HFIR
[DE84-014080] 05 p0617 N85-13948
Influence of the shape and distribution of inclusions of the fatigue strength of bearing steels in rotary bending
[BLL-FNR-60243-(6019.3153)] 08 p0768 N85-14912
Strength and aging behaviour of soft soldered joints
[BLL-T6365/BG/WH600/84] 07 p0925 N85-15862
On heat-treatable copper-chromium alloy, 1
[NASA-TM-77753] 07 p0927 N85-15879
Mechanical property data 7050-t736511 alloy
[AD-A147365] 07 p0928 N85-15882
Imide modified epoxy matrix resins
[NASA-CR-174695] 07 p0930 N85-15892
Laboratory investigation on adhesives for Naval facilities construction
[AD-A147453] 07 p0932 N85-15909
Hydrogen embrittlement of nickel
[AD-A146322] 08 p1129 N85-17119
Tensile test of pressureless-sintered silicon nitride at elevated temperature
[NASA-TM-77777] 08 p1172 N85-17390
Effect of tempering on the strength and toughness of 2 1/4 Cr-1 Mo steel weldments
[DE85-003818] 09 p1296 N85-18140
Ti-6Al-4V alloy castings prepared in zircon sand molds and the effect of hot isostatic pressing
[PB85-109932/GAR] 09 p1298 N85-18150
Studies of structure and mechanical properties of carbon-reinforced plastic based on spirally reinforced fiber 10 p1444 N85-19100
Influence of extension rate on strength and deformation characteristics of titanium alloys over a broad temperature range 10 p1448 N85-19121
Effects of chromium and aluminum on mechanical and oxidation properties of iron-nickel-base superalloys based on CG-27
[NASA-TP-2443] 12 p1805 N85-21323
The strength and characteristics of VPPA welded 2219-T87 aluminum alloy 12 p1946 N85-22224
Structural strenght of strip D16T aluminum alloy with low copper and magnesium content 13 p2025 N85-22691
New deformable secondary aluminum alloys 13 p2026 N85-22694
Effect of operating medium on cyclic durability of AD33-W composite 13 p2029 N85-22716
Analysis of strength and ductility of welded joints in AMtsS and AMg5 aluminum alloys 13 p2033 N85-22737
Experimental investigation of crippling strength of Chinese aluminum alloy (LY12CZ) sections 13 p2041 N85-22779
Effect of oxygen on mechanical properties of Nb-V alloy
[DE85-002681] 14 p2256 N85-23982
Cast-iron technology: Metallographic and mechanical testing results
[DE85-002684] 14 p2257 N85-23984
Environmental effects on the tensile strength of chemically vapor deposited silicon carbide fibers
[NASA-TM-86981] 14 p2259 N85-24000
Hydrogen resistance of VT1-0 titanium under 150 MPa pressure at room temperature 15 p2499 N85-25414
Development of high strength ship hull steel for high heat input welding — controlled rolling and accelerated cooling 15 p2565 N85-25827
Tensile and fracture toughness properties of Mirage III spars
[AR-003-019] 15 p2578 N85-25899
Magnetic method of inspecting mechanical properties of general purpose tubes
[BLL-M-36084-(5828.4)] 16 p2796 N85-27235
Mechanical properties of lunar materials under anhydrous, hard vacuum conditions: Applications of lunar glass structural components
[DE85-006682] 16 p2801 N85-27271
SRB filament wound case material property study
[NASA-CR-171469] 17 p2910 N85-27940
Role of hydrogen and structure on CMSX-2 17 p2915 N85-27967
High tensile strength, punchable, hot rolled strips with good plasticity
[BMFT-FB-T-84-256] 18 p3078 N85-29040
Load-carrying capabilities of refractory alloys for space reactor power applications
[DE85-010666] 19 p3240 N85-30067
-Long range ordered alloys modified by addition of niobium and cerium
[DE85-011661] 20 p3431 N85-31285
Orientation and strength of semi-crystalline polymers 20 p3432 N85-31294
Long-term strength of glass fibre/phenolic resin composites
[NPL-DMA(A)-98] 22 p3742 N85-33195
Tensile fatigue of glass fibers and composites with conventional and surface compressed fibers
[RR-84-4] 22 p3742 N85-33196
Strength properties of glassfiber reinforced thermoplastics 23 p3908 N85-34212
Study on fracture behavior of epoxy resin 23 p3909 N85-34216
Effects of temperature on the tensile strength and elastic modulus of composite material
[AD-A156112] 24 p4075 N85-35251
Crystallization of Polyetheretherketone (PEEK) in carbon fiber composites
[AD-A156316] 24 p4075 N85-35252
Effect of microstructure on the fatigue behavior of Fe-C-X alloys
[DE85-011749] 24 p4080 N85-35285

TENSILE STRESS
Contributions to the 7th International Acoustic Emission Symposium
[AD-A145388] 02 p0275 N85-11792
Stress concentration due to axial tension of loaded nonsymmetric-shaped grooves
[AD-A149425] 10 p1496 N85-19442
Tether fundamentals 11 p1643 N85-20345
Simplified theory for the behaviour of buried flexible cylinders under the influence of uniform hoop compression
[PB85-116531] 11 p1654 N85-20419
Longitudinal splitting in unidirectional composites, analysis and experiments
[NASA-CR-3881] 13 p2015 N85-22639
Orientation and temperature dependence of some mechanical properties of the single-crystal nickel-base superalloy Rene N4. 3: Tension-compression anisotropy
[NASA-TM-86982] 13 p2021 N85-22660
Origin of Martian polygonal terrain: Preliminary results 13 p2191 N85-23591
Determination of permissible heating rate of metal
[BLL-M-36107-(5828.4)] 16 p2748 N85-26957
Magnetic method of inspecting mechanical properties of general purpose tubes
[BLL-M-36084-(5828.4)] 16 p2796 N85-27235
Matrix fracture in fiber-reinforced ceramics
[AD-A154704] 21 p3589 N85-32197
A continuous damage model based on stepwise-stress creep rupture tests
[NASA-CR-174941] 21 p3597 N85-32341
Apparatus producing constant cable tension for intermittent demand
[DE85-006434] 23 p3938 N85-34412

TENSILE TESTS
Tensile and crack propagation tests on aluminum alloys of the 2000 and 7000 series in laminated plate and forged products
[M2-678300] 03 p0373 N85-12383
Composite materials characterization and development at AFWAL 04 p0464 N85-12944
Finite element method calculation of a necking tension specimen including heat transfer influence
[RUB-IFM-MITT-40] 05 p0648 N85-14162
Special features of the deformation of molybdenum at high temperatures
[BLL-M-36027-(5828.4)] 07 p0924 N85-15856
Tensile testing of SiC whiskers
[DE85-003712] 11 p1593 N85-20025
Strength properties of unidirectionally reinforced hybrid composites 11 p1599 N85-20056
Reduced-chromium stainless steel substitutes containing silicon and aluminum
[PB85-160786] 15 p2513 N85-25502
Magnetic method of inspecting mechanical properties of general purpose tubes
[BLL-M-36084-(5828.4)] 16 p2796 N85-27235
MM2 LRSLA testing stage 3 propellant
[AD-A152540] 17 p2937 N85-28126
Short term determination of the creep properties of high temperature materials
[CRIF-MT-160] 20 p3432 N85-31288
Graphite/PMR polyimide composites with improved toughness
[NASA-TM-87081] 21 p3561 N85-32148
Tensile testing apparatus
[NASA-CASE-LAR-13243-1] 23 p3933 N85-34375
Effect of temperature and ionic impurities at very low concentrations on stress corrosion cracking of Type 304 stainless steel
[TI85-003048] 24 p4079 N85-35283

TENSIOMETERS
A strain gauge manual
[AD-A151802] 16 p2787 N85-27197

TENSION
Psychological states (mood, affect or emotion) experienced by JASDF pilots through flying duties. 3: Flying conditions causing pilots psychological disturbances 01 p0090 N85-10606
Evaluation of failure criterion for graphite/epoxy fabric laminates
[NASA-CR-172547] 10 p1431 N85-19025

TENSOR ANALYSIS
Linear and bilinear infinite-dimensional representations of finite-dimensional nonlinear systems
[RR-259] 02 p0254 N85-11661
Trust region methods for minimization
[AD-A147073] 07 p1030 N85-16540
Alternatives for jet engine control
[NASA-CR-175831] 16 p2709 N85-26713
Alternatives for jet engine control
[NASA-CR-175832] 16 p2709 N85-26714
Alternatives for jet engine control
[NASA-CR-175833] 16 p2709 N85-26715
Boundary layer and parabolic flows
[DFVLR-FB-84-46] 17 p2960 N85-28285
Reduction techniques for infinite-dimensional Hamiltonian systems: Some ideas and applications
[PREPRINT-424] 18 p3173 N85-29666

TENSOR FIELDS
U TENSORS

TENSORS
NT STRESS TENSORS
Linear conformal gravitation 02 p0265 N85-11735
Microwave measurement of the complex dielectric tensor at anisotropic slab materials
[DE84-017050] 04 p0493 N85-13144
Interacting Boson approximation
[DE85-003016] 22 p3837 N85-33756
Scalar/Vector potential formulation for compressible viscous unsteady flows
[NASA-CR-3921] 23 p3893 N85-34113

TEREPHTHALATE
NT POLYETHYLENE TEREPHTHALATE

TERMINAL BALLISTICS
Penetrator/armour interactions: Background to Australian work
[MRL-R-936] 03 p0367 N85-12353
An introduction to fuzzy regression analysis with a ballistic application
[AD-A148093] 03 p0411 N85-12629
Nondestructive deceleration of a rocket sled — target penetration tests
[FOA-C-20549-D3] 07 p0912 N85-15771
A computerized study of rigid cones penetrating aluminum targets
[FOA-C-20561-D4] 11 p1648 N85-20384
An orthogonal grid technique for studying internal deformation and energy absorption in target penetration
[AD-A149989] 12 p1860 N85-21665
OMEGA: An optronic device to measure the incidence angle of a projectile
[ISL-CO-207/83] 14 p2306 N85-24274
A method for the evaluation of the residual energy of a metallic fragment after perforation of a thin target
[ISL-R-113/83] 16 p2794 N85-27233
Holographic assembly for measuring velocity fields of supersonic ballistic splinters at a large distance
[ISL-CO-203/84] 20 p3459 N85-31487
Numerical simulation of interior and terminal ballistics phenomena. Investigation of the effects of the parameters and application examples
[ISL-R-112/84] 22 p3831 N85-33731
Presentation of numerical simulation work in terminal ballistics using a few examples. Applications of the calculation model Program for Elastoplastic Simulation of Impacts (PEPSI) of the Franco-German Research Institute Saint Louis (ISL)
[ISL-CO-209/84] 22 p3834 N85-33741
Experimental data for characterizing perforating impacts: Fragmentation processes
[AD-A156370] 24 p4102 N85-35427

TERMINAL GUIDANCE
NT LASER GUIDANCE
Dual mode radio frequency-infrared frequency system
[AD-D011402] 08 p1061 N85-16850
Integration of ground and on-board system for terminal count 08 p1092 N85-16898
AN investigation into the control limitations of a bank to turn missile in the terminal homing phase
[AD-A152193] 16 p2704 N85-26696
Dispersion sensitivity of the eight inch advanced ramjet munitions technology projectile due to wind and minor thrust errors
[AD-A152145] 16 p2727 N85-26835
Automatic assembly of space stations 20 p3409 N85-31153

TERMINALS
BBC receiving terminal for the European orbital test satellite
[BBC-RD-1984/15] 08 p1142 N85-17205
TERMINATOR LINES
Near Earth space sporadic radio emission bursts occurring during sunrise
[SH-10.1-9] 23 p4054 N85-35140
TERMINOLOGY
An operational system for subject switching between controlled vocabularies: A computational linguistics approach
[NASA-CR-3838] 02 p0293 N85-11903
Error and uncertainty — metrology
[NPL-DPMA-2] 08 p1137 N85-17161
Online database search strategies and thesaural relationship models 09 p1402 N85-18822
Systematic nomenclature of the nitrogen, oxygen and sulfur functional polycyclic aromatic hydrocarbons
[DE85-007426] 17 p2916 N85-27974
Coping with computer terminology
[DE85-006076] 18 p3161 N85-29579
Spanish language equivalents for a glossary of terms used in the field of space exploration
[NASA-TM-86211] 19 p3379 N85-30961
Re-evaluation of cosmic ray cutoff terminology
[SH-6.1-11] 23 p4045 N85-35084
TERNARY ALLOYS
Re-evaluation of phase separation in Ti-Zr-Be metallic glasses
[DE84-015603] 03 p0338 N85-12176
Zero-flux planes and flux reversals in multicomponent diffusion
[DE84-015212] 05 p0618 N85-13950
High temperature properties of equiatomic FeAl with ternary additions
[NASA-TM-86938] 10 p1439 N85-19072
Clustering and ordering in 3-5 alloys
[AD-A150604] 13 p2022 N85-22870
Influence of composition on the microstructural evolution and mechanical properties of irradiated Fe-Ni-Cr ternaries
[DE85-007462] 17 p2931 N85-28094
Amorphous alloys of ion-implanted Fe-Ti-C
[DE85-010656] 19 p3360 N85-30634
A fractographic study on mode 2 and mode 3 SCC crack growth in an Al-Zn-Mg alloy 23 p3905 N85-34191
Enthalpies of formation of liquid Fe-Ce-Si and Fe-Ce-Al three-component alloys
[BLL-M-36296-(5828.4)] 23 p3913 N85-34247
TERNARY SYSTEMS
Transport properties and distribution functions in 3-5 semiconductors
[AD-A147525] 07 p1049 N85-16660
Formation of a limiting composition in the preparation of ternary 3-5 semiconductors by the VPE (Vapor Phase Epitaxy) Hydride technique
[AD-A147639] 08 p1225 N85-17713
High temperature properties of equiatomic FeAl with ternary additions
[NASA-TM-86938] 10 p1439 N85-19072
A study of interdiffusion in beta + gamma/gamma + gamma prime Ni-Cr-Al
[NASA-CR-174852] 11 p1597 N85-20041
Characterization of high temperature electrically conducting oxides
[DE85-004296] 12 p1803 N85-21307
Process for making a heterojunction source-drain insulated gate field-effect transistors utilizing diffusion to form the lattice
[AD-D011536] 12 p1939 N85-22176
A study of liquid-vapor equilibria of the bromine-hydrobromic acid-water system
[NASA-TM-77748] 14 p2249 N85-23940
Dual species ion implantation of ternary compounds based on In-Ga-As
[AD-D011617] 16 p2959 N85-27698
Three body abrasive wear in various metal combinations 23 p3906 N85-34200
TERNARY SYSTEMS (DIGITAL)
U DIGITAL SYSTEMS
TERRACES (LANDFORMS)
NT PIEDMONTS
NT PLATEAUS
Quaternary stratigraphy of the lower Iowa and Cedar River Valleys, southeast Iowa 09 p1352 N85-18504
Morphology and mechanics of terraces in lunar craters 13 p2182 N85-23543
Newly discovered Martian impact basins 13 p2182 N85-23544
Interaction of Martian flow ejecta blankets with pre-existing impact craters: Morphological observations 13 p2183 N85-23546
TERRAIN
A one-level mesoscale model suitable for nowcasting and short-term forecasting in regions of complex terrain 01 p0081 N85-10541
Digital Terrain Elevation Data (DTED) anomaly removal through the use of an interactive Fourier frequency filtering process
[AD-A145433] 02 p0219 N85-11445
Digital elevation models improve processing of Alaskan gravity data 04 p0515 N85-13285
Stratigraphy, petrology, and structure of the Pingston terrane, Mount Hayes C-5 and C-6 quadrangles, eastern Alaska Range, Alaska 04 p0517 N85-13301
Relationship between model complexity and data base quality for complex terrain tracer experiments
[DE84-015022] 04 p0539 N85-13429
Potential geological natural landmarks of the East Gulf Coastal Plain
[PB84-230317] 06 p0635 N85-15316
Simple mesoscale models for operational use in regions of topographic and thermal forcing: Development and evaluation
[AD-A146667] 06 p0639 N85-15325
On the long range propagation of sound over irregular terrain
[NASA-CR-3862] 07 p1038 N85-16589
Automatic terrain elevation mapping and registration 08 p1148 N85-17242
Interactive digital image processing for terrain data extraction
[AD-A146580] 08 p1176 N85-17417
Soil compliance influence on tyre performance
[AD-P004260] 09 p1404 N85-18836
Dynamic simulation of track laying vehicles
[AD-P004266] 09 p1405 N85-18842
A comparison between a conventional method and an improved method for predicting tracked vehicle performance
[AD-P004276] 09 p1406 N85-18852
Effect of hitch positions on the performance of track-grouser systems
[AD-P004277] 09 p1406 N85-18853
Ride comfort of off-road vehicles
[AD-P004279] 09 p1406 N85-18855
Further development in ride quality assessment
[AD-P004280] 09 p1406 N85-18856
Comparison of measured and simulated ride comfort for an agricultural tractor and influence of travel speed and tyre-inflation pressure on dynamic response
[AD-P004281] 09 p1407 N85-18857
Characteristics of farm field profiles as sources of tractor vibration
[AD-P004282] 09 p1407 N85-18858
Smoother terrain-machine
[AD-P004286] 09 p1409 N85-18873
Natural environment analysis
[NASA-CR-171333] 10 p1428 N85-19010
A comparison between predicted and measured propagation loss in the VHF/UHF range in rugged terrain 10 p1471 N85-19285
Control of mammals at airports
[AD-P004192] 11 p1580 N85-19957
Landscape management on airports for reduction of bird populations
[AD-P004194] 11 p1581 N85-19960
Inexpensive multipurpose landscaping 11 p1581 N85-19961
Atmospheric diffusion in hilly region on middle reaches of the Chang Jiang 11 p1620 N85-20196
Mean flow and turbulence in complex terrain NPS (Naval Postgraduate School)/Vandenberg measurement system
[AD-A150184] 13 p2138 N85-23274
The ASCOT Data Analysis Workshop
[DE85-004407] 13 p2139 N85-23283
Low altitude texture comparison data base and smooth shaded texture
[AD-A150342] 13 p2146 N85-23323
Dark halo craters and the thickness of grooved terrain on Ganymede 13 p2173 N85-23484
Formation of bright terrain bands on Ganymede by unstable lithosphere extension 13 p2173 N85-23485
Basaltic pressure ridges: Formation and relationship to flow emplacement 13 p2186 N85-23567
Paleohydrologic implications of valley networks of Mars 13 p2190 N85-23585
Relative time-scale for channeling events within chaotic terrains, Margaritifer Sinus, Mars 13 p2190 N85-23588
Terrestrial analog studies for Martian patterned ground 13 p2190 N85-23590
Origin of Martian polygonal terrain: Preliminary results 13 p2191 N85-23591
Investigations of the Mars cratered terrain: Smooth plains boundary in the eastern equatorial region 13 p2191 N85-23596
Martian fretted terrain morphometry interpreted using principal components analysis 13 p2192 N85-23597
Distribution and properties of large symmetric knobs on Mars 13 p2192 N85-23598
Enigmatic hills of the mottled plains, Mare Acidalium quadrangle (MC-4), Mars 13 p2192 N85-23599
Importance of the tectonic motions on Ganymede 13 p2202 N85-23681
Evaluation of carrying capacity and landscape damage in northern Kenya by multistage remote sensing
[DFVLR-FB-84-47] 14 p2347 N85-24514
A study of terrain reductions, density anomalies and geophysical inversion methods in gravity field modelling
[AD-A150788] 14 p2373 N85-24668
Technical development to improve satellite sounding over radiatively complex terrain
[NASA-CR-175746] 15 p2583 N85-25929
Mean conditions and turbulence statistics at Vandenberg AFB, California
[AD-A151986] 15 p2665 N85-26449
Radar return from vegetation covered terrains
[INPE-3470-PRE/713] 16 p2770 N85-27093
A study of the effect of gently varying terrain on atmospheric flow near the surface 16 p2823 N85-27411
Structural analysis of terrane accretions in the eastern Brooks Range and adjacent areas in central Alaska and Canada
[DE85-006279] 17 p2993 N85-28501
Application of artificial intelligence (AI) to radar image understanding
[AD-A152519] 17 p3017 N85-29654
The AFTI/F16 terrain-aided navigation system
[DE85-008411] 18 p3060 N85-29935
Influence of land surface processes on the Indian monsoon: A numerical study 18 p3146 N85-29478
Influence of land-surface roughness on atmospheric circulation and rainfall: A sensitivity study with a GCM 18 p3146 N85-29479
Categorization of nocturnal drainage flows within the Brush Creek valley in western Colorado and the variability of sigma theta in complex terrain
[DE85-011291] 19 p3300 N85-30461
MELSAR: A mesoscale air quality model for complex terrain. Volume 2: Appendices
[DE85-010991] 19 p3310 N85-30519
The use of the glistening surface concept in rough surface scattering
[AD-A154922] 21 p3575 N85-32234
Geomorphological similarity and uniqueness 21 p3601 N85-32361
Ancient landscapes: Their nature and significance for the question of inheritance 21 p3601 N85-32364
Landscape inheritance: Report of Working Group Number 2 21 p3604 N85-32383
Process thresholds: Report of Working Group Number 3 21 p3604 N85-32384
Microcomputer processing of LANDSAT Thematic Mapper data for the acquisition of military tactical terrain data
[AD-A154781] 21 p3605 N85-32389
Mean flow and turbulence in complex terrain
[AD-A155136] 21 p3636 N85-32583
A transportable, machine oriented library of european sky and terrain radiance distributions with contemporary radiometric and meteorological profiles
[AD-A155254] 21 p3637 N85-32590
A review of tectonic aspects of the Limpopo belt and other Archean high-grade gneissic terranes 21 p3720 N85-33080
Implementation of the SITAN algorithm in the digital terrain management and display system
[DE85-010659] 22 p3729 N85-33115
Terrain illumination conditions when taking scanning photographs from space 22 p3736 N85-33159
MELSAR: A mesoscale air quality model for complex terrain. Volume 1: Overview, technical description and user's guide
[DE85-010943] 22 p3811 N85-33606
Evaluation of the 2DFLOW and hybrid complex-terrain dispersion models with the 1980 ASCOT data base from the Geysers
[DE85-012980] 22 p3812 N85-33613
A user-friendly computer-aided construction of boundaries 23 p3982 N85-34564
Three-dimensional gravity ideal body studies in rough terrain
[DE85-014097] 24 p4118 N85-35525
Turbulent structure of stably stratified nocturnal slope flows
[AD-A155845] 24 p4123 N85-35559
TERRAIN ANALYSIS
Geomorphology 02 p0214 N85-11411
Terrain analysis procedural guide for surface configuration
[AD-A145637] 02 p0219 N85-11446

Remote sensing for landforms and soils in the arid southwest United States 03 p0378 N85-12410
Comparison between tracer measurements and model calculations for nighttime drainage flows in complex terrain
[DE84-014709] 04 p0539 N85-13431
Atmospheric studies in complex terrain
[DE84-006553] 05 p0676 N85-14345
A brief investigation into the validity of SEASAT radar altimeter data acquired over land
[AD-A146580] 06 p0827 N85-15254
Evaluation of the L-band scattering characteristics of volcanic terrain in aid of lithologic identification, assessment of SIR-B calibration, and development of planetary geomorphic analogs 06 p1146 N85-17232
Investigation of SIR-B images for lithologic mapping 06 p1148 N85-17241
Mathematical aspects of digital terrain information; Report from International Society for Photogrammetry and Remote Sensing (ISPRS) working group 3:3, 1980 - 1984 — photogrammetry 06 p1175 N85-17407
Natural environment analysis
[NASA-CR-174390] 06 p1180 N85-17433
Automated and interactive data base generation
[AD-P004316] 09 p1268 N85-17970
CIG (Computer image generation) data bases in an instance: Bits and pieces
[AD-P004318] 09 p1269 N85-17972
The generation of three-dimensional data bases using a building block approach
[AD-P004319] 09 p1269 N85-17973
SIR-A imagery in geologic studies of the Sierra Madre Oriental, northeastern Mexico. Part 1 (Regional stratigraphy): The use of morphostratigraphic units in remote sensing mapping
[NASA-CR-175457] 10 p1505 N85-19497
The accuracy in calculations of intervisibility with digital terrain models — digital models
[FOA-C-20557-D6(E1)] 12 p1909 N85-21983
Stagnation zone impaction on a simple terrain feature in stable flow 13 p2130 N85-23255
Using SM-4 Omega system in checking and editing digital terrain information 15 p2487 N85-25350
Structural analysis of terrane accretions in the eastern Brooks Range and adjacent areas in central Alaska and Canada
[DE85-008279] 17 p2993 N85-28501
Scattering from foliage covered terrain
[AD-A154724] 21 p3574 N85-32228
Planning for VRM: Radar and sonar studies of volcanic terrains on Earth, Venus and Mars 22 p3857 N85-33684

TERRAIN FOLLOWING AIRCRAFT
Observations of physiological and psychological effects of terrain following flight based on in-flight test experience 10 p1532 N85-19657

TERRESTRIAL MAGNETISM
U GEOMAGNETISM

TERRESTRIAL PLANETS
NT EARTH (PLANET)
NT MARS (PLANET)
NT MERCURY (PLANET)
NT VENUS (PLANET)
Development of a Global 3-D magnetohydrodynamic computational model for solar wind-cometary and planetary studies
[NASA-CR-175490] 12 p1962 N85-22331
Accumulation of the terrestrial planets 13 p2179 N85-23524
Implications of convection in the Moon and the terrestrial planets 13 p2183 N85-23548
Terrestrial Planets: Comparative Planetology
[NASA-CR-176093] 22 p3851 N85-33849
Noble gases in meteorites and terrestrial planets 22 p3851 N85-33850
Terrestrial Xe isotopic contraints on the early history of the Earth 22 p3852 N85-33852
Oxidation states of iron in the terrestrial planets: Evidence and implications for accretion models 22 p3852 N85-33854
The distribution of compositional classes in the asteroid belt: A cosmochemical fingerprint? 22 p3852 N85-33856
Late-stage planetesimals: How big? 22 p3852 N85-33857
What determines the location of satellites and planets? 22 p3853 N85-33858
Interrelationships among the terrestrial planets 22 p3853 N85-33859
Impact processes and their implications for planetary formation and early evolution 22 p3853 N85-33860
Origin of the atmosphere and hydrosphere of the terrestrial planets 22 p3853 N85-33863
A solid-state framework for terrestrial upper mantles 22 p3856 N85-33878
Crustal development in the terrestrial planets 22 p3856 N85-33879
Magnetic field generation in the cores of terrestrial bodies 22 p3859 N85-33894

TERRESTRIAL RADIATION
A sphere-scanning radiometer for rapid directional measurements of sky and ground radiance: The PARABOLA field instrument
[NASA-TM-86171] 03 p0363 N85-12329
Simple formula to estimate carbon dioxide gas effect in radiation balance of underlying surface 06 p0823 N85-15226
Deciduous forest radiation regimes: Effects of forest structure, phenology and Earth-Sun geometry upon their spatial, temporal and spectral variability
[AD-A146804] 07 p0996 N85-16327
Diurnal variations in terrestrial magnetic field and structure of magnetosphere 14 p2344 N85-24493
Comparison of measurement and simulation results of radiation temperatures applied to the thermal mapping of Munich
[DFVLR-FB-85-06] 17 p2984 N85-28442
Ion waves generated by ion loss-cone distributions or drifting particles
[KGI-PREPRINT-070] 20 p3549 N85-32067
Empirical model for the Earth's cosmic ray shadow at 400 KM: Prohibited cosmic ray access
[SH-6.1-14] 23 p4046 N85-35067
Cosmic ray secular variations in terrestrial records and aurorae
[SH-7.1-3] 23 p4047 N85-35096

TESSERAL HARMONICS
Geopotential harmonics of order 15 and 30, from analysis of the orbit of satellite 1971-10B
[RAE-TR-84008] 02 p0165 N85-11121
Individual geopotential coefficients of order 15 and 30, from resonant satellite orbits
[RAE-TR-84021] 08 p1105 N85-16985

TEST BEDS
U TEST EQUIPMENT

TEST CHAMBERS
NT ANECHOIC CHAMBERS
NT HYPERBARIC CHAMBERS
NT PRESSURE CHAMBERS
NT VACUUM CHAMBERS
Natural exposure versus chamber simulation
[AD-A149598] 10 p1495 N85-19437
An environmentally-controlled extended-use small animal hypobaric chamber
[AD-A153735] 19 p3221 N85-29974
A prototype test chamber for fit testing of protective masks in the field
[FOA-C-40208-C1(C2)] 20 p3512 N85-31834
Analysis of performance of dynamic thermal diffusion chamber 21 p3642 N85-32625
A thermal diffusion chamber for the measurement of cloud condensation nuclei 21 p3642 N85-32627
Stable generation of highly monodisperse aerosols 21 p3642 N85-32628
Development of a chemical kinetic mechanism for the US EPA (Environmental Protection Agency) regional oxidant model
[PB85-185858] 22 p3813 N85-33618
Modeling of auto exhaust smog chamber data for EKMA development
[PB85-186492] 22 p3813 N85-33619
Multidimensional analysis of data obtained in experiments with X-ray emulsion chambers and extensive air showers
[HE-3.6-2] 24 p4184 N85-35951

TEST EQUIPMENT
Economic model of calibration improvements for automatic test equipment
[PB84-217627] 01 p0051 N85-10335
A machine for weight-lift testing
[AD-A146816] 07 p0973 N85-16182
Random pattern tracking acceleration tolerance tester
[AD-D011404] 07 p1017 N85-16459
Heater block assembly for use in thermal oxidation testing of jet fuel
[AD-D011430] 08 p1123 N85-17077
Seven-wavelength pyrometer for determining surface temperature of ablation materials
[NASA-TM-77832] 14 p2305 N85-24266
Electromagnetic inspection of wire ropes using sensor arrays
[AD-A155412] 22 p3795 N85-33509
The design and analysis of single flank transmission error tester for loaded gears
[NASA-CR-176163] 23 p3937 N85-34404

TEST FACILITIES
NT ANECHOIC CHAMBERS
NT BLOWDOWN WIND TUNNELS
NT CASCADE WIND TUNNELS
NT CRYOGENIC WIND TUNNELS
NT ENVIRONMENTAL LABORATORIES
NT HYDRAULIC TEST TUNNELS
NT HYPERSONIC WIND TUNNELS
NT LOW SPEED WIND TUNNELS
NT ROCKET TEST FACILITIES
NT SLOTTED WIND TUNNELS
NT SUBSONIC WIND TUNNELS
NT SUPERSONIC WIND TUNNELS
NT TEST RANGES
NT TEST STANDS
NT TRANSONIC WIND TUNNELS
NT WIND TUNNELS
Aeronautical systems technology needs: Escape, rescue and survival, test facilities and test equipment and training-simulation equipment
[AD-A145059] 01 p0001 N85-10002
Characteristics of controlled-oscillating annular cascade test facility with Freon gas
[NAL-TR-812] 01 p0003 N85-10014
Evaluation of hollow fiber ultrafiltration as a pretreatment for reverse osmosis desalination of seawater
[PB84-212406] 01 p0026 N85-10160
The NBS tri-directional test facility
[PB84-217462] 01 p0051 N85-10334
HOST liner cyclic facilities: Facility description 02 p0146 N85-10988
Atmospheric and pressurized low speed wind tunnel performance and cost comparisons
[ARL/AERO-R-160] 02 p0149 N85-11006
Performance of a large area flash chamber prototype
[NOTA-INTERNA-807] 02 p0201 N85-11338
Accelerated stress facility 1976-1983
[AD-A146101] 03 p0359 N85-12303
Space power distribution system technology. Volume 3: Test facility design
[NASA-CR-171230] 04 p0463 N85-12936
Calibration and use of filter test facility orifice plates
[DE84-016851] 04 p0500 N85-13190
The European Space Tribology Laboratory (ESTL) activities report
[ESA-ESTL-61] 05 p0646 N85-14146
Measuring system and data evaluation methods of the test field for wind energy units at Pellworm 05 p0668 N85-14296
High pressure combustion test facility for gas turbine research
[NAL-TR-801] 06 p0757 N85-14845
Heat transfer results and operational characteristics of the NASA Lewis Research Center Hot Section Cascade Test Facility
[NASA-TM-86890] 06 p0808 N85-15133
Advanced mass spectrometers for hydrogen isotope analyses
[DE85-000716] 06 p0811 N85-15150
Visibility monitoring in the southern California desert for the Department of Defense: Research on operations-limiting visual extinction, RESOLVE protocol
[AD-A146617] 06 p0835 N85-15315
The Western Aeronautical Test Range of NASA Ames Research Center
[NASA-TM-85924] 07 p0909 N85-15756
Facility safety study
[NASA-CR-174280] 07 p0910 N85-15759
Equipment for preflight test of an Electronic Countermeasures (ECM) avionic system 07 p0939 N85-15949
National Bureau of Standards passive solar test facility: Instrumentation and site handbook
[PB85-100451/GAR] 07 p0968 N85-16148
Langley Mach 4 scramjet test facility
[NASA-TM-86277] 08 p1089 N85-16883
Electronics systems test laboratory testing of shuttle communications systems 08 p1101 N85-16958
Sensitiveness and explosiveness assessment at Perme Waltham Abbey 08 p1115 N85-17029
On the frontier: Flight research at Dryden 1946-1981
[NASA-SP-4303] 09 p1263 N85-17934
Activities at MI Experimental Design Bureau 09 p1278 N85-18036
High pressure combustion test facility for gas turbine research
[NAL-TR-801] 09 p1283 N85-18065
NASA-VCOSS dynamic test facility
[NASA-TM-86491] 10 p1427 N85-18998
Ground test experiment for large space structures
[NASA-TM-86489] 10 p1429 N85-19013
Theory versus experiment for the rotordynamic coefficients of annular gas seals. Part 1: Test facility and apparatus
[NASA-CR-174409] 10 p1491 N85-19417
Facilities for studing radiation damage in nonmetals during irradiation
[DE85-000590] 10 p1554 N85-19801
New air supply-prime mover facility for engine tests detailed 11 p1621 N85-20204

Use of laser flow visualization techniques in reactor component thermal-hydraulic studies
[DE84-014768] 11 p1639 N85-20330
Major facilities for materials research and related disciplines
[PB85-106850] 11 p1739 N85-20934
A history of full-scale testing of aircraft structures at the National Aeronautical Establishment
[NAE-AN-24] 12 p1777 N85-21153
Heat Cycle Research Experimental Program report, FY-84
[DE85-003558] 12 p1882 N85-21811
AIRLAB: A laboratory for flight-crucial-electronics system research 13 p1968 N85-22362
Activities of the Jet Propulsion Laboratory, 1 January - 31 December 1983
[NASA-CR-175555] 13 p2167 N85-23447
Electric vehicle test program: INEL transition qualification test plan
[DE85-005171] 13 p2169 N85-23456
Welcome to the Saclay Propeller Testing Center
[NASA-TM-77648] 14 p2225 N85-23799
Dynamic verification of large space structures 14 p2234 N85-23847
Modifications to the nozzle test chamber to extend nozzle static-test capability
[NASA-TM-86368] 15 p2464 N85-25216
The design and construction of a flow channel and rig for corrosion studies
[AERE-M-3455] 15 p2508 N85-25474
French consulting firm develops own robotics 15 p2535 N85-25642
Parameterization of a transient electromagnetic facility and test antennas from transient data
[DE85-006231] 15 p2545 N85-25710
Influence of surface roughness on compressor blades at high reynolds number in a two-dimensional cascade
[AD-A151855] 15 p2557 N85-25777
Space reactor ground tests, assessment of facility needs
[DE85-008614] 15 p2650 N85-26345
An assessment of the suitability of the BHGA structural test rig for aerodynamic testing of hang gliders
[CA-8505] 17 p2896 N85-27853
Rotorcraft research testing in the National Full-Scale Aerodynamics Complex at NASA Ames Research Center
[NASA-TM-86687] 17 p2896 N85-27854
Experience with oepration of a large magnet system in the international fusion superconducting magnet test facility
[DE85-009288] 17 p3027 N85-28721
An Impurity Control Test Facility (ICTF) for the study of fusion reactor/plasma edge materials
[DE85-007946] 17 p3040 N85-28810
Research test facility for evaporation and combustion of alternative jet fuels at high air temperatures
[AD-A153830] 18 p3083 N85-29073
New technologies to improve laboratory testing
[DE85-008151] 18 p3110 N85-29257
Operation of HFTF to test the MIT 12 T coil
[DE85-010409] 18 p3195 N85-29821
The DREO (Defence Research Establishment Ottawa) Inertial Navigation Laboratory: Development and test capabilities
[AD-A154425] 19 p3216 N85-29945
Opacity control technique for jet engine test cells
[AD-D011668] 19 p3220 N85-29968
Air Force bid sample testing 20 p3437 N85-31323
MFTF-(alpha) + T shield design
[DE85-010496] 20 p3529 N85-31946
Simulation of automatic control of MFTF-B neutral beams
[DE85-010640] 20 p3530 N85-31960
MHD generator CDIF
[DE85-011389] 20 p3536 N85-32001
Decomposition of sulfuric acid using solar thermal energy
[DE85-012288] 21 p3584 N85-32170
Georgetown University Photovoltaic Higher Education National Exemplar Facility (PHENEF)
21 p3607 N85-32400
Low temperature experimental capability for use with gas guns
[DE85-010418] 22 p3801 N85-33548
Description of a test site for large-scale heavy gas dispersion and combustion experiments
[DE85-004987] 23 p3911 N85-34231
The 1984 biotic studies of Yucca Mountain, Nevada test site, Nye County, Nevada
[DE85-011715] 23 p3951 N85-34487
Design and testing of an energy-absorbing crewseat for the F/FB-111 aircraft. Volume 2: Data from seat testing
[NASA-CR-3917] 24 p4064 N85-35184
A study of the control of particulate emissions from turbine engine test cells 24 p4067 N85-35205

TEST FIRING
NT STATIC FIRING
A metallographic investigation of rotating bands for 7.5 cm artillery projectiles
[FOA-C-20551-D2] 07 p0929 N85-15888
Using a data base management system for modelling SSME test history data 12 p1944 N85-22211
Detonation velocity measurements of the explosives Datasheet C and Amatol
[AD-A152298] 18 p2757 N85-27015
Use of the computer programs PARA 80 to study results from firing the railgun ERGS-1M
[MRL-R-900] 22 p3738 N85-33167
A 1984 environmental summary: Sandia National Laboratories Tonopah Test Range, Tonopah, Nevada
[DE85-011145] 22 p3812 N85-33812

TEST RANGES
The Western Aeronautical Test Range of NASA Ames Research Center
[NASA-TM-85924] 07 p0909 N85-15756
A 1984 environmental summary: Sandia National Laboratories Tonopah Test Range, Tonopah, Nevada
[DE85-011145] 22 p3812 N85-33812

TEST STANDS
DFVLR rotorcraft: Construction and engineering
[NASA-TM-77740] 01 p0006 N85-10035
HOST liner cyclic facilities: Facility description
02 p0146 N85-10988
Possibilities of increasing the simulation quality of multiaxial test stands — vehicle testing
05 p0649 N85-14169
Synthesis of load-time histories resulting from statistical analysis 05 p0650 N85-14171
A tracked vehicle test plant for the simulation of dynamic operation
[AD-P004305] 09 p1410 N85-18682
The detonation of aerosols and vapors of combustible substances under controlled conditions. Part 1: Construction of a test installation
[ISL-R-109/83-PT-1] 14 p2254 N85-23986
Test devices for aeronautical research and technology
[NASA-TM-77651] 17 p2905 N85-27914
Data processing on the rotor test stand at DFVLR in Brunswick: Microprogrammable interfaces and array processor as key components in a PDP 11 real time data acquisition and processing system
[DFVLR-MITT-85-03] 17 p2906 N85-27921
Comparison of simulation with experiment in an RFQ
[DE85-010770] 19 p3349 N85-30757
The design and analysis of single flank transmission error tester for loaded gears
[NASA-CR-176163] 23 p3937 N85-34404

TEST VEHICLES
NT FLIGHT TEST VEHICLES
Energy efficient engine ICLS Nacelle detail design report
[NASA-CR-167870] 02 p0146 N85-10993
A functional vehicle for autonomous mobile robot research
[AD-A150052] 12 p1660 N85-21668
Test plan for performance testing of the Eaton AC-3 electric vehicle
[DE85-011954] 23 p3927 N85-34341

TESTERS
U TEST EQUIPMENT

TESTING
U TESTS

TESTING MACHINES
U TEST EQUIPMENT

TESTS
Experiments on the influence of active walls on the initial amplitudes and growths of instability waves
[AD-A154630] 21 p3583 N85-32275

TETHERED BALLOONS
Preliminary investigation of the electrodynamics of a conducting tether 13 p1997 N85-22521

TETHERED SATELLITES
Proceedings of a Workshop on Applications of Tethers in Space, Executive Summary
[NASA-CR-171195] 03 p0322 N85-12075
Proceedings of a Workshop on the Applications of Tethers in Space, Volume 1
[NASA-CR-171196] 03 p0322 N85-12076
Proceedings of a Workshop on Applications of Tethers in Space, Volume 2
[NASA-CR-171197] 03 p0322 N85-12077
Global matrix of thermospheric density values for selected solar/geomagnetic conditions and spacecraft orbital attitudes
[NASA-TM-86478] 04 p0533 N85-13409
Electrodynamic tethers. 1: Power generator in LEO. 2: Thrust for propulsion and power storage
05 p0611 N85-13901
The investigation of tethered satellite system dynamics
[NASA-CR-171278] 07 p0912 N85-15772
Investigation of dynamic noise affecting geodynamics information in a tethered subsatellite
[NASA-CR-174292] 08 p1174 N85-17405
Applications of Tethers in Space, volume 1
[NASA-CP-2364] 11 p1642 N85-20339
Tethers open new space options
11 p1642 N85-20340
Tethered satellite system project overview
11 p1642 N85-20341
Shuttle tethered satellite system program overview
11 p1642 N85-20342
TSS Satellite overview 11 p1642 N85-20343
Satellite module design 11 p1642 N85-20344
Tether fundamentals 11 p1643 N85-20345
Science Applications, part 1 11 p1643 N85-20346
Science Applications, part 2 11 p1643 N85-20347
Transportation applications, part 2
11 p1643 N85-20350
Technology and test 11 p1643 N85-20353
Summary presentation of the Science Applications Panel 11 p1644 N85-20355
Summary presentation of the technology and test panel 11 p1644 N85-20360
Applications of Tethers in Space, volume 2
[NASA-CP-2365] 11 p1644 N85-20361
Space science and applications
11 p1644 N85-20362
Report of the Electrodynamic Interactions Panel
11 p1645 N85-20363
Report of the Technology and Test Panel
11 p1646 N85-20370
Pultrusion process for fabrication of tethers (preliminary concepts) 11 p1646 N85-20371
Instrumentation for Application Number 1: Mass spectrometric analysis of the boundary layer associated with the tethered satellite 11 p1646 N85-20372
Application Number 3: Using tethers for attitude control 11 p1646 N85-20373
Study proposal for the possible use of ISS as an aerodynamic facility for aerospace applications
11 p1646 N85-20374
Transport processes in the upper atmosphere
11 p1648 N85-20375
Applications of Tethers in Space
[NASA-CP-2366] 12 p1859 N85-21659
Excitation of low-frequency plasma waves by a conducting, tethered satellite 13 p2171 N85-23470
The investigation of tethered satellite system dynamics
[NASA-CR-171433] 15 p2492 N85-25375
The investigation of tethered satellite system dynamics
[NASA-CR-175855] 16 p2731 N85-26854
Shuttle-tethered satellite system definition study extension
[NASA-CR-171473] 17 p2907 N85-27923
Shuttle-tethered satellite system definition study. Volume 1: Executive study
[NASA-CR-171474] 17 p2907 N85-27924
Dynamics and control of tethers in elliptical orbits
20 p3399 N85-31087
Shuttle Molecular Gun: Smog. Potential experiment for the electrodynamic Tethered Satellite System (TSS) mission
[IFSI-84-17] 20 p3419 N85-31221
Investigation of dynamic noise affecting geodynamics information in a tethered subsatellite
[NASA-CR-176031] 20 p3476 N85-31602
Recoverable Plasma Diagnostics Package (RPDP)
23 p3902 N85-34167
Electrodynamic tether 23 p3902 N85-34168
The investigation of tethered satellite system dynamics
[NASA-CR-176180] 24 p4069 N85-35215

TETHERING
Selected tether applications in space: An analysis of five selected concepts
[NASA-CR-171222] 04 p0460 N85-12921
Propellant transfer: Tethered depot
06 p1106 N85-17006
Applications of Tethers in Space, volume 1
[NASA-CP-2364] 11 p1642 N85-20339
Tethers open new space options
11 p1642 N85-20340
Electrodynamic interactions 11 p1643 N85-20348
Transportation applications, part 1
11 p1643 N85-20349
Physiological considerations of artificial gravity
11 p1643 N85-20351
Constellations 11 p1643 N85-20352
Where are we going in tethers
11 p1644 N85-20354

Summary presentation of the Science Applications Panel 11 p1644 N85-20355
Summary presentation of the Electrodynamics Interactions Panel 11 p1644 N85-20356
Summary presentation of the Transportation Panel 11 p1644 N85-20357
Summary presentation to the Artificial Gravity Panel 11 p1644 N85-20358
Summary presentation of the Constellations Panel 11 p1644 N85-20359
Summary presentation of the technology and test panel 11 p1644 N85-20360
Report of the Transportation Panel 11 p1645 N85-20364
Report of the Artificial Gravity Panel 11 p1645 N85-20365
Physiological considerations of artificial gravity 11 p1645 N85-20366
Artificial gravity: Tethers and containers 11 p1645 N85-20367
Report of the Constellations Panel 11 p1645 N85-20368
Some aspects of attitude stability of tethered space stations 11 p1646 N85-20369
The Satellite sail 11 p1647 N85-20376
A functional vehicle for autonomous mobile robot research [AD-A150062] 12 p1860 N85-21666
Selected tether applications in space: Phase 2. Executive summary [NASA-CR-171421] 13 p1987 N85-22462
Selected tether applications in space: Phase 2 [NASA-CR-171422] 13 p1987 N85-22463
Preliminary assessment of power-generating tethers in space and of propulsion for their orbit maintenance 13 p1997 N85-22520
Preliminary investigation of the electrodynamics of a conducting tether 13 p1997 N85-22521
Attitude control tradeoff study between the use of a flexible beam and a tether configuration for the connection of two bodies in orbit 20 p3412 N85-31174
The role of tethers on space station [NASA-TM-86519] 23 p3900 N85-34154

TETHERLINES
Electrodynamic tethers. 1: Power generator in LEO. 2: Thrust for propulsion and power storage 05 p0611 N85-13901
Tether fundamentals 11 p1643 N85-20345
Pultrusion process for fabrication of tethers (preliminary concepts) 11 p1646 N85-20371
Applications of Tethers in Space [NASA-CP-2368] 12 p1859 N85-21659
Stratospheric ClO: In-situ detection with a new approach 16 p2824 N85-27416
Shuttle-tethered satellite system definition study. Volume 1: Executive study [NASA-CR-171474] 17 p2907 N85-27924
Non-backdriveable free wheeling coupling [NASA-CASE-MSC-20475-1] 18 p3116 N85-29290
Dynamics and control of tethers in elliptical orbits 20 p3399 N85-31087

TETRACHLOROMETHANE
U CARBON TETRACHLORIDE

TETRAGONS
NT RECTANGLES

TETRAHYDROFURAN
Development of a lithium secondary battery separator 20 p3444 N85-31378

TETRANITROTETRAZACYCLOOCTANE
U HMX

TETROONS
U SUPERPRESSURE BALLOONS

TEXAS
Hurricane Alicia, Galveston and Houston, Texas, 17-18 August 1983 [PB84-237056] 04 p0541 N85-13441
Stratigraphy of early ordovician El Paso group of the southern Hueco Mountains, Hudspeth County, Texas 09 p1353 N85-18510
On the formation of the nocturnal coastal surface wind speed maximum 09 p1356 N85-18528
Radioactive waste isolation in salt: Peer review of the Office of Nuclear Waste Isolation's report on the organic geochemistry of deep groundwaters from the Palo Duro Basin, Texas [DE85-001439] 10 p1556 N85-19811
Analysis of SMIRR data for volcanic and sedimentary terrains of the trans-Pecos region, Texas 13 p2197 N85-23626
Report on regional groundwater flow modeling for the Palo Duro Basin, Texas [DE85-007490] 16 p2815 N85-27370
Surface hydrologic characteristics of proposed repository locations in the Palo Duro Basin of the Texas Panhandle [DE85-010530] 18 p3126 N85-29355

TEXTILES
Improved uniformity of viscous textile fibers obtained by altering drying procedures 06 p0762 N85-14871
Synthesis of antimicrobial chemical fibers and fibrous materials containing quaternary ammonium compounds and their utilization 06 p0762 N85-14872
Preparation of fire-resistant infusible polycaproamide fiber 06 p0763 N85-14877
Ceramic fabric material testing [DE84-012014] 09 p1300 N85-18185
Italy invents robot to compete with Asea, Hitachi 15 p2535 N85-25643
Substitution of asbestos by aramid fibers and fiber blends in industrial textiles and composites with organic binders [BMFT-FB-T-85-006] 23 p3920 N85-34294
Re-designing a mechanism for higher speed: A case history from textile machinery 23 p3923 N85-34310
A versatile computer package for mechanism analysis 23 p3924 N85-34314

TEXTS
Formats for numerical and textual data in data processing [DFVLR-MITT-84-07] 04 p0551 N85-13504
Electronic generation of text for television [BBC-RD-1984/14] 13 p2053 N85-22856
The acquisition of procedures from text. A production-system analysis of transfer of training [AD-A151029] 14 p2392 N85-24732
A network-based approach to text handling for the online scientific community 15 p2664 N85-26444
NAPGEN: Automatic NAPLPS page generator 23 p3964 N85-34575

TEXTURES
Visual representations subserving texture perception [AD-A145412] 02 p0236 N85-11538
Ion contrasting chamber for discrimination of grains and textures [BMFT-FB-T-84-151] 04 p0477 N85-13036
Late oligocene gabbro near Ketchikan, southeastern Alaska 04 p0518 N85-13307
Microstructure, texture and formability of thin aluminium sheets 06 p0796 N85-15068
Size dependence of chondrule textural types 06 p0862 N85-15606
Texture classification using autoregressive filtering 07 p0984 N85-16254
A wind-tunnel study of the saltation of heterogeneous (size, density) sands 08 p1162 N85-17449
Optical flow and texture variables useful in detecting decelerating and accelerating self-motion [AD-A148716] 09 p1384 N85-18703
Microwave remote sensing of soil moisture 13 p2125 N85-23235
Low altitude texture comparison data base and smooth shaded texture [AD-A150342] 13 p2146 N85-23323
Textural transformations taking place during heat and mechanical treatment in triplex steels [BLL-BISI-TRANS-22404-(6022.06)] 17 p2927 N85-28063
Texture perception and shape from texture [AD-A154276] 19 p3336 N85-30672

TF-34 ENGINE
Nonlinear global stability analysis of compressor stall phenomena [NASA-CR-174908] 19 p3219 N85-29960

TFX AIRCRAFT
U F-111 AIRCRAFT

THAILAND
Ex-minister urges communications satellite development 10 p1476 N85-19316
Communications satellite needs examined 10 p1476 N85-19317
Satellite-computer interface 10 p1476 N85-19318

THALAMUS
Influence of limboreticular complex on some reactions of rabbits 19 p3326 N85-30607

THALLIUM
Abundancies of Ni, Cr, CO and major elements in the silicate portion of the Moon: Constraints from primary lunar magmas 04 p0582 N85-13720

THAWING
U MELTING

THEMATIC MAPPING
Evaluating effectiveness of using space information in specialized hydrogeological research 02 p0164 N85-11114
Technological approach to automation of specialized processing of survey data 02 p0165 N85-11116
Relationships between grass canopy characteristics and LANDSAT Thematic Mapper bands 02 p0213 N85-11402
The Multispectral Imaging Science Working Group. Volume 1: Executive summary [E85-10001] 02 p0213 N85-11404
The Multispectral Imaging Science Working Group. Volume 2: Working group reports [E85-10002] 02 p0213 N85-11405
Geographic science: Executive summary 02 p0214 N85-11408
Geographic science 02 p0214 N85-11409
Land use/land cover 02 p0214 N85-11410
Geomorphology 02 p0214 N85-11411
Cartography 02 p0214 N85-11412
A prospectus for Thematic Mapper research in the Earth sciences [E85-10003] 02 p0215 N85-11416
Executive report: Results of the IRGA-CNPq/INPE experimental project [E85-10011] 02 p0216 N85-11424
Remote sensing applied to forest resources [E85-10012] 02 p0216 N85-11425
A report on the training course at Fortaleza (Ceara) [E85-10013] 02 p0216 N85-11426
Basic principles, methodology, and applications of remote sensing in agriculture [E85-10016] 02 p0217 N85-11429
Mapping land use changes in the carboniferous region of Santa Catarina, report 2 [E85-10017] 02 p0217 N85-11430
Remote sensing applications program [E85-10022] 02 p0218 N85-11435
Application of digital analysis of MSS to agro-environmental studies [E85-10024] 02 p0218 N85-11437
Thematic mapping of likely target areas for the occurence of cassiterite in the Serra do Mocambo (GO) granitic massifs using LANDSAT 2 digital imaging [E85-10027] 02 p0219 N85-11440
The mapping of the Sun at 8 mm wavelength and tracking of the active regions in the period 23 May - 5 June 1983 [REPT-S-149] 02 p0297 N85-11924
Assessment of computer techniques for processing digital LANDSAT MSS data for lithological discrimination of Serra do Ramalho, State of Bahia [E85-10033] 03 p0378 N85-12412
LANDSAT instruments characterization [E85-10029] 05 p0654 N85-14198
Integration of multiple thematic data with LANDSAT data: Some results about the feasibility of Mediterranean land cover inventories 05 p0655 N85-14205
The integrated use of digital cartographic data and remotely sensed imagery 05 p0655 N85-14206
Monitoring and mapping global vegetation cover using data from meteorological satellites 05 p0656 N85-14211
Statistics and mapping of land uses by means of LANDSAT MSS imagery 05 p0657 N85-14219
The use of Thematic Mapper data for land cover survey 05 p0657 N85-14220
Metric evaluation of SAR-580 optical images for cartographic purposes 05 p0659 N85-14231
Combining Heat Capacity Mapping Mission (HCMM) LANDSAT and thematic map information into a unique high precision merged multichannel system — climatology 05 p0660 N85-14239
A field control methodology of remotely sensed data for statistical purposes: An example of SPOT simulated data in eastern Belgium — land use statistics 05 p0660 N85-14241
Evaluation of SIR-B imagery for geologic and geomorphic mapping, hydrology, and oceanography in Australia 08 p1146 N85-17229
Structural investigation of the Grenville Province by radar and other imaging and nonimaging sensors 08 p1147 N85-17237
Investigation of SIR-B images for lithologic mapping 08 p1148 N85-17241
Analysis of terrestrial conditions and dynamics [E85-10063] 08 p1174 N85-17401
Advanced technology for hydrographic mapping [FOA-C-30371-E1] 08 p1176 N85-17418
Analysis of data acquired by synthetic aperture radar and LANDSAT Multispectral Scanner over Kershaw County, South Carolina, during the summer season [E85-10071] 10 p1503 N85-19485
Study of spectral/radiometric characteristics of the Thematic Mapper for land use applications [E85-10075] 10 p1504 N85-19489
Spectroradiometric calibration of the Thematic Mapper and Multispectral Scanner system [E85-10077] 10 p1504 N85-19491
Thematic Mapper: Design through flight evaluation [E85-10078] 10 p1504 N85-19492
LANDSAT-4 Science Characterization Early Results. Volume 2, part 1: Thematic Mapper (TM) [E85-10066] 11 p1668 N85-20508
An overview of LANDSAT-4 and the Thematic Mapper 11 p1668 N85-20509

Radiometric calibration and processing procedure for reflective bands on LANDSAT-4 protoflight Thematic Mapper 11 p1668 N85-20510
An overview of the Thematic Mapper geometric correction system 11 p1668 N85-20511
TM digital image products for applications 11 p1668 N85-20512
Canadian plans for Thematic Mapper data 11 p1668 N85-20513
Characterization of radiometric calibration of LANDSAT-4 reflective bands 11 p1669 N85-20516
LANDSAT-4 Science Characterization Early Results. Volume 3, part 2: Thematic Mapper (TM) [E85-10089] 12 p1869 N85-21724
Thermal band characterization of the LANDSAT-4 Thematic Mapper 12 p1869 N85-21727
A preliminary assessment of LANDSAT-4 Thematic Mapper data — Windsor, Ontario and Medicine Hat areas, Canada 12 p1869 N85-21728
Preliminary evaluation of the radiometric calibration of LANDSAT-4 Thematic Mapper data by the Canada Centre for Remote Sensing 12 p1870 N85-21729
A preliminary analysis of LANDSAT-4 Thematic Mapper radiometric performance 12 p1870 N85-21730
A preliminary evaluation of LANDSAT-4 Thematic Mapper data for their geometric and radiometric accuracies 12 p1871 N85-21739
Spatial resolution estimation of LANDSAT-4 Thematic Mapper data 12 p1872 N85-21741
An analysis of the high frequency vibrations in early Thematic Mapper scenes 12 p1872 N85-21742
Tests of low-frequency geometric distortions in LANDSAT 4 images 12 p1872 N85-21744
Investigation of TM band-to-band registration using the JSC registration processor 12 p1872 N85-21745
Geodetic accuracy of LANDSAT 4 Multispectral Scanner and Thematic Mapper data 12 p1873 N85-21746
Investigations of vegetation and soils information contained in LANDSAT Thematic Mapper and Multispectral Scanner data [E85-10082] 12 p1873 N85-21747
Remote sensing research for agricultural applications — San Joaquin County, California and Snake River Plain and Twin Falls area, Idaho [E85-10090] 12 p1873 N85-21752
LANDSAT 4 band 6 data evaluation [E85-10093] 12 p1874 N85-21755
Spectroradiometric calibration of the Thematic Mapper and Multispectral Scanner system [E85-10094] 12 p1874 N85-21756
LANDSAT 4 investigations of Thematic Mapper and Multispectral Scanner applications — Drum Mountains, Utah and Tonopath, Nevada [E85-10095] 12 p1874 N85-21757
Review of computer mapping and display techniques applicable to regional analysis [DE85-003545] 12 p1875 N85-21764
Experience in combined special mapping using space information 13 p1984 N85-22449
LANDSAT-4 Science Characterization Early Results. Volume 4: Applications — agriculture, soils land use, geology, hydrology, wetlands, water quality, biomass identification, and snow mapping [E85-10070] 13 p2117 N85-23186
Overview of TM applications research reports 13 p2117 N85-23187
Impact of Thematic Mapper sensor characteristics on classification accuracy — suburban Washington, D.C., Maryland, and the Chesapeake Bay 13 p2117 N85-23188
Analysis and evaluation of the LANDSAT-4 MSS and TM sensors and ground data processing systems: Early results 13 p2117 N85-23189
Characterization of LANDSAT-4 TM and MSS image quality for the interpretation of California's agricultural resources — Central Valley 13 p2118 N85-23190
Evaluation of Thematic Mapper performance as applied to hydrocarbon exploration — Ontario, Canada; Cement, Oklahoma; and Death Valley, California 13 p2118 N85-23191
Geologic utility of LANSDAT-4 TM data — Death Valley, California and the Silver Bell area of southern Arizona 13 p2118 N85-23192
An initial analysis of LANDSAT-4 Thematic Mapper data for the discrimination of agricultural, forested wetlands, and urban land cover — Poinsett County, Arkansas; and Reelfoot Lake and Union City, Tennessee 13 p2118 N85-23193
Preliminary evaluation of Thematic Mapper image data quality 13 p2118 N85-23194
Assessment of computer based geologic mapping of rock units in the LANDSAT-4 scene of northern Death Valley, California 13 p2119 N85-23195
A concept for the processing and display of Thematic Mapper data 13 p2119 N85-23196
Quick look analysis of TM data of the Washington, District of Columbia, area 13 p2119 N85-23197
Remote sensing of coastal wetlands biomass using Thematic Mapper wavebands — Lewes, Delaware 13 p2119 N85-23198
A preliminary comparison of the information content of data from the LANDSAT 4 Thematic Mapper and Multispectral Scanner — Arkansas 13 p2119 N85-23199
Early results of investigations of LANDSAT 4 Thematic Mapper and Multispectral Scanner applications — Washington, D.C. 13 p2119 N85-23200
Thematic Mapper data quality and performance assessment in renewable resources/agriculture/remote sensing 13 p2120 N85-23201
Preliminary comparisons of the information content and utility of TM versus MSS data 13 p2120 N85-23202
A first evaluation of LANDSAT TM data to monitor suspended sediments in lakes — Lake Chicot, Arkansas 13 p2120 N85-23204
Snow reflectance from Thematic Mapper 13 p2120 N85-23205
Preliminary evaluation of TM for soils information 13 p2121 N85-23206
Preliminary study of information extraction of LANDSAT TM data for a suburban/regional test site 13 p2121 N85-23208
Comparative techniques used to evaluate Thematic Mapper data for land cover classification in Logan County, West Virginia 13 p2121 N85-23209
Comparison of MSS and TM data for landcover classification in the Chesapeake Bay area: A preliminary report — Taylor's Island, Maryland 13 p2121 N85-23210
Comparison of land cover information from LANDSAT Multispectral Scanner (MSS) and airborne Thematic Mapper simulator (TMS) data for hydrologic applications — Clinton River Basin, Michigan 13 p2122 N85-23211
Relative accuracy assessment of LANDSAT-4 MSS and TM data for level 1 land cover inventory — Washington, D.C. 13 p2122 N85-23212
An investigation of several aspects of LANDSAT-5 data quality — Palmer County, Shelby, mt; White sands, NM; Great Salt Lake, UT; San Matted Bridge and Sacramento, California [E85-10096] 13 p2122 N85-23214
Studies on physical properties of snow based on multi channel microwave radiometer 13 p2125 N85-23231
Analysis of NIMBUS-7 SMMR data — Hokkaido, Japan snow cover 13 p2125 N85-23232
CNPq/INPE LANDSAT system: Report of activities from October 1, 1983 to September 30, 1984 — Brazil [E85-10097] 16 p2808 N85-27318
Shuttle imaging radar-A (SIR-A) data analysis — geology of the Ozark Plateau of southern Missouri, land use in western Illinois, and vegetation types at Koonamore Station, Australia [NASA-CR-175785] 16 p2809 N85-27324
Raster or vector processing. Experience with the application of programs for the construction of thematic maps with boundary design in the Lower Saxony (West Germany) Land Administration for ground research 16 p2815 N85-27365
Microcomputer processing of LANDSAT Thematic Mapper data for the acquisition of military tactical terrain data [AD-A154781] 21 p3605 N85-32389
Comprehensive mapping of arid territories of Arizona using space photography 22 p3737 N85-33164
How map designers can represent their ideas in thematic maps: Effective user interfaces for thematic map design 23 p3952 N85-34562
LANDSAT-4/5 image data quality analysis [E85-10105] 24 p4107 N85-35463
Study of spectral/radiometric characteristics of the Thematic Mapper for land use applications [E85-10106] 24 p4107 N85-35464
Geology and geomorphology of the Roraima group, southeastern Venezuela 24 p4115 N85-35511

THEODOLITES
Testing of a field portable GPS (Global Positioning System) geodetic receiver [AD-A148336] 08 p1082 N85-16859
Experience in use of optical theodolite for machine construction 14 p2267 N85-24049

THEOREM PROVING
Cores of tangent cones and Clarke's tangent cone [CSIR-TWISK-314] 01 p0108 N85-10727
Boundary behavior of analytic functions, analytic wave front sets and the intersection problem of Ehrenpreis [PREPRINT-809] 01 p0114 N85-10778
Simplified proofs of some basic theorems for quasiregular mappings 10 p1535 N85-19677
The Chinese remainder theorem and multi-PRF radars [AD-A141375] 13 p2054 N85-22858

THEOREMS
NT BAYES THEOREM
NT BERNOULLI THEOREM
NT DUALITY THEOREM
NT EQUIPARTITION THEOREM
NT EXISTENCE THEOREMS
NT FLOQUET THEOREM
NT GAUSS-MARKOV THEOREM
NT POYNTING THEOREM
NT RECIPROCITY THEOREM
NT SIMILARITY THEOREM
NT STOKES THEOREM (VECTOR CALCULUS)
NT UNIQUENESS THEOREM
NT VIRIAL THEOREM
Cores of tangent cones and Clarke's tangent cone [CSIR-TWISK-314] 01 p0108 N85-10727
A non-commutative quasi subadditive ergodic theorem [AD-A146810] 07 p1037 N85-16581
A theorem on the optimal allocation of effort [AD-A148028] 08 p1211 N85-17623
Signal reconstruction from Fourier transform sign information [AD-A148039] 08 p1211 N85-17624
Dynamics and control of general linear lumped-parameter systems 09 p1372 N85-18623
Computing the Kac determinant using dual mode techniques and more about the No-ghost theorem [DE85-001329] 09 p1375 N85-18640
Simplified proofs of some basic theorems for quasiregular mappings 10 p1535 N85-19677
Statistical analysis techniques for small sample sizes [NASA-CR-171872] 15 p2639 N85-26279
Extension of three theorems of Fourier series on the disc to the torus [AD-A153017] 17 p3019 N85-28609
Central limit theorems in the area of large deviations for some dependent random variables [AD-A153125] 17 p3043 N85-28831
Some relations among directions of curves at an invariant point on a thermodynamic phase diagram 19 p3312 N85-30530
A note on a theorem of R. Duffin [AD-A154786] 21 p3676 N85-32838
A system of magnetohydrodynamic-type equations 21 p3693 N85-32946

THEORETICAL PHYSICS
NT NEWTON THEORY
NT QUANTUM THEORY
Research program in theoretical high-energy physics [DE84-013717] 01 p0119 N85-10817
USSR report: Physics and mathematics [JPRS-UPM-84-006] 02 p0256 N85-11678
Research in elementary particle physics [DE84-013520] 02 p0279 N85-11815
Theoretical studies in tandem mirror physics [DE84-015634] 04 p0566 N85-13604
Activities report in nuclear physics 05 p0728 N85-14680
Testing theories of superluminal motion — QUASAT 07 p1058 N85-16714
Experimental and theoretical high energy physics [DE85-000844] 11 p1726 N85-20858
Theoretical nuclear physics [DE85-003486] 12 p1932 N85-22135
Research in theoretical physics [DE85-004286] 12 p1944 N85-22207
Theoretical aspects of electroweak and other interactions in medium-energy nuclear physics [DE85-003821] 13 p2157 N85-23392
Research in theoretical nuclear physics [DE85-006172] 14 p2418 N85-24920
Field near the front of a signal in a waveguide accomplished with dispersive plasma [REPT-11/1984] 16 p2768 N85-27083
Activities report in nuclear physics and particle acceleration 20 p3532 N85-31977
Bergson and the unification of the sciences [DE85-009961] 20 p3538 N85-32018
USSR report: Physics and mathematics [JPRS-UPM-85-004] 21 p3680 N85-32860

THEORIES
On the validation of computer science theories [AD-A148637] 08 p1203 N85-17572

THERAPY
NT CHEMOTHERAPY
NT RADIATION THERAPY
Influence of activation of ASFS-2 on human emotional status 08 p1194 N85-17522
Management of vibration sickness in coal mines by hyperbaric oxygenation 10 p1523 N85-19809
Comparative assessment of different treatment modalities in miners with vibration- and noise-induced disease 10 p1524 N85-19810

Management of microcirculatory disorders in vibration sickness 10 p1524 N85-19611
Modulated sinusoidal currents in management of vibration sickness 10 p1524 N85-19612

THERMAL ABSORPTION
Selective coatings for solar-to-thermal energy converters 14 p2280 N85-24127
Thickness-insensitive selective surface paint [DE85-010568] 19 p3250 N85-30150
Heat-mass flow enhancement system for a metal hydride assembly [DE85-010698] 22 p3783 N85-33441

THERMAL AGITATION
U THERMAL ENERGY

THERMAL ANALYSIS
Energy efficient engine combustor test hardware detailed design report [NASA-CR-167945] 02 p0140 N85-10950
Simulation of solidification in a Bridgman cell [NASA-CR-3643] 02 p0197 N85-11314
HIP glassmaking for high nitrogen compositions in the Y-Si-Al-O-N system [DE84-015546] 03 p0336 N85-12175
An experimental investigation and numerical simulation of the thermomechanical phenomena in compressor rotor tip rubbing 03 p0367 N85-12352
Technical activities 1983, Office of Nondestructive Evaluation [PB84-217074] 03 p0370 N85-12360
Accurate measurement of heat capacity by differential scanning calorimetry 04 p0468 N85-12975
Thermal and mechanical analysis of major components for the advanced adiabatic diesel engine 04 p0508 N85-13243
Special soft solder TK-3 (L-SnCu 3 - DIN 1707) [BLL-T6384/BG/WH799/84(9022.48)] 06 p0767 N85-14907
Semicrystalline casting process development and verification 06 p0832 N85-15289
Reduction method for thermal analysis of complex aerospace structures [NASA-TP-2373] 07 p0957 N85-16066
A critical analysis of ocean thermal analysis models in operation at FNOC (Fleet Numerical Oceanography Centers) [AD-A148731] 09 p1359 N85-18547
Development of media for dynamic latent heat storage for the low-temperature range. Part 1: Thermal analyses of selected salt hydrate systems [NASA-TM-77778] 10 p1507 N85-19510
Theoretical interpretation of thermal arrest data from differential thermal analysis measurements 12 p1949 N85-22241
Applications of high pressure differential scanning calorimetry to aviation fuel thermal stability research [NASA-TM-87002] 14 p2249 N85-23941
NASTRAN's application in agricultural engineering 15 p2575 N85-25680
Analysis of physical-chemical processes governing SSME internal fluid flows [NASA-CR-175693] 17 p2957 N85-28261
Electrical conductivity and phase diagram of binary alloys. 21: The system palladium-chromium [NASA-TM-77863] 18 p3073 N85-29009
Binary phase diagram determinations [DE85-010856] 19 p3235 N85-30058
Improved Nominal Operating Cell Temperature (NOCT) test procedure 21 p3612 N85-32449

THERMAL BATTERIES
Synthesis and properties of Hexachloromolybdates(5) and related species [AD-A139599] 07 p0924 N85-15852
Thermal design requirements of a 50-kW zinc/redox flow battery for solar electrical energy storage [DE84-017088] 09 p1345 N85-18483
Robotic thermal battery pellet fabrication [DE85-007755] 16 p2779 N85-27154
Additional experiments relative to the shelf life of Li(Si)/FeS2 thermal batteries [DE85-006482] 18 p3095 N85-29162
Burn front velocity as a function of pellet density in iron-potassium perchlorate heat powders [DE85-011448] 21 p3572 N85-32214

THERMAL BLOOMING
Ground-up-to-Space (GUTS) laser propagation code description and manual [AD-A150783] 14 p2309 N85-24295
Ship-to-ship propagation: Maritime data analyses [AD-A155484] 21 p3592 N85-32325

THERMAL BOUNDARY LAYER
Qualification of the T2 wind tunnel in cryogenic operation. A: Thermal field, preliminary study of a schematic model [NASA-TM-77761] 14 p2227 N85-23805
Structure of cold film in water-air boundary layer 14 p2335 N85-24443

THERMAL CONDUCTIVITY
Simulation of solidification in a Bridgman cell [NASA-CR-3643] 02 p0197 N85-11314
Thermal conductivity of iron/potassium perchlorate heat powder [DE84-017071] 04 p0476 N85-13035
Thermal conductivity and interface resistance of particle-filled silicone resin [DE84-011681] 04 p0479 N85-13056
Insulating polymer concrete [DE84-017239] 04 p0480 N85-13057
Geothermal studies in Alaska: Conditions at Prudhoe Bay 04 p0516 N85-13290
Thermal properties of soils and soils testing [DE84-015312] 04 p0525 N85-13360
Megaregolith thickness, heat flow, and the bulk composition of the Moon 04 p0583 N85-13723
High temperature thermoelectric energy conversion 05 p0610 N85-13894
Thermal contact conductance measurements on Doublet 3 armor tile graphite [DE84-013554] 05 p0613 N85-13916
Thermal diffusivity and conductivity of chromium-manganese alloying compositions [BLL-M-35925-(5828.4)] 05 p0616 N85-13938
Salt-gradient solar ponds: Summary of US Department of Energy sponsored research [NASA-CR-174183] 05 p0667 N85-14286
Solar pond research at Argonne National Laboratory 05 p0667 N85-14291
Thermal conductivity of aluminum, copper, iron and tungsten for temperature from 1 K to the melting point [PB84-235878] 06 p0770 N85-14924
Test your contacts by measuring their constriction resistance [BLL-WH-611-(9091.9F)] 07 p0944 N85-15978
Analysis of the heating process of a body in a melt [BLL-M-36014-(5828.4)] 07 p0956 N85-16057
Thermal evaporation in blast waves: A model for aneurism formation in the NRL (Naval Research Laboratory) LASER-HANE simulation experiment [AD-A147006] 07 p0978 N85-16210
Computer program to compute soil thermal conductivity from transient temperature measurements [PB85-100550] 07 p0998 N85-16341
Wave absorption and transport studies on Electron Cyclotron Resonance (ECR) heated stellarator plasmas in W 7-A [IPF-84-9] 09 p1395 N85-18782
Transport properties of the outer crust of magnetic neutron stars 09 p1415 N85-18927
Analysis of compact heat exchanger performance [DE84-012624] 10 p1485 N85-19377
Some specifics of methods for mass detailed studies of rock heat conductivity 10 p1502 N85-19477
U, Th, K content, heat production and thermal conductivity of Sao Paulo, Brazil continental shelf sediments: A reconnaissance work [INPE-3401-PRE/670] 10 p1515 N85-19558
Generation of Alfven waves due to thermal modulation of the electrical conductivity [AD-A149389] 10 p1558 N85-19826
Thickness effect in low-density insulation [DE85-003065] 11 p1631 N85-20273
Theoretical and experimental analysis of vertical, concentric-tube ground-coupled heat exchangers [DE85-000474] 11 p1633 N85-20286
Operational characteristics of the OMEGA short-wavelength laser fusion facility [DE85-002819] 11 p1640 N85-20334
Temperature responses of composite panels [AD-A150053] 12 p1798 N85-21277
Update of thermal conductivity and electrical resistivity of electrolytic iron, tungsten and stainless steel [PB85-115814] 12 p1803 N85-21311
Simulation of thermal and electromagnetic processes in induction plasmatrons 12 p1841 N85-21552
Effect of variable solid phase thermal properties on propellant combustion 13 p2002 N85-22547
Thermally stimulated conductivity in semi-insulating gallium arsenide 13 p2088 N85-23036
Time resolved X-ray studies during pulsed laser irradiation of Ge [DE85-005263] 13 p2097 N85-23083
Electrical and thermal transport property studies of high-temperature thermoelectric materials [AD-A150167] 13 p2163 N85-23417
H-division materials physics progress [DE85-004990] 13 p2165 N85-23430
Electrical and thermal transport property studies of high-temperature thermoelectric materials [AD-A150900] 14 p2427 N85-24957
Transformation toughened ceramics: A potential material for light diesel engine applications [AD-A151413] 15 p2518 N85-25525
Transformation toughened ceramics: A potential material for light diesel engine application [AD-A151421] 15 p2518 N85-25526
Directional thermal conductivities of graphite-epoxy composites: 0/90 and 0/+ or - 45/90 [AD-A152209] 16 p2743 N85-26929
Characterization-curing-property studies of HBRF 55A resin formulations [NASA-CR-175836] 16 p2753 N85-26989
Conducting a thermal conductivity survey [NASA-CR-175792] 16 p2782 N85-27166
In situ Tuff water migration/heater experiment [DE85-010415] 18 p3101 N85-29200
Development of a high-temperature coolant for advanced diesel engines [AD-A153680] 18 p3117 N85-29297
Thermophysical properties correlations and pseudocomponent characterization parameter estimation for fossil fluids [DE85-009297] 19 p3230 N85-30024
Clearing of polydisperse aqueous aerosol by laser radiation pulses 19 p3298 N85-30445
Approximate solution to the problem of heating massive bodies by radiation [BLL-M-36272-(5828.4)] 20 p3450 N85-31422
Basic cryogenics and materials. Phase 1 [NASA-CR-177932] 21 p3572 N85-32215
In-situ measurement of wall thermal performance: Data interpretation and apparatus design recommendations [DE85-011979] 21 p3586 N85-32289
The design, construction and operation of a large-area, high-temperature, thermal conductance apparatus — furnace insulation [NPL-DMA(A)-84] 22 p3786 N85-33455
The properties of thin-section, four-point-contact ball bearings in space 22 p3797 N85-33521
Development of improved thermoelectric materials for space nuclear power systems [DE85-013079] 22 p3844 N85-33807
Poly-functional building material from fiberglass (its fabrication and properties) 23 p3908 N85-34209
Finding the roots of the transcendental equations in problems in determining the thermal conductivity of spheres with heterogeneous boundary conditions [BLL-M-35878-(5828.4)] 23 p3929 N85-34347
Calculation of roots of transcendental equations in problems of determining thermal conductivity of cylinder with non-uniform boundary conditions [BLL-M-35788-(5828.4)] 23 p3929 N85-34349
Sequential regularization solution of the inverse heat conduction problem [DE85-010657] 23 p3931 N85-34362
Confinement experiments on ISX-B [DE85-012346] 23 p3984 N85-34709

THERMAL CONTROL COATINGS
Optimization of the NiCrAl-Y/ZrO-Y2O3 thermal barrier system [NASA-TM-86905] 07 p0927 N85-15878
Evaluation of colorless polyimide film for thermal control coating applications [NASA-TM-86341] 07 p0930 N85-15894
Challenges in the development of the orbiter active thermal control subsystem 08 p1096 N85-16923
Thermal design of the space shuttle solid rocket booster 08 p1103 N85-16976
Thermal design of the space shuttle external tank 08 p1103 N85-16977
Space environment simulation to test satellite thermal control coatings, volume 1 [CERT-4128-VOL-1] 08 p1109 N85-17012
Space environment simulation to test satellite thermal control coatings. Volume 2: Annex 1 [ESA-CR(P)-1870-VOL-2] 08 p1109 N85-17013
Space environment simulation to test satellite thermal control coatings. Volume 2: Annexes 2, 3, 4 [ESA-CR(P)-1870-VOL-3] 08 p1109 N85-17014
An investigation of enhanced capability thermal barrier coating systems for diesel engine components [NASA-CR-174820] 09 p1298 N85-18154
Antifriction properties of gas thermal coatings of clad carbine powders 10 p1447 N85-19115
Influence of temperature on wear resistance of detonation coatings of alloy powders 10 p1447 N85-19116
Method of determining thermal stability of heat-resistant coatings on graphite 10 p1447 N85-19117
Contactless determination of the conductivity of the white paint PCB-Z — Giotto spacecraft thermal control coating 14 p2243 N85-23907
Rocket thrust chamber thermal barrier coatings 16 p2734 N85-26867
Vacuum plasma coatings for turbine blades 16 p2734 N85-26869
Erosion of corrosion-resistant surface treatments on alloy steels [DE85-006446] 17 p2932 N85-28100

Advanced thermal barrier system bond coatings for use on Ni, Co-, and Fe-base alloy substrates
[NASA-TM-87062] 20 p3431 N85-31283
Energy efficient engine, high pressure turbine thermal barrier coating. Support technology report
[NASA-CR-168037] 24 p4066 N85-35199

THERMAL CONVECTION
U FREE CONVECTION

THERMAL CURRENTS
U CONVECTIVE FLOW

THERMAL CYCLING TESTS
HOST instrumentation R and D program overview
02 p0141 N85-10957
Validation of structural analysis methods using the in-house liner cyclic rigs 02 p0146 N85-10987
HOST liner cyclic facilities: Facility description
02 p0146 N85-10988
Influence of thermal cycling on the behavior of CFRP material for space structures 05 p0626 N85-14013
In-flight evalution of LCF life consumption of critical rotor components subjected to high transient thermal stress
07 p0906 N85-15734
Ion implantation and laser processing of III-V compound semiconductors with applications to the fabrication of microwave devices
[AD-A146846] 07 p1047 N85-16851
Damage to boron fibers during thermal cycling and annealing 10 p1445 N85-19107
NASA welding assessment program
[NASA-CR-175512] 12 p1859 N85-21661
Change in microstructure of heat-resistant nickel alloys upon thermal cycling in a current of gas
13 p2031 N85-22725
The cyclic stress-strain behavior of nickel-base superalloy poly- and single crystals
14 p2254 N85-23969
Rocket thrust chamber thermal barrier coatings
16 p2734 N85-26867
Downdraw extrusion of ULE(TM) glass
[AD-A153783] 18 p3079 N85-29048
Thermal-cycle testing of the G-tunnel heated block
[DE85-008408] 18 p3126 N85-29359
Effect of heating temperature in a vacuum on state of surface layers of welded OT4 titanium alloy
19 p3245 N85-30123
Electrical resistivity and hysteresis of the equiatomic nickel-titanium alloy near the martensitic transformation temperature 23 p3904 N85-34161
X-ray measurement of thermal stresses in tungsten fiber-copper composites 23 p3907 N85-34205

THERMAL DECOMPOSITION
NT PYROLYSIS
Fire retardant cellulosehydrate fibers
06 p0761 N85-14870
Critical analysis of nitramine decomposition data. Preliminary comments on autoacceleration and autoinhibition in HMX and RDX decomposition
[AD-A146570] 06 p0774 N85-14946
Description and operation of a thermal decomposition unit-gas chromatographic system
[PB84-246362] 07 p0968 N85-16148
Synthesis, static and reactive characterization of supported organometallics
[DE85-004265] 12 p1808 N85-21340
The use of hydrazine as an alternate source of energy
[NASA-CR-175535] 12 p1817 N85-21397
A computer controlled mass spectrometer system for investigating the decomposition of non-metallic materials under atmospheric conditions 12 p1948 N85-22237
Kinetics of mechanism of the thermal decomposition of dimethylnitramine and dimethylnitrosamine
13 p2004 N85-22559
Theory of relaxation processes in decomposing polymer materials during high-intensity convective heating
13 p2028 N85-22710
Metallic and metalloceramic coating by thermal decomposition
[NASA-TM-86992] 13 p2036 N85-22755

THERMAL DEFOCUSING
U THERMAL BLOOMING

THERMAL DEGRADATION
Thermal ageing studies of 9%Cr 1%Mo steel
[AERE-R-11100] 03 p0333 N85-12149
Liquid phase products and solid deposit formation from thermally stressed model jet fuels
[NASA-TM-86874] 04 p0481 N85-13066
Pathophysiological study of poisoning due to thermal degradation of materials — aircraft cabins
[CERMA-84-15] 11 p1692 N85-20640
Material thermolysis product toxicity: Definition of a hazard evaluation methodology
[CERMA-84-09] 11 p1692 N85-20641
Evaluation of infrared reflectance as a technique for measuring absorber materials degradation
[DE85-002171] 11 p1729 N85-20874
Laboratory studies of Kapton degradation in an oxygen ion beam 13 p1990 N85-22477
Structure-property relationships in polymeric matrix materials
[AD-A153929] 18 p3080 N85-29050
Absorber coatings degradation
[DE85-008628] 18 p3128 N85-29367
CP DDT detonators. 4: Thermal aging
[DE85-011172] 19 p3251 N85-30160
Photothermal degradation studies of encapsulants
21 p3606 N85-32403
Micromolecular modeling 21 p3606 N85-32405

THERMAL DIFFUSION
Stresses and strains in lithosphere caused by Earth's thermoconvective oscillations 06 p0822 N85-15217
Noncontact photo-thermal probe-beam deflection measurement of thermal diffusivity in an confined hot gas
[AD-A147481] 07 p0971 N85-16170

THERMAL DIFFUSIVITY
Analysis of performance of dynamic thermal diffusion chamber 21 p3642 N85-32625
A thermal diffusion chamber for the measurement of cloud condensation nuclei 21 p3642 N85-32627
Noncontact photo-thermal probe-beam deflection measurement of thermal diffusivity in an confined hot gas
[AD-A147481] 07 p0971 N85-16170
Optical beam deflection detection of thermal waves in opaque solids 19 p3374 N85-30927
Characterization of the optical and thermal properties of matter by photothermal techniques
[DE85-012607] 24 p4076 N85-35260

THERMAL DISSOCIATION
Jet fuel property changes and their effect on producibility and cost in the U.S., Canada, and Europe
[NASA-CR-174840] 16 p2757 N85-27012

THERMAL EFFECTS
U TEMPERATURE EFFECTS

THERMAL EFFICIENCY
U THERMODYNAMIC EFFICIENCY

THERMAL EMISSION
NT THERMIONIC EMISSION
Surface coatings for low emittance in the thermal surveillance band
[MRL-R-937] 03 p0336 N85-12158
Absorption and emission of EUV radiation by the local ISM 06 p0876 N85-15563
Exploration of the solar system by airborne astronomy
08 p1244 N85-17851
Continuous laminar smoke generator
[NASA-CASE-LAR-13014-1] 12 p1781 N85-21178
Hot spots on Io: Correlation of infrared emission and visible reflectance 13 p2172 N85-23475
Pressed boride cathodes
[NASA-TM-77821] 17 p2918 N85-27984

THERMAL ENERGY
Control and performance of a photovoltaic-thermal energy system 03 p0367 N85-12475
Possibilities of conjugating binary solutions for thermal energy storage
[DE84-016704] 04 p0531 N85-13392
Deputy Minister discusses plans for geothermal power
07 p0994 N85-16313
Electrodynamic interactions 11 p1643 N85-20348
Solar Thermal Research Program
[DE85-000514] 18 p3131 N85-29388
Advanced evacuated tube collectors
[DE85-010271] 19 p3274 N85-30302
Thermal Energy Storage Program annual operating plan FY 1985
[DE85-008745] 19 p3307 N85-30499
Decomposition of sulfuric acid using solar thermal energy
[DE85-012288] 21 p3564 N85-32170
Design and development of a linear thermal actuator
22 p3796 N85-33518
Study of alternative system conversions for the Solar One pilot plant
[DE85-010026] 22 p3809 N85-33594
Heat transfer coefficients for particles in liquid in axially rotating cans 24 p4093 N85-35370

THERMAL ENERGY STORAGE
U HEAT STORAGE

THERMAL ENVIRONMENTS
Thermal management technology status
05 p0610 N85-13895
In-flight testing of the space shuttle orbiter thermal control system 08 p1103 N85-16074
NASA welding assessment program
[NASA-CR-175683] 15 p2568 N85-25845
Thermal annealing of Fe implanted Al2O3 in oxidizing and reducing environment: Revised version
[DE85-007548] 16 p2752 N85-26983
The study of thermal forecasting for gliding
16 p2830 N85-27453
Downdraw extrusion of ULE(TM) glass
[AD-A153783] 18 p3079 N85-29048
Improved Nominal Operating Cell Temperature (NOCT) test procedure 21 p3612 N85-32449
Filament wound structures in PSP carbon composite
[RV10/84424] 22 p3743 N85-33198
A kinetic model for predicting oxidative degradation rates in combined radiation-thermal environments
[TI85-002629] 24 p4100 N85-35414

THERMAL EXPANSION
Self-similar expansion of dense matter due to heat transfer by nonlinear conduction
[MPQ-81] 01 p0048 N85-10297
Method for calculating linear shrinkage and expansion of metals and alloys
[BLL-M-35747-(5828.4)] 02 p0175 N85-11173
Thermal deformation measurements of heat-resistant structural materials for aircraft by electro optical displacement transducer
[NAL-TR-810] 03 p0325 N85-12092
Investigation of the relations between neat resin and advanced composite mechanical properties. Volume 1: Results
[NASA-CR-172303] 05 p0612 N85-13911
The dimensional stability of advanced composite antenna reflectors: Analytical and test evaluation — satellite antennas 05 p0626 N85-14014
Thermal stress-dependent dilation of concrete
[DE84-014688] 11 p1653 N85-20412
Fracture mechanics evaluation of GaAs
[NASA-CR-175857] 13 p2102 N85-23101
Extreme precision antenna reflector study results
14 p2232 N85-23630
Density and thermal expansion measurements of several mixed oxide glasses in the solid and liquid regions
[DE85-006134] 14 p2261 N85-24014
Enhanced thermal-structural analysis by integrated finite elements
[AD-A151103] 15 p2636 N85-26258
Low-temperature thermal expansion of glass
15 p2645 N85-26315
Thermal expansion effects in electrical transport in amorphous metals
[AD-A152477] 17 p2930 N85-28089
Daze fasteners
[NASA-CASE-LAR-13009-1] 18 p3116 N85-29285
Thermal-cycle testing of the G-tunnel heated block
[DE85-008408] 18 p3126 N85-29359
Thermal expansion coefficients of a 30% glass fiber filled PEEK pyrotechnic charge holder
[DE85-010806] 19 p3251 N85-30155
Thermal expansion of selected graphite reinforced polyimide-, epoxy-, and glass-matrix composite
[NASA-TM-87572] 21 p3561 N85-32149
Temperature sensitivity of fiber-optic transmission line
22 p3764 N85-33331
Design and development of a linear thermal actuator
22 p3796 N85-33518
Hermetic chip carrier compliant soldering pads
[AD-D011722] 23 p3938 N85-34410
Search for acoustic signals from high energy cascades
[HE-7.1-1] 24 p4213 N85-36155
Experimental investigation of radiative-acoustic effects in the water by the thermodynamical conditions of Dumand
[HE-7.1-2] 24 p4213 N85-36156
Acoustic detection of air shower cores
[HE-7.1-4] 24 p4213 N85-36158

THERMAL FATIGUE
Stress corrosion of pressure vessel steel A533-B in high temperature water
[BLL-RISLEY-TR-4600-(9091.9F)]
03 p0330 N85-12125
Cumulative damage modeling of fatigue crack growth
07 p0907 N85-15741
Engine cyclic durability by analysis and material testing 07 p0907 N85-15744
Thermal-mechanical fatigue crack growth in Inconel X-750
[NASA-CR-174740] 07 p0927 N85-15877
Analytical and experimental investigation of rubbing interaction in labyrinth seals for a liquid hydrogen fuel pump — space shuttle main engine
[NASA-CR-174657] 09 p1287 N85-18084
Fatigue resistance of welded joints of high strength steels produced by electron beam welding
10 p1449 N85-19127
High-thermal-gradient superalloy crystal growth
17 p2914 N85-27966
Gas turbines: Operating conditions, material selection and development
[NLR-MP-83046-U] 20 p3395 N85-31082
Basic cryogenics and materials. Phase 1
[NASA-CR-177932] 21 p3572 N85-32215

THERMAL GRAVIMETRY
U THERMOGRAVIMETRY
THERMAL INSTABILITY
Ionospheric and magnetospheric modifications caused by VLF waves
[AD-A148210] 08 p1186 N85-17475
THERMAL INSULATION
Insulating polymer concrete
[DE84-017239] 04 p0480 N85-13057
Description of the insulation system for the Langley 0.3-Meter Transonic Cryogenic Tunnel
[NASA-TM-86274] 07 p0909 N85-15755
Thermal and mechanical properties of polyurethane foams and a survey of insulating concretes at cryogenic temperatures
[PB85-100949/GAR] 07 p0934 N85-15918
Thermal design of the space shuttle external tank
08 p1103 N85-16977
FRG ceramic engine components (PET)
08 p1141 N85-17193
A systems analysis of alternative concepts for aircrew cold weather clothing
[AD-A148805] 09 p1365 N85-18580
Insulation bonding test system
[NASA-CASE-MFS-25862-1] 11 p1610 N85-20126
Thickness effect in low-density insulation
[DE85-009065] 11 p1631 N85-20273
Envelope thermal test unit: Technical description
[DE84-012254] 11 p1674 N85-20548
Integrated insulation wall assembly — for a solid rocket motor case
[AD-D011553] 12 p1794 N85-21257
Environmental cycling of cellulosic thermal insulation and its influence on fire performance
[DE85-004295] 13 p2041 N85-22776
Development of a polystyrene insulation system
[DE85-006950] 16 p2784 N85-27180
Heat resistant sheathed insulated electrical conductors
[AD-D011644] 17 p2951 N85-28219
Ceramic coatings for heat engine materials: Status and future needs
[DE85-008758] 18 p3080 N85-29053
Ceramic coatings for heat engine materials
[DE85-005238] 18 p3080 N85-29054
Design and operation of solar thermal heat transfer systems
[DE85-009837] 19 p3257 N85-30263
Performance analysis of mixed passive solar heating systems
[DE85-009824] 21 p3613 N85-32455
The design, construction and operation of a large-area, high-temperature, thermal conductance apparatus — furnace insulation
[NPL-DMA(A)-84] 22 p3766 N85-33455
Carbon/carbon combustor external insulation
[AD-D011719] 23 p3910 N85-34224
High temperature structural insulating material
[DE85-006361] 23 p3920 N85-34291
SRB attach ring phenolic TPS fishtail seal evaluation tests
[NASA-CR-170667] 24 p4098 N85-35407
Study of NSI and related cable performance during tests performed in the NASA Hot Gas Facility
[NASA-CR-170668] 24 p4101 N85-35423
THERMAL MAPPING
Application of digital analysis of MSS to agro-environmental studies
[E85-10024] 02 p0218 N85-11437
Contributions to remote sensing : Applications of thermal infrared
[COMMUN-34/1984] 05 p0654 N85-14196
The need for integrating ground thermal measurements with thermal aircraft imagery 05 p0680 N85-14243
The use of principal components analysis techniques Nimbus-7 coastal zone color scanner data to define mesoscale ocean features through a warm humid atmosphere
[AD-A148567] 08 p1176 N85-17416
Examples of environment services: Hydrological and pollution measurements in the Po River (Italy)
[CISE-2290] 11 p1679 N85-20578
Evaluation of the radiometric quality of the TM data using clustering, linear transformations and multispectral distance measures — Illinois 12 p1870 N85-21731
Geologic interpretation of remote sensing data for the Martian volcano, Ascraeus Mons
13 p2194 N85-23608
Water-ice clouds on Mars: Location and seasonal variation 13 p2194 N85-23611
Proposed use of system ARGOS with data buoys for calibration of thermal infrared imagery of North British waters for sea surface temperature maps
14 p2240 N85-23889
Temperature anomalies above ore bodies
14 p2345 N85-24500
Comparison of measurement and simulation results of radiation temperatures applied to the thermal mapping of Munich
[DFVLR-FB-85-06] 17 p2984 N85-28442
Modeling of geothermal systems
[DE85-012553] 23 p3943 N85-34439
THERMAL NEUTRONS
Method and apparatus for determining the content and distribution of a thermal neutron absorbing material in an object
[DE84-014319] 01 p0117 N85-10801
Fine structure analysis with thermal neutrons and development and construction of a multidetector system
03 p0422 N85-12698
Sputtering of gold irradiated with thermal neutrons
03 p0429 N85-12738
Two phases of neutron production in the POSEIDON plasma focus
[IPF-84-10] 09 p1395 N85-18783
Apparatus and method for identification of matrix materials in which transuranic elements are embedded using thermal neutron capture gamma-ray emission
[DE85-011659] 22 p3786 N85-33454
Properties of 10 (16)-10 (19)eV EAS at far core distance
[HE-4.7-3] 24 p4198 N85-36054
THERMAL NOISE
Realization of noise power in the microwave range by thermal noise standards 05 p0629 N85-14034
Adaptive antenna arrays for weak interfering signals
[NASA-CR-174336] 08 p1150 N85-17258
Mathematical model of discriminator for signals with fluctuations and thermal noise 13 p2072 N85-22943
An excitation mechanism for solar 5-minute oscillation of intermediate and high degree
14 p2444 N85-25085
THERMAL PLASMAS
Bremsstrahlung radiation from longitudinal plasma waves caused by subthermal electrons in plasma
02 p0264 N85-11730
Power law X- and gamma-ray emission from relativistic thermal plasmas 06 p1241 N85-17829
Physics of nonmagnetic relativistic thermal plasmas
09 p1386 N85-18715
Modeling thermal plasma material processing experiments
[DE85-001551] 10 p1580 N85-19838
Excitation of impurities by heavy particles and radiative losses of thermonuclear plasma
11 p1719 N85-20616
Plasma processing of materials
[AD-A152398] 17 p3039 N85-28800
Thermal ion heating in the vicinity of the plasmapause
[NASA-CR-176030] 20 p3535 N85-31993
A retarding ion mass spectrometer for the Dynamics Explorer-1
[NASA-CR-171588] 21 p3589 N85-32303
Integral representation for nonlinear heat transport
23 p3961 N85-34683
Synthesis of ultrafine ceramic and metallic powders in a thermal argon rf plasma
[DE85-009834] 23 p3983 N85-34696
THERMAL POWER
U TURBOGENERATORS
THERMAL PROPERTIES
U THERMODYNAMIC PROPERTIES
THERMAL PROTECTION
Testing of three different flight suits in fire environment — fuel fire
[FOA-C-56012-H1] 02 p0236 N85-11552
Verification tests of durable TPS concepts
[NASA-TM-86313] 03 p0323 N85-12085
Integral boost, heat protection, port covers and transition 07 p0916 N85-15813
Space Shuttle Technical Conference, part 2
[NASA-CP-2342-PT-2] 08 p1098 N85-16937
Thermal design of the space shuttle solid rocket booster 08 p1103 N85-16976
Orbiter thermal protection system
08 p1104 N85-16979
Rolls-Royce experience with thermal barrier coatings — in aircraft engines
[PNR-90222] 08 p1135 N85-17152
Process for preparing essentially colorless polyimide film containing phenoxy-linked diamines
[NASA-CASE-LAR-13353-1] 11 p1611 N85-20128
Study of outgassing and decomposition of space shuttle heat protection tiles, fillers and adhesive
[NASA-CR-175565] 12 p1791 N85-21242
Impacts of Space Shuttle thermal protection system tile on F-15 aircraft vertical tile
[NASA-TM-85904] 12 p1792 N85-21245
Process for preparing highly optically transparent-colorless aromatic polyimide film
[NASA-CASE-LAR-13351-1] 12 p1811 N85-21360
Electron beam charging of Space Shuttle thermal protection system tiles 13 p1990 N85-22478
National Space Transportation Systems Program mission report
[NASA-TM-87454] 14 p2242 N85-23899
Development of acceptance criteria for batches of silane primer for external tank thermal protection system bonding applications
[NASA-CR-171428] 14 p2259 N85-23998
Seven-wavelength pyrometer for determining surface temperature of ablation materials
[NASA-TM-77832] 14 p2305 N85-24268
Development of acceptance criteria for batches of silane primer for external tank thermal protection system bonding applications
[NASA-CR-171436] 15 p2518 N85-25523
Development of acceptance criteria for batches of silane primer for external tank thermal protection system bonding applications
[NASA-CR-175850] 16 p2754 N85-26995
Artificial and natural icing tests YEH-60A quick fix helicopter
[AD-A155147] 21 p3555 N85-32116
Experimental aerodynamic heating to simulated space shuttle tiles in laminar and turbulent boundary layers with variable flow angles at a nominal Mach number of 7
[NASA-TP-2307] 23 p3929 N85-34351
Upgrading auxiliary facility outleakage and combustion detection
[DE85-012796] 23 p3934 N85-34386
Investigation of experimental lightweight firewall materials for A/C engine bay applications
[AD-A155765] 24 p4062 N85-35175
Verification of the SRB motor case pin retainer band tips
[NASA-CR-170682] 24 p4070 N85-35220
SRB TPS closeout materials characterization
[NASA-CR-170685] 24 p4070 N85-35222
Results of tests of the SRB aft skirt heat shield curtain in the MSFC Hot Gas Facility
[NASA-CR-170688] 24 p4070 N85-35223
Results of tests of MTA-2 TPS on the SRB hold-down bolt blast container
[NASA-CR-170691] 24 p4070 N85-35224
SRB thermal protection systems materials test results in an arc-heated nitrogen environment
[NASA-CR-170681] 24 p4072 N85-35236
Results of tests of K5NA and a revised formulation of EPDM/cork patch material in MSFC Hot Gas Facility
[NASA-CR-170690] 24 p4073 N85-35238
Results of tests of weathered K5NA closeout material in the MSFC Hot Gas Facility
[NASA-CR-170693] 24 p4073 N85-35239
Evaluation of SRB phenolic TPS material made by an alternate vendor
[NASA-CR-170694] 24 p4073 N85-35240
Space shuttle SRB TPS protective paint test and evaluation in NASA Hot Gas Facility and AEDC Tunnel C
[NASA-CR-170684] 24 p4081 N85-35294
Results of tests of Insta-Foam Thermal Protection System (TPS) material for protection of equipment inside the SRB aft skirt
[NASA-CR-170692] 24 p4081 N85-35295
THERMAL RADIATION
Thick film radiation detector
[AD-D011211] 01 p0048 N85-10318
Infrared thermal radiation of Venus
02 p0163 N85-11101
Investigation of cloud feedback in the GLAS model
05 p0685 N85-14404
Modeling influence of three layer cloud cover on outgoing thermal radiation 06 p0825 N85-15242
The adsorption of CO and oxygen on Cu layers on a W(110) surface
[AD-A147345] 07 p0923 N85-15847
Support for the Naval Research Laboratory Passive Microwave Clutter Analysis Program
[AD-A146771] 07 p0939 N85-15951
Self-generated magnetic fields and thermal flux inhibition
[AD-A147405] 07 p0971 N85-16166
Thermal radiation hazards from Liquified Petroleum Gas (LPG) fireballs
[VTT-304] 09 p1293 N85-18122
Influence of aerosol on formation of outgoing thermal radiation 14 p2342 N85-24483
Lidar and radiometer observations of thunderstorm tops 15 p2595 N85-25994
Technique to reduce scattered light in optical systems
[AD-D011597] 18 p3185 N85-29752
Enhanced thermal coupling by a repetitively pulsed laser
[AD-A154435] 19 p3276 N85-30317

Nuclear thermal transmittance in the atmosphere using LOWTRAN-6 computer code
[AD-A154669] 21 p0630 N85-32553
Enhancing precision of remote temperature sensing data from satellites under cloudy atmospheric conditions
22 p3734 N85-33148
Instrumentation for sensing moisture content of material using a transient thermal pulse
[NASA-CASE-NPO-15493-2] 23 p3933 N85-34373
Fire research publications, 1984
[PB85-208502] 24 p4166 N85-35827

THERMAL RESISTANCE
Silicon nitride powder
[NASA-TM-77731] 01 p0022 N85-10132
Thermal conductivity and interface resistance of particle-filled silicone resin
[DE84-011661] 04 p0479 N85-13056
High specific heat dielectrics and Kapitza resistance at dielectric boundaries
[AD-A148476] 08 p1217 N85-17666
Vapor pressure and evaporation rate of certain heat-resistant compounds in a vacuum at high temperatures
[NASA-TM-77607] 10 p1434 N85-19036
Oxidation of PT-7M and OT4-1 titanium alloys in air
11 p1600 N85-20063
Thermal barrier coating system
[NASA-CASE-LEW-13324-2] 12 p1796 N85-21266
Fire resistant polymers based on 1-(diorgano oxyphosphony)methyl-2,4- and 2,6-diamino benzenes
[NASA-CASE-ARC-11512-2] 12 p1811 N85-21362
Fire and heat resistant laminating resins based on maleimido and citraconimido substituted 1-(diorgano oxyphosphony)methyl-2,4- and 2,6-diaminobenzenes
[NASA-CASE-ARC-11533-1] 12 p1812 N85-21364
Temperature-insensitive optical fibers
[AD-D011551] 12 p1933 N85-22142
Possibility of producing monolithic composite materials based on niobium carbide 13 p2028 N85-22707
System for forming and focusing high current beam of deuterium ions 13 p2045 N85-22798
Measurement of internal thermal resistance for quality control of semiconductor devices
13 p2074 N85-22953
Heat resistant Carbon Fiber Reinforced Plastics (CFRP) hardening equipment
[MBB/LFA33/CFK/PUB/007] 17 p2916 N85-27976
Dispersion-strengthened powder-metallurgical chromium steels
[BLL-BISI-TRANS-22323-(9022.06)]
17 p2929 N85-28081
Investigations of the material factors in the adiabatic shearing of steels
[AD-A153084] 17 p2979 N85-28418
A simple power meter for high energy pulsed lasers
[AD-D011661] 18 p3113 N85-29271
Thermodynamics of high temperature materials
[AD-A154269] 19 p3378 N85-30658
Solid-state resistance welding cylinders and spheres
[DE85-010084] 20 p3469 N85-31555
Investigation of experimental lightweight firewall materials for A/C engine bay applications
[AD-A155765] 24 p4062 N85-35175

THERMAL RESOURCES
NT GEOTHERMAL RESOURCES
NT GEYSERS
The United States Geological Survey in Alaska: Accomplishments during 1983
[USGS-CIRC-945] 23 p3948 N85-34468

THERMAL SHIELDING
U HEAT SHIELDING

THERMAL SHOCK
Thermal shock as a carbide grade development tool
[DE84-016939] 04 p0509 N85-13251
Impact of NDE unreliability on pressure vessel fracture predictions
[DE84-015586] 05 p0647 N85-14151
Computation of thermal shock-free straightening conditions for aluminum-magnesium alloy welded structures 10 p1449 N85-19131
Possibility of producing monolithic composite materials based on niobium carbide 13 p2028 N85-22707
Dispersed-metal-toughened alumina
[NASA-CR-174687] 13 p2037 N85-22758
Creep ratcheting simplified methods experience from structural design of elevated temperature components
[DE85-007433] 15 p2580 N85-25915

THERMAL SIMULATION
Simulation of the coupled atmospheric and oceanic boundary layer model during MILDEX
[AD-A155166] 21 p3655 N85-32705

THERMAL STABILITY
NT TEMPERATURE DEPENDENCE
Development of new and improved polymer matrix resin systems, phase 1
[NASA-CR-166595] 01 p0017 N85-10104
Heat treatment of welded joints in OT4 and VT20 titanium alloys 01 p0020 N85-10119
Stability of bromine intercalated graphite fibers
[NASA-TM-86859] 01 p0031 N85-10187
A new heat-resistant polymer from dimer diamine bismaleimide. Part 1: Preparation and free radical cure of dimer diamine bismaleimide
[AD-A145664] 02 p0186 N85-11247
External fuel vaporization study, phase 2
[NASA-CR-174079] 02 p0187 N85-11252
The KZD-85 engine test. Engine type: 1 cylinder, 2 stroke motor 2100 Husquarna
[FWE-FO-1717] 02 p0205 N85-11354
Study of application of organic semiconductors to electronic components
[BMFT-FB-T-84-142] 02 p0289 N85-11890
Reinforcement of molybdenum disilicide with nematic crystals of aluminum oxide 03 p0353 N85-12269
Construction of a bacterium to convert cellulose to ethanol
[TI84-901639] 04 p0481 N85-13068
Thermally stable thermoset resin compositions
[AD-D011274] 05 p0620 N85-13963
Structural design and thermal stability of TELE-X antenna tower 05 p0627 N85-14016
Vaporization behavior, phase equilibria, and thermodynamic stabilities of nickel phosphides
[AD-A146883] 06 p0765 N85-14897
Hazard Studies for Solid Propellant Rocket Motors
[AGARD-CP-367] 08 p1114 N85-17025
Heater block assembly for use in thermal oxidation testing of jet fuel
[AD-D011430] 08 p1123 N85-17077
Phase formation and stability in the pseudobinary Ni3Al-Ni3V alloy system
[DE85-001117] 09 p1296 N85-18143
Strength and failure of ceramic-metallic material
10 p1448 N85-19112
Method of determining thermal stability of heat-resistant coatings on graphite 10 p1447 N85-19117
Study of advanced fuel system concepts for commercial aircraft and engines
[NASA-CR-174752] 10 p1456 N85-19176
A review of hazard assessment procedures for liquid gun propellants
[AD-A149470] 10 p1457 N85-19182
Properties and thermal stabilities of amorphous transition metal hydrides
[DE85-002117] 11 p1607 N85-20104
High-temperature-stable detonators
[DE85-005188] 12 p1818 N85-21402
SAW oscillator with digital compensation for the temperature related frequency changes
[AD-D011537] 12 p1833 N85-21500
Stability of three-layer glass-reinforced plastic shells of rotation 13 p2047 N85-22813
NASA space materials research
14 p2232 N85-23831
Some observations of heated gallium arsenide heteroface solar cells
[NASA-TM-86368] 14 p2246 N85-23925
Applications of high pressure differential scanning calorimetry to aviation fuel thermal stability research
[NASA-TM-87002] 14 p2249 N85-23941
Surface composition, properties and thermal stability of massive and fine metallic glasses
15 p2513 N85-25506
Thermal stability of titanium alloys after cold plastic deformation 15 p2515 N85-25515
Simulation studies for surfaces and materials strength
[NASA-CR-175766] 16 p2800 N85-27262
Thermally stable elastomers: Review of silarylene-siloxane polymers and polysilmethylenes
[AD-A152323] 17 p2934 N85-28111
Atomic hydrogen maser measurements with wall surfaces of carbon tetrafluoride
18 p3108 N85-29243
Graphite/PMR polyimide composites with improved toughness
[NASA-TM-87081] 21 p3561 N85-32148
Basic research in novel inorganic reagents and fluorocarbon chemistry
[AD-A155340] 21 p3584 N85-32185
Basic cryogenics and materials. Phase 1
[NASA-CR-177932] 21 p3572 N85-32215
Experimental characterization and stability of salt- and nonsalt-containing grouts and mortars (BCT-1F- and BCT-1FF-related)
[DE85-012339] 22 p3753 N85-33263
Review of zirconium-zircaloy pyrophoricity
[DE85-011169] 23 p3916 N85-34270
A theoretical study of non-adiabatic surface effects for a model in the NTF cryogenic wind tunnel
[NASA-CR-3924] 23 p3929 N85-34352

THERMAL STRESSES
Burner liner thermal/structural load modelling
02 p0143 N85-10970
Features of plastic deformation and fracture of EP 741 nickel alloy under thermal strain
03 p0349 N85-12250
Liquid phase products and solid deposit formation from thermally stressed model jet fuels
[NASA-TM-86874] 04 p0481 N85-13066
In-flight evalution of LCF life consumption of critical rotor components subjected to high transient thermal stress
07 p0906 N85-15734
Monitoring engine thermal stresses
07 p0906 N85-15735
Thermal-stress analysis for a wood composite blade
[NASA-CR-174794] 08 p1178 N85-17421
Thermal striping downstream of a horizontal elbow under thermally stratified transient flow conditions
[DE84-014687] 09 p1320 N85-18302
The response of explosive systems to thermal stimuli: A state-of-the-art assessment
[DE85-000919] 11 p1614 N85-20148
Thermal stress-dependent dilation of concrete
[DE84-014688] 11 p1653 N85-20412
Temperature responses of composite panels
[AD-A150053] 12 p1798 N85-21277
Stress compensation crystal device
[AD-D011497] 12 p1941 N85-22189
Optimization of overall dimensions of enclosures for low-voltage devices and equipment
13 p2087 N85-23033
Estimating defectiveness buildup during service in metal of welded runner in low-pressure cylinder of turbine
14 p2271 N85-24070
Enhanced thermal-structural analysis by integrated finite elements
[AD-A151103] 15 p2636 N85-26258
Thrust chamber life prediction
16 p2733 N85-26865
Finite element thermal-structural analysis of cable-stiffened space structures
[AD-A153822] 16 p3066 N85-28963
Daze fasteners
[NASA-CASE-LAR-13009-1] 18 p3116 N85-29285
Gas turbines: Operating conditions, material selection and development
[NLR-MP-83046-U] 20 p3395 N85-31062
Accelerated stress factors and failure/degradation mechanisms in terrestrial solar cells
21 p3613 N85-32451
Effects of residual stresses and distortion on the nickel 200 and stainless steel 304 weldments
[DE85-011668] 22 p3748 N85-33233
X-ray measurement of thermal stresses in tungsten fiber-copper composites 23 p3907 N85-34205
Influence of cyclic thermal loading on internal stress in casted epoxy resin 23 p3908 N85-34211
Thermal stress analysis of a new turbine shroud seal concept
[NASA-TM-87082] 23 p3938 N85-34406
Mach 14 flow restrictor thermal stress analysis
[AD-A156215] 24 p4067 N85-35208

THERMAL VACUUM TESTS
Seven-year thermal-vacuum real-life test of a solar array drive mechanism manufactured by Marconi Space and Defence Systems (Model No. 002)
[ESA-ESTL-62] 11 p1618 N85-20161

THERMALIZATION (ENERGY ABSORPTION)
Monte Carlo simulation of thermalization of subexcitation electrons in molecular hydrogen
[NAL-TR-815T] 01 p0117 N85-10798
Efficient heating and confinement of ions in an axisymmetric magnetic mirror supplemented with dc electric field
[IPPJ-707] 12 p1935 N85-22180
Monte Carlo simulation of thermalization of subexcitation electrons in He, Ne, Ar, Kr and Xe
[NAL-TR-843T] 18 p3178 N85-29702

THERMICONS
Preliminary study for an IR-vidicon for the 8 to 14 micron range, phase 1
[BMFT-FB-W-84-025] 05 p0633 N85-14057

THERMIONIC CATHODES
Pressed boride cathodes
[NASA-TM-77821] 17 p2918 N85-27984
The effect of metal overlayers of thermionic dispenser cathodes
[AD-A154795] 21 p3701 N85-32995

THERMIONIC CONVERSION SYSTEMS
U THERMIONIC POWER GENERATION

THERMIONIC CONVERTERS
NT SOLAR BLANKETS
Technology status of thermionic fuel elements for space nuclear power 05 p0610 N85-13893
China report: Science and technology
[JPRS-CST-84-039] 11 p1621 N85-20208

Thermionic converter for space reactor described
11 p1621 N85-20206
SP-100 Thermionic Technology Program
[DE85-012311] 23 p3972 N85-34625
THERMIONIC EMISSION
AlAs/GaAs superlattice barrier unipolar diode structure
[DE85-001904] 11 p1736 N85-20921
THERMIONIC EMITTERS
Technology status of thermionic fuel elements for space nuclear power 05 p0610 N85-13893
Research on thermionic plasmas
[AD-A150663] 14 p2423 N85-24944
Multi-channel pulser for the SLC thermionic electron source
[DE85-014222] 24 p4160 N85-35792
THERMIONIC POWER GENERATION
Thermoelectric and thermionic conversion technology
05 p0611 N85-13905
Close-spaced high temperature Knudsen flow
[AD-A148477] 08 p1176 N85-17424
High thermal power density heat transfer apparatus providing electrical isolation at high temperature using heat pipes
[NASA-CASE-LEW-12950-2] 18 p3096 N85-29179
Thermionic photovoltaic energy converter
[NASA-CASE-LEW-14077-1] 23 p3944 N85-34441
THERMIONIC REACTORS
U ION ENGINES
THERMISTORS
A variable length and sensor spacing thermistor array
[AD-D011416] 06 p1113 N85-17017
Temperature sensors for OTEC applications
[DE85-009807] 18 p3110 N85-29254
THERMITES
Thermite and Fe/KClO4: Some thermodynamic calculations
[DE84-016945] 04 p0573 N85-13653
Consolidation of thermites by pressing and sintering
[DE84-016943] 09 p1297 N85-18146
Parameters affecting hot wire ignition of thermite mixtures
[DE84-016941] 09 p1301 N85-18176
A program to develop thermite reactions to produce refractory borides and carbides
[AD-A148972] 10 p1434 N85-19037
Thermal profiles of thermite reactions
[DE85-003306] 10 p1438 N85-19061
THERMOCHEMICAL PROPERTIES
NT HEAT OF FORMATION
NT HEAT OF FUSION
NT HEAT OF VAPORIZATION
Compiled and thermodynamic data sources for aqueous and biochemical systems: An annotated bibliography, 1930 - 1983
[PB85-137693] 12 p1944 N85-22206
Influence of thermochemical treatment on properties of low-carbon steel
[BLL-BISI-TRANS-22410-(9022.06)]
17 p2927 N85-28055
Hydrolysis, formation and ionization constants at 25(0)C, and at high temperature-high ionic strength
[DE85-010645] 19 p3236 N85-30081
THERMOCHEMISTRY
NT AEROTHERMOCHEMISTRY
Experimental and theoretical study of a solar thermochemical receiver module
[NASA-CR-174107] 04 p0528 N85-13374
Blanket materials for fusion reactors: Comparisons of thermochemical performance
[DE84-016240] 04 p0568 N85-13622
Laminar heat-transfer distributions on biconics at incidence in hypersonic-hypervelocity flows
[NASA-TP-2213] 07 p0957 N85-16065
Application of computer methods for calculation of multicomponent phase diagrams of high temperature structural ceramics
[AD-A148138] 08 p1133 N85-17140
Dynamics and mechanisms of catalytic processes and hot chemistry
[DE85-002699] 09 p1292 N85-18114
Carbon vaporization/condensation effects
[NASA-TM-87430] 10 p1436 N85-19048
Some specifics of methods for mass detailed studies of rock heat conductivity 10 p1502 N85-19477
Solar thermochemical process interface study
[NASA-CR-174442] 10 p1510 N85-19527
Direct contact heat recovery from molten salt
[DE85-002690] 11 p1674 N85-20550
Combustion kinetics of metal atoms and metallic radicals over wide temperature ranges 13 p1999 N85-22530
Mechanical properties of TiN deposits obtained by PVD and TiN, TiC, TiC + TiN obtained by CVD
[BLL-RISLEY-TR-5097-(9091.9F)]
15 p2506 N85-25471
Gas phase ion-molecule chemistry of carbon, nitrogen and oxygen compounds
[AD-A152876] 17 p2919 N85-27996
Elementary reactions of importance in oxidation, combustion ignition and flame inhibitions
[AD-A153139] 17 p2921 N85-28004
Influence of preliminary thermomechanical treatment on depth and hardness of nitrided layers
[BLL-BISI-TRANS-22468-(9022.06)]
17 p2929 N85-28078
Alcohol Fuels Program technical review, spring 1984
[DE85-002919] 17 p2936 N85-28134
Light scattering and spectroscopic studies of polymerization processes
[AD-A153407] 18 p3069 N85-28984
Thermochemical energy transport using a hydrogen rich working fluid
[AD-D011696] 19 p3233 N85-30042
Theoretical studies of combustion chemistry
[DE85-010284] 19 p3237 N85-30069
High temperature solar electrothermal processing 2. Zinc from zinc oxide
[AD-A154747] 21 p3562 N85-32159
Biomass thermochemical conversion program
[DE85-011867] 21 p3572 N85-32213
Process for improving the quality of epitaxial silicon films grown on insulating substrates
[AD-D011730] 22 p3847 N85-33828
Thermodynamics of the corrosion of chromium in molten carbonates
[DE85-011407] 24 p4079 N85-35282
THERMOCHROMATIC MATERIALS
Electrochromic and thermochromic materials for solar energy applications with emphasis on niobium and vanadium oxides
[DE85-010830] 19 p3249 N85-30147
THERMOCLINES
The effect of stochastic surface heat fluxes on the climatology of the seasonal thermocline
[AD-A149957] 12 p1889 N85-21857
Frontal nature of Cromwell Current
14 p2336 N85-24445
Local mechanism of equatorial countercurrents
14 p2336 N85-24446
Most important geochemical barrier zones in ocean (with example of Atlantic Ocean basin)
14 p2343 N85-24491
Real-time enhancement of a climatology or forecast of ocean thermal structure using observed ocean temperatures
[AD-A151118] 15 p2604 N85-26049
Thermal evolution of coastal California with implications for hydrocarbon maturation 24 p4115 N85-35509
THERMOCOUPLE PYROMETERS
Thin-film sensors for space propulsion technology
17 p2915 N85-27968
THERMOCOUPLES
Dynamic gas temperature measurement system
02 p0141 N85-10958
Evaluation of thermocouple junction temperature
[DE84-015159] 04 p0502 N85-13206
Field installed brazed thermocouple feedthroughs for high vacuum experiments
[DE84-013556] 04 p0503 N85-13207
Development of a feasibility model for a thin-film precision power meter
[BMFT-FB-T-84-161] 04 p0504 N85-13217
Effects of temperature on the response time of thermocouples and resistance thermometers
[DE84-016855] 06 p0811 N85-15154
High temperature thermocouple and heat flux gauge using a unique thin film-hardware hot juncture
[NASA-TM-86898] 07 p0962 N85-16096
Calibration of thermocouples based on two state points of water and BS 4937; part 5, 1974
09 p1324 N85-18317
Problems in high temperature thermocouple thermometry
[DE85-000808] 10 p1488 N85-19397
Advanced thin film thermocouples
[NASA-CR-175541] 12 p1850 N85-21607
Performance of Chromel versus Alumel and Nicrosil versus Nisil thermocouple assemblies in vacuum and argon between 1000 deg C and 1200 deg C
[DE85-000810] 12 p1853 N85-21624
Results of aeroheating DFI and ET design-data test on a 0.0175-scale model 60-OTS conducted in the Von Karman Gas Dynamics Facility (VKF) 40' supersonic and the 50' hypersonic wind tunnels A and C
[NASA-CR-167693] 13 p1988 N85-22466
Low temperature calibration fixture
[DE85-003960] 13 p2094 N85-23071
Qualification of the T2 wind tunnel in cryogenic operation. A: Thermal field, preliminary study of a schematic model
[NASA-TM-77781] 14 p2227 N85-23805
Thermocouple modeling
[DE85-005172] 14 p2306 N85-24273
Development of a temperature measurement system with application to a jet in a cross flow experiment
[NASA-CR-174896] 15 p2472 N85-25262
Design and construction of a computer controlled microthermocouple probe for the study of buoyant jets
[AD-A152224] 16 p2788 N85-27199
A ten channel temperature controller
[AD-A152664] 17 p2967 N85-28326
Heating parameter estimation using coaxial thermocouple gages in wind tunnel test articles
[AD-A153039] 17 p2968 N85-28328
The effects of extreme temperatures on thermocouples
[DE85-006650] 18 p3110 N85-29258
Imbedded thermocouples as a solid propellant combustion probe
[AD-A155630] 21 p3564 N85-32167
Resolution of thermal striping issue downstream of a horizontal pipe elbow in stratified pipe flow
[DE85-006195] 21 p3586 N85-32292
Failure mechanisms in metal-sheathed thermocouples
[DE85-011929] 21 p3590 N85-32317
IEA-SSPS CRS calibration report: Calibration of relevant measuring sensors
[DE85-010174] 22 p3788 N85-33468
THERMODYNAMIC COUPLING
Survey of mixing in metal/insulator systems
[DE85-011938] 23 p3985 N85-34714
THERMODYNAMIC CYCLES
NT BRAYTON CYCLE
NT CARNOT CYCLE
NT OTTO CYCLE
NT RANKINE CYCLE
NT STIRLING CYCLE
Liquid-piston Stirling machines
[DE84-014255] 02 p0205 N85-11351
Standardized efficiency terms: Comparison of some Stirling engine performance figures
[DE84-015407] 02 p0205 N85-11352
Noise reduction of the exhaust from pneumatic tools
[BMFT-FB-HA-83-021] 02 p0276 N85-11799
Magnetic heat pump cycles for industrial waste heat recovery
[DE84-017016] 04 p0499 N85-13183
Evaluation of heat engine for hybrid vehicle application
[NASA-CR-174163] 04 p0508 N85-13245
Heat cycle research program
[DE84-017015] 09 p1344 N85-18455
Initial results for supercritical cycle experiments using pure and mixed-hydrocarbon working fluids
[DE84-017008] 09 p1345 N85-18460
Available energy method for evaluating thermodynamic performance of heat pump systems
[DE84-017223] 09 p1400 N85-18814
DOE/ORNL electric systems program overview
[DE85-003334] 10 p1459 N85-19197
Initial testing of a variable-stroke Stirling engine
[NASA-TM-86875] 10 p1569 N85-19695
Heat Cycle Research Experimental Program report, FY-84
[DE85-003558] 12 p1882 N85-21611
Power plants of modular construction with quasi-paraboloidal concentrators of solar energy
14 p2266 N85-24036
A mathematical model of reciprocating combustion engine dynamics for the diagnosis of deficient energy conversion 19 p3280 N85-30339
Adiabatic thermal models for planetary bodies
22 p3857 N85-33881
THERMODYNAMIC EFFICIENCY
Combustion modeling of a 2 cylinder cycle reciprocating engine
[AD-A144782] 01 p0055 N85-10364
Available energy method for evaluating thermodynamic performance of heat pump systems
[DE84-017223] 09 p1400 N85-18814
Influence of fuel properties on gas turbine combustion performance
[AD-A151464] 15 p2504 N85-25448
Development of a coal-water slurry-fueled diesel engine for industrial cogeneration. Task 1.0 topical report: Thermodynamic analysis
[DE85-010455] 19 p3236 N85-30062
Historical perspective of barriers to achieving high-efficiency silicon solar cells
20 p3479 N85-31616
Fuel cell applications literature review
[DE85-011691] 22 p3809 N85-33592
THERMODYNAMIC EQUILIBRIUM
An interactive computer code for calculation of gas-phase chemical equilibrium (EQLBRM)
[NASA-CR-168337] 02 p0140 N85-10948

Thermodynamic conditions of the Earth's atmosphere with pollution processes 04 p0523 N85-13345
ECUT, Energy Conversion and Utilization Technologies program: Isothermal separation processes update [NASA-CR-175463] 10 p1433 N85-19033
Adsorption thermodynamics and surface transport of metal catalyst poisons [DE85-002868] 10 p1441 N85-19084
Nucleation of phase transitions in the vicinity of phase boundary. Part 1: Comparison of various idolated mechanisms. Part 2: Coupled cluster growth processes [N-0208-5658] 12 p1938 N85-22174
Compiled and thermodynamic data sources for aqueous and biochemical systems: An annotated bibliography, 1930 - 1983 [PB85-137893] 12 p1944 N85-22208
Thermodynamic calculations of equilibrium states in metal-carbon-hydrogen-oxygen system [BLL-BISI-TRANS-22092-(9022.06)] 17 p3045 N85-28844
The interactions of composition and stress in crystalline solids [PB85-179075] 20 p3473 N85-31583
Current understanding of point defects and diffusion processes in silicon 20 p3481 N85-31632
Condensation properties of atmospheric aerosol 21 p3649 N85-32672

THERMODYNAMIC PROPERTIES
NT CRITICAL POINT
NT CRITICAL PRESSURE
NT CRITICAL TEMPERATURE
NT EMISSIVITY
NT ENTHALPY
NT ENTROPY
NT FREE ENERGY
NT HEAT OF FORMATION
NT HEAT OF FUSION
NT HEAT OF VAPORIZATION
NT MELTING POINTS
NT PYROELECTRICITY
NT SPECIFIC HEAT
NT SUPERCRITICAL PRESSURES
NT SURFACE ENERGY
NT THERMAL CONDUCTIVITY
NT THERMAL DIFFUSION
NT THERMAL DIFFUSIVITY
NT THERMAL EXPANSION
NT THERMAL INSTABILITY
NT THERMAL STABILITY
NT THERMOCHEMICAL PROPERTIES
NT THERMOPHYSICAL PROPERTIES
NT VAPOR PRESSURE
NT VOLATILITY

Combustion gas properties I-ASTM jet A fuel and dry air [NASA-TP-2359] 01 p0010 N85-10064
Granular boundary segregation in low-alloyed titanium-vanadium alloys 01 p0019 N85-10117
A thermodynamic surface for the critical region of ethylene [PB84-217850] 01 p0025 N85-10159
Thermodynamic properties of isobutane-isopentane mixtures from -40 to +600(0)F and up to 1000 psia [DE84-015137] 01 p0124 N85-10850
Dynamic gas temperature measurement system 02 p0141 N85-10958
Laser speckle technique for burner liner strain measurements 02 p0142 N85-10960
Thermodynamics of reactions of deoxidation of nickel melts [BLL-M-35729-(5828.4)] 02 p0175 N85-11168
A case study of a convective outbreak using VAS-derived thermodynamic parameters [AD-A145560] 02 p0232 N85-11512
NBS (National Bureau of Standards): Materials measurements [NASA-CR-174038] 03 p0332 N85-12143
Surface coatings for low emittance in the thermal surveillance band [MRL-R-937] 03 p0336 N85-12158
Critical evaluation of binary rare Earth diagrams [DE84-014880] 04 p0470 N85-12991
Electrochemical investigations of novel electrode materials [DE84-014352] 04 p0495 N85-13158
Thermal properties of soils and soils testing [DE84-015312] 04 p0525 N85-13360
Thermite and Fe/KClO4: Some thermodynamic calculations [DE84-016945] 04 p0573 N85-13653
Americium thermodynamic data for the EQ3/6 database [DE84-017065] 04 p0573 N85-13656
Analytical thermal formulations for antenna dishes -- satellite antennas 05 p0627 N85-14017
Strain rate effects and temperature history effects for three different tempers of 4340 VAR steel [AD-A146372] 06 p0768 N85-14915
Effects of surface interactions and mechanical properties of PBXs (plastic bonded explosives) on explosive sensitivity [AD-A146368] 06 p0773 N85-14944
Aerodynamic and thermal characteristics of stellate bodies in hypersonic flow of rarefied gas at angle of attack 06 p0778 N85-14974
Thermodynamical characteristics of heat storage reactors using metal hydrides [NAL-TR-822] 06 p0869 N85-15524
Thermal and mechanical properties of polyurethane foams and a survey of insulating concretes at cryogenic temperatures [PB85-100949/GAR] 07 p0934 N85-15918
Thermal evaporation in blast waves: A model for aneurism formation in the NRL (Naval Research Laboratory) LASER-HANE simulation experiment [AD-A147006] 07 p0978 N85-16210
A virial equation of state option for the TIGER computer program [AD-A147490] 07 p1025 N85-16507
Temperature dependence of the crystal structures of Nylon 11 [AD-A147563] 07 p1049 N85-16661
Computer program for calculation of complex chemical equilibrium compositions and applications. Supplement 1: Transport properties [NASA-TM-86885] 07 p1049 N85-16663
In-flight testing of the space shuttle orbiter thermal control system 08 p1103 N85-16974
Photoacoustic microscopy of oxygen contaminated titanium alloys [AD-P004127] 08 p1127 N85-17102
A research proposal for the theoretical study of the thermodynamic and transport properties of dense plasmas [AD-A148040] 08 p1224 N85-17706
Proceedings of the AFOSR/AFRPL Rocket Propulsion Research Meeting: Abstracts and Agenda [AD-A148818] 09 p1268 N85-18085
Thermodynamic properties of aqueous NaCl from 273 to 823 K with estimates for higher temperatures [DE85-000392] 09 p1292 N85-18116
Physical characterization of magma [DE85-000568] 09 p1354 N85-18519
Materials physics [DE84-017103] 09 p1377 N85-18658
Acoustic microscopy at cryogenic temperatures [AD-A148755] 09 p1384 N85-18704
Magnetic fusion energy plasma interactive and high heat flux components. Volume 2: Technical assessment of the critical issues and problem areas in high heat flux materials and component development [DE85-001155] 09 p1393 N85-18764
Pulsed photothermal radiometry for remote sensing of spectroscopic and physical properties of thin film [AD-A149060] 10 p1435 N85-19041
Quasi-thermodynamic prediction of hydrogen reemission behavior from titanium films [DE85-003657] 10 p1584 N85-19664
Application of Monte Carlo and molecular dynamics methods to the calculation of thermodynamic properties of molten salts [AD-A148897] 10 p1565 N85-19669
Thermophysical properties of porous fiber materials 11 p1601 N85-20068
The physical modelling of transition metal alloying: The roles that different levels of theory play [DE85-000591] 11 p1607 N85-20105
Report of the Technology and Test Panel 11 p1646 N85-20370
User's manual for GRIZZLY [DE85-001405] 11 p1702 N85-20702
Novel photo-thermal technique for flow and spectroscopic measurements in a dense aerosol stream [AD-A149745] 12 p1800 N85-21287
Chemical approach for controlling nadimide cure temperature and rate [NASA-CASE-LEW-13770-5] 12 p1810 N85-21352
Fine-grained, isotropic graphite for use as NBS (National Bureau of Standards) thermophysical property RM's from 5 to 2500 K [PB85-112986] 12 p1814 N85-21381
Mathematical simulation of thermal processes involved in electron-beam treatment 12 p1843 N85-21565
Normal coordinate monolithic crystal filter [AD-D011496] 12 p1941 N85-22188
Ideal gas thermodynamic properties for the phenyl, phenoxy, and o-biphenyl radicals [NASA-TM-83800] 12 p1943 N85-22204
Green's function solution of the Kondo problems and universality of the thermodynamic properties [DE85-002739] 12 p1943 N85-22206
Efficiency of algorithms for gas-air channel diagnostics in gas turbine engines based on gas thermodynamic parameters 13 p2048 N85-22823
Thermodynamic and kinetic studies of pulsed laser annealing from transient conductivity measurements [DE85-009677] 13 p2096 N85-23078
Thermal response of aircraft cabin ceiling materials during a post-crash, external fuel-spill, fire scenario [PB85-145847] 14 p2220 N85-23764
Thermal deformation of flexible rotors in friction bearings 14 p2280 N85-24123
Analysis and testing of the thermal properties of space battery cells, phase B, draft [ESA-CR(P)-1971] 15 p2560 N85-25741
On thermomechanical testing in support of constitutive equation development for high temperature alloys [NASA-CR-174879] 15 p2577 N85-25894
Development of new materials for turbopump bearings 16 p2735 N85-26877
Effect of nickel addition on the thermal, magnetic and magnetomechanical properties of Fe(80)B(15)Si(5) [AD-A152281] 16 p2749 N85-26967
Computer program for the calculation of multicomponent convective diffusion deposition rates from chemically frozen boundary layer theory [NASA-CR-166329] 16 p2781 N85-27164
Design and construction of a computer controlled microthermocouple probe for the study of buoyant jets [AD-A152224] 16 p2788 N85-27199
The study of thermal forecasting for gliding 16 p2830 N85-27453
Thermal and magnetic properties of neutron stars 16 p2880 N85-27774
Investigation of heat transfer to a turbine blade cascade using a shock tube [AD-A153090] 17 p2896 N85-27871
Thermodynamic analysis of the plasma nitriding of ferrovanadium [BLL-BISI-TRANS-22237-(9022.06)] 17 p2924 N85-28032
Analysis and modeling for thermal focal plane arrays [AD-A153158] 17 p2968 N85-28329
Thermodynamic calculations of equilibrium states in metal-carbon-hydrogen-oxygen system [BLL-BISI-TRANS-22092-(9022.06)] 17 p3045 N85-28844
High-temperature oxidation of alloys in mixed oxidants [DE85-009706] 18 p3077 N85-29035
Preparation of sinteractive silicon nitride powders [BMFT-FB-T-84-303] 18 p3082 N85-29066
Reliability derating procedures [AD-A153744] 18 p3119 N85-29309
Materials research for passive solar systems: Solid-state phase-change materials [DE85-009779] 18 p3132 N85-29395
Growth mechanism and properties of the thermal and anodic oxides of the 3-5 compound semiconductors [AD-A153406] 18 p3193 N85-29803
Electronic states in silicon and on its interfaces [AD-A153684] 18 p3193 N85-29807
Thermodynamic properties of liquid Li-Pb, Na-Pb and K-Pb alloys: Similarities and Differences [DE85-004074] 18 p3197 N85-29830
Thermodynamic systematics of oxides of americium, curium and neighboring elements [DE85-009704] 18 p3197 N85-29831
Thermophysical properties correlations and pseudocomponent characterization parameter estimation for fossil fluids [DE85-009297] 19 p3230 N85-30024
Self-developing polysilane deep-UV resists: Photochemistry, photophysics and submicron lithography [DE85-007606] 19 p3237 N85-30067
Structure and properties of VT23 alloy welded joints after thermocyclic processing 19 p3246 N85-30125
Thermo-mechanical and thermal behavior of high-temperature structural materials [AD-A154154] 19 p3266 N85-30251
Activities of Rutgers - The State University Department of Mathematics [AD-A154158] 19 p3370 N85-30904
Thermodynamics of high temperature materials [AD-A154269] 19 p3378 N85-30958
Special materials: Carbons [SNIAS-851-551-104] 20 p3421 N85-31235
Method for determining Wagner parameters of interaction of first and second orders [BLL-M-36261-(5828.4)] 20 p3430 N85-31278
Meteorological weapons [AD-A154735] 21 p3635 N85-32575
Numerical modeling of sea ice dynamics and ice thickness characteristics [AD-A154600] 21 p3654 N85-32700
Thermodynamic data for mineral technology [PB85-184331] 22 p3903 N85-33560

Refractive indices and thermo-optic coefficients of nonlinear crystals isomorphic to KH2PO4
[DE85-012968] 22 p3847 N85-33831
Experimental evaluation of the thermodynamic properties of concentrated aqueous potassium hydroxide solutions
[DE85-010628] 23 p3912 N85-34238
Calculation of activities of components in liquid alloys of iron with yttrium
[BLL-M-35866-(5828.4)] 23 p3914 N85-34253
Design and lubrication of high-speed rolling-element bearings
[NASA-TM-87107] 23 p3938 N85-34409
Determination of properties of zeolite/refrigerant combinations for solar refrigeration systems
[DE85-012009] 23 p3945 N85-34448
Characterization of the optical and thermal properties of matter by photothermal techniques
[DE85-012607] 24 p4076 N85-35260
Analysis of the nonlinear equations describing the elastic, thermal, and electromagnetic behavior of solids: Existence of solutions of semi-inverse problems
24 p4100 N85-35415

THERMODYNAMICS
NT AEROTHERMODYNAMICS
NT COMBUSTION PHYSICS
Compressibility and fugacity of gaseous hydrogen
[NLR-TR-83079-U] 01 p0025 N85-10154
Theory of nonlocal elasticity and some applications
[AD-A145201] 01 p0062 N85-10412
Reduction of nonlinear problems to Schroedinger or heat equations: Formation of Kepler orbits, singular solutions for hydrodynamical equations
[REPT-72] 01 p0129 N85-10892
Thermodynamics of decarburization of niobium-bearing high-alloy melts
[BLL-M-35728-(5828.4)] 02 p0175 N85-11169
Thermodynamic calculations and the chemical vapour deposition of hard materials 02 p0179 N85-11200
Analysis and simulation of the I C engine Otto cycle using the second law of thermodynamics
02 p0291 N85-11891
Thermomechanical cracking in layered media from moving friction load
[AD-A146022] 03 p0373 N85-12379
Difference schemes for equations of Schrodinger type
[AD-A145812] 03 p0410 N85-12622
The development of new methods for solving the target identification or inverse scattering problem for time-harmonic acoustic and electromagnetic waves
[AD-A145821] 03 p0415 N85-12657
Thermodynamics and phase equilibria in the vanadium-silicon system
[AD-A145870] 03 p0435 N85-12769
Thermodynamic study of CO2-organic compound interaction at high pressures and temperatures
[DE84-015777] 04 p0573 N85-13654
Linear harmonic analysis for Stirling machines and second law analysis of four important losses
[DE84-016595] 04 p0573 N85-13655
Linear harmonic analysis of Stirling engine thermodynamics
[DE84-016646] 04 p0574 N85-13657
On experimental equations of state for Boson gases
[PTB-ME-61] 04 p0574 N85-13659
Answering thermodynamic questions with three-dimensional viscous flow calculations
05 p0636 N85-14081
Variational principles in thermoplasticity. Part 2: Coupled thermomechanical processes
[RUB-IFM-MITT-37-PT-2] 05 p0648 N85-14161
Process Modeling Applied to Metal Forming and Thermomechanical Processing
[AGARD-LS-137] 06 p0796 N85-15066
Intercomparison between West Germany and US thermodynamic codes
[AD-A146822] 06 p0869 N85-15525
Aqueous alteration of meteorite parent bodies: Possible role of unfrozen water and the Antarctic meteorite analogy 06 p0884 N85-15617
Interaction between chromium oxide and carbon
[BLL-M-36002-(5828.4)] 07 p0926 N85-15667
Target detection using microwave irradiances from natural sources: A passive, local and global surveillance system
[NASA-CR-174290] 07 p0946 N85-15991
Assessment of the operating characteristics of the SSME LOX turbopump pump-end bearing
[NASA-CR-171287] 08 p1167 N85-17362
Impact and collisional processes in the solar system
[NASA-CR-174297] 08 p1255 N85-17914
A thermal-mechanical model of deflagration-to-detonation in granular energetic materials
[AD-P004346] 10 p1455 N85-19170
Thermodynamics of the reactive flow model
[DE85-004405] 10 p1565 N85-19870
Explorations into thermodynamics analogies and critical points in reference to gas-solid transport
[DE85-000816] 11 p1738 N85-20929
Viscoplastic constitutive relationships with dependence on thermomechanical history
[NASA-CR-174836] 12 p1864 N85-21691
Atmospheric environment for Space Shuttle (STS-51A) launch
[NASA-TM-86497] 12 p1892 N85-21875
Clustering and ordering in 3-5 alloys
[AD-A150604] 13 p2022 N85-22670
Thermodynamics of copper-nickel alloys containing aluminum, silicon, titanium, and chromium relative to their use in ceramic brazing
[DE85-004787] 13 p2023 N85-22674
Some unique features of isentrophic flow of gas under high pressures 13 p2043 N85-22788
Impact and collisional processes in the solar system
13 p2180 N85-23530
Theoretical thermodynamics of mixtures at high pressures 13 p2183 N85-23550
Chemical-mechanical interaction in gears
14 p2223 N85-23785
Thermodynamic calculations and the chemical vapour deposition of hard materials 14 p2431 N85-24991
Get Away Special (GAS) thermal design summary
[X-732-83-8] 15 p2475 N85-25278
Separating polymer solutions using high pressure LCST Lower Critical Solution Temperature) phenomena
[AD-A151538] 15 p2518 N85-25528
Entropy production during fatigue as a criterion for failure. A local theory of fracture in engineering materials
[AD-A151289] 15 p2578 N85-25902
Numerical simulation of North Atlantic Sea ice variability, 1951 - 1980 15 p2603 N85-26040
Origin of the Greenland ice sheet
15 p2604 N85-26048
USSR report: Physics and mathematics
[JPRS-UPM-85-003] 15 p2642 N85-26300
Stream dynamics between 1 AU and 2 AU: A detailed comparison of observations and theory
[NASA-TM-86086] 15 p2684 N85-26578
Analytical fuel property effects--small combustors
[NASA-CR-174738] 16 p2706 N85-26709
Study of the kinetics and thermodynamics of hydrogen in Pd-based alloys
[DE85-007341] 16 p2750 N85-26960
Eigenvalue approximation methods for quantum lattice Hamiltonians 16 p2858 N85-27627
Dynamic creep buckling: Analysis of shell structures subjected to time-dependent mechanical and thermal loading 17 p2913 N85-27959
Designing for fiber composite structural durability in hygrothermomechanical environment
[NASA-TM-87045] 17 p2917 N85-27978
Silica problem in the design of geothermal power plants
[DE85-006245] 17 p2986 N85-28453
Homogeneous processes of atmospheric interest
[NASA-CR-175770] 17 p2989 N85-28475
Effects of level broadening on the magnetothermal oscillations in two-dimensional electron systems
[AD-A152639] 17 p3029 N85-28732
Rolling contact fatigue testing of thermomechanically processed M-50 steel
[AD-A153640] 18 p3122 N85-29327
Implications about in situ stress at Yucca Mountain
[DE85-006066] 18 p3126 N85-29356
Solar rocket component study
[AD-A154186] 19 p3227 N85-30007
Thermo-mechanical and thermal behavior of high-temperature structural materials
[AD-A154154] 19 p3266 N85-30251
Evaluation of the eigenvalue method in the solution of transient heat conduction problems
[AD-A154434] 19 p3266 N85-30256
Thermodynamic study of CO2-organic compound interaction at high pressures and temperatures
[DE85-010699] 19 p3268 N85-30266
Some relations among directions of curves at an invariant point on a thermodynamic phase diagram
19 p3312 N85-30530
Thermodynamics of high temperature materials
[AD-A154269] 19 p3378 N85-30958
Thermomigration in porous media. Study of the development of a drying zone 20 p3456 N85-31462
Physical concepts in the development of constitutive equations 20 p3467 N85-31537
Effects of weak interfaces on thermostructural behavior of carbon-carbon composites
[AD-A155330] 21 p3562 N85-32154
Polymer solution-supercritical fluid behavior
[AD-A154514] 21 p3568 N85-32192
Sintering studies project
[AD-A154750] 21 p3572 N85-32216
The sound field of a moving laser-induced acoustic array (theory)
[AD-A154553] 21 p3699 N85-32981
Chemical evolution of the Earth: Equilibrium or disequilibrium process? 21 p3721 N85-33088
Technical assessment of thermal-hydraulics for high heat flux fusion components
[DE85-013178] 23 p3930 N85-34359
Thermodynamics of the corrosion of chromium in molten carbonates
[DE85-011407] 24 p4079 N85-35262
Hadron thermodynamics in relativistic nuclear collisions
[HE-1.1-8] 24 p4171 N85-35856

THERMOELASTICITY
Finite element analysis of thermoelasticity problems
02 p0208 N85-11369
New aspects of thermoelastic contact
[AD-A147554] 07 p0979 N85-16217
An electro-optic spatial light modulator for thermo-elastic generation of programmably focused ultrasound
[AD-A149078] 10 p1553 N85-19794
Translational and extensional energy release rates (the J- and M-integrals) for a crack layer in thermoelasticity
[NASA-CR-174872] 12 p1863 N85-21685
Effects of triazine components on physicochemical properties of polybutadiene: urethane block copolymers
13 p2014 N85-22635
A review of path-independent integrals in elastic-plastic fracture mechanics, task 4
[NASA-CR-174956] 22 p3799 N85-33541

THERMOELECTRIC CONVERSION SYSTEMS
U THERMOELECTRIC POWER GENERATION

THERMOELECTRIC GENERATORS
NT SOLAR SEA POWER PLANTS
Space nuclear safety program
[DE84-015074] 04 p0463 N85-12939
Space nuclear safety program
[DE84-015084] 04 p0463 N85-12940
Technical support services for space and terrestrial systems programs
[DE84-009031] 05 p0597 N85-13806
Radioisotope space power programs
05 p0609 N85-13887
Power flattening techniques for radioisotopic thermoelectric generators
[AD-A146365] 06 p0833 N85-15299
Development of a prototype times wastewater recovery subsystem, addendum
[NASA-CR-171823] 07 p1019 N85-16468
General-purpose heat source development: Safety test program. Postimpact evaluation, design iteration test 4
[LA-10217-SR] 12 p1930 N85-22128
Development of advanced thermoelectric materials
[NASA-CR-175684] 14 p2351 N85-24532
Long-term exposure of pressed plutonium oxide heat sources to aquatic environments
[DE85-007365] 15 p2495 N85-25392
LPCVD tungsten deposition on Si-Ge alloy
[DE85-005588] 16 p2750 N85-26970
Liquid metal thermoelectric converter (LMTEC) for solar applications
[DE85-008405] 18 p3129 N85-29378
Thermoelectric generator and method for the fabrication thereof
[DE85-011650] 22 p3760 N85-33302

THERMOELECTRIC MATERIALS
Electrical and thermal transport property studies of high-temperature thermoelectric materials
[AD-A150167] 13 p2163 N85-23417
Development of advanced thermoelectric materials
[NASA-CR-175684] 14 p2351 N85-24532
Electrical and thermal transport property studies of high-temperature thermoelectric materials
[AD-A150900] 14 p2427 N85-24967
Development of improved thermoelectric materials for space nuclear power systems
[DE85-013079] 22 p3844 N85-33807

THERMOELECTRIC POWER GENERATION
Emerging space nuclear power needs
05 p0608 N85-13882
High temperature thermoelectric energy conversion
05 p0610 N85-13894
Thermoelectric and thermionic conversion technology
05 p0611 N85-13905
Power flattening techniques for radioisotopic thermoelectric generators
[AD-A146365] 06 p0833 N85-15299
General-purpose heat source development: Safety test program. Postimpact evaluation, design iteration test 5
[LA-10232-SR] 12 p1931 N85-22129
General-purpose heat source development: Safety test program. Postimpact evaluation, design iteration test 1
[LA-9680-SR] 12 p1931 N85-22131

Spaceborne power systems preference analyses. Volume 2: Decision analysis
[NASA-CR-175645] 14 p2349 N85-24518

THERMOELECTRICITY
Mechanisms of electrical conductivity in olivine
[DE84-014333] 04 p0495 N85-13159
Power flattening techniques for radioisotopic thermoelectric generators
[AD-A146365] 06 p0833 N85-15299
Evaluation of the thermoelectric method for determination of interstitial gases in titanium
[AD-P004132] 08 p1127 N85-17107
Thermally induced quasiparticle branch imbalance in thin film superconductors 09 p1396 N85-18786
Electrothermal transducer with short time constant
13 p2068 N85-23040
Electrical and thermal transport property studies of high-temperature thermoelectric materials
[AD-A150167] 13 p2163 N85-23417
Transport studies of several novel organic conductors
[DE85-003950] 14 p2429 N85-24979
Thermo-electric valve
[AD-D011682] 19 p3252 N85-30165
Cells for measuring thermoelectromotive force and electrical resistance of metals in temperature range of 20-950 degrees Celsius
[BLL-M-36240-(5828.4)] 20 p3457 N85-31473

THERMOGRAMS
U RECORDING INSTRUMENTS
U TEMPERATURE MEASURING INSTRUMENTS

THERMOGRAPHY
Infrared thermography of burn front propagation in heat powders
[DE85-003307] 10 p1438 N85-19060
Thermal profiles of thermite reactions
[DE85-003308] 10 p1438 N85-19061
Fast times at high temperatures
[DE85-003306] 12 p1943 N85-22205

THERMOGRAVIMETRY
Development of acceptance criteria for batches of silane primer for external tank thermal protection system bonding applications
[NASA-CR-171266] 04 p0478 N85-13043
Instruments for characterization of carbon black and polymers
[AD-A146475] 06 p0810 N85-15146
Applications of high pressure differential scanning calorimetry to aviation fuel thermal stability research
[NASA-TM-87002] 14 p2249 N85-23941
Supercritical solvent extraction of lignite to form carbonaceous chars
[DE85-010159] 19 p3229 N85-30019

THERMOHYDRAULICS
Thermohydrodynamic model: Hydrothermal system, shallowly seated magma chamber
13 p2115 N85-23173
Coolant mixing in LMFBR rod bundles and outlet plenum mixing transients
[DE85-010336] 19 p3268 N85-30268
Technical assessment of thermal-hydraulics for high heat flux fusion components
[DE85-013178] 23 p3930 N85-34359
Mathematical modeling of ultimate heat sink cooling ponds
[TI85-009747] 23 p3932 N85-34369
Ocean thermal energy conversion
[DE85-012291] 23 p3946 N85-34456
MATADOR (Methods for the Analysis of Transport And Deposition Of Radionuclides) code description and user's manual
[TI85-901402] 23 p3966 N85-34592

THERMOLUMINESCENCE
The observation of a single thermoluminescence glow peak described by kinetics more general than the usual 1st and 2nd order kinetics
[DE84-014697] 02 p0173 N85-11160
Investigation of basic characteristics of laser heating in thermoluminescence and of laser-stimulated luminescence
[AD-A152143] 16 p2790 N85-27212
Dosimeasurements with thermoluminescence dosimeters at a Febetron 701, 600 kV in room 022 of the Interuniversity Reactor Institute (IRI)
[IRI-190-84-02] 18 p3111 N85-29262
Symposium on Luminescent Radiation Receivers and Converters 19 p3295 N85-30430
Research on the experimental verification of dosimetry calculations
[DE85-011282] 19 p3331 N85-30637
Error evaluation in measurements with thermoluminescent dosimeters
[ISS-T-84/6] 22 p3788 N85-33471
The read-out system of spatial distribution of thermoluminescence in meteorites
[SH-9.1-16] 23 p4052 N85-35131
Detection threshold energy of high energy cascade showers using thermoluminescence PTFE-sheet and hot-gas reader
[HE-7.1-5] 24 p4213 N85-36159
Application of thermoluminescence for detection of cascade shower 1: Hardware and software of reader system
[HE-7.1-6] 24 p4213 N85-36160
Spatial distribution read-out system for thermoluminescence sheets
[HE-7.1-7] 24 p4213 N85-36161
Application of thermoluminescence for detection of cascade shower 2: Detection of cosmic ray cascade shower at Mount Fuji
[HE-7.1-12] 24 p4214 N85-36162

THERMOMAGHADYNAMICS
U THERMOMAGNETIC EFFECTS

THERMOMAGNETIC EFFECTS
Thermomagnetic generator
[DE84-017018] 04 p0530 N85-13388
The formation of isolated phase precipitates during the decomposition of high-coercive force Fe-Cr-Co alloys
[BLL-M-36028-(5828.4)] 07 p0924 N85-15855

THERMOMAGNETISM
U THERMOMAGNETIC EFFECTS

THERMOMECHANICAL TREATMENT
Directional nature of strengthening during thermomechanical treatment
[BLL-M-35746-(5828.4)] 02 p0175 N85-11174
Cavitation phenomenon in superplastic creep
[DE84-015484] 04 p0513 N85-13271
The creep and creep rupture of SMC-R50 under different thermomechanical conditions 05 p0648 N85-14160
Back stress in dislocation creep. Part 1: Basic concepts and measuring techniques
[NASA-TM-77773] 07 p0977 N85-16206
Developing procedures for thermomechanical processing of high-durability VT22 titanium alloy
13 p2031 N85-22726
Compositional control of plate steels
15 p2565 N85-25826
Fatigue life, fatigue crack propagation and fracture toughness study of 7075 aluminum alloy subjected to thermomechanical processing 15 p2573 N85-25862
Analysis of shell type structures subjected to time dependent mechanical and thermal loading
[NASA-CR-175747] 15 p2577 N85-25898
Multiaxial and thermomechanical fatigue considerations in damage tolerant design
[NASA-TM-87022] 16 p2749 N85-26964
Thermomechanical softening treatment for bearing and tool steels
[BLL-BISI-TRANS-22432-(9022.06)]
17 p2925 N85-28035
Thermomechanical treatment aimed at the protection of type 316 stainless steel from IGC and IGSCC
[BLL-BISI-TRANS-22498-(9022.06)]
17 p2925 N85-28040
Investigation of fatigue strength of spring steel after high-temperature thermomechanical working (HTMW) by helical drawing
[BLL-M-36274-(5828.4)] 20 p3465 N85-31525
Thermomechanical deformation in the presence of metallurgical changes 20 p3466 N85-31533
Thermomechanically induced pre- and postbuckling of general structure 20 p3467 N85-31540
Development and application of a unified viscoelastic constitutive model for the prediction of material response under thermomechanical loading
24 p4101 N85-35420

THERMOMECHANICS
U THERMODYNAMICS

THERMOMETERS
NT RESISTANCE THERMOMETERS
Heat flux sensors for burner liners and turbine blades and vanes 02 p0142 N85-10961
Digital thermometer with linearizer on slide wire
07 p0954 N85-16049
Germanium resistance thermometer calibration at superfluid helium temperatures
12 p1947 N85-22228
Low temperature calibration fixture
[DE85-003969] 13 p2094 N85-23071
The gamma thermometer: A new type of fixed internal instrumentation developed by EDF
[BLL-CE-TRANS-8080-(9022.09)]
15 p2560 N85-25791
Fiber optic Raman thermometer for Space Shuttle main engine preburner profiling 16 p2739 N85-26904

THERMOMETRY
U TEMPERATURE MEASUREMENT

THERMONUCLEAR ENERGY
U THERMONUCLEAR POWER GENERATION

THERMONUCLEAR EXPLOSIONS
On the design of a global detection system for airborne radioactivity
[CM-68] 20 p3487 N85-31670

THERMONUCLEAR POWER GENERATION
SPECTER: Neutron damage calculations for materials irradiations
[DE85-005791] 18 p3180 N85-29716
Modeling and experiments on tritium permeation in fusion reactor blankets
[DE85-006439] 18 p3183 N85-29741
Tokamak ignition/burn experimental research device
[DE85-009999] 18 p3190 N85-29785
Alloy development for irradiation performance
[DE85-010454] 19 p3240 N85-30091
Report to the Working Group on Technology, Growth and Employment
[DE85-010320] 19 p3372 N85-30920
Nuclear data needs for fusion energy development
[DE85-010445] 20 p3536 N85-32000
Technical assessment of thermal-hydraulics for high heat flux fusion components
[DE85-013178] 23 p3930 N85-34359

THERMONUCLEAR REACTIONS
NT CONTROLLED FUSION
NT NUCLEAR FUSION
Ion-density correlations and enhancement of thermonuclear reaction rate in dense, inertially confined fusion plasmas 02 p0284 N85-11849
Solar neutrinos: Prospects for detection and implications
[DE84-015522] 02 p0304 N85-11966
Inertial confinement fusion: Present status and future potential
[DE84-016177] 04 p0567 N85-13618
X-ray bursts: Observation versus theory
[NASA-CR-174415] 10 p1573 N85-19916
Numerical analysis of thermonuclear detonation in dense plasma 11 p1719 N85-20814
Fusion Energy Division
[DE85-001701] 11 p1731 N85-20884
Whist code calculations of ignition margin in an ignition Tokamak
[DE85-009507] 18 p3180 N85-29784
Advances in ICF power reactor design
[DE85-010930] 19 p3361 N85-30041
X-ray spectra of bursting neutron stars
23 p3961 N85-34688

THERMOPHILES
Construction of a bacterium to convert cellulose to ethanol
[TI84-901639] 04 p0481 N85-13068

THERMOPHILIC PLANTS
NT BLUE GREEN ALGAE

THERMOPHYSICAL PROPERTIES
NT CRITICAL POINT
NT CRITICAL PRESSURE
NT CRITICAL TEMPERATURE
NT EMISSIVITY
NT HEAT OF FUSION
NT MELTING POINTS
NT PYROELECTRICITY
NT SPECIFIC HEAT
NT SUPERCRITICAL PRESSURES
NT TEMPERATURE DEPENDENCE
NT THERMAL CONDUCTIVITY
NT THERMAL DIFFUSION
NT THERMAL DIFFUSIVITY
NT THERMAL STABILITY
NT VAPOR PRESSURE
NT VOLATILITY
USSR report: Materials science and metallurgy, no. 93
[JPRS-84810] 01 p0018 N85-10110
Solidification and crystal growth of solid solution semiconducting alloys 02 p0155 N85-11046
Exothermic processes in solids under low temperatures, their physics and their cryogenic implications
[JUEL-1919] 03 p0414 N85-12651
PRIAMUS, a computer program for the calculation of thermophysical properties of gas mixtures containing O2, N2, CO, CO2, He, H2O, H2, CH4
[JUEL-1916] 04 p0472 N85-13002
National Bureau of Standards passive solar test facility: Instrumentation and site handbook
[PB85-100451/GAR] 07 p0968 N85-16148
Thermophysical property testing using transient techniques
[AD-A147085] 07 p1049 N85-16884
Weldability of alloy ABM1 to alloy 1201
11 p1603 N85-20080
China report: Science and technology
[JPRS-CST-84-025] 11 p1620 N85-20197
Thermophysical properties of matter
11 p1620 N85-20199

Fine-grained, isotropic graphite for use as NBS (National Bureau of Standards) thermophysical property RM's from 5 to 2500 K
[PB85-112866] 12 p1614 N85-21381
Simulation of thermal and electromagnetic processes in induction plasmatrons 12 p1841 N85-21552
Nested subcritical flows within supercritical systems
[NASA-TM-86960] 12 p1845 N85-21574
Thermophysical properties of working fluids for binary geothermal cycles
[DE85-000385] 12 p1881 N85-21804

THERMOPHYSICS
U THERMODYNAMICS

THERMOPLASTIC FILMS
Induction heating gun
[NASA-CASE-LAR-13181-1] 18 p3085 N85-29083

THERMOPLASTIC RESINS
NT THERMOPLASTIC FILMS
Thermoplastic-carbon fiber hybrid yarn
[NASA-CR-3849] 03 p0325 N85-12093
Constituent property - composite property relationships in thermoset matrices 04 p0465 N85-12950
Free volume considerations in thermoplastic and thermosetting resins 04 p0465 N85-12952
Solvent resistant thermoplastic composite matrices 04 p0466 N85-12960
Thermoplastic/melt-processable polyimides 04 p0466 N85-12961
Aliphatic-aromatic heterocyclics as potential thermoplastics for composite matrices 04 p0466 N85-12962
Characterization of a thermoplastic polyimidesulfone
[NASA-TM-86358] 10 p1450 N85-19135
Characterization and adhesive bonding of poly(etheretherketone) resins and composites
[DE85-002526] 11 p1593 N85-20023
Hot melt adhesive attachment pad
[NASA-CASE-LAR-12894-1] 11 p1610 N85-20125
Broadband thermoplastic radomes
[AD-P004369] 12 p1827 N85-21483
Stability of three-layer glass-reinforced plastic shells of rotation 13 p2047 N85-22813
Finland, Sweden cooperate in composites research 17 p2946 N85-28184
Phenoxy resins containing pendent ethynyl groups and cured resins obtained therefrom
[NASA-CASE-LAR-13262-1] 18 p3068 N85-28973
Laminated thermoplastic radome
[AD-D011664] 18 p3079 N85-29045
Adhesive evaluation of LARC-TPI and a water-soluble version of LARC-TPI
[NASA-TM-86428] 19 p3248 N85-30136
Development of an impact- and solvent-resistant thermoplastic composite matrix, phase 3
[NASA-CR-172568] 20 p3422 N85-31239
Structure-property relationships in thermoplastic elastomers. Part 3: Segmented polyacetal-polyurethanes
[AD-A154897] 21 p3569 N85-32200
Strength properties of glassfiber reinforced thermoplastics 23 p3908 N85-34212
Determination of the viscosity number of thermoplastics in dilute solution; polyamides (PA)
[NASA-TM-77673] 24 p4081 N85-35296

THERMOPLASTICITY
Nonlinear structural and life analyses of a combustor liner 02 p0141 N85-10955
Variational principles in thermoplasticity. Part 2: Coupled thermomechanical processes
[RUB-IFM-MITT-37-PT-2] 05 p0648 N85-14161
Finite element method calculation of a necking tension specimen including heat transfer influence
[RUB-IFM-MITT-40] 05 p0648 N85-14162
Structure-property relationships in thermoplastic elastomers. Part 1: Segmented polyether-polyurethanes
[AD-A148043] 08 p1133 N85-17138
Characterization of novel binders based on energetic thermoplastic elastomers
[AD-A146993] 10 p1451 N85-19139
Thermoset-thermoplastic aromatic polyamide containing N-propargyl groups
[NASA-CASE-LAR-12723-1] 11 p1610 N85-20123
Process for preparing solvent resistant, thermoplastic aromatic poly(imidesulfone)
[NASA-CASE-LAR-12858-2] 11 p1610 N85-20124
Chemoviscosity modeling for thermosetting resins, 2
[NASA-CR-177958] 24 p4073 N85-35243

THERMOREGULATION
Thermoregulatory consequences of long-term microwave exposure at controlled ambient temperatures
[PB84-236603] 05 p0697 N85-14484
Effects of body mass and morphology on thermal responses in water
[AD-A147558] 07 p1016 N85-16455
Specifics of human thermal regulatory reactions upon exposure to coriolis acceleration 10 p1525 N85-19617
Sleep deprivation and exercise tolerance
[AD-A150566] 13 p2142 N85-23296
Exercise-heat strain during hypohydration: Interaction with heat acclimation and aerobic fitness
[AD-A151023] 14 p2369 N85-24717
Thermoregulatory and vestibular systems in the rat 15 p2610 N85-26082
Mathematical models relating to human thermoregulation: Basic assumptions, validation, and application. Parts A and B
[AD-A151556] 15 p2618 N85-26130
Primate experiments on SLS-1 15 p2687 N85-26592
Microwave radiation and thermoregulation
[AD-A155718] 22 p3818 N85-33654
Electroanesthesia as a means of controlling cold stress of local hypothermia 22 p3823 N85-33687

THERMOSETTING RESINS
NT EPOXY RESINS
NT KEVLAR (TRADEMARK)
NT NYLON (TRADEMARK)
NT PHENOLIC RESINS
NT POLYAMIDE RESINS
Chemoviscosity modeling for thermosetting resins - I
[NASA-CR-172443] 03 p0326 N85-12096
Constituent property - composite property relationships in thermoset matrices 04 p0465 N85-12950
Free volume considerations in thermoplastic and thermosetting resins 04 p0465 N85-12952
Thermally stable thermoset resin compositions
[AD-D011274] 05 p0620 N85-13963
The use of microdielectrometry in monitoring the cure of resins and composites
[AD-A148619] 08 p1119 N85-17055
Synthesis of hydrophobic, crosslinkable resins
[AD-A150858] 14 p2260 N85-24002
NASA/aircraft industry standard specification for graphite fiber toughened thermoset resin composite material
[NASA-RP-1142] 16 p2742 N85-26923
Structure-property relationships in polymeric matrix materials
[AD-A153929] 18 p3080 N85-29050
Synthesis and properties of arylethersulfone thermoset systems
[AD-A154811] 21 p3569 N85-32198
Chemoviscosity modeling for thermosetting resins, 2
[NASA-CR-177958] 24 p4073 N85-35243

THERMOSIPHONS
Investigation of crisis phenomena in thermosyphons with internal heat-dissipation
[BLL-M-35765-(5628.4)] 02 p0197 N85-11313

THERMOSPHERE
NT TURBOPAUSE
Global matrix of thermospheric density values for selected solar/geomagnetic conditions and spacecraft orbital attitudes
[NASA-TM-86478] 04 p0533 N85-13409
Dynamics of the low-latitude thermosphere and ionosphere 09 p1351 N85-18501
Middle Atmosphere Program. Handbook for MAP, volume 10
[NASA-CR-175477] 11 p1658 N85-20450
Coupling between the thermosphere and the stratosphere: The role of nitric oxide 11 p1662 N85-20472
Basic features of global circulation in the mesopause lower thermosphere region 11 p1662 N85-20475
Investigation of aeronomic processes on the basis of ionospheric sporadic E 11 p1663 N85-20482
High time resolution thermospheric temperature and wind studies in the Arctic
[AD-A150114] 12 p1890 N85-21860
Experiment for measuring electric fields within the sounding rocket project Energy Budget
[BMFT-FB-W-84-048] 12 p1891 N85-21866
Models of the upper atmosphere 12 p1945 N85-22217
Analysis and interpretation of observations of airglow at 297 nm in the Venus thermosphere 13 p2172 N85-23473
Mechanism of formation of low temperatures in nighttime Venusian thermosphere 16 p2723 N85-26807
Thermospheric winds observed by OI6300A Doppler shifts at 23 deg S in the Brazilian sector
[INPE-3384-RPE/470] 16 p2834 N85-27479
Circulation and transport in the middle atmosphere: Mesosphere and lower thermosphere 18 p3148 N85-29492
Additional possibilities of radiometeor azimuthal method for measuring wind velocity in lower thermosphere 19 p3296 N85-30438
Venus thermospheric circulation
[PB85-180420] 19 p3384 N85-30997
Further developments of EISCAT as an MST radar 21 p3627 N85-32534

THERMOSTABILITY
U THERMAL STABILITY

THERMOSTATS
German payloads for EURECA 1
[BMFT-FB-W-85-003] 20 p3419 N85-31223
TEMO and TEB thermoelectronic devices 22 p3779 N85-33415

THERMOTROPISM
U ANISOTROPY
U TEMPERATURE EFFECTS

THERMOVISCOELASTICITY
Thermoviscoelastic analysis of dimensionally stable fiber composite space structures
[AD-A149275] 11 p1593 N85-20021
The initiation and growth of adiabatic shear bands
[AD-A154459] 19 p3287 N85-30382

THESAURI
An operational system for subject switching between controlled vocabularies: A computational linguistics approach
[NASA-CR-3838] 02 p0293 N85-11903
NASA Thesaurus supplement: A 3-part cumulative supplement to the 1982 edition of the NASA Thesaurus
[NASA-SP-7051(SUPPL-2)] 03 p0437 N85-12765
Online database search strategies and thesaural relationship models 09 p1402 N85-18822
Keyword thesaurus: A list of terms and codes to identify areas of interest for research and other types of sponsored programs (revised October 1984)
[PB85-136893] 10 p1568 N85-19860
NASA Thesaurus supplement, a three part cumulative supplement to the 1982 edition of the NASA Thesaurus
[NASA-SP-7051(SUPPL-3)] 14 p2432 N85-25002
Energy data base: Subject thesaurus
[DE84-010568] 16 p2878 N85-27761

THETA PINCH
The origin of plasma rotation in the early phase of an FRC produced by a reversed field theta pinch
[IPPJ-698] 06 p0663 N85-15482
Theta pinch discharges for solids vaporization and elemental chemical analysis
[DE85-002966] 11 p1733 N85-20899

THIAZINE (TRADEMARK)
The electrochemistry of azine, oxazine and thiazine dyes
[AD-A152394] 17 p2918 N85-27990

THICK FILMS
Conductor structure for thick film electrical device
[AD-D011240] 01 p0043 N85-10281
Thick film radiation detector
[AD-D011211] 01 p0048 N85-10318
Structural studies of sputtered MOS(2) films by angle-resolved photoelectron spectroscopy
[AD-A146052] 03 p0433 N85-12759
Transport processes during the growth of oxide films at elevated temperature
[AERE-R-11293] 03 p0434 N85-12766
Qualification of a thick film hybrid
[BMFT-FB-W-84-024] 04 p0497 N85-13170
Viscosity measurements for thick-film pastes 06 p0631 N85-15280
The replacement of precious metal thick film inks using conductive polymer technology. Phase 1: Feasibility study
[AD-A147614] 07 p0933 N85-15913
Ink jet printing of silver metallization for photovoltaics
[NASA-CR-175798] 15 p2586 N85-25943
The replacement of precious metal thick film inks using conductive polymer technology
[AD-A152002] 16 p2749 N85-26965
MOD silver metallization for photovoltaics
[NASA-CR-175773] 16 p2818 N85-27381
MOD silver metallization for photovoltaics 21 p3610 N85-32428

THICK PLATES
On some exact solutions in elastostatics in terms of harmonic functions 09 p1332 N85-18367
Assessment of effectiveness of electron beam welding of titanium alloys up to 40 mm in thickness by vertical or horizontal beam 11 p1603 N85-20078
Method of separately determining electrophysical properties of bulky conductor 13 p2073 N85-22951
Method of fabricating acceleration resistant crystal resonators and acceleration resistant crystal resonators so formed
[AD-D011630] 16 p2778 N85-27145
The nonlinear analysis of thick composite plates using a cubic spline function 16 p2798 N85-27252
A refinement of the transverse shear deformation theory for multilayered anisotropic plates
[STN-5] 20 p3471 N85-31571

THICK WALLS
Allowing for the temperature field in the wall thickness of checkerwork in thermal calculation
[BLL-M-36015-(5828.4)] 07 p0956 N85-16058
Development of a floating element wall shear transducer
[AD-A148450] 08 p1164 N85-17346
Radiographic inspection of butt welds described 11 p1620 N85-20196
Methods of first wall structural analysis with applications to the long pulse commercial Tokamak reactor design
[DE85-004915] 15 p2657 N85-26397
Experimental study of collapse of thick-walled tube under external pressure and axial force 23 p3904 N85-34186

THICKNESS
Evaluation of moduli and thicknesses of pavement systems by spectral-analysis-of-surface-waves method
[PB84-219112] 03 p0342 N85-12205
Variation of resin properties through the thickness of cured samples 04 p0468 N85-12974
Synthesis study of nondestructive testing devices for use in overlay thickness design of flexible pavements
[PB84-218080] 06 p0774 N85-14950
Stability of circular cylindrical shell with piecewise constant thickness subjected to radial pressure 06 p0779 N85-14982
Method for non contacting gauging of the wall thickness of tubes by backscattering radiation
[OEFZS-4274] 07 p0968 N85-16144
Lithography radiation effects study
[AD-A149552] 10 p1468 N85-19260
New method for studying surface crack growth in laminated polymer composite materials 11 p1598 N85-20051
Thickness effect in low-density insulation
[DE85-003065] 11 p1631 N85-20273
Liquid thickness gage
[NASA-CASE-LAR-13342-1] 11 p1635 N85-20297
AEM with a convergent beam
[DE85-000667] 11 p1714 N85-20784
An investigation of compressible flows over open cavities including shear layer thickness effects
[AD-A150086] 12 p1847 N85-21588
Analysis of optimum front cover thickness for lightweight solar arrays 13 p2010 N85-22606
Composition and thickness of oxide coatings on granule surfaces of aluminum alloys 13 p2030 N85-22719
Spectral frequency of eigenvalues in optimal problems of stability of cylindrical shells of variable thickness 13 p2047 N85-22815
Thickness of ridged plains materials in Hesperia Planum, Mars 13 p2185 N85-23561
Apparent thickness of Saturn's rings from the observations of the ring plane crossing 15 p2671 N85-26477
Specimen thickness effects for elastic-plastic CTOD toughness of A36 steel
[DE85-006992] 18 p3077 N85-29038
Electrodynamic transducers for ultrasonic reception 18 p3119 N85-29306
Effect of confinement on failure in 95 TATB/5 KEL-F
[DE85-010790] 19 p3251 N85-30158
Heat flow through ocean floor and its relationship to lithosphere structure and thickness 19 p3294 N85-30422
X-ray diffractometric measurements and calculations of limiting values of discrepancy between lattices and layer thicknesses, preventing generation of dislocations during growth of multilayer heterostructures 21 p3681 N85-32966
The longitudinal thickness of air-shower fronts
[OG-9.5-1] 23 p4030 N85-34978
Solid neon sources for plasma and X-ray lasers
[DE85-011347] 24 p4096 N85-35402

THIN AIRFOILS
NT THIN WINGS
Aerodynamics of airfoils subject to 3-dimensional periodic gusts
[AD-A145149] 01 p0003 N85-10018
Technology for pressure-instrumented thin airfoil models, phase 1
[NASA-CR-3691] 14 p2227 N85-23804

THIN FILMS
NT ENERGY ABSORPTION FILMS
NT FERROMAGNETIC FILMS
NT MONOMOLECULAR FILMS
Research on large, highly accurate, inflatable reflectors
[AD-A145080] 01 p0016 N85-10099
Analysis of glow discharges for understanding the process of film formation
[NASA-TM-83750] 01 p0022 N85-10138
Platinum thin film resistors as accurate and stable temperature sensors
[NASA-TM-77728] 01 p0049 N85-10322
Time resolved calorimetry of 30 nm Te-films during laser annealing
[AD-A145047] 01 p0052 N85-10346
Conversion of microwave signals by superconducting films in the resistive state
[NASA-TM-77595] 01 p0123 N85-10843
Preparation and properties of evaporated CdTe films compared with single crystal CdTe
[DE85-000502] 02 p0222 N85-11452
DOE/SERI polycrystalline thin-film photovoltaic research
[DE84-004516] 02 p0223 N85-11464
Thin film (Al, Ga)As heterojunction solar cells 02 p0258 N85-11691
Materials modification by ion beam mixing
[AD-P003948] 02 p0266 N85-11864
Relationships between electronic structure and stability of metallic glasses
[AD-A145508] 02 p0287 N85-11874
Diffusion of Cr-51 tracer in Cr-2O-3 and the growth of Cr-2O-3 films
[AERE-R-11314] 03 p0333 N85-12148
Twisted domain wall in very thin magnetic films with perpendicular anisotropy 03 p0350 N85-12252
Effect of heat treatment on phase composition and crystal structure of thin WSi2 films on silicon substrates 03 p0350 N85-12253
One-dimensional model of thin films. Analysis of aluminum surface 03 p0350 N85-12254
Development of the production technology of Cu2S/CdS solar generators
[BMFT-FB-T-84-137] 03 p0386 N85-12469
Dielectric and optical properties of sputtered thin films
[AD-A146210] 03 p0420 N85-12661
Fast ions as probes in solid state research 03 p0430 N85-12740
Center for dielectric studies
[AD-A146163] 03 p0434 N85-12761
The effect of thin-film growth mode on XPS/UPS/AES intensities
[AD-A146284] 03 p0434 N85-12763
Transport processes during the growth of oxide films at elevated temperature
[AERE-R-11293] 03 p0434 N85-12766
Research activities of the Illinois University Coordinated Science Laboratory
[AD-A145589] 03 p0449 N85-12856
Contamination problems during surface cleaning for thermocompression bonding
[DE84-013066] 04 p0475 N85-13023
Development of a feasibility model for a thin-film precision power meter
[BMFT-FB-T-84-161] 04 p0504 N85-13217
Thin polymer film collectors as a contribution to the solar industry
[DE84-015299] 04 p0529 N85-13363
Advanced amorphous materials for photovoltaic conversion
[DE84-017196] 04 p0529 N85-13384
Development and utilization of CdS/Cu2S 05 p0662 N85-14256
Contamination analysis of Ti-O2 thin films deposited using ion assisted deposition
[DE84-014944] 05 p0732 N85-14705
Stability of lubricant film in gas dynamic bearing 06 p0778 N85-14977
Recording holograms on thin films of titanium dioxide 06 p0789 N85-15039
Oxide charge characteristics of low temperature MOS (Metal-Oxide-Silicon) oxide films
[AD-A146447] 06 p0803 N85-15113
Amorphous metallic layers in Si metallization systems 06 p0830 N85-15277
Recent developments in photovoltaics
[DE84-004528] 06 p0833 N85-15305
Electronic transport processes in refractory metal silicides
[AD-A146495] 06 p0861 N85-15468
Effects of monolayer coverages on substrate sputtering yields 06 p0865 N85-15496
Synergistic sputtering properties of binary alloys 06 p0865 N85-15497
Arc-evaporated carbon films: Optical properties and electron mean free paths
[DE85-001246] 06 p0867 N85-15510
Substrate preparation for thin film deposition: A survey
[DE84-016119] 06 p0868 N85-15514
Evaluation of colorless polyimide film for thermal control coating applications
[NASA-TM-86341] 07 p0930 N85-15804
Sputtering in thin film technology for optics — laser systems 07 p0938 N85-15948
Fast granular superconducting bolometer
[AD-D011332] 07 p0961 N85-16093
High temperature thermocouple and heat flux gauge using a unique thin film-hardware hot juncture
[NASA-TM-86898] 07 p0962 N85-16096
Research on electroluminescence in thin film yttrium oxysulfide
[AD-A146909] 07 p1037 N85-16582
Electronic structure, chemical bonding, and electron conductivity of thin-film transition-metal silicides
[AD-A147721] 08 p1226 N85-17718
Thin film transistors for addressing flat panel displays
[BMFT-FB-T-84-210] 08 p1227 N85-17726
An inexpensive vector thin film magnetometer
[AD-A148725] 09 p1323 N85-18310
Light scattering studies of lower dimensional colloidal particle and critical fluid systems
[DE85-002087] 09 p1377 N85-18854
Thermally induced quasiparticle branch imbalance in thin film superconductors 09 p1396 N85-18786
Amorphous materials and recrystallization
[DE85-001873] 09 p1398 N85-18801
Pulsed photothermal radiometry for remote sensing of spectroscopic and physical properties of thin film
[AD-A149080] 10 p1435 N85-19041
Bondability of Al-Si thin film in thermosonic gold wire bonding — integrated circuits
[NASA-TM-77795] 10 p1439 N85-19071
Lithography radiation effects study
[AD-A149552] 10 p1468 N85-19260
Mod silver metallization for photovoltaics
[NASA-CR-174444] 10 p1509 N85-19518
Use of alternative solvents for low-temperature LPE growth of CdTe films
[AD-A149418] 10 p1562 N85-19853
Photon scattering and interaction analysis of interfacial corrosion and catalysis
[DE85-002534] 11 p1608 N85-20114
Deposition of diamondlike carbon films
[NASA-CASE-LEW-14060-1] 11 p1615 N85-20183
Chemically amplified laser direct-writing of aluminum
[DE85-000308] 11 p1639 N85-20324
Fabrication of monocrystalline GaAs solar cells utilizing NaCl sacrificial substrates
[DE84-013016] 11 p1673 N85-20544
Observation of standing spinwaves in thin Fe-films by means of Raman spectroscopy
[DE85-003036] 11 p1735 N85-20913
A computer simulation of thin film nucleation and growth: The Volmer-Weber case
[NASA-TM-86968] 12 p1796 N85-21264
A process to produce fine line metallic collection patterns on semiconductors devices
[NASA-CASE-NPO-16413-1] 12 p1805 N85-21325
Monolithic thin film SAW (Surface Acoustic Wave) structures
[AD-A149782] 12 p1835 N85-21511
Advanced thin film thermocouples
[NASA-CR-175541] 12 p1850 N85-21607
Ultrasensitive measuring devices
[DE85-000672] 12 p1853 N85-21622
Development of a CdSe thin film solar cell 12 p1880 N85-21796
Thin film technology of high-critical-temperature superconducting electronics
[AD-A150010] 12 p1940 N85-22186
Mass spectra of neutral particles released during electrical breakdown of thin polymer films 13 p1996 N85-22511
Microscopic magnetic structure of multiple bilayers of thin films of Fe and Ge
[DE85-004188] 13 p2024 N85-22682
Structure of amorphous films of alloys based on Fe, condensed from laser erosion products 13 p2035 N85-22749
Planar ferroelectric microcapacitors for microwave devices 13 p2067 N85-23032
Non-linear optical techniques for visible and UV lasers and thin film deposition
[AD-A150489] 13 p2096 N85-23077
Silicon-sheet and thin-film cell and module technology potential: Issue study
[NASA-CR-175654] 14 p2349 N85-24520
Tunneling in magnetic superconducting systems
[AD-A150677] 14 p2426 N85-24963
Ferroelectric tungsten bronze bulk crystals and epitaxial thin films for electro-optic device applications
[AD-A151044] 14 p2427 N85-24970
Structure of condensed aluminum thin film metallizations 15 p2512 N85-25501
Recording of acoustic wave in gaseous medium with thin-film pyroelectric transducers 15 p2525 N85-25571
Thin film cadmium telluride and zinc phosphide solar cells
[DE85-002904] 15 p2587 N85-25950
In situ thin film measurements
[AD-A151379] 15 p2652 N85-26353

Experimental and theoretical study of the infrared reflectance of thin oxide films on metals
[DE85-005799] 15 p2653 N85-26386
Applications of piezoelectric and pyroelectric thin films: Opportunities for Langmuir-Blodgett technology
[AD-A149239] 15 p2659 N85-26408
Synthesis and characterization of superconducting electronic materials
[AD-A151112] 15 p2659 N85-26409
In situ thin film measurement
[AD-A151365] 15 p2659 N85-26411
Fundamental studies of growth, doping and transformation in beta silicon carbide
[AD-A152047] 15 p2660 N85-26416
Characterization of thin films and layered structures using X-ray absorption and reflection at grazing incidence
[DE85-006580] 15 p2662 N85-26429
Thin-film polycrystalline silicon research
[DE85-002908] 15 p2663 N85-26434
Thin-film sensors for space propulsion technology
17 p2915 N85-27968
In situ HVEM studies of electron beam-driven composition changes in thin film alloys: Displacement-rate gradient effects
[DE85-007992] 17 p2931 N85-28092
Thin films properties of sputtered niobium silicide on SiO2, SiSN4 and on n+ poly-Si
[AD-A152378] 17 p2952 N85-28228
Technology development for thin-film-trace humidity sensors
[BMFT-FB-T-84-268] 17 p2969 N85-28338
Research and developmental study on MIS thin film solar cells of amorphous hydrogenated silicon, part 2
[BMFT-FB-T-84-290] 17 p2988 N85-28467
The structure of ion plated films in relation to coating properties
[NASA-TM-87055] 18 p3085 N85-29085
Dynamics of thin-film breakup in a constricted pore
[DE85-008442] 18 p3101 N85-29199
SERI photovoltaic advanced research and development project: FY 1984 accomplishments
[DE85-002939] 18 p3128 N85-29368
Thin layered interference mirrors to reduce radiation damage
[DE85-009765] 18 p3185 N85-29756
Ion beam sputter-deposited thin film coatings for protection of spacecraft polymers in low Earth orbit
[NASA-TM-87051] 19 p3248 N85-30137
Mechanical protection of DLC films on fused silica slides
[NASA-TM-87056] 19 p3248 N85-30138
Method for production of ceramic oxide and carbide bodies by polymer inclusion and decomposition
[DE85-011666] 19 p3250 N85-30152
Thin film phase transition materials development program
[AD-A154260] 19 p3259 N85-30209
VUV synchrotron light as a technique for studying the interface quality and properties of thin overlayers
[DE85-006822] 19 p3262 N85-30227
High temperature Raman studies of phase transitions in thin film dielectrics
[DE85-010973] 19 p3263 N85-30234
Cadmium sulfide/copper ternary heterojunction cell research
[DE85-008778] 19 p3305 N85-30486
Optical effects of thin film adhesives in multijunction solar cells
[DE85-010120] 19 p3305 N85-30488
Photoeffects of semiconductor electrolyte interfaces
[AD-A154163] 20 p3449 N85-31411
Nitridation of SiO2 for surface passivation
20 p3480 N85-31627
Recent improvements in materials for thin GaAs and multibandgap solar cells
[DE85-006600] 20 p3484 N85-31651
New metal coating method developed
21 p3568 N85-32191
Multilayer capacitor dielectrics produced from metallo-organic precursors
[AD-A154592] 21 p3580 N85-32254
Development of wide band recording materials
[AD-A154981] 21 p3589 N85-32309
Microwave-enhanced thin-film deposition
21 p3611 N85-32431
Failure analysis of thin-film amorphous-silicon solar-cell modules
21 p3613 N85-32452
Electrotransport in thin films
[AD-A155584] 21 p3710 N85-33034
Structure and functions of ultra-thin films of organic compounds
[DRIC-T-7481] 22 p3741 N85-33188
Examination of anisotropic films by resonance method
22 p3776 N85-33412
Advances in sputtered and ion plated solid film lubrication
22 p3797 N85-33524
1985 Amorphous Silicon Review Meeting
[DE85-008794] 22 p3807 N85-33582
Development and demonstration of a spiral-wound thin-film composite membrane system for the economical production of oxygen-enriched air, phase 4
[DE85-012360] 23 p3920 N85-34288
Polarisation insensitive achromatic cube beamsplitter — binocular microscopes
[NPL-MOM-72] 23 p3973 N85-34630

THIN PLATES
A triangular finite element for thin plates and shells
01 p0058 N85-10386
Composite laminate optimization program suitable for microcomputers
01 p0059 N85-10389
Scattering of H10-mode wave by narrow conducting plate inside rectangular waveguide
06 p0788 N85-15036
Microstructure, texture and formability of thin aluminium sheets
06 p0796 N85-15088
Silicon-sheet surface studies
06 p0831 N85-15287
Investigation of structural and electrical properties of low-angle silicon sheet
06 p0831 N85-15288
Static and dynamic fracture toughness characterization of SA508 forging and SA533B welded plate — pressure vessel steels
[CISE-2258] 08 p1131 N85-17127
The problem of protecting the structure of a packet composite of optimal thinwall elements
10 p1444 N85-19101
Assessment of effectiveness of electron beam welding of titanium alloys up to 40 mm in thickness by vertical or horizontal beam
11 p1603 N85-20078
Potential of high-average-power solid state lasers
[DE85-003884] 11 p1639 N85-20329
A new model for thin plates with rapidly varying thickness. Part 3: Comparison of different scalings
[AD-A149748] 12 p1866 N85-21704
Scattered data interpolation using thin plate splines with tension
[AD-A149803] 12 p1866 N85-21705
Experimental and numerical analysis of electric currents and electromagnetic blunting of cracks in thin plates
[AD-A150418] 13 p2022 N85-22669
Breakdown of thin plates by radiation
13 p2028 N85-22709
Pre- and post-processing for stream-function eddy current calculations
[AD-A150417] 13 p2065 N85-22896
Measurement of damping of graphite epoxy materials
[NASA-CR-175663] 14 p2248 N85-23931
The effect of low sheet thicknesses on the fracture toughness of an Al alloy (7075-T6) — Aramid Reinforced Aluminum Laminate (ARALL)
[VTH-LR-425] 16 p2752 N85-26984
A method for the evaluation of the residual energy of a metallic fragment after perforation of a thin target
[ISL-R-113/83] 16 p2794 N85-27233
An experimental study of the magnetoelastic bending of thin plates made of soft ferromagnetic material
19 p3282 N85-30352
Method of preparing thin porous sheets of ceramic material
[DE85-006399] 24 p4062 N85-35300

THIN WALLED SHELLS
A triangular finite element for thin plates and shells
01 p0058 N85-10386
Initial postbuckling analysis of elastoplastic thin-shear structures
01 p0059 N85-10393
Numerical improvement of asymptotic solutions and nonlinear shell analysis
05 p0648 N85-14158
Nonlinear finite element analysis of elastic and elastic-plastic buckling of cylinders under complex combined loads
09 p1332 N85-18373
The problem of protecting the structure of a packet composite of optimal thinwall elements
10 p1444 N85-19101
A new NDE (Non-Destructive Evaluation) capability for thin-shelled structures
[AD-A149625] 12 p1862 N85-21678
Elasticity formulas for thin-walled shells with piezoceramic layers
13 p2047 N85-22816
Fabrication of ceramic substrate-reinforced and free forms
[NASA-TM-86994] 14 p2247 N85-23926
Strength computation of thin walled shell by discreet-continuous model
14 p2268 N85-24181
Dynamic creep buckling: Analysis of shell structures subjected to time-dependent mechanical and thermal loading
17 p2913 N85-27959
Initial imperfection surveys on conical shells at Hoechst AG
[VTH-LR-407] 17 p2981 N85-28429

THIN WALLS
Interactive buckling of thin-walled structural components under static and dynamic loads
01 p0059 N85-10392
Analysis of thin-walled airframe members in geometrically nonlinear statement
06 p0780 N85-14995
Stability of hollow shafts under torsion
06 p0780 N85-14996
Effect of protective medium on durability and fracture structure on seam zones of thin-walled titanium articles produced by diffusion welding
13 p2033 N85-22738
Theory of diaphragm light modulators with electrical input signal
13 p2082 N85-23002
Head-on scattering of a tubular cylinder of finite length for radar target identification purposes
[AD-A155608] 21 p3577 N85-32246

THIN WINGS
ESP (External-Stores Program): A pilot computer program for determining flutter-critical external-store configurations. Volume 2: Final report on program enhancement and delivery
[AD-A152269] 16 p2711 N85-26726
A computational method for wings of arbitrary planform
[AD-A153788] 18 p3059 N85-28929
A supersonic potential gradient method for the calculation of unsteady aerodynamic pressures on harmonically oscillating wings
[DFVLR-FB-85-11] 20 p3390 N85-31026

THINNERS
U SOLVENTS

THIOLS
Formation of high molecular weight products from benzene during boundary lubrication
[NASA-TM-86966] 13 p2017 N85-22644
Distribution and abundance of organic thiols
21 p3657 N85-32717

THOMAS-FERMI MODEL
Theoretical thermodynamics of mixtures at high pressures
13 p2183 N85-23550

THOMAS-FERMI THEORY
U THOMAS-FERMI MODEL

THOMSON EFFECT
U THERMOELECTRICITY

THOMSON SCATTERING
A high transmission, 20 channel polychromator for the Thomson scattering diagnostic of TORTUR 3 — plasma diagnostics
[REPT-84-156] 03 p0422 N85-12694
Lidar-Thomson scattering — nuclear fusion
[IPP-1/299] 08 p1221 N85-17693
Feasibility of alpha particle measurement by CO2 laser Thomson scattering
[DE85-001764] 09 p1326 N85-18334
Lidar-Thomson scattering — Joint European Torus
[IPF-84-3] 09 p1394 N85-18777
Feasibility of alpha particle measurement by CO2 laser Thomson scattering
[DE85-004938] 13 p2097 N85-23061
System for lower hybrid current startup
15 p2654 N85-26373
Electron temperature measurements from induced toroidal current in ELMO Bumpy Torus scale
[DE85-006549] 18 p3189 N85-29779
Thomson scattering on Elmo Bumpy Torus
[DE85-010584] 20 p3527 N85-31941
Instrument to synchronize Thomson scattering diagnostic measurements with MHD activity in a Tokamak
[DE85-012082] 23 p3984 N85-34708

THORIUM
NT THORIUM ISOTOPES
Contribution to the radiogeology of Sao Roque, SP, granites
[INPE-3079-PRE/492] 03 p0391 N85-12503
U, Th, K content, heat production and thermal conductivity of Sao Paulo, Brazil continental shelf sediments: A reconnaissance work
[INPE-3401-PRE/670] 10 p1515 N85-19558
Uranium, thorium isotopic analyses and uranium-series ages of calcite and opal and stable isotopic compositions of calcite from drill cores UE25a no. 1, USR G-2 and USW G-3/GU-3, Yucca Mountain, Nevada
[DE85-013039] 23 p3948 N85-34471

THORIUM ISOTOPES
Development of solid thorium-232 reference materials
[DE85-011453] 22 p3841 N85-33785

THORIUM 228
U THORIUM ISOTOPES

THORIUM 230
U THORIUM ISOTOPES

THORIUM 234
U THORIUM ISOTOPES

THORON
U RADON ISOTOPES

THREADS
Improvement of gas-tightness of OTTG and TBO-5 threaded pipe couplings
[BLL-M-35993-(5828.4)] 07 p0972 N85-16175
The design and development of a spacecraft appendage tie down mechanism 22 p3797 N85-33522
THREAT EVALUATION
Dual band radome wall design
[AD-P004357] 12 p1825 N85-21451
Generation of flight paths using heuristic search
[AD-A151949] 16 p2704 N85-26894
Fiber reinforcement of gun propellant
[AD-A152296] 16 p2757 N85-27014
Space Station crew safety alternatives study. Volume 5: Space Station safety plan
[NASA-CR-3858] 17 p2908 N85-27930
Space station crew safety alternatives study. Volume 3: Safety impact of human factors
[NASA-CR-3856] 19 p3223 N85-29984
Space station crew safety alternatives study, volume 1
[NASA-CR-3854] 19 p3223 N85-29985
Space Station crew safety alternatives study. Volume 2: Threat development
[NASA-CR-3855] 21 p3558 N85-32133
Evaluation of a software design approach: Develop a threat resolution module in Ada (trademark)
[AD-A155599] 21 p3672 N85-32815
THREE AXIS STABILIZATION
Fluid slosh dynamics of surface tension tanks in three axis stabilized spacecraft
[MBB-UR-E-739-84-O] 11 p1634 N85-20291
The attitude control model tests for the Infrared Astronomical Satellite (IRAS)
[B6580071] 18 p3067 N85-28967
THREE BODY PROBLEM
Sturmian expansion approximation to three-body scattering
[CSIR-TWISK-309] 01 p0109 N85-10731
Spline-Galerkin solution of integral equations for 3-body scattering above break-up
[TWISK-327] 01 p0109 N85-10738
Rapid nonresonant rotation of a spacecraft in nominally periodic orbits in limited 3 body problem
02 p0160 N85-11083
Quasi-three dimensional modeling of functionally-integrated elements of large-scale integrated circuits 04 p0490 N85-13122
The restricted problem of 2 + N bodies
09 p1414 N85-18925
Lagrangian solutions in photogravitational restricted circular three-body problem 13 p1979 N85-22416
Computation of elliptical functions in problems of celestial mechanics 13 p1979 N85-22418
Stability of steady motions of dynamically symmetrical solid at a triangular libration point
14 p2279 N85-24120
On an assymetric choice for a cluster expansion of the three-body problem
[CSIR-TWISK-339] 14 p2408 N85-24844
Applications of three-body resonances to satellites and planetary rings 15 p2676 N85-26518
Integrable cases of restricted doubly averaged 3-body problem 16 p2718 N85-26778
The 6 pi-periodic solutions of plane restricted elliptical 3-body problem in neighborhood of libration points
16 p2718 N85-26779
Configuration space Faddeev calculations
[DE85-005813] 16 p2872 N85-27721
THREE DIMENSIONAL BODIES
Recent advances in hybrid/mixed finite elements
[NASA-CR-175574] 12 p1863 N85-21687
Three-dimensional sensing and interpretation
[AD-A150800] 14 p2311 N85-24304
Three-dimensional photochemical machining with lasers
[AD-A154711] 21 p3591 N85-32320
On the dependence of the convergence of Gummel's algorithm on the regularity of the solution
[AD-A154826] 21 p3675 N85-32832
Mathematical modeling of ultimate heat sink cooling ponds
[TI85-009747] 23 p3932 N85-34369
A simple but systematic CSG system
23 p3963 N85-34569
Building an octree from a set of parallelepipeds
23 p3964 N85-34572
Low cost geometric modelling system for CAM
23 p3964 N85-34578
Generative design in architecture using an expert system 23 p3965 N85-34582
THREE DIMENSIONAL BOUNDARY LAYER
On the instability of a 3-dimensional attachment line boundary layer: Weakly nonlinear theory and a numerical approach
[NASA-CR-172504] 07 p0957 N85-16063
Theoretical contributions to transonic flow analysis for transport aircraft
[BMFT-FB-W-84-036] 08 p1078 N85-16838
A 3-dimensional turbulent boundary layer upstream and around a junction vortex flow 08 p1160 N85-17319
A finite difference method for inverse mode calculations of a three-dimensional boundary layer
[ESA-TT-863] 09 p1274 N85-18007
Influence of turbulence of incident stream on three dimensional boundary layer 14 p2278 N85-24113
An exploratory investigation of sharp fin-induced shock wave/turbulent boundary layer interactions at high shock strengths
[AD-A151571] 15 p2558 N85-25772
Three-Dimensional Boundary Layers
[AGARD-R-719] 15 p2558 N85-25784
Three-dimensional boundary layers and shear flows activities at ONERA/CERT 15 p2558 N85-25785
Three-dimensional boundary layers: A report on work in Germany 15 p2559 N85-25786
Three-dimensional boundary layer research at NLR
15 p2559 N85-25787
Brief review of current work in the UK on three dimensional boundary layers 15 p2559 N85-25788
Problems and opportunities with three-dimensional boundary layers — aircraft, missile, and ship components 15 p2559 N85-25789
Three-dimensional wing boundary layer analysis program BLAY and its application
16 p2694 N85-26832
THREE DIMENSIONAL FLOW
NT SECONDARY FLOW
Numerical analysis of the 3-dimensional inviscid hypersonic flow around capsule-type bodies by the alternate directional implicit method
[NAL-TR-799] 01 p0002 N85-10012
Aerodynamics of airfoils subject to 3-dimensional periodic gusts
[AD-A145149] 01 p0003 N85-10018
Transonic wing and far field test data on a high aspect ratio transport wing for three dimensional computational method evaluation 01 p0004 N85-10021
Oil flow patterns of separated flow on a hemispherical cylinder at incidence
[DFVLR-FB-84-20] 01 p0048 N85-10313
Characteristic boundary conditions for three-dimensional transonic unsteady aerodynamics
[NASA-TM-86292] 02 p0134 N85-10915
Three dimensional separation and vortex formation
02 p0196 N85-11308
Two- and three-dimensional model and wall data from a flexible-walled transonic test section
03 p0312 N85-12015
A data base for three-dimensional all-interference code evaluation 03 p0312 N85-12017
Minimization of wall interference for three-dimensional models with two-dimensional wall adaptation — wind tunnel walls
[VKI-TN-149] 03 p0321 N85-12070
Turbomachinery blade design using advanced calculation methods
[PNR-90218] 04 p0456 N85-12896
Fundamental study of three dimensional two phase flow in combustion systems
[AD-A142886] 04 p0498 N85-13177
Flow calculation on a thin wing, with specific attention to separation point at the trailing edge
[FTW-FO-1721] 05 p0594 N85-13787
Accuracy of preparation of three-dimensional reference grid
[BLL-M-35921-(5828.4)] 05 p0616 N85-13939
Answering thermodynamic questions with three-dimensional viscous flow calculations
05 p0636 N85-14061
Theoretical approach to labyrinth seal forces - cross-coupled stiffness of a straight-through labyrinth seal 05 p0643 N85-14127
Turbulent bubbles behind airfoils and wings at high angle of attack 06 p1069 N85-16779
Aerodynamic issues in the design of high-lift systems for transport aircraft 06 p1069 N85-16780
Application of two and three-dimensional criteria for calculating transitions and boundary layers over swept wings 06 p1070 N85-16783
Application of the vortex-lattice concept to flows with smooth-surface separation 08 p1160 N85-17320
Research done at DERAT (October 1982 through September 1983); summary of principal results obtained
[NASA-TM-77786] 08 p1226 N85-17730
Three-dimensional vortex methods
[DE85-000391] 09 p1320 N85-18299
Averaging effects in models of three-dimensional two-phase flows
[AD-A149313] 10 p1484 N85-19371
Developments in the simulation of compressible inviscid and viscous flow on supercomputers
[NASA-TM-86674] 11 p1575 N85-19924
Three-dimensional analysis of heat transfer and gas flow in a radiant furnace
[DE84-011732] 11 p1633 N85-20284
A study of degenerate and nondegenerate critical points in three-dimensional flow fields
[DFVLR-FB-84-36] 11 p1633 N85-20288
Dynamic investigations of a spherical tank structure filled with liquid using ANSYS three-dimensional fluid elements
[MBB-UR-E-737-83-O] 11 p1654 N85-20418
Three-dimensional unsteady lifting surface theory in the subsonic range
[NASA-TM-77812] 12 p1770 N85-21111
The split-coefficient matrix method for supersonic three dimensional flow 12 p1821 N85-21425
A three-dimensional spectral algorithm for simulations of transition and turbulence
[NASA-CR-172561] 12 p1845 N85-21575
Solution of the three-dimensional Navier-Stokes equations for a steady laminar horseshoe vortex flow
[AD-A149851] 12 p1846 N85-21582
Turbulent convecting flow in a square duct with a 180 deg bend: An experimental and numerical study
[AD-A149969] 12 p1846 N85-21583
Experimental studies of Quasi-Two-Dimensional and three-dimensional viscous interaction regions induced by skewed-shock and swept-shock boundary layer interactions
[AD-A150080] 12 p1847 N85-21587
Robust calculation of three-dimensional transonic potential flow based on the nonlinear gas multigrid method and a mixed incomplete lower upper decomposition/strongly implicit procedure (ILU/SIP) algorithm
[NLR-MP-84003-U] 12 p1848 N85-21593
On the solution of the three-dimensional flowfield about a flow-through nacelle
[NASA-TM-87448] 13 p1969 N85-22371
Preliminary development of an approximation procedure for supercritical wing design optimization applications
[AD-A150177] 13 p1972 N85-22383
Calculation of three-dimensional, viscous flow through turbomachinery blade passages by parabolic marching
[NASA-TM-86684] 14 p2211 N85-23711
Mixing, chemical reaction and flow field development in ducted rockets
[DE85-004083] 14 p2247 N85-23928
Fundamental study of three dimensional two phase flow in combustion systems
[AD-A150739] 14 p2250 N85-23945
Discrete models for the numerical analysis of time-dependent multidimensional gas dynamics
[NASA-CR-172574] 14 p2300 N85-24239
Three-dimensional current systems and electric fields during active aurora 14 p2362 N85-24599
The generation of three-dimensional body-fitted coordinate systems for viscous flow problems
[AD-A150861] 14 p2408 N85-24848
Unsteady transonic aerodynamic and aeroelastic calculations about airfoils and wings
15 p2459 N85-25185
Natural convection in cylindrical containers
15 p2555 N85-25763
Two computational methods for cascade flows
16 p2692 N85-26817
Numerical example of three-dimensional flying object in shockless transonic flow 16 p2693 N85-26823
Turbulence characteristics of swirling flowfields
[NASA-CR-174918] 16 p2709 N85-26717
Study of the primary zone of gas turbine hearths
[ONERA-RTS-22/3256-EY] 16 p2709 N85-26719
Numerical analysis of flow non-uniformity in the hot gas manifold of the Space Shuttle main engine
16 p2738 N85-26899
Fuel and oxidizer turbine loss analysis
16 p2739 N85-26900
Redistribution of the inlet temperature profile through the SSME fuel turbine 16 p2739 N85-26901
Report on regional groundwater flow modeling for the Palo Duro Basin, Texas
[DE85-007490] 16 p2815 N85-27370
A three-dimensional turbulent separated flow and related measurements
[NASA-CR-175913] 18 p3098 N85-29181
A method for computing the core flow in three-dimensional leading-edge vortices
[NASA-TM-87489] 19 p3214 N85-29932
KIVA: A computer program for two- and three-dimensional fluid flows with chemical reactions and fuel sprays
[DE85-010334] 19 p3339 N85-30693
Numerical simulation of potential flow in transonic steady regimes 20 p3389 N85-31018

Extension of the small perturbations method in three-dimensional transonic, unsteady flow to the case of real wings
[ONERA-NT-17/3064-RY-070-R] 20 p3389 N85-31017
An implicit finite-difference code for a two-equation turbulence model for three-dimensional flows
[NASA-TM-86752] 20 p3454 N85-31448
A new finite element approach: Progress in inviscid flow computations
[NASA-TM-86434] 20 p3454 N85-31450
Three-Dimensional Techniques Applied to Internal Flows in Propulsion Systems
[AGARD-LS-140] 21 p3586 N85-32293
An analysis of flow models: From Navier-Stokes to potential flow equations 21 p3587 N85-32295
Computation of three-dimensional, inviscid, rotational flows 21 p3587 N85-32296
An elliptic calculation procedure for 3-D viscous flow 21 p3587 N85-32297
A 3-D Euler method for internal transonic flows computation with a multi-domain approach 21 p3587 N85-32298
Performance evaluation of flow in turbomachinery blade rows 21 p3587 N85-32299
Numerical solution of the Navier-Stokes equations for 3-D internal flows: An emerging capability 21 p3588 N85-32300
Simulation of complex three-dimensional flows
[NASA-TM-86773] 21 p3675 N85-32831
A three-dimensional viscous flow analysis for the helicopter tip vortex generation problem
[NASA-CR-3806] 23 p3893 N85-34114
Integral equation formulation for three-dimensional unsteady transonic flow
[ARL/STRUC-R-416] 23 p3894 N85-34119
Block-implicit calculations of three-dimensional laminar flow in strongly curved ducts
[DE85-003047] 23 p3931 N85-34363
System maintenance manual for master modeling of aerodynamic surfaces by three-dimensional explicit representation
[NASA-CR-178224] 23 p3956 N85-34517
Unsteady flow in a supersonic cascade with two in-passage shocks
[NASA-CR-3925] 24 p4060 N85-35158
General design method for 3-dimensional, potential flow fields. Part 2: Computer program DIN3D1 for simple, unbranched ducts
[NASA-CR-3928] 24 p4060 N85-35159
The lateral distributions of charged particles of energy greater than 0.3 E sub crit in electron-photon cascades in lead and air
[HE-3.6-10] 24 p4185 N85-35957

THREE DIMENSIONAL MOTION
NT SECONDARY FLOW
NT THREE DIMENSIONAL FLOW
Recognition of complex 3-dimensional objects using 3-dimensional moment invariants
[AD-A148119] 06 p1212 N85-17625
Ill-posed problems and regularization analysis in early vision
[AD-A147753] 06 p1222 N85-17696
Collision detection for moving polyhedra
[AD-A148961] 10 p1544 N85-19735
Cyclic industrial robots with mechanical energy storing devices: Multipositional system with one or several degrees of freedom 13 p2045 N85-22803
Stability of Rossby waves within framework of three-component analysis 13 p2109 N85-23142
New method for compensating and measuring any motion of three-dimensional objects in holographic interferometry
[ISL-CO-216/84] 22 p3789 N85-33474
Three-dimensional hydrodynamic hot-spot model
[DE85-009587] 23 p3922 N85-34301
Computation of three-dimensional shock wave and boundary-layer interactions
[NASA-TM-86780] 24 p4093 N85-35372
Analytical-numerical methods of calculations of energy and three-dimensional particle distributions in electromagnetic cascades
[HE-3.5-13] 24 p4184 N85-35950
On mini-cluster observed by Chacaltaya emulsion chamber experiment
[HE-3.6-12] 24 p4185 N85-35959
Peculiarities of gamma-quanta distribution at 20 TeV energy
[HE-3.7-10] 24 p4186 N85-35967

THRESHOLD CURRENTS
Determination of threshold and maximum operating electric stresses for selected high voltage insulation. Task 3: Investigation of high voltage capacitor insulation
[DE84-017051] 09 p1316 N85-18274
Threshold electron studies of gas-surface interactions
[AD-A151271] 15 p2647 N85-26328
Inter-zone auger recombination in GaSb laser structures 21 p3682 N85-32875

THRESHOLD DETECTORS (DOSIMETERS)
Search for anomalous C-jets in Chacaltaya emulsion chamber experiment
[HE-3.2-5] 24 p4179 N85-35913
Exotic interactions among C-jets and Pb-jets
[HE-3.2-6] 24 p4179 N85-35914
Detection threshold energy of high energy cascade showers using thermoluminescence PTFE-sheet and hot-gas reader
[HE-7.1-5] 24 p4213 N85-36159

THRESHOLD GATES
High-power gate turn-off thyristors 06 p0793 N85-15071

THRESHOLD LOGIC
Estimation of the threshold in fatigue crack initiation models: A Bayesian approach
[AD-A144847] 01 p0062 N85-10410

THRESHOLD SHIFT
U THRESHOLDS

THRESHOLDS
Analysis of threshold effects during estimation of arrival time of optical signals 07 p0951 N85-16030
The role of nuclei size in transient cavitation threshold measurements
[AD-A148334] 08 p1162 N85-17332
Optimal threshold and weight sorting of elevation angle readings under conditions of fadeouts of a directed signal 12 p1840 N85-21547
An evaluation of discretized conditional probability and linear regression threshold techniques in model output statistics forecasting of visibility over the north Atlantic Ocean
[AD-A151955] 16 p2857 N85-27619
Threshold effects and cellular recognition
[DE85-010616] 19 p3327 N85-30614

THRESHOLDS (PERCEPTION)
Thresholds of perception of whole body linear oscillation: Modification by spaceflight 05 p0694 N85-14467
Inner ear characteristics during 7 day antiorthostatic bedrest (6 deg head down tilt) 05 p0695 N85-14470
Quantitative measurement of human auditory acuity 10 p1524 N85-19614
Auditory impairment and the onset of disability and handicap in noise-induced hearing loss
[ISVR-TR-126] 20 p3507 N85-31801
Thresholds for detection of linear oscillation following prolonged weightlessness 20 p3508 N85-31810
Auditory fatigue caused by exposure to different frequency sounds presented at equivalent intensity
[ISL-R-101/84] 20 p3525 N85-31923

THROATS
Multiple steady states for characteristic initial value problems
[NASA-CR-172486] 06 p0749 N85-14800
Mixing characteristics of an underexpanded multiple jet ejector
[AD-A149557] 10 p1485 N85-19375
Characteristics of flow of oscillatory-relaxing gas in nozzles with constant cross-sections in throat region 11 p1716 N85-20794

THROTTLING
Nonintrusive shaft speed sensor 16 p2740 N85-28908

THRUST
NT JET THRUST
NT LOW THRUST
NT ROCKET THRUST
NT VARIABLE THRUST
Three degree of freedom steady state point performance program: Updated version 1
[CSIR-NIAST-83/48] 01 p0001 N85-10005
Development of the Engineering Test Satellite-3 (ETS-3) ion engine system
[NASA-TM-77538] 01 p0017 N85-10101
Energy efficient engine ICLS engine bearings, drives and configuration: Detail design report
[NASA-CR-167871] 02 p0147 N85-10997
Thrust characterization of very high burning rate propellants
[AD-A145891] 03 p0340 N85-12186
On selecting bypass mixers for turbofan engines 09 p1306 N85-18207
An investigation of the driving wheel thrust of paddy field tractors
[AD-P004284] 09 p1407 N85-18661
Summary presentation of the Electrodynamics Interactions Panel 11 p1644 N85-20356
Report of the Electrodynamic Interactions Panel 11 p1645 N85-20363
Application of an aerodynamic analysis method including attainable thrust estimates to low speed leading-edge flap design for supersonic cruise vehicles
[NASA-CR-165843] 19 p3212 N85-29918
Measurement of turbofan-turbojet thrust from tailpipe static pressure
[AD-A154036] 19 p3220 N85-29967
Docking simulation analysis of range data requirements for the orbital maneuvering vehicle
[NASA-TM-86510] 20 p3407 N85-31143
Voyager 0.2-lbf thruster valve assembly short pulse test report
[NASA-CR-176121] 22 p3741 N85-33185

THRUST AUGMENTATION
An engine trade study for a supersonic STOVL fighter-attack aircraft, volume 1
[NASA-CR-166304] 02 p0133 N85-10910
Viscous-inviscid aerodynamic analysis of two-dimensional thrust augmentors
[NASA-CR-177321] 04 p0451 N85-12861
An experimental investigation of two-dimensional thrust augmenting ejectors, part 1
[NASA-CR-174111] 04 p0456 N85-12864
A theoretical study of two stage thrust augmenting ejectors
[ARL/AERO-R-166] 19 p3218 N85-29954
Discussion of the paper, Some Aspects of Propulsion for the Augmenter-Wing Concept, by D. C. Whittley
[NASA-TM-77884] 22 p3727 N85-33108

THRUST BEARINGS
Comparison of predicted and measured friction for a tilt-pad thrust bearing with crown and roughness under hydrodynamic and mixed lubrication
[AD-A145752] 03 p0371 N85-12371
Axial bearings with lever-type equalizer system 14 p2267 N85-24048
Work of axial bearing under dynamic loading 14 p2288 N85-24182
Calculation of friction at spherical bearing journals in turbomachines 17 p2940 N85-28150

THRUST CHAMBERS
Extended performance technology study 30-cm thruster
[NASA-CR-168259] 07 p0917 N85-15806
SSME thrust chamber simulation using Navier-Stokes equations
[NASA-CR-171349] 10 p1430 N85-19017
Thrust chamber performance using Navier-Stokes solution --- space shuttle main engine viscous nozzle calculation
[NASA-CR-171346] 10 p1430 N85-19019
Effective specific impulse of secondary flow injected into a rocket nozzle
[NAL-TR-848T] 18 p3067 N85-28970

THRUST CONTROL
NT THRUST VECTOR CONTROL
Aircraft thrust control scheme for terrain following system
[AD-D011387] 07 p0901 N85-15711
Design evolution of the orbiter reaction control subsystem 08 p1099 N85-16944

THRUST DISTRIBUTION
Space Shuttle booster thrust imbalance analysis
[NASA-TM-86493] 12 p1791 N85-21241

THRUST FAULTS
U GEOLOGICAL FAULTS

THRUST LOADS
Calculation of friction at spherical bearing journals in turbomachines 17 p2940 N85-28150
Characteristics of a confined jet thrust vector control nozzle
[AD-A153067] 17 p2958 N85-28268

THRUST MEASUREMENT
Vacuum chamber pressure effects on thrust measurements of low Reynolds number nozzles
[NASA-TM-86955] 12 p1794 N85-21259
Measurement of turbofan-turbojet thrust from tailpipe static pressure
[AD-A154036] 19 p3220 N85-29967
Two-plane balance and slip-ring design 22 p3799 N85-33536

THRUST POWER
U THRUST

THRUST REVERSAL
Experimental study of aerodynamic shielding of turbojet engine air intake against exhaust gases 09 p1307 N85-18210

THRUST VECTOR CONTROL
Gyrodynamic fixture for measuring thrust force components
[AD-D011258] 06 p0760 N85-14660
The solid rocket booster auxiliary power unit: Meeting the challenge 08 p1099 N85-16946
Static internal performance of a two-dimensional convergent nozzle with thrust-vectoring capability up to 60 deg
[NASA-TP-2391] 10 p1419 N85-18951

Preliminary performance of a vertical-attitude takeoff and landing, supersonic cruise aircraft concept having thrust vectoring integrated into the flight control system
[NASA-CR-172530] 10 p1423 N85-18977
Relative control effectiveness technique with application to airplane control coordination
[NASA-TP-2416] 14 p2218 N85-23753
Minimum time turns using vectored thrust
[AD-A151693] 15 p2471 N85-25256
Characteristics of a confined jet thrust vector control nozzle
[AD-A153087] 17 p2958 N85-28268
Static investigation of several yaw vectoring concepts on nonaxisymmetric nozzles
[NASA-TP-2432] 18 p3058 N85-28924
Thrust vectoring apparatus for maneuvering missile in flight
[AD-D011693] 19 p3226 N85-30004

THRUSTORS
Modeling the exhaust of the pulsed plasma thruster
[AD-A155344] 21 p3707 N85-33018

THUNDERSTORMS
On the nowcasting of mountain-generated thunderstorm systems 01 p0074 N85-10489
The microburst as a hazard to aviation: Structure, mechanisms, and nowcasting 01 p0074 N85-10491
A scheme for the delineation and extrapolation of thunderstorms from GOES satellite data 01 p0076 N85-10507
A lightning detection system in Sweden 01 p0078 N85-10519
A short-term forecast model for thunderstorm rotation 01 p0081 N85-10542
Nowcasting using lightning location techniques 01 p0084 N85-10568
Investigation of summertime convection over the upper Current River valley of southeast Missouri
[PB84-222389] 01 p0086 N85-10578
A case study of a convective outbreak using VAS-derived thermodynamic parameters
[AD-A145560] 02 p0232 N85-11512
Effects of a lightning strike on a civil defense operation center
[FOA-A-30035-A3] 02 p0232 N85-11514
NASA thunderstorm overflight program: Atmospheric electricity research. An overview report on the optical lightning detection experiment for spring and summer 1983
[NASA-TM-86468] 03 p0363 N85-12330
Investigations of severe/tornadic thunderstorm development and evolution based on satellite and AVE/SESAME/VAS data
[NASA-CR-174154] 04 p0536 N85-13424
Aircraft accident report Air Canada, Lockheed L-1011, C-FTNJ, near Charleston, South Carolina, November 24, 1983
[PB84-910413] 05 p0594 N85-13790
Synoptic observations of the radio noise background in the frequency range 150-160 kHz to provide design data for the low frequency communications designer
[AD-A147438] 07 p0941 N85-15965
Sea breeze-induced mesoscale systems and severe weather
[NASA-CR-174317] 08 p1187 N85-17480
Direct-strike lightning photographs, swept-flash attachment patterns, and flight conditions for storm hazards 1982
[NASA-TM-86347] 12 p1892 N85-21877
Mesoscale Atmospheric Processes Research Program Science Review
[NASA-TM-87465] 15 p2594 N85-25987
Anvil structure of severe thunderstorms 15 p2595 N85-25993
Lidar and radiometer observations of thunderstorm tops 15 p2595 N85-25994
Modeling of midwest severe thunderstorms 15 p2596 N85-25995
Satellite detection of severe thunderstorms 15 p2596 N85-25996
Severe storm detection with passive 37 GHz observations 15 p2596 N85-25997
Soil moisture and evapotranspiration estimates based on satellite data 15 p2596 N85-25998
Sea breeze-induced mesoscale systems and severe weather 15 p2598 N85-26012
Comparison of wind velocity in thunderstorms determined from measurements by a ground-based Doppler radar and an F-106B airplane
[NASA-TM-86348] 16 p2703 N85-26687
Fluid-dynamic model of a downburst
[UTIAS-271] 16 p2829 N85-27441
The electric current densities beneath thunderstorms 20 p3494 N85-31726
Thunderstorm phenomena and weather radar scanning strategies
[DOT/FAA/PM-85/14] 21 p3634 N85-32573

THYMUS GLAND
Distinctions of rat lymphatic organ reactions to acute stress factor during hypokinesia 19 p3324 N85-30596

THYRATRONS
Non-self-maintained high-voltage low-pressure discharge 13 p2088 N85-23037

THYRISTORS
NT SILICON CONTROLLED RECTIFIERS
High-speed power thyristors with excellent switching and load characteristics 06 p0793 N85-15070
High-power gate turn-off thyristors 06 p0793 N85-15071
High-speed power devices with field control 06 p0794 N85-15073
New methods of fast switching of high power by means of semiconductor devices 06 p0794 N85-15075
Allowable surge currents and failure mechanisms in semiconductor power devices in various modes of operation 06 p0795 N85-15080
Semiconductor submicrosecond power commutator switches 06 p0795 N85-15081
Analysis of inverter models and harmonic propagation. Part 3. Transient processes in inverter models
[DE85-000191] 10 p1510 N85-19530
High-voltage, high-power, solid-state remote power controllers for aerospace applications
[NASA-TP-2437] 12 p1795 N85-21263
New types of power supplies for ultrasonic processing equipment 12 p1843 N85-21566
The performance of an alternating-current thyristor-controlled motor 15 p2546 N85-25716
Fast transient behavior of thyristor switches
[AD-A154109] 19 p3259 N85-30206
Standard series of direct-current motors for regulated electric drives 22 p3772 N85-33375
Photothyristor optrons and optron microcircuits, part 1 22 p3781 N85-33424

THYROID GLAND
Structural changes in thyroid due to high-altitude adaptation in Kirghizia 22 p3820 N85-33666

TID
U TRAVELING IONOSPHERIC DISTURBANCES

TIDAL OSCILLATION
U TIDES

TIDAL WAVES
Tide tables 1985, high and low water predictions, central and western Pacific Ocean and Indian Ocean
[PB84-238393] 04 p0542 N85-13451
Recent observations of tides and tidal currents from the northeastern Bering Sea shelf
[PB84-241785] 04 p0543 N85-13452
Rip in White Sea 19 p3290 N85-30401
An objective analysis technique for extrapolating tidal fields 20 p3493 N85-31715

TIDE POWERED GENERATORS
Progress in developing tidal electric power plants reported 07 p0994 N85-16314

TIDES
NT ATMOSPHERIC TIDES
NT EARTH TIDES
NT LUNAR TIDES
Tide tables 1985. High and low ater predictions: Europe and West Coast of Africa including the Mediterranean Sea
[PB84-230093] 08 p0841 N85-15343
Spectral model for subtidal variability in the Chesapeake Bay
[PB84-226879] 06 p0842 N85-15345
Tides and tidal currents of the inland waters of Western Washington
[PB84-237379] 06 p0842 N85-15346
Monitoring of the tidal dynamics of the Dutch Waddensea by SIR-B 08 p1147 N85-17235
Altimetry, orbits and tides
[E85-10066] 08 p1174 N85-17404
Field-work report: Medway Estuary, 28 June - 18 July 1983
[RNC/NS/TR8] 13 p2041 N85-22773
Stability of the Galilean satellites in deep orbital resonance 13 p2172 N85-23477
Two-cycle mechanism of dissipation of tidal energy in ocean 14 p2335 N85-24438
Tidal breakup and origin of the Uranian ring system 15 p2578 N85-26535
Tidal rectification in lateral viscous boundary layers of a semienclosed basin
[CWI-AM-R8415] 17 p2960 N85-28284
Dynamic theory of polar tide 19 p3292 N85-30414
An objective analysis technique for extrapolating tidal fields 20 p3493 N85-31715
Ocean tidal parameters from LAGEOS 20 p3493 N85-31716
Interactions of galaxies and their nuclear activity 20 p3545 N85-32060
Reverification of the Chesapeake Bay model
[AD-A155486] 21 p3655 N85-32706
Coastal erosion along Monterey Bay
[AD-A155610] 21 p3655 N85-32707
On the importance of viscous dissipation in Io 22 p3855 N85-33873
Bibliography on tidal hydraulics. Report 2. Supplement 9: Supplementary material compiled from June 1950 - June 1983. Tidal flows in rivers and harbors
[AD-A155990] 24 p4125 N85-35574

TIG WELDING
U GAS TUNGSTEN ARC WELDING

TIGHTNESS
Improvement of gas-tightness of OTTG and TBO-5 threaded pipe couplings
[BLL-M-35993-(5828.4)] 07 p0972 N85-16175

TILES
Thermal contact conductance measurements on Doublet 3 armor tile graphite
[DE84-013554] 05 p0613 N85-13916
The challenging scales of the bird: Shuttle tile structural integrity 08 p1095 N85-16919
Study of outgassing and decomposition of space shuttle heat protection tiles, fillers and adhesive
[NASA-CR-175565] 12 p1791 N85-21242
Photovoltaic roofing tile systems 12 p1878 N85-21783
Electron beam charging of Space Shuttle thermal protection system tiles 13 p1990 N85-22478
Mechanical fastener
[NASA-CASE-LAR-12738-2] 19 p3279 N85-30335
Experimental aerodynamic heating to simulated space shuttle tiles in laminar and turbulent boundary layers with variable flow angles at a nominal Mach number of 7
[NASA-TP-2307] 23 p3929 N85-34351

TILT
U ATTITUDE (INCLINATION)

TILT ROTOR AIRCRAFT
Speed benefits of tilt-rotor designs for LHX
[NASA-CR-166437] 07 p0902 N85-15717
Helicopter aeromechanics: Introduction and historical review 18 p3057 N85-28914

TILTING
U ATTITUDE (INCLINATION)

TILTING ROTORS
Speed benefits of tilt-rotor designs for LHX
[NASA-CR-166437] 07 p0902 N85-15717

TILTMETERS
Soil tilt measurement: First results of the comparative analysis of the response of two different tiltmeters
[NOTA-INTERNA-818] 02 p0228 N85-11494

TIMBER IDENTIFICATION
Remote sensing applications program
[E85-10022] 02 p0218 N85-11435
An initial analysis of LANDSAT-4 Thematic Mapper data for the discrimination of agricultural, forested wetlands, and urban land cover — Poinsett County, Arkansas; and Reelfoot Lake and Union City, Tennessee 13 p2118 N85-23193

TIMBER INVENTORY
Some principles of plant resources evaluation using remotely sensed data 04 p0543 N85-13459
Forest cover monitoring by remote sensing in Great Britain 05 p0656 N85-14214

TIME
NT EPHEMERIS TIME
NT FLIGHT TIME
NT REACTION TIME
NT RELAXATION TIME
NT RESPONSE TIME (COMPUTERS)
NT SIDEREAL TIME
NT UNIVERSAL TIME
Microseism level, time variations at Turkmen seismic stations studied 07 p0981 N85-16231
Efficient computation of optimal time for transaction processing in a database system
[AD-A147566] 07 p1054 N85-16699
A theorem on the optimal allocation of effort
[AD-A148028] 08 p1211 N85-17623
A power transformation exponential regression model for censored failure time data
[AD-A148377] 08 p1212 N85-17632
Historical cost curves for hydrogen masers and cesium beam frequency and timing standards 10 p1465 N85-19245
Space and time variations and turbopause dynamical structure 11 p1683 N85-20483
High time resolution thermospheric temperature and wind studies in the Arctic
[AD-A150114] 12 p1890 N85-21880
Annals of the New York Academy of Sciences, Volume 423 — timing and time perception
[AD-A150031] 12 p1909 N85-21881
The measurement of human time estimating ability using a modified jerison device
[AD-A151870] 15 p2620 N85-26141

Piloted simulation of an algorithm for onboard control of time-optimal intercept
[NASA-TP-2445] 18 p3063 N85-28949
Proceedings of the Sixteenth Annual Precise Time and Time Interval (PTTI) Applications and Planning Meeting
[NASA-TM-87561] 18 p3105 N85-29221
The Rubidium-Crystal Oscillator Hybrid Development Program 18 p3106 N85-29230
The timing of noise-sensitive activities in residential areas
[NASA-CR-177937] 20 p3524 N85-31918
The sound field of a moving laser-induced acoustic array (theory)
[AD-A154553] 21 p3699 N85-32981
Digital matched filter 22 p3765 N85-33339
Dual optical mechanical position tracker
[AD-D011739] 22 p3844 N85-33811
An internally consistent gamma ray burst time history phenomenology
[OG-1.2-6] 22 p3862 N85-33916

TIME CONSTANT
Control of lateral conjectory motion of spacecraft in atmosphere 02 p0160 N85-11065
Development of a temperature measurement system with application to a jet in a cross flow experiment
[NASA-CR-174896] 15 p2472 N85-25262
Sub-optimal control of nonlinear flexible space structures 20 p3414 N85-31190

TIME DELAY
U TIME LAG

TIME DEPENDENCE
Time variability of directionality properties of pulsed EB-EDL (Electron Beam-Electric Discharge Laser) N2-CO2 lasers
[AD-A145546] 02 p0202 N85-11344
Time-temperature dependence of the strength of commercial zirconia ceramics
[AD-A146233] 03 p0336 N85-12173
Optimum replacement of a system subject to shocks
[AD-A145811] 03 p0372 N85-12374
A proposed reference set of scenarios for radiatively active atmospheric constituents
[DOE/NBB-0086] 03 p0388 N85-12483
Time-dependent chemistry of molecular clouds 03 p0443 N85-12822
Time dependent effects at the foot of the chromosphere
[NASA-CR-174143] 04 p0589 N85-13762
Volatility of vanadium from a candidate fusion tractor alloy
[DE84-015277] 05 p0618 N85-13955
Titanium-potassium heat pipe corrosion studies
[DE84-015528] 05 p0637 N85-14090
Components of the time variation of sea surface height from SEASAT altimeter data 05 p0658 N85-14227
The effect of pressure on the mechanical properties of polymers. Part 2: Measurement of the time-dependent Poisson's ratio
[DE85-002139] 06 p0772 N85-14938
Splitting methods for the numerical solution of the incompressible Navier-Stokes equations
[AD-A147463] 07 p1032 N85-16554
Effect of integration time on precision of absorbances measured with a diode array UV-VIS spectrophotometer
[AD-A146952] 07 p1043 N85-16624
A moving finite element method for time dependent partial differential equations with error estimation and refinement
[AD-A147710] 08 p1210 N85-17617
Can the singularity be removed in time-dependent flow?
[AD-P004185] 09 p1265 N85-17950
Influence of normalized frequency on time-dependent aerodynamic characteristics of vane blading profiles 09 p1306 N85-18204
Numerical investigation of phase change heat transfer in a horizontal cylinder including effects of natural convection 09 p1318 N85-18286
The vertical structure and stability of alpha model accretion disks 09 p1417 N85-18938
Electromagnetic braking of a metallic projectile in flight
[AD-A149424] 10 p1480 N85-19345
Mechanisms of damage accumulation in time-dependent cyclic deformation
[DE85-001004] 10 p1498 N85-19443
The relevance of averaging period to wind power measurements and efficiency of Wind Energy Conversion Systems (WECS)
[GKSS-84-E-35] 11 p1676 N85-20562
X-ray spectroscopy of laser-produced plasmas
[DE85-002170] 11 p1733 N85-20697
Unsteady flows around 3-dimensional wings
[AD-A148993] 12 p1772 N85-21124
Study of the kinetics of hydrogenation using aged catalysts
[DE85-004373] 12 p1802 N85-21302
Rheology of dissemination
[AD-A150006] 12 p1813 N85-21373
Surface forward scattering and reflection
[AD-A150115] 12 p1926 N85-22112
Research program on the effect of pressure on the mechanical properties of polymers, part 2
[DE85-000995] 13 p2037 N85-22761
Time-dependent flow of stream swirled in vortex chamber 13 p2043 N85-22786
Time dependent interaction of internal pressure wave with system of two spherical shells 13 p2046 N85-22809
Time-resolved ellipsometry and reflectivity measurements of the optical properties of silicon during pulsed excimer laser irradiation
[DE85-005091] 13 p2096 N85-23079
Nonrelativistic Kapitza-Dirac scattering
[AD-A150622] 13 p2159 N85-23405
Discrete models for the numerical analysis of time-dependent multidimensional gas dynamics
[NASA-CR-172574] 14 p2300 N85-24239
High time-resolution studies of the auroral ionosphere
[AD-A150945] 14 p2409 N85-24850
Nonrelativistic Kapitza-Dirac scattering
[AD-A150649] 14 p2417 N85-24911
A study of the time dependence in fracture processes relating to service prediction of adhesive joints and advanced composites
[AD-A152064] 15 p2579 N85-25910
Gravity perception and response in shoot of cereal grasses 15 p2611 N85-26091
A practical system for collecting reliable data on the space-time behavior of people
[AD-A151174] 15 p2619 N85-26140
Time dependent and steady-state solutions of the electron energy distribution in a weakly ionized gas subject to an ac or dc electric field
[AD-A151829] 15 p2658 N85-26391
Identification and control of structures in space
[NASA-CR-175790] 16 p2731 N85-26850
An incremental multigrid strategy for the fluid dynamics equations
[AD-A151953] 16 p2783 N85-27172
Some advances in experimentation supporting development of viscoplastic constitutive models
[NASA-CR-174855] 16 p2799 N85-27260
Evaluation of an algorithm for the solution of the time-dependent Euler equations
[AD-A151993] 16 p2854 N85-27600
Optimum convection conditions for Czochralski growth of semiconductors
[INPE-3395-PRE/665] 16 p2870 N85-27703
Analysis of time dependent dielectric failures
[AD-A153200] 17 p2954 N85-28243
New time and frequency services at the National Bureau of Standards 17 p2961 N85-28259
Distributed elections in a ring of processors using Archimedean time
[CWI-CS-R8416] 17 p3016 N85-28653
The temperature dependence of diffracted beam intensities in atom-surface scattering
[AD-A152782] 17 p3029 N85-28736
Model computations of radon, and radon decay product, concentrations in an open system; the Hewlett-Packard 41C program RNSS, version 02
[IRI-190-83-12] 17 p3035 N85-28775
The strategy for time dependent quantum mechanical calculations using a Gaussian wave packet representation of the wave function
[AD-A152709] 17 p3046 N85-28845
Drift mobilities by time-of-flight methods and time-dependent phototransport in the nanosecond regime in amorphous semiconductors
[DE85-006729] 18 p3194 N85-29815
A first-order time-domain Green's function approach to supersonic unsteady flow
[NASA-CR-172206] 19 p3214 N85-29930
On spectral multigrid methods for the time-dependent Navier-Stokes equations
[NASA-CR-172613] 19 p3344 N85-30725
Exact invariants in resonance form for time-dependent potentials
[DE85-010733] 19 p3346 N85-30739
Some advances in experimentation supporting development of viscoplastic constitutive models 20 p3468 N85-31545
Time-implicit Monte-Carlo collision algorithm for particle-in-cell electron transport models
[DE85-010758] 20 p3521 N85-31900
Source-term considerations for a potential radioactive-waste repository located in unsaturated tuff
[DE85-010090] 20 p3529 N85-31953
Magnetospheric response to solar wind variations
[DE85-010762] 20 p3547 N85-32074
Variations in the small-scale galactic magnetic field and short time-scale intensity variations of extragalactic radio sources 20 p3549 N85-32084
Use of MIMLE3 to determine lower order equivalent systems in the time domain
[AD-A154700] 21 p3554 N85-32112
MPS solidification model. Analysis and calculation of macrosegregation in a casting ingot
[NASA-CR-171589] 21 p3566 N85-32178
In-situ measurement of wall thermal performance: Data interpretation and apparatus design recommendations
[DE85-011979] 21 p3586 N85-32289
Mean flow and turbulence in complex terrain
[AD-A155138] 21 p3636 N85-32583
Calculation of steady and unsteady airfoil flow fields via the Navier-Stokes equations
[NASA-CR-3699] 22 p3727 N85-33105
Analysis of solution of Bloch's equations in time domain 22 p3771 N85-33371
Model projections of time-dependent response to increasing carbon dioxide
[DE85-013326] 22 p3816 N85-33641
Implicit Monte Carlo methods and non-equilibrium Marshak wave radiative transport
[DE85-010711] 22 p3835 N85-33743
Multiple collision solutions for time-dependent neutron transport in slabs of finite thickness
[OEFZS-4312] 22 p3838 N85-33762
Evidence for long-term variability in the ultra high energy photon flux from Cygnus X-3
[OG-2.1-10] 22 p3863 N85-33926
Variability in the high energy gamma ray emission from Cyg X-3 over a two-year period (1983 - 1984) at E 4 x 10(11) eV
[OG-2.1-11] 22 p3864 N85-33927
Experimental study on time and temperature dependent behavior of crack growth in viscoelastic strip 23 p3905 N85-34193
Time and temperature dependence of fracture surface in soft epoxy resin 23 p3908 N85-34213
Preliminary SPR thermal model description and results for WH-11 and BM-4
[DE85-013171] 23 p3931 N85-34360
Compressible two-phase flow instabilities simulated with a hybrid Lagrange-Euler pseudospectral method
[DE85-009904] 23 p3931 N85-34361
Thermal transport measurements of UV laser irradiated spherical targets
[DE85-011038] 23 p3931 N85-34365
New semi-implicit method for solving the time-dependent conservation equations for incompressible flow
[DE85-010926] 23 p3931 N85-34367
Guiding center distribution function and longitudinal invariant 23 p3978 N85-34663
The dependence of solar modulation on the sign of the cosmic ray particle charge
[SH-4.2-23] 23 p4009 N85-34860
Time-dependent nonlinear cosmic ray shocks confirming abstract
[OG-8.1-3] 23 p4017 N85-34893
Selfsimilar time dependent shock structures
[OG-8.1-4] 23 p4017 N85-34894
A new approach to evaluate gamma-ray measurements
[OG-9.5-11] 23 p4031 N85-34988
Diagnostic of electromagnetic conditions in space using cosmic rays
[SH-4.5-19] 23 p4038 N85-35036
Time and energy dependence of the cosmic ray gradient in the outer heliosphere
[SH-4.7-2] 23 p4040 N85-35047
Identification and control of structures in space
[NASA-CR-176175] 24 p4069 N85-35214
Subcritical fracture propagation in rocks: An examination using the methods of fracture mechanics and non-destructive testing 24 p4116 N85-35516
Time-dependent response of the climate to increasing atmospheric carbon dioxide 24 p4119 N85-35532
DEPTH-CHARGE static and time-dependent perturbation/sensitivity system for nuclear reactor core analysis, revision 1
[DE85-013103] 24 p4139 N85-35859
A graph theoretic procedure for the design of feedback patterns
[REPT-110] 24 p4142 N85-35573
Decentralized stabilization by high gain feedback
[BU-115] 24 p4144 N85-35689
Structure of air shower disc near the core
[HE-4.7-2] 24 p4198 N85-36053
Longitudinal development of muons in large air showers studies from the arrival time distributions measured at 900m above sea level
[HE-4.7-4] 24 p4199 N85-36055

Arrival time distributions of electrons in air showers with primary energies above 10 (18)eV observed at 900m above sea level
[HE-4.7-5] 24 p4199 N85-36056
A note on some statistical properties of rise time parameters used in muon arrival time measurements
[HE-4.7-12] 24 p4199 N85-36062
Study of the time-differentiated particle flux density at various distances from EAS axis
[HE-4.7-15] 24 p4200 N85-36065

TIME DISCRIMINATION
Estimating number, time and length; a baseline study
05 p0695 N85-14473

TIME DIVISION MULTIPLE ACCESS
SLIM TDMA ANIK B pilot project
[CRC-REPT-1366] 03 p0354 N85-12278
The Telecom 1 satellite telecommunication system
04 p0493 N85-13147
Analytical modeling of a polling protocol — airline information network
[ENST-84H001] 09 p1277 N85-18029
Multimission advanced configurations study — telecommunication satellites
[MATRA-DM.51/CC/FL/0151.83] 12 p1790 N85-21237
Assessment of effectiveness of signal-code constructions in time division-multi-access satellite systems 13 p2066 N85-22906
Onboard demand scheduling of a multibeam SS/TDMA satellite with integrated circuit and packet switching
14 p2229 N85-23812

TIME DIVISION MULTIPLEXING
Digital correlator speed improvement by multiplexing
[AD-A145207] 01 p0100 N85-10662
Multiplexing the ethernet interface among VAX/VMS users
[AD-A145539] 02 p0243 N85-11588
Contribution to the study and realization of the CARTHAGE multiservice local network
[ENST-84E006] 05 p0716 N85-14595
Electro-optic techniques for VLSI interconnect
18 p3186 N85-29774

TIME FUNCTIONS
Long-time tail in the two-wave model
02 p0282 N85-11837
Determination of crustal and upper mantle structure from analysis of broadband teleseismic P-waveforms
08 p1181 N85-17440
Effects of heterogeneities on the propagation, scattering and attenuation of seismic waves and the characterization of seismic source
[AD-A148284] 08 p1186 N85-17476
Reflected wave travel-time curves in stratified media with vertically heterogeneous layers and slightly sloping curved boundaries 13 p2114 N85-23167
Optimal sensor locations for structural identification
20 p3417 N85-31209
Use of MMLE3 to determine lower order equivalent systems in the time domain
[AD-A154700] 21 p3554 N85-32112
Art of programming programmable microcalculators: Calculation of response from current values of action
22 p3767 N85-33348
SIG: A general-purpose signal processing program. User's manual: Revision 1
[DE85-013035] 24 p4140 N85-35662

TIME LAG
A nonlinear filter for compensating for time delays in manual control systems 05 p0700 N85-14493
A method for measuring the effective throughput time delay in simulated displays involving manual control
05 p0701 N85-14497
Effects of transport delays of manual control system performance 05 p0701 N85-14498
Measurements of pilot time delay as influenced by controller characteristics and vehicles time delays
05 p0701 N85-14500
Optimal stochastic LQ control with measurements displaced in time
[OUEL-1547/84] 08 p1209 N85-17605
A note on the prediction error for small time lags into the future
[AD-A148221] 08 p1215 N85-17654
Adaptive signal processing for radio communications
10 p1473 N85-19295
In-flight investigation of the effects of time delay in control system on flying qualities in landing approach
[DFVLR-FB-84-35] 11 p1586 N85-19989
Signal propagation delay, wire length distribution and the efficiency of VLSI circuits
[CWI-CS-R8412] 11 p1630 N85-20266
Circuit topology, signal propagation delay and the efficiency of VLSI circuits
[CWI-CS-R8414] 11 p1630 N85-20267
On the application of compatibility checking techniques to dynamic flight test data
[ARL/AERO-R-161] 12 p1776 N85-21151
The effects of cooling on delay-time limits in IC's
14 p2297 N85-24224
Wavelength dependent, tunable, optical time delay system for electrical signals
[AD-D011584] 15 p2548 N85-25725
Mode dependent, optical time delay system for electrical signals
[AD-D011596] 15 p2553 N85-26363
Digital RF delay line for ECM (electronic countermeasure) look-through
[AD-A152120] 16 p2774 N85-27120
Topics in time delay estimation
[AD-A152231] 16 p2855 N85-27607
Proceedings of the Fifteenth Annual Precise Time and Time Interval (PTTI) Applications and Planning Meeting
[AD-A149163] 17 p2961 N85-28287
Timing accuracy of LF and TV synchronization techniques 17 p2961 N85-28288
International time comparison by a GPS timing receiver 17 p2962 N85-28293
First results of GPS time transfer to Australia
17 p2962 N85-28294
The role of a low Earth orbiter in intercontinental time synchronization via GPS satellites
17 p2964 N85-28306
Ionospheric limitations to time transfer by satellite
18 p3107 N85-29234
Atmospheric limitations to clock synchronization at microwave frequencies 18 p3107 N85-29236
Probabilistic analysis of combinational circuits with random delays 19 p3257 N85-30192
Use of MMLE3 to determine lower order equivalent systems in the time domain
[AD-A154700] 21 p3554 N85-32112
In-flight evaluation of pure time delays in pitch and roll
[NASA-TM-86744] 21 p3556 N85-32123
Robust detection and classification of regional seismic signals using a two mode/two stage cascaded adaptive arma (CAARMA) model
[AD-A154710] 21 p3630 N85-32554
Sub-luminal pulses from cosmic ray air showers
[HE-4.7-13] 24 p4200 N85-36063

TIME MARCHING
Spectral methods in time for parabolic problems
[NASA-CR-172539] 11 p1706 N85-20730
Time marching numerical solution of the dynamic response of nonlinear systems
[NAF-AN-25] 12 p1885 N85-21696
Thermodynamic evaluation of transonic compressor rotors using the finite volume approach
[NASA-CR-175811] 16 p2708 N85-26712

TIME MEASUREMENT
Timing performance of phase-locked loops in optical pulse position modulation communication systems
[AD-A145403] 02 p0190 N85-11271
Late Paleozoic and early Mesozoic radiolarians in the Circle quadrangle, east-central Alaska
04 p0517 N85-13297
Time comparison with GPS technique and first results with the DFVLR C/A code receiver
[DFVLR-MITT-84-05] 05 p0595 N85-13794
References in space and time
05 p0598 N85-13809
Measurements of pilot time delay as influenced by controller characteristics and vehicles time delays
05 p0701 N85-14500
Mobility and trapping time measurements in HgI2
[DE84-015954] 06 p0869 N85-15522
Effects of aircraft and flight parameters on energy-efficient profile descents in time-based metered traffic
[NASA-CR-172338-ADD] 07 p0901 N85-15706
Construction, testing of 1-MW nitrogen laser
08 p1140 N85-17182
A system for measuring the characteristics of the ionospheric channel by digital transmissions
10 p1472 N85-19287
Operating time meter for tape recorder
12 p1838 N85-21537
Location and synchronization — space-time coordinates 14 p2397 N85-24788
Development of simulation procedures for VLSI systems (timing simulation)
[BMFT-FB-T-84-297] 15 p2550 N85-25743
Analysis of short-period changes in intensity of hard X-radiation of solar flares registered aboard Venera-13 and Venera-14 spacecraft 16 p2723 N85-26806
Proceedings of the Fifteenth Annual Precise Time and Time Interval (PTTI) Applications and Planning Meeting
[AD-A149163] 17 p2961 N85-28287
Recent improvements in the atomic time scales of the National Bureau of Standards 17 p2962 N85-28290
Improved master clock reference system at USNO
17 p2963 N85-28300
Spread spectrum time transfer experiment via INTELSAT 17 p2964 N85-28304
Timing-system design considerations for a mobile astrolabe 17 p2965 N85-28309
Clock characterization tutorial
17 p2965 N85-28311
Methods for optimal recursive estimation of non-stationary time series, applications to atomic time and frequency metrology 17 p2965 N85-28312
Kalman filter estimates of the NAVSTAR satellite clock parameters 17 p2965 N85-28315
The measurement of linear frequency drift in oscillators 17 p2966 N85-28316
A plan for the development of inertial reconstruction of initial state clock (IRIS) 17 p2966 N85-28317
Prospects for atomic frequency standards
18 p3105 N85-29222
Time transfer techniques: Historical overview, current practices and future capabilities
18 p3108 N85-29245
Maintenance of time and frequency in the Jet Propulsion Laboratory's Deep Space Network using the Global Positioning System 18 p3109 N85-29249
Using GPS and VLBI technology to maintain 14 digit synchronization 18 p3109 N85-29250
Performance test results of a low cost GPS time and frequency monitor 18 p3109 N85-29252
Drift mobilities by time-of-flight methods and time-dependent photoitransport in the nanosecond regime in amorphous semiconductors
[DE85-008729] 18 p3194 N85-29815
Time comparisons using the Global Positioning System (GPS). Method and first results obtained using the DFVLR C/A receiver
[ESA-TT-894] 20 p3460 N85-31480
Investigation of space-time structure of glow of laser plasma colliding with flat screen
21 p3693 N85-32947
The sound field of a moving laser-induced acoustic array (theory)
[AD-A154553] 21 p3699 N85-32981
Method of characterizing critical timing paths and analyzing timing related failure modes in very large scale integrated circuits
[AD-D011731] 22 p3759 N85-33296
Hit-size effectiveness theory applied to high doses of low LET radiation for pink mutations in Tradescantia
[DE85-011835] 22 p3819 N85-33857
Observations of Cygnus X-3 above 10(15) eV from 1979 - 1984
[OG-2.1-6] 22 p3863 N85-33923
On gamma and neutrino radiation from Cyg X-3
[OG-2.1-7] 22 p3863 N85-33924
Observations of the Crab Nebula at energies 4.10(11)
[OG-2.3-1] 22 p3865 N85-33936
Spectra and positions of galactic gamma-ray sources
[OG-2.5-7] 22 p3869 N85-33963
Mini and super mini arrays for the study of highest energy cosmic rays
[OG-9.4-9] 23 p4029 N85-34976
Shower disc sampling and the angular resolution of gamma-ray shower detectors
[OG-9.5-2] 23 p4030 N85-34980
The use of the McIlwain L-parameter to estimate cosmic ray vertical cutoff rigidities for different epochs of the geomagnetic field
[SH-6.1-12] 23 p4045 N85-35085
Characterization of microstrip discontinuities in the time and frequency domains
[NASA-CR-176190] 24 p4088 N85-35342
The system of EAS time analysis
[HE-4.4-10] 24 p4193 N85-36018

TIME MEASURING INSTRUMENTS
NT ATOMIC CLOCKS
NT AUTONOMOUS SPACECRAFT CLOCKS
NT CHRONOMETERS
NT CLOCKS
NT TIMING DEVICES
Optical pin apparatus for measuring the arrival time and velocity of shock waves and particles
[DE84-014501] 01 p0120 N85-10624
The steering of GPS time 17 p2964 N85-28301
Spread spectrum time transfer experiment via INTELSAT 17 p2964 N85-28304

TIME OF FLIGHT SPECTROMETERS
Time-of-flight spectroscopy of ionic and metastable fragments from dissociating molecules
[AD-A148068] 08 p1220 N85-17683
A compact time-of-flight energy analyzer of high resolution — for Tokamaks
[REPT-84-154] 09 p1324 N85-18318
An operational test of a time-of-flight analyzer at the ASDEX Tokamak
[REPT-84-155] 09 p1324 N85-18319

In-beam tests of an air-core superconducting-solenoid particle spectrometer
[DE85-004029] 12 p1853 N85-21625
Carbon foil secondary electron emission during ion passage through the 40 to 500 keV energy field
[MPE-190] 18 p3184 N85-29747
Time-resolved energy spectrum of the ion beam generated in the plasma focus 19 p3369 N85-30892
Gas composition and molecule velocity in the detonation products of pentaerythritol tetranitrate (PETN) in expansion in a high vacuum container. Analysis by mass spectroscopy and time of flight spectrometry
[ISL-R-100/84] 22 p3747 N85-33226
An improved time of flight gamma-ray telescope to monitor diffuse gamma-ray in the energy range 5 MeV - 50 MeV
[OG-9.3-2] 23 p4027 N85-34957
The Nagoya cosmic-ray muon spectrometer 3, part 1: Preliminary observations
[HE-5.2-2] 24 p4202 N85-36080
The Nagoya cosmic-ray muon spectrometer 3, part 2: Track detector
[HE-5.2-3] 24 p4202 N85-36081
The Nagoya cosmic-ray muon spectrometer 3, part 3: Automatic film scanning equipment
[HE-5.2-4] 24 p4202 N85-36082
The Nagoya cosmic-ray muon spectrometer 3, part 4: Track reconstruction method
[HE-5.2-5] 24 p4202 N85-36083

TIME OPTIMAL CONTROL
Optimal control of waiting time in a M/G/1 queue
[INPE-2767-PRE/340] 02 p0255 N85-11671
Development and certification of a new stall warning and avoidance system 05 p0702 N85-14507
Inverse modelling to obtain head movement controller signal 05 p0706 N85-14525
A control model: Interpretation of Fitts' law 05 p0706 N85-14526
Improvement of the transient response in the finite settling time control
[NAL-TR-823] 06 p0757 N85-14843
Minimum time turns using vectored thrust
[AD-A151693] 15 p2471 N85-25256
High specific power aircraft turn maneuvers: Tradeoff of time-to-turn versus change in specific energy
[AD-A151701] 15 p2471 N85-25257
Wavelength dependent, tunable, optical time delay system for electrical signals
[AD-D011584] 15 p2548 N85-25725

TIME RESPONSE
Machine computation of delay and capacitance of transistor structures of subnanosecond large integrated circuits 04 p0490 N85-13120
Generalization of discrete Fourier transform for interpolation in time domain 22 p3775 N85-33396
Generalization of discrete Fourier transformation for interpolation in time domain 22 p3776 N85-33400

TIME SERIES ANALYSIS
Kolmogorov-Smirnov goodness-of-fit test: Corrected for use with EEG-like data
[AD-A143711] 01 p0110 N85-10745
Influential observations in time series
[AD-A144719] 01 p0112 N85-10763
Estimation in nonlinear time series model II: Some nonstationary series
[AD-A145708] 02 p0255 N85-11668
On-line fatigue life prediction under stochastic loading by the time series modeling 03 p0370 N85-12362
Time series modeling of human operator dynamics in manual control tasks 05 p0699 N85-14488
Statistical time series models of pilot control with applications to instrument discrimination 05 p0700 N85-14489
Utilization of historic information in an optimization task 05 p0700 N85-14490
Time series analysis programs for stratigraphic data
[AD-A146827] 06 p0854 N85-15429
Electronics research at the University of Texas at Austin
[AD-A146600] 07 p0947 N85-15696
Autoregressive spectral estimation for two dimensional time series 07 p0965 N85-16258
The ocean and the dynamics of the tropical atmosphere; its possible predictability 07 p1002 N85-16366
A factor analysis for time series
[AD-A147495] 07 p1036 N85-16574
Time series analysis of closed-loop pilot vehicle dynamics 08 p1067 N85-16876
Robust linear filtering for multivariable stationary time series, part 3
[AD-A146169] 08 p1212 N85-17627
Methods and applications of time series analysis. Part 2: Linear stochastic models
[AD-A147292] 08 p1214 N85-17645
On the ergodicity of bilinear time series models and some applications
[AD-A148032] 08 p1215 N85-17651
Internal variables in the lattice for cholesky factorization. Kalman filtering and model identification
[AD-A149431] 10 p1547 N85-19757
Modelling and residual analysis of nonlinear auto-regressive time series in exponential variables
[AD-A149047] 10 p1550 N85-19776
Asymptotic distributions of the sample mean, autocovariances and autocorrelations of long-memory time series
[AD-A149409] 10 p1551 N85-19781
Statistical analysis of autoregressive spectral estimates for noise corrupted autoregressive series
[AD-A149543] 11 p1706 N85-20747
Simulation of estimating periodicity of seasonally stationary time series
[DE85-003517] 11 p1708 N85-20748
Bayesian analysis of time series 1: Householder transformation analyses
[DE85-004449] 11 p1708 N85-20749
Analysis of selective chopper radiometer data
[NASA-CR-175157] 12 p1895 N85-21894
A review of some aspects of robust inference for time series
[AD-A149706] 12 p1923 N85-22062
Approaches and algorithms for robust signal processing 13 p2062 N85-22878
Markov method for simulating non-Gaussian wind speed time series
[DE85-003450] 13 p2139 N85-23284
Studies of the initiation of pitting corrosion on stainless steels
[AERE-M-3400] 14 p2254 N85-23967
Dynamic spectra of mean monthly values of geomagnetic field elements based on spectral-time analysis data 14 p2344 N85-24496
Annual report on electronics research at the University of Texas at Austin
[AD-A150836] 14 p2415 N85-24901
Analysis and interpretation of synthetic time strings of oscillation data 14 p2444 N85-25079
Spectral information from gapped data. A comparison of technique 14 p2444 N85-25080
A comparison of alternative analytic models for event related potential records
[AD-A151977] 15 p2618 N85-26134
A practical system for collecting reliable data on the space-time behavior of people
[AD-A151174] 15 p2619 N85-26140
Kalman filtering and exponential smoothing in economics 15 p2635 N85-26248
Higher order residual analysis for nonlinear time series with autoregressive correlation structures
[AD-A149232] 15 p2636 N85-26257
Study of longitudinal landing flying qualities evaluation using pilot model theory
[AD-A152194] 16 p2706 N85-26702
A Markov method for simulating non-Gaussian wind speed time series
[DE85-007131] 16 p2835 N85-27485
Methods for optimal recursive estimation of non-stationary time series, applications to atomic time and frequency metrology 17 p2965 N85-28312
Towards a study of synoptic-scale variability of the California current system
[NASA-CR-175871] 17 p2997 N85-28529
Transverse vorticity measurements in an excited two-dimensional mixing layer 19 p3264 N85-30241
Rayleigh scattering for density measurements in premixed flames: One point, time series data 20 p3424 N85-31253
Numerical considerations in the development and implementation of constitutive models 20 p3467 N85-31541
Magnetospheric response to solar wind variations
[DE85-010762] 20 p3547 N85-32074
On the spectrum of atmospheric velocity fluctuations seen by MST/ST radar and their interpretation 21 p3622 N85-32504
On the transformation regularities of time series of solid aerosol concentrations in the surface atmospheric layer 21 p3645 N85-32648
Kalman filter time series analysis of gamma-ray data from NaI(T1) detectors for the ND6620 computer
[AD-A154995] 21 p3705 N85-33014
The conjecture concerning time variations in the solar neutrino flux
[SH-8.1-6] 23 p4049 N85-35111
Methods and software for cosmic ray scintillation studies
[SH-8.1-17] 23 p4052 N85-35132
Signal space models for antenna arrays
[AD-A156063] 24 p4087 N85-35335

TIME SHARING
Normal approximation for response time in a processor-shared computer system model
[AD-A144997] 01 p0103 N85-10690
The effects of task structure on time-sharing efficiency and resource allocation optimality 05 p0711 N85-14562
Passive maser using timesharing for control of the cavity and control of the oscillator on the line of stimulated emission
[AD-D011326] 07 p0969 N85-16151
Development and evaluation of a Fault-Tolerant Multiprocessor (FTMP) computer. Volume 2: FTMP software
[NASA-CR-166072] 19 p3341 N85-30706

TIME SIGNALS
Portable real-time clock
[AD-A146218] 03 p0364 N85-12336
Digital raster timing encoder-decoder
[AD-D011279] 06 p0604 N85-15120
Clock synchronization by the Symphonie and Laser Synchronization from Stationary Orbit (LASSO) geostationary satellites 14 p2398 N85-24778
Maintenance of time and frequency in the DSN using the global positioning system 16 p2771 N85-27105
Proceedings of the Fifteenth Annual Precise Time and Time Interval (PTTI) Applications and Planning Meeting
[AD-A149163] 17 p2961 N85-28287
Timing accuracy of LF and TV synchronization techniques 17 p2961 N85-28288
New time and frequency services at the National Bureau of Standards 17 p2961 N85-28289
Recent improvements in the atomic time scales of the National Bureau of Standards 17 p2962 N85-28290
Automation of Precise Time Reference Stations (PTRS) 17 p2962 N85-28291
International time comparison by a GPS timing receiver 17 p2962 N85-28293
A new precision time and frequency source for stationary PTTI applications 17 p2963 N85-28297
On-orbit frequency stability analysis of the GPS NAVSTAR's 3 and 4 rubidium clocks and NAVSTAR's 5 and 6 cesium clocks 17 p2963 N85-28298
Improved master clock reference system at USNO 17 p2963 N85-28300
The steering of GPS time 17 p2964 N85-28301
Test results for prototype GPS rubidium clocks 17 p2964 N85-28302
Spread spectrum time transfer experiment via INTELSAT 17 p2964 N85-28304
Unattended TV time transfer results 17 p2964 N85-28305
The role of a low Earth orbiter in intercontinental time synchronization via GPS satellites 17 p2964 N85-28306
Timing of spacecraft data: Time accuracy requirements and timing facilities of the European Space Agency (ESA) 17 p2964 N85-28307
UHF IRIG G distribution system 17 p2965 N85-28308
Precise time transfer using MKIII VLBI technology 17 p2965 N85-28310
Kalman filter estimates of the NAVSTAR satellite clock parameters 17 p2965 N85-28315
Time synchronization experiments with APPLE 17 p2967 N85-28323
Prospects for atomic frequency standards 18 p3105 N85-29222
Atmospheric limitations to clock synchronization at microwave frequencies 18 p3107 N85-29236
Relationship between Allan variances and Kalman Filter parameters 18 p3107 N85-29236
Development of hydrogen masers for K-3 VLBI system 18 p3108 N85-29239

TIMERS
U TIMING DEVICES

TIMING
U TIME MEASUREMENT

TIMING DEVICES
Proceedings of the Fifteenth Annual Precise Time and Time Interval (PTTI) Applications and Planning Meeting
[AD-A149163] 17 p2961 N85-28287
New time and frequency services at the National Bureau of Standards 17 p2961 N85-28289
Recent improvements in the atomic time scales of the National Bureau of Standards 17 p2962 N85-28290
International time comparison by a GPS timing receiver 17 p2962 N85-28293
International time transfer and portable clock evaluation using GPS timing receivers: Preliminary results 17 p2964 N85-28303
Prospects for atomic frequency standards 18 p3105 N85-29222
Atmospheric limitations to clock synchronization at microwave frequencies 18 p3107 N85-29236

Development of hydrogen masers for K-3 VLBI system
18 p3108 N85-29239
New GOES satellite synchronized time code generation
18 p3109 N85-29247
Numerical optical computing at the Ohio State University
18 p3188 N85-29775

TIN
Thematic mapping of likely target areas for the occurence of cassiterite in the Serra do Mocambo (GO) granitic massifs using LANDSAT 2 digital imaging
[E85-10027] 02 p0219 N85-11440
Study of vibrational energy transfer at a liquid tin surface
[AD-A145741] 02 p0277 N85-11804
Effects of tin on microstructure and mechanical behavior of Inconel 718
[NASA-TM-86866] 03 p0330 N85-12129
Geology and geochemical evolution of the Lost River, Alaska, tin deposit
04 p0533 N85-13405
Float zone experiments in space
[NASA-CR-171284] 07 p0911 N85-15766
Investigations into the improvement of processing of Bolivian tin ores
[BMFT-FB-T-84-184] 07 p0917 N85-15807
Interpretation of 119 Sn isomer shifts and 3d 5/2-core-level shifts based on Dirac-Slater calculations on a number of ionic states
[USIP-85-06] 20 p3532 N85-31973
Development of metallization process: FSA project, cells and module formation research area
[NASA-CR-176136] 23 p3945 N85-34447
The Conterminous United States Mineral Assessment Program
24 p4106 N85-35458
The Alaska Mineral Resources Assessment Program
24 p4107 N85-35460

TIN ALLOYS
Electron-irradiated effects in metals
[DE84-016869] 09 p1297 N85-18147
Electron-diffraction structural examination of amorphous iron-tin alloys
11 p1604 N85-20084
Properties of Ti alloyed multifilamentary Nb3Sn wires by internal tin process
[DE85-003212] 12 p1941 N85-22191
Basis and pyramidal slipping in single crystals of alpha-alloy Ti-Al-Sn
13 p2032 N85-22730
Critical current density and microstructural state of an internal tin multifilamentary superconducting wire
[DE85-009966] 22 p3761 N85-33308

TIN COMPOUNDS
NT NIOBIUM STANNIDES
NT TIN OXIDES
NT TIN TELLURIDES
Magnetization measurements on multifilamentary Nb3Sn and NbTi conductors
[DE85-001237] 11 p1737 N85-20923
Marine environmental quality assessment program, five-year plan (FY 1984 - 1988)
[AD-A154715] 21 p3613 N85-32459

TIN OXIDES
Process for preparation of crosslinked poly(tri-n-butyltin) methacrylate with simultaneous particle size reduction
[AD-D011313] 07 p0932 N85-15905
Development of materials for open-cycle MHD
[DE84-017293] 09 p1393 N85-18770

TIN TELLURIDES
The behavior of Pb(1-x)Sn(x)Te semiconductor laser diodes in a magnetic field
[AD-A145431] 02 p0267 N85-11872

TIP DRIVEN ROTORS
Experimental study of main rotor tip geometry and tail rotor interactions in hover. Volume 1: Text and figures
[NASA-CR-177336-VOL-1] 13 p1965 N85-22344
Experimental study of main rotor tip geometry and tail rotor interactions in hover. Volume 2: Run log and tabulated data
[NASA-CR-177336-VOL-2] 13 p1965 N85-22345
Application of two-dimensional unsteady aerodynamic to a free-tip rotor response analysis
[NASA-CR-177348] 19 p3215 N85-29933
Performance comparison between NACA 23024 and NACA 64(3)-618 airfoil configurated rotors for horizontal-axis wind turbines
[NASA-TM-83471] 19 p3303 N85-30477

TIP SPEED
Shutdown characteristics of the Mod-O wind turbine with aileron controls
[NASA-TM-86916] 07 p0992 N85-16299
Study of controlled diffusion stator blading
[NASA-CR-167995] 09 p1281 N85-18058
Further comparison of wind tunnel and airplane acoustic data for advanced design high speed propeller models
[NASA-TM-86935] 12 p1927 N85-22106
Energy efficient engine. Fan and quarter-stage component performance report
[NASA-CR-168070] 23 p3897 N85-34141

TIPS
NT BLADE TIPS
NT CRACK TIPS
NT WING TIPS
Approximation methods for inverse problems involving the vibration of beams with tip bodies
[NASA-CR-172468] 02 p0209 N85-11379

TIRES
NT AIRCRAFT TIRES
Predictor model for seasonal variations in skid resistance. Volume 2: Comprehensive report
[PB84-226620] 01 p0037 N85-10230
Numerical analysis of some problems related to the mechanics of pneumatic tires: Finite deformation/rolling contact of a viscoelastic cylinder and finite deformation of cord-reinforced rubber composites
01 p0060 N85-10397
Orbiter wheel and tire certification
08 p1101 N85-16969
Modelling of off-road tyres and soil for improved traction
[AD-P004258] 09 p1404 N85-18834
Soil compliance influence on tyre performance
[AD-P004260] 09 p1404 N85-18836
Performance prediction of pneumatic tyres on sand
[AD-P004262] 09 p1404 N85-18838
Effects of slip on energy distribution between tyre and soil
[AD-P004263] 09 p1404 N85-18839
Traction forces of drive tyre on the compacted soil
[AD-P004264] 09 p1404 N85-18840
Prediction of in-sand tire and wheeled vehicle drawbar performance
[AD-P004265] 09 p1404 N85-18841
Comparison of measured and simulated ride comfort for an agricultural tractor and influence of travel speed and tyre-inflation pressure on dynamic response
[AD-P004281] 09 p1407 N85-18857
Proceedings of the 8th International Conference on the Performance of Off-Road Vehicles and Machines, volume 2
[AD-A148835] 09 p1407 N85-18859
Pressure tests in soil below tires of agricultural vehicles
[AD-P004294] 09 p1408 N85-18871
Flotation tires and subsurface compaction
[AD-P004299] 09 p1409 N85-18876
Forces on undriven, angled wheels
[AD-P004303] 09 p1409 N85-18880
Influence of tire on resistance and steering forces of tires
[AD-P004306] 09 p1410 N85-18883
Tire inflation/deflation system
[AD-D011459] 10 p1493 N85-19426
Tire deflation mechanism
[AD-D011460] 10 p1493 N85-19427
Techniques to analyze vehicle coastdown data
[DE85-005159] 12 p1772 N85-21127

TIROS N SERIES SATELLITES
NT NOAA 6 SATELLITE
Report of the First Session of the International Working Group on Data Management for the International Satellite Cloud Climatology Project (ISCCP)
[WCP-42] 01 p0073 N85-10483
ISCCP Cloud Algorithm Intercomparison Workshop
01 p0073 N85-10485
ISSCP Cloud Algorithm Intercomparison Workshop
01 p0073 N85-10486
A comparison of TIROS-N series satellite data and LANDSAT data over Scotland
05 p0656 N85-14210
The ARGOS Platform Transmitter Terminals (PTTs)
14 p2237 N85-23872
Hydrometric telemetry in Canada
14 p2239 N85-23882
Data Collection and Platform Location by Satellite: ARGOS Users' Conference
14 p2239 N85-23883
Some experience from ARGOS stations in the open sea
14 p2240 N85-23891
The experience of the Swedish Meteorological and Hydrological Institute (SMHI) with the ARGOS system (PM-U1/81)
14 p2240 N85-23892
Improvements brought about to the system since 1978 and statements on future development
14 p2323 N85-24349
New directions in ARGOS instrumentation at Polar Research Lab (PRL)
14 p2323 N85-24350
Automatic weather stations in Antarctica
14 p2324 N85-24360
NOAA'S role in support of service ARGOS
14 p2328 N85-24394
Long term drifting float for measuring mean oceanic circulation using ARGOS system
16 p2611 N85-27339
Availability of the ARGOS system based on the orbital characteristics of the TIROS-N satellites — oceanographic/meteorological data
16 p2613 N85-27352
Location and data collection satellite system ARGOS. User's guide — satellite based localization
16 p2616 N85-27371

TIROS PROJECT
Data Collection and Platform Location by Satellite: ARGOS Users' Conference
14 p2237 N85-23869
The ARGOS system status report after 2 years operation
14 p2237 N85-23870
System performance, data distribution and technical files — ARGOS project
14 p2237 N85-23871
The ARGOS VHF direct readout mini-station and CML-80-MP data collection Platform Transmitter Terminals (PTTs)
14 p2238 N85-23873
The ARGOS system status report
14 p2239 N85-23884
Equipment for the ARGOS system from Eldevoll Electronics A.S.
14 p2239 N85-23885
ARGOS VHF direct readout mini-station
14 p2239 N85-23886
The ARGOS system after 3 years operation
14 p2325 N85-24368
The ARGOS program — satellite based localization
14 p2397 N85-24775

TIROS SATELLITES
NT TIROS N SERIES SATELLITES
Satellites and politics: Weather, communications, and earth resources
23 p4057 N85-35144

TISSUES (BIOLOGY)
NT EPITHELIUM
Determination of bound water in biological tissue and energy dissipated in bound water by low level microwaves
[AD-A143101] 03 p0399 N85-12547
Alterations in skeletal muscle with disuse atrophy
[NASA-CR-174195] 06 p0843 N85-15349
Interactions of ketones and hexacarbons
[AD-P004019] 06 p0843 N85-15353
Workshop on membrane biophysics
[AD-A148238] 08 p1192 N85-17512
Bioelectrochemistry 2: Membrane phenomena
[AD-A149132] 10 p1522 N85-19602
Characteristics of human masseter under conditions of hypokinesia
11 p1691 N85-20630
Morphological study of monkeys submitted to antiortho-static hypokinesia
12 p1902 N85-21942
Gravitropism in leafy dicot stems
15 p2610 N85-26086
Chemicals identified in human biological media, a data base. Volume 6, part 2: Records 7586-8694
[DE85-008767] 18 p3154 N85-29528
Method for thermal monitoring subcutaneous tissue
[NASA-CASE-LAR-13026-1] 19 p3328 N85-30618
Development annd testing of electrophoresis solutions. Task I.1: Development of optimal buffer system
20 p3500 N85-31755
Physicnl chemical state of water in living cells
[AD-A154566] 21 p3662 N85-32749

TITAN
Do the satellites of Uranus control its magnetosphere?
02 p0301 N85-11952
Outer satellite atmospheres: Their nature and planetary interactions
[NASA-CR-174146] 04 p0589 N85-13759
Extended atmospheres of outer planet satellites and comets
[NASA-CR-174398] 09 p1416 N85-18933
Research in planetary studies and operation of Mauna Kea Observatory
[NASA-CR-175618] 13 p2189 N85-23460
Giant planets and their satellites: Cosmochemistry, evolution and structure
13 p2175 N85-23494
Extended atmospheres of outer planet satellites and comets
[NASA-CR-175673] 14 p2440 N85-25058
The eccentric ringlet at 1.29 R sub S — Saturn radius (RS)
15 p2573 N85-26496
Volatiles in the outer solar system. 1: Thermodynamics of clathrate hydrates. 2: Ethane ocean on Titan. 3: Evolution of primordial Titan atmosphere
19 p3362 N85-30964

TITAN CENTAUR LAUNCH VEHICLE
Assessment of candidate-expendable launch vehicles for large payloads
[NASA-CR-175540] 14 p2237 N85-23867

TITANATES
NT BARIUM TITANATES
NT LEAD ZIRCONATE TITANATES
NT PEROVSKITES
NT PIEZOELECTRIC CERAMICS
NT STRONTIUM TITANATES

TITANIUM
Optimization of mechanical/corrosion properties of Ticode-12 plate and sheet. Part 1: Compositional effects, stage 1
[DE84-015935] 02 p0184 N85-11231
Characterization of amorphous surface layers in Fe implanted with Ti and C
[DE84-014960] 02 p0289 N85-11865
Study of structure of sponge titanium varieties 03 p0350 N85-12256
Structural recrystallization in titanium 03 p0351 N85-12258
Causes of strength reduction in welded titanium-steel joints 03 p0352 N85-12262
Effect of oxide coated thickness on thermal ignition of titanium-based pyrotechnics
[DE84-013061] 04 p0461 N85-13065
Oxygen diffusion from anodic surface oxide films on titanium subhydride studies by auger electron spectroscopy and electron energy loss spectroscopy
[DE84-016942] 04 p0572 N85-13648
Testing of production of silicon-titanium-magnesium alloying composition
[BLL-M-35904-(5828.4)] 05 p0616 N85-13937
Nitriding of titanium and its alloys by N2, NH3 or mixtures of N2 + H2 in a dc arc plasma at low pressures (or = to torr)
[NASA-TM-83803] 06 p0814 N85-15168
Evaluation of the alkaline peroxide pre-bond surface treatment for titanium
[AD-A147352] 07 p0929 N85-15881
Ultrasonic evaluation of titanium contamination with correlation techniques
[AD-P004128] 08 p1126 N85-17101
Feasibility study to demonstrate detection of low levels of oxygen contaminant in titanium using eddy current and ultrasonic NDE (Nondestructive Evaluation) techniques
[AD-P004129] 08 p1127 N85-17104
Neutron activation analysis of titanium with oxygen contamination
[AD-P004134] 08 p1128 N85-17109
The influence of strain rate and porosity on the deformation and fracture of titanium and nickel
[AD-A148670] 08 p1130 N85-17123
Implantation of Ti + C for reduced friction and wear of steels
[DE85-001606] 09 p1295 N85-18135
Fiber composite materials with titanium matrix 10 p1445 N85-19105
Kinetics of saturation of porous titanium with low melting point metals 10 p1446 N85-19114
Quasi-thermodynamic prediction of hydrogen reemission behavior from titanium films
[DE85-003667] 10 p1564 N85-19884
USSR report: Materials science and metallurgy
[JPRS-UMS-84-005] 11 p1597 N85-20044
Structure and properties of copper-titanium-aluminum composites obtained by thermoreactive sintering 11 p1600 N85-20061
Effect of silicon and titanium properties on N08Co9Mb5Ti steel 11 p1601 N85-20069
Mechanism of titanium impact on brittle tendency in delayed deformation of martensite-aging steels 11 p1604 N85-20087
Chemisorption theory: Adsorption on copper-nickel alloys and titanium surface embrittlement
[DE85-001815] 12 p1607 N85-21334
Rational use of tatanium in nonferrous metallurgy 13 p2031 N85-22728
Studies of electrical properties of surface films and localization during electrochemical dimensional working of titanium 13 p2032 N85-22729
Study of structural changes of dual-phase titanium alloy during shock wave loading 15 p2496 N85-25406
Possible use of rapid heating for improving mechanical properties of titanium alloys 15 p2496 N85-25409
Study of oxidized surface coating on titanium after annealing 15 p2496 N85-25412
Residual oxygen pressure in contact gap upon diffusion welding of titanium 15 p2490 N85-25418
Titanium diffusion method prevents metal corrosion 15 p2514 N85-25510
Inhibiting titanium corrosion in hot nitrogen nitrate solutions using sulfate ions 15 p2514 N85-25511
Hydrogen induced crack growth in Grade-12 Titanium
[BNL-NUREG-35596] 16 p2751 N85-26976
Experimental investigation of the pulsed photoacoustic effect produced on a solid surface
[AD-A152114] 16 p2660 N85-27640
Mechanical properties of polycrystalline alpa titanium
[BLL-BISI-TRANS-21923-(9022.08)] 17 p2924 N85-28029
Study of the influence of metallurgical factors on fatigue and fracture of aerospace structural materials
[AD-A153913] 18 p3122 N85-29326
The physical and mechanical properties of near-equiatomic titanium-nickel 19 p3237 N85-30072
Microstructures and mechanical properties of microalloyed medium carbon steels 19 p3238 N85-30074
The microstructural state of Nb3Sn in a multifilamentary titanium doped bronze-process wire
[DE85-010979] 19 p3240 N85-30089
Vacuum pressure welding of commercial titanium with 2Kh13 and 12Kh18N10T steels 19 p3246 N85-30124
Producing titanium-sapphire items by solid-phase bonding through aluminum gasket 19 p3246 N85-30127
Electrochemical reduction of titanium in dimethyl sulphoxide
[BLL-OA-TRANS-3225-(6196.300)] 20 p3429 N85-31267
Long range ordered alloys modified by addition of niobium and cerium
[DE85-011661] 20 p3431 N85-31285
Precision measurements of solar energetic particle elemental composition
[PAPER-SH-2.1-4] 21 p3715 N85-33052
Properties of Ti-6Al-4V spun formed fuze supports
[DE85-011968] 22 p3792 N85-33498
Joint design for improved fatigue life of diffusion-bonded box-stiffened panels
[NASA-TP-2480] 22 p3799 N85-33537
The development of titanium production in the USSR
[BLL-OA-TRANS-3226-(6196.3)] 23 p3913 N85-34244
Calculating the interatomic pair potential allowing for resonance interaction in titanium, nickel and vanadium
[BLL-M-35843-(5828.4)] 23 p3913 N85-34249
The properties of VSt3sp inoculated steel
[BLL-M-35894-(5828.4)] 23 p3915 N85-34263
An X-ray diffraction study of titanium oxidation
[NASA-CR-176263] 23 p3915 N85-34264
Applications of the mineral resources data system and the international strategic minerals inventory in mineral-resource assessments by region and commodity 24 p4105 N85-35451

TITANIUM ALLOYS
NT NITINOL ALLOYS
Granular boundary segregation in low-alloyed titanium-vanadium alloys 01 p0019 N85-10117
Influence of annealing on properties of AT3 alloy welded joints 01 p0019 N85-10118
Heat treatment of welded joints in OT4 and VT20 titanium alloys 01 p0020 N85-10119
Strength of welded joints in VT23 alloy upon repeated static loading 01 p0020 N85-10120
Fracture toughness characteristics of welded joints in VT65 and AT6 titanium alloys 01 p0020 N85-10121
Nonlinear ultrasonic characterization of oxygen impurities in titanium, 2
[AD-A144857] 01 p0027 N85-10171
Effect of microstructure and trapping on the hydrogen embrittlement susceptibility of a titanium bearing HSLA steel 02 p0174 N85-11166
Re-evaluation of phase separation in Ti-Zr-Be metallic glasses
[DE84-015603] 03 p0336 N85-12176
Kinetics of fatigue factor of AT3 titanium alloys in air, distilled water and 3.5% aqueous NaCl solution 03 p0350 N85-12255
Structure of two-phase titanium alloys with different microstructures 03 p0351 N85-12257
Energy of stacking fault and dislocation structure of titanium alloys 03 p0351 N85-12259
Structure and properties of titanium alloys after isothermal deformation at low speeds 03 p0351 N85-12260
Structure and ductility of fracture of joints produced by electron-beam welding of VT6ch titanium alloy parts 03 p0351 N85-12261
Fatigue crack propagation in metastable titanium alloys
[AD-A145824] 03 p0372 N85-12376
The TA6Zr5D (IMI 685) characterization in strain controlled tests. (Specimens obtained from a forged spinning wheel) no. M4-45870
[M4-45870] 03 p0373 N85-12384
Swelling behavior of titanium-modified AISI 316 alloys
[DE84-013940] 05 p0618 N85-13958
Flow-based analyses of metal deformation processes: An overview 06 p0796 N85-15087
Pulsed electric discharge laser technology. Electron beam window foil material
[AD-A146420] 06 p0813 N85-15162
Nitriding of titanium and its alloys by N2, NH3 or mixtures of N2 + H2 in a dc arc plasma at low pressures (or = to torr)
[NASA-TM-83803] 06 p0814 N85-15168
Disc fatigue life predictions for gas turbine engines 07 p0907 N85-15743
Titanium Matrix/Continuous Fiber/Continuous fiber composite interface interactions and their influence on mechanical properties
[AD-A147504] 07 p0920 N85-15829
Study of residual stresses introduced into TA6ZrD (685) cylinders by quenching
[BLL-PNR-90240-(8019.3153)] 07 p0925 N85-15859
Pulsed electric discharge laser technology. Electron beam window foil material
[AD-A147488] 07 p0972 N85-16171
Proceedings of the 2nd Workshop on Nondestructive Evaluation (NDE) of Titanium Alloys
[AD-A147626] 08 p1125 N85-17095
NDE (Nondestructive Evaluation) of oxygen contaminated titanium alloys and weldments
[AD-P004121] 08 p1126 N85-17096
Effects of oxygen on the microstructure and properties of titanium 6211 alloys
[AD-P004122] 08 p1126 N85-17097
Nonlinear ultrasonic characterization of oxygen impurities in titanium
[AD-P004123] 08 p1126 N85-17098
Effects of oxygen-contamination-induced microstructural changes on the reverberation of ultrasound in Ti-6211 alloys
[AD-P004124] 08 p1126 N85-17099
Acoustical characterization of Ti-6211 weldments and oxygen contamination Ti-6211 plate
[AD-P004125] 08 p1126 N85-17100
Photoacoustic microscopy of oxygen contaminated titanium alloys
[AD-P004127] 08 p1127 N85-17102
High resolution acoustic microstructural characterization of titanium with interstitial contamination
[AD-P004128] 08 p1127 N85-17103
Evaluation of interstitial gas contamination in titanium alloys using induced magnetic field analysis
[AD-P004130] 08 p1127 N85-17105
Electromagnetic NDE of interstitial contamination in titanium alloy weldments
[AD-P004131] 08 p1127 N85-17106
Evaluation of the thermoelectric method for determination of interstitial gases in titanium
[AD-P004132] 08 p1127 N85-17107
Measurement of oxygen contamination in titanium alloy ingots by fast neutron activation analysis
[AD-P004133] 08 p1128 N85-17108
Nondestructive evaluation of titanium alloys. ESCA (Electron Spectroscopy for Chemical Analysis), ISS (Ion Scattering Spectroscopy), and SIMS (Secondary Ion Mass Spectrometry) examination of titanium alloy solid surfaces
[AD-P004135] 08 p1128 N85-17110
Effect of microstructure and trapping on the hydrogen embrittlement susceptibility of a ti-bearing HSLA steel
[AD-A148610] 08 p1130 N85-17122
Deformation and fracture of P/M (Powder/Metallurgy) titanium alloys
[AD-A148672] 09 p1294 N85-18128
Ion implantation of surgical Ti-6Al-4V alloy
[DE85-000943] 09 p1296 N85-18142
Ti-6Al-4V alloy castings prepared in zircon sand molds and the effect of hot isostatic pressing
[PB85-109932/GAR] 09 p1298 N85-18150
Study of residual stresses introduced into TA6ZrD (685) cylinders by quenching — compressor disk alloy
[PNR-90240] 09 p1341 N85-18435
Impact toughness of composites with layered microstructure of OT4 titanium alloy 10 p1445 N85-19104
Optimization of production of composite diamond-containing materials using titanium carbide-steel alloys 10 p1446 N85-19113
Influence of extension rate on strength and deformation characteristics of titanium alloys over a broad temperature range 10 p1448 N85-19121
Kinetics of oxidation of titanium alloy upon heating to 1000 deg C 10 p1448 N85-19122
Kinetics of joint formation during diffusion welding of VT5 titanium alloys 10 p1448 N85-19125
Calculation of mode field in electron beam welding of VT6 titanium alloy 10 p1449 N85-19129
Oxidation of PT-7M and OT4-1 titanium alloys in air 11 p1600 N85-20063
Fractographic features of titanium alloy fatigue failure under repeated static stress and high frequency vibration 11 p1601 N85-20070
Effect of hydrogen on fatigue of VT6 alloy 11 p1601 N85-20071
Dependence of mechanical properties of large VT3-1 alloy forgings on microstructure parameters 11 p1602 N85-20072

Phase transformations in vanadium alloys of titanium during quenching and tempering
11 p1602 N85-20073
Sensitivity of titanium alloys to stress concentration during repeated static loads 11 p1602 N85-20074
Improving operational properties of titanium alloys by diffusion silicking 11 p1602 N85-20075
Assessment of effectiveness of electron beam welding of titanium alloys up to 40 mm in thickness by vertical or horizontal beam 11 p1603 N85-20078
Amorphous Ni-Ti alloys: A new method of synthesis [DE85-002744] 11 p1605 N85-20094
MBB uses superplastic forming, diffusion bonding for alloys 11 p1618 N85-20177
Method for refining microstructures of cast titanium articles [AD-D011518] 12 p1804 N85-21316
Alloy development, processing and characterization of devitrified titanium base microcrystalline alloys [AD-A149609] 12 p1806 N85-21327
Proton NMR and susceptibility measurements in TiCoH/sub x [DE85-003309] 12 p1807 N85-21336
Comparison of the fatigue resistance (initiation, propagation) of cast TA6V with hot rolled TA6V — titanium alloy [DGT-25369-PT-1] 12 p1808 N85-21341
Properties of Ti alloyed multifilamentary Nb3Sn wires by internal tin process [DE85-003212] 12 p1941 N85-22191
Effect of phase state of TiC-NiTi powder composite materials on nature of failure and mechanical properties 13 p2027 N85-22702
Decomposition of VTAN alloy solid solution upon irradiation and thermal aging 13 p2029 N85-22712
High temperature antifriction properties of Ti sub 1-sub xNb sub x C sub 0.5N sub 0.5 alloys 13 p2029 N85-22715
Developing procedures for thermomechanical processing of high-durability VT22 titanium alloy 13 p2031 N85-22726
Influence of annealing on cyclic and short-term strength of thin sheets of VT1-0 titanium and OTR4 alloy 13 p2031 N85-22727
Basis and pyramidal slipping in single crystals of alpha-alloy Ti-Al-Sn 13 p2032 N85-22730
Specifics of structure and mechanical properties of metastable beta-titanium alloys after deformation and aging 13 p2032 N85-22731
Properties of welded joints in argon arc welding of titanium alloy using a protective coating 13 p2032 N85-22733
Thermal hardening of welded joints in titanium alloys with various structures 13 p2032 N85-22734
Effect of protective medium on durability and fracture structure on seam zones of thin-walled titanium articles produced by diffusion welding 13 p2033 N85-22738
Technological parameters of diffusion welding processes in honeycomb titanium alloy structures 13 p2033 N85-22739
Fatigue strength of alpha-titanium alloys under cophasal action of variable normal and tangential stresses 15 p2498 N85-25407
Study of structural changes of dual-phase titanium alloy during shock wave loading 15 p2498 N85-25408
Possible use of rapid heating for improving mechanical properties of titanium alloys 15 p2498 N85-25409
Effect of annealing procedures on structure and properties of VT6 alloy with initial large-grained structure 15 p2498 N85-25410
Effect of aluminum on nature of titanium alloy failure 15 p2498 N85-25411
Resistance of hydrogenated alpha-titanium alloys to corrosion-fatigue fracture 15 p2499 N85-25413
Hydrogen resistance of VT1-0 titanium under 150 MPa pressure at room temperature 15 p2499 N85-25414
Ways of improving level and stability of mechanical characteristics of diffusion-welded joints of OT4 titanium alloy 15 p2499 N85-25417
Brittle fracture resistance of electron beam-welded joints in titanium Alpha alloys 15 p2500 N85-25419
Increasing seam formation stability in electron beam welding of very thick titanium alloys 15 p2500 N85-25420
Development of coating for protection of backside of seam in welding of titanium alloys 15 p2500 N85-25421
Thermocompression welding of parts made from AMts and VT1 alloys 15 p2501 N85-25430
USSR report: Materials science and metallurgy [JPRS-UMS-85-004] 15 p2513 N85-25503
Hardening of titanium alloy electric-arc welded joints 15 p2514 N85-25513
Mechanical properties of cast Martensitic high-strength multicomponent titanium alloys 15 p2514 N85-25514
Thermal stability of titanium alloys after cold plastic deformation 15 p2515 N85-25515
Dependence of plasticity of VT1-00 titanium alloy on microstructure 15 p2515 N85-25516
Structure and properties of VT20L titanium alloy with 0.1-0.3 percent content 15 p2515 N85-25517
Effect of initial structure on texture of pressed titanium alloy bars 15 p2515 N85-25518
Anode formation of passivating films on titanium alloy at temperatures up to 200 deg C 15 p2515 N85-25519
West Europe report: Science and technology [JPRS-WST-84-012] 15 p2523 N85-25552
MBB uses new CFC form tool for titanium alloy air intake 15 p2523 N85-25553
Titanium alloys, products, standards listed 15 p2533 N85-25626
Solid state bonding of molybdenum and TZM [BLL-T6439/BG/LRS/LRST751/85] 16 p2792 N85-27220
Effects of the phase compositions of cast low-pearlite steels micro-alloyed with vanadium and titanium of their structure and properties [BLL-BISI-TRANS-22301-(9022.06)] 17 p2928 N85-28067
Titanium metal-matrix composites [AD-D011643] 17 p2930 N85-28086
The disordering process in an L12 ordered alloy [DE85-006152] 17 p2931 N85-28093
Fundamental studies of beta phase decomposition modes in titanium alloys [AD-A154122] 19 p3236 N85-30078
Wear improvement in titanium alloys by ion implantation [AD-D011694] 19 p3239 N85-30081
Effect of thermochemical processing on fatigue resistance of titanium alloys 19 p3244 N85-30112
Determining partial molar volume of hydrogen in titanium alloys 19 p3245 N85-30119
Fatigue resistance of VT3-1 titanium alloy related to surface cold working 19 p3245 N85-30120
Effect of protective method on cyclic durability and nature of failure of titanium alloy welded joints 19 p3245 N85-30122
Effect of heating temperature in a vacuum on state of surface layers of welded OT4 titanium alloy 19 p3245 N85-30123
Fatigue resistance of homogeneous and heterogeneous welded joints of TS5 titanium alloy 19 p3246 N85-30126
concentration variation of work function of alloys in the system nickel-titanium-aluminum 19 p3247 N85-30134
CO adsorption on (111) and (100) surfaces of the Pt sub 3 Ti alloy. Evidence for parallel binding and strong activation of CO [NASA-CR-176077] 21 p3585 N85-32176
Fundamental investigations of failure during superplastic forming process [AD-A154647] 21 p3588 N85-32194
Thermodynamic properties of alloys in the Fe-Ti system [NPL-DMA(A)-96] 22 p3748 N85-33229
Electrical resistivity and hysteresis of the equiatomic nickel-titanium alloy near the martensitic transformation temperature 23 p3904 N85-34181
Influence of particle erosion on the microstructural changes in metals and alloys [TI85-901364] 23 p3917 N85-34276
Laser welding of 6Al-4V titanium alloy [DE85-012019] 23 p3938 N85-34413
The stress pattern analysis of coarse grain titanium specimens [PNR-90250] 23 p3942 N85-34433

TITANIUM BORIDES
Development and testing of TiB2, used as cathode material in Al-electrolysis cells [BMFT-FB-T-84-176] 05 p0633 N85-14060
Surface mechanical properties and wear behavior of ion implanted TiB2 [DE85-001130] 09 p1295 N85-18133
Secondary fluorescence effects on X-ray microanalysis [DE85-005585] 15 p2506 N85-25457
Study of self-propagating condensed phase reactions TiB(2) synthesis [AD-A153198] 17 p2921 N85-28005

TITANIUM CARBIDES
New titanium carbide grade for metal cutting 02 p0181 N85-11214
Optimization of production of composite diamond-containing materials using titanium carbide-steel alloys 10 p1446 N85-19113
Antifriction properties of gas thermal coatings of clad carbine powders 10 p1447 N85-19115
Particulate toughened silicon carbide [DE85-004797] 13 p2016 N85-22843
Comparative sinterability of combustion synthesized and commercial titanium carbides [DE85-006255] 15 p2512 N85-25498
Joining of sintered composite TiC-steel materials by welding [BLL-M-36253-(5828.4)] 20 p3461 N85-31502

TITANIUM CHLORIDES
Electrochemical behaviour of TiCl4 solutions in low melting point organic media [BLL-OA-TRANS-3174-(6196.3)] 06 p0764 N85-14868
Electrochemical reduction of titanium in dimethyl sulphoxide [BLL-OA-TRANS-3225-(6196.300)] 20 p3429 N85-31267
The determination of dinitrotoluene in single base propellants [AD-A154672] 21 p3571 N85-32209

TITANIUM COMPOUNDS
NT BARIUM TITANATES
NT LEAD ZIRCONATE TITANATES
NT PEROVSKITES
NT PIEZOELECTRIC CERAMICS
NT RUTILE
NT STRONTIUM TITANATES
NT TITANIUM BORIDES
NT TITANIUM CARBIDES
NT TITANIUM CHLORIDES
NT TITANIUM NITRIDES
NT TITANIUM OXIDES
Critical current measurements on an NbTi superconducting wire standard reference material [PB85-118594] 13 p2066 N85-22906
The mechanisms of phenylacetylene polymerization by molybdenum and titanium initiators [AD-A150993] 14 p2260 N85-24007
Pressure-dependence of TiS(2) and TiSe(2) bandstructures [AD-A151200] 15 p2659 N85-26410
New catalysts and new electrolytes for acid fuel cells [DE85-009940] 19 p3307 N85-30498
Geosynchronous performance of a lithium-titanium disulfide battery 20 p3444 N85-31377
The development of titanium production in the USSR [BLL-OA-TRANS-3228-(6196.3)] 23 p3913 N85-34244
Development of metallization process: FSA project, cells and module formation research area [NASA-CR-176136] 23 p3945 N85-34447

TITANIUM DIOXIDE
U TITANIUM OXIDES

TITANIUM NITRIDES
Deposition of titanium nitride coatings by reactive evaporation and electrically activated reactive evaporation [BLL-TRANS-5043-(9091.9F)] 07 p0925 N85-15858
Structural distortions of ultra-dispersed titanium nitride powders 13 p2029 N85-22717
Gear-cutting tools made of ultra high speed steel coated with TiN [BLL-RISLEY-TR-5109-(9091.9F)] 15 p2567 N85-25837
New metal coating method developed 21 p3588 N85-32191

TITANIUM OXIDES
NT RUTILE
The development of CVD oxide coatings for the protection of metal surfaces — chemical vapor deposition (CVD) 03 p0332 N85-12142
Contamination analysis of Ti-O2 thin films deposited using ion assisted deposition [DE84-014944] 05 p0732 N85-14705
Recording holograms on thin films of titanium dioxide 06 p0789 N85-15039
Time resolved Raman studies of laser induced damage in TiO2 optical coatings [DE85-003166] 11 p1640 N85-20332
Degradation mechanisms in ceramic dielectrics [AD-A149791] 12 p1813 N85-21369
Electron stimulated desorption and the role of secondary electrons [AD-A150974] 14 p2252 N85-23955
Fracture surface analysis in composite and titanium bonding: Part 1: Titanium bonding [NASA-CR-175750] 15 p2502 N85-25434
Photoeffects of semiconductor electrolyte interfaces [AD-A154163] 20 p3449 N85-31411
Characterization of catalysts with metal-support effects and of the species adsorbed on their surfaces [DE85-012254] 24 p4096 N85-36394

TITRATION
Mononitration of durene [NASA-TM-77774] 06 p0765 N85-14892

Aromatics determination in middle distillate petroleum fractions by spectrophotometric titration
[PNR-90239] 09 p1293 N85-18123
Computer-assisted Gran titration procedure for strong acid determination
[DE85-006801] 15 p2507 N85-25462
Increase of total CO2 in the World ocean
[DE85-007756] 23 p3950 N85-34484

TNT (TRINITROTOLUENE)
U TRINITROTOLUENE

TOBACCO
Plant cell cultures in biological space experiments
05 p0690 N85-14434

TOKAMAK DEVICES
MHD instabilities in simple plasma configuration
[AD-A144936] 01 p0121 N85-10629
Polarized electron cyclotron emission in the Tokapole 2 Tokamak
[DE84-014953] 01 p0122 N85-10638
Plasma surface interactions in magnetic fusion systems
[DE84-015255] 01 p0123 N85-10642
Measuring local ion energy distribution function in Tuman-3 Tokamak plasma 02 p0271 N85-11768
Relaxation of plasma rotation in a Tokamak in the presence of extraneous forces and corrugation of the magnetic field
[DE84-015628] 02 p0284 N85-11854
Theory of resistive ballooning modes in Tokamaks
[DE84-015626] 04 p0566 N85-13606
Internal helical mode m = 1 of a Tokamak in the plateau and banana regimes
[DE84-015623] 04 p0566 N85-13607
Fusion plasma theory. Task 1: Magnetic confinement fusion plasma theory
[DE84-014941] 04 p0566 N85-13608
Fusion plasma theory. Task 3: Auxiliary heating in Tokamaks and tandem mirrors
[DE84-014940] 04 p0566 N85-13609
Rotation of a tenuous plasma with a high toroidal velocity in a Tokamak
[DE84-012990] 04 p0567 N85-13615
High-Beta Tokamak research
[DE84-016470] 04 p0568 N85-13618
High-Beta plasma theory
[DE84-016471] 04 p0568 N85-13619
Proceedings of the US-Japan Theory Workshop on 3-D MHD Studies
[DE84-012019] 04 p0568 N85-13620
Imaging polarimeter-interferometer arrays for Tokamak measurements
[DE84-015016] 05 p0730 N85-14693
Passive stabilization of vertical instability in Tokamak reactor 06 p0775 N85-14958
Generation of suprathermal electrons during plasma current startup by lower hybrid waves in a Tokamak
[IPPJ-697] 06 p0863 N85-15483
Alpha-particle diagnostics with high energy neutral beams
[IPPJ-695] 06 p0863 N85-15485
Limits of possible operation of the R-Tokamak due to ideal MHD instabilities
[IPPJ-694] 06 p0863 N85-15486
Experimental results on Tokamak beta limits from ISX-B
[DE84-015372] 07 p1046 N85-16844
High-performance TF coil design for the Toroidal Fusion Core Experiment (TFCX)
[DE85-001127] 08 p1159 N85-17315
Subcable test facility
[DE85-002103] 09 p1315 N85-18269
A compact time-of-flight energy analyzer of high resolution — for Tokamaks
[REPT-84-154] 09 p1324 N85-18318
An operational test of a time-of-flight analyzer at the ASDEX Tokamak
[REPT-84-155] 09 p1324 N85-18319
Slow wave antenna coupling to ion Bernstein waves for plasma heating in ICRF
[AD-B089084L] 09 p1386 N85-18717
Proceedings on US-Japan Workshop on Tokamak Diagnostics by X-ray, VUV and Optical Radiations
[IPPJ-703] 09 p1386 N85-18719
X-rays spectroscopy on the PLT and TFTR Tokamaks
09 p1386 N85-18720
Radial profiles of high resolution X-ray spectra from the Alcator C Tokamak 09 p1387 N85-18723
Recent activities on JIPP T-IIU Tokamak
09 p1387 N85-18724
Impurity control by additional current rise and gas puffing during ICRF heating in JIPP T-IIU Tokamak
09 p1387 N85-18725
X-ray spectroscopy of high-Z and high-density plasmas 09 p1387 N85-18726
Spectra of highly-ionized atoms for the diagnostics of the new generation of Tokamaks
09 p1388 N85-18730
Sources, densities, and transport of impurities in neutral-beam injected Tokamaks
09 p1388 N85-18731
Spectroscopic instrumentation for Tokamak diagnostics 09 p1388 N85-18732
Determination of ion temperature and rotation velocity profiles by visible, UV and X-ray spectroscopy on Doublet 3 09 p1388 N85-18734
Transport experiments in the Texas experimental Tokamak 09 p1389 N85-18741
Radiation data and standards for Tokamak diagnostics
09 p1390 N85-18742
Impact of atomic data on Tokamak modeling
09 p1390 N85-18743
Compilation of atomic data for diagnostics of Tokamak
09 p1390 N85-18744
Beam-foil spectroscopy of highly ionized aluminum atoms 09 p1390 N85-18746
MHD equilibrium and stability for stellarator/torsatron configurations
[DE85-001139] 09 p1391 N85-18750
Extended abstract: Ergodic magnetic limiter experiments on TEXT with a 7/3 resonance
[DE85-001390] 09 p1391 N85-18754
Discharge initiation experiments in the Tokapole II Tokamak
[DE84-017345] 09 p1391 N85-18755
Experimental investigations of driven Alfven wave resonances in a Tokamak plasma using carbon dioxide laser interferometry
[DE85-001049] 09 p1392 N85-18758
Effects of q and high beta on Tokamak stability
[DE84-016650] 09 p1393 N85-18767
Background calculations for the measurement of the ion temperature in a deuterium plasma
[DE84-016546] 09 p1393 N85-18768
Versator divertor experiment: Preliminary designs
[DE84-017159] 09 p1393 N85-18769
Studies on impurity control and hydrogen pumping with chromium gettering in ISX-B
[DE85-001896] 09 p1394 N85-18771
The energy spectra of slowed-down neutrals from the heating beams in ASDEX — tokamak
[REPT-84-157] 09 p1394 N85-18772
Sequentially-framing soft X-ray pinhole camera for Tokamak plasma studies
[DE85-001717] 10 p1489 N85-19399
CO2 laser interferometer array for Big Dee
[DE85-001718] 10 p1490 N85-19411
Far-infrared interferometry/polarimetry on the ISX-B Tokamak
[DE84-015401] 10 p1558 N85-19827
Space-time statistics of the turbulence in a Tokamak edge plasma
[DE85-002667] 10 p1559 N85-19834
A proposed method for fast determination of plasma parameters
[IPP-1/228] 11 p1730 N85-20877
Fusion Energy Division
[DE85-001701] 11 p1731 N85-20884
FIR interferometer/polarimeter system on ISX-B Tokamak
[DE85-001129] 11 p1731 N85-20887
Control of surface composition and hydrogen recycling by plasma conditioning
[DE85-001859] 11 p1731 N85-20889
Driven global Alfven eigenmodes
[DE85-001056] 11 p1732 N85-20890
Fluctuations and transport in fusion plasmas
[DE85-003612] 11 p1732 N85-20893
Determination of experimental Tokamak plasma properties using maximum entropy analysis
[DE85-001723] 12 p1936 N85-22165
Tritium catalyzed deuterium Tokamaks
[DE85-004825] 12 p1936 N85-22166
Observations of bulk electron heating due to return current in a tokamak discharge started up by lower hybrid waves
[IPPJ-708] 12 p1937 N85-22172
Winding insulation in electromagnetic systems for Tokamak reactor plants 13 p2087 N85-23035
Lower hybrid heating and current drive, and ion cyclotron heating experiments on the Alcator C and the Versator II Tokamaks
[DE85-004918] 13 p2161 N85-23412
East Europe report: Science and technology
[JPRS-ESA-85-015] 14 p2289 N85-24189
Design, theoretical innovations in Tokamaks systems
14 p2289 N85-24190
Noninductive current drive in Tokamaks
[DE85-005427] 14 p2424 N85-24951
ICRF antenna coupling theory for a cylindrically stratified plasma
[DE85-004960] 14 p2424 N85-24952
Self-substaining low-Z coatings for impurity control. Part 1: General considerations
[DE85-000427] 14 p2425 N85-24956
Magnetohydrodynamic considerations for the design of self-cooled liquid-metal fusion reactor blankets
[DE85-000242] 14 p2425 N85-24957
Breakthrough in container confinement of ultracold neutrons 15 p2644 N85-26311
Annual Review, April 1983 - March 1984
[ISSN-0547-1567] 15 p2654 N85-26369
Scientific activities. A: Reacting plasma physics. 1: Introduction and overview 15 p2654 N85-26370
Outline of alternative design of R-Tokamak
15 p2654 N85-26371
Plasma heating 15 p2654 N85-26372
Preparatory experiments. 1: JIPP T-IIU
15 p2654 N85-26374
MHD fluctuations in ISX-B
[DE85-004800] 15 p2657 N85-26395
New directions in Tokamak reactors
[DE85-002548] 15 p2657 N85-26396
Methods of first wall structural analysis with applications to the long pulse commercial Tokamak reactor design
[DE85-004915] 15 p2657 N85-26397
Toroidal equilibrium with low frequency wave driven currents
[DE85-005790] 15 p2658 N85-26401
Self-sustaining low-Z coatings for fusion applications 2 - copper-lithium
[DE85-002553] 15 p2658 N85-26403
Ballooning beta limits of dee and bean shaped Tokamaks
[IPPJ-713] 16 p2866 N85-27676
TOKASTAR: A Tokamak stellarator hybrid with possible bean-shaped operation
[IPPJ-718] 16 p2866 N85-27680
Computational plasma physics and supercomputers, revision 1
[DE85-007228] 16 p2867 N85-27687
Spherical torus, compact fusion at low field
[DE85-006983] 16 p2867 N85-27689
Time-resolving electron temperature diagnostic for ALCATOR C
[DE85-004916] 16 p2868 N85-27690
A four-field model for Tokamak plasma dynamics
[DE85-007111] 16 p2868 N85-27694
Coupled plasma-neutral transport model for the scrape-off region
[DE85-007559] 16 p2868 N85-27695
Tokamak systems code
[DE85-008147] 16 p2869 N85-27696
Accelerator-based plasma-wall interaction studies on the TEXTOR Tokamak
[DE85-007540] 17 p3040 N85-28806
Tokamak fusion core experiment maintenance study
[DE85-008040] 17 p3040 N85-28813
The transport of neutral H, D, T and He and O in the boundary layers of a Tokamak plasma
[REPT-84-153] 17 p3041 N85-28817
New concept for a wall detector for alpha particles
[DE85-009037] 18 p3183 N85-29740
Whist code calculations of ignition margin in an ignition Tokamak
[DE85-009507] 18 p3190 N85-29784
Tokamak ignition/burn experimental research device
[DE85-009999] 18 p3190 N85-29785
Feasibility study of a fission-suppressed Tokamak fusion breeder
[DE85-009099] 18 p3190 N85-29786
Toroidal viscosity and ambipolarity in the neoclassical transport theory of axisymmetric tori
[DE85-010622] 19 p3358 N85-30820
TFCX shielding optimization
[DE85-010503] 19 p3359 N85-30826
Magnetic fusion 1985: What next?
[DE85-009953] 19 p3365 N85-30868
Impurity and particle control systems for tokamak reactor experiments
[DE85-006124] 19 p3366 N85-30873
ICRF antenna coupling and wave propagation in a tokamak plasma 19 p3369 N85-30893
Effects of a radial electric field on tokamak edge turbulence
[DE85-010401] 19 p3371 N85-30910
Ballooning instabilities on a magnetic separatrix
[DE85-010655] 19 p3372 N85-30915
Neutronics activities for next generation devices
[DE85-010488] 20 p3527 N85-31939
Superconducting toroidal field coil current densities for the TFCX
[DE85-010285] 20 p3530 N85-31958

Runaway electrons and plasma turbulence in current ramping by lower hybrid waves in tokamak plasmas
[DE85-011390] 20 p3535 N85-31997
Injection of hydrogen macroparticles into T-10 tokamak 21 p3692 N85-32937
Influence of ECR-heating on MHD activity of plasma in tokamak-10 installation 21 p3694 N85-32949
System and method of operating toroidal magnetic confinement devices
[DE85-011670] 22 p3845 N85-33814
Possibility of potential generation by lower hybrid wave 23 p3977 N85-34654
Observation of mode-converted by ion Bernstein wave by an HCN laser scattering
[IPPJ-724] 23 p3979 N85-34668
Compact DT fusion spherical tori at modest field
[DE85-011568] 23 p3982 N85-34692
Experimental measurements of the ion cyclotron antennas' coupling and RF characteristics
[DE85-011569] 23 p3982 N85-34694
Shield design for next-generation, low-neutron-fluence, superconducting tokamaks
[DE85-011409] 23 p3982 N85-34695
Observation of helical sawtooth oscillations in a tokamak
[DE85-012062] 23 p3983 N85-34703
ECH tokamak
[DE85-012074] 23 p3984 N85-34707
Neutral pumping rates for a next step tokamak ignition device
[DE85-012780] 24 p4157 N85-35776
Generalized reduced fluid model with finite ion-gyroradius effects
[DE85-013123] 24 p4157 N85-35777
Resonance localization in tokamaks excited with ICRF waves
[DE85-014559] 24 p4160 N85-35791

TOLERANCES (MECHANICS)
NT IMPACT TOLERANCES
Development of powder metallurgy 2XXX series Al alloys for high temperature aircraft structural applications
[NASA-CR-172408] 02 p0182 N85-11220
Array sidelobes, error tolerance, gain, and beamwidth
[AD-A147004] 07 p0940 N85-15956
Tolerance synthesis of multilayer radome walls 07 p0953 N85-16041
Advances in composites technology
[NASA-TM-86353] 08 p1118 N85-17048
Defect tolerance in pipeline girth welds
[ERS-E.353] 09 p1328 N85-18347
Construction tolerances for low loss, dielectric coated, metallic waveguide for transmission optical radiation
[DE85-004056] 10 p1558 N85-19822
Method for increasing linearity of load cell 11 p1623 N85-20221
Advanced life analysis methods. Volume 1: Cracking data survey and NDI (nondestructive inspection) assessment for attachment lugs
[AD-A150419] 13 p2103 N85-23108
Advanced life analysis methods. Volume 2: Crack growth analysis methods for attachment lugs
[AD-A150420] 13 p2103 N85-23109
Advanced life analysis methods. Volume 4: Tabulated test data for attachment lugs
[AD-A151016] 14 p2219 N85-23760
Advanced life analysis methods. Volume 5: Executive summary and damage tolerance criteria recommendations for attachment lugs
[AD-A151017] 14 p2219 N85-23761
Dimensions of smooth mating parts with protective coatings 14 p2280 N85-24124
Multiaxial and thermomechanical fatigue considerations in damage tolerant design
[NASA-TM-87022] 16 p2749 N85-26964
Probabilistic structural analysis of SSME turbopump blades: Probabilistic geometry effects 17 p2913 N85-27958

TOLERANCES (PHYSIOLOGY)
NT ACCELERATION TOLERANCE
NT ALTITUDE TOLERANCE
NT COLD TOLERANCE
NT HEAT TOLERANCE
NT HUMAN TOLERANCES
NT RADIATION TOLERANCE
General resistance of organism of rats under hypokinesia 05 p0694 N85-14462
A crew exposure study. Volume 1: Offshore
[AD-A146884] 07 p1015 N85-16449
Effects of restricted water intake on performance in a cold environment
[AD-A146904] 07 p1015 N85-16[illegible]
Aviation-related cardiorespiratory effects of blood donation in female pilots
[AD-A148045] 08 p1195 N85-17529
Analysis of head motion during simulated, rough water operation of a 2200 ton surface effect ship 11 p1695 N85-20656
The current status of the RAF programme of densensitisation for motion sick aircrew 11 p1695 N85-20658
Role of mental work in human tolerance in total-body vibration 12 p1901 N85-21940
Investigation of adaptive distinctions of mechanism of controlled glycemia in Macaca rheseus monkeys 12 p1902 N85-21946
Multiple regression method used to assess animal adaptation to hypoxic hypoxia 12 p1902 N85-21947
The medical results of human exposures to radio frequency radiation
[AD-A149718] 12 p1905 N85-21962
Sleep deprivation and exercise tolerance
[AD-A150180] 13 p2142 N85-23295
Sleep deprivation and exercise tolerance
[AD-A150566] 13 p2142 N85-23296
Sleep deprivation and exercise tolerance
[AD-A150626] 13 p2142 N85-23297
Simulation of a G-tolerance curve using the pulsatile cardiovascular model
[NASA-CR-171873] 15 p2616 N85-26120
Fluid-electrolyte responses during prolonged space flight: A review and interpretation of significant findings
[NASA-CR-171878] 15 p2617 N85-26124
Functional impairment and structureal cervical injuries in human surrogates
[PB85-167436] 15 p2619 N85-26137
Effects of dehydration or cold exposure and restricted fluid intake upon cognitive performance
[AD-A151973] 16 p2842 N85-27525
An in vitro method for the screening of trichothecene mycotoxin cytotoxicity and the study of mycotoxin countermeasures
[AD-A153663] 18 p3152 N85-29517
Acclimatization to far north 20 p3506 N85-31792
The role of sulfur in osmoregulation and salinity tolerance in cyanobacteria, algae, and plants 21 p3660 N85-32736
A crew exposure study. Phase II. Volume 2. At sea. Part A
[AD-A155233] 21 p3666 N85-32774
Effects of low level carbon monoxide (CO) on tracking and monitoring. An attempt to replicate the findings of Putz et al. (1976) protocol 2
[AD-A155722] 22 p3825 N85-33694
Tolerance to +Gz and +Gx accelerations of individuals in older age groups in good health and with early signs of arteriosclerosis 23 p3952 N85-34496

TOLLMIEN-SCHLICHTING WAVES
Generation and development of small-amplitude disturbances in a laminar boundary layer in the presence of an acoustic field
[NASA-TM-77826] 14 p2299 N85-24237

TOLUENE
Effect of toluene on the solubility of bichezardous volatile synthetic organic compounds
[AD-A145188] 01 p0018 N85-10109
Deuteron NMR (Nuclear Magnetic Resonance) in relation to the glass transition in polymers
[AD-P003910] 01 p0032 N85-10196
Influence of structural parameters of zeolite catalysts on their activity and selectivity
[BMFT-FB-T-83-253] 03 p0329 N85-12119
Determination of Toluene's degradation products under simulated atmospheric conditions 05 p0674 N85-14331
Research in phase transfer catalysis
[AD-A148286] 08 p1121 N85-17068
Supersonic molecular jet study of the liquid state
[AD-A147416] 09 p1379 N85-18671
Polymer solution-supercritical fluid behavior
[AD-A154514] 21 p3568 N85-32192
Thermal reactions of aromatics with CaO
[DE85-010688] 22 p3742 N85-33193
Modeling of auto exhaust smog chamber data for EKMA development
[PB85-186492] 22 p3813 N85-33619
Carcinogenesis of nitrated toluenes and benzenes skin and lung tumor assays in mice
[AD-A155723] 22 p3818 N85-33655
Studies in photochemical smog chemistry. 1: Atmospheric chemistry of toulene. 2: Analysis of chemical reaction mechanisms for photochemical smog 24 p4113 N85-35497

TOMOGRAPHY
NT COMPUTER AIDED TOMOGRAPHY
Tomographic reconstruction of neutron radiograph images
[AD-A145882] 02 p0280 N85-11826
Time-resolved tomographic images of a relativistic electron beam
[DE84-015021] 04 p0565 N85-13597
Tomographic reconstruction of axially symmetric objects from a single radiograph
[DE84-016783] 04 p0565 N85-13599
Field implementation of geophysical diffraction tomography
[DE84-017594] 09 p1343 N85-18449
Acoustic tomographic reconstrution of anomalies in three-dimensional bodies
[DE84-017035] 09 p1378 N85-18666
Simultaneous determination of cerebral blood flow and partition coefficient with a freely diffusable tracer
[DE85-001226] 11 p1690 N85-20625
Reconstruction of a 3-dimensional transonic rotor flow field from holographic interferogram data
[NASA-TM-86690] 12 p1770 N85-21112
Research in image understanding as applied to 3-D tomographic imaging with near optical resolution
[AD-A150098] 12 p1829 N85-21483
A new NDE (Non-Destructive Evaluation) capability for thin-shelled structures
[AD-A149625] 12 p1862 N85-21678
NDE methods for green ceramics
[DE85-004019] 13 p2038 N85-22766
Optical processing in radon space
[AD-A150289] 13 p2159 N85-23402
Axial topography from digitized real time radiography
[DE85-006767] 18 p3091 N85-29130
Three-dimensional and tomographic imaging device for X-ray and gamma-ray emitting objects
[NASA-CASE-GSC-12851-1] 19 p3271 N85-30261
Preliminary evaluation of alterant geophysical tomography in welded tuff
[DE85-010626] 19 p3302 N85-30469
Arctic acoustic tomography MIZEX 84
[AD-A154426] 19 p3320 N85-30580
Biology and Medicine Division
[DE85-010638] 19 p3327 N85-30613
Radiation interactions for tomography
[DE85-008961] 19 p3355 N85-30799
Advanced instrumentation for Positron Emission Tomography
[DE85-011147] 22 p3840 N85-33779

TONOMETRY
U INTRAOCULAR PRESSURE
U PRESSURE MEASUREMENT

TONUS
U MUSCULAR TONUS

TOOLING
New tooling for plasma cutting technology 13 p2051 N85-22842
MBB automates aircraft production in many FRG facilities 14 p2289 N85-24188
An analysis of machine tool systems suitable for laser profiling 14 p2308 N85-24282

TOOLS
NT BORING MACHINES
NT DRILL BITS
NT GRINDING MACHINES
NT LATHES
NT MACHINE TOOLS
NT MILLING MACHINES
NT SAWS
NT SPACE TOOLS
NT TURRET LATHES
Utility of the M.I.T. (Massachusetts Institute of Technology) underwater stud welding gun
[AD-A144793] 01 p0055 N85-10365
Prediction accuracy of the torques for rotary tillage by an analog tool
[AD-P004288] 09 p1408 N85-18865
Connection system — insuring against loss of a tool component without using multiple tethers
[NASA-CASE-MSC-20319-1] 12 p1857 N85-21649
Aircraft skin penetrator and agent applicator. Volume 2: Test and evaluation
[AD-A151609] 15 p2456 N85-25225
Gear-cutting tools made of ultra high speed steel coated with TiN
[BLL-RISLEY-TR-5109-(9091.9F)] 15 p2567 N85-25637
Classification and types of diamond wear in honing 15 p2567 N85-25842
Printed wiring board circuit isolator tool
[AD-D011638] 17 p2968 N85-28333
The blind and the paralyzed. The notion of the tool revealed and integrated in a different organization environment
[SNIAS-851-422-104] 20 p3513 N85-31835
Action of wear-inhibiting Al2O3-coatings when applied to hard metal cutting tools
[BLL-RISLEY-TR-5041-(9091.9F)] 24 p4081 N85-35292
Wear-resistant coatings for tools intended for cold working
[BLL-RISLEY-TR-5040-(9091.9F)] 24 p4081 N85-35293

TOPEX
Topex Gravity Model Development Team activities during fiscal year 1984
[NASA-TM-86208] 16 p2804 N85-27285
Status of the observational data sets — TOPEX
16 p2804 N85-27286
Satellite selection criteria 16 p2804 N85-27288
Optical best arc RMS test results
16 p2804 N85-27290
Ocean tide models for Topex analysis
16 p2805 N85-27291
Radial orbit error spectrum for Topex
16 p2805 N85-27292
The size of a gravitational field model for Topex
16 p2805 N85-27293
Numerical integration through force discontinuities: Solar radiation pressure 16 p2805 N85-27296
Station coordinates and Earth rotation parameters from Lageos laser ranging 16 p2806 N85-27299
TOPEX error budget 20 p3493 N85-31717
TOPOGRAPHY
NT LUNAR TOPOGRAPHY
NT TERRAIN
The SANCOR programme on coastal processes, April 1982 - March 1988
[REPT-88] 01 p0069 N85-10455
Investigation of summertime convection over the upper Current River valley of southeast Missouri
[PB84-222389] 01 p0086 N85-10578
The application of principal component analysis in a study of rainfall 02 p0212 N85-11396
Geomorphology 02 p0214 N85-11411
Cartography 02 p0214 N85-11412
Hypothesis on the origin of lineaments in the LANDSAT and SLAR images of precambrian soil in the low Contas River Valley (southern Bahia)
[E85-10007] 02 p0215 N85-11420
Terrain analysis procedural guide for surface configuration
[AD-A145837] 02 p0219 N85-11446
Satellite altimetry for sea-surfacing topography determination and geoid improvement
03 p0362 N85-12444
Modelling of altimeter tracking over topographical surfaces — satellite antennas 03 p0363 N85-12450
The structure of the Iceland-Faeroe ridge, derived from geophysical measurements
[DRIC-T-7255] 03 p0397 N85-12535
Comparison between tracer measurements and model calculations for nighttime drainage flows in complex terrain
[DE84-014709] 04 p0539 N85-13431
The 1984 NASA/ASEE summer faculty fellowship program
[NASA-CR-174136] 04 p0574 N85-13663
Mars polar volatiles: Topographic and geologic setting
[NASA-CR-174089] 04 p0581 N85-13708
Atmospheric studies in complex terrain
[DE84-008553] 05 p0676 N85-14345
Potential geological natural landmarks of the East Gulf Coastal Plain
[PB84-230317] 06 p0835 N85-18316
Statistical relationships between meteorological data stations and implications to diagnostic models in complex terrain
[DE84-014380] 06 p0839 N85-15328
Relationship between forest clearing and biophysical factors in tropical environments: Implications for the design of a forest change monitoring approach — Costa Rica
[E85-10051] 07 p0983 N85-16247
A Computer-generated topographic display system for navigation and mission planning in helicopters
08 p1073 N85-16600
SIR-B interferometric topography
08 p1145 N85-17224
Interlobate comparison of glacial-depositional style as evidenced by small-relief glacial landscape features in Illinois, Indiana, and Ohio, utilizing SIR-B
08 p1146 N85-17231
SIR-B cartography and stereo topographic mapping
08 p1147 N85-17234
Monitoring of the tidal dynamics of the Dutch Waddensea by SIR-B 08 p1147 N85-17235
Application and calibration of the subsurface mapping capability of SIR-B in desert regions
08 p1148 N85-17244
Mathematical aspects of digital terrain information; Report from International Society for Photogrammetry and Remote Sensing (ISPRS) working group 3:3, 1980 - 1984 — photogrammetry 08 p1175 N85-17407
Post-Laramide history of North Central Wyoming
08 p1181 N85-17444
A method for determining mesoscale dynamic topography
[AD-D011412] 08 p1191 N85-17506
Gravity anomaly map of Mars and Moon and analysis of Venus gravity field: New analysis procedures
[NASA-CR-174295] 08 p1258 N85-17919
The pleistocene geology of Vilas County, Wisconsin
09 p1353 N85-18509
Venus 09 p1411 N85-18891
A comparison between predicted and measured propagation loss in the VHF/UHF range in rugged terrain 10 p1471 N85-19285
Climate of Salt Lake City, Utah
[PB85-123675] 10 p1521 N85-19589
Application of SLF (Standard Linear Format) to digital hydrographic products
[AD-A149509] 10 p1522 N85-19596
Microstrain analysis in bent single crystal silicon by double crystal X-ray topography technique
[DE85-000422] 10 p1564 N85-19883
Analysis of slope stability, Wilmington to Lindenkohl Canyons, US mid-Atlantic margin
[DE84-012276] 12 p1899 N85-21921
Planetary cartography in the next decade (1984 - 1994)
[NASA-SP-475] 12 p1960 N85-22323
Physiography of the Martian west equatorial uplift
12 p1961 N85-22325
Hypsometric features on Venus
13 p1983 N85-22439
Evaluating accuracy in orientation of topographic photograph and satellite-centered direction from star photograph 13 p1983 N85-22442
Development, achievements in China's cartography work 13 p2166 N85-23434
Topographic evidence for shield volcanism on Io
13 p2172 N85-23478
The support of long wavelength loads on Venus
13 p2178 N85-23515
Newly discovered Martian impact basins
13 p2182 N85-23544
Mapping structures characteristic of the highland boundary scarp on Mars 13 p2191 N85-23595
Mercury radar altimetry: A preliminary analysis
13 p2196 N85-23631
Unsupervised classification of global radar units on Venus 13 p2196 N85-23632
Mapping and geological analysis of Mercury and Venus radar ranging data 13 p2196 N85-23633
Correction and geological analysis of lunar 3.8 cm radar data 13 p2196 N85-23634
Mars radar catalog 13 p2196 N85-23636
The deep structure of lunar basins: Clues to the understanding of basin formation and modification
13 p2200 N85-23647
Mars: Stratigraphy of western highlands and polar regions 13 p2201 N85-23653
The Galilean Satellite Geological Mapping Program, 1984 13 p2203 N85-23664
Fatigue Crack Topography
[AGARD-CP-376] 14 p2318 N85-24321
Fatigue fracture topography 14 p2318 N85-24323
A study of terrain reductions, density anomalies and geophysical inversion methods in gravity field modelling
[AD-A150788] 14 p2373 N85-24668
Studies of deformation in niobium by X-ray topographic methods
[AD-A150726] 14 p2427 N85-24965
Contamination of the fetch-limited directional wave spectrum by waves emanating from an embayment
[NASA-TM-84441] 15 p2604 N85-26048
Tenth Conference of Working Group of Socialist Countries on Remote Sensing of Earth under Intercosmos Program 16 p2725 N85-26820
Reports on cartography and geodesy. Series 1: Original reports, no. 94
[ISSN-0468-4236] 16 p2814 N85-27357
Use of vector processors in cartographic raster data processing, with special regard to the AP-120B vector processor 16 p2814 N85-27358
Testing of scanner-assisted revision of the topographic map 1:25,000 (TK 25) 16 p2814 N85-27359
Automatic engraving of map frames in the revision of the TK 25, 1:25,000 topographical map
16 p2814 N85-27362
Groundwater model for an island aquifer: Bribie Island groundwater study
[CE-44] 16 p2821 N85-27398
System analysis of a field Army Topographic Support System
[AD-A153318] 17 p2984 N85-28439
A discussion of adaptive grids and their applicability in numerical hydrodynamic modeling
[AD-A151843] 17 p3017 N85-28659
Derivation of model topography
18 p3141 N85-29449
Sigma filter 18 p3142 N85-29450
Comparison of two orographical data sets for the GLAS Fourth Order GCM 18 p3142 N85-29452
Engineering geology of selected areas, US army engineer division, lower Mississippi valley. The American bottom area, MO-IL. Volume 1
[AD-A154256] 19 p3299 N85-30455
Sand dispersion from an ephemeral river delta on the wave-dominated central California coast
[AD-A154352] 19 p3300 N85-30458
Stratigraphic analysis of Pennsylvania rocks using hierarchy of transgressive-regressive units
19 p3312 N85-30531
Evolution of the oceanic upper mantle and effects on sea floor subsidence geoid height and heat flow
19 p3319 N85-30575
HANDTC: A FORTRAN program to calculate inner-zone terrain corrections
[DE85-011196] 19 p3340 N85-30699
Video discs - what are they and where do they fit in?
[AD-A154166] 20 p3456 N85-31479
Comparative study of fracture planes computed from topography and lineaments from imagery with structures and mineralization in the magnetic belt of Washington State
[DE85-010972] 20 p3477 N85-31606
The application of computer imaging techniques to ocean topography and geophysical data
20 p3492 N85-31711
Geophysical interpretation of Venus gravity data
[NASA-CR-176063] 20 p3547 N85-32071
The measurement of strain fields by X-ray topographic contour mapping
[AD-A154870] 21 p3599 N85-32348
Geomorphological similarity and uniqueness
21 p3601 N85-32361
Regional landform thresholds
21 p3601 N85-32362
Some observations on paleogeomorphology
21 p3601 N85-32363
Ancient landscapes: Their nature and significance for the question of inheritance 21 p3601 N85-32364
Quantitative analysis in megageomorphology
21 p3603 N85-32376
Landscape inheritance: Report of Working Group Number 2 21 p3604 N85-32383
Process thresholds: Report of Working Group Number 3 21 p3604 N85-32384
Frequency and site selection criteria for MST radars, part 5.1A 21 p3624 N85-32512
Upward continuation of surface gravity anomalies
[AD-A154973] 21 p3631 N85-32560
An enhanced photoresponse at dislocation subgrain boundaries revealed by X-ray topography of polysilicon solar cells 22 p3806 N85-33572
Planetary surface processes: A review
22 p3855 N85-33869
Evaluation: Close-range photogrammetry for slope inventory and monitoring
[PB85-192755] 24 p4106 N85-35470
Three-dimensional gravity ideal body studies in rough terrain
[DE85-014097] 24 p4118 N85-35525
TOPOLOGY
NT FIXED POINTS (MATHEMATICS)
NT HOMOTOPY THEORY
NT LINKS (MATHEMATICS)
NT METRIC SPACE
Planarity criteria in electromagnetic topology
[AD-A145279] 01 p0036 N85-10241
Birkhoff orbits for non-monotone twist maps
[AD-A144718] 01 p0110 N85-10747
Fractals: From snow flakes to galactic clusters
[NOTA-INTERNA-796] 02 p0296 N85-11918
A topological approach to database theory
03 p0437 N85-12781
Lectures on generalized solutions to the minimal surface equation
[DE84-016882] 05 p0722 N85-14642
Invariant measures and the equicontinuous structure relation 1
[CWI-PM-R8403] 05 p0723 N85-14645
Invariant measures and the equicontinuous structure relation 2: The relative case
[CWI-PM-R8404] 05 p0723 N85-14646
Disturbance propagation in structural networks; control of large space structures 06 p0759 N85-14856
Chemical applications of topology and group theory. 18: Polyhedral isomerizations of seven-coordinate complexes
[AD-A149461] 10 p1436 N85-19047
Advanced inverter technology
[AD-A149335] 10 p1480 N85-19343
A circuit grammar for operational amplifier design
[AD-A149566] 10 p1481 N85-19346
Diffeomorphic approximation of quasiconformal and quasisymmetric homeomorphisms
10 p1536 N85-19678

Shielded enclosures for experimental studies of shielding topology
[AD-A149292] 11 p1624 N85-20227
Circuit topology, signal propagation delay and the efficiency of VLSI circuits
[CWI-CS-R8414] 11 p1630 N85-20267
Annals of the Fourier Institute, volume 34, no. 4 11 p1698 N85-20668
Topological triviality of versal unfoldings of complete intersections 11 p1699 N85-20678
The origin and evolution of terrestrial and Martian rock labyrinths
[NASA-CR-175511] 12 p1961 N85-22326
Relationship between topological and magnetic order in small metal clusters
[AD-A150547] 13 p2018 N85-22651
Method for processing broad-profile data 13 p2117 N85-23185
Surfaces with canonical hyperplane sections
[CWI-TRACT-1] 14 p2410 N85-24858
Topology and Order Structures, part 2
[MCT-169-PT-2] 14 p2413 N85-24879
Twenty questions on ordered spaces 14 p2413 N85-24880
A note on perfect normality in generalized ordered spaces 14 p2413 N85-24881
Metrization theorems for continuous images of compact ordered spaces 14 p2413 N85-24882
A pathological homogeneous subspace of the real line 14 p2413 N85-24883
A note on topological groups with dense orderable subspaces 14 p2413 N85-24884
The Kappa sub n property in small Omega sub 1 trees 14 p2413 N85-24885
On compactifications of generalized order GO-spaces 14 p2413 N85-24886
The orderability of compact scattered spaces 14 p2413 N85-24887
Submetrizable topologies on the ordinals 14 p2414 N85-24888
When is a GO-space JO(2)? 14 p2414 N85-24889
Local bases and product partial order II 14 p2414 N85-24890
Mappings of finite oscillations at local separating points 14 p2414 N85-24891
Orderable subspaces of compact F-spaces 14 p2414 N85-24892
Fake topological Hilbert spaces and characterizations of dimension in terms of negligibility
[CWI-TRACT-2] 14 p2414 N85-24893
Isoparametric 3-D finite element mesh generation using interactive computer graphics 15 p2574 N85-25573
Point processes associated with extreme value theory
[AD-A151211] 15 p2640 N85-26280
Mathematical programming in computer network design
[AD-A152275] 16 p2848 N85-27558
A study of topologies and protocols for fiber optic local area network
[NASA-CR-175771] 16 p2864 N85-27669
Chemical applications of topology and group theory. 17: An information theoretical approach to polyhedral symmetry
[AD-A152821] 17 p2919 N85-27995
The definition and computation of a metric on plane curves. The meaning of a face on a geometric model 17 p3004 N85-28571
Some negative results in N-sided patches 17 p3004 N85-28572
Contouring trivariate data 17 p3005 N85-28582
On the definition of topological susceptibility via lattice anomalous Ward identities and its perturbative tail
[PREPRINT-416] 18 p3184 N85-29744
Nested dissection on a mesh-connected processor array
[AD-A154088] 19 p3342 N85-30711
Global Mega-Geomorphology
[NASA-CP-2312] 21 p3600 N85-32357
Broadcasting topology and routing information in computer networks
[AD-A155668] 21 p3674 N85-32827
Synthesis of metrico-topological model for layout of topology of large-scale-integration arrays 22 p3781 N85-33427
Graph-theoretical exorcism
[DE85-011916] 23 p3955 N85-34512
Cosmic ray secondary nuclei and the structure of the galaxy
[OG-7.2-4] 23 p4014 N85-34876
Alfven wave scattering and the secondary to primary ratio
[OG-7.2-9] 23 p4015 N85-34878
Edge detection and geometric methods in computer vision
[AD-A155873] 24 p4135 N85-35630

TORCHES
Cosmonauts report on space welding at conference 15 p2484 N85-25329
Paton comments on results of space welding tests 15 p2484 N85-25330

TORNADO AIRCRAFT
U MRCA AIRCRAFT

TORNADOES
Recent examples of mesoscale numerical forecasts of severe weather events along the east coast
[NASA-TM-86172] 03 p0395 N85-12523
Investigations of severe/tornadic thunderstorm development and evolution based on satellite and AVE/SESAME/VAS data
[NASA-CR-174154] 04 p0538 N85-13424
TVENT1P user's manual, a computer code for analyzing tornado induced gas dynamic transients in flow networks
[DE85-002346] 10 p1486 N85-19379
Hurricane Research Division, fiscal year 1984 programs, fiscal year 1985 projections 16 p2836 N85-27491
J. P. Finley: The first severe storms forecaster
[PB85-17453] 19 p3318 N85-30566
Automated cell detection as a mesocyclone precursor tool
[AD-A154952] 21 p3635 N85-32577
Real-time automated detection of mesocyclones and tornado vortex signatures
[AD-A154966] 21 p3635 N85-32578

TOROIDAL PLASMAS
Means of varying conditions in the expanded boundary divertor without affecting energy confinement
[DE84-013840] 01 p0122 N85-10636
Plasma drift equilibrium (gyration) in toroidal systems with complex magnetic-field geometry
[DE84-015627] 01 p0122 N85-10639
Destruction of magnetic surfaces in three-dimensional MHD equilibria 02 p0282 N85-11838
Elimination of stochasticity in stellarators 02 p0282 N85-11839
Study of plasma convection and wall interactions in magnetic confinement systems
[DE84-013959] 03 p0421 N85-12692
Compact toroid development, activity plan for spheromaks
[DE84-016736] 04 p0567 N85-13617
Monte Carlo studies of transport in stellarators
[DE84-017833] 04 p0568 N85-13625
Elmo Bumpy Torus physics
[DE84-015909] 05 p0730 N85-14694
Generation of suprathermal electrons during plasma current startup by lower hybrid waves in a Tokamak
[IPPJ-697] 06 p0863 N85-15483
Shear-Alfven dynamics of toroidally confined plasmas, part A
[DE85-001590] 06 p0866 N85-15502
X-rays spectroscopy on the PLT and TFTR Tokamaks 09 p1386 N85-18720
Recent activities on JIPP T-IIU Tokamak 09 p1387 N85-18724
Density measurements of atomic hydrogen in NBT-IM by laser-induced fluorescence spectroscopy 09 p1389 N85-18739
Transport experiments in the Texas experimental Tokamak 09 p1389 N85-18741
Design and construction details of the FRX-C/T device: A compact toroid plasma translation experiment
[DE85-001527] 09 p1390 N85-18749
Discharge initiation experiments in the Tokapole II Tokamak
[DE84-017345] 09 p1391 N85-18755
Effects of q and high beta on Tokamak stability
[DE84-016650] 09 p1393 N85-18767
Analysis of Jovian low frequency radio emissions
[NASA-CR-174449] 10 p1571 N85-19908
Observations of low frequency plasma fluctuations in ELMO Bumpy Torus
[DE85-003796] 11 p1732 N85-20895
Long term variability of the IO torus 11 p1760 N85-21070
The continuous spectrum of an axisymmetric equilibrium with a mixed poloidal and toroidal magnetic field with gravity included 14 p2450 N85-25128
Preparatory experiments. 1: JIPP T-IIU 15 p2654 N85-26374
Toroidal equilibrium with low frequency wave driven currents
[DE85-005790] 15 p2658 N85-26401
Spherical torus, compact fusion at low field
[DE85-006963] 16 p2867 N85-27689
Time-resolving electron temperature diagnostic for ALCATOR C
[DE85-004916] 16 p2868 N85-27690
Comparison study of toroidal-field divertors for a compact reversed-field pinch reactor
[DE85-009501] 18 p3189 N85-29781
Toroidal viscosity and ambipolarity in the neoclassical transport theory of axisymmetric tori
[DE85-010822] 19 p3358 N85-30820
Poloidal variations in toroidal fusion reactor wall power loadings
[DE85-009505] 19 p3362 N85-30848
Radiation-cooled helicity-injecting reversed field pinch formed with relativistic electrons
[IPPJ-721] 19 p3370 N85-30901
System and method of operating toroidal magnetic confinement devices
[DE85-011670] 22 p3845 N85-33614
Compact DT fusion spherical tori at modest field
[DE85-011568] 23 p3982 N85-34692
Advanced Toroidal Facility (ATF)
[DE85-011587] 23 p3983 N85-34699
Observation of helical sawtooth oscillations in a tokamak
[DE85-012062] 23 p3983 N85-34703
Proposed FRX-D experiment
[DE85-012766] 24 p4158 N85-35778

TOROIDAL SHELLS
Poloidal variations in toroidal fusion reactor wall power loadings
[DE85-009505] 19 p3362 N85-30848
Alternating current OHMIC heating in a toroidal stellerator 20 p3534 N85-31986

TOROIDS
Self potentials of an electron ring in a torus for large ring displacement from the minor axis
[AD-A146088] 03 p0421 N85-12691
The evaluation of a deformable diffraction grating for a stigmatic EUV spectroheliometer
[NASA-CR-174248] 07 p1042 N85-16621
Experience highlights from the design and manufacture of US LCT coils
[DE84-017504] 10 p1482 N85-19354
Experience with oepration of a large magnet system in the international fusion superconducting magnet test facility
[DE85-009268] 17 p3027 N85-28721
Recent progress in stellarator reactor conceptual design
[DE85-009592] 18 p3189 N85-29780
TFCX shielding optimization
[DE85-010503] 19 p3359 N85-30826
Steady-state spheromak reactor studies
[DE85-009585] 19 p3372 N85-30916
Design of aggressive superconducting TFCX magnet systems
[DE85-010003] 19 p3376 N85-30943
Confinement and heating of high beta plasma with emphasis on compact toroids. Compact toroid research
[DE85-011463] 22 p3846 N85-33821

TORPEDO ENGINES
NT TURBOROCKET ENGINES

TORQUE
Cylinder power fault diagnosis in military diesel engines
[TT-8405] 01 p0053 N85-10354
The in-flight estimation and indication of cumulative fatigue damage to helicopter gears
[ARL/AERO-R-164] 03 p0317 N85-12050
Autonomous momentum management for space station
[NASA-CR-174065] 04 p0462 N85-12931
Autonomous momentum management for space station, exhibit A
[NASA-CR-171256] 04 p0462 N85-12933
Torque command steering law for double-gimbaled control moment gyros applied to rotor energy storage 05 p0606 N85-13679
Speed governor for diesel engine 09 p1307 N85-18214
Prediction accuracy of the torques for rotary tillage by an analog tool
[AD-P004288] 09 p1408 N85-18885
Antenna axis drive torques for the 70-meter antenna 10 p1484 N85-19237
Advanced gearbox technology in small turbo propeller engines 14 p2221 N85-23771
Influence of axial shaft load on operation of magnetoelastic torque transducer 14 p2270 N85-24065
Selection of optimum corrections torque for vertical gyro according to special-purpose program 14 p2273 N85-24082
Superconducting gyroscope research
[NASA-CR-171406] 15 p2560 N85-25795
How a shepherd guides a sheep herd — satellite-planetary ring interaction 15 p2674 N85-26503
Calculation of friction at spherical bearing journals in turbomachines 17 p2940 N85-28150
Load-induced rotordynamic instabilities in turbomachinery 19 p3280 N85-30340

Estimation of dynamic rotor loads for the rotor systems research aircraft: Methodology development and validation
[NASA-CR-177362] 20 p3393 N85-31045
Test evaluation of the Honeywell GG1111 Single-Degree-of-Freedom (SDF) strapdown gyroscope
[AD-A154766] 21 p3589 N85-32307
Drag-compensated, precision-powered hinge system 22 p3796 N85-33517
Application of traction drives as servo mechanisms 22 p3797 N85-33520
The properties of thin-section, four-point-contact ball bearings in space 22 p3797 N85-33521
Two-plane balance and slip-ring design 22 p3799 N85-33536
Dual towline spin-recovery device
[NASA-CASE-LAR-13076-1] 24 p4066 N85-35200

TORQUE CONVERTERS
Advanced inverter technology
[AD-A149335] 10 p1480 N85-19943

TORQUE MEASURING APPARATUS
U TORQUEMETERS

TORQUE MOTORS
Brush and commutator segment torquer motor
[AD-D011728] 23 p3927 N85-34340

TORQUEMETERS
Torque sensor
[AD-D011276] 05 p0639 N85-14096
Load-induced rotordynamic instabilities in turbomachinery 19 p3260 N85-30340
Two-plane balance and slip-ring design 22 p3799 N85-33536
Development of contactless sensors for industrial and automotive applications
[BMFT-FB-T-85-031] 24 p4097 N85-35400

TORQUERS
A dual spin space station design 20 p3408 N85-31152

TORSION
Design proposals for torsional buckling of stiffeners
[AD-A144783] 01 p0062 N85-10409
Fatigue in composite materials 04 p0467 N85-12966
Initial sailplane project: The RP-1 04 p0468 N85-12976
A geometrical theory of spin motion
[DE84-016537] 04 p0574 N85-13658
Damping capacity of multilayer tube during torsion
[BLL-M-36011-(5828.4)] 07 p0977 N85-16202
Modelling and identification of the structural properties of an astromast
[CRC-1574] 09 p1329 N85-18352
Evaluation of failure criterion for graphite/epoxy fabric laminates
[NASA-CR-172547] 10 p1431 N85-19025
Rheology of dissemination
[AD-A150006] 12 p1813 N85-21373
Fatigue damage and small crack growth during biaxial loading 16 p2797 N85-27247
Buckling and bracing of cantilevers
[CE-42] 17 p2979 N85-28413
Torsion-tension coupling in rods 18 p3120 N85-29315
Application of traction drives as servo mechanisms 22 p3797 N85-33520

TORSIONAL STRESS
Stability of hollow shafts under torsion 06 p0760 N85-14966
Steady-state reaction of three-layered cylindrical shell to effect of moving load 13 p2047 N85-22611
Influence of axial shaft load on operation of magnetoelastic torque transducer 14 p2270 N85-24065
Twisting of segmental shafts 14 p2279 N85-24119
On the radial structure of planetary rings 15 p2675 N85-26512
An improved torsional method for determining the fracture toughness of stiff materials and of adhesive joints
[AD-A152091] 16 p2800 N85-27267

TORSIONAL VIBRATION
Cylinder power fault diagnosis in military diesel engines
[TT-8405] 01 p0053 N85-10354
Damping capacity of multilayer tube during torsion
[BLL-M-36011-(5828.4)] 07 p0977 N85-16202
Measurement and evaluation of the loading of shafts by torsional vibrations 07 p0980 N85-16222
Optimization of vibrating beams including the effects of coupled bending and torsional modes 09 p1331 N85-18364
A pole-free reduced-order characteristic determinant method for linear vibration analysis based on sub-structuring 09 p1338 N85-18412
Effect of coupled torsional-flexural vibration of a geared shaft system on the dynamic tooth load 09 p1338 N85-18415
Precision measurement of torsional oscillations induced by gear errors 09 p1338 N85-18416
Journal of Research of the National Bureau of Standards, volume 89, number 2, March - April 1984
[PB85-115426] 12 p1926 N85-22103

TORSO
Torso sizing ring construction for hard space suit
[NASA-CASE-ARC-11616-1] 12 p1910 N85-21987
Torso restraint system
[AD-D011609] 16 p2702 N85-26684

TORUSES
A modeling analysis program for the JPL Table Mountain Io sodium cloud data
[NASA-CR-175493] 11 p1661 N85-20589
Torus data flow for parallel computation of missized matrix problems
[DE85-006761] 17 p3026 N85-28715
Alternating current OHMIC heating in a toroidal stellerator 20 p3534 N85-31988
Effect of ECH and ICH on ambipolar potential in NBT-1M 23 p3978 N85-34661
Transports studies of ECH and ICRH-heated bumpy torus plasma in NBT-1M 23 p3978 N85-34662
Simulation studies on stability of hot electron plasma 23 p3978 N85-34664
Behavior of helically-trapped fast ion orbits in heliotron E 23 p3976 N85-34666
Observation of mode-converted by ion Bernstein wave by an HCN laser scattering
[IPPJ-724] 23 p3979 N85-34668

TOTAL ENERGY SYSTEMS
NT SOLAR TOTAL ENERGY SYSTEMS
Develop and test fuel cell powered on-site integrated total energy systems. Phase 3: Full-scale power plant development
[NASA-CR-174887] 15 p2586 N85-25941

TOUCH
NT TACTILE DISCRIMINATION
The acquisition, processing, and use of tactile sensor data in robot control 05 p0641 N85-14114
The touch panel system: Design and development
[AD-A153014] 17 p3008 N85-28598
Ergonomic problems regarding the interactive touch input via screens in onboard and ground-based flight control
[NASA-TM-77814] 20 p3512 N85-31832
Issues and techniques in touch-sensitive tablet input (executive summary) 23 p3960 N85-34543
A multi-touch three dimensional touch-sensitive tablet (executive summary) 23 p3961 N85-34553

TOUGHNESS
NT NOTCH SENSITIVITY
A study of vacuum melting to increase the toughness of maraging steels
[AD-A145017] 01 p0028 N85-10175
Fundamental studies of structure property relationship in transformation toughened ceramics
[DE84-015344] 01 p0033 N85-10204
Microstructural basis of strength and toughness in hardmetals 02 p0177 N85-11185
The inter-relation of microstructure, toughness and fatigue crack growth behaviour in WC-Co hardmetals 02 p0177 N85-11188
Design of strong, ductile, duplex low alloy steels 02 p0177 N85-11189
Tough Composite Materials
[NASA-CP-2334] 04 p0463 N85-12941
Fundamental studies of composite toughness 04 p0464 N85-12948
Development of a heterogeneous laminating resin 04 p0465 N85-12956
Constituent properties and interrelationships 04 p0467 N85-12964
Inclusion formation during solidification of steels with improved machinability
[BMFT-FB-T-84-160] 05 p0619 N85-13957
Imide modified epoxy matrix resins
[NASA-CR-174695] 07 p0930 N85-15892
Effect of tempering on the strength and toughness of 2 1/4 Cr-1 Mo steel weldments
[DE85-003618] 09 p1296 N85-18140
Interlaminar fracture toughness in resin matrix composites
[AD-A150565] 13 p2015 N85-22640
Particulate toughened silicon carbide
[DE85-004797] 13 p2016 N85-22643
Simultaneous chemical vapor deposition of SiC-dispersed phase composites
[DE85-007751] 16 p2744 N85-26931
Strength versus toughness relation in Fe-high manganese alloys
[DE85-007662] 18 p3074 N85-29013
Aging study of copper alloy 172
[DE85-009648] 18 p3075 N85-29023
Specimen thickness effects for elastic-plastic CTOD toughness of A36 steel
[DE85-006992] 18 p3077 N85-29036
The mechanics of internal stress and microcrack toughening mechanisms in ceramics
[AD-A154049] 19 p3248 N85-30139
Controlled indentation flaws for the construction of toughness and fatigue master maps
[PB85-179067] 20 p3473 N85-31582
Graphite/PMR polyimide composites with improved toughness
[NASA-TM-87061] 21 p3561 N85-32148
Development of a high strength isothermally heat-treated nodular iron road wheel arm
[AD-A155755] 24 p4099 N85-35406

TOWED BODIES
A dynamical model for a towed linear sonar antenna
[REPT-6-84] 04 p0512 N85-13263
The rolling resistance and sinkage of towed dual wheel combination in sand
[AD-P004261] 09 p1404 N85-18837
A Lagrange-D'Alembert formulation of the equations of motion of a helicopter carrying an externally suspended load
[NASA-TM-85864] 12 p1776 N85-21149
A towed instrument vehicle for deep ocean sampling
[AD-A156322] 24 p4125 N85-35576

TOWED TARGETS
U TARGETS
U TOWED BODIES

TOWERS
NT AIRPORT TOWERS
Some considerations on Aeroelastic instabilities caused by coupling between propeller-type rotor and its supporting structure
[NAL-TR-804] 01 p0003 N85-10013
Structural design and thermal stability of TELE-X antenna tower 05 p0627 N85-14016
Dynamic testing of NOVA laser switchyard tower
[DE84-014450] 05 p0640 N85-14103
A novel type of stayed tower for wind turbines
[ISD-295] 15 p2587 N85-25952
Structural analysis and cost estimate of an eight-leg space frame as a support structure for horizontal axis wind turbines
[NASA-TM-83470] 19 p3284 N85-30361
New corrosion protection concept for very high voltage line towers
[BLL-OA-TRANS-2691-(6196.300)] 20 p3429 N85-31270

TOWING
Compaction of sand using ordinary off-road vehicles
[AD-P004297] 09 p1409 N85-18874

TOWNSEND DISCHARGE
NT GAS DISCHARGES

TOXIC DISEASES
NT CARBON MONOXIDE POISONING
NT LEAD POISONING
Proceedings of the 14th Conference on Environmental Toxicology
[AD-A146400] 06 p0843 N85-15350
Neurotoxicology: A new scientific challenge
[AD-P004017] 06 p0843 N85-15351

TOXIC HAZARDS
Effect of toluene on the solubility of biohazardous volatile synthetic organic compounds
[AD-A145186] 01 p0016 N85-10109
Polychlorinated biphenyls (PCBs) in transit system electrical equipment
[PB84-222207] 01 p0045 N85-10291
The pyrolysis toxic gas analysis of aircraft interior materials
[AD-A146285] 03 p0328 N85-12115
A biological sensor for the detection of toxicants
[AD-D011304] 07 p0967 N85-16141
Toxic hazards research
[AD-A147857] 07 p1011 N85-16425
A scanning alarm electronic processor
[AD-D011419] 08 p1158 N85-17309
Strategies for preparing and submitting a part B application for a DoD facility
[AD-P004139] 09 p1347 N85-18475
Practical application of earth resistivity methods in phase 2 of the installation restoration program
[AD-P004148] 09 p1348 N85-18484
The Hazardous Materials Technical Center
[AD-P004149] 09 p1349 N85-18485
Protocol for aquifer cleanup decision making at military installations
[AD-P004151] 09 p1349 N85-18487
Analysis of geohydrologic data by kriging
[AD-P004152] 09 p1349 N85-18488

Test report for Getty Synthetic Fuels, Inc., Calumet City, Illinois
[PB85-119493] 10 p1459 N85-19191
Improved techniques for removal of sediments contaminated with hazardous materials
[PB85-116093] 11 p1679 N85-20560
Methods/materials matrix of ultimate disposal techniques for spilled hazardous materials
[PB85-116853] 12 p1885 N85-21833
Assessment of hazardous waste surface impoundment technology case studies and perspectives of experts
[PB85-117059] 12 p1886 N85-21834
Summary report of the Workshop on Structure Activity Concepts in Environmental Sciences
[PB85-137339] 12 p1887 N85-21841
Effect of high ammonia content in closed environment on some parameters of human nitrogen and carbohydrate metabolism against background of a controlled diet
12 p1903 N85-21948
Analysis and model/data comparisons of large-scale releases of nitrogen tetroxide
[DE85-009969] 18 p3133 N85-29406
Toxic hazards tests for vehicles and other equipment
[AD-A149164] 20 p3506 N86-31797
Hydrazine and the F-16 20 p3511 N85-31826
Space Station crew safety alternatives study. Volume 2: Threat development
[NASA-CR-3855] 21 p3558 N85-32133
Review of hazardous waste cleanup and disposal efforts at Tinker Air Force Base
[GPO-43-294] 21 p3613 N85-32457
Hazardous air pollutants
[GPO-43-064] 21 p3613 N85-32458
Emergency modeling of hazardous air pollutants
[AD-A155441] 21 p3614 N85-32461
Air force technical objective document, Aerospace Medical Division, Fiscal Year 1986
[AD-A155196] 21 p3664 N85-32762
A crew exposure study. Phase II. Volume 2. At sea. Part A
[AD-A155233] 21 p3666 N85-32774
Practical consequences of the assessment of different energy health risks
[DE85-004538] 22 p3825 N85-33696
Proceedings of the 7th Joint Panel Meeting of the UJNR Panel on Fire Research and Safety
[PB85-199545] 24 p4085 N85-35317
Land Disposal of Hazardous Waste
[PB85-196376] 24 p4113 N85-35500

TOXICITY
NT CARBON MONOXIDE POISONING
NT LEAD POISONING
Aquatic plant control research program. Evaluation of Fusarium roseum Culmorum as a biological control agent for Hydrilla verticillata
[AD-A145228] 01 p0069 N85-10459
Toxicological evaluation of Columbia spacecraft
01 p0094 N85-10631
Modeling effects of toxicants on aquatic systems
[DE84-016594] 04 p0531 N85-13396
Toxicology and metabolism of nickel compounds
[DE84-014919] 05 p0696 N85-14478
The toxicity of complex mixtures
[AD-P004033] 06 p0844 N85-15363
Toxicology of natural and man-made toxicants in drinking water
[AD-P004035] 06 p0845 N85-15365
Aspects of solvent toxicity in mixtures
[AD-P004036] 06 p0845 N85-15366
Toxic hazards research
[AD-A147857] 07 p1011 N85-16425
A crew exposure study. Volume 1: Offshore
[AD-A148884] 07 p1015 N85-16449
Acute oral toxicity (LD50) of 4-nitrophenyl monochloromethyl (Phenyl) phosphinate (TA009) in male rats
[AD-A148337] 08 p1192 N85-17513
Manned testing of two closed-circuit oxygen underwater breathing apparatus: US Navy Emerson Rig and Fenzy PO.68
[AD-A148300] 08 p1200 N85-17560
Role of biological assessment in effluent control
[PB85-116101] 12 p1885 N85-21830
Toxicity, mutagenesis and aging due to endogenous oxygen radicals
[AD-A150121] 12 p1900 N85-21928
Determination of toxicity of combustion products of habitability foams concurrently with flammability studies of these materials
[AD-A149647] 12 p1905 N85-21961
Chemical characterization and toxicologic evaluation of airborne mixtures. Inhalation toxicology of diesel fuel obscurant aerosol in Sprague-Dawley rats. Phase 3. Subchronic exposures
[AD-A150100] 12 p1905 N85-21966
Interaction of metals and metalloids with biomembranes
[DE85-004902] 13 p2141 N85-23293
Toxicity of TNT wastewaters to aquatic organisms. Volume 4: Chronic toxicity of 2,4-dinitrotoluene and condensate water
[AD-A153536] 18 p3132 N85-29400
Formation and fate of toxic chemicals in California's atmosphere
[PB85-172609] 18 p3134 N85-29414
An in vitro method for the screening of trichothecene mycotoxin cytotoxicity and the study of mycotoxin countermeasures
[AD-A153663] 18 p3152 N85-29517
Chemicals identified in human biological media, a data base. Volume 6, part 2: Records 7568-8694
[DE85-008767] 18 p3154 N85-29528
Information science in toxicology
[DE85-007746] 18 p3200 N85-29651
Pollutant body burdens and reproduction in Platichthys stellatus from San Francisco Bay
[DE85-010407] 19 p3308 N85-30509
Polyesters: A review of the literature on products of combustion and toxicity
[NBSIR-85-3139] 20 p3433 N85-31298
Hydrazine and the F-16 20 p3511 N85-31826
Distribution and abundance of organic thiols
21 p3657 N85-32717
Effects of low level carbon monoxide (CO) on tracking and monitoring. An attempt to replicate the findings of Putz et al. (1976) protocol 2
[AD-A155722] 22 p3825 N85-33694
Anaerobic microbial transformations in subsurface environments: Project description
[DE85-012789] 23 p3951 N85-34486
Estimating risks of lead-induced hemoglobin decrements under conditions of uncertainty: Methodology, pilot judgments and illustrative calculations
[DE85-012293] 23 p3952 N85-34493

TOXICITY AND SAFETY HAZARD
Portable microprocessor-controlled instrument for sensing, identifying and monitoring gaseous chemicals
[DE84-013431] 04 p0504 N85-13214
Immobilization of toxic waste by embedding it in bitumen
[OEFZS-4277] 07 p0995 N85-16322
Health assessment document for carbon tetrachloride
[PB85-124196] 10 p1526 N85-19638
Material thermolysis product toxicity: Definition of a hazard evaluation methodology
[CERMA-84-08] 11 p1692 N85-20641
Use of environmental health-risk analysis for managing toxic substances
[DE85-008964] 18 p3160 N85-29574

TOXICOLOGY
Proceedings of the 14th Conference on Environmental Toxicology
[AD-A146400] 06 p0843 N85-15350
Neurotoxicology: A new scientific challenge
[AD-P004017] 06 p0843 N85-15351
Review of the toxicokinetics of n-hexane
[AD-P004018] 06 p0843 N85-15352
Interactions of ketones and hexacarbons
[AD-P004019] 06 p0843 N85-15353
Molecular mechanisms of n-hexane neurotoxicity
[AD-P004020] 06 p0843 N85-15354
Pathology and axonal transport in hexacarbon neuropathies
[AD-P004021] 06 p0843 N85-15355
Organophosphorus-induced delayed neurotoxicity: Syndrome and experimental models
[AD-P004022] 06 p0844 N85-15356
Chemistry and metabolism of delayed neurotoxic organophosphorus esters
[AD-P004023] 06 p0844 N85-15357
Pathology of organophosphorus-induced delayed neurotoxicity
[AD-P004024] 06 p0844 N85-15358
Electrophysiologic changes in organophosphorus-induced delayed neurotoxicity
[AD-P004025] 06 p0844 N85-15359
Biochemistry and pathogenic hypotheses of organophosphorus-induced delayed neurotoxicity
[AD-P004026] 06 p0844 N85-15360
Critical overview of hexacarbons and organophosphates
[AD-P004027] 06 p0844 N85-15361
Pharmacokinetic interactions of mixtures
[AD-P004032] 06 p0844 N85-15362
The toxicity of complex mixtures
[AD-P004033] 06 p0844 N85-15363
Teratogenicity studies of carbaryl and malathion alone and in combination in various laboratory animals
[AD-P004034] 06 p0845 N85-15364
Toxicology of natural and man-made toxicants in drinking water
[AD-P004035] 06 p0845 N85-15365
Aspects of solvent toxicity in mixtures
[AD-P004036] 06 p0845 N85-15366
An update on the capabilities of the Air Force Computerized Occupational Health Program (COHP)
[AD-P004037] 06 p0845 N85-15367
The epidemiology and toxicology of Agent Orange
[AD-P004038] 06 p0845 N85-15368
Early detection of environmental exposure
[AD-P004039] 06 p0845 N85-15369
USSR report: Life sciences. Biomedical and behavioral sciences
[JPRS-UBB-84-015] 07 p1010 N85-16416
Material thermolysis product toxicity: Definition of a hazard evaluation methodology
[CERMA-84-08] 11 p1692 N85-20641
Air quality criteria for ozone and other photochemical oxidants. External review draft, volume 4
[PB85-126068] 12 p1898 N85-21838
Chemical characterization and toxicologic evaluation of airborne mixtures. Inhalation toxicology of diesel fuel obscurant aerosol in Sprague-Dawley rats. Phase 3. Subchronic exposures
[AD-A150100] 12 p1905 N85-21966
Role and fate of ozone in the atmosphere
18 p2824 N85-27421
Information science in toxicology
[DE85-007746] 18 p3200 N85-29651
Molecular toxicology of chromatin: The role of Poly(ADP-Ribose) in gene control
[AD-A154415] 19 p3327 N85-30611
EPA (Environmental Protection Agency) research program guide, FY-1985, October 1, 1984 - September 30, 1985
[PB85-181681] 20 p3487 N85-31676

TOXINS AND ANTITOXINS
Induction of immunity to toxins with anti-idiotypic antibody
[AD-A146793] 07 p1014 N85-16445
Bibliography of venomous and poisonous marine animals and their toxins
[AD-A148409] 08 p1192 N85-17514
Structural-functional changes in bacterial cells under spaceflight conditions 18 p2724 N85-26812
An in vitro method for the screening of trichothecene mycotoxin cytotoxicity and the study of mycotoxin countermeasures
[AD-A153663] 18 p3152 N85-29517
Differences in susceptibility of inbred mice to bacillus anthracis
[AD-A155846] 21 p3662 N85-32750

TRACE CONTAMINANTS
Aircraft measurements of tracer gas during the 1983 cross Appalachian tracer experiment (CAPTEX)
[DE84-015292] 04 p0531 N85-13395
Atmospheric tracer experiments in a deep narrow valley
[PB84-234590] 04 p0532 N85-13402
Cross-Appalachian Tracer Experiment (CAPTEX '83)
[PB84-236641] 06 p0834 N85-15307
Modeling of turbulent dispersion of neutral and buoyant contaminants released from two dimensional sources — air pollution
[VKI-TN-150] 06 p1180 N85-17438
Methodology for the collection and analysis of trace metals in atmospheric precipitation
[CM-67] 09 p1350 N85-18491
Nebulization reflux concentrator
[NASA-CASE-LAR-13254-1] 11 p1615 N85-20154
One-dimensional nonstationary model of photochemical transformations of gas impurities in stratosphere
14 p2342 N85-24484
Vertical redistribution of a pollutant tracer due to cumulus convection
[PB85-172971] 18 p3134 N85-29415
Diffusion of trace gases in the ground level boundary layer 18 p3148 N85-29489
Internal contamination in the space station
18 p3157 N85-29549
Space station trace contaminant control
18 p3157 N85-29550
Some problems associated with trace contaminant removal systems for spacecabins
18 p3158 N85-29554
Contamination control for increased crew productivity
18 p3158 N85-29555
Human productivity program definition
18 p3158 N85-29556
X-ray fluorescence analysis of uranium concentrates
[DE85-013189] 24 p4148 N85-35717

TRACE ELEMENTS
Minor element effects on gas tungsten arc weld penetration
[PB84-222579] 01 p0068 N85-10370

Green River air quality model development: Meteorological and tracer data, July/August 1982. Field study in Brush Valley, Colorado
[DE84-014975] 02 p0225 N85-11474

COST 50 - materials for gas turbines, part 1 and 2
[NPL-DMA(A)-74] 05 p0617 N85-13943

The effect of trace elements on the properties at high temperature of a Ni-Cr-base alloy
05 p0617 N85-13944

The use of tracers for the study of atmospheric chemical and physical transformation processes
[DE84-015267] 05 p0671 N85-14313

Aspects of the comparison of stratospheric trace species measurements with photochemical models
[DE84-017028] 05 p0672 N85-14317

The Georges Bank monitoring program 1983: Analysis of trace metals in bottom sediments
[CIRC-915] 05 p0686 N85-14423

Dark matter near the sun: Simulated star counts and the Oort limit 06 p0880 N85-15592

Atmospheric heating of meteorites: Results from nuclear track studies 06 p0882 N85-15607

Application of tunable monochromatic synchrotron radiation to the quantitative determination of trace elements
[DE85-001271] 09 p1291 N85-18106

Tracer diffusion in an ordered alloy: Application of the path probability and Monte Carlo methods
[DE85-002768] 14 p2257 N85-23986

Resonant coherent anti-Stokes Raman scattering
[ESA-TT-876] 15 p2507 N85-25466

Trace metal determinations in nickel-plating baths by polarographic methods
[DE85-007064] 15 p2511 N85-25488

Upper-air data collection during CAPTEX
[DE85-006300] 16 p2827 N85-27438

Use of a network of telemetered meteorological stations for prediction of the distribution of an atmospheric tracer
16 p2831 N85-27458

An ultrasensitive and element specific photoionization detection system for environmental analysis
[AD-A153365] 17 p2966 N85-28332

Data base of all known, published data on trace elements in oil shale and its products
[DE85-003399] 18 p3128 N85-29357

Elemental tracers of source regions of contaminants in precipitation
[DE85-007366] 18 p3133 N85-29407

Atmospheric Tracer Workshop
[DE85-010573] 20 p3466 N85-31666

Marine aerosols at the Dutch North Sea coast: Size distributions and fractionation of trace elements
21 p3648 N85-32664

Anorthositic oceanic crust in the Archean Earth
21 p3719 N85-33077

Ultra-trace analysis of sintar tantalum with SIMS
[BLL-RARDE-TR-1220-(7291.7965)]
23 p3913 N85-34245

Evaluation of low-temperature geothermal potential in Utah and Goshen Valleys and adjacent areas, Utah. Part 2: Water temperature and chemistry
[DE85-009344] 23 p3943 N85-34438

The identification of compounds in mustard hydrolysate
[AD-A156381] 24 p4076 N85-35258

Interaction of trace elements and welding parameters on GTA weld shape
[DE85-004046] 24 p4080 N85-35264

Elemental tracers of source regions of contaminants in precipitation
[DE85-012858] 24 p4113 N85-35499

TRACERS

Analysis techniques for tracer studies of oxidation
[NASA-CR-174798] 03 p0336 N85-12162

Relationship between model complexity and data base quality for complex terrain tracer experiments
[DE84-015022] 04 p0539 N85-13429

A new physical Lagrangian tracer
[DE84-016212] 05 p0687 N85-14419

Mechanisms of impurity diffusion in rutile
[DE84-014741] 06 p0766 N85-14902

Air quality assessment model validation in complex terrain
[AD-A147690] 08 p1180 N85-17434

Chlorine isotopes as environmental tracers in Columbia River basalt groundwaters
[DE85-011392] 19 p3302 N85-30473

Atmospheric Tracer Workshop
[DE85-010573] 20 p3466 N85-31666

A strategy for calibrating atmospheric transport models
[CSIRO-DAR-TP-9] 24 p4116 N85-35516

TRACKED VEHICLES

Proceedings of the International Conference on the Performance of Off-Road Vehicles and Machines, (8th), volume 1
[AD-A148634] 09 p1403 N85-18833

Dynamic simulation of track laying vehicles
[AD-P004266] 09 p1405 N85-18842

Stresses in situ generating by bulldozers
[AD-P004270] 09 p1405 N85-18846

Finite element analysis of ground deformation beneath moving track loads
[AD-P004271] 09 p1405 N85-18847

A rig for testing the soft soil performance of track systems
[AD-P004272] 09 p1405 N85-18848

The dependence of soil bearing capacity and drawbar pull on the spacing between track
[AD-P004273] 09 p1406 N85-18849

The dynamic interaction between track and soil
[AD-P004274] 09 p1406 N85-18850

Analysis of ground pressure distribution beneath tracked model with respect to external loading
[AD-P004275] 09 p1406 N85-18851

A comparison between a conventional method and an improved method for predicting tracked vehicle performance
[AD-P004276] 09 p1406 N85-18852

Effect of hitch positions on the performance of track-grouser systems
[AD-P004277] 09 p1406 N85-18853

Grouser effect studies
[AD-P004278] 09 p1406 N85-18854

Proceedings of the 8th International Conference on the Performance of Off-Road Vehicles and Machines, volume 2
[AD-A148635] 09 p1407 N85-18859

Mobility of the small combine (track type) on soft ground-relationship between the position of the center of gravity and the mobility
[AD-P004285] 09 p1407 N85-18862

Study on controllability and stability of high speed tracked vehicles
[AD-P004302] 09 p1409 N85-18879

A tracked vehicle test plant for the simulation of dynamic operation
[AD-P004305] 09 p1410 N85-18882

Basic study on the turning resistance of track
[AD-P004307] 09 p1410 N85-18884

Study on steerability of articulated tracked vehicles
[AD-P004308] 09 p1410 N85-18885

Skid steering of wheeled and tracked vehicles: Analysis with Coulomb friction assumptions
[AD-A149826] 12 p1860 N85-21864

Improvements in tank tread assemblies
[NASA-CASE-NPO-16321-1] 18 p3117 N85-29291

TRACKING (POSITION)

NT CCD STAR TRACKER
NT INFRARED TRACKING
NT OPTICAL TRACKING
NT POLYSTATION DOPPLER TRACKING SYSTEM
NT PURSUIT TRACKING
NT RADAR TRACKING
NT RADIO TRACKING
NT RANGE AND RANGE RATE TRACKING
NT SATELLITE TRACKING
NT SPACECRAFT TRACKING
NT STAR TRACKERS
NT WILDLIFE RADIOLOCATION

Distributed sensor networks
[AD-A146209] 03 p0355 N85-12286

Biaxial tracking solar generator
05 p0663 N85-14259

Model estimation and identification of manual controller objectives in complex tracking tasks
05 p0700 N85-14494

Types of tracking errors induced by concurrent secondary manual task 05 p0711 N85-14561

Device for measuring relative axial expansion of turbine rotor employing space-vector tracking method
06 p0776 N85-14962

Annual energy spectrum for tracking arrays
06 p0832 N85-15297

Stereo Electro-optical Tracking System (SETS)
[NASA-CR-172471] 07 p0962 N85-16098

Automatic camera tracking for remote manipulators
[DE85-001897] 07 p0974 N85-16187

An interactive FORTRAN program for determining reliability of pseudo-range geodetic point positioning using the global positioning system
[AD-A147133] 07 p0988 N85-16275

Random pattern tracking acceleration tolerance tester
[AD-D011404] 07 p1017 N85-16459

JPL Robotics Laboratory computer vision software library
[NASA-CR-174272] 07 p1023 N85-16491

Ocean acoustics
[AD-A147062] 07 p1038 N85-16591

Dual mode scanner-tracker
[AD-D011417] 08 p1113 N85-17018

Deep water mass circulation in the Western Alboran Basin: Measurements in July and September 1980 (Alboran I experiment)
[AD-A148566] 08 p1191 N85-17504

Mobility of the small combine (track type) on soft ground-relationship between the position of the center of gravity and the mobility
[AD-P004285] 09 p1407 N85-18862

Development of mass-producible line-focus tracking concentrating solar collectors. Category 2: Trackers
[DE85-002673] 10 p1512 N85-19543

Wind-weighting for sounding rockets with a telemetry system
[NASA-TP-2438] 12 p1792 N85-21246

Observational study of transport in the free troposphere
[PB85-144145] 12 p1887 N85-21845

Numerical methods for tracking interfaces
[LA-9917-MS] 12 p1919 N85-22052

Technical manual: Description and operation Slaved Tracking System
[DE85-004807] 13 p2094 N85-23070

Main features of Antarctic Ocean circulation as revealed by satellite tracking of icebergs
14 p2325 N85-24372

Some methods of computing platform transmitter terminal location estimates — ARGOS system; whale tracking 14 p2332 N85-24420

Digital computer applications of Kalman filter in target tracking
[AD-A150770] 14 p2404 N85-24821

Investigation of a failure detection/identification system for a tactical aircraft navigation system
[AD-A151846] 15 p2469 N85-25240

Swedish equipment for automatic docking in space
15 p2489 N85-25363

Sonars with high noise and clutter rejection for use with adaptive robots
[AD-A151875] 15 p2543 N85-25701

Automatic tracking of crack growth via finite elements
16 p2797 N85-27246

An evaluation of the performance of a new storm tracking methodology
[AD-A152234] 16 p2835 N85-27484

Development of mass-producible line-focus tracking concentrating solar collectors. Category 2: Control systems
[DE85-007873] 17 p2967 N85-28459

Automatic detection of gust fronts
[FAA-PM-85-11] 17 p2995 N85-28516

Tracking algorithm performance analysis program (TRAPP)
[DE85-007304] 17 p3009 N85-28601

Adaptive aiding for symbiotic human-computer control: Conceptual model and experimental approach
[AD-A153870] 19 p3332 N85-30644

Department of Energy gear drive unit final prototype testing and design evaluation
[DE85-003296] 22 p3793 N85-33499

Airborne cloud tracking measurements during the Three Mile Island nuclear station accident, Middletown, Pennsylvania. Date of survey: March - June 1979
[DE85-012060] 22 p3816 N85-33638

Operator's functional comfort zone when controlling moving object 22 p3821 N85-33670

Effects of low level carbon monoxide (CO) on tracking and monitoring. An attempt to replicate the findings of Putz et al. (1976) protocol 2
[AD-A155722] 22 p3825 N85-33694

Comparative analysis of operational forecasts versus actual weather conditions in airline flight planning, volume 1
[NASA-CR-167862] 24 p4119 N85-35534

Comparative analysis of operational forecasts versus actual weather conditions in airline flight planning, volume 2
[NASA-CR-167863] 24 p4119 N85-35535

TRACKING AND DATA RELAY SATELLITES

U TDR SATELLITES

TRACKING ANTENNAS

U DIRECTIONAL ANTENNAS

TRACKING FILTERS

Design and performance of sampled data loops for subcarrier and carrier tracking 05 p0623 N85-13988

Improved carrier tracking by smoothing estimators
05 p0623 N85-13989

Algorithm for tracking maneuvering object with ambiguous measurements 06 p0791 N85-15057

Trilatic tracking filter used by the multistatic measurement system
[AD-A146885] 07 p0911 N85-15769

Synthesis of digital nonrecursive band-elimination filters for moving-target selectors 12 p1840 N85-21545
Synthesis of optimum algorithms for secondary processing 13 p2080 N85-22992
Investigation of a failure detection/identification system for a tactical aircraft navigation system
[AD-A151646] 15 p2469 N85-25240
Theory and Applications of State Estimation. NRIMS Summer Seminar Series
[CSIR-SWISK-37] 15 p2635 N85-26244
Tracking filters 15 p2635 N85-26252
Estimation of maneuvering targets 15 p2636 N85-26253
Synthesis of adaptive filters for tracking radio systems 22 p3763 N85-33325

TRACKING NETWORKS
NT DEEP SPACE NETWORK
NT GLOBAL TRACKING NETWORK
NT MATTS (SYSTEMS)
NT POLYSTATION DOPPLER TRACKING SYSTEM
NT RADAR NETWORKS
Evaluation of the RSTN (Regional Seismic Test Network) network and further improvement to automatic association
[AD-A146395] 06 p0835 N85-15312
Distributed sensor networks
[AD-A147636] 06 p1151 N85-17262

TRACKING PROBLEM
Suppression of biodynamic interference by adaptive filtering 05 p0706 N85-14530
Models for the effects of G-seat cuing on roll-axis tracking performance 05 p0707 N85-14532
Some effects of digital sampling on orbiter flight control system operation 08 p1092 N85-16903

TRACKING RADAR
Turnaround control for mechanically scanned radar antennas
[AD-D011236] 01 p0039 N85-10246
A proof-of-principle getaway special free-flying satellite demonstration 02 p0155 N85-11051
Avionics Flight Evaluation System (AFES) 13 p1967 N85-22357
Angular tracking error in A phase comparison monopulse tracking radar: A critical review and extension of the phase front distortion approach
[AD-A152628] 17 p2949 N85-28205

TRACKING STATIONS
NT GLOBAL TRACKING NETWORK
NT POLYSTATION DOPPLER TRACKING SYSTEM
Survey of VLF-OMEGA transmissions received during summer at Antarctic peninsula
[INPE-3399-PRE/666] 10 p1462 N85-19223

TRACKING STUDIES
U TRACKING (POSITION)

TRACKS
An evaluation of the 64-meter antenna radial bearing for use on the 70-meter antenna 10 p1464 N85-19236

TRACTION
Modelling of off-road tyres and soil for improved traction
[AD-P004258] 09 p1404 N85-18834
Soil compliance influence on tyre performance
[AD-P004260] 09 p1404 N85-18836
Traction forces of drive tyre on the compacted soil
[AD-P004264] 09 p1404 N85-18840
The stress-strain-time graph of rheological soils and its application
[AD-P004266] 09 p1407 N85-18863
Thermal traction contact performance evaluation under fully flooded and starved conditions
[NASA-CR-168173] 15 p2568 N85-25848
Rolling, slip and traction measurements on low modulus materials
[NASA-CR-174909] 22 p3791 N85-33491
Application of traction drives as servo mechanisms 22 p3797 N85-33520

TRACTORS
NT TRACKED VEHICLES
Converting gasoline farm tractors to run efficiently on farm-produced alcohol
[DE84-015796] 02 p0205 N85-11350
Effects of slip on energy distribution between tyre and soil
[AD-P004263] 09 p1404 N85-18839
A theoretical investigation of an active suspension system for wheeled tractors
[AD-P004268] 09 p1405 N85-18844
Increase in performance and improvement of ride comfort of self-propelled construction machinery by reducing pitch and vertical vibration
[AD-P004269] 09 p1405 N85-18845
Comparison of measured and simulated ride comfort for an agricultural tractor and influence of travel speed and tyre-inflation pressure on dynamic response
[AD-P004261] 09 p1407 N85-18857
Characteristics of farm field profiles as sources of tractor vibration
[AD-P004262] 09 p1407 N85-18858
The research of driving wheel with movable lugs of the paddy field floating tractor
[AD-P004283] 09 p1407 N85-18860
An investigation of the driving wheel thrust of paddy field tractors
[AD-P004284] 09 p1407 N85-18861
Behaviour of soil under a lugged wheel
[AD-P004287] 09 p1407 N85-18864
The analysis on the dynamic performance of a single lug
[AD-P004289] 09 p1408 N85-18866
Some stability and control problems with trailed farm tankers on slopes
[AD-P004291] 09 p1408 N85-18868
Control of tractors on sloping ground
[AD-P004292] 09 p1408 N85-18869
Tractor power selection with compaction constraints
[AD-P004300] 09 p1409 N85-18877
Turning behaviour of articulated frame steering tractor
[AD-P004304] 09 p1409 N85-18881

TRACTS
U SITES

TRADEOFFS
Hydrologic and economic models for watershed evaluation and research
[PB84-222371] 01 p0066 N85-10438
BIT/BITE tradeoff analysis model
[AD-A149345] 11 p1701 N85-20697
High specific power aircraft turn maneuvers: Tradeoff of time-to-turn versus change in specific energy
[AD-A151701] 15 p2471 N85-25257
Trade-off between land vehicle antenna cost and gain for satellite mobile communications
[NASA-CR-175732] 15 p2540 N85-25681
Space Station man-machine automation trade-off analysis
[NASA-CR-176046] 20 p3408 N85-31147

TRADESCANTIA
Hit-size effectiveness theory applied to high doses of low LET radiation for pink mutations in Tradescantia
[DE85-011635] 22 p3819 N85-33657

TRAFFIC
NT AIR TRAFFIC
Study of annoyance due to urban automobile traffic
[NASA-TM-77514] 01 p0069 N85-10458
Study of annoyance due to urban automobile traffic. Annex 4: A catalog of the characteristics of noise at different measuring points
[NASA-TM-77516] 03 p0387 N85-12478
Patterns of behavior in lodgings exposed to traffic noise
[NASA-TM-77750] 03 p0387 N85-12479
Proceedings of the 8th International Conference on the Performance of Off-Road Vehicles and Machines, volume 2
[AD-A149635] 09 p1407 N85-18859
Basic study on the turning resistance of track
[AD-P004307] 09 p1410 N85-18884
Base communications issues for the 1990s
[AD-A149764] 12 p1828 N85-21474
Overlays for plain jointed concrete pavements
[PB85-156297] 15 p2523 N85-25557
An electron microscopic study of urban aerosol 21 p3651 N85-32659

TRAFFIC CONTROL
NT AIR TRAFFIC CONTROL
NT AUTOMATED EN ROUTE ATC
NT RADAR APPROACH CONTROL
US Army human Engineering Laboratory Communications Survey: A Pilot Study (HELCOMS-PS)
[AD-A151434] 15 p2521 N85-25544

TRAILERS
Some stability and control problems with trailed farm tankers on slopes
[AD-P004291] 09 p1408 N85-18868

TRAILING EDGE FLAPS
Pressure distribution data from tests of 2.29 M (7.5 feet) span EET high-lift transport aircraft model in the Ames 12-foot pressure tunnel
[NASA-TM-84517] 19 p3211 N85-29912
Low-speed tests of a high-aspect-ratio, supercritical-wing transport model equipped with a high-lift flap system in the Langley 4- by 7-meter and Ames 12-foot pressure tunnels
[NASA-TP-2097] 20 p3388 N85-31010

TRAILING EDGES
Experimental studies of transonic airfoil trailing edge and wake flowfield properties 05 p0592 N85-13773
Simultaneous flow visualization and unsteady lift measurement on an oscillating lifting surface
[AD-P004157] 09 p1264 N85-17942
Current status of trailing edge loss calculation for a turbine blade
[PNR-90244] 09 p1282 N85-19081
Aerodynamic heating rate distributions induced by trailing edge controls on hypersonic aircraft configurations at Mach 8
[NASA-TM-87453] 13 p1986 N85-22370
Low-speed characteristics of a circulation control airfoil with AFT camber and a spiral trailing edge
[AD-A150851] 14 p2213 N85-23725
Turbulent flow of fluid near trailing edge of plate in stream at zero angle of attack 16 p2764 N85-27057
Flame acceleration mechanisms under conditions of partial confinement
[PB85-184063] 18 p3073 N85-29004
Analysis of the turbulent near wake at a sharp trailing edge 20 p3387 N85-31008
Trailing edge flow and aerodynamic sound. Part 1: Tonal pressure and velocity fluctuations. Part 2: Random pressure and velocity fluctuations
[AD-A154947] 21 p3552 N85-32097
On the application of a hairpin vortex model of wall turbulence to trailing edge noise prediction
[NASA-CR-177936] 22 p3728 N85-33109
A design procedure to modify the trailing edge upper surface pressure gradient of a given aerofoil
[GU-AERO-8408] 23 p3894 N85-34120
Reflection plane tests of a wind turbine blade tip section with ailerons
[NASA-TM-87018] 23 p3945 N85-34444

TRAILS
U TRACKS

TRAINEES
U STUDENTS

TRAINERS
U TRAINING DEVICES

TRAINING
U EDUCATION

TRAINING AIRCRAFT
NT CL-41 AIRCRAFT
NT DH 115 AIRCRAFT
NT JAGUAR AIRCRAFT
NT JET PROVOST AIRCRAFT
NT T-33 AIRCRAFT
Analysis of the flow field about a T-45 using PANAIR
[AD-A148811] 07 p0899 N85-15699
Can the Aggressors continue to be effective in the F-5E?
[AD-A148661] 07 p1019 N85-16465
Collision avoidance for Naval training aircraft
[FAA-PM-84-4] 12 p1774 N85-21136
Aircraft structure for application to training aircraft
[CH-635286-A5] 15 p2469 N85-25244
RAFTS: A T-38 replacement for the 21st century
[AD-A156103] 24 p4065 N85-35191

TRAINING ANALYSIS
Factors critical to the implementation of self-paced instruction: A background review
[AD-A145143] 01 p0097 N85-10648
Artificial intelligence contributions to training and maintenance
[AD-P003934] 02 p0247 N85-11614
An analysis of the technical training of enlisted minuteman missile maintenance personnel
[AD-A147078] 07 p0912 N85-15775
Pilot education and safety awareness programs 09 p1277 N85-19026

TRAINING DEVICES
Aeronautical systems technology needs: Escape, rescue and survival, test facilities and test equipment and training-simulation equipment
[AD-A145069] 01 p0001 N85-10002
Training effectiveness evaluation and utilization demonstration of a low cost cockpit procedures trainer
[AD-A145179] 01 p0013 N85-10076
Factors critical to the implementation of self-paced instruction: A background review
[AD-A145143] 01 p0097 N85-10648
Ada (trademark) training curriculum. Real-time concepts t303 teacher's guide
[AD-A145093] 01 p0104 N85-10694
Ada (trademark) training curriculum. Software engineering for managers m101 teacher's exercise guide
[AD-A145094] 01 p0104 N85-10695
GUIDON
[AD-P003925] 02 p0246 N85-11605
Designing an expert system for training automotive electrical troubleshooting
[AD-P003926] 02 p0246 N85-11606
The psychology of technical devices and technical discourse
[AD-P003929] 02 p0246 N85-11609
Artificial intelligence contributions to training and maintenance
[AD-P003934] 02 p0247 N85-11614

Training capabilities test of Electronics Equipment Maintenance Trainer (EEMT): Findings and conclusions
[AD-A146075] 03 p0359 N85-12302
Information Center handbook
[PB84-211341] 03 p0439 N85-12795
Determining training device requirements in Army aviation systems 05 p0711 N85-14558
The design and use of subtasks in part training and their relationship to the whole task 05 p0711 N85-14559
Simulating speed and height cues in the C-130 weapon system trainer
[AD-P004313] 09 p1268 N85-17967
Dynamic training devices in CRM training 09 p1276 N85-18018
Use of airplanes for loft training 09 p1276 N85-18019
Cockpit resources management and the theory of the situation 09 p1276 N85-18022
Cockpit resource management training 09 p1276 N85-18023
Simulation 09 p1277 N85-18024
Low cost training aids and devices 09 p1277 N85-18025
Pilot education and safety awareness programs 09 p1277 N85-18026
Initiative uses of aircraft for flight training 09 p1277 N85-18027
Study of cognitive styles of students in automated teaching system 10 p1525 N85-19620
New flight simulators at Vnukovo permit less in-flight training 12 p1769 N85-21107
Maintenance training simulators prime item development specification. Model specification and handbook
[AD-A154106] 19 p3330 N85-30628
Models for multidimensional tests and hierarchically structured training materials
[AD-A155231] 21 p3666 N85-32768

TRAINING EVALUATION
Training effectiveness evaluation and utilization demonstration of a low cost cockpit procedures trainer
[AD-A145179] 01 p0013 N85-10078
Factors critical to the implementation of self-paced instruction: A background review
[AD-A145143] 01 p0097 N85-10648
Overview of training and aiding
[AD-P003917] 02 p0245 N85-11597
Individual differences in automatic and controlled information processing
[AD-A146245] 03 p0401 N85-12559
An analysis of the technical training of enlisted minuteman missile maintenance personnel
[AD-A147078] 07 p0912 N85-15775
Concept paper for the development of a DOD Ada (trademark) software engineering education and training plan
[AD-A146774] 08 p1206 N85-17592
Simulation 09 p1277 N85-18024
Low cost training aids and devices 09 p1277 N85-18025
Innovative approaches to recurrent training 09 p1277 N85-18028
Research needs on the interaction between information systems and their users: Report of a workshop
[PB85-121523] 10 p1588 N85-19691
NASA Ames Summer High School Apprenticeship Research Program
[NASA-TM-86006] 15 p2686 N85-28590
A review of safety practices and safety training for the explosives field
[AD-A152295] 16 p2759 N85-27028
Welder training/welder testing
[BLL-WI-TRANS-683-(9312.57)] 16 p2792 N85-27223
Guidelines of the Federal Minister of Transportation for the formation and examination of airline personnel, part 4 17 p3002 N85-28556
The use of flight simulators in measuring and improving training effectiveness
[AD-A153617] 18 p3084 N85-29954
Simulation for human factors research. A central question: Fidelity 18 p3159 N85-29568
Microcomputers in transportation: Software and source book, February 1985
[PB85-181022] 20 p3517 N85-31868

TRAINING SIMULATORS
NT COCKPIT SIMULATORS
NT FLIGHT SIMULATORS
NT SPACECRAFT CABIN SIMULATORS
The design, fabrication and delivery of a spacelab neutral buoyancy Instrument Pointing System (IPS) mockup — underwater training simulator
[NASA-CR-171233] 04 p0462 N85-12934
The use of flight simulators in measuring and improving training effectiveness
[AD-A153617] 18 p3084 N85-29954
Maintenance training simulators prime item development specification. Model specification and handbook
[AD-A154106] 19 p3330 N85-30628

TRAJECTORIES
NT ABORT TRAJECTORIES
NT ASCENT TRAJECTORIES
NT BALLISTIC TRAJECTORIES
NT DESCENT TRAJECTORIES
NT EARTH-VENUS TRAJECTORIES
NT ELECTRON TRAJECTORIES
NT INTERORBITAL TRAJECTORIES
NT INTERPLANETARY TRAJECTORIES
NT MISSILE TRAJECTORIES
NT PARTICLE TRAJECTORIES
NT REENTRY TRAJECTORIES
NT ROUND TRIP TRAJECTORIES
NT SPACECRAFT TRAJECTORIES
Moment induced by liquid payload during spin-up without a critical layer
[AD-A145716] 02 p0199 N85-11327
Trajectory estimation using combined time-of-arrival and velocity measurements
[DE84-015872] 02 p0242 N85-11582
Arctic ice island and sea ice movements and mechanical properties
[DE84-016323] 04 p0542 N85-13450
A numerical investigation of planetesimal collision trajectories with a Moon accumulating in Earth orbit 04 p0588 N85-13740
A Generalized Escape System Simulation (GESS) computer program. Volume 2: GESS programmer's manual, version 2
[AD-A148363] 08 p1081 N85-16845
An investigation of the driving wheel thrust of paddy field tractors
[AD-P004284] 09 p1407 N85-18861
Electromagnetic braking of a metallic projectile in flight
[AD-A149424] 10 p1480 N85-19345
Atmospheric profile imprint in firewall ablation coefficient 11 p1662 N85-20473
A user's manual for AMEER flight path trajectory simulation code
[DE85-006580] 15 p2472 N85-25260
Numerical calculation of subsonic jets in crossflow with reduced numerical diffusion
[NASA-TM-87003] 15 p2472 N85-25263
Inference and state estimation for stochastic point processes
[AD-A151216] 15 p2640 N85-26281
Dispersion sensitivity of the eight inch advanced ramjet munitions technology projectile due to wind and minor thrust errors
[AD-A152145] 16 p2727 N85-26835
The mean trajectory approximation for charge and energy transfer processes at surfaces
[AD-A152708] 17 p3043 N85-28830
Lattice actions improved by block-spin renormalisation group and maximally symmetric lattices
[DE85-007416] 17 p3045 N85-28841
Global coordinate system
[AD-A153878] 19 p3299 N85-30454
Effect of vertical shear on regional-scale trajectories in near-frontal conditions
[DE85-007554] 19 p3317 N85-30561
Emittance growth caused by current variation in a beam-transport channel
[DE85-010743] 19 p3363 N85-30649
Use of a minimum-ellipse criterion in the study of ion-beam extraction systems
[DE85-012670] 24 p4148 N85-35721

TRAJECTORY ANALYSIS
Trajectory estimation using combined time-of-arrival and velocity measurements
[DE84-015872] 02 p0242 N85-11582
Relationships between Ariane trajectories and satellite orbits 05 p0599 N85-13615
Interplanetary trajectories 05 p0600 N85-13627
Algorithm for tracking manuevering object with ambiguous measurements 06 p0791 N85-15057
Flow visualization study of the effect of injection hole geometry on an inclined jet in crossflow
[NASA-TM-86936] 11 p1631 N85-20269
Rejection of anomalous observations when determining spacecraft trajectories 13 p1979 N85-22421
Approximate analytic method of calculating trajectories of movement of a flight vehicle in the atmosphere 14 p2279 N85-24121
Space Mathematics for the Preparation and Development of satellite Exploitation
[ISBN-2-85428-115-2] 14 p2395 N85-24753
Orbit reconstitution — satellite orbits 14 p2396 N85-24765
Towards the Halley Comet 14 p2399 N85-24783
Minimax problem of estimating trajectory parameters in continuous formulation 15 p2479 N85-25301
Computer program for prediction of capture maneuver probability for an on-off reaction controlled upper stage
[NASA-CR-165937] 17 p3010 N85-28611
The role of thermal motions of air particles for fireballs
[PUBL-59] 17 p3053 N85-28900
Calculation of trajectories of detached wind turbine blades and prediction of site risk levels associated with failures of HAWT's 24 p4110 N85-35475

TRAJECTORY CONTROL
NT TRAJECTORY OPTIMIZATION
Space interception guidance with uncertain factors 13 p2042 N85-22781
User's manual of the BNDSCO computer program for solving constrained optimal control problems
[DFVLR-MITT-85-05] 20 p3516 N85-31865
A method of accurizing rail guns
[LA-10028-MS] 22 p3737 N85-33186

TRAJECTORY MEASUREMENT
Trajectory estimation using combined time-of-arrival and velocity measurements
[DE84-015872] 02 p0242 N85-11582
Rejection of anomalous observations when determining spacecraft trajectories 13 p1979 N85-22421
Trajectory measurements for take-off and landing tests and other short-range applications, volume 16
[AGARD-AG-160-VOL-16] 15 p2561 N85-25801
Method for evaluating perturbation in algorithms for solving navigational problems 16 p2718 N85-26763

TRAJECTORY OPTIMIZATION
Interplanetary trajectories 05 p0600 N85-13627
Optimal multiple-impulse nonlinear orbital rendezvous 08 p1105 N85-16984
Planning of minimum-time trajectories for robot arms
[AD-A148956] 10 p1492 N85-19418
Algorithm for determining optimal three impulse point-to-orbit transfer with limited transfer time 13 p1979 N85-22419
Synthesis of optimum algorithms for secondary processing 13 p2060 N85-22992
Optimal space trajectories 14 p2396 N85-24756
Minimum time turns using vectored thrust
[AD-A151693] 15 p2471 N85-25256
A numerical study of the mean trajectory approximation in a non-adiabatic process
[AD-A152763] 17 p3030 N85-28737
Piloted simulation of an algorithm for onboard control of time-optimal intercept
[NASA-TP-2445] 18 p3063 N85-28949
SIGMA - A stochastic-integration global minimization algorithm
[AD-A154878] 21 p3671 N85-32806

TRANQUILIZERS
Primate equilibrium performance and diazepam: A behavioral tolerance effect
[AD-A145156] 01 p0094 N85-10634

TRANSATMOSPHERIC VEHICLES
NASA R and T aerospace plane vehicles: Progress and plans
[NASA-TM-86429] 15 p2491 N85-25368

TRANSCEIVERS
U TRANSMITTER RECEIVERS

TRANSCENDENTAL FUNCTIONS
NT EXPONENTIAL FUNCTIONS
NT LOGARITHMS
NT PERIODIC FUNCTIONS
NT TANGENTS
On the spherical derivative of a meromorphic function with a Nevanlinna deficient value 10 p1535 N85-19676
Solutions of problems of miller and rubel 10 p1536 N85-19685
Collision detection for moving polyhedra
[AD-A148961] 10 p1544 N85-19735
Arithmetic and elementary functions on mini and microcomputers 14 p2396 N85-24761
Calculation of roots of transcendental equations in problems of determining thermal conductivity of cylinder with non-uniform boundary conditions
[BLL-M-35788-(5628.4)] 23 p3929 N85-34349

TRANSDUCERS
NT ELECTROACOUSTIC TRANSDUCERS
NT ELECTRONIC TRANSDUCERS
NT HYDROPHONES
NT IMAGE TRANSDUCERS
NT INTERDIGITAL TRANSDUCERS
NT LOUDSPEAKERS
NT MAGNETIC TRANSDUCERS
NT MICROPHONES
NT MODE TRANSFORMERS
NT PIEZOELECTRIC GAGES
NT PIEZOELECTRIC TRANSDUCERS
NT PIEZORESISTIVE TRANSDUCERS
NT PRESSURE SENSORS
NT SOUND TRANSDUCERS
NT TORQUERS
NT ULTRASONIC WAVE TRANSDUCERS

A miniature urethane molded acoustic transducer
[AD-A146459] 06 p0804 N85-15114
Unsteady pressure measurements on a biconvex airfoil in a transonic oscillating cascade
[NASA-TM-86914] 07 p0896 N85-15689
Digital thermometer with linearizer on slide wire 07 p0954 N85-16049
Ultrasonic transducers, performance variability, design, and manufacturing procedures
[AD-A148575] 08 p1158 N85-17306
Development of a floating element wall shear transducer
[AD-A148450] 08 p1164 N85-17346
Modeling of real UT transducer field/flaw interactions
[DE85-000341] 09 p1329 N85-18351
Stress waves in an isotropic elastic plate excited by a circular transducer
[NASA-CR-3877] 11 p1650 N85-20390
Compensation of skew passband of a SAW filter using predistortion 12 p1821 N85-21422
Thin film strain transducer — suitable for in-flight measurement of scientific balloon strain
[NASA-CASE-WLP-10055-2] 12 p1849 N85-21598
Rocket body charge neutralization processes in ARAKS experiment (data from two launches) 13 p1980 N85-22426
Programmable filter with fanned interdigital surface acoustic wave transducer 13 p2063 N85-23008
Electrothermal transducer with short time constant 13 p2086 N85-23040
Influence of axial shaft load on operation of magnetoelastic torque transducer 14 p2270 N85-24085
Transducer of linear displacements 14 p2281 N85-24130
A transduction path method of solid state sensor analysis and investigation
[AD-A152123] 16 p2870 N85-27707
Liquid-metal transducers for strain measurement during in-pile materials testing 17 p2945 N85-28176
Automatic liquid-metal temperature monitoring with the use of immersed transducers
[BLL-BISI-TRANS-22427-(9022.06)] 18 p3104 N85-29215
Gravity enhanced acoustic levitation method and apparatus
[NASA-CASE-NPO-16147-1-CU] 18 p3177 N85-29693
Microwave bandstop filter
[AD-D011716] 19 p3261 N85-30222
Fiber optic sensors operating at dc
[AD-D011674] 19 p3271 N85-30283
Fiber optics in transient radiation fields
[DE85-010721] 19 p3368 N85-30686
Wideband disturbance accomodation in precision flexible space structures 20 p3415 N85-31194
Ultrasonic flowmetering with reflected pulses
[PB85-179885] 20 p3460 N85-31492
R and D activities of the Systems Engineering Division 20 p3540 N85-32027
Experimental and theoretical assessment of a new technique for the non-destructive evaluation of laminated panels
[AD-A155622] 21 p3562 N85-32155
Shear wave transducer for boreholes
[DE85-011662] 22 p3787 N85-33461
Device for frequency modulation of a laser output spectrum
[DE85-011634] 22 p3790 N85-33479
Non-bonded ultrasonic transducer
[DE85-011008] 22 p3794 N85-33504
Electromagnetic inspection of wire ropes using sensor arrays
[AD-A155412] 22 p3795 N85-33509
Fast shutter apparatus
[DE85-006501] 23 p3926 N85-34343
Acoustic cross-correlation flowmeter for solid-gas flow
[DE85-005988] 23 p3935 N85-34391
A multi-touch three dimensional touch-sensitive tablet (executive summary) 23 p3961 N85-34553

TRANSEQUATORIAL PROPAGATION
Propagation and amplification of Ion Cyclotron Waves (ICW's) in a multicomponent plasma. The Earth magnetosphere as a giant maser for Alfven waves 14 p2368 N85-24634

TRANSFER
U TRANSFERRING

TRANSFER FUNCTIONS
NT MODULATION TRANSFER FUNCTION
NT OPTICAL TRANSFER FUNCTION
Definition of acceptable levels of mismatch for equivalent systems of augmented CTOL (Conventional Take-Off and Landing) aircraft
[AD-A145619] 02 p0149 N85-11007
Gain-phase structures for linear multivariable systems
[RR-256] 02 p0256 N85-11674
Dual (GaAl) As-heterostructure based injection laser traveling wave amplifier 02 p0261 N85-11708
Transfer function of multilayered magnetooptical space-time modulator 02 p0264 N85-11726
CONTROL: A suite of interactive transfer-function analysis programs
[OUEL-1527/84] 03 p0408 N85-12609
Coupling of airborne sound into the Earth
[AD-A146231] 03 p0416 N85-12663
Introduction to the subjective transfer function approach to analyzing systems
[AD-A145617] 03 p0436 N85-12774
Investigation of several aspects of LANDSAT 4/5 data quality
[E85-10038] 04 p0525 N85-13357
Mars polar volatiles: Topographic and geologic setting
[NASA-CR-174089] 04 p0581 N85-13706
A very efficient transfer function bounding technique on bit error rate for Viterbi decoded, rate 1/N convolutional codes 05 p0624 N85-13991
Derivation of recursive digital filters by the step-invariant and the ramp-invariant transformations
[AD-A146500] 06 p0857 N85-15452
EMC (Electromagnetic compatibility) spec criteria in Volterra systems
[AD-A147659] 06 p1151 N85-17263
Optically induced intervalence-band transitions in germanium by the absorption of 1.06 micrometers picosecond pulses
[DE85-000948] 09 p1399 N85-18803
Further results on rate 1/N convolutional code constructions with minimum required SNR criterion 10 p1464 N85-19235
Imaging through a multiple scattering medium
[DE85-002051] 10 p1557 N85-19821
Journal of Research of the National Bureau of Standards, volume 89, number 2, March - April 1984
[PB85-115426] 12 p1926 N85-22103
Modal synthesis of multidimensional PI-regulators for objects with inertial sections 14 p2270 N85-24064
Tutorial discussion of electronic sampling systems for recording wide-bandwidth transient signals
[DE85-006577] 15 p2549 N85-25735
Development of graphical pole-zero, root-locus, Bode, Nyquist, and Nichols responses using the OPTSYSX program
[AD-A152148] 16 p2847 N85-27555
Generalised translation invariance and systems theory
[CRIM-8501] 17 p3017 N85-28657
An interactive computer aid for the design and analysis of linear, single input/single output digital and continuous control systems
[AD-A153704] 18 p3162 N85-29589
A study of interior noise levels, noise sources and transmission paths in light aircraft
[NASA-CR-172152] 19 p3350 N85-30766
Matrix transfer function design for flexible structures: An application 20 p3416 N85-31199
Basic EMC (Electromagnetic Compatibility) technology advancement for C3 systems. Volume 1B: Demodulation radio frequency interference effects in operational amplifier circuits
[AD-A154121] 20 p3440 N85-31350
Synthesis of high-speed devices using integrated operational amplifiers 22 p3781 N85-33426
Method and apparatus for transfer function simulator for testing complex systems
[NASA-CASE-NPO-15696-1] 23 p3926 N85-34333
A multi-touch three dimensional touch-sensitive tablet (executive summary) 23 p3961 N85-34553

TRANSFER OF TRAINING
China report: Science and technology
[JPRS-CST-85-003] 13 p2166 N85-23433
The role of prior knowledge in operating equipment from written instructions
[AD-A151007] 14 p2392 N85-24730
The acquisition of procedures from text. A production-system analysis of transfer of training
[AD-A151029] 14 p2392 N85-24732

TRANSFER ORBITS
NT INTERPLANETARY TRANSFER ORBITS
Commercializing the transfer orbit stage 02 p0155 N85-11049
Relationships between Ariane trajectories and satellite orbits 05 p0599 N85-13815
Satellite positioning — in geosynchronous orbit 05 p0600 N85-13823
Transportation applications, part 1 11 p1643 N85-20349
Space debris protection for a reusable orbital transfer vehicle 12 p1786 N85-21208
The long term behaviour of Earth orbits and the implications for debris control 12 p1786 N85-21213
Radiation exposure and performance of multiple burn LEO-GEO orbit transfer trajectories
[NASA-TM-86948] 12 p1788 N85-21228
Algorithm for determining optimal three impulse point-to-orbit transfer with limited transfer time 13 p1979 N85-22419
Optimal space trajectories 14 p2396 N85-24756
Manrating orbital transfer vehicle propulsion
[NASA-TM-87019] 15 p2494 N85-25385
Telescope in lunar orbit 15 p2662 N85-26588
Analysis of orbit transfer vehicles for GPS Block 3 satellites
[AD-A152021] 16 p2732 N85-26660
Primary propulsion of electrothermal, ion and chemical systems for space-based radar orbit transfer
[NASA-TM-87043] 17 p2916 N85-27972
Optimal low thrust transfer using a first-order perturbation model
[AD-A154761] 21 p3676 N85-32835

TRANSFERRING
Voltage dependence of the relative AC-DC transfer difference for HF voltage-transfer standards 05 p0630 N85-14038
Chemical and photographic evaluation of rigid explosive transfer lines
[AD-A149303] 11 p1613 N85-20145
A new technique for system-to-system transfer of surface data 17 p3007 N85-28699

TRANSFORM INTEGRALS
U INTEGRAL TRANSFORMATIONS

TRANSFORMATION TENSORS
U TENSORS

TRANSFORMATIONS
Tests of fit based on normalized spacings
[AD-A149749] 12 p1921 N85-22062
Transformation of charged particle beams by concentrating electro-optical systems 21 p3690 N85-32925

TRANSFORMATIONS (MATHEMATICS)
NT COORDINATE TRANSFORMATIONS
NT FAST FOURIER TRANSFORMATIONS
NT HOUSEHOLDER TRANSFORMATIONS
NT INTEGRAL TRANSFORMATIONS
NT LAPLACE TRANSFORMATION
Reducing spectral dimension of remotely sensed data using principal components analysis and a Peano scanning 02 p0212 N85-11399
Utilization of interpolation and transformation for the compression of digital image data
[INPE-3081-PRE/479] 02 p0240 N85-11566
Lie-transformation action principle for classical plasma dynamics
[DE84-014576] 02 p0265 N85-11858
Comparison of free component mode synthesis techniques using MSC/NASTRAN
[DE84-014451] 04 p0514 N85-13278
Derivation of recursive digital filters by the step-invariant and the ramp-invariant transformations
[AD-A146500] 06 p0857 N85-15452
New technology high efficiency and high stability color motion video compression system
[AD-A147523] 07 p0941 N85-15968
Use of shanks transformation for speeding up adaptation process in antenna arrays 07 p0951 N85-16029
A power transformation exponential regression model for censored failure time data
[AD-A148377] 08 p1212 N85-17632
Modeling relationships using groups and items 09 p1367 N85-18591
Investigation of three-dimensional mesh generation with precise controls
[AD-A148759] 09 p1374 N85-18636
Diffeomorphic approximation of quasiconformal and quasisymmetric homeomorphisms 10 p1536 N85-19678
A conformal mapping suitable for problems involving interaction between given geometries and known far fields
[AD-A149060] 10 p1545 N85-19744
Triple matrix product optical processors using combined time-and-space integration
[AD-D011483] 10 p1557 N85-19820
Bayesian analysis of time series 1: Householder transformation analyses
[DE85-004449] 11 p1708 N85-20749
Functional equation for the embedding of a homomorphism of the interval into a flow
[DE85-000655] 11 p1713 N85-20780
Nonlinear sigma-models and integration methods
[DE85-004447] 12 p1922 N85-22071
Harmonic analysis and Radon transforms on pencils of geodesics
[CWI-PM-R8413] 12 p1922 N85-22074
A simple and efficient algorithm to compute tail probabilities from transforms
[AD-A150928] 14 p2409 N85-24849

The omni-transform in single-channel queues
[AD-A151019] 14 p2409 N85-24852
Control of a flexible beam
[DE85-007243] 15 p2580 N85-25014
Old and new in Moebius groups
15 p2634 N85-26235
Solution to eigenvalue problems of antisymmetric cross-ply and antisymmetric angle-ply laminated plates using affine transformations
[AD-A153040] 17 p2917 N85-27980
Curved finite elements and curve approximation
17 p3007 N85-28590
Investigation and implementation of a tree transformation system for user friendly programming
[AD-A152716] 17 p3011 N85-28617
Generalised translation invariance and systems theory
[CRM-8501] 17 p3017 N85-28657
On approximating a set-valued function locally
[AD-A153540] 18 p3170 N85-29641
On the transformation of derivatives of distributions on surfaces
[PREPRINT-434] 18 p3173 N85-29670
Application of Floquet theory to helicopter blade flapping stability
[AD-A154460] 19 p3218 N85-29952
Nonlinear dynamics: A personal perspective
[DE85-010982] 20 p3521 N85-31869

TRANSFORMERS
NT MODE TRANSFORMERS
NT VOLTAGE CONVERTERS (AC TO AC)
Developments in space power components for power management and distribution 05 p0608 N85-13677
Pulse transformer package for impedance matching a laser diode to a transmission line
[AD-D011499] 12 p1656 N85-21632
Design and performance of etched polarisation transformers for microwave frequencies
[R-NIAS-26] 14 p2297 N85-24218
Detection and location of partial discharges in transformer windings using electrical methods
15 p2551 N85-25760
Research on design of cryotransformers and its prospects for the future
[AD-A152400] 17 p2952 N85-28230
High voltage isolation transformer
[NASA-CASE-GSC-12817-1] 18 p3093 N85-29146
Design and testing of a pulsed current transformer
[AD-A154228] 19 p3259 N85-30206
T/R switch design for short-range measurements, part 6.1A
21 p3624 N85-32515
Calculation of external magnetic field of a shielded transformer 22 p3771 N85-33373

TRANSFORMS
U TRANSFORMATIONS (MATHEMATICS)

TRANSIENT HEATING
NT PULSE HEATING
NT SHOCK HEATING
Instrumentation for sensing moisture content of material using a transient thermal pulse
[NASA-CASE-NPO-15493-2] 23 p3933 N85-34373

TRANSIENT LOADS
NT BLAST LOADS
NT GUST LOADS
NT IMPACT LOADS
NT LANDING LOADS
NT SHOCK LOADS
Transient vibration test criteria for spacecraft hardware — galileo spacecraft 09 p1338 N85-18418
Crack growth geometry in aluminum alloy sheet material under flight simulation loading. 1: A comparison between TWIST and miniTWIST FALSTAFF and short FALSTAFF. 2: Effect of truncating high loads
[VTH-LR-441] 11 p1609 N85-20119
Symmetric primal-dual variational formulations of coupled dynamic systems: Three-dimensional elasticity, shells, fluid-structure interaction
[ONERA-1983-91] 12 p1663 N85-21684
Analysis of shell type structures subjected to time dependent mechanical and thermal loading
[NASA-CR-175747] 15 p2577 N85-25896
Transient behavior of a single-blade horizontal-axis wind turbine
[MSB-UD-421/84-O] 16 p2675 N85-27737

TRANSIENT OSCILLATIONS
Thresholds of perception of whole body linear oscillation: Modification by spaceflight 05 p0694 N85-14467
Transient voltage oscillations in coils
[DE85-006715] 15 p2550 N85-25738
Analysis of transient radiation upset in a 16K SRAM
[DE85-009442] 23 p3965 N85-34586

TRANSIENT PRESSURES
Finite element method for a class of viscoelastic flows in deforming domains applied to jet breakup
[DE84-014571] 04 p0500 N85-13166
Surge transient simulation in turbo-jet engine
05 p0596 N85-13796
Experimental investigations of the unsteady turbulent friction behavior with pressure impulses in a circular pipe
[IWAWI-MITT-102] 18 p3103 N85-29210
Response of steam-water mixtures to pressure transients
[DE85-010798] 19 p3267 N85-30262

TRANSIENT RESPONSE
A generalized mathematical solution for transient off tracking of single vehicles and truck combinations
[DM-2] 01 p0107 N85-10719
The transient behavior of networks with infinite server nodes
[CWI-OS-R8408] 05 p0722 N85-14640
Improvement of the transient response in the finite settling time control
[NAL-TR-823] 06 p0757 N85-14843
Sensitivity analysis of discrete structural systems: A survey
[NASA-TM-86333] 06 p0817 N85-15186
Data and results of a laboratory investigation of microprocessor upset caused by simulated lightning-induced analog transients
07 p0999 N85-16345
Transient response of a small-signal microwave GaAs FET to X-rays
[DE85-000066] 09 p1315 N85-18265
The Shock and Vibration Bulletin 54. Part 2: Ship shock, shock and blast and ground shock
[AD-A148132] 09 p1334 N85-18388
Two-dimensional shock response of a mass on energy-absorbing shock mounts
09 p1334 N85-18389
Optimum design for nonlinear shock mounts for transient inputs 09 p1334 N85-18390
An objective error measure for the comparison of calculated and measured transient response histories
09 p1335 N85-18395
Analysis of inverter models and harmonic propagation. Part 3. Transient processes in inverter models
[DE85-000191] 10 p1510 N85-19530
Analysis of the transient response of temporal artery blood flow data relative to various anti-G suit pressure schedules 10 p1533 N85-19660
TRACR3D: A model of flow and transport in porous/fractured media
[LA-9667-MS] 12 p1645 N85-21576
Symmetric primal-dual variational formulations of coupled dynamic systems: Three-dimensional elasticity, shells, fluid-structure interaction
[ONERA-1983-91] 12 p1663 N85-21684
Laboratory studies of spacecraft response to transient discharge pulses 13 p1995 N85-22506
Hydrodynamic simulation of transient processes in injection system of aircraft engines during pump unswirling 13 p2050 N85-22829
Transient analysis of loaded thin-wire antennas and transmission lines 13 p2053 N85-22852
Research efforts in support of resonance extraction studies. Volume 1: Improvement and validation of TWFD (Thin-Wire Frequency-Domain): A thin-wire frequency-domain scattering code
[AD-A150296] 13 p2054 N85-22864
Tutorial discussion of electronic sampling systems for recording wide-bandwidth transient signals
[DE85-006577] 15 p2549 N85-25735
Transient analysis of a magnetic heat pump
15 p2576 N85-25891
Continuum modeling of latticed structures
17 p2977 N85-28399
A state variable approach to transient creep deformation in stress reduction experiments
[DE85-009492] 18 p3122 N85-29331
Dynamical study of flat plates by nonlinear elasticity theory
[STN-8] 20 p3471 N85-31572
Analysis of the transient response of temporal artery blood flow data relative to various anti-G suit pressure schedules
[AD-A155242] 21 p3666 N85-32775
Numerical simulation of nonisothermal transient processes in GaAs diode structures
22 p3767 N85-33350
Synthesis of high-speed devices using integrated operational amplifiers 22 p3781 N85-33428
Substructure coupling in the frequency domain
[NASA-CR-178140] 22 p3800 N85-33543
The transient electromagnetic depth sounding technique applied to hydrocarbons and geothermal exploration
[MITT-42] 23 p3949 N85-34476

TRANSIENTS (SURGES)
U SURGES

TRANSISTOR AMPLIFIERS
Isolated load switching with surge suppression
[AD-D011216] 01 p0042 N85-10274
Dual-gate MESFET variable gain constant output power amplifier
[AD-D011334] 07 p0945 N85-15982
Playback amplifier with high interference immunity
13 p2077 N85-22970
KT3127A, KT3128A transistors
22 p3779 N85-33414

TRANSISTOR CIRCUITS
Machine computation of delay and capacitance of transistor structures of subnanosecond large integrated circuits 04 p0490 N85-13120
Computer investigation of effects of high injection in transistor large integrated circuit structures
06 p0793 N85-15068
Transistor-transistor logic microcircuit tester
12 p1642 N85-21556
Recommendation on use of series K157UL1 microcircuits 13 p2071 N85-22936
USSR report: Electronics and electrical engineering
[JPRS-UEE-84-015] 22 p3762 N85-33314
Noise in stages and in interstage couplings of various transistor circuits 22 p3765 N85-33334

TRANSISTOR LOGIC
Development of a planar heterojunction bipolar transistor for very high speed logic
[AD-A150374] 13 p2064 N85-22895

TRANSISTOR-TRANSISTOR-LOGIC INTEG CIRCUITS
U TTL INTEGRATED CIRCUITS

TRANSISTORS
NT BIPOLAR TRANSISTORS
NT FIELD EFFECT TRANSISTORS
NT JFET
NT JUNCTION TRANSISTORS
NT PHOTOTRANSISTORS
NT SILICON TRANSISTORS
Solution of the Boltzmann transport equations for a permeable base transistor
[AD-A144999] 01 p0112 N85-10757
Electron traps in the GaAs permeable base transistor
[AD-A145399] 02 p0287 N85-11871
Circuit engineering and technological optimization of very high speed LSI logic elements and transistor structures 03 p0347 N85-12237
Developments in space power components for power management and distribution 05 p0608 N85-13677
Qualitative of analysis of MOS circuits
[AD-A149267] 10 p1480 N85-19341
Code lock with microcircuit 13 p2071 N85-22935
Study of 1/f noise in solids
[AD-A151069] 14 p2428 N85-24972
Computer-aided identification of complete constitution model of transistor structure for design of subnanosecond large-scale-integrated circuits 15 p2529 N85-25594
Energy considerations in second breakdown
[AD-A152380] 17 p2952 N85-28229
Leading-edge microelectronics research at Sweden's Chalmers 20 p3438 N85-31337
Millimetre wave pulse technology — satellite mapping
[ESA-CR(P)-2004] 20 p3478 N85-31611

TRANSIT SATELLITES
The TRANSIT and Global Positioning System (GPS) systems. Precision navigation and localization
14 p2398 N85-24777

TRANSITION
Deuteron NMR (Nuclear Magnetic Resonance) in relation to the glass transition in polymers
[AD-P003910] 01 p0032 N85-10196

TRANSITION FLOW
First cryogenic test of the CAST 7 profile in the T2 wind tunnel. Comparison with calculations — airfoils
[ONERA-RTS-58/1685-AY-035-D]
04 p0577 N85-13682
Transition and mixing in axisymmetric jets and vortex rings 05 p0591 N85-13769
Boundary layer control by transition fixing — conference
[DFVLR-MITT-84-17] 14 p2211 N85-23712
Investigation of the conditions for tripping transition with roughness elements and their influence on boundary layer development 14 p2212 N85-23720
Transition fixing and simulation of high Reynolds number flow at transonic velocities 14 p2212 N85-23721
Investigations of the experimental detection of boundary layer transitions 14 p2213 N85-23723
Cone drag in the transition from continuum to free molecular flow
[OUEL-1538/84] 20 p3390 N85-31023
Experimental observation of transition behavior on a flat plate 20 p3452 N85-31437
Development of a temperature-compensated hot-film anemometer system for boundary-layer transition detection on high-performance aircraft
[NASA-TM-86732] 22 p3730 N85-33121
Nozzle wall roughness effects on free-stream noise and transition in the pilot low-disturbance tunnel
[NASA-TM-86369] 23 p3930 N85-34355

TRANSITION METALS
NT CADMIUM
NT CHROMIUM
NT CHROMIUM ISOTOPES
NT COBALT
NT COBALT 60
NT GOLD
NT HAFNIUM
NT IRIDIUM
NT IRON
NT IRON ISOTOPES
NT IRON 59
NT MANGANESE
NT MANGANESE ISOTOPES
NT MOLYBDENUM
NT NICKEL
NT NICKEL ISOTOPES
NT NIOBIUM
NT OSMIUM
NT OSMIUM ISOTOPES
NT PALLADIUM
NT PLATINUM
NT REFRACTORY METALS
NT RHENIUM
NT RHODIUM
NT RUTHENIUM
NT SCANDIUM
NT SCANDIUM ISOTOPES
NT SILVER
NT TANTALUM
NT TECHNETIUM
NT TITANIUM
NT TUNGSTEN
NT VANADIUM
NT YTTRIUM
NT ZINC
NT ZIRCONIUM
The oxidation of transition-metal ions by molecular oxygen
[BLL-M-29593-(5828.4)] 02 p0175 N85-11172
Calculations of optical properties of transition metals
[BLL-M-35744-(5828.4)] 02 p0175 N85-11175
Lattice dilation in metal-hydrogen systems
[BLL-M-35758-(5825.4)] 02 p0176 N85-11176
Lattice defects in body centered cubic transition metals 03 p0427 N85-12727
Evidence for d-band conduction in metallic glasses containing transition metal elements
[DE84-014822] 04 p0570 N85-13635
Theoretical methods for the study of transition metals in crystals
[DE84-015606] 05 p0732 N85-14709
Electronic and magnetic properties of transition-metal surfaces, interfaces and overlayers
[DE84-016886] 06 p0733 N85-14713
A nonnoble front metallization process
06 p0830 N85-15279
Theoretical research program to study transition metal trimers and embedded clusters
[NASA-CR-174296] 06 p1125 N85-17083
Electronic structure, chemical bonding, and electron conductivity of thin-film transition-metal silicides
[AD-A147721] 08 p1226 N85-17718
Comparisons between computed and observed grain boundary structures and properties in metals
[DE85-002596] 10 p1442 N85-19085
Properties and thermal stabilities of amorphous transition metal hydrides
[DE85-002117] 11 p1607 N85-20104
The physical modelling of transition metal alloying: The roles that different levels of theory play
[DE85-000591] 11 p1607 N85-20105
Studies of metal/carbon surface chemistry
[DE85-005513] 15 p2507 N85-25463
Synthesis and characterization of superconducting electronic materials
[AD-A151112] 15 p2659 N85-26409
Transitional metal activation and functionalization of C-H bonds
[DE85-006816] 16 p2746 N85-26949
Survey of experimental and theoretical electron-impact ionization cross sections for transition metal ions in low stages of ionization
[DE85-007605] 16 p2863 N85-27658
Thermodynamic analysis of the plasma nitriding of ferrovanadium
[BLL-BISI-TRANS-22237-(9022.06)]
17 p2924 N85-28032
Clusters of transition metal atoms
[AD-A153126] 17 p3030 N85-28740
New examples of clusters, extended metal-metal bonding and interstitial derivatives
[DE85-005926] 17 p3044 N85-28837
Coadsorption studies on transition metals
[PB85-183713] 18 p3072 N85-29003
Local density theory of heats of formation and short-range order parameters in substitutionally disordered alloys
[DE85-009811] 18 p3075 N85-29021
Transition metal catalyzed transformations of unsaturated molecules
[DE85-009531] 18 p3080 N85-29055
Spectroscopic investigation of materials for tunable infrared lasers
[AD-A154124] 19 p3272 N85-30291
The influence of temperature on the compositon density of the transition metals
[BLL-M-35896-(5828.4)] 23 p3915 N85-34262
Noble metals as incipient transition metals
[DE85-013283] 24 p4080 N85-35286
TRANSITION POINTS
Combustion-deflagration-detonation transition in a confined spherical powder
[ISL-R-108/84] 22 p3747 N85-33223
Combustion-deflagration-detonation transition
[ISL-CO-221/84] 22 p3747 N85-33225
TRANSITION PRESSURE
Experiments with phase transitions at very high pressure
[NASA-CR-174029] 02 p0172 N85-11148
Analysis of Shock to Detonation Transition (SDT) of porous high energy propellant from ramp-wave compression loading
[AD-A149333] 10 p1457 N85-19180
TRANSITION PROBABILITIES
Studies of the chemistry of vibrationally and electronically excited species in planetary upper atmospheres
[NASA-CR-174134] 03 p0449 N85-12851
Absolute transition probabilities of lines in the spectra of astrophysical atoms, molecules, and ions
[NASA-CR-174141] 04 p0580 N85-13705
Radiation data and standards for Tokamak diagnostics
09 p1390 N85-18742
Sensitivity of conditions for lumping finite Markov chains
[AD-A152122] 16 p2855 N85-27604
Field theory of the metal-insulator transitions in restricted symmetries
[NOTA-INTERNA-829] 18 p3196 N85-29826
Variational transition state theory
[DE85-010685] 19 p3235 N85-30059
Probabilistic analysis of automatic control systems for detection systems 22 p3765 N85-33335
Vacuum ultraviolet laser
[DE85-011632] 22 p3790 N85-33478
TRANSITION TEMPERATURE
Nuclear Magnetic Resonance of Polymeric Materials
[AD-A145078] 01 p0032 N85-10192
Structural evolution during the gel to glass conversion
[DE84-014954] 06 p0772 N85-14939
Ferromagnetism in metals at finite temperatures
[DE85-000898] 09 p1377 N85-18656
Connector/nitinol delta contact force device
[AD-D011467] 10 p1481 N85-19349
Development of media for dynamic latent heat storage for the low-temperature range. Part 1: Thermal analyses of selected salt hydrate systems
[NASA-TM-77778] 10 p1507 N85-19510
Synthesis and properties of arylethersulfone thermoset systems
[AD-A154811] 21 p3569 N85-32198
Importance and significance of transition temperatures
[AD-A154871] 21 p3569 N85-32199
TRANSITS
NT THEODOLITES
TRANSLATING
NT MACHINE TRANSLATION
The portable LISP translation tool
[AD-A149765] 12 p1915 N85-22023
The design and analysis of a complete hierarchical interface for the multi-backend database system
[AD-A151550] 15 p2629 N85-26203
Spanish language equivalents for a glossary of terms used in the field of space exploration
[NASA-TM-86211] 19 p3379 N85-30961
TRANSLATIONAL MOTION
NT SECONDARY FLOW
NT THREE DIMENSIONAL FLOW
NT THREE DIMENSIONAL MOTION
Translational control of a graphically simulated robot arm by kinematic rate equations that overcome elbow joint singularity
[NASA-TP-2376] 08 p0956 N85-15446
Processing dynamic image sequences from a moving sensor
[AD-A149984] 12 p1934 N85-22148
Absolute movement of Pacific Ocean plate during last 120 million years 13 p2107 N85-23126
The unsteady boundary layer on an elliptic cylinder following the impulsive onset of translational and rotational motion — dynamic stall 14 p2209 N85-23699
Construction of conditionally periodic solutions of problem of reciprocating motion of axially symmetric satellite of triaxial planet 15 p2480 N85-25304
TRANSLUCENCE
Light transmitting window assembly
[NASA-CASE-MSC-18417-1] 18 p3185 N85-29750
TRANSLUNAR SPACE
U INTERPLANETARY SPACE
TRANSMISSION
NT ACOUSTIC PROPAGATION
NT AERODYNAMIC HEAT TRANSFER
NT CODE DIVISION MULTIPLE ACCESS
NT CONDUCTIVE HEAT TRANSFER
NT CONVECTIVE HEAT TRANSFER
NT DATA TRANSMISSION
NT DEMULTIPLEXING
NT DIFFRACTION PROPAGATION
NT ELECTRIC POWER TRANSMISSION
NT ELECTROMAGNETIC WAVE TRANSMISSION
NT FREQUENCY DIVISION MULTIPLE ACCESS
NT FREQUENCY DIVISION MULTIPLEXING
NT GROUND WAVE PROPAGATION
NT HALOS
NT HEAT TRANSFER
NT HEAT TRANSMISSION
NT HYPERSONIC HEAT TRANSFER
NT IONOSPHERIC PROPAGATION
NT LAMINAR HEAT TRANSFER
NT LIGHT SCATTERING
NT LIGHT TRANSMISSION
NT MICROWAVE ATTENUATION
NT MICROWAVE TRANSMISSION
NT MULTIPATH TRANSMISSION
NT MULTIPLE ACCESS
NT MULTIPLEXING
NT PCM TELEMETRY
NT RADAR TRANSMISSION
NT RADIATIVE HEAT TRANSFER
NT RADIO TRANSMISSION
NT SATELLITE TRANSMISSION
NT SCATTER PROPAGATION
NT SELF PROPAGATION
NT SHOCK WAVE PROPAGATION
NT SHORT WAVE RADIO TRANSMISSION
NT SIGNAL TRANSMISSION
NT SINGLE CHANNEL PER CARRIER TRANSMISSION
NT SINGLE SIDEBAND TRANSMISSION
NT SOUND TRANSMISSION
NT SPREAD SPECTRUM TRANSMISSION
NT STRESS PROPAGATION
NT TELEPHONY
NT TELEVISION TRANSMISSION
NT TIME DIVISION MULTIPLEXING
NT TRANSEQUATORIAL PROPAGATION
NT TURBULENT HEAT TRANSFER
NT WAVE PROPAGATION
NT WAVELENGTH DIVISION MULTIPLEXING
Characterization of atmospheric conditions along transmission paths from a remotely piloted vehicle
[AD-A145527] 02 p0232 N85-11511
A new leaky wave antenna for millimeter waves based on the groove guide
[AD-A146428] 06 p0799 N85-15102
Multiple scattering effects on transmission through the atmosphere
[AD-A147527] 07 p0941 N85-15969
Low-loss flexible dielectric waveguide for millimeter-wave transmission and its application to devices
[AD-A147848] 07 p0948 N85-16006
Temperature dependence of propagation of high-current electron beam through drift space
13 p2079 N85-22982
Journal of Research of the National Bureau of Standards, volume 90, number 1, January - February 1985
[PB85-179083] 20 p3522 N85-31908
Conjugated symmetrical coupler curves, produced by 4-bar linkages having the same transmission angles
23 p3924 N85-34322
Hologram-like transmission of pictures
23 p3961 N85-34552
TRANSMISSION CIRCUITS
Interface structures for millimeter-wave circuits
[AD-A146557] 06 p0804 N85-15118
Beam forming network
[NASA-CASE-NPO-15743-1] 16 p3069 N85-29118
TRANSMISSION EFFICIENCY
Effects of transport delays of manual control system performance 05 p0701 N85-14498
Automated radome testing
[AD-P004362] 12 p1826 N85-21456

Recommendation on use of series K157UL1 microcircuits
[AD-D011229] 13 p2071 N85-22936

Interference immunity of optical radar system with phased antenna array
[NASA-CR-175734] 15 p2526 N85-25575

Land mobile satellite transmission measurements at 869 MHz: Selected results from the dedicated stratospheric balloon experiment of November 12 and 13, 1984
[NASA-CR-175764] 15 p2541 N85-25685

A brief comparison of Egyptian with West German atmospheric transmission data in the 8 to 11.5 micron waveband
[BAE-BT-12829] 15 p2594 N85-25983

Meteorological factors in Earth-Satellite propagation
[NASA-CR-175764] 16 p2769 N85-27089

Correlation of rheological characteristics of lubricants with transmission efficiency measurements
[NASA-TM-86988] 19 p3280 N85-30342

Serial Minimum Shift Keying (SMSK) follow-on study — spacecraft communication
[ESA-CR(P)-2026] 20 p3399 N85-31083

TRANSMISSION LINES
NT BEAM WAVEGUIDES
NT CIRCULAR WAVEGUIDES
NT COAXIAL CABLES
NT COMMUNICATION CABLES
NT FLUID TRANSMISSION LINES
NT MICROSTRIP TRANSMISSION LINES
NT OPTICAL WAVEGUIDES
NT PLASMAGUIDES
NT POWER LINES
NT RECTANGULAR WAVEGUIDES
NT STRIP TRANSMISSION LINES
NT SUBMARINE CABLES
NT UNDERGROUND TRANSMISSION LINES
NT WAVEGUIDES

Broadband transverse field interaction continuous beam amplifier
[AD-D011229] 01 p0043 N85-10279

Transverse field interaction multibeam amplifier
[AD-D011241] 01 p0043 N85-10282

Laboratory evaluation of Electromagnetic Pulse (EMP) hardness testing concepts for electrical conduit systems
[AD-A145466] 02 p0190 N85-11273

Fiber cable in optical system with brightness amplifier
02 p0263 N85-11724

Electrical parameters in 60-Hz biological exposure systems and their measurement: A primer
[PB84-217793] 03 p0400 N85-12548

Development of intercalated wire and cable
[AD-A146502] 06 p0774 N85-14949

Safety requirements for wiring systems and connectors for photovoltaic systems
[NASA-CR-174211] 06 p0803 N85-15110

Holographic directional coupler for fiber optic systems
[AD-D011365] 07 p0937 N85-15939

Multiwavelength bidirectional coupler-decouplers
[AD-A147009] 07 p1043 N85-16625

Operational characteristics of a 1000 MVA superconducting power transmission system
[DE85-000232] 09 p1314 N85-18263

Feasibility study for a 34 GHz (Ka band) gyroamplifier
[NASA-CR-174439] 10 p1477 N85-19325

Experimental investigation of certain beam transport issues in a pulsed transmission line linear accelerator
[DE85-002310] 10 p1555 N85-19605

Effect of interfacial characteristics of metal clad polymeric substrates on electrical high frequency interconnection performance
[NASA-TM-86948] 11 p1824 N85-20223

Effects of electromagnetic fields produced by high voltage transmission lines
[DE85-900034] 11 p1625 N85-20230

Calculation of transmission line impedances using the ANSYS finite element program
[DE84-016715] 11 p1629 N85-20261

A process to produce fine line metallic collection patterns on semiconductors devices
[NASA-CASE-NPO-16413-1] 12 p1805 N85-21325

Pulse transformer package for impedance matching a laser diode to a transmission line
[AD-D011499] 12 p1855 N85-21632

Transient analysis of loaded thin-wire antennas and transmission lines
13 p2053 N85-22852

Interference immunity of fiber-optic communication lines with spectral multiplexing of channels
13 p2069 N85-22924

AL-124 light-emitting diode in 30 Mbit/s fiber-optic communication line
13 p2069 N85-22925

Synthesis of low-pass filters using coupled lines with unmatched loads
13 p2071 N85-22938

Possibilities of aerial electric prospecting by long cable method for detecting poorly conducting strata
13 p2115 N85-23177

A compact, aperture-matched, balanced transmission line antenna
[R-NIAS-28] 14 p2290 N85-24196

Basic EMC (Electromagnetic Compatibility) technology advancement for C3 systems. Volume 4E: Modeling of transmission lines. A comparison of lumped-circuit iterative models and the transmission line model
[AD-A150652] 14 p2291 N85-24201

Preliminary estimation of mutual interference between fixed satellite service systems
15 p2528 N85-25586

Asymptotic solutions of MHD equations with finite conductivity
[REPT-12/1984] 16 p2852 N85-27581

Multiconductor flat cable
[AD-D011635] 17 p2950 N85-28218

Performance analysis of radiation cooled dc transmission lines for high power space systems
[NASA-TM-87040] 17 p2951 N85-28222

Reliability report for communication networks
[AD-A153764] 18 p3090 N85-29127

Electrical line source and point source interactions with anomalies in the ground
[DE85-009777] 18 p3095 N85-29161

Energizing arrangement for charge coupled device control electrodes
[AD-D011712] 19 p3261 N85-30220

Development of power system measurements
[PB85-182582] 20 p3450 N85-31420

Ultrasonic flowmetering with reflected pulses
[PB86-179885] 20 p3460 N85-31492

Fin line filters technology and electronic warfare
[AD-A154975] 21 p3576 N85-32237

Microcomputer network: Investigation and implementation
[AD-A155631] 21 p3674 N85-32826

Temperature sensitivity of fiber-optic transmission line
22 p3764 N85-33331

Maximally flat approximation of attenuation characteristics of coupled-line filters
22 p3775 N85-33393

Injector losses on Mite
[DE85-012356] 24 p4090 N85-35355

RFQ modeling computer program
[DE85-012665] 24 p4140 N85-35661

TRANSMISSION LOSS

Performance loss with shorted cells
06 p0832 N85-15294

Analytic models for radiation induced loss in optical fibers 2: A physical model
[AD-A147442] 07 p1044 N85-16632

Optical frequency domain reflectometry
08 p1222 N85-17695

Studies on reactive mufflers. Part 2: Mufflers with air flow
09 p1303 N85-18184

Propagation measurements for land-mobile satellite services in the 800 MHz band
[CRC-TN-724] 09 p1310 N85-18231

Propagation measurements for land-mobile satellite systems at 1541 MHz
[CRC-TN-723] 09 p1310 N85-18232

Subcable test facility
[DE85-002103] 09 p1315 N85-18269

A critical analysis of ocean thermal analysis models in operation at FNOC (Fleet Numerical Oceanography Centers)
[AD-A146731] 09 p1359 N85-18547

A comparison between predicted and measured propagation loss in the VHF/UHF range in rugged terrain
10 p1471 N85-19285

Construction tolerances for low loss, dielectric coated, metallic waveguide for transmission optical radiation
[DE85-004056] 10 p1558 N85-19822

Measurements and predictions of HF ground wave radio propagation over irregular, inhomogeneous terrain
[PB85-110666] 12 p1830 N85-21467

Noise transmission loss of a rectangular plate in an infinite baffle
[NASA-TP-2398] 12 p1927 N85-22109

Optical reflectometer for multimode fiber lightpipes
13 p2075 N85-22961

Ice statistics and acoustic scattering in the Arctic basin
[AD-A150141] 13 p2140 N85-23289

Development of a modified time delay spectrometry technique for underwater acoustic measurements in a multipath environment
[AD-A152111] 16 p2860 N85-27639

Effects of Formvar coating and copper-nickel outer sheath on the ac losses of multi-strand subsize cables
[DE85-010413] 18 p3096 N85-29166

Airborne sound transmission loss characteristics of wood-frame construction
[AD-A154174] 20 p3524 N85-31919

TRANSMISSIONS (MACHINE ELEMENTS)

The in-flight estimation and indication of cumulative fatigue damage to helicopter gears
[ARL/AERO-R-164] 03 p0317 N85-12050

The monitoring of machines
[CETIM-15-J-041] 04 p0510 N85-13253

Investigation on experimental techniques to detect, locate and quantify gear noise in helicopter transmissions
[NASA-CR-3847] 08 p1217 N85-17667

Feasibility demonstration of a novel, flat-belt, continuously variable transmission or automotive and electric-hybrid vehicle application
[NASA-CR-174430] 10 p1569 N85-19894

Design of tightening device and calculation of forces in manipulator transmissions with base-drive mounted
13 p2046 N85-22804

Gears and Power Transmission Systems for Helicopters and Turboprops
[AGARD-CP-369] 14 p2220 N85-23765

Summary of drive-train component technology in helicopters
14 p2220 N85-23766

Current transmission systems
14 p2220 N85-23767

Helicopter transmission lubricants
14 p2220 N85-23768

Special power train requirements for the next generation of rotary-wing aircraft
14 p2220 N85-23769

A state of the art assessment of turboprop transmission technology and projected needs for the next generation
14 p2220 N85-23770

The helicopter transmission design process
14 p2221 N85-23772

Software for designing teeth for reduction gears and transmissions
14 p2221 N85-23773

Fine filtration: An attractive route towards lower helicopter operating costs
14 p2221 N85-23774

Manufacturing considerations related to aircraft gearboxes
14 p2222 N85-23778

Possible technological answers to new design requirements for power transmission systems
14 p2222 N85-23779

Transmission efficiency measurements and correlations with physical characteristics of the lubricant
14 p2222 N85-23781

Problems of elastic hydrodynamic lubrication of helicopter transmission gears
14 p2222 N85-23784

Evolution of the design techniques for helicopter main transmission gearboxes
14 p2223 N85-23789

Do new aircraft need new technologies and certification rules?
14 p2224 N85-23795

Establishment and maintenance of certification standards for helicopter and turboprop power transmission systems
14 p2224 N85-23796

A system-level mathematical model for evaluation of power train performance of load-leveled electric-vehicles
[NASA-CR-175852] 14 p2434 N85-25009

Correlation of rheological characteristics of lubricants with transmission efficiency measurements
[NASA-TM-86988] 19 p3280 N85-30342

Estimation of dynamic rotor loads for the rotor systems research aircraft: Methodology development and validation
[NASA-CR-177362] 20 p3393 N85-31045

The design and analysis of single flank transmission error tester for loaded gears
[NASA-CR-176163] 23 p3937 N85-34404

TRANSMISSIVITY

Seasonal variations of reflexibility and transmissibility of ULF waves propagating through the ionosphere of geomagnetic mid-latitudes
[REPT-560] 03 p0376 N85-12403

Fine structure of vertical distribution of light attenuation index of sea water
13 p2109 N85-23140

The geostatistical approach to the inverse problem in two-dimensional steady state groundwater modeling
24 p4107 N85-35462

TRANSMISSOMETERS

Atmospheric transmissometer
[AD-D011540] 12 p1932 N85-22140

Comparison of 8 to 12 micrometer and 3 to 5 micrometer CVF transmissometer data with LOWTRAN calculations
[AD-A154216] 19 p3350 N85-30763

TRANSMITTANCE

Changes in spectral properties of detached leaves
[E85-10042] 07 p0983 N85-16243

Carbon dioxide laser radar for monitoring atmospheric transmittance and atmospheric aerosol
09 p1354 N85-18516

An HF communications frequency-management procedure for forecasting the frequency of optimum transmission
[AD-A149191] 10 p1467 N85-19254

A new CO2 transmittance parameterization and its impact on the GLA GCM
18 p3146 N85-29476

Measurement of permittivity and permeability of microwave materials
[AD-D011656] 18 p3176 N85-29688

Light transmitting window assembly
[NASA-CASE-MSC-18417-1] 18 p3185 N85-29750

Comparison of 8 to 12 micrometer and 3 to 5 micrometer CVF transmissometer data with LOWTRAN calculations
[AD-A154218] 19 p3350 N85-30763
Ship-to-ship propagation: Maritime data analyses
[AD-A155484] 21 p3592 N85-32325
Nuclear thermal transmittance in the atmosphere using LOWTRAN-6 computer code
[AD-A154669] 21 p3630 N85-32553
Characteristic modes for slots in a ground plane TE case
[AD-A155757] 24 p4086 N85-35326
Feasibility study of radar-transmitting materials
[AD-A155839] 24 p4087 N85-35329
Linear absorption and scattering of laser beams
[AD-A156167] 24 p4098 N85-35401

TRANSMITTER RECEIVERS
Quartz filter transceiver 12 p1838 N85-21538
Firefighters' communication transceiver test plan
[NASA-CR-171419] 13 p2053 N85-22864
Transceiver test device
[AD-D011726] 22 p3786 N85-33458

TRANSMITTERS
NT EMERGENCY LOCATOR TRANSMITTERS
NT IONOSONDES
NT RADAR TRANSMITTERS
NT RADIO BEACONS
NT RADIO TRANSMITTERS
NT RADIOSONDES
NT RADIOTELEPHONES
NT RAWINSONDES
NT REPEATERS
NT TRANSMITTER RECEIVERS
Lightweight, broadband Rayleigh wave transducer
[AD-D011345] 07 p1037 N85-16584
A variable length and sensor spacing thermistor array
[AD-D011416] 08 p1113 N85-17017
Methodical approaches to determination of sanitation protective zone dimensions around TV centers and TV retransmitters 09 p1361 N85-18563
Data acquisition, measurement devices at 1984 Leipzig Spring Fair 09 p1378 N85-18661
Performance assessment of Class 1E pressure transmitters subjected to environmental stresses
[DE85-001623] 12 p1854 N85-21626
A compact, aperture-matched, balanced transmission line antenna
[R-NIAS-28] 14 p2290 N85-24196
Satellite reception of reentry vehicle telemetry
[AD-A151851] 15 p2492 N85-25372
Cophasal horizontal wideband array antennas for transmitting with asymmetric output 15 p2526 N85-25576
Measurement results from a balloon experiment simulating land mobile satellite transmissions
[NASA-CR-175740] 15 p2540 N85-25683
On the throughput of channel access algorithms with limited sensing
[AD-A151984] 15 p2630 N85-26206
Digital RF delay line for ECM (electronic countermeasure) look-through
[AD-A152120] 16 p2774 N85-27120
A communications link for an implantable electrode array
[AD-A152238] 16 p2840 N85-27510
High switching speed electrically tuned microwave magnetic resonance devices
[AD-D011699] 19 p3260 N85-30217
Multitrunk high-frequency multiplexing of antenna-waveguide channels 22 p3774 N85-33385
Transmitter spectrum analyzer 22 p3774 N85-33389
Microcomputer controlled image processor
[AD-D011734] 22 p3833 N85-33735

TRANSONIC AIRCRAFT
U SUPERSONIC AIRCRAFT

TRANSONIC COMPRESSORS
A finite element method for the solution of two-dimensional transonic flows in cascades
[PNR-90216] 03 p0316 N85-12045
Study of controlled diffusion stator blading
[NASA-CR-167995] 09 p1281 N85-18058

TRANSONIC FLIGHT
Joined wing transonic design and test validation
[AD-A148355] 08 p1078 N85-16834
Experiences with transition fixation in the high-speed regime at NLR 14 p2211 N85-23715
Design of a basic airfoil for a slightly swept wing. Part 1: Theoretical transonic airfoil design
[ESA-TT-892] 20 p3394 N85-31054

TRANSONIC FLOW
An experimental study of the transonic equivalence rule with lift, part 2
[AR-LR-614-PT-2] 01 p0001 N85-10004
Development and applications of algorithms for calculating the transonic flow about harmonically oscillating wings
[NASA-CR-172376] 01 p0002 N85-10007
Computational methods for complex flowfields
[AD-A145219] 01 p0004 N85-10019
Transonic flow analysis for rotors. Part 1: Three-dimensional quasi-steady, full-potential calculation
[NASA-TP-2375-PT-1] 02 p0134 N85-10914
Further development of a transonic cascade analysis
[AD-A145410] 02 p0196 N85-11319
Inverse design technique for cascades
[NASA-CR-3838] 03 p0311 N85-12008
Performance of two transonic airfoil wind tunnels utilizing limited ventilation 03 p0313 N85-12020
Experiments suitable for wind tunnel wall interference assessment/correction 03 p0313 N85-12021
Development in UK of a method for calculating tunnel wall corrections from flow measurements 03 p0314 N85-12026
Design of a basic airfoil for a slightly swept wing. Part 1: Theoretical transonic airfoil design
[DFVLR-FB-84-19-PT-1] 03 p0316 N85-12043
A finite element method for the solution of two-dimensional transonic flows in cascades
[PNR-90216] 03 p0316 N85-12045
Investigations of boundary layers in the Emmen Federal Aircraft works transonic tunnel, Switzerland
[FW-FO-1641] 04 p0453 N85-12877
Comparative flow calculation on transonic cone/cylinder standard models in connection with the wall interference problem
[FW-FO-1689] 04 p0453 N85-12878
A local slot boundary condition for transonic flow calculations in slotted-wall test sections of wind tunnels
[FFA-TN-1984-34] 04 p0453 N85-12879
Investigation for the improvement of the transonic tunnel working section of the Emmen Federal Aircraft Works (Switzerland)
[FW-FO-1661] 04 p0458 N85-12904
Simulation of separated transonic airfoil flow by finite-difference viscous-inviscid interaction 05 p0591 N85-13768
The numerical simulation of steady transonic rotational flow using a dual potential formulation 05 p0591 N85-13770
Experimental studies of transonic airfoil trailing edge and wake flowfield properties 05 p0592 N85-13773
Transonic jets: A numerical approach in the hodograph plane 05 p0592 N85-13774
Navier-Stokes computational study of axisymmetric transonic turbulent flows with a two-equation model of turbulence 05 p0634 N85-14068
Development of the code NSFOIL for analyzing high Reynolds number transonic flow around an airfoil
[NAL-TR-816] 06 p0749 N85-14801
A theoretical design method for 3-dimensional transonic wings
[NAL-TR-830] 06 p0754 N85-14834
Transonic flow of elastic medium past slender solid body 06 p0778 N85-14976
Review of requirements and status of simulation and scaling of transonic, viscous flows
[AD-A146357] 06 p0808 N85-15137
A comparative study of the nonuniqueness problem of the potential equation
[NASA-TP-2385] 07 p0898 N85-15684
An exploratory study of finite difference grids for transonic unsteady aerodynamics
[NASA-TM-84583] 07 p0899 N85-15696
A method for solving the inverse problem of transonic cascade flow
[AD-A146739] 07 p0899 N85-15698
Transonic shock interaction with a tangentially-injected turbulent boundary layer 08 p1072 N85-16796
Shock waves in transonic flows at moderate Reynolds Number 08 p1076 N85-16823
Vectorizable multigrid algorithms for transonic flow calculations
[NASA-CR-174326] 08 p1077 N85-16827
Research into topics in transonic flow theory
[AD-A148526] 08 p1078 N85-16837
Theoretical contributions to transonic flow analysis for transport aircraft
[BMFT-FB-W-84-036] 08 p1078 N85-16838
Analysis of inviscid transonic flow around an airfoil by diagonal form of IAF scheme
[NAL-TR-831] 10 p1420 N85-18955
Effects of airfoil shape, thickness, camber, and angle of attack on calculated transonic unsteady airloads
[NASA-TM-86320] 10 p1420 N85-18957
Efficient self-consistent viscous-inviscid solutions for unsteady transonic flow
[NASA-TM-86335] 10 p1420 N85-18959
Unsteady transonic flow calculations for two-dimensional canard-wing configurations with aeroelastic applications
[NASA-TM-86375] 10 p1420 N85-18960
Viscous effects on transonic airfoil stability and response
[NASA-TM-86374] 10 p1421 N85-18961
Unsteady transonic pressure measurements on a semispan wind-tunnel model of a transport-type supercritical wing (Lann model). Part 2: Pressure distributions (plotted) and plots of the vibration modes
[AD-A130488] 10 p1421 N85-18965
Contribution to the study of a numerical implicit method for solving the Euler equations
[ESA-TT-872] 10 p1549 N85-19771
A fast algorithm of the finite difference method for computation of the transonic flow past an arbitrary airfoil with the conservative full-potential equation 11 p1619 N85-20191
A mixed finite difference analysis of the internal and external transonic flow fields of inlets with centerbody 11 p1619 N85-20192
A locally linearized panel method for tran-/subsonic flow past an oscillating wing 11 p1622 N85-20212
Transonic pressure distribution computations of a flexible wing 11 p1622 N85-20213
On relaxation of transonic flows around zero-lift airfoils and convergence of self-correcting wing tunnels 11 p1622 N85-20214
Finite difference computation of the flow around airfoils in two-dimensional transonic slotted wall wind tunnel 11 p1623 N85-20216
Reconstruction of a 3-dimensional transonic rotor flow field from holographic interferogram data
[NASA-TM-86690] 12 p1770 N85-21112
Transonic interactions of unsteady vortical flows
[NASA-TM-86658] 12 p1770 N85-21113
Measured unsteady transonic aerodynamic characteristics of an elastic supercritical wing with an oscillating control surface
[NASA-TM-86376] 12 p1771 N85-21116
Pseudospectral calculations of two-dimensional transonic flow (Task 1). Numerical investigation of VTOL aerodynamics (Task 2)
[AD-A150123] 12 p1772 N85-21126
Unsteady transonic pressure measurements on a semi-span wind-tunnel model of a transport-type supercritical wing (Lann model). Part 2: Pressure distributions (plotted) and plots of the vibration modes
[AD-A130488] 12 p1846 N85-21579
Robust calculation of three-dimensional transonic potential flow based on the nonlinear gas multigrid method and a mixed incomplete lower upper decomposition/strongly implicit procedure (ILU/SIP) algorithm
[NLR-MP-84003-U] 12 p1848 N85-21593
Preliminary development of an approximation procedure for supercritical wing design optimization applications
[AD-A150177] 13 p1972 N85-22383
F-14A aircraft high-speed flow simulations
[NASA-CR-172559] 14 p2209 N85-23702
Calibration of sonic valves for the laminar flow control, leading-edge flight test
[NASA-TP-2423] 14 p2210 N85-23707
Recent transonic unsteady pressure measurements at the NASA Langley Research Center
[NASA-TM-86408] 14 p2210 N85-23710
The influence of transition strips on the pressure distribution on transonic profiles 14 p2212 N85-23716
Transition fixing and simulation of high Reynolds number flow at transonic velocities 14 p2212 N85-23721
Transonic merging separated flows
[AD-A150867] 14 p2213 N85-23724
Calculation of an unsteady transonic flow with shock waves and separation in Laval nozzles
[MPIS-14/1984] 14 p2213 N85-23728
Application possibilities of laser Doppler anemometry in the investigation of the transonic interaction between shock wave and boundary layer
[ISL-R-131/83] 14 p2304 N85-24265
Transonic Unsteady Aerodynamics and its Aeroelastic Applications
[AGARD-CP-374] 15 p2457 N85-25171
Transonic pressure distributions on a two-dimensional 0012 and supercritical MBB-A3 profile oscillating in heave and pitch 15 p2457 N85-25173
Numerical studies of unsteady transonic flow over oscillating airfoil 15 p2458 N85-25174
Analysis of transonic aerodynamic characteristics for a supercritical airfoil oscillating in heave, pitch and with oscillating flap 15 p2458 N85-25175
Calculation of harmonic aerodynamic forces of aerofoils and wings from the Euler equations 15 p2458 N85-25177

Calculation of unsteady transonic separated flows by viscous-inviscid interaction 15 p2458 N85-25178
A semi-empirical unsteady transonic method with supersonic free stream 15 p2458 N85-25179
Improvement and extension of a numerical procedure for the three dimensional unsteady transonic flows 15 p2459 N85-25181
Application of time-linearized methods to oscillating wings in transonic flow and flutter 15 p2459 N85-25182
Computation of unsteady transonic flows about two-dimensional and three-dimensional AGARD standard configurations 15 p2459 N85-25183
Calculation of unsteady transonic flow around a high swept wing 15 p2459 N85-25184
Unsteady transonic aerodynamic and aeroelastic calculations about airfoils and wings 15 p2459 N85-25185
The development of unsteady transonic 3-D full potential code and its aeroelastic applications 15 p2460 N85-25187
A new implicit plus minus splitting method for the solution of the Euler equations in the transonic flow regime 15 p2461 N85-25200
Transonic aerodynamic and aeroelastic characteristics of a variable sweep wing
[NASA-TM-86677] 15 p2462 N85-25203
Numerical analyses in aerodynamic design of aero-engine fan 16 p2692 N85-26618
Numerical example of three-dimensional flying object in shockless transonic flow 16 p2693 N85-26623
A numerical design method for three-dimensional transonic wings 16 p2694 N85-26631
Description of a computer program treating transonic steady state aeroelastic effects for a canard or tail airplane
[FFA-TN-1983-23] 16 p2700 N85-26674
Measurements of the symmetric aerodynamic coefficients for flat faced cylinders in the angle of attack regime 0 to 90 deg for transonic and supersonic speeds
[FFA-TN-1984-04] 16 p2700 N85-26675
Numerical solution of transonic normal shock wave-boundary layer interaction using the Bohning-Zierep model — wind tunnel flow
[VTH-LR-416] 16 p2701 N85-26683
Numerical study of porous airfoils in transonic flow
[NASA-TM-86713] 17 p2892 N85-27828
Transonic Mach number determination in a blow-down wind tunnel with solid walls and a downstream throat
[VTH-LR-402] 17 p2893 N85-27835
Navier-Stokes computational study of axisymmetric transonic turbulent flows with a two-equation model of turbulence
[AD-A152653] 17 p2958 N85-28265
Proceedings of the 9th US Air Force and the Federal Republic of Germany Data Exchange Agreement Meeting, Viscous and Interacting Flow Field Effects
[AD-A153020] 17 p2958 N85-28266
Subsonic and transonic aerodynamics of a wraparound fin configuration
[AD-A153646] 18 p3059 N85-28927
Flow quality of National Aerospace Laboratory two-dimensional transonic wind tunnel. Part 3: Flow turbulence level and measuring method
[NAL-TR-842-PT-3] 18 p3064 N85-28952
Hyperbolic phenomena in the flow of viscoelastic fluids
[AD-A153533] 18 p3099 N85-29186
Inviscid analysis of two supercritical laminar-flow-control airfoils at design and off-design conditions
[NASA-TM-84657] 19 p3212 N85-29920
Unsteady transonic flow calculations for interfering lifting surface configurations
[NASA-TM-86432] 19 p3214 N85-29931
Selected topics in experimental aeroelasticity at the NASA Langley Research Center
[NASA-TM-86436] 19 p3284 N85-30364
Floating shock-fitting in transonic potential flow calculations 20 p3367 N85-31007
Calculation of transonic flows around an aircraft configuration with motorized nacelle
[SNIAS-851-111-106] 20 p3367 N85-31008
Transonic calculations for a flexible supercritical wing and comparison with experiment
[NASA-TM-86439] 20 p3368 N85-31012
Numerical simulation of potential flow in transonic steady regimes 20 p3369 N85-31016
Data set 9: LANN wing. Pitching oscillation 20 p3390 N85-31030
The application of laser anemometry to the study of transonic shock boundary-layer interactions
[ISL-CO-204/84] 20 p3396 N85-31057
R and D activities of the Aerodynamics Division 20 p3539 N85-32023
Calculation of transonic steady and oscillatory pressures on a low aspect ratio model and comparison with experiment
[NASA-TM-86449] 21 p3551 N85-32092
Notes on unsteady transonic cascade flows
[AD-A154829] 21 p3552 N85-32096
Design of a generator for near-tangential transonic swirling outflow
[AD-A155163] 21 p3584 N85-32280
An elliptic calculation procedure for 3-D viscous flow 21 p3587 N85-32297
Exact solutions of singular equations for viscous transonic flows 21 p3683 N85-32882
Integral equation formulation for three-dimensional unsteady transonic flow
[ARL/STRUC-R-416] 23 p3894 N85-34119
A review of spectral methods
[NASA-CR-172502] 23 p3929 N85-34350
Unsteady transonic heat transfer in a transient facility
[NASA-CR-176145] 23 p3930 N85-34354
System maintenance manual for master modeling of aerodynamic surfaces by three-dimensional explicit representation
[NASA-CR-178224] 23 p3956 N85-34517
A stream function approach to solving the conservative Euler equations for transonic flows 24 p4059 N85-35156
Numerical studies of 2-dimensional flows
[NASA-CR-3930] 24 p4060 N85-35160

TRANSONIC FLUTTER
Experimental study on transonic flutter characteristics of sweptback wing with core composite plates having different fiber orientations
[NAL-TR-827] 06 p0756 N85-14842
A study of transonic flutter of a two-dimensional airfoil using the U-g and p-k methods
[LR-615] 12 p1771 N85-21121
Experience with transonic unsteady aerodynamic calculations 15 p2458 N85-25178
A semi-empirical unsteady transonic method with supersonic free stream 15 p2458 N85-25179
A study of transonic flutter of a two-dimensional airfoil using the U-g and p-k methods
[AD-A151463] 15 p2473 N85-25268
Numerical simulation of transonic flutter of a high-aspect ratio transport wing 16 p2694 N85-26630
Selected topics in experimental aeroelasticity at the NASA Langley Research Center
[NASA-TM-86436] 19 p3284 N85-30364
Verification of calculation methods for unsteady airloads in the precipitation of transonic flutter
[NLR-MP-84016-U] 20 p3390 N85-31027

TRANSONIC INLETS
U SUPERSONIC INLETS

TRANSONIC SPEED
Effect of upstream sidewall boundary layer removal on an airfoil test — conducted in Langley 0.3-m transonic cryogenic tunnel 03 p0313 N85-12019
Asymptotic methods for wind tunnel wall corrections at transonic speed 03 p0313 N85-12022
Effect of a variable camber and twist wing at transonic Mach numbers
[NASA-TM-86281] 04 p0452 N85-12869
Prediction of cruciform all-movable control characteristics at transonic speeds
[AD-A147291] 08 p1078 N85-16832
On detached shock wave of sphere moving with transonic velocities 11 p1622 N85-20215
Analysis of unsteady pressure measurements on a supercritical airfoil with a harmonically oscillating trailing edge flap at subsonic and transonic speeds
[DFVLR-FB-84-49] 17 p2893 N85-27837
Flow quality of National Aerospace Laboratory two-dimensional transonic wind tunnel. Part 3: Flow turbulence level and measuring method
[NAL-TR-842-PT-3] 18 p3064 N85-28952
An experimental investigation of propfan installations on an upswept supercritical wing at transonic Mach numbers
[NASA-CR-172605] 20 p3368 N85-31013
Development of a temperature-compensated hot-film anemometer system for boundary-layer transition detection on high-performance aircraft
[NASA-TM-86732] 22 p3730 N85-33121

TRANSONIC WIND TUNNELS
Pressure distributions measured on research wing M100 mounted on an axisymmetric body 01 p0004 N85-10023
Pressure distributions measured on research wing M86 mounted on an axisymmetric body 01 p0004 N85-10024
The data processing system of the NAL 2m x 2m transonic wind tunnel
[NAL-TR-811] 01 p0012 N85-10075
Computations for the 16-foot transonic tunnel, NASA, Langley Research Center
[NASA-TM-86319] 02 p0149 N85-11009
Wind Tunnel Wall Interference Assessment and Correction, 1983
[NASA-CP-2319] 03 p0311 N85-12011
Wall interference measurements for three-dimensional models in transonic wind tunnels: Experimental difficulties 03 p0311 N85-12012
Survey of ONERA activities on adaptive-wall applications and computation of residual corrections 03 p0312 N85-12013
Two- and three-dimensional model and wall data from a flexible-walled transonic test section 03 p0312 N85-12015
Assessment of lift- and blockage-induced wall interference in a three-dimensional adaptive-wall tunnel 03 p0312 N85-12016
A data base for three-dimensional all-interference code evaluation 03 p0312 N85-12017
Investigations of flow field perturbations induced on slotted transonic-tunnel walls 03 p0312 N85-12018
Review of the advanced technology airfoil test program in the 0.3-meter transonic cryogenic tunnel 03 p0315 N85-12033
Some experience with Barnwell-Sewall type correction to two-dimensional airfoil data 03 p0315 N85-12034
Adaptation of a four-wall interference assessment/correction procedure for airfoil tests in the 0.3-m TCT 03 p0315 N85-12035
Parametric determination of blockage interference of 3-dimensional models in the Emmen Federal Aircraft works transonic tunnel (Switzerland)
[FW-FO-1636] 04 p0453 N85-12876
Investigation for the improvement of the transonic tunnel working section of the Emmen Federal Aircraft Works (Switzerland)
[FW-FO-1681] 04 p0456 N85-12904
Description of the insulation system for the Langley 0.3-Meter Transonic Cryogenic Tunnel
[NASA-TM-86274] 07 p0909 N85-15755
Flow quality of NAL 2-dimensional transonic wind tunnel. Part 2: Extensive and systematic pressure fluctuations study in the settling chamber, test section and second throat of the NAL 2-D transonic wind tunnel
[NAL-TR-836-PT2] 09 p1283 N85-18066
The S2MA wind tunnel at the Modane-Avrieux aerodynamic test center
[ESA-TT-862] 09 p1284 N85-18071
Aeronautical facilities catalogue. Volume 1: Wind tunnels
[NASA-RP-1132] 10 p1426 N85-18991
Finite difference computation of the flow around airfoils in two-dimensional transonic slotted wall wind tunnel 11 p1623 N85-20216
Exploratory flutter test in a cryogenic wind tunnel
[NASA-TM-86380] 12 p1863 N85-21689
Calibration of wind tunnel flow quality 13 p1976 N85-22399
Harbin's subsonic, transonic wind tunnel detailed 14 p2283 N85-24143
Measurements in the flow field of a cylinder with a laser transit anemometer and a drag rake in the Langley 0.3 m transonic cryogenic tunnel
[NASA-TM-86399] 14 p2305 N85-24270
Mathematical modeling of the AEDC (Arnold Engineering Development Center) propulsion wind tunnel (16T)
[AD-A151293] 15 p2475 N85-25275
Investigation to optimize the passive shock wave/boundary layer control for supercritical airfoil drag reduction
[NASA-CR-175788] 16 p2699 N85-26665
A curved test section for research on transonic shock wave-boundary layer interaction
[VTH-LR-414] 16 p2701 N85-26682
Study on needs for a magnetic suspension system operating with a transonic wind tunnel
[NASA-CR-3900] 16 p2715 N85-26759
Design of a basic profile for a low sweep airfoil. Part 2: Experimental investigation on the DFVLR-W1 airfoil profile in the Brunswick transonic wind tunnel
[DFVLR-FB-85-01-PT-2] 17 p2892 N85-27833
Transonic Mach number determination in a blow-down wind tunnel with solid walls and a downstream throat
[VTH-LR-402] 17 p2893 N85-27835
Flow quality of National Aerospace Laboratory two-dimensional transonic wind tunnel. Part 3: Flow turbulence level and measuring method
[NAL-TR-842-PT-3] 18 p3064 N85-28952
On power effecient operation of the 2m x 2m transonic wind tunnel at the National Aerospace Laboratory
[NAL-TR-847] 18 p3064 N85-28953
High Reynolds number tests of a NASA SC(3)-0712(B) airfoil in the Langley 0.3-meter transonic cryogenic tunnel
[NASA-TM-86371] 19 p3213 N85-29926

Transonic and supersonic wind tunnel tests on control effectiveness on schematic missile configurations
[FFA-TN-1983-20] 20 p3389 N85-31020
Transonic and supersonic wind tunnel tests on control effectiveness on schematic missile configurations: Supplement
[FFA-TN-1983-20-SUPPL] 20 p3389 N85-31021
Sidewall boundary-layer effects in two-dimensional airfoil testing
[NASA-CR-176034] 20 p3396 N85-31065

TRANSONICS
U TRANSONIC FLOW

TRANSPARENCE
Method for measuring haze in transparencies
[AD-D011233] 01 p0120 N85-10823
Effect of aberration in optical system on illuminance distribution over image of strip in semicoherent light 06 p0777 N85-14970
Evaluation of colorless polyimide film for thermal control coating applications
[NASA-TM-86341] 07 p0930 N85-15894
Demonstration of transparent solar array module design
[NASA-CR-174257] 07 p0992 N85-16302
Aircraft transparency bird impact analysis using the MAGNA computer program
[AD-P004186] 11 p1579 N85-19948
Process for preparing essentially colorless polyimide film containing phenoxy-linked diamines
[NASA-CASE-LAR-13353-1] 11 p1611 N85-20128
Process for preparing highly optically transparent-colorless aromatic polyimide film
[NASA-CASE-LAR-13351-1] 12 p1811 N85-21360
Progress on transparent yttria
[AD-P004370] 12 p1827 N85-21464
Effect of transparent coatings on generation of laser-induced shock waves in metals 13 p2026 N85-22711
Nonuniform interference coatings with thickness-dependent refractive index 14 p2281 N85-24131
Error in laser correlation wind speed meters resulting from variable atmospheric transparency 14 p2338 N85-24457
Choice of optimum pairs of spectral intervals for IR-range survey of Earth's surface 15 p2486 N85-25344
Measurement of ultrasonic fields in transparent media using a scanning differential interferometer
[NASA-CR-175921] 17 p3028 N85-28726
Light transmitting window assembly
[NASA-CASE-MSC-18417-1] 18 p3185 N85-29750
Optical stability, atmospheric transparency and aerosol absorption 19 p3297 N85-30442
The measurement of aircraft windscreen haze and its effect on visual performance
[AD-A154949] 21 p3555 N85-32114
Transparency of water 9n 186 - 500 nm region 21 p3690 N85-32923
Digital holographic synthesis of pattern-forming transparencies for ring antenna arrays 22 p3763 N85-33326
Implicit Monte Carlo methods and non-equilibrium Marshak wave radiative transport
[DE85-010711] 22 p3835 N85-33743

TRANSPARENT MATERIALS
U TRANSPARENCE

TRANSPIRATION
Study of deposition control using transpiration
[DE85-002339] 10 p1485 N85-19378
Study of deposition control using transpiration
[DE85-003463] 11 p1585 N85-19964
Pressure drop and coefficients of internal heat transfer necessary for transpiration cooling 13 p2050 N85-22831
Small gas turbine combustor study: Fuel injector performance in a transpiration-cooled liner
[NASA-TM-86989] 15 p2473 N85-25264
Study of a constricted electric arc cooled by transpiration
[NASA-TM-77846] 17 p3038 N85-28798

TRANSPIRATION COOLING
U SWEAT COOLING

TRANSPLANTATION
The EM algorithm for censored data
[AD-A148136] 08 p1212 N85-17026

TRANSPONDERS
Investigation of the ice dynamics in the marginal ice zone
[AD-A146729] 07 p1009 N85-16411
Margin leveling algorithm for fully saturated satellite transponder with CDMA (Code Division Multiple Access) signalling
[AD-A151710] 15 p2543 N85-25699
Channel multiplexers for broadcast satellite transponders in the 12 GHz band
[NHK-LABS-NOTE-310] 18 p3090 N85-29122
Performance interface document for the S-band diplexer for space users of NASA networks
[NASA-TM-86224] 23 p3900 N85-34155

TRANSPORT AIRCRAFT
NT A-310 AIRCRAFT
NT A-320 AIRCRAFT
NT ALADIN 2 AIRCRAFT
NT BOEING 727 AIRCRAFT
NT BOEING 737 AIRCRAFT
NT BOEING 747 AIRCRAFT
NT BOEING 767 AIRCRAFT
NT C-5 AIRCRAFT
NT C-135 AIRCRAFT
NT C-141 AIRCRAFT
NT CARGO AIRCRAFT
NT CH-47 HELICOPTER
NT CONCORDE AIRCRAFT
NT DC 8 AIRCRAFT
NT DC 9 AIRCRAFT
NT DC 10 AIRCRAFT
NT DHC 2 AIRCRAFT
NT EUROPEAN AIRBUS
NT F-27 AIRCRAFT
NT L-1011 AIRCRAFT
NT UH-60A HELICOPTER
Design of a digital ride quality augmentation system for commuter aircraft
[NASA-CR-172419] 01 p0006 N85-10037
Analysis of a transport fuselage section drop test 01 p0060 N85-10400
Experimental trim drag values and flow-field measurements for a wide-body transport model with conventional and supercritical wings
[NASA-TP-2071] 02 p0135 N85-10920
Advanced composite stabilizer for Boeing 737 aircraft
[NASA-CR-168451] 02 p0137 N85-10934
Aircraft surface coatings
[NASA-CR-3661] 02 p0137 N85-10935
Simulator study of flight characteristics of several large, dissimilar, cargo transport airplanes during approach and landing
[NASA-TP-2357] 02 p0148 N85-11002
Integrated Application of Active Controls (IAAC) technology to an advanced subsonic transport project-longitudinal handling qualities study of a relaxed-stability airplane
[NASA-CR-3660] 02 p0148 N85-11005
Design of a basic airfoil for a slightly swept wing. Part 1: Theoretical transonic airfoil design
[DFVLR-FB-84-19-PT-1] 03 p0316 N85-12043
Flutter parametric studies of cantilevered twin-engine-transport type wing with and without winglet. Volume 1: Low-speed investigations
[NASA-CR-172410-VOL-1] 04 p0513 N85-13259
Flight test results on stall characteristics of a large jet transport
[NAL-TR-817] 06 p0754 N85-14835
Integrated Application of Active Controls (IAAC) technology to an advanced subsonic transport project. ACT/Control/Guidance System study, volume 1
[NASA-CR-165963-VOL-1] 06 p0754 N85-14837
Integrated Application of Active Controls (IAAC) technology to an advanced subsonic transport project. ACT/Control/Guidance System study. Volume 2: Appendices
[NASA-CR-165963-VOL-2] 06 p0754 N85-14838
Ground-effect analysis of a jet transport airplane
[NASA-TM-85920] 07 p0897 N85-15687
Integrated technology wing study (oral presentation)
[NASA-CR-169497] 07 p0902 N85-15718
Design and test requirements for development of today's engines 07 p0906 N85-15737
Documentation and separate test program development is most important for test/maintenance 08 p1065 N85-16745
Aerodynamic issues in the design of high-lift systems for transport aircraft 08 p1069 N85-16780
Technology developments for laminar boundary layer control on subsonic transport aircraft 08 p1071 N85-16787
Theoretical contributions to transonic flow analysis for transport aircraft
[BMFT-FB-W-84-036] 08 p1078 N85-16836
The visibility climatology of McMurdo Sound-Williams Field, Antarctica
[AD-A148108] 08 p1180 N85-17492
Initiative uses of aircraft for flight training 09 p1277 N85-18027
Review of engine ingestions to wide body transport aircraft
[AD-P004185] 11 p1579 N85-19947
New runway enables IL-76 flights to Tenkeli in far north 12 p1760 N85-21106
Integrated paratroop door
[AD-D011507] 12 p1776 N85-21148
Analytically redundant output feedback scheme for reduction of structural loads of a flexible transport aircraft
[TT-8303] 12 p1777 N85-21154
Guidance and control research flight testing with HFB 320 test aircraft 13 p1967 N85-22356
Study for the optimization of a transport aircraft wing for maximum fuel efficiency. Volume 1: Methodology, criteria, aeroelastic model definition and results
[NASA-CR-172551] 13 p1971 N85-22378
China report: Science and technology
[JPRS-CST-84-009] 13 p1972 N85-22384
Improved Y-11 general-purpose transport designated Y-12 13 p1972 N85-22385
Assessing the behavior and performance of teams in organizations: The case of air transport crews
[AD-A150359] 13 p2143 N85-23902
Experiences with transition fixation in the high-speed regime at NLR 14 p2211 N85-23715
Demonstration of relaxed stability on a commercial transport 16 p2713 N85-26745
Realisation of relaxed static stability on a commercial transport 16 p2713 N85-26746
Wing buffeting active control testing on a transport aircraft configuration in a large sonic tunnel 16 p2714 N85-26750
How to handle failures in advanced flight control systems of future transport aircraft 16 p2714 N85-26752
Methods for design aerodynamics of modern transport aircraft
[DFVLR-FB-85-05] 17 p2893 N85-27836
Friction and wear behavior of aluminum and composite I-beam stiffened airplane skins
[NASA-TM-86416] 17 p2895 N85-27852
Demonstration of relaxed static stability on a commercial transport 17 p2903 N85-27896
Realisation of relaxed static stability on a commercial transport 17 p2903 N85-27899
Wing buffeting active control testing on a transport aircraft configuration in a large sonic windtunnel 17 p2904 N85-27903
How to handle failures in advanced flight control systems of future transport aircraft 17 p2904 N85-27905
Advanced secondary power system for transport aircraft
[NASA-TP-2483] 18 p3062 N85-29044
Pressure distribution data from tests of 2.29 M (7.5 feet) span EET high-lift transport aircraft model in the Ames 12-foot pressure tunnel
[NASA-TM-84517] 19 p3211 N85-29912
Nacelle/pylon/wing integration on a transport model with a natural laminar flow nacelle
[NASA-TP-2439] 19 p3213 N85-29924
Crew systems and flight station concepts for a 1995 transport aircraft
[NASA-CR-166068] 19 p3221 N85-29973
Low-speed tests of a high-aspect-ratio, supercritical-wing transport model equipped with a high-lift flap system in the Langley 4- by 7-meter and Ames 12-foot pressure tunnels
[NASA-TP-2097] 20 p3388 N85-31010
Seat experiments for the full-scale transport aircraft controlled impact demonstration
[AD-A155024] 21 p3553 N85-32106
Energy efficient transport technology: Program summary and bibliography
[NASA-RP-1135] 22 p3729 N85-33116
Application of frequency domain handling qualities criteria to the longitudinal landing task
[NASA-TM-86729] 22 p3730 N85-33124
Development of an energy-absorbing passenger seat for a transport aircraft 22 p3796 N85-33515
Guidelines for the evaluation of visual approach slope indicators
[ARL/SYS-R-32] 23 p3896 N85-34132
Ground-based and in-flight simulator studies of flight characteristics of a twin-fuselage passenger transport airplane during approach and landing
[NASA-TP-2451] 23 p3898 N85-34144

TRANSPORT COEFFICIENTS
U TRANSPORT PROPERTIES

TRANSPORT PROPERTIES
NT ATMOSPHERIC CONDUCTIVITY
NT CARRIER MOBILITY
NT DIFFUSION COEFFICIENT
NT EDDY VISCOSITY
NT ELECTRICAL RESISTIVITY
NT ELECTRON MOBILITY
NT GAS VISCOSITY
NT GASEOUS DIFFUSION
NT GASEOUS SELF-DIFFUSION
NT HOLE MOBILITY
NT IONIC MOBILITY
NT IONOSPHERIC CONDUCTIVITY
NT KONDO EFFECT
NT MAGNETORESISTIVITY

NT PHOTOCONDUCTIVITY
NT PLASMA CONDUCTIVITY
NT SUPERCONDUCTIVITY
NT THERMAL CONDUCTIVITY
NT THERMAL DIFFUSIVITY
NT VISCOSITY
Plasma surface interactions in magnetic fusion systems
[DE84-015255] 01 p0123 N85-10642
Transport properties of multiphase systems
[DE84-015560] 02 p0173 N85-11159
Electrocatalysis of fuel cell reactions: Investigation of alternate electrolytes
[NASA-CR-174753] 02 p0222 N85-11455
Diffusion and intermittency in an extended one-dimensional maps 02 p0282 N85-11834
Stochasticity and transport in Hamiltonian systems 02 p0282 N85-11836
Fundamental electronic properties of donor-type graphite intercalated compounds
[AD-A146148] 03 p0326 N85-12069
Electrochemical and surface science research on fuel cells
[DE84-015962] 03 p0359 N85-12307
Static and quasielastic neutron scattering for the investigation of structure, dynamics and transport properties of lipid layers and lipid/protein compounds 03 p0432 N85-12753
Novel transport and recombination processes in semiconductors
[AD-A145969] 03 p0433 N85-12757
Transport processes during the growth of oxide films at elevated temperature
[AERE-R-11293] 03 p0434 N85-12766
High temperature thermoelectric energy conversion 05 p0610 N85-13694
Three dimensional global modeling of atmospheric CO2 05 p0652 N85-14189
Transport and relaxation processes in supercritical fluids
[DE84-006591] 05 p0731 N85-14608
Pathology and axonal transport in hexacarbon neuropathies
[AD-P004021] 06 p0843 N85-15355
Electronic transport processes in refractory metal silicides
[AD-A146495] 06 p0861 N85-15468
Preparation and electronic properties of MoS(2) and WS(2) single crystals grown in the presence of cobalt
[AD-A146508] 06 p0866 N85-15506
Strained-layer superlattice emitter and detector structures using modulation-doped active regions
[DE85-000064] 06 p0867 N85-15511
Anomalous electronic transport in boron carbides
[DE84-015620] 06 p0868 N85-15518
Transport properties and distribution functions in 3-5 semiconductors
[AD-A147525] 07 p1049 N85-16660
Computer program for calculation of complex chemical equilibrium compositions and applications. Supplement 1: Transport properties
[NASA-TM-86885] 07 p1049 N85-16663
Application of electrochemical engineering methods and theory to solving corrosion and adhesion problems with organic coatings
[AD-A147799] 08 p1129 N85-17115
The fundamentals of dislocation transport of hydrogen in bcc iron
[AD-A148143] 08 p1129 N85-17117
A research proposal for the theoretical study of the thermodynamic and transport properties of dense plasmas
[AD-A148040] 08 p1224 N85-17706
Resistivity of alloys
[DE85-000906] 09 p1296 N85-18138
Analysis of geohydrologic data by kriging
[AD-P004152] 09 p1349 N85-18486
Ionic and molecular transport in beta- and beta''-alumina
[DE85-000984] 09 p1360 N85-18680
Transport experiments in the Texas experimental Tokamak 09 p1389 N85-18741
Transport relaxation processes in supercritical fluids
[DE85-002076] 09 p1398 N85-18798
Transport properties of the outer crust of magnetic neutron stars 09 p1415 N85-18927
Finite-(beta) optimization of tandem mirrors
[DE85-002658] 10 p1560 N85-19635
Transport processes in the upper atmosphere 11 p1648 N85-20375
MCNP code
[DE85-002565] 11 p1702 N85-20705
TRACRSD: A model of flow and transport in porous/fractured media
[LA-9667-MS] 12 p1845 N85-21576
ELECT groundwater transport research code
[DE85-003284] 12 p1884 N85-21824
Stochastic convective-dispersive transport model for wastes disposed at the 106-mile ocean disposal site
[PB85-116176] 12 p1885 N85-21831
SS-3 ONR-116 data analysis
[AD-A149725] 12 p1889 N85-21855
User's guide for TWOHEX: A code package for two-dimensional, neutral-particle transport in equilateral triangular meshes
[DE85-004462] 12 p1930 N85-22125
The ASCOT Data Analysis Workshop
[DE85-004407] 13 p2139 N85-23263
Electrical and thermal transport property studies of high-temperature thermoelectric materials
[AD-A150167] 13 p2163 N85-23417
Transport properties of silica thermally grown on silicon
[AD-A150304] 13 p2163 N85-23418
Ion transporting composite membranes. 1: Nafion impregnated gore-tex
[AD-A151020] 14 p2252 N85-23960
Electrical and thermal transport property studies of high-temperature thermoelectric materials
[AD-A150900] 14 p2427 N85-24967
Transport studies of several novel organic conductors
[DE85-003950] 14 p2429 N85-24979
Experimental check of ion transport mechanism in Earth's radiation belt with exposure to nonsteady-state electric fields 15 p2480 N85-25308
Two-phase fluid thermal transport for spacecraft
[AD-A151316] 15 p2493 N85-25376
Mixing across a gas-gas interface
[AD-A151471] 15 p2556 N85-25770
Development of algorithms for using satellite meteorological data sets to study global transport of stratospheric aerosols and ozone
[NASA-CR-172540] 15 p2591 N85-25974
Polyamines as possible modulators of gravity induced calcium transport in plants 15 p2606 N85-26060
Electrical resistivity in amorphous metals: Consequences of phonon ineffectiveness in the diffraction model
[AD-A152130] 16 p2779 N85-27150
Computer program for the calculation of multicomponent convective diffusion deposition rates from chemically frozen boundary layer theory
[NASA-CR-168329] 16 p2781 N85-27164
Coupled plasma-neutral transport model for the scrape-off region
[DE85-007550] 16 p2868 N85-27695
Polycrystalline semiconductor heterojunction modelling (CdS/CuInSe(sub)2)
[DE85-002913] 16 p2871 N85-27713
Variability of short term eddy-correlation estimates of mass exchange
[PB85-172841] 18 p3138 N85-29431
Turbulent transport and length scale measurement experiments with confined coaxial jets
[NASA-CR-174831] 19 p3265 N85-30245
Transport properties of Topopah Spring tuff
[DE85-010448] 19 p3270 N85-30278
Sand dispersion from an ephemeral river delta on the wave-dominated central California coast
[AD-A154352] 19 p3300 N85-30458
Monte Carlo electron/photon transport
[DE85-010799] 19 p3364 N85-30661
Hadley circulation in planetary atmospheres 20 p3546 N85-32067
Silicon refinement by chemical vapor transport 21 p3609 N85-32412
Influence of chemical form, feeding regimen, and animal species on the gastrointestinal absorption of plutonium
[DE85-010291] 21 p3682 N85-32751
Electrotransport in thin films
[AD-A155584] 21 p3710 N85-33034
The relation between the age of the subconducting slab and the recycling of sediments into the mantle 21 p3717 N85-33063
Comments on two matters related to turbulent combustion 22 p3743 N85-33204
New and revised methods of purifying mercuric iodide
[DE85-011684] 22 p3749 N85-33237
Estimation of Sr90 and Cs137 activity introduced and accumulation in the Po basin until 1983
[CISE-2515] 22 p3813 N85-33617
Subduction zone tectonic studies to develop concepts for the occurrence of sediment subduction
[DE85-011794] 22 p3815 N85-33632
Nuclear data for MCNP
[DE85-010794] 22 p3840 N85-33782
Proceedings of the US-Japan Workshop on Transport in Open-Ended Systems
[IPPJ-727] 23 p3975 N85-34644
Potential effect in transport due to non-axisymmetric confining field 23 p3975 N85-34645
Radial transport phenomena for TMX-upgrade 23 p3976 N85-34647
Induced azimuthal electric field effects on tandem transport and ambipolarity 23 p3976 N85-34650
Radial transport caused by collision 23 p3976 N85-34652
Bounce resonance heating and radial transport of electrons 23 p3977 N85-34655
Electron dynamics and transport in a mirror field 23 p3977 N85-34656
Azimuthal uniformity and current balance study of ICRH-produced plasma in RFC-XXM 23 p3977 N85-34659
Effect of ECH and ICH on ambipolar potential in NBT-1M 23 p3978 N85-34661
Transports studies of ECH and ICRH-heated bumpy torus plasma in NBT-1M 23 p3978 N85-34662
Workshop report on Simulation Techniques for Shock Wave Phenomena and Characteristics of Plasmas in Inertial Confinement Fusion
[IPPJ-725] 23 p3979 N85-34670
Helios 1 energetic particle observations of the solar gamma ray flare events of 7, 21 June 1980 and 3 June 1982
[SH-1.3-8] 23 p3993 N85-34755
Source energy spectra from demodulation of solar particle data by interplanetary and coronal transport
[SH-1.3-13] 23 p3994 N85-34756
Constraints of solar flare particle transport models from anisotropy observations at Voyager 1
[SH-3.1-8] 23 p4002 N85-34812
Radial transport of approximately 1 MeV/nucleon ions during the 22 November 1977 solar particle event
[SH-3.2-5] 23 p4003 N85-34821
Cosmic-ray transport in the galactic magnetosphere
[OG-7.2-17] 23 p4016 N85-34884
Subseasonal variability in a two-level atmospheric general circulation model 24 p4114 N85-35504
A strategy for calibrating atmospheric transport models
[CSIRO-DAR-TP-9] 24 p4116 N85-35518
Calculation of heavy-ion tracks in liquid water
[DE85-012101] 24 p4149 N85-35725
Beam intensity increases at the intense pulsed neutron source accelerator
[DE85-012377] 24 p4155 N85-35764
Neutral pumping rates for a next step tokamak ignition device
[DE85-012760] 24 p4157 N85-35776
TRANSPORT THEORY
NT CHAPMAN-ENSKOG THEORY
NT MIXING LENGTH FLOW THEORY
Solution of contaminant transport equations using an orthogonal-upstream finite element scheme
[DE84-014266] 01 p0070 N85-10463
Experimental observation of neoclassical currents
[DE84-015113] 01 p0122 N85-10634
A finite element projection method for the solution of particle transport problems with anisotropic scattering
[AD-A145362] 02 p0250 N85-11637
A simple transport model 02 p0284 N85-11853
On the co-variant formulation of the law of motion of passive particles in a field of turbulence
[REPT-564] 03 p0377 N85-12407
Proceedings of a Workshop on Atmospheric Research Needs for the Western United States
[DE84-015069] 04 p0534 N85-13412
Parallel processing of numerical transport algorithms
[DE84-016825] 04 p0555 N85-13534
Theoretical studies of Field-Reversed Configurations (FRC) and experimental study of the FRC during translation
[DE84-016467] 04 p0566 N85-13603
Fusion plasma theory. Task 3: ECRH and transport modeling in tandem mirrors and divertor physics
[DE84-014939] 04 p0567 N85-13612
Rotation of a tenuous plasma with a high toroidal velocity in a Tokamak
[DE84-012990] 04 p0567 N85-13615
Monte Carlo studies of transport in stellarators
[DE84-017633] 04 p0568 N85-13625
Theoretical investigations relevant to magnetic fusion research
[DE85-001777] 06 p0866 N85-15503
Hydrologic characteristics of the Mediterranean and Black Sea 07 p0961 N85-16228
The (20)Ne interaction in extended matter
[NASA-TM-86312] 07 p1061 N85-16728
Spectroscopic measurement on Heliotron E 09 p1387 N85-18722
Radial profiles of high resolution X-ray spectra from the Alcator C Tokamak 09 p1387 N85-18723
Applied mathematics of transport theory
[DE85-000848] 11 p1633 N85-20283

Finite element method for solving neutron transport problems
[DE85-001075] 11 p1722 N85-20829
ITS: The integrated TIGER Series of coupled electron/photon Monte Carlo transport codes
[DE85-003719] 11 p1725 N85-20847
Magnetic fluctuations, field reversal maintenance, and anomalous thermal transport in the reversed field pinch
[DE85-003804] 11 p1732 N85-20892
Fluctuations and transport in fusion plasmas
[DE85-003612] 11 p1732 N85-20893
A linear characteristic-nodal transport method for the two-dimensional (X,Y)-geometry multigroup discrete ordinates equations over an arbitrary triangle mesh
[LA-10092-T] 12 p1913 N85-22008
Polar cap formation on Ganymede 13 p2174 N85-23486
Active Magnetospheric Particle Tracing Explorers (AMPTE)
[AD-A151072] 14 p2374 N85-24674
Synthetic acceleration of coarse-mesh S/sub n/ transport calculations
[DE84-014721] 14 p2409 N85-24855
Image formation in terms of the transport equation
[DE85-004993] 15 p2653 N85-26365
Limiting profiles in contaminant transport through porous media — ground water pollution
[REPT-84-31] 17 p2960 N85-28282
Projected discrete ordinates methods for numerical transport problems
[DE85-005832] 17 p3020 N85-28678
Augmented weighted diamond force of the linear nodal scheme for Cartesian coordinate systems
[DE85-005831] 17 p3020 N85-28679
Examination of a method for predicting the properties of railgun plasmas
[AR-004-322] 17 p3039 N85-28799
Electron multiple, plural and single scattering
[DE85-010325] 18 p3181 N85-29721
Low plasma edge temperatures for the self-pumped limiter
[DE85-010155] 18 p3189 N85-29782
MCNP: A general Monte Carlo code for neutron and photon transport
[DE85-010764] 19 p3348 N85-30753
Low-discrepancy point sets in transport codes
[DE85-010786] 19 p3348 N85-30755
Toroidal viscosity and ambipolarity in the neoclassical transport theory of axisymmetric tori
[DE85-010622] 19 p3358 N85-30820
A new slab geometry radiation transport differencing scheme
[DE85-006681] 19 p3366 N85-30874
Monte Carlo learning-biasing experiment with intelligent random numbers
[DE85-010713] 22 p3834 N85-33742
Collisional transport for a superthermal ion species in a plasma
[DE85-011943] 22 p3845 N85-33818
Theoretical and computational research on the focused transport of intense charged particle beams
[DE85-012980] 23 p3972 N85-34621
Why do leaky-box models work so fine?
[OG-7.2-8] 23 p4014 N85-34877
Exact solutions for sporadic acceleration of cosmic rays
[OG-8.3-7] 23 p4022 N85-34925
Relativistic transport theory for cosmic-rays
[OG-8.3-8] 23 p4022 N85-34926

TRANSPORT VEHICLES
Test methods for cable cars
[CETIM-1-5K-45-1] 04 p0515 N85-13282

TRANSPORTATION
NT AIR TRANSPORTATION
NT CHALLENGER (ORBITER)
NT COLUMBIA (ORBITER)
NT DISCOVERY (ORBITER)
NT ENTERPRISE (ORBITER)
NT MARINE TRANSPORTATION
NT RAIL TRANSPORTATION
NT SPACE SHUTTLE BOOSTERS
NT SPACE SHUTTLE MISSION 31-C
NT SPACE SHUTTLE MISSION 41-B
NT SPACE SHUTTLE MISSION 41-C
NT SPACE SHUTTLE MISSION 41-G
NT SPACE SHUTTLE MISSION 51-A
NT SPACE SHUTTLE MISSION 51-C
NT SPACE SHUTTLE MISSIONS
NT SPACE SHUTTLE ORBITERS
NT SPACE TRANSPORTATION
NT SPACE TRANSPORTATION SYSTEM
NT URBAN TRANSPORTATION
Summary of activities pertaining to utilization of grant purchase of batteries for electric van
[DE84-015793] 02 p0195 N85-11305
USSR report: Transportation
[JPRS-UTR-84-026] 03 p0310 N85-12002
Proceedings of a Workshop on the Applications of Tethers in Space, Volume 1
[NASA-CR-171196] 03 p0322 N85-12076
Proceedings of a Workshop on Applications of Tethers in Space, Volume 2
[NASA-CR-171197] 03 p0322 N85-12077
ECUT energy data reference series: Lightweight materials for ground transportation
[DE84-015269] 05 p0621 N85-13974
Determining training device requirements in Army aviation systems 05 p0711 N85-14558
Risks in the transport and storage of liquefied natural gas. Sub-project 5-2: Investigation into building damage
[BLL-RISLEY-TR-4608-(9091.9F)] 07 p0935 N85-15826
USSR report: Transportation
[JPRS-UTR-85-001] 08 p1067 N85-16783
USSR report: Transportation
[JPRS-UTR-85-003] 09 p1277 N85-18032
The Hazardous Materials Technical Center
[AD-P004149] 09 p1349 N85-18485
Electric-Hybrid Vehicle (E-HV) demonstration-test project
[DE85-002370] 10 p1570 N85-19699
Transportation
[JPRS-UTR-85-004] 12 p1769 N85-21105
Current development, applications of airships in USSR 12 p1769 N85-21100
USSR report: Transportation
[JPRS-UTR-84-015] 15 p2460 N85-25192
US Army human Engineering Laboratory Communications Survey: A Pilot Study (HELCOMS-PS)
[AD-A151434] 15 p2521 N85-25544
Structures and Dynamics Division research and technology plans for FY 1985 and accomplishments for FY 1984
[NASA-TM-86417] 15 p2577 N85-25895
USSR report: Transportation
[JPRS-UTR-84-025] 17 p2894 N85-27841
Test devices for aeronautical research and technology
[NASA-TM-77851] 17 p2905 N85-27914
Tribological sinks: Money down the drain
[DE85-010019] 17 p2974 N85-28376
Microcomputers in transportation: Software and source book, February 1985
[PB85-181022] 20 p3517 N85-31868
Shuttle car loading system
[NASA-CASE-NPO-15948-1] 23 p3987 N85-34722

TRANSPORTATION ENERGY
Hybrid propulsion technologies for urban bus transit
[PB85-157469] 16 p2880 N85-27773

TRANSPORTATION NETWORKS
Relationship between forest clearing and biophysical factors in tropical environments: Implications for the design of a forest change monitoring approach — Costa Rica
[E85-10051] 07 p0983 N85-16247
Microwave methods for paving
[DE85-004194] 14 p2285 N85-24032
Information technology applications in voluntary sector transport operations. SP1: Objectives and programme of work
[TT-8501] 15 p2667 N85-26457
Design and implementation of an interactive route editor 23 p3982 N85-34559

TRANSPORTER
An air-breathing ballistic space transporter for Europe
[NASA-TM-77845] 12 p1792 N85-21244

TRANSURANIUM ELEMENTS
NT AMERICIUM
NT AMERICIUM ISOTOPES
NT AMERICIUM 241
NT CALIFORNIUM ISOTOPES
NT CURIUM
NT CURIUM 244
NT PLUTONIUM
NT PLUTONIUM ISOTOPES
NT PLUTONIUM 238
NT PLUTONIUM 239
Volume compressibilities of transuranium elements compounds, especially of neptunium compounds 03 p0431 N85-12744
TRU decontamination of high-level PUREX waste by solvent extraction using a mixed octyl(phenyl)-N,N-diisobutyl-carbamoyl methylphosphine oxide/TBP/NPH (TRUEX) solvent
[DE85-010251] 19 p3235 N85-30054
Apparatus and method for identification of matrix materials in which transuranic elements are embedded using thermal neutron capture gamma-ray emission
[DE85-011659] 22 p3786 N85-33454

TRANSVERSE ACCELERATION
Axisymmetrical oscillations of shell systems subjected to impulse loads 13 p2047 N85-22814
Relation between gamma-ray family and EAS core: Monte-Carlo simulation of EAS core
[HE-3.6-7] 24 p4185 N85-35955
Structured events in Pamir carbon X-ray chambers
[HE-3.7-7] 24 p4186 N85-35965
Structure of air shower disc near the core
[HE-4.7-2] 24 p4198 N85-36053

TRANSVERSE OSCILLATION
A Galerkin method for the estimation of parameters in hybrid systems governing the vibration of flexible beams with tip bodies
[NASA-CR-172537] 10 p1544 N85-19734

TRANSVERSE VIBRATION
U TRANSVERSE OSCILLATION

TRANSVERSE WAVES
Acoustoelectric interaction in double-layer semiconductors 06 p0786 N85-15023
Quantitative acoustic emission techniques
[AERE-R-11282] 07 p0977 N85-16203
Tunable microwave transversal filters
[AD-A148370] 08 p1158 N85-17304
Automated TEM (Transverse electromagnetic) cell calibration system
[PB85-134377] 11 p1638 N85-20319
Explosive transverse electric field and particle acceleration during magnetic collapse — cosmic plasma 12 p1956 N85-22292
Surface acoustic wave structure and volume waves 15 p2525 N85-25568
Transverse periodic boundary conditions in molecular dynamics with uniaxial strain shock waves
[DE85-006497] 16 p2863 N85-27658
Guided-mode launching in a slab waveguide by way of diffraction at the edge of a conducting screen residing on one surface of the slab
[AD-A154666] 21 p3575 N85-32232
Transverse momentum distribution of pion deg in the fragmentation region of super high energy interactions 24 p4180 N85-35921
Radio wave emitted by an extensive air showers in 10KHz to 1MHz region
[HE-4.6-15] 24 p4196 N85-36051

TRANSVERSELY EXCITED ATMOSPHERIC LASERS
U TEA LASERS

TRAPATT DIODES
U AVALANCHE DIODES

TRAPPED MAGNETIC FIELDS
Simulation of the ion-beam-driven drift instability in a magnetic trap, 1
[AD-A149451] 10 p1452 N85-19147
Simulation of the ion-beam-driven drift instability in a magnetic trap, 2
[AD-A149452] 10 p1554 N85-19798
Beam trapping in high current cyclic accelerators with strong focusing fields
[AD-A151392] 15 p2648 N85-26331

TRAPPED PARTICLES
NT INNER RADIATION BELT
NT MAGNETICALLY TRAPPED PARTICLES
NT OUTER RADIATION BELT
NT PROTON BELTS
NT RADIATION BELTS
Laser cooling and trapping of neutral atoms
[AD-A146048] 03 p0366 N85-12345
Charge trapping in low temperature MOS (Metal-Oxide-Silicon) oxides
[AD-A148450] 06 p0860 N85-15467
Simulation of the ion-beam-driven drift instability in a magnetic trap, 2
[AD-A149452] 10 p1554 N85-19798
SCATHA (spacecraft charging at high altitudes) plasma interaction experiment: SC-3 high energy particle spectrometer; SC-8 energetic ion composition experiment
[AD-A149728] 12 p1793 N85-21252
S3-3 ONR-118 data analysis
[AD-A149725] 12 p1889 N85-21855
Intermolecular energy transfer between the individual zero-field levels of triplet traps in an orientationally disordered solid
[AD-A150751] 14 p2417 N85-24914
Reduction of the trapping of positrons in dislocated single crystals of iron when charged with hydrogen
[DE85-010235] 19 p3377 N85-30950
Proton ring trapping in a magnetic mirror 20 p3534 N85-31990
CYLTRAN calculations of electron effects on XD detectors
[LA-10264-MS] 23 p3989 N85-34601
HgCdTe surface and defect study program
[AD-A156079] 24 p4161 N85-35799

TRAPPING
Trapping for Newtonian diffusion processes
[REPT-73] 01 p0130 N85-10893

Effect of microstructure and trapping on the hydrogen embrittlement susceptibility of a titanium bearing HSLA steel
02 p0174 N85-11166
Impurity trapping during gas phase epitaxy of gallium arsenide
02 p0257 N85-11686
Deceleration, cooling, and trapping of atoms
[AD-A146234] 03 p0418 N85-12672
Mobility and trapping time measurements in HgI2
[DE84-015954] 06 p0869 N85-15522
Effect of microstructure and trapping on the hydrogen embrittlement susceptibility of a ti-bearing HSLA steel
[AD-A148610] 08 p1130 N85-17122
Hydrogen trapping, diffusion, and recombination in austenitic stainless steels
[DE85-001871] 09 p1294 N85-18129
Effect of hydrostatic pressure on trapping centers in strained-layer superlattice structures
[DE85-001362] 09 p1399 N85-18807
Enhanced diffusion from interstitial trapping during solid-phase-epitaxial growth of silicon alloys
[DE85-001285] 12 p1941 N85-22193
Trapping model analysis of annihilation line narrowing in some plastically deformed metals and alloys
[AERE-R-10593] 14 p2258 N85-23995
Energy trapping, release, and transport in three-dimensional energetic solids and molecular crystals: Theory of defects and impurities
[AD-A151071] 14 p2428 N85-24973
Frequency and time standards based on stored ions
18 p3105 N85-29223
Theory of positron annihilation in vacancies in concentrated disordered alloys
[DE85-010267] 18 p3163 N85-29734
Carrier loss in dispersive transport in amorphous semiconductors
[DE85-009122] 18 p3194 N85-29811
Trapping of ion conics by downward parallel electric fields
[AD-A155306] 21 p3633 N85-32568

TRAPS
Electron traps in the GaAs permeable base transistor
[AD-A145399] 02 p0267 N85-11871
Characterization of ion implanted deuterium traps in nickel by equilibration with deuterium gas
[DE84-014958] 02 p0288 N85-11879
Deceleration, cooling, and trapping of atoms
[AD-A146234] 03 p0418 N85-12672
Forces on neutral atoms due to electromagnetic fields
[AD-A146984] 07 p1040 N85-16603
Theoretical issues involving traps for neutral spin-polarized atoms
[AD-A148035] 08 p1220 N85-17682

TRAVELING IONOSPHERIC DISTURBANCES
Medium- and large-scale wave disturbances and heterogeneities of electron concentration in outer ionosphere in middle and low latitudes
08 p0825 N85-15241
Dispersion properties of moving ionospheric perturbations
07 p0952 N85-16038
On the dynamics of the westward traveling surge
14 p2364 N85-24607

TRAVELING SALESMAN PROBLEM
Statistical analysis of some traveling salesman algorithms
[AD-A145788] 03 p0410 N85-12620
The traveling salesman problem on a graph and some related integer polyhedra
[AD-A147953] 08 p1211 N85-17621
Local search in routing problems with time windows
[CWI-OS-R8409] 12 p1922 N85-22075

TRAVELING SOLVENT METHOD
Automatic Monoellipsoidal Mirror Furnace Facility (AMMFF), volume 1 — spaceborne crystal growth
[AMF-RP.100-DS-015-VOL-1] 09 p1285 N85-18073

TRAVELING WAVE MASERS
Millimeter-wave range masers: A review
13 p2089 N85-23042
Propagation and amplification of Ion Cyclotron Waves (ICW's) in a multicomponent plasma. The Earth magnetosphere as a giant maser for Alfven waves
14 p2368 N85-24634

TRAVELING WAVE MODULATION
Advanced infrared laser modulator development
[NASA-CR-172479] 06 p0662 N85-15479

TRAVELING WAVE TUBES
NT HELITRONS
Dual (GaAl) As-heterostructure based injection laser traveling wave amplifier
02 p0261 N85-11708
Spectrally matched modulation of radiation of injection laser in traveling-wave amplifier below 2 GHz
02 p0262 N85-11712
Millimeter-wave travelling-wave IMPATT diode
[AD-A146545] 06 p0804 N85-15117
Development of a 30 GHz/1 kW broadband traveling wave tube with suppression of band edge oscillations
[BMFT-FB-W-84-035] 07 p0948 N85-16011
Traveling wave tube for broadcast satellites
10 p1475 N85-19310
Design of low loss helix circuits for interference fitted and brazed circuits
[NASA-CR-166313] 10 p1478 N85-19328
Construction techniques of a molecular hydrogen laser
[AD-A152928] 17 p2970 N85-28343

TRAVELING WAVES
NT SOLITARY WAVES
On the asymptotic analysis of travelling shocks and phase boundaries in elastic bars
[AD-A147239] 07 p0959 N85-16076
Performance ranges of helical antenna made of conductor with extra bends
12 p1838 N85-21536
Behavior of small ferromagnetic particles in traveling magnetic field
12 p1843 N85-21564
Reflected wave travel-time curves in stratified media with vertically heterogeneous layers and slightly sloping curved boundaries
13 p2114 N85-23167
Dynamic response of shells and plates subjected to variable magnitude traveling loads
16 p2796 N85-27250
Experiments on the influence of active walls on the initial amplitudes and growths of instability waves
[AD-A154630] 21 p3583 N85-32275

TRAYS
A robotic system for preparing reagent and dilution vials
[DE85-006262] 16 p2793 N85-27231

TREADS
Improvements in tank tread assemblies
[NASA-CASE-NPO-16321-1] 18 p3117 N85-29291

TREE RING DATING
U DENDROCHRONOLOGY

TREES (MATHEMATICS)
NT FAULT TREES
Model-based probabilistic reasoning for electronics troubleshooting
[AD-P003937] 02 p0247 N85-11617
Synthesis of tree-structured computing systems through use of closures
[AD-A150502] 13 p2147 N85-23326
Parallel update of minimum spanning trees in logarithmic time
[AD-A150497] 13 p2151 N85-23357
The Kappa sub n property in small Omega sub 1 trees
14 p2413 N85-24885
Generation and termination of binary decision trees for nonparametric multiclass classification
[AD-A151361] 15 p2640 N85-26283
Investigation and implementation of a tree transformation system for user friendly programming
[AD-A152716] 17 p3011 N85-28617
Embedding graphs in lines, trees and grids
19 p3334 N85-30652
A theoretical and empirical analysis of coherent ray-tracing
23 p3957 N85-34524
A new approach to linear quadtrees
23 p3961 N85-34550

TREES (PLANTS)
NT CONIFERS
NT DECIDUOUS TREES
Nonparametric analysis of Minnesota spruce and aspen tree data and LANDSAT data
07 p0964 N85-16253
Simulating responses to expected climate change in eastern North America: Applications to decision-making in the forest industry
[DE85-001272] 07 p1008 N85-16406
UHF radiowave propagation through forests
[AD-A149518] 10 p1467 N85-19256
Response of unmanaged forests to CO2-induced climate change: Available information, initial tests and data requirements
[DOE/NSB-0053] 12 p1883 N85-21817
Combined effects of atmospheric deposition, internal acid production, and harvesting on nutrient gains and losses from forest ecosystems
[DE85-002325] 12 p1884 N85-21821
Areas with forest soils sensitive to acidic deposition under alternative damage hypotheses
[DE85-005257] 13 p2130 N85-23257
Use of forest modeling to project acid rain effects
[DE85-005251] 16 p2821 N85-27400
Interactive effects of acid rain and gaseous air pollutants on natural terrestrial vegetation
[DE85-005255] 16 p2821 N85-27401
Screening Prosopis (mesquite) species for biofuel production on semi-arid lands
[DE85-010048] 19 p3302 N85-30471
Insights into the phylogenetic positions of photosynthetic bacteria obtained from 5S rRNA and 16S rRNA sequence data
21 p3658 N85-32719
Effects of acid rain on forest nutrient status
[DE85-012486] 23 p3947 N85-34463

TREMORS
Study of earthquake preparation processes from distribution of weak tremor epicenters
14 p2345 N85-24501

TRENDS
Future directions in operations research
[REPT-84-24] 17 p3026 N85-28711
Avionics and civil aircraft systems: The present and the future
[SNIAS-851-111-104] 20 p3392 N85-31036
Evolution of spacecraft design methods as a function of environmental and geometrical constraints
[ESA-CR(P)-2012] 20 p3418 N85-31216

TRESCA FLOW
Removal of singularities in Tresca and Mohr-Coulomb yield functions
[OUEL-1528/84] 03 p0413 N85-12642

TRIAMINOGUANIDINIUM AZIDE
The crystal and molecular structure of a new propellant compound: Triaminoguanidium Azide Nitrate (TAZN)
13 p2002 N85-22551

TRIAMINOTRINITROBENZENE
U TATB

TRIANGULAR WINGS
U DELTA WINGS

TRIANGULATION
A triangular finite element for thin plates and shells
01 p0058 N85-10386
The 1980 diagnostic adjustment of the German main triangulation network. 4: Network adjustment (part 3)
[SER-B-267-PT-3-MITT-168] 11 p1665 N85-20494
The 1980 diagnostic adjustment of the German main triangulation network. 4: Network adjustment (part 1)
[SER-B-267-PT-1-MITT-168] 11 p1670 N85-20525
The 1980 diagnostic adjustment of the German main triangulation network. 4: Network adjustment (part 2)
[SER-B-267-PT-2-MITT-168] 11 p1670 N85-20526
The 6 pi-periodic solutions of plane restricted elliptical 3-body problem in neighborhood of libration points
16 p2718 N85-26779
Standards and specifications for geodetic control networks
[PB85-166478] 16 p2816 N85-27374

TRIAXIAL STRESSES
Creep deformation of compacted decomposed granite soils
09 p1303 N85-18187
Influence of grain size distribution on the undrained dynamic properties of saturated sand
[PB85-102362/GAR] 09 p1305 N85-18197

TRIAXIALITY
U TRIAXIAL STRESSES

TRIBOLOGY
Plasma variables and tribological properties of coatings in low pressure (0.1 - 10.0 torr) plasma systems
[NASA-TM-83798] 02 p0189 N85-11261
Microscopic aspects of the effect of friction reducers at the lubrication limit
[NASA-TM-77413] 03 p0367 N85-12354
Roller crosshead analysis
04 p0507 N85-13238
The European Space Tribology Laboratory (ESTL) activities report
[ESA-ESTL-61] 05 p0646 N85-14146
Effect of asperity interactions on scuffing
[AD-A146544] 06 p0814 N85-15170
Tribological properties of graphite-fiber-reinforced, partially fluorinated polyimide composites
[NASA-TM-86926] 09 p1298 N85-18153
Effect of implantation species on the tribological response of stainless steel surfaces
[DE85-003530] 10 p1493 N85-19432
The role of silver in self-lubricating coatings for use at extreme temperatures
[NASA-TM-86943] 11 p1611 N85-20127
Tribological properties of boron nitride synthesized by ion beam deposition
[NASA-TM-86962] 12 p1810 N85-21355
Tribological systems as applied to aircraft engines
[NASA-TM-86965] 12 p1858 N85-21657
Thermal and thermoelastic effects in rolling/sliding contacts
[AD-A150435] 13 p2165 N85-23429
Gears and Power Transmission Systems for Helicopters and Turboprops
[AGARD-CP-369] 14 p2220 N85-23765
Chemical-mechanical interacti..n in gears
14 p2223 N85-23785
Wear reduction by lubricants in confined contacts
14 p2223 N85-23786
Summaries of FY 1984 engineering research
[DE85-006273] 15 p2664 N85-26442
Effect of counterface material type and its topography on the tribological properties of polyimide composites
[NASA-TM-87036] 16 p2754 N85-26993
Tribological sinks: Money down the drain
[DE85-010019] 17 p2974 N85-28376

European Space Tribology Laboratory: Facilities, services, capabilities
[ESA-BR-12] 20 p3398 N85-31080
Activities report of the European Space Tribology Laboratory
[ESA-ESTL-66] 20 p3484 N85-31653
Hertzian contact in two and three dimensions
[NASA-TP-2473] 21 p3596 N85-32331
Aluminum work function: Effect of oxidation, mechanical scraping and ion bombardment
[NASA-TM-87079] 23 p3915 N85-34265
TRICHLORIDES
U CHLORIDES
TRIGGER CIRCUITS
Low jitter trigger for an excimer laser
[DE85-005732] 13 p2097 N85-23080
Construction techniques of a molecular hydrogen laser
[AD-A152928] 17 p2970 N85-28343
Coordinated research program in pulsed power physics
[AD-A154629] 21 p3679 N85-32858
Fast shutter apparatus
[DE85-006501] 23 p3928 N85-34343
Synchronous timing of multi-energy fast beam extraction during a single AGS cycle
[DE85-011829] 24 p4158 N85-35781
Arrival time distributions of electrons in air showers with primary energies above 10 (18)eV observed at 900m above sea level
[HE-4.7-5] 24 p4199 N85-36058
Methods for roof-top mini-arrays
[HE-4.7-7] 24 p4199 N85-36058
Progress report on a new search for free e/3 quarks in the cores of 10(15) - 10(16) eV air showers
[HE-6.2-15] 24 p4212 N85-36151
TRIGGERS
U ACTUATORS
TRIGONOMETRIC FUNCTIONS
NT TANGENTS
TRIM (BALANCE)
U AERODYNAMIC BALANCE
TRIMERS
Polymerization and halogen scrambling behavior of phenyl-substituted cyclotriphosphazenes
[AD-A146368] 06 p0771 N85-14930
Theoretical research program to study transition metal trimers and embedded clusters
[NASA-CR-174296] 08 p1125 N85-17093
TRIMETHYL COMPOUNDS
Effects of heteroatom substituents on the properties of 1,2-dioxetanes
[AD-A148727] 09 p1290 N85-18100
TRINITROTOLUENE
Treatment of wastewater (red water) resulting from TNT (trinitrotoluene) purification
[AD-P004146] 09 p1348 N85-18482
Voltammetric analysis of ordnance materials. Part 2: A portable digital voltammeter for use with a silver wire working electrode
[AD-A152480] 17 p2967 N85-28325
Toxicity of TNT wastewaters to aquatic organisms. Volume 4: Chronic toxicity of 2,4-dinitrotoluene and condensate water
[AD-A153536] 18 p3132 N85-29400
TRINITROTRIAZOCYCLOHEXANE
U RDX
TRIODES
Textured carbon surfaces on copper
[NASA-CASE-LEW-14130-1] 11 p1615 N85-20156
Multi-channel pulser for the SLC thermionic electron source
[DE85-014222] 24 p4160 N85-35792
TRIPHENYLS
Stable polymeric carbon radicals. Part 2: Attempts at the preparation of polyradicals of the triphenylmethyl type linked by P-phenylene units
[NASA-TM-77799] 10 p1450 N85-19134
TRIPLE AXIS SPECTROMETERS
U NEUTRON SPECTROMETERS
TRIPLET EXCITATION
U ATOMIC ENERGY LEVELS
TRIPLET STATE
U ATOMIC ENERGY LEVELS
TRIPROPELLANTS
U LIQUID ROCKET PROPELLANTS
TRITIUM
Blanket materials for fusion reactors: Comparisons of thermochemical performance
[DE84-016240] 04 p0568 N85-13622
Evaluation of arctic test of improved tritium radioluminescent lighting
[DE84-014887] 05 p0597 N85-13805
Tritium catalyzed deuterium Tokamaks
[DE85-004825] 12 p1936 N85-22166
Scientific activities. A: Reacting plasma physics. 1: Introduction and overview 15 p2654 N85-26370
Two-dimensional TBR calculations for conceptual compact reversed-field pinch reactor blanket
[DE85-007636] 17 p3040 N85-28812
Use of environmental health-risk analysis for managing toxic substances
[DE85-008964] 18 p3160 N85-29574
New concept for a wall detector for alpha particles
[DE85-009037] 18 p3183 N85-29740
Modeling and experiments on tritium permeation in fusion reactor blankets
[DE85-008439] 18 p3183 N85-29741
Counter current extraction system for tritium recovery from 17Li-83Pb
[DE85-010519] 19 p3240 N85-30090
Quantitative passive technique for assay of near-surface tritium in materials
[DE85-010661] 19 p3360 N85-30833
Tritium system design for the mirror reactors FPD-1, FPD-2 and FPD-3
[DE85-010490] 19 p3363 N85-30852
Current state of development and expected performance of copper-lithium alloys as an impurity control system in fusion applications
[DE85-009673] 19 p3372 N85-30917
Tables of generalized hydrogen diffusion profiles and permeating fluxes for fusion applications
[DE85-008876] 19 p3372 N85-30919
MFTF-(alpha) + T shield design
[DE85-010496] 20 p3529 N85-31948
Tritium technology review
[DE85-010504] 21 p3703 N85-33006
Tritium-helium effects in metals
[DE85-011507] 22 p3749 N85-33235
Environmental surveillance at Los Alamos during 1984
[DE85-011666] 22 p3811 N85-33605
The 1984 environmental monitoring report, Sandia National Laboratories, Albuquerque, New Mexico
[DE85-011175] 22 p3811 N85-33607
Technology of off-gas treatment for liquid-fed ceramic melters
[DE85-012467] 22 p3812 N85-33610
Global environmental transport models for tritium
[DE85-011437] 22 p3816 N85-33639
Ultraviolet radiation-damage absorption peak in solid deuterium-tritium, revision 1
[DE85-012969] 22 p3844 N85-33806
Key issues of fusion nuclear technology development (FINESSE)
[DE85-012599] 22 p3845 N85-33817
Compact DT fusion spherical tori at modest field
[DE85-011566] 23 p3962 N85-34692
Tritium hazard via the ingestion pathway
[DE85-012897] 24 p4133 N85-35618
TRITON
Physical properties of Neptune and Triton inferred from the Orbit of Triton 02 p0300 N85-11942
Physical properties of the satellites of Neptune 02 p0300 N85-11945
Seasonal variations in Triton's atmospheric mass and composition 02 p0301 N85-11948
Research in planetary studies and operation of Mauna Kea Observatory
[NASA-CR-175618] 13 p2169 N85-23460
On the origin of Triton and Pluto 13 p2175 N85-23497
TRIVALENT IONS
Trivalent ion exchange in beta alumina
[AD-A145373] 02 p0172 N85-11151
Trivalent cerium doped crystals as tunable laser systems: Two bad apples
[DE85-006168] 22 p3790 N85-33482
TROILITE
The low-energy secondary cosmic ray flux: Detectors in iron meteorites 06 p0667 N85-15635
TROMBE WALLS
Short duration winter-time performances of different passive solar systems
[DE85-000850] 11 p1675 N85-20557
Thickness-insensitive selective surface paint
[DE85-010568] 19 p3250 N85-30150
Performance analysis of mixed passive solar heating systems
[DE85-009624] 21 p3613 N85-32455
TROPICAL METEOROLOGY
Planetary scale interactions 05 p0684 N85-14397
Diagnostics of rainfall anomalies in the nordeste during the global weather experiment 05 p0685 N85-14405
Frequency and motion of western North Pacific tropical cyclones
[PB85-106466/GAR] 06 p0839 N85-15331
Ocean and climate, an example. The interannual variability of the tropical Pacific Ocean 07 p1002 N85-16365
The ocean and the dynamics of the tropical atmosphere; its possible predicability 07 p1002 N85-16366
The Amazon and climate 07 p1003 N85-16376
Meridional penetration of frontal systems in South America and its relation to organized convection in the Amazon
[INPE-3407-PRE/676] 10 p1518 N85-19572
Accuracy of typhoon center determined by GMS imagery 12 p1894 N85-21887
Tropical Oceans-Global Atmosphere (TOGA) experiment planning for the Brazilian participation in TOGA global climate program
[INPE-3499-PRE/735] 16 p2834 N85-27477
Tropical ozone: Seasonal variations in the troposphere at 6 deg S
[INPE-3555-PRE/766] 19 p3313 N85-30535
Mariners weather log, volume 29, number 1, winter 1985
[PB85-177483] 19 p3318 N85-30570
Mariners weather log, volume 28, number 4, fall 1984
[PB85-176408] 19 p3318 N85-30571
Southern oscillation/El Nino excitation of the Earth's Chandler wobble 20 p3490 N85-31695
Forecast of Atlantic seasonal hurricane activity for 1985 20 p3495 N85-31732
Tropical Ocean and Global Atmosphere (TOGA) heat exchange project: A summary report
[NASA-CR-176039] 20 p3496 N85-31738
TROPICAL REGIONS
NT AMAZON REGION (SOUTH AMERICA)
Resonance model of Pc3 in subtropical regions — geomagnetism 04 p0520 N85-13323
Monthly and seasonal climatology over the global tropics and subtropics for the decade 1973 to 1983. Volume 1: 200 mb winds
[AD-A146521] 06 p0838 N85-15322
Razrezy program research in the tropical Atlantic 07 p0981 N85-16229
Relationship between forest clearing and biophysical factors in tropical environments: Implications for the design of a forest change monitoring approach — Costa Rica
[E85-10051] 07 p0983 N85-16247
Natural exposure versus chamber simulation
[AD-A149538] 10 p1495 N85-19437
Slow motions in the tropical troposphere 13 p2131 N85-23262
A theoretical study of the ozone quasi-biennial oscillation in the tropical stratosphere 13 p2132 N85-23264
Cumulus effects on the large-scale vorticity and momentum fields in the tropical atmosphere 13 p2137 N85-23270
Surface currents in the tropical Pacific during 1979-1980 using drifting buoys 14 p2323 N85-24354
The Tropical Ocean and Global Atmosphere program (TOGA) 14 p2330 N85-24411
Deuteron whistlers at low latitudes in the low altitude topside ionosphere 14 p2366 N85-24625
Low-latitude ducted whistlers observed at Sanya, Hainan, China 14 p2367 N85-24626
Whistler observation at Okinawa, Japan during the IMS 14 p2367 N85-24627
Biophysical evaluation of the wet globe temperature index (Botsball) at high air movements and constant dew point temperature
[AD-A151065] 14 p2378 N85-24683
Chemical, biological, and physical measurements from the subtropical western North Atlantic Ocean. Summer 1982, USNS Lynch, cruise 710-82
[AD-A153823] 18 p3201 N85-29657
Tropical ozone: Seasonal variations in the troposphere at 6 deg S
[INPE-3555-PRE/766] 19 p3313 N85-30535
An examination of the Southern Oscillation in the upper tropospheric tropical and subtropical wind field 20 p3488 N85-31680
Moist barotropic instability in the tropics 20 p3489 N85-31683
Aircraft observations of condensation and ice nuclei at a tropical station 21 p3640 N85-32613
Formation of particles in the air of the humid tropical forests 21 p3644 N85-32639
A statistical study of CCN concentration in subequatorial climate: The particular case of the tropical wet forest 21 p3649 N85-32673
Properties of forest derived cloud condensation nuclei 21 p3650 N85-32682
Sulfates in marine aerosols over the tropical Western Pacific Ocean 21 p3651 N85-32690
Observation of energy spectrum of electron albedo in low latitude region at Hyderabad, India
[SH-6.1-7] 23 p4045 N85-35081
Proton albedo spectrum observation in low latitude region at Hyderabad, India
[SH-6.1-8] 23 p4045 N85-35082
Mean cloudiness over the global tropics from satellite observations
[AD-A156188] 24 p4123 N85-35561

TROPICAL STORMS
NT HURRICANES
NT TYPHOONS
Digital radar data as an aid in nowcasting in Hong Kong 01 p0079 N85-10525
Statistical tropical cyclone forecasting techniques for the Southern Hemisphere
[AD-A144752] 01 p0085 N85-10569
A tropical cyclone precipitation estimation technique using geostationary satellite data
[PB84-226703] 01 p0086 N85-10579
Summary of 1984 Atlantic seasonal tropical cyclone activity and verification of author's forecast 03 p0395 N85-12520
A possible mechanism for the diurnal oscillations of tropical cyclones 09 p1356 N85-18530
Tropical cyclone data tape for the Eastern and Central North Pacific Basins, 1949-1983: Contents, limitations and uses
[PB85-110054] 10 p1520 N85-19585
Intensification of tropical instabilities
[AD-A149985] 12 p1896 N85-21899
Mesoscale Atmospheric Processes Research Program Science Review
[NASA-TM-87465] 15 p2594 N85-25987
Monitoring tropical cyclone growth using GOES VISSR/VAS and Nimbus-7 TOMS data 15 p2595 N85-25989
Convection modeling and application to severe storms 15 p2595 N85-25991
Forecast of Atlantic seasonal hurricane activity for 1985 16 p2833 N85-27470
Technique that uses satellite, radar, and conventional data for analyzing and short-range forecasting of precipitation from extratropical cyclones
[PB85-164994] 16 p2837 N85-27499
Characteristics of North Indian Ocean tropical cyclone activity
[AD-A153085] 17 p2997 N85-28524
Forecasting of tropical cyclone motion using an EOF (Empirical Orthogonal Function) representation of wind forcing
[AD-A155034] 21 p3636 N85-32580
TROPICS
U TROPICAL REGIONS
TROPISM
NT GEOTROPISM
NT GRAVITROPISM
Polyamines as possible modulators of gravity induced calcium transport in plants 15 p2606 N85-26060
Calcium and calmodulin localization in gravitropically-responding plant organs 15 p2606 N85-26061
Role of Ca++ in shoot gravitropism — avena 15 p2607 N85-26065
Gravistimulus production in roots of corn 15 p2607 N85-26066
A possible explanation of why gravitropic growth is detected earlier than straight growth 15 p2607 N85-26067
Gravitropism in leafy dicot stems 15 p2610 N85-26086
Mutant peas as probes in the understanding of growth and gravitropism 15 p2611 N85-26088
TROPOPAUSE
Applications of TOMS ozone data and clustering techniques in satellite soundings 05 p0681 N85-14379
Applications of fuzzy clustering techniques to stratified by tropopause MSU temperature retrievals 18 p3141 N85-29444
Comparison of tropopause altitude determination by the Platteville Radar, Sunset Radar and the NWS Rawinsonde 21 p3617 N85-32477
Practical use of a tropopause height determination algorithm on an MST radar data set, part 1.8B 21 p3618 N85-32479
The Ponape ST radar 21 p3629 N85-32549
TROPOSPHERE
The inducement of planetary boundary layer mass convergence associated with varying vorticity beneath tropospheric wind maximum 01 p0074 N85-10494
Observed rate of tropospheric diffusion
[DE84-016047] 02 p0224 N85-11470
Assessment of Techniques for Measuring Tropospheric H sub x O sub y
[NASA-CP-2332] 05 p0675 N85-14336
Assessment of Techniques for Measuring Tropospheric H sub x O sub y: Summary 05 p0675 N85-14337
Detailed performance calculations: Goddard Group, appendix D 05 p0676 N85-14341
Detailed performance calculations: Georgia Institute of Technology Group, appendix E 05 p0676 N85-14342
Detailed performance calculations: Harvard Group, appendix G 05 p0676 N85-14344
Jet stream errors and tropospheric-stratospheric interactions in the GLAS general circulation model 05 p0683 N85-14392
Linear studies of stationary, extratropical anomalies in the troposphere 05 p0686 N85-14410
Revised Uniform Summary of Surface Weather Observations (RUSSWO). Spangdahlem AB, Germany, parts A-F
[AD-A147166] 07 p1006 N85-16392
Tropospheric and ionospheric phase perturbations and Doppler frequency shift effects
[AD-A148579] 08 p1154 N85-17283
Propagation of wide bandwidth signals in a tropospheric ducting system 10 p1469 N85-19271
Observational study of transport in the free troposphere
[PB85-144145] 12 p1887 N85-21845
Global tropospheric chemistry: A plan for action
[NASA-CR-175545] 12 p1891 N85-21865
Varying structure and intensity change characteristics of 4 Western North Pacific tropical cyclones
[AD-A149628] 12 p1895 N85-21895
Intensification of tropical instabilities
[AD-A149985] 12 p1896 N85-21899
Slow motions in the tropical troposphere 13 p2131 N85-23262
Cumulus cloud venting of mixed layer ozone
[NASA-TM-87429] 13 p2132 N85-23269
Cumulus effects on the large-scale vorticity and momentum fields in the tropical atmosphere 13 p2137 N85-23270
Comparison of observations of orographic disturbances in the troposphere and upper atmosphere 14 p2341 N85-24479
Survey of developments in tropospheric communication apparatus 15 p2528 N85-25587
An investigation of tropospheric ions 16 p2823 N85-27412
Radon concentration inversion in the troposphere: Still unexplained
[INPE-3360-PRE/636] 16 p28 .8 N85-27431
The seasonal cycle of atmospheric CO in the Southern Hemisphere 16 p2830 N85-27447
A review of tropospheric refraction effects on Earth-to-satellite systems 18 p3107 N85-29235
Field measurements with the TAMS-2B and development of methods for measuring HCHO, HC3 and HONO in real air
[PB85-172955] 18 p3135 N85-29419
Investigation of the reaction system NOX/ClOX/HOX under tropospheric and stratospheric conditions
[BPT-11/84] 18 p3137 N85-29427
Circulation and transport in the middle atmosphere: Troposphere and lower atmosphere 18 p3148 N85-29491
Tropical ozone: Seasonal variations in the troposphere at 6 deg S
[INPE-3555-PRE/766] 19 p3313 N85-30535
Short meridional scale anomalies in the lower stratosphere and upper troposphere 20 p3489 N85-31684
Troposphere-stratosphere (surface-55 km) monthly general circulation statistics for the Northern Hemisphere-four year averages
[NASA-TM-86182] 20 p3495 N85-31730
Meteorological and aeronomical requirements for MST radar networks (keynote paper), part 1 21 p3615 N85-32467
Tropospheric-stratospheric exchange, part 1.1A 21 p3615 N85-32468
A numerical analysis of transient planetary waves and the vertical structure in a meso-strato-troposphere model, part 1.4A 21 p3617 N85-32473
Performance of the Colorado wind-profiling network, part 1.5A 21 p3617 N85-32475
Vertical transport in the atmosphere: Measurement capabilities and requirements of VHF radars, part 1.6A 21 p3617 N85-32476
Morphology of the scattering targets: Fresnel and turbulent mechanisms, part 2.1A 21 p3618 N85-32481
Antenna induced range smearing in MST radars 21 p3620 N85-32495
Frequency and site selection criteria for MST radars, part 5.1A 21 p3624 N85-32512
Urbana radar systems: Possibilities and limitations 21 p3628 N85-32540
Progress and plans for the Colorado Wind Profiler Network 21 p3628 N85-32542
Millstone Hill radar: Capabilities for S/T observations 21 p3629 N85-32548
The Ponape ST radar 21 p3629 N85-32549
Measurements of vertical velocity over flat terrain by ST radar and other related uses of the radar data set 21 p3630 N85-32550
Eleventh International Conference on Atmospheric Aerosols, Condensation and Ice Nuclei, volume 1
[PB85-162400] 21 p3644 N85-32636
A new hypothesis for the observed vertical distribution of atmospheric aerosols 21 p3645 N85-32646
On the mechanisms responsible for the formation of typical size spectra and vertical distribution of tropospheric aerosol particles 21 p3645 N85-32647
Application of Particle Induced X-ray Emission analysis (PIXE) to aerosol long range transport studies 21 p3648 N85-32665
Aircraft observations of cloud condensation nuclei in maritime and continental environments 21 p3650 N85-32680
Sulfur Cycle 21 p3662 N85-32748
TROPOSPHERIC SCATTERING
Field coherence function in layerwise nonhomogeneous troposphere 06 p0784 N85-15012
Influence of propagation in digital wireless beam, microwave links 10 p1470 N85-19277
Measurements and predictions of multipath dispersion for troposcatter links 10 p1472 N85-19289
Tropospheric scatter communication system having angle diversity
[AD-D011448] 14 p2291 N85-24200
Microwave propagation studies, measurements and education in Surabaya, Indonesia
[B8464633] 24 p4068 N85-35339
TROPOSPHERIC WAVES
NT PLANETARY WAVES
Tropospheric gravity waves observed by three closely spaced ST radars 21 p3623 N85-32509
Elimination of range-aliased echoes in the VHF radars 21 p3625 N85-32521
TROUBLESHOOTING
U MAINTENANCE
TROUGHS
Prediction of wave height of wind-generated seas in finite water depth
[AD-A145996] 03 p0398 N85-12539
The origin and evolution of terrestrial and Martian rock labyrinths
[NASA-CR-175511] 12 p1961 N85-22326
TRUCKS
NT TANK TRUCKS
A generalized mathematical solution for transient off tracking of single vehicles and truck combinations
[DM-2] 01 p0107 N85-10719
Evaluation of the particulate levels occurring under 1.0/1.2 g/mi nitrogen oxide standards for light duty diesel vehicles and light duty diesel trucks
[PB85-115939/GAR] 09 p1350 N85-18494
Comparison of measured and simulated ride comfort for an agricultural tractor and influence of travel speed and tyre-inflation pressure on dynamic response
[AD-P004281] 09 p1407 N85-18857
Electric vehicle demonstration project
[DE85-003124] 11 p1741 N85-20944
Test plan for acceptance, verification and performance testing of the Bedford Lucas Chloride Electric Van. Part 1: Acceptance and verification testing at EG and G Automotive Research. Part 2: INEL performance testing, revision 1
[DE85-005157] 17 p3051 N85-28888
Three-dimensional finite element impact analysis of a nuclear waste truck cask
[DE85-010653] 19 p3288 N85-30389
TRUNCATION (MATHEMATICS)
U APPROXIMATION
TRUNCATION ERRORS
Crack growth geometry in aluminum alloy sheet material under flight simulation loading. 1: A comparison between TWIST and minTWIST FALSTAFF and short FALSTAFF. 2: Effect of truncating high loads
[VTH-LR-441] 11 p1609 N85-20119
Sigma filter 18 p3142 N85-29450
TRUNKS (LINES)
U TRANSMISSION LINES
TRUNNIONS
U SHAFTS (MACHINE ELEMENTS)
TRUSSES
The evolution of small payload carrier systems 02 p0153 N85-11038
Effects of member imperfections on the behavior of space trusses 02 p0207 N85-11363
Conceptual design for scaled truss antenna flight experiment
[NASA-TM-85804] 04 p0462 N85-12932
Space Station truss structures and construction considerations
[NASA-TM-86338] 07 p0916 N85-15796
Alternative approximation concepts for space frame synthesis
[NASA-CR-172526] 12 p1776 N85-21150
Variable geometry truss concept
[REPT-614] 12 p1865 N85-21697

Synchronously deployable tetrahedral truss reflector
14 p2231 N85-23827
Deployable controllable geometry truss beam
[NASA-TM-86366] 17 p2909 N85-27934
Buckling and post-buckling behavior of sparsely connected built-up columns 19 p3283 N85-30358
Application of the ADAMS program to deployable space truss structures
[NASA-CR-177927] 19 p3284 N85-30366
Environmental background measurement program
[AD-A153860] 19 p3319 N85-30577
Parametric stiffness control of flexible structures
20 p3414 N85-31187
Deployable-erectable trade study for space station truss structures
[NASA-TM-87573] 22 p3740 N85-33181
Structural dynamics model and response of the deployable reference configuration space station
[NASA-TM-86366] 22 p3799 N85-33539
Box truss analysis and technology development. Task 1: Mesh analysis and control
[NASA-CR-172570] 23 p3900 N85-34156

TRYPSIN
Effects of method of detachment on electrophoretic mobility of mammalian cells grown in monolayer culture
20 p3500 N85-31757

TRYPTOPHAN
Laboratory note: Effect on sleep latency of pre-sleep AEP (Auditory Evoked Potential) procedures
[AD-A147620] 08 p1194 N85-17527

TSUNAMI WAVES
Catalog of submarine volcanoes and hydrological phenomena associated with volcanic events: 1500 BC to 31 Dec. 1899
[PB85-117984] 12 p1891 N85-21869
Atmospherically forced, coastally trapped, long period gravity waves off the south coast of southern Africa
16 p2832 N85-27461
Plane Tsunami wave caused by elastic oscillations of ocean floor 19 p3290 N85-30403

TTL INTEGRATED CIRCUITS
AL-124 light-emitting diode in 30 Mbit/s fiber-optic communication line 13 p2069 N85-22925

TUBE ANODES
On-line monitoring of the true corrosion rate in problems related to power plants
[CISE-2335] 08 p1131 N85-17126

TUBE CATHODES
NT COLD CATHODES
NT HOT CATHODES
NT PHOTOCATHODES
NT THERMIONIC CATHODES
Improved materials and processes of dispenser cathodes
[AD-A148610] 09 p1314 N85-18262
The effect of metal overlayers of thermionic dispenser cathodes
[AD-A154795] 21 p3701 N85-32995

TUBE HEAT EXCHANGERS
Internal heat transfer and pressure drop measurements in a variously baffled shell and tube heat exchanger
03 p0360 N85-12310
Fluidelastic instability in shell and tube heat exchangers: A framework for a prediction method
[DE84-006518] 10 p1496 N85-19444
Acoustic resonance in heat exchanger tube banks
[DE85-004395] 11 p1632 N85-20281
Flow-induced tube vibration thresholds in heat exchangers from shellside water tests
[DE84-006603] 11 p1652 N85-20407
Computer-aided thermohydraulic design of TEMA type E shell and tube heat exchangers for use in low pressure, liquid-to-liquid, single phase applications
[AD-A153779] 18 p3100 N85-29191

TUBES
Apparatus for producing diamond-like carbon flakes
[NASA-CASE-LEW-13837-3] 11 p1615 N85-20155
Dynamic models of flux tubes in the interpretation of polarization measurements 18 p3206 N85-29891
Electrostatic astigmatic tubular lens
21 p3695 N85-32955

TUBING
U PIPES (TUBES)

TUMBLING MOTION
Optimal open loop and nonlinear feedback control for remote orbital capture
[AD-A151967] 16 p2732 N85-26859

TUMORS
NT CANCER
NT LEUKEMIAS
Radiation physics, biophysics, and radiation biology
[DE84-014885] 09 p1360 N85-18557
Carcinogenesis of nitrated toluenes and benzenes skin and lung tumor assays in mice
[AD-A155723] 22 p3818 N85-33655

TUNABLE LASERS
Tunable CW semiconductor platelet laser
[AD-D011215] 01 p0052 N85-10341
Using two-beam interference method for measuring wavelength of tunable pulse lasers
02 p0272 N85-11772
Advanced infrared laser modulator development
[NASA-CR-172479] 06 p0862 N85-15479
Visible and ultraviolet lasers based on excimer transitions in the homonuclear halogens
[AD-D011311] 07 p0971 N85-16163
A new free electron laser using a relativistic beam with spiralling electron
[AD-D011318] 07 p0971 N85-16165
Characterization of CNRS Fizeau wedge laser tuner
[NASA-CR-174357] 09 p1325 N85-18328
Carbon dioxide laser radar for monitoring atmospheric transmittance and atmospheric aerosol
09 p1354 N85-18516
Developments and applications of laser fluorescence spectroscopy for studies of particle behaviours in fusion plasmas 09 p1389 N85-18735
Optically bistable devices using semiconductor materials
[AD-A149551] 11 p1628 N85-20253
Progress toward free-electron lasers for applications
[DE85-002208] 11 p1639 N85-20326
Portable remote laser sensor for methane leak detection
[NASA-CASE-NPO-15790-1] 12 p1855 N85-21631
Advanced crystalline laser materials
[DE85-003142] 12 p1857 N85-21647
Principle and design of a medium-enhanced free-electron laser 15 p2561 N85-25802
Calculations of collision-induced optical gain in high-density mixtures of D2 or HD with a buffer gas
[AD-A151372] 15 p2648 N85-26330
Spectroscopic investigation of materials for frequency agile laser systems
[AD-A151731] 16 p2790 N85-27208
High resolution spectroscopy of C13O16 in gas mixtures
[AD-A152625] 17 p2919 N85-27991
The construction and study of improved Al(x)Ga(1-x)As-GaAs heterostructure devices
[AD-A153264] 17 p2954 N85-28244
Digital control of diode laser for atmospheric spectroscopy
[NASA-CASE-NPO-16000-1] 18 p3112 N85-29264
Intense ion beam diode diagnostics using a tunable dye laser
[DE85-006079] 18 p3113 N85-29272
Measurement of radical species concentrations and polycyclic aromatic hydrocarbons in flames by fluorescence and absorption using a tunable dye laser
[DE85-006624] 18 p3113 N85-29274
Field measurements with the TAMS-2B and development of methods for measuring HCHO, HCl and HONO in real air
[PB85-172955] 18 p3135 N85-29419
Spectroscopic investigation of materials for tunable infrared lasers
[AD-A154124] 19 p3272 N85-30291
Lifetime and quenching measurements of C2H emission produced by vacuum ultraviolet photolysis of C2H2
[DE85-010789] 19 p3278 N85-30330
Generation of single nanosecond high-contrast radiation pulses (lambda=10.6 micrometers)
21 p3684 N85-32886
Lasing on LiF:F(-)2 - dye centers with transverse pumping 21 p3684 N85-32890
Tunable lasers with high conversion efficiency
21 p3687 N85-32906
Identification of vibrational-rotational transitions of Os-192O4 within frequency tuning limits of high pressure CO2 waveguide laser 21 p3689 N85-32917
Trivalent cerium doped crystals as tunable laser systems: Two bad apples
[DE85-008168] 22 p3790 N85-33482
High-resolution spectroscopy and dynamics of multiphoton processes in atoms and molecules
[AD-A155862] 24 p4147 N85-35714

TUNDRA
The ecology of tundra ponds of the Arctic coastal plain: A community profile
[TI85-900650] 15 p2589 N85-25958

TUNERS
NT WAVEGUIDE TUNERS
Characterization of CNRS Fizeau wedge laser tuner
[NASA-CR-174357] 09 p1325 N85-18328
Imaging apparatus for transverse electrode electro-optic tunable filter
[AD-D011524] 12 p1832 N85-21487
Wavelength dependent, tunable, optical time delay system for electrical signals
[AD-D011564] 15 p2548 N85-25725

TUNGSTATES
Spectral-luminescence characteristics and induced emission of Nd-3(+) ion in Gd(2-x)Nd(x)(WO4)3 crystals
21 p3688 N85-32912
Electronic structure and lattice dynamics of dimensionally constrained and disordered solids
[AD-A155927] 24 p4161 N85-35797

TUNGSTEN
Microstructural basis of strength and toughness in hardmetals 02 p0177 N85-11185
Magnetic properties of the cobalt matrix in WC-Co compacts 02 p0177 N85-11186
The inter-relation of microstructure, toughness and fatigue crack growth behaviour in WC-Co hardmetals
02 p0177 N85-11188
Hydrogen absorption on (110) tungsten planes at 30 K: An atom-probe field-ion microscope study
[DE84-015659] 04 p0560 N85-13565
Thermal conductivity of aluminum, copper, iron and tungsten for temperature from 1 K to the melting point
[PB84-235878] 06 p0770 N85-14924
The adsorption of CO and oxygen on Cu layers on a W(110) surface
[AD-A147345] 07 p0923 N85-15847
Influence of volumetric fiber content on some matrix damage factors during thermal cycling of tungsten-El 765 composite 10 p1443 N85-19087
Influence of melting conditions on strength of transition zone between steel and composite material
10 p1450 N85-19133
Influence of plastic deformation on structural stability of nichrome-tungsten composite materials
11 p1599 N85-20060
Negative lithium emission from a tungsten surface in a plasma
[DE85-003456] 12 p1936 N85-22167
Gigantic lithium deposit discovered in France
14 p2289 N85-24184
Ferroelectric tungsten bronze bulk crystals and epitaxial thin films for electro-optic device applications
[AD-A151044] 14 p2427 N85-24970
Influence of oxygen traces on the properties of tungsten heavy metals
[BLL-RARDE-TR-1177-(7291.7965)]
15 p2508 N85-25470
Corrosion inhibitor formulation for molybdenum, tungsten and other metals
[AD-D011593] 15 p2510 N85-25486
LPCVD tungsten deposition on Si-Ge alloy
[DE85-005586] 16 p2750 N85-26970
Positron annihilation studies of vacancy formation in tungsten, chromium, and niobium
[DE85-006837] 16 p2871 N85-27710
Continued development and testing of tungsten controlled porosity dispenser cathodes
[AD-A152595] 17 p2931 N85-28090
Influence of microstructure on mechanical properties in cemented tungsten-carbides 19 p3230 N85-30029
PAS determination of the vacancy formation enthalpy in tungsten
[DE85-010283] 19 p3240 N85-30066
Properties of tungsten-free steel for cutting tools
[BLL-M-35808-(5828.4)] 23 p3915 N85-34259
Detonation in tungsten-loaded HMX
[DE85-009806] 23 p3922 N85-34299
Dynamic compaction of a monosized spherical tungsten powder
[DE85-014808] 24 p4080 N85-35289
Applications of the mineral resources data system and the international strategic minerals inventory in mineral-resource assessments by region and commodity
24 p4105 N85-35451
The Conterminous United States Mineral Assessment Program 24 p4106 N85-35458

TUNGSTEN ALLOYS
The Palmqvist test and its applications in WC-Co alloys 02 p0177 N85-11187
Ultrasonic inspection of alloyed tungsten bars
[AD-A148900] 10 p1495 N85-19435
Fabrication and properties of tungsten heavy metal alloys containing 30% - 90% tungsten
[DE85-000152] 11 p1607 N85-20103
Stress corrosion cracking behavior of tungsten heavy alloys
[AD-A149843] 12 p1806 N85-21329
Development of reduced activation alloys for fusion service: Draft
[DE85-007464] 18 p3074 N85-29014

TUNGSTEN CARBIDES
Microstructure and deformation aspects of some specialty steels and hard metals
02 p0176 N85-11182
Erosion of sintered WC-Co alloys
02 p0179 N85-11201
Erosion of multiphase materials
[DE84-015616] 04 p0474 N85-13018

Calibration method for acoustic scattering measurements using a spherical target
[AD-D011521] 12 p1927 N85-22106
Phase size distribution in WC/Co hardmetal
[NPL-DMA(A)-93] 20 p3431 N85-31261
TUNGSTEN COMPOUNDS
NT TUNGSTATES
NT TUNGSTEN CARBIDES
Preparation and electronic properties of MoS(2) and WS(2) single crystals grown in the presence of cobalt
[AD-A146508] 06 p0866 N85-15506
TUNGSTEN INERT GAS WELDING
U GAS TUNGSTEN ARC WELDING
TUNING
A high resolution spectroscopic study of the oxygen molecule
[NASA-CR-174061] 02 p0172 N85-11150
Tunable microwave transversal filters
[AD-A148370] 08 p1158 N85-17304
Approximate models in multivariable process control: An inverse Nyquist array and robust tuning regulator interpretation
[RR-261] 08 p1216 N85-17663
Integrated circuit tunable cavity oscillator
[AD-D011474] 10 p1481 N85-19351
Precision tunable resonant microwave cavity
[NASA-CASE-LEW-13935-1] 11 p1628 N85-20248
Aircraft rotor blade with passive tuned tab
[NASA-CASE-ARC-11444-1] 19 p3217 N85-29947
Longitudinal tune control in synchrotrons
[DE85-010745] 20 p3527 N85-31937
Gradiential adaptive corrector with optimum tuning step 22 p3776 N85-33403
Tuning system for capacitively loaded 1/4 accelerating cavity
[DE85-012516] 24 p4091 N85-35358
TUNISIA
Tunisian climate seen through a Markov process
[CT-585] 23 p3950 N85-34482
TUNNEL DIODES
Spectroscopy of surface adsorbed molecules
[DE85-009452] 17 p3034 N85-28768
TUNNEL RESISTORS
U ELECTRON TUNNELING
U RESISTORS
TURBIDITY
Active remote sensing of ocean parameters, an engineering study 02 p0213 N85-11403
Influence scattering and Q in the lithosphere
[AD-A150939] 14 p2293 N85-24213
Visibility of small objects in turbid atmosphere 14 p2342 N85-24482
Rapid rate-kinetic turbidometric assay for quantitation of antiviral complement-fixing antibodies
[AD-A153644] 18 p3152 N85-29516
Determination of low chloride values in Rocky Flats scrub alloy solutions and other complex matrices
[DE85-011506] 23 p3911 N85-34234
TURBINE BLADES
The effect of channel convergence on heat transfer in a passage with short pin fins
[NASA-TM-83801] 01 p0046 N85-10303
Nonlinear structural and life analyses of a turbine blade 02 p0141 N85-10954
Heat flux sensors for burner liners and turbine blades and vanes 02 p0142 N85-10961
Studies on the hot corrosion of a nickel-base superalloy, Udimet 700
[NASA-TM-86882] 02 p0183 N85-11224
Preliminary results of a study of the relationship between free stream turbulence and stagnation region heat transfer
[NASA-TM-86884] 02 p0197 N85-11317
A finite element method for the solution of two-dimensional transonic flows in cascades
[PNR-90216] 03 p0316 N85-12045
Materials for advanced turbine engines. Project 2: Rene 150 directionally solidified superalloy turbine blades, volume 2
[NASA-CR-167993] 03 p0319 N85-12059
Cyclic endurance testing of the RB211-22B cast HP turbine blade — high pressure (HP)
[PNR-90210] 03 p0320 N85-12063
A study of the effect of wake-passing on turbine blades
[OUEL-1515/84] 03 p0363 N85-12326
Turbine blade damping study
[NASA-CR-171255] 04 p0456 N85-12890
Turbine blade damping study, introduction 04 p0456 N85-12891
Forced vibrations of friction-damped beam structures in two dimensions
[UDR-TM-82-08] 04 p0456 N85-12892
COST 50 - materials for gas turbines, part 1 and 2
3UK9
[NPL-DMA(A)-74] 05 p0617 N85-13943
The microstructural characteristics of revert superalloys — for turbine blades 05 p0617 N85-13945
Use of least-squares method for estimating errors of turbine blade type parts during fabrication 06 p0776 N85-14963
Random vibrations of aircraft engine blades 06 p0777 N85-14967
Turbine blade test cascade modifications and orations, August 1982 - April 1983
[DE84-009268] 06 p0833 N85-15303
Problems and possibilities for life extension in gas turbine components 07 p0907 N85-15742
Experiences with the material bevaviour and high temperature low cycle fatigue life prediction of the IN 738 blading alloy 07 p0908 N85-15746
Cyclic endurance testing of the RB211-22B cast HP turbine blade 07 p0908 N85-15747
Verification of life prediction through component testing 07 p0908 N85-15748
Repair welding and brazing procedures for turbine components and investigation of the brazing behavior of thin filler foils
[MTU-TB-908/84] 07 p0974 N85-16190
SSME lifetime prediction and verification, integrating environments, structures, materials: The challenge 08 p1095 N85-16918
Thermal-stress analysis for a wood composite blade
[NASA-CR-174794] 08 p1178 N85-17421
Life assessment and damage tolerance of wind turbines
[AD-B088148L] 08 p1179 N85-17427
Current status of trailing edge loss calculation for a turbine blade
[PNR-90244] 09 p1282 N85-18061
Replaceable blade turbine and stationary specimen corrosion testing facility
[NASA-TM-86931] 09 p1294 N85-18126
USSR report: Engineering and equipment
[JPRS-UEQ-85-001] 09 p1305 N85-18200
Designing the profile of turbine blades using an iteration technique 09 p1305 N85-18201
Calculating secondary nonviscous gas flows in spatial cascades of turbines 09 p1305 N85-18202
Influence of secondary flow rate on dynamic stresses in turbine rotor blades 09 p1306 N85-18205
Experimental study of influence of size of upper and lower laps on operational efficiency of centripetal full-inlet air driven microturbines 09 p1307 N85-18211
Calculating heat transfer coefficients for turbine profiles taking surface curvature and elevated flow turbulence into account 09 p1307 N85-18212
Correction of engraving stamp for forming blanks of gas turbine engine blades 09 p1307 N85-18213
Determination of blade service life under irregular loading conditions 09 p1309 N85-18222
The analysis by the lumped parameter method of slade platform friction dampers used in the high pressure fuel turbopump on the space shuttle main engine 09 p1338 N85-18417
One-piece HPTR blade squealer tip
[AD-D011452] 10 p1425 N85-18989
Nonlinear analysis for high-temperature multilayered fiber composite structures — turbine blades
[NASA-TM-83754] 12 p1797 N85-21273
High pressure turbine rotor two-piece blade retainer
[AD-D011498] 12 p1858 N85-21653
Cooled turbine blade tip closure
[AD-D011525] 12 p1858 N85-21654
Computer analysis of wind turbine blade dynamic loads
[DE85-000530] 12 p1867 N85-21714
Energy losses at leading edge of turbine blade during multirow jet cooling 13 p2049 N85-22826
effect of gas stream sweeping past the effluent of a perforated plate on heat transfer inside the perforations 13 p2051 N85-22836
Mechanization and automation of production processes in turbine building 14 p2269 N85-24057
Construction of profiles of intermediate blade sections from master profiles given on conical surfaces 14 p2272 N85-24075
Automating the study of error in discrete aerodynamic fairing design 14 p2288 N85-24176
Unified constitutive material models for nonlinear finite-element structural analysis — gas turbine engine blades and vanes
[NASA-TM-86985] 14 p2320 N85-24338
Cyclic structural analyses of anisotropic turbine blades for reusable space propulsion systems — ssme fuel turbopump
[NASA-TM-86990] 14 p2320 N85-24339
Advanced High Pressure O2/H2 Technology
[NASA-CP-2372] 16 p2733 N85-26862
Vacuum plasma coatings for turbine blades 16 p2734 N85-26869
Material technology 16 p2734 N85-26870
Design overview of fiber-reinforced superalloy composites for the Space Shuttle main engine 16 p2734 N85-26871
Materials for advanced rocket engine turbopump turbine blades 16 p2734 N85-26872
High-pressure hydrogen testing of single crystal superalloys for advanced rocket engine turbopump turbine blades 16 p2735 N85-26875
Turbine blade friction damping study 16 p2736 N85-26886
Nonlinear structural analysis for fiber-reinforced superalloy turbine blades 16 p2737 N85-26887
Redistribution of the inlet temperature profile through the SSME fuel turbine 16 p2739 N85-26901
Reusable rocket engine turbopump condition monitoring 16 p2740 N85-26907
Response of a wind turbine blade to seismic and turbulent wind excitations 16 p2817 N85-27375
Investigation of heat transfer to a turbine blade cascade using a shock tube
[AD-A153090] 17 p2898 N85-27871
Testing of materials and coatings for jet engine components under simulated operational conditions
[B8580073] 17 p2899 N85-27873
SSME turbopump turbine computations 17 p2911 N85-27944
Probabilistic structural analysis of SSME turbopump blades: Probabilistic geometry effects 17 p2913 N85-27958
Structural tailoring of SSME blades (vanes) 17 p2913 N85-27960
Cyclic structural analyses of SSME turbine blades 17 p2914 N85-27963
Effects of high mean stress on high-cycle fatigue behavior of PWA 1480 17 p2914 N85-27964
Post-stall wind tunnel data for NACA 44XX series airfoil sections
[DE85-002948] 18 p3060 N85-28931
Long-Term Materials Test Program
[DE85-003248] 18 p3077 N85-29034
Acoustic noise associated with the MOD-1 wind turbine: its source, impact, and control
[DE85-002947] 18 p3178 N85-29700
Turbine blade-tip clearance excitation forces
[NASA-CR-171534] 19 p3220 N85-29963
Effect of prolonged high temperature on durability of coated high-temperature nickel alloys 19 p3243 N85-30105
Effects of high mean stress on the high-cycle fatigue behavior of PWA 1480
[NASA-CR-176020] 19 p3287 N85-30388
Realization by vapor deposition of turbine blades covered with a silicon nitride layer 20 p3395 N85-31061
Preliminary results of a study of the relationship between free-stream turbulence and stagnation region heat transfer 20 p3452 N85-31435
Influence of moisture and elevated temperature on the fatigue properties of WTS-3 glass fiber blade material — wind turbine blade (WTS-3)
[FFA-TN-1984-58] 20 p3470 N85-31558
Design and fabrication of durable owner-built wind turbine blades
[DE85-009200] 20 p3484 N85-31650
R and D activities of the Propulsion Division 20 p3539 N85-32025
Component-specific modeling
[NASA-CR-174925] 21 p3556 N85-32119
Three-Dimensional Techniques Applied to Internal Flows in Propulsion Systems
[AGARD-LS-140] 21 p3586 N85-32293
A 3-D Euler method for internal transonic flows computation with a multi-domain approach 21 p3587 N85-32298
Calculation of 3-D flow without numerical mixing 21 p3588 N85-32301
Local heat-transfer measurements on a large, scale-model turbine blade airfoil using a composite of a heater element and liquid crystals
[NASA-TM-86900] 22 p3782 N85-33435
Design, development and operation of a high simultaneous capacity digital telemetry system — turbomachine blade flutter
[PNR-90261] 23 p3899 N85-34151
Calculation of trajectories of detached wind turbine blades and prediction of site risk levels associated with failures of HAWT's 24 p4110 N85-35475
TURBINE ENGINES
NT GAS TURBINE ENGINES
NT J-52 ENGINE
NT J-85 ENGINE
NT JET ENGINES
NT RAMJET ENGINES
NT SUPERSONIC COMBUSTION RAMJET ENGINES

NT TURBOFAN ENGINES
NT TURBOJET ENGINES
NT TURBOPROP ENGINES
Chemistry of fuel deposits and sediments and their predursors
[NASA-CR-174778] 01 p0034 N85-10209
HOST instrumentation R and D program overview 02 p0141 N85-10957
Hot section laser anemometry 02 p0142 N85-10962
Laser anemometer optimization 02 p0142 N85-10963
Turbine heat transfer 02 p0142 N85-10964
Life prediction and constitutive behavior: Overview 02 p0143 N85-10973
Dilution jet mixing 02 p0145 N85-10985
Combustion system for radiation investigations 02 p0145 N85-10986
Validation of structural analysis methods using the in-house liner cyclic rig 02 p0146 N85-10987
HOST liner cyclic facilities: Facility description 02 p0146 N85-10988
Energy efficient engine. Low pressure turbine test hardware detailed design report
[NASA-CR-167956] 02 p0147 N85-10994
Materials for advanced turbine engines. Project 2: Rene 150 directionally solidified superalloy turbine blades, volume 2
[NASA-CR-167993] 03 p0319 N85-12059
Heat transfer and pressure drop in blade cooling channels with turbulence promoters
[NASA-CR-3837] 03 p0361 N85-12315
Parametric estimates of propulsion system maintenance manhours
[AD-A147120] 07 p0894 N85-15662
Improvement of the corrosion resistance of turbine engine bearings
[AD-A147430] 07 p0905 N85-15731
Engine Cyclic Durability by Analysis and Testing
[AGARD-CP-368] 07 p0905 N85-15733
The application of a technology index to aircraft turbine engine cost estimating relationships
[AD-A147701] 08 p1087 N85-16874
Design description of a microprocessor based Engine Monitoring and Control unit (EMAC) for small turboshaft
[NASA-TM-86860] 09 p1283 N85-17935
Experimental and analytical study of ceramic-coated turbine-tip shroud seals for small turbine engines
[NASA-TM-86861] 09 p1281 N85-18057
An analytic model of gas turbine engine installations
[AD-A148708] 09 p1281 N85-18059
USSR report: Engineering and equipment
[JPRS-UEQ-85-001] 09 p1305 N85-18200
Use of braking stages for control of turbine speed 09 p1308 N85-18215
Advanced stress analysis methods applicable to turbine engine structures
[NASA-CR-175573] 12 p1778 N85-21165
Pressure drop and coefficients of internal heat transfer necessary for transpiration cooling 13 p2050 N85-22831
Composition and photochemical reactivity of turbine engine exhaust
[AD-A150559] 13 p2130 N85-23256
Design of piping for oil drain from turbine bearings 14 p2271 N85-24073
Ignition/combustion processes 16 p2740 N85-26909
New facility to study unsteady wake effects on turbine airfoil heat transfer 17 p2911 N85-27948
USSR report: Engineering and equipment
[JPRS-UEQ-85-004] 17 p2939 N85-28142
Flow characteristics of a partially submerged liquid pickup
[DE85-008744] 17 p2959 N85-28276
Improved statistical analysis method for prediction of maximum inlet distortion
[AD-A153767] 18 p3063 N85-28947
Ceramic Technology for Advanced Heat Engines Project
[DE85-008755] 18 p3080 N85-29052
Ceramic coatings for heat engine materials: Status and future needs
[DE85-008759] 18 p3080 N85-29053
Ceramic coatings for heat engine materials
[DE85-005238] 18 p3080 N85-29054
Component-specific modeling
[NASA-CR-174925] 21 p3556 N85-32119
Energy efficient engine, high pressure turbine thermal barrier coating. Support technology report
[NASA-CR-168037] 24 p4066 N85-35199
A study of the control of particulate emissions from turbine engine test cells 24 p4067 N85-35205

TURBINE PUMPS
Rotordynamic analysis of the SSME turbopumps using reduced models
[NASA-CR-171170] 01 p0054 N85-10355
Non-intrusive speed sensor — space shuttle main engine turbopumps
[NASA-CR-171204] 03 p0364 N85-12331
Analysis of physical-chemical processes governing SSME internal fluid flows
[NASA-CR-174245] 06 p0760 N85-14862
Assessment of the operating characteristics of the SSME LOX turbopump pump-end bearing
[NASA-CR-171287] 08 p1167 N85-17362
Calculation of flow about posts and powerhead model — space shuttle main engine
[NASA-CR-171344] 10 p1483 N85-19362
Cyclic structural analyses of anisotropic turbine blades for reusable space propulsion systems — ssme fuel turbopump
[NASA-TM-86990] 14 p2320 N85-24339
Advanced High Pressure O2/H2 Technology
[NASA-CP-2372] 16 p2733 N85-26862
Ceramics for advanced O2/H2 application 16 p2734 N85-26868
Design overview of fiber-reinforced superalloy composites for the Space Shuttle main engine 16 p2734 N85-26871
Materials for advanced rocket engine turbopump turbine blades 16 p2734 N85-26872
Development of new materials for turbopump bearings 16 p2735 N85-26877
Bearings working group 16 p2735 N85-26878
Advanced rocket engine cryogenic turbopump bearing thermal model 16 p2735 N85-26879
Hybrid bearings for LH2 and LO2 turbopumps 16 p2736 N85-26880
Rolling contact fatigue life of chromium ion plated 440C bearing steel 16 p2736 N85-26882
Signal analysis techniques for incipient failure detection in turbomachinery 16 p2736 N85-26884
Turbine blade friction damping study 16 p2736 N85-26886
Preliminary results on passive eddy current damper technology for SSME turbomachinery 16 p2737 N85-26890
Damping seal verification setup 16 p2738 N85-26893
Damping seals for turbomachinery 16 p2738 N85-26894
Vibration characteristics of the HPOTP (High Pressure Oxygen Turbopump) of the SSME (Space Shuttle Main Engine) 16 p2738 N85-26895
Analytical study of flow phenomena in SSME turnaround duct geometries 16 p2739 N85-26902
Reusable rocket engine turbopump condition monitoring 16 p2740 N85-26907
Nonintrusive shaft speed sensor 16 p2740 N85-26908
SSME fuel preburner two-dimensional analysis 17 p2911 N85-27943
SSME turbopump turbine computations 17 p2911 N85-27944
Probabilistic structural analysis of SSME turbopump blades: Probabilistic geometry effects 17 p2913 N85-27958
Cyclic structural analyses of SSME turbine blades 17 p2914 N85-27963
Constitutive cyclic deformation behavior in single-crystal and directionally solidified SSME high-pressure fuel turbopump airfoil materials 17 p2914 N85-27965
Improved turbopump dynamics
[NASA-TM-86514] 20 p3462 N85-31509

TURBINE WHEELS
Unsteady aerodynamic response of cascades and turborotors 03 p0319 N85-12058
Comparison between the properties of conventional wrought and powder metallurgical alloys for turbine disc applications 07 p0906 N85-15739
Problems and possibilities for life extension in gas turbine components 07 p0907 N85-15742
Clearance flow-generated transverse forces at the rotors of thermal turbomachines
[NASA-TM-77292] 07 p0973 N85-16180
Influence of setting angle of jet cooling nozzles on temperature and stress state of a turbine wheel 09 p1306 N85-18208
Causes and means of prevention of erosion of exit edges of drive vanes in final stages of K-300-240 turbine 14 p2272 N85-24076
Some problems of optimum journal design for disk-drum rotors under antisymmetric loading 14 p2286 N85-24167
Properties and microstructures for dual alloy combinations of three superalloys with alloy 901
[NASA-TM-86987] 16 p2749 N85-26963
Aerodynamic forces developing in channels between vanes in turbine drive wheels 16 p2765 N85-27082
Unsteady heat transfer due to time-dependent free stream velocity 17 p2911 N85-27947
Experimental measurements and analysis of heat transfer and gas dynamics in a rotating turbine stage 17 p2911 N85-27949
A comparison of experimental and theoretical results for rotordynamic coefficients of four annular gas seals
[NASA-CR-176086] 21 p3596 N85-32332

TURBINES
NT GAS TURBINES
NT SHROUDED TURBINES
NT STEAM TURBINES
NT WIND TURBINES
Characteristics of controlled-oscillating annular cascade test facility with Freon gas
[NAL-TR-812] 01 p0003 N85-10014
Energy efficient engine high pressure turbine ceramic shroud support technology report
[NASA-CR-168036] 02 p0147 N85-10996
Further development of a transonic cascade analysis
[AD-A145410] 02 p0198 N85-11319
Turbine test report, addendum
[DE84-015130] 02 p0205 N85-11353
Device for measuring relative axial expansion of turbine rotor employing space-vector tracking method 06 p0776 N85-14962
Influence of secondary flow rate on dynamic stresses in turbine rotor blades 09 p1306 N85-18205
On vortex transport in turbine channels 09 p1308 N85-18217
Gear case vibration isolation in a geared turbine generator 09 p1338 N85-18414
Assessing expired fatigue life in large turbine shafts
[DE84-016876] 09 p1340 N85-18427
Initial results for supercritical cycle experiments using pure and mixed-hydrocarbon working fluids
[DE84-017006] 09 p1345 N85-18460
Fabrication of turbine parts with transportable tools 14 p2267 N85-24046
Conservation of turbines by inhibited air 14 p2268 N85-24054
Manufacture of drive wheel vanes for hydraulic turbines on program controlled machine tools 14 p2269 N85-24058
Dependents of velocity distribution in exit section of converging channel on shape of inlet channel in regulating valve 14 p2277 N85-24106
Study of axial bearings without oil bath with radial cooling of blocks 14 p2286 N85-24164
Unsteady gas dynamics problems related to flight vehicles
[AD-A151187] 15 p2464 N85-25218
Aviation turbine fuels from tar sands bitumen and heavy oils. Part 1: Process analysis
[AD-A151319] 15 p2521 N85-25539
Exploratory wind-tunnel investigation of a wingtip-mounted vortex turbine for vortex energy recovery
[NASA-TP-2468] 16 p2699 N85-26867
Qualification of a wall gage for the SIMA wagon, adapted to the test of half models motorized by compressed air turbines — SIMA wind tunnel
[ONERA-PV-1/8068-GY] 16 p2701 N85-26877
Water brake convertor: A simple device to convert mechanical energy into heat energy
[DE85-006021] 16 p2716 N85-26766
Fuel and oxidizer turbine loss analysis 16 p2739 N85-26900
USSR report: Engineering and equipment
[JPRS-UEQ-84-006] 16 p2760 N85-27035
Quasi-steady vibrations of a rotating shaft grazing an obstacle: Spiral vibration
[BLL-CE-TRANS-7962-(9022.09)] 16 p2799 N85-27256
Ceramic turbochargers: A case study of a near-term application of high-strength ceramics
[DE85-006495] 17 p2975 N85-28379
Method for driving two-phase turbines with enhanced efficiency
[NASA-CASE-NPO-15037-2] 18 p3115 N85-29282
Variable cycle engine for high altitude aircraft
[AD-D011705] 19 p3221 N85-29969
Combustor turbulence 20 p3452 N85-31434
Heat transfer in aeropropulsion systems
[NASA-TM-87066] 20 p3453 N85-31444
Microprocessor control design for a low-head crossflow turbine
[AD-A155477] 21 p3556 N85-32121
Observations of the use of the setapoint detector
[AD-A154533] 21 p3571 N85-32208

TURBOCHARGERS
U SUPERCHARGERS
U TURBOCOMPRESSORS

TURBOCOMPRESSORS
Energy efficient engine component development and integration program
[NASA-CR-170934] 02 p0146 N85-10990
Full load testing in the platform module prior to tow-out: A case history of subsynchronous instability
05 p0642 N85-14117
Current problems in turbomachinery fluid dynamics
[AD-A147127] 07 p0958 N85-16074
Study of residual stresses introduced into TA6ZrD (685) cylinders by quenching — compressor disk alloy
[PNR-90240] 09 p1341 N85-18435
A theory of post-stall transients in multistage axial compression systems
[NASA-CR-3878] 12 p1771 N85-21117
Some unique features in operation of two-stage turbojet engine with afterburner 13 p2049 N85-22828
HPFTP flow diverter analysis
[NASA-CR-171424] 13 p2091 N85-23057
T700 cutter life improvement program
[AD-A150450] 13 p2099 N85-23089
Simulation of multistage turbine flows
17 p2911 N85-27945
Unsteady flow in multistage turbines
17 p2911 N85-27946
Precision die forging of blades or gas turbines
17 p2940 N85-28148
Ceramic turbochargers: A case study of a near-term application of high-strength ceramics
[DE85-006495] 17 p2975 N85-28379
Future of ceramic turbochargers: Promises and pitfalls
[DE85-006209] 17 p2975 N85-28380
TURBOCONVERTERS
U TURBOGENERATORS
TURBOELECTRIC CONVERSION
U TURBOGENERATORS
TURBOFAN AIRCRAFT
NT A-7 AIRCRAFT
NT BOEING 727 AIRCRAFT
NT BOEING 737 AIRCRAFT
NT BOEING 767 AIRCRAFT
NT C-141 AIRCRAFT
NT CONCORDE AIRCRAFT
NT CV-990 AIRCRAFT
NT DC 8 AIRCRAFT
NT F-111 AIRCRAFT
Aerodynamic detuning analysis of an unstalled supersonic turbofan cascade
[NASA-TM-87001] 16 p2700 N85-26670
A computer program for the drag prediction of subsonic, turbine powered aircraft in the en-route configuration
[VTH-LR-412] 16 p2701 N85-26681
TURBOFAN ENGINES
NT TF-34 ENGINE
Characteristics of controlled-oscillating annular cascade test facility with Freon gas
[NAL-TR-812] 01 p0003 N85-10014
Stall elimination and restart enhancement device
[AD-D011217] 01 p0010 N85-10062
Development trends and requirements of propulsion system technology for civil aircraft
01 p0011 N85-10066
Effect of combined pressure and temperature distortion orientation on high-bypass-ratio turbofan engine stability
[NASA-TM-83771] 01 p0011 N85-10067
Energy efficient engine. Volume 1: Component development and integration program
[NASA-CR-173084] 02 p0146 N85-10992
Energy efficient engine ICLS engine bearings, drives and configuration: Detail design report
[NASA-CR-167871] 02 p0147 N85-10997
Turbofan noise generation. Volume 2: Computer programs
[NASA-CR-167952] 02 p0275 N85-11791
Static jet noise test results of four 0.35 scale-model QCGAT mixer nozzles
[NASA-TM-86571] 04 p0558 N85-13551
Applications of finite and wave envelope element approximations to acoustic radiation from turbofan engine inlets in flight 05 p0726 N85-14664
Effect of steady-state temperature distortion on inlet flow to a high-bypass-ratio turbofan engine
[NASA-TM-86896] 07 p0904 N85-15725
Flow measurement device
[AD-D011432] 08 p1168 N85-17369
Research and development for semi-spherical inflow control device
[NAL-TR-833] 09 p1281 N85-18056
On selecting bypass mixers for turbofan engines
09 p1306 N85-18207
Preliminary performance of a vertical-attitude takeoff and landing, supersonic cruise aircraft concept having thrust vectoring integrated into the flight control system
[NASA-CR-172530] 10 p1423 N85-18977
Fluctuating pressures on fan blades of a turbofan engine, flight test investigation
[NASA-TP-2381] 10 p1553 N85-19790
Review of engine ingestions to wide body transport aircraft
[AD-P004185] 11 p1579 N85-19947
On the solution of the three-dimensional flowfield about a flow-through nacelle
[NASA-TM-87448] 13 p1969 N85-22371
Effects of inlet distortion on a static pressure probe mounted on the engine hub in an F-15 airplane
[NASA-TP-2411] 13 p1974 N85-22394
Hover test results of a small-scale twin-tilt nacelle model
[NASA-TM-86685] 14 p2210 N85-23706
Performance and surge limits of a TF30-P-3 turbofan engine/axisymmetric mixed-compression inlet propulsion system at Mach 2.5
[NASA-TP-2461] 15 p2472 N85-25261
Transient technique for measuring heat transfer coefficients on stator airfoils in a jet engine environment
[NASA-TM-87005] 15 p2560 N85-25794
Spacer structure
[AD-D011641] 17 p2897 N85-27866
Fan noise suppression in turbofan engines
[B8580076] 17 p2898 N85-27872
DEAN: A program for dynamic engine analysis
[NASA-TM-87033] 18 p3062 N85-28945
Energy efficient engine component development and integration program
[NASA-CR-172846] 19 p3219 N85-29958
Fault detection and accommodation testing on an F100 engine in an F-15 airplane
[NASA-TM-86735] 19 p3219 N85-29962
Measurement of turbofan-turbojet thrust from tailpipe static pressure
[AD-A154036] 19 p3220 N85-29967
Energy Efficient Engine Program technology benefit/cost study, volume 1
[NASA-CR-174766-VOL-1] 24 p4066 N85-35197
Energy Efficient Engine Program technology benefit/cost study, volume 2
[NASA-CR-174766-VOL-2] 24 p4066 N85-35198
TURBOFANS
Energy efficient engine component development and integration program
[NASA-CR-170034] 02 p0146 N85-10990
Turbofan noise generation. Volume 2: Computer programs
[NASA-CR-167952] 02 p0275 N85-11791
CFM 56-2. Oligocyclic fatigue of the turbofan disk: Dimensionning and tests for verification and improvements 07 p0908 N85-15750
Structural response of a rotating bladed disk to rotor whirl
[NASA-CR-175605] 13 p1973 N85-22391
Energy efficient engine. Fan and quarter-stage component performance report
[NASA-CR-168070] 23 p3897 N85-34141
TURBOGENERATORS
Operating experience with potassium systems — thermal power stations
[OEFZS-4275] 03 p0387 N85-12473
Monitoring environmental and related performance parameters for a Rankine-cycle turbine electric generator utilizing geothermal energy at the Gila Hot Springs, New Mexico
[DE84-901772] 09 p1345 N85-18465
Conceptual design of a 10 MW shore-based OTEC plant
[DE84-015808] 10 p1511 N85-19532
USSR report: Engineering and equipment
[JPRS-UEQ-84-001] 14 p2265 N85-24034
Study of axial bearings without oil bath with radial cooling of blocks 14 p2266 N85-24164
Conceptual design of a fixed-pitch wind turbine generator system rated at 400 kilowatts
[NASA-CR-174877] 18 p3127 N85-29383
ASME performance test on TVA Sequoyah unit 1
[DE85-901316] 19 p3358 N85-30815
TURBOJET AIRCRAFT
U JET AIRCRAFT
TURBOJET ENGINE CONTROL
Man-vehicle systems research facility advanced aircraft flight simulator throttle mechanism
22 p3798 N85-33527
TURBOJET ENGINES
NT J-52 ENGINE
NT J-85 ENGINE
NT TURBOFAN ENGINES
NT TURBOPROP ENGINES
Surge transient simulation in turbo-jet engine
05 p0596 N85-13796
Exploratory development of advanced surface flaw detection methods
[AD-A148757] 09 p1281 N85-18060
Experimental study of aerodynamic shielding of turbojet engine air intake against exhaust gases
09 p1307 N85-18210
Experimental study of ceramic coated tip seals for turbojet engines
[NASA-TM-86939] 10 p1483 N85-19363
Propagation of three-dimensional turbulent jet from lobar nozzle through surrounding stream
13 p2042 N85-22785
Exergetical analysis of turbojet engine cycle
13 p2049 N85-22825
Some unique features in operation of two-stage turbojet engine with afterburner 13 p2049 N85-22828
Influence of fuel properties on gas turbine combustion performance
[AD-A151464] 15 p2504 N85-25448
Transient technique for measuring heat transfer coefficients on stator airfoils in a jet engine environment
[NASA-TM-87005] 15 p2560 N85-25794
Preliminary wind tunnel study of the influence of a jet on the unsteady aerodynamics of a turbojet engine
[ONERA-RT-12/5115-RY-230-R-231G]
16 p2701 N85-26679
Measurement of turbofan-turbojet thrust from tailpipe static pressure
[AD-A154036] 19 p3220 N85-29967
Variable cycle engine for high altitude aircraft
[AD-D011705] 19 p3221 N85-29969
China has developed a new version of fighter aircraft
[AD-A155293] 21 p3555 N85-32118
TURBOMACHINE BLADES
NT COMPRESSOR BLADES
NT ROTOR BLADES (TURBOMACHINERY)
NT STATOR BLADES
NT TURBINE BLADES
Characteristics of controlled-oscillating annular cascade test facility with Freon gas
[NAL-TR-812] 01 p0003 N85-10014
Analysis of turbomachine blades: A review
02 p0208 N85-11374
Model equation for simulating flows in multistage turbomachinery
[NASA-TM-86869] 03 p0315 N85-12036
Performance deterioration of cascades exposed to solid particles 03 p0319 N85-12057
Unsteady aerodynamic response of cascades and turborotors 03 p0319 N85-12058
Turbomachinery blade design using advanced calculation methods
[PNR-90218] 04 p0456 N85-12896
Incorporation of viscous-inviscid interactions in turbomachinery design
[PNR-90219] 04 p0457 N85-12897
Modelling viscous flow in turbomachinery
[PNR-90220] 04 p0457 N85-12898
An improved computer model for prediction of axial gas turbine performance losses
[NASA-CR-174246] 07 p0904 N85-15724
Tailored airfoils for vertical axis wind turbines
[DE85-004628] 12 p1772 N85-21128
Current problems in turbomachinery fluid dynamics
[AD-A150533] 13 p1974 N85-22397
Experimental and analytical investigation of fan flow interaction with downstream struts
[NASA-CR-175756] 15 p2462 N85-25201
A study of internal and distributed damping for vibrating turbomachiner blades
[NASA-CR-175901] 17 p2898 N85-27868
Unsteady heat transfer due to time-dependent free stream velocity 17 p2911 N85-27947
Experimental measurements and analysis of heat transfer and gas dynamics in a rotating turbine stage
17 p2911 N85-27949
Composite loads spectra for select space propulsion structural components 17 p2912 N85-27953
Directionally solidified gas turbine alloys
[PNR-90284] 23 p3917 N85-34279
TURBOMACHINERY
NT CENTRIFUGAL COMPRESSORS
NT CENTRIFUGAL PUMPS
NT GAS TURBINES
NT SHROUDED TURBINES
NT STEAM TURBINES
NT TURBINE PUMPS
NT TURBINES
NT TURBOCOMPRESSORS
NT TURBOFANS
NT TURBOGENERATORS
NT WIND TURBINES
Advanced blade tip seal system, volume 2
[NASA-CR-167851] 02 p0147 N85-10999
Model equation for simulating flows in multistage turbomachinery
[NASA-TM-86869] 03 p0315 N85-12036
Performance deterioration of cascades exposed to solid particles 03 p0319 N85-12057

Unsteady aerodynamic response of cascades and turborotors 03 p0319 N85-12058
Comparative review of laser Doppler and laser two-focus anemometry in turbomachinery applications [VKI-TM-34] 03 p0367 N85-12350
Incorporation of viscous-inviscid interactions in turbomachinery design [PNR-90219] 04 p0457 N85-12897
Modelling viscous flow in turbomachinery [PNR-90220] 04 p0457 N85-12898
Rotordynamic Instability Problems in High-Performance Turbomachinery [NASA-CP-2338] 05 p0642 N85-14116
Analysis of dynamic characteristics of fluid force induced by labyrinth seal 05 p0643 N85-14129
Prediction of force coefficients for labyrinth seals 05 p0644 N85-14130
An Iwatsubo-based solution for labyrinth seals - comparison with experimental results 05 p0644 N85-14131
Preliminary investigation of labyrinth packing pressure drops at onset of swirl-induced rotor instability 05 p0644 N85-14132
Identification of dynamic coefficients of annular turbulent seals 05 p0644 N85-14133
Effects of fluid inertia and turbulence on force coefficients for squeeze film dampers 05 p0645 N85-14137
Squeeze-film dampers for turbomachinery stabilization 05 p0645 N85-14138
Influence of stationary components on unsteady flow in industrial centrifugal compressors 05 p0645 N85-14140
USSR report: Engineering and equipment [JPRS-UEQ-84-007] 06 p0775 N85-14954
The use of an optical data acquisition system for bladed disk vibration analysis [NASA-TM-86891] 06 p0817 N85-15184
Development of a Navier-Stokes rotor and stator analysis [AD-A146967] 07 p0958 N85-16070
Clearance flow-generated transverse forces at the rotors of thermal turbomachines [NASA-TM-77292] 07 p0973 N85-16180
Turbo fluid machinery and diffusers [NASA-TM-77467] 08 p1167 N85-17363
Calculating secondary nonviscous gas flows in spatial cascades of turbines 09 p1305 N85-18202
Analysis of experimental shaft seal data for high-performance turbomachines, as for Space Shuttle main engines [NASA-TM-86928] 12 p1844 N85-21569
Current problems in turbomachinery fluid dynamics [AD-A150533] 13 p1974 N85-22397
Future directions in aeropropulsion technology [NASA-TM-87010] 14 p2207 N85-23685
Experimental and analytical investigation of fan flow interaction with downstream struts [NASA-CR-175756] 15 p2462 N85-25201
Material technology 16 p2734 N85-26870
Monitoring of turbo-machines by shaft vibration measurement [BLL-CE-TRANS-7900-(9022.09)] 16 p2799 N85-27255
Simulation of multistage turbine flows 17 p2911 N85-27945
Vibrations of rotors connected through couplings with backlash 17 p2940 N85-28147
Calculation of friction at spherical bearing journals in turbomachines 17 p2940 N85-28150
Load-induced rotordynamic instabilities in turbomachinery 19 p3260 N85-30340
Damping seal for turbomachinery [NASA-CASE-MFS-25842-2] 19 p3280 N85-30341
Numerical and experimental investigation of turbomachinery rotor flow fields 20 p3451 N85-31429
A device for generating motive force through the expansion of a non-elastic dense fluid [NASA-TM-77664] 20 p3454 N85-31446
Three-Dimensional Techniques Applied to Internal Flows in Propulsion Systems [AGARD-LS-140] 21 p3586 N85-32293
An analysis of flow models: From Navier-Stokes to potential flow equations 21 p3587 N85-32295
Calculation of 3-D flow without numerical mixing 21 p3588 N85-32301
A comparison of experimental and theoretical results for rotordynamic coefficients of four annular gas seals [NASA-CR-176066] 21 p3596 N85-32332
A geometric modeller for turbomachinery applications 23 p3962 N85-34556

TURBOPAUSE

Space and time variations and turbopause dynamical structure 11 p1663 N85-20483
Turbopause as source of internal gravity waves 16 p2808 N85-27314

TURBOPROP AIRCRAFT

NT F-27 AIRCRAFT
NT OV-1 AIRCRAFT
Observations from varying the lift and drag inputs to a noise prediction method for supersonic helical tip speed propellers [NASA-TM-83797] 01 p0115 N85-10788
Installed nacelle drag-improvement tests of an M = 0.8 turboprop transport configuration [NASA-TM-84302] 07 p0902 N85-15716
Transmission error measurements in gearbox development 14 p2224 N85-23794
Establishment and maintenance of certification standards for helicopter and turboprop power transmission systems 14 p2224 N85-23796
Fundamental studies of structure borne noise for advanced turboprop applications [NASA-CR-175737] 15 p2646 N85-26320
A computer program for the drag prediction of subsonic, turbine powered aircraft in the en-route configuration [VTH-LR-412] 16 p2701 N85-26681
Effects of propeller rotation direction on airplane interior noise levels [NASA-TP-2444] 19 p3350 N85-30787

TURBOPROP ENGINES

An improved source model for aircraft interior noise studies [NASA-CR-172517] 08 p1217 N85-17668
Analytical fuel property effects: Small combustors, phase 2 [NASA-CR-174848] 10 p1458 N85-19175
Gears and Power Transmission Systems for Helicopters and Turboprops [AGARD-CP-369] 14 p2220 N85-23785
A state of the art assessment of turboprop transmission technology and projected needs for the next generation 14 p2220 N85-23770
Advanced gearbox technology in small turbo propeller engines 14 p2221 N85-23771
Fatigue life analysis of a turboprop reduction gearbox [NASA-TM-87014] 16 p2793 N85-27228
Wind tunnel results of advanced high speed propellers in the takeoff, climb and landing operating regimes [NASA-TM-87054] 19 p3213 N85-29925
Low-speed wind-tunnel tests of an advanced eight-bladed propeller [NASA-TM-86364] 19 p3214 N85-29926
Large-scale Advanced Propfan (LAP) program [NASA-TM-87067] 19 p3220 N85-29964
Two-plane balance and slip-ring design 22 p3799 N85-33536

TURBOPUMPS

U TURBINE PUMPS

TURBOROCKET ENGINES

Aerojet advanced engine concept 08 p1107 N85-16999

TURBOROTORS

U TURBINE WHEELS

TURBOSHAFTS

Temperature distortion generator for turboshaft engine testing [NASA-TM-83748] 07 p0893 N85-15658
Variable cycle engine for high altitude aircraft [AD-D011705] 19 p3221 N85-29969

TURBULENCE

NT ATMOSPHERIC TURBULENCE
NT CLEAR AIR TURBULENCE
NT GUSTS
NT HOMOGENEOUS TURBULENCE
NT ISOTROPIC TURBULENCE
NT LOW LEVEL TURBULENCE
NT MAGNETOHYDRODYNAMIC TURBULENCE
NT PLASMA TURBULENCE
Limiting effects during turbulent combustion 02 p0274 N85-11784
Chaotic behavior induced by solitons in perturbed integrable systems 02 p0283 N85-11844
Vorticity amplification in viscous flow around a body 03 p0360 N85-12309
Heat transfer and pressure drop in blade cooling channels with turbulence promoters [NASA-CR-3837] 03 p0361 N85-12315
Numerical studies of unsteady transonic flow over an oscillating airfoil [NASA-TM-86011] 03 p0361 N85-12316
On the co-variant formulation of the law of motion of passive particles in a field of turbulence [REPT-564] 03 p0377 N85-12407
A spatial model of wind shear and turbulence for flight simulation 03 p0395 N85-12518
Automatic recognition and turbuling objects [AD-A145908] 03 p0419 N85-12676
The role of freestream turbulence scale in subsonic flow separation [NASA-CR-174172] 04 p0452 N85-12870
Laminar separation bubble with transition: Prediction test with local interaction [BLL-PNR-90231-(8019.3153)] 06 p0808 N85-15132
Characteristic scale of inner mixing layers in stably stratified atmosphere 06 p0824 N85-15235
A scanning laser velocimeter for turbulence research [NASA-CR-172493] 07 p0897 N85-15686
The structure of dilute combusting sprays [NASA-CR-174838] 07 p0905 N85-15726
Dynamical characteristics of weak turbulence [AD-A147186] 07 p0959 N85-16075
Turbulence measurement interferometer apparatus [AD-D011377] 07 p0970 N85-16156
Recent advances in computational methods to solve the high-lift multi-component airfoil problem 08 p1068 N85-16774
Basic instability mechanisms in chemically reacting subsonic and supersonic flows [AD-A148408] 08 p1122 N85-17071
Nonradiative heating and enhanced mass-loss due to shear turbulence in massive hot stars 08 p1235 N85-17780
Analysis of pressure gradient-velocity correlation in turbulent, premixed flames 09 p1272 N85-17994
Flame propagation and stabilization studies using Rayleigh scattering and laser Doppler velocimetry [AD-A148802] 09 p1290 N85-18102
Turbulent premixed flame study [DE85-003220] 09 p1292 N85-18112
A free shear layer prediction of the turbulent wake of a flat plate towed below a free surface [AD-A148699] 09 p1319 N85-18293
Natural environment analysis [NASA-CR-171333] 10 p1428 N85-19010
Effects of a periodic disturbance on structure and mixing in turbulent shear layers and wakes [AD-A149278] 10 p1484 N85-19370
Internal Gravity Waves and Small-Scale Turbulence: Proceedings of the 2nd 'Aha Hulko'a Hawaiian Winter Workshop [AD-A149510] 10 p1522 N85-19597
Fragmentation and turbulence in collapsing gas clouds [DE85-003745] 11 p1633 N85-20282
Pre-turbulence: Transitional Laminar-turbulent flows 11 p1716 N85-20793
Frequency spectra of turbulent pulsations in stability of laminar boundary layer 11 p1716 N85-20795
Fluctuations and transport in fusion plasmas [DE85-003612] 11 p1732 N85-20893
Theory of resistivity-gradient-driven turbulence [DE85-002175] 11 p1733 N85-20896
Skin friction measurements for 2 relatively thick airfoil sections at high Reynolds number [AD-A150021] 12 p1772 N85-21125
Time and space variability of turbulent concentration fluctuations [AD-A149963] 12 p1896 N85-21898
Methods of progressing waves in turbulent media with applications to acoustics [AD-A149599] 12 p1920 N85-22055
Plasma performance of TFCX and jet with sawtoothing [DE85-003335] 12 p1936 N85-22186
Processes and problems in secondary star formation [DE85-003623] 12 p1960 N85-22322
Intensity fluctuations of focused laser beam during reflection in turbulent atmosphere 13 p2078 N85-22975
Mean flow and turbulence in complex terrain NPS (Naval Postgraduate School)/Vandenberg measurement system [AD-A150184] 13 p2138 N85-23274
Evolution of grains in a turbulent solar nebula 13 p2179 N85-23525
Estimating unsteady aerodynamic forces on a cascade in a three-dimensional turbulence field [NASA-TM-86701] 14 p2209 N85-23704
Factors affecting dwell times on digital displaying [NASA-TM-86406] 14 p2390 N85-24722
On the influence of turbulent motions on non-radial oscillations 14 p2444 N85-25083
Numerical studies of unsteady transonic flow over oscillating airfoil 15 p2458 N85-25174
Studies on the interference of wings and propeller slipstreams [NASA-CR-175753] 15 p2483 N85-25210
An experimental study of hairpin-type vortices as a potential flow structure of turbulent boundary layers 15 p2553 N85-25751
Mixing across a gas-gas interface [AD-A151471] 15 p2556 N85-25770
High-capacity real-time computer system for processing hydrophysical data 15 p2625 N85-26178

Measurement and theory of turbulence in RR Lyrae
[DE85-005899] 15 p2669 N85-26471
Voyage to Uranus 15 p2687 N85-26506
Observations, theoretical ideas and modeling of turbulent flows: Past, present and future
[NASA-TM-86679] 16 p2782 N85-27167
A Markov method for simulating non-Gaussian wind speed time series
[DE85-007131] 16 p2835 N85-27485
Kolmogorov and scalar spectral regimes in numerical turbulence
[NASA-TM-86699] 17 p2957 N85-28264
Parameterization of subgrid-scale fluxes in mesoscale meteorological models
[AD-A153016] 17 p2998 N85-28523
Flame acceleration mechanisms under conditions of partial confinement
[PB85-184063] 18 p3073 N85-29004
Applications of Canuto's method to Rayleigh-Taylor-initiated turbulence
[DE85-010835] 18 p3102 N85-29202
An experimental investigation of curvature and freestream turbulence effects on heat transfer and fluid mechanics in transitional boundary layer flows
19 p3264 N85-30240
Experimental determination of the mixing frequency parameter for coalescence/dispersion modeling of turbulent combustion
[DE85-011468] 19 p3270 N85-30280
Excitation of turbulence by density waves
[NASA-CR-3905] 19 p3314 N85-30548
Measurements of folded path optical scintillation using a corner cube, a cat's eye and a flat mirror reflector
[AD-A154044] 19 p3367 N85-30679
Ion-acoustic double layer in a magnetic picket fence configuration
[INPE-3552-PRE/764] 19 p3369 N85-30696
Two-point theory of current-driven ion-cyclotron turbulence
[DE85-010114] 19 p3372 N85-30918
Transition in Turbines
[NASA-CP-2386] 20 p3452 N85-31433
Preliminary results of a study of the relationship between free-stream turbulence and stagnation region heat transfer 20 p3452 N85-31435
Flat-plate transition 20 p3452 N85-31436
Sandia Cooperative Group on the Aerothermochemistry of Turbulent Combustion
[DE85-004720] 20 p3455 N85-31453
Sandia Cooperative Group on the Aerothermochemistry of Turbulent Combustion
[DE85-007493] 20 p3455 N85-31454
Progress in the development of a two-fluid model of turbulence: A set of 42 lecture panels
[CFD/84/20] 20 p3457 N85-31469
Verification of theoretically computed spectra for a point rotating in a vertical plane
[DE85-011967] 20 p3520 N85-31893
Mean and large-scale turbulence characteristics of the noise-producing region of an acoustically excited round jet 20 p3523 N85-31911
R and D activities of the Propulsion Division
20 p3539 N85-32025
Large eddy structures in transitional and turbulent flames
[AD-A154520] 21 p3562 N85-32157
Experiments on the influence of active walls on the initial amplitudes and growths of instability waves
[AD-A154630] 21 p3583 N85-32275
Velocity and transient measurements in a shock tube using a hot-wire anemometer
[AD-A154694] 21 p3589 N85-32305
Observations of mesospheric turbulence by rocket probe and VHF radar, part 2.4A 21 p3619 N85-32484
Mesospheric measurements of irregularity patches using a 3-antenna interferometer, part 3.6B
21 p3621 N85-32498
Techniques for the study of gravity waves and turbulence (keynote paper), part 4 21 p3621 N85-32499
Spectral measurements of turbulence and gravity waves, part 4.2A 21 p3622 N85-32501
Relationship of isolated turbulent regions to the general turbulent background, part 4.4A
21 p3623 N85-32506
Multiparameter conditionally sampled laser velocimetry measurements during flame propagation in a spark ignition engine
[DE85-009850] 22 p3793 N85-33502
A simulation of high energy cosmic ray propagation 1
[OG-5.4-1] 22 p3885 N85-34078
Interstellar turbulence, random density variations, and scintillation measurements
[OG-7.2-13] 23 p4015 N85-34880
On the cosmic ray diffusion in a violent interstellar medium
[OG-7.2-14] 23 p4015 N85-34881
The role of cosmic rays in magnetic hydrodynamics of interstellar medium
[OG-7.2-15] 23 p4015 N85-34882
Noise-sustained structure, intermittency and the Ginzburg-Landau equation
[DE85-009626] 24 p4094 N85-35379
Study of the parameters affecting the collapse of a rotating protostellar cloud 24 p4168 N85-35837

TURBULENCE EFFECTS
Application of two and three-dimensional criteria for calculating transitions and boundary layers over swept wings 08 p1070 N85-16783
Magnetohydrodynamic (MHD) turbulence in radio galaxies 12 p1958 N85-22305
Influence of turbulence of incident stream on three dimensional boundary layer 14 p2278 N85-24113
An excitation mechanism for solar 5-minute oscillation of intermediate and high degree
14 p2444 N85-25085
The effects of atmospheric turbulence on an air-to-air optical communication link
[AD-A151840] 15 p2543 N85-25700
A three-dimensional turbulent separated flow and related measurements
[NASA-CR-175913] 18 p3098 N85-29181
Radio wave scattering and intermittency of turbulence in the atmosphere 19 p3268 N85-30392
Radio wave scattering and turbulence intermittence in atmosphere 19 p3298 N85-30446
The Terrain-Responsive Atmospheric Code (TRAC) for plume growth and dispersion in complex terrain
[DE85-010541] 19 p3309 N85-30513
Fluctuations in light intensity during backscattering in turbulent medium 21 p3695 N85-32956
Compressible two-phase flow instabilities simulated with a hybrid Lagrange-Euler pseudospectral method
[DE85-009904] 23 p3931 N85-34361
The physical and empirical basis for a specific clear-air turbulence risk index
[NASA-CR-178522] 24 p4120 N85-35540

TURBULENCE METERS
Lidar measurements of structural characteristics of atmospheric turbulence 06 p0824 N85-15229
Turbulence measurements in shock induced flows
13 p2091 N85-23055
Surface shear stress characteristics in turbulent flows
19 p3211 N85-29914

TURBULENT BOUNDARY LAYER
Turbulent boundary layers over rough surfaces hypersonic flow
[AD-A145040] 01 p0003 N85-10016
An integral method for analyzing incompressible two dimensional turbulent boundary layers with separation
02 p0196 N85-11309
Design, manufacture, and testing of compliant coatings for reduction of turbulent drag
[AD-A145510] 02 p0196 N85-11323
Similarity criteria of spectra of pressure pulsations of turbulent boundary layer near wall
02 p0256 N85-11679
Developed turbulent flow under conditions of internal and external problems 02 p0260 N85-11700
Geometric characteristics of turbulent boundary layer separation upon action with direct shock wave in conical flows 02 p0269 N85-11755
A study of the critical layer in a rotating liquid payload
[AD-A146094] 03 p0362 N85-12321
Laminar and turbulent boundary layers in a plane of symmetry
[AD-A146261] 03 p0362 N85-12323
Turbulent boundary layers with secondary flow
[NASA-TM-77494] 04 p0498 N85-13176
The aerodynamics of bluff bodies in turbulent shear layers 05 p0593 N85-13760
Friction and heat exchange in laminar and turbulent boundary layers with axisymmetrical bodies exposed to heterogeneous supersonic flow
05 p0724 N85-14655
Channel constructed to provide well defined boundary layers for vorticity optical probe measurements
[AD-A146679] 06 p0809 N85-15140
Design studies of thick laminar flow airfoils for low speed flight employing turbulent boundary layer suction over the rear part 06 p1070 N85-16786
On the relaxation of a turbulent boundary layer after an encounter with a forward facing step
06 p1071 N85-16789
Full scale experiments into the use of large eddy breakup devices for drag reduction on aircraft
06 p1071 N85-16790
Oblique shock wave-turbulent boundary layer interaction on a porous wall with suction 06 p1072 N85-16794
Transonic shock interaction with a tangentially-injected turbulent boundary layer 06 p1072 N85-16796
A 3-dimensional turbulent boundary layer upstream and around a junction vortex flow 06 p1160 N85-17319
Aerothermal tests of a 12.5 percent cone at Mach 6.7 for various Reynolds numbers, angles of attack and nose shapes --- conducted in Langley 8-foot high temperature tunnel
[NASA-TP-2345] 06 p1161 N85-17322
Comparison of techniques to measure the low wavenumber wall pressure spectrum of a turbulent boundary layer
[AD-A148074] 06 p1162 N85-17331
Development of a floating element wall shear transducer
[AD-A148450] 06 p1164 N85-17346
Some structural features of unsteady separating turbulent shear flows
[AD-P004164] 09 p1265 N85-17949
Experiments on controlled, unsteady, separated turbulent boundary layers
[AD-P004172] 09 p1266 N85-17957
A finite difference method for inverse mode calculations of a three-dimensional boundary layer
[ESA-TT-863] 09 p1274 N85-18007
Comparison of two-dimensional laser and hot-wire velocimetry for a supersonic turbulent boundary layer
11 p1576 N85-19927
Experimental investigation of a turbulent incompressible boundary layer on a curved wall
11 p1577 N85-19936
Finite difference method for solving turbulent boundary layer equations 11 p1619 N85-20193
A survey of the turbulent drag reduction using passive devices
[NMI-R-193] 11 p1630 N85-20268
Flight-measured laminar boundary-layer transition phenomena including stability theory analysis
[NASA-TP-2417] 12 p1771 N85-21118
A study of the turbulent layer in the water at an air-water interface 14 p2378 N85-24679
An experimental study of hairpin-type vortices as a potential flow structure of turbulent boundary layers
15 p2553 N85-25751
Computational models of the viscous sublayer and limiting behavior of turbulence near a wall
[AD-A151198] 15 p2556 N85-25767
An exploratory investigation of sharp fin-induced shock wave/turbulent boundary layer interactions at high shock strengths
[AD-A151571] 15 p2556 N85-25772
Viscous effects on blast wave flowfields
[AD-A152013] 15 p2558 N85-25779
Three-dimensional boundary layers and shear flows activities at ONERA/CERT 15 p2558 N85-25785
Three-dimensional boundary layer research at NLR
15 p2559 N85-25787
Brief review of current work in the UK on three dimensional boundary layers 15 p2559 N85-25788
Thermodynamic evaluation of transonic compressor rotors using the finite volume approach
[NASA-CR-175811] 16 p2708 N85-26712
An experimental study of compressible turbulent reattaching free shear layers 16 p2781 N85-27161
Vortex studies relating to boundary layer turbulence and noise
[NASA-TM-87475] 16 p2782 N85-27169
Theoretical investigation of three-dimensional shock wave turbulent boundary layer interactions. Part 3
[AD-A152251] 16 p2783 N85-27177
An experimental investigation of the interaction between a shock wave and a turbulent boundary layer on a convex wall
[VTH-LR-426] 16 p2785 N85-27187
Navier-Stokes computational study of axisymmetric transonic turbulent flows with a two-equation model of turbulence
[AD-A152653] 17 p2958 N85-28265
Numerical simulation of unsteady motion in a turbulent mixing layer
[NAL-TR-849T] 18 p3099 N85-29183
On the origin of streamwise vortices in a turbulent boundary layer
[AD-A153651] 18 p3100 N85-29188
An experimental study of plane mixing layer development
[NASA-TM-86698] 19 p3221 N85-29971
Transverse vorticity measurements in an excited two-dimensional mixing layer 19 p3264 N85-30241
Acrosswind response of towers and stacks of circular cross-section 19 p3282 N85-30354
A survey of the turbulence in the marine surface layer for the operation of low-Reynolds number aircraft
[AD-A154133] 19 p3316 N85-30558
Analysis of the turbulent near wake at a sharp trailing edge 20 p3387 N85-31006
The effects of microbubbles on turbulent boundary layer skin friction 20 p3451 N85-31425
Transition in Turbines
[NASA-CP-2386] 20 p3452 N85-31433

Transition in a disturbed environment
20 p3452 N85-31436
Experimental observation of transition behavior on a flat plate
20 p3452 N85-31437
On the evaluation of boundary layer measurements on boattailed bodies of revolution in axisymmetric compressible subsonic flow
[ESA-TT-883] 20 p3457 N85-31471
Trailing edge flow and aerodynamic sound. Part 1: Tonal pressure and velocity fluctuations. Part 2: Random pressure and velocity fluctuations
[AD-A154947] 21 p3552 N85-32097
An evaluation of four methods of numerical analysis for two-dimensional airfoil flows
[AD-A155202] 21 p3552 N85-32098
Recession of graphitic nozzles in rocket motors
21 p3560 N85-32144
Investigations of micro-turbulence in the bottom of the boundary layer
[AD-A155148] 21 p3636 N85-32585
Thermal contraction of current flow through electrode turbulent boundary layer 21 p3690 N85-32926
On the application of a hairpin vortex model of wall turbulence to trailing edge noise prediction
[NASA-CR-177938] 22 p3728 N85-33109
Experimental aerodynamic heating to simulated space shuttle tiles in laminar and turbulent boundary layers with variable flow angles at a nominal Mach number of 7
[NASA-TP-2307] 23 p3929 N85-34351
A three-dimensional turbulent boundary layer undergoing transverse strain and streamwise pressure gradient
[NASA-TM-86768] 23 p3930 N85-34358
Adverse pressure gradient and separating turbulent boundary-layer flows: The effect of disequilibrium in initial conditions 24 p4059 N85-35155
Vortex boundary-layer interactions
[NASA-CR-176192] 24 p4093 N85-35373
Pressure cross spectra in turbulent boundary layers in water
[AD-A156153] 24 p4094 N85-35378

TURBULENT DIFFUSION

Engineering method of calculating a turbulent diffusion flame
[BLL-M-35761-(5828.4)] 02 p0171 N85-11147
On the co-variant formulation of the law of motion of passive particles in a field of turbulence
[REPT-564] 03 p0377 N85-12407
Combustion driven oscillation of ducted diffusion flame
09 p1289 N85-18094
Influence of turbulence on erosion by a particle-laden fluid jet
[DE84-014365] 09 p1320 N85-18301
Atmospheric diffusion in hilly region on middle reaches of the Chang Jiang 11 p1620 N85-20196
Continued research in mesoscale air pollution simulation modeling. Volume 6. Further studies in the modeling of microscale phenomena
[PB85-137370] 12 p1887 N85-21844
Constraints of observations of solar oscillations on solar models with mixing by turbulent diffusion
[DE85-003741] 13 p2205 N85-23678
An equation of profile of snow drift density during snowfall 15 p2581 N85-25919
Field validation of 6-particle puff model
[DE85-004073] 15 p2589 N85-25962
Estimation of vertical diffusion from observations of Atmospheric turbulence layers, part 4.4B
21 p3623 N85-32507
MST radar data management
21 p3627 N85-32532
Application of a turbulent closure model to the parameterization of the vertical diffusion of heat, momentum, and humidity in the ECMWF model — European Center for Medium Term Weather Forecasting (ECMWF)
[MITT-41] 24 p4095 N85-35387

TURBULENT FLOW

NT CAVITATION FLOW

A review and analysis of boundary layer transition data for turbine application
[NASA-TM-86880] 01 p0047 N85-10306
Analytical modeling of random thermal fluctuations in the NORDA high-frequency sound scattering facility
[AD-A145024] 01 p0116 N85-10790
Accelerated convergence for incompressible flow calculations
[NASA-TM-86883] 02 p0140 N85-10949
Direct numerical simulation of curved turbulent channel flow
[NASA-TM-86974] 02 p0197 N85-11316
Preliminary results of a study of the relationship between free stream turbulence and stagnation region heat transfer
[NASA-TM-86884] 02 p0197 N85-11317
The CMC/3DPNS computer program for prediction of three-dimensional, subsonic, turbulent aerodynamic juncture region flow. Volume 3: Programmers' manual
[NASA-CR-165996] 02 p0197 N85-11318
Design, manufacture, and testing of compliant coatings for reduction of turbulent drag
[AD-A145510] 02 p0198 N85-11323
Computer simulation techniques for turbulent flows
[CFD/84/11] 02 p0199 N85-11331
Developed turbulent flow under conditions of internal and external problems 02 p0260 N85-11700
Laminar-to-turbulent flow transition under influence of acoustic oscillations 02 p0260 N85-11701
Second order modeling of scalar turbulent flows
03 p0360 N85-12311
The structure of the vorticity field in turbulent channel flow. Part 2: Study of ensemble-averaged fields
[NASA-TM-86657] 03 p0361 N85-12317
Numerical simulations of compliant material response to turbulent flow, revision 1
[AD-A145801] 03 p0372 N85-12373
Study of the structure of turbulent shear flows at supersonic speeds and high Reynolds number
[NASA-CR-174144] 04 p0452 N85-12865
Fundamental study of three dimensional two phase flow in combustion systems
[AD-A142886] 04 p0498 N85-13177
Numerical calculation of steady turbulent flows in adverse pressure gradients
[CFD/83/9] 04 p0501 N85-13195
Progress in the development of a two-fluid model of turbulence for near-wall flows, part 1
[CFD/84/7-PT-1] 04 p0501 N85-13196
Progress in the development of a two-fluid model of turbulence for near-wall flows. Part 3: Preliminary investigation of a stably-stratified boundary layer
[CFD/84/9-PT-3] 04 p0501 N85-13197
Navier-Stokes computational study of axisymmetric transonic turbulent flows with a two-equation model of turbulence 05 p0634 N85-14068
Direct numerical simulation of curved turbulent channel flow 05 p0635 N85-14072
Experiments on the structure of turbulent reattaching flow 05 p0635 N85-14074
Identification of dynamic coefficients of annular turbulent seals 05 p0644 N85-14133
Analysis and testing for rotordynamic coefficients of turbulent annular seals with different, directionally homogeneous surface-roughness treatment for rotor and stator elements 05 p0644 N85-14134
Effects of fluid inertia and turbulence on force coefficients for squeeze film dampers
05 p0645 N85-14137
A three-dimensional axisymmetric calculation procedure for turbulent flows in a radial vaneless diffuser
[NASA-TM-86903] 06 p0749 N85-14798
Investigation of the local mass transfer of a laminar and turbulent falling liquid film
[BLL-T6368/BG/WH792/84] 06 p0807 N85-15130
Channel constructed to provide well defined boundary layers for vorticity optical probe measurements
[AD-A146579] 06 p0809 N85-15140
A scanning laser velocimeter for turbulence research
[NASA-CR-172493] 07 p0897 N85-15686
Studies of the wall shear stress in a turbulent pulsating pipe flow
[AD-A146772] 07 p0957 N85-16068
Turbulence measurement interferometer apparatus
[AD-D011377] 07 p0970 N85-16156
Ionospheric turbulence: Interchange instabilities and chaotic fluid behavior
[AD-A147810] 07 p0998 N85-16337
Turbulent drag reduction research
08 p1071 N85-16788
Combustion in high speed air flows
[AD-A148371] 08 p1122 N85-17070
The two-fluid model of turbulence applied to combustion phenomena
[CFD/84/15] 08 p1124 N85-17089
Computation of flow and heat transfer in flow around a 180 deg bend
[AD-A148065] 08 p1162 N85-17330
A 2-dimensional second order closure model of the upper atmosphere 08 p1182 N85-17450
Closure problem and numerical studies of turbulence
08 p1209 N85-17606
Research done at DERAT (October 1982 through September 1983); summary of principal results obtained
[NASA-TM-77786] 08 p1228 N85-17730
USSR report: Engineering and equipment
[JPRS-UEQ-85-001] 09 p1305 N85-18200
Calculating heat transfer coefficients for turbine profiles taking surface curvature and elevated flow turbulence into account 09 p1307 N85-18212
Analysis of sudden expansion flow in a two-dimensional duct with and without side-wall injection using the k-epsilon turbulence model 09 p1317 N85-18282
Turbulent buoyant flow and pressure variations around a circular cylinder in a cross uniform flow near the ground 09 p1318 N85-18287
The sensitivity analysis in k-epsilon turbulence modeling applied to jet flows 09 p1318 N85-18288
A turbulent closure model for the free atmosphere
09 p1351 N85-18502
Turbulence in pure superfluid flow
09 p1397 N85-18790
A multistage time-stepping scheme for the Navier-Stokes equations
[NASA-CR-172527] 10 p1483 N85-19365
Momentum and heat transfers in a complex, but well-defined turbulent fluid flow
[DE85-002857] 10 p1486 N85-19381
Discovery about temperature fluctuations in turbulent air flows 10 p1500 N85-19466
Modeling turbulent flow in compressible fluids: Metrological aspects — conferences
11 p1575 N85-19926
Characterization of jet turbulence using infrared radiometry 11 p1576 N85-19928
Laser Raman techniques for studying flows and flames 11 p1576 N85-19929
Experimental approach to terms within grids — turbulent flow calculations 11 p1576 N85-19930
Fourier densitometry: A new optical method for measuring density fluctuations by Rayleigh scattering — turbulent jets 11 p1576 N85-19932
Research in nonlinear problems of energy: Informal technical report
[DE85-001529] 11 p1595 N85-20031
Numerical simulation of turbulent reacting flows
[DE84-016777] 11 p1632 N85-20278
Calculation of oscillating turbulent flows in open channels
[KU-SFB-80/T/228] 11 p1633 N85-20289
Pre-turbulence: Transitional Laminar-turbulent flows
11 p1716 N85-20793
An investigation of turbulence mechanisms in V/STOL upwash flow fields
[AD-A149786] 12 p1772 N85-21123
Investigation of flowfields found in typical combustor geometries
[NASA-CR-3869] 12 p1779 N85-21187
Two-dimensional measurements of OH concentration and temperature in reactive flows
[AD-A149849] 12 p1800 N85-21292
Kinetics of nitric oxide formation in laminar and turbulent methane combustion
[PB85-149696] 12 p1804 N85-21313
Application of large eddy interaction model to channel flow
[NASA-TM-86891] 12 p1844 N85-21572
Theoretical and empirical studies of the basic structure of turbulent shear flows, including separated flows and effects of wall curvature
[AD-A149657] 12 p1846 N85-21580
Turbulent convecting flow in a square duct with a 180 deg bend: An experimental and numerical study
[AD-A149969] 12 p1846 N85-21583
Time and space variability of turbulent concentration fluctuations
[AD-A149963] 12 p1896 N85-21896
Hydrodynamic stability problem formulated by numerical solutions of the Navier-Stokes equations
12 p1948 N85-22223
Turbulent flows of surfactant solutions
[AD-B089137L] 13 p2092 N85-23058
Flow-induced vibrations of a circular cylinder due to turbulent internal flows
[DE85-002766] 13 p2103 N85-23110
Evolution of set of Rossby waves toward anisotropic equilibrium state 13 p2109 N85-23141
Investigation of the turbulent separated flow behind a spoiler
[ISL-CO-240/83] 14 p2213 N85-23726
Turbulent flow around circular cylinder uniformly rotating in infinite incompressible fluid 14 p2277 N85-24109
Hydraulic drag of rod with artificial microroughness in longitudinal flow 14 p2278 N85-24111
Calculating boundary layer on profile with laminar and turbulent flow zone 14 p2288 N85-24177
Problem of reduction to ideal tube in experimental aerodynamics 14 p2288 N85-24179
Block-implicit multigrid solution of Navier-Stokes equations in primitive variables
[DE85-004071] 14 p2301 N85-24250
Energy structure of atmospheric boundary layer above waves 14 p2335 N85-24442
Modeling of shear flow in a stratified fluid
14 p2340 N85-24469

Unsteady transonic aerodynamic and aeroelastic calculations about airfoils and wings
15 p2459 N85-25185
Analysis of selected problems involving vortical flows
[NASA-CR-177347] 15 p2463 N85-25212
On the structure of the turbulent vortex
15 p2463 N85-25213
Heat transfer and fluid mechanics measurements in the turbulent reattaching flow behind a backward-facing step
15 p2553 N85-25753
A critical evaluation of various turbulence models as applied to internal fluid flows
[NASA-TP-2474] 15 p2554 N85-25757
The influence of jet-grid turbulence on heat transfer from the stagnation region of a cylinder in crossflow
[NASA-TM-87011] 15 p2554 N85-25760
Turbulence effects on a glow discharge as derived from continuity and energy considerations
[AD-A151838] 15 p2557 N85-25775
An experimental study of the noise generated by vaporous cavitation in turbulent shear flows produced by confined orifice plates
15 p2645 N85-26316
La Recherche Aerospatiale Bimonthly Bulletin Number 1984-3, 220/May-June
[ESA-TT-882] 16 p2695 N85-26696
Low Reynolds number vehicles
[AGARD-AG-288] 16 p2699 N85-26666
Rotor blade flap-lag stability and response in forward flight in turbulent flows
16 p2705 N85-26698
Thermodynamic evaluation of transonic compressor rotors using the finite volume approach
[NASA-CR-175811] 16 p2708 N85-26712
Confined turbulent swirling recirculating flow predictions
[NASA-CR-174917] 16 p2709 N85-26716
Turbulence characteristics of swirling flowfields
[NASA-CR-174918] 16 p2709 N85-26717
Turbulent flow of fluid near trailing edge of plate in stream at zero angle of attack
16 p2764 N85-27057
Observations, theoretical ideas and modeling of turbulent flows: Past, present and future
[NASA-TM-86679] 16 p2782 N85-27167
Dynamic response of fluid transmission lines
[AD-A151926] 16 p2782 N85-27171
Study of the coupling between average, coherent and turbulent fields in a circular excited free jet
[ISL-R-115/83] 16 p2785 N85-27184
Computation model of turbulent free flow: Application to axisymmetric jets
[ISL-R-126/83] 16 p2785 N85-27185
The development of a computational model for a two-dimensional turbulent flow. Part 1: Mathematical background — solid fuel combustion
[VTH-LR-436-PT-1] 16 p2785 N85-27186
A study of the effect of gently varying terrain on atmospheric flow near the surface
16 p2823 N85-27411
An introduction to vortex breakdown and vortex core bursting
[NAE-AN-28] 17 p2892 N85-27829
SSME turbopump turbine computations
17 p2911 N85-27844
An experimental investigation of a turbulent junction vortex
[NASA-CR-175915] 17 p2957 N85-28259
Heat transfer in pipes
[NASA-TM-77638] 17 p2957 N85-28262
Navier-Stokes computational study of axisymmetric transonic turbulent flows with a two-equation model of turbulence
[AD-A152653] 17 p2958 N85-28265
Coherent structure reflective turbulent viscous flow modeling
[AD-A153066] 17 p2958 N85-28267
A three-dimensional turbulent separated flow and related measurements
[NASA-CR-176913] 18 p3098 N85-29181
Surface shear stress characteristics in turbulent flows
19 p3211 N85-29914
Nacelle/pylon/wing integration on a transport model with a natural laminar flow nacelle
[NASA-TP-2439] 19 p3213 N85-29924
Decay of a coherent scalar disturbance in a turbulent flow
[NASA-TM-86700] 19 p3264 N85-30244
Turbulent transport and length scale measurement experiments with confined coaxial jets
[NASA-CR-174831] 19 p3265 N85-30245
One mechanism for generation of wave disturbances in spectra of turbulent flows near ocean surface
19 p3269 N85-30397
A study of the turbulent layer in the water at an air-water interface
[AD-A154117] 19 p3319 N85-30578
Sandia Cooperative Group on the Aerothermochemistry of Turbulent Combustion. Discussion record of fourth meeting
[DE85-004720] 20 p3423 N85-31248
Intermittency, conditional sampling and turbulent combustion
20 p3424 N85-31249
Conditional modelling in turbulent shear flows
20 p3424 N85-31250
The microstructure approach to conserved scalar pdf models
20 p3424 N85-31251
Rayleigh scattering for density measurements in premixed flames: One point, time series data
20 p3424 N85-31253
Blowout of turbulent diffusion flames
20 p3425 N85-31256
Non-equilibrium effects in turbulent diffusion flames
20 p3425 N85-31258
Vortex simulation of v-shaped flame
20 p3425 N85-31259
Mechanisms of exhaust pollutants and plume formation in continuous combustion
[AD-A154169] 20 p3435 N85-31310
The effect of injection-stream turbulence on film cooling effectiveness and heat transfer coefficients
20 p3451 N85-31424
Turbulent reacting flows 20 p3451 N85-31427
A mathematical analysis of the effect of free stream turbulence on the Blasius boundary layer
20 p3451 N85-31430
Combustor turbulence 20 p3452 N85-31434
Heat transfer and fluid mechanics measurements in transitional boundary layer flows
20 p3453 N85-31439
A review and analysis of boundary layer transition data for turbine application
20 p3453 N85-31440
Turbulent solutions of equations of fluid motion
20 p3453 N85-31441
An implicit finite-difference code for a two-equation turbulence model for three-dimensional flows
[NASA-TM-86752] 20 p3454 N85-31448
On the multifractal nature of fully developed turbulence and chaotic systems
[PREPRINT-413] 20 p3455 N85-31458
Progress in the development of a two-fluid model of turbulence: A set of 42 lecture panels
[CFD/84/20] 20 p3457 N85-31469
Optimization of a numerical method to calculate elliptic flows
[ESA-TT-889] 20 p3457 N85-31472
Injection of drag reducing additives into turbulent water flows: Two-component velocity measurements and mixing length model predictions
[AD-A154604] 21 p3583 N85-32274
Numerical solutions of turbulent models for flow over a flat plate with angle of attack
[DE85-010380] 21 p3585 N85-32286
Determination of billows and other turbulent structures, part 4.1A
21 p3621 N85-32500
Recent results at the Sunset radar
21 p3627 N85-32536
Theoretical foundations of turbulent flows
21 p3683 N85-32680
On the application of a hairpin vortex model of wall turbulence to trailing edge noise prediction
[NASA-CR-177936] 22 p3728 N85-33109
Sandia Cooperative Group on the Aerothermochemistry of Turbulent Combustion. Discussion record of the second meeting
[DE85-007493] 22 p3743 N85-33203
Comments on two matters related to turbulent combustion
22 p3743 N85-33204
Pressure correlations in turbulent reacting flows
22 p3744 N85-33205
Second order modelling in non-constant density flows
22 p3744 N85-33206
Turbulent mixing and combustion
22 p3744 N85-33207
Jet flows: Modelling and experiments
22 p3744 N85-33208
Simultaneous measurement of velocity and density in a turbulent nonpremixed flame 22 p3744 N85-33209
Vortex dynamics simulation of conserved scalar dissipation
22 p3745 N85-33210
Nonequilibrium chemistry in an isothermal turbulent flow
22 p3745 N85-33211
Modeling of turbulent recirculating combusting flows
22 p3745 N85-33212
Turbulence modelling for the prediction of turbulent jets: Wakes and plumes
[CFD/84/5] 22 p3784 N85-33447
The calculation of two-dimensional buoyant surface jets with the k-W model of turbulence — kinetic energy-vorticity fluctuations (k-W)
[CFD/84/21] 22 p3785 N85-33448
Experimental aerodynamic heating to simulated space shuttle tiles in laminar and turbulent boundary layers with variable flow angles at a nominal Mach number of 7
[NASA-TP-2307] 23 p3929 N85-34351
A study of the second and third order closure models of turbulence for prediction of separated shear flows
[NASA-CR-176127] 23 p3929 N85-34353
Adverse pressure gradient and separating turbulent boundary-layer flows: The effect of disequilibrium in initial conditions
24 p4059 N85-35155
Prediction of turbulent internal recirculating flows with K-epsilon models
24 p4092 N85-35366
Studies on effects of boundary conditions in confined turbulent flow predictions
[NASA-CR-3929] 24 p4093 N85-35371
Turbulent structure of stably stratified nocturnal slope flows
[AD-A155845] 24 p4123 N85-35559
Two-point closure study of covariance budgets for turbulent Rayleigh-Benard convection
[PB85-189108] 24 p4124 N85-35568

TURBULENT HEAT TRANSFER

A study of the effect of wake-passing on turbine blades
[OUEL-1515/84] 03 p0363 N85-12326
Convective heat transfer coefficients for pipe flow with curvature induced secondary motion
09 p1318 N85-18285
An experimental investigation of flap turbulent heat transfer and pressure characteristics in hypersonic flow
12 p1821 N85-21426
Coupling between velocity oscillations and solid propellant combustion
[AD-A151081] 14 p2247 N85-23927
Design and construction of a computer controlled mirothermocouple probe for the study of buoyant jets
[AD-A152224] 16 p2788 N85-27199
Experimental investigation of turbulent heat transfer in straight and curved rectangular ducts
[AD-A154413] 19 p3266 N85-30255
Bypass transition to turbulence and research Desiderata
20 p3453 N85-31442
Scale separation closure and Alfven wave turbulence
[DE85-013124] 24 p4095 N85-35385

TURBULENT JETS

The properties of plane turbulent buoyant jet
[NAL-TR-798] 01 p0046 N85-10304
Characteristics of a turbulent plane offset jet
02 p0196 N85-11310
An experimental study of jet impingement on a circular cylinder
[AD-A145583] 02 p0198 N85-11326
Mass and momentum transport in a turbulent buoyant vertical axisymmetric jet
05 p0635 N85-14070
Design of swirled axisymmetric turbulent jets
05 p0724 N85-14657
The properties of a round turbulent buoyant jet
[NAL-TR-826] 06 p0808 N85-15136
Turbulent jet flow in a channel with a circulation region
09 p1306 N85-18218
An experimental study of single and multiple turbulent buoyant jets in crossflow
09 p1317 N85-18281
Deflected jet experiments in a turbulent combustor flowfield
[NASA-CR-174863] 13 p1973 N85-22390
Behavior of turbulent gas jets in an axisymmetric confinement
[NASA-CR-174829] 15 p2473 N85-25265
An experimental investigation of unexcited and excited elliptic jets
15 p2554 N85-25755
Buoyant jet entrainment in stratified fluids
19 p3263 N85-30238
Conditional modelling in turbulent shear flows
20 p3424 N85-31250
Recent measurements in turbulent jet flames at Sandia Combustion Research Facility 20 p3424 N85-31254
Assessment of superlayer contribution to the conserved scalar PDF in a hydrogen turbulent jet diffusion flame
20 p3425 N85-31255
Strong turbulence chemistry interaction in a piloted turbulent jet diffusion flame 20 p3425 N85-31257
Jet flows: Modelling and experiments
22 p3744 N85-33208
Turbulence modelling for the prediction of turbulent jets: Wakes and plumes
[CFD/84/5] 22 p3784 N85-33447

TURBULENT MIXING

Further developments of a nongradient theory of premixed turbulent flames
[NAL-TR-802T] 01 p0023 N85-10143
Experiments on turbulent mixing and chemical reactions in a liquid mixing layer
02 p0134 N85-10912
Effects of core mixing on solar oscillation frequencies
[DE84-015540] 03 p0449 N85-12853

Long range effect of turbulent pressure pulsations in plane-parallel flows at different velocities with various flame fronts 09 p1308 N85-18220
Mixing chemical reaction and flow field development in ducted rockets
[DE85-002710] 11 p1591 N85-20009
Propagation of three-dimensional turbulent jet from lobar nozzle through surrounding stream 13 p2042 N85-22785
Time-dependent flow of stream swirled in vortex chamber 13 p2043 N85-22786
Behavior of turbulent gas jets in an axisymmetric confinement
[NASA-CR-174829] 15 p2473 N85-25265
An experimental investigation of confined, multiple, turbulent jet mixing with recirculation — flow distribution in combustors with injection plates 15 p2555 N85-25764
Mixing across a gas-gas interface
[AD-A151471] 15 p2556 N85-25770
Kolmogorov and scalar spectral regimes in numerical turbulence
[NASA-TM-86699] 17 p2957 N85-28264
Numerical simulation of unsteady motion in a turbulent mixing layer
[NAL-TR-849T] 18 p3099 N85-29183
Transverse vorticity measurements in an excited two-dimensional mixing layer 19 p3264 N85-30241
Destruction of density jumps in ocean by turbulence 19 p3291 N85-30407
Slow chemistry effects in a turbulent mixing layer 20 p3424 N85-31252
Recent measurements in turbulent jet flames at Sandia Combustion Research Facility 20 p3424 N85-31254
Strong turbulence chemistry interaction in a piloted turbulent jet diffusion flame 20 p3425 N85-31257
Mechanisms of exhaust pollutants and plume formation in continuous combustion
[AD-A154169] 20 p3435 N85-31310
An experimental investigation of confined, multiple, turbulent jet mixing with recirculation 20 p3451 N85-31426
Errors and parameterizations of sub-grid scale processes in regional-scale atmospheric models 20 p3488 N85-31682
Mean and large-scale turbulence characteristics of the noise-producing region of an acoustically excited round jet 20 p3523 N85-31911
Vertical transport in the atmosphere: Measurement capabilities and requirements of VHF radars, part 1.6A 21 p3617 N85-32476
Morphology of the scattering targets: Fresnel and turbulent mechanisms, part 2.1A 21 p3618 N85-32481
Turbulent mixing and combustion 22 p3744 N85-33207
Jet flows: Modelling and experiments 22 p3744 N85-33208

TURBULENT WAKES
NT PROPELLER SLIPSTREAMS
NT SLIPSTREAMS
A study of the effect of wake-passing on turbine blades
[OUEL-1515/84] 03 p0363 N85-12326
Experimental studies of transonic airfoil trailing edge and wake flowfield properties 05 p0592 N85-13773
Wake flow behind bluff bodies 05 p0593 N85-13783
A free shear layer prediction of the turbulent wake of a flat plate towed below a free surface
[AD-A148699] 09 p1319 N85-18293
Method for the prediction of the installation aerodynamics of a propfan at subsonic speeds
[NASA-CR-3857] 15 p1969 N85-22369
Calculating isothermal flow in wake beyond injection zone 14 p2287 N85-24175
Periodic vortex shedding in the supersonic wake of a planar plate
[NASA-TM-77854] 15 p2483 N85-25207
Development of a rotor wake-vortex model, volume 1
[NASA-CR-174849] 16 p2699 N85-26668
New facility to study unsteady wake effects on turbine airfoil heat transfer 17 p2911 N85-27948
Turbulent wake of a submerged flat plate
[AD-A153776] 18 p3100 N85-29190
Across-wind response of towers and stacks of circular cross-section 19 p3282 N85-30354
Analysis of the turbulent near wake at a sharp trailing edge 20 p3387 N85-31006
Turbulence modeling in a two-dimensional wake 20 p3452 N85-31431
Trailing edge flow and aerodynamic sound. Part 1: Tonal pressure and velocity fluctuations. Part 2: Random pressure and velocity fluctuations
[AD-A154947] 21 p3552 N85-32097
Turbulence modelling for the prediction of turbulent jets: Wakes and plumes
[CFD/84/5] 22 p3784 N85-33447
Laser Doppler Anemometer (LDA) measurements in the turbulent near-wake of blunt bodies
[ISL-CO-212/84] 22 p3785 N85-33450

TURING MACHINES
One queue or two pushdown stores take square time on a one-head tape unit
[CWI-CS-R8406] 05 p0717 N85-14601
Counting is easy — Turing machines
[CWI-CS-R8423] 17 p3009 N85-28606

TURKEY
Delineation of major geologic structures in Turkey using SIR-B data 08 p1149 N85-17249

TURNAROUND (STS)
Overview od STS ground operations/orbiter turnaround STS-1 through STS-7 08 p1096 N85-16926

TURNING FLIGHT
Robust rate control system designs for a submersible
[AD-A144792] 01 p0111 N85-10753
High specific power aircraft turn maneuvers: Tradeoff of time-to-turn versus change in specific energy
[AD-A151701] 15 p2471 N85-25257

TURRET LATHES
Production turret lathe retrofitted with robot 10 p1461 N85-19214

TURTLES
Transatlantic migration study of the leathery turtle using the ARGOS system. Transatlantic turtle race 14 p2326 N85-24379

TUTOR AIRCRAFT
U CL-41 AIRCRAFT

TVC (CONTROL)
U THRUST VECTOR CONTROL

TWILIGHT GLOW
Twilight intensity variation of the infrared hydroxyl airglow 11 p1683 N85-20481

TWINNING
The growth of twins and twin lamellae in synthetic diamond crystals 02 p0181 N85-11213
Development of high-efficiency solar cells on silicon web
[NASA-CR-174212] 08 p0828 N85-15259
Method of fabricating acceleration resistant crystal resonators and acceleration resistant crystal resonators so formed
[AD-D011630] 16 p2778 N85-27145

TWISTED WINGS
Effect of a variable camber and twist wing at transonic Mach numbers
[NASA-TM-86281] 04 p0452 N85-12869
Detailed pressure distribution measurements obtained on several configurations of an aspect-ratio-7 variable twist wing
[NASA-TM-86306] 10 p1419 N85-18950

TWISTING
Indications of twist in the Epsilon rings of Uranus 15 p2572 N85-26490
Effects of shepherd conjunctions on Saturn's F-ring 15 p2575 N85-26511

TWO BODY ORBITS
U TWO BODY PROBLEM

TWO BODY PROBLEM
Nonlinear oscillations of 2 body system relative to center of mass in elliptical orbit 02 p0159 N85-11082
Constraints on the origin of viscoelastic bodies 04 p0584 N85-13732
Accumulation of the terrestrial planets 13 p2179 N85-23524

TWO DIMENSIONAL BODIES
Forced vibrations of friction-damped beam structures in two dimensions
[UDR-TM-82-08] 04 p0456 N85-12692
Current status of one- and two-dimensional numerical models: Successes and limitations 20 p3482 N85-31636
On the dependence of the convergence of Gummel's algorithm on the regularity of the solution
[AD-A154628] 21 p3575 N85-32832
Adaptive rezoner in a two-dimensional Lagrangian hydrodynamic code
[DE85-010108] 24 p4094 N85-35381
Use of a minimum-ellipse criterion in the study of ion-beam extraction systems
[DE85-012670] 24 p4148 N85-35721

TWO DIMENSIONAL BOUNDARY LAYER
Stability of heated boundary layers 02 p0196 N85-11311
Boundary condition effects in the energy loss spectrum of layered systems
[NOTA-INTERNA-602] 02 p0269 N85-11867
Influence of turbulence of incident stream on three dimensional boundary layer 14 p2278 N85-24113
Stability calculations of the two-dimensional boundary layer along a concave wall: Part 1: A numerical method of solution for the simultaneous ordinary differential equations governing disturbances
[NAL-TR-841] 15 p2554 N85-25758

TWO DIMENSIONAL FLOW
NT COUETTE FLOW
An integral method for analyzing incompressible two dimensional turbulent boundary layers with separation 02 p0196 N85-11309
Stability of heated boundary layers 02 p0196 N85-11311
Large structure in the far wakes of two-dimensional bluff bodies 05 p0592 N85-13771
Unsteady flow characteristics in the near-wake of a two-dimensional obstacle
[NASA-TM-77782] 07 p0897 N85-15684
Laminar flow over a backward-facing step
[AD-A147469] 07 p0960 N85-16084
Unsteady free-convection heat transfer inside an annular cavity
[CFD/84/16] 08 p1183 N85-17339
Weakly-reflective boundary conditions for two-dimensional shallow water flow problems
[PUBL-322] 08 p1183 N85-17341
Modeling of turbulent dispersion of neutral and buoyant contaminants released from two dimensional sources — air pollution
[VKI-TN-150] 08 p1180 N85-17438
A 2-dimensional second order closure model of the upper atmosphere 08 p1182 N85-17450
Flow instabilities in transonic small disturbance theory
[NASA-TM-86251] 09 p1273 N85-18000
Analysis of sudden expansion flow in a two-dimensional duct with and without side-wall injection using the k-epsilon turbulence model 09 p1317 N85-18282
Numerical predictions for unsteady viscous flow past an array of cylinders 09 p1318 N85-18284
SSME thrust chamber simulation using Navier-Stokes equations
[NASA-CR-171349] 10 p1430 N85-19017
Transonic interactions of unsteady vortical flows
[NASA-TM-86658] 12 p1770 N85-21113
Pseudospectral calculations of two-dimensional transonic flow (Task 1). Numerical investigation of VTOL aerodynamics (Task 2)
[AD-A150123] 12 p1772 N85-21126
Numerical integration of the unsteady full-potential equation with applications to transonic flow about a two-dimensional airfoil
[NLR-MP-84022-U] 12 p1773 N85-21130
Experimental studies of Quasi-Two-Dimensional and three-dimensional viscous interaction regions induced by skewed-shock and swept-shock boundary layer interactions
[AD-A150090] 12 p1847 N85-21587
A linear characteristic-nodal transport method for the two-dimensional (X,Y)-geometry multigroup discrete ordinates equations over an arbitrary triangle mesh
[LA-10092-T] 12 p1913 N85-22008
Propagation of three-dimensional turbulent jet from lobar nozzle through surrounding stream 13 p2042 N85-22785
Evolution of set of Rossby waves toward anisotropic equilibrium state 13 p2109 N85-23141
Stability of Rossby waves within framework of three-component analysis 13 p2109 N85-23142
Wave motion of three-component medium under load moving on plane boundary 14 p2277 N85-24105
Discrete models for the numerical analysis of time-dependent multidimensional gas dynamics
[NASA-CR-172574] 14 p2300 N85-24239
Laser anemometry two dimensional measurement of velocity fluctuations in an excited jet
[ISL-CO-213/83] 14 p2302 N85-24254
Unsteady transonic aerodynamic and aeroelastic calculations about airfoils and wings 15 p2459 N85-25185
A finite element, Navier-Stokes study of the confined, laminar flow over a downstream facing step 15 p2553 N85-25754
Influence of surface roughness on compressor blades at high reynolds number in a two-dimensional cascade
[AD-A151855] 15 p2557 N85-25777
The development of a computational model for a two-dimensional turbulent flow. Part 1: Mathematical background — solid fuel combustion
[VTH-LR-436-PT-1] 16 p2785 N85-27186
Supersonic flow around weak radiation sources 17 p2942 N85-28162
Flow quality of National Aerospace Laboratory two-dimensional transonic wind tunnel. Part 3: Flow turbulence level and measuring method
[NAL-TR-842-PT-3] 18 p3084 N85-28952

Time-averaged and time-dependent computations of isothermal flowfields in a canterbody combustor
[AD-A153662] 18 p3100 N85-29189
Screening phase transitions in two-dimensional Coulomb gas
[NOTA-INTERNA-830] 18 p3192 N85-29798
Use of a two-dimensional flow model to quantify aquatic habitat
[AD-A154287] 19 p3266 N85-30253
KIVA: A computer program for two- and three-dimensional fluid flows with chemical reactions and fuel sprays
[DE85-010334] 19 p3339 N85-30693
A numerical method for the solution of the inverse problem in external aerodynamics
[STN-7] 20 p3390 N85-31025
Turbulent reacting flows 20 p3451 N85-31427
Turbulence modeling in a two-dimensional wake
20 p3452 N85-31431
Two-dimensional separation in an incompressible fluid — boundary layer separation
[ONERA-RTS-16/3232-RY-060-R]
20 p3456 N85-31459
An evaluation of four methods of numerical analysis for two-dimensional airfoil flows
[AD-A155202] 21 p3552 N85-32098
Finite element methods for viscoelastic flow
[AD-A154877] 22 p3783 N85-33437
Two-dimensional simulation of instability growth due to shocks
[DE85-011869] 22 p3784 N85-33442
Turbulence modelling for the prediction of turbulent jets: Wakes and plumes
[CFD/84/5] 22 p3784 N85-33447
The calculation of two-dimensional buoyant surface jets with the k-W model of turbulence — kinetic energy-vorticity fluctuations (k-W)
[CFD/84/21] 22 p3785 N85-33448
Unsteady flow in a supersonic cascade with two in-passage shocks
[NASA-CR-3925] 24 p4060 N85-35158
Numerical studies of 2-dimensional flows
[NASA-CR-3930] 24 p4060 N85-35160

TWO DIMENSIONAL JETS
Large amplitude forcing of a high speed 2-dimensional jet
[NASA-CR-175846] 13 p1974 N85-22393

TWO FLUID MODELS
Progress in the development of a two-fluid model of turbulence for near-wall flows, part 1
[CFD/84/7-PT-1] 04 p0501 N85-13196
Progress in the development of a two-fluid model of turbulence for near-wall flows. Part 3: Preliminary investigation of a stably-stratified boundary layer
[CFD/84/9-PT-3] 04 p0501 N85-13197
The two-fluid model of turbulence applied to combustion phenomena
[CFD/84/15] 08 p1124 N85-17069
Direct electron and ion fluid computation of high electrostatic fields in dense inhomogeneous plasma with subsequent nonlinear optical and dynamical laser interaction 15 p2656 N85-26388
Progress in the development of a two-fluid model of turbulence: A set of 42 lecture panels
[CFD/84/20] 20 p3457 N85-31469

TWO PHASE FLOW
Void fraction measurements performed in a vertical large diameter tube compared to different predicting correlations
[GKSS-84-E-24] 01 p0048 N85-10315
Visualization of the diverging two-phase flow pattern in a horizontal T-junction with vertical branch
[GKSS-84-E-25] 01 p0048 N85-10316
Investigation of the gas-content of gas-liquid systems
[BLL-M-35748-(5828.4)] 02 p0171 N85-11146
One-dimensional two-phase constant lag flow in combustion chamber of solid propellant rocket motors
[AD-A145679] 02 p0173 N85-11157
Investigation of crisis phenomena in thermosyphons with internal heat-dissipation
[BLL-M-35765-(5828.4)] 02 p0197 N85-11313
Combustion waves in dispersed-2-phase mixtures
[CFD/84/13] 04 p0472 N85-13003
Fundamental study of three dimensional two phase flow in combustion systems
[AD-A142866] 04 p0498 N85-13177
Similarity considerations in 1-component 2-phase flow
[DE84-016370] 04 p0499 N85-13184
Deterministic sensitivity analysis of two-phase flow systems: Forward and adjoint methods
[DE84-016276] 04 p0499 N85-13185
Theoretical description of film boiling in a two phase flow calculation
[IKE-2-66] 05 p0838 N85-14092
VORT: A computer code for bubbly two-phase flow
[DE84-017076] 06 p0809 N85-15142
Flow of nitrogen-pressurized Halon 1301 in fire extinguishing systems
[NASA-CR-174271] 07 p0900 N85-15701
Influence of turbulence on erosion by a particle-laden fluid jet
[DE84-014365] 09 p1320 N85-18301
Averaging effects in models of three-dimensional two-phase flows
[AD-A149313] 10 p1484 N85-19371
TRACR3D: A model of flow and transport in porous/fractured media
[LA-9667-MS] 12 p1845 N85-21576
Two-phase flow in geothermal systems
[DE85-004692] 12 p1848 N85-21591
Fundamental study of three dimensional two phase flow in combustion systems
[AD-A150739] 14 p2250 N85-23945
A fundamental study of liquid phase particle breakup. Revision
[AD-A150791] 14 p2301 N85-24249
Two-phase fluid thermal transport for spacecraft
[AD-A151316] 15 p2493 N85-25378
Application of the Van Leer method to the solution of one-dimensional volume fraction equations
[CFD/84/17] 15 p2558 N85-25781
Two-phase flow in centrifugal pumps
[BLL-CE-TRANS-8065-(9022.09)]
15 p2605 N85-26053
Measurements of two-phase exhaust flow parameters of a small caliber gun associated with muzzle flash phenomena
[ISL-CO-212/83] 16 p2784 N85-27182
Flow characteristics of a partially submerged liquid pickup
[DE85-008744] 17 p2959 N85-28276
Two phase discharge of liquefied gases through pipes. Field experiments with ammonia and theoretical model
[FOA-B-40139-C1] 18 p3103 N85-29209
Method for driving two-phase turbines with enhanced efficiency
[NASA-CASE-NPO-15037-2] 18 p3115 N85-29282
Effect of nonuniform size on internal stresses in a rapid, simple shear flow of granular materials. Part 2: Multiple grain sizes
[AD-A154046] 19 p3285 N85-30373
Droplet deposition in vertical two-phase flow
[CFD/84/22] 20 p3456 N85-31460
Intermittent gas-liquid flow modeling in horizontal or weakly inclined pipes
[EME-132] 20 p3456 N85-31465
Some remarks on the constitutive equations of stratified gas-liquid flow
[EME-137] 20 p3456 N85-31466
Enthalpy transients in fractured two-phase geothermal systems
[DE85-011988] 22 p3808 N85-33587
Compressible two-phase flow instabilities simulated with a hybrid Lagrange-Euler pseudospectral method
[DE85-009904] 23 p3931 N85-34361
Stability of two-dimensional immiscible flow to viscous fingering
[DE85-011403] 23 p3931 N85-34364
A two-phase flow and heat transfer model for zero gravity
[AD-A156097] 24 p4094 N85-35377

TWO PHASE SYSTEMS
U BINARY SYSTEMS (MATERIALS)

TWO REFLECTOR ANTENNAS
Attempts to contruct two-dimensional image of Sun from observations made with RATAN-600 radiotelescope by relay race method 06 p0783 N85-15005
The 20 GHz proof-of-concept test model results for a multiple scan beam dual reflector antenna
[NASA-CR-174268] 07 p0938 N85-15944
BBC receiving terminal for the European orbital test satellite
[BBC-RD-1984/15] 08 p1142 N85-17205
Interpolation methods for GTD analysis of shaped reflectors 10 p1463 N85-19231

TWO-WAVELENGTH LASERS
Spectral evolution of the pulse of a dual frequency dye laser
[CNES-83/168/T/CT/DRT/TIT/10]
20 p3461 N85-31497
High-power two-frequency CW dye laser
21 p3586 N85-32900

TYPE 3 BURSTS
Interplanetary radio storms. 2: Emission levels and solar wind speed in the range 0.05-0.8 AU
[NASA-TM-84946] 04 p0589 N85-13761
Arguments for fundamental emission by the parametric process L yields T + S in interplanetary type III bursts — langmuir, electromagnetic, ion acoustic waves (L, T, S) 12 p1958 N85-22311
Evidence concerning the generation mechanism of solar type 3 radio bursts 16 p2686 N85-27802
Type 3 solar radio bursts and 3HE-rich events
[SH-2.2-3] 23 p4000 N85-34798

TYPE 4 BURSTS
The longitudinal asymmetry of the interplanetary perturbation producing Forbush decreases
[IFSI-84-18] 20 p3546 N85-32065
Interplanetary disturbances during Forbush decreases
[IFSI-84-10] 20 p3547 N85-32075
The flare origin of Forbush decreases not associated with solar flares on the visible hemisphere of the Sun
[SH-5.1-4] 23 p4041 N85-35058

TYPEWRITERS
The representation of action plans in long term memory 05 p0709 N85-14545

TYPHOONS
Frequency and motion of western North Pacific tropical cyclones
[PB85-106466/GAR] 06 p0839 N85-15331
Meteorological Satellite Center Technical Note No. 10, 1984
[MSC-TN-10] 12 p1894 N85-21884
On the relative motion of typhoons: In the case of Typhoon 8305 and Typhoons 8306 and 8307
12 p1894 N85-21885
On the error of typhoon intensity estimation by means of IR Dvorak technique occurring when the eye is very small 12 p1894 N85-21886
Accuracy of typhoon center determined by GMS imagery 12 p1894 N85-21887
Hurricane Research Division, fiscal year 1984 programs, fiscal year 1985 projections 16 p2836 N85-27491

U

U TUBES
U MANOMETERS

U.S.S.R.
Development of powder metallurgy in various sections of USSR 01 p0019 N85-10116
Report on high-precision jig-boring machines
01 p0035 N85-10215
Growth, future of Soviet robotics sector analyzed
01 p0035 N85-10217
USSR report: Space
[JPRS-USP-84-005] 02 p0156 N85-11060
Features and uses of progress cargo ships
02 p0157 N85-11061
USSR report: Physics and mathematics
[JPRS-UPM-84-006] 02 p0256 N85-11676
USSR report: Transportation
[JPRS-UTR-84-028] 03 p0310 N85-12002
Ministry wants better commo facilities for agroaviation
03 p0310 N85-12003
Start-2 ATC system installation progresses at Leningrad 03 p0311 N85-12007
USSR report: Electronics and electrical engineering
[JPRS-UEE-84-014] 03 p0344 N85-12215
Bibliography of Soviet laser developments, number 65, May - June 1983
[AD-A146189] 03 p0366 N85-12347
USSR report: Electronics and electrical engineering
[JPRS-UEE-84-010] 04 p0485 N85-13095
USSR report: Physics and mathematics
[JPRS-UPM-84-007] 05 p0723 N85-14651
Manganese in recent sediments of Ukrainian SSR Black Sea shelf 06 p0619 N85-15200
Thermal energy resources of thermal waters in Kazakhstan 06 p0620 N85-15208
Deep structure of terrestrial crust and upper mantle in southeastern Siberia and Far East according geological-geophysical data 06 p0621 N85-15212
Automated Lavina collects data on snow
07 p0980 N85-16224
New data on presence of ores in salt dome structures of Dnieper-Donets Basin 07 p0981 N85-16234
Deep structure of Western Siberia
07 p0981 N85-16235
Deputy Minister discusses plans for geothermal power
07 p0994 N85-16313
USSR report: Life sciences. Biomedical and behavioral sciences
[JPRS-UBB-84-027] 07 p1012 N85-16426
USSR report: Transportation
[JPRS-UTR-85-001] 08 p1067 N85-16783
Director on institute's civil aviation projects
08 p1067 N85-16784
International projects, other work of Aeroproyekt Institute 08 p1068 N85-16787
Designer on civil aircraft design trends in USSR
08 p1068 N85-16788
Regional and seasonal variations in snow-cover density in the USSR
[AD-A148429] 08 p1189 N85-17496

USSR report: Life sciences. Biomedical and behavioral sciences
[JPRS-UBB-85-001] 06 p1193 N85-17515
USSR report: Transportation
[JPRS-UTR-85-003] 09 p1277 N85-18032
First deputy minister on 1984 civil aviation performance 09 p1277 N85-18033
Collegium on aviation fuel conservation efforts 09 p1278 N85-18034
Activities at MII Experimental Design Bureau 09 p1278 N85-18038
Improvements under way at Gorkiy airport 09 p1278 N85-18040
USSR report: Engineering and equipment
[JPRS-UEQ-85-001] 09 p1305 N85-18200
USSR report: Life sciences. Biomedical and behavioral sciences
[JPRS-UBB-85-007] 09 p1362 N85-18566
USSR report: Materials science and metallurgy
[JPRS-UMS-84-008] 10 p1442 N85-19088
French commentary on Soviet industrial espionage 10 p1461 N85-19210
Types of placer formation of eastern Arctic shelf 10 p1498 N85-19452
Relationship of gold content to gravity fields in Far East 10 p1501 N85-19475
USSR report: Life sciences. Biomedical and behavioral sciences
[JPRS-UBB-85-008] 10 p1523 N85-19605
USSR report: Life sciences. Biomedical and behavioral sciences
[JPRS-UBB-85-011] 10 p1525 N85-19616
USSR report: Life sciences. Biomedical and behavioral sciences
[JPRS-UBB-85-009] 10 p1526 N85-19625
Soviet National Middle Atmosphere Program 11 p1655 N85-20429
USSR report: Physics and mathematics
[JPRS-UPM-85-001] 11 p1715 N85-20786
Transportation
[JPRS-UTR-85-004] 12 p1769 N85-21105
Current development, applications of airships in USSR 12 p1769 N85-21109
New method of reconstructing conditions of recent differentiation of oil and gas in the Amudarya Basin (based on results of interpretation of space photographs) 13 p1984 N85-22446
Current plans for development of chemical industry 13 p2014 N85-22633
USSR report: Electronics and electrical engineering
[JPRS-UEE-85-002] 13 p2066 N85-22907
Possibilities of aerial electric prospecting by long cable method for detecting poorly conducting strata 13 p2115 N85-23177
Minister Bugayev on civil aviation in 1984, plans for 1985 14 p2208 N85-23689
1st deputy minister on civil aviation support of economy 14 p2208 N85-23690
Deputy minister on civil aviation fuel conservation efforts 14 p2208 N85-23691
Deputy minister on civil aviation construction projects 14 p2208 N85-23692
Improvements in personnel needed for better flight safety 14 p2208 N85-23693
USSR report: Engineering and equipment
[JPRS-UEQ-84-005] 14 p2285 N85-24157
Results of comparison of long-wave radiation fluxes measured by Soviet and Japanese actinometric radiosounds 14 p2333 N85-24427
Second Soviet-French Symposium on Space Cytology 14 p2366 N85-24699
USSR report: Cybernetics, computers, and automation technology
[JPRS-UCC-85-002] 14 p2400 N85-24794
The astrometry network of observers in USSR 14 p2436 N85-25029
USSR report: Transportation
[JPRS-UTR-85-006] 15 p2460 N85-25189
Official on Soviet research in deicing techniques 15 p2460 N85-25191
USSR report: Transportation
[JPRS-UTR-84-015] 15 p2460 N85-25192
Civil air code international flights section explained 15 p2460 N85-25194
Study of Volga river delta using space photosurvey materials 15 p2485 N85-25340
Use of space information in petroleum- and gas-prospecting work (example of Southern Mangyshlak) 15 p2485 N85-25341
USSR report: Materials science and metallurgy
[JPRS-UMS-85-001] 15 p2496 N85-25395
USSR report: Electronics and electrical engineering
[JPRS-UEE-85-005] 15 p2524 N85-25565
USSR report: Cybernetics, computers and automation technology
[JPRS-UCC-85-003] 15 p2625 N85-26174
USSR report: Physics and mathematics
[JPRS-UPM-85-003] 15 p2642 N85-26300
USSR report: Space
[JPRS-USP-85-004] 16 p2717 N85-26772
Study and mapping of anthropogenic effect on environment in different regions of USSR on basis of space photographs 16 p2726 N85-26824
USSR report: Engineering and equipment
[JPRS-UEQ-84-006] 16 p2760 N85-27035
Cloud-seeding for regulating precipitation in Moscow area 16 p2807 N85-27308
USSR report: Transportation
[JPRS-UTR-84-025] 17 p2894 N85-27841
Science and Technology in the Soviet Union
[AD-A152828] 17 p3047 N85-28856
Soviet weapons development and the scientific community
[AD-P004562] 17 p3047 N85-28857
Computing in the Soviet general economy: An introductory overview
[AD-P004563] 17 p3047 N85-28858
The outlook for Soviet advanced technologies
[AD-P004564] 17 p3048 N85-28859
Social and political problems in Soviet basic research
[AD-P004565] 17 p3048 N85-28860
Technology and Soviet political choices
[AD-P004566] 17 p3048 N85-28861
Technology and technical efficiency in the Soviet Union: Dominant patterns of constrained optimization in a noncompetitive economic regime
[AD-P004567] 17 p3048 N85-28862
The revolution in military affairs and the Soviet system
[AD-P004568] 17 p3048 N85-28863
Close encounters with S/T (science and technology) in the Soviet Union
[AD-P004570] 17 p3048 N85-28864
R/D contracts in the Soviet Union
[AD-P004569] 17 p3048 N85-28865
Permafrost, seasonally frozen ground, snow cover and vegetation in the USSR
[AD-A153828] 18 p3124 N85-29346
Search and rescue at sea in the USSR 20 p3400 N85-31094
COSPAS-SARSAT demonstration and evaluation phase: COSPAS tests in the USSR and their results 20 p3405 N85-31130
Microwave hydrology: A trilogy
[NASA-CR-176042] 20 p3477 N85-31603
on the transport of large condensation nuclei in the atmosphere at various altitudes over the territory of the USSR 21 p3653 N85-32696
USSR Space Life Sciences Digest
[NASA-CR-3922] 21 p3656 N85-32709
USSR report: Electronics and electrical engineering
[JPRS-UEE-84-003] 22 p3773 N85-33361
The development of titanium production in the USSR
[BLL-OA-TRANS-3226-(6196.3)] 23 p3913 N85-34244
Space activities in the Soviet Union, Japan, and the People's Republic of China 23 p4057 N85-35149

U.S.S.R. SPACE PROGRAM
Soviet space programs, 1976-1980, with supplementary data through 1983. Part 2: Manned space programs and space life sciences
[S-REPT-98-235-PT-2] 01 p0014 N85-10088
Tass reports medical, materials studies aboard Salyut-7 02 p0158 N85-11071
25th anniversary of the Gagarin Cosmonaut Training Center
[NASA-TM-77644] 09 p1286 N85-18076
The space flight of the Soviet-Indian crew
[NASA-TM-77615] 12 p1788 N85-21226
USSR report: Space Biology and Aerospace Medicine, volume 18, no. 6, November - December 1984
[JPRS-USB-85-002] 12 p1900 N85-21931
Feoktistov says manned lunar, Mars flights lack justification 13 p1985 N85-22452
U.S., Soviet space program aims contrasted 13 p1985 N85-22455
USSR report: Space
[JPRS-USP-85-003] 15 p2476 N85-25284
List of recent Soviet space launches 15 p2480 N85-25361
Interkosmos program of space communication development 15 p2528 N85-25585
Forecasts on long-range development of space programs 16 p2727 N85-26830
International cooperation in space exploration 16 p2766 N85-27079
Soviet space programs, 1976-1980 (with supplementary data through 1983). Part 3: Unmanned space activities
[S-PRT-98-235-PT-3] 16 p2879 N85-27765

U-2 AIRCRAFT
NASA thunderstorm overflight program: Atmospheric electricity research. An overview report on the optical lightning detection experiment for spring and summer 1983
[NASA-TM-86488] 03 p0383 N85-12330
Discovery of nuclear tracks in interplanetary dust 06 p0889 N85-15647

UBV SPECTRA
UBV photometry of E region stars: Some intercomparisons 01 p0128 N85-10880

UDIMET ALLOYS
The response of cobalt-free Udimet 700 type alloy to modified heat treatments
[NASA-TM-86942] 11 p1587 N85-20043

UH-1 HELICOPTER
Navigation and flight director guidance for the NASA/FAA helicopter MLS curved approach flight test program
[NASA-CR-177350] 16 p2704 N85-26691

UH-60A HELICOPTER
UH-60A external stores support system fixed provision fairings drag determination
[AD-A147188] 07 p0902 N85-15719
A comparison of lightning and nuclear electromagnetic pulse response of a helicopter 07 p1000 N85-16349
Assessment of simulation fidelity using measurements of piloting technique in flight 08 p1075 N85-16817

UHTREX (NUCLEAR REACTORS)
U HIGH TEMPERATURE NUCLEAR REACTORS

UK SATELLITES
NT MIRANDA SATELLITE
UK Skynet 4 communications satellites 11 p1710 N85-20757
Minimization of system vulnerability in Naval satellite communication networks 11 p1710 N85-20758

ULM (LIGHT MODULATION)
U ULTRASONIC LIGHT MODULATION

ULTRA SHORT WAVE RADIO EQUIPMENT
U VERY HIGH FREQUENCY RADIO EQUIPMENT

ULTRAHIGH FREQUENCIES
Wave multiple scattering by a finite number of uncloaed circular cylinders
[NASA-TM-77593] 01 p0037 N85-10232
VHF/UHF radar and its application in nowcasting 01 p0078 N85-10516
DRG theory on the basis of a discrete interaction model
[PR-215] 03 p0358 N85-12297
Shuttle S-band communications technical concepts 08 p1099 N85-16948
Using the global positioning system (GPS) phase observable for relative geodesy: Modeling, processing, and results 09 p1341 N85-18437
Dissemination of ERS-1 low bit rate data and the use of L-band receiving stations
[NLR-TR-83049-U] 09 p1358 N85-18542
Effect of modulated ultrahigh frequency field on behavior and hormone level in female rats under emotional stress 09 p1361 N85-18562
Broad-band UHF dipole array
[NASA-TM-86373] 10 p1482 N85-19222
UHF radiowave propagation through forests
[AD-A149518] 10 p1487 N85-19256
UHF communications through forested propagation channels 10 p1470 N85-19250
Measurements of propagation at 900 MHz in an urban zone for establishing a digital radiomobile system 10 p1472 N85-19288
Shuttle S-band high gain switched beam breadboard antennas
[NASA-CR-171852] 10 p1478 N85-19327
Assessment of satellite power flux-density limits in the 2025-2300 MHz frequency range, part 2
[PB85-101244] 11 p1625 N85-20236
Spectrum resource assessment of the fixed and mobile services in the 947-17,700 MHz band, phase 1
[PB85-126288] 11 p1626 N85-20243
The ARGOS Platform Transmitter Terminals (PTTs) 14 p2237 N85-23672
Propagation considerations in land mobile satellite transmission
[NASA-CR-175733] 15 p2540 N85-25684
Optimal frequencies for broadcast transmitters in the UHF domain: Report
[TUM-M8404] 16 p2769 N85-27088
A phase modulation evaluation procedure for an ARGOS type signal 16 p2811 N85-27336
FAA (Federal aviation administration) assessment of satellite concepts and aviation spectrum requirements
[AD-A152338] 17 p2948 N85-28189
Measurements of VHF/UHF radio propagation in a maritime temperate climate
[CRC-1380] 18 p3089 N85-29119
Improved high performance television receiver
[PB85-170751] 18 p3092 N85-29139

Dielectric resonator stabilized microstrip oscillator
[AD-D011706] 19 p3261 N85-30219
The CCIR satellite EPIRB coordinated trials programme — Emergency Position Indicating Radio Beacon (EPIRB); International Radio Consultative Committee (CCIR) 20 p3402 N85-31111
The International Radio Consultative Committee (CCIR) recommended satellite Emergency Position Indicating Radio Beacon (EPIRB) system operating through geostationary satellites at 1.6 GHz 20 p3402 N85-31112
A 406 MHz geostationary satellite SARSAT experiment 20 p3403 N85-31113
A 406 MHz ELT processor for geostationary satellites — Emergency Locator Transmitter (ELT) 20 p3403 N85-31114
Evolution of 406 MHz Search and Rescue (SAR) processor 20 p3403 N85-31116
A micro/PDP-11 system for 406 MHz COSPAS/SARSAT processing 20 p3403 N85-31117
Search and rescue satellite (SARSAT) error analysis of the 406 MHz system 20 p3403 N85-31118
The 121.5/243 MHz ELT identification — Emergency Locator Transmitter (ELT) 20 p3404 N85-31119
SARSAT 406 MHz system technical evaluation 20 p3404 N85-31124
SARSAT 121.5/243 MHz technical evaluation 20 p3405 N85-31126
Potential advantages of the spaced antenna method for operational wind profiling, part 3.1B 21 p3620 N85-32490
Hadron cross sections at ultra high energies and unitarity bounds on diffraction dissociation
[HE-1.1-3] 24 p4170 N85-35851
1Single particle momentum and angular distributions in hadron-hadron collisions at ultrahigh energies
[HE-1.2-1] 24 p4171 N85-35860

ULTRAHIGH VACUUM
Precision manipulator heating and cooling apparatus for use in UHV systems with sample transfer capability
[NASA-CASE-LAR-13040-1] 18 p3116 N85-29286
Space shuttle molecular and wake vacuum measurements
[NASA-TM-86509] 19 p3222 N85-29978

ULTRALIGHT AIRCRAFT
Parachute extraction device for ultralight gliders
[CH-643499-A5] 16 p2699 N85-26883

ULTRALOW FREQUENCIES
U EXTREMELY LOW RADIO FREQUENCIES

ULTRALOW TEMPERATURES
Thermal and mechanical properties of polyurethane foams and a survey of insulating concretes at cryogenic temperatures
[PB85-100948/GAR] 07 p0934 N85-15918

ULTRASHORT PULSED LASERS
Coherent amplification of ultrasonic pulses in activated crystals 05 p0724 N85-14853
Clock synchronization by the Symphonie and Laser Synchronization from Stationary Orbit (LASSO) geostationary satellites 14 p2398 N85-24778
Optical inhomogeneities in a nanosecond-pulse iodine photodissociation laser with slow UV radiation pumping 21 p3686 N85-32902

ULTRASONIC CLEANING
Cleaning procedures of laser mirror substrates
[DFVLR-MITT-84-06] 06 p0640 N85-14108

ULTRASONIC FLAW DETECTION
Ultrasonic synthetic aperture focusing using unfocused pulse-echo transducers
[AERE-R-11230] 01 p0057 N85-10374
Modernization of IDTs-6 ultrasonic installation
[BLL-M-35716-(5628.4)] 02 p0206 N85-11356
High-frequency asymptotic behavior of reflected and transmitted waves during scattering of sound by hollow elastic sphere filled with fluid 02 p0268 N85-11738
Identification of pulse-echo rays in austenitic steels
[AERE-R-11265] 03 p0369 N85-12356
Ultrasonic and metallurgical examination of a cracked type 304 stainless steel BWR pipe weldment
[TI84-014968] 04 p0511 N85-13254
Defect detection threshold in riveted joints, test report no.44-833/F — in aircraft 04 p0511 N85-13260
The detection and assessment of defects in automatic ultrasonic inspection
[BLL-RISLEY-TR-4597-(9091.9F)] 05 p0647 N85-14150
Pulse-echo method for flaw detection in concrete
[PB84-234509] 06 p0775 N85-14953
NDE (Nondestructive Evaluation) of oxygen contaminated titanium alloys and weldments
[AD-P004121] 08 p1126 N85-17096
Leak monitoring in high pressure preheaters by a noninvasive ultrasonic method
[CISE-2373] 11 p1650 N85-20394
Leak detection by acoustic emission monitoring in power plant high pressure preheaters
[CISE-2392] 11 p1650 N85-20395
Defect characterisation and monitoring by acoustic emission
[AERE-R-11409] 12 p1863 N85-21683
An amplitude correlation and differencing method for the monitoring of flaws in repeat ultrasonic inspections
[AERE-R-11416] 15 p2571 N85-25854
Sizing capability of automated ultrasonic time-of-flight diffraction in thick section steel and aspects of reliable inspection in practice
[AERE-R-11548] 15 p2571 N85-25855
Laser-based non-destructive testing techniques for the ultrasonic characterization of sub-surface flaws
[AERE-R-11562] 15 p2572 N85-25856
Nondestructive tests of ceramic components for aircraft turbines 16 p2709 N85-26718
Echo-response from crack-like two-dimensional reflectors in focused ultrasonic fields. Ultrasonic crack tip method for the determination of crack depth
[BLL-BISI-22062-(9022.06)] 16 p2796 N85-27236
Ultrasonic testing of carbon fiber reinforced plastics (CFRP) using pattern recognition methods
[MBB-BB-563/84-0] 16 p2873 N85-27726
Ultrasonic flaw detector with microcomputer interpretation
[BMFT-FB-T-84-272] 17 p2977 N85-28395
Detecting and analyzing crack defects
[BLL-BISI-TRANS-22062-(9022.06)] 17 p3027 N85-28723
Echo-response from crack-like two-dimensional reflectors in focused ultrasonic fields 17 p3027 N85-28724
Ultrasonic crack tip method for the determination of crack depth 17 p3028 N85-28725
Ultrasonic testing of tubes
[BLL-BISI-TRANS-22337-(9022.06)] 18 p3119 N85-29304
Characteristic features of testing equipment: Application to the ultrasonic inspection of tubes 18 p3119 N85-29305
Study of an ultrasonic detection method to inspect bonding effects in light alloy bonded structures, test report no. 43-954/F — aircraft structures
[PV-43-954/F] 22 p3795 N85-33510
Ultrasonic inspection of carbon fiber reinforced plastic by means of sample-recognition methods
[NASA-TM-77896] 24 p4074 N85-35245

ULTRASONIC LIGHT MODULATION
Four-wave hypersonic reversing mirrors in saturated mode 11 p1719 N85-20812

ULTRASONIC RADIATION
Polarization of ultrasound transmitted through boundary of magnetically inactive and equatorially magnetized media 02 p0257 N85-11682
Theory of harmonic generation of finite amplitude ultrasonic waves in solids of hexagonal symmetry
[AD-A146636] 06 p0660 N85-15465
Superlattice ultrasonic wave generator
[AD-D011383] 07 p1038 N85-16585
Effects of scatterer spacing statistics on ultrasonic backscatter signal spectra
[DE85-003259] 12 p1928 N85-22114
Investigations of ultrasonic wave interactions at boundaries separating anisotropic materials
[DE85-003506] 13 p2155 N85-23384
Connection between time- and frequency-domain three-dimensional inverse problems for the Schroedinger equation
[DE85-005914] 15 p2639 N85-26274
An electro-optic spatial light modulator for thermoelastic generation of programmably focused ultrasound
[AD-A152066] 15 p2646 N85-26323
Acoustooptic pulse-echo transducer system
[NASA-CR-175919] 17 p2951 N85-28224
Dual differential interferometer
[NASA-CASE-LAR-12966-1] 19 p3271 N85-30262
Method for thermal monitoring subcutaneous tissue
[NASA-CASE-LAR-13028-1] 19 p3328 N85-30618
Development of ultrasonic modeling techniques for the study of crustal inhomogeneities
[AD-A155206] 21 p3632 N85-32565
Second Colloquim on the Scattering of Ultrasonic Waves
[AD-A156298] 24 p4145 N85-35697

ULTRASONIC SCANNERS
Study and realization of a Doppler system with pulsed, directional, multiport (128) emission and sequential signal treatment — ultrasonic echography, blood flow
[ENST-84E008] 05 p0639 N85-14102
Ultrasonic measurements, X-ray photographs and image processing
[BLL-RISLEY-TR-4586-(9091.9F)] 07 p1037 N85-16583
Measurement of ultrasonic fields in transparent media using a scanning differential interferometer
[NASA-CR-175921] 17 p3028 N85-28726
Study of requirements for and method of multidimensional acoustic imaging — spaceborne experiments
[ESA-CR(P)-2020] 20 p3525 N85-31924

ULTRASONIC SPECTROSCOPY
Second Colloquim on the Scattering of Ultrasonic Waves
[AD-A156298] 24 p4145 N85-35697

ULTRASONIC TESTS
Nonlinear ultrasonic characterization of oxygen impurities in titanium, 2
[AD-A144857] 01 p0027 N85-10171
Ultrasonic nondestructive evaluation, microstructure, and mechanical property interrelations
[NASA-TM-86876] 01 p0056 N85-10371
Evaluation of interfacial stresses from the amplitude of reflected ultrasonic signal
[DE84-015472] 02 p0276 N85-11798
Technical activities 1983, Office of Nondestructive Evaluation
[PB84-217074] 03 p0370 N85-12360
Nondestructive evaluation of residual stress in low-carbon steel, introduction 04 p0512 N85-13265
Nondestructive determination of mechanical properties — aluminum alloys 04 p0512 N85-13266
Measurement of the preloading of bolted joints by the ultrasonic method
[CETIM-1-5H-38-6] 04 p0558 N85-13556
Ultrasonic girth weld evaluation for aluminum substrate of spherical Kevlar-epoxy test specimens
[DE85-001592] 06 p0616 N85-15181
Nondestructive inspection: Improved capabilities of technicians
[AD-A147388] 07 p0975 N85-16196
Ultrasonic analysis of spherical composite test specimens
[DE85-001591] 07 p0976 N85-16197
Use of the analytic signal in ultrasonic imaging
[DE84-016843] 07 p1039 N85-16598
Effects of oxygen-contamination-induced microstructural changes on the reverberation of ultrasound in Ti-6211 alloys
[AD-P004124] 08 p1126 N85-17099
Ultrasonic evaluation of titanium contamination with correlation techniques
[AD-P004126] 08 p1126 N85-17101
Modeling of real UT transducer field/flaw interactions
[DE85-000341] 09 p1329 N85-18351
Emerging technology of synthetic aperture focusing for ultrasonic testing
[DE85-000373] 09 p1378 N85-18664
Ultrasonic inspection of alloyed tungsten bars
[AD-A148900] 10 p1495 N85-19435
Ultrasonic analysis of Kevlar-epoxy filament wound spherical test specimens
[DE85-005198] 11 p1593 N85-20024
Ultrasonic large-diameter pipe weld testing installations 11 p1603 N85-20061
Quantitative non-destructive evaluation of damage in composite materials using transmitted and reflected ultrasound
[NASA-CR-175550] 12 p1796 N85-21269
The role of dislocations in ultrasonic attenuation
[AERE-R-11384] 12 p1804 N85-21317
Application of homomorphic signal processing to stress wave factor analysis
[NAS 1.26:174871] 12 p1861 N85-21673
Defect characterisation and monitoring by acoustic emission
[AERE-R-11409] 12 p1863 N85-21683
The measurement of residual stresses using ultrasonics
[AERE-R-11415] 12 p1868 N85-21722
Effects of scatterer spacing statistics on ultrasonic backscatter signal spectra
[DE85-003259] 12 p1928 N85-22114
Investigation of steel structures using ultrasonic waves
[BR93258] 13 p2101 N85-23091
Standing of industrial radiography in South Africa 14 p2316 N85-24311
Ultrasonic non-destructive testing technique 14 p2316 N85-24313
Laser-based non-destructive testing techniques for the ultrasonic characterization of sub-surface flaws
[AERE-R-11562] 15 p2572 N85-25856
An electro-optic spatial light modulator for thermoelastic generation of programmably focused ultrasound
[AD-A152066] 15 p2646 N85-26323

Ultrasonic dispersion of soils for routine particle size analysis: Recommended procedures
[DE85-005530] 16 p2861 N85-27643
Ultrasonic test evaluation of the insert bond on hermetic connectors
[DE85-008394] 18 p3120 N85-29310
Grain structure identification by ultrasound frequency averaging and deconvolution
[AD-A154332] 19 p3352 N85-30777
Advanced ultrasonic imaging of piping in Dresden and Vermont Yankee reactors
[TI85-010049] 20 p3464 N85-31520
The use of ultrasound to monitor incipient failure of rolling element bearings 23 p3924 N85-34317
Calculations on the feasibility of ultrasonic inspection of steam generator tubing in pressurized water reactors
[AERE-R-10960] 23 p3940 N85-34419
Quantitative non-destructive evaluation of composite materials based on ultrasonic wave propagation
[NASA-CR-176176] 24 p4074 N85-35244

ULTRASONIC WAVE TRANSDUCERS
Multiple passband transducers for tone selection from a frequency comb generator
[RSRE-MEMO-3647] 02 p0194 N85-11295
Qualification of noninvasive systems for on-line leak detection in high pressure feed water preheaters
[CISE-2341] 04 p0558 N85-13555
New types of power supplies for ultrasonic processing equipment 12 p1843 N85-21566
Piezoelectric and electrostatic polymeric tranducers for acoustic emission detection
[AD-A150863] 14 p2306 N85-24272
A multi-element ultrasonic ranging array
[AD-A150898] 14 p2416 N85-24906
Ultrasonic testing of tubes
[BLL-BISI-TRANS-22337-(9022.06)] 18 p3119 N85-29304
Electrodynamic transducers for ultrasonic reception 18 p3119 N85-29306
The use of ultrasound to monitor incipient failure of rolling element bearings 23 p3924 N85-34317

ULTRASONIC WAVES
U ULTRASONIC RADIATION

ULTRASONIC WELDING
Non-destructive testing of HF-welded pipe
[BLL-BISI-TRANS-22182-(9022.06)] 17 p2976 N85-28386
Ultrasonic seam welding on thin silicon solar cells
[NASA-CR-176116] 22 p3805 N85-33570

ULTRASONICS
Collapse of cavitation bubbles between two walls in ultrasonic field 02 p0266 N85-11739
Propagation of acoustic shear waves through active periodic structure 04 p0490 N85-13125
Optical method of measuring velocity of shear waves 06 p0787 N85-15029
Nondestructive measurement of bulk residual stresses
[AD-A147063] 07 p0978 N85-16211
Optical fibers with reduced pressure sensitivity to high frequency acoustic field
[AD-D011306] 07 p1043 N85-16627
Nonlinear ultrasonic characterization of oxygen impurities in titanium
[AD-P004123] 08 p1126 N85-17098
Ultrasonic transducers, performance variability, design, and manufacturing procedures
[AD-A148575] 08 p1158 N85-17306
Journal of Research of the National Bureau of Standards, Volume 89, Number 1, January-February, 1984
[PB84-235530] 08 p1262 N85-17931
An electro-optic spatial light modulator for thermo-elastic generation of programmably focused ultrasound
[AD-A149078] 10 p1563 N85-19794
Stress waves in an isotropic elastic plate excited by a circular transducer
[NASA-CR-3877] 11 p1650 N85-20390
Elastic compliance of imperfect interfaces: Review and relationship to ultrasonic scattering
[DE85-003066] 11 p1652 N85-20404
Dynamic world modeling for an intelligent mobile robot using a rotating ultra-sonic ranging device
[AD-A149979] 12 p1775 N85-21143
Continuous measurement of zircaloy corrosion in air with an ultrasonic corrosion monitor
[DE85-003663] 12 p1807 N85-21337
Journal of Research of the National Bureau of Standards, volume 89, number 2, March - April 1984
[PB85-115426] 12 p1926 N85-22103
Elastic wave scattering from cavities and sound inclusions analyzed by the resonance method
[AD-A150315] 13 p2155 N85-23381
Applications of ultrasonic technology 14 p2283 N85-24144
A multi-element ultrasonic ranging array
[AD-A150898] 14 p2416 N85-24906
Ultrasonic SH wave velocity in textured aluminum plates
[AERE-R-11516] 15 p2509 N85-25475
Sonars with high noise and clutter rejection for use with adaptive robots
[AD-A151875] 15 p2543 N85-25701
The development of a transducer system for the accurate measurement of ultrasonic phase delay of SH plate waves
[AERE-R-11598] 15 p2559 N85-25790
Ultrasonic characterization of porosity: Theory
[DE85-005922] 15 p2646 N85-26325
Evaluation of experimental epoxy monomers
[NASA-TM-87476] 16 p2754 N85-26996
Creating a Mobile Autonomous Robot Research System (MARRS)
[AD-A151963] 16 p2793 N85-27229
Method for ultrasonic bonding to soft microelectronic substrates
[NASA-CASE-NPO-16087-1] 18 p3094 N85-29151
Electrodynamic transducers for ultrasonic reception 18 p3119 N85-29306
Ultrasonic testing of plates containing edge cracks
[NASA-CR-3904] 18 p3119 N85-29307
Dual differential interferometer
[NASA-CASE-LAR-12966-1] 19 p3271 N85-30282
Method for thermal monitoring subcutaneous tissue
[NASA-CASE-LAR-13028-1] 19 p3328 N85-30618
Grain structure identification by ultrasound frequency averaging and deconvolution
[AD-A154332] 19 p3352 N85-30777
Ultrasonic flowmetering with reflected pulses
[PB85-179885] 20 p3460 N85-31492
Propagation and reflection of a finite amplitude ultrasonic beam including harmonic content: A numeric model 20 p3523 N85-31914
Reliability of void detection in structural ceramics using scanning laser acoustic microscopy
[NASA-TM-87035] 21 p3587 N85-32337
USSR report: Electronics and electrical engineering
[JPRS-UEE-84-009] 22 p3773 N85-33381
Non-bonded ultrasonic tranducer
[DE85-011006] 22 p3794 N85-33504
Analytical ultrasonics for structural materials
[TI85-006132] 23 p3968 N85-34600
Sound speed measurements in liquid oxygen-liquid nitrogen mixtures
[NASA-TP-2464] 24 p4083 N85-35307

ULTRAVIOLET ABSORPTION
Solar radiation in the ozone layer 04 p0522 N85-13342
Measuring EUV line emission from the hot interstellar medium 06 p0880 N85-15595
Cumulus cloud venting of mixed layer ozone
[NASA-TM-87429] 13 p2132 N85-23269
Multiple product channels in the collision free UV photodissociation of 2-nitropropane
[AD-A150886] 14 p2251 N85-23951
Studies on radiative collisional and ultraviolet lasers
[AD-A151004] 14 p2310 N85-24296
Ground-based remote sensing of atmospheric pollution 16 p2832 N85-27462
Micromolecular modeling 21 p3608 N85-32405
Heating of the deep chromosphere during solar flares
[AD-A155256] 21 p3723 N85-33100
Ultraviolet radiation-damage absorption peak in solid deuterium-tritium, revision 1
[DE85-012969] 22 p3844 N85-33806

ULTRAVIOLET ASTRONOMY
UBV photometry of E region stars: Some intercomparisons 01 p0128 N85-10880
Ultraviolet observations of Uranus and Neptune below 3000 Angstrom 02 p0298 N85-11932
Documentation for the machine-readable version of the ANS Ultraviolet Photometry Catalogue of Point Sources (Wesselius et al 1982)
[NASA-TM-87379] 03 p0406 N85-12589
Observations of local ISM emission with the Berkeley EUV/FUV shuttle telescope 06 p0880 N85-15594
X-ray and UV Emission from Active Galactic Nuclei — conference
[MPE-184] 08 p1236 N85-17790
Ultraviolet spectroscopy of selected astronomical sources
[NASA-CR-174379] 09 p1413 N85-18912
Future of Ultraviolet Astronomy Based on Six Years of IUE Research
[NASA-CP-2349] 11 p1743 N85-20961
IUE absorption line studies of highly ionized interstellar gas 11 p1743 N85-20962
Hot stars: Six years of progress 11 p1743 N85-20963
Ultraviolet and X-ray observations of active galactic nuclei: Constraints on models of the broad emission line region 11 p1744 N85-20966
Interacting binary systems 11 p1744 N85-20967
Outer atmospheres of cool stars observed with IUE 11 p1744 N85-20968
Future ultraviolet experiments, including FUSE/COLUMBUS 11 p1744 N85-20969
UV observations and results on pre-main sequence stars 11 p1744 N85-20970
White dwarf stars at ultraviolet wavelengths 11 p1744 N85-20971
Supernova remnants and the carbon abundance in M33 11 p1745 N85-20972
Comments on the origins and variations of carbon and nitrogen in the ISM of galaxies as evident from IUE spectroscopy of H 2 regions 11 p1745 N85-20973
IUE spectroscopy of extragalactic H II regions 11 p1745 N85-20974
The usual hot stars in unusual galaxies 11 p1745 N85-20975
Highly ionized gas associated with the small Magellanic cloud 11 p1745 N85-20976
Galactic absorption lines measured from the IUE low dispersion spectra of active galaxies 11 p1745 N85-20977
Observations of Mg 1 and Mg 2 in the local ISM 11 p1748 N85-20997
Observations of RR Lyrae and X Arietis with the IUE satellite 11 p1754 N85-21030
The spatial dependence of the Jovian auroral emissions 11 p1759 N85-21068
Ultraviolet observations of Uranus and Neptune below 3000 A 11 p1760 N85-210*1
Stellar ultraviolet flux distributions in the 912-1200 A wavelength range 11 p1762 N85-21081
Current ideas on the nature of comets 14 p2435 N85-25017
Winds in cataclysmic variable stars
[DE85-006708] 15 p2669 N85-26470
Research in extreme ultraviolet and far ultraviolet astronomy
[NASA-CR-176068] 21 p3716 N85-33060
Astron X-ray experiment 22 p3732 N85-33137

ULTRAVIOLET LASERS
Interaction of UV-laser radiation with molecular surface-films
[AD-A146311] 03 p0366 N85-12349
Development of prototypes for versatile fast discharge systems for pulsed gas lasers, especially excimer lasers
[BMFT-FB-T-84-174] 06 p0613 N85-15165
Visible and ultraviolet lasers based on excimer transitions in the homonuclear halogens
[AD-D011311] 07 p0971 N85-16163
Investigations of vacuum ultraviolet and soft X-ray lasers
[AD-A148277] 08 p1167 N85-17358
Laser-Electron-Gamma-Source (LEGS)
[DE85-003204] 11 p1638 N85-20322
Operational characteristics of the OMEGA short-wavelength laser fusion facility
[DE85-002819] 11 p1640 N85-20334
Non-linear optical techniques for visible and UV lasers and thin film deposition
[AD-A150489] 13 p2098 N85-23077
Studies on radiative collisional and ultraviolet lasers
[AD-A151004] 14 p2310 N85-24296
Laser with a hollow copper cathode
[ISL-R-119/83] 14 p2310 N85-24300
The application of laser resonance saturation to the development of efficient short wavelength lasers
[AD-A153951] 18 p3113 N85-29270
Vacuum ultraviolet laser
[DE85-011632] 22 p3790 N85-33478
Thermal transport measurements of UV laser irradiated spherical targets
[DE85-011038] 23 p3931 N85-34365

ULTRAVIOLET LIGHT
U ULTRAVIOLET RADIATION

ULTRAVIOLET MICROSCOPY
Interaction of solutes with stretched polymers
[AD-A154662] 21 p3569 N85-32196

ULTRAVIOLET PHOTOMETRY
Documentation for the machine-readable version of the ANS Ultraviolet Photometry Catalogue of Point Sources (Wesselius et al 1982)
[NASA-TM-87379] 03 p0406 N85-12589
Local interstellar extinction with an emphasis on uvby beta results 06 p0875 N85-15559
Research in extreme ultraviolet and far ultraviolet astronomy
[NASA-CR-176068] 21 p3716 N85-33060

ULTRAVIOLET RADIATION
NT EXTREME ULTRAVIOLET RADIATION
NT FAR ULTRAVIOLET RADIATION
NT LYMAN ALPHA RADIATION
Temporal and spatial variations in the intensity of ultraviolet emissions from Jupiter and the Io torus 03 p0448 N85-12848

Absolute transition probabilities of lines in the spectra of astrophysical atoms, molecules, and ions
[NASA-CR-174141] 04 p0580 N85-13705
Search for the radiative decay of a cosmic relic particle with IUE
[PREPRINT-410] 04 p0580 N85-13707
Plant responses to solar UV-B radiation
05 p0690 N85-14436
Properties of ultra-violet cured poly(dimethylsiloxane)-urea acrylates
[AD-A148570] 06 p1134 N85-17148
Active inner regions of isolated galaxies
06 p1237 N85-17795
The unidentified emission features: A study of the Orion Bar and planetary nebulae 06 p1246 N85-17862
Effect of ultraviolet radiation on transparent polymer films as determined using in situ FTIR-RA spectroscopy. Volume 2: Photophysics of poly(vinylidene fluoride) films
[DE84-013040] 09 p1299 N85-18159
Functional and structural changes in human erythrocyte surface after irradiation by UV waves of various wavelengths. Report 1: Expression of ABO and Rhesus system antigen 09 p1361 N85-18564
Functional and structural changes in human erythrocyte surface after irradiation by UV waves of various wavelenghts. Report 2: Adsorption of alcyan blue by external premembranous components
09 p1361 N85-18565
Design of VUV monochromator systems
09 p1368 N85-18733
Genetic effects of microwave exposure on mammalian cells in vitro. Volume 2, Appendix B: Cytogenetics and growth kinetics data, 1.2 GHz
[AD-A148867] 10 p1522 N85-19800
Parametric processes in underdense UV laser-produced plasmas
[DE85-002812] 10 p1559 N85-19830
Temperature-dependent surface states and transitions of Si(111)-7x7
[AD-A149156] 10 p1562 N85-19850
Report on the Workshop on Intercomparison of Solar UV Irradiance Measurements and Related Instrument Calibration 11 p1658 N85-20448
MSG-7: Molecular absorption processes related to the penetration of ultraviolet solar radiation into the middle atmosphere 11 p1658 N85-20449
The variation of galactic interstellar extenction in the ultraviolet 11 p1749 N85-21000
Interstellar extinction in the nucleus of H PER
11 p1749 N85-21001
New results on PU VUL 11 p1753 N85-21023
Temporal UV emission from the peculiar star RX Puppis 11 p1753 N85-21026
Effect of ultraviolet radiation on transparent polymer films as determined using in situ FTIR-RA spectroscopy. Volume 1: Photodegradation of transparent polymer films
[DE84-013039] 12 p1814 N85-21377
Determination of ionospheric electron density profiles from satellite UV (ultraviolet) emission measurements
[AD-A150734] 14 p2373 N85-24667
Photoreactivation and other ultraviolet/visible light effects on DNA in human skin
[DE85-005135] 14 p2300 N85-24719
Evaluation of pyrotechnic fire suppression system for six pyrotechnic compositions
[AD-A152995] 17 p2937 N85-26130
Definition of requirements for injection locking of pulsed UV lasers
[DE85-010126] 18 p3113 N85-29275
The photochemical oxidation of GaAs
[AD-A153689] 19 p3233 N85-30045
Method for the preparation of photochromic insulating crystals
[DE85-011606] 19 p3262 N85-30229
Lidar techniques for search and rescue
[DE85-009586] 19 p3278 N85-30327
Molecular toxicology of chromatin: The role of Poly(ADP-Ribose) in gene control
[AD-A154415] 19 p3327 N85-30611
Photon-counting image sensors for the ultraviolet
[NASA-CR-176062] 20 p3458 N85-31478
Polymerizable ultraviolet stabilizers
21 p3608 N85-32406
Photoinduced active sites on ice nucleating aerosol of silver iodide 21 p3639 N85-32601
Excimer-laser generator of powerful UV picosecond pulses synchronized with picosecond pulses in visible and IR bands 21 p3686 N85-32903
Investigation of some aspects of amino acid metabolism in man during brief exposure to antiorthostatic hypokinesia combined with ultraviolet radiation
22 p3822 N85-33678
Ultraviolet radiation-damage absorption peak in solid deuterium-tritium, revision 1
[DE85-012968] 22 p3844 N85-33806
Solar Ultraviolet Spectral Irradiance Monitor (SUSIM)
23 p3901 N85-34160
Process for functionalizing alkanes
[DE85-006420] 23 p3909 N85-34219
Using the information of cosmic rays to predict influence epidemic
[SH-10.1-2] 23 p4053 N85-35134
The 2nd European Conference on Atomic and Molecular Physics
[AD-A155863] 24 p4148 N85-35715
Surface discharges as intense photon sources in the extreme ultraviolet
[DE85-012593] 24 p4158 N85-35782

ULTRAVIOLET SPECTRA

Search for the radiative decay of a cosmic relic particle with IUE
[PREPRINT-410] 04 p0580 N85-13707
X-ray and ultraviolet observations of BL Lacertae objects 05 p0741 N85-14767
Observations of absorption lines from highly ionized atoms 06 p0876 N85-15562
Ultraviolet spectral morphology of O-type stellar winds
06 p1232 N85-17782
The ultraviolet spectra of the narrow line active galaxies NGC 3081 and NGC 4507 06 p1237 N85-17799
UV and X-ray observations of AGN: Two comparisons with other wave lengths — Active Galactic Nuclei (AGN)
06 p1240 N85-17819
Extended atmospheres of outer planet satellites and comets
[NASA-CR-174338] 08 p1258 N85-17916
Excimer laser photofragmentation of organophosphonates. 1: Detection of the PO radical from dimethyl methyl phosphonate (DMMP)
[AD-A149471] 10 p1490 N85-19407
International Ultraviolet Explorer observations of amorphous hot galaxies
[NASA-CR-174354] 10 p1571 N85-19904
Structure of the Seyfert broad line region and absorption region of NGC 4151 11 p1746 N85-20978
The UV spectra of intermediate redshift quasars
11 p1746 N85-20980
Very recent IUE observations of 2 BL lacertae objects
11 p1746 N85-20982
A model for the variable continuum of the Seyfert 1 galaxy NGC 5548 11 p1747 N85-20985
IUE observations of planetary nebulae in the Magellanic Clouds 11 p1747 N85-20986
IUE observations of the jet emission feature in R Aquarii 11 p1747 N85-20986
The changing ultraviolet spectrum of Herbig-Haro object No. 1 11 p1747 N85-20989
Short-wavelength observations of HH-2H and HH-24A
11 p1747 N85-20990
Ultraviolet studies of the young populous cluster NGC 2100 in the LMC 11 p1748 N85-20995
IUE observations of interstellar lines
11 p1748 N85-20996
High-velocity interstellar gas in the line-of-sight to HD 50896 11 p1749 N85-20999
Coronal effects of the winds of early-type stars
11 p1749 N85-21002
Superionized species and winds in low luminosity B and Be stars 11 p1749 N85-21003
Main sequence B stars with strong winds
11 p1750 N85-21005
IUE and ESO observations of the P Cyg star AG Carinae and its ring nebula 11 p1750 N85-21006
Coordinated ultraviolet and visual observations of Omega Orionis 1982-1983 11 p1750 N85-21007
The spectroscopic antics of S 18/SMC
11 p1750 N85-21008
An episodic red-wing structure of SiIV, lambda 1394A, in gamma Cas 11 p1750 N85-21009
IUE and Voyager observations of very hot O-type subdwarfs 11 p1751 N85-21010
Analysis of high-depression IUE spectra of subdwarf B stars 11 p1751 N85-21011
The fading of R coronae borealis
11 p1753 N85-21029
Observations of RR Lyrae and X Arietis with the IUE satellite 11 p1754 N85-21030
Atmospheric properties of RU Lupi derived from high- and low-resolution IUE spectra
11 p1754 N85-21031
Mg 2 emission of Pop. 2 long-period Cepheids
11 p1754 N85-21032
Blue companions of Cepheids
11 p1754 N85-21033
Ultraviolet observations of Population 2 Cepheids
11 p1754 N85-21034
Ultraviolet analysis of the peculiar F supergiant HD 112374 11 p1754 N85-21035
Eclipse observations of Epsilon Aurigae
11 p1755 N85-21037
The stellar wind in the BO V-type eclipsing binary Y Cygni 11 p1755 N85-21040
Multi-year and possibly periodic variations in the UV spectrum of 56 Pegasi 11 p1756 N85-21046
Physical models for the UV continua of symbiotic stars
11 p1756 N85-21048
MU Sagittarii and Beta Lyrae: Combined IUE/Voyager observations 11 p1757 N85-21052
Chromospheric activity in M giants
11 p1757 N85-21056
A progress report on the analysis of long exposure SWP high resolution spectra of cool stars
11 p1758 N85-21057
Chromospheric emission lines in high-resolution LWR spectra (220 - 3000 alpha) of gamma CRU (M3 3) and alpha ORI (M2 Iab) 11 p1758 N85-21058
Rotational modulation of chromospheric emission in cool giants and hybrid stars 11 p1759 N85-21064
Ultraviolet and optical spectroscopy and polarimetry of the helium weak star HD 21699: Evidence for a magnetically controlled stellar wind
11 p1759 N85-21065
IUE spectrophotometry of helium weak and silicon stars 11 p1759 N85-21067
The Jovian Stratosphere in the ultraviolet
11 p1760 N85-21069
Long term variabil"y of the IO torus
11 p1760 N85-21070
IUE low-dispersion reference atlas
11 p1760 N85-21073
An IUE high-resolution atlas of O-type spectra
11 p1760 N85-21074
Statistical classification of IUE low-despersion stellar spectra: Progress report 11 p1760 N85-21075
The ultraviolet excess of quasars 3: The highly polarized quasars PKS 0736+017 and PKS 1510-089
[NASA-CR-175576] 12 p1953 N85-22268
A survey of Mg II h and k emission in near-solar type stars
[NASA-CR-175572] 12 p1953 N85-22269
Plasma processes in Herbig-Haro objects
12 p1957 N85-22301
NIMBUS-7 SBUV (Solar Backscatter Ultraviolet) observations of solar UV spectral irradiance variations caused by solar rotation and active-region evolution for the period November 7, 1978 - November 1, 1980
[NASA-CR-175544] 12 p1962 N85-22334
A survey for galactic plane ultraviolet-excess objects: Space densities for white dwarfs, subdwarfs, and cataclysmic variables 13 p2169 N85-23458
Ultraviolet spectral diagnostics of solar flares and heating events 13 p2205 N85-23675
Self-developing polysilane deep-UV resists: Photochemistry, photophysics and submicron lithography
[DE85-007606] 19 p3237 N85-30067
The ultraviolet spectra of intermediate redshift quasars
20 p3544 N85-32056

ULTRAVIOLET SPECTROGRAPHS

U ULTRAVIOLET SPECTROMETERS

ULTRAVIOLET SPECTROMETERS

Oblique focus ICCD laboratory evaluation
[NASA-CR-174205] 06 p0862 N85-15480
Voyager EUV and FUV observations
06 p0875 N85-15554
A new generation of spectrometer designs for ultraviolet astronomy 11 p1761 N85-21079
Ozone Correlative Measurements Workshop
[NASA-CP-2362] 13 p2105 N85-23112
Scientific requirements for ozone measurements
13 p2105 N85-23113
Method for determining the number of correlative measurements required to validate the SBUV/2 ozone retrievals 13 p2105 N85-23114
Ultraviolet Spectrometer and Polarimeter (UVSP) software development and hardware tests for the solar maximum mission
[NASA-CR-175279] 14 p2305 N85-24271
Measurements with an auroral spectrometer in the Energy Budget Campaign
[BMFT-FB-W-84-050] 14 p2374 N85-24677
Voyager UVS observations of stellar occultations by the rings of Saturn — ultraviolet spectrometer (UVS)
15 p2673 N85-26497
French and West German equipment for Vega Project
16 p2722 N85-26805
Ground-based remote sensing of atmospheric pollution 16 p2832 N85-27462
Studies of hot B subdwarfs. Part 2: Energy distributions of three bright sdB/sdOB stars in the 950-5500 angstrom range
[NASA-CR-175854] 16 p2881 N85-27775
Solar Ultraviolet Spectral Irradiance Monitor (SUSIM)
23 p3901 N85-34160
High Resolution Telescope and Spectrograph (HRTS)
23 p3901 N85-34162

ULTRAVIOLET SPECTROPHOTOMETERS
Effect of integration time on precision of absorbances measured with a diode array UV-VIS spectrophotometer
[AD-A146952] 07 p1043 N85-16624
Winds in cataclysmic variable stars
[DE85-006708] 15 p2669 N85-26470
ULTRAVIOLET SPECTROSCOPY
Optical and UV emission of active galactic nuclei
08 p1236 N85-17791
Determination of ion temperature and rotation velocity profiles by visible, UV and X-ray spectroscopy on Doublet 3
09 p1388 N85-18734
UV observations of epsilon aurigae during ingress and totality
11 p1755 N85-21038
Egress spectra of the new eclipsing supergiant 22 Vulpeculae
11 p1755 N85-21039
Ultraviolet spectroscopy of the interacting binary U Sagittae
11 p1755 N85-21042
The essence of binary star coalescence: A coordinated ground-based photometric and IUE ultraviolet study of FK Comae
11 p1756 N85-21044
Strange F + Be binary star systems
11 p1756 N85-21045
Characterization of multiphoton ionization processes in the ultraviolet
[AD-A151427] 15 p2652 N85-26354
Transparency of water 9n 186 - 500 nm region
21 p3890 N85-32923
The 2nd European Conference on Atomic and Molecular Physics
[AD-A155863] 24 p4148 N85-35715
ULTRAVIOLET TELESCOPES
Observations of local ISM emission with the Berkeley EUV/FUV shuttle telescope 06 p0880 N85-15584
UMBRAS
Linear models of acoustic waves in sunspot umbrae
14 p2450 N85-25130
Solar cycle variations of sunspot temperatures
14 p2452 N85-25141
UNCONSCIOUSNESS
NT BLACKOUT (PHYSIOLOGY)
UNCONTROLLED REENTRY (SPACECRAFT)
Natural atmospheric reentry --- satellite orbit decay
05 p0800 N85-13829
Orbital debris policy issues: Battelle involvement and some personal observations 12 p1787 N85-21218
Natural reentry of satellites 14 p2397 N85-24774
UNDERCARRIAGES
Deflection model of a CT4-A undercarriage
[AD-A149778] 12 p1777 N85-21156
Selection of effective arrangement of heavy undercarriage systems for use with concrete runways
14 p2285 N85-24158
UNDERGROUND ACOUSTICS
Sidereal variations deep underground in Tasmania
[SH-4.4-4] 23 p4033 N85-35002
The effect of the interplanetary magnetic field on sidereal variations observed at medium depth underground detectors
[SH-4.4-5] 23 p4033 N85-35003
Corrected sidereal anisotropy for underground muons
[SH-4.4-7] 23 p4033 N85-35005
Cosmic ray intensity variations observed at Matsushiro (220 M.W.E. in depth)
[SH-4.4-9] 23 p4034 N85-35007
UNDERGROUND EXPLOSIONS
Seismology 1983: Nuclear test ban verification, earthquake and Earth resource investigation
[FOA-C-20537-T1] 02 p0229 N85-11495
Micro-deformation of quartz under dynamic action and its applications 11 p1620 N85-20201
Surface wavesseismic yields as measured by the Regional Seismic Test Network
[DE85-010532] 18 p3137 N85-29425
A multiphase continuum model to describe dynamic loading effects in nonlinear porous media
[DE85-010102] 19 p3301 N85-30463
Seismic discrimination
[AD-A154167] 20 p3494 N85-31722
Experimental and analytic characterization of nonlinear seismic attenuation
[AD-A154760] 21 p3631 N85-32556
Investigation of the lightning vulnerability of nuclear explosive test systems at the Nevada Test Site
[DE85-011761] 24 p4124 N85-35563
Ground motion measurements for the QUESO nuclear event
[DE85-014806] 24 p4151 N85-35743
UNDERGROUND STORAGE
Hybrid system for producing and storing ice
[DE84-017474] 09 p1304 N85-18195
Natural convection experiments about a finite-length cylindrical heat source in a liquid-saturated porous medium
[DE84-012657] 09 p1320 N85-18298
Nevada nuclear waste storage investigations preliminary repository concepts report
[DE85-002132] 09 p1383 N85-18696
Rock mechanics: Issues and research needs in the disposal of wastes in hydraulic fractures
[DE85-001399] 10 p1556 N85-19809
Index to published geologic maps in the region around the potential Yucca Mountain nuclear waste repository site, southern Nye County, Nevada
[DE85-000260] 11 p1669 N85-20518
Underground pumped hydroelectric storage
[DE85-000288] 11 p1676 N85-20560
Consolidation around a point heat source
[PB85-116549] 11 p1682 N85-20601
High-level waste processing and disposal
[DE85-003564] 11 p1728 N85-20865
Shallow land burial technology: Humid
[DE85-004432] 12 p1932 N85-22136
Occurrence of uranium in ground water in the vicinity of the US Department of Energy Feed Materials Production Center, Fernald, Ohio
[DE85-010340] 19 p3364 N85-30862
Preliminary SPR thermal model description and results for WH-11 and BM-4
[DE85-013171] 23 p3931 N85-34360
UNDERGROUND STRUCTURES
Finite element modelling of buried structures
01 p0061 N85-10403
Study for a large area underground detector made with organic scintillators for searching for magnetic monopoles
[NOTA-INTERNA-814] 02 p0201 N85-11339
An underground search for massive slow particles (hunting Grand Unified Theory (GUT) monopoles)
[NOTA-INTERNA-821] 02 p0292 N85-11894
Underground engineering (selected articles)
[AD-A141053] 04 p0483 N85-13082
Development of the GASCOPACT (R) pipe and cable tracer
[ERS-E.340] 09 p1324 N85-18320
GASCOPACT: A new approach to pipe and cable location
[ERS-E.383] 09 p1325 N85-18324
Simplified theory for the behaviour of buried flexible cylinders under the influence of uniform hoop compression
[PB85-116531] 11 p1654 N85-20419
Behavior of buried flexible cylinders under the influence of nonuniform hoop compression
[PB85-116523] 12 p1868 N85-21718
Constitutive modeling for blast-induced wave propagation
[AD-A153576] 18 p3099 N85-29187
Commercial feasibility of underground gasification of Texas lignite to produce synthetic gas
[DE85-001998] 18 p3127 N85-29361
Literature survey of underground construction methods for application to hardened facilities
[AD-A155212] 21 p3599 N85-32351
Method for determining depth and shape of a sub-surface conductive object
[DE85-006502] 23 p3935 N85-34389
New Matsushiro underground cosmic ray station (220 M.W.E. in depth)
[SH-9.1-14] 23 p4052 N85-35129
An underground cosmic ray muon telescope for observation of cosmic ray anisotropy
24 p4196 N85-36037
A possible EAS array above the Soudan 2 detector
[HE-4.6-9] 24 p4197 N85-36046
Upper limit on magnetic monopole flux from Baksan experiment
[HE-6.1-11] 24 p4210 N85-36136
UNDERGROUND TRANSMISSION LINES
The HEMP (High-altitude Electromagnetic Pulse) response of a long transmission line buried in the earth
[AD-A148517] 06 p0800 N85-15106
Development of the GASCOPACT (R) pipe and cable tracer
[ERS-E.340] 09 p1324 N85-18320
GASCOPACT: A new approach to pipe and cable location
[ERS-E.383] 09 p1325 N85-18324
UNDERWATER ACOUSTICS
A description and discussion of FREDDEX oceanographic measurements
[AD-A145032] 01 p0068 N85-10598
The numerical solution of the Helmholtz equation for wave propagation problems in underwater acoustics
[NASA-CR-172454] 02 p0250 N85-11634
The acoustic pressure in a wedge-shaped water layer overlying a fast fluid bottom
[AD-A145517] 02 p0276 N85-11795
Acoustic scattering cross sections for truly composite wind-wave surfaces. Scattering without bubbles
[AD-A145672] 03 p0415 N85-12655
Signal characteristics of an underwater explosive acoustic telemetry system
[DE84-016053] 05 p0726 N85-14668
Wave-wave interactions, microseisms, and infrasonic ambient noise in the ocean
[AD-A146529] 06 p0859 N85-15483
Research on acoustical and optical scattering, optics of bubbles, diffraction catastrophes, laser generation of sound, and shock induced cavitation
[AD-A146703] 06 p0860 N85-15486
Ocean acoustics
[AD-A147062] 07 p1038 N85-16591
Arctic marine acoustics
[AD-A147492] 07 p1039 N85-16594
Current and current shear effects in the parabolic approximation for underwater sound channels
[AD-A147833] 07 p1039 N85-16597
An efficient numerical solution technique for wave propagation in horizontally stratified ocean environments
[AD-A148537] 08 p1190 N85-17502
SAI (Science Applications, Inc.) Interim Scattering Model/Ice (SISM/ICE)
[AD-A148596] 08 p1213 N85-17638
A broadband matching network
[AD-D011406] 08 p1219 N85-17675
A 3-dimensional mass conserving element for compressible flows
[NASA-CR-172513] 09 p1373 N85-18626
Specifics of backscattering of sound by bottom of bank in open sea 10 p1499 N85-19460
Average sound intensity decrease rule in irregular hydroacoustical waveguide 10 p1499 N85-19461
Linear and nonlinear ultrasonic interaction on liquid-solid boundaries
[AD-A148679] 10 p1553 N85-19793
A stochastic-mechanical approach to acoustic pulse propagation in the deep ocean sound channel
[AD-A149598] 12 p1928 N85-22110
Twenty-five sound propagation tests on the continental shelf between Long Island, New York and Cape Canaveral, Florida
[AD-A149869] 12 p1928 N85-22111
Numerical results of acoustic radiation, transmission and reflection of steel plate in water
[AMTE(N)-TM-84037] 13 p2155 N85-23378
Vertical discrimination in the sound channel
[AD-A150254] 13 p2155 N85-23380
Recent progress in the development and application of the parabolic equation
[AD-A151475] 15 p2637 N85-26265
Development of a modified time delay spectrometry technique for underwater acoustic measurements in a multipath environment
[AD-A152111] 16 p2860 N85-27639
Multiple array processors for ocean acoustic problems
[AD-A152174] 16 p2860 N85-27641
Metrology and Oceanology Institutes' underwater acoustics R and D 19 p3289 N85-30394
Arctic acoustic tomography MIZEX 84
[AD-A154426] 19 p3320 N85-30580
Well-posedness of one-way wave equations and absorbing boundary conditions
[NASA-CR-172619] 19 p3345 N85-30727
Development of computer programs using the method of images to predict the sound field in a wedge overlaying a fast fluid and comparison with laboratory experiments
[AD-A154580] 21 p3670 N85-32797
The moving thermoacoustic array: A theoretical feasibility study
[AD-A154510] 21 p3699 N85-32980
Discrete-element acoustic analysis of submerged structures using doubly asymptotic approximations
[AD-A154959] 21 p3700 N85-32987
A random layer model for reflection from ocean bottom sediments
[AD-A155019] 21 p3700 N85-32988
Propagation of sound in a layered laboratory model
[AD-A155141] 21 p3700 N85-32989
Understanding coherence losses incurred by bottom-retained signals
[AD-A155559] 21 p3701 N85-32992
Mean intensity of wave reflected by wavefront reversing mirror in turbulent medium 22 p3782 N85-33432
Pressure cross spectra in turbulent boundary layers in water
[AD-A156153] 24 p4094 N85-35378
A comparison of multipath arrival structures observed in the presence of a surface duct with predictions obtained using classical ray techniques and the parabolic equation method
[AD-A156024] 24 p4145 N85-35696
UNDERWATER BREATHING APPARATUS
Manned testing of two closed-circuit oxygen underwater breathing apparatus: US Navy Emerson Rig and Fenzy PO.86
[AD-A148300] 08 p1200 N85-17560

The use of austenitic stainless steel versus monel (Ni-cu) alloy in pressurized Gaseous Oxygen (GOX) life support systems
[AD-A156306] 24 p4134 N85-35625
UNDERWATER ENGINEERING
Utility of the M.I.T. (Massachusetts Institute of Technology) underwater stud welding gun
[AD-A144793] 01 p0055 N85-10385
French firms develop artificial intelligence robot 03 p0341 N85-12192
Evaluation of the Kerle Cable thermal arc cutting equipment
[AD-A147813] 07 p0974 N85-16166
Underwater pipeline: Welding by high frequency induction
[BLL-WI-TRANS-662-(9312.57)] 16 p2792 N85-27221
The dynamics of slack marine cables
[AD-A155022] 21 p3599 N85-32349
UNDERWATER EXPLOSIONS
Signal characteristics of an underwater explosive acoustic telemetry system
[DE84-016653] 05 p0726 N85-14668
The development of a method for the shock-resistant securing of large batteries in submarines 09 p1335 N85-16391
Shipboard shock response of the model structure DSM: Experimental results versus responses predicted by eight participants 09 p1335 N85-16392
An experimental investigation into the dynamic response of a stiffened flat plate loaded impulsively by an underwater shockwave
[AD-A151321] 15 p2578 N85-25903
Underwater shock-induced responses of stiffened flat plates: An investigation into the predictive capabilities of the USA-STAGS code
[AD-A154245] 19 p3286 N85-30377
An investigation into the comparisons of the underwater shock effects on a stiffened flat plate to the predictive nature of a computer model
[AD-A156612] 21 p3600 N85-32355
UNDERWATER PHOTOGRAPHY
East Europe report: Science and technology
[JPRS-ESA-84-030] 01 p0101 N85-10670
Underwater television equipment described 01 p0101 N85-10672
The use of in-situ photography in studies of the deep-sea benthos at IOS — Institute of Oceanographic Sciences (IOS)
[IOS-182] 09 p1360 N85-16553
Processing of underwater photographs 10 p1499 N85-19462
UNDERWATER PHYSIOLOGY
Hyperbaric physiology (status and prospects) 08 p1194 N85-17521
Hydrogen-oxygen (hydrox) breathing at 1.3MPa
[FOA-C-56015-H1] 09 p1364 N85-16577
Pressure chamber simulation of 450-meter dive 20 p3505 N85-31788
UNDERWATER RESEARCH LABORATORIES
Preliminary results of an ALVIN dive program on active hydrothermal vents at the southern Juan de Fuca Ridge 24 p4106 N85-35454
UNDERWATER RESOURCES
Maritime prospecting, mining discussed 07 p0990 N85-16226
Technical and cost analyses of manganese nodule processing techniques and their significant variations
[PB85-148815] 14 p2258 N85-23992
Massive sulfide deposits from the southern Juan de Fuca Ridge 24 p4105 N85-35446
UNDERWATER SOUND
U UNDERWATER ACOUSTICS
UNDERWATER STRUCTURES
Discrete-element acoustic analysis of submerged structures using doubly asymptotic approximations
[AD-A154959] 21 p3700 N85-32987
UNDERWATER TESTS
The design, fabrication and delivery of a spacelab neutral buoyancy Instrument Pointing System (IPS) mockup — underwater training simulator
[NASA-CR-171233] 04 p0462 N85-12934
NOAA OTEC CWP (National Oceanic and Atmospheric Administration Ocean Thermal Energy Conversion Cold Water Pipe) at-sea test. Volume 3, part 1: Tabulation of the power spectra for selected channels
[PB84-236955] 09 p1346 N85-16467
The Deep Drifter Program — deep ocean sensors 14 p2329 N85-24400
Predicting electrical performance parameters of underwater cables 22 p3775 N85-33391
Modular detector for deep underwater registration of muons and muon groups
[HE-5.4-15] 24 p4208 N85-36125
UNDERWATER VEHICLES
NT SUBMARINES
NT UNDERWATER RESEARCH LABORATORIES
Technology development for unmanned untethered submersible vehicle systems
[AD-A148794] 09 p1304 N85-16190
The ARGOS system aboard research vehicles: 1981 experiment aboard the Le Suroit oceanographic vessel and the outlook
[CNEXO/DFT/OPNAV/82-05] 14 p2327 N85-24382
Environmental background measurement program
[AD-A153860] 19 p3319 N85-30577
A towed instrument vehicle for deep ocean sampling
[AD-A156322] 24 p4125 N85-35576
UNIAXIAL STRAIN
U AXIAL STRAIN
UNIFIED FIELD THEORY
On the nature of the baryon asymmetry
[NASA-TM-86156] 05 p0746 N85-14784
Thin end of the wedge
[DE84-016439] 09 p1401 N85-16816
Supersymmetric inflationary cosmology
[DE85-001332] 09 p1415 N85-16929
Experimental and theoretical high energy physics
[DE85-000844] 11 p1726 N85-20658
Superheavy magnetic monopoles and the standard cosmology
[DE85-003922] 15 p2686 N85-26587
Dark matter, galaxies, and large scale structure in the universe
[DE85-008053] 16 p2862 N85-27786
Study for a large area acrylic scintillator detector — magnetic monopoles
[NOTA-INTERNA-827] 18 p3097 N85-29174
Cosmology in theories with extra dimensions 18 p3202 N85-29864
The dimensional reduction transition
[DE85-003948] 19 p3383 N85-30990
Charge 4/3 leptons in cosmic rays
[HE-6.2-14] 24 p4212 N85-36150
UNIFORM FLOW
NT BLASIUS FLOW
Comparison of uniform perturbation solutions and numerical solutions for some potential flows past slender bodies
[NASA-CR-172485] 06 p0749 N85-14799
UNIPOLAR TRANSISTORS
U FIELD EFFECT TRANSISTORS
UNIQUENESS
On existence and uniqueness of solutions of Hamilton-Jacobi equations
[AD-A147507] 07 p1033 N85-16560
Existence, uniqueness and stability conditions for general finite element methods in linear elasticity 09 p1332 N85-16372
Hamilton-Jacobi equations in infinite dimensions. Part 1. Uniqueness of viscosity solutions
[AD-A149094] 10 p1546 N85-19749
Construction of solutions for two-dimensional Riemann problems
[DE85-003136] 10 p1549 N85-19770
Uniqueness and stability in nonlinear elasticity and viscoelasticity
[AD-A151470] 15 p2637 N85-26264
UNIQUENESS THEOREM
On two concepts of fundamental matching
[CSIR-TWISK-395] 01 p0110 N85-10743
Existence and non-uniqueness of similarity solutions of a boundary layer problem
[NASA-CR-172503] 07 p0957 N85-16064
UNITED KINGDOM
NT ENGLAND
The United Kingdom Meteorological Office mesoscale forecasting system 01 p0080 N85-10533
Revised Uniform Summary of Surface Weather Observations (RUSSWO). Alconbury RAF United Kingdom, parts A-F
[AD-A146913] 07 p1004 N85-16384
Revised Uniform Summary of Surface Weather Observations (RUSSWO). Mildenhall RAF, United Kingdom, parts A-F
[AD-A146915] 07 p1005 N85-16386
Air traffic management concepts for the UK in the 1990's: A review of recent RSRE work
[AD-A147850] 08 p1062 N85-16853
United Kingdom report on space research 08 p1231 N85-17752
Innovation in British industry (notably the aircraft industry) and its value: Collected papers
[BAE-KRS-N-GEN-256] 09 p1263 N85-17933
Assessment of wave power available at key United Kingdom sites
[IOS-186] 09 p1346 N85-16466
British aerospace studies HOTOL satellite launcher 10 p1460 N85-19206
Meteorological and oceanographic support during the Falklands conflict 11 p1712 N85-20769
A review of fatality, impairment of consciousness and head and neck injury on Royal Air Force ejections 1968-1981 12 p1907 N85-21975
Brief review of current work in the UK on three dimensional boundary layers 15 p2559 N85-25788
Information technology applications in voluntary sector transport operations. SP1: Objectives and programme of work
[TT-8501] 15 p2667 N85-26457
British super-shuttle 18 p3067 N85-29104
The contribution of an operational SAR satellite system to the UK SAR organisation — search and rescue (SAR) 20 p3400 N85-31095
UK experience with COSPAS-SARSAT and INMARSAT distress systems 20 p3408 N85-31132
Environmental aspects of large-scale wind-power systems in the UK 24 p4110 N85-35478
UNITED KINGDOM SATELLITES
U UK SATELLITES
UNITED NATIONS
International cooperation in remote sensing applications 05 p0656 N85-14209
UNITED STATES
NT ALABAMA
NT ALASKA
NT ARIZONA
NT ARKANSAS
NT CALIFORNIA
NT COLORADO
NT CONNECTICUT
NT DELAWARE
NT FLORIDA
NT GEORGIA
NT HAWAII
NT IDAHO
NT ILLINOIS
NT INDIANA
NT IOWA
NT KANSAS
NT KENTUCKY
NT LOUISIANA
NT MAINE
NT MARYLAND
NT MASSACHUSETTS
NT MICHIGAN
NT MISSISSIPPI
NT MISSOURI
NT MONTANA
NT NEBRASKA
NT NEVADA
NT NEW HAMPSHIRE
NT NEW JERSEY
NT NEW MEXICO
NT NEW YORK
NT NORTH CAROLINA
NT NORTH DAKOTA
NT OHIO
NT OKLAHOMA
NT OREGON
NT PENNSYLVANIA
NT SOUTH CAROLINA
NT SOUTH DAKOTA
NT TENNESSEE
NT TEXAS
NT UTAH
NT VIRGINIA
NT WASHINGTON
NT WISCONSIN
NT WYOMING
Geology and geomorphology of the southern central Blue Ridge: An indexed bibliography
[PB84-225119] 01 p0072 N85-10480
The south-central United States magnetic anomaly
[E85-10025] 02 p0218 N85-11438
International cooperation and competition in space
[GPO-38-001] 02 p0295 N85-11911
Statement of Otho E. Eskin, Director, Office of Advanced Technology, Department of State 02 p0295 N85-11914
Statement of John H. McElroy, Assistant Administrator for Environmental Satellite, Data and Information Services, National Oceanic and Atmospheric Administration 02 p0295 N85-11915
International cooperation and competition in civilian space activities, summary, appendix 1 02 p0295 N85-11916
NESDIS international activities, appendix 2 02 p0295 N85-11917
US energy for the rest of the century, 1984 edition
[PB84-207406] 04 p0531 N85-13393
The evolution of civilian in-space infrastructure, i.e., space station concepts in the United States 07 p0914 N85-15788

International involvement in a civilian space station program 07 p0915 N85-15789
Synopsis of the OTA Workshop on Cost Containment of Civilian Infrastructure (Civilian Space Station) Elements 07 p0915 N85-15790
Title 2: National Commission on Space (Public Law 98-361) 07 p0915 N85-15791
Financing considerations and Federal budget impacts 07 p0915 N85-15792
Government contract contingent liabilities. The anti-deficiency act, and the hobgoblin of little minds [AD-A147919] 07 p1053 N85-16684
Evaluation of the radar response to land surfaces and volumes: Examination of theoretical models, target statistics, and applications 08 p1149 N85-17250
Outlook for expanding the Federal research in progress system [AD-A148354] 08 p1229 N85-17737
High-technology ceramics in Japan [TI85-900380] 09 p1299 N85-18157
Comparison of energy storage systems in the United States chilled water versus two types of ice storage systems [DE85-001102] 09 p1344 N85-18452
Petrography, diagenesis and depositional models of the St. Louis limestone, valmeyeran (middle Mississippian), Illinois Basin, USA 09 p1352 N85-18506
Birds and airport agriculture in the conterminous United States: A review of literature [AD-P004208] 11 p1583 N85-19975
The FAA grant-in-aid assurances: FAR part 139, and airport hazards [AD-P004209] 11 p1583 N85-19976
MAP-related activities in the United States 11 p1655 N85-20427
Shallow magma targets in the western US [DE85-003274] 12 p1881 N85-21809
Response of unmanaged forests to CO2-induced climate change: Available information, initial tests and data requirements [DOE/NSB-0053] 12 p1883 N85-21817
A review of neck injury and impaired consciousness associated with US Navy ejections 1 January 1969 - 31 December 1979 12 p1906 N85-21973
Twenty-five sound propagation tests on the continental shelf between Long Island, New York and Cape Canaveral, Florida [AD-A149869] 12 p1928 N85-22111
Militarization of space activity in United States 15 p2488 N85-25360
Military journal on US intelligence satellites 16 p2727 N85-28832
AWS (Air Weather Service) climatic briefs: North America [AD-A152161] 16 p2835 N85-27483
Great Lakes winter weather and ice conditions for 1982-83 [PB85-165009] 16 p2837 N85-27498
Potential climatic impacts of increasing atmospheric CO2 with emphasis on water availability and hydrology in the United States [NASA-TM-87479] 17 p2995 N85-28517
Close encounters with S/T (science and technology) in the Soviet Union [AD-P004570] 17 p3048 N85-28864
Experimental philosophy leading to a small scale digital data base of the conterminous United States for designing experiments with remotely sensed data [NASA-TM-85009] 17 p3049 N85-28877
US restrictions on technology transfer reviewed 18 p3088 N85-29115
Shales and other argillaceous strata in the United States [DE85-010453] 18 p3125 N85-29353
The COSPAS/SARSAT demonstration and evaluation. Results of the first year in the United States 20 p3405 N85-31128
The south-central United States magnetic anomaly 20 p3474 N85-31591
The south-central United States magnetic anomaly 20 p3475 N85-31592
Helicopter noise survey for selected cities in the contiguous US [AD-A154893] 21 p3699 N85-32985
Magnetic Fusion Program plan [DE85-009661] 22 p3846 N85-33823
The role of regional subsurface geochemistry in resource assessment in the central United States 24 p4104 N85-35440
New silver resource map of the United States: Potential for increased domestic silver production 24 p4105 N85-35445
Early and middle Cenozoic volcanic synthesis 24 p4105 N85-35449

UNITY
Partitions of unity and approximation [AD-A144717] 01 p0110 N85-10746

UNIVAC COMPUTERS
NT UNIVAC 1100 SERIES COMPUTERS
Sperry Univac System 80, Model 6, OS/3 BASIC, Version 10.01 [PB85-108066] 10 p1542 N85-19722

UNIVAC 1100 SERIES COMPUTERS
R and D activities of the Computer Centre 20 p3540 N85-32029

UNIVERSAL TIME
Universal time effects in polar ionosphere 14 p2338 N85-24461

UNIVERSE
Decaying particles do not heat up the Universe [DE85-002191] 11 p1763 N85-21091
Cosmology, galactic astronomy and elementary particle physics 12 p1956 N85-22269
Dark matter, galaxies, and large scale structure in the universe [DE85-008053] 16 p2682 N85-27786
Constructing a bit string universe [DE85-006317] 18 p3197 N85-29629

UNIVERSITIES
An investigation of the use, cost, perceived value and social context of telecommunications tools in two-year college libraries in the southeastern United States 02 p0293 N85-11901
Improving the research infrastructure at US universities and colleges [GPO-35-290] 04 p0574 N85-13661
Research report 1979-1982. Part 2: Projects [ISBN-3-7983-0960-4] 04 p0575 N85-13667
Optical computer studies at UK's Heriot-Watt University 09 p1309 N85-18227
NASA Lewis Research Center/University Graduate Research Program on Engine Structures [NASA-TM-86916] 09 p1333 N85-18375
Renewal request for high energy physics at Texas A and M University [DE85-004469] 11 p1724 N85-20843
Research in surface sciences, disordered materials, and solidification and growth [PB85-132140] 11 p1737 N85-20927
Air Force Academy Aeronautics Digest [AD-A149814] 12 p1789 N85-21104
Academic science and engineering: R and D funds, fiscal year 1982 (detailed statistical tables) [PB85-154763] 15 p2664 N85-26443
Selected university laboratory needs in support of national security [AD-A153511] 18 p3197 N85-29633
NASA initiatives with historically black colleges and universities [NASA-EP-210] 19 p3379 N85-30960
The Department of Defense report on the technology base and support of university research [AD-A154309] 20 p3540 N85-32030
Spin-offs from technical scientific infrastructures, no. 1 20 p3540 N85-32034
The Naval Postgraduate School Flight Mechanics Laboratory: A feasibility study [AD-A154578] 21 p3557 N85-32127
New innovative businesses from industry. Experiences in the Netherlands in the successful transfer of technology from university to industry 22 p3849 N85-33843

UNIVERSITY PROGRAM
Canada report to COSPAR 01 p0131 N85-10906
Summary and analysis of hearing on improving the research infrastructure at US universities and colleges [GPO-36-854] 04 p0574 N85-13660

UNLOADING
Mechanical features of the shuttle rotating service structure 08 p1102 N85-16967
New applications for robot loaders, unloaders 08 p1139 N85-17175
Mathematical model for rollout of planet roving vehicle from landing craft 15 p2484 N85-25334
Application of the unloading compliance methods in fracture toughness measurements of a quenched and tempered steel [BLL-CE-TRANS-7963-(9022.09)] 20 p3465 N85-31523
Responses of skeletal muscle to unloading, a review [NASA-CR-176177] 24 p4128 N85-35594

UNMANNED SPACECRAFT
NT BIOSATELLITES
NT EXOSAT SATELLITE
NT GALILEO PROBE
NT GALILEO SPACECRAFT
NT GEODETIC SATELLITES
NT GEOS 1 SATELLITE
NT GEOS 2 SATELLITE
NT GEOS 3 SATELLITE
NT GIOTTO MISSION
NT HEAO 1
NT HEAO 2
NT HEAO 3
NT HELIOS 1
NT HELIOS 2
NT JUPITER PROBES
NT LAGEOS (SATELLITE)
NT LUNIK LUNAR PROBES
NT MARINER 5 SPACE PROBE
NT MARINER 9 SPACE PROBE
NT MARS PROBES
NT NAVIGATION SATELLITES
NT NAVSTAR SATELLITES
NT PASSIVE SATELLITES
NT PIONEER SPACE PROBES
NT PIONEER VENUS SPACECRAFT
NT PIONEER 10 SPACE PROBE
NT PIONEER 11 SPACE PROBE
NT SOLAR OBSERVATORIES
NT SPACE PROBES
NT TRANSIT SATELLITES
NT VENERA SATELLITES
NT VENERA 11 SATELLITE
NT VENUS PROBES
NT VOYAGER 1 SPACECRAFT
NT VOYAGER 2 SPACECRAFT
Winged first stages of space transport appliances [TUM-RT-TB-84/3] 02 p0167 N85-11125
A study of spacecraft technology and design concepts, volume 1 [NASA-CR-172579-VOL-1] 16 p2730 N85-26844
A study of spacecraft technology and design concepts. Volume 2: Appendices [NASA-CR-172579-VOL-2] 16 p2730 N85-26845
Soviet space programs, 1976-1980 (with supplementary data through 1983). Part 3: Unmanned space activities [S-PRT-98-235-PT-3] 16 p2879 N85-27765
Far travelers: The exploring machines [NASA-SP-480] 22 p3731 N85-33126
Noiseless coding for the Gamma Ray spectrometer [NASA-CR-176201] 24 p4069 N85-35219

UNSATURATION (CHEMISTRY)
Stabilized unsaturated polyesters [NASA-CASE-NPO-16103-1] 18 p3078 N85-29043

UNSTEADY FLOW
NT OSCILLATING FLOW
Development and applications of algorithms for calculating the transonic flow about harmonically oscillating wings [NASA-CR-172376] 01 p0002 N85-10007
A study of the effect of wake-passing on turbine blades [OUEL-1515/84] 03 p0363 N85-12328
Evaluation of the unsteady effects for a class of wind turbines 05 p0592 N85-13772
Experiences with nonsynchronous forced vibration in centrifugal compressors 05 p0642 N85-14119
Two-dimensional unsteady analysis of fluid forces on a whirling centrifugal impeller in a volute 05 p0643 N85-14126
Influence of stationary components on unsteady flow in industrial centrifugal compressors 05 p0645 N85-14140
An experimental study of airfoil-spoiler aerodynamics [NASA-CR-177328] 06 p0748 N85-14796
Unsteady flow characteristics in the near-wake of a two-dimensional obstacle [NASA-TM-77762] 07 p0897 N85-15684
A scanning laser velocimeter for turbulence research [NASA-CR-172493] 07 p0897 N85-15686
Comparison of analytical and experimental steadyand unsteady-pressure distributions at Mach number 0.78 for a high-aspect-ratio supercritical wing model with oscillating control surfaces [NASA-TM-84589] 07 p0899 N85-15697
Some important problems in unsteady boundary layers including separation. 2: Unsteady boundary layers close to the stagnation region of slender bodies [AD-A148964] 07 p0968 N85-16069
A comparison of measured and predicted unsteady pressure on a fan blade in unstalled supersonic flutter [PNR-90223] 08 p1079 N85-16639
Proceedings of the workshop on unsteady separated flow held at the United States Air Force Academy on August 10-11, 1983 [AD-A148249] 09 p1263 N85-17937
Wing rock flow phenomena [AD-P004154] 09 p1264 N85-17939
Potential applications of forced unsteady flows [AD-P004155] 09 p1264 N85-17940
Numerical solution of the Navier-Stokes equations for unsteady separated flows [AD-P004161] 09 p1265 N85-17946
Unsteady aerodynamic loading of an airfoil due to vortices released intermittently from its upper surface [AD-P004162] 09 p1265 N85-17947

Can the singularity be removed in time-dependent flows?
[AD-P004165] 09 p1265 N85-17950
Unsteady separated flow: Forced and common vorticity about oscillating airfoils
[AD-P004167] 09 p1265 N85-17952
Unsteady separated flows: Generation and use by insects
[AD-P004168] 09 p1266 N85-17953
Theoretical study of non-linear unsteady aerodynamics of a non-rigid lifting body
[AD-P004169] 09 p1266 N85-17954
Theoretical investigation of dynamic stall using a momentum integral method
[AD-P004170] 09 p1266 N85-17955
Preliminary results from the unsteady airfoil model USTAR2
[AD-P004171] 09 p1266 N85-17956
Experiments on controlled, unsteady, separated turbulent boundary layers
[AD-P004172] 09 p1266 N85-17957
Flow separation induced by periodic aerodynamic interference
[AD-P004174] 09 p1266 N85-17959
Numerical predictions for unsteady viscous flow past an array of cylinders 09 p1318 N85-18284
On the flow processes in sharply inclined and stalled airfoils in parallel movement and rotation
[NASA-TM-77509] 10 p1419 N85-18952
Unsteady transonic flow calculations for two-dimensional canard-wing configurations with aeroelastic applications
[NASA-TM-86375] 10 p1420 N85-18960
A probe for direct measurement of flow direction
[ESA-TT-853] 11 p1637 N85-20310
Parachute inflation dynamics 11 p1715 N85-20792
Unsteady aerodynamic characterization of a military aircraft in vertical gusts
[NASA-TM-77810] 12 p1770 N85-21110
Three-dimensional unsteady lifting surface theory in the subsonic range
[NASA-TM-77812] 12 p1770 N85-21111
Transonic interactions of unsteady vortical flows
[NASA-TM-86658] 12 p1770 N85-21113
Unsteady flows around 3-dimensional wings
[AD-A149993] 12 p1772 N85-21124
Numerical integration of the unsteady full-potential equation with applications to transonic flow about a two-dimensional airfoil
[NLR-MP-84022-U] 12 p1773 N85-21130
Estimating unsteady aerodynamic forces on a cascade in a three-dimensional turbulence field
[NASA-TM-86701] 14 p2209 N85-23704
Recent transonic unsteady pressure measurements at the NASA Langley Research Center
[NASA-TM-86408] 14 p2210 N85-23710
Calculation of an unsteady transonic flow with shock waves and separation in Laval nozzles
[MPIS-14/1984] 14 p2213 N85-23726
Interactions of unstable shear layers with leading edges and associated pressure fields 14 p2299 N85-24236
Stability of an oscillating boundary layer
[NASA-TM-77827] 14 p2299 N85-24236
Unsteady flows in a tube with combustion reaction
[ISL-R-116/83] 14 p2303 N85-24261
Transonic Unsteady Aerodynamics and its Aeroelastic Applications
[AGARD-CP-374] 15 p2457 N85-25171
Trends in computational capabilities for fluid dynamics 15 p2457 N85-25172
Transonic pressure distributions on a two-dimensional 0012 and supercritical MBB-A3 profile oscillating in heave and pitch 15 p2457 N85-25173
Analysis of transonic aerodynamic characteristics for a supercritical airfoil oscillating in heave, pitch and with oscillating flap 15 p2458 N85-25175
Experience with transonic unsteady aerodynamic calculations 15 p2458 N85-25176
Calculation of unsteady transonic separated flows by viscous-inviscid interaction 15 p2458 N85-25178
A semi-empirical unsteady transonic method with supersonic free stream 15 p2458 N85-25179
Improvement and extension of a numerical procedure for the three dimensional unsteady transonic flows 15 p2459 N85-25181
Computation of unsteady transonic flows about two-dimensional and three-dimensional AGARD standard configurations 15 p2459 N85-25183
Calculation of unsteady transonic flow around a high swept wing 15 p2459 N85-25184
The development of unsteady transonic 3-D full potential code and its aeroelastic applications 15 p2460 N85-25187
Unsteady analysis of rotor blade tip flow
[NASA-CR-3868] 15 p2462 N85-25202
Transonic aerodynamic and aeroelastic characteristics of a variable sweep wing
[NASA-TM-86677] 15 p2462 N85-25203
Numerical solutions of 3-dimensional Navier-Stokes equations for closed bluff-bodies
[NASA-CR-175755] 15 p2636 N85-26255
Recent progress in computational aerodynamics 16 p2693 N85-26826
LDA study of non-steady flame propagation in a constant volume duct
[DE85-007233] 16 p2746 N85-26948
Experimental investigations of prismatic cylinders in flow with harmonic pulsations
[KU-SFB-210/E/4] 16 p2785 N85-27186
Background noise measurements from jet exit vanes designed to reduced flow pulsations in an open-jet wind tunnel
[NASA-TM-86383] 17 p2906 N85-27916
Unsteady flow in multistage turbines 17 p2911 N85-27946
New facility to study unsteady wake effects on turbine airfoil heat transfer 17 p2911 N85-27948
Numerical simulation of unsteady motion in a turbulent mixing layer
[NAL-TR-849T] 18 p3099 N85-29183
Experimental investigations of the unsteady turbulent friction behavior with pressure impulses in a circular pipe
[IWAWI-MITT-102] 18 p3103 N85-29210
A first-order time-domain Green's function approach to supersonic unsteady flow
[NASA-CR-172208] 19 p3214 N85-29930
Unsteady transonic flow calculations for interfering lifting surface configurations
[NASA-TM-86432] 19 p3214 N85-29931
Verification of calculation methods for unsteady airloads in the precipitation of transonic flutter
[NLR-MP-84016-U] 20 p3390 N85-31027
Compendum of unsteady aerodynamic measurements, addendum 1
[AGARD-R-702-ADD-1] 20 p3390 N85-31028
Data set 9: LANN wing. Pitching oscillation 20 p3390 N85-31030
Nonnewtonian, unsteady flow in a convergent divergent duct 20 p3456 N85-31463
Identification of unsteady aerodynamics and aeroelastic integro-differential systems
[NASA-TM-86749] 21 p3678 N85-32851
Toward the propagation of waves in unsteady media 21 p3683 N85-32881
One method of solving the problem of unsteady heat exchange of a body and its ablation 22 p3733 N85-33146
Scalar/Vector potential formulation for compressible viscous unsteady flows
[NASA-CR-3921] 23 p3893 N85-34113
Integral equation formulation for three-dimensional unsteady transonic flow
[ARL/STRUC-R-416] 23 p3894 N85-34119
Modelling of unsteady, incompressible separation on an aerofoil using an inviscid flow algorithm
[GU-AERO-8412] 23 p3894 N85-34122
Unsteady transonic heat transfer in a transient facility
[NASA-CR-176145] 23 p3930 N85-34354
Unsteady flow in a supersonic cascade with two in-passage shocks
[NASA-CR-3925] 24 p4060 N85-35158

UNSTEADY STATE
Autoregressive nonsteady methods for the analysis and synthesis of the human voice
[FUB-3-1984] 01 p0041 N85-10266
Instability in semiconductors exposed to ionizing radiation 02 p0267 N85-11747
Full load testing in the platform module prior to tow-out: A case history of subsynchronous instability 05 p0642 N85-14117
Subsynchronous vibrations in a high pressure centrifugal compressor: A case history 05 p0642 N85-14118
Control of rotordynamic instability in a typical gas turbine's power system 05 p0642 N85-14120
Experimental on-stream elimination of resonant whirl in a large centrifugal compressor 05 p0642 N85-14121
MPS solidification model. Analysis and calculation of macrosegregation in a casting ingot
[NASA-CR-171589] 21 p3586 N85-32178
Toward the propagation of waves in unsteady media 21 p3683 N85-32881

UNSWEPT WINGS
NT RECTANGULAR WINGS
Turbulent bubbles behind airfoils and wings at high angle of attack 08 p1069 N85-16779

UP-CONVERTERS
Distortion of temporal characteristics during parametric up-conversion of ultrashort laser pulses 11 p1717 N85-20603

UPDRAFTS
U VERTICAL AIR CURRENTS

UPGRADING
The properties of VSt3sp inoculated steel
[BLL-M-35894-(5828.4)] 23 p3915 N85-34263

UPLINKING
Polarization angles of linearly polarized antennas and radio waves in satellite communications
[PB85-131613] 11 p1628 N85-20240
Remote control of an impact demonstration vehicle
[NASA-TM-85925] 14 p2225 N85-23797
The IRAS end-to-end data system
[NLR-MP-83056-U] 17 p3051 N85-28883
Receive shaping filter manufacture --- QPSK uplinks
[ESA-CR(P)-1998] 20 p3449 N85-31412

UPPER AIR
U UPPER ATMOSPHERE

UPPER ATMOSPHERE
NT D REGION
NT E REGION
NT EXOSPHERE
NT F REGION
NT F 2 REGION
NT GEOMAGNETIC TAIL
NT IONOSPHERE
NT LOWER IONOSPHERE
NT MAGNETOPAUSE
NT MAGNETOSPHERE
NT MESOPAUSE
NT MESOSPHERE
NT SPORADIC E LAYER
NT THERMOSPHERE
NT TURBOPAUSE
NT UPPER IONOSPHERE
MERIT: A man/computer data management and enhancement system for upper air nowcasting/forecasting in the United States --- Minimum Energy Routes using Interactive Techniques (MERIT) 01 p0063 N85-10558
Aeronomy 02 p0296 N85-11930
Upper Atmosphere Research Satellite (UARS) trade analysis
[NASA-CR-175269] 07 p0912 N85-15774
A 2-dimensional second order closure model of the upper atmosphere 08 p1182 N85-17450
Application of Fabry-Perot spectrometers for measurement of upper atmosphere temperatures and winds 08 p1183 N85-17454
The influence of deep cumulus convection on large-scale flow during AVE/SESAME 1, 10-11 April 1979 09 p1355 N85-18526
Survey of VLF-OMEGA transmissions received during summer at Antarctic peninsula
[INPE-3399-PRE/666] 10 p1462 N85-19223
Upper atmosphere research at INPE
[INPE-3281-PRE/604] 10 p1515 N85-19557
Brazil future plans in upper atmosphere research in Antarctica
[INPE-3400-PRE/669] 10 p1515 N85-19559
Transport processes in the upper atmosphere 11 p1646 N85-20375
Orographic disturbances of upper atmosphere emissions 11 p1663 N85-20480
Increase in hydrogen emission of upper atmosphere following launches of space vehicles 13 p1981 N85-22431
Comparison of observations of orographic disturbances in the troposphere and upper atmosphere 14 p2341 N85-24479
Magnetospheric effects on the upper atmosphere 14 p2365 N85-24616
Investigation of the daytime lunar atmosphere
[NASA-CR-175636] 14 p2440 N85-25057
Atmospheric density model 16 p2805 N85-27297
Full shadow phenomenon in Earth's upper atmosphere 16 p2808 N85-27316
Homogeneous processes of atmospheric interest
[NASA-CR-175770] 17 p2989 N85-28475
Observations of mesospheric turbulence by rocket probe and VHF radar, part 2.4A 21 p3619 N85-32484
The MU radar now partly in operation 21 p3628 N85-32543
Geologic processes on Venus: An update 22 p3857 N85-33883
Wide Angle Michelson Doppler Imaging Interferometer (WAMDII) 23 p3902 N85-34172
Additional flux of particles and albedo-electrons in upper atmosphere
[SH-6.1-6] 23 p4045 N85-35080
Space Station Polar Platform: Integrating research and operational missions
[PB85-195279] 24 p4069 N85-35218

UPPER IONOSPHERE
NT F REGION
NT F 2 REGION

Medium- and large-scale wave disturbances and heterogeneities of electron concentration in outer ionosphere in middle and low latitudes
06 p0625 N85-15241
Spreading of greatly extended inhomogeneities in upper ionosphere 14 p2339 N85-24462
Determining effective rate of plasma heating in outer equatorial ionosphere using data from ISIS-1 and ISIS-2 satellites 16 p2721 N85-26797

UPPER STAGE ROCKET ENGINES
Experiments on residual thrust and prediction for upper-stage solid propellant rockets
[NAL-TR-800] 03 p0324 N85-12087
LOX/LH2 propulsion system for launch vehicle upper stage, test results
[NASA-TM-77727] 03 p0324 N85-12089
Shuttle/Centaur project perspective
06 p1106 N85-16991
Shuttle/Centaur upper stage capability
11 p1712 N85-20773

UPPER SURFACE BLOWING
A study of lift characteristics of an upper surface blown jetwing with a rectangular nozzle
05 p0591 N85-13767
Low-speed wind tunnel tests of the NAL fan-jet STOL research aircraft model with ground simulation by tangential blowing
[NAL-TR-828] 10 p1423 N85-18976

UPSTREAM
Effect of upstream sidewall boundary layer removal on an airfoil test — conducted in Langley 0.3-m transonic cryogenic tunnel 03 p0313 N85-12019

UPWASH
Integral equation of lifting surfaces in Laplace domain and analytic continuation of its pressure kernel
[NAL-TR-795T] 01 p0002 N85-10009
An investigation of turbulence mechanisms in V/STOL upwash flow fields
[AD-A149786] 12 p1772 N85-21123
Fuselage upwash effects on RSRA rotor systems
[NASA-CR-177349] 20 p3388 N85-31015

UPWELLING
U UPWELLING WATER

UPWELLING WATER
Salinity driven oceanographic upwelling
[DE85-011664] 22 p3618 N85-33652

URANIUM
NT URANIUM ISOTOPES
NT URANIUM 235
Progress in lead/uranium zircon studies of lower paleozoic rocks of the southern Alexander terrane
04 p0518 N85-13304
U, Th, K content, heat production and thermal conductivity of Sao Paulo, Brazil continental shelf sediments: A reconnaissance work
[INPE-3401-PRE/670] 10 p1515 N85-19558
Approaches to ultrafast neutron detectors
[DE85-001206] 11 p1636 N85-20307
Compact L-edge densitometer for uranium concentration assay
[DE85-010344] 18 p3110 N85-29261
Occurrence of uranium in ground water in the vicinity of the US Department of Energy Feed Materials Production Center, Fernald, Ohio
[DE85-010340] 19 p3364 N85-30982
Reaction of uranium and the fluorocarbon FC-75
[DE85-012322] 22 p3843 N85-33602
Shape memory effect in uranium-niobium alloys below room temperature
[DE85-012964] 23 p3916 N85-34266
Method for preparing hydride configurations and reactive metal surface
[DE85-006443] 23 p3917 N85-34274
Uranium, thorium isotopic analyses and uranium-series ages of calcite and opal and stable isotopic compositions of calcite from drill cores UE25a no. 1, USR G-2 and USW G-3/GU-3, Yucca Mountain, Nevada
[DE85-013039] 23 p3948 N85-34471
Separation of uranium from technetium in recovery of spent nuclear fuel
[DE85-006499] 23 p3972 N85-34627
Lead and uranium group abundances in cosmic rays [OG-7.1-3] 23 p4013 N85-34885
X-ray fluorescence analysis of uranium concentrates
[DE85-013189] 24 p4148 N85-35717
Measurement of uranium enrichment for gaseous uranium at low pressure
[DE85-012697] 24 p4150 N85-35733
Stopping relativistic Xe, Ho, Au and U nuclei in nuclear emulsions 24 p4173 N85-35876

URANIUM ALLOYS
Cerium compounds in the fashion of the light actinides
[DE84-014642] 04 p0475 N85-13024
The corrosion resistance of zinc coatings on depleted uranium and uranium alloys
[DE85-007216] 15 p2510 N85-25487
Neutron scattering study of the heavy fermion system UBe-13
[DE85-010955] 19 p3356 N85-30804
Experimental attempt to achieve microstructure variations through temperature/time permutations for a nonwrought powder metallurgy uranium-6 niobium alloy
[DE85-013166] 23 p3916 N85-34272

URANIUM CARBIDES
Loss-of-flow transient characterization in carbide-fueled LMFBRs
[DE85-009552] 19 p3269 N85-30270

URANIUM COMPOUNDS
NT URANIUM CARBIDES
NT URANIUM FLUORIDES
Growth and magnetic investigations of single crystals of intermetallic compounds of rare earths and uranium — magnetic properties 03 p0425 N85-12712
Measurement of uranium enrichment for gaseous uranium at low pressure
[DE85-012697] 24 p4150 N85-35733

URANIUM FLUORIDES
Liquid-phase compositions from vapor-phase analyses 2: Adaptation of the Prausnitz program to UF6 and some of its potential impurities
[DE85-011521] 21 p3673 N85-32619

URANIUM ISOTOPES
NT URANIUM 235
Methodology for economic evaluation of process technologies in the early research and development stages
[DE84-015863] 05 p0736 N85-14731
Environmental surveillance at Los Alamos during 1984
[DE85-011866] 22 p3611 N85-33605
The 1984 environmental monitoring report, Sandia National Laboratories, Albuquerque, New Mexico
[DE85-011175] 22 p3611 N85-33607
Gamma-ray line intensities for depleted uranium
[DE85-012674] 22 p3843 N85-33604

URANIUM 235
Technology for increasing the uranium-235 isotopic abundance in natural uranium feed on a productive scale
[DE85-011252] 19 p3357 N85-30810
Application of evaluated fission-product delayed-neutron precursor data in reactor kinetics calculations
[DE85-012728] 23 p3972 N85-34624
Measurement of uranium enrichment for gaseous uranium at low pressure
[DE85-012697] 24 p4150 N85-35733

URANUS (PLANET)
NT URANUS RINGS
Uranus and Neptune
[NASA-CP-2330] 02 p0296 N85-11927
The origin and evolution of Uranus and Neptune
02 p0296 N85-11928
Atmospheres of Uranus and Neptune
02 p0296 N85-11929
Aeronomy 02 p0296 N85-11930
Temperature structures and infrared-derived properties of the atmosphere of Uranus and Neptune
02 p0296 N85-11931
Interior structure of Uranus 02 p0296 N85-11939
Rotational properties of Uranus and Neptune
02 p0299 N85-11940
Oblatenesses of Uranus and Neptune
02 p0300 N85-11941
Origin and evolution of the Uranian and Neptunian satellites: Some dynamical considerations
02 p0300 N85-11943
Composition, structure and evolution of Uranian and Neptunian satellites 02 p0300 N85-11944
Physical properties of the Uranian satellites
02 p0300 N85-11946
Satellite masses in the Uranus and Neptune systems [PSI-CONTRIB-198] 02 p0301 N85-11947
Magnetospheric structures: Uranus and Neptune
02 p0301 N85-11949
Magnetosphere, rings, and moons of Uranus
02 p0301 N85-11951
Do the satellites of Uranus control its magnetosphere?
02 p0301 N85-11952
The structure of the Uranian rings and the search for rings around Neptune 02 p0302 N85-11954
Infrared images of the Uranian rings
02 p0302 N85-11955
Dynamics of the Uranian rings
02 p0302 N85-11956
Research in planetary studies and operation of Mauna Kea Observatory
[NASA-CR-175618] 13 p2169 N85-23460
Giant planets and their satellites: Cosmochemistry, evolution and structure 13 p2175 N85-23494
The structure and composition of Uranus and Neptune
13 p2175 N85-23495
Studies of icy bodies: Uranian satellites and cometary nuclei 13 p2175 N85-23496
Voyage to Uranus 15 p2687 N85-26598
Magnetospheres of the outer planets
[AD-A154354] 19 p3364 N85-30986

URANUS ATMOSPHERE
Properties of the upper tropospheres of Uranus and Neptune derived from observations at visible to near-infrared wavelengths 02 p0296 N85-11933
Near infrared imaging of Uranus and Neptune
02 p0299 N85-11934
A review of the millimeter and centimeter observations of Uranus 02 p0299 N85-11935
Atmospheric dynamics of Uranus and Neptune: Theoretical considerations 02 p0299 N85-11936
The possibility of detection and measurement of cloud structure in the atmosphere of Uranus
02 p0299 N85-11937
Ultraviolet observations of Uranus and Neptune below 3000 A 11 p1760 N85-21071
Possible period of Jovian activity and possibility of seasons 16 p2723 N85-26810
Monodeuterated methane in the outer solar system. 2. Its detection on Uranus at 1.6 microns
[NASA-CR-175782] 16 p2982 N85-27782

URANUS RINGS
Magnetosphere, rings, and moons of Uranus
02 p0301 N85-11951
The structure of the Uranian rings and the search for rings around Neptune 02 p0302 N85-11954
Infrared images of the Uranian rings
02 p0302 N85-11955
Dynamics of the Uranian rings
02 p0302 N85-11956
The rings of Uranus 15 p2672 N85-26486
Inclinations of the Uranian rings
15 p2672 N85-26487
Infrared observations of the Uranian rings
15 p2672 N85-26488
Stellar occultations by Uranus rings on 15 August 1980 and 22 April 1982 15 p2672 N85-26489
Indications of twist in the Epsilon rings of Uranus
15 p2672 N85-26490
The gravitational interaction between inclined, elliptical rings — Uranus rings 15 p2675 N85-26514
On planetary rings as sources and sinks of magnetospheric plasmas 15 p2677 N85-26526
Tidal breakup and origin of the Uranian ring system
15 p2678 N85-26535
Future studies of planetary rings by spaceprobes
15 p2679 N85-26541

URBAN AREAS
U CITIES

URBAN DEVELOPMENT
Department of Housing and Urban Development, and certain independent agencies appropriations for fiscal year 1985, part 2
[S-REPT-98-889-PT-2] 01 p0127 N85-10870
National Aeronautics and Space Administration
01 p0127 N85-10871
Study of the urban evolution of Brasilia with the use of LANDSAT data
[E85-10101] 16 p2909 N85-27321

URBAN PLANNING
Nationwide urban runoff program. Relationship of urban runoff to land use and groundwater resources
[PB85-114692] 10 p1506 N85-19505
Experience of the Institute of Space Research with the use of remote sensing in urban planning studies
[INPE-3150-PRE/533] 16 p2880 N85-27770
Hydrodynamics and sanitation
[CT-579] 20 p3487 N85-31872

URBAN RESEARCH
Study of annoyance due to urban automobile traffic
[NASA-TM-77514] 01 p0069 N85-10458
Land use/land cover 02 p0214 N85-11410
Astronomy and sodium lighting
[RAND/N-2089-RC] 09 p1413 N85-18914
An initial analysis of LANDSAT-4 Thematic Mapper data for the discrimination of agricultural, forested wetlands, and urban land cover — Poinsett County, Arkansas; and Reelfoot Lake and Union City, Tennessee
13 p2118 N85-23199
Urban vehicle research project
[DE85-005444] 17 p3052 N85-28889
The timing of noise-sensitive activities in residential areas
[NASA-CR-177937] 20 p3524 N85-31918
Solar energy meteorological research and training program: Region 4
[DE85-011763] 22 p3616 N85-33640

URBAN TRANSPORTATION
Electric and hybrid vehicle demonstration project
[DE84-014622] 06 p0671 N85-15535
ElectriFleet Project
[DE85-001598] 10 p1570 N85-19898
Electric vehicle demonstration project
[DE85-003124] 11 p1741 N85-20944

In-vehicle evaluation of the Globe EV 2300 lead-acid, Delco Remy 150 nickel-zinc, and Eagle-Picher NIF 270 nickel-iron battery systems
[NASA-CR-175653] 14 p2349 N85-24521
Hybrid propulsion technologies for urban bus transit
[PB85-157469] 16 p2880 N85-27773

UREAS
Crystalline structure of urea ice sheets used in modeling experiments in the CRREL test basin
[AD-A148434] 06 p1226 N85-17722
Long term durability of urea formaldehyde glued joints removed from Vampire aircraft
[AD-A149053] 10 p1424 N85-18985

URETHANES
A miniature urethane molded acoustic transducer
[AD-A148450] 06 p0804 N85-15114
Plasticizer system for propellant compositions
[AD-D011502] 12 p1816 N85-21390
Plasticizer system for propellant compositions
[AD-D011517] 12 p1817 N85-21395

URINALYSIS
Circadian dynamics of potassium excretion in urine as related to working on one and two shifts
19 p3325 N85-30598

URINE
Urokinase production by electrophoretically separated cultured human embryonic kidney cells
20 p3501 N85-31765
A critical synopsis: Continuous growth of proximal tubular kidney epithelial cells in hormone-supplemented serum-free medium
20 p3501 N85-31767
The Fibrin slide assay for detecting urokinase activity in human fetal kidney cells
20 p3502 N85-31768
Composition and dynamics of bacteriocenosis associated with algae in human life-support systems
22 p3823 N85-33684

USA (UNITED STATES)
U UNITED STATES

USER MANUALS (COMPUTER PROGRAMS)
High frequency radar software reference manual for Product Two
[PB84-210079] 01 p0041 N85-10270
Manual of phosphoric acid fuel cell power plant optimization model and computer program
[NASA-CR-174721] 01 p0067 N85-10445
IAC user manual
[NASA-CR-175300] 01 p0102 N85-10677
PDSS/IMC CIS user's guide
[NASA-CR-171179] 01 p0102 N85-10682
MICROSCOPE: A software system for multivariate analysis
[AD-A144720] 01 p0103 N85-10688
HULL users' manual
[AD-A145000] 01 p0103 N85-10691
AGS-880 menu system user guide
[DE84-014338] 01 p0104 N85-10699
PASCAL-MP algebraic and numerical manipulator for polynomials
[INPE-3229-TDL/178] 02 p0240 N85-11582
SMILE user's guide: A macro preprocessor for extending FORTRAN
[DE84-015984] 02 p0243 N85-11584
Programmer's guide for ASKF 77: A tool for programming of dialogs in FORTRAN and PASCAL
[FOA-C-30366-E1] 02 p0243 N85-11585
A user's guide to the Flexible Spacecraft Dynamics and Control Program
[NASA-TM-87360] 03 p0405 N85-12586
Computer center introductory reference manual for CDC CYBER
[AD-A145796] 03 p0406 N85-12593
Effective date (E-DATE) model documentation. Changes to reflect model enhancement
[AD-A146050] 03 p0407 N85-12599
NATFREQ users manual: A FORTRAN 4 program for computing natural frequencies, mode shapes and drag coefficients for taut strumming cables with attached masses and spring-mass combinations
[AD-A146058] 03 p0407 N85-12600
Advanced Ada (trademark)
[AD-A146257] 03 p0407 N85-12602
Real-time Ada (trademark)
[AD-A146258] 03 p0407 N85-12603
Turbine blade damping study
[NASA-CR-171255] 04 p0456 N85-12690
Users manual for a computer program for dynamic response analysis of bladed systems
[UDR-TR-84-39] 04 p0456 N85-12693
NIKE3D: An implicit, finite-deformation, finite element code for analyzing the static and dynamic response of three-dimensional solids, revision 1
[DE84-017161] 04 p0514 N85-13277
Users manual for BRGLM: Interactive general linear model regression, version 3
[DE84-017366] 04 p0550 N85-13501
Preliminary user's guide for BIGONE on the Cray
[DE84-017075] 04 p0568 N85-13623
Automated Library Search System (ALSS) user's manual
[DE84-015952] 04 p0576 N85-13672
Computer programs to predict induced effects of jets exhausting into a crossflow
[NASA-CR-166591] 05 p0592 N85-13776
PROGRAM VSAERO: A computer program for calculating the non-linear aerodynamic characteristics of arbitrary configurations: User's manual
[NASA-CR-166476] 06 p0749 N85-14902
VLSI design tools, reference manual, release 2.0
[AD-A146444] 06 p0803 N85-15112
Investigative findings of image enhancement techniques
[AD-A146392] 06 p0853 N85-15424
High altitude chemically reacting gas particle mixtures. Volume 3: Computer code user's and applications manual — rocket nozzle and orbital plume flow fields
[NASA-CR-171828] 07 p0917 N85-15603
Interactive Signal Analysis Software (ISAS). User's manual
[AD-A146999] 07 p1022 N85-16485
RATFOR user's guide version 2.0
[NASA-CR-166601] 07 p1023 N85-16490
NYU Ada/Ed user's guide: Version 1.4 for VAX/VMS systems
[AD-A146759] 07 p1024 N85-16495
NOISEMAP 4.4 computer program update, operator's manual, addendum 1
[AD-A147091] 07 p1025 N85-16503
FORTRAN version of the quantitative energy-dispersive electron beam X-ray analysis program FRAME C
[PB84-240936] 07 p1027 N85-16519
A FORTRAN plotting package for graphic VDUs
[AD-A148469] 08 p1204 N85-17577
MC68CRX cross-assembler users manual
[AD-A148031] 08 p1205 N85-17584
Operating system for a real-time multiprocessor propulsion system simulator. User's manual
[NASA-TP-2426] 08 p1207 N85-17596
Boring information and subsurface data base package user's guide
[AD-A148623] 08 p1230 N85-17747
Computer center CDC libraries/utility (programs)
[AD-A148680] 09 p1368 N85-18593
FLAD user's manual: FLAD file contents
[AD-A148700] 09 p1368 N85-18594
User's guide to MIX: A computer code for fitting mixture distributions to data
[DE85-001451] 09 p1369 N85-18603
User/programmer guide for UCMD 108 multi-vertex polyarc/path integrity verifier
[DE84-017173] 09 p1369 N85-18604
User's manual: Menu-driven data graphing program for the Tektronix 7912AD and 7612D transient digitizer system
[DE85-002151] 09 p1370 N85-18610
UKIRT spectro-photometry system — United Kingdom Infrared Telescope (UKIRT)
[UKIRT-23] 09 p1414 N85-18921
TVENT1P user's manual, a computer code for analyzing tornado induced gas dynamic transients in flow networks
[DE85-002345] 10 p1486 N85-19379
Ada (trademark) primer
[AD-A148855] 10 p1539 N85-19703
FORTRAN 66 analyser: User's manual
[PB85-111748] 10 p1542 N85-19724
User's manual for GRIZZLY
[DE85-001405] 11 p1702 N85-20702
User's guide for the computer program response factor (REFAC)
[PB85-136600] 11 p1705 N85-20726
A GC/MS (Gas Chromatograph/Mass Spectrometer) data management process. Part 1: User's guide, version 1.0
[PB85-116051] 12 p1803 N85-21309
NOAA-AISC user's guide for implementing CERES maize model for large area yield estimation
[E85-10063] 12 p1873 N85-21748
User's guide to the TAMW wheat model as implemented on the IBM 360/195 computer
[E85-10064] 12 p1873 N85-21749
NOAA-AISC user's guide for implementing CERES wheat model for large area yield estimation
[E85-10065] 12 p1873 N85-21750
User's manual for the University of Houston individual heliostat layout and performance code
[DE85-004643] 12 p1882 N85-21606
A user's guide to sensitivity testing on computer models at Los Alamos National Laboratory
[LA-10104-M] 12 p1914 N85-22018
Implementation of the computer program-system MOSS (Map Overlay and Statistical System) on a VAX-11 series computer under VMS
[AD-A149612] 12 p1914 N85-22019
User's guide for NPSOL (Version 2.1): A FORTRAN package for quadratic programming
[AD-A150078] 12 p1916 N85-22028
METC VAX-IBM guide to ASPEN
[DE85-001974] 12 p1916 N85-22031
VAX-ASPEN installation guide
[DE85-001973] 12 p1916 N85-22032
Microcomputers in transit: A software handbook
[PB85-136414] 12 p1916 N85-22042
User's guide for TWOHEX: A code package for two-dimensional, neutral-particle transport in equilateral triangular meshes
[DE85-004482] 12 p1930 N85-22125
ROSA: A computer model for optical power ratio calculations
[DE85-005174] 13 p2129 N85-23251
M68000 RNF text formatter user's manual
[NASA-TM-86327] 13 p2146 N85-23320
SIGPI: A user's manual for the fast computation of the probabilistic performance of a complex system
[DE85-005447] 13 p2148 N85-23336
User's and programmer's guide to the mechanics of moving finite element code
[DE85-006165] 13 p2152 N85-23365
User's guide to calibration of analog electronic controllers in HVAC systems
[AD-A150803] 14 p2296 N85-24229
Users guide: The LaRC human-operator-simulator-based pilot model
[NASA-TM-86367] 14 p2390 N85-24721
The HORNE reasoning system, revision
[AD-A150963] 14 p2405 N85-24827
Computer Visual System (CVS) reference manual
[DE85-006328] 14 p2407 N85-24837
Automatic Dynamic Aircraft Modeler (ADAM), volume 1
[AD-A151410] 15 p2471 N85-25252
A user's manual for AMEER flight path trajectory simulation code
[DE85-006580] 15 p2472 N85-25260
A new NASTRAN capability for data reduction
15 p2574 N85-25874
The interactive plotting program: GRAPH
[AD-A151371] 15 p2623 N85-26165
Design specifications for IMAGER: The DREO (Defence Research Establishment Ottawa) image processing system
[AD-A151752] 15 p2624 N85-26168
Backend control processor for a multi-processor relational database computer system
[AD-A151892] 15 p2624 N85-26169
Programming the digital computer ODRA-1204 in MOST-2 language
[NASA-TM-87462] 15 p2627 N85-26191
Advanced life analysis methods. Volume 6: User's manual for LUGRO computer program to predict crack growth in attachment lugs
[AD-A151235] 15 p2628 N85-26195
Preliminary design of the Ada programming support environment configuration manager
[AD-A151845] 15 p2629 N85-26206
GEMINI: A computer program for two and three dimensional linear static and seismic structural analysis, CDC 7600 version
[DE85-007496] 15 p2631 N85-26218
User manual for IMAGER: The DREO (Defence Research Establishment Ottawa) image processing system
[AD-A151754] 15 p2653 N85-26362
ESP (External-Stores Program): A pilot computer program for determining flutter-critical external-store configurations. Volume 1: User's manual
[AD-A152268] 16 p2710 N85-26725
An interactive computer package for use with simulation models which performs multidimensional sensitivity analysis by employing the techniques of response surface methodology
[AD-A151956] 16 p2846 N85-27548
Users manual for coordinate generation code CRDSRA
[NASA-CR-172584] 17 p2891 N85-27824
User's manual for airfoil flow field computer code SRAIR
[NASA-CR-172585] 17 p2891 N85-27825
Airport and airway system cost allocation model. Volume 7: User's manual
[AD-A152877] 17 p2906 N85-27917
FLOWPLOT 2: A fluid dynamics and heat transfer plotting package
[DE85-009602] 17 p2959 N85-28277

Documentation of PHOTO: A user's manual for the analysis of photographic and X-ray negatives
[AD-A152968] 17 p2967 N85-28327
COSMIC Software Catalog, 1985 edition
[NASA-CR-174070] 17 p3010 N85-28608
Real-Time Multiprocessor Programming Language (RTMPL) user's manual
[NASA-TP-2422] 17 p3010 N85-28610
VULTURE manual
[DE85-008873] 17 p3013 N85-28631
ODIN: An extensible software environment. Report and user's reference manual
[DE85-008459] 18 p3164 N85-29600
Nimbus 7 Coastal Zone Color Scanner (CZCS). Level 2 data product users' guide
[NASA-TM-86202] 19 p3299 N85-30452
An interim user's manual for the advanced scavenging module version 1.2
[PB85-173904] 19 p3318 N85-30572
Cultural data base implementation study and computer-aided scene modeling system users manual
[AD-A154232] 19 p3333 N85-30646
MC TRICOMP user's guide
[AD-A154339] 19 p3337 N85-30673
BP (Basic Processor) TRICOMP user's guide
[AD-A154340] 19 p3337 N85-30674
VAX TRICOMP user's guide
[AD-A154341] 19 p3337 N85-30675
Computer Performance Modeling Tool (CPMT)
[AD-A154438] 19 p3338 N85-30682
T sub EX font tables
[DE85-011394] 19 p3339 N85-30687
Apollo multiplexer operations manual
[DE85-011293] 19 p3343 N85-30719
Nonequilibrium air radiation (Nequair) program: User's manual
[NASA-TM-86707] 19 p3353 N85-30780
User's guide for the Mk-3 D-coronameter data system
[PB85-181204] 19 p3365 N85-31002
A set of subroutines for masked three-dimensional plotting with rotations
[MEAH-33] 20 p3514 N85-31846
SCAP: A Shaped Charge Analysis Program. User's manual for SCAP 1.0
[DE85-011182] 20 p3515 N85-31854
User's manual of the BNDSCO computer program for solving constrained optimal control problems
[DFVLR-MITT-85-05] 20 p3516 N85-31865
Manual for the computer program for the Gaussian plume model with percentile calculations
[KNMI-TR-60] 20 p3517 N85-31867
Tip vortex computer code SRATIP. User's guide
[NASA-CR-172603] 21 p3551 N85-32093
User's guide for computer program CGFAG, Concrete General Flexure Analysis with Graphics
[AD-A155555] 21 p3570 N85-32204
BLAF: A blast field reconstruction program from pressure histories
[AD-A155300] 21 p3585 N85-32283
CARE 3 user friendly interface user's guide
[NASA-CR-172606] 21 p3669 N85-32791
Research on an expert system for database operation of simulation-emulation math models. Volume 2, Phase 1: Results
[NASA-CR-176088] 21 p3669 N85-32793
Praxis release notes, version 7.3
[DE85-011862] 21 p3673 N85-32820
Aerodynamic analysis of a horizontal axis wind turbine by use of helical vortex theory, volume 2: Computer program users manual
[NASA-CR-174921] 22 p3804 N85-33563
QKPLT users guide, version 2.0
[L-10094-M] 22 p3828 N85-33707
CARE 3 MENU maintenance manual
[NASA-CR-172609] 22 p3828 N85-33708
DECODE: A software manual for use with the Serial ASCII Instrumentation Loop (SAIL) system
[AD-A155358] 22 p3828 N85-33709
SMACS: A system of computer programs for probabilistic seismic analysis of structures and subsystems. Volume 1: User's manual
[DE85-011853] 22 p3830 N85-33724
User's operating procedures. Volume 1: Scout project information programs
[NASA-CR-177948] 23 p3956 N85-34518
User's operating procedures. Volume 1: Scout project financial analysis program
[NASA-CR-177949] 23 p3956 N85-34519
User's guide to the MATHEW/ADPIC models
[DE85-012952] 23 p3966 N85-34587
User's manual for the FLORA equilibrium and stability code
[DE85-013182] 23 p3966 N85-34590
Development of NATOPS performance software for the SH-3D and SH-3H helicopters
[AD-A156140] 24 p4065 N85-35192
User's guide: A computer program for strength analysis of non-hydraulic concrete structural elements. Report 2. Strength design of reinforced concrete column sections (PCAUC)
[AD-A156393] 24 p4102 N85-35429
Users guide for optimum interpolation method of global data assimilation
[AD-A155929] 24 p4138 N85-35648
SIG: A general-purpose signal processing program. User's manual: Revision 1
[DE85-013035] 24 p4140 N85-35662
LOCAT: A data retrieval program
[AD-A156004] 24 p4165 N85-35822

USER REQUIREMENTS

User requirements for very-short-range weather forecasts: Some key issues 01 p0084 N85-10562
Benefits resulting from tailored very-short-range forecasts in Sweden 01 p0084 N85-10564
Some aspects of matching nowcasting and Very-Short-Range Forecasting (VSRF) products with the need of a multilingual community of a mountainous country — Swiss Alps 01 p0084 N85-10566
Evaluating a scientific workstation computer
[DE84-014764] 01 p0100 N85-10683
AGS-680 menu system user guide
[DE84-014336] 01 p0104 N85-10699
Microcomputer management guidelines
[PB84-212174] 01 p0105 N85-10704
Information requirements analysis: An application
[AD-A144896] 01 p0125 N85-10858
Implications of artificial intelligence for a user defined technical information system
[AD-P003938] 02 p0248 N85-11618
An effective graphics user interface for rules and inference mechanisms
[AD-P003942] 02 p0248 N85-11622
Intelligent information retrieval from on-line technical documentation
[AD-P003946] 02 p0249 N85-11626
Design of a scientific information collation and dissemination system, volumes 1 thru 3
[AD-A146002] 03 p0438 N85-12791
Definition of technology development missions for early Space Station satellite servicing. Volume 2: Technical
[NASA-CR-171229] 04 p0481 N85-12923
Calms processor (CALMPRO) user's guide
[PB84-229467] 04 p0540 N85-13439
User-oriented development and production of integrated circuits in small and medium quantities
[BMFT-FB-T-84-171] 05 p0633 N85-14059
ERS-1 and its potential for industrial utilization 05 p0659 N85-14235
Civil law enforcement missions 06 p0751 N85-14812
Specification of a transport protocol for computer communications. Volume 1: Overview and Services. Volume 2: Class 2 protocol. Volume 3: Class 4 protocol
[PB84-222850] 06 p0848 N85-15380
Specification of a transport protocol for computer communications. Volume 4: Service specifications. Volume 5: Guidance for the implementor. Volume 6: Guidance for implementation selection
[PB84-222868] 06 p0848 N85-15385
Specification of a transport protocol for computer communications. Volume 7: Testing OSI protocols, a compendium of papers. Volume 8: User's guide to the testing system for implementations of the ICST transport protocol. Volume 9: A test suite for implementations of the ICST transport protocol. Volume 10: Specification of a remote scenario interpreter for implementations of the ICST transport protocol
[PB84-222876] 06 p0848 N85-15386
Beginner's guide to blocked records on magnetic tape
[DE85-001691] 06 p0855 N85-15433
Design and analysis of an SQL (Structured Query Language) interface for a multi-backend database system
[AD-A146534] 06 p0856 N85-15447
Commerce Laboratory: Mission analysis payload integration study
[NASA-CR-171296] 07 p0911 N85-15764
Results of principal NASA studies on space station uses and functional requirements 07 p0914 N85-15787
What do we want: Increased speed, resolution, contrast or DOE? — astronomical photography 07 p0964 N85-16115
Climatological information and water resources 07 p1002 N85-16357
Mental models and cooperative problem solving with expert systems
[AD-A147843] 07 p1021 N85-16479
A study of the relationship between user attitudes and the success of the MAJCOM and AFRCE work information management system
[AD-A146956] 07 p1051 N85-16671
ATE user's view on design for maintainability 08 p1064 N85-16737
Commerce Lab: Mission analysis. Payload integration study
[NASA-CR-171285] 08 p1104 N85-16982
Shuttle/Centaur project perspective 08 p1106 N85-16991
Space Station needs, attributes, and architectural option study
[NASA-CR-174316] 08 p1109 N85-17011
Space Station engineering and technology development
[NASA-CR-174383] 09 p1287 N85-18079
Commerce lab: Mission analysis and payload integration study
[NASA-CR-174361] 10 p1426 N85-18993
Sector suite man-machine functional capabilities and performance requirements
[AD-A148881] 10 p1531 N85-19847
Microcomputers in transit: A hardware handbook
[PB85-113880] 10 p1536 N85-19700
Research needs on the interaction between information systems and their users: Report of a workshop
[PB85-121523] 10 p1566 N85-19891
Development of computer centers, equipment described: Problems of computer centers 11 p1700 N85-20686
GPS system field testing 11 p1711 N85-20762
Evaluation of the vocabulary switching systems
[PB85-127157] 12 p1951 N85-22260
Introduction to the Space Physics Analysis Network (SPAN)
[NASA-TM-86499] 14 p2290 N85-24196
Commercial data base management system for geonames data base
[AD-A150835] 14 p2433 N85-25007
Study on needs for a magnetic suspension system operating with a transonic wind tunnel
[NASA-CR-3900] 16 p2715 N85-26759
Design of computer-related workstations in relation to job functions and productivity
[AD-A151938] 16 p2844 N85-27534
Management considerations for an information center
[AD-A151774] 16 p2875 N85-27742
Personal computer aided decision analysis
[AD-A151911] 16 p2875 N85-27743
Further development of high voltage SIPMOS FET's to fulfill market needs
[BMFT-FB-T-84-255] 17 p3045 N85-28843
Automated Weather Observing System (AWOS) demonstration program
[AD-A153463] 18 p3148 N85-29493
BREED: A CDC-7600 computer program for the automation of breeder reactor design analysis (LWBR Development Program)
[DE85-010327] 19 p3338 N85-30686
SPAR improved structural-fluid dynamic analysis capability
[NASA-CR-171549] 20 p3454 N85-31449
Design guidelines for user-system interface software
[AD-A154907] 21 p3671 N85-32807
The effect of communication-language designs on software specifications
[AD-A155173] 21 p3672 N85-32809
Praxis release notes, version 7.3
[DE85-011862] 21 p3673 N85-32820
The flow of scientific and technical information in the US Army Research Laboratories
[AD-A155050] 21 p3713 N85-33043
Fracture detection and characterization for geothermal reservoir definition
[DE85-006677] 22 p3815 N85-33630
DECODE: A software manual for use with the Serial ASCII Instrumentation Loop (SAIL) system
[AD-A155358] 22 p3828 N85-33709
Product definition: Technical specification of needs
[SNIAS-851-430-104] 23 p3910 N85-34228
Graphics interaction in databases 23 p3958 N85-34534
A model for graphics interface tool development 23 p3960 N85-34545
Using percent-done program indicators to enhance user interfaces 23 p3960 N85-34546
Architecture of languages for large CAD systems development 23 p3962 N85-34557
How map designers can represent their ideas in thematic maps: Effective user interfaces for thematic map design 23 p3962 N85-34562

UTAH

Summary of salt gradient solar pond research 05 p0557 N85-14292
Geology and resources of the Tar Sand Triangle, southeastern Utah
[DE84-012017] 05 p0677 N85-14346

A geographic information system for resource managers based on multi-level remote sensing data
[E85-10047] 06 p0827 N85-15249
Geothermal assessment of a portion of the Escalante Valley, Utah
[DE84-015964] 06 p0828 N85-15257
Detecting agricultural to urban land use change from multi-temporal MSS digital data — Salt Lake County, Utah
[E85-10049] 07 p0983 N85-16245
An integrated remote sensing approach for identifying ecological range sites — parker mountain
[E85-10050] 07 p0983 N85-16246
Revised Uniform Summary of Surface Weather Observations (RUSSWO). Hill AFB, Utah, parts A-F
[AD-A147184] 07 p1006 N85-16395
Petrography, sedimentology, diagenesis, and reservoir characteristics of some Pennsylvanian phylloid algal limestones: Kansas and Utah, USA
09 p1352 N85-16507
Assessment of LANDSAT for rangeland mapping, Rush Valley, Utah
[E85-10072] 10 p1503 N85-19486
An integrated GIS/remote sensing data base in North Cache soil conservation district, Utah: A pilot project for the Utah Department of Agriculture's RIMS (Resource Inventory and Monitoring System)
[E85-10073] 10 p1504 N85-19487
LANDSAT 4 investigation of Thematic Mapper and Multispectral Scanner applications
[E85-10076] 10 p1504 N85-19490
Climate of Salt Lake City, Utah
[PB85-123675] 10 p1521 N85-19589
Low-temperature geothermal assessment of the Jordan Valley Salt Lake County, Utah
[DE85-000816] 11 p1670 N85-20524
Aeromagnetic and radiometric signatures of a possible porphyry system in the western Tushar Mountains, Utah
24 p4103 N85-35437
Evaluation of low-temperature geothermal potential in north-central Box Elder County, Utah
[DE85-009541] 24 p4112 N85-35490

UTILITIES
Analysis of wind energy systems for selected electric utilities
[DE84-013025] 04 p0530 N85-13369
Photovoltaic Systems Development and Evaluation Projects Integration Meeting
[DE84-008530] 11 p1673 N85-20542
Experimental investigation of a variable speed constant frequency electric generating system from a utility perspective
[NASA-CR-174950] 21 p3579 N85-32251

UTILITY AIRCRAFT
NT BO-105 HELICOPTER
NT DO-28 AIRCRAFT
NT P-531 HELICOPTER
NT U-2 AIRCRAFT
NT UH-1 HELICOPTER
NT UH-60A HELICOPTER

UTILIZATION
NT COAL UTILIZATION
NT GEOTHERMAL ENERGY UTILIZATION
NT LASER APPLICATIONS
NT LASER CUTTING
NT LASER FUSION
NT REUSE
NT WASTE ENERGY UTILIZATION
NT WASTE UTILIZATION
NT WINDPOWER UTILIZATION
The Palmqvist test and its applications in WC-Co alloys 02 p0177 N85-11187
Radio telemetry formula applications. A practical users guide
[AD-A146247] 03 p0356 N85-12288
Technical order managers handbook: Utilization assessment
[AD-A147579] 07 p1055 N85-16604
Space station propulsion: The advanced development program at Lewis
[NASA-TM-86999] 15 p2494 N85-25386
Mathematical programming in the Netherlands
[REPT-ARW-03-THE-BDK/ORS/83/10] 20 p3517 N85-31866
Applications of CdTe to nuclear medicine
[DE85-011877] 23 p3952 N85-34492

UV CETI STARS
U FLARE STARS

UV LASERS
U ULTRAVIOLET LASERS

V

V BAND
U EXTREMELY HIGH FREQUENCIES

V/STOL AIRCRAFT
NT BO-105 HELICOPTER
NT CH-47 HELICOPTER
NT FLYING PLATFORMS
NT HELICOPTERS
NT MILITARY HELICOPTERS
NT P-531 HELICOPTER
NT RIGID ROTOR HELICOPTERS
NT ROTARY WING AIRCRAFT
NT SHORT TAKEOFF AIRCRAFT
NT TILT ROTOR AIRCRAFT
NT UH-1 HELICOPTER
NT UH-60A HELICOPTER
NT VERTICAL TAKEOFF AIRCRAFT
Inlet and airframe compatibility for a V/STOL fighter/attack aircraft with top-mounted inlets
[NASA-TM-84252] 01 p0003 N85-10015
Computer programs to predict induced effects of jets exhausting into a crossflow
[NASA-CR-166591] 05 p0592 N85-13776
An investigation of turbulence mechanisms in V/STOL upwash flow fields
[AD-A149786] 12 p1772 N85-21123
Some aspects of the design of a fly-by-wire flying control system for a supersonic V/STOL fighter aircraft
[COLL-AERON-8413] 12 p1780 N85-21175
Special course on V/STOL aerodynamics: An assessment of European jet lift aircraft
[AGARD-R-710-ADDENDUM] 15 p2460 N85-25188
Future of V/STOL aircraft systems: A survey of opinions
[NASA-TM-86689] 18 p3061 N85-28937

VACANCIES (CRYSTAL DEFECTS)
Application of positron annihilation in materials science
[DE84-014733] 02 p0288 N85-11883
Investigation of the interaction of atoms with lattice defects using probe methods 03 p0429 N85-12737
Defective nature of the crystalline lattice of nickel ferrite-based solid solutions
[BLL-TRANS-WH-595-(9091.9F)] 10 p1439 N85-19068
Resolvability of defect ensembles with positron annihilation studies
[DE85-010041] 18 p3196 N85-29823
PAS determination of the vacancy formation enthalpy in tungsten
[DE85-010283] 19 p3240 N85-30066

VACCINES
Induction of immunity to toxins with anti-idiotypic antibody
[AD-A146793] 07 p1014 N85-16445
Progress, goals in biotechnology summarized 17 p2945 N85-28182
Genetic and physiological control of protective antigen synthesis by bacillus anthracis
[AD-A156324] 24 p4133 N85-35617

VACUUM
NT HIGH VACUUM
NT ULTRAHIGH VACUUM
The Boltzmann equation: Global existence for a rare gas in an infinite vacuum
[PREPRINT-78] 01 p0124 N85-10851
Gravitational vacuum 02 p0265 N85-11734
Simulation of the interaction of single-pulsed optical lasers with targets in a vacuum
[DE84-016476] 05 p0640 N85-14107
Performance of Chromel versus Alumel and Nicrosil versus Nisil thermocouple assemblies in vacuum and argon between 1000 deg C and 1200 deg C
[DE85-000810] 12 p1853 N85-21824
Review of anode phenomena in vacuum arcs
[DE85-002736] 12 p1926 N85-22101
High temperature antifriction properties of Ti sub 1-sub xNb sub x C sub 0.5N sub 0.5 alloys
13 p2029 N85-22715
ANTENA user guide
[DE85-004961] 14 p2424 N85-24953
Spray applicator for spraying coatings and other fluids in space
[NASA-CASE-MSC-18852-1] 18 p3115 N85-29283
Magnetics calculations for an ELMO Bumpy Square
[DE85-010442] 18 p3191 N85-29792
The photochemical oxidation of GaAs
[AD-A153689] 19 p3233 N85-30045
Prospective uses for diffusion welding in vacuum
22 p3733 N85-33145
The 2nd European Conference on Atomic and Molecular Physics
[AD-A155863] 24 p4148 N85-35715
SU(2) x U(1) vacuum and the Centauro events
24 p4175 N85-35885

VACUUM APPARATUS
NT ION PUMPS
NT IONIZATION GAGES
NT MOLECULAR PUMPS
NT VACUUM CHAMBERS
NT VACUUM FURNACES
NT VACUUM PUMPS
High temperature ultra-high vacuum infrared window seal
[AD-D011333] 07 p0929 N85-15890
Cryogenic glass-to-metal seal
[AD-D011370] 07 p0933 N85-15911
Metal vapor arc switch electromagnetic accelerator technology
[NASA-CR-174380] 09 p1314 N85-18259
Instrumentation for particle-beams research using excited merging beams
[AD-A154155] 19 p3356 N85-30807
Effective brightness of zero-point fluctuations of the electromagnetic vacuum accompanying parametric scattering of light 21 p3694 N85-32951

VACUUM CHAMBERS
Final magnetic shimming of vacuum chamber suspension holes on the sector magnets
[CSIR-NAC-83-02] 01 p0117 N85-10796
Electrostatic wave observation during a space simulation Beam-Plasma-Discharge (BPD)
[NASA-CR-174286] 07 p1045 N85-16639
Tailored vacuum chambers for ac magnets
[DE85-010767] 21 p3591 N85-32319
Dual-chamber plasma deposition of A-Si:H solar cells at high rates using disilane
[DE85-011626] 23 p3946 N85-34451
Monitoring dosage of volatile compounds in tests at low barometric pressure 23 p3954 N85-34508
Size effects of vacuum chamber for H- (D-) ion volume production by sheet plasma 1
[IPPJ-731] 23 p3974 N85-34639

VACUUM DEPOSITION
Apparatus for producing diamond-like carbon flakes
[NASA-CASE-LEW-13837-3] 11 p1615 N85-20155
Diamondlike flakes
[NASA-CASE-LEW-13837-2] 12 p1796 N85-21267
Peculiarities of MgF2 film formation and optimization of MgF2 film deposition process 14 p2281 N85-24132
In situ thin film measurements
[AD-A151379] 15 p2652 N85-26353
Synthesis and characterization of superconducting electronic materials
[AD-A151112] 15 p2659 N85-26409
Vacuum plasma coatings for turbine blades
16 p2734 N85-26869
New metal coating method developed
21 p3568 N85-32191
Advances in sputtered and ion plated solid film lubrication 22 p3797 N85-33524
Polarisation insensitive achromatic cube beamsplitter — binocular microscopes
[NPL-MOM-72] 23 p3973 N85-34630

VACUUM EFFECTS
Density distribution in supersonic jet discharged into vacuum from nozzle with bevel tip
02 p0269 N85-11757
Spacelab 1 experiment: Microorganisms in space hard environment 05 p0691 N85-14443
Evaluation and prediction of long-term environmental effects of nonmetallic materials
[NASA-CR-171353] 10 p1450 N85-19137
Cutting structural materials in vacuum
14 p2286 N85-24165
Mechanical properties of lunar materials under anhydrous, hard vacuum conditions: Applications of lunar glass structural components
[DE85-006682] 16 p2801 N85-27271
Effective specific impulse of secondary flow injected into a rocket nozzle
[NAL-TR-848T] 18 p3067 N85-28970
Prospective uses for diffusion welding in vacuum
22 p3733 N85-33145

VACUUM FURNACES
West Europe report: Science and technology
[JPRS-WST-84-008] 15 p2531 N85-25606
France develops new continuous vacuum treatment method 15 p2531 N85-25611
Studies on the processing methods for extraterrestrial materials
[NASA-CR-175778] 16 p2716 N85-26768

VACUUM GAGES
NT IONIZATION GAGES

VACUUM MELTING
A study of vacuum melting to increase the toughness of maraging steels
[AD-A145017] 01 p0028 N85-10175
Effect of prior warm rolling on the retained austenite content and hardening response of VIM-VAR (vacuum-induction melted-vacuum-arc remelted) AISI M-50 steel
[AD-A156145] 24 p4079 N85-35281
X-ray fluorescence analysis of 304L stainless steel
[DE85-013254] 24 p4080 N85-35286

VACUUM PUMPS
NT ION PUMPS
NT MOLECULAR PUMPS
Electron storage ring beam lifetime dependence on pressure and pumping speed
[DE85-003208] 11 p1724 N85-20845
Impurity control and vacuum pumping system design and analysis for next-generation Tokamaks
[DE85-009291] 17 p3041 N85-26815
VACUUM SYSTEMS
Design study of the vacuum pump of the ESRP — synchrotron radiation
[NIKHEF-MTG-21] 08 p1138 N85-17167
Electron storage ring beam lifetime dependence on pressure and pumping speed
[DE85-003208] 11 p1724 N85-20845
Measurement of NSLS distributed diode sputter ion pump characteristics
[DE85-006550] 16 p2760 N85-27031
Management of vacuum leak-detection processes, standards and calibration
[DE85-006705] 16 p2788 N85-27202
Vacuum interface flashover with bipolar electric fields
[DE85-012027] 22 p3755 N85-33275
Supermite vacuum interface design
[DE85-012861] 22 p3837 N85-33759
Ultrahigh vacuum system of the heavy ion transport line at Brookhaven
[DE85-011838] 22 p3840 N85-33778
Key issues of fusion nuclear technology development (FINESSE)
[DE85-012599] 22 p3845 N85-33817
Experimental lithium system
[DE85-013252] 24 p4094 N85-35382
High vacuum portable pumping station suitable for accelerator use
[DE85-011840] 24 p4155 N85-35759
Vacuum system for the Argonne 6 GeV synchrotron light source
[DE85-012286] 24 p4157 N85-35773
Neutral pumping rates for a next step tokamak ignition device
[DE85-012780] 24 p4157 N85-35776
VACUUM TESTS
NT THERMAL VACUUM TESTS
The performance of Fomblin Z25 oil in ball bearings operating in vacuum — spacecraft lubricant
[ESA-ESTL-056] 08 p1134 N85-17150
The wear of small polyacetal and polymide gears in vacuum — spacecraft gears
[ESA-ESTL-058] 08 p1169 N85-17374
Vapor pressure and evaporation rate of certain heat-resistant compounds in a vacuum at high temperatures
[NASA-TM-77807] 10 p1434 N85-19036
Measurement of damping of graphite epoxy materials
[NASA-CR-176073] 21 p3596 N85-32334
VACUUM TUBE OSCILLATORS
NT CATHODE RAY TUBES
NT COLD CATHODE TUBES
NT GAS DISCHARGE TUBES
NT HELITRONS
NT KLYSTRONS
NT MAGNETRONS
NT MICROWAVE OSCILLATORS
NT MICROWAVE TUBES
NT PHOTOMULTIPLIER TUBES
NT PICTURE TUBES
NT THERMICONS
NT THYRATRONS
NT TRAVELING WAVE TUBES
NT VIDICONS
VACUUM TUBES
NT CATHODE RAY TUBES
NT COLD CATHODE TUBES
NT GAS DISCHARGE TUBES
NT HELITRONS
NT KLYSTRONS
NT MAGNETRONS
NT MICROWAVE OSCILLATORS
NT MICROWAVE TUBES
NT PHOTOMULTIPLIER TUBES
NT PICTURE TUBES
NT THERMICONS
NT THYRATRONS
NT TRAVELING WAVE TUBES
NT VIDICONS
Laser welder for fabricating neutron tubes
[DE85-009965] 17 p2974 N85-28377
Advanced evacuated tube collectors
[DE85-010271] 19 p3274 N85-30302
VACUUM ULTRAVIOLET RADIATION
U FAR ULTRAVIOLET RADIATION
VALENCE
Actinides, the narrowest bands
[DE84-016463] 05 p0733 N85-14710
Basic studies of atomic dynamics
[DE84-015661] 09 p1380 N85-19675
Angle-resolved photoemission study of AuGa2 and AuIn2 intermetallic compounds
[AD-A150000] 12 p1940 N85-22183
The Valence- and conduction-band structure of the sapphire (1102) surface
[AD-A150001] 12 p1940 N85-22184
Mixed valence materials
[AD-A151009] 14 p2252 N85-23959
Strained-layer superlattices and strain-induced light holes
[DE85-003675] 14 p2431 N85-24990
VALIDATION
U PROVING
VALIDITY
AFOS (Automation of Field Operations and Services)-ERA forecast verification, September 1984
[PB85-137578] 12 p1897 N85-21912
A note on validity generalization procedures
[AD-A150065] 12 p1924 N85-22085
VALKYRIE AIRCRAFT
U B-70 AIRCRAFT
VALLEYS
NT DEATH VALLEY (CA)
NT IMPERIAL VALLEY (CA)
NT SACRAMENTO VALLEY (CA)
Paleohydrology and geomorphology of selected reaches of the upper Wabash Valley, Indiana
02 p0226 N85-11481
Love and Rayleigh waves in irregular ground
04 p0523 N85-13348
Atmospheric tracer experiments in a deep narrow valley
[PB84-234500] 04 p0532 N85-13402
Geothermal assessment of a portion of the Escalante Valley, Utah
[DE84-015964] 06 p0826 N85-15257
Towing tank studies of stratified flow over ridges and valleys
[DE84-011418] 06 p0839 N85-15329
A numerical method for interface problems in elastodynamics
[NASA-TM-86486] 08 p1172 N85-17391
Mesozoic ophiolitic olistostromes and Cenozoic imbricate thrust faulting in the northern California coast ranges: Geology of the Mysterious Valley area, Napa County 08 p1182 N85-17445
Low-temperature geothermal assessment of the Jordan Valley Salt Lake County, Utah
[DE85-000618] 11 p1670 N85-20524
Paleohydrologic implications of valley networks of Mars 13 p2190 N85-23585
Geomorphology and geology of the Southwestern Margaritifer Sinus and Argyre regions of Mars. Part 1: Geological and geomorphological overview 13 p2192 N85-23600
Geomorphology and geology of the Southwestern Margaritifer Sinus and Argyre regions of Mars. Part 3: Valley types and distribution 13 p2193 N85-23602
Late Tertiary and Quaternary river systems of the eastern Sahara as mapped on shuttle radar and LANDSAT images 13 p2199 N85-23641
The rifted margin of Saudi Arabia 17 p2990 N85-28483
VALMET: A valley air pollution model
[DE85-010820] 21 p3614 N85-32483
VALSALVA EXERCISE
Main component method used to study variations of cardiovascular parameters 12 p1901 N85-21939
VALSALVA MANEUVER
U VALSALVA EXERCISE
VALUE
NT Q VALUES
Point processes associated with extreme value theory
[AD-A151211] 15 p2640 N85-26280
Computing the singular value decomposition of a product of two matrices
[DE85-006977] 16 p2659 N85-27631
VALUE ENGINEERING
Introduction to the subjective transfer function approach to analyzing systems
[AD-A145817] 03 p0436 N85-12774
Value analysis — industrial competition
[CNES-NT-110] 04 p0577 N85-13684
Mini-Seminar on Non-Destructive Testing
[CSIR-TSD-0009/83] 14 p2316 N85-24308
New materials needs in aeronautics
[SNIAS-851-502-101] 22 p3729 N85-33120
DOD Value Engineering Conference report. Value Engineering (VE): A tool that benefits line management held at Leesburg, Virginia on 1-2 November 1984. Part 1. Executive summary
[AD-A156067] 24 p4163 N85-35810
DOD Value Engineering Conference report. Value Engineering (VE): A tool that benefits line management held at Leesburg, Virginia on 1-2 November 1984. Part 2. Plenary session
[AD-A156068] 24 p4163 N85-35811
DoD Value Engineering conference report. Value Engineering (VE): A tool that benefits line management. Part 3, Workshop A: VE in the program office
[AD-A156069] 24 p4163 N85-35812
DoD Value Engineering conference report. Value Engineering (VE): A tool that benefits line management. Part 4, Workshop B: VE on spare parts
[AD-A156070] 24 p4163 N85-35813
DoD Value Engineering conference report. Value Engineering (VE): A tool that benefits line management. Part 5, Workshop C: VEP/VECP administration, negotiation, and implementation
[AD-A156071] 24 p4163 N85-35814
DoD Value Engineering conference report. Value Engineering (VE): A tool that benefits line management. Part 6, Workshop D: VE training-orientation
[AD-A156072] 24 p4164 N85-35815
DoD Value Engineering conference report. Value Engineering (VE): A tool that benefits line management. Part 7, Workshop E: VE in construction and architect engineer contracts
[AD-A156073] 24 p4164 N85-35816
VALVES
NT AUTOMATIC CONTROL VALVES
NT COCKS
NT CONTROL VALVES
NT DAMPERS (VALVES)
NT FUEL VALVES
NT GAS VALVES
NT PRESSURE REGULATORS
NT SOLENOID VALVES
Back end valves: History and modifications
[DE84-009272] 05 p0846 N85-14145
Turbine blade test cascade modifications and orations, August 1982 - April 1983
[DE84-009268] 06 p0833 N85-15303
Airspeed sensing pressure valve system
[AD-D011472] 10 p1425 N85-18987
Tire inflation/deflation system
[AD-D011459] 10 p1493 N85-19425
Tire deflation mechanism
[AD-D011460] 10 p1493 N85-19427
Performance of the 10 KSI Wilson valve breech
[DE85-000258] 10 p1493 N85-19430
Pneumatic clamping device
[AD-D011544] 12 p1958 N85-21656
Hydraulic characteristics of reduction installation valves 14 p2269 N85-24060
Dependents of velocity distribution in exit section of converging channel on shape of inlet channel in regulating valve 14 p2277 N85-24106
Fracture mechanics analysis of cold drawn SI-Cr valve steel
[BLL-BISI-TRANS-22216-(9022.06)] 17 p2978 N85-28405
Automatic volume calibration system
[DE85-006955] 18 p3102 N85-29204
Moisture content and gas sampling device
[NASA-CASE-MSC-18665-1] 18 p3103 N85-29213
Linear motion valve
[NASA-CASE-MSC-20148-1] 18 p3115 N85-29284
Thermo-electric valve
[AD-D011682] 19 p3252 N85-30165
Sobolev-Poincare's inequality and the Neumann problem for u sub t = divergence of the absolute value of the gradient u to the p-2 power x the gradient u
[AD-A154788] 21 p3676 N85-32839
Automatic rotary valve actuator
[DE85-012797] 22 p3794 N85-33505
Reactant pressure differential control for fuel cell gases
[NASA-CASE-MSC-20127-2] 23 p3937 N85-34403
VAMPIRE AIRCRAFT
U DH 115 AIRCRAFT
VAN ALLEN RADIATION BELTS
U RADIATION BELTS
VAN DER WAAL FORCES
Infrared excitation of clusters and ions of atmospheric interest
[DE85-002098] 10 p1516 N85-19564
Explorations into thermodynamics analogies and critical points in reference to gas-solid transport
[DE85-000816] 11 p1738 N85-20929
Many-body processes in atomic and molecular physics
[DE85-009750] 19 p3354 N85-30791
VANADIUM
Granular boundary segregation in low-alloyed titanium-vanadium alloys 01 p0019 N85-10117
The effect of replacing molybdenum with vanadium on the corrosion resistant properties of stainless steels 02 p0178 N85-11197

Electrolytic lapping technique for vanadium
[DE84-014710] 02 p0183 N85-11227
Review: Role of refractory metal alloys in fusion reactor applications
[AERE-R-11317] 03 p0422 N85-12695
Thermodynamics and phase equilibria in the vanadium-silicon system
[AD-A145870] 03 p0435 N85-12769
Preparation of low-silicon vanadium metal
[DE84-014818] 04 p0476 N85-13031
Volatility of vanadium from a candidate fusion tractor alloy
[DE84-015277] 05 p0618 N85-13955
Investigation of vanadium solid solution and zeta phase regions of vanadium-carbon system
[DE85-002678] 11 p1605 N85-20092
Improvement in magnetic field properties of vanadium-gallium superconductors by enhancement of spin-orbit scattering
[DE85-002693] 13 p2164 N85-23422
Thermodynamic analysis of the plasma nitriding of ferrovanadium
[BLL-BISI-TRANS-22237-(9022.06)] 17 p2924 N85-28032
Microstructures and mechanical properties of microalloyed medium carbon steels 19 p3238 N85-30074
Properties of Ti-6Al-4V spun formed fuze supports
[DE85-011968] 22 p3792 N85-33498
Method for preparing high purity vanadium
[DE85-006412] 23 p3913 N85-34242
Calculating the interatomic pair potential allowing for resonance interaction in titanium, nickel and vanadium
[BLL-M-35843-(5828.4)] 23 p3913 N85-34249
Flux-line lattice anisotropy in V3Si: Observation and interpretation
[DE85-011935] 23 p3985 N85-34713
Applications of the mineral resources data system and the international strategic minerals inventory in mineral-resource assessments by region and commodity 24 p4105 N85-35451

VANADIUM ALLOYS
The use of vanadium in low alloy structural steels 02 p0160 N85-11207
Ion implantation of surgical Ti-6Al-4V alloy
[DE85-000943] 09 p1296 N85-18142
Ti-6Al-4V alloy castings prepared in zircon sand molds and the effect of hot isostatic pressing
[PB85-109032/GAR] 09 p1296 N85-18150
Phase transformations in vanadium alloys of titanium during quenching and tempering 11 p1602 N85-20073
Partial replacement of chromium in austenitic stainless steels by molybdenum, copper, and vanadium, report of investigations 1984
[PB85-116508] 12 p1809 N85-21346
Decomposition of VTAN alloy solid solution upon irradiation and thermal aging 13 p2029 N85-22712
Effect of oxygen on mechanical properties of Nb-V alloy
[DE85-002681] 14 p2256 N85-23982
Conversions in amorphous zirconium-vanadium alloy 15 p2496 N85-25400
Effects of the phase compositions of cast low-pearlite steels micro-alloyed with vanadium and titanium of their structure and properties
[BLL-BISI-TRANS-22301-(9022.06)] 17 p2928 N85-28067
The disordering process in an L12 ordered alloy
[DE85-008152] 17 p2931 N85-28093
Development of reduced activation alloys for fusion service: Draft
[DE85-007464] 18 p3074 N85-29014
Long range ordered alloys modified by addition of niobium and cerium
[DE85-011681] 20 p3431 N85-31285
Reliability of welds to repair defects in cast components made from CrMoV steel
[BLL-CE-TRANS-8054-(9022.09)] 20 p3461 N85-31501

VANADIUM COMPOUNDS
NT VANADIUM OXIDES
Scale-up of vanadium trineodecanoate
[AD-A149935] 12 p1813 N85-21370

VANADIUM OXIDES
A study of the K-edge absorption spectra of selected vanadium compounds
[AD-A149334] 10 p1435 N85-19045
Metal-semiconductor phase transition and its application
[DRIC-T-7149] 13 p2021 N85-22685
Electrochromic and thermochromic materials for solar energy applications with emphasis on niobium and vanadium oxides
[DE85-010830] 19 p3249 N85-30147

Thin film phase transition materials development program
[AD-A154260] 19 p3259 N85-30209
Photoeffects of semiconductor electrolyte interfaces
[AD-A154163] 20 p3449 N85-31411
The Konstantinov effect and absorption of sound in inhomogeneous media 21 p3680 N85-32861

VANELESS DIFFUSERS
Vaneless diffusers — flow in centrigal compressors 05 p0637 N85-14084
Lateral fluid forces acting on a whirling centrifugal impeller in vaneless and vaned diffuser 05 p0643 N85-14123
A three-dimensional axisymmetric calculation procedure for turbulent flows in a radial vaneless diffuser
[NASA-TM-86903] 06 p0749 N85-14798

VANES
NT GUIDE VANES
NT JET VANES
NT WIND VANES
Heat flux sensors for burner liners and turbine blades and vanes 02 p0142 N85-10961
Studies on the hot corrosion of a nickel-base superalloy, Udimet 700
[NASA-TM-86882] 02 p0183 N85-11224
Preliminary results of a study of the relationship between free stream turbulence and stagnation region heat transfer
[NASA-TM-86884] 02 p0197 N85-11317
Comparison of options for reduction of noise in the test section of the NASA Langley 4x7m wind tunnel, including reduction of nozzle area
[NASA-CR-172446-VOL-2] 05 p0726 N85-14667
Replaceable blade turbine and stationary specimen corrosion testing facility
[NASA-TM-86931] 09 p1294 N85-18126
Effects of vane/blade ratio and spacing on fan noise, volume 1
[NASA-CR-174664] 10 p1553 N85-19791
Effects of vane/blade ratio and spacing on fan noise. Volume 2: Data supplement
[NASA-CR-174665] 10 p1553 N85-19792
Manufacture of drive wheel vanes for hydraulic turbines on program controlled machine tools 14 p2269 N85-24058
Causes and means of prevention of erosion of exit edges of drive vanes in final stages of K-300-240 turbine 14 p2272 N85-24076
Prediction of vortex-induced loads on wind-tunnel turning vanes
[NASA-TM-86678] 15 p2462 N85-25204
Vortex shedding flowmeters for liquids at high flow velocities 16 p2740 N85-26906
Aerodynamic forces developing in channels between vanes in turbine drive wheels 16 p2765 N85-27062
Long-Term Materials Test Program
[DE85-003248] 18 p3077 N85-29034
Preliminary results of a study of the relationship between free-stream turbulence and stagnation region heat transfer 20 p3452 N85-31435
Design of a generator for near-tangential transonic swirling outflow
[AD-A155163] 21 p3584 N85-32280

VANS
U TRUCKS

VAPOR DEPOSITION
NT VACUUM DEPOSITION
Hot hollow cathode gun assembly
[DE84-014312] 01 p0121 N85-10832
Chemical vapor deposition of amorphous silicon films produced by using higher order silanes
[DE84-004519] 01 p0123 N85-10847
Laser spectroscopy and gas-phase chemistry in CVD
[DE84-014959] 02 p0173 N85-11158
Thermodynamic calculations and the chemical vapour deposition of hard materials 02 p0179 N85-11200
The development of CVD oxide coatings for the protection of metal surfaces — chemical vapor deposition (CVD) 03 p0332 N85-12142
Deposition in the human lung during respiration of small particles suspended in the air
[BLL-RISLEY-TR-5021-(9091.9F)] 03 p0400 N85-12549
CVD parameter study using strategy of experimentation
[DE84-015900] 04 p0473 N85-13011
Development of a polysilicon process based on chemical vapor deposition of dichlorosilane in an advanced Siemen's reactor
[NASA-CR-174148] 04 p0483 N85-13083
Glow discharge amorphous silicon tin alloys
[DE84-013001] 05 p0618 N85-13952
Creep of chemically vapor deposited SiC fibers
[NASA-TM-86897] 06 p0763 N85-14878

Electrical properties of 10-50 nm TEOS (Tetraethoxysilane) LPCVD (Low Pressure Chemical Vapor Deposition) films
[AD-A146416] 06 p0803 N85-15111
Investigation of silicon surface passivation by silicon nitride deposition 06 p0829 N85-15266
Preparation and electronic properties of MoS(2) and WS(2) single crystals grown in the presence of cobalt
[AD-A146506] 06 p0866 N85-15506
Alloys and method of making
[AD-D011337] 07 p0927 N85-15874
Method of preparing single crystalline cubic silicon carbide layers
[AD-D011305] 07 p1048 N85-16653
Preparation and evaluation of ZnSe and ZnS sub X Se sub 1-x epitaxial layers on Ge substrates for applications in surface passivation and heterojunction devices
[AD-A147432] 07 p1048 N85-16657
Fabrication of ceramic-ceramic composites by chemical vapor deposition
[DE85-000981] 09 p1298 N85-18155
Advanced high-efficiency concentrator cells
[DE84-013020] 09 p1344 N85-18459
Fabrication of fiber-reinforced ceramic composites by chemical vapor infiltration
[DE85-003809] 11 p1611 N85-20132
Chemically amplified laser direct-writing of aluminum
[DE85-000308] 11 p1639 N85-20324
Development of a polysilicon process based on chemical vapor deposition of dichlorosilane in an advanced Siemen's reactor
[NASA-CR-174445] 11 p1672 N85-20532
Fabrication of monocrystalline GaAs solar cells utilizing NaCl sacrificial substrates
[DE84-013016] 11 p1673 N85-20544
High-temperature, solid oxide electrolyte fuel cell power generation system
[DE85-002978] 11 p1675 N85-20552
Method for the preparation of epitaxial films of mercury cadmium telluride
[AD-D011532] 12 p1938 N85-22175
Environmental effects on the tensile strength of chemically vapor deposited silicon carbide fibers
[NASA-TM-86981] 14 p2259 N85-24000
Laser-assisted solar cell metallization processing
[NASA-CR-175686] 14 p2350 N85-24528
Producible alternative to CdTe for epitaxy (PACE-2) of LWIR (Long Wave Infrared) HgCdTe
[AD-A150678] 14 p2426 N85-24964
Thermodynamic calculations and the chemical vapour deposition of hard materials 14 p2431 N85-24991
Mechanical properties of TiN deposits obtained by PVD and TiN, TiC, TiC + TiN obtained by CVD
[BLL-RISLEY-TR-5097-(9091.9F)] 15 p2508 N85-25471
Vapor sensing by means of a ZnO-on-Si surface acoustic wave resonator
[DE85-003250] 15 p2646 N85-26324
Fundamental studies of growth, doping and transformation in beta silicon carbide
[AD-A152047] 15 p2660 N85-26416
Chemical vapor deposition of amorphous semiconductor films
[DE85-002917] 15 p2661 N85-26421
Computer program for the calculation of multicomponent convective diffusion deposition rates from chemically frozen boundary layer theory
[NASA-CR-168320] 16 p2761 N85-27164
Morphology of GaAs/sub 1-x/P/sub x/ superlattices grown by MOCVD and chloride VPE
[DE85-002944] 17 p3045 N85-28842
Corrosion resistant coating
[NASA-CASE-NPO-15828-1] 18 p3073 N85-29005
Limiting processes laser CVD
[DE85-008846] 18 p3114 N85-29279
Crystal growth from the vapor in low gravity environments
[DE85-009628] 18 p3195 N85-29616
Chemistry and physics of silicon-based amorphous semiconductors
[DE85-001931] 19 p3377 N85-30949
Realization by vapor deposition of turbine blades covered with a silicon nitride layer 20 p3395 N85-31061
New metal coating method developed 21 p3568 N85-32191
Improved process for the preparation of fiber-reinforced ceramic composites by chemical vapor deposition
[DE85-011564] 22 p3752 N85-33255
1985 Amorphous Silicon Review Meeting
[DE85-008794] 22 p3807 N85-33582
An impact-induced terrestrial atmosphere and iron-water reactions during accretion of the Earth 22 p3854 N85-33864

Tests on zirconium nitride coatings applied to SW 18 steel using the chemical vapor deposition method
24 p4078 N85-35271

VAPOR GENERATORS
U VAPORIZERS

VAPOR JETS
A new theory aiming to define the mechanisms of material removal in electroerosion
[NASA-TM-77875] 18 p3176 N85-29689

VAPOR LIQUID EQUILIBRIUM
U LIQUID-VAPOR EQUILIBRIUM

VAPOR PHASE EPITAXY
Impurity trapping during gas phase epitaxy of gallium arsenide 02 p0257 N85-11686
Preparation and evaluation of ZnSe and ZnS sub X Se sub 1-x epitaxial layers on Ge substrates for applications in surface passivation and heterojunction devices
[AD-A147432] 07 p1048 N85-16657
Formation of a limiting composition in the preparation of ternary 3-5 semiconductors by the VPE (Vapor Phase Epitaxy) Hydride technique
[AD-A147639] 08 p1225 N85-17713
Fundamental studies of growth, doping and transformation in beta silicon carbide
[AD-A149339] 10 p1562 N85-19851
Preparation of crystal growth experiments in Spacelab: Si (FSLP), CdTe (D1), ZnS (D1)
[BMFT-FB-W-84-045] 12 p1788 N85-21227
1.5 to 1.7 micrometers LEDs (Light-Emitting Diode)
[AD-A149685] 12 p1834 N85-21508
Process for the epitaxial deposition of III-V compounds utilizing a continuous in-situ hydrogen chloride etch
[AD-D011557] 12 p1939 N85-22177
Morphological stability and fluid dynamics of vapor crystal growth
[NASA-CR-175879] 17 p3042 N85-28822
Morphological stability and fluid dynamics of vapor crystal growth
[NASA-CR-175880] 17 p3042 N85-28823
Development of photodetectors
[AD-A153773] 18 p3095 N85-29158
Process for the epitaxial deposition of 3-5 compounds utilizing a binary alloy as the metallic source
[AD-D011663] 18 p3193 N85-29801
Doping superlattices in organometallic VPE InP
[AD-A155151] 21 p3710 N85-33029

VAPOR PHASES
CREKID: A computer code for transient, gas-phase combustion of kinetics
[NASA-TM-83906] 01 p0011 N85-10068
NaK chemiluminescence
[AD-A146077] 03 p0328 N85-12110
Sintering behavior of ultrafine silicon carbide powders obtained by vapor phase reaction
[NASA-TM-77422] 03 p0336 N85-12161
Numerical modelling of the drying of porous materials
[DE84-013056] 04 p0499 N85-13181
Attempted measurement of gaseous H-2O-2 in the ambient atmosphere
[DE85-001937] 06 p0834 N85-15306
Reactions of metal ions and their cluster in the gas phase using laser ionization: Ion cyclotron resonance spectroscopy
[DE84-016491] 09 p1293 N85-18120
Effective antireflection coatings of transparent polymeric materials by gas-phase surface fluorination
[DE84-013027] 09 p1385 N85-18711
Desorption efficiences of vapor phase polynuclear aromatic compounds on solid adsorbents
[DE85-001303] 10 p1436 N85-19052
Determination of vapor phase content when metals are struck by laser radiation pulses of various densities
10 p1445 N85-19106
Numerical simulations of liquid propellant combustion instability: Onset and growth
[DE85-000743] 10 p1458 N85-19186
Analysis of phase composition of products of laser destruction of metallic surfaces
11 p1600 N85-20064
Chemical kinetics of gas phase decomposition products of nitramine propellants 13 p2003 N85-22558
Procedure for certifying quantity of volatile organic compounds emitted by paint, ink and other coatings
[PB85-159044] 15 p2520 N85-25537
Vapor sensing by means of a ZnO-on-Si surface acoustic wave resonator
[DE85-003250] 15 p2646 N85-26324
Research on the kinetics of phase changes in solids
[AD-A152387] 17 p2918 N85-27980
Gas phase ion-molecule chemistry of carbon, nitrogen and oxygen compounds
[AD-A152876] 17 p2919 N85-27996
The decomposition of gas phase formaldehyde by plasma discharge
[AD-A153202] 17 p2921 N85-28007
Chemical transformation modules for Eulerian acid deposition models. Volume 1: The gas-phase chemistry
[PB85-173714] 18 p3072 N85-29001
Electron irradiation of light emitting diodes
[AD-A154441] 19 p3260 N85-30213
Chemical transformation in acid rain. Volume 1: New methodologies for sampling and analysis of gas-phase peroxide
[PB85-173425] 19 p3311 N85-30527
Reactions of metal ions and their clusters in the gas phase using laser ionization-ion cyclotron resonance spectroscopy
[DE85-009478] 19 p3361 N85-30838
Modeling of chemical transformations of SO(x) and NO(x) in the polluted atmosphere: An overview of approaches and current status
[PB85-173169] 20 p3487 N85-31677
Liquid-phase compositions from vapor-phase analyses 2: Adaptation of the Prausnitz program to UF6 and some of its potential impurities
[DE85-011521] 21 p3673 N85-32819
Microwave semiconductor research: Materials, devices and circuits and gallium arsenide ballistic electron transistors
[AD-A154698] 21 p3709 N85-33024
Method for preparing Pb-(beta)-aluminum ceramic
[DE85-011685] 22 p3752 N85-33256
Volatile loss following very large impacts
22 p3853 N85-33862
Volatiles on satellites of the outer solar system
22 p3854 N85-33868
Vapor phase heat transport concepts
[DE85-009550] 23 p3931 N85-34366
Heats of formation of gas phase organosulfur molecules, radicals and ions measured by PEPICO and application of (17)O and (33)S NMR spectroscopy to structure determination of organosulfur compounds
[DE85-010558] 24 p4071 N85-35229

VAPOR PRESSURE
Mathematical models for the boiling diagram of the ideal two-component mixture
[DFVLR-FB-84-22] 04 p0471 N85-13000
Stable isotope studies
[DE84-016752] 04 p0562 N85-13583
Metal vapor arc switch electromagnetic accelerator technology
[NASA-CR-174380] 09 p1314 N85-18250
Vapor pressure and evaporation rate of certain heat-resistant compounds in a vacuum at high temperatures
[NASA-TM-77807] 10 p1434 N85-19036
Vapor pressure studies of the solubilization of hydrocarbons by surfactant micelles
[DE85-004319] 12 p1803 N85-21306
Trends of petroleum fuels
[DE85-000116] 14 p2263 N85-24023
Entropy of He 2 and universality near the superfluid in He(4)
19 p3378 N85-30957

VAPORIZATION HEAT
U HEAT OF VAPORIZATION

VAPORIZERS
NT EVAPORATORS
Nonlinear control model of an H2O steam reactor
[DFVLR-FB-84-30] 07 p0975 N85-16192
Solar thermochemical process interface study
[NASA-CR-174442] 10 p1510 N85-19527
Continuous laminar smoke generator
[NASA-CASE-LAR-13014-1] 12 p1781 N85-21178
Forced convective, nonequilibrium, post-CHF heat transfer experiment data and correlation comparison report
[TIS5-009331] 23 p3932 N85-34371

VAPORIZING
NT BOILING
NT COAL GASIFICATION
NT EVAPORATION
NT EVAPOTRANSPIRATION
NT FILM BOILING
NT FLASHING (VAPORIZING)
NT NUCLEATE BOILING
NT PROPELLANT EVAPORATION
NT SUBLIMATION
NT TRANSPIRATION
Vaporization behavior of chromium phosphides. The solid 2-phase regions CrP-Cr12P7, Cr12P7-Cr3P, and Cr3P-Cr
[AD-A145481] 02 p0172 N85-11152
Volatile elements in and on lunar volcanic glasses: What do they tell us about lunar genesis?
04 p0584 N85-13728
Vaporization behavior, phase equilibria, and thermodynamic stabilities of nickel phosphides
[AD-A146683] 06 p0765 N85-14897
Methanol vaporization: Effects on volumetric efficiency and on determination of optimum fuel delivery system
[PB84-243914] 09 p1302 N85-18151
Initial results for supercritical cycle experiments using pure and mixed-hydrocarbon working fluids
[DE84-017008] 09 p1345 N85-18460
Carbon vaporization/condensation effects
[NASA-TM-87430] 10 p1436 N85-19048
Dissociated methanol citation
[DE85-000505] 10 p1458 N85-19188
Analysis of phase composition of products of laser destruction of metallic surfaces
11 p1600 N85-20064
Theta pinch discharges for solids vaporization and elemental chemical analysis
[DE85-002968] 11 p1733 N85-20899
Studies on the processing methods for extraterrestrial materials
[NASA-CR-175778] 18 p2716 N85-26768
Crystal growth from the vapor in low gravity environments
[DE85-009628] 18 p3195 N85-29816
Effects of ambient pressure on the instability of a liquid boiling explosively at the superheat limit
[DE85-009476] 23 p3932 N85-34370
Monitoring dosage of volatile compounds in tests at low barometric pressure 23 p3954 N85-34506

VAPORS
NT METAL VAPORS
NT SODIUM VAPOR
NT WATER VAPOR
Experimental and theoretical study of condensation in multicomponent vapors
[DE84-015610] 02 p0174 N85-11164
VOC emissions from volatile organic liquid storage tanks: Background information for proposed standards
[PB84-237320] 04 p0532 N85-13403
Pharmacokinetic interactions of mixtures
[AD-P004032] 06 p0844 N85-15382
Mass spectrometry/mass spectrometry as a screening method for detecting explosive vapors
[DE85-001276] 09 p1292 N85-18110
Experimental and theoretical study of condensation in multicomponent vapors
[DE85-000843] 10 p1485 N85-19376
Photo-thermal detection of the onset of photo-chemical nucleation (laser-snow) in vapor
[AD-A150111] 12 p1801 N85-21295
The detonation of aerosols and vapors of combustible substances under controlled conditions. Part 1: Construction of a test installation
[ISL-R-109/83-PT-1] 14 p2254 N85-23966
Vapor explosions in superheated liquids and fundamental studies of the physics of detonation
[AD-A151362] 15 p2504 N85-25447
Development of a new faster process for the fabrication of ceramic fiber-reinforced ceramic composites by chemical vapor infiltration
[DE85-007550] 16 p2756 N85-27007
Performance of an active/passive hybrid solar system utilizing vapor transport
[DE85-006627] 17 p2968 N85-28466
Dynamics of vapor explosions
[DE85-006845] 18 p3101 N85-29194
Surface acoustic wave devices as chemical vapor microsensors
[AD-A153752] 18 p3177 N85-29698
Vapor-screen technique for flow visualization in the Langley Unitary Plan Wind Tunnel
[NASA-TM-86364] 19 p3214 N85-29929
Catalytic hydrotreatment studies with model compounds
[DE85-010167] 19 p3236 N85-30064
Enhanced thermal coupling by a repetitively pulsed laser
[AD-A154435] 19 p3276 N85-30317
Laser-induced fluorescence measurement of vapor concentration surrounding evaporating droplets
[DE85-009409] 19 p3277 N85-30320
Status of boron combustion research
[AD-A154782] 21 p3563 N85-32160
Silicon refinement by chemical vapor transport
21 p3609 N85-32412
A crew exposure study. Phase II. Volume 2. At sea. Part A
[AD-A155233] 21 p3666 N85-32774
Photofragment fluorescence as a sensitive probe for gas-phase alkali compounds and their photochemistry
[DE85-010707] 22 p3748 N85-33219
New and revised methods of purifying mercuric iodide
[DE85-011684] 22 p3749 N85-33237
Drying of pulverized material with heated condensible vapor
[DE85-011656] 22 p3783 N85-33438

VARACTOR DIODES
Maser cavity servo-tuning system
[NASA-CASE-NPO-15890-1-CU]
18 p3093 N85-29143

VARACTORS
U VARACTOR DIODES
VARIABILITY
Variability of major organic components in aircraft fuels. Volume 3: Sample data package for the reference JP-4 fuel
[AD-A145483] 02 p0188 N85-11254
Climatological variability in modeling of long-term regional transport and deposition of air pollutants
[DE84-014726] 04 p0539 N85-13430
An analysis of kinetic response variability
05 p0707 N85-14533
A survey for photometric variability from space
09 p1251 N85-17897
Evaluating the variability of ceramics with X-ray fluorescence
[DE85-002028] 10 p1453 N85-19155
Variability of cardiac rhythm during information loading
10 p1525 N85-19619
Middle Atmosphere Program. Handbook for MAP, volume 5
[NASA-CR-175481] 11 p1656 N85-20434
A catalogue of dynamic parameters describing the variability of the middle stratosphere during the northern winters
11 p1656 N85-20435
Long term variability of the IO torus
11 p1760 N85-21070
Ozone Correlative Measurements Workshop
[NASA-CP-2362] 13 p2105 N85-23112
Scientific requirements for ozone measurements
13 p2105 N85-23113
Influence of spatial variability of hydraulic characteristics of soils on surface parameters obtained from remote sensing data in infrared and microwaves
[NASA-TM-77902] 20 p3477 N85-31604
Observations of Cygnus X-3 above 10(15) eV from 1979 - 1984
[OG-2.1-8] 22 p3863 N85-33923
Variability in the high energy gamma ray emission from Cyg X-3 over a two-year period (1983 - 1984) at E 4 x 10(11) eV
[OG-2.1-11] 22 p3864 N85-33927
A search in the COS-B data base for correlated time variability in regions containing objects of interest
[OG-2.5-9] 22 p3869 N85-33964
Effect of precipitation variables on the specific surface and explosion characteristics of pentaerythritol tetranitrate
[DE85-009620] 23 p3922 N85-34302
VARIABLE AREA WINGS
U TRAILING EDGE FLAPS
VARIABLE CYCLE ENGINES
Supersonic cruise technology
[NASA-SP-472] 18 p3057 N85-28912
Variable cycle engine for high altitude aircraft
[AD-D011705] 19 p3221 N85-29869
VARIABLE GEOMETRY STRUCTURES
Variable geometry Darrieus wind machine
[PB84-207281] 01 p0068 N85-10453
Variable geometry truss concept
[REPT-614] 12 p1865 N85-21697
Stability of cylindrical shells with variable thickness under external pressure 17 p2943 N85-28164
VARIABLE LIFT
U LIFT
VARIABLE MASS SYSTEMS
The fragmentation of molecular clouds and the IMF
05 p0740 N85-14759
The influence of stellar luminosity and temperature calibration on the determination of the initial mass function 05 p0740 N85-14760
VARIABLE PITCH PROPELLERS
Circulation control propellers for general aviation, including a BASIC computer program
[NASA-CR-165968] 19 p3219 N85-29959
VARIABLE STARS
NT CATACLYSMIC VARIABLES
NT CEPHEID VARIABLES
NT DWARF NOVAE
NT HERCULES NOVA
NT NOVAE
NT SUPERNOVAE
NT SYMBIOTIC STARS
NT T TAURI STARS
Simultaneous photometry and radial velocities of dwarf cepheids and Delta Scuti stars
01 p0128 N85-10876
Spectroscopic data for globular cluster giants. 1: Stars of the red giant tip 01 p0129 N85-10885
Nonradial pulsation and mass loss in early B stars
08 p1232 N85-17759
EXO 1102.8+2539, an X-ray variable Active Galactic Nucleus (AGN) 08 p1239 N85-17816
A statistical evaluation of the limitations of single-channel intermediate-band photoelectric stellar photometry 08 p1251 N85-17900
Study of the pulsations of the ZZ Ceti stars
09 p1414 N85-18923
White dwarf stars at ultraviolet wavelengths
11 p1744 N85-20971
IUE observations of the jet emission feature in R Aquarii 11 p1747 N85-20966
IUE and ESO observations of the P Cyg star AG Carinae and its ring nebula 11 p1750 N85-21006
Coordinated ultraviolet and visual observations of Omega Orionis 1982-1983 11 p1750 N85-21007
The outburst and long term behavior of the triple period cataclysmic variable TV Col 11 p1752 N85-21021
New results on PU VUL 11 p1753 N85-21023
The UV extinction of HR 5999
11 p1753 N85-21026
The fading of R coronae borealis
11 p1753 N85-21029
Observations of RR Lyrae and X Arietis with the IUE satellite 11 p1754 N85-21030
Atmospheric properties of RU Lupi derived from high- and low-resolution IUE spectra
11 p1754 N85-21031
Mg 2 emission of Pop. 2 long-period Cepheids
11 p1754 N85-21032
Blue companions of Cepheids
11 p1754 N85-21033
Observations of cataclysmic variable star winds
11 p1755 N85-21041
Three short-period binaries seen at high-dispersion UX ARI, ICTA TRI and HA5110 11 p1756 N85-21047
A model for eclipsing cataclysmic variables
13 p2171 N85-23467
Offerings of the Astronomical Institute of Bonn
15 p2667 N85-26459
Photoelectric observations of the eclipsing binary V 836 Cygni
[REPT-98] 15 p2668 N85-26462
Measurement and theory of turbulence in RR Lyrae
[DE85-005899] 15 p2669 N85-26471
Long-term observations of Cyg X-3 with Vela 5B
[DE85-005556] 15 p2686 N85-26586
Galactic gamma-ray sources, SNOBs, and giant H2 regions
[OG-2.5-4] 22 p3869 N85-33961
VARIABLE SWEEP WINGS
Transonic aerodynamic and aeroelastic characteristics of a variable sweep wing
[NASA-TM-86677] 15 p2462 N85-25203
VARIABLE THRUST
Orbital maneuvers with finite thrust. Volume 1: Mathematical formulation, numerical methods, catalog concept
[ESA-CR(P)-1910-VOL-1] 06 p0758 N85-14848
Orbit maneuvers with finite thrust. Volume 2: Reference manual, part 1
[ESA-CR(P)-1910-VOL-2-PT-1]
06 p0758 N85-14849
Orbit maneuvers with finite thrust. Volume 3: User's guide, part 2
[ESA-CR(P)-1910-VOL-3-PT-2]
06 p0758 N85-14850
Orbit maneuvers with finite thrust. Volume 3: Reference catalog, parts 1 and 2
[ESA-CR(P)-1910-VOL-3-PT-1/2]
06 p0758 N85-14851
Orbit maneuvers with finite thrust. Volume 3: Reference catalog, part 3
[ESA-CR(P)-1910-VOL-3-PT-3]
06 p0758 N85-14852
VARIANCE (STATISTICS)
NT ANALYSIS OF VARIANCE
NT BIVARIATE ANALYSIS
NT COVARIANCE
NT MULTIVARIATE STATISTICAL ANALYSIS
NT REGRESSION ANALYSIS
Construction of a confidence region for linear functions with unknown parameters
[CTH-MATH-1984-17] 05 p0721 N85-14830
Geostatistics for resource and reserve estimation
[PB85-105781/GAR] 07 p0989 N85-16286
Screwi plots, and letter and blettter strips
[DE85-001409] 11 p1707 N85-20739
Optimal designs for comparisons between two sets of treatments
[AD-A150621] 13 p2152 N85-23360
Censored observations, repeated measures and mixed effects models: An approach using the EM algorithm and normal errors
[MATHEMATICS-RESEARCH-183]
15 p2636 N85-26256
Studies in quality improvement. Part 1: Dispersion effects from fractional designs, revised
[AD-A153516] 18 p3119 N85-29308
VARIATION METHOD
U CALCULUS OF VARIATIONS
VARIATIONAL PRINCIPLES
Variational principles in thermoplasticity. Part 2: Coupled thermomechanical processes
[RUB-IFM-MITT-37-PT-2] 05 p0648 N85-14161
Surface reconstruction preserving discontinuities
[AD-A146741] 07 p1028 N85-16526
The principle of virtual work and associated variational principles
[ESA-TT-873] 09 p1340 N85-18428
Symmetric primal-dual variational formulations of coupled dynamic systems: Three-dimensional elasticity, shells, fluid-structure interaction
[ONERA-1983-91] 12 p1863 N85-21684
On Hybrid and mixed finite element methods
[NASA-CR-175551] 13 p2101 N85-23096
On an iterative scheme for the solution of constrained variational equations
[CSIR-TWISK-341] 13 p2149 N85-23342
Lyapunov stability of very simple steady solutions of prognostic systems 14 p2333 N85-24429
Finite element methods in space mathematics
14 p2396 N85-24757
Axisymmetric magnetofluidistatic (MFS) equilibria of solar coronal loops: An integral equation approach
14 p2449 N85-25118
Variational bounds on Darcy's constant
[DE85-006638] 15 p2580 N85-25916
Variational bounds on Darcy's constant
[DE85-008959] 18 p3101 N85-29195
VARIATIONS
NT ANNUAL VARIATIONS
NT DIURNAL VARIATIONS
NT GEOMAGNETIC PULSATIONS
NT MAGNETIC VARIATIONS
NT NOCTURNAL VARIATIONS
NT PERIODIC VARIATIONS
NT SECULAR VARIATIONS
NT WIND VARIATIONS
Measurement of areal mass variation in Rayleigh-Taylor unstable targets
[AD-A145541] 02 p0198 N85-11325
Determination of geoid undulations and ocean heights from ERS-1 radar altimetry data
03 p0361 N85-12432
Spectral model for subtidal variability in the Chesapeake Bay
[PB84-226679] 06 p0842 N85-15345
Efficient scores, variance decompositions and Monte Carlo swindles
[AD-A146673] 06 p0858 N85-15458
Fluctuation phenomena studies in chemically sensitive field effect transistors. Part 2: Corrosion of silicon oxynitride
[AD-A148227] 08 p1157 N85-17302
The ground based photometric limitations to the search for light variations due to 5-minute solar-type oscillations in other stars 08 p1251 N85-17898
NMR study on rotational fluctuation in solid hydrogen and deuterium 09 p1289 N85-18093
Discovery about temperature fluctuations in turbulent air flows 10 p1500 N85-19466
Twilight intensity variation of the infrared hydroxyl airglow 11 p1663 N85-20481
Space and time variations and turbopause dynamical structure 11 p1663 N85-20483
Variability of ultraviolet emission lines in the carbon star TX Psc 11 p1753 N85-21027
The portable LISP translation tool
[AD-A149765] 12 p1915 N85-22023
Observation of cosmic ray flux variations in stratosphere 13 p1981 N85-22430
Variations in resistivity of upper crustal layer
13 p2113 N85-23164
Method for processing broad-profile data
13 p2117 N85-23165
The relationship between marine aerosol particles and satellite-detected radiance 13 p2131 N85-23263
VAS/model impact study 15 p2597 N85-26006
Measuring electrical field fluctuations by Langmuir Double Probe Method 16 p2720 N85-26789
Probabilistic finite element: Variational theory
17 p2913 N85-27957
Energy sources of the dominant frequency dependent 3-dimensional atmospheric modes
18 p3143 N85-29462
On the characterization of nonnegatively estimable linear combinations of variance components
[AD-A153786] 18 p3174 N85-29678
Emittance growth caused by current variation in a beam-transport channel
[DE85-010743] 19 p3363 N85-30849
Intermittency, conditional sampling and turbulent combustion 20 p3424 N85-31249
Magnetospheric response to solar wind variations
[DE85-010762] 20 p3547 N85-32074

On the transformation regularities of time series of solid aerosol concentrations in the surface atmospheric layer
21 p3645 N85-32648
Object identification and manipulation using silhouette moments
[AD-A154755] 21 p3705 N85-33011
Optical output stabilization method for direct current arc lamps
[AD-A154987] 21 p3705 N85-33013
Impact of fluctuations in optical properties of atmosphere on the ratio of spectral brightness from remote sensing of agricultural land 22 p3734 N85-33149
Gamma-ray burst variability above 4 MeV
[OG-1.2-7] 22 p3862 N85-33917
Cosmic ray intensity variations at primary rigidities near 1900 GV
[OG-5.3-0] 22 p3885 N85-34075
The final COS-B database: In-flight calibration of instrumental parameters
[OG-9.3-9] 23 p4026 N85-34964
The effect of the interplanetary magnetic field on sidereal variations observed at medium depth underground detectors
[SH-4.4-5] 23 p4033 N85-35003
Corrected sidereal anisotropy for underground muons
[SH-4.4-7] 23 p4033 N85-35005
Sidereal anisotropy of cosmic rays
[SH-4.4-8] 23 p4034 N85-35006
A study of periodicities and recurrences in solar activity and cosmic ray modulation
[SH-4.4-14] 23 p4034 N85-35010
Altitude variations of cosmic-ray soft and hard components observed by airborne detectors
[SH-8.1-5] 23 p4045 N85-35079
The effects of parameter variation on helicopter performance
[AD-A156027] 24 p4064 N85-35189
Cluster variation study of coherent ordering in FCC and BCC solid solutions
[AD-A156039] 24 p4079 N85-35260
The measurement of nitrogen oxide (NO, NO2) exchange over plant/soil surfaces
[CSIRO-DAR-TP-8] 24 p4127 N85-35587
Muon fluctuation studies of EAS 10(17) eV
[HE-4.3-9] 24 p4191 N85-36003

VARIOMETERS
Primary processing of experimental magnetovariation sounding data using spline functions
13 p2115 N85-23175

VARISTORS
Advanced metal oxide varistor concepts
[DE84-016877] 09 p1316 N85-18276
Effects of processing chemistry on electrical properties of high field ZnO varistors
[DE85-007688] 17 p2956 N85-28254
A study of Co and Mn in ZnO varistors
[DE85-011193] 19 p3263 N85-30233
Long-term research in Japan: Amorphous metals, metal oxide varistors, high-power semiconductors and superconducting generators
[DE85-010827] 22 p3748 N85-33230

VARNISHES
Evaluation of properties of varnishes, exterior stains and exterior primers
[PB84-243948] 08 p0772 N85-14940

VASCULAR SYSTEM
NT ARTERIES
NT BLOOD VESSELS
NT VEINS
Modulated sinusoidal currents in management of vibration sickness 10 p1524 N85-19612
Specifics of human thermal regulatory reactions upon exposure to coriolis acceleration
10 p1525 N85-19617

VASOCONSTRICTION
Endocrine responses to hypotensive gravitational stress: Catecholamines, pancreatic polypeptide, and vasopressin 05 p0693 N85-14460

VASOMOTOR NERVOUS SYSTEM
U NERVOUS SYSTEM

VATOL AIRCRAFT
Preliminary performance of a vertical-attitude takeoff and landing, supersonic cruise aircraft concept having thrust vectoring integrated into the flight control system
[NASA-CR-172530] 10 p1423 N85-18977
Ground effect on helicopter aerodynamics and stability
20 p3395 N85-31063

VAX COMPUTERS
NT VAX-11 SERIES COMPUTERS
NT VAX-11/780 COMPUTER
Introduction to LBL graphics
[DE85-000389] 09 p1369 N85-18600
Scientific data bases on a VAX-11/780 running VMS
[DE85-007925] 16 p2878 N85-27760
Report on the SLC control system
[DE85-013078] 24 p4148 N85-35722

VAX-11 SERIES COMPUTERS
NT VAX-11/780 COMPUTER
Digital Equipment Corp., VAX-11/782, VAX FORTRAN version 4.0
[PB84-227701] 03 p0406 N85-12582
Implementation of the computer program-system MOSS (Map Overlay and Statistical System) on a VAX-11 series computer under VMS
[AD-A149612] 12 p1914 N85-22019
A system identification package for VAX and LSI 11
[OUEL-1569/85] 20 p3516 N85-31862
Parallel processing on the Livermore VAX 11/780-4 parallel processor system with compatability to Cray Research, Inc. (CRI) multitasking, version 1
[DE85-011856] 23 p3967 N85-34595

VAX-11/780 COMPUTER
Multiplexing the ethernet interface among VAX/VMS users
[AD-A145539] 02 p0243 N85-11568
Digital Equipment Corporation VAX Ada Compiler Version T0.6-2 VAX-11/785, 11/750, 11/730, using VMS, Version 4.0 and MicroVAX 1, using MicroVMS Version 1.0
[AD-A149375] 10 p1538 N85-19696
Integrated Support Software System (ISSS)
[AD-A155715] 22 p3829 N85-33710

VCE
U VARIABLE CYCLE ENGINES

VCO
U VOLTAGE CONTROLLED OSCILLATORS

VECTOR ANALYSIS
NT COLLINEARITY
NT COPLANARITY
NT VORTICITY
Cores of tangent cones and Clarke's tangent cone
[CSIR-TWISK-314] 01 p0108 N85-10727
Constrained optimization using iterated partial Kuhn-Tucker vectors
[AD-A145476] 02 p0251 N85-11641
Wind shear measuring on board an airliner
[NASA-TM-77463] 03 p0395 N85-12521
Techniques for vector quantization
[AD-A147052] 07 p1030 N85-18539
Belief structures
[AD-A147526] 07 p1098 N85-18575
Robust prediction and interpolation for vector stationary processes, part 3
[AD-A147660] 07 p1036 N85-18579
Development of a 20/30 GHz receiving station for propagation experiments with L-SAT
[AD-A148261] 08 p1152 N85-17271
A moving finite element method for time dependent partial differential equations with error estimation and refinement
[AD-A147719] 08 p1210 N85-17617
Vectorization and implementation of an efficient multigrid algorithm for the solution of elliptic partial differential equations
[AD-A149049] 10 p1545 N85-19743
Characteristic vector analysis of inflection ratio spectra: New technique for analysis of ocean color data
[NASA-TP-2428] 13 p2126 N85-23237
Dynamics of solid body with ellipsoidal cavity containing magnetic fluid 14 p2279 N85-24116
Proposal for an extended set of FORTRAN Basic Linear Algebra subprograms
[DE85-007241] 16 p2848 N85-27582
The role of ellipticity and normality assumptions in formulating live-boundary conditions in elasticity
[AD-A153475] 18 p3168 N85-29630
Magnetic field-vector measurements in quiescent prominences via the Hanle effect: Analysis of prominences observed at Pic-du-Midi and at Sacramento Peak
18 p3208 N85-29898
Inferred flows of electric currents in solar active regions 18 p3208 N85-29899
Comparisons of simultaneous vector magnetograms
18 p3208 N85-29900
Evidence for submergence of magnetic flux in a growing active region 18 p3208 N85-29902
Graphic displays of vector magnetograph data
18 p3209 N85-29904
High accuracy digital acousto-optic matrix computer
[AD-D011692] 19 p3343 N85-30716
Vector calculation of particle code
23 p3981 N85-34688
Invariant tests and likelihood ratio tests for multivariate elliptically contoured distributions
[AD-A155844] 24 p4142 N85-35679

VECTOR CALCULUS
U VECTOR SPACES

VECTOR CONTROL
U DIRECTIONAL CONTROL

VECTOR MESONS
Skyrmions and vector mesons: A symmetric approach
[DE84-015297] 04 p0563 N85-13584
Does low-energy physics depend on the potential of a heavy Higgs-particle
[NIKHEF-H/85-1] 22 p3838 N85-33763

VECTOR SPACES
NT ADJOINTS
NT BANACH SPACE
NT CANONICAL FORMS
NT EIGENVALUES
NT EIGENVECTORS
NT HILBERT SPACE
NT JORDAN FORM
NT MATRICES (MATHEMATICS)
NT SOBOLEV SPACE
NT STATE VECTORS
NT STIFFNESS MATRIX
NT STOKES THEOREM (VECTOR CALCULUS)
NT VECTORS (MATHEMATICS)
NT VORTICITY
Aerospatiale's experimentations of vectorization on supercomputers for aircraft structural problems
01 p0007 N85-10041
Comparative analysis of the clustering of the LPC coefficients in phoneme recognition
[FUB-39-1983] 01 p0041 N85-10284
Trilinear alternating forms on a vector space of dimension 7
[CWI-PM-R8402] 05 p0722 N85-14844
Schubert varieties are arithmetically Cohen-Macaulay
16 p2853 N85-27592
The vector potential in a branched Riemann space
[VTH-LR-395] 16 p2856 N85-27614
The global structure of magnetic fields which support quiescent prominences 18 p3204 N85-29876
A classification vocoder: A very low rate speech transmission by vector quantization of the spectrum
[ENST-84D003] 20 p3441 N85-31356
Study of new computing algorithms for supercomputers. Application to parallel processing computation
[SNIAS-440-070/84] 20 p3516 N85-31860
Simulation of complex three-dimensional flows
[NASA-TM-86773] 21 p3675 N85-32831
On the convergence of an iterative formulation of the electromagnetic scattering from an infinite grating of thin wires 24 p4065 N85-35319

VECTORS (MATHEMATICS)
NT EIGENVECTORS
NT STATE VECTORS
NT VORTICITY
Some concepts in multi-criteria optimization
[CSIR-TWISK-299] 01 p0108 N85-10722
What is principal components analysis?
02 p0211 N85-11389
The information in the minor principal components
02 p0211 N85-11391
Techniques for vector quantization
[AD-A147052] 07 p1030 N85-18539
Determining vector of radiointerferometer base from observations of natural radio emission with narrow spectrum 13 p2112 N85-23158
Schur-Ostrowski theorems for functionals on l1(0,1)
[AD-A150193] 13 p2150 N85-23348
Organization of conveyor processing of vector commands in multiprocessor computer systems with a reorganizable structure 14 p2401 N85-24799
Spline techniques for magnetic fields
[DE85-004919] 14 p2415 N85-24902
Recent trends in software technology for vector processors 16 p2891 N85-28615
Recent developments in nonlinear normal mode initialization 18 p3142 N85-29451
Development of an optimum interpolation analysis method for the CYBER 205 18 p3143 N85-29456
Measurements of Solar Vector Magnetic Fields
[NASA-CP-2374] 18 p3203 N85-29869
The vector structure of active magnetic fields
18 p3203 N85-29870
Trends in measurement of solar vector magnetic fields using the Zeeman effect 18 p3204 N85-29877
Measurements of vector fields with diode array
18 p3204 N85-29880
Analysis of the new polarimeter for the Marshall Space Flight Center vector magnetograph
18 p3205 N85-29881
The solar vector magnetograph of the Okayama Astrophysical Observatory 18 p3205 N85-29882
Generation and transfer of polarized radiation in the solar atmosphere: Physical mechanisms and magnetic-field diagnostics 18 p3206 N85-29890
Optimizing data access in the LAMPF control system
[DE85-012653] 24 p4140 N85-35663

VEGA LAUNCH VEHICLE
Kovtunenko comments on Vega flight plan, instrumentation 15 p2482 N85-25318

VEGA PROJECT
The Venus Balloon Project 10 p1465 N85-19243

The International VEGA 'Venus-Halley' (1984-1986 experiment: Description and scientific objectives
[NASA-TM-77536] 12 p1980 N85-22324
USSR report: Space
[JPRS-USP-85-001] 13 p1977 N85-22403
Comments on Vega mission 15 p2462 N85-25319
Press conference on flight of Vega spacecraft 15 p2462 N85-25320
TASS update on flights of Vega-1 and Vega-2 16 p2722 N85-26803
Kovtunenko discusses Vega Project 16 p2722 N85-26804
French and West German equipment for Vega Project 16 p2722 N85-26805

VEGA ROCKET VEHICLE
U VEGA LAUNCH VEHICLE

VEGETABLES
NT POTATOES
Multi crop area estimation in Idaho using EDITOR
[E85-10054] 06 p0827 N85-15251
Packaging for food service 14 p2394 N85-24747

VEGETATION
NT CANOPIES (VEGETATION)
The Multispectral Imaging Science Working Group. Volume 1: Executive summary
[E85-10001] 02 p0213 N85-11404
The Multispectral Imaging Science Working Group. Volume 2: Working group reports
[E85-10002] 02 p0213 N85-11405
Botanical sciences team 02 p0214 N85-11407
Late quarterly glaciolacustrine and vegetational history of the Copper River Basin, south-central Alaska 03 p0391 N85-12499
Scattering models in the microwave regime
[NASA-CR-174001] 04 p0525 N85-13361
Scattering from randomly oriented scatterers of arbitrary shape in the low-frequency limit with application to vegetation 04 p0525 N85-13362
Scattering from randomly oriented circular discs with application to vegetation 04 p0525 N85-13363
A comparison between active and passive sensing of soil moisture from vegetated terrains 04 p0526 N85-13364
Monitoring and mapping global vegetation cover using data from meteorological satellites 05 p0656 N85-14211
Integration of multispectral data obtained at different view angles for vegetation analysis 05 p0657 N85-14218
Classification of vegetation communities in the Battle Mountain SE quadrangle, Nevada with MSS digital data
[E85-10043] 06 p0826 N85-15246
An integrated LANDSAT/ancillary data classification of desert rangeland
[E85-10046] 06 p0826 N85-15248
An integrated remote sensing approach for identifying ecological range sites — parker mountain
[E85-10050] 07 p0983 N85-16246
Microwave and optical remote sensing of forest vegetation 06 p1146 N85-17228
Remote sensing of soil moisture 06 p1149 N85-17252
North American vegetation patterns observed with the NOAA-7 advanced very high resolution radiometer — North America
[E85-10062] 08 p1174 N85-17400
Shortwave infrared detection of vegetation
[E85-10064] 08 p1174 N85-17402
An integrated GIS/remote sensing data base in North Cache soil conservation district, Utah: A pilot project for the Utah Department of Agriculture's RIMS (Resource Inventory and Monitoring System)
[E85-10073] 10 p1504 N85-19487
Preliminary evaluation of the airborne imaging spectrometer for vegetation analysis
[NASA-CR-174440] 10 p1505 N85-19488
Vegetation analysis for arid lands geobotany
[NASA-CR-175455] 10 p1506 N85-19500
Thematic Mapper spectral dimensionality and data structure 12 p1871 N85-21736
Investigations of vegetation and soils information contained in LANDSAT Thematic Mapper and Multispectral Scanner data
[E85-10082] 12 p1873 N85-21747
Air quality criteria for ozone and other photochemical oxidants, external review draft, volume 3
[PB85-126050] 12 p1886 N85-21837
Preliminary comparisons of the information content and utility of TM versus MSS data 13 p2120 N85-23202
The microwave propagation and backscattering characteristics of vegetation — wheat, sorghum, soybeans and corn fields in Kansas
[E85-10088] 13 p2122 N85-23213
Microwave remote sensing of soil moisture 13 p2125 N85-23235
Atlas of archived vegetation, land-use and seasonal Albedo data sets
[NASA-TM-86199] 14 p2346 N85-24506
Soil moisture and evapotranspiration estimates based on satellite data 15 p2596 N85-25998
Use of Goudrian model in studying laws of reflection in vegetation-soil system in optical range. 2: Influence of illumination conditions on spectral brightness coefficients 16 p2726 N85-26827
Microwave model prediction and verifications for vegetated terrain
[E85-10102] 16 p2809 N85-27322
Function of remote sensing in Brazil
[INPE-3314-PRE/621] 16 p2810 N85-27329
Impact of ozone on vegetation
[PB85-159937] 16 p2821 N85-27403
Airphoto interpretation of vegetation and landforms for soil mapping 17 p2963 N85-28436
Permafrost, seasonally frozen ground, snow cover and vegetation in the USSR
[AD-A153628] 18 p3124 N85-29346
Influence of land surface processes on the Indian monsoon: A numerical study 18 p3146 N85-29478
Space imagery and some geomorphological problems of the Guiana Shield, South America 21 p3602 N85-32368

VEGETATION GROWTH
NT CROP GROWTH
Remote sensing applied to forest resources
[E85-10012] 02 p0216 N85-11425
Terrestrial nitrogen cycles: Some unanswered questions 05 p0653 N85-14192
Image texture study for the operational meteorological satellites NOAA 6 and NOAA 7 and its variation with time. Application to the Beauce region
[ENST-84E009] 05 p0661 N85-14249
Simulating responses to expected climate change in eastern North America: Applications to decision-making in the forest industry
[DE85-001272] 07 p1008 N85-16406
Effects of low temperatures on the growth and unfrozen water content of an aquatic plant
[AD-A147107] 07 p1011 N85-16424
Controlled ecological life support system higher plant flight experiments
[NASA-CR-177323] 07 p1020 N85-16471
Spectral characterization of the LANDAT-4 MSS sensors 11 p1666 N85-20499
NOAA-AISC user's guide for implementing CERES wheat model for large area yield estimation
[E85-10085] 12 p1873 N85-21750
Estimating solar radiation for plant simulation models
[E85-10089] 12 p1873 N85-21751
Modular plant culture systems for life support functions
[NASA-CR-171853] 12 p1899 N85-21924
Transduction of the root gravitropic stimulus: Can apical calcium regulate auxin distribution? 15 p2606 N85-26063
Attempts to localize and identify the gravity sensing device of plant seedlings 15 p2607 N85-26064
Daylily as a system to study effects of space flight on plant development 15 p2607 N85-26068
Importance of gravity for plant growth and behavior 15 p2608 N85-26070
Mechanical stress regulation of plant growth and development 15 p2610 N85-26087
Mutant peas as probes in the understanding of growth and gravitropism 15 p2611 N85-26088
Plant growth biophysics: The basis for growth asymmetry induced by gravity 15 p2611 N85-26089
An indirect role for ethylene in shoot-inversion release of apical dominance in Pharbitis nil 15 p2611 N85-26090
Gravity perception and response in shoot of cereal grasses 15 p2611 N85-26091
Participation of ethylene in two modes of gravistimulation of shoots 15 p2613 N85-26101
Isolation of hybridomas for golgi-associated proteins and a plant calmodulin 15 p2613 N85-26103
Differential wall growth in gravistimulated corn roots: Its timing and regulation 15 p2614 N85-26105
Use of forest modeling to project acid rain effects
[DE85-005251] 16 p2821 N85-27400
Hydroponics developments for spaceship garden 21 p3663 N85-32754
Regression analysis of aircraft and ground measurement data on vegetation cover 22 p3735 N85-33156

VEGETATIVE INDEX
Effects of atmospheric water vapor and clouds on NOAA (National Oceanic and Atmospheric Administration) AVHRR (Advanced Very High Resolution Radiometer) satellite data
[AD-A145425] 02 p0280 N85-11824
Remote sensing of coastal wetlands biomass using Thematic Mapper wavebands — Lewes, Delaware 13 p2119 N85-23198

VEHICLE WHEELS
Performance evaluation of automotive wheel bearing greases
[AD-A145948] 03 p0337 N85-12168
Orbiter wheel and tire certification 08 p1101 N85-16959
Prediction of in-sand tire and wheeled vehicle drawbar performance
[AD-P004265] 09 p1404 N85-18841
Proceedings of the 8th International Conference on the Performance of Off-Road Vehicles and Machines, volume 2
[AD-A148635] 09 p1407 N85-18859
The research of driving wheel with movable lugs of the paddy field floating tractor
[AD-P004283] 09 p1407 N85-18860
An investigation of the driving wheel thrust of paddy field tractors
[AD-P004284] 09 p1407 N85-18861
Behaviour of soil under a lugged wheel
[AD-P004287] 09 p1407 N85-18864
The analysis on the dynamic performance of a single lug
[AD-P004289] 09 p1408 N85-18866
A simple prediction model for soil compaction under various wheel loads and geometries as an aid to vehicle design
[AD-P004298] 09 p1409 N85-18875
The guidelines to design the lever turning gears in articulated vehicles
[AD-P004301] 09 p1409 N85-18878
Skid steering of wheeled and tracked vehicles: Analysis with Coulomb friction assumptions
[AD-A149626] 12 p1860 N85-21664

VEHICULAR TRACKS
Improvements in tank tread assemblies
[NASA-CASE-NPO-16321-1] 18 p3117 N85-29291

VEINS
Reaction of cerebral ventricles to antiorthostatic position and occlusion of jugular veins 01 p0093 N85-10626
Effect of maximum physical load on oxygen-transport properties of blood 01 p0093 N85-10627
The influence of angiotensin on the maintenance of venous tone. The effect of Lower Body Negative Pressure (LBNP) and angiotensin blockade 05 p0693 N85-14457
Hemodynamics and plasma arginine vasopressin during water immersion in normal man 05 p0693 N85-14458

VELA SATELLITES
X-ray emission from Centaurus A — Vela 5B; radio galaxy 08 p1239 N85-17813
Long-term observations of Cyg X-3 with Vela 5B
[DE85-005556] 15 p2686 N85-26586

VELOCITY
NT ACOUSTIC VELOCITY
NT AIRSPEED
NT ANGULAR VELOCITY
NT CRITICAL VELOCITY
NT EXHAUST VELOCITY
NT FLOW VELOCITY
NT GROUND SPEED
NT GROUP VELOCITY
NT HIGH SPEED
NT HYPERSONIC SPEED
NT LIGHT SPEED
NT LOW SPEED
NT ORBITAL VELOCITY
NT PHASE VELOCITY
NT PROPAGATION VELOCITY
NT RADIAL VELOCITY
NT RELATIVISTIC VELOCITY
NT ROTOR SPEED
NT SOLAR VELOCITY
NT SOLAR WIND VELOCITY
NT SUBSONIC SPEED
NT SUPERSONIC SPEEDS
NT TIP SPEED
NT TRANSONIC SPEED
NT WIND VELOCITY
Turbine test report, addendum
[DE84-015130] 02 p0205 N85-11353
The influence of inert particulate material on the properties of RDX/polyethylene wax compositions
[MRL-R-929] 03 p0336 N85-12159
Dynamic compression and volatile release of carbonates
[NASA-CR-174076] 03 p0391 N85-12504
Speed test results and hardware/software study of computational speed problem, appendix D 05 p0603 N85-13843
Transonic flow of elastic medium past slender solid body 06 p0778 N85-14976

Speed benefits of tilt-rotor designs for LHX
[NASA-CR-166437] 07 p0902 N85-15717
Free surface effects on the wake of a flat plate
[AD-A146968] 07 p0958 N85-16071
Nondestructive measurement of bulk residual stresses
[AD-A147063] 07 p0978 N85-16211
A low perturbation electron injector for cyclic accelerators
[AD-D011312] 07 p1040 N85-16604
Investigation of the pressure-and velocity-coupled responses of solid propellants using impedance tube method 09 p1300 N85-18168
Metallographic grinding efficiency
[DE85-001520] 09 p1304 N85-18194
The axial velocity spread acceptance of free electron lasers
[AD-A149024] 10 p1489 N85-19403
Initial velocity of the emerging free boundary in a two-phase Stefan problem with imposed flux
[DE85-003813] 11 p1631 N85-20272
Digital temperature and velocity control of mach 0.3 atmospheric pressure durability testing burner rigs in long time, unattended cyclic testing
[NASA-TM-86959] 12 p1805 N85-21321
Speed and accuracy in automated manufacture
[DE85-003913] 12 p1819 N85-21410
Basic studies of gases for fast switches
[AD-A149628] 12 p1835 N85-21514
The performance of an alternating-current thyristor-controlled motor 15 p2546 N85-25716
Empirical development of ground acceleration, velocity and displacement for accidental explosions at J5 or the proposed large altitude rocket cell at Arnold Engineering Development Center
[DE85-008324] 16 p2758 N85-27020
BLAF: A blast field reconstruction program from pressure histories
[AD-A155300] 21 p3585 N85-32283
Numerical solutions of turbulent models for flow over a flat plate with angle of attack
[DE85-010380] 21 p3585 N85-32286
Horizontal and vertical structure of velocity, potential vorticity and energy in the gulf stream
[AD-A154753] 21 p3655 N85-32702
Experimental studies of chemical reactivity during shock initiation of hexanitrostilbene
[DE85-011726] 22 p3754 N85-33270
The design and development of a constant-speed solar array drive 22 p3796 N85-33519
Detonation in tungsten-loaded HMX
[DE85-009606] 23 p3922 N85-34299
Comparison of experimental data on detonation velocity and Chapman-Jouget pressure vs initial HE density with predictions from Ree's model equation of state
[DE85-007268] 23 p3922 N85-34304
Design and lubrication of high-speed rolling-element bearings
[NASA-TM-87107] 23 p3938 N85-34409
Crustal structure in southern California from array data 24 p4115 N85-35512

VELOCITY COUPLING

Coupling between velocity oscillations and solid propellant combustion 13 p2000 N85-22536
Coupled acoustic and hydrodynamic wave instabilities 13 p2000 N85-22538
Investigation of the characteristics of the velocity-coupled response functions of solid propellants 13 p2001 N85-22540
Analysis of combustion oscillations in heterogeneous systems
[AD-A151999] 16 p2745 N85-26942
Measurement of mode interaction due to waveguide surface roughness
[AD-A154039] 19 p3255 N85-30183

VELOCITY DISTRIBUTION

Monte Carlo simulation of thermalization of subexcitation electrons in molecular hydrogen
[NAL-TR-815T] 01 p0117 N85-10798
Numerical analysis of flow and heat transfer in the VAFB LOX storage Dewar tank
[NASA-CR-171203] 02 p0197 N85-11315
NLR activities in the field of wind tunnel wall interference 03 p0313 N85-12024
On the co-variant formulation of the law of motion of passive particles in a field of turbulence
[REPT-564] 03 p0377 N85-12407
Laser anemometer study of separated flow on wing profiles
[ISL-CO-214/83] 04 p0453 N85-12872
Finite element method for a class of viscoelastic flows in deforming domains applied to jet breakup
[DE84-014571] 04 p0500 N85-13186
Study of the velocity-acoustic pressure correlation in a cold jet, centered on the sign and the amplitude of the velocity fluctuations
[ISL-R-124/83] 04 p0501 N85-13193
Experiments on the structure of turbulent reattaching flow 05 p0635 N85-14074
The evolution of a sparse stellar system 05 p0740 N85-14758
The fragmentation of molecular clouds and the IMF 05 p0740 N85-14759
The velocity-age relation for B and A stars 05 p0740 N85-14782
Stability of stellar disk and ratio of halo to disk masses in the galaxy 05 p0740 N85-14783
Laminar separation bubble with transition: Prediction test with local interaction
[BLL-PNR-90231-(8019.3153)] 06 p0808 N85-15132
Molecular clouds within 100 pc 06 p0877 N85-15573
The smallest sizes of diffuse interstellar clouds 06 p0878 N85-15578
Kinematics of nearby gas and stars 06 p0880 N85-15591
Dark matter near the sun: Simulated star counts and the Oort limit 06 p0880 N85-15592
Calculation of the velocity field generated by a helicopter main and tail rotors in hover
[AD-A147731] 08 p1078 N85-16833
On the virtual wall height in open channel flow with large relative roughness 09 p1303 N85-18186
Determination of total pressure losses in stepped annular diffusors with curvilinear outer walls and uniform velocity field at inlet 09 p1306 N85-18203
Feasibility of alpha particle measurement by CO2 laser Thomson scattering
[DE85-001764] 09 p1326 N85-18334
Monte Carlo simulation of electron thermalization in rare gases
[NAL-TR-834T] 09 p1375 N85-18643
Determination of ion temperature and rotation velocity profiles by visible, UV and X-ray spectroscopy on Doublet 3 09 p1388 N85-18734
Behavior of mode frequency characteristics in shallow sea with variation of P-wave veocity in bottom sediment layer and sonic velocity profile in water layer 10 p1498 N85-19457
Surface-slip equations for multicomponent nonequilibrium air flow
[NASA-TM-85820] 12 p1845 N85-21573
Velocity distributions of solar wind ions and electrons 12 p1954 N85-22273
Plasma in the clusters of galaxies 12 p1957 N85-22299
Dilution jet configurations in a reverse flow combustor
[NASA-CR-174886] 13 p1974 N85-22392
Size and velocity distributions of particles and droplets in spray combustion systems
[AD-A150355] 13 p2017 N85-22648
More precise curve of dependance between density and velocity of longitudinal waves in consolidated crust and top of mantle in oceanic structures 13 p2110 N85-23143
Progress on Experimental impact studies 13 p2181 N85-23534
Ring-diameter ratios for multi-ring basins average 2.0(0.5)D 13 p2182 N85-23542
Dependents of velocity distribution in exit section of converging channel on shape of inlet channel in regulating valve 14 p2277 N85-24106
Effect of drag behind nozzle array on its force and energy characteristics 14 p2277 N85-24107
Laser anemometry two dimensional measurement of velocity fluctuations in an excited jet
[ISL-CO-213/83] 14 p2302 N85-24254
Visualization of velocity fields with Doppler images
[ISL-CO-218/83] 14 p2302 N85-24256
Energy structure of atmospheric boundary layer above waves 14 p2335 N85-24442
Localization of sources of equivalent noise in fast cold jets, excited and nonexcited
[ISL-CO-201/83] 14 p2416 N85-24910
Sensitivity of inferred subphotospheric velocity field to mode selection, analysis technique and noise 14 p2442 N85-25065
The effects of image motion on the l-nu diagram 14 p2443 N85-25076
The effects of seeing on noise 14 p2443 N85-25077
Global solar oscillations in irradiance and velocity: A comparison 14 p2446 N85-25094
Investigation of potential and viscous flow effects contributing to dynamic stall
[AD-A151696] 15 p2557 N85-25773
Study of the coupling between average, coherent and turbulent fields in a circular excited free jet
[ISL-R-115/83] 16 p2785 N85-27184
Multinomial form of the solution of problems of the statistics of elastic rectangular disks
[REPT-17/1984] 16 p2797 N85-27244
Feasibility of mapping velocity flow fields in SSME powerhead by laser anemometry techniques 17 p2915 N85-27971
Least squares inversion of Stokes profiles in the presence of velocity gradients 18 p3207 N85-29992
Generation of capillary instabilities by external disturbances in a liquid jet
[NASA-TM-87041] 19 p3265 N85-30248
Geometry, velocity structure and penetration depths of descending slabs in the western Pacific 19 p3319 N85-30574
A comparison of laser Doppler anemometry and probe measurements within the boundary layer of an airfoil at subsonic flow
[ISL-CO-219/84] 23 p3895 N85-34127
Real time analysis of PETN detonation products
[DE85-009581] 23 p3922 N85-34303
Collisional relaxation of electron tail distribution
[IPPJ-729] 23 p3974 N85-34635
Electron loss process and cross section of multiply charged ions by neutral atoms 23 p3981 N85-34685
High resolution Cherenkov detectors for cosmic ray isotope experiment
[OG-9.1-4] 23 p4023 N85-34930
Workshop Proceedings: Interpretation of Seismic Wave Propagation in Laterally Heterogeneous Structures
[BMR-258] 24 p4118 N85-35530
Analysis of two-parameter constant background born inversion for acoustic synthetic data
[AD-A156394] 24 p4145 N85-35698

VELOCITY FIELDS

U VELOCITY DISTRIBUTION

VELOCITY MEASUREMENT

NT WIND VELOCITY MEASUREMENT
Optical pin apparatus for measuring the arrival time and velocity of shock waves and particles
[DE84-014501] 01 p0120 N85-10824
Hot section laser anemometry 02 p0142 N85-10962
Laser anemometer optimization 02 p0142 N85-10963
Trajectory estimation using combined time-of-arrival and velocity measurements
[DE84-015872] 02 p0242 N85-11582
Project review on geophysical and ocean sound speed profile inversion
[AD-A145717] 02 p0278 N85-11797
Non-intrusive speed sensor — space shuttle main engine turbopumps
[NASA-CR-171204] 03 p0364 N85-12331
Hyadas moving group 05 p0740 N85-14757
Kinematics of B and A stars 05 p0741 N85-14766
Optical method of measuring velocity of shear waves 06 p0787 N85-15029
Axisymmetric electromagnetic field influence on the characteristic velocity of an arc-jet
[NASA-TM-77475] 07 p0938 N85-15942
Experiments on controlled, unsteady, separated turbulent boundary layers
[AD-P004172] 09 p1286 N85-17957
Analysis of pressure gradient-velocity correlation in turbulent, premixed flames 09 p1272 N85-17994
Velocity measurements in a 3D shock wave laminar boundary layer interaction. Part 1: Low speed 2D LDV measurements
[AD-A149533] 10 p1485 N85-19373
Study of submicron particle size distributions by laser Doppler measurement of Brownian motion
[AD-A149139] 10 p1487 N85-19388
Ion velocity distributions from spherical 1064 nm and 351 nm laser plasmas
[DE85-002816] 10 p1559 N85-19833
Comparison of two-dimensional laser and hot-wire velocimetry for a supersonic turbulent boundary layer 11 p1576 N85-19927
Experimental investigation of a turbulent incompressible boundary layer on a curved wall 11 p1577 N85-19936
Assessment of satellite collision hazards by simulated sampling in space 12 p1784 N85-21195
In situ orbital debris experiment concepts 12 p1784 N85-21198
Use of ground radar to detect reentering debris 12 p1784 N85-21200
Solid particle receiver experiments: Velocity measurements
[DE85-000257] 12 p1853 N85-21623
Dilution jet configurations in a reverse flow combustor
[NASA-CR-174886] 13 p1974 N85-22392
Large space antenna technology applied to radar-imaging, rain-rate measurements, and ocean wind sensing 14 p2230 N85-23620
Laser anemometry two dimensional measurement of velocity fluctuations in an excited jet
[ISL-CO-213/83] 14 p2302 N85-24254

Interferometric velocity measurements in ballistics
[ISL-CO-239/83] 14 p2306 N85-24276
New methods for interpreting seismic time fields in media with variable velocities 14 p2343 N85-24490
A brief summary of results derived from Scandinavian Twin Aurcral Radar Experiment (STARE) observations during IMS — ionospheric electric fields 14 p2362 N85-24585
The Fourier tachometer 2: An instrument for measuring global solar velocity fields 14 p2442 N85-25068
Investigation of a failure detection/identification system for a tactical aircraft navigation system
[AD-A151846] 15 p2469 N85-25240
An experimental technique for the study of velocity profiles in a laminar jet using a pulsed nitrogen laser
[AD-A151496] 15 p2556 N85-25771
Voyage to Uranus 15 p2687 N85-26596
Method of calculating separation flow of subsonic gas stream around wings 17 p2942 N85-28161
Apparatus for measuring velocity of sound in fluids 17 p2944 N85-28175
Least squares inversion of Stokes profiles in the presence of velocity gradients 18 p3207 N85-29092
Geomagnetic velocimeter
[AD-D011672] 19 p3218 N85-29953
Effect of confinement on failure in 95 TATB/5 KEL-F
[DE85-010790] 19 p3251 N85-30158
Improved fluid flow meter for measuring the rate of fluid flow in a conduit
[NASA-CASE-MFS-28030-1] 19 p3271 N85-30286
Using synchro-ballistic cameras to determine the velocity and spin rate of high-velocity projectiles
[DE85-010629] 19 p3367 N85-30884
Velocity visualization in gaseous flows
[NASA-CR-174954] 20 p3453 N85-31445
Holographic assembly for measuring velocity fields of supersonic ballistic splinters at a large distance
[ISL-CO-203/84] 20 p3459 N85-31487
New optical satellite data 20 p3492 N85-31705
Free-zone electrophoresis of animal cells. 1: Experiments on cell-cell interactions 20 p3499 N85-31754
Improvement of vertical velocity measurements, part 3.4B 21 p3620 N85-32494
Problems and solutions in analyzing partial-reflection drift data by correlation techniques 21 p3626 N85-32529
Simultaneous measurement of velocity and density in a turbulent nonpremixed flame 22 p3744 N85-33209
Optical-fiber/microprocessor-based remote velocity sensor
[DE85-010071] 22 p3788 N85-33470
Nonsimultaneous coupled laser velocimeter measurement technique: Error prediction for spatially noncoincident measurements
[NASA-TM-86718] 23 p3934 N85-34379
Noise-sustained structure, intermittency and the Ginzburg-Landau equation
[DE85-009626] 24 p4094 N85-35379
Determination of vertical air velocity using measurements of the aircraft motion 24 p4121 N85-35545

VELOCITY MODULATION
Velocity-changing collisional effects in nonlinear atomic spectroscopy and photon echo decay in gases
[NASA-CR-174159] 04 p0559 N85-13559
Profile of a relativistic electron beam propagated through a linear wiggler and an axial guide field
[AD-A154403] 19 p3353 N85-30783

VELOCITY PROFILES
U VELOCITY DISTRIBUTION

VENERA SATELLITES
NT VENERA 11 SATELLITE
Results on volcanism, surface geology from Venera-15, -16 15 p2482 N85-25321

VENERA 11 SATELLITE
Microstructure of Venus cloud layer based on spectrophotometric data from Venera-11 spacecraft 13 p1982 N85-22436

VENTILATION
Hangar destratification investigation
[AD-A145049] 01 p0012 N85-10076
Performance of two transonic airfoil wind tunnels utilizing limited ventilation 03 p0313 N85-12020
Interaction between lung mechanics and gas exchange by low volume high frequency pulmonary ventilation in patients with respiratory failure
[AD-A146604] 06 p0846 N85-15372
Active and passive shock/boundary layer interaction control on supercritical airfoils 08 p1072 N85-16795
TVENT1P user's manual, a computer code for analyzing tornado induced gas dynamic transients in flow networks
[DE85-002346] 10 p1486 N85-19379
Theoretical and experimental investigations of dust loaded flow fields in industrial halls
[BMFT-FB-HA-84-044] 12 p1819 N85-21411
Spiroll-2 instrument used to test pulmonary ventilation 12 p1903 N85-21950
New control design principles based on measured performance and energy analysis of HVAC (Heating, Ventilating, and Air-Conditioning) systems
[AD-A151708] 15 p2522 N85-25546
Ventilation flow: Submerged 18 p3156 N85-29545

VENTING
The effect of 2 strength reducing techniques on the ultimate tensile strength of AISI 4130 steel: Rocket motor case venting
[AD-A145526] 02 p0169 N85-11134
External tank GH2 vent arm 08 p1102 N85-16988
Cumulus cloud venting of mixed layer ozone
[NASA-TM-87429] 13 p2132 N85-23269
Opacity control technique for jet engine test cells
[AD-D011668] 19 p3220 N85-29988

VENTS
Numerical simulations of the effect of floor and ceiling venting on fire and smoke spread in aircraft cabins
[PB85-178333] 19 p3216 N85-29939
Preliminary results of an ALVIN dive program on active hydrothermal vents at the southern Juan de Fuca Ridge 24 p4106 N85-35454

VENTURI TUBES
Certain optimal parameters of high-velocity Venturi ejection tubes
[BLL-M-35924-(5828.4)] 05 p0634 N85-14066

VENUS (PLANET)
NT VENUS SURFACE
Infrared thermal radiation of Venus 02 p0163 N85-11101
Impact cratering: The process and its effects on planetary evolution — and silicate-carbonate reactions on Venus
[NASA-CR-174016] 02 p0228 N85-11488
Mars exploration, Venus swingby and conjunction class mission modes, time period 2000 to 2045
[NASA-TM-86477] 02 p0303 N85-11961
Gravity anomaly map of Mars and Moon and analysis of Venus gravity field: New analysis procedures
[NASA-CR-174295] 08 p1258 N85-17919
The geology of the terrestrial planets
[NASA-SP-469] 09 p1410 N85-18888
Venus 09 p1411 N85-18891
The Venus Balloon Project 10 p1465 N85-19243
The international VEGA 'Venus-Halley' (1984-1986 experiment: Description and scientific objectives
[NASA-TM-77536] 12 p1960 N85-22324
Volcanism on Venus as connecting link 13 p1962 N85-22433
Preliminary photomaps of Venus surface in the Maxwell Mountains and adjacent areas 13 p1982 N85-22438
Analysis and interpretation of observations of airglow at 297 nm in the Venus thermosphere 13 p2172 N85-23473
Characteristics of basaltic lava flows on Venus 13 p2177 N85-23508
Venus surface composition from radio/radar measurements 13 p2177 N85-23509
Surface units on Venus derived from Pioneer-Venus altimetry, roughness, and reflectivity measurements 13 p2177 N85-23510
Classification of circular features on Venus 13 p2177 N85-23511
Venus gravity: Global field results 13 p2177 N85-23512
Geophysical interpretation of Venus gravity data 13 p2178 N85-23513
Gravity field of Venus and comparison with Earth 13 p2178 N85-23514
The support of long wavelength loads on Venus 13 p2178 N85-23515
Venus chasmata: A lithosphere stretching model 13 p2178 N85-23516
A statistical treatment of the regional slope characteristics of Venus and Earth 13 p2178 N85-23517
The effect of particle density on aeolian transport 13 p2189 N85-23581
Potential bedforms on Venus: Wind tunnel simulations 13 p2189 N85-23583
Analyses of radar images of small craters 13 p2199 N85-23642
Planetary interior modeling and tectonic implications 13 p2200 N85-23649
TASS update on flights of Vega-1 and Vega-2 16 p2722 N85-26803
Kovtunenko discuses Vega Project 16 p2722 N85-26804
French and West German equipment for Vega Project 16 p2722 N85-26805
Venus thermospheric circulation
[PB85-180420] 19 p3384 N85-30997
Geophysical interpretation of Venus gravity data
[NASA-CR-176063] 20 p3547 N85-32071
Extended atmospheres of outer planet satellites and comets
[NASA-CR-176137] 22 p3851 N85-33848
Venus, Earth and Mars: Present bounds on similarities and differences in bulk composition 22 p3856 N85-33876
Contrasts in evolution of Venus and Earth 22 p3857 N85-33880
Geologic processes on Venus: An update 22 p3857 N85-33883
Planning for VRM: Radar and sonar studies of volcanic terrains on Earth, Venus and Mars 22 p3857 N85-33884
Dynamic compensation of Venus's geoid: A comparison with Earth 22 p3858 N85-33885
Admittance functions from Venus vertical gravity and modes of topographic support 22 p3858 N85-33889
A dynamic model of Venus's gravity field
[NASA-CR-176173] 24 p4169 N85-35845

VENUS ATMOSPHERE
NT VENUS CLOUDS
Two-level model for formation of night ionosphere of Venus from radio occulation experiments 02 p0162 N85-11100
H2O profile in lower atmosphere of Venus based on effective radiation flux measurements 02 p0163 N85-11102
Change in Venusian atmosphere absorption coefficient with altitude 02 p0163 N85-11103
Theoretical study of electron concentration in Venusian atmosphere as function of zenith angle of sun and solar activity in areas of photochemical equilibrium 02 p0163 N85-11104
Laboratory evaluation of microwave absorption properties under simulated conditions for planetary atmospheres
[NASA-CR-174060] 02 p0303 N85-11960
Studies of the chemistry of vibrationally and electronically excited species in planetary upper atmospheres
[NASA-CR-174134] 03 p0449 N85-12851
Construction of a superheterodyne receiver for 10 micron waves to be put on a Cassegrain optics telescope for spectroscopic research on the Mars and Venus atmospheres
[MPE-183] 06 p0872 N85-15538
Exploration of the solar system by airborne astronomy 08 p1244 N85-17951
Response of Earth's atmosphere to increases in solar flux and implications for loss of water from Venus 13 p2178 N85-23518
The effect of particle density on aeolian transport 13 p2189 N85-23581
Mechanism of formation of low temperatures in nighttime Venusian thermosphere 16 p2723 N85-26807
Venus thermospheric circulation
[PB85-180420] 19 p3384 N85-30997
Water loss from Venus: Implications for the Earth's early atmosphere 21 p3721 N85-33067
Laboratory evaluation and application of microwave absorption properties under simulated conditions for planetary atmospheres
[NASA-CR-176078] 22 p3851 N85-33847

VENUS CLOUDS
Microstructure of Venus cloud layer based on spectrophotometric data from Venera-11 spacecraft 13 p1982 N85-22436

VENUS PROBES
NT MARINER 5 SPACE PROBE
NT VENERA SATELLITES
NT VENERA 11 SATELLITE
Kovtunenko comments on Vega flight plan, instrumentation 15 p2482 N85-25318
Comments on Vega mission 15 p2482 N85-25319
Press conference on flight of Vega spacecraft 15 p2482 N85-25320
Results on volcanism, surface geology from Venera-15, -16 15 p2482 N85-25321
Interpretation of Venus gravitational anomalies 15 p2483 N85-25322
Laboratory evaluation and application of microwave absorption properties under simulated conditions for planetary atmospheres
[NASA-CR-176078] 22 p3851 N85-33847

VENUS RADAR ECHOES
Progress in planetary radarclinometry 13 p2198 N85-23630

VENUS SURFACE
Venus 09 p1411 N85-18891
Visualization of radar altimetry data for Venus 13 p1982 N85-22437
Preliminary photomaps of Venus surface in the Maxwell Mountains and adjacent areas 13 p1982 N85-22438

Hypsometric features on Venus
13 p1983 N85-22439
Volcanism and rift formation in Beta Regio, Venus: New radar results
13 p2176 N85-23507
Characteristics of basaltic lava flows on Venus
13 p2177 N85-23508
Venus surface composition from radio/radar measurements
13 p2177 N85-23509
Surface units on Venus derived from Pioneer-Venus altimetry, roughness, and reflectivity measurements
13 p2177 N85-23510
Classification of circular features on Venus
13 p2177 N85-23511
Venus gravity: Global field results
13 p2177 N85-23512
Geophysical interpretation of Venus gravity data
13 p2178 N85-23513
The support of long wavelength loads on Venus
13 p2178 N85-23515
Venus chasmata: A lithosphere stretching model
13 p2178 N85-23516
A statistical treatment of the regional slope characteristics of Venus and Earth
13 p2178 N85-23517
Potential bedforms on Venus: Wind tunnel simulations
13 p2189 N85-23583
Microdunes and other aeolian bedforms on Venus: Wind tunnel simulations
13 p2189 N85-23584
Unsupervised classification of global radar units on Venus
13 p2198 N85-23632
Analyses of radar images of small craters
13 p2199 N85-23642
Geological analyses of the surface of Venus and Mars from lander spacecraft images and orbital radar observations
19 p3384 N85-30993
Geophysical interpretation of Venus gravity data
[NASA-CR-176063] 20 p3547 N85-32071

VERBAL COMMUNICATION
Crew communication as a factor in aviation accidents
05 p0710 N85-14555
A full mission simulator study of aircrew performances: The measurement of crew coordination and decisionmaking factors and their relationships to flight task performance
05 p0710 N85-14556
Communication on the flight deck
05 p0711 N85-14557
Neuro-linguistic programming: Eye movements as indicators of representational systems
[AD-A147541] 07 p1016 N85-18454
Multiple resources and brain laterality
[AD-A148912] 10 p1530 N85-19643
Verbal information processing paradigms: A review of theory and methods
[AD-A153229] 17 p3050 N85-28880

VERIFICATION (PROVING)
U PROVING

VERTEBRAE
Analysis of long bone and vertebral failure patterns
[AD-A154798] 21 p3663 N85-32758

VERTEBRAL COLUMN
The effects of helicopter vibration on the spinal system
[AD-A146274] 03 p0402 N85-12562
Analysis of long bone and vertebral failure patterns
[AD-A154798] 21 p3663 N85-32758

VERTEBRATES
NT AMPHIBIA
NT BABOONS
NT BEARS
NT BIRDS
NT CATS
NT DEER
NT DOGS
NT DOLPHINS
NT FISHES
NT FROGS
NT GUINEA PIGS
NT HUMAN BEINGS
NT MAMMALS
NT MICE
NT MONKEYS
NT PRIMATES
NT RABBITS
NT RATS
NT SEALS (ANIMALS)
NT SHARKS
NT SHEEP
NT TURTLES
NT WHALES

VERTICAL AIR CURRENTS
Diurnal and seasonal patterns of temperature and wind flow in the planetary boundary layer for ten locations in complex terrain
[PB85-106698/GAR] 06 p0840 N85-15333
The sensitivity of mesoscale cyclogenesis forecasts to detailed three-dimensional isentropic initial analyses and varied vertical model resolution
15 p2598 N85-26015
The study of thermal forecasting for gliding
16 p2830 N85-27453
Approximate method for computing wind velocity in atmosphere
19 p3298 N85-30444
Tropospheric gravity waves observed by three closely spaced ST radars
21 p3623 N85-32509
Thunderstorm phenomena and weather radar scanning strategies
[DOT/FAA/PM-85/14] 21 p3634 N85-32573
Determination of vertical air velocity using measurements of the aircraft motion
24 p4121 N85-35545
Measurements for the determination of the vertical structure of the convective boundary layer — atmospheric boundary layer
24 p4122 N85-35550

VERTICAL ATTITUDE TAKEOFF-LANDING AIRCRAFT
U VATOL AIRCRAFT

VERTICAL DISTRIBUTION
NT STAR DISTRIBUTION
Wave phase velocity in a wind gradient — gravity waves
04 p0523 N85-13343
The z-dependance of the spin temperature of HI
06 p0878 N85-15580
Measurements of H2O in Jupiter's atmosphere from 5 microns airborne observations
08 p1244 N85-17854
The vertical structure and stability of alpha model accretion disks
09 p1417 N85-18938
Aerosol limb absorption — stratosphere
[NASA-TM-77733] 10 p1515 N85-19582
Measurement of the vertical gradient of the semidiurnal tidal wind phase in winter at the 95 km level
11 p1662 N85-20478
Peat resources of Maine. Volume 1: Aroostook County
[DE85-004196] 11 p1669 N85-20519
Peat resources of Maine. Volume 4: Southern and western Maine
[DE85-004198] 11 p1670 N85-20520
Special features of computations of vertical distribution of concentration of suspended sediments under marine conditions
13 p2106 N85-23125
An equation of profile of snow drift density during snowfall
15 p2581 N85-25919
An experimental study of brine upward migration in thin sea ice
15 p2582 N85-25923
Vertical redistribution of a pollutant tracer due to cumulus convection
[PB85-172971] 18 p3134 N85-29415
Development and testing of the variable vertical resolution Fourth Order GCM
18 p3142 N85-29453
Parameterization of surface fluxes in the VVR Fourth Order GCM
18 p3142 N85-29454
Observations of mesospheric turbulence by rocket probe and VHF radar, part 2.4A
21 p3619 N85-32484
Visibility and vertical structure measurements in southern Germany
[AD-A154714] 21 p3635 N85-32574
A new hypothesis for the observed vertical distribution of atmospheric aerosols
21 p3645 N85-32646
On the mechaniams responsible for the formation of typical size spectra and vertical distribution of tropospheric aerosol particles
21 p3645 N85-32647
Drying of pulverized material with heated condensible vapor
[DE85-011656] 22 p3783 N85-33438
Application of nonlinear least squares methods to the analysis of solar spectra
[NASA-CR-176122] 22 p3816 N85-33637
Estimating the change in asymptotic direction due to secular changes in the geomagnetic field
[SH-6.1-13] 23 p4045 N85-35088
Partitioning of the vertical turbulent energy transport into positive and negative contributions — meteorology
24 p4122 N85-35551
Aircraft measurements during the Bonn Experiment (BONEX 1) — meteorology
24 p4122 N85-35552

VERTICAL FINS
U FINS

VERTICAL JUNCTION SOLAR CELLS
Apparatus for etching vertical junction solar cell wafers
[AD-D011653] 17 p2984 N85-28443

VERTICAL LANDING
Why vertical landing — aircraft
[BAE-KRS-N-GEN-301] 09 p1279 N85-18048

VERTICAL MOTION
Vertical crustal movements in southern California, 1974 to 1978
[GS-CIRC-905] 02 p0228 N85-11491
Increase in performance and improvement of ride comfort of self-propelled construction machinery by reducing pitch and vertical vibration
[AD-P004269] 09 p1405 N85-18845
Vertical movements and structure formation within island systems of northeast Asia
10 p1501 N85-19471
Diagnosis of vertical motions from VAS retrievals during a convective outbreak
[NASA-CR-171569] 19 p3316 N85-30554
A simple model for testing the effects of gravity-wave-produced vertical oscillations of scattering irregularities on spaced-antenna, horizontal drift measurements
21 p3619 N85-32489
Estimation of vertical diffusion from observations of Atmospheric turbulence layers, part 4.4B
21 p3623 N85-32507

VERTICAL ORIENTATION
Observations of the vertical structure of the eddy field in the Kuroshio extension
[AD-A145178] 01 p0069 N85-10599
Mass and momentum transport in a turbulent buoyant vertical axisymmetric jet
05 p0635 N85-14070
Lateral fluid forces acting on a whirling centrifugal impeller in vaneless and vaned diffuser
05 p0643 N85-14123
Experimental investigation of lateral forces induced by flow through model labyrinth glands
05 p0643 N85-14128
The growth of large diameter single crystals by vertical solidification of the melt
[AD-A148756] 09 p1397 N85-18792
Along-track deflection of the vertical from SEASAT: GEBCO (General Bathymetric Chart of the Oceans) overlays
[PB85-129641] 12 p1876 N85-21767
Vertical discrimination in the sound channel
[AD-A150254] 13 p2155 N85-23380
High-frequency acoustic variability in the arctic
[AD-A150550] 13 p2155 N85-23383
Six-inch HYGE vertical impact facility
[AD-A150665] 14 p2228 N85-23809
Observation of precipitating clouds by a vertically pointing radar at Morino in the Iburi District, Hokkaido, Japan
15 p2582 N85-25922
Scheme for atmospheric thermal sensing from satellites with enhanced vertical resolution
16 p2726 N85-26823
The theoretical response of a vertical line array to wind-generated noise in shallow water
[AD-A151730] 16 p2880 N85-27638
Structural design of the Sandia 34-meter vertical-axis wind turbine
[DE85-011146] 18 p3118 N85-29300
Natural convection in square partitioned enclosures
[AD-A153707] 18 p3197 N85-29828
Improvement of vertical velocity measurements, part 3.4B
21 p3620 N85-32494
Determination of horizontal and vertical wavelengths of gravity waves in the mesosphere by spaced wind measurements
21 p3623 N85-32510
Trapping of ion conics by downward parallel electric fields
[AD-A155306] 21 p3633 N85-32568
Visibility and vertical structure measurements in southern Germany
[AD-A154714] 21 p3635 N85-32574
Horizontal and vertical structure of velocity, potential vorticity and energy in the gulf stream
[AD-A154753] 21 p3655 N85-32702
Admittance functions from Venus vertical gravity and modes of topographic support
22 p3858 N85-33869

VERTICAL PERCEPTION
Prediction of seasickness susceptibility
11 p1693 N85-20647
Amyloplast sedimentation kinetics in corn roots
15 p2606 N85-26059
Polyamines as possible modulators of gravity induced calcium transport in plants
15 p2606 N85-26060
Role of Ca++ in shoot gravitropism — avena
15 p2607 N85-26065
A possible explanation of why gravitropic growth is detected earlier than straight growth
15 p2607 N85-26067
Dissociation of autonomic and sensory vestibular reactions
23 p3953 N85-34501

VERTICAL STABILIZERS
U STABILIZERS (FLUID DYNAMICS)

VERTICAL TAILS
U STABILIZERS (FLUID DYNAMICS)
U TAIL ASSEMBLIES

VERTICAL TAKEOFF AIRCRAFT
NT FLYING PLATFORMS
An engine trade study for a supersonic STOVL fighter-attack aircraft, volume 1
[NASA-CR-166304] 02 p0133 N85-10910

Simulation evaluation of two VTOL control/display systems in IMC approach and shipboard landing
[NASA-TM-85996] 08 p0756 N85-14841
Circulation control: A bibliography of DTNSRDC research and selected outside references: Update
[AD-A146066] 07 p0693 N85-15661
International aviation (selected articles)
[AD-A148704] 08 p1067 N85-16782
Pseudospectral calculations of two-dimensional transonic flow (Task 1). Numerical investigation of VTOL aerodynamics (Task 2)
[AD-A150123] 12 p1772 N85-21126
Analysis of control system from a viewpoint of desired pole placement and desired degree of robustness
[AD-A152627] 17 p2699 N85-27876

VERTICAL TAKEOFF AND LANDING
U VERTICAL LANDING

VERTICES
U APEXES

VERY HIGH FREQUENCIES
VHF/UHF radar and its application in nowcasting
01 p0078 N85-10516
Study of factors affecting an HF/VHF direct broadcasting satellite service
[PB85-120669/GAR] 09 p1313 N85-18255
Improvement of VHF(MB) model
[AD-A150067] 12 p1829 N85-21480
A fully distributed approach to the design of a 16 K bit/sec VHF packet radio network
[AD-A141282] 13 p2054 N85-22859
Alternatives for satellite sound broadcast systems at HF and VHF 14 p2229 N85-23815
The ARGOS VHF direct readout mini-station and CML-80-MP data collection Platform Transmitter Terminals (PTTs) 14 p2238 N85-23873
ARGOS VHF direct readout mini-station
14 p2239 N85-23886
Generalized graph coloring: A frequency assignment method for VHF broadcasting
[TUM-M8405] 16 p2844 N85-27535
Measurements of VHF/UHF radio propagation in a maritime temperate climate
[CRC-1380] 18 p3089 N85-29119
Field antenna handbook
[AD-A155204] 21 p3576 N85-32242
A modified Fresnel scattering model for the parameterization of Fresnel returns, part 2.3A
21 p3618 N85-32483
Observations of mesospheric turbulence by rocket probe and VHF radar, part 2.4A 21 p3619 N85-32484
Usefulness of multifrequency MST radar measurements, part 2.6B 21 p3619 N85-32487
Potential advantages of the spaced antenna method for operational wind profiling, part 3.1B
21 p3620 N85-32490
Improvement of vertical velocity measurements, part 3.4B 21 p3620 N85-32494
Interferometer applications of VHF radars, part 3.6A
21 p3621 N85-32497
Testing and optimizing MST coaxial collinear arrays, part 6.4A 21 p3625 N85-32516
Elimination of range-aliased echoes in the VHF radars
21 p3625 N85-32521
A note on the proposed UK VHF radar
21 p3629 N85-32545
Radar wind profilers in the Colorado network
[PB85-185486] 22 p3617 N85-33647

VERY HIGH FREQUENCY RADIO EQUIPMENT
Preliminary investigation of the performance of repeater technology for satellite sound broadcasting
[SSP/017/82] 18 p3092 N85-29137

VERY HIGH SPEED INTEGRATED CIRCUITS
U VHSIC (CIRCUITS)

VERY LARGE SCALE INTEGRATION
Routing the power and ground wires on a VLSI chip
[AD-A145956] 02 p0194 N85-11296
The application of microprocessors in the command and control of satellites by the MECB stations
[INPE-3282-RPE/466] 02 p0239 N85-11553
Supercomputers and VLSI: The effect of large scale integration on computer architecture
[AD-A145406] 02 p0239 N85-11555
Circuit engineering and technological optimization of very high speed LSI logic elements and transistor structures 03 p0347 N85-12237
Application of a silicon compiler to VLSI (Very Large Scale Integrated circuits) design of digital pipelined multipliers
[AD-A146328] 03 p0403 N85-12569
VLSI (Very Large Scale Integration) design tools reference manual, release 1.0
[AD-A146273] 03 p0408 N85-12604
Ion beam lithography
[BMFT-FB-T-84-182] 04 p0504 N85-13219
VLSI architectures for the multiplication of integers modulo a Fermat number 05 p0624 N85-13993
Practical application of electron beam testing in LSI and VLSI circuits
[BMFT-FB-T-84-185] 05 p0633 N85-14061
VLSI design tools, reference manual, release 2.0
[AD-A146444] 06 p0803 N85-15112
Specialized silicon compilers for language recognition
[AD-A146526] 06 p0853 N85-15425
Built-in test and self repair mechanisms in a digital correlator integrated circuit 08 p1064 N85-16741
Electronics component R and D, production capability reviewed 08 p1140 N85-17181
Electrical characterization of VLSI (Very Large Scale Integration) memories
[AD-A147657] 08 p1156 N85-17296
Restructurable VLSI program
[AD-A148145] 08 p1157 N85-17301
DDL system: Design systhesis of digital systems
[NASA-CR-170759] 09 p1356 N85-18584
Researchers, projects at French intelligent machine center 10 p1480 N85-19207
Siemens' CAD system designs VLSI circuits
10 p1481 N85-19209
Research into self-timed VLSI circuits
[AD-A149140] 10 p1479 N85-19339
Method of examining microcircuit patterns
[NASA-CASE-NPO-16299-1] 11 p1628 N85-20250
Signal propagation delay, wire length distribution and the efficiency of VLSI circuits
[CWI-CS-R8412] 11 p1630 N85-20266
Design of a bit-sliced processor array with built-in-self-test
[AD-A149785] 12 p1835 N85-21513
Built-in tests for VLSI (Very Large Scale Integration) finite-state machines
[AD-A149784] 12 p1911 N85-21997
X-ray lithography and VLSI circuits
13 p2052 N85-22846
Periodic binary sequence generators: VLSI circuits considerations
[NASA-CR-175649] 13 p2063 N85-22886
EOS (electrical overstress) protection for VLSI (Very Large Scale Integration) devices
[AD-A150333] 13 p2064 N85-22891
UW/NW (University of Washington/Northwest) VLSI Consortium
[AD-A150740] 14 p2404 N85-24818
Developments in microelectronics: Past and future
15 p2530 N85-25597
Designing VLSI (Very Large Scale Integrated) circuits for testability
[AD-A151834] 15 p2549 N85-25729
Development of simulation procedures for VLSI systems (timing simulation)
[BMFT-FB-T-84-297] 15 p2550 N85-25743
Influence and possibilities of Very Large Scale Integration (VLSI) in pattern recognition and image processing 15 p2622 N85-26160
Techniques for computing the DFT using the residue Fermat number systems and VLSI
16 p2770 N85-27097
An integrated UNIX-based CAD system for the design and testing of custom VLSI chips
16 p2771 N85-27102
System design of automated VLSI (Very Large Scale Integrated) test station and implementation of selected system aspects
[AD-A151961] 16 p2778 N85-27147
Radiation hardening for VLSI applications
[DE85-005493] 16 p2780 N85-27155
VLSI workshop and project: February - November 1982
[WSRL-0374-TR] 17 p2951 N85-28223
Restructurable VLSI (Very large scale integration) program
[AD-A152340] 17 p2951 N85-28226
Efficient VLSI (Very Large Scale Integration) fault simulation
[AD-A152661] 17 p2953 N85-28233
VLSI (Very large scale integrated circuits) device reliability models
[AD-A153268] 17 p2954 N85-28245
Speed-up techniques for complementary metal oxide semiconductor very large scale integration
[AD-A152466] 17 p3043 N85-28829
Microstore: The Stanford analog memory unit
[DE85-005534] 18 p3095 N85-29160
Evaluation of VLSI technology — space applications
[CD.6501702] 18 p3096 N85-29177
The use of VLSI technology for the real-time generation of graphics displays: A proposal
[AD-A153766] 18 p3160 N85-29578
Electro-optic techniques for VLSI interconnect
18 p3188 N85-29774
Split-cross-bridge resistor for testing for proper fabrication of integrated circuits
[NASA-CASE-NPO-16021-1] 19 p3258 N85-30187
A single chip VLSI architecture for radar signal processing 19 p3257 N85-30195
A comparison of the radiation hardness of various VLSI technologies for defense applications
[DE85-006973] 19 p3263 N85-30238
Fault-tolerant computing research
[AD-A154082] 19 p3342 N85-30710
Implementation of a serial communication process for a fault tolerant, real time, multitransputer operating system
[AD-A154237] 19 p3343 N85-30714
VLSI structures for numerical and digital signal processing computations 20 p3439 N85-31340
Basic development of a 1.5 micrometer very large scale integrated technique, part 1-4
[BMFT-FB-T-85-032-PT-1-4] 20 p3449 N85-31417
VLSI (Very Large Scale Integrated) tutorials through the video-computer courseware implementation system
[AD-A155889] 24 p4135 N85-35631
Computer Aided Design (CAD) methods for very large scale integration systems
[BMFT-FB-T-85-029] 24 p4141 N85-35668

VERY LONG BASE INTERFEROMETRY
Measurement of pulsar parallax by Very Long Baseline Interferometry 03 p0444 N85-12830
The Telecommunications and Data Acquisition Report
[NASA-CR-174149] 05 p0622 N85-13980
Submilliarcsecond VLBI using compact close pairs of radio sources: Error analysis 05 p0622 N85-13981
VLBI solutions for the time variation of DSN baselines: 1978 - 1983 05 p0623 N85-13983
The performance of differential VLBI delay during interplanetary cruise 05 p0623 N85-13984
VLBI system (BLK I) IF-video down conversion design
05 p0625 N85-13998
Interferometry with decametric waves (review)
06 p0781 N85-14996
Software for Crimea-Pushchino radiointerferometer
06 p0783 N85-15007
Primary data processing in very long baseline radiointerferometer 06 p0783 N85-15008
QUASAT: A VLBI observatory in space — conferences
[ESA-SP-213] 07 p1056 N85-16700
The galaxy scene and QUASAT — VLBI satellite
07 p1056 N85-16703
The QUASAT mission: An overview
07 p1056 N85-16704
Some prospects of space VLBI
07 p1056 N85-16705
QUASAT: Technical aspects of the proposed mission — VLBI satellite 07 p1057 N85-16706
A study on the imaging potential of QUASAT — spaceborne VLBI 07 p1057 N85-16707
Potential affiliate stations to work with the EVN — European VLBI Network; QUASAT
07 p1057 N85-16708
Correlator and data processing requirements for QUASAT 07 p1057 N85-16709
Limitation of VLBI angular resolution
07 p1057 N85-16710
Processing system for space VLBI
07 p1057 N85-16711
Testing theories of superluminal motion — QUASAT
07 p1058 N85-16714
QUASAT, gravitational lenses, and studies of the interstellar, intracluster and intergalactic medium
07 p1058 N85-16715
Very Long Base Interferometry (VLBI) in space and X-ray observations of compact sources in active galactic nuclei 07 p1058 N85-16716
The wide-range space radio interferometer
07 p1058 N85-16717
The relevance of QUASAT to the star formation problem 07 p1058 N85-16718
Galactic OH and H2O masers — QUASAT project
07 p1058 N85-16719
Water masers and distance measurements: The impact of QUASAT 07 p1059 N85-16721
A short note on the high precision navigation of QUASAT 07 p1059 N85-16722
Opportunities for high angular and temporal resolutions of galactic objects at radio frequencies — QUASAT
07 p1059 N85-16723
Very long base interferometry (VLBI) and X-ray observations of complete samples of radio selected active galactic nuclei 08 p1243 N85-17847
VLBI observations of compact double radio sources
09 p1417 N85-18940
The Telecommunications and Data Acquisition Report
[NASA-CR-174366] 10 p1462 N85-19224
Arcsecond positions for milliarcsecond VLBI nuclei of extragalactic radio sources. Part 3: 74 sources
10 p1463 N85-19225
The accuracy of radio interferometric measurements of Earth rotation 10 p1465 N85-19246

Utilization of mobile VLBI for geodetic measurements
10 p1466 N85-19248
Studies of galactic HI in 21-centimeter absorption
13 p2170 N85-23466
QUASAT: An orbiting very long baseline interferometer program using large space antenna systems
14 p2230 N85-23822
Antenna Technology for QUASAT application — radio antenna for very long base interferometry missions
14 p2231 N85-23826
Observation model and parameter partials for the JPL VLBI parameter estimation software MASTERFIT-F 2.0
[NASA-CR-175640] 14 p2347 N85-24509
Station coordinates and Earth rotation parameters from Lageos laser ranging 16 p2606 N85-27299
Basic research for the geodynamics program
[NASA-CR-175751] 16 p2625 N85-27424
Precise time transfer using MKIII VLBI technology
17 p2965 N85-28310
Using GPS and VLBI technology to maintain 14 digit synchronization 18 p3109 N85-29250
New stations supporting crustal dynamics project VLBI measurements 20 p3491 N85-31701
New VLBI technology developments
20 p3491 N85-31702
Comparing SLR and VLBI geodetic parameters
20 p3491 N85-31703
Milliarcsecond morphology of the twin quasar 0957 + 56A,B: The view through a gravitational lens
20 p3544 N85-32054
Mapping with QUASAT (quasar satellite) using short observation times
[AD-A155155] 21 p3559 N85-32141
Crustal dynamics project data analysis fixed station VLBI geodetic results
[NASA-TM-86229] 21 p3615 N85-32465
Crustal Dynamics Project: Catalogue of site information
[NASA-TM-86218] 22 p3801 N85-33552

VERY LOW FREQUENCIES

The case for concern about very low frequency fields from visual display terminals: The need for further research and shielding of VDTs
[CCOHS-P83-2E] 02 p0234 N85-11526
Impedance measurements on a VLF multi-turn loop antenna in a space plasma simulation chamber
[AD-A145104] 04 p0492 N85-13141
Human reactions to ELF (Extremely Low Frequency) electric and magnetic fields. An annotated bibliography of current literature, fourth edition
[PB84-230358] 04 p0545 N85-13472
Infralow-frequency digital phase meter
06 p0787 N85-15031
Ionospheric and magnetospheric modifications caused by VLF waves
[AD-A148210] 08 p1186 N85-17475
Survey of VLF-OMEGA transmissions received during summer at Antarctic peninsula
[INPE-3399-PRE/666] 10 p1462 N85-19223
The ULF/ELF/VLF electromagnetic fields generated in a sea of finite depth by elevated dipole sources
[AD-A149638] 12 p1828 N85-21470
A new radio emission at 3 kHz in the outer heliosphere 12 p1959 N85-22312
VLF emissions observed by ISIS Satellites during the IMS 14 p2366 N85-24621
VLF wave-particle interaction experiments by EXOS-B/Siple station transmissions
14 p2366 N85-24622
Magnetospheric wave characteristics derived from cross-spectral analysis 14 p2371 N85-24659
Hazards of VLF electromagnetic fields
16 p2776 N85-27136
VLF (Very low frequency) workshop held at San Diego California, 24-25 January 1985
[AD-A154652] 21 p3573 N85-32224
Numerical modeling of subsurface communication
[DE85-012818] 21 p3577 N85-32249

VESTA ASTEROID

Asteroid collisional evolution studies
13 p2176 N85-23501

VESTIBULAR NYSTAGMUS

Caloric stimulation of the vestibular system in microgravity 05 p0695 N85-14469
Problems of space biology. Volume 50: Nystagmometry for evaluation of the status of the vestibular function
[NASA-TM-77616] 14 p2385 N85-24694

VESTIBULAR TESTS

The European vestibular experiments in the Spacelab 1 mission 05 p0694 N85-14466
Thresholds of perception of whole body linear oscillation: Modification by spaceflight 05 p0694 N85-14467
The adaptation of vestibulo-spinal reflexes as a function of spaceflight and their relationship to space motion sickness 05 p0694 N85-14468
Caloric stimulation of the vestibular system in microgravity 05 p0695 N85-14469
Visual-vestibular interaction in human motion perception 05 p0695 N85-14471
Thermoregulatory and vestibular systems in the rat
15 p2610 N85-26082
Influence of limbosreticular complex on some reactions of rabbits 19 p3326 N85-30607
The European vestibular experiments of the Spacelab-1 mission 20 p3508 N85-31808
Some results of the European vestibular experiments in the Spacelab-1 mission 20 p3508 N85-31809
Spatial orientation in weightlessness and readaptation to Earth's gravity 20 p3509 N85-31811
Mission operations requirements document for D-1 Experiment 102, Vestibular Experiments in Spacelab
[NASA-TM-87495] 21 p3557 N85-32129
Effect of experimental motion sickness on postrotory nystagmus and counterrotation illusion
22 p3824 N85-33690
Dissociation of autonomic and sensory vestibular reactions 23 p3953 N85-34501

VESTIBULES

The development of the vestibular apparatus under conditions of weightlessness
[NASA-TM-77517] 07 p1011 N85-16422
Neurophysiological correlates of motion sickness: Role of vestibulocerebellum and 'vomiting center' reanalyzed
11 p1693 N85-20643
Influence of gravitoinertial force level on apparent magnitude of coriolis cross-coupled angular accelerations and motion sickness 11 p1693 N85-20644
Vestibular and oculomotor function during Gz variations 11 p1693 N85-20645
Quantitation of Na+, K+-ATPase enzyme activity in tissues of the mammalian vestibular system
15 p2613 N85-26102
Anatomy of the vestibulo-automatic outflow to the gut
15 p2614 N85-26106
Mission operations requirements document for D-1 Experiment 102, Vestibular Experiments in Spacelab
[NASA-TM-87495] 21 p3557 N85-32129
Effect of experimental motion sickness on postrotory nystagmus and counterrotation illusion
22 p3824 N85-33690
Dissociation of autonomic and sensory vestibular reactions 23 p3953 N85-34501

VETERINARY MEDICINE

USSR report: Life sciences. Biomedical and behavioral sciences
[JPRS-UBB-84-015] 07 p1010 N85-16416

VFR (RULES)

U VISUAL FLIGHT RULES

VHF OMNIRANGE NAVIGATION

Use of microprocessor techniques and new antenna systems to improve the navigation aids very high frequency omnidirectional radar (VOR), Doppler VOR and Instrument Landing System (ILS)
[BMFT-FB-W-84-026] 02 p0137 N85-10930
Evaluation of radio navigation systems and their configuration with respect to minimum cost
[ESA-TT-847] 20 p3392 N85-31043

VHSIC (CIRCUITS)

Circuit engineering and technological optimization of very high speed LSI logic elements and transistor structures 03 p0347 N85-12237
USSR report: Electronics and electrical engineering
[JPRS-UEE-84-010] 04 p0485 N85-13095
Life cycle cost model for very high speed integrated circuits
[AD-A147798] 08 p1157 N85-17296
Signal propagation delay, wire length distribution and the efficiency of VLSI circuits
[CWI-CS-R8412] 11 p1630 N85-20266
Circuit topology, signal propagation delay and the efficiency of VLSI circuits
[CWI-CS-R8414] 11 p1630 N85-20267
Research in the design of high-performance reconfigurable systems
[NASA-CR-175705] 15 p2621 N85-26153
VLSI (Very large scale integrated circuits) device reliability models
[AD-A153266] 17 p2954 N85-28245
GAO (General Accounting Office) assessment of DOD's Very High Speed Integrated Circuits (VHSIC) technology program
[AD-A155109] 21 p3581 N85-32261

VIBRATION

NT BENDING VIBRATION
NT COMBUSTION VIBRATION
NT FLUTTER
NT FORCED VIBRATION
NT FREE VIBRATION
NT LATTICE VIBRATIONS
NT LINEAR VIBRATION
NT MISSILE VIBRATION
NT POGO EFFECTS
NT RANDOM VIBRATION
NT RESONANT VIBRATION
NT SELF INDUCED VIBRATION
NT STRUCTURAL VIBRATION
NT SUBSONIC FLUTTER
NT SUPERSONIC FLUTTER
NT TORSIONAL VIBRATION
NT TRANSONIC FLUTTER

Helicopter rotor blade design for minimum vibration
[NASA-CR-3825] 01 p0006 N85-10032
Rotordynamic analysis of the SSME turbopumps using reduced models
[NASA-CR-171170] 01 p0054 N85-10355
Human response to vibroacoustic environments of space vehicles
[NASA-TM-86316] 01 p0116 N85-10789
The Shock and Vibration Digest, volume 16, no. 8
[AD-A145663] 02 p0206 N85-11372
Analysis of turbomachine blades: A review
02 p0206 N85-11374
Approximation methods for inverse problems involving the vibration of beams with tip bodies
[NASA-CR-172468] 02 p0209 N85-11379
Interactions among system stiffness, wear and vibrations 03 p0370 N85-12364
Studies of the chemistry of vibrationally and electronically excited species in planetary upper atmospheres
[NASA-CR-174134] 03 p0449 N85-12851
Structural properties of amorphous metals by Raman scattering
[DE84-016947] 04 p0475 N85-13027
Computation of the nonequilibrium flow in a gasdynamic laser
[AD-A141022] 04 p0505 N85-13224
Vibration data analysis system for SNLA area 3 reference manual
[DE84-016207] 04 p0514 N85-13275
Subsynchronous vibrations in a high pressure centrifugal compressor: A case history 05 p0642 N85-14118
Experiences with nonsynchronous forced vibration in centrifugal compressors 05 p0642 N85-14119
Internal hysteresis experienced on a high pressure syn gas compressor 05 p0642 N85-14122
Experimental investigation of lateral forces induced by flow through model labyrinth glands
05 p0643 N85-14128
An Iwatsubo-based solution for labyrinth seals - comparison with experimental results
05 p0644 N85-14131
Influence of stationary components on unsteady flow in industrial centrifugal compressors
05 p0645 N85-14140
Propulsive efficiency of vibrating wing in supersonic flow 05 p0724 N85-14856
Linear problem of harmonic vibrator acting at supercritical frequencies in subsonic boundary layer
06 p0779 N85-14978
F-8 refueling boom ground vibration test
[NASA-TM-84914] 07 p0902 N85-15713
Analysis of the surface load and radiated sound of a vibrating airfoil with application to the experiment of Brooks
[NASA-CR-3864] 07 p1038 N85-16690
Development of a pressure transducer for usage in high-temperature and vibration environments. Phase 1: Feasibility investigation
[AD-A148695] 08 p1165 N85-17349
Eigenvalues of rotating machinery
08 p1167 N85-17361
Vibration analysis of a multipurpose platform
[NAL-TR-803] 09 p1286 N85-18078
Identification of vibration parameters of flexible structures 09 p1331 N85-18360
Coriolis effects on the vibrations of rotating beams, plates and shells 09 p1331 N85-18366
Impact of 810D on dynamic test laboratories
09 p1334 N85-18368
The Shock and Vibration Bulletin 54. Part 2: Ship shock, shock and blast and ground shock
[AD-A148132] 09 p1334 N85-18369
Direct energy minimization approach to whipping analysis of pressure hulls 09 p1335 N85-18393
The Shock and Vibration Bulletin 54. Part 3: Structural dynamics, machinery dynamics and vibration problems
[AD-A148133] 09 p1337 N85-18408
Increase in performance and improvement of ride comfort of self-propelled construction machinery by reducing pitch and vertical vibration
[AD-P004289] 09 p1405 N85-18845
Ride comfort of off-road vehicles
[AD-P004279] 09 p1406 N85-18855
Further development in ride quality assessment
[AD-P004280] 09 p1406 N85-18856

Characteristics of farm field profiles as sources of tractor vibration
[AD-P004262] 09 p1407 N85-18858
Integrated Technology Rotor/Flight Research Rotor (ITR/FRR) concept definition study
[NASA-CR-166444] 10 p1424 N85-18981
Fluidelastic instability in shell and tube heat exchangers: A framework for a prediction method
[DE84-006516] 10 p1496 N85-19444
Health standards for general vibration
10 p1523 N85-19607
Effects of overall vibration and noise on operational personnel 10 p1523 N85-19608
Acta Aeronautica et Astronautic Sinica (selected articles)
[AD-A148830] 11 p1575 N85-19922
Fractographic features of titanium alloy fatigue failure under repeated static stress and high frequency vibration 11 p1601 N85-20070
Modal testing and analysis of NOVA laser structures
[DE84-017569] 11 p1638 N85-20321
On the coupling of an anchored flame with an acoustic field
[COLL-AERON-8434] 12 p1799 N85-21282
Applications of vibration analysis to the condition monitoring of rolling element bearings
[ARL/AERO-R-163] 12 p1859 N85-21663
An analysis of the high frequency vibrations in early Thematic Mapper scenes 12 p1872 N85-21742
Nonlinear rotordynamics analysis
[NASA-CR-171425] 13 p1968 N85-22384
Normal mode calculations for fuselage type intricate structures by regarding them as systems with superposed constraints 13 p2048 N85-22817
The Shock and Vibration Digest, volume 16, no. 12
[AD-A150594] 13 p2102 N85-23102
Machine tool vibrations: A review
13 p2102 N85-23104
Flow-induced vibrations of a circular cylinder due to turbulent internal flows
[DE85-002766] 13 p2103 N85-23110
Condition monitoring of helicopter gearboxes using automatic vibration analysis techniques
14 p2223 N85-23790
Gear noise origins 14 p2224 N85-23791
Transmission error measurements in gearbox development 14 p2224 N85-23794
Some problems in improving reliability and accuracy of regulators with hydraulic amplifiers in main channel of power turbine 14 p2271 N85-24071
Oscillations of gas turbine installation rotors under operating conditions 14 p2272 N85-24077
Abatement of noise and vibration in pipelines of hydro systems 14 p2276 N85-24102
Effect of apparent fluid masses on natural vibration frequencies of impellers of multistage centrifugal pumps
14 p2277 N85-24108
Recent developments in the dynamics of advanced rotor systems
[NASA-TM-86859] 14 p2317 N85-24320
Flow induced vibration of the SSME LOX posts
[NASA-CR-175608] 15 p2495 N85-25391
Frequency/period estimation and adaptive rejection of periodic disturbances
[AD-A149229] 15 p2632 N85-26226
Raman scattering of light in epitaxial films of solid phosphide-gallium arsenide solutions
15 p2643 N85-26301
Stability and vibrations of internal windings of high-current superconducting solenoid magnets
[AD-A151465] 15 p2656 N85-26390
Identification and control of structures in space
[NASA-CR-175790] 16 p2731 N85-26850
The effect of inaccuracies in structural models on the control of large space structures
[AD-A151794] 16 p2732 N85-26858
Flow dynamic environment data base development for the SSME 16 p2736 N85-26885
Vibration characteristics of the HPOTP (High Pressure Oxygen Turbopump) of the SSME (Space Shuttle Main Engine) 16 p2736 N85-26885
Flow-induced vibration of the SSME LOX posts: Additional issues
[DE85-007339] 16 p2741 N85-26916
Measurement of damping of graphite epoxy materials
[NASA-CR-175793] 16 p2743 N85-26925
Suppression of vibration effects on piezoelectric crystal resonators
[AD-D011625] 16 p2778 N85-27142
Quasi-steady vibrations of a rotating shaft grazing an obstacle: Spiral vibration
[BLL-CE-TRANS-7962-(9022.09)]
16 p2790 N85-27256
Quantum statistical theory of vibrational dynamics in a laser-driven admolecule-surface system
[AD-A152022] 16 p2872 N85-27719
Natural vibrations of reinforced spherical shells
17 p2943 N85-28165
DOE/ANL/HTRI heat exchanger tube vibration data bank: Addendum 5
[DE85-007730] 17 p2980 N85-28425
Telescoping low vibration pulling mechanism for Czochralski crystal growth
[AD-D011655] 17 p3044 N85-28836
Turbine blade-tip clearance excitation forces
[NASA-CR-171534] 19 p3220 N85-29963
Forced structural response using component mode synthesis
[DE85-006479] 19 p3287 N85-30383
Vibration control experiment design for the 15-m hoop/column antenna 20 p3409 N85-31159
Time-optimal bang-bang slew of rigidized SCOLE configuration 20 p3410 N85-31164
Numerical and experimental evaluation for single-axis control of an LSS laboratory model
20 p3411 N85-31168
On the measurement of material damping in a simulated space environment 20 p3411 N85-31169
A phase-locked frequency multiplier for the signal averaging of the vibration of the Wessex helicopter input spiral bevel pinion
[AD-A154914] 21 p3555 N85-32113
Proposal for modifications to the Wessex helicopter main rotor gearbox vibration monitoring program
[AD-A155196] 21 p3555 N85-32117
Calculation of molecular constants potential energy curves and Franck-Condon factors for lead oxide
[AD-A154521] 21 p3562 N85-32158
Development of a temperature-compensated hot-film anemometer system for boundary-layer transition detection on high-performance aircraft
[NASA-TM-86732] 22 p3730 N85-33121
A modal parameter extraction procedure applicable to linear time-invariant dynamic systems
[NASA-CR-176120] 22 p3835 N85-33747
Accelerator vibration issues
[DE85-010766] 22 p3842 N85-33791
Dual optical mechanical position tracker
[AD-D011739] 22 p3844 N85-33811
Generated spiral bevel gears: Optimal machine-tool settings and tooth contact analysis
[NASA-TM-87075] 23 p3937 N85-34405
Nonlinear flap-lag-extensional vibrations of rotating, pretwisted, preconed beams including Coriolis effects
[NASA-TM-87102] 23 p3941 N85-34427
Laboratory vibration schedules
[AD-A155856] 24 p4064 N85-35188
Vibrations of free hollow circular cylindrical bodies
24 p4100 N85-35418
A normal incidence X-ray telescope sounding rocket payload
[NASA-CR-176169] 24 p4153 N85-35749

VIBRATION DAMPERS
U VIBRATION ISOLATORS

VIBRATION DAMPING
Modular design attitude control system
[NASA-CR-171182] 01 p0016 N85-10098
Highlights of the Institute of Sound and Vibration Research 01 p0131 N85-10905
Simulation of vibration processes in damped structures with allowance for temperature-frequency characteristics of vibration absorbing materials
02 p0257 N85-11680
Basic study of bladed disk structural response
[AD-A146226] 03 p0319 N85-12061
An appraisal of an out-of-phase feed-back system for the variation of damping of dynamic wind-tunnel models
[NMI-189] 03 p0320 N85-12065
Turbine blade damping study
[NASA-CR-171255] 04 p0456 N85-12890
Turbine blade damping study, introduction
04 p0456 N85-12891
Forced vibrations of friction-damped beam structures in two dimensions
[UDR-TM-82-08] 04 p0456 N85-12892
Experiments in control of flexible structures with uncertain parameters 05 p0602 N85-13837
Damping capacity of a sealed squeeze film bearing
05 p0645 N85-14139
F-8 refueling boom ground vibration test
[NASA-TM-84914] 07 p0902 N85-15713
Study to eliminate ground resonance using active controls
[NASA-CR-166609] 07 p0902 N85-15715
Damping capacity of multilayer tube during torsion
[BLL-M-36011-(5828.4)] 07 p0977 N85-16202
Photoemission, vibrational and stimulated desorption studies of metal-semiconductor interfaces and of chemisorbed atoms and molecules
[AD-A147709] 08 p1225 N85-17717
Shock response analysis by personal computer using the extended IFT algorithm 09 p1335 N85-18397
Experimental investigation of vibroimpact of two cantilever beams 09 p1336 N85-18399
The Shock and Vibration Bulletin 54. Part 3: Structural dynamics, machinery dynamics and vibration problems
[AD-A148133] 09 p1337 N85-18406
Structural modifications by viscoelastic elements
09 p1337 N85-18407
Stochastic dynamic analysis of a structure with frictional joints 09 p1337 N85-18408
The experimental performance of an off-road vehicle utilizing a semi-active suspension — off-road motorcylas
09 p1339 N85-18421
A theoretical investigation of an active suspension system for wheeled tractors
[AD-P004268] 09 p1405 N85-18844
Variable friction secondary seal for face seals
[NASA-CASE-LEW-14170-1] 11 p1647 N85-20377
The effect of an elastic foundation and of dissipative forces on the stability of fluid conveying pipes
[TAE-563] 12 p1883 N85-21688
A quantitative comparison of active and passive damping for large space structures
[UTIAS-TN-249] 13 p1998 N85-22524
Dynamic verification of large space structures
14 p2234 N85-23847
Passive and Active Control of Space Structures (PACOSS)
14 p2234 N85-23848
ACOSS 11 (Active Control Of Space Structures)
[AD-A150639] 14 p2246 N85-23922
Measurement of damping of graphite epoxy materials
[NASA-CR-175663] 14 p2248 N85-23931
Selection of bearing type for large steam turbines
14 p2271 N85-24069
Modeling and control of large flexible structures, phase 1
[AD-A150736] 14 p2403 N85-24817
Preliminary results on passive eddy current damper technology for SSME turbomachinery
16 p2737 N85-26890
A study of internal and distributed damping for vibrating turbomachiner blades
[NASA-CR-175901] 17 p2898 N85-27868
Stressed-strained state of tightening buckles in sectional runners of gas turbines 17 p2940 N85-28149
Continuum modeling of latticed structures
17 p2977 N85-28399
Vibration control of rotor shaft
[NASA-TM-87053] 18 p3117 N85-29292
Spillover minimization: An approach for actuators and sensors placement in distributed parameter study
[INPE-3525-PRE/746] 19 p3272 N85-30289
Variable force, eddy-current or magnetic damper
[NASA-CASE-LEW-13717-1] 19 p3279 N85-30333
A dual spin space station design
20 p3408 N85-31152
Stiffness control of large space structures
20 p3414 N85-31189
Sub-optimal control of nonlinear flexible space structures 20 p3414 N85-31190
Adaptive filtering for large space structures: A closed-form solution 20 p3417 N85-31206
A comparison of experimental and theoretical results for rotordynamic coefficients of four annular gas seals
[NASA-CR-176066] 21 p3596 N85-32332
Modelling and parameter estimation for distributed vibratory systems
[AD-A154518] 21 p3598 N85-32344
Fixed gain and adaptive techniques for rotorcraft vibration control
[NASA-CR-177344] 22 p3728 N85-33111
Flutter clearance of the Schweizer 1-36 deep-stall sailplane
[NASA-TM-85917] 22 p3729 N85-33118
A substructure coupling procedure applicable to general linear time-invariant dynamic systems
[NASA-CR-176144] 22 p3800 N85-33542
Multishaker modal testing
[NASA-CR-176139] 22 p3800 N85-33544

VIBRATION EFFECTS
NT POGO EFFECTS
Singular asymptotic expansions in nonlinear rotordynamics
[NASA-CR-174012] 01 p0017 N85-10100
The effects of helicopter vibration on the spinal system
[AD-A146274] 03 p0402 N85-12582
Experimental investigation of vibroimpact of two cantilever beams 09 p1336 N85-18399
Structural modifications by viscoelastic elements
09 p1337 N85-18407
Propeller propulsion system integration: State of technology survey
[NASA-CR-3882] 12 p1771 N85-21119
Role of mental work in human tolerance to total-body vibration 12 p1901 N85-21940

Singular asymptotic expansions in nonlinear rotordynamics 12 p1945 N85-22218
Suppression of vibration effects on piezoelectric crystal resonators
[AD-D011625] 16 p2778 N85-27142
Dual species ion implantation of ternary compounds based on In-Ga-As
[AD-D011617] 16 p2869 N85-27696
Flow-induced vibration of SSME main injector liquid-oxygen posts 17 p2912 N85-27951
Vibrations of rotors connected through couplings with backlash 17 p2940 N85-28147
Stressed-strained state of tightening buckles in sectional runners of gas turbines 17 p2940 N85-28149
A mechanical model of the human body and its application 24 p4129 N85-35598

VIBRATION ISOLATORS
Extended aeroelastic analysis for helicopter rotors with prescribed hub motion and blade appended penduluum vibration absorbers
[NASA-CR-172455] 03 p0315 N85-12036
Optimum design for nonlinear shock mounts for transient inputs 09 p1334 N85-18390
Gear case vibration isolation in a geared turbine generator 09 p1338 N85-18414
The analysis by the lumped parameter method of slade platform friction dampers used in the high pressure fuel turbopump on the space shuttle main engine 09 p1338 N85-18417
Vibrational loading mechanism of unitized corrugated containers with cushions and non-load-bearing contents 09 p1339 N85-18419
Vibration isolated cold plate assembly
[AD-D011444] 10 p1484 N85-19368
Evaluation of air and ground launched cruise missile navigational element containers
[AD-A149654] 12 p1774 N85-21138
Vibration isolator actuator
[AD-D011574] 14 p2321 N85-24343
Helicopter rotor
[CH-637890-A5] 15 p2470 N85-25245
Frequency/period estimation and adaptive rejection of periodic disturbances
[AD-A149229] 15 p2632 N85-26226
Preliminary results on passive eddy current damper technology for SSME turbomachinery 16 p2737 N85-26890
Consolidation theory with consideration of frame plasticity
[REPT-9/1984] 16 p2796 N85-27240
Aircraft rotor blade with passive tuned tab
[NASA-CASE-ARC-11444-1] 19 p3217 N85-29947
Variable force, eddy-current or magnetic damper
[NASA-CASE-LEW-13717-1] 19 p3279 N85-30333
Fast scintillation counter preamplifier for the observation of Linsley effect
[HE-4.7-9] 24 p4199 N85-36060
A mini-array for large air showers
[HE-4.7-10] 24 p4199 N85-36061

VIBRATION MEASUREMENT
The monitoring of machines
[CETIM-15-J-041] 04 p0510 N85-13253
Measuring large amplitudes of mechanical vibrations with laser interferometers 06 p0787 N85-15028
Emitted vibration measurement device and method
[NASA-CASE-MFS-25981-1] 11 p1635 N85-20299
Applications of the vibration probe to localized current measurements
[DE85-004702] 13 p2023 N85-22675
Ultrafast holography using optical fibers
[ISL-CO-238/83] 16 p2788 N85-27204
Monitoring of turbo-machines by shaft vibration measurement
[BLL-CE-TRANS-7900-(9022.09)] 16 p2799 N85-27255
Measurement of damping of graphite epoxy materials
[NASA-CR-176073] 21 p3596 N85-32334

VIBRATION METERS
NT SEISMOGRAPHS
System for automatic recording of vibration parameters 14 p2282 N85-24135

VIBRATION MODE
Helicopter rotor blade design for minimum vibration
[NASA-CR-3825] 01 p0006 N85-10032
Theoretical and experimental modal analysis of a rotor test rig — shipboard equipment
[AMTE(N)-TM-83079] 03 p0371 N85-12370
The use of an optical data acquisition system for bladed disk vibration analysis
[NASA-TM-86891] 06 p0817 N85-15184
The Shock and Vibration Digest, volume 16, no. 10
[AD-A147588] 09 p1331 N85-18361
A review of approximate methods for determining the vibrational modes of membranes 09 p1331 N85-18363
Optimization of vibrating beams including the effects of coupled bending and torsional modes 09 p1331 N85-18364
Leakage-flow-induced vibration of a tube-in-tube slip joint
[DE84-007301] 11 p1652 N85-20406
Unsteady transonic pressure measurements on a semi-span wind-tunnel model of a transport-type supercritical wing (Lann model). Part 2: Pressure distributions (plotted) and plots of the vibration modes
[AD-A130488] 12 p1846 N85-21579
Spline-based Rayleigh-Ritz methods for the approximation of the natural modes of vibration for flexible beams with tip bodies
[NASA-CR-172586] 13 p2102 N85-23100
Effect of axisymmetric vibration modes on sensitivity and directivity characteristics of piezoceramic sphere — hydrophones 15 p2525 N85-25589
Ultrafast holography using optical fibers
[ISL-CO-238/83] 16 p2788 N85-27204
A natural modes formulation and modal identities for structures with linear viscous damping
[CRC-1382] 18 p3120 N85-29312

VIBRATION PROTECTION
U VIBRATION ISOLATORS

VIBRATION SIMULATORS
The changing vibration simulation for military ground vehicles 09 p1334 N85-18387

VIBRATION TESTING MACHINES
U VIBRATION SIMULATORS

VIBRATION TESTS
NT DAMPING TESTS
Vibration, acoustic, and shock design and test criteria for components on the Solid Rocket Boosters (SRB), Lightweight External Tank (LWT), and Space Shuttle Main Engines (SSME)
[NASA-RP-1127] 01 p0061 N85-10405
F-8 refueling boom ground vibration test
[NASA-TM-84914] 07 p0902 N85-15713
Transient vibration test criteria for spacecraft hardware — galileo spacecraft 09 p1338 N85-18418
Flow-induced tube vibration thresholds in heat exchangers from shellside water tests
[DE84-006603] 11 p1652 N85-20407
Steam generator tube vibration tests
[DE85-003599] 12 p1867 N85-21712
Vibroacoustic study of the NASA Goddard Space Flight Center OSS-1 payload
[NASA-CR-175320] 13 p1968 N85-22465
Investigation of gas-turbine engine blower impeller vibrations with change in engine intake conditions 14 p2287 N85-24170
Vibrations of rotors connected through couplings with backlash 17 p2940 N85-28147
Seakeeping and vibration tests of the Coast Guard 110 foot surface effect ship SEA BIRD class (WSES)
[AD-A154150] 19 p3252 N85-30166

VIBRATIONAL FREQUENCIES
U VIBRATIONAL SPECTRA

VIBRATIONAL RELAXATION
U MOLECULAR RELAXATION

VIBRATIONAL SPECTRA
Vibrational power transmission of an idealised gearbox
[ISVR-TR-124] 02 p0204 N85-11346
Optimizing CW CO2 lasers with respect to output power in different bands 02 p0271 N85-11766
Structure of vibrational spectrum and selection rules in Raman and hyper-Raman light scattering spectra of inorganic glasses 02 p0271 N85-11769
Molecular beam scattering 03 p0417 N85-12666
Investigation on experimental techniques to detect, locate and quantify gear noise in helicopter transmissions
[NASA-CR-3847] 08 p1217 N85-17867
Quantum mechanical and semiclassical approaches to molecular dynamics
[DE85-003458] 10 p1555 N85-19803
An analysis of short-to-medium-range seismic attenuation tests using a multilayered viscoelastic seismic propagation model
[AD-A149771] 12 p1869 N85-21856
Adsorption site, adsorption energy and normal vibration frequency of H/Ni(100) via total energy calculations
[AD-A150555] 13 p2156 N85-23386
Observation of surface vibrational resonances on (110) surfaces of FCC metals
[AD-A150469] 13 p2163 N85-23419
Dipole active surface vibrational resonances on clean and hydrogen covered Ni(110)
[AD-A150546] 13 p2163 N85-23420
Calculations of collision-induced optical gain in high-density mixtures of D2 or HD with a buffer gas
[AD-A151372] 15 p2648 N85-26330
A measurement of the vibrational band strength for the upsilon sub 3 band of the HO2 radical
[NASA-CR-175858] 16 p2744 N85-26936
Vibrational spectra of a-Fe(.78)P(.22) by inelastic neutron scattering
[DE85-008296] 17 p2922 N85-28016
Investigation of several low-lying levels of X doublet pi state of NCO using argon laser excited fluorescence
[AD-A153693] 18 p3071 N85-28994
Vibrational properties of disordered solids: Far infrared studies
[DE85-010400] 19 p3377 N85-30951
Requirements for attaining Treanor's distribution of vibrational energy among CO2 levels in CW gasdynamic laser flows
[STN-3] 20 p3461 N85-31499
Modelling and parameter estimation for distributed vibratory systems
[AD-A154518] 21 p3598 N85-32344
Time-resolved spectroscopic studies of detonating heterogeneous explosives
[DE85-009760] 23 p3921 N85-34297
The photodissociation of acetylene at 193.3 NM
[AD-A155775] 24 p4075 N85-35255
Circumstellar shells of late-type stars: A study at millimeter and infrared wavelengths 24 p4167 N85-35836

VIBRATIONAL STRESS
Influence of secondary flow rate on dynamic stresses in turbine rotor blades 09 p1306 N85-18205
Comparison of measured and simulated ride comfort for an agricultural tractor and influence of travel speed and tyre-inflation pressure on dynamic response
[AD-P004281] 09 p1407 N85-18857
Investigation of gas-turbine engine blower impeller vibrations with change in engine intake conditions 14 p2287 N85-24170

VIBRATORY LOADS
Damping capacity of multilayer tube during torsion
[BLL-M-36011-(5628.4)] 07 p0977 N85-16202
Measurement and evaluation of the loading of shafts by torsional vibrations 07 p0980 N85-16222
Vibrational loading mechanism of unitized corrugated containers with cushions and non-load-bearing contents 09 p1339 N85-18419

VIBROMETERS
U VIBRATION METERS

VIDEO COMMUNICATION
Videotex and weather services: Finnish applications 01 p0084 N85-10567
Video concepts in CRM training 09 p1276 N85-18015
Combined processing method and matched filter for discrete composite frequency phase-shift keyed signal 13 p2070 N85-22931
Development of thin film hybrid IC active filter for video band use
[NHK-LABS-NOTE-312] 18 p3094 N85-29153
Optical multiplexing on monomode fibers
[ENST-83E016] 20 p3533 N85-31982

VIDEO DATA
Flight demonstration of new NRL real-time data acquisition system and laser video waveform sampler
[AD-A145126] 01 p0053 N85-10350
Videotex and weather services: Finnish applications 01 p0084 N85-10567
High-speed videography for optical and X-ray imaging
[DE84-012661] 04 p0564 N85-13595
Atmospheric wind and diffusion from analysis of an SF6 release at 350 km altitude
[AD-A147965] 08 p1185 N85-17471
Producing high scene content with perspective validity
[AD-P004314] 09 p1268 N85-17968
Automated and interactive data base generation
[AD-P004316] 09 p1268 N85-17970
Geographic subdivision and top level data structures, Columbus, Magellan, and expanding CIG (Computer Image Generation) horizons
[AD-P004317] 09 p1268 N85-17971
CIG (Computer Image generation) data bases in an instance: Bits and pieces
[AD-P004318] 09 p1269 N85-17972
Extracting digital data from a bus and multiplexing it with a video signal
[AD-D011491] 11 p1636 N85-20302
Television animation store: Digital chroma, key and mixer units
[BBC-RD-1984/16] 12 p1824 N85-21442
Performance of time-position discriminator of composite signal 13 p2072 N85-22941
Evaluating identifiability in remote sensing problems 15 p2486 N85-25347
Processing speech for analysis using optical Fourier techniques
[AD-A151898] 15 p2544 N85-25704
Design issues in video disc map display
[AD-A153531] 18 p3109 N85-29253
Video discs - what are they and where do they fit in?
[AD-A154166] 20 p3458 N85-31479

Balloon-borne video cassette recorders for digital data storage
[OG-9.3-11] 21 p3715 N85-33050
Relaxation techniques
[AD-A156248] 24 p4133 N85-35621
Aeronautical Systems Division Manufacturing/Quality assurance orientation
[AD-A156128] 24 p4164 N85-35817

VIDEO DISKS
Requirements and specifications for cartographic video discs
[AD-A144906] 01 p0049 N85-10325
Analog disc recorder system: Operator's reference manual
[DE84-016026] 04 p0503 N85-13209
Low altitude high speed flight simulation using video disc technology
[AD-P004312] 09 p1268 N85-17966
Design issues in video disc map display
[AD-A153531] 18 p3109 N85-29253
Video discs - what are they and where do they fit in?
[AD-A154166] 20 p3458 N85-31479
Realizing the full potential of the video disc for mapping applications
[AD-A154966] 21 p3606 N85-32391
Electronic file system on an SM 90 minicomputer: The SARDE project
[ENST-84E018] 22 p3828 N85-33705
Balloon-borne video cassette recorders for digital data storage
[OG-9.3-11] 23 p4028 N85-34966

VIDEO EQUIPMENT
NT PICTURE TUBES
Development of a dynamic radiographic capability using high-speed video
[DE84-016477] 04 p0511 N85-13256
Visual systems for remotely controlled vehicles 05 p0703 N85-14512
VICOM technical description
[REPT-611-0012-REV-A] 06 p1202 N85-17563
Television animation store: Recording pictures on a parallel transfer magnetic disc
[BBC-RD-1984/17] 10 p1462 N85-19220
Video animation system
[DE85-005494] 14 p2405 N85-24831
Operation of autotracking system in various video playback modes 16 p2764 N85-27055
Atmospheric Emission Photometric Imaging (AEPI) 23 p3902 N85-34170

VIDEO SIGNALS
Transient currents of ideally conducting body of revolution with transient diffraction 06 p0785 N85-15019
Electrooptical sensor for automatic detection of objects 06 p0789 N85-15040
New technology high efficiency and high stability color motion video compression system
[AD-A147523] 07 p0941 N85-15968
Analysis of threshold effects during estimation of arrival time of optical signals 07 p0951 N85-16030
Extracting digital data from a bus and multiplexing it with a video signal
[AD-D011491] 11 p1636 N85-20302
Television camera video level control system
[NASA-CASE-MSC-18578-1] 12 p1821 N85-21427
Operation of autotracking system in various video playback modes 16 p2764 N85-27055
Hardware test program for evaluation of baseline range-range rate sensor concept
[NASA-CR-175794] 16 p2787 N85-27193
Synthesis of optimum receiver and processor for interfering radio pulse signals 22 p3769 N85-33761

VIDICONS
NT RETURN BEAM VIDICONS
NT THERMICONS
Programmable optical sensor
[AD-D011244] 02 p0281 N85-11829
Mars polar volatiles: Topographic and geologic setting
[NASA-CR-174089] 04 p0581 N85-13708
The development of new techniques in laser spectroscopy 19 p3233 N85-30041
LI481 and LI482 vidicons for two-tube color TV cameras with improved image quality 22 p3764 N85-33333

VIEW EFFECTS
Integration of multispectral data obtained at different view angles for vegetation analysis 05 p0657 N85-14218

VIEWING
NT FIELD OF VIEW
Improved radiographic viewing system
[AD-A147587] 07 p1016 N85-16456
Double window viewing chamber assembly
[NASA-CASE-MFS-28057-1] 18 p3063 N85-28951

VIKING LANDER SPACECRAFT
NT VIKING LANDER 1
Conclusion of Viking Lander Imaging Investigation: Picture catalog of experiment data record
[NASA-RP-1137] 11 p1765 N85-21099
The search for igneous materials at the Viking landing sites 13 p2194 N85-23609

VIKING LANDER 1
Analysis of the Viking Lander 1 surface wind vector for sols 45 to 375
[NASA-CR-174349] 09 p1416 N85-18932
Observed changes at Viking Lander 1 13 p2188 N85-23575

VIKING MARS PROGRAM
The Mars ancient cratered terrain, smooth plains boundary: Implications of Viking color data for evolution of the Amenthes Region 15 p2682 N85-26564

VIKING ORBITER SPACECRAFT
Geomorphic classification of Icelandic and Martian volcanoes: Limitations of comparative planetology research from LANDSAT and Viking orbiter images 21 p3603 N85-32372

VIKING SPACECRAFT
NT VIKING LANDER SPACECRAFT
NT VIKING LANDER 1
NT VIKING ORBITER SPACECRAFT
Participation in the Mars Data Analysis Program: Analysis of cloud forms in Viking and Mariner 9 images
[NASA-CR-175604] 13 p2204 N85-23673

VIKING 1 SPACECRAFT
NT VIKING LANDER SPACECRAFT
NT VIKING LANDER 1
NT VIKING ORBITER SPACECRAFT

VIKING 2 SPACECRAFT
NT VIKING LANDER SPACECRAFT
NT VIKING ORBITER SPACECRAFT

VINYL COPOLYMERS
Vinyl citrates from citric acid as new monomers
[BMFT-FB-T-83-256] 03 p0338 N85-12178
Ferroelectric homopolymer PVF2 and P (VDF-TrFe) copolymers 24 p4089 N85-35347

VINYL CYANIDE
U ACRYLONITRILES

VINYL ETHYLENE
U BUTADIENE

VINYL POLYMERS
NT POLYVINYL FLUORIDE
Development of new and improved polymer matrix resin systems, phase 1
[NASA-CR-166595] 01 p0017 N85-10104
Dynamic polymer pressure transducer with temperature compensation
[AD-D011373] 07 p0967 N85-16142
Chiral polymers
[AD-A150366] 13 p2037 N85-22760
A new large-scale, high-resolution multicolor software display concept
[AD-A155404] 22 p3827 N85-33703
Development and demonstration of a spiral-wound thin-film composite membrane system for the economical production of oxygen-enriched air, phase 4
[DE85-012380] 23 p3920 N85-34288
High temperature polymer concrete
[DE85-005756] 23 p3920 N85-34290

VINYL RADICAL
(Vinyloxy)fluorocyclotriphosphazenes
[AD-A147448] 07 p0924 N85-15850

VINYLIDENE
Synthesis and characterization of poly(vinylidene fluoride)
[AD-A150291] 13 p2037 N85-22759
C2H(n) fragments on metal surfaces
[AD-A151474] 15 p2505 N85-25449

VIOLENCE
NT ATTACKING (ASSAULTING)

VIRGINIA
Late precambrian to ordovician metamorphism and orogenesis in the Blue Ridge and western Piedmont, Virginia Appalachians 09 p1352 N85-18503
Intraband radiometric performance of the LANDSAT 4 Thematic Mapper — Washington, DC, Arkansas, Massachusetts, Virginia, and Arizona 12 p1871 N85-21738

VIRGO GALACTIC CLUSTER
Virgo cluster as a high energy cosmic rays source
[OG-5.4-8] 22 p3886 N85-34085

VIRGO STAR CLUSTER
U VIRGO GALACTIC CLUSTER

VIRIAL COEFFICIENTS
A virial equation of state option for the TIGER computer program
[AD-A147490] 07 p1025 N85-16507
Measurement of gas compressibility factor data for natural gas and synthetic gas components and their mixtures
[PB85-129047] 11 p1614 N85-20151
Observations of current pulsations of characteristics in atmosphere with period of about 1.5 hours 14 p2341 N85-24480

VIRIAL THEOREM
On experimental equations of state for Boson gases
[PTB-ME-61] 04 p0574 N85-13659
Potential at atomic boundaries in the TF (or TFD) model and equations of states 12 p1820 N85-21419

VIRTUAL PROPERTIES
The principle of virtual work and associated variational principles
[ESA-TT-873] 09 p1340 N85-18428

VIRUSES
Molecular interactions of high energy fuels and jet fuels with oncogenic viruses and endogenous viruses
[AD-A145484] 02 p0188 N85-11255
The effects of simulated weightlessness on susceptibility to viral and bacterial infections using a murine model 15 p2613 N85-26100
Using the information of cosmic rays to predict influence epidemic
[SH-10.1-2] 23 p4053 N85-35134

VISCERA
NT ADRENAL GLAND
NT BLADDER
NT INTESTINES
NT KIDNEYS
NT LIVER
NT LUNGS
NT ORGANS
NT PANCREAS
NT PARATHYROID GLAND
NT PITUITARY GLAND
NT RECTUM
NT SPLEEN
NT THYMUS GLAND
NT THYROID GLAND

VISCOELASTIC DAMPING
A quantitative comparison of active and passive damping for large space structures
[UTIAS-TN-249] 13 p1998 N85-22524
Finite element prediction of loss factors for structures with frequency-dependent damping treatments 15 p2576 N85-25889

VISCOELASTIC FLOW
U VISCOELASTICITY

VISCOELASTICITY
NT PHOTOVISCOELASTICITY
NT THERMOVISCOELASTICITY
Nuclear Magnetic Resonance of Polymeric Materials
[AD-A145078] 01 p0032 N85-10192
NMR (Nuclear Magnetic Resonance) and macromolecular migration in a melt or in concentrated solutions
[AD-P003908] 01 p0032 N85-10194
On wave propagation in linear viscoelasticity
[AD-A144739] 01 p0111 N85-10750
Determination of nonlinear viscoelasticity parameters for polymeric and composite materials by numerical methods
[AD-A145311] 02 p0185 N85-11240
Acceleration waves 02 p0207 N85-11367
Accelerated viscoelastic characterization of T300/5208 graphite-epoxy laminates 03 p0325 N85-12091
Numerical simulations of compliant material response to turbulent flow, revision 1
[AD-A145801] 03 p0372 N85-12373
Finite element method for a class of viscoelastic flows in deforming domains applied to jet breakup
[DE84-014571] 04 p0500 N85-13186
Dynamics of liquid filament breakup
[DE84-016008] 04 p0500 N85-13187
Constraints on the origin of viscoelastic bodies 04 p0584 N85-13732
Existence of slow steady flows of viscoelastic fluids with differential constitutive equations
[AD-A147240] 07 p0959 N85-16077
Study of reaction kinetics and development of elastic properties in network polymerization systems by the impulse technique
[AD-A148187] 08 p1133 N85-17141
An efficient numerical solution technique for wave propagation in horizontally stratified ocean environments
[AD-A148537] 08 p1190 N85-17502
A finite element analysis of viscoelastic materials with varying time scales 09 p1330 N85-18355
Structural modifications by viscoelastic elements 09 p1337 N85-18407
Recent developments and open problems in the mathematical theory of viscoelasticity
[AD-A149043] 10 p1545 N85-19742
Single integral constitutive equations for viscoelastic fluids
[AD-A149410] 10 p1547 N85-19756
Stability of viscoelastic constructions subjected to steady random compressing loads 11 p1720 N85-20819

Accelerated viscoelastic characterization of T300-5208 graphite-epoxy laminates
[NASA-CR-3871] 12 p1797 N85-21271
Algorithm for the simulation of transient viscoelastic flows with free surfaces
[DE85-002713] 12 p1848 N85-21590
Journal of Research of the National Bureau of Standards, volume 89, number 2, March - April 1984
[PB85-115426] 12 p1926 N85-22103
Mechanics of polymers and composites: Research opportunities
[DE85-007052] 15 p2503 N85-25442
Fracture problems in power law viscoelastic materials
[AD-A149221] 15 p2578 N85-25900
Uniqueness and stability in nonlinear elasticity and viscoelasticity
[AD-A151470] 15 p2637 N85-26264
Dynamic response of shells and plates subjected to variable magnitude traveling loads
16 p2798 N85-27250
Vortices in non-Newtonian fluids
[AD-A153169] 17 p2958 N85-28269
Theoretical and experimental studies of the mechanics of viscoelastic liquids
[AD-A153505] 18 p3070 N85-28967
Hyperbolic phenomena in the flow of viscoelastic fluids
[AD-A153533] 18 p3099 N85-29186
Prediction of lifetime for ceramic materials in the elastic and viscoelastic region by fracture mechanical methods
[ESA-TT-825] 20 p3434 N85-31305
Finite element methods for viscoelastic flow
[AD-A154877] 22 p3783 N85-33437
Experimental study on time and temperature dependent behavior of crack growth in viscoelastic strip
23 p3905 N85-34193
Viscoelastic behavior of short-fiber composite materials
[DE85-011233] 23 p3910 N85-34225
Three-dimensional finite deformation viscoelastic model accounting for damage effects
[DE85-012951] 24 p4139 N85-35660

VISCOMETRY
Interpolation formulas for viscosity of six gases: Air, nitrogen, carbon dioxide, helium, argon and oxygen
[PB84-217801] 01 p0026 N85-10161

VISCOPLASTIC FLOW
U VISCOPLASTICITY

VISCOPLASTICITY
Viscoplastic finite element analysis of rapid fracture
03 p0370 N85-12365
Life prediction at high temperature under multiaxial loading
07 p0907 N85-15745
Viscoplastic constitutive relationships with dependence on thermomechanical history
[NASA-CR-174836] 12 p1864 N85-21691
On thermomechanical testing in support of constitutive equation development for high temperature alloys
[NASA-CR-174879] 15 p2577 N85-25894
Uniqueness and stability in nonlinear elasticity and viscoelasticity
[AD-A151470] 15 p2637 N85-26264
Some advances in experimentation supporting development of viscoplastic constitutive models
[NASA-CR-174855] 16 p2799 N85-27260
Interaction of large amplitude stress waves in layered elasto-plastic materials
[AD-A153519] 18 p3121 N85-29323
Nonlinear Constitutive Relations for High Temperature Application, 1984
[NASA-CP-2369] 20 p3465 N85-31530
Viscoplasticity based on overstress with a differential growth law for the equilibrium stress
20 p3466 N85-31532
Constitutive modeling of superalloy single crystals and directionally solidified materials
20 p3466 N85-31535
On the use of internal state variables in thermoviscoplastic constitutive equations
20 p3466 N85-31536
Physical concepts in the development of constitutive equations
20 p3467 N85-31537
Some advances in experimentation supporting development of viscoplastic constitutive models
20 p3468 N85-31545
Creep crack growth predictions in INCO 718 using a continuum damage model
20 p3469 N85-31551
Short-time creep of ice
[NRC/CNR-TT-2111] 23 p3941 N85-34428
Development and application of a unified viscoelastic constitutive model for the prediction of material response under thermomechanical loading
24 p4101 N85-35420

VISCOSITY
NT EDDY VISCOSITY
NT GAS VISCOSITY
Interpolation formulas for viscosity of six gases: Air, nitrogen, carbon dioxide, helium, argon and oxygen
[PB84-217801] 01 p0026 N85-10161
Laminar flow heat exchangers. Viscosity induced non-uniform flow
[AD-A144777] 01 p0047 N85-10307
External fuel vaporization study, phase 2
[NASA-CR-174079] 02 p0187 N85-11252
An investigation of the suitability of using a Seiglaff-McKelvey high shear rate melt rheometer for the measurement of low viscosity polymer solutions
[AD-A146275] 03 p0338 N85-12174
Numerical simulations of fuel droplet flows using a Lagrangian triangular mesh
[AD-A146087] 03 p0382 N85-12320
Development of acceptance criteria for batches of silane primer for external tank thermal protection system bonding applications
[NASA-CR-171266] 04 p0478 N85-13043
Toughening mechanism in elastomer-modified epoxy resins, part 2
[NASA-CR-3852] 04 p0478 N85-13046
A simple extension to multidimensional problems of the artificial viscosity due to Lapidus
06 p0808 N85-15134
Viscosity measurements for thick-film pastes
06 p0831 N85-15280
Structural relaxation and isoconfigurational flow of a metallic glass near equilibrium
[AD-A147888] 07 p0933 N85-15915
Viscosity solutions of Hamilton-Jacobi equations at the boundary
[AD-A147444] 07 p1032 N85-16553
On existence and uniqueness of solutions of Hamilton-Jacobi equations
[AD-A147597] 07 p1033 N85-16560
Research into topics in transonic flow theory
[AD-A148526] 08 p1078 N85-16837
A Van Leer shock capturing algorithm for the Euler equations
[AD-A148761] 08 p1163 N85-17335
New discovery in supersonic flight research
09 p1278 N85-18041
Metallographic grinding efficiency
[DE85-001520] 09 p1304 N85-18194
Blood viscosity responses to acute exercise and aerobic conditioning in women 09 p1363 N85-18573
Neumann type boundary conditions for Hamilton-Jacobi equations
[AD-A149069] 10 p1546 N85-19746
Hamilton-Jacobi equations in infinite dimensions. Part 1. Uniqueness of viscosity solutions
[AD-A149094] 10 p1546 N85-19749
Structure-phase state and properties of high-durability VAL8 alloy 11 p1597 N85-20046
Trends of petroleum fuels
[DE85-000116] 14 p2263 N85-24023
Mixing in the solar interior 14 p2446 N85-25095
Models of solar differential rotation
14 p2446 N85-25097
Possible use of rapid heating for improving mechanical properties of titanium alloys 15 p2498 N85-25409
Mean free paths, viscosity, and the limitations of perfect fluid hydrodynamics in the description of the quark-gluon plasma
[DE85-005501] 15 p2649 N85-26339
Viscosity in Saturn's rings 15 p2674 N85-26507
Characterization-curing-property studies of HBRF 55A resin formulations
[NASA-CR-175836] 16 p2753 N85-26989
Aerodynamic performance of a wing in ground effect using the PANAIR program
[AD-A153303] 17 p2892 N85-27832
Evaluation of used crankcase oils using computerized infrared spectrometry
[AD-A152993] 17 p2920 N85-27999
Thermophysical properties correlations and pseudocomponent characterization parameter estimation for fossil fluids
[DE85-009297] 19 p3230 N85-30024
Synthesis and characterization of novel polymers from non-petroleum sources for use in enhanced oil recovery
[DE85-010922] 19 p3250 N85-30151
On spectral multigrid methods for the time-dependent Navier-Stokes equations
[NASA-CR-172613] 19 p3344 N85-30725
Floating shock-fitting in transonic potential flow calculations 20 p3387 N85-31007
Large-time behavior of viscous surface waves
[AD-A154805] 21 p3584 N85-32278
Thermophysical properties of fluids for the gas industry
[PB85-196471] 22 p3747 N85-33227
Dynamic compensation of Venus's geoid: A comparison with Earth 22 p3858 N85-33688
Method for controlling the viscosity of siloxane oils
[DE85-011586] 23 p3909 N85-34221
Measurement and correlation of jet fuel viscosities at low temperatures
[NASA-CR-174911] 23 p3921 N85-34295
Chemoviscosity modeling for thermosetting resins, 2
[NASA-CR-177958] 24 p4073 N85-35243
Determination of the viscosity number of thermoplastics in dilute solution; polyamides (PA)
[NASA-TM-77673] 24 p4081 N85-35296
Study of the parameters affecting the collapse of a rotating protostellar cloud 24 p4166 N85-35837

VISCOUS DAMPING
NT VISCOELASTIC DAMPING
Results for second order hyperbolic systems with viscous dumping
[AD-A151100] 15 p2555 N85-25765
Viscosity in Saturn's rings 15 p2674 N85-26507
A natural modes formulation and modal identities for structures with linear viscous damping
[CRC-1382] 18 p3120 N85-29312

VISCOUS DRAG
Aircraft drag reduction technology
06 p1070 N85-16782
Numerical study of large-eddy breakup and its effect on the drag characteristics of boundary layers
[NASA-CR-3884] 12 p1797 N85-21272

VISCOUS FLOW
NT BOUNDARY LAYER FLOW
NT BOUNDARY LAYER SEPARATION
NT COUETTE FLOW
NT REATTACHED FLOW
NT SECONDARY FLOW
NT SEPARATED FLOW
NT STOKES FLOW
Prediction of aerodynamic characteristics of fighter wings at high angles of attack
[AD-A145107] 01 p0003 N85-10017
Gas flow environment and heat transfer nonrotating 3D program 02 p0142 N85-10966
Nonsteady motion of solid sphere in compressible viscous fluid 02 p0269 N85-11753
Model equation for simulating flows in multistage turbomachinery
[NASA-TM-86869] 03 p0315 N85-12036
Vorticity amplification in viscous flow around a body
03 p0360 N85-12309
Viscous-inviscid aerodynamic analysis of two-dimensional thrust augmentors
[NASA-CR-177321] 04 p0451 N85-12861
Numerical calculations of stratified Ekman layer flow over ridges with a finite element model
[DE84-014482] 04 p0499 N85-13179
Bicomponent flow problems in rheological fluid mechanics 05 p0635 N85-14073
Answering thermodynamic questions with three-dimensional viscous flow calculations
05 p0636 N85-14081
Review of requirements and status of simulation and scaling of transonic, viscous flows
[AD-A148357] 06 p0908 N85-15137
Analytical modeling of circuit aerodynamics in the new NASA Lewis wind tunnel
[NASA-TM-86912] 07 p0897 N85-15688
Recent advances in computational methods to solve the high-lift multi-component airfoil problem
08 p1068 N85-16774
Aerodynamic issues in the design of high-lift systems for transport aircraft 08 p1069 N85-16780
Research done at DERAT (October 1982 through September 1983); summary of principal results obtained
[NASA-TM-77786] 08 p1228 N85-17730
Theoretical study of non-linear unsteady aerodynamics of a non-rigid lifting body
[AD-P004169] 09 p1288 N85-17954
Numerical approach for the aerodynamic analysis of airfoils with laminar separation
[NASA-CR-172496] 09 p1273 N85-18001
Numerical predictions for unsteady viscous flow past an array of cylinders 09 p1316 N85-18284
Viscous effects on transonic airfoil stability and response
[NASA-TM-86374] 10 p1421 N85-18981
Thrust chamber performance using Navier-Stokes solution — space shuttle main engine viscous nozzle calculation
[NASA-CR-171346] 10 p1430 N85-19019
A multistage time-stepping scheme for the Navier-Stokes equations
[NASA-CR-172527] 10 p1483 N85-19365
Flow and plasticity via nonequilibrium molecular dynamics
[DE85-001011] 10 p1555 N85-19804
Calculation of three-dimensional, viscous flow through turbomachinery blade passages by parabolic marching
[NASA-TM-86984] 14 p2211 N85-23711

Stability of steady rotation of a cylinder filled with a stratified viscous incompressible fluid
14 p2278 N85-24112
Computations for segmented radial bearings
14 p2268 N85-24180
Contribution to the theory of stationary separation areas
[NASA-TM-77825] 14 p2300 N85-24244
The generation of three-dimensional body-fitted coordinate systems for viscous flow problems
[AD-A150861] 14 p2408 N85-24848
Numerical calculation of subsonic jets in crossflow with reduced numerical diffusion
[NASA-TM-87003] 15 p2472 N85-25203
Investigation of potential and viscous flow effects contributing to dynamic stall
[AD-A151696] 15 p2557 N85-25773
Viscous effects on blast wave flowfields
[AD-A152013] 15 p2558 N85-25779
Numerical solutions of 3-dimensional Navier-Stokes equations for closed bluff-bodies
[NASA-CR-175756] 15 p2636 N85-26255
A numerical procedure on three-dimensional parabolic flow in duct
16 p2692 N85-26620
Computational aerodynamics in designing aircraft
16 p2693 N85-26622
Recent progress in computational aerodynamics
16 p2693 N85-26626
The role of computational fluid dynamics in aeronautical engineering
16 p2694 N85-26629
Numerical analysis of flow non-uniformity in the hot gas manifold of the Space Shuttle main engine
16 p2738 N85-26699
Proceedings of the 9th US Air Force and the Federal Republic of Germany Data Exchange Agreement Meeting, Viscous and Interacting Flow Field Effects
[AD-A153020] 17 p2958 N85-28286
A second-order pressure-correction method for viscous incompressible flow
[REPT-84-15] 17 p2960 N85-28280
Numerical computation of space shuttle orbiter flow field
[NASA-CR-175912] 18 p3058 N85-28921
Instability at the interface between two shearing fluids in a channel
[AD-A153532] 18 p3099 N85-29185
Application of computational fluid dynamics to complex inlet ducts
[NASA-TM-87060] 19 p3265 N85-30247
Viscous flows in rotating pipes with internal cavities and related vortex breakdowns
[NASA-TM-86761] 20 p3454 N85-31447
A new finite element approach: Progress in inviscid flow computations
[NASA-TM-86434] 20 p3454 N85-31450
Tip vortex computer code SRATIP. User's guide
[NASA-CR-172603] 21 p3551 N85-32093
Large-time behavior of viscous surface waves
[AD-A154805] 21 p3584 N85-32278
Computation of three-dimensional, inviscid, rotational flows
21 p3587 N85-32296
A 3-D Euler method for internal transonic flows computation with a multi-domain approach
21 p3587 N85-32298
Exact solutions of singular equations for viscous transonic flows
21 p3683 N85-32682
On the importance of viscous dissipation in Io
22 p3855 N85-33873
Scalar/Vector potential formulation for compressible viscous unsteady flows
[NASA-CR-3921] 23 p3893 N85-34113
A three-dimensional viscous flow analysis for the helicopter tip vortex generation problem
[NASA-CR-3906] 23 p3893 N85-34114
Stability of two-dimensional immiscible flow to viscous fingering
[DE85-011403] 23 p3931 N85-34364
Elastohydrodynamic lubrication calculations used as a tool to study scuffing
[NASA-TM-87097] 23 p3938 N85-34408
Cooling high intensity atomic hydrogen beams to liquid helium temperatures
[DE85-012515] 24 p4148 N85-35718

VISCOUS FLUIDS
Fluctuation spectrum for linear gyroviscous MHD
[IPP-6/237] 01 p0121 N85-10828
Wave propagation in compliant tubes containing a heat-conducting viscous fluid
[WTHD-163] 05 p0638 N85-14094
Sedimentation of two arbitrarily oriented spheroids in a viscous fluid
[AD-A147303] 07 p0960 N85-16082
Analysis of the surface load and radiated sound of a vibrating airfoil with application to the experiment of Brooks
[NASA-CR-3864] 07 p1038 N85-16590
Boundary layer at moving cylinder surface
16 p2765 N85-27064
Theoretical and experimental studies of the mechanics of viscoelastic liquids
[AD-A153505] 18 p3070 N85-29867
Instability at the interface between two shearing fluids in a channel
[AD-A153532] 18 p3099 N85-29185
Couette flow of two fluids between concentric cylinders
[AD-A155827] 24 p4093 N85-35376

VISIBILITY
Shipboard measurement of cloud bases and average surface visibility with an eye-safe lidar
[AD-A144869] 01 p0052 N85-10345
Joint probability of selected cloud and visibility thresholds around Koblenz, Germany
[AD-A145294] 02 p0231 N85-11506
Air-to-air visual acquisition performance with TCAS 2
[FAA-PM-84-17] 02 p0236 N85-11537
Visibility of various target-background color combinations under different chromatic ambient illuminations
[AD-A146348] 03 p0420 N85-12684
Revised Uniform Summary of Surface Weather Observations (RUSSWO). Alconbury RAF United Kingdom, parts A-F
[AD-A146913] 07 p1004 N85-16384
Revised Uniform Summary of Surface Weather Observations (RUSSWO). McChord AFB, Washington, parts A-F
[AD-A146914] 07 p1005 N85-16385
Revised Uniform Summary of Surface Weather Observations (RUSSWO). Mildenhall RAF, United Kingdom, parts A-F
[AD-A146915] 07 p1005 N85-16386
Revised Uniform Summary of Surface Weather Observations (RUSSWO). Dobbins AFB, Georgia, parts A-F
[AD-A146916] 07 p1005 N85-16387
Experiments in forecasting atmospheric marine horizontal visibility using model output statistics with conditional probabilities of discretized parameters
[AD-A147574] 07 p1006 N85-16404
Evaluation of nose, roof, and mast mounted sensor platforms for piloting and sighting, integrated in future combat helicopters
08 p1074 N85-16808
The visibility climatology of McMurdo Sound-Williams Field, Antarctica
[AD-A148108] 08 p1189 N85-17492
Selecting one among the many: A simple network implementing shifts in selective visual attention
[AD-A148989] 10 p1530 N85-19644
Analysis of a visual performance experiment
[DE85-000710] 10 p1530 N85-19645
Impact of aerosols on visibility and climate: A report prepared for Panel 3, Environmental Impact, of the NATO/CCMS Air Pollution Pilot Study on Air Pollution Control Strategies and Impact Modelling
[PB85-106744] 12 p1897 N85-21906
The accuracy in calculations of intervisibility with digital terrain models — digital models
[FOA-C-20557-D8(E1)] 12 p1909 N85-21983
Visibility of small objects in turbid atmosphere
14 p2342 N85-24482
Retroreflective armbands: Influences of wearing mode, aging and other factors on the visibility distance
[IZF-1984-26] 14 p2422 N85-24942
Determination of the observation conditions of celestial bodies with the aid of the DISPO system
[NAS 1.15:77632] 14 p2436 N85-25044
Comparison of some West German cloud height and visibility data — weapon test sites
[BAE-BT-12734] 15 p2593 N85-25982
Poisson and multinomial shadowing processes
[AD-A151600] 15 p2640 N85-26286
Air quality benefit analysis for Los Angeles and San Francisco based on housing values and visibility
[PB85-166049] 16 p2822 N85-27409
Spatial and temporal visual masking and visibility
[AD-A151966] 16 p2842 N85-27524
An evaluation of discretized conditional probability and linear regression threshold techniques in model output statistics forecasting of visibility over the north Atlantic Ocean
[AD-A151955] 16 p2857 N85-27619
Quality assurance for RESOLVE (Research on Operations-Limiting Visual Extinction). A visibility study in the California desert
[AD-A152383] 17 p2992 N85-28494
The measurement of aircraft windscreen haze and its effect on visual performance
[AD-A154949] 21 p3555 N85-32114
Forecasting atmospheric visibility over the summer north Atlantic using the principal discriminant method
[AD-A155537] 21 p3637 N85-32593
Ice fog as an electro-optical obscurant
[AD-A155059] 21 p3705 N85-33015
Immediate visibility after red and white adaptation
[AD-A156271] 24 p4132 N85-35618

VISIBLE INFRARED SPIN SCAN RADIOMETER
An evaluation and comparison of vertical profile data from the VISSR Atmospheric Sounder (VAS)
[NASA-TP-2425] 07 p1000 N85-16351
VISSR infrared calibration by means of calculated radiances
12 p1894 N85-21889
GMS operational calibration procedure and status
12 p1895 N85-21893
Sea surface temperatures from VAS MSI data
[NASA-CR-175706] 14 p2382 N85-24689
Review of VAS demonstration
15 p2596 N85-26002
Nowcasting applications of VAS
15 p2597 N85-26003

VISIBLE RADIATION
U LIGHT (VISIBLE RADIATION)

VISIBLE SPECTRUM
Spectral components at visual and infrared wavelengths in active galactic nuclei
[NASA-CR-174133] 03 p0445 N85-12832
IUE and ESO observations of the P Cyg star AG Carinae and its ring nebula
11 p1750 N85-21006
Coordinated ultraviolet and visual observations of Omega Orionis 1982-1983
11 p1750 N85-21007
The spectroscopic antics of S 18/SMC
11 p1750 N85-21008
Ultraviolet and optical spectroscopy and polarimetry of the helium weak star HD 21699: Evidence for a magnetically controlled stellar wind
11 p1759 N85-21065
Non-linear optical techniques for visible and UV lasers and thin film deposition
[AD-A150489] 13 p2096 N85-23077
Spectral units on Europa and Ganymede
13 p2196 N85-23621
Spectral reflectance of carbonate minerals and rocks in the visible and near infrared (0.35 - 2.55 microns) and its applications in carbonate petrology
[NASA-CR-175763] 15 p2591 N85-25973
Estimation of convective rainfall from visible and infrared satellite data
15 p2596 N85-25999
In situ thin film measurements
[AD-A151379] 15 p2652 N85-26353
Alkali atom - SbCl(5) reactions: Blue-green chemiluminescence from an inverted population in SbCl
[AD-A154371] 19 p3276 N85-30315
Absorption and scattering properties of aerosols of aggregated particles in the infrared spectral region
[AD-A155475] 21 p3637 N85-32591
Transparency of water 9n 186 - 500 nm region
21 p3690 N85-32923
The ISAVF opto-mechanical test bed
[NASA-TM-87505] 24 p4067 N85-35206

VISION
NT BINOCULAR VISION
NT COLOR VISION
NT NIGHT VISION
NT PERIPHERAL VISION
Pattern reversal visual evoked potentials and reaction time
[CSIR-SR-PERS-354] 01 p0097 N85-10644
Development and evaluation of a performance-based test of saccadic and vestibulo-ocular control
[AD-A145367] 02 p0237 N85-11545
Visually evoked responses from non-occipital areas of the human cortex
[AD-A146079] 03 p0400 N85-12553
Visual selective attention
[AD-A146220] 03 p0401 N85-12556
Spatiotemporal characteristics of visual localization
[AD-A146013] 08 p1200 N85-17555
Ill-posed problems and regularization analysis in early vision
[AD-A147753] 08 p1222 N85-17696
Human assembly time versus levels of visual and tactile sensory input: Experimental results for five devices
[AD-A149982] 12 p1909 N85-21980
Italy's Fiat uses Sweden's Asea seeing robot
15 p2536 N85-25650
Vision algorithms and psychophysics
[AD-A151886] 15 p2620 N85-26142
Retinally stabilized differential resolution television display
[NASA-CASE-NPO-15432-1] 18 p3089 N85-29117
Discovery regarding visual neuron adaptation applicable to robot use
20 p3504 N85-31786
Some results of the European vestibular experiments in the Spacelab-1 mission
20 p3508 N85-31809
Visual phenomena produced by binocularly disparate dynamic visual noise
[AD-A154758] 21 p3663 N85-32757

The development and evaluation of color display systems for airborne applications. Phase 1: Fundamental visual, perceptual, and display system considerations
[FAA/PM-85-19] 22 p3826 N85-33700
Heuristic rules for visualization 23 p3965 N85-34584

VISUAL ACUITY
Using gross outline features in long range target identification
[FOA-C-53018-H2] 02 p0237 N85-11543
Electrophysiological correlates of Vernier acuity in human visual cortex
[AD-A146533] 06 p0846 N85-15371
Immediate visibility after red and white adaptation
[AD-A156271] 24 p4132 N85-35616

VISUAL AIDS
Dialog system of preparation and presentation of visual information 10 p1526 N85-19622

VISUAL CONTROL
The two modes of visual processing: Implications for spatial orientation 01 p0008 N85-10047
Neurocognitive pattern analysis of an auditory and visual numeric motor control task. Part 1: Development of methods
[AD-A148809] 09 p1364 N85-18578
Guidelines for the evaluation of visual approach slope indicators
[ARL/SYS-R-32] 23 p3896 N85-34132

VISUAL DISCRIMINATION
The two modes of visual processing: Implications for spatial orientation 01 p0008 N85-10047
A human visual system investigation applicable to image contour coding
[FUB-36-1983] 01 p0095 N85-10640
The perceptual quality of smoke screens: An analysis of the Oldebroek 2 trials, May 1981
[IZF-1984-20] 01 p0095 N85-10641
The prediction of observer responses from photometric data on smoke screens; an analysis of the Oldebroek 2 trials, May 1981
[IZF-1984-21] 01 p0095 N85-10642
Discriminability of signals from noise in a dynamic stereoscopic space
[AD-A148406] 08 p1196 N85-17535
Color measurement and discrimination
[NASA-CR-3824] 09 p1365 N85-18579
Human assembly time versus levels of visual and tactile sensory input: Experimental results for five devices
[AD-A149982] 12 p1909 N85-21980
Visual search strategy predictions: The use of aspect ratio as a cue
[BAE-BT-12565] 15 p2619 N85-26136
Individual observer data for the 1955 Stiles-Burch 2 deg pilot investigation — color vision
[NPL-QU-68] 20 p3512 N85-31830
An error-dependent model of instrument-scanning behavior in commercial airline pilots
[NASA-CR-3908] 21 p3665 N85-32765
Discrimination of linear contour elements of space photographs based on visual perception model 22 p3736 N85-33161

VISUAL DISPLAYS
U DISPLAY DEVICES

VISUAL FIELDS
The two modes of visual processing: Implications for spatial orientation 01 p0008 N85-10047

VISUAL FLIGHT RULES
National airspace review: Airport radar service area operational confirmation report
[DOT/FAA/AT-84/2] 07 p0901 N85-15707
Analysis of estimation algorithms for CDTI and CAS applications
[NASA-CR-172444] 13 p1973 N85-22387

VISUAL OBSERVATION
Procedures for precap visual inspection
[NASA-RP-1122] 04 p0495 N85-13156
Statistical analysis of visual wave observations and gage/radar measurements
[AD-A146358] 06 p0798 N85-15100
The state of the art in printed wiring board inspection
[AD-A149871] 12 p1862 N85-21879
An MRTD-compatible bar pattern response model for TV and direct view sighting systems
[BAE-BT-12090] 15 p2620 N85-26146
A preliminary human factors planning and design outline of parameters related to space station windows and CCTV monitoring 18 p3158 N85-29559

VISUAL PERCEPTION
NT SPACE PERCEPTION
NT VISUAL DISCRIMINATION
The Malcolm horizon: History and future 01 p0008 N85-10046
The peripheral visual cue assessment facility at Ames Research Center 01 p0008 N85-10050
Peripheral vision displays: The future 01 p0009 N85-10058
Image signals encoding techniques oriented towards the reduction of perceptive redundance
[FUB-23-1983] 01 p0040 N85-10256
Effects of repetitive, small-spot, incoherent light flashes on pursuit tracking performance
[AD-A144848] 01 p0095 N85-10637
Inhibition of return: Neural basis and function
[AD-A145242] 01 p0098 N85-10652
The effect of sleep loss on the human visual event-related potential
[AD-A145364] 02 p0234 N85-11528
Eyelid motion sequences predictive of decision errors
[AD-A145702] 02 p0235 N85-11531
Air-to-air visual acquisition performance with TCAS 2
[FAA-PM-84-17] 02 p0236 N85-11537
Visual representations subserving texture perception
[AD-A145412] 02 p0236 N85-11538
Toward a computational neuropsychology of high-level vision
[AD-A145711] 02 p0236 N85-11540
The Beatrice experiment and the luminance concept in Dante
[NOTA-INTERNA-823] 02 p0281 N85-11831
A mathematical model of visual perception regarding peripheral vision and its application to the Hermann's illusion 04 p0483 N85-13080
Visual-vestibular interaction in human motion perception 05 p0695 N85-14471
Representing multidimensional systems using visual displays 05 p0711 N85-14560
Central regulation of sensory flow in human visual system 07 p1013 N85-16435
Lateral specifics of visual perception 07 p1013 N85-16436
Testing changes in visual function due to orbital environment
[AD-A147259] 07 p1016 N85-16453
Vision by man and machine: How the brain processes visual information may be suggested by studies in computer vision (and vice versa)
[AD-A147890] 07 p1017 N85-16458
Discriminability of signals from noise in a dynamic stereoscopic space
[AD-A148406] 08 p1196 N85-17535
Spatiotemporal characteristics of visual localization
[AD-A148013] 08 p1200 N85-17555
The IMAGE 3 Conference Proceedings
[AD-A148636] 09 p1267 N85-17962
Altitude control using action-demanding interactive displays: Toward an active psychophysics
[AD-P004311] 09 p1267 N85-17965
Considerations in an optical variable acuity display system
[AD-P004323] 09 p1269 N85-17977
Progress report on an eye-slaved area-of-interest visual display
[AD-P004326] 09 p1270 N85-17980
Baffled eye and confounded brain or using visual illusions to train blind pilots
[AD-P004332] 09 p1271 N85-17986
Global optical metrics for self-motion perception
[AD-P004333] 09 p1271 N85-17987
AVTS (Advanced Visual Technology System): A high fidelity visual simulator
[AD-P004338] 09 p1271 N85-17992
Restructuring of the process of visual recognition as perception conditions alter 10 p1526 N85-19624
Multiple resources and brain laterality
[AD-A148912] 10 p1530 N85-19643
Selecting one among the many: A simple network implementing shifts in selective visual attention
[AD-A148989] 10 p1530 N85-19644
Some effects of display format variables on the perception of aircraft spatial orientation 10 p1534 N85-19666
A method for reduction of ambiguity in segmentation of images
[INPE-3394-TDL/186] 11 p1697 N85-20664
The accuracy in calculations of intervisibility with digital terrain models — digital models
[FOA-C-20557-D8(E1)] 12 p1909 N85-21963
Visual simulation requirements for aircraft aspect recognition at real world distances
[AD-A151040] 14 p2228 N85-23810
The effect of set size on color matching
[AD-A150699] 14 p2368 N85-24713
Visual recognition of simple objects by a connection network
[AD-A151043] 14 p2369 N85-24718
Survey of remote sensing techniques for wave measurement
[NASA-TM-84429] 15 p2583 N85-25928
A portable battery for objective, non-obstrusive measures of human performance
[NASA-CR-171868] 15 p2586 N85-25942
Vision algorithms and psychophysics
[AD-A151888] 15 p2620 N85-26142
Spatial and temporal visual masking and visibility
[AD-A151968] 16 p2842 N85-27524
Perception of roll rate from an artificial horizon and peripheral displays
[VTH-LR-403] 17 p3002 N85-29557
Effect of background/foreground color coding on detection in acoustic data displays
[AD-A154105] 19 p3352 N85-30774
The measurement of aircraft windscreen haze and its effect on visual performance
[AD-A154949] 21 p3555 N85-32114
Visual phenomena produced by binocularly disparate dynamic visual noise
[AD-A154758] 21 p3663 N85-32757
Discrimination of linear contour elements of space photographs based on visual perception model 22 p3736 N85-33161
Heterodyne holographic interferometry for visualization of surface acoustic waves
[AD-A155405] 22 p3836 N85-33753
Image synthesis: Optical identity or pictorial communication? 23 p3963 N85-34585
Heuristic rules for visualization 23 p3965 N85-34584
Visual impact of GROWIAN and resulting recommendations for siting of large wind energy converters 24 p4112 N85-35486
Matched filtering of visual evoked potentials to detect acceleration (+Gz) induced blackout
[AD-A155912] 24 p4131 N85-35609
The human engineering eye movement measurement research facility
[AD-A156099] 24 p4132 N85-35613
Immediate visibility after red and white adaptation
[AD-A156271] 24 p4132 N85-35616

VISUAL PHOTOMETRY
The prediction of observer responses from photometric data on smoke screens; an analysis of the Oldebroek 2 trials, May 1981
[IZF-1984-21] 01 p0095 N85-10642
Photometric study of the Saturn E ring 15 p2571 N85-25483
A manual of methods for the continuous flow determination of ammonia, nitrate-nitrite, phosphate and silicate in seawater
[IOS-177] 23 p3913 N85-34243

VISUAL SIGNALS
Discriminability of signals from noise in a dynamic stereoscopic space
[AD-A148406] 08 p1196 N85-17535
Changing system and display concepts and their impact on aircrew performance 10 p1533 N85-19665

VISUAL STIMULI
The two modes of visual processing: Implications for spatial orientation 01 p0008 N85-10047
The peripheral visual cue assessment facility at Ames Research Center 01 p0008 N85-10050
Pattern reversal visual evoked potentials and reaction time
[CSIR-SR-PERS-354] 01 p0097 N85-10644
Neural control of the direction of covert visual orienting
[AD-A145189] 01 p0097 N85-10650
An in-flight investigation of a twin fuselage configuration in approach and landing
[NASA-CR-172366] 05 p0696 N85-13801
Spontaneous motility of goldfish in absence of terrestrial zeitgebers: Space flight simulation in a mine 05 p0699 N85-14432
Use of linear perspective scene cues in a simulated height regulation task 05 p0704 N85-14517
Cockpit window edge proximity effects on judgements of horizon vertical displacement 05 p0704 N85-14518
Mean and random errors of visual roll rate perception from central and peripheral visual displays 05 p0704 N85-14519
Direction judgement errors in perspective displays 05 p0705 N85-14520
The interaction of focused attention with flow-field sensitivity 05 p0705 N85-14521
Accuracy of system step response roll magnitude estimation from central and peripheral visual displays and simulator cockpit motion 05 p0705 N85-14522
Lateral specifics of visual perception 07 p1013 N85-16436
Visual evoked potentials with disrupted functioning of nonspecific cerebral systems 07 p1013 N85-16437
Random pattern tracking acceleration tolerance tester
[AD-D011404] 07 p1017 N85-16459
Functional inter-hemisphere asymmetry in recognition of visual stimuli of various classes 08 p1193 N85-17517

Spatiotemporal characteristics of visual localization
[AD-A148013] 08 p1200 N85-17555
Determination of functional mobility of human nervous system with the PHN-3 instrument
10 p1525 N85-19618
Susceptibility of cat and squirrel monkey to motion sickness induced by visual stimulation: Correlation with susceptibility to vestibular stimulation
11 p1694 N85-20650
Visual simulation requirements for aircraft aspect recognition at real world distances
[AD-A151040] 14 p2228 N85-23610
The effect of set size on color recognition
[AD-A150968] 14 p2391 N85-24726
Visual phenomena produced by binocularly disparate dynamic visual noise
[AD-A154758] 21 p3663 N85-32757

VISUAL TASKS
Effects of repetitive, small-spot, incoherent light flashes on pursuit tracking performance
[AD-A144848] 01 p0095 N85-10637
The effect of set size on color matching
[AD-A150899] 14 p2388 N85-24713

VISUAL TRACKING
U OPTICAL TRACKING

VISUALIZATION OF FLOW
U FLOW VISUALIZATION

VITAMIN D
U CALCIFEROL

VITAMIN K
U PHYLLOQUINONE

VITAMINS
NT CALCIFEROL
NT PHYLLOQUINONE
Vitamin metabolism in cosmonauts following short-term flights 01 p0091 N85-10615
The effects of prolonged feeding meal, ready-to-eat (MRE) operational rations
[AD-A154763] 21 p3666 N85-32773

VITREOUS MATERIALS
Microtektite discovered in Beijing
[NASA-TM-77765] 01 p0130 N85-10695
Effect of light pulses on film of chalcogenide vitreous semiconductors 02 p0258 N85-11687

VITRIFICATION
Stabilization of contaminated soils by in situ vitrification
[AD-P004144] 09 p1348 N85-18480
High level radioactive waste vitrification process equipment component testing
[DE85-011143] 19 p3273 N85-30298
Development of HWVP melter/turntable components for canyon-remote maintenance and replacement
[DE85-010308] 19 p3273 N85-30298
Technology of off-gas treatment for liquid-fed ceramic melters
[DE85-012467] 22 p3812 N85-33610

VLASOV EQUATIONS
Hamiltonian and Lagrangian theory of gyrokinetic equations 02 p0283 N85-11845
Theory of ponderomotive forces
02 p0283 N85-11847
Covariant Poisson brackets for classical fields
[DE85-010085] 18 p3171 N85-29654
High harmonic rectangular gyrotron
19 p3256 N85-30189
Guiding center distribution function and longitudinal invariant 23 p3978 N85-34663
Numerical solutions of the Vlasov equation
23 p3979 N85-34672

VLBI
U VERY LONG BASE INTERFEROMETRY

VLSI
U VERY LARGE SCALE INTEGRATION

VOCODERS
Literature review of voice recognition and generation technology for Army helicopter applications
[AD-A146878] 07 p0939 N85-15954
Comparative architectures for a multiple function speech processor
[AD-A150873] 14 p2292 N85-24211
Survey of narrow band vocoder technology
[AD-A151919] 16 p2773 N85-27114
The design of an adaptive predictive coder using a single-chip digital signal processor
[AD-A152461] 17 p2952 N85-28231
A classification vocoder: A very low rate speech transmission by vector quantization of the spectrum
[ENST-84D003] 20 p3441 N85-31356

VOICE COMMUNICATION
NT TELEPHONY
NT VOICE DATA PROCESSING
Improvement of the narrowband linear predictive coder. Part 2: Synthesis improvements
[AD-A145031] 01 p0038 N85-10237
Interaction of voice and data traffic in a packet switching communication network and virtual circuit
[FUB-83-1982] 01 p0039 N85-10249
Voice communication handling in X 25 packet switching networks
[FUB-30-1983] 01 p0040 N85-10260
Royal Signals and Radar Establishment speech database recordings 1983: Part 2: Recordings made for automatic speech recognition assessment and research
[RSRE-84008-PT-2] 02 p0190 N85-11267
Identification as a function of familiarity for known voices talking over an unprocessed channel and an LPC (Linear Predictive Coding) voice processor
[AD-A145545] 02 p0191 N85-11276
Technological Institute director views artificial intelligence 03 p0341 N85-12197
Wideband integrated voice/data technology
[AD-A146054] 03 p0355 N85-12283
Hearing protection and speech intelligibility of two nonstandard inflight communication headsets
[AD-A146110] 03 p0355 N85-12284
Rech-1 speech synthesizer for man-machine dialog
04 p0543 N85-13456
VOTAN V5000 speech recognition system performance test report
[AD-A146726] 07 p0939 N85-15950
Literature review of voice recognition and generation technology for Army helicopter applications
[AD-A146878] 07 p0939 N85-15954
Man-machine communication research for robotics reported
08 p1139 N85-17177
Transmission scheduling to reduce convex delay costs in packet networks
[AD-A148451] 08 p1153 N85-17278
A voice-actuated wind tunnel model leak checking system
[NASA-TM-86359] 09 p1263 N85-17936
EHF air-to-air communications
10 p1469 N85-19273
Fast data and voice transmission for mobile services with high immunity against multipath and co-channel interference 10 p1475 N85-19306
Overview of leading-edge research at French CNRS lab
11 p1618 N85-20179
Base communications issues for the 1990s
[AD-A149764] 12 p1828 N85-21474
Automatic speech recognition in severe environments
[PB85-121697] 12 p1830 N85-21490
Tubes and transistors in audio amplifiers
12 p1837 N85-21532
Low-bit rate speech encoders based on Line-Spectrum Frequencies (LSF)
[AD-A150518] 13 p2056 N85-22871
Interference effects of vocalization on dual task performance
[AD-A150667] 14 p2291 N85-24203
Secure digital speech communication
[AD-D011572] 14 p2293 N85-24215
A preliminary investigation into the intelligibility of Microspeech-2, a speech synthesiser
[BAE-BT-12284] 15 p2539 N85-25675
Wideband integrated voice/data technology
[AD-A152329] 17 p2947 N85-28197
Oral discussion, group-to-individual transfer and achievement in cooperative learning groups
[AD-A153209] 17 p3001 N85-28552
Secure digital voice communications in the Defense Data Network (DDN)
[AD-A154677] 21 p3574 N85-32226
Interactive on-line conferences
[AD-A154723] 21 p3574 N85-32227
Application of adaptive noise cancellation to Coast Guard voice communications
[AD-A154798] 21 p3574 N85-32230
Software for interactive on-line conferences
[AD-A154742] 21 p3670 N85-32801
Speech analysis system for assessing pilots' working fitness 22 p3819 N85-33661

VOICE CONTROL
Voice command weapons launching system
[AD-D011378] 07 p0937 N85-15940
Automatic speech recognition in severe environments
[PB85-121697] 12 p1830 N85-21490
A description of the process of elaborating man-machine dialog in an aircraft equipped with cathode tubes: Rules and specifications of piloted simulation methods
16 p2666 N85-26658
Wideband integrated voice/data technology
[AD-A152329] 17 p2947 N85-28197
Study to determine potential flight applications and human factors design guidelines for voice recognition and synthesis systems
[NASA-CR-172590] 20 p3440 N85-31349

VOICE DATA PROCESSING
Classification methods for Italian vowels — speech recognition
[FUB-61-1982] 01 p0039 N85-10248
Description of a semiannual selection procedure of vowel parts of the voice signal using a PDP 11/34 computer
[FUB-4-1983] 01 p0039 N85-10250
Determination of vowel zones in speech — speech recognition
[FUB-16-1983] 01 p0040 N85-10253
Vowel phoneme identification in speech
[FUB-26-1983] 01 p0040 N85-10257
Voice phonetic coding and decoding processes
[FUB-29-1983] 01 p0040 N85-10259
Voice communication handling in X 25 packet switching networks
[FUB-30-1983] 01 p0040 N85-10260
Autoregressive nonsteady methods for the analysis and synthesis of the human voice
[FUB-3-1984] 01 p0041 N85-10266
Measures of distance between speech signals in the frequency domain — speech recognition
[FUB-5-1984] 01 p0041 N85-10267
Analog voice processing for FM transmission in a telephone channel
[INPE-2798-PRE/359] 03 p0354 N85-12279
Voice data processing in packet switching modes
[FUB-44-1983] 09 p1312 N85-18248
Speech analysis by parametric methods: A survey
[ENST-84C004] 09 p1313 N85-18251
Automatic speech recognition in severe environments
[PB85-121697] 12 p1830 N85-21490
Comparative architectures for a multiple function speech processor
[AD-A150873] 14 p2292 N85-24211
Preliminary assessment of the Heuristics H2000 speechlink - speech recognition device — voice data input for Apple 2 computer
[BAE-BT-12276] 15 p2539 N85-25674
A review of speech systems
[BAE-BT-12285] 15 p2539 N85-25676
Processing speech for analysis using optical Fourier techniques
[AD-A151898] 15 p2544 N85-25704
Wideband integrated voice/data technology
[AD-A152329] 17 p2947 N85-28197
A method and apparatus for operating on companded PCM voice data
[NASA-CASE-KSC-11285-1] 18 p3089 N85-29120
A classification vocoder: A very low rate speech transmission by vector quantization of the spectrum
[ENST-84D003] 20 p3441 N85-31356
Introduction to adaptive techniques for voice signal processing
[FUB-52-1983] 22 p3756 N85-33267

VOID RATIO
Void fraction measurements performed in a vertical large diameter tube compared to different predicting correlations
[GKSS-84-E-24] 01 p0048 N85-10315
A note on the G-space version of Glicksberg's theorem
[CWI-PM-R8405] 08 p1217 N85-17665

VOIDS
Radiation effects on structural materials
[DE84-014771] 01 p0029 N85-10178
Induction voidmeter
[DE84-014321] 01 p0050 N85-10329
Experimental determination of the critical cavity radius in Fe-10% Cr for ion irradiation
[DE84-016570] 04 p0571 N85-13646
Collapse and removal of discontinuities in joint zone during diffusion welding 11 p1602 N85-20077
Effect of diaphragm leakage on turbine stage characteristics 14 p2286 N85-24168
Swelling behavior of titanium-modified AISI 316 alloys
[DE85-007470] 16 p2752 N85-26982
Theory of positron annihilation in vacancies in concentrated disordered alloys
[DE85-010267] 18 p3183 N85-29734
Determination of the vacancy formation enthalpy in chromium by positron annihilation
[DE85-010266] 19 p3239 N85-30084
Reliability of void detection in structural ceramics using scanning laser acoustic microscopy
[NASA-TM-87035] 21 p3597 N85-32337

VOIGT EFFECT
Voigt line profile computation of infrared lines in the stratosphere and mesosphere
[AERONOMICA-ACTA-A-294-1985]
22 p3813 N85-33622

VOLATILITY
Effect of toluene on the solubility of biohazardous volatile synthetic organic compounds
[AD-A145188] 01 p0018 N85-10109

Dynamic compression and volatile release of carbonates
[NASA-CR-174076] 03 p0391 N85-12504
Origin of the Moon: Constraints from volatile elements 04 p0584 N85-13727
Volatility of vanadium from a candidate fusion tractor alloy
[DE84-015277] 05 p0618 N85-13955
Volatile organic emissions from adhesives with indoor applications
[DE84-015965] 05 p0620 N85-13966
Volatility of in-use gasoline and gasoline-methanol blends
[PB85-117976] 10 p1459 N85-19189
Magmas as selective filters of volatiles between planetary mantles and surfaces
13 p2185 N85-23557
Procedure for certifying quantity of volatile organic compounds emitted by paint, ink and other coatings
[PB85-159044] 15 p2520 N85-25537
Limiting factor of flame propagation in mono-sized sprays of low-volatility fuels
[NAL-TR-839T] 15 p2521 N85-25538
Volatiles in the outer solar system. 1: Thermodynamics of clathrate hydrates. 2: Ethane ocean on Titan. 3: Evolution of primordial Titan atmosphere
19 p3382 N85-30084
Nebular volatile fractionations associated with chondrule formation 22 p3852 N85-33855
Volatile loss following very large impacts
22 p3853 N85-33862
Volatiles on satellites of the outer solar system
22 p3854 N85-33868
Monitoring dosage of volatile compounds in tests at low barometric pressure 23 p3954 N85-34506

VOLATILIZATION
U VAPORIZING

VOLCANICS
U VOLCANOLOGY

VOLCANOES
NT MARS VOLCANOES
The petrology and geochemistry of high cascade volcanics in southern Washington: Mount Saint Helens volcano and the Indian Heaven basalt field
02 p0227 N85-11487
Geology and geochemistry of early Tertiary submarine volcanic rocks of the Aleutian Islands, and their bearing on the development of the Aleutian Island Arc
03 p0369 N85-12493
Reconnaissance geology of the northern part of the Unalakleet quadrangle 04 p0516 N85-13291
Paleomagnetic latitude of paleocene volcanic rocks of the Cantwell Formation, central Alaska
04 p0517 N85-13302
Paleogene volcanic rocks of the Matanuska Valley area and the displacement history of the Castle Mountain fault 04 p0518 N85-13303
Models for volcanic processes in Long Valley, California: Testing by continental drilling
[DE84-014943] 04 p0534 N85-13414
Satellite photographs suggest arctic volcano
07 p0982 N85-16239
Evaluation of the L-band scattering characteristics of volcanic terrain in aid of lithologic identification, assessment of SIR-B calibration, and development of planetary geomorphic analogs 08 p1148 N85-17232
Correlation and petrological interpretation of abyssal and terrestrial tephra layers 09 p1353 N85-18512
Tectonic lineaments in the cenozoic volcanics of southern Guatemala: Evidence for a broad continental plate boundary zone
[NASA-CR-175456] 10 p1505 N85-19499
Airborne lidar measurements of El Chichon stratospheric aerosols, October 1982 to November 1982
[NASA-RP-1136] 10 p1514 N85-19550
Catalog of submarine volcanoes and hydrological phenomena associated with volcanic events: 1500 BC to 31 Dec. 1899
[PB85-117984] 12 p1891 N85-21869
Volcanism on Venus as connecting link
13 p1982 N85-22433
Sulfur volcanoes on Io? 13 p2173 N85-23479
Geomorphic classification of lava flows on Io
13 p2173 N85-23480
Volcanism and rift formation in Beta Regio, Venus: New radar results 13 p2176 N85-23507
Volcanic debris flows in the Elysium region of Mars
13 p2185 N85-23560
Estimates of lava eruption rates at Alba Patera, Mars
13 p2185 N85-23562
Thermal infrared observations of lava flows during the 1984 Mauna Loa eruption 13 p2186 N85-23564
Field measurements of the 1983 Royal Gardens lava flows, Kilauea Volcano, and 1984 Mauna Loa lava flows, Hawaii 13 p2186 N85-23565
Surface structures of Hawaiian lavas
13 p2186 N85-23566
Morphologic evolution of the Mount St. Helens crater area, Washington 13 p2187 N85-23568
Volcanism of the Colorado Plateau (basin and range transition): Implications for crustal processes
13 p2187 N85-23569
The geology of East Butte, a rhyolitic volcanic dome on the Eastern Snake River Plain, Idaho
13 p2187 N85-23570
A silicic shield volcano in Bolivia
13 p2187 N85-23572
Submarine volcanic eruptions and potential analogs for Venus 13 p2187 N85-23573
Terrestrial analogs for planetary wrinkle ridges
13 p2199 N85-23844
Skywave radar detectability of volcanic aerosols
[AD-A151448] 15 p2542 N85-25604
The impact ejection of living organisms into space
15 p2682 N85-26566
Closer look at lunar volcanism
[DE85-006663] 15 p2683 N85-26576
Evolution of stratospheric aerosol size distribution from ground-based radiometric measurements: A study of El Chichon aerosol
[DE85-007555] 16 p2827 N85-27439
Thermal-cycle testing of the G-tunnel heated block
[DE85-008408] 18 p3126 N85-29359
Pacific Northwest solar radiation data
[DE85-009773] 18 p3149 N85-29496
Influence of underwater volcanic mountains of Atlantic on microplankton distribution 19 p3294 N85-30424
Melt zones beneath five volcanic complexes in California: An assessment of shallow magma occurrence
[DE85-010844] 19 p3305 N85-30489
Source-term considerations for a potential radioactive-waste repository located in unsaturated tuff
[DE85-010090] 20 p3529 N85-31953
Data analysis for lidar and quartz crystal microbalance systems
[NASA-CR-172601] 21 p3615 N85-32484
Changes in the organic material in lakes in the blast zone of Mount St. Helens, Washington: Hydrologic effects of the eruptions
[GS-CIRC-850-1] 21 p3630 N85-32551
Early and middle Cenozoic volcanic synthesis
24 p4105 N85-35449
Preliminary results of an ALVIN dive program on active hydrothermal vents at the southern Juan de Fuca Ridge
24 p4106 N85-35454

VOLCANOLOGY
Magnetic characteristics of some volcanic rocks of the west Carpathians
[REPT-557] 03 p0376 N85-12400
Electric properties of neovolcanic rocks of central and east Slovakia
[REPT-558] 03 p0376 N85-12401
Volatile elements in and on lunar volcanic glasses: What do they tell us about lunar genesis?
04 p0584 N85-13728
Tectonic, volcanic, and climatic geomorphology study of the Sierras Pampeanas Andes, northwestern Argentina 08 p1144 N85-17215
Structure of Iceland and ocean floor spreading
13 p2112 N85-23159
Magmatism in continent-ocean transition zone (development of ideas of A. N. Zavaritskiy)
13 p2113 N85-23161
Planetary geology in the 1980s
[NASA-SP-467] 13 p2169 N85-23457
Reports of the Planetary Geology and Geophysics Program, 1984
[NASA-TM-87563] 13 p2172 N85-23474
Topographic evidence for shield volcanism on Io
13 p2172 N85-23478
Estimates of lava eruption rates at Alba Patera, Mars
13 p2185 N85-23562
Emplacement of long lava flows on Mauna Loa (Hawaii) and Alba (Mars)
13 p2186 N85-23563
Thermal infrared observations of lava flows during the 1984 Mauna Loa eruption 13 p2186 N85-23564
Volcanism of the Colorado Plateau (basin and range transition): Implications for crustal processes
13 p2187 N85-23569
The geology of Mt. Hope, a silicic volcanic center in West Central Arizona 13 p2187 N85-23571
Hydrovolcanism 13 p2188 N85-23574
Results on volcanism, surface geology from Venera-15, -16 15 p2482 N85-25321
Closer look at lunar volcanism
[DE85-006663] 15 p2683 N85-26576
Andrean examples of mega-geomorphology themes
21 p3602 N85-32367
Planetary surface processes: A review
22 p3855 N85-33869
Planning for VRM: Radar and sonar studies of volcanic terrains on Earth, Venus and Mars
22 p3857 N85-33884
Workshop on Recent Research in the Valles Caldera
[DE85-010569] 23 p3949 N85-34472

VOLT-AMPERE CHARACTERISTICS
Planar ferroelectric microcapacitors for microwave devices 13 p2087 N85-23032
Solar cells with distributed parameters: Current-voltage characteristics under uniform and nonuniform illumination 14 p2275 N85-24093
Pressed boride cathodes
[NASA-TM-77821] 17 p2918 N85-27984
Electrochemistry of Hexanitroazobenzene (HNAB)
[DE85-010607] 21 p3565 N85-32171

VOLTAGE
U ELECTRIC POTENTIAL

VOLTAGE BREAKDOWN
U ELECTRICAL FAULTS

VOLTAGE CONTROLLED OSCILLATORS
Analog to digital converter
[AD-D011338] 07 p0945 N85-15983
Image line voltage controlled oscillator with replaceable components
[AD-D011436] 10 p1479 N85-19333
Wide-band phase locked loop amplifier apparatus
[AD-D011720] 23 p3927 N85-34337

VOLTAGE CONVERTERS (AC TO AC)
Automatic ac/dc thermal voltage converter and ac voltage calibration system
[PB85-182574] 19 p3274 N85-30304
Outline of CCVT (Coupling Capacitor Voltage Transformer) calibration procedure, EPRI-NBS (Electric Power Research Institute/National Bureau of Standards) prototype system. Supplement to EPRI report EL-690 (Field Calibration System for CCVTs, April 1978)
[PB85-182566] 20 p3450 N85-31418

VOLTAGE CONVERTERS (DC TO DC)
Control of energy-storage dc-to-dc converters: The large-signal time-domain approach
19 p3257 N85-30196

VOLTAGE GENERATORS
NT PHOTOVOLTAIC CELLS

VOLTAGE MEASUREMENT
U ELECTRICAL MEASUREMENT

VOLTAGE REGULATORS
Problems with electrical interference between solar generators and shunt type regulators
13 p2010 N85-22807
Autonomous uninterruptable power supply apparatus
[AD-D011571] 14 p2298 N85-24232
Method of improving dynamic characteristics of DC voltage stabilizers with compound regulation
15 p2528 N85-25589
Spark gap electrode erosion
[AD-A152802] 17 p2953 N85-28237
High voltage isolation transformer
[NASA-CASE-GSC-12817-1] 18 p3093 N85-29146
Batteryless magneto-driven portable radiac
[DE85-011622] 22 p3760 N85-33300

VOLTAGE VARIATION INDICATORS
U VOLTMETERS

VOLTERRA EQUATIONS
Linear autonomous retarded functional differential equations; a sharp version of Henry's theorem
[CWI-AM-R8405] 05 p0720 N85-14625
EMC (Electromagnetic compatibility) spec criteria in Volterra systems
[AD-A147859] 08 p1151 N85-17263
Stability results for discrete Volterra equations: Numerical experiments
[CWI-NM-R8409] 11 p1707 N85-20743
Solving Volterra integral equations with ODE codes
[DE85-011216] 19 p3345 N85-30740

VOLTMETERS
China report: Science and technology
[JPRS-CST-84-001] 04 p0557 N85-13545
Present status, future prospects of domestic acoustical instruments 04 p0557 N85-13548
Pulsed-power system diagnostics: Electromagnetic data interpretation along pulse lines
[AD-A146807] 06 p0810 N85-15148
Microprocessor-controlled anodic stripping voltammeter for trace metal analysis in tap water
[DE85-002781] 12 p1852 N85-21619
Application of modulated hydrodynamic voltammetry to the study of anodic electrocatalysis
[DE85-004182] 13 p2018 N85-22953
R, L, C, G measurement 21 p3668 N85-32784

VOLUME
NT BODY VOLUME (BIOLOGY)
The analysis of tank calibration data from several runs
[DE84-015529] 02 p0200 N85-11337
Characteristics of aerosol volume distributions measured at Meppen, W. Germany
[AD-A146136] 03 p0396 N85-12528

Free volume considerations in thermoplastic and thermosetting resins 04 p0465 N85-12952
Reflection of volume waves in multilayer structures 04 p0485 N85-13097
Precision volume measuring system [DE85-002599] 11 p1636 N85-20305
Optimization of pressure vessels with standard intercepting spheres [INPE-3276-PRE/600] 11 p1651 N85-20397
Application of the Van Leer method to the solution of one-dimensional volume fraction equations [CFD/84/17] 15 p2558 N85-25781
Determining partial molar volume of hydrogen in titanium alloys 19 p3245 N85-30119

VOLUMETRIC ANALYSIS
Chemistry of ore-forming fluids 24 p4103 N85-35436

VOLUMETRIC EFFICIENCY
Methanol vaporization: Effects on volumetric efficiency and on determination of optimum fuel delivery system [PB84-243914] 09 p1302 N85-18181

VOMITING
Neurophysiological correlates of motion sickness: Role of vestibulocerebellum and 'vomiting center' reanalyzed 11 p1693 N85-20643
Prediction of the space adaptation syndrome 11 p1693 N85-20646

VON MISES THEORY
U STRESS FUNCTIONS

VOR SYSTEMS
U VHF OMNIRANGE NAVIGATION

VORTEX ALLEVIATION
Wake effects on the aerodynamic performance of horizontal axis wind turbines [NASA-CR-174920] 18 p3127 N85-29364

VORTEX AVOIDANCE
Experimental research on electric propulsion. Note 7: Analysis of the performance of an arc-jet driven by means of hydrogen and nitrogen [NASA-TM-77473] 06 p0760 N85-14861

VORTEX BREAKDOWN
Turbulent drag reduction research 08 p1071 N85-16788
Full scale experiments into the use of large eddy breakup devices for drag reduction on aircraft 08 p1071 N85-16790
Experimental investigation of a breakdown criterion for a vortex in an incompressible flow — delta wing [ONERA-RT-27/1147-AY] 11 p1577 N85-19935
La Recherche Aerospatiale Bimonthly Bulletin, Number 1984-4, 221/July-August [ESA-TT-884] 16 p2695 N85-26837
An introduction to vortex breakdown and vortex core bursting [NAE-AN-28] 17 p2892 N85-27829
Viscous flows in rotating pipes with internal cavities and related vortex breakdowns [NASA-TM-86781] 20 p3454 N85-31447

VORTEX COLUMNS
U VORTICES

VORTEX DISTURBANCES
U VORTICES

VORTEX FLAPS
The lateral-directional characteristics of a 74-degree Delta wing employing gothic planform vortex flaps [NASA-CR-3848] 03 p0311 N85-12009
Calculation of vortex-flap aerodynamic characteristics [NASA-CR-175624] 13 p1969 N85-22367
Investigation of the Vortex Tab [NASA-CR-172586] 15 p2483 N85-25209

VORTEX FLOW
U VORTICES

VORTEX GENERATION
U VORTEX GENERATORS

VORTEX GENERATORS
An experimental investigation of the parallel blade-vortex interaction [NASA-TM-86005] 05 p0592 N85-13777
On the generation of trailing vortices by surface mounted obstacles 05 p0593 N85-13785
On vortex transport in turbine channels 09 p1308 N85-18217
Generation of a pair of symmetric eddies behind a slender axisymmetric body with pitch angle [ISL-R-121/83] 11 p1577 N85-19934
An experimental investigation of two-dimensional flame-vortex interactions 16 p2744 N85-26934
Vortex generating flow passage design for increased film cooling effectiveness [NASA-CASE-LEW-14039-1] 22 p3782 N85-33433
Wingtip vortex propeller [NASA-CASE-LAR-13019-1] 24 p4065 N85-35194
Vortex boundary-layer interactions [NASA-CR-176192] 24 p4093 N85-35373

VORTEX RINGS
Transition and mixing in axisymmetric jets and vortex rings 05 p0591 N85-13769

VORTEX SHEDDING
An experimental study of airfoil-spoiler aerodynamics [NASA-CR-177328] 06 p0748 N85-14796
Wing rock flow phenomena [AD-P004154] 09 p1264 N85-17939
Unsteady aerodynamic loading of an airfoil due to vortices released intermittently from its upper surface [AD-P004162] 09 p1265 N85-17947
A Navier-Stokes calculation of the airfoil dynamic stall process [AD-P004163] 09 p1265 N85-17948
On the shedding of vorticity at separation [AD-P004166] 09 p1265 N85-17951
Acoustic resonance in heat exchanger tube banks [DE85-004395] 11 p1632 N85-20281
Nonlinear interactions between vortices and acoustic waves in a rocket combustion chamber 13 p1999 N85-22533
Acoustic energy exchange in sheared mean flows — solid rocket motors 13 p1999 N85-22534
Periodic vortex shedding in the supersonic wake of a planar plate [NASA-TM-77854] 15 p2463 N85-25207
Vortex shedding flowmeters for liquids at high flow velocities 16 p2740 N85-26906
Trailing edge flow and aerodynamic sound. Part 1: Tonal pressure and velocity fluctuations. Part 2: Random pressure and velocity fluctuations [AD-A154947] 21 p3552 N85-32097

VORTEX SHEETS
Physics on aircraft wakes [NASA-CR-174105] 04 p0453 N85-12871
Unsteady flows around 3-dimensional wings [AD-A149993] 12 p1772 N85-21124
A study of aerodynamic control in stalled flight leading-edge vortex formation analysis [AD-A153758] 18 p3059 N85-28928
A method for computing the core flow in three-dimensional leading-edge vortices [NASA-TM-87489] 19 p3214 N85-29932
Vortex sheet modeling with higher order curved panels 20 p3451 N85-31428
A panel method study of vortex sheets with special emphasis on sheets of axisymmetric geometry [NASA-CR-177365] 21 p3552 N85-32095

VORTEX STREETS
NT KARMAN VORTEX STREET

VORTEX TUBES
U HILSCH TUBES
U VORTICES

VORTICES
NT WING TIP VORTICES
On vortex bursting [NASA-TM-77567] 01 p0002 N85-10008
Results of tests of advanced flexible insulation vortex and flow environments in the North American Aerodynamics Laboratory lowspeed wind tunnel using 0.0405-scale Space Shuttle Orbiter model 16-0 (test OA-309) [NASA-CR-167692] 01 p0015 N85-10096
Stability of fluid flow in a cylindrical annulus [NASA-TM-77720] 01 p0046 N85-10300
Review of some vortex relations [NASA-CR-172452] 01 p0046 N85-10302
Induction voidmeter [DE84-014321] 01 p0050 N85-10329
Observations of the vertical structure of the eddy field in the Kuroshio extension [AD-A145178] 01 p0089 N85-10599
Numerical studies of mesoscale eddies using quasigeostrophic and primitive equation ocean models [PB84-214048] 01 p0089 N85-10602
Experiments on turbulent mixing and chemical reactions in a liquid mixing layer 02 p0134 N85-10912
Force and moment measurements on a 74 deg delta wing with an apex flap [NASA-CR-166081] 02 p0134 N85-10918
VORCOR: A computer program for calculating characteristics of wings with edge vortex separation by using a vortex-filament and-core model [NASA-CR-165902] 02 p0135 N85-10921
Three dimensional separation and vortex formation 02 p0196 N85-11306
Flow visualization study of a vortex-wing interaction [NASA-TM-86656] 03 p0316 N85-12040
Interaction between an airfoil and a streamwise vortex [AD-A145823] 03 p0316 N85-12041
Vorticity amplification in viscous flow around a body 03 p0360 N85-12309
Vortex-generating coolant-flow-passage design for increased film-cooling effectiveness and surface coverage [NASA-TP-2388] 03 p0361 N85-12314
The structure of the vorticity field in turbulent channel flow. Part 2: Study of ensemble-averaged fields [NASA-TM-86657] 03 p0361 N85-12317
Eddy detection in the Norwegian, Greenland, and Barents Seas with a radar altimeter 03 p0382 N85-12442
Particle entrainment in a compressible vortex [ISL-CO-230/83] 04 p0500 N85-13192
The numerical simulation of steady transonic rotational flow using a dual potential formulation 05 p0591 N85-13770
An experimental investigation of the parallel blade-vortex interaction [NASA-TM-86005] 05 p0592 N85-13777
On the generation of trailing vortices by surface mounted obstacles 05 p0593 N85-13785
Aircraft accident report Air Canada, Lockheed L-1011, C-FTNJ, near Charleston, South Carolina, November 24, 1983 [PB84-910413] 05 p0594 N85-13790
The effect of grazing flow on the impedance of the Helmholtz resonator 05 p0635 N85-14076
A collection of flow visualization techniques used in the Aerodynamic Research Branch [NASA-TM-85998] 06 p0808 N85-15135
Channel constructed to provide well defined boundary layers for vorticity optical probe measurements [AD-A146879] 06 p0809 N85-15140
VORT: A computer code for bubbly two-phase flow [DE84-017076] 06 p0809 N85-15142
Large-eddy simulation. Guidelines for its application to planetary boundary layer research [AD-A146381] 06 p0690 N85-15651
An investigation of vortex-induced aerodynamic characteristics of supersonic cruise configurations [NASA-CR-174299] 07 p0898 N85-15690
Numerical studies of interacting vortices [NASA-TM-86325] 07 p0957 N85-16062
Current problems in turbomachinery fluid dynamics [AD-A147127] 07 p0958 N85-16074
Free-surface boundary layer and the origin of bow vortices [AD-A147427] 07 p0960 N85-16083
Laminar flow over a backward-facing step [AD-A147469] 07 p0960 N85-16084
Interactions between mean flow and finite-amplitude mesoscale eddies in a barotropic ocean [AD-A147249] 07 p1009 N85-16413
Modelling circulation control by blowing — airfoils 08 p1069 N85-16778
Full scale experiments into the use of large eddy breakup devices for drag reduction on aircraft 08 p1071 N85-16790
Helicopter model rotor-blade vortex interaction impulsive noise: Scalability and parametric variations [NASA-TM-86007] 08 p1077 N85-16826
Prediction of dynamic stall characteristics using advanced non-linear panel methods [AD-A148453] 08 p1078 N85-16836
New Zealand SIR-B science investigations 08 p1144 N85-17218
A 3-dimensional turbulent boundary layer upstream and around a junction vortex flow 08 p1160 N85-17319
Application of the vortex-lattice concept to flows with smooth-surface separation 08 p1160 N85-17320
Secondary flow in cascades [AD-A148415] 08 p1162 N85-17333
A 2-dimensional second order closure model of the upper atmosphere 08 p1182 N85-17450
Unsteady aerodynamic loading of an airfoil due to vortices released intermittently from its upper surface [AD-P004162] 09 p1265 N85-17947
Unsteady separated flow: Forced and common vorticity about oscillating airfoils [AD-P004167] 09 p1265 N85-17952
New discovery in supersonic flight research 09 p1278 N85-18041
Three-dimensional vortex methods [DE85-000391] 09 p1320 N85-18299
Turbulence in pure superfluid flow 09 p1397 N85-18790
A study for calculating rotor loads using free vortex concept 11 p1620 N85-20194
A study of eddy-mean flow interactions using Eliassen-Palm diagnostics: FGGE SOP-1 data and the NASA GLAS general circulation model compared [NASA-CR-175508] 11 p1686 N85-20604
Frequency spectra of turbulent pulsations in stability of laminar boundary layer 11 p1716 N85-20795
Transonic interactions of unsteady vortical flows [NASA-TM-86658] 12 p1770 N85-21113
Numerical study of large-eddy breakup and its effect on the drag characteristics of boundary layers [NASA-CR-3884] 12 p1797 N85-21272

A calculation of slender delta wing with leading-edge separation by quasi-vortex-lattice method
12 p1821 N85-21423
Calculation of the flow around thick wings with separation vortices 12 p1821 N85-21424
Solution of the three-dimensional Navier-Stokes equations for a steady laminar horseshoe vortex flow
[AD-A149651] 12 p1846 N85-21582
A supplement study on the subsynoptic cloud system off the south coast of Japan 12 p1895 N85-21892
Study for prediction of rotor/wake/fuselage interference, part 1
[NASA-CR-177340-VOL-1] 13 p1965 N85-22346
Study for prediction of rotor/wake/fuselage interference. Part 2: Program users guide
[NASA-CR-177340-VOL-2] 13 p1966 N85-22347
Method for the prediction of the installation aerodynamics of a propfan at subsonic speeds
[NASA-CR-3687] 13 p1969 N85-22369
Deflected jet experiments in a turbulent combustor flowfield
[NASA-CR-174863] 13 p1973 N85-22390
Propagation of three-dimensional turbulent jet from lobar nozzle through surrounding stream
13 p2042 N85-22785
Time-dependent flow of stream swirled in vortex chamber 13 p2043 N85-22786
Experimentally determined characteristics of vortex heaters 13 p2050 N85-22833
Grid generation for a pump collector
[AD-A150217] 13 p2092 N85-23059
Double and inverse Taylor-Hogg vortices in a stratified ocean 13 p2108 N85-23137
An experimental investigation of the chopping of helicopter main rotor tip vortices by the tail rotor
[NASA-CR-177338] 13 p2154 N85-23376
Computations of two-dimensional airfoil-vortex interactions --- helicopter rotor flowfields
[NASA-CR-3885] 14 p2210 N85-23709
Stability of vortex structures during separation flow past array of wings 14 p2278 N85-24110
Experimental and theoretical investigation of the motion of particles in a compressible vortex
[ISL-R-129/83] 14 p2303 N85-24264
Modeling evolution of unstable geostropic eddies in barotropic ocean 14 p2336 N85-24447
Hydromagnetic vortices: An interpretation for dawnside events as on December 11, 1977 — magnetotail
14 p2371 N85-24653
Prediction of vortex-induced loads on wind-tunnel turning vanes
[NASA-TM-86678] 15 p2482 N85-25204
An exploratory study of apex fence flaps on a 74 deg delta wing
[NASA-CR-172463] 15 p2483 N85-25208
Analysis of selected problems involving vortical flows
[NASA-CR-177347] 15 p2483 N85-25212
On the structure of the turbulent vortex
15 p2483 N85-25213
Flow past a flat plat with a vortex/sink combination
[JIAA-TR-58] 15 p2484 N85-25215
An experimental study of hairpin-type vortices as a potential flow structure of turbulent boundary layers
15 p2553 N85-25751
Stability calculations of the two-dimensional boundary layer along a concave wall: Part 1: A numerical method of solution for the simultaneous ordinary differential equations governing disturbances
[NAL-TR-841] 15 p2554 N85-25758
Vortex dynamics
[AD-A151278] 15 p2637 N85-26260
Dust devils on Mars 15 p2663 N85-26573
La Recherche Aerospatiale Bimonthly Bulletin Number 1984-2, 219/March-April
[ESA-TT-878] 16 p2694 N85-26635
Exploratory wind-tunnel investigation of a wingtip-mounted vortex turbine for vortex energy recovery
[NASA-TP-2468] 16 p2699 N85-26667
Development of a rotor wake-vortex model, volume 1
[NASA-CR-174849] 16 p2699 N85-26668
An experimental investigation of two-dimensional flame-vortex interactions 16 p2744 N85-26934
Vortex studies relating to boundary layer turbulence and noise
[NASA-TM-87475] 16 p2782 N85-27189
An experimental investigation of a turbulent junction vortex
[NASA-CR-175915] 17 p2957 N85-28259
Vortices in non-Newtonian fluids
[AD-A153169] 17 p2958 N85-28269
The effect of the Benthic Boundary Layer on the physics of intense mesoscale eddies
[AD-A153193] 17 p2958 N85-28270
Tidal rectification in lateral viscous boundary layers of a semienclosed basin
[CWI-AM-R8415] 17 p2960 N85-28284
Kinetic energy and vorticity of lee cyclones
[MITT-40] 17 p2993 N85-28502
Flame acceleration mechanisms under conditions of partial confinement
[PB85-184083] 18 p3073 N85-29004
On the origin of streamwise vortices in a turbulent boundary layer
[AD-A153651] 18 p3100 N85-29188
Turbulent wake of a submerged flat plate
[AD-A153776] 18 p3100 N85-29190
The hydroelastic infundibulum
[AD-A153849] 18 p3100 N85-29192
Transient eddies in the UCLA GCM
18 p3145 N85-29470
Singularity solutions for ellipsoids in Low-Reynolds-Number flows: With applications to the calculation of hydrodynamic interactions in suspensions of ellipsoids
[AD-A153503] 18 p3168 N85-29632
Wake effects of the aerodynamic performance of horizontal axis wind turbines 19 p3211 N85-29915
Aerodynamic analysis of a horizontal axis wind turbine by use of helical vortex theory. Volume 1: Theory
[NASA-CR-168054] 19 p3212 N85-29916
Lee-side flow over delta wings at supersonic speeds
[NASA-TP-2430] 19 p3212 N85-29921
A method for computing the core flow in three-dimensional leading-edge vortices
[NASA-TM-87489] 19 p3214 N85-29932
Transverse vorticity measurements in an excited two-dimensional mixing layer 19 p3264 N85-30241
Shock waves in adjacent engine inlets
[ISL-R-104/84] 20 p3396 N85-31068
Vortex simulation of v-shaped flame
20 p3425 N85-31259
Viscous flows in rotating pipes with internal cavities and related vortex breakdowns
[NASA-TM-86761] 20 p3454 N85-31447
Large eddy structures in transitional and turbulent flames
[AD-A154520] 21 p3562 N85-32157
Determination of billows and other turbulent structures, part 4.1A 21 p3621 N85-32500
On the application of a hairpin vortex model of wall turbulence to trailing edge noise prediction
[NASA-CR-177936] 22 p3728 N85-33109
Vortex dynamics simulation of conserved scalar dissipation 22 p3745 N85-33210
Drying of pulverized material with heated condensible vapor
[DE85-011656] 22 p3783 N85-33438
Aerodynamic analysis of a horizontal axis wind turbine by use of helical vortex theory, volume 2: Computer program users manual
[NASA-CR-174921] 22 p3804 N85-33563
A three-dimensional viscous flow analysis for the helicopter tip vortex generation problem
[NASA-CR-3908] 23 p3893 N85-34114
Comments on the prediction of dynamic stall
[GU-AERO-8501] 23 p3894 N85-34125

VORTICITY

The inducement of planetary boundary layer mass convergence associated with varying vorticity beneath tropospheric wind maximum 01 p0074 N85-10494
Spatial and temporal interpolation of NEROS radiosonde winds
[PB84-232545] 04 p0540 N85-13436
Numerical modeling of the atmosphere
05 p0680 N85-14370
Channel constructed to provide well defined boundary layers for vorticity optical probe measurements
[AD-A146679] 06 p0809 N85-15140
Calculating secondary nonviscous gas flows in spatial cascades of turbines 09 p1305 N85-18202
Behavior and characteristics of storm cold outflows
09 p1356 N85-18529
A frozen vorticity approach to the axisymmetric strong interaction problem
[AD-A149101] 10 p1484 N85-19369
Planetary scale circulation anomalies associated with droughts over northeast Brazil
[INPE-3351-PRE/630] 10 p1518 N85-19570
Cumulus effects on the large-scale vorticity and momentum fields in the tropical atmosphere
13 p2137 N85-23270
Natural convection in cylindrical containers
15 p2555 N85-25763
Numerical experiments of jet streak ageostrophic circulations using pseudo-geostrophic initialization and perspectives 15 p2590 N85-25969
The vector potential in a branched Riemann space
[VTH-LR-395] 16 p2856 N85-27614
Transverse vorticity measurements using an array of four hot-wire probes
[FSFL-R-85-006] 18 p3099 N85-29184
On Fofonoff's mode 18 p3145 N85-29471
Transverse vorticity measurements in an excited two-dimensional mixing layer 19 p3264 N85-30241
Horizontal and vertical structure of velocity, potential vorticity and energy in the gulf stream
[AD-A154753] 21 p3665 N85-32702
Maintenance of blocking anticyclones in a general circulation model
[PB85-190866] 24 p4104 N85-35587

VORTICITY EQUATIONS

Hyperbolic phenomena in the flow of viscoelastic fluids
[AD-A153533] 18 p3099 N85-29186
Multiple equilibria of the barotropic vorticity equation on a sphere 18 p3146 N85-29475
A numerical study of Taylor-Vortex flow
[AD-A154787] 21 p3584 N85-32277
The calculation of two-dimensional buoyant surface jets with the k-W model of turbulence --- kinetic energy-vorticity fluctuations (k-W)
[CFD/84/21] 22 p3765 N85-33448

VORTICITY TRANSPORT HYPOTHESIS

Behavior of small ferromagnetic particles in traveling magnetic field 12 p1843 N85-21564

VOWELS

Classification methods for Italian vowels --- speech recognition
[FUB-61-1982] 01 p0039 N85-10248
Description of a semiannual selection procedure of vowel parts of the voice signal using a PDP 11/34 computer
[FUB-4-1983] 01 p0039 N85-10250
Determination of vowel zones in speech --- speech recognition
[FUB-16-1983] 01 p0040 N85-10253
Vowel phoneme identification in speech
[FUB-26-1983] 01 p0040 N85-10257

VOYAGER PROJECT

Uranus and Neptune
[NASA-CP-2330] 02 p0298 N85-11927
Atmospheric dynamics of Uranus and Neptune: Theoretical considerations 02 p0299 N85-11936
Charged particle erosion of icy satellites: Coronal atmospheres and surface redistribution
03 p0448 N85-12945
Multispectral and geomorphic studies of processed Voyager 2 images of Europa
[NASA-CR-174075] 03 p0448 N85-12948
Mission science value-cost savings from the Advanced Imaging Communication System (AICS)
[NASA-CR-174170] 04 p0458 N85-12905
The performance of differential VLBI delay during interplanetary cruise 05 p0623 N85-13964
Lower atmospheric composition of Jupiter from Voyager infrared measurements
[NASA-CR-174196] 05 p0745 N85-14779
Analysis of Jovian decametric data: Study of radio emission mechanisms
[NASA-CR-174208] 08 p1258 N85-17917
MU Sagittarii and Beta Lyrae: Combined IUE/Voyager observations 11 p1757 N85-21052
Radio scintillations observed during atmospheric occultations of Voyager: Internal gravity waves at Titan and magnetic field orientations at Jupiter and Saturn
[NASA-CR-175554] 12 p1981 N85-22327
Sulfur volcanoes on Io? 13 p2173 N85-23479
Geomorphic classification of lava flows on Io
13 p2173 N85-23480
Sulfur oxygen processes on Io
13 p2173 N85-23481
The violet absorber on Io: Disulfur monoxide derivatives 13 p2173 N85-23482
Dark halo craters and the thickness of grooved terrain on Ganymede 13 p2173 N85-23484
Formation of bright terrain bands on Ganymede by unstable lithosphere extension 13 p2173 N85-23485
Investigations of planetary ring phenomena
13 p2174 N85-23487
Dynamical studies of Saturn's rings
13 p2174 N85-23489
Jupiter/Voyager data analysis
[NASA-CR-175723] 15 p2679 N85-26545
Stream dynamics between 1 AU and 2 AU: A detailed comparison of observations and theory
[NASA-TM-86086] 15 p2984 N85-26578
Voyager 0.2-lbf thruster valve assembly short pulse test report
[NASA-CR-176121] 22 p3741 N85-33185

VOYAGER 1 SPACECRAFT

Voyager EUV and FUV observations
06 p0875 N85-15554
Hot spots on Io: Correlation of infrared emission and visible reflectance 13 p2172 N85-23475

The eccentric ringlet at 1.29 R sub S — Saturn radius (RS) 15 p2673 N85-26496
Voyager UVS observations of stellar occultations by the rings of Saturn — ultraviolet spectrometer (UVS) 15 p2673 N85-26497
Voyager planetary radio astronomy: Grain and particle impacts shot noise in Saturn's ring plane 15 p2673 N85-26498
Shocks in the solar wind between 1 and 8.5 AU: Voyager 1 observations [NASA-CR-175911] 18 p3209 N85-29905
Analysis of Jovian decametric data: Study of radio emission mechanisms [NASA-CR-176057] 22 p3851 N85-33846
The energy spectrum of Jovian electrons in interplanetary space [SH-1.5-18] 23 p3997 N85-34781

VOYAGER 2 SPACECRAFT
Pioneer 10 and Voyager observations of the interstellar medium in scattered emission of the He 584 A and H Lya 1216 A lines 06 p0873 N85-15541
Voyager EUV and FUV observations 06 p0875 N85-15554
Patterns of fracture and tidal stresses due to nonsynchronous rotation: Implications for fracturing on Europa 13 p2173 N85-23483
Voyager UVS observations of stellar occultations by the rings of Saturn — ultraviolet spectrometer (UVS) 15 p2673 N85-26497
Voyager planetary radio astronomy: Grain and particle impacts shot noise in Saturn's ring plane 15 p2673 N85-26498
Future studies of planetary rings by spaceprobes 15 p2679 N85-26541
Voyage to Uranus 15 p2687 N85-26596
Cosmic ray modulation and turbulent interaction regions near 11 AU [NASA-TM-86193] 18 p3209 N85-29909
Acceleration of ions and electrons to near-cosmic ray energies in a perpendicular shock: The January 6, 1978 event [SH-1.5-4] 23 p3996 N85-34773
The energy spectrum of Jovian electrons in interplanetary space [SH-1.5-18] 23 p3997 N85-34781

VTOL
U VERTICAL LANDING

VTOL AIRCRAFT
U VERTICAL TAKEOFF AIRCRAFT

VULCANIZATES
U VULCANIZED ELASTOMERS

VULCANIZED ELASTOMERS
Simple EOS for the silicone rubber Sylgard 184 [DE85-001394] 12 p1814 N85-21376
Development of nitrile rubbers and foams having a high static modulus and low creep [BR91465] 14 p2259 N85-24001

VULNERABILITY
The vulnerability of cast double base rocket motors to thermomechanical attack 08 p1115 N85-17033
A methodology for the determination of rotary wing aircraft vulnerabilities in air-to-air combat simulation [AD-A146984] 10 p1424 N85-18994
Survivable local area network [AD-D011453] 10 p1466 N85-19262
Minimization of system vulnerability in Naval satellite communication networks 11 p1710 N85-20758
Systems vulnerability and lethality in the development phase [AD-A149737] 12 p1924 N85-22089
Elastic-workhardening SDF (Single-Degree-of-Freedom) system subjected to random blast excitations [AD-A151666] 15 p2579 N85-25909
Survivable ground base sensor [AD-D011647] 17 p2950 N85-28213
Literature survey of underground construction methods for application to hardened facilities [AD-A155212] 21 p3599 N85-32351
Investigation of the lightning vulnerability of nuclear explosive test systems at the Nevada Test Site [DE85-011761] 24 p4124 N85-35563

W

W WINGS
U VARIABLE SWEEP WINGS

W-R STARS
U WOLF-RAYET STARS

WAFERS
Ion beam lithography [BMFT-FB-T-84-182] 04 p0504 N85-13219
Silicon-sheet surface studies 06 p0831 N85-15267
Restructurable VLSI program [AD-A148145] 08 p1157 N85-17301
Pulsed excimer laser processing for cost-effective solar cells [NASA-CR-174429] 10 p1509 N85-19517
Pulsed excimer laser processing for cost-effective solar cells [NASA-CR-175465] 10 p1509 N85-19520
Stress studies in EFG [NASA-CR-175464] 10 p1509 N85-19522
Lithium counterdoped silicon solar cell [NASA-CASE-LEW-14177-1] 11 p1672 N85-20535
Factors affecting SOS (Silicon-On-Sapphire) yield and reliability [AD-A150004] 12 p1835 N85-21515
Ingot slicing machine and method [NASA-CASE-NPO-15483-1] 12 p1857 N85-21650
A low cost approach with larger diameter silicon wafer — solar cells 13 p2006 N85-22572
Multifunctional elements for integrated optics 13 p2066 N85-22918
Time-resolved reflectivity measurement of extrinsic silicon during pulsed laser irradiation [AD-A150350] 13 p2159 N85-23403
Uses of, experiences in production of custom designed IC's 17 p2945 N85-28180
Interfacial bonding stability 21 p3608 N85-32409
Sixty GHz IMPATT diode development [NASA-CR-174969] 22 p3758 N85-33293

WAKEFULNESS
Effects of partial deprivation of slow-wave sleep on sleep-wakefulness cycles 10 p1524 N85-19613
Sleep and wake physiology in weightlessness 20 p3510 N85-31819

WAKES
NT AIRCRAFT WAKES
NT HELICOPTER WAKES
NT LAMINAR WAKES
NT NEAR WAKES
NT PROPELLER SLIPSTREAMS
NT SLIPSTREAMS
NT SUPERSONIC WAKES
NT TURBULENT WAKES
Turbofan noise generation. Volume 2: Computer programs [NASA-CR-167952] 02 p0275 N85-11791
Large structure in the far wakes of two-dimensional bluff bodies 05 p0592 N85-13771
Energy spread in SLC linac with Landau damping [DE84-016259] 05 p0727 N85-14675
SEASAT 3 and 4 [AD-A148343] 08 p1152 N85-17274
Second order Bragg scattering in a SAR [AD-A148395] 08 p1152 N85-17275
Solitons and SEASAT [AD-A148396] 08 p1176 N85-17414
Preliminary results from the unsteady airfoil model USTAR2 [AD-P004171] 09 p1266 N85-17956
A study for calculating rotor loads using free vortex concept 11 p1620 N85-20194
Unsteady flows around 3-dimensional wings [AD-A149993] 12 p1772 N85-21124
Electron and ion density depletions measured in the STS-3 orbiter wake 13 p1989 N85-22474
Polar orbit electrostatic charging of objects in shuttle wake 13 p1992 N85-22487
Ram-wake effects on plasma current collection of the PIX 2 Langmuir probe 13 p1993 N85-22496
Oscillating airfoils and their wake [NASA-TM-77831] 14 p2209 N85-23701
Prediction of vortex-induced loads on wind-tunnel turning vanes [NASA-TM-86678] 15 p2462 N85-25204
Analysis of selected problems involving vortical flows [NASA-CR-177347] 15 p2463 N85-25212
On the structure of the turbulent vortex 15 p2463 N85-25213
SEASAT report [AD-A151283] 15 p2583 N85-25931
A study of aerodynamic control in stalled flight leading-edge vortex formation analysis [AD-A153758] 18 p3059 N85-28928
Wake effects on the aerodynamic performance of horizontal axis wind turbines [NASA-CR-174920] 18 p3127 N85-29364
Space shuttle molecular and wake vacuum measurements [NASA-TM-86509] 19 p3222 N85-29978
Preliminary investigation of dispersion of pollutants in model building wake flows using bipolar space charge [IC-AERO-84-04] 20 p3487 N85-31671
Using ship wake patterns to evaluate SAR (Synthetic Aperture Radar) ocean wave imaging mechanisms. Joint US-Canadian Ocean Wave Investigation Project [AD-A154633] 21 p3573 N85-32223

WALKING
Locomotion research for the analysis of the human gait and for the determination of the maximum loads of the pelvis-leg skeleton. Volume 1: Two-dimensional analysis [BMFT-FB-T-83-187-VOL-1] 02 p0236 N85-11535
Locomotion research for the analysis of the human gait and for the determination of the maximum loads of the pelvis-leg skeleton. Volume 2: Three-dimensional analysis [BMFT-FB-T-83-188-VOL-2] 02 p0236 N85-11536
The energy cost of women walking and running in shoes and boots [AD-A151022] 14 p2389 N85-24716
Diet of first Soviet expedition on Mount Everest 19 p3323 N85-30586

WALKING MACHINES
Machine Mechanics Institute builds walking vehicle 04 p0543 N85-13455
Control of walking: Local control and real time systems 05 p0715 N85-14583
3D (Three-Dimensional) sensor for adaptive suspension vehicle [AD-A150921] 14 p2311 N85-24305

WALL FLOW
Design, manufacture, and testing of compliant coatings for reduction of turbulent drag [AD-A145510] 02 p0198 N85-11323
Similarity criteria of spectra of pressure pulsations of turbulent boundary layer near wall 02 p0256 N85-11679
Developed turbulent flow under conditions of internal and external problems 02 p0260 N85-11700
Progress in wind tunnel wall interference assessment/correction procedures at the NAE 03 p0314 N85-12025
Tunnel constraint for a jet in crossflow 03 p0314 N85-12027
Interference from slotted walls 03 p0314 N85-12028
Wind tunnel wall interference correction for aircraft models 03 p0314 N85-12029
Determination of equivalent model geometry for tunnel wall interference assessment/correction 03 p0314 N85-12031
Minimization of wall interference for three-dimensional models with two-dimensional wall adaptation — wind tunnel walls [VKI-TN-149] 03 p0321 N85-12070
Wall effects on the slow steady motion of a particle in a viscous incompressible fluid [PREPRINT-828] 03 p0363 N85-12327
Wall influence corrections in wind tunnels: Blockage correction according to the wall pressure signature method [FW-FO-1613] 04 p0453 N85-12875
Parametric determination of blockage interference of 3-dimensional models in the Emmen Federal Aircraft works transonic tunnel (Switzerland) [FW-FO-1636] 04 p0453 N85-12876
A local slot boundary condition for transonic flow calculations in slotted-wall test sections of wind tunnels [FFA-TN-1984-34] 04 p0453 N85-12879
Investigation for the improvement of the transonic tunnel working section of the Emmen Federal Aircraft Works (Switzerland) [FW-FO-1681] 04 p0458 N85-12904
Turbulent boundary layers with secondary flow [NASA-TM-77494] 04 p0498 N85-13176
Progress in the development of a two-fluid model of turbulence for near-wall flows, part 1 [CFD/84/7-PT-1] 04 p0501 N85-13196
Progress in the development of a two-fluid model of turbulence for near-wall flows. Part 3: Preliminary investigation of a stably-stratified boundary layer [CFD/84/9-PT-3] 04 p0501 N85-13197
Proposal for wall function for friction and heat transfer in the presence of roughness and mass transfer [CFD/84/12] 04 p0501 N85-13198
Experiments on the structure of turbulent reattaching flow 05 p0635 N85-14074
Studies of the wall shear stress in a turbulent pulsating pipe flow [AD-A146772] 07 p0957 N85-16068
Corrections for attached sidewall boundary-layer effects in 2-dimensional airfoil testing [NASA-CR-3873] 09 p1272 N85-17997
Experimental investigation of a turbulent incompressible boundary layer on a curved wall 11 p1577 N85-19936
An investigation of turbulence mechanisms in V/STOL upwash flow fields [AD-A149786] 12 p1772 N85-21123
A three-dimensional spectral algorithm for simulations of transition and turbulence [NASA-CR-172561] 12 p1845 N85-21575

An experimental investigation of the interaction between a shock wave and a turbulent boundary layer on a convex wall
[VTH-LR-428] 16 p2785 N85-27187
Adaptive wall wind tunnels and wall interference correction methods
[DFVLR-IB-222-84-A-37] 17 p2905 N85-27912
Coherent structure reflective turbulent viscous flow modeling
[AD-A153066] 17 p2958 N85-28267
Wall effect on lateral migration of spherical particles in a linear shear flow 20 p3452 N85-31432
Injection of drag reducing additives into turbulent water flows: Two-component velocity measurements and mixing length model predictions
[AD-A154604] 21 p3583 N85-32274
Experiments on the influence of active walls on the initial amplitudes and growths of instability waves
[AD-A154630] 21 p3583 N85-32275

WALL JETS
Modelling circulation control by blowing — airfoils 06 p1069 N85-16778

WALL PRESSURE
Experimental study of Mach reflection of weak shock waves 02 p0260 N85-11703
Wind tunnel wall interference in closed, ventilated and adaptive test sections 03 p0312 N85-12014
Experiments suitable for wind tunnel wall interference assessment/correction 03 p0313 N85-12021
Tunnel constraint for a jet in crossflow 03 p0314 N85-12027
An interference assessment approach for a three-dimensional slotted tunnel with sparse wall pressure data 03 p0314 N85-12030
Review of the advanced technology airfoil test program in the 0.3-meter transonic cryogenic tunnel 03 p0315 N85-12033
Singularity model for the analysis of wall interference in closed wind tunnels according to the wall pressure signature method (blockage and lift)
[FW-FO-1612] 04 p0453 N85-12874
Comparative flow calculation on transonic cone/cylinder standard models in connection with the wall interference problem
[FW-FO-1689] 04 p0453 N85-12878
Comparison of techniques to measure the low wavenumber wall pressure spectrum of a turbulent boundary layer
[AD-A148074] 06 p1162 N85-17331
Experimental investigation of a turbulent incompressible boundary layer on a curved wall 11 p1577 N85-19936
Sidewall boundary-layer effects in two-dimensional airfoil testing
[NASA-CR-176034] 20 p3396 N85-31085

WALL TEMPERATURE
Laminar flow heat exchangers. Viscosity induced non-uniform flow
[AD-A144777] 01 p0047 N85-10307
High temperature thermocouple and heat flux gauge using a unique thin film-hardware hot juncture
[NASA-TM-86898] 07 p0962 N85-16096
The effect of air holes on combustor liner wall temperature profile: Experiments
[NAL-TR-840] 15 p2504 N85-25443
Study of a constricted electric arc cooled by transpiration
[NASA-TM-77846] 17 p3038 N85-28798
Numerical solutions of turbulent models for flow over a flat plate with angle of attack
[DE85-010390] 21 p3585 N85-32286

WALLS
NT NOZZLE WALLS
NT POROUS WALLS
NT THICK WALLS
NT THIN WALLS
NT TROMBE WALLS
NT WIND TUNNEL WALLS
Development of a floating element wall shear transducer
[AD-A144794] 01 p0049 N85-10324
Direct numerical simulation of curved turbulent channel flow
[NASA-TM-85974] 02 p0197 N85-11316
Performance of two transonic airfoil wind tunnels utilizing limited ventilation 03 p0313 N85-12020
Modeling of propulsive jet plumes--extension of modeling capabilities by utilizing wall curvature effects
[AD-A146262] 03 p0362 N85-12324
Complex frequency analysis of damped thin-walled beams with open cross sections 03 p0371 N85-12366
Architecture of dermatophyte cell Walls: Electron microscopic and biochemical analysis
[NASA-TM-77441] 03 p0399 N85-12546
Study of plasma convection and wall interactions in magnetic confinement systems
[DE84-013959] 03 p0421 N85-12692
Laminar flame propagation/quench for a parallel-wall duct
[DE84-009773] 04 p0470 N85-12993
Response measurements for two building structures excited by noise from a large horizontal axis wind turbine generator
[NASA-CR-172482] 04 p0558 N85-13552
JPL in-house fluidized-bed reactor research 06 p0832 N85-15291
Proceedings of Workshop on Synergistic Effects in Surface Phenomena Related to Plasma-Wall Interactions
[IPPJ-AM-35] 06 p0864 N85-15488
Synergistic effects in fusion machines, session summary 06 p0864 N85-15489
Plasma surface interaction processes and possible synergisms 06 p0864 N85-15490
Synergisms in hydrogen recycling, session summary 06 p0864 N85-15491
Steady state hydrogen transport in solids 06 p0864 N85-15492
Synergisms in surface erosion, session summary 06 p0864 N85-15493
Synergistic effects related to surface composition, session summary 06 p0865 N85-15495
Effects of monolayer coverages on substrate sputtering yields 06 p0865 N85-15496
Synergestic sputtering properties of binary alloys 06 p0865 N85-15497
Tolerance synthesis of multilayer radome walls 07 p0953 N85-16041
Oblique shock wave-turbulent boundary layer interaction on a porous wall with suction 08 p1072 N85-16794
Transonic shock interaction with a tangentially-injected turbulent boundary layer 08 p1072 N85-16796
Studies on seismic earth pressure of cohesive backfill 09 p1303 N85-18186
Determination of total pressure losses in stepped annular diffusors with curvilinear outer walls and uniform velocity field at inlet 09 p1306 N85-18203
Plasma surface interaction processes and possible synergisms
[DE85-001861] 09 p1391 N85-18752
Heat transfer and mechanical interactions in fusion nuclear systems
[DE84-016233] 09 p1392 N85-18761
OTEC (Ocean Thermal Energy Conversion) Cold Water Pipe At-Sea Test Program. Phase 2: Suspended pipe test
[PB85-119931] 10 p1512 N85-19542
Envelope thermal test unit: Technical description
[DE84-012254] 11 p1674 N85-20548
Vibrational relaxation in H-2 molecules by wall collisions: Applications to negative ion source processes
[DE85-000852] 11 p1721 N85-20828
Control of surface composition and hydrogen recycling by plasma conditioning
[DE85-001859] 11 p1731 N85-20889
Integrated insulation wall assembly — for a solid rocket motor case
[AD-D011553] 12 p1794 N85-21257
Method and apparatus for mapping the distribution of chemical elements in an extended medium
[NASA-CASE-GSC-12906-1] 12 p1798 N85-21279
Theoretical and empirical studies of the basic structure of turbulent shear flows, including separated flows and effects of wall curvature
[AD-A149657] 12 p1846 N85-21580
Turbulent convecting flow in a square duct with a 180 deg bend: An experimental and numerical study
[AD-A149969] 12 p1846 N85-21583
Apparatus and method to keep the walls of a free-space reactor free from deposits of solid materials
[NASA-CASE-NPO-15851-1] 12 p1858 N85-21652
Experimental studies of low temperature surface interactions of atomic hydrogen using maser technique
[AD-A150218] 13 p2017 N85-22647
Optimization of overall dimensions of enclosures for low-voltage devices and equipment 13 p2087 N85-23033
Overview of latent storage for passive solar applications
[DE85-005354] 13 p2129 N85-23249
Confinement properties of high energy density plasmas in the Wisconsin levitated octupole 13 p2161 N85-23408
Heat transfer to vertical flat plates in a rectangular gas-fluidized bed
[AD-A150785] 14 p2301 N85-24248
Stability calculations of the two-dimensional boundary layer along a concave wall: Part 1: A numerical method of solution for the simultaneous ordinary differential equations governing disturbances
[NAL-TR-841] 15 p2554 N85-25758
Plasma-wall interactions in tandem mirror machines
[DE85-006387] 15 p2657 N85-26399
Accelerator-based plasma-wall interaction studies on the TEXTOR Tokamak
[DE85-007540] 17 p3040 N85-28606
Atomic hydrogen maser measurements with wall surfaces of carbon tetrafluoride 18 p3108 N85-29243
New concept for a wall detector for alpha particles
[DE85-009037] 18 p3183 N85-29740
Airborne sound transmission loss characteristics of wood-frame construction
[AD-A154174] 20 p3524 N85-31919
Wall flames and implications for upward flame spread
[FAA-CT-85-2] 21 p3553 N85-32103
Construction of University of Missouri, Rolla's full scale cloud simulation chamber and applied research
[AD-A154682] 21 p3557 N85-32128
In-situ measurement of wall thermal performance: Data interpretation and apparatus design recommendations
[DE85-011979] 21 p3586 N85-32289

WALSH FUNCTION
Algorithm in Walsh function basis for analysis of integrated microcircuits on MOS-structures 13 p2083 N85-23006
Use of Walsh functions for calculating characteristics of digital filters with impulse response of finite duration 13 p2083 N85-23011
Investigation of influence of communications link and synchronization error on noise tolerance of group transmission of binary information based on orthogonal Walsh function 13 p2086 N85-23026

WAR GAMES
Command control group behaviors. Objective 1: A methodology for and identification of command control group behaviors
[AD-A145690] 02 p0191 N85-11279
Automated CPX support system preliminary design phase
[NASA-CR-175784] 16 p2769 N85-27091
An extended two-target differential game model for medium-range air combat game analysis
[NASA-CR-175968] 18 p3175 N85-29687

WARFARE
NT ANTISHIP WARFARE
NT ANTISUBMARINE WARFARE
NT CHEMICAL WARFARE
NT COMBAT
NT ELECTRONIC WARFARE
Materials for emergency repair of runways
[AD-A146139] 03 p0320 N85-12068
A framework for the development of Navy computer-based systems: Combat system architecture and combat system engineering put into perspective
[AD-A146460] 06 p0956 N85-15445
Can the Aggressors continue to be effective in the F-5E?
[AD-A146661] 07 p1019 N85-16485
The value and utility of inflight onboard simulation
[AD-A148033] 08 p1196 N85-17543
A methodology for the determination of rotary wing aircraft vulnerabilities in air-to-air combat simulation
[AD-A148984] 10 p1424 N85-18964
Servo operated anti-G suit pressurization system
[AD-D011468] 10 p1531 N85-19651
Impact of future aircombat characteristics on pilot performance and cockpit design 10 p1533 N85-19661
PRC journal discusses 'Star Wars' space program 11 p1621 N85-20207
Military applications of meteorological satellite (METSAT) data 11 p1711 N85-20767
Civil weather satellite systems 11 p1711 N85-20768
Meteorological and oceanographic support during the Falklands conflict 11 p1712 N85-20769
Development of satellite data presentation for environmental forecasting 11 p1712 N85-20770
Ground evaluation of helicopter air-to-air warfare 13 p1967 N85-22360
Visual simulation requirements for aircraft aspect recognition at real world distances
[AD-A151040] 14 p2228 N85-23810
Equilibrium solutions, stabilities and dynamics of Lanchester's equations with optimization of initial force commitments
[AD-A151510] 15 p2637 N85-26288
Equipment development for rapid detection of microorganisms in air and water
[FOA-A-40046-B2] 18 p3134 N85-29410
Transceiver test device
[AD-D011728] 22 p3786 N85-33458
Arms control and The President's Strategic Defense Initiative
[AD-A156334] 24 p4068 N85-35212

WARHEADS
Penguin warhead safety tests
06 p1115 N85-17031
Calculation through Fault Tree Analysis of the probability of a warhead being armed prior to launch
[AD-P004339] 10 p1454 N85-19163
Preventing explosive propagation in racks or containers of tactical missiles
[AD-P004342] 10 p1455 N85-19166
WARMING
U HEATING
WARNING DEVICES
U WARNING SYSTEMS
WARNING SIGNALS
U WARNING SYSTEMS
WARNING SYSTEMS
NT MINE DETECTORS
Flight phase status monitor study. Phase 1: Systems concepts
[DOT/FAA/PM-84/18] 03 p0317 N85-12048
A model for the effectiveness of aircraft alerting and warning systems 05 p0702 N85-14506
Development and certification of a new stall warning and avoidance system 05 p0702 N85-14507
Statistics from the operation of the low-level wind shear alert system (LLWAS) during the Joint Airport Weather Studies (JAWS) Project
[DOT/FAA/PM-84/32] 06 p0750 N85-14804
Human factors in cockpit automation
06 p0752 N85-14819
A biological sensor for the detection of toxicants
[AD-D011304] 07 p0967 N85-16141
Battery control and fault detection method
[AD-D011384] 07 p0993 N85-16307
LPI-radar for helicopter obstacle warning
06 p1074 N85-16810
History, design and performance of the space shuttle hazardous gas detection system
06 p1098 N85-16936
A scanning alarm electronic processor
[AD-D011419] 06 p1158 N85-17309
The use of synthetic aperture radar imagery to detect hazards to navigation
[AD-A149324] 10 p1422 N85-18971
Large natural geophysical events: Planetary planning
[DE85-000859] 11 p1783 N85-21092
Extraction of signals from background interference with unknown parameters in quantized sample
13 p2084 N85-23013
Helicopter user survey: Traffic alert and collision avoidance system (TCAS)
[FAA-PM-85-6] 15 p2466 N85-25236
Preliminary airworthiness evaluation of a National Aeronautics and Space Administration automated stall warning system for an OV-1 aircraft
[AD-A152010] 16 p2707 N85-26706
Reusable rocket engine turbopump condition monitoring 16 p2740 N85-26907
Information presentation in power plant control rooms
[VTT-320] 16 p2864 N85-27668
Seismic discrimination
[AD-A154167] 20 p3494 N85-31722
Function of a device for detection of biological aerosols in field testing
[FOA-C-40194-B2] 20 p3504 N85-31782
Automated cell detection as a mesocyclone precursor tool
[AD-A154952] 21 p3635 N85-32577
ARAC status report, 1985
[DE85-012935] 22 p3810 N85-33603
Solar system fault detection
[DE85-005967] 23 p3946 N85-34458
An approach to determining computer security requirements for Navy systems
[AD-A155750] 24 p4135 N85-35627
WARPAGE
Determination of shear coefficient of a general beam cross section by finite element method
09 p1338 N85-18413
WASHING
In situ washing procedures for the UKIRT 3.8 meter primary mirror — United Kingdom Infrared Telescope (UKIRT)
[UKIRT-20] 09 p1414 N85-18918
Control of acid deposition precursors through dry scrubbing
[DE85-010261] 19 p3235 N85-30056
WASHINGTON
Glacier dynamics and the development of glacial landforms in the eastern Puget lowland, Washington
03 p0389 N85-12490
Stratigraphy, sedimentology and tectonic significance of the Upper Cretaceous Virginian Ridge formation, Method Basin, Washington: Implications for tectonic history of the North Cascades 03 p0390 N85-12494
Tides and tidal currents of the inland waters of Western Washington
[PB84-237379] 06 p0842 N85-15346
Revised Uniform Summary of Surface Weather Observations (RUSSWO). McChord AFB, Washington, parts A-F
[AD-A146914] 07 p1005 N85-16385
Preliminary survey of wind generation in Washington: Site studies and selected wind speed data
[DE85-000058] 09 p1345 N85-18462
Structural morphology and associated strain within parts of the US section of the Kootenay Arc, NE, Washington
09 p1352 N85-18505
Changes in the organic material in lakes in the blast zone of Mount St. Helens, Washington: Hydrologic effects of the eruptions
[GS-CIRC-850-1] 21 p3630 N85-32551
WASHOUT (RADIOACTIVITY)
U FALLOUT
WASPALOY
An electrochemical study of hydrogen uptake and elimination by bare and gold-plated waspaloy
[NASA-TM-86479] 02 p0182 N85-11222
Possibilities for a more accurate life prediction of components — gas turbine disks
07 p0976 N85-16196
WASTE DISPOSAL
NT HAZARDOUS MATERIAL DISPOSAL (IN SPACE)
Depot modernization at the Defense Logistics Agency
[AD-P004008] 03 p0308 N85-11988
Crystalline rocks of the northeastern United States
[DE84-013674] 05 p0677 N85-14347
Description and operation of a thermal decomposition unit-gas chromatographic system
[PB84-246362] 07 p0968 N85-16146
Design concept definition study for an improved shuttle waste collection subsystem
[NASA-CR-171834] 08 p1198 N85-17546
Improved orbiter waste collection system study
[NASA-CR-171830] 08 p1199 N85-17548
Improved orbiter waste collection system study, appendix D
[NASA-CR-171833] 08 p1199 N85-17549
Waste collection subsystem study
[NASA-CR-171836] 08 p1199 N85-17552
Space Shuttle Orbiter waste collection system conceptual study
[NASA-CR-171844] 08 p1199 N85-17553
Ground-water level data and preliminary potentiometric-surface maps, Yucca Mountain and vicinity, Nye County, Nevada
[DE85-001771] 09 p1343 N85-18448
Proceedings of the Environmental Systems Symposium (13th) held at Bethesda, Md., 20-22 March 1984
[AD-A148194] 09 p1346 N85-18471
Strategies for preparing and submitting a part B application for a DoD facility
[AD-P004139] 09 p1347 N85-18475
Assessment of environmental costs at ordnance activities
[AD-P004140] 09 p1347 N85-18476
Remedial action of hazardous waste US Army Corps of Engineers, Anniston, Alabama
[AD-P004141] 09 p1347 N85-18477
Polymeric liner selection for military waste impoundments
[AD-P004143] 09 p1348 N85-18479
Applying an innovative approach to field investigations at a remedial action site
[AD-P004145] 09 p1348 N85-18481
The Hazardous Materials Technical Center
[AD-P004149] 09 p1349 N85-18485
Community relations activities at Department of Defense sites
[AD-P004150] 09 p1349 N85-18486
Protocol for aquifer cleanup decision making at military installations
[AD-P004151] 09 p1349 N85-18487
Analysis of geohydrologic data by kriging
[AD-P004152] 09 p1349 N85-18488
Consideration of future climatic changes in three geologic settings
[DE85-001704] 09 p1357 N85-18537
Measurements of sediment temperatures, conductivity and heat flow in the North Atlantic and their relevance to radioactive waste disposal
[IOS-172] 09 p1359 N85-18551
An assessement of biological processes close to the sea bed in a slope region and its significance to the assessment of sea-bed disposal of radioactive waste
[IOS-185] 09 p1360 N85-18554
Rockwell Hanford operations defense waste and byproducts management
[DE85-000553] 09 p1382 N85-18694
Nevada nuclear waste storage investigations preliminary repository concepts report
[DE85-002132] 09 p1383 N85-18696
Planning for greater-confinement disposal
[DE85-002143] 09 p1383 N85-18697
Perspective on demonstrations of compliance for high-level waste disposal
[DE85-000989] 09 p1383 N85-18698
Commission operation. National Low-Level Radioactive Waste Management Program
[DOE/LLW-33T] 09 p1383 N85-18699
Rock mechanics: Issues and research needs in the disposal of wastes in hydraulic fractures
[DE85-001399] 10 p1556 N85-19809
FAA policy regarding solid waste disposal facilities
[AD-P004196] 11 p1581 N85-19963
Airport bird hazards associated with solid waste disposal facilities
[AD-P004197] 11 p1581 N85-19964
Effectiveness of an overhead wire barrier in deterring gulls from feeding at a sanitary landfill
[AD-P004199] 11 p1582 N85-19966
Effectiveness of an overhead wire barrier system in reducing gull use at the BFI Jedburg sanitary landfill, Berkeley and Dorchester counties, South Carolina
[AD-P004200] 11 p1582 N85-19967
Effect of host-rock dissolution and precipitation on permeability in a nuclear waste repository in tuff
[DE85-000675] 11 p1727 N85-20660
Radioactive waste isolation in salt: Peer review of the D'Appolonia report on schematic designs for penetration seals for a repository in the Permian Basin, Texas
[DE85-000693] 11 p1727 N85-20661
Field lysimeter facility for evaluating the performance of commercial solidified low-level waste
[DE85-003886] 11 p1727 N85-20663
High-level waste processing and disposal
[DE85-003564] 11 p1728 N85-20665
ELECT groundwater transport research code
[DE85-003284] 12 p1884 N85-21824
Role of biological assessment in effluent control
[PB85-116101] 12 p1885 N85-21830
Stochastic convective-dispersive transport model for wastes disposed at the 106-mile ocean disposal site
[PB85-116176] 12 p1885 N85-21831
Methods/materials matrix of ultimate disposal techniques for spilled hazardous materials
[PB85-116853] 12 p1885 N85-21833
Assessment of hazardous waste surface impoundment technology case studies and perspectives of experts
[PB85-117059] 12 p1886 N85-21834
Shallow land burial technology: Humid
[DE85-004432] 12 p1932 N85-22136
Research and development related to the Nevada nuclear waste storage investigations
[DE85-002303] 12 p1932 N85-22138
Application of far-field models to the disposal of nuclear waste in geologic formations
[DE85-005489] 14 p2420 N85-24932
Protecting the nation's groundwater from contamination, volume 1
[PB85-154201] 15 p2590 N85-25965
Protecting the nation's groundwater from contamination, volume 2
[PB85-154219] 15 p2590 N85-25966
Shales and other argillaceous strata in the United States
[DE85-010453] 18 p3125 N85-29353
Region-to-area screening methodology for the Crystalline Repository Project
[DE85-000892] 18 p3125 N85-29354
Implications about in situ stress at Yucca Mountain
[DE85-008068] 18 p3126 N85-29356
Thermal-cycle testing of the G-tunnel heated block
[DE85-008408] 18 p3126 N85-29359
Advanced regenerative environmental control and life support systems: Air and water regeneration
18 p3155 N85-29595
Radionuclide mobility in the shallow portion of an active high-temperature geothermal system
[DE85-010293] 18 p3182 N85-29729
Experimental program to determine maximum temperatures for dry storage of spent fuel
[DE85-010307] 19 p3236 N85-30060
Hydrolysis, formation and ionization constants at 25(0)C, and at high temperature-high ionic strength
[DE85-010645] 19 p3236 N85-30061
Mixtures experiment where the amount of the mixture is a factor under study
[DE85-010974] 19 p3250 N85-30153
Reference data source documentation for performance assessment studies, Basalt Waste Isolation Project, Hanford Site, Washington
[DE85-010543] 19 p3301 N85-30468

Preliminary evaluation of alterant geophysical tomography in welded tuff
[DE85-010828] 19 p3302 N85-30469
Petrologic and geochemical characterization of the Topopah Spring Member of the Paintbrush Tuff: Outcrop samples used in waste package experiments
[DE85-010449] 19 p3302 N85-30470
Environmental Sciences Division report
[DE85-010452] 19 p3308 N85-30506
Radioactive liquid wastes discharged to ground in the 200 areas during 1984
[DE85-010619] 19 p3310 N85-30517
Analysis of leachate production in closed hazardous waste landfills
[DE85-010978] 19 p3310 N85-30520
Bulk and thermal properties of the functional Tuffaceous Beds in holes USW G-1, UE-25 no. 1, and USW G-2, Yucca Mountain, Nevada
[DE85-011181] 19 p3365 N85-30866
Dispersal From Deep Ocean Sources: Physical and Related Scientific Processes
[DE85-010420] 20 p3497 N85-31740
Development of processes for the inclusion of radioactive waste in glass-metal compounds and ceramic materials
[BLL-CE-TRANS-8014-(9022.09)] 20 p3526 N85-31931
Geologic and hydrologic characterization and evaluation of the basin and range province relative to the disposal of high-level radioactive waste. Part 1: Introduction and guidelines
[GS-CIRC-904-A] 20 p3526 N85-31932
Geologic and hydrologic characterization and evaluation of the basin and range province relative to the disposal of high-level radioactive waste. Part 2: Geologic and hydrologic characterization
[GS-CIRC-904-B] 20 p3526 N85-31933
Geologic and hydrologic characterization and evaluation of the basin and range province relative to the disposal of high-level radioactive waste. Part 3: Geologic and hydrologic evaluation
[GS-CIRC-904-A] 20 p3526 N85-31934
Source-term considerations for a potential radioactive-waste repository located in unsaturated tuff
[DE85-010090] 20 p3529 N85-31953
Review of hazardous waste cleanup and disposal efforts at Tinker Air Force Base
[GPO-43-294] 21 p3613 N85-32457
Centrifugal castings of stainless steel spiked with radioactive tracers
[DE85-012003] 22 p3748 N85-33234
WIPP horizon in situ permeability measurements
[DE85-012687] 22 p3802 N85-33557
Technology of off-gas treatment for liquid-fed ceramic melters
[DE85-012467] 22 p3812 N85-33610
Corrosion resistant storage container for radioactive material
[DE85-011666] 22 p3838 N85-33765
Office of Civilian Radioactive Waste Management
[DE85-012585] 22 p3839 N85-33774
Review of zirconium-zircaloy pyrophoricity
[DE85-011169] 23 p3916 N85-34270
Method for making a low density polyethylene waste form for safe disposal of low level radioactive material
[DE85-006401] 23 p3920 N85-34292
Research at the Institute of Oceanographic Sciences related to the possible disposal of radioactive waste on or beneath the seafloor
[IOS-204] 23 p3973 N85-34828
Simulated effects of increased recharge on the ground-water flow system of Yucca Mountain and vicinity, Nevada-California
[DE85-012985] 24 p4106 N85-35469
Land Disposal of Hazardous Waste
[PB85-196376] 24 p4113 N85-35500

WASTE ENERGY UTILIZATION

Evaluation of selected advanced heat exchangers for waste heat recuperation of high temperature streams
[DE84-016299] 04 p0499 N85-13180
Magnetic heat pump cycles for industrial waste heat recovery
[DE84-017016] 04 p0499 N85-13183
Detailed performance analysis of the A.A.D. - concept B
04 p0507 N85-13237
Overview of waste heat utilization systems
[NASA-TM-86901] 04 p0578 N85-13692
Challenges in the development of the orbiter radiator system
08 p1096 N85-16925
Available energy method for evaluating thermodynamic performance of heat pump systems
[DE84-017223] 09 p1400 N85-18814
Comparative evaluation of three alternative power cycles for waste heat recovery from the exhaust of adiabatic diesel engines
[NASA-TM-86953] 20 p3542 N85-32043
Feasibility study for small group water desalination equipment
[AD-A155106] 21 p3563 N85-32164
Woven heat exchanger
[DE85-011633] 22 p3783 N85-33439
Advanced regenerative heat recovery system
[PB85-196602] 24 p4084 N85-35315

WASTE HEAT

Evaluation of selected advanced heat exchangers for waste heat recuperation of high temperature streams
[DE84-016299] 04 p0499 N85-13180
Magnetic heat pump cycles for industrial waste heat recovery
[DE84-017016] 04 p0499 N85-13183
Open-cycle vapor compression heat pump
[PB85-101475/GAR] 08 p0775 N85-14951
Available energy method for evaluating thermodynamic performance of heat pump systems
[DE84-017223] 09 p1400 N85-18814
Development and test of a high COP Rankine heat pump for generation of process steam. Phase 2: Fabrication and test
[DE85-002600] 11 p1632 N85-20275
Technology for industrial waste heat recovery by organic Rankine cycle systems
[DE85-006719] 18 p3102 N85-29206
Comparative evaluation of three alternative power cycles for waste heat recovery from the exhaust of adiabatic diesel engines
[NASA-TM-86953] 20 p3542 N85-32043
Woven heat exchanger
[DE85-011633] 22 p3783 N85-33439
Energy from low temperature differences
[DE85-008817] 24 p4112 N85-35492

WASTE TREATMENT

HS and E environmental sciences
[DE84-016183] 05 p0672 N85-14314
Immobilization of toxic waste by embedding it in bitumen
[CEFZS-4277] 07 p0995 N85-16322
Proceedings of the Environmental Systems Symposium (13th) held at Bethesda, Md., 20-22 March 1984
[AD-A148194] 09 p1346 N85-18471
Strategies for preparing and submitting a part B application for a DoD facility
[AD-P004139] 09 p1347 N85-18475
Stabilization of contaminated soils by in situ vitrification
[AD-P004144] 09 p1348 N85-18480
Treatment of wastewater (red water) resulting from TNT (trinitrotoluene) purification
[AD-P004146] 09 p1348 N85-18482
Rockwell Hanford operations defense waste and byproducts management
[DE85-000553] 09 p1382 N85-18694
Hydrolysis of plastic wastes with the aim of recovering and reprocessing the starting components (recycling)
[BMFT-FB-T-84-250] 12 p1885 N85-21828
Controlled Ecological Life Support Systems (CELSS)
15 p2688 N85-26804
Survey of CELSS concepts and preliminary research in Japan
18 p3155 N85-29533
Publications of the NASA CELSS (Controlled Ecological Life Support Systems) program
[NASA-CR-3911] 19 p3326 N85-30606
Anaerobic microbial transformations in subsurface environments
[DE85-012790] 22 p3819 N85-33659
Method for extracting lanthanides and actinides from acid solutions by modification of Purex solvent
[DE85-005763] 23 p3909 N85-34220

WASTE UTILIZATION

Development of a preprototype times wastewater recovery subsystem, addendum
[NASA-CR-171823] 07 p1019 N85-16468
Technology for industrial waste heat recovery by organic Rankine cycle systems
[DE85-006719] 18 p3102 N85-29206
Qualitative comparison of fusion reactor materials for waste handling and disposal
[DE85-010473] 19 p3360 N85-30830

WASTE WATER

Development of a preprototype times wastewater recovery subsystem
[NASA-CR-171815] 03 p0388 N85-12480
Addendum: Development of a preprototype times wastewater recovery subsystem
[NASA-CR-171816] 03 p0388 N85-12481
Development of a preprototype times wastewater recovery subsystem: Appendices
[NASA-CR-171817] 03 p0388 N85-12482
Mechanism and process of flocculation by polymeric flocculant
09 p1303 N85-18185
Polymeric liner selection for military waste impoundments
[AD-P004143] 09 p1348 N85-18479
Treatment of wastewater (red water) resulting from TNT (trinitrotoluene) purification
[AD-P004146] 09 p1348 N85-18482
Removal of heavy metals by artificial wetlands
[PB85-116127] 10 p1513 N85-19548
Literature review for development of the master analytical scheme for organic compounds in water
[PB85-152874] 15 p2507 N85-25468
Toxicity of TNT wastewaters to aquatic organisms. Volume 4: Chronic toxicity of 2,4-dinitrotoluene and condensate water
[AD-A153536] 18 p3132 N85-29400
EPA (Environmental Protection Agency) research program guide, FY-1985, October 1, 1984 - September 30, 1985
[PB85-181861] 20 p3487 N85-31676
The degradation of pollutants in water and waste water by means of electron or gamma irradiation
[OEFZS-4317] 22 p3812 N85-33615

WASTES

NT FECES
NT GARBAGE
NT HUMAN WASTES
NT INDUSTRIAL WASTES
NT LIQUID WASTES
NT METABOLIC WASTES
NT RADIOACTIVE WASTES
NT SOLID WASTES
NT URINE
NT WASTE WATER
Proceedings of the Environmental Systems Symposium (13th) held at Bethesda, Md., 20-22 March 1984
[AD-A148194] 09 p1346 N85-18471
Strategies for preparing and submitting a part B application for a DoD facility
[AD-P004139] 09 p1347 N85-18475
Location of volatile buried wastes by field portable instrumentation
[AD-P004147] 09 p1348 N85-18483
Practical application of earth resistivity methods in phase 2 of the installation restoration program
[AD-P004148] 09 p1348 N85-18484
Organic solvent alteration of hydraulic properties of sedimentary rocks of low permeability: A review
[DE85-012537] 22 p3815 N85-33635

WATCHES

U CLOCKS

WATER

NT COASTAL WATER
NT COLD WATER
NT FRESH WATER
NT GROUND WATER
NT INLAND WATERS
NT NEARSHORE WATER
NT POTABLE WATER
NT SEA WATER
NT SHALLOW WATER
NT SPRINGS (WATER)
NT SURFACE WATER
NT WASTE WATER
Compilation of elemental concentration data for NBS (National Bureau of Standards) biological, geological and environmental standard reference materials, 1982
[PB84-218336] 01 p0025 N85-10158
Resonant frequencies and mode shapes for single and double cylindrical shells
[AD-A144778] 01 p0062 N85-10408
Effect of fluid and salt supplements to food allowance on endurance of head-to-pelvis accelerations following 7-day dry immersion and under ordinary motor activity conditions
01 p0092 N85-10618
Determination of bound water in biological tissue and energy dissipated in bound water by low level microwaves
[AD-A143101] 03 p0399 N85-12547
Prediction of long term strength of glass reinforced plastics in wet environments
[NPL-DMA(A)-80] 04 p0477 N85-13041
Ice-soil mixtures: Visual and near-infrared remote sensing techniques
[NASA-CR-174087] 04 p0525 N85-13358
Effect of water on hydrogen permeability --- Stirling engines
[NASA-TM-86904] 06 p0761 N85-14864
Deuterium diffusion in a soil-water-ice mixture
[AD-A148457] 08 p1178 N85-17415
Ground-based measurements of mesosphere temperatures by optical means
08 p1183 N85-17453
A method for automatic water mass classification
[AD-D011405] 08 p1191 N85-17505
Prototype wash water renovation system integration with government-furnished wash fixture
[NASA-CR-171829] 08 p1196 N85-17547
Measurements of H2O in Jupiter's atmosphere from 5 microns airborne observations
08 p1244 N85-17854

Water impact laboratory and flight test results for the space shuttle solid rocket booster aft skirt
09 p1335 N85-16394
A model for the climatic behavior of water on Mars
09 p1415 N85-18931
Factors influencing the ball milling of SiSN4 in water
[NASA-TM-86932] 10 p1450 N85-19136
Water absorption and conductivity in poly(ethylene oxide)-lithium tetrafluoroborate films
[AD-A147969] 10 p1450 N85-19138
A 10/sup 11/W high current pulse electron beam accelerator described
11 p1620 N85-20200
Photosynthetic water splitting
[DE85-002460] 11 p1690 N85-20627
Alternative anodic reactions in water splitting
[DE85-004150] 12 p1802 N85-21500
Parametric evaluation of ball milling of SiC in water
[NASA-TM-86974] 12 p1811 N85-21356
Microprocessor-controlled anodic stripping voltammeter for trace metal analysis in tap water
[DE85-002781] 12 p1852 N85-21619
Development and evaluation of a procedure for the rapid analysis of fresh concrete
[AD-A149741] 12 p1866 N85-21703
Gas-liquid chemistry of natural waters, volume 2
[DE85-002457] 12 p1864 N85-21623
Polar cap formation on Ganymede
13 p2174 N85-23486
The evolution of CO2 on Mars
13 p2185 N85-23558
Hydrovolcanism
13 p2186 N85-23574
Mars: Long term changes in the state and distribution of H2O
13 p2191 N85-23593
Radar and the detection of liquid water on Mars
13 p2199 N85-23638
Ammonia formation caused by the presence of water in the wet grinding of silicon nitride powder
[NASA-TM-77746] 14 p2249 N85-23937
Long-term exposure of pressed plutonium oxide heat sources to aquatic environments
[DE85-007385] 15 p2495 N85-25382
The effects of water and hydrogen on materials used in integrated circuit packages
[AD-A151693] 15 p2518 N85-25529
Physics effects of accidental submersion of space power reactors in water
[DE85-005020] 15 p2650 N85-26344
The Martian climate: Energy balance models with CO2/H2O atmospheres
[NASA-CR-175722] 15 p2679 N85-26547
Mars: Seasonally variable radar reflectivity
15 p2683 N85-26570
Combustion and micro-explosion of water/oil emulsions in high pressure environments
[AD-A152960] 17 p2919 N85-27997
Alternative heat sources for heat pumps
[DE85-007610] 17 p2959 N85-28275
Inspection evaluation and repair of the flawed feedwater nozzle of the 50 MWe Dodewaard GKN boiling water reactor
[ISBN-90-353-0017-3] 17 p2977 N85-28394
Potential climatic impacts of increasing atmospheric CO2 with emphasis on water availability and hydrology in the United States
[NASA-TM-87479] 17 p2995 N85-28517
Modeling and experiments on tritium permeation in fusion reactor blankets
[DE85-008439] 18 p3183 N85-29741
Adhesive evaluation of LARC-TPI and a water-soluble version of LARC-TPI
[NASA-TM-86426] 19 p3248 N85-30136
Response of steam-water mixtures to pressure transients
[DE85-010796] 19 p3267 N85-30262
Activities of the Wind Energy Programme
20 p3540 N85-32028
Two-phase flow visualization in a transparent, atmospheric pressure, boiling water loop
[DE84-016857] 21 p3586 N85-32268
Polymer-water interaction studies
21 p3609 N85-32411
Mechanism of heterogeneous deposition ice nucleation near water-saturation
21 p3638 N85-32597
Ice nucleation of single water droplet by silver iodide: A laboratory observation
21 p3643 N85-32630
Critical supersaturations with respect to water for fast condensation-freezing ice nucleation
21 p3643 N85-32632
Monte Carlo studies of H2O layers adsorbed on a model basal face of AgI
21 p3643 N85-32633
Cloud condensation on insoluble particles
21 p3648 N85-32670
Interactions among sulfide-oxidizing bacteria
21 p3661 N85-32741
Physical chemical state of water in living cells
[AD-A154566] 21 p3662 N85-32749
Transparency of water 9n 186 - 500 nm region
21 p3690 N85-32923
Activation analysis of natural water using neutrons of various energies
21 p3690 N85-32924
Nonsaturable microdryer
[DE85-005760] 23 p3946 N85-34457
Multi-solute subsurface transfer modeling for energy solid wastes: Highlights FY 1984
[DE85-012788] 23 p3966 N85-34591
Pressure cross spectra in turbulent boundary layers in water
[AD-A156153] 24 p4094 N85-35378
Calculation of heavy-ion tracks in liquid water
[DE85-012101] 24 p4149 N85-35725
Observation of EAS using a large water tank
24 p4189 N85-35986
An experiment to detect gut monopoles
[HE-6.1-7] 24 p4210 N85-36133

WATER BALANCE
The water balance and climate — Amazon region
07 p1003 N85-16370
Modeling interception of rainfall by forests and the role of interception in the water balance
[DE85-002822] 12 p1884 N85-21625
Fluid metabolism of monkeys during two-week antiorthostatic hypokinesia
12 p1902 N85-21943

WATER CIRCULATION
NT COASTAL CURRENTS
NT EL NINO
NT GULF STREAM
NT OCEAN CURRENTS
NT WATER CURRENTS
Synthesis of current measurements in Puget Sound, Washington. Volume 1: Index to current measurements made in Puget Sound from 1908-1980 with daily and record averages for selected measurements
[PB84-214105] 01 p0069 N85-10603
Deep water mass circulation in the Western Alboran Basin: Measurements in July and September 1980 (Alboran I experiment)
[AD-A148566] 08 p1191 N85-17504
North Atlantic Deep Water Formation
[NASA-CP-2367] 15 p2601 N85-26028
Review of North Atlantic source waters
15 p2601 N85-26029
Deep water formation
15 p2601 N85-26030
Destruction of density jumps in ocean by turbulence
19 p3291 N85-30407

WATER COLOR
Analysis of suspended sediment distributions in the surface waters of Delaware Bay using remote sensing of optical properties
15 p2582 N85-25926

WATER CONSUMPTION
Uncertainty in water resource planning: An economic evaluation of a water use reduction alternative
[PB84-202605] 01 p0065 N85-10430

WATER CONTENT
U MOISTURE CONTENT

WATER COOLED REACTORS
NT BOILING WATER REACTORS
NT LIGHT WATER REACTORS
NT PRESSURIZED WATER REACTORS
NT ZERO POWER REACTORS
Emerging technology of synthetic aperture focusing for ultrasonic testing
[DE85-000373] 09 p1378 N85-18864
Technical assessment of thermal-hydraulics for high heat flux fusion components
[DE85-013178] 23 p3930 N85-34359

WATER COOLING
U LIQUID COOLING

WATER CURRENTS
NT COASTAL CURRENTS
NT EL NINO
NT GULF STREAM
NT OCEAN CURRENTS
Spectral model for subtidal variability in the Chesapeake Bay
[PB84-226679] 06 p0842 N85-15345
Slope water intrusions within the nearshore waters off Long Island, New York
[DE85-001386] 09 p1359 N85-18549
Analysis of flow within the coastal boundary layer off Long Island, New York
[DE85-001384] 09 p1359 N85-18550
Field-work report: Medway Estuary, 28 June - 18 July 1983
[RNC/NS/TR8] 13 p2041 N85-22773
Temporal and spatial scales of Labrador Sea water formation
15 p2601 N85-26031
Frequency of recurrence and critical conditions for generation of Langmuir circulations
19 p3291 N85-30409

WATER DEPTH
Satellite altimetric measurements of lake levels
03 p0383 N85-12447
Evolution of nonlinear wave groups on water of slowly-varying depth
[AD-A147947] 08 p1162 N85-17329

WATER EROSION
Paleohydrology and geomorphology of selected reaches of the upper Wabash Valley, Indiana
02 p0226 N85-11461
Experiments and analyses of the formation of erosional scour marks with implications to the origin of the Martian outflow channels
13 p2190 N85-23588

WATER FLOW
Water resources data for Maine, water year 1983
[PB84-225143] 01 p0066 N85-10440
Water resources data for Ohio, water year 1983. Volume 1: Ohio River basin
[PB84-224690] 01 p0066 N85-10441
Water resources data for Michigan, water year 1983
[PB84-225176] 01 p0066 N85-10442
Coso Monitoring Program, January 1981 through December 1983
[AD-A147894] 07 p0998 N85-16338
Subcooled flow boiling at high heat flux
[OUEL-1540/84] 08 p1163 N85-17338
Weakly-reflective boundary conditions for two-dimensional shallow water flow problems
[PUBL-322] 08 p1163 N85-17341
Analysis of geohydrologic data by kriging
[AD-P004152] 09 p1349 N85-18486
World ocean level oscillations and their relationship to change in inflow of continental waters
13 p2108 N85-23133
A computer program to calculate the supersonic flow over a solid cone in air or water
[AD-A151102] 15 p2464 N85-25217
Applications of Kalman filtering and recursive least-squares in river flow modelling
15 p2636 N85-26254
Tidal rectification in lateral viscous boundary layers of a semienclosed basin
[CWI-AM-R8415] 17 p2960 N85-28284
The hydrosynclastic infundibulum
[AD-A153849] 18 p3100 N85-29192
Injection of drag reducing additives into turbulent water flows: Two-component velocity measurements and mixing length model predictions
[AD-A154604] 21 p3583 N85-32274
Reverification of the Chesapeake Bay model
[AD-A155486] 21 p3655 N85-32706
Computer and water-model simulation of flow through poppet valves
[CFD/85/2] 22 p3785 N85-33449
Military hydrology. Report 9: State-of-the-art review and annotated bibliography of dam-breach flood forecasting
[AD-A155383] 22 p3801 N85-33553
Stochastic groundwater flow modeling using the second-order method
[DE85-011250] 22 p3802 N85-33556
National program for inspection of non-federal dams. Woodward reservoir dam (VT 00209), Connecticut River Basin, Plymouth, Vermont. Phase 1 inspection report
[AD-A156256] 24 p4144 N85-35693

WATER HEATING
Test methods and standards development for active solar heating and cooling systems
[PB84-217447] 03 p0343 N85-12209
Qualification of noninvasive systems for on-line leak detection in high pressure feed water preheaters
[CISE-2341] 04 p0558 N85-13555
Actual versus design performance of solar systems in the National Solar Data Network
[DE85-001190] 09 p1344 N85-18456
A review of development and application of heat pump technology
[CSIR-RR-585] 14 p2300 N85-24241
Thermal performance testing and mathematically modeling of integral collector storage solar hot water systems
[PB85-166906] 18 p3132 N85-29398
Energy and Technology Review
[DE85-011767] 21 p3716 N85-33061
Advanced heat pump research and development
[DE85-009540] 23 p3932 N85-34372

WATER IMMERSION
Effects of body mass and morphology on thermal responses in water
[AD-A147558] 07 p1016 N85-16455

WATER INJECTION
Geothermal wells drilled in Transcarpathians
07 p0994 N85-16315
Description of a technique to measure spray distribution in an air stream
[AD-A149780] 12 p1771 N85-21122
Estimation of gas turbine engine boost provided by injecting water behind compressor
13 p2051 N85-22838

Steamflood pilots in the O'Connell Ranch field and the T-4 Ranch field
[DE85-001363] 24 p4108 N85-35468
WATER JETS
U HYDRAULIC JETS
WATER LANDING
NT DITCHING (LANDING)
Air carrier overwater emergency equipment and procedures
[PB85-917006] 21 p3553 N85-32105
Aircraft accident report: World Airways Inc., Flight 30H, McDonnell Douglas DC-10-30CF, N113WA, Boston-Logan International Airport, Boston, Massachusetts, January 23, 1982
[PB85-910406] 22 p3728 N85-33114
WATER MANAGEMENT
Water resources data, Mississippi, water year 1982
[PB84-224559] 01 p0065 N85-10434
Water resources data for Maine, water year 1983
[PB84-225143] 01 p0066 N85-10440
Water resources data for Ohio, water year 1983. Volume 1: Ohio River basin
[PB84-224690] 01 p0066 N85-10441
Remote sensing applications program
[E85-10022] 02 p0218 N85-11435
Water Science and Technology Board
[PB84-216571] 03 p0384 N85-12460
Photovoltaic pump systems 05 p0664 N85-14269
The ARGOS system and hydrology. Results obtained by ORSTROM and benefits of a degree of standardization 14 p2239 N85-23681
Hydrometric telemetry in Canada
14 p2239 N85-23682
Water quantity and quality research for the Rhine Meuse estuary
[PUBL-325] 17 p2988 N85-28470
Great Lakes hydrometeorologic and hydraulic data needs 20 p3496 N85-31739
Empirical methods for predicting eutrophication in impoundments. Report 3. Phase 2. Model refinements
[AD-A155483] 21 p3614 N85-32462
WATER MASERS
Masers associated with regions of recent star formation 03 p0443 N85-12820
Galactic OH and H2O masers — QUASAT project
07 p1058 N85-16719
Water maser outburst 07 p1058 N85-16720
Water masers and distance measurements: The impact of QUASAT 07 p1059 N85-16721
WATER POLLUTION
NT OIL POLLUTION
Solution of contaminant transport equations using an orthogonal-upstream finite element scheme
[DE84-014266] 01 p0070 N85-10463
Response of algal populations to changes in stream water quality
[PB84-202464] 01 p0070 N85-10465
Acid Deposition: Processes of Lake Acidification
[PB84-216175] 01 p0070 N85-10466
The use of fixed-bed adsorber models to predict the fluxes of toxic substances in groundwaters and soil environments
[PB84-202563] 01 p0071 N85-10468
Reverse osmosis treatment to control inorganic and volatile organic contamination
[PB84-223528] 01 p0071 N85-10470
East Europe report: Science and technology
[JPRS-ESA-84-029] 01 p0115 N85-10783
Radiotracer studies of the dispersion of solid pollutants in marine and estuarial environment: Measurement of diffusion coefficients and the phenomenon of dispersion by currents
[BLL-DRIC-TRANS-7104-(3623.66)]
02 p0224 N85-11468
Potential for acidification of six remote ponds in the White Mountains of New Hampshire
[PB84-207349] 02 p0225 N85-11475
Polycyclic aromatic hydrocarbons on the inner surfaces of copper tubing
[AD-A146979] 03 p0337 N85-12169
NODC/1983: National Oceanographic Data Center report
[PB84-222231] 04 p0542 N85-13449
Fate and disposition of trichloroethylene in surface soils
[AD-A147918] 07 p0995 N85-16321
Remote sensing of rice fields and sea pollution by SIR-B 08 p1145 N85-17222
Applying an innovative approach to field investigations at a remedial action site
[AD-P004145] 09 p1348 N85-18481
Protocol for aquifer cleanup decision making at military installations
[AD-P004151] 09 p1349 N85-18487
Intrusion of radioactive industrially polluted water from North Sea into central Baltic Sea
10 p1498 N85-19454
Removal of heavy metals by artificial wetlands
[PB85-116127] 10 p1513 N85-19548
Examples of environment services: Hydrological and pollution measurements in the Po River (Italy)
[CISE-2299] 11 p1679 N85-20578
Isolation, concentration and subsequent analysis by capillary gas chromatography of trace amounts of organophosphorus compounds from aqueous samples
[AD-B089301L] 12 p1803 N85-21308
Role of biological assessment in effluent control
[PB85-116101] 12 p1885 N85-21830
Standard analytical procedures of the NOAA National Analytical Facility, 1984-85: Extractable toxic organic compounds
[PB85-126282] 12 p1887 N85-21840
Determining adsorption of surface-active substances by sea bottom deposits 13 p2107 N85-23128
Protecting the nation's groundwater from contamination, volume 1
[PB85-154201] 15 p2590 N85-25965
Protecting the nation's groundwater from contamination, volume 2
[PB85-154219] 15 p2590 N85-25966
Acid rain: Effects on fish and wildlife
[PB85-154672] 16 p2821 N85-27402
Limiting profiles in contaminant transport through porous media — ground water pollution
[REPT-84-31] 17 p2960 N85-28282
Radiation-induced degradation of trichloroethylene and tetrachloroethylene in drinking water
[OEFZS-4298] 18 p3134 N85-29409
Equipment development for rapid detection of microorganisms in air and water
[FOA-A-40046-B2] 18 p3134 N85-29410
Pollutant body burdens and reproduction in Platichthys stellatus from San Francisco Bay
[DE85-010407] 19 p3308 N85-30509
Radioactive liquid wastes discharged to ground in the 200 areas during 1984
[DE85-010819] 19 p3310 N85-30517
State-of-the-art of aquifer restoration. Volume 1: Sections 1 through 6
[PB85-181071] 20 p3478 N85-31612
State-of-the-art of aquifer restoration. Volume 2: Appendices A through G
[PB85-181089] 20 p3478 N85-31613
Chemoreception and detection of micropollutants by means of a telemetric bionic detector
[DRIC-T-7460] 22 p3810 N85-33600
Acid rain in Europe
[COMMITTEE-PRINT-99-F] 22 p3810 N85-33601
The 1984 effluent and environmental monitoring report for the Bettis Atomic Power Laboratory
[DE85-011533] 22 p3810 N85-33602
Environmental summary for calendar year 1984
[DE85-012020] 22 p3810 N85-33604
The 1984 environmental monitoring report, Sandia National Laboratories, Albuquerque, New Mexico
[DE85-011175] 22 p3811 N85-33607
The degradation of pollutants in water and waste water by means of electron or gamma irradiation
[OEFZS-4317] 22 p3812 N85-33615
WATER PRESSURE
Fine structure of vertical distribution of light attenuation index of sea water 13 p2109 N85-23140
WATER PURIFICATION
U WATER TREATMENT
WATER QUALITY
Application guide for Hydrological Simulation Program FORTRAN (HSPF)
[PB84-215763] 01 p0064 N85-10427
Major institutional arrangements affecting ground water in New York state
[PB84-202506] 01 p0065 N85-10429
Water resources data, Florida, water year 1982. Volume 4: Northwest Florida
[PB84-223445] 01 p0066 N85-10437
Water resources data for Maine, water year 1983
[PB84-225143] 01 p0066 N85-10440
Water resources data for Ohio, water year 1983. Volume 1: Ohio River basin
[PB84-224690] 01 p0066 N85-10441
Water resources data for Michigan, water year 1983
[PB84-225176] 01 p0066 N85-10442
Response of algal populations to changes in stream water quality
[PB84-202464] 01 p0070 N85-10465
Acid Deposition: Processes of Lake Acidification
[PB84-216175] 01 p0070 N85-10466
Multispectral Imaging Science Working Group for Hydrologic Science: Executive summary
02 p0214 N85-11414
Water resources data for California, water year 1982. Volume 1: Southern Great Basin from Mexican border to Mono Lake Basin and Pacific Slope Basins from Tijuana River to Santa Maria River
[PB84-220670] 03 p0384 N85-12461
Water resources data for Florida, water year 1982. Volume 3A: Southwest Florida surface water
[PB84-223060] 03 p0384 N85-12462
Water resources data for Nebraska, water year 1982
[PB84-223668] 03 p0385 N85-12463
Water resources data for California, water year 1982. Volume 3: Southern Central Valley Basins and Great Basins from Walker River to Truckee River
[PB84-223726] 03 p0385 N85-12464
In-lake water quality management for Lake Eureka: Highlights of third year (1983) operation
[PB85-104149/GAR] 07 p0990 N85-16289
Climate and water quality 07 p1002 N85-16388
Development of a preprototype times wastewater recovery subsystem, addendum
[NASA-CR-171823] 07 p1019 N85-16468
Water resources data for Alabama, water year 1983
[PB85-123642] 10 p1507 N85-19507
Water resources data for Illinois, water year 1983. Volume 1: Illinois except Illinois River Basin
[PB85-125755] 10 p1507 N85-19508
Monitoring approaches for assessing quality of high altitude lakes: Colorado Flat Tops Wilderness Area
[PB85-117232] 11 p1679 N85-20579
Role of biological assessment in effluent control
[PB85-116101] 12 p1885 N85-21830
Drifting ice as mechanical factor in purifying and polluting hydrosphere 13 p2106 N85-23132
A first evaluation of LANDSAT TM data to monitor suspended sediments in lakes — Lake Chicot, Arkansas
13 p2120 N85-23204
Literature review for development of the master analytical scheme for organic compounds in water
[PB85-152674] 15 p2507 N85-25488
Water quantity and quality research for the Rhine Meuse estuary
[PUBL-325] 17 p2988 N85-28470
Surface hydrologic characteristics of proposed repository locations in the Palo Duro Basin of the Texas Panhandle
[DE85-010530] 18 p3128 N85-29355
Toxicity of TNT wastewaters to aquatic organisms. Volume 4: Chronic toxicity of 2,4-dinitrotoluene and condensate water
[AD-A153536] 18 p3132 N85-29400
Modeling water resources systems for water quality
[AD-A154298] 19 p3300 N85-30457
Annual environmental monitoring report, January-December 1984
[DE85-011689] 20 p3486 N85-31685
EPA (Environmental Protection Agency) research program guide, FY-1985, October 1, 1984 - September 30, 1985
[PB85-181681] 20 p3487 N85-31676
Offshore oceanographic and environmental monitoring services for the Strategic Petroleum Reserve, volume 3
[DE85-009907] 20 p3487 N85-31741
Empirical methods for predicting eutrophication in impoundments. Report 3. Phase 2. Model refinements
[AD-A155483] 21 p3614 N85-32462
Soil extraction kit
[AD-D011736] 22 p3742 N85-33190
The 1984 effluent and environmental monitoring report for the Bettis Atomic Power Laboratory
[DE85-011533] 22 p3810 N85-33602
Environmental surveillance at Los Alamos during 1984
[DE85-011666] 22 p3811 N85-33605
The 1984 environmental monitoring report, Sandia National Laboratories, Albuquerque, New Mexico
[DE85-011175] 22 p3811 N85-33607
Legionnaires' disease bacteria in power plant cooling systems: Phase 2
[DE85-011546] 22 p3825 N85-33695
WATER RECLAMATION
Development of a preprototype times wastewater recovery subsystem
[NASA-CR-171815] 03 p0388 N85-12480
Addendum: Development of a preprototype times wastewater recovery subsystem
[NASA-CR-171816] 03 p0388 N85-12481
Development of a preprototype times wastewater recovery subsystem: Appendices
[NASA-CR-171817] 03 p0388 N85-12482
Development of a preprototype times wastewater recovery subsystem, addendum
[NASA-CR-171823] 07 p1019 N85-16468
Prototype wash water renovation system integration with government-furnished wash fixture
[NASA-CR-171829] 08 p1198 N85-17547

Space station ECLSS integration analysis: Simplified General Cluster Systems Model, ECLS System Assessment Program enhancements
[NASA-CR-176089] 21 p3670 N85-32796
Experimental validation of allowable concentrations of sodium and potassium in recycled drinking water
22 p3823 N85-33685

WATER RECOVERY
U WATER RECLAMATION

WATER RESOURCES
NT AQUIFERS
Major institutional arrangements affecting ground water in New York state
[PB84-202506] 01 p0065 N85-10429
Uncertainty in water resource planning: An economic evaluation of a water use reduction alternative
[PB84-202605] 01 p0065 N85-10430
Water resources data, Maryland and Delaware, water year 1983
[PB84-225135] 01 p0065 N85-10431
Water resources data, California, water year 1982. Volume 4: Northern central valley basins and the Great Basin from Honey Lake Basin to Oregon state line
[PB84-225127] 01 p0065 N85-10432
Water resources data, California, water year 1982. Volume 2: Pacific slope basins from Arroyo Grande to Oregon state line except Central Valley
[PB84-224706] 01 p0065 N85-10433
Water resources data, Mississippi, water year 1982
[PB84-224559] 01 p0065 N85-10434
Water resources data, Virginia, water year 1983
[PB84-224542] 01 p0066 N85-10435
Water resources data, Ohio, water year 1983. Volume 2: St. Lawrence River basin statewide project data
[PB84-223676] 01 p0066 N85-10436
Water resources data, Florida, water year 1982. Volume 4: Northwest Florida
[PB84-223445] 01 p0066 N85-10437
Water resources data for Maine, water year 1983
[PB84-225143] 01 p0066 N85-10440
Water resources data for Ohio, water year 1983. Volume 1: Ohio River basin
[PB84-224690] 01 p0066 N85-10441
Water resources data for Michigan, water year 1983
[PB84-225176] 01 p0066 N85-10442
Estuaries of the Cape. Part 2: Synopses of available information on individual systems. Report 13: Silvermine (CSW 3)
[CSIR-RR-412-PT-2] 01 p0066 N85-10582
Water resources by orbital remote sensing: Examples of applications
[E85-10015] 02 p0217 N85-11428
Water resources data for Florida, water year 1983. Volume 3B: Southwest Florida ground water
[PB84-220862] 03 p0384 N85-12459
Water Science and Technology Board
[PB84-216571] 03 p0384 N85-12460
Water resources data for California, water year 1982. Volume 1: Southern Great Basin from Mexican border to Mono Lake Basin and Pacific Slope Basins from Tijuana River to Santa Maria River
[PB84-220870] 03 p0384 N85-12461
Water resources data for Florida, water year 1982. Volume 3A: Southwest Florida surface water
[PB84-223080] 03 p0384 N85-12462
Water resources data for Nebraska, water year 1982
[PB84-223668] 03 p0385 N85-12463
Water resources data for California, water year 1982. Volume 3: Southern Central Valley Basins and Great Basins from Walker River to Truckee River
[PB84-223726] 03 p0385 N85-12464
Activities of the Coastal Research Center
[PB84-231323] 05 p0672 N85-14320
Climatological information and water resources
07 p1002 N85-16367
Water and climate, study of one case
07 p1002 N85-16368
The water balance and climate — Amazon region
07 p1003 N85-16370
Closed-loop concepts for the Army: Water conservation, recycle, and reuse
[AD-A146839] 09 p1365 N85-18581
Water resources data for Alabama, water year 1983
[PB85-123842] 10 p1507 N85-19507
Water resources data for Illinois, water year 1983. Volume 1: Illinois except Illinois River Basin
[PB85-125755] 10 p1507 N85-19508
Water resources data for Colorado, water year 1983. Volume 1: Missouri River Basin, Arkansas River Basin and Rio Grande Basin
[PB85-123859] 11 p1671 N85-20528
Water resources data for Colorado, water year 1983. Volume 2: River Basin above Dolores River
[PB85-123867] 11 p1671 N85-20529
Building a functional, integrated GIS/remote sensing resource analysis and planning system — Utah
[E85-10092] 12 p1874 N85-21754
Hydrology and climatic conditions in Greenland
14 p2327 N85-24387
Protecting the nation's groundwater from contamination, volume 1
[PB85-154201] 15 p2590 N85-25965
Groundwater model for an island aquifer: Bribie Island groundwater study
[CE-44] 16 p2821 N85-27398
Water quantity and quality research for the Rhine Meuse estuary
[PUBL-325] 17 p2988 N85-28470
Modeling water resources systems for water quality
[AD-A154268] 19 p3300 N85-30457
Radioactive liquid wastes discharged to ground in the 200 areas during 1984
[DE85-010619] 19 p3310 N85-30517
Microwave hydrology: A trilogy
[NASA-CR-176042] 20 p3477 N85-31603
Great Lakes hydrometeorologic and hydraulic data needs
20 p3496 N85-31739
Feasibility study for small group water desalination equipment
[AD-A155106] 21 p3563 N85-32164

WATER RUNOFF
Remote Sensing of Snow and Evapotranspiration
[NASA-CP-2363] 13 p2123 N85-23223
General report of the researches of snowpack properties, snowmelt runoff and evapotranspiration in Japan
13 p2124 N85-23225
Snowmelt-runoff model utilizing remotely-sensed data
13 p2124 N85-23226
Snowmelt runoff model in Japan
13 p2124 N85-23227
Distribution of snow and maximum snow water equivalent obtained by LANDSAT data and degree day method
13 p2124 N85-23229

WATER TABLES
Ground-water level data and preliminary potentiometric-surface maps, Yucca Mountain and vicinity, Nye County, Nevada
[DE85-001771] 09 p1343 N85-18448

WATER TAKEOFF AND LANDING AIRCRAFT
NT SEAPLANES

WATER TEMPERATURE
NT OCEAN TEMPERATURE
NT SEA SURFACE TEMPERATURE
Water resources data for Michigan, water year 1983
[PB84-225176] 01 p0066 N85-10442
Forecasting water temperature decline and freeze-up in rivers
[AD-A147068] 07 p0987 N85-16274
Coso Monitoring Program, January 1981 through December 1983
[AD-A147894] 07 p0998 N85-16338
Geothermal assessment of part of the east shore area, Davis and Weber Counties, Utah
[DE84-016817] 09 p1342 N85-18446
Water resources data for Illinois, water year 1983. Volume 1: Illinois except Illinois River Basin
[PB85-125755] 10 p1507 N85-19508
Fine structure of vertical distribution of light attenuation index of sea water
13 p2109 N85-23140
A first evaluation of LANDSAT TM data to monitor suspended sediments in lakes — Lake Chicot, Arkansas
13 p2120 N85-23204
Physiochemically controlled scour jet array system
[AD-D011688] 19 p3306 N85-30505
Evaluation of low-temperature geothermal potential in Utah and Goshen Valleys and adjacent areas, Utah. Part 2: Water temperature and chemistry
[DE85-009344] 23 p3943 N85-34438
Geothermal resources of the Washakie and Great Divide basins, Wyoming
[DE85-013004] 24 p4112 N85-35491

WATER TREATMENT
An evaluation of the electrodialysis reversal process (Edr) for the desalination of brackish water from the Omaruru delta (SWA/Namibia)
01 p0023 N85-10141
Operating experiences of reverse osmosis plants treating Rand Water Board (RWB) water: Pitfalls and problems
01 p0023 N85-10142
Reverse osmosis treatment to control inorganic and volatile organic contamination
[PB84-223528] 01 p0071 N85-10470
Ultrafiltration as pretreatment for the preparation of drinking water by reverse osmosis onboard ships
[PML-1984-32] 01 p0098 N85-10654
Evaluation of survival straws (pocket purifier)
[AD-A146240] 03 p0328 N85-12114
Development of a preprototype times wastewater recovery subsystem
[NASA-CR-171815] 03 p0388 N85-12480
Addendum: Development of a preprototype times wastewater recovery subsystem
[NASA-CR-171816] 03 p0388 N85-12481
Development of a preprototype times wastewater recovery subsystem: Appendices
[NASA-CR-171817] 03 p0388 N85-12482
Solar energy supplied mobile water purification unit
05 p0664 N85-14270
USSR report: Chemistry
[JPRS-UCH-84-012] 06 p0761 N85-14865
In-lake water quality management for Lake Eureka: Highlights of third year (1983) operation
[PB85-104149/GAR] 07 p0990 N85-16289
Development of a preprototype times wastewater recovery subsystem, addendum
[NASA-CR-171823] 07 p1019 N85-16468
Prototype wash water renovation system integration with government-furnished wash fixture
[NASA-CR-171829] 08 p1198 N85-17547
Mechanism and process of flocculation by polymeric flocculant
09 p1303 N85-18185
Treatment of wastewater (red water) resulting from TNT (trinitrotoluene) purification
[AD-P004146] 09 p1348 N85-18482
Removal of heavy metals by artificial wetlands
[PB85-116127] 10 p1513 N85-19548
Radiation-induced degradation of trichloroethylene and tetrachloroethylene in drinking water
[OEFZS-4296] 18 p3134 N85-29409
Hydrodynamic solutions for the diffusion of components in confined media
20 p3458 N85-31484
State-of-the-art of aquifer restoration. Volume 1: Sections 1 through 8
[PB85-181071] 20 p3478 N85-31612
State-of-the-art of aquifer restoration. Volume 2: Appendices A through G
[PB85-181089] 20 p3478 N85-31613
Oxidation of formaldehyde solutions used for the preservation of reverse osmosis membranes
[PB85-185585] 22 p3742 N85-33194
The degradation of pollutants in water and waste water by means of electron or gamma irradiation
[OEFZS-4317] 22 p3812 N85-33615
Experimental validation of allowable concentrations of sodium and potassium in recycled drinking water
22 p3823 N85-33685

WATER TUNNEL TESTS
Design, manufacture, and testing of compliant coatings for reduction of turbulent drag
[AD-A145510] 02 p0198 N85-11323
Multi-ducted inlet combustor research and development
[AD-A153753] 18 p3063 N85-28946
Circulation control lift generation experiment: Hardware development
22 p3799 N85-33535

WATER TUNNELS
U HYDRAULIC TEST TUNNELS

WATER VAPOR
H2O profile in lower atmosphere of Venus based on effective radiation flux measurements
02 p0163 N85-11102
The water vapor resistances of some clothing assemblies used by flying personnel of the Swedish Armed Forces: A series of model studies
[FOA-C-59011-H1] 02 p0238 N85-11551
Effects of atmospheric water vapor and clouds on NOAA (National Oceanic and Atmospheric Administration) AVHRR (Advanced Very High Resolution Radiometer) satellite data
[AD-A145425] 02 p0260 N85-11824
Measurement of range-resolved water vapor concentration by coherent CO2 differential absorption lidar
[PB84-236892] 04 p0535 N85-13420
Development and evaluation of cloud water collectors
[PB84-232529] 04 p0540 N85-13437
Aspects of the comparison of stratospheric trace species measurements with photochemical models
[DE84-017028] 05 p0672 N85-14317
Comparison of optimum interpolation and Cressman analyses
05 p0680 N85-14371
Water vapor profile retrievals from the HIRS/MSU satellite sounder
05 p0681 N85-14378
Studies of atmospheric water in storms with the Nimbus 7 scanning multichannel microwave radiometer
05 p0682 N85-14382
Hydrogen production employing high-temperature solid oxide cells
[DE84-014559] 06 p0766 N85-14901
Nonlinear control model of an H2O steam reactor
[DFVLR-FB-84-30] 07 p0975 N85-16192
Continuum absorption by H2O in the 700-1200 cm(-1) and 2400-280 cm(-1) windows
[AD-A147391] 07 p0997 N85-16334
The atmospheric extinction problem
08 p1251 N85-17901

An analysis of the seasonal variations in the water vapor transport fields over the Southern Hemisphere
09 p1356 N85-16531
Effect of water vapor and water droplets on the RAM-1 (Real-Time Aerosol Monitor): Preliminary results
[PB85-109429] 11 p1637 N85-20313
Electrochemical cell to measure corrosion rates in noncondensing environments
[DE85-003148] 12 p1807 N85-21338
The effects of atmospheric water vapor on infrared propagation
[AD-A150030] 12 p1934 N85-22150
An atlas of nitrogen-broadened water vapor spectra from 500 to 5000 cm(-1), volume 1
[AD-A150527] 13 p2018 N85-22650
Absorption of radiation by water vapor in windows of relative transparency of 95-145 micrometer range
13 p2076 N85-22968
Below-room-temperature water-vapor continuum absorption within the 8- to 10 micron atmospheric transmission window
[TR-0084(4945-09)-1] 13 p2132 N85-23266
A study of liquid-vapor equilibria of the bromine-hydrobromic acid-water system
[NASA-TM-77748] 14 p2249 N85-23940
Diffusion of water vapor in Carbon Fiber Reinforced Plastics (CFRP). Measurement of the diffusion coefficient under influence of concentration
[DFVLR-FB-84-41] 14 p2262 N85-24018
Determining atmosphere moisture content from differences in two-frequency microwave radiation measurements 14 p2341 N85-24474
Study of integral and spectral direct solar radiation over Atlantic 14 p2341 N85-24475
Biophysical evaluation of the wet globe temperature index (Botsball) at high air movements and constant dew point temperature
[AD-A151065] 14 p2378 N85-24683
An atlas of pure water vapor spectra from 500 to 5000/cm, volume 1
[AD-A151756] 15 p2505 N85-25454
Development of hydrogen resistant alloys
16 p2735 N85-26873
An atlas of pure water vapor spectra from 500 to 5000/cm, Volume 2
[AD-A151757] 16 p2745 N85-26940
Water vapor 16 p2824 N85-27420
Precipitable water in the atmosphere, determined from surface dewpoint values 16 p2831 N85-27457
Atmospheric frontal zone studies
[NASA-CR-175293] 16 p2833 N85-27489
Experimental and theoretical study of condensation in multicomponent vapors
[DE85-009357] 17 p2923 N85-28021
Water vapor radiometry research and development phase
[NASA-CR-175887] 17 p2995 N85-28512
Comparison of optimum interpolation and Cressman analyses 18 p3141 N85-29448
Ship-to-ship propagation: Maritime data analyses
[AD-A155484] 21 p3592 N85-32325
On the efficiency of the mechanism of ice particles formation in the vapor supersaturation field around a freezing droplet 21 p3639 N85-32606
Basic ice nucleation mechanisms on mono and microcrystals and ice forming nuclei. Theoretical analysis and experimental results achieved in the laboratory over the past ten years: Review paper
21 p3642 N85-32629
A simple model to investigate the activation process in waterclouds 21 p3649 N85-32675
The interaction of polynuclear aromatic hydrocarbons PAH's with water vapor and their role as condensation nuclei in the formation of haze and fog
21 p3652 N85-32695
Distinctions in formation of microflora on construction materials used in habitable pressurized compartments
22 p3823 N85-33633
Potential spin-offs of the carbon dioxide observational platform system (CO-OPS) for remote sensing opportunities
[NASA-TP-2510] 23 p3899 N85-34149
Millimeter-wave propagation in moist air: Model versus path data
[AD-A156040] 24 p4087 N85-35331
Air chemistry measurements 2
[AD-A156041] 24 p4117 N85-35520

WATER VEHICLES
NT AIRCRAFT CARRIERS
NT BOATS
NT LIFEBOATS
NT SHIPS
NT SUBMARINES
NT SURFACE EFFECT SHIPS
NT TANKER SHIPS
NT UNDERWATER RESEARCH LABORATORIES
NT UNDERWATER VEHICLES
Corrosion problems in the Canadian maritime forces
[AD-A151594] 15 p2509 N85-25481

WATER WAVES
NT TIDAL WAVES
Return wave heights off South Uist estimated from seven years of data
[IOS-164] 01 p0089 N85-10601
Paleoenvironmental interpretation of the upper cretaceous Point Lookout sandstone: Implications for shoreline progradation and basin tectonic history, San Juan basin, New Mexico 02 p0227 N85-11486
Ocean wave parameters extraction using satellite short-pulse radar altimeters 03 p0360 N85-12425
The impact of satellite altimeter data on wave research 03 p0360 N85-12427
International banking of satellite and in-situ wave data by the Marine Information and Advisory Services (MIAS)
03 p0381 N85-12434
Impact of ERS-1 observations on wave forecasting in the North Sea 03 p0381 N85-12437
Intercomparison of GEOS 3/SEASAT wave data and wave model data 03 p0381 N85-12438
Extraction of wave period from altimeter data
03 p0382 N85-12439
Simulation of wavefronts returned by realistic surfaces
03 p0383 N85-12448
The altimeter as a support to the scatterometer in the representation of winds and derived wave fields in coastal waters and enclosed seas: A research at its onset
03 p0383 N85-12453
The estimation of persistance statistics from cumulative probabilities of wave height
[NMI-R183] 03 p0397 N85-12534
Prediction of wave height of wind-generated seas in finite water depth
[AD-A145996] 03 p0396 N85-12539
Parameterizing extreme still water levels and waves in design level studies
[IOS-163] 03 p0396 N85-12542
Statistical analysis of visual wave observations and gage/radar measurements
[AD-A146358] 06 p0798 N85-15100
Two-dimensional lake wave prediction system
[PB84-231034] 06 p0841 N85-15342
Wave-wave interactions, microseisms, and infrasonic ambient noise in the ocean
[AD-A146529] 06 p0859 N85-15463
The interpretation of SIR-B imagery of surface waves and other oceanographic features using in-situ, meteorological satellite, and infrared satellite data
08 p1143 N85-17212
The spatial evolution of t he directional wave spectrum in the Southern Ocean: Its relation to extreme waves in Agulhas Current 08 p1144 N85-17213
Evolution of nonlinear wave groups on water of slowly-varying depth
[AD-A147947] 08 p1182 N85-17329
Assessment of wave power available at key United Kingdom sites
[IOS-166] 09 p1346 N85-18466
Field studies of run-up generated by wind waves on dissipative beaches
[AD-A148793] 09 p1359 N85-18548
Quantization study for ERS-1 wave mode
[DFVLR-FB-84-39] 11 p1625 N85-20234
The imaging of internal waves by the SEASAT-A synthetic aperture radar
[AD-A149808] 12 p1875 N85-21761
Hurricane alicia storm surge and wave data
[AD-A149666] 12 p1895 N85-21896
Relationship between brightness spectrum of photographic image and spectrum of rises on a water surface with waves 13 p2115 N85-23171
Fourier transform of wave data on ARGOS buoys
14 p2323 N85-24351
Low-frequency oscillations of sea level and group structure of wind waves 14 p2335 N85-24441
Remote sensing of directional wave spectra using the surface contour radar
[NASA-TM-84440] 14 p2347 N85-24510
Water wave propagation over uneven bottoms
[AD-A151450] 15 p2556 N85-25789
Survey of remote sensing techniques for wave measurement
[NASA-TM-84429] 15 p2563 N85-25928
Contamination of the fetch-limited directional wave spectrum by waves emanating from an embayment
[NASA-TM-84441] 15 p2604 N85-26048
Deepwater wind wave growth with fetch and duration
[AD-A151604] 15 p2604 N85-26051
Sound propagation through directional internal wave fields
[AD-A151168] 15 p2646 N85-26321
Wave directional spectra via ARGOS
16 p2812 N85-27343
Routine wave and meteorological measurements in offshore areas using ARGOS data surveillance
16 p2812 N85-27344
Atmospherically forced, coastally trapped, long period gravity waves off the south coast of southern Africa
16 p2832 N85-27461
Internal waves in marine straits
[PREPRINT-415] 18 p3151 N85-29510
A laser slope gauge and a spar buoy wave gauge: Tools for the validation of microwave remote sensors
[AD-A154038] 19 p3272 N85-30290
One mechanism for generation of wave disturbances in spectra of turbulent flows near ocean surface
19 p3289 N85-30397
Plane Tsunami wave caused by elastic oscillations of ocean floor 19 p3290 N85-30403
Discovery of a nonpropagating hydrodynamic soliton
[AD-A155589] 21 p3582 N85-32269
Coastal erosion along Monterey Bay
[AD-A155610] 21 p3655 N85-32707
Theory of soliton waves
[AD-A154784] 21 p3676 N85-32837
Basic properties and interpretation of synthesized radar images of sea waves with long synthetization time
22 p3773 N85-33384
Atlantic coast hindcast. Phase 2: Wave information, additional extremal estimates
[AD-A156137] 24 p4125 N85-35575

WATERPROOFING
Shallow land burial technology: Humid
[DE85-004432] 12 p1932 N85-22136
Results of the AFRSI rewaterproofing systems screening test in the NASA/Ames Research Center (ARC) 2 x 2-foot transonic wind tunnel
[NASA-CR-167694] 13 p1988 N85-22467
Land vehicle corrosion management
22 p3750 N85-33246

WATERSHEDS
Hydrologic and economic models for watershed evaluation and research
[PB84-222371] 01 p0066 N85-10438
Erosion and sedimentation chronology of three watersheds in Maryland
[PB84-207356] 01 p0071 N85-10467
Estuaries of the Cape. Part 2: Synopses of available information on individual systems. Report 13: Silvermine (CSW 3)
[CSIR-RR-412-PT-2] 01 p0086 N85-10582
Estuaries of the Cape. Part 2: Synopses of available information on individual systems. Report no. 18: Eerste (CSW 6)
[CSIR-RR-415-PT-2] 01 p0087 N85-10585
Potential for acidification of six remote ponds in the White Mountains of New Hampshire
[PB84-207349] 02 p0225 N85-11475
The 1984 NASA/ASEE summer faculty fellowship program
[NASA-CR-174138] 04 p0574 N85-13863
Multispectral remote sensing of inland wetlands in South Carolina: Selecting the appropriate sensor
[DE84-013951] 05 p0661 N85-14247
Identification and characterization of watershed models for evaluation of impacts of climate change on hydrology
[DE85-008575] 18 p3125 N85-29348
Synthetic rainfall and its use in hydrologic modeling
19 p3314 N85-30542
Geologic and hydrologic characterization and evaluation of the basin and range province relative to the disposal of high-level radioactive waste. Part 1: Introduction and guidelines
[GS-CIRC-904-A] 20 p3526 N85-31932
Hydrology
[PB85-182954] 23 p3944 N85-34440

WATERWAVE ENERGY
Assessment of wave power available at key United Kingdom sites
[IOS-166] 09 p1346 N85-18466
Evaluation of wave energy resources on the French Atlantic seaboard 14 p2325 N85-24369

WATERWAVE ENERGY CONVERSION
Research recommendations for ac interfacing between electric utility transmission and distribution systems and wind, photovoltaics, and OTEC energy systems
[DE85-002942] 18 p3096 N85-29169

WATERWAYS
NT HARBORS

WATTMETERS
Development of a feasibility model for a thin-film precision power meter
[BMFT-FB-T-84-161] 04 p0504 N85-13217
The Mk.1 NPL digital sampling ac wattmeter
[NPL-DES-82] 22 p3758 N85-33290

WAVE AMPLIFICATION
Radiative amplification of acoustic waves in hot stars
08 p1235 N85-17786
Propagation and amplification of Ion Cyclotron Waves (ICW's) in a multicomponent plasma. The Earth magnetosphere as a giant maser for Alfven waves
14 p2368 N85-24634
Microwave tubes: Literature survey no. 5 comprising year 1983
[FOA-C-30377-E] 15 p2550 N85-25739
Amplification of electromagnetic wave by electron stream with negative velocity differences
21 p3692 N85-32941
Electromagnetic wave amplification during cyclotron resonance in a medium 21 p3693 N85-32942

WAVE ATTENUATION
NT ACOUSTIC ATTENUATION
NT MANDELSTAM REPRESENTATION
NT RADAR ATTENUATION
NT RADIO ATTENUATION
NT SHOCK WAVE ATTENUATION
Atmospheric channel performance measurements at 10 to 100 GHz
[PB84-211325] 01 p0042 N85-10271
Elastic wave propagation through polycrystals
[DE84-016772] 04 p0558 N85-13554
Measuring transient radiation effects in optical fibers
[DE84-015044] 04 p0565 N85-13698
Applicability of log-normal model to probabilistic description of quasi-pulse interference
13 p2084 N85-23014
Effects of contact area of an interface on acoustic wave transmission characteristics
[DE85-009935] 20 p3524 N85-31920
Maximally flat approximation of attenuation characteristics of coupled-line filters
22 p3775 N85-33393

WAVE DIFFRACTION
Scattering of electromagnetic waves by plasma half-space after initiation of motion
02 p0264 N85-11729
Diffraction of plane polarized waves by noncircular cylindrical cavity 02 p0269 N85-11754
Diffraction of electromagnetic wave by screen of arbitrary shape 02 p0273 N85-11776
Diffraction of plane electromagnetic waves on semiinfinite grid of parallel conductors arranged at angle to its edge 03 p0344 N85-12217
Ionospheric scintillation: A brief review
04 p0522 N85-13337
Scattering of electromagnetic waves by surface with small asperities 06 p0784 N85-15013
Approach to solution of diffraction problem for waves at rough surface 06 p0784 N85-15014
Optimization piezoelectric transducer width of acousto-optical devices 07 p0950 N85-16024
Spontaneous diffraction of sequence of supershort light pulses in dye solution 11 p1718 N85-20811
Measurement of the configuration of a concave surface by the interference of reflected light
[NASA-TM-77796] 11 p1728 N85-20867
Diffraction of plane TM-wave on continuously irregular elliptical plasma 13 p2067 N85-22914
Calculation of amplitude-phase characteristics of signal scattered obliquely on meteor trail
13 p2073 N85-22948
Intensity fluctuations of focused laser beam during reflection in turbulent atmosphere
13 p2078 N85-22975
Problem of diffraction by wavy surface: Comparison of numerical methods of solution
13 p2079 N85-22985
Diffraction of periodic grounding system of finite length
13 p2081 N85-22994
Accuracy of random signal spectral parameter estimation against interference background in acoustooptical spectrum analyzers
13 p2090 N85-23052
An examination of the use of wave packets for the calculation of atom diffraction by surface
[AD-A152760] 17 p3029 N85-28735
Asymmetry of diffraction orders with light diffraction at surface acoustic wave 22 p3782 N85-33431
Holoswitch
[AD-A155841] 24 p4096 N85-35392

WAVE DISPERSION
Elastic dispersion effects on dynamics and control of large modular antennas — spacecraft antennas
05 p0627 N85-14019
Dispersion curves for normal waves in cylindrical shell and conditions for spatial coincidence in vicinity of critical frequencies 06 p0775 N85-14973
Structure of frequency modulated and phase-shift keyed signals reflected from ionosphere at near-critical frequencies 07 p0952 N85-16035
Dispersion properties of moving ionospheric perturbations 07 p0952 N85-16036
Measurements and predictions of multipath dispersion for troposcatter links 10 p1472 N85-19289
Observations of RR Lyrae and X Arietis with the IUE satellite 11 p1754 N85-21030
Magnetostatic-wave propagation in a finite YIG-Loaded rectangular waveguide
[AD-A150332] 13 p2055 N85-22865
Intensity fluctuations of focused laser beam during reflection in turbulent atmosphere
13 p2078 N85-22975
Generation and propagation of electron cyclotron harmonic waves 14 p2367 N85-24630
Theoretical studies of electric cyclotron harmonic (ECH) waves based on experimental data from GEOS 1
14 p2367 N85-24631
Modifications to a propagation model for the combinded refraction-diffraction of stokes waves; shallow water, large angle and breaking wave effects
[AD-A151428] 15 p2556 N85-25768
A method of solving the dispersion equation for electrostatic electron waves in magnetized plasma
[KGI-PREPRINT-071] 16 p2869 N85-27697
Beam diffusion in linear ionospheric layer
21 p3695 N85-32958
Methods for measuring and analyzing dispersion properties of multimode fiber optic lightpipes (a review)
21 p3695 N85-32960
Optical image of bounded objects
21 p3697 N85-32968
Observation of mode-converted by ion Bernstein wave by an HCN laser scattering
[IPPJ-724] 23 p3979 N85-34668
Transient analysis of electromagnetic reflection from dispersive materials
[PB85-200186] 24 p4154 N85-35753

WAVE DRAG
NT INTERFERENCE DRAG
An investigation of vortex-induced aerodynamic characteristics of supersonic cruise configurations
[NASA-CR-174299] 07 p0898 N85-15690

WAVE EQUATIONS
NT DIRAC EQUATION
NT EIKONAL EQUATION
NT KORTEWEG-DEVRIES EQUATION
NT LAME WAVE EQUATIONS
NT SCHROEDINGER EQUATION
Integral of wave kinetic equation of drift waves
02 p0283 N85-11848
Current status of blast wave theory and computations. Volume 2: The quasi-similar solution
[AD-A146538] 06 p0808 N85-15138
Nonlinear wave propagation
[AD-A148114] 08 p1152 N85-17269
Solitons and SEASAT
[AD-A148396] 08 p1176 N85-17414
An invariant measure for the equation u sub tt - u sub xx + u3 = 0
[AD-A147300] 08 p1210 N85-17612
High order difference schemes with reduced dispersion for hyperbolic differential equations
[CWI-NM-R8408] 11 p1634 N85-20293
Research in theoretical nuclear physics
[DE85-004349] 12 p1932 N85-22137
A mathematical formulation of the Scole control problem, part 1
[NASA-CR-172561] 14 p2243 N85-23903
Wave description of sound propagation through stratified moving atmosphere 15 p2525 N85-25567
Scattering of sounds by piezoceramic cylindrical shell near rigid surface 17 p2943 N85-28168
Pattern selection and instability in nonlinear wave equation: An aspect of soliton and chaos
[DE85-009578] 18 p3101 N85-29197
Reverberation effects on directionality and response of stationary monopole and dipole sources in a wind tunnel
[NASA-TM-87063] 20 p3453 N85-31443
Wave propagation and methods of solution of the wave equation for moving disturbances sources
[ESA-TT-824] 20 p3522 N85-31906
Qualitative analysis of sign-bit processing
[AD-A154776] 21 p3671 N85-32804
Generalized string amplitude and wave equation for hadrons
[DE85-011492] 22 p3842 N85-33798
Absorbing boundary conditions for exterior problems
[NASA-CR-177944] 24 p4142 N85-35676

WAVE EXCITATION
NT ACOUSTIC EXCITATION
Investigation of RF excited CW CO2 waveguide lasers
[NASA-CR-174106] 04 p0505 N85-13221
Surface wave excitation study
[DE85-005301] 13 p2056 N85-22875
Numerical simulations of convectively excited gravity waves 14 p2444 N85-25082
An excitation mechanism for solar 5-minute oscillation of intermediate and high degree
14 p2444 N85-25085
Antenna with outboard exciter for 3.4-13.25 GHz frequency range 15 p2526 N85-25577
Study of the coupling between average, coherent and turbulent fields in a circular excited free jet
[ISL-R-115/83] 16 p2785 N85-27184
Vibrational stabilization of flexible structures
20 p3414 N85-31188
Excitation of some alkaline Earth-like ions
[DE85-010737] 20 p3529 N85-31951

WAVE FRONT DEFORMATION
Fast Hartmann method for problems in astronomical adaptive optics 02 p0161 N85-11094
Degenerate four-wave mixing lineshapes in sodium vapor under pulsed excitation
[AD-A148211] 08 p1222 N85-17698

WAVE FRONT RECONSTRUCTION
Algorithms for reconstruction of partially known, band limited Fourier transform pairs from noisy data
[AD-A150194] 13 p2150 N85-23347
Methods for design aerodynamics of modern transport aircraft
[DFVLR-FB-85-05] 17 p2893 N85-27838

WAVE FRONTS
NT SHOCK FRONTS
Boundary behavior of analytic functions, analytic wave front sets and the intersection problem of Ehrenpreis
[PREPRINT-809] 01 p0114 N85-10778
Simulation of wavefronts returned by realistic surfaces
03 p0383 N85-12448
Performance of Bayes-optimal angle-of-arrival estimators
[AD-A146594] 06 p0858 N85-15454
Modeling of real UT transducer field/flaw interactions
[DE85-000341] 09 p1329 N85-18351
Experimental investigation of wavefront conjugation during Mandelstam-Brillouin scattering of focused laser beams in condensed media 11 p1716 N85-20796
Four-wave hypersonic reversing mirrors in saturated mode 11 p1719 N85-20812
Double pinhole spatial phase correlator apparatus
[AD-D011495] 11 p1729 N85-20872
Ruby wavefront-conjugation laser for obtaining high temperature plasma 13 p2044 N85-22795
Sphericity gauge for wavefront of laser radiation
14 p2275 N85-24096
Stability of high energy particle plasmas to MHD-like modes
[DE85-007879] 17 p3039 N85-28803
Mean intensity of wave reflected by wavefront reversing mirror in turbulent medium 22 p3782 N85-33432
Heterodyne holographic interferometry for visualization of surface acoustic waves
[AD-A155405] 22 p3836 N85-33753
The longitudinal thickness of air-shower fronts
[OG-9.5-1] 23 p4030 N85-34978

WAVE FUNCTIONS
NT MOLECULAR ORBITALS
Sturmian expansion approximation to three-body scattering
[CSIR-TWISK-309] 01 p0109 N85-10731
Dirac single particle wave functions in inelastic electron scattering
[DE84-015129] 02 p0279 N85-11814
Long-time tail in the two-wave model
02 p0282 N85-11837
Oscillator strengths for OII ions
[NASA-CR-174153] 04 p0559 N85-13558
Aharonov-Bohm effect in absorption of electromagnetic wave 06 p0786 N85-15022
An extension of the multiconfiguration Hartree-Fock program for continuum functions
[DE85-002080] 09 p1379 N85-18672
Quasiparticle aggregation in the Fractional Quantum Hall Effect
[DE85-001574] 10 p1565 N85-19668
Computer modeling of vibrational energy levels of potential laser candidates (diatomic molecules)
[AD-A151765] 16 p2790 N85-27209
Microscopic analysis of angular momentum projected HFB-states in terms of interacting bosons
[DE85-007629] 16 p2863 N85-27661
The strategy for time dependent quantum mechanical calculations using a Gaussian wave packet representation of the wave function
[AD-A152709] 17 p3046 N85-28845
Experimental and theoretical investigations of open resonators — precipitation measurement
[DFVLR-FB-85-12] 20 p3449 N85-31414
Excitation of some alkaline Earth-like ions
[DE85-010737] 20 p3529 N85-31951
Overlap integrals for atom-metal surface interactions
[AD-A155038] 21 p3702 N85-32998

WAVE GENERATION
Waves and instabilities in collisionless shocks
[AD-A146689] 06 p0881 N85-15587
Superlattice ultrasonic wave generator
[AD-D011363] 07 p1038 N85-16585
Evolution of nonlinear wave groups on water of slowly-varying depth
[AD-A147947] 08 p1162 N85-17329
Generation of longitudinal acoustic waves by modulated helicon waves — nonlinear steady state waves in metals 13 p2090 N85-23049
Generation and development of small-amplitude disturbances in a laminar boundary layer in the presence of an acoustic field
[NASA-TM-77826] 14 p2299 N85-24237
Pc 1-2 pulsations and related phenomena: A review — geomagnetic pulsations 14 p2364 N85-24611
Generation and propagation of electron cyclotron harmonic waves 14 p2367 N85-24630
Microwave tubes: Literature survey no. 5 comprising year 1983
[FOA-C-30377-E] 15 p2550 N85-25739
On gravitational waves 16 p2759 N85-27026
Millimeter wave generation by relativistic electron beams
[AD-A153980] 18 p3179 N85-29706
Ion waves generated by ion loss-cone distributions or drifting particles
[KGI-PREPRINT-070] 20 p3549 N85-32087

WAVE INTERACTION
NT SHOCK WAVE INTERACTION
Broadband transverse field interaction continuous beam amplifier
[AD-D011229] 01 p0043 N85-10279
Chaotic behavior induced by solitons in perturbed integrable systems 02 p0283 N85-11844
Wave-wave interactions, microseisms, and infrasonic ambient noise in the ocean
[AD-A146529] 06 p0859 N85-15463
Ionospheric and magnetospheric modifications caused by VLF waves
[AD-A148210] 08 p1186 N85-17475
PMP-2: Equatorial wave dynamics 11 p1655 N85-20422
Coupling between velocity oscillations and solid propellant combustion 13 p2000 N85-22536
Measurements of distributed combustion 13 p2001 N85-22542
Stability of Rossby waves within framework of three-component analysis 13 p2109 N85-23142
An analytical and numerical study of the interaction of rarefaction waves with area changes in ducts. Part 2: Area enlargements
[UTIAS-273] 14 p2300 N85-24242
ICRF antenna coupling theory for a cylindrically stratified plasma
[DE85-004960] 14 p2424 N85-24952
The resonant count diagram and solar g mode oscillations 14 p2445 N85-25086
Interaction of large amplitude stress waves in layered elastic-plastic materials
[AD-A153519] 18 p3121 N85-29323
Guided and radiation wave interactions in periodic dielectric waveguides 19 p3253 N85-30173
Frequency-spreading coupler
[AD-D011683] 19 p3258 N85-30200
Finite-perturbation intermediate neglect of differential overlap molecular orbital calculations of nuclear magnetic resonance spin-spin coupling constants for polycyclic aromatic hydrocarbons and aromatic nitrogen heterocyclics
[NASA-TM-87486] 20 p3525 N85-31927
Wave/particle interactions in the plasma sheet
[NASA-CR-171537] 20 p3547 N85-32072
Some recent developments in the interpretation of MST radar returns from clear air (keynote paper), part 2 21 p3618 N85-32480
Computation of three-dimensional shock wave and boundary-layer interactions
[NASA-TM-86780] 24 p4093 N85-35372
Resonance localization in tokamaks excited with ICRF waves
[DE85-014559] 24 p4160 N85-35791

WAVE MOTION
U WAVES

WAVE OSCILLATORS
U OSCILLATORS

WAVE PACKETS
Reduction of the wavepacket: How long does it take?
[DE84-016778] 09 p1400 N85-18815
Directional analysis of wave packets of magnetotelluric field 14 p2344 N85-24495
Propagation of wave packet in a dissipative dielectric medium
[IPPJ-710] 15 p2655 N85-26385
An examination of the use of wave packets for the calculation of atom diffraction by surface
[AD-A152760] 17 p3029 N85-28735
The strategy for time dependent quantum mechanical calculations using a Gaussian wave packet representation of the wave function
[AD-A152709] 17 p3048 N85-28845
Electrostatic ion cyclotron instability due to a nonuniform electric field perpendicular to the external magnetic field
[AD-A155474] 21 p3707 N85-33019

WAVE PROPAGATION
NT ACOUSTIC PROPAGATION
NT DIFFRACTION PROPAGATION
NT GROUND WAVE PROPAGATION
NT HALOS
NT IONOSPHERIC PROPAGATION
NT LIGHT SCATTERING
NT MANDELSTAM REPRESENTATION
NT SCATTER PROPAGATION
NT SHOCK WAVE PROPAGATION
NT TRANSEQUATORIAL PROPAGATION
Implementation of the supersonic triplet singularity into the USTORE computer code
[CSIR-NIAST-83/47] 01 p0001 N85-10006
Problems on the diffraction and propagation of waves (selected articles)
[AD-A145139] 01 p0038 N85-10240
Atmospheric channel performance measurements at 10 to 100 GHz
[PB84-211325] 01 p0042 N85-10271
Transverse field interaction multibeam amplifier
[AD-D011241] 01 p0043 N85-10282
On wave propagation in linear viscoelasticity
[AD-A144739] 01 p0111 N85-10750
Fast waves near the lower hybrid frequency
[DE84-015217] 01 p0123 N85-10841
Acceleration waves 02 p0207 N85-11367
Finite element analysis of thermoelasticity problems 02 p0208 N85-11369
Paleoenvironmental interpretation of the upper cretaceous Point Lookout sandstone: Implications for shoreline progradation and basin tectonic history, San Juan basin, New Mexico 02 p0227 N85-11486
The propagation and growth of whistler mode waves generated by electron beams in Earth's bow shock
[AD-A145572] 02 p0226 N85-11492
The numerical solution of the Helmholtz equation for wave propagation problems in underwater acoustics
[NASA-CR-172454] 02 p0250 N85-11634
Polarization of ultrasound transmitted through boundary of magnetically inactive and equatorially magnetized media 02 p0257 N85-11682
Propagation of longitudinal elastic waves in multilayered half-space 02 p0273 N85-11779
Stochastic property of K-dV solitons perturbed by random forces — Korteweg-Devries equation 02 p0283 N85-11843
Computer molecular dynamics of 2-D water (ice) structures under shock
[AD-A145818] 03 p0372 N85-12375
Specific phenomena associated with the propagation of seismic waves in central Europe
[REPT-548] 03 p0375 N85-12391
Hole shots along refraction profile R4/78 recorded at the temporary seismic station near Stary Plzenec (west Bohemia)
[REPT-549] 03 p0375 N85-12392
Seasonal variations of reflexibility and transmissibility of ULF waves propagating through the ionosphere of geomagnetic mid-latitudes
[REPT-560] 03 p0376 N85-12403
Finite-difference synthetic seismograms for SH waves
[AD-A145834] 03 p0392 N85-12508
Millimeter-wave propagation and remote sensing of the atmosphere
[AD-A146339] 03 p0393 N85-12512
Coupling of airborne sound into the Earth
[AD-A146231] 03 p0416 N85-12663
Gyrotron beam generation with helical magnetic fields
[AD-A145987] 03 p0417 N85-12670
Studies of ignition and combustion wave propagation in exothermic systems using high-speed photography
[DE84-016482] 04 p0471 N85-12905
Digital radio link: Wave propagation measurements using narrow band technique
[FOA-C-30964-E2] 04 p0494 N85-13152
Wave phase velocity in a wind gradient — gravity waves 04 p0523 N85-13343
Elastic wave propagation through polycrystals
[DE84-016772] 04 p0558 N85-13554
Wave propagation in compliant tubes containing a heat-conducting viscous fluid
[WTHD-163] 05 p0639 N85-14094
Characteristic impedance of a porous center during transmission of quasi-static sinusoidal vibrations
[ISSN-0208-5658] 05 p0647 N85-14155
Signal characteristics of an underwater explosive acoustic telemetry system
[DE84-016653] 05 p0726 N85-14668
Disturbance propagation in structural networks; control of large space structures 06 p0759 N85-14856
Acoustoelectric interaction in double-layer semiconductors 06 p0786 N85-15023
Investigating phase structure of electromagnetic field in local inhomogeneities by modeling method 06 p0822 N85-15220
Longitudinal current before westward propagating auroral bend 06 p0823 N85-15223
Limits of applicability of long wave theory in studies of oscillations of n-layer fluid 06 p0824 N85-15234
Theory of harmonic generation of finite amplitude ultrasonic waves in solids of hexagonal symmetry
[AD-A146636] 06 p0860 N85-15465
Reverse wave suppression in unstable ring resonator
[AD-A148825] 07 p0939 N85-15952
A quasi-optical method for measuring the complex permittivity of materials
[AD-A147483] 07 p0941 N85-15966
Multiple scattering effects on transmission through the atmosphere
[AD-A147527] 07 p0941 N85-15969
Slow surface magnetoplasma waves in oblique magnetic field 07 p0952 N85-16034
Transformation of electromagnetic waves in plasma with randomly-heterogeneous magnetic field 07 p0953 N85-16039
Quantitative acoustic emission techniques
[AERE-R-11262] 07 p0977 N85-16203
Nonlinear waves in a rod. Results for incompressible elastic materials
[AD-A147485] 07 p0979 N85-16216
Nonlinear wave propagation study
[AD-A147011] 07 p0996 N85-16329
Short period guided waves over oceanic and continental paths
[AD-A147053] 07 p0997 N85-16331
On the long range propagation of sound over irregular terrain
[NASA-CR-3662] 07 p1036 N85-16589
Electrostatic wave observation during a space simulation Beam-Plasma-Discharge (BPD)
[NASA-CR-174286] 07 p1045 N85-16639
Acoustical characterization of Ti-6211 weldments and oxygen contamination Ti-6211 plate
[AD-P004125] 08 p1126 N85-17100
Nonlinear wave propagation
[AD-A148114] 08 p1152 N85-17269
Propagation and scattering considerations for the 0.2-3.0 GHz frequency range for a space-based radar
[AD-A148504] 08 p1153 N85-17282
Tunable microwave transversal filters
[AD-A148370] 08 p1158 N85-17304
On seismic waves 08 p1171 N85-17383
Effects of heterogeneities on the propagation, scattering and attenuation of seismic waves and the characterization of seismic source
[AD-A148284] 08 p1186 N85-17476
An efficient numerical solution technique for wave propagation in horizontally stratified ocean environments
[AD-A148537] 08 p1190 N85-17502
Optical wave propagation and imaging in the atmosphere 08 p1222 N85-17694
Short range order-long range order in superconducting materials
[AD-A148764] 08 p1227 N85-17724
A leaky waveguide model for MHD wave driven winds from coronal holes 08 p1235 N85-17781
Wave propagation in periodic, composite structures 09 p1332 N85-18370
Penetration of short duration airblast into protective structures 09 p1336 N85-18404
Acoustic tomographic reconstruction of anomalies in three-dimensional bodies
[DE84-017035] 09 p1378 N85-18666
UHF radiowave propagation through forests
[AD-A149518] 10 p1467 N85-19256
Propagation of electromagnetic fields along the sea/sea-bed interface
[AD-A149523] 10 p1467 N85-19257
Propagation Influences on Digital Transmission Systems: Problems and Solutions
[AGARD-CP-363] 10 p1469 N85-19269
Propagation of wide bandwidth signals in a tropospheric ducting system 10 p1469 N85-19271
Influence of propagation in digital wireless beam, microwave links 10 p1470 N85-19277
Design criteria for limited scan antennas at digital microwave line of sight links 10 p1471 N85-19284
A comparison between predicted and measured propagation loss in the VHF/UHF range in rugged terrain 10 p1471 N85-19285

A review of transmission and channel evaluation techniques for digital communication systems
10 p1474 N85-19301
Shock propagation in the exhaust gas handling system of the proposed large altitude rocket cell: Methods and preliminary analysis
[DE85-003055] 11 p1591 N85-20010
Digital controller for the Wave Propagation Laboratory's VHF and UHF wind-profiling radars
[PB85-112142] 11 p1626 N85-20238
Soviet National Middle Atmosphere Program
11 p1655 N85-20428
Seasonal characteristics of mesospheric plasma and their transitions 11 p1660 N85-20464
Midwinter disturbances in the middle atmosphere
11 p1661 N85-20465
Numerical investigation of propagation of radiation pulse at xxx 11 p1718 N85-20809
Wavecode constitutive models: Nonhomogeneous mixtures
[DE85-000838] 12 p1798 N85-21278
Waveform control and application of detonation wave in explosives 12 p1820 N85-21420
Aerosol multiple-scanning code, ASCAT
[LA-10046-MS] 12 p1823 N85-21440
Double reference pulsed phase locked loop (DRP-2L-2)
[NASA-CASE-LAR-13310-1] 12 p1824 N85-21441
Survivable propagation
[AD-A150070] 12 p1829 N85-21478
An analysis of short-to-medium-range seismic attenuation tests using a multilayered viscoelastic seismic propagation model
[AD-A149771] 12 p1889 N85-21856
Structure and forcing of teleconnection patterns occurring in general circulation model simulations
[DE85-002434] 12 p1890 N85-21862
Methods of progressing waves in turbulent media with applications to acoustics
[AD-A149599] 12 p1920 N85-22055
Magnetostatic-wave propagation in a finite YIG-Loaded rectangular waveguide
[AD-A150332] 13 p2055 N85-22665
Two-and-one-half dimensional in-plane wave propagation
[AD-A150467] 13 p2055 N85-22667
USSR report: Electronics and electrical engineering
[JPRS-UEE-85-002] 13 p2066 N85-22907
Mode control and wavelength tuning in open ended Michelson interferometric semiconductor laser
13 p2095 N85-23073
Applications of the conformal mapping method to the solution of mechanical vibrations problems
13 p2102 N85-23103
Regions of propagation of short-wave perturbations in spherical layer of rotating fluid 13 p2107 N85-23130
Geomagnetic precursors of intensive earthquakes in the 1-0,-2 Hz frequency range of geomagnetic pulsations
13 p2116 N85-23178
Seismic waves and dispersion relations
13 p2116 N85-23181
Vertical discrimination in the sound channel
[AD-A150254] 13 p2155 N85-23380
Investigations of ultrasonic wave interactions at boundaries separating anisotropic materials
[DE85-003506] 13 p2155 N85-23384
Wave propagation in heterogeneous media
[AD-A150800] 14 p2321 N85-24341
Possibility of retrieving dynamics of reflected wave method records beneath low-velocity zone
14 p2346 N85-24603
Generation and propagation of electron cyclotron harmonic waves 14 p2367 N85-24630
Regional seismic wave propagation
[AD-A150801] 14 p2373 N85-24671
Surface acoustic wave structure and volume waves
15 p2525 N85-25568
Water wave propagation over uneven bottoms
[AD-A151450] 15 p2556 N85-25769
Reflection and transmission of flexural waves at discontinuities 15 p2572 N85-25861
Contamination of the fetch-limited directional wave spectrum by waves emanating from an embayment
[NASA-TM-84441] 15 p2604 N85-26048
Recent progress in the development and application of the parabolic equation
[AD-A151475] 15 p2637 N85-26265
Field near the front of a signal in a waveguide accomplished with dispersive plasma
[REPT-11/1984] 16 p2768 N85-27083
Characteristic functionals of stochastic wave processes
[REPT-14/1984] 16 p2768 N85-27084
Wave propagation in density stratified fluids
16 p2781 N85-27162
Two-dimensional beat wave acceleration simulation
[DE85-005961] 16 p2791 N85-27214
Principles of wave formation along web of H-beams
[BLL-M-36041-(5826.4)] 16 p2798 N85-27253
Numerical resolution calculation for elastic-plastic impact problems
[AD-A152292] 16 p2801 N85-27270
Born inversion with a stratified reference velocity
[AD-A149222] 16 p2853 N85-27594
Research and development of subsurface acoustic wave devices for sensor applications
[AD-A152197] 16 p2861 N85-27642
Propagation of non-axisymmetric elastic waves through shell with filler under radial load at one end
17 p2943 N85-28169
Radiometer integrated into a communication terminal
[AD-A151746] 17 p2947 N85-28195
A transport theory of millimeter wave propagation in woods and forests
[AD-A151883] 17 p2947 N85-28196
The weighting function for scintillation on a folded path
[AD-A152659] 17 p2949 N85-28206
A crustal section for the Arabian Shield and adjacent Red Sea margin derived from first-arrival data
17 p2990 N85-28480
Measurements of VHF/UHF radio propagation in a maritime temperate climate
[CRC-1380] 18 p3089 N85-29119
Some further aspects of the influence of raindrop-size distributions on millimeter-wave propagation
[PB85-165334] 18 p3092 N85-29138
Hyperbolic phenomena in the flow of viscoelastic fluids
[AD-A153533] 18 p3099 N85-29186
Constitutive modeling for blast-induced wave propagation
[AD-A153576] 18 p3099 N85-29187
Propagation of gravity waves in the atmosphere and around critical levels
[KNMI-WR-85-1] 18 p3137 N85-29428
On the global distribution of three-dimensional Eliassen-Palm fluxes by stationary waves
18 p3145 N85-29469
Anderson localization for large disorder or low energy
[PREPRINT-426] 18 p3176 N85-29692
Theoretical investigations of the propagation and interactions of surface waves
[AD-A153548] 18 p3185 N85-29753
Measurement of mode interaction due to waveguide surface roughness
[AD-A154039] 19 p3255 N85-30183
Clearing of polydisperse aqueous aerosol by laser radiation pulses 19 p3298 N85-30445
Use of Omega radio navigation system in geophysical work in Antarctica 19 p3298 N85-30448
Linear time-invariant, space-variant filters and the WKB approximation with applications to underwater acoustic signal processing
[AD-A154250] 19 p3352 N85-30775
Heating of electrons in a high density tokamak by a micro-wave near second harmonic frequency
[DE85-010682] 19 p3359 N85-30822
Application of single and multiple scattering techniques to optical properties of dielectric media
19 p3366 N85-30877
ICRF antenna coupling and wave propagation in a tokamak plasma 19 p3369 N85-30893
Electromagnetic lateral waves in layered media
19 p3369 N85-30894
Localization of waves in a disordered medium
19 p3373 N85-30926
Scattering models in signal processing
20 p3439 N85-31339
Field antenna handbook
[AD-A155204] 21 p3576 N85-32242
Numerical modeling of subsurface communication
[DE85-012818] 21 p3577 N85-32249
Dynamic fracture of concrete and other heterogeneous materials
[AD-A154513] 21 p3598 N85-32343
Gravity waves from the stratosphere to the mesosphere, part 1.3B 21 p3616 N85-32471
Gravity-wave spectra in the atmosphere observed by MST radar, part 4.2B 21 p3622 N85-32502
Experimental and analytic characterization of nonlinear seismic attenuation
[AD-A154760] 21 p3631 N85-32556
Development of ultrasonic modeling techniques for the study of crustal inhomogeneities
[AD-A155206] 21 p3632 N85-32565
The effects of subrefractive layers and elevated ducts on airborne radar and ESM (Electronic Surveillance Measures)
[AD-A155524] 21 p3637 N85-32592
New approximations and findings of theory of nonlinear acoustic beams 21 p3660 N85-32663
Reflection of acoustic beam from inhomogeneous boundary 21 p3660 N85-32664
Toward the propagation of waves in unsteady media
21 p3683 N85-32881
Laser radiation propagation in inertialess nonlinear medium 21 p3686 N85-32686
Variation in radiowave propagation conditions in corona during solar activity cycle 22 p3763 N85-33327
USSR report: Electronics and electrical engineering
[JPRS-UEE-84-003] 22 p3773 N85-33361
Calculating dominant (quasi-t) mode group velocity in shielded microstrip line 22 p3780 N85-33422
Gradient scaling for nonuniform meshes
[DE85-009625] 22 p3784 N85-33443
Numerical experiment of elastic wave propagation by framework model
[DRIC-T-7462] 22 p3795 N85-33511
Surface wave modes of a multilayered medium backed by a perfectly conducting ground plane: Computation of propagation constants
[DE85-011454] 22 p3829 N85-33715
A measurement of the cosmic ray elements C to Fe in the two energy intervals 0.5-2.0 GeV/n and 20-60 GeV/n
[OG-4.1-6] 22 p3876 N85-34012
Interstellar propagation and the isotopic composition of hydrogen in the galactic cosmic rays
[OG-4.2-1] 22 p3877 N85-34021
Galactic propagation models consistent with the cosmic ray lifetime derived from Be-10 measurements
[OG-4.3-1] 22 p3878 N85-34026
Implications of new measurements of O-16 + p + C-12,13, N-14,15 for the abundances of C, N isotopes at the cosmic ray source
[OG-4.3-2] 22 p3878 N85-34027
A simulation of high energy cosmic ray propagation 1
[OG-5.4-1] 22 p3885 N85-34078
Behaviors of stress waves in a conical bar
23 p3904 N85-34182
Computational study on excitation, propagation and 3 omega -heating due to the ion Bernstein wave
[IPPJ-733] 23 p3975 N85-34641
Cosmic ray modulatin and merged interaction regions
[SH-4.1-11] 23 p4005 N85-34834
Propagation of the phase of solar modulation
[SH-4.1-12] 23 p4005 N85-34835
Cosmic ray modulation in a random anisotropic magnetic field
[SH-4.1-20] 23 p4006 N85-34839
Diffusion of strongly magnetized cosmic ray particles in a turbulent medium
[OG-7.2-16] 23 p4015 N85-34883
Measurements of the fragmentation of (40)Ar, (28)Si and (12)C in CH2C and H targets between 300 and 1500 MeV/nuc at the Bevalac
[OG-7.2-19] 23 p4016 N85-34886
Interactions of heavy nuclei, Kr, Xe and Ho, in light targets
[OG-7.2-21] 23 p4016 N85-34888
Perturbation-iteration theory for analyzing microwave striplines
[NASA-CR-176189] 24 p4085 N85-35321
Millimeter-wave propagation in moist air: Model versus path data
[AD-A156040] 24 p4087 N85-35331
Workshop Proceedings: Interpretation of Seismic Wave Propagation in Laterally Heterogeneous Structures
[BMR-258] 24 p4118 N85-35530
A comparison of multipath arrival structures observed in the presence of a surface duct with predictions obtained using classical ray techniques and the parabolic equation method
[AD-A156024] 24 p4145 N85-35696
Propagation of cosmic rays through the atmosphere in the quark-gluon strings model 24 p4173 N85-35873

WAVE RADIATION
U ELECTROMAGNETIC RADIATION

WAVE REFLECTION
NT MACH REFLECTION
An improved analytical theory of Rossby wave driven Eulerian and Lagrangian mean flows along non-zonal barriers with application to the Hawaiian Ridge
[AD-A144951] 01 p0088 N85-10593
Scattering matrix of antenna array with Joule losses in radiators 06 p0791 N85-15053
An extension of the Born inversion method to a depth dependent reference profile
[AD-A146469] 06 p0859 N85-15461
Reflection theorems for some anisotropic media
07 p0953 N85-16038
Application of homomorphic signal processing to stress wave factor analysis
[NAS 1.26:174871] 12 p1861 N85-21673

Three-mirror open resonator for millimeter wave band
13 p2077 N85-22972
Interference flux during reflection of heterogeneous waves
13 p2078 N85-22977
Axial focusing of signal from distant point radiator reflected twice in deep paraboloid
13 p2078 N85-22979
Experimental verification of beam deflection from hybrid reflector antenna within wide-angle sector
13 p2079 N85-22984
Water wave propagation over uneven bottoms
[AD-A151450] 15 p2556 N85-25769
Reflection and transmission of flexural waves at discontinuities
15 p2572 N85-25861
Results of simultaneous measurements of absorption and polarization of radio waves reflected from ionosphere
16 p2807 N85-27313
Kirchhoff modeling via wave equation datuming
[AD-A152399] 17 p3028 N85-28727
Most desirable terrain, e.g., flat vs valley location, part 5.1B
21 p3624 N85-32513
A random layer model for reflection from ocean bottom sediments
[AD-A155019] 21 p3700 N85-32988
Transient analysis of electromagnetic reflection from dispersive materials
[PB85-200186] 24 p4154 N85-35753

WAVE RESISTANCE
Nonrelativistic Kapitza-Dirac scattering
[AD-A150649] 14 p2417 N85-24911
Reactanceless synthesized impedance bandpass amplifier
[NASA-CASE-GSC-12788-1] 18 p3093 N85-29145

WAVE SCATTERING
NT ACOUSTIC SCATTERING
NT ATMOSPHERIC SCATTERING
NT ELECTROMAGNETIC SCATTERING
NT HALOS
NT LIGHT SCATTERING
NT MICROWAVE SCATTERING
NT MIE SCATTERING
NT RAMAN SPECTRA
NT RAYLEIGH SCATTERING
NT REVERBERATION
NT THOMSON SCATTERING
NT TROPOSPHERIC SCATTERING
NT X RAY SCATTERING
Wave multiple scattering by a finite number of unclosed circular cylinders
[NASA-TM-77593] 01 p0037 N85-10232
Wave guide branchings (n-port) types of representation of linear, time-independent and sourceless n-ports
[NASA-TM-77770] 01 p0037 N85-10233
Scattering of plane wave on cylindrical shell in low-frequency region
02 p0256 N85-11677
Transformation of heterogeneous surface waves by skewed streams
02 p0259 N85-11697
Modeling rain polarization effects to millimeter wave frequencies
[PB84-231042] 03 p0357 N85-12296
Elastic compliance of imperfect interfaces: Review and relationship to ultrasonic scattering
[DE85-003068] 11 p1652 N85-20404
Calculation of amplitude-phase characteristics of signal scattered obliquely on meteor trail
13 p2073 N85-22948
Use of Bigaussian approximation to describe fading in scattering communications channel
13 p2084 N85-23017
Elastic wave scattering from an interface crack in a layered half space
13 p2101 N85-23095
Scattering of elastic waves on fractures randomly distributed in a three-dimensional medium
13 p2111 N85-23151
Nonrelativistic Kapitza-Dirac scattering
[AD-A150649] 14 p2417 N85-24911
Field near the front of a signal in a waveguide accomplished with dispersive plasma
[REPT-11/1984] 16 p2768 N85-27083
A transport theory of millimeter wave propagation in woods and forests
[AD-A151883] 17 p2947 N85-28196
The temperature dependence of diffracted beam intensities in atom-surface scattering
[AD-A152782] 17 p3029 N85-28736
Laser forward and backscattering in particulate media
[AD-A154138] 19 p3275 N85-30312
Application of single and multiple scattering techniques to optical properties of dielectric media
19 p3366 N85-30877
Optical beam deflection detection of thermal waves in opaque solids
19 p3374 N85-30927
Scattering models in signal processing
20 p3439 N85-31339
Development of ultrasonic modeling techniques for the study of crustal inhomogeneities
[AD-A155206] 21 p3632 N85-32585
Acoustic wave scattering by round cylindrical shell reinforced with stringers
21 p3688 N85-32916
Investigation of ion-acoustic plasma turbulence in field of powerful electromagnetic wave by CO2-laser radiation scattering
21 p3691 N85-32935
Characteristics of optical information-measurement channels with utilization of scattering effects
22 p3781 N85-33429
Method and apparatus for Delta Kappa synthetic aperture radar measurement of ocean current
[NASA-CASE-NPO-15704-1] 23 p3925 N85-34327
Attenuation properties of the Petatlan region, Mexico, and a local magnitude scale for microearthquakes in this area
24 p4116 N85-35513
Second Colloquim on the Scattering of Ultrasonic Waves
[AD-A156298] 24 p4145 N85-35697

WAVEFORMS
NT PULSE AMPLITUDE
NT PULSE DURATION
NT SAWTOOTH WAVEFORMS
NT SQUARE WAVES
Flight demonstration of new NRL real-time data acquisition system and laser video waveform sampler
[AD-A145126] 01 p0053 N85-10350
Detection and estimation of image contours
[FUB-35-1983] 01 p0112 N85-10760
Notes on NAC report NAC-83-05: Beam Pulse Length Determination by Spectral Analysis
[CSIR-NAC-83-06] 01 p0119 N85-10816
Simulation of wavefronts returned by realistic surfaces
03 p0383 N85-12448
Acoustic emission waveforms in a half space
[AD-A146322] 03 p0417 N85-12664
Beam profiling in gigawatt 1064-nm lasers used in research on optical materials at Livermore
[DE84-007226] 04 p0505 N85-13223
On estimating the phase of periodic waveform in additive Gaussian noise, part 2
05 p0622 N85-13982
Pulsed-power system diagnostics: Electromagnetic data interpretation along pulse lines
[AD-A146607] 06 p0810 N85-15148
Electromagnetic resonances of cylinders and aircraft model with resistive wires
[NASA-CR-174203] 06 p0838 N85-15319
Theoretical and experimental analyses of laser altimeters for barometric measurements over the ocean
08 p1165 N85-17351
Determination of crustal and upper mantle structure from analysis of broadband teleseismic P-waveforms
08 p1181 N85-17440
The ambiguity function of random binary-phase-coded waveforms
[AD-A148906] 10 p1466 N85-19249
Transient waveform acquisition system for the ELMO Bumpy Torus
[DE85-000154] 11 p1733 N85-20901
Waveform control and application of detonation wave in explosives
12 p1820 N85-21420
Estimation of the impulse response of television channels from digitized waveforms
[CRC-1376] 12 p1822 N85-21429
The use of a high-speed 12-bit A/D converter for digital sampling of communication signal carriers
[AD-A150578] 13 p2056 N85-22872
Invariance of probability characteristics of detector to shape of optical pulse signals
13 p2090 N85-23048
Generation of longitudinal acoustic waves by modulated helicon waves --- nonlinear steady state waves in metals
13 p2090 N85-23049
Secure digital speech communication
[AD-D011572] 14 p2293 N85-24215
Modifications to a propagation model for the combinded refraction-diffraction of stokes waves; shallow water, large angle and breaking wave effects
[AD-A151428] 15 p2556 N85-25768
A comparison of alternative analytic models for event related potential records
[AD-A151977] 15 p2618 N85-26134
An analysis of jamming effects on noncoherent digital receivers
[AD-A153791] 18 p3090 N85-29126
Huffman-coded pulse compression waveforms
[AD-A155322] 21 p3576 N85-32243
Transceiver test device
[AD-D011728] 22 p3786 N85-33458
Fast scintillation counter system and performance
[HE-4.6-10] 24 p4197 N85-36047
Search for acoustic signals from high energy cascades
[HE-7.1-1] 24 p4213 N85-36155

WAVEGUIDE ANTENNAS
NT HORN ANTENNAS
Analysis of flat finite antenna consisting of waveguide radiators
06 p0790 N85-15048
A new leaky wave antenna for millimeter waves based on the groove guide
[AD-A146428] 06 p0799 N85-15102

WAVEGUIDE FILTERS
Dual mode directionally coupled band reject filter apparatus
[AD-D011359] 07 p0945 N85-15984
Optimal synthesis of surface acoustic wave filters
13 p2070 N85-22933
Fin line filters technology and electronic warfare
[AD-A154975] 21 p3576 N85-32237
Waveguide dielectric millimeter band filter with enhanced selectivity
22 p3780 N85-33421

WAVEGUIDE LASERS
Investigation of RF excited CW CO2 waveguide lasers
[NASA-CR-174106] 04 p0505 N85-13221
Life study of RF excited Hg arc lamps and CO2 waveguide lasers
[AD-A149618] 12 p1856 N85-21640
Ground slot waveguide laser
[AD-D011600] 15 p2563 N85-25813

WAVEGUIDE TUNERS
Micro-waveguide transformers of coherent optical signals
07 p0950 N85-16022

WAVEGUIDE WINDOWS
Analysis of waveguide discontinuities by the method of moments
[AD-A151499] 15 p2547 N85-25721

WAVEGUIDES
NT BEAM WAVEGUIDES
NT CIRCULAR WAVEGUIDES
NT OPTICAL WAVEGUIDES
NT PLASMAGUIDES
NT RECTANGULAR WAVEGUIDES
Wave guide branchings (n-port) types of representation of linear, time-independent and sourceless n-ports
[NASA-TM-77770] 01 p0037 N85-10233
Parabolic tapers for overmoded waveguides
[DE84-014237] 01 p0039 N85-10247
Biaxial-crystal laser with waveguide resonator
02 p0262 N85-11717
Using fiber-optics light guides in diagnosing intense shock waves
02 p0272 N85-11773
Scattering of electromagnetic waves in flat waveguide with bilateral diaphragms
03 p0347 N85-12235
The S-matrix and acoustic signal structure in simple and compound waveguides
[PP-583] 03 p0415 N85-12652
Implementing waveguide bandwidth six-port reflectometer circuits at millimetric wavelengths
[RSRE-MEMO-3678] 04 p0495 N85-13155
Technology for the ERS-1 SAR antenna
05 p0626 N85-14006
Field coherance function in layerwise nonhomogeneous troposphere
06 p0784 N85-15012
Interface structures for millimeter-wave circuits
[AD-A146557] 06 p0804 N85-15118
Investigating phase structure of electromagnetic field in local inhomogeneities by modeling method
06 p0822 N85-15220
Advanced infrared laser modulator development
[NASA-CR-172479] 06 p0862 N85-15479
MMIC devices for active phased array antennas
[NASA-CR-174281] 07 p0938 N85-15943
NBS (National Bureau of Standards) and WR62 and WR90 reference noise standards
[PB84-235704] 07 p0942 N85-15977
Investigation of planar waveguides and components for millimeter-wave integrated circuits
[AD-A147380] 07 p0948 N85-16005
Low-loss flexible dielectric waveguide for millimeter-wave transmission and its application to devices
[AD-A147848] 07 p0948 N85-16006
Acoustic transducers for fast reactor instrumentation
[BLL-RISLEY-TR-4979-(9091.9F)]
07 p0961 N85-16091
Upgrading flexible infrared waveguides
[AD-A146763] 07 p0970 N85-16160
A leaky waveguide model for MHD wave driven winds from coronal holes
08 p1235 N85-17781
The Shock and Vibration Digest, volume 16, no. 10
[AD-A147588] 09 p1331 N85-18361
Sound transmission in ducts
09 p1331 N85-18362
Multihole couplers for overmoded waveguide systems
[IPF-83-8] 09 p1394 N85-18773
Design of mode converters from TE circular om modes in circular waveguides to TE rectangular mo modes in rectangular waveguides for high power applications in the frequency range 1 to 30 GHz
[IPF-84-7] 09 p1395 N85-18781
Interleaved array antenna technology development
[NASA-CR-171845] 10 p1477 N85-19326

Design of low loss helix circuits for interference fitted and brazed circuits
[NASA-CR-166313] 10 p1478 N85-19326
Filter reflection image guide oscillator and solid state line scanning device
[AD-D011440] 10 p1479 N85-19336
Integrated circuit tunable cavity oscillator
[AD-D011474] 10 p1481 N85-19351
Average sound intensity decrease rule in irregular hydroacoustical waveguide 10 p1489 N85-19461
Construction tolerances for low loss, dielectric coated, metallic waveguide for transmission optical radiation
[DE85-004056] 10 p1558 N85-19822
Numerical methods for analyzing electromagnetic scattering
[NASA-CR-175507] 12 p1823 N85-21438
Single-cavity SLED device
[DE85-002567] 12 p1929 N85-22117
Variational and moment method solutions of the fields in a parallel-plate waveguide-aperture system
[DE85-006288] 13 p2057 N85-22876
A 60 GHz 200 kW CW gyrotron with high output mode purity
[DE85-005283] 13 p2066 N85-22905
Diffraction of periodic grounding system of finite length 13 p2081 N85-22994
Microstrip comb array design
[R-NIAS-24] 14 p2290 N85-24195
Millimeter-wave diffraction devices and materials
[AD-A150676] 14 p2418 N85-24917
Space processing of acoustic signals in plane-parallel waveguide — antenna arrays 15 p2525 N85-25572
Analysis of the electromagnetic scattering from an inlet geometry with lossy walls
[NASA-CR-175743] 15 p2541 N85-25686
Analysis of waveguide discontinuities by the method of moments
[AD-A151499] 15 p2547 N85-25721
Monolithic planar doped barrier limiter
[AD-D011578] 15 p2548 N85-25723
Waveguide phenomena in dense relaxing gases and their use in chemical and gas-dynamic lasers 15 p2644 N85-26308
Field near the front of a signal in a waveguide accomplished with dispersive plasma
[REPT-11/1984] 16 p2788 N85-27083
Design of the waveguide for microwave heating of solid lithium ceramic blankets
[DE85-009776] 17 p2935 N85-28120
Fiber optics in high dose radiation fields
[DE85-008649] 18 p3185 N85-29755
Analysis of systems of waveguide discontinuities by the method of moments 19 p3253 N85-30171
Guided and radiation wave interactions in periodic dielectric waveguides 19 p3253 N85-30173
Measurement of mode interaction due to waveguide surface roughness
[AD-A154039] 19 p3255 N85-30183
High harmonic rectangular gyrotron 19 p3256 N85-30189
Frequency-spreading coupler
[AD-D011683] 19 p3258 N85-30200
A computation of fin-line impedance
[AD-A154060] 19 p3258 N85-30204
Controlled-linewidth laser source
[AD-D011681] 19 p3274 N85-30306
Propagation of acoustic pulse in atmospheric waveguide 19 p3297 N85-30443
Guided-mode launching in a slab waveguide by way of diffraction at the edge of a conducting screen residing on one surface of the slab
[AD-A154686] 21 p3575 N85-32232
Multitrunk high-frequency multiplexing of antenna-waveguide channels 22 p3774 N85-33385
Miniature two-mode filters 22 p3775 N85-33394
Strongly coupled millimeter-band waveguide directional couplers 22 p3779 N85-33418
Fundamentals of radio optical theory of resonant and directional quasi-optical devices 22 p3780 N85-33420
Normal modes in an overmoded circular waveguide coated with lossy material
[NASA-CR-176186] 24 p4085 N85-35320

WAVELENGTH DIVISION MULTIPLEXING
Multiwavelength bidirectional coupler-decouplers
[AD-A147009] 07 p1043 N85-16625
NGC 2024: Multi-wavelength infrared and radio observations 08 p1246 N85-17865
Optical multiplexing on monomode fibers
[ENST-83E016] 20 p3533 N85-31982

WAVELENGTHS
Influence of radiation wavelength on elastic pulse shape during laser excitation 02 p0257 N85-11681
The 248 nm - new short wavelength for pumping lasers employing vapors of complex molecules 02 p0261 N85-11705
Using two-beam interference method for measuring wavelength of tunable pulse lasers 02 p0272 N85-11772
Variability of Neptune 02 p0299 N85-11938
Extinction by dielectric particles at optical and infrared wavelengths
[AD-A146305] 03 p0413 N85-12640
Wavelength coded image transmission and holographic optical elements
[AD-A146490] 06 p0810 N85-15147
Calibrations of wavelengths in SWP echelle spectra 11 p1761 N85-21077
Enhancing the performance of a high-gain free electron laser operating at millimeter wavelengths
[DE85-000862] 12 p1857 N85-21646
Phase function, backscatter, extinction, and absorption for standard radiation atmosphere and El Chichon aerosol models at visible and near-infrared wavelengths
[NASA-TM-86379] 12 p1892 N85-21874
Regions of propagation of short-wave perturbations in spherical layer of rotating fluid 13 p2107 N85-23130
Development of global model for atmospheric backscatter at CO2 wavelengths
[NASA-CR-175679] 15 p2591 N85-25971
Population inversion in laser-initiated vacuum arcs
[AD-A151958] 16 p2790 N85-27210
An evaluation and preparation of ferromagnetic liquid composites for use at millimeter wavelengths
[AD-A153939] 16 p3069 N85-28980
The application of laser resonance saturation to the development of efficient short wavelength lasers
[AD-A153951] 18 p3113 N85-29270
Development and application of a high power ND-glass laser instrument
[AD-A154366] 19 p3276 N85-30314
Reduced to pole long-wavelength magnetic anomalies of Africa and Europe 20 p3475 N85-31595
Long-wavelength magnetic and gravity anomaly correlations on Africa and Europe 20 p3476 N85-31597
Increase of antenna area instead of transmitter power, part 6.3A 21 p3624 N85-32517
Investigation of reproducibility of emission wavelength of helium-neon laser with external neon absorption cell (0.63 micrometers) 21 p3683 N85-32884

WAVES
A numerical method for interface problems in elastodynamics
[NASA-TM-86488] 08 p1172 N85-17391
Special features of computations of vertical distribution of concentration of suspended sediments under marine conditions 13 p2106 N85-23125
Energy structure of atmospheric boundary layer above waves 14 p2335 N85-24442
High-frequency wind wave spectrum in storm basin 14 p2336 N85-24444
The development of a transducer system for the accurate measurement of ultrasonic phase delay of SH plate waves
[AERE-R-11598] 15 p2559 N85-25790
Behavior of the porous bed in a combustion-deflagration-detonation transition
[ISL-CO-220/84] 22 p3747 N85-33224
Shear wave transducer for boreholes
[DE85-011662] 22 p3787 N85-33461

WEAK ENERGY INTERACTIONS
NT WEAK INTERACTIONS (FIELD THEORY)
Results on weak current from CHARM collaboration — neutrino interactions
[NOTA-INTERNA-810] 02 p0279 N85-11817
Theoretical aspects of electroweak and other interactions in medium-energy nuclear physics
[DE85-003821] 13 p2157 N85-23392
Strong-coupling approximations
[DE85-007829] 19 p3353 N85-30785
Search for neutrino oscillations at the Brookhaven AGS
[DE85-009766] 20 p3530 N85-31957
Effects of CP violation in SU(2) sub L x SU(2) sub R x U(1) electroweak models
[DE85-010601] 20 p3531 N85-31965

WEAK INTERACTIONS (FIELD THEORY)
Thin end of the wedge
[DE84-016439] 09 p1401 N85-18816
Shell-model Lanczos-method studies of the Gamow-Teller strength function in astrophysics
[DE85-004205] 11 p1763 N85-21093
Theoretical nuclear physics
[DE85-003466] 12 p1932 N85-22135
Weak interactions of quarks and leptons: Experimental status
[DE85-006171] 18 p3181 N85-29723
The effects of weak turublence on parametric processes in an unmagnetized plasma 19 p3369 N85-30896
Phenomenology of the standard and nonstandard Higgs particles
[USIP-85-03] 20 p3532 N85-31971
Systematics of quark mass matrices in the Standard Electroweak Model
[USIP-85-05] 20 p3532 N85-31972
Spatial parity violation in elastic neutron-nuclei interaction channel 21 p3691 N85-32932
Does low-energy physics depend on the potential of a heavy Higgs-particle
[NIKHEF-H/85-1] 22 p3838 N85-33763

WEAPON SYSTEMS
NT LASER WEAPONS
NT MISSILE SYSTEMS
Analysis of on-board CIG (Computer Image Generator) applications for aircrew training
[AD-A145214] 01 p0013 N85-10079
Directed energy missile defense in space
[PB84-210111] 01 p0015 N85-10095
The need for improvements in weapon system maintenance: What can AI (Artificial Intelligence) contribute?
[AD-P003913] 02 p0244 N85-11593
Artificial intelligence applications to maintenance
[AD-P003914] 02 p0244 N85-11594
Knowledge based tools for electronic equipment maintenance
[AD-P003940] 02 p0248 N85-11620
Avionics/crew station integration 06 p0752 N85-14818
Attack helicopter (AH-1T) cockpit systems integration 06 p0753 N85-14826
ILIR task of digital recoil travel measurement system
[AD-A147102] 07 p0967 N85-16140
An analysis of the effect of process controls on productivity and weapon system costs in DoD procurement
[AD-A147496] 07 p1052 N85-16678
Estimating wartime support resource requirements. Statistical and related policy issues
[AD-A147923] 07 p1053 N85-16685
Effective life cycle software support: A study in discipline and versatility 08 p1065 N85-16748
A weapon system design approach to diagnostics 08 p1066 N85-16752
A simulator for studying helicopter weapons systems 08 p1075 N85-16816
On estimating the cost growth of weapon systems
[AD-A147297] 08 p1230 N85-17749
Simulating speed and height cues in the C-130 weapon system trainer
[AD-P004313] 09 p1268 N85-17967
Air Force space technology center space technology: Emphasis 84 09 p1333 N85-18381
Assuring structural integrity in Army systems
[NASA-CR-175492] 11 p1651 N85-20398
BIT/BITE tradeoff analysis model
[AD-A149345] 11 p1701 N85-20697
Supersonic Tactical Missile (STM) radome development
[AD-P004360] 12 p1825 N85-21454
Air combat simulation: Methods, models, trends 13 p1967 N85-22359
Using NASTRAN to model missile inertia loads 15 p2576 N85-25886
Studies of electro-optical attenuation in the vicinity of cloud base
[AD-A151745] 15 p2653 N85-26360
Design adequacy: An effectiveness factor 16 p2695 N85-26642
Design-To-Cost (DTC) methodology to achieve affordable avionics 16 p2696 N85-26645
Military journal on US intelligence satellites 16 p2727 N85-26832
Presentations at the Tri-Service Cloud Modeling Workshop (2nd), held at the Naval Surface Weapons Center, White Oak, Maryland, 26-27 June 1984, volume 1
[AD-A152735] 17 p2996 N85-28522
The Department of Defense statement on the Science and Technology Program by Colonel Donald I. Carter, USAF Acting Deputy Under Secretary of Defense for Research and Advanced Technology before the Subcommittee on Research and Development of the Committee on Armed Services of the United States House of Representatives, 99th Congress, first session
[AD-A152467] 17 p3046 N85-28850
Soviet weapons development and the scientific community
[AD-P004562] 17 p3047 N85-28857
The revolution in military affairs and the Soviet system
[AD-P004568] 17 p3048 N85-28863
Assessment of computer resource management plan for division support weapon system
[AD-A154142] 19 p3342 N85-30712

Producibility Engineering and Planning (PEP): Program management guidelines
[AD-A153730] 19 p3379 N85-30966
Cost and schedule implications of multinational coproduction
[AD-A154356] 19 p3380 N85-30969
SAFEORD: Safety of explosive ordnance databank
[AD-A154058] 19 p3380 N85-30972
Meteorological weapons
[AD-A154735] 21 p3635 N85-32575
Next generation gunship
[AD-A156361] 24 p4065 N85-35193
Proceedings of the 14th Army Science Conference. Volume 3: Principal authors P through Z
[AD-A149202] 24 p4144 N85-35691

WEAPONS
NT ARTILLERY
NT GUNS (ORDNANCE)
NT LASER WEAPONS
NT NUCLEAR WEAPONS
NT SPACE WEAPONS
NT WARHEADS
Evolution of the NWC (Naval Weapons Center) thermal standard. Part 5: Thermal standard development and applications
[AD-A146173] 03 p0364 N85-12334
Naval surface weapons center technology transfer report (FY83)
[AD-A146501] 06 p0871 N85-15534
Design of explosive logic elements
[DE84-009511] 11 p1614 N85-20146
China report: Science and technology
[JPRS-CST-84-025] 11 p1620 N85-20197
Phenomenology of microwave coupling, part 1
[DE85-003097] 11 p1624 N85-20229
Theory of lethality
[DE85-000457] 11 p1721 N85-20826
A proportional-plus-integral controller for a particle beam weapon
[AD-A153213] 17 p3035 N85-28778
Toxic hazards tests for vehicles and other equipment
[AD-A149164] 20 p3506 N85-31797

WEAPONS DELIVERY
Content, variety, and augmentation of simulated visual scenes for teaching air-to-ground attack
[AD-A145218] 01 p0013 N85-10080

WEAPONS DEVELOPMENT
Soviet weapons development and the scientific community
[AD-P004562] 17 p3047 N85-28857
Technology and technical efficiency in the Soviet Union: Dominant patterns of constrained optimization in a noncompetitive economic regime
[AD-P004567] 17 p3048 N85-28862

WEAR
Structure and wear workshop colloquium
01 p0054 N85-10356
The influence of surface layers on the friction and wear behavior of materials 01 p0054 N85-10357
The influence of the carbide distribution on the abrasive wear of ledeburitic chromium steels
01 p0054 N85-10359
Structure and abrasive resistance of iron based alloys rich in hardening components 01 p0054 N85-10360
Friction and wear of polymers and polymer composite materials 01 p0054 N85-10361
Friction, wear and structure of heterogeneous materials 01 p0055 N85-10362
Wear properties of rapidly solidified surfaces of a pseudo-binary Fe-TiC alloy 02 p0179 N85-11204
The constitution as the basis for recent and future developments of wear resistant materials
02 p0179 N85-11205
Surface segregation of sulfur during oscillatory pin-on-plate wear studies of precious metal electrical contact alloys. 1: Friction and electrical contact resistance
[DE84-006962] 02 p0195 N85-11303
Lubricity of well-characterized jet and broad-cut fuels by ball-on-cylinder machine
[NASA-TM-83807] 03 p0339 N85-12183
Interactions among system stiffness, wear and vibrations 03 p0370 N85-12364
Wear and corrosion of components under stress and subjected to motion
[AD-A145781] 03 p0372 N85-12372
Effect of humidity on fretting wear of several pure metals
[NASA-TP-2403] 04 p0472 N85-13006
Microstructural effects in abrasive wear
[DE84-016155] 04 p0509 N85-13247
Wear of anodic oxide films on aluminum alloys in cryogenic liquids
[NAL-TR-818] 06 p0768 N85-14914
Effects of silver and group 2 fluorides addition to plasma sprayed chromium carbide high temperature solid lubricant for foil gas bearing to 650 deg C
[NASA-TM-86895] 06 p0770 N85-14926
A study of wear characteristics due to pressure for hydraulic fixed displacement vane pumps
[AD-A146023] 06 p0814 N85-15189
Mechanical aspects of high temperature coatings
07 p0906 N85-15749
Fundamental tribological properties of ceramics
[NASA-TM-86915] 07 p0930 N85-15893
Surface effects of corrosive media on hardness, friction, and wear of materials
[NASA-TM-83711] 07 p0930 N85-15896
Effect of five lubricants on life of AISI 9310 spur gears
[NASA-TP-2419] 07 p0962 N85-16099
Structure of solids surfaces in wear situations
[AD-A148480] 08 p1168 N85-17366
The wear of small polyacetal and polymide gears in vacuum — spacecraft gears
[ESA-ESTL-058] 08 p1169 N85-17374
Surface mechanical properties and wear behavior of ion implanted TiB2
[DE85-001130] 09 p1295 N85-18133
Implantation of Ti + C for reduced friction and wear of steels
[DE85-001606] 09 p1295 N85-18135
Influence of temperature on wear resistance of detonation coatings of alloy powders
10 p1447 N85-19116
Characteristics of the elevation drive suspension of the 64-meter antennas 10 p1464 N85-19240
Effect of implantation species on the tribological response of stainless steel surfaces
[DE85-003530] 10 p1493 N85-19432
Engine wear and cold startability of methanol fueled engines.
[DE85-001206] 11 p1647 N85-20381
Ion-beam nitriding of steels
[NASA-CASE-LEW-14104-1] 12 p1805 N85-21324
Tribological systems as applied to aircraft engines
[NASA-TM-86965] 12 p1858 N85-21657
Applications of vibration analysis to the condition monitoring of rolling element bearings
[ARL/AERO-R-163] 12 p1859 N85-21663
Rational use of tatanium in nonferrous metallurgy
13 p2031 N85-22728
Durability of VT16 alloy compounds obtained by diffusion welding 13 p2034 N85-22740
Sliding seal materials for adiabatic engines
[NASA-CR-174893] 13 p2037 N85-22757
Use of optical techniques in studies of wear rates of anodized aluminum and polymer coatings on aluminum
14 p2259 N85-23997
Sweden invents new ceramic for more durable cutting tools 15 p2536 N85-25845
Classification and types of diamond wear in honing
15 p2567 N85-25842
Metal armatures for railguns
[AD-A152129] 16 p2728 N85-26838
Reusable rocket engine turbopump condition monitoring 16 p2740 N85-26907
Effects of wear on structure-sensitive magnetic properties of ceramic ferrite in contact with magnetic tape
[NASA-TM-87007] 16 p2753 N85-26991
Effect of counterface material type and its topography on the tribological properties of polyimide composites
[NASA-TM-87036] 16 p2754 N85-26993
Breakway friction and dynamic friction/wear measurements of various ceramic materials from 25 C (75 F) to 650 C (1200 F)
[NASA-CR-174803] 16 p2754 N85-26994
Tooth wear in worm gears in vacuum
16 p2766 N85-27070
Extreme evaluation of reliability indices for components of metallurgical equipment
[BLL-M-36070-(5828.4)] 16 p2796 N85-27234
Friction and wear behavior of aluminum and composite I-beam stiffened airplane skins
[NASA-TM-86418] 17 p2895 N85-27852
Tribological sinks: Money down the drain
[DE85-010019] 17 p2974 N85-28378
Studies on surface processes during friction and wear
[AD-A153509] 18 p3117 N85-29296
Wear improvement in titanium alloys by ion implantation
[AD-D011694] 19 p3239 N85-30081
Microstructure-abrasive wear characteristics of low carbon dual phase steels
[DE85-010988] 19 p3239 N85-30083
Geothermal COMPAX drill bit development
[DE85-011353] 20 p3489 N85-31556
Rolling, slip and traction measurements on low modulus materials
[NASA-CR-174909] 22 p3791 N85-33491
Application of traction drives as servo mechanisms
22 p3797 N85-33520
Three body abrasive wear in various metal combinations 23 p3906 N85-34200

WEAR INHIBITORS
The role of molybdenum as an alloy element in adhesive wear resistance 02 p0181 N85-11212
The effect of heat treatment on wear resistance of gas-plasma eutectic coatings
[BLL-M-35756-(5828.4)] 03 p0329 N85-12122
Deposition of titanium nitride coatings by reactive evaporation and electrically activated reactive evaporation
[BLL-TRANS-5043-(9091.9F)] 07 p0925 N85-15858
Effect of zero-wear in friction pairs operating in abrasive media 13 p2045 N85-22601
Wear reduction by lubricants in confined contacts
14 p2223 N85-23786
Gear-cutting tools made of ultra high speed steel coated with TiN
[BLL-RISLEY-TR-5109-(9091.9F)]
15 p2567 N85-25837
Non-contact hydrostatic bearings
16 p2782 N85-27048
Lubricant and additive effects on spur gear fatigue life
[NASA-TM-87044] 17 p2974 N85-28373
Physical-mechanical characteristics and wear resistance of coatings applied by microarc oxidation
19 p3242 N85-30104
Anti wear property of two phasic metal composite
23 p3906 N85-34199
Action of wear-inhibiting Al2O3-coatings when applied to hard metal cutting tools
[BLL-RISLEY-TR-5041-(9091.9F)]
24 p4081 N85-35292
Wear-resistant coatings for tools intended for cold working
[BLL-RISLEY-TR-5040-(9091.9F)]
24 p4081 N85-35293

WEAR TESTS
The monitoring of machines
[CETIM-15-J-041] 04 p0510 N85-13253
The wear of small polyacetal and polymide gears in vacuum — spacecraft gears
[ESA-ESTL-058] 08 p1169 N85-17374
Implantation of Ti + C for reduced friction and wear of steels
[DE85-001606] 09 p1295 N85-18135
Cutting structural materials in vacuum
14 p2295 N85-24165
Classification and types of diamond wear in honing
15 p2567 N85-25842
Determination of wear intensity and resource of crankshafts and cylinder liners of ZIL-130 and ZMZ-53 engines
[BLL-BISI-TRANS-21393-(9022.06)]
17 p2072 N85-28355
Examples of application of machinability tests
[BLL-BISI-TRANS-22346-(9022.06)]
17 p2973 N85-28363
Lubricant and additive effects on spur gear fatigue life
[NASA-TM-87044] 17 p2974 N85-28373
Sintering reactions, structure and properties of a cobalt free nonconventional hard material
[DE85-007704] 18 p3076 N85-29025
Study of the chemical mechanism in lubrication
[DE85-010768] 19 p3228 N85-30013
Mechanical protection of DLC films on fused silica slides
[NASA-TM-87056] 19 p3248 N85-30138

WEATHER
NT COLD WEATHER
NT HOT WEATHER
National solar-terrestrial research program
[PB84-216183] 01 p0072 N85-10479
Weather satellite products in the Flight Service Automation System (FSAS)
[AD-A146520] 06 p0759 N85-14855
Revised Uniform Summary of Surface Weather Observations (RUSSWO). Alconbury RAF United Kingdom, parts A-F
[AD-A146913] 07 p1004 N85-16384
Revised Uniform Summary of Surface Weather Observations (RUSSWO). McChord AFB, Washington, parts A-F
[AD-A146914] 07 p1005 N85-16385
Revised Uniform Summary of Surface Weather Observations (RUSSWO). Mildenhall RAF, United Kingdom, parts A-F
[AD-A146915] 07 p1005 N85-16386
Revised Uniform Summary of Surface Weather Observations (RUSSWO). Dobbins AFB, Georgia, parts A-F
[AD-A146916] 07 p1005 N85-16387

Revised Uniform Summary of Surface Weather Observations (RUSSWO). Shemya AFB, Alaska, parts A-F
[AD-A146917] 07 p1005 N85-16388
Revised Uniform Summary of Surface Weather Observations (RUSSWO). Pope AFB, Fayetteville, North Carolina, parts A-F
[AD-A146918] 07 p1005 N85-16389
Revised Uniform Summary of Surface Weather Observations (RUSSWO). Sondestrom AB, Greenland, parts A-F
[AD-A146919] 07 p1005 N85-16390
Revised Uniform Summary of Surface Weather Observations (RUSSWO). England AFB, Alexandria, Louisiana, parts A-F
[AD-A146920] 07 p1006 N85-16391
Revised Uniform Summary of Surface Weather Observations (RUSSWO). Spangdahlem AB, Germany, parts A-F
[AD-A147166] 07 p1006 N85-16392
Limited surface observations climatic summary (USOCS). Hohenfels, AAF, West Germany
[AD-A147167] 07 p1006 N85-16393
Revised Uniform Summary of Surface Weather Observations (RUSSWO). Offutt AFB, Nebraska, parts A-F
[AD-A147183] 07 p1006 N85-16394
Revised Uniform Summary of Surface Weather Observations (RUSSWO). Hill AFB, Utah, parts A-F
[AD-A147184] 07 p1006 N85-16395
Revised Uniform Summary of Surface Weather Observations (RUSSWO). Parts A-F: Homestead AFB, Florida
[AD-A147203] 07 p1007 N85-16396
Propagation and scattering considerations for the 0.2-3.0 GHz frequency range for a space-based radar
[AD-A148504] 08 p1153 N85-17282
Two-dimensional modeling for lineal and areal probabilities of weather conditions
[AD-A147970] 08 p1188 N85-17486
Denver ARTCC (Air Route Traffic Control Center) evaluation of PROFS (Program for Regional Observing and Forecasting Services) mesoscale weather products
[PB85-120301/GAR] 09 p1279 N85-18045
Revised Uniform Summary of Surface Weather Observations (RUSSWO). Parts A-F Zweibrucken AB, Germany
[AD-A147165] 09 p1357 N85-18536
Weather data for simplified energy calculation methods. Volume 4: United States, WYEC data
[DE85-000491] 09 p1357 N85-18539
Equations and algorithms for meteorological applications in air weather service
[AD-A148694] 10 p1519 N85-19575
OBLOG: Designed to create and maintain a 49 hour observation log file
[PB85-109526] 10 p1519 N85-19579
Monthly and Seasonal Weather Outlook for November, 1984, Volume 38, Number 27, October 30, 1984
[PB85-118800] 10 p1521 N85-19588
Digital and color energy maps for graphic display of hourly data
[DE85-000586] 11 p1673 N85-20543
Weather data for simplified energy calculation methods. Volume 2: Middle United States. TRY data
[DE86-000494] 11 p1687 N85-20606
Monthly and seasonal weather outlook for October 1984, volume 38, number 19, 29 September 1984
[PB85-113538] 11 p1687 N85-20610
Monthly and seasonal weather outlook for January 1985, volume 39, number 1
[PB85-148799] 12 p1898 N85-21915
El Nino, the capricious child 13 p2106 N85-23121
Possibility of determining atmospheric weather parameters by radio and radiooptical measurements of refraction of cosmic sources 13 p2110 N85-23146
Summary of Meteorological Observations, Surface (SMOS), Fallon, Nevada
[AD-A150481] 13 p2136 N85-23276
Summary of Meteorological Observations, Surface (SMOS) Camp Pendleton, California
[AD-A150482] 13 p2136 N85-23277
Summary of Meteorological Observations, Surface (SMOS), Bermuda
[AD-A150637] 13 p2136 N85-23278
Summary of Meteorological Observations, Surface (SMOS), Alameda, California
[AD-A150609] 13 p2136 N85-23281
An introduction to USAFETAC (USAF Environmental Technical Applications Center)
[AD-A150971] 14 p2378 N85-24682
The impact of weather on aviation safety
[GPO-35-520] 16 p2703 N85-26685
Regularities in recent changes in surface air temperature and atmospheric precipitation fields 16 p2807 N85-27311
Effect of precipitation on wind turbine performance
[NASA-TM-86666] 16 p2818 N85-27385
AWS (Air Weather Service) climatic briefs: Asia
[AD-A151944] 16 p2835 N85-27481
Comparison of circulation statistics based on FGGE (First GARP Global Experiment) level 3-B analyses produced by GFDL (Geophysics Fluid Dynamics Laboratory) and ECMWF (European Centre for Medium Range Weather Forecasts) for special observing periods
[PB85-153948] 16 p2836 N85-27492
Monthly and seasonal weather outlook for mid-January to mid-February 1985, volume 39, number 2, January 15, 1985
[PB85-164572] 16 p2837 N85-27500
Monthly and seasonal weather outlook for February 1985, volume 39, number 3, January 30, 1985
[PB85-159424] 16 p2838 N85-27502
Flying in spite of the weather
[NLR-MP-84021-U] 17 p2895 N85-27847
Air Weather Service (AWS) climatic briefs: Europe
[AD-A152528] 17 p2996 N85-28519
Experiments on the assimilation of patches of data using a barotropic model 18 p3140 N85-29441
Mariners weather log, volume 29, number 1, winter 1985
[PB85-177483] 19 p3318 N85-30570
Mariners weather log, volume 28, number 4, fall 1984
[PB85-178408] 19 p3318 N85-30571
Middle Atmosphere Program. Handbook for MAP. Volume 14: URSI/SCOSTEP Workshop on Technical Aspects of MST Radar
[NASA-CR-176085] 21 p3615 N85-32466
Investigations of micro-turbulence in the bottom of the boundary layer
[AD-A155148] 21 p3636 N85-32585
A simulation of weather in 3D space
[AD-A155221] 21 p3636 N85-32586
Satellites and politics: Weather, communications, and earth resources 23 p4057 N85-35144

WEATHER CHARTS
U METEOROLOGICAL CHARTS

WEATHER CONDITIONS
U WEATHER

WEATHER CONTROL
U WEATHER MODIFICATION

WEATHER DATA RECORDERS
Thermosonde C2N measurements in Hawaii–August 1982
[AD-A148016] 08 p1189 N85-17489
Annual cycle. Part 1: The annual variation of surface temperatures over the United States and Canada
[PB85-147676] 15 p2600 N85-26026
Fog advection in the Namib 16 p2831 N85-27454

WEATHER FORECASTING
NT LONG RANGE WEATHER FORECASTING
NT NOWCASTING
NT NUMERICAL WEATHER FORECASTING
NT STATISTICAL WEATHER FORECASTING
Operational evaluation of 5 cm Doppler radar. Two contributions: Review of WSR-74C Doppler radar operations at WSO Montgomery, Alabama (April 1982 - August 1983). The Johnson-Effect resolving ambiguous Doppler velocities
[PB84-207521] 01 p0041 N85-10269
Large-scale ocean-atmosphere interactions in the mid-latitudes and equatorial regions: A literature review
[CSIR-T/SEA-8302] 01 p0073 N85-10482
Remote sensing of atmospheric particulates: Technological innovation and physical limitations in applications to short-range weather prediction
[NSF ATM-82-09684] 01 p0077 N85-10511
The use of dual polarisation radar for observing and predicting convective activity 01 p0077 N85-10512
The PROMIS Doppler radar system; design and operational experience 01 p0077 N85-10513
Nowcasting with Doppler radar: The forecaster-computer relationship 01 p0077 N85-10514
PROFS: An approach to improved operational weather services — Program for Regional Observing and Forecasting Services (PROFS) 01 p0083 N85-10555
Statistical tropical cyclone forecasting techniques for the Southern Hemisphere
[AD-A144752] 01 p0085 N85-10569
Setting hurricane conditions of readiness with high confidence
[AD-A144785] 01 p0085 N85-10570
Automated aircraft icing forecast technique
[AD-A144853] 01 p0085 N85-10571
Some aspects of post-frontal convective areas along the west coast of the united states
[AD-A144895] 01 p0085 N85-10572
Investigation of summertime convection over the upper Current River valley of southeast Missouri
[PB84-222389] 01 p0086 N85-10576
Joint probability of selected cloud and visibility thresholds around Koblenz, Germany
[AD-A145294] 02 p0231 N85-11506
Handbook for sea ice analysis and forecasting
[AD-A145286] 02 p0233 N85-11516
Report of the Division of Atmospheric Physics, 1980-1983 03 p0391 N85-12501
Plotting TDL coastal wind forecasts
[PB84-220789] 03 p0397 N85-12533
Use of photographs of meteorologic satellites in synoptic analysis
[SESIT-5] 05 p0679 N85-14357
Very short range statistical forecasting of automated weather observations
[DOT/FAA/PM-84/31] 05 p0679 N85-14359
Global Scale Atmospheric Processes Research Program Review
[NASA-CP-2344] 05 p0679 N85-14360
GLAS fourth order model 05 p0679 N85-14361
Massively parallel processor 05 p0680 N85-14366
Studies of atmospheric water in storms with the Nimbus 7 scanning multichannel microwave radiometer 05 p0682 N85-14382
The influence of synoptic scales on low-frequency modes of variability 05 p0687 N85-14412
Convective scale weather analysis and forecasting
[NASA-CR-174185] 06 p0838 N85-15320
Mariners weather log, volume 28, no. 3, July-August-September 1984
[PB85-107266] 06 p0840 N85-15334
Trends in skill and accuracy of National Weather Service pop forecasts
[PB84-229053] 06 p0840 N85-15335
Environmental research laboratories (of the National Oceanic and Atmospheric Administration) programs and plans: FY 1983 programs and FY 1984 plans
[PB84-226729] 06 p0840 N85-15336
AFOS (Automation of Field Operations and Services) display of MDR (Manually Digitized Radar) data on local map backgrounds
[PB84-220797] 06 p0840 N85-15338
NOAA (National Oceanic and Atmospheric Administration) Aircraft Satellite Data Link (ASDL)
[PB84-243773] 07 p0942 N85-15976
Automated Lavina collects data on snow 07 p0980 N85-16224
Experiments in forecasting atmospheric marine horizontal visibility using model output statistics with conditional probabilities of discretized parameters
[AD-A147574] 07 p1008 N85-16404
The 500 millibar sign frequency teleconnection charts: Winter
[PB85-106276/GAR] 07 p1009 N85-16410
Estimations of diabatic heating for an explosively-developing maritime cyclone
[AD-A147678] 08 p1188 N85-17483
Two-dimensional modeling for lineal and areal probabilities of weather conditions
[AD-A147970] 08 p1188 N85-17486
A scheme for short-term prediction of hydrometeors using advection and physical forcing
[AD-A148011] 08 p1188 N85-17487
Index of Air Weather Service technical publications, 1 July 1983-30 June 1984
[AD-A148051] 08 p1189 N85-17491
The visibility climatology of McMurdo Sound-Williams Field, Antarctica
[AD-A148108] 08 p1189 N85-17492
Denver ARTCC (Air Route Traffic Control Center) evaluation of PROFS (Program for Regional Observing and Forecasting Services) mesoscale weather products
[PB85-120301/GAR] 09 p1279 N85-18045
Rain volume estimation over areas using satellite and radar data
[NASA-CR-174434] 10 p1518 N85-19568
Frozen precipitation and concurrent weather: A case study for Munchen-Riem, West Germany
[AD-A149227] 10 p1519 N85-19577
Monthly and Seasonal Weather Outlook for November, 1984, Volume 38, Number 27, October 30, 1984
[PB85-118800] 10 p1521 N85-19588
Climate of Salt Lake City, Utah
[PB85-123875] 10 p1521 N85-19589
Hurricane plotting program
[PB85-121432] 10 p1521 N85-19592
Improved models for increasing wind penetration, economics and operating reliability
[NASA-CR-175538] 11 p1674 N85-20545
Monthly and seasonal weather outlook for mid-October to mid-November 1984, volume 38, number 20, 13 October 1984
[PB85-113546] 11 p1687 N85-20611
The 500 millibar sign frequency teleconnection charts: Fall
[PB85-110930] 11 p1687 N85-20612

The 500 millibar sign frequency teleconnection charts: Summer
[PB85-111359] 11 p1688 N85-20613
The 500 millibar sign frequency teleconnection charts: Spring
[PB85-111367] 11 p1688 N85-20614
Isentropic objective analysis
[PB85-112167] 11 p1688 N85-20617
Use and interpretation of isentropic analyses
[PB85-132694] 11 p1688 N85-20618
Development of satellite data presentation for environmental forecasting 11 p1712 N85-20770
21 Layer troposphere-stratosphere climate model
[NASA-TM-86183] 12 p1892 N85-21871
Space Shuttle interactive meteorological data system study
[NASA-CR-171418] 12 p1892 N85-21876
Hurricane storm surge research
[GPO-40-048] 12 p1893 N85-21880
On the error of typhoon intensity estimation by means of IR Dvorak technique occurring when the eye is very small 12 p1894 N85-21886
Varying structure and intensity change characteristics of 4 Western North Pacific tropical cyclones
[AD-A149628] 12 p1895 N85-21895
Navy tactical applications guide. Volume 4. Part 1. Eastern North Pacific weather analysis and forecast applications
[AD-A150097] 12 p1896 N85-21900
FTASUM: Aviation forecast summaries
[PB85-112977] 12 p1897 N85-21908
SAOSUM: A short summary of observations
[PB85-120384] 12 p1897 N85-21909
Preliminary results of associating cloud-to-ground lightning with surface convergence and radar reflectivity at Kennedy Space Center in 1983
[NASA-CR-175543] 12 p1897 N85-21910
TRAJ: Single station trajectory plot
[PB85-135002] 12 p1897 N85-21911
AFOS (Automation of Field Operations and Service) surface observation decoding
[PB85-137566] 12 p1898 N85-21913
New atmospheric sensor analysis study
[NASA-CR-171426] 13 p2094 N85-23089
Summary of Meteorological Observations Surface (SMOS), Sigonella, Sicily/Navy
[AD-A150539] 13 p2138 N85-23280
Tactical deployment of satellite-reporting drifting data buoys for environmental data acquisition 14 p2332 N85-24423
Influence of interaction between ocean and atmosphere on intensity of moving tropical cyclone 14 p2333 N85-24431
Monthly and Seasonal Weather Outlook for mid-December 1984 mid-January 1985, volume 38, number 24, 14 December 1984 14 p2379 N85-24687
Convection modeling and application to severe storms 15 p2595 N85-25991
Mesoscale analysis and modeling group 15 p2596 N85-26001
Nowcasting applications of VAS 15 p2597 N85-26003
Recent failures of weather satellites
[S-HRG-98-1070] 16 p2731 N85-26855
Lightweight aerological radiosonde MARZ 16 p2807 N85-27309
Symposium on Atmospheric Sciences in South Africa
[CSIR-S-331] 16 p2829 N85-27442
The study of thermal forecasting for gliding 16 p2830 N85-27453
Use of a network of telemetered meteorological stations for prediction of the distribution of an atmospheric tracer 16 p2831 N85-27458
Forecast of Atlantic seasonal hurricane activity for 1985 16 p2833 N85-27470
A survey of major east coast snowstorms, 1960-1983. Part 2: Case studies of eighteen storms
[NASA-TM-86196] 16 p2833 N85-27472
SINOGRAFO: A system for influencing and forecasting weather
[INPE-3349-PRE/628] 16 p2834 N85-27475
Simulation of a synchronously coupled atmosphere-ocean prediction model
[AD-A152020] 16 p2835 N85-27482
Hurricane Research Division, fiscal year 1984 programs, fiscal year 1985 projections 16 p2836 N85-27491
SCPP (Sierra Cooperative Pilot Project) Forecasting Support 16 p2837 N85-27493
Evaluation of the PROFS (Program for Regional Observing and Forecasting Services) 1982, real-time forecast experiment
[PB85-159747] 16 p2837 N85-27495
Technique that uses satellite, radar, and conventional data for analyzing and short-range forecasting of precipitation from extratropical cyclones
[PB85-164994] 16 p2837 N85-27499
Centralized Storm Information System (CSIS)
[NASA-CR-175898] 17 p2994 N85-28506
A report from the Space Science and Engineering Center, the University of Wisconsin-Madison, Madison, Wisconsin 17 p2994 N85-28507
Test and evaluation plan for the Centralized Storm Information System 17 p2994 N85-28508
CSIS test and evaluation 17 p2994 N85-28509
Functional and performance requirements of the next NOAA-Kansas City computer system 17 p2994 N85-28510
Spectral decomposition and verification of NOGAPS 500MB medium-range forecasts
[AD-A152550] 17 p2996 N85-28520
Weather radar studies
[AD-A152563] 17 p2996 N85-28521
Airborne research meteorological data collected by the National Hurricane Research Laboratory (Hurricane Research Division/AOML) during the 1982-1983 hurricane seasons: Inventory and availability
[PB85-163681] 17 p2997 N85-28528
Research Review, 1983
[NASA-TM-86219] 18 p3139 N85-29433
Forecast impact simulation studies 18 p3139 N85-29435
The contrasting Northern Hemisphere winters of 1980-81 and 1981-82 18 p3144 N85-29468
Some recent developments in numerical modelling at ECMWF 18 p3147 N85-29481
Automated Weather Observing System (AWOS) demonstration program
[AD-A153463] 18 p3148 N85-29493
Environmental Research Laboratories (of the National Oceanic and Atmospheric Administration) programs and plans: FY 1984 programs and FY 1985 plans
[PB85-171494] 18 p3149 N85-29501
Application of climatological analysis to minimize air pollution impacts in California
[PB85-172963] 18 p3149 N85-29502
Isotropic plotter
[PB85-175651] 18 p3150 N85-29504
Monthly and seasonal weather outlook for mid-March to mid-April 1985, March 14, 1985, volume 39, no. 6
[PB85-174751] 19 p3317 N85-30565
J. P. Finley: The first severe storms forecaster
[PB85-17453] 19 p3318 N85-30566
VIDTEX
[PB85-175689] 19 p3318 N85-30567
Forecast of Atlantic seasonal hurricane activity for 1985 20 p3495 N85-31732
Carbon dioxide and climate: Potential impacts
[DE85-009473] 20 p3496 N85-31734
Automated cell detection as a mesocyclone precursor tool
[AD-A154952] 21 p3635 N85-32577
Forecasting of tropical cyclone motion using an EOF (Empirical Orthogonal Function) representation of wind forcing
[AD-A155034] 21 p3636 N85-32580
Monthly and seasonal weather outlook for April 1985, March 30, 1985, volume 39, no. 7
[PB85-183804] 22 p3817 N85-33648
Dynamics of Mesoscale Weather Systems: 1984 Summer Colloquium
[PB85-186266] 22 p3817 N85-33649
Application of a turbulent closure model to the parameterization of the vertical diffusion of heat, momentum, and humidity in the ECMWF model — European Center for Medium Term Weather Forecasting (ECMWF)
[MITT-41] 24 p4095 N85-35387
Comparative analysis of operational forecasts versus actual weather conditions in airline flight planning, volume 1
[NASA-CR-167862] 24 p4119 N85-35534
Comparative analysis of operational forecasts versus actual weather conditions in airline flight planning, volume 2
[NASA-CR-167863] 24 p4119 N85-35535
Comparative analysis of operational forecasts versus actual weather conditions in airline flight planning, volume 3
[NASA-CR-167864] 24 p4120 N85-35536
Comparative analysis of operational forecasts versus actual weather conditions in airline flight planning, volume 4
[NASA-CR-167865] 24 p4120 N85-35537
Comparative analysis of operational forecasts versus actual weather conditions in airline flight planning: Summary report
[NASA-CR-167866] 24 p4120 N85-35538
A preliminary intercomparison between numerical upper wind forecasts and research aircraft measurements of jet streams
[NASA-CR-167864] 24 p4120 N85-35539
The physical and empirical basis for a specific clear-air turbulence risk index
[NASA-CR-178522] 24 p4120 N85-35540
Project Skywater, 1983-84 SCPP (Sierra Cooperative Pilot Project) data inventory
[PB85-187052] 24 p4124 N85-35565
Surface cyclogenesis as indicated by satellite imagery
[PB85-191815] 24 p4124 N85-35566
Program for Regional Observing and Forecasting Services (PROFS)
[PB85-186050] 24 p4124 N85-35569

WEATHER FRONTS
U FRONTS (METEOROLOGY)

WEATHER MAPS
U METEOROLOGICAL CHARTS

WEATHER MODIFICATION
NT CLOUD DISPERSAL
NT CLOUD SEEDING
NT RAINMAKING

International Conference on Physics of Clouds 06 p0619 N85-15198
The management of atmospheric resources in food production 07 p1002 N85-16362
Satellite support to the Sierra Cooperative Pilot Project: 1979/80 and 1980/81
[PB85-115079] 10 p1520 N85-19583
Ice multiplication in summertime cumulus clouds in the BEWMEX area 16 p2829 N85-27445
Effects of cloud seeding on precipitation development in cumulus clouds 16 p2831 N85-27456
Meteorological weapons
[AD-A154735] 21 p3635 N85-32575
Experimental studies of the kinetics of deposition nucleation on an ice nucleant used in weather modification 21 p3638 N85-32598
Ice nucleating characteristics of Capparis Aphylla, an Indian herb 21 p3641 N85-32619
Project Skywater, 1983-84 SCPP (Sierra Cooperative Pilot Project) data inventory
[PB85-187052] 24 p4124 N85-35565

WEATHER RADAR
U METEOROLOGICAL RADAR

WEATHER STATIONS
NT AUTOMATIC WEATHER STATIONS

The climate of Denmark. Summaries of observations from light vessels. 3: Sea temperature
[ISBN-87-7478-215-0] 01 p0073 N85-10481
The pluviometric recording stations in the 11 GHz radio link at Inviolatella Monte S. Pancrazio — Italy
[FUB-6-1983] 01 p0086 N85-10575
Use of prototyping for man-machine interface requirements definition on the AWDS (Automated Weather Distribution System) program
[AD-A146033] 03 p0398 N85-12526
Acquisition and storage of Cabauw measurements: A system proposal
[KNMI-TR-48] 04 p0540 N85-13434
Statistical relationships between meteorological data stations and implications to diagnostic models in complex terrain
[DE84-014380] 06 p0839 N85-15328
Mariners weather log, volume 28, no. 3, July-August-September 1984
[PB85-107266] 06 p0840 N85-15334
Automated Lavina collects data on snow 07 p0980 N85-16224
Climate of Salt Lake City, Utah
[PB85-123675] 10 p1521 N85-19589
Cabauw (Netherlands) meteorological data tapes 1973-1984: Description of instrumentation and data processing for continuous measurements
[KNMI-WR-84-6] 14 p2379 N85-24685
Wind observation station description for Den Helder (period 1843-1972) and De Kooy (period 1955-1980)
[KNMI-TR-42] 14 p2379 N85-24686
Fog advection in the Namib 16 p2831 N85-27454
Use of a network of telemetered meteorological stations for prediction of the distribution of an atmospheric tracer 16 p2831 N85-27458
Ground-based remote sensing of atmospheric pollution 16 p2832 N85-27462
AWS (Air Weather Service) climatic briefs: North America
[AD-A152161] 16 p2835 N85-27483
SCPP (Sierra Cooperative Pilot Project) data collection and analysis. Volume 1: Executive summary
[PB85-158065] 16 p2837 N85-27494
Evaluation of the PROFS (Program for Regional Observing and Forecasting Services) 1982, real-time forecast experiment
[PB85-159747] 16 p2837 N85-27495

Climatological data of stations in the Netherlands No. 11: Frequency tables and tables with runs according to measurements at principal climatological stations 1951-1960, sunshine stations 1956-1960, precipitation stations 1951-1960
[KNMI-150-11] 18 p3149 N85-29499
Reports from the German Meteorological Service. No. 155: The optimal spectral density of climatological station networks
[ISBN-3-88148-214-8] 23 p3950 N85-34478

WEATHERING
Impact cratering: The process and its effects on planetary evolution — and silicate-carbonate reactions on Venus
[NASA-CR-174016] 02 p0228 N85-11488
Durability and behavior of prestressed concrete beams. Posttensioned concrete beam investigation, supplemental laboratory tests of beams exposed from 1961 to 1962
[AD-A148821] 09 p1304 N85-18191
NBS solar collector durability/reliability test program
[DE85-003489] 12 p1881 N85-21801
Planetary analogs in Antarctica: Mars 13 p2193 N85-23604
Iron oxides of Mars: Evidence for contemporary weathering 13 p2195 N85-23613
New corrosion protection concept for very high voltage line towers
[BLL-OA-TRANS-2691-(6196.300)] 20 p3429 N85-31270

WEATHERPROOFING
New corrosion protection concept for very high voltage line towers
[BLL-OA-TRANS-2691-(6196.300)] 20 p3429 N85-31270

WEBBING
Large-area sheet task advanced dendritic web growth development
[NASA-CR-174021] 02 p0223 N85-11483

WEBS (MEMBRANES)
U MEMBRANES

WEBS (SHEETS)
Development of high-efficiency solar cells on silicon web
[NASA-CR-174212] 06 p0828 N85-15259
Advanced dendritic web growth development 06 p0831 N85-15286
Aircraft barricade
[AD-D011316] 07 p0910 N85-15761
Solid/melt interface studies of high-speed silicon sheet growth
[NASA-CR-175698] 14 p2350 N85-24525
Development of high-efficiency solar cells on silicon web
[NASA-CR-175707] 15 p2585 N85-25939
Stress and efficiency studies in EFG
[NASA-CR-176125] 22 p3751 N85-33251
Instrumentation for sensing moisture content of material using a transient thermal pulse
[NASA-CASE-NPO-15493-2] 23 p3933 N85-34373
Flat-plate solar array project process development area process research of non-CZ silicon material
[NASA-CR-176117] 23 p3945 N85-34445

WEBS (SUPPORTS)
Principles of wave formation along web of H-beams
[BLL-M-36041-(5628.4)] 16 p2798 N85-27253

WEDGE FLOW
Pseudo-stationary oblique-shock-wave reflections in a polyatomic gas, sulfur hexafluoride
[UTIAS-TN-253] 12 p1845 N85-21577
Tabular and graphical solutions of regular and Mach reflections in pseudo-stationary frozen and vibrational-equilibrium flows, part 1
[UTIAS-283-PT-1] 23 p3893 N85-34117
Tabular and graphical solutions of regular and Mach reflections in pseudo-stationary frozen and vibrational-equilibrium flows, part 2
[UTIAS-283-PT-2] 23 p3894 N85-34118

WEDGES
Aircraft chocks
[AD-A145135] 01 p0012 N85-10077
Wedge with crack in bilastic medium 02 p0273 N85-11760
Design of two-mirror scanner with axes of rotation not in plane of mirrors 06 p0777 N85-14969
Modeling of large-scale accretionary wedge and thin-skinned trust-and-fold belt mechanics 06 p1181 N85-17442
Experimental study of the effect of moist environments on epoxy resin chocks
[AD-A152052] 15 p2568 N85-25849
An experimental study of the pressure in a fast bottom beneath the apex of an overlying fluid wedge
[AD-A153618] 18 p3177 N85-29696

WEIBEL INSTABILITY
Reliability prediction of the series system with spares subject to Weibull failure 24 p4100 N85-35413

WEIBULL DENSITY FUNCTIONS
Return wave heights off South Uist estimated from seven years of data
[IOS-164] 01 p0089 N85-10601
The estimation of persistance statistics from cumulative probabilities of wave height
[NMI-R183] 03 p0397 N85-12534
Brownian motion with quadratic killing and some implications: Revision
[AD-A151323] 15 p2642 N85-26296
Rolling contact fatigue testing of thermomechanically processed M-50 steel
[AD-A153640] 18 p3122 N85-29327
On the confidence limits for Weibull reliability and quantiles: The case of maximum likelihood estimation from small size censored samples
[REPT-84-RR-345] 20 p3521 N85-31896
Weibull distribution based on maximum likelihood with interval inspection data
[NASA-TM-86515] 21 p3678 N85-32847
Reliability of two sintered silicon nitride materials
[NASA-TM-87092] 23 p3919 N85-34264

WEIGHT (MASS)
NT ATOMIC WEIGHTS
NT BIOMASS
NT BODY WEIGHT
NT STRUCTURAL WEIGHT
Silicon nitride powder
[NASA-TM-77731] 01 p0022 N85-10132
Potential of flywheels for spacecraft energy storage 05 p0609 N85-13890
A machine for weight-lift testing
[AD-A146816] 07 p0973 N85-16182
Advances in composites technology
[NASA-TM-86353] 08 p1118 N85-17048
Primer for mass metrology
[PB85-121424/GAR] 09 p1305 N85-18199
The optimal control and design of a flexible manipulator arm 09 p1327 N85-18340
A study of the effect of mass loading on the shock environment 09 p1336 N85-18401
Tractor power selection with compaction constraints
[AD-P004300] 09 p1409 N85-18877
Integrated Technology Rotor/Flight Research Rotor (ITR/FRR) concept definition study
[NASA-CR-166444] 10 p1424 N85-18981
State measurement laboratories: Program description (part 1). Directory (part 2)
[PB85-137651] 11 p1739 N85-20935
Gears and Power Transmission Systems for Helicopters and Turboprops
[AGARD-CP-369] 14 p2220 N85-23765
Advanced gearbox technology in small turbo propeller engines 14 p2221 N85-23771
The physical effects of different stress situations on graphite/epoxy compounds 15 p2687 N85-26594
Some aspects of how to design cost-effective flight control systems 16 p2695 N85-26639
Study of Kapton under simulated shuttle environment
[NASA-CR-176003] 19 p3225 N85-29997
Preliminary sizing and performance of aircraft
[NASA-TM-86357] 21 p3554 N85-32111
On high strain rate fragmentation of a closed vessel 23 p3904 N85-34187

WEIGHT FACTORS
U WEIGHT (MASS)

WEIGHT INDICATORS
NT MICROBALANCES
Rain rate meter
[AD-D011381] 07 p0999 N85-16342
Numerical analysis of the first static calibration of the RSRA helicopter active-isolator rotor balance system
[NASA-TM-85975] 08 p1083 N85-16863
Effect of superconducting solenoid model cores on spanwise iron magnet roll control
[NASA-TM-86378] 17 p2905 N85-27915

WEIGHT MEASUREMENT
Portable pallet weighing apparatus
[NASA-CASE-GSC-12789-1] 11 p1635 N85-20294

WEIGHT REDUCTION
Flight simulation fatigue crack propagation in metal/carbon-epoxy laminates
[NLR-TR-83006-U] 01 p0063 N85-10416
Modern structural materials. Present situation and evolution prospects — aircraft materials
[SNIAS-842-551-101] 04 p0455 N85-12886
Space shuttle external tank performance improvements: The challenge 08 p1094 N85-16916
Preventing explosive propagation in racks or containers of tactical missiles
[AD-P004342] 10 p1455 N85-19166
Development of Halley's Comet explorer PLANET-A solar array 13 p2010 N85-22608
Filmwise condensation of steam on low integral-finned tubes
[AD-A152220] 16 p2783 N85-27176
Application of lightweight composite materials to naval weapons systems
[PB85-173607] 18 p3069 N85-28981
Multi-kW solar arrays for Earth orbit applications
[NASA-CR-171538] 20 p3406 N85-31139
Aeroelastic constraints for a wing weight minimization procedure
[FFA-TN-1985-4] 23 p3895 N85-34126

WEIGHTING FUNCTIONS
Solution of contaminant transport equations using an orthogonal-upstream finite element scheme
[DE84-014266] 01 p0070 N85-10463
A combined logistic regression and Zionts-Wallenius methodology for multiple criteria linear programming
[TWISK-314] 01 p0102 N85-10679
A weighted polynomial inequality
[CSIR-TWISK-332] 01 p0110 N85-10741
Definition of acceptable levels of mismatch for equivalent systems of augmented CTOL (Conventional Take-Off and Landing) aircraft
[AD-A145619] 02 p0149 N85-11007
Weighted distributions arising out of methods of ascertainment
[AD-A145615] 02 p0252 N85-11648
Long-range predictive control using weighting-sequence models
[OUEL-1542/84] 04 p0553 N85-13521
Synthesis of systems for coherent weighted signal processing against background of correlated interference 06 p0790 N85-15045
A noise-suppressing digital frequency meter 06 p0796 N85-15084
An adaptive Fast Fourier Transform weighting technique to increase small target sensitivity
[AD-D011424] 08 p1154 N85-17286
On the binary weight distribution of some Reed-Solomon codes
[NASA-CR-174375] 09 p1373 N85-18628
Optimal threshold and weight sorting of elevation angle readings under conditions of fadeouts of a directed signal 12 p1840 N85-21547
Investigation of the numerical method of moments for digital computer determination of differential equations
[AD-A151696] 15 p2636 N85-26268
Locally-weighted-regression scatter-plot smoothing (LOWESS): A graphical exploratory data analysis technique
[AD-A152239] 16 p2855 N85-27609
The weighting function for scintillation on a folded path
[AD-A152659] 17 p2949 N85-28206
Fuzzy hierarchical analysis
[DE85-008149] 17 p3021 N85-28685
Experimental investigations of the unsteady turbulent friction behavior with pressure impulses in a circular pipe
[IWAVI-MITT-102] 18 p3103 N85-29210
Evaluation of densities and distributions via hermite and generalized laguerre series employing high-order expansion coefficients determined recursively via moments or cumulants
[AD-A153950] 18 p3175 N85-29682
MCNP variance reduction overview
[DE85-010765] 19 p3346 N85-30741
Measurements of folded path optical scintillation using a corner cube, a cat's eye and a flat mirror reflector
[AD-A154044] 19 p3367 N85-30879
Monte Carlo learning-biasing experiment with intelligent random numbers
[DE85-010713] 22 p3834 N85-33742

WEIGHTLESSNESS
Second All-Union Seminar on Hydromechanics and Heat and Mass Exchange in Weightlessness, summaries of reports
[NASA-TM-77590] 01 p0047 N85-10305
Circulatory orthostatic instability: Role of deconditioning of relative vessels 01 p0091 N85-10512
Hemopoiesis in rats submitted to weightlessness 01 p0091 N85-10513
Compensatory and adaptive regional hemodynamic reactions to weightlessness during long-term spaceflights 01 p0091 N85-10516
Effect of spaceflight factors on rat bone marrow cells 01 p0092 N85-10520
Developing commercial users of space 02 p0154 N85-11044
Post buckling behavior of a circular rod constrained within a circular cylinder 02 p0207 N85-11365
A survey of space biology and space medicine
[ESA-BR-17] 04 p0545 N85-13466
Three-dimensional ballistocardiography in weightlessness (experiment 1ES 026) — Spacelab 05 p0691 N85-14447
The European vestibular experiments in the Spacelab 1 mission 05 p0694 N85-14468
Sleep physiology in weightlessness (experiment 1ES 030) — Spacelab 05 p0695 N85-14474

The effect of part-simulation of weightlessness on human control of bilateral teleoperation: Neuromotor considerations 05 p0703 N85-14510
The development of the vestibular apparatus under conditions of weightlessness
[NASA-TM-77517] 07 p1011 N85-16422
Distinctions of SPF rats used in experiments aboard biosatellites 07 p1012 N85-16427
Testing changes in visual function due to orbital environment
[AD-A147259] 07 p1016 N85-16453
Controlled ecological life support system higher plant flight experiments
[NASA-CR-177323] 07 p1020 N85-16471
Gravity and biological systems: Emphasis on human physiology
[ESA-BR-21] 09 p1360 N85-18558
Physiological considerations of artificial gravity 11 p1645 N85-20366
Influence of gravitoinertial force level on apparent magnitude of coriolis cross-coupled angular accelerations and motion sickness 11 p1693 N85-20644
Space adaptation syndrome: Incidence and operational implications for the space transportation system program 11 p1695 N85-20655
USSR report: Space Biology and Aerospace Medicine, volume 18, no. 6, November - December 1984
[JPRS-USB-85-002] 12 p1900 N85-21931
External respiration, gas exchange and energy expenditures of man in weightlessness 12 p1900 N85-21932
Circadian rhythm of human body temperature during spaceflights 12 p1901 N85-21934
Comparative analysis of effects of weightlessness and its models on velocity and strength properties and tone of human skeletal muscles 12 p1901 N85-21936
LBNP training of crew members on main missions aboard Salyut-6 orbital station 12 p1901 N85-21938
Human lung fluid content during 7-day head-down tilt 12 p1902 N85-21941
Fluid metabolism of monkeys during two-week antiorthostatic hypokinesia 12 p1902 N85-21943
Parameters of carbohydrate metabolism and blood serum enzyme activity after short-term spaceflights 12 p1903 N85-21951
Alterations in gut transport of minerals and in binding proteins during simulated weightlessness
[NASA-CR-175637] 14 p2368 N85-24709
Effects of weightlessness of Aurelia Ephyra differentiation and statolith synthesis 15 p2605 N85-26056
Transduction of the root gravitropic stimulus: Can apical calcium regulate auxin distribution? 15 p2606 N85-26063
Daylily as a system to study effects of space flight on plant development 15 p2607 N85-26068
The role of vitamin D in the bone changes associated with simulated weightlessness 15 p2608 N85-26072
Quantitative alterations in the function of bone forming cells due to reduced weight bearing 15 p2609 N85-26075
Blood pressure responses and mineral ocorticoid levels in the suspended rat model for weightlessness 15 p2609 N85-26079
Development and maturation of the neuromuscular junciton in cell culture under conditions of simulated zero-gravity 15 p2611 N85-26093
Effects of simulated weightlessness on mammalian development. Part 2: Meiotic maturation of mouse oocytes during clinostat rotation 15 p2612 N85-26094
Evidence that resorption of bone by rat peritoneal macrophages occurs in an acidic environment 15 p2612 N85-26096
The effects of simulated weightlessness on susceptibility to viral and bacterial infections using a murine model 15 p2613 N85-26100
Analysis of head-down tilt as an analog of weightlessness using a mathematical simulation model
[NASA-CR-171870] 15 p2616 N85-26118
Predictions of cardiovascular responses during STS reentry using mathematical models
[NASA-CR-171871] 15 p2616 N85-26119
Simulation of a G-tolerance curve using the pulsatile cardiovascular model
[NASA-CR-171873] 15 p2616 N85-26120
Description, validation, and modification of the Guyton model for space-flight applications. Part A. Guyton model of circulatory, fluid and electrolyte control. Part B. Modification of the Guyton model for circulatory, fluid and electrolyte control
[NASA-CR-171876] 15 p2616 N85-26122
The behavior of renal-regulating hormones during hypogravic stress
[NASA-CR-171877] 15 p2616 N85-26123
Fluid-electrolyte responses during prolonged space flight: A review and interpretation of significant findings
[NASA-CR-171878] 15 p2617 N85-26124
Mathematical modeling of fluid-electrolyte alterations during weightlessness
[NASA-CR-171881] 15 p2617 N85-26125
Aerosol deposition along the respiratory tract at zero gravity: A theoretical study
[DE85-006703] 15 p2619 N85-26136
Primate experiments on SLS-1 15 p2687 N85-26592
USSR report: Space
[JPRS-USP-85-004] 16 p2717 N85-26772
Free-surface phenomena under low- and zero-gravity conditions
[NASA-CR-175835] 16 p2782 N85-27168
Free-surface phenomena under low- and zero-gravity conditions
[NASA-CR-175885] 17 p2907 N85-27922
Changes in bone structure and metabolism during simulated weightlessness: Endocrine and dietary factors
[NASA-CR-175961] 18 p3153 N85-29521
Crystal growth from the vapor in low gravity environments
[DE85-009626] 18 p3195 N85-29816
Crystallization of aluminum-based alloys in weightlessness 19 p3242 N85-30101
Cosmonauts' postural reactions after long-term missions aboard Salyut-6 orbital station 19 p3323 N85-30585
A systems analysis of the erythropoietic responses to weightlessness. Volume 1: Mathematical model simulations of the erythropoietic responses to weightlessness
[NASA-CR-171890] 20 p3506 N85-31794
A systems analysis of the erythropoietic responses to weightlessness. Volume 2: Description of the model of erythropoiesis regulation. Part A: Model for regulation of erythropoiesis. Part B: Detailed description of the model for regulation of erythropoiesis
[NASA-CR-171891] 20 p3506 N85-31795
An integrated analysis of the physiological effects of space flight: Executive summary
[NASA-CR-171892] 20 p3506 N85-31796
Results of Space Experiments in Physiology and Medicine and Informal Briefings by the F-16 Medical Working Group
[AGARD-CP-377] 20 p3507 N85-31805
Thresholds for detection of linear oscillation following prolonged weightlessness 20 p3508 N85-31810
Spatial orientation in weightlessness and readaptation to Earth's gravity 20 p3509 N85-31811
Reinterpretation of otolith input as a primary factor in space motion sickness 20 p3509 N85-31812
Postural adjustments associated with arm movements in weightlessness 20 p3509 N85-31813
Mass-discrimination during prolonged weightlessness 20 p3509 N85-31814
Changes in cardiovascular function: Weightlessness and ground-based studies 20 p3509 N85-31815
Cardiovascular research in space: Problems and results 20 p3510 N85-31817
Sleep and wake physiology in weightlessness 20 p3510 N85-31819
Sensitivity of human lymphocytes to microgravity in-vitro 20 p3510 N85-31820
Mission operations requirements document for D-1 Experiment 102, Vestibular Experiments in Spacelab
[NASA-TM-87495] 21 p3557 N85-32129
Analysis of the transient response of temporal artery blood flow data relative to various anti-G suit pressure schedules
[AD-A155242] 21 p3688 N85-32775
Intracardiac hemodynamics and human heart function in simulated weightlessness 22 p3733 N85-33140
Mechanisms of osteodystrophy in weightlessness 22 p3733 N85-33143
USSR report: Space Biology and Aerospace Medicine, volume 19, no. 2, March - April 1985
[JPRS-USB-85-004] 22 p3820 N85-33667
Labyrinthine and extralabyrinthine mechanisms of development of motion sickness in weightlessness 22 p3821 N85-33668
Effect of body position and immobilization on intensity of spatial illusions in weightlessness 22 p3821 N85-33672
Vascular mechanisms of adaptation to antiorthostatic position 22 p3822 N85-33675
Cerebral hemodynamics and ventricular function in -15 deg antiorthostatic position 22 p3822 N85-33676
Effect of short-term antiorthostatic hypokinesia on dynamics of cardiorespiratory parameters during graded physical exercise 22 p3822 N85-33677
Investigation of some aspects of amino acid metabolism in man during brief exposure to antiorthostatic hypokinesia combined with ultraviolet radiation 22 p3822 N85-33678
General description of experiment dealing with rat ontogenesis aboard Cosmos-1514 biosatellite 22 p3822 N85-33679
Morphological study of antiorthostatic hypokinesia in monkeys 22 p3822 N85-33680
Rat plasma hormone levels following flight aboard Cosmos-1129 biosatellite 22 p3823 N85-33681
Morphological manifestations of hemodynamic changes in lungs of monkeys submitted to antiorthostatic hypokinesia 22 p3824 N85-33686
Effect of substrate moisture on growth and structure of corn leaf 22 p3824 N85-33692
Spacelab 1 hematology experiment (INS103): Influence of space flight on erythrokinetics in man
[NASA-TM-58288] 22 p3824 N85-33693
Fluid-electrolyte metabolism and renal function in cosmonauts following 185-day spaceflight 23 p3952 N85-34495
Effect of hypokinesia and +Gz accelerations on transport function of human blood 23 p3952 N85-34497
Effect of water immersion of parameters of central hemodynamics in individuals over 45 years old 23 p3953 N85-34499
Rat skeletal muscles with simulation of physiological effects of weightlessness (morphological study) 23 p3953 N85-34502
Lipogenesis in rat liver after flight aboard Cosmos-1129 biosatellite 23 p3954 N85-34508
Problems of aviation and space medicine and psychology discussed at 14th Gagarin lectures 23 p3954 N85-34509
A two-phase flow and heat transfer model for zero gravity
[AD-A156097] 24 p4094 N85-35377
The use of a laser Doppler velocimeter in a standard flammability tube
[NASA-CR-174960] 24 p4096 N85-35389
Possible mechanism for changes in glycogen metabolism in unloaded soleus muscle
[NASA-CR-176164] 24 p4127 N85-35588
Response of amino acids in hindlimb muscles to recovery from hypogravity and unloading by tail-cast suspension
[NASA-CR-176183] 24 p4128 N85-35589
Muscle protein and glycogen responses to recovery from hypogravity and unloading by tail-cast suspension
[NASA-CR-176181] 24 p4128 N85-35591
Cardiovascular responses to orthostatism and weightlessness 24 p4130 N85-35601

WEIGHTLESSNESS SIMULATION

Influence of simulated weightlessness on the motility of the acellular slime mold Physarum polycephalum 05 p0689 N85-14430
Plant cell cultures in biological space experiments 05 p0690 N85-14434
The use of horizontal clinostats in studies of plant statocyte development 05 p0690 N85-14435
Left heart ventricular function during a 7 day zero-g simulation (6 deg head down tilt) 05 p0691 N85-14448
Physical performance capacity after a 7 day head-down tilt (-6 deg) 05 p0692 N85-14451
Leg volume changes. Responses to Lower Body Negative Pressure (LBNP) during 7 days of zero-g simulation (6 deg Head-Down Tilt (HDT))
05 p0692 N85-14452
Heart rate variability during 7 day head-down tilt (6 deg) 05 p0692 N85-14453
Comparison of simulation of weightlessness by Head Down Tilt (HDT) and Water Immersion (WI) 05 p0692 N85-14454
Hemodynamics and plasma arginine vasopressin during water immersion in normal man 05 p0693 N85-14458
Glucose tolerance in trained and untrained subjects during head-down tilt (6 deg) 05 p0693 N85-14461
Inner ear characteristics during 7 day antiorthostatic bedrest (6 deg head down tilt) 05 p0695 N85-14470
The role of gravity on the reproduction of arabidopsis plants 15 p2607 N85-26069
The salutary effect of dietary calcium on bone mass in a rat model of simulated weightlessness 15 p2608 N85-26073
Actual and simulated weightlessness inhibit osteogenesis in long bone metaphysis by different mechanisms 15 p2608 N85-26074
Cardiovascular effects of weightlessness 15 p2688 N85-26607
Chromosome aberrations in Crepis capillaris exposed to gamma radiation and clinostat 19 p3325 N85-30600
Morphological study of primate hypothalamus and hypophysis after experiment with antiorthostatic hypokinesia 19 p3325 N85-30603

Study of the cardiovascular system in microgravity: Results and perspectives 20 p0509 N85-31616

WELD STRENGTH

Strength of welded joints in VT23 alloy upon repeated static loading 01 p0020 N85-10120

Fracture toughness characteristics of welded joints in VT6S and AT6 titanium alloys 01 p0020 N85-10121

Influence of residual stresses resulting from manufacturing on the fatigue strength of welded joints 05 p0650 N85-14177

Repair welding and brazing procedures for turbine components and investigation of the brazing behavior of thin filler foils [MTU-TB-908/84] 07 p0974 N85-16190

Static and dynamic fracture toughness characterization of SA508 forging and SA533B welded plate — pressure vessel steels [CISE-2258] 08 p1131 N85-17127

Mechanical properties of Shielded Metal Arc (SMA) and Submerged Arc (SA) welded joints for quenched and tempered steel StE 470. [VTT-319] 09 p1328 N85-18346

Defect tolerance in pipeline girth welds [ERS-E.353] 09 p1328 N85-18347

The effect of filler wire and flux compositions on the microstructure and properties of microalloyed steel weld metal [AD-A149529] 10 p1492 N85-19423

Kinetics of reaction of metals and non-metals during diffusion welding 11 p1602 N85-20076

Collapse and removal of discontinuities in joint zone during diffusion welding 11 p1602 N85-20077

Weldability of alloy ABM1 to alloy 1201 11 p1603 N85-20080

Effects of neutron irradiation on the fracture properties of HT-9 weld [DE85-001066] 12 p1807 N85-21339

Influence of welding defects at melting boundary on static strength of welded joint in large-diameter pipe 13 p2033 N85-22735

Technological parameters of diffusion welding processes in honeycomb titanium alloy structures 13 p2033 N85-22739

Durability of joints of 30KhGSA and 12Kh18N10T steels made by diffusion welding 15 p2501 N85-25428

Mechanical properties of welded joints of 1201 aluminum alloy 15 p2502 N85-25431

Fillet weld stress using finite element methods 15 p2576 N85-25864

Paton Institute expert on GDR-USSR welding research 16 p2768 N85-27078

Local heat treatment of welded joints of pipes and rotary vessels [BLL-BISI-TRANS-22197-(9022.06)] 17 p2972 N85-28354

Technical information: Weldability of stainless steel. Part 1: Austenitic stainless steel [BLL-BISI-TRANS-22456-(9022.06)] 17 p2973 N85-28362

Load-carrying capabilities of refractory alloys for space reactor power applications [DE85-010566] 19 p3240 N85-30087

Structure and properties of VT23 alloy welded joints after thermocyclic processing 19 p3246 N85-30125

Diffusion welding of Cassegrainian concentrator cell stack assemblies [NASA-CR-176104] 22 p3805 N85-33566

Ultrasonic seam welding on thin silicon solar cells [NASA-CR-176116] 22 p3805 N85-33570

WELD TESTS

Electromagnetic-acoustic-transducer e system for thick-weld inspection [PB84-219492] 01 p0051 N85-10336

Prediction of weld defects using welding condition data [VTT-RR-264] 03 p0370 N85-12359

Comparative investigation of testing methods to determine hot crack susceptibility during welding [BAM-ERP-2415] 07 p0979 N85-16218

Static and dynamic fracture toughness characterization of SA508 forging and SA533B welded plate — pressure vessel steels [CISE-2258] 08 p1131 N85-17127

Mechanical properties of Shielded Metal Arc (SMA) and Submerged Arc (SA) welded joints for quenched and tempered steel StE 470. [VTT-319] 09 p1328 N85-18346

Ultrasonic large-diameter pipe weld testing installations 11 p1603 N85-20081

Structure of transient zone in diffusion welding of TsTS-19 piezoceramic with AMg6 alloy 11 p1603 N85-20082

Effects of neutron irradiation on the fracture properties of HT-9 weld [DE85-001066] 12 p1807 N85-21339

The strength and characteristics of VPPA welded 2219-T87 aluminum alloy 12 p1946 N85-22224

Paton comments on results of space welding tests 15 p2484 N85-25330

Durability of joints of 30KhGSA and 12Kh18N10T steels made by diffusion welding 15 p2501 N85-25428

Weldability of Ni3Al-type aluminide alloys [DE85-006932] 15 p2512 N85-25496

Welder training/welder testing [BLL-WI-TRANS-683-(9312.57)] 16 p2792 N85-27223

Local heat treatment of welded joints of pipes and rotary vessels [BLL-BISI-TRANS-22197-(9022.06)] 17 p2972 N85-28354

Statistical models used in analyzing the quality of welded tubes [BLL-BISI-TRANS-22232-(9022.06)] 17 p2976 N85-28384

Non-destructive testing of HF-welded pipe [BLL-BISI-TRANS-22182-(9022.06)] 17 p2976 N85-28388

Mechanical properties of Shielded Metal Arc (SMA) and Submerged Arc (SA) welded joints in a steel Raex 388 P Arctic [VTT-339] 22 p3801 N85-33551

WELDABILITY

Weldability of aged heat resistant nickel alloys 01 p0021 N85-10125

Effect of iron on the performance of IN 625 weld deposits [BR91456] 08 p1169 N85-17376

Weldability of alloy ABM1 to alloy 1201 11 p1603 N85-20080

Weldability and mechanical property characterization of weld clad alloy 800H tubesheet forging [DE85-001737] 11 p1609 N85-20116

The strength and characteristics of VPPA welded 2219-T87 aluminum alloy 12 p1946 N85-22224

Laser spot welding in the electronics industry 14 p2308 N85-24287

Weldability of Ni3Al-type aluminide alloys [DE85-006932] 15 p2512 N85-25496

Development of high strength ship hull steel for high heat input welding — controlled rolling and accelerated cooling 15 p2565 N85-25827

Relationships between microstructure and microfissuring in alloy 718 16 p2735 N85-26878

Paton Institute expert on GDR-USSR welding research 16 p2768 N85-27078

Weldability of micro-alloy steels as reaction of structure and inclusions [BLL-BISI-TRANS-22196-(9022.06)] 17 p2924 N85-28027

High-strength weldable steel 03G4N2MAF Sh with improved ductility [BLL-BISI-TRANS-22233-(9022.06)] 17 p2924 N85-28031

Stainless steels: Application and welding [BLL-BISI-TRANS-22357-(9022.06)] 17 p2927 N85-28059

Welding of 11 458.1 steel in shielding atmospheres [BLL-BISI-TRANS-21763-(9022.06)] 17 p2972 N85-28353

Submerged arc welding of new Czechoslovak micro-alloy steels [BLL-BISI-TRANS-22193-(9022.06)] 17 p2972 N85-28356

Technical information: Weldability of stainless steel. Part 1: Austenitic stainless steel [BLL-BISI-TRANS-22456-(9022.06)] 17 p2973 N85-28362

Tests of low-cycle fatigue of elected steels of class 11 [BLL-BISI-TRANS-22039-(9022.06)] 17 p2978 N85-28404

Weldability/microstructure relationships of high nickel alloys for header applications [DE85-009337] 19 p3241 N85-30094

Plasma arc welding, equipment, installation and process control [DE85-008481] 19 p3373 N85-30921

Ultrasonic seam welding on thin silicon solar cells [NASA-CR-176116] 22 p3805 N85-33570

WELDED JOINTS

NT SPOT WELDS

Influence of annealing on properties of AT3 alloy welded joints 01 p0019 N85-10118

Heat treatment of welded joints in OT4 and VT20 titanium alloys 01 p0020 N85-10119

Strength of welded joints in VT23 alloy upon repeated static loading 01 p0020 N85-10120

Fracture toughness characteristics of welded joints in VT6S and AT6 titanium alloys 01 p0020 N85-10121

Suppressing porosity in weld joints of 1420 aluminum alloy 01 p0020 N85-10123

Effect of welding method on corrosion resistance of welded compositions made of 1201 alloy 01 p0020 N85-10124

Research on high-strength steels with an improved resistance against weld cracking [AD-A144830] 01 p0027 N85-10170

Electromagnetic-acoustic-transducer e system for thick-weld inspection [PB84-219492] 01 p0051 N85-10336

Minor element effects on gas tungsten arc weld penetration [PB84-222579] 01 p0056 N85-10370

Materials studies for magnetic fusion energy applications at low temperatures, 7 [DE84-013487] 01 p0122 N85-10837

Design, construction, demonstration and delivery of an automated narrow gap welding system [AD-A145497] 02 p0204 N85-11348

Strain distribution in a type 316/16-8-2 stainless steel weldment during cyclic loading [DE84-015844] 02 p0210 N85-11384

Effect of rhenium on the structure and properties of the weld metal of a molybdenum alloy [NASA-TM-77491] 03 p0330 N85-12128

Causes of strength reduction in welded titanium-steel joints 03 p0352 N85-12262

Localized corrosion and stress corrosion cracking behavior of stainless steel weldments [DE84-016095] 04 p0474 N85-13017

Solidification and aging behavior of types 308 and 308CRE stainless steel welds [DE84-016552] 04 p0476 N85-13029

Influence of residual stresses resulting from manufacturing on the fatigue strength of welded joints 05 p0650 N85-14177

Ultrasonic girth weld evaluation for aluminum substrate of spherical Kevlar-epoxy test specimens [DE85-001592] 06 p0816 N85-15181

Residual stresses at small diffusion welds [DE84-014982] 07 p0974 N85-16189

Comparison of the sensitivities of ultrasonic, radiographic and acoustic emission test methods for the examination of a thick weld [BLL-RISLEY-TR-4547-(9091.9F)] 07 p0975 N85-16194

Ultrasonic evaluation of titanium contamination with correlation techniques [AD-P004126] 08 p1126 N85-17101

Electrodes for repairing power engineering equipment made from creep resisting steel [BLL-CE-TRANS-8064-(9022.09)] 08 p1167 N85-17360

Effect of tempering on the strength and toughness of 2 1/4 Cr-1 Mo steel weldments [DE85-003818] 09 p1296 N85-18140

Mechanical properties of Shielded Metal Arc (SMA) and Submerged Arc (SA) welded joints for quenched and tempered steel StE 470. [VTT-319] 09 p1328 N85-18346

Fracture toughness of austenitic stainless steel weld metal at 4 K [DE84-016638] 09 p1340 N85-18425

Kinetics of joint formation during diffusion welding of VT5 titanium alloys 10 p1448 N85-19125

Fatigue resistance of welded joints of high strength steels produced by electron beam welding 10 p1449 N85-19127

Estimate of quality of aluminum alloy surface preparation for arc welding 10 p1449 N85-19128

Calculation of mode field in electron beam welding of VT6 titanium alloy 10 p1449 N85-19129

Diffusion welding with forced deformation of heat-resistant nickel-based dispersion hardened alloy 10 p1449 N85-19130

Collapse and removal of discontinuities in joint zone during diffusion welding 11 p1602 N85-20077

Assessment of effectiveness of electron beam welding of titanium alloys up to 40 mm in thickness by vertical or horizontal beam 11 p1603 N85-20078

Distribution of hydrogen in multi-layer welded joints of alloyed steels 11 p1603 N85-20079

Ultrasonic large-diameter pipe weld testing installations 11 p1603 N85-20081

Structure of transient zone in diffusion welding of TsTS-19 piezoceramic with AMg6 alloy 11 p1603 N85-20082

China report: Science and technology [JPRS-CST-84-025] 11 p1620 N85-20197

Radiographic inspection of butt welds described 11 p1620 N85-20198

NASA welding assessment program [NASA-CR-175512] 12 p1859 N85-21661

The strength and characteristics of VPPA welded 2219-T87 aluminum alloy 12 p1946 N85-22224

Problem of pore formation mechanism in welded joints of aluminum alloys in the system aluminum-magnesium-lithium 13 p2032 N85-22732
Properties of welded joints in argon arc welding of titanium alloy using a protective coating 13 p2032 N85-22733
Thermal hardening of welded joints in titanium alloys with various structures 13 p2032 N85-22734
Influence of welding defects at melting boundary on static strength of welded joint in large-diameter pipe 13 p2033 N85-22735
Mechanical properties and brittle fracture resistance of welded multilayer elements for high pressure vessels 13 p2033 N85-22736
Analysis of strength and ductility of welded joints in AMtsS and AMg5 aluminum alloys 13 p2033 N85-22737
Effect of protective medium on durability and fracture structure on seam zones of thin-walled titanium articles produced by diffusion welding 13 p2033 N85-22738
Durability of VT16 alloy compounds obtained by diffusion welding 13 p2034 N85-22740
Structure and mechanical characteristics of heterogeneous joints produced by laser welding 13 p2034 N85-22742
Method of calculating strength of joint produced by cold welding of aluminum under discrete loading 13 p2034 N85-22743
Effect of moisture in inert gases on density of seam metal and on mechanical characteristics of welded joints of aluminum and aluminum alloys 13 p2034 N85-22744
Automatic multi-layer welding of thick cylindrical structures under flux 13 p2035 N85-22746
Softening of metal near seam during welding of heat-resistant nickel alloys 13 p2035 N85-22747
Microstructure and properties of ferrous alloy weldments [DE85-005582] 14 p2257 N85-23987
Laser spot welding in the electronics industry 14 p2308 N85-24287
Ways of improving level and stability of mechanical characteristics of diffusion-welded joints of OT4 titanium alloy 15 p2499 N85-25417
Structure and mechanical properties of dispersion-hardened nickel alloy joints welded by diffusion 15 p2500 N85-25422
Evaluation of stress concentration coefficients in butt-welded joints with displaced edges 15 p2501 N85-25425
Pressure welding of corrosion-resistant steel with AMg6 aluminum 15 p2501 N85-25426
Durability of joints of 30KhGSA and 12Kh18N10T steels made by diffusion welding 15 p2501 N85-25428
Contact point and seam welding of heat-resistant alloys 15 p2501 N85-25429
Thermocompression welding of parts made from AMts and VT1 alloys 15 p2501 N85-25430
Mechanical properties of welded joints of 1201 aluminum alloy 15 p2502 N85-25431
Effect of protective atmosphere composition on durability of welded joints of niobium alloys 15 p2502 N85-25432
Hardening of titanium alloy electric-arc welded joints 15 p2514 N85-25513
Evaluation of the corrosion properties of aluminum alloy 5083 weldments [DE85-007729] 16 p2751 N85-26977
Method of investigating accumulations of damage to weld joints in the case of low-cycle creep [BLL-CE-TRANS-8088-(9022.09)] 16 p2792 N85-27219
Special features of the one-sided automatic welding of structures of Al-Mg alloys 16 p2792 N85-27222
Sources of improvement in quality of contact butt welding of wire [BLL-M-36085-(5828.4)] 16 p2793 N85-27225
An X-ray study of residual stresses in narrow groove TIG weldments [DE85-006485] 16 p2802 N85-27274
Local heat treatment of welded joints of pipes and rotary vessels 17 p2924 N85-28028
Welding of 11 458.1 steel in shielding atmospheres [BLL-BISI-TRANS-21763-(9022.06)] 17 p2972 N85-28353
Local heat treatment of welded joints of pipes and rotary vessels [BLL-BISI-TRANS-22197-(9022.06)] 17 p2972 N85-28354
Formation of a fine structure during shock wave welding [BLL-BISI-TRANS-22401-(9022.06)] 17 p2973 N85-28366
Examination of the regions of the joint of sheets bonded by the explosive welding technique [BLL-BISI-TRANS-22352-(9022.06)] 17 p2973 N85-28370
Differential between crack and pseudo-crack indications by means of objective magnetic flux leakage testing [BLL-BISI-TRANS-22033-(9022.06)] 17 p2976 N85-28386
Inspection of welds and the factors improving its effectiveness in welded structure fabrication [BLL-BISI-TRANS-22194-(9022.06)] 17 p2976 N85-28387
Non-destructive testing of HF-welded pipe [BLL-BISI-TRANS-22182-(9022.06)] 17 p2976 N85-28388
The fatigue properties of welds at low temperature, according to the type of steel [BLL-BISI-TRANS-22455-(9022.06)] 17 p2978 N85-28410
Fatigue strength of Inconel 625 plate and weldments used in the DIII-D configuration vacuum vessel [DE85-006276] 17 p2981 N85-28427
Fatigue behavior of HY-130 steel weldments containing fabrication discontinuities [AD-A153630] 18 p3122 N85-29326
Effect of protective method on cyclic durability and nature of failure of titanium alloy welded joints 19 p3245 N85-30122
Vacuum pressure welding of commercial titanium with 2Kh13 and 12Kh18N10T steels 19 p3246 N85-30124
Structure and properties of VT23 alloy welded joints after thermocyclic processing 19 p3246 N85-30125
Fatigue resistance of homogeneous and heterogeneous welded joints of TS5 titanium alloy 19 p3246 N85-30126
Hot cracking of austenitic stainless steels: The debut of the Sigmajg [DE85-010560] 20 p3431 N85-31287
Determination of local deformation during explosive welding [BLL-M-36279-(5828.4)] 20 p3462 N85-31503
Production verification of the acoustic emission weld monitor [AD-A154168] 20 p3464 N85-31519
Effects of residual stresses and distortion on the nickel 200 and stainless steel 304 weldments [DE85-011868] 22 p3748 N85-33233
Mechanical properties of Shielded Metal Arc (SMA) and Submerged Arc (SA) welded joints in a steel Rsex 366 P Arctic [VTT-339] 22 p3801 N85-33551
Gas shielding apparatus [DE85-005992] 23 p3939 N85-34416
X-ray fluorescence analysis of 304L stainless steel [DE85-013254] 24 p4080 N85-35288

WELDED STRUCTURES

NT STEEL STRUCTURES
Weld metal solidification cracking in a carbon-manganese steel 03 p0330 N85-12126
Ultrasonic and metallurgical examination of a cracked type 304 stainless steel BWR pipe weldment [TI84-014968] 04 p0511 N85-13254
NDE (Nondestructive Evaluation) of oxygen contaminated titanium alloys and weldments [AD-P004121] 08 p1126 N85-17096
Effects of oxygen-contamination-induced microstructural changes on the reverberation of ultrasound in Ti-6211 alloys [AD-P004124] 08 p1126 N85-17099
Acoustical characterization of Ti-6211 weldments and oxygen contamination Ti-6211 plate [AD-P004125] 08 p1126 N85-17100
Electromagnetic NDE of interstitial contamination in titanium alloy weldments [AD-P004131] 08 p1127 N85-17106
Computation of thermal shock-free straightening conditions for aluminum-magnesium alloy welded structures 10 p1449 N85-19131
Institute's contribution to Soviet welding technology noted 16 p2767 N85-27072
Local heat treatment of welded joints of pipes and rotary vessels [BLL-BISI-TRANS-22197-(9022.06)] 17 p2972 N85-28354
Steel Tubes [BLL-BISI-TRANS-22064-(9022.06)] 17 p2973 N85-28369
Inspection of welds and the factors improving its effectiveness in welded structure fabrication [BLL-BISI-TRANS-22194-(9022.06)] 17 p2976 N85-28387
Hot cracking of austenitic stainless steels: The debut of the Sigmajg [DE85-010560] 20 p3431 N85-31287

WELDING

NT ARC WELDING
NT BRAZING
NT COLD WELDING
NT DIFFUSION WELDING
NT ELECTRIC WELDING
NT ELECTRON BEAM WELDING
NT ELECTROSLAG WELDING
NT EXPLOSIVE WELDING
NT FRICTION WELDING
NT FUSION WELDING
NT GAS TUNGSTEN ARC WELDING
NT LASER WELDING
NT LOW TEMPERATURE BRAZING
NT PLASMA ARC WELDING
NT PRESSURE WELDING
NT ULTRASONIC WELDING
Future robotics program at San Antonio ALC (Air Logistics Center) [AD-P004011] 03 p0309 N85-11991
USSR report: Materials science and metallurgy [JPRS-UMS-84-007] 03 p0348 N85-12244
Compact welding apparatus with solar power supply 03 p0352 N85-12263
Comparative investigation of testing methods to determine hot crack susceptibility during welding [BAM-ERP-2415] 07 p0979 N85-16218
Robotics application in construction industry assessed 08 p1139 N85-17178
Technical data on new engineering products 10 p1460 N85-19201
Interaction between a crack and a soft inclusion [NASA-CR-172533] 10 p1495 N85-19439
Investigation of welded interconnection of large area wraperound contacted silicon solar cells [NASA-CR-174436] 10 p1509 N85-19519
USSR report: Materials science and metallurgy [JPRS-UMS-84-005] 11 p1597 N85-20044
Evaluation of residual stress in laminated metallic composites 11 p1598 N85-20052
Chemical cleaning of 304 and 304-L stainless steel surfaces by the nitradd passivation process [DE85-003714] 11 p1615 N85-20158
Automatic multi-layer welding of thick cylindrical structures under flux 13 p2036 N85-22746
USSR report: Materials science and metallurgy [JPRS-UMS-85-001] 15 p2496 N85-25395
USSR report: Materials science and metallurgy [JPRS-UMS-85-004] 15 p2513 N85-25503
Soviet institute director on GDR-USSR welding technology 15 p2538 N85-25662
Applicability of modular versus universal robots discussed 15 p2538 N85-25664
Welding technology: Japan — Conference [ISBN-0-85300177-4] 15 p2565 N85-25823
The development and implementation of advanced welding technology 15 p2566 N85-25824
Studies of ferritic filler metals for welding 9 percent nickel steel 15 p2565 N85-25825
Application of new welding technology in the fabrication of nuclear power plant 15 p2566 N85-25829
NASA welding assessment program [NASA-CR-175683] 15 p2568 N85-25845
Special features of the one-sided automatic welding of structures of Al-Mg alloys 16 p2792 N85-27222
Hazards in welding due to oxygen changes in the workplace atmosphere [BLL-WI-TRANS-684-(9312.57)] 16 p2792 N85-27224
The characteristic structure of weld metal of high temperature alloy X20CrMoV 121 [BLL-BISI-TRANS-21823-(9022.06)] 17 p2926 N85-28069
Formation of a fine structure during shock wave welding [BLL-BISI-TRANS-22401-(9022.06)] 17 p2973 N85-28368
Principal quality assurance measures in the manufacture of HF-welded high-pressure linepipe [BLL-BISI-TRANS-21690-(9022.06)] 17 p2976 N85-28389
Fatigue crack propagation characteristics and fatigue fracture toughness in 780 MPa grade high strength steel weldments at low temperature [BLL-BISI-TRANS-22369-(9022.06)] 17 p2979 N85-28411
Alignment and assembly tool for very large diameter cylinders [NASA-CASE-MFS-28001-1] 18 p3116 N85-29269
Brittle fracture behaviour of cold formed, welded 10mm to 20 mm thick plate manufactured from plain carbon structural steels [BLL-BISI-TRANS-21678-(9022.06)] 18 p3120 N85-29311

Chemical composition and kinetics of libration of gases upon welding of aluminum alloys
19 p3247 N85-30131
Reliability of welds to repair defects in cast components made from CrMoV steel
[BLL-CE-TRANS-8054-(9022.09)]
20 p3461 N85-31501
Joining of sintered composite TiC-steel materials by welding
[BLL-M-36253-(5828.4)] 20 p3461 N85-31502
Production verification of the acoustic emission weld monitor
[AD-A154188] 20 p3464 N85-31519
Analytical simulation of weld effects in creep range
20 p3466 N85-31550
United States Army welding research and development topical and coordination meeting
[AD-A155834] 24 p4099 N85-35409

WELDING MACHINES
Compact welding apparatus with solar power supply
03 p0352 N85-12263
New welding equipment for mechanized welding and trends in further development 03 p0352 N85-12264
Laser and diffusion welding equipment R and D
03 p0352 N85-12265
Design features, applications of new robots
08 p1139 N85-17174
Characterization of the heat source distribution of a typical GTAW welding arc
[DE85-004322] 12 p1861 N85-21670
Automatic multi-layer welding of thick cylindrical structures under flux 13 p2035 N85-22746
Cosmonauts report on space welding at conference
15 p2484 N85-25329
Paton comments on results of space welding tests
15 p2484 N85-25330
Sources of improvement in quality of contact butt welding of wire
[BLL-M-36085-(5828.4)] 16 p2793 N85-27225
Laser welder for fabricating neutron tubes
[DE85-009965] 17 p2974 N85-28377

WELLS
Similarity considerations in 1-component 2-phase flow
[DE84-016370] 04 p0499 N85-13184
Geothermal wells drilled in Transcarpathians
07 p0994 N85-16315
Geothermal assessment of part of the east shore area, Davis and Weber Counties, Utah
[DE84-016817] 09 p1342 N85-18446
Technical support for geopressured-geothermal well activities in Louisiana
[DE85-010462] 18 p3102 N85-29203
Hot Dry Rock Geothermal Energy Developement Program
[DE85-010570] 19 p3268 N85-30264
Lost circulation in geothermal wells: Research and development status
[DE85-009936] 19 p3268 N85-30267
Linear boundary detection using pressure buildup tests
[DE85-009926] 22 p3784 N85-33444
Geologic, technical, and economic sensitivity analysis in support of the GRI (Gase Research Institute) tight gas reservoirs project area
[PB85-192276] 22 p3802 N85-33559
Proposed resource evaluation plan. Salton Sea scientific drilling program
[DE85-011294] 22 p3815 N85-33633
Method for determining depth and shape of a sub-surface conductive object
[DE85-006502] 23 p3935 N85-34389
Depletion modeling of liquid dominated geothermal reservoirs
[DE85-009823] 23 p3943 N85-34437
Evaluation of low-temperature geothermal potential in north-central Box Elder County, Utah
[DE85-009541] 24 p4112 N85-35490

WEST GERMANY
Colloquium about Joint Projects within DFVLR/ISRO Cooperation
[DFVLR-MITT-84-12] 04 p0458 N85-12907
Presentation of Indian Space Research Organization (ISRO)/DFVLR cooperation 04 p0459 N85-12912
German domestic scheduled air transport in the year 2000
[ESA-TT-826] 05 p0595 N85-13792
Global radiation in West Germany — solar generators
05 p0662 N85-14253
Overview of German microgravity activities in the field of life science 05 p0696 N85-14476
BDLI memorandum on the future of space flight in the Federal Republic of Germany
[NASA-TM-77624] 07 p0911 N85-15765
Revised Uniform Summary of Surface Weather Observations (RUSSWO). Spangdahlem AB, Germany, parts A-F
[AD-A147166] 07 p1006 N85-16392
Limited surface observations climatic summary (LISOCS). Hohenfels, AAF, West Germany
[AD-A147167] 07 p1006 N85-16393
Activities report on West German civil airports. Part 1: Text
[ISBN-3-87977-055-7-PT-1] 08 p1090 N85-16887
Activities report for the West German Civil Airports. Part 2: Tables
[ISBN-3-87977-055-7-PT-2] 08 p1090 N85-16888
The Prandtl Hergesell project of a national research establishment for aeronautics
[ESA-TT-835] 09 p1272 N85-17993
Space research in the Federal Republic of Germany
09 p1285 N85-18074
Activities report of the Department of Applied Research 78 for satellite geodesy of the Technical University, Munich
[ASTRON-GEODAET-ARB-45]
09 p1342 N85-18440
Revised Uniform Summary of Surface Weather Observations (RUSSWO). Parts A-F Zweibrucken AB, Germany
[AD-A147165] 09 p1357 N85-18536
Activities report in aerospace in West Germany
[ISSN-0070-3966] 09 p1418 N85-18947
FRG's DFVLR ready for participation in space station
11 p1616 N85-20176
The 1980 diagnostic adjustment of the German main triangulation network. 4: Network adjustment (part 3)
[SER-B-267-PT-3-MITT-168] 11 p1665 N85-20494
The 1980 diagnostic adjustment of the German main triangulation network. 4: Network adjustment (part 1)
[SER-B-267-PT-1-MITT-168] 11 p1670 N85-20525
The 1980 diagnostic adjustment of the German main triangulation network. 4: Network adjustment (part 2)
[SER-B-267-PT-2-MITT-168] 11 p1670 N85-20526
List of head/neck injury on ejection in the German Armed Forces from 1972-1981 12 p1906 N85-21972
D-1 report: The first German spacelab mission
[NASA-TM-77637] 13 p1977 N85-22402
West Europe report: Science and technology
[JPRS-WST-84-007] 15 p2530 N85-25600
Three-dimensional boundary layers: A report on work in Germany 15 p2559 N85-25786
Comparison of some West German cloud height and visibility data — weapon test sites
[BAE-BT-12734] 15 p2593 N85-25982
A brief comparison of Egyptian with West German atmospheric transmission data in the 8 to 11.5 micron waveband
[BAE-BT-12829] 15 p2594 N85-25983
Proceedings of the 9th US Air Force and the Federal Republic of Germany Data Exchange Agreement Meeting, Viscous and Interacting Flow Field Effects
[AD-A153020] 17 p2958 N85-28266
Investigation of air pollution impact in Eastern Bavaria: Measurement results from August and September, 1984
[DFVLR-FB-85-03] 17 p2988 N85-28471
Documentation for the West German Federal Cabinet's space policy decision 17 p3051 N85-28886
Investigation of the transferability of measures of passive solar energy utilization in the USA to the Federal Republic of Germany
[BMFT-FB-T-84-264] 18 p3132 N85-29396
International space research perspectives of commercialization for German industry
[NASA-TM-77657] 19 p3222 N85-29979
Maritime mobile satellite techniques as an integral part of the Future Global Maritime Distress and Safety System (FGMDSS): The position of the Federal Republic of Germany 20 p3406 N85-31136
Reports from the German Meteorological Service. No. 167: Results of aerological soundings in the model area upper Rhine: Heat release project upper Rhine area, part 3
[ISBN-3-88148-216-4] 23 p3950 N85-34479
Special questions of siting wind turbine arrays and networks — West Germany 24 p4111 N85-35484

WEST INDIES
NT CUBA
NT PUERTO RICO

WEST PAKISTAN
U BANGLADESH

WESTLAND AIRCRAFT
NT P-531 HELICOPTER

WESTLAND P-531 HELICOPTER
U P-531 HELICOPTER

WETLANDS
Multispectral remote sensing of inland wetlands in South Carolina: Selecting the appropriate sensor
[DE84-013951] 05 p0661 N85-14247
Removal of heavy metals by artificial wetlands
[PB85-116127] 10 p1513 N85-19548
An initial analysis of LANDSAT-4 Thematic Mapper data for the discrimination of agricultural, forested wetlands, and urban land cover — Poinsett County, Arkansas; and Reelfoot Lake and Union City, Tennessee
13 p2118 N85-23193
Remote sensing of coastal wetlands biomass using Thematic Mapper wavebands — Lewes, Delaware
13 p2119 N85-23196
Comparison of MSS and TM data for landcover classification in the Chesapeake Bay area: A preliminary report — Taylor's Island, Maryland
13 p2121 N85-23210

WETNESS
U MOISTURE CONTENT

WETTABILITY
Preliminary evaluation of a liquid belt radiator for space applications
[NASA-CR-174807] 07 p0917 N85-15804
Contact angle and surface tension measurements of a five-ring polyphenyl ether
[NASA-TM-86827] 07 p0930 N85-15897

WETTING
Critical point wetting drop tower experiment
02 p0155 N85-11045
The chemical nature of the fiber/resin interface in composite materials 04 p0465 N85-12953
A nonnoble front metallization process
06 p0830 N85-15279
Investigation of surface tension phenomena using the KC-135 aircraft
[NASA-TM-82506] 10 p1426 N85-18995
Factors influencing the ball milling of Si3N4 in water
[NASA-TM-86932] 10 p1450 N85-19136
Modeling of transient heat pipe operation
[NASA-CR-175496] 12 p1844 N85-21571
Examination of the contact wetting angle in the vicinity of critical temperature
[BLL-T6416/BG/CRS/LR-ST735/84]
13 p2091 N85-23054
Statistical mechanics of adsorption and wetting
[DE85-010093] 19 p3269 N85-30271
Mechanics of a gaseous film barrier to lubricant wetting of elastohydrodynamically lubricated conjunctions
[NASA-TP-2500] 21 p3595 N85-32330

WHALES
Tracking whale migrations with the ARGOS satellite system 14 p2330 N85-24403
Some methods of computing platform transmitter terminal location estimates — ARGOS system; whale tracking 14 p2332 N85-24420
The ARGOS system used for tracking gray whales
14 p2332 N85-24421
The ARGOS system used for tracking gray whales
16 p2812 N85-27347

WHEAT
Multi crop area estimation in Idaho using EDITOR
[E85-10054] 06 p0827 N85-15251
Growth/reflectance model interface for wheat and corresponding model
[E85-10058] 07 p0987 N85-16269
Growth and reflectance characteristics of winter wheat canopies
[E85-10080] 10 p1505 N85-19494
User's guide to the TAMW wheat model as implemented on the IBM 360/195 computer
[E85-10084] 12 p1873 N85-21749
NOAA-AISC user's guide for implementing CERES wheat model for large area yield estimation
[E85-10085] 12 p1873 N85-21750
Modeling the backscattering and transmission properties of vegetation canopies
[E85-10099] 16 p2809 N85-27320
Regression analysis of aircraft and ground measurement data on vegetation cover 22 p3735 N85-33156

WHEATSTONE BRIDGES
The constant current strain gauge bridge
[ARL/STRUC-TM-385] 07 p0962 N85-16097
Developing a flowmeter for streams with high solids content
[DE84-016643] 09 p1323 N85-18316
Instrumentation for sensing moisture content of material using a transient thermal pulse
[NASA-CASE-NPO-15493-2] 23 p3933 N85-34373

WHEEL BRAKES
Development of carbon based brake lining materials without asbestos content in the form of carbon-carbon composites and carbon-metal or carbon-carbide composites
[BMFT-FB-T-85-014] 18 p3082 N85-29067

WHEELS
NT COUNTER-ROTATING WHEELS
NT FLYWHEELS
NT REACTION WHEELS
NT TURBINE WHEELS
NT VEHICLE WHEELS

Grease versus oil lubrication of wheel bearings in Army equipment
[AD-A147546] 07 p0973 N85-16184
Space shuttle wheels and brakes
06 p1101 N85-16962
Development of a soil-wheel interaction model
[AD-P004259] 09 p1404 N85-18835
The rolling resistance and sinkage of towed dual wheel combination in sand
[AD-P004261] 09 p1404 N85-18837
Forces on undriven, angled wheels
[AD-P004303] 09 p1409 N85-18880
An evaluation of the 64-meter antenna radial bearing for use on the 70-meter antenna
10 p1464 N85-19238
Manufacture of drive wheel vanes for hydraulic turbines on program controlled machine tools
14 p2269 N85-24058
Modernization of running gear of crane
14 p2286 N85-24163
Assessing the machinability of gearwheel steels during manufacture
[BLL-BISI-TRANS-22343-(9902.06)]
17 p2973 N85-28365
Non-backdriveable free wheeling coupling
[NASA-CASE-MSC-20475-1] 16 p3116 N85-29290
Development of a high strength isothermally heat-treated nodular iron road wheel arm
[AD-A155755] 24 p4099 N85-35408

WHIP ANTENNAS
HF broadband whip antenna evaluation
[AD-A149527] 10 p1467 N85-19258

WHIRL
U ROTATION

WHIRL INSTABILITY
U ROTARY STABILITY

WHIRLING
U ROTATION

WHISKER COMPOSITES
Fabrication of SiC whiskers and composites
[DE85-002038] 09 p1289 N85-18091
Tensile testing of SiC whiskers
[DE85-003712] 11 p1583 N85-20025
Particulate and whisker toughened alumina composites
[DE85-005239] 16 p2743 N85-26930

WHISKERS (CRYSTALS)
Tensile testing of SiC whiskers
[DE85-003712] 11 p1583 N85-20025

WHISTLERS
The propagation and growth of whistler mode waves generated by electron beams in Earth's bow shock
[AD-A145572] 02 p0228 N85-11492
Inference of equatorial field-line integrated electron density values using whistlers
[AD-A145822] 03 p0362 N85-12507
Asymptotic orbit theory for trapped electrons in inhomogeneous Whistler field
[AD-A146178] 03 p0392 N85-12510
Three dimensional ray tracing of the Jovian magnetosphere in the low frequency range
[NASA-CR-175462] 10 p1571 N85-19909
Excitation of low-frequency plasma waves by a conducting, tethered satellite 13 p2171 N85-23470
Deuteron whistlers at low latitudes in the low altitude topside ionosphere 14 p2366 N85-24625
Low-latitude ducted whistlers observed at Sanya, Hainan, China 14 p2357 N85-24626
Whistler observation at Okinawa, Japan during the IMS 14 p2357 N85-24627
Whistler mode waves near the plasmapause: Results from the IMS VLF experiment at Halley, Antarctica
14 p2357 N85-24628

WHITE DWARF STARS
Search for white dwarf companions of cool stars with peculiar element abundances
[NASA-CR-174030] 02 p0297 N85-11923
Voyager EUV and FUV observations
06 p0875 N85-15554
Stromgren trails of hot white dwarfs
06 p0879 N85-15589
Ultraviolet spectroscopy of selected astronomical sources
[NASA-CR-174379] 09 p1413 N85-18912
On the progenitors of white dwarfs
[NASA-CR-174378] 09 p1413 N85-18913
Study of the pulsations of the ZZ Ceti stars
09 p1414 N85-18923
White dwarf stars at ultraviolet wavelengths
11 p1744 N85-20971
Mass distribution and evolutionary scheme for central stars of planetary nebulae 11 p1751 N85-21012
Further investigation of mass loss phenomena in hot white dwarfs and O subdwarfs 11 p1751 N85-21014
Self-consistent recalibration of IUE determination of hot DA white dwarf effective temperatures
11 p1751 N85-21016
Carbon, silicon, and oxygen in the white dwarf star GD 40 11 p1752 N85-21017
Analysis of white dwarf Lyman alpha profiles
11 p1752 N85-21018
A search for white-dwarf companions of subgiant CH stars 11 p1752 N85-21019
The white dwarf companion of the mild BA star Xi1 Cet 11 p1752 N85-21020
The outburst and long term behavior of the triple period cataclysmic variable TV Col 11 p1752 N85-21021
Hydrodynamic simulations of recurrent novae
11 p1753 N85-21025
Egress spectra of the new eclipsing supergiant 22 Vulfeculae 11 p1755 N85-21039
A survey for galactic plane ultraviolet-excess objects: Space densities for white dwarfs, subdwarfs, and cataclysmic variables 13 p2169 N85-23458
Photoelectric observations of the dwarf nova VW Hydri during the November 1977 supermaximum
[REPT-97] 15 p2667 N85-26461
On gamma and neutrino radiation from Cyg X-3
[OG-2.1-7] 22 p3863 N85-33924

WHITE LIGHT HOLOGRAPHY
White-light optical information processing and holography
[AD-A148938] 07 p0967 N85-16138
The utilization of optical fibers in holography
[ISL-R-102/83] 16 p2787 N85-27196

WHITE NOISE
NT THERMAL NOISE
Non-Gaussian approach for parametric random vibration of non-linear structures 01 p0060 N85-10395
Spectral noise density and random errors of pulse frequency characteristic meters
03 p0346 N85-12231
Flight test technique for evaluation of gust load alleviation analysis methodology
[NASA-TM-86344] 06 p0754 N85-14833
On the probability density of signal-to-noise ratio in an improved adaptive detector, part 1
[AD-A148856] 10 p1550 N85-19772
Statistical analysis of autoregressive spectral estimates for noise corrupted autoregressive series
[AD-A149543] 11 p1708 N85-20747
Methods of digital correction for channels of multichannel radar receivers 13 p2082 N85-23005
On the probability density of signal-to-noise ratio in an improved detector
[AD-A152529] 17 p2952 N85-28232
Random vibration of nonlinear, parametrically excited systems 19 p3282 N85-30351
Noise in stages and in interstage couplings of various transistor circuits 22 p3765 N85-33334
Nonlinear filtration of clutter 22 p3777 N85-33404

WICKS
Monogroove heat pipe design: Insulated liquid channel with bridging wick
[NASA-CASE-MSC-20497-1] 18 p3098 N85-29180

WIDE ANGLE LENSES
A second generation WAVIDS (Wide Angle Virtual Image Display System)
[AD-P004328] 09 p1270 N85-17962
Wide-angle optics with strong magnetic fields for efficient generation of secondary-particle beams
[DE85-007727] 18 p3179 N85-29713
Evidence for long-term variability in the ultra high energy photon flux from Cygnus X-3
[OG-2.1-10] 22 p3863 N85-33926

WIDEBAND
U BROADBAND

WIDEBAND COMMUNICATION
Interference immunity of digital equipment for coherent processing of wideband signals
04 p0486 N85-13100
Digital simulation of communications channels: An overview 10 p1472 N85-19290
Fast synchronization model for UHF spread-spectrum communication system 10 p1473 N85-19296
Overview of RADC adaptive antenna developments for communications 10 p1474 N85-19299
Ionospheric distortions of digital signals with wideband modulation 13 p2072 N85-22945
Cophasal horizontal wideband array antennas for transmitting with asymmetric output
15 p2526 N85-25578
Adaptation of bit error rate by coding — spacecraft transmissions
[ESA-CR(P)-1970] 15 p2545 N85-25711

WIENER FILTERING
Recursive algorithms for adaptive arrays based on estimates
[REPT-5-84] 01 p0107 N85-10718

WIENER HOPF EQUATIONS
Random equations in aerodynamics
[NASA-CR-174279] 06 p1077 N85-16825

WIGGLER MAGNETS
A free electron laser with two-component wiggler
11 p1623 N85-20217
Progress toward free-electron lasers for applications
[DE85-002208] 11 p1630 N85-20326
Note of the dynamic behavior of a magnet system suspended by a thin fiber, with special reference to the Quartz Horizontal Magnetometer (QHM)
[DMI-GEOPHYS-PAPERS-R-70]
11 p1714 N85-20785
Application of permanent magnets in accelerators and electron storage rings
[DE85-004981] 15 p2642 N85-26297
Permanent magnets for production and use of high energy particle beams
[DE85-009934] 20 p3522 N85-31905
Electron trajectories in a combined wiggler and alternating gradient quadrupole field
[DE85-010727] 22 p3842 N85-33794
Breeding new light into old machines (and new)
[DE85-013055] 24 p4155 N85-35783

WIGHTMAN THEORY
U FIELD THEORY (PHYSICS)
U QUANTUM THEORY
U RELATIVISTIC THEORY

WIGNER COEFFICIENT
A packed storage program for angular momentum coupling coefficients
[TWISK-316] 01 p0102 N85-10680
The ambiguity function and the Wigner distribution
[AD-A150095] 12 p1829 N85-21482

WILDLIFE
NT BABOONS
NT BIRDS
NT MONKEYS
Control of mammals at airports
[AD-P004192] 11 p1580 N85-19957
Airport site selection and design
[AD-P004193] 11 p1581 N85-19959
Acid rain: Effects on fish and wildlife
[PB85-154672] 16 p2821 N85-27402

WILDLIFE RADIOLOCATION
Tracking pelagic dolphins by satellite
14 p2324 N85-24364
Polar bear telemetry results from the Nimbus-6 system
14 p2325 N85-24365
Development of ARGOS platforms for tracking of basking sharks, Cetorhinus maximus
14 p2326 N85-24378
Transatlantic migration study of the leathery turtle using the ARGOS system. Transatlantic turtle race
14 p2326 N85-24379
Tracking whale migrations with the ARGOS satellite system 14 p2330 N85-24403
Drifting buoy development and future programs — Japanese ARGOS program 14 p2330 N85-24406
Some methods of computing platform transmitter terminal location estimates — ARGOS system; whale tracking 14 p2332 N85-24420
The ARGOS system used for tracking gray whales
14 p2332 N85-24421
Motivation for satellite tracking of southern elephant seals Mirounga leonina at sea 16 p2812 N85-27346
The ARGOS system used for tracking gray whales
16 p2812 N85-27347

WINCHES
The orbiter mate/demate device
06 p1103 N85-16972
Improvements in linked-spar motion-compensated lifting system
[AD-D011413] 08 p1138 N85-17165

WIND (METEOROLOGY)
NT CYCLOGENESIS
NT GEOSTROPHIC WIND
NT GROUND WIND
NT GUSTS
NT JET STREAMS (METEOROLOGY)
NT MONSOONS
NT SEA BREEZE
NT SQUALLS
NT WINDS ALOFT
Alpine meteorology: Translations of classic contributions by Wagner, A., Ekhart, E. and Defant, F.
[DE84-014929] 01 p0065 N85-10574
Microburst wind structure and evaluation of Doppler radar for wind shear detection
[DOT/FAA/PM-84/29] 02 p0230 N85-11501
Wind shear measuring on board an airliner
[NASA-TM-77483] 03 p0395 N85-12521
Plotting TDL coastal wind forecasts
[PB84-220789] 03 p0397 N85-12533

Aircraft measurements of tracer gas during the 1983 cross Appalachian tracer experiment (CAPTEX)
[DE84-015292] 04 p0531 N85-13395
Effect of mountain wave dynamics on orographic storms
[DE84-014713] 04 p0540 N85-13433
Comparison of wind derived from the LIMS (Limb Infrared Monitor of the Stratosphere) satellite instrument with rocket observations
[NASA-CR-174083] 04 p0541 N85-13444
Investigation of satellite measurements in the presence of clouds, forcing influences on clouds and feedback to the large scale following convection
05 p0682 N85-14381
Large scale rossby waves during FGGE
05 p0684 N85-14396
Statistical relationships between meteorological data stations and implications to diagnostic models in complex terrain
[DE84-014360] 06 p0839 N85-15328
Limited surface observations climatic summary (LISOCS). Camp Casey, Tong Du Chon, Korea
[AD-A147204] 07 p1007 N85-16397
Limited surface observatins climatic summary (LISOCS). Ansbach AHP, Germany
[AD-A147205] 07 p1007 N85-16398
Studies of coastal mesoscale winds using SIR-B
08 p1147 N85-17238
MWR, Meteor Wind Radars 08 p1184 N85-17462
Development of guidance forecasts at the Royal Netherlands Meteorological Institute (KNMI). Part 2: Extreme wind speed at IJmuiden
[KNMI-TR-84-PT-2] 08 p1190 N85-17500
Modeling stochastic wind loads on vertical axis wind turbines
[DE85-001148] 09 p1340 N85-18426
The wobble of the Earth and the low frequency dynamics of the ocean 09 p1358 N85-18546
Field studies of run-up ger...rated by wind waves on dissipative beaches
[AD-A148793] 09 p1359 N85-18548
MAP in Japan: Organization and projects
11 p1655 N85-20425
MAP activities in Hungary 11 p1657 N85-20440
Variation of derived mesospheric nitric oxide in relation to wind and temperature in winter
11 p1658 N85-20452
Large scale winter time disturbances in meteor winds over central and eastern Europe
11 p1661 N85-20467
VHF radar observations in the stratosphere and mesosphere during a stratospheric warming
11 p1661 N85-20468
Changes in the ozone content over central Europe during reversals of stratospheric circulation in late winter
11 p1661 N85-20469
Some aspects of general circulation and tides in the middle atmosphere 11 p1661 N85-20470
Meteor wind results from Atlanta, USA, and Ramey, Puerto Rico 11 p1662 N85-20474
Basic features of global circulation in the mesopause lower thermosphere region 11 p1662 N85-20475
Winds and waves (4 min - 11 yrs) in the upper middle atmosphere (60-110 km) at Saskatoon, Canada (52 deg N, 107 deg W): MF radar (2.2 MHz) soundings 1973 - 1983 11 p1662 N85-20476
Measurement of the vertical gradient of the semidiurnal tidal wind phase in winter at the 95 km level
11 p1662 N85-20478
Stratwarm effects in the ionospheric D region wind field 11 p1663 N85-20479
Orographic disturbances of upper atmosphere emissions 11 p1663 N85-20480
Turbulence parameters impacting dispersion in an urban convection boundary layer
[PB85-116036] 11 p1662 N85-20598
High time resolution thermospheric temperature and wind studies in the Arctic
[AD-A150114] 12 p1890 N85-21660
Los Alamos MINI-Review: Tracking Antarctic winds
[DE85-004597] 12 p1896 N85-21903
Summary of Meteorological Observations Surface (SMOS), Sigonella, Sicily/Navy
[AD-A150539] 13 p2138 N85-23290
Summary of Meteorological Observations, Surface (SMOS), Alameda, California
[AD-A150609] 13 p2138 N85-23291
Determination of gravity wave envelope solitons on surface of stratified fluid interacting with wind
14 p2334 N85-24433
High-frequency wind wave spectrum in storm basin
14 p2336 N85-24444
Field of point source of low-frequency sound in atmosphere with altitudinally nonuniform wind
15 p2524 N85-25566
Nowcasting applications of VAS
15 p2597 N85-26003
Wind modelling for increased aircraft operational efficiency 16 p2697 N85-26852
Use of a network of telemetered meteorological stations for prediction of the distribution of an atmospheric tracer
16 p2831 N85-27458
A Markov method for simulating non-Gaussian wind speed time series
[DE85-007131] 16 p2835 N85-27485
Propagation of gravity waves in the atmosphere and around critical levels
[KNMI-WR-85-1] 18 p3137 N85-29428
Analysis of ocean surface wind fields using SEASAT-A scatterometer data 18 p3139 N85-29434
Application of climatological analysis to minimize air pollution impacts in California
[PB85-172963] 18 p3149 N85-29502
A survey of the turbulence in the marine surface layer for the operation of low-Reynolds number aircraft
[AD-A154133] 19 p3316 N85-30558
A survey of wind and turbulence modeling methods
[AD-A154470] 20 p3498 N85-31733
Aeolian geomorphology from the global perspective
21 p3603 N85-32373
Diagnostics of severe convection and subsynoptic scale ageostrophic circulations
[NASA-CR-171581] 21 p3634 N85-32571
Notes on atmospheric stability, turbulence, and its measurements
[AD-A155230] 21 p3637 N85-32586
Radar wind profilers in the Colorado network
[PB85-185486] 22 p3817 N85-33647
Evaluation of source strength and dispersion model predications with data from large nitrogen tetroxide field experiments
[DE85-011855] 23 p3947 N85-34465
Program for Regional Observing and Forecasting Services (PROFS)
[PB85-188050] 24 p4124 N85-35569

WIND CIRCULATION
U ATMOSPHERIC CIRCULATION

WIND DIRECTION
Multisensor satellite data integration for sea surface wind speed and direction determination
[NASA-CR-174162] 04 p0542 N85-13446
Development and verification of MCD-2 and MOD-OA simulation models
[DE84-017389] 04 p0550 N85-13499
A diagnostic approach to obtaining planetary boundary layer winds using satellite-derived thermal data
05 p0674 N85-14330
Climate at CRREL (Cold Regions Research and Engineering Laboratory) Hanover, New Hampshire
[AD-A148400] 08 p1189 N85-17495
Analysis of the Viking Lander 1 surface wind vector for sols 45 to 375
[NASA-CR-174349] 09 p1416 N85-18932
Isentropic objective analysis
[PB85-112167] 11 p1688 N85-20617
Portable Automated Mesonet (PAM) data from the 1980 experiment in Anderson Creek Valley
[DE85-004361] 13 p2139 N85-23282
Analysis of the inflow and air-sea interactions in hurricane Frederic 15 p2595 N85-25990
Mean conditions and turbulence statistics at Vandenberg AFB, California
[AD-A151366] 15 p2665 N85-26449
Urban climate and air hygiene before, during, and after the lifework of Helmut Berg. Overview of a branch of applied meteorology 18 p3147 N85-29457
Acrosswind response of towers and stacks of circular cross-section 19 p3282 N85-30354
Practicality of electronic beam steering for MST/ST radars, part 6.2A 21 p3624 N85-32516
Mean flow and turbulence in complex terrain
[AD-A155138] 21 p3636 N85-32583

WIND EFFECTS
Natural environment analysis
[NASA-CR-171333] 10 p1428 N85-19010
Cut-off lows and their influence on the weather in Switzerland
[REPT-45] 10 p1519 N85-19574
Study of pollutant dispersion in an urban street canyon
[DE85-002648] 11 p1677 N85-20571
Algorithms for automatic four-dimensional aircraft guidance, considering the momentary wind situation
[DFVLR-FB-84-40] 12 p1775 N85-21146
Evaluating wind flow around buildings on heliport placement
[FAA-PM-84-25] 12 p1893 N85-21881
On the wind error of the Finnish raingauge
[REPT-37] 12 p1893 N85-21883
The clinical and biomedical evaluation of trauma and fatalities associated with aircrew ejection and crash. A Working Group report
[AGARD-AR-194] 12 p1906 N85-21969
Introduction: The clinical and biomedical evaluation for trauma and fatalities associated with aircrew ejection and crash 12 p1906 N85-21970
List of head/neck injury on ejection in the German Armed Forces from 1972-1981 12 p1906 N85-21972
Portable Automated Mesonet (PAM) data from the 1980 experiment in Anderson Creek Valley
[DE85-004361] 13 p2139 N85-23282
Seasonal and secular variation of the Solis Lacus albedo feature: Relation to the Martian dust-transport cycle
13 p2188 N85-23576
The effect of particle density on aeolian transport
13 p2189 N85-23581
A comparison of terrestrial saltation flux in the laboratory and the field 13 p2189 N85-23582
Statistics of Aeolian surface of Mars
13 p2199 N85-23637
Sea-ice motion in response to geostrophic winds
14 p2323 N85-24357
Local mechanism of equatorial countercurrents
14 p2336 N85-24446
Sound propagation studies for a large horizontal axis wind turbine
[NASA-CR-172564] 14 p2415 N85-24804
Sea breeze-induced mesoscale systems and severe weather 15 p2598 N85-26012
Dynamic and aeroelastic action of guy cables
[VTT-18] 16 p2802 N85-27276
Response of a wind turbine blade to seismic and turbulent wind excitations 16 p2817 N85-27375
On the wind-induced vibrations of a mass-spring system
[REPT-84-04] 17 p2981 N85-28428
Experimental and theoretical determination of the wing-induced lateral wind on the tail surfaces in oscillating rolling motion. Part 2: Theoretical investigations for calculation of the lateral wind
[IFD-1/84-PT-2] 18 p3061 N85-28940
Experiments on the assimilation of patches of data using a barotropic model 18 p3140 N85-29441
Study of drift currents in initial stage of generation of wind waves by laser Doppler anemometer
19 p3291 N85-30408
Frequency of recurrence and critical conditions for generation of Langmuir circulations
19 p3291 N85-30409
Sea surface radio emission at wavelengths 0.86 and 1.3 cm near Brewster angle 19 p3293 N85-30418
Comparative analysis of operational forecasts versus actual weather conditions in airline flight planning, volume 4
[NASA-CR-167865] 24 p4120 N85-35537

WIND ENERGY
U WINDPOWER UTILIZATION

WIND EROSION
Venus 09 p1411 N85-18891
Observed changes at Viking Lander 1
13 p2188 N85-23575
Seasonal and secular variation of the Solis Lacus albedo feature: Relation to the Martian dust-transport cycle
13 p2188 N85-23576
Eolian erosion on Mars: Three scales
13 p2188 N85-23577
Planetary analogs in Antarctica: Mars
13 p2193 N85-23604

WIND MEASUREMENT
NT WIND VELOCITY MEASUREMENT
Detailed analysis of the structure of local wind systems in Canterbury, New Zealand 01 p0075 N85-10501
The altimeter as a support to the scatterometer in the representation of winds and derived wave fields in coastal waters and enclosed seas: A research at its onset
03 p0383 N85-12453
Wind shear measuring on board an airliner
[NASA-TM-77483] 03 p0395 N85-12521
A feasibility study on the use of wind profilers to support Space Shuttle launches
[NASA-CR-3861] 04 p0538 N85-13423
Spatial and temporal interpolation of NEROS radiosonde winds
[PB84-232545] 04 p0540 N85-13436
Measurement-Technical Investigations of Wind Energy Units
[JUEL-SPEZ-244] 05 p0667 N85-14293
Measurement-technical investigations of wind energy units in the short-time range --- spectrum analysis
05 p0668 N85-14294
Measurement-technical problems in the investigation of wind energy units 05 p0668 N85-14295
Measuring system and data evaluation methods of the test field for wind energy units at Pellworm
05 p0668 N85-14296

Measuring methods to determine the static and dynamic behavior of wind energy converters
05 p0668 N85-14297
Measuring-technical investigation of wind energy units from the control-technical, electrical and energetic point of view
05 p0668 N85-14301
Existing measuring systems for wind energy units
05 p0669 N85-14302
Measuring techniques in the measuring program for the windpowered unit GROWIAN
05 p0669 N85-14303
Application of Fabry-Perot spectrometers for measurement of upper atmosphere temperatures and winds
08 p1183 N85-17454
Partial reflection spaced antenna wind measurements
08 p1185 N85-17467
D1 LF wind measurements in the 90 to 100 km height range
08 p1185 N85-17468
Data catalog for the 1982 DFVLR observational Foehn experiment — alpine wind
[DFVLR-FB-84-33] 09 p1358 N85-18543
The effect of the arbitrary level assignment of satellite cloud motion wind vectors on wind analyses in the pre-thunderstorm environment
[NASA-TM-86186] 10 p1517 N85-19565
Cut-off lows and their influence on the weather in Switzerland
[REPT-45] 10 p1519 N85-19574
An evaluation of wind measurements by four Doppler sodars
[PB85-115301] 10 p1520 N85-19586
Measurement of the vertical gradient of the semidiurnal tidal wind phase in winter at the 95 km level
11 p1662 N85-20478
Stratwarm effects in the ionospheric D region wind field
11 p1663 N85-20479
Improved models for increasing wind penetration, economics and operating reliability
[NASA-CR-175538] 11 p1674 N85-20545
The relevance of averaging period to wind power measurements and efficiency of Wind Energy Conversion Systems (WECS)
[GKSS-84-E-35] 11 p1676 N85-20562
Wind-weighting for sounding rockets with a telemetry system
[NASA-TP-2438] 12 p1792 N85-21246
Atmosphere ice-ocean interactions in the Antarctic (IAGO)
14 p2326 N85-24375
An overview of NDBC drifting buoy development programs — NOAA Data Buoy Center (DBC)
14 p2332 N85-24422
Low-frequency oscillations of sea level and group structure of wind waves
14 p2335 N85-24441
Experimental results of temperature-wind soundings of the atmosphere by the radio acoustical method
14 p2340 N85-24471
Wind observation station description for Den Helder (period 1843-1972) and De Kooy (period 1955-1980)
[KNMI-TR-42] 14 p2379 N85-24686
Application of infrared radiometers for airborne detection of clear air turbulence and low level wind shear, airborne infrared low level wind shear detection test
[NASA-CR-175725] 15 p2594 N85-25985
Wind modelling for increased aircraft operational efficiency
16 p2697 N85-26652
Analysis of the NASA/MSFC airborne Doppler lidar results from San Gorgonio Pass, California
[NASA-CR-3901] 16 p2832 N85-27463
Influence of coherent mesoscale structures on satellite-based Doppler lidar wind measurements
[NASA-CR-175853] 16 p2833 N85-27467
Analysis of ocean surface wind fields using SEASAT-A scatterometer data
16 p3139 N85-29434
Using regression analysis for determining air data sensor errors by means of an inertial navigation system
[ESA-TT-886] 20 p3392 N85-31041
Tropical Ocean and Global Atmosphere (TOGA) heat exchange project: A summary report
[NASA-CR-178038] 20 p3496 N85-31738
Facility for large-scale hazardous gas testing
[DE85-011852] 21 p3564 N85-32169
Performance of the Colorado wind-profiling network, part 1.5A
21 p3617 N85-32475
Potential advantages of the spaced antenna method for operational wind profiling, part 3.1B
21 p3620 N85-32490
Determination of horizontal and vertical wavelengths of gravity waves in the mesosphere by spaced wind measurements
21 p3623 N85-32510
Elimination of range-aliased echoes in the VHF radars
21 p3625 N85-32521
Data base for the Colorado profiling network
21 p3627 N85-32533
Verification of Doppler sodar measurements — atmospheric boundary layer
[KNMI-WR-85-2] 22 p3817 N85-33645

WIND PRESSURE
The relevance of averaging period to wind power measurements and efficiency of Wind Energy Conversion Systems (WECS)
[GKSS-84-E-35] 11 p1676 N85-20562
The theoretical response of a vertical line array to wind-generated noise in shallow water
[AD-A151730] 16 p2860 N85-27636

WIND PROFILES
Structural design guidelines for heliports
[FAA-PM-84-23] 02 p0149 N85-11010
Wave phase velocity in a wind gradient — gravity waves
04 p0523 N85-13343
A feasibility study on the use of wind profilers to support Space Shuttle launches
[NASA-CR-3861] 04 p0538 N85-13429
Spatial and temporal interpolation of NERIS radiosonde winds
[PB84-232545] 04 p0540 N85-13438
Calms processor (CALMPRO) user's guide
[PB84-229467] 04 p0540 N85-13439
Error analysis of wind determined using a VLF Omega sonde
[WSRL-0361-TM] 06 p0838 N85-15321
Diurnal and seasonal patterns of temperature and wind flow in the planetary boundary layer for ten locations in complex terrain
[PB85-106696/GAR] 06 p0840 N85-15333
Atmospheric environment for Space Shuttle (STS-41G) launch
[NASA-TM-86486] 07 p0995 N85-16320
Natural environment analysis
[NASA-CR-174330] 08 p1180 N85-17433
Global scale diagnoses of FGGE data
[NASA-CR-174356] 09 p1356 N85-18533
Spring changeover of the middle atmosphere circulation compared with rocket wind data up to 80 km
11 p1661 N85-20466
Measurement of the vertical gradient of the semidiurnal tidal wind phase in winter at the 95 km level
11 p1662 N85-20478
Stratwarm effects in the ionospheric D region wind field
11 p1663 N85-20479
Phased antenna array for wind profiling applications
[PB85-132884] 12 p1837 N85-21529
Oceanographic and meteorological research based on the data products of SEASAT
[E85-10091] 12 p1874 N85-21753
High time resolution thermospheric temperature and wind studies in the Arctic
[AD-A150114] 12 p1890 N85-21860
Atmospheric environment for Space Shuttle (STS-51A) launch
[NASA-TM-86497] 12 p1892 N85-21875
Preliminary study of inphase gusts and moment force wind loads over the first 150 meters at KSC, Florida
[NASA-TM-86501] 13 p2137 N85-23273
Thermospheric winds observed by OI6300A Doppler shifts at 23 deg S in the Brazilian sector
[INPE-3384-RPE/470] 16 p2834 N85-27479
Analysis of ocean surface wind fields using SEASAT-A scatterometer data
18 p3139 N85-29434
Specification of surface roughness over oceans in the GLAS Fourth Order GCM
18 p3142 N85-29455
Additional possibilities of radiometeor azimuthal method for measuring wind velocity in lower thermosphere
19 p3296 N85-30438
The micrometeorology of an Amazonian rainforest
[INPE-3515-PRE/740] 19 p3315 N85-30551
An examination of the Southern Oscillation in the upper troposheric tropical and subtopical wind field
20 p3488 N85-31680
Performance of the Colorado wind-profiling network, part 1.5A
21 p3617 N85-32475
Potential advantages of the spaced antenna method for operational wind profiling, part 3.1B
21 p3620 N85-32490
High resolution evidence for the Garrett-Munk spectrum of stratospheric gravity waves
21 p3622 N85-32503
On the spectrum of atmospheric velocity fluctuations seen by MST/ST radar and their interpretation
21 p3622 N85-32504
Relationship of isolated turbulent regions to the general turbulent background, part 4.4A
21 p3623 N85-32508
Testing and optimizing MST coaxial collinear arrays, part 6.4A
21 p3625 N85-32518
Elimination of range-aliased echoes in the VHF radars
21 p3625 N85-32521
Data base for the Colorado profiling network
21 p3627 N85-32533
Recent results at the Sunset radar
21 p3627 N85-32536
Progress and plans for the Colorado Wind Profiler Network
21 p3628 N85-32542
Method and apparatus for four-beam radar
[PB85-181477] 22 p3757 N85-33289
Verification of Doppler sodar measurements — atmospheric boundary layer
[KNMI-WR-85-2] 22 p3817 N85-33645
Radar wind profilers in the Colorado network
[PB85-185486] 22 p3817 N85-33647
User's guide to the MATHEW/ADPIC models
[DE85-012952] 23 p3966 N85-34587
Determination of vertical air velocity using measurements of the aircraft motion
24 p4121 N85-35545
Control variables in vertical wind determination using simple flight-mechanical equations
24 p4121 N85-35546

WIND SHEAR
The microburst as a hazard to aviation: Structure, mechanisms, and nowcasting
01 p0074 N85-10481
Microburst wind structure and evaluation of Doppler radar for wind shear detection
[DOT/FAA/PM-84/29] 02 p0230 N85-11501
A spatial model of wind shear and turbulence for flight simulation
03 p0395 N85-12518
Wind shear measuring on board an airliner
[NASA-TM-77463] 03 p0395 N85-12521
Conditional symmetric instability and mesoscale rainbands
05 p0678 N85-14356
Jet stream errors and tropospheric-stratospheric interactions in the GLAS general circulation model
05 p0683 N85-14382
Statistics from the operation of the low-level wind shear alert system (LLWAS) during the Joint Airport Weather Studies (JAWS) Project
[DOT/FAA/PM-84/32] 06 p0750 N85-14804
Critical conditions for the automatic control of landing from decision height in variable winds
[UTIAS-284] 06 p0753 N85-14830
Combined effects of baroclinic and barotropic instability in a nonlinear low order model
[DM-41] 09 p1358 N85-18544
The effect of the arbitrary level assignment of satellite cloud motion wind vectors on wind analyses in the pre-thunderstorm environment
[NASA-TM-86186] 10 p1517 N85-19565
Wind shear detection technology
[GPO-38-920] 12 p1893 N85-21879
Intensification of tropical instabilities
[AD-A149985] 12 p1896 N85-21899
Total energy-rate feedback for automatic glide-slope tracking during wind-shear penetration
[NASA-TP-2412] 14 p2226 N85-23801
Long nonlinear waves in layers of sudden changes in wind velocity
14 p2340 N85-24470
Application of infrared radiometers for airborne detection of clear air turbulence and low level wind shear, airborne infrared low level wind shear detection test
[NASA-CR-175725] 15 p2594 N85-25985
Radar turbulence estimates. Effects of wind shear and reflectivity factor gradients
[AD-A151875] 15 p2599 N85-26023
The use of pressure sensing taps on the aircraft wing as sensor for flight control systems
16 p2698 N85-26660
Contributions on the subject of longhudinal movements of aircraft in wind shears
[NASA-TM-77837] 18 p3139 N85-29432
Effect of vertical shear on regional-scale trajectories in near-frontal conditions
[DE85-007554] 19 p3317 N85-30561
A survey of wind and turbulence modeling methods
[AD-A154470] 20 p3496 N85-31733

WIND TUNNEL APPARATUS
Preliminary results using a rapid photographic wake traverse system — in a wind tunnel
[RAE-TM-AERO-1987] 02 p0200 N85-11332
Measurement data acquisition and processing system for wind rotor measurements in the wind channel of Bremen University
05 p0668 N85-14298
Procedural aspects of testing aerodynamic models with combustion in high-enthalpy transient-mode installations
05 p0725 N85-14858
Analytical and physical modeling program for the NASA Lewis Research Center's Altitude Wind Tunnel (AWT)
[NASA-TM-86919] 07 p0909 N85-15757
The NASA Altitude Wind Tunnel (AWT): Its role in advanced icing research and development
[NASA-TM-86920] 07 p0910 N85-15758
Six-component strain gage block scale 167-6B. Part 1: Calibration, September 1983
[F+W-FO-1899] 07 p0968 N85-16143
Numerical analysis of the first static calibration of the RSRA helicopter active-isolator rotor balance system
[NASA-TM-85975] 08 p1083 N85-16863
A new fast response probe for diffusion studies in atmospheric air — pollution modeling
[IC-AERO-84-01] 08 p1180 N85-17437

The S2MA wind tunnel at the Modane-Avrieux aerodynamic test center
[ESA-TT-862] 09 p1284 N85-18071
Development of an artificial boundary layer for different outlet flows 14 p2212 N85-23719
Investigation of the conditions for tripping transition with roughness elements and their influence on boundary layer development 14 p2212 N85-23720
Transition detection using surface pressure holes 14 p2212 N85-23722
Investigations of the experimental detection of boundary layer transitions 14 p2213 N85-23723
Prediction of vortex-induced loads on wind-tunnel turning vanes
[NASA-TM-86678] 15 p2462 N85-25204
The ONERA establishment at Cannes in the service of aeronautical research
[ESA-TT-875] 15 p2475 N85-25276
Qualification of a wall gage for the SIMA wagon, adapted to the test of half models motorized by compressed air turbines — SIMA wind tunnel
[ONERA-PV-1/6068-GY] 16 p2701 N85-26677
Study on needs for a magnetic suspension system operating with a transonic wind tunnel
[NASA-CR-3900] 16 p2715 N85-26759
An automatic traversing system for Laser Doppler Anemometer (LDA) applications to wind tunnels and to free jets
[ISL-CO-225/83] 16 p2936 N85-27490
Construction 1976-1980: Design, manufacturing, calibration of the German-Dutch wind tunnel (DNW)
17 p2905 N85-27913
Effect of superconducting solenoid model cores on spanwise iron magnet roll control
[NASA-TM-86378] 17 p2905 N85-27915
Cryogenic test technology, 1984
[AGARD-AR-212] 18 p3068 N85-29116
A computer-controlled traverse gear for the Oxford wind engineering research group's 4 metre x 2 metre wind tunnel
[OUEL-1525/84] 20 p3463 N85-31514
Gust simulation for flight mechanical wind tunnel tests
24 p4062 N85-35172

WIND TUNNEL BALANCES
U WEIGHT INDICATORS
U WIND TUNNEL APPARATUS

WIND TUNNEL CALIBRATION
Wind tunnel calibration of a hemispherical head angle of attack and angle of sideslip indicator
[FFA-TN-1984-11] 02 p0135 N85-10923
Langley Mach 4 scramjet test facility
[NASA-TM-86277] 08 p1089 N85-16883
Calibration of wind tunnel flow quality
13 p1976 N85-22389
A preliminary investigation of the dynamic force-calibration of a magnetic suspension and balance system
[NASA-CR-172580] 14 p2228 N85-23808

WIND TUNNEL MODELS
Pressure distributions measured on research wing M100 mounted on an axisymmetric body
01 p0004 N85-10023
Problem of reduction to ideal wind tunnel in experimental aerodynamics 02 p0260 N85-11702
An appraisal of an out-of-phase feed-back system for the variation of damping of dynamic wind-tunnel models
[NMI-189] 03 p0320 N85-12065
Singularity model for the analysis of wall interference in closed wind tunnels according to the wall pressure signature method (blockage and lift)
[FW-FO-1612] 04 p0453 N85-12874
Comparative flow calculation on transonic cone/cylinder standard models in connection with the wall interference problem
[FW-FO-1689] 04 p0453 N85-12878
Manufacturing report of an augmented lift, variable deflection half wing
[ONERA-RT-25/1736-AY-108-A]
05 p0591 N85-13766
Procedural aspects of testing aerodynamic models with combustion in high-enthalpy transient-mode installations
05 p0725 N85-14658
A preliminary study of using a strain-gauged balance and parameter estimation techniques for the determination of aerodynamic forces on a model in a very short duration wind tunnel
[AD-A146473] 06 p0810 N85-15145
Analysis of the flow field about a T-45 using PANAIR
[AD-A146811] 07 p0899 N85-15699
Experiences with the use of a side-strut model support system for high angles of attack in the Trinsonik wind tunnel TMK
[DFVLR-MITT-84-09] 07 p0910 N85-15763
Joined wing transonic design and test validation
[AD-A146355] 08 p1078 N85-16834
A voice-actuated wind tunnel model leak checking system
[NASA-TM-86359] 09 p1263 N85-17936
The generation of rolling moments with the superconducting solenoid model
[NASA-CR-172520] 09 p1283 N85-18068
Initial investigation of cryogenic wind tunnel model filler materials
[NASA-TM-86363] 09 p1283 N85-18069
Unsteady transonic pressure measurements on a semispan wind-tunnel model of a transport-type supercritical wing (Lann model). Part 2: Pressure distributions (plotted) and plots of the vibration modes
[AD-A130488] 10 p1421 N85-18965
Wall interference estimation of the NAL's two-dimensional wind tunnel
[NAL-TR-829] 10 p1426 N85-18992
Flight mechanics analysis of dynamic derivatives of the Dornier variable wind tunnel model
[ESA-TT-854] 11 p1577 N85-19937
Technology for pressure-instrumented thin airfoil models, phase 1
[NASA-CR-3891] 14 p2227 N85-23804
An exploratory study of apex fence flaps on a 74 deg delta wing
[NASA-CR-172463] 15 p2463 N85-25208
The design and operation of a simple low-speed flutter-suppression model
[AD-A151610] 15 p2474 N85-25269
Synthesis study: Validation of a gust generator in the presence of a model in a wind tunnel
[ONERA-RT-16/5108-RY-051]
16 p2701 N85-26678
The application of numerical control (NC) in manufacturing wind tunnel models
[B6580078] 17 p2939 N85-28140
Analysis of heat-transfer measurements from 2 AEDC wind tunnels on the Shuttle external tank
[NASA-CR-171470] 17 p2957 N85-28263
Heating parameter estimation using coaxial thermocouple gages in wind tunnel test articles
[AD-A153039] 17 p2968 N85-28328
Materials and techniques for model construction
[NASA-CR-172620] 20 p3396 N85-31066
Experiences with the use of a side-strut model support system for high angles for attack in the TMK Trinsonik Wind Tunnel
[ESA-TT-895] 20 p3396 N85-31069
Preliminary investigation of dispersion of pollutants in model building wake flows using bipolar space charge
[IC-AERO-84-04] 20 p3487 N85-31671
A systematic plan for the continued study of dimensional stability of metallic alloys considered for the fabrication of cryogenic wind tunnel models
[NASA-CR-172449] 21 p3565 N85-32172
Machining-induced deformation in stepped specimens of PH 13-8 Mo, 18 nickel maraging steel grade 200T1 and grain-refined HP 9-4-20
[NASA-CR-172450] 21 p3565 N85-32177
Two-plane balance and slip-ring design
22 p3799 N85-33536

WIND TUNNEL STABILITY TESTS
Experimental and theoretical determination of the wing-induced lateral wind on the tail surfaces in oscillating rolling motion. Part 1: Application of the Mobile Oscillating Derivatives (MOD) on an experimental part
[IFD-1/84-PT-1] 18 p3061 N85-28939

WIND TUNNEL TESTS
Transonic wing and far field test data on a high aspect ratio transport wing for three dimensional computational method evaluation 01 p0004 N85-10021
Transonic wing and far field test data on a moderate aspect ratio wing for three dimensional computational method evaluation 01 p0004 N85-10022
Pressure distributions measured on research wing M100 mounted on an axisymmetric body
01 p0004 N85-10023
Pressure distributions measured on research wing M86 mounted on an axisymmetric body
01 p0004 N85-10024
DFVLR rotorcraft: Construction and engineering
[NASA-TM-77740] 01 p0006 N85-10035
Results of tests of advanced flexible insulation vortex and flow environments in the North American Aerodynamics Laboratory lowspeed wind tunnel using 0.0405-scale Space Shuttle Orbiter model 16-0 (test OA-309)
[NASA-CR-167692] 01 p0015 N85-10096
Planar jets impinging on various obstacles and some modes of flow oscillation
[MPIS-MITT-78] 01 p0048 N85-10317
Data input, processing and presentation — helicopter rotor balance measurement
[NASA-TM-77739] 01 p0125 N85-10858
Design and wind tunnel evaluation of a symmetric airfoil series for large wind turbine applications
[NASA-CR-174764] 02 p0135 N85-10919
Results of winglet development studies for DC-10 derivatives
[NASA-CR-3677] 02 p0138 N85-10936
Space Shuttle wind tunnel testing program
[NASA-RP-1125] 02 p0167 N85-11127
Experimental study of Mach reflection of weak shock waves 02 p0260 N85-11703
Analysis of noise measured from a propeller in a wake
[NASA-TP-2358] 02 p0274 N85-11788
Wall interference measurements for three-dimensional models in transonic wind tunnels: Experimental difficulties 03 p0311 N85-12012
Survey of ONERA activities on adaptive-wall applications and computation of residual corrections
03 p0312 N85-12013
Assessment of lift- and blockage-induced wall interference in a three-dimensional adaptive-wall tunnel
03 p0312 N85-12016
Wind tunnel wall interference correction for aircraft models 03 p0314 N85-12029
Determination of equivalent model geometry for tunnel wall interference assessment/correction
03 p0314 N85-12031
Experiences with a high-blockage model tested in the NASA Ames 12-foot pressure wind tunnel
03 p0315 N85-12032
Experimental and predicted heating distributions for biconics at incidence in air at Mach 10
[NASA-TP-2334] 03 p0361 N85-12313
Laser anemometer study of separated flow on wing profiles
[ISL-CO-214/83] 04 p0453 N85-12872
Wall adaptation at Mach 1.2 — wind tunnel tests
[ONERA-RTS-26/3075-AY-402]
04 p0453 N85-12873
Singularity model for the analysis of wall interference in closed wind tunnels according to the wall pressure signature method (blockage and lift)
[FW-FO-1612] 04 p0453 N85-12874
Wall influence corrections in wind tunnels: Blockage correction according to the wall pressure signature method
[FW-FO-1613] 04 p0453 N85-12875
Parametric determination of blockage interference of 3-dimensional models in the Emmen Federal Aircraft works transonic tunnel (Switzerland)
[FW-FO-1636] 04 p0453 N85-12876
Investigations of boundary layers in the Emmen Federal Aircraft works transonic tunnel, Switzerland
[FW-FO-1641] 04 p0453 N85-12877
Comparative flow calculation on transonic cone/cylinder standard models in connection with the wall interference problem
[FW-FO-1689] 04 p0453 N85-12878
Flight and wind-tunnel comparisons of the inlet-airframe interaction of the F-15 airplane
[NASA-TP-2374] 04 p0455 N85-12884
Evaluation of the Langley 4- by 7-meter tunnel for propeller noise measurements
[NASA-TM-85721] 04 p0558 N85-13553
First cryogenic test of the CAST 7 profile in the T2 wind tunnel. Comparison with calculations — airfoils
[ONERA-RTS-58/1685-AY-035-D]
04 p0577 N85-13682
Amiet shear layer correction with an additional temperature gradient considered: Nomograms for the correction of noise signatures from open jet wind tunnel tests
[DFVLR-MITT-84-11] 05 p0726 N85-14669
Static internal performance of single-expansion-ramp nozzles with various combinations of internal geometric parameters
[NASA-TM-86270] 06 p0749 N85-14797
A preliminary study of using a strain-gauged balance and parameter estimation techniques for the determination of aerodynamic forces on a model in a very short duration wind tunnel
[AD-A146473] 06 p0810 N85-15145
Effects of body shape on the aerodynamics of a body of revolution at Mach numbers from 1.6 to 4.6
[NASA-TM-86345] 07 p0893 N85-15657
Analytical modeling of circuit aerodynamics in the new NASA Lewis wind tunnel
[NASA-TM-86912] 07 p0897 N85-15688
Aileron effectiveness for a subsonic transport model with a high-aspect-ratio supercritical wing
[NASA-TM-85674] 07 p0898 N85-15695
The UH-1H helicopter icing flight test program: An overview
[NASA-TM-86925] 07 p0900 N85-15702
Installed nacelle drag-improvement tests of an M = 0.8 turboprop transport configuration
[NASA-TM-84302] 07 p0902 N85-15716

Analytical and physical modeling program for the NASA Lewis Research Center's Altitude Wind Tunnel (AWT)
[NASA-TM-86919] 07 p0909 N85-15757
The NASA Altitude Wind Tunnel (AWT): Its role in advanced icing research and development
[NASA-TM-86920] 07 p0910 N85-15758
Stereo Electro-optical Tracking System (SETS)
[NASA-CR-172471] 07 p0962 N85-16098
Investigations into the effects of scale and compressibility on lift and drag in the RAE 5m pressurized low-speed wind tunnel 08 p1068 N85-16773
Results of S5 CH tests with an ARL (Aerospace Research Laboratory) cascade
[NASA-TM-77510] 08 p1089 N85-16882
A wind-tunnel study of the saltation of heterogeneous (size, density) sands 08 p1182 N85-17449
Research done at DERAT (October 1982 through September 1983); summary of principal results obtained
[NASA-TM-77786] 08 p1228 N85-17730
Corrections for attached sidewall boundary-layer effects in 2-dimensional airfoil testing
[NASA-CR-3673] 09 p1272 N85-17997
Effect of jet exit vanes on flow pulsations in an open-jet wind tunnel
[NASA-TM-86299] 09 p1273 N85-17999
Subsonic and transonic pressure measurements on a high-aspect-ratio supercritical-wing model with oscillating control surfaces
[NASA-TM-83201] 09 p1273 N85-18004
The Altitude Wind Tunnel (AWT): A unique facility for propulsion system and adverse weather testing
[NASA-TM-86921] 09 p1283 N85-18067
Static internal performance of a two-dimensional convergent nozzle with thrust-vectoring capability up to 60 deg
[NASA-TP-2391] 10 p1419 N85-18951
Space Shuttle Orbiter trimmed center-of-gravity extension study. Volume 9: Effects of configuration modifications on the aerodynamic characteristics of the 140 A/B Orbiter at Mach numbers of 1.5, 2.0, and 2.5 — wind tunnel tests
[NASA-TM-72661-VOL-9] 10 p1420 N85-18956
Unsteady transonic pressure measurements on a semispan wind-tunnel model of a transport-type supercritical wing (Lann model). Part 2: Pressure distributions (plotted) and plots of the vibration modes
[AD-A130486] 10 p1421 N85-18965
Low-speed wind tunnel tests of the NAL fan-jet STOL research aircraft model with ground simulation by tangential blowing
[NAL-TR-826] 10 p1423 N85-18976
Study of several factors affecting crew escape trajectories from the Space Shuttle Orbiter at low-subsonic speeds
[NASA-TM-86303] 10 p1428 N85-19008
Post stall airfoil data for wind turbines: Wind tunnel test results
[DE85-004052] 10 p1511 N85-19534
Fluctuating pressures on fan blades of a turbofan engine, flight test investigation
[NASA-TP-2381] 10 p1553 N85-19790
Wind-tunnel investigation of a full-scale canard-configured general aviation airplane
[NASA-TP-2382] 11 p1575 N85-19925
Flight mechanics analysis of dynamic derivatives of the Dornier variable wind tunnel model
[ESA-TT-854] 11 p1577 N85-19937
Unsteady aerodynamic characterization of a military aircraft in vertical gusts
[NASA-TM-77810] 12 p1770 N85-21110
Measured unsteady transonic aerodynamic characteristics of an elastic supercritical wing with an oscillating control surface
[NASA-TM-86376] 12 p1771 N85-21116
Unsteady transonic pressure measurements on a semi-span wind-tunnel model of a transport-type supercritical wing (Lann model). Part 2: Pressure distributions (plotted) and plots of the vibration modes
[AD-A130486] 12 p1846 N85-21579
Exploratory flutter test in a cryogenic wind tunnel
[NASA-TM-86380] 12 p1863 N85-21689
Further comparison of wind tunnel and airplane acoustic data for advanced design high speed propeller models
[NASA-TM-86935] 12 p1927 N85-22106
Dynamic wind tunnel testing for active control research 13 p1966 N85-22352
Dynamic wind-tunnel testing of active controls by the NASA Langley Research Center
13 p1966 N85-22353
Effects of leading-edge devices on the low-speed aerodynamic characteristics of a highly-swept arrow-wing
[NASA-CR-172531] 13 p1968 N85-22365
Investigations into the effects of scale and compressibility on lift and drag in the RAE 5m pressurised low-speed wind tunnel
[RAE-TM-AERO-2006] 13 p1969 N85-22372
Deflected jet experiments in a turbulent combustor flowfield
[NASA-CR-174863] 13 p1973 N85-22390
Cryogenic wind tunnels: A selected annotated bibliography
[NASA-TM-86346] 13 p1976 N85-22401
Results of aeroheating DFI and ET design-data test on a 0.0175-scale model 60-OTS conducted in the Von Karman Gas Dynamics Facility (VKF) 40° supersonic and the 50° hypersonic wind tunnels A and C
[NASA-CR-167693] 13 p1988 N85-22466
Results of the AFRSI rewaterproofing systems screening test in the NASA/Ames Research Center (ARC) 2 x 2-foot transonic wind tunnel
[NASA-CR-167694] 13 p1988 N85-22467
Results of a M = 5.3 heat transfer test of the integrated vehicle using phase-change paint techniques on the 0.0175-scale model 56-OTS in the NASA/Ames Research Center 3.5-foot hypersonic wind tunnel
[NASA-CR-167695] 13 p1988 N85-22468
CARD's low-speed wind tunnel described
13 p2052 N85-22849
Wind tunnel acoustic study of a propeller installed behind an airplane empennage: Data report
[NASA-CR-177335] 13 p2154 N85-23377
The effect of particle density on aeolian transport
13 p2189 N85-23581
Potential bedforms on Venus: Wind tunnel simulations
13 p2189 N85-23583
Microdunes and other aeolian bedforms on Venus: Wind tunnel simulations 13 p2189 N85-23584
Estimating unsteady aerodynamic forces on a cascade in a three-dimensional turbulence field
[NASA-TM-86701] 14 p2209 N85-23704
Low-speed stability and control wind-tunnel investigations of effects of spanwise blowing on fighter flight characteristics at high angles of attack — Langely 12-ft low-speed tunnel and 30- by 60-ft tunnel
[NASA-TP-2431] 14 p2210 N85-23708
Recent transonic unsteady pressure measurements at the NASA Langley Research Center
[NASA-TM-86406] 14 p2210 N85-23710
Boundary layer control by transition fixing — conference
[DFVLR-MITT-84-17] 14 p2211 N85-23712
Problems of the application of wind tunnel results to aerodynamic performance of large aircraft
14 p2211 N85-23713
Transition fixing on wings in industrial wind tunnels and associated problems 14 p2212 N85-23717
Transition detection using surface pressure holes
14 p2212 N85-23722
Investigations of the experimental detection of boundary layer transitions 14 p2213 N85-23723
Investigation of the aerodynamic forces on bluff bodies at high Reynolds numbers
[DFVLR-MITT-84-19] 14 p2213 N85-23727
Qualification of the T2 wind tunnel in cryogenic operation. B: Flow fluctuations, particle detection and qualification
[NASA-TM-77782] 14 p2227 N85-23806
Space Shuttle aerothermodynamic data report, phase C
[NASA-CR-171858] 14 p2241 N85-23897
China report: Science and technology
[JPRS-CST-84-012] 14 p2263 N85-24140
Harbin's subsonic, transonic wind tunnel detailed
14 p2263 N85-24143
Transonic pressure distributions on a two-dimensional 0012 and supercritical MBB-A3 profile oscillating in heave and pitch 15 p2457 N85-25173
Analysis of transonic aerodynamic characteristics for a supercritical airfoil oscillating in heave, pitch and with oscillating flap 15 p2458 N85-25175
An exploratory study of apex fence flaps on a 74 deg delta wing
[NASA-CR-172463] 15 p2463 N85-25208
Investigation of the Vortex Tab
[NASA-CR-172586] 15 p2463 N85-25209
Behavior of turbulent gas jets in an axisymmetric confinement
[NASA-CR-174829] 15 p2473 N85-25265
Experiments in dilution jet mixing effects of multiple rows and non-circular orifices
[NASA-TM-86996] 15 p2473 N85-25266
The ONERA establishment at Cannes in the service of aeronautical research
[ESA-TT-875] 15 p2475 N85-25276
An evaluation of proposed acoustic treatments for the NASA LaRC 4 x 7 meter wind tunnel
[NASA-CR-172577] 15 p2646 N85-26319
La Recherche Aerospatiale Bimonthly Bulletin Number 1984-2, 219/March-April
[ESA-TT-878] 16 p2694 N85-26635
Low Reynolds number vehicles
[AGARD-AG-288] 16 p2699 N85-26666
Exploratory wind-tunnel investigation of a wingtip-mounted vortex turbine for vortex energy recovery
[NASA-TP-2468] 16 p2699 N85-26667
An experimental and analytical study of the aerodynamic interference effects between two Sears-Haack bodies at Mach 2.7
[NASA-TM-85729] 16 p2700 N85-26673
Measurements of the symmetric aerodynamic coefficients for flat faced cylinders in the angle of attack regime 0 to 90 deg for transonic and supersonic speeds
[FFA-TN-1984-04] 16 p2700 N85-26675
Measurements in low pressure flow using an electronic beam detector — wind tunnel tests
16 p2701 N85-26676
Synthesis study: Validation of a gust generator in the presence of a model in a wind tunnel
[ONERA-RT-16/5108-RY-051]
16 p2701 N85-26678
Preliminary wind tunnel study of the influence of a jet on the unsteady aerodynamics of a turbojet engine
[ONERA-RT-12/5115-RY-230-R-231G]
16 p2701 N85-26679
Wing buffeting active control testing on a transport aircraft configuration in a large sonic tunnel
16 p2714 N85-26760
An experimental study of compressible turbulent reattaching free shear layers 16 p2781 N85-27181
Wing tunnel investigation of dynamic stall of an NACA 0018 airfoil oscillating in pitch
[NAE-AN-27] 17 p2892 N85-27830
Design of a basic profile for a low sweep airfoil. Part 2: Experimental investigation on the DFVLR-W1 airfoil profile in the Brunswick transonic wind tunnel
[DFVLR-FB-85-01-PT-2] 17 p2892 N85-27833
Rotorcraft research testing in the National Full-Scale Aerodynamics Complex at NASA Ames Research Center
[NASA-TM-86687] 17 p2896 N85-27854
Wing buffeting active control testing on a transport aircraft configuration in a large sonic windtunnel
17 p2904 N85-27903
Background noise measurements from jet exit vanes designed to reduced flow pulsations in an open-jet wind tunnel
[NASA-TM-86383] 17 p2906 N85-27916
The gust simulation apparatus of the 3m x 3m low speed wind tunnel of the DFVLR in Goettingen, West Germany
[DFVLR-FB-85-04] 17 p2908 N85-27920
Analysis of heat-transfer measurements from 2 AEDC wind tunnels on the Shuttle external tank
[NASA-CR-171470] 17 p2957 N85-28263
Heating parameter estimation using coaxial thermocouple gages in wind tunnel test articles
[AD-A153039] 17 p2968 N85-28328
Wind-tunnel evaluation of a 21-percent-scale powered model of a prototype advanced scout helicopter
[NASA-TP-2420] 18 p3058 N85-28923
Static investigation of several yaw vectoring concepts on nonaxisymmetric nozzles
[NASA-TP-2432] 18 p3058 N85-28924
Gust load alleviation of a cantilevered rectangular elastic wing. Wind tunnel experiment and analysis
[NAK-TR-66] 18 p3063 N85-28950
Cryogenic test technology, 1984
[AGARD-AR-212] 18 p3088 N85-29116
Activities of the Department of Aerospace Engineering
18 p3109 N85-29844
Inviscid analysis of two supercritical laminar-flow-control airfoils at design and off-design conditions
[NASA-TM-84657] 19 p3212 N85-29920
Effect of leading-edge load constraints on the design and performance of supersonic wings
[NASA-TP-2446] 19 p3213 N85-29923
Nacelle/pylon/wing integration on a transport model with a natural laminar flow nacelle
[NASA-TP-2439] 19 p3213 N85-29924
High Reynolds number tests of a NASA SC(3)-0712(B) airfoil in the Langley 0.3-meter transonic cryogenic tunnel
[NASA-TM-86371] 19 p3213 N85-29926
Pressure distribution from high Reynolds number tests of a NASA SC(3)-0712(B) airfoil in the Langley 0.3-meter transonic cryogenic tunnel
[NASA-TM-86370] 19 p3213 N85-29927
Low-speed wind-tunnel tests of an advanced eight-bladed propeller
[NASA-TM-86364] 19 p3214 N85-29928
A numerical solution of a nonisothermal wall using the two-dimensional Navier-Stokes equations
[AD-A154467] 19 p3266 N85-30257

Acrosswind response of towers and stacks of circular cross-section 19 p3262 N85-30354
Selected topics in experimental aeroelasticity at the NASA Langley Research Center
[NASA-TM-86436] 19 p3284 N85-30364
Computer program for plotting and fairing wind-tunnel data
[NASA-TM-85648] 20 p3387 N85-31009
Low-speed tests of a high-aspect-ratio, supercritical-wing transport model equipped with a high-lift flap system in the Langley 4- by 7-meter and Ames 12-foot pressure tunnels
[NASA-TP-2097] 20 p3388 N85-31010
Real scale test of the Petit Canard aircraft in the number 3 section, 47 sqm, of the SIMA wind tunnel, May 1984
[ONERA-PV-1/8136-GY] 20 p3389 N85-31018
Aerodynamic measurement of the wind flow in the number two section of the SIMA wind tunnel
[ONERA-PV-1/8138-GY] 20 p3389 N85-31019
Transonic and supersonic wind tunnel tests on control effectiveness on schematic missile configurations
[FFA-TN-1983-20] 20 p3389 N85-31020
Transonic and supersonic wind tunnel tests on control effectiveness on schematic missile configurations: Supplement
[FFA-TN-1983-20-SUPPL] 20 p3389 N85-31021
Data set 8: ZKP wing, oscillating aileron
20 p3390 N85-31029
Reverberation effects on directionality and response of stationary monopole and dipole sources in a wind tunnel
[NASA-TM-87063] 20 p3453 N85-31443
Preliminary wind tunnel experiments to investigate the effect of heat transfer on the dispersion of cold dense gases
[OUEL-1546/84] 20 p3456 N85-31467
Amiet shear layer correction with an additional temperature gradient considered: Nomograms for the correction of noise signatures from open jet wind tunnel tests
[ESA-TT-897] 20 p3525 N85-31926
Aerodynamic characteristics of the standard dynamics model in coning motion at Mach 0.6
[NASA-TM-86717] 21 p3552 N85-32094
Wind tunnel drag evaluations of helicopter nose sections
[AD-A155489] 21 p3553 N85-32100
The collected data for ramp function tests on a NACA 23012 aerofoil. Volume 1: Description and pressure data
[GU-AERO-8413-VOL-1] 23 p3894 N85-34123
An investigation into the three-dimensional stall development on a modified NACA 23012 aerofoil
[GU-AERO-8414] 23 p3894 N85-34124
Prediction of the flow-field interference induced by the long-range laser velocimeter in the Ames 40- by 80-foot and the 80- by 120-foot wind tunnels
[NASA-TM-86763] 23 p3898 N85-34148
Reflection plane tests of a wind turbine blade tip section with ailerons
[NASA-TM-87016] 23 p3945 N85-34444
Presentation of the acoustic and aerodynamic results of the Aladin 2 concept qualification testing
[NASA-TM-77683] 24 p4060 N85-35161
Gust simulation for flight mechanical wind tunnel tests
24 p4062 N85-35172
The influence of helicopter tail shape on drag: An aerodynamic study using a low speed wind tunnel
[AD-A156304] 24 p4062 N85-35174
Miniature infra-red data acquisition and telemetry system
[NASA-CR-177953] 24 p4096 N85-35390

WIND TUNNEL WALLS

Wind Tunnel Wall Interference Assessment and Correction, 1983
[NASA-CP-2319] 03 p0311 N85-12011
Wall interference measurements for three-dimensional models in transonic wind tunnels: Experimental difficulties 03 p0311 N85-12012
Survey of ONERA activities on adaptive-wall applications and computation of residual corrections
03 p0312 N85-12013
Wind tunnel wall interference in closed, ventilated and adaptive test sections 03 p0312 N85-12014
Two- and three-dimensional model and wall data from a flexible-walled transonic test section
03 p0312 N85-12015
Assessment of lift- and blockage-induced wall interference in a three-dimensional adaptive-wall tunnel
03 p0312 N85-12016
A data base for three-dimensional all-interference code evaluation 03 p0312 N85-12017
Effect of upstream sidewall boundary layer removal on an airfoil test — conducted in Langley 0.3-m transonic cryogenic tunnel 03 p0313 N85-12019
Experiments suitable for wind tunnel wall interference assessment/correction 03 p0313 N85-12021
Asymptotic methods for wind tunnel wall corrections at transonic speed 03 p0313 N85-12022
Effect of boundary layers on solid walls in three-dimensional subsonic wind tunnels
03 p0313 N85-12023
NLR activities in the field of wind tunnel wall interference 03 p0313 N85-12024
Progress in wind tunnel wall interference assessment/correction procedures at the NAE
03 p0314 N85-12025
Development in UK of a method for calculating tunnel wall corrections from flow measurements
03 p0314 N85-12026
Tunnel constraint for a jet in crossflow
03 p0314 N85-12027
Interference from slotted walls
03 p0314 N85-12028
Adaptation of a four-wall interference assessment/correction procedure for airfoil tests in the 0.3-m TCT 03 p0315 N85-12035
Minimization of wall interference for three-dimensional models with two-dimensional wall adaptation — wind tunnel walls
[VKI-TN-149] 03 p0321 N85-12070
Wall adaptation at Mach 1.2 — wind tunnel tests
[ONERA-RTS-26/3075-AY-402]
04 p0453 N85-12873
Singularity model for the analysis of wall interference in closed wind tunnels according to the wall pressure signature method (blockage and lift)
[FW-FO-1612] 04 p0453 N85-12874
Wall influence corrections in wind tunnels: Blockage correction according to the wall pressure signature method
[FW-FO-1613] 04 p0453 N85-12875
Parametric determination of blockage interference of 3-dimensional models in the Emmen Federal Aircraft works transonic tunnel (Switzerland)
[FW-FO-1636] 04 p0453 N85-12876
A local slot boundary condition for transonic flow calculations in slotted-wall test sections of wind tunnels
[FFA-TN-1984-34] 04 p0453 N85-12879
On the relaxation of a turbulent boundary layer after an encounter with a forward facing step
08 p1071 N85-16789
Wall interference estimation of the NAL's two-dimensional wind tunnel
[NAL-TR-829] 10 p1426 N85-18992
Aerodynamic behavior of ventilated wind tunnel walls
13 p1968 N85-22363
Unsteady gas dynamics problems related to flight vehicles
[AD-A151187] 15 p2464 N85-25218
Wind tunnel wall interference
[AD-A151212] 15 p2474 N85-25273
A curved test section for research on transonic shock wave-boundary layer interaction
[VTH-LR-414] 16 p2701 N85-26682
Adaptive wall wind tunnels and wall interference correction methods
[DFVLR-IB-222-84-A-37] 17 p2905 N85-27912
Effect of ground and/or ceiling planes on thrust of rotors in hover
[NASA-TM-86754] 20 p3388 N85-31014
Reverberation effects on directionality and response of stationary monopole and dipole sources in a wind tunnel
[NASA-TM-87063] 20 p3453 N85-31443

WIND TUNNELS

NT BLOWDOWN WIND TUNNELS
NT CASCADE WIND TUNNELS
NT CRYOGENIC WIND TUNNELS
NT HYPERSONIC WIND TUNNELS
NT LOW SPEED WIND TUNNELS
NT SLOTTED WIND TUNNELS
NT SUBSONIC WIND TUNNELS
NT SUPERSONIC WIND TUNNELS
NT TRANSONIC WIND TUNNELS

Investigations of boundary layers in the Emmen Federal Aircraft works transonic tunnel, Switzerland
[FW-FO-1641] 04 p0453 N85-12877
Evaluation of the Langley 4- by 7-meter tunnel for propeller noise measurements
[NASA-TM-85721] 04 p0558 N85-13553
Sources, paths, and concepts for reduction of noise in the test section of the NASA Langley 4x7m wind tunnel
[NASA-CR-172446-VOL-1] 05 p0726 N85-14666
Comparison of options for reduction of noise in the test section of the NASA Langley 4x7m wind tunnel, including reduction of nozzle area
[NASA-CR-172446-VOL-2] 05 p0726 N85-14667
Ultrasound instrumentation for the 7 inch Mach seven tunnel
[NASA-CR-174277] 07 p1038 N85-16586
On relaxation of transonic flows around zero-lift airfoils and convergence of self-correcting wing tunnels
11 p1622 N85-20214
The ONERA establishment at Cannes in the service of aeronautical research
[ESA-TT-875] 15 p2475 N85-25276
Post-stall wind tunnel data for NACA 44XX series airfoil sections
[DE85-002948] 18 p3060 N85-28931
Vapor-screen technique for flow visualization in the Langley Unitary Plan Wind Tunnel
[NASA-TM-86364] 19 p3214 N85-29929
Practical aspects of laser holographic interferometry in wind tunnels
[NASA-TM-86788] 23 p3933 N85-34378
Langley aeronautics and space test highlights, 1984
[NASA-TM-87585] 23 p4057 N85-35151

WIND TURBINES

Some considerations on Aeroelastic instabilities caused by coupling between propeller-type rotor and its supporting structure
[NAL-TR-804] 01 p0003 N85-10013
Variable geometry Darrieus wind machine
[PB84-207281] 01 p0068 N85-10453
Design and wind tunnel evaluation of a symmetric airfoil series for large wind turbine applications
[NASA-CR-174764] 02 p0135 N85-10919
Aileron controls for wind turbine applications
[NASA-TM-86867] 02 p0222 N85-11458
Development and demonstration of a vertical axis wind turbine POWERHOUSE
[DE84-901449] 04 p0527 N85-13389
Tailored airfoils for vertical axis wind turbines
[DE84-013618] 04 p0529 N85-13380
Analysis of wind energy systems for selected electric utilities
[DE84-013025] 04 p0530 N85-13389
Meteorological analysis for clusters of wind turbines
[DE84-013164] 04 p0539 N85-13425
Subhourly wind forecasting techniques for wind turbine operations
[DE84-016205] 04 p0539 N85-13427
Development and verification of MCD-2 and MOD-OA simulation models
[DE84-017389] 04 p0550 N85-13499
Response measurements for two building structures excited by noise from a large horizontal axis wind turbine generator
[NASA-CR-172482] 04 p0558 N85-13552
Evaluation of the unsteady effects for a class of wind turbines 05 p0592 N85-13772
Measurement-Technical investigations of Wind Energy Units
[JUEL-SPEZ-244] 05 p0667 N85-14293
Measurement-technical investigations of wind energy units in the short-time range — spectrum analysis
05 p0668 N85-14294
Measurement-technical problems in the investigation of wind energy units 05 p0668 N85-14295
VOITH: Wind energy converter WEC 520
05 p0668 N85-14299
Shutdown characteristics of the Mod-O wind turbine with aileron controls
[NASA-TM-86918] 07 p0992 N85-16299
Development of large wind energy power generation system
[NASA-TM-77779] 07 p0992 N85-16301
Design criteria for small wind turbines
[NLR-MP-83054-U] 07 p0994 N85-16310
Verification of the fatigue properties of (small) wind turbines
[NLR-MP-83055-U] 07 p0994 N85-16311
Detection of low frequency impulsive noise from large wind turbine generators
[NASA-CR-172511] 07 p1038 N85-16588
Blade technology program for large wind turbines, phase 1
[BMFT-FB-T-84-217] 08 p1179 N85-17426
Life assessment and damage tolerance of wind turbines
[AD-B088148L] 08 p1179 N85-17427
Modeling stochastic wind loads on vertical axis wind turbines
[DE85-001148] 09 p1340 N85-18426
Preliminary survey of wind generation in Washington: Site studies and selected wind speed data
[DE85-000058] 09 p1345 N85-18462
Variable speed generator technology options for wind turbine generators
[RR-84-4] 10 p1478 N85-19331
Post stall airfoil data for wind turbines: Wind tunnel test results
[DE85-004052] 10 p1511 N85-19534
Rocky Flats Wind Energy Research Center FY 1983 report
[DE85-004500] 10 p1511 N85-19535
Mini-modal testing of wind turbines using novel excitation
[DE85-000668] 11 p1654 N85-20417

Improved models for increasing wind penetration, economics and operating reliability
[NASA-CR-175538] 11 p1674 N85-20545
Tailored airfoils for vertical axis wind turbines
[DE85-004628] 12 p1772 N85-21128
Computer analysis of wind turbine blade dynamic loads
[DE85-000530] 12 p1867 N85-21714
Aerodynamic research efforts at SERI Wind Energy Research Center at Rocky Flats
[DE85-000529] 12 p1881 N85-21805
Development of large, horizontal-axis wind turbines
[NASA-TM-86950] 13 p2128 N85-23242
Structural design of the Sandia 34-M Vertical Axis Wind Turbine
[DE85-002631] 13 p2129 N85-23247
Investigation of doubly-fed machine in variable speed application
[DE85-004378] 14 p2299 N85-24234
Sound propagation studies for a large horizontal axis wind turbine
[NASA-CR-172584] 14 p2415 N85-24904
NASTRAN-based software for the structural dynamic analysis of vertical and horizontal axis wind turbines
[DE85-001712] 15 p2580 N85-25911
Inviscid upwind finite difference model for two dimensional vertical axis wind turbines
15 p2585 N85-25933
A novel type of stayed tower for wind turbines
[ISD-295] 15 p2587 N85-25952
Response of a wind turbine blade to seismic and turbulent wind excitations 16 p2617 N85-27375
Effect of precipitation on wind turbine performance
[NASA-TM-86986] 16 p2618 N85-27385
Transient behavior of a single-blade horizontal-axis wind turbine
[MBB-UD-421/84-O] 16 p2875 N85-27737
Wind energy systems: Program summary for fiscal year, 1983
[DE85-002927] 17 p2985 N85-28451
Field test report of the Department of Energy's 100-kW vertical axis wind turbine
[DE85-006475] 17 p2987 N85-28458
A 5-year research plan, 1985-1990. Wind energy technology: Generating power from the wind
[DE85-006427] 17 p2987 N85-28463
Post-stall wind tunnel data for NACA 44XX series airfoil sections
[DE85-002948] 18 p3060 N85-28931
Structural design of the Sandia 34-meter vertical-axis wind turbine
[DE85-011146] 18 p3118 N85-29300
Conceptual design of a fixed-pitch wind turbine generator system rated at 400 kilowatts
[NASA-CR-174877] 18 p3127 N85-29363
Wake effects on the aerodynamic performance of horizontal axis wind turbines
[NASA-CR-174920] 18 p3127 N85-29364
Government review of the Mod-2 wind turbine (as-built)
[NASA-TM-86963] 18 p3127 N85-29365
Acoustic noise associated with the MOD-1 wind turbine: Its source, impact, and control
[DE85-002947] 18 p3178 N85-29700
Wake effects of the aerodynamic performance of horizontal axis wind turbines 19 p3211 N85-29915
Aerodynamic analysis of a horizontal axis wind turbine by use of helical vortex theory. Volume 1: Theory
[NASA-CR-168054] 19 p3212 N85-29916
Structural analysis and cost estimate of an eight-leg space frame as a support structure for horizontal axis wind turbines
[NASA-TM-83470] 19 p3284 N85-30361
Analytical model for predicting emergency shutdown of a two-bladed horizontal axis wind turbine
[NASA-TM-83472] 19 p3303 N85-30476
Performance comparison between NACA 23024 and NACA 64(3)-618 airfoil configurated rotors for horizontal-axis wind turbines
[NASA-TM-83471] 19 p3303 N85-30477
The Federal Wind Program at NASA Lewis Research Center
[NASA-TM-83480] 19 p3304 N85-30478
Operational results for the experimental DOE/NASA Mod-OA wind turbine project
[NASA-TM-83517] 19 p3304 N85-30479
Influence of moisture and elevated temperature on the fatigue properties of WTS-3 glass fiber blade material — wind turbine blade (WTS-3)
[FFA-TN-1984-58] 20 p3470 N85-31558
Design and fabrication of durable owner-built wind turbine blades
[DE85-009200] 20 p3484 N85-31650
Wind energy in the north Netherlands region
20 p3455 N85-31661
Wind turbines and environment management
[CP-MEMO-1983-11] 20 p3485 N85-31662
Verification of theoretically computed spectra for a point rotating in a vertical plane
[DE85-011967] 20 p3520 N85-31693
Experimental investigation of a variable speed constant frequency electric generating system from a utility perspective
[NASA-CR-174950] 21 p3579 N85-32251
Aerodynamic analysis of a horizontal axis wind turbine by use of helical vortex theory, volume 2: Computer program users manual
[NASA-CR-174921] 22 p3804 N85-33563
Reflection plane tests of a wind turbine blade tip section with ailerons
[NASA-TM-87018] 23 p3945 N85-34444
General environmental aspects of large scale wind energy utilization 24 p4110 N85-35474
Calculation of trajectories of detached wind turbine blades and prediction of site risk levels associated with failures of HAWT's 24 p4110 N85-35475
GROWIAN: First observations of the environmental impact at the GROWIAN site — wind energy converter
24 p4110 N85-35476
Wind turbine noise: Prediction tools and design parameter dependence 24 p4110 N85-35477
Environmental Monitoring Burger Hill, Orkney wind turbine generator site and similar work at other UK WTG sites 24 p4111 N85-35482
Siting of large scale wind turbines in Denmark
24 p4111 N85-35483
Special questions of siting wind turbine arrays and networks — West Germany 24 p4111 N85-35484
Environmental aspects of the Netherlands wind farm project 24 p4111 N85-35485
Visit to test facility Stoetten (West Germany) May 9, 1984, including the Voith Wind Energy Converter (WEC) 520 turbine. The annual production of various wind energy plants in selected locations 24 p4112 N85-35487

WIND VANES

R and D activities of the Systems Engineering Division
20 p3540 N85-32027

WIND VARIATIONS

Development and verification of MCD-2 and MOD-OA simulation models
[DE84-017389] 04 p0550 N85-13499

WIND VELOCITY

NT SOLAR WIND VELOCITY

Helium atoms in interstellar and interplanetary media, part 3: Temperature and velocity of interstellar wind
02 p0160 N85-11088
Fastest-mile wind speeds in Hurricane Alicia
[PB84-220771] 03 p0397 N85-12532
Bipolar molecular outflows: T Tauri stars and Herbig-Haro objects 03 p0446 N85-12837
Subhourly wind forecasting techniques for wind turbine operations
[DE84-016205] 04 p0539 N85-13427
Multisensor satellite data integration for sea surface wind speed and direction determination
[NASA-CR-174162] 04 p0542 N85-13446
Development and verification of MCD-2 and MOD-OA simulation models
[DE84-017389] 04 p0550 N85-13499
Study of the improvement in analyzing passive microwave remote sensing data by integrated use of ground data 05 p0958 N85-14226
A diagnostic approach to obtaining planetary boundary layer winds using satellite-derived thermal data
05 p0974 N85-14330
Variability of short-term eddy-correlation estimates of mass exchange
[DE84-007271] 05 p0977 N85-14349
Atmospheric wind and diffusion from analysis of an SF6 release at 350 km altitude
[AD-A147965] 08 p1185 N85-17471
Climate at CRREL (Cold Regions Research and Engineering Laboratory) Hanover, New Hampshire
[AD-A148400] 08 p1189 N85-17495
Regional and seasonal variations in snow-cover density in the USSR
[AD-A148429] 08 p1189 N85-17496
Preliminary survey of wind generation in Washington: Site studies and selected wind speed data
[DE85-000058] 09 p1345 N85-18462
Dynamics of the low-latitude thermosphere and ionosphere 09 p1351 N85-18501
On the formation of the nocturnal coastal surface wind speed maximum 09 p1356 N85-18528
Analysis of the Viking Lander 1 surface wind vector for sols 45 to 375
[NASA-CR-174349] 09 p1416 N85-18932
Antenna axis drive torques for the 70-meter antenna
10 p1464 N85-19237
Tropical cyclone data tape for the Eastern and Central North Pacific Basins, 1945-1983: Contents, limitations and uses
[PB85-110054] 10 p1520 N85-19585
A catalogue of dynamic parameters describing the variability of the middle stratosphere during the northern winters 11 p1658 N85-20435
Wind: Measuring for energy
[DE85-900227] 11 p1687 N85-20607
Observations of cataclysmic variable star winds
11 p1755 N85-21041
Study of effective physiological temperature
13 p2042 N85-22780
Preliminary study of inphase gusts and moment force wind loads over the first 150 meters at KSC, Florida
[NASA-TM-86501] 13 p2137 N85-23273
Portable Automated Mesonet (PAM) data from the 1980 experiment in Anderson Creek Valley
[DE85-004361] 13 p2139 N85-23282
Markov method for simulating non-Gaussian wind speed time series
[DE85-003450] 13 p2139 N85-23284
Design considerations for high-altitude, long-endurance, microwave-powered aircraft
[NASA-TM-86403] 14 p2218 N85-23751
Large space antenna technology applied to radar-imaging, rain-rate measurements, and ocean wind sensing 14 p2230 N85-23820
Low-frequency oscillations of sea level and group structure of wind waves 14 p2335 N85-24441
Error in laser correlation wind speed meters resulting from variable atmospheric transparency
14 p2338 N85-24457
Long nonlinear waves in layers of sudden changes in wind velocity 14 p2340 N85-24470
Wave description of sound propagation through stratified moving atmosphere 15 p2525 N85-25567
Mean conditions and turbulence statistics at Vandenberg AFB, California
[AD-A151366] 15 p2985 N85-28449
Comparison of wind velocity in thunderstorms determined from measurements by a ground-based Doppler radar and an F-106B airplane
[NASA-TM-86348] 16 p2703 N85-28687
Formulation and implementation of nonstationary adaptive estimation algorithm with applications to air-data reconstruction
[NASA-TM-86727] 16 p2706 N85-28699
Variability of short term eddy-correlation estimates of mass exchange
[PB85-172641] 18 p3138 N85-29431
Urban climate and air hygiene before, during, and after the lifework of Hellmut Berg. Overview of a branch of applied meteorology 18 p3147 N85-29487
Utilization of the SEASAT scatterometer winds for ocean mixed layer modeling
[AD-A153746] 18 p3150 N85-29506
Study of drift currents in initial stage of generation of wind waves by laser Doppler anemometer
19 p3291 N85-30408
Approximate method for computing wind velocity in atmosphere 19 p3298 N85-30444
Comparison of wind and turbulence measurements from Doppler lidar and instrumented aircraft
[NASA-CR-171535] 20 p3495 N85-31729
Improved Nominal Operating Cell Temperature (NOCT) test procedure 21 p3612 N85-32449
Synoptic-scale dynamics with vertical velocity, part 1.8A 21 p3617 N85-32478
Relationship of spaced antenna and Doppler techniques for velocity measurements (keynote paper), part 3
21 p3619 N85-32488
Effects of line-of-sight velocity on spaced-antenna measurements, part 3.5A 21 p3621 N85-32496
Use of the VAD technique and measurements of momentum flux in the stratosphere at Aerobo, part 4.3A
21 p3622 N85-32505
Tropospheric gravity waves observed by three closely spaced ST radars 21 p3623 N85-32509
Data base for the Colorado profiling network
21 p3627 N85-32533
Status of the Jicamarca radar
21 p3627 N85-32535
Recent results at the Sunset radar
21 p3627 N85-32536
Mean flow and turbulence in complex terrain
[AD-A155138] 21 p3636 N85-32583
Method and apparatus for four-beam radar
[PB85-181477] 22 p3757 N85-33289
Air-sea interaction with SSM/I and altimeter
[NASA-CR-176105] 22 p3818 N85-33650
Comparative analysis of operational forecasts versus actual weather conditions in airline flight planning, volume 1
[NASA-CR-167862] 24 p4119 N85-35534

Comparative analysis of operational forecasts versus actual weather conditions in airline flight planning, volume 2
[NASA-CR-167863] 24 p4119 N85-35535
Comparative analysis of operational forecasts versus actual weather conditions in airline flight planning, volume 3
[NASA-CR-167864] 24 p4120 N85-35536
Comparative analysis of operational forecasts versus actual weather conditions in airline flight planning, volume 4
[NASA-CR-167865] 24 p4120 N85-35537
Comparative analysis of operational forecasts versus actual weather conditions in airline flight planning: Summary report
[NASA-CR-167866] 24 p4120 N85-35538

WIND VELOCITY MEASUREMENT
Performance evaluation and estimation of a laser time-of-flight velocimeter 03 p0363 N85-12326
Wind speed determination from radar altimeters 03 p0360 N85-12424
Laser Doppler Anemometer (LDA) wind velocity measurements: Possibilities for measurements on windpower units 05 p0668 N85-14300
Wind sheltering correction — anemometry
[KNMI-TR-82] 07 p1009 N85-16408
Recent methods for calibrating the anemometry of helicopters at low speeds 08 p1074 N85-16809
Radiosonde system for remote synchronous measurements of wind speed, temperature and its fluctuations 13 p2110 N85-23145
Science opportunities using the NASA scatterometer on N-ROSS
[NASA-CR-175639] 13 p2123 N85-23222
Intermediate results of the NORDSEE experiment
[AD-A151383] 15 p2542 N85-25693
The use of pressure sensing taps on the aircraft wing as sensor for flight control systems 16 p2698 N85-26660
Conducting a wind sensing study
[NASA-CR-175782] 16 p2832 N85-27465
Feasibility study on Laser Doppler Anemometer (LDA) wind velocity measurements using pulsed visible laser light
[ISL-CO-224/83] 16 p2836 N85-27489
Additional possibilities of radiometeor azimuthal method for measuring wind velocity in lower thermosphere 19 p3296 N85-30438
Aerodynamic measurement of the wind flow in the number two section of the SIMA wind tunnel
[ONERA-PV-1/8138-GY] 20 p3389 N85-31019
Relationship of spaced antenna and Doppler techniques for velocity measurements (keynote paper), part 3 21 p3619 N85-32488
The Adelaide VHF radar: Capabilities and future plans 21 p3629 N85-32546
Millstone Hill radar: Capabilities for S/T observations 21 p3629 N85-32548
Air-sea interaction with SSM/I and altimeter
[NASA-CR-176105] 22 p3818 N85-33650
Kinematic analysis of Hurricane Frederick (1979) using satellite, aircraft and rawinsonde data
[NASA-CR-176167] 24 p4119 N85-35533
Control variables in vertical wind determination using simple flight-mechanical equations 24 p4121 N85-35546
The principles of wind measurement with the help of aircraft 24 p4123 N85-35558

WINDING
NT FILAMENT WINDING
NT WIRE WINDING
Stability and vibrations of internal windings of high-current superconducting solenoid magnets
[AD-A151495] 15 p2656 N85-26360
Optimization of design parameters for alternating current stabilizer based on magnetic suspension 22 p3772 N85-33374
Apparatus producing constant cable tension for intermittent demand
[DE85-006434] 23 p3938 N85-34412

WINDMILLS (WINDPOWERED MACHINES)
Investigations on the dynamic loading of wind energy converters with vertical axis and problems of control during starting and overload conditions
[BMFT-FB-T-84-155] 03 p0386 N85-12472
Government review of the Mod-2 wind turbine (as-built)
[NASA-TM-86963] 18 p3127 N85-29365
Aerodynamic analysis of a horizontal axis wind turbine by use of helical vortex theory. Volume 1: Theory
[NASA-CR-168054] 19 p3212 N85-29916
Activities of the Wind Energy Programme 20 p3540 N85-32028
Television interference measurement at Kalkugnen (Sweden) test windmill 24 p4111 N85-35481

WINDOWS (APERTURES)
Response measurements for two building structures excited by noise from a large horizontal axis wind turbine generator
[NASA-CR-172482] 04 p0558 N85-13552
Cockpit window edge proximity effects on judgements of horizon vertical displacement 05 p0704 N85-14518
Preliminary design criteria and certification test specifications for blast resistant windows 09 p1337 N85-18405
Calculation of Si(Li) X-ray detector efficiencies
[DE85-002732] 10 p1489 N85-19400
Hypervelocity impacts on Skylab 4/Apollo windows 12 p1785 N85-21202
Millimeter wave dielectric property measurement of gyrotron window materials
[DE85-004430] 12 p1802 N85-21304
Improvements in glazings: SERI materials research in progress
[DE84-013049] 12 p1814 N85-21378
Double window viewing chamber assembly
[NASA-CASE-MFS-28057-1] 18 p3063 N85-28951
A preliminary human factors planning and design outline of parameters related to space station windows and CCTV monitoring 18 p3158 N85-29559
Light transmitting window assembly
[NASA-CASE-MSC-18417-1] 18 p3185 N85-29750
Laser sealed evacuated window glazings
[DE85-000512] 22 p3754 N85-33273
Diamondlike carbon protective coatings for IR materials
[NASA-TM-87083] 23 p3973 N85-34631

WINDOWS (INTERVALS)
NT LASER WINDOWS
NT LAUNCH WINDOWS
The Jovian atmospheric window at 2.7 microns: A search for H2S
[NASA-TM-86661] 03 p0445 N85-12836
The effects of a nearly 100% duty cycle in observations of solar oscillations 14 p2443 N85-25078
China report: Science and technology
[JPRS-CST-85-007] 15 p2533 N85-25621
Professional Committee on Solid Propulsion hold conference 15 p2533 N85-25623
Extent to which least-squares cross-validation minimizes integrated square error in nonparametric density estimation
[AD-A153789] 18 p3174 N85-29679
Search of the VAXintosh customizing VMS V4.0 for DCL windows
[DE85-011306] 22 p3831 N85-33729

WINDPOWER UTILIZATION
Aileron controls for wind turbine applications
[NASA-TM-86867] 02 p0222 N85-11458
Operational behavior of wind energy converters. Control and dynamic and types of generators, volume 1
[BMFT-FB-T-84-154-VOL-1] 03 p0386 N85-12470
Operational behavior of wind energy converters: Control and dynamic and types of generators, volume 2
[BMFT-FB-T-84-154-VOL-2] 03 p0386 N85-12471
Investigations on the dynamic loading of wind energy converters with vertical axis and problems of control during starting and overload conditions
[BMFT-FB-T-84-155] 03 p0386 N85-12472
Analysis of wind energy systems for selected electric utilities
[DE84-013025] 04 p0530 N85-13389
Measurement-Technical investigations of Wind Energy Units
[JUEL-SPEZ-244] 05 p0667 N85-14293
Measurement-technical problems in the investigation of wind energy units 05 p0668 N85-14295
Measuring system and data evaluation methods of the test field for wind energy units at Pellworm 05 p0668 N85-14296
Measuring-technical investigation of wind energy units from the control-technical, electrical and energetic point of view 05 p0668 N85-14301
Wind-powered electric generation runway lighting system demonstration project
[DE84-014962] 05 p0670 N85-14311
Development of large wind energy power generation system
[NASA-TM-77779] 07 p0992 N85-16301
Preliminary survey of wind generation in Washington: Site studies and selected wind speed data
[DE85-000058] 09 p1345 N85-18462
Rocky Flats Wind Energy Research Center FY 1983 report
[DE85-004500] 10 p1511 N85-19535
Improved models for increasing wind penetration, economics and operating reliability
[NASA-CR-175538] 11 p1674 N85-20545
Wind generator for Solar Office Complex, Luna Vocational Technical Institute, Las Vegas, New Mexico
[DE85-900103] 11 p1674 N85-20547
The relevance of averaging period to wind power measurements and efficiency of Wind Energy Conversion Systems (WECS)
[GKSS-84-E-95] 11 p1676 N85-20562
Wind: Measuring for energy
[DE85-900227] 11 p1687 N85-20607
Aerodynamic research efforts at SERI Wind Energy Research Center at Rocky Flats
[DE85-000529] 12 p1861 N85-21805
The transpacific experimental sailing by YASEIGO 3 14 p2327 N85-24360
Wind energy technology program summary
[DE85-007349] 16 p2820 N85-27392
Transient behavior of a single-blade horizontal-axis wind turbine
[MBB-UD-421/84-O] 16 p2875 N85-27737
Wind energy systems: Program summary for fiscal year, 1983
[DE85-002927] 17 p2985 N85-28451
Field test report of the Department of Energy's 100-kW vertical axis wind turbine
[DE85-008475] 17 p2987 N85-28458
A 5-year research plan, 1985-1990. Wind energy technology: Generating power from the wind
[DE85-008427] 17 p2987 N85-28463
Research recommendations for ac interfacing between electric utility transmission and distribution systems and wind, photovoltaics, and OTEC energy systems
[DE85-002942] 18 p3086 N85-29169
Government review of the Mod-2 wind turbine (as-built)
[NASA-TM-86963] 18 p3127 N85-29365
Aerodynamic analysis of a horizontal axis wind turbine by use of helical vortex theory. Volume 1: Theory
[NASA-CR-168054] 19 p3212 N85-29916
The Federal Wind Program at NASA Lewis Research Center
[NASA-TM-83480] 19 p3304 N85-30478
Renewable technologies program summaries
[DE85-001509] 19 p3307 N85-30500
Wind energy in the north Netherlands region 20 p3485 N85-31661
Wind turbines and environment management
[CP-MEMO-1983-11] 20 p3485 N85-31662
Verification of theoretically computed spectra for a point rotating in a vertical plane
[DE85-011967] 20 p3520 N85-31893
R and D programmes at the National Aeronautical Laboratory
[AR-22] 20 p3539 N85-32022
Activities of the Wind Energy Programme 20 p3540 N85-32028
Wind energy battery storage, phase 2
[DE85-009753] 23 p3945 N85-34450
Solar energy education. Renewable energy: A background text
[DE85-010365] 23 p3946 N85-34452
Implementing agreement for cooperation in the development of large scale wind energy conversion systems
[JUEL-SPEZ-278] 24 p4110 N85-35473
General environmental aspects of large scale wind energy utilization 24 p4110 N85-35474
GROWIAN: First observations of the environmental impact at the GROWIAN site — wind energy converter 24 p4110 N85-35476
Environmental aspects of large-scale wind-power systems in the UK 24 p4110 N85-35478
Environmental Monitoring Burger Hill, Orkney wind turbine generator site and similar work at other UK WTG sites 24 p4111 N85-35482
Visit to test facility Stoetten (West Germany) May 9, 1984, including the Voith Wind Energy Converter (WEC) 520 turbine. The annual production of various wind energy plants in selected locations 24 p4112 N85-35487

WINDPOWERED GENERATORS
Operational behavior of wind energy converters. Control and dynamic and types of generators, volume 1
[BMFT-FB-T-84-154-VOL-1] 03 p0386 N85-12470
Operational behavior of wind energy converters: Control and dynamic and types of generators, volume 2
[BMFT-FB-T-84-154-VOL-2] 03 p0386 N85-12471
Development and demonstration of a vertical axis wind turbine POWERHOUSE
[DE84-901449] 04 p0527 N85-13369
Measurement-Technical Investigations of Wind Energy Units
[JUEL-SPEZ-244] 05 p0667 N85-14293
Measurement-technical investigations of wind energy units in the short-time range — spectrum analysis 05 p0668 N85-14294
Measurement-technical problems in the investigation of wind energy units 05 p0668 N85-14295

Measuring system and data evaluation methods of the test field for wind energy units at Pellworm
05 p0668 N85-14296
Measuring methods to determine the static and dynamic behavior of wind energy converters
05 p0668 N85-14297
Measurement data acquisition and processing system for wind rotor measurements in the wind channel of Bremen University
05 p0668 N85-14298
Laser Doppler Anemometer (LDA) wind velocity measurements: Possibilities for measurements on windpower units
05 p0668 N85-14300
Measuring-technical investigation of wind energy units from the control-technical, electrical and energetic point of view
05 p0668 N85-14301
Existing measuring systems for wind energy units
05 p0669 N85-14302
Measuring techniques in the measuring program for the windpowered unit GROWIAN
05 p0669 N85-14303
Measuring and control tasks in OPTIWA
05 p0669 N85-14304
The upwind power plant Manzanares
05 p0669 N85-14305
Wind-powered electric generation runway lighting system demonstration project
[DE84-014962]
05 p0670 N85-14311
A modified unit commitment and generation control for utilities with large wind generation penetrations
[DE84-015362]
06 p0606 N85-15129
Development of large wind energy power generation system
[NASA-TM-77779]
07 p0992 N85-16301
A preliminary assessment of environmental noise from large Wind Energy Conversion Systems (WECS) based on experiences from Swedish prototypes
[FFA-TN-1984-48]
09 p1379 N85-18668
Variable speed generator technology options for wind turbine generators
[RR-84-4]
10 p1478 N85-19331
Wind generator for Solar Office Complex, Luna Vocational Technical Institute, Las Vegas, New Mexico
[DE85-900103]
11 p1674 N85-20547
Development of large, horizontal-axis wind turbines
[NASA-TM-86950]
13 p2128 N85-23242
Field test report of the Department of Energy's 100-kW vertical axis wind turbine
[DE85-008475]
17 p2987 N85-28458
Government review of the Mod-2 wind turbine (as-built)
[NASA-TM-86983]
18 p3127 N85-29365
Structural analysis and cost estimate of an eight-leg space frame as a support structure for horizontal axis wind turbines
[NASA-TM-83470]
19 p3284 N85-30361
The Federal Wind Program at NASA Lewis Research Center
[NASA-TM-83480]
19 p3304 N85-30478
Operational results for the experimental DOE/NASA Mod-OA wind turbine project
[NASA-TM-83517]
19 p3304 N85-30479
Activities of the Wind Energy Programme
20 p3540 N85-32026
Implementing agreement for cooperation in the development of large scale wind energy conversion systems
[JUEL-SPEZ-278]
24 p4110 N85-35473
General environmental aspects of large scale wind energy utilization
24 p4110 N85-35474
Calculation of trajectories of detached wind turbine blades and prediction of site risk levels associated with failures of HAWT's
24 p4110 N85-35475
GROWIAN: First observations of the environmental impact at the GROWIAN site — wind energy converter
24 p4110 N85-35476
Wind turbine noise: Prediction tools and design parameter dependence
24 p4110 N85-35477
Environmental aspects of large-scale wind-power systems in the UK
24 p4110 N85-35478
A Programmable Automatic Noise Data and Other Related parameter Acquisition system (PANDORA) — wind energy converters
24 p4111 N85-35479
Television interference at the Maglarp (Sweden) wind turbine
24 p4111 N85-35480
Environmental Monitoring Burger Hill, Orkney wind turbine generator site and similar work at other UK WTG sites
24 p4111 N85-35482
Special questions of siting wind turbine arrays and networks — West Germany
24 p4111 N85-35484
Environmental aspects of the Netherlands wind farm project
24 p4111 N85-35485
Visual impact of GROWIAN and resulting recommendations for siting of large wind energy converters
24 p4112 N85-35486
Visit to test facility Stoetten (West Germany) May 9, 1984, including the Volth Wind Energy Converter (WEC) 520 turbine. The annual production of various wind energy plants in selected locations
24 p4112 N85-35487

WINDPOWERED PUMPS
Activities of the Wind Energy Programme
20 p3540 N85-32026

WINDS ALOFT
NT GEOSTROPHIC WIND
NT JET STREAMS (METEOROLOGY)
A feasibility study on the use of wind profilers to support Space Shuttle launches
[NASA-CR-3861]
04 p0538 N85-13423
Cut-off lows and their influence on the weather in Switzerland
[REPT-45]
10 p1519 N85-19574
Atmospheric environment for space shuttle (STS-51C) launch
[NASA-TM-86508]
19 p3315 N85-30547

WINDSCREENS
U WINDSHIELDS

WINDSHIELDS
Method for measuring haze in transparencies
[AD-D011233]
01 p0120 N85-10823
Evaluation of the birdstrike threat to the F-15 present fleet, rapid deployment force, and dual role fighter transparencies
[AD-A148954]
10 p1421 N85-18966
Avoiding serious bird strike incidents
[AD-P004178]
11 p1578 N85-19940
1983 Air Force bird strikes
[AD-P004182]
11 p1579 N85-19944
Aircraft transparency bird impact analysis using the MAGNA computer program
[AD-P004186]
11 p1579 N85-19948
Bird impact evaluation of the F/RF-4 transparency system
11 p1579 N85-19949
The measurement of aircraft windscreen haze and its effect on visual performance
[AD-A154949]
21 p3555 N85-32114

WING CAMBER
Automatic flight control modes for the AFTI/F-111 mission adaptive wing aircraft
17 p2905 N85-27909

WING FLAPS
NT LEADING EDGE FLAPS
NT LEADING EDGE SLATS
NT TRAILING EDGE FLAPS
NT VORTEX FLAPS
Force and moment measurements on a 74 deg delta wing with an apex flap
[NASA-CR-166081]
02 p0134 N85-10918
Recent progress of development and understanding of high lift systems
08 p1068 N85-16772
Analysis of transonic aerodynamic characteristics for a supercritical airfoil oscillating in heave, pitch and with oscillating flap
15 p2458 N85-25175
Airfoil wing with flap
[CH-634787-A5]
15 p2469 N85-25243
Simulator study of the stall departure characteristics of a light general aviation airplane with and without a wing-leading-edge modification
[NASA-TM-86309]
15 p2470 N85-25250

WING FLOW METHOD TESTS
Flow visualization study of a vortex-wing interaction
[NASA-TM-86656]
03 p0316 N85-12040
Transition fixing on wings in industrial wind tunnels and associated problems
14 p2212 N85-23717
Transonic calculations for a flexible supercritical wing and comparison with experiment
[NASA-TM-86439]
20 p3388 N85-31012

WING LOADING
Design of a digital ride quality augmentation system for commuter aircraft
[NASA-CR-172419]
01 p0006 N85-10037
Numerical simulation of the subsonic wing-rock phenomenon
03 p0320 N85-12084
Crack resistance of pressed and rolled semifinished goods of aluminum alloys used in load-bearing aircraft wing structures
03 p0348 N85-12245
Flight test technique for evaluation of gust load alleviation analysis methodology
[NASA-TM-86344]
06 p0754 N85-14833
Structural load measurements on a Northrop NF-5A
07 p0894 N85-15667
Downwash in the plane of symmetry of an elliptically loaded wing
[NASA-TP-2414]
07 p0898 N85-15693

WING NACELLE CONFIGURATIONS
Installed nacelle drag-improvement tests of an M = 0.8 turboprop transport configuration
[NASA-TM-84302]
07 p0902 N85-15716
Nacelle/pylon/wing integration on a transport model with a natural laminar flow nacelle
[NASA-TP-2439]
19 p3213 N85-29924

WING OSCILLATIONS
Graphics software for the display of body deformation motion
[FW-FO-1640]
04 p0455 N85-12866
Propulsive efficiency of vibrating wing in supersonic flow
05 p0724 N85-14858
Wing rock flow phenomena
[AD-P004154]
09 p1264 N85-17939
Transonic steady- and unsteady-pressure measurements on a high-aspect-ratio supercritical-wing model with oscillating control surfaces
[NASA-TM-81868]
09 p1273 N85-18003
A locally linearized panel method for tran-/subsonic flow past an oscillating wing
11 p1622 N85-20212
Oscillating airfoils and their wake
[NASA-TM-77831]
14 p2209 N85-23701
Transonic Unsteady Aerodynamics and its Aeroelastic Applications
[AGARD-CP-374]
15 p2457 N85-25171
Analysis of transonic aerodynamic characteristics for a supercritical airfoil oscillating in heave, pitch and with oscillating flap
15 p2458 N85-25175
Calculation of harmonic aerodynamic forces of aerofoils and wings from the Euler equations
15 p2458 N85-25177
A semi-empirical unsteady transonic method with supersonic free stream
15 p2458 N85-25179
Application of time-linearized methods to oscillating wings in transonic flow and flutter
15 p2459 N85-25182
The development of unsteady transonic 3-D full potential code and its aeroelastic applications
15 p2460 N85-25187
Propulsion efficiency of vibrating bodies in subsonic gas stream
17 p2942 N85-28159
Data set 9: LANN wing. Pitching oscillation
20 p3390 N85-31030

WING PANELS
Solar Array Experiment (SAE) flight experience
14 p2236 N85-23861

WING PLANFORMS
NT DELTA WINGS
NT SWEPT FORWARD WINGS
NT SWEPTBACK WINGS
NT VARIABLE SWEEP WINGS
A method for estimating the rolling moment due to spin rate for arbitrary planform wings
[NASA-TM-86365]
10 p1425 N85-18990
Calculation of the flow around thick wings with separation vortices
12 p1821 N85-21424
Supersonic aerodynamic characteristics of canard, tailless, and aft-tail configurations for 2 wing planforms
[NASA-TP-2434]
17 p2891 N85-27822
Some effects of sweep direction and strakes for wings with sharp leading edges
[CA-8421]
17 p2892 N85-27826
A method to calculate the parameters of wings of arbitrary planform
[AD-A152689]
17 p2892 N85-27831

WING PROFILES
NT WING SPAN
Laser anemometer study of separated flow on wing profiles
[ISL-CO-214/83]
04 p0453 N85-12872
Manufacturing report of an augmented lift, variable deflection half wing
[ONERA-RT-25/1736-AY-108-A]
05 p0591 N85-13796
Numerical method for computing supersonic flow over wings of flight vehicles
05 p0725 N85-14859
Integrated technology wing study (oral presentation)
[NASA-CR-169497]
07 p0902 N85-15718
Transition fixing in the high speed range for the development of civil aircraft wings
14 p2211 N85-23716
The influence of transition strips on the pressure distribution on transonic profiles
14 p2212 N85-23718
Investigation of the conditions for tripping transition with roughness elements and their influence on boundary layer development
14 p2212 N85-23720
Studies on the interference of wings and propeller slipstreams
[NASA-CR-175753]
15 p2483 N85-25210
Unsteady transonic flow calculations for interfering lifting surface configurations
[NASA-TM-86432]
19 p3214 N85-29931
Low-speed tests of a high-aspect-ratio, supercritical-wing transport model equipped with a high-lift flap system in the Langley 4- by 7-meter and Ames 12-foot pressure tunnels
[NASA-TP-2097]
20 p3388 N85-31010
A numerical method for the solution of the inverse problem in external aerodynamics
[STN-7]
20 p3390 N85-31025

Design of a basic airfoil for a slightly swept wing. Part 1: Theoretical transonic airfoil design
[ESA-TT-862] 20 p3394 N85-31054

WING ROOTS
Optimum design of nonplanar wings: Minimum induced drag for a given lift and wing root bending moment
[NAL-TR-797] 01 p0002 N85-10011

WING SLATS
U LEADING EDGE SLATS

WING SPAN
Integrated technology wing study (oral presentation)
[NASA-CR-169497] 07 p0902 N85-15718
Aerodynamic analysis of a horizontal axis wind turbine by use of helical vortex theory, volume 2: Computer program users manual
[NASA-CR-174921] 22 p3804 N85-33563

WING TANKS
Fuel containment and damage tolerance in large composite primary aircraft structures
[NASA-CR-166093] 19 p3231 N85-30032

WING TIP VORTICES
Prediction of aerodynamic characteristics of fighter wings at high angles of attack
[AD-A145107] 01 p0003 N85-10017
Aerodynamic improvements by discrete wing tip jets
[AD-A149861] 10 p1421 N85-18964
Investigation of the Vortex Tab
[NASA-CR-172586] 15 p2463 N85-25209
Interaction of a turbulent vortex with a lifting surface
15 p2464 N85-25214
Tip vortex computer code SRATIP. User's guide
[NASA-CR-172603] 21 p3551 N85-32093

WING TIPS
Integrated technology wing study (oral presentation)
[NASA-CR-169497] 07 p0902 N85-15718
Determination of corrections to flow direction measurements obtained with a wing-tip mounted sensor
[NASA-CR-174412] 10 p1421 N85-18962
Exploratory wind-tunnel investigation of a wingtip-mounted vortex turbine for vortex energy recovery
[NASA-TP-2488] 18 p2699 N85-26667
Wingtip vortex propeller
[NASA-CASE-LAR-13019-1] 24 p4065 N85-35194

WINGED VEHICLES
An overview of some monoplanar missile programs
[NASA-TM-86330] 06 p0747 N85-14786

WINGLETS
Optimum design of nonplanar wings: Minimum induced drag for a given lift and wing root bending moment
[NAL-TR-797] 01 p0002 N85-10011
Natural laminar flow airfoil design considerations for winglets on low-speed airplanes
[NASA-CR-3653] 04 p0452 N85-12663
Flutter parametric studies of cantilevered twin-engine-transport type wing with and without winglet. Volume 1: Low-speed investigations
[NASA-CR-172410-VOL-1] 04 p0513 N85-13269
Flutter parametric studies of cantilevered twin-engine transport type wing with and without winglet. Volume 2: Transonic and density effect investigations
[NASA-CR-172410-VOL-2] 04 p0513 N85-13270
Study of winglets applied to biplanes
[NASA-TM-86350] 08 p1083 N85-18882
DC-10 winglet flight evaluation
[NASA-CR-3704] 19 p3217 N85-29949

WINGS
NT AEROELASTIC RESEARCH WINGS
NT BEARINGLESS ROTORS
NT CAMBERED WINGS
NT DELTA WINGS
NT FIXED WINGS
NT FLEXIBLE WINGS
NT LIFTING ROTORS
NT LOW ASPECT RATIO WINGS
NT RECTANGULAR WINGS
NT RIGID ROTORS
NT RIGID WINGS
NT ROTARY WINGS
NT SLENDER WINGS
NT SUPERCRITICAL WINGS
NT SWEPT FORWARD WINGS
NT SWEPT WINGS
NT SWEPTBACK WINGS
NT THIN WINGS
NT TILTING ROTORS
NT TIP DRIVEN ROTORS
NT TWISTED WINGS
NT UNSWEPT WINGS
NT VARIABLE SWEEP WINGS
Integral equation of lifting surfaces in Laplace domain and analytic continuation of its pressure kernel
[NAL-TR-795T] 01 p0002 N85-10009
Optimum design of nonplanar wings: Minimum induced drag for a given lift and wing root bending moment
[NAL-TR-797] 01 p0002 N85-10011
Deposition in the human lung during respiration of small particles suspended in the air
[BLL-RISLEY-TR-5021-(9091.9F)]
03 p0400 N85-12549
A study of lift characteristics of an upper surface blown jetwing with a rectangular nozzle
05 p0591 N85-13767
Reduction method for thermal analysis of complex aerospace structures
[NASA-TP-2373] 07 p0957 N85-16066
Recent progress of development and understanding of high lift systems 08 p1068 N85-16772
Design of an airfoil leading edge slat using an inverse aerodynamic calculation method
08 p1069 N85-16777
Aerodynamic issues in the design of high-lift systems for transport aircraft 08 p1069 N85-16780
An update of the Canada/USA augmentor-wing project 08 p1070 N85-16781
Aerodynamic-structural study of canard wing, dual wing, and conventional wing systems for general aviation applications
[NASA-CR-172529] 08 p1077 N85-16829
Theory of wing rock 09 p1282 N85-18064
Unsteady transonic flow calculations for two-dimensional canard-wing configurations with aeroelastic applications
[NASA-TM-86375] 10 p1420 N85-18960
Remote pivot decoupler pylon: Wing/store suppression
[NASA-CASE-LAR-13173-1] 11 p1584 N85-19981
A locally linearized panel method for tran-/subsonic flow past an oscillating wing 11 p1622 N85-20212
Fatigue crack propagation in mirage 1110 wing main spar specimens and the effects of spectrum truncation on life
[ARL/STRUC-R-405] 12 p1776 N85-21152
Study for the optimization of a transport aircraft wing for maximum fuel efficiency. Volume 1: Methodology, criteria, aeroelastic model definition and results
[NASA-CR-172551] 13 p1971 N85-22378
Some optimization problems in static aeroelasticity for wings made of composite materials
14 p2277 N85-24104
Computation of unsteady transonic flows about two-dimensional and three-dimensional AGARD standard configurations 15 p2459 N85-25183
The application of transonic unsteady methods for calculation of flutter airloads 15 p2460 N85-25186
Studies on the interference of wings and propeller slipstreams
[NASA-CR-175753] 15 p2463 N85-25210
Aircraft structure for application to training aircraft
[CH-635266-A5] 15 p2469 N85-25244
Learjet Model 55 wing analysis with landing loads
15 p2575 N85-25883
Computational aerodynamics for aircraft wing design
16 p2693 N85-26627
A numerical design method for three-dimensional transonic wings 16 p2694 N85-26631
Hypersonic nonequilibrium gas flow past zero-aspect wing 16 p2765 N85-27063
Wing buffeting active control testing on a transport aircraft configuration in a large sonic windtunnel
17 p2904 N85-27903
Method of calculating separation flow of subsonic gas stream around wings 17 p2942 N85-28161
Further investigations to improve the fatigue life of the Mirage 1110 wing main span
[ARL/STRUC-TM-397] 18 p3061 N85-26938
Gust load alleviation of a cantilevered rectangular elastic wing. Wind tunnel experiment and analysis
[NAK-TR-86] 18 p3063 N85-26950
Application of an aerodynamic analysis method including attainable thrust estimates to low speed leading-edge flap design for supersonic cruise vehicles
[NASA-CR-165843] 19 p3212 N85-29918
Data set 8: ZKP wing, oscillating aileron
20 p3390 N85-31029
Data set 9: LANN wing. Pitching oscillation
20 p3390 N85-31030
Vortex sheet modeling with higher order curved panels
20 p3451 N85-31428
R and D activities of the Structural Sciences Division
20 p3539 N85-32026
Aerodynamic characteristics of a distinct wing-body configuration at Mach 6: Experiment, theory, and the hypersonic isolation principle
[NASA-TP-2467] 22 p3727 N85-33107
Aeroelastic constraints for a wing weight minimization procedure
[FFA-TN-1985-4] 23 p3895 N85-34126
Fuel containment and damage tolerance for large composite primary aircraft structures. Phase 1: Testing
[NASA-CR-166091] 24 p4073 N85-35241

WINTER
The winter anomaly in ionospheric absorption (with special reference to the results obtained in Spain)
04 p0522 N85-13338
Possible anomaly prediction system for the middle atmosphere — ionospheric absorption
04 p0522 N85-13339
Mean maximum mixing heights for northern Asia for the winter of 1978
[DE84-015980] 05 p0672 N85-14315
Forecast impact of components of the FGGE observing system 05 p0681 N85-14373
Results of the carbon monoxide study in Washington, D.C. and Denver, Colorado, in the winter of 1982-83
[PB84-230069] 06 p0834 N85-15309
Trends in skill and accuracy of National Weather Service pop forecasts
[PB84-229053] 06 p0840 N85-15335
The 500 millibar sign frequency teleconnection charts: Winter
[PB85-106276/GAR] 07 p1009 N85-16410
Regional and seasonal variations in snow-cover density in the USSR
[AD-A148429] 08 p1189 N85-17496
Frozen precipitation and concurrent weather: A case study for Munchen-Riem, West Germany
[AD-A149227] 10 p1519 N85-19577
Precipitation gage network operations for wintertime research in the Central Sierra Nevada
[PB85-115020] 10 p1520 N85-19582
Ground-based snow and ice crystal observation system used in Sierra Nevada winter orographic storms
[PB85-115343] 10 p1520 N85-19584
California coastal erosion and storm damage during the winter 1982 - 1983, a reconnaissance report
[PB85-121705] 10 p1521 N85-19591
PMP-1: A coordinated study of the behavior of the middle atmosphere in winter 11 p1654 N85-20421
The Middle Atmosphere Program: Winter in Northern Europe (MAP/WINE) 11 p1655 N85-20429
Middle Atmosphere Program. Handbook for MAP, volume 5
[NASA-CR-175481] 11 p1656 N85-20434
A catalogue of dynamic parameters describing the variability of the middle stratosphere during the northern winters 11 p1656 N85-20435
Middle Atmosphere Program. Handbook for MAP, volume 7
[NASA-CR-175479] 11 p1656 N85-20437
Winter in Northern Europe (WINE) project
11 p1657 N85-20439
PMP-1 report: The fourth winter of PMP-1, 1981 - 1982: A winter with several interesting features
11 p1657 N85-20441
Workshop on Comparison of Data and Derived Dynamical Quantities During Northern Hemisphere (PMP-1) Winters 11 p1657 N85-20444
The first winter of MAP-dynamics, 1982-1983: A winter with three different warming periods
11 p1657 N85-20446
Variation of derived mesospheric nitric oxide in relation to wind and temperature in winter
11 p1658 N85-20452
Abnormal circulation changes in the winter stratosphere, detected through variations of D region ionospheric absorption 11 p1659 N85-20458
Winter anomaly of the lower ionosphere and its possible causes 11 p1660 N85-20459
Autumn and winter anomalies in ionospheric absorption as measured by riometers 11 p1660 N85-20460
Winter anomaly 1982/83 in comparison with earlier winters (1960-82) 11 p1660 N85-20461
A model of the influence of neutral air dynamics on the seasonal variation in the low ionosphere
11 p1660 N85-20462
Explanation of the normal winter anomaly from the seasonal variation of short wave absorption
11 p1660 N85-20463
Midwinter disturbances in the middle atmosphere
11 p1661 N85-20465
Large scale winter time disturbances in meteor winds over central and eastern Europe
11 p1661 N85-20467
Changes in the ozone content over central Europe during reversals of stratospheric circulation in late winter
11 p1661 N85-20469
Measurement of the vertical gradient of the semidiurnal tidal wind phase in winter at the 95 km level
11 p1662 N85-20478
Stratwarm effects in the ionospheric D region wind field 11 p1663 N85-20479
Middle Atmosphere Program. Handbook for MAP, Volume 12: Coordinated Study of the Behavior of the Middle Atmosphere in Winter (PMP-1) Workshops
[NASA-CR-175475] 11 p1665 N85-20492

Short duration winter-time performances of different passive solar systems
[DE85-000850] 11 p1675 N85-20557
Sector analysis of relevant meteorological parameters for long range transport of air pollutants
[NR-27] 12 p1893 N85-21882
Mountain barrier baroclinity effects on surface winds along the Alaskan Arctic coast 14 p2236 N85-23677
Data collection and winter ice dynamics in the Beaufort Sea 14 p2236 N85-23878
Response of winter forecasts made with the GLA Fourth Order GCM to Changes in the horizontal grid resolution 18 p3143 N85-29458
Energy sources of the dominant frequency dependent 3-dimensional atmospheric modes 18 p3143 N85-29462
The contrasting Northern Hemisphere winters of 1980-81 and 1981-82 18 p3144 N85-29468
Transient eddies in the UCLA GCM 18 p3145 N85-29470
Circulation and transport in the middle atmosphere: Troposphere and lower atmosphere 18 p3148 N85-29491
Airborne measurements of atmospheric ice nuclei 21 p3640 N85-32612
Snow cover in the Siberian forest-steppe
[NASA-TM-77914] 23 p3943 N85-34435
Project Skywater, 1983-84 SCPP (Sierra Cooperative Pilot Project) data inventory
[PB85-187052] 24 p4124 N85-35565

WIRE
NT ELECTRIC WIRE
NT EXPLODING WIRES
NT GUY WIRES
Finitely conducting, infinitely long, cylindrical wire in the presence of a plane wave (EMP)
[DE84-015363] 02 p0192 N85-11282
Impact toughness of wire after cold deformation and annealing
[BLL-M-35941-(5628.4)] 05 p0615 N85-13930
Galvanized wire protected against corrosion by chromate passivization
[BLL-M-35906-(5628.4)] 05 p0616 N85-13936
Development of intercalated wire and cable
[AD-A146502] 06 p0774 N85-14949
Electromagnetic resonances of cylinders and aircraft model with resistive wires
[NASA-CR-174203] 06 p0836 N85-15319
Electromagnetic inspection of wire ropes using sensor arrays
[AD-A148317] 08 p1170 N85-17379
Characterization of Nb-8 wt % Al wires by analytical electron microscopy
[DE85-002726] 10 p1442 N85-19086
Double pinch-push contact insertion end-effector
[AD-D011485] 10 p1459 N85-19196
Effectiveness of an overhead wire barrier in deterring gulls from feeding at a sanitary landfill
[AD-P004199] 11 p1582 N85-19966
Multiple parallel wires above a finitely conducting plane earth in the presence of a plane wave (EMP)
[DE85-001116] 11 p1625 N85-20231
A moment solution for an arbitrary configuration of partly shielded wires above a ground plane
[AD-A149762] 12 p1828 N85-21473
Method and apparatus for detecting acoustic emissions from metal matrix wire
[AD-D011556] 12 p1927 N85-22107
Investigation of the conditions for tripping transition with roughness elements and their influence on boundary layer development 14 p2212 N85-23720
Basic EMC (Electromagnetic Compatibility) technology advancement for C3 systems: Model revision for IEMCAP (Intrasystem Electromagnetic Compatibility Analysis Program)
[AD-A150795] 14 p2292 N85-24208
Research on design of cryotransformers and its prospects for the future
[AD-A152400] 17 p2952 N85-28230
Basic EMC (Electromagnetic compatibility) technology advancement for C3 systems. Volume 4D: Modeling crosstalk in balanced twisted pairs
[AD-A153678] 18 p3000 N85-29125
The microstructural state of Nb3Sn in a multifilamentary titanium doped bronze-process wire
[DE85-010979] 19 p3240 N85-30089
Electromagnetic inspection of wire ropes using sensor arrays
[AD-A155412] 22 p3795 N85-33509
Features of the solar array drive mechanism for the space telescope 22 p3798 N85-33532
Towards the development of technological processes for the preparation of cadmium plated steel articles
[BLL-M-36315-(5628.4)] 23 p3913 N85-34248
Apparatus producing constant cable tension for intermittent demand
[DE85-006434] 23 p3938 N85-34412
Effect of Cu4Ti compound formation on the characteristics of NbTi accelerator magnet wire
[DE85-014226] 24 p4159 N85-35788

WIRE BRIDGE CIRCUITS
NT WHEATSTONE BRIDGES
Modular detonator device
[AD-D011232] 03 p0340 N85-12184

WIRE CLOTH
Explosion-proof properties and hydraulic resistance of fire-barrier elements based on knitted metallic screens 11 p1601 N85-20067
Flow through very porous screens
[NASA-TP-2436] 11 p1631 N85-20270
Flow around rotating and nonmoving circular cylinder near flat screen. Report 1: Aerodynamic forces in cylinder 16 p2765 N85-27059

WIRE MESH
U WIRE CLOTH

WIRE WINDING
Detection and location of partial discharges in transformer windings using electrical methods 15 p2551 N85-25750

WIRELESS COMMUNICATION
NTT (Nippon Telegraph and Telephone Public Corporation) develops new optical fiber 10 p1476 N85-19311

WIRING
NT BEAM LEADS
Bondability of Al-Si thin film in thermosonic gold wire bonding — integrated circuits
[NASA-TM-77795] 10 p1439 N85-19071
Safety requirements for wiring systems and connectors for photovoltaic systems
[NASA-CR-174431] 10 p1477 N85-19324
Reducing gull use of some attractions near airports
[AD-P004195] 11 p1581 N85-19962

WIRING SYSTEMS
U WIRING

WISCONSIN
Compilation of annual reports of the Navy ELF (Extremely Low Frequency) communications system ecological monitoring program. Volume 1: Tabs A-E
[AD-A146326] 08 p1152 N85-17272
Compilation of annual reports of the Navy ELF (Extremely Low Frequency) communications system ecological monitoring program (1983). Volume 2: Tabs F-J
[AD-A146327] 08 p1152 N85-17273
Glacial geology of Barron County, Wisconsin 09 p1351 N85-18500
The pleistocene geology of Vilas County, Wisconsin 09 p1353 N85-18509
Rationale and basic design for experimental acidification of a lake ecosystem in Northern Wisconsin
[PB85-116077] 12 p1885 N85-21829

WOLF-RAYET STARS
Observations of nonthermal radio emission from early-type stars 08 p1232 N85-17758
Departures from LTE populations versus anomalous abundances: The effects of heating 08 p1234 N85-17776
Spectroscopic observations of selected stellar systems
[NASA-CR-174288] 08 p1255 N85-17915
High-velocity interstellar gas in the line-of-sight to HD 50896 11 p1749 N85-20999
Gamma-ray line emission from Al-26 produced by Wolf-Rayet stars
[OG-3.2-5] 22 p3875 N85-34003
Neutron-rich nuclei in cosmic rays and Wolf-Rayet stars
[OG-8.2-6] 23 p4019 N85-34906
Bursting star formation and the overabundance of Wolf-Rayet stars
[OG-8.2-8] 23 p4019 N85-34907

WOLFRAM
U TUNGSTEN

WOMEN
U FEMALES

WOOD
NT CORK (MATERIALS)
NT PLYWOOD
Thermal-stress analysis for a wood composite blade
[NASA-CR-174794] 08 p1178 N85-17421
Flash pyrolysis of biomass with reactive and non-reactive gases
[DE85-010982] 19 p3308 N85-30496
Airborne sound transmission loss characteristics of wood-frame construction
[AD-A154174] 20 p3524 N85-31919

WOODEN STRUCTURES
Seismic performance of low-rise light-framed wood buildings 08 p1171 N85-17384

WOOL
Properties of polycaproamide fibers modified by grafted polyacrylonitrile 06 p0761 N85-14867
Pathophysiological study of poisoning due to thermal degradation of materials — aircraft cabins
[CERMA-84-15] 11 p1692 N85-20640

WORD PROCESSING
Bulletin of the Faculty of Engineering, Hokkaido University, no. 123
[ISSN-0385-602-X] 04 p0482 N85-13075
Document interchange format
[PB84-217093] 07 p1027 N85-18517
M68000 RNF text formatter user's manual
[NASA-TM-86327] 13 p2148 N85-23320
The Record of Electrical and Communication Engineering Conversazione, volume 53, no. 2, November 1984
[ISSN-0365-7719] 16 p2758 N85-27022
The design of an English word-processor for scientific and technical use in which superscripts, subscripts and Greek characters are operated by screen-edit. 3 16 p2759 N85-27025
A procedure for communications with PDP-10 and PDP-11 (IS/1 UNIX) type computers through use of CPT word processing equipment, revision 1
[DE85-007596] 16 p2845 N85-27540

WORDS (LANGUAGE)
Keyword thesaurus: A list of terms and codes to identify areas of interest for research and other types of sponsored programs (revised October 1984)
[PB85-136893] 10 p1568 N85-19690
Spanish language equivalents for a glossary of terms used in the field of space exploration
[NASA-TM-86211] 19 p3379 N85-30961

WORK
NT PHYSICAL WORK
An update on the capabilities of the Air Force Computerized Occupational Health Program (COHP)
[AD-P004037] 06 p0845 N85-15367
Human aspects in office automation
[PB84-240736] 06 p0847 N85-15376
The principle of virtual work and associated variational principles
[ESA-TT-873] 09 p1340 N85-18428
Sector suite man-machine functional capabilities and performance requirements
[AD-A148881] 10 p1531 N85-19647
Computing environments for data analysis. Part 1: Introduction
[DE85-007919] 17 p3009 N85-28603
Computing environments for data analysis. Part 2: Hardware
[DE85-008320] 17 p3009 N85-28604

WORK CAPACITY
Work capacity of heat and electric power plant operations working 12 hour day and night shifts 09 p1362 N85-18567
Human assembly time versus levels of visual and tactile sensory input: Experimental results for five devices
[AD-A149662] 12 p1909 N85-21980
The relationship between performance and satisfaction: A utility analysis
[AD-A152342] 17 p3000 N85-28548
Cosmonauts' cardiovascular system function during long-term orbital flights aboard Salyut-6 station 22 p3733 N85-33141
Responses of skeletal muscle to unloading, a review
[NASA-CR-176177] 24 p4128 N85-35594
Physiological responses to unvarying (steady) and 2-2-1 shifts: Miami International Flight Service Station
[AD-A155751] 24 p4133 N85-35619

WORK FUNCTIONS
Amorphous metallic layers in Si metallization systems 06 p0830 N85-15277
Energy relations on the small oscillations excitation in the stars 14 p2450 N85-25125
concentration variation of work function of alloys in the system nickel-titanium-aluminum 19 p3247 N85-30134
Study of nonlinear distortion in microwave amplifiers using Schottky gate field effect transistors 22 p3780 N85-33423

WORK HARDENING
NT STRAIN HARDENING
Crack tip opening displacement for work hardening materials
[GKSS-84-E-25] 01 p0063 N85-10415
Work hardening of simple two phase composites
[DE84-014629] 04 p0488 N85-12978
Effect on work-hardening in dynamic deformation of beryllium
[DE85-002691] 11 p1608 N85-20111

WORK-REST CYCLE
Effects of partial deprivation of slow-wave sleep on sleep-wakefulness cycles 10 p1524 N85-19613

Human performance in continuous/sustained operations and the demands of extended work/rest schedules. An annotated bibliography
[AD-A155619] 21 p3668 N85-32771
Psychophysiological distinctions of organization and regulation of daily cyclograms of crew activities during long-term spacecraft 22 p3821 N85-33669
Physiological responses to unvarying (steady) and 2-2-1 shifts: Miami International Flight Service Station
[AD-A155751] 24 p4133 N85-35619
WORKING FLUIDS
NT FERROFLUIDS
Technical Review of the Solid Particle Receiver Program
[DE84-015181] 01 p0068 N85-10451
Method and apparatus for determining the content and distribution of a thermal neutron absorbing material in an object
[DE84-014319] 01 p0117 N85-10801
Analysis of dynamic characteristics of fluid force induced by labyrinth seal 05 p0643 N85-14129
Working medium for sorption heat pumps
[BLL-T6360/BG/WH785/84] 06 p0807 N85-15131
Preliminary evaluation of a liquid belt radiator for space applications
[NASA-CR-174807] 07 p0917 N85-15804
Initial results for supercritical cycle experiments using pure and mixed-hydrocarbon working fluids
[DE84-017008] 09 p1345 N85-18480
Performance of solar thermal systems with liquid metal MHD conversion
[DE85-002758] 11 p1675 N85-20655
Leak detectors for organic Rankine cycle power plants: On-line and manual methods
[DE85-002792] 12 p1852 N85-21617
Thermophysical properties of working fluids for binary geothermal cycles
[DE85-000385] 12 p1881 N85-21804
Effect of operating medium on cyclic durability of AD33-W composite 13 p2029 N85-22716
Advanced radiator concepts
[NASA-TM-87008] 14 p2300 N85-24245
Intrinsically irreversible acoustic heat engines
[DE85-007672] 19 p3270 N85-30276
WORKLOADS (PSYCHOPHYSIOLOGY)
An investigation of the use of steady-state evoked potentials for human performance and workload assessment and control
[AD-A145727] 02 p0237 N85-11541
Decision tree rating scales for workload estimation: Theme and variations
[NASA-CR-174062] 02 p0237 N85-11544
Measuring workload differences between short-term memory and long-term memory scenarios in a simulated flight environment 05 p0703 N85-14513
POPCORN: A supervisory control simulation for workload and performance research
05 p0704 N85-14515
Twentieth Annual Conference on Manual Control, volume 2
[NASA-CP-2341-VOL-2] 05 p0707 N85-14535
Measurement of workload: Physics, psychophysics, and metaphysics 05 p0708 N85-14539
Subjective workload assessment and voluntary control of effort in a tracking task 05 p0708 N85-14540
Decision tree rating scales for workload estimation: Theme and variations 05 p0708 N85-14541
Assessing the subjective workload of directional orientation tasks 05 p0708 N85-14542
Classification systems for individual differences in multiple-task performance and subjective estimates of workload 05 p0708 N85-14543
Measuring pilot workload in a moving-base simulator. Part 2: Building levels of workload
05 p0712 N85-14566
The Sternberg task as a workload metric in flight handling qualities research 05 p0712 N85-14568
Blood pressure levels of active pilots compared with those of air traffic controllers
[AD-A146845] 06 p0846 N85-15373
Dynamic training devices in CRM training
09 p1276 N85-18018
Research at automated ATC Scientific-Experimental Center 09 p1278 N85-18037
Improvement of workload estimation techniques in piloting tasks
[NASA-CR-174374] 10 p1531 N85-19646
Aircrew and avionics: Friends or Foes?
10 p1532 N85-19654
Impact of future aircombat characteristics on pilot performance and cockpit design
10 p1533 N85-19661
Grasp of information by the pilot in future combat aircraft 10 p1533 N85-19662
Pilot workload, performance and aircraft control automation 10 p1534 N85-19670
Aircrew-aircraft integration issues in future US Army helicopters 10 p1535 N85-19672
Operations concept for the advanced automation system man-machine interface
[AD-A149797] 12 p1774 N85-21139
Human assembly time versus levels of visual and tactile sensory input: Experimental results for five devices
[AD-A149982] 12 p1909 N85-21980
Plans for adaptation research during Antarctic expedition 14 p2333 N85-24426
Complex program of ergonomic studies Pilot described 14 p2366 N85-24698
Analysis of team performance in a programmed environment
[NASA-CR-175634] 14 p2392 N85-24728
Dual-task timesharing using a projected attitude display (Malcolm horizon)
[AD-A150789] 14 p2395 N85-24750
Mental workload measurement: Event-related potentials and ratings of workload and fatigue
[NASA-CR-177354] 15 p2619 N85-26139
A comparison of pictorial and speech warning messages in the modern cockpit
[AD-A151917] 16 p2707 N85-26706
Aspects of application of ACT systems for pilot workload alleviation 16 p2712 N85-26734
Statistical study of the dynamic analysis of the workload in the A310 certification campaign
16 p2844 N85-27531
Aspects of application of ACT systems for pilot workload alleviation 17 p2901 N85-27887
The relationship between performance and satisfaction: A utility analysis
[AD-A152342] 17 p3000 N85-28546
Investigation of biochemical and psychological parameters of air traffic controllers in prestart state before beginning to work 19 p3325 N85-30599
Adaptive aiding for symbiotic human-computer control: Conceptual model and experimental approach
[AD-A153670] 19 p3332 N85-30644
Guide on workload forecasting
[PB85-177632] 19 p3341 N85-30704
Speech analysis system for assessing pilots' working fitness 22 p3819 N85-33661
Cardiorespiratory function and work performance during adaptation to industrial labor in midalpine conditions
22 p3820 N85-33665
Models for assessing workload of aircrews on long distance flights 24 p4129 N85-35599
Physiological responses to unvarying (steady) and 2-2-1 shifts: Miami International Flight Service Station
[AD-A155751] 24 p4133 N85-35619
WORKSTATIONS
Extension of the software development workbench to include microcomputer workstations
[AD-A151903] 15 p2630 N85-26207
Design of computer-related workstations in relation to job functions and productivity
[AD-A151938] 16 p2844 N85-27534
NASA space station automation: AI-based technology review. Executive summary
[NASA-CR-176096] 21 p3558 N85-32135
WORLD
U EARTH (PLANET)
WORLD DATA CENTERS
Use of Ebro Observatory data at Word Data Center A for Solar-Terrestrial Physics 04 p0518 N85-13310
On the study of ionospheric disturbances
04 p0522 N85-13335
WORLD METEOROLOGICAL ORGANIZATION
Review of climate problems in Latin America and the Caribbean 07 p1001 N85-16354
The potential contributions of the World Climate Program (WCP) to the economies of developing countries
07 p1003 N85-16371
International list of selected, supplementary and auxiliary ships --- WMO
[WMO-47-ED-84] 11 p1687 N85-20609
Commission for Marine Meteorology
[WMO-640] 20 p3496 N85-31735
The 2nd World Meteorological Association Regional Association (Asia), 8th session
[WMO-642] 22 p3817 N85-33643
WRAPAROUND CONTACT SOLAR CELLS
U SOLAR CELLS
WRINKLING
NT FLANGE WRINKLING
WRIST
Kinematic rate control of simulated robot hand at or near wrist singularity
[NASA-TP-2440] 16 p2851 N85-27575
The compliance of end effector force sensors for robot manipulator control 24 p4098 N85-35406
WROUGHT ALLOYS
Characterization of modified 9 r-1 Mo steel sand castings
[DE85-012057] 24 p4080 N85-35287
WU-2 AIRCRAFT
U U-2 AIRCRAFT
WYOMING
Geothermal resources of the Laramie, Hanna, and Shirley Basins, Wyoming
[DE84-016104] 01 p0064 N85-10423
Subsurface temperatures in northeastern Wyoming measured by bottom hole temperature records
[TI84-901610] 04 p0534 N85-13413
Chronologic and climatic control on soil development, northern Bighorn Basin, Wyoming and Montana
08 p1181 N85-17443
Post-Laramide history of North Central Wyoming
08 p1181 N85-17444
Geothermal resources of the Laramie, Hanna and Shirley Basins, Wyoming
[DE85-005006] 23 p3943 N85-34436
Depositional systems and coal occurrence in the Fort Union Formation (Paleocene), Powder River Basin, Wyoming and Montana 24 p4114 N85-35505

X

X BAND
U SUPERHIGH FREQUENCIES
X RAY ABSORPTION
EXAFS studies of sodium silicate glasses containing dissolved actinides
[DE84-015835] 04 p0479 N85-13051
Extended X-ray absorption fine structure (Exafs) studies of the actinides
[DE84-015833] 04 p0559 N85-13561
X-ray absorption in perfect crystals
[DE84-016034] 05 p0732 N85-14706
Measurement of soft X-ray absorption spectra with a fluorescent ion chamber detector
[AD-A142213] 07 p0922 N85-15838
Synchrotron X-ray fluorescence and extended X-ray absorption fine structure analysis
[DE85-003606] 10 p1438 N85-19063
Characterization of thin films and layered structures using X-ray absorption and reflection at grazing incidence
[DE85-006560] 15 p2662 N85-26429
X RAY ANALYSIS
NT LAUE METHOD
X-radiography of slices of the Allende Meteorite
06 p0885 N85-15822
FORTRAN version of the quantitative energy-dispersive electron beam X-ray analysis program FRAME C
[PB84-240936] 07 p1027 N85-16519
Recent investigations at INPE in magnetospheric physics and geomagnetism
[INPE-3280-PRE/603] 10 p1514 N85-19555
K and L-shell cross-sections for X-ray microanalysis in an AEM
[DE85-002733] 11 p1721 N85-20822
The clinical and radiological assessment of cervical injury, Annex A 12 p1907 N85-21976
Head/neck injury: Post mortem procedures, Annex B
12 p1907 N85-21977
In-situ burning rate determination using flash radiography 13 p2002 N85-22550
EXAFS of monolayers on silver electrodes: SSRL proposal number 717M
[AD-A150823] 13 p2018 N85-22652
Application of field X-ray: Radiometric analysis in exploratory geology and means for its improvement
13 p2115 N85-23176
Uniaxial orientation of linear low density polyethylene
[AD-A151037] 14 p2261 N85-24009
Flash radiography 14 p2317 N85-24316
Studies of deformation in niobium by X-ray topographic methods
[AD-A150726] 14 p2427 N85-24965
Secondary fluorescence effects on X-ray microanalysis
[DE85-005585] 15 p2506 N85-25457
La Recherche Aerospatiale Bimonthly Bulletin Number 1984-3, 220/May-June
[ESA-TT-862] 16 p2695 N85-26636
Elemental analysis of aerosols in Transvaal urban and power-producing areas using time and size-resolved samples 16 p2829 N85-27443
Atom location by electron channeling analysis
[DE85-007549] 16 p2872 N85-27716
East Europe report: Science and technology
[JPRS-ESA-85-017] 17 p2945 N85-28177
Proton induced X-ray emission method, its application in analytics 17 p2945 N85-28178

Cosmic X-ray physics
[NASA-CR-175906] 17 p3055 N85-28610
X-ray satellite
[NASA-TM-77696] 20 p3407 N85-31144
Application of Particle Induced X-ray Emission analysis (PIXE) to aerosol long range transport studies 21 p3648 N85-32665
An enhanced photoresponse at dislocation subgrain boundaries revealed by X-ray topography of polysilicon solar cells 22 p3806 N85-33572
X-ray residual stress analysis on the coarse grain of copper and its application to the brazed copper 23 p3907 N85-34202
Study on the correlation between grinding conditions and residual stresses in ground surface of steel by the X-ray method 23 p3907 N85-34203
X-ray measurement of thermal stresses in tungsten fiber-copper composites 23 p3907 N85-34205
X-ray fluorescence analysis of 304L stainless steel
[DE85-013254] 24 p4080 N85-35298
Detection threshold energy of high energy cascade showers using thermoluminescence PTFE-sheet and hot-gas reader
[HE-7.1-5] 24 p4213 N85-36159
Application of thermoluminescence for detection of cascade shower 2: Detection of cosmic ray cascade shower at Mount Fuji
[HE-7.1-12] 24 p4214 N85-36162

X RAY APPARATUS
NT X RAY TUBES
DoD Robotics Application Workshop Proceedings
[AD-A145867] 03 p0307 N85-11978
Robotics in nondestructive inspection at Sacramento Air Logistics Center
[AD-P004012] 03 p0309 N85-11992
Characterizing X-ray machines
[AD-A146532] 06 p0662 N85-15461
X rays from the aurora
[AD-A148828] 06 p1186 N85-17477
Flash X-ray diffraction
[ISL-CO-227/84] 23 p3936 N85-34396

X RAY ASTRONOMY
NT X RAY BINARIES
NT X RAY SOURCES
Rocket observations 01 p0014 N85-10084
Study of a coded mask telescope for astronomical measurements in the hard X-ray domain
[MPE-182] 01 p0129 N85-10999
X-ray observations of the Seyfert 1 galaxies AKN120 and MCG8-11-11
[NASA-TM-86863] 03 p0446 N85-12839
A large scale height galactic component of the diffuse 2-60 keV background
[NASA-TM-83837] 03 p0446 N85-12841
A model of the soft X-ray background as a blast wave viewed from inside 06 p0879 N85-15586
Very Long Base Interferometry (VLBI) in space and X-ray observations of compact sources in active galactic nuclei 07 p1058 N85-16716
Design and fabrication of a CCD camera for use with relay optics in solar X-ray astronomy
[NASA-CR-174334] 08 p1164 N85-17344
Theory tested by means of the stars — viability of the alpha-omega dynamo model 08 p1233 N85-17770
X-ray and UV Emission from Active Galactic Nuclei — conference
[MPE-184] 08 p1236 N85-17790
X-ray emission from active galactic nuclei 08 p1236 N85-17806
EXOSAT observations of active galactic nuclei 08 p1236 N85-17809
Very long base interferometry (VLBI) and X-ray observations of complete samples of radio selected active galactic nuclei 08 p1243 N85-17847
X-ray bursts: Observation versus theory
[NASA-CR-174415] 10 p1573 N85-19018
Contributions of the X-ray astronomy group — conference
[MPE-PREPRINT-28] 11 p1741 N85-20947
Contributions of the X-ray astronomy group — conference
[MPE-PREPRINT-29] 11 p1742 N85-20952
Development of high resolution imaging detectors for X-ray astronomy
[NASA-CR-175505] 12 p1953 N85-22266
X-ray astronomy and plasma astrophysics 12 p1958 N85-22296
Solar and stellar coronal plasmas
[NASA-CR-175823] 13 p2205 N85-23676
Solar maximum mission results on the energetics of the impulsive phase of solar flares 14 p2454 N85-25159
Professional Committee on Solid Propulsion hold conference 15 p2633 N85-25823
A program of ground-based astronomy to complement einstein observations
[AD-A151111] 15 p2668 N85-26466
Spectral constraints on models of gas in clusters of galaxies
[NASA-TM-86188] 15 p2669 N85-26468
Analysis of short-period changes in intensity of hard X-radiation of solar flares registered aboard Venera-13 and Venera-14 spacecraft 16 p2723 N85-26806
Optical pulsar in the Large Magellanic Cloud remnant 0540-69.3
[DE85-006707] 16 p2863 N85-27766
The soft X-ray background as a supernova blast wave viewed from inside: Solar abundance models
[NASA-CR-175767] 16 p2867 N85-27813
Observation of the Crab nebula in the hard X-ray
[MPE-186] 17 p3053 N85-28697
Axion mass limits from pulsar X-rays
[DE85-010634] 18 p3202 N85-29665
The Extended Range X-Ray Telescope center director's discretionary fund report
[NASA-TM-86507] 19 p3362 N85-30983
X-ray satellite
[NASA-TM-77662] 20 p3407 N85-31145
The design, development, testing, fabrication, calibration and integration of a High Resolution Imager (HRI) for the Roentgen Satellite (ROSAT)
[NASA-CR-175302] 22 p3741 N85-33184
Cyg X-3: Not seen in high-energy gamma rays by COS-B
[OG-2.2-2] 22 p3864 N85-33929
Relevance of the observation of UHE gammas to hard X-ray astronomy
[OG-2.2-6] 22 p3865 N85-33932
High-resolution spectroscopic observation of Vela X-1 in the hard X-ray energy range
[OG-2.2-10] 22 p3865 N85-33936
Quasiperiodic oscillations in bright galactic-bulge X-ray sources
[NASA-CR-176136] 23 p3987 N85-34723
Lapec: A Phoswich balloon experiment for hard X-ray astronomy
[OG-9.3-1] 23 p4027 N85-34956
Research of advanced techniques for X-ray detectors and telescopes with applications to rockets and the LAMAR facility
[NASA-CR-176161] 23 p4054 N85-35141

X RAY ASTROPHYSICS FACILITY
Natural environment design criteria for the Advanced X-ray Astrophysics Facility (AXAF) definition and preliminary design
[NASA-TM-86461] 01 p0014 N85-10089
Study of the potential usefulness of superfine holographic x-ray gratings in AXAF and astrophysics in general 12 p1945 N85-22215

X RAY BINARIES
Search for millisecond rotational periods in some low-mass X-ray binaries observed by EXOSAT 11 p1741 N85-20949
Spectral studies of low-mass X-ray binaries observed by EXOSAT 11 p1743 N85-20959
IUE and optical observations of LMC X-ray binaries 11 p1757 N85-21050
Ultra high energy gamma rays, cosmic rays and neutrinos from accreting degenerate stars
[OG-2.2-5] 22 p3864 N85-33931
500 TeV gamma rays from Hercules X-1
[OG-2.2-7] 22 p3865 N85-33933
High-resolution spectroscopic observation of Vela X-1 in the hard X-ray energy range
[OG-2.2-10] 22 p3865 N85-33936

X RAY DENSITY MEASUREMENT
Non-local origin of a substantial portion of the soft X-ray background 06 p0877 N85-15567
X-ray gauge measures areal density variations as small as 0.1%
[DE85-003774] 12 p1854 N85-21829

X RAY DIFFRACTION
Applications of synchrotron X-ray diffraction topography to fractography
[DE84-016257] 04 p0513 N85-13274
X-ray polarization in highly oriented pyrolytic graphite
[DE84-015573] 05 p0613 N85-13917
Microstructural origins of hot spots in RDX explosive and a reference inert material
[AD-A146865] 06 p0774 N85-14847
Mossbauer spectroscopy and X-ray diffraction of samples from the Santa Catharina iron meteorite 06 p0865 N85-15624
Gallium arsenide compounds tested nondestructively with X-rays 07 p0936 N85-15834
X-ray and backscattering analysis of ion implantation phenomena in GaAs and related compounds
[AD-A147449] 07 p1048 N85-16659
Temperature dependence of the crystal structures of Nylon 11
[AD-A147563] 07 p1049 N85-16661
Structural studies of amorphous Mo-Ge alloys using synchrotron radiation
[DE85-002061] 08 p1131 N85-17125
Determination of the elastic constants of inhomogeneous materials with X-ray diffraction
[AD-A148469] 08 p1173 N85-17393
Application of layered synthetic microstructures to high temperature plasma diagnostics
[DE85-002035] 10 p1559 N85-19828
Microscopic magnetic structure of multiple bilayers of thin films of Fe and Ge
[DE85-004188] 13 p2024 N85-22662
Characterization of supported metal catalysts by imaging, microdiffraction and microanalysis techniques
[DE85-005567] 14 p2253 N85-23961
Structural, morphological and optical characteristics of KGd(WO4)2 crystals 14 p2260 N85-24128
Crystallinity determination by curvefit procedure for a semi-crystalline polymer
[NASA-TM-86412] 15 p2517 N85-25520
Ca-Ga, Sr-Ga and Ba-Ga binary systems
[DE85-006454] 16 p2751 N85-26960
X-ray crystallography of steel U8 after pulsed laser hardening
[BLL-BISI-22444-(9022.06)] 17 p2925 N85-29036
X-ray diffraction study of changes in stress-strain distributions during fatigue of a 2-phase alloy
[AD-A152367] 17 p2930 N85-29067
An X-ray diffraction study of the residual stress-strain distribution in shot-peened 2-phase brass
[AD-A152418] 17 p2930 N85-29068
The synthesis and structure of polyphosphazenes
[AD-A153134] 17 p2934 N85-29112
Properties of defects in Hg(1-x)Cd(x)Te
[AD-A153243] 17 p3044 N85-29836
Age hardening and atomic structure of an aluminum-6 at. % silver alloy
[DE85-009977] 18 p3077 N85-29931
A new high-resolution pickup tube for live X-ray topography
[NHK-LABS-NOTE-309] 18 p3193 N85-29802
Application of the reference intensity method to coal analysis
[DE85-009526] 19 p3228 N85-30015
Highly dispersed metal atoms in zeolites
[DE85-010515] 19 p3354 N85-30792
Debye temperature and static displacements in LuH sub x single crystals from energy dispersive X-ray diffraction
[DE85-010961] 19 p3376 N85-30948
Modification of the grain size of sputtered copper with additions of oxygen, krypton, silver, or yttrium
[DE85-010975] 21 p3567 N85-32189
The measurement of strain fields by X-ray topographic contour mapping
[AD-A154870] 21 p3599 N85-32348
Quantitative determination of mineral composition by powder X-ray diffraction
[DE85-011654] 22 p3780 N85-33901
An X-ray diffraction study of titanium oxidation
[NASA-CR-176263] 23 p3915 N85-34264
Flash X-ray diffraction
[ISL-CO-227/84] 23 p3936 N85-34396

X RAY FLUORESCENCE
Synchrotron X-ray fluorescence and extended X-ray absorption fine structure analysis
[DE85-003606] 10 p1436 N85-19063
Evaluating the variability of ceramics with X-ray fluorescence
[DE85-002028] 10 p1453 N85-19155
Highly dispersed metal atoms in zeolites
[DE85-010515] 19 p3354 N85-30792
Variations of particulate sulfur concentrations in a coastal atmospheric environment in connection with the change of air masses origin 21 p3552 N85-32592
X-ray fluorescence analysis of 304L stainless steel
[DE85-013254] 24 p4080 N85-35298
Measurement of uranium enrichment for gaseous uranium at low pressure
[DE85-012697] 24 p4150 N85-35733

X RAY IMAGERY
Development of a dynamic radiographic capability using high-speed video
[DE84-016477] 04 p0511 N85-13256
FLACS: A new sensitometer for measurement of extreme low intensity reciprocity in a controlled environment — X-ray film 07 p0983 N85-16104
The physical implications of an isothermal model for the hot intracluster medium
[NASA-TM-86174] 11 p1783 N85-21099
Development of high resolution imaging detectors for X-ray astronomy
[NASA-CR-175505] 12 p1953 N85-22266
New developments in industrial radiography 14 p2317 N85-24317

Documentation of PHOTO: A user's manual for the analysis of photographic and X-ray negatives
[AD-A152986] 17 p2967 N85-26327
A new high-resolution pickup tube for live X-ray topography
[NHK-LABS-NOTE-309] 18 p3193 N85-29602
Development of observational and instrumental techniques in hard X-ray and medium energy gamma-ray astronomy
[NASA-CR-176172] 24 p4168 N85-35841
High sensitive X-ray films to detect electron showers in 100 GeV region
[HE-3.1-13] 24 p4176 N85-35911
X-ray film chamber with carbon target of Tien-Shan complex array 24 p4179 N85-35915
A new method of differential structural analysis of gamma-family basic parameters
[HE-3.6-3] 24 p4184 N85-35952

X RAY INSPECTION
Quantitative roughness analysis of treated surfaces with higher-class finish by methods of X-ray reflectometry
14 p2282 N85-24136

X RAY IRRADIATION
Lithography radiation effects study
[AD-A146552] 10 p1468 N85-19260
Hit-size effectiveness theory applied to high doses of low LET radiation for pink mutations in Tradescantia
[DE85-011835] 22 p3819 N85-33957
Applications of holography to X-ray imaging
[DE85-010984] 23 p3934 N85-34364
The read-out system of spatial distribution of thermoluminescence in meteorites
[SH-9.1-16] 23 p4052 N85-35131
Neutrino astronomy and the atmospheric background
[HE-5.3-17] 24 p4207 N85-36111

X RAY LASERS
Particle physics
[DE84-013834] 05 p0727 N85-14673
Estimate of nuclear-pumped X-ray laser mechanism
06 p0748 N85-14795
Investigations of vacuum ultraviolet and soft X-ray lasers
[AD-A148277] 08 p1167 N85-17358
Imploding plasma X-ray laser research
[DE85-000067] 09 p1328 N85-18331
KMSF X-ray laser experiments, task no. 1
[DE85-001002] 11 p1639 N85-20325
KMSF X-ray laser experiments, task no. 2
[DE85-000291] 11 p1640 N85-20335
Time resolved X-ray studies during pulsed laser irradiation of Ge
[DE85-005283] 13 p2097 N85-23083
Population inversion in laser-initiated vacuum arcs
[AD-A151958] 16 p2790 N85-27210
Progress in inertial fusion at LLNL
[DE85-010931] 19 p3277 N85-30321
Strong coupling effects on bound states in plasmas
[AD-A154353] 19 p3370 N85-30805
Novette diagnostic support
[DE85-012937] 23 p3934 N85-34363
Photoionization-pumped, Ne 2, X-ray laser studies project
[DE85-012973] 23 p3936 N85-34399
Summary of activities, 1983
[LBL-16600] 23 p3969 N85-34605
Solid neon sources for plasma and X-ray lasers
[DE85-011347] 24 p4066 N85-35402

X RAY SCATTERING
High energy-resolution inelastic X-ray scattering
[DE84-014665] 01 p0118 N85-10804
X-ray and neutron scattering and X-ray spectroscopy for the study of defects in solid state materials
03 p0430 N85-12741
Microstructural analysis of ion containing polymers
[DE85-001694] 10 p1453 N85-19157
Magnetic X-ray scattering studies of the rare Earth metal holmium
[DE85-003608] 12 p1607 N85-21335
Comparison of findings of theories describing reflection from real surface with experiments in region of ultrasoft X-radiation 21 p2984 N85-32950
On gamma and neutrino radiation from Cyg X-3
[OG-2.1-7] 22 p3863 N85-33824
Gamma rays of 0.3 to 30 MeV from PSR 0531+21
[OG-2.3-8] 22 p3866 N85-33845

X RAY SOURCES
NT X RAY BINARIES
X-ray observations of the Seyfert 1 galaxies AKN120 and MCG8-11-11
[NASA-TM-80663] 03 p0446 N85-12839
On syntheses of the X-ray background with power-law sources
[NASA-TM-82173] 03 p0446 N85-12840
Einstein solid state spectrometer observation of the peculiar red dwarf Wolf 630 AB
[NASA-TM-83947] 03 p0447 N85-12843
Ultrasoft X-ray background observations of the local interstellar medium 06 p0677 N85-15571
Preliminary results on the ultraviolet observations of a complete X-ray selected sample of Active Galactic Nuclei (AGN) — HEAO 2 08 p1237 N85-17800
The extragalactic nature of H0323+022
08 p1237 N85-17802
Spatially resolved optical spectroscopy of the radio jet of the X-ray galaxy NGC 2110 08 p1236 N85-17804
X-ray surveys of quasars with the Einstein observatory
08 p1236 N85-17807
Characteristics of X-ray spectra from galactic and extragalactic X-ray sources 08 p1239 N85-17811
EXO 1102.8+2539, an X-ray variable Active Galactic Nucleus (AGN) 08 p1239 N85-17816
Comments on the physics of active galactic nuclei
08 p1240 N85-17823
The ROSAT all-sky survey in X-rays
08 p1243 N85-17843
The ROSAT XUV wide field camera
08 p1243 N85-17844
On the unique capabilities of the Hubble space telescope for studies of ROSAT deep-survey X-ray sources
08 p1243 N85-17846
A survey of fast X-ray transients using the HEAO A-1 Sky Survey experiment 09 p1411 N85-18895
X-ray emission from Centaurus A
[DE85-002030] 09 p1417 N85-18943
Design, construction and initial evaluation of an absolute, time-integrating/time-resolving spectrometer for the diagnostics of pulsed, high temperature plasma X-ray sources in the 100-10,000 eV region
[DE85-003526] 11 p1732 N85-20686
The X-ray structure of the Crab Nebula
11 p1741 N85-20948
Search for millisecond rotational periods in some low-mass X-ray binaries observed by EXOSAT
11 p1741 N85-20949
Optical and X-ray observations of 4U2129+47/V1727 CYG in a quiescent state 11 p1742 N85-20950
EXOSAT observations of the galactic bulge X-ray source GX17+2 — X ray binary star 11 p1742 N85-20951
The X-ray structure of the Crab Nebula
11 p1742 N85-20954
Recent results on the Crab Pulsar X-ray light curve
11 p1742 N85-20955
EXOSAT observations of the 35d intensity variations of Her X-1 — X ray binary source
11 p1742 N85-20956
Pulse phase spectroscopy of Her X-1 with EXOSAT — X ray binary source 11 p1743 N85-20957
Simultaneous EXOSAT and optical observations of the pulsing X-ray binary H2252-035 / AO Psc
11 p1743 N85-20958
Spectral studies of low-mass X-ray binaries observed by EXOSAT 11 p1743 N85-20959
EXOSAT observations of 4U1705-44 — X ray binary
11 p1743 N85-20960
Very recent IUE observations of 2 BL lacertae objects
11 p1748 N85-20962
Considerations for upgrading modifications to the Marshall Space Flight Center's X-ray calibration facility
12 p1946 N85-22226
X-ray experiment on Prognoz-9 artificial Earth satellite
15 p2478 N85-25295
Optical observations of HEAO-B objects
17 p3052 N85-28695
A high energy X-ray study of the galactic center
[AD-A153852] 18 p3202 N85-29862
One-frequency laser interferometer using the optic fiber as a polarization-independent interference phase detector
[DE85-010544] 19 p3277 N85-30326
Salyut-7 cosmonauts work with RS-17 and GSPS X-ray telescopes 22 p3731 N85-33131
Comments on RS-17 X-ray telescope
22 p3731 N85-33132
Astron X-ray experiment 22 p3732 N85-33137
Observation of hard X-rays from the Crab pulsar and A0535+26
[OG-2.3-7] 22 p3866 N85-33844
Search for periodicities near 59 s in the COS-B gamma-ray data of 2CG195+04 (Geminga)
[OG-2.4-3] 22 p3867 N85-33950
A search in the COS-B data base for correlated time variability in regions containing objects of interest
[OG-2.5-9] 22 p3869 N85-33964
Radio observations of four anticenter 2CG gamma-ray sources
[OG-2.5-10] 22 p3869 N85-33965
Balloon observations of hard X-rays from some galactic X-ray sources
[OG-2.5-11] 22 p3870 N85-33966
Further studies of X-ray structure of the Perseus cluster
[OG-2.5-12] 22 p3870 N85-33967
Observation of gamma-rays from LMC X-4 above 10(16) eV
[OG-2.6-10] 22 p3870 N85-33972
The 4U 0115+63: Another energetic gamma ray binary pulsar
[OG-2.6-11] 22 p3870 N85-33973
Balloon observations of hard X-rays from NGC 4151 and an X-ray transient source
[OG-2.7-6] 22 p3871 N85-33979
An extended superhot solar flare X-ray source
[SH-1.2-6] 23 p3991 N85-34743
Capabilities of the GRO/BATSE for monitoring of discrete sources
[OG-9.2-16] 23 p4026 N85-34965
Lapex: A Phoswich balloon experiment for hard X-ray astronomy
[OG-9.3-1] 23 p4027 N85-34966

X RAY SPECTRA
X-ray observations of the Seyfert 1 galaxies AKN120 and MCG8-11-11
[NASA-TM-80663] 03 p0446 N85-12839
On syntheses of the X-ray background with power-law sources
[NASA-TM-82173] 03 p0446 N85-12840
The X-ray spectrum and time variability of narrow emission line galaxies
[NASA-TM-83959] 03 p0446 N85-12842
Secondary fluorescence effects on X-ray microanalysis
[DE84-016600] 05 p0618 N85-13951
Non-LTE considerations in spectral diagnostics of thermal transport and implosion experiments
[DE84-015187] 05 p0730 N85-14689
X-ray and ultraviolet observations of BL Lacertae objects 06 p0741 N85-14767
Measurements of X-ray spectra from laser produced plasma 06 p0748 N85-14794
The nature of the soft X-ray emitting region in the direction of the North Polar spur
06 p0677 N85-15568
HEAO-1 diffuse soft X-ray sky maps
06 p0677 N85-15570
Ultrasoft X-ray background observations of the local interstellar medium 06 p0677 N85-15571
Evidence for non-radiative activity in stars with T sub eff 10000 K 08 p1231 N85-17757
Coronal temperatures 08 p1233 N85-17766
Effect of scattering on instabilities in line-driven stellar winds 08 p1235 N85-17784
Radiative amplification of acoustic waves in hot stars
08 p1235 N85-17786
X-ray emission from active galactic nuclei
08 p1236 N85-17806
Soft X-ray emission from BL Lac objects
08 p1239 N85-17810
Characteristics of X-ray spectra from galactic and extragalactic X-ray sources 08 p1239 N85-17811
X-ray emission from PKS 2155-304 — BL Lac object
08 p1239 N85-17812
X-ray emission from Centaurus A — Vela 5B; radio galaxy 08 p1239 N85-17813
X-ray spectra of accretion disks — active galactic nuclei 08 p1239 N85-17814
The X-ray spectra of NGC 4151 — Seyfert galaxy
08 p1239 N85-17815
One to eight month X-ray light curves for active extragalactic objects 08 p1239 N85-17817
The high energy X-ray spectrum of 3C 273 — quasar
08 p1240 N85-17818
UV and X-ray observations of AGN: Two comparisons with other wave lengths — Active Galactic Nuclei (AGN)
08 p1240 N85-17819
The X-ray properties of high-redshift, optically selected QSOs 08 p1240 N85-17821
On the surface density of X-ray selected BL Lacertae objects 08 p1240 N85-17822
An inverse Compton model of the X-ray emission in Seyfert galaxies 08 p1241 N85-17827
Power law X- and gamma-ray emission from relativistic thermal plasmas 08 p1241 N85-17829
Pair production at moderate optical depths — galactic nuclei X ray spectra 08 p1241 N85-17830
X-ray spectra of accretion disks — active galactic nuclei 08 p1242 N85-17838
The origin of the X-ray background
08 p1243 N85-17841
Temporal and spectral characteristics of solar flare hard X-ray emission
[NASA-TM-86187] 08 p1259 N85-17923
Application of tunable monochromatic synchrotron radiation to the quantitative determination of trace elements
[DE85-001271] 09 p1291 N85-18106
X-ray spectra of supernova remnants
[NASA-TM-86169] 09 p1413 N85-18909

Sequentially-framing soft X-ray pinhole camera for Tokamak plasma studies
[DE85-001717] 10 p1489 N85-19399
Design, construction and initial evaluation of an absolute, time-integrating/time-resolving spectrometer for the diagnostics of pulsed, high temperature plasma X-ray sources in the 100-10,000 eV region
[DE85-003528] 11 p1732 N85-20896
Contributions of the X-ray astronomy group — conference
[MPE-PREPRINT-29] 11 p1742 N85-20952
X-ray coronae of late type stars: Theoretical implications 11 p1742 N85-20953
EXOSAT observations of the 35d intensity variations of Her X-1 — X ray binary source 11 p1742 N85-20956
Spectral studies of low-mass X-ray binaries observed by EXOSAT 11 p1743 N85-20959
IUE and optical observations of LMC X-ray binaries 11 p1757 N85-21050
X-ray emission from active galactic nuclei
[NASA-TM-86175] 11 p1783 N85-21088
Plasma in the clusters of galaxies 12 p1957 N85-22299
A soft X-ray survey of galactic supernova remnants with the Einstein Observatory 14 p2434 N85-25013
High resolution hard X-ray spectra of solar and cosmic sources 14 p2455 N85-25183
Spectroscopy of quasimolecular X-rays with H-like decelerated ions
[DE85-006565] 15 p2649 N85-26337
Spectral constraints on models of gas in clusters of galaxies
[NASA-TM-86188] 15 p2669 N85-26468
X-ray emission and the winds of cataclysmic variables
[DE85-007663] 17 p3053 N85-28902
The solar coronal X-ray spectrum 5.5-12 A
[AD-A152334] 17 p3054 N85-28908
Opticals constant at X-ray wavelengths
[DE85-009743] 19 p3355 N85-30795
Simultaneous Solar Maximum Mission and Very Large Array (VLA) observations of solar active regions
[NASA-CR-176090] 22 p3859 N85-33897
CEN A observation at MeV-energies
[OG-2.7-7] 22 p3871 N85-33980
Investigations of the cyclotron resonance effects in the X ray spectrum of the neutron star Hercules X-1
[MPE-191] 22 p3890 N85-34112
Workshop report on Simulation Techniques for Shock Wave Phenomena and Characteristics of Plasmas in Inertial Confinement Fusion
[IPPJ-725] 23 p3979 N85-34670
X-ray spectra of bursting neutron stars 23 p3981 N85-34686
Multiple inner shell vacancies in laser-irradiated Au plasma 23 p3981 N85-34687
Helios 1 energetic particle observations of the solar gamma ray flare events of 7, 21 June 1980 and 3 June 1982
[SH-1.3-8] 23 p3993 N85-34755
Injection of energetic particles following the gamma-ray flares on June 7, 1980, as observed on Helios 1
[SH-1.3-9] 23 p3993 N85-34756
Multidimensional analysis of data obtained in experiments with X-ray emulsion chambers and extensive air showers
[HE-3.6-2] 24 p4184 N85-35951

X RAY SPECTROGRAPHY
U X RAY SPECTROSCOPY

X RAY SPECTROMETRY
U X RAY SPECTROSCOPY

X RAY SPECTROSCOPY
The X-ray Absorption Coefficient Fine Structure (EXAFS) study on precipitates in AlCu
[DESY-SR-84-15] 01 p0025 N85-10153
X-ray and neutron scattering and X-ray spectroscopy for the study of defects in solid state materials 03 p0430 N85-12741
Space observations of solar flares 04 p0519 N85-13313
Non equilibrium ionization in the local hot bubble 06 p0679 N85-15587
Measurement of soft X-ray absorption spectra with a fluorescent ion chamber detector
[AD-A142213] 07 p0922 N85-15838
An auroral X-ray imaging spectrometer
[AD-A147758] 08 p1185 N85-17469
Simulation of bent crystal spectrometers
[DE85-002042] 09 p1385 N85-18709
X-rays spectroscopy on the PLT and TFTR Tokamaks 09 p1386 N85-18720
Radial profiles of high resolution X-ray spectra from the Alcator C Tokamak 09 p1387 N85-18723
Soft X-ray spectroscopy of laser produced plasmas 09 p1387 N85-18727
X-ray spectroscopy of high-Z and high-density plasmas 09 p1387 N85-18726
Determination of ion temperature and rotation velocity profiles by visible, UV and X-ray spectroscopy on Doublet 3 09 p1388 N85-18734
X-ray spectra of supernova remnants
[NASA-TM-86189] 09 p1413 N85-18909
Characterization of CO binding sites on Rh(111) and Rh(331) surfaces by XPS and LEED (Low Energy Electron Diffraction): Comparison to EELS (Electron Energy Loss Spectroscopy) results
[AD-A149331] 10 p1435 N85-19044
Synchrotron X-ray fluorescence and extended X-ray absorption fine structure analysis
[DE85-003606] 10 p1436 N85-19063
Calculation of Si(Li) X-ray detector efficiencies
[DE85-002732] 10 p1489 N85-19400
X-ray spectroscopy of laser-produced plasmas
[DE85-002170] 11 p1733 N85-20897
Pulse phase spectroscopy of Her X-1 with EXOSAT — X ray binary source 11 p1743 N85-20957
Description of the SSB/A (Special Sensor B/Aerospace X-ray spectrometer
[AD-A150040] 12 p1790 N85-21236
Some unique aspects of fouling on copper as compared to titanium or nickel
[AD-A150072] 12 p1806 N85-21332
Development and application of low energy X-ray and electron physics
[AD-A149983] 12 p1926 N85-22099
The Valence- and conduction-band structure of the sapphire (1102) surface
[AD-A150001] 12 p1940 N85-22184
Magnetic field structures of hard X-ray flares observed by HINOTORI spacecraft — solar flares 14 p2455 N85-25181
X-ray spectroscopy of solids under pressure
[DE85-006939] 15 p2507 N85-25465
Soft X-ray diagnostics of laser-produced plasmas (HALNA) 15 p2655 N85-26382
Cosmic X-ray physics
[NASA-CR-175808] 17 p3055 N85-28910
Proceedings of the Fifth International Conference on Nuclear Methods in Environmental and Energy Research
[DE84-017348] 19 p3310 N85-30521
An empirical technique to measure X-ray production and detection efficiencies in the analytical electron microscope
[DE85-010270] 19 p3361 N85-30837
Chemical structure of interfaces 20 p3480 N85-31629
CCD-based X-ray spectrometry for on-line determination of laser plasma electron temperature 21 p3692 N85-32908
Soft X-ray polychromator for the Solar Maximum Mission
[NASA-CR-175297] 21 p3723 N85-33096
Salyut-7 cosmonauts work with RS-17 and GSPS X-ray telescopes 22 p3731 N85-33131
Astron X-ray experiment 22 p3732 N85-33137
X-ray spectroscopy of solids under pressure
[DE85-011486] 22 p3745 N85-33213
Thermal transport measurements of UV laser irradiated spherical targets
[DE85-011038] 23 p3931 N85-34365
Elliptical X-ray analyzer spectrograph application to a laser-produced plasma
[DE85-013790] 24 p4097 N85-35368
Size and shape dependence of CO adsorption sites on sapphire supported Fe microcrystals
[NASA-CR-176171] 24 p4160 N85-35794

X RAY STRESS ANALYSIS
Multiaxial stress analysis taking account of penetration depth of X-rays. A solution by means of polynomial approximation 23 p3907 N85-34204

X RAY TELESCOPES
A normal incidence, high resolution X-ray telescope for solar coronal observations
[NASA-CR-174145] 04 p0579 N85-13699
Considerations for upgrading modifications to the Marshall Space Flight Center's X-ray calibration facility 12 p1946 N85-22228
A normal incidence, high resolution X-ray telescope for solar coronal observations
[NASA-CR-176822] 13 p2199 N85-23461
A rocket-borne X-ray observation of SN1006 with the imaging gas scintillation proportional counter 14 p2435 N85-25014
The Extended Range X-Ray Telescope center director's discretionary fund report
[NASA-TM-86507] 19 p3382 N85-30883
Salyut-7 cosmonauts work with RS-17 and GSPS X-ray telescopes 22 p3731 N85-33131
Comments on RS-17 X-ray telescope 22 p3731 N85-33132
Astron X-ray experiment 22 p3732 N85-33137
Coordinated study of solar-terrestrial payloads on space station
[NASA-CR-176180] 23 p3900 N85-34158
Soft X-Ray Telescope (SXT) 23 p3900 N85-34159
A comparison of calculated and measured background noise rates in hard X-ray telescopes at balloon altitude
[OG-9.3-7] 23 p4028 N85-34882
A normal incidence X-ray telescope sounding rocket payload
[NASA-CR-176169] 24 p4153 N85-35749

X RAY TUBES
Considerations for upgrading modifications to the Marshall Space Flight Center's X-ray calibration facility 12 p1946 N85-22228

X RAYS
NT COSMIC X RAYS
NT SOLAR X-RAYS
Determining composition in surface region of semiconductor crystals by method of sudden changes in X-ray photoelectric effect 02 p0257 N85-11748
Experimental capabilities and prospects for measuring soft X-ray photoabsorption
[DE84-015498] 02 p0278 N85-11813
Energetic electrons in impulsive solar flares 02 p0900 N85-11962
Flash radiography as a quantitative tool
[DE84-016465] 04 p0503 N85-13211
Real space solution to the phase problem in X-ray crystallography: ALCAMPS (Ames Laboratory Computer-aided Analysis of Multi-solution Patterson Superpositions)
[DE84-015476] 04 p0572 N85-13651
A neutral gas jet in a low velocity shock front at the boundary of the Draco Nebula 06 p0878 N85-15576
Improved radiographic viewing system
[AD-A147587] 07 p1018 N85-16456
X rays from the aurora
[AD-A149628] 08 p1186 N85-17477
X-ray activity in pre-main sequence stars 08 p1233 N85-17764
Is the ratio of observed X-ray luminosity to bolometric luminosity in early-type stars really a constant? 08 p1234 N85-17777
Non-radiative energy from differential rotation in hot stars 08 p1234 N85-17778
Bipolar flows and X-ray emission from young stellar object 08 p1234 N85-17779
A microchannel plate pinhole camera for 20 to 100 keV X-ray imaging
[DE85-001572] 10 p1488 N85-19396
X-ray holography of biological specimens
[DE85-002437] 10 p1489 N85-19398
Coronal effects of the winds of early-type stars 11 p1740 N85-21002
Development and application of low energy X-ray and electron physics
[AD-A149983] 12 p1926 N85-22099
X-ray lithography and VLSI circuits 13 p2052 N85-23846
Utilization of microchannel plates in the flash X-ray technique
[ISL-CO-226/83] 14 p2308 N85-24275
Basic principles of industrial radiography 14 p2316 N85-24310
Auroral X-rays and equatorial electrons in the morning sector — substorm 14 p2361 N85-24590
On the location of the source for X-ray microbursts 14 p2361 N85-24591
Workshop report on new directions in soft X-ray photoabsorption
[DE85-006150] 14 p2419 N85-24923
X-ray emission in heavy ion collisions
[DE85-006350] 14 p2419 N85-24927
X-ray polarimetry: The measurement of the polarization of solar flare X-rays and the design of a Compton polarimeter 14 p2441 N85-25059
Annual Review, April 1983 - March 1984
[ISSN-0547-1567] 15 p2654 N85-26360
An X-ray study of residual stresses in narrow groove TIG weldments
[DE85-006485] 16 p2802 N85-27274
Software for reflectivity calculations of X-ray mirrors, revision 1
[DE85-006942] 16 p2867 N85-27668
A synchrotron/inverse Compton interpretation of a solar burst producing fast pulses at lambda 3 mm and hard X-rays 16 p2867 N85-27815
Documentation of PHOTO: A user's manual for the analysis of photographic and X-ray negatives
[AD-A152988] 17 p2967 N85-29027
Coherent X-rays and vacuum-ultraviolet radiation from storage-ring-based undulators and free electron lasers
[DE85-009998] 18 p3183 N85-29736

Design consideration for the X-ray Cerenkov experiment
[AD-A153636] 18 p3189 N85-29777
Three-dimensional and tomographic imaging device for X-ray and gamma-ray emitting objects
[NASA-CASE-GSC-12851-1] 19 p3271 N85-30261
Symposium on Luminescent Radiation Receivers and Converters 19 p3295 N85-30430
Opticals constant at X-ray wavelengths
[DE85-009743] 19 p3355 N85-30795
An empirical technique to measure X-ray production and detection efficiencies in the analytical electron microscope
[DE85-010270] 19 p3361 N85-30837
Comparison of findings of theories describing reflection from real surface with experiments in region of ultrasoft X-radiation 21 p3694 N85-32950
Contributions to the 19th International Cosmic Ray Conference
[NASA-CR-176000] 21 p3714 N85-33044
Salyut-7 cosmonauts work with RS-17 and GSPS X-ray telescopes 22 p3731 N85-33131
Results from Astron orbiting telescope 22 p3732 N85-33134
Gamma-ray burst variability above 4 MeV
[OG-1.2-7] 22 p3862 N85-33917
Observations on TeV gamma rays from Geminga and PSR 0950+08
[OG-2.4-6] 22 p3868 N85-33953
Balloon observations of hard X-rays from some galactic X-ray sources
[OG-2.5-11] 22 p3870 N85-33966
Further studies of X-ray structure of the Perseus cluster
[OG-2.5-12] 22 p3870 N85-33967
Some evidence for large gravitational redshift in Seyfert galaxy NGC 4151
[OG-2.7-11] 22 p3872 N85-33984
Spectrum of the gamma-ray diffuse component observed from HEAO-1
[OG-3.1-12] 22 p3874 N85-34000
Applications of holography to X-ray imaging
[DE85-010984] 23 p3934 N85-34384
Quasiperiodic oscillations in bright galactic-bulge X-ray sources
[NASA-CR-176136] 23 p3967 N85-34723
A position sensitive phoswich hard X-ray detector system
[OG-9.3-12] 23 p4028 N85-34967
Generation of stimulated emission in the soft X-ray range by nonlinear processes with excimer lasers
[DE85-012465] 24 p4098 N85-35403
On a possibility of inelasticity partial coefficient K sub gamma determination in pi C and pi Pb interactions at 10 to the 14th power eV (experiment PAMIR 1)
[HE-1.1-12] 24 p4171 N85-35859
Experiment Pamir-3. Coplanar emission of high energy gamma-quanta at interaction of hadrons with nuclei of air atoms at energies above 10 to the 7th power GeV
[HE-1.4-12] 24 p4177 N85-35899
Hadrons registration in emulsion chamber with carbon block
[HE-3.7-3] 24 p4186 N85-35962
Structured events in Pamir carbon X-ray chambers
[HE-3.7-7] 24 p4186 N85-35965
Ultra high energy events in ECHOS series and primary energy spectrum
[HE-3.7-9] 24 p4186 N85-35966

X-15 AIRCRAFT
Low-speed longitudinal orbiter qualities 08 p1092 N85-16905

X-29 AIRCRAFT
Multivariable control law design for the X-29 aircraft
[AD-A151828] 15 p2472 N85-25259
X-29 digital flight control system design 17 p2901 N85-27889

XB-70 AIRCRAFT
U B-70 AIRCRAFT

XBQM-108A AIRCRAFT
U VATOL AIRCRAFT

XENON
NT XENON ISOTOPES
NT XENON 129
Where is the Earth's missing xenon?
06 p0886 N85-15641
Kinetic studies following state selective laser excitations
[DE85-007173] 15 p2564 N85-25816
Double photon excitation of high-Rydberg atoms as a long-lived submillimeter detector
[NASA-CASE-NPO-16372-1] 19 p3352 N85-30779
Energy transfer and excimer formation in rare gas solids 19 p3374 N85-30930
Powerful XeCl excimer electric discharge laser with good temporal stability and fast response time
21 p3688 N85-32911
Interactions of heavy nuclei, Kr, Xe and Ho, in light targets
[OG-7.2-21] 23 p4016 N85-34888
Stopping relativistic Xe, Ho, Au and U nuclei in nuclear emulsions 24 p4173 N85-35876
Experimental basis for the models of cascade propagation in atmosphere
[HE-3.6-6] 24 p4185 N85-35954

XENON CHLORIDE LASERS
Electric discharge excitation and energy source integration
[AD-A151502] 15 p2562 N85-25808
Discharge characteristics of high-pressure, fast-discharge XeCl excimer laser
15 p2564 N85-25820

XENON FLUORIDE LASERS
Investigation of plasma processes in electronic transition lasers
[AD-A149682] 12 p1834 N85-21506

XENON ISOTOPES
NT XENON 129
The I-Pu-Xe age of the Moon
04 p0584 N85-13729
The degassing history of the Earth: Noble gas studies of Archaean cherts and zero age glassy submarine basalts 21 p3718 N85-33072
Nuclear reactions in shock wave front during supernova events
[OG-8.2-19] 23 p4021 N85-34915

XENON 129
When did the average cosmic ray flux increase?
[SH-7.1-4] 23 p4047 N85-35097

Y

YAG (GARNET)
U YTTRIUM-ALUMINUM GARNET

YAG LASERS
Optical recording of information on paper by CO2 and YAG-lasers 02 p0261 N85-11710
Optimization of ultrashort pulse generation mode of YAG laser 02 p0262 N85-11713
Anomalies in frequency characteristics of solid-state ring laser 02 p0271 N85-11765
Laser balancing system for high material removal rates
[NASA-CR-174731] 03 p0365 N85-12341
Design and testing of a refractive laser beam homogenizer
[AD-A146997] 07 p0970 N85-16162
Highly efficient Nd:YAG lasers for free-space optical communications 10 p1483 N85-19229
Solid state luminescent light filters for neodymium lasers 11 p1716 N85-20799
Lasing characteristics of YAG: Nd(3+)-laser with LiF passive shutter with F2 color centers
11 p1717 N85-20802
Stability of temporal and energy parameters of picosecond lanthanum beryllate laser
11 p1717 N85-20804
Neodymium YAG laser pumped with radiation from high frequency electrodeless discharge
13 p2044 N85-22796
Laser Welding, Cutting and Surface Treatment
14 p2306 N85-24278
Laser welding in the manufacture of heart pacemakers
14 p2306 N85-24286
Lasers in the nuclear industry
14 p2309 N85-24289
Laser drilling of aeroengine components
14 p2309 N85-24290
Future trends in the use of lasers in manufacturing
14 p2309 N85-24291
Amplification of scattered induced radiation flux in high-gain laser rods 15 p2644 N85-26309
Raman studies of surface temperature in laser-heated semiconductors
[AD-A151377] 15 p2659 N85-26412
Conducting a wind sensing study
[NASA-CR-175782] 16 p2832 N85-27465
Feasibility study on Laser Doppler Anemometer (LDA) wind velocity measurements using pulsed visible laser light
[ISL-CO-224/83] 16 p2836 N85-27489
Design and construction of a CW ND:YAG laser using a single elliptical cavity and water cooled krypton arc lamp pumping
[AD-A152657] 17 p2970 N85-28340
Laser machining and some applications
[NHK-LABS-NOTE-307] 18 p3112 N85-29266
Development and application of a high power ND-glass laser instrument
[AD-A154366] 19 p3276 N85-30314
Choice of optimum saturating absorber for YAG passive mode-locking laser 21 p3685 N85-32893
Operation of solid state lasers exposed to electron beam 21 p3685 N85-32895
Passive Q-modulation of optical cavities by KCl crystals containing OH(-) -ions 21 p3686 N85-32915
Holographic cinematography with the help of a pulse YAG laser
[ISL-CO-213/84] 22 p3788 N85-33472
Cineholography
[ISL-CO-214/84] 22 p3788 N85-33473

YANG-MILLS FIELDS
Supersymmetric Yang-Mills fields as an integrable system and connections with other non-linear systems
[DE84-013231] 04 p0556 N85-13539

YARNS
The effects of radial yarns, 3-dimensionally reinforced carbon-carbon composite
[AD-A144751] 01 p0022 N85-10134
Thermoplastic-carbon fiber hybrid yarn
[NASA-CR-3849] 03 p0325 N85-12093

YAW
Robust rate control system designs for a submersible
[AD-A144792] 01 p0111 N85-10753
Oil-flow study of a Space Shuttle orbiter tip-fin controller
[NASA-TM-86276] 04 p0460 N85-12920
Hypothetical zero yaw drag trajectory of spinning projectiles between M = 5 and M = 10
[AD-A148699] 10 p1421 N85-18903
Static investigation of several yaw vectoring concepts on nonaxisymmetric nozzles
[NASA-TP-2432] 18 p3058 N85-28924

YAWING MOMENTS
Liquid moment on a filled coning cylinder during spin-up: Ad hoc model
[AD-A150280] 13 p2092 N85-23060

YAWMETERS
U ATTITUDE INDICATORS
U YAW

YEAST
Microbial ecology of extreme environments: Antarctic yeasts and growth in substrate-limited habitats
[NASA-CR-175810] 16 p2839 N85-27509
Microbial ecology of extreme environments: Antarctic yeasts and growth in substrate-limited habitats
[NASA-CR-176005] 19 p3326 N85-30609

YF-17 AIRCRAFT
U F-17 AIRCRAFT

YHU-1 HELICOPTER
U UH-1 HELICOPTER

YIELD
Crop yield forecasting 07 p1001 N85-16360
NOAA-AISC user's guide for implementing CERES maize model for large area yield estimation
[E85-10083] 12 p1873 N85-21748
Electron yields from spacecraft materials
13 p1996 N85-22512
Surface wave seismic yields as measured by the Regional Seismic Test Network
[DE85-010532] 18 p3137 N85-29425

YIELD POINT
Removal of singularities in Tresca and Mohr-Coulomb yield functions
[OUEL-1528/84] 03 p0413 N85-12642
A simple engineering treatment of center cracked tension panels in the regime of nonlinear fracture mechanics under plane stress conditions
[GKSS-84-E-38] 08 p1173 N85-17398
The influence of mechanical damage on transmission pipeline integrity
[ERS-E.351] 09 p1340 N85-18431
Recent studies of the significance of mechanical damage in pipelines
[ERS-E.367] 09 p1341 N85-18433
Dynamic pressure test unit-ratio method
[AD-D011466] 10 p1488 N85-19392
Yield joint condition for three-dimensional I-beams
[ILR-MITT-137] 12 p1867 N85-21716
Magnetic method of inspecting mechanical properties of general purpose tubes
[BLL-M-36084-(5828.4)] 16 p2796 N85-27235
Fuel containment and damage tolerance in large composite primary aircraft structures
[NASA-CR-166063] 19 p3231 N85-30032
Effect of edge distance on yield initiation in a remotely loaded half-plane containing interference-fit disc of the same material
[ARL/STRUC-R-413] 19 p3285 N85-30369
Fuel containment and damage tolerance for large composite primary aircraft structures. Phase 1: Testing
[NASA-CR-166091] 24 p4073 N85-35241

YIELD STRENGTH
NT MICROYIELD STRENGTH
Multiaxial yield behavior of 1100 aluminum following various magnitudes of prestrain
[DE84-013904] 05 p0617 N85-13949

Defining effect of hardening on mean yield strength in deformation zone
[BLL-M-35934-(5828.4)] 05 p0647 N85-14154
Yield joint condition for three-dimensional I-beams
[ILR-MITT-137] 12 p1867 N85-21716
Structural strenght of strip D16T aluminum alloy with low copper and magnesium content
13 p2025 N85-22691
New deformable secondary aluminum alloys
13 p2026 N85-22694
Experimental investigation of crippling strength of Chinese aluminum alloy (LY12CZ) sections
13 p2041 N85-22779
Effect of oxygen on mechanical properties of Nb-V alloy
[DE85-002681] 14 p2256 N85-23982
Cast-iron technology: Metallographic and mechanical testing results
[DE85-002684] 14 p2257 N85-23984
Elastic-plastic analysis for cyclic loading using a linearized yield condition
[PB85-149607] 14 p2322 N85-24346
Magnetic method of inspecting mechanical properties of general purpose tubes
[BLL-M-36084-(5828.4)] 16 p2796 N85-27235
The Mises yield condition for thin rotationally symmetric shells
[BLL-BISI-TRANS-22047-(9022.06)]
17 p2978 N85-28409
Strength versus toughness relation in Fe-high manganese alloys
[DE85-007682] 18 p3074 N85-29013
Aging study of copper alloy 172
[DE85-009648] 18 p3075 N85-29029
Yield stress determination from miniaturized disk bend test data
[DE85-009495] 18 p3122 N85-29330
Effect of edge distance on yield initiation in a remotely loaded half-plane containing interference-fit disc of the same material
[ARL/STRUC-R-413] 19 p3285 N85-30369
Fatigue-crack growth and ductile fracture toughness behavior of ASTM A387 Grade 91 steel
[DE85-006495] 20 p3431 N85-31286
Mechanical properties of plasma arc cut steel
23 p3905 N85-34186

YIG (GARNET)
U YTTRIUM-IRON GARNET

YJ-85 ENGINE
U J-85 ENGINE

YOUNG MODULUS
U MODULUS OF ELASTICITY

YTTERBIUM
Optimization of the NiCrAl-Y/ZrO-Y2O3 thermal barrier system
[NASA-TM-86905] 07 p0927 N85-15678
Thermal barrier coating system
[NASA-CASE-LEW-14057-1] 24 p4072 N85-35233

YTTRIUM
High-temperature erosion of plasma-sprayed, yttria-stabilized zirconia in a simulated turbine environment
[NASA-TP-2406] 04 p0478 N85-13045
Compatibility experiments of facilities, materials, and propellants for electrothermal thrusters
[NASA-TM-86958] 12 p1795 N85-21260
Magnetovolume effects in some Y-Ni intermetallic compounds
[ISSN-0066-2003] 13 p2021 N85-22663
Improvement by cerium and yttrium ion implantation of oxidation behaviour of stabilised stainless steel in carbon dioxide
[AERE-R-11523] 14 p2259 N85-23996
A study of adherent oxide scales
[AD-A155554] 21 p3567 N85-32186
Modification of the grain size of sputtered copper with additions of oxygen, krypton, silver, or yttrium
[DE85-010975] 21 p3567 N85-32189
Calculation of activities of components in liquid alloys of iron with yttrium
[BLL-M-35868-(5828.4)] 23 p3914 N85-34253
Influence of yttrium on eutectoid transformation in irons
[BLL-M-35787-(5828.4)] 24 p4078 N85-35270

YTTRIUM COMPOUNDS
NT YTTRIUM OXIDES
NT YTTRIUM-ALUMINUM GARNET
NT YTTRIUM-IRON GARNET
Research on electroluminescence in thin film yttrium oxysulfide
[AD-A146809] 07 p1037 N85-16582

YTTRIUM OXIDES
Fundamental studies of structure property relationship in transformation toughened ceramics
[DE84-015344] 01 p0033 N85-10204
Study of the reactive-element effect in oxidation of Fe-Cr alloys using transverse section analytical electron microscopy
[DE84-016237] 04 p0571 N85-13841
Densification of submicron YSZ (Yttria-Stabilized Zirconia) powders with alumina and borate additives
[AD-A149520] 10 p1452 N85-19150
Progress on transparent yttria
[AD-P004370] 12 p1627 N85-21464
High-temperature X-ray diffraction study of coating-substrate compatibility in yttria-coated graphite
[DE85-005916] 14 p2262 N85-24016
Passivation on high Q acoustic strain sensor for accelerometer
[AD-A153565] 18 p3177 N85-29695
Process for improving the quality of epitaxial silicon films grown on insulating substrates
[AD-D011730] 22 p3847 N85-33828

YTTRIUM-ALUMINUM GARNET
Phonon-impurity relaxation and acoustic wave absorption in yttrium-aluminum garnet crystals with impurities
11 p1715 N85-20790
Electron-oscillatory spectra of yttrium-erbium-aluminum garnet of crystals and their role in laser pumping
11 p1715 N85-20791

YTTRIUM-IRON GARNET
Symmetry of exchange interaction in crystalline magnetic films
02 p0259 N85-11694

YUGOSLAVIA
The time and frequency comparisons via Loran-C and National TV Network in Yugoslavia
18 p3109 N85-29248

YUH-1 HELICOPTER
U UH-1 HELICOPTER

YUH-60A HELICOPTER
U UH-60A HELICOPTER

Z

ZEEMAN EFFECT
Development of novel lamps for study of enhanced production of resonance by low-density mercury discharges
[DE84-016889] 05 p0632 N85-14053
EPR linewidth studies of unpaired electrons at the Si-SiO2
[DE84-016727] 05 p0733 N85-14712
Nonlinear optical studies of rydberg atoms using degenerate four-wave mixing
[AD-A146827] 07 p1043 N85-16623
Basic studies of atomic dynamics
[DE84-015661] 09 p1380 N85-18675
Trends in measurement of solar vector magnetic fields using the Zeeman effect
18 p3204 N85-29677
Contribution functions for Zeeman-split lines, and line formation in photospheric faculae
18 p3207 N85-29693

ZENER DIODES
U AVALANCHE DIODES

ZENITH
Winter anomaly 1982/83 in comparison with earlier winters (1960-82)
11 p1660 N85-20461
Development of a portable zenith chamber and its use on the 47th parallel
[SER-C-287] 11 p1741 N85-20946
Simultaneous Earth observations from 2 satellites
[NASA-TM-86204] 16 p2810 N85-27325
The thickness of the shower disc as observed in showers produced by primaries above 10 (19)eV
[HE-4.7-6] 24 p4199 N85-36057
Thickness of the particle swarm in cosmic ray air showers
[HE-4.7-14] 24 p4200 N85-36064
Energy spectrum of cascades generated by muons in Baksan underground scintillation telescope
[HE-5.1-15] 24 p4202 N85-36077
Geophysical searches for three-neutrino oscillations
[HE-5.3-9] 24 p4205 N85-36103

ZEOLITES
Influence of structural parameters of zeolite catalysts on their activity and selectivity
[BMFT-FB-T-83-253] 03 p0329 N85-12119
Neutron diffraction studies of the hydrogen bonding and water molecules in zeolites
[DE84-016431] 06 p0786 N85-14900
Catalytic oxidation by transition metal ions in zeolites
[AD-A146826] 07 p0922 N85-15842
Advanced NMR characterization of zeolite catalysts
[DE85-000456] 09 p1291 N85-18104
Cation promotion effects in zeolite-supported F-T catalysts
[DE85-001708] 09 p1291 N85-18108
Zeolites on Mars: Prospects for remote sensing
13 p2195 N85-23615
Chemical weathering of soils from the dry valleys of Antarctica: A terrestrial analog of Martian weathering processes
13 p2197 N85-23628
Experimental testing of cooling by low pressure adsorption in a zeolite
[DE85-007509] 16 p2716 N85-26783
Correlation of zeolite ZSM-5 acid strength with catalytic activity and selectivity
[DE85-005415] 17 p2922 N85-29013
High resolution powder diffraction
[DE85-008287] 17 p2922 N85-29015
Cation promotion effects in zeolite-supported F-T catalysts
[DE85-009699] 19 p3233 N85-30044
Advanced NMR characterization of zeolite catalysts
[DE85-010143] 19 p3363 N85-30853
Rigid zeolite containing polyurethane foams
[DE85-006406] 23 p3919 N85-34286
Determination of properties of zeolite/refrigerant combinations for solar refrigeration systems
[DE85-012009] 23 p3945 N85-34448
FTIR studies of hydrocarbon synthesis on Pd/ZSM5 catalysts
[DE85-012430] 24 p4071 N85-35230

ZERO CROSSINGS
U ROOTS OF EQUATIONS

ZERO GRAVITY
U WEIGHTLESSNESS

ZERO LIFT
On relaxation of transonic flows around zero-lift airfoils and convergence of self-correcting wing tunnels
11 p1622 N85-20214

ZERO POINT ENERGY
Effective brightness of zero-point fluctuations of the electromagnetic vacuum accompanying parametric scattering of light
21 p3694 N85-32951
Evaluation of parameters for particles acceleration by the zero-point field of quantum electrodynamics
[OG-8.2-16] 23 p4020 N85-34912

ZERO POWER REACTORS
Monte Carlo alpha calculation
[DE85-010720] 19 p3349 N85-30758
Sulfur activation at the Little Boy-Comet Critical Assembly: A replica of the Hiroshima bomb
[DE85-010261] 20 p3527 N85-31938

ZETA AURIGAE STAR
Accretion in the zeta Aurigae and 32 Cygni shock cones
11 p1754 N85-21096
Egress spectra of the new eclipsing supergiant 22 Vulpeculae
11 p1755 N85-21039

ZETA PINCH
Finite orbit analysis for long wavelength modes in a plasma with a hot component
[DE85-006696] 15 p2658 N85-26404

ZINC
Universal binding energy relations in metallic adhesion
[NASA-TM-86669] 03 p0331 N85-12132
Alabama Tin Belt: Metallogenesis and mineral resource evaluation. Year-end report
[DE84-901335] 07 p0669 N85-16263
Thermal design requirements of a 50-kW zinc/redox flow battery for solar electrical energy storage
[DE84-017068] 09 p1345 N85-18463
Humidity effects on adhesion of nickel-zinc ferrite in elastic contact with magnetic tape and itself
[NASA-TP-2449] 12 p1811 N85-21359
Research on separators for alkaline zinc batteries
[DE85-003062] 12 p1836 N85-21523
New deformable secondary aluminum alloys
13 p2026 N85-22694
Aluminum alloy ATs5K5 (5% Zn + 5% Ca) for superplastic forming
13 p2026 N85-22697
Observation of a novel low-lying excited state in zinc complexes
[AD-A150188] 13 p2156 N85-23395
Thin film cadmium telluride and zinc phosphide solar cells
[DE85-002904] 15 p2587 N85-25950
Characteristics of polyacrylic acid-complexed zinc phosphate conversion films deposited on metal surfaces
[DE85-004057] 16 p2750 N85-26974
New approaches to functionalized fluorocarbons
[AD-A154205] 19 p3348 N85-30141
Photoelectronic properties of zinc phosphide crystals and heterojunctions
[DE85-006777] 19 p3307 N85-30501
Zinc: Biological effects. Facts and fiction
[USIP-84-12] 20 p3507 N85-31798
Plasma mass and effective inductance in a small railgun
[AD-A154644] 21 p3589 N85-32304
Environmental surveillance at Los Alamos during 1984
[DE85-011886] 22 p3811 N85-33605
The Conterminous United States Mineral Assessment Program
24 p4106 N85-35458

ZINC ALLOYS
Sea water rope batteries
[AD-A144775] 01 p0042 N85-10275
Application of the diffraction model to amorphous magnesium zinc alloys
[AD-A147369] 07 p0928 N85-15883
Influence of excess phases on fracture toughness of cast alumiun-magnesium-zinc alloy
10 p1442 N85-19091
Study of superplastic alloys based on Al-Zn-Ca
10 p1442 N85-19092
The role of hydrogen in the stress corrosion failure of high strength Al-Zn-Mg alloys
[AD-A150801] 14 p2258 N85-23978
Temperature variation of resistivity of certain alloys based on transition and simple metals in amorphous and crystalline states 15 p2496 N85-25399
Thermal expansion effects in electrical transport in amorphous metals
[AD-A152477] 17 p2930 N85-28069
Study of phase equilibria and crystallization processes in Al-Zn-Mg alloy systems 19 p3241 N85-30098
Resistance to corrosion fatigue in aluminum alloy 1561 in sea water 19 p3243 N85-30108
ZINC CHLORIDES
Transport in aqueous battery systems
[DE85-007246] 17 p2955 N85-28251
ZINC COATINGS
Galvanized wire protected against corrosion by chromate passivization
[BLL-M-95908-(5828.4)] 05 p0616 N85-13936
High strength steel sheet with dual phase structure
[BMFT-FB-T-84-219] 12 p1808 N85-21342
Corrosion of aircraft Al and Al-Zn ion plated steel fasteners 13 p2021 N85-22666
The effect of water chemistry on the rates of hydrogen generation for galvanized steel corrosion at post-loca conditions
[NUREG/CR-3361] 14 p2253 N85-23963
The corrosion resistance of zinc coatings on depleted uranium and uranium alloys
[DE85-007216] 15 p2510 N85-25487
New corrosion protection concept for very high voltage line towers
[BLL-OA-TRANS-2691-(6196.300)] 20 p3429 N85-31270
Effects of humidity cycles on the corrosion of galvanised reinforcements in carbonated and uncarbonated mortars
[BLL-CE-TRANS-8039-(9022.09)] 20 p3430 N85-31272
ZINC COMPOUNDS
NT ZINC CHLORIDES
NT ZINC OXIDES
NT ZINC SELENIDES
NT ZINC SULFIDES
The alpha-form of the hydroxides of bivalent metals
[NASA-TM-77506] 04 p0473 N85-13009
Magnetic and structural properties of shock-synthesized zinc ferrite
[DE85-000469] 11 p1736 N85-20915
Properties of chromate coatings formed on electrolytic zinc substrates
[BLL-BISI-TRANS-22349-(9022.06)] 17 p2926 N85-29052
ZINC NICKEL BATTERIES
U NICKEL ZINC BATTERIES
ZINC OXIDES
Solid state, surface and catalytic properties of oxides
[DE85-002006] 06 p0667 N85-15512
Advanced metal oxide varistor concepts
[DE84-016877] 09 p1316 N85-18276
Stability of highly nonlinear oxide-zinc resistors under continuous voltage of industrial frequency
13 p2087 N85-23030
Vapor sensing by means of a ZnO-on-Si surface acoustic wave resonator
[DE85-003250] 15 p2646 N85-26324
Effects of processing chemistry on electrical properties of high field ZnO varistors
[DE85-007688] 17 p2956 N85-28254
A study of Co and Mn in ZnO varistors
[DE85-011193] 19 p3263 N85-30233
Gas sensing with surface acoustic wave devices
[DE85-009125] 20 p3524 N85-31921
High temperature solar electrothermal processing 2. Zinc from zinc oxide
[AD-A154747] 21 p3562 N85-32159
Development and evaluation of sulfonated polysulfone membranes for the zinc-ferricyanide battery
[DE85-009104] 24 p4090 N85-35357
ZINC SELENIDES
Effect of oxidizing medium and heat treatment on stoichiometry of ZnSe crystal surface
03 p0353 N85-12272
Zn3P2 as an improved semiconductor for photovoltaic solar cells
[DE85-006772] 18 p3097 N85-29171
ZINC SULFIDES
Laser induced damage of zinc sulphide
[BAE-BT-13363] 15 p2562 N85-25803
Zn3P2 as an improved semiconductor for photovoltaic solar cells
[DE85-006772] 18 p3097 N85-29171
Prospects for parallel nonlinear optical signal processing using GaAs etalons and ZnS interference filters
18 p3187 N85-29765
Vectorial electron transfer on designed surfaces
[PB85-204600] 24 p4076 N85-35263
ZINC-BROMIDE BATTERIES
Prospects for advanced storage battery technologies
[DE84-015706] 09 p1345 N85-18464
ZINC-CHLORINE BATTERIES
Baseline cycle testing of a 500-kWh zinc chloride battery at the Battery Energy Storage Test (BEST) Facility
[DE85-006948] 17 p2955 N85-28249
Transport in aqueous battery systems
[DE85-007246] 17 p2955 N85-28251
ZIRCALOYS (TRADEMARK)
Continuous measurement of zircaloy corrosion in air with an ultrasonic corrosion monitor
[DE85-003663] 12 p1807 N85-21337
ZIRCONIUM
Effects of cobalt, boron, and zirconium on the microstructure of Udimet 738
[NASA-CR-174762] 01 p0027 N85-10166
High-temperature erosion of plasma-sprayed, yttria-stabilized zirconia in a simulated turbine environment
[NASA-TP-2406] 04 p0478 N85-13045
A soluble linear Schiff-base coordination polymer containing eight-coordinate zirconium(4)
[AD-A151446] 15 p2518 N85-25527
Characterization of the fatigue and slow crack growth behavior of partially stabilized zirconia ceramics
[DE85-005240] 17 p2934 N85-28113
Long range ordered alloys modified by addition of niobium and cerium
[DE85-011661] 20 p3431 N85-31285
Chemical constraints on the evolution of Archean continental crust 21 p3722 N85-33093
Thermal barrier coating system
[NASA-CASE-LEW-14057-1] 24 p4072 N85-35233
ZIRCONIUM ALLOYS
NT ZIRCALOYS (TRADEMARK)
Re-evaluation of phase separation in Ti-Zr-Be metallic glasses
[DE84-015603] 03 p0338 N85-12176
On reversion phenomena in Cu-Zr-Cr alloys
[NASA-TM-77791] 08 p1125 N85-17092
Effects of hydrogen on magnetic properties of amorphous zirconium alloys
[DE85-003303] 11 p1607 N85-20107
Conversions in amorphous zirconium-vanadium alloy
15 p2496 N85-25400
Manufacturing process to reduce large grain growth in zirconium alloys
[DE85-011649] 23 p3915 N85-34267
ZIRCONIUM CARBIDES
Combustion of zirconium carbide
13 p1999 N85-22532
Measurements of distributed combustion
13 p2001 N85-22542
ZIRCONIUM COMPOUNDS
NT ZIRCONIUM CARBIDES
NT ZIRCONIUM HYDRIDES
NT ZIRCONIUM NITRIDES
NT ZIRCONIUM OXIDES
Progress in lead/uranium zircon studies of lower paleozoic rocks of the southern Alexander terrane
04 p0518 N85-13304
Dating Archean zircon by ion microprobe: New light on an old problem 21 p3722 N85-33094
ZIRCONIUM HYDRIDES
Effects of hydrogen on magnetic properties of amorphous zirconium alloys
[DE85-003303] 11 p1607 N85-20107
ZIRCONIUM NITRIDES
Corrosion study on zirconium refractory coatings. 1: Oxidation of zirconium nitride coatings by oxygen
[BLL-RISLEY-TR-5044-(9091.9F)] 07 p0925 N85-15857
Tests on zirconium nitride coatings applied to SW 18 steel using the chemical vapor deposition method
24 p4078 N85-35271
ZIRCONIUM OXIDES
Fundamental studies of structure property relationship in transformation toughened ceramics
[DE84-015344] 01 p0033 N85-10204
Microfluorescence studies of zirconium oxide
[DE84-016116] 03 p0329 N85-12118
Time-temperature dependence of the strength of commercial zirconia ceramics
[AD-A146233] 03 p0339 N85-12173
An investigation of enhanced capability thermal barrier coating systems for diesel engine components
[NASA-CR-174820] 09 p1296 N85-18154
Study of charge transport in the thermoelectret state of some ceramics and glasses
[DE85-001763] 09 p1300 N85-18163
Densification of submicron YSZ (Yttria-Stabilized Zirconia) powders with alumina and borate additives
[AD-A149520] 10 p1452 N85-19150
Laser processing of ceramics
[DE85-001184] 11 p1612 N85-20135
High-temperature, solid oxide electrolyte fuel cell power generation system
[DE85-002976] 11 p1675 N85-20552
Transformation toughened ceramics: A potential material for light diesel engine applications
[AD-A151413] 15 p2518 N85-25525
Rocket thrust chamber thermal barrier coatings
16 p2734 N85-26857
Fracture toughness of MgCr(sub)2O(sub)4-ZrO(sub)2
[DE85-007945] 17 p2917 N85-27962
Indirect brazing of structural ceramics for uncooled diesels
[DE85-005589] 17 p2935 N85-28116
Microstructure-mechanical property relationships in transformation-toughened ceramics
[DE85-009722] 17 p2935 N85-28117
Study of synthesis gas conversion over metal oxides
[DE85-010136] 18 p3072 N85-28999
Process for improving the quality of epitaxial silicon films grown on insulating substrates
[AD-D011730] 22 p3847 N85-33829
ZODIACAL DUST
Zodiacal light: A replica of the interplanetary dust cloud — Helios space probe 16 p2685 N85-27796
ZODIACAL LIGHT
Zodiacal light: A replica of the interplanetary dust cloud — Helios space probe 16 p2685 N85-27796
ZONAL HARMONICS
Diurnal variation harmonics and spatial change in cosmic ray flux 06 p0624 N85-15230
First zonal harmonic component of cosmic ray neutron intensity
[SH-4.3-13] 23 p4032 N85-34997
ZONE MELTING
Stress studies of EFG
[NASA-CR-174078] 05 p0651 N85-14179
German payloads for EURECA 1
[BMFT-FB-W-85-003] 20 p3419 N85-31223
Striation free doped silicon
[AD-A155730] 22 p3847 N85-33827
ZONE REFINING
U ZONE MELTING
ZONES
U REGIONS
ZPR REACTORS
U ZERO POWER REACTORS

VOLUME 23 NUMBERS 1-6

Scientific and Technical Aerospace Reports

Abstracts January – March 1985

TABLE OF CONTENTS

STAR Issue	Page
1	1
2	133
3	307
4	451
5	591
6	747

VOLUME 23 NUMBERS 7-12

Scientific and Technical Aerospace Reports

Abstracts April – June 1985

TABLE OF CONTENTS

STAR Issue	Page
7	893
8	1063
9	1263
10	1419
11	1575
12	1769

VOLUME 23 NUMBERS 13-18

Scientific and Technical Aerospace Reports

Abstracts July – September 1985

TABLE OF CONTENTS

STAR Issue	Page
13	1965
14	2207
15	2457
16	2691
17	2891
18	3057



VOLUME 23 NUMBERS 19-24

Scientific and Technical Aerospace Reports

Abstracts October – December 1985

TABLE OF CONTENTS

STAR Issue	Page
19	3211
20	3387
21	3551
22	3727
23	3893
24	4059

☆U.S. GOVERNMENT PRINTING OFFICE: 1986—498—188 42457



FEDERAL DEPOSITORY LIBRARY PROGRAM

The Federal Depository Library Program provides Government publications to designated libraries throughout the United States. The Regional Depository Libraries listed below receive and retain at least one copy of nearly every Federal Government publication, either in printed or microfilm form, for use by the general public. These libraries provide reference services and inter-library loans; however, they are *not* sales outlets. You may wish to ask your local library to contact a Regional Depository to help you locate specific publications, or you may contact the Regional Depository yourself.

ARKANSAS STATE LIBRARY
One Capitol Mall
Little Rock, AR 72201
(501) 371-2326

AUBURN UNIV. AT MONTGOMERY LIBRARY
Documents Department
Montgomery, AL 36193
(205) 279-9110, ext. 253

UNIV. OF ALABAMA LIBRARY
Documents Dept.—Box S
University, AL 35486
(205) 348-7369

DEPT. OF LIBRARY, ARCHIVES AND PUBLIC RECORDS
Third Floor—State Cap.
1700 West Washington
Phoenix, AZ 85007
(602) 255-4121

UNIVERSITY OF ARIZONA LIB.
Government Documents Dept.
Tucson, AZ 85721
(602) 626-5233

CALIFORNIA STATE LIBRARY
Govt. Publications Section
P.O. Box 2037
Sacramento, CA 95809
(916) 322-4572

UNIV. OF COLORADO LIB.
Government Pub. Division
Campus Box 184
Boulder, CO 80309
(303) 492-8834

DENVER PUBLIC LIBRARY
Govt. Pub. Department
1357 Broadway
Denver, CO 80203
(303) 571-2131

CONNECTICUT STATE LIBRARY
Government Documents Unit
231 Capitol Avenue
Hartford, CT 06106
(203) 566-4971

UNIV. OF FLORIDA LIBRARIES
Library West
Documents Department
Gainesville, FL 32611
(904) 392-0367

UNIV. OF GEORGIA LIBRARIES
Government Reference Dept.
Athens, Ga 30602
(404) 542-8951

UNIV. OF HAWAII LIBRARY
Govt. Documents Collection
2550 The Mall
Honolulu, HI 96822
(808) 948-8230

UNIV. OF IDAHO LIBRARY
Documents Section
Moscow, ID 83843
(208) 885-6344

ILLINOIS STATE LIBRARY
Information Services Branch
Centennial Building
Springfield, IL 62706
(217) 782-5185

INDIANA STATE LIBRARY
Serials Documents Section
140 North Senate Avenue
Indianapolis, IN 46204
(317) 232-3686

UNIV. OF IOWA LIBRARIES
Govt. Documents Department
Iowa City, IA 52242
(319) 353-3318

UNIVERSITY OF KANSAS
Doc. Collect—Spencer Lib.
Lawrence, KS 66045
(913) 864-4662

UNIV. OF KENTUCKY LIBRARIES
Govt. Pub. Department
Lexington, KY 40506
(606) 257-3139

LOUISIANA STATE UNIVERSITY
Middleton Library
Govt. Docs. Dept.
Baton Rouge, LA 70803
(504) 388-2570

LOUISIANA TECHNICAL UNIV. LIBRARY
Documents Department
Ruston, LA 71272
(318) 257-4962

UNIVERSITY OF MAINE
Raymond H. Fogler Library
Tri-State Regional Documents Depository
Orono, ME 04469
(207) 581-1680

UNIVERSITY OF MARYLAND
McKeldin Lib.—Doc. Div.
College Park, MD 20742
(301) 454-3034

BOSTON PUBLIC LIBRARY
Government Docs. Dept.
Boston, MA 02117
(617) 536-5400 ext. 226

DETROIT PUBLIC LIBRARY
Sociology Department
5201 Woodward Avenue
Detroit, MI 48202
(313) 833-1409

MICHIGAN STATE LIBRARY
P.O. Box 30007
Lansing, MI 48909
(517) 373-0640

UNIVERSITY OF MINNESOTA
Government Pubs. Division
409 Wilson Library
309 19th Avenue South
Minneapolis, MN 55455
(612) 373-7813

UNIV. OF MISSISSIPPI LIB.
Documents Department
University, MS 38677
(601) 232-5857

UNIV. OF MONTANA
Mansfield Library
Documents Division
Missoula, MT 59812
(406) 243-6700

NEBRASKA LIBRARY COMM.
Federal Documents
1420 P Street
Lincoln, NE 68508
(402) 471-2045
In cooperation with University of Nebraska-Lincoln

UNIVERSITY OF NEVADA LIB.
Govt. Pub. Department
Reno, NV 89557
(702) 784-6579

NEWARK PUBLIC LIBRARY
5 Washington Street
Newark, NJ 07101
(201) 733-7812

UNIVERSITY OF NEW MEXICO
Zimmerman Library
Government Pub. Dept.
Albuquerque, NM 87131
(505) 277-5441

NEW MEXICO STATE LIBRARY
Reference Department
325 Don Gaspar Avenue
Santa Fe, NM 87501
(505) 827-2033, ext. 22

NEW YORK STATE LIBRARY
Empire State Plaza
Albany, NY 12230
(518) 474-5563

UNIVERSITY OF NORTH CAROLINA AT CHAPEL HILL
Wilson Library
BA/SS Documents Division
Chapel Hill, NC 27515
(919) 962-1321

UNIVERSITY OF NORTH DAKOTA
Chester Fritz Library
Documents Department
Grand Forks, ND 58202
(701) 777-2617, ext. 27
(In cooperation with North Dakota State Univ. Library)

STATE LIBRARY OF OHIO
Documents Department
65 South Front Street
Columbus, OH 43215
(614) 462-7051

OKLAHOMA DEPT. OF LIB.
Government Documents
200 NE 18th Street
Oklahoma City, OK 73105
(405) 521-2502

OKLAHOMA STATE UNIV. LIB.
Documents Department
Stillwater, OK 74078
(405) 624-6546

PORTLAND STATE UNIV. LIB.
Documents Department
P.O. Box 1151
Portland, OR 97207
(503) 229-3673

STATE LIBRARY OF PENN.
Government Pub. Section
P.O. Box 1601
Harrisburg, PA 17105
(717) 787-3752

TEXAS STATE LIBRARY
Public Services Department
P.O. Box 12927—Cap. Sta.
Austin, TX 78753
(512) 471-2996

TEXAS TECH UNIV. LIBRARY
Govt. Documents Department
Lubbock, TX 79409
(806) 742-2268

UTAH STATE UNIVERSITY
Merrill Library, U.M.C. 30
Logan, UT 84322
(801) 750-2682

UNIVERSITY OF VIRGINIA
Alderman Lib.—Public Doc.
Charlottesville, VA 22901
(804) 924-3133

WASHINGTON STATE LIBRARY
Documents Section
Olympia, WA 98504
(206) 753-4027

WEST VIRGINIA UNIV. LIB.
Documents Department
Morgantown, WV 26506
(304) 293-3640

MILWAUKEE PUBLIC LIBRARY
814 West Wisconsin Avenue
Milwaukee, WI 53233
(414) 278-3000

ST. HIST LIB. OF WISCONSIN
Government Pub. Section
816 State Street
Madison, WI 53706
(608) 262-4347

WYOMING STATE LIBRARY
Supreme Ct. & Library Bld.
Cheyenne, WY 82002
(307) 777-6344

National Aeronautics and
Space Administration
Code NIT-4
Washington, D.C.
20546

Official Business

Penalty for Private Use, $300

SPECIAL FOURTH-CLASS RATE
POSTAGE & FEES PAID
NASA
WASHINGTON, D.C.
PERMIT No. G 27

NASA

POSTMASTER: If Undeliverable (Section 158
Postal Manual) Do Not Return